

SYMPOSIUM BI01

Developing an Open Source Introductory Textbook for the Materials Community
November 30 - December 7, 2021

Symposium Organizers

Marc De Graef, Carnegie Mellon University
Kevin Jones, University of Florida
Amy Moll, Boise State University
Steven Yalisove, University of Michigan

* Invited Paper

SESSION BI01.01: Flexible Textbooks for the Materials Community I

Session Chair: Scott Beckman
Tuesday Morning, November 30, 2021
Sheraton, 2nd Floor, Grand Ballroom

10:30 AM *BI01.01.01

Materials Education and the Need for Modular, Flexible Textbooks M. Stanley Whittingham; Binghamton University, The State University of New York, United States

A challenge in teaching materials science is the rapid pace at which the field is changing and the different audiences that want educated. Two decades ago Binghamton planned an MS in MS&E that could be taken on-line with all the material on-line and could be taken at the student's pace. Today, there are continuous demands for a materials primer for advanced materials in the energy field, or for biomaterials. To satisfy those audiences an open-source textbook that could be readily modified and where modules could be plucked out to suit the audience level is needed. At Binghamton, we have begun such an effort in the areas of materials for energy storage and for electronics packaging. However, to achieve success a coordinated effort across several universities is necessary.

11:00 AM BI01.02.01

Spotlight Talk—Integrating Interactive Computing Experiences into Materials Science and Engineering Curricula Using Open-Source Jupyter Authoring Tools Enze Chen¹, Michelle H. Wilkerson¹ and Mark Asta^{1,2}; ¹University of California, Berkeley, United States; ²Lawrence Berkeley National Laboratory, United States

The ability for computational models and informatics techniques to rapidly provide scientific insights has led to their adoption across all areas of materials research, and there now exists tremendous opportunity to integrate these tools into materials science curricula [1]. However, even as advances in computing have made such tools accessible for teaching and learning, barriers to integration still exist partly due to the incoherent interface between research software (e.g., C++, Python, Julia) and curriculum design platforms (e.g., HTML, JavaScript, Microsoft Office). We show how the Jupyter Book platform [2] can be used to bridge this divide and create a digital textbook that synthesizes multiple sources of content, including rich computational narratives in Jupyter notebooks [3] that are widely used in the materials research community. The software is open source and the final textbook is accessible for not only readers, who engage with it dynamically in an internet browser or statically as a PDF, but also authors, who compile it directly from familiar file formats like Markdown and Jupyter notebooks.

We share our experience using Jupyter Book to design an open-source, introductory materials informatics curriculum [4] for a remote summer research internship at Lawrence Berkeley National Laboratory for UC Berkeley undergraduates in engineering. To accommodate their relative inexperience with programming and materials science, we support the Python programming exercises with prose, graphics, slides, polls, and discussion questions, all of which are seamlessly embedded into a common web interface as a digital textbook. In this way, the textbook is a one-stop-shop where the course information can be easily organized, accessed, and perused, which facilitates remote learning, user experience, and expansion to larger audiences. Most prominently, Jupyter Books have interactive programming capabilities, which we enable through the JupyterHub cloud infrastructure [5], that provide active learning opportunities in these digital spaces for students to interrogate the code, test their own hypotheses, and deepen their comprehension of the material. Through a combination of group-based exercises and self-directed research projects on data-driven design of photoactive materials, students are engaged in authentic learning experiences that demonstrate the broad utility of the Jupyter ecosystem in sustaining the growth of materials science education into new frontiers.

[1] Raúl A. Enrique, Mark Asta, and Katsuyo Thornton. "Computational materials science and engineering education: An updated survey of trends and needs," JOM, 70, 9, 2018, pp. 1644-1651.

[2] Executable Books Community. Jupyter Book, v0.10, 2020. Zenodo. DOI:10.5281/zenodo.4539666

[3] Thomas Kluyver et al. "Jupyter Notebooks - a publishing format for reproducible computational workflows," in Positioning and power in academic publishing: Players, agents and agendas (IOS Press, Netherlands), 2016, pp. 87-90.

[4] Enze Chen and Mark Asta. Introduction to Materials Informatics. 2021. Retrieved from <https://enze-chen.github.io/mi-book>

[5] Division of Computing, Data Science, and Society. DataHub. 2020. Retrieved from <https://datahub.berkeley.edu/>

11:05 AM BI01.02.02

Spotlight Talk—Interactive, Reactive, Web-Based Media for Sharing and Exploring Materials Knowledge [Michael Deagen](#) and Linda Schadler; University of Vermont, United States

An open-source digital textbook presents an opportunity to envision dynamic, model-based representations of materials knowledge unbounded by many of the limitations of traditional print media. With an emphasis on reactive computational notebooks that run in-browser, we discuss the ideation and development of supplementary modules, exercises, and other learning activities for students entering the field of materials science and engineering in the 21st century. Authors of these notebooks—which blend code, prose, and other digital media—can demonstrate foundational concepts with parameterized explanations that allow readers to actively delve into models through embedded interactive elements. By facilitating exploration of domain models through a combination of *enactive*, *iconic*, and *symbolic* representations (Bruner, 1966), these interactive environments promote the formation of robust mental models around a given topic. While platforms such as *Observable* illustrate the state-of-the-art, they embody a decades-long trend toward literate programming, computational essays, “explorations,” and other forms of dynamic expression with computational media. In addition to the pedagogical advantages of this approach with respect to reproducibility and modularity, we examine some of the practical considerations around managing scope, editorial quality, and maintenance of these notebooks.

SESSION BI01.02: Poster Session I
Tuesday Afternoon, November 30, 2021
8:00 PM - 10:00 PM
Hynes, Level 1, Hall B

BI01.02.01

Spotlight Talk—Integrating Interactive Computing Experiences into Materials Science and Engineering Curricula Using Open-Source Jupyter Authoring Tools [Enze Chen](#)¹, Michelle H. Wilkerson¹ and Mark Asta^{1,2}; ¹University of California, Berkeley, United States; ²Lawrence Berkeley National Laboratory, United States

The ability for computational models and informatics techniques to rapidly provide scientific insights has led to their adoption across all areas of materials research, and there now exists tremendous opportunity to integrate these tools into materials science curricula [1]. However, even as advances in computing have made such tools accessible for teaching and learning, barriers to integration still exist partly due to the incoherent interface between research software (e.g., C++, Python, Julia) and curriculum design platforms (e.g., HTML, JavaScript, Microsoft Office). We show how the Jupyter Book platform [2] can be used to bridge this divide and create a digital textbook that synthesizes multiple sources of content, including rich computational narratives in Jupyter notebooks [3] that are widely used in the materials research community. The software is open source and the final textbook is accessible for not only readers, who engage with it dynamically in an internet browser or statically as a PDF, but also authors, who compile it directly from familiar file formats like Markdown and Jupyter notebooks.

We share our experience using Jupyter Book to design an open-source, introductory materials informatics curriculum [4] for a remote summer research internship at Lawrence Berkeley National Laboratory for UC Berkeley undergraduates in engineering. To accommodate their relative inexperience with programming and materials science, we support the Python programming exercises with prose, graphics, slides, polls, and discussion questions, all of which are seamlessly embedded into a common web interface as a digital textbook. In this way, the textbook is a one-stop-shop where the course information can be easily organized, accessed, and perused, which facilitates remote learning, user experience, and expansion to larger audiences. Most prominently, Jupyter Books have interactive programming capabilities, which we enable through the JupyterHub cloud infrastructure [5], that provide active learning opportunities in these digital spaces for students to interrogate the code, test their own hypotheses, and deepen their comprehension of the material. Through a combination of group-based exercises and self-directed research projects on data-driven design of photoactive materials, students are engaged in authentic learning experiences that demonstrate the broad utility of the Jupyter ecosystem in sustaining the growth of materials science education into new frontiers.

[1] Raúl A. Enrique, Mark Asta, and Katsuyo Thornton. “Computational materials science and engineering education: An updated survey of trends and needs,” JOM, 70, 9, 2018, pp. 1644–1651.

[2] Executable Books Community. Jupyter Book, v0.10, 2020. Zenodo. DOI:10.5281/zenodo.4539666

[3] Thomas Kluyver et al. “Jupyter Notebooks - a publishing format for reproducible computational workflows,” in Positioning and power in academic publishing: Players, agents and agendas (IOS Press, Netherlands), 2016, pp. 87–90.

[4] Enze Chen and Mark Asta. Introduction to Materials Informatics. 2021. Retrieved from <https://enze-chen.github.io/mi-book>

[5] Division of Computing, Data Science, and Society. DataHub. 2020. Retrieved from <https://datahub.berkeley.edu/>

BI01.02.02

Spotlight Talk—Interactive, Reactive, Web-Based Media for Sharing and Exploring Materials Knowledge [Michael Deagen](#) and Linda Schadler; University of Vermont, United States

An open-source digital textbook presents an opportunity to envision dynamic, model-based representations of materials knowledge unbounded by many of the limitations of traditional print media. With an emphasis on reactive computational notebooks that run in-browser, we discuss the ideation and development of supplementary modules, exercises, and other learning activities for students entering the field of materials science and engineering in the 21st century. Authors of these notebooks—which blend code, prose, and other digital media—can demonstrate foundational concepts with parameterized explanations that allow readers to actively delve into models through embedded interactive elements. By facilitating exploration of domain models through a combination of *enactive*, *iconic*, and *symbolic* representations (Bruner, 1966), these interactive environments promote the formation of robust mental models around a given topic. While platforms such as *Observable* illustrate the state-of-the-art, they embody a decades-long trend toward literate programming, computational essays, “explorations,” and other forms of dynamic expression with computational media. In addition to the pedagogical advantages of this approach with respect to reproducibility and modularity, we examine some of the practical considerations around managing scope, editorial quality, and maintenance of these notebooks.

BI01.02.03

Functional Materials—Electronic, Magnetic, Optic, Thermal and Elastic [Scott Beckman](#); Washington State University, United States

The purpose of this session is to discuss the administrative and academic details needed to coordinate writing a chapter addressing functional materials,

which may include the electronic, magnetic, optic, thermal, and elastic properties and their cross-interactions. Our goal is to organize a working group that can engage in the writing and editing of content and create a rough outline for the chapter that will guide the development of content.

BI01.02.04

Teaching Materials Science Concepts Using a Web-Based Force-Directed Graph Framework [George Varnavides](#), Amina Matt and W. C. Carter; Massachusetts Institute of Technology, United States

Recent developments in just-in-time compilers for dynamic languages have significantly improved the performance of web-based physics engines. Combined with the prevalence of interactive visualizations and the level of maturity of Document Object Model (DOM) manipulation libraries¹, this provides a unique opportunity to leverage such client-side physics engines for education. Force-directed graph layouts describe a broad class of algorithms which attempt to visualize the relationships between nodes in undirected graphs and hierarchical trees, via means of a physical simulation^{2,3}. Such graph layouts have recently enjoyed increased popularity in the domain of information visualization, given the rise of interactive visualizations and advancements in just-in-time compilers for Javascript⁴.

In this talk, we explore the use of physical simulations interactively on the client-side in the context of undergraduate education. We present an extension module to a popular open-source force-directed graph layout library which uses energy-conserving velocity Verlet integration to teach materials science concepts based on the Lennard Jones interatomic potential⁵. We find the ability to seamlessly integrate our numerical integrator with interaction techniques familiar to users, such as clicking, dragging, and brushing to improve the pedagogy of the simulations. The interactive exposition is deployed using a reactive notebook environment, which effectively intertwines textual explanations with multiple interactive visualizations⁶.

¹ M. Bostock, V. Ogievetsky, and J. Heer, IEEE (Proc. InfoVis) 2011

² W.T. Tutte Proc London Math Soc. s3-13(1) 1963

³ P. Eades Congressus Numerantium 42:149-160 1984

⁴ B. Hackett and S. Guo Sigplan Not. 47(6):239-250 2012

⁵ <https://www.npmjs.com/package/d3-force-md>

⁶ <https://observablehq.com/@gvarnavi/teaching-materials-science-concepts-using-the-d3-force>

BI01.02.08

Materials—A More Central Science [Ilija Rasovic](#); University of Birmingham, United Kingdom

Chemistry has long rested on its laurels as “the central science”: the fulcrum about which all scientific endeavours pivot. Yet this view is based on the (arguably outdated) delineation of long-established traditional scientific disciplines and their associated *epistemological* hierarchy. This is limiting, for it doesn’t take into account the *technological* dimension of scientific research (not to mention the final element of the Aristotelian triumvirate: *phronesis*). Were we to do so, I contend that Materials Science and Engineering (MSE) would be a more viable candidate for “the central science”. This is not only important for raising the profile of the subject, but also for shaping what should be included in an undergraduate introductory text.

MSE, as a formalised subject with dedicated university departments, is a young discipline. It emerged out of the chaos of the Second World War to become the primary innovation and technology driver, with the recognition that the material realisation of advanced scientific, technological and, indeed, societal visions could not be achieved without dedicated research on understanding materials themselves. This understanding fundamentally boils down to the relationship between processing, structure and properties. As such, the subject inherently demands an intimate relationship with a vast array of characterisation techniques. It covers a huge range of length scales and spans all technology readiness levels. It is this explicit link between fundamental scientific understanding (*episteme*) and technological implementation (*techne*)—and the complete embedding of the subject in the tangible, physical, *material* world—that sets MSE apart from all other physical sciences.

This research endeavour unified scientists and engineers from across disciplines—physics; chemistry; mineralogy; chemical, mechanical and electrical engineering—giving rise to a highly interdisciplinary field that continues to this day to sprawl across boundaries. Indeed, it now defines itself adjacent to a plethora of even more diverse disciplines—computer science, medicine, the life sciences, sustainability, conservation, archaeology, and more—and its methodologies are propelling the establishment of a crucial new discipline in its own right: nanoscience and nanotechnology.

None of the above is news to an audience of materials science researchers and academic staff. But it would be remiss to assume that undergraduates had such a holistic overview and appreciation of the centrality of MSE in the networks of modern scientific research and contemporary human existence. This is especially true when considering audiences such as first-generation students and those majoring in other disciplines but who might require knowledge of some aspect of MSE. I anticipate that such knowledge would help *all* students to understand better their chosen subject and succeed in their MSE education. As such, I would like to take this opportunity to provoke discussion around how an open-access introductory undergraduate textbook can best incorporate such insights. I will offer some initial thoughts on how this might be achieved through, for example, the structure and content of the text, as well as embedding examples and problems.

SESSION BI01.03: Morning Session—Flexible Textbooks for the Materials Community II/Panel Discussion, Needs and Best Practices

Session Chairs: Kevin Jones and Steven Yaliso

Tuesday Morning, December 7, 2021

BI01-Virtual

8:30 AM *BI01.03.01

Materials Education and the Need for Modular, Flexible Textbooks [M. Stanley Whittingham](#); Binghamton University, The State University of New York, United States

A challenge in teaching materials science is the rapid pace at which the field is changing and the different audiences that want educated. Two decades ago Binghamton planned an MS in MS&E that could be taken on-line with all the material on-line and could be taken at the student’s pace. Today, there are continuous demands for a materials primer for advanced materials in the energy field, or for biomaterials. To satisfy those audiences an open-source textbook that could be readily modified and where modules could be plucked out to suit the audience level is needed. At Binghamton, we have begun such an effort in the areas of materials for energy storage and for electronics packaging. However, to achieve success a coordinated effort across several

universities is necessary.

9:00 AM *BI01.03.02

Vision Panel Discussion Amy Moll¹, Marc De Graef², Kevin Jones³ and Steven M. Yalisove⁴; ¹Boise State University, United States; ²Carnegie Mellon University, United States; ³University of Florida, United States; ⁴University of Michigan, United States

Vision Panel Discussion

9:30 AM *BI01.04.01

University Materials Council: MSE Department Chairs' Perspective on Open Source Test Book Amit Misra; University of Michigan—Ann Arbor, United States

Not available.

9:50 AM *BI01.04.02

Open Source Presentation of Topics in Electronic Properties of Materials and Their Applications Angus Rockett; Colorado School of Mines, United States

A key element of materials is their electronic properties. However, this topic is rarely covered in detail in conventional introductory materials textbooks and there is a general lack of good coverage even in more advanced books. The topic as covered in Materials departments but without good textbook support includes the following: fundamental concepts in electronic structure, conduction (electricity, light, heat, ions, superconductivity, etc), magnetism and magnetic properties, dielectric properties, and semiconductors. These should be accompanied by applications of each of these concepts. A particular advantage of an open source textbook is that additional background can be added as needed. This is particularly important to the topic of electronic properties as it relies significantly on physics and chemistry concepts.

10:10 AM BREAK

10:30 AM *BI01.04.03

Filling the Capability Gap in Materials, Processing and Manufacturing Glenn Daehn; The Ohio State University, United States

Critical issues of supply chain, sustainability and jobs are all directly tied to the United States' ability to manufacture what it needs and uses. Its widely recognized that even if through economic means like tariffs and taxes US-based manufacturing were completely competitive with overseas manufacturing, the US does not have the talent needed to rapidly ramp up manufacturing. The inability to execute an effective manufacturing policy have led to a shortage of essential workers in welding, machining, equipment maintenance and installation, leading to bottlenecks in new technology deployment and innovation in the US. Multiple studies and technical society initiatives have focused on this problem, but with only modest success.

There are bright spots that we will focus on. The ASM Materials Education Foundation has successfully provided professional development to K-12 teachers at scale, leading to many new materials courses in high schools, and the broader problem is well understood. I will issue a call to action to bring together the stakeholders, largely through the technical societies to coordinate on one roadmap and use collective action to plow through the roadblocks.

10:50 AM *BI01.04.05

Growing Materials Science in Africa Samuel Chigome; Botswana Institute for Technology Research and Innovation, Botswana

Africa is the world's second largest and second most populous continent in the world. Generally, it has a rich concentration of a wide range of natural resources such as oil, copper, diamonds, bauxite, lithium, gold, graphite, iron ore, coal, hardwood forests, tropical fruits among others. It is estimated that 30% of the earth's mineral resources are found in Africa. However, there is underutilization of the resources partly because materials science has not been embraced effectively across the continent. This is evidenced by the fact that there some countries that do not have materials science programmes at any of their Universities.

The presentation will give an overview of the status of materials science in Africa, the efforts of the African Materials Research Society to close the materials science development gaps and the need for open access to materials science literature.

11:10 AM *BI01.04.06

Open Course Material Development, Distribution, and Usage Anthony Palmiotto; Rice University, United States

Not available.

11:30 AM *BI01.04.07

Recap - All Speakers Steven M. Yalisove; University of Michigan, United States

A recap of the day including a chance for Q&A with the Speakers.

SESSION BI01.05: Afternoon Session—Working Groups, Working Groups Breakout Rooms and Logistics, Version Control and Server Needs
Session Chairs: Kevin Jones and Amy Moll
Tuesday Afternoon, December 7, 2021
BI01-Virtual

1:30 PM *BI01.05.01

Taking a Scientific Approach to Science Education Carl Wieman; Stanford University, United States

Not available.

2:00 PM *BI01.05.02**Working Groups Fundamentals** [Anton Van der Ven](#); University of California, Santa Barbara, United States

An overview of what will be done in the five Working Groups:

Math and Computation—[Michael Falk](#)Inorganic Functional Materials and Electronic Properties—[Scott Beckman](#)Structural Materials and Mechanical Properties—[Amy Clark](#)Organic Functional Materials—[Dave Martin](#)Characterization—[Marc DeGraef](#)**3:00 PM BREAK****3:15 PM *BI01.05.03****Working Groups Breakout Rooms Math and Computation—[Michael Falk](#) Inorganic Functional Materials and Electronic Properties—[Scott Beckman](#) Structural Materials and Mechanical Properties—[Amy Clark](#) Organic Functional Materials—[Dave Martin](#) Characterization—[Marc DeGraef](#)** [Michael L. Falk](#)¹, [Scott Beckman](#)², [David Martin](#)³, [Amy Clarke](#)⁴ and [Marc De Graef](#)⁵; ¹Johns Hopkins University, United States; ²Washington State University, United States; ³University of Delaware, United States; ⁴Colorado School of Mines, United States; ⁵Carnegie Mellon University, United States

Not available.

4:15 PM BREAK**4:30 PM BI01.06.01****Approaches for Data Management and Version Control in Materials Science** [Marcus D. Hanwell](#); Brookhaven National Laboratory, United States

Research in materials science in the modern age involves far more data and software code than ever before. This makes it ever more important that researchers in materials science develop a good grasp of approaches for data management for their data and version control for their software code, scripts and other artifacts. There are also circumstances where data itself may need to be version controlled which presents unique challenges, along with the challenges of expressing the interplay between data and the software code/scripts used to analyze it.

An overview of some of the existing approaches to data management will be presented, along with discussions of the use of metadata, data, and programming interfaces that can be used to expose these things to the wider world. Approaches for small, medium and large data will be discussed including how data management approaches can document the links between raw data, reduced data and analyzed/derived data. The use of licenses to encourage sharing will be discussed along with the pros and cons of different licensing schemes.

Approaches to version control will look at pragmatic approaches to version control using mainstream version control projects, command-line, graphical interfaces and some embedded integrations in code editors. The interplay of version control and data along with some practical advice on different approaches there, along with the importance of licensing, documentation, and using standard development practices. Some discussion of licensing, distribution, archiving and the generation of digital object identifiers and similar using integrations with platforms/minting of identifiers to increase the citability of data and code.

Organizations to encourage better data management are an important component of the community, along with those that encourage better coding practices in the sciences and alternative career paths to better address these areas. It is important to consider how the community can better scope proposals and projects in order to fully cover not only the capital equipment costs, but also the data management and software/coding requirements to fully support instruments/projects is an important emerging area.

4:50 PM *BI01.06.02**OpenChapters—How an Open Source Textbook Might Work** [Marc De Graef](#); Carnegie Mellon University, United States

Not available.

5:10 PM *BI01.06.03**Recap—All Speakers** [Steven M. Yalisove](#); University of Michigan, United States

A group discussion with the speakers of the session.

SESSION BI01.07: Poster Session II
Session Chairs: [Amy Moll](#) and [Steven Yalisove](#)
Tuesday Afternoon, December 7, 2021
BI01-Virtual

9:00 PM BI01.07.01**Materials Science—Who Cares? Why Should You?** [Mark Atwater](#); Liberty University, United States

I had no plan to be a materials science educator and researcher. It was only after seeing, experiencing, and applying the concepts that I even became interested. Too often we assume others have the natural inclinations we have to study and be motivated by the fundamentals of materials, and we under emphasize the reasons we became interested and still are. As an educator in manufacturing, mechanical, and materials engineering, I have sought to incorporate the principles of materials science within broader contexts so that there is reason for each of my students to care. Distilling concepts to ensure the weakest student understands and highlighting current research to give the strongest student opportunity for growth is a difficult but valuable approach

to presenting such a diverse topic. This presentation has three suggestions for future materials education: 1) It should be relatable, 2) it should be unique, and 3) it should accommodate both the student and professor. The basis for these aspects comes from my own experience writing an introductory materials and manufacturing textbook including more than 500 figures of original artwork and photography. I will share the struggles and successes I encountered along the way, and how that may help shape open-source materials education initiatives.

9:05 PM BI01.07.02

A Text Book on Materials Degradation on Earth and Outer Space Kalathur S. Santhanam; Rochester Institute of Technology, United States

The development of innumerable number of technologies of the twenty first century is based on the knowledge generated through the subject of Materials Science and Engineering, paving the way for our comfortable living. The materials are classified into the following categories. a) Metals b) Ceramics c) Polymers and d) Composites. A number of books (1-4) have been written on these materials for teaching undergraduate and graduate level courses. Our understanding of their behavior has been increasing over the years by constant research activities; this has resulted in the discovery and development of nanomaterials. The planned text book is an e-book with power point illustrations with vocal lectures. The book addresses a basic question on the stability of the materials; do they remain in the same virgin state over a long period of time or degrade with time. If they do not remain in virgin state, what are the causes for the change and how to overcome this problem. Our curiosity has driven us to explore interstellar planets which requires utilization of the above mentioned materials driving us to understand the behavior of materials in different atmospheric conditions. Will their behavior on our planet (earth) different from outer interstellar space due to the presence of meteorites and high energy radiation such as X-rays, g-rays and ultraviolet rays. On earth, we have besides moisture, atmospheric gases like oxygen, nitrogen and carbon dioxide and sunlight that are free from high energy radiation except for small quantities of ultra violet, visible and infra red radiations. In addition, there is hydrodynamical and mechanical effects that would be imposed on the materials. With metals, there has been well focused degradation processes (3,4) that are based on electrochemical theories providing solutions to greater stability of metals. Today, we have durable materials starting from microelectronics chips to large scale industrial processes for the betterment of humanity. Polymers fall into a different class and the degradation occurs by a) swelling and distortion b) bond rupture caused by radiation/chemical/thermal processes c) weathering d) mechanical oxidation and e) biodegradation. The mechanism of degradation is complex and contrasts metals and ceramics. The composites provide unique answers to many of the problems faced with metals and polymers; here composites with nanomaterials appear to offer distinctive advantages (5). Overall, the text book amalgamates the behavior of materials on earth and in outer space, in a combined fashion to bring the relative merits of the earth and outer space.

1. W.D. Callister Jr., D.G. Rethwisch, Materials Science and Engineering: An Introduction, Wiley PLUS, 10th Edition, 2018; ISBN-13: 978-1119721772.
2. Donald R. Askeland (Author), Wendelin J. Wright, The Science and Engineering of Materials, 7th Edition, CENGAGE learning, 2015.
3. M.G. Fontana, Corrosion Engineering, 3Ed, Mc Graw Hill India, (2005); ISBN-13 978-0070607446
4. R.W. Revie and H.H. Uhling, Corrosion and Corrosion Control, John Wiley and sons, 2008; ISBN 978-0-471-73279-2
5. Book review: K.S.V. Santhanam, "Graphene: Preparations, Properties, Applications, and Prospects Kazuyuki Takai, Seiya Tsujimura, Feiyu Kang, and Michio Inagaki Elsevier, 2019,." Rev. of Graphene, by Kazuyuki Takai, Seiya Tsujimura, Feiyu Kang, and Michio Inagaki. Materials Research Society Bulletin, 15 Oct. 2020

9:10 PM BI01.07.03

Late News: Incorporating nanoHUB's Free Simulation Apps for Materials Science Education into an Open Source Online Textbook Tanya A. Falten and Alejandro Strachan; Purdue University, United States

Simulation plays a valuable role in engineering education, allowing students to explore phenomena and gain a greater comprehension of physical systems. Cloud-based simulation can also level the playing field by making powerful simulation tools available to students across a variety of institutions. nanoHUB provides free access to a wide range of simulation tools and computational resources that can be accessed online by users from around the world. Via easy-to-use nanoHUB apps, computational scientists can put powerful scientific software in the hands of instructors and students. This frictionless access lowers access barriers and accelerates innovation. Importantly, nanoHUB apps can be accessed via a standard web-browser and run in the cloud, so no downloading or installation of software for classroom use is required. With recent developments, nanoHUB apps can now be consumed as a web-service and be seamlessly incorporated into online courses and textbooks.

While many powerful, research-grade computational engines such as LAMMPS, OOF2 and Quantum Espresso are installed and available in nanoHUB, they are made accessible to a wide range of users, from beginner to advanced, through apps that are designed with interactive graphical user interfaces. Students can select input parameters and generate engaging images, atomic-level visualizations, graphs, trajectories, animations, and other types of data to explore and analyze, and thus engage more interactively in their learning. There are nanoHUB apps designed to explore a wide range of materials science topics, including, but not limited to: bonding, crystal and electronic structure, polymer structures, tensile testing, dislocations, plastic deformation, crack propagation, thermal transport, phase transformations, phase diagrams, microstructural analysis, optical properties, and magnetic properties. nanoHUB provides instructor-friendly features such as the ability to share a simulation session with an entire class, or smaller groups within a class, and assign control of the shared simulation to any student. Caching of simulation runs allows the rapid retrieval of simulation results if a specific set of inputs has previously been run, significantly reducing the time required. Jupyter notebooks in nanoHUB come with a wide range of libraries and packages to provide a powerful platform for interactive computing. These tools have been used to deploy learning modules in data science and machine learning in the field of materials.

This presentation will demonstrate some of the interactive nanoHUB apps that have been used to teach materials science skills and concepts, illustrate nanoHUB features that are beneficial for the classroom use of simulation apps, and show how nanoHUB apps can be incorporated into an online electronic materials science textbook.

9:15 PM BI01.07.04

Teaching Basic Crystallography and Diffraction Using Open Access Structure Visualization Software Matt Beekman; California Polytechnic State University, United States

The understanding of basic concepts in crystallography and diffraction is foundational for the study of solid-state physics, chemistry, and materials science. In this talk, I will describe how open access structure visualization software, such as VESTA (<https://jp-minerals.org/vesta/en/>), can be used to help make learning the fundamentals of crystallography and X-ray diffraction active, engaging, and effective. The ability for 3D visualization of crystal structures, bonding, lattice planes, and simulation of powder X-ray diffraction patterns in a single software package allows students to discover and explore important concepts such as Bragg's law, symmetry, Miller indices, systematic absences, and the relation between the location and type of atoms in the unit cell influence and relative intensity in the diffraction pattern. Learning modules using such open access software give students familiarity with tools that are also used in authentic research and could be readily integrated with an open access introductory textbook.

9:25 PM ADDITIONAL POSTER PRESENTATION RECORDING

SYMPOSIUM BI02

Women in Materials Science—Pioneers and a Vision for a More Inclusive Future
November 30 - December 7, 2021

Symposium Organizers

Raffaella Buonsanti, Ecole Polytechnique Federale de Lausanne
Betar Gallant, Massachusetts Institute of Technology
Jennifer Hollingsworth, Los Alamos National Laboratory
Fang Liu, University of California, Los Angeles

Symposium Support

Silver

Science Advances | AAAS

Bronze

APL Materials | AIP Publishing

* Invited Paper

SESSION BI02.01: Women in Materials Science I

Session Chair: Jennifer Hollingsworth

Tuesday Morning, November 30, 2021

Hynes, Level 1, Room 107

10:30 AM *BI02.01.01

The Importance of Being a "Bad Scientist"—Towards a More Inclusive Future for Women in Materials Science [Julia R. Greer](#)^{1,2}; ¹California Institute of Technology, United States; ²Kavli Nanoscience Institute, United States

I am a Professor of Mat Sci, Mechanics, and Medical Engineering at Caltech, and apparently I am a bad scientist. At least that's what my advisor told me when I was a Master's student at Stanford. Is there anything you are bad at? Because it turns out that sometimes being told that you are bad at something can make you excel at that very thing. I finished my Ph.D. degree at Stanford and spent a couple of years working at Intel, after which I had decided that if I were a bad scientist, at the very least I should be one with a Ph.D. I was lucky enough to become a Ph.D. student at Stanford in a research group of Prof. William D. Nix, affectionately known as "the Boss." At that time, Stanford's Materials Science department did not have a single woman faculty member. Together with the Boss we discovered that tiny little crystals of common metals – like gold, copper, and nickel, which we know to be quite malleable – become exceptionally strong when their dimensions are reduced to ~ 200nm, or ~1000th of your hair diameter. We coined this phenomenon a "smaller is stronger" size effect. Working with Bill Nix had a tremendous impact on my life; to this day, he is quite possibly the most influential person in my professional career – he saw me transform from being a young "bad scientist" into a decent thinker. Most importantly, he believed in me, as he did in all of his graduate students, many of whom were women. And we rose to the occasion.

At the end of my third year in graduate school, I did everything backwards: I first had two faculty interviews for professorships at Caltech and MIT, I then interviewed for a post-doc, and finally defended my Ph.D. dissertation on May 16, 2005.

I built my professorial career at Caltech in Materials Science "option" (in the Division of Engineering and Applied Sciences) to study all things nano (materials and architectures) – much because of our discovery during my Ph.D. that materials behave differently at nano-scale. In the back of my mind, I had always wondered if there was a way to somehow harness these unique properties offered by nanomaterials and proliferate them onto larger scale so that we can have materials that behave as though they were nanomaterials but they look like our regular, macroscopic objects.

Fast forward a decade – I am now an endowed, chaired professor at Caltech, having accumulated multiple national and international recognitions and awards. I run a research group with 20+ incredibly smart, talented, and motivated Ph.D. students, undergraduate students, and post-docs. In the course of my career, have graduated 29 Ph.D. students, 7 of whom are tenure-track professors at US universities (not counting post-docs). And what gets me going every morning is that I know that my work, in part, that in the world where our children will live there will be no need for hearing aids because we will be able to synthetically "write" the cochlear bone directly into the ear, where the batteries their iPhone 83's will be able to hold charge for a year without needing re-charging, where balloons will not have to be filled up with He or any other gas but instead will be evacuated to make vacuum balloons, and where chocolate will have 100% taste, 99.9% air, and 0.01% calories. My success comes *from* being a woman, not *in spite* of being a woman. One of my key missions in life is to inspire as many young women to pursue a career in science, and especially in materials science, through mentoring, encouragement, and passing on the legacy of Bill Nix.

11:00 AM *BI02.01.02

Perspectives on a Career in Electrochemistry and Hydrogen—Translating R&D into Commercial Products [Katherine Ayers](#); Nel Hydrogen, United

States

To reach global sustainability goals, renewable sources of hydrogen are urgently needed. Regardless of the debate over various electrochemical energy solutions and the end mix for the electrical and transportation sectors, even decarbonizing many existing chemical manufacturing processes is a large challenge directly related to existing hydrogen generation. Most industrially produced hydrogen is used for manufacturing chemicals such as ammonia, methanol, ethylene, and other hydrocarbons, and this hydrogen currently comes from fossil sources. Any effort to convert this industrial hydrogen stream to a fully renewable resource at scale will involve significant deployment of existing commercial technologies in the near term (5-10 years), while emerging technologies may play a larger role in the future.

Both liquid alkaline and proton exchange membrane-based electrolyzers have been scaled to multi-megawatt systems and are growing business segments. Both also have continued room for cost reduction and efficiency improvements, especially the PEM technology. However, fundamental understanding and process development are required to get to the targets. While most of the cell stack materials in fuel cells have been optimized for the application, electrolyzers still largely adapt existing materials for hydrogen generation. In addition, significant work has been done in developing roll to roll manufacturing methods and related quality control for PEM fuel cells, which has not yet been translated to electrolysis. Much of the learning from fuel cells can be leveraged, but needs to be applied to electrolyzer specific requirements and materials.

Collaborations will be a major element in this transition. At this stage of development, close interaction between the supply chain, electrolyzer manufacturers, and project developers all contribute to advancing towards the needed cost and performance levels. Fundamental research conducted by academia and National Labs also play a critical role. Leveraging contacts and networks built over several years in electrochemical technologies helps to bring these partners together. As a female in the field, understanding partners that value diversity and teamwork is an especially important part of this network building.

Major areas of research and development for PEM electrolysis include the polymer membrane, catalyst thrifting, automated component fabrication and assembly, and porous transport layer development. In this talk, some historical perspective on development of alkaline and PEM electrolysis will be described, with details presented on paths forward, especially in the PEM systems. Career experiences in the electrochemistry field including how to manage obstacles and opportunities from the perspective of a female scientist will also be discussed.

SESSION BI02.02: Women in Materials Science II

Session Chair: Betar Gallant

Tuesday Afternoon, November 30, 2021

Hynes, Level 1, Room 107

1:30 PM *BI02.02.01

Superprotonic Solid Acids for Sustainable Energy Technologies [Sossina M. Haile](#); Northwestern University, United States

The compound CsH_2PO_4 (cesium dihydrogen phosphate) has emerged as a viable electrolyte for intermediate temperature electrochemical cells, devices for interconversion between electricity and value-added chemical compounds. Cesium dihydrogen phosphate is a member of the general class of materials known as solid acids or acid salts, in which polyanion groups are linked together via hydrogen bonds and monoatomic cations provide overall charge balance. Several such solid acids display a superprotonic transition, at which the material transforms to a high conductivity phase with a high degree of polyanion rotational disorder. At the transition the conductivity jumps by as much as 5 orders of magnitude and the activation energy for proton transport drops to 0.35 eV or less. In the case of CsH_2PO_4 the transition occurs at 228 °C and the conductivity reaches $\sim 10^{-2}$ S/cm at 240 °C, enabling electrochemical device operation at temperatures between 230 and 260 °C. The physical characteristics of CsH_2PO_4 imply a number of realized and potential advantages for their application in fuel cells, electrolyzers, and electrochemical hydrogen pumps relative to polymer, solid oxide, and liquid electrolyte alternatives. We present here an overview of the transport characteristics of superprotonic solid acids and the current status of electrochemical technologies based on these electrolytes.

2:00 PM *BI02.02.02

Becoming WISE—Women In Science and Engineering [Y. Shirley Meng](#); University of California, San Diego, United States

I will share my personal perspective on the challenge and joy of being a woman in science and engineering. High energy long life rechargeable battery is considered as key enabling technology for deep de-carbonization. Energy storage in the electrochemical form is attractive because of its high efficiency and fast response time. Besides the technological importance, electrochemical devices also provide a unique platform for fundamental and applied materials research since *ion* movement is often accompanied by inherent complex phenomena related to phase changes, electronic structure changes and defect generation. In this seminar, I will discuss a few new perspectives for energy storage materials including new fast ion conductors, new intercalation compounds and their interfacial engineering. With recent advances in characterization tools and computational methods, we are able to explore ionic mobility, charge transfer and phase transformations in electrode materials *in-operando*, and map out the structure-properties relations in functional materials for next generation energy storage and conversion. Moreover, I will discuss a few future priority research directions for electrochemical energy storage.

2:30 PM *BI02.02.03

Nucleating a New Culture in STEM [Debra R. Rolison](#); U.S. Naval Research Laboratory, United States

The research-intensive STEM (science/technology/engineering/math) environment—for all its renowned innovation and productivity—has only glacially incorporated the STEM talent endemic to humankind. And science really is too important to be left just to men [1]. Besides, we have never run the control experiment to assess just how well science and society will be served by inclusion, retention, and celebration of the STEM talent endemic to humankind. In short: we need a better culture. We have four mechanistic levers to work the problem: Revolution (such as when I proposed Title IX assessments of STEM departments in 2000 [2,3] and the General Accountability Office agreed in 2004); Subversion (always in fashion); Climate Change (creating a human-centric, innovative microclimate); and Market Forces (steering the talent and the funds to healthy, productive microclimates). Our team at the U.S. Naval Research Laboratory* has created such a microclimate. A key component of our success (recognized by awards and eager collaborators) is inclusion of full-time undergraduate researchers who step away from campus to spend six-to-twelve months working with a scrum (because we love disordered materials) of Ph.D. staff and postdoctoral associates on frontier research in nanomaterials, energy storage and conversion, catalysis, and chemical threat

mitigation. And we have great fun doing so.

* Rolison heads the Advanced Electrochemical Materials Section at the U.S. Naval Research Laboratory (NRL). The views are those of the author and are not necessarily those of the NRL or the U. S. Department of Defense.

[1] D.R. Rolison in L.D. Madsen: *Successful Women Ceramic and Glass Scientists and Engineers: 100 Inspirational Profiles*, Wiley (2016), pp. 467–472.

[2] D.R. Rolison, *C&EN* **2000**, 78(11), 5 (13 March).

[3] D.R. Rolison, “A ‘Title IX’ challenge to academic chemistry... or... Isn’t a millennium of affirmative action for white men sufficient??” in *Women in the Chemical Workforce*, National Academy Press (2000), Ch. 6, pp. 74–88.

3:00 PM *BI02.02.04

Understanding Dynamics at Solid-Solid and Solid-Liquid Interfaces for Separations and Energy Storage [Kelsey B. Hatzell](#); Princeton University, United States

Understanding transport mechanisms in geometrically confined layered conducting inorganic membranes and solid electrolytes is paramount for next generation batteries and separation application. Ion transport is widely studied in an array of applications from batteries, to colloid science, to biological applications, and separations. Each of these applications rely on ion mobility in confined regions where the pore sizes are comparable to the Debye screening length. At these dimensions, biophysicists have observed efficient transport and selectivity mechanisms. Yet, it is still not understood how water and ions move in structural domains between 1-10 nm. Electrically tunable solid-state nanochannels may offer additional pathways for tailoring transport and controlling fundamental interactions that govern separations processes (desolvation, adsorption, selectivity, etc.). This talk intends to describe the role long-range microstructural (tortuosity, constriction, etc.) and short-range (electric double layer, confined water) structural properties impact transport in solid electrolytes and separation membranes. To accomplish this goal, this talk will discuss a range of non-equilibrium techniques (spectroscopy, imaging, etc.) to probe solid/liquid and solid-solid interfaces in order to directly observe water and ion transport processes. The talk will also give a broader lens on women in engineering and tools to finding your community.

3:30 PM BREAK

SESSION BI02.03: Women in Materials Science III

Session Chair: Fang Liu

Tuesday Afternoon, November 30, 2021

Hynes, Level 1, Room 107

4:00 PM *BI02.03.01

Microwave Sintering Faux Moondust for NASA [Holly Shulman](#)^{1,2}; ¹Alfred University, United States; ²DrHollyShulman, LLC, United States

For the symposium subject of "Women in Materials Science", my experiences as a scientist contracting with NASA may be of interest. My first interaction with NASA was through my previous company, Ceralink Inc., in 2010. I founded Ceralink in 2000 to provide feasibility and scale up studies for energy saving processes, including the use of microwave energy. Ceralink demonstrated feasibility of microwave sintering for lunar and Martian regolith sintering through SBIR grants (Small Business Innovative Research). Ceralink's work resulted in the largest dense samples of microwave sintered lunar simulant (JSC-1A) to date. NASA is moving forward with construction on the moon and invited me to define a scope of work to lead the Microwave Sintering team. In my current role as a Professor of Ceramic Engineering at Alfred University, I am engaging undergraduate and graduate engineering students in this mission. This includes the development of synthetic lunar minerals, as well as process design for energy efficient and uniform microwave heating. I would be delighted to share some stories of getting out of my own way, accepting my position as a world expert in microwave and materials and interactions, and getting comfortable with how much I don't know and don't have to know to still be a valuable member of an amazing NASA team.

4:30 PM BI02.03.02

A Sustainable Future for Materials Science and Engineering—Enabling Scalable Manufacturing of Polymer Nanocomposites and Addressing Underrepresentation of Women in the Field [Cecile Chazot](#) and John Hart; Massachusetts Institute of Technology, United States

Polymer nanocomposites have been proposed as next-generation lightweight structural materials for applications ranging from aerospace to automotive and sports equipment. However, their processing often requires high temperatures for hours (or sometimes days), contributing to their energy footprint.[1] Additionally nanocomposite manufacturing techniques, such as dispersion of nanofillers in polymer solutions and resin infusion in nanoporous assemblies, often result in composite systems with heterogeneous morphologies and therefore reduced mechanical properties. We present a scalable, low-temperature nanocomposite manufacturing method called in-situ interfacial polymerization (ISIP), which is based on interfacial polycondensation of high-performance polymers in nanoporous assemblies. For example, we demonstrate that dense carbon nanotube (CNT)-polymer composites can be obtained by ISIP within CNT networks.[2] Uniform aramid-CNT composite sheets obtained by this method have a Young's modulus of 31 GPa and a tensile strength of 776 MPa, which is a two-fold increase compared to the pristine CNT sheets. We also present how ISIP can be extended to a broad range of polymers and matrices including nanofiber mats and 3D printed lattices. A macrokinetics model describing the simultaneous fluid flow and polymerization reaction is used to predict final composite morphology and performance. We also demonstrate the implementation of ISIP as a roll-to-roll process, where the nanoporous substrate is continuously drawn through the series of liquid immersion steps to produce the final composite fiber.

We also share the personal experience of a woman in STEM and Materials Science and Engineering (MSE) from technical high school in France to graduate school in the United States. While women represent 44% of the total workforce in the US, they constitute 39% of materials scientists and chemists, and only 16% of materials engineers.[3,4] Notably, the proportion of women decreases with increasing degree level in higher education in MSE in both France and the US. We will put the underrepresentation at the highest level of the field in relation with the social psychology topic of stereotype threat: a type of social identity threat that occurs when one fears being judged in terms of a group-based stereotype.[5,6] Last, we will discuss current ongoing initiatives at MIT targeted at mitigating stereotype threat and reducing these inequalities in the laboratory and the classroom.

[1] C. A. C. Chazot and A. J. Hart, “Understanding and control of interactions between carbon nanotubes and polymers for manufacturing of high-performance composite materials,” *Compos. Sci. Technol.*, vol. 183, p. 107795, Oct. 2019, doi: 10.1016/J.COMPSCITECH.2019.107795.

[2] C. A. C. Chazot, C. K. Jons, and A. J. Hart, “In Situ Interfacial Polymerization: A Technique for Rapid Formation of Highly Loaded Carbon Nanotube-

Polymer Composites,” *Adv. Funct. Mater.*, vol. 30, no. 52, p. 2005499, Dec. 2020, doi: 10.1002/adfm.202005499.

[3] “A Report on the Workshop on Gender Equity in Materials Science and Engineering,” College Park, Maryland, 2008. Accessed: Jun. 15, 2021. [Online]. Available: <https://www.nsf.gov/mps/dmr/BroadeningPresentations/gewreport.pdf>.

[4] C. Corbett and C. Hill, *Solving the equation: The Variables for Women’s Success in Engineering and Computing*. Washington, DC: American Association for University Women, 2015.

[5] M. C. Murphy, C. M. Steele, and J. J. Gross, “Signaling threat: How situational cues affect women in math, science, and engineering settings,” *Psychol. Sci.*, vol. 18, no. 10, pp. 879–885, Oct. 2007, doi: 10.1111/j.1467-9280.2007.01995.x.

[6] S. J. Spencer, C. M. Steele, and D. M. Quinn, “Stereotype Threat and Women’s Math Performance,” *J. Exp. Soc. Psychol.*, vol. 35, no. 1, pp. 4–28, Jan. 1999, doi: 10.1006/jesp.1998.1373.

SESSION BI02.04: Women in Materials Science IV

Session Chair: Fang Liu

Wednesday Morning, December 1, 2021

Hynes, Level 1, Room 107

10:30 AM *BI02.04.01

Semiconductor Quantum Dots—A Journey from the Flask to Photonic Devices Jennifer Hollingsworth; Los Alamos National Laboratory, United States

Solution-processed quantum dots (QDs) are finding real-world applications in a wide-range of technologies from displays and lighting to photovoltaics and photodetectors. We take advantage of an expanded “structural toolbox” to synthesize QDs with novel and optimized photophysical properties relevant for device implementation. We use advanced heterostructuring that employs interfacial alloying, bandgap engineering, thick (“giant”) or asymmetric shell growth, etc. In this way, we have synthesized QDs for which non-radiative processes, such as blinking, Auger recombination and photobleaching, have been suppressed or even “turned off” at room temperature,¹⁻⁷ or at elevated temperatures while exposed to atmospheric oxygen.⁸⁻⁹ This has required simultaneous development of new methods for evaluating correlations between synthesis, resulting nanostructure and realized functionality toward the ideal of a materials-by-design approach to the next generation of useful QDs. In this talk, I will review highlights of our work in this area, as well as some of the enabled device demonstrations. I will also discuss the integration of QDs with other functional nanomaterials for multifunctionality or emergent properties, as well as into devices, especially scanning-probe-enabled fabrication of single-photon sources.¹⁰

The journey from materials discovery to demonstrated application is long and complex, but equally so are the personal journeys of the scientists and engineers pursuing this path. In the theme of this symposium, I will conclude my presentation with some observations, concerns and aspirations for women in science made over the course of more than 20 years as a national lab technical staff member.

Krishnamurthy, S. et al. PbS/CdS Quantum Dot Room-Temperature Single-Emitter Spectroscopy Reaches the Telecom O and S Bands via an Engineered Stability. *ACS Nano* **2021**, *15*, 575.

McBride, J. R. et al. Role of shell composition and morphology in achieving single-emitter photostability for green-emitting “giant” quantum dots. *J. Chem. Phys.* **2020**, *152*, 124713.

Dennis, A. M., et al. Role of Interface Chemistry in Opening New Radiative Pathways in InP/CdSe Giant Quantum Dots with Blinking-Suppressed Two-Color Emission. *Adv. Funct. Mater.* **2019**, *29*, 1809111.

Hanson, C. J. et al. Giant PbSe/CdSe/CdSe Quantum Dots: Crystal-Structure-Defined Ultrastable Near-Infrared Photoluminescence from Single Nanocrystals. *J. Am. Chem. Soc.* **2017**, *139*, 11081.

Mishra, N. et al. Using shape to turn off blinking for two-colour multiexciton emission in CdSe/CdS tetrapods. *Nature Commun.* **2017**, *8*, 15083.

Dennis, A. M. et al. Suppressed Blinking and Auger Recombination in Near-Infrared Type-II InP/CdS Nanocrystal Quantum Dots. *Nano Lett.* **2012**, *12*, 5545.

Ghosh, Y. et al. New Insights into the Complexities of Shell Growth and the Strong Influence of Particle Volume in Non-Blinking “Giant” Core/Shell Nanocrystal Quantum Dots. *J. Am. Chem. Soc.* **2012**, *134*, 9634.

11:00 AM *BI02.04.02

Colloidal Semiconductor Nanocrystals—(Un)Conventional and Quantum Materials and Devices Cherie R. Kagan; University of Pennsylvania, United States

Colloidal semiconductor nanocrystals (NCs) are typically 2-20 nm diameter fragments of the bulk solid. They are known as “artificial atoms” or quantum dots since electrons, holes, and excitons are quantum-mechanically confined and occupy discrete electronic states. The research community has celebrated >30 years of study of the synthesis, assembly, structure, properties, and applications of colloidal semiconductors NCs, and I have enjoyed the opportunity to contribute to the field in my career. Advances in wet-chemical synthetic methods enable the preparation of NCs tailorable in size, shape, composition, and surface chemistry. As colloids, these NCs are readily dispersed in solvents and deposited using solution-based methods. They can self-assemble to form glassy or crystalline NC solids or be directed to assemble to deterministically position single or countable numbers of NCs. I will focus on routes to design solid-state NC materials by manipulating the NC surface chemistry to strengthen electronic coupling, by exchanging the ligands used in synthesis for more compact chemistries, and NC doping, by introducing atoms and ions that serve as impurities or modify stoichiometry. Ultimately, I will connect NC material design to their physical properties and their application in (un)conventional electronic and optoelectronic devices. I will also give an outlook on the opportunity to exploit NCs as platforms for quantum information science, in particular as optically addressable qubits.

11:30 AM BI02.04.03

A Bioinspired, Bioinorganic Approach to Materials Design—Using Fe and V Coordination to Create Photoresponsive Materials Alexis D. Ostrowski; Bowling Green State Univ, United States

In bioinorganic chemistry, metal ions play important roles in the structure and function of a variety of systems. Using this as inspiration, our approach is to design materials that exploit metal coordination bonding to create materials with unique properties. Of particular interest, are materials that coordinate Fe and V ions, since once coordinated, the metal-ligand bonding in the material can be controlled with light using photochemical processes. Both Fe(III) and V(V) coordination in polysaccharide materials can be used to create hydrogels. Once irradiated, photo-induced charge transfer processes change the Fe and V coordination environments in the gel, and disrupting the intermolecular forces in the material, changing the viscosity and modulus of the gels. These photoresponsive materials can be used for a variety of applications, including encapsulation and delivery of bioactive molecules or nutrients.

11:45 AM BI02.04.04

Designing Nanoparticles for Self-Assembly of Novel Photonic Materials Rose K. Cersonsky^{1,2}, James Antonaglia¹, Bradley D. Dice¹ and Sharon C. Glotzer¹; ¹University of Michigan, United States; ²École Polytechnique Fédérale de Lausanne, Switzerland

The design of new materials has often relied on crystal structure as a primary source for design complexity and innovation, requiring new crystal structures and new manners of constructing and synthesizing these structures. Within the photonics community, where the goal is a photonic crystal, i.e., a crystal that reflects a range of wavelengths, the literature points to a handful of targets, most commonly the diamond or inverse opal structures. Nanoparticle self-assembly, or the spontaneous emergence of order due to particle interactions, has been identified as a favorable synthesis route, as photonic nanocrystals reflect wavelengths within the visible range due to the scale-covariance of photonic band structures. Yet, the effort to self-assemble photonic crystals has been fraught with obstacles — from difficulty synthesizing diamond to the degradation of photonic band gaps based upon thermal noise within the assembly. This begs the question: if we look beyond the known set of photonic crystal structures, which other structures are worth targeting? We discuss the unexpectedly diverse range of crystallographic structures that will support a photonic band gap, as determined by more than 150,000 photonic band structure calculations. These calculations identify nearly 300 previously unstudied targets for photonic crystals—including targets achievable via colloidal self-assembly [1]. We demonstrate avenues to predict the polyhedral nanoparticles that can cleanly self-assemble these targets and the implications, both good and bad, that small changes to nanoparticle shape have on the resulting crystal's behavior [2-4].

Finally, we discuss the topic of scientific communication, which is fundamental in encouraging underrepresented populations in STEM by deterring the imposter syndrome for those who may glean a sense of “otherness” from poorly communicated work. We will focus on two programs at the University of Michigan to connect higher education institutions with primary and secondary school educators [5],[6]. These programs facilitate and promote discourse between graduate students and K-12 STEM educators, pushing students to communicate and contextualize their research and extending access to cutting-edge science to populations typically harder to reach via other outreach efforts.

[1] R. K. Cersonsky, J. Antonaglia, B. D. Dice, S. C. Glotzer, "Unexpected Diversity of Three-Dimensional Photonic Crystals," (2021). Nature Communications. <https://www.nature.com/articles/s41467-021-22809-6>

[2] R. K. Cersonsky, G. van Anders, P. M. Dodd, and S. C. Glotzer, "Relevance of Packing in Colloidal Self-Assembly," (2018). Proceedings of the National Academy of Sciences. <https://doi.org/10.1073/pnas.1720139115>.

[3] R. K. Cersonsky, J. Dshemuchadse, J. Antonaglia, G. van Anders, S. C. Glotzer, "Pressure-Tunable Band Gap in an Entropic Crystal", (2018). Phys. Rev. Mat. <https://doi.org/10.1103/PhysRevMaterials.2.125201>.

[4] Y. Zhou, R. K. Cersonsky, S. C. Glotzer, "A New Route to the Diamond Colloidal Crystal." In preparation.

[5] R.K. Cersonsky, LL Foster, T Ahn, RJ Hall, HL Van Der Laan, TF Scott. "Augmenting Primary and Secondary Education with Polymer Science and Engineering," (2017). Journal of Chemical Education 94 (11), 1639-1646. <https://pubs.acs.org/doi/full/10.1021/acs.jchemed.6b00805>

[6] A Travitz, A Muniz, JK Beckwith, R.K. Cersonsky. "Bringing Science Education and Research together to REACT," (2021). American Society for Engineering Education, 1-13. <https://doi.org/10.18260/1-2--35030>

SESSION BI02.05: Women in Materials Science V
Session Chair: Jennifer Hollingsworth
Wednesday Afternoon, December 1, 2021
Hynes, Level 1, Room 107

1:30 PM *BI02.05.02

Barriers to Electrons in Nanocrystal Films and Barriers Arising from Gender Stereotypes Delia Milliron; The University of Texas at Austin, United States

Colloidal nanocrystals are attractive as solution-processable precursors to make conductive thin films for electronic and optoelectronic devices. However, in most cases electrons move through nanocrystal films by thermally activated hopping, behaving as insulators even when the nanocrystals themselves are metallic. We synthesize indium tin oxide transparent conducting nanocrystals to fabricate conductive thin films and show how the contact resistance between them controls the metal-insulator transition. Our results establish a “phase diagram” for electron transport, mapping conditions for hopping, thermally activated granular metallic, and classical metallic conduction.

From the perspective I now have – participating regularly in faculty recruiting, promotion, and mentorship – I have started to see experiences from my own early career in a broader context. Reflecting on these, I'll talk briefly about the ways that prevalent stereotypes present barriers to the development and advancement of women and people from underrepresented groups in STEM.

2:00 PM *BI02.05.03

Rethinking our Approach to Developing Inorganic Nanoparticles for *In Vivo* Imaging Allison M. Dennis; Boston University, United States

Although semiconductor quantum dots (QDs) are excellent fluorophores for biosensing and biomedical imaging, their translation to clinical applications is stymied by toxicity concerns. While materials developed for optoelectronic applications such as displays and photovoltaics exhibit excellent photophysical properties, their elemental composition is often contraindicated for use in human subjects. The current solution to elemental toxicity is to cap the core nanoparticle in a shell, usually of zinc sulfide, to prevent the release of the offending elements into the biological environment. This sequestration approach also results in the accumulation and persistence of the nanoparticles in the liver, an outcome that would preclude FDA approval for a diagnostic contrast agent. This combination of toxic compositions and bioaccumulation is a persistent barrier to the clinical translation of semiconductor nanoparticles.

In our new approach to developing inorganic nanoparticles for biomedical imaging and in vivo biosensing applications, we have shifted our focus to consider biological interactions first and optical properties second to identify the best materials for the application. Developing inorganic nanomaterials that can be used as contrast agents in humans requires addressing issues of toxicity, bioaccumulation, and function. We are inspired by the composition of the only FDA-approved inorganic nanoparticle: iron oxide. Iron oxide nanoparticles degrade in vivo into biocompatible and bioessential elements, coincidentally treating the patient's anemia. To develop biocompatible inorganic nanoparticles (bioNPs), we are synthesizing nanocrystals comprising bioessential elements and assessing their optical properties, degradation, and nanotoxicity. These iron- and copper-based semiconductors are often understudied with regards to both their optoelectronic properties and biocompatibility. For example, we have demonstrated that while copper indium

sulfide (CIS) QDs exhibit appropriate optical properties for in vivo luminescence imaging, ZnS shell-free CIS particles degrade rapidly with high toxicity in mice. Alloying zinc into the particles (CISZ) improves their optical properties, maintains a reasonable degradation rate, and substantially reduces toxicity. In comparison, copper iron sulfide nanoparticles (chalcopyrite or bornite; abbreviated CFS) biodegrade and exhibit localized surface plasmon resonance (LSPR) in the NIR, showing promise for photoacoustic imaging and photothermal therapy applications. As we expand the compositions of the bioNPs tested, we are developing a framework to relate the degradation rate and degradation products to toxicity. This information is being used together with the optoelectronic properties of the new materials to change the way we develop semiconductor nanoparticles for in vivo applications.

SESSION BI02.06: Women in Materials Science VI—Panel Discussion
Session Chairs: Betar Gallant, Jennifer Hollingsworth and Fang Liu
Wednesday Afternoon, December 1, 2021
Sheraton, 2nd Floor, Grand Ballroom

4:15 PM WOMEN IN MATERIALS SCIENCE VI—PANEL DISCUSSION

SESSION BI02.07: Women in Materials Science VII
Session Chair: Raffaella Buonsanti
Tuesday Morning, December 7, 2021
BI02-Virtual

9:00 AM *BI02.07.01

Advancement of Battery Technology for EVs Mei Cai; General Motors, United States

Despite the current battery technology evolution, battery chemistries have not changed much in the last two decades. Highly emerged EV market evokes the demands on advanced batteries with high energy density. Among the future chemistries, lithium metal batteries have great advantages over state-of-the-art lithium ion batteries in term of energy density and cost, which bring huge opportunity for long-range and low-cost electrical vehicles in the future. However, automotive industry has critical requirements on specific characteristics of battery cells. In this talk, I will discuss the requirements for future electrical vehicle application and the impact of Li-metal batteries on automotive industry. As a women scientist working in the automotive industry, I will also describe the range of opportunities available to women in this field. Some concerns and challenges will also be discussed.

9:30 AM *BI02.07.02

Using Multidisciplinary Science to Drive Healthcare Innovations Molly Stevens; Imperial College London, United Kingdom

This talk will provide an overview of our multidisciplinary approach to elucidate the interfaces between living and non-living matter, and how we use this fundamental knowledge to design innovative materials and technologies with impactful applications in regenerative medicine, advanced therapeutic delivery and disease diagnostics.

We engineer simple conceptually novel biosensing approaches using designer bio-nanomaterials for ultrasensitive diagnostic assays that are simple, cost-effective and easy deploy to the point-of-care. We are exploiting the sensing capabilities of nanoparticles to engineer paper-based lateral flow immunoassays (LFIA) for the detection of infectious diseases such as HIV [2], Ebola, tuberculosis and Covid-19, and we can integrate our assays with smartphone technology for patient self-monitoring, geographical tagging and epidemic surveillance [3]. Harnessing our knowledge of the bio-interfaces, we also engineer complex 3D architectures with spatially arranged biochemical cues and cell interfacing nanoneedles for multiplexed intracellular biosensing at sub-cellular resolution and modulation of biological processes [4].

I will also speak about the breakthroughs, innovations and aspirations that shape who we are and what we do, and how we strive to create an inclusive and stimulating environment where science and scientists flourish.

[1] P. D. Howes... M. M. Stevens. "Colloidal nanoparticles as advanced biological sensors." *Science*. 2014. 346: 53-63.

[2] C. Loynachan... M. M. Stevens. "Platinum nanocatalyst amplification: redefining the gold standard for lateral flow immunoassays with ultra-broad dynamic range." *ACS Nano*. 2018. 12(1): 279-288.

[3] C. S. Wood... M. M. Stevens. "Taking connected mobile-health diagnostics of infectious diseases to the field." *Nature*. 2019. 566: 467-474.

[4] C. Chiappini... M. M. Stevens, E. Tasciotti. "Biodegradable silicon nanoneedles delivering nucleic acids intracellularly induce localized in vivo neovascularization." *Nature Materials*. 2015. 14: 532-539.

SESSION BI02.08: Women in Materials Science VIII
Session Chair: Raffaella Buonsanti
Tuesday Morning, December 7, 2021
BI02-Virtual

10:30 AM *BI02.08.01

From Flexible Electronics to Skin Inspired Electronics a Personal Reflection Zhenan Bao; Stanford University, United States

In this talk, I will reflect on my journey working with flexible electronics from my early career to defining a new field of skin-inspired electronics. I will talk about lessons learned through this journey.

11:00 AM *BI02.08.02

Emerging Nanophotonic Platforms for Infectious Disease Diagnostics—Re-Imagining the Conventional Microbiology Toolkit Jennifer A. Dionne; Stanford University, United States

We present our research, education, outreach, and translational work to control light at the nanoscale for infectious disease diagnostics, including detecting bacteria at low concentration, screening for viral gene sequences, and visualizing in-vivo inter-cellular forces. First, we combine Raman spectroscopy and deep learning to accurately classify bacteria by both species and antibiotic resistance in a single step. We design a convolutional neural network (CNN) for spectral data and train it to identify 30 of the most common bacterial strains from single-cell Raman spectra, achieving antibiotic treatment identification accuracies exceeding 99% and species identification accuracies similar to leading mass spectrometry identification techniques. Our combined Raman-CNN system represents a proof-of-concept for rapid, culture-free identification of bacterial isolates and antibiotic resistance. Second, we describe resonant nanophotonic surfaces, known as “metasurfaces” that enable multiplexed detection of SARS-CoV-2 gene sequences. Our metasurfaces utilize guided mode resonances excited in high refractive index nanostructures. The high quality factor modes produce a large amplification of the electromagnetic field near the nanostructures that increase the response to targeted binding of nucleic acids; simultaneously, the optical signal is beam-steered for multiplexed detection. We describe how this platform can be manufactured at scale for portable, low-cost assays. Finally, we introduce a new class of *in vivo* optical probes to monitor biological forces with high spatial resolution. Our design is based on upconverting nanoparticles that, when excited in the near-infrared, emit light of a different color and intensity in response to nano-to-microNewton forces. The nanoparticles are sub-30nm in size, do not bleach or photoblink, and can enable deep tissue imaging with minimal tissue autofluorescence. We present the design, synthesis, and characterization of these nanoparticles both in vitro and in vivo, focusing on the forces generated by the roundworm *C. elegans* as it feeds and digests its bacterial food. Beyond the rigor of research, I also describe how I am reliving my childhood with my two young sons, and exploring the country as an avid cyclist and long-distance runner.

11:30 AM BI02.08.03

A Computational Framework for Studying CoCrFeNiTi High Entropy Alloys—My Path to Computational Materials Science as a Young Egyptian Woman Geraldine Anis¹, Mostafa Youssef¹, Moataz Attallah² and Hanadi Salem¹; ¹The American University in Cairo, Egypt; ²University of Birmingham, United Kingdom

In my presentation, I will talk about my academic journey as a young Egyptian woman and the path that led me to studying and working in computational materials science. I will describe our recent work on a multiscale modeling and simulation study of a high entropy alloy (HEA) system by combining continuum level thermodynamic modeling, atomic scale quasi-random structures, and electronic structure density functional theory (DFT). The main aim of this study is to provide a framework that can aid with and potentially accelerate the exploration of the massive HEA composition space through guiding experimental efforts.

Computational phase diagrams of four subsystems of the CoCrFeNiTi HEA system were constructed using the calculation of phase diagrams (CALPHAD) method. Our efforts were focused on the single phase face-centered cubic (FCC) regions in the obtained diagrams, due to the potentially favorable properties of alloys with this structure. A thermodynamic analysis was also carried out, in which we studied the variations in the mixing enthalpies and entropies within the studied systems. From our analysis, we were able to determine the main stabilizing factor (enthalpy vs. entropy) of the single FCC phase as a function of temperature. Furthermore, we tested the possibility of changing the thermodynamic phase diagram of this alloy system upon dissolution of impurities such as carbon and oxygen.

The constructed phase diagrams were then used to guide composition selection for an alloy to study its mechanical properties using first-principles DFT calculations. The selected alloy with composition CoCrFeNi_{1.75}Ti_{0.25} was modeled using the special quasi-random structure (SQS) approach and DFT calculations were used to determine the elastic constants matrix of this alloy composition in addition to its stress-strain response under a uniaxial load. Additionally, we analyzed the hypothesis of sluggish diffusion in HEA via computing the formation energies of all possible vacancies in the alloy. Our coupled CALPHAD-SQS-DFT approach provides a general methodology for understanding the thermodynamics and mechanics of non-equiatomic HEAs.

In addition to the technical aspects related to the HEA work, I will be sharing my experience and some aspects of my personal life, with an emphasis on the things that have helped me overcome the obstacles that women in STEM face. My interest in materials science was sparked early on when I was still an undergraduate student, which led me to volunteer as a research assistant on a project focused on synthesizing and characterizing aluminum-graphene composites. Although I started my M.Sc. thesis as an experimentalist working on studying HEAs, the Covid-19 pandemic imposed a shift of my project to a fully computational study, after which I successfully obtained my M.Sc. degree. Upon finishing my thesis and facing a delay in my PhD plans due to the Covid-19 pandemic, I worked on a research project at the interface between materials science and biochemistry in which I employed molecular dynamics simulations to study the effect of certain small molecules on the binding affinity of the SARS-CoV-2 virus to the ACE2 human enzyme.

Finally, I will conclude my presentation with a discussion of my future plans, which include obtaining a PhD degree in modeling of heterogeneous systems, as well as how my goals have been shaped by my experiences and previous research.

11:45 AM BREAK

SESSION BI02.09: Women in Materials Science IX
Session Chair: Fang Liu
Tuesday Afternoon, December 7, 2021
BI02-Virtual

1:00 PM *BI02.09.01

The Growing Role of Women in Materials Science—Personal Experiences and My Recent Research in Oxide Thin Films Judith L. MacManus-Driscoll; University of Cambridge, United Kingdom

Women have, throughout history, played an important role in materials science. In recent times, our role has grown strongly and we have become more prominent. So things are improving, but I believe we still face many challenges, some well recognized and spoken about openly, but others that are more hidden and hence not addressed or spoken about. Based on my own experiences, I will try to address some of challenges I have faced and will discuss how I have (or have tried to) overcome them. I will move on from here to show examples of my recent work demonstrating the important role of materials science in the engineering of oxide electronic thin films for low power electronics and energy applications.

1:30 PM *BI02.09.02

Imaging, Understanding and Controlling of Nanoscale Materials Transformations Haimei Zheng^{1,2}; ¹Lawrence Berkeley National Laboratory, United States; ²University of California, Berkeley, United States

The development of liquid cells for transmission electron microscopy (TEM) has enabled breakthroughs in our ability to follow nanoscale structural, morphological, or chemical changes during materials growth and applications. Time-resolved high-resolution imaging and chemical analysis through liquids have opened the opportunity to capture nanoscale dynamic processes of materials, including reaction intermediates and the transformation pathways. In this talk, I will present a series of work in my group on liquid cell developments and in situ liquid cell TEM study of nanocrystal growth and transformations, lithium dendrite formation and suppression and using liquid cell TEM in other studies on materials dynamics. The understanding garnered accelerates the discovery of novel materials for applications in energy storage, catalysis, and other functional devices.

2:00 PM *BI02.09.03

Empowering Women's Leadership in the Energy Sector Mihrimah Ozkan; University of California, Riverside, United States

The Energy sector has low diversity and gender equality into its workspaces and boardrooms. Based on some statistics, only 14% of energy engineers are women. This testifies that we need to take serious steps to improve the gender diversity in the energy sector. Women at leadership positions, in boardrooms and in factory floors can be achieved in two ways: 1) male dominant hiring managers can help to promote women engineers for the leadership positions, 2) mentoring and supporting younger women generations in engineering and helping them to become more visible and confident. In my presentation, I will focus on my research about Li-ion batteries and their applications in electric vehicles and my journey as a women academic engineer being the first women tenure-track faculty hired for the engineering college in 2001, and also being the only women full-professor in the engineering college today.

2:30 PM *BI02.09.04

Engineering an Inclusive Future Aditi Risbud Bartl; Stanford University, United States

At the UC Davis College of Engineering, we've launched a new communications platform titled Engineering an Inclusive Future: <https://engineering.ucdavis.edu/engineering-inclusive-future>. This new platform highlights how much we've done—and how much more we will be doing—to move the College of Engineering toward “inclusion excellence,” in which all members of a community are encouraged and supported to work, study and learn in a way that allows each of us to reach our full potential. For this effort, I wanted to take a chance and show not just our best work but areas where we can improve, so we've employed first-person storytelling from our students, faculty, staff and postdocs. We post one to two stories a month and share these on our social media channels. Sometimes these stories are less than rosy, but this transparency helps stimulate conversation and reveals a deeper need to discuss challenges faced by women and underrepresented groups across our constituencies.

In addition, I've been part of a larger effort in collaboration with colleagues at the Northern California UC campuses (Davis, Berkeley, Santa Cruz, San Francisco), as well as Berkeley Lab, titled Imagining an Anti-Racist UC: https://www.ucop.edu/human-resources/coro/2020_forms/coro_nor-cal_2020_executive_summary.pdf. This effort aims to facilitate learning, reflection and performance assessment processes with respect to anti-racism among UC supervisors/leaders. Despite being the third largest employer in California, the racial/ethnic demographics of our senior professionals and management do not reflect the racial/ethnic demographics of the UC workforce, or our state.

To address this need, we developed an Anti-Racism Learning and Reflection Tool that establishes guiding anti-racism principles and practices that can be applied uniformly across the UC system by leaders, supervisors and managers to better communicate and carry out anti-racist core values and cultivate a climate of belonging for our staff. While each UC campus has a performance review process and evaluation tool that includes consideration of diversity, equity and inclusion, these materials do not currently incorporate a focus on anti-racist principles and practices. This tool aims to support the life-long learning of managers by offering a framework for them to advance racial equity principles and practices in hiring, performance review, promotion, and workplace climates for staff. I will present this tool and share learnings from its implementation at UC Davis.

SYMPOSIUM CH01

In Situ and Operando Techniques Applied to Electrochemical Systems—A Key Toolkit for Deep Understanding
November 29 - December 8, 2021

Symposium Organizers

Kristina Edstrom, Uppsala University
Christian Masquelier, Université de Picardie Jules Verne
Y. Shirley Meng, University of California, San Diego
Claire Villevieille, CEA

* Invited Paper

SESSION Tutorial CH01: Electrochemical Impedance Spectroscopy Applied to Interfacial Battery Investigation
Session Chairs: Sylvain Franger, Fabio La Mantia and Claire Villevieille
Monday Morning, November 29, 2021
Virtual

8:30 AM

Electrochemical Impedance Spectroscopy (EIS) Applied to Battery Characterization [Sylvain Franger](#); Université Paris-Saclay, France

EIS is one of the most practical in situ analysis technique, which can discriminate electrochemical processes by their time constant. EIS gives information from the electrode/electrolyte interface (MHz) to the bulk electrode (μ Hz). The frequency region scanned mainly concerns ionic mobility and is thus well adapted to evidence matter transport limitations (both in electrolyte and in active materials).

In that way, EIS is particularly interesting to check the interface since it is a non-destructive investigation method, giving access to several electrochemical parameters of major interest (charge transfer, passivation film, adsorption, corrosion, ionic diffusion...).

However, interpreting EIS data still requires specific attention.

For that purpose, in this tutorial, some fundamentals of Electrochemical Impedance Spectroscopy will be reminded. Different examples (from liquid-based and solid-state batteries) will be shown in order to illustrate the tutorial's theoretical aspects.

The goal of this tutorial is actually to give some keys for:
convenient experimental set-up in order to record unambiguous EIS data
use of adequate EIS signal (a special attention will be given to GEIS and PEIS)
data analysis through the use of both Nyquist and Bode diagrams
understanding the interest and limits of equivalent electrical circuit models

10:00 AM BREAK

10:15 AM

Dynamic Impedance Spectroscopy for Operando Battery Materials Characterization [Fabio La Mantia](#); Universität Bremen, Germany

Electrochemical impedance spectroscopy is a very powerful tool, however its actual implementation in standard electrochemical instrumentation does not allow looking into the dynamic behavior of the electrochemical systems. For this reason, classic impedance spectroscopy fails for the investigation of aging of materials, corrosion, self-oscillation, poisoning and others. In order to achieve an understanding of the effect of such degradation mechanisms on the materials and their electrochemical properties, it is necessary to use a methodology, which is able to look at systems while they are changing. The tutorial will start by introducing the concept of dynamic impedance and its connection to the Volterra series of the electrochemical system will be given. An overview of the experimental methodologies for the measurement and extraction of dynamic impedance spectra will follow, accompanied by an analysis of the experimental artefacts related to the electrochemical instrumentation. Different examples of dynamic impedance spectra acquired for different electrochemical reactions will be shown: redox couple in solution; intercalation of ions in host structures; hydrogen evolution on platinum electrodes. The data will be analyzed using at first a statistical approach based on the concept of Pade' approximants, using as weighting factor the theoretical variance of the admittance. The connection between equivalent circuits and Pade' approximants will be explored, as well as their connection to the Kramers-Kronig transformations. Finally, a physico-chemical model will be established in order to describe the phenomena occurring during the electrochemical reaction and the dynamic impedance spectra will be fitted using such model, in order to quantify the kinetic constants of the reaction. The tutorial will close with an summary of the main important points and an overview of the possible applications in the field of energy storage and energy conversion.

SESSION CH01.01: Cathode Materials Investigation
Session Chairs: Joshua Gallaway and Brett Lucht
Tuesday Morning, November 30, 2021
Hynes, Level 3, Room 304

10:30 AM *CH01.01.01

Nanostructure Formation as a Signature of Oxygen Redox in Li-Rich Cathodes [Karina Chapman](#)¹, Antonin Grenier¹, Gabrielle Kamm¹, Y. Shirley Meng², Yixuan Li² and Hyeseung Chung²; ¹Stony Brook University, United States; ²University of California, San Diego, United States

Lithium-rich nickel manganese cobalt oxide (LRNMC) is being explored as an alternative to stoichiometric nickel manganese cobalt oxide (NMC) cathode materials due to its higher, initially accessible, energy-storage capacity. This higher capacity has been associated with reversible O oxidation, however, the mechanism through which the change in O chemistry is accommodated by the surrounding cathode structure remains incomplete, making it challenging to design strategies to mitigate poor electrode performance resulting from extended cycling. Focusing on LRNMC cathodes, we identify nanoscale domains of lower electron density within the cathode as a structural consequence of O oxidation using small-angle X-ray scattering (SAXS) and operando X-ray diffraction (XRD). A feature observed in the small angle scattering region suggest the formation of nanopores, which first appear during O oxidation, and is partially reversible. This feature is not present in traditional cathode materials, including stoichiometric NMC and lithium nickel cobalt aluminum oxide (NCA), but appears to be common to other Li-rich systems tested here, Li_2RuO_3 and $\text{Li}_{1.3}\text{Nb}_{0.3}\text{Mn}_{0.4}\text{O}_2$.

11:00 AM CH01.01.02

Regeneration of Degraded Li-rich Layered Oxide Materials Through Heat Treatment-Induced Transition Metal Reordering [Yixuan Li](#)¹, Mateusz Zuba², Shuang Bai¹, Zachary Lebens-Higgins², Bao Qiu³, Zhaoping Liu³, Minghao Zhang¹, Louis Piper² and Y. Shirley Meng¹; ¹University of California, San Diego, United States; ²Binghamton University, United States; ³Ningbo Institute of Materials Technology and Engineering, Chinese Academy of Sciences, China

Lithium-rich layered oxides (LRLO) have drawn great attention recently as a high energy density cathode material. However, the practical deployment of these materials is hindered by voltage and capacity decay during electrochemical cycling. Applying mild thermal energy to cycled LRLO materials allows to recover the voltage profile and to alleviate the voltage decay problem in the following cycling. In this work, a detailed mechanism study of the voltage

and structure recovery is conducted through various analytical tools. The recovery of the lattice structure is investigated through in-situ neutron powder diffraction and synchrotron X-ray diffraction. The reordering of the transition metal environment is explored by in-situ extended X-ray absorption fine structure and pair distribution function. A transition metal reordering pathway is proposed and evaluated through computation methodology. Heat treatment provides the necessary energy for the transition metal to overcome the kinetic barrier to move from the honeycomb center to the honeycomb vertex and recover the honeycomb ordering in the transition metal layer. An ambient-air relithiation using Li^+ molten salt was also conducted along with the heat treatment to the cycled LRLO cathode and lead to a material regeneration in both the voltage and capacity. This work identifies the transition metal reordering as the key factor under the structure recovery of degraded LRLO materials. It opens a door for promising strategies to mitigate the voltage and capacity degradation problem in LRLO and provides the potential routes to recycle degraded LRLO materials.

11:15 AM CH01.01.04

Late News: Established and Emerging Methodologies for *Operando* X-Ray Total Scattering and Pair Distribution Function Analysis for Rechargeable Batteries [Martin A. Karlsen](#)¹, Simon J. Billinge^{2,3} and Dorthé B. Ravnsbæk¹; ¹University of Southern Denmark, Denmark; ²Columbia University, United States; ³Brookhaven National Laboratory, United States

The inevitable and necessary green transition towards sustainable energy sources depends completely on the ability to store energy. One possibility is to store the excess energy from renewable energy sources electrochemically in rechargeable batteries. A possibility that has also been realized for the substitution of combustion engines in vehicles.

To develop the rechargeable batteries of tomorrow, fundamental understanding of relations between material structure and properties is essential. Here, *operando* experiments are essential, as they provide insight into material behavior under the true dynamic conditions relevant for real applications. For the material structure at the atomic and nano length scales, x-rays, neutrons, and electrons are excellent probes.

If materials are crystalline and well-ordered on the atomic and nano length scales, traditional diffraction methods are ideal to probe the long-range order of the material structure, as the relevant information lies in the Bragg peaks. In recent years, it has been realized that crystallinity is not a given for all battery materials at all states-of-charge or at all stages of a battery's lifetime. However, for non-crystalline materials, whether they are nanocrystalline, disordered, or even amorphous, the more traditional diffraction methods fall short. Now, the relevant information does not lie *in* the Bragg peaks but *underneath* them in the diffuse scattering.

To probe the material structure of crystallographically challenged materials, total scattering experiments, which involve both the Bragg and diffuse scattering, hold the key. From total scattering data, the reduced atomic pair distribution function (PDF) can be obtained, which takes the scattering data from reciprocal space and into real space. The PDF can be thought of as a probability distribution of the interatomic distances in the material and the very local structure down to nearest-neighbor distances in materials can now be probed. Everything is seen in the PDF, which is a blessing as well as a curse for battery scientists, as batteries are multicomponent systems with complicated PDFs, which calls for battery-specific PDF methodologies.

This contribution will address how to obtain *operando* PDFs for battery materials during cycling and especially how to analyze data.

In our studies, we utilize model-dependent PDF analysis, sometimes referred to as 'real-space Rietveld refinement', via a least-square optimization method, like Rietveld refinement, where an input model is refined against experimental data, such that the residual between the two is minimized. The user-friendly PDFgui and the more versatile and advanced DiffPy Complex Modelling Interface (DiffPy-CMI) software are two examples on tools to conduct model-dependent, quantitative PDF analysis. In addition, we employ novel tools for model-free PDF analysis.

During summer 2021, 'PDF in the cloud' (PDFfitc) was launched at 'pdfitc.org', where multiple apps for PDF analysis are available to users. This includes the model-free 'similarityMapping' app, which is a statistical analysis based on Pearson correlation. During fall 2021, another model-free statistical method will become available as an app: non-negative matrix factorization (NMF), which is somewhat like principal component analysis (PCA). Automated methods are also starting to enter the ballpark of PDF analysis. The 'structureMining', 'spacegroupMining', and 'clusterMining' apps at PDFfitc mine structural databases and guide users in their PDF analyses to enable the users to explore the atomic level structure of their materials.

11:30 AM CH01.01.05

Operando Single Particle Diffraction of $\text{Na}_x[\text{Ni}_{1/3}\text{Mn}_{2/3}]\text{O}_2$ [Jason J. Huang](#)¹, Daniel B. Weinstock¹, Hayley Hirsch², Ryan Bouck¹, Oleg Gorobtsov¹, Malia Okamura³, Ross Harder⁴, Wonsuk Cha⁴, Jacob Ruff¹, Y. Shirley Meng² and Andrej Singer¹; ¹Cornell University, United States; ²University of California, San Diego, United States; ³Carnegie Mellon University, United States; ⁴Argonne National Laboratory, United States

The prevalence of both structural and sodium-ion ordering phase transitions in sodium-ion intercalation materials limits their useful cycle life. The multitude of transitions creates complex phase behavior that is difficult to investigate, especially on the single nanoparticle scale and under operating conditions. Here, we develop operando single particle x-ray diffraction to observe single particle rotation, interlayer spacing, and layer misorientation. We apply the technique, during charge, to a model P2-type sodium ion cathode material, $\text{Na}_x[\text{Ni}_{1/3}\text{Mn}_{2/3}]\text{O}_2$ (NNMO), where $0 < x < 2/3$, which exhibits the detrimental P2-O2 transition. From operando observations of single particle misorientation and layer spacing changes, we propose a model for the phase evolution of NNMO that includes a localized to correlated Jahn-Teller distortion phase transformation. Through this work, the proposed model can serve to guide further characterization of NNMO and other materials with P2-O2 type transitions, and operando single particle x-ray diffraction has the demonstrated potential to be used in other systems to reveal phase behavior at the nanoscale.

11:45 AM CH01.01.06

The Impact of Alkali-Ion Intercalation on Redox Chemistry and Mechanical Deformations—Case Study on Intercalation of Li, Na and K Ions into FePO_4 Cathode Bertan Ozdogru and [Omer O. Capraz](#); Oklahoma State University, United States

Development of cathode structures suitable for Na-ion and K-ion batteries is still one of the major challenges on the way to the design of next-generation alkali metal-ion batteries. Although Li, Na and K belong to the same alkali metal group with a single charge in their cation form, intercalation of Na^+ and K^+ ions in electrodes is difficult since ionic radii of Na^+ (0.98 Å) and K^+ (1.38 Å) are larger than that of Li^+ (0.69 Å). Therefore, physical, and electrochemical behavior of the cathode materials in response to Na^+ and K^+ ion intercalation is expected to be fundamentally different than the response to Li^+ ion. However, there is not much known about how electrochemical reactions and transport of ions take place in cathode materials with different alkali metal ions. There have been several studies focusing on electrochemical characterization and investigation of the structural changes in the electrode materials. Lack of insight into these reaction-transport mechanisms limits the design of novel cathode materials for Na-ion and K-ion batteries. Comparative studies between Li-ion, Na-ion and K-ion battery cathodes are critical to identify fundamental similarities and differences during intercalation. Even modest expansions in brittle cathodes can cause particle fracturing in a larger crystalline-size scale. Intercalation of larger ions can cause structural collapse and amorphization induced by continuous strains and distortions. Although the amorphization in the structure can be easily

identified by conventional diffraction or electron microscopy techniques, quantitative analysis of the physical changes in the structure during and after amorphization while cycling the battery electrode is critical.

In the first part of the talk, we will first report the utilization of in situ digital image correlation and in-operando X-ray diffraction (XRD) techniques to probe dynamic changes in the amorphous phase of iron phosphate during potassium intercalation¹. A new experimental approach allows to monitor dynamic physical and structural changes in the amorphous phase of the electrodes. In-operando XRD demonstrates amorphization in the electrode's nanostructure during the first charge / discharge cycle. In situ strain analysis detects the reversible deformations associated with redox reactions in the amorphous phases. This method offers new insights to study mechanics of ion intercalation in the amorphous nanostructures.

In the second part of the talk, we will compare the electrochemical and mechanical response of the iron phosphate cathodes upon Li, Na and K ion intercalation by using electrochemical techniques and *in situ* digital image correlation. Iron phosphate model electrodes were prepared by electrochemical displacement technique in order to ensure identical morphology, structure and chemistry in the pristine iron phosphate electrodes. Strain evolution during Li and Na intercalation results in more linear dependence on the state of charge / discharge. However, strains generated in the electrode shows nonlinear behavior during insertion / extraction of K ions. Interestingly, when the same amount of K and Na ions are intercalated, similar chemomechanical expansions were observed. However, strain rate calculations showed that K ion intercalation results in a progressive increase in the strain rate, whereas Li and Na intercalation induce nearly constant strain rates. Potential-dependent behaviors also demonstrate more sluggish redox reactions during K intercalation, compared to the Li and Na intercalation. These observations provide a fundamental insight into the impact of alkali ions on the redox chemistry and associated chemomechanical deformations.

Reference

1. B. Ozdogru, Y. Cha, V. Murugesan, M-K Song, Ö. Çapraz. *In Situ Probing Potassium-ion Intercalation-induced Amorphization in Crystalline Iron Phosphate Cathode Materials*. ChemRxiv. Cambridge: Cambridge Open Engage; 2021.

SESSION CH01.02: Electrolyte Characterization

Session Chair: Karena Chapman

Tuesday Afternoon, November 30, 2021

Hynes, Level 3, Room 304

1:30 PM *CH01.02.01

Electrolyte Oxidation and the Role of Acidic Fluorophosphates in Capacity Loss for Lithium-Ion Batteries [Brett Lucht](#); University of Rhode Island, United States

Cycling lithiated metal oxides to high potential (>4.5 V vs Li) is of significant interest for the next generation of lithium ion batteries. Cathodes cycled to high potential suffer from rapid capacity fade due to a combination of thickening of the anode solid electrolyte interphase (SEI) and impedance growth on the cathode. While transition metal catalyzed degradation of the anode SEI has been widely proposed as a primary source of capacity loss, we propose a related acid induced degradation of the anode SEI. A systematic investigation of LMO, LNMO, NMC622, and MNC811 cathodes will be presented. The role of potential on the generation of soluble acidic fluorophosphates crossover species and the impact of these species on the structure and stability of the SEI will be presented.

2:00 PM CH01.02.02

In Operando Visualization and Data-Driven Modeling of Ion Transport in Electrolytes for Lithium Metal Batteries [Yuan Yang](#); Columbia University, United States

In-operando Visualization of ion transport in electrolyte provides fundamental understandings of electrolyte dynamics and electrolyte-electrode interaction, shedding light on material designs to enhance device performance, such as batteries and fuel cells. However, this task is extremely challenging for existing techniques, since it is difficult to capture the low ionic concentration (<1 M) and the fast dynamics (1-10 s) of the electrolyte. Here we show that an emerging Stimulated Raman Scattering (SRS) microscopy offers the required spatial (sub-micrometer optical resolution), temporal (faster than 1 s per frame) and chemical (around mM) sensitivities to address this challenge.

The SRS microscopy has been used to study ion depletion and lithium dendrite growth in both liquid and polymer electrolyte, and distinct behaviors are observed. In liquid electrolyte, we observe a three-stage lithium deposition process, each corresponding to no-depletion, partial-depletion and full-depletion regime of Li⁺, respectively. A positive feedback mechanism between the inhomogeneous growth of lithium and the local ionic concentration or flux. In polymer electrolyte, we clearly see phase separation due to ion depletion and observe the accompanying transport of plasticizer inside, which was not observed in the past. These new understanding also leads to new strategies to suppress lithium dendrites. Moreover, the high-speed image acquisition also enables data-driven modeling to understand the relation between local material properties (e.g. salt concentration) and dendrite growth. A neural network modeling is built to understand how different factors affect dendrite growth.

2:15 PM CH01.02.03

Operando AFM and Electrochemical Characterization of the Growth of the Solid Electrolyte Interphase [Harry Thaman](#)^{1,2}, Che-Ning Yeh¹, Justin Rose¹ and William C. Chueh¹; ¹Stanford University, United States; ²SLAC National Accelerator Laboratory, United States

Understanding the formation and operation of the solid electrolyte interphase (SEI) is critical to the development of lithium metal batteries because of the continuous evolution of new surface area which necessitates a rapidly passivating SEI to minimize capacity loss. However, because of the highly sensitive, heterogeneous, and continuously evolving nature of the SEI, it remains challenging to develop a fundamental understanding of how SEI morphology relates to key metrics such as ionic conductivity and formation rate. To probe the role of these parameters in the SEI evolution, we combine operando atomic force microscopy (AFM) with electrochemical characterization to extract the relationships between the SEI's roughness and its efficacy at forming a self-passivating layer.

Using a combination of electrochemical impedance spectroscopy (EIS) and capacity measurement during constant voltage holds, we observe formation process in which the initially deposited SEI substantially increases the ionic impedance while subsequently grown SEI produces limited impedance increases despite consuming significant amounts of lithium. These observations are supported by operando AFM measurements taken during the SEI formation process. The AFM topography measurements reveal a two part SEI microstructure composed of a compact film interspersed with large nuclei

that make up a substantial fraction of the SEI volume but cover relatively little of the surface area. This observation matches our electrochemical observation of SEI composed of both passivating and non-passivating components.

To further investigate the morphology and composition of the SEI layer, we leverage the AFM system to scrape away the soft outer layer of the solid electrolyte interphase and quantify roughness and thickness properties of both the inner and outer layers of the SEI to further understand the role the SEI components play in the previously measured EIS and SEI growth rate measurements. Ultimately, by relating electrochemical properties of the SEI - both in steady state and EIS measurement modes - to its morphology and thickness we provide correlations between easily measured average electrochemical properties and critical but hard-to-measure nanoscale properties that we hope will inform the development of advanced electrolytes and formation protocols for anode free and lithium metal batteries.

2:30 PM CH01.02.04

In Situ Characterization of Solid Liquid Interface by Infrared Nanospectroscopy Xiao Zhao^{1,2}, Yi-Hsien Lu¹ and Miquel Salmeron^{1,2}; ¹Lawrence Berkeley National Laboratory, United States; ²University of California, Berkeley, United States

The solid-liquid interface plays a crucial role in many natural process and practical applications, such as corrosion, electrochemical catalysis and energy storage. Fundamental insights of solid-liquid interface are necessary to understand these processes, but currently these studies are hampered by the shortage of appropriate characterization tools. Extensive efforts have been made to develop or improve *in-situ* or *operando* characterization techniques to study the information of solid phase near interface, while the knowledge on the liquid layers at interface, including ion concentration, double layer structure and speciation, is still limited.

Here we present a new nondestructive methodology that enables molecular study of liquid layer near interface with nanoscale spatial resolution. It is based on Fourier transform infrared nanospectroscopy (nano-FTIR), where the infrared (IR) field is plasmonically enhanced near the tip apex of an atomic force microscope (AFM). Ultra-thin freestanding membrane (single layer graphene or 2-5nm thick metal oxide film grown by atomic layer deposition (ALD)) separates AFM tip and electrolyte while acting as working electrode. We illustrate this method by comparing interface-sensitive nano-FTIR spectra with bulk-sensitive spectra obtained by ATR-FTIR and demonstrate its capability to determine changes in chemical composition and molecular structure near solid-liquid interface under electrochemical condition. These membranes can be further functionalized with synthesized nanoparticles to study the catalytic microenvironment under electrochemical condition. This platform developed and presented here will open up new avenues for the study of catalytic, electrochemical, geochemical, and other reactions at interfaces in practical conditions.

2:45 PM CH01.02.05

Energy Dispersive X-Ray Diffraction (EDXRD) as a Synchrotron Technique for Spatially-Resolved *Operando* Study of Buried Materials and Interfaces Within Batteries Joshua W. Galloway; Northeastern University, United States

Energy dispersive X-ray diffraction (EDXRD) from a high energy source enables *operando* study of battery materials within their real-world form factor and containment. This is thanks to the (a) use of a highly penetrating incident X-ray white beam (20-200 keV) and (b) placement of the detector and sample to define a well-controlled diffraction gauge volume in space. The shape of this gauge volume allows spatial resolution of ten of microns when positioned inside a battery, and movement of the battery along a scanning direction allows construction of diffraction profiles across electrodes, all with time resolution of tens of seconds. This technique can identify formation of new phases as well as map fine changes in active material lattice parameters, the latter of which is equivalent to obtaining spatially resolved state-of-charge information in the case of intercalation electrodes. Because development of both high energy density and low cost batteries is enabled by designs with thick electrodes, the types of material profiles provided by EDXRD are highly relevant for the present day thrust of battery engineering. Thick electrodes, while desirable, bring extra challenges because they can cause inhomogeneities within the battery that lead to uneven active material utilization and/or battery failure. While the fundamental electrochemistry of battery active materials can be known from laboratory experiments, system-level phenomena not necessarily inherent to the active materials can have an equally profound impact on battery performance. EDXRD is a powerful tool for probing this information, with no need to adjust the cell construction, which could alter the resultant electrochemistry. Due to its highly penetrating nature, EDXRD is also ideally suited for collecting *operando* data from within batteries at high temperature or under high pressure. Some current solid-state battery designs require high cell compression to ensure good interfacial contact, and this makes *operando* data collection challenging using techniques other than EDXRD.

This talk will address the fundamentals of EDXRD, as well as provide examples of its use to establish mechanistic knowledge in several types of batteries, including (1) rechargeable alkaline batteries with electrodes of thicknesses of >1mm, (2) sulfide all solid-state batteries tested under high compression, and (3) multivalent ion batteries tested at elevated temperature within unmodified coin cells. In alkaline rechargeable batteries, EDXRD was used to establish a catalytic effect by Bi-containing additives to favor formation of rechargeable Mn(OH)₂ over terminal Mn₂O₄. In all solid-state batteries, EDXRD demonstrated a crystalline instability of a sulfide solid-state electrolyte, Li_{6.6}Ge_{0.6}Sb_{0.4}S₅I (LGSSI), which was observed only in the cathode and not elsewhere in the cell. This was due to reduction of the LGSSI when in contact with active material and conductive carbon in the cathode during discharge. It was also shown that this crystalline change was reversible if the cell lower voltage limit was correctly chosen. Finally, *operando* observation of the intercalation reaction of both Al³⁺ and Zn²⁺ was collected for Chevrel Mo₆S₈ and Mo₆Se₈ cathode hosts. This was accomplished from within unaltered, sealed coin cells, which was important as previous literature has suggested that the fully intercalated species can be inadvertently oxidized during destructive sample preparation.

Acknowledgments

This work was supported by the U.S. Department of Energy (DOE) Office of Electricity Delivery and Energy Reliability, Dr. Imre Gyuk, Energy Storage Program Manager. We also acknowledge financial support from the National Science Foundation under Award Number CBET-ES-1924534.

3:00 PM CH01.02.06

In Situ and *Operando* Characterization of Capacity and Efficiency Limiting Phenomena in Electrochemical Energy Storage Systems Amy Marschilok^{1,2}, Esther S. Takeuchi^{1,2} and Kenneth Takeuchi^{1,2}; ¹Stony Brook University, United States; ²Brookhaven National Laboratory, United States

Parasitic side reactions can limit the capacity and efficiency of the energy storage system, via formation of resistive interfaces and consumption of redox active material/s. Transport limitations can also impact functional capacity of systems, and can manifest at different states of (dis)charge and as a function of time over extended cycling. In this presentation, insights in elucidating and quantifying productive and parasitic processes from complementary *in situ*, and *operando* spectroscopy, diffraction and electrochemistry studies will be highlighted.

4:00 PM *CH01.03.01

Looking into Key Components for Next Generation Batteries with *Operando* X-Ray Tomography Aleksandar Matic, Matthew Sadd and Shizhao Xiong; Chalmers University of Technology, Sweden

New configurations and chemistries for next generation batteries are currently in focus as a response to needs from sustainable energy technologies and transport applications. The electrochemical mechanism for next generation batteries is often based on conversion reactions and transport of active material, which is different from the “Rocking Chair” concept in current state-of-the-art, the Li-ion battery. To probe these processes *operando* computed X-ray tomography is a powerful technique which allows nondestructive and quantitative imaging in 3D of materials and components during operation. A particular advantage is the possibility to quantitatively correlate the 3D morphology to electrochemical data recorded simultaneously if the whole cell can be within the field of view. With the high flux of 3rd and 4th generation synchrotron sources rapid acquisition (sub minute for a full tomogram with sub μm resolution) opens the possibility for *operando* studies, even at high discharge rates.

In this contribution we show how X-ray tomography can be used to provide insights on processes in Li-sulfur (LiS) cells and the Li-plating process in Li-metal batteries, two promising next generation battery concepts. In LiS-cells the electrochemical conversion of elemental sulfur delivers a very high theoretical specific capacity (1672 mAh/g). The conversion takes place through a series of soluble intermediate polysulfide species (Li_2S_n) whereas the end product, Li_2S , is insoluble in the common electrolytes used [1]. This mechanism leads to continuous dissolution/precipitation processes during cycling which are closely related to the difficulty in reaching a high specific capacity in practice due to poor active material utilization. This can be related to elemental sulfur in the cathode not being converted, dissolved polysulfides diffusing out of the cathode and not being further converted, or Li_2S forming a continuous insulating layer that blocks access to the conducting part of the cathode matrix and stops the conversion reaction. With an *operando* X-ray tomography experiment we are able to directly follow the dissolution/precipitation processes at discharge with the whole cathode within field of view using a capillary *operando* cell. This enables us to quantitatively correlate the sulfur conversion/dissolution process to the charge delivered by the cell. In a multi-modal approach we also follow the diffusion of polysulfides species in the electrolyte with an *operando* optical imaging experiment in the same cell.

Common for several of the high-capacity concepts is the use of Li-metal as the anode. However, preferred electrodeposition of Li-metal can lead to a mossy or dendritic morphology, as a result of depletion of Li-ions at the electrode surface [2,3]. In combination with the high reactivity of Li this results in a continuous breakdown of the electrolyte during cycling and the formation of “dead Li”, manifesting in a low coulombic efficiency. These phenomena are accelerated at low operating temperatures, in dilute electrolytes or high applied current densities. To build an understanding of the plating process we use *operando* X-ray tomography to reveal the 3D-geometry and kinetics of dendrite growth during cycling to build a connection between the properties of the new electrolytes, and the microstructure formed on the Li-metal anode. These results are correlated to phase-field modelling to provide a mechanistic understanding of the plating process.

References

- [1] M. Agostini, J. Y. Hwang, H. M. Kim, P. Bruni, S. Brutti, F. Croce, A. Matic, Y. K. Sun, Adv. Energy Mater. 8, 1801560 (2018)
- [2] Y. Liu, X. Xu, M. Sadd, O. O. Kapitanova, V. A. Krivchenko, J. Ban, J. Wang, X. Jiao, Z. Song, J. Song, S. Xiong, A. Matic, Adv. Sci. 8, 2003301 (2021)
- [3] X. Xu, Y. Liu, J. Y. Hwang, O. O. Kapitanova, Z. Song, Y. K. Sun, A. Matic, S. Xiong, Adv. Energy Mater. 10, 2002390 (2020)

4:30 PM CH01.03.02

Unveiling the Relation Between Electrochemical Performance and Nanostructure of Fuel Cell Electrode Materials via Scanning SAXS and Ptychographic X-Ray Nanotomography Christian Appel¹, Katharina Jeschonek², Kai Brunnengräber², Bastian J.M. Etzold², Marianne Liebi^{3,4} and Manuel Guizar-Sicairos¹; ¹Paul Scherrer Institute, Switzerland; ²Technische Universität Darmstadt, Germany; ³Empa–Swiss Federal Laboratories for Materials Science and Technology, Switzerland; ⁴Chalmers University of Technology, Sweden

Future energy solution require development of advanced composite materials. Such materials are for example catalyst layers of polymer electrolyte membrane fuel cells (PEMFCs) where electricity is generated by electrochemical reactions that take place in a complex environment. These layers are porous materials built up from three different components; chemically active sites, electron conducting support and proton conducting binder. This study focusses on investigating Pt nanoparticles on carbon black support (PTC, HiSPEC 3000), spray-coated on a polymer membrane with varying amounts of binder (PTFE – ionomer) but an equal loading of catalyst ($m_{\text{Pt}} = 0.2 \text{ mg/m}^2$).

The meso and nanoscale structure of the catalyst is investigated by a correlative approach based on two techniques; scanning small-angle X-ray scattering (SAXS) and ptychographic X-ray computed nanotomography (PXCT). From scanning SAXS we obtain statistical information about the nanostructure, in the range of 1 to 300 nm, probed in local areas of $10 \times 10 \mu\text{m}^2$ which correspond to the scanning step size over macroscopic areas of $1 \times 1 \text{ mm}^2$. X-ray fluorescence spectra were simultaneously collected, with which we can then map the Pt content in the layers based on the Pt- M_{α} emission line at 2.05 keV. 2D maps of X-ray scattering and XRF, integrated over a specific q-range and energy-range, respectively, were processed and allow quantification of sample homogeneity in terms of nanostructure and Pt distribution across the macroscopic length scale. This data was further used to choose specific representative areas to mill out cylindrical $20 \mu\text{m}$ sized pillars using FIB/SEM. These pillars were investigated under cryogenic temperatures to avoid radiation damage with the OMNY setup at the cSAXS beamline to reveal the 3D nanostructure with PXCT down to a 3D half-period resolution of 26 nm.

PXCT measures the 3D electron density from $20 \mu\text{m}$ down to 26 nm, which perfectly bridges the gap between the macroscopic domains probed by scanning SAXS (1 mm to $10 \mu\text{m}$), and the statistically averaged information of the nanoscale probed by SAXS (1 nm to 300 nm) for local areas of $10 \times 10 \mu\text{m}^2$. PXCT measurements alone are already able to provide valuable information to distinguish structural features of the three different catalysts. Threshold segmentation reveals differences in the pore size distribution as well as connectivity of pores. This information is crucial for a better understanding of gas and liquid transport mechanisms within the catalyst. However PXCT cannot reveal the chemically active sites due to limitations in spatial resolution, namely the Pt nanoparticles of 2-3 nm diameter where the electrochemical reaction takes place. In this work, we explore different approaches to correlate the imaging data from PXCT with the statistical data from SAXS and XRF. Our vision is to generate 3D representative models for catalyst layers based on its imaged structure by PXCT, but further complemented with statistical data from SAXS and XRF measured from the exact same sample. Such models are strongly desired in flow simulations on PEMFCs to further understand limiting factors for their performance. In addition, our study also explores novel routes in correlative data analysis combining imaging with scattering experiments. These insights may further lead to new approaches and studies in investigating porous materials.

This project has received funding from the European Union’s Horizon 2020 research and innovation program under the Marie Skłodowska-Curie grant

agreement No 701647 (PSI-FELLOW-III-3i) and funding from the Chalmers initiative for advancement of neutron and x-ray techniques. The authors acknowledge the funding from the European Research Council (ERC) under the European Union's Horizon 2020 research and innovation program (grant agreement No. 681719). We also acknowledge the Paul Scherrer Institut, Villigen, Switzerland for provision of synchrotron radiation beamtime at beamline cSAXS of the SLS.

4:45 PM OPEN DISCUSSION

5:00 PM CH01.03.04

***In Situ* XANES of Non-Stoichiometric Vanadium Oxide During Electrochemical Cycling of Aqueous Zn-Ion Battery** Christopher J. Patridge, D'youville College, United States

Multivalent ion batteries represent a unique approach to increasing energy capacity for electrochemical storage. While Li-ion batteries (LIB) are the dominant technology that continues to advance with novel architectures and engineering, there still exists serious issues of thermal sensitivity and runaway. Aqueous systems would significantly reduce these thermal concerns and also drop the economic costs associated with the organic solvents that compose the electrolytes in LIBs. The Zn ion (+2) gives twice the capacity and the ionic radii (0.78 angstroms) matches closely to the Li ion. The increased electronic/structural disruption imposed by intercalating a +2 ion finds some relief by co-intercalation of H₂O along with sandwich layered structures often associated with the multitude of vanadium oxide polymorphs.

Synchrotron work at NSLS-II BM-6 looked at the XANES and EXAFS dependence on voltage. Using crystal structure data for the material, theoretical XAFS scattering was compared to the experimental data to establish possible local site occupancy for the intercalated Zn ion. Further in-situ experiments on both Zn_{0.25}V₂O₅ and Ca_{0.25}V₂O₅ were performed using a novel electrochemical cell. Both materials exhibit a clear change in the local geometry and oxidation state of the vanadium in the active material with early cycle reversibility. Integrated XANES difference spectra are correlated with the approximate shift of vanadium from a nominal oxidation state of +4.75 down to +4.00 if assuming an approximate fully discharged state stoichiometry of Zn₁V₂O₅ or Ca_{0.25}V₂O₅.

5:15 PM CH01.03.07

Kelvin Probe Force Microscopy Provides New Insights into Electrochemical Reactions via Suspended Graphene Irit Rosenhek Goldian¹, Salma Khatun¹, Sidney R. Cohen¹, Sa'ar Shor Peled¹, Robert S. Weatherup² and Baran Eren¹; ¹Weizmann Institute of Science, Israel; ²University of Oxford, United Kingdom

Probing processes at electrode-electrolyte interfaces promises new insights into electrochemical reactions, which are inherent to many sustainable energy storage and conversion technologies.

Kelvin Probe Force Microscopy (KPFM) is widely used to map work function (surface potential) variations at the nanoscale in ambient or vacuum conditions. KPFM could be of great importance for electrochemical systems, but is impractical in polar liquids due to screening and interference from surrounding fluid. Capping a liquid-cell by free-standing single-layer graphene (SLG) serving as the working electrode, enables a stable KPFM measurement on the SLG working electrode to monitor its Fermi-level shift and is sensitive to processes occurring at the liquid-solid interface. The graphene-membrane physically separates the scanning tip from the conducting solution. With KPFM, localized information can be obtained for single SLG regions, unlike techniques like cyclic voltammetry (CV), where the signal is averaged over the entire reactor-cell.

We have applied this approach to study small electrochemical cells of 500 nm diameter capped by SLG under electrochemical reaction conditions. We used a polymer-free transfer method in order to avoid the presence of polymer residues that would alter the measured WF and the interfacial activity of the graphene. Measurement at different alkaline pH values enabled investigation of the influence of the electrical double layer (edl). This method enabled us to perform statistical measurements by monitoring several cells, following them through a few cycles while correlating the different signals recorded simultaneously (Topography, phase, KPFM).

Our experimental results correlate well with a simple electrochemical gating model, shedding light on the interplay between electronic and electrochemical doping (through redox of water) processes in the suspended graphene. The observed topographical changes in the suspended graphene in the form of bulging are attributed to electro-wetting of graphene induced by charge-carrier doping.

The experimental approach and results presented here serve as a benchmark for future studies of the electrochemical behavior of two-dimensional materials both in aqueous and organic electrolytes, and the underlying mechanisms of doping.

SESSION CH01.04: Poster Session I
Tuesday Afternoon, November 30, 2021
8:00 PM - 10:00 PM
Hynes, Level 1, Hall B

CH01.04.02

Li Deposition in a Highly Concentrated Electrolyte Studied by *In Situ* Neutron Reflectometry Josef Rizell¹, Anton Zubayer², Matthew Sadd¹, Filippa Lundin¹, Nataliia Mozhzhukhina¹, Alexei Vorobiev^{3,4}, Shizhao Xiong¹ and Aleksandar Matic¹; ¹Chalmers University of Technology, Sweden; ²Linköping University, Sweden; ³Uppsala University, Sweden; ⁴Institut Laue-Langevin, France

Li-metal has a theoretical specific capacity of 3860 mAh/g, ten times larger than that of graphite (372 mAh/g). In combination with the low reduction potential of Li, this entails Li-metal batteries (LMB) with significantly higher energy densities compared to Li-ion batteries. [1] However, the long-term cycling of LMBs is hindered by several parasitic effects linked to Li deposition. In the worst case scenario, uncontrolled Li-plating results in dendrites that can pierce the separator and short circuit the cell. Lithium plated in a dendritic morphology is also more prone to lose contact with the electrode, forming so called dead Li, leading to loss of active material and poor coulombic efficiency. Furthermore, uneven Li-morphologies expose more fresh Li to the electrolyte, leading to continuous electrolyte consumption in side reactions.

To stabilize the Li-metal anode, one of several routes is to tune the electrolyte composition. Recently, we have shown that electrolytes with higher salt concentrations can enable stable cycling and uniform Li-plating [2]. This improvement in electrochemical performance can be rationalized by (1) a mitigated risk of Li-ion depletion at the electrode surface (Li-ion depletion would cause rapid dendrite growth) (2) the tendency for these electrolytes to form a stable surface layer at the anode. However, more work is needed to fully understand the mechanism for the improved efficiency of Li-plating in highly concentrated electrolytes.

Due to the very low potential of the anode during Li plating, the electrolyte will tend to decompose on the electrode surface to form a surface layer, the solid electrolyte interphase (SEI). This layer is an important factor for efficient Li plating and stripping. [3] However, the sensitivity of the SEI makes several characterization methods elusive. Any ex situ characterization, like x-ray photoelectron spectroscopy, is associated with large uncertainties regarding the stability of the SEI under a change of environment.

Instead, in situ and operando characterization of the SEI layer becomes important for building a better understanding of its role in Li deposition. In this contribution we report on a neutron reflectometry study of SEI formation and early stages of Li-metal plating, performed with the reflectometer SuperADAM at ILL. Due to the weak interaction of neutrons with matter it is possible to build an in-situ sample environment where the neutron beam can enter the cell through the back side of the working electrode. Using a custom made Li-Cu cell, we probe the formation of surface layers on the Cu working electrode. By measuring the reflectivity as a function of momentum transfer, we detect the changes in the neutron scattering length density arising as a result of a changing surface layer, thickness and composition, on the working electrode. In this study we compare Li deposition in a highly concentrated electrolyte (4M salt concentration) with an electrolyte with conventional salt concentration (1M) and discuss how the electrode/electrolyte interface evolves and influences the Li deposition.

[1] Li, L.; Basu, S.; Wang, Y.; Chen, Z.; Hundekar, P.; Wang, B.; Shi, J.; Shi, Y.; Narayanan, S.; Koratkar, N. *Science* **2018**, *359* (6383), 1513-1516.

[2] Xu, X., Liu, Y., Hwang, J.-Y., Kapitanova, O. O., Song, Z., Sun, Y.-K., Matic, A., Xiong, S. *Adv. Energy Mater.* 2020, 2002390.
<https://doi.org/10.1002/aenm.202002390>

[3] Lin, D.; Liu, Y.; Cui, Y. *Nat. Nanotechnol.* **2017**, *12* (3), 194-206.

CH01.04.03

Direct Insight into Electrochemical Processes in Alkali-Ion Cathodes from Operando Electron Spin Probes Howie Nguyen, Daniil Kitchaev, Emily Foley, Allyson Ee, Yuefan Ji and Raphael J. Clement; University of California, Santa Barbara, United States

Operando electron paramagnetic resonance (EPR) enables to monitor the evolution of the local crystal and electronic structure of lithium-ion electrodes in real time, by following changes in EPR spectral linewidth and intensity.¹ These spectral changes are induced by the evolving magnetic-exchange interactions between transition metal species in the electrode material during battery operation. However, ambiguities can still arise as to the exact interpretation of *operando* EPR datasets since different charge-compensation reactions can lead to similar trends in linewidth and intensity. Additionally, traditional EPR detection is limited to transition metal species with spin-allowed transitions (spin ½ species) and favorable spin relaxation times. We address these shortcomings by conducting *operando* EPR in tandem with *operando* magnetometry, where the bulk magnetic susceptibility is used as an additional filter to parse out different local redox processes. This combined *operando* electron spin probe approach is applied to the LiNi_{0.5}Mn_{0.5}O₂ cathode, and complemented with DFT calculations of magnetic J-couplings. EPR results show an evolving signal that disappears at high potentials and Mn dissolution after the initial cycle. *Operando* magnetometry is used to decipher electrode changes during the regions of undetectable EPR. Other applications of our *operando* magnetometry cell include probing reaction mechanisms and estimating irreversibility in the conversion-type Na₃FeF₆ cathode. Magnetic susceptibility changes during cycling suggest Na-ion initially intercalates into carbon additives before the active material is converted into NaF and Fe. The reaction products are unable to convert back to Na₃FeF₆ as indicated by an irreversible change in magnetic susceptibility. Furthermore, the instability of this system is highlighted by a growing magnetic susceptibility during a relaxation period after cycling.

(1) Nguyen, H.; Clément, R. J. *Rechargeable Batteries from the Perspective of the Electron Spin.* *ACS Energy Lett.* **2020**.

<https://doi.org/10.1021/acsenerylett.0c02074>.

CH01.04.04

Isothermal Microcalorimetry Characterization of Lithium Battery Storage Materials and Mechanisms Wenzao Li¹, Lisa House², Calvin D. Quilty¹, Mallory Vila¹, Lei Wang², Christopher Tang¹, David Bock², Kenneth Takeuchi^{1,2}, Esther S. Takeuchi^{1,2} and Amy Marschilok^{1,2}; ¹Stony Brook University, United States; ²Brookhaven National Laboratory, United States

Li ion batteries, one of the most popular energy conversion and storage devices, are widely applied as power sources for electronics, electric vehicles, and medical devices. However, when current flows through Li ion batteries upon charge or discharge, heat is triggered and can lead to many undesirable consequences: (1) heat is considered wasted energy that is typically not converted to useful electrical work; (2) heat could provoke a local temperature increase within the battery that accelerates the ageing of electrodes and electrolyte for those with poor thermal stability; (3) the accumulation of heat, especially in large-scale battery packs, may cause safety hazards. Therefore, monitoring thermal behavior of Li ion batteries under load currents is an insightful way to understand electrochemical mechanisms, diagnose batteries' failure mechanisms, and navigate safety management.

Operando isothermal microcalorimetry (IMC) is a precise characterization method that can measure the real-time heat flow dissipated from batteries while cells are undergoing synchronous electrochemical cycling. We applied the IMC method to investigate multiple lithium storage systems covering both conversion and insertion type electrode materials. Heat flow features visualized by the IMC provide information on the kinetics and thermodynamics of electrode materials' chemistry and electrode-electrolyte interactions. Among sources of cell's heat generation, the heat flow associated with parasitic reactions can be quantified as an indicator of interfacial reactions, mainly the formation and evolution of the SEI. Further, the structural change of electrode materials was also found to be a factor governing the heat generation. These results inspire us to pave new ways of understanding phase evolution of Li storage materials via thermodynamics.

SESSION CH01.05: Multiscale Techniques
Session Chairs: Kent Griffith and Aleksandar Matic
Wednesday Morning, December 1, 2021
Hynes, Level 3, Room 304

10:30 AM *CH01.05.01

Insights into Battery Processes from the Perspective of the Electron Spin Howie Nguyen, Emily Foley, Daniil Kitchaev, Allyson Ee, Yuefan Ji and Raphael J. Clement; University of California, Santa Barbara, United States

Advances in rechargeable batteries rely on the discovery of high power, high energy density electrode materials, but also on mitigating degradation mechanisms. Understanding how a battery works and why it fails requires the development of cutting-edge characterization tools capable of monitoring structural changes and redox reactions at the surface and in the bulk of the electrodes as the battery is (dis)charged. The fundamental insights thereby

gained are key to designing new compounds for high performance batteries.

Electron paramagnetic resonance (EPR) and magnetometry offer a rare perspective on structural and redox processes from the standpoint of electron spins and magnetic interactions between redox-active species, holding promise for breakthroughs in our understanding of charge-discharge phenomena in battery materials. Our group has recently developed *operando* EPR and magnetometry cells to investigate such processes in real time. In this talk, I will briefly discuss when EPR and magnetometry are best used and how *operando* datasets are analyzed. Specifically, our recent work has shown that the interpretation of the broad EPR spectra obtained on paramagnetically-concentrated electrodes is challenging and requires the tandem use of magnetometry.¹ I will also present our recent (and preliminary) work on both intercalation and conversion electrodes using these powerful tools.

References

1. H. Nguyen and R. J. Clément, *ACS Energy Letters*, **5**, 3848–3859 (2020).

11:00 AM CH01.05.02

Operando Surface Enhanced Raman Spectroelectrochemistry for Mechanistic Understanding of Energy Storage in Lithium/Sodium/Potassium Ion-Batteries Containing Few-Layered 2D Anodes Mariusz Radtke and Christian Hess; Technical University of Darmstadt, Germany

Reaction mechanisms underlying energy storage and intercalation in lithium/sodium/potassium-ion batteries (LIB, NIB, KIB) were investigated in few layers 2D FeS₂, SnS₂, TiS₂ and MoS₂ by means of *operando* surface enhanced Raman spectroelectrochemistry (SERSEC).

The few-layers 2D materials were prepared by anodic exfoliation from bulk in mild K₂SO₄ media and characterized by HRTEM, XPS, Raman and EDX. Each sample exhibited similar Raman signature of two most prominent modes- A_{1g} and E_g, which were basis for the *operando* experiments. During the *operando* SERSEC A_{1g} mode in SnS₂ exhibited considerable red shift by 20 cm⁻¹ in the anodic oxidation scan, due to the generation of Sn-S-Li bond, as evaluated by the post-mortem XPS after the reaction. On the contrary the intercalation of Li⁺-ion in FeS₂, TiS₂ and MoS₂ was purely physical, as based on ion insertion between the the layers of 2D materials.

All *operando* electrochemical and SERSEC measurements were performed in a specially-designed spectroelectrochemical cell equipped with borosilicate windows modified with mercaptosilicate gold clusters of varying sizes attached covalently to the window, which were able to create hot-spots with localized plasmon resonances (LPR). The clusters were designed to be electrochemically inert (silicate shell) and LPR Raman active (gold core), as proven by the electrochemical DPV scan. The MALDI-TOF/TOF MS analysis has revealed that the gold clusters were created in mostly icosahedral shapes, as based on m/z analysis. The electrochemically inert borosilicate windows have allowed for performing of highly precise *operando* experiments (analytical enhancement factor: 4282).

In addition we discuss the potential of expanding SERSEC with the spectroscopic LPR windows by introduction of e.g. time-resolved *operando* 4D and 5D electrochemical impedance spectroscopy (EIS) for exact Raman mapping of bulk RedOx reactions with spatial resolution at the Abbé limit.

References

C. Hess, *Chem. Soc. Rev.*, 2021,50, 3519-3564

M. Radtke, C. Hess *Operando* Raman shift replaces current in Butler-Volmer analysis of Li-ion batteries: a comparative study (submitted) 2021

M. Radtke, C. Hess, K. Kopp Coupling long-range Raman with X-ray Photoelectron Spectroscopy for complementary bulk and surface characterization of battery materials (submitted) 2021

11:15 AM CH01.05.03

Elucidating the Role of Halides and Iron During Radiolysis Driven Oxidative Etching of Gold Nanocrystals Using Liquid Cell TEM and Pulse Radiolysis Michelle Crook¹, Christian Laube¹, Ivan Moreno-Hernandez¹, Axel Kahnt², Stefan Zahn², Justin C. Ondry¹, Aijia Liu¹ and A. Paul Alivisatos¹; ¹University of California, Berkeley, United States; ²Leibniz Institute of Surface Engineering (IOM), Germany

Graphene liquid cell transmission electron microscopy (TEM) has enabled the observation of a variety of nanoscale transformations. Yet understanding the chemistry of the liquid cell solution and its impact on the observed transformations remains an important step towards translating insights from liquid cell TEM to bench-top chemistry. Gold nanocrystal etching can be used as a model system to probe the reactivity of the solution. FeCl₃ has been widely used to promote gold oxidation in bulk and liquid cell TEM studies, but the roles of the halide and iron species have not been fully elucidated. In this work, we observed the etching trajectories of gold nanocrystals in different iron halide solutions. We observed an increase in gold nanocrystal etch rate going from Cl⁻ to Br⁻ to I⁻-containing solutions. This is consistent with a mechanism in which the dominant role of halides is as complexation agents for oxidized gold species. Additionally, the mechanism through which FeCl₃ induces etching in liquid cell TEM remains unclear. Ground state bleaching of the Fe(III) absorption band observed through pulse radiolysis indicates that iron may react with Cl₂⁻ radicals to form an oxidized transient species under irradiation. Complete active space self-consistent field (CASSCF) calculations indicate that the FeCl₃ complex is oxidized to an Fe species with an OH radical ligand. Together our data indicates that an oxidized Fe species may be the active oxidant, while halides modulate the etch rate by tuning the reduction potential of gold nanocrystals.

11:30 AM CH01.05.04

Nanoscale Chemical and Structural Analysis During In Situ Scanning/Transmission Electron Microscopy in Liquids Rui F. Serra-Maia¹, Pawan Kumar¹, Andrew C. Meng¹, Alexandre Foucher¹, Yijin Kang², Deep M. Jariwala¹, Khim Karki³ and Eric A. Stach^{1,3}; ¹University of Pennsylvania, United States; ²Northwestern University, United States; ³Hummingbird Scientific, United States

Liquid-cell scanning/transmission electron microscopy (S/TEM) has emerged as an effective in-situ / *operando* approach to characterize electrochemical systems. This approach confines both the sample of interest, electrolyte and microfabricated electrodes between two silicon nitride membranes to allow materials characterization in aqueous environments. While powerful, the thickness of the liquid layer and the nitride membranes inhibits high-resolution characterization. We will show that it is possible to overcome these limits to a great extent by utilizing electrochemical water splitting to generate a gas bubble that reduces the liquid to a film that is approximately 30 nm thick and which remains on the sample. This reduction in liquid thickness permits the acquisition of atomically resolved S/TEM images, electron diffraction patterns, and electron energy loss spectra with sufficiently high signal to noise to allow characterization of valence. After high-resolution characterization, the gas bubble can be eliminated by water oxidation. This allows us to alternate between a full cell and thin-film condition so that we can obtain optimal electrochemical cycling (full cell) and intermittent, controllable analytical characterization. We will show how we use this method to advance our understanding of several different electrochemically driven processes, including dealloying of nanoporous AuAg alloys and CO₂-driven shape changes in copper nanoparticle systems.

SESSION CH01.06: Spectroscopy Techniques I
Session Chair: Raphael Clement
Wednesday Afternoon, December 1, 2021
Hynes, Level 3, Room 304

1:30 PM *CH01.06.01

Exploring Complex Oxide Structural Motifs in Lithium-Ion Battery Anodes with Diffraction and Spectroscopy Kent J. Griffith, G. J. Snyder and Kenneth R. Poeppelmeier; Northwestern University, United States

Complex early transition metal oxides have emerged as leading candidates for fast charging lithium-ion battery anode materials. Framework crystal structures with frustrated topologies are good electrode candidates because they may intercalate large quantities of guest ions with minimal structural response. Starting from the empty perovskite (ReO₃) framework, shear planes and filled pentagonal columns are examples of motifs that decrease the structural degrees of freedom. As a consequence, many early transition metal oxide shear and bronze structures do not readily undergo the tilts and distortions that lead to phase transitions and/or the clamping of lithium diffusion pathways that occur in a purely corner-shared polyhedral network.

In this work, we explore the relationship between composition, crystal structure, and reduction pathway in a variety of mixed transition metal and main group oxides. The electrochemical properties of a series of sodium and lithium niobates are studied as new fast-charging lithium-ion battery electrode materials. High-resolution neutron diffraction is used to resolve structural questions in the host materials related to sodium disorder, space group subtleties, lithium positions, and second-order Jahn-Teller distortions of the d⁰ Nb⁵⁺ redox centers. Structural evolution is followed in real-time at rapid discharge/charge rates with *operando* synchrotron X-ray diffraction, collecting high-resolution diffraction patterns in a few seconds. The structure models from diffraction are informed by the local structure perspective from solid-state NMR spectroscopy and *operando* X-ray absorption spectroscopy (XANES and EXAFS), while the structural (meta)stability and ionic properties are probed through density functional theory (DFT) calculations. A comprehensive picture of the charge storage mechanisms in these complex oxides are described. Prospects for tunability and implications for charge rate and structural stability will be discussed.

2:00 PM CH01.06.02

Quantifying Electron-Beam Induced Electrochemistry Using *In Situ* KPFM Evgheni Strelcov^{1,2}, William McGehee¹, Vladimir Oleshko¹, Nikolai Zhitenev¹, Jabez McClelland¹ and Andrei Kolmakov¹; ¹National Institute of Standards and Technology, United States; ²University of Maryland, United States

Nanoscale characterization of solid-state electrochemical devices is crucial for understanding functional mechanisms and limiting factors in device operation. Many characterization techniques use electron microscopy and associated electron and X-ray spectroscopies, but these techniques are limited by electron- or X-ray-radiation-induced modification of the device. While the standard solution to this problem is to limit the irradiation dose to a minimum, we demonstrate the utility of some electron-beam-induced changes to probe nanoscale electrochemistry. Careful selection of electron beam parameters allows the employment of the electron beam not just as a probe, but as an active electron source to create a nanoscopic virtual anode and cathode to study *in situ* and *in vacuo* solid-state electrochemistry. We quantify electron-beam-induced variation in surface potential in electrochemical systems using *in situ* Kelvin probe force microscopy. Correlation of the surface potential and material's work function changes with the electron beam dose and energy as well as with the amount of the reaction products, revealing details of the electrochemical transformation mechanisms. We compare local oxidation and reduction in several systems, including lithiated silicon, a Li-ion conductor, metallic lithium, magnesium and platinum, to establish the transformation mechanism.

2:15 PM CH01.06.03

Illuminating Porous Electrodes via 4D *In Situ* Fluorescent Electrochemical Microscopy Anton M. Graf¹, Thomas Cochard¹, Meisam Bahari¹, Shmuel Rubinstein² and Michael Aziz¹; ¹Harvard University, United States; ²The Hebrew University of Jerusalem, Israel

Porous electrodes are a crucial hardware for many sustainable electrochemical energy devices. They are broadly used in redox flow batteries and fuel cells as well as in electrochemical synthesis and separation. Although porous electrodes with many different internal fibre architectures have been studied, there is no clear consensus as to what structural features affect electrode performance. Recent results revealing heterogeneities on length scales an order of magnitude greater than the pore size challenge the common assumption that transport in porous electrodes can be approximated by a homogeneous Darcy-like permeability, particularly at the length scales relevant to many electrochemical systems. [1]

In this study, we investigate various porous electrodes with different fibre architectures by visualization of the electrolyte charging process *via in-situ* confocal microscopy at length scales down to the single digit micron scale. We present fluorescent electrochemical microscopy, a strategy to couple confocal fluorescence microscopy with electrochemical monitoring as a new analytical method to investigate electrochemical flow systems *in operando*. The fluorescent signature of quinone electrolytes differs for the charged and discharged redox states, which enables us to map the local state of charge in three spatial and one temporal dimension (4D imaging). In addition, we use 4D fluorescent particle tracking to evaluate local velocity fields, fluid streamlines, and spatial heterogeneities. The correlation between flow fields and electrochemical concentration maps shows that not only the surface area limits the electrode efficiency but also the fibre arrangement affecting the overall electrolyte flow.

Literature cited:

[1] A.A. Wong, S.M. Rubinstein and M.J. Aziz, "Direct visualization of electrochemical reactions and heterogeneous transport within porous electrodes *in operando* by fluorescence microscopy" *Cell Reports Phys. Sci.* **2021**, 100388; <https://doi.org/10.1016/j.xcrp.2021.100388>

SESSION CH01.11: Structural Characterization
Session Chair: Claire Villevieille
Monday Morning, December 6, 2021
CH01-Virtual

8:00 AM *CH01.11.01

In Situ and Operando Neutron Powder Diffraction at the ILL on Li-Ion Batteries—How Can We Help You? Emmanuelle Suard; Institut Laue Langevin, France

Li-ion batteries structure and purity have been characterized ex-situ classically by neutron powder diffraction for a long time. More recently, there has been a huge effort to provide scientists with a tool to study Li-ion batteries operando, in order to obtain better insights of the processes involved during charge and discharge. Several electrochemical cells have been developed in various facilities [1]

At the ILL, we have designed our own custom-made electrochemical cell to respond to some specific requirements (cell fully transparent to neutrons, sample amount between 100mg to 300mg, easy to use, extremely good quality neutron powder diffraction patterns) #ILLBAT1 [2].

We showed that this cell could function properly electrochemically, whilst enabling, at the same time, the acquisition of NPD patterns of high quality for Rietveld structural refinements using D20 at the ILL. We have used this cell to study different classes of materials and it has proven very effective. We therefore decided to give users access to this new, powerful tool.

The next step was the development of similar electrochemical cells for operando studies on all-solid-state lithium batteries. This cell #ILLBAT2 has a similar design as the original one, the main difference being that it can be used at non-ambient temperature (either high or low temperature) [3].

We are now still working on improving our cells in order to fulfill our users requests. ILLBAT#3 is a cell designed to work on ASSB as ILLBAT#2, but its specificity is that it will be possible to maintain a high pressure on the sample while measuring. And finally a cylindrical cell will also be soon available. All made in TiZy alloys. These two last cells are still prototypes but they will be soon available for our users community.

In parallel, in order to give more beamtime available for such studies we are developing the possibility to perform operando experiments using such cells on D19 which is a single-crystal diffractometer with a large bi-dimensionnal detector. The results of the preliminary tests are extremely positive and there is no doubt that D19 will be a good alternative to D20.

Finally, to give the best possible experimental conditions to our users, we are now building a Small Electrochemistry Laboratory (SEL) near D20, for the purpose of preparing these cells in a clean environment.

Of course, Operando experiments are not the only measurements using NPD. In-situ experiments using furnaces, cryostats are also common to study phase transformations or follow the phase diagram depending during the synthesis.

This conference is an opportunity to present the possibilities offered by the ILL to characterize the crystallographic structure and monitor the Li atoms position and content either *operando* or in-situ in Li-ion batteries using Neutron Powder Diffraction

[1] L. Vitoux, M. Reichardt, S. Sallard, P. Novák, D. Sheptyakov, C. Villevieille *Frontiers in Energy Research*, 6 (2018).

[2] M. Bianchini, J.B. Leriche, J.L. Laborier, L. Gendrin, E. Suard, L. Croguennec, C. Masquelier, *Journal of the Electrochemical Society*, 160 (2013) A2176-A2183.

[3] Tatiana Renzi PhD manuscript (in preparation)

8:30 AM *CH01.11.02

CELLS-ALBA Synchrotron, a Versatile Facility Offering Wide Panel of In Situ and/or Operando Synchrotron Techniques Applied to Electrochemical Systems Francois Fauth; CELLS-ALBA synchrotron, Spain

CELLS-ALBA is the Spanish synchrotron located in the Barcelona area. The facility started in 2011 and is now prospecting machine upgrade. Along last years, several synchrotron techniques were applied using *In Situ* data collection on Operando electrochemical systems. Synchrotron X-ray Powder Diffraction (SXRPD) performed on BL04-MSPD has been the most productive tool in the study of new electrode materials and in particular the realized crystallographic phases settling in during (des-)insertion of alkaline ions. Typical example is the $\text{Na}_3\text{V}_2(\text{PO}_4)_2\text{F}_3$ system for which the high angular resolution allowed whole structure determination of all occurring phases in the charge/discharge process [1]. The same system was studied using hard X-ray Absorption (XAS) techniques on the BL22-CLEASS beamline highlighting the electronic configuration of the V pairs when desinserting two Na^+ [2]. The presentation will cover selected examples for which both SXRPD and XAS has been applied to electrochemical systems as well an insight to the presently commissioned BL16-NOTOS beamline principally offering the possibility to collect both SXRPD and XAS data "quasi" simultaneously. Soft X-ray spectroscopy and Imaging techniques have been applied using the BL09-MISTRAL beamline in the study of Ca intercalation in TiS_2 . Differential absorption tomography allowed reconstruction in direct space of Ca distribution at several steps of intercalation.[3] In the same trend of multivalent based batteries, the identification, quantification and morphology of materials built at solid electrolyte interphase (SEI) has been tackled by InfraRed (IR) spectroscopy techniques on BL01-MIRAS beamline [4]. So far soft X-ray techniques are only available on *Ex Situ* prepared samples but development of *In Situ* cells is ongoing at ALBA. Details on development will be presented.

The move towards All Solid State batteries focus now the search on solid electrolytes exhibiting high ionic conductivity and stable crystal structures.

Temperature dependent SXRPD sounds a valuable technique in the understanding of such materials as demonstrated in studies of Na_3PS_4 [5] and $\text{Li}_6\text{Zn}(\text{P}_2\text{O}_7)_2$ [6] performed on BL04-MSPD.

Another approach in optimization and better understanding of cathode material production involves *In Situ* synthesis studies as recently exemplified in temperature dependent SXRPD under controlled gas atmosphere performed during synthesis of LiNiO_2 [7] and Ni-rich layered $\text{Li}(\text{NiCoMn})\text{O}_2$ oxides [8].

[1] Bianchini *et al*, Comprehensive Investigation of the $\text{Na}_3\text{V}_2(\text{PO}_4)_2\text{F}_3$ - $\text{NaV}_2(\text{PO}_4)_2\text{F}_3$ System by Operando High Resolution Synchrotron X-ray Diffraction, 10.1021/acs.chemmater.5b00361

[2] Broux *et al*, VIV Disproportionation Upon Sodium Extraction From $\text{Na}_3\text{V}_2(\text{PO}_4)_2\text{F}_3$ Observed by Operando X-ray Absorption Spectroscopy and Solid-State NMR 10.1021/acs.jpcc.6b11413

[3] Tchitchekova *et al*, Electrochemical Intercalation of Calcium and Magnesium in TiS_2 : Fundamental Studies Related to Multivalent Battery Applications, 10.1021/acs.chemmater.7b04406

[4] Forero-Saboya *et al*, Understanding the nature of the passivation layer enabling reversible calcium plating, 10.1039/d0ee02347g

[5] Famprikis *et al*, A New Superionic Plastic Polymorph of the N^{th} Conductor Na_3PS_4 , 10.1021/acsmaterialslett.9b00322

[6] Saha *et al*, Influence of Temperature-Driven Polymorphism and Disorder on Ionic Conductivity in $\text{Li}_6\text{Zn}(\text{P}_2\text{O}_7)_2$, 10.1021/acs.inorgchem.8b01800

[7] Bianchini *et al*, From LiNiO_2 to Li_2NiO_3 : Synthesis, Structures and Electrochemical Mechanisms in Li-Rich Nickel Oxides

9:00 AM CH01.11.03

Resolving Structural Deterioration in Ni-Rich Layered Cathode Materials at Higher Operating Potentials in Operando [Anastasiia Mikheenkova](#)¹, Olof Gustafsson¹, Casimir Misiewicz¹, William Brant¹, Matthew Lacey², Maria Hahlin¹ and Erik Berg¹; ¹Uppsala University, Sweden; ²Scania CV AB, Sweden

Aiming for high capacity and high energy density batteries, combined with the strive to reduce the use of Co has resulted in significant demand for Ni-rich cathode layered materials (Li[Ni_{1-x}Co_xAl_y]O₂, so-called NCA, and Li[Ni_{1-x}Mn_xCo_y]O₂, so-called NMC) on the EV market. Structure driven deterioration together with mechanical degradation hinder the full potential of the NCA and NMC materials. During cycling to higher voltages (above 4.2 V) the layered oxide materials exhibit significant reactivity of the active material with electrolyte with further gas evolution¹. Along with studies demonstrating structural fatigue facilitating rapid degradation while reaching high potentials, the high relevance of studies focused on the dependence of oxygen release and structural degradation is justified². We will present insights into the relation of structural changes coupled with gas evolution and advanced electrochemical characterisation that expand understanding of the limits of Ni-rich cathode material and clarify strategies for surmounting these limits. Specifically, the current study is focused on investigating the origins of NCA cathode material degradation at higher operating potentials in commercial electrodes. We use a combination of intermittent current interruption technique³ with *operando* XRD and *operando* gas analysis on electrodes extracted from commercial cells (Tesla Model 3 18650 cylindrical cells). This work allows to expound the degradation processes in Ni-rich layered oxides at high operating potentials.

1. Tao, Q. *et al.* Understanding the Ni-rich layered structure materials for high-energy density lithium-ion batteries. *Materials Chemistry Frontiers* **5**, 2607–2622 (2021).
2. Xu, C. *et al.* Bulk fatigue induced by surface reconstruction in layered Ni-rich cathodes for Li-ion batteries. *Nat. Mater.* **20**, 84–92 (2021).
3. Chien Y-C, Liu H, Menon AS, Brant WR, Brandell D, Lacey MJ. A fast alternative to the galvanostatic intermittent titration technique. ChemRxiv. Cambridge: Cambridge Open Engage; 2021; This content is a preprint and has not been peer-reviewed.

9:15 AM CH01.11.04

Li_xMoO₂ and Na_xMoO₂ Systems Studied by Operando Pair Distribution Function Analysis During Lithium or Sodium Electrochemical (De)Intercalation [Marie Guignard](#) and Matthew Suchomei; Institute of Condensed Matter Chemistry of Bordeaux (ICMCB), France

For many years already, we have shown that the electrochemical intercalation and deintercalation of alkali ions in a battery is a very powerful technique for determining phase diagrams in MO₂-AMO₂ systems (where A is an alkali ion and M is a 3d or 4d transition metal ion) by combining in situ powder X-ray diffraction and electrochemistry. In the molybdenum systems MoO₂-LiMoO₂ and MoO₂-NaMoO₂, it has been found that many phase transitions occur during the deintercalation of alkali ions without being able to determine the origin. We proposed that these phase transitions arose in part from the rearrangement of molybdenum atoms in MoO₂ sheets formed of MoO₆ octahedra.

In order to validate this hypothesis, we performed operando pair distribution function analysis (PDF) experiments during battery cycling using Li_{2/3}MoO₂ and Na_{2/3}MoO₂ phases as positive electrode materials in lithium batteries and sodium, respectively. These experiments were performed at the XPDF beamline of the Diamond synchrotron using the electrochemical cells specifically dedicated to PDF analysis designed by Diamond. These experiments confirmed that molybdenum atoms shifted slightly from the center of MoO₆ octahedra during electrochemical (de)intercalation of alkali ions and thus formed short (approximately 2.5 Å) and long (approximately 3.2 Å) Mo-Mo bonds. The length and the distribution of the different Mo-Mo bonds have been analyzed. We concluded that different geometries of molybdenum clusters can be observed in the Li_xMoO₂ and Na_xMoO₂ phases during the alkali electrochemical deintercalation (for example, zig-zag chains or diamond-like chains).

9:30 AM *CH01.11.05

Operando Characterization of Silicon-Based Battery Anodes by Neutron and Synchrotron Techniques [Sandrine Lyonard](#); CEA-IRIG, France

Understanding lithiation and ageing mechanisms in Li-ion batteries requires ad hoc tools to probe the real-time evolution of active materials during charge and discharge of a battery. Neutron & synchrotron techniques have been widely employed to probe the structural, morphological and chemical changes occurring in electrodes, as both high energy X-rays and neutrons can deeply penetrate into matter, therefore enabling to monitor key processes in realistic devices with ultimate space and time resolutions. Recently, composite anodes made of (nano)silicon and graphite have attracted attention due to the high specific capacity of silicon. However, these are extremely complex materials where the volume changes due to silicon alloying with lithium generate ageing on the long-term, therefore hindering their potential use towards viable high energy density anodes. We will present in this talk a toolkit of techniques employed to quantify strain in crystalline silicon by operando synchrotron XRD [1], nanoscale morphological changes in composite anodes by synchrotron SAXS and SANS [2,3], 3D lithiation heterogeneities and microstructural ageing by SAXS/WAXS synchrotron tomography and synchrotron mXCT [4]. These investigations established the details of core-shell lithiation mechanism as well as the correlations between electrochemistry, materials design and ageing process, allowing to highlight the key features for a better engineering of novel silicon-based anodes.

[1] S. Tardif *et al.*, ACS Nano, 2017, 11, 11306–11316.

[2] C. Berhaut *et al.*, ACS Nano, 2019, 13, 10, 11538-11551.

[3] C. Berhaut *et al.*, Energy Storage Materials, 2020, 29, 190–197.

[4] Vorauer *et al.*, Comm. Chemistry, 2020, 3, 141.

SESSION CH01.12: Electrochemical Mechanisms
Session Chairs: Kristina Edstrom and Sandrine Lyonard
Monday Morning, December 6, 2021
CH01-Virtual

10:30 AM *CH01.12.01

Towards Holistic Understanding of Electrochemical Energy Conversion and Storage Systems Using High Energy X-Rays [Jakub Drnec](#); ESRF, France

Complete physico-chemical operando characterization of electrochemical devices in whole, or its constituent materials separately, is necessary to guide the development and to improve the performance. High brilliance synchrotron X-ray sources play a crucial role in this respect as they act as a probe with relatively high penetration power and low damage potential. Synchrotron sources will undergo major upgrades in next decade and will provide even higher brilliance and, more importantly, coherence. These upgrades will be particularly advantageous for beamlines providing high energy X-rays as they will allow use of advanced scattering techniques with highly penetrating probe. Therefore, the techniques typically used for ex-situ measurements or at lower X-ray energies could be used on materials in liquid half-cells and operating electrochemical devices. In this contribution the new possibilities of using high energy, high intensity, coherent X-rays to probe model systems and whole electrochemical devices will be presented. The focus will be on defects tracking, local structure determination and correlative multimodal characterization using advanced WAXS, SAXS and surface scattering techniques.

To study fuel cells or batteries as a whole, elastic scattering techniques such as wide angle and small angle scattering are typically employed, as they can provide important complementary information to more standard X-ray imaging and tomography. The advantage is that the chemical contrast and sensitivity at atomic and nm scales is superior. Coupling these technique with the tomographic reconstruction (XRD-CT and SAXS-CT) is much less common as it requires bright synchrotron sources, fast 2D detectors and advanced instrumentation [1]. However, such combination allows spatial reconstruction of materials important atomic parameters in operando conditions. This will be demonstrated on imaging of standard 5 cm² PEM fuel cell during operation. Furthermore, local atomic and mesoscale structure, together with defect content, can also be determined by using Rietveld fitting, Pair Distribution Function (PDF) analysis and advanced SAXS theory. This in principle allows holistic investigations of interfaces at the device level, specification of defects' role in catalysis and determination of interplay between different phases during operation. These are critical questions needed to be answered in order to incorporate novel materials into the electrochemical devices. Examples will be given on studies of the defectious ORR catalysts [2,3] and amorphous Li-ion anodes.

HESXRD (High Energy Surface X-ray Diffraction) [4] and TDS (Transmission Surface Diffraction) [5] provide ideal tools to study structural changes during reaction conditions on single crystal model electrodes. The main advantage of both techniques is the possibility to follow the surface structural changes precisely with atomic resolution. While HESXRD is ideally used to determine exact atomic position, the TSD is easier from experimental perspective and allows studies with high spatial resolution. Advantages and disadvantages of both approaches will be discussed and examples of measurements on ORR and OER catalysts will be given. The future possibility to use high energy coherent beams will open new opportunities for both techniques to study single defects and surface dynamics in operando conditions.

References :

- 1) A. Vamvakeros et al., Nat. Commun., 9, 4751 (2018)
- 2) R. Chattot et al., Nat. Matter., 17(2018)
- 3) C.J. Gommers et al., J. Appl. Cryst., 52(2019)
- 4) J. Gustafson et al., Science 343, 758 (2014)
- 5) F. Reikowski et al., J. Phys. Chem. Lett., 5, 1067-1071 (2017)

11:00 AM CH01.12.02

Advances in *In Situ* Liquid Phase TEM to Study Electrochemical Processes in Li-Ion Batteries and Beyond Yevheniy Pivak, Hongyu Sun, Anne F. Beker and Hugo H. Pérez Garza; Denssolutions, Netherlands

In situ liquid phase transmission electron microscopy (LPTM) is a promising technique to visualize and study real-time dynamic processes happening during electrochemical cycling of Li-, Zn-, Na- and other types of ion batteries. The in situ LPTM allows to reveal morphological and structural changes occurring in the sample in a liquid environment and to correlate it with the electrochemistry. On the other hand, this method has a number of drawbacks which reduces its success rate and limits wide practical application. First of all, high resolution (~ nm scale) and analytical capabilities (Electron Diffraction-ED, Energy Dispersive X-ray Spectroscopy-EDXS and Electron Energy Loss Spectroscopy-EELS) are substantially hindered by the uncontrolled thick liquid layer (≥ 500 nm). Furthermore, the current designs of the liquid flow cells used for in situ liquid phase TEM have no direct control over the liquid flow as they possess multiple fluidic pathways with considerably higher fluidic resistance in the sample area. This prevents measuring the flow rate around the sample and studying the effect of the flow on the dendrite growth. Furthermore, bubbles, often created in the imaging area while performing electrochemical cycling abort the whole experiment as these are impossible to remove from the current liquid cells.

To solve the above-mentioned limitations and to increase the success rate, we revolutionized the design of the liquid cell. Unlike existing solutions, where the liquid inlet and the outlet are located in the TEM holder, the new design has the liquid inlet/outlet directly in the liquid cell. The spacers inside the cell guide the liquid from the inlet to the outlet, forming a fluidic channel that goes through the imaging area. This innovation made it possible to have a direct flow control over the sample. In combination with a new type of liquid delivery system based on pressure-driven flow, the new liquid cell has a well-defined flow direction, allows to control the pressure of the liquid inside the cell and thus the liquid thickness, enables quantification of liquid flow rates, enables bubbles removal and much more.

In this work we are going to present the design of the new liquid cell together with the new liquid delivery setup and show how this new system can be used to remove bubbles from the region of interest by means of the liquid flow or the liquid pressure, how it is possible to minimize the effect of the electron beam with the flow, how to make high resolution imaging and enable elemental mapping in liquid and how to define the mass transport in the electrochemical cell and to study kinetics of redox reactions.

11:15 AM *CH01.12.03

Unriddling the Complex Battery Chemistry by Rationally Designed High-Performance Liquid Electrolytes Isidora Cekic-Laskovic; Helmholtz-Institute Muenster, IEK-12 Forschungszentrum Juelich, Germany

Materials science in the field of batteries as dominating electrochemical energy storage systems is forced to follow a systems approach as the interactions between active materials, the electrolyte, the separator and various inactive materials (binder, current collector, conductive fillers, cell housing, etc.), are of similar or even higher importance as the properties and performance parameters of the individual materials. Successful operation of batteries relies significantly on a series of interrelated mechanisms, some involving instability of the constituting components induced by charge/discharge cycles and some also encompassing formation/reaction of metastable phases. With this in line, the ability to achieve long-term stability requires careful elucidation of the physical and chemical processes governing charge/discharge cycling and storage. The key performance requirements of a battery for different applications might look very similar at first sight, however, each application calls for different requirement prioritization. Frequently, they conflict with one another and call for inevitable trade-offs. The objective of advanced battery research and development relates to obtaining the best compromise among the determined goals, followed by a decision whether the balanced system should be implemented instead of a competing technology. In all types of batteries, electrolyte as the only component in direct contact with all other active and inactive parts, plays a key role in terms of overall performance, life and safety. Chemistry of liquid electrolytes and their interaction with anode and cathode materials is complex and yet not fully understood, thus representing a delicate balance of various properties. Despite our limited knowledge, modern needs for battery electrolytes require the development of sophisticated electrolyte solutions with multifunctional components, able to simultaneously fulfill several duties. Typical requirements include combined roles as salt dissolution

enhancers, viscosity decrease, flame-retardants or effective electrolyte interphase formers at the electrodes. The introduction of these modern components can be regarded as a paradigm shift in order to increase the efficiency and safety of lithium-based and post-lithium-based batteries, when compared with nowadays technologies.

This talk is an invitation to a journey of the scientific development, technology as well as engineering of selected classes of advanced liquid electrolytes for lithium-based batteries under systematic approach that allows to understand the structure-property-performance relationships of the selected compounds/formulations, their impact on the overall battery chemistry, performance and safety, thus helping to further tailor relevant properties of electrolyte components/formulations for targeted applications.

11:45 AM CH01.12.04

Operando GC/MS Gas Analysis for Monitoring Complex Electrolyte Decomposition Products in Lithium-Ion Batteries Jürgen Kahr¹, Christiane Groher¹, Maria Antoniadou², Erwin Rosenberg² and Marcus Jahn¹; ¹AIT, Austria; ²Technische Universität Wien, Austria

Lithium Ion Batteries (LIB) find not only wide use in portable devices and consumer electronics, but also attract increasing attention in stationary energy storage and the automotive sector. In this regard, LIBs play a significant role as intermediate energy storage due to their high volumetric and gravimetric energy, high power density, and long cycle life. With respect to larger battery packs safety became a major concern and attracted increasing research interest in this field.

To achieve the required performance, the interaction of novel anode and high-voltage cathode materials with the electrolyte is of paramount interest. Safety and performance issues arise from degradation reactions of the conducting salt and electrolyte solvent, due to the formation of flammable, corrosive and toxic gas species. Particularly, the safety must be assessed with respect to the formation of volatile and reactive species during cell operation which can negatively alter cell components. Gas chromatography / mass spectroscopy (GC/MS) has proven to be a reliable tool for species detection. Unfortunately, conventional GC systems lack time resolution for operando gas analysis regarding fast processes, for example battery failure. Therefore, developing operando testing methods with improved time resolution is key to giving insight into electrolyte alterations during battery operation.

Here one of them, an operando GC/MS for LIBs is presented as a gas monitoring technique for volatile organic species arising from the decomposition of conventional LIB electrolytes. The combination of a continuous sampling technique with GC/MS allows an increased time resolution for the analysis of products from fast decomposition processes. Commercially produced NMC-based pouch cells and coin cell-sized batteries were monitored with respect to evolving gas species during battery operation. Especially, the degradation products of organic carbonate-based electrolytes, such as derivatives that appear in the presence of decomposed LiPF₆, have been evaluated in respect to the cell potential.

The author gratefully acknowledges the FFG (Austrian Research Promotion Agency) for funding this research within project No. 879613.

12:00 PM *CH01.12.05

Investigating Li Metal Anodes with Operando Neutron Depth Profiling and Solid-State NMR Marnix Wagemaker, Ming Liu, Qidi Wang, Chao Wang, Tomas Verhallen and Swapna Ganapathy; Delft Univ of Technology, Netherlands

Li-metal is the ultimate anode for Li-batteries from the perspective of energy density. However, reversible cycling is challenged by dendrite formation and the irreversible reactions with the electrolyte, a topic that is intensively investigated for many decades. Here we show the use of operando Neutron Depth Profiling (NDP) and Solid State NMR to monitor some of the aspects of Li-metal deposition. Neutron Depth Profiling provides the Li density profile perpendicular to the electrode plane in modified pouch cells. Solid state NMR is able to monitor the evolution of dead Li metal in a full cell geometry, as well as the nature of the deposited Li metal. Both techniques are applied to different solution strategies, such as electrolyte/solvent additives and a host scaffold for Li metal plating. Operando NDP is employed on a regular LiPF₆ EC/DMC electrolyte [1], to illustrate the NDP principle and the type of data that can be extracted, as well as on an amide electrolyte [2], highlighting how this changes the Li metal plating and stripping. Operando 7Li solid state NMR on full anodeless cells is performed [3], with and without a high dielectric scaffold that is intended to induce more compact Li metal growth. These examples provide insight in the underlying mechanism of these strategies, illustrating the value of these operando techniques in Li metal studies.

[1] Operando monitoring the lithium spatial distribution of lithium metal anodes, S. Lv et al., <https://doi.org/10.1038/s41467-018-04394-3>

[2] Interface chemistry of an amide electrolyte for highly reversible lithium metal batteries, Q. Wang et al., <https://doi.org/10.1038/s41467-020-17976-x>

[3] Under review

SESSION CH01.13: Interfacial Characterizations

Session Chairs: Jordi Cabana and Jakub Drnec

Monday Afternoon, December 6, 2021

CH01-Virtual

1:00 PM *CH01.13.01

Using X-Rays to Locate Chemical Phenomena in Battery Materials Jordi Cabana; University of Illinois at Chicago, United States

The evolution of local chemistry determines the performance of electrodes and electrolytes used in batteries because limitations can be tracked to slow kinetics and transport, and irreversibilities in the storage reaction. Tools that provide insight into local chemistry are critical for identifying the underpinnings of electrochemical function. This information must be resolved within architectures, from individual particles to microscale domains, to pinpoint the relationship between local phenomena and their role in macroscopic metrics and degradation. Technical developments in X-ray microscopy and mapping have built a flexible suite of tools that combine the desired spatial resolution and 3D capabilities with a suite of possible contrast mechanisms, such as diffraction and spectroscopy. In this talk, we will discuss our recent research that demonstrates the diversity of length scales at which important chemical heterogeneity can be induced in battery electrodes. For this purpose, the systems of study will be the leading cathodes for Li-ion batteries, but the insight is expected to be generalizable to “beyond” technologies, such as Na-ion or Mg. We will highlight the new fundamental insight generated by the tools. The mechanisms of transformation will be related to their impact on material and architecture properties. Along the way, we will also provide a glimpse into the future by showing how emerging synchrotron techniques can enhance the impact of X-ray microscopy in fundamental battery science. Particularly, in the spirit of this Symposium, we will discuss the prospects of probing time-resolved phenomena using operando measurements to avoid uncertainty due to relaxation under open circuit conditions.

1:30 PM CH01.13.02

Imaging Phase Segregation in Nanostructured Li_xCoO_2 Islands with Conductive Atomic Force Microscopy Elliot J. Fuller¹, David Ashby¹, Celia Polop², Enrique Vasco³, Joshua Sugar³ and A. A. Talin¹; ¹Sandia National Laboratories, United States; ²Universidad Autónoma de Madrid, Spain; ³Instituto de Ciencia de Materiales de Madrid, Spain

Li_xCoO_2 (LCO) is a common battery cathode material that exhibits phase transformations that are significantly complicated by the coupling of correlated electronic effects, strain and diffusional anisotropy. At compositions $0.96 < x < 1$ LCO remains insulating, while at compositions $x < 0.75$ it is metallic. Between these two compositions, the insulating and metallic phases coexist. While the bulk phase diagram has been studied extensively [1, 2], it remains unclear how the electronic and structural phases scale to nanometer particle dimensions, and the effects of strain and diffusional anisotropy on the phase morphology [3]. We have investigated nanoscale, epitaxial LiCoO_2 islands grown by pulsed laser deposition onto SrTiO_3 substrates. After charge cycling of the islands, conductive atomic force microscopy (c-AFM) is used to image the spatial distribution of conductive and insulating phases at various states of charge and under strain conditions. Above island thicknesses of 25 nm, we resolve a diffusion-limited intercalation wavefront propagating along the Li-planes. Thinner islands (~1 nm) are found to exhibit a striping pattern which suggests the surface energy plays a critical role in the phase morphology when particles are scaled below a critical dimension. The effects of strain are investigated through the application of force with the c-AFM tip. Above a critical force threshold, the insulating regions of the islands are found to undergo an insulator-metal transition. The results suggest that the morphology of phase segregation and strain play a critical role in charge-cycling of nanoscale particles.

[1] K. Mizushima, P.C. Jones, P.J. Wiseman and J.B. Good-enough, *Mater. Res. Bull.* 55, 783 (1980)

[2] A. Van der Ven, M.K. Aydinol and G. Ceder, *Phys. Rev. B* 58, 2975 (1998)

[3] Nadkarni et al., *Adv. Funct. Mater.*, 29, 1902821 (2019)

1:45 PM CH01.13.03

In Situ X-Ray Multimodal Characterization for Insights into Synthesis/Processing of High-Ni Cathode Materials Sizhan Liu, Jianming Bai and Feng Wang; Brookhaven National Laboratory, United States

Driven by the increasing need for energy storage, especially for electric vehicles and electronic devices, the technological advancements of lithium-ion batteries (LIBs) are urgently in demand to increase energy density while reducing the cost. Battery performance is largely determined by the phase constitution and properties of electrodes and electrolytes and, therefore, can be advanced by synthesis/processing, in making certain phases with controlled structure and material properties. This is particularly true for high-Ni layered oxides, $\text{LiNi}_x\text{Mn}_y\text{Co}_{1-x-y}\text{O}_2$ (NMC; $x > 0.7$), the most promising low-cost, high energy density cathodes for next-generation LIBs. In such cathode materials, the increasingly high Ni loading worsens the surface instability and, consequently, lowers the cells' lifespan and brings issues to materials production and storage, posing a practical challenge to their commercial deployment. In this work, a multimodal *in situ* synchrotron X-ray characterization approach is employed to investigate the thermodynamic and kinetic pathways in the synthesis/processing of high-Ni NMC materials. A combination of *in situ* X-ray diffraction, total scattering (coupled with pair distribution function analysis), X-ray absorption spectroscopy, and imaging is applied to tracking structural/chemical evolution at short, intermediate, and long-range ordering of intermediates in preparing NMC811, LiNiO_2 , and other layered oxides from their hydroxide counterparts. Results of our recent studies reveal the strong composition dependence of the structure and morphology evolution as a result of the preferential oxidation of Mn/Co over Ni. We show Mn and Co play an important role in facilitating Li/O incorporation, consequently leading to more continuous structural ordering and crystal growth in Mn/Co containing high-Ni NMC compared to the pure LiNiO_2 . Those findings shed light on the rational design of synthesis/processing in preparing high-Ni layered cathodes of optimized performance for next-generation LIBs.

2:00 PM CH01.13.04

Advancing Nondestructive In Situ Characterizations of Buried Electrochemical Interfaces—Infrared Nanospectroscopy at Electrode/Liquid-Electrolyte and Electrode/Polymer-Electrolyte Interfaces Jonathan Larson, Xin He, Hans Bechtel and Robert Kostecki; Lawrence Berkeley National Laboratory, United States

Paving new pathways for *in situ* and/or *operando* characterizations of buried and intact electrochemical interfaces is critically important for, in the least, (i) advancing basic energy storage science and for (ii) optimizing the efficacy of engineered interfaces/interphases in batteries. In this talk, we first present a brief overview of near-field based infrared nanospectroscopy (true nanoscale Fourier transform infrared spectroscopy) and nanoimaging. We follow this by sharing how we have demonstrated such techniques can be utilized to study graphene/liquid-electrolyte interfaces, with sensitivity to even species within the electric double layer. Finally, we discuss our most recent data in which we extend such near-field methods to characterize buried and intact electrode/electrolyte interface evolution in solid-state polymer battery (SPB) devices, *in situ*. The SPB devices are capped with graphene, which operates as both infrared transparent window and current collector for Li plating and stripping (similar in function to anode-less batteries). *In situ* infrared imaging and spectroscopic measurements are performed at pristine, heated, plated, and stripped interfaces, where we find that the interfacial solid-state polymer-electrolyte (SPE) intrinsically possesses nanoscale heterogeneities that contribute to plating inhomogeneities on a similar length scale. Additionally, we find that a mosaic-like solid-electrolyte interphase forms at the Li/SPE interface consisting of decomposition products amongst SPE. Our approach paves a way for SPB optimization (or other chemistries), by providing a method for unprecedented nanoscale measurements of crystallinity, structure, conductivity, and chemistry of intact and buried electrochemical interfaces in their native environments.

2:15 PM CH01.13.05

In Situ/Operando Soft X-Ray Absorption Spectroscopy Probing of the Electrode/Electrolyte Interfacial Dynamics Influenced by the Electrolyte Anions and Cations Feipeng Yang¹, Xuefei Feng¹, Hui Li¹, Scott A. McClary², Ana Sanz-Matias¹, Nathan M. Hahn², David Prendergast¹, Kevin Zavadil² and Jinghua Guo¹; ¹Lawrence Berkeley National Laboratory, United States; ²Sandia National Laboratories, United States

There is considerable interest in the study of electrochemical processes in calcium batteries since the demonstration of room temperature plating and stripping of calcium with high capacities and low polarization using $\text{Ca}(\text{BH}_4)_2$ as the electrolyte. The greater polarizability of Ca^{2+} over Mg^{2+} represents greater configurational flexibility, facilitating ionic cluster formation and rapid delivery of Ca^{2+} ions to the electrode interface. To promote the development of calcium batteries, it is critical to probe the solvation and charge transfer mechanism at the electrode/electrolyte interface. It has been reported that when $\text{Ca}(\text{BH}_4)_2$ is substituted by the weakly coordinated calcium hexafluoroisopropoxyborate ($\text{Ca}(\text{Bhfiip})_2$), ionic conductivity increases by an order of magnitude, which demonstrates the strong coordination of BH_4^- compared to Ca^{2+} in THF. In this work, the coordination of Ca^{2+} at this electrolyte/electrode interface as a function of the type of anions is probed by the *in-situ/operando* soft X-ray absorption (XAS) spectroscopy under *operando* electrochemical conditions. The total electron yield (TEY) mode XAS is sensitive to the interfacial speciation under *in-situ* and *operando* conditions. It was observed that the $\text{Ca}(\text{Bhfiip})_2$ in THF shows a small shoulder on the right side of the L_2 -edge and a pre-edge peak on the left side of the L_2 -edge peak. A less prominent pre-edge peak is also observed on the left side of the L_3 -edge peak. These signatures become more prominent when the potential is swept negatively and are not reversible when the potential is swept positively in a cyclic voltammetry cycle. On the other hand, the $\text{Ca}(\text{BH}_4)_2$ in THF is more reversible, and no shoulder peak on the right side of the L_2 -edge peak was observed. The effect of cations was also compared by investigation

of the calcium L-edge and fluorine K-edge TEY mode XAS from the 0.5M calcium bis(trifluoromethanesulfonyl)imide (Ca(TFSI)₂) in THF vs. 0.45M Ca(TFSI)₂ + 0.05M LiTFSI in THF. The TEY-XAS spectra from these operando studies indicate their differences in the Ca²⁺ coordination chemistry at the electrode/electrolyte interface as a result of the anions and cations, and will path the way for the future development of electrolytes for calcium batteries.

2:30 PM CH01.13.06

In Situ and Operando XPS Studies of the Si-Anode Solid-Electrolyte Interphase Sarah Frisco, Yeyoung Ha, David Moore, Andrew Colclasure and Glenn Teeter; National Renewable Energy Laboratory, United States

Laboratory-based x-ray photoelectron spectroscopy (XPS) is a ubiquitous, powerful technique for analyzing surfaces and interfaces to reveal compositions and chemical states. Beyond these typical applications, in recent years there has been growing interest around *in situ* and *operando* XPS approaches that can elucidate dynamic interfacial phenomena, including charge- and mass-transfer processes relevant to renewable technologies including lithium-ion batteries (LIBs). This presentation will discuss recent efforts to develop and apply *in situ* and *operando* approaches to probe interfacial charge transfer and phase transformations relevant to the formation and evolution of the solid-electrolyte interphase (SEI) in silicon-anode LIBs. These experiments are enabled by the so-called virtual electrode (VE) approach [1,2], in which electrochemical currents are driven during VE-XPS measurements on exposed interfaces via a combination of low-energy Li⁺ ion and electron guns and ultraviolet-based photoemission. Key recent findings that will be discussed include: (i) conversion of native SiO_x to Li_ySiO_x phases; (ii) lithium-induced band-alignment shifts at the SiO_x/silicon interface; (iii) observed correlations between lithium chemical potential (m_{Li}) and ionic vs. electronic conductivities of SEI constituent phases such as LiF and Li₂CO₃; and (iv) *in situ* reduction of ethylene carbonate (EC) on various model-system electrodes.

[1] K.N. Wood, K.X. Steirer, S.E. Hafner, C. Ban, S. Santhanagopalan, S.-H. Lee, G. Teeter, "Operando X-ray photoelectron spectroscopy of solid electrolyte interphase formation and evolution in Li₃S-P₂S₅ solid-state electrolytes," Nature Communications **9**, 2490 (2018).

[2] A.L. Davis, R. Garcia-Mendez, K.N. Wood, E. Kazyak, K.-H. Chen, G. Teeter, J. Sakamoto, N.P. Dasgupta, "Electro-chemo-mechanical evolution of sulfide solid electrolyte/Li metal interfaces: operando analysis and ALD interlayer effects," Journal of Materials Chemistry A **8**, 6291 (2020).

2:45 PM CH01.13.07

Operando Spectroscopic Ellipsometry—A Non-Destructive Optical Technique Offering Insights into Lithium Intercalation and Solid Electrolyte Interphase Formation Juan Carlos Gonzalez-Rosillo¹, Valerie Siller¹, Marc Nuñez Eroles¹, Michel Stchakovsky², Alex Morata¹ and Albert Tarancón^{1,3}; ¹Catalonia Institute of Energy Research, Spain; ²HORIBA Scientific, France; ³ICREA, Spain

Vast efforts have been devoted over the last decade to develop new techniques and approaches to obtain critical information about interfacial phenomena during device operation to establish direct correlations towards their electrochemical performance. However, the sophistication of some of the most powerful techniques, such as isotopic ion exchange methods, *in situ* TEM and synchrotron radiation based techniques, limits the routine access to essential information for developing next-generation batteries. In addition, commonly available techniques have also been explored including X-ray diffraction, atomic force microscopy, Raman spectroscopy and Fourier transform infrared (FTIR) spectroscopy showing different compromises between spatial and time resolutions. Surprisingly, and despite the well-known capabilities of Spectroscopic Ellipsometry (SE) to infer the properties of thin film systems (including multilayers), the use of this affordable, non-destructive technique in the field of Li-ion batteries is very limited. In short, SE measures the change in the polarization state of a light beam reflected in the sample. By comparing with a suitable model, the relevant optical properties of the material, such as the dielectric function and extinction coefficients, are extracted as a function of the wavelength. This technique is typically sensitive to parameters such as crystallinity, materials ratio in mixtures, roughness, structure of the interfaces, etc

In this talk, we will discuss the basic theory and our implementation of Spectroscopic Ellipsometry to perform operando experiments thanks to its fast response and the strong effect of the oxidation state on the optical properties of the films. We will exemplify the power of the technique with two examples. First, we have used SE to monitor Li⁺ transport properties through real-time tracking of the valence changes associated with lithium insertion and extraction along LiMn₂O₄ thin films and interfaces¹. Second, we have employed SE to interrogate the formation of a Solid Electrolyte Interphase (SEI) during the first cycle on spinel-based anode and cathodes over the extended voltage range. Here, we link the changes in the optical properties of the films with the capacity losses associated with the first cycle, and provide guidelines for SEI-resistant coatings at the cathode and anode interfaces².

References

1 A. Morata, V. Siller, F. Chiabrera, M. Nuñez, R. Trocoli, M. Stchakovsky and A. Tarancón, *J. Mater. Chem. A*, 2020, **8**, 11538–11544.

2 J.C. Gonzalez-Rosillo, V. Siller, M. Nuñez, M. Stchakovsky, A. Morata and A. Tarancón, *In preparation*

SESSION CH01.14: Dynamic Investigations
Session Chairs: Jordi Cabana and Y. Shirley Meng
Monday Afternoon, December 6, 2021
CH01-Virtual

4:00 PM *CH01.14.01

Operando Studies of Lithium-Ion Battery Electrodes Under Fast Charge Conditions Daniel Abraham; Argonne National Laboratory, United States

Fast charging of lithium-ion batteries (LIBs), being developed for electric vehicles, is needed to meet customer demands of time-parity with today's gasoline-powered cars. The U.S. Department of Energy (DOE) has set a target charging time of 15 minutes (4C rate) as a near-term goal, further indicating that a 10-minute charge (6C rate) could be a long-term goal. This talk will present an overview of fast charge studies being conducted at Argonne National Laboratory as part of projects funded by the U.S. DOE. *In-situ* and *operando* methods to examine electrode and cell behavior will be discussed: results from cells containing layered oxide cathodes and graphite anodes will be highlighted. The use of a microprobe reference electrode to monitor the onset of Li plating conditions and to determine develop cycling protocols that minimize cell performance degradation will be presented. X-ray methodologies to characterize spatial distribution of the active materials and investigate lithium concentration gradients that develop in electrodes will be examined. The heterogeneities that develop and persist in the electrodes cause non-uniform degradation across the electrodes thus making it a challenge to predict cell life.

4:30 PM CH01.14.03

In Situ Dynamic Measurements of Ti₃C₂ MXene Thin Films During Voltage Cycling at Variable Sweep Rates Thomas Sobyra¹, Tyler Mathis², Yury

Gogotsi² and Paul Fenter¹; ¹Argonne National Laboratory, United States; ²Drexel University, United States

X-ray reflectivity and crystal truncation rod measurements, performed at the Advanced Photon Source at Argonne National Laboratory, monitored structural changes of Ti₃C₂ MXene films as a function of applied potential between 0.3 and -0.7 V in an aqueous 0.1 M Li₂SO₄/H₂O electrolyte. Static measurements show negative potential sweeps lead to a contraction in the interlayer spacing of 1.2 Å upon Li insertion and a net loss of electron density between the layers (Sobyra et al. *ACS AMI*, **2021**, Under Review). The layer spacing changes continuously, except for an additional discrete contraction that occurs near -0.35 V having the characteristics of a first-order transition. The continuous change in the MXene layer spacing is associated with the capacitive charge, while the discrete change in structure correlated with the weak feature in the cyclic voltammogram at -0.35 V can be interpreted as either a pseudocapacitive charging process or a potential-dependent change in capacity.

New dynamic *in-situ* measurements observe the change in lattice spacing and MXene layer widths in real-time as a function of sweep rate to provide insight into the mechanisms of intercalation as the system is forced to respond to the rapidly changing environment. Potential sweep rates were varied from 1 mV/s to 500 mV/s. The Ti₃C₂ MXene response at slow sweep rates, less than 10 mV/s is similar to the static charging, but at faster rates, the system shows less contraction in the Ti₃C₂ layer spacing as the Li insertion becomes transport limited.

Analysis of the MXene electrochemical response reveals a charging mechanism that is sweep rate-dependent and not diffusion-limited as the Li⁺ ions diffuse slower than the bulk diffusion rate through the interlayer spacing. These measurements with varying sweep rates, in conjunction with the dynamic X-ray measurements, confirm the rapid change in layer spacing that occurs below -0.3 V is directly associated with the broad redox peak seen in the cyclic voltammogram.

4:45 PM *CH01.14.04

***In Situ* Magnetic Resonance Studies of Electrochemical Processes in Li-Ion Cells Using Novel Probes** Gillian R. Goward¹, Kevin Sanders¹, Amanda A. Ciezki¹, Zoya Sadighi¹, Annica Freytag¹, Andres Ramirez Aguilera² and Bruce J. Balcom²; ¹McMaster University, Canada; ²University of New Brunswick, Canada

Magnetic resonance tools for *in situ* and *in operando* investigations of electrochemical processes have provided many new insights into electrochemical processes in lithium ion batteries. We have recently reported the application of a parallel-plate NMR probe to monitor Li metal deposition on a graphite anode during the charging of a single layer prismatic cell.^[1] The probe provides an enhanced sensitivity and an ideal orientation of the cell relative to the applied electromagnetic fields, and allows the quantification of the lithiation of the graphite anode throughout the duration of cell charging.

A new version of this parallel-plate resonator for ⁷Li ion cell studies is introduced along with a removable cartridge-like electrochemical cell for studies of LIBs.^[2] This geometry separates the RF probe from the electrochemical cell permitting charge/discharge of the cell outside the magnet and introduces the possibility of multiplexing samples. The cell and RF probe dramatically increase the sample volume compared to traditional MR compatible battery designs. The cell and RF probe may be employed for spectroscopy, imaging, and relaxation studies.

Here we report the application of this probe, together with a custom electrochemical cell assembly, to monitor Li plating on a graphite anode of a full-cell LIB using *in operando* NMR spectroscopy and imaging. We are able to quantify the amount of Li metal deposited on the anode surface and correlate it to the relative amounts of Li species within the graphite anode with high time resolution relative to the high charging rate of 1C. Our data demonstrate that most of the Li metal deposited on the anode surface can be intercalated into graphite during rest periods when no current is applied, and that the formation of Li metal correlates to the loss of capacity of the cell over multiple high-rate charge cycles. Moreover, we demonstrate that this methodology can be extended to a variety of battery chemistries, with an emphasis on full-cell behaviour.

Finally, we demonstrate a magic-angle spinning (MAS) based *in situ* electrochemical NMR method that offers significantly improved resolution over conventional static NMR experiments. We demonstrate that it is possible to monitor both the anode and cathode simultaneously making it possible to track the Li distribution in a full cell.^[3] The state of charge, metallic Li plating and SEI formation was captured for the first charge/discharge cycle of a full electrochemical cell using conventional liquid electrolytes. The use of a polymer electrolyte membrane offers improvements over the original design.

References:

- [1] Krachkovskiy, S. A., Reza, M., Ramirez Aguilera, A. R., Halalay, I. C., Balcom, B. J., Goward, G. R. *J. Electrochem Soc.* 167(13), 130514 (2020)
- [2] Ramirez Aguilera, A. MacMillan B., Krachkovskiy, S., Sanders, K.J., Alkhayri, F., Dyker, A., Goward, G.R., Balcom, B.J., *J. Magn. Reson.* 325, 106943 (2021).
- [3] Freytag, A., Pauric, A., Krachkovskiy, S., and Goward, G.R. *J. Am. Chem. Soc.* 141 (35), 13758-13761 (2019).

5:15 PM CH01.14.05

Structural Dynamics of Metallic Nanocatalysts for Fuel Cells by *In Situ* Total X-Ray Scattering Valeri Petkov; Central Michigan University, United States

Many catalysts for energy related applications, in particular metallic nanoalloys, undergo atomic-level changes during electrochemical reactions. The nature and dynamics of the changes and their impact on the catalyst performance, however, are not well understood. This is largely because they are studied on model nanocatalysts under controlled laboratory conditions. We will present results from recent studies [1, 2, 3] on the dynamic behavior of metallic nanoalloy catalysts inside an operating proton exchange membrane fuel cell. Results show that the nanocatalyst change profoundly, from their initial state to the active form and further along the cell operation. Their electrocatalytic activity also changes, as reflected by the cell's performance. We will also show that the rate and magnitude of the changes may be rationalized when the limits of traditional relationships used to connect the composition and structure of nanoalloys with their electrocatalytic activity and stability, such as Vegard's law, are taken into account. The new insight into the atomic-level evolution of nanoalloy electrocatalysts is likely to inspire new efforts to stabilize transient structure states beneficial to their activity and stability under operating conditions, if not synthesize them directly.

V. Petkov et al. *Nanoscale* 11, 5512 (2019).
Zh. Kong et al. *J. Am. Chem. Soc.* 142, 1287 (2020).
Z. -P. Wu et al. *Nature Commun.* 12, 8597 (2021)

5:30 PM CH01.14.06

***In Operando* Study of Electrochemical Strain and Charge Storage in Nanosheet Oxide Electrodes** Scott T. Misture, Madeleine N. Flint, Peter Metz, Peng Gao and Robert Koch; Alfred University, United States

MnO₂ nanosheets demonstrate an interesting response to reduction of Mn⁴⁺ to Mn³⁺, where Jahn-Teller distorted Mn³⁺ is displaced out of the plane of the nanosheet forming a "surface Frenkel" defect. Atomic scale point defects enhance capacitance beyond 300F/g while lowering charge transfer resistance of δ-MnO₂ nanosheets by a factor of 10. X-ray total scattering was teamed with X-ray absorption spectroscopy and Raman spectroscopy probe the local

atomic structure, defect chemistry, and strain during electrochemical cycling. All methods employed in-situ or real-time in-operando study using custom sample environment cells and porous agglomerated nanosheet active materials. Specimens prepared by exfoliation of pristine powder grains to form nanosheet clusters with 2-5 individual layers were processed into nanosheet floccules, which are of high surface area (over 200 square meters per gram) and can be deposited as thick films using electrophoretic deposition. The result of the studies is a description of the charging mechanism in high surface area MnO₂ nanosheet electrodes and related nanosheet oxides: in-plane strains of up to 0.7% occur during charging, accompanied by Mn reduction. The initial number of Mn³⁺ defects determines the magnitude of the charge stored and consequently the electrochemical strain. In-situ XANES showed 16% of the Mn in MnO₂ reduced from Mn⁴⁺ to Mn³⁺ during electrochemical cycling. In agreement, in-situ Raman spectra demonstrate an increase in the number of Jahn-Teller distorted MnO₆ octahedra in the charged state as well as changes in the polarizability of vibrational modes that are affected by interlayer cations and interlayer water, though there is only very limited restacking of a few nanosheets. The excellent cycling stability of the nanosheet electrodes vs. bulk solids is attributed to the free space in the floccules that allows electrochemically-driven expansion and contraction without degrading the charge transfer pathways and without microcracking the active electrode. Another new discovery is Mn³⁺ defects also induce enhanced mass transport, resulting in formation of tunnel-like fragments which disrupt the sheet-like motif. Heat treatments expedite this layer-to-tunnel conversion which has a profound impact on the electrochemical properties and cycling stability. At low scan rates the capacitance of δ -MnO₂ heat treated at 60°C is ~6 times larger than the 400°C samples indicating a change in the charge storage mechanism that cannot be detected by diffraction studies alone, and requires PDF analyses. Kinetic analysis paired with PDF refinements demonstrate tunnel formation hinders the intercalative ion diffusion, reaching a percolation threshold around 25-30% tunnel structured MnO₂.

SESSION CH01.15: Morphological and Structural Characterization
Session Chairs: Daniel Abraham and Gillian Goward
Monday Afternoon, December 6, 2021
CH01-Virtual

6:30 PM *CH01.15.01

Advanced Neutron Characterisation of Rechargeable Batteries [Vanessa K. Peterson](#)^{1,2}; ¹ANSTO, Australia; ²University of Wollongong, Australia

The performance of rechargeable batteries is determined largely by materials structure- and dynamic-function relations. During battery function, materials undergo change, such as the experienced by electrode materials during the compositional change that occurs during battery cycling. Robust characterization methods that quantitatively and accurately capture structure- and dynamic-function relations across the relevant length and timescales for batteries are essential to the strategic design of materials with superior function.

Neutrons have attributes that make them exceptionally useful for this purpose. The predominantly nuclear interaction of neutrons with matter results in both high penetration, allowing the analysis of materials within whole commercial batteries, as well as an elemental sensitivity that is particularly well suited to battery materials composition.

This talk will give examples of neutron characterization of rechargeable battery materials, with a focus on instrumentation at the Australian Centre for Neutron Scattering, and much of which examines materials within whole batteries during operation. Examples using neutron powder diffraction,¹⁻⁵ neutron imaging,^{6,7} small and ultra small angle neutron scattering,⁸ and quasielastic neutron scattering,⁹ will be presented.

¹ N. Sharma, V. K. Peterson, M. M. Elcombe, M. Avdeev, A. J. Studer, N. Blagojevic, R. Yusoff, N. Kamarulzaman, *J. Power Sources*, 2010.

² C. Didier, W. K. Pang, Z. Guo, S. Schmid, V. K. Peterson, *Chem. Mater.*, 2020.

³ G. Liang, C. Didier, Z. Guo, W. K. Pang, V. K. Peterson, *Adv. Mater.*, 2020.

⁴ W. K. Pang, V. K. Peterson, N. Sharma, J. -J. Shiu, S. -h. Wu, *Chem. Mater.*, 2014.

⁵ W. K. Pang, V. K. Peterson, *J. Appl. Cryst.*, 2015.

⁶ D. Petz, M. J. Mühlbauer, A. Schökel, K. Achterhold, F. Pfeiffer, T. Pirling, M. Hofmann, A. Senyshyn, *Batteries & Supercaps*, 2021.

⁷ D. Petz, M. J. Mühlbauer, V. Baran, M. Frost, A. Schökel, C. Paulmann, Y. Chen, D. Garcés, A. Senyshyn, *J. Power Sources*, 2020.

⁸ S. Seidlmayer, J. Hattendorff, I. Buchberger, L. Karge, H. A. Gasteiger, R. Gilles, *J. Electrochem. Soc.* 2015

⁹ M. J. Klenk, S. E. Boeberitz, J. Dai, N. H. Jalarvo, V. K. Peterson, W. Lai, *Solid State Ionics*, 2017

7:00 PM CH01.15.02

In Situ TEM Corrosion Study and Anti-Corrosion Control of Pd@Pt Core-Shell Electrocatalysts [Fenglei Shi](#); Shanghai Jiao Tong University, China

Platinum (Pt)-based electrocatalysts are widely used in many fields such as energy, environment, medicine, and so on. The activity can be improved by composition, structure, morphology control while the performance degradation still occurs during the operation. Therefore, it is of great importance to investigate the degradation mechanism of the Pt-based electrocatalysts. Herein, we chose Pd@Pt core-shell structure, a promising electrocatalyst toward oxygen reduction reaction (ORR) as the study system. In-situ liquid cell transmission electron microscopy (LC-TEM) technique was utilized to explore the nanoscale corrosion kinetics of the electrocatalysts. The corrosion of Pd@Pt core-shell nanoparticles with different morphology like cube and octahedra were studied. The results indicate that the defects are the inducing factors of corrosion and the sequential corrosion process is controlled by both the local strain and evolving curvature. Strain plays a major role in the early process, and the local curvature dominates gradually in the later process. In addition, the sites with high surface energy like corners are the preferential etching areas. We sequentially designed and synthesized corner-protected Pd@Pt nanocubes and small size octahedral nanoparticles with fewer defects and smaller strains based on these insights in nanoscale corrosion behaviors. Both in-situ LC-TEM study and ex-situ stability tests confirmed that the newly designed electrocatalysts were much more corrosion-resistant.

References

1 Shi, F. et al. *Nat. Commun.* **9**, 1011, 2018.

2 Shi, F. et al. *Chem* **6**, 2257-2271, 2020.

3 Shi, F. et al. *ChemNanoMat* **5**, 1439-1455, 2019.

4 Shi, F. et al. *Adv. Mater.* accepted, 2021.

7:15 PM CH01.15.03

Operando Visualization of Mass Transport Behavior in Electrolytes During Electrochemical Device Operation by Phase-Contrast X-Ray

Imaging Daiko Takamatsu, Akio Yoneyama and Jun Hayakawa; Hitachi, Ltd., Japan

A fundamental understanding of mass transport properties in electrolytes during electrochemical reaction is important for optimal operation and design of energy conversion/storage devices, including batteries, fuel cells and water electrolysis. It is known that internal resistance of the lithium-ion batteries (LIBs) temporarily rises by repeating high-rate charge/discharge cycles and that it decreases by stopping the battery operation and rest. Because such a reversible resistance rise occurs only during the battery operation, this phenomenon is speculated to be related to the ion concentration distributions in the electrolyte. Such ion concentration distributions in the electrolyte give also serious effect on the performance of lead-acid batteries (LABs). The development of a vertical ion concentration gradient of sulfuric acid is called electrolyte stratification, which causes inhomogeneous current distribution in the vertical distribution of the electrodes by frequent charging-discharging, reducing the life of LABs. However, there are few techniques that can be used to quantitatively characterize ion concentration distribution that arise in electrolytes during the battery operation.

Phase-contrast X-ray imaging is a technique that can be used to visualize density differences by detecting the X-ray phase shift caused by an X-ray passing through a sample. The sensitivity of the phase-contrast X-ray imaging is about 1000 times higher than that of conventional X-ray absorption imaging in a hard X-ray region for light elements. Since the electrolytes of batteries are composed of light elements, the phase-contrast X-ray imaging is expected to be effective in visualizing small density differences in an electrolyte during battery operation. We have demonstrated that phase-contrast X-ray imaging technique can quantitatively visualize ion concentration distributions that arise in electrolytes during battery operation (cf. LIBs [1], LABs [2]).

Recently, hydrogen energy systems that use hydrogen as an energy carrier, such as fuel cells (hydrogen-to-power) and water electrolysis cells (power-to-hydrogen), is a growing interest to realize carbon emission-free energy technologies. Among the various types of hydrogen energy devices, the proton exchange membrane fuel cell (PEFC) and water electrolysis (PEM-WE), which use solid polymer membrane as electrolyte, have been used in practical applications. For further improvement of PEFC and PEM-WE performance, there are several obstacles to be solved include sluggish reaction kinetics, complex water management, limited lifetime due to membrane degradation. However, characterization of mass transport phenomena (e.g., ion transport, thermal transport, etc.) in polymer electrolyte membrane under device operating conditions remains insufficient because of the lack of suitable observation techniques. We have demonstrated that phase-contrast X-ray imaging can visualize the behavior of the water distribution of polymer electrolyte membranes during water electrolysis operations [3].

In this presentation, we will introduce operando phase-contrast X-ray imaging technique can quantitatively evaluate mass transport phenomena in the electrolyte simultaneously during electrochemical device operation with high temporal (a few seconds) and spatial (a few microns) resolutions.

References: [1] Takamatsu, et al. J. Am. Chem. Soc., 140, 1608 (2018). [2] Takamatsu, et al. Chem. Commun., 56, 9553 (2020). [3] Takamatsu, et al., submitted.

7:30 PM *CH01.15.04

Structural-Electrochemical Studies of Sodium-Ion Battery Positive Electrodes Neeraj Sharma; UNSW, Australia

A significant challenge in sodium-ion batteries relative to lithium-ion batteries is the larger size of the sodium cation especially for host structures. An ideal electrode should be able to reversibly insert/extract large quantities of sodium ions with minimal structural distortions or with distortions that can be managed. The positive electrode active material is a significant source of the sodium ions during battery function and can be one of the most expensive and toxic components. Layered transition metal (TM) oxides of the general formula, Na_xTMO_2 have shown excellent electrochemical properties but are plagued in part by the structural changes during battery function. Our work has utilized *in situ* and *operando* synchrotron X-ray diffraction to probe the relationship between structure and electrochemistry during battery function in this class of materials with a variety of compositions.

Here, the focus will be on Mn-rich compositions which represent one of the cheapest and least toxic candidates for positive electrodes. The parameter space covered in this talk will include the structural and phase evolution of - Mn-rich P2 $\text{Na}_{2/3}\text{Fe}_{1-x}\text{Mn}_x\text{O}_2$ highlighting the differences based on composition, P2- $\text{Na}_{2/3}\text{Mn}_{0.8}\text{M}'_{0.1}\text{O}_2$ ($M = \text{Zn}, \text{Fe}$ and $M' = \text{Cu}, \text{Al}, \text{Ti}$) showing how the choice of transition metals influences structural evolution, and P2/O3- $\text{Na}_{2/3}\text{Li}_{0.18}\text{Mn}_{0.8}\text{Fe}_{0.2}\text{O}_2$ illustrating the role of a multi-component electrode.

8:00 PM *CH01.15.05

Operando Analysis of Lithium-Ion Battery Electrodes and Cells Featuring Neutron Diffraction Hajime Arai, Tetsuya Omiya and Atsunori Ikezawa; Tokyo Institute of Technology, Japan

Operando analysis under both in-situ and non-equilibrium conditions offers information on how battery materials actually function during battery operation. The behavior of interest includes not only continuous status changes during discharging and charging but relaxation phenomena and even degradation.

The time resolutions of analytical methods limit their application to operando analysis; 6 min is required to observe each 10% change of battery materials during 1C rate operation. Electrochemical analysis generally shows high time resolutions but offers only limited physico-chemical information of the material. To support the phenomena observed by electrochemical analysis, a variety of operando methods have been proposed and applied such as X-ray diffraction, X-ray absorption and neutron magnetic resonances.

Operando analysis of practical cells has been difficult due to the limited penetration depths of the analytical probes. Neutron analysis can be applied to look through the practical cells while it generally lacks sufficient time resolutions. SPICA, a diffractometer installed at Material and Life Science Experimental Facility of Japan Proton Accelerator Research Complex [1], uses strong neutron beam to enable operando analysis of 18650 cells during battery operation up to 1C [2,3] to allow simultaneous observation of positive and negative electrodes.

In this study, we apply the operando neutron analysis to clarify the degradation behavior of commercially available 18650 lithium-ion cells under float-charging, cycling and the mixture of them. We first anticipated that occasional cycling releases the cell from continuous float-charging to decrease side reactions and thus prolong the life. Against our expectations, it turned out that there is a negative synergy effect on the cell life when the float-charging and cycling were mixed. The dV/dQ curve [4] of the degraded cell was totally different from the original one, showing the limitation of the dV/dQ analysis to clarify the origin of the degradation. Neutron diffraction analysis indicated that the serious degradation chiefly originated from the positive electrode side, with its resistance increase. This is in contrast to the soft degradation caused by either float-charging or cycling, which can be attributed to loss of lithium inventory due to side reactions at the negative electrode [5] (clarified by the dV/dQ curve analysis and the neutron diffraction).

It is noted that the degraded positive electrode showed reaction inhomogeneity during discharging, which has rarely been reported by neutron diffraction. Such reaction inhomogeneity can be ascribed to the ion transportation limitation, as shown by X-ray diffraction [6] and optical measurement [7]. We assume that the surface film formation caused by the float-charging was accelerated by the particle cracking due to cycling, and considerable ion transportation limitation finally resulted in the high resistance of the positive electrode. These results prove that operando neutron analysis is a powerful tool for clarifying the degradation mode of practical cells.

Acknowledgment

The authors acknowledge the collaborative work by NTT facilities, Inc. and by High Energy Accelerator Research Organization.

References

- [1] M. Yonemura et al., *J. Phys.: Conf. Ser.*, **502**, 012053 (2014).
- [2] S. Taminato et al., *Sci. Rep.*, **6**, 28843 (2016).
- [3] S. Shiotani et al., *J. Power Sources*, **325**, 404 (2016).
- [4] I. Bloom et al., *J. Power Sources*, **139**, 295-303 (2005).
- [5] J. Vetter et al., *J. Power Sources*, **147**, 269-281 (2005).
- [6] H. Murayama et al., *J. Phys. Chem. C*, **118**, 20750 (2014).
- [7] H. Arai et al., *J. Phys. Chem. C*, **125**, 3776 (2021).

SESSION CH01.16: Imaging and Structural Characterization
Session Chairs: Francois Fauth and Emmanuelle Suard
Tuesday Morning, December 7, 2021
CH01-Virtual

10:30 AM *CH01.16.01

Understanding the Interplay of Electrode Microstructure, Crystallography and Performance Using Advanced X-Ray and Correlative Imaging Methods Paul Shearing^{1,2}; ¹University College London, United Kingdom; ²The Faraday Institution, United Kingdom

The past decade has seen the rapid development and proliferation of three-dimensional X-ray imaging tools applied to Li-ion batteries, providing a framework to improve the understanding of electrode morphology and its influence on transport processes, electrochemistry and mechanical behaviour. The non-destructive, and multi-scale characteristics of X-ray imaging tools provide benefits to quantify hierarchical complexity from the particle to the electrode and device level. Through the application of image-based modelling tools, it has become possible to simulate a range of phenomena using a computational framework derived directly from tomographic images. Here, we will review this progress and reflect on recent developments using multi-modal methods to understand the performance of Li-batteries: this includes XRD-CT to reconcile chemical, crystallographic and morphological behaviour, Bragg Coherent Diffraction Imaging to access sub-particle behaviour and complementary neutron and X-ray imaging techniques, leveraging the benefits of the alternative contrast modes possible.

In concert, the portfolio of imaging and modelling tools provides a platform to explore the performance, degradation and failure of Li-ion batteries and post Li-ion chemistries, including LiS and solid state batteries, which will also be presented here.

11:00 AM CH01.16.02

Revealing a Dissolution and Reprecipitation Process of Copper Catalysts During CO₂ Reduction Reaction Jan Vavra, Tzu-Hsien Shen, Dragos Stoian, Vasiliki Tileli and Raffaella Buonsanti; EPFL, Switzerland

Electrochemical CO₂ reduction reaction (CO₂RR) aims at reusing waste CO₂ and turning it into fuels and chemical feedstock. Ongoing development of catalysts focuses at reducing overpotentials and improving selectivity and stability. Cu is the most promising catalyst for multi-carbon products. Here, we describe a mechanism responsible for evolution of a Cu-based catalyst during CO₂RR by relying on in-situ techniques. Liquid cell electrochemical transmission electron microscopy is complemented by x-ray absorption near edge structure.

Metallic Cu nanospheres were shown to evolve into larger particles selective for C₂ products during CO₂RR.¹ We describe a series of subsequent stages responsible for the catalyst reconstruction. Initially, the catalyst oxidizes to Cu₂O upon exposure to the cell environment at open circuit voltage, while releasing Cu ions into the electrolyte. During the cell startup, the dissolved Cu ions redeposit, while the bulk of the catalyst is reduced back to metallic Cu. Surprisingly, the catalyst dissolution and redeposition continues under cell operation at reductive potential, despite the absence of oxidized phases. We exclude a previously proposed process of particle migration and coalescence by resolving individual particles in an operating CO₂RR cell. The observed process is instead similar to Ostwald ripening and proceeds through a soluble intermediate.²

The observed dissolution/reprecipitation process does rationalize the reported evidence of catalyst activation¹ as well as the loss of initial selectivity in precision synthesized nanocrystals.³ By understanding the processes responsible for CO₂RR catalyst reconstruction, we direct the efforts in synthesis of long-term stable catalysts and motivate future research aimed at controlling the redeposition to continuously refresh the catalysts active sites.

1. Kim, D. et al., *Proc. Natl. Acad. Sci.* **114**, 10560-10565 (2017).

2. Vavra, J. et al., *Angew. Chem. Int. Ed.* **60**, 1347-1354 (2021).

3. Huang, J. et al., *Nat. Commun.* **9**, 3117 (2018).

11:15 AM *CH01.16.03

Atoms in Motion—Operando M-Ion Battery Monitoring Using X-Ray Techniques Damien Saurel, Marine Reynaud, María Jáuregui, Montserrat Galcerán and Montserrat Casas-Cabanas; CIC Energígune, Spain

The use of operando methods for the study of electrochemical processes occurring in energy storage systems has become increasingly popular in recent years. Operando experiments represent a powerful tool for the monitoring of internal processes upon battery cycling that provide valuable insights regarding the fundamental electrochemical redox mechanisms and ageing phenomena in battery materials. Nevertheless, obtaining high-quality, representative and exploitable data from *operando* measurements requires careful control of many experimental parameters (i.e. cell configuration, electrode preparation, optical/goniometer geometry, data acquisition protocols and data interpretation methodology).

In this talk we aim to share our experience and draw the attention into several aspects that we consider important for effective data acquisition and exploitation using both lab-scale and synchrotron powder X-ray diffraction (PXRD) and Small Angle X-ray Scattering (SAXS) instruments. The impact of several key factors, related to the cell design, the experimental setup as well as the sample and experiment preparation, will be discussed.¹ Next, several case studies will be shown to illustrate the effectiveness of operando experiments to understand the electrochemical signature of several Na-ion battery materials,²⁻³ including asymmetric reaction mechanisms and order-disorder transitions.

1. Damien Saurel, Afshin Pendashteh, María Jáuregui, Marine Reynaud, Marcus Fehse, Montserrat Galceran, Montse Casas-Cabanas, Experimental Considerations for Operando Metal-Ion Battery Monitoring using X-ray Techniques, *Chemistry methods*, 1(6), 249-260, 2021.

2. Damien Saurel, Montserrat Galceran, Marine Reynaud, Henri Anne, Montse Casas-Cabanas, Rate dependence of the reaction mechanism in olivine

NaFePO₄ Na-ion cathode material, *Int. J. Energy Res.*, 42(10), 3258-3265, 2018.

3. Benoit Mortemard de Boisse, Marine Reynaud, Jiangtao Ma, Jun Kikkawa, Shin-ichi Nishimura, Montse Casas-Cabanas, Claude Delmas, Masashi Okubo, Atsuo Yamada, Coulombic self-ordering upon charging a large-capacity layered cathode material for rechargeable batteries, *Nat Commun* 10, 2185, 2019.

11:45 AM *CH01.16.04

Visualizing Electrochemical Reactions at the Nano- and the Atomic Scale by *In Situ* TEM Huolin Xin, Chunyang Wang, Lili Han and Peichao Zou; University of California, Irvine, United States

Over the past decade, we have witnessed a rapid growth in liquid and gas phase, heating and electrochemistry holders for transmission electron microscopy. These holders have enabled direct imaging of material transformations in liquid and gaseous environments with submicron-scale to atomic-scale spatial resolution under operando conditions. In particular, research regarding electrode materials in lithium ion batteries and nanocatalysts in heterogeneous catalysis has greatly benefited from the emergence of these capabilities. In this talk, I will showcase the capability of direct nanoscale visualization of electrochemical nucleation, growth and degradation of electrode materials and electrocatalysts utilizing operando and in-situ TEM techniques and discuss the insights extracted from these experiments for improving the electrochemical devices.

12:15 PM CH01.16.05

***In Situ* NMR Guided Electrochemical Regeneration of Anthraquinone Flow Batteries** Yan Jing¹, Evan Wenbo Zhao², Marc-antonio Goulet¹, Meisam Bahari¹, Eric Fell¹, Shijian Jin¹, Erlendur Jónsson², Ali Davoodi¹, Min Wu¹, Clare Grey², Roy Gordon¹ and Michael Aziz¹; ¹Harvard University, United States; ²University of Cambridge, United Kingdom

Organic molecules used for aqueous redox flow batteries hold great promise in significantly lowering levelized costs of electricity storage and potentially outperforming their inorganic counterparts, representing one class of promising candidates for grid-scale electricity storage.^[1] Short lifetime of aqueous organic redox flow batteries, caused by the instability of organic molecules, has been considered the biggest obstacle for successful commercialization. *In situ* NMR metrology offers a unique, non-invasive opportunity to observe dissolved redox-active organic molecules undergoing electrochemical reactions in an operating flow battery.^[2]

2,6-Dihydroxyanthraquinone (DHAQ²⁻) shows a fast instantaneous temporal fade rate (~5%/day) due to the instability of the reduced form (DHAQ⁴⁻), which disproportionates to 2,6-dihydroxyanthrone (DHA) along with its tautomer, 2,6-dihydroxyanthranol (DHAL), and DHAQ²⁻.^[3] In the present work, we employ *in situ* NMR to observe reversible and irreversible reactions among these DHAQ-related species as we vary the cell voltage. DHAQ (100 mM) was first charged at 30 mA/cm² and held at 1.7 V vs. Fe(CN)₆^{3-/4-} (100 mM) in a full cell, then it was discharged at 30 mA/cm² while the voltage decreased from 0.9 V to a cut-off voltage of 0.5 V, followed by a voltage hold at 0.5 V for 7.4 hours. During the voltage hold at 1.7 V, ¹H NMR signals of DHAQ⁴⁻ are visible; signals from DHA(L) were also observed. During discharge, the fast electron transfer between DHAQ³⁻ radical and DHAQ⁴⁻ anions causes the corresponding aromatic peak broadening, allowing the DHA²⁻ and DHAL²⁻ signals to be revealed as they remain unaffected. During the voltage hold at 0.5 V, aromatic peaks of DHAQ²⁻ and the new signals at 6.36, 6.41, 7.40 and 7.41 ppm grow in, accompanied by the decrease of signal intensities of DHA(L). The chemical shifts of these new signals were assigned to (DHA)₂. These results indicate that, at 0.5 V, DHA(L) can be electrochemically oxidized to (DHA)₂.

To determine whether (DHA)₂ can be further oxidized, the cell voltage was decreased from 0.1 V to -0.3 V, stepping in decrements of 0.1 V, holding for 2 hours at each voltage step. The intensity of the (DHA)₂ signals remains unchanged at 0.1 V and starts to decrease at 0 V, and the signals disappear completely at -0.2 V, accompanied by the increase of signal intensities of DHAQ²⁻. This observation indicates that (DHA)₂ has been electrochemically oxidized to DHAQ²⁻.

The concentration of DHAQ²⁻ as a function of battery voltage has been quantified. It remains at 72 mM at 0.1 V, starts to increase to 80 mM, 95 mM and 100 mM at 0 V, -0.1 V and -0.2 V, respectively. A comparison of the initial concentration of DHAQ²⁻ (*i.e.*, 100.4 mM 0.25 mM) with the concentration after electrochemical regeneration (*i.e.*, 99.9 mM 0.44 mM) indicates complete regeneration within the experimental resolution. This result demonstrates the circularity of the electrochemical reactions from DHAQ to DHA(L), to (DHA)₂ and back to DHAQ at different potentials.

The electrochemical regeneration technique rejuvenates not only DHAQ, but also the positive electrolyte – rebalancing the states of charge of both electrolytes without introducing extra ions. The strategy should extend to other water-soluble anthraquinones susceptible to anthrone formation; it may also be applicable for other redox-active organic molecules. The strategy could permit redox-active organic molecules to reach the combination of performance, cost, and lifetime necessary for AORFBs to become an attractive solution to the intermittent renewable electricity storage problem.

Reference:

[1] D. G. Kwabi, et al., *Chem. Rev.*, 2020, 120, 6467–6489.

[2] E. W. Zhao, et al., *Nature*, 2020, 579, 224–228.

[3] M.-A. Goulet, et al., *J. Am. Chem. Soc.*, 2019, 141, 8014–8019.

SESSION CH01.17: Microscopy and Imaging Techniques & Poster Session II
Session Chairs: Jean-Noel Chotard, Arnaud Demortiere and Claire Villevieille
Tuesday Afternoon, December 7, 2021
CH01-Virtual

1:00 PM *CH01.17.01

Fast X-Ray Operando Measurements “at Home” Jean-Noel Chotard, Vincent Seznec, Arina Nadeina, Tristan Lombard and Christian Masquelier; Lab de Reactivite Chimie-Solides, France

One of the weak point of batteries is their low cycling rate. It takes tens of minutes to charge a mobile phone (in the best cases) and even hours to charge an Electrical Vehicle and they fail delivering instant high power. **High rate materials**, *i.e.* materials able to be charge and discharge in the scale of the minutes or seconds, are of most interest. Some cathode materials such as Na₃V₂(PO₄)₂F₃ (NVPF) can be cycled at high rate (10C) with a limited loss of capacity [1]. A key point to develop such materials is the understanding of the cycling mechanisms involved. **Fast operando measurements are thus crucial**. Such measurements on electrode materials can easily be performed thanks to the high photons brilliance provided by third generation synchrotron light sources and the fast detection modes. In this field, the LRCS already demonstrated its ability to innovate by developing cells allowing concomitant measurement of the electrochemical and structural properties of electrode materials. Since the first operando-cell developed 15 years ago (for Lab X-ray diffraction), continuous improvements have been made. More recently, the cell was updated for transmission measurements in transmission mode [2] successfully used at both **SOLEIL (France) and ALBA (SPAIN) synchrotrons**. Additionally, this cell can be utilized for both absorption

(EXAF/XANES) and diffraction measurements. In parallel, a cell suitable for neutron diffraction has also been developed (collaboration between LRCS, the ICMCB in Bordeaux, France and the Laue Langevin Institute (ILL) in Grenoble) [3]. These various innovations shed lights on the reaction mechanism as well as Li/Na diffusion paths into the electrode material as demonstrated by some of our experiences in ALBA [4].

However, it is not easy to access large-scale facilities and beam time is rare. Being able to perform x-ray diffraction measurements in the time scale of a minute “at home” would indeed be a strong asset.

Thanks to a new diffractometer equipped with a Molybdenum rotating anode source, a highly efficient detector and a specific operando cell, those measurements are now doable in laboratories.

As it will be shown in this talk, fast measurements (less than a minute per diagram) can be performed allowing following the different phase changes during the charge or discharge of high rate electrode materials and identifying the formation of new metastable phases. Moreover, thanks to the high energy of the molybdenum radiation, we can do X-Ray diffraction in transmission mode through full All Solid State Batteries and study at the same time the anode and cathode.

1. Wang, M. *et al.* Synthesis and electrochemical performances of Na₃V₂(PO₄)₂F₃/C composites as cathode materials for sodium ion batteries. *RSC Adv.* **9**, 30628–30636 (2019).
2. Leriche, J. B. *et al.* An electrochemical cell for operando study of lithium batteries using synchrotron radiation. *J. Electrochem. Soc.* **157**, A606–A610 (2010).
3. Bianchini, M. Spinel materials for Li-ion batteries: new insights obtained by operando neutron and synchrotron X-ray diffraction.
4. Bianchini, M. *et al.* Comprehensive Investigation of the Na₃V₂(PO₄)₂F₃–NaV₂(PO₄)₂F₃ System by Operando High Resolution Synchrotron X-ray Diffraction. *Chem. Mater.* **27**, 3009–3020 (2015).

1:30 PM CH01.17.02

Operando X-Ray Nano-CT Coupling with XANES for Monitoring the (De)Lithiation Dynamics Inside NMC Secondary Particle Tuan-Tu Nguyen¹, Zeliang Su¹, Vincent De Andrade², Charles Delacourt¹ and Amaud Demortiere¹; ¹CNRS RS2E/LRCS, France; ²Argonne National Laboratory, United States

Over the last decades, with increasing energy demand along with the shift towards greener energy solutions, Li-ion batteries have gained attraction for energy storage applications.^[1] Due to the high complexity in the hierarchical architecture of composite electrodes, it is extremely challenging to ensure a homogenous electrode structure. The non-uniform distribution of phases, leading to microstructural heterogeneities, has been shown to induce a non-uniform electrochemical behavior, which can deteriorate the performance, and cause macroscopic failures.^[2,3] Therefore, the identification of these microstructural heterogeneities and understanding their effects on the dynamics of (de)lithiation is crucial to improve electrode design.

Lithium compositional distributions in composite electrodes can also be investigated using various techniques such as Raman microscopy,^[4] X-ray diffraction,^[5] or 2D X-ray absorption near-edge structure spectroscopy (XANES).^[6] However, these methods have been restricted to low spatial resolution or spatially integrated signal along the depth direction and cannot accurately capture the spatial distributions and can lead to a limited interpretation of the mechanism.

Several works have combined XANES and X-ray tomography^[7] to generate a rich data set that allows a direct correlation of the chemical information and the microstructure. Meirer *et al.*^[8] used 3D XANES to probe the conversion of NiO to Ni metal in a partly reduced electrode. They found significant inhomogeneities in terms of chemical states across particles as well as evidence of fracturing caused by volume expansion during the reaction. More recently, Wang *et al.*^[9] collected a 46-point spectrum across the iron K-edge of a LiFePO₄ cathode particle and developed a run-out correction system to enable automated tomography.

Here, we perform XANES coupled with transmission X-ray computed tomography at nanoscale in *operando* mode to investigate LiNi_{0.5}Mn_{0.3}Co_{0.2}O₂ (NMC) positive electrodes. In this work, we demonstrate that *operando* XANES-TXM nanoCT allows access to the Li distribution at nanoscale within the LiB electrodes during the operation. We also proposed a method that relies on just three energy levels located at pre-edge, edge, post-edge for minimization of radiation damage to the sample. Also, a specific electrochemical cell and a sample preparation process were introduced, which make the use of electrodes typical to those used in real-life applications possible.

Our experimental results unveil the non-uniformity of the Li repartition throughout the LiB porous electrodes during operation. As a result, there are regions being more active than the others as well as preference spots on the particle surface where the reactions are more likely to occur. The Li repartition across the electrode depth is adequately uniform, which indicates a negligible effect from porous electrode. In addition, some of the reconstructed slices also revealed that the lithiation process could also happen from internal pores of the AM particles. This observation also implies that the electrolyte along with the carbon conductive can penetrate some internal pores through the AM grain boundaries and allow the (de)lithiation process to occur from the inside of the NMC secondary particles. This multiscale insight can shed light to the optimization of the electrode design to improve the electrode performance.

[1] J. B. Goodenough, *Energy Environ. Sci.* 2014, 7, 14.

[2] Y. Yang, *et al. Adv. Energy Mater.* 2019, 9, 1900674.

[3] X. Lu, *et al. Nat. Commun.* 2020, 11, 1.

[4] J. Nanda, *et al. Adv. Funct. Mater.* 2011, 21, 3282.

[5] J. Liu, *et al. J. Phys. Chem. Lett.* 2010, 1, 2120.

[6] K. Chen, *et al. J. Phys. Chem. C* 2019, 123, 3292.

[7] D. P. Finegan, *et al. Nat. Commun.* 2020, DOI 10.1038/s41467-020-14467-x.

[8] Meirer, F *et al. Journal of Synchrotron Radiation* 2011, 18 (5), 773–781.

[9] Wang, J *et al. J. Nature Communications* 2016, 7, 1–7.

1:45 PM CH01.17.03

Late News: Advances in Direct Detectors for In Situ Electron Microscopy Barnaby D. Levin; Direct Electron LP, United States

In situ transmission electron microscopy (TEM) experiments on electrochemical systems require highly sensitive detectors in order to minimize the electron beam dose incident on the specimen, and thereby minimize the potential effects of electron beam damage. Highly sensitive detectors are also advantageous for *in situ* and *operando* experiments that aim to observe phenomena on millisecond timescales, where electron beam dose per frame is necessarily limited¹.

Monolithic active pixel sensor (MAPS) based direct detectors such as the DE-12 and DE-16 offer higher detective quantum efficiency (DQE) and sensitivity compared to conventional, scintillator-coupled detectors, and have been employed in a variety of *in situ* TEM experiments²⁻⁴, including studies of lithiation and delithiation⁵, sodium electrodeposition⁶, and CO₂ reduction⁷. More recently, Direct Electron has developed two new MAPS detectors, Apollo and Celeritas, that offer significant advances in the capability of direct detectors with potential applications to *in situ* experiments.

The event-based Apollo detector provides a fast-imaging speed whilst operating in an electron counting mode. Although MAPS based detectors achieve greater DQE than conventional TEM detectors when operating in charge integrating mode, DQE is further enhanced when performing electron counting. For frame-based MAPS based detectors, electron counting requires a very sparse signal per frame (~1 electron per 50 pixels), meaning that many frames must be summed to obtain interpretable images, effectively reducing imaging speed by one or two orders of magnitude. At the same time, enormous computational power is required to identify and count sparse events in individual frames. Instead of generating frames of data, event-based detectors only generate data from pixels in which an event occurs, causing intensity to exceed a threshold level. The generation of data from select pixels, rather than entire frames means fewer computational resources are needed to generate interpretable data, yielding a potential increase in speed. In the Apollo detector, events occur when pixels are excited by an electron hitting the sensor. These events are compiled into interpretable counting mode images, which are output at a rate of 60 images per second in 8192 x 8192 super-resolution mode.

The Celeritas detector offers very fast frame rates compared to previous TEM detectors. The physical sensor is 1024 x 1024 pixels with a 15 μm pixel size. At full frame size the frame rate exceeds 1950 fps, allowing phenomena to be observed with a time step of just 512 μs between images. With a reduced sub-area of 256 x 64 pixels, a frame rate of up to 87,000 fps can be achieved. This allows the Celeritas detector to be used to collect *in situ* 4D STEM datasets, where a time step of less than 0.2 seconds between entire 128 x 128 probe position datasets is possible. This is a comparable speed to conventional 2D STEM imaging and is one to two orders of magnitude faster than is currently possible with typical 4D STEM detectors.

The speed and sensitivity of the Celeritas and Apollo detectors may be advantageous for *in situ* electrochemical TEM experiments, such as studies of dendrite growth and formation, or of atomic structural fluctuations in electrocatalysts, where high-speed imaging will be valuable for understanding fundamental mechanisms.

References:

- B.D.A. Levin *J. Phys. Mater.* **4** 042005 (2021).
Chee et al. *Nano Letters*, **19**, 5, 2871-2878 (2019)
Liu et al. *PNAS*, **118** (10) e2008880118 (2021)
Gavhane et al. *npj 2D Materials and Applications*, **5**, 24 (2021)
Zeng et al. *Nano Letters*, **15**, 5214-5220 (2015)
Zeng et al. *Nano Energy*, **72**, 104721 (2020)
Vavra et al. *Angewandte Chemie*, **60**, 1347-1354 (2021)

Acknowledgements: This material is based upon work supported by the US Department of Energy, Office of Science under award numbers DE-SC0020577 & DE-SC0018493

2:00 PM CH01.17.04

Late News: Anisotropy of Lithium Metal Stripping Explored with *Operando* 3D Microscopy [Adrian J. Sanchez](#), Eric Kazyak, Yuxin Chen, Jose Lasso and Neil P. Dasgupta; University of Michigan, United States

A promising pathway to surpass the energy storage capabilities of Li-ion is to incorporate a Lithium (Li) metal anode into a rechargeable battery. However, challenges, such as poor cycle life and safety concerns, severely hinder the performance of Li metal anodes. Dendritic growth has been shown to contribute to poor cycle life, but the impact pit formation has performance is not fully understood. In our previous work, we implemented *operando* video microscopy to study the nucleation of Li metal and demonstrated the impact pits have on Li metal cycling¹. The edges of pits were observed to be “hot” spots for dendrite nucleation¹. Furthermore, the size of the pits was observed to influence the reversibility of dendrites when nucleation occurred in a pit¹. However, a mechanistic understanding of how pit formation influences dendrite nucleation and reversibility is lacking. To better understand how pits evolve and how this evolution impacts dendrites, we have enabled focus variation microscopy in our *operando* visualization platform². This technique captures the areal surface topography of sample with sufficient temporal resolution for *operando* measurements.

Using this capability, we: (1) explore the morphological evolution of individual pits; (2) demonstrate the anisotropic expansion of pits; (3) correlate electrode surface microstructure and crystallographic orientation with stripping anisotropy; and (4) demonstrate pit faceting. The results of this study highlight the anisotropic nature of Li metal stripping and identify the critical role of electrode crystallographic orientation and microstructure on stripping. Furthermore, this study illuminates how the observed anisotropic stripping can promote dead Li formation and suggests potential pathways to improve reversibility.

- A. J. Sanchez et al., *ACS Energy Lett.*, **5**, 994–1004 (2020).
A. J. Sanchez, E. Kazyak, Y. Chen, J. Lasso, and N. P. Dasgupta, *J. Mater. Chem. A* (2021).

2:15 PM CH01.17.05

Late News: *In Situ* Transmission Electron Microscopy of High-Temperature Corrosion by Chloride Salts [Prachi Pragnya](#), Daniel Gall and Robert Hull; Rensselaer Polytechnic Institute, United States

Understanding high temperature corrosion of molten salt containment materials is of great importance to improve energy-efficiency and reduce cost of thermal energy storage systems used with concentrating solar power plants. We have developed and implemented an *in situ* high-temperature transmission electron microscopy (TEM) diffraction and imaging approach to monitor corrosion of Inconel-625 alloy by molten eutectic MgCl₂-NaCl-KCl with 3 ± 1 nm spatial resolution and sub-second temporal resolution in real time. The experimental setup uses a micro-environmental cell (MEC) assembly inside a TEM with a gas flow channel and substrate heating (25-1000 °C), manufactured by Hummingbird Scientific. We also developed procedures involving a mobile vacuum transfer vessel and encapsulation in inert gas in a glove box to avoid incorporation of significant H₂O and O₂ in a Mg-chloride based salt-stack to be used for controlled corrosion studies. Quantitative *in situ* diffraction pattern analysis is implemented using a numerical clustering algorithm and 2D Gaussian fit functions to determine diffraction spot intensities as a function of space and time. This facilitates determination of overall corrosion rates as well as quantitative observation of the evolution of individual grains, providing microscopic insight into the nucleation and growth of the corrosion process. Multi-layered salt films (25 nm MgCl₂, 13 nm NaCl, and 12 nm KCl) on 50 nm-thick Inconel-625 layers on TEM heater-chips are assembled into a MEC for corrosion experiments at various temperatures and ambients inside a TEM. The isothermal corrosion rate for an anhydrous, unoxidized salt-stack is 25 ± 3 nm hr⁻¹ (220 ± 30 μm year⁻¹) at 700 °C. It increases to 40 ± 2 nm hr⁻¹ (350 ± 20 μm year⁻¹) at 800 °C. The corrosion rate at 700 °C increases five-

fold to $114 \pm 19 \text{ nm hr}^{-1}$ ($1000 \pm 170 \text{ } \mu\text{m year}^{-1}$) when the salt stack is air-exposed. These isothermal corrosion rates indicate that the molten chloride corrosion is significantly accelerated by salt hydration from air exposure. Real-time imaging of the microstructure suggests that corrosion is initiated at grain-boundaries.

<svg id="zcomponents__svg" style="display: none;"></svg>

2:30 PM CH01.17.07

Reaction Rate Constant Parameterization Methods for Simplified Electrochemical Lithium-Ion Models Alain Goussian¹, Sylvain Franger¹, Loïc Assaud¹ and Issam Baghdadi²; ¹Université Paris-Saclay, France; ²Stellantis, France

The modeling of lithium ion batteries (LIB) requires to fulfill two main aspects to: i) finding a system of relevant equations and ii) defining adequate unambiguous parameters. Actually, the parameterization of an electrochemical LIB model could be time consuming and the choice of the inputs is thus crucial. However, among all the parameters needed for an accurate model, the kinetic rate constants is often forgotten in the literature, when it comes to identify its value and dependency, whereas it takes a major part in electrochemical processes. Moreover, this parameter is believed to have a huge sensitivity over the entire model. Thus, our study is exploring, suggesting and comparing different approaches to estimate this reaction rate constant value and its dependency over other state variables, in order to identify an efficient method to determine this important parameter while accelerating parameterization phase and getting a more trustful result of the overall model.

2:35 PM CH01.17.08

Solid-Liquid Interactions of Oxygen Evolving Oxide Catalysts Probed in Real-Time Tzu-Hsien Shen¹, Liam Spillane², Jiayu Peng³, Yang Shao-Horn³ and Vasiliki Tileli¹; ¹Ecole Polytechnique Federale de Lausanne, Switzerland; ²Gatan, United States; ³Massachusetts Institute of Technology, United States

The improvement of the electrocatalyst performance for the oxygen evolution reaction (OER, $4\text{OH}^- \rightarrow \text{O}_2 + 2\text{H}_2\text{O} + 4\text{e}^-$) requires fundamental understanding of the active sites during operation [1]. Here, we use electrochemical liquid-phase transmission electron microscopy (TEM) in combination with electron energy-loss spectroscopy (EELS) to probe solid-liquid interfacial interactions of the OER catalysts in real-time. The wetting behavior of Co-oxide particles is revealed and the catalytic products during the oxygen evolution reaction are detected at a single particle level. Three different crystal structures were evaluated: the rocksalt CoO, the spinel Co_3O_4 , and the highly OER-active perovskite $\text{Ba}_{0.5}\text{Sr}_{0.5}\text{Co}_{0.8}\text{Fe}_{0.2}\text{O}_{3-\delta}$ (BSCF) [2]. By analyzing the contrast of sequences of TEM images, the oxide surfaces are found to switch from hydrophobic to hydrophilic character under anodic potential due to electro-wetting induced by OH^- accumulation at the interface [3]. The process is fully reversible and the extent of its stability is linked to the underlying $\text{Co}^{2+/3+}$ redox reaction as well as the oxyhydroxide phase transformation on the spinel surfaces [4]. At high anodic applied potential, the evolution of molecular oxygen, probed site-specifically from areas surrounding the single particles, enhances the apparent hydrophilicity of the surfaces. These observations, performed in real-time and at a single particle level, provide unique nanoscale insights into the solid-liquid interactions of catalysts in their native environment.

[1] J. T. Mefford, A. R. Akbashev, M. Kang, C. L. Bentley, W. E. Gent, H. D. Deng, D. H. Alsem, Y. S. Yu, N. J. Salmon, D. A. Shapiro, P. R. Unwin, and W. C. Chueh, *Nature* **593**, 67 (2021).

[2] J. Suntivich, K. J. May, H. A. Gasteiger, J. B. Goodenough, Y. Shao-horn, F. Calle-vallejo, A. D. Oscar, M. J. Kolb, M. T. M. Koper, J. Suntivich, K. J. May, H. A. Gasteiger, J. B. Goodenough, and Y. Shao-horn, *Science* (80-.), **334**, 2010 (2011).

[3] T. H. Shen, L. Spillane, J. Peng, Y. Shao-Horn, and V. Tileli, *submitted* (2021).

[4] T. H. Shen, L. Spillane, J. Vavra, T. H. M. Pham, J. Peng, Y. Shao-Horn, and V. Tileli, *J. Am. Chem. Soc.* **142**, 15876 (2020).

SESSION CH01.18: Imaging and Surface Characterization
Session Chairs: Jean-Noel Chotard and Arnaud Demortiere
Wednesday Morning, December 8, 2021
CH01-Virtual

8:00 AM *CH01.18.01

Mapping Lithium with Operando Synchrotron X-Ray and Neutron Imaging Techniques Ingo Manke¹, Markus Osenberg¹, Nikolay Kardjilov¹, Robert Bradbury¹, Wolfgang Zeier², Ohno Saneyuki³, Alessandro Tengattini⁴, André Hilger¹, Joachim Binder⁵, Kang Dong¹ and Fu Sun⁶; ¹Helmholtz-Zentrum Berlin, Germany; ²University Münster, Germany; ³Kyushu University, Japan; ⁴Universite Grenoble, France; ⁵Karlsruhe Institute of Technology, Switzerland; ⁶Chinese Academy of Sciences, China

The three-dimensional structure and morphology of the electrode has a strong influence on the performance characteristics of a battery. Optimizing 3D structure and morphology is one of the key issues in the development of battery materials. Good electrical conductivity and sufficient Li-ion transport must be ensured at every point of the entire electrode at all times. Furthermore, changes of the 3D structure during cycling are often a main reason for capacity fading. The 3D structure has to be stable over hundreds of cycles. Therefore, a well designed 3D structure is essential for improving storage capacities and longevity. Radiographic and tomographic measurement techniques based on (synchrotron) X-rays and neutrons are ideally suited to obtain detailed information on the electrode structures. If properly used these techniques are non-destructive and allow for operando studies of structural changes during cycling in the cell.

This presentation will give an overview of recent developments in the field of operando imaging on batteries at Helmholtz-Zentrum Berlin (HZB) with a special focus on lithium mapping. To study the distribution of lithium and/or the lithiation process in a battery electrode different imaging techniques are of particular importance: 1. Synchrotron X-ray phase contrast imaging is well suited for analysis of lithium degradation when no strong X-ray absorbers are nearby. The high spatial resolutions allow studying small effects at interfaces of Li anodes or inside of a separator material. Some examples for Li anode degradation and Li dendrite formation will be shown. 2. X-ray absorption edge spectroscopic imaging at a synchrotron provides spatially resolved chemical information on the lithiation process even inside strong X-ray absorbers like NMC particles. The high spatial resolution also allows the analysis of individual battery particles. 3. Neutron imaging has a high sensitivity to lithium and allows studying in particular solid state electrolyte batteries during cycling. Some results will be presented and the use of Li isotopes for contrast enhancement will be discussed.

Finally, the talk will give some insights into the use of machine learning tools and the training of neural networks for optimized data segmentation and data analysis.

8:30 AM CH01.18.02

Operando Atomic Force Microscope-Scanning Electrochemical Microscopy (AFM-SECM) of pH Gradients at Gas Diffusion Electrodes [Nathan T. Nesbitt](#)^{1,2}, Thomas Burdyny², Divya Bohra², Recep Kas^{3,2} and Wilson Smith^{1,3,2}; ¹National Renewable Energy Laboratory, United States; ²TU Delft, Netherlands; ³University of Colorado Boulder, United States

Electrochemical carbon dioxide reduction (CO₂R) to renewable chemical feedstocks and fuels at high current density creates a high local concentration of hydroxide near the cathode. Due to diffusion limitations of hydroxide and homogeneous carbonate/bicarbonate reactions being out of equilibrium, this creates a pH gradient in the electrolyte between the cathode and the electrolyte bulk. Knowing this gradient is important for accurate analysis of CO₂R mechanisms, but it has yet to be measured in industrially relevant conditions. Using atomic force microscope-scanning electrochemical microscopy, we have measured this pH gradient above a gas diffusion electrode (GDE) and compared it with different transport models to determine the models' accuracy.

8:45 AM *CH01.18.03

Operando Kerr Gated Raman Spectroscopy to Investigate Ageing Processes on Lithium-Ion Electrode Interfaces [Laurence J. Hardwick](#)¹, Alex Neale¹, David Costa-Milan¹, Laura Cabo-Fernandez¹, Filipe Braga¹ and Igor Sazanovich²; ¹University of Liverpool, United Kingdom; ²Central Laser Facility, United Kingdom

Ageing mechanisms have a great impact into batteries calendar life and performance. A better understanding of these complex processes is critical to improve the lifetime of the battery. Electrolyte ageing plays a key role in the decrease of capacity since insoluble species and gas by-products are formed during the electrochemical cycling of the battery. Fluorescent species are formed during cycling of lithium ion batteries as a result of electrolyte decomposition due to the instability of the non-aqueous electrolytes and side reactions that occur at the electrode surface. The increase in the background fluorescence due to the presence of these components makes it harder to analyse data due to the spectroscopic overlap of Raman scattering and fluorescence. Herein we will demonstrate both *ex situ* and operando Kerr gated Raman spectroscopy as an effective technique for the isolation of the scattering effect from the fluorescence. This enabled the collection of the Raman spectra of LiPF₆ salt and LiPF₆-based organic carbonate electrolyte, without the interference of the fluorescence component and the measurement of Raman bands of graphite carbon at high states of lithiation.

9:15 AM CH01.18.04

Improved Operando Raman Cell Configuration for Commercially-Sourced Li-Ion and Na-Ion Battery Electrodes [Andy Wain](#)¹, Tim Rosser¹, Edmund Dickinson¹, Rinaldo Raccichini¹, Katherine Hunter², Andrew Searle², Christopher Kavanagh², Peter Curran², Gareth Hinds¹ and Juyeon Park¹; ¹National Physical Laboratory, United Kingdom; ²Deregallera Ltd, United Kingdom

Operando Raman spectroscopy is a powerful analytical technique for observing real-time chemical changes in energy storage materials under electrochemical cycling conditions. However, the requirement for optical access to the sample surface of interest places constraints on cell geometry, leading to an unavoidable trade-off between electrochemical performance and spectral data quality. This issue is particularly prominent in the case of commercially-sourced electrode samples that have been densely processed onto metal foil current collectors, for which spectro-electrochemical cycling at industrially relevant current densities is highly challenging.

In this work we present an improved configuration for performing *operando* Raman spectroscopy on commercially-sourced alkali-ion battery electrodes, in which a spacer is used to alleviate electrolyte ion accessibility limitations and improve electrochemical cell performance compared to a previously established spectro-electrochemical cell configuration. Electrochemical simulation predicts an improvement in lithiation homogeneity and electrochemical cycling performance at higher specific currents, and this is corroborated experimentally for a foil-backed graphite Li-ion negative electrode. The wider applicability of this configuration is also demonstrated by way of a case study of hard carbon Na-ion negative electrodes measured over 50 cycles. We show that this approach enables reliable *operando* Raman spectroscopy on commercial battery electrodes under conditions of more practical relevance to industry than previous cell configurations.

9:30 AM CH01.18.06

Revisiting the Ethylene Carbonate–Propylene Carbonate Mystery with Operando Characterization [Tim Melin](#) and Erik Berg; Uppsala University, Sweden

The “EC-PC mystery” has puzzled electrochemists for decades. The historically persistent use of propylene carbonate (PC) rather than ethylene carbonate (EC) as electrolyte solvent in lithium based batteries significantly delayed their realization. The additional methyl group in PC is surprisingly the root cause of the failure of PC to form a stable solid electrolyte interphase (SEI) on the negative Li-ion electrode, but the underlying reason remains debated.¹ Several explanations have been hypothesized, mostly based on *ex situ* measurements of electrolytes and electrodes.^{1,2} However, in order to obtain a detailed mechanistic understanding of the highly elusive interphase formation, *in situ* and *operando* techniques are needed.

In the presented study, electrode interphases formed as a result of EC and PC reduction are analyzed by two state-of-the-art *operando* techniques, Online Electrochemical Mass Spectroscopy (OEMS) and Electrochemical Quartz Crystal Microbalance with Dissipation monitoring (EQCM-D). OEMS and EQCM-D are techniques highly dedicated for analyzing volatile species³ as well as viscoelastic properties of electrode interphases during their formation in operating Li-ion cells.⁴ Both EC and PC based electrolytes show similar evolution profiles of H₂ and CO₂ while the extent of propylene (in the PC-based electrolyte) was significantly larger than the corresponding amount of ethylene (in the EC-based electrolyte). The findings correlate well with the EQCM measurements where a clear dissolution behavior of SEI in the PC-electrolyte was observed, while electrode mass deposition was irreversible when EC was present. Clearly, solubility of the various SEI components (primarily the dicarbonate) leads to dramatic differences in performance of PC as opposed to EC.¹ The presented study serves as a model for how *operando* techniques may provide deeper insights into well studied subjects, such as the EC-PC mystery.

1. Xu, K. Whether EC and PC Differ in Interphasial Chemistry on Graphitic Anode and How. *J. Electrochem. Soc.* **156**, A751 (2009).
2. Spahr, M. E. *et al.* Exfoliation of Graphite during Electrochemical Lithium Insertion in Ethylene Carbonate-Containing Electrolytes. *J. Electrochem. Soc.* **151**, A1383 (2004).
3. Lundström, R. & Berg, E. J. Design and validation of an online partial and total pressure measurement system for Li-ion cells. *J. Power Sources* **485**, (2021).
4. Kitz, P. G., Lacey, M. J., Novák, P. & Berg, E. J. Operando EQCM-D with Simultaneous *in situ* EIS: New Insights into Interphase Formation in Li Ion Batteries. *Anal. Chem.* **91**, 2296–2303 (2019).

9:45 AM CH01.19.05

Elucidating Performance-Limiting Side-Reactions in Large-Format Li-Ion Cells with Operando Electrochemical Mass Spectrometry [Casimir Misiewicz](#); Uppsala University, Sweden

Advances in methodologies for real-time analysis of batteries have come an extraordinarily long way [1], especially with the development of *Operando* Electrochemical Mass Spectrometry (OEMS). These approaches allow for the determination of side reactions during battery cycling with unprecedented selectivity and sensitivity, thus providing vital information necessary for determination of lifetime-limiting processes. However, the work thus far has primarily been carried out on model battery systems, where cell configurations and atmospheres are largely tampered with (through continuous flow [2] [3] in the *open* approach and purging [4] in the *semi-closed* approach [5]) and the operation conditions are therefore not comparable with real-life situations. Herein, the development and validation of an entirely *closed* OEMS system adapted for readily available commercial batteries is showcased. We provide a detailed description of two unique analysis designs with subsequent comparisons between them and other existing OEMS setups. Additionally, time-resolution modelling is applied to the data to determine precise gas onset points, ultimately eliminating diffusion related time delays. The prospects of utilizing OEMS for the study of commercially available rechargeable batteries after production or usage is evaluated.

[1] A. M. Tripathi, W. N. Su, and B. J. Hwang, "In situ analytical techniques for battery interface analysis," *Chem. Soc. Rev.*, vol. 47, no. 3, pp. 736–751, 2018, doi: 10.1039/c7cs00180k.

[2] P. Novák *et al.*, "Advanced in situ characterization methods applied to carbonaceous materials," *J. Power Sources*, vol. 146, no. 1–2, pp. 15–20, 2005, doi: 10.1016/j.jpowsour.2005.03.129.

[3] N. Tsiouvaras, S. Meini, I. Buchberger, and H. A. Gasteiger, "A Novel On-Line Mass Spectrometer Design for the Study of Multiple Charging Cycles of a Li-O₂ Battery," *J. Electrochem. Soc.*, vol. 160, no. 3, pp. A471–A477, 2013, doi: 10.1149/2.042303jes.

[4] R. Lundström and E. J. Berg, "Design and validation of an online partial and total pressure measurement system for Li-ion cells," *J. Power Sources*, vol. 485, no. December 2020, 2021, doi: 10.1016/j.jpowsour.2020.229347.

[5] L. A. Kaufman and B. D. McCloskey, "Surface Lithium Carbonate Influences Electrolyte Degradation via Reactive Oxygen Attack in Lithium-Excess Cathode Materials," *Chem. Mater.*, pp. 1–7, 2021, doi: 10.1021/acs.chemmater.1c00935.

SESSION CH01.19: Bulk and Interfacial Investigation
Session Chair: Ingo Manke
Wednesday Morning, December 8, 2021
CH01-Virtual

10:30 AM *CH01.19.01

Effective Transport in Li-S Solid-State Batteries Wolfgang Zeier; University of Muenster, Germany

The advent of solid-state batteries has spawned a recent increase in interest in lithium conducting solid electrolytes, especially in the lithium thiophosphates. However, many open questions remain when trying to optimize electrolytes and understand solid state battery chemistries. Among the interesting solid-state battery systems, the conversion reaction of sulfur has been recently of interest.

In this presentation, we will show how an understanding of the chemomechanical changes as well as the interfacial decomposition reactions in Li-S solid state batteries help to better understand and design these systems.

Further, we will show that fast ionic conduction is paramount within solid state battery composites. Measuring the effective ionic transport in cathode composites provides an avenue to explore transport and stability limitations that in turn provide better criteria for solid state battery performance

11:00 AM CH01.19.02

***Operando* Surface Enhanced Raman Spectroscopy of the Stepwise Formation of Solid Electrolyte Interphases in Li-Ion Batteries** Neeha Gogoi and Erik Berg; Uppsala University, Sweden

Solid electrolyte interphase (SEI) formed due to the reductive decomposition of electrolytes on the graphite negative electrode is one of the most widely studied phenomenon in Li-ion batteries[1]. Yet, no real consensus of the governing processes has been established due to their inherent complexity and lack of dedicated characterisation techniques[2]. Herein we have employed *Operando* surface enhanced Raman spectroscopy (SERS) to investigate the SEI formation in a model electrolyte based on Lithium bis(trifluoromethanesulfonyl)imide (LiTFSI) in ethylene carbonate (EC). We observe a stepwise potential-dependent reaction process involving decomposition of both electrolyte impurities and the EC solvent. The SERS enhancement has enabled us to also identify several metastable intermediates. For instance, Li₂CO₃ is observed as an interphasial component formed primarily due to the electrochemical reduction of residual contaminants in the electrolyte. SERS provides a deeper understanding of the underlying processes during SEI formation and the dynamics of the interfacial composition during the battery cycling. Challenges when analysing the SEI and prospects for development of this approach will further be highlighted.

Reference:

[1] M. Winter, "The solid electrolyte interphase - The most important and the least understood solid electrolyte in rechargeable Li batteries," *Zeitschrift fur Phys. Chemie*, vol. 223, no. 10–11, pp. 1395–1406, 2009, doi: 10.1524/zpch.2009.6086.

[2] A. J. Cowan and L. J. Hardwick, "Advanced Spectroelectrochemical Techniques to Study Electrode Interfaces Within Lithium-Ion and Lithium-Oxygen Batteries," *Annu. Rev. Anal. Chem.*, vol. 12, pp. 323–346, 2019, doi: 10.1146/annurev-anchem-061318-115303.

11:15 AM CH01.19.03

The Effects of Residual Water in Li-Ion Battery Model Systems Studied with Online Gas Analysis Robin Lundström and Erik Berg; Uppsala University, Sweden

The solid electrolyte interphase (SEI) is key to battery performance. The composition of the SEI is an assortment of decomposition products, mainly from reduced electrolyte species but also from residual contaminants, such as H₂O. The SEI both forms and changes during operation of a Li-ion battery. A full understanding of the SEI is challenging to attain with only post-mortem analysis. Therefore, analytical techniques monitoring the battery during operation, or *operando*, are needed to deconvolute the SEI formation in Li-ion batteries.

Many side-reactions, including SEI formation, in Li-ion batteries have volatile species forming as some of the decomposition products. Online Electrochemical Mass Spectrometry (OEMS) can sample the gas composition of a battery.¹ By sampling the volatile species from a battery cell during operation, a voltage-dependent gas evolution profile is gained. The result is a holistic overview of side-reactions in Li-ion batteries.

In this presentation, we deepen the study of the SEI formation on carbon electrodes and demonstrate how it is impacted by residual H₂O. Glassy carbon electrodes in carbonate-based electrolyte are studied using OEMS. More H₂O present in the battery cell has been linked to an increase² in CO₂ and decrease in C₂H₄ evolution³. We show that CO₂ and C₂H₄ evolution are connected with a linear relationship in relative amounts depending on H₂O content. The thermal reaction between H₂O and electrolyte components can result in HF forming over time. A high HF concentration in the electrolyte breaks the linear relationship of CO₂ and C₂H₄ gas evolution, as a new major decomposition reaction affects the SEI formation. Different stages of CO₂ evolution and consumption during the formation cycle will be shown, where multiple processes are present. Unintended reactions taking place in the glassy carbon model system will be shown to have a significant impact on the SEI composition.⁴ The influence of H₂O on the SEI formation in Li-ion battery systems and especially in model systems are highlighted.

(1) Lundström, R.; Berg, E. J. Design and Validation of an Online Partial and Total Pressure Measurement System for Li-Ion Cells. *J. Power Sources* **2021**, *485*, 229347.

(2) Bernhard, R.; Metzger, M.; Gasteiger, H. A. Gas Evolution at Graphite Anodes Depending on Electrolyte Water Content and SEI Quality Studied by On-Line Electrochemical Mass Spectrometry. *2015*, *162* (10), 1984–1989.

(3) Joho, F. et al. Key Factors for the Cycling Stability of Graphite Intercalation Electrodes for Lithium-Ion Batteries. *J. Power Sources* **1999**, *81–82*, 243–247.

(4) Lundström, R.; Berg, E. J. *In manuscript*.

11:30 AM *CH01.19.04

Using *In Situ* X-Ray Spectroscopy to Study Metal-Sulfur Batteries Lorenzo Stievano^{1,2}; ¹Univ. Montpellier, France; ²RS2E, France

Metal-sulfur batteries have been proposed in the last years as a promising energy storage technology for the future, due to the high theoretical capacity, remarkable energy density, and low cost. However, the major drawbacks of sulfur positive electrodes, such as the well known polysulfide shuttle effect and the low electrical conductivity of elemental sulfur, add to those specific of each negative electrode, such as the side reactions between metal anodes and electrolytes, are currently preventing their possible commercialization. All these effects are often interconnected, and strongly depend upon the type and the amount of electrolyte used in the cells. Therefore a thorough understanding of the mechanisms of all these processes, both in the bulk and at the interfaces, during the lifetime of metal-sulfur batteries is necessary for mastering them and producing a viable metal-sulfur system. Among the different techniques that have been developed for understanding these processes, *in situ* X-ray spectroscopies are among the most interesting ones. For instance, sulfur K-edge X-ray absorption and X-ray emission spectroscopies have been used to follow the evolution and the dynamics of the sulfur species in a working battery, while *ex situ* X-ray photoelectron spectroscopy was employed to study the evolution of the interfaces and the aging mechanisms of the metal-sulfur cells.

In this presentation, an overview of the application of X-ray spectroscopy methods to the study of metal-sulfur batteries is presented. It will be shown how these techniques together provide a unified view of metal-sulfur systems, suggesting possible strategies to circumvent their main drawbacks and thus enabling their practical applications.

12:00 PM CH01.19.06

***Operando* X-Ray Scattering with Stochastic Modelling to Quantify the Nanoscale Phase Evolution in Post-Lithium-Ion Batteries** Christian Prehal^{1,2}, Heinz Amenitsch², Stefan A. Freunberger^{3,2} and Vanessa Wood¹; ¹ETH Zurich, Switzerland; ²Graz University of Technology, Austria; ³IST Austria (Institute of Science and Technology Austria), Austria

Properties and function of beyond intercalation-type batteries are not only rooted in the chemistry but at least as much in the structure all the way from atomic to sub-micrometer length scales. This concerns specifically complex transformations such as the electrodeposition of insulating materials in conversion-type lithium-sulfur (Li-S) or lithium-air (Li-O₂) battery electrodes. Substantial performance improvements, therefore, rely on a quantitative physico-chemical understanding at all relevant length scales, which puts high demands on (*operando*) analytical techniques.

Here we present *operando* small and wide angle X-ray scattering (SAXS / WAXS) as a suitable method to study the nanoscale phase evolution of solid Li₂O₂ during charging and discharging a custom-built *operando* Li-O₂ cell. For data analysis, our recently developed method used for supercapacitors was adapted [1] and synergistically combined with modelling of Li₂O₂ nucleation and growth in a realistic 3D carbon pore model generated via stochastic modelling. This allows visualizing the nanoscale product formation in real-time and distinguishing between Li₂O₂ formed via disproportionation (solution mechanism) or direct electroreduction (surface mechanism). Contrary to what current knowledge predicts, we find that Li₂O₂ is formed to the widest extent via solution mediated disproportionation of LiO₂, even under conditions previously considered prototypical for Li₂O₂ surface growth [2]. Results were backed up by hydrodynamic voltammetry, electron microscopy and numerical modelling, and question significant parts of the currently accepted reaction model in Li-O₂ batteries [3].

Next to Li-O₂ batteries, the potential of the method is demonstrated by quantifying the reversible electrodeposition of solid reaction products during charging and discharging a custom-built *operando* Li-S cell. *In situ* SAXS / WAXS data analysis was combined with stochastic modelling of the three-phase nanostructure Li₂S / Li₂S₄ / electrolyte using the concept of PluriGaussian random fields [4]. The hierarchical Li₂S₄ – Li₂S composite nanostructures formed during Li-S discharge indicate that Li₂S forms via solid-state disproportionation of higher-order polysulfides rather than direct electroreduction at the carbon-electrolyte interface. Structural information derived from X-ray scattering was complemented by cryo (scanning and transmission) electron microscopy and small angle Neutron scattering. The found mechanism provides novel design criteria for improved capacities and improved cycle life in Li-S batteries.

References:

1 Prehal, C., Koczwara, C. *et al.* Quantification of ion confinement and desolvation in nanoporous carbon supercapacitors with modelling and *in situ* X-ray scattering. *Nature Energy* **2**, 16215, (2017).

2 Aurbach, D., McCloskey, B. D., Nazar, L. F. & Bruce, P. G. Advances in understanding mechanisms underpinning lithium-air batteries. *Nature Energy* **1**, 16128, (2016).

3 Prehal, C., Samojlov, A. *et al.* *In situ* small angle X-ray scattering reveals solution phase discharge of Li-O₂ batteries with weakly solvating electrolytes. *PNAS* **118**, e2021893118, (2021).

4 Prehal, C., Fitzek H. *et al.* Persistent and reversible solid iodine electrodeposition in nanoporous carbons. *Nature Communications* **11**, 4838, (2020).

12:15 PM BREAK

1:00 PM *CH01.20.01

Probing Interface Stability and Charge Distribution in Solid-State Batteries via STEM Miaofang Chi; Oak Ridge National Laboratory, United States

Solid-state batteries hold the promise of safer, cheaper, and longer-lasting batteries. Its largest bottleneck lies in their interfaces, including both interfaces with electrodes and internal grain boundaries. For example, many current solid electrolytes either involve concerning interfacial stability with electrodes and/or an unexpected dendrite growth along their grain boundaries. The associated underlying origins however remain unknown. To understand the interfacial mechanisms at play, the electrochemical stability, mechanical stability, and local potential variations, must be studied correlatively and ideally, under simulated operation. In this talk, I will show several examples of elucidating the interface stability, overpotential, and dendrite growth mechanism in model solid electrolytes, including lithium phosphorus oxynitride (LiPON), $\text{Li}_x\text{La}_{2/3-x/3}\text{TiO}_3$ (LLTO) and Al- $\text{Li}_7\text{La}_3\text{Zr}_2\text{O}_{12}$ (LLZO). This presentation will also demonstrate the power of utilizing a suite of scanning transmission electron microscopy techniques, including cryogenic high-resolution imaging, in situ biasing microscopy, differential phase-contrast imaging, and low loss electron energy loss spectroscopy (EELS) to probe features defining the function of interfaces in solid-state batteries.

This research was supported by an Early Career project supported by the DOE Office of Science FWP #ERK CZ55. All microscopy technique development was performed and supported by Oak Ridge National Laboratory's (ORNL) Center for Nanophase Materials Sciences (CNMS), which is a DOE Office of Science User Facility.

1:30 PM CH01.20.04

Modelling X-Ray Absorption Spectra for Dynamic Interfaces in Multivalent Electrolytes Ana Sanz-Matias and David Prendergast; Lawrence Berkeley National Laboratory, United States

The increasing demand of large-scale energy storage with improved performance, safety and sustainability for renewable variable energy sources drives the search for post-Li-ion batteries based on multivalent cation chemistries (e.g., Mg, Zn and Ca). However, poor electrolyte stability against metal anodes and high voltage cathodes has been so far one of many barriers to the development of multivalent cation rechargeable batteries. (Electro)chemistry at the electrolyte-electrode interface is critical to battery performance. Multivalent cations are prone to complex formation with solvent molecules and anions, leading to different interfacial species with characteristic (electro)chemical properties. Although multivalent cation solvation/complexation structures have been investigated in the bulk, fundamental understanding of speciation at the interface is lacking.

Fluorinated anions are often used in multivalent and other post-Li-ion electrolytes. Fluorine K-edge X-ray Absorption Spectroscopy provides access to a surprising level of detailed electronic structure information about the anion coordination and decomposition process, despite the relatively predictable oxidation state and ionicity of the fluoride ion. In this work, we examine the sensitivity of the F K-edge to the fluorine bonding environment in solid, liquid and interfacial species relevant to energy applications. Utilizing a combination of Molecular Dynamics simulations and a recently developed many-body approach based on the Δ SCF method, we calculate the X-ray absorption spectra of multiple fluoride salts using density functional theory. Thin films and surfaces are also explored to establish whether they provide distinct spectral signatures that might be observable in the solid electrolyte interphase of working electrodes. At last, the solid-liquid interface of non-aqueous, Mg based electrolytes with fluorinated anions are examined.

1:45 PM CH01.04.01

Nucleation and Growth of Transition Metal Alloy Nanoparticles from Transition Metal Hydroxide Complexes Observed in Graphene Liquid Cells Azadeh Amiri, Abhijit H. Phakatkar and Reza Shahbazian-Yassar; University of Illinois Chicago, United States

The nucleation and growth of crystalline nanoparticles is an important fundamental process of synthesis in many applications to better control and engineer the properties of nanoparticles. In-situ studies of electron beam-induced formation of metal nanoparticles from the precursor solution in the liquid-cell transmission electron microscopy (LCTEM) is one of the helpful methods to reveal the nucleation and growth mechanism.^{1,2} Especially, employing graphene liquid-cell (GLC) which encapsulates the liquid solution between thin graphene layers allows high-resolution imaging and better visualization of the important steps of nanocrystals nucleation and growth.^{3,4} In this work, using the GLC microscopy technique, nucleation and growth of transition metal alloys in an equimolar aqueous mixture of Mn, Fe, Ni, and Zn chloride salt precursor solution under electron beam is studied.

The radio-chemistry formation of metallic particles commonly involves three major steps of (1) production of metal atoms in solution by electron beam-induced reduction of metal ions; (2) nucleation of solid-phase by atom clustering; and (3) growth of nucleated particles by monomer addition and particle coalescing. Solvated electron (e^-_{aq}) produced by the radiolysis of water is a very strong reducing agent to reduce the transition metal ions with negative reduction potential to their zerovalent state. However, other ionic and radical species products of water radiolysis present in the solution can also react with metal atoms and oxidize them back to positive valence ionic states. Polyvinylpyrrolidone (PVP) is added to precursor solution can act as a strict stabilizer and a scavenger of OH radicals and minimize their oxidizing effect.

The transition metal salts dissolved in water were initially found as nanorod shape crystalline precipitates inside the GLC (Figure 1a). The analysis of the *fast Fourier transforms (FFT)* diffraction pattern matches the monoclinic crystalline structure of used transition metal hydroxide ($\text{TM}(\text{OH})_2$). (Figure 1b). The direct transformation of metal hydroxide nanorods to metal nanoparticles was observed by focusing the electron beam on a smaller screening area. As a result of increasing the magnification, the electron dose increases, and metal ions are reduced to metal atoms. The nucleation of nanoparticles is detected in few seconds at two sides of the long rods and they grow to 2 nm size particles in 10 s. Then 3-4 adjacent small particles start to coalesce and make the bigger particles. The growth of particles is slowed down after reaching 5 nm in less than 60 s. (Figure 2). The in-situ formed nanoparticles have a FCC crystalline structure close to the FCC structure of transition metals used which shows a single-phase multi-metallic alloy is formed in the solution and at room temperature. (Figure 2c-d)

References

- (1) Ngo, T.; Yang, H. Toward Ending the Guessing Game: Study of the Formation of Nanostructures Using in Situ Liquid Transmission Electron Microscopy. *J. Phys. Chem. Lett.* **2015**, *6* (24), 5051–5061. <https://doi.org/10.1021/acs.jpcclett.5b02210>.
- (2) Woehl, T. J. Metal Nanocrystal Formation during Liquid Phase Transmission Electron Microscopy: Thermodynamics and Kinetics of Precursor Conversion, Nucleation, and Growth. *Chem. Mater.* **2020**, *32* (18), 7569–7581. <https://doi.org/10.1021/acs.chemmater.0c01360>.
- (3) Fendler, J. H.; Kholkin, A.; Kingon, A.; Tokumoto, H.; Sinnamon, L. J.; Gregg, J. M.; Sharma, P.; Ke, X.; Rzechowski, M.; Eom, C. B.; Anglada, M.; Sharma, P.; Cross, L. E. References and Notes **1**. **2012**, No. April, 61–65.

- (4) Ghodsi, S. M.; Megaridis, C. M.; Shahbazian-Yassar, R.; Shokuhfar, T. Advances in Graphene-Based Liquid Cell Electron Microscopy: Working Principles, Opportunities, and Challenges. *Small Methods* **2019**, *3* (5), 1–16. <https://doi.org/10.1002/smt.201900026>.
- (5) The authors gratefully acknowledge the financial support from National Science Foundation (NSF Award number DMR-1809439)

1:50 PM CH01.04.05

In Situ Transmission Electron Microscopy Studies of Multi-Elemental Nanoparticles Synthesis in Liquid Flow Cells Azadeh Amiri, Abhijit H. Phakatkar and Reza Shahbazian-Yassar; University of Illinois Chicago, United States

Multi-element alloy nanoparticles are important materials for different catalysis and energy conversion applications due to the compositional complexity and lattice distortion.[1-2] Yet, fabrication of homogenous multi-metallic particles composed of miscible and immiscible elements is challenging and needs special kinetically controlled synthesis methods. [3-4]

In this work, we studied the in-situ colloidal synthesis of multi-element alloys through different equilibrium and non-equilibrium growth mechanisms. An equimolar aqueous mixture of Au, Pt, Ir, Cu and Ni chloride is used as the precursor solution and polyvinylpyrrolidone (PVP) is added as a stabilizer. A liquid flow holder integrated with microfluidic tubing is used to gradually inject the precursor solution into the liquid cell. The time-lapse series of TEM images show the fast formation of particles in solution entered into the liquid cell by electron beam reduction of metal ions, followed by nucleation of and growth of particles. The crystalline phase structure, elemental composition and distribution of formed nanoparticles are identified by ex-situ aberration-corrected scanning transmission electron microscopy (STEM), energy-dispersive X-ray spectroscopy (EDS) and high angle annular dark field imaging (HAADF) characterization techniques.

Due to the difference in miscibility and reduction rate kinetics of metallic elements, particles formed in liquid cells have different sizes, morphologies, and compositions. Three different types of particles are detected as AuCu alloy, PtCuIrNi alloy and Ni@Cu core-shell nanoparticles. Larger particles with a size of 20-30 nm are gold-rich AuCu alloy with near hexagonal morphologies. The second type of detected particles are Ni@Cu core-shell 8-10 nm in size. Nickel has the lowest reduction potential and is more likely to be oxidized by oxidizing radicals and ions product of water radiolysis. The formation of Ni@Cu core-shell nanoparticles can be explained by the slower reduction rate of transition metal elements compare to noble metals used in the mixture. The third type of particle has the smallest size and most complex composition. The PtCuIrNi particle are 2-3 nm in size and have a single FCC crystal structure. The crystal of these multicomponent nanoparticles is composed of atoms with different size and binding energies which results in lattice distortion and complex surface energies of lattice planes. This complex structure and surface energies of crystal facets hinder the fast coalescence of nanoparticles and further growth of particles. This is a promising mechanism for the synthesis of small nanoparticles with increased surface area and highly active surface sites for many catalysis applications.

- (1) Buck, M. R.; Schaak, R. E. Emerging Strategies for the Total Synthesis of Inorganic Nanostructures. *Angew. Chemie - Int. Ed.* **2013**, *52* (24), 6154–6178. <https://doi.org/10.1002/anie.201207240>.
- (2) Amiri, A.; Shahbazian-Yassar, R. Recent Progress of High-Entropy Materials for Energy Storage and Conversion. *J. Mater. Chem. A* **2021**, *9* (2), 782–823. <https://doi.org/10.1039/d0ta09578h>.
- (3) Chen, P.-C.; Liu, X.; Hedrick, J. L.; Xie, Z.; Wang, S.; Lin, Q.-Y.; Hersam, M. C.; Dravid, V. P.; Mirkin, C. A. Targets. In This Way, We Can Characterize Cross-Talk and Extract Errors per Gate from Errors per Gate Pair. For Target Atoms, E. *Nanoscale* **2015**, *352* (6293), 0–5.
- (4) Kwon, S. G.; Krylova, G.; Phillips, P. J.; Klie, R. F.; Chattopadhyay, S.; Shibata, T.; Bunel, E. E.; Liu, Y.; Prakapenka, V. B.; Lee, B.; Shevchenko, E. V. Heterogeneous Nucleation and Shape Transformation of Multicomponent Metallic Nanostructures. *Nat. Mater.* **2015**, *14* (2), 215–223. <https://doi.org/10.1038/nmat4115>.

- The authors acknowledge the financial support from National Science Foundation (NSF Award number DMR-1809439)

1:55 PM CH01.01.03

Operando XRD and Lattice Models as Tools to Determine Phase Diagrams—The Case of LiNiO₂ Matteo Bianchini^{1,2}, Markus Mock¹, Francois Fauth³, Karsten Albe⁴ and Sabrina Sicolo¹; ¹BASF SE, Germany; ²Karlsruhe Institute of Technology, Germany; ³ALBA Synchrotron, Spain; ⁴Technische Universität Darmstadt, Germany

Operando X-ray diffraction (XRD) is an established technique to observe cathode active materials (CAMs) and their crystallographic transformations upon Li (de)intercalation in Li-ion batteries.¹ With synchrotron radiation, high intensity and excellent temporal and angular resolution can be obtained, yielding accurate Rietveld refinement results.² This allows tracking unit cell symmetry and volume, atomic positions and even site occupancy factors; in other words it allows real-time investigations of compositional phase diagrams as a function of lithium content. In this respect, a complex and still debated CAM is LiNiO₂, which benefits nowadays of a wave of renewed interest fueled by the industry moving towards high-Ni layered CAMs.³ In this respect, it also becomes important to study LNO with operando XRD in electrochemical setups resembling commercial applications, such as unmodified pouch cells. In this presentation we will show that synchrotron XRD can indeed be used to measure pouch half cells in transmission mode to investigate CAMs, with a focus on LiNiO₂. Despite the fact that its phase diagram has been the object of numerous experimental and computational studies over the last two decades, even between recent experimental studies inconsistencies emerge on the position and width of single- and two-phase fields^{4,5}. Modelling of the phase diagram has always been a daunting task and resulted in the prediction of several stable Li phases that were not observed experimentally. Aiming at resolving the sources of discrepancy among experiments and between experiments and theory, we combine operando synchrotron XRD and Rietveld refinement with Monte-Carlo Simulation using a modified cluster expansion formalism at the Density Functional Theory (DFT) level⁶. A surrogate lattice model pinpoints the influence of off-stoichiometry (Li_{1-x}Ni_{1+x}O₂) and elemental substitution on the phase diagram and yields an unprecedented match to experimental ones. The dominant effect of both off-stoichiometry and elemental substitution is to disrupt Li ordering, suppressing phase transitions and promoting solid-solution behavior and the corresponding smoothing of voltage curves. Our model is particularly effective at reproducing the monoclinic domain and allows to draw a correspondence between electrochemical features (dx/dV curve) and Li-vacancy orderings (including the first identification of a Li_{5/8}NiO₂ superstructure). Deviations from experiments at both ends of the phase diagram are resolved and attributed to faulting and sluggish kinetics at high and low state of charge, respectively. The formation of stacking faults, in particular, known from ex situ observations⁷, is investigated for the first time under operando conditions.

Bibliography

1. Liu et al., Review of Recent Development of In Situ/Operando Characterization Techniques for Lithium Battery Research. *Adv Mater* **2019**, *31* (28), e1806620.
2. Bianchini et al., Comprehensive Investigation of the Na₃V₂(PO₄)₂F₃–NaV₂(PO₄)₂F₃ System by Operando High Resolution Synchrotron X-ray Diffraction. *Chemistry of Materials* **2015**, *27* (8), 3009–3020.
3. Bianchini et al., There and Back Again—The Journey of LiNiO₂ as a Cathode Active Material. *Angew Chem Int Ed Engl* **2019**, *58* (31), 10434–10458.
4. Li et al., Updating the Structure and Electrochemistry of Li_xNiO₂ for 0 ≤ x ≤ 1. *Journal of The Electrochemical Society* **2018**, *165* (13), A2985–A2993.
5. De Biasi et al., Phase Transformation Behavior and Stability of LiNiO₂ Cathode Material for Li-Ion Batteries Obtained from In Situ Gas Analysis and Operando X-Ray Diffraction. *ChemSusChem* **2019**, *12* (10), 2240–2250.
6. Mock et al., Atomistic understanding of the LiNiO₂–NiO₂ phase diagram from experimentally-guided lattice models. *Journal of Materials Chemistry A* **2021**, <https://doi.org/10.1039/D1TA00563D>.

7. Croguennec et al., Structural characterisation of the highly deintercalated $\text{Li}_x\text{Ni}_{1.02}\text{O}_2$ phases (with $x \leq 0.30$). *Journal of Materials Chemistry* **2001**, *11* (1), 131-141.

2:10 PM CH01.03.03

Structural Evolution of All-Solid-State Li-Ion Battery Using *Operando* TEM and X-Ray Micro-CT Sorina Cretu^{1,2,3}, Martial Duchamp² and Arnaud Demortiere^{1,3,4}; ¹Laboratoire de Réactivité et de Chimie des Solides, France; ²Nanyang Technological University, Singapore; ³RS2E-French Research Network on Electrochemical Energy Storage, France; ⁴ALISTORE- European Research Institute, France

Conventional lithium-ion batteries (LiB)¹ are the most efficient energy storage devices that triggered the transformation of our lifestyle into a digital nomad with the revolution of portable electronics. Compare to conventional liquid electrolyte, inorganic solid-state electrolytes (SSE) represent a promising alternative due to their nonflammable nature, broader temperature operating range and larger electrochemical window. Therefore, all-solid-state-batteries (ASSB) made an important step toward new-generation in electrochemical energy storage systems². However, several limitations still impact the performances of ASSBs such as SSE ionic conductivity, chemical evolution of SSE/active-materials interface, lithium dendrite growth, grain boundary conductivity and solid/solid interfacial resistance³.

To get a better insight into the limiting parameters of the performances of the ASSBs, a better quantification of the relationship between the structural and electrochemical properties is strongly required. In this study, we propose an approach to carry out *Operando* Transmission Electron Microscopy (TEM) measurements⁴ and X-ray micro computed tomography (XCT)⁵ to study the chemical and morphological modifications while operating the ASSB focusing on the multiple solid/solid interfaces at a local scale using the TEM, but also having a general view using the XCT.

For this study ASSB using an oxide solid electrolyte, $\text{Li}_{1.5}\text{Al}_{0.5}\text{Ge}_{1.5}(\text{PO}_4)_3$ (LAGP)⁶ was used due to their high stability in the air. Different batteries configuration was used for the *operando* TEM experiment and XCT. In the case of *Operando* TEM a LiFePO_4 (LFP)/LAGP/ $\text{Li}_3\text{V}_2(\text{PO}_4)_3$ (LVP) battery was studied where LFP was chosen as cathode material due to its safety and price attractions. One of the most difficult part in the realization process of the *operando* TEM experiment was represented by the production nanobattery process where the electrolyte layer must be thin enough (maximum 20 nm) to allow a full battery to be connected to the chip which allows applying bias. In the case of *operando* XCT NMC/LAGP/Li metal battery was studied where NMC and Li metal were chosen due to their high energy density.

A home-made electrochemical cell designed for tomography requirements has been used for monitoring Li dendrite, cracks formation, LAGP degradation in real-time during (de)lithiation process. The contact between lithium metal and solid electrolyte generated the formation of an instable interface where dendrites penetration in the solid electrolyte throw a delamination effect was spotted. Lithium exchange process produced extra stress and volume increase in the material which generated the production of the cracks in the battery. Once the irreversible process of the cracks started, lithium metal penetrated inside the cracks and slowly filled them, in the end producing the short-circuit the battery.

Operando TEM analysis allowed us a more local analysis where the solid/solid interface between cathode and solid electrolyte was studied at nanoscale. The appearance of cracks while cycling that was noticed using XCT was confirmed also with the TEM analysis. The migration of the cathode elements inside the solid electrolyte at the local scale upon cycling was noticed after the bias was applied offering us insights of the solid/solid interface in the ASSB at a local scale. The quantification of the dynamics of Li dendrite formation and the morphological changes within ASSB open new opportunities to attenuate failure processes occurring during the (de)lithiation mechanism.

1. J.M. Tarascon and M. Armand. *Nature* **414**, 359–367 (2001).
2. Takada, K. *et al. J. Power Sources* **394**, 74–85 (2018).
3. Bachman, J. C. *et al. Chem. Rev.* **116**, 140–162 (2016).
4. Nomura, Y. *et al. Nanoletters.* (2018)
5. Nguyen, T. *et al. Advanced Energy Materials.* *11*(8), 2003529, (2021).
6. Yang, G *et al. ACS Omega* **5**, 18205–18212 (2020).

2:25 PM BREAK

SYMPOSIUM CH02

Solid-State Chemistry of New Materials
November 29 - December 7, 2021

Symposium Organizers

Craig Brown, National Institute of Standards and Technology
Amparo Fuertes, ICMAB-CSIC
Hiroshi Kageyama, Kyoto University
Brent Melot, University of Southern California

Symposium Support

Bronze

Chemistry of Materials | ACS Publications
Hiden Analytical, Inc
Inorganic Chemistry | ACS Publications
Journal of Solid State Chemistry | Elsevier
Quantum Design, Inc.

* Invited Paper

SESSION CH02.01: Functional Porous Materials
Session Chairs: Craig Brown and Brent Melot
Monday Afternoon, November 29, 2021
Hynes, Level 3, Room 302

1:30 PM *CH02.01.01

Dynamically-Controlled Optoelectronic Behavior of Metal-Organic Materials Natalia Shustova; University of South Carolina, United States

Modulation of electronic properties as a function of external stimuli is driven by multifunctional device development. For instance, optical control over material electronic structures offers a powerful approach for optical switch integration, memory device evolution, and photocatalyst development. Tailoring electronic properties of metal-organic frameworks (MOFs) was previously achieved through metal node engineering, redox-active linker installation, or guest incorporation. We coupled previously applied synthetic strategies in this research area with the possibility of dynamically modulating electronic properties through integration of photoresponsive moieties within a framework.¹⁻³ In this presentation, a photophysics–electronics correlation will be discussed as a function of external stimuli. Optical cycling, modeling of density of states near the Fermi edge, conductivity measurements, and photoisomerization kinetics were employed to shed light on the process of tailoring MOF optoelectronic properties. This talk will also cover our recent efforts for engineering the first photochromic MOF-based field-effect transistor, in which the field-effect response could be changed through light exposure. As a demonstration, the change in current upon light exposure was sufficient to operate a two-LED fail-safe indicator circuit.¹

References:

1. Martin, C. R.; Leith, G. A.; Kittikhunnatham, P.; Park, K. C.; Ejegbavwo, O. A.; Mathur, A.; Callahan, C. R.; Desmond, S. L.; Keener, M. R.; Ahmed, F.; Pandey, S.; Smith, M. D.; Phillpot, S. R.; Greytak, A. B.; Shustova, N. B. *Angew. Chem. Int. Ed.* **2021**, *60*, 8072–8080.
2. Dolgoplova, E. A.; Berseneva, A. A.; Faillace, M. S.; Ejegbavwo, O. A.; Leith, G. A.; Choi, S. W.; Gregory, H. N.; Rice, A. M.; Smith, M. D.; Chruszcz, M.; Garashchuk, S.; Myhre, K.; Shustova, N. B. *J. Am. Chem. Soc.* **2020**, *142*, 4769–4783.
3. Dolgoplova, E. A.; Galitskiy, V. A.; Martin, C. R.; Gregory, H. N.; Yarbrough, B. J.; Rice, A. M.; Berseneva, A. A.; Ejegbavwo, O. A.; Stephenson, K. S.; Kittikhunnatham, P.; Karakalos, S. G.; Smith, M. D.; Greytak, A. B.; Garashchuk, S.; Shustova, N. B. *J. Am. Chem. Soc.* **2019**, *141*, 5350–5358.

2:00 PM CH02.01.02

Late News: Host-Guest Catalyst Systems for CO₂ Conversion Using Transition Metal Complexes Encapsulated in Metal-Organic Frameworks Jeffery Byers¹, Chia-Kuang Tsung¹, Zhehui Li¹, Thomas Rayer^{1,2}, Enric Adillon^{1,3}, Banruo Li¹ and William Thompson¹; ¹Boston College, United States; ²The Ohio State University, United States; ³California Institute of Technology, United States

The construction of host-guest catalyst systems for CO₂ hydrogenation reactions is described wherein molecular ruthenium-based complexes are encapsulated in the metal-organic framework (MOF) UiO-66. Encapsulation of the molecular complexes is made possible by utilizing an aperture-opening methodology that capitalizes on the dissociative ligand exchange process that occurs for the UiO-66 MOF. Through this method, host-guest catalyst constructs can be synthesized that decouple the synthesis of the transition metal complex, which serves as the catalytically active subunit, with the MOF host material. This advantage was used to develop a variety of catalysts used for the hydrogenation of carbon dioxide to useful fuels, such as formic acid and methanol. The method enables multicomponent catalytic systems that benefit from cascade catalysis. Additionally, the method is amenable for installing functional groups that modulate catalytic function through second-sphere interactions, which come about through modifications made to the MOF host material.

2:15 PM CH02.01.03

An Architectural Perspective on Heterogeneous Catalysis Debra R. Rolison, Paul A. DeSario, Catherine L. Pitman, Jeremy J. Pietron, Ashley M. Pennington, Todd Brintlinger, Evan R. Glaser, Travis G. Novak, Rhonda Stroud and Michelle D. Johannes; U.S. Naval Research Laboratory, United States

Our team investigates transport functionality—ion, electron, and mass—using aerogels as an ultraporous mesoscale platform that innately wires in three dimensions these three necessary mobilities for catalysis [1]. We track performance with a model bifunctional catalytic reaction: oxidation of carbon monoxide at metal nanoparticles (NPs) supported on reducing oxides. We can use the flexibility of sol–gel routes to prepare oxide aerogels as a means to site Au NPs either in the covalently bonded oxide network of TiO₂ or supported on the network using conventional routes to oxide-supported metals. We find that Au|TiO₂ interfacial design strongly impacts charge carrier (electron and proton) transport over mesoscale distances in the metal guest–oxide host architecture with implications for catalytic oxidations and controls the activity of CO oxidation under broadband illumination [2]. The intimacy of interfacial contact between Cu NPs supported on either TiO₂ or CeO₂ aerogels maintains the Cu NPs in a sufficiently metallic state to sustain a plasmonic response without ligand stabilization or during exposure to water/O₂ conditions or CO oxidation. The CeO₂ support also markedly increases activity for the thermal catalysis of CO oxidation over that obtained for Cu NPs supported on titania aerogels enabling Cu-based rather than Au-based oxidative catalysis [3].

[1] D.R. Rolison, J.J. Pietron, E.R. Glaser, T.H. Brintlinger, J.P. Yesinowski, P.A. DeSario, J.S. Melinger, A.D. Dunkelberger, J.B. Miller, C.L. Pittman, J.C. Owrutsky, R.M. Stroud, M.D. Johannes, *ACS Applied Materials & Interfaces* **2020**, *12*, 41277–41287.

[2] A.M. Pennington, C.L. Pittman, P.A. DeSario, T.H. Brintlinger, R.B. Balow, S. Jeon, J.J. Pietron, R.M. Stroud, and D.R. Rolison, *ACS Catalysis* **2020**, *10*, 14834–14846.

[3] C.L. Pitman, A.M. Pennington, T.H. Brintlinger, D.E. Barlow, L.F. Esparraguera, R.M. Stroud, J.J. Pietron, P.A. DeSario, D.R. Rolison, *Nanoscale Advances*, **2020**, *2*, 4547–4556

2:30 PM *CH02.01.05

Enhancing MOF Performance Through the Introduction of Polymer Guests Shuliang Yang, Daniel T. Sun, Li Peng, Vikram V. Karve, Natalia Gasilova, Mehrdad Asgari, Emad Oveisi, Olga Trukhina and Wendy L. Queen; École Polytechnique Fédérale de Lausanne (EPFL), Switzerland

Abstract: Among several classes of porous materials, metal-organic frameworks (MOFs) are particularly attractive due to their unprecedented internal surface areas (up to 7800 m²/g),^[1] easy chemical tunability, and strong, selective binding of a host of guest species. Through judicious selection of MOF

building blocks, which include metal ions and organic ligands, one can readily modify their properties for a variety of potential applications. Despite these attractive features, there are still challenges in the field that limit our ability to use MOFs as a solution for a wide range of industrial problems. For instance, some MOFs have limited mechanical and chemical stability, particularly in highly humid, acidic or basic environments. Overcoming this problem could lead to extended lifetimes and hence increased feasibility for their use in areas where such conditions are required.

In response to these needs, we have recently begun to combine MOFs and polymers in an effort to boost MOF performance and extend their stability. Our recent work demonstrates that selected polymers can significantly enhance MOF performance in a number of important liquid and gas separations^[2-4] as well as extend catalyst lifetimes in selected reactions.^[5] In addition to this, controlled polymerization processes were employed to enhance the mechanical stability^[6] of large pore frameworks and extend the chemical stability of a number of structurally diverse MOFs not only in humid environments, but also in acidic and basic media.^[7] We hope such work can help bring these frameworks a few steps closer to their deployment into a range of ecologically and economically important applications. In this presentation, our recent work, devoted to the development of novel MOF polymer composites, will be outlined.

References

1. Hönigle, I. M.; Bon, I. S. V.; Baburin, I. A.; Bönisch, N.; Raschke, S.; Evans, J. D.; Kaskel, S. *Angew. Chem. Int. Ed.* **2018**, *57*, 13780.
2. Sun, D.; Peng, L.; Reeder, W. R.; Britt, D. K.; Moosavi, M.; Tiana, D.; Oveisi, E.; Queen, W. L.; *ACS Central Sci.* **2018**, *4*, 3, 349.
3. Sun, D.; Yang, S.; Oveisi, E.; Gasilova, N.; Queen, W. L. *J. Am. Chem. Soc.* **2018**, *140*, 48, 16697.
4. Peng, L.; Yang, S.; Sun, D.; Asgari, M.; Queen, W. L. *Chem. Commun.* **2018**, *54*, 10602.
5. Karve, V. V.; Sun, D. T.; Trukhina, O.; Yang, S.; Oveisi, E.; Luterbacher, J.; Queen, W. L. *Green Chemistry* **2020**, *22*, 368.
6. Peng, L.; Yang, S.; Jawahery, S.; Moosavi, S. M.; Huckaba, A. J.; Asgari, M.; Oveisi, E.; Nazeeruddin, Md K.; Smit, B.; Queen, W. L. *J. Am. Chem. Soc.*, **2019**, *141*, 12397.
7. Yang, S.; Peng, L.; Sun, D.; Asgari, M.; Oveisi, E.; Trukhina, O.; Bulut, S.; Jamali, A.; Queen, W. L. *Chem. Sci.* **2019**, *10*, 4542.

3:30 PM CH02.01.06

Clathrate Behavior from a Molten Hydrogen-Bonded Organic Framework Adam H. Slavney and Jarad A. Mason; Harvard University, United States

Solid-state framework materials represent a unique class of solids in which chemists are able to exercise fine control of the crystalline structure through a carefully tuned combination of strong, directional bonding interactions and rigid organic struts. This level of control has enabled the design of highly effective materials for uses as varied as ion transport and gas capture and storage. However, despite these achievements, normal liquids remain the media of choice for many industrial adsorption applications as their fluidity greatly simplifies process design. As a means of bridging the liquid and solid adsorption paradigms we are interested in investigating the molten phases of framework materials. Due to their strong bonds, most framework materials decompose prior to melting. The few zeolitic imidazolate frameworks (ZIFs) which have been shown to melt do so at ~400 °C, temperatures too high to observe appreciable physisorptive interactions with guest molecules. We hypothesized that replacing the strong metal-ligand coordination bonds used in many frameworks with weaker hydrogen bonds would lead to significantly lowered melting points.

I will discuss our work on creating hydrogen-bonded frameworks (HOFs) with low melting points. By borrowing anti-crystal engineering strategies from the ionic liquid literature, we successfully lowered the melting point of a guanidinium sulfonate HOF from ~200 °C to as low as 70 °C. In fact, our molten HOF is itself an ionic liquid, albeit a very viscous one. The melting point of the framework is strongly dependent on its interactions with physisorbed guest species and can vary from 70 – 140 °C with different guests. In the absence of guests molecules, the HOF ionic liquid does not crystallize instead vitrifying into a glassy state at 45 °C. This phase behavior is strongly reminiscent of the clathrate hydrates; where water crystallizes into a network of hydrogen-bonded cages with encapsulated non-polar guests at low temperatures and high gas pressures. We demonstrate that the phase diagram of our HOF-guest system is isomorphic with that of a typical clathrate hydrate, emphasizing this connection. We suspect that the clathrate-like behavior we observe in our HOF may be a general phenomenon of molten frameworks at sufficiently low temperatures and this conceptual framework might be useful for future studies on molten framework materials.

3:30 PM BREAK

3:45 PM *CH02.01.07

Reactivity and Catalysis with Hydride Compounds Yoji Kobayashi; King Abdullah University of Science and Technology, Saudi Arabia

Hydrogenations are an integral part of many catalytic reactions. It is also natural to ask, then, whether this reaction can be catalyzed by hydride compounds. In solid state chemistry, the development of many new hydrides and related mixed-anion compounds has been reported; these advances form an excellent basis for developing new catalysts. We are interested in how these hydrides interact with small molecules, and whether they can lead to novel catalytic materials. Often, these are active as bulk materials, even without any supported metal. We will present how these materials can be used for ammonia synthesis/decomposition and CO₂ hydrogenation, while examining how the bulk structure/composition is involved.

SESSION CH02.02: Dielectric, Magnetic and Superconducting Materials I
Session Chairs: Brent Melot and Katharine Page
Tuesday Morning, November 30, 2021
Hynes, Level 3, Room 302

10:30 AM *CH02.02.01

Dielectric Behavior to Identify New Electronic Materials David J. Singh¹, Xin He², Patsorn Boon-on³, Ming-Way Lee³ and Lijun Zhang²; ¹University of Missouri, United States; ²Jilin University, China; ³National Chung Hsing University, Taiwan

Dielectric screening plays an important role in reducing the strength of carrier scattering and trapping by point defects for many semiconductors such as the halide perovskite solar materials. However, it was rarely considered as a screen to find new electronic semiconductors. We performed a material search study using the dielectric properties as a screen to identify potential electronic materials in the class of metal-pnictide ternary sulfosalts, containing Bi or Sb. These salts are basically ionic due to the electronegativity difference between the S and both the metal and pnictogen elements. However, we do find significant cross-gap hybridization between the S p-derived valence bands and pnictogen p-derived conduction bands in many of the materials. This leads to enhanced Born effective charges and, in several cases, highly enhanced dielectric constants. We additionally find a series of compounds with low effective mass, high dielectric constant, and other properties that

suggest good performance as electronic materials and also several potential thermoelectric compounds.

11:00 AM CH02.02.02

Tuning La₂O₃-Type Structure Magnetic Topological Candidates [Madalynn Marshall](#)¹, Antonio Moreira dos Santos², Huibo Cao² and Weiwei Xie¹; ¹Rutgers, The State University of New Jersey, United States; ²Oak Ridge National Laboratory, United States

Within the condensed matter science community, interest in topological materials has grown rapidly. An exciting direction is the combination of topological electronic states with additional quantum phases including magnetic topological materials, which have a range of applications including spintronics, thermoelectric and photovoltaics. Previously, our group discovered the trigonal La₂O₃-type Mg₃Bi₂ material to be a type-II nodal-line semimetal. The strong spin orbit coupling (SOC) Bi layers in this structure create an ideal environment for the topological electronic states. To drive this material even further magnetic elements can be introduced, potentially leading to a coupling between the magnetism and topological quasiparticles that can be additionally enhanced through pressure techniques. Widely accepted as a beneficial clean tool, pressure has the ability to tune the electronic interactions in quantum materials through the atomic distances. In this work we explore various La₂O₃-type structure magnetic topological candidates consisting of either 3d or 4f magnetic elements. Various pressure techniques have been utilized to observe the intricate tuning of the magnetic and electronic properties in these materials including high-pressure neutron diffraction, revealing evident nuclear and magnetic structure transitions. Manipulating these materials will result in a further understanding of our ability to control the magnetic and topological properties.

11:15 AM CH02.02.03

Highly Improved Ferroelectricity and Reliability in Hf_{0.5}Zr_{0.5}O₂ Films Using a HfO_xN_y Interfacial Layer [Beom Yong Kim](#)¹, Hyeon Woo Park¹, Yong Bin Lee¹, Suk Hyun Lee¹, Minsik Oh¹, Seung Kyu Ryoo¹, In Soo Lee¹, Doosup Shim¹, Min Hyuk Park^{2,1} and Cheol Seong Hwang¹; ¹Seoul National University, Korea (the Republic of); ²Pusan National University, Korea (the Republic of)

Since the ferroelectric (FE) property was first reported in the fluorite-structured Si-doped HfO₂ thin film in 2011, numerous researches on this emerging material have been conducted for memory and energy-related applications. The FE characteristic appears in the HfO₂ thin film because of the formation of the polar orthorhombic (o) phase. Although the non-polar monoclinic (m) phase is a thermodynamically stable phase in bulk HfO₂, it has been reported that the o-phase can be formed in HfO₂ thin films by controlling various factors such as dopants, surface energy, mechanical encapsulation, oxygen vacancies, and cooling rate. Meanwhile, the chemically reactive TiN bottom electrode (BE) has a tendency to induce a chemical reaction with the growing HfO₂ film, which can cause defects in the film and produce an unwanted interfacial dielectric layer. The former could significantly degrade the reliability through a leakage current flow and the eventual breakdown of the film during the endurance cycle tests, whereas the latter may degrade the remanent polarization (P_r) by inducing the depolarization effect. In this regard, the nitride interfacial layers, especially HfN_x (or HfO_xN_y) and ZrN_x (or ZrO_xN_y), are noteworthy. The inclusion of nitrogen may suppress the unwanted chemical between the (Hf, Zr)O₂ (HZO) film and the TiN BE, which could improve the reliability of the HZO film and suppress the depolarization effect. Among the HfN_x and ZrN_x, HfN_x could be more promising because it may suppress the in-situ crystallization of the HZO film during its atomic layer deposition (ALD), which adversely interfere with the o-phase formation.

In this study, the enhancements in the FE performance of the HZO-based TiN/HZO/TiN device with the insertion of HfO_{0.61}N_{0.72} interfacial layer (IL) were examined in detail. After optimizing the growth condition of the HfO_xN_y layer by the reactive sputtering, a 2-nm-thick HfO_{0.61}N_{0.72} IL was deposited on the TiN BE, which was oxidized in-situ to the HfO_{1.62}N_{0.34} during the subsequent ALD of the HZO thin film. The adoption of the 2-nm-thick HfO_{0.61}N_{0.72} IL suppressed the uncontrolled growth of larger HZO grains during the subsequent rapid thermal annealing process, which was accompanied by a more than 60% decrease in the inclusion of the undesirable m-phase compared to the structure without the IL. This improvement resulted in a ~30% increase in $2P_r$ without any change in the coercive field. Such improvement was maintained up to the HZO thickness of 20 nm. This could be ascribed to the formation of an amorphous HfO_{1.62}N_{0.34} IL on the TiN BE, which suppressed the unwanted in-situ inclusion of the crystalline nuclei in the HZO film during the ALD of the HZO film. Also, the slight inclusion of the nitrogen atoms at the bottom interface enhanced the reaction barrier property against the adverse chemical reaction with the reactive TiN BE, which crucially improved the electrical reliability of the HZO film. As a result, the 10-nm-thick HZO film showed an endurance cycle of 1.5×10^{11} cycles with a $2P_r$ value of $23.3 \mu\text{C cm}^{-2}$ when the endurance cycle test was performed at 3.0 MV cm^{-1} . This is among the highest endurance performance levels even without cation doping. Therefore, HfO_{0.61}N_{0.72} IL was highly promising in various FE HfO₂-based devices.

11:30 AM CH02.02.04

Low-Dimensional Magnetism with Triangular “CuV2” Motifs [Yiran Wang](#)¹, Masayuki Fukuda², Romain Gautier¹, Atsushi Miyake³, Sergey Nikolaev², Hena Das², Masashi Tokunaga³, Masaki Azuma² and Kenneth R. Poeppelmeier¹; ¹Northwestern University, United States; ²Tokyo Institute of Technology, Japan; ³The University of Tokyo, Japan

Owing to the interesting spin gap behavior, low-dimensional magnetic systems attract considerable attention. Transition metals, such as Cu²⁺ and V⁴⁺ with spin $S = 1/2$, are often used to construct such systems. Recently, we synthesized two crystalline compounds which contain both Cu²⁺ and V⁴⁺ ions by the hydrothermal pouch method. Single crystal X-ray diffraction reveals that triangular “CuV2” motifs with different arrangements forms in the infinite one-dimensional chain compound [H₃N(CH₂)₂NH₃]Cu(H₂O)₂[V₂O₂F₈] (**1**) and the molecular tetramer compound [Cu(H₂O)(4,4'-dimethyl-2,2'-bipyridyl)]₂[V₂O₂F₈] (**2**). Magnetization measurement in a pulsed high-magnetic field suggests a presence of a spin gap of 48.6 and 57.6 K in compound **1** and compound **2**, respectively. First-principles calculations indicate the presence of strong and weak antiferromagnetic interactions between Cu²⁺ and V⁴⁺, and weak ferromagnetic interactions between V⁴⁺ and V⁴⁺ in both systems. As a result, the quasi-one-dimensional chain compound **1** can be regarded as a chain of weakly coupled linear $S = 1/2$ spin trimers, and the molecular tetramer compound **2** can be decoupled into two weakly coupled $S = 1/2$ spin dimers.

SESSION CH02.04: Dielectric, Magnetic and Superconducting Materials II

Session Chairs: Craig Brown and David Singh

Tuesday Afternoon, November 30, 2021

Hynes, Level 3, Room 302

4:00 PM *CH02.04.01

Tuning Chemical Short Range Order in High-Entropy Oxide Perovskite and Spinel Lattices [Katharine Page](#)^{1,2}, Xin Wang¹, Palani Raja Jothi¹ and Bo Jiang²; ¹The University of Tennessee, United States; ²Oak Ridge National Laboratory, United States

Next generation materials of nearly every kind rely on chemical, electronic, and/or magnetic heterogeneity for creating, harnessing, and controlling functionality. High entropy oxides (HEOs), materials exhibiting a single-phase crystal structure containing five or more different cations on single

crystallographic lattice sites, have attracted great interest in diverse fields because of their inherent opportunities to tailor and combine materials functionalities. The control of local order/disorder in the class is by extension a grand challenge towards realizing their vast potential. We present detailed investigation of the cation site preferences, chemical short range order, and magnetic and thermal properties achieved in specific transition metal-based manganite perovskite and ferritic spinel HEO families through compositional tuning and variation in synthesis/processing conditions. A combination of local to long-range electron, X-ray and neutron scattering probes are employed to investigate their complex configurational diversity and associated structure-property trends. Experimentally derived models are supported by Density Functional Theory calculations and Metropolis Monte Carlo simulations. This work hints at the exquisite level of detail that may be required in computational and experimental approaches to guide structure-property tuning in emerging HEO materials.

4:30 PM CH02.04.02

Late News: Crystal Growth and Design of Defect Pyrochlores and Related High Entropy Oxides [Lucas Pressley](#)^{1,1}, [Angela Torrejon](#)¹, [W A. Phelan](#)² and [Tyrel McQueen](#)^{1,1,1}; ¹Johns Hopkins University, United States; ²Los Alamos National Laboratory, United States

A family of high entropy oxides with the formula $Mg_2Ta_3Ln_3O_{14}$ ($Ln = La, Pr, Nd, Sm, Eu, Gd$) has been discovered and synthesized. Single crystals, 5 mm OD \times 2.5 cm, for $Ln = Nd$ have been grown using the laser optical floating zone technique. Crystal orientations are confirmed by Laue diffraction, and structure solutions were obtained via single crystal X-ray diffraction. The structure is found to be a partially disordered pyrochlore, space group $Fd-3m$, fractional chemical formula $(Mg_{0.25}Nd_{0.75})_2(Mg_{0.25}Ta_{0.75})_2O_7$. Magnetization measurements indicate ordinary paramagnetic behavior in all compounds down to $T = 2$ K, except in the Eu variant which possesses Van Vleck paramagnetism. Specific heat measurements for $Ln = Nd$ shows no phase transitions between $T = 300$ and 2 K. We demonstrate the ability to prepare magnetically disordered materials by substitution of Mg with Ni, Mn, and Co, demonstrating the flexibility of this family in accommodating defects. The stabilization of these compounds could be due to the entropy gain associated with defects, showcasing a "materials by design" approach by using disorder to stabilize novel magnetic and optical materials. Further work has been done targeting high entropy versions of other families of oxides, with particular focus on the perovskite structure.

4:45 PM CH02.04.04

Intermediate Twinning, Abnormal Grain Growth and Chemical Inhomogeneity—Challenges and Opportunities in Lead-Free Ferroelectrics [Patricia Pop-Ghe](#)¹, [Monika Amundsen](#)², [Niklas Wolff](#)³, [Amna Rubab](#)³, [Lorenz Kienle](#)³, [Anette Gunnæs](#)², [Eckhard Quandt](#)³ and [Richard James](#)¹; ¹University of Minnesota, United States; ²University of Oslo, Norway; ³Kiel University, Germany

Recently, changing political and environmental demands are being met by an intense growth of research on efficient, environmentally friendly and ecological technologies. Among these technologies, lead-free ferroelectric ceramics have been widely studied, as possible applications range from the substitution of lead-based materials in piezoelectric devices and innovative cooling technologies to energy harvesting and conversion applications. However, their full potential remains unexploited for both bulk materials and thin films, the latter being a major driving force in today's key technology sectors. In this context, the ferroelectric potassium sodium niobate (KNN) ceramic is assumed to bear great potential ever since its discovery in the 1950's due to its combination of material properties i.e., its perovskite structure and correlated first-order phase transformations and ferroelectricity, as well as its high Curie temperature. However, composition and microstructure control are major challenges due to the material's multi-scale chemical heterogeneity, including high volatility, as well as varying diffusion constants and leading to an insufficient electrical performance as compared to lead derivatives.

The focus of this work is on the analysis, optimization and theory-guided synthesis of KNN, based on the geometrically nonlinear theory of martensite (GNLTM). The latter gives precise rules for the minimization of structural fatigue, but its applicability to complex ceramic materials is unclear. For KNN a major goal is the suppression of abnormal grain growth and the bimodal grain size distribution that lead to degradation of thermal and electronic properties. We show that the GNLTM correctly predicts favorable lattice structures and thus improved material properties for the homogeneous ceramic in which abnormal grain growth has been successfully suppressed. We achieve excellent thermal stability and repeatability of the tuned ceramic as seen from temperature-dependent X-ray diffraction (XRD), temperature-dependent transmission electron microscopy (TEM), and energy dispersive X-ray spectroscopy (EDS). These investigations reveal that the GNLTM together with advanced synthesis and characterization techniques provides a useful strategy for the improvement of the reversibility and functionality of phase-change materials with complex chemistry and structure.

SESSION CH02.05: Poster Session I
Tuesday Afternoon, November 30, 2021
8:00 PM - 10:00 PM
Hynes, Level 1, Hall B

CH02.05.01

Toward Durable Multimetal Oxyhalide Intergrowths for Solar Water Splitting [Kaustav Chatterjee](#)¹, [Roberto dos Reis](#)², [Jaye K. Harada](#)², [Jette K. Mathiesen](#)³, [Sandra L. Atehortua Bueno](#)¹, [Kirsten M. Jensen](#)³, [James M. Rondinelli](#)², [Vinayak Dravid](#)² and [Sara E. Skrabalak](#)¹; ¹Indiana University, United States; ²Northwestern University, United States; ³University of Copenhagen, Denmark

Metal heteroanionic photocatalysts have gained attention for their visible-light absorption; however, they are also plagued by photocorrosion, which limits their long-term use. Such photocorrosion occurs from the photooxidation of the less electronegative non-oxide ions, leading to decomposition of the material's lattice. In this presentation, new intergrowth oxyhalide photocatalysts composed of tantalum and gadolinium will be shown to be stable materials under visible light for photocatalytic water splitting. These intergrowths were prepared using a halide flux method, with their crystal structures analyzed by Rietveld refinement of powder X-ray diffraction data and scanning transmission electron microscopy. These analyses support intergrowth formation. The Ta:Gd molar ratio was systematically varied in the intergrowths to rationalize the effect of charge separation and changes in band structure towards photocatalytic water splitting activity. Furthermore, these intergrowths are capable of sustained overall water splitting in a Z-scheme with Ru/SrTiO₃:Rh as a hydrogen evolution catalyst. The high stability of these intergrowth materials is attributed to O 2p orbitals at the valance band edge rather than Cl 3p orbitals, as discerned from electronic structure calculations. These results provide new strategies for designing durable artificial photosynthetic systems by rational modulation of crystal and electronic structure.

CH02.05.05

Stable Water-Soluble Complexes with Picolinamide as a Solubilizing Ligand [Raúl Castañeda](#), [Tatiana Kornilova](#), [Michael S. Petronis](#) and [Tatiana Timofeeva](#); New Mexico Highlands University, United States

In pursuit to obtain water-stable MRI contrast agents, the bidentate ligand picolinamide (**PIAm**) was used to make complexes with copper, nickel, and zinc. The bidentate coordination of **PIAm** is analogous to that observed in 2,2'-bipyridine, but **PIAm** has an additional nitrogen atom which can act as both hydrogen bond donor, and acceptor, helping to improve the aqueous solubility of the target complexes. In this work seven different complexes with one, or two **PIAm** ligands, as well different geometries were obtained with $\text{Cu}^{\text{II}}\text{Cl}_2$, $\text{Cu}^{\text{II}}\text{ClBr}$, $\text{Ni}^{\text{II}}\text{Cl}_2$, $\text{Ni}^{\text{II}}2\text{H}_2\text{O}$ and $\text{Zn}^{\text{II}}\text{Cl}$. Interestingly these complexes are water-soluble, and they can be promising for some applications such as aqueous polymerization, hydrogen splitting, and MRI contrast agents. The stability of these complexes in water was tested using two different approaches: (i) using UV-vis, and (ii) by recovering the initial complex from an aqueous solution after the evaporation of water. Both approaches lead us to conclude that **PIAm** remains coordinated to the metal ion in an aqueous environment, although in some cases the chlorine ligands can be displaced. The geometry, chemistry, and similarities or differences in the crystal packing of these complexes will be discussed in detail in this work. Finally, the accurate measure of solubility and the EPR data of these complexes are underway and will be presented during the congress.

CH02.05.06

CeO₂ Aerogel-Supported Nickel for Highly Active and Stable Oxidation of Carbon Monoxide Travis G. Novak, Paul A. DeSario, Todd Brintlinger, Christopher N. Chervin, Rhonda Stroud and Debra R. Rolison; U.S. Naval Research Laboratory, United States

Nickel-based heterogeneous catalysts are widely researched as cost-effective alternatives to Pt or Au based materials for many reactions related to carbon chemistry, with ongoing efforts focused on improving stability and specific activity. Dispersing Ni on or within a highly porous oxide – such as Al_2O_3 , TiO_2 , or CeO_2 – can improve performance by both exposing more active sites and promoting metal-support interactions. However, the surface chemistry and stability of the active Ni phase is often unclear, as is the potential effect of the supporting oxide on the presence and persistence of certain phases. In this work, we photodeposit nickel nanoparticles (NPs) onto CeO_2 aerogels, an architecture that provides high surface area and a mesoporous structure allowing facile permeation of gas to interior active sites. Through *ex-situ* XPS analysis, we show that intimate contact between Ni and CeO_2 stabilizes Ni as $\text{Ni}(\text{OH})_2$, the highly active phase for CO oxidation. Conversion to NiO that occurs in higher weight loading with aggregated Ni is prevented. Activity for Ni/ CeO_2 aerogels is far greater than that of either unsupported Ni or Ni supported by structurally similar TiO_2 aerogels, indicating that this system benefits from a unique interaction between CeO_2 and Ni rather than simply the high surface area of the aerogel. CeO_2 aerogels with 2.5 wt.% Ni have both higher activity per mol of Ni and greater stability than higher weight loadings, with 95% CO conversion at 200 °C and no decline in activity after 12 h of continuous reaction. Our results reveal CeO_2 aerogels serve as an ideal supporting oxide for Ni catalysts and provide important insights regarding the effect of Ni phase for CO oxidation.

CH02.05.09

In Situ Synchrotron XRD Studies of Microstructure Evolution During the Salt-Mediated Coarsening of Nanoporous Metals Adam A. Corrao^{1,2}, Gerard S. Mattej^{1,2}, Christopher M. Coaty³, Victoria Petrova³, Zhuo Li^{1,2}, Monty R. Cosby^{1,2}, Taewoo Kim³, David P. Fenning^{3,3,4}, Ping Liu^{3,3,4} and Peter G. Khalifah^{1,2}; ¹Stony Brook University, United States; ²Brookhaven National Laboratory, United States; ³University of California, San Diego, United States; ⁴University of California San Diego, United States

Conversion reaction synthesis (CRS) methods provide a scalable and versatile route to nanoporous metals (NPMs) of both noble and non-noble metals with a morphology that is highly desirable for catalysis and other applications that benefit from a high surface area. CRS-derived NPMs can exhibit enhancements in catalytic activity relative to conventional metal nanoparticles, though the optimal surface area will be system-specific and represents a compromise between the demands for activity (higher surface areas are better) and stability (which the highest surface area morphologies may lack). For this reason, it is important to gain both a fundamental understanding and practical control over processes that can be used to tune particle and pore sizes in NPMs.

While thermal annealing is generally suitable for tuning porosity, it has been observed that CRS-prepared NPMs often collapse during heating, resulting in the loss of surface area and particle interior accessibility. We have found that the collapse can be avoided by heating not the pure NPMs, but instead heating the NPMs when they are in the form of a CRS intermediate nanocomposite phase in which salt (typically LiCl) fills the NPM pores. *In situ* synchrotron X-ray diffraction studies with fine time resolution (~1 sec step size) have been used to quantitatively follow the rapid evolution in microstructure that occurs when Fe, Co, and Cu NPM-salt nanocomposites are heated. Intriguingly, the most rapid growth in the metal particle size occurs concurrently with a sharp reduction in lattice strain within the salt phase, indicating a non-innocent role of the solid salt in the coarsening process. This work provides the first quantitative mechanistic insights into the coarsening behavior of CRS-prepared NPMs.

Work has also been carried out to extend the CRS methodology from simple homogeneous metal systems to more complex heterogeneous systems that can have improved catalytic properties. One example of this is a ZnO-supported Co catalyst, which has an advantageous anisotropic morphology that provides better access to the interior porosity of the nanoporous Co metal than traditional isotropic NPM morphologies. It was found that the combination of the ZnO support and the anisotropic morphology led to a 3x improvement in H_2 production during the steam reformation of ethanol relative to chemically analogous isotropic nanoparticles.

CH02.05.10

Phase Transition Pathway by a Co-Operative Pseudo-Jahn Teller Effect Under Microwave Radiation Kelvin Dsouza and Daryoosh Vashae; North Carolina State University, United States

Microwave interaction in materials has been studied, debated, and extensively used for its exciting effects in the last two decades. Applications for microwave processing have grown over the years, especially for material sintering, waste processing, organic and inorganic material synthesis, and the rate enhancement of chemical reactions.

The intrinsic dielectric loss in a material can be explained by lifetime broadened two-phonon difference processes. At temperatures near phase transition, this absorption due to phonon relaxation can result in different structural orientations of the crystal leading to order-disordered phases and phase retention in the crystal structure.

In this work, we investigate the effect of microwave radiation on structural phase transitions and present the results for the case of bismuth oxide. Bismuth oxide has numerous applications in solid oxide fuel cells, gas sensors, photocatalyst, and optoelectronics for its attractive properties of wide bandgap, ionic conductor, and high refractive index. There have been five polymorphs of Bi_2O_3 reported so far, including α , β , δ , γ , and ϵ , with α - Bi_2O_3 being the stable phase at room temperature. However, under microwave radiation, we were able to synthesize the metastable β phases at room temperature. The sample is characterized using X-ray diffraction, Raman spectroscopy, Differential Scanning Calorimetry, and UV-Vis spectroscopy to evaluate the structure and different phases in the sample. These metastable states are structurally related, and different phases can emerge depending on the temperature and intensity at which the sample is irradiated with the microwave. Lone pair activity plays a crucial role in the crystal structure, and the position and direction of these lone pairs explain the orientation of the crystal. The underlying electronic phenomena can be attributed to the co-operative pseudo-Jahn teller effect, which is the interaction of active pseudo-Jahn teller centers. By evaluating the symmetry descent in the crystal lattice for the phases adopted by bismuth oxide through heat treatment, one can justify the hypothesis of a co-operative effect. As phonons carry the interaction between these centers, we hypothesize that

the intrinsic microwave absorption leads to multi-phonon relaxation, disrupting the interaction between the centers. To calculate the intrinsic microwave absorption and support the hypothesis, we evaluate the phonon dispersion and the two phonon relaxation using first-principle calculations.

CH02.05.11

Tunable Novel Magnetic System in an Anti-CeCoIn₃ Structure Type [Ranuri S. Dissanayaka](#) [Mudiyanselage](#)¹, Chang-Jong Kang¹, Kaya Wei², Tai Kong³, Gabriel Kotliar¹ and Weiwei Xie¹; ¹Rutgers, The State University of New Jersey, United States; ²National High Magnetic Field Laboratory, United States; ³The University of Arizona, United States

The materials science community is constantly striving to discover new critical materials that meet future technological demands. Exploring rare-earth free magnetic materials is one direction, where Mn-based compounds have been identified as a promising candidate to replace the rare-earth elements. Here we have designed and synthesized Mn-based novel rare-earth free magnetic materials in the anti-CeCoIn₃ structure type by using chemical bonding concepts. Physical property measurements have confirmed that the magnetic behavior of these compounds range from room temperature ferromagnetic to an antiferromagnetic. Furthermore, theoretical assessments indicate that by including a strong spin orbit coupling and manipulating the lattice parameters, in particular the *c/a* ratio, a magnetic transformation from antiferromagnetic to ferromagnetic state or vice versa can be observed. Various pressure dependent techniques are being utilized to investigate this predicted behavior. Overall, these materials provide an ideal platform to enhance the understanding of intricate structure-magnetic relationships. Fundamental knowledge on the manipulation of magnetic properties will accelerate the discovery of new critical materials.

CH02.05.12

Structural Investigation of Cu-Pd, Cu-Pt, and Cu-Ru Nanoparticles [Alexandre Foucher](#) and Eric A. Stach; University of Pennsylvania, United States

Bimetallic structures are advantageous to reduce the use of precious metals and diminish the cost of catalysts for critical chemical reactions. For instance, Pd is used for alkyne hydrogenation, Ru for the Fischer-Tropsch process, and Pt is an excellent catalyst for CO or methanol oxidation. However, these metals are expensive, and monometallic particles are not always very stable. To this end, Pt, Pd, and Ru are often incorporated with Cu to create optimized intermetallic or core-shell structures. The combination of these three expensive metals and Cu also yield a unique electronic configuration at the surface of the particles. Alloying leads to increased stability, activity, and selectivity compared to monometallic compounds. However, dynamical restructuring effects during chemical reactions may alter the property of the bimetallic nanocatalysts. Change in valence states, composition, and crystallography will influence the physical properties of innovative alloys for catalysis.

In this study, three Cu-based alloys were synthesized and characterized. In-situ transmission electron microscopy (TEM) and electron energy-loss spectroscopy (EELS) were performed to understand structural and compositional changes upon exposure to elevated temperatures and O₂/H₂. Modification of the crystal structure at the surface of the nanoparticles and changes in the oxidation numbers can be correlated with increased or reduced chemical properties. Differences between alloyed and monometallic systems are investigated with EELS and electron pair-distribution function (ePDF) analysis. Results are also supported with density functional theory (DFT) calculations to understand the effect of crystallography, valence state, and composition on reactions.

Hence, bimetallic nanocatalysts' chemical and physical properties can be described by a combination of innovative characterization techniques supported by electronic structure calculation. This approach can be expanded to an extensive range of new materials to understand the origin of their properties.

CH02.05.13

Ternary Ti-Mo-Fe Nanotubes as Efficient Photoanodes for Solar-Assisted Water Splitting [Nageh K. Allam](#); American University in Cairo, Egypt

Designing efficient and stable water splitting-photocatalysts is an intriguing challenge for energy conversion systems. We report on the optimal fabrication of perfectly aligned nanotubes on trimetallic Ti-Mo-Fe alloy with different compositions prepared via the combination of metallurgical control and facile electrochemical anodization in organic media. The X-ray diffraction (XRD) patterns revealed the presence of composite oxides of anatase TiO₂ and magnetite Fe₃O₄ with better stability and crystallinity. With the optimal alloy composition Ti- (5.0 at.%) Mo- (5.0 at.%) Fe anodized for 16 h, enhanced conductivity, improved photocatalytic performance, and remarkable stability were achieved in comparison with Ti- (3.0 at.%) Mo- (1.0 at.%) Fe samples. Such optimized nanotube films attained an enhanced photocatalytic activity of ~0.272 mA/cm² at 0.9 V_{SCE}, which is approximately four times compared to the bare TiO₂ nanotubes fabricated under the same conditions (~0.041 mA/cm² at 0.9 V_{SCE}). That was mainly correlated with the emergence of Mo and Fe impurities within the lattice, providing excess charge carriers. Meanwhile, the nanotubes showed outstanding stability with a longer electron lifetime. Moreover, carrier density variations, lower charge transfer resistance, and charge carriers dynamics features were demonstrated via the Mott-Schottky and electrochemical impedance analyses.

CH02.05.14

Engineering Random Dielectric Nanoscale Strains on Silicon Surface to Enhance Light Emission [Sufian Abedrabbo](#)¹, El Mostafa Benchafia¹, Ahmad Al-Qawasmeh¹, Nuggehalli M. Ravindra² and Anthony T. T. Fiory³; ¹Khalifa University of Science and Technology, United Arab Emirates; ²New Jersey Institute of Technology, United States; ³Integron Solutions, United States

Engineered materials and devices typically involve interfaces of various forms that introduce property modifications of interfaced materials by introduction of stresses and strains. In this study, we focus on interfaces created in silicon associated with inhomogeneous stresses and specifically address their strong effect on radiative properties of indirect bandgaps. In particular, attention is drawn to the sol-gel based dielectric coatings catalyzed by various acids on silicon that modulates the indirect bandgap of Si favorably towards radiative recombination of free-carriers. A hypothesis on the role of random nanoscale stresses is presented. Photoluminescence and strain levels properties of surface engineered interfaces via colloidal coatings is compared to those of thermal and chemical deposited coatings. Appreciable improvements of band edge light emission is revealed. Other techniques and structures that results also in inhomogeneous bulk strains and expected efficient radiative recombination properties will be presented. One of these include formation of ordered nanoscale dislocation loops below the silicon surface.

CH02.05.15

Na₂FePO₄F—A Computational Investigation into a Promising Cathode Material for Sodium-Ion Batteries [Daniel N. Sykes](#)^{1,2}, Yong-Seok Choi^{1,2} and David O. Scanlon^{1,2,3}; ¹University College London, United Kingdom; ²Faraday Institution, United Kingdom; ³Diamond Light Source, United Kingdom

Long-term viability of Li-ion battery energy storage may be limited by global lithium reserves. Recently, sodium-ion batteries (NIBs) have garnered a great deal of attention, partially because of sodium's natural abundance, its more even distribution across the earth and it costs less than lithium. NIBs are especially attractive for large-scale energy storage systems where cost and life cycle are essential. To this end, Na₂FePO₄F has been a material of interest as

a viable cathode material for sodium-ion storage due to the high discharge voltage and favourable theoretical capacity.¹ Recent work has shown the potential for doping in Na₂FePO₄F cathodes to increase average voltage, reduce band gap and Na-ion diffusion barrier.² In this work we will present work completed on computationally investigating Na₂FePO₄F using Density Functional Theory (DFT) with the periodic code, VASP (Vienna Ab Initio Simulation Package), and the hybrid HSE06³ (Heyd-Scuseria-Ernzerhof) functional. Here we elucidated the bulk geometric structure of the material through relaxation as well as the most stable magnetic configuration. The electronic structure of the material has also been examined with a Density of States (DOS) and band structure being obtained. Furthermore, to examine the defect landscape of the material properly later, the different stable phases of Na₂FePO₄F have been investigated. Calculating the phase stability of Na₂FePO₄F builds a foundation for a detailed understanding of its defect chemistry at given chemical potentials.

References

- B. L. Ellis, W. R. M. Makahnouk, Y. Makimura, K. Toghill, L. F. Nazar, *Nature Mater*, 2007, **6**, 749-753
D. Jin, H. Qui, F Du, Y. Wei, X Meng, *Solid State Sciences*, 2019, **93**, 63-69
A. V. Krukau, O. A. Vydrov, A. F. Izmaylov, G. E. Scuseria, *J. Chem. Phys.*, 2006, **6**, 224106

CH02.05.16

Chemical Bonding Revisited—The Potential of Property Maps Carl-Friedrich Schön, Steffen van Bergerem, Christian Mattes, Leif Kobbelt, Martin Grohe and Matthias Wuttig; RWTH Aachen University, Germany

Physicists and chemists share a common belief. The properties of solids are determined by the arrangement of its constituting atoms, which is governed by the chemical bonding mechanism present in the material at hand. It should therefore be possible to revert this relation and infer from a material's properties which bonding mechanism is employed. This is no simple feat, as there is a multitude of physical properties which might be an indicator for the relevant bonding mechanism in the corresponding solid. We therefore utilize means of computer science by using classification algorithms to sort a database of materials to a priori arbitrary groups, which we aim to link to bonding mechanisms.

In our study, we have composed a database of elements and binary compounds, containing for example Aluminum, Gallium Arsenide, Diamond, Sodium Chloride, Germanium Telluride etc. For all compounds in the database, the corresponding values of a set of properties were included. This set contains the conductivity σ , the Born Effective Charge Z^* , the Effective Coordination Number (ECoN) and the Bandgap EG, the melting point T_M , the density ρ and the atomic density ρ_A . To further increase the size of the dataset, miscible compounds were alloyed and the parameters interpolated accordingly, resulting in a total of about 330 compounds used for the classification.

A Gaussian mixture algorithm was utilized to separate the compounds in the database into n clusters, where each value from 2-6 was tested for the number of allowed clusters n . For three clusters, the traditional separation into covalent, ionic and metallic compounds could be reproduced, as no compounds with Hydrogen bonds or Van-der-Waals bonding were added to the database. Only few materials were wrongly classified, with the majority being mix-ups between covalent and ionic compounds. Interestingly, with the number of allowed clusters n set to 4, exactly those materials that have recently been proposed to utilize a novel chemical bond, named metavalent bond, are being assigned to the fourth cluster. We hence conclude, that our results support the concept of metavalent bonding by an a priori computational method. More importantly, this classification provides a close link between chemical bonding mechanisms and properties enabling novel routes to materials design.

CH02.05.17

Copper(II) Metal-Organic Framework (MOF) with Excellent Antifungal Activity So-Hyeon Yang¹, Mayura Veerana², Gyungsoon Park², Youngmee Kim¹ and Sung-Jin Kim¹; ¹Ewha Womans University, Korea (the Republic of); ²Kwangwoon University, Korea (the Republic of)

Metal-Organic Frameworks (MOFs) have been of great interest for decades due to their porosity and wide application possibilities, such as gas sorption, separation, catalysis, luminescence sensing, and biomedical applications. Among them, MOFs have been utilized as materials with antimicrobial properties against microorganisms. In this work, our group synthesized a Cu-MOF containing glutarate (Glu) and 4,4'-azopyridine (azpy) by solvothermal method. We tested its antifungal activity against two fungi, *C. albicans* and *A. niger*, and found that the Cu-MOF shows great antifungal properties for these two fungi. Based on this antifungal ability, it is expected that the material we synthesized can be used for purposes such as food storage and antifungal agents used for various contamination and infection. Detailed results and mechanisms will be discussed.

SESSION CH02.06: Materials for Energy and Environment
Session Chairs: Brent Melot and Sara Thoi
Wednesday Morning, December 1, 2021
Hynes, Level 3, Room 302

10:30 AM *CH02.06.01

Barocaloric Effects in Metal-Organic Materials for Solid-State Cooling Jarad A. Mason, Jinyoung Seo, Jason Braun, Ryan McGillicuddy, Adam Slavney and Selena Zhang; Harvard University, United States

With more than 20% of the world's electricity currently used for cooling and a growing population demanding more comfortable living conditions amid an ever warming global climate, the need for sustainable cooling technologies is expected to increase dramatically over the next several decades. Most commercial cooling systems rely on vapor-compression cycles of environmentally harmful refrigerants that are prone to leakage. As an alternative, caloric effects can drive solid-state cooling cycles that feature a high energy efficiency and zero direct emissions, as well as faster start-up times, quieter operation, easier recyclability, and greater amenability to miniaturization than conventional vapor-compression technologies. Here, we will describe how pressure-induced thermal changes—barocaloric effects—mediated by order-disorder or spin-crossover phase transitions can be leveraged for solid-state cooling. In particular, we will discuss the structural and chemical factors that contribute to entropy changes, sensitivity to hydrostatic pressure, and thermal hysteresis in a series of metal-organic materials that exhibit large barocaloric effects.

11:00 AM *CH02.06.02

Design Strategies in Functional Porous Materials for Energy Storage Sara Thoi; Johns Hopkins Univ, United States

Despite their high theoretical specific energy of 2,600 Wh kg⁻¹, the commercialization of Li-S devices is hindered by irreversible capacity loss from the dissolution of polysulfide intermediates in the electrolyte solution. Inspired by the rich chemistry in solid-state materials, we integrate molecular units capable of tethering polysulfides into metal-organic frameworks (MOFs) to improve cycling stability and charge conductivity. Incorporation of redox-

active moieties in the framework further enable fast charge and discharge capabilities. Identification of structure-property-function relationships in tunable molecular platforms provide a pathway for translatable strategies across materials types and battery technologies.

11:30 AM CH02.06.04

Looking for Glazer Tilts in the Local Structure of Perovskites [Sandra Skjaerboe](#) and Simon J. Billinge; Columbia University, United States

Crystallographically determined long-range ordered structures of materials are often taken for granted when investigating properties and functionalities. Although this simplifies our lives, there is a growing awareness of the fact that short-range deviations from the long-range order is not only common but also determining for many of the properties, such as bandgap and magnetic order. As an example, many oxides with the perovskite structure, ABO_3 , have well-defined crystalline order, but their properties can in some cases be explained better if one accounts for the local disorder.

To be able to understand how properties are affected by the short-range deviations, or local structure, we first have to properly describe what that local structure looks like. Just as with long-range ordered crystal structures, we can determine the local structure using scattering experiments and subsequently fitting the data to models. To obtain the local structure, however, we must also analyze the diffuse scattering in addition to the Bragg scattering, which is best done in real space as the pair distribution function (PDF). We build on the many already existing PDF studies on perovskites and constrain our structure model further by taking advantage of the knowledge that the structure tends to distort in ways that keep its BO_6 octahedra intact. The resulting distortions, collective or not, can therefore often be described by one of 23 unique tilting patterns of the rigid octahedra, identified by Glazer in the '70s [1]. In our implementation, fitting a model of any of the tilting patterns to scattering data requires refinement of no more than four variables at once – one lattice parameter and a maximum of three tilt amplitudes. Here we present our PDF analysis of a selection of perovskites and determine their degree and type of structural tilting disorder.

PDF analysis and modeling in the Billinge group was supported by the U.S. National Science Foundation through grant DMREF-1922234.

[1] Glazer, A. M. 'The Classification of Tilted Octahedra in Perovskites'. *Acta Cryst. B* **28**, no. 11 (1972): 3384–92.

SESSION CH02.07: Computational Characterization

Session Chairs: Craig Brown and Seán Kavanagh

Wednesday Afternoon, December 1, 2021

Hynes, Level 3, Room 302

4:00 PM *CH02.07.01

Rutile Rules—Lessons on the Mott-Peierls Transitions [James M. Rondinelli](#); Northwestern University, United States

Transition metal compounds based on the structurally simple rutile structure exhibit a range of collective electronic phenomena, including metal-insulator transitions, superconductivity, and nontrivial fermions. The ability to manipulate such electronic states through structure is key to realizing new classes of adaptive and low-power microelectronics. Here I briefly overview our progress in understanding the structural contributions to driving metal-insulator transitions in binary and ternary rutile and trirutile compounds using electronic structure based methods. I will first describe our understanding of how geometric and bonding constraints determine the crystallization of compounds in the trirutile structure as opposed to other ternary structures in this space. Here, we predict several previously unreported candidate trirutile oxides, and one is successfully synthesized. I will then present results on vanadium-free rutile and trirutile phases, focusing on the stability and transformations in the electronic structure of 4d and 5d compounds where strong electron-electron interactions are expected to be weak. Our main finding is that one can control the conducting or insulating state by structural design through inductive control over metal-metal interactions with multiple cations or anions. Last, I will describe our recent progress in utilizing this structure-function understanding to automate the discovery process of electronic transitions with Bayesian optimization techniques.

This work was performed in collaboration with Ram Seshadri, Stephen Wilson, Emily Schueller, Kyle Miller, Jaye Harada, Lauren Walters, and Danilo Puggioni and financially supported by the National Science Foundation under awards DMR-1729489, DMR-1729303, and DMR-2011208.

4:30 PM CH02.07.02

Late News: Identifying New Inorganic Solar Absorbers with Long Carrier Lifetime Using High-Throughput Computational Screening [Geoffroy Hautier](#)^{1,2}, [Diana Dahliah](#)², [Guillaume Brunin](#)², [Janine George](#)², [Viet-Anh Ha](#)² and [Gian-Marco Rignanese](#)²; ¹Dartmouth College, United States; ²University Catholique de Louvain, Belgium

Current solar absorbers for thin film technologies (e.g., CIGS or perovskites) can show good efficiencies above 20% but show limitations in terms of toxicity, earth-abundance or long-term stability. Finding new solar absorber is a cumbersome process involving complex synthesis and characterization steps. Computational modeling using density functional theory (DFT) on the other hand offers an attractive way to speed up this process. Here, we will report on a large scale high-throughput computational search for new solar absorbers among known inorganic materials. The originality of our approach lies in the consideration of intrinsic defects that are essential in controlling carrier lifetime.[1] More precisely, we searched among 7,000 copper-based known inorganic materials for materials presenting adequate band gap, transport (effective masses) and intrinsic defects (i.e., defects that will not act as important non-radiative recombination centers). We will report on a series of candidates and identify the copper phosphides and especially the alkali copper phosphides as very promising potential new solar absorbers. We will present the compounds of interest which have been synthesized before but have never been considered for solar applications and discuss the intrinsic chemical reasons for their adequate PV properties.

[1] Dahliah D., Brunin G., George J., Ha V.-A., Rignanese G.-M., Hautier G., "High-throughput computational search for high carrier lifetime, defect-tolerant solar absorbers", *Energy Environ. Sci.*, accepted (2021)

4:45 PM *CH02.07.03

A Super Fast and Efficient High-Throughput Search Method for Near Room Temperature Superconductors Under High Pressure [Tianran Chen](#)^{1,2} and [Taner Yildirim](#)²; ¹University of Maryland, United States; ²National Institute of Standards and Technologies, United States

Due to the low atomic mass and high phonon frequencies of hydrogen, hydride compounds under extreme pressures are most promising in the search for near room temperature superconductors. First-principles based computational search has become extremely important not only predicting new materials but

also guiding high-pressure experimental measurements. However, the calculation of electron-phonon coupling and the corresponding T_c for a given system is usually computationally very expensive, limiting the application of computational search to a few numbers of candidate systems.

In this work, we have developed a super-efficient and fast high-throughput method for searching high- T_c hydride superconductors. We introduce new "metrics" that are strongly correlated to strong electron-phonon coupling and T_c but it is much faster to calculate them. Using our new method, we have searched more than 100,000 binary hydride superconductors and discovered many new high- T_c systems. Among them, we report our prediction of high-temperature superconductivity at relatively low pressure of 50 GPa in a novel binary metal hydride which may break the current record. A detailed mechanism of the superconductivity, phonons and electron-phonon coupling, anharmonicity, as well as the abnormal T_c -pressure dependence, will be also discussed. Our work will not only greatly accelerate the discovery of new hydride superconductors but also give a detailed understanding of important factors that yield superconductivity near room temperature at high pressures.

5:15 PM CH02.07.04

The Electronic Entropy Contribution to Some Congruent and Allotropic Phase Transitions [Jonathan Paras](#) and Antoine Allanore; Massachusetts Institute of Technology, United States

Knowledge of the entropy change at a phase transition remains critical for engineering materials. For allotropic phase transformations in transition metals and congruent transitions in intermetallic compounds, computation of the electronic structure, and by extension the entropy, has remained particularly difficult. We introduce a formalism that links electronic transport properties with the state electronic entropy to circumvent these difficulties in compounds like Cu_3Au and transition metals including Fe and Co. Our formalism connects materials chemistry and the partial molar entropy of electrons in solution, opening the door for quantitative engineering of the phase transition entropy via chemistry. Application to allotropic phase transitions in some transition metals at atmospheric pressure suggest a possible electron-driven origin of hexagonal close packed stability.

SESSION CH02.08: Poster Session II
Wednesday Afternoon, December 1, 2021
8:00 PM - 10:00 PM
Hynes, Level 1, Hall B

CH02.08.01

Development of Sodium Hybrid Quasi-Solid Electrolytes Based on Porous NASICON and Ionic Liquids C.S. Martínez-Cisneros¹, B. Pandit¹, B. Levenfeld¹, J.Y. Sanchez^{1,2} and [Alejandro Varez](#)¹; ¹University Carlos III of Madrid, Spain; ²Univ. Grenoble Alpes, Univ. Savoie Mont Blanc, CNRS, Grenoble INP, France

Sodium batteries emerge as an alternative to produce the new, so called, post-lithium batteries (1). In this study, we explore (i) the effect of sodium content and sintering temperature in solid electrolytes based in NASICON-type compounds and (ii) the use of two methodologies to obtain porous NASICON samples: application of natural substances and organic materials as pore-formers and freeze casting. The main purpose is the attainment of hybrid quasi-solid state electrolytes (2), with enhanced room temperature conductivity, based on porous ceramic electrolyte layers infiltrated with ionic liquids. Using this approach, porous samples with different microstructure and porous morphology and distribution were achieved, providing an enhancement in conductivity (ranging from 0.45 to 0.96 mS cm⁻¹ at 30°C) of one order of magnitude for infiltrated samples respect to pore-free samples. Preliminary electrochemical test on thick electrode showed a specific capacity higher than 80% respect to the theoretical one, which is quite promising considering the thickness of the electrolyte. According to these results the porous NASICON might be considered as a functional macroporous inorganic separator that can act as a Na⁺ reservoir.

The authors would like to thank the Agencia Española de Investigación /Fondo Europeo de Desarrollo Regional (FEDER/UE) for funding the projects PID2019-106662RBC43. This work has also been supported by Comunidad de Madrid (Spain) - multiannual agreement with UC3M ("Excelencia para el Profesorado Universitario" - EPUC3M04) - Fifth regional research plan 2016-2020.

References

- [1] N. Yabuuchi, K. Kubota, M. Dahbi, S. Komaba, Research development on sodium-ion batteries, Chem. Rev. 114 (2014) 11636–11682
- [2] M. Keller, A. Varzi an S. Passerini, J. Power Sources, 392, (2018), 206-225

CH02.08.03

As-Synthesized Alkyne-Coated CdSe Quantum Dots for Site-Directed Nanoparticle-Substrate Chemical Linkage [Lucas Tortella](#) and J. S. Niezgoda; Saint Joseph's University, United States

Site-directed and robust chemical binding of the nanocrystalline surface to a substrate is of utmost importance in the fields of printable electronics, fluorescence assays and catalysis, among others. Historically, nanocrystal preparation methods have involved chemically inert ligands than are post-synthetically exchanged from the surface of the crystal—whether in colloidal solution or in the solid film—to a more useful and/or fitting molecule for the given application. Here, in line with the overarching theme of the Niezgoda lab, we present our findings on the development of a preparation for CdSe quantum dots (QDs) prepared with a native terminal alkyne ligand, 10-undecynoic acid (UDYA), as the lone surface-bound molecule. Further, core/shell architectures of these particles have been prepared with decent quantum yields in the visible spectrum. High-resolution TEM images with elemental mapping show well-formed and monocrystalline particles, and the presence of the alkyne on the surface is verified with FTIR and NMR spectroscopies. These first-of-their kind native alkyne-coated fluorescent QDs are immediately useful in alkyne-azide click chemistry applications, wherein the QDs can be site-directed to any substrate decorated with azide moieties. Examples of colloidal, thin film and 3D-printed systems involving alkyne-azide click cyclization of the novel QDs to substrate are shown as proof-of-principle demonstrations of the wide applicability of these particles. We emphasize that the fundamental innovation of this project is that it effectively circumvents the need for a post-synthetic ligand exchange to accomplish robust QD-substrate chemical linkage, while still providing QDs with suitable quantum yield and stability.

CH02.08.04

High-Performance Supercapacitors by the Infiltration of Gel Polymer Electrolytes into Porous Electrodes [Pado Kim](#), Min Guk Gu and Sung-Kon Kim; Jeonbuk National University, Korea (the Republic of)

The development of materials used for electrodes brings advances in energy storage technology. In addition, research on how to maximize the efficiency of electrodes with a combination with solid-state electrolytes, one of the key elements of energy storages. Polymer-based electrolytes such as solid polymer

electrolytes (SPEs) and gel polymer electrolytes (GPEs) are of great interest due to their flexibility in creating flexible energy storages. It also solves the weakness of liquid electrolytes: liquid leakage, volatility, flammability, weak chemistry properties, and electrochemical properties. Herein, we demonstrate a way to improve the electrochemical performances of the supercapacitor (SC) by infiltrating GPEs with high ion conductivity into electrode made of multi-walled carbon nanotube (MWCNT). GPEs are synthesized through polymerization of poly(ethylene glycol) methyl ether acrylate (PEGMA) in the presence of trimethylolpropane ethoxylate triacrylate (ETPTA) in LiPF_6 organic solution. By changing the chemical composition of PEGMA, ETPTA, and lithium solution we can adjust the mechanical properties and ionic conductivity of GPEs. Electrode-infilling gel polymer electrolyte (EI-GPE) with high ionic conductivity improves the characteristics of the electrode-electrolyte interface and creates a high-performance SCs. The SCs produced in this way exhibit excellent performance in capacitance and energy density, and exhibit a long cycle life even under mechanical deformation.

CH02.08.05

Insights to Electronic and Nanoscale Structure of Durable Multimetal Oxychloride Intergrowth Photocatalysts [Kaustav Chatterjee](#)¹, Roberto dos Reis², Jared Stanley¹, Vinayak Dravid² and Sara E. Skrabalak¹; ¹Indiana University, United States; ²Northwestern University, United States

Structure-property connections are a key theme in heterogeneous catalysis such as photocatalytic water splitting. Bismuth-based layered perovskite compounds such as $\text{Bi}_4\text{MO}_8\text{X}$ ($\text{M}=\text{Nb, Ta}$; $\text{X}=\text{Cl, Br}$) have emerged as promising durable photocatalysts for visible-light driven water splitting. The unique electronic structure of these oxyhalides in the valence band suppresses the self-oxidation of non-oxide anions by photogenerated holes. The unique combination of electronic and optical properties in these oxyhalide perovskite materials lies in their rich structural complexity. In this study, the electronic and nanoscale structure of multimetal oxyhalide intergrowth oxychloride: $\text{Bi}_4\text{TaO}_8\text{Cl-Bi}_2\text{GdO}_4\text{Cl}$ have been systematically investigated. We have varied the amount of $\text{Bi}_4\text{TaO}_8\text{Cl}$ in the intergrowths to rationalize the effect changes in the local crystal and electronic structure. A combination of Ultraviolet Photoelectron Spectroscopy, UV-Visible Diffuse Reflectance Spectroscopy and Electron Energy Loss Spectroscopy techniques were used to determine and investigate the electronic structure of the oxyhalide intergrowths. The obtained conduction and valence band energy levels elucidate the possibility of photocatalytic water splitting as well as carbon dioxide reduction. By virtue of aberration-corrected scanning transmission electron microscopy and converged-beam electron diffraction (CBED), the nanoscale structure of the intergrowth materials was elucidated with atomic displacements at an accuracy of several picometers. Based on the high-order Laue zone reflections of CBED patterns, the local symmetry and tilting of TaO_6 octahedra in the intergrowth crystal structure were revealed. We believe our approach demonstrated here opens up opportunities for understanding the atomic-scale structure-property phenomena of novel photocatalytic systems.

CH02.08.06

High-Performance Microsupercapacitor Based on Laser-Induced Fluorinated Polyimide Films with Organic Gel Polymer Electrolytes [Min Guk Gu](#)¹, Pado Kim¹, Minsu Kim², Byoung Gak Kim² and Sung-Kon Kim¹; ¹Jeonbuk National University, Korea (the Republic of); ²Korea Research Institute of Chemical Technology, Korea (the Republic of)

Due to the need for small-scale electronic devices, many studies are in progress on energy storage devices. In particular, in the case of microsupercapacitors (MSCs), they can be embedded in small electronic devices and are being used as energy storage devices that can temporarily supply power to rechargeable batteries. For this reason, in this study, MSCs are fabricated by laser photothermal method of 3D porous laser-induced graphene (LIG) electrodes. A fluorine-based polyimide (fPI) film is used as substrates for LIG electrode (LIG-fPI). During the graphitization process caused by the laser, gaseous products including fluorine are released from fPI to form a microporous structure, which can overcome the disadvantage of a small electrode specific surface area seen in conventional LIGs, and increasing the specific surface area is a way to improve the energy density of MSCs. As the electrolyte used in this study, we choose an organic gel polymer electrolyte (o-GPE). MSCs with o-GPE are mechanically flexible and have excellent electrochemical performance. For o-GPE, poly(ethylene glycol) methyl ether methacrylate (PEGMA), trimethylol propane ethoxylate triacrylate (ETPTA) are used, and 2-hydroxyl-2-methyl-1-phenyl-1-propanone (HMPP) is used as a photo-initiator. UV-cured o-GPE impregnated with a liquid electrolyte containing lithium salt is made into a pouch cell with LIG-fPI, which is flexible and bendable. It exhibits very high energy and power densities of 0.58 mW cm^{-2} and 0.01 mWh cm^{-2} , respectively, at a high voltage window of 3 V. The resulting LIG-fPI-MSC is promising for use in rechargeable power supplies in various applications such as wearable microelectronics and the Internet of Things.

CH02.08.08

Late News: Generation of Zinc Oxide Nanoparticles in Presence of Ethylene Glycol [Kerianys N. Torres](#)¹, Veronica I. Nash-Montes¹, Josian Luciano Velazquez² and Sonia J. Bailón- Ruíz¹; ¹University of Puerto Rico at Ponce, United States; ²University of Puerto Rico at Mayagüez, United States

Nanomaterials as zinc oxide have potential applications in nanomedicine, biosensors, catalysts and biomedical bio-imaging because of their intrinsic optical properties. We report the synthesis and characterization of zinc oxide nanostructures in presence of ethylene glycol and the effect of the zinc precursor on the particle. Zinc oxide nanoparticles were produced in presence of ethylene glycol and zinc precursors at 197°C by using a reflux system. The reaction time was ranged from two to six hours and the precursors evaluated were zinc sulphate heptahydrate (II) and zinc acetate dehydrated (II). As-synthesized nanostructures were characterized by Absorption and Photoluminescence spectroscopies. Besides, the presence of ethylene glycol on the ZnO was corroborated by Infrared Spectroscopy. Results evidenced that nanostructures exhibited strong emission peaks at 400 nm which comes from the recombination of their pars electron-hole. Whereas the absorption spectra exhibited shoulder peaks at approximately 360 nm which is attributed to the band gap. Also, preliminary studies evidenced that ZnO nanostructures have catalytic properties to destroy contaminants in aqueous matrices.

CH02.08.09

Late News: Antiferro- and Meta-Magnetism in the $S=7/2$ Hollandite Analog EuGa_2Sb_2 [Tanya Berry](#)¹, Sean R. Parkin² and Tyrel McQueen¹; ¹Johns Hopkins University, United States; ²University of Kentucky, United States

Recent work analyzing the impact of non-symmorphic symmetries on electronic states has given rise to the discovery of multiple types of topological matter. Here we report the single crystal synthesis and magnetic properties of EuGa_2Sb_2 , an Eu-based antiferromagnet structurally consisting of pseudo-1D chains of Eu ions related by a non-symmorphic glide plane. We find the onset of antiferromagnetic order at $T_N = 8 \text{ K}$. Above T_N ; the magnetic susceptibility is isotropic. Curie-Weiss analysis suggests competing ferromagnetic and antiferromagnetic interactions, with $\mu_{\text{eff}} = 8.1 \mu_B$ as expected for $4f7 J = S = 7/2 \text{ Eu}^{2+}$ ions. Below T_N and at low applied magnetic fields, an anisotropy develops linearly, reaching $\chi_{\perp}/\chi_{\parallel} = 6$ at $T = 2 \text{ K}$. There is concomitant metamagnetic behavior along χ_{\parallel} , with a magnetic field of $\mu_0 H \approx 0.5 \text{ T}$ sufficient to suppress the anisotropy. Independent of crystal orientation, there is a continuous evolution to a field polarized paramagnetic state with $M = 7 \mu_B/\text{Eu}^{2+}$ at $\mu_0 H = 2 \text{ T}$ as $T \rightarrow 0 \text{ K}$. Specific heat measurements show a recovered magnetic entropy of $\Delta S_{\text{mag}} \approx 16.4 \text{ J.mol}^{-1}\text{K}^{-1}$ from $T \sim 0 \text{ K}$ to $T = T_N$, close to the expected value of $R \ln(8)$ for an $S = 7/2$ ion, indicating little low dimensional spin fluctuations above T_N . We find no evidence of unusual behaviors arising either from the dimensionality or the presence of the non-symmorphic symmetries.

CH02.08.10

Late News: Effect of the Capping Agent on the Photocatalytic Performance of ZnS Nanostructures [Veronica I. Nash-Montes](#)¹, Kevin Correa²,

Kerianys N. Torres¹, Josian Luciano Velazquez² and Sonia J. Bailón- Ruíz¹; ¹University of Puerto Rico in Ponce, United States; ²University of Puerto Rico at Mayagüez, United States

Tons of pollutants from textile industries are lost to effluents every year due to the inefficiency of dyeing processes. In this regard, conventional techniques as adsorption or coagulation have been used in water treatment to concentrate pollutants by transferring them to other phases. Alternative destructive techniques are needed to obtain a fast destruction of pollutants in wastewater treatment. In this way, photo-catalysis is an advanced oxidation process that includes a quick oxidation of the pollutant molecules, lack of production of polycyclic products, and final degradation of contaminants in the ppb range. This technology is based on the activation of nanomaterials (i.e. semiconductors) in presence of electromagnetic radiation and subsequent generation of radicals from water to directly oxidize many organic pollutants. Based on the above considerations, this research is an attempt at the use of Zn-based nanomaterials (i.e. as ZnS and ZnO NPs) for the degradation of environmental pollutants from aqueous matrices. The specific goals of this project are: i) Generate and characterize nanomaterials with photoactive properties, ii) Study the photochemical stability of photoactive nanomaterials, and iii) Demonstrate the degradation of environmental pollutants in presence of photoactive nanomaterials and the reuse of the nanostructures. Optical properties showed a luminescent peak at 420 nm and 442 nm and an absorption peak at 270 nm and 307 nm. Photodegrading capacities of quantum dots were evaluated in presence of Acid Red 14 at different concentrations (250 ppm and 500 ppm). Bare ZnS nanomaterials degraded Acid Red 14 successfully (75%) after 180 minutes.

CH02.08.11

Late News: Theoretical and Experimental Properties of Ag₂SeO₄ and Ag₂SeO₃ for Photoluminescent and Photocatalytic Applications Ivo M. Pinatti^{1,2}, Ana C. Tello³, Marcio D. Teodoro³, Ieda L. Rosa³, Elson Longo³, Juan Andres² and Alexandre Z. Simões¹; ¹UNESP, Brazil; ²UIJ, Spain; ³UFSCar, Brazil

Theoretical and experimental study of inorganic crystals is an interdisciplinary subject that is attracting intense research and development due to both fundamental and applied scientific value. Metallic selenites present different chemical structures and advanced physical properties such as pyroelectricity, ferroelectricity and piezoelectricity. Also, selenium-silver based matrices exhibit interesting structural, optical, and photoluminescent properties, which accounts for potential materials in many research fields like physics, chemistry and materials science. Moreover, the chemistry of selenium and silver is very prominent in biological systems, mainly because of their interactions with molecules like proteins. In this work, silver selenate (Ag₂SeO₄) and silver selenite (Ag₂SeO₃) microcrystals were prepared by the sonochemistry (SC), ultrasonic probe (UP), coprecipitation (CP), and microwave assisted hydrothermal (MH) methodologies. X-ray powder diffraction patterns results showed intense and sharp peaks related to the orthorhombic Ag₂SeO₄ and monoclinic Ag₂SeO₃ structures, attesting that materials are crystalline and present structural long-range order. It was also observed experimental Raman modes for both phase, which corroborated to the theoretical ones calculated indicating structural short-range order. The morphologies were confirmed by FE-SEM microscopy and Wulff construction, showing distinct shapes of different width and length due to the different methodologies of synthesis. Optical properties were attested by UV-vis spectroscopy which showed the characteristic semiconductor band gap value for both materials. Photoluminescence spectroscopy showed an intense band in the visible region with maximum at around 700 nm for all samples. Further trapping experiments prove that the holes and hydroxyl radical, in minor extent, are responsible for the photocatalytic degradation of dyes. The geometry, electronic properties of the bulk, and surface energies of these materials were evaluated using first-principles quantum mechanical calculations based on the density functional theory (DFT/B3LYP) to provide information at the atomic level. In this sense, experimental results were correlated to theoretical studies and enabled a deep understanding between structure and property. Inspired by the above considerations, these materials may present superior characteristics for new compounds with photoluminescent and photocatalytic applications.

CH02.08.12

Late News: Investigating Semiconductor Photocatalysts for C-C Bond Formation via First Principles Computations Arun Kumar Mannodi Kanakkithodi, Shukai Yao, Jiaqi Yang and Peilin Liao; Purdue University, United States

Semiconductor-based photocatalytic systems have been frequently used for small molecule activation and transformation reactions, such as water splitting for H₂ and O₂ evolution, CO₂ reduction, and N₂ reduction. During photocatalysis, light-irradiation on semiconductors leads to the generation of excited electrons which compete to recombine with co-generated excited holes, resulting in lower reaction yields. The simultaneous utilization of excited electrons and holes, for example via a cross-coupling mechanism, is thus of critical importance for useful organic transformations, such as C-C bond forming reactions. To realize cross-coupling for C-C bond formation, the redox potentials of carbonyls and alcohols must match the reduction (conduction band minimum) and oxidation (valence band maximum) power of the semiconductor, respectively.

In this work, we perform first principles-based density functional theory (DFT) computations to rationally design semiconductors with proper band-edge positions for photochemistry through varying facets and thicknesses, as well as introducing co-catalysts. We model surface slab structures with different facets for several important semiconductors of interest, such as CdS, ZnIn₂S₄, Cu₂ZnSnS₄ and Ag₂ZnSnS₄ (as well as related compounds with replacement or mixing at cation/anion sites), with different thicknesses of the bulk region. Relative electronic band edges are thus computed for multiple pseudo-2D semiconductors as a function of surface termination and thickness, and compared with redox potentials of relevant alcohols, carbonyls, amines and imines. We further study the formation energies of intrinsic point defects as a function of chemical potential conditions and charge states in selected compounds, namely Cu₂ZnSnS₄ and Ag₂ZnSnS₄, and suggest strategies to suppress the formation of harmful anti-site defects. Finally, we model the adsorption of organic molecules on selected semiconductor surfaces, and study photocatalytic coupling reaction mechanisms in the presence of H atoms or added electrons and determine energy barriers using nudged elastic band (NEB) calculations. Complementary experimental synthesis and characterization of ultrathin 2D semiconductor-based photocatalytic systems and the production of ketyl radicals from carbonyls are carried out by our collaborators. The computational screening undertaken in this work reveals novel ways of tuning the photocatalytic properties of semiconductors via modification of slab thickness and surface termination, composition engineering, and defect manipulation.

CH02.08.13

Late News: Enhancement of Thermoelectric Properties in CuCrSnS₄/Cu₂SnS₃ Nanocomposite by Exchange Interaction of Itinerant Carrier and Superparamagnetism of CuCrSnS₄ Precipitation Sujin Kim¹, Junphil Hwang¹, Tae Soo You², Mi-kyug Han¹, Minju Lee¹ and Sung-Jin Kim¹; ¹Ewha Womans University, Korea (the Republic of); ²Chungbuk National University, Korea (the Republic of)

Thermoelectric materials have attracted considerable research attention in recent decades due to their ability of reversible conversion between heat and electricity. The enhancement of thermoelectric performance is challenging due to the strong interrelation of Electrical conductivity and Seebeck coefficient. In this work, we studied eco-friendly Cr-doped Cu₂SnS₃ with CuCrSnS₄ nanoparticles. Our experiments and theoretical calculation(DFT) proved that doping Cr atom in Sn site of Cu₂SnS₃ enhanced electrical conductivity by modifying electron density of state. Moreover, by DFT calculation, it is found that doping Cr atom in Sn site makes chemical bonding soften resulting in lattice thermal conductivity decrease. Using XRD analysis, the solubility limit of Cr impurity in Cu₂SnS₃ is around 5 at%. Doping Cr atom above the solubility limit induced the spinel CuCrSnS₄ nanoprecipitations. The superparamagnetic fluctuation of spin angular momentum of spinel CuCrSnS₄ results in exchange interaction with itinerant carrier spin. The synergetic

effect of Cr doping made the power factor increase from 1.12 to 6.67 $\mu\text{W}/\text{cm}/\text{K}^2$. The CuCrSnS_4 were verified that second phase in Cu_2SnS_3 matrix by XRD and TEM analysis. The size of CuCrSnS_4 confirmed that 50 nm. Finally, Cr-doped- Cu_2SnS_3 with magnetic nanoparticles showed the highest zT value of 0.8 at 723 K comparing with pristine zT of 0.08 at 723 K.

CH02.08.14

Gas Solubility in Water Confined within Microporous Materials Malia Wenny and Jarad A. Mason; Harvard University, United States

The solubility of gases in water—despite being relatively low compared to other solvents—is key to many biological and industrial processes. Bulk water's highly structured hydrogen bonding arrangement is thought to impede the formation of transient voids large enough to accommodate gas molecules. However, when water is confined to the nanoscale, such as in a protein cavity, a carbon nanotube, or a microporous material, its structure and properties can differ dramatically from those observed in the bulk. In particular, the solubility of gases in confined water can be at least an order of magnitude higher than in bulk water, possibly due to differences in the density and hydrogen bonding arrangement of confined water. Understanding the origin and extent of this increase in gas solubility is important for biological and industrial gas-dependent processes that involve water, but experimental investigation of the structure of confined water within micropores and its impact on gas solubility is limited. Microporous materials such as metal–organic frameworks and zeolites provide excellent tools to study the structure and gas solubility of water confined to nanoscopic dimensions due to their chemical and structural tunability and well-studied gas adsorption behavior. This work examines the impact of pore size, shape, and chemistry on the structure and gas solubility of confined water, with particular emphasis on solid-state features such as the relative hydrophilicity of pore walls and the presence of open metal coordination sites capable of binding water molecules.

CH02.08.15

Simple Technique to Generate Small Cerium Oxide Nanoparticles Natalie M. Lopés Velasco¹, Eduardo Chaparro² and Sonia J. Bailón-Ruiz¹; ¹University of Puerto Rico at Ponce, Puerto Rico; ²University of Puerto Rico at Mayagüez, Puerto Rico

The generation of small Cerium Oxide Nanoparticles (CeO_2 NPs) was performed by a simple precipitation method in the presence of CETAB (hexadecyltrimethylammonium bromide), cerium nitrate hexahydrate ($(\text{Ce}(\text{NO}_3)_3 \cdot 6\text{H}_2\text{O})$) and ammonium hydroxide solution (NH_4OH). An amount of cerium precursor was added to CTAB and under constant agitation NH_4OH was added until the pH was at a basic of 10.0. The colloidal solution was heated in a reflux system at the range of 55 to 65 Celsius during 3 hours and 6 hours. The final solutions were purified using the centrifugation system twice for 15 minutes on 7,000 rpm using deionized water. High resolution transmission electron microscopy (HRTEM) studies evidenced mainly spherical-shape and highly crystalline structures for both samples and average sizes of 6 nm and 8 nm for synthesis of 3 hours and 6 hours, respectively. The presence of CTAB as surfactant material would be controlling the growth and particle size of the material. Electron diffraction (ED) patterns evidenced cubic structures for both sizes in the (111), (200), (220), and (311) reflections which are indexes as face centered cubic (fcc) arrangements. Studies of Energy dispersive X-ray Spectroscopy (EDX) indicated Ce (25.6%) and O (74.4%) in the synthesis of 6 hours, and Ce (29.2%) and O (70.8%) at the synthesis of 3 hours. Generated nanoparticles because of their small sizes and high surface area will be evaluated in photodegradation studies to destroy organic pollutants in aqueous matrices.

CH02.08.16

Modeling Stabilization of Reactive Oxygen Species on Defect-Rich Ceria for Toxin Destruction Janna Domenico¹, Nam Q. Le¹, Travis G. Novak², Jeffrey Long² and Paul A. DeSario²; ¹Johns Hopkins University Applied Physics Laboratory, United States; ²U.S. Naval Research Laboratory, United States

Materials based on ceria (CeO_2) show promising degradative activity towards a variety of pollutants and toxins including organophosphorus pesticides or chemical warfare agents. CeO_2 is highly reducible, leading to oxygen vacancy defects that assist in the formation and stabilization of reactive oxygen species (ROS). These persistent reactive species may later degrade toxic compounds over long timescales. We use density functional theory (DFT) to calculate the energies of binding and formation of ROS at multiple types of defect sites on low-index surfaces of CeO_2 . Differences in the calculated energies, which should correlate with ROS lifetimes, originate in the geometry and electronic structure of these surfaces. We compare the predicted trends with the spectroscopic characterization of ROS at CeO_2 aerogels and defect-rich Gd-doped CeO_2 aerogels. The combined modeling and experimental results suggest strategies to engineer longer ROS lifetimes for enhanced toxin destruction through controlled nanoparticle morphology and doping.

CH02.08.17

The Coexistence or Absence of Magnetic Interactions and Superconductivity in Highly Doped $\text{YSr}_2\text{Cu}_3\text{O}_{7-d}$ Cuprates—The Fe and Mo Cases Miguel Angel Alario-Franco¹, Xabier Martínez de Irujo-Labalde², Sara A. López-Paz¹ and Susana García Martín²; ¹Universidad Complutense, Spain; ²University of Oxford, United Kingdom

The total or even partial replacement of copper in the charge reservoir block in the well-known $\text{YSr}_2\text{Cu}_3\text{O}_{7-d}$ cuprate by other transition metals (TM) allows one to extend the hole doping range with respect to the conventional phase diagram (1). In particular, the introduction of highly valent cations such as $\text{TM}=\text{Fe}^{3+}/\text{Fe}^{4+}$ or Mo^{5+} results in unusually high nominal hole concentrations at the CuO_2 planes (2,3).

Quite interestingly, despite the elevated doping levels, superconductivity with *relatively high* critical temperatures of $T_c = 83$ and 70 K are observed in the resulting $\text{Mo}_{0.3}\text{Cu}_{0.7}\text{Sr}_2\text{TmCu}_2\text{O}_{7+\delta}$ and $\text{FeSr}_2\text{YCu}_2\text{O}_{7+\delta}$ compounds, respectively. Besides the realization of unusually high hole doping levels, the chemical modification of the charge reservoir blocks allows one the study of the *effect of chemical disorder* in the superconducting properties, providing interesting structure-hole doping- T_c relations (4). Also, in the *case of the iron* by copper substitution, *additional complexity arises from the coexistence of magnetic and superconducting interactions* (5). Here we present a broad outlook on the unusual properties of these TM substituted cuprates.

References:

- [1] S.D. Conradson, T.H. Geballe, A. Gauzzi, M. Karppinen, C. Jin, G. Baldinozzi, W. Li, L. Cao, E. Gilioli, J.M. Jiang, M. Latimer, O. Mueller, V. Nasretdinova, *Proc. Natl. Acad. Sci.* 117 (2020) 4559–4564.
- [2] X.M. de Irujo-Labalde, S.A. López-Paz, S. García-Martín, M.Á. Alario-Franco, *J. Solid State Chem.* 286 (2020).
- [3] S.A. López-Paz, X. Martínez De Irujo-Labalde, J. Sánchez-Marcos, C. Ritter, E. Moran, M.A. Alario-Franco, *Inorg. Chem.* 58 (2019) 12809–12814.
- [4] X. Martínez de Irujo-Labalde, E. Urones-Garrote, S. García-Martín, M.Á. Alario-Franco, *Inorg. Chem.* 57 (2018) 12038–12049.
- [5] S.A. López-Paz, D.P. Sari, A.D. Hillier, M.A. Alario-Franco, *AIP Adv.* 11 (2021) 015011.

Authors thank Dr. Romero de Paz and Dr. Fernandez-Sanjulian for the magnetic and electric measurements and Dr. Ritter(ILL) for the neutron diffraction measurements. X.M.d.I.-L. thanks MECD for the grant FPU014/05971; S.A.L-P. also thanks MECD for an FPU-016/00732 grant. This work has also been supported by REE (Project No. REE: 44-2014) Fundación Ramón Areces, Projects MAT2016-78362-C4-4-R and MAT2017-84385-R, and CAM project MATERYENER3CM-S2013/MIT-2753.

CH02.08.18

Late News: TiO₂/Ag Nanoparticles Synthesized by Self-Combustion Used as Alternatives for Postharvest Fruit Ripening Control [Carlos Paucar](#), Paula Nevado and Claudia Garcia; National University of Colombia, Colombia

Fruits reach its maturity several days after its harvest, this process is highly complex since it is associated with biochemical changes that increase the levels of ethylene, which influences its maturation and quality parameters. Ethylene, in its role as an enzyme, is one of the variables with the greatest influence on the ripening and deterioration process in avocado. However, there are also other pathologies and to face pathologies of biotic origin, its management is made with products like imidazole which is toxic and is already banned in some countries. At present, materials such as TiO₂, ZnO, Ag and SiO₂ Nanoparticles could give them the ability to intervene in the amount of free ethylene, and on the other hand they have been found to have antimicrobial activity. TiO₂ nanoparticles are the most widely used at an industrial level due to their photocatalytic activity and properties such as biocompatibility, corrosion resistance and zero toxicity, and Ag nanoparticles due to their photoactivity are promoted as an antimicrobial agents. This work seeks to obtain TiO₂ / Ag nanoparticles by combustion synthesis to search for nanotechnology-based alternatives that can be used in the post-harvest process. Considering the photocatalytic properties of TiO₂ and its relationship with the absorption of ethylene and the antimicrobial properties of Ag, its potential for the postharvest process can be studied. TiO₂ nanoparticles with different concentrations of silver (0%, 0.75%, 1.5%, 3% and 4.5% mole percentage) were obtained by the burning combustion solution method using titanium isopropoxide and silver nitrate as precursors, nitric acid as oxidizing agent and glycine as fuel. Rhodamine-B dye degradation test was performed to verify its photocatalytic activity under visible light and it was observed that indeed the particles obtained have photocatalytic activity. An FTIR study has also been performed on each type of particle and it is observed that there are functional groups such as OH in a peak of 3452.5 cm⁻¹, which is vital for photocatalysis, there are peaks between 836.8 cm⁻¹ and 530.2 cm⁻¹ that corresponds to vibrations of Ti-O and there is a peak that can be associated with the interaction of OH with AgNO₃ between 1669.3 cm⁻¹ and 1313.4 cm⁻¹ since it occurs only in the particles that were synthesized to obtain them with Ag. XRD has been performed to test anatase and rutile with Ag⁺ inclusions in crystallographic phases present after combustion synthesis. As results of this study Ag-TiO₂ particles were obtained by the burning combustion solution method with photocatalytic activity under visible light and having ethylene absorption capacity. The presence of OH, Ti-O groups and the interaction of OH with Ag⁺ can be observed, thereby the presence of silver in the sample and its photocatalytic activity is higher in samples with OH peak is more intense.

CH02.05.07

Mechanistic Investigation on the Solid-State Transformation of One-Dimensional Sb₂Se₃ Nanorods to SbSeI Nanorods [Eran Edri](#) and Subila Kurukkal Balakrishna; Ben-Gurion University of the Negev, Israel

Metal trichalcogenides and chalcogenides establishes a class of semiconducting materials with a quasi-one-dimensional crystal structure. These low-symmetry semiconductors have shown favorable optoelectronic properties for photovoltaic and photoelectrocatalysis: an optical bandgap in the visible-NIR region, and a relatively small electron affinity. However, there are limited synthetic strategies for nanostructured chalcogenides. Here we report a facile route for transformation of Sb₂Se₃ to SbSeI nanorods. The Sb₂Se₃ nanorods acted as templates to form small diameter SbSeI nanorods. The aspect ratio of SbSeI nanorods could be varied by changing the aspect ratio of the template. A detailed investigation of the transformation process reveals favorable thermodynamics and proceeds through a topotactic mechanism that may be suitable for other trichalcogenide-chalcogenide transformations. These ID materials show good charge transport and a band gap (E_g) of 1.7 eV, which are suitable for photocathodes for hydrogen evolution reactions.

SESSION CH02.09: Chalcogenides
Session Chair: Brent Melot
Thursday Morning, December 2, 2021
Hynes, Level 3, Room 302

10:30 AM *CH02.09.01

Chemistry of Chiral and Polar Transition Metal Silicon-Phosphides [Kirill Kovnir](#)^{1,2}; ¹Iowa State University, United States; ²US DOE Ames Laboratory, United States

Non-centrosymmetric intermetallic compounds with antisymmetric spin-orbit coupling exhibit a plethora of emergent properties, such as unconventional superconductivity, topologically non-trivial quantum properties, and quasiparticle behaviour. Chemical bonding preferences in the transition metal silicon-phosphides T-S-P create the asymmetric environment around metal atoms resulting in high abundance of non-centrosymmetric chiral and polar crystal structures. The synthesis of those phases is hampered by inertness of T and Si in contrast to high reactivity and vapor pressure of phosphorus. We developed a comprehensive synthetic strategy allowing to produce single crystals and phase-pure polycrystalline samples of metal tetrel-pnictides. The correlation between the crystal structure, chemical bonding, and optical and transport properties will be discussed.

11:00 AM CH02.09.02

Thermoelectric Transport and Crystal Morphology of the Quasi-1D Zintl Ca₅M₂Sb₆ [Alexandra Zevalkin](#); Michigan State University, United States

Zintl phases, with their vast range of structural patterns in non-cubic space groups and their excellent high-temperature thermoelectric performance, stand out as an intriguing subject area for the study of transport anisotropy. The covalently-bonded polyanions exemplified by Zintl phases crystallize in a diverse range of highly anisotropic sub-structures, including isolated moieties, 1D chains, 2D sheets and 3D networks. Despite ample theoretical evidence of light band mass and enhanced thermoelectric efficiency in the covalently-bonded direction in Zintl phases, experimental confirmation is still largely lacking. This knowledge gap is exacerbated by the difficulty of growing single crystals large enough for complete characterization of transport properties. In the present study, we use a combination of theory and experiment to investigate the anisotropic electronic structure, transport properties, and growth habit of Ca₅M₂Sb₆ (M=Al, Ga, In), which is characterized by anionic sub-structures resembling infinite 1D chains of corner-linked MSb₄ tetrahedra. Ca₅M₂Sb₆ single crystals grown from an Sb-rich molten flux were found to form long, needle-like crystals oriented parallel to the polyanionic chains. Due to the small cross-section of the crystals, characterization of transport properties in the direction perpendicular to the chains is challenging. For this purpose, micro-ribbons were extracted from single crystals using focused ion beam milling, and laser photolithography was used to deposit contacts to measure electrical resistivity and Hall coefficients. The resistivity measured parallel to the growth direction was found to be nearly 20 times higher than the perpendicular direction, confirming predictions. In addition, we investigated the surface energies of various terminations of Ca₅Ga₂Sb₆, revealing that the calcium content plays a central role in surface reconstruction, leading to the formation or breaking of surface covalent bonds. The relative surface energies are a strong function of growth conditions (either Ca rich or Ca poor), suggesting that the flux composition can be used to tune the growth habit, perhaps guiding future crystal growth of Zintl phases.

11:15 AM CH02.09.03

High-Pressure Structure and Bonding of AMg_2Pn_2 Thermoelectrics ($A=Ca, Mg, Yb$; $Pn=Bi, Sb$) [Mario R. Calderon Cueva](#)¹, Allison Pease¹, Wanyue Peng¹, Jingxuan Ding², Tyson Lanigan-Atkins², Olivier Delaire², Susannah Dorfman¹ and Alexandra Zevalkink¹; ¹Michigan State University, United States; ²Duke University, United States

Compounds in the structure type $CaAl_2Si_2$, in particular Mg_3Sb_2 and Mg_3Bi_2 , have attracted great interest in recent years for their remarkable thermoelectric performance. Their impressive thermoelectric figure of merit (zT) stems, in part, from their anomalously low thermal conductivity. In the present study, in situ high-pressure synchrotron X-ray diffraction was used to investigate the structure and bonding of binary and ternary AM_2X_2 ($A=Ca, Mg, Yb$; $X=Bi, Sb$) compounds at pressures up to 50 GPa. These experiments allowed us to develop trends between bond compressibility and cation size and to study the stability of the $CaAl_2Si_2$ structure type. Our results for binary compounds confirm prior predictions of isotropic in-plane and out-of-plane compressibility but reveal large disparities between the bond strength of the two distinct Mg sites. We show that the octahedral Mg–Sb bonds are significantly more compressible than the tetrahedral Mg–Sb bonds. Conversely, the discrepancy in the polyhedral compressibility for the ternaries is not as pronounced as for the binaries. These results indicate that the bonds of the octahedrally-coordinated Mg are responsible for the ultralow Mg_3Sb_2 and Mg_3Bi_2 . Further, we report the discovery of phases transitions above 4.0, 7.8, 11.3, and 18.0 GPa for Mg_3Sb_2 , Mg_3Bi_2 , $YbMg_2Bi_2$, and $CaMg_3Sb_2$, respectively.

11:30 AM CH02.09.04

Measurements of Thermal Conductivity of Materials at High Pressures and High Temperatures Using Flash Laser Heating Method with Pockels Cell [Irina Chuvashova](#)^{1,2}, Zachary Geballe¹, Sergey Lobanov³, Lukas Schifferle³ and Alexander Goncharov¹; ¹Carnegie Science, United States; ²Florida International University, United States; ³Helmholtz Centre Potsdam, Germany

Thermal conductivity is the intrinsic property of a material that expresses its ability to conduct heat. The process of heat conduction depends on four basic factors: the temperature gradient, the cross section of the materials involved, their path length, and the properties of those materials. There are two categories of measurement techniques: steady-state and transient. Steady-state techniques infer the thermal conductivity from measurements on the state of a material once a steady-state temperature profile has been reached, whereas transient techniques operate on the instantaneous state of a system during the approach to steady state.

Thermal transport properties of minerals and melts at high pressures and temperatures is of central importance to the evolution and dynamics of planets. The pressure of the Earth's interior continuously increases with the depth from the surface of the Earth: several hundred MPa at the region of the crust, ~20 GPa at the upper mantle and ~130 GPa at the lower mantle. Precise data of thermal conductivity and/or thermal diffusivity for minerals at elevated pressure make it possible to estimate the heat budget in the Earth.

Direct measurements of thermal conductivity of Earth minerals at extreme pressures and temperatures are very challenging; the available experimental data are limited and inconclusive, causing geodynamical studies to rely on theoretical calculations and/or large extrapolations.

In the present work, we demonstrate the optimized technique to perform direct measurements of thermal conductivity of materials in diamond anvil cells at high pressures and high temperature. We used a continuous 100-Watt infrared laser for heating sample from both sides to a desired temperature and a pulsed 300-Watt infrared laser creating a microsecond long heat wave from one sample side. Thermal conductivity can be determined by measuring temperature of sample radiometrically using a streak camera coupled to a spectrograph from both sample sides as a function of time and fitting the results with FE calculations. KCl was used as PTM, Ir was used for absorption of the laser if the absorption of the sample was small. Pulse was shaped to a square shape by a Pockels cell, which simplified and improved the accuracy of FE calculations. Furthermore, we significantly improved FE analysis by introducing automatic procedures based on python codes enabling the fitting parameter optimization. Fast measurements of thermal emissions allowed us to resolve the heating response through the sample enabling direct measurements of thermal conductivity of Earth's lower mantle minerals and Fe alloys in the core.

This complex system can be used for pressures in the range of 5 to 150 GPa for materials with any laser absorption properties. We used this system to obtain the values of thermal conductivity of ferropericlase, bridgmanite, and iron-silicon alloys which correspond well with literature data albeit mainly measured at room temperature.

11:45 AM CH02.09.06

Exploring Ultralow Thermal Conductive Heteroanionic Materials Hydrothermal Synthesis [Chi Zhang](#), Jiangang He, Rebecca McClain, Hongyao Xie, Songting Cai, Lauren Walters, Jiahong Shen, James M. Rondinelli, Mercurio G. Kanatzidis, Christopher Wolverton, Vinayak Dravid and Kenneth R. Poeppelmeier; Northwestern University, United States

Owing to large lattice anharmonicity from interface interactions between adjacent layers, layered heteroanionic materials have the potential to realize ultralow thermal conductivity[1-3]. As an analog of well-known ultralow thermal conductive phase $BiCuOSe$, $BiAgOSe$ has been predicted to be a better ultralow thermal conductive material by DFT calculations[4,5]. Utilizing both DFT calculations and Pourbaix diagrams[6], we have optimized the hydrothermal reaction conditions and developed an efficient, high yield synthesis to obtain the $BiAgOSe$ phase. Moreover, we have investigated the thermal transport behavior of $BiAgOSe$, and demonstrated that it has a lower lattice thermal conductivity compared to $BiCuOSe$. To study the origin of the ultralow thermal conductivity of $BiAgOSe$, we combined lattice dynamic calculations and synchrotron x-ray diffraction measurements and found that the low lattice thermal conductivity results from strong lattice anharmonicity and low phonon velocities which are associated with the vibrations of the silver ions.

References:

1. Chang, C. *et al.* 3D charge and 2D phonon transports leading to high out-of-plane ZT in n-type SnSe crystals. *Science* 360, 778–783 (2018).
2. Zhao, L.-D. *et al.* Ultrahigh power factor and thermoelectric performance in hole-doped single-crystal SnSe. *Science* 351, 141–144 (2016).
3. Zhao, L.-D. *et al.* Ultralow thermal conductivity and high thermoelectric figure of merit in SnSe crystals. *Nature* 508, 373–377 (2014).
4. Li, J. *et al.* Predicting excellent anisotropic thermoelectric performance of the layered oxchalcogenides $BiAgOCh$ ($Ch = S, Se, \text{ and } Te$). *Computational Materials Science* 171, 109273 (2020).
5. He, J. *et al.* Computational Discovery of Stable Heteroanionic Oxchalcogenides $ABXO$ ($A, B = \text{metals}$; $X = S, Se, Te$) and Their Potential Applications. *Chemistry of Materials* 32(19), 8229–8242 (2020).
6. Walters, L. N., Zhang, C., Dravid, V. P., Poeppelmeier, K. R. & Rondinelli, J. M. First-Principles Hydrothermal Synthesis Design to Optimize Conditions and Increase the Yield of Quaternary Heteroanionic Oxchalcogenides. *Chemistry of Materials* 16.

1:30 PM CH02.10.01

Tetranuclear Copper(I) Clusters as Highly Efficient Blue Phosphors—Tunable Emissions via Remote Steric Effects Yuichiro Watanabe, Benjamin Washer, Matthias Zeller, Sergei Savikhin, Lyudmila Slipchenko and Alexander Wei; Purdue University, United States

Flexible and lightweight optoelectronic displays depend on luminophores that emit brightly at red, green, and blue wavelengths, but access to the latter is hindered by the limited availability or high cost of phosphors that can produce deep-blue emission. Here, we describe solid-state phosphorescence from a series of tetranuclear copper(I)-pyrazolate (Cu_4pz_4) clusters with high quantum yields and blue emission with color coordinates of [0.15, 0.11]. These emissions are remarkably sensitive to structural effects far from the Cu_4 core: When 3,5-di-*tert*-butylpyrazoles are used as bridging ligands, adding a C4 substituent can cause a blueshift in photoluminescence by over 100 nm. X-ray crystal structures of several Cu_4pz_4 clusters reveal C4 substitution (H, F, Cl, or Br) to have modest effects on solid-state geometries, yet structure-property trends and time-dependent density functional theory (TD-DFT) calculations show the impact of these remote substituents on phosphorescence to be entirely steric in nature. The size of the C4 unit controls the conformations of adjacent *tert*-butyl groups and can increase the rigidity of the Cu_4pz_4 metallacycle, which can diminish Jahn-Teller distortion and prevent the excited-state structure from adopting lower energy states prior to photoluminescence. Such remote steric effects on photophysical processes are unprecedented, and may offer a novel approach toward the design of molecular phosphors with tunable optoelectronic properties.

1:45 PM CH02.10.02

Systematic Bandgap Tuning of 2D Silver Phenylselenide Derivatives Through Organic Modification Tomoaki Sakurada, Watcharaphol Paritmongkol, Woo Seok Lee and William Tisdale; Massachusetts Institute of Technology, United States

Silver phenylselenide (AgSePh), a two-dimensional (2D) member of the broader class of hybrid organic-inorganic metal organochalcogenide (MOC) family, has gained a renewed interest as a novel class of hybrid organic-inorganic 2D semiconductors. AgSePh features multiple exciting properties such as narrow blue luminescence, in-plane anisotropy, large exciton binding energy, earth abundant elemental composition, and a scalable synthesis. In contrast to 2D layered perovskites and transition metal dichalcogenides, AgSePh has strong covalent bonding between organic and inorganic components. This unique covalent interaction makes AgSePh a *truly hybrid* organic-inorganic semiconductor and opens a new door to control the properties of 2D semiconductors through organic functionalization. In this presentation, we will show the unique bandgap tuning of AgSePh and its derivatives by systematically introduce para-substituted functional groups with varied electron-donating and electron-withdrawing capabilities. These newly synthesized derivatives adopt 2D layered structures and exhibit strong excitonic characteristics. We will discuss the effect of organic functionalization on the optical and electronic properties, and show the application of this knowledge on designing new MOC compounds with excellent optical properties.

2:00 PM CH02.10.03

Interaction Between 1D Defects and Dopants in La-Doped BaSnO_3 and Its Impact on Material Properties Hwanhui Yun and Andre Mkhoyan; University of Minnesota, United States

Interaction between lattice defects and dopants in crystalline materials has long been recognized, and its influence on the materials' properties has been evidenced in a wide range of materials(1). In thin-film semiconductors, significant density of 1D defects, from well-known dislocations to new types of line defect(2), are formed and interact with dopants, and it has received increasing research interest as the interplay of the crystalline defects and solute atoms can alter the electronic and optical properties of the thin films. Despite its significance, the study of the defect-dopant interaction has remained challenging due to the atomic-scale defect structures and low concentration of dopants. Here, analytical scanning transmission electron microscopy (STEM) and *ab initio* calculations are employed to directly examine the effects of dopants on 1D defects in promising perovskite La-doped BaSnO_3 (3, 4). The local atomic and chemical configurations of two representative dislocations, single ($b=a\langle 100 \rangle$) and dissociated ($b=a\langle 110 \rangle$) dislocations, in La-doped BaSnO_3 thin films are characterized via STEM imaging and energy dispersive X-ray (EDX) spectroscopy. In both single and dissociated dislocations, a substantial amount of dopant segregation inside and outside dislocation cores as well as dopant-driven atomic re-arrangement is observed. Core-loss electron energy-loss spectroscopy (EELS) analysis is used to probe the local chemical and electronic structure variation at the dislocations, and structural optimization and electronic ground state calculations provide insight into the origin of the dopant-induced atomic and electronic modifications. Finally, the dopant behavior at dislocations is compared with dopant segregation observed in unique Sn-core line defects in La-doped BaSnO_3 (2), highlighting the complex but predictable nature of dopants at 1D defects and potential applications of these atomic-scale disorders(5). La-doped BaSnO_3 films were grown on SrTiO_3 and LaAlO_3 substrates by hybrid molecular beam epitaxy method(6). Plan-view STEM samples were prepared by mechanical polishing, and STEM experiments were carried out using an FEI Titan G2 60-300 (S)TEM equipped with EDX and EELS detectors. *Ab-initio* calculations were performed using the Quantum Espresso package(7) for structural relaxation and WIEN2K code(8) for ground-state calculations.

- (1) N. F. Fiore, C. L. Bauer, *Prog. Mater. Sci.* 13, 85-134 (1968).
- (2) H. Yun et al., *Sci. Adv.* 7, eabd4449 (2021).
- (3) K. Hyung Joon et al., *Appl. Phys. Exp.* 5, 061102 (2012).
- (4) A. Prakash et al., *Nat. Commun.* 8, 15167 (2017).
- (5) H. Yun et al., *Nano Lett.* 21, 4357-4364 (2021).
- (6) A. Prakash et al., *J. Vac. Sci. Technol. A* 33, 060608 (2015).
- (7) P. Giannozzi et al., *J. Phys.: Condens. Matter.* 21, 395502 (2009).
- (8) K. Schwarz et al., *Comput. Phys. Commun.* 147, 71-76 (2002).

2:15 PM CH02.10.04

Hidden Spontaneous Polarisation in the Chalcogenide Photovoltaic Absorber $\text{Sn}_2\text{SbS}_2\text{I}_3$ Seán R. Kavanagh¹, Christopher Savory², Aron Walsh³ and David O. Scanlon²; ¹University College London & Imperial College London, United Kingdom; ²University College London, United Kingdom; ³Imperial College London, United Kingdom

Perovskite-inspired materials aim to replicate the optoelectronic performance of lead-halide perovskites, while eliminating issues with stability and toxicity.¹⁻³ Recently, chalcogenides of group IV/V elements have attracted attention, due to enhanced stability provided by stronger metal-chalcogen bonds, alongside compositional flexibility and ns^2 lone pair cations — a performance-defining feature of halide perovskites.⁴ A rigorous description of their atomistic properties and performance potential is lacking, however.

Following the first experimental report of solution-grown tin-antimony sulfoiodide ($\text{Sn}_2\text{SbS}_2\text{I}_3$) solar cells,⁵ with power conversion efficiencies above 4%

(exceeding the first reported solar efficiency of methylammonium lead-iodide (MAPI)),⁶ we assess the structural and electronic properties of this emerging earth-abundant PV material.⁷ We find that the experimentally reported centrosymmetric *Cmcm* crystal structure represents an average over multiple polar *Cmc2₁* configurations. The instability is confirmed through a combination of lattice dynamics and molecular dynamics simulations. We predict a large spontaneous polarisation of 37 $\mu\text{C}/\text{cm}^2$ that could be active for electron-hole separation in operating solar cells. The resemblance of this dynamic crystal structure and ferroelectric behavior to that of MAPI begs the question of its importance in high-performance defect-tolerant solar materials.

Moreover, using state-of-the-art *ab-initio* methods (hybrid Density Functional Theory including spin-orbit coupling effects), we rigorously assess the efficiency limits of this material on the basis of its electronic structure and predicted defect behaviour, calculating $\eta_{\text{max}} > 30\%$ for film thicknesses $t > 0.5\ \mu\text{m}$.

The results shine a spotlight on the largely-unexplored class of $\text{A}_2\text{BCh}_2\text{X}_3$ mixed-metal chalcogenides. These are candidates for solution-processed ferroelectric and optoelectronic devices, with the substitutional flexibility for engineering band gaps, band energies, and lattice polarisation. Our work provides insight regarding both the potential success of this emerging class of optoelectronic materials and structure-property relationships in perovskite-inspired materials, guiding design strategies and expanding the compositional space of candidate materials.

1 Y.-T. Huang, S. R. Kavanagh, D. O. Scanlon, A. Walsh and R. L. Z. Hoye, *Nanotechnology*, 2021, **32**, 132004.

2 Z. Li, S. R. Kavanagh, M. Napari, R. G. Palgrave, M. Abdi-Jalebi, Z. Andaji-Garmaroudi, D. W. Davies, M. Laitinen, J. Julin, M. A. Isaacs, R. H. Friend, D. O. Scanlon, A. Walsh and R. L. Z. Hoye, *J. Mater. Chem. A*, 2020, **8**, 21780–21788.

3 M. Buchanan, *Nature Physics*, 2020, **16**, 996–996.

4 R. Nie, R. R. Sumukam, S. H. Reddy, M. Banavoth and S. I. Seok, *Energy Environ. Sci.*, 2020, **13**, 2363–2385.

5 R. Nie, K. S. Lee, M. Hu, M. J. Paik and S. I. Seok, *Matter*, 2020, S2590238520304471.

6 A. Kojima, K. Teshima, Y. Shirai and T. Miyasaka, *Journal of the American Chemical Society*, 2009, **131**, 6050–6051.

7 S. R. Kavanagh, C. N. Savory, D. O. Scanlon and A. Walsh, *Materials Horizons*, 2021 (Accepted).

2:30 PM CH02.10.05

Organohalide Precursors for the Continuous Production of Photocatalytic Bismuth Oxyhalide Nanoplates Matthew N. Gordon, Kaustav Chatterjee, Alison L. Lambright, Sandra L. Atehortua Bueno and Sara E. Skrabalak; Indiana University, United States

Metal heteroanionic materials, such as oxyhalides, are promising photocatalysts in which band positions can be engineered for visible-light absorption by changing the halide identity. Advancing the synthetic routes towards these materials, bismuth oxyhalides of the form BiOX ($X = \text{Cl}, \text{Br}$) have been prepared using rapid and scalable ultrasonic spray synthesis (USS). Central to this advance was the identification of small organohalide molecules as halide sources. When these precursors are spatially and temporally confined in the aerosol phase with molten salt fluxes, powders composed of single-crystalline BiOX nanoplates can be produced continuously. A mechanism highlighting the in situ generation of halide ions is detailed. These materials can be used as photocatalysts and provide proof-of-concept of USS as a route to more complex bismuth oxyhalide materials.

SESSION CH02.18: On-Demand
Sunday Morning, December 5, 2021
On-Demand

8:00 AM CH02.18.01

An Insight into the Phase Dependent Photocatalytic Activity of Bulk and Exfoliated Defect-Controlled 2D Flakes of Copper Sulfide System Under Simulated Solar Light Madina Telkhozhayeva, Rajashree Konar, Eti Teblum and Gilbert D. Nessim; Bar-Ilan University, Israel

Sunlight-driven photocatalysis is an environmentally friendly approach to solve ecological issues and energy crisis. The development of simple, yet sufficiently stable, photocatalytic materials responsible for harvesting full-spectrum light remains a significant challenge so far. With regard to the design of advanced photocatalysts, low-dimensional materials show tremendous prospects due to their unique surface and electronic properties, which are not seen in their bulk counterparts. Among the various inorganic semiconductors, copper sulfides (Cu_2xS , $0 \leq x \leq 1$) have attracted great interest in applications linked to photovoltaic devices and photocatalysis due to their low cost, high element abundance, non-toxic nature, structural and compositional versatility.¹ However, the properties of copper sulfides are sensitive to the Cu-S stoichiometry, which determines the density of copper vacancies, thus the hole concentration; therefore it is critical to finely tune their phases for use in applications.

Herein, we first demonstrate the phase transformations of bulk copper sulfides from digenite (Cu_9S_5) to djurleite ($\text{Cu}_{1.97}\text{S}$) and low-chalcocite (Cu_2S) by the continuous reactive thermal annealing in ambient pressure chemical vapor deposition (CVD), followed by their top-down exfoliation. XRD, HRTEM, and XPS analyses confirm that monoclinic Cu_2S is primarily formed at higher temperatures or greater reaction times and using reducing atmosphere owing to its lower free energy of formation and greater symmetry in its crystal structure. Although copper sulfide does not have a typical MX_2 structure common for transition metal chalcogenides (TMCs), we successfully exfoliated it into 2D flakes using high-frequency liquid-phase exfoliation (LPE) due to its layered morphology.² From AFM, we measured the average thickness of approximately 4 nm of the exfoliated flakes with relatively large lateral size up to 10 μm . We tested the three phases of bulk copper sulfides and their exfoliated forms as photocatalysts for dye degradation under simulated solar light irradiation. Exfoliated Cu_2S flakes exhibited superior photocatalytic activity with a rate constant roughly twice higher than that of bulk chalcocite, which could be predominantly attributed to their unique 2D structure and layered morphology, where the exfoliated flakes can provide an ultrahigh fraction of surface atoms, which could serve as the active sites for dye photodegradation. In addition, the enhanced photocatalytic activity could be attributed to the 2D planar defects such as stacking faults in different portions of exfoliated Cu_2S that were introduced during the annealing in reducing atmosphere without altering its structure and crystallinity. Furthermore, optical spectroscopy results demonstrate that the 2D Cu_2S has sufficient bandgap energy for simultaneously absorbing across the whole solar spectrum. Photocatalytic mechanism experiments and electron-spin resonance (ESR) data indicate that both superoxide radicals and holes served as dominant active species during the photocatalytic reaction. Our study provides a better understanding of possible phase transformations in the copper sulfide system and paves the way for developing next-generation 2D copper sulfide photocatalysts to capture a broad range of the solar spectrum for environmental decontamination.

References

(1) Coughlan, C.; Ibáñez, M.; Dobrozhan, O.; Singh, A.; Cabot, A.; Ryan, K. M. Compound Copper Chalcogenide Nanocrystals. *Chem. Rev.* **2017**, *117* (9), 5865–6109.

(2) Telkhozhayeva, M.; Teblum, E.; Konar, R.; Girshevitz, O.; Perelshtein, I.; Aviv, H.; Tischler, Y. R.; Nessim, G. D. Higher Ultrasonic Frequency Liquid

8:15 AM CH02.01.09

Novel Metal–Organic Glasses and Liquids from Metal–Bis(acetamide) Frameworks with Low Melting Temperatures Mandy Liu¹, Ryan McGillicuddy¹, Hung Vuong², Songsheng Tao², Adam Slavney¹, Miguel I. Gonzalez¹, Simon J. Billinge² and Jarad A. Mason¹; ¹Harvard University, United States; ²Columbia University, United States

Molten phases of metal–organic networks offer exciting opportunities for using coordination chemistry principles and reticular synthesis to access liquids and glasses with unique and tunable structures and properties. Here, we discuss general thermodynamics strategies to design extended coordination solid structures with an increased enthalpic and entropic driving force for reversible, low-temperature melting transitions and illustrate this approach through a systematic study of novel bis(acetamide)-based networks with record-low melting temperatures. The low melting temperatures of these compounds are the result of weak coordination bonds, conformationally flexible bridging ligands, and weak electrostatic interactions between spatially separated cations and anions, which collectively reduce the enthalpy and increase the entropy of fusion.

Through a combination of crystallography, spectroscopy, and calorimetry, we demonstrate that trends in enthalpy of fusion are dictated by the strength of coordination bonds and hydrogen bonds within each extended coordination solid, while trends in entropy of fusion are strongly influenced by the degree to which residual motion and positional disorder are restricted in the crystalline state. Pair distribution function (PDF) and extended X-ray absorption fine structure (EXAFS) analysis of Co(bba)₃[CoCl₄] [bba = *N,N'*-1,4-butylenebis(acetamide)], which features a record-low melting temperature for a three-dimensional metal–organic network of 124 °C, provide evidence of metal–ligand coordination in the liquid phase, as well as intermediate- and extended-range order that support its network-forming nature. Glass formation is observed from the metal–organic liquids with various chemical compositions, and rheological measurements are used to rationalize differences in glass-forming ability and relaxation dynamics. These findings reveal exciting potential of manipulating melting thermodynamics of extended coordination solids by controlling structural and chemical factors in their crystalline state, as well as accessing metal–organic glass and liquid phases with unique structures and properties.

SESSION CH02.11: Physical Properties of Inorganic Solids I
Session Chairs: Craig Brown and Brent Melot
Monday Morning, December 6, 2021
CH02-Virtual

8:00 AM *CH02.11.01

Chiral Organic Semiconductors—Predicting Molecules and Motifs Kim E. Jelfs; Imperial College London, United Kingdom

Recent years have seen a surge in interest throughout the materials science community in the rational design of crystal structures that maximise a material's suitability as an organic semiconductor. Predicting the spatial arrangement of molecules in the solid state and, therefore being able to compute the resulting electronic properties, provides insights into structure-property relationships to guide the material design process. We have been predicting polymorphs and charge mobilities for a myriad of [6]helicenes. Helicenes are a class of axially chiral twisted graphene-like molecules, with potential applications as organic semiconductors. Due to their discernible molecular geometry, helicenes tend to pack in recurring structural motifs. The ubiquity of certain motifs across polymorphs can be exploited to screen a vast pool of helicenes for the best charge transport material along a specific motif. We generated approximately 1400 different [6]helicene molecules, packing in the most frequently encountered translational dimer motif. We computed the transfer integral and inner reorganisation energy to screen for good semiconductors. For the most promising [6]helicene molecules, a CSP search was performed and the lowest energy polymorphs' charge carrier mobility was computed. We observed very low inner reorganisation energies for symmetrically disubstituted [6]helicenes containing side groups with a triple bond. The most promising candidates have been selected for full crystal structure prediction and are being synthesised by our experimental collaborators. More recent work analysing the packing of helicenes on surfaces using coarse-graining methods will also be discussed.

8:30 AM CH02.11.07

Lone-Pair-Induced Structural Ordering in the Mixed-Valent 0D Metal-Halides Rb₂₃Bi^{III}_xSb^{III}_{7-x}Sb^V₂Cl₅₄ (0 ≤ x ≤ 7) Kyle M. McCall^{1,2}, Bogdan M. Benin^{1,2}, Michael Woerle¹, Dominique Borgeaud dit Advocat¹, Thomas Vonderach¹, Kostiantyn Sakhatskyi^{1,2}, Sergii Yakunin^{1,2}, Detlef Guenther^{1,2} and Maksym V. Kovalenko^{1,2}; ¹ETH Zurich, Switzerland; ²Empa–Swiss Federal Laboratories for Materials Science and Technology, Switzerland

Mixed-valent solid-state compounds have long been known for their vibrant colors, and the pnictogen-halide semiconductors containing *ns*² lone pairs are no exception, exhibiting intense absorption bands with unusual colors. In contrast, zero-dimensional (0D) *ns*²-based metal-chlorides without mixed-valency are generally colorless but have recently demonstrated unique properties that are promising for optoelectronic applications such as broadband lighting, thermometry, and radiation detection.

Here, a new family of mixed-valent alkali pnictogen halides with composition Rb₂₃Bi^{III}_xSb^{III}_{7-x}Sb^V₂Cl₅₄ (0 ≤ x ≤ 7) is discovered through solvothermal synthesis. Single-crystal X-ray diffraction reveals that the deep red Rb₂₃Sb^{III}₇Sb^V₂Cl₅₄ crystallizes in an orthorhombic space group (*Cmcm*) with a unique, layered 0D structure driven by the repulsion of the 5s² lone pairs of the Sb^{III}Cl₆ octahedra. In contrast to the prototypical Cs₃Sb^{III}Sb^VCl₁₂ tetragonal structure with highly symmetric octahedral environments, here the Sb^{III}Cl₆ octahedra exhibit trigonal or disphenoidal distortion from the lone pair, yielding layers with distinct orientations of the octahedra as these asymmetric units pack around the Sb^VCl₆ octahedra. Partially or fully substituting Sb^{III} with isoelectronic Bi^{III} yields the series Rb₂₃Bi^{III}_xSb^{III}_{7-x}Sb^V₂Cl₅₄ (0 < x ≤ 7), with a similar layered 0D structure but exhibiting rotational disorder that yields a trigonal crystal system with a polar space group (*R32*). Second harmonic generation of 532 nm light from a 1064 nm laser using Rb₂₃Bi^{III}₇Sb^V₂Cl₅₄ powder confirms the non-centrosymmetry of this compound. As with the prototypical mixed-valent pnictogen halides, the visible absorption bands of the Rb₂₃Bi^{III}_xSb^{III}_{7-x}Sb^V₂Cl₅₄ family are the result of intervalent Sb^{III}-Sb^V and mixed-valent Bi^{III}-Sb^V charge transfer bands, with a blueshift of the absorption edge as Bi^{III} substitution increases. No PL is observed from this family of semiconductors, but a crystal of Rb₂₃Bi^{III}₇Sb^V₂Cl₅₄ exhibits a high resistivity of 1.0 × 10¹⁰ Ωcm and weak X-ray photoconductivity with a μτ product of 8.0 × 10⁻⁵ cm² s⁻¹ V⁻¹. Beyond simply adding a new entry to the growing library of 0D metal halides, the unique 0D layered structures of the Rb₂₃Bi^{III}_xSb^{III}_{7-x}Sb^V₂Cl₅₄ family highlight the versatility of the *ns*² lone pair and offer ripe opportunities for tuning and improving these materials; namely, the ability to tune both lone-pair expression as well as the charge transfer absorption band characteristic of mixed-valent materials within the same structure.

8:35 AM CH02.11.02

Reversible Phase Transformations in Novel Dual-Phase Ce-Substituted Perovskite Oxide Composites for Solar Thermochemical CO₂ Redox Splitting J. Madhusudhan Naik¹, Clemens Ritter², Brendan Bulfin³, Aldo Steinfeld³, Rolf Erni⁴ and Greta R. Patzke¹; ¹University of Zurich,

Switzerland; ²Institut Laue-Langevin, France; ³ETH Zurich, Switzerland; ⁴Empa–Swiss Federal Laboratories for Materials Science and Technology, Switzerland

Solar thermochemical (STC) splitting of CO₂ and/or H₂O via two-step metal oxide redox cycles is a promising approach to generate large-scale quantities of synthetic liquid hydrocarbon fuels. STC pathway utilizes the entire spectrum of solar radiation as a source of high-temperature process heat to split CO₂ and/or H₂O into CO and/or H₂.^[1] The CO and H₂ (*syngas*) produced may be directly used as a fuel or further processed into synthetic liquid hydrocarbon fuels by the Fischer-Tropsch process. The two-step thermochemical temperature-swing cycle involves an endothermic reduction step of a redox metal oxide at high temperatures (1300–1500 °C), generating lattice oxygen vacancies, followed by an exothermic re-oxidation step with CO₂ and H₂O at low temperatures (800–1000 °C).^[2] Perovskite-type (ABO_{3-δ}) oxides are being considered as an attractive redox material class alternative to the state-of-the-art material ceria (CeO_{2,δ}), due to their high structural and thermodynamic tunability. However, these advantages are offset by the unfavorable re-oxidation equilibria due to their low entropy change compared to pure ceria, leading to lower mass specific fuel productivity under most conditions relevant for STC cycles. This work reports a novel dual-phase Ce-substituted Mn-deficient perovskite oxide (LSC25M75), La³⁺_{0.48}Sr²⁺_{0.52}(Ce⁴⁺_{0.06}Mn³⁺_{0.79})O_{2.55} (*R-3c*, 70 %) and pyrochlore Ce⁴⁺_{2.6}La³⁺_{1.4}O_{6.28} (*Fd-3m*, 30 %) composite material, aiming to overcome individual thermodynamic limitations of perovskite oxide and ceria based redox materials. Thermochemical CO₂ redox splitting and long-term cyclability of LSC25M75 evaluated with a thermogravimetric analyzer and an IR furnace reactor over 100 consecutive redox cycles demonstrated a two-fold higher CO₂ conversion extent than the current state-of-the-art perovskite oxide, La_{0.60}Sr_{0.40}MnO_{3-δ} (LSM). Improved understanding of the true phases and the structure-property relationship of materials under operational conditions is necessary for developing high performance STC redox materials. The underlying reaction mechanism for the obtained high performance were elucidated for the first time using complementary diffraction techniques. Based on in situ high temperature neutron, ex situ synchrotron X-ray and electron diffraction experiments, we obtained an unprecedented structural insight into thermochemical perovskite oxide materials. We propose a novel CO₂ splitting reaction mechanism involving a reversible temperature induced phase transition from the *n* = 1 Ruddlesden-Popper phase (Sr_{1.10}La_{0.64}Ce_{0.26})MnO_{3.88} (*I4/mmm*, K₂NiF₄-type) at reduction temperature (1350 °C) to the *n* = 2 Ruddlesden-Popper phase (Sr_{2.60}La_{0.22}Ce_{0.18})Mn₂O_{6.6} (*I4/mmm*, Sr₃Ti₂O₇-type) at re-oxidation temperature (1000 °C) after the CO₂ splitting step.^[3]

References

- [1] M. Romero, A. Steinfeld, *Energy Environ. Sci.* **2012**, *5*, 9234.
- [2] D. Marxer, P. Furler, M. Takacs, A. Steinfeld, *Energy Environ. Sci.* **2017**, *10*, 1142.
- [3] J. M. Naik, C. Ritter, B. Bulfin, A. Steinfeld, R. Emi, G. R. Patzke, *Adv. Energy Mater.* **2021**, *11*, 2003532.

8:40 AM CH02.11.03

Local Order—A New Control Parameter for Optimizing Material Properties Arkadiy Simonov and Yevheniia Kholina; ETH Zurich, Switzerland

Disorder is commonly used in chemistry for designing functional materials. For instance, preparation of solid solutions is nothing else than the introduction of a controlled number of point defects in a crystal. Disordered systems, though, provide more degrees of freedom: not only the number of defects, but also their distribution can be used to optimise the functional properties of materials, however up until now, defect distribution was hard to control and thus was rarely used in practice.

In this talk we will show how to precisely tune distribution of point defects by changing various chemical parameters during crystal growth, and characterise it with the single crystal diffuse scattering.

We will use Prussian Blue Analogues (PBAs) as our model system. PBAs is a class of cyanide materials with the general formula M[M'(CN)₆]_{1-δ} · xH₂O where M and M' are transition metals. Depending on the nature of transition metals, PBAs can accommodate a large number of vacancies on the M'(CN)₆ site (for instance δ=0.33 for M=Mn and M'=Co) which makes them highly porous and, as a result, attractive for hydrogen storage applications. Distribution of M'(CN)₆ vacancies is important for the performance of this material, since more disordered vacancy configurations provide more diffusion pathways through the structure, larger accessible volume, and easier transport.

8:45 AM CH02.11.05

Rare Earth Doped Nanoscale Upconverting Fluorides Na_{1.5}Yb_{1.5}F₆ and SrF₂ and Their Application for Dosimetry and Thermal Supervision Michael Arnold, Julia Katzmann, Christiane Schuster and Thomas Härtling; Fraunhofer IKTS, Germany

A recent approach to measure electron radiation doses in the kGy range is the use of phosphors with an irradiation dose-dependent luminescence decay time. NaYF₄:Yb³⁺:Er³⁺ is limited as it shows pronounced fading. Therefore, in this work a modified synthesis of three fluorides is presented that results in nanoparticles co-doped Yb and Er, Ho or Tm that is shown to be a promising dosimeter material. Upon excitation with a 980 nm laser a typical upconversion luminescence is observed. For all these materials a dose dependency of the luminescence decay time is observed. However, of the most importance is the very low fading effect of the luminescence decay time. In the case of SrF₂ that is as low as 5 % in the 30 days after irradiation and beyond. This makes this type of materials attractive for electron beam dosimetry in spite of lower upconversion intensity compared to NaYF₄ or BaYbF₅. In addition all two materials show Na_{1.5}Yb_{1.5}F₆ and SrF₂ shows thermoluminescent properties.

Experimental: The precipitation (SrF₂)^[1] is done with an ammonium fluoride solution (all Sigma Aldrich) in distilled water. The hydrothermal syntheses of Na_{1.5}Yb_{1.5}F₆:RE run in a PTFE autoclave with a stainless steel envelop. All compounds were characterized by x-ray powder diffractometry and micro structure photography. The samples were irradiated in an EBLab 200 electron irradiator (Comet) using 200 KV acceleration voltage. Doses of 5 kGy up to 50 kGy were applied to the samples. To measure luminescence decay curves, the phosphor samples were excited by a 1 ms light pulse from a 980 nm laser diode (max. 80 mW, Roithner SPL980-100-105M-PD) and the temporal upconversion luminescence decay was recorded by a silicon photodiode (Osram SFH2200). Ten consecutive curves were averaged and then exponentially fitted to obtain the decay time.

Results: After electron beam irradiation (200 keV) of a thin immobilized phosphor layer the luminescence decay time of the SrF₂: 2%Er, 2...20% Yb phosphor decreases from 1520 μs to values between 1250 μs and 1020 μs, depending on the irradiation dose as shown in Figure 1a. For samples irradiated with 5, 10 and 20 kGy, respectively, the luminescence decay times were repeatedly measured until 50 days after irradiation (Figure 1b). The material Na_{1.5}Yb_{1.5}F₆:Ho,Yb shows a decay time dependence of the temperature (Figures 2a and 2b) in case of the radiated materials. The altered decay time after electron beam radiation is similar low fading in 30 days than SrF₂:Er,Yb.

Conclusion: In this work, a series of fluoride sub-micron powders co-doped with different amounts of Yb³⁺ sensitizer and trivalent Er, Ho Tm activator ions were synthesized. For SrF₂:Er,Yb(2%/20%), a dose-dependent reduction of the material's luminescence decay time after electron irradiation is observed. This allows the use of the powder as a dosimeter material. Encouragingly, SrF₂:Er,Yb(2%/20%) shows reduced fading of the luminescence decay time compared to the previously studied NaYF₄:Yb³⁺, Er³⁺. The thermal response of the radiated Na_{1.5}Yb_{1.5}F₆:Ho,Yb make this material suitable for temperature supervision^[2] on electronic boards e.g.

Figure 1: a) end point of the decay time (TCSPC) after different electron beam doses, b) fading of different radiated SrF₂:Er Yb samples (a fifty days storage shows the same)

Figure 2: thermal response of the decay time with radiated SrF₂:Er Yb (a) and Na_{1.5}Yb_{1.5}F₆:Ho, Yb (b) by the same dose

[1] Kuznetsov, S.; Ermakova, Y.; Voronov, V.; Fedorov, P.; Busko, D.; Howard, I. A.; Richards, B. S.; Turshatov, A. Up-conversion quantum yields of SrF₂:Yb³⁺, Er³⁺ sub-micron particles prepared by precipitation from aqueous solution. *Journal of Materials Chemistry C* **2018**, *6* (3), 598–604.

[2] Schuster, C.; Kuntz, F.; Strasser, A.; Härtling, T.; Dornich, K.; Richter, D. 3D relative dose measurement with a μm thin dosimetric layer. *Radiation Physics and Chemistry* **2020** (in submission).

8:50 AM CH02.11.06

Doping by Design—Enhanced Thermoelectric Performance of GeSe-Based Alloys Through Metavalent Bonding Yuan Yu, Carl-Friedrich Schön, Oana Cojocaru-Mirédin and Matthias Wuttig; RWTH Aachen University, Germany

For thermoelectrics doping is usually the first step to tailor the charge carrier concentration and concomitant properties. Doping should also turn GeSe, which features intrinsically a low concentration, into a competitive thermoelectric. Yet, elemental doping fails to adjust the charge carrier concentration. Doping with AgSbSe₂, on the contrary, works and causes a remarkable enhancement of thermoelectric performance. This improvement is closely related to a change of bonding mechanism, as evidenced by sudden alterations of the optical dielectric constant ϵ_{∞} , the Born effective charge Z^* and the bond breaking mechanism. These property changes signal the formation of metavalent bonds. These bonds lead to an octahedral-like atomic arrangement and a favorable band structure featuring small effective masses. A quantum-mechanical map distinguishes the different types of chemical bonding. It reveals that orthorhombic GeSe is located in a map region where covalent bonding prevails, while cubic and rhombohedral GeSe are located in the region characterized by metavalent bonding. These assignments are in line with the measured properties and thermoelectric performance of the different phases. Our work thus redefines doping rules and provides a 'treasure map' to tailor thermoelectric properties of chalcogenides and related p-bonded materials.

8:55 AM *CH02.11.08

Towards Reversible High-Voltage Multi-Electron Reactions in Alkali-Ion Batteries Using Vanadium Phosphate Positive Electrode Materials Laurence Croguennec¹, Edouard Boivin^{2,1}, Long H.B. Nguyen^{1,2}, Jacob Olchowka¹, Dany Carlier¹, Jean-Noël Chotard² and Christian Masquelier²; ¹ICMCM, CNRS, Bordeaux Univ., Bordeaux INP, France; ²LRCS, Picardie Jules Verne Univ., France

Vanadium phosphate positive electrode materials attract great interest in the field of Alkali-ion (Li, Na and K-ion) batteries due to their ability to store several electrons per transition metal. These multi-electron reactions (from V²⁺ to V⁵⁺) combined with the high voltage of corresponding redox couples (e.g., 4.0 V vs. Na⁺/Na for V³⁺/V⁴⁺ in Na₃V₂(PO₄)₂F₃) could allow the achievement of the 1 kWh/kg milestone at the positive electrode level in Alkali-ion batteries. However, a massive divergence in the voltage reported for the V³⁺/V⁴⁺ and V⁴⁺/V⁵⁺ redox couples as a function of crystal structure is noticed. Moreover, vanadium phosphates that operate at high V³⁺/V⁴⁺ voltages are usually unable to reversibly exchange several electrons in a narrow enough voltage range. During this talk, through the review of redox mechanisms and structural evolutions occurring upon electrochemical operation of selected widely studied materials, we will identify the crystallographic origin of this trend: the distribution of PO₄ groups around vanadium octahedra, that allows or prevents the formation of the vanadyl distortion (O . . . V⁴⁺=O or O . . . V⁵⁺=O).¹⁻⁴ While the vanadyl entity massively lowers the voltage of the V³⁺/V⁴⁺ and V⁴⁺/V⁵⁺ couples, it considerably improves the reversibility of these redox reactions. Therefore, anionic substitutions, mainly O²⁻ by F⁻, have been identified as a strategy allowing for combining the beneficial effect of the vanadyl distortion on the reversibility with the high voltage of vanadium redox couples in fluorine rich environments.

References

1. Boivin, E.; Chotard, J.-N.; Masquelier, C.; Croguennec, L., Towards Reversible High-Voltage Multi-Electron Reactions in Alkali-Ion Batteries Using Vanadium Phosphate Positive Electrode Materials. *Molecules* **2021**, *26*, 1428.
2. Boivin, E.; Iadecola, A.; Fauth, F.; Chotard, J.N.; Masquelier, C.; Croguennec, L. Redox Paradox of Vanadium in Tavorite LiVPO₄F_{1-y}O_y. *Chem. Mater.* **2019**, *31*, 7367–7376.
3. Nguyen, L.H.B.; Broux, T.; Sanz Camacho, P.; Denux, D.; Bourgeois, L.; Belin, S.; Iadecola, A.; Fauth, F.; Carlier, D.; Olchowka, J.; Masquelier, C.; Croguennec, L. Stability in water and electrochemical properties of the Na₃V₂(PO₄)₂F₃ – Na₃(VO)₂(PO₄)₂F solid solution. *Energy Storage Materials* **2019**, *20*, 324–334.
4. Nguyen, L.H.B.; Iadecola, A.; Belin, S.; Olchowka, J.; Masquelier, C.; Carlier, D.; Croguennec, L. A Combined Operando Synchrotron X-ray Absorption Spectroscopy and First-Principles Density Functional Theory Study to Unravel the Vanadium Redox Paradox in the Na₃V₂(PO₄)₂F₃-Na₃V₂(PO₄)₂FO₂ Compositions. *J. Phys. Chem. C* **2020**, *124*, 23511–23522.

9:25 AM CH02.11.09

Understanding the Short-Range Order Preference in the Antiperovskite Cathode Material Li₂FeSO Samuel W. Coles^{1,2}, Kit McColl^{1,2}, Alexander Squires^{1,2}, Conn O'Rourke^{1,2}, Saiful Islam^{1,2} and Benjamin J. Morgan^{1,2}; ¹University of Bath, United Kingdom; ²Faraday Institution, United Kingdom

In cation disordered cathode materials the presence of any short-range ordering of cations can have a strong influence on their function, in particular their electrochemical behaviour on cycling[1]. The recently discovered anti-perovskite cathode material Li₂FeSO has a promising theoretical capacity[2], but still encounters issues with capacity fade and long-term structural degradation[3].

This theoretical study seeks to explore the short range ordering of cations in Li₂FeSO by using a DFT+U based cluster expansion. It will be shown that there is a strong preference for the formation of OLi₄Fe₂ of oxygen octahedra, which we postulate is due to equidistribution of charge. More curiously we find that the asymmetric arrangement of lithium and iron ions around the sulfur and oxygen anions is favoured versus symmetric arrangements. Subsequent Wannier analysis of DFT calculations shows that this stabilisation has its origins in the generation of dipoles on the anions. We conclude that these anion dipoles are not only the origins of the short-range order in Li₂FeSO but also induce disorder in this material.

[1] A. Abdellahi, A. Urban, S. Dacek, and G. Ceder, *Chem. Mater.* **28**, 5373.

[2] K. T. Lai, I. Antonyshyn, Y. Prots, and M. Valldor, *J. Am. Chem. Soc.* **139**, 9645.

[3] M. V. Gorbunov, S. Carrocci, S. Maletti, M. Valldor, T. Doert, S. Hampel, I. G. G. Martinez, D. Mikhailova, and N. Gräßler, *Inorg. Chem.* **59**, 15626.

9:40 AM CH02.11.10

Tunable Phase Transitions in a Two-Dimensional Superionic Conductor Alex Rettie; University College London, United Kingdom

Superionic conductors (SICs) possess liquid-like ionic diffusivity in the solid state, finding wide applicability from electrolytes in energy storage to

materials for thermoelectric energy conversion. Type I SICs, where high ionic diffusivity is linked to the crystal structure *via* a first-order transition and is therefore either on or off, are attractive for energy storage and conversion applications providing the transition temperature can be controlled. However, such SICs (e.g., AgI, Ag₂Se, etc.) have been found exclusively in 3D crystal structures so far, limiting existing approaches to applied pressure and nanoscale size effects – which affect the transition temperature in one direction – while the effects of chemical substitution cannot be easily decoupled from 3D ion-conducting pathways. Layered materials have spatially separated mobile and immobile sublattices, potentially facilitating wide tunability and functioning as platforms to study two-dimensional superionic conduction.

We previously identified a first-order, order-disorder phase transition in 2D KAg₃Se₂ – a dimensionally-reduced derivative of 3D Ag₂Se – at ~695 K using in-situ XRD and DSC [1]. Here, we use quasi-elastic neutron scattering and AIMD simulations reveal that a-KAg₃Se₂ is a type I SIC with a highly disordered Ag sublattice restricted to 4 Å thick layers [2]. The superionic local structure was probed by in-situ XPDF analysis, confirming the defect dynamics from AIMD simulations. Thermal analyses of cation-substituted AAg₃Se₂ (A = Li-Cs) compounds indicate that the superionic transition temperature can be tuned by the composition of the immobile charge-balancing layers. Future directions to design materials with tailored ionic conductivities and phase transitions will be discussed.

References

- 1) A.J.E. Rettie et al., *J. Am. Chem. Soc.*, **2018**, 140, 9193–9202.
- 2) A.J.E. Rettie et al., *Nat. Mater.*, **2021** (accepted), ChemRxiv preprint.

SESSION CH02.12: Physical Properties of Inorganic Solids II
Session Chairs: Amparo Fuertes and Hiroshi Kageyama
Monday Afternoon, December 6, 2021
CH02-Virtual

1:00 PM *CH02.12.01

Complex Halide Perovskites Kurt Lindquist¹, Bridget Connor¹, Michael Boles¹, Stephanie Mack^{2,3}, Jeffrey Neaton^{2,3} and Hemamala Karunadasa^{1,4}; ¹Stanford University, United States; ²UC Berkeley, United States; ³LBNL, United States; ⁴SLAC National Accelerator Laboratory, United States

I will present our recent studies on further increasing the accessible electronic structures of the versatile family of halide perovskites by synthesizing mixed-metal compositions. Our work on halide double perovskites has prompted us to explore still more complex perovskites. In particular, I will discuss unusual new architectures that combine sublattices of different dimensionality and the consequences of incorporating three distinct stoichiometric metals in the octahedral sites.

1:30 PM CH02.12.02

Atomistic Investigation of Uranium Oxycarbide (UCO) Phase Stability, Point Defects and Fission Products Properties Ibrahim Cheik Njifon and Edmanuel Torres; Canadian Nuclear Laboratories, Canada

We present atomistic modelling of uranium oxycarbide (UCO), a candidate fuel kernel for TRISO particles in the high temperature gas reactors (HTGRs). The use of UCO aims at mitigating the formation and release of CO gas [1] which is associated with the TRISO particle failure. Under operation, UCO microstructure evolves to form the high atomic mass UC(O) phase with rocksalt structure and the low atomic mass UO₂(C) phase with fluorite structure [2, 3]. This study sheds light on phase stability, structural and thermodynamic quantities of both UCO phases. Defects stability, atomic self-diffusion and fission products incorporation are also investigated in the UO₂(C) phase. Our results demonstrate a strong dependence on carbon content, which may have a significant impact on the fuel chemistry under operation, thereby playing an important role in the fuel performance properties such as fission products retention and release in UCO fuel kernel of TRISO particles.

- [1] J. W. McMurray, T. B. Lindemer, N. R. Brown, T. J. Reif, R. N. Morris, J. D. Hunn, *Ann. Nucl. Energy* 104 (2017) 237 – 242.
- [2] I. J. Van Rooyen, Z. Fu, Y. Yang, T. Holesinger, M. Bachhav, in: *Proceedings of HTR 2018*, Warsaw, Poland.
- [3] J. A. Phillips, S. G. Nagley, E. L. Shaber, *Nucl. Eng. Des.* 251 (2012) 261 –281

1:35 PM CH02.12.03

Development of Noble Metal Free Bi-Functional Electrocatalysts for Hydrogen Evolution Reaction on Porous Carbon Support and Performance Study Sanju Gupta; University of Central Florida, United States

Developing bi-functional electrocatalysts for both oxygen reduction reaction (ORR) and hydrogen evolution reaction (HER) is crucial for enhancing the energy transfer efficiency of metal-air batteries and fuel cells, as well as producing hydrogen with high purity. Herein, a series of Ni-Co alloyed nanoparticles encapsulated in or decorated on activated charcoal and porous carbon support (BAX) synthesized using electrodeposition and employed as a bifunctional electrocatalyst for both ORR and HER. The scanning electron microscopy measurements showed optimal loading of Ni-Co nanoparticles, with a size of approximately 5–10 nm, which were uniformly dispersed on the nanoporous carbons support, with occasional aggregated nanoparticles. The as-prepared samples exhibited effective ORR activity in alkaline media and excellent HER activity in both alkaline and acid solutions. While the cobalt nanoparticles showed an overpotential of 54 mV dec⁻¹, Ni-Co_{0.3:1} showed higher current density and higher overpotential of 130 mV dec⁻¹ at 10 mA cm⁻² in 1 M KOH, respectively suggesting Volmer-Tafel and Volmer-Herovskiy mechanism, respectively, for HER. Overall, Ni: Ni:Co_{0.3:1}/BAX on graphite rod samples displayed the best activity and stability among the series, which is comparable and superior to that of commercial 10% Pd/C. The strategy for encapsulating bimetallic alloys within porous carbon materials is promising for fabricating sustainable energy toward electrocatalysts with multiple electrocatalytic activities for alternative energy-related applications.

1:40 PM CH02.12.04

Multimodal Structure Solution with ¹⁹F NMR Crystallography of Spin Singlet Molybdenum Oxyfluorides Fenghua Ding, Kent J. Griffith and Kenneth R. Poeppelmeier; Northwestern University, United States

Complex crystal structures with subtle atomic scale details are now routinely solved using complementary tools such as X-ray and/or neutron scattering combined with electron diffraction and imaging. Identifying unambiguous atomic models for oxyfluorides, needed for materials design and structure-property control, is often still a considerable challenge. In this work, NMR crystallography and single-crystal X-ray diffraction are combined for the

complete structure solution of three new compounds featuring a rare triangular early transition metal oxyfluoride cluster $[\text{Mo}_3\text{O}_4\text{F}_9]^{5-}$. After framework identification by single-crystal X-ray diffraction, 1D and 2D solid-state ^{19}F NMR spectroscopy supported by *ab initio* calculations are used to solve the structures of (1) $\text{K}_5[\text{Mo}_3\text{O}_4\text{F}_9]\bullet 3\text{H}_2\text{O}$, (2) $\text{K}_5[\text{Mo}_3\text{O}_4\text{F}_9]\bullet 2\text{H}_2\text{O}$, and (3) $\text{K}_{16}[\text{Mo}_3\text{O}_4\text{F}_9]_2[\text{TiF}_6]_3\bullet 2\text{H}_2\text{O}$ and to assign the nine distinct fluorine sites in the oxyfluoride clusters. Furthermore, ^{19}F NMR identifies selective fluorine dynamics in $\text{K}_{16}[\text{Mo}_3\text{O}_4\text{F}_9]_2[\text{TiF}_6]_3\bullet 2\text{H}_2\text{O}$. These dual scattering and spectroscopy methods are used to demonstrate the generality and sensitivity of ^{19}F shielding to small changes in bond length—on the order of 0.01 Å or less—even in the presence of hydrogen-bonding, metal–metal bonding, and electrostatic interactions. Starting from the structure models, the nature of chemical bonding in the molybdates is explained from molecular orbital theory and electronic structure calculations. The average Mo–Mo distance of 2.505 Å and diamagnetism in (1), (2) and (3) are attributed to a metal–metal bond order of unity along with a $1a^2 1e^4$ electronic ground state configuration for the $[\text{Mo}_3\text{O}_4\text{F}_9]$ cluster, leading to a rare trimeric spin singlet involving d^2 Mo^{4+} ions. The approach to structure solution and bonding analysis is a powerful strategy to understand the structures and chemical properties of complex fluorides and oxyfluorides.

1:45 PM CH02.12.05

New Atomistic Framework for Identifying, Optimizing and Extrapolating Structure-Property Relationships in Inorganic Solids Olivier C. Gagné¹ and Frank Hawthorne²; ¹Carnegie Institution for Science, United States; ²University of Manitoba, Canada

Growing interest in the design of functional materials with increasingly complex crystal structures calls for a more detailed understanding of structure-property relationships in inorganic solids. Whereby functional material properties are often linked to irregular bond distances, deciphering the causal mechanisms underlying bond-length variation, and the *extent* to which bond lengths vary in solids, has important implications in the design of new materials and the optimization of their functional properties.

Investigation of the relation between bond-length variation and the expression of functional material properties begins with systematization of chemical-bonding behavior via large-scale bond-length dispersion analysis. Completion of the largest bond-length dispersion analysis to date for inorganic solids (177,446 bond lengths hand-picked from 9210 crystal-structure refinements for oxides; 6,770 bond lengths from 720 crystal-structure refinements for nitrides; 33,626 bond lengths from 1832 crystal-structure refinements for chalcogenides) recently enabled straightforward identification of anomalous (i.e. irregular) bonding behavior for all ions of the periodic table observed bonding to O^{2-} , N^{3-} , and $\text{S}^{2-}/\text{Se}^{2-}/\text{Te}^{2-}$. In addition to comprehensive description of bond-length variations in inorganic solids, the large amount of data on anomalous coordination environments provided by this undertaking allows (1) conclusive resolution of the causal mechanisms underlying bond-length variation in inorganic solids, and (2) quantification of the extent to which these causal mechanisms result in bond-length variation.

In a sample of 266 highly irregular coordination polyhedra covering 85 transition-metal ion configurations bonded to O^{2-} , the most common cause of bond-length variation is observed to be *non-local bond-topological asymmetry* — a widely overlooked phenomenon whose associated bond-length variation results from asymmetric patterns of *a priori* bond valences — followed closely by the pseudo Jahn-Teller effect (PJTE). Two new indices, Δ_{topol} and Δ_{cryst} , calculated on the basis of crystallographic site, are proposed to quantify bond-length variation arising from bond-topological and crystallographic mechanisms in extended solids; Δ_{topol} is defined as the mean weighted deviation between the bond valences of a given polyhedron and that of its regular variant with equal bond lengths, while Δ_{cryst} similarly quantifies the difference between *a priori* and observed bond valences. Bond-topological mechanisms of bond-length variation are (1) non-local bond-topological asymmetry and (2) multiple-bond formation, while crystallographic mechanisms are (3) electronic effects (e.g. vibronic mixing, lone-pair stereoactivity), and (4) crystal-structure effects (e.g. structural strain).

Comprehensive bond-length dispersion analyses for inorganic nitrides and chalcogenides reveal several “phenomenological gaps” compared to their oxide counterparts, thus providing synthetic opportunities via the transposing of anomalously bonded coordination units bearing functional properties into new compositional and/or structural spaces. Resolving the contribution of (static) bond-topological *vs* (tunable) crystallographic mechanisms of bond-length variation via the Δ_{topol} and Δ_{cryst} indices, combined with their spatial resolution within the coordination polyhedron and unit cell, is proposed to quantify the *effective* tunable extent of a functional property for a given crystal structure, e.g. via alteration of the responsible coordination unit(s). The known extent for which bond-topological and crystallographic mechanisms materialize into bond-length variations, provided by large-scale bond-length dispersion analyses, guides optimization of these properties within the constraints of physically realistic crystal structures. Such information is essential to the design of new materials with (1) increasingly complex crystal structures, and (2) superior functional properties.

1:50 PM CH02.12.06

Photocatalytic Degradation of Lignin Using Gold Nanorod Immobilized TiO_2 Photoanode Under Mild Conditions Hai Nguyen¹, Shuya Li¹, Saerona Kim¹, Gyu Leem¹, Benjamin Sherman², Chang G. Yoo¹ and Jingshun Zhuang³; ¹SUNY College of Environmental Science and Forestry, United States; ²Texas Christian University, United States; ³The Michael M. Szwarc Polymer Research Institute, United States

Lignin is an alternative source of petroleum production, which consists of useful aromatic functional groups in lignocellulosic biomass. The aromatic-rich fraction in lignin is converted to biofuel through fermentation. Past studies have focused on lignin valorization under harsh conditions such as high temperature, pressure and/or additional oxidants. However, our research group has developed the dye-sensitized photoelectrochemical cells (DPECs) system for visible light induced lignin degradation at room temperature. Here, we introduce DSPECs incorporated with gold nanorods (Au NRs) for the application of lignin depolymerization. The Au NRs can be a promising candidate to increase the performance of the photocatalytic system and enhance light-harvesting efficiency. The Au NRs are immobilized to TiO_2 electrodes by using bifunctional L-glutathione (GSH) featuring dicarboxylic acid and thiol moieties. These moieties allow to anchor Au NRs to the surface of TiO_2 . The TiO_2 -based photoanode incorporates a surface-bound Au NRs-based photocatalyst and solution-dissolved nitroxyl mediators (e.g., 4-acetamido 2,2,6,6-tetramethylpiperidine-1-oxy) to perform solar-driven photocatalytic oxidation of the lignin model compounds under aerobic conditions with simulated solar illumination.

1:55 PM CH02.12.08

Phase Analysis of Titanium Oxide Nanoparticles by the Application of Attenuated Crystal Models on X-Ray Pair Distribution Functions Songsheng Tao¹, Jonas Billet², Jonathan De Roo³ and Simon J. Billinge^{1,4}; ¹Columbia University, United States; ²University of Ghent, Belgium; ³University of Basel, Switzerland; ⁴Brookhaven National Laboratory, United States

Metal oxide nanoparticles have a number of important technological applications in electronic devices. In particular, titanium(IV) oxide nanoparticles have potential applications in lithium ion batteries. A particular synthesis challenge with titanium(IV) oxide nanoparticles is that it has multiple possible structural phases. Differentiating between the various phases is particularly challenging when they are nanoparticles and it is crucial to be able to identify the structural phases of synthesized nanoparticles. Beyond knowing the phase distribution in the sample, it is also important to study crystallite sizes and shapes, as well as the presence of common defects, since these factors have an important impact on the functionalities. X-ray atomic pair distribution function (PDF) analysis is an important and powerful tool to use for this purpose because it reveals the local structure on nanometer length-scales, revealing quantitative information about the structural phase, particle morphology and defects in nanoparticulate materials, which is beyond the capability of traditional x-ray diffraction methods when the nanoparticles are small (< 10nm in diameter). One of the common methods for studying nanoparticles

using PDF analysis is to use attenuated crystal model (ACM) to test candidate structures and extract quantitative information about them. Given the growing importance of the PDF approach in nano-materials science and chemistry, we feel that it is helpful to the community to discuss the approach in a pedagogical way. Here we address a gap in the literature and present a detailed workflow for applying ACM in a robust and accurate way, using titanium(IV) oxide nanoparticles as an example. Using this approach we find that the nanoparticles contain the bronze phase as the major phase and the anatase phase as the minor phase, obtain the structural parameters of both phases, and that the particle sizes of the major phase are probably following a lognormal distribution. This work was supported by the U.S. Department of Energy, Office of Science, Office of Basic Energy Sciences (DOE-BES) under contract No. DE-SC0012704.

2:00 PM CH02.12.09

Strength and Toughness Variation in Transition Metal Carbides Due to Electronic Structure and Hybridization Jenny G. Ziegler, Katelyn Young and Zubaer M. Hossain; University of Delaware, United States

Ultra high temperature ceramics, or uhtc have various applications, especially in aircrafts and spacecrafts. They must have outstanding refractory properties at elevated temperatures. However a key limitation is in the toughness of these materials, which severely limits its applications. This is why they are used to make rocket engine nozzles and thermal barrier coatings. The most common example of a uhtc is silicon carbide, SiC. SiC is an important uhtc since it has a high melting temperature, high strength and is very lightweight. Yet it is still not perfect since it has low toughness like uhtcs. On the other hand many transition metal carbides have very low melting temperatures, but they are extremely tough. One of the key differences between transition metal carbides and SiC is the hybridization of the molecule. Using a combination of density function simulations and analytical analysis we examine the toughness, strength, Young's modulus of SiC with diamond-crystal structure and HfC, ZrC, TaC, TiC, VC, and NbC with rock-salt crystal structures under symmetry-preserving and symmetry-breaking deformations. In this presentation we will discuss how certain electronic structures and hybridizations create materials with variable toughness, young's modulus, and strength. By examining the patterns in electron redistribution we will see how the type of orbital (p,d,s) and hybridization (sp³, spd) affect the mechanical properties. By examining how mechanical properties are developed due to the electronic structure we can find alternatives or supplements to SiC. This new understanding will help us create better materials for nozzles of rockets and other elements of rockets.

2:05 PM *CH02.12.10

Reversible Sulfide Oxidation in Alkali-Rich Li-Ion Battery Cathodes Kimberly A. See; California Institute of Technology, United States

Current Li-ion batteries store charge by intercalation and deintercalation of Li⁺ into a host material such as a transition metal oxide. Capacities are typically limited to less than one equivalent of Li⁺ per transition metal and the charge compensation is largely localized on the transition metal. Utilizing the electronic states of the anions represents an interesting way to increase the Li⁺ that can be stored to reach so-called "Li-rich" regimes in which greater than one equivalent of Li⁺ is stored per transition metal. We will discuss a family of Li-rich sulfides that undergo reversible multi-electron redox involving both the transition metal (*M*) and the sulfide. Anion substitution allows us to tune the covalency of the M-anion bond, systematically control the voltage of anion oxidation, and control the distribution of electroactive atoms in the material during the charge. Anion oxidation causes interesting structural changes that will be discussed, along with the structure-property relationships that control anion oxidation reversibility.

2:35 PM CH02.12.11

Electronic Phase Segregation in the Hexagonal Perovskite Ba₃SrMo₂O₉ Struan Simpson and Abbie McLaughlin; University of Aberdeen, United Kingdom

Strongly correlated transition metal oxides are renowned for their ability to phase-segregate into multiple competing states with distinct electronic properties. Prominent examples include colossal magnetoresistant (CMR) manganites, where chemical disorder mediates segregation into ferromagnetic metallic and antiferromagnetic charge/orbital-ordered states¹. This phenomenon has drawn considerable attention in oxides containing 3*d* transition metals, yet reports are comparatively scarce for their 4*d*/5*d* counterparts.

In recent years, 6H-perovskites of the form Ba₃B'*M*₂O₉ (B' = rare earth, *M* = 4*d*/5*d* transition metal) have been investigated for their potential to exhibit spin-liquid ground states². This structure type is distinguished by bioctahedral M₂O₉ dimers; short distances between the *M* cations, combined with spatially diffuse 4*d*/5*d* orbitals, can facilitate the formation of quasi-molecular M₂O₉ clusters with spin-gapped excitations³. However, most Ba₃B'*M*₂O₉ compositions feature magnetic moments localised on the *M* cations so that the formation of quasi-molecular clusters is suppressed.

We have observed an unprecedented electronic phase segregation (EPS) in the new 6H-perovskite Ba₃SrMo₂O₉. This is the first report of a Ba₃B'*M*₂O₉ composition where *M* = Mo. Below 230 K, Ba₃SrMo₂O₉ segregates into two electronically distinct phases: a hexagonal P6₃/m phase consisting of weakly interacting Mo⁵⁺₂O₉ spin dimers, and a monoclinic P2₁/m phase containing a 50:50 mixture of quasi-molecular Mo⁵⁺₂O₉ clusters and localised Mo⁵⁺ spins. We propose this segregation has a unique origin related to competition between direct Mo–Mo bonding and Mo–O–Mo superexchange. In contrast to established electronic materials like CMR manganites, EPS appears to manifest without the aid of charge order or chemical disorder. Accordingly, Ba₃SrMo₂O₉ comprises a seemingly unique electronic material.

References

- [1] Y. Zhu *et al.*, *Nat. Commun.*, 2016, **7**, 11260.
- [2] A. Nag *et al.*, *Phys. Rev. Lett.*, 2016, **116**, 097205.
- [3] S. A. J. Kimber *et al.*, *Phys. Rev. Lett.*, 2012, **108**, 217205.

2:50 PM CH02.12.12

Unravelling the Effect of Superficial Rh Depletion on Shallow d-States of Gallium-Rhodium Liquid Metal Alloys Tzung-En Hsieh¹, Haiko Wittkämper², Johannes Frisch^{1,3}, Mihaela Gorgoi^{1,3}, Regan Wilks^{1,3}, Christian Papp² and Marcus Baer^{1,2,4}; ¹Helmholtz-Zentrum Berlin für Materialien und Energie GmbH (HZB), Germany; ²Friedrich-Alexander Universität Erlangen-Nürnberg (FAU), Germany; ³Helmholtz-Zentrum Berlin für Materialien und Energie GmbH, Germany; ⁴Helmholtz Institute for Renewable Energy (HI ERN), Germany

In this study, we report on the investigation of the electronic and chemical structure of supported GaRh alloys as model systems for the active phase in Supported Catalytically Active Liquid Metal Solutions (SCALMS). SCALMS is a novel class of single atom catalysts comprised of a liquid metal matrix and a diluted catalytically active transition metal. We prepared a series of gallium-rhodium samples with different Ga/Rh molar ratios and tracked the evolution of the surface electronic structure decreasing Rh concentration (from 100 % to 1 %). We employed Photoemission Spectroscopy (PES) to probe the shallow core levels of the top layers of the GaRh alloys. Our results reveal a narrowing of the rhodium 4d-band and the formation of Ga-Rh intermetallic compounds (IMCs). Furthermore, we discuss annealing and surface oxidation effects. We observe the dissolution of GaRh IMCs during

annealing and the incorporation of Rh into the formed gallium oxide (GaO_x) layers as a result of surface oxidation. These results contribute to a more fundamental understanding of the valence band structure of GaRh SCALMS and its relation to the catalytic reactivity.

SESSION CH02.13: Physical Properties of Inorganic Solids III
Session Chairs: Hiroshi Kageyama and Brent Melot
Monday Afternoon, December 6, 2021
CH02-Virtual

9:00 PM *CH02.13.01

Cyanide-Anion Based Dynamic Solid-State Materials Ryo Ohtani; Kyushu university, Japan

Our group investigates new materials synthesized by the anionic four-coordinate/penta-coordinate molecules with cyanides as building units, combined with various metal ions or organic cations. They often exhibit interesting dynamic structural characteristics such as thermal expansion and melting. Recently, we synthesized a cyanide-bridged three-dimensional framework FePd(CN)₄ incorporating four-coordinate iron(II) ions. FePd(CN)₄ was synthesized by a thermal treatment to remove waters from a two-dimensional six-coordinate iron(II) coordination polymer Fe(H₂O)₂Pd(CN)₄·4H₂O. FePd(CN)₄ consists of a two-fold interpenetrated PtS topology three-dimensional structure where four-coordinate iron(II) ions has intermediate geometry between tetrahedral and square planar geometries. FePd(CN)₄ exhibits large anisotropic thermal expansion behavior including uniaxial colossal TE and negative 2D-TE. Moreover, we are also focusing on the penta-coordinate mixed-anion units to construct polar skeletons. Such compounds achieved a characteristic polarity switching via anion manipulation along polar axis in crystals.

9:30 PM *CH02.13.02

New Mixed-Anion Semiconductor Photocatalysts for Visible-Light-Induced Water Splitting Ryu Abe; Kyoto University, Japan

Photo-induced water splitting using semiconductor photocatalysts has attracted considerable attention for producing H₂ as a clean energy carrier, while the effective utilization of visible light is imperative to achieve the desired efficiency for practical applications.[1] Various mixed-anion compounds such as oxynitrides, oxysulfides, and oxyhalides have been extensively studied as promising photocatalysts for visible light-induced water splitting, because their valence band maximum (VBM) values are generally more negative than those of conventional oxides, due to the significant contribution of high-energy p orbitals of the non-oxide anions (e.g., N-2p, S-3p, Br-4p, and I-5p) mixed with O-2p. Some tantalum oxynitrides (TaON and BaTaO₂N) have been successfully employed as a H₂-evolving photocatalyst in Z-scheme water splitting systems, combined with another O₂-evolving photocatalyst such as WO₃. [2] However, most of mixed-anion compounds suffer from facile self-oxidative deactivation of non-oxide anions by photogenerated holes, thereby imposing surface modifications such as loading some cocatalysts to circumvent the oxidative deactivation. For example, we have demonstrated that the loading of IrO₂ or CoOx nanoparticles as a cocatalyst for water oxidation on such oxynitrides suppress the self-oxidative deactivation to some extent, and thus enable us to employ such surface modified (oxy)nitrides (TaON and Ta₃N₅) as O₂-evolving photocatalysts in Z-scheme systems with (IO₃⁻/I⁻) redox. [2] Such surface modification has been proven effective for the fabrication of (oxy)nitride-based photoanode. The porous tantalum oxynitrides (TaON or BaTaO₂N) electrode prepared on conducting substrates showed relatively stable O₂ evolution with significantly high quantum efficiency in an aqueous solution, after loading of effective cocatalyst nanoparticles for water oxidation. [3,4]

We have recently demonstrated that Sillén–Aurivillius type perovskite oxyhalides such as Bi₄NbO₈Cl can stably and efficiently oxidize water to O₂ under visible light without any surface modifications, and also exhibits a stable Z-scheme water splitting [5] when coupled with a H₂-evolving photocatalyst. [4] It was revealed that the VBMs of these materials consist mainly of O-2p orbitals, instead of Cl-3p (or Br-4p), but their positions CBMs are much more negative than those of conventional oxides. Thus, they possess narrow bandgaps for visible light absorption as well as sufficiently negative CBMs for water reduction. DFT calculation visualized a fairly strong hybridization between the Bi-6s and O-2p orbitals, which can explain why the O-2p orbitals are elevated in energy, combined with the result on Madelung site potential analysis that can rationalize the origin of high energy of O-2p orbital in these materials. [6, 7] Since O⁻ anions are known to be relatively stable, photogenerated holes populated at the O-2p orbitals will not lead to self-decomposition but to oxidize water. These results could provide new strategies for developing durable materials for water splitting under visible light, by manipulating the interaction between post-transition metal s orbitals and O-2p orbitals.

[1] R. Abe, J. Photochem. Photobiol. C: Photochem. Rev. 2011, 11, 179.

[2] R. Abe, J. Tang et al. Chem. Rev. 2018, 118, 5201.

[3] M. Higashi, K. Domen, R. Abe, J. Am. Chem. Soc. 2012, 134, 6968.

[4] M. Higashi, K. Domen, R. Abe, J. Am. Chem. Soc. 2013, 135, 10238.

[5] H. Fujito, H. Kunioku, H. Kageyama, R. Abe et al., J. Am. Chem. Soc. 2016, 38, 2082.

[6] D. Kato, H. Kunioku, R. Abe, H. Kageyama et al. J. Am. Chem. Soc. 2017, 139, 18725.

[7] H. Kunioku, H. Kageyama, R. Abe et al., J. Mater. Chem. A 2018, 6, 3100.

10:00 PM CH02.13.03

Crystal Structure and Electronic Properties of Cation-Ordered Non-Cubic Pentavalent Fullerides Keisuke Matsui and Kosmas Prassides; Osaka Prefecture University, Japan

Metal fullerides are molecule-based strongly correlated electron systems, whose properties can be tuned by both changes in bandfilling and bandwidth (or equivalently interfullerene separation). The electronic properties of trivalent cubic fullerides, A₃C₆₀ (A = alkali metal) vary with lattice volume, resulting in a dome-shaped superconducting transition temperature (*T_c*) dependence adjacent to an antiferromagnetic (AFM) insulating phase - fingerprint of strong electron correlations. As evidenced by the maximum *T_c* ~ 38 K (highest among molecular superconductors) and upper critical magnetic field *H_{c2}* ~ 90 T (highest among isotropic superconductors), fullerene is a unique materials platform in condensed matter physics. The flexible volume tunability of fullerides by chemical/physical means has inspired the search for possible emergence of superconductivity at other bandfillings. Indeed, there are superconducting fullerides in octavalent (Ba₄C₆₀, *T_c* ~ 7.7 K) and nonavalent (A₃Ba₃C₆₀, *T_c* ≤ 6 K) materials in which the Fermi level lies in the *t_{1g}* (LUMO+1)-derived band.

The properties of pentavalent fullerides M₂AC₆₀ (M = divalent cation) have not been explored systematically although some theories do suggest the emergence of superconductivity. Two decades ago, studies showed that non-superconducting Ba₂AC₆₀ (A = K, Rb, Cs) [1, 2] form a cation-ordered face-centered-cubic (*fcc*) structure, in which Ba²⁺ and A⁺ ions occupy small tetrahedral and large octahedral holes, respectively. In particular, there was little change in the lattice volume with changing the A⁺ ion (= K, Rb, Cs) size in Ba₂AC₆₀ because the octahedral holes are of a much larger size (~ 2.06 Å) than

that of the A^+ ions (e.g. $Cs^+ \sim 1.67 \text{ \AA}$). Therefore, substituting the tightly-packed Ba^{2+} ion in the small tetrahedral hole ($\sim 1.14 \text{ \AA}$) with other divalent cations may allow access to unexplored regions in the pentavalent fulleride phase field. Here we present our recent work on the families of ternary fullerides, M_2AC_{60} ($M = \text{alkaline-earth or rare-earth metal}$). We have successfully prepared cation-ordered M_2AC_{60} phases via solid-state synthesis, systematically varying both M^{2+} and A^+ ions. Interestingly, X-ray diffraction profiles show that smaller M^{2+} ions lead to non-cubic crystal structures (orthorhombic) in which the M^{2+} ions are shifted to off-centered positions, in contrast to isoelectronic *fcc*- Ba_2AC_{60} . Both the reduction in symmetry and the pentavalent character of the fulleride units are confirmed by Raman spectroscopy. The electronic properties of the materials have been studied by SQUID magnetometry, and EPR and NMR spectroscopy. Complementary synchrotron X-ray absorption studies reveal intriguing mixed valence behavior in the rare-earth fulleride systems.

[1] A. C. Duggan *et al.*, *Chem. Commun.* **10**, 1191-1192 (1996)

[2] T. Yildirim *et al.*, *Phys. Rev. B* **54**, 11981-11984 (1996)

10:05 PM CH02.13.04

First-Principles Analysis on Electronic Structure of 10H Long-Period Stacking Ordered Phases in Mg-Zn-Y Alloys Riku Sato¹, Shinya Ogane¹, Kazumasa Tsutsui², Yuta Tanaka² and Koji Moriguchi^{1,2}; ¹Tohoku University, Japan; ²Nippon Steel Corporation, Japan

Since the functionalities of materials usually originate from the spatial inhomogeneity in the associated systems, the local inhomogeneities such as defect, surface, interface, and nanostructure often play an important role for developing sophisticated materials. In this paper, among the many phenomena related to inhomogeneity in materials, we will report our computational research on the modulation of electronic structure by the solute elements for the long period stacking ordered (LPSO) phases.

In 2001, Kawamura *et al.* have developed a novel $Mg_{97}Zn_1Y_2$ (at. %) alloy using rapidly solidified powder metallurgy processing [1]. It has extremely high tensile yield strength of 610 MPa and elongation of 5% mechanical strength at room temperature. After that, other high-strength Mg alloys have been reported one after another [2-5] which alloys are usually composed of Mg, transition metal (TM) elements, and rare earth (RE) ones. It has also been reported that the reinforced phases in these Mg alloys contain stacking faults (SF) with long periodicity along the *c*-axis, and solute elements of TM and RE segregate into these SF regions [1-5]. Since the structural modulation and the chemical modulation are experimentally confirmed to be synchronized in the reinforced phases, the associated phases in these Mg alloys are called the synchronized long period stacking ordered (LPSO) phases.

Some investigations on the thermodynamic stability for LPSO phases have also been reported so far [6-8]. Egami *et al.* have recently examined the thermodynamic behaviors of dilute Mg-Zn-Y ternary alloys to form a unique solute-enriched stacking-fault based on the calculation of phase diagrams (CALPHAD) method along with the first-principles analyses [8]. They have found that the co-segregations of Zn and Y solute elements at the stacking faults make the fault layers more stable than the hcp-Mg matrix-base configuration. Furthermore, within the stacking faults, spinodal-like decomposition into the Mg-rich solid-solution and the Zn/Y-rich L12-type order phase is also reported to cause a significant reduction of the total Gibbs energy of the system. These results based on the CALPHAD method stimulate our curiosity as to how alloying elements associated bring about the changes of atomistic interactions in the LPSO structures.

We have presented the theoretical studies on the energetics of metallic polytypes including the LPSO structures from the viewpoint of interlayer interactions [9, 10]. Our theoretical analyses have suggested that the relatively long-distance interatomic interaction is a significant factor for the energetic stabilization of the LPSO composed of the close-packed structures [10]. Since the phase stability is generally determined by the electronic states, the associated electronic structure can provide a more basic knowledge on the thermodynamic phase stability for the LPSO phases. In the present work, comparative studies are carried out on the electronic structure of $Mg_{92}Zn_{12}Y_{16}$, $Mg_{108}Zn_{12}$, $Mg_{104}Y_{16}$, and Mg_{120} with two and/or ten stacking layers based on first-principles calculations within the density functional theory. In our presentation, we will discuss the correlation between the modulation of electronic structure by Zn and Y solute elements and the phase stability of the LPSO-Mg structures.

[1] Y. Kawamura *et al.*, *Mater. Trans.* **42** (2001) 1172-1176.

[2] S. Yoshimoto *et al.*, *Mater. Trans.* **47** (2006) 959-965.

[3] Y. Kawamura *et al.*, *Scr. Mater.* **55** (2006) 453-456.

[4] T. Homma *et al.*, *Scr. Mater.* **61** (2009) 644-647.

[5] S. Izumi *et al.*, *Mater. Sci. Forum* **654-656** (2010) 767-770.

[6] A. Datta *et al.*, *Acta. Mater.* **56** (2008) 2531-2539

[7] S. Iikubo *et al.*, *Phys. Rev. B* **86** (2012) 054105

[8] M. Egami *et al.*, *Mater. Des.* **188** (2020) 108452.

[9] K. Moriguchi *et al.*, *MRS Advances* **6**, 163-169 (2021).

[10] S. Ogane and K. Moriguchi, *MRS Advances* **6**, 170-175 (2021).

10:10 PM CH02.13.05

Development of an EAM Type Potential with a Long-Range Cutoff Radius for Describing Metallic Polytype Energetics Shinya Ogane¹, Riku Sato¹, Yuta Tanaka², Kazumasa Tsutsui² and Koji Moriguchi¹; ¹Tohoku University, Japan; ²Nippon Steel Corporation, Japan

The Kepler conjecture in 1611 states that no arrangement of equally sized spheres filling space has a greater average density than that of the face-centered cubic and/or hexagonal close packing arrangements [1]. This conjecture has been only recently proved by the Flyspeck project team [2]. The polytypes are characterized by a stacking order with a given repeating unit along a directional axis and are theoretically possible to have endless permutations of the sequences. The close-packed (CP) polytypes in which the associated stacking is composed of the CP planes are, therefore, considered to be the crystalline systems realizing the Kepler conjecture. Significant changes in physical properties due to the intentional polytype formation have also been reported in various fields of metallic and semiconductive systems [3-5].

Predicting polytype phase stability for a material has still been a long-standing issue in condensed matter physics and/or materials science [6, 7]. This situation stems from the fact that the atomistic interactions on polytype energetics might be quite complex and delicate despite the simplicity of their geometrical structure. We have recently presented a theoretical consideration on the CP polytype total energetics using the geometrical analysis for the correlation between interlayer interactions and interatomic ones [8]. These results suggest that short-range interactions are not enough to describe the CP polytype energetics and provide significant insights for creating interatomic models successfully showing the polytypes other than 3C and 2H structures as a ground state, those have never yet been implemented as far as the authors know.

Since the ground state for metallic lanthanum (La) is the double hexagonal CP structure (DHCP), the La can be an important reference system for studying polytype formation mechanism. It is, therefore, possible to investigate the essential factors determining the polytype selection rule through the dynamical analyses for metallic La. In the present work, we report on the process of constructing an interatomic potential for metallic La, that can be used for molecular dynamics (MD) simulations. The Embedded Atom Method (EAM) type functions reported by Mishin *et al.* [9] are adopted for constructing the numerical potential model in this study. Since our previous theoretical studies have shown that the long-range nature of interactions is an important factor for determining the ground state of polytype [7, 8], the cutoff radius has been carefully selected considering the computational cost.

Our interatomic potential can well describe the total energy vs. volume curves for various crystal structures and the Bain path energetics along the fcc-bcc

structures deduced by the first-principles calculations. This potential is, therefore, an interaction model for metallic polytypes that can describe not only the energetics but also the lattice dynamics such as lattice dynamical instability, which is generally significant for the phase transition phenomena [10, 11]. Our research is at the stage of working on MD analyses for the polytype formation mechanism using this potential. In the presentation, other basic properties, transferability of the potential constructed, and some results of the MD analyses will be also discussed.

- [1] J. Kepler, *The Six-Cornered Snowflake*, 1966 translation by C. Hardie (Clarendon Press, Oxford, 1611), ISBN: 0198712499.
- [2] T. C. Hales et al., *Forum of Mathematics*, Pi, 5, E2 (2017).
- [3] E. M. T. Fadaly et al., *Nature*, 580, 205 (2020).
- [4] Z. Fan et al., *Nat. Commun.* 6, 7684 (2015).
- [5] E. Abe et al. *Philos. Mag. Lett.* 91, 690 (2011).
- [6] C. H. Loach et al., *Phys. Rev. Lett.* 119, 205701 (2017).
- [7] K. Moriguchi et al., *MRS Advances* 6, 163 (2021).
- [8] S. Ogane and K. Moriguchi, *MRS Advances* 6, 170 (2021).
- [9] Y. Mishin et al., *Phys. Rev. B* 59, 3393(1999).
- [10] K Moriguchi and M Igarashi, *Phys. Rev. B* 74, 024111 (2006).
- [11] G. Grimvall et al., *Rev. Mod. Phys.* 84, 945 (2012).

10:15 PM CH02.13.06

Atomic-Scale Observation of Electrostatic Origin Octahedral Distortion in Ruddlesden-Popper Phases [Youngjae Hong](#) and Sung-Yoon Chung; Korea Advanced Institute of Science and Technology, Korea (the Republic of)

Precise identification of the distortion, tilt, and rotation of octahedra is an essential step toward understanding the structure-property correlation in view of the fact that the physical properties of ABX_3 perovskite-based oxides strongly depend on the geometry of oxygen octahedra containing B site cations. In this work, we find out a crucial electrostatic origin responsible for Jahn-Teller-type tetragonal elongation of oxygen octahedra during atomic-level direct observation of two-dimensional [AX] interleaved shear faults in five different perovskite-type materials. When the [AX] sublayer has a net charge, for instance $[LaO]^+$ in $LaNiO_3$, significant tetragonal elongation of oxygen octahedra at the fault plane is observed and it blocks the strong repulsion between the consecutive $[LaO]^+$ layers. Moreover, our findings on the distortion induced by local charge are identified to be a striking common feature in $A_{n+1}B_nX_{3n+1}$ -type Ruddlesden-Popper structure with charged [AX] sublayers. This study thus demonstrates that electrostatic origin local charge is a crucial factor significantly affecting the crystal structure of complex oxides.

10:20 PM CH02.13.07

Late News: Gap-State Engineering for Enhanced Ferroelectric Photovoltaic Effect Under Visible Light Irradiation [Hiroki Matsuo](#) and Yuji Noguchi; Kumamoto University, Japan

Ferroelectric materials exhibit the characteristic photovoltaic (PV) effect that can generate photovoltage far exceeding their bandgap energy (E_g)^[1]. The ferroelectric photovoltaic (FPV) effect arises from polarization-driven carrier separation under light irradiation and the absence of limitation in the photovoltage by the bandgap is a great advantage of the FPV effect over the conventional PV effect in $p-n$ junctions of semiconductors. Since typical ferroelectric oxides have wide bandgap, a vanishingly small photoresponse under visible light has been an issue to be overcome. Though bandgap tuning can partly improve the photoresponse, narrowing of the bandgap is, in principle, accompanied by a substantial loss of ferroelectric polarization. In this study, to enhance the visible-light activity of the ferroelectric materials without sacrificing the ferroelectric polarization, we propose an approach, 'gap-state' engineering, in which defect states within the bandgap act as a stepping stone for photocarrier generation^[2,3]. We investigate the FPV effect in ferroelectric $BiFeO_3$ (BFO) epitaxial thin films doped with various transition metals (TMs). Impact of the TM doping on electronic structures and the PV response were investigated by combined analysis using the density functional theory (DFT) calculations and experimental measurements for the TM-doped BFO epitaxial thin films.

The DFT calculations revealed that substitution of Mn^{3+} for Fe^{3+} generates doubly degenerated half occupied defect level derived from $Mn-3d$ orbitals within the bandgap of BFO. The defect level i.e., gap states, locates at 0.8 eV above the valence band maximum, which corresponds to 1.9 eV below the conduction band minimum. Experimental analyses of the PV properties were performed for epitaxial thin films of undoped BFO and 5% Mn-doped BFO (BFMO) with a single domain structure prepared by the pulsed-laser deposition (PLD). We found that both the photocurrent density and the photovoltage were markedly enhanced by the introduction of small amount of Mn especially under illumination with photon energy lower than E_g . These results present that the gap states formed within the bandgap enables two-photon excitation and provides the enhanced PV response over a broad spectral range. This approach utilizing the gap states will be promising route to the development of visible-light-active ferroelectrics without sacrificing the ferroelectric polarization.

- [1] A. M. Glass et al., *Appl. Phys. Lett.*, **25**, 233 (1974).
- [2] H. Matsuo et al., *Nat. Commun.*, **8**, 207 (2017).
- [3] Y. Noguchi et al., *Nat. Commun.*, **11**, 966 (2020).

10:25 PM CH02.13.08

Atomic-Scale Direct Observation of Pre-Melting of RP Faults in Perovskite Oxide System [Ji-Sang An](#) and Sung-Yoon Chung; Korea Advanced Institute of Science and Technology, Korea (the Republic of)

Melting is a common phenomenon in our daily life and it is fundamental to daily life, basic science and technology. Therefore, understanding and controlling the melting phenomenon becomes important in various disciplines. In particular, pre-melting which occurs below the melting temperature has been studied for in-depth understanding of melting and numerous studies have shown that pre-melting usually occurs in 2-dimensional defects like surface, grain boundaries and dislocations. In this study, using atomic-scale direct observation of scanning transmission electron microscopy (STEM) and acceptor doped $BaCeO_3$ as model system, pre-melting phenomena also can occur in Ruddlesden Popper (RP) faults in ABO_3 type perovskite oxide. Chemical composition analysis and STEM images demonstrate that the amorphous phase is the RP-mediated liquid phase and as sintering temperature goes up, the thickness of amorphous phase in RP faults getting thick. And with electron beam irradiation, re-crystallization of the amorphous layer can occur. To the best of our knowledge, the present study demonstrates for the first time ever observation of pre-melting in RP faults providing a broader academic depth to pre-melting or melting.

10:30 PM *CH02.13.09

Discovery of Two-Dimensional van der Waals Materials and Topological Dirac Semimetal in the Class of ABC Zintl Phases [Sung Wng Kim](#); Sungkyunkwan university, Korea (the Republic of)

The discovery of new families of two-dimensional (2D) van der Waals (vdW) layered materials has always attracted great attention to pursue beyond

graphene. It has been challenging to artificially develop the van der Waals bonded layer structure that is constructed by the stacking of honeycomb atomic lattice composed of two elements as in hexagonal boron nitride. In this talk, a new class of 2D vdW materials, layered Zintl phases will be introduced. These new 2D layered Zintl phases can allow unlimited extent of 2D science in terms of the diversity of materials and their physical properties. A new class of 2D materials was developed from a 3D structured material that has (1) a multicomponent system, (2) primary atomic bonds in three-dimensionality, (3) thermodynamic and chemical stability, and (4) diversity in chemical compositions. Through the dimensional manipulation of crystal structure, we create an unprecedented 2D vdW zinc antimonide (2D-ZnSb), which is the layered Zintl phase with sp^2 -hybridized bonding characters in Zn-Sb honeycomb atomic layers [1]. The vdW layered structure of 2D-ZnSb is evolved by selectively etching the lithium cations from the layered LiZnSb Zintl phase that is formulated by alloying the lithium atoms into sp^3 -hybridized bonded three-dimensional ZnSb (3D-ZnSb), demonstrating the bidimensional polymorphism of 3D- and 2D-ZnSb. Finally, the recent experimental and theoretical studies on diverse physical properties obtained in the new 2D materials will be discussed with the focus on the three-dimensional topological Dirac semimetal of KZnBi compound [2].

[1] J. S. Song et al., *Sci. Adv.* 2019;5 : eaax0390.

[2] J.S. Song et al., *Phys. Rev. X*, online published, <https://journals.aps.org/prx/accepted/7b077K0c12f1550f853344b9421091d5157265e34>

SESSION CH02.14: Physical Properties of Inorganic Solids IV
 Session Chairs: Amparo Fuertes and Hiroshi Kageyama
 Tuesday Morning, December 7, 2021
 CH02-Virtual

8:00 AM *CH02.14.01

Design and Topochemical Synthesis of Metastable (oxy-)Chalcogenide Materials Laurent Cario, Shunsuke Sasaki, Louis Béni Mvélé, Catherine Guillot-Deudon, Maria Teresa Caldes, Isabelle Braems, Benoit Corraze, Etienne Janod and Stephane Jobic; CNRS, Université de Nantes, France

Layered transition metal compounds have been extensively investigated due to their unconventional electronic/magnetic properties. Topochemical reactions, which introduce/withdraw ions into/from host materials retaining their lamellar structures, serve as one of the most effective tools to design such low-dimensional materials. Despite their huge advances during the recent decade, most of topochemical reactions rely on redox activities of transition metal cations in host lattices so that their charge balance are respected throughout the process. Conversely the redox activity of molecular anions for topochemical syntheses remains almost unexplored. This study demonstrates the topochemical reaction of layered polychalcogenides or oxychalcogenides containing pre-formed (Sn)₂ (n=2,3) oligomers with transition metals or alkali metals to form (metastable) layered compounds at low temperature [1,2,3]. Structure prediction calculations and advanced electron microscopy techniques confirms that depending on the metal nature the reaction with the oligomers lead either to the intercalation of the metallic species [1,2], or to the deintercalation of part of the chalcogen atoms [3]. This study paves therefore the way to the design of (oxy-)chalcogenide compounds with interesting potential applications.

[1] S. Sasaki, D. Driss, E. Grange, J.-Y. Mevellec, M. T. Caldes, C. G.-Deudon, S. Cadars, B. Corraze, E. Janod, S. Jobic, L. Cario, *Angew. Chem. Int. Ed.*, 57, 13618-13623 (2018).

[2] S. Sasaki, M. Lesault, E. Grange, E. Janod, B. Corraze, S. Cadars, M. Teresa Caldes, C. Guillot-Deudon, S. Jobic, L. Cario, *Chemical Communications* 55, 6189 (2019).

[3] S. Sasaki, M. T. Caldes, C. Guillot-Deudon, I. Braems, G. Steciuk, L. Palatinus, E. Gautron, G. Frapper, E. Janod, B. Corraze, S. Jobic, L. Cario, *Nat. Commun.* 12, 3605 (2021).

8:30 AM *CH02.14.02

Divalent Magnetic Cations to Generate Magnetoelectric Properties in Corundum-Derived Structures Antoine Maignan^{1,2}, Christine Martin^{1,2} and Françoise Damay^{1,3}, ¹CNRS, France; ²crismat, France; ³CEA, France

Several ways can be used to achieve magnetoelectric (ME) effects [1 and references herein] such as strain-mediated coupling between ferroelectric and (anti)ferromagnetic composites, compounds hosting both d^0 ferroelectricity and $4f$ or d^0 magnetism and lone-pair cation (such as BiFeO₃ [2]). In general, for the latter, the electric polarization is large but the ME coupling weak. Another class of multiferroics (MF), also called spin-induced MF, gathers the $3d^0$ magnetic compounds whose magnetic symmetry breaks both space-inversion and time-reversal. These type-II MFs are very often compounds exhibiting large ME coupling. Searching for large ME coupling, the linear ME (LME) compounds are also attracting as a third class of ME. Though these centrosymmetric compounds are not MF, a magnetic field application induces a polarization, with P proportional to H, as the prototype α -Cr₂O₃ corundum [3,4].

For solid state chemists, this structural type forms a very broad field to play with, as illustrated for instance by the numerous isomorphous transition metal niobates and tantalates of composition M₄A₂O₉ (429), with M a divalent cation (M = Co, Fe, Mn) [5]. Recent re-investigations of Co₄Nb₂O₉ magnetic structure [6-8], a LME exhibiting one of the largest ME coefficient (≈ 30 ps/m [6]), triggered a surge of interest for these M₄A₂O₉ crystallizing in a trigonal structure (SG: *P*-3c1) and which magnetic structure is still a matter of debate [5-8].

Among the 429, solely cobalt and manganese niobates and tantalates were known to be LME till 2018 [9-12], after which the Fe₄Nb₂O₉ [13] and Fe₄Ta₂O₉ [14-15] ME were reported. From the synthesis side, these oxides containing divalent iron are difficult to prepare as pure phases.

Interestingly, there exist M_{4-x}M'_xA₂O₉ solubility ranges, involving a careful control of the (PO₂,T) synthesis conditions depending on M and M' and on x, which open the route to produce new LME and ME behaviours. In particular, to exacerbate the P response to H, the M/M' magnetic cations disorder can be exploited to modify the magnetization H dependence. The preliminary results obtained by mixing divalent Fe and Co have allowed us to produce a much steeper P(H) dependence, the Fe₂Co₂Nb₂O₉ compound exhibiting ME properties overpassing those of the Co₄Nb₂O₉ and Fe₄Nb₂O₉ end members.

On the opposite, considering that Ni₄Nb₂O₉ is orthorhombic, ferrimagnetic and not ME [16], the Ni solubility in M_{4-x}Ni_xNb₂O₉ with M=Co or Fe has been investigated. These magnetic substitutions by Co or Ni are now compared to those by diamagnetic ones.

The synthesis, characterizations of the crystal/magnetic structures and magneto(di)electric properties of several such corundum - derived compounds, including Mn₃WO₆ [17], will be presented to illustrate the richness of these systems to generate new (L)ME candidates.

[1] N. A. Spaldin et al., *Nature Materials* **18**, 203–212 (2019).

[2] J. Wang et al., *Science* **29**, 1719-1722 (2003).

[3] I. E. Dzyaloshinskii, *Zh. Eksp. Teor. Fiz.* **37**, 881 (1959).

[4] D.N. Astrov, *Zh. Eksp. Teor. Fiz.* **38**, 984 (1960).

[5] E. F. Bertaut et al., *J. Phys. Chem. Solids* **21**, 234 (1961).

- [6] N. D. Khanh et al., *Phys. Rev. B* **93**, 075117 (2016).
 [7] N. D. Khanh et al., *Phys. Rev. B* **96**, 094434 (2017).
 [8] G. Deng et al., *Phys. Rev. B* **97**, 085154 (2018).
 [9] Y. M. Cao et al., *Scientific Reports* **7**, 14079 (2017).
 [10] N. D. Khan et al., *Applied Physics Letters* **114**, 102905 (2019).
 [11] B. B. Liu et al., *Materials Letters* **164**, 425 (2016).
 [12] N. Narayanan et al., *Physical Review B* **98**, 134438 (2018).
 [13] A. Maignan et al., *Physical Review B* **97**, 161106 (2018).
 [14] A. Maignan et al., *Physical Review Materials* **2**, 091401 (2018).
 [15] S. N. Panja et al., *Physical Review B* **98**, 024410 (2018).
 [16] E. Tailleux et al., *J. of Appl. Phys.* **127**, 063902 (2020).
 [17] A. Maignan et al., *Chem. Mater.* **32**, 5664 (2020).

9:00 AM CH02.14.03

Spectroscopic and First Principles Characterization of Electronic, Optical and Defect Properties of P-Type CuBi₂O₄ Sebastian E. Reyes-Lillo¹, Zemin Zhang² and Jason K. Cooper³; ¹Universidad Andres Bello, Chile; ²Lanzhou University, China; ³Lawrence Berkeley National Laboratory, United States

CuBi₂O₄ is an emerging p-type semiconductor for applications as a photocathode in photoelectrochemical (PEC) solar fuel production. Recently, we have examined p-CuBi₂O₄ thin films with a comprehensive spectroscopic and first principles characterization methodology to describe its fundamental electronic and optical properties while addressing intrinsic limitations in the observed PEC performance [1]. In this talk, connections will be established between electronic structure, optical properties, and PEC performance through a combination of X-ray spectroscopies (X-ray absorption spectroscopy, X-ray emission spectroscopy, and resonant inelastic X-ray scattering) and density functional theory (DFT) based modeling. The results provide the basis for the understanding of the observed polaron limitations in CuBi₂O₄. In addition, we investigate the presence and working mechanism of natural defects, through experimental and first principles approaches. Two main types of defects, oxygen vacancies and hydrogen impurities, are found in CuBi₂O₄ thin films with a high level. Our DFT results show that oxygen and hydrogen defects act as donor impurities, and therefore, their suppression increases the carrier density and enhance the performance of CuBi₂O₄. Our work aims at broadening the understanding of materials governed by polaronic limitations as well as the investigation of defects in p-type metal oxide semiconductors to further advance their application in solar-fuels generating systems.

References:

- [1] Cooper *et al.*, *Chem. Mater.* **33**, 934 (2021).

9:05 AM CH02.14.04

Impact of Surface Area on Capacity Retention in the LiNi_{0.5}Mn_{0.5-x}Co_xO₂ (x = 0.1 - 0.3) Series—Tradeoffs from the Ni²⁺/Ni³⁺ Ratio Rajalakshmi Senthil Arumugam, Ramesh Shunmugasundaram and Vanessa Wood; ETH Zürich, Switzerland

The most commonly used cathode materials in Li-ion batteries are layered lithium metal oxides (LiTMO₂, TM = transition metal ion) due to their large theoretical capacities (~280 mAh/g).^[1] Among the layered cathode materials, lithium nickel manganese cobalt oxides (Li(Ni_xMn_yCo_{1-x-y})O₂ or NMC) exhibit promising electrochemical properties, which primarily depends on the atomic composition of Ni, Mn and Co in the structure.^[2] Several NMC compositions such as NMC 111, 442, 532, 622 and 811 (the three numbers denote the ratio of Ni to Mn to Co) have been studied extensively. This study systematically studies the effect of TM ratio on the electrochemical behavior of cathode materials and why these particular TM ratios have emerged to be of highest commercial interest.

To do so, this study focuses on cathode material compositions in the series LiNi_{0.5}Mn_{0.5-x}Co_xO₂ (0 ≤ x ≤ 0.3) that includes LiNi_{0.5}Mn_{0.5}Co_{0.2}O₂ or NMC 532. Three cathode materials NMC 541, NMC 532 and NMC 523 were synthesized by systematically varying the concentrations of Mn and Co but keeping the Ni content constant. This systematic variation in atomic percentages of Mn and Co leads to different Ni²⁺ to Ni³⁺ ratios (4:1 for NMC 541, 3:2 for NMC 532, and 2:3 for NMC 523). For each composition, two morphological variants with different surface areas were made. The compounds were structurally and electrochemically characterized. The results of this study show that NMC 532 achieves a balance between a larger number of antisite defects with increasing Ni²⁺ (e.g. NMC 541) and the higher surface reactivity found with increasing Ni³⁺ (e.g., NMC 523), both of which lead to capacity fade. This explains why NMC 532 is the highest performing material in the LiNi_{0.5}Mn_{0.5-x}Co_xO₂ series.

References:

- [1]. C. M. Julien, A. Mauger, K. Zaghib, H. Groult, *Inorganics*. **2** (2014) 132–154.
 [2]. R. Van Noorden, *Nature*. **507** (2014) 26–28.

9:10 AM CH02.14.05

Functional Materials by Design—Developing Treasure Maps with Quantum Chemistry Matthias Wuttig¹, Carl-Friedrich Schön¹ and Jean-Yves Raty²; ¹RWTH Aachen University, Germany; ²Universite de Liege, Belgium

Scientists and practitioners have long dreamt of designing materials with novel properties. Yet, a hundred years after quantum mechanics lay the foundations for a systematic description of the properties of solids, it is still not possible to predict the best material in applications such as photovoltaics, superconductivity or thermoelectric energy conversion. This is a sign of the complexity of the problem, which is often exacerbated by the need to optimize conflicting material properties. Hence, one can ponder if design routes for materials can be devised.

In recent years, the focus of our work has been on designing advanced functional materials with attractive opto-electronic properties, including phase change materials, thermoelectrics, photonic switches and materials for photovoltaics. To reach this goal, one can try to establish close links between material properties and chemical bonding. However, until recently it was quite difficult to adequately quantify chemical bonds. Some developments in the last decades, such as the quantum theory of atoms in molecules [1] have provided the necessary tools to describe bonds in solids quantitatively. Using these tools, it has been possible to devise a map which separates different bonding mechanisms [2]. This map can now be employed to correlate chemical bonding with material properties [3]. Machine learning and property classification demonstrate the potential of this approach. These insights are subsequently employed to design phase change as well as thermoelectric materials [4,5]. Yet, the discoveries presented here also force us to revisit the concept of chemical bonds and bring back a history of vivid scientific disputes about 'the nature of the chemical bond'.

9:15 AM CH02.14.06

Structure/Function Relationship in Luminescent Pure and Ti-Doped HfO₂ Nanocrystals Alessandro Lauria; ETH Zürich, Switzerland

Intense recent research efforts are directed toward the development of novel materials morphologies, such as nanoparticles, able to efficiently convert ionizing radiation into light. Fluorescent or scintillating materials attract great interest in lighting technology, solar applications, theranostics and self-lighting photodynamic therapy. Moreover, additive manufacturing advancements suggest the possibility to fabricate nanoparticle-based materials applicable in several fields. Therefore, novel luminescent nanomaterials free from toxic or expensive elements, such as rare earths, are desirable building blocks for promoting future developments in all these fields.

In this work, the structural and morphological properties of pure and Ti-doped HfO₂ nanoparticles are studied in dependence of calcination temperatures leading to a fine tuning of either morphology and functional defect configuration. Indeed, tuneable optical features are observed in undoped monoclinic HfO₂ nanocrystals and their dependence on the structural properties of the material at the nanoscale are disclosed. TEM, XRD, XPS, and surface area data combined with the analysis of the luminescence allowed us to identify the dual nature of the broad emission at 2.5 eV, where an ultrafast defect-related intrinsic luminescence overlaps with a slower emission ascribed to extrinsic Ti impurities.[1]

When titanium is employed as luminescence activator, a bright emission is observed under excitation with both UVC radiation and X-rays. [2] These results represent useful insights toward the design of novel promising nanomaterials suitable for rare-earth-free UV pumped white LEDs based on intrinsic defect engineering, and for X-ray triggered oncological therapies by using the Ti (IV)-related bright radioluminescence to excite photosensitizer molecules for singlet oxygen generation.

[1] Villa, I.; Vedda, A.; Fasoli, M.; Lorenzi, R.; Kränzlin, N.; Rechberger, F.; Ilari, G.; Primc, D.; Hattendorf, B.; Heiligtag, F. J.; Niederberger, M.; Lauria, A., Size-Dependent Luminescence in HfO₂ Nanocrystals: Toward White Emission from Intrinsic Surface Defects. *Chem. Mater.* 2016, 28 (10), 3245-3253.

[2] Villa, I.; Moretti, F.; Fasoli, M.; Rossi, A.; Hattendorf, B.; Dujardin, C.; Niederberger, M.; Vedda, A.; Lauria, A., The Bright X-Ray Stimulated Luminescence of HfO₂ Nanocrystals Activated by Ti Ions. *Advanced Optical Materials* 2020, 8 (1), 1901348.

9:20 AM CH02.14.07

Growth of Branched Nanowires via Solution Based Au Particle Deposition for Charge Carrier Diffusion Induced Nanowire Light Emitting Diodes Kristi Adham, Lukas Hrachowina, David Alcer and Magnus T. Borgström; Lund University, Sweden

Conventional LEDs consist of heterojunction structures in which the active region (usually a multi quantum well stack (MQW)) is embedded in-between the layers in a p-n junction. Recent developments have made it possible to decouple the active region from the p-n junction and demonstrate a working LED where electron and holes are injected by carrier diffusion into the MQW. [1] In order to improve this architecture further we propose to implement it in nanowire (NW) structures. From theoretical simulations it has been shown that NWs with diameter below a threshold value, trap light very poorly because the electric field is not kept inside the NW [2]. To make use of this property and to separate the active region from the p-n junction we aim to make heterostructures with branched nanowires, where core p-i-n NWs with a high bandgap are grown, followed by a subsequent growth of NW branches with lower bandgap. The difference in bandgap would induce carrier diffusion towards the branches, which have a small diameter (~25-50 nm), where the carriers can recombine, and as a consequence light is emitted. The benefits of using nano scale building blocks in this architecture is not only that lattice matching requirements are relieved, but opens up to completely avoid the challenge of total internal reflection as the light emitted has much longer wavelength than the nanowire diameter.

We have developed a cost beneficial method to deposit Au particles along the entire length of the core nanowires which act as catalyst for the growth of the branches. A stock solution of HAuCl₄·3H₂O (10 mM) was prepared, in order to deposit Au particles on the sidewalls of the cores by submerging the substrates inside the solution. To study the deposition of the Au particles, core p-i-n InP NWs in a hexagonal pattern with a pitch of 1 μm and a length of approximately 2 μm were grown on InP(111):Zn substrates by Metal Organic Vapor Phase Epitaxy. For our study we have varied the concentration of the solution by diluting the stock solution into concentrations of 0.25, 0.5, 1, 2 and 4 mM and we have varied the temperature of the solution during deposition and the time which we submerge the substrates to find the optimal deposition parameters. To study the nucleation and growth of the branches we have grown InP branches by varying the trimethylindium (TMIn) flow and keeping growth time constant at 1 minute. By changing the concentration of the solution, we can control the growth direction of the branches to (111B) or the (110) direction.

In conclusion, we have deposited Au catalyst particles on the sidewalls of core NWs. We have studied the parameters for the deposition such as the solution concentration and temperature and the time of deposition. We have successfully grown InP branches on p-i-n InP cores and aim to develop heterostructures as the next step with InGaP p-i-n cores and InP branches leading to the intended charge carrier diffusion needed for these type of light emitting diodes with promise to high efficiency at low cost.

[1] Riittanen, L., et al. Diffusion injected multi-quantum well light-emitting diode structure. *Applied Physics Letters*, 104(8), 081102, (2014). [2] Anttu, N., & Xu, H. Q. *Journal of nanoscience and nanotechnology*, 10(11), 7183-7187, (2010).

9:25 AM *CH02.14.08

Microwave-Assisted Routes for Rapid and Efficient Topochemical Modification of Layered Perovskites John B. Wiley; The University of New Orleans, United States

Microwave processing methods have greatly decreased the times needed to topochemically modify layered perovskites. Reactions involving ion exchange, intercalation, grafting, and exfoliation have all been impacted. Here we find that quality products can often be obtained in hours instead of days. In this presentation, methods and products will be highlighted in terms of the utility of this approach, not only in the formation of bulk materials, but also in the production and modification of exfoliated nanosheets.

SESSION CH02.15: Physical Properties of Inorganic Solids V
Session Chairs: Amparo Fuertes and Hiroshi Kageyama
Tuesday Afternoon, December 7, 2021
CH02-Virtual

1:00 PM *CH02.15.01

The Role of Dimensionality on the Spin and Charge Transport Properties of Metal Halide Semiconductors Luisa L. Whittaker-Brooks; University of Utah, United States

Metal halide semiconductors while highly desirable for a host of applications, present several challenges that remain unresolved, including the ability to control their dimensionality at the molecular level (orientation and mode of attachment), matching of phonon band structure in inorganics with discrete vibrations within the molecule, and tuning energetic offsets for effective charge and spin transfer. Each of these parameters ultimately governs charge transport, the preservation of coherence, and energy transfer.

In this talk, I will discuss fundamental guidelines for the design of dimensionally stable metal halide heterostructures with controlled morphology and interfaces that serve as conduits for deterministic and coherent spin and charge transfer. I will divide my talk into two different sub-topics, i.e., (1) how matching phonon structure across interfaces through control of mode and site of attachment of molecules to surfaces allow for efficient coherent charge transfer and (2) how topologically protected electronic states can be defined by 2D assembly of pi-conjugated molecules and layered metal halide materials on surfaces for spin-coherent electronic transport. Here, I will emphasize the role that dimensionality plays in modulating the spin and charge properties of metal halide heterostructures.

1:30 PM CH02.15.03

Tailoring the Structure and Morphology of Mesoporous High Entropy MCo_2O_4 Spinel Oxide Nanoparticles [Xin Wang](#)¹, Palani Raja Jothi¹ and Katharine Page^{1,2}; ¹The University of Tennessee, Knoxville, United States; ²Oak Ridge National Laboratory, United States

The unique structure diversity, tunable compositions, and physical-chemical properties of high entropy oxides (HEOs) attract wide research interests. At the same time, there are vast economic and environmental needs for obtaining stable, high-capacity, and low-cost catalysts for automotive and industrial exhaust applications; in particular, high surface areas and high thermal stability of oxygen storage capacity catalysts are often incompatible. Here, an eco-friendly soft-templating route is applied to form mesoporous HEO spinel nanostructures (MCo_2O_4 , M= Mn^{2+} , Fe^{2+} , Ni^{2+} , Mg^{2+} , Zn^{2+} , etc.), in which high surface area, thermal stability, and compositionally tuned catalysis behavior can be simultaneously achieved. The structural order/disorder in the HEO spinel lattice can be achieved through M cation selection and the morphology (ranging from highly faceted octahedron to highly mesoporous nanocrystalline agglomerates) can be tuned through the selection of templates and reaction conditions. We apply a wide array of characterization techniques, including electron microscopy, and neutron and X-ray total scattering probes, to correlate these characteristics with thermal and catalytic properties. Identifying the role of specific lattice defects, chemical short-range order, and nanoscale heterogeneity in this MCo_2O_4 spinel family will promote design principles and strategies for HEO nanostructured catalysts.

1:35 PM CH02.15.04

Bulk Synthesis of Ternary Metal Nitrides Through Low-Temperature Ion Exchange Reactions [Paul K. Todd](#); National Renewable Energy Lab, United States

Ternary nitrides are an emerging class of inorganic materials for use in a variety of optical, electronic, and refractory applications. In preparing inorganic nitrides, selection of precursors and reaction conditions is dependent on controlling the reactivity of the nitride anion, as decomposition to yield N_2 is thermodynamically favorable at high temperatures used in traditional ceramic processes. While high pressures or reactive environments like ammonia can change the chemical potential of nitrogen to favor a nitride product, reactions that occur under low-temperatures and mild reaction conditions are desired. Here we present on low-temperature ion-exchange reactions that yield magnesium metal nitrides and zinc metal nitrides at low-temperatures and pressures. First, we report on the synthesis of rocksalt MgZrN_2 , rocksalt Mg_2NbN_3 , and hexagonal MgMoN_2 using magnesium nitrochloride and the corresponding transition metal halides as precursors. Key to these preparations is a low-temperature anneal (300-450 °C), which calorimetry experiments show results in Mg-M-N product formation. Then, we present on additional experiments using these magnesium metal nitrides as a structural template to perform selective ion-exchange reactions with zinc halide precursors to yield metastable zinc metal nitrides: rocksalt $\text{Zn}_x\text{Mg}_{1-x}\text{ZrN}_2$, rocksalt $\text{Zn}_x\text{Mg}_{2-x}\text{NbN}_3$, and layered $\text{Zn}_x\text{Mg}_{1-x}\text{MoN}_2$. Overall, these low-temperature ion exchange reactions hold promise to increased discovery of new ternary metal nitrides.

1:40 PM CH02.15.05

Thermodynamic Investigation of LiFePO_4 in Triphylite, Heterosite and Solid Solution Phases [Hillary Smith](#), Alexandra Specht and Aleah Wilson; Swarthmore College, United States

The electrochemical properties of a battery cathode material depend on the structural and associated thermodynamic changes that are induced by ion intercalation and deintercalation. Despite the prevalence of LiMPO_4 cathodes (M represents Mn, Fe, Co, Ni, or a mixture of multiple of these elements), some aspects of local structural characteristics and thermodynamics are not thoroughly understood in these materials. Li_xFePO_4 undergoes a transformation from a two-phase mixture of triphylite and heterosite to a distinct solid solution phase at elevated temperatures. In this work, the phase transformation in Li_xFePO_4 $x=0.6$ is investigated using neutron powder diffraction, inelastic neutron scattering, and calorimetry. We report contributions to the vibrational and configurational entropy as a function of temperature, both above and below the phase transformation. Results are compared to first-principles calculations of phonon spectra. New insights into the how the electronic and ionic conductivity differs in each phase will be discussed.

1:55 PM CH02.15.06

Nanofluids' Evaluation for Enhanced Recovery in the Oil Industry [Ana Paulina Gomora Figueroa](#); Universidad Nacional Autónoma de México, Mexico

Nanotechnology has the potential to upgrade the oil and gas industry within different areas such as exploration, drilling, production, and enhanced oil recovery (EOR). For instance, the use of nanoparticles as an EOR method exhibit many advantages since:

The size and shape of nanoparticles can be easily modified during fabrication.

Nanoparticles' surface chemical properties can be easily adapted to turn them hydrophobic or hydrophilic and modify the chemical interaction with specific types of surfaces.

Nanoparticles may resist more complex conditions in comparison with conventional EOR chemical methods.

During the last decade, numerous studies have been conducted employing nanoparticles for EOR purposes. Although different types of nanoparticles, both organic and inorganic, show a significant increase in the additional recovery factor (RF) of crude oil, these results are encouraging, specifically for mature fields.

This work presents the synthesis of inorganic nanoparticles and their performance evaluation in oil displacement tests under different conditions: water-oil ratios, the concentration of nanoparticles, temperature, and salinity of various synthetic brines. Tests were carried out with sandstone to evaluate the interactions between rock-nanoparticles and brine-nanoparticles. During these tests, the nanoparticles displaced up to 50 % of the oil, compared to 26 % of oil displaced by synthetic brines. Additionally, we demonstrated that nanoparticles are helpful to reduce the water-oil interfacial tension, resulting in the formation and stabilization of Pickering-type emulsions, which have shown the ability to be formed in-situ and improve oil recovery in crude oil reservoirs. The results opened the door to future experiments for assessing the wettability alteration promoted by nanofluids and the efficiency of displacement of oil contained in a porous media.

2:00 PM CH02.15.07

Late News: Growth and Structure of the Topological Semimetal Candidate SmMnBi₂ [Tiglet Besara](#) and Sudha Krishnan; Missouri State University, United States

The $MMn(\text{Bi,Sb})_2$ (M —rare earth or alkaline earth) family has emerged as a fertile ground for exploration of topological semimetals. Topological semimetals are charge-balanced compounds that host Dirac or Weyl fermions and with electronic excitations protected by topology. Several members of this family have been explored, such as $(\text{Ca,Sr,Ba,Eu,Yb})\text{Mn}(\text{Sb,Bi})_2$, all with divalent oxidation state of the rare earth or alkaline earth metal. Here, we report on the discovery of a new member of the family, SmMnBi_2 , and compare its structure to other compounds in the family. Surprisingly, despite the near-identical ionic sizes of Eu^{2+} and Sm^{2+} , the structural layers in SmMnBi_2 differ from that of EuMnBi_2 .

2:05 PM CH02.15.09

Structure-Property Relationships in Na-Si Clathrates—Old and New Questions from a (Deceptively) Simple Binary Phase [Matt Beekman](#)¹, Antti J. Karttunen², Winnie Wong-Ng³, James A. Kaduk^{4,5}, Ethan Cruse¹, Christian Posadas¹ and George Nolas⁶; ¹California Polytechnic State University, United States; ²Aalto University, Finland; ³National Institute of Standards and Technology (NIST), United States; ⁴Illinois Institute of Technology, United States; ⁵North Central College, United States; ⁶University of South Florida, United States

$\text{Na}_x\text{Si}_{136}$ ($0 \leq x \leq 24$) materials with the clathrate-II crystal structure provide a unique opportunity to investigate the direct effect of guest content on physical properties of intermetallic clathrates in a chemically simple system with only two elements. The preferential filling of two framework cages with very different sizes is accompanied by very different guest-framework interactions, resulting in a non-monotonic structural response to cage filling that is correlated with a metal-insulator transition near $x = 8$. Temperature-dependent single-crystal and powder X-ray diffraction experiments show that the room temperature linear coefficient of thermal expansion increases by nearly a factor of 3 upon filling, attributed to an increase in the anharmonicity in the interatomic interactions. Furthermore, negative thermal expansion, present at low temperature ($T < 150$ K) in Si_{136} and $\text{Na}_x\text{Si}_{136}$ at lower Na contents, disappears for $x > 16$. Extremely large atomic displacement parameters obtained from structure refinements, as well as dynamic instability observed in first principles calculation of phonon dispersion, suggest the Na guest in the larger cage is displaced off-center, but the exact nature of the off-centering and dynamical behavior remains difficult to elucidate. Thus, modeling and understanding the physical mechanisms underlying the effects of guest content on electrical, thermal, and mechanical properties of these silicon clathrates is non-trivial.

2:10 PM *CH02.14.09

Oxychalcogenide Building Blocks Toward Nonlinear Optical Properties [Houria Kabbour](#)¹, Batoul Almoussawi¹, Hiroshi Kageyama², Mike Whangbo^{3,4} and Shuiquan Deng⁴; ¹Univ. Lille, CNRS, Centrale Lille, ENSCL, Univ. Artois, UMR 8181 – UCCS – Unité de Catalyse et Chimie du Solide, France; ²Kyoto University, Japan; ³North Carolina State University, United States; ⁴Chinese Academy of Sciences, China

Among the versatile mixed anion compounds [1], oxychalcogenides are emerging as promising alternative candidates for a variety of applications including for energy. Recently, they have been pointed as interesting systems for mid IR nonlinear optical (NLO) properties [2]. In particular, strong second harmonic generation (SHG) responses are found for NLO compounds with functional groups composed of mixed anions such as in BaGeSe_2O with GeO_2Se_2 tetrahedra [3] (compared to its oxide analogue with GeO_4 tetrahedra). Here we will discuss, through several structure types based on thiovanadates $\text{V}(\text{O,S})_4$ building blocks, the possibility to tune the symmetry and engineer the band gap. $\text{Ba}_5(\text{VO}_2\text{S}_2)_2(\text{S}_2)_2$ [4] with third-harmonic generation properties and $\text{Ba}_7\text{S}(\text{VOS}_3)_2(\text{S}_2)_3$ and its selenide-derivatives [5] will be discussed with support of density functional theory (DFT). We will see that the presence of Q–Q bonds (Q= chalcogenide) lead to original lattices with multiple anionic species and add greater structure and electronic structure versatility to design functional materials. On another hand, we will present unprecedented oxysulfide building block for SHG active materials and give a comprehension of the SHG response mechanism with support of DFT calculations [6].

References :

- [1] Kageyama, H. *et al. Nature Communications* **2018**, 9 (1), 772.
- [2] Li, Y. Y. *et al. Cryst. Growth Des.* **2019**, 19 (7), 4172–4192.
- [3] Liu, B. *et al. Chemistry of Materials* **2015**, 27 (24), 8189–8192.
- [4] Almoussawi, B. *et al. Inorganic Chemistry* **2020**, 59 (9), 5907–5917.
- [5, 6] submitted (2021)

SESSION CH02.16: Physical Properties of Inorganic Solids VI

Session Chairs: Hiroshi Kageyama and Brent Melot

Tuesday Afternoon, December 7, 2021

CH02-Virtual

4:00 PM *CH02.16.01

Towards Solid–State Electrolytes—Complex Halides and Hydrides as New Fast Li-Ion Conductors [Duncan Gregory](#); Univ of Glasgow, United Kingdom

Many of the most widespread and commercially successful materials in Li-ion batteries are oxides. Nevertheless, some of the best performing materials contain elements from elsewhere in the periodic table (e.g. chalcogenides, pnictides). Although halide salts have long been employed as electrolytes in solution or in the molten state, there are few examples of halides as solid-state cationic conductors and until recently, still fewer in terms of hydrides.

This contribution focuses principally on the possibilities for designing fast Li-ion conducting (pseudo-)halides as potential electrolytes in all-solid-state batteries. In switching the materials design emphasis from cations to anions, it will be shown how both static and dynamic disorder might be exploited to enhance Li-ion transport and how diffusion pathways might be modified in terms of anion geometry and electronegativity (polarizability). Concepts of lattice “softness” and complex anion dynamics become crucial components of such a design strategy. Synthesis (often of metastable solids) can be challenging, but mechanochemistry and other “soft” chemical approaches, can provide a means to access such materials, while facilitating nanostructuring and generating defects.

This contribution covers several exemplar systems of promising complex hydride and halide Li fast-ion conductors, including $\text{Li}(\text{BH}_4)_{1-y}\text{X}_y$, LiAlX_4 and $\text{LiCe}(\text{BH}_4)_3\text{X}$; $X = \text{Cl, Br, I}$, among others. In each case a raft of techniques including neutron diffraction and muon spin relaxation spectroscopy have been fundamental in elucidating the structure-property relationships in these systems. A synergic combination of experiment and computational calculations are

beginning to shed light on the mechanisms for Li-ion conduction in these families of non-oxide materials and their prospects as solid state electrolytes will be evaluated.

4:30 PM CH02.16.02

Group VI Metalates as Thermosensitive Phosphors [Federico A. Rabuffetti](#); Wayne State University, United States

Group VI metal oxides featuring MoO_4^{2-} and WO_4^{2-} anions are ideal semiconducting host materials for thermosensitive phosphors activated by Mn^{4+} and/or rare-earth metals. A distinct feature of these materials is their structural diversity in terms of metal coordination and connectivity, which makes them an ideal platform to exercise compositional control over their temperature-dependent luminescence response. In this talk, I will highlight the potential of molybdate and tungstate phosphors as luminescent thermometers. I will show that selected Mn^{4+} -activated metalates serve as bandshift thermometers with a temperature sensitivity comparable to that of quantum dots but with a much broader usable temperature range. Further, I will show how the crystal-chemistry of group VI metalates may be exploited to generate thermochromic phosphors via codoping Mn^{4+} - Tb^{3+} pairs. Findings presented in this talk expand the scope of applicability of Mn^{4+} -activated thermosensitive phosphors beyond ratiometric bandshape and lifetime thermometry. They also provide structural guidelines for discovering and screening novel oxide hosts for dual-activator luminescent thermometers.

4:45 PM CH02.16.03

A General Method for Reconstructing the Orientation Ordering of Materials Constituents from Their Scattering Anisotropy [Guan-Rong Huang](#)¹, Jan-Michael Carrillo¹, Yangyang Wang¹, Changwoo Do¹, Yuya Shinohara¹, Takeshi Egami^{1,2}, Lionel Porcar³, Yun Liu⁴, Bobby Sumpter¹ and Wei-Ren Chen¹; ¹Oak Ridge National Laboratory, United States; ²The University of Tennessee, Knoxville, United States; ³Institut Laue-Langevin, France; ⁴National Institute of Standards and Technology, United States

We outline a state-of-the-art approach for reconstructing the orientation distribution function (ODF) of materials from their scattering anisotropy using real spherical harmonics (RSH) expansion. Without assuming the functional form of ODF, we perform the reconstruction through the RSH decomposition of their scattering intensity and ODF subject to certain constraints from symmetries and orientation order parameters. We demonstrated its validity by the quantitative agreement between case studies of molecular dynamics simulations and numerical computations. Our proposed method is applicable for general materials subject to various external conditions. Material's properties usually reflect on the coarse-grained averages of the relative orientation and separation at molecular levels over a characteristic length scale. One of the well-known examples is the magnetic response of materials is the ensemble average of magnetic moments over all the possible configuration distributions in phase space. Knowing how the molecular orientation distributes enables us to investigate the fundamental mechanism between the microscopic variables and macroscopic properties of interest in response to the applied fields. It can facilitate us with materials design and characterization for its practical use under different conditions. These can be exemplified by the magnetization alignment induced by the applied magnetic field or the orientational ordering of anisotropic nanoparticles in composites undergoing mechanical deformation. Typically, the microscopic information of material's orientation is conceived in its corresponding scattering spectra, which is an ensemble average in momentum space. Under the external fields without rotational symmetry, the constituent of materials would possess a preferred orientation, which will reflect on the anisotropy of their scattering signature. Therefore, how to reconstruct the ODF of materials from their scattering anisotropy is inevitably important.

5:00 PM DISCUSSION TIME

5:15 PM CH02.04.03

Multipolar Hidden Orders in 5d¹ Double Perovskites [Aria Mansouri Tehrani](#) and Nicola Spaldin; ETH Zurich, Switzerland

We present a density functional theory study of the interplay between multiple hidden and established charge, magnetic and structural orders in 5d¹ double perovskites. The ordering of structural distortions, magnetic dipole moments, atomic orbital occupancies, and electronic charges is widespread in materials and leads to well-known behaviors such as changes in the crystal structure, the onset of ferromagnetism, or metal-insulator transitions. While such orderings have been extensively investigated, there remain many materials that show intriguing changes in behavior indicating the onset of order, but for which the nature of the order is not yet known. Double perovskite oxides (halides) with 5d¹ transition magnetic ion have been of particular interest recently to explore these multipolar hidden orders which stem from their unique crystal chemistry and the interplay of spin-orbit coupling, crystal-field splitting, and electron-electron repulsion. Here, we present a density functional theory study of multipolar ordering (e.g. charge quadrupoles and magnetic octupoles) and their coupling with the dipolar magnetic and the crystal structure of two 5d¹ double perovskites, $\text{Ba}_2\text{MgReO}_6$ and Cs_2TaCl_6 . Both of these compounds are spin-orbit-driven Mott insulators with a symmetry-lowering structural phase transition at low temperatures driven by the ordering of charge quadrupoles. Our primary goal is to provide an understanding of the interplay between the structural distortions, the charge quadrupole ordering, and the magnetic dipole ordering in these compounds. In addition to shedding light on the detailed behavior of $\text{Ba}_2\text{MgReO}_6$ and Cs_2TaCl_6 , our analysis provides a novel insight into the crystal structure-multipolar order relationship of 5d¹ double perovskites.

5:30 PM BREAK

SESSION CH02.17: Physical Properties of Inorganic Solids VII

Session Chair: Craig Brown

Tuesday Afternoon, December 7, 2021

CH02-Virtual

9:00 PM *CH02.17.02

Porous Ionic Crystals Based on Polyoxometalates as a Tunable Platform for Functional Materials [Sayaka Uchida](#); The University of Tokyo, Japan

Porous crystalline materials such as zeolites and metal-organic frameworks (MOFs) have attracted wide attention due to their well-defined porous structures and high surface area, which are useful in gas storage and separation, ion exchange and conduction, and heterogeneous catalysis. Polyoxometalates (POMs) are nano-sized metal-oxide molecular anions with unique catalytic, electrochemical, magnetic, and luminescent properties and have stimulated research in broad fields of science. Recently, the incorporation of POMs in nano-sized cavities of MOFs has been reported; these POM-MOFs show unique functions such as oxidative removal of hydrogen sulfide, selective adsorption of cationic dyes, and visible-light-driven hydrogen production. In contrast, we have reported that the complexation of POMs with molecular cations with appropriate elements, charges, sizes, symmetry, ligands, etc., results in the formation of voids and channels in the crystal lattice. The properties of porous ionic crystals (PICs) based on POMs can be

summarized as follows. (a) POMs show reversible redox properties, which can lead to the formation of “redox-active” PICs. (b) Guest binding and catalytically active sites can be incorporated beforehand into the ionic components. These functions can be maintained and utilized in the PICs since the ionic components still exist as discrete molecules in the crystal lattice. (c) The ionic components create strong electrostatic fields at the internal surfaces of PICs, which are suitable for accommodating and stabilizing polar guests and reaction intermediates. (d) POMs can transport protons as counter cations efficiently because the negative charge of POMs is smeared over the external oxygen atoms decreasing the effective surface charge density. These properties lead to interesting functions in selective ion-uptake/exchange, proton conduction, heterogeneous catalysis, formation of luminescent mixed-valence metal clusters, etc., which are unique to PICs.¹⁻¹²

Recent papers: (1) *ACS Appl. Mater. Interfaces* 13, 19138 (2021), selected as ACS editor's choice, (2) *Nanoscale* 13, 8049 (2021), selected as backside cover. (3) *Eur. J. Inorg. Chem.* 1531 (2021), selected as frontside cover. (4) *Chem. Lett.* 50, 21-39 (2021), highlight review. (5) *Dalton Trans.* 49, 10328 (2020), selected as backside cover. (6) *Langmuir* 36, 6277 (2020). (7) *Chem. Sci.* 10, 7670 (2019), selected as frontside cover. (8) *ChemCatChem* 11, 3745 (2019), selected as frontside cover. (9) *Communications Chemistry* Article number: 9 (2019). (10) *Inorg. Chem.* 56, 15187 (2017). (11) *Angew. Chem. Int. Ed.* 55, 3987 (2016). (12) *Chem. Mater.* 27, 2092 (2015).

9:30 PM CH02.17.03

Tri-Phase Photocatalysis for CO₂ Reduction and N₂ Fixation with Efficient Electron Transfer on a Hydrophilic Surface of Transition-Metal-Doped MIL-88A (Fe) Niwesh Ojha; IIT Patna, India

Efficient transfer of charges at the interface of transition-metal and semiconductor can improve efficiency of photocatalyst. Herein, we examined the photoactivity of Mn and Zn-doped MIL-88A for CO₂ reduction and N₂ fixation by water under UV-visible irradiation and ambient conditions. Gaseous-phase photo-reduction of CO₂ generated CO, H₂, and CH₄. Apparent quantum yield of Zn-MIL-88A was found to be 2.16-folds higher than that of pristine MIL-88A catalyst. Also, the highest NH₄⁺ generation rate was for Zn-MIL-88A catalyst. Dissecting the underlying mechanism discloses that electrons efficiently transferred from doped transition-metals to the Fe-O cluster of MIL-88A. The hydrophilic surface of the tested catalysts in a tri-phase photocatalyst system led the process to be controlled by mass-transport; which governed the product distribution and limited the kinetics of the process. Experimental results also unveil that the addition of transition metals improved stability, charge-separation, and efficiency of the resulting photocatalysts.

9:35 PM CH02.17.04

Analysis of Chemical and Electronic States Related to Hydration Reactivity of Lime Phase Coexisting with Other Oxides to Utilize Steelmaking Slag Hiroimi Eba, Ryosuke Serigano, Kousuke Yonemoto and Yuuki Suzuki; Tokyo City University, Japan

In steelmaking processes that refine pig iron into tough steel, calcined lime (CaO) is added to remove unwanted components, such as Si, P, and S, and steelmaking slag is produced as a by-product. This slag consists primarily of CaO and SiO₂ and is effectively used as recycled materials for construction and civil engineering. However, part of the CaO in the slag remains in the unreacted form, *i.e.* as free lime, which expands to about double volume by hydration. Therefore, fresh slags that contain free lime must undergo aging. In general, slags containing high amounts of free lime have higher expansibility than their counterparts, which have lower CaO contents. The expansibility, however, varies with the particle size, physical state of the free lime, and the corresponding chemical composition. Therefore, estimating the expansibility solely as a function of the free lime content is difficult. In this study, to promote the utilization of steelmaking slag, the hydration reactivity and electronic state of free lime were observed. It was confirmed by X-ray diffraction (XRD) and thermal analysis that the hydration reactivity decreases when CaO forms a lime-phase solid solution with FeO, and it was revealed by X-ray photoelectron spectroscopy (XPS) observations and DV-X α calculation that the decrease in reactivity occurs due to deepening of the energy levels of the electron orbitals. The morphology and hydration reactivity of the free lime contained in a synthesized slag were observed by XRD and electron probe microanalysis. Fe-containing phases and double oxides were found to be adjacent to free lime; the former is considered to be related to the formation of a solid solution with FeO, and the latter closely surrounds the free lime and shields it from the outside; thus, both contribute to suppressing the hydration reaction. Furthermore, it was found that simply mixing lime with double oxides suppressed the hydration reaction. XPS and thermal analysis confirmed that a chemical change occurred on the surface of the free lime; that is, the energy levels of the electron orbitals are deepened and the hydration reaction is suppressed due to chemical interactions with the double oxides to stabilize the lime surface. It was clarified that in order to effectively promote the hydration of free lime, it must be exposed by breaking the structure of the slag that protects the free lime and suppresses hydration.

9:40 PM CH02.17.05

Tuning of Mixed Valency in Rare-Earth Fullerides at Ambient and Elevated Pressures Naoya Yoshikane¹, Keisuke Matsui¹, Hitoshi Yamaoka², John Arvanitidis³ and Kosmas Prassides¹; ¹Osaka Prefecture University, Japan; ²RIKEN, Japan; ³Aristotle University of Thessaloniki, Greece

The electronic properties of rare-earth elements, RE are dominated by the 3+ oxidation state, but 2+ can be also stabilized for Sm, Eu, and Yb due to their comparable energy^[1]. As a result, mixed valency phenomena are encountered in compounds of these rare-earths (Kondo insulators, heavy fermions) with the average RE valence strongly affected by changes in external stimuli (temperature, pressure). Research in elastic, conducting, optical, and magnetic properties triggered by such valence changes remains at the frontier of solid-state chemistry.

The RE fullerides with stoichiometry, RE_{2.75}C₆₀ (RE=Sm, Yb) constitute an intriguing class of electronic systems due to the strong electronic coupling between the highly-correlated mixed-valence RE cation and C₆₀ anion sublattices. Past work pointed towards strong coupling of lattice and electronic degrees of freedom with the occurrence of pressure-induced lattice collapse and concomitant insulator-metal transition around 4 GPa^[2,3]. However, to-date there has been no direct study of the RE electronic states – all information about valence changes has come indirectly from diffraction and Raman spectroscopic measurements.

Here we report the results of element-specific synchrotron X-ray absorption spectroscopic (XAS) measurements of the average Sm valence in binary and ternary Sm fullerides, authenticating the mixed valence character of the materials for the first time. In addition, we directly address the evolution of the Sm electronic states both by chemical pressure induced by progressive introduction of smaller-in-size valence-precise Ca²⁺ ions and by external physical pressure^[4,5]. Following this spectroscopic work, we address the structural behavior of this family of materials by high-resolution synchrotron X-ray powder diffraction measurements at elevated pressures – the observed lattice collapse with increasing pressure sensitively depends on the level of Ca²⁺ substitution and perfectly mirrors the Sm valency transition authenticated by synchrotron XAS. The pressure-induced phase transition is isostructural but is accompanied by well-defined renormalization of the rare-earth metal positions and their shift towards high-symmetry positions. The results provide a rationalization of the pressure-induced drastic changes in structural, conducting and optical properties of RE fullerides that are coupled with the extreme fragility of the rare-earth valence.

[1] P. Strange, A. Svane, W. M. Temmertman, Z. Szotek & H. Winter, *Nature*, **399**, 756-758 (1999)

[2] J. Arvanitidis, K. Papagelis, S. Margadonna, and K. Prassides, *Dalton Trans.*, **19**, 3144-3146 (2004)

[3] S.M. Souliou, J. Arvanitidis, D. Christofilos, K. Papagelis, S.Ves, G.A. Kourouklis, K. Prassides, Y. Iwasa and K. Syassen, *High Pressure Research*, **31**, 13-17 (2011)

[4] N. Yoshikane, T. Nakagawa, K. Matsui, H. Yamaoka, N. Hiraoka, H. Ishii, J. Arvanitidis, K. Prassides*, *J. Phys. Chem. Solids* **150**, 109822/1-6 (2021).

[5] N. Yoshikane, K. Matsui, T. Nakagawa, A. G. V. Terzidou, Y. Takabayashi, H. Yamaoka, N. Hiraoka, H. Ishii, J. Arvanitidis, K. Prassides*, *Mater.*

9:45 PM *CH02.17.06

High Pressure Synthesis of Novel Perovskite-Related Cuprates Shintaro Ishiwata; Osaka University, Japan

The discovery of high temperature superconductivity in cuprates has spurred the search for novel low dimensional cuprates such as spin ladder compounds. On the other hand, less attention has been paid for the three dimensional counterpart, the perovskite-type cuprates ACuO₃, presumably because of the difficulty in high pressure synthesis. In this talk, a novel orthorhombic perovskite PrCuO₃ obtained by high pressure synthesis will be introduced[1]. Synchrotron x-ray diffraction and x-ray absorption spectroscopy reveal that PrCuO₃ consists of quasi-one-dimensional chains of Cu-O with square-planar coordination, and the oxidation state of Cu ions is about 2.2+. The formation of the Cu-O chain reflects the cooperative Jahn-Teller distortion of nearly divalent Cu ions. Upon the La substitution for Pr, we found the abrupt change in structure and electrical conductivity, from the orthorhombic semimetal to rhombohedral metal, which is accompanied by the AB site charge transfer. This system offers a unique opportunity to explore novel quantum phases of correlated electrons as the simplest one-dimensional counterpart of the high temperature superconducting cuprates. In addition, we will introduce a computational structure prediction for novel oxygen-deficient perovskite-type cuprates on the basis of the density functional theory and Bayesian optimization[2].

References

- [1] M. Ito, H. Takahashi, H. Sakai, H. Sagayama, Y. Yamasaki, Y. Yokoyama, H. Setoyama, H. Wadati, K. Takahashi, Y. Kusano and S. Ishiwata, Chem. Commun. **55**, 8931 (2019).
[2] A. Seko and S. Ishiwata, Phys. Rev. B **101**, 134101 (2020).

10:15 PM CH02.17.07

Why Lattices and High Valence States are Stabilized in Perovskite-Type Oxides by Madelung Lattice Site Potentials Masahiro Yoshimura^{1,2} and Kripasindhu Sardar¹; ¹National Cheng Kung University, Japan; ²Tokyo Institute of Technology, Japan

Perovskite-type oxides (ABO₃) are quite common for various Ferroelectric, Piezoelectric, Conducting Electrode and/or even Superconducting oxides. However, it has not been clear why they will take perovskite-type structure(s). For the stability of Perovskite Lattices, classic Tolerance Factors based upon ion packing model have been considered even now. One of the present authors proposed another concept: Madelung lattice energy should be the key factor of the Lattice and Valence Stability.^{1,2)} The total Madelung Lattice energy (U) could be considered by the summation of Sub-Lattices Energies of A, B and O sites. Since they are given each lattice site potential (Φ) and its valence (q): that is, $U = \Phi_A \times q_A + \Phi_B \times q_B + 3\Phi_O \times q_O$. Using a recent Program: VESTA³⁾, we have confirmed 1) U_{ABO_3} is always larger than the summation of $U_{AO} + U_{BO_2}$ or $U_{AO_{1.5}} + U_{BO_{1.5}}$. 2) U_{ABO_3} become larger when valence pairs are shifted from 3+ and 3+ to, 4+ and 2+ then 1+ and 5+ or 0+ and 6+. 3) Furthermore, those large B Sublattice potential can be strongly related to high valence state of B ions in Perovskite ABO₃. Since the ionization potential [loss] can be compensated by high lattice site potential [gain], high valence ion(s) can be stabilized in B site with high lattice-site potential. For example, Ce⁴⁺, Pr⁴⁺, and Tb⁴⁺ can be stabilized in a Fluorite lattice, and more stabilized in the B site of Perovskite ABO₃ lattice. Un-common high-valence ions like Co³⁺, Ni³⁺, Fe⁴⁺ in the B-sites of the Perovskite ABO₃ lattices can be explained similarly. On the other hand, those high-valence ions cannot be stabilized in the A site of Perovskites nor various A₂O₃, like A-type and C-type M₂O₃, or corundum, lattices thus they take rather common valence states in those cases. The Madelung Lattice energy (U) is Enthalpy at 0 K, thus it consists of ca. 90% of total free energy (G) of the compound. Therefore the valence stability of certain ions in particular lattices is directly related to the Madelung self-site potential (Φ) of the lattice site. The entropy term by Temperature and P_{O₂} can contribute < 10% of U at 1000K. Therefore it might be rather minor effects for those internal lattice potential energy. Vacancy formation energies can also be estimated by Madelung Lattice Site Potentials. More precise data can be calculated by recent First Principle Calculation using several additional parameters, but they should include several hypothetical parameters and much longer times for calculation.

Reference

- [1] M. YOSHIMURA, et al.: Stabilization of High valence States of Ions at B site of Perovskite Structure ABO₃: Electrostatic Potential in Perovskite Structure; Bull. Tokyo Inst. Tech., 120, 1327, (1974).
[2] M. YOSHIMURA, Valence Stability of Rare Earth Ions, (in Japanese), Chapter 34, pp 851-862, Kidorui (Rare Earth) Handbook, Edited by G. Adachi, NTS Book Co. Ltd. Tokyo, 2008.
[3] M. Yoshimura and K. Sardar, Revisiting Valence Stability and Preparation of Perovskite-type Oxides ABO₃ with the Use of Madelung Electrostatic Potential Energy and Lattice Site Potential, RSC Advance. 2021, 11, 20737-20745.

10:30 PM BREAK

SYMPOSIUM CH03

Frontiers in Scanning Probe Microscopy—Beyond Imaging of Soft Materials
November 30 - December 8, 2021

Symposium Organizers

Philippe Leclere, University of Mons
Zoya Leonenko, University of Waterloo
Ken Nakajima, Tokyo Institute of Technology
Igor Sokolov, Tufts University

Symposium Support

Gold
Bruker

Silver
Oxford Instruments, Asylum Research

Bronze
Nanosurf

* Invited Paper

SESSION CH03.01: Electrical Properties I
Session Chairs: Udo Schwarz and Igor Sokolov
Tuesday Morning, November 30, 2021
Hynes, Level 3, Room 301

10:30 AM *CH03.01.01

Quantifying Nano-Electromechanical and Nano-Mechanical Measurements with a Metrological Atomic Force Microscope Roger Proksch; Asylum Research and Oxford Instruments, United States

Voltage modulation (VM) of atomic force microscopy (AFM) has been used to quantify a host of electronic, electrochemical and electromechanical functionalities across nanometer length scales. The critical importance of such information has resulted in the development of a plethora of VM-AFM techniques for exploration of either long or short-range forces. Of relevance for ferroelectrics, piezoresponse force microscopy (PFM) imaging and associated spectroscopies have effectively opened the door to the exploration of nanoscale ferroelectric properties. The rise of PFM, however, has also brought about claims of ferroelectricity in materials which were subsequently thought to be not ferroelectric,[1] even unlikely materials such as soda-lime glass. Explanations for the origins of these unexpected nanoscale phenomena have not been in short supply, including new material properties, surface-mediated polarization changes and/or spatially resolved behavior that is not present in bulk measurements. At the same time, it is well known that VM-AFM measurements are susceptible to numerous forms of crosstalk and despite efforts within the AFM community, a global approach for quantitative, crosstalk-free techniques remains elusive. In an effort to understand the true origins of the measured VM-AFM signals we demonstrate the presence of hysteretic ("false ferroelectric") long-range interactions between the sample and cantilever body and show that these are intrinsic to traditional VM-AFM detection methods. However, we show that with interferometric displacement sensor (IDS) [2] it is possible to separate the true tip motion from the cantilever dynamics. Using the IDS we have established a rapid and simple flagging routine of false piezo and ferroelectric responses and are able to demonstrate fully quantitative and repeatable nanoelectromechanical characterization. These quantitative measurements are critical for a wide range of devices ranging from mems actuators, memristor devices, energy storage and dynamic computer memory. While our initial work was focused on electromechanical measurements, we have extended this microscope to improved quantification of force-based mechanical measurements. Quantifying the force and displacement with this metrological AFM has enabled improved quantitative and high speed modulus mapping in a variety of environments. [3, 4]

References

- [1] Vasudevan, Rama K., et al. "Ferroelectric or non-ferroelectric: Why so many materials exhibit "ferroelectricity" on the nanoscale." *Applied Physics Reviews* 4.2 (2017): 021302.
- [2] Labuda, Aleksander, and Roger Proksch. "Quantitative measurements of electromechanical response with a combined optical beam and interferometric atomic force microscope." *Applied Physics Letters* 106.25 (2015): 253103.
- [3] M. Kocun et al., "Fast, High Resolution, and Wide Modulus Range Nanomechanical Mapping with Bimodal Tapping Mode", *ACS Nano* 11 10097 (2017).
- [4] V. G. Gisbert et al., "High-Speed Nanomechanical Mapping of the Early Stages of Collagen Growth by Bimodal Force Microscopy" *ACS Nano*, 15 1850 (2021).

11:00 AM CH03.01.02

Controlled Manipulation of Benzene and Phenyl Groups Across Different Energy Landscapes Chao Zhou¹, Omur E. Dagdeviren^{1,2}, Milica Todorović³, Eric Altman¹ and Udo Schwarz¹; ¹Yale University, United States; ²University of Quebec, Canada; ³Aalto University, Finland

With the continued development of scanning probe microscopy techniques, manipulation of single molecules has become possible. Thereby, the manipulation path can be chosen at will and the energy landscape around the molecule can be quantified before and after manipulation. This not only allows to extract the energy barriers between potential minima along the manipulation pathway but may more generally provide unprecedented insight into the chemical interaction of individual molecules with their surroundings. To further explore the approach's potential, we conducted controlled manipulation experiments with benzene on a Cu (100) surface as a model system using a novel manipulation protocol that despite not requiring any active feedback during execution provides the normal and lateral forces at the instance of the jump with piconewton accuracy, which leads to very robust operation. The results indicate that the molecules were either pushed, pulled, jumped to the tip, or did not move depending on the chemical surroundings of the molecules and the chemical identity of the tip. We then compared the experimentally obtained energy landscapes and barrier heights with computational results obtained by combining density functional theory with machine learning approaches. The Bayesian Optimization Structure Search (BOSS) protocol suggests that the presence of the tip lowers the energy barrier the molecule has to overcome during its motion, which evolves with the chemical identity of the tip. In addition, phenyl groups were produced from iodobenzene precursors, from which the iodine atom was split off by applying a controlled bias voltage. We then manipulated the phenyl group away from the iodine atom and measured the required energy barrier, which was found to decrease with increasing distance from the iodine atom. Calculations indicate that there are different ways the molecules can move that have different barriers, so the finding of different barrier heights may simply reflect different processes. Overall, our results indicate that a reliable methodology where surface reactions can be induced by the tip of a scanning probe microscope and the reaction pathway is chosen at will could be in reach, which would

ultimately enable an individualized, site-specific understanding of single-molecule surface chemistry.

11:15 AM CH03.01.03

Theoretical Models for KPFM with Flexible Tip Apices Ondrej Krejci¹ and Adam Foster^{1,2,3}; ¹Aalto University, Finland; ²Kanazawa University, Japan; ³Graduate School Materials Science in Mainz, Germany

More than 10 years ago two types of Scanning Probe Microscopy (SPM) – Scanning Tunneling Microscopy (STM) [1] and non-contact Atomic Force Microscopy (nc-AFM) [2] – showed a possibility to reveal positions of atoms on small flat organic molecules in real space without any damage to the sample. These two works noticeably enhanced the field of molecular, 1 and 2D material studies in surface science (i.e. [3]). The sub-molecular resolution was achieved by usage of non-reactive and flexible tip-apices like CO-molecule [4]. Kelvin Probe Force Microscopy (KPFM)[5] is a technique proceeded with combined nc-AFM/STM instrument, which basically measures the effect of applied voltage between the microscope tip and sample on the measured force. It has possibility to measure the changes of work-function on the microscale and electric field above the sample on the nanoscale. However, the physics behind KPFM signal with flexible-tip apices showing the sub-molecular resolution, which could help with elemental recognition, remain unknown. In this work, we will summarize up-to-date knowledge about KPFM [5,6] focusing mainly on measurements with simultaneous frequency modulation - Atomic Force Microscopy / Scanning Tunneling Microscopy instruments. Based upon this, we will present a new model for electrostatic field, which is describing the experiments with CO-metal tips [7] and metal substrates. This new electrostatic model is applied in a Density Functional Theory (DFT) calculations simulating the full tip-sample system. The results of the DFT calculations will be compared with simple mechanistic models capturing various sources of achieved signal. All these models and simulations have aim to recover the physics behind KPFM with flexible tip apices. This knowledge can help to get more information about the sample with SPM and is possibly a further step towards reliable chemical resolution in SPM.

References:

- [1] R. Temirov, S. Soubatch, O. Neucheva, A. C. Lassise and F. S. Tautz, *New J. Phys.* **10**, 053012 (2008).
- [2] L. Gross, F. Mohn, N. Moll, P. Liljeroth and G. Meyer., *Science* **325**, 1110 (2009).
- [3] A. Mistry, B. Moreton, B. Schuler, F. Mohn, G. Meyer, L. Gross, A. Williams, P. Scott, G. Costantini and D. J. Fox, *Chem. Eur. J.* **21**, 2011-2018 (2015).
- [4] P. Hapala, G. Kichin, C. Wagner, F. S. Tautz, R. Temirov, and P. Jelínek, *Phys. Rev. B* **90**, 085421 (2014).
- [5] M. Nonnenmacher, M. P. O'Boyle, and H. K. Wickramasinghe, *Appl. Phys. Lett.* **58**, 2921 (1991).
- [6] L. Gross, B. Schuler, F. Mohn, N. Moll, N. Pavliček, W. Steurer, I. Scivetti, K. Kotsis, M. Persson, and G. Meyer, *Phys. Rev. B* **90**, 155455 (2014).
- [7] F. Schulz, J. Ritala, O. Krejci, A. P. Seitsonen, A. S. Foster, and P. Liljeroth, *ACS Nano* **12**, 5274–5283 (2018).

11:30 AM CH03.01.04

Imaging Ballistic and Viscous Flow of Carriers in Graphene Using Scanning Tunneling Potentiometry Zachary Krebs, Wyatt Behn and Victor Brar; University of Wisconsin - Madison, United States

The flow of electrical current through a material can, in special circumstances, mimic the flow of a viscous fluid. This so-called 'hydrodynamic' regime occurs when the rate of momentum-conserving collisions between charge carriers is larger than the momentum-relaxing rate due to other scattering sources. Until very recently this condition has been difficult to satisfy in real materials, hampering experimental studies of electronic transport in this unique regime. Ultraclean graphene has emerged as an ideal platform for studying hydrodynamic flow, opening up the possibility of directly imaging fluid-like behavior such as vortex formation. In this talk, I will show scanning tunneling potentiometry (STP) measurements of quasiparticle flow around tunable electrostatic barriers in graphene on a hexagonal boron nitride substrate. Measurements are performed as carriers pass through μm -scale channels that are continuously narrowed until they are blocked entirely, forming 'electrostatic dams'. Local STP measurements of the electrochemical potential allow for direct characterization of the evolving flow profile near the channels, which is observed to be non-Ohmic, and highly dependent on the sample temperature and the channel width. Under all flow conditions, we observe the formation of Landauer resistivity dipoles across the barriers due to scattering. However, at low temperatures (4.5 K) the channel conductance is observed to be consistent with ballistic transport, while at elevated temperatures (77 K) the conductance is observed to increase. We attribute this 'superballistic' transport to a viscous enhancement of the conductance originally predicted by Gurzhi, a hallmark of hydrodynamic flow. We further use these measurements to extract the electron-electron scattering length at a range of carrier densities. We compare our measurements to finite-element simulations of a Stokesian fluid with different parameters, finding good agreement at 77 K for a fluid with a kinematic viscosity of $0.7 \text{ m}^2/\text{s}$. Our results demonstrate the incredible utility of STP in distinguishing between different electronic transport regimes, and quantifying the interaction length scales that lead to a distinct flow profiles.

11:45 AM CH03.01.05

Sub-Molecular Resolution nc-AFM and KPFM Imaging of Dipolar Molecule Assemblies on Si(111):B Natalia Turek¹, Sylvie Godey¹, Dominique Deresmes¹, Christophe Krzeminski¹, Judicael Jeannoutot², Younes Makoudi², Frank Palmino², Frederic Cherioux², David Gao³ and Thierry Melin¹; ¹IEMN-CNRS, France; ²FEMTO ST-CNRS, France; ³NANOLAYERS, United Kingdom

We studied by non-contact AFM (nc-AFM) the formation of molecular self-assemblies on the passivated surface of boron doped silicon B-Si(111)- $(\sqrt{3}\times\sqrt{3})R30^\circ$. The investigated molecules (1-(4'-cyanophenyl)-2,5-bis(decyloxy)-4-(4'-iodophenyl)benzene) possesses aliphatic chains attached to a triphenyl core ended with two possible different terminations (either iodine or cyano group). The use of a passivated semiconductor substrate enables creating regular and extended structures without significant change in electronic properties of molecules [1]. Scanning tunneling microscopy and nc-AFM imaging have been performed using a low-temperature (AFM/STM (JT AFM/STM, SPECS) operated at T=4K with high stiffness Kolibri sensors ($k=540 \text{ kN/m}$, $f_0=1 \text{ MHz}$). The growth of a periodic molecular network is observed, formed by parallel lines made by molecule aromatic cores and interdigitated aliphatic chains placed between adjacent rows. We obtain submolecular resolution in the constant height δf images without intentional tip functionalization, but only by conditioning the tip on the silicon surface [2]. We will discuss the high-resolution AFM imaging, as well as the conformation of the molecules in the observed assemblies (e.g. changes in the interdigitated aliphatic chains ordering). Kelvin Probe Force Microscopy (KPFM) images of single molecules and molecular assemblies with sub-elementary charge sensitivity [3] and submolecular resolution will be provided and discussed, in particular with respect to the choice of the molecular terminations. They reveal the dipolar character of asymmetric molecules and are consistent with the formation of dipole-driven molecular arrays, in the case of self-assemblies. Density functional theory calculations as well as molecular dynamics simulations will be compared with experimental results.

- [1] Makoudi Y, Beyer M, Lamare S, Jeannoutot J, Palmino F, Chérioux F, *Nanoscale* 2016, 8, 12347.
- [2] Berger J, Spadafora EJ, Mutombo P, Jelínek P, Švec M, Small, 2015, 113686-3693.
- [3] Turek N, Godey S., Deresmes D, Melin T, *Phys. Rev. B* 2020 102, 245433.

12:00 PM CH03.01.06

Late News: Anomalous Tip-Sample Interaction on Soft 2D Materials Revealing Inter-Layer van der Waals (VDW) Strength by Scanning Tunneling Microscopy (STM) Nirjhar Sarkar, Prab Bandaru and Robert C. Dynes; UC San Diego, United States

A new solution is offered to understand an instrumental artifact which is the anomalously high atomic amplitudes on graphite surface measured by Scanning Tunneling Microscopy (STM) using the local elastic deformation theory. This is demonstrated by a series of simple experiments done to measure atomic topography of various 2D surfaces like Niobium diselenide, monolayer graphene and graphite across their monatomic step heights to show how tip-sample interaction causing the anomalous atomic amplitudes is of purely mechanical nature and not electronic. The underlying physics of Van der Waal bonding playing a major role in these interactions with 'soft' 2D surfaces will be uncovered.

12:15 PM CH03.01.07

A Graphene-Based Platform for Investigation of Protein Assembly by Infrared Nanospectroscopy Xiao Zhao^{1,2}, Dong Li¹, Yi-Hsien Lu¹, Paul Ashby¹ and Miquel Salmeron^{1,2}; ¹Lawrence Berkeley National Laboratory, United States; ²University of California, Berkeley, United States

The nanoscale structures and dynamical processes of proteins have been extensively studied by various imaging techniques such as electron microscopy and atomic force microscopy (AFM) in liquid. However, these imaging techniques can damage or perturbate the samples and do not provide chemical identification. This prevents a direct monitoring of structural and chemical evolution under physiological conditions. Herein, we demonstrate a new nondestructive platform that enables nanoscale Infrared (IR) spectroscopy for protein at graphene-aqueous solution interface by combining graphene liquid cell and Fourier Transform Infrared Nanospectroscopy (nano-FTIR). Single layer graphene separating the assembly solution and the tip minimize the sample damage and tip contamination. The S-layer protein structural evolution during and after assembling process is monitored by recording the amide I and II vibration bands, which provides unique and complimentary information to the AFM morphology in liquid. Our platform opens up broad opportunities for *operando* study of soft materials or nanostructures (enzyme, other membrane protein, virus, and plastic material) in their realistic condition and under external stimuli.

SESSION CH03.02: New Developments I
Session Chairs: Roger Proksch and Igor Sokolov
Tuesday Afternoon, November 30, 2021
Hynes, Level 3, Room 301

2:00 PM CH03.02.02

Using High-Speed, Molecularly Resolved AFM to Investigate Nucleation from Solution James J. De Yoreo^{1,2}, Benjamin A. Legg¹, Marcel D. Baer¹, Christopher J. Mundy^{1,2}, Jaehun Chun^{1,3} and Kislou Voitchofsky⁴; ¹Pacific Northwest National Laboratory, United States; ²University of Washington, United States; ³City University of New York, United States; ⁴University of Durham, United Kingdom

Investigating nucleation from solutions is challenging, because it is a consequence of unstable density fluctuations, making the structures and events that must be probed both transient in nature and small in spatial extent. Thus high-speed, molecularly resolved AFM provides a powerful and unrivalled method to investigate nucleation from solution by choosing systems that nucleate onto surfaces. Here we illustrate the deep level of fundamental insight into the pathways and energetics of nucleation made possible by this method by using it to investigate epitaxial nucleation of gibbsite (Al(OH)₃) on muscovite mica (001). AFM results combined with streaming potential measurements reveal a surface population of ions that is dominated by hydrolyzed species (Al(OH)₂⁺ and Al(OH)₂²⁺) even though Al³⁺ vastly dominates the bulk solution. These adsorbed ions evolve into subcritical clusters with increasing saturation state and temperature, constituting a population whose size distribution and fluctuations exhibit many similarities to the predictions of classical nucleation theory (CNT). However, severe discrepancies with CNT emerge when the values of key thermodynamic parameters are extracted from the AFM data. Moreover, the resulting gibbsite film forms simultaneously across the surface, rather than through the appearance of rare critical-size nuclei. Using kinetic Monte-Carlo (KMC) simulations, we demonstrate how this behavior can arise from electrostatic interactions between positively charged aluminum clusters and the negatively charged mica surface. Our results indicate that surface charging can dynamically modify both the chemical potential for accumulating ions on the surface, and the edge tension of the clusters. As the film grows, these interactions stabilize a nanostructured surface mesophase, which evolves gradually via a process of cluster growth and coalescence and is not limited by the classical formation of a critically sized nucleus. Our results show that high speed AFM provides a direct molecular view of nucleation at surfaces that reveals both consistencies and deviations from the simple classical picture and highlights the inherent role of surface charge in determining pathways and outcomes of nucleation.

2:15 PM CH03.02.03

Enhancing the Force Stability, Force Precision and Time Resolution of BioAFM with Focused-Ion-Beam Modified Cantilevers Thomas Perkins^{1,2}; ¹University of Colorado Boulder, United States; ²National Institute of Standards and Technology, United States

Atomic force microscopy (AFM)-based single-molecule force spectroscopy enables a wide array of studies, from measuring the strength of a ligand-receptor bond to elucidating the complex unfolding pathway of individual membrane proteins. Such studies and, more generally, the diverse applications of AFM across biophysics and nanotechnology are improved by enhancing the force stability, force precision, and time resolution of bioAFM. For an advanced, small-format commercial AFM, we uncovered how these three metrics were limited by the cantilever itself rather than the larger microscope structure, and then describe three increasingly sophisticated cantilever modifications using a focused ion beam that yielded enhanced data quality. For example, our most recent cantilever design, a "Warhammer," achieved a sub-pN force precision and stability over 5 decades of time (1 ms – 100 s) coupled with 8- μ s time resolution in liquid when positioned just above a surface. High-precision single-molecule studies of membrane proteins—the target for over 50% of current and future drugs—have lagged analogous studies of globular proteins due to instrumental limitations. We revisited the unfolding of the canonical membrane protein bacteriorhodopsin with a 100-fold improvement in time resolution and a 10-fold improvement in force precision. The resulting data revealed the unfolding pathway in unprecedented detail. I will conclude by discussing extensions of this capability to other diverse biomolecules, including nucleic-acid structures and globular proteins involved in hereditary heart disease. The metrological enhancements enabled by modified AFM cantilevers are not limited to single-molecule force spectroscopy but are broadly applicable across diverse AFM studies. Importantly, these modified cantilevers are robust, reusable over multiple days and, in our lab, typically modified by undergraduates. Thus, they are neither too costly nor too challenging to modify for routine use.

2:30 PM CH03.02.04

Direct Probing of the Interfacial Hydrogen Bonding and Dynamics of PMMA Confined in Porous Organosilicate Using Correlative Scanning Probe Microscopy David W. Collinson and Reinhold H. Dauskardt; Stanford University, United States

Understanding the chemistry and dynamics of polymers at the nanoscale and under confinement is of utmost importance for high performance and emerging materials and composites. Scanning probe microscopy (SPM) techniques promise extremely high resolution and direct, sensitive measurement of

polymer chemical and mechanical properties down to 1-10 nm. However, collection and interpretation of SPM data remains complicated due to the difficulty in interpreting measured properties at such fine scales. Correlative approaches using both mechanical and chemical SPM techniques, in conjunction with modelling of tip-surface interactions, can enable discovery even at the limits of SPM resolution and performance.

Here, we demonstrate the ability to directly measure the loss tangent of poly(methyl methacrylate) (PMMA) confined to 7 nm diameter pores in an organosilicate (OCS) matrix utilizing dynamic atomic force microscopy (AFM) and modelling of the tip-sample interactions. Further, we identify a decrease in the loss tangent of PMMA when confined to an OCS matrix treated to increase silanol density on the pore surfaces. At the nanoscale, X-ray photoelectron spectroscopy as well as other optical spectroscopy techniques demonstrate that the increased silanol density leads to an increase in hydrogen bonding between the carbonyl groups in the PMMA chains and the surface silanols. The increased bonding reduces chain mobility and consequentially decreases the observed loss tangent as the surface interaction strength increases. The correlative microscopy approach enables a direct link between the observed decrease in the loss tangent of PMMA as measured by AFM and the underlying change in polymer chemistry responsible.

The highly sensitive measurements and findings described above are enabled by a technique known as gas cluster ion beam (GCIB) etching. Previously, it has been challenging to prepare composite surfaces that consist of soft polymers and hard ceramic components that are sufficiently smooth to enable high resolution mechanical property measurements. To overcome these challenges a GCIB procedure is presented that allows for damage free removal of the PMMA and OCS to produce a surface with an R_a of approximately 0.3 nm. GCIB is a promising sample preparation method that has not been extensively used in the preparation of polymer composite samples for SPM. Expanded use of GCIB should enable a broader range of samples, particularly in-situ samples, to be probed with SPM techniques.

SESSION CH03.03: Poster Session I
Tuesday Afternoon, November 30, 2021
8:00 PM - 10:00 PM
Hynes, Level 1, Hall B

CH03.03.03

Using Electrostatic Force Microscopy to Investigate Localized Charges on Single-Walled Carbon Nanotubes Erin E. Christensen, Trevor M. Tumiel, Mitesh Amin and Todd D. Krauss; University of Rochester, United States

Electrostatic force microscopy (EFM) is a modification of atomic force microscopy (AFM) which allows for a quantitative determination of localized charges and dielectric constants at the nanometer scale. In our implementation of EFM, the tip is lifted off the surface and scanned at a constant height under an applied AC and DC voltage, thereby providing sensitivity to extremely small capacitive and coulombic forces. By modeling the surface charge-cantilever force through a coulombic interaction, quantitative determinations of surface charge magnitude and location are possible down to less than 0.1 e at room temperature. In this presentation we have used EFM to study the spatial distribution and magnitude of charged regions along individual single-walled carbon nanotubes (SWCNTs). For dozens of long NTs dispersed with ionic surfactant we found surprisingly large charge density variations all along the NT with magnitudes on the order of 1 e to 15 e per 25 nm², which is roughly the EFM spatial resolution. Also, the charges had both positive and negative signs. Acquiring EFM data from before and after photoexcitation suggests that the ionic surfactant actually creates local electrostatic perturbations that act as barriers for exciton transport, which leads to distinct localized regions of charge. Additionally, we have been able to correlate single molecule photoluminescence (PL) spectroscopy and AFM microscopy images of the same individual SWCNTs. We found a highly unexpected localization of PL at sites of significant surfactant coverage. From our EFM measurements, we know these sites routinely display greater static charge accumulation, which suggests a connection between the electrostatic and optical characteristics of SWCNTs. Current efforts in our laboratory aim to provide a more detailed comparison of the charge and emissive profiles of individual NTs by correlating single molecule spectroscopy with EFM.

SESSION CH03.04: Technical Developments
Session Chairs: Igor Sokolov and Dalia Yablon
Wednesday Morning, December 1, 2021
Hynes, Level 3, Room 301

10:30 AM CH03.04.01

Late News: Magnetic Mapping of Iron Using Magnetic Force Microscopy Kevin J. Walsh¹, Stavan Shah¹, Angie Blissett¹, Binbin Deng¹, Ping Wei¹, Josh Sifford¹, Sheng Tong², Samuel Oberdick³, Doug Scharre¹, Gang Bao², David McComb¹, Dana McTigue¹ and Gunjan Agarwal¹; ¹The Ohio State University, United States; ²Rice University, United States; ³University of Colorado Boulder, United States

Iron (Fe) is an essential metal involved in a wide spectrum of physiological functions in the body, including oxygen transport, enzymatic reactions and amino acid synthesis. Ferritin, the major iron storage protein in the mammalian body, consists of ~8 nm iron cores in the form of the iron-oxide crystal ferrihydrite. The size, distribution and oxidation state of ferritin(iron) has been shown to play an important role in health and disease. Histochemical staining, the routinely used approach to characterize iron distribution, offers limited insight into the chemical environment and composition of tissue iron. One of the properties of ferritin(iron) which has not been adequately exploited in histology is the magnetic behavior of tissue iron.

In this study we elucidate, how magnetic force microscopy (MFM), an atomic force microscopy (AFM)-based technique, can be used to map (magnetic) iron deposits in histological sections. MFM analysis was conducted on physiologically present ferritin(iron) deposits in naïve rodent spleen. To examine ferritin(iron) deposits in pathological tissues, an acutely injured rodent tissue (spinal cord) as well as tissues from chronic injury as present in brain tissue (hippocampus) from patients with Alzheimer's disease (AD) were used. Perl's histochemical staining was used to confirm the presence of ferric iron (Fe³⁺) and analytical transmission electron microscopy was used to verify ferritin(iron) deposits at the ultrastructural level. MFM images were analyzed to ascertain the size of magnetic deposits, the strength of the magnetic signal (phase), and fluctuations (roughness) of the MFM signal.

Our results show that while Perl's histological staining is sensitive to the use of chemical fixatives, MFM analysis is not affected between fixed and unfixed tissues. Further, the size(s) of the magnetic deposits ascertained using MFM corresponded to that of ferritin(iron) rich lysosomal iron ascertained using electron microscopy. The size of these iron-rich deposits was significantly smaller in the diseased tissues (injured spinal cord and AD brain tissue) as compared to naïve spleen. Further naïve spleen exhibited significantly higher strength of the MFM signal when compared to injured spinal cord and brain

tissue. Interestingly, the roughness of MFM signal was similar across all tissues. TEM analysis indicated that the density of lysosomal ferritin(iron) deposits, was the major factor accounting for variances in MFM phase differences in mice tissue. Thus, rich and physiologically relevant information can be obtained through MFM mapping of histological iron.

To enable a multimodal analysis of iron we further developed an indirect MFM technique where TEM, MFM and fluorescence microscopy could be performed on the very same sample. In indirect MFM the sample is physically separated from the MFM probe by an ultrathin membrane. Further studies along these directions can allow for a high throughput and multimodal analysis of the quantity and quality of iron in AD. This can be of special relevance in neurodegenerative diseases where a transition of ferrihydrite into magnetite/maghemite is reported as the two minerals differ in their magnetic properties. Finally, the high sensitivity and spatial resolution offered by MFM makes it an attractive technique for a label free mapping of iron deposits in histology.

1) Blissett, A. R., et. al. Sub-cellular In-situ Characterization of Ferritin(iron) in a Rodent Model of Spinal Cord Injury. *Sci. Rep.* (2018)

2) Sifford, J., et. al. Indirect magnetic force microscopy. *Nanoscale Advances.* (2019)

3) Walsh, K. J., et. al. Effects of fixatives on histomagnetic evaluation of iron in rodent spleen. *JMMM.* (2020)

10:45 AM CH03.04.02

Time-Resolved Scanning Ion Conductance Microscopy for Three-Dimensional Tracking of Nanoscale Cell Surface Dynamics Samuel Leita¹, Barney Drake¹, Katarina Pinjusic¹, Xavier Pierrat¹, Vytautas Navikas¹, Adrian Nievergelt¹, Charlene Brillard¹, Denis Djekic², Aleksandra Radenovic¹, Alex Persat¹, Daniel Constam¹, Jens Anders² and Georg Fantner¹; ¹EPFL, Switzerland; ²Universität Stuttgart, Germany

Dynamic nanoscale information of cell structures and organelles plays a vital role in understanding cellular function. Nanocharacterization techniques, such as super-resolution optical microscopy, electron microscopy, and atomic force microscopy (AFM), have been applied to image the structure of cells in great detail. The major challenge is to obtain three-dimensional (3D) information at nanometer resolution without affecting the viability of the cells and avoiding interference with the process. Scanning probe microscopy methods such as AFM can generate high-resolution characterization of stiff cell surfaces, such as bacteria [1]. However, the mechanical contact between the tip and the sample deforms soft membranes, disturbing the native state of eukaryotic cells and prevents long time-lapse imaging. Here, we show a scanning ion conductance microscope (SICM) for high-speed and long-term nanoscale imaging of soft cells [2]. By implementing advances in nanopositioning, nanopore fabrication, microelectronics, and controls engineering we developed a microscopy method that can resolve spatiotemporally diverse 3D processes on the cell membrane at sub-5nm axial resolution. Moreover, we combine 3D surface data from SICM with volumetric super-resolution optical fluctuation imaging (SOFI), to generate correlative high-resolution information of live cell morphology [3]. This true non-contact technique enables a detailed look at long-period membrane events with sub-second resolution and may offer insights into cell-cell interactions for infection, immunology, and cancer research.

1: Pascal Odermatt *et al.* Overlapping and essential roles for molecular and mechanical mechanisms in mycobacterial cell division. *Nature Physics* (2019). doi:10.1038/s41567-019-0679-1

2: Samuel M. Leita *et al.* Time-resolved scanning ion conductance microscopy for three-dimensional tracking of nanoscale cell surface dynamics. *bioRxiv* (2021). doi:10.1101/2021.05.13.444009v1

3: Vytautas Navikas, Samuel M. Leita *et al.* Correlative 3D imaging of single cells using super-resolution and scanning ion-conductance microscopy. *bioRxiv* (2020). doi:10.1101/2020.11.09.374157

11:00 AM CH03.04.03

Fully Motorized, Tip-Scanning AFM with Photothermal Excitation for Improved Imaging and Cell Measurement Methods Jonathan Adams¹, Christian Bippes¹, Lukas Howald¹, Simon Fricker¹, Patrick Frederix¹, Pieter van Schendel¹, Hans Gunstheimer¹, Laura Gonzalez¹, Gabriel König¹, Gotthold Fläschner^{1,2} and Dominik Ziegler¹; ¹Nanosurf AG, Switzerland; ²ETH Zürich, Switzerland

Since its invention, atomic force microscopy (AFM) has become a widely used technique in many different research disciplines from physics, through materials science to life sciences. Instruments and measurement methods alike have been developed that allow for imaging surface structures and probing the mechanical and electrical properties of samples at high spatial resolution. Along with new methods, a major aim in recent AFM development is towards improved ease of use, reliability, and integration with complementary techniques. Our newly developed DriveAFM addresses these topics by including several technological features that improve the ease of use and extend the capabilities of the instrument. It features a fully-motorized, tip-scanning design that allows for integration with optical microscopy, flexibility regarding sample size and weight, and the possibility for automated system operation from laser adjustment to sample translation. Most importantly, we implemented photothermal cantilever excitation in this tip-scanning AFM and used this feature in several new imaging and measurement methods.

Photothermal excitation directly excites the cantilever by locally heating it at its base, and thus allows stable and clean excitation in almost any environment [1]. Here, we will show the technical difficulties and concepts implemented to include photothermal excitation in a fully motorized tip scanning AFM employing a new optomechanical design [2] as well as measurement data enabled by this implementation. The clean and unambiguous photothermal excitation of the cantilever and its textbook-like response, especially liquids, allows new kinds of measurements, e.g. time-resolved measurement of mass changes [3] or probing the nanomechanical properties of cells over a wide range of frequencies [4]. The ability to effectively drive small, fast cantilevers with photothermal excitation also below their resonance frequency allows off-resonance imaging modes being operated at higher actuation frequencies compared to typically used piezo-based actuation schemes [5].

[1] A. P. Nievergelt *et al.*, *Beilstein J. Nanotech.* (2014) 5: 2459–2467

[2] J.D. Adams. U.S. Patent 10,564,181B2 (2020)

[3] D. Martinez-Martin *et al.*, *Nature* (2017) 550: 500–505

[4] G. Fläschner *et al.*, *Nat. Comm.* (2021) 12:2922

[5] A. P. Nievergelt *et al.*, *Nat. Nanotech.* (2018) 13: 696-701

11:15 AM CH03.04.04

Massively Parallel, Cantilever-free Atomic Force Microscopy Wenhan Cao¹, Nourin Alsharif¹, Zhongjie Huang², Alice White¹, YuHuang Wang² and Keith A. Brown¹; ¹Boston University, United States; ²University of Maryland, United States

Resolution and field-of-view present a challenging tradeoff in microscopy. Atomic force microscopy (AFM), in which a cantilevered probe deflects under the influence of local forces as it scans across a substrate, is a key example of this tradeoff with high resolution imaging being largely limited to small areas. Here, we show that nanoscale motion of cantilever-free probes can be imaged using conventional optical microscopy to enable massively parallel AFM. Specifically, we realize optically reflective rigid probes on a compliant film that comprises a distributed optical lever that reports local deformation.

By observing the optical contrast on each probe in an array as it is raster scanned across a sample, we demonstrate parallel imaging of surface topography with 1,088 probes with 100 nm lateral resolution and sub 10-nm vertical precision across 0.5 mm. The scalability of this approach makes it well suited for imaging applications that require high resolution over large areas such as integrated circuit quality control, optical metasurface inspection, and multi-scale characterization of biological tissue.

[1] Cao, W.; Alsharif, N.; Huang, Z.; White, A. E.; Wang, Y.; Brown, K. A., Massively parallel cantilever-free atomic force microscopy. *Nat. Commun.* **2021**, *12* (1), 393.

11:30 AM CH03.04.05

A Novel Scheme to Interpret Linear and Non-Linear Interactions in Dynamic Atomic Force Microscopy [Jaime Colchero](#)¹, Pablo Contreras Vélez¹, Jesus Sanchez Lacasa^{2,1} and Juan Francisco Gonzalez Martinez^{3,1}; ¹University de Murcia, Spain; ²Weizmann Institute of Science, Israel; ³University of Malmo, Sweden

In practical applications Dynamic Atomic Force Microscopy (DAFM) a (highly) non-linear oscillator, since the oscillation amplitude is (much) larger than the typical length scale of tip-sample interactions. However, it is mostly modelled as a (multifrequency) harmonic oscillator. This very simple approximation works surprisingly well, also for cases where the DAFM system is clearly operated in a large oscillation regime, and therefore non-linearity should be important. In this work, we will discuss why this apparent contradiction is in fact possible. For this, a new scheme to interpret and unify linear and nonlinear interactions is proposed. Using the classical model for the driven damped harmonic oscillator, its response is described by means of a complex number. We explicitly calculate how the time dependence of the deflection is processed by a typical Lock-In setup to obtain a point in the complex plane representing the oscillation state.

Using the Virial Theorem and work of San Paulo et al. [1] as starting point, we show how a linear DSFM system can be easily interpreted in terms of "Circles". Essentially, as the drive frequency is tuned through the resonance frequency the outputs of a typical DSFM electronics describe to a very good approximation a "Circle" when visualized in xy-mode on an oscilloscope. Interestingly, our model shows that this "Circle" remains essentially invariant when including the non-linearity of typical tip-sample interactions. These "Circles" are distorted only by dissipation which varies with tip-sample distance. We therefore propose that this representation scheme allows a very sensitive method to separate the effect of conservative interactions (linear as well as non-linear) from the effect of dissipative interactions.

[1] A. San Paulo and R. García. PRB 66:041406 (2002).

SESSION CH03.05: Nanomechanics I
Session Chairs: Greg Haugstad and Igor Sokolov
Wednesday Afternoon, December 1, 2021
Hynes, Level 3, Room 301

1:30 PM *CH03.05.01

The Impact of Nanostructure on Viscoelastic Properties of Polymer Composites [Bede Pittenger](#), Sergey Osechinskiy, John Thornton, Sophie Loire and Thomas Mueller; Bruker, United States

The mechanical behavior of polymer composites is controlled by the properties of the components as well as the microstructure of the material. Because confinement effects and interphase formation can alter properties of the microphases, only measurements performed directly on the composite can provide a complete picture of this local property distribution.

In contrast, the bulk viscoelastic properties of these materials targeted during material development are usually measured using dynamic mechanical analysis, DMA (also known as dynamic mechanical spectroscopy, DMS). This measurement involves application of an oscillating stress or strain to a macroscopic sample, with the response of the sample measured as a function of oscillation frequency). When heterogeneous samples are measured using this macroscopic technique, no information about the properties of the microstructure is available – only the spatially averaged properties of the whole sample.

Atomic Force Microscopy (AFM) has the resolution and mechanical sensitivity to provide the needed local mechanical property information. However, previous AFM measurements of viscoelastic properties [1,2] have suffered from several drawbacks, making it impossible to compare directly with DMA. To address this issue, we have developed a mode combining the benefits of AFM and DMA [3]. Like bulk DMA, AFM-nDMA provides spectra of storage and loss modulus at low frequencies. Unlike bulk DMA, it can localize the measurements and generate maps with resolution of a few nanometers.

In this presentation we will demonstrate how AFM-nDMA spectra can be compared directly to bulk DMA spectra. We will review insights gained when time-temperature superposition [4] is applied to AFM-nDMA data to generate master curves, including for materials that only exist in microscopic domains within the sample. Finally, we will discuss how comparing this nanoscale viscoelastic data with that of the bulk can clarify structure-property relationships in polymer composites.

[1] B. Pittenger and D. G. Yablon, *Bruker Application Note*, 2017, AN149, doi: 10.13140/RG.2.2.15272.67844.

[2] M. Chyasnachyus, S. L. Young, and V. V Tsukruk, *Langmuir*, 2014, 30, 10566.

[3] B. Pittenger, S. Osechinskiy, D. Yablon, and T. Mueller, *JOM*, 2019, 71, 3390.

[4] M. L. Williams, R. F. Landel, and J. D. Ferry, *J. Am. Chem. Soc.*, 1955, 77, 3701.

2:00 PM *CH03.05.02

Physical Interpretations of Multimodal AFM Contrast on Soft Materials [Greg D. Haugstad](#)¹, Andrew Avery², Brad Hauser³, Stephen Hubig⁴, Rachel Rahn⁴ and Melinda Shearer⁵; ¹University of Minnesota, United States; ²Unilever Research, United Kingdom; ³Donaldson, United States; ⁴Ecolab, United States; ⁵PPG Industries, United States

In this work we quantitatively analyze up to eight AFM measurables that can generate materials contrast on soft matter, including (i) sliding friction force in contact mode; (ii, iii) adhesion and contact stiffness in force-distance curve mapping (both slow and fast variants, e.g. "force volume" and "peakforce" modes), (iv, v) phase imaging in net attractive- and net repulsive-regime dynamic/AC mode (aka traditional amplitude-modulation "tapping mode"); (vi, vii) contact resonance amplitude and frequency under pulsed-IR excitation (aka resonance-enhanced mode on a Bruker NanoIR3 AFM-IR system); (viii) Fourier-reconstructed conservative and dissipative force versus distance relationships analyzed and mapped using machine learning in intermodulation mode (i.e., Intermodulation Products AB Multi Lockin Analyzer / software system).

We apply select combinations of these methods to polymer blends, nanostructured single-layer and multi-layer coatings, two-surfactant and surfactant/nanoparticle ultrathin films, and polymer/small-molecule (e.g., drug) mixtures, all being systems of interest to our industrial as well as academic collaborators. We seek improved understandings of (i) complementary information obtained (mechanical, tribological, surface energy, chemical) as well as (ii) methodological limitations and optimizations.

2:30 PM CH03.05.03

Multidimensional Tomography of Soft Materials by Atomic Force Microscopy and Dynamic Mechanical Spectroscopy Renato C. Aguilera¹, Maxim Dokukin^{1,2}, Nadia Makarova¹ and Igor Sokolov^{1,1,1}; ¹Tufts University, United States; ²NanoScience solutions, Inc., United States

Material fate and degradation *in situ* is regulated not only by chemical interactions but also the stress and strain from coupled mechanical systems. Strain defects and breakage of nanoscale soft materials such as tissue scaffolds, biopolymers, and cells are elusive to characterize due to their subtle and slow viscoelastic response. Here, we present the application of our new technique, FT-NanoDMA, to create a multidimensional tomography of the dynamical mechanical properties of such soft materials. FT-NanoDMA stands for Fourier transformed nano dynamical mechanical analysis, which is implemented in conjunction with atomic force microscopy (AFM). It allows for simultaneous recordings at different frequencies of multiple dynamical mechanical properties of soft materials, such as the storage and loss moduli, loss tangent, etc. The FT-nanoDMA is a modality that allows for mechanical analysis of nanointerfaces and single cells with a nanoscale spatial resolution (up to 10-70 nm when recorded on fixed cells) and spans the entire biological spectroscopic range (up to 300 Hz). The images of the distribution of these parameters can be recorded at each particular depth, thereby creating a stack of images suitable to create a multidimensional tomography of single cells. We demonstrate examples, which show that the tomographic images show unique features not present in the complementary fluorescent/optical images of cells.

3:45 PM CH03.05.05

AFM Based Nanomechanical Experiments to Capture Interphasial Property Gradients in Poly(methyl methacrylate)-Polyrotaxane Blends Suzanne Peterson, Glendimar Molero, Zewen Zhu, Hung Jue Sue and Pavan Kolluru; Texas A&M University, United States

Poly (methyl methacrylate) (PMMA) is often used as a lightweight, shatter resistant alternative to glass, but exhibits low scratch resistance and poor ductility. It was recently shown that blending PMMA with a very low concentrations (1 wt%) of two different polyrotaxanes (PR) - unmodified PR (uPR) and modified PR (mPR) improves these properties. uPR was created by grating cyclodextrin (CD) rings onto a polycaprolactone (PCL) backbone, while the mPR had methacrylate functional groups at the end of the PCL to facilitate miscibility with PMMA. Although bulk scale dynamic mechanical analysis (DMA) and dielectric spectroscopy on these PMMA-PR blends have indicated that significant PMMA-PR interactions in these systems lead to different molecular mobility changes, which eventually contribute to the observed mechanical property changes at the bulk scale, a direct understanding of the local interfacial interactions is missing. This presentation will discuss the use of Atomic Force Microscope (AFM) based nanomechanical spectroscopic methods to directly map the local time-dependent mechanical property gradients at the interphase regions in PMMA-uPR and PMMA-mPR blends, which in turn will provide direct insights into how PMMA-PR interactions affect their mechanical behavior.

3:00 PM BREAK

4:00 PM CH03.05.06

Direct Evidence for the Polymeric Nature of Polydopamine Katerina Malollari, Peyman Delparastan and Phillip Messersmith; University of California, Berkeley, United States

Inspired by the adhesive proteins of mussels, polydopamine (PDA) has emerged as one of the most widely employed materials for surface functionalization. Despite numerous attempts at characterization, little consensus has emerged regarding whether PDA is a covalent polymer or a noncovalent aggregate of low molecular weight species. Here, we employed single-molecule force spectroscopy (SMFS) to characterize PDA films. Retraction of a PDA-coated cantilever from an oxide surface shows the characteristic features of a polymer with contour lengths of up to 200 nm. PDA polymers are generally weakly bound to the surface through much of their contour length, with occasional “sticky” points. Our findings represent the first direct evidence for the polymeric nature of PDA and provide a foundation upon which to better understand and tailor its physicochemical properties.

SESSION CH03.06: Cells and Biological Samples I
Session Chairs: Keith Brown and Igor Sokolov
Thursday Morning, December 2, 2021
Hynes, Level 3, Room 301

10:30 AM CH03.06.01

How to Combine AFM with Machine Learning Analysis Igor Sokolov and Siona Prasad; Tufts University, United States

Recent large interest in machine learning (ML) analysis has been extended to atomic force microscopy (AFM). In this talk, I will address three questions which typically arise when AFMers start applying ML to classify the AFM images:

1. What mode is the best to use?
2. How many images is sufficient to run machine learning classifiers and believe the results?
3. How do I know that the obtained classification is not an artifact of some fine-tuning?

In this talk, I will suggest answers to the questions. In short, the mode of operation should be robust, repeatable. This is the key. The number of images required for classification can be roughly estimated using “the rule of 10”. A more precise algorithm to identify the required number of images will be described. To be confident that one doesn’t deal with an artifact of fine-tuning or overtraining a classifier, we suggest a rather simple yet powerful method of estimating the exact amount of overtraining by using randomization of the initial classification. Examples will be given.

10:45 AM CH03.06.02

Carbon Nanotube Penetration of Cell Membranes Fabio Priante¹, Ygor Jaques¹, Takeshi Fukuma² and Adam Foster^{1,2}; ¹Aalto University, Finland; ²Nano Life Science Institute (WPI-NanoLSI), Kanazawa University, Japan

The possibility of non-destructively measuring living cells and their internal structures with nanoscale resolution would allow for a much greater understanding of numerous biological phenomena. To realize this goal, the use of carbon nanotube (CNT)-terminated tips in atomic force microscopy

(AFM) has been shown to hold promise [1].

However, even in the very first step of the proposed “nanoendoscopic” process, consisting in the penetration of the plasma membrane, it is not always easy to give a precise interpretation of the experimental signal, which is a convolution of cell dynamics, tip shape and buffer solution.

Here, we use coarse-grained (CG) molecular dynamics simulations to investigate the effect that different widths, thicknesses and functionalization of the CNT tip can have in the penetration process. To simulate the membrane and the solvent dynamics we use the Martini 2 Force Field [2], while the CNT is simulated with a Martini-compatible force-field [3] which is more accurate in reproducing multi-layer graphene mechanical properties.

We carry out the membrane penetration by steering the CNTs downwards with constant velocity, then extracting the system's free energy using umbrella sampling, finally obtaining simulated force profiles. Additionally, we probe the possible role of the membrane skeleton mesh size [4] by emulating its effect as a position restraint on the lipids at the membrane's edge. We directly compare our results to experimental measurements using an equivalent setup and outline the successes and limitations of the model.

[1] - Singhal, R., Orynbayeva, Z., Kalyana Sundaram, R., Niu, J., Bhattacharyya, S., & Vitol, E. et al. (2010). Multifunctional carbon-nanotube cellular endoscopes. *Nature Nanotechnology*, 6(1), 57-64.

[2] - Marrink, S., Risselada, H., Yefimov, S., Tieleman, D., & de Vries, A. (2007). The MARTINI Force Field - Coarse Grained Model for Biomolecular Simulations. *The Journal Of Physical Chemistry B*, 111(27), 7812-7824.

[3] - Ruiz, L., Xia, W., Meng, Z., & Keten, S. (2015). A coarse-grained model for the mechanical behavior of multi-layer graphene. *Carbon*, 82, 103-115.

[4] - Morone, N., Fujiwara, T., Murase, K., Kasai, R., Ike, H., & Yuasa, S. et al. (2006). Three-dimensional reconstruction of the membrane skeleton at the plasma membrane interface by electron tomography. *Journal Of Cell Biology*, 174(6), 851-862.

11:00 AM CH03.06.03

Mechanobiology of Cancer Metastasis to Bone Using Direct Nanoindentation Dinesh R. Katti, Kalpana Katti, Sumanta Kar, MD Shahjahan Molla and Sharad V. Jaswandkar; North Dakota State University, United States

According to the World Cancer Research Fund, Breast cancer and Prostate cancer are among the most prevalent cancers in women and men, respectively. World Health Organization estimates that about 3.4 million breast and prostate cancer cases are reported each year, and about a million deaths occur worldwide due to these cancers. These cancers are almost entirely curable if detected in the early stage at the primary sites. However, most deaths occur due to metastasis when the cancer cells from the primary site migrate to a distant organ. Bone appears to be a niche for both cancers. We have developed a novel testbed using a bone mimetic nanoclay based scaffold to regenerate human bone using human mesenchymal stem cells followed by seeding prostate and breast cancer cells to generate tumors. Extensive analysis of the tumors using gene and protein expression assays and imaging confirm that the testbeds can replicate tumors during mesenchymal to epithelial transition (MET) for both cancers. Mechanical properties of cells have been used to describe the disease state for a variety of diseases. The confocal imaging of the cells from tumors shows significant changes to the cytoskeleton in terms of the quantity and organization within the cells as cancer progresses at the bone metastasis site. In the present work, for the first time, we have used mechanical response from cells from direct nanoindentation experiments on cancer cells from tumors generated on the testbeds to describe the evolution of cell properties during cancer progression at the bone metastasis sites. The nanoindentation experiments are conducted in static and dynamic modes to evaluate elastic moduli, hardness, and viscoelastic properties of cancer tumor cells. We report the evaluation of mechanical properties of cells from tumors grown on the testbed, over time, with two breast cancer cell lines (MCF-7 and MDA-MB231) at the bone metastases site using static and dynamic nanoindentation modes. A new fixture was designed and fabricated to conduct live-cell nanoindentation experiments. The force-displacement response, elastic moduli, hardness, plastic deformation, viscoelastic properties, and other mechanics characteristics were captured, along with confocal imaging of the cytoskeleton and gene and protein expressions at the same time points. Our results indicated a significant reduction in elastic modulus and increased fluid-like behavior of bone metastasized MCF-7 cells caused by depolymerization and reorganization of F-actin. On the other hand, bone metastasized MDA-MB-231 cells showed insignificant changes in elastic modulus and F-actin reorganization over time. We also measured changes to nanomechanical properties of MDA PCa2b prostate cancer cells during the MET and cancer bone metastasis progression over time. The stiffness of PCa cells decreases with metastasis; however, the mechanical plasticity increases during the same time, suggesting that PCa cells become softer on undergoing MET and softer with metastasis progression. In all cases, the imaging and gene, protein expression studies, and computational modeling point towards the depolymerization of actin and reorganization of the cytoskeleton as key factors in the evolution of cell mechanics. These studies present the use of direct nanoindentation as a potential new biomarker for metastasis progression.

11:15 AM CH03.06.04

Effect of Rapid-Solidification Induced Cellular Structures on the Corrosion Behavior of an Additively Manufactured 316L Stainless Steel Investigated by High-Speed AFM Yuliang Zhang, Thomas Voisin, Zhen Qi, Rongpei Shi, Tuan Anh Pham, Nathan Keilbart, Yu-Ting Hsu, Xiao Chen, Roger Qiu and Brandon Wood; Lawrence Livermore National Laboratory, United States

Additively manufactured 316L stainless steels (AM 316L SS) using laser powder bed fusion exhibit outstanding mechanical properties such as high strength and high ductility. The rapid-solidification induced sub-grain cellular structures, a dominant microstructural feature present in the as-built material, are largely responsible. However, in term of corrosion properties, the effect of these cellular structures has yet to be confirmed. A difference in metal dissolution rate between cell walls and cell interior has been reported but the underlying mechanisms remain unclear. To certify the use of AM 316L SS in corrosive environment, it is necessary to observe, understand, and predict the local effect of the microstructure on the resistance to corrosion, notably the initiation mechanisms. Here, we combine in-situ high-speed AFM (HS-AFM) during corrosion in HCl and NaCl solution, TEM, and SEM/EBSD to try and capture the native oxide breakdown, re-passivation, pit nucleation, and metal dissolution. We quantitatively measure and map, in-situ, the metal dissolution rates in the cellular structure for different grain orientations and compare to the conventional, well annealed material.

11:30 AM CH03.06.05

Robustness of AFM-based Method to Identify Mechanical Properties of the Cell Body and Pericellular Coat Nadia Makarova and Igor Sokolov; Tufts University, United States

The atomic force microscopy (AFM) combined with the force volume mode allows measurement of both indentation force curves and sample topography and is used to study cell mechanics. As was demonstrated in multiple publications, the Hertz mechanical model is not sufficient to describe cell mechanical properties in a self-consistent way. Self-consistency can be attained when using a relatively dull AFM probe and processing the data through the brush model. The brush model allows determination of both the mechanical properties of the cell body and the physical properties of the pericellular (glycocalyx) layer. Separation of the mechanical response of the pericellular layer from deformation of the cell body has demonstrated its utility in multiple studies, such as mechanics of cancerous and aging cells, and endothelial cells associated with various cardiovascular diseases. Despite its utility, the brush model has not yet been tested for its robustness with respect to the uncertainties within the model and experimental data. In other words, there is a need to demonstrate how unambiguous and precise the parameters extracted with the brush model are, when considering the uncertainty within the model and possible ambiguities of the collected force curves.

Here we address this need. We present the calculation of the elastic modulus of the cell and characteristics of the pericellular layer for a diverse set of cells:

fibroblasts of zebrafish, mouse neuroblastoma cells, and human cervical epithelial cells. We perform the analysis and demonstrate that the brush model is robust. Errors in defining the modulus, which come from both model and experimental uncertainties, are within 3%, which is substantially smaller than a typical uncertainty in the spring constant of the AFM cantilever. To quantify the uncertainties in the extracted force due to the brush layer, we characterize the brush with Alexander de Gennes model, which is described by the equilibrium size of the brush layer and grafting density of the brush molecules. Although it is an obviously oversimplified approximation, we see the uncertainty in those parameters is not larger than 25%. It is worth noting that the brush parameters calculated in this way is completely independent of the calculation of the modulus.

SESSION CH03.07: Nanomechanics II
Session Chairs: Philippe Leclere, Ken Nakajima and Igor Sokolov
Monday Afternoon, December 6, 2021
CH03-Virtual

1:00 PM *CH03.07.01

Measuring Mechanical Properties Of Developing Embryo with AFM Takaharu Okajima; Hokkaido University, Japan

It is widely recognized that embryogenesis is strongly associated with cell mechanical properties [1]. However, little is known about how embryonic single cells change their mechanical properties during their developing process due to a lack of technique. I will present our recent studies regarding the stiffness of cells in developing ascidian embryos with AFM [2] and the rheological measurements. The results showed that the force-distance curves measured in upper regions of embryonic cell surfaces were well fitted to the conventional Hertzian contact model, and the apparent Young's modulus was calibrated using a modified Hertzian contact model [3] considering the tilt angle of the sample surface. The cell shapes in the height and the Young's modulus images were almost identical, and the cell locations were in good agreement with the 3D virtual embryo model determined from confocal microscopic images, indicating that the embryonic cell stiffness measured by AFM mainly reflected the mechanical properties of cells that directly contacted the AFM probe. Furthermore, the cell stiffness exhibited a remarkable increase at the onset of cell division and then decreased after cell division, which is reminiscent of changes in an *in vitro* dividing single cell forming cortical actin filaments [4]. The results indicate that AFM is useful for measuring the embryonic cell stiffness in the developing process and can facilitate a better understanding of how embryonic single cells in animals are spatiotemporally regulated via mechanical cues.

References:

[1] D. Gilmour et al. Nature 541, 311 (2017). [2] Y. Fujii, et al, Commun. Biol. 4, 341 (2021). [3] Y. Fujii and T. Okajima, AIP Adv. 9, 015028 (2019). [4] R. Matzke et al. Nat. Cell. Biol. 3, 607 (2001).

1:30 PM CH03.07.02

Viscoelasticity of Single Polymer Chains Investigated by Single-Molecule Force Spectroscopy Xiaobin Liang¹ and Ken Nakajima^{1,2}; ¹Tokyo Institute of Technology, Japan; ²The University of Tokyo, Japan

In single-molecule force spectroscopy (SMFS), many studies have focused on the elasticity and conformation of polymer chains, but little attention has been devoted to the dynamic properties of single polymer chains. In this study, we measured the energy dissipation and elastic properties of single polystyrene (PS) and poly(N-isopropylacrylamide) (PNIPAM) chains in different solvents using a homemade piezo-control and data acquisition system, which provided more accurate information regarding the dynamic properties of the polymer chains. We quantitatively measured the chain length-dependent changes in the stiffness and viscosity of a single chain using a phenomenological model consistent with the theory of viscoelasticity for polymer chains in dilute solution. The effective viscosity of a polymer chain can be determined using the Kirkwood model, which is independent of the intrinsic viscosity of the solvent and dependent on the interaction between the polymer and solvent.

1:45 PM CH03.07.03

EUV Photoresist Dissolution Using Microperfusion Stage for High-Speed AFM Jiajun Chen¹, Luke Long², Andrew Neureuther², Patrick Naulleau¹ and Paul Ashby¹; ¹Lawrence Berkeley National Laboratory, United States; ²University of California, Berkeley, United States

The push towards high-resolution lithography in the semiconductor industry has yielded the introduction of extreme ultraviolet (EUV) into high-volume manufacturing. However, looking forward to future technology nodes, further improvements are required in photoresist materials to keep pace with and fully utilize improvements in the EUV source and scanner. One of the critical steps is to understand the role of the dissolution process, which converts latent exposure chemistry in the photoresist into a developed pattern. This process is particularly challenging to follow due to the requirement of nanometer spatial and sub-second temporal resolution simultaneously. Most metrology of the patterning process thus ignores either the temporal component of the dissolution process by measuring just the final developed structure or the spatial component as is done in most dissolution rate monitoring techniques. In our study, a microfluidic sample stage is designed to enable the delivery of full-strength developer within fractions of a second with better concentration control and smaller dead volume for less lag and more accurate time zero determination. Moreover, our microfluidic design minimizes the mixing problem of the full-strength developer and water, which usually disrupts laser-based detection mechanism, allowing us to monitor the development process with high-speed atomic force microscopy (AFM) at the nanoscale. Thus, our system offers the ability to probe the spatially-dependent nature of the dissolution process in a fab-like environment, providing insight into exposure-dependent dissolution rate gradient, material swelling, and polymer entanglement.

2:00 PM CH03.07.04

High Contrast Atomic Force Microscopy for Additive Filled Through-Thickness Vertical Block Copolymer Morphologies for High Permeability Oil-Water Separation Membranes Kshitij Sharma¹, Khadar B. Shaik¹, Ali Ammar¹, Mohammad K. Hassan², Samer Adham³, Mariam Al Ali Al-Maadeed² and Alamgir Karim¹; ¹University of Houston, United States; ²Qatar University, Qatar; ³Qatar Science and Technology Park, Qatar

Block copolymers with mechanically identical blocks having identical glass transitions such as Polystyrene-*b*-Poly(methyl methacrylate) (PS-*b*-PMMA) show poor contrast between domains, especially in vertically ordered microstructure. Addition of plasticizers that segregate into selective domains and significantly reduce the glass transition temperature of that block also increase its contrast for detection through atomic force microscopy. These additives also enhance the chemical incompatibility between blocks producing sharp interfaces that can be easily detected for the additive swollen domains. In this study, we demonstrate producing vertical domain assembly in as-cast block copolymer (BCP) thin films by controlling the casting environment using solvent mixtures and plasticizing additives. The combined interaction between the plasticizer segregated into selective domains and the solvent mixture drives the ordering front to produce through film vertical assembly in PS-*b*-PMMA films with cylindrical and lamellar volume fractions. The morphology

is probed with atomic force microscopy to analyze the effect of additive volume fraction on domain sizes and film morphologies. Ultrafiltration membranes are an energy-efficient alternative to overcome the environmental challenges occurring from the rising amounts of mixed oil and water through oil-spills and industrial wastewater etc. Ultrafiltration membranes were fabricated from these vertically oriented structures and are promising candidates for oil-water separation applications. In addition to the uniform pore size of the membranes, the membranes have been designed to function as highly permeable as well as selective active layers on top of the polyethersulfone (PES) support membranes. This has been accomplished during the membrane preparation stage by the addition of varying amounts of plasticizing and homopolymer additives to further modify the membranes. The influence of these additives on the pore characteristics and membrane performance have accordingly been analyzed as a function of their mass ratio with respect to BCP. The created asymmetric membranes were demonstrated to be effective for oil/water separation when plasticizing additives were added in the 50%-60% mass ratio.

2:15 PM CH03.07.05

Amplitude Nanofriction Spectroscopy [Antoine Lainé](#)¹, Andrea Vanossi², Antoine Nigues³, Erio Tosatti² and Alessandro Siria³; ¹Lawrence Berkeley National Laboratory, United States; ²SISSA, Italy; ³ENS - PSL, France

Macroscopic friction behaviors originate from the mechanical and tribological response of asperities at the microscopic and nanometric level. As a consequence atomic scale friction stands as a cornerstone for the field of tribology. At such small scale, materials exhibit mechanical properties reminiscent of soft materials, such as adhesion and high deformability, thus making similar experimental challenges arise. From a sliding friction perspective, the dynamics undergo different successive steps from elastic pinning to large velocity kinetic friction. Atomic force microscopy usually only probes the steady state response leaving the early sliding response unexplored. Here, we unveil a combined experimental and simulation framework based on a high-frequency oscillatory strained interface to resolve the onset of sliding as well as the large velocity steady-state at once. A model contact of a few atoms formed between a gold tip and graphite is used to demonstrate our experimental ability to explore the different sliding regimes. We uncover peculiar behaviors, from thermolubricity for the smaller contact, to superlubricity as the contact gets larger than the unit cell of graphite. This new experimental methodology paves the way for a better understanding of sliding friction and its different dynamic stages.

2:30 PM CH03.07.06

Developing a Framework for the Forward Prediction of the Mechanical Properties of Polymer Nanocomposites [Heer Majithia](#), Boran Ma and L. Catherine Brinson; Duke University, United States

To enable the forward prediction of mechanical properties of polymer nanocomposites, we have developed a novel framework that uses experimental methods and finite element analysis and we demonstrate it for a nanocomposite made of a polydimethylsiloxane (PDMS) matrix and silica particles (SiO₂). We have experimentally determined the microstructure distribution and the local mechanical properties of the extent of the interphase between the silica particles and the PDMS matrix via atomic force microscopy (AFM), and the macroscale properties of the PDMS matrix via dynamic mechanical analysis (DMA). We hypothesize that by accurately determining the local properties in the interphase we can predict the behavior of the macroscale nanocomposite as the interphase between the polymer matrix and filler has altered properties that are thought to be responsible for the enhanced properties observed in thin films and polymer nanocomposites. A key challenge in accurately determining the extent of the interphase around a nanoparticle via AFM occurs as a result of the complex contact conditions between the AFM tip and the polymer near an interphase. To address this we have developed a method similar to one used in nanoindentation experiments to eliminate the indentation depth dependence of the local property measurements and calculating depth independent properties that are not convoluted by extraneous influences. Consequently, we have performed finite element analysis (FEA) simulations to predict the macroscale properties of PDMS-SiO₂ nanocomposites and validated them against experimental data for PDMS-SiO₂ nanocomposites. This framework provides a method to achieve the forward prediction of mechanical properties of polymer nanocomposites with limited experimental work, optimizing the process to discover and develop materials with desired properties.

2:35 PM BREAK

SESSION CH03.08: New Developments II
Session Chairs: Philippe Leclere and Ken Nakajima
Tuesday Morning, December 7, 2021
CH03-Virtual

8:00 AM *CH03.08.01

Quantifying Nanoscale Electromechanical Properties of Polymeric and Soft Materials via Advanced Modes of Piezoresponse Force Microscopy [Liam Collins](#); Oak Ridge National Laboratory, United States

Electromechanical coupling underlies a broad range of diverse applications from energy harvesting to biotechnology. Voltage modulated (VM) AFM techniques including piezoresponse force microscopy (PFM) are uniquely positioned to probe electromechanical properties with spatial resolution from micrometers to nanometers. As with all AFM techniques, the goal of any PFM measurement should be towards quantification of the local material properties. Unfortunately, quantification of PFM signals remains a significant challenge. Indeed, with the growing popularity of PFM there has been a congruent rise in reports of nanoscale electromechanical functionality, including ferroelectric hysteresis, in materials that should be incapable of exhibiting piezo- or ferroelectric response. This presentation will evaluate the appropriateness of advanced modes of PFM, including interferometric and multifrequency methods, for quantification of soft and hybrid materials. A particular focus will be overcoming the susceptibility of PFM measurements to crosstalk, a pre-requisite for quantification of piezoelectric coupling coefficients. Throughout the presentation examples of quantitative measurements on soft and polymeric materials including PVDF-TrFE and hybrid organic inorganic perovskites will be described. *This work was conducted at the Center for Nanophase Materials Sciences, which is a DOE Office of Science User Facility.*

8:30 AM *CH03.08.02

Multimodal Chemical and Surface Potential Nano-Imaging Through Peak Force Infrared-Kelvin Probe Force Microscopy [Xiaoji Xu](#); Lehigh University, United States

Multimodal measurements of chemical composition, electrical properties, mechanical properties, and topography by scanning probe microscopy (SPM) deliver correlations across properties at the nanoscale and provide clues to the structure-function relationship of materials. In the past, measurements with these modalities are operated separately with different operational modes of SPM. Not only do the sequential measurements require additional operation time, subject to scanner/sample drift, but also, different modalities of SPM have different spatial resolutions, which undermine correlative analysis. For

example, the popular frequency-modulated Kelvin Probe Force Microscopy measures the surface potential with 30–50 nm spatial resolution under the ambient conditions, whereas the SPM measurements of chemical composition, mechanical properties, and topography can routinely achieve < 10 nm spatial resolution.

At the MRS conference, we will present our invention of an integrated SPM mode that can simultaneously provide chemical, surface potential, mechanical, and topographic imaging at < 10 nm spatial resolution under ambient conditions. First, we will present our development of pulsed force Kelvin probe force microscopy (PF-KPFM) that delivers 10 nm spatial resolution from surface potential measurement under ambient conditions. Second, we will briefly describe the peak force infrared (PFIR) microscopy on infrared nano-imaging and spectroscopy. Finally, we will introduce our invention of peak force infrared-Kelvin probe force microscopy (PFIR-KPFM) that combines PFIR and PF-KPFM in one unified SPM mode. In a single scan, the integrated PFIR-KPFM delivers simultaneous multimodal measurement at a comparable and high spatial resolution of < 10 nm. We demonstrated the PFIR-KPFM on a range of samples, from perovskite photovoltaics to protein aggregates, and revealed correlations among modalities.

9:00 AM CH03.08.03

Scanning Probe Microscopy—Are There Even Best Practices? Richard J. Sheridan¹, David W. Collinson², Marc Palmeri¹ and L. Catherine Brinson¹; ¹Duke University, United States; ²Stanford University, United States

Scanning probe microscopy encompasses techniques that span length scales, time scales, and operational complexity scales. Because of the existence and value of these complex measurements, it is typical for an eager, new user to require extended training together with an expert to reliably acquire the advanced, precise data they hope to collect.

In our new review in *Progress in Polymer Science* [1], we attempt to address the nuances of extended training by providing a resource in the form of a collection of recommendations and best practices in the nanomechanical characterization of polymers and other soft/heterogeneous materials. The review discusses and compares the variety of nanomechanical techniques available, provides details and practical considerations for real nanomechanical experiments, and summarizes notable published works as case studies for the application of available modes for nanoscale property mapping. This presentation selects a very small subset of the content to demonstrate the utility of the review as a guide, but also to draw attention to some unanswered questions that were raised as this domain continues to mature.

Our review is concentrated on nanomechanical AFM of polymers, both because that system is one of our group's competencies, and also because it prevented the scope of the review from growing without limit. But already the narrow scope raises questions: Are these recommendations applicable to other materials, like hydrogels or metals? Can they be applied to other scanning probe microscopy techniques, like scanning tunneling microscopy or single molecule force spectroscopy? To what extent? In this presentation, we seek to lay a foundation for a greater discussion and collaboration between groups and sub-fields regarding best practices, training, and converting individual or even institutional knowledge into common knowledge.

[1] Collinson DW, Sheridan RJ, Palmeri MJ, Brinson LC (2021) Best practices and recommendations for accurate nanomechanical characterization of heterogeneous polymer systems with atomic force microscopy. *Progress in Polymer Science*, 101420. <https://doi.org/10.1016/j.progpolymsci.2021.101420>

9:15 AM CH03.08.04

Automated Scanning Probe Microscopy Based on Deep Kernel Learning Yongtao Liu¹, Stephen Jesse¹, Susan E. Trolier-McKinstry^{2,2}, Maxim A. Ziatdinov^{1,1} and Sergei V. Kalinin¹; ¹Oak Ridge National Laboratory, United States; ²The Pennsylvania State University, United States

Ferroelectric materials remain a source of physical discovery through the long history of the field. On-going development has pointed to the crucial role of domains and domain walls in ferroelectric materials. The development of scanning probe microscopy (SPM) allows visualization of domain structure and its evolution under external fields, such as electric bias applied through tip and electrodes, strain, light illumination, and heating. However, the behaviors of interest mostly are related to domain structures and concentrated in specific locations. This initializes the opportunities of automated microscopy with an automatically defined workflow for scanning sequence and data acquisition. Here, we used a Deep Kernel Learning (DKL) framework to explore the domain structure and physical properties of ferroelectric materials. We further developed a workflow based on the DKL for Piezoresponse Force Microscopy (PFM) that allows problem-specific tuning of workflow and operation in real-time, which allows exploring polarization switching and domain structure in ferroelectric materials. The structure of the DKL kernel provides insight into the physics of the process. We further build the relationship between domain wall geometry and presence of ferroelastic domain walls, as well as topography, and hysteresis loop shape. Previously in the post-experiment approach, this was accomplished via im2spec and rotational variational autoencoder (rVAE) approaches. The DKL allows to learn these relationships during the experiment. This workflow can also be adapted to other microscopy systems, such as electron microscopy and optical microscopy.

Acknowledgments: This work is supported by the U.S. Department of Energy, Office of Science, Office of Basic Energy Sciences Energy Frontier Research Centers program under Award Number DE-SC0021118. This work is conducted at the Center for Nanophase Materials Sciences, a US Department of Energy Office of Science User Facility.

9:30 AM CH03.08.05

Conductive Hotspots in Hf_{0.5}Zr_{0.5}O₂—An Automated Experiment Investigation Yongtao Liu¹, Shelby S. Fields², Kyle P. Kelley¹, Stephen Jesse¹, Susan E. Trolier-McKinstry^{3,3}, Maxim A. Ziatdinov^{1,1}, Jon Ihlefeld^{2,2} and Sergei V. Kalinin¹; ¹Oak Ridge National Laboratory, United States; ²University of Virginia, United States; ³The Pennsylvania State University, United States

HfO₂-based materials have attracted a great deal of interest because they exhibit robust ferroelectricity at extremely thin thickness and are thermodynamically compatible with conventional semiconductors, leading to a wide range of applications in ferroelectric-based devices, such as field-effect transistors, random-access memory, and tunnel junctions. However, the local uniformity of HfO₂-based materials is rarely investigated, which is important for their application. In this work, we developed an automated experiment (AE) workflow in scanning probe microscopy (SPM) to investigate the local conductivity of a Hf_{0.5}Zr_{0.5}O₂ (HZO) thin film. This AE workflow maps a large field of view of material first and automatically locates the regions of interest (ROI); then, detailed zoom-in measurements are automatically performed in the ROIs to systematically understand the material under study. Further, to solve a universal problem—measurement drift—in microscopes, we embedded a drift correction algorithm to maintain the in-situ measurement. This drift correction method is based on a recently developed shift-invariant variational autoencoder (shift-VAE). Finally, we investigated the heterogeneous conductivity of the HZO thin films by this AE workflow, revealing the evolution of conductive hotspots around several tens of nanometers in HZO with bias voltage and time. The hotspots show complex spatiotemporal dynamics as a function of time and bias during the scanning, suggesting the presence of complex conduction mechanisms. These results underpin a wide range of HZO-based applications. We believe that the AE approach developed in this work will be universally useful for microscopy measurements.

Acknowledgments: This work is supported by the U.S. Department of Energy, Office of Science, Office of Basic Energy Sciences Energy Frontier Research Centers program under Award Number DE-SC0021118. This work is conducted at the Center for Nanophase Materials Sciences, a US

SESSION CH03.09: Cells and Biological Samples II
Session Chairs: Philippe Leclere and Ken Nakajima
Tuesday Afternoon, December 7, 2021
CH03-Virtual

1:00 PM *CH03.09.01

Infrared Nanospectroscopy at the Single Molecule Scale for Bio- and Materials Science [Francesco Simone Ruggeri](#); Wageningen University, Netherlands

Biological processes at the base of life rely on a wide class of biomolecular machines that have characteristic nanoscale physical dimensions and whose function emerges from a correlation between their chemical and structural properties. Therefore, a fundamental objective of modern analytical methods in Physics and Chemistry is to unravel the heterogeneous chemical and physical properties of single biomolecules and relevant bio-surfaces at the nanoscale. While innovative imaging methods have been developed to characterise biomolecular processes at the nanoscale, imaging microscopies are to the most part chemically blind; thus hampering the characterisation of inhomogeneous and complex systems.

Here, we first demonstrate that Atomic Force Microscopy (AFM) provides detailed information not only on the morphological, but also on the mechanical properties of biomolecular processes and functional materials at the nanoscale [1,2]. Then, to overcome the limitations of conventional imaging microscopies, we show a real breakthrough with the development and application of Infrared Nanospectroscopy (AFM-IR) in bio- and materials science. AFM-IR combines the high spatial resolution of AFM (~1 nm) with the chemical analysis power of infrared (IR) spectroscopy to retrieve unprecedented correlative information at the nanoscale on the structural, mechanical and chemical properties of heterogeneous bio-molecular processes and functional biomaterials.[3] As most recent advances in the field, we demonstrate the achievement of single protein molecule chemical identification and structural determination.[4] Then, we show the application of this single molecule sensitivity to unravel the molecular interaction fingerprint between a small molecule and its target [3], the surface properties of artificial model membranes [6] and the structure of functional protein self-assemblies to be exploited as a novel class of biomaterials in bioscience [7-8].

Overall, the aim of our present and future research is to expand the capabilities of nanoscience for chemistry and biology to open a new window of observation on the fundamental biomolecular processes at the core of life and ageing, to shed light on the structure-activity relationship of biomolecules, and characterises functional surfaces and materials for nano- and bio- science applications.

References

- [1] Ruggeri, *ACS Nano*, 2020.
- [2] Ruggeri, *PNAS*, 2018.
- [3] Ruggeri, *Nature Comm.*, 2015.
- [4] Ruggeri, *Nature Comm.*, 2020.
- [5] Ruggeri, *Nature Comm.*, 2021.
- [6] Marchesi, *Advanced Functional Materials*, 2020.
- [7] Shen, Ruggeri, *Nature Nanotechnology*, 2020.
- [8] Qamar*, Wang*, Randle*, Ruggeri*, *Cell*, 2018.

1:30 PM CH03.09.02

Deciphering the Effect of Matrix Stiffness on Mechanical Properties of Human Umbilical Vein Endothelial Cells [Quynh T. Tran](#), Abir Kazan, Sylvain Gabriele and Philippe E. Leclere; University of Mons, Belgium

In the field of cell mechanics, a change in physicochemical properties of the extracellular matrix (ECM) can cause profound functional modifications, such as differentiation, replication, migration, and apoptosis. Thus the physicochemical properties of culture substrates were modulated in order to mimic in vitro the complexity of physiological environments. In this work, polydimethylsiloxane and hydroxy-polyacrylamide hydrogel (hydroxy-PAAm) were used to study the impact of matrix stiffness on endothelial cell mechanics. Firstly, the viscoelastic properties were estimated in physiological conditions by nano Dynamic Mechanical Analysis, based on single force curves, while the probe is indenting the surface with nano-Newton forces. Our findings show a linear stiffness gradient while the bis-acrylamide/acrylamide ratio increases. In addition, we show that the adhesion from PeakForce Quantitative NanoMechanics (PF QNM) is higher significantly than the value obtained in Force Volume. Then we quantitatively mapped the nanomechanical properties of human umbilical vein endothelial cells (HUVECs) plated on polydimethylsiloxane and hydrogels. We found that the elastic modulus of the cell body is about 12-18 kPa which is higher than the cell lamellipodia (5-10 kPa) with $\tan \delta$ approximately 0.5 for cell body.

1:45 PM *CH03.09.03

Understanding Biomechanics of Bladder Cancer Cells [Malgorzata Lekka](#)¹, Nadia Makarova², Joanna Pabijan¹, Kajangi Gnanachandran¹ and Igor Sokolov^{2,2,2}; ¹Institute of Nuclear Physics PAN, Poland; ²Tufts University, United States

The bladder is a highly variable mechanical microenvironment expanding from a few to hundreds of kPa due to functional reasons. Interestingly, such a large range of functional stiffness seems not to influence the mechanical properties of urothelial cancer cells as they become more deformable already at the early stages of cancer progression as measured by atomic force microscopy (AFM). Several structural components contribute to the mechanical properties of bladder cancer cells. Primarily, they are related to the organization of polymerized actin form (actin filaments) and the overall actin content. Cell mechanics alter dynamically in response to external or internal stimuli, including the organization of cells (single cells, monolayers or more complex structures) and the interplay of cellular deformability with the surrounding microenvironment (i.e., extracellular matrix, ECM). All steps of cancer progression involve specific interactions between cell surface receptors and multiple components of the ECM, including basement membranes (BMs), mainly composed of laminins or type IV collagen. This structural scaffold, making a physical barrier, contributes to such phenomena as cell adhesion, proliferation, and migration. Laminin binding to receptors present on a cell surface initiates cell invasion through BMs. The actin cytoskeleton is linked with the focal adhesion molecules, thus altered expressions of related molecules will affect cell deformability. This leads to glycocalyx as the other component contributing to bladder cancer mechanics at the cellular level. By applying the brush model, the mechanical properties of the cells studied under specific cleavage conditions were correlated with the presence of the particular type of the pericellular glycocalyx layer. Distinct contributions of cell structural elements to cell biomechanics form a question of the leading cause of the alterations in mechanical properties of cells. The working hypothesis can be summarized as follows: mechanical properties of local cellular microenvironment define the invasive and migratory phenotype of cancerous cells

through irreversible changes in composition and structure of both proteoglycan's component of the glycocalyx and expression of the adhesive molecules leading to cytoskeleton reorganization. Cells leaving the primary tumour site carry this information and use it to form a secondary, metastatic site.

2:15 PM *CH03.09.04

Verification of Microscale Modulus Control in Photopolymer 3D Printing [Jason Killgore](#); National Institute of Standards and Technology, United States

Atomic force microscopy (AFM) is uniquely capable of characterizing the 3-dimensional modulus variations that arise in vat photopolymerization additive manufacturing processes such as stereolithography, digital light processing and inkjet. 3D control of part shape and properties is essential to realize additive manufacturing opportunities in critical applications such as organ printing and dentistry. We will discuss how AFM can be used both ex-situ and in-situ to the printing process to inform where heterogeneity and shape deviation arise in printed parts. We will then employ and verify various models to correct and control for such variations, yielding geometrically and mechanically precise parts. Ex site characterization of as-printed parts, both pristine and cryo-ultramicrotomed reveals true process control of properties based on light exposure and feature size. In-situ characterization complements ex-situ by revealing differences between resin, green-state and final part properties. Overall, the interplay between characterization and control enables new freedoms in 3D printed part design, particularly at the smallest length scales.

2:45 PM BREAK

SESSION CH03.10: Electrical Properties II
Session Chair: Philippe Leclere
Wednesday Morning, December 8, 2021
CH03-Virtual

8:00 AM CH03.10.01

Customized MFM Probes Based on Magnetic Nanorods [Miriam Jaafar](#)¹, Javier Pablo Navarro², Eider Berganza³, Pablo Ares¹, Cesar Magen⁴, Julio Gómez-Herrero¹, Jose De Teresa¹ and Agustina Asenjo⁵; ¹Autonomous University of Madrid and Condensed Matter Physics Center, Spain; ²Helmholtz-Zentrum Dresden Rossendorf, Germany; ³Karlsruhe Institute of Technology, Germany; ⁴Instituto de Nanociencia y Materiales de Aragón (INMA), Universidad de Zaragoza-CSIC, Spain; ⁵Instituto de Ciencia de Materiales de Madrid, Spain

Atomic Force Microscopy (AFM) is a powerful technique in biophysics and nanomedicine, since it allows imaging and manipulating nanostructures in physiological conditions on a single molecule level [1]. Magnetic Force Microscopy (MFM) is an AFM-based technique where a nanometric magnetic probe is scanned in close proximity to a surface detecting the local magnetic fields gradients near it. MFM has been applied to the study of a variety of magnetic systems, including magnetic nanoparticles. Despite the importance of studying magnetic nanostructures with biological applications in physiological conditions, the applicability of MFM to these systems was limited up to now because of the difficulty in developing MFM for detecting magnetic interactions in liquids. This is a consequence of the higher damping forces acting on the cantilever when working in liquid environment, as compared to air, which results in a significant loss of sensitivity of the MFM signal. In the work presented here, we start by introducing the necessary development for MFM imaging in liquid media [2] and discussing the influence of the chosen cantilever on the obtained MFM signal-to-noise ratio. Then, we present the development of new magnetic probes fabricated by Focused Electron Beam Induced Deposition (FEBID) using specially designed cantilevers for liquid medium and demonstrating that further improvement on the performance can be gained [3].

[1] Y. F. Dufre'ne et al. *Nature Nanotechnology* 12, 295–307 (2017).

[2] P. Ares et al. *Small* 11, 36, 4731–4736 (2015).

[3] M. Jaafar et al, *Nanoscale*, 12, 10090–10097 (2020).

8:15 AM CH03.10.03

Three-Dimensional Fast Force Mapping as a Means for Understanding Interfacial Solution Structure and Its Impact on Interparticle

Forces [Sakshi Yadav](#)¹, Elias Nakouzi¹, Jaehun Chun^{1,2} and James DeYoreo^{1,3}; ¹Pacific Northwest National Laboratory, United States; ²The City University of New York, United States; ³University of Washington, United States

Many of the processes occurring at electrolyte-solid interfaces, such as corrosion, catalysis and heterogeneous nucleation, as well as the interactions and response dynamics of colloidal systems, are mediated by the solution near the interface. However, our knowledge of interfacial solution structure (ISS) has been limited by a dearth of experimental techniques that can visualize ISS at the atomic scale. AFM-based three-dimensional fast force mapping (3D FFM) is a recently developed method that provides this ability. During FFM, changes in phase and amplitude (or frequency) of an oscillating AFM tip due to interactions with its surroundings is recorded as the tip approaches and retreats from the surface. By collecting these 1D force curves over a 2D area, a 3D map of solution structure is created. As part of an effort to understand the interactions and dynamics leading to growth of nanomaterials through the process of oriented attachment (OA), we are using 3D FFM to visualize solution structure at a variety of crystal interfaces. Here we report on studies of the Zn (0001) interface in which we pursue three novel directions. First, we attempt to understand how the ISS depends on the nature of the solvent by examining both water and ethanol. Second, we utilize the polar nature of ZnO to investigate how differences in surface termination — O vs Zn — impact the ISS. Third, we introduce custom-made nanocrystal AFM probes fabricated by depositing ZnO onto commercial silicon probes to understand the structure seen by ZnO particles as they approach one another during OA. Our results to date demonstrate distinct differences between 3D FFM data collected in water and ethanol. In particular, a strong attractive force at a tip-sample separation of ~1nm is measured in water, yet absent in ethanol. Measurements on Zn- and O-terminated surfaces reveal differences in both the surface morphology and the interfacial structure. We successfully used the ZnO tips to execute FFM; the initial data show that the tip chemistry strongly influences the solution structure confined between the two surfaces. In summary, our findings reveal a complex dependence of ISS on surface termination, solvent composition and tip chemistry. By resolving the key limitation of conventional 3D FFM — namely the discrepancy between the tip and sample materials — we provide a more straightforward basis for predicting long-range interactions between ZnO particles, delineating the solution structure, and advancing the quantitative interpretation of 3D FFM data.

8:30 AM CH03.10.04

Single-Molecule Conductance of Discrete, π -Stacked Pyridinium Dimers [Hao Yu](#), Jialing Li, Songsong Li, Charles Schroeder and Jeff Moore; University of Illinois at Urbana-Champaign, United States

Charge transport in π -stacked aromatic rings is central to biological processes and organic electronics. However, direct experimental investigation of

intermolecular charge transport between aromatics at molecular level is challenging. In this work, we use a supramolecular self-assembly approach to control the stacking geometry of two pyridinium molecules, thereby providing a promising model system to investigate intermolecular charge transport behaviors in discrete pyridinium dimers. The charge transport properties of free and dimerized pyridiniums were characterized using a scanning tunneling microscope-break junction (STM-BJ) technique, thereby enabling direct measurement of single-molecule conductance. Our results show that π -stacked pyridinium dimers exhibit up to 10-fold enhanced molecular conductance compared to single pyridinium. The experimental results were further analyzed with insights from density function theory (DFT) calculations. From a broad perspective, we anticipate that merging supramolecular chemistry and single-molecule conductance experiments will afford new functional molecular electronics.

8:45 AM CH03.10.05

Hydrogen Depassivation Lithography with a MEMS-Based Scanning Tunneling Microscope Afshin Alipour¹, Emma L. Fowler¹, S. O. Reza Moheimani¹, James H. Owen², Ehud Fuchs² and John Randall²; ¹The University of Texas at Dallas, United States; ²Zyvx Labs, United States

About ten years after invention of Scanning Tunneling Microscope (STM), scientists found that STM can be used to modify sample surfaces at atomic scale. This led to the invention of STM-based lithography in which the STM tip is used as a source of a very fine and low energy electron beam to pattern a monolayer resist adsorbed on the sample surface with ultimate atomic resolution and precision. As a result, STM has been proposed as a viable alternative to conventional e-beam lithography whose resolution and precision is fundamentally limited to a few nanometers.

Despite this superiority in resolution, slow speed and low throughput have been major downsides of the STM which hinder its widespread use. A key contributor to these limitations is its relatively large nanopositioner, i.e. the piezotube. For this drawback, miniaturization stands out as a practical solution for the bulkiness of the STM piezotube. A Microelectromechanical-System (MEMS) STM nanopositioner can offer higher bandwidth and an opportunity for parallel operation of a multi-tip STM due to its small footprint.

In our previous work [1], we presented a MEMS-based STM system. There, we integrated a one-degree-of-freedom MEMS STM nanopositioner into a commercial Ultrahigh-Vacuum (UHV) STM system to replace the Z axis of its piezotube. As a result, a hybrid system is achieved in which the MEMS device provides the Z-axis motion which requires higher sensitivity, while the XY-plane motions are still delivered by the piezotube during the scan. Compared to the Z-axis of the piezotube, the MEMS device features tenfold higher bandwidth (i.e. 10 kHz) with the same range of motion (1-2 μm). In this work, we further examine the practical benefits of this hybrid system over a conventional piezo-based STM. Thanks to the MEMS nanopositioner, higher scan speeds are achieved during both imaging and lithography compared to the original UHV STM system. Dimer row resolution images of Si(001):H were obtained at scan speeds over 2 $\mu\text{m/s}$ with the hybrid STM in conjunction with the improved control loop [2].

STM-based lithography was also tested with the proposed hybrid system. With the greater sensitivity of the MEMS Z-actuator and the improved control loop, it is expected that lithography can operate at much higher tunnel current setpoints, allowing for much faster lithography. In our experiments, the sample used was a H-terminated Si(100)-2 \times 1 surface. First, the sample surface was imaged, and its lattice was detected based on the image. Then, H atoms were selectively desorbed by moving the tip along a predefined trajectory over the sample surface using an appropriate bias voltage (+4 V) and tunnel currents up to 40 nA, providing write speeds up to 100 nm/s. The results obtained in this work demonstrate that the proposed MEMS-based STM system is conducive to high-speed atomic-scale lithography.

Acknowledgements

This work is supported by the U.S. Department of Energy's Office of Energy Efficiency and Renewable Energy under the Advanced Manufacturing Office Award No. DEEE0008322. The authors wish to thank Zyvx Labs members, William R. Owen and Robin Santini for their assistance in setting up the experimental testbeds.

References

- [1] Alipour, Afshin, et al. "Atomic-precision imaging with an on-chip scanning tunneling microscope integrated into a commercial ultrahigh vacuum STM system." *Journal of Vacuum Science & Technology B* (2021) (Accepted for publication).
- [2] Tajaddodianfar, Farid, et al. "Scanning tunneling microscope control: a self-tuning PI controller based on online local barrier height estimation." *IEEE Transactions on Control Systems Technology* 27.5 (2018): 2004-2015.

9:00 AM CH03.10.06

Dynamic Ferroelectric Domain Manipulation via Automated Experimentation in Piezoresponse Force Microscopy Kyle P. Kelley, Stephen Jesse, Rama K. Vasudevan and Sergei V. Kalinin; Oak Ridge National Laboratory, United States

Domain structures and topological defects in ferroelectric materials underpin a broad range of applications ranging from materials with giant electromechanical responses to domain wall electronics. Correspondingly, exploring the functionalities of domain walls and controlled modifications of domain structures is of interest for a broad spectrum of applications. However, the dynamic nature of these objects severely constrains piezoresponse force microscopy approaches to explore their functionality. Here, to overcome this challenge, a real space image-based feedback approach is utilized to control the atomic force microscope tip bias during ferroelectric switching allowing for modification routes triggered by domain states under the tip. Specifically, the complex trigger system (i.e., "FerroBot") is to used study frustrated and metastable domain and domain-wall dynamics in a $\text{Pb}_x\text{Sr}_{(1-x)}\text{TiO}_3$ system. We have demonstrated that microscopic mechanisms of the domain-wall dynamics can be identified, i.e., domain-wall bending can be separated from irreversible domain reconfiguration regimes. In conjunction, phase-field modeling was used to corroborate the observed mechanisms. This study highlights a new pathway toward discovery and control of metastable states in ferroelectrics, and more generally paves way for automated systems for controlled modification of domain walls and defects to improve material properties. This work was supported by the U.S. Department of Energy, Office of Science, Basic Energy Sciences, Materials Sciences and Engineering Division at Oak Ridge National Laboratory's Center for Nanophase Materials Science, which is a U.S. DOE Office of Science User Facility.

9:15 AM CH03.10.07

Determination of Doping Profiles in Semiconductor Nanowires by Electrical Modes from Scanning Probe Microscopy Georges E. Bremond^{1,2}; ¹INSA de Lyon, France; ²Université de Lyon, France

Recently, semiconductor nanowires (NW) have gained more and more attention, as they are the building blocks of various future functional devices at the nanoscale. The measurement and quantitative determination of doping and doping profile within semiconductor nanowires (NW) are crucial in order to develop the technology using them. Specific methods and techniques are in high demand to understand the incorporation of doping into such one-dimensional structures. In the last two decades, scanning capacitance microscopy (SCM) and scanning spreading resistance microscopy (SSRM) based on atomic force microscopy, has emerged as promising tools for two-dimensional high resolution carrier/dopant profiling. In SCM, the capacitance change providing by an alternating bias applied between the tip/sample system under a DC bias to alternately accumulate and deplete carriers within the semiconductor underneath the local tip is dependent on the local carrier concentration of the semiconductor. In SSRM, the local resistivity, allowing the determination of the doping concentration, is determined via the spreading resistance measurement at the tip/sample system, applying an additional DC bias on the sample and using a logarithmic current amplifier. As multi-parameter experiments, these two techniques need of an accurate calibration method

for a quantitative doping analysis.

In this study we present first a doping calibration method based on cross-sectional scanning of multilayers samples, with, for pedagogic demonstration, different Ga doping concentration in n-type ZnO allowing the quantitative measurement by SCM and SSRM. Then, to study NWs, we have developed a methodology of sample preparation, based on dip-coating filling of NWs field. The dip-coating parameters as coating solution, removal rate and NW field morphology have been controlled by SEM, ellipsometry and atomic force microscopy topography in order to optimize the filling and polishing process. As examples, some results are presented on ZnO and GaN NW: One important result has been to be able to measure using SCM and SSRM, the non-intentionally n-type doping (nid) of ZnO nanowires, well estimated at 210^{18}cm^{-3} , explaining the difficulty to turn these NWs into p-type during p-type doping experiments, a crucial problematic in ZnO. Using antimony (Sb) doping in nid ZnO core/ Sb ZnO shell NW structures, we have successfully determined the decrease of carrier concentration with respect to the nid ZnO core, which can be ascribed to the formation of Sb-related acceptors compensating the native donors. The understanding of this electric compensation mechanism is the clear signature of a p-type Sb doping feasibility in ZnO NW. This important result opens the way to succeed in the p-type doping in ZnO. The generalization of this doping profiling methodology to other NW semiconductors is also pointed out for instance to study the non homogeneity of Si and Mg doping in GaN NWs.

9:30 AM CH03.01.08

Direct Observation of the Double-Layering Quantized Growth of Mica-Confined Ionic Liquids [Bingchen Wang](#)^{1,2} and Lei Li¹; ¹University of Pittsburgh, United States; ²University of Wisconsin–Madison, United States

Since the interface between ionic liquids (ILs) and solids always plays a critical role in important applications such as coating, lubrication, energy storage, and catalysis, it is essential to uncover the molecular structure and dynamics of ILs confined to solid surfaces. Here, we present our direct observation of a unique double-layering quantized growth of three IL (i.e., [Emim][FAP], [Bmim][FAP] and [Hmim][FAP]) nanofilms on mica. AFM results show that the IL nanofilms initially grow only by covering more surface areas at the constant film thickness of 2 monolayers (ML) until a quantized increase in the film thickness by another 2 ML. Based on the AFM results, we propose a double-layering model describing the molecular structure of IL cations and anions on the mica surface. The interesting double-layering structure can be explained as the result of several competing interactions at the IL-mica interface. Meanwhile, the time-dependent AFM results indicate that the topography of IL nanofilms could change with time, and the mobility of the nanofilm is lower for ILs with longer alkyl chains, which can be attributed to the more ordered packing between longer alkyl chains. Our findings have important implications on the molecular structure and dynamics of ILs confined to solid surfaces.

SESSION CH03.11: Cells and Biological Samples III
Session Chairs: Philippe Leclere and Zoya Leonenko
Wednesday Morning, December 8, 2021
CH03-Virtual

10:30 AM *CH03.11.01

Nanoscale Viscoelasticity of Living Tissues with AFM—Physics of Biological Growth and Shape Across Temporal and Spatial Scales [Sonia Contera](#), Jacob Seifert, Alba Rosa Piacenti and Casey Adam; University of Oxford, United Kingdom

The dynamic shapes of biological tissues emerge from a complex interplay of physics, chemistry and genetics, which determines—at each temporal and spatial scale—the mechanical properties that eventually form the adaptive structures of living organisms. Shape and mechanical stability of living organisms rely on precise control in time and space of growth, which is achieved by dynamically tuning the mechanical (viscous and elastic) properties of their hierarchically built structures from the nanometer up. It is now well-established that cellular behaviour (including stem cell differentiation) crucially depends on the mechanical properties of the cells' environment. Attention has been directed towards the importance of the *stiffness* of the natural (extracellular matrix, ECM) or artificial matrices where cells grow, with the purpose of either understanding mechanotransduction, or controlling the behaviour of cells in tissue engineering. While stiffness (i.e. the capacity of a material to elastically store mechanical energy) has been the focus of most experimental research, neither cells or matrices are elastic. Biological systems dissipate energy (i.e. they are viscous) and hence they do not respond to mechanical deformations instantaneously (like an ideal Hookean spring), but present different time responses at different spatial scales that characterise their responses to external stimuli. Measuring viscoelasticity (especially at the nanoscale) has remained experimentally challenging [1,2]. I will present atomic force microscopy (AFM)- based techniques developed in my lab to measure and map the nano-viscoelasticity of living organisms, cells, membranes, collagen, ECMs, and tissue engineering matrices across the spatial and temporal (from Hz to 100s of kHz) scales, and chirp-based spectroscopic techniques to assess viscoelasticity from Hz to 100s kHz at the nano and micro scale developed in my lab. I will also present tests for assessing which viscoelastic model better fits the experimental AFM results. Our results have uncovered that extracellular matrices of both plants [3] and tumours present an almost perfect linear viscoelastic behaviour.

References:

- [1] "Multifrequency AFM reveals lipid membrane mechanical properties and the effect of cholesterol in modulating viscoelasticity" 2019. Z Al-Rekabi, S Contera; Proceedings of the National Academy of Sciences 115 (11), 2658-2663.
- [2] "Mapping nanomechanical properties of live cells using multi-harmonic atomic force microscopy" 2011 A Raman, S Trigueros, A Cartagena, APZ Stevenson, M Susilo, E Nauman, S Contera. Nature Nanotechnology 6 (12), 809.
- [3] "Mapping cellular nanoscale viscoelasticity and relaxation times relevant to growth of living Arabidopsis thaliana plants using multifrequency AFM" 2021 J Seifert, C Kirchhelle, I Moore, S Contera. Acta Biomaterialia 121, 371-382

11:00 AM *CH03.11.02

Nanocorresopy—Unravelling Multifactorial Properties of Biomaterials at Nanoscale [Wojciech Chrzanowski](#); The University of Sydney, Australia

Nanoimaging and probing of physical-chemical characteristics is central to the development of new nanomaterials for energy and environment, communication, computing and security as well as for health and medicine. While all these areas are of significant importance, health and medical applications remain the most challenging because they involve interactions with living organisms. Inherently, such interactions are less predictable and directly linked to human health, which highlights their societal impact. Therefore, resolving the principles that govern biological behaviours and developing modern technologies that exploit new capabilities offered by nanomaterials to control multicellular environment is likely to result in significant advances in a quest for innovative therapies for major health threats including multi drug resistance, cancer and diabetes.

We know that biological responses are not controlled by a single material parameter. It is rather an interplay of many parameters such as size, shape, surface charge, chemistry and mechanical properties that defines the biological outcome. Therefore, correlative characterisation of structural, physical and

biological interactions at the nanoscale is paramount in order to correlate nanomaterials to their biological modulatory capabilities. Precise knowledge of key characteristics of nanomaterials will ultimately allow us to predict their safety and fate in biological systems and in the environment. It will unlock new opportunities to create safe-by-design systems for various biomedical applications.

To overcome limitations of current methods we proposed a correlative approach that uses nanoscale infrared spectroscopy, Lorentz contact resonance spectroscopy and Molecular force probe spectroscopy to interrogate nanoscale mechanical properties and map chemical structure of nanoparticles. To demonstrate strength of the nanocorrescopy in nanomaterials characterisation we used a copolymer composite mPEG-PLGA (methoxy-poly (ethylene glycol)-b-poly (lactic-co-glycolic) acid) nanorods. We demonstrated that the nanocorrescopy is capable of characterising precisely distribution of viscoelastic and chemical properties with the spatial resolution of <150 nm and <20 nm respectively. We further showed that this methodology enable characterisation of the corona formation on nanoparticles and for the first time assess its evolution in real time. We believe that the nanocorrescopy provides new opportunities to characterise variety of biomaterials used in biomedicine to ensure their safety, reliability, and sustainability.

11:30 AM CH03.11.03

Late News: Ex Situ AFM-Molecule Chip Technique for Single-Molecule Detection of Antibody-Antigen Bindings on a Semiconductor Chip Surface Ming-Pei Lu¹, Ying-Ya Weng² and Yuh-Shyong Yang³; ¹Taiwan Semiconductor Research Institute, National Applied Research Laboratories, Taiwan; ²Institute of Biomedical Engineering, National Yang Ming Chiao Tung University, Taiwan; ³Department of Biological Science and Technology, National Yang Ming Chiao Tung University, Taiwan

In-situ AFM typically possesses the single-molecule detection sensitivity of the antibody-antigen binding, however, yielding inevitably great limitations due to operational issues from a practical application viewpoint. Here, we propose a method of an ex-situ AFM-molecule chip technique with the feature of graphically superimposed alignment that enables ex-situ AFM analysis of an immobilized antibody at the same location on a semiconductor chip surface before and after incubation with its antigen, which makes all required chemical/biological treatments feasibly executed in the standard laboratory manner, allowing the single-molecule ex-situ AFM detection in a way with more practicality, flexibility, and versatility. Accordingly, by taking the hepatitis B virus X protein (HBx) for instance, the individual information of the topographical characteristics for the immobilized IgG antibodies/aggregates on the chip surface can be extracted using this ex-situ AFM analysis method, and further analyzed statistically. Experimental observations revealed that individual IgG antibodies covalently immobilized on the aldehyde-terminated chip surface, presumably featuring a predominately head-on orientation, possessed an AFM height of approximately 5.416 nm in statistical analysis. Furthermore, information regarding the AFM height change of individual IgG antibody/aggregate arising from the conformational change in the IgG-HBx complex formation was investigated in a statistical manner as well, leading to an increased height of approximately 1 nm. To broaden the application spectrum of the ex-situ AFM-molecule chip technique, we attempted to apply this technique to identify the locations and spatial distributions of the immobilized molecules on the bioFET surfaces. The surface topographical measurements at the same location on the nanowire bioFET surface were recorded after the chip cleaning, antibody modification, and antigen incubation steps, respectively. As a result, information regarding the correlation between the spatial distributions of the biological molecules on the bioFET surface and the corresponding electrical characteristics of the nanowire bioFETs can be obtained, highlighting that the single-molecule ex-situ analysis method can be beneficial to the development of bioFET applications. More importantly, other analysis modules in the SPM family can also be employed to simultaneously record various fundamental characteristics of the molecules on the chip surface at the single-molecule level while recording the topographical information of the chip surface using an AFM module, significantly revealing versatile applications of the ex-situ SPM-molecule chip technique (here using the SPM to replace the AFM for highlighting the potentials of multi-functional applications) in multidisciplinary areas across materials, chemistry, physics, and biology.

11:45 AM BREAK

SESSION CH03.12: On-Demand
Sunday Morning, December 5, 2021
On-Demand

8:00 AM CH03.03.01

Predicting Hydration Layers over Surfaces Yashasvi S. Ranawat¹, Ygor Jaques¹ and Adam Foster^{1,2}; ¹Aalto University, Finland; ²Kanazawa University, Japan

Several technological and natural processes are dominated by the mineral-water interactions, for example biomineralisation, corrosion etc, and hence, characterization of such interfaces is vital. Atomic Force Microscopy (AFM) has gained prominence in characterizing such surfaces. However, the complex interplay of the tip with the hydration layers over the surface govern the AFM tip's interaction with the hydration layers, and impede high resolution requirements needed for characterization. The theoretical molecular dynamics (MD) approaches have helped with the surface characterization. Given a hydration layer image, the search space is wide and the MD approach becomes prohibitively expensive. Here we introduce deep learning methods to reliably predict the hydration layer over a given surface.

SYMPOSIUM CH04

Accelerating Materials Characterization, Modeling and Discovery by Physics-Informed Machine Learning
November 29 - December 8, 2021

[Symposium Organizers](#)

Maria Chan, Argonne National Laboratory
Kamal Choudhary, National Institute of Standards and Technology
Sebastian Schmitt, Helmholtz Zentrum Berlin
Rama Vasudevan, Oak Ridge National Laboratory

* Invited Paper

SESSION Tutorial CH04: Machine Learning and AI Methods for Materials—Applications to Theory, Characterization, and Smart Experiments
Session Chairs: Sergei Kalinin, Sebastian Schmitt and Maxim A. Ziatdinov
Monday Morning, November 29, 2021
Virtual

8:30 AM

Machine Learning and AI Methods for Materials Science—Applications to Theory, Characterization, and Smart Experiments - Morning Session [Sergei V. Kalinin](#) and Maxim A. Ziatdinov; Oak Ridge National Laboratory, United States

The morning session will cover:

ML to theory (force fields, generic property predictions, visualization, accessing the different databases, etc.)
Deep learning introduction and use to segment images from electron or scanning probe microscopy

12:30 PM BREAK

1:00 PM

Machine Learning and AI Methods for Materials Science—Applications to Theory, Characterization, and Smart Experiments - Afternoon session [Sergei V. Kalinin](#) and [Maxim A. Ziatdinov](#); Oak Ridge National Laboratory, United States

The afternoon session will cover:

Spectral processing with matrix/tensor factorization and deep learning methods (including autoencoders) for extracting data from large multidimensional datasets
Reinforcement learning and Bayesian optimization for efficient and smart experiments

SESSION CH04.01: Accelerating Materials Science by Natural Language Processing, Machine Learning and High-Throughput Studies
Session Chair: Hannah Barad
Tuesday Morning, November 30, 2021
Hynes, Level 3, Room 303

10:30 AM *CH04.01.01

Linking Text Extracted Data and Existing Resources Towards Predictive Models [Elsa Olivetti](#); Massachusetts Institute of Technology, United States

Data continues to be a fundamental ingredient for accelerating and optimizing materials design and synthesis. Advances in applying natural language processing (NLP) to material science text has greatly increased the size and acquisition speed of materials science data from the published literature. This presentation will describe work to extract information from peer reviewed academic literature across a range of materials and explicit links between text-derived data and physics-based simulation data to inform materials discovery. We will present cases from microelectronics, catalysis and solid-state electrolytes.

11:00 AM CH04.01.03

Simultaneous Electrochemical Analysis of Material Libraries with Real Combinatorial High-Throughput Characterization [Hannah N. Barad](#), Björn Miksch and Peer Fischer; Max Planck Institute for Intelligent Systems, Germany

Fabrication of CMLs with variations in deposition parameters, composition, thickness, oxidation state, and even nanostructure morphology have been demonstrated, but measuring and analyzing their properties is not straightforward. Typically, the measurements entail serial methods that measure samples point-by-point on pre-determined positions on the CMLs. While these measurements are often termed 'high-throughput' they are only so in the sense of processing large amounts of data. Especially, in the case of electrochemical measurements, the analysis can take a very long time, even days, to complete for one CML.

Here, we present a real high-throughput parallel method for determination of electrochemical properties. We do this using an array of ion-sensing field effect transistors (ISFETs) that was specifically designed for high-throughput measurements. ISFET sensors are used to detect changes in concentrations of specific ions in a solution, and as such can follow changes in electrochemical reactions. For this work we chose to examine CMLs of electrolyzers for oxygen evolution reaction (OER), which may form OH^- or H^+ intermediates during the reaction. In our setup, the sensor array is placed in solution directly above the studied CML, and we examine the changes in H^+ concentration as a result of the OER. The ISFET array allows us to quickly screen for material combinations of interest for OER, and generate large amounts of data in a short period of time, enabling parallel high-throughput CML characterization. We will share our most recent results in the generation of high-throughput CMLs [1] and analyzing these with similarly high-throughput parallel electrochemical measurements.

Reference:

[1] Hannah-Noa Barad, Mariana Alarcón-Correa, Gerardo Salinas, Eran Oren, Florian Peter, Alexander Kuhn and Peer Fischer; Combinatorial growth of multinary nanostructured thin functional films, *Accepted to Materials Today*, 2021.

11:15 AM CH04.01.04

Machine Learning Assisted Metal-Insulator Compound Transition Discovery and Understanding—Database, New Features and Online Classifier Tool Alexandru Georgescu¹, Peiwen Ren¹, Aubrey R. Toland², Shengtong Zhang¹, Kyle Miller¹, Daniel Apley¹, Elsa Olivetti³, Nicholas Wagner¹ and James M. Rondinelli¹; ¹Northwestern University, United States; ²Georgia Institute of Technology, Georgia; ³Massachusetts Institute of Technology, United States

Understanding, and predicting new materials with relevant electronic properties is a key task in materials science. This task is complicated in the case of materials with complex electronic interactions, particularly in the case of materials with an open d-shell of a transition metal ion known as correlated materials. This is due to the limitations of current theoretical methods, as well as the scarcity and heterogeneity of known materials. Of these materials, materials that exhibit a thermally driven metal-insulator transition (MIT) are particularly important for technological applications, yet only around 60 are known. To accelerate materials discovery and understanding, we have built, with the assistance of natural language processing techniques, the first materials database of MIT and related compounds which is now available for scientists' use (1,2). We have trained a machine learning model on this database, allowing us to extract new relevant features for this class of materials, including generalized tolerance factors, the Ewald energy, as well as confirmed the importance of well-known ones such as the Hubbard U (1). Finally, we provide this model in a user-friendly binder format that scientists can run in their browser and obtain new predictions on whether a material is a metal, insulator, or MIT in seconds based on .cif structure files - without installing any software on their machine (1,3). Our work shows how machine learning can be used to accelerate materials discovery and understanding at every step of the research process. If time permits, I will present results on newly identified metal-insulator transition compounds.

References:

- 1) <https://arxiv.org/abs/2010.13306> ; in press at Chemistry of Materials
- 2) <https://mtd.mccormick.northwestern.edu/mit-classification-dataset/>
- 2) <https://tinyurl.com/mit-classifiers>

The information, data, or work presented herein was also funded in part by the Advanced Research Projects Agency-Energy (ARPA-E), U.S. Department of Energy, under Award Number DE-AR0001209. The views and opinions of authors expressed herein do not necessarily state or reflect those of the United States Government or any agency thereof.

SESSION CH04.02: Physics-Assisted ML Methods for Knowledge Extraction I

Session Chair: Elsa Olivetti

Tuesday Afternoon, November 30, 2021

Hynes, Level 3, Room 303

1:30 PM CH04.02.02

Decoding Reactive Structures in Dilute Alloy Catalysts Nicholas Marcella¹, Jin Soo Lim², Anna Plonka¹, George Yan³, Cameron J. Owen², Jessi van der Hoeven^{2,2}, Alexandre Foucher⁴, Hio Tong Ngan³, Steven B. Torrisi², Nebojsa S. Marinkovic⁵, Eric A. Stach⁴, Jason Weaver⁶, Philippe Sautet^{3,3}, Boris Kozinsky^{2,7} and Anatoly Frenkel^{1,8}; ¹Stony Brook University, The State University of New York, United States; ²Harvard University, United States; ³University of California, Los Angeles, United States; ⁴University of Pennsylvania, United States; ⁵Columbia University, United States; ⁶University of Florida, United States; ⁷Robert Bosch LLC, Research and Technology Center, United States; ⁸Brookhaven National Laboratory, United States

Fundamental atomic-level understanding of the active site structure is a central requirement of rational catalyst design. Due to the large configurational space inherent to many catalytic systems, it is very challenging to resolve the active sites directly. Moreover, these structures often exhibit dynamical behavior in response to the reactive environment. Here, we propose a multipronged strategy of decoding reactive structures at the atomic level, combining catalysis, characterization, machine learning, and first-principles based kinetic modeling. We unambiguously demonstrate the effect of catalyst treatment on its nanostructure and reactivity toward the prototypical hydrogen-deuterium (HD) exchange reaction, using a dilute alloy Pd₈Au₉₂ supported on highly stable raspberry colloid template SiO₂. Remarkably, the Sabatier optimum is established with small Pd_n ensembles, where the reactivity is tuned by modulating the active site on the order of only a few atoms ($n = 1-3$) through catalyst pretreatment.

The catalyst is activated by O₂ treatment and decreases in activity upon H₂ treatment. These observations are explained in terms of catalyst restructuring induced by the treatments, as evidenced by X-ray absorption spectroscopy and coordination numbers extracted from neural network inversion of the spectra. A quasi-random alloy is revealed: the majority of Pd remains dispersed inside Au, with a small amount of Pd segregating toward the surface upon O₂ treatment and dissolving into the bulk upon H₂ treatment. Extensive theoretical modeling of the HD exchange reaction network on several model surfaces establishes Pd monomers, dimers, and trimers as decisive candidate structures for the active site. Very good agreement is found between theory and experiment in terms of the apparent activation energy: O₂-treated samples are dominated by desorption-limited Pd trimers, whereas H₂-treated samples are characterized by dissociation-limited Pd dimers & monomers. These dilute Pd ensembles numerically satisfy the observed coordination numbers for all of our samples, thereby fulfilling both the kinetic and structural criteria of the active site. Our multidisciplinary approach enables precise identification of the active site at atomic resolution with fully consistent structure-activity relationship.

1:45 PM CH04.02.04

Encoding Dynamical Information in Graph Representation Learning for Large-Scale Protein Function Prediction Yuan Chiang and Shu-Wei Chang; National Taiwan University, Taiwan

Understanding the protein structure-function relationship is essential for broad biological fields, with important applications in the design of new functional biomaterials, drugs, and antibiotics for biotechnology and pharmaceutical industries. Recent advances in protein function prediction take advantage of graph-based deep learning approaches to correlate protein 3D structure and topological features with molecular functions. The latest end-to-end model PersGNN had achieved a boost in Gene Ontology classification compared with baseline graph neural networks (GNNs). However, proteins in nature are not static but dynamic molecules interacting with the environment, constantly alternating conformation, and even forming assemblies of quaternary complexes. This talk will present the expressiveness and robustness of GNNs to encode information from spatial proximity, persistence homology, together

with normal mode analysis across protein residues. The learned representation aggregates node-level features from local to global hierarchy and provides graph-level embedding with inter-residue dynamical couplings for downstream function prediction. High throughput classification tasks for over 100,000 proteins and 1,000 function tags from Protein Data Bank and Gene Ontology demonstrate remarkable performance gain in the discriminatory power based on such dynamics-informed representation. The proposed method can be readily extended to wide crystalline and amorphous materials that can be represented as graph-structured data and be incorporated with particle-based dynamics.

2:00 PM CH04.02.05

Ab Initio Modeling of Configurational Disorder in Complex Systems by Combining Machine Learning and Cluster Expansions [Julia Yang](#)¹ and [Gerbrand Ceder](#)^{1,2}; ¹University of California, Berkeley, United States; ²Lawrence Berkeley National Laboratory, United States

Disordered multicomponent systems have immense engineering design flexibility and a subsequently rich space of properties. A lattice cluster expansion is one powerful computational tool to obtain precise, detailed configurational and energetic resolution, but in practice has primarily been used in binary systems or ternary alloys. In this presentation we will discuss approaches to significantly increase the complexity of systems to which the cluster expansion can be applied, including a high number of species, different valence states of ions, complex underlying lattices, and large off-lattice relaxations. We demonstrate this approach to a multicomponent, multi-sublattice lithium manganese oxyfluoride electrode system, setting up the largest cluster expansion ever attempted to our knowledge. In order to bridge the vastly under-determined configurational space observed by neutron diffraction with computation, we apply the sparse group lasso statistical method to reduce model complexity from over 4500 features to fewer than 200. We also use Bayesian optimization via Gaussian Processes in oxidation state assignments during data cleaning, demonstrating its success in high dimensional spaces with limited training data. Lastly, we extend existing theoretical cluster expansion methods and derive how to analytically calculate and characterize local structural and chemical orderings in any state of disorder. Our developments make the fitting and analysis of complex systems tractable and provide guidance for thorough, high-throughput computational studies of multi-component, disordered systems.

2:15 PM CH04.02.03

Topology-Informed Machine Learning for Predicting Glasses' Properties [Mathieu Bauchy](#); University of California, Los Angeles, United States

Although machine learning offers a unique, largely untapped opportunity to accelerate the discovery of novel glasses with exotic functionalities, it faces several challenges. Since they are usually only driven by data and do not embed any mechanistic knowledge, machine learning models can sometimes violate physical and chemical laws. For these reasons, machine learning techniques are usually good at “interpolating” data but have thus far a limited potential for “extrapolating” predictions far from their initial training set, which prevents the efficient exploration of new unknown compositional domains. Here, we present a new machine learning framework aiming to predict the properties of oxide glasses. As expected, we show that “blind machine learning” (i.e., which does not embed any physical or chemical knowledge) can successfully interpolate data but fails at extrapolating predictions far from its training set. As an alternative route, we report a new “topology-informed machine learning” framework that addresses this limitation. This framework relies on artificial neural networks and embeds a topological description of the connectivity of the atomic network. We show that our “topology-informed machine learning” model allows us to extrapolate predictions far from the training set. More generally, topology-informed machine learning offers a promising route to overcome the tradeoff between accuracy, simplicity, and interpretability—which are otherwise often mutually exclusive in traditional “blind machine learning” models.

2:30 PM CH04.02.06

Identifying High-Stability Motifs of Structural Patterns in Molecular Crystals [Rose K. Cersonsky](#)¹, [Maria Pahknova](#)¹, [Edgar A. Engel](#)² and [Michele Ceriotti](#)¹; ¹École Polytechnique Fédérale de Lausanne, Switzerland; ²University of Cambridge, United Kingdom

Molecular crystals play an important role in various fields of science and industry, with applications in the pharmaceutical, electronics, and food industries. Predicting the stability of crystal structures formed from molecular components is non-trivial, given the complexity inherent to the multiscale nature of their structure and the subtle balance of weak intermolecular interactions governing the structure-property relations. We have curated a dataset containing over 3'000 molecular crystals, their constituent molecules, and their related properties. We use it to demonstrate the use of machine-learning techniques to estimate the stability of the crystalline structures. We use general-purpose descriptors of atomic structure and modify them to explicitly incorporate information on the molecular nature and thermodynamics of the material. In combination with a principal covariates regression analysis that explicitly determines the best low-dimensional representation of structure-property relations, we demonstrate how to identify the atomic motifs associated with a strong stabilizing effect on molecular packing.

2:45 PM CH04.02.07

Spanning the 5D Space of Grain Boundaries—A Comprehensive Database of Grain Boundary Structures and Their Interface Energy [Eric R. Homer](#), [Gus L. Hart](#), [Derek Hensley](#), [Jay Spendlove](#), [Braxton Owens](#) and [Lydia Serafini](#); Brigham Young Univ, United States

The space of possible grain boundary structures is vast, with 5 macroscopic, crystallographic degrees of freedom that define the character of a grain boundary. While numerous datasets of grain boundaries have been created to examine this space, none has systematically examined the full range of possibilities. We will present a dataset of more than 4200 unique grain boundaries in the 5D crystallographic space. Our sampling includes a range of possible microscopic, atomic configurations for each unique 5D crystallographic structure, which we refer to as metastable grain boundary structures. In all, the number of metastable structures associated with the 4200 unique grain boundaries is over 31 million. We will present an overview of the methods used to generate this dataset, an initial examination of the raw data, as well as methods and insights gained in machine learning of grain boundary energy structure-property relationships.

3:00 PM CH04.02.08

Learning with Delayed Rewards—A Case Study on Inverse Defect Design in 2D Materials [Suvo Banik](#)¹, [Troy Loeffler](#)², [Rohit Batra](#)², [Harpal Singh](#)³, [Mathew J. Cherukara](#)² and [Subramanian Sankaranarayanan](#)²; ¹University of Illinois at Chicago, United States; ²Argonne National Laboratory, United States; ³Sentient Science Corporation, United States

Defect dynamics in materials are of central importance to a broad range of technologies from catalysis to energy storage systems to microelectronics. Material functionality depends strongly on the nature and organization of defects – their arrangements often involve intermediate or transient states that present a high barrier for transformation. The lack of knowledge of these intermediate states and the presence of this energy barrier presents a serious challenge for inverse defect design, especially for gradient-based approaches. Here, we present a reinforcement learning (Monte Carlo Tree Search) based on delayed rewards that allow for efficient search of the defect configurational space and allows us to identify optimal defect arrangements in low dimensional materials. Using a representative case of 2D MoS₂, we demonstrate that the use of delayed rewards allows us to efficiently sample the defect configurational space and overcome the energy barrier for a wide range of defect concentrations (from 1.5% to 8% S vacancies) – the system evolves from an initial randomly distributed S vacancies to one with extended S line defects consistent with previous experimental studies. Detailed analysis in the

feature space allows us to identify the optimal pathways for this defect transformation and arrangement. Comparison with other global optimization schemes like genetic algorithms suggests that the MCTS with delayed rewards takes fewer evaluations and arrives at a better quality of the solution. The implications of the various sampled defect configurations on the 2H to 1T phase transitions in MoS₂ are discussed. Overall, we introduce a Reinforcement Learning (RL) strategy employing delayed rewards that can accelerate the inverse design of defects in materials for achieving targeted functionality.

3:15 PM CH04.02.09

Predictive Computational Frameworks to Guide the Solid-State Synthesis of Novel Materials [Wenhao Sun](#); University of Michigan, United States

Solid-state synthesis from powder precursors is the primary processing route to multicomponent ceramic materials. The black-box nature of the reaction vessel typically precludes an understanding of the solid-state reaction mechanisms that govern phase evolution, leading to trial-and-error approaches to synthesis. In the age of autonomous laboratories, better theories of materials synthesis are needed to predict and guide robotic synthesis approaches to novel materials. Here, we combine *ab initio* thermodynamics with *in situ* synchrotron X-ray scattering and TEM to build predictive theories for which non-equilibrium phases form during solid-state ceramic synthesis, and why. I will present examples from the ceramic synthesis of Na_xMO₂ (M = Co, Mn) layered oxides [1] and also the classic high-temperature superconductor YBa₂Cu₃O_{6+x} (YBCO) [2]. We derive an interfacial reaction model to predict the first-phase-to-form between two powder precursors, which can consume a large fraction of the reaction energy and can topotactically template structural transformations to other non-equilibrium intermediates. Our insights can help guide the choice of precursors and parameters employed in the solid-state synthesis of ceramic materials, and constitutes a step forward in building predictive thermodynamics and kinetics-informed machine-learning strategies for the autonomous synthesis of novel materials.

[1] M. Bianchini, J. Wang, W. Sun, G. Ceder et al., "The interplay between thermodynamics and kinetics in the solid-state synthesis of layered oxides" *Nature Materials* 2020

[2] A. Miura, C. Bartel, W. Sun et al., "Observing and modeling the sequential pairwise reactions that drive solid-state ceramic synthesis" *Advanced Materials* (2021)

3:30 PM CH04.02.10

Late News: Parsimonious Neural Networks Learn Interpretable Physical Laws [Alejandro Strachan](#); Purdue University, United States

Machine learning is playing an increasing role in the physical sciences and significant progress has been made towards embedding domain knowledge into models. Less explored is its use to discover interpretable physical laws from data. We propose parsimonious neural networks (PNNs) that combine neural networks with evolutionary optimization to find models that balance accuracy with parsimony. The power and versatility of the approach is demonstrated by developing models for classical mechanics and to predict melting temperature of materials, and performance of energetic materials from fundamental properties. In the first example, the resulting PNNs are easily interpretable as Newton's second law, expressed as a non-trivial time integrator that exhibits time-reversibility and conserves energy, where the parsimony is critical to extract underlying symmetries from the data. In the case of melting, the PNNs not only find the celebrated Lindemann melting law, but also new relationships that outperform it in the pareto sense of parsimony vs. accuracy.

SESSION CH04.03: Image and Spectral Analysis by Computer Vision and Related Methods I

Session Chair: Suvo Banik

Wednesday Morning, December 1, 2021

Hynes, Level 3, Room 303

10:30 AM CH04.03.01

Reconstructing the Exit Wave in High-Resolution Transmission Electron Microscopy Using Machine Learning [Jakob Schiøtz](#)¹, Frederik Dahl¹, Matthew Helmi Leth Larsen¹, Christian Kisielowski², Stig Helveg¹, Ole Winther¹ and Thomas W. Hansen¹; ¹Technical University of Denmark, Denmark; ²Lawrence Berkeley National Laboratory, United States

High-resolution Transmission Electron Microscopy (HRTEM) is a powerful technique for examining matter at the atomic scale. In particular, the ability to acquire single projection images of the sample volume in a parallel fashion employing low electron doses and dose-rates makes HRTEM attractive to detect the atomic-scale realm of matter [1]. However, interpreting the image is not always straightforward, as images are formed by phase contrast.

A focal series of HRTEM images enables reconstruction of the exit wave function, which provides the most informative measure of the sample. A series of typically 20-50 images acquired with varying defocus is used to numerically reconstruct the most likely exit wave, which is then interpreted as it corresponds closely to the structure of the sample [2,3].

Here we show that a convolutional neural network is able to reconstruct the exit wave function from a focal series of only two or three images – but not from a single image. The convolutional neural network is based on the U-Net architecture [4] and is almost the same as the one we have previously used to identify the positions of atomic columns in single images of metallic nanoparticles [5].

We train the neural networks on simulated images. The simulated images are produced with the multislice algorithm, using pyqstem [6], both the exit wave function and images produced with three different values of the defocus are saved. The exit waves are then blurred slightly by folding with a gaussian, and a neural network is trained to reconstruct the exit wave from the images. The network is validated on a different set of simulated images.

In all cases we work with thin flakes of 2D materials, although the methods should generalize to other classes of materials. We train and validate networks based on three different types of samples of increasing difficulty. The first two are unsupported nanoflakes of molybdenum disulphide (MoS₂), and molybdenum disulphide supported on a graphene substrate. MoS₂ is an active catalyst for photooxidation, hydrogen evolution and hydrodesulphurization reactions. The third type is a diverse collection of existing and proposed quasi-two-dimensional materials, taken from the Computational 2D Materials Database (C2DB) [7]. In all cases the neural network is able to learn to reconstruct the exit wave function of the vast majority of the samples in the validation sets.

Finally, we demonstrate that the network trained on simulated data for graphene-supported molybdenum disulphide can also be used to analyze images

from an experimental focus series taken on a sample of a realistic model of an industrial MoS₂ based hydrodesulphurization catalyst. The neural network is able to reconstruct the exit wave with such fidelity that the atomic structure of both the MoS₂ nanoparticle and the supporting graphene is clearly recovered.

1. Kisielowski, C., Frei, H., Specht, P., Sharp, I. D., Haber, J. A., Helveg, S., *Adv Struct Chem Imag* **2**, 13 (2016). doi:10.1186/s40679-016-0027-9
2. de Beeck, M.O., Van Dyck, D., Coene, W., *Ultramicroscopy* **64**, 167–183 (1996). doi:10.1016/0304-3991(96)00058-7
3. Tiemeijer, P.C., Bischoff, M., Freitag, B., Kisielowski, C., *Ultramicroscopy* **118**, 35–43 (2012). doi:10.1016/j.ultramic.2012.03.019
4. Ronneberger, O., Fischer, P., Brox, T., in: *Medical Image Computing and Computer-Assisted Intervention – MICCAI 2015*, pp. 234–241. Springer, Cham (2015). doi:10.1007/978-3-319-24574-4_28
5. Madsen, J., Liu, P., Kling, J., Wagner, J.B., Hansen, T.W., Winther, O., Schiøtz, J., *Adv. Theory Simul.* **1**, 1800037 (2018). doi:10.1002/adts.201800037
6. Madsen, J., Liu, P., Wagner, J. B., Hansen, T. W., Schiøtz, J., *Adv. Struct. Chem. Imag.* **3**, 14 (2017). doi:10.1186/s40679-017-0047-0
7. Hastrup, S. et al., *2D Materials* **5**, 042002 (2018). doi:10.1088/2053-1583/aacfc1 See also <https://cmr.fysik.dtu.dk/c2db/c2db.html>

10:45 AM CH04.03.02

Machine Learning for Information Extraction from Transmission Electron Microscopy Data Xingzhi Wang^{1,2}, Jie Li^{1,1}, Chang Yan², Justin C. Ondry³, Jakob Dahl^{1,2}, Teresa Head-Gordon^{1,1,2}, Peter Ercius² and A. Paul Alivisatos^{1,3}; ¹University of California, Berkeley, United States; ²Lawrence Berkeley National Laboratory, United States; ³The University of Chicago, United States

Recent advancements in transmission electron microscopy (TEM) have significantly improved the information-richness and efficiency of acquisition of TEM data. Traditional methods for TEM data analysis based on manual interpretations of TEM images are often found insufficient to take full advantages of the richness of information contained in these data. Here, we will demonstrate how machine learning can be used to provide potential solutions for this problem. First, we will demonstrate an unsupervised machine learning algorithm for classifying the shapes of gold nanoparticles from TEM images. The algorithm is capable of extracting shape parameters of nanoparticles from TEM images, and classify the particles based on their shapes, requiring minimum human input in the process. The algorithm's performance will be tested on two datasets of gold nanoparticles with different morphologies, and compared to human analysis of the same datasets to validate its accuracy and efficiency. We will show that the algorithm provides a method for efficient extraction and interpretation of statistical morphological information of metal nanoparticles, while introducing minimum human biases into the results. We will then demonstrate the use of machine learning to identify and track atomic movements during the oriented attachment and annealing processes of semiconductor nanocrystals observed by *in-situ* TEM. We will show how advancements in the automation of electron microscope imaging has allowed the acquisition of this dataset in high-throughput, and how machine learning can provide an efficient method to extract information from such a highly complex dataset. We hope that the two applications we show here will serve as examples of how machine learning can be incorporated into the analysis of large and/or complex TEM datasets, enabling the extraction of information that may not be obtainable otherwise.

11:00 AM CH04.03.04

Convolutional Neural Networks for Recognizing Superconducting Phases in Powder X-Ray Diffraction Nam Q. Le¹, Janna Domenico¹, Eddie Gienger¹, Timothy Montalbano¹, Ian McCue¹, Alexander New¹, Christine Chung¹, Elizabeth Pogue², Tyrel McQueen² and Christopher Stiles¹; ¹Johns Hopkins University Applied Physics Laboratory, United States; ²Johns Hopkins University, United States

X-ray diffraction (XRD) is indispensable in high-throughput materials screening, both for confirming the synthesis of expected phases and for revealing new structures in unexplored material systems. As a case study, samples synthesized from binary and ternary intermetallic systems were screened for A15-type phases based on XRD measurements. These compositions span both known and unknown phase diagram compositions. Many A15 phases are Type-II superconductors at comparatively high temperatures relative to other metallic alloys, motivating a hypothesis that screening novel A15 phases will lead to a high proportion of novel superconductors. A bottleneck in this approach is identification of relevant phases from the XRD patterns, which, even using current software, requires human intervention and is thus not suitable for fully automated workflows. We report results of a convolutional neural network (CNN) trained to classify A15-like phases based on a large database of synthetic data with simulated noise, and show strategies needed to address class imbalance challenges intrinsic to identification of single classes of phases. This enables high-throughput sample screening and allows focusing of human time only on the most interesting materials. These approaches can extend readily to other materials discovery settings where properties are strongly tied to particular phases that are distinguishable based on XRD patterns.

SESSION CH04.04: AI for Materials Design I

Session Chair: Suvo Banik

Wednesday Afternoon, December 1, 2021

Hynes, Level 3, Room 303

1:30 PM *CH04.04.02

Materials Project and Data-Driven Materials Design Kristin A. Persson^{1,2}; ¹UC Berkeley, United States; ²Lawrence Berkeley National Laboratory, United States

The powerful combination of supercomputing resources, robust algorithms for solving the laws of physics and state-of-the-art software infrastructure are enabling rapid, systematic calculations of real materials properties from quantum mechanics across chemistry and structure. A result of this paradigm change are databases like the *Materials Project* (www.materialsproject.org) which is charting the properties of all known inorganic materials and beyond, designing novel materials and offering the data free of charge to the community together with online analysis and design algorithms. The growing body of available, reliable data has reached the stage where automated learning algorithms can be effectively trained and utilized to accelerate all aspects of the materials design cycle: from property prediction to materials synthesis and characterization. In 2021, the Materials Project has rolled out a completely revamped infrastructure to meet growing demands on data accessibility and user experience. A stand-alone data portal has been launched for community data contributions, which is designed to automatically connect contributed materials data with the organization and users of the Materials Project. We will present the new infrastructure and exemplify the approach of data-driven materials design using in-house case studies as well as community-driven research. The data spans design, characterization and synthesis - closing the loop and showcasing rapid iteration between ideas, computations, insight and new materials development.

2:00 PM CH04.04.03

Enhancing Discovery and Characterization of Materials Far From Equilibrium with ML Duncan Sutherland¹, R. Van Dover¹, Carla Gomes¹, Michael O. Thompson¹, Maximilian Amsler¹, Aine Connolly¹, Sebastian Ament¹, John M. Gregoire² and Ming-Chiang Chang¹; ¹Cornell University,

United States; ²California Institute of Technology, United States

Materials processed under conditions that are far from equilibrium can yield new metastable materials with uncommon and valuable properties. Exhaustive exploration of the material space is often intractable due to the many synthesis degrees of freedom, e.g., processing time, temperature, and multiple composition variables. To explore this complex space most efficiently, our workflow employs high-throughput experimentation along with powerful machine learning algorithms. Our experiments consist of lateral gradient laser spike annealing of thin films characterized by micron scale analytics. To rapidly interpret these data, we use a combination of complementary active learning schemes: Gaussian process regression to map out phase boundaries and NMF/compressive sensing to label phases where possible. For a wide range of material systems (oxides, nitrides, and chalcogenides), we demonstrate the richness of the processing phase diagrams and identify methods to address the challenges that arise when executing completely autonomous interpretation.

2:15 PM CH04.04.04

CASTING—A Continuous Action Space Tree search for INverse desiGn Suvo Banik¹, Srilok Srinivasan², Troy Loeffler², Sukriti Manna¹, Rohit Batra², Henry Chan², Pierre Darancet² and Subramanian Sankaranarayanan^{2,1}; ¹University of Illinois at Chicago, United States; ²Argonne National Laboratory, United States

The most common and popular methods for structure search and optimization are based on evolutionary design. This can often be cumbersome, limited to few tens of parameters, and fails for large structural configurations or design problems with high degrees of freedom. Reinforcement learning approaches mostly operate in discrete action space such as in Go game but the applications of that to inverse problems is limited since most inverse problems deal with continuous action space. There are a large number of inverse structural search problems ranging from crystal structure search in material sciences to topology design in Quantum information, where it is highly desirable to optimize structure/configuration to target desired properties or functionalities. This talk will provide an overview of our current efforts to perform scalable crystal structure search to discover and design metastable or non-equilibrium phases with desired functionality. We will demonstrate select use cases that highlight the efficacy of CASTING for molecular, crystal structure, defects, topology, device, and component design.

2:30 PM CH04.04.05

Discovery of Novel Inorganic Crystal Structures via Generative Adversarial Networks. Taylor D. Sparks, Michael Alverson and Ryan Murdock; Univ of Utah, United States

The idea of material discovery has excited and perplexed scientists for centuries. Several methods have been employed to find new types of materials, ranging from replacement of atoms in a crystal structure to advanced machine learning methods for predicting entirely new crystal structures. In this work, we investigate the performance of various Generative Adversarial Network (GAN) architectures to find innovative ways of generating theoretical crystal structures that are synthesizable and stable. Over 300,000 entries from Pearson's Crystal Database are used for the training of each GAN. The space group number, atomic positions, and lattice parameters are parsed and used to construct an input tensor for each of the network architectures. Several different GAN layer configurations are designed and analyzed, including Wasserstein GANs with weight clipping and gradient penalty, in order to identify a model that can adequately discern symmetry patterns that are present in known material crystal structures.

SESSION CH04.05: Poster Session: Accelerating Materials Characterization, Modeling and Discovery by Physics-Informed Machine Learning
Wednesday Afternoon, December 1, 2021
8:00 PM - 10:00 PM
Hynes, Level 1, Hall B

CH04.05.02

Understanding Gold Nanorod Synthesis from Experiments and Literature Using Quantitative Analysis of Plasmonic Absorption Spectra Samuel P. Gleason¹, Jakob Dahl¹, Mahmoud Elzouka², Xingzhi Wang¹, Sean Lubner², Ravi Prasher² and A. Paul Alivisatos¹; ¹University of California, Berkeley, United States; ²Lawrence Berkeley National Laboratory, United States

Gold nanorods (AuNRs) have found applications in cancer imaging and treatment, catalysis, and solar technology due to their size dependent and highly tunable optical properties. The utilization of these applications requires the synthesis of AuNRs of specific sizes and shapes. The determination of the sizes and shapes of AuNRs produced by a colloidal synthesis is commonly achieved using TEM analysis. This procedure requires a significant time investment and expensive instrumentation to attain the volume and quality of images necessary to produce statistically significant distributions. Our method extracts quantitative information about AuNR size distributions from absorption spectra. We treat an absorption spectrum as a linear combination of single particle spectra, and use numerically simulated spectra to determine the length, diameter, and aspect ratio distributions of simulated AuNRs which reproduce the experimental spectrum. This model has been used as an automated tool on AuNRs synthesized using robotic high throughput synthesis, which utilizes a modified one step seedless AuNR synthesis procedure. The accuracy of this model is verified using TEM analysis of samples of this dataset and by the extraction of well labeled spectra from the AuNR synthesis literature. This project demonstrates an effective method to extract population level size distribution information from a colloidal nanocrystal sample. Through using this model on high throughput samples and literature spectra where quantitative information about the size distributions is unknown, the quantitative impact of synthetic procedure on the size distributions of AuNRs can be determined, further developing the fundamental knowledge of AuNR synthesis. In principle, this approach can be extended to any other nanocrystal system where the absorption spectra are size dependent and accurate numerical simulation of the absorption spectra is possible.

CH04.05.04

Real-Time 3D Analysis During Tomographic Experiments on tomviz Jonathan Schwartz¹, Chris Harris², Jacob Pietryga¹, Huihuo Zheng³, Prashant Kumar⁴, Anastasiia Vishneratina⁴, Nicholas Kotov^{1,4}, Yi Jiang³, Marcus D. Hanwell⁵ and Robert Hovden^{1,1}; ¹University of Michigan, United States; ²Kitware, United States; ³Argonne National Laboratory, United States; ⁴University of Michigan—Ann Arbor, United States; ⁵Brookhaven National Laboratory, United States

Three-dimensional (3D) characterization across the nanoscale is now possible using scanning / transmission electron microscopes (S/TEM). Unfortunately, tomographic reconstructions can take one to several days to complete depending upon the dataset size or algorithm(s) employed. Even worse, the reconstruction occurs offline, long after all the data has been collected, preventing immediate interpretation during an ongoing experiment. While

advancements in detector hardware have boosted throughput with digital data collection, substantial human effort and computational resources are still required to process the deluge of raw data. Thus, it has been a longstanding goal to begin 3D analysis of specimens in real-time allowing immediate assessment of nanoscale structure. Continuous 3D feedback provides early diagnosis of specimens to bridge material synthesis with accelerated characterization. Achieving high-throughput electron tomography requires an integrated pipeline that links the microscope hardware to optimized reconstruction algorithms and efficient 3D volumetric visualization. Moreover, this pipeline should be multi-threaded to run dynamic visualizations that updates as new data is collected or reconstruction algorithms proceed.

Here we present interactive 3D visualization that seamlessly runs while experimental projections are collected in an electron microscope using the tomviz platform (www.tomviz.org). Tomviz presents 3D materials structure to scientists in real-time enabling high-throughput specimen interpretation with immediate tomogram visualization. During the experimental acquisition, tomviz monitors for new projections which are continuously appended into the reconstruction process. After a reconstruction updates, tomviz immediately renders the 3D volume. We demonstrate real-time tomography on a helical nanoparticle comprised of a Cysteine amino-acid coordinated with Cadmium (Cys/Cd). The specimen's left-handed chirality is discerned in the first twenty minutes and a high-resolution volume is available within 50% of the experiment (20-30 minutes). Real-time tomography demands maximally efficient computational speed to ensure the optimization runs faster than the experimental data acquisition rate. Tomograms are reconstructed in parallel with data acquisition and a high-quality 3D reconstruction is available before the experiment ends. Tomviz contains novel real-time algorithms that are compatible with high-performance computing clusters to produce and visualize large 3D volumes (>1024 voxels).

The multithreaded pipeline in tomviz enables interactive 3D analysis of the current reconstruction state with minimal impact on performance. A robust graphical interface allows for 3D objects to be rendered as shaded contours or volumetric projections and these objects can be rotated, cropped, or sliced as the reconstruction evolves. Thus, scientists can go beyond superficial inspection to quantify specimen features or internal structure while simultaneously operating the microscope. This immediate feedback can save researchers days of effort as reconstructions are no longer processed offline.

Tomviz offers unparalleled electron tomography throughput with real-time 3D analysis — it is an open-source repository that is available to all institutions for download at www.tomviz.org

CH04.05.05

Identifying Unknown Organic Molecules in Atomic Force Microscopy Images Through Deep Generative Models [Fabio Priante](#)¹, Niko Oinonen¹, Fedor Urtev¹ and Adam Foster^{1,2}; ¹Aalto University, Finland; ²Nano Life Science Institute (WPI-NanoLSI), Kanazawa University, Japan

The use of functionalized tips in Atomic Force Microscopy (AFM) has enabled the investigation of organic molecules with atomic resolution [1]. To more easily interpret the resulting images - which is often a non-trivial task, even for experts - a machine-learned approach based on Convolutional Neural Networks (CNN) has been recently proposed [2]. This method associates unique descriptors to a high-resolution AFM image, allowing automatic extraction of the spatial configuration of the molecule being probed, even for highly three-dimensional cases.

However, if no previous knowledge is available about the identity of the molecule in question, it is very difficult to draw meaningful conclusions.

Here, we approach the problem of recognizing both the identity and the configuration of unknown molecules in high-resolution AFM by using the CNN-extracted descriptors to guide the latent space optimization of a deep generative model for molecular graphs.

These models have seen a rapid development over the past few years, as a way to generate plausible small-molecule drug candidates [3]. Usually, once a generative architecture has been trained to reproduce sufficiently well the distribution of the training data (e.g. the QM9 dataset), optimization of the model's latent space can then be carried out to maximize a property of interest, such as drug-likeness, obtaining a list of best candidates.

In the context of AFM, we optimize the latent space of a state of the art generative model using a score which gives the alignment of each generated molecule with the original CNN-extracted descriptors. As a result, a ranked list of best-fit, chemically valid molecules is proposed as possibly underlying the starting AFM image.

[1] - Gross L., Mohn F., Moll N., Liljeroth P. and Meyer G. 2009 Science **325** 1110

[2] - Alldritt B., Hapala P., Oinonen N., Urtev F., et al 2020 Science Adv **6** 6913

[3] - Gómez-Bombarelli R. et al., 2018 ACS Cent Sci **4** 268–276

SESSION CH04.06: Machine Learning for Material Processing and Synthesis

Session Chair: Jakob Dahl

Thursday Morning, December 2, 2021

Hynes, Level 3, Room 303

10:30 AM CH04.06.01

Elucidating the Weakly Reversible Cs–Pb–Br Perovskite Nanocrystal Reaction Network with High-Throughput Maps and Transformations [Jakob Dahl](#)^{1,2,2}, Xingzhi Wang^{1,2}, Xiao Huang¹, Emory Chan² and A. Paul Alivisatos^{1,2}; ¹University of California, Berkeley, United States; ²Lawrence Berkeley National Laboratory, United States

Advances in automation and data analytics can aid exploration of the complex chemistry of nanoparticles. Lead halide perovskite colloidal nanocrystals provide an interesting proving ground: there are reports of many different phases and transformations, which has made it hard to form a coherent conceptual framework for their controlled formation through traditional methods. In this work, we systematically explore the portion of Cs–Pb–Br synthesis space in which many optically distinguishable species are formed using high-throughput robotic synthesis to understand their formation reactions. We deploy an automated method that allows us to determine the relative amount of absorbance that can be attributed to each species in order to create maps of the synthetic space. These in turn facilitate improved understanding of the interplay between kinetic and thermodynamic factors that underlie which combination of species are likely to be prevalent under a given set of conditions. Based on these maps, we test potential transformation routes between perovskite nanocrystals of different shapes and phases. We find that shape is determined kinetically, but many reactions between different phases show equilibrium behavior. We demonstrate a dynamic equilibrium between complexes, monolayers, and nanocrystals of lead bromide, with substantial impact on the reaction outcomes. This allows us to construct a chemical reaction network that qualitatively explains our results as well as previous reports and can serve as a guide for those seeking to prepare a particular composition and shape. The dataset shown here is openly accessible, has already resulted in several follow-on publications and has been used in a classroom setting to help undergraduate students learn how to explore questions at the intersection of materials chemistry and data analytics.

10:45 AM CH04.06.02

Predicting Synthesizability of Double Perovskite Halide via Machine Learning [Joonchul Kim](#); Soongsil University, Korea (the Republic of)

Double perovskite structure has brought significant attention due to its great potentials for applications of rechargeable batteries, lighting-devices, and energy harvesting materials. Despite of its importance, it is difficult to find the thermodynamically stable structure satisfying target properties due to its enormous chemical space. Conventionally, the tolerance factor is used to predict the stability of the perovskite materials, but its usage has not been fully validated for the double perovskite structures. For example, the halide-type double perovskite structures have demonstrated exceptional physicochemical properties, but its search space is enormous; the chemical formula of the halide-type of double perovskite is $ABB'X_3$ and the number of atomic elements, which can locate at A and B site, reaches 70 and 4 elements to X site, leading to 1,400,000 structures. In this regard, applying the high-throughput materials screening to this type of material cannot be performed with the conventional method such as experiments or *ab initio* calculations.

In this study, to overcome above-mentioned issues, machine learning algorithm is employed to search for new stable double perovskite halide materials. First, the inorganic materials properties are adopted from well-established Materials Project database and double perovskite oxide database that we constructed in our previous work and they are used as a training set (around 120,000 structures and 11,000 double perovskite oxide). Then, the chemical features are constructed to describe given materials. We used the regression as well as the classification method for optimizing the surrogate model. Finally, trained machine learning model is applied to the whole chemical space of the double perovskite halide material (13,542 structures; they are chosen based on previous tolerance factor for validation of the current model). Initially, the prediction accuracy for the formation energy was obtained to be r-squared score of 0.77 and RMSE of 0.399 (eV/atom) when trained only with previous data sets. Finally, to further improve the prediction accuracy more efficiently, we employed the optimization method; exploration by quantifying the prediction uncertainty. This method clearly validated that the r-squared value is increased to 0.90, only by adding 6.5% of selected halide data to the training data.

In this study, the actual formation energy and convex hull energy of the Double perovskite candidate material were calculated using DFT. Machine learning models performed using DFT computational results were successfully able to predict formation energy and convex hull energy of double perovskite halide.

11:00 AM CH04.06.03

“Big Data” Characterization of Material Properties and High Temperature Kinetics [James Horwath](#)¹, Peter Voorhees² and Eric A. Stach¹; ¹University of Pennsylvania, United States; ²Northwestern University, United States

Deactivation of supported metal nanocatalysts under harsh reaction conditions limits the feasibility and efficiency of important industrial reactions. High reaction temperatures and reactive environments enable nanoparticle evolution to reduce the particles' high surface energy, while simultaneously reducing the number of available reaction sites and catalytic activity overall. While research aimed to describe coarsening and degradation processes in nanoscale systems has been undertaken for decades, the difficulty of *in situ* observation and the analysis of *in situ* experimental data has inhibited the development of a theory which comprehensively describes the evolution of supported nanoparticles.

With the goal of understanding coarsening and degradation kinetics in model catalyst systems, we used *in situ* Transmission Electron Microscopy (TEM) to track the evolution of supported gold nanoparticles heated to 900C under vacuum. Using unsupervised machine learning to automatically process TEM images, nanoparticles sizes and positions as a function of time were extracted from experimental images. Using detailed characterization from both ensemble- and particle-scale measurements, we present an analytical model describing nanoparticle degradation as a competition between evaporation into the surrounding vacuum and diffusion between particles along the support. Moreover, we can fit our model to the evolution trajectories of hundreds of individual nanoparticles to determine statistically validated values for fundamental physical properties such as the diffusion coefficient, solid-vapor surface energy, and the equilibrium vapor pressure for gold nanoparticles at high temperature. By comparing these values with literature references, and thereby affirming the validity our model, we can investigate the physical meaning of the remaining parameters which are not measurable by traditional experimental methods. As an example, we are able to use our rich dataset describing nanoparticle evolution to characterize mean diffusion distances for gold adatoms on the silicon nitride support to show that, while nearest neighbor interactions dominate the role of diffusion in nanoparticle growth, there is a measurable contribution for long range interactions across the system of supported particles. This finding demonstrates how a traditional mean-field kinetic model paired with novel data analysis methods can yield results which could not be obtained by either method alone and motivates further study into new physical models which can describe coarsening and evaporation without relying on mean field assumptions.

11:15 AM CH04.06.05

Reconstruction of Low-Index Au Surfaces Using Large-Scale Machine Learning Molecular Dynamics with Many-Body Bayesian Force Fields [Cameron J. Owen](#), Lixin Sun, Yu Xie and Boris Kozinsky; Harvard University, United States

Gold surfaces have a long history of microscopic studies due to their propensity to reconstruct in complex patterns depending on the terminating surface facet and the environment (temperatures and atmosphere). However, the details of restructuring processes and metastable intermediate structures, which could be critical for catalytic reactions, remain unknown due to the limits of microscopy time resolution and accuracy of classical force field simulations.

This work demonstrates a robust many-body Bayesian potential trained with an on-the-fly active learning framework implemented using Gaussian process regression in the FLARE code [1]. The active learning module uses molecular dynamics (MD) simulations of low-index surfaces to sample important configurations and runs density functional theory (DFT) calculations when the prediction Bayesian uncertainty exceeds a threshold. The trained Bayesian force field is then used to perform a large-scale MD to study surface diffusion and reconstructions of various surface facets, e.g., semi-hexagonal reconstruction on (100), Herringbone reconstruction on (111), and missing-row reconstruction on (110).

[1] J. Vandermause et al, *NPJ Computational Materials* **6** (2020).

SESSION CH04.07: Advanced ML/AI Assisted Material Characterization I
Session Chair: Adam Foster
Thursday Afternoon, December 2, 2021
Hynes, Level 3, Room 303

1:30 PM *CH04.07.01

Structure Discovery in Atomic Force Microscopy [Adam Foster](#)^{1,2}; ¹Aalto University, Finland; ²Kanazawa University, Japan

Atomic force microscopy (AFM) with molecule-functionalized tips has emerged as the primary experimental technique for probing the atomic structure of organic molecules on surfaces [1]. Most experiments have been limited to nearly planar aromatic molecules, due to difficulties with interpretation of highly distorted AFM images originating from non-planar molecules [2]. Here we develop a deep learning infrastructure that matches a set of AFM images with a unique descriptor characterizing the molecular configuration, allowing us to predict the molecular structure directly in a few seconds on a laptop [3]. We apply this methodology to resolve several distinct adsorption configurations and conformations of molecules based on low-temperature AFM measurements. In general, we find high success rates in predicting the atomic and chemical structure of molecules. This approach opens the door to apply high-resolution AFM to a large variety of systems for which routine atomic and chemical structural resolution on the level of individual objects/molecules would be a major breakthrough. We also look at applications of similar approaches to the imaging of biomaterials and AFM imaging in liquids.

[1] N. Pavliček and L. Gross, *Nat. Rev. Chem.* **1**, 0005 (2017)

[2] P. Jelinek, *J. Phys.:Condens. Mat.* **29**, 343002 (2017)

[3] B. Alldritt, P. Hapala, N. Oinonen, F. Urtev, O. Krejci, F. F. Canova, J. Kannala, F. Schulz, P. Liljeroth, and A. S. Foster, *Sci. Adv.* **6** (2020) eaay6913

2:00 PM CH04.07.03

Autonomous Identification of X-Ray Diffraction Spectra Using Probabilistic Deep Learning Nathan Szymanski^{1,2}, Christopher Bartel^{1,2}, Yan Zeng², Qingsong Tu² and Gerbrand Ceder^{1,2}; ¹University of California, Berkeley, United States; ²Lawrence Berkeley National Laboratory, United States

To enable the development of self-driving laboratories and their application to the synthesis of inorganic materials, we designed a deep learning approach that automates the analysis of diffraction spectra and identifies chemical reaction products. Using a convolutional neural network, our model was trained on simulated spectra that were augmented with physics-informed perturbations to account for possible experimental artifacts left over from sample preparation and synthesis. These diffraction spectra were derived from experimentally reported phases as well as hypothetical solid solutions with off-stoichiometric compositions. For the analysis of spectra obtained from mixtures of materials, we developed a branching algorithm to evaluate suspected mixtures and identify the set of phases that maximize the probabilities given by the neural network. Our model was tested on simulated and experimental data from materials in a five-component system, achieving accuracies up to 92% and 87% for the identification of single- and multi-phase spectra, respectively. These results show an improvement greater than 10% when compared to previously reported methods based on profile matching and deep learning. To extend the application of our approach to arbitrary sets of materials, we provide a software suite that facilitates the training of new models, which we hope may be used to automate the characterization step in high-throughput and autonomous experimental workflows.

2:15 PM CH04.07.04

High-Fidelity Retrieval of Nanoscale Short-Range Order Distribution in GeSn Alloys Guided by Statistical Methods in Atom Probe Tomography Shang Liu, Alejandra V. Covian, Cory T. Cline and Jifeng Liu; Dartmouth College, United States

GeSn alloys on Si have been an attractive research area given their capability to engineer the bandgap for mid-infrared applications and compatibility with Si-based integrated circuits. Recently, short-range order (SRO) in GeSn alloys has been theoretically predicted [1] especially for >15 at.% Sn composition, which profoundly impacts the band structure of GeSn alloys. In principle, atom probe tomography (APT) is a powerful experimental technique to study SRO (e.g., via radial distribution function, RDF) by offering 3D atomic reconstruction of the alloy. In reality, however, high-fidelity retrieval of lattice information and accurate RDF has been limited to metals [2,3]. Deriving SRO of semiconductor alloys from APT has been a significant challenge due to larger measurement error in atomic positions as well as lower detection efficiency compared to elemental metals. In fact, the APT data of semiconductor alloys resembles a significantly perturbed lattice, and ~50% of the atomic sites are empty due to the limited detection efficiency. Therefore, one can no longer identify the lattice from the raw APT data. Currently, SRO analyses in alloys are limited to relatively crude methods such as artificially cutting a line midway between the theoretical distances of the k th and $(k+1)$ th nearest neighbor shells to accommodate the perturbed atomic positions [4]. To overcome this limit and retrieve SRO at high fidelity, here we demonstrate a new method that only requires the input of crystal structure to derive SRO in GeSn alloys from the nonideal APT data by combining Poisson distribution and k -nearest neighbors (KNN) analysis. This approach establishes a statistical correlation between the nominal KNN directly obtained from the nonideal APT data to the *true* KNN shell for diamond cubic structure, thereby regrouping the former to reconstruct the latter at high fidelity. Lattice constants can also be derived using an iterative approach given the crystal structure. We demonstrate that our method can retrieve lattice constants with ~1.5% accuracy from the APT data of Ge and GeSn alloys. For GeSn alloys, we define SRO parameter α_{Sn-Sn}^{KNN} as the probability for a Sn atom to have another Sn atom in the *true* KNN shell divided by the Sn at.% in the same region. For example, $\alpha_{Sn-Sn}^{KNN} > 1$ indicates more Sn-Sn clustering than a random alloy. This way, we were able to study nanoscale SRO distribution along the depth of the GeSn thin films. Our study shows that α_{Sn-Sn}^{KNN} decreases from 1.052±0.051 to 1.026±0.045 as the depth increase from 150 to 800 nm under the surface, with 18 10 nm×10 nm×10 nm blocks examined at each depth. These results indicate more preference towards Sn-Sn clustering near the surface where the Sn composition is higher due to strain relaxation [5]. The discovery of a relatively large fluctuation in SRO in GeSn, together with the theoretical prediction of large band structure variation with SRO, explains why the photoluminescence (PL) peaks are broad even at low T for GeSn (i.e., width $\gg k_B T$). Furthermore, we propose an algorithm based on least square fit to rearrange atoms to nearby perfect lattice sites, which show a very good consistency with the aforementioned results before rearrangement. A great advantage of APT-based SRO analyses is that we can map the SRO at nanoscale in a relatively large region with millions of atoms (e.g., 30x30x800 nm³), while other methods either give an average (EXAFS) or only analyze a very small region (STEM). Our method can be extended to other material systems such as high-entropy alloys.

[1] Cao, B., et al. *ACS Applied Materials & Interfaces* **12**, 51, (2020): 57245–57253.

[2] Gault, B., et al. *Microscopy and Microanalysis* **16.1** (2010): 99-110.

[3] Geiser, B.P., et al. *Microscopy and Microanalysis* **13.6** (2007): 437-447.

[4] Ceguerra, A. V., et al. *Acta Crystallographica Section A: Foundations of Crystallography* **68.5** (2012): 547-560.

[5] Dou, W., et al. *Scientific reports* **8.1** (2018): 1-11.

2:30 PM CH04.07.05

Machine-Learning Prediction of Structural Transition Temperature in Multialloy MTX Alloys with Model Interpretability Analysis Timothy Hartnett¹, Vaibhav Sharma², Radhika Barua² and Prasanna Balachandran^{1,1}; ¹University of Virginia, United States; ²Virginia Commonwealth University, United States

The global rise of environmental concern has highlighted the need to switch from harmful vapor-compression-based cooling technologies to more friendly options. Solid-state cooling devices based on multicaloric materials are one promising option. Multicaloric materials undergo a reversible thermal change driven by more than one external energy source. One promising multicaloric materials family of interest is the intermetallic MTX compounds.

The MTX materials [where M = transition metal (Mn, Fe, Ni, Co); T = transition metal (Mn, Fe, Ni, Co); X = main group p-block element (Si, Ge, Sn, Al, Ga)] undergo a martensitic phase transition from the low temperature, martensitic Pnma (TiNiSi-type) phase to the high temperature, austenitic P6₃/mmc (Ni₂In-type) phase. Nominally, in the stoichiometric parent compound, MnNiSi, the martensitic phase transition (T_m) occurs at 1200 K. The Pnma phase is

also ferromagnetic and has a Curie temperature (T_c) of 662 K. Through alloying with other transition metals and p-block elements, T_m and T_c can be tuned to coincide resulting in a hysteretic magnetostructural phase transformation that is first-order in thermodynamic character. There is significant interest in identifying alloy compositions where the magnetostructural transition temperature (T_t) is observed near room temperature with minimal hysteresis so that devices can be built with maximum cooling efficiency.

Here, we develop a data-driven machine learning (ML) approach to predict the T_t and hysteresis of solid solutions of MTX alloys. We compiled a dataset of experimentally synthesized and characterized MTX solid solutions from surveying the published literature. We represented each composition using three sets of features: (1) compositions, (2) elemental descriptors, and (3) those generated from density functional theory calculations. Four separate ML methods were considered for regression (1 linear, 3 non-linear), and the best method was selected based on test set performance quantified by R^2 goodness-of-fit. The top-performing model was then validated experimentally on new solid solutions.

In addition to prediction, we also implemented a novel post hoc interpretability technique to understand model behavior. Typically, many ML algorithms are treated as black-box models. While ML-based approaches have been demonstrated to optimize materials design and discovery, the lack of model interpretability means that it is very difficult to extract valuable scientific insights from the trained models. To address this problem, we implement a common model interpretability technique, global feature importance, along with less common, local instance-level variable attribution techniques. The results show that the model prioritizes features that are known to impact the T_t in the system. The results of the local analysis also show that the variable attribution varies significantly for different compositions highlighting the limitations of global feature importance.

2:45 PM CH04.07.06

Time-Resolved Phase Formation Studies Inform Machine Learning Algorithms During Autonomous Materials Discovery [Aine Connolly](#), Ming-Chiang Chang, Katie Gann, Maximilian Amsler, Duncan Sutherland, Michael O. Thompson and R. Van Dover; Cornell University, United States

High-throughput experimentation today explores not only compositional space, but also process space. In our work, we use micro- to milli-second thermal processing to synthesize metastable phases in binary and ternary systems, and a combination of optical spectroscopy and synchrotron x-ray diffraction (XRD) to characterize them. However, post-processing analysis constrains understanding to the terminal structures only, without identifying transient structures that may develop during synthesis. The search for autonomous materials using ML and AI algorithms would be enhanced by incorporating time-resolved information regarding the phase evolution alongside the characterization of the final phases.

The unique experimental characteristics of the lateral-gradient Laser Spike Annealing technique allows this temporal structural evolution to be mapped onto a spatial dimension, enabling a wide range of characterization techniques. For initial studies, optical imaging has been used to track the phase formation sequence as a function of both time and temperature during IgLSA in materials such as Bi_2O_3 and Ga_2O_3 . In single-composition Bi_2O_3 , for example, initial nucleation of the δ phase occurs early during heating with transformation to the β phase also observed during the temperature ramp; in this system, no subsequent transformations have been identified during cooling to ambient conditions. Behaviors across a number of binary systems will also be discussed. Ultimately, these data can be integrated into closed-loop experiments to inform the autonomous search for new materials.

3:00 PM CH04.07.07

Late News: Analytical Methods to Characterize Dynamics of Individual Dislocations with DFXM [Leora E. Dresselhaus-Marais](#); Stanford University, United States

Dislocation boundaries dominate the multiscale structure and properties of metals, setting the complex dynamics that determine how they respond to external stresses or heating. Characterization of these intricate multiscale dynamics is extremely difficult at the single-dislocation level, due to experimental and analytical challenges. Dark-field X-ray microscopy (DFXM) was recently demonstrated to resolve the dynamics of populations of deep subsurface dislocations at the single-dislocation level, but challenges persist in assigning the positions and character. We have developed a suite of computer-vision methods to identify and track dislocations in DFXM movies collected on single-crystal aluminum during annealing. This talk will present our new methods and the opportunities they hold to quantify statistically significant defect dynamics in crystalline materials at the mesoscale.

3:15 PM CH04.03.03

Deep Learning-Based Analysis of Optical and Morphological Properties of Chiral Micron-Scale Helices [Anastasiia Vishseratina](#)¹, Alexander Vishseratin², Prashant Kumar¹ and Nicholas Kotov¹; ¹University of Michigan–Ann Arbor, United States; ²Beehive AI, United States

Chiral nano- and micron-scale inorganic structures have potential in many technological fields, including biosensing, chiral catalysis, enantioselective separation, and quantum computing. While they have numerous unique physico-chemical properties, their ability to exhibit high chiroptical activity is the key characteristic that spurs research in this area. To date, many researchers are focused on the development of materials with hierarchical chirality since the combination of nano-, meso-, and micron-scale chiral elements in one structure can allow to rotate light polarization in a wide spectral range. However, top-down approaches, such as ion-beam lithography, extensively used for growing such helices, are limited for the fabrication of nanoscale elements and have a low mass production efficiency. Also, there is a need for novel methods for the structural characterization of chiral nano- and micron-scale inorganic structures.

Here we developed a facile bottom-up approach for the formation of microscale helices of bowtie shape. Depending on the enantiomer of chiral molecules used, bowties have a right- or left-handed twist with 100% enantiomeric excess. Transmission electron microscopy of bowties allowed to establish that bowties are self-assembled from nanoparticles with 3.4 nm diameter that are then arranged into stacked twisted nanosheets. The latter have a thickness of about 100 nm and a 50 nm separation between each other. Careful adjustment of synthesis conditions allows growing bowties with desired length, width, thickness, and twist, which, in turn, lead to the strong chiroptical activity that could be carefully tuned in a from UV-Vis to NIR spectral range. Computations of bowties chiroptical activity have shown that the circular dichroism and g-factor spectra blue-shift as the pitch of bowties decreases. Varying synthesis conditions, we synthesized more than 600 different samples and obtained more than 1200 scanning electron microscopy (SEM) images to study their nucleation, growth, and final morphology. Analysis and characterization of SEM images can be significantly improved and fastened by using artificial intelligence approaches. We developed a convolutional neural network model for the recognition of bowties on SEM images and the determination of their handedness (right-handed, left-handed). Our next step is to advance the model and make it able to calculate the enantiomeric excess of bowties and their dimensions.

Also, to predict the optical properties based on the concentrations of chemicals used, we developed a multi-layer fully connected neural network. The approach that was chosen is to model target parameters independently to get better accuracy. The model has four hidden layers with the following number of neurons in each - 400, 2000, 1000, 400. The developed neural network allows to predict bowties parameters (length, width, thickness, and twist angle) and their optical properties (circular dichroism peak wavelength and g-factors) with good accuracy.

We believe that these results open new horizons for designing, characterization, and engineering of chiroptical materials and metamaterials with a strong and tunable polarization rotation essential for multiple emerging technologies.

8:00 AM CH04.08.01

Low-Uncertainty Condensation Heat Transfer Characterization Using Intelligent Vision Siavash Khodakarami and Nenad Miljkovic; University of Illinois at Urbana-Champaign, United States

Vapor condensation is of great significance to a plethora of applications such as power generation, thermal management, and water desalination. Over the past century, many hydrophobic coatings have been developed to promote dropwise condensation (DWC) on surfaces of interest. DWC on hydrophobic coatings is preferred as it has heat transfer coefficients (HTC) one order of magnitude higher than filmwise condensation (FWC) on an uncoated surface. Quantification of the heat transfer performance during condensation is normally done in vacuum systems to limit the presence of the non-condensable gases (NCG), and to enable high-fidelity temperature measurements for heat transfer quantification. Numerous difficulties exist with these classical techniques mainly related to the high uncertainties in the measured heat flux and calculated HTC when proper experimental conditions are not used. Here, we demonstrate a visualization-based method for rigorous and high-fidelity heat transfer characterization during DWC. State-of-the-art computer vision techniques are used to extract physical features which are used to predict the heat transfer performance of hydrophobic tubes undergoing DWC. We demonstrate the utility of our visual approach by using it to estimate the local axially-varying heat flux on a tube with spatially varying wettability without using any temperature measurement. Unlike classical methods, we demonstrate that our method has a fixed heat flux estimation uncertainty of 13% of the measured value. In contrast, we show that the measurement uncertainty of classical techniques is a function of sensor uncertainty, geometrical parameters such as length and diameter of the sample, and the heat flux itself, and is generally several times higher than the uncertainty associated with our vision-based method. Our visualization-based method does not require high-speed imaging and can be applied with regular 30 FPS imaging. Our computer-vision method demonstrates significant utility for conditions where conventional temperature-based methods fail such as DWC with short or small diameter tubing, experiments with laminar cooling flows, small heat flux condensation, or obtaining local heat flux measurements.

8:15 AM CH04.08.02

Towards Automation of Particle Size Distribution Analysis of Catalyst Layers for Polymer Electrolyte Fuel Cells André Colliard Granero^{1,2}, Mohammad Javad Eslamibidgoli¹, Mariah Batool³, Jasna Jankovic³, Michael Eikerling¹ and Kourosh Malek¹; ¹Forschungszentrum Jülich, Germany; ²University of Cologne, Germany; ³The University of British Columbia, Canada

Accelerating the development of electrochemical devices is pivotal for the societal shift towards a sustainable and de-fossilized energy economy. Imaging is crucial to quantify structural characteristics of materials, as well as to detect and monitor structural changes during fabrication and normal operating cycles of the device (battery, fuel cell, electrolysis cell). The escalating use of imaging infrastructure in the energy materials domain drives a significant growth of data in terms of their amount and complexity. This leaves the applications of standard machinery for image processing often ad hoc, indiscriminate, and empirical which in turn makes the quantification metrics for analysis elusive. Moreover, the use of standard techniques for materials characterization is expensive, slow and often involves several pre-processing steps. In this contribution, we present a deep learning-based approach to automate the analysis of particle size distribution (PSD) from Transmission Electron micrographs (TEM) of carbon supported catalyst electrodes for Polymer Electrolyte Membrane (PEM) Fuel Cells or PEM electrolyzers. The catalyst layer components are fabricated based on catalyst nanoparticles (e.g. Pt) on a high-surface-area carbon support material. The automation was enabled via a multi-step approach based on supervised learning, by 1. manual annotation of TEM images [1], 2. training a U-Net model for instance segmentation [2] of catalyst nanoparticles, followed by 3. employing computer vision techniques for the diameter measurement of individual particles and 4. generating particle size distribution plots. Results on the validation set are in well agreement with PSD analysis by our experimental experts, presenting an efficient use case of ML-enabled materials characterization.

References:

- [1] P. Bankhead, et al, *Scientific Reports* **2017**, 7, 16878.
- [2] Ronneberger, et al. In International Conference on Medical image computing and computer-assisted intervention, Springer, Cham, **2015**, 234.

8:30 AM CH04.08.03

A Statistical Study of Corrosion Dynamics in Atomically-Thin Nanomaterials Utilising *In Situ* SEM Ryo Mizuta¹, Ye Fan¹, Peter Voorhees² and Stephan Hofmann¹; ¹University of Cambridge, United Kingdom; ²Northwestern University, United States

The 'lifetime' of materials is a central topic in the field of corrosion science and is a crucial consideration for any real-world use of emerging materials. Recent years have witnessed a surge in the development of low-dimensional nanomaterials (e.g. 2D materials) towards commercial applications, driven by discoveries of novel, record-breaking material properties. However, systematic studies on their ageing dynamics are comparatively rare and the fundamental processes that dictate their lifetime remain poorly understood [1]. Meanwhile, statistical variations are expected to significantly impact dynamic processes at the nanoscale, including ageing. Despite this, the collection of sufficiently large datasets that permit their statistical analysis remains challenging and is commonly not emphasised when studying the properties of low dimensional nanomaterials. Recent reports which combine high-throughput image processing workflows with large electron microscopy datasets of "static" nanomaterials, illustrate a promising approach for rapidly extracting quantitative datasets of statistically relevant sizes [2,3]. However, such methods have rarely been extended to studies of nanoscale dynamics, given the lack of suitable characterisation platforms that can probe nanomaterials *in-situ*, under realistic working conditions. Here, we combine a custom *in-situ* environmental scanning electron microscope (ESEM), equipped with localised gas injection and heating capabilities, with automated image analysis to observe and collect statistically large datasets that quantify nanoscale dynamics. The formation of corrosion pits during the thermal oxidation of atomically-thin 2D materials is selected as a prototype system to demonstrate the capabilities of our workflow. By leveraging the ESEM's large field of view and our high-throughput experimental design, the expansion dynamics of $10^3 - 10^4$ corrosion pits are tracked and quantified simultaneously in each experiment. Our statistically relevant datasets of pit formation permit conventional corrosion theories to be statistically tested in the 2D limit. The collection and analysis of gigabyte to terabyte levels of kinetic data are semi-automated, with heavy reliance on developing suitable computer image recognition algorithms. Our research paradigm, in which the statistical analysis of large *in-situ* experimental data is emphasized, promises a more repeatable and reliable experimental analysis of nanoscale processes.

References

- [1] Li et al., *J. Mater. Chem. A*, 2019, 7(9), 4291
- [2] Lee et al., *ACS Nano*, 2020, 14(12), 17125
- [3] Laramy et al., *ACS Nano*, 2015, 9(12), 12488

8:45 AM CH04.08.04

Deep Learning for On-the-Fly Visualization of Large Datasets and Out-of-Distribution Data Detection Lars Banko¹, Phillip M. Maffettone², Daniel Olds² and Alfred Ludwig¹; ¹Ruhr-Universität Bochum, Germany; ²Brookhaven National Laboratory, United States

Artificial intelligence agents offer great opportunities for accelerating materials discovery by autonomous data analysis. With advanced methods of high-throughput experimentation producing increasingly larger datasets, autonomous analysis and decision making by AI is required in collaboration with the deep reasoning provided by expert scientists. While AI should be focused on autonomously analyzing the standard cases, expert scientist resources should be centered around the most interesting or challenging tasks. A persistent issue of AI models is associated with drawing conclusions from uncertain settings, e.g. when the information stored in the data does not allow for a definite decision or the training data does not support aberrations encountered in experimental data.

In this contribution, we demonstrate that variational autoencoders (VAE) provide a powerful toolset for the analysis of large X-ray diffraction datasets. Visualization of the latent vectors can reveal intrinsic features of the dataset that allow for an assessment of possible failure modes during a classification task. The representation can further be used for on-the-fly visualization of a dataset distribution across different structures. Here, latent space proximity can be used as a structural estimator. A strategy based on the evaluation of the reconstruction error and the clustering of latent variables for the detection of out-of-distribution data is reported and demonstrated on experimental data. By inclusion of experiment specific domain knowledge (e.g. chemical composition) the model can be tuned to produce valid solutions under awareness of constraints. Transferability to other experimental sources of spectral data is demonstrated. We envision the VAE working cooperatively together in a federation of specialized AI agents.

9:00 AM CH04.08.05

Decoding the Shift-Invariant Data—Applications for Band-Excitation Scanning Probe Microscopy Yongtao Liu¹, Rama K. Vasudevan¹, Kyle P. Kelley¹, Dohyung Kim², Yogesh Sharma³, Mahshid Ahmadi², Sergei V. Kalinin¹ and Maxim A. Ziatdinov^{1,1}; ¹Oak Ridge National Laboratory, United States; ²The University of Tennessee, Knoxville, United States; ³Los Alamos National Laboratory, United States

In this work, we introduced a shift-invariant variational autoencoder (shift-VAE), which is an unsupervised method developed for analyzing 1D spectra data disentangling the physically-relevant shifts from other latent variables. Using synthetic datasets, we show that the shift-VAE latent variables are linear functions of the ground truth parameters, indicating the strength of shift-VAE in disentangling physically-relevant variables in a model-free unsupervised manner. The application of shift-VAE is illustrated for band-excitation piezoresponse force microscopy (BE-PFM) data. From two BE-PFM data sets, we consistently observed that shift-VAE successfully disentangles ferroelectric polarization and crosstalk-induced resonance frequency peak shift from BE curves. In addition, shift-VAE also shows the strength in denoising raw curves without sacrificing real response. Overall, shift-VAE proves to be a powerful technique for learning spectra, which should have very broad applications in many fields. This approach can also be extended to analysis of X-ray diffraction, photoluminescence, Raman spectra, and other data sets.

Acknowledgments: This work is supported by the U.S. Department of Energy, Office of Science, Office of Basic Energy Sciences Energy Frontier Research Centers program under Award Number DE-SC0021118. This work is conducted at the Center for Nanophase Materials Sciences, a US Department of Energy Office of Science User Facility.

9:15 AM CH04.08.07

Late News: Machine Learning Assisted Identification of Threading Dislocations Bohdan J. Starosta and Benjamin Hourahine; University of Strathclyde, United Kingdom

Electron channeling contrast imaging (ECCI) is a non-destructive scanning electron microscope (SEM) surface imaging technique that is sensitive to distortion of planes in crystal lattices. It detects the diffraction intensity of electrons incident on a sample, where the angles between detector, sample normal, and the SEM electron beam, are carefully chosen so that the orientation of diffracting planes with respect to the incident electron beam is approaching their Bragg angle, creating strong contrast in the image. Local lattice strain induced deviations to the crystallographic orientation or lattice constant will then affect the intensity of the back scattered electrons, and produce a variation in contrast in the resulting surface image that indicates the presence of a defect. These images are over a relatively wide area (~100 μm^2), with a spatial resolution of ~20 nm, and allow us to detect and classify threading dislocations, grain boundaries, and other defects at semiconductor surfaces [1].

Of particular interest is the ability to conduct a quantitative analysis of threading dislocations (TDs) present in a GaN thin film, which manifest an ECC image as spots with a dipolar black-white (B-W) contrast. One obstacle to this is the need for the painstaking marking and manual analysis of each individual experimental image by a skilled researcher. Bulk epitaxial GaN thin films often have TD area densities of 10^8 to 10^9 cm^{-2} [2], adding to the scale of the problem. This creates a need for a fast, automated, and relatively accurate method of extracting defect data from multiple images.

Supervised machine learning techniques have been proven in recent years to be able to achieve a high degree of success in detecting predetermined features, particularly in the medical imaging field [3]. We have utilized previously documented techniques for quickly identifying TDs on III-Nitrides [1,4] to build a training dataset for a U-Net based deep fully convolutional network architecture [5,6]. This includes images of defects both with a strong B-W contrast as well as dislocations at close to the invisibility criteria which are faintly resolved.

The neural network that is trained on this set can then relatively reliably detect the positions of TDs in ECCI of GaN with an accuracy on the order of 75-90% for independent testing data (i.e. marked images unseen by the network during training), with the main source of errors being false positives due to strong non-TD features, and false negatives due to either TD faintness at certain diffraction conditions, or overlapping, closely spaced TDs affecting the predictive binary mask. The recognition process for a 2576x1936px image currently takes around 90 seconds when using a modern 8-core consumer grade CPU. For our current dataset size the network can be trained to convergence in 30±10 minutes when using a single NVIDIA V100 GPU. Fig. 1 shows the marked locations for a cluster of dislocations in GaN.

- [1] Trager-Cowan, C. et al. *Semicond. Sci. Technol.* 35, 054001 (2020).
- [2] Kopolnek, D. et al. *Appl. Phys. Lett.* 67, 1541–1543 (1995).
- [3] Arganda-Carreras, I. et al. *Front. Neuroanat.* 9, (2015).

[4] Naresh-Kumar, G. et al. *Phys. Rev. Lett.* 108, 135503 (2012).

[5] Wiehman, S. & Villiers, H. de. Semantic segmentation of bioimages using convolutional neural networks. in 2016 International Joint Conference on Neural Networks (IJCNN) 624–631 (2016).

[6] Ronneberger, O., Fischer, P. & Brox, T. U-Net: Convolutional Networks for Biomedical Image Segmentation. in MICCAI 2015 234–241 (Springer, 2015). doi:10.1007/978-3-319-24574-4_28.

9:20 AM CH04.08.08

A Physics-Based Model to Index Crystal Orientation Using Directional Reflectance Microscopy [Chenyang Zhu](#) and Matteo Seita; Nanyang Technological University, Singapore

Characterizing crystallographic quantities in crystalline materials—including crystal structure, grain orientation, and defects character—is the realm of diffraction-based techniques. We have developed a simple and affordable method—which we call directional reflectance microscopy (DRM)—to capture this information using an optical microscope. DRM relies on producing orientation-dependent features on the surface of crystalline solids and measuring the reflectance they generate when illuminated from different angles. Point-by-point indexing of optical reflectance across the sample surface enables mapping the underlying crystallographic orientation in a similar fashion to electron backscatter diffraction. Here we discuss the advantages of indexing the optical signal using a forward model approach. Our method consists of producing a dictionary of reflectance patterns generated by a discrete sampling of orientation space using a physics-based reflection model. We then compare these simulated patterns with the experimental one to find the best match, which is selected as the nominal orientation. This dictionary indexing method overcomes limitations that are inherent to previous approaches, which relied on fitting good quality patterns. We demonstrate the improved accuracy of the forward-model method on a centimeter-scale aluminum sample.

9:25 AM CH04.08.09

Late News: Machine Learning for Optimization of Optical Super-Resolution Microstructure Analysis [Alex Ulyanenko](#)¹, Alexander Mikhalychev^{2,3}, Konstantin Zhevno², Svetlana Vlasenko³ and Dmitri Mogilevsev³; ¹Atomicus LLC, United States; ²Atomicus OOO, Belarus; ³B.I.Stepanov Institute of Physics, NAS of Belarus, Belarus

Optical methods are appealing for application to microstructure analysis due to their simplicity, direct observation of details, and availability of versatile elemental base. However, diffraction of light blurs the collected images and sets the fundamental limit on the achievable resolution [1]. Recently, a number of super-resolving techniques based on nano-particles fluorescence were developed for overcoming the classical resolution limit, for instance stimulated-emission depletion (STED) microscopy [2], photoactivated localization microscopy (PALM) [3], and structured illumination microscopy (SIM) [4]. Super-resolution optical fluctuation imaging (SOFI) is also among promising quantum-inspired techniques [5]. The resolution enhancement in SOFI stems from special statistical analysis of the intensity correlations of randomly fluctuating fluorescent sources: quantum dots [5], organic dyes [6], or other fluorescent particles. Namely, a cumulant image is formed instead of usual intensity images and provides a narrower point-spread function (weaker blurring of the image). The approach is applicable for both investigation of inorganic samples and imaging of living cells and subcellular structures.

Initially, SOFI was believed to provide infinite growth of resolution with the increase of cumulants order. Recently, it has been shown that the inevitable statistical noise imposes fundamental limits on the achievable resolution; the optimal cumulant order is finite (and depends on the imaged object); and combined analysis of several cumulant orders may be profitable [7,8]. The research was based on maximization of Fisher information and included some simplifying limitations: either just two point emitters were considered [8], or the statistical switching noise of the fluorescent sources themselves was neglected [7]. In the current contribution, we follow that line of Fisher information-based research, but consider a general case of several emitters, finite observation time, and realistic fluctuations model.

A measurement in SOFI is fast and provides an image with a large number of pixels (up to 1 million). To benefit from those advantages of the technique (especially, when fast living-cell processes are analyzed), one needs to be able to perform fast on-the-fly processing of the acquired data. For that reason, it is desirable to know and process the optimal cumulant order soon after the dataset is collected. While Fisher information approach is much faster and more reliable than direct Monte-Carlo simulations, it is still computationally expensive for taking such real-time decisions. Here, we show that machine learning is capable of solving that issue. An artificial neural network (a 5-layer perceptron) takes an intensity image of the object (easily generated from a SOFI dataset) as an input and decides, which cumulant order or combination of cumulant orders would yield the maximal information gain for the same computational resources. The training datasets are prepared with the help of Fisher information approach. The preliminary results show that the probability of taking the correct decision among 4 options with approximately equal probabilities exceeds 80%. The proposed tandem approach of Fisher information and machine learning is universal and applicable to many other techniques for optimization of on-the-fly analysis or taking real-time decisions which measurement to perform next.

1. Abbe, E., *Archiv für mikroskopische Anatomie*, 1873, 9, 413.
2. Hell, S. W. and Wichmann, J., *Opt. Lett.*, 1994, 19, 780.
3. Hess, S. T. et al., *Biophys. J.*, 2006, 91, 4258.
4. Classen, A. et al., *Optica*, 2017, 4, 580.
5. Dertinger, T. et al., *Proc. Natl. Acad. Sci. U.S.A.*, 2009, 106, 22287.
6. Dertinger, T. et al., M., *Angew. Chem. Int. Ed.*, 2010, 49, 9441.
7. Vlasenko, S. et al., *Phys. Rev. A*, 2020, 102, 063507.
8. Kurdzialek, S. and Demkowicz-Dobrzanski, R., *J. Opt.*, 2021, 23, 075701.

SESSION CH04.09: Machine Learning for Material Processing and Synthesis II

Session Chair: Rama Vasudevan
Monday Morning, December 6, 2021
CH04-Virtual

10:30 AM CH04.09.01

Twining Network Graph Analysis on Ingot-Scale Multicrystalline Structure [Takuto Kojima](#)¹, Kentaro Kutsukake², Tetsuya Matsumoto¹, Hiroaki Kudo¹ and Noritaka Usami¹; ¹Nagoya University, Japan; ²RIKEN, Japan

Multicrystalline materials can be relatively easily fabricated with a large crystal growth furnace leading to cost-effective yield, whereas non-uniformity of

crystal properties is a problem for large ingots. Therefore, it is important to extract the ingot-scaled features of the multicrystalline structure. The multicrystalline structure grown by the unidirectional solidification method develops from the nucleus at the bottom of the crucible into a columnar structure, and successive twinning inside the columnar structure causes various grain boundaries. The orientation relationship between the individual nuclei is random, while the orientation relationship due to twinning is crystallographically determined, which consequently contains information about the grain development relationship. We have developed a method to analyze multicrystalline structures using network graphs where edges represent successive twinning from crystal orientations of grains in 30×40 mm² multicrystalline silicon, obtained by electron backscatter diffraction pattern (EBSD) method [1-3]. In this study, we attempted to extract ingot-scaled features of multicrystalline structures by performing network analysis on crystal orientations obtained by the Laue scanner method [4] on 156×156 mm² substrates sliced from the bottom, middle, and top parts of a multicrystalline silicon ingot. The network analysis was performed by coding with a Python package NetworkX [5].

The crystal orientations of 1918, 1490, and 1390 grains (at the center of gravity of each grain) were obtained from the bottom, center, and top of the ingot, respectively. The orientation relationship between grains was attributed to an n th-order ($0 \leq n \leq 3$) twinning relationship ($\Sigma 3^n$) that gives the minimum residual angle θ . A graph G was generated with edges for the twinning relation satisfying $\theta/\theta_{th} + d/d_{th} \leq 1$, where $\theta_{th} = 2^\circ$ and $d_{th} = 40$ mm were thresholds for θ and the distance d between grains. Connected subgraphs contained four or more nodes were plotted on the grain boundary mapping extracted from the optical image, where grains in the same subgraph are considered to have grown from the same nucleus. As the crystal growth proceeded, the number of nodes in a subgraph and the area occupied by a subgraph with a large number of nodes also tended to increase. The analysis using network graphs made it possible to extract ingot-scaled features of multicrystalline structures.

References

- [1] T. Kojima et al., Abstr. 66th JSAP Spring Meeting, 9a-W611-3, 2019.
- [2] T. Kojima et al., Abstr. 80th JSAP Autumn Meeting, 20a-E314-4, 2019.
- [3] T. Kojima et al., Abstr. 67th JSAP Spring Meeting, 14a-A205-3, 2020.
- [4] T. Lehman et al., *Acta Materialia* **69**, 1 (2014).
- [5] A. A. Hagberg et al., *Proc. SciPy2008*, pp. 11-15.

10:45 AM CH04.09.02

Quasi-Continuous Representation of Crystal Structure of Thin Films with Two-Dimensional X-Ray Diffraction and Non-Negative Matrix Factorization Akihiro Yamashita^{1,2}, Takahiro Nagata², Shinjiro Yagyu², Toru Asahi¹ and Toyohiro Chikyow²; ¹Waseda University, Japan; ²National Institute for Materials Science, Japan

Materials informatics (MI) is a data-driven approach to discover novel materials. In this approach, structure information such as crystal structure is one of important information because it has strong relationship to inorganic materials' properties. In conventional MI approaches, crystal structure is often represented in form of a categorical variable of corresponding space group, but this limits applicable machine learning (ML) methods compared to a continuous variable. Therefore, other representations of structure, such as crystal graph [1], have been proposed to convert structure information into quasi-continuous variable. To apply this kind of methods, crystal structure must be known, this means that structure of sample is analyzed by experts in advance. However, this is time-consuming and will be bottleneck in data-driven materials discovery.

We propose to use ML results of direct application to measurement data as crystal structure representations instead of experts-analyzed data. To proof our concept, we used non-negative matrix factorization (NMF) [2]. NMF approximates non-negative matrix V , a set of measurement data, with multiplication of two non-negative matrices W and H . This method is already studied with one-dimensional X-ray diffraction (1D-XRD) patterns from single composition spread [3]. We studied under more practical situation: we used 2D-XRD patterns from multiple samples with variety in substrate types and fabrication conditions. 2D-XRD is convenient in thin film research compared for 1D-XRD because it includes reflections from various out of planes.

2D-XRD patterns of In-Ga-O thin films were studied. We first analyzed NMF results in terms of generative model to confirm that NMF converts 2D-XRD patterns into variables which follows a continuous probability distribution. NMF results can be recognized that W is a set of factor vectors and H is that of feature vectors. The feature vectors were evaluated whether they represent propensities in original 2D-XRD patterns. We also compared results of samples fabricated by pulsed laser decomposition and those by sputtering. The detail will be discussed in the presentation.

References

- [1] T. Xie and J. C. Grossman, "Crystal Graph Convolutional Neural Networks for an Accurate and Interpretable Prediction of Material Properties," *Physical Review Letters*, vol. 120, no. 14, p. 145301, Apr. 2018, doi: 10.1103/PhysRevLett.120.145301.
- [2] D. D. Lee and H. S. Seung, "Learning the parts of objects by non-negative matrix factorization," *Nature*, vol. 401, no. 6755, pp. 788–791, Oct. 1999, doi: 10.1038/44565.
- [3] C. J. Long, D. Bunker, X. Li, V. L. Karen, and I. Takeuchi, "Rapid identification of structural phases in combinatorial thin-film libraries using x-ray diffraction and non-negative matrix factorization," *Review of Scientific Instruments*, vol. 80, no. 10, p. 103902, Oct. 2009, doi: 10.1063/1.3216809.

11:10 AM BREAK

SESSION CH04.10: Bayesian and Related Optimization Methods for Materials

Session Chair: Rama Vasudevan

Monday Afternoon, December 6, 2021

CH04-Virtual

1:00 PM CH04.10.01

Active Learning of Reactive Bayesian Force Fields—Application to Heterogeneous Catalysis Dynamics of H/Pt Jonathan Vandermause, Yu Xie, Jin Soo Lim, Cameron J. Owen and Boris Kozinsky; Harvard University, United States

Atomistic modeling of chemically reactive systems has traditionally relied on either expensive ab initio methods or bond-order force fields requiring arduous parametrization. Here, we introduce FLARE++, a Bayesian active learning method for training reactive many-body force fields "on the fly" during molecular dynamics (MD) simulations. At each timestep, the predictive uncertainties of a sparse Gaussian process (SGP) are evaluated to automatically determine whether additional ab initio data are needed. The resulting SGP is mapped onto a polynomial model whose prediction cost is independent of the training set size. Using this method, we perform large-scale MD simulations of a prototypical system in heterogeneous catalysis—H₂ chemisorption on Pt(111)—at chemical accuracy. The model, trained within three days of wall time, performs at twice the simulation speed of an available ReaxFF model while maintaining ab initio accuracy to a much higher fidelity. Our method enables efficient automated training of fast and accurate reactive force fields for

chemically complex systems.

1:15 PM CH04.10.03

Bayesian Inverse Design of High-Strength Aluminum Alloys at High Temperatures [Shimpei Takemoto](#)¹, Takeshi Kaneshita¹, Kenji Nagata², Yoshishige Okuno¹, Junya Inoue³ and Manabu Enoki³; ¹Showa Denko K.K., Japan; ²National Institute for Materials Science, Japan; ³The University of Tokyo, Japan

2000 series aluminum alloys or Al-Cu-Mg series are high-strength alloys, but it is known that their strength decreases rapidly at high temperatures above 150°C. Therefore, improving the strength at high temperatures is essential for industrial applications, especially automotive and aircraft applications. In this study, we perform a Bayesian inverse design of high-strength aluminum alloys at high temperatures.

We build a neural network to predict mechanical properties from process parameters, including additive elements and heat treatment. By choosing the appropriate activation function and features, neural networks show high prediction accuracy even at high temperatures. Specifically, we show that the hyperbolic tangent or sigmoidal activation functions well reproduce the rapid decrease in strength of aluminum alloys at high temperatures. We also show that by treating the holding temperature and holding time as input nodes in the neural network, we can predict mechanical properties measured at various temperatures. The neural network constructed with this approach can even perform extrapolation prediction, learning the mechanical properties at lower temperatures and predicting at higher temperatures.

In this study, Bayesian inference of neural network parameters is performed using the replica-exchange Monte Carlo method, an extended Markov chain Monte Carlo (MCMC) method. This approach allows us to evaluate the probability distribution and uncertainty of mechanical property predictions. By maximizing the probability of satisfying the desired properties, we explore combinations of process parameters for designing high-strength aluminum alloys at high temperatures.

The thermodynamic calculations are also performed using the Thermo-Calc software to analyze the strengthening mechanism of the alloy designs proposed by the neural network. We investigate how a fine grain structure caused by the Mn addition and the competition between the Al-Cu, Al-Cu-Mg, and Mg-Si compounds formation affect the alloy strength.

1:30 PM CH04.10.04

Incorporating Physical Priors Into Probabilistic Models in Bayesian Framework [Ayana Ghosh](#), Sergei V. Kalinin and Maxim A. Ziatdinov; Oak Ridge National Laboratory, United States

Progress in any scientific research area in physical and life sciences is primarily driven by assessments produced by numerous experimental and simulation-based techniques. Computational approaches ranging from lattice models and molecular dynamics to advanced density functional theory and quantum Monte Carlo methods provides a wealth of information on electronic, magnetic, thermodynamics properties, phase transitions of materials, to name a few. Electron and scanning probe microscopies and neutron and X-ray scattering methods provide huge volumes of structural and functional data leading to fundamental insights into structural properties and high-temperature superconductivity, visualization of the light elements, and many others. Both theoretical and experimental aspects of research require search over broad parameter spaces to discover optimal experimental conditions, regions of interest in the image space, or parameter space of computational models. The direct grid search of the parameter space tends to be exceedingly time consuming, leading towards advancing strategies to balance between exploration of unknown parameter spaces and exploitation towards required performance metrics. The classical approach for this is Gaussian process (GP)-based Bayesian optimization (BO).

However, classical BO strategies do not readily allow for the incorporation of the known physical behaviors or past knowledge.

Here, we explore hybrid approaches combining unstructured (non-parametric) and structured (semi-parametric and parametric) BO approaches. The former utilizes Gaussian process (GP) as the surrogate model while the latter one uses GP augmented with a probabilistic model of the system's physical behavior based on partially known analytical, hierarchical, or numerical models. Hence, this approach seeks to guide the exploration of parameter space when refining the physical understandings describing functional behavior over this space and using combined aleatoric and estimated epistemic uncertainty to guide the exploration. This approach is demonstrated for Ising model followed by looking at magnetism in 2D materials. We further discuss extending this capability towards perform automated experiment in the context of automated materials synthesis, scanning probe microscopy, and electron microscopy by injecting prior knowledge in the form of physical models and past data in this BO framework.

This effort (machine learning) is based upon work supported by the U.S. Department of Energy (DOE), Office of Science, Office of Basic Energy Sciences Data, Artificial Intelligence and Machine Learning at DOE Scientific User Facilities (A.G., S.V.K.) and was also supported (STEM experiment) by the DOE, Office of Science, Basic Energy Sciences (BES), Materials Sciences and Engineering Division (O.D.), and was performed and partially supported (M.Z.) at the Oak Ridge National Laboratory's Center for Nanophase Materials Sciences (CNMS), a DOE Office of Science User Facility.

1:45 PM CH04.10.05

Physics-Informed CoKriging Model of a Redox Flow Battery [Amanda Howard](#)¹, Alexandre Tartakovsky^{1,2} and Panagiotis Stinis¹; ¹Pacific Northwest National Laboratory, United States; ²University of Illinois at Urbana-Champaign, United States

Redox flow batteries (RFBs) offer the capability to store large amounts of energy cheaply and efficiently, however, there is a need for fast and accurate models of the charge-discharge curve of a RFB to potentially improve the battery capacity and performance. We develop a multifidelity model for predicting the charge-discharge curve of a RFB. In the multifidelity model, we use the Physics-informed CoKriging (CoPhIK) machine learning method trained on experimental data and constrained by the so-called "zero-dimensional" physics-based model. In this talk, we demonstrate that the CoPhIK model shows good agreement with experimental results and significant improvements over existing zero-dimensional models. We show that the proposed model is robust as it is not sensitive to the input parameters in the zero-dimensional model. We also show that only a small amount of high-fidelity experimental datasets are needed for accurate predictions for the range of considered input parameters, which include current density, flow rate, and initial concentrations.

2:00 PM CH04.10.06

A Facile Method to Extract a Constitutive Relation for Granular Materials Using Bayesian Optimization-Based Analysis [Kyuhoo Jang](#) and In-Suk Choi; Seoul National University, Korea (the Republic of)

Granular materials are widely used in various fields such as sintering process, tablet manufacturing, and geotechnical engineering. To predict its constitutive behavior in the finite element method (FEM), the modified Drucker-Prager/Cap model (DPC model) is commonly adopted. However, the conventional method requires multiple triaxial compression experiments and even heuristic approaches to determine a great number of parameters in the DPC model. In this study, we propose an alternative method for the DPC model that utilizes the entire stress-strain curves from triaxial compression testing and the Bayesian optimization algorithm to extract the parameters. The method was applied to acquire the constitutive relation of FE simulation for unsaturated sand-bentonite mixtures which successfully predicted experimental depth-sensing indentation results. Since our method dramatically reduces

the number of experiments and even eliminates heuristic determination of some parameters, we believe that it will facilitate efficient exploration of the mechanical behavior of granular materials.

2:20 PM BREAK

SESSION CH04.11: AI for Materials Design II
Session Chair: Sebastian Schmitt
Tuesday Morning, December 7, 2021
CH04-Virtual

8:00 AM CH04.11.01

Identifying the Activity Origin of a Cobalt Single-Atom Catalyst for Hydrogen Evolution Using Supervised Learning [Xinghui Liu](#); Department of Chemistry, Sungkyunkwan University (SKKU), 2066 Seoburo, Jangan-Gu, Suwon 16419, Republic of Korea., Korea (the Republic of)

Single-atom catalysts (SACs) have become the forefront of energy conversion studies, but unfortunately, the origin of their activity and the interpretation of the synchrotron spectrograms of these materials remain ambiguous. Here, systematic density functional theory computations reveal that the edge sites—zigzag and armchair—are responsible for the activity of the graphene-based Co (cobalt) SACs toward hydrogen evolution reaction (HER). Then, edge-rich (E)-Co single atoms (SAs) were rationally synthesized guided by theoretical results. Supervised learning techniques are applied to interpret the measured synchrotron spectrum of E-Co SAs. The obtained local environments of Co SAs, 65.49% of Co-4N-plane, 13.64% in Co-2N-armchair, and 20.86% in Co-2N-zigzag, are consistent with Athena fitting. Remarkably, E-Co SAs show even better HER electrocatalytic performance than commercial Pt/C at high current density. Using the joint effort of theoretical modeling, thorough characterization of the catalysts aided by supervised learning, and catalytic performance evaluations, this study not only uncovers the activity origin of Co SACs for HER but also lays the cornerstone for the rational design and structural analysis of nanocatalysts.

8:15 AM CH04.11.02

ALIGNN—Atomistic Line Graph Neural Network for Improved Materials Property Predictions [Kamal Choudhary](#) and Brian L. DeCost; National Institute of Standards and Technology, United States

Graph neural networks (GNN) have been shown to provide much improved performance for representing and modeling atomistic materials compared with descriptor-based machine-learning models. While most existing GNN models for atomistic predictions are based on atomic distance information, they do not explicitly incorporate bond angles, which are critical for distinguishing many atomic structures. Furthermore, many material properties are known to be sensitive to slight changes in bond angles. We develop Atomistic Line Graph Neural Network (ALIGNN) using a GNN architecture that performs message passing on both the interatomic bond graph and its line graph corresponding to bond angles. We demonstrate that angle information can be explicitly and efficiently included for materials to provide much improved performance. We train 44 models for predicting several solid-state material properties available in the JARVIS-DFT and materials-project databases. ALIGNN can outperform some of the previously known GNN models by up to 43.8 %.

8:30 AM CH04.11.03

Late News: Predicting the Heat Storage Properties of Salt Hydrates Using Density Functional Theory and Machine Learning [Steven G. Kiyabu](#)¹ and Donald Siegel²; ¹University of Michigan, United States; ²The University of Texas at Austin, United States

Salt hydrates demonstrate promise as heat storage materials as they possess high energy densities and reversibility at moderate temperatures. Despite their promise, a great number of salt hydrate compositions have not been explored. The goal of this work is to identify new salt hydrates that can outperform known materials in terms of energy density and are predicted to be thermodynamically stable. Around ten thousand hypothetical salt hydrates were generated by substituting cations and anions into salt hydrate crystal structures mined from the Inorganic Crystal Structure Database. These hypothetical hydrates were characterized according to their enthalpy of dehydration (from which stability, energy density, and heat-storing temperature are derived) using high-throughput density functional theory calculations. Machine learning models were then trained on this large dataset. Many different compositional and structural feature sets from the Matminer library were attempted, as well as several different machine learning algorithms, such as random forests, support vector machines, and neural networks. Several models were highlighted, either for their ability to predict the heat storage characteristics of other hypothetical salt hydrates or their identification of property-performance relationships in salt hydrates. In addition to this, several promising hypothetical hydrates were identified with higher energy densities than experimentally-known salt hydrates.

8:45 AM CH04.11.04

Uranium Compounds with High Thermal Conductivity Proposed by Machine Learning [Meigyoku Kin](#)¹, Masaya Kumagai^{1,2,3}, Yuji Ohishi⁴ and Ken Kurosaki^{1,5}; ¹Kyoto University, Japan; ²SAKURA internet Inc., Japan; ³RIKEN, Japan; ⁴Osaka University, Japan; ⁵University of Fukui, Japan

In recent years, materials informatics (MI), which is a fusion of materials science and information science, has been attracting attention. Although MI is becoming a mainstream research field such as magnetic materials and thermoelectric materials, there are few reports on MI in materials research in nuclear fields. In this study, we propose a method to comprehensively explore uranium compounds with high thermal conductivity by using machine learning in order to apply MI to nuclear fuel development in the nuclear field.

We constructed a machine learning model using Starrydata, a database of experimental properties developed by our research group. The features were designed using the basic physical properties based on chemical composition, and the target variable is thermal conductivity. The model was trained using Random Forest, and the prediction accuracy of 93% was obtained. Using the trained machine learning model, the thermal conductivity of uranium compounds that could exist in the world was comprehensively predicted. Based on the predicted thermal conductivities, 20 uranium compounds were extracted from the top and bottom of the list, respectively. Uranium compounds experimentally synthesizable are going to be synthesized, and the relevance of the machine learning model is going to be evaluated by comparing the measured values with the predicted values. Based on the evaluation, we are going to propose a new uranium compound with high thermal conductivity.

9:00 AM CH04.11.06

Reinforcement Learning in Materials Science—Atomic Fabrication and Materials Design in Simulated Environments [Rama K. Vasudevan](#), Ayana Ghosh, Erick Orozco, Maxim A. Ziatdinov and Sergei V. Kalinin; Oak Ridge National Laboratory, United States

Although by now machine learning is commonplace within virtually all sectors of materials science, the use of reinforcement learning (RL) agents is only now gaining traction. This is partly because of the extensive compute requirements for RL, and the paucity of scalable algorithms. Recent advances in the field have enabled the training of agents to tackle previously difficult challenges in fields such as online gameplay and board games, but their application to the physical sciences has been very limited. Here, we explored the use of RL agents for two particular tasks: one of atomic fabrication by an electron beam, and another of design of ferroelectric materials by defect engineering.

For both situations, we created a virtual environment in which the RL agent can interact and learn by trial and error, and designed reward functions to achieve specific gains. We then trained agents using both policy gradient and implicit (Q learning) methods, in a model-free setting. For the atomic fabrication case, we employed an environment utilizing molecular dynamics simulations, and trained agents to move multiple Si dopants towards each other on a graphene lattice by specifying quantities of momentum transfer at different steps during the episode. For the second case, we explored RL agents for moving and manipulating defects in a ferroelectric sample, simulated via a discrete Landau model, to affect the type and quantity of topological defects generated. We argue that not only are these agents capable of discovering policies that are novel, but also that the policies encode important information regarding the dynamics of the system, and thus inspection of policies can be an important source of physics knowledge discovery. This work was conducted at and supported by the Center for Nanophase Materials Sciences, a US DOE Office of Science User Facility.

9:15 AM CH04.11.07

Molecularly Resolved Segmentation of Non-Fullerene Acceptor Bulk Heterojunction—Lessons from Manifold Learning and Ensemble Clustering Jochen A. Kammerer^{1,2}, Wolfgang Köntges¹, Pavlo Perkhun³, Christin Videtot-Ackermann³, Jörg Ackermann³, Rasmus R. Schröder¹ and Martin Pfannmöller¹; ¹Heidelberg University, Germany; ²Karlsruhe Institute of Technology, Germany; ³Aix-Marseille Université, France

High performing devices often rely on multiphase nanostructures with complex interfacial effects. Transmission electron microscopy (TEM) has proven indispensable to understand these effects and reveal the structure-property-relationship of these devices. One example are bulk heterojunctions (BHJs) for organic solar cells, where the excitons are split at the interface between donor and acceptor domains.¹ A precise segmentation of the donor and acceptor domains is crucial for understanding the process of charge separation. However, low contrast between chemically similar donor and acceptor materials makes classical imaging challenging and does not allow for molecular resolution at the interface. The combination of low loss energy loss signal based hyperspectral imaging and machine learning has proven to efficiently overcome this challenge.² However, the spectral difference for modern non-fullerene acceptor (NFA) systems is weak.³ Thus, the segmentation becomes obscured by experimental influences (such as noise, signal delocalization, multiple scattering and non-isochromaticity of the imaging tool). More sophisticated approaches are needed to obtain molecular resolution for non-fullerene acceptor BHJs.

Unsupervised segmentation and spectral unmixing of the hyperspectral datasets are typically approached by linear dimensionality reduction alone — e.g. principal component analysis (PCA), independent component analysis (ICA) and non-negative matrix factorization (NMF)—, by clustering algorithms alone, or the combination of both.^{4,5} For the latter, the influence of linear dimensionality reduction on the cluster result is not clear, especially in the context of the given experimental influences. Furthermore, unequally performing cluster algorithms introduce non-negligible uncertainties.

We use an ensemble clustering approach to obtain a more robust unsupervised segmentation of hyperspectral low loss TEM datasets. Furthermore, we systematically investigate experimental influences as well as the effects of linear and nonlinear dimensionality reduction on the clustering results.

Nonlinear dimensionality reduction (manifold learning) improves the tolerance to experimental restrictions from multiple scattering and non-isochromaticity. The combination of the manifold learning algorithm UMAP⁶ and ensemble clustering enables segmentations with an unrivaled tolerance against noise.

We applied this combination of manifold learning and ensemble clustering to hyperspectral images in the TEM low loss regime from PBDB-T:ITIC non-fullerene acceptor BHJs. Segmentations at molecular resolution allowed us to exclude a mixed materials phase at the NFA donor acceptor interface. This contrasts with their fullerene acceptor predecessors and sheds new light on the charge separation in modern BHJs. The combination of TEM based hyperspectral imaging and the machine learning workflow with UMAP and ensemble clustering can be applied to other low contrast material combinations. The machine learning workflow itself is unsupervised, fully automated⁷ and has already been successfully applied to non-TEM hyperspectral datasets.

1. Liu, Q. *et al. Sci. Bull.* **65**, 272–275 (2020).
2. Pfannmöller, M. *et al. Nano Lett.* **11**, 3099–3107 (2011).
3. Köntges, W. *et al. Energy Environ. Sci.* **13**, 1259–1268 (2020).
4. de la Peña, F. *et al. Ultramicroscopy* **111**, 169–176 (2011).
5. Torruella, P. *et al. Ultramicroscopy* **185**, 42–48 (2018).
6. McInnes, L. & Healy, J. *ArXiv180203426 Cs Stat* (2018).
7. Potapov, P. & Lubk, A. *Adv. Struct. Chem. Imaging* **5**, 4 (2019).

9:30 AM CH04.15.03

Late News: Accessing Negative Poisson's Ratio of Graphene by Machine Learning Interatomic Potentials Jing Wu¹, E Zhou¹, Zhenzhen Qin², Xiaoliang Zhang³ and Guangzhao Qin¹; ¹Hunan University, China; ²Zhengzhou University, China; ³Dalian, China

The negative Poisson's ratio (NPR) is a novel property of materials, which enhances the mechanical feature and creates a wide range of application prospects in lots of fields, such as aerospace, electronics, medicine, etc. Fundamental understanding on the mechanism underlying NPR plays an important role in designing advanced mechanical functional materials. However, with different methods used, the origin of NPR is found different and conflicting with each other, for instance, in the representative graphene. In this study, based on machine learning technique, we constructed a moment tensor potential (MTP) for molecular dynamics (MD) simulations of graphene. By analyzing the evolution of key geometries, the increase of bond angle is found to be responsible for the NPR of graphene instead of bond length. The results on the origin of NPR are well consistent with the start-of-art first-principles, which amend the results from MD simulations using classic empirical potentials. Our study facilitates the understanding on the origin of NPR of graphene and paves the way to improve the accuracy of MD simulations being comparable to first-principle calculations. Our study would also promote the applications of machine learning interatomic potentials in multiscale simulations of functional materials.

10:30 AM *CH04.12.01

To Mix or not to Mix? Settling the Matter of the Role of Vibrations in the Stability of High-Entropy Carbides [Stefano Curtarolo](#); Duke University, United States

Disordered multicomponent systems occupying the mostly uncharted centers of phase diagrams, have been studied for the last two decades as innovative materials. By maximizing their entropy (configurational and/or vibrational) and stabilizing (near) equimolar mixtures, it has been possible to achieve robust systems with promising applications. Still, effective computational discovery of useful materials remains challenged by the immense number of configurations: the synthesizability of high-entropy ceramics is typically assessed using ideal entropy along with the formation enthalpies from density functional theory, with simplified descriptors or machine learning methods. With respect to vibrations — even if they may have significant impact on phase stability — the contributions are drastically approximated to reduce the high computational cost, or often avoided with the hope of them being negligible, due to the technical difficulties posed in calculating them for disordered systems. As such, in high-entropy ceramics, the vibrational contributions remain a matter of conjecture — their inclusion left to researchers' guesswork. In this presentation we illustrate the problem, its implications, and suggest simple solutions.

11:00 AM CH04.12.03

Continuous Evaluation of Carrier Recombination Velocity of Grain Boundaries in Multicrystalline Si Using Machine Learning [Kentaro Kutsukake](#)¹, Kazuki Mitamura², Takuto Kojima² and Noritaka Usami²; ¹RIKEN, Japan; ²Nagoya University, Japan

Grain boundaries (GBs) in multicrystalline Si (mc-Si) are still of interest in research because mc-Si will maintain a certain share in the substrate for solar cells to consume low-grade Si raw materials that cannot be used for Czochralski Si in addition to its importance as fundamental physics. One of the research issues is a quantitative evaluation of spatially local electrical activities to reveal the influence of local structures such as atomically reconstructed structures at curved GBs. Measurable spatial images of electrical activities, such as photoluminescence (PL) and electron beam induced current (EBIC) images, provide qualitative distributions, however, quantitative analysis of the images, in which parameter fitting is required, needs a large calculation cost. In this study, we developed a fast and continuous evaluation method of carrier recombination velocity (V_{GB}) along a GB from a photoluminescence image using carrier simulation and its machine learning. A dataset of 3000 PL profiles was made through PL image simulation, which was developed incorporating the influence of inclination angle of GB (θ) [1], using random values of parameters of V_{GB} , θ , and carrier diffusion length in left and right crystal grains (L_{left} and L_{right}). A fully connected feedforward neural network model was constructed with the inputs of the PL profile and θ , which is determined by measuring the position shift of the GB between the front and rear surface [1], and the outputs of V_{GB} , L_{left} , and L_{right} . The coefficient of determination and the root mean squared error of the trained model for V_{log} , which is the common logarithm of V_{GB} , for the test dataset were 0.97 and 0.24, respectively. This prediction error was sufficiently low for the practical estimation of V_{GB} . The calculation time for the prediction is less than 0.01 seconds. By utilizing this fast prediction method, continuous evaluation of V_{GB} along a GB was demonstrated. V_{GB} was clearly visualized, and small fluctuations were detected quantitatively. V_{GB} increases around the curved region and fluctuates even in straight regions. This quantitative and high spatial resolution evaluation of the property will lead to a deep and quantitative understanding of defects by combining it with microscopic structural and computational analysis.

[1] K. Mitamura, K. Kutsukake, T. Kojima, and N. Usami, Journal of Applied Physics 128, 125103 (2020).

11:15 AM CH04.12.04

Disentangling Ferroelectric Wall Dynamics and Identification of Pinning Mechanisms via Deep Learning [Yongtao Liu](#)¹, Roger Proksch², Chun Yin Wong³, Maxim A. Ziatdinov^{1,1} and Sergei V. Kalinin¹; ¹Oak Ridge National Laboratory, United States; ²Asylum Research, An Oxford Instruments Company, United States; ³The University of Tennessee, Knoxville, United States

Field-induced domain wall dynamics in ferroelectric materials underpins multiple applications ranging from actuators to information technology devices and necessitates a quantitative description of the associated mechanisms including giant electromechanical couplings, controlled non-linearities, or low coercive voltages. While the advances in dynamic Piezoresponse Force Microscopy measurements over the last two decades have rendered visualization of polarization dynamics relatively straightforward, the associated insights into the local mechanisms have been elusive. Here we use a workflow combining deep learning-based segmentation of the domain structures with non-linear dimensionality reduction using multilayer rotationally-invariant autoencoders (rVAE). A Canny filter and ResHED network were utilized to detect domain walls based on the PFM images. Then, sub-images centered at 180° domain walls were used for rVAE analysis to encode information of domain switch and wall dynamics. Through analyzing the time dynamics of domain switch and interactions between ferroelastic and ferroelectric domain walls by rVAE, we discovered new factors affecting the ferroelectric wall dynamics and pinning mechanism. We believe that the approach developed in this work will be universally useful for time-dependent dynamics of complex materials.

Acknowledgments: This work is supported by the U.S. Department of Energy, Office of Science, Office of Basic Energy Sciences Energy Frontier Research Centers program under Award Number DE-SC0021118. This work is conducted at the Center for Nanophase Materials Sciences, a US Department of Energy Office of Science User Facility.

11:30 AM CH04.12.05

Deep Learning Enables Crystallographic Information from Electron Diffraction Images [Joydeep Munshi](#)¹, Alexander Rakowski², Benjamin Savitzky², Colin Ophus² and Maria K. Chan¹; ¹Argonne National Laboratory, United States; ²Lawrence Berkeley National Laboratory, United States

We present one of the targeted analysis pipelines, *4D>Crystal*, in an aim to generate a series of reduced crystalline diffraction vectors from a given combination of STEM probe in vacuum with typical 4D-STEM diffraction dataset. *4D>Crystal* pipeline is composed of three main workflows namely – 1) crystal selection and data scraping (4D-MANIPULATT), 2) training data generation (4D-MAKE) and 3) Bragg disk detection network training and evaluation (4D-DISK). We use python-based pymatgen package and the materials project (MP) API to fetch crystal structures from more than 120,000 materials present in the MP database. Additionally, AFLOW library is leveraged to fetch structure prototypes from over 250 different structure types of crystals based on their structural similarity. Finally, we select a fraction of structures from the MP database, resembling each structure prototype, following the square-root distribution law. Following the crystal structure selection, we employ supercell manipulation algorithm (4D-MANIPULATT) to manipulate unit cell structures to create randomly rotated supercells. Finally, simulated electron diffraction data (CBED) and the simulated atomic potential for each of these supercells are simulated leveraging the Multislice algorithm implemented. For the deep learning training to predict Bragg disks locations and their intensities we implement a modified complex U-Net type encoder-decoder based network. Complex convolution based network in this work showed improved performance of disk predictions for overlapped diffraction disks at larger thickness.

12:00 PM BREAK

1:00 PM CH04.13.01

Design of Features Based on X-ray Diffraction Patterns for Prediction of Mechanical Properties Naoki Hato¹, Masaya Kumagai^{1,2,3} and Ken Kurosaki^{1,4}; ¹Kyoto University, Japan; ²SAKURA internet Inc., Japan; ³RIKEN, Japan; ⁴University of Fukui, Japan

The development of new materials requires many steps, such as sample preparation, X-ray diffraction measurement and analysis, property measurement, and performance evaluation, and requires an enormous amount of time. In recent years, high-throughput material synthesis and high-speed X-ray diffraction measurements have made sample preparation and X-ray diffraction measurements more efficient. However, the analysis of crystal structures has not yet become efficient. In this study, we constructed an optimal feature vector based on the X-ray diffraction pattern to predict the crystal structure with high accuracy, and also predicted the mechanical properties that are highly related to the crystal structure.

Various feature vectors based on the intensity, angle, and number of peaks in the X-ray diffraction pattern were constructed and their effects on the prediction accuracy were clarified. Since the number of diffraction peaks varied greatly among the different crystal systems, it was confirmed that the number of peaks made a difference in the prediction accuracy. The prediction accuracy for Cubic among the seven crystal systems was about 97% at maximum. On the other hand, the prediction accuracies of Monoclinic and Triclinic were lower than that of the other crystal systems due to the similarity of their X-ray diffraction patterns. By constructing an optimal feature vector that can predict crystal structures with high accuracy, highly accurate prediction of mechanical properties such as volume modulus can also be expected.

1:15 PM CH04.13.02

Combinatorial Synthesis of Heteroepitaxial, Functional Thin Films of Complex Materials with High-Throughput, *In Situ*, Chemical and Structural Characterization Eun Ju Moon and Amit Goyal; University at Buffalo, The State University of New York, United States

Materials informatics applied to a range of advanced materials applications can identify a range of compositions of complex materials (having multiple cations and anions) within which combinatorial synthesis is needed to obtain materials with ideal compositions for optimized properties. Combinatorial synthesis via a continuous composition spread is an excellent route to develop thin-film libraries from a single experiment on a single wafer, which is both time- and cost-efficient for developing new materials with ideal compositions and having optimized properties for next-generation applications. A reliable, high-throughput, *in-situ* characterization analysis method is required to meet the crucial need to screen materials libraries. Creating libraries of functional multi-component complex oxide films requires excellent control over the synthesis parameters combined with high-throughput analytical feedback across a given substrate area. Here, we report on the use of a newly developed *in-situ* compositional analysis technique, called low-angle x-ray spectroscopy (LAXS), to map the chemical composition profile of combinatorial heteroepitaxial complex oxide film deposited in a continuous composition spread using pulsed laser molecular beam epitaxy (MBE). This state-of-the-art combinatorial growth system facilitates a fully synchronized four-axis mechanical substrate stage without shadow masks, alternating acquisition of chemical compositional data using LAXS at various different positions on the ~41mm x 41mm range and sequential deposition of multilayers of SrTiO₃ and SrTi_{0.8}Ru_{0.2}O₃ on a 2-inch (50.8mm) LaAlO₃ wafer in a single growth. Reflection high-energy electron diffraction (RHEED) and x-ray diffraction (XRD) are used to confirm the epitaxy of the combinatorial oxide films, SrTi_{1-x}Ru_xO_{3-δ}, deposited across the wafer. Rutherford backscattering spectrometry (RBS) is used to calibrate and validate the measurement data produced by the LAXS on the composition spread across the substrate. The calibrated LAXS data exhibits a gradual composition elevation, thus showing a good agreement with the RBS results (0 ≤ x ≤ 0.2). This study shows the feasibility of combinatorial synthesis extended to heteroepitaxial, functional complex oxide films at wafer-scale using a new *in-situ* high-throughput characterization technique. The combination of laser-MBE growth with high-throughput LAXS for probing composition and RHEED for epitaxy is a powerful route to obtain new materials with optimized compositions, epitaxy, and functional properties.

1:30 PM CH04.13.03

Advanced Feature Extraction with Machine Learning and Combinatorial Methodologies for Thin-Film Photovoltaic Materials Enric Tomas T. Grau-Luque¹, Maxim Guc¹, Fabien Atlan¹, Andreas Zimmermann², Sergio Giraldo¹, Ignacio Becerril-Romero¹, Alejandro Perez-Rodriguez^{1,3} and Victor Izquierdo-Roca¹; ¹IREC, Spain; ²Sunplugged GmbH, Austria; ³Universitat de Barcelona, Spain

Spectroscopic characterization techniques, such as Raman spectroscopy (RS), photoluminescence (PL), or X-ray fluorescence (XRF) are becoming widely spread for advanced material characterization due to their easy application and highly informative output about different materials properties in a fast and non-destructive manner. Spectroscopic data is mostly processed through simple analytical procedures that are time-consuming and undermine their potential. This is especially critical in the context of research in new material-based technologies which often present a high degree of complexity (e.g. multilayer, multiscale or multiprocess) and require the use of several characterization techniques in a combinatorial way in order to obtain an advanced understanding of their fundamental properties and failure mechanisms. The use of simple analytical procedures for this complex analysis results in long conception-to-market development times (normally 10-20 years) using large amounts of resources.

Recently, combinatorial analysis (CA) and machine learning (ML) have started to become common methodologies in the analysis of complex systems. It is foreseen that these advanced methodologies will shorten technology development times by a factor of 10. However, they require deep theoretical, analytical, and programming knowledge as well as big-data experimental generation which sets a barrier for their widespread implementation. In this context, the development of practical methodologies is paramount to accelerate the broad adoption of CA and ML and ultimately shorten technology development times.

This work proposes a novel methodology based on ML and CA to accelerate experimentation, analysis, and development. We present a step-by-step explanation of the methodology that includes the following key aspects: i) defining features and targets, ii) pre-processing and scaling experimental data, iii) selecting and using a ML algorithm, iv) analyzing and interpreting the outputs, v) visualizing the results, and vi) combining ML with CA for feature extraction. When applied successfully, this workflow produces consistent results that offer impactful insights into materials research. We illustrate this methodology by presenting its application to two practical examples of complex materials with high relevance for the thin-film PV community: the development of the earth-abundant Cu₂ZnGeSe₄ (CZGSe) at laboratory scale and of mature Cu(In,Ga)Se₂ (CIGSe) PV technologies. These materials exhibit several difficulties in their development due to the high amount of parameters involved in their multi-step fabrication and their impact on material properties. In the case of CZGSe, it is a high band gap absorber material with a high potential for tandem or semitransparent PV applications. The study was carried out in a combinatorial sample with graded composition characterized by XRF, RS, and current-voltage (I-V). In the case of CIGSe, it is a mature PV technology but with high improvement and cost reduction potential. In this study, CA (using RS, PL, and I-V) and ML methodologies were applied to optimize the fabrication of solar modules on flexible substrates in SUNPLUGGED GmbH's innovative roll-to-roll (RtR) production line. In both cases, the applied CA and ML methodologies are demonstrated to enable defining the critical deposition parameters and conditions that allow reaching the

optimum material properties in terms of their application in PV devices.

Finally, we also introduce a free open-source library based on Python for the presented methodologies to facilitate researchers and developers to perform CA and ML analysis of spectroscopic data. We strongly believe that this work represents the foundations for the future research of complex materials, which aims for more robust, faster, and automated work structures. In the particular case of thin-film PV, this will lead to a more efficient, versatile, and cheaper production of PV devices for a greener future.

1:45 PM CH04.13.04

signac—Data Management and Workflows for Computational Materials Discovery and Design [Bradley D. Dice](#), Brandon Butler and Sharon C. Glotzer; University of Michigan, United States

The open-source signac data management framework (<https://signac.io>) helps researchers execute reproducible computational studies, scaling from laptops to supercomputers and emphasizing portability and fast prototyping. With signac, users can track, search, and archive data and metadata for file-based workflows and automate workflow submission on high performance computing (HPC) clusters. We will showcase current research by the materials community using signac, and discuss how recent improvements to the software's feature set, scalability, and usability are enabling new scientific applications of the framework. Newly implemented synced data structures, workflow subgraph execution, and performance optimizations will be covered. Motivated by the needs of computational materials scientists for heterogeneous data processing with bespoke parallel execution patterns on widely varying hardware, we will demonstrate how these new capabilities enhance signac's integrated approach to materials simulations and facilitate the high level of flexibility required by this domain of research.

2:00 PM CH04.13.05

Combining Crystal Structure Prediction and High-throughput Powder Pattern Refinement for Organic Solid Form Selection [Kiran Sasikumar](#), Jacco van de Streek and Marcus Neumann; Avant-garde Materials Simulation GmbH, Germany

On some occasions, a crystal structure that has been prepared and marketed for years is unexpectedly superseded by a thermodynamically more stable polymorph, rendering the initial crystal structure almost impossible to obtain—a so-called “disappearing polymorph” [1]. Despite the relative rarity of such events, famous cases such as the drug compounds Ritonavir and Rotigotine, where costly reformulations were required to manufacture the product again, underlined the commercial need for extensive screening of solid-state forms. Sometimes christened virtual polymorph screening, crystal structure prediction (CSP) emerged as a complement to experimental solid-form screens in order to evaluate the risk of a “disappearing polymorph” event. With the technology achieving maturity, CSP is now increasingly being used in the pharmaceutical industry to predict the relative thermodynamic stability of solid-state forms and to guide small-molecule solid form selection [2, 3].

A key component of the risk assessment and solid form selection workflow is to map the experimentally synthesized solid forms onto the predicted crystal-energy landscape. As CSP is increasingly used early in the drug development cycle, experimental single crystal structures are often unavailable, and X-ray powder diffraction patterns are the best available experimental representation of the synthesized solid form. Furthermore, several factors can affect the pattern quality, such as preferred orientation of crystallites in the powder sample, amorphous background or peak position offset. The available powder sample may also correspond to disordered crystal structures and/or be phase mixtures of multiple solid forms. Hence, it is imperative to have a sophisticated high-throughput matching functionality to place the experimentally observed forms on the predicted landscape.

In this contribution, we present the results of high-throughput refinement of powder diffraction patterns involving phase mixtures of pharmaceutically relevant compounds. Specifically, we compare the powder diffraction pattern against an extensive list of input crystal structures from an early-stage CSP study by refining or optimizing ~1 million parameter-sets that involve different combinations of structures, phase volume fractions and preferred orientation directions. Further, we discuss the ambiguities inherent to structure solution from powder diffraction data and the importance of calculated lattice energies (often also free energies where vibrational contributions are factored in) in the robust bridging of experimental and computational data.

References

- [1] D.-K. Bučar, R. W. Lancaster & J. Bernstein (2015), “Disappearing Polymorphs Revisited” *Angew. Chem., Int. Ed.* 54, 6972-6993.
- [2] M. A. Neumann & J. van de Streek (2018), “How Many Ritonavir Cases Are There Still out There?” *Faraday Discuss.* 211, 441-458.
- [3] J. Hoja, Hsin-Yu Ko, M. A. Neumann, R. Car, R. A. DiStasio Jr. & A. Tkatchenko (2019), “Reliable and Practical Computational Description of Molecular Crystal Polymorphs” *Sci. Adv.* 5, eaau3338.

2:15 PM *CH04.13.06

Similarity of Materials and Data-Quality Assessment by Unsupervised Learning [Claudia Draxl](#), Simon Gabaj, Martin Kuban, Santiago Rigamonti and Markus Scheidgen; Humboldt-Universität zu Berlin, Germany

Data-centric approaches are already complementing our daily research and will even significantly change materials science in the near future. In this respect, data-analytics and machine-learning approaches are being developed and applied to various problems, and high-throughput screening (HTS) is going hand in hand with the establishment of small- and large-scale data collections. These resources allow us finding trends and patterns that cannot be obtained from individual investigations. Moreover, one can search for materials which exhibit features that are similar to those of other materials but are superior with respect to other criteria.

We have developed a platform that implements various similarity measures and employ this tool to explore the materials available in the NOMAD Encyclopedia [1]. Besides finding materials that resemble each other, e.g. in their electronic properties, this toolbox can also be used for assessing data quality. As such, one can compare the performance of different methodologies for one and the same material or the impact of approximations and computational parameters on calculated properties. We also make use of an unsupervised learning to find trends in the data and rationalize their physical origin. We will also discuss how we are currently expanding our efforts towards other materials properties of interest and developments towards inclusion of experimental data.

- [1] C. Draxl and M. Scheffler, *The NOMAD Laboratory: From Data Sharing to Artificial Intelligence*, *J. Phys. Mater.* 2, 036001 (2019); <https://nomad-lab.eu>.

2:45 PM CH04.13.07

High-Throughput Study of Antisolvents on the Stability of Multicomponent Metal Halide Perovskites Through Robotics-Based Synthesis and Machine Learning Approaches Kate Higgins¹, Maxim A. Ziatdinov², Sergei V. Kalinin² and [Mahshid Ahmadi](#)¹; ¹University of Tennessee, Knoxville, United States; ²Oak Ridge National Laboratory, United States

Considerable research attention has focused on metal halide perovskites (MHPs) over the recent years because of the combination of exceptional optoelectronic properties and low fabrication cost, making them ideal candidates for a variety of applications¹⁻⁴. Even so, the development of MHPs for commercialization must overcome an obstacle, namely stability in the pure or device-integrated form⁵. Overcoming adverse effects stemming from external stimuli can be minimized or avoided by utilizing established encapsulation techniques and device engineering^{6,7}. Simultaneously, another strategy is to improve the intrinsic stability by cation and/or halide alloying to synthesis multicomponent MHPs^{8,9}. A multitude of studies have demonstrated how the incorporation of other cations, particularly Cs⁺ and formamidinium (FA⁺) into methylammonium (MA⁺) systems, leads to improve stability in ambient and operational conditions. Mixing halides, has also proven to be an effective strategy toward stable perovskite materials. Antisolvent crystallization methods are frequently used to fabricate high quality perovskite thin films, to produce sizable single crystals, and to synthesize nanoparticles at room temperature. However, a systematic exploration of the effect of specific antisolvents on the intrinsic stability of multicomponent metal halide perovskites has yet to be demonstrated. We have previously reported the development of a workflow for materials discovery utilizing both automated synthesis and machine learning (ML)^{10,11}. Similarly in this study, we develop a high-throughput experimental workflow that incorporates robotic synthesis, automated characterization, and ML techniques to explore how the choice of antisolvent affects the intrinsic stability of binary perovskite systems in ambient conditions¹². Different combinations of the endmembers are used to synthesize 15 combinatorial libraries, each with 96 unique combinations. In total, roughly 1100 different compositions are synthesized. Each library is fabricated twice using two different antisolvents: toluene and chloroform. Once synthesized, photoluminescence spectroscopy is automatically performed every 5 minutes for approximately 6 hrs. Non-negative Matrix Factorization (NMF) is then utilized to map the time- and compositional-dependent optoelectronic properties. Through the utilization of this workflow for each library, we demonstrate that the selection of antisolvent is critical to the stability of MHPs in ambient conditions. We explore possible dynamical processes, such as halide segregation, responsible for either the stability or eventual degradation as caused by the choice of antisolvent. Overall, this high-throughput study demonstrates the vital role that antisolvents play in the synthesis of high quality multicomponent MHP systems.

References:

- 1 Park, N.-G., Grätzel, M., Miyasaka, T., Zhu, K., Emery, K. *Nature Energy* **1** (2016).
- 2 Ahmadi, M., Wu, T., Hu, B. *Adv Mater* **29** (2017).
- 3 Lukosi, E. *et al. Nuclear Instruments and Methods in Physics Research Section A*, **927**, 401 (2019).
- 4 Zou, Y., Yuan, Z., Bai, S., Gao, F., Sun, B. *Materials Today Nano* **5**, (2019).
- 5 Liu, W. W., Wu, T. H., Liu, M. C., Niu, W. J. & Chueh, Y. L. *Advanced Materials Interfaces* **6**, (2019).
- 6 Lee, J.-W. *et al. Advanced Energy Materials* **5**, (2015).
- 7 Seo, S., Jeong, S., Bae, C., Park, N. G., Shin, H. *Adv Mater*, e1801010 (2018).
- 8 Xu, F., Zhang, T., Li, G., Zhao, Y. *Journal of Materials Chemistry A* **5**, 11450 (2017).
- 9 David P. McMeekin, G. S., Waqaas Rehman, Giles E. Eperon, Michael Saliba, Maximilian T. Hörantner, Amir Haghghirad, Nobuya Sakai, Lars Korte, Bernd Rech, Michael B. Johnston, Laura M. Herz, Henry J. Snaith. *Science* **351** (2016).
- 10 Higgins, K., Valletti, S. M., Ziatdinov, M., Kalinin, S. V., Ahmadi, M. *ACS Energy Letters* **5**, 3426 (2020).
- 11 Heimbrook, A., Higgins, K., Kalinin, S. V., Ahmadi, M. *Nanophotonics*, (2021).
- 12 Higgins, K., Ziatdinov, M., Kalinin, S. V., Ahmadi, M. *arXiv:2106.03312* (2021).

SESSION CH04.14: Physics-Assisted ML Methods for Knowledge Extraction II

Session Chair: Sebastian Schmitt

Wednesday Morning, December 8, 2021

CH04-Virtual

8:00 AM CH04.14.02

A Fundamental Training Paradigm for Graph Neural Networks to Characterize Complex Features in Atomic Microstructures Yu-Ting Hsu, James Chapman, Penghao Xiao, Xiao Chen and Brandon Wood; Lawrence Livermore National Laboratory, United States

Graph neural networks (GNNs) are an emerging machine learning methodology for processing irregularly structured data. They have shown promise in learning/predicting properties of atomistic structures due to their intrinsically physically-informed nature, with graph nodes representing atoms and graph edges symbolizing interatomic bonds. In atomistic modelling, the application of GNNs has generally been limited to small-scale molecular structures or crystalline materials represented by small unit cells. In contrast, describing more complex structural and microstructural features such as grain boundaries, voids, and surfaces requires scaling the application space of GNNs to vastly larger atomistic microstructures. To this end, we have developed a GNN training paradigm to characterize microstructural features without the need for GNN to explicitly identify such information during training. Our methodology aims to capture a fundamental aspect of complex atomic environments, in which one can generalize local geometries on a scale from fully ordered (perfect crystal) to completely disordered. This atomic-level classification system allows our GNN to extrapolate widely to configurations that it has not explicitly seen before. Our methodology also overcomes limitations associated with existing methods where the local environments are predefined to a “hard-coded” reference of specific structural motifs, which often leads to incorrect classification of complex structural environments such as grain boundaries. The notion of scaling between order and disorder presents a much smoother classification system of these geometric domains. We highlight the application of our GNN scheme to the automated detection and characterization of aluminum microstructures, derived from polycrystalline structures containing a variable number of grains and temperatures. We show that with a limited training set, our method correctly identifies and characterizes microstructural features such as surfaces, grain boundaries, voids, or other defect-like environments on a much larger scale than that encountered during training. The examples presented here showcase the ability of our GNN methodology to characterize atomistic structures with unprecedented accuracy and transferability, opening the door to understanding structure-property relationships in complex materials in greater detail.

8:15 AM CH04.14.03

Physics-Informed Machine Learning Enhances Predictive Design of Fluorescent DNA-Stabilized Silver Clusters Peter Mastracco¹, Joshua Evans², Anna Gonzalez-Rosell¹, Petko Bogdanov³ and Stacy Copp¹; ¹University of California, Irvine, United States; ²Chaffey College, United States; ³University at Albany, State University of New York, United States

DNA-stabilized silver clusters (Ag_N-DNAs) are a model system for developing machine learning approaches to materials discovery. These clusters of 10-30 Ag atoms are encapsulated in short DNA strands, whose nucleobase sequences tune fluorescence emission from 500 nm to at least 1000 nm by selection of cluster size and morphology. With high quantum yield fluorescence, unique rod-like geometries, compatibility with DNA, and sensitivity to certain analytes, Ag_N-DNAs are promising for applications including sensing, bioimaging, and nanophotonics. However, the complex relationship between DNA sequence and Ag_N-DNA fluorescence color and the enormous combinatorial space of DNA sequences to choose from has hindered rational design of Ag_N-

DNAs for such applications. Previously, we applied supervised machine learning classification together with high-throughput experiments to learn the connection between DNA sequence and Ag_N -DNA color, using data mining together with feature selection to engineer features for these models. Here, we present new efforts to engineer physically motivated features, presenting new features hypothesized based on observations from the first reported crystal structures of Ag_N -DNAs. We show that models using these physics-informed features perform comparably well or better than more complex models with features engineered by naive data mining, and the dimensionality of the new models is one order of magnitude less than the previous naive models. Furthermore, we rank features by a metric of importance to further reduce the dimensionality of our learned models and to inform the understanding of how DNA stabilizes silver clusters. This work demonstrates the importance of merging first-principles knowledge with machine learning and high throughput experimentation for the discovery of sequence-encoded biomolecular materials.

8:30 AM *CH04.14.04

Automating Data Interpretation with Deep Reasoning Networks John M. Gregoire¹, Di Chen², Yiwei Bai², Sebastian Ament², Wenting Zhao², Lan Zhou¹, Bart Selman², R. Van Dover², Carla Gomes² and Dan Guevarra¹; ¹California Institute of Technology, United States; ²Cornell University, United States

As materials discovery efforts increasingly expand in high-order composition spaces and/or far-from-equilibrium syntheses, characterizing the phase behavior of the materials becomes increasingly challenging. The limited ability of algorithms to automate phase mapping – the generation of the composition map of crystalline phases from a set of x-ray diffraction patterns – creates a bottleneck in high throughput and autonomous materials discovery. For properties where only phase-pure materials are of interest one needs to screen out the mixed-phase diffraction patterns, although properties from catalysis to light harvesting materials may be optimized through interfaces and other multi-phase interactions. As a result, mixed-phase x-ray diffraction patterns must be de-mixed, which can be very challenging when candidate structures contain overlapped features and the diffraction patterns of prototype structures vary due to, for example, alloying. In such cases, experts analyze the data by collectively considering a collection of related mixed-phase diffraction patterns and invoking thermodynamic rules that govern phase mixtures in the given materials space. Previous methods have used such rules to “fix” phase mapping solutions from de-mixing patterns, but when dozens of phase mixtures exist within a dataset and the materials space has multiple degrees of freedom that require hundreds of diffraction patterns to characterize, the data complexity exceeds the capabilities of both human experts and state of the art algorithms. In such cases, the prior knowledge about phase prototypes of thermodynamic rules must be integrated into the demixing process. Application of the rules inherently involves computational reasoning and recognition of the phase-pure patterns in the data inherently involves computational learning. The combination of reasoning and learning to solve challenging problems is a hallmark of human intelligence, and we introduce Deep Reasoning Networks (DRNets) to seamlessly integrate reasoning and learning. DRNets are designed with an interpretable latent space for encoding prior-knowledge domain constraints and integrating constraint reasoning into neural network optimization. DRNets are demonstrated for solving complex phase behavior in 3-cation oxide composition spaces.

9:00 AM CH04.14.05

Predicting Temperature-Dependent Oxide Redox Reactions with Machine-Learning Augmented First-Principles Calculations José A. Garrido Torres, Vahe Gharakhanyan, Tobias Hoffmann Eegholm, Nongnuch Artrith and Alexander Urban; Columbia University, United States

Understanding the conditions for the formation and reduction of metal oxides at high temperatures is of great industrial relevance, e.g., for corrosion prevention and for metal production. However, the experimental characterization of high-temperature redox chemistry is challenging and requires specialized equipment. Simulations with the Calculation of Phase Diagrams (CALPHAD) method can be an alternative but require assessed phase diagrams for the system of interest. First-principles calculations, on the other hand, can provide robust estimates of redox potentials at zero Kelvin without experimental input, but simulating redox reactions at high temperatures is computationally demanding and often too approximate.

Here, we will discuss initial progress towards the efficient computational prediction of high-temperature redox chemistry using machine-learning augmented first-principles calculations. We show that a combination of results from zero-Kelvin density-functional theory (DFT) calculations and a machine-learning model trained on temperature-dependent reaction free energies allows predicting reduction temperatures of metal oxides that the model was not trained on. Hence, this initial application for crystalline binary and ternary oxides demonstrates that the temperature dependence of the free energy can indeed be cross-learned from other oxides, thereby removing the limitation to compounds that have previously been thermodynamically assessed.

9:15 AM CH04.14.07

Machine Learning for Revealing Spatial Dependence Among Nanoparticles: Understanding Catalyst Film Dewetting via Gibbs Point Process Models Ahmed Aziz Ezzat¹ and Mostafa Bedewy²; ¹Rutgers, The State University of New Jersey, United States; ²University of Pittsburgh, United States

How can we simulate a complex nanoscale phenomena involving coupled physical and chemical processes and interactions that are hard to model? In this work we show that combining *in situ* environmental transmission electron microscopy (E-TEM) with automated image processing and statistical machine learning uniquely enables formulating interpretable mathematical models as well as creating accurate simulation tools. In particular, there is a need for a better understanding, characterization, and prediction of the proximity effects among dense populations of metal nanocatalysts as they form and evolve over time. Here, we leverage point process theory—a branch of statistical machine learning—to “learn” the spatial dependencies among ensembles of adjacent alumina-supported iron nanoparticles from a time sequence of E-TEM images. We construct a set of point process models to make statistical inferences about the nature of spatial dependencies that govern the rapid formation, or “popping” of nanoparticles during thin film dewetting, concomitant with metal reduction in the presence of acetylene at 750 °C. We show that nanoparticles exhibit strong dispersion behavior, i.e. new nanoparticles pop in dispersed locations at a predictable distance from their existing territorial neighbors. We also show that the Softcore model, a class of Gibbs point processes, adequately describes the pairwise interactions underlying such time-dependent spatial variations. Further, we leverage the probabilistic nature of our statistical models to develop a computational simulation tool capable of producing accurate simulations of the spatio-temporal evolution of formation patterns of nanoparticles at both finer time resolutions and larger spatial domains than experimental observations. This is a much needed capability, wherein the behavior of hard-to-model coupled nanoscale phenomena involving complex chemical and physical processes are accurately captured in machine-learned mathematical formulations; thus overcoming current limitations in computational methods supporting the design and analysis of collective nanocatalyst populations.

9:20 AM CH04.14.08

Defects Engineering to Design Tough Graphene Chang-Yan Wu¹, Markus J. Buehler² and Chi Hua Yu^{1,2}; ¹National Cheng Kung University, Taiwan; ²Massachusetts Institute of Technology, United States

Fracture behaviors of brittle materials have been a crucial problem when it comes to safety and reliability. Unlike the one-sided understanding that defects result in a negative effect on materials, a new perspective from recent studies indicates that nano-defects could strengthen the material if rationally designed. Nevertheless, fracture behaviors of graphene under defective conditions remain unclear and need more comprehensive studies. With deep learning (DL) recently drawing attention in the material field, several studies have applied machine learning techniques on predicting crack growth of

brittle materials. This study aims to use a deep sequential model to predict the fracture path of graphene under two systems of defective configuration. One involves graphene with different crystalline, and the other involves graphene with various porous defects. First, we built 20 nm 16 nm graphene sheets with different orientations or pores defects. The 20 nm pre-existing crack is set at the edge of each graphene sheet. Subsequently, we performed uniaxial tensile tests by implementing molecular dynamics simulation and process the results into grayscale images. We sliced every single image into pieces so that the ConvLSTM-based model can learn the spatiotemporal features from the sequential images. The input matrices are mapped from the sequential images, and the output matrices are mapped from the crack images of the next timestep. After iterating the prediction process, we can obtain the final crack path of the graphene. We first used 100 crack images (graphene with ten different orientations in 10 sets) to train the model. The model shows 99.45% binary accuracy and can predict the crack path of graphene under different orientations, whether it is single crystal or bicrystal. We used other 300 crack images (arbitrary porous graphene) to train another model. The model shows 94.50% binary accuracy and can predict crack propagation of arbitrary porous graphene. This study applied deep learning on graphene fracture predictions, which work as a more efficient tool than conventional simulation methods, which is potential for next-generation material design.

SESSION CH04.15: Physics-Assisted ML Methods for Knowledge Extraction III

Session Chair: Rama Vasudevan

Wednesday Morning, December 8, 2021

CH04-Virtual

10:30 AM *CH04.02.01

Realizing Physical Discovery in Imaging with Machine Learning [Sergei V. Kalinin](#), Yongtao Liu, Ayana Ghosh, Kyle P. Kelley, Kevin Roccapriore and Maxim A. Ziatdinov; Oak Ridge National Laboratory, United States

Machine learning and artificial intelligence (ML/AI) are rapidly becoming an indispensable part of physics research, with domain applications ranging from theory and materials prediction to high-throughput data analysis. In parallel, the recent successes in applying ML/AI methods for autonomous systems from robotics through self-driving cars to organic and inorganic synthesis are generating enthusiasm for the potential of these techniques to enable automated and autonomous experiment (AE) in imaging. The implementation of this vision requires the synergy of three intertwined components, including the engineering controls of the imaging tools, the algorithmic developments that allow to define non-trivial exploratory patterns, and physics-driven interpretation.

In this presentation, I will discuss recent progress in automated experiment in electron and scanning probe microscopy, ranging from feature to physics discovery via active learning. The applications of classical deep learning methods in streaming image analysis are strongly affected by the out of distribution drift effects, and the approaches to minimize though are discussed. We further present invariant variational autoencoders as a method to disentangle affine distortions and rotational degrees of freedom from other latent variables in imaging and spectral data. The analysis of the latent space of autoencoders further allows establishing physically relevant transformation mechanisms. Extension of encoder approach towards establishing structure-property relationships will be illustrated on the example of plasmonic structures. Finally, I illustrate transition from post-experiment data analysis to active learning process. Here, the strategies based on simple Gaussian Processes often tend to produce sub-optimal results due to the lack of prior knowledge and very simplified (via learned kernel function) representation of spatial complexity of the system. Comparatively, deep kernel learning (DKL) methods allow to realize both the exploration of complex systems towards the discovery of structure-property relationship, and enable automated experiment targeting physics (rather than simple spatial feature) discovery. The latter is illustrated via experimental discovery of the edge plasmons in STEM/EELS and ferroelectric domain dynamics in PFM.

This research is supported by the by the U.S. Department of Energy, Basic Energy Sciences, Materials Sciences and Engineering Division and the Center for Nanophase Materials Sciences, which is sponsored at Oak Ridge National Laboratory by the Scientific User Facilities Division, BES DOE.

11:00 AM *CH04.15.01

Learning Rules for Materials Properties and Functions by Artificial Intelligence [Matthias Scheffler](#); The NOMAD Laboratory at the FHI, Germany

In materials science and engineering, one is typically searching for materials that exhibit exceptional performance for a certain function, and all these searches face the following situation[1]

-- The number of possible materials is practically infinite.

-- The electronic and atomistic processes that rule a desired materials function are many, and their concerted action is typically highly complex and intricate, resulting in an immense number of possibly relevant mechanisms.

-- The number of data that are “clean” (i.e. comprehensively characterized and high-quality) and relevant for the function of interest are typically very low.

Under these daunting conditions we aim to identify the rules that govern the rare phenomena corresponding to particularly exceptional materials. Thus, the scientific discovery typically resembles the proverbial hunt for the needle in a haystack.

This talks describes two methods that guide the way towards solutions of the challenge: *Subgroup Discovery* [2] and *Sure Independent Screening and Sparcifying Operator* (SISSO) [3]. Both methods enable us to identify the “materials genes”, i.e. the basic physico-chemical parameters that are relevant for the property of interest. In analogy to biology, these “materials genes” are correlated to processes that trigger, actuate, or facilitate, or hinder the property of interest.

In the coordinate systems of these genes we identify maps of materials properties, i.e. (small) regions where the desired high-performance materials can be found.

The talk describes the concepts and illustrates them with specific examples, e.g. crystal-structure prediction, topological semiconductors, materials that may convert green-house gases into useful chemicals and fuels, and more.

1) C. Draxl and M. Scheffler, Big-data-driven materials science and its FAIR data infrastructure. Handbook of Materials Modeling, eds. S. Yip and W. Andreoni (Basel: Springer International Publishing) p. 49 (2020).

2) B. R. Goldsmith, M. Boley, J. Vreeken, M. Scheffler, L. M. Ghiringhelli, Uncovering structure-property relationships of materials by subgroup

discovery, New J. Phys. 19, 013031 (2017).

3) R. Ouyang, S. Curtarolo, E. Ahmetcik, M. Scheffler, and L. M. Ghiringhelli, SISSO: a compressed-sensing method for identifying the best low-dimensional descriptor in an immensity of offered candidates. Phys. Rev. Mat. 2, 083802 (2018).

11:30 AM *CH04.04.01

Matrices, Graphs and Natural Language—Ways to Represent Materials for Machine Learning Keith T. Butler^{1,2}, Ricardo Grau-Crespo², Luis Antunes², Scott Midgley², Jeyan Thiyagalingam¹, Johannes Allotey³, Aron Walsh⁴ and Alexander Moriarty⁴; ¹Rutherford Appleton Laboratory, United Kingdom; ²University of Reading, United Kingdom; ³University of Bristol, United Kingdom; ⁴Imperial College London, United Kingdom

In this talk I will present some of our recent work on different ways of representing materials for various machine learning applications. Starting with a simple case of using the well-known Coulomb matrix representation for solid-solutions and alloys, I will demonstrate how this significantly outperforms the cluster expansion approach, which has been the standard method for atomistic modelling of alloys for several decades. The Coulomb matrix representation, in combination with neural networks is shown to be highly effective in predicting non-linear relationships, exemplified by the case of band gaps in a solid-solution of (Zn, Mg)O. Next I will consider graph-neural networks (GNNs), which encode the topology of a material as a message passing graph – typically these GNNs are coupled with a standard neural network to predict a given material property. I will demonstrate how GNNs can be used instead to learn a representation of the material as a compressed vector, which can then be used in a Bayesian approach to predict properties, but with added value of a principled estimate of the uncertainty in the estimation. By using this GNN-fed Gaussian process, we are then able to develop an active learning protocol whereby we select the next best experiment (or high-level calculation) to obtain new labelled data. We find that this active learning process leads to model improvement at twice the rate of adding data without guidance. Finally I will demonstrate how principles from natural language processing (NLP) can be applied to learn representations of atoms and then to assemble these atoms into compounds. Using this approach we can leverage existing databases, such as the Materials Project to rapidly learn distributed embeddings and then apply these embeddings to predict compound properties – I will show how this NLP-inspired approach outperforms many existing approaches on a number of standard materials science benchmark tests.

12:00 PM *CH04.15.02

Statistical Physics of Machine Learning Bruno Loureiro, Lenka Zdeborová and Florent Krzakala; École Polytechnique Fédérale de Lausanne, Switzerland

The past decade has witnessed a surge in the development and adoption of machine learning algorithms to solve day-a-day computational tasks. Yet, a solid theoretical understanding of even the most basic tools used in practice is still lacking, as traditional statistical learning methods are unfit to deal with the modern regime in which the number of model parameters are of the same order as the quantity of data - a problem known as *the curse of dimensionality*. Curiously, this is precisely the regime studied by Physicists since the mid 19th century in the context of interacting many-particle systems. This connection, which was first established in the seminal work of Elisabeth Gardner and Bernard Derrida in the 80s, is the basis of a long and fruitful marriage between these two fields.

In this talk I will motivate and review the connections between Statistical Physics and problems in high-dimensional Statistics, such as the ones stemming from the fields of Machine Learning and Signal Processing. Finally, I will exemplify this discussion with some recent concrete applications of the Statistical Physics toolbox to different problems of interest.

SYMPOSIUM DS01

Accelerating Experimental Materials Research with Machine Learning
November 29 - December 6, 2021

Symposium Organizers

Kristen Brosnan, Superior Technical Ceramics
Keith Brown, Boston University

A. Gilad Kusne, National Institute of Standards and Technology
Alfred Ludwig, Ruhr-University Bochum

Symposium Support

Bronze

Matter | Cell Press

* Invited Paper

SESSION Tutorial DS01: E-MRS/MRS: Deep, Reinforcement, Active Learning for Materials Science and Competition
Monday Morning, November 29, 2021
Hynes, Level 2, Room 203

8:30 AM**Introduction to Machine Learning and Materials Data Science** [A. Gilad Kusne](#); National Institute of Standards and Technology, United States

A high level introduction to the basic concepts of Machine Learning and central challenges in applying these concepts to materials data.

9:15 AM**Introduction to Gaussian Processes for Regression and Classification** [A. Gilad Kusne](#); National Institute of Standards and Technology, United States

A high level introduction to the basics of Gaussian Processes (GP), their applications to regression and classification tasks, and their relationship to deep learning and linear regression. We will also have a brief hands-on demonstration of GPs applied to materials data. For attendees interested in following along, please bring a laptop and have a Google account.

10:00 AM BREAK**10:30 AM****A Gentle Introduction to Deep Learning** [Stefan Sandfeld](#); Forschungszentrum Jülich GmbH, Germany

A brief introduction to artificial neural networks (Neural Network Definition and Elements, Custom layers, Activation Functions, Loss functions) as well as to Deep Neural Networks (CNN, RNN) will be given. This is complemented by examples that focus on materials science applications, such as semantic segmentation of images.

12:00 PM BREAK**1:30 PM****Sequential Bayesian Experimental Design** [Kris Reyes](#); University at Buffalo, The State University of New York, United States

In this module, we shall discuss sequential experimental design, and the Bayesian modeling of experimental responses. Key to this is the idea of a decision-making policy. We shall give many examples of such policies for various design tasks. Topics discussed will include Gaussian Processes, Multi-armed Bandits and Bayesian Optimization.

3:00 PM BREAK**3:30 PM****Active Learning Competition** [Shijing Sun](#); Toyota Research Institute, United States

A hands-on demonstration of active learning in action. This includes a competition where attendees will compete in using Bayesian Optimization to identify the global extrema of a hidden function. Attendees who would like to participate in the competition should bring a laptop and have a Google account. Prizes will be awarded.

SESSION DS01.01: Human Machine Partnership
Session Chairs: Jason Hattrick-Simpers and Mrigi Munjal
Tuesday Morning, November 30, 2021
Sheraton, 5th Floor, Riverway

10:30 AM *DS01.01.01**Applied Machine Learning in Industry—Case Studies, Successes and Challenges** [Andrew Deter](#), Vipul Gupta, Nathaniel McKeever and Daniel Ruscitto; GE Research, United States

Access to machine learning methods has grown significantly over the past decade. Robust, open-source tools are readily available allowing materials scientists to explore the benefits of a modern materials informatics approach. Here, we present a selection of recent case studies covering a range of problems intended to test the application of machine learning to accelerate materials research at GE. New alloy and coating development projects, component life prediction, and part inspection are all discussed. Successes are highlighted where machine learning has directly led to new insights, but we also address challenges in applying these methods to complex industrially relevant problems. We cover the perennial lack-of-data issue and ongoing efforts at GE to tackle this problem through a deliberate data strategy, integrating both internal and external sources of information to improve model performance. The role of high-throughput experiments is also discussed as a critical enabler for machine learning. While many successes have been published in the academic literature, we cover some of the unique challenges in applying a modern materials informatics framework in industry and ongoing work at GE to modernize the way we conduct materials research and development.

11:00 AM DS01.01.02**Experiments and Data-Driven Modeling of Graphene Synthesis by Chemical Vapor Deposition** [Aagam Shah](#), Mitisha Surana, Jad Yaacoub, Elif Ertekin and Sameh Tawfik; University of Illinois at Urbana-Champaign, United States

Despite that graphene synthesis via chemical vapor deposition (CVD) was first demonstrated in 2009, today economically-viable manufacturing of continuous single crystals of graphene is still elusive. Hundreds of coupled synthesis parameters and complex kinetic pathways impede the development of recipes that, for instance, are reproducible, environmentally sustainable and compatible with electronics fabrication. Building an accurate model for synthesis is challenging due to the coupled chemistry-multi-physics, multi-time and -length scale nature of the growth process. To overcome these challenges, we have adopted a data driven approach to address the complexities of CVD synthesis of graphene. First, we will present a data project called Gr-ResQ (Graphene Recipes for Synthesis of High-Quality Materials). Gr-ResQ is a platform enabling the sharing and use of synthesis data towards building a more accurate predictive model for graphene synthesis. At the core of Gr-ResQ is a crowd-sourced database of CVD recipes and characterization. A suite of associated tools enable fast, automated, and standardized processing of Raman spectra and scanning electron microscopy images. To facilitate community-based efforts, Gr-ResQ provides tools for cyber-physical collaborations among research groups, allowing experiments to

be designed, executed, and analyzed by different teams. Second, we present a data set of synthesis experiments where the selected parameters have a reasonably trackable influence on the outcome. Finally, we apply a Bayesian optimization technique to exploit the results of these experiments. This data-driven approach could facilitate more efficient discovery of complex synthesis recipes, where experimentation is time or capital intensive. This technique can guide the selection of the next experiment and iterate through the process till a predictive model is prepared.

11:15 AM DS01.01.03

From Instruments to Insights—A Platform Approach to Lab Data Automation [Max Petersen](#) and Rob Brown; Dotmatics, United States

The ability to deliver innovative products to the marketplace is at the core of many chemicals and materials companies. One of the main obstacles in doing so are high R&D cost and long development timelines. As a promising solution, data-driven R&D has made its way on executive agendas. At the same time, the underlying IT infrastructure required to provision R&D data to these data-modeling initiatives is often overlooked and/or under resourced. Consequently, many initiatives that aim at implementing data-driven R&D are facing data accessibility challenges, including insufficient data quality, lack of data contextualization or incomplete data sets because of poor system adoption.

The solution to this problem is a uniform platform approach that can directly ingest data from their point of creation and serve up these data to lab managers, scientists, or directly to data modeling tools. This approach is a departure from traditional R&D IT infrastructure designs, as it avoids compartmentalizing data in silos e.g., in LIMS, ELN, or SDMS databases. This is especially important for materials innovation, as workflows are highly variable and generated by scientists from multiple disciplines, leading to data aggregation and curation issues across data silos.

Our unified, data-driven platform that allows for flexible configuration of workflows and roles that naturally contextualizes R&D data. This is paired with a set of scientific data intelligence capabilities, that spans data querying across heterogeneous data sources, data analytics, and advanced scientific data visualization applications. The platform can operate in conjunction with other IT systems and data sources or as a standalone system that includes lab digitalization. This presentation reviews the general aspects of this approach and discusses various customer scenarios of digitalization efforts in the chemicals and materials space.

11:30 AM DS01.01.04

Interactive Graphical Software for the Automatic Characterization of Nanoscale Objects Using Computer Vision [Phillip Williams](#), Joseph H. Absi and Benoit Lessard; University of Ottawa, Canada

In previous work¹, it was established that the use of Artificial Intelligence (AI) and Computer Vision (CV) can augment the current approaches used for thin film analysis. By applying cutting edge Machine Learning techniques to Atomic Force Microscopy (AFM) images, fast, accurate and reproducible analysis can be done at much larger scales and levels of detail than previously feasible. The analysis pipeline uses the AFM height data to calculate metrics that are currently collected manually – such as linear density – as well as providing entirely new information not available from any machine or manual technique, such as the positions, orientations, and lengths of each individual carbon nanotubes in a device.

However, the main drawback of my previous work¹ is that an experienced Machine Learning practitioner is required to properly operate the software and algorithms. In practice, there are many parameters and configurations possible for each algorithm, and processing the data requires a very specific software environment as well as access to the source code. In this work, the previous approaches are implemented in a graphical interface, allowing chemists and materials scientists to leverage the cutting edges techniques without any technical support from a Machine Learning researcher. Various parameters can be tuned, configurations explored, and the results can be computed and visualized in near real-time.

In the analysis software, there are several steps to the data analysis procedure. First, the AFM height data is ingested in the form of a color or black-and-white image. Next, there are several pre-processing steps available; the image can be cropped, converted to black-and-white and even remove outliers (pixels that are particularly bright or dark). Once the image has been preprocessed, a scientist can apply various segmentation algorithms to the AFM data, this segmentation will produce a bitmap which represents the presence or absence of a nanoscale object at a given position in the microscope image. The segmentation processes consist of several steps which are designed to identify if a given point in a film belongs to a nanoscale object or not. In the previous work¹ this is accomplished by using adaptive thresholding techniques such as Otsu's method or Yen thresholding. However, improved algorithms have been added to augment the capabilities of m Thresholding techniques and more sophisticated algorithms such as Deep Neural Networks. The final output of this segmentation process is a matrix of true and false values, indicating if a given pixel belongs to a nanotube (true) or if belongs to the substrate that the nanotube was deposited on (false). Once the segmentation is complete, a variety of solvers can be applied to extract quantitative measures of the nanoscale objects (or film morphologies in the case of thin film devices). We even propose the use of an algorithm in which a scientist can select automatic segmentation or manually specify points of interest, which are then used to segment and extract the polygonal boundary of crystal grains. Using our graphical interface, materials scientist will be able to quickly and easily apply a wide range of cutting-edge Machine Learning techniques to extract detailed quantitative descriptors of their thin film devices or nanoscale objects without the need for any special hardware or Machine Learning expertise.

1. Mirka, B. et al. ACS Nano 15, 8252–8266 (2021)

SESSION DS01.02: Data—Born Digital and Ingested
Session Chairs: Daniel Schwalbe Koda and Duncan Sutherland
Tuesday Afternoon, November 30, 2021
Sheraton, 5th Floor, Riverway

1:30 PM *DS01.02.01

Hard Fought Lessons on Open Data and Code Sharing and the *Terra Infirma* of Ground Truth [Jason R. Hattrick-Simpers](#)^{1,2}, Zachary Trautt³, Brian L. DeCost³ and Howie Jorress³; ¹University of Toronto, Canada; ²NRCan CanmetMATERIALS, Canada; ³National Institute of Standards and Technology, United States

The use of artificial intelligence (AI) or machine learning (ML) in the physical sciences has exploded over the past 5 years - 10 years. In that time frame several truly remarkable discoveries have been made including the discovery of new phase change materials, amorphous alloys, and catalysts. The continued success of these methods relies upon the availability of open data, meta-data and scientific code conforming to the findable, accessible, interoperable and reusable (F.A.I.R.) guidelines. Here I will briefly discuss successes and failures at NIST in collaboration with NREL, SLAC and the

University of Maryland to create the first multi-institution combinatorial dataset and code repository to comply with F.A.I.R. guidelines. But even scientifically sound AI models built from open data sets can only be as trusted as the labels and values contained within them. The second part of my talk will focus on the tenuousness of ground truth and the need for an honest and open accounting for experimental uncertainties within our data sets. An example to be discussed will be of phase attribution from x-ray diffraction data. This will drive home the difficulties in forming unanimous expert consensus and how a consensus with variance impacts the perceived performance of ML model attributions.

2:00 PM DS01.02.02

Data Driven Framework for Development of Large Scale ‘Virtual’ Battery Material Databases [Scott Broderick](#)¹, [Kaito Miyamoto](#)^{2,1} and [Krishna Rajan](#)¹; ¹University at Buffalo, United States; ²Toyota Research Institute of North America, United States

We introduce an approach for the prediction of capacity for over 100,000 spinel compounds relevant for battery materials, from which we propose the few most promising candidate materials. In the design of batteries, selecting the proper material is difficult because there are so many metrics to consider, including capacity which is a fundamental engineering property. Using reported experimental data as our starting point, we demonstrate how we can build a dataset that provides a guide for the selection of battery materials. Although we focus on capacity of Li based spinel structures for electrode materials relevant for usage in batteries, the methodology developed and demonstrated here can be adapted to other properties, structures, and site occupancies. This work integrates non-linear manifold learning, prediction approaches accounting for co-linearity in the data, and uncertainty assessments. This addresses important issues in design of materials, where often the underlying physics is complex and difficult to visualize, while also accounting for challenges with limited data. Our methodology provides a reasonably accurate computational representation of experimental data while accounting for model uncertainty.

2:15 PM DS01.02.03

A Framework for Shared, Distributed Autonomy in Additive Manufacturing Research and High-Mix Low-Volume Manufacture [James O. Hardin](#)¹, [Robert Weeks](#)², [Nicholas Arn](#)^{3,1}, [Jennifer Ruddock](#)^{3,1}, [Jennifer Lewis](#)² and [J. D. Berrigan](#)¹; ¹Air Force Research Laboratory, United States; ²Harvard University, United States; ³UES Inc, United States

The future of research and manufacturing is autonomous and data-driven. Well-curated data is the fuel for this change, but research and high-mix low-volume manufacturing tend to produce highly dynamic and complex data. To date, most solutions have been limited to single pieces of equipment in highly controlled environments, thus limiting the applicability of solutions to the originating environments. Despite this limit, standardized portions of the data can be added to communal material data repositories like NOMAD or Materials Cloud. The tools to interact with the data in these cloud repositories are growing quickly, but there is very limited support for the process data, non-standardized data, and integration of the repository into closed-loop control of research or manufacturing automation. The authors propose that the ROSEDA (Repository of Operations & Subject Expertise for Decision Autonomy) framework may close these gaps, enabling autonomous learning, not just as a lab, but as a national manufacturing/research system. The ROSEDA framework includes an agile cyber-physical framework involving automation, dynamic database engineering, cloud/edge computing, human-machine interfacing, and artificial intelligence. As a first demonstration, the authors are attempting to give a ROSEDA system an "intuition" about new inks similar to the intuition possessed by expert print technicians. This presentation will cover the structure of the ROSEDA framework and current progress toward this demonstration.

2:30 PM DS01.02.04

Text-Mined Dataset of Solution-Based Inorganic Materials Synthesis Recipes for Predictive Synthesis [Zheren Wang](#)^{1,2}, [Olga Kononova](#)^{1,2}, [Kevin Cruse](#)^{1,2}, [Tanjin He](#)^{1,2}, [Haoyan Huo](#)^{1,2}, [Yuxing Fei](#)^{1,2}, [Yan Zeng](#)², [Yingzhi Sun](#)^{1,2}, [Zijian Cai](#)^{1,2}, [Wenhao Sun](#)³ and [Gerbrand Ceder](#)^{1,2}; ¹University of California, Berkeley, United States; ²Lawrence Berkeley National Laboratory, United States; ³University of Michigan–Ann Arbor, United States

In the past decade, the Materials Genome Initiative (MGI) effort has significantly facilitated and accelerated materials discovery and design by deploying large-scale ab-initio computation and building computational databases of structure-property relationships, thereby significantly accelerating the design of novel compounds. In contrast, important experimental properties aspects of materials research are only available in manually curated databases, or are not collected at all as large data sets. In this presentation, we focus on inorganic synthesis recipes, as a comprehensive large-scale collection of synthesis formulations would assist in the development of more quantitative and AI-driven approaches to synthesis routes for novel compounds.

Scientific publications represent the largest repository of knowledge about material synthesis and could be used as a reliable source of data. However, human-written descriptions of syntheses require additional levels of interpretation in order to be converted into a codified, machine-operable format. In this work, we built an extraction pipeline consisting of algorithms and models which use various advanced machine learning and natural language processing techniques to extract essential solution-based inorganic materials synthesis information from the scientific literature. By applying the extraction pipeline, we extracted 35,675 codified solution-based inorganic materials synthesis "recipes" from over 4 million papers. Each recipe includes precursors, targets, the quantities of materials used, and synthesis actions with the corresponding attributes. Information about targets and precursors was used to build the reaction formula for every synthesis procedure. This work has created the first large-scale, freely available dataset of solution-based inorganic materials synthesis recipes. The dataset not only paves the way for future data-driven approaches to investigate inorganic materials synthesis and synthesizability, but also allows researchers to design optimized synthesis procedures for automated experimentation.

2:45 PM DS01.02.05

Estimation of Flory- Huggins Interaction Parameter Using Machine Learning [Janhavi Nistane](#), [Lihua Chen](#) and [Rampi Ramprasad](#); Georgia Institute of Technology, United States

For crude oil separation, polymer membranes consume as little as 10 percent of the total energy as required by thermal distillation processes, hence showing potential to surpass traditional distillation processes in terms of carbon emissions and energy efficiency. To build a polymer membrane, it is of utmost importance to investigate thermodynamic properties like solubility, miscibility, diffusivity, absorption, etc. The Flory-Huggins Interaction Parameter (χ) is often used to describe the polymer-solvent behavior in terms of these thermodynamic quantities.

This work focuses on building a temperature-dependent machine learning model for the prediction of χ for a given polymer-solvent pair, by making use of existing experimental data from numerous literature sources.

The experimental data was collected from over 130 research articles, to build a database of temperature-dependent χ , for over 50 polymers and 130 solvents. This dataset was also augmented with a dataset of Hildebrand solubility parameters for polymers and solvents. Both datasets were used to build a Gaussian Process Regression (GPR) based model in the "multi-task" learning mode. To further boost the performance of the model, feature engineering using Recursive Feature Elimination (RFE) and LASSO reduction was employed. Multi-task learning, which involves dataset fusion, has recently proved powerful in treating situations with data sparsity. We show that the resultant model is superior in performance to the conventional approach of estimating χ using empirical relationships.

3:00 PM *DS01.02.06**Informing Manufacturing Scalability with Text and Data Mining** Elsa Olivetti and [Mrigi Munjal](#); Massachusetts Institute of Technology, United States

This presentation will cover learnings around the manufacturing scalability of experimental research through automatic mining of published text for key phrases and facet similarity across multiple disciplines. In this way we inform at least three principal consequences of materials selection: (1) the availability, scaling capacity, and price volatility of the chosen materials' constituents, (2) the manufacturing processes needed to integrate the chosen materials towards manufacturable devices, and (3) the performance that may be practically achieved with the chosen materials and processes. While each of these factors is, in isolation, a pivotal determinant of manufacturing scalability, we show that consideration and optimization of their collective effects and trade-offs is necessary to more completely chart a scalable pathway towards experimental research that moves more rapidly towards manufacturability. Successful scale up and integration of these novel materials is conditioned on a multitude of factors that are difficult to simultaneously optimize, particularly given the wide range of chemical and structural archetypes currently under investigation. Here we discuss key materials and processing considerations that could impact the scale up to production.

3:30 PM BREAK

SESSION DS01.03: Hard Matter

Session Chairs: Scott Broderick and Tony Wu

Tuesday Afternoon, November 30, 2021

Sheraton, 5th Floor, Riverway

4:00 PM DS01.03.01**A priori Control of Zeolite Synthesis with High-Throughput Simulations** [Daniel Schwalbe Koda](#)¹, Soonhyoung Kwon¹, Cecilia Paris², Estefania Bello-Jurado², Zachary Jensen¹, Elsa Olivetti¹, Tom Willhammar³, Avelino Corma², Yuriy Román-Leshkov¹, Manuel Moliner² and Rafael Gómez-Bombarelli¹; ¹Massachusetts Institute of Technology, United States; ²Universitat Politècnica de València-Consejo Superior de Investigaciones Científicas, Spain; ³Stockholm University, Sweden

Computational methods can guide materials discovery by screening relevant compositions and structures prior to experimentation. Despite the acceleration provided by these approaches, synthesis efforts still rely on trial-and-error to realize computationally designed materials. Here, we combine high-throughput simulations, automated literature extraction, human-computer interaction, and experimentation to control materials synthesis from first principles. We focus on zeolite structures, whose challenging synthesis hinders the discovery of new catalysts. We start developing algorithms that accelerate zeolite simulations by two orders of magnitude when compared to traditional methods. Then, we compute more than half a million zeolite-molecule pairs, thus simulating relevant synthesis conditions for these materials. The calculations explain synthesis outcomes from more than one thousand articles extracted from the literature. In addition, computational predictions enable the design of organic structure-directing agents (OSDAs) with tailored selectivity towards the materials of interest. To visualize the generated data, we developed a web-based platform that provides a visual interface for data exploration by human experts. This human-computer partnership enables researchers to compare templates, obtain information on prior art and literature for zeolite-OSDA pairs, and downselect molecules based on their selectivity, synthetic accessibility, or physical descriptors prior to attempting the synthesis. Experimental results show that the proposed synthesis routes are effective in crystallizing the target materials and additionally enhance the catalytic properties of the obtained frameworks. This work offers a design platform for zeolite synthesis and can be extended to other classes of materials.

4:15 PM DS01.03.02**Machine Learning Design of Low-Cost, Selective Organic Templates for Zeolites** [Omar A. Santiago Reyes](#), Daniel Schwalbe Koda and Rafael Gómez-Bombarelli; Massachusetts Institute of Technology, United States

Zeolites are porous, crystalline aluminosilicate materials that have a wide range of industrial uses. These materials exhibit a variety of pore sizes and shapes, which enable them to selectively and efficiently catalyze specific chemical reactions. To template the formation of target frameworks, organic structure-directing agents (OSDAs) are incorporated into the zeolite synthesis route. However, selecting appropriate OSDAs to synthesize a desired zeolite often requires exhaustive experimentation and trial-and-error. While atomistic simulations can suggest favorable OSDAs for zeolites, their computational cost hinders a vast exploration of the combinatorial host-guest space. Here, we developed a machine learning approach to address this combinatorial design challenge. We started by creating an interpretable representation to capture OSDA shapes and sizes. Then, we trained machine learning models on more than 500,000 simulated zeolite-OSDA pairs to predict binding energies at a fraction of the computational cost from simulations. To thoroughly explore the chemical space of OSDAs, we created a library of candidates using a computational synthesis approach. The molecules were combinatorially generated from known precursors taken from vendors and ranked by their final cost. Finally, we evaluated the potential of millions of molecules as selective OSDAs for hundreds of zeolites using the ML-predicted energies. Our library covers a wide portion of the OSDA molecular-shape space and can drastically accelerate zeolite discovery.

4:30 PM DS01.03.03**Discovering New Concrete Materials by Machine Learning and Bayesian Optimization** [Mathieu Bauchy](#); University of California, Los Angeles, United States

Concrete—which is by far the most manufactured material in the world—is responsible for 5-to-10% of human CO₂ emissions. Here, we present an uncertainty-aware, machine-learning-enabled optimization scheme that aims to accelerate the discovery of new optimized concrete mixes featuring minimum embodied CO₂ while meeting target performance and manufacturing constraints. We first develop an unprecedented dataset comprising more than 10,000 concretes with varying mixture proportions, together with their measured properties (compressive strength, slump, etc.). The dataset is used to train a series of Gaussian Process regression (GPR) models that accurately map concretes' mixture proportions to their properties, and uncertainty thereof. We then adopt Bayesian optimization to guide the discovery of new concrete mixtures featuring minimum embodied CO₂ while presenting required performance metrics (e.g., with a strength meeting or exceeding a given target) and obeying manufacturing constraints (e.g., with compliant slump). This pipeline leads to the discovery of several new concrete mixtures presenting a >50% decrease in embodied CO₂.

4:45 PM DS01.03.04**Unified GNN Architecture Design for High-Throughput Material Screening** [Petar Griggs](#), Lin Li and Rajmonda Caceres; MIT Lincoln Laboratory,

United States

Given the natural graph structure in crystalline materials, numerous graph neural network (GNN) architectures have been developed to learn robust and generalizable representations that enable fast property prediction and accelerate the design of crystalline materials. However, with a vast array of material properties of interest, many of which differ from one another in fundamental ways, a one-size-fits-all approach to designing machine learning (ML) models is ill-suited to property prediction tasks. In this work, we develop the Integrated Graph Neural Network (I-GNN) framework to systematically explore the architecture design space for GNNs over a wide range of material property prediction tasks, ranging from mechanical properties, thermal properties to electronic properties. We construct an expansive design space of GNNs to enable methodical exploration of design choices. We show how the design space can be searched to find a task-specific optimal architecture by performing Bayesian optimizations over the model architecture itself. We demonstrate that the I-GNN framework is able to find architectures that outperform existing GNN architectures, such as CGCNN, MEGNet and GATGNN, on a wide range of properties, and the optimal architecture is indeed property-dependent. To provide insights into individual GNN designs for predicting specific material properties, we analyze the correlation between property similarities and the associated optimal architecture similarities, and study the transferability of the best GNN design across different properties. In summary, the I-GNN framework offers a methodical and scalable approach to explore the GNN design space, identifies the relationship between the best GNN designs and the target material properties, and provides insights into selecting the appropriate GNN to train given the target prediction task.

5:00 PM DS01.03.05

Bayesian Experimental Optimization of Photonic Curing Process for Flexible Perovskite Photovoltaics Devices Zhe Liu¹, Robert Piper², Weijie Xu² and Julia Hsu²; ¹Northwestern Polytechnical University, China; ²The University of Texas at Dallas, United States

Perovskite solar cells have attracted significant attention in the PV community, because >25% power conversion efficiency was recently demonstrated in lab-scale small-area devices. However, manufacturing scale-up of perovskite solar cells is one of the critical areas requiring further innovations [1]. Photonic curing process is an industrially compatible technique that could facilitate crystallization of large-area perovskite thin films in milliseconds without heating the substrate [2]. This key feature enables perovskite device manufacturing on a flexible substrate that cannot sustain high temperature at high web speed. Due to the vast number of possible experimental combinations, process optimization typically requires a systematic effort of experimental planning to find an optimal window of process conditions.

In this work, we demonstrate rapid optimization of photonic curing with four process variables (namely, MAPbI₃ precursor concentration, additive concentration, exposure time and radiant energy during photonic curing) and aim at achieving the power conversion efficiency improvement from the current baseline of 10% on 100 μm thick Willow glass substrates [3]. Machine-learning-based Bayesian optimization framework is deployed to search the optimal process conditions in a high-dimensional experimental space. Using this framework, we can quickly establish the numerical regression model between process variables and device efficiency, and suggest new experimental planning based on evaluating an acquisition function that balances between exploitation and exploration. Especially, to increase human-machine interactions and reduce the possibility of potential mistakes in the model, we provide human-understandable 2D visualization (e.g., contour plot, tSNE plot) in every iteration and produce real-time feature importance ranking by the Shapley Additive Explanation (SHAP) method. The Bayesian optimization framework is shown to be efficient in process optimization and could accelerate the transition from the conventional thermal annealing process to photonic curing. Furthermore, we explore the potential of transferring the knowledge of fabricating the perovskite absorber layer to the hole and electron transport layers. We envision machine learning could be a useful tool to accelerate the development of manufacturing scale-up in perovskite PV devices.

Reference:

- [1] Z. Li, T. R. Klein, D. H. Kim, M. Yang, J. J. Berry, M. F. A. M. Van Hest, and K. Zhu, "Scalable fabrication of perovskite solar cells," *Nature Reviews Materials*, vol. 3, pp. 1–20, 2018.
- [2] Weijie Xu, Trey B. Daunis, Robert T. Piper, Julia W.P. Hsu. Effects of Photonic Curing Processing Conditions on MAPbI₃ Film Properties and Solar Cell Performance. *ACS Applied Energy Materials* 2020, 3 (9) , 8636-8645.
- [3] R. T. Piper, T. B. Daunis, W. Xu, K. A. Schroder, and J. W. P. Hsu, "Photonic Curing of Nickel Oxide Transport Layer and Perovskite Active Layer for Flexible Perovskite Solar Cells: A Path towards High-throughput Manufacturing," *Frontiers in Energy Research* 9, 640960 (2021)

SESSION DS01.04: Soft Matter
Session Chairs: Tyler Martin and Abigail Rendos
Wednesday Morning, December 1, 2021
Sheraton, 5th Floor, Riverway

10:30 AM DS01.04.01

Design of Polymers for High-Temperature Capacitors via a Migration-Assisted Evolutionary Algorithm, Machine Learning, and Retrosynthetic Analysis Joseph D. Kern, Lihua Chen, Chiho Kim and Rampi Ramprasad; Georgia Institute of Technology, United States

Polymer film capacitors are favored by engineers because of their graceful failure mechanisms and low cost. However, certain applications, such as electrified aircraft, require capacitors that can withstand temperatures over 250 C, which is at least 100 C higher than the operating temperature of state-of-the-art polymer film capacitors. We combined machine learning with a genetic algorithm to predict hypothetical polymers with bandgaps above 5 eV, glass transition temperatures above 500 K, and dielectric constants above 4 at 100 Hz. These are useful properties, as a large bandgap can be used as a proxy for dielectric breakdown field strength, a high glass transition temperature indicates the polymer is thermally stable at high temperatures, and a high dielectric constant improves energy density per volume.

Basic genetic algorithms, however, suffer from low chemical diversity. To solve this challenge, we implemented a migration-assisted genetic algorithm where polymers evolved on separate islands, with each island enforcing a different design criterion, and then migrated. This increased the chemical space explored and improved the speed at which polymers achieving target properties were discovered. This is a robust design that could be used for other design applications as well. After predicting polymers that achieved target properties, a retrosynthetic algorithm was used to screen them for ease of synthesizability and likely reactants. A list of synthesis-friendly polymers achieving target properties and their likely reactants is shown.

10:45 AM DS01.04.02

Machine Learning for Accelerated Discovery of Polymer Electrolytes Gabriel Bradford, Jeffrey Lopez, Richard Osterude, Tian Xie, Jeffrey C.

Grossman, Rafael Gómez-Bombarelli and Yang Shao-Horn; Massachusetts Institute of Technology, United States

Polymer electrolytes (PEs) have the potential to improve safety and enable higher energy densities in energy storage devices. However, PEs suffer from significantly lower ionic conductivity than liquid electrolytes¹, preventing their adoption in functional devices. Additionally, because PE synthesis and characterization are time consuming, relatively few PE formulations have been experimentally tested despite decades of study. In this work we leverage advances in machine learning (ML) and high throughput experimentation² to accelerate the design and discovery of PEs. The ML model we've developed incorporates Arrhenius behavior into a state-of-the-art message passing neural network³ to predict ionic conductivity of PEs. To train the model, we've compiled the largest known PE ionic conductivity dataset with nearly 15,000 values, which were gathered from experimental PE characterization publications and hand checked for quality. Ionic conductivity values were predicted for several thousand previously untested PE formulations, from which promising candidates—subject to synthesizability and processability requirements—will be selected for high throughput testing. The resulting data from high throughput experiments will be used to retrain the ML model, improving model predictions in an active learning fashion. The ML model shows marked improvement with increasing training data, indicating that data scarcity is a key limitation in machine learning PE ionic conductivity that our high throughput experimental setup addresses. This work offers an integrated computational-experimental platform to accelerate materials discovery for energy storage applications.

References

1. Xue, Z., He, D. & Xie, X. Poly(ethylene oxide)-based electrolytes for lithium-ion batteries. *Journal of Materials Chemistry A* vol. 3 19218–19253 (2015).
2. Ren, F. *et al.* Accelerated discovery of metallic glasses through iteration of machine learning and high-throughput experiments. *Sci. Adv.* **4**, eaaq1566 (2018).
3. Yang, K. *et al.* Analyzing Learned Molecular Representations for Property Prediction. *J. Chem. Inf. Model.* **59**, 3370–3388 (2019).

11:00 AM DS01.04.03

polyG2G—A Novel Machine Learning Algorithm Applied to the Generative Design of Polymer Dielectrics Rishi Gurnani, Deepak Kamal, Huan Tran, Harikrishna Sahu and Ramamurthy Ramprasad; Georgia Institute of Technology, United States

Polymers, due to advantages such as low-cost processing, chemical stability, low density and tunable design, have emerged as a powerhouse class of materials for a wide range of applications, including dielectrics. In certain applications, the performance of dielectrics is limited by low electric breakdown strength. Using this real-world application as a technology driver, we describe a novel artificial intelligence (AI) based approach for the design of polymers. We call this *polyG2G*. The key concept underlying *polyG2G* is graph-to-graph translation. In graph-to-graph translation, the distribution of subtle chemical differences between high- and low-performing polymers is learned and then sampled to generate novel, high-performing, hypothetical materials. Our approach, with respect to a host of presently adopted design methods, exhibits a favorable trade-off between generation of chemically valid materials and available chemical search space. *polyG2G* finds thousands of potentially high-value targets (in terms of glass-transition temperature, band gap, and electron injection barrier) from an otherwise intractable search space. Density functional theory simulations of band gap and electron injection barrier confirm that a large fraction of the polymers designed by *polyG2G* are indeed high-value. Finally, we find that *polyG2G* is able to learn established structure-property relationships.

11:15 AM DS01.04.04

Multi-Task Predictor for Homopolymers, Copolymers and Polymer Blends Shivank S. Shukla, Christopher B. Kuenneth and Rampi Ramprasad; Georgia Institute of Technology, United States

Polymer blends is one of the most rapidly growing fields in the plastics industry. These multicomponent systems can satisfy complex material requirements by blending known polymers. There is a huge demand for property prediction models to find superior materials in the vast chemical space of polymer blends. In this study, we train a multi-task deep neural network to predict the glass transition, melting, and degradation temperature of homopolymers, copolymers, and polymer blends in a single model. For this, we propose a universal fingerprinting scheme applicable to all three polymer types that shows excellent performance. Our models were built on a joint dataset of more than 20,000 data points containing experimental values of the thermal properties of homopolymers, copolymers, and polymer blends. Our developed models are accurate, fast, flexible, and scalable, and aim to supersede previously developed models for only homopolymers and copolymers.

11:30 AM DS01.04.05

Machine Learning Models to Predict Properties Relevant to Depolymerization of Polymers Aubrey R. Toland, Huan Tran, Lihua Chen, Yinghao Li, Chao Zhang and Rampi Ramprasad; Georgia Institute of Technology, United States

High performance polymers which can exhibit controlled degradation to monomer feedstock at end-of-use are essential to solve the global polymeric waste problem. This work focuses on polymers which undergo ring-opening-polymerization (ROP), as these polymers have shown promise within the context of high performance, depolymerizable polymers. We attempt to accelerate the development of such ROP depolymerizable polymers using machine learning to predict properties indicative of whether or not a polymer can undergo stable depolymerization. These properties, which include ceiling temperature (T_c), enthalpy of polymerization (ΔH_p), and entropy of polymerization (ΔS_p), are reported in literature for only a small subset of ROP polymers. In order to overcome this problem of data scarcity, classical molecular dynamics and density functional theory based simulations were utilized to compute ΔH_p for several hundreds of ROP polymers spanning a much larger chemical diversity than studied thus far. The computational dataset (treated as a “low-fidelity” version of the true measured ΔH_p) was combined with the much smaller dataset of experimentally measured ΔH_p (treated as the “high-fidelity” data) to develop predictive models of ΔH_p at the high-fidelity level. A variety of multi-fidelity learning approaches, including co-kriging and multi-task learning, were adopted. Finally, the computed ΔH_p , measured ΔH_p , and T_c datasets were utilized together to develop predictive models of T_c , the temperature above which depolymerization will be thermodynamically favored. A critical analysis of the performance of the models, challenges that remain in terms of data sparsity and diversity, the true benefits and limitations of the information fusion approaches, and guidelines on chemical factors that control ΔH_p and T_c will also be presented.

1:30 PM *DS01.05.01

Accelerated Development of Colloidal Nanomaterials Enabled by Autonomous Robotic Experimentation in Flow Milad Abolhasani; North Carolina State University, United States

Despite the intriguing properties and widespread applications of colloidal nanomaterials in energy and chemical technologies, their discovery, synthesis, and manufacturing are still based on Edisonian trial-and-error-based techniques. Existing nanomaterials development strategies using resource-intensive batch reactors with irreproducible and uncontrollable heat/mass transport rates very often fail to overcome the demands of the vast synthesis and processing universe of colloidal nanomaterials, resulting in a slow and expensive discovery and development timeframe (8-10 years). Recent advances in lab automation and machine learning (ML)-guided modeling/decision-making strategies provide an exciting opportunity to reshape the discovery and manufacturing of colloidal nanomaterials.¹ In this talk, I will present an intelligent closed-loop nanomaterial synthesizer for on-demand development, formulation optimization, and manufacturing of colloidal nanomaterials through the convergence of robo-fluidic experimentation and *in-situ* nanomaterial characterization with machine learning.² I will discuss how modularization of different stages of colloidal nanomaterials synthesis and processing in tandem with a modular neural network ensemble modeling and decision-making under uncertainty can enable resource-efficient navigation through an experimentally accessible high dimensional space. An application of the developed modular robotic experimentation workflow for the autonomous synthesis of colloidal metal halide perovskite nanocrystals will be presented.

References

1. (a) Volk, A. A.; Abolhasani, M., *Trends in Chemistry* **2021**, Advance Article, DOI: 10.1016/j.trechm.2021.04.001; (b) Volk, A. A., et al., *Advanced Materials* **2020**, *33* (4), 2004495.
2. (a) Abdel-Latif, K., et al., *Advanced Intelligent Systems* **2021**, *3* (2), 2000245; (b) Epps, R. W., et al., *Chemical Science* **2021**, *12* (17), 6025-6036.

2:00 PM DS01.05.02

Autonomous Discovery of Perovskite Nanocrystals and Nanoplatelets Tony C. Wu, Andrew Johnston, Daniel Flam-Shepherd, Yitong Dong, Edward H. Sargent and Alan Aspuru-Guzik; University of Toronto, Canada

Halide perovskite materials have gained significant interest in recent years for their optoelectronic applications such as photovoltaics and light-emitting diodes. Colloidal perovskite nanocrystals (NCs) and nanoplatelets (NPLs) are promising specifically for light-emitting applications, due to bright luminescence, tunable energy levels, narrow emission spectrum, confined excitons, and facile synthetic process. Perovskite NCs and NPLs are in the form of ABX_3 or $L_2[ABX_3]_{n-1}BX_4$, where A is a monovalent cation, B is a divalent cation, X is a halide ion, and L is a ligand for stabilization. There is a large combinatorial space of ions, ligands, concentration, ratios, solvents for optimizing perovskite NCs and NPLs. An autonomous system that combines parameter exploration and automated experimentation can accelerate the development of perovskite NCs and NPLs.

In this work, we will demonstrate our automated system for Ligand Assisted Reprecipitation (LARP) synthesis. This system has the advantage of using batch synthesis conditions, compared to other flow synthesis approaches. The system can also easily include a wide variety of reagents, ligands, and solvents. For characterization, a custom-built optical setup with flow cells is used for measuring absorption, emission, and photoluminescence quantum yield (PLQY). The system also features a wash design protocol to clean the reactors and flow cells for the next experimental cycle. We use Bayesian Optimization to search for perovskite synthesis conditions that maximize PLQY, color, or emission widths. For the results, we demonstrate how the system can help us optimize experimental conditions autonomously.

2:15 PM DS01.05.03

AI-Guided Autonomous Continuous Flow Synthesis for Accelerated Colloidal Quantum Dot Discovery Paul Kenis; University of Illinois at Urbana-Champaign, United States

Semiconducting colloidal quantum dots hold promise for and are starting to be applied in a number of applications ranging from optoelectronics and photovoltaics to bioimaging. Their properties can be tuned by controlling their composition, structure, size, and size distribution. Given the vastness of synthesis parameter space, identifying optimal compositions and structures as well as associated optimal synthesis recipes for them, however, remains a major hurdle for accelerated screening and discovery. The implementation of modular flow reactors, integrated with real-time reaction monitoring, automation and data science, for resource-efficient synthesis has the potential to accelerate this material discovery and synthesis screening process.

This presentation will highlight the development and application of a modular continuous flow reactor platform for synthesis of heavy-metal-free colloidal quantum dots with improved size-uniformity and enhanced optical properties. For example, our efforts, in collaboration with experts from industry and academia, have led to multiple promising insights into the synthesis of InP-based quantum dots. Second, the presentation will feature the development of a flow reactor platform that integrates inline spectroscopy with artificial intelligence-based feedback algorithms for efficient exploration of the multidimensional chemical synthesis parameter space. This platform autonomously learns the parameter space from a small number of experiments (<100), develops a predictive model, and synthesizes InP quantum dots of targeted bandgap and polydispersity (with no-prior-knowledge of the reaction space) all through self-driven experiments in less than 30 hours. Our results underscore the promise and critical role of data-science-assisted experimentation for accelerating the screening and discovery of semiconducting colloidal nanocrystals with desired properties, but also for maximizing synthesis insights across multidimensional parameter space for different classes of colloidal materials.

2:30 PM DS01.05.04

Machine Learning with Knowledge Constraints Accelerates Process Optimization of Perovskite Solar Cell Manufacturing Nicholas Rolston¹, Zhe Liu², Austin Flick¹, Thomas W. Colburn¹, Zekun Ren², Justin Chen¹, Tonio Buonassisi² and Reinhold H. Dauskardt¹; ¹Stanford University, United States; ²Massachusetts Institute of Technology, United States

Perovskite solar cell technology has achieved rapid, unprecedented development in the research lab in terms of its record power conversion efficiency (PCE); however, successful commercialization requires the development of low-cost, scalable, and high-throughput manufacturing techniques. One of the key challenges to develop a new fabrication technique is the high-dimensional process optimization. Sequential learning, an iterative framework of machine learning for experimental planning, has been adopted for high-dimensional optimization tasks in many fields of physical science. This framework has been adopted to achieve research autonomy for optimization tasks, which is often combined with robotic research equipment, and in some research studies, sequential learning method can overperform the experimental plan made by human experts.

The current reports of sequential learning studies for process optimization have some common drawbacks: e.g., disregarding knowledge from related background studies, or neglecting qualitative insights from human experts. For example, during manual optimization of perovskite thin films, a visual assessment of film thickness, color, and large asperities has been used as an effective screening method. Based on this idea, we introduce an ML

manufacturing process optimization framework that combines the output of a regression-based model (learning by doing) with probabilistic knowledge constraints (physical intuition and previously collected data) in sequential learning.

We optimized six parameters in the rapid spray plasma processing (RSPP) technique — substrate temperature, linear process speed, spray flow rate, plasma gas flow rate, plasma height, and plasma duty cycle. Process optimization enables 19% efficiency, which is on par with the highest performance reported to date for open-air spray coating processing technique. The resulting acceleration factor to achieve this highest efficiency is > 3X compared to conventional pseudo-random or factorial design of experiments sampling methods. Additionally, the model has an enhancement factor of greater than 30X in finding the top-one-percentile process conditions, identifying 10 new conditions that produce efficiencies comparable to previous top performing devices before implementing the machine learning approach.

In closing, we observe a disconnection between the machine learning community and photovoltaics research community, where machine learning methods tend to take human out of the loop. Herein, we developed this sequential learning framework to provide an alternative demonstration, where researchers' inputs and background data can be easily incorporated with decision making during the iterative experimental planning.

2:45 PM DS01.05.05

Joint Property-Process Optimization of Halide Perovskites: Active Learning on Computed Property Manifolds in High-Throughput Experiments [Rishi Kumar](#)¹, Deniz N. Cakan¹, Moses Kodur¹, Connor Dolan¹, Maria K. Chan², Gal Mishne¹, Arun Kumar Mannodi Kanakkithodi³ and David P. Fenning¹; ¹University of California, San Diego, United States; ²Argonne National Laboratory, United States; ³Purdue University, United States

The path from computational prediction to realization of new materials is clouded by processing parameters and kinetics. We present a new approach to unify computational and experimental data sets, wherein the computed material properties and processing parameters form a joint property+process space for experimental efforts. Active learning over the manifold defined by computed properties utilizes their topology rather than their absolute values. This approach leverages similarities in computed and measured property manifolds while sidestepping problems arising from absolute errors in computed properties.

We demonstrate high-throughput optimization of composition and processing conditions for hybrid halide perovskites thin-films using a robotic platform guided by active learning on a joint property-process manifold. The property manifold is constructed using a limited set of density functional theory (DFT) calculations, augmented by trained materials graph networks (MEGNet [1]). The graph network densely interpolates the DFT-computed properties over the compositional search space, the manifold of which forms the “property space”. Process variables (annealing temperature, solvent, antisolvent, etc) form the “process space”. The joint property+process space constitutes our overall search space.

We search this property+process space using a high-throughput, automated thin-film deposition platform, Automated Materials by Solution Synthesis (AMaSS). AMaSS deposits solution-based thin films and characterizes them by darkfield, brightfield, and photoluminescence imaging and transmission and photoluminescence spectroscopy. These characterizations are processed to extract features describing film morphology, homogeneity, and optoelectronic behavior. AMaSS experiments are guided by Bayesian Optimization, in which the inputs are points in property+process space and the outputs are features extracted from the in-line characterization.

We will present several examples of validation of the approach, using optimizations within well understood search spaces, followed by results from discovery in new materials spaces. By simultaneously optimizing over property predictions and process variables, we bridge computational and experimental results. Our approach is broadly applicable to materials systems for which properties can be computed and offers a framework for translation of computed property manifolds into experimentally realized materials.

[1] Chen, Chi, Weike Ye, Yunxing Zuo, Chen Zheng, and Shyue Ping Ong. “Graph Networks as a Universal Machine Learning Framework for Molecules and Crystals.” *Chemistry of Materials* 31, no. 9 (2019): 3564–72.

SESSION DS01.06: Mechanics

Session Chairs: Milad Abolhasani and Keith Brown
Wednesday Afternoon, December 1, 2021
Sheraton, 5th Floor, Riverway

4:00 PM DS01.06.01

Accelerated Design of Architected Solids with Bayesian Optimization for Optimal Failure Properties [Chengyang Mo](#), Xiaoheng Zhu, Paris Perdikaris and Jordan R. Rane; University of Pennsylvania, United States

With the widespread adoption of 3D printing processes, it is now a simple matter to build architected solids with complex geometries, such as cellular structures with non-uniform struts and non-periodic arrangements, to achieve desirable mechanical properties. However, finding the structures that optimize a set of mechanical properties, particularly nonlinear and/or failure properties, is challenging due to the large number of parameters that arise. To design more complex architected lattices, machine learning algorithms such as neural networks can help in the design process by generating all possible geometric patterns and finding candidates that match the desired properties. However, this approach is limiting, as it is only feasible for low dimensions and can only be experimentally validated for a few design candidates that have been identified. Here, we discuss the use of a framework based on Bayesian optimization which accelerates the convergence process. Bayesian optimization is a closed-loop design process based on Gaussian process regression which guides the choice of design variables for each iteration of experiments. We show the efficacy of the framework by first examining 3D-printed single edge notched bend bars with embedded cellular inclusions that act as defects. These defect regions can deflect cracks and lead to higher energy absorption during bending-induced fracture. Our Bayesian optimization framework explores the entire parameter space to find the geometry that leads to the globally optimal energy absorption, thereby identifying the parameters to use for the next experimental specimen. In a second application, we apply this framework to maximize energy absorption of cellular solids during in-plane compression. Groups of struts in the cellular solid are allowed to have non-uniform thickness, resulting in sixteen parameters. To accelerate the convergence process we use multiple data streams, including “high-fidelity” (but costly) experimental sources and “low-fidelity” (but inexpensive) finite element simulations using ABAQUS. We show that by including low-fidelity sources, the framework can converge more quickly than by using high-fidelity sources alone, thereby reducing the time and cost needed to discover an optimal design.

4:15 PM DS01.06.02

A Data-Driven Framework for Accelerating Mechanical Characterization at Small Scales [Christos E. Athanasiou](#)¹, Xing Liu¹, Nitin P. Padture¹,

Brian W. Sheldon¹ and Huajian Gao²; ¹Brown University, United States; ²Nanyang Technological University, Singapore

Investigating mechanical properties at small scales is a challenging endeavor. It requires sophisticated micro-/nano-scale experimental methods combined with laborious/time-intensive finite element computations. In this talk, a new framework for materials characterization at small scales using the latest developments in machine learning will be presented. This framework involves multi-fidelity deep learning and active learning methods limiting the need for finite element simulations. Its application for predicting the fracture toughness of microscale pentagonal cross-sectional ceramic cantilevers will be showcased, demonstrating that it can significantly accelerate fracture toughness characterizations at small scales.

4:30 PM DS01.06.03

Late News: PRESTO: Rapid Protein Mechanical Strength Prediction with an End-to-End Deep Learning Model Frank Y. Liu, Bo Ni and Markus J. Buehler; Massachusetts Institute of Technology, United States

Proteins can form biomaterials with exceptional mechanical properties equal or even superior to synthetic materials. Currently, using experimental atomic force microscopy or computational molecular dynamics to evaluate protein mechanical strength remains costly and time-consuming, limiting large-scale *de novo* protein investigations. Therefore, there exists a growing demand for fast and accurate prediction of protein mechanical strength. To address this challenge, here we present PRESTO, a rapid end-to-end deep learning model to predict protein resistance to pulling directly from sequences. By integrating a natural language processing model with simulation-based protein stretching data, we first demonstrate that PRESTO can accurately predict the maximal pulling force, F_{max} , for given protein sequences with unprecedented efficiency, bypassing the costly steps of conventional methods. Enabled by this rapid prediction power, we further find that PRESTO can successfully identify specific mutation locations that may greatly change protein strength in a biologically plausible manner, such as at the center of polyalanine regions. Finally, we apply PRESTO to design *de novo* protein sequences by randomly mixing two known sequences at varying ratios. Interestingly, PRESTO predicts that the strength of these mixed proteins follows up- or down-opening “banana curves”, breaking away from the general law of mixtures in conventional material systems. By discovering key insights and optimal sequences, we demonstrate the versatility of PRESTO as a tool in a rapid protein design pipeline. Our model may offer new pathways for protein material science that focus on analysis and testing of large-scale novel protein sets, as a discovery tool that can be complemented with other modeling methods, and ultimately, experimental synthesis and testing.

4:45 PM DS01.06.04

Direct Ink Writing—An *In Situ* Platform for Measuring Ink Rheology Robert Weeks¹, Jennifer Ruddock², Ezra Ameperosa³, James Hardin³, J. D. Berrigan³ and Jennifer Lewis¹; ¹Harvard University, United States; ²UES, Inc., United States; ³Air Force Research Laboratory, United States

Direct ink writing (DIW) is capable of patterning viscoelastic structural, functional, and biological inks into planar and 3D architectures. During extrusion-based printing, these inks are fluidized under an applied stress enabling their flow through fine nozzles. However, upon exiting the nozzle, they rapidly recover a solid-like state allowing the extruded filaments to retain their shape. For identical printing conditions (i.e., nozzle size, printing pressure, and speed), modest changes in ink rheology can significantly impact the printed feature size and fidelity. However, the optimization of key printing parameters for a given ink is time consuming. Here, we describe a data-driven approach to estimate the critical rheological parameters from images of printed standardized patterns. Our model is trained on data generated with automated experimentation using multiple samples of several different inks that exhibit a wide range of flow behavior. Using oscillatory shear rheometry, we collect sets of data that serve as “truth” for a machine learning model. Our work represents a significant step towards the establishment of autonomous, material-aware 3D printing platforms.

5:00 PM DS01.06.05

Using Machine Learning to Study Classification and Correlation of AFM Images with Bulk Properties Dalia G. Yablou¹ and Ishita Chakraborty²; ¹SurfaceChar LLC, United States; ²Stress Engineering, United States

AFM images were collected on a variety of polymer blend samples that differ in bulk mechanical properties and microstructure. A deep learning model based on a convolutional neural net (CNN) successfully classified various combinations of images pointing to real and meaningful differences in their microstructure. A separate regression-based CNN was built to correlate the AFM images with various bulk mechanical properties. The results observed from the deep learning model reveal a relationship between the microstructures as captured by the AFM images with the different bulk material properties.

SESSION DS01.07: Poster Session
Session Chairs: Keith Brown and Amanda Krause
Wednesday Afternoon, December 1, 2021
8:00 PM - 10:00 PM
Hynes, Level 1, Hall B

DS01.07.02

Inorganic Synthesis Planning for Zeolites Enabled by Data Extraction and Generative Modeling Zachary Jensen¹, Soonhyoung Kwon¹, Daniel Schwalbe Koda¹, Rafael Gómez-Bombarelli¹, Yuriy Román-Leshkov¹, Manuel Moliner² and Elsa Olivetti¹; ¹Massachusetts Institute of Technology, United States; ²Instituto de Tecnología Química, Spain

Zeolites are crystalline, nanoporous materials extensively studied for a variety of industrial applications including catalysis, absorption, and separations. Zeolites are typically synthesized hydrothermally using an organic structure-directing agent in combination with other inorganic precursors. While a number of studies have used simulation and data-driven methods to examine the effect of the organic component of zeolite studies, very little research has studied the inorganic aspects including the gel composition, reaction conditions, and precursor selection with similar techniques. Through data extraction and generative modeling, we examine and develop tools to improve these inorganic aspects of zeolite synthesis. We use natural language processing and human-in-the-loop data cleaning to optimize data extraction from the literature resulting in an exhaustive data set of approximately 20,000 zeolite synthesis routes. We then construct a conditional variational autoencoder trained to generate the inorganic synthesis components including gel composition, reaction conditions, and precursors given an OSDA and zeolite structure. This model is capable of generating synthesis conditions for newly predicted OSDA-zeolite pairs and can be paired with other models and simulations designed to optimize the organic aspect of zeolite synthesis. Additionally, we estimate basic kinetic information including the nucleation and growth rates by fitting crystallization curves found in the data set. We estimate synthesis systems missing intermediate crystallization points by fitting the parameters of existing curves as a function of the synthesis variables. We then examine the effect of various synthesis variables on these kinetic variables.

DS01.07.03

An Informatics Approach for Designing Doped Conjugated Polymers [Hongmo Li](#), Harikrishna Sahu, Lihua Chen, Arunkumar C. Rajan, Chiho Kim, Natalie Stingelin and Rampi Ramprasad; Georgia Institute of Technology, United States

Conjugated polymers have garnered great interest as potential candidates for a wide variety of applications, ranging from electronics to biomedical usages. Doping conjugated polymers is an effective strategy for manipulating their electrical conductivity by generating charge carriers via addition of p-type or n-type dopants. However, identifying a suitable polymer:dopant combination generally relies on heuristic experimental approaches, and is exceptionally time- and labor-consuming due to the vastness of the chemical, configurational and morphological space. Here, we present high-performance surrogate models that are developed to predict the electrical conductivity of p-type and n-type doped polymers. Based on support vector machine (SVM) and Gaussian process regression (GPR) algorithms, the models are trained with available experimentally measured data, and are subsequently used to screen more than 800,000 polymer and dopant candidates to identify promising polymer:dopant combinations. Additionally, we extract new design guidelines that extend knowledge on important molecular fragments that correlate to high conductivity. Our work, thus, provides a roadmap towards robust and rapid material discoveries for doped conjugated polymers. Models are deployed at www.polymergenome.org for broader open-access community use.

DS01.07.04

Comparison of State-of-the-Art Machine Learning Descriptors for Property Prediction of Materials [Janna Domenico](#)¹, Nam Q. Le¹, Alexander New¹, Ian McCue¹, Christine Piatko¹, Michael Pekala¹, Elizabeth Pogue¹, Tyrel McQueen² and Christopher Stiles¹; ¹Johns Hopkins University Applied Physics Laboratory, United States; ²Johns Hopkins University, United States

Machine learning (ML) approaches have the potential to accelerate and transform materials discovery and property prediction. One challenge is the development of accurate material descriptors, i.e., accurate ways to describe the characteristics of a real material to a ML model. Several techniques to generate descriptors have already been developed, such as RooSt and Magpie, which convert a material's composition string to a long-form descriptor: a weighted graph or a matrix of attributes. In contrast, Crystal Graph Convolutional Neural Networks (CGCNN) ML framework develops a descriptor using a material's full crystal structure – its crystallographic information file (CIF) – creating a multigraph. Until now, no rigorous comparison of descriptors has been performed. We assess these descriptors and their performance in ML models for predicting band gap, formation energy, and crystal system, for a database of ~800,000 material composition strings and CIFs. Insights into relative performance of descriptors can help assess what level of materials knowledge is required for accurate prediction of specific materials properties.

DS01.07.05

Accelerate Synthesis of Metal-Organic Frameworks by an Automated Robot and Machine Learning Algorithms [Yunchao Xie](#), Chi Zhang, Heng Deng and Jian Lin; University of Missouri-Columbia, United States

Synthesis of materials with desired structures, e.g. metal-organic frameworks (MOFs), involves optimization of highly complex chemical and reaction spaces due to multiple choices of chemical elements and reaction parameters/routes. Traditionally, realizing such an aim requires rapid screening of these nonlinear spaces by experimental conduction under human intuition, which is quite inefficient and may cause errors or bias. In this work, we report a platform that integrates a synthesis robot with machine learning algorithms to accelerate the synthesis of MOFs. The robotic platform consists of an automatic direct laser writing apparatus, precursors injecting and Joule-heating components. It can automate the synthesis upon fed reaction parameters which are recommended by the genetic algorithm or the Bayesian optimization algorithm. Without any prior knowledge, this integrated platform continuously improves the crystallinity of ZIF-67, a demo MOF employed in this study, as the operation iterations of the two algorithms increase. This work represents a methodology enabled by a data-driven synthesis robot which achieves the goal of material synthesis with improved crystal structures, thus greatly shortening the reaction time and reducing energy consuming. It can be easily generalized to other material systems and paves a new route to the autonomous discovery of a variety of materials in a cost-effective way in future.

DS01.07.06

Application of Bayesian Optimization and Regression Analysis to Ferromagnetic Materials Development [Alexandria Will-Cole](#)¹, A. Gilad Kusne^{2,3}, Peter Tonner², Cunzhen Dong¹, Xianfeng Liang¹, Huaihao Chen¹ and Nian Sun¹; ¹Northeastern University, United States; ²National Institute of Standards and Technology, United States; ³University of Maryland, United States

Bayesian optimization is a well-developed machine learning field for black box function optimization. In Bayesian optimization a surrogate predictive model, here a Gaussian process, is used to approximate the black box function. The estimated mean and uncertainty of the surrogate model are paired with an acquisition function to decide where to sample next. Bayesian optimization with Gaussian processes can be used for structure-property relationship optimization in materials systems with second order phase transitions or gradual disordering without a distinct phase transition. In this study we applied this technique to known ferromagnetic thin film materials such as ferromagnetic $(\text{Fe}_{100-y}\text{Ga}_y)_{1-x}\text{B}_x$ ($x=0-21$ & $y=9-17$) and $(\text{Fe}_{100-y}\text{Ga}_y)_{1-x}\text{C}_x$ ($x=1-26$ and $y=2-18$) to demonstrate optimization of structure-property relationships, specifically the dopant concentration or stoichiometry effect on magnetostriction and ferromagnetic resonance linewidth. These systems both experience gradual disordering without distinct phase transition with increase in boron and carbon concentration, thus are great case systems for Bayesian optimization with Gaussian processes. We have shown that using simulated Bayesian optimization methods to guide experiments, the number of samples required to statistically determine the optimum was reduced by 50 % compared with traditional research methods. Our results suggest that Bayesian optimization can be used to save time and resources to optimize ferromagnetic films. This method is transferrable to other ferromagnetic material structure-property relationships, providing an accessible implementation of machine learning to magnetic materials development.

DS01.07.08

Phase Classification of High Entropy Alloys Using Interpretable Machine Learning [Kyungtae Lee](#)¹, Mukil Ayyasamy¹, Timothy Hartnett¹, Paige Delsa² and Prasanna Balachandran¹; ¹University of Virginia, United States; ²Louisiana School for Math, Science, and the Arts, United States

High entropy alloys (HEAs) are multicomponent materials with nearly equal amount of four or more principal elements. Compared to conventional metal alloys, HEAs exhibit excellent mechanical, thermal, and electrochemical properties with immense potential for materials design due to a vast compositional space. HEAs are typically solid solutions with face centered cubic (FCC), body centered cubic (BCC), or hexagonally closed packed (HCP) phases. There is a long-standing in the application of machine learning (ML) methods to accurately classify the HEA phases as a function of chemistry and composition.

In this work, we develop an ML model with post hoc interpretability capability for HEA phase prediction. We accomplished our objective by combining an ensemble support vector machines (eSVM) algorithm with a variable attribution method. A dataset of 1,821 compositions was compiled from surveying the published literature. Each composition was represented by a high-dimensional space of 125 features that include atomic size, electronegativity, valence electron number, enthalpy of formation, and mixing entropy to name a few. The purpose of eSVM was to build a data-driven multi-class classification

learning model that establishes a quantitative relationship between chemical composition and experimentally determined phase information. We also compared the performance of the eSVM model with a random forest model. Both models had an accuracy of ~85% on the independent test set. We then performed post hoc interpretability of the trained eSVM models to quantify the relative contribution of each feature to the ML prediction score with respect to each instance in the training data. We developed a new clustering algorithm that identifies the similarity between training instances based on the variable attribution scores. Our analysis uncovers previously unknown phase-specific correlations between key features and the HEA phases.

SESSION DS01.08: Data-Driven Analysis I
Session Chairs: A. Gilad Kusne and Kris Reyes
Thursday Morning, December 2, 2021
Sheraton, 5th Floor, Riverway

10:30 AM *DS01.08.01

Building a Grain Growth Model by Deep Reinforcement Learning [Amanda Krause](#)¹, [Weishi Yan](#)¹, [Lin Yang](#)¹, [Michael S. Kesler](#)², [Michael R. Tonks](#)¹ and [Joel B. Harley](#)¹; ¹University of Florida, United States; ²Oak Ridge National Laboratory, United States

Abnormal grain growth, where a few grains grow faster at the expense of their neighbors, is hypothesized to occur because of anisotropic grain boundary (GB) character and unique GB networks. In a polycrystalline material, there are thousands of potential GB types and unlimited combinations of those GBs that makeup the 3D topology of a GB network. This combinatorial, high-complex space is too large for conventional data analysis methods to identify the physical descriptors that are necessary to build anisotropic grain growth models. Reinforcement learning is a machine learning tool that can capture the underlying behavior of an evolving Markov decision process and “teach” it to maximize the “rewards” regarding the agreement between prediction and simulation. Here, we applied a deep reinforcement model to emulate grain growth by conducting learning on Monte Carlo Potts grain growth simulations. Relative to other machine learning networks, reinforcement learning is a relatively interpretable model since the outputs of the models are tied directly to action. The developed reinforcement model can also be used to test different microstructural architectures and, thus, identify how GBs evolve over time. The accuracy of our short and long-term predictions for grain growth will be evaluated. Additionally, the potential and challenges associated with this method for exploring the cause of abnormal grain growth will be discussed.

11:00 AM DS01.08.02

Late News: Predicting Stability of Alloying Si Electrodes for Multivalent Cations by Support Vector Regression [Joy Datta](#), [Vidushi Sharma](#) and [Dibakar Datta](#); New Jersey Institute of Technology, United States

Data driven methodology has become a key tool in predicting material properties computationally at low cost. We present a detailed analysis on predicting stability of Si electrodes for multivalent ion batteries using Support Vector Regression (SVR). Emphasis is on transferability of machine learning (ML) SVR model trained on a set of Si alloys to new Si electrodes for multivalent ion batteries. SVR has the ability to deal with non-linear higher dimensional data in feature space by using kernel trick. We utilize previously reported Si based alloys derived from database for training and testing. Hyperparameters are tuned using two different approaches namely, Grid search CV and Bayesian optimization. The performance of the two approaches is compared in predicting energies and packing fraction of the structures. Furthermore, dependence of these two output properties on the crystal structures calls for an additional analysis on structural representation to the ML model. Three different featurizers are used to represent material structures as input features for ML. Our results show that featurizer Orbital Field Matrix performed best on validation dataset against featurizers X-Ray Diffraction and Sine Coulomb Matrix, while it predicted poor energy values of test data. In contrast, Sine Coulomb Matrix data achieved the lowest error between actual energies and predicted energies of test structures. Our work highlights the potential of ML methodologies in accurately foretelling the stability of reaction intermediates in alloying electrodes for ion batteries beyond Li and guides the experimental studies in selecting appropriate battery materials.

11:15 AM DS01.08.03

Recovering Atomic-Scale Chemistry from Multi-Modal Electron Microscopy [Jonathan Schwartz](#)¹, [Yi Jiang](#)², [Zichao Wendy Di](#)², [Steve Rozeveld](#)³ and [Robert Hovden](#)^{1,1}; ¹University of Michigan, United States; ²Argonne National Laboratory, United States; ³Dow, United States

Modern scanning transmission electron microscopes (STEM) can focus sub-angstrom electron probes to extract quantitative atomic structure and chemistry from elastic and inelastic scattering processes. The chemical composition of specimens is revealed by spectroscopic techniques produced by inelastic interactions in the form of energy dispersive X-rays (EDX) or electron energy loss of the transmitted electrons (EELS). Each atom's chemical identity and coordination provides essential information about the performance of nanomaterials across a wide range of applications from clean energy, batteries, and optoelectronics, among many others. Unfortunately, the dose requirements for high-resolution chemical-spectroscopy (e.g. 10^6 e/Å²) often far exceeds the dose limits of a specimen—chemical maps are noisy or missing entirely. More reliable interpretation of material structure is made in combination with elastically scattered electrons that can measure structure, but not chemistry, at high signal-to-noise ratios (SNR). These inelastic and elastic signals (i.e. modalities) are typically analyzed separately. However, inspired by machine learning and compressed sensing methods, we show high-SNR recovery of chemical maps down to atomic resolution can be achieved by linking information between modalities.

Here we introduce multi-modal electron microscopy, a technique that offers high SNR recovery (500% increase in favorable cases) of nanoscale material chemistry by leveraging correlated information encoded within both high-angle annular dark-field (HAADF) and EDX / EELS. We recover chemical maps by reformulating the inverse problem as an optimization that seeks a solution which surpasses traditional dose limits. First, we model the physics of elastic scattering process to the inelastic spectroscopic chemistries. Second, we ensure the recovered chemical maps maintain a high degree of agreement with the initial measurements using a maximum log-likelihood. Lastly, following recent achievements in compressed sensing, we ensure the recovered chemical maps are maximally sparse in the gradient domain.

We demonstrate chemical recovery at the nanoscale in commercial CoS₂ catalysts for oxygen-reduction and atomic length scales for Co_{0.51}Mn_{1.49}O₃ and ZnS/Cu_{1.81}S interfaces. In all cases, noise in the raw chemical maps is dramatically reduced, even at lower doses, while maintaining structure at and around interfaces. Moreover, our multi-modal approach also recovers the specimen's chemical relative concentration, allowing researchers to measure local stoichiometry. Uncertainty can be further quantified using confidence intervals from Fisher Information maps. This data-driven approach opens new pathways for high-throughput chemical characterization and the investigation of radiation sensitive specimens.

As a result, multi-modal electron microscopy reveals atomic scale chemistry with enhanced clarity at significantly lower electron doses than traditionally allowed.

11:30 AM DS01.08.04

A Real-Time, Physically Informed, Probabilistic Phase Labeling Algorithm for High-Throughput X-Ray Diffraction Studies [Ming-Chiang Chang](#), Sebastian Ament, Maximilian Amsler, Duncan Sutherland, Carla Gomes, R. Van Dover and Michael O. Thompson; Cornell University, United States

High-throughput experimentation is widely used to rapidly assess phase behavior across composition and processing space. Fast and accurate phase identification (on the timescales of active learning loops) from synchrotron-based X-ray diffraction data is a critical step in many of these experiments. In contrast to conventional nonnegative matrix factorization(NMF) algorithms or modern neural network(NN) methods, we have developed a probabilistic algorithm to search and label the specific phases existing in processed libraries. The algorithm builds from a database of potential phases, exploiting the crystallography space group to model physically possible peak shifts (e.g., due to alloying or strain). This makes this method training free, lightweight and flexible. Finally, by modeling the peak shifting, peak ratio deviation, and other variations in the spectrum using Bayesian statistics, we are able to give a probabilistic prediction of the phases that are presented in each diffraction pattern, including the probability of an uncatalogued phase. The algorithm has been benchmarked using a range of binary and ternary oxide systems, with analysis speeds that are commensurate with the lateral-gradient Laser Spike Annealing high throughput technique.

11:45 AM DS01.08.05

In Situ Phase Determination Through Deep Learning Analysis of RHEED Data [Haotong Liang](#)¹, Valentin Stanev¹, A. Gilad Kusne^{2,1}, Alex Wang¹, Logan M. Saar¹, Mikk Lippmaa³ and Ichiro Takeuchi¹; ¹University of Maryland, United States; ²National Institute of Standards and Technology, United States; ³The University of Tokyo, Japan

A key challenge in materials development is the ability to identify material phase in-situ during synthesis and processing. In this talk we present a phase mapping and phase determination method based on Reflection High Energy Electron Diffraction (RHEED) data. RHEED is an in-situ surface-structure characterization technique commonly used to observe the growth of thin films that produces diffraction patterns containing a wealth of static and dynamic information. However, the ability to extract this information is limited by the lack of versatile systems for automated analysis of the patterns. We used a Deep Learning-based tool for automating the analysis of RHEED diffraction patterns. Our method combines several supervised and unsupervised learning methods and permits the extraction of important qualitative and quantitative information characterizing the structure. As a test of the developed pipeline, we applied it to map the phase diagram of hematite structures grown under different conditions. With the increased robustness of the information extracted from the RHEED measurements, one would be able to attain quantitative insight as to the underlying structural phase as well as how the surface structure of a thin film is evolving during the deposition.

SESSION DS01.09: Closed-Loop and Autonomous II
Session Chairs: A. Gilad Kusne and Ichiro Takeuchi
Thursday Afternoon, December 2, 2021
Sheraton, 5th Floor, Riverway

1:30 PM *DS01.09.01

Autonomous Research Systems Current and Future Directions [Benji Maruyama](#); AFRL/RXA, United States

The current materials research process is slow and expensive; taking decades from invention to commercialization. The Air Force Research Laboratory pioneered ARES™, the first autonomous research systems for materials development. A rapidly growing number of researchers are now exploiting advances in artificial intelligence (AI), autonomy & robotics, along with modeling and simulation to create research robots capable of doing iterative experimentation orders of magnitude faster than today. We will discuss concepts and advances in autonomous experimentation in general, and associated hardware, software and autonomous methods.

We expect autonomous research to revolutionize the research process, and propose a “Moore’s Law for the Speed of Research,” where the rate of advancement increases exponentially, and the cost of research drops exponentially. We also consider a renaissance in “Citizen Science” where access to online research robots makes science widely available. This presentation will highlight advances in autonomous research and consider the implications of AI-driven experimentation on the materials landscape.

2:00 PM *DS01.09.02

Decision-Making Under Uncertainty for Multi-Stage Experimental and Computational Pipelines [Kris Reyes](#); SUNY Buffalo, United States

Many experiments in materials science and chemistry are executed within multi-stage experimental and computational pipelines. Examples of such pipelines include the sequential screening and filtering of candidate materials or drugs through a sequence of computer models of increasing fidelity, or multi-step materials synthesis and characterization. In this talk, we present some models and algorithms for executing multi-stage experimental and computational pipelines under the context of optimal experimental design and decision-making under uncertainty. In particular, we present techniques that capture the multi-stage nature of the experimental procedure, including both the need to model experimental decisions for intermediate stages and the ability to characterize the outputs of such stages. We demonstrate how such models and decision-making algorithms can lead to improvements over other methods that treat the experimental structure as a black box, or techniques that perform sequential screening without measuring and mitigating uncertainty.

2:30 PM DS01.09.03

Scientific AI for Autonomous Neutron Diffraction Experiments [Austin McDannald](#)¹, William Ratcliff^{1,2}, Daniel Samarov¹, Efrain Rodriguez², Ichiro Takeuchi², Matthias Frontzek³, Andrei Savici³, Mathieu Doucet³ and A. Gilad Kusne^{1,2}; ¹National Institute of Standards and Technology, United States; ²University of Maryland, United States; ³Oak Ridge National Laboratory, United States

Beamtime at neutron diffraction instruments is a valuable resource uniquely capable of characterizing the magnetic structure of materials but with very limited availability. Here we develop a Scientific AI (SciAI) that is able to autonomously discover the magnetic transition temperature, and thus make efficient use of the beamtime. Several physical principles of the problem are encoded into this Bayesian algorithm, such as the Poissonian-like detector physics and the relationship between diffraction intensity and material magnetization. Furthermore, this system demonstrates hypothesis testing wherein the algorithm identifies which physical principles govern the magnetic transition. This SciAI has been implemented on the BT-4 beamline at NCNR at NIST as well as at WAND² at the HB-2C beamline at HIFR at ORNL, and has been used to autonomously discover the magnetic transition temperature of

both MnO and Fe_{1.09}Te, materials with different magnetic behaviors. Compared to an *a priori* scheduled experiments, this system reduced the number of measurements needed for the experiment by a factor of approximately 5.

2:45 PM DS01.09.04

Physics-Informed Bayesian Approach for Autonomous Grain Map Discovery with EBSD [Austin McDannald](#)¹, Amit Verma², Sukbin Lee³, Gregory Rohrer² and A. Gilad Kusne^{1,4}; ¹National Institute of Standards and Technology, United States; ²Carnegie Mellon University, United States; ³Ulsan National Institute of Science and Technology, Korea (the Republic of); ⁴University of Maryland, United States

Electron Backscatter Diffraction (EBSD) mapping is a powerful technique that can be used to study the crystal grain orientations in a material, but it can be time consuming to exhaustively collect diffraction data at every location in the sample. Here we present a Scientific AI (SciAI) that autonomously discovers the grain map, collecting data at the most informative locations. This SciAI encodes physics to predict the grain map such as: the crystal symmetry of the material under study, and the rule that crystal grains should be contiguous. Crucial to the success of the active learning scheme employed in this SciAI is the quantification of uncertainty in the assigned grain membership and propagation of that uncertainty to the prediction of the grain map. This SciAI is able to discover a grain map for ZnO with only ~10% of the data used in a traditional measurement.

3:00 PM DS01.09.05

Autonomous Synthesis of Metastable Materials Maximilian Amsler¹, Sebastian Ament¹, [Duncan Sutherland](#)¹, Ming-Chiang Chang¹, Dan Guevarra², Aine Connolly¹, John M. Gregoire², Michael O. Thompson¹, Carla Gomes¹ and R. Van Dover¹; ¹Cornell University, United States; ²California Institute of Technology, United States

Autonomous experimentation enabled by artificial intelligence (AI) offers a new paradigm for accelerating scientific discovery. Non-equilibrium materials synthesis is emblematic of complex, resource-intensive experimentation whose acceleration would be a watershed for materials discovery and development. The mapping of non-equilibrium synthesis phase diagrams has recently been accelerated via high throughput experimentation but still limits materials research because the parameter space is too vast to be exhaustively explored.

In this talk we will present our efforts to accelerate synthesis and exploration of metastable materials through hierarchical autonomous experimentation governed by the Scientific Autonomous Reasoning Agent (SARA). SARA integrates robotic materials synthesis and characterization along with a hierarchy of AI methods that efficiently reveal the structure of processing phase diagrams. SARA designs lateral gradient laser spike annealing (lg-LSA) experiments for parallel materials synthesis and employs optical spectroscopy to rapidly identify phase transitions. Efficient exploration of the multi-dimensional parameter space is achieved with nested active learning (AL) cycles built upon advanced machine learning models that incorporate the underlying physics of the experiments as well as end-to-end uncertainty quantification. With this, and the coordination of AL at multiple scales, SARA embodies AI harnessing of complex scientific tasks. We demonstrate its performance by autonomously mapping synthesis phase boundaries for the Bi₂O₃ system, leading to orders-of-magnitude acceleration in establishment of a synthesis phase diagram that includes conditions for kinetically stabilizing δ -Bi₂O₃ at room temperature, a critical development for electrochemical technologies such as solid oxide fuel cells.

SESSION DS01.10: Closed-Loop and Autonomous III
Session Chairs: Keith Brown and Austin McDannald
Thursday Afternoon, December 2, 2021
Sheraton, 5th Floor, Riverway

4:00 PM *DS01.10.01

Closed-Loop Autonomous Combinatorial Experimentation for Streamlined Materials Discovery [Ichiro Takeuchi](#); University of Maryland, United States

We are incorporating active learning in screening of combinatorial libraries of functional materials. The array format with which samples of different compositions are laid out on combinatorial libraries is particularly conducive to active learning driven autonomous experimentation. For some physical properties, each characterization/measurement requires time/resources long/large enough that true "high"-throughput measurement is not possible. Examples include detection of martensitic transformation and superconducting transitions in thin film libraries. By incorporating active learning into the protocol of combinatorial characterization, we can streamline the measurement and the analysis process substantially. We have previously demonstrated discovery of a new phase change memory (PCM) material using the closed-loop autonomous materials exploration and optimization (CAMEO) strategy. The discovered PCM material has been tested in various scaled-up device formats and continues to exhibit superior performance to industrial standards. Recent efforts in developing synthesis – measurement closed loops on a combinatorial thin film platform will be discussed. This work is performed in collaboration with A. Gilad Kusne, V. Stanev, H. Yu, H. Liang, M. Li, E. Pop, and A. Mehta. This work is funded by SRC, ONR, AFOSR, and NIST.

4:30 PM DS01.10.02

A Low-Cost Education Platform for Teaching Autonomous Physical Science [Logan M. Saar](#)¹, Haotong Liang¹, Alex Wang¹, Austin McDannald², Ichiro Takeuchi¹ and A. Gilad Kusne^{2,1}; ¹University of Maryland, United States; ²National Institute of Standards and Technology, United States

Autonomous physical sciences is a rapidly developing field, where artificial intelligence controls experiment design, execution, and analysis in a closed-loop. The field promises to revolutionize the physical sciences, with the next generation of scientists using autonomous systems to address research challenges that are out of reach of Edisonian trial and error methods. However, as of yet, there are no education platforms for teaching the necessary skills to the next generation workforce. In this talk, we present a low-cost education platform which was used during an undergraduate course on machine learning for materials science at the University of Maryland. Through python code, students are taught the fundamentals of machine learning to identify trends from chemistry experiments. Students can also deploy active learning to guide sequential experiments to investigate chemical reactions and perform hypothesis testing.

4:45 PM DS01.10.03

CAMEO 2.0—Physics-Informed Machine Learning for Materials Exploration, Optimization and Discovery [A. Gilad Kusne](#)^{1,2}, Austin McDannald¹, Brian L. DeCost¹, Apurva Mehta³ and Ichiro Takeuchi²; ¹National Institute of Standards and Technology, United States; ²University of Maryland, United States; ³SLAC National Accelerator Laboratory, United States

Technology motivates the perpetual need for novel advanced materials. As a result, materials scientists are driven to investigate materials of increasing complexity. However, with each new synthesis or processing parameter, the materials search space grows exponentially, making human-driven exhaustive experimentation infeasible. In this talk we will compare the use of physics-informed machine learning to off-the-shelf machine learning in their ability to accelerate materials exploration, optimization, and discovery. We will explore different levels of physics integration in the updated Closed-Loop Autonomous Materials Exploration and Optimization 2.0 (CAMEO) algorithm and its impact on the coupled challenges of phase mapping and materials optimization. In particular, we will look at the use of probabilistic priors based on exogenous data, the integration of phase mapping and functional property physics and heuristics, and exploiting mutual information shared between phase mapping and materials optimization for physics-informed active learning. Performance is evaluated on combinatorial library data including the Fe-Ga-Pd benchmark dataset.

SESSION DS01.11: Closed-Loop and Autonomous IV
Session Chairs: Jason Hatrick-Simpers and Austin McDannald
Monday Morning, December 6, 2021
DS01-Virtual

8:00 AM *DS01.11.01

Materials Discovery Using an Artificially Intelligent Mobile Robotic Scientist Benjamin Burger, Phillip M Maffettone, Vladimir V Gusev, Catherine M Aitchison, Yang Bai, Xiaoyan Wang, Xiaobo Li, Ben M Alston, Buyi Li, Rob Clowes, Nicola Rankin, Brandon Harris, Reiner Sebastian Sprick and [Andrew I Cooper](#); University of Liverpool, United Kingdom

Technologies such as batteries, biomaterials, and heterogeneous catalysts have functions that are defined by mixtures of molecular and mesoscale components. As yet, this multi-length scale complexity cannot be fully captured by atomistic simulations, and the design of such materials from first principles is still rare. Likewise, experimental complexity scales exponentially with the number of variables, restricting most searches to narrow areas of materials space. Robots can assist in experimental searches but their widespread adoption in materials research is challenging because of the diversity of operations, instruments and measurements that is required. Here we use a mobile robot to search for improved photocatalysts for hydrogen production from water (*Nature*, **2020**, 583, 237). The robot operated autonomously over 8 days, performing 688 experiments within a 10-variable experimental space that has more than 46 million points, driven by a batched Bayesian search algorithm. This autonomous search identified photocatalyst mixtures that were six times more active than the initial formulations, selecting beneficial components and deselecting negative ones. Our strategy uses a dexterous free-roaming robot, automating the researcher rather than the laboratory instruments, which are largely unmodified. This modular approach may have applications across a broad range of research problems. The mobility and non-linearity of the robot scientist offers the potential to unlock the power of artificial intelligence and machine learning – for example, to make complex, conditional decisions about what measurements and experiments to do next.

8:30 AM DS01.11.02

Machine-Learning-Accelerated Experimental Characterization and Multiobjective Design Optimization of Natural Porous Materials [Giulia Lo Dico](#)^{1,2,3}, [Veronica Carcelén](#)² and [Maciej Haranczyk](#)¹; ¹Foundation IMDEA Materials, Spain; ²Tolsa Company, Spain; ³University of Carlos III, Madrid, Spain

Natural porous materials such as nanoporous clays are recognized as green and low-cost adsorbents and catalysts. The industrial development of novel products requires properties optimization tailored to specific application. Machine learning-aided material design cut time and costs accelerating the experimental research. In our approach we apply predictive algorithms to diverse experimental datasets, obtained by a clay-manufacturer company, for multiobjective optimization. The methods were exploited for the development of (1) acid nanocatalyzers, (2) mycotoxin detoxifiers (3) and rheological additives for drilling fluid application.

In the (1) project, we applied tree-based algorithms trained on experimental datasets to accelerate the characterization of the morphology and the surface activity of processed clay-based materials. We proposed a design function finding optimal processing conditions for clays exploitable in acid catalysis. One of such identified materials was synthesized and tested in catalytic degradation of chlorophyll-a, achieving the 79% of removal.

In the (2) project, we explored promising mycotoxin detoxifiers which form bulky non-absorbable complexes with toxic molecules, reducing their bioavailability. The machine learning models were trained using an extensive set of *in vitro* adsorption experiments imitating the gastrointestinal tract of the animals. The powerfulness of the models allowed to identify high performing formulations for the regulated toxins, predict the detoxification of a wide set of yet-unregulated mycotoxins, and gain insights into the *in vitro* detoxification mode of action through model feature importance analysis. Furthermore, the machine learning algorithms were used to design the *in vivo* experiment for validating the performance of the selected composite material, i.e., the most challenging detoxification experiment. The biomarker detection-based *in vivo* detoxification of deoxynivalenol in broiler chickens confirmed the outcomes of our approach.

The (3) project was focused on the optimization of the thixotropic properties (apparent viscosity and yield point) of clay-based additives for drilling fluid process. In this case we generated experimental data by advanced space-filling design of experiments (latin hypercube sampling with multidimensional uniformity). The latter provided a powerful solution to generate the maximum information by the minimum number of needed experiments. The homogenous dataset allowed to build high predictive models enabling exploration of novel optimal formulations by multiobjective optimization based on pareto-front. Four optimal materials were prepared and tested finding correspondence with the virtual experiments.

8:45 AM DS01.11.03

Benchmarking Active Learning Strategies for Materials Optimization and Discovery [Alex Wang](#)¹, [Austin McDannald](#)², [Logan M. Saar](#)¹, [Haoteng Liang](#)¹, [Ichiro Takeuchi](#)¹ and [A. Gilad Kusne](#)^{2,1}; ¹University of Maryland, United States; ²National Institute of Standards and Technology, United States

Autonomous physical science has the ability to revolutionize how materials science is performed: algorithmically searching materials systems for optimal materials. This reduces the time and cost of the experiments by optimally collecting knowledge-rich data. Such an approach is becoming ever more popular with developments in active learning and scientific AI. We present a benchmarking study to compare the efficacy of popular off-the-shelf active learning methods and those designed with incorporated knowledge of the materials optimization challenge. A primary focus is the data fusion of structural and functional properties information. In this study we benchmark the active learning methods on 5 ternary composition materials datasets containing composition, structure, and functional property data and evaluate the impact of prior knowledge on materials optimization.

9:00 AM DS01.11.04

Towards the Automation of Structural Discovery in Scanning Transmission Electron Microscopy [Nicole Creange](#), [Ondrej Dyck](#), [Rama K. Vasudevan](#), [Maxim A. Ziatdinov](#) and [Sergei V. Kalinin](#); Oak Ridge National Laboratory, United States

Electron microscopy has been on the forefront of materials discovery in numerous fields ranging from ceramics to biology [1-3]. Advancements in instrument controls and detectors have expanded the available pathways for uncovering physical phenomenon. However, despite the technological progression, the fundamental principle of scanning microscopies has remained largely the same, namely the sequential acquisition of data and the data collection workflow. The majority of workflows remain human operated, vastly limiting the data acquisition and feature identification through the latency time of a human operator. Thus, the integration of artificial intelligence and automated manipulation of microscope parameters opens new avenues for experiments with higher control, lower beam damage, and an overall decreased time per experiment. Here, we develop various approaches for automated experiment workflows in scanning transmission electron microscopy (STEM) based on building feature of interest descriptors using the raw image, image segmentation, deep convolutional neural networks (DCNN), and rotationally-invariant variational autoencoders (rVAE). The descriptor is used as a basis for the acquisition function which guides the Bayesian optimization algorithm. Each workflow is applied to three datasets, with a range of feature sizes, comprised of NiO pillars within a La: SrMnO₃ matrix, ferroelectric domains in BiFeO₃, and topological defects in graphene. This approach is compared with the simpler method based on the linear transform-based AE workflows. This work was performed at the Center for Nanophase Materials Sciences, a US Department of Energy Office of Science User Facility.

1. S. J. Pennycook, et al., in *Advances in Imaging and Electron Physics, Vol 153*, (2008), p. 327.
2. S. J. Pennycook, et al., *Journal of Electron Microscopy* **58** (2009), p.87.
3. Y. Jiang, et al., *Nature* **559** (2018) p.343.

9:15 AM *DS01.10.04

Better Batteries and Catalysts by Automation, Data Management and Integration of Machine Learning Helge S. Stein; Karlsruhe Institute of Technology, Germany

Scaling electrochemical energy storage to TWh/a requires the proliferation of new post-Li ion battery chemistries to overcome materials supply constraints. Identification of lead materials for electrodes, electrolytes and the associated optimal electrochemical protocols do, however, remain elusive for many emergent chemistries like Na-, Mg-, Ca- or Al-ion batteries. This talk will present first results obtained from the platform for accelerated electrochemical energy storage research located at the Helmholtz Institute in Ulm as part of the Karlsruhe Institute of Technology. The talk will showcase transfer learning from high-throughput millimeter scale electrochemistry towards high-throughput coin and pouch cell manufacturing and beyond. The talk will also highlight bottlenecks in deploying a highly integrated laboratory and demonstrate how strict implementation of data management protocols and analysis servers fast track machine learning guided experimentation across the entire battery research value chain.

SESSION DS01.12: Data-Driven Analysis II
Session Chairs: Austin McDannald and Helge Stein
Monday Morning, December 6, 2021
DS01-Virtual

10:30 AM *DS01.12.01

Materials Representation and Transfer Learning for Prediction in New Composition Spaces John M. Gregoire¹, Shufeng Kong², Dan Guevarra¹ and Carla Gomes²; ¹California Institute of Technology, United States; ²Cornell University, United States

Active or sequential learning holds great promise for accelerating materials experiments, although full realization of this promise relies on the ability of machine learning models to be predictive in new composition spaces where no training data is available. Expert scientists make such predictions based on their materials chemistry knowledge, i.e. how the individual elements and interactions among them give rise to properties in composition spaces that have not been measured. Additionally, experts transfer knowledge about materials chemistry from other domains. To emulate these aspects of expert extrapolative predictions, we introduce the Hierarchical Correlation Learning for Multi-property Prediction (H-CLMP) framework that seamlessly integrates (i) prediction using only a material's composition, (ii) learning and exploitation of correlations among target properties in multi-target regression, and (iii) leveraging training data from tangential domains via generative transfer learning. H-CLMP accurately predicts non-linear composition-property relationships in composition spaces for which no training data is available, which broadens the purview of machine learning to the discovery of materials with exceptional properties. This achievement results from the principled integration of latent embedding learning, property correlation learning, generative transfer learning, and attention models. The best performance is obtained using H-CLMP with Transfer learning (H-CLMP(T)) wherein a generative adversarial network is trained on computational density of states data and deployed in the target domain to augment prediction of optical absorption from composition. H-CLMP(T) aggregates multiple knowledge sources with a framework that is well-suited for multi-target regression across the physical sciences.

11:00 AM DS01.12.02

Molecular Transformer-Aided Biocatalysed Synthesis Planning Daniel Probst, Matteo Manica, Yves G. Nana Teukam, Alessandro Castrogiovanni, Federico Paratore and Teodoro Laino; IBM Research Europe, Switzerland

Enzyme catalysts are an integral part of green chemistry strategies towards a more sustainable and resource-efficient chemical synthesis. However, the retrosynthesis of given targets with biocatalysed reactions remains a significant challenge: the substrate specificity, the potential to catalyse unreported substrates, and the specific stereo- and regioselectivity properties are domain-specific knowledge factors that hinders the adoption of biocatalysis in daily laboratory works. [1,2]

Here, we use the molecular transformer architecture [3] to capture the latent knowledge about enzymatic activity from a large data set of publicly available enzymatic data, extending forward reaction and retrosynthetic pathway prediction to the domain of biocatalysis. We introduce class tokens based on the EC classification scheme that allows to capture catalysis patterns among different enzymes belonging to same hierarchical families. The forward prediction model achieves a top-5 accuracy of 62.7%, while the single step retrosynthetic model shows a top-1 round-trip accuracy of 39.6%. The enzymatic data and the trained models are available through the RXN for Chemistry platform (<https://rxn.res.ibm.com> and <https://github.com/rxn4chemistry>).

- [1] Katrin Hecht et al., *Catalysts*, 2020, 10(12), 1420
- [2] Shuke Wu et al., *Angewandte Chemie*, 2021, 60(1), 88-119
- [3] Philippe Schwaller et al., *ACS Central Science*, 2019, 5(9), 1572–1583

11:15 AM DS01.12.03

Uncertainty Prediction for Machine Learning Models of Material Properties [Francesca Tavazza](#), Kamal Choudhary and Brian L. DeCost; National Institute of Standards and Technology, United States

Uncertainty quantification in AI-based predictions of material properties is of immense importance for the success and reliability of AI applications in material science. While confidence intervals are commonly reported for machine learning (ML) models, prediction intervals, i.e. the evaluation of the uncertainty on each prediction, are seldomly available. In this work we compare 3 different approaches to obtain such individual uncertainty, testing them on 12 ML-physical properties. Specifically, we investigated using the Quantile loss function, machine learning the prediction intervals directly, and using Gaussian Processes. We identify each approach's advantages and disadvantages and compare their results. All data for training and testing were taken from the publicly available JARVIS-DFT database, and the codes developed for computing the prediction intervals are available through JARVIS-tools.

11:20 AM DS01.12.04

AI for Material Formulations Victor Viterbo, [Federico Zipoli](#), Oliver Schilter and Leonid Kahle; IBM Research Zurich, Switzerland

Over the years a tremendous amount of data on materials have been gathered whether by academic experimentalists building up databases, or during manufacturing process investigations. The sheer amount of data makes the use of it intractable by humans at a global scale and is hence limited to very specific uses by specialists. We present a data-driven approach for formulations of novel materials via autoencoders-based models. Using deep-learning techniques, we are trying to find important correlations and patterns in the underlying data and by doing so, improve existing products and design new ones¹, using the groundwork laid by Kingma² and Bombarelli.³ Starting from data that can consist of various inputs like compositions, processes or even aging conditions, and as outputs, product properties. We encoded the input into three latent representations utilizing encoder-decoder neural-network structures. From these trained latent space vector, the property can be predicted by a separate feed-forward neural network. Alternatively, one can optimize any given property with a given target value, by searching the latent space using a Gaussian process, to retrieve the corresponding compositions and processes. The scheme has been successfully applied to various material case studies in the past: ranging from polymers and epoxy resin to different alloys and it is general enough to be applied to much broader types of industrial problems. As an example of the broad potential use of such an algorithm, we present an application to the phase prediction of ceramic materials. We used commercially available databases consisting of binary and ternary diagrams to train an AI system able to predict properties such as the phases resulting from the mixture of compounds at any given temperatures and pressures conditions.

References:

- 1) T. Gaudin, O. Schilter, F. Zipoli and T. Laino, <https://ercim-news.ercim.eu/en122/special/advanced-data-driven-manufacturing>.
- 2) D. P. Kingma and M. Welling, Auto-encoding Variational Bayes, ICRL 2014, <https://arxiv.org/abs/1312.6114>
- 3) R. Gómez-Bombarelli, J. N. Wei, D. Duvenaud, J. M. Hernández-Lobato, B. Sánchez-Lengeling, D. Sheberla, J. Aguilera-Iparraguirre, T. D. Hirzel, R. P. Adams and A. Aspuru-Guzik, ACS Central Science, 2018, 4, 268–276.

11:35 AM DS01.12.05

Prediction of Solid-State Synthesizability for Ternary Metal Oxides Using Information from the Literature [Yincet Chung](#), David J. Payne and Aron Walsh; Imperial College London, United Kingdom

Material discovery is bottlenecked by the validation of the vast number of promising hypothetical materials generated from high-throughput calculations. The main reason is that the traditional experimental approach relies on trial-and-error. Therefore, time is wasted in attempting to synthesize non-synthesizable material or using the wrong conditions or methods. In recent years, natural language processing (NLP) techniques have been utilized to extract material synthesis conditions from the literature. By leveraging text mined dataset (TMD), researchers have developed data-driven approaches for experiment planning and synthesizability prediction, such as predicting the synthesis outcomes¹ and choosing the correct precursors for solid state reaction (SSR)², in hopes to reduce the number of failed synthesis attempts and accelerate material discovery. High quality data is required for any data-driven approaches to avoid error propagation. While it is generally agreed that the accuracies of TMD are lower than their manually collected counterparts³, there is no quantitative comparison between the two in the material domain.

In this study, SSR information of 4103 ternary metal oxides was manually collected from the literature. The information includes whether the oxide has been synthesized via SSR in the past and the SSR conditions. The accuracy of this dataset was quantitatively compared with reported performances of recent TMDs in materials, which highlights the limitation of current NLP to extract relatively complicated synthesis information. An example is the mixing/grinding conditions, where the manually collected dataset has a precision of 0.96 as opposed to 0.62-0.82 for a TMD⁴. The accuracy of this manually extracted dataset can serve as a milestone for future NLP applications in materials. A filter based on the distribution of heating temperature and binary oxide melting point of the manually collected dataset was created to identify over 100 erroneous entries in a subset of the TMD of solid state reaction⁴. Aside from common errors observed in the literature, some issues with the NLP set up and their implications to the TMD usages were found and discussed.

As a demonstration, this manually collected dataset was used to train a positive-unlabelled learning model to predict the solid state synthesizability of hypothetical ternary oxides. This approach can aid researchers to decide the suitability of using SSR to synthesize new materials.

1. Malik, S. A., Goodall, R. E. A. & Lee, A. A. Predicting the Outcomes of Material Syntheses with Deep Learning. *Chem. Mater.* (2021). doi:10.1021/acs.chemmater.0c03885
2. Kim, E. *et al.* Inorganic Materials Synthesis Planning with Literature-Trained Neural Networks. *J. Chem. Inf. Model.* **60**, 1194–1201 (2020).
3. Kononova, O. *et al.* Opportunities and challenges of text mining in materials research. *iScience* **24**, 1–20 (2021).
4. Kononova, O. *et al.* Text-mined dataset of inorganic materials synthesis recipes. *Sci. data* **6**, 203 (2019).

11:40 AM DS01.12.07

Connecting Pathways of Microscopic Images and First-Principles Simulations via Deep Learning [Ayana Ghosh](#), Sergei V. Kalinin and Maxim A. Ziatdinov; Oak Ridge National Laboratory, United States

Over the last decades, electron and scanning probe microscopies have evolved as one of the primary tools to study systems in the domain of physical and life sciences on the atomic and mesoscale levels. These measurements give rise to highly reliable structural and spectral data containing a wealth of information on structures and functionalities of the systems. On the other hand, development and availability of more computational capabilities including accessible CPU/GPUs, efficient algorithms and corresponding implementations have significantly boosted the advancement of physical simulations. Physical models constructed using first-principle calculations to quantum Monte Carlo and finite-element methods, spanning over quantum-mechanical to

continuum scales leads to abundance of insights on thermodynamic, and electronic properties of materials. There has also been a surge in applications of deep learning and data-driven techniques in each of these avenues in recent years. However, studies utilizing a combination of all three of these avenues to establish a bridge between such learnings is still in its infancy.

In this work, we show how deep learning can bridge together the knowledge learned from microscopic images and first-principles simulations to develop a comprehensive understanding of the physics of the materials of interest. Here we focus on how deep convolutional neural networks can be employed to identify atomic features (type and position) in graphene, use them to construct supercells perform density functional theory simulations to find optimized geometry of the structures followed by studying temperature-dependent dynamics of system evolutions with ad-atoms and defects. The results along with associated uncertainties in predictions at various levels as obtained utilizing this framework may be used to evaluate and modify experimental conditions and regions of interest. We aim to further expand this approach to incorporate edge-computing involving direct transfer of image-based data from microscopes via Jetson AGX Xavier and then analyze, train deep neural networks using a GPU-based platform followed by performing simulations using CPU-based high-performance computing resources and feed back to the human in the loop, altogether on-the-fly, to better guide experiments while learning from theoretical models.

This effort (machine learning) is based upon work supported by the U.S. Department of Energy (DOE), Office of Science, Office of Basic Energy Sciences Data, Artificial Intelligence and Machine Learning at DOE Scientific User Facilities (A.G., S.V.K.) and was also supported (STEM experiment) by the DOE, Office of Science, Basic Energy Sciences (BES), Materials Sciences and Engineering Division (O.D.), and was performed and partially supported (M.Z.) at the Oak Ridge National Laboratory's Center for Nanophase Materials Sciences (CNMS), a DOE Office of Science User Facility.

11:45 AM DS01.12.08

Understanding the Composition–Property Relationships of Glasses Using Interpretable Machine Learning Ravinder Bhattoo, Suresh Bishnoi, Mohd Zaki and N M Anoop Krishnan; Indian Institute of Technology Delhi, India

The stoichiometry of inorganic glasses controls their material property. Therefore, understanding the compositional dependence of glass properties is critical in developing novel glasses. Herein, we use a glass database (>450,000 glass compositions) with up to 232 glass components to train XGBoost (Extreme Gradient Boosting) models for 25 glass properties (including optical, physical, electrical, and mechanical properties). Further, we determine the role of each input glass component in controlling the glass property us SHAP (Shapely additive explanations) analysis. The SHAP analysis reveals a strong interdependence among the glass components for properties like liquidus temperature and glass transition, whereas no such interdependence for properties like density. While some of this interdependence can be explained as “boron anomaly” and “mixed modifier effect”, the others need further exploration. Thus, our work is critical in understanding the component–structure–property relationship of inorganic glasses and discovering novel inorganic glasses.

12:05 PM BREAK

SESSION DS01.13: Closed-Loop and Autonomous V
Session Chairs: Keith Brown and Alfred Ludwig
Monday Afternoon, December 6, 2021
DS01-Virtual

1:30 PM DS01.13.02

Autonomous Microfluidic Synthesis of Metal Cation-Doped Perovskite Quantum Dots Fazel Bateni, Kameel Abdel-Latif, Robert Epps and Milad Abolhasani; North Carolina State University, United States

All-inorganic lead halide perovskite (LHP) quantum dots (QDs) have recently emerged as a promising class of semiconducting nanomaterials for a wide range of solution-processed photonic devices, including color-tunable light-emitting diodes (LEDs), solar cells, and lasers. Despite the outstanding optoelectronic properties of LHP QDs, their widespread adoption in chemical and energy technologies has been limited due to the health and environmental concerns associated with the high amount of lead ions (Pb^{2+}) present in their crystalline network. Partial cation exchange of Pb^{2+} ions with less toxic impurity dopants (i.e., manganese, Mn^{2+}) has been promoted as an effective strategy to simultaneously mitigate the toxicity concerns associated with Pb and incorporate new optical/magnetic properties into the pristine LHP QDs.

The synthesis, fundamental studies, and development of metal cation-doped LHP QDs, similar to other colloidal QDs, are conventionally conducted using time-, material- and labor-intensive flask-based techniques. In contrast, microfluidic synthesis strategies with their tunable and reproducible heat/mass transport rates as well as their reduced chemical consumption and waste generation compared to batch reactors (e.g., round-bottom flasks) have been demonstrated as a reliable time- and material-efficient tool for accelerated fundamental and applied studies of colloidal QDs. Despite the high-throughput nature of microfluidic QD synthesis strategies, the user-guided experiment selection restricts a comprehensive mapping of the multivariable chemical universe and complicates the search for the optimal formulation of metal cation-doped LHP QDs. Recently, the use of deep neural networks (DNNs) and reinforcement learning algorithms have enabled accelerated chemical space exploration in organic syntheses and discovery and optimization of advanced LHP QDs. In this work, we present a self-driven modular robotic QD synthesizer for closed-loop metal cation doping of LHP QDs with desired optoelectronic properties. The robotic QD synthesizer is equipped with (i) a formulation, (ii) multiple flow synthesis reactors, and an (iii) *in-situ* spectral monitoring module. Through convergence of automated robotic QD synthesis with machine learning (ML)-guided modeling (DNN ensemble) and decision-making under uncertainty, we demonstrate accelerated formulation discovery of high-quality Mn-doped LHP QDs. We study the effect of black-box vs modular ML modeling and decision-making on the overall experimental cost for multiple formulation optimization campaigns of Mn-doped LHP QDs. Additionally, we demonstrate the role of in-house-generated prior knowledge within the same modular flow reactor on the performance of the autonomous QD synthesizer. The developed ML-guided material synthesis strategy provides a smart workflow for data-driven formulation optimization and continuous manufacturing of metal cation-doped LHP QDs.

1:45 PM DS01.13.03

A Supervised Machine Learning Approach Towards Accelerating the Development of High-Performance Non-Pb Perovskite Solar Devices Md S. Islam¹, Md T. Islam², Saugata Sarker¹, Sadiq S. Nishat³, Md R. Jani¹, Abrar Rauf¹, Hasan A. Jame¹, Sumaiyatul Ahsan¹, Kazi M. Shorowordi¹, Sankha Banerjee⁴, Deidra Hodges⁵, Haralabos Efstathiadis⁶, Joaquin Carbonara⁷ and Saqui Ahmed⁷; ¹Bangladesh University of Engineering and Technology, Bangladesh; ²University at Buffalo, The State University of New York, United States; ³Rensselaer Polytechnic Institute, United States; ⁴California State University, Fresno, United States; ⁵The University of Texas at El Paso, United States; ⁶State University of New York Polytechnic Institute, United States; ⁷Buffalo State College, United States

In this research, SCAPS (Solar Cell Capacitance Simulator) was utilized to build and probe non-toxic Cs-based perovskite solar devices, and investigate modulations of key materials parameters on ultimate power conversion efficiency (PCE). The input materials parameters of the absorber Cs-perovskite layer were incrementally changed, and with the various resulting combinations, 63,500 unique devices were formed and probed to produce device PCE. Versatile and well-established machine learning algorithms were thereafter utilized to train, test and evaluate the output dataset with a focused goal to delineate and rank the input materials parameters for their impact on ultimate device performance and PCE. The most impactful parameters were then tuned to showcase unique ranges that would ultimately lead to higher device PCE values. As a validation step, the predicted results were confirmed against SCAPS simulated results as well, highlighting high accuracy and low error metrics. Overall, the results from this investigation provide much-needed insight and guidance for researchers at large, and experimentalists in particular, towards fabricating commercially viable non-toxic inorganic perovskite alternatives for the burgeoning solar industry.

2:00 PM DS01.13.04

Late News: AI Accelerated Asynchronous Experimentation for Battery Materials Discovery [Fuzhan Rahmanian](#)^{1,2}, Jackson K. Flowers^{1,2}, Dan Guevarra³, John M. Gregoire³ and Helge S. Stein^{1,2}; ¹Karlsruhe Institute of Technology, Germany; ²Helmholtz-Zentrum Ulm, Germany; ³Institute of Technology, United States

The optimization space for battery materials is vast, requiring better instrumentation and orchestration for efficient exploration. Herein, we present a hierarchical experimental laboratory automation and orchestration (HELAO) framework that is capable of operating multiple distributed and resource sharing instruments at once. HELAO is a versatile, highly modular, user-friendly, lightweight framework that incorporates active learning, AI-assisted data analysis, and high-level hardware abstraction to support globally distributed laboratories. We will demonstrate the open source HELAO framework both through a distributed multi-instrument active learning run and through a combinatorial investigation of multi-cation electrodeposition optimization for battery electrodes using a scanning droplet cell. We will demonstrate the development and discovery of a Lithium and a Mg-cathode post-Li ion battery material and optimal charging protocols. These demonstrations will illustrate the processes required in partially autonomous workflows as envisioned for the Platform for accelerated electrochemical energy storage research (PLACES/R) at the Karlsruhe Institute of Technology and Helmholtz Institute Ulm.

2:15 PM DS01.07.07

SPM at the Edge—Bayesian Optimization with Prior Knowledge for Accelerating Spectroscopy in Scanning Probe Platforms [Rama K. Vasudevan](#), Jacob Hinkle, Kyle P. Kelley, Arpan Biswas, Stephen Jesse, Maxim A. Ziatdinov and Sergei V. Kalinin; Oak Ridge National Laboratory, United States

Scanning probe microscopy (SPM) has become a mainstay of nanoscience, enabling nanoscale measurements of a vast array of different materials. SPM hosts an immense number of modalities of both imaging as well as spectroscopy, to enable functional property measurements to then be correlated with nanoscale (or atomic scale) features of the sample. Despite over three decades since the initial SPM developments, the method of spectroscopy acquisition has remained largely the same, restricted to either individual point measurements, or those on a uniformly spaced grid. This is problematic both due to high levels of redundancy (neighboring pixels are likely to contain the same behavior) as well as inefficiency (time taken per spectra can be prohibitive), thus resulting in tradeoffs between spectral and spatial resolution.

Here, we explored methods to improve the efficiency of spectroscopy in SPM via utilization of Bayesian optimization schemes, implemented via incorporation of edge hardware in the form of GPU servers connected to SPM instrumentation. We first collect hysteresis loops on a ferroelectric thin film from random locations, and then train a surrogate model via Gaussian process regression to predict specific spectral features at the unmeasured sites with quantified uncertainty. We then use an acquisition functions in the Bayesian optimization algorithm to determine the optimal locations to sample to maximize the target spectral feature of interest. We find efficiency gains on the order of 2-3x over conventional grid-based methods. We further incorporate prior knowledge into the algorithm through use of high-resolution imaging, via deep kernel learning, to further improve the predictions of the surrogate model. The tradeoffs between the cost of computation of the more advanced approaches and the cost of actual measurements are discussed. In sum, we show that it is possible to substantially reduce the quantity of spectra captured whilst maintaining highly accurate spectral reconstructions with sparse data on samples with a significant degree of spatial correlation. Notes on how to extend the framework to other spectroscopies will be discussed. This work was conducted at and supported by the Center for Nanophase Materials Sciences, a US DOE Office of Science User Facility.

SESSION DS01.14: Recommendation Engines
Session Chairs: A. Gilad Kusne and Alexandria Will-Cole
Monday Afternoon, December 6, 2021
DS01-Virtual

4:00 PM *DS01.14.01

The Transition from Automated to Autonomous Material Optimization at the Hand of Semiconducting Materials [Christoph J. Brabec](#)^{1,2} and Larry Lueer¹; ¹FAU Erlangen-Nuremberg, Germany; ²Research Center Julich, Germany

Evaluating the potential of novel functional materials and devices for industrial viability is a multi-dimensional large parameter space exploration. Manual experimentation is extremely limited in throughput and reproducibility. Automated platforms for fabricating and characterizing complete functional devices can accelerate experimentation speed within tight processing parameter variations. In this talk I will introduce the concept for the automated research platform AMANDA Line 1 and outline the R&D challenges such a research platform is able to address by today in the broad scope of semiconducting materials

As a first test case I will demonstrate a multi-target evaluation of photovoltaic materials at full device level. About 100 processing variations and nearly 1000 devices have been tested for one photovoltaic absorber on AMANDA Line 1 and evaluated by a Gaussian process regression-based data evaluation. The unique data quality in combination with GPR allowed to discover hidden structure – property relationships within 70 hours only which otherwise would have taken months to establish. Similar acceleration factors are found for further material systems. Engineering efficient and stable perovskite devices was recently demonstrated as well, and the automated material research quest is now directed towards Pb free perovskites. The outlook projects the transition from high throughput engineering towards autonomous optimization. The design, synthesis, testing and optimization of hundreds of interface materials out of a library with more than a million candidates is discussed as a real world scenario for ML guided and autonomous material invention.

4:30 PM DS01.14.02

Developing Active Learning Enabled Materials Exploration System with Enhanced Crystal Structure Representation [Guangshuai Han](#), Yining

Feng and Na Lu; Purdue University, United States

Materials discovery from infinite earth repository is always considered as the bottleneck of each revolutionary technological progress. The technique is hindered by the labor-intensive and time-consuming process. Although the collection of the machine learning techniques has shown excellent capability for speeding up materials discovery, the material feature representation, especially crystal structural information, is still a challenge.

This work focuses on developing an active learning-enabled adaptive materials exploration system for accelerating piezoelectric materials discovery. The system works in a closed-loop mode, which starts from the material's stoichiometry and crystal structure representation. As the piezoelectric properties highly depend on the materials crystal structure, this work graphically encodes crystal structure by newly adopted adjacency matrix. Further, the system learned the materials' properties by the implemented machine learning algorithm and well-established piezoelectric properties database. In this way, the materials exploration system could provide general guidance for piezoelectric properties optimization. Evaluated by the realistic experimental data, the system outcome will yield feedback within each cycle. This adaptive materials exploration system has demonstrated the efficiency of optimizing piezoelectric properties. The presented work mode can also be utilized when speeding up the material exploration system for properties other than piezoelectricity, such as photovoltaic, thermoelectricity, etc. This knowledge will have a broad interest in materials science and the machine learning community.

4:45 PM DS01.14.03

Inverse Design of High Entropy Alloys with Exceptional Properties Using Generative Deep Learning [Arindam Debnath](#) and Wesley Reinhart; The Pennsylvania State University, United States

Ni-based superalloys are the preferred choice of materials for high temperature applications like turbines due to their exceptional properties at such elevated temperatures. However, the current generation of Ni-based components are operating at close to their melting point (1100 °C). Therefore, there has been an increase in the demand for metallic alloys that display superior mechanical properties at temperatures as high as 1600 °C. High-Entropy Alloys (HEAs) are suitable candidates as they show promising properties at these operational temperatures. However, very few HEAs have been discovered so far that surpass the performance of Ni based superalloys. Designing new HEAs that can meet these requirements is therefore a challenging task that not only requires domain knowledge, but also depends on fortuitous discovery from expensive experiments and computation.

Due to the complexity of the problem, generative deep learning is a prime candidate to accelerate the discovery of HEAs. Generative Adversarial Networks (GANs) are a promising method for learning complex distributions and have been demonstrated to great success in the field of computer vision. When trained on HEA compositions, these models can generate candidate materials rapidly as well as interpolate continuously between desirable structures. Our approach involves training a continuous conditional GAN (ccGAN) model on the HEA compositions with their corresponding figures of merit (such as high-temperature mechanical properties) as the conditioning vector. This allows us to generate novel HEAs which approach the desired figure of merit by querying the network for new samples with a given conditioning vector. We train the model on composition-property pairs found in the literature and evaluate the results using cross-validation and DFT calculations.

5:00 PM BREAK

SESSION DS01.15: Closed-Loop and Autonomous VI
Session Chairs: Kamal Choudhary and A. Gilad Kusne
Monday Afternoon, December 6, 2021
DS01-Virtual

9:00 PM *DS01.15.01

Integrating Knowledge Representations into Machine Learning for Materials Research [Tonio Buonassisi](#); Massachusetts Institute of Technology, United States

Machine learning (ML) has evolved to become a powerful cognitive assistant for optimizing processes and materials, as evidenced by numerous academic examples and industrial applications. However, the ability of ML to integrate and generate generalizable scientific knowledge generally still requires a human. In this talk, I'll review the state of the art of ML-based knowledge representation in scientific research broadly. Then, I'll discuss nascent examples applying knowledge representations to materials for sustainability, including elucidating the root cause(s) of perovskite degradation. In conclusion, I'll summarize by sharing a personal perspective of where the field can evolve over the coming years, what classes of discovery may be enabled by further evolution of knowledge representations, and the ethical imperatives associated with this evolution.

9:30 PM DS01.15.02

Informatics for Functional Materials: A User-Friendly Implementation of Multi-Objective Bayesian Optimization [Kyohei Hanaoka](#)¹ and Junichi Kuwata²; ¹Showa Denko Materials Co., Ltd., Japan; ²Hitachi, Ltd., Japan

In past several years, the material industry has paid much effort to accelerate material design by introducing data driven methods. Usually design problems attacked by the material industry are more challenging than those reported in the literature in some aspects. For example, in functional materials design, there are often more than three target properties (usually 5 to 10) whose experimental errors are not negligible, and this situation is much more complex than most data-driven material design studies reported in the literature. Moreover, in most cases, the number of possible experiments for functional materials design is extremely limited, because the evaluation of some target properties, such as the durability, requires extremely long-time experiments, and the speed of materials design is always important in order to win the competition among material manufacturers. Furthermore, efficient screening methods, such as virtual and real-world high throughput screenings, are still not available for most functional material design problems, due to the complexity and diversity of their experimental systems. Multi-objective Bayesian optimization is promising for such design problems, which can be applied to any multi-objective design problems requiring time-consuming experiments in order to accelerate their design processes. However, in contrast to single objective Bayesian optimization, which is rapidly spreading in the materials industry, the industrial application of multi-objective Bayesian optimization remains in its nascent stages, and trials and errors by experienced data scientists are required to design materials that satisfy multiple customer requirements using multi-objective Bayesian optimization.

In this study, we developed a straightforward graphical user interface (GUI) based system for multi-objective Bayesian optimization. This system was designed for a common situation of industrial functional materials design where there are multiple target properties with quantitative goals that are defined to satisfy customer requirements and material design efforts will be stopped after finding materials achieving quantitative goals for all target properties.

The developed system employs the joint probability of the achievement of all goals (PA) as an acquisition function¹⁾. This allows users to easily control Bayesian optimization with many objectives and to efficiently achieve the goals only by inputting the target value for each objective. This system also provides users an interpretable visualization of the progress of multi-objective Bayesian optimization based on the PA, which allows material scientists not familiar with data science to see whether optimization efforts should be continued, whether the current choice of the design space is promising, and which material is the best solution. Furthermore, using this system, material scientists can easily feed experimental data obtained in past material design projects to the machine learning model driving Bayesian optimization, which further accelerates multi-objective Bayesian optimization. The development of the straightforward GUI-based system, which does not require experienced data scientists, will popularize multi-objective Bayesian optimization in the material industry. The developed system will be used for the actual functional material design of Showa Denko Materials Co., Ltd. from the beginning of 2022.

Hanaoka, K.; Bayesian Optimization for Goal-Oriented Multi-Objective Inverse Material Design, *iScience* 2021, in press.

9:35 PM DS01.15.03

Informatics for Functional Materials—Finding the Global Optimal Solution from a Vast Experimental Space of Functional Materials. Yuuki Nagai and Kyohei Hanaoka; Showa Denko Materials Co., Ltd, Japan

Many products called functional materials are made by mixing multiple raw materials in order to achieve various properties. The design of such materials requires both tuning of the composition ratio of materials and selection of optimal combination of raw materials from many candidate materials. However, it is difficult to optimize both raw material combination and their composition ratio simultaneously due to their vast experimental space. Therefore, experimenter usually fix compositional or combinational freedom in order to optimize the other freedom. However, such experiment largely limits accessible experimental space even with acceleration by data-driven methods, and true global minimum in the vast experimental space is difficult to be found. It is expected that Bayesian optimization employing machine learning model that can learn both structural and compositional information of functional materials can be a potential solution to this problem, however, its efficiency remains unclear due to difficulty in data acquisition. Unlike other material systems, for functional materials, it is difficult to generate data by simulation, because, functional materials are extremely complex systems that are usually consisted of such as multiple polymeric raw materials and nano-particles. Moreover, for real experiments, it is difficult to acquire many data due to experimental costs and time issues. In this study, we demonstrate the efficiency of Bayesian optimization for tuning of both structural and compositional freedoms of functional materials by developing an experimental system specially designed for the rapid evaluation of the performances of optimization approaches. The developed experimental system is a multi-component polymeric film consisting of around 20 raw materials in maximum and was tuned to allow rapid evaluation of target properties. The target property chosen for the demonstration is the adhesiveness of the film which is expected to show non-linear responses to compositions of materials and is also expected to be difficult to optimize. As expected, by using machine learning model that can learn both structural and compositional freedoms of materials, we successfully found the optimal design within the large experimental space of the developed system. Additionally, we compared the performances of optimization strategies employing Bayesian optimization, classical design of experiment method, and experiments based on knowledge of materials experts, and we report both advantages and disadvantages of each strategy. From the early 2022, we plan to release the PA system as in-house platform for speeding up the actual functional material design.

9:40 PM DS01.15.04

Informatics for Functional Materials—Demonstration of Multi-Objective Inverse Design for Functional Materials by Newly Developed Bayesian Optimization Naotaka Tanaka, Yuuki Nagai and Kyohei Hanaoka; Showa Denko Materials Co.,Ltd., Japan

Data-driven materials design methods are rapidly spreading in the functional materials industry. Among them, Bayesian optimization is especially helpful for inverse design problems of materials. Single-objective (single target property) Bayesian optimization is known to work well under common situations in the materials industry where the amount of available data is small and the number of experiments that can be conducted is also small. However, we actually need to overcome trade-off for multiple target properties in order to satisfy several customer demands. Currently, most applications of Bayesian optimization are limited to single-objective systems or computational problems, and the efficiency of multi-objective Bayesian optimization in industrial functional material design remains unclear.

In previous our study, we proposed a new Bayesian optimization method for tuning the multiple target properties with quantitative goals that satisfy customer demands¹⁾. The proposed method employs the joint probability of achievement (PA) of predefined quantitative target values for all objective properties as the acquisition function. We have represented the efficiency of Bayesian optimization with the PA for a virtual multi-objective inverse design of functional materials employing regression models obtained from the previous experimental study²⁾.

In this study, we actually demonstrated a real-world multi-objective inverse design for functional materials using Bayesian optimization with the PA. Only by inputting the quantitative goal values for each target properties, the PA efficiently navigated the multi-objective optimization trajectory in the space of multiple target properties. We therefore successfully designed the film-shaped polymeric functional materials that satisfy three desired properties within moderate number of experiments. As far as we know, this is the first achievement that validates multi-objective inverse design for the functional material targeting multiple quantitative goals by Bayesian optimization. We plan to release the PA system as the in-house platform in the early 2022 for speeding up the actual functional material design.

1) Hanaoka, K.; Bayesian Optimization for Goal-Oriented Multi-Objective Inverse Material Design, *iScience* 2021, in press.

2) Wang, B., Cai, J., Liu, C., Yang, J., and Ding, X.; Harnessing a Novel Machine-learning-assisted Evolutionary Algorithm to Co-optimize Three Characteristics of an Electrospun Oil Sorbent. *ACS Appl. Mater. Interfaces* 12, 2020, p42842–42849.

9:45 PM DS01.15.05

Prediction of Discharge Characteristics of Lead-Acid Batteries by Machine Learning Utilizing a Part of Time Series Data Hiroshi Ohkubo; Showa Denko Materials Co., Ltd., Japan

Lead-acid batteries are a type of rechargeable battery that uses lead, lead dioxide, and dilute sulfuric acid. They are used in batteries for automobiles, uninterruptible power supplies (UPS) for industrial use (for example, in data centers, in hospitals) and other infrastructure facilities, and main power supplies for electric vehicles such as battery-powered electric forklifts.

One of the important characteristics of lead-acid batteries and other storage batteries is their discharge characteristics, such as battery capacity and internal resistance. Discharge characteristics are evaluated from the transition of voltage values as time series data, which are obtained from measurements that a fully charged storage battery is discharged to the end-of-discharge voltage at a certain temperature and current. Since the battery capacity is evaluated from the above discharge data, the measurement is a time-consuming process.

For lithium-ion batteries, which are a type of rechargeable battery like lead-acid batteries and are widely used in the world, researches on time series analytics (for example, residual life prediction) has been actively conducted. However, there have been few reports of research on time series prediction for lead-acid batteries.

The purpose of this study was to shorten the measurement time of data required to evaluate the discharge characteristics of lead-acid batteries. Therefore,

we focused on whether it is possible to predict the actual discharge characteristics from the first half of the time series data obtained in the discharge experiment.

In this study, we used about 11,000 discharge data obtained from in-house measurements. These data consist of a time series data of voltage values every second. A machine learning model for discharging time prediction was developed using support vector regression (SVR).

As a result, it was found that the SVR model can accurately predict the time from start to finish discharge by using both the first 30% or 50% of the time series data and the difference every 10 seconds as an explanatory variable.

This result suggests that the measurement time required to predict battery characteristics can be shortened and that the present method has a potential to speed up the evaluation and development process of lead-acid battery materials.

9:50 PM DS01.15.06

Development of the Efficient Optimization Method for High Dimensional Incomplete Datasets [Ryosuke Arai](#)^{1,2}; ¹Showa Denko Materials, Japan; ²Research Association of High-Throughput Design and Development for Advanced Functional Materials, Japan

Regression-based optimization methods are known to be effective tools in the field of material developments. However, in practical applications, we often face methodological problems of the poor performance in the case of utilizing high dimensional and incomplete datasets. Bayesian Optimization (BO) is a well-known regression-based optimization method. Although BO works well to reach global minimum/maximum to objective functions in many cases, its efficiency decreases as the dimension of design spaces become higher, such as molecular descriptors. Furthermore, BO cannot deal with incomplete initial datasets without arbitrary treatments for missing values, such as imputation. Gaussian mixture regression-based optimization (GMRBO) is proposed as an efficient optimization method with direct inverse analysis, which works better than BO in high dimensional design space [1]. However, GMRBO also has the same drawback as BO, that it cannot deal with incomplete datasets.

In this study, we have developed an optimization method by extending GMRBO to deal with incomplete datasets. The performance of the extended GMRBO (exGMRBO) was investigated and compared with BO and GMRBO. For the investigation, we used the benchmark function ZDT1 with 30 design variables and two objective functions. The percentage of missing data in the initial dataset was maintained from 10% to 70%.

The results show that while the exGMRBO performance difference between GMRBO and BO was smaller for higher missing rates (above 60%), it achieved a higher performance difference for missing rates between 10 to 50%. However, the performance of exGMRBO outperformed that of GMRBO and that of BO in all cases. Therefore, it was verified that exGMRBO indicates a better performance than BO and GMRBO when the initial dataset contains missing values.

We have also applied the exGMRBO to find Pareto front of the conflict properties of polymers.

* This work was supported by a grant from the New Energy and Industrial Technology Development Organization (NEDO) of Japan (JPNP16010).

[1] H. Kaneko, *Chemometrics and Intelligent Laboratory Systems*, Volume 208, 104226 (2021)

9:55 PM DS01.15.07

Web Platform of a Molecular Generative Model for Experimental Chemists [Seiji Takeda](#), Toshiyuki Hama, Hsianghan Hsu, Akihiro Kishimoto, Lisa Hamada and Daiju Nakano; IBM Research Tokyo, Japan

1. Introduction

Meticulous design of molecules is a key of material development. However, molecular design processes heretofore has been driven by human expert's trial-and-error cycles, therefore, a typical lead time to design new material takes more than 10 years. Over the past half a decade, data-driven approaches leveraging artificial intelligence (AI) have been introduced to this field, especially on the context of generative model. The primary requirement for molecular generative models is industrial practicality, including high speed design with large structural variety. Another important requirement is that a model should be accessible for researchers and engineers of experimental chemistry, who are not necessarily familiar with software-related works; writing Python scripts, using a command line interface, etc. Releasing a state-of-the-art molecular generative model to a wide variety of potential users is important.

In this paper, we will present on our web application (webapp) – based molecular design platform that has practical advantages in terms of speed and diversity of molecule generation, interpretability of model, no requirement of pre-training. The user interface (UI) is designed so to make the tool accessible for experimental chemists.

2. Method

The main workflow is composed of four steps. (1) Training a model: the system encodes input molecular structures to a set of feature vectors by graph kernel approaches. Those feature vectors are used to build a regression model to predict target properties. (2) Setting target properties: a user sets target properties values that should be satisfied by new molecules. (3) Structure generation: molecular graphs are built by repeatedly connecting *graph resources*, which consists of atoms, rings, and user-defined substructures, while avoiding isomorphic duplications. (4) Online evaluation : during running the graph generation algorithm, each generated structure is encoded to a feature vector and then evaluated on the regression model. If the predicted property satisfies the user-set target value, the structure is accepted and stored in the candidate list. Repeating the above process (3) and (4), molecular structures satisfying target properties are generated.

3. Results

First, we used a small subset (300 sample) of QM9 dataset to evaluate the performance. We trained a property prediction model on the energy of the highest occupied molecular orbital (HOMO); E_{homo} . Carrying out property prediction by changing models and sweeping hyper parameters, the system produced reasonable accuracy when using kernel ridge regression. We use this model for the following molecular generation process. In structure generation, we used three target properties; $E_{\text{homo}} \sim -0.28$ (Ha), -0.25 (Ha), and -0.20 (Ha). Depending on the target E_{homo} value, the generation speed (i.e. the number of molecules generated per second) ranges from 29 to 77 per sec. The speed of other state-of-the-art molecular generative models is typically 1 to 10 per sec when QM9 is used, that confirms our method's significant acceleration in terms of speed.

For more practical use, we design new photoacid generator (PAG). We trained our model with $\sim 1,300$ PAG structures extracted from U.S. patents, and corresponding property data which we calculated by DFT simulation. We targeted five properties; LogW, LogP, T_{bio} , LD50, and λ_{max} , satisfying specific ranges set by a PAG chemist. After running MolGX for 6 hours, more than 2,000 molecular structures were generated, that is more than 100 time of acceleration in design speed. The designed PAG structures were experimentally synthesized.

4. Web Application

We implemented the algorithms as a GUI-based web application for a wide variety of users especially experimental chemists. We designed the workflow from a viewpoint of user experience (UX), developed API set, and implemented it on a Kubernetes-based cloud environment. The system is today in-service on IBM Cloud.

10:10 PM DS01.15.08

Training Data Optimization and Error Analysis for Machine Learning-Based Crystal Orientation Estimation [Kyoka Hara](#)¹, Takuto Kojima¹, Kentaro Kutsukake², Hiroaki Kudo¹ and Noritaka Usami¹; ¹Nagoya University, Japan; ²RIKEN, Japan

Multicrystalline materials are often the most immediate choice for various applications including solar cells because of their affordable price and productivity. As for solar cells, the conversion efficiency based on multicrystalline materials is generally inferior to that based on monocrystalline ones. This is mainly explained by the presence of dislocation clusters, which is closely related to crystal structure components such as crystal orientations. We aim to control the formation of dislocation clusters by clarifying the generation mechanisms with the aid of an ingot-scale analysis of crystal orientations, grain boundaries, and dislocation clusters.

For this purpose, we have developed a machine learning-based method for estimating crystal orientations from multiple optical images of textured multicrystalline wafers and reported that the estimation accuracy can be improved by data augmentation. In this study, we report on further improvement of the prediction accuracy by optimizing training data through statistical analysis of the estimation results in different conditions.

In the first step, we perform alkaline texturing on the wafer surface. This shaves off some surface particles and leaves only {111} planes on the surface, creating a pyramid-like structure. Shining light on this pyramid will generate specific reflection patterns that inherit crystal orientation information. A house-made apparatus is used to generate and capture these patterns. The apparatus mainly consists of a camera, a rotating collimate light for illumination, and a stage. As the illumination light rotates around the sample, optical images are taken within every 5 degrees of rotation. We integrate these 72 images into a 72-dimensional signal intensity matrix which we call the "reflection profile."

In the second step, we carry out the machine learning-based orientation estimation. An LSTM neural network and some connected layers constitute our model. The pre-obtained reflection profile is used as the input to the model, and quaternions as the output. Correct grain orientations are measured by the Laue scanner method as teacher data. Note that the training, validation, and test datasets consist of the reflection profiles of 3838, 960, and 6373 grains, respectively.

Successful training of the model resulted in an estimation error median of 8.61 degrees. Based on the assumption that a diverse reflection profile should enhance estimation accuracy, we increased the size and diversity of the training data. Diverse data was created by a variety of incident light angles. We set the elevation angle of the incident light to three different values; 30, 45, and 60 degrees. Using all three elevation data we improved accuracy by 15%. Comparing the results trained on each angle, we discovered that there is an optimal elevation angle. The estimation accuracy varied by ~30% depending on the elevation angle. To acquire the best results most efficiently, we then performed double angle training using two elevations to train the model.

Considering results from single angle training, we selected the two angles with higher accuracy; 30 and 45 degrees, and trained the model, expecting better results compared to other selections. However, this resulted in a poorly trained model, indicating that the combination of angles with good results alone does not always train the model effectively. Further evaluation of results revealed that the three elevations were capable of correctly estimating different orientations. For example, at 30 degrees, planes {100} were correctly estimated while {111}~{101} were poorly estimated. At 60 degrees, {111}~{100} were poorly estimated. By calculating the correlation coefficient between each two elevations, we revealed that the selection of angles with smaller correlation resulted in a better-trained model. This indicates that the selection of angles with different estimation capabilities should train the model most effectively.

10:25 PM DS01.15.10

Automating the Design of Dendronized Vesicles—The PACE² Framework [Akash Banerjee](#), Srinivas Mushnoori, Ethan Zang and Meenakshi Dutt; Rutgers, The State University of New Jersey, United States

Nanoparticles that block fundamental bacterial functions like quorum sensing could potentially replace conventional antibiotic therapies. Vesicles that bind interfacially to charged biomolecules could be used to block these quorum sensing pathways. Here, lipid-based vesicles consisting of dipalmitoyl-sn-glycero-3-phosphocholine lipids and polyamidoamine dendron-grafted amphiphiles (PDAs) are studied. PDAs have charged terminal groups that can electrostatically bind to oppositely charged biomolecules. Variation of the generation and relative concentration of PDAs could affect the functionality and stability of the vesicle. To identify the optimal control parameters, i.e., PDA generation and concentration, a large phase space of vesicles is studied as a function of the two parameters. For each model, a flat membrane is simulated under conditions that forces the membrane to bend its edges, eventually forming a spherical vesicle. This process, also known as membrane closing, entails several structural changes and hence there are numerous fluctuations in the system. This often leads to simulation failure. In this situation, a new set of conservative parameters, e.g. a smaller integration timestep, could be used to successfully proceed with the simulation. However, if the conservative parameter is used for the remaining duration of the simulation, the entire process will turn out to be computationally expensive and time consuming. In this study, a computational workflow is designed to divide the entire membrane closing process into multiple stages, each associated with a short simulation. Each simulation has a predetermined set of regular and conservative parameters. Analysis routines are weaved into the design of this workflow. On the basis of the performance of the previous simulation (success/failure), the analysis routines adaptively decide on an appropriate set of parameters (regular/conservative) for the next simulation. In this way, the membrane closing process is conducted efficiently without any human intervention. The workflow is generalized for biomolecular simulations and has been named PACE² (Pipeline for Automating Compliance Based Elimination and Extension). The PACE² framework lays out the process to investigate a large molecular parameter phase space to identify optimal designs for nanoparticles.

10:30 PM DS01.15.11

Machine Learning for Polyamide Carbon Nanotube Composite Membranes [Aaron Morelos-Gomez](#) and Morinobu Endo; Shinshu University, Japan

Given the increase in global population and the continuous depletion of fresh water sources, it is necessary to keep developing technologies to provide fresh water. Thus, seawater desalination is increasing in adoption and development. For this, membrane technology is capable of removing salts from water and providing fresh water, the most common membranes for this task are based on polyamide. Membrane desalination is characterized by permeate flux and salt rejection. Previously we have developed polyamide carbon nanotube composite membranes, with enhanced antifouling properties. In this work, we developed a machine learning (ML) model to predict permeate flux and salt rejection according to membrane synthesis conditions such as carbon nanotube concentration, m-phenylenediamine concentration, trimesoyl chloride concentration, and others. To construct the machine learning model we used feature selection and soft voting ensemble using data collected through two years of experimentation with salt rejections above 90%. The obtained ML model could predict permeate flux and salt rejection with R² of 0.8 and 0.4, respectively. Furthermore, we used Shapley additive explanations to extract feature importance that could give further insights of the ML model and membrane synthesis.

10:35 PM DS01.15.12

Autonomous Thin-Film Fabrication System for Exploring Solid Electrolytes [Shigeru Kobayashi](#)¹, Ryota Shimizu¹, Yasunobu Ando² and Taro Hitosugi¹; ¹Tokyo Institute of Technology, Japan; ²National Institute of Advanced Industrial Science and Technology (AIST), Japan

We recently developed a system that autonomously searches for the best conditions to fabricate thin-film materials. The system integrates a sputter deposition system, electrical resistance measurement system, and Bayesian optimization algorithm; the samples are transferred using robots to perform the closed-loop optimization. The system autonomously optimizes the deposition conditions to obtain the TiO₂ thin film with minimum electrical resistance.

[1]

In this study, the autonomous system was used to search for new lithium solid electrolyte materials. Two target materials, Li_3PO_4 and Li_2CO_3 , were co-sputtered onto a quartz substrate with comb-shaped Au electrodes. The sputtering power of each target was separately tuned to control the composition of films. The sputtering power and the flow rate of Ar/ N_2 process gas were optimized using the Bayesian optimization algorithm. The ionic conductivity of thin films was evaluated using AC impedance spectroscopy.

The ionic conductivity of thin films improved to 2~3 times higher than the simple amorphous Li_3PO_4 or Li_2CO_3 solid electrolytes within twelve experimental cycles. Such an autonomous system will accelerate the development of new materials from an expanded chemical space.

[1] R. Shimizu, T. Hitosugi *et al.*, APL Mater 2020, **8**, 111110.

10:55 PM BREAK

SYMPOSIUM DS02

Advanced Atomistic Algorithms in Materials Science
November 29 - December 8, 2021

Symposium Organizers

David Aristoff, Colorado State University
Enrique Martinez, Clemson University
Jutta Rogal, New York University
Gideon Simpson, Drexel University

* Invited Paper

SESSION DS02.01: Electronic Structure Models I
Session Chair: William Curtin
Monday Morning, November 29, 2021
Hynes, Level 2, Room 209

8:30 AM *DS02.01.01

Recent Advances in the PAOFLOW Method—Electronic and Optical Properties of Real Materials from Projections on Atomic Orbital Bases Marco Buongiorno Nardelli; University of North Texas, United States

First-principles electronic structure calculations are the state-of-the-art for solid-state physics, chemistry, and materials science; however, their predictive capability is constrained by the limitations on simulated length- and time-scale due to computational cost and the unfavorable scaling of the algorithms. In this talk, I will review recent progress in theoretical and computational tools for data generation and advanced characterization, and in particular, discuss the development and validation of the PAOFLOW framework for the generation of local basis representations for effective ab-initio tight-binding schemes. PAOFLOW is a software tool to efficiently post-process standard first principles electronic structure plane-wave pseudopotential calculations in order to promptly compute, from interpolated band structures and density of states, several quantities that provide insight on transport, optical, magnetic and topological properties such as anomalous and spin Hall conductivity, magnetic circular dichroism, spin circular dichroism, and topological invariants. After reviewing recent advances in the establishment of theoretical framework, including the generation of efficient atomic basis sets, I will illustrate the method with a few recent examples from our research on 2D ferroelectric materials, including the demonstration of a transistor prototype based on electrically switchable persistent spin helix and a memory device that exploits the domains of switchable spin textures and spin-to-charge conversion.

9:00 AM DISCUSSION TIME

9:15 AM DS02.01.05

Explanation of the Pressure Induced Invar Effect in Ni-Rich $\text{Fe}_{1-x}\text{Ni}_x$ Alloys Using Non-Collinear Magneto-Structural Relaxations from First Principles Amanda Ehn, Bjorn Alling and Igor A. Abrikosov; Linköping University, Sweden

Fcc structured Fe-Ni alloys containing 36 at.% Ni are known as Invar alloys. They are characterized by an anomalous low, practically zero, thermal expansion at room temperature and ambient pressure, a finding that awarded C.E Guillaume the Nobel Prize in Physics already 1920. It is clear that the origin of the Invar effect is linked to the magnetic properties of the material but a complete explanation for the effect is not yet agreed on. Phenomena such as Fe-moment spin flips, high-to-low-spin transitions, non-collinear magnetism, local chemical environments, and strong electron correlations have been considered as possible origins, which together possess a challenge for the state-of-the-art first-principles methods for disordered magnetic alloys. [1,2]

The Invar effect is known to disappear when the Ni composition is even slightly increased.[2] However, it was observed that the Invar effect could be

induced by high pressure also for Fe-Ni alloys with high Ni concentrations.[3]

In this study we investigate the origin of the pressure induced Invar effect in the disordered fcc $\text{Fe}_{1-x}\text{Ni}_x$ alloy for $x = 0.36, 0.50,$ and 0.75 from first principles calculations. We perform a large pool of different non-collinear supercell electronic structure calculations, and let the magnetic state and atomic structure gradually relax towards their most preferred states. Using this approach we observe a transition from ferromagnetic states to noncollinear or almost collinear spin-flipped states as the volume decreases for all three compositions. The volumes at which the transitions occur correspond to the volumes observed to display volume-pressure anomalies in previous experiments. Our study confirms that the pressure induced Invar effect is a result of a magnetic transition from a ferromagnetic state to a complex magnetic state in Fe-Ni alloys.

[1] van Schilfhaarde, M., Abrikosov, I. & Johansson, B. Origin of the Invar effect in iron–nickel alloys. *Nature* **400**, 46–49 (1999)

[2] E.F. Wassermann. The Invar problem. *Journal of Magnetism and Magnetic Materials*, 100(1):346-362, 1991

[3] Leonid Dubrovinsky, Natalia Dubrovinskaja, Igor A. Abrikosov, Marie Vennström, Frank Westman, Stefan Carlson, Mark van Schilfhaarde, and Börje Johansson. Pressure-induced Invar effect in Fe-Ni alloys. *Phys. Rev. Lett.*, 86:4851-4854, 2001

9:30 AM DS02.01.08

Transferable Models and Efficient Nonlocal Descriptors for Machine Learning Exchange-Correlation Functionals Kyle W. Bystrom and Boris Kozinsky; Harvard University, United States

Machine Learning (ML) is a promising approach to improve the accuracy of exchange-correlation (XC) functionals for Density Functional Theory (DFT). Two key developments are necessary to successfully leverage ML for XC functionals. First, because of the limited information provided by semi-local ingredients like the density and its gradient, computationally efficient, physically relevant, and nonlocal descriptors of the density or density matrix must be designed as input to the model. Building on our recently developed CIDER functional for the exchange energy, we explore possible improvements to the model as well as its computationally efficient implementation. We also investigate the application of ML to efficient, orbital-dependent ingredients like Rung 3.5 functionals [1]. Second, robust ML architectures and workflows must be developed to train functionals that are both accurate and transferable. We discuss how Gaussian Processes yield smooth and transferable models and how different regularization and training schemes impact the performance of parametric functionals.

[1] B. G. Janesko, *J. Chem. Phys.* 133, 104103 (2010); <https://doi.org/10.1063/1.3475563>

SESSION DS02.02: Electronic Structure Models II

Session Chair: Danny Perez

Monday Afternoon, November 29, 2021

Hynes, Level 2, Room 209

1:45 PM DS02.02.02

Late News: *Ab Initio* Electron Dynamics in High Electric Fields—Accurate Predictions of Velocity-Field Curves Ivan Maliyov, Jinsoo Park and Marco Bernardi; California Institute of Technology, United States

Electron dynamics in external electric fields governs the behavior of solid-state electronic devices. First-principles calculations enable precise predictions of charge transport in low electric fields. However, studies of high-field electron dynamics remain elusive due to a lack of accurate and broadly applicable methods. Here we develop an efficient approach to solve the real-time Boltzmann transport equation with both the electric field term and *ab initio* electron-phonon collisions. These nanosecond-long simulations provide field-dependent electronic distributions with a femtosecond resolution, allowing us to investigate both transient and steady-state transport in electric fields ranging from low to high (>10 kV/cm). The broad capabilities of our approach are shown by computing nonequilibrium electron occupations and velocity-field curves in Si, GaAs, and graphene, obtaining results in quantitative agreement with experiment. Our approach sheds light on microscopic details of transport in high electric fields, including dominant scattering mechanisms and valley occupation dynamics. Our results demonstrate quantitatively accurate calculations of electron dynamics in low-to-high electric fields. This method, implemented in our open-source code Perturbo [1], provides a timely and robust tool to advance the discovery and design of novel electronic materials.

[1] J.-J. Zhou, J. Park, I-Te Lu, I. Maliyov, X. Tong, M. Bernardi. *Comput. Phys. Commun.* **2021**, 264, 107970.

SESSION DS02.03: Molecular Dynamics Models

Session Chair: Marco Buongiorno Nardelli

Monday Afternoon, November 29, 2021

Hynes, Level 2, Room 209

2:45 PM DS02.03.01

Late News: Voltage Equilibration for Reactive Atomistic Simulations of Electrochemical Processes Alejandro Strachan¹, Nicolas Onofrio², Xavier Cartoixa³ and Laura Urquiza⁴; ¹Purdue University, United States; ²Institut Européen des Membranes, IEM, UMR 5635, Université Montpellier, France; ³Universitat Autònoma de Barcelona, Spain; ⁴Laboratoire des Solides Irradiés, École Polytechnique, Institut Polytechnique de Paris, France

We introduce electrochemical dynamics with implicit degrees of freedom (EChemDID), a model to describe electrochemical driving force in reactive molecular dynamics simulations. The method describes the equilibration of external electrochemical potentials (voltage) within metallic structures and their effect on the self-consistent partial atomic charges used in reactive molecular dynamics. An additional variable assigned to each atom denotes the local potential in its vicinity and we use fictitious, but computationally convenient, dynamics to describe its equilibration within connected metallic structures on-the-fly during the molecular dynamics simulation. This local electrostatic potential is used to dynamically modify the atomic electronegativities used to compute partial atomic changes via charge equilibration. Validation tests show that the method provides an accurate description of the electric fields

generated by the applied voltage and the driving force for electrochemical reactions. We demonstrate EChemDID via simulations of the operation of electrochemical metallization and valence change cells. The simulations predict the switching of the device between a high-resistance to a low-resistance state as a conductive filament is formed and resistive currents that can be compared with experimental measurements. In addition to applications in nanoelectronics, EChemDID could be useful to model electrochemical energy conversion devices.

3:00 PM DS02.03.02

Late News: All-Atom Simulation Method for Zeeman and Dipolar Assembly of Magnetic Nanoparticles [Akhlak-ul Mahmood](#) and Yaroslava Yingling; North Carolina State University, United States

Magnetic Nanoparticles (MNPs) can organize into novel structures in solutions with excellent order and geometry that are important for many industrial and biomedical applications. Studies of self-assembly of smaller MNPs is challenging due to the complicated interplay between VDW, electrostatic, dipolar, steric, hydrodynamic, and external magnetic field interactions. An all-atom molecular dynamics (AMD) simulation technique can decipher such complex interactions and can account for the effect of the MNP core, surfactant layers, solvent molecules. Here we present a novel AMD simulation method to study the dynamics, self assembly and properties of MNPs structures with various particles size and shapes, surfactant and solvents. We demonstrate the use and effectiveness of the model by simulating the self-assembly of several commonly obtained equilibrium structures like ring, line, chain, clusters by oleic acid surfactants coated spherical and cubic Magnetite (Fe_3O_4) nanoparticles in vacuum and in explicit solvents and under the presence of a uniform external magnetic field. We found that the long-range electrostatic interactions can favor chain formation over rings, the VDW and steric interactions by the surfactants promote MNPs cluster growth and the interplay of solvent and increased surface energy can reduce the rotational diffusion of the MNPs. The algorithm has been parallelized to take advantage of multiple processors of a modern computer and can be used as a plugin for the popular LAMMPS simulation software to study the behavior of small magnetic nanoparticles and gain insights into the physics and chemistry of different magnetic assembly processes with atomistic details.

SESSION DS02.04: Molecular Dynamics I

Session Chair: Steven Kenny

Tuesday Morning, November 30, 2021

Sheraton, 5th Floor, Public Garden

10:30 AM DS02.04.01

REACTER 2.0: Quantum-Informed Reaction Constraints and Automated Interaction Typing [Jacob Gissing](#) and Kristopher E. Wise; NASA Langley Research Center, United States

REACTER is a heuristic method for modeling chemical reactions in classical molecular dynamics simulations, implemented in LAMMPS as *fix bond/react*. The authors recently extended LAMMPS to support alphanumeric labels for atom types, bond types etc., which enables the pre- and post-reaction templates required by the REACTER protocol to be portable between different simulations and greatly simplifies the task of creating simulation-ready reaction templates. To further increase the generality of reaction templates, support for wildcard characters within atom types has been added, along with the automatic assignment of interaction types for new bonds, angles, etc. based on the involved atom types. In some cases, this feature can express a class of reactions with one pair of reaction templates, where previously dozens may have been required. Advanced reaction constraints have also been added, including an Arrhenius constraint to enforce an effective activation energy, a root-mean-square-deviation option for complex geometrical constraints, as well as a custom constraint that leverages LAMMPS' powerful built-in variable framework. Other new features include variable support for various inputs (e.g. to allow reaction rates or cutoffs to be dependent on overall conversion), on-the-fly update of molecule IDs, and the ability to create new atoms positioned with respect to the reaction site. The new features are applied to modeling polymeric, thermosetting and composite materials, and advanced applications of the new reaction constraints are demonstrated. For example, REACTER is shown to accurately reproduce mechanically-induced bond breaking, as characterized by third-order DFT-based tight-binding (DFTB3) simulations, via a constraint on the total potential energy of the involved atoms.

10:45 AM DS02.04.02

Extension of an Atomistic Grain Tracking Algorithm for Analysis of CdTe/CdS Structures [Sharmin Abdullah](#)¹, Xiaowang Zhou², Rodolfo Aguirre¹ and David Zubia¹; ¹The University of Texas at El Paso, United States; ²Sandia National Laboratories, United States

Grain structures impact Cadmium Telluride/ Cadmium Sulfide (CdTe/CdS) solar cells since grain boundaries can act as recombination centers for carriers. Computer simulations such as molecular dynamics (MD) can be a convenient and cost-effective method for investigating the evolution of grain structures during the growth of materials. Recently, MD simulations have been successfully applied to study the growth of polycrystalline CdTe/CdS structures, revealing complex zincblende and wurtzite grains along with highly disordered atoms that are often observed in experiments. However, little efforts have been made to quantify the grain structures observed in MD simulations in literature. In this work, the grain tracking algorithm originally developed by Panzarino et al. has been extended for polycrystalline CdTe/CdS structures. Specifically, we focus on the face-centered-cubic (fcc) sublattice of the zincblende crystal structure. The common neighbor analysis and centrosymmetric parameter values are used to calculate the orientation of each atom in the grain tracking algorithm. We then apply this modified approach to analyze the CdTe/CdS films obtained from our MD polycrystalline growth simulations. We demonstrate that our method can provide a variety of useful information such as grain domains, grain orientations, plane indices, and sample texture. Moreover, kinetic analysis of microstructure evolution of the materials can be performed. These results will add to the understanding of granular microstructure that can describe physical, chemical, mechanical, and electronic properties.

11:00 AM DS02.04.03

Atom-Centered Electronic Heat Transport Within Electron-Ion Coupled Classical Molecular Dynamics [Artur Tamm](#) and Alfredo A. Correa; Lawrence Livermore National Laboratory, United States

Atomistic modeling of metallic systems needs the inclusion of electron-ion interactions in order to have realistic dynamics. For example, it is generally known that around 20% of the projectile's kinetic energy could be absorbed by the electrons and redistributed within the metallic system outside the collision cascade. Capturing this in classical molecular dynamics is rather challenging as these simulations usually do not include explicit electrons. We present a novel model that captures both the electron-ion interactions as well as energy transport within the electronic system. Our Langevin based stochastic model is able to capture the non-adiabatic collective dynamics of phonons. Moreover, we have demonstrated that we can also apply the same model to the high energy events, such as radiation damage. In this work, we present an important aspect of electronic heat transport - we have developed an

atom based diffusion model where energy is transferred directly between atoms, taking into account convective transport of electronic energy. Our model reproduces the macroscopic heat diffusion behaviour, but is also able to incorporate environment dependent and hydrodynamics effects. Furthermore, the model is coupled to the Langevin based electron-ion model, thus creating a unified approach for enabling classical molecular dynamics with electronic effects. We will present the theoretical aspects of the model as it is implemented in an extension for LAMMPS code. Finally, we present an application of compression shockwave dynamics through a system consisting of a metal and an insulator. This example demonstrates the strength of our approach, as electronic heat is transported both by diffusion and convection.

This work performed under the auspices of the U.S. Department of Energy by Lawrence Livermore National Laboratory under Contract DE-AC52-07NA27344.

11:15 AM DS02.04.04

Using Virtual Sites for Coarse-Grained Simulations of Conjugated Polymers and Organic Semiconductors Puja Agarwala, Shreya Shetty, Enrique D. Gomez and Scott T. Milner; The Pennsylvania State University, United States

The local structure of conjugated polymers is vital for many optoelectronic properties, such as charge conduction and charge photogeneration at donor-acceptor interfaces. We perform molecular dynamics simulation in Gromacs to study the local arrangement of these polymers. Conjugated polymers have aromatic rings as repeat units. Due to the stiffness and large size of these polymers, atomistic simulations are computationally expensive. Hence, to increase simulation efficiency, we exploit the stiffness of aromatic moieties using virtual sites to represent multiple atoms within each ring. These virtual sites do not have mass but contain electronic properties; hence, we significantly reduce degrees of freedom while retaining the shapes and dipole moments of the aromatic rings. As a result, these simulations are ~10 times faster compared to atomistic simulations. We simulate poly(3-hexylthiophene-2,5-diyl) (P3HT) and rhodanine-benzothiadiazole-coupled indacenodithiophene (O-IDTBR), as well as mixtures of these two materials. Our simulations predict a persistence length of 3.8 nm, a density of 0.91 kg/m³ for P3HT, and an amorphous scattering profile that compare well to experimental results. In addition, the crystal structure of IDTBR is stable when arranged in experimentally-determined unit cell parameters. Our simulations allow us to examine equilibrated molecular configurations at the interface of P3HT and IDTBR, and reveal preferences in terms of contacts between specific moieties.

SESSION DS02.05: Machine Learning Potentials I

Session Chair: Laura Lopes

Tuesday Afternoon, November 30, 2021

Sheraton, 5th Floor, Public Garden

1:30 PM DS02.05.01

Machine-Learning-Aided Development of Analytical Empirical Forcefields for Glasses Mathieu Bauchy; University of California, Los Angeles, United States

Modeling glasses requires extended timescales—since their simulation involves the slow cooling of a liquid into an out-of-equilibrium disordered solid. As such, reliable, yet computationally efficient empirical interatomic forcefields are key to facilitate the modeling of glasses. Although analytical forcefields offer optimal computational efficiency, their parametrization is challenging as the high number of parameters renders traditional optimization methods inefficient or subject to bias. Here, we present a new parametrization method based on machine learning, which combines *ab initio* molecular dynamics simulations, Gaussian Process Regression, and Bayesian optimization. By taking the examples of silicate and chalcogenide glasses, we show that our method yields new interatomic forcefields that offer an unprecedented agreement with *ab initio* simulations, at a fraction of computational cost. This method offers a new route to efficiently parametrize new interatomic forcefields for disordered solids in a non-biased fashion.

1:45 PM *DS02.05.02

An Entropy-Maximization Approach for the Generation of Training Sets for Machine-Learned Potentials Joshua Brown¹, Mariia Karabin² and Danny Perez¹; ¹Los Alamos National Laboratory, United States; ²Oak Ridge National Laboratory, United States

The last few years have seen considerable advances in the development of machine-learned interatomic potentials. A very important aspect of the parameterization of transferable potentials is the generation of training sets that are sufficiently diverse, yet compact enough to be affordably characterized with high-fidelity reference methods. We formulate the generation of a training set as an optimization problem where the figure of merit is the entropy of the distribution of atom-wise descriptors. This can be used to create a fictitious potential to explicitly drive the generation of new configurations that maximally improve the diversity of the training set. I will show how this strategy can provide an automated and scalable solution to generate large training sets without human intervention.

2:15 PM DS02.05.03

Active Learning of Many Body Coarse Grained Potentials with Gaussian Process Regression Blake Duschatko, Jonathan Vandermause, Nicola Molinari and Boris Kozinsky; Harvard University, United States

In recent years, machine learning has been used to improve the training and simulation efficiency of “bottom-up” coarse grained potentials, which guarantee the preservation of thermodynamic quantities in the coarse grained space [1]. While these potentials can be used to capture the physics of systems on large length and time scales that are traditionally inaccessible with molecular dynamics, they are known to generally have a high degree of complexity.

It has been shown that Gaussian process regression can be used as a framework for active learning of force fields from *ab initio* data [2], and we extend this idea to coarse grained models. In particular, we study the utility of active learning over passive learning schemes in the efficient modeling of coarse grained potentials. Moreover, we examine how Gaussian processes can be used as a tool to better understand the importance of model complexity in coarse grained problems.

[1] W. G. Noid, Jih-Wei Chu, Gary S. Ayton, Vinod Krishna, Sergei Izvekov, Gregory A. Voth, Avisek Das and Hans C. Andersen. “The multiscale coarse-graining method. I. A rigorous bridge between atomistic and coarse-grained models,” *J. Chem. Phys.* 128, 244114 (2008).

[2] Jonathan Vandermause, Steven B. Torrisi, Simon Batzner, Alexie M. Kolpak, and Boris Kozinsky. Submitted. “On-the-Fly Bayesian Active Learning of Interpretable Force-Fields for Atomistic Rare Events,” *NPJ Computational Materials* 6 (2020).

2:30 PM *DS02.05.04

Empirical Potentials for Complex Systems [Steven D. Kenny](#), Iain Brown, Jiawei Zhou and Roger Smith; Loughborough University, United Kingdom

Many Materials Science problems of interest involve a number of atomic species and this often makes deriving potentials for these systems very challenging. In this work we will present simulations on dopants and interfaces in systems based on ZnO that have been modelled using a ReaxFF potential approach, using machine learning methods to fit the potentials. This is an important transparent conducting oxide system and the doping of it and the interfaces of it and other materials are often critical in the mechanical performance of devices that utilise this. We will also present work on using a machine learning potential to study high entropy ceramic materials and compare this with ab-initio calculations on these systems.

SESSION DS02.06: Machine Learning Aided Modeling I

Session Chair: Danny Perez

Tuesday Afternoon, November 30, 2021

Sheraton, 5th Floor, Public Garden

4:00 PM DS02.06.01

Building Useful Machine-Learned Interatomic Potentials [Gus L. Hart](#)¹, Hayden Oliver¹, Brayden Bekker¹, Alexander Shapcev², van der Oord Cas³ and Gabor Csanyi³; ¹Brigham Young University, United States; ²Skolkovo Institute of Science and Technology, Russian Federation; ³University of Cambridge, United Kingdom

Machine-learned interatomic potentials are far more expressive than traditional physically motivated interatomic potentials like Lennard-Jones, Stillinger-Weber, Embedded Atom Potentials, etc. While they can be far more accurate, they are also more likely to be completely wrong outside of the training domain, are more difficult to train reliably, and are computationally expensive. We have developed MLIPs for the Hf-Ni-Ti shape memory alloy. We share cautionary tales, best practices for generating training sets, and demonstrate how community tools make for "easy entry" to realistic thermodynamic modeling with these potentials.

4:15 PM DS02.06.02

Unsupervised Machine Learning for Autonomous Parameterization of Classical Hamiltonian [Aditya Koneru](#)^{1,2}, Henry Chan^{1,2}, Sukriti Manna^{1,2}, Troy Loeffler^{1,2} and Subramanian Sankaranarayanan^{1,2}; ¹University of Illinois at Chicago, United States; ²Argonne National Laboratory, United States

We introduce an unsupervised machine learning workflow to autonomously parameterize Tersoff Bond Order Potential using two-dimensional (2D) materials as a representative example. This is a 14-dimensional space and even with the state-of-the-art techniques, the decision of fixing the search boundaries still remains a daunting task. This has been tackled by continually sampling the potential energy surface using the Latin Hypercube Sampling (LHS) technique starting with an arbitrary search bounds. The high dimensional parameter space is projected into a low-dimensional space using Principal Component Analysis (PCA) and are tagged with corresponding energy values estimated from molecular dynamic simulations using LAMMPS. We next employ clustering techniques to identify the range of parameter sets that fall in the desired energy space. A simplex optimization is performed next to identify the parameter set with energies close to the actual energies and guide the range selection for the next iteration. We demonstrate that the search can autonomously achieve target minima on the potential energy surface - a bond order model developed for Carbon 2D polymorphs outperforms existing parameterizations. Our workflow represents an elegant method to overcome issues with selection of parameter ranges and weights for multiobjective high-dimensional optimization of force-field parameters.

4:30 PM DS02.06.03

Graph Attention Networks for Predicting Materials Properties [Taylor D. Sparks](#)¹, Debjit Sarkar² and Sourodeep Roy²; ¹Univ of Utah, United States; ²Jadavpur University, India

Graph neural networks are powerful tools for representing a wide variety of subjects. In recent years these tools have become state of the art for the social network domains and elsewhere. However, they are relatively new in the field of materials science. Prior approaches utilizing graphs such as CGCNN or MolCLR do not utilize the breadth of feature tools available in social networks and these could offer advantages when representing compounds. In this work, we apply graph attention networks (a variant of graph neural networks) on a graph representation of inorganic compounds including unique global, edge, and node features to create representation vectors for the whole graph. Emphasis is placed on learning relations of bonds rather than nearest neighbors by relying on chemical domain knowledge such as dipoles and electronegativity. Node features are extracted through clustering algorithms and neighbor-based encoding. Global features will include bonding motifs, structural topology characteristics, composition-based feature vector, clustering coefficients, and thermodynamic descriptors. Models are constructed to predict material properties and the attention map attribute of the graph attention network is used to learn and visualize the importance of the information obtained from neighboring nodes.

4:45 PM *DS02.06.04

Estimation of Errors in the Prediction of Long Time Scale Properties with Machine Learning Potentials for Fusion Materials [Laura J. Lopes](#) and Danny Perez; Los Alamos National Laboratory, United States

In the development of new machine learning potentials, it is essential to guarantee the correct description of the properties of interest. Our goal is to correctly describe long time scale properties of fusion materials to simulate the surface degradation caused by the contact with the plasma. In order for that to be accomplished, it is necessary to estimate the errors made for those properties by candidate potentials. In this work we developed a method to estimate confidence intervals for the calculation of energy barriers using the SNAP potential.

5:15 PM DS02.06.05

Multitask Machine Learning of Collective Variables for Enhanced Sampling of Rare Reaction Events [Lixin Sun](#), Jonathan Vandermause, Simon L. Batzner, Yu Xie, Steven B. Torrisi, Wei Chen and Boris Kozinsky; Harvard University, United States

Collective variables (CVs), a low dimensional representation of atomic structures, are the cornerstone of many enhanced sampling techniques that enable efficient free energy landscape explorations. Conventionally, CVs are simple geometric descriptors, such as atomic bonds and angles. However, it often needs intuition and trial-and-error testing to determine which CV can lead to accurate free energy calculations and efficient sampling.

In this work, we demonstrate a data-driven method to learn CV with a multitask learning framework. Short molecular dynamics simulations around the transition states and basins are used to train a multitask network consisting of an encoder that encodes atomic structures to a low dimensional latent space and two separate downstream parts that map the latent space to predictions of basin class labels and potential energies. The trained latent space can be used as an effective CV for umbrella sampling bias and free energy calculations. This learning framework is demonstrated on model systems, small molecules, and metal surfaces.

[1] L Sun et al., Multitask machine learning of collective variables for enhanced sampling of rare events, arXiv preprint arXiv:2012.03909

SESSION DS02.07: Poster Session
Session Chair: Gang Lu
Tuesday Afternoon, November 30, 2021
8:00 PM - 10:00 PM
Hynes, Level 1, Hall B

DS02.07.01

Investigating the Protein Corona and Bio-Nanointerface Interactions of the CNT-BSA with Molecular Dynamics Simulations Ankarao Kalluri¹, [Catherine Tang](#)², Bhushan V. Dharmadhikari³, Prabir Patra^{4,4} and Challa V. Kumar^{1,2,2}; ¹University Of Connecticut, United States; ²University of Connecticut, United States; ³University of Minnesota, United States; ⁴University of Bridgeport, United States

Fundamental understanding of the nanotube-protein interactions at the interface is a crucial issue for the development and rational design of the various biocompatible and hybrid bionanomaterials for applications in bio-sensing, biocatalysis, and drug delivery. We investigated the interactions of bovine serum albumin (BSA) with multi-walled carbon nanotubes (MWCNT) by all-atom molecular dynamics (MD) simulation. MD simulations indicated that hydrophobic, van der Waals (VDW), electrostatic, and hydrogen bonding interactions contribute to the total binding, and these components have been separated out in our work. As a cutoff distance of 5\AA used to see the bio-nano surface interactions observed between CNT and BSA surface for 80 ns MD simulation. Analysis of binding components of the total interaction energy (-63 Kcal/mol) shows that the driving force of the binding is mainly hydrophobic (-30 Kcal/mol) interactions by the non-polar side chain residues (valine314, proline302 & 303, ala311). CNT interacts with positively charged residues (Arg and lysine312) negatively charged residues (Glu 299 & 310, Asp 311) in proteins through the cation- π and anionic- π interactions, respectively. Notably, the BSA molecular structure and function preserved largely after its adsorption on the CNT surface. By investigation of the protein adsorption on the CNT surface would be helpful to better understand the stability and bio-nanosurface interactions at a molecular level.

Keywords: protein corona, carbon nanotubes molecular dynamics, hybrid bionanomaterials

SESSION DS02.08: Coarse Grain Models I
Session Chair: Kristen Fichthorn
Wednesday Morning, December 1, 2021
Sheraton, 5th Floor, Public Garden

10:30 AM *DS02.08.01

Time-Scale Decoupling in Mass Transport Computations Reveals a Law of Total Diffusion [Manuel Athenes](#)¹, Gilles Adjanor² and Jérôme Creuze³; ¹Université Paris-Saclay, CEA, France; ²EDF Lab, France; ³Université Paris-Saclay, CNRS, France

Directly computing mass transport coefficients in stochastic models requires integrating over time the equilibrium correlations between atomic displacements. Here, we show how to accelerate the computations by decoupling short- and long-time correlations, which statistically amounts to conditioning the mass transport estimator through a law of total diffusion. We illustrate the approach with kinetic path sampling simulations of atomic diffusion in alloys where percolating solute clusters trap the mediating vacancy. There, Green functions serve to generate first-passage paths escaping the traps and to propagate the long-time dynamics. When they also serve to estimate mean-squared displacements via conditioning, colossal reductions of statistical variance are achieved.

11:00 AM DS02.08.02

Energy Renormalization for Coarse-Graining of Conjugated Polymer for Prediction Thermomechanical Behaviors [Zhaofan Li](#); North Dakota State University, United States

Conjugated polymers (CPs) possessing the characterization of relatively rigid conjugation backbone and peripheral flexible side chain have attracted considerable attention toward the application of organic electronic and optoelectronic devices. The computational prediction of the thermomechanical behavior of CPs to serve the needs of materials design and prediction of their functional performance is a grand challenge due to the prohibitive computational times of all-atomistic (AA) molecular dynamic (MD) simulations. Atomistically informed coarse-grained (CG) modeling is an essential strategy for making progress on this problem. In this work, focusing on the widespread explored regioregular poly(3-hexylthiophene) (P3HT), we develop a temperature-transferable CG model based upon the energy-renormalization (ER) approach that allows for modeling of CPs dynamics over a wide temperature range and accessing greater spatiotemporal scales. The results show that the CG model faithfully and accurately capturing the short- and long-timescale dynamics, *i.e.*, Debye-Waller factor and segmental relaxation time. Systematically exploration of the mechanical properties, such as tensile and shear, reveals that the cohesive interaction exhibits a great impact on the mechanical response. Our work highlights the necessity and feasibility of ER when modeling a conjugated polymer that possesses branched architecture, and sheds new light on the rational design of the temperature-transferable CG model of complex polymers for their thermomechanical and conformational prediction.

11:15 AM DS02.08.03

Late News: Combined Molecular Dynamics/Monte Carlo Simulation Study of the Mechanism(s) of Cu Thin Film Growth on TiN Substrates [Reza](#)

Namakian, Brian R. Novak, Xiaoman Zhang, Wen Jin Meng and Dorel Moldovan; Louisiana State University, United States

We tailored and calibrated a sequential molecular dynamics (MD)/time-stamped force-bias Monte Carlo (tfMC) simulation methodology to investigate the growth mode, the resulting crystalline structure, and orientation of Cu thin films obtained by sputter deposition on epitaxial TiN substrates. Our studies reveal for the first time that at the very early stage of growth, BCC-Cu grows pseudomorphically on the TiN(001) substrate as a very thin continuous film with the BCC-Cu[001]/TiN[001] growth direction. As the Cu thin film thickness increases the film transforms, through the Nishiyama-Wasserman mechanism, from BCC into predominantly FCC-Cu with abundant nanotwins, which is the same type of structure obtained in the experiment conducted here via a dc magnetron sputter deposition technique to grow Cu on TiN001 at 105 °C [1]. The MD/tfMC simulations also reveal that on the N-terminated TiN(111), Cu shows a very poor wettability and the FCC-Cu(111) film grows vertically in the form of tall 3D islands. On Ti-terminated TiN(111) surface, however, FCC-Cu(111) initially grows in the form of 2D islands with high wettability. With additional Cu deposition, a triangular misfit dislocation network is generated at the Cu(111)/Ti terminated TiN(111) interface with subsequent formation of a two-layer nanotwin with its twinning plane parallel to the surface substrate. The present simulation results provide deep insights into some complexities of the growth mechanisms operating during Cu growth on TiN and shed light on related thin film growth in weakly-interacting metal/substrate systems.

[1] X.M. Zhang, S. Shao, A.S.M. Miraz, C.D. Wick, B.R. Ramachandran, W.J. Meng, Low temperature growth of Cu thin films on TiN(001) templates: Structure and energetics, *Materialia*, 12, 100748 (2020).

* Work funded in part by the NSF EPSCoR program, awards OIA-1541079 and OIA-1946231.

11:30 AM DS02.08.04

An Efficient Computational Framework for Prediction of Charge Density Symmetry in Twisted Bilayer Graphene Tawfiqur Rakib¹, Elif Ertekin¹, Pascal Pochet² and Harley Johnson¹; ¹University of Illinois at Urbana-Champaign, United States; ²Univ. Grenoble-Alpes and CEA, France

The discovery of correlated insulating states at half filling at a twist angle of 1.08° known as the magic angle has stirred tremendous interest in twisted bilayer graphene (TBG). Such exotic physics and electronic properties are intrinsically dependent on the atomic structure of the material. In TBG, a periodic variation of different stacking regions emerges from the relative rotation between the graphene layers. At large twist angles (> 1.47°), the positions of the atoms are well-described by considering a rigid rotation between the individual graphene layers. However, the symmetry changes significantly for low twist angles (< 1.47°) due to atomistic relaxations that expand the stable AB stacking region while shrinking the size of the AA and SP stacking regions. While this atomic relaxation is very well-described in the literature, the effect of the symmetry change on the charge density of TBG remains unexplored since electronic structure calculations at small twist angles require large, and often computationally infeasible, supercells. Therefore, we develop a computationally efficient framework that enables the exploration of the charge density symmetry of low twist angle TBG. Our approach is based on the evolution of the high intensity Bragg peaks in the Fourier representation of the charge density, obtained from density functional theory, as the twist angle decreases. The structural relaxation is found to correspond to low intensity satellite peaks in the Fourier representation. By accounting for these satellite peaks, it is possible to observe the transformation of symmetry in the charge density distribution from high to low twist angle TBG. One striking outcome of our framework is the observation of electron localization in the AA region of low twist angle TBG. The framework shows clearly the effects of atomistic relaxations on the symmetry of the charge density of TBG at small twist angles, which may be useful for better understanding of the exotic physics of TBG.

11:45 AM DS02.08.05

Photopolymer Resin Design with Reactive Coarse-Grained Molecular Dynamics—Reaction Mechanism as a Variable John J. Karnes¹, Todd H. Weisgraber¹, Caitlyn C. Cook¹, Daniel N. Wang¹, Jonathan C. Crowhurst¹, Christina A. Fox^{1,2}, Bradley Harris², James S. Oakdale¹, Roland Faller² and Maxim Shusteff¹; ¹Lawrence Livermore National Laboratory, United States; ²University of California, Davis, United States

Coarse-graining (CG) approaches reduce the total number of particles in molecular dynamics (MD) simulations and often enable the use of longer integration time steps. Both of these effects serve to reduce computational expense and therefore provide access to larger length and time scales for a given system. The Martini model is a widely used CG force field, flexible and transferrable enough to find applications ranging from biological to polymer-based systems, including reactive CG MD simulations. However, CG models like Martini typically combine several atoms into a representative 'bead,' meaning that individual reaction sites effectively disappear as atomic identities are absorbed into the Martini beads. In this work we use this loss of specificity as a tool that enables the simulation of different chemical reaction mechanisms that may arise from the same CG model. This approach therefore isolates reaction mechanism as the variable in these simulations.

As proof of concept, we consider monomers that share a similar molecular mechanical description but polymerize by different mechanisms: radical chain-growth polymerization and radical step-growth polymerization. We represent these physically similar monomers with the same CG model, a 'Universal Monomer,' and use reactive CG MD simulations to prepare highly crosslinked thermosets of each monomer. Since the monomers are represented by precisely the same model, differences observed in the polymerization reactions or in the mechanical properties of the resulting thermosets are a function of the reaction mechanism. We compare on-the-fly simulated polymerization, network topology, and simulated mechanical testing of the two reactive CG MD systems and discuss related experimental results. Further, we suggest that this Universal Monomer approach is a reasonable survey of 'mechanism-space' with application to the rational design of chemical feedstocks for photopolymerization-based additive manufacturing techniques.

This work was performed under the auspices of the U.S. Department of Energy by Lawrence Livermore National Laboratory under Contract DE-AC52-07NA27344, IM release number LLNL-ABS-823466.

SESSION DS02.09: Accelerated Methods I
Session Chair: Manuel Athenes
Wednesday Afternoon, December 1, 2021
Sheraton, 5th Floor, Public Garden

1:30 PM DS02.09.01

Atomistic Propagation of the Aluminum Oxide/Aluminum Interface Vrinda Somjit and Bilge Yildiz; Massachusetts Institute of Technology, United States

Identifying the aluminum oxide/aluminum ($\text{Al}_2\text{O}_3/\text{Al}$) interfacial structure is important to improve the performance of the wide range of applications that employ this interface, such as to mitigate sources of noise in superconducting electronic devices and to improve the chemical and mechanical properties of corrosion coatings and structural composites. It will also help gain deeper understanding of oxide propagation into the metal in this fundamental system. However, the structure of the interface has not been resolved at the atomic scale, and the stages of growth of the oxide into the metal are unknown. Experimental studies claim that the interface is sharp, coherent and indicate the presence of undercoordinated aluminum atoms, but provide no information on the atomic arrangement at the interface. Computational studies have primarily only looked into the stability of different terminations of the oxide on the metal, computed the work of adhesion, electronic structure, etc. Given that the interface presents an environment vastly different from either the bulk oxide or metal, it is likely that it has different structural features and properties. In this study, we utilize ab initio Grand Canonical Monte Carlo, a physically motivated, bias-free method, to accurately search the interface configuration space and understand the structure and evolution of the interface. We show that 12.5% aluminum vacancies are present at the interface at the oxide/metal equilibrium. As the oxygen chemical potential is gradually increased, the interface propagation appears to occur in a layer-by-layer fashion. Oxygen is first incorporated at the FCC hollow sites at the interface, and then at the tetrahedral interstitial sites. This resembles oxygen incorporation at the Al(111) surface, after which the stacking sequence of Al_2O_3 is regained. We also discuss the trends in bond lengths, coordination environment and electronic structures of these interfacial configurations. The results of this study have implications for interfacial defect transport, charge trapping and adhesion.

1:45 PM DS02.09.02

Kinetic Monte Carlo Simulations of Nanowin Formation in FCC Metal Thin Films [Shefford P. Baker](#), Nathaniel G. Rogers and Derek H. Warner; Cornell University, United States

FCC metal thin films produced by atom-by-atom deposition methods can be formed with dense arrays of parallel coherent twin boundaries (CTB's) having average spacings in the nanometer regime. There has been great interest in these nanotwinned structures due to their expected unusual properties. To access those properties, it must be possible to control the average CTB spacing. Yet demonstrations of experimental control remain elusive and existing models (molecular dynamics simulations, phase field and analytical models) provide conflicting predictions. We have simulated nanotwin formation as a function of deposition rate and temperature on (111) surfaces in FCC metal thin films using a rejection-free kinetic Monte Carlo (KMC) approach. In our simulations, atoms are added to a 2-D hexagonal lattice and moved according to an energy landscape that accounts for the differences in transitions between twin and FCC sites using an adaptation of the variable step size method. Rates and temperatures that mimic experimental conditions are used. Layer growth occurs by nucleation, growth, and island interaction. However, interactions with simulation cell boundaries strongly influence results and a choice between cell sizes small enough to run many times for good statistics and large enough to obtain realistic behavior limited predictive capabilities. We find that for experimentally relevant rates, temperatures, and grain sizes, nanotwin formation takes place in the nucleation-dominated regime and developed an analytical model based on the KMC methods to describe this. Predictions for nanotwin formation are described.

2:00 PM *DS02.09.03

An Adaptive Hyperdynamics Method [Kristen A. Fichthorn](#); The Pennsylvania State University, United States

Accelerated molecular dynamics methods have the capability to increase the time scales probed in rare-event simulations by orders of magnitude, with no loss in accuracy. However, these methods have not been widely applied because of several drawbacks. In hyperdynamics, one of these drawbacks is the appropriate choice of the boost potential. If the boost is too high, the simulation can be inaccurate. If the boost is too low, the method is ineffective. Obtaining an optimal boost requires detailed knowledge of the underlying free-energy surface, which is computationally demanding. However, with advances in parallel computing, this problem is becoming tractable. In this work, we introduce an adaptive hyperdynamics method for global hyperdynamics that can predict optimal parameters for the bond-boost potential. By quantifying the probability distribution for a rare event to occur within a time t as a function of the boost, we observe a stair-like property. We can correlate stair steps with features of the boosted potential surface in a way that allows us to avoid inaccuracies associated with too large of a boost. We have implemented this method using a Python wrapper that allows us to test boosts for many replicas of a system in parallel, so a near-optimal boost can be identified relatively rapidly. The method is currently applicable to rare events governed by a potential-energy barrier, but extensions are possible in the future. We demonstrate the method in simulations of metal nanostructures in solvent with adsorbed capping molecules, a problem relevant to the shape-selective growth of metal nanocrystals.

2:30 PM DS02.09.04

Generalizable Kinetics Models of Hydrocarbon Pyrolysis from Molecular Dynamics Simulations for Combined Solid and Molecular Phases [Vincent Dufour-Decieux](#)¹, Rodrigo Freitas² and Evan Reed¹; ¹Stanford University, United States; ²Massachusetts Institute of Technology, United States

Building a chemical kinetics model traditionally requires conducting many experiments over the course of several years. Recently developed atomistic simulations had made it possible to develop kinetics models within months, using the large amount of data generated by these simulations. These kinetics models allow scientists to predict the chemical evolution of complex systems that can involve several thousands of reactions and species, while reducing computation time by up to four orders of magnitude compared against atomistic simulations. When building these kinetics models, there are usually two frameworks depending on the size of the species that are being studied. First, a kinetics model usually used for gas phase systems: this type of kinetics model has been thoroughly studied and can involve several thousands of molecules and reactions. The reactions are described using molecules, but this description prevents such a kinetics model from studying larger molecules, because these kinetics models fail to predict the creation and the reactivity of unobserved molecules. The second type is used for long chains or solids, like in polymer growth or soot formation. These models are usually simplified to include only a few reactions occurring at some reacting sites. This description is not adapted to smaller molecules, and the reduced number of reactions cannot always reflect the complexity that these processes have. These two frameworks have shown successes throughout the years, but there is a lack of kinetics models that would span across all these different systems, starting from small molecules and going all the way to solid particles.

In this work, we propose a new description for reactions in kinetics models that allows us to study small particles and large clusters: the atomic-level features. In our proposed approach, the reactions are described by the atoms surrounding the reactive site. This description resonates with the approach used for long chains and solids, but it is also applied to small molecules, resulting in a model that can describe both sizes. To demonstrate the efficiency of our approach, we study carbon particle growth in the atmosphere of icy giant planets. In this application, the initial composition is liquid methane which then grows into long hydrocarbons chains. The mechanism here is not fully understood, and a kinetics model that could describe accurately the three different states that this system goes through is needed. We demonstrate that the atomic description of reactions outperforms the molecular description on the prediction of the larger chain growth, while maintaining similar accuracy on the small molecules. This is achieved because the atomic features allow the creation of molecules unobserved in the training set, in addition to accurately predicting their reactivity. Furthermore, the atomic-level model requires fewer unique reactions than a conventional molecular-level model. This induces a more accurate estimation of the reaction rates and the ability to parametrize the kinetics model with less data. A corollary of this ability is that it is possible to extrapolate in time and in size using the atomic-level features. Finally, the atomic kinetics model can be transferred to different starting molecules while maintaining a high level of accuracy. Therefore, we find

that our proposed atomic featurization of reactions enables simultaneous description of small molecules and large clusters.

2:45 PM DS02.09.05

Atomistic Multi-Lattice Kinetic Monte Carlo (KMC) Modeling of Hyperthermal Oxidation of Multi-Layer Graphene [Sharon Edward](#) and Harley Johnson; University of Illinois at Urbana Champaign, United States

Thermal protection systems (TPS) in hypersonic vehicles are primarily made from carbon-based materials, due to the high heat capacity and high energy of vaporization of carbon, which protects the vehicles from damage in reentry conditions. However, at very high temperatures, reactions with oxygen cause the erosion of the TPS through formation of CO and CO₂. In this work, we model defect generation in multi-layer graphene due to adsorption and diffusion of oxygen using an atomic scale multi-lattice KMC approach. Simulations based on this KMC model reveal details of the pitting process driven by atomic oxygen in multi-layer graphene for specific temperatures and partial pressures of atomic and molecular oxygen. The model is developed using separate, interacting lattices for the carbon and oxygen sites. The carbon lattice includes all possible carbon sites in a multilayer graphene structure representative of an HOPG material. In every time step of the simulation, a change in the state of a site in the oxygen lattice affects the possible states of the neighboring sites in the carbon lattice. The use of separate lattices makes it possible to effectively distinguish the oxygen and carbon sites and allow them to communicate throughout the simulation as various chemical interactions are tracked. The model implemented here consists of 20 surface reactions and 23 reactions on graphene edge sites, for a total of 43 reactions. Surface groups such as lactone-ethers and ether-lactone-ethers are formed on the surface as a result of reactions between neighboring epoxies and are shown to have a low energy barriers to CO and CO₂ formation. These groups are thus crucial to the initial formation of defects as they lead to formation of CO and CO₂ from initially defect free surfaces. For computational efficiency, only active oxygen sites around the previously executed site in the last timestep are checked for available events and are updated to the existing list of available events. We use the approach to show the effects of high symmetry grain boundaries and terraces on the formation and growth of defects in the oxidation process, and we observe pit formation enhanced by the presence of the exposed edges. Using the multi-lattice KMC model it is possible to simulate much longer times than in direct MD simulation. Scales of milliseconds are easily reached on a laptop computer without significant effort to optimize efficiency. Thus, the approach enables analyses of relatively large domains over experimental laboratory time scales.

3:00 PM BREAK

4:00 PM *DS02.09.06

Self-Interstitial-Based Diffusion in Concentrated Binary Alloys Simulated Using Classical Molecular Dynamics and Accelerated Dynamics [Laurent K. Béland](#)¹, [Keyvan Ferasat](#)¹, [Thomas D. Swinburne](#)², [Yuri Osetsky](#)³, [Alexander Barashev](#)⁴, [Peyman Saidi](#)¹ and [Mark Daymond](#)¹; ¹Queen's University, Canada; ²CNRS/CINaM, France; ³Oak Ridge National Laboratory, United States; ⁴University of Michigan, United States

Self-interstitial atoms (SIAs) are almost exclusively observed in irradiated materials. In part because of their presence, unique materials science phenomena occurs during irradiation of materials, such as radiation-induced segregation and radiation-induced (dis)ordering. While SIAs in pure metals typically diffuse very rapidly, within the timescale accessible by molecular dynamics, SIA kinetics in disordered alloys can be inhibited by configurational traps. In this talk, I will present two examples. First, I will present the case of SIA diffusion in Ni(x)Fe(1-x) concentrated solid solution alloys. Second, I will present the case of SIA-based reordering of irradiated Ni3Al alloys. In the case of the Ni(x)Fe(1-x) alloys, we use a mix of micro-second scale molecular dynamics, the kinetic Activation Relaxation Technique and accelerated lattice kinetic Monte Carlo to explain why the SIA diffusion coefficient is a non-monotonic function of alloy chemical composition. In the case of Ni3Al, we use molecular dynamics and temperature-accelerated Markov models with Bayesian estimation of rates (TAMMBER), which show that even though the SIA diffusion coefficient increases as it re-orders the system, the re-ordering kinetics, counterintuitively, slow down. We demonstrate that a relatively simple mean-field rate theory is able to quantitatively predict this behavior.

SESSION DS02.10: Coarse Grain Models II
Thursday Morning, December 2, 2021
Sheraton, 5th Floor, Public Garden

10:30 AM *DS02.10.01

Multiscale Atom-Continuum Coupling Using Lattice Greens Functions [William A. Curtin](#) and [Ankit Gupta](#); Ecole Polytechnique Federale Lausanne, Switzerland, Switzerland

Atomistic/Continuum coupling methods have now been developed for over 25 years. However, methods in which non-elastic behavior is occurring in the continuum domain remain computationally challenging due to the need for full 3d solutions in the continuum domain using finite elements. Greens function methods have the potential to greatly reduce the computational costs and enable large multiscale simulations. Here, progress toward a GFM method is described. First, the Flexible Boundary Condition Method of Sinclair et al., which is a GFM for an atomistic region in an infinite elastic space, does not give unique solutions even for linear problems. Second, efficient/usable GFM methods require a transition from a full lattice GF to a continuum GF, and this is shown to create numerical errors. However, these errors can be controlled and reduced. Third, starting from a fully-atomistic description, a coarse-graining of the outer (continuum) boundary is presented that greatly reduces the computational costs with essentially no loss of accuracy. These results show that an emerging GFM method will solve the bottleneck of current multiscale methods.

11:00 AM DS02.10.02

Spectral Denoising for Accelerated Analysis of Correlated Ionic Transport [Nicola Molinari](#)¹, [Yu Xie](#)¹, [Ian Leifer](#)¹, [Aris Marcolongo](#)², [Mordechai Kornbluth](#)³ and [Boris Kozinsky](#)^{1,3}; ¹Harvard University, United States; ²Universität Bern, Switzerland; ³Robert Bosch LLC, United States

In this work, we propose a new general method for analyzing and calculating diffusivity and ionic conductivity in media with strong ionic correlations from molecular trajectories [1]. Previously, the only two options were the dilute uncorrelated approximation, which converges rapidly but it is inaccurate, and the exact Green-Kubo method that is prohibitively expensive for complex and large systems. The herein presented approach automatically extracts and utilizes the collective diffusion eigenmodes of the displacement correlation matrix to denoise the calculation of the transport properties. The proposed approach is universally applicable, simple, and provably superior to previously available methods, exhibiting speed ups of several orders of magnitude. Thus, it opens wide opportunities to study correlated diffusion in previously inaccessible complex electrolytes.

[1] N Molinari, Y Xie, I Leifer, A Marcolongo, M Kornbluth, and B Kozinsky, "Spectral denoising for accelerated analysis of correlated ionic transport",

SESSION DS02.11: Electronic Structure Methods I
Session Chairs: Maytal Caspary Toroker and Vikram Gavini
Monday Morning, December 6, 2021
DS02-Virtual

8:00 AM *DS02.11.01

Calculations of Electronic Excited States Using Time Independent Functional Approach [Hannes Jonsson](#); University of Iceland, Iceland

A method is presented for time independent density functional calculations of excited electronic states using direct orbital optimization [1,2]. The calculations are variational and converge on stationary states, so they provide estimates of atomic forces in the excited state. Calculations of materials can be calculated using either a real space grid or a plane wave basis set. The functional can be orbital density dependent (ODD) as in self-interaction corrected functionals or be of the Kohn-Sham (KS) form as in the generalized gradient approximation. The implementation for KS functionals involves two nested loops: (1) An inner loop for finding a stationary point in a subspace spanned by the occupied and a few virtual orbitals corresponding to the excited state; (2) an outer loop for minimizing the energy in a tangential direction in the space of the orbitals. For ODD functionals, a third loop is used to find the unitary transformation that minimizes the energy functional among occupied orbitals only. Combined with the maximum overlap method, the algorithm converges in challenging cases where conventional self-consistent field algorithms tend to fail. The benchmark tests presented include charge-transfer excitations, defect states in diamond and excitons in silica.

[1] 'Variational Density Functional Calculations of Excited States via Direct Optimization', G. Levi, A. Ivanov and H. Jónsson, J. Chem. Theory Comput. 16, 6968 (2020).

[2] 'Direct Optimization Method for Variational Excited-State Density Functional Calculations Using Real Space Grid or Plane Waves', A. V. Ivanov, G. Levi, E. Ö. Jónsson and H. Jónsson, J. Chem. Theory Comput. (in press, 2021). Manuscript available on arXiv.

8:30 AM DS02.11.02

Discrete Discontinuous Basis Projection (DDBP) Method for Large-Scale Electronic Structure Calculations [Qimen Xu](#)¹, Phanish Suryanarayana¹ and John Pask²; ¹Georgia Institute of Technology, United States; ²Lawrence Livermore National Laboratory, United States

The large number of grid points per atom required for accurate real-space Kohn-Sham Density Functional Theory (DFT) calculations restricts their efficiency. In this work, we present an approach to accelerate such calculations severalfold, without loss of accuracy, by systematically reducing the cost of the key computational step: the determination of the Kohn-Sham orbitals spanning the occupied subspace. This is achieved by systematically reducing the dimension of the discrete eigenproblem that must be solved, through projection into a highly efficient discrete discontinuous basis. In calculations of quasi-1D, quasi-2D, and bulk metallic systems, we find that accurate energies and forces are obtained with 8–25 basis functions per atom, reducing the dimension of full-matrix eigenproblems by 1–3 orders of magnitude.

8:45 AM DS02.11.03

SPARC—Real-Space Density Functional Theory for Large Length and Time Scales [Phanish Suryanarayana](#); Georgia Institute of Technology, United States

In this talk, the speaker will present SPARC: Simulation Package for Ab-initio Real-space Calculations. SPARC can perform Kohn-Sham density functional theory calculations for isolated systems such as molecules as well as extended systems such as crystals and surfaces, in both static and dynamic settings. It is straightforward to install/use and highly competitive with state-of-the-art planewave codes, demonstrating comparable performance on a small number of processors and increasing advantages as the number of processors grows. Notably, SPARC brings solution times down to a few seconds for systems with O(100-500) atoms on large-scale parallel computers, outperforming planewave counterparts by an order of magnitude and more.

9:00 AM DS02.11.04

Late News: Cu Atoms Induce a New Reconstruction in the MnGa(001) Surface—An Ab Initio Study [Ricardo M. Ruvalcaba](#)¹, Joseph P. Corbett² and Jonathan Guerrero¹; ¹National Autonomous University of Mexico, Mexico; ²The Ohio State University, United States

MnGa alloys possess a set of properties that give them a wide range of highly interesting applications: from magnetic tunnel junctions [1] to semiconductor-magnetic hybrid devices [2]. In the present study, we report a first-principles investigation on a surface reconstruction based on the L1₀-ordered MnGa (001) with Cu atoms incorporated at the surface. We present a comprehensive analysis of the viability of all the possible reconstructions, as well as the structural, electronic, and magnetic properties of the most stable one: a 1 × 2 reconstruction with a Cu-by-Ga substitution at the surface, similar to the one reported in a previous study [3]. We propose that this structure may pose as a magnetic catalyst, adding yet another interesting application to MnGa alloys.

Acknowledgements

The authors would like to thank the support provided by the following DGAPA-UNAM projects: IN101019 and IA100920, as well as the CONACYT concession A1-S-9070. The calculations were performed in the supercomputing center DGCTIC-UNAM, through the projects LANCAD-UNAM-DGTIC-051 and LANCAD-UNAM-DGTIC-368. We thank *Laboratorio Nacional de Supercómputo del Sureste de México*, CONACYT, member of the national web of laboratories for providing computational resources and technical support. We would also like to thank the computing center THUBAT KAAL IPICYT for providing its computational resources. Finally, we thank Eduardo Murillo and Aldo Rodríguez Guerrero for their technical support.

References

- [1] Q. L. Ma, T. Kubota, S. Mizukami, X. M. Zhang, H. Na-ganuma, M. Oogane, Y. Ando, and T. Miyazaki, Phys. Rev. B **87**, 184426 (2013).
- [2] M. Tanaka, J. P. Harbison, T. Sands, B. Philips, T. L. Cheeks, J. De Boeck, L. T. Florez, and V. G. Keramidis, Applied Physics Letters **63**, 696 (1993).
- [3] J. Corbett, J. Guerrero-Sanchez, A. Richard, D. Ingram, N. Takeuchi, and A. Smith, Applied Surface Science **422**, 985 (2017).

9:15 AM DS02.11.05

Spectral Quadrature for Large Scale First Principles Simulations of Crystal Defects [Swarnava Ghosh](#); Oak Ridge National Laboratory, United States

Defects in crystalline solids play a crucial role in determining properties of materials at the nano, meso- and macroscale, such as the coalescence of vacancies at the nanoscale to form voids and prismatic dislocation loops or diffusion and segregation of solutes to nucleate precipitates. First principles Density Functional Theory (DFT) simulations can provide a detailed understanding of these phenomena, however the number of atoms needed to correctly simulate these systems is often beyond the reach of current DFT codes. We present an accurate and efficient finite-difference formulation and parallel implementation of Linear Scaling Kohn-Sham Density (Operator) Functional Theory (DFT) for non-periodic systems embedded in a bulk environment. We discuss the parallel scalability of the framework, acceleration on the state-of-the-art Graphics Processing Units, and will present the results of applying the framework to study isolated defects in lightweight Magnesium alloys. Finally, we will talk about integrating Machine Learning methods into the framework to further extend the scope of simulations.

Acknowledgements:

Part of this research was carried out when S.G. held a position at the California Institute of Technology. Some of the computations were carried out on the Caltech High Performance Cluster partially supported by a grant from the Gordon and Betty Moore Foundation. This research was also funded in part by the U. S. Department of Energy, Office of Science, Basic Energy Sciences, Materials Sciences and Engineering Division and it used resources of the Oak Ridge Leadership Computing Facility, which is supported by the Office of Science of the U.S. Department of Energy under Contract No. DE-AC05-00OR22725.

9:30 AM *DS02.11.06

A New *Ab Initio* Tool for Uncovering the Ultrafast Response of Functional Correlated Materials Volodymyr Turkowski, Shree Ram Acharya and Talat S. Rahman; University of Central Florida, United States

Accurate description of the temporal evolution of correlated electron materials, when perturbed by an external field, is a challenging and sought-after problem in condensed matter physics and material science. This is particularly the case for the ultrafast (femtosecond) response of the system since it may be dominated by electron correlations, unhindered by interactions, for example with the lattice. Suitable *ab initio* computational methods would thus need to extend beyond the standard density functional theory (DFT). Time-dependent density-functional theory (TDDFT) when equipped with appropriate exchange-correlation (XC) functional offers a way forward. This necessarily implies development of XC functionals beyond the standard local density or the generalized gradient approximations because of the need to treat on-site orbital-resolved correlations and/or time dependent interactions. In this presentation, we first provide some details of our new methodology in which we combine dynamical mean-field theory (DMFT) and TDDFT to examine the ultrafast response of materials in which electron-electron correlations play an important role. We obtain a non-adiabatic XC kernel (potential for nonlinear response) from the electron charge susceptibility (self-energy) by solving an effective Hubbard model using DMFT. This XC kernel or potential when implemented in TDDFT provides a computationally feasible approach for examination of nonequilibrium properties of systems in question. We next demonstrate the viability of the approach through computation of the ultrafast demagnetization of Ni [1], for which we calculate the pre-thermalization of the electron and hole subsystems and related spin-resolved properties. We show that the system magnetic moment reaches its lower, transient-state value (demagnetized) in tens of femtoseconds, and that the charge (electron and hole) pre-thermalization occurs after ~10 femtoseconds, both results in agreement with experimental data. Since at such short time scales electron-electron interaction is the only source of scattering in the system, these results capture the power of the TDDFT+DMFT methodology for isolating the femtosecond physics of strongly correlated materials.

This work was supported in part by DOE grant DE-FG02-07ER46354.

[1] S. R. Acharya, V. Turkowski, G-p Zhang, and T. S. Rahman, Phys. Rev. Lett. 125, 017202 (2020).

<https://doi.org/10.1103/PhysRevLett.125.017202>

SESSION DS02.12: Electronic Structure Methods II

Session Chair: Talat Rahman

Monday Morning, December 6, 2021

DS02-Virtual

10:30 AM *DS02.12.01

Modeling Polaron Transport in Defected Spinel Oxides Maytal Caspary Toroker; Technion-Israel Institute of Technology, Israel

The small-polaron hopping model has been used for several decades for modeling electronic charge transport in oxides. Despite its significance, the model was developed for binary oxides, and its accuracy has not been rigorously tested for higher-order oxides. To investigate this issue, we chose the $\text{Mn}_x\text{Fe}_{3-x}\text{O}_4$ spinel system, which has exciting electrochemical and catalytic properties, and mixed cation oxidation states that enable us to examine the mechanisms of small-polaron transport. Using a combination of experimental results and DFT+*U* calculations, we find that the charge transport occurs only between like-cations (Fe/Fe or Mn/Mn). And due to asymmetric hopping barriers and formation energies, we find that the polaron is energetically preferred to the polaron, resulting in an asymmetric contribution of the Mn/Mn pathways. The effect of vacancies near and far from the polaron will be emphasized in this talk.

Reference:

A. Bhargava, R. Eppstein, J. Sun, M. A. Smeaton, H. Paik, L. F. Kourkoutis, D. G. Scholm, M. Caspary Toroker*, R. D. Robinson*, "Breakdown of the small-polaron hopping model in higher-order spinels", Adv. Mat., 2004490 (2020).

11:00 AM *DS02.12.03

Large-Scale Real-Space Electronic Structure Calculations Sambit Das¹, Bikash Kanungo¹, Phani Motamarri² and Vikram Gavini¹; ¹University of Michigan, United States; ²Indian Institute of Science, India

Electronic structure calculations, especially those using density functional theory (DFT), have been very useful in understanding and predicting a wide range of materials properties. Despite the success of DFT, and the tremendous progress in theory and numerical methods over the decades, the following challenges remain. Firstly, the state-of-the-art implementations of DFT suffer from cell-size and geometry limitations, with the widely used codes in solid state physics being limited to periodic geometries and typical simulation domains containing a few thousand electrons. This limits the complexity of materials systems that are accessible to DFT calculations. Further, there are many materials systems (such as strongly-correlated systems) where the widely used model exchange-correlation functionals are inaccurate. Addressing these challenges will enable large-scale quantum-accuracy DFT calculations, and can significantly advance our predictive modeling capabilities of complex materials systems.

This talk will discuss our recent advances towards addressing the aforementioned challenges. In particular, the development of computational methods and numerical algorithms for large-scale real-space DFT calculations using adaptive finite-element discretization will be presented, which form the basis for the recently released DFT-FE open-source code. The computational efficiency, scalability and capability of DFT-FE will be presented, and contrasted with other widely used codes. Further, ongoing efforts, and related thoughts, on developing a framework for a data-driven approach to improve the exchange-correlation description in DFT will be discussed.

11:30 AM DS02.12.04

Systematic Evaluation of First Principles DFT+U+J Algorithms for the Fast and Accurate Modelling of Transition Metal Oxides [Daniel S. Lambert](#) and David D. O'Regan; Trinity College Dublin, Ireland

Hubbard U corrections are a widely used approach for overcoming the characteristic band gap underestimation in approximate Density Functional Theory (DFT) calculations, without incurring significant computational costs. However, Hubbard U corrections for transition metal oxides (TMOs) are often chosen on a somewhat arbitrary basis and tend to over-correct. This has led to a search for improvements to the U correction such as DFT+U+J, which includes a correction based on the Hund's coupling parameter J that accounts for the dependence of interactions on the spin orientation.

In our research, a standardised first-principles algorithm is implemented for calculating U and J for both metal and oxygen subspaces, based on the linear response to an applied potential. This procedure is benchmarked with several TMO materials to assess the effect of DFT+U+J on the band gap, effective mass, bond lengths and unit cell volume.

We find that in certain materials, first-principles DFT+U+J can give band gap values that are close to experimental values, out-performing PBE and standard DFT+U and, in some cases, even outperforming hybrid functional results. It is also shown that DFT+U+J does not appear to introduce significant distortions in material ionic geometry or band-structures, suggesting that this methodology could be useful for the computationally efficient modelling of TMOs.

11:45 AM DS02.12.05

Symmetry-Adapted Density Functional Theory [Abhiraj Sharma](#) and Phanish Suryanarayana; Georgia Institute of Technology, United States

One-dimensional nanostructures such as nanotubes, nanowires, nanohelices, nanospirals, and nanocoils have received increased attention over the past three decades due to their fascinating elastic, electronic, vibrational, optical, and thermal properties. In this work, we present a cyclic and helical symmetry-adapted formulation and large-scale parallel implementation of real-space Kohn-Sham DFT for 1D nanostructures, with application to the mechanical and electronic response of carbon nanotubes subject to torsional deformations. Specifically, we derive symmetry-adapted variants for the energy functional, electronic ground state's variational problem, Kohn-Sham equations, atomic forces, and axial stress, all posed on the fundamental domain, while employing a semilocal exchange-correlation functional and a local electrostatic formulation. Within this framework, we develop a representation for nanotubes of arbitrary chirality subject to external twists. We develop a high-order finite-difference parallel implementation capable of performing cyclic and helical symmetry-adapted Kohn-Sham calculations in both the static and dynamic settings. Using this implementation, we study the mechanical and electronic response of carbon nanotubes to twist-controlled deformations, at both small and large deformations.

12:00 PM DS02.12.06

Ab Initio Random Structure Searching for Nonhydrostatic Environments [William C. Witt](#) and Chris J. Pickard; University of Cambridge, United Kingdom

Thermodynamics dictates that a crystal under pressure will prefer the structure of lowest enthalpy, provided the temperature is sufficiently low. Structure prediction techniques like random structure searching rely on this insight, optimizing candidate structures to balance the applied pressure, then ranking them by enthalpy. This procedure becomes more complicated when the applied stress is nonhydrostatic. Numerous formulations of enthalpy for nonhydrostatic environments appear in the literature, tracing back to early work by Gibbs, but many are unsuitable for large deformations or have other undesirable features. We illustrate the various difficulties and present our solution in a form suitable for random structure searching, illustrating it with a few simple examples.

12:15 PM DS02.01.04

Computational Modeling of Materials for Organic Light Emitting Diodes [Alexander Yakubovich](#), Alexey Odinokov and Hyeonho Choi; Samsung Advanced Institute of Technology, Russian Federation

Rational design of novel materials for organic light emitting diodes (OLED) requires deep understanding of the processes accompanying device operation at the molecular scale, such as charge and energy transfer, generation and relaxation of excited states, photochemical reactions leading to the degradation of the material, etc. Modern computational chemistry provides versatile tools to study morphology and properties of the OLED materials that often cannot be accurately addressed with experimental techniques.

We present an overview of theoretical methods applied for computational OLED materials development and intend to cover the following subjects:

- prediction of photoluminescence efficiency and CIE coordinates for cyclometalated Platinum and Iridium complexes, which requires evaluation of radiative and non-radiative decay constants, Frank-Condon progressions [1, 2]
- simulations of functional materials using quantum mechanically derived force fields, including modeling of sublimation process of large organometallic compounds, which is an essential step in OLED device fabrication [3-4]
- computational prediction of photochemical stability of OLED materials and more general problem of OLED devices operational stability, including the isotope effects and the problem of charge recombination rate prediction in OLED emitting layers [5-7]
- computational design of OLED materials using generative artificial neural networks: application to triplet-triplet fusion materials

References

- [1] Kim. I. et al. "Predicting phosphorescence quantum yield for Pt(II)-based OLED emitters from correlation function approach" J. Phys. Chem. C 123(17), 11140-11150 (2019).
- [2] Osipov A. et al. "Tetradentate Pt(II) Phosphors – a Computational Analysis of Nonradiative Decay Rates and Luminescent Efficiency" J. Phys. Chem. C, 124(22), 12039–12048 (2020).
- [3] Yakubovich A. et al. "Accurate vapor pressure prediction for large organic molecules utilized in organic light-emitting diodes (OLED)", J. Chem. Theory Comput. 2020, 16(9), 5845–5851

- [4] Odinkov. et al. "Exploiting the Quantum Mechanically Derived Force Field for Functional Materials Simulations", submitted (2021).
- [5] Odinkov A. et al. "Charge recombination in polaron pairs: a key factor for operational stability of blue-phosphorescent light-emitting devices", *Adv. Theory and Sim.* 3(8), 2000028 (2020).
- [6] Freidzon A. Ya. et al. "Predicting the operational stability of phosphorescent OLED host molecules from first principles: a case study" *J. Phys. Chem. C* 121, 22422-22433 (2017).
- [7] Hyejin Bae et. al. "Protecting benzylic C–H bonds by deuteration doubles the operational lifetime of deep blue Ir-phenylimidazole dopants in phosphorescent OLEDs", *Adv. Opt. Mat.* Doi: 10.1002/adom.202100630 (2021).

SESSION DS02.13: Machine Learning
Session Chair: Milica Todorovic
Monday Afternoon, December 6, 2021
DS02-Virtual

1:00 PM *DS02.13.01

Atomic Cluster Expansion: Practice and Theory [Christoph Ortner](#); University of British Columbia, Canada

Accurate molecular simulation requires computationally expensive quantum chemistry models that makes simulating complex material phenomena or large molecules intractable. The relatively recent trend of "data-driven" models intended to overcome this barrier. I will focus on a specific class, based on the Atomic Cluster Expansion (Drautz, 2019) and explain how such models are constructed from symmetry-adapted "features" which can be used in regression schemes including classical linear regression, kernel ridge regression or ANNs, and show some concrete examples highlighting successes and potentials. I will then discuss some of the more theoretical aspects and try to explain *why* the ACE approach (and ML in general) has been so successful: a necessary condition is that there must be a relatively low-dimensional representation of the potential energy landscape. I will focus on three aspects, locality, low body-order and self-consistency, and try to explain rigorously how these occur in the potential energy landscape of ab initio models, and connect this back to the ACE model.

1:30 PM DS02.13.02

A Machine Learning Based Inorganic Crystal Forcefield Optimizer [Filip Dinic](#), Zhibo Wang and Oleksandr Voznyy; University of Toronto, Canada

For expansive structures, the individual energy calculations per optimization step becomes non-trivial and therefore rapidly expands the computational resources required for full optimization. In comparison, ML predictions can be agile even on small machines as many computationally expensive matrix diagonalization algorithms are substituted with neural network layers. The model was trained on a wide range of materials, which were systematically stretched/compressed to simulate unoptimized structures. In order to speed up structural optimization, a gradient descent is applied and used to continually adjust atomic positions in order to minimize the total energy of the material. This presentation will discuss the universality of the optimizer generated and the overall accuracy achieved.

There are several potential applications of this optimizer, such as speeding up costly energy relaxation calculations. Furthermore, it can be used as a pre-cleaning tool for novel materials before being further analyzed by other ML models. In addition, a similar strategy of employing stretched/compressed materials was used to improve the performance of bandgap prediction. This presentation will demonstrate the capabilities of the optimizer in improving bandgap predictions for inorganic materials, and how this can be applied in the search for novel blue-UV emitting materials.

1:45 PM DS02.13.03

Active Learning of Surrogate Interatomic Potentials from Large-Scale Simulations [Max Hodapp](#) and Alexander Shapeev; Skolkovo Institute of Science and Technology, Russian Federation

One of the main open challenges in computational materials science is the construction of interatomic potentials which achieve quantitative agreement with fully—but infeasible—ab initio models for large-scale problems, possibly involving tens of thousands of atoms. Empirical potentials, arguably the most popular type of interatomic potentials, generally fail in making quantitative predictions. Therefore, they largely remain inadequate for a predictive modeling of multicomponent systems and, thus, for a computational discovery of new materials.

The advent of machine learning interatomic potentials (MLIPs) for small systems of order 10–100 yet holds promise that overcoming these limitations appear within sight (see [1] for a review). On the other hand, a well-known drawback of state-of-the-art MLIPs is their poor ability to extrapolate beyond the training domain. This demands for carefully chosen, problem-dependent training data which can hardly be defined by the user prior to a simulation due to the vast amount of possible atomic neighborhoods to be considered. Therefore, solution algorithms for atomistic problems using MLIPs have to incorporate error estimators which measure the degree of extrapolation in order to "find" the right training data during a simulation.

Here, we present such an algorithm based on active learning and apply it to screw dislocation motion in bcc tungsten [2,3]. Using structural identification methods, we locate the dislocation line, check the extrapolation grade of the MLIP around its core, and construct new training configurations, sufficiently small to be computable with plane-wave density functional theory, if the extrapolation grade exceeds some threshold. We show that the algorithm reproduces classical results from the literature (i.e., core structure, Peierls barrier/stress), in addition to its anticipated application to more complex problems involving interactions of dislocations with other types of defects, e.g., interstitials, which are out of scope with ab initio methods solely.

[1] Y. Zuo et al., 2019. Performance and Cost Assessment of Machine Learning Interatomic Potentials. *J. Phys. Chem. A* 124, 731–745

[2] E. Podryabinkin, A. Shapeev, 2017. Active learning of linearly parametrized interatomic potentials. *Comput. Mater. Sci.* 140, 171–180

[3] M. Hodapp, A. Shapeev, 2020. In operando active learning of interatomic interaction during large-scale simulations. *Mach. Learn.: Sci. Technol.* 1 045005

2:00 PM DS02.13.04

Late News: Ultra-Fast Force Fields (UF3) Framework for Fitting Interpretable Machine-Learning Potentials Stephen R. Xie^{1,2}, Matthias Rupp³ and [Richard Hennig](#)¹; ¹University of Florida, United States; ²NASA Ames Research Center, United States; ³University of Konstanz, Germany

Although *ab initio* methods are indispensable tools for predicting properties of materials and simulating chemical processes, the tradeoff between computational efficiency and predictive accuracy limits their application to large systems and long simulation times. The Ultra-fast Force Fields (UF3) framework is an open-source software package for fitting machine-learning models of the energy landscape that are fast to train and evaluate, interpretable in form, and accurate even for relatively small training sets. Specifically, these interatomic potentials are based on a general many-body expansion combined with a cubic B-spline basis and regularized linear regression. We benchmark speed and accuracy using a bcc tungsten dataset, including melting point calculations with thousands of atoms. We find that our potential is two to four orders of magnitude faster than state-of-the-art machine-learning potentials while achieving comparable accuracy. Finally, we discuss the application of the introduced potentials in accelerating structure prediction.

2:15 PM *DS02.13.05

A Density-Based Machine Learning Force Field for Nonbond Interactions Lin-Wang Wang; Lawrence Berkeley National Laboratory, United States

Using machine learning model to yield a machine learning force field (ML-FF) from *ab initio* calculation data has becoming a powerful approach to simulate material properties with both size and temporal scales much larger than what can be handled by direct *ab initio* methods. The common ML-FF approach describes the energy of one atom as a function of its neighboring atom positions. This however cannot describe the long range electrostatic interactions. Furthermore, the point charge based electrostatic model in classical force field might not be accurate enough due to the lack of dipole moment, as well as the polarization. Besides, the nonbonding interaction can be rather complicated in terms of its atomic configuration, which makes direct machine learning training difficult. Here, we present an electron charge density based machine learning model to deal with the nonbond interactions. In this model, the electron charge density is fitted, and used for nonbond interactions directly, including electrostatic and exchange-correlation interactions. We also developed an accurate polarization model, describing the polarization energy of a molecule under external potential. We have used battery organic electrolyte as our testing example for this development.

2:45 PM DS02.13.06

Machine Learning the Local Yield Surface in Model Glasses Rahul Meena, Spencer Fajardo, Dihui Ruan, Yannis Kevrekidis, Michael Shields and Michael L. Falk; Johns Hopkins University, United States

The Local Yield Stress (LYS) method involves directly probing local regions of atoms in atomistic simulations to quantify the incremental stress necessary to induce plastic rearrangements [1,2]. This quantity is key to informing meso-scale and continuum models of plastic deformation and flow in glasses and other amorphous solids. In doing so the LYS seeks to quantify scalar functions of a tensor quantity, the normalized applied shear strain, for a given assemblage of a few tens to hundreds of atoms. While the LYS algorithm is scalable and highly generalizable, it is also computationally intensive. This is particularly true in 3D, which is most relevant for practical application. For this reason, we seek to develop a machine learning methodology to utilize the direct simulation data obtained on a given material to enable efficient and highly generalizable quantification of the LYS. We begin by developing a novel distance metric to quantify the relatedness of atomistic assemblages. We then apply a dimension reduction scheme to the atomistic data in order to determine the most relevant degrees of freedom for our learning algorithm. We make a direct comparison between the atomistic quantification and the learned results in order to validate the method.

[1] Patinet, S., Vandembroucq, D. and Falk, M.L., 2016. Connecting local yield stresses with plastic activity in amorphous solids. *Physical review letters*, 117(4), p.045501.

[2] Barbot, A., Lerbinger, M., Hernandez-Garcia, A., García-García, R., Falk, M.L., Vandembroucq, D. and Patinet, S., 2018. Local yield stress statistics in model amorphous solids. *Physical Review E*, 97(3), p.033001.

SESSION DS02.14: Machine Learning Aided Models II

Session Chair: Thomas Swinburne

Tuesday Morning, December 7, 2021

DS02-Virtual

8:00 AM DS02.14.01

Exciton-Phonon Coupling of Real-Size Quantum Dots by Machine-Learning Potential—An Excellent Agreement Between Theory and Experiment Sungwoo Kang¹, Youngho Kang² and Seungwu Han¹; ¹Seoul National University, Korea (the Republic of); ²Incheon National University, Korea (the Republic of)

Recently, quantum dots (QDs) have acquired much attention as promising materials for optical applications. To fully realize the potential of QD, it requires to exhibit a sharp luminescence spectrum. Therefore, many efforts have been taken into minimizing the luminescence line widths of QDs. While it is well known that the luminescence linewidth of a single QD arises from exciton-phonon coupling (EPC), the mechanism and origin of EPC are not fully resolved yet. For example, it is still controversial which mode between acoustic and optical phonon dominates EPC in QDs. A theoretical investigation by density functional theory (DFT) calculations can provide fundamental insights into EPC as well as its impact on the line broadening at an atomic scale. In our previous study, we reported an *ab initio* method to evaluate luminescence line shapes of QDs due to EPC, combining the DFT and Frank-Condon approximation [1]. However, DFT calculations require large computational time so that the size of QD is restricted to ~500 atoms while real-size QDs are much larger (usually consist of 1,000-100,000 atoms).

In this study, we combine DFT and machine-learning potential to simulate real-size InP/ZnSe QD which consists of ~4000 atoms. The calculated lineshape and its temperature dependence are in excellent agreement with the experiments. In addition, we also find that acoustic phonon modes significantly couple with an exciton in core/shell QDs, which is in stark contrast to the widely accepted perception that exciton-optical phonon coupling dominates the luminescence line broadening.

[1] S. Kang, et al. ACS Appl. Mater. Interfaces, 12, 22012 (2020).

8:15 AM DS02.14.02

Synergistic Coupling in QM/MM Simulations of Dislocations via Machine Learning Petr Grigorev¹, James Kermod², Mihai-Cosmin Marinica³ and Thomas D. Swinburne¹; ¹CINaM Centre Interdisciplinaire de Nanoscience de Marseille, France; ²School of Engineering, University of Warwick, United Kingdom; ³CEA, Service de Recherches de Métallurgie Physique, France

Ab initio modelling of dislocations is essential to gain quantitative insight into a vast range of important material phenomena, from elementary glide or

climb mechanisms to predictive models of solute solution strengthening or post irradiation annealing. The simulation data can be used directly in phenomenological micro-structural models or in the construction of empirical interatomic potentials in a multi-scale framework. With some notable exceptions, ab initio size limitations mean that most dislocations cannot be contained in periodic supercells, requiring the use of flexible boundary techniques which either couple to an elastic Green's function or an empirical interatomic potential in QM/MM simulations. In the latter case, the potential should ideally have identical elastic properties as the ab initio medium. A key limitation of these flexible boundary methods is that whilst the ionic positions and forces can be extracted, the total energy becomes ill-defined.

In recent work [1,2], we showed how this information could be used to extract energetic barriers for glide or segregation through the principle of virtual work. A very good agreement was found with special cases treatable with periodic supercells, whilst in general our ab initio results deviate significantly from predictions of empirical potentials, particularly for prismatic (edge) dislocations. In this work, we show how linear-in-descriptor machine learning (ML) potentials [3] can be used to exactly match ab initio elastic properties, typically leading to efficiencies over "traditional" empirical potentials during QM/MM relaxations. We then go further, using the ionic positions and forces to train the ML potential, showing that the resultant "classical" migration barriers are in excellent agreement with that obtained from QM/MM. Our work shows that QM/MM methods can qualitatively expand the range of atomic structures in the training database of machine learning interatomic potentials, with significant impact on their transferability, or predictive power, for materials modelling.

References:

- [1] Swinburne, T. D., & Kermode, J. R. (2017). Computing energy barriers for rare events from hybrid quantum/classical simulations through the virtual work principle. *Phys. Rev. B*, 96(14), 144102.
- [2] Grigorev, P., Swinburne, T. D., & Kermode, J. R. (2020). Hybrid quantum/classical study of hydrogen-decorated screw dislocations in tungsten: Ultrafast pipe diffusion, core reconstruction, and effects on glide mechanism. *Phys. Rev. Materials*, 4(2), 23601.
- [3] Dérès J, Goryaeva A. M., Lapointe C., Grigorev P., Swinburne, T. D., Kermode, J. R., Ventelon L., Baima J., and Marinica M.-C. Efficient and transferable machine learning potentials for the simulation of crystaldefects in bcc Fe and W. Submitted to *Phys. Rev. Materials*

8:30 AM *DS02.01.02

Realistic Description of Processes at Solid/Liquid Interfaces by *Ab Initio* Molecular Dynamics Simulations with Potential Control Mira Todorova, Sudarsan Surendralal, Stefan Wippermann, Florian Diessenbeck and Jorg U. Neugebauer; Max Planck Institute fuer Eisenforschung, Germany

Many present day technological challenges related to battery materials, electro-catalysis, fuel cells, corrosion and others, centre around understanding and controlling processes at solid/liquid interfaces. A targeted design of desired functionalities critically relies on understanding and quantifying the underlying fundamental mechanisms. However, understanding them is equally challenging to both theoretical modelling and experimental characterisation.

The presentation will discuss our recent advances achieved by developing a novel potentiostat design [Surendralal *et al.*, *Phys. Rev. Lett.* **120**, 246801 (2018)] and a canonical thermopotentiostat [Deißenbeck *et al.*, *Phys. Rev. Lett.* **126**, 136803 (2021)] approach. These enable us to control the electrode potential of the system by tuning the excess charge of the working electrode and use ab-initio molecular dynamics simulations to study solid/liquid interfaces under realistic conditions of applied bias. The opportunities opened by the availability of these new approaches will be discussed for a few prototype examples related to electro-catalysis and corrosion: The mechanisms leading to the onset of the hydrogen evolution reaction (HER) in the H/Pt/H₂O system [Surendralal *et al.*, *Phys. Rev. Lett.* **126**, 166802 (2021)] and corrosion at the Mg/water interfaces.

9:00 AM BREAK

SESSION DS02.15: Accelerated Methods II
Session Chairs: Richard Henning and Manon Michel
Tuesday Morning, December 7, 2021
DS02-Virtual

10:30 AM *DS02.15.01

How to Compute Transition Times? Tony Lelièvre; Ecole des Ponts, France

We illustrate how the Hill relation and the notion of quasi-stationary distribution can be used to analyse the error introduced by many algorithms that have been proposed in the literature, in particular in molecular dynamics, to compute mean reaction times between metastable states for Markov processes. The theoretical findings are illustrated on various examples demonstrating the sharpness of the error analysis as well as the applicability of our study to elliptic diffusions. This is a joint work with Manon Baudel and Arnaud Guyader. Reference: M. Baudel, A. Guyader, and T. Lelièvre, *On the Hill relation and the mean reaction time for metastable processes*, <https://arxiv.org/abs/2008.09790>.

11:00 AM DS02.15.02

Predicting Hydrogen Diffusivity in Amorphous Titania using Machine Learning-Assisted Adaptive Markov Chain Kinetic Monte Carlo Simulations James Chapman, Kyoung E. Kweon and Nir Goldman; Lawrence Livermore National Laboratory, United States

Understanding hydrogen transport is vital to industries focused on discovering new materials for energy storage and corrosion mitigation. However, knowledge of the physical nature of hydrogen's diffusion pathways is often limited, especially for materials that exhibit a multitude of phases/defect classes. These materials typically have three rate-limiting structural domains: (1) bulk (2) grain boundaries, and (3) surfaces. In this work we have chosen to study hydrogen diffusion through titania due to its importance in the aforementioned application spaces. Here, we aim to understand diffusion through titania grain boundaries, which are approximated via the amorphous phase. Density functional theory (DFT) was used to calculate thousands of activation energies of hydrogen diffusion in the amorphous phase via nudged elastic band (NEB) calculations using an automated hydrogen pathway generation scheme. Amorphous structures, on the order of tens of nanometers, were generated using a machine learning force field via classical molecular dynamics (MD). Markov chains (MC) were generated using the MD-derived atomic structures as their reference. The MC edge weights, which employ the activation energy between hydrogen hopping sites, were calculated via a Gaussian process regression model, which was trained on the DFT-NEB data. Kinetic Monte Carlo simulations were then performed over a variety of temperatures and amorphous structures. Both stoichiometric and non-stoichiometric amorphous structures were chosen to understand the relationship between hydrogen diffusion and oxygen concentration. The machine learning-assisted adaptive Markov Chain Kinetic Monte Carlo scheme employed in this work allows us to quantitatively describe hydrogen diffusion rates for systems without pre-defined sites and/or activation energies. This work sets the stage for one to perform long time-scale and/or length-scale simulations of transport phenomena

for practically any material system, removing the need to simplify the system either structurally and/or kinetically.

11:15 AM DS02.15.03

Degradation Evolution of Pt Alloy Nanoparticle via Kinetic Monte Carlo Simulation Driven by Neural Network Potentials Jisu Jung, Suyeon Ju, Purun-hanul Kim, Jisu Kim and Seungwu Han; Seoul National University, Korea (the Republic of)

Global warming caused by the excess use of fossil fuels has become a critical issue in modern society. The proton-exchange membrane fuel cell (PEMFC) has attracted wide attention as the environmentally friendly renewable energy device that is used in hydrogen-fueled vehicles. The performance of PEMFC relies on the nanoscale electrocatalyst on the cathode electrode. Over the last several decades, experimental and computational researches have focused on the sluggish oxygen reduction reaction (ORR) and the cost of a precious metal catalyst. However, as the activity of the catalyst increases, their low durability problem also rises. Therefore, an atomistic picture of the degradation of nanoscale catalysts is needed to improve the stability of nanoscale catalysts.

While several works describe the long-term degradation evolution with kinetic Monte Carlo (kMC) simulation, they are limited due to the inaccurate classical potential or computationally expensive quantum calculation. Recently, neural network potential (NNP) has been applied to various systems, delivering the accuracy of quantum calculation at a much lower cost.

In this talk, we combine NNP and kMC simulation to explore the degradation of various shapes of Pt alloy nanoparticles with 3–5 nm under electric bias. We found that our simulation results agree with the experimental observation. This work would pave the way to design more durable nanoparticle electrocatalysts.

11:20 AM DS02.15.04

Kinetic Monte Carlo Study of the Atomic Layer Deposition of Titanium Nitride Sangtae Kim, Hyungmin An, Sangmin Oh, Jiho Lee and Seungwu Han; Seoul National University, Korea (the Republic of)

Titanium nitride (TiN) belongs to the family of refractory transition metal nitrides and represents useful properties such as chemical inertness, thermodynamic stability, extreme hardness, good thermal and electrical conductivity. Atomic layer deposition (ALD) of TiN has been used for protecting layers in tungsten as the minimum feature size of the devices decreased and a high aspect ratio was required. Accordingly, experimental and theoretical research on the TiN-ALD thin film process using various reducing agents (NH_3 , H_2) based on the TiCl_4 precursor was published. However, observations on the sub-nanometer scale surface reaction are limited due to the characteristics of the ALD process that grows at the atomic scale. In the case of previous theoretical studies, there is a gap in understanding the actual process because it is limited to indirect analysis through thermodynamic energy based on density functional theory (DFT) calculation. So in this study, we introduce the multi-scale modeling for TiN-ALD. We investigate the overall growth of the TiN thin films grown via $\text{TiCl}_4/\text{NH}_3$. Multi-scale modeling with DFT and on-lattice kinetic Monte Carlo (kMC) is adopted to reproduce the whole ALD process. To determine the most probable pathway, all individual reactions are considered and calculated with DFT, and a set of corresponding activation energies are implemented in the kMC code as a transition probability for the surface reactions on the TiN (111) surface. To verify the compatibility with the experiment ALD process, the growth rate and mass gain according to the process conditions (temperature, pulse time, pressure) were compared with the simulation results. The temperature-dependent growth profile obtained from our model is in good qualitative agreement with the experimental data. These kinetic results should help to explain TiN ALD growth rates observed at different reactant exposures and substrate temperatures.

11:25 AM *DS02.15.05

Active Learning for Accelerated Structure Search with BOSS Milica Todorovic; University of Turku, Finland

Atomistic structure search for organic/inorganic heterostructures is made complex by the many degrees of freedom and the need for accurate but costly density-functional theory (DFT) simulations. To accelerate structure determination in heterogeneous functional materials across lengthscales, we employ active learning with the Bayesian Optimization Structure Search (BOSS) approach [1].

Here, Bayesian optimization is employed to build N-dimensional surrogate models for the energy or property landscapes and infer global minima. The models are iteratively refined by sequentially sampling DFT data points that are promising and/or have high information content. Representing heterogeneous materials with compact chemical ‘building blocks’ allowed us to build in prior knowledge and reduce search dimensionality. The uncertainty-led exploration/exploitation sampling strategy delivers global minima with modest sampling, but also ensures visits to less favorable regions of phase space to gather information on rare events and energy barriers.

We applied this active learning scheme to study adsorption at the organic/inorganic interfaces: C_{60} on $\text{TiO}_2(101)$ anatase [1] and camphor on $\text{Cu}(111)$ [2,3]. At larger lengthscales, we investigated the substrate-decoupled F4TCNQ-TTF charge transfer complexes. Global minima configurations in 6 dimensions are identified with reasonable computational efficiency. BOSS produces chemically-intuitive adsorption energy landscapes that are parsed for local minima and the minimum energy paths between them, allowing us to extract complex barrier-related atomistic pathways. With a recent batch implementation for active learning, BOSS can make use of exascale computing resources to solve largescale structural problems without sacrificing quantum-mechanical accuracy.

[1] M. Todorović, M.U. Gutmann, J. Corander and P. Rinke, ‘Efficient Bayesian Inference of Atomistic Structure in Complex Functional Materials’, *npj Comput. Mater.* **5**, 35 (2019).

[2] J. Järvi, P. Rinke and M. Todorović, ‘Detecting stable adsorbates of (1S)-camphor on $\text{Cu}(111)$ with Bayesian optimization’ *Beilstein J. Nanotechnol.* **11**, 1577 (2020).

[3] J. Järvi, B. Aldritt, O. Krejčí, M. Todorović, P. Liljeroth and P. Rinke, ‘Integrating Bayesian Inference with Scanning Probe Experiments for Robust Identification of Surface Adsorbate Configurations’, *Adv. Func. Mater.* 2010853 (2021).

11:55 AM DS02.15.06

Evaluation of Sampling Methods on Performance of Bayesian Parameter Estimation During Refinement of Empirical Molecular Dynamics Potentials Troy Gustke¹, Abhishek T. Sose¹, Gaurav Anand¹, Fangxi Wang¹, Aditya (Ashi) Savara² and Sanket Deshmukh¹; ¹Virginia Tech, United States; ²Oak Ridge National Laboratory, United States

Uncertainty quantification (UQ) methods such as Bayesian methods have been recently used to quantify the uncertainty associated with the force-field parameters and their predictions. However, the reliability and accuracy of these UQ algorithms depend on the sampling methods used to perform the analysis. Here, as a test case, we have performed UQ on a new all-atom (AA) embedded atom method (EAM) potential of gold developed in our group. The AA model itself was aimed at reproducing physical, thermodynamic, and mechanical properties of interest obtained through experimental methods and/or density functional theory. The robustness and parametric sensitivity of the gold model was analyzed using Sobol sequencing and calculating sensitivity indices. Bayesian Parameter Estimation with UQ was performed using different sampling methods including Metropolis-Hastings (MH),

Ensemble-slice (ESS), Uniform, and Grid as implemented in CheKiPEUQ, an open-source Bayesian parameter estimation package. This allowed us to investigate the performance and dependence of Bayesian predictions on these sampling methods. The sampling process was accelerated through surrogate modeling by developing Gaussian Process Regression (GPR) models trained with data obtained from molecular dynamics (MD) simulations. The Bayesian framework was used to obtain the highest posterior density interval and the highest probability parameter set, which better reproduces the properties with respect to the confidence levels of experimental and/or DFT observations.

12:10 PM DS02.15.07

Extending the KineCluE Code to the Computation of Transport Coefficients in Concentrated Alloys Pamela Camilos, Thomas Schuler and Maylise Nastar; Commissariat à l'énergie atomique et aux énergies alternatives, France

Modeling diffusion from the atomic scale is necessary because experimental studies are only feasible at high temperatures and in most systems, it is not possible to measure the full Onsager matrix. The problem is mostly solved in pure and dilute alloys, for instance using the KineCluE code. Computing the full Onsager matrix in concentrated alloys remains a challenge due to the vastness and complexity of the configuration space and the connected ones associated with jump sequences. Current approaches rely either on mean-field approximations or atomic kinetic Monte Carlo simulations, however each of them has its own limitations; with the former, kinetic correlations are not fully taken into account while with the latter statistical errors arise, especially when calculating off-diagonal transport coefficients. Therefore, a comprehensive deterministic diffusion model is needed. In this work, we aim to extend the kinetic cluster expansion formalism to concentrated alloys in order to get an efficient evaluation of transport coefficients, time life and mobility of clusters in concentrated alloys based on atomic-scale data. Our formalism relies on the Self-Consistent Mean Field Theory and it is implemented in the KineCluE code. We treat the local configuration of the diffusing species exactly, while further away atoms are replaced by a homogeneous mean-field. This allows us to treat short-range kinetic correlations exactly and to construct the long-range kinetic paths under controlled approximations while reducing the computational load and keeping the calculations feasible. In the case of a random alloy, we compare our model's performance to previous analytical theories and Monte Carlo simulations. The model will also be tested in the case of Fe-Cr concentrated alloys where thermodynamic short-range order cannot be neglected, and the results will be compared to Monte Carlo simulations as well as experimental studies.

12:25 PM BREAK

SESSION DS02.16: Accelerated Methods III
Session Chairs: Youping Chen and Tony Lelièvre
Tuesday Afternoon, December 7, 2021
DS02-Virtual

1:00 PM *DS02.16.01

Accelerated Sampling in Bidimensional Particle Systems Manon Michel and Arnaud Guillin; CNRS - Université Clermont-Auvergne, France

In the context of the high-dimensionality and multimodality of the potentials encountered in chemical physics, massive efforts have been devoted into the development of efficient simulation methodologies. Since the first works of Molecular dynamics (MD) and Markov-chain Monte Carlo (MCMC) methods, bidimensional particle systems, in particular with hard-core interactions, have played the role of a challenging test bed. In spite of their apparent simplicity, they exhibit a rich behavior where topological defects bind or unbind themselves in pair, ruling by doing so the transition phases. I will first review successful MCMC simulation strategies in sphere systems. These methods are based on the introduction of non-reversibility in the underlying stochastic sampling processes, upgrading them into piecewise deterministic Markov processes (PDMP) and competitors to their MD counterparts. Then I will present how to adapt these strategies in the context of anisotropic particles by exploiting recent progress in PDMP-based sampling.

1:30 PM DS02.16.02

Late News: Predictive Monte Carlo Modeling of Secondary Electron Emission Based on First Principles Calculations Maciej Polak¹, Ivana Matanovic², Raul Gutierrez², John Booske¹, Edl Schamiloglu² and Dane Morgan¹; ¹University of Wisconsin - Madison, United States; ²The University of New Mexico, United States

Monte Carlo modeling of secondary electron emission from metal surfaces usually requires information on material properties obtained from experimental measurements, in particular the energy loss function, a quantity derived from the dielectric function is needed, as well as the Fermi energy and the work function. In addition, the momentum space representation of the energy loss function is often approximated with the use of extrapolation schemes. Here we present a new approach and a first open-source Monte Carlo code for secondary electron yield modeling [1], where all the necessary quantities are calculated from first principles, density functional theory (DFT) methods. In particular, the energy and momentum dependent dielectric function is obtained from time-dependent DFT calculations explicitly, removing the necessity for experimentally measured quantities as well as momentum space extrapolation. In addition DFT calculated density of states is used in secondary electron generation, and DFT obtained work functions are used. This approach allows for predictive modeling of systems where experimental measurements are not available or are very challenging to obtain with high accuracy, such as metal alloys [2]. Successful verification of the approach on well known systems such as Cu and Al, encouraged calculations of secondary electron emission from elemental metals across the whole periodic table. The calculations revealed clear periodic trends in the maximum secondary electron yield, which has not been shown previously, and provided the largest computational database of secondary electron yield curves for elemental metals up to date.

[1] M. P. Polak and D. Morgan, "MAST-SEY: MAterial Simulation Toolkit for Secondary Electron Yield. A monte carlo approach to secondary electron emission based on complex dielectric functions", Computational Materials Science 193, 110281 (2021), <https://doi.org/10.1016/j.commatsci.2021.110281>.
[2] R. E. Gutierrez, I. Matanovic, M. P. Polak, R. S. Johnson, D. Morgan, and E. Schamiloglu, "First principles inelastic mean free paths coupled with Monte Carlo simulation of secondary electron yield of Cu-Ni, Cu-Zn, and Mo-Li", Journal of Applied Physics 129, 175105 (2021), <https://doi.org/10.1063/5.0049522>

1:45 PM DS02.16.03

Langevin Processes in Bounded-in-Position Domains—Application to Quasi-Stationary Distributions Mouad Ramil; CEA, France

Quasi-stationary distributions can be seen as the first eigenvector associated with the generator of the stochastic differential equation at hand, on a domain with Dirichlet boundary conditions (which corresponds to absorbing boundary conditions at the level of the underlying stochastic processes). Many results on the quasi-stationary distribution hold for non degenerate stochastic dynamics, whose associated generator is elliptic. The case of degenerate dynamics is

less clear. In this work, together with T. Lelièvre and J. Reygner (Ecole des Ponts, France) we generalize well-known results on the probabilistic representation of solutions to parabolic equations on bounded domains to the so-called kinetic Fokker Planck equation on bounded domains in positions, with absorbing boundary conditions. Furthermore, a Harnack inequality, as well as a maximum principle, is provided for solutions to this kinetic Fokker-Planck equation, as well as the existence of a smooth transition density for the associated absorbed Langevin dynamics. The continuity of this transition density at the boundary is studied as well as the compactness, in various functional spaces, of the associated semigroup. This work is a cornerstone to prove the consistency of some algorithms used to simulate metastable trajectories of the Langevin dynamics, for example the Parallel Replica algorithm.

2:00 PM *DS02.16.04

Nested Sampling—Finding the Stable Phases and Calculating Phase Transitions Without a Fuss [Livia Bartok-Partay](#)¹, Noam Bernstein², Albert P. Bartok¹, Gyorgy Hantal³ and Gabor Csanyi⁴; ¹University of Warwick, United Kingdom; ²U.S. Naval Research Laboratory, United States; ³University of Natural Resources and Life Sciences, Austria; ⁴University of Cambridge, United Kingdom

In recent years we have been working on adapting a novel Bayesian statistical approach, called nested sampling, for studying atomistic systems. Nested sampling automatically generates all the relevant atomic configurations, unhindered by high barriers, and one of its most appealing advantages is that the global partition function can be calculated very easily, thus thermodynamic properties, such as the heat capacity or compressibility becomes accessible.

Nested sampling is a top-down sampling technique, starting from the high-energy region of the potential energy landscape (gas phase) and progressing towards the ground state structure through a series of nested energy levels, estimating the corresponding phase space volume of each. This way the method samples the different basins proportional to their volume, and instead of providing an exhaustive list of the local minima, it identifies the thermodynamically most relevant states without any prior knowledge of the structures or phase transitions. This means that unlike other methods, nested sampling may be fully automated, allowing high-throughput calculations of novel materials.

The use and advantages of the nested sampling method has been demonstrated in sampling the potential energy landscape of simple model system, calculating the pressure-temperature phase diagram of several metals and alloys[1]. Studying phase transitions and structural properties of small Lennard-Jones[2] and water clusters[3] highlighted the importance of identifying those local minimum basins which contribute the most to the total partition function. Our recent work on the core softened double ramp potential, the Jagla-model, has demonstrated that nested sampling plays an important role in discovering high temperature thermodynamically stable phases, redrawing what we knew about the system's liquid-liquid transitions[4].

[1] RJN Baldock, LB Partay, AP Bartok, MC Payne and G Csanyi, Phys. Rev. B 93, 174108 (2016); RJN Baldock, N Bernstein, KM Salerno, LB Partay and G Csanyi, Phys. Rev. E 96, 043311 (2017); LB Partay, Comp. Mat. Sci. 149 153 (2018)

[2] LB Partay, AP Bartok and G Csanyi, J. Phys. Chem. B 114 10502 (2010)

[3] J Dorrell and LB Partay, Phys. Chem. Chem. Phys. 21 7305 (2019)

[4] AP Bartok, G Hantal and LB Partay, arXiv:2103.03406

2:30 PM DS02.16.05

Optimal Resource Allocation in Parallel Trajectory Splicing [Andrew Garmon](#), Vinay Ramakrishnaiah and Danny Perez; Los Alamos National Laboratory, United States

Widely considered a workhorse in materials simulation, MD has struggled to maintain strong-scalability as it only weak-scales with traditional parallelization methods. One method aimed towards improving the strong-scalability of MD is Parallel Trajectory Splicing (ParSplice); a specialized MD method designed to accelerate the dynamics of rare-event systems without compromising the accuracy of MD. It works by generating a large number of independently-generated trajectory "segments" in such a way that they can later be assembled into a single statistically-correct state-to-state trajectory. Due to the impossibility of deterministically forecasting the future evolution of the trajectory (which would be required to perfectly assign the execution of segments), ParSplice relies on stochastic speculation as it assigns segments via a KMC-like model that is parameterized on-the-fly. In this talk we present a method for extracting an estimate of the likelihood that any given segment will be used as part of the simulation. Then, using these probabilities, we derive an optimization framework for dynamically allocating resources among the set of possible tasks (i.e. potential segments). We detail the improvements in performance resulting from our optimized framework as compared to more naive allocation schemes including the maximum-task-throughput and minimum-time allocations. Performance results are illustrated through the use of several models of varying complexity, lending to fully interpretable results. These models enable an understanding as to when and why other allocation schemes fail, thus further highlighting the versatility/importance of our optimized allocation method. We observe that this new strategy can improve throughput up to 20x, thus greatly improving the scalability of a traditionally scale-limited application.

2:45 PM BREAK

SESSION DS02.17: Molecular Dynamics II
Session Chair: Nikolas Provatas
Tuesday Afternoon, December 7, 2021
DS02-Virtual

4:00 PM *DS02.17.01

Transport Flux, One Unified Concept, Numerous Formulations and One Common Mistake [Youping Chen](#) and Adrian Diaz; University of Florida, United States

Irving and Kirkwood (IK) derived the transport equations from the principles of classical statistical mechanics using the Dirac delta to define local densities. Thereby, formulas for fluxes (local stress and heat flux) were obtained as point functions in terms of molecular variables. The IK formalism has inspired numerous formulations. Many of the later developments, however, believed it more rigorous to replace the Dirac delta with a continuous volume-weighted averaging function and subsequently define fluxes as a volume density. Although these volume-averaged (VA) flux formulas have dominated the literature for decades and are widely implemented in popular molecular dynamics (MD) software, they are a fundamental departure from the well-established physical concept of fluxes.

In this talk, we review the historical developments that led to the unified physical concept of transport fluxes. We then use MD simulations to show that replacing the Dirac delta with a volume weighting function changes the fundamental nature of fluxes as a surface density. As a result, the dynamic balance

between the rate of change of the total momentum or energy in a volume element and the fluxes across the surface boundary cannot be established. This then leads to the failure of VA flux formulas in satisfying the momentum and energy conservation laws or typical transport boundary conditions. We also use two different approaches to derive fluxes for general many-body potentials. The results show that atomistic formulas for fluxes can be fully consistent with the physical definitions of fluxes and conservation laws.

4:30 PM DS02.17.03

Simulation of Bistable [2]Rotaxane for Molecular Memory Application Peiqiao Wu¹, Prabir Patra¹, Bhushan V. Dharmadhikari² and Xingguo Xiong¹; ¹University of Bridgeport, United States; ²Minnesota State University Mankato, United States

VLSI (Very-Large Scale Integration) industry is shifting the paradigm from microelectronics to nanoelectronics so that Moore's law can be extended. Molecular electronics directly utilizes individual molecules to construct circuits and systems, leading to ultra-high efficiency and device density. For digital molecular electronics, a suitable molecule with controllable and stable electrical switching between "ON" and "OFF" states is desired. Among various potential candidates, bistable [2]rotaxane has attracted extensive attention from researchers due to its repeatable switching characteristics and the ability to be driven electrically. Many studies have been performed on characterizing the [2]rotaxane molecule, its I-V characteristics, and molecular dynamics mechanism. In this paper, we reported our findings of molecular simulation of [2]rotaxane utilizing Nanoscale Molecular Dynamics (NAMD) and Visual Molecular Dynamics (VMD) platforms. The simulation illustrates the switching mechanism of [2]rotaxane between its two stable states, and what factors might affect the switching process. The simulation shows the switching process of [2]rotaxane is repeatable and controllable, resulting it to be an excellent candidate for molecular memory application. The signal "crosstalk" – interference between neighboring [2]rotaxane molecules, is also investigated with simulation. A mathematical model is proposed to describe the minimum pitch of the memory array to ensure the reliability of the data stored in the memory. Based on this, a set of design rules, the analogy to DRC (Design Rule Check) in CMOS VLSI, are proposed to tolerate the process variation and signal interference of the [2]rotaxane-based molecular memory. The simulation results verify [2]rotaxane as a promising candidate for molecular memory application.

4:35 PM DS02.17.04

Understanding the Molecular-Level Interactions Between Polymers and Functionalized Metal-Organic Frameworks Abhishek T. Sose, Fangxi Wang and Sanket Deshmukh; Virginia Tech, United States

The need to develop environmentally friendly and energy efficient technology for gas separations can be fulfilled by polymer mixed matrix membranes (MMMs) of metal-organic frameworks (MOFs). In these MMMs, polymers, MOFs and the polymer-MOF interface are known to play an important role in determining the gas separation mechanism. However, fundamental understanding of the parameters determining the compatibility of the polymer-MOF interface is still unknown. In this study, we have performed all-atom (AA) molecular dynamics (MD) simulation of a model polymer-MOF MMMs of hydrophobic/hydrophilic polymers with IRMOF-1 and IRMOF-10 as fillers. These systems include the polymer matrix of hydrophobic polymers *viz.* polyvinylidene fluoride (PVDF), polyethylene (PE), and hydrophilic polymers *viz.* polymethylmethacrylate (PMMA), polyethylene glycol (PEG). To understand the effect of MOF functionalization on the polymer-MOF interface, we decorated IRMOF-1 with the four functional groups *viz.* methyl (-CH₃), amine (-NH₂), hydroxy (-OH) and fluorine (-F). A stronger structural correlation for the polymer-MOF interface was observed in the systems with functionalized MOFs compared to unfunctionalized MOFs embedded in hydrophilic (or hydrophobic) polymer matrix. Thus, different functional groups can be added to control the compatibility of polymer-MOF interfaces.

4:50 PM *DS02.17.05

Molecular Dynamics Using Non-Linear Charge Relaxation Models Anders M. Niklasson; Los Alamos National Laboratory, United States

Molecular dynamics simulations are currently undergoing a revolution thanks to modern machine learning tools that can provide very accurate short-range interatomic potentials. Unfortunately, without a dramatic increase in the computational cost, these new techniques fail to account for the critically important long-range electrostatic interactions and their associated polarization and charge relaxations – rendering them practically useless for many real-world problems. In this talk I will show how the computational overhead associated with the long-range charge equilibration problem in molecular dynamics simulations based on non-linear charge relaxation models can be avoided. The technique relies on the construction of approximate shadow energy functionals whose relaxed ground state charge distributions closely follow the fully equilibrated solutions of the corresponding exact non-linear charge relaxation models. This makes it possible to perform accurate molecular dynamics simulations with non-linear charge relaxation models using only a single Coulomb summation per time step.

5:20 PM DS02.17.06

Molecular Dynamics Simulations to Explore Crack Tip Behaviour in High Entropy Alloys Sandeep K. Singh and Avinash Parashar; Indian Institute of Technology, India

In the last couple of decades, high entropy alloys (HEAs) or multi-element alloys are emerging as potential candidates for many diversified structural applications. Molecular dynamics based simulations were performed in conjunction with 2NN MEAM potential to study the fracture behaviour in ternary, quaternary, and quinary alloy configurations. Simulations were performed after aligning the crack plane with three different principle planes of FCC crystal. Deformation in each of the orientations was primarily governed by dislocations, twinning, and stacking faults emanating from the crack tips or from the surface of the crack plane. Medium and high entropy alloys have shown higher resistance to fracture and were capable of retaining strength up to a larger extent as compared to low entropy alloy and pure Ni crystal. The higher dislocation density and uniform distribution of dislocation in medium and high entropy alloys lead to plasticity in the crystal after the onset of yielding. Blunting of the crack tip in medium and high entropy alloys was predicted in orientation 1 and 2, whereas crack propagates in orientation 3. This study will help in elucidating the capabilities of medium and high entropy alloys in resisting the opening mode of crack propagation, which can be further utilized to enhance the diversified structural applications of these emerging multi-elemental alloys.

5:35 PM DS02.17.07

Interaction of Electron Beam and Gold Nanoparticles Cuauhtémoc N. Valencia, Jakob Schiotz, Matthew Helmi Leth Larsen, Thomas W. Hansen, William Bang Lomholdt and Pei Liu; Denmark Technical University, Denmark

Beam damage in High-Resolution Transmission Electron Microscopy (HRTEM) is poorly understood theoretically, and not yet well described phenomenologically. For example, it is not yet known whether it is the total dose (electrons per area) or the dose rate (electrons per area per time) that is most critical for inducing beam damage [1,2]. In order to study the dependence of the total dose, a molecular dynamics simulation can be an appropriate tool to understand the atomic level behavior, when coupled to experimental observations. Using molecular dynamics, we study the beam damage in gold nanoparticles caused by high-energy electron beam irradiation. We assume that the main damage mechanism in metallic nanoparticles is knock-on damage, where an energetic electron transfers momentum and energy to an atom through

Rutherford scattering.

In this work, we focus on the simplest mechanism for beam damage: direct transfer of momentum between the energetic electrons and the nuclei through Rutherford scattering. Several molecular dynamics studies have previously focused on electron head-on collision in carbon nanomaterials [3,4]. Here, we extend these methods to include collisions with non-zero impact parameter, and build a model including both complete removal of atoms as well as beam-induced surface diffusion on the nanoparticle, in the context of HRTEM. We use a stochastic approach for the momentum transfer to the atoms in the nanoparticle, focusing on momentum transfer to the easily removed surface atoms. In this way, for each nanoparticle size, we get a rate of atom removal and a rate of induced surface diffusion proportional to the beam intensity. We compare these rates with observation of beam induced surface diffusion and beam induced damage in gold nanoparticles on a cerium dioxide (CeO₂) substrate, as observed in HRTEM. The analysis of the experimental data leverages convolutional neural networks to identify when the structure changes [5].

If the momentum transferred to an atom is insufficient (such as non-zero impact parameters) to remove the atom from the nanoparticle, the induced motion will be primarily in the beam direction. In this case the nanoparticle may heal through thermal diffusion processes. We model this qualitatively through a short molecular dynamics annealing step between each energy transfer event. This may lead to a dependency on not only the total dose, but also on the dose rate.

In addition, effects of the dose rate are expected to be shown predominantly through the heating of the nanoparticle due to the increase of the events per unit of time as we increase the dose rate. In addition to heating from the many Rutherford scattering events with too low momentum transfer to inflict direct damage, there may also be a heating effect due to interactions between the beam electrons and the conduction electrons of the metals. Simple models can be made for these effects, and rough estimates of the heating of the nanoparticle can then be used to extend the current molecular dynamics simulations to higher temperatures, where beam damage will occur more readily.

REFERENCES:

- [1] Kisielowski, Christian, et al. *Physical Review B* 88.2 (2013): 024305.
- [2] Kisielowski, C., et al. *Advanced structural and chemical imaging* 2.1 (2016): 1-14.
- [3] Yasuda, Masaaki, et al. *MRS Online Proceedings Library* 1700.1 (2014): 29-35.
- [4] Pregler, Sharon K., and Susan B. Sinnott. *Physical Review B* 73.22 (2006): 224106.
- [5] Madsen, Jacob, et al. *Advanced Theory and Simulations* 1.8 (2018): 1800037.

5:55 PM BREAK

SESSION DS02.18: Molecular Dynamics III
Session Chairs: Livia Bartok-Partay and Anders Niklasson
Wednesday Morning, December 8, 2021
DS02-Virtual

8:00 AM DS02.18.02

Late News: Multiscale Simulation of Atomic Structure in the Vicinity of Nanovoids and Evaluation of the Shifting Rates of the Void Surface Elements in bcc and fcc Metals Andrei V. Nazarov^{1,2}, Aleksey P. Melnikov¹, Alexander A. Mikheev³ and Irina V. Ershova¹; ¹National Research Nuclear University MEPhI, Russian Federation; ²Institute for Theoretical and Experimental Physics named by A.I. Alikhanov of NRC "Kurchatov Institute", Russian Federation; ³The Kosygin State University of Russia, Russian Federation

We simulate structure in the vicinity of different size nanovoids using a new variant of the Molecular Statics, wherein atomic structure in the vicinity of nanovoids and the parameters that define the displacements of atoms placed in elastic continuum around main computation cell are determined in a self-consistent manner. Atomic structure are calculated in vicinity of nanovoids for bcc and fcc metals. Should pay attention that in bcc structures displacements of atoms located in the direction <100> or close to it are positive, whereas the atom displacements located in other directions is negative [1,2,3]. For fcc structures all displacements are negative but may vary significantly in value depending on the direction. Strain fields calculated based on the displacement fields lead to anisotropy of vacancy fluxes. Then we simulate structure of the surface of different crystallographic planes. Kinetic equations for shifting rate of void surface elements are obtained [2] that take into account the dependence of the vacancy flux on strain fields and the surface energies of the crystallographic planes that located normal to the void surface. The shifting rates of void surface elements are calculated for different crystallographic directions in a wide range of temperatures and different supersaturations of vacancies. Rates of displacements in different crystallographic directions for bcc and fcc metals differ significantly, and for the <100> direction they are greatly lower than for other directions. This effect can lead to a change in the shape of the initially spherical nanovoids and cause their transformation into pores of a cuboid shape. The influence of the calculated values of the surface energies for various crystallographic planes on the shifting rates in the corresponding directions is also evaluated.

[1] A.V. Nazarov, I. V. Ershova, and Y. S. Volodin, *KnE Materials Science*, p. 451, (2018) DOI 10.18502/50.

[2] Andrei V. Nazarov, Alexander A. Mikheev, Aleksey P. Melnikov, *Journal of Nuclear Materials*, 532, 152067 (2020).

[3] A V Nazarov et al 2020 *IOP Conf. Ser.: Mater. Sci. Eng.* **1005** 012026-6
DOI 10.1088/1757-899X/1005/1/012026

8:15 AM DS02.18.03

Late News: Simulation Features of Atom Jumps at Constant Temperature and Under Different Pressure by Molecular Dynamics Madina Boboqambarova¹ and Andrei V. Nazarov^{1,2}; ¹National Research Nuclear University MEPhI, Russian Federation; ²Institute for Theoretical and Experimental Physics named by A.I. Alikhanov of NRC "Kurchatov Institute", Russian Federation

At present, Molecular Dynamics (MD) is the most suitable approach to gain information at the atomic scale. However, a simulation of diffusion by MD faces some difficulties in implementation. In particular, we noticed that when modeling diffusion by MD and molecular statics (MS) using the same potentials, the found values of the migration energy differ markedly [1]. In our work we discuss features of atomic jump simulation. Then we present a new approach (approach of natural thermostat) that fully takes into account the fluctuating character of atomic jumps at the constant temperature MD simulation. In addition the combination of MD and modified method of MS [2] allowed within this model to take into account thermal expansion of the lattice and long-range elastic displacement of the atoms in the vicinity of defects. With the developed model, we study features of atom diffusion in iron by

vacancy mechanism at different temperatures using a many-body potential [3]. Migration energy and pre-exponential factor are obtained and a comparison of the calculated diffusion parameters with the results of the other authors' work whose used various modeling methods is carried out. We then developed our approach to take into account the effect of pressure on diffusion jumps of atoms. This approach made it possible to calculate the temperature dependence of the migration volume. In addition, the model developed by us makes it possible to select and construct the trajectories of motion of atoms making a diffusion jump, and therefore to analyze the features of various types of diffusion jumps, in particular, to detect such events as double jumps of atoms and jumps leading to the return of an atom to a vacancy. Analysis of a large number of diffusion jump trajectories allows us to estimate the contribution of double jumps in the diffusion mobility at different temperatures.

[1] Mikhlin A.G., Osetsky Yu.N., J. Phys.: Condens. Matter, –1993 –Vol.5 – p.9121.

[2] Valikova I.V., Nazarov A.V., Defect Diffus. Forum, – 2008 – Vol. 277 – p.125.

[3] Ackland G.J., Bacon D.J., Calder A.F., Harry T. , Phil. Mag. A. – 1997. – Vol. 75. – N 3. –p. 713.

8:30 AM DS02.18.04

Unraveling Mechanisms of Interface Diffusion and Interfacial Creep in Metals, Semiconductors and Metal-Ceramic Composites [Ian Chesser](#), Raj Koju and Yuri Mishin; George Mason University, United States

Interface diffusion and interfacial slip are two key processes controlling the high-temperature creep deformation of metal-matrix composites. Fundamental understanding of these processes remains poor. Atomistic simulations are a promising route toward understanding, but reliable methodology for measuring kinetic coefficients and disentangling competing mechanisms has not been developed in this context. In this work, we compare interface diffusion and sliding coefficients in pure Al and Si grain boundaries to those in AlSi phase boundaries using direct molecular dynamic simulations at high and intermediate homologous temperatures. Diffusion along AlSi phase boundaries is found to be quite fast, depending on interface orientation and structure, with activation energies on par with GB diffusion in pure Al. Clusters of highly mobile Si atoms at these phase boundaries often have activation energies similar to Al. Interface diffusion and interface slip are found to be distinct, but correlated processes with characteristic fractal dimensions, cluster size distributions, and nucleation and growth dynamics. Universal and system dependent features of atomic motion during diffusion and sliding are identified over a large parameter space including multiple interface geometries, temperatures and strain rates. Key results are verified with an accurate PINN potential.

8:45 AM *DS02.18.05

Diffusion in Stationary and Moving Interfaces in Alloys Raj K. Koju, Ian Chesser and [Yuri Mishin](#); George Mason Univ, United States

While it is well-established that atoms diffuse along interfaces much faster than in the perfect lattice, atomistic understanding of this “short-circuit” diffusion phenomenon remains incomplete. This talk will discuss several topics related to interface diffusion: atomic mechanisms of grain boundary (GB) diffusion, the effect of GB segregation on the GB diffusion rate, and the role of GB diffusion in the solute drag phenomenon. These effects are studied by atomistic computer simulations combining molecular dynamics, Monte Carlo methods, and other computational approaches. It is shown that solute segregation can cause either acceleration or retardation of GB diffusion, depending on the thermodynamics of the system, GB structure, and the segregation mechanism. In a solute-drag study, the drag force has been investigated systematically as a function of temperature, alloy composition, and the GB velocity. It is shown that solute diffusion along the GB can dramatically impact the GB mobility by redistributing the solute atoms non-uniformly in the form of nano-clusters or islands and causing additional pinning. GB diffusion coefficients and diffusion mechanisms are compared with those for metal/semiconductor phase boundaries with different orientation relationships between the phases.

9:15 AM DS02.18.06

Charge Equilibration Model with Shielded Long-Range Coulomb for Molecular Dynamics Simulations [Udoka, Nwankwo](#), Nicolas Onofrio and Chi-Hang Lam; The Hong Kong Polytechnic University, Hong Kong

Dynamic charge distribution and polarization effects are often difficult to describe using traditional force field models, especially for crystalline and amorphous systems. Reactive molecular dynamics has become a panacea for describing the potential chemistry between atoms and molecules, and the environment-dependent charge distribution and polarization effects. Charge equilibration as well reactive force field models such as ReaxFF can include these effects in large systems. However, the numerical implementation of these models include Coulomb interaction up to a “short-distance” cutoff for computational speed, limiting their application to devices with unrealistic small sizes. Although designing an effective atomic charge model to reproduce the electrostatic fields in electrochemical systems has always been a challenge, ignoring long-range Coulomb interaction affects the ability to describe charge distribution and polarization effects in electrochemical systems. We include long-range effects to partial charge calculations (QEq) using shielded long-range Coulomb potential and then evaluate long-range effect between charged particles. By including long-range effect, we anticipate better account of Coulomb interaction for dynamic charge distribution and polarization in atomic and molecular systems. The accuracy of our model to compute charges on a number of metal organic frameworks and simple systems compare to conventional QEq and quantum mechanics (QM) shows that charges computed without long-range are slightly overestimated. A test of our QEq technique against standard QEq on a simple capacitor configuration under external potential shows some significant differences between charges computed with/without long-range Coulomb. The difference results from long-range influence on ions of the capacitor. The difference indicates clearly that the excluded ions via short-distance cut-off treatment of conventional QEq coupled molecular dynamics affect the interaction potential. Further improved investigation of our approach shows that inclusion of orbital overlap function and/or bond-dependent electronegativity as in split charge (SQE) method correctly exhibits dissociation property for largely separated atoms. The later improvement would enable the atomic description of electrochemical systems involving bond breaking while preserving long-range Coulomb interaction effect on charged electrodes throughout the dielectric layer such as in battery and emerging solid-state memory.

9:20 AM DS02.18.07

Energy Absorption Capabilities of BNNS Reinforced Polyethylene Nanocomposites—A Compressive Shock Behavior [Ankur Chaurasia](#) and Avinash Parashar; Indian Institute of Technology Roorkee, India

The present study aims to investigate the effect of two-dimensional (2D) inorganic nanofiller boron nitride nanosheet (BNNS) on the shock compressive response of polyethylene (PE) based nanocomposites. A non-equilibrium molecular dynamics (NEMD) based simulations were performed in conjunction with reactive force field (Reaxff) parameters to capture the interatomic interactions within 2D nanofiller BNNS and polyethylene chains, whereas interfacial properties were triggered with the help of non-bonded interactions. Nanocomposite reinforced with monolayer BNNS is predicted to be a superior nanofiller for attenuating the shock strength across the interface BNNS/PE nanocomposites as compared to pristine PE. In continuation with the monolayer reinforced nanocomposites, compressive shock hughoniot response of dispersed BNNS reinforced nanocomposites were also predicted and compared with the monolayer BNNS reinforced nanocomposites. It was reported that dispersed BNNS significantly increases the energy dissipation capability via deformation and temperature rise of the dispersed BNNS nanosheet. These present study outcomes will help developing inorganic nanofiller reinforced nanocomposites with superior shock mitigation for lightweight armor and space structures.

9:40 AM BREAK

SESSION DS02.19: Coarse Grain Models V
Session Chair: Lin-Wang Wang
Wednesday Morning, December 8, 2021
DS02-Virtual

10:30 AM DS02.19.01

Recent Theoretical Development of Py-Chemshell for Calculating Vibrational Properties of Transition Metal Containing Zeolites [Jingcheng Guan](#)¹, You Lu², Thomas W. Keal², Andrew Beale³, C. Richard A. Catlow¹ and Alexey A. Sokol¹; ¹University College London, United Kingdom; ²Daresbury Laboratory, STFC, United Kingdom; ³Rutherford Appleton Laboratory, STFC, United Kingdom

We report a theoretical development of a fully anharmonic method for the calculation of local vibrational properties of transition metal-containing zeolites modelled by the hybrid QM/MM approach. The scheme is closely related to the vibrational self-consistent field (VSCF) method [1] applied to localised modes in gas-phase molecules [2] but includes the effects of the environments and accurate numerical solutions of the VSCF equations in real space using Schrödinger solvers. The method is implemented as a new module/library of the Py-Chemshell (PCS) [3]. These zeolites calculations are integrated with the QM/MM models, which have been reported previously [4] and implemented in PCS. This work continues the recent extension in PCS to support calculations of infrared and Raman intensities based on the harmonic approximations. Our VSCF implementation tackles anharmonicities, coupling and delocalisation of normal modes - these are recognised as key challenges for first-principle computations of vibrational properties. We carry on from the VSCF calculations to talk about how to assign band positions for intermediates of a selective catalytic redox cycle over Cu-SSZ-13 [5]. We conclude with a discussion of further intermodal correlation and evolution effects.

References:

- [1] J. Bowman, et al. *Molecular Physics*. 2010, 106, 16-18, 2145-2182.
- [2] X. Cheng, et al. *J. Chem. Phys.* 2014, 141.10, 104105.
- [3] L. You, et al. *J. Chem. Theory Comput.* 2019, 1317-1328.
- [4] P. Sherwood, et al. *Faraday Discuss.* 1997, 106, 79-92.
- [5] A. Greenaway, et al. *Chem. Sci.* 2020, 447-455.

10:45 AM *DS02.19.03

Multiscale Quantum-Atomistic and Atomistic-Continuum Modelling of Crack Propagation and Dislocation Motion [James Kermode](#); University of Warwick, United Kingdom

I will review recent progress on the development and application of advanced atomistic algorithms to simulate chemomechanical systems where local chemistry and long-range stress are tightly coupled, e.g. at the tip of a propagating crack or the core of a dislocation. I will discuss two general approaches (i): hybrid quantum/classical approaches where bond-breaking is treated at the DFT level embedded within a large-scale classical atomistic model to capture elastic relaxation, including recent applications to tungsten [1] and polymer nanocomposites [2]; (ii) atomistic-to-continuum modelling for crack propagation, either through extracting effective continuum models from large-scale atomistic simulations of fracture [3], or by flexibly embedding an atomistic domain within a continuum model, using a new algorithm to compute bifurcation diagrams for fracture systems [4].

- [1] P. Grigorev, T. Swinburne and J. R. Kermode, QM/MM study of hydrogen-decorated screw dislocations in tungsten: ultrafast pipe diffusion, core reconstruction and effects on glide mechanism, *Phys. Rev. Materials* **4** 023601 (2020)
- [2] J. R. Golebiowski, J. R. Kermode, P. D. Haynes and A. A. Mostofi, Atomistic QM/MM simulations of the strength of covalent interfaces in carbon nanotube-polymer composites, *Phys. Chem. Chem. Phys.* **22** 12007 (2020)
- [3] S. M. Khosrownejad, J. R. Kermode, and L. Pastewka, Quantitative Prediction of the Fracture Toughness of Amorphous Carbon from Atomic-Scale Simulations, *Phys. Rev. Materials* **5**, 023602 (2021)
- [4] M. Buze and J. R. Kermode, Numerical-Continuation-Enhanced Flexible Boundary Condition Scheme Applied to Mode-I and Mode-III Fracture, *Phys. Rev. E* **103**, 033002 (2021)

11:15 AM *DS02.19.04

Phase Field Crystal Modelling of Orientation Gradients in Rapidly Solidified Aluminum Paul Jreidini¹, Tatu Pinomaa², Jörg M.K. Wiezorek³, Joseph McKeown⁴, Anssi Laukkanen² and [Nikolas Provatas](#)¹; ¹McGill University, Canada; ²VTT Technical Research Centre of Finland Ltd, Finland; ³University of Pittsburgh, United States; ⁴Lawrence Livermore National Laboratory, United States

This talk discusses recent rapid solidification experiments on thin film aluminum samples that reveal the presence of lattice orientation gradients within crystallizing grains. To study this phenomenon, a new phase-field crystal (PFC) model that captures the properties of solid, liquid, and vapor phases is proposed to model pure aluminum quantitatively. A coarse-grained representation of this model is used to study rapid solidification in samples approaching micrometer scales. We present recent results of this model that reproduce the experimentally observed orientation gradients within crystallizing grains grown at experimentally relevant rapid quenches, discussing a causal connection between defect formation and orientation gradients.

11:45 AM DS02.19.06

Computing the Local Yield Surface in 3D Model Glasses to Predict Plastic Events [Spencer Fajardo](#)¹, Dihui Ruan¹, Sylvain Patinet² and Michael L. Falk¹; ¹Johns Hopkins University, United States; ²École Supérieure de Physique et de Chimie Industrielles, France

Using 2D model glasses as a theoretical base for studying amorphous materials, the Local Yield Stress (LYS) method has ranked highly among available predictors for determining the location of plastic events. By probing local regions of atoms, the LYS method quantifies the amount of incremental stress

necessary to induce plastic rearrangements. In 2D, the computed local yield stress ($\Delta\tau_c$) is dependent on the direction in which the stress was applied on the local region. Thus, a more accurate prediction is made by sampling multiple loading directions in each local region. In 3D, in order to fully quantify the local yield surface, we sample 432 distinct loading orientations. The resulting yield surface can be used to calculate the projected local yield stress ($\Delta\tau_y$) with respect to the loading on the boundary. We then quantify the difference in predictive capabilities of the LYS method when using the full local yield surface, compared to predictions made using only a single local probing direction aligned with the loading on the boundary.

SESSION DS02.20: Coarse Grain Models III
Session Chair: Enrique Martinez
Wednesday Afternoon, December 8, 2021
DS02-Virtual

1:00 PM *DS02.20.01

High-Performance Quasicontinuum for Multilattice 3D Systems [Ellad B. Tadmor](#)¹, Stephen M. Whalen¹ and Woo Kyun Kim²; ¹University of Minnesota, United States; ²University of Cincinnati, United States

The quasicontinuum (QC) method is a multiscale method that extends the length and time scales accessible to fully-atomistic simulations by orders of magnitude. This talk will describe the development over recent years of a high-performance implementation of QC for three-dimensional (3D) polycrystalline materials of arbitrary multilattice crystal structures. Features include finite temperature support (hot-QC), temporal acceleration via hyperdynamics (hyper-QC), and support for the KIM API (allowing usage of interatomic potentials archived on <https://openkim.org>). The code is optimized for a heterogeneous computing infrastructure including a mix of shared memory (OpenMP) and distributed memory (MPI) parallelism. A graph partitioning load balancing algorithm has been developed for efficient resource usage. State-of-the-art software engineering techniques are applied including Git revision control, test-driven development (TDD), and continuous integration (CI) to minimize errors in this complex software platform (120K lines of code). The code features, structure and performance will be discussed as well as example applications to fracture, nanoindentation and friction in semiconductors, metals and thermal shielding materials.

1:30 PM DS02.20.02

Novel Methodology for Computing Interactions Between Curved Fibers [Anirban Pal](#); West Texas A&M University, United States

Simulating athermal fiber-networks involves the computation of cohesive energies between fiber segments. A general fiber in three-dimensional space can be represented as a connected sequence of straight-line segments or as an assembly of Bezier curves. The former can result in poor representation of fiber curvature and has been addressed in previous work. The latter is treated in this work. The computation of energy (and force) between two Bezier curves can be implemented using a distance distribution function. This distribution function lacks a closed form expression and is computed using a mix of contouring techniques, interval trees and quadrees. This method reduces some of the artificial friction associated with the discretization of continuous fibers.

1:45 PM *DS02.20.03

Towards Predicting Non-Equilibrium Material Response [Celia Reina](#)¹, Shenglin Huang¹ and Steve Fitzgerald²; ¹University of Pennsylvania, United States; ²University of Leeds, United Kingdom

Non-equilibrium material behavior is still riddled with many open questions: is it possible to predict the far-from-equilibrium material behavior under arbitrary loading from equilibrium data? Is it possible to predict the effect of element transmutation in the mechanical behavior of materials? In this talk, a statistical mechanics framework for non-equilibrium material response will be presented to address these questions.

2:15 PM DS02.20.04

Coarse-Grained Molecular Dynamics Simulations of poly(N-isopropylacrylamide)-Peptide Conjugates [Soumil Y. Joshi](#) and Sanket Deshmukh; Virginia Tech, United States

Polymer-peptide conjugates have been of great interest over the years because of their proposed applications in biotechnology, medicine and nanotechnology. Conjugation of peptides and polymers can result in hybrid materials with increased biological functions like enzymatic action or receptor recognition as well as suppressed surface activity to prevent its degradation by proteolytic enzymes. Thermosensitive polymers like poly(N-isopropylacrylamide) (PNIPAM) that have a lower critical solution temperature (LCST = ~305 K) can undergo a reversible coil-to-globule transition in response to changes in temperature. When conjugated with peptides, PNIPAM has been shown to create temperature-induced phase switches to alter the substrate activity of the peptide, self-assembled mesoglobules etc. However, precise molecular details of these PNIPAM-peptide architectures as well as the effects of PNIPAM chain lengths and peptide type are largely unexplored, especially using computational methods. In this study, we employ coarse grained (CG) molecular dynamics (MD) simulations to simulate PNIPAM-peptide systems using PNIPAM and amino acid models previously developed in the group. We explore a number of peptides formed using combinations of hydrophobic (Leu, Phe, Trp etc.), hydrophilic (Arg, Lys, Asn etc.) and neutral (Gly, Ser, His etc.) amino acids like Gly-Arg-Lys-Phe-Gly. By performing detailed structural analysis, we investigate the molecular-level structure of these conjugates and solvent at the interface.

2:30 PM DS02.20.05

Bayesian Uncertainty Quantification of Coarse-Grained (CG) Embedded Atom Method (EAM) Potentials for FCC Metals [Abhishek T. Sose](#)¹, Troy Gustke¹, Fangxi Wang¹, Aditya (Ashi) Savara² and Sanket Deshmukh¹; ¹Virginia Tech, United States; ²Oak Ridge National Laboratory, United States

New coarse-grained (CG) embedded atom method (EAM) potentials have been developed to describe the interatomic interaction for face-centered cubic (FCC) metals *viz.* Gold (Au), Palladium (Pd), Nickel (Ni), Copper (Cu), Aluminum (Al) and Platinum (Pt). These CG metal models could reproduce several physical, mechanical, and thermodynamic properties obtained from experimental and/or quantum methods. The reliability and robustness of each EAM potential is assessed by performing sensitivity analysis using Sobol sampling. Subsequently, the model was refined with the Bayesian parameter estimation (BPE) and further uncertainty quantification (UQ) using CheKiPEUQ, a Bayesian parameter estimation tool. The refinement and UQ process was accelerated by integrating Gaussian Process (GP) based machine learning (ML) models. The Bayesian refined CG model predicted the metal properties within reasonable confidence levels of experimental data. This improved computational framework can be extended to develop the reliable and accurate CG interatomic potentials for other hard- and soft-materials.

SESSION DS02.00: General Session
Session Chairs: David Aristoff and Enrique Martinez
Wednesday Afternoon, December 8, 2021
DS02-Virtual

4:00 PM *DS02.09.07

Bounding and Propagating Uncertainty in Atomistic Exploration [Thomas D. Swinburne](#)^{1,2}; ¹CNRS, France; ²CINaM, Aix-Marseille Université, France

Atomistic models of materials are always approximate, giving rise to uncertainty. One source is from the cohesive model, due to e.g. the treatment of electronic correlation in density functional theory or the functional form / descriptor basis of an empirical interatomic potential. In many cases, some form of error bound can be derived, and a variety of propagation schemes have been developed.

An equally common, but often unquantified, uncertainty arises when targeting some observable whose mechanism is *a priori* unknown. As this requires computational exploration, via sampling methods such as accelerated molecular dynamics or saddle search routines, any estimate will be vulnerable to additional sampling data (namely, the discovery of new mechanisms). This complicates how results from atomistic simulations can be confidently used for direct predictions or the parametrization of higher-scale models.

I will discuss some recent efforts to quantify sampling uncertainties when system trajectories can be considered metastable, allowing a rigorous Markov chain / kinetic Monte Carlo representation[1]. Using examples of point defect diffusion in alloys and structural transformations of atomic clusters, I will show how the bounding and propagation of sampling uncertainty depends critically on both the quantity of interest and the sampling method. In particular, errors from dynamic sampling methods can be rigorously bounded[2], whilst static methods have approximate bounds that benefit from a committee approach[3]. Some of these ideas are exploited by the TAMMBER code[4], which optimally manages thousands of simulation tasks in parallel, autonomously distributing (dynamic) sampling effort such that the target uncertainty, propagated through the Markov chain, reduces maximally fast. If time allows I will also discuss how this same framework can be used to propagate and target model form uncertainty in empirical potentials.

[1] TD Swinburne, *Comp. Mat. Sci.* 2021, 10.1016/j.commatsci.2020.110256

[2] TD Swinburne and D Perez, *NPJ Comp. Mat.* 2020, 10.1038/s41524-020-00463-8

[3] TD Swinburne and DJ Wales, *JCTC* 2020, 10.1021/acs.jctc.9b01211

[4] github.com/tomswinburne/tamMBER

4:30 PM *DS02.01.03

Many-Body Approaches for Excitations In Solids—Current Limitations and Perspectives Towards Exascale Performance [Claudia Draxl](#)¹, Ronaldo Pela¹, Benedikt Maurer¹, Andris Gulans² and Felix Henneke³; ¹Humboldt-Universität zu Berlin, Germany; ²University of Latvia, Latvia; ³Freie Universität Berlin, Germany

The Bethe-Salpeter equation (BSE) of many-body perturbation theory (MBPT) is the state-of-the-art approach to determine optical, UV, and x-ray absorption spectra of crystalline materials. Likewise, time-dependent density functional theory (TDDFT) enables the study of excitations in molecules and solids either via time propagation or by computing their response to external perturbations in the linear regime. Such high-level approaches are, however, compute-intensive, often hampering their application to complex systems. This is in particular so, if highly accurate basis sets are employed to solve the underlying DFT problem and to expand the non-local operators appearing in excited-state methodology. In this talk, we will discuss current limitations and present various algorithms to overcome some of the bottlenecks. All this is realized in the all-electron linearized augmented plane-wave + local orbital (LAPW+lo) code **exciting** [1]. The first example concerns (i) an iterative solver for diagonalizing huge sparse matrices that appear when treating low-dimensional systems in codes that apply periodic boundary conditions. Making use of this method, allows us to reach microHartree precision for the energies of atoms and molecules [2]. Building on this, we are (ii) extending this approach towards the time domain in TDDFT [3]. Moreover, we make use of a (iii) recently developed algorithm for substantially speeding up the solution of the BSE [4], and (iv) demonstrate the successful implementation in **exciting** by applications to complex systems. Finally, we will discuss how to bring high-level approaches to exascale as envisioned in the European Center of Excellence NOMAD [5].

[1] A. Gulans, S. Kontur, C. Meisenbichler, D. Nabok, P. Pavone, S. Rigamonti, S. Sagmeister, U. Werner, and C. Draxl, *exciting: a full-potential all-electron package implementing density-functional theory and many-body perturbation theory*, *J. Phys: Condens. Matter (Topical Review)* 26, 363202 (2014).

[2] A. Gulans, A. Kozhevnikov, and C. Draxl, *Microhartree precision in density functional theory calculations*, *Phys. Rev. B* 97, 161105(R) (2018).

[3] R. Rodrigues Pela and C. Draxl, *All-electron full-potential implementation of real-time TDDFT in exciting*, *Electronic Structure* (2021); in print.

[4] F. Henneke, L. Lin, C. Vorwerk, C. Draxl, R. Klein, and C. Yang, *Fast optical absorption spectra calculations for periodic solid state systems*, *Commun. Appl. Math. Comp. Sci.* 15, 89 (2020).

[5] NoMAD Center of Excellence, <https://nomad-coe.eu>. NOMAD CoE receives funding from the European Union's Horizon 2020 research and innovation program under the grant agreement 951786.

5:00 PM DS02.01.07

New Methods for the Theory of Spin-Lattice Coupling in Magnetic Materials at High Temperature [Bjorn Alling](#); Linköping University, Sweden

We have developed a method, the combines atomistic spin dynamics and *ab-initio* molecular dynamics (ASD-AIMD) to investigate magnetic materials at high temperature.[1] We apply the method to study the mutual coupling of spin fluctuations and lattice vibrations in paramagnetic CrN and elemental Fe. The two degrees of freedom can be dynamically coupled, and our method allows for observations of nonadiabatic effects. In CrN, those effects is found to suppress the phonon lifetimes at low temperature compared to an adiabatic, fast-magnetism approximation. The dynamic coupling identified here provides an explanation for the experimentally observed unexpected temperature dependence of the thermal conductivity of CrN and other magnetic semiconductors at and above the magnetic ordering temperature.

Our method is based on an alternating scheme of ASD and AIMD steps. In every step of AIMD, constrained non-collinear magnetic moments are used in

the density functional theory calculations. The obtained forces are used to update the atomic positions by a single-step propagation of the atoms. With the new atomic positions, new distance dependent magnetic exchange interactions are obtained and used to propagate the magnetic state for the same time-step in the ASD simulation together giving a coupled ASD-AIMD step that are repeated until convergence of studied quantities.

The dynamics of the CrN spin system impacts atomic lattice vibrations and the quantities related to it, in particular phonon lifetimes. The magnetic state and its dynamics are influenced by the lattice vibrations. Slightly above the transition temperature (300K), the dynamical coupling, is found to significantly reduce the phonon lifetimes of the acoustic modes. In contrast, at high temperatures (1000 K) the dynamical coupling and its impact on phonon lifetimes are largely reduced.

Our ASD-AIMD method provides access to magnetic materials at high temperature with AIMD- level accuracy previously only existing for non-magnetic materials. We demonstrate its reliability by deriving the free energy differences between alpha- gamma- and delta-Fe as a function of temperature and investigate paramagnetic Fe under Earth-core conditions.

[1] *Anomalous Phonon Lifetime Shortening in Paramagnetic CrN Caused by Spin-Lattice Coupling: A Combined Spin and Ab Initio Molecular Dynamics Study*

Irina Stockem, Anders Bergman, Albert Glensk, Tilmann Hickel, Fritz Körmann, Blazej Grabowski, Jörg Neugebauer, and Björn Alling
Physical Review Letters 121, 125902 (2018)

5:15 PM *DS02.01.06

From Moiré Excitons to Charge and Energy Transfer in 2D van der Waals Heterostructures [Gang Lu](#); California State University Northridge, United States

When 2D materials are stacked to form a van der Waals (vdW) heterostructure with a small angular and/or lattice mismatch, a moiré superlattice may appear, which could lead to novel quantum phenomena, driven by an interplay of flat energy bands and strong electron-electron interactions. In particular, the moiré superlattices comprised of 2D semiconductors, such as transition metal dichalcogenides (TMDs), could host localized, long-lived and valley-polarized moiré excitons, which are envisioned as single-photon emitters in quantum information and optoelectronic applications. In this talk, we provide an overview of our recent effort to elucidate the properties of moiré excitons in twisted 2D vdW heterostructures from first principles. We predict that moiré excitons can be formed in twisted 2D organic-inorganic halide perovskites, group IV monochalcogenides, in addition to the well-known TMD bilayers. In conjunction with localized moiré excitons, nearly flat bands are also formed in these vdW heterostructures. 1D flat bands, anisotropic and 1D moiré excitons are also predicted to emerge in some of the vdW heterostructures, specially, when defects are present. We explore how vertical electric field can be tuned to control the position, polarity, emission energy, and hybridization strength of the moiré excitons. In the second part of the talk, we will shed light on exciton dynamics in TMD vdW heterostructures. In particular, we unravel the competition of charge and energy transfer in type-II WS₂/MoSe₂ heterostructures. Incorporating excitonic effect in non-adiabatic electronic dynamics, our first-principles study uncovers a two-step process in ultrafast energy and charge transfer, unravel their relative efficiencies and explore the means to control their competition. The excitonic effect is revealed to drive the efficient energy and charge transfer in the heterostructures.

5:45 PM BREAK

SESSION DS02.21: Coarse Grain Models IV
Session Chair: Ellad Tadmor
Wednesday Afternoon, December 8, 2021
DS02-Virtual

4:00 PM DS02.21.01

Investigation of Molecular Mechanism of MOF-5 Self-Assembly Using Coarse-Grained Models [Fangxi Wang](#)¹, Abhishek T. Sose¹, Praveen Thallapally² and Sanket Deshmukh¹; ¹Virginia Tech, United States; ²Pacific Northwest National Laboratory, United States

The self-assembly of porous structures including metal-organic frameworks (MOFs) is a complex process. Even though MOF-5 is one of the most widely studied structures in the literature, very little is known about its self-assembly. In this study, the growth of 3-D structure of MOF-5 is successfully investigated using coarse-grained (CG) molecular dynamics (MD) simulations by employing different growth pathways. Interactions between metal nodes, linker, and solvent molecules were developed to reproduce their structure obtained from all-atom MD simulations. These building blocks were self-assembled by employing four different pathways from which only one resulted in a 3-D MOF-5 structure that resembled experimentally reported structure. We will discuss these approaches and our results in detail. This computational approach can be used to study self-assembly of other MOFs to provide insights into their growth and self-assembly process.

4:15 PM DS02.21.02

Development of Nonbonded Interactions Between Coarse-Grained Metal and Solvents [Fangxi Wang](#), Soumil Y. Joshi, Abhishek T. Sose and Sanket Deshmukh; Virginia Tech, United States

Metal nanoparticles (NPs) and their self-assembled functionalized hybrid structures have received huge interest due to their wide application in catalysis, sensors, and optics. In general interactions between these NP hybrids and solvents play an important role in their processing as well as in determining their self-assembled structures. To understand the role of these interactions at the molecular-level, coarse-grained (CG) molecular dynamics (MD) simulations can be employed. However, a key to generate reliable results is to use accurate and robust force-field (FF) parameters of all the components involved. In this study, we will present our methodology and FF parameters to define the interactions between CG models of metals (e.g. gold, silver, copper, etc.) with solvents (water, DMF, etc.) developed in our group. These interactions were developed to reproduce experimental (macroscopic contact angle, interfacial energies, surface tensions) and computational (binding energies) properties.

4:30 PM DS02.21.03

Development of Temperature and Solvent Transferable Coarse-Grained Polystyrene Model [Fangxi Wang](#), Yaxin An, Soumil Y. Joshi and Sanket Deshmukh; Virginia Tech, United States

Due to its exceptional strength and compatibility with blood, polystyrene (PS) is one of the most widely used commercial polymers in the fields ranging from packaging to medical devices. Hence, understanding the structure of PS in different solvents used for its processing as well as in water becomes important to improve the quality of these products. Here, we have integrated our previous coarse-grained (CG) hydrocarbon models (J. Phys. Chem. B, 2018, 122, 7143–7153) and benzene model (J. Phys. Chem. B 2018, 122, 6, 1958–1971) to develop a new CG model of PS. The bonded interactions between hydrocarbon and benzene model were tuned such that the new PS CG model can successfully reproduce its physical properties such as density at 300 K and glass transition temperature (T_g). Then, the non-bonded interaction parameters are optimized between this new PS CG model with pure solvents (water and DMF), also developed in our group, to reproduce the radius of gyration (R_g) from all-atom molecular dynamics (MD) simulation. The conformation of PS in the DMF/water solvent mixture indicates that the globule-to-coil transition happened with the increased concentration of DMF. The radial distribution functions (RDF) analysis of PS with solvent beads suggests the water molecules are repelled far away from the PS side chains when the DMF concentration increases, which leads to the stretch of the PS chains to form a coil-like structure.

4:35 PM DS02.21.04

Permeability of Bicontinuous Nanoporous Media [Chang Liu](#) and Paulo Brancio; University of Southern California, United States

It is challenging to describe the fluid flow behavior in natural nanoporous materials due to inherent complexities of the porous network topology. In nanoporous medium, collisions and interactions between particles and walls are as important as the collisions and interactions between particles as the molecular mean free path is comparable to the characteristic length scale of the medium. In this work, we employ Many-body Dissipative Particle Dynamics (mDPD) simulations to investigate the fluid flow process through realistic bicontinuous nanoporous media, which are representative models for a wide class of nanoporous materials. Bicontinuous nanoporous models are constructed considering a defined morphology at 0.65 porosity level and varying pore sizes from 30 to 120 nm. The models provide a stochastic description of the morphology and pore size distribution and allow for a direct investigation of the dependence of permeability on average pore-size. Simulation results from fluid obtained by imposing different pressure differences on the nanoporous model by the action of two confining pistons, indicate a linear pressure drop within the nanoporous model, regardless of pore size. The steady state fluid flow through the nanoporous models is proportional to the pressure gradient applied in agreement with the Darcy's law, in spite of the complexities and different scales of the porous media considered. The predicted pore-size dependence of the permeability is well described by the Hagen-Poiseuille law considering a single shape correction factor that accounts for the flow resistance due to the complex nanoporous morphology.

4:40 PM DS02.21.05

Predicting Plasticity in 2D Model Metallic Glasses Using the Local Yield Stress and Diffusion Maps [Rahul Meena](#)¹, Michael Shields¹, Dimitris G. Giovanis¹, Michael L. Falk¹, Dihui Ruan¹, Spencer Fajardo¹, Yannis Kevrekidis¹, Thomas J. Hardin² and Michael E. Chandross²; ¹Johns Hopkins University, United States; ²Sandia National Laboratories, United States

Shape Failure in amorphous solids arises from local rearrangements in the material's atomic configurations and how these respond to stress. To this end, the Local Yield Stress (LYS) method was recently developed to probe local regions and quantify their susceptibilities to plasticity by measuring the incremental stress required to trigger a local rearrangement. While this methodology shows great potential for enhancing predictive plastic theories, it is not a practical means for characterizing materials structure due to its computationally intensive nature. We propose a manifold learning-based framework to extract microstructural descriptors from atomistic configurations. More specifically, we deploy Diffusion Maps (a nonlinear manifold learning technique) to systematically extract the structural information features from the high-dimensional data (cartesian coordinates of local clusters of atoms and relate this structure to LYS). Due to the nature of the problem, a "point" corresponds to a geometric conformation of atoms, and thus meaningful similarity measure between configurations must be devised for capturing the actual distance between two points. Therefore, we utilize the Grassmann manifold to measure the similarity between the cluster of atoms. We start with a "proof of concept" example crystalline system where our aim is to identify known defects (vacancies and dislocation) using the machine learning approach trained to the geometric conformation of atoms before moving on to amorphous materials to demonstrate its practicability. Finally, our application is a two-dimensional binary glass-forming system, deformed with an incremental Athermal Quasistatic Shear (AQS) method.

4:45 PM DS02.21.06

Late News: (Garcia High School Student) Investigating the Atomistic Mechanism of Fibrinogen Inhibition by P12 [Sophia Cai](#)¹, LeAnn Tai² and Bernard Essuman³; ¹Barrington High School, United States; ²Arnold O. Beckman High School, United States; ³Stony Brook University, The State University of New York, United States

Fibrinogen is a plasma-soluble glycoprotein responsible for blood clot formation. After an injury to the blood vessels, fibrinogen molecules are polymerized into fibrin through binding and interactions at their α C domains, forming a fibrin mesh that completes a blood clot. Previous studies indicate that excessive coagulation can lead to harmful diseases and health conditions like strokes and pulmonary embolism. P12, a peptide derived from fibronectin, can mitigate fibrinogen formation and reduce thrombogenesis. In this study, we investigated the properties of the distortion of the α C domain by P12, which inhibits fibrinogen polymerization and prevents the formation of a fiber network. To test this, an in silico model of the α C domain and potential models of the P12- α C interaction were collected from multiple docking servers. The top models from each server were further evaluated using protein-ligand affinity prediction software. The top scores were all located within residues 518 to 584, which we hypothesized to be the binding site of P12 in the α C domain. To understand the binding interactions between P12 and the α C domain, hydrogen bonding sites were mapped through Cytoscape detection. Six residues displayed hydrogen bonding with the P12 ligand, and VMD analysis indicated that two salt bridges broke due to the change in the structure of the α C domain. Furthermore, the introduction of P12 increased the overall flexibility of the α C domain complex, as indicated by higher RMSF values. The hydrophobicity of the α C domain and P12 complex was mapped using UCSF Chimera to observe the forces that keep the complex intact and determine the degree of hydrophobicity at the P12 binding sites on the α C domain. On both the P12 molecule and the α C domain, the specific sites of interaction were shown to be very hydrophobic. This research suggests that P12 is an effective inhibitor of fibrinogen polymerization due to its interactions with the α C domain.

8:00 AM DS02.02.03

Late News: Quantum Computing for New Materials and Chemistry Applications [Nicolas P. Sawaya](#); Intel Corporation, United States

Usually when one thinks of calculating the properties of a material or molecule, the first calculation that comes to mind is electronic structure, which can be approximated on traditional computers using techniques such as density functional theory. Appropriately, most materials-related quantum algorithms developed so far have targeted electronic degrees of freedom. However, there are other types of materials simulation that would require the use of a quantum computer for accurate results. These include problems for which one is simulating vibrational, excitonic, or nuclear degrees of freedom. Though these types of simulations are relatively unexplored in the quantum computation community, they are relevant to many industrial applications. Here, we present recent work on designing quantum algorithms for important industrial applications such as microscopic energy transfer, spectroscopy, thermal properties, and analytical chemistry. We begin with an overview of general quantum computing methods for materials and chemistry simulation. Next, we discuss the design of efficient low-level quantum data structures for these applications. Metrics related to computational complexity are compared between electronic structure and these new application areas, leading us to postulate that simulating these alternative degrees of freedom will be possible before simulating electronic structure. Finally, we discuss the mathematical ways in which the problem goals are different for each application, with an eye toward guiding quantum algorithm design in these areas of materials simulation.

SYMPOSIUM DS03

Combining Machine Learning with Simulations for Materials Modeling
November 30 - December 7, 2021

Symposium Organizers

Mathieu Bauchy, University of California, Los Angeles
Sumanta Das, University of Rhode Island
Christian Hoover, Arizona State University
N M Anoop Krishnan, Indian Institute of Technology Delhi

* Invited Paper

SESSION DS03.01: Machine Learning for Accelerating Simulations I
Session Chair: Mathieu Bauchy
Tuesday Morning, November 30, 2021
Sheraton, 5th Floor, The Fens

10:30 AM *DS03.01.01

Bioinspired Artificial Intelligence and Protein Materials by Design [Markus J. Buehler](#); Massachusetts Institute of Technology, United States

Nature produces a variety of materials with many functions, often out of simple and abundant materials, and at low energy. Such systems - examples of which include silk, tendon, bone, nacre or diatoms - provide broad inspiration for engineering. Here we explore the translation of biological composites to engineering applications, using a variety of tools including molecular modeling, AI and machine learning, and experimental synthesis and characterization. We review a series of studies focused on the mechanical behavior of materials, especially deformation and fracture, and how these phenomena can be modeled using a combination of molecular dynamics and machine learning, to generate a novel simulated evolutionary process that offers directed adaptation of biomaterial properties. We also present case studies of protein material optimization using genetic algorithms, applied to 3D printed composites, molecular design, and a translation of protein folding to music and back. We also review a close integration of music and materials, and review our recent research on a new bio-inspired compositional technique called materiomics.

11:00 AM DS03.01.03

Per-Atom Magnetic Moment Prediction in Transition Metal Oxides [Jaclyn Lunger](#), Jessica Karaguesian, Daniel Schwalbe Koda, Yang Shao-Horn and Rafael Gómez-Bombarelli; Massachusetts Institute of Technology, United States

Inorganic crystalline materials with a magnetic ground state are of interest in various applications such as spintronics, memristors, and data-storage. Even when magnetism is not the key property of interest, studying magnetic materials with Density Functional Theory requires spin-polarized calculations to find the ground state structure and energy. However, computational exploration of magnetic materials is challenging due to the complexity of their electronic and magnetic states. In particular, calculating the ground state of a magnetic material requires careful initialization because spin-polarized DFT calculations are prone to getting trapped in local minima. Previous efforts to resolve this challenge have included high-throughput workflows wherein many possible magnetic orderings are enumerated and calculated. However, this workflow is computationally intensive and requires many spin-polarized DFT optimizations to correctly identify the magnetic ground state of a single material. In this work we present a graph convolutional neural network for predicting per-atom magnetic moment magnitudes given crystal structure. This model is trained on ~ 30,000 magnetic transition metal oxides retrieved from the Materials Project and in-house calculations, and is able to estimate per-atom magnetic moment within an MAE of 0.33 bohr magnetons. We see

significant speed-ups for spin-polarized DFT calculations initialized with per-atom magnetic moments predicted by our model. Finally, we extend our model to predict collinear magnetic orderings by attaching a +/- classification to each atom. After training this extended model on the transition metal oxides that have been analyzed through a magnetic ordering workflow, we are able to predict the magnitude and sign of the magnetic moment on each atom with high accuracy and thus significantly decrease the number of calculations required to find the ordered magnetic ground state. We anticipate the use of our model to screen materials for interesting magnetic behavior and for the inverse design of novel materials with desired magnetic properties. We also propose the generalization of the presented model to predict other per-site properties—such as band structures and Bader charges—thus enabling fine-tuned exploration and design in varied materials problems.

11:15 AM DS03.01.04

Benchmarking Descriptors, Models and Systems for Many-Body Machine Learned Force Fields in Molten Transition Metals Steven B. Torrisi^{1,2}, Cameron J. Owen², Isabel Diersen², Lixin Sun², Jin Soo Lim², Yu Xie², Jonathan Vandermause² and Boris Kozinsky^{2,3}; ¹Toyota Research Institute, United States; ²Harvard University, United States; ³Bosch, United States

The development of accurate and efficient molecular dynamics force fields are a crucial step in an overall materials discovery workflow that complements experiments with theoretical simulations. In order to facilitate the ongoing development of automated machine-learned force fields using tools like FLARE++ and Nequip, we have generated a benchmarking dataset of molten single-element bulk structures with a vacancy defect in order to study the interplay between many body behavior and model performance. This dataset contains ab initio molecular dynamics simulations capturing high-temperature crystalline and melted phases. We attempt to explain the difference in model performance across implementation, levels of descriptor fidelity, and individual systems based on differences in elemental properties, and using interpretable machine learning models, reveal the interplay between elemental properties and many-body character revealed by these differences in performance.

SESSION DS03.02: Machine Learning for Targeted Material Design I

Session Chairs: Sumanta Das and Christian Hoover

Tuesday Afternoon, November 30, 2021

Sheraton, 5th Floor, The Fens

1:30 PM DS03.02.01

Integrating High-Performance Computing and Machine Learning-Enabled Design of Materials Nathan Frey, Lin Li and Vijay Gadepally; Massachusetts Institute of Technology, United States

As machine learning (ML) workflows become more prevalent and computationally demanding in materials science, there is an emerging need to integrate deep domain expertise with efficient high-performance computing and appropriate ML methods. In cases where design goals require explorations of vast areas of chemical/material space, or target properties are prohibitively expensive to compute, efficient use of resources and careful choice of method enable previously inaccessible capabilities for material design. Here, we explore interactive supercomputing for applying ML to challenges in materials and chemistry. We discuss the scaling of ML methods for materials and molecular design, with respect to supercomputing resources and dataset size. We present two workflows for high-throughput virtual screening (HTVS) and ML to engineer quantum states in layered materials. An approach based on deep transfer learning, machine learning, and first-principles calculations is shown to rapidly predict key properties of point defects in 2D materials. Properties including band gap and bulk formation energy are predicted for over 4,000 2D materials using deep transfer learning. 10,000 dopant, vacancy, divacancy, and antisite defect structures are generated in 150 wide band-gap materials and more than 1,000 defect band structures are computed via first-principles methods. We identify over 100 promising, unexplored dopant defect structures in layered metal chalcogenides, hexagonal nitrides, and metal halides including GeS, h-AIN, and MgI₂. The hybrid HTVS/ML approach is also used to discover 18 transition metal oxide materials with coexisting magnetic and topological quantum orders.

DISTRIBUTION STATEMENT A. Approved for public release. Distribution is unlimited.

This material is based upon work supported by the Under Secretary of Defense for Research and Engineering under Air Force Contract No. FA8702-15-D-0001. Any opinions, findings, conclusions or recommendations expressed in this material are those of the author(s) and do not necessarily reflect the views of the Under Secretary of Defense for Research and Engineering.

1:45 PM DS03.02.02

Hybrid Multi-Scale and Data-Driven Models for Designing the Smart Properties of Nanocomposite Materials Atta Muhammad¹, Rajat Srivastava¹, Eliodoro Chiavazzo¹, Pietro Asinari^{1,2} and Matteo Fasano¹; ¹Politecnico di Torino, Italy; ²Istituto Nazionale di Ricerca Metrologica, Italy

The enhanced properties of composite materials are exploited in many fields, from aerospace to electronics industries, from automotive to biomedical applications. Furthermore, smart properties (i.e. material responses influenced by external stimuli) of composites are highly desirable to design next-generation devices in a broad variety of industries. Composites are typically made of polymeric matrices reinforced with macroscopic fillers, e.g. carbon or glass fibers. Recently, nanostructured fillers have been also employed to further improve the effective and smart properties of composites. Carbon nanostructures such as graphene or carbon nanotubes are particularly suitable for that, since they show superior thermal, mechanical and electrical properties. Nevertheless, the properties of nanocomposites are determined by phenomena spanning from the nano to the macro scale and, thus, should be simulated by tailored multi-scale modelling techniques.

In this presentation, hybrid multi-scale and data-driven models to predict the properties of polymer nanocomposites reinforced with carbon nanofillers are presented and experimentally validated. Firstly, the coarse-grained interaction potentials describing some thermoset and thermoplastic polymer matrices obtained from atomistic simulations are compared between each other, to define the mesoscopic configuration more suitable to mimic the thermal-physical properties measured experimentally. Secondly, carbon nanofillers with high thermal, mechanical, and electrical properties are coarse-grained as well, and then introduced in a representative volume element of the nanocomposite to be simulated. Thirdly, sensitivity analyses are carried out by means of the coarser mesoscopic model, to identify the geometrical and physical-chemical features influencing more the thermomechanical response of the considered nanocomposites. Results are compared against both experiment and continuum simulations, to validate the proposed approach and highlight its advantages with respect to consolidated modelling strategies. Finally, data-driven algorithms based on machine learning are employed to improve the prediction capability of the multi-scale model, in order to account for the nonlinear effects in the heat transfer processes. In perspective, such hybrid data- and physics-driven methods should allow to investigate also other properties of nanocomposites, for instance electromagnetic ones.

This work has received funding from the European Union's Horizon 2020 research and innovation program SMARTFAN under grant agreement N. 760779.

2:00 PM DS03.02.03

Transforming Automated Quantum Chemistry Calculation Workflows with Machine Learning—Towards Faster and More Accurate Materials Discovery Chenru Duan and Heather J. Kulik; Massachusetts Institute of Technology, United States

Machine learning (ML) has begun to accelerate materials discovery by providing advances in efficiency needed to overcome the combinatorial challenge of computational materials design. In ML-assisted materials discovery, an automated quantum chemistry (QC) calculation workflow is used to generate datasets to train surrogate models, which serve as alternatives to rapidly explore a large space to identify candidate materials. However, current workflows with density functional theory (DFT) as workhorse leads to many attempted calculations that are doomed to fail and brings biases/inaccuracy to the training data that may be out of the domain of applicability of DFT. This includes many compelling functional materials and catalytic processes that are difficult because of their complex electronic structure, such as systems involving strained chemical bonds, open-shell radicals and diradicals, or metal-organic bonds to open-shell transition-metal centers. We address these challenges of computation efficiency and accuracy by integrating ML approaches into conventional DFT-based QC workflows.

More than half of the computational resource and time is wasted on unfruitful geometry optimizations during the transitional metal complex (TMC) design. To address this issue, we built two types of classifiers to predict the likelihood of calculation success: 1. static model prior to calculations and 2. dynamic model on-the-fly monitoring calculations. The static classifier is a near zero-cost model that rapidly filters out candidate calculations most likely to fail, while the dynamic model monitors and terminates an already running calculation if it is predicted to fail with high confidence. The prediction of the dynamic classifier is interpretable and helps reveal the failure modes in geometry optimizations. Together, these classifiers save half of the computation resources. We have also demonstrated the usefulness of these classifiers on the active learning discovery of candidate catalysts for small alkane activation.

Many interesting functional materials may have complex electronic structures difficult for DFT. We developed multiple types of classifiers to predict the presence of strong correlation, which is usually a sign of a system being out of the domain of applicability of DFT. Our models only require calculations at DFT cost and can classify which systems in a dataset will require more expensive but accurate wavefunction theory calculations, leading to overall high fidelity of the entire dataset. These models far outperform the existing unsupervised learning (i.e., clustering) methods and conventional cutoff-based approach widely used in the chemistry community in distinguishing systems that contain strong MR character. In addition, since electronic structure information is encoded as the inputs, our models are readily transferable to larger systems and systems with unseen elements. All these classifier models represent the first efforts toward autonomous workflows that move past the need for expert determination of the robustness of DFT-based materials discoveries.

2:15 PM DS03.02.04

Davis Computational Spectroscopy Workflow—From Structure to Spectra Lucas Samir Ramalho Cavalcante¹, Luke L. Daemen², Nir Goldman³, Ambarish Kulkarni¹ and Adam J. Moule¹; ¹University of California, Davis, Brazil; ²Oak Ridge National Laboratory, United States; ³Lawrence Livermore National Laboratory, United States

Metal-organic frameworks (MOF) hold great promise in applications on gas adsorption, catalysis, and supercapacitors because of their porous structure and modularity. Despite having a symmetrical and apparently well-organized structure formed by metal clusters connected via organic linkers, these materials have low thermal, mechanical, and chemical stability, yielding a high defect density and disorder. To overcome the stability problem, a zirconium-based MOF called UiO-66 was presented as a solution due to its high connectivity with 12 connected clusters in the face-centered-cubic topology. However, a better understanding of the nature of defects and disorder in UiO-66 MOFs is still required.

Inelastic Neutron Scattering (INS) has been proven to be a good ally in the investigation of structural and dynamic disorder but it requires detailed modeling of the system in order to characterize peak positions and intensities, and subsequently materials properties. The high computational cost of the electronic modeling has limited investigations with INS to crystalline materials, dampening the study of disordered large systems such as MOFs.

To address the trade-off between simulation cost and accuracy, we developed an automated workflow that connects various atomic simulation tools in order to investigate the relationship between material properties, lattice dynamics, and INS spectra. This workflow allows an accurate and efficient method of calculating phonon modes and the INS spectrum with the use of a broad range of quantum mechanical approximations, including density functional theory (DFT) and density functional tight-binding (DFTB). We have also implemented a machine-learned force field based on Chebyshev polynomials (Chebyshev Interaction Model for Efficient Simulation - ChIMES) to improve the accuracy of the DFTB simulations with ~100x reduction in computational expense while retaining most of the accuracy of DFT. Besides the benefits of a tool that automates the simulation and consequent analysis of the INS spectrum, our efforts expand the possibilities of investigating more complex structures that would be unfeasible with *ab initio* methods.

2:30 PM DS03.02.05

Materials from Fire—A New Approach to Design Material from Nature Mario Milazzo and Markus J. Buehler; Massachusetts Institute of Technology, United States

Fire has fascinated humankind since the prehistoric era and, according to different traditions, was selected as one of the four main elements that “make of all things in Nature”. Science and art have both used fire as a tool and inspiration over the years. From a scientific-technological standpoint, fire is one of the fundamental agents to enable chemical reactions, and its controlled dynamics have been widely studied to optimize and control combustion processes. Another field of interest concerns fire detection and monitoring for safety purposes since an efficient control of fire since its activation has a huge impact not only on people and animal protection but also on environmental sustainability.

As for visual and music arts, fire has been used as a tool and inspiration for creating paintings but, more interestingly, has inspired composers to create melodies able to evoke its power and perpetual shape mutation without using the audible dull sounds emitted from the interaction with air.

Rooted in the interactions between sound and flames, here we report a new method to use fire for a variety of purposes, including sonification, art, and the design and manufacturing of nature-inspired materials. At the root of the work is a new method to sonify fire, thereby offering a translation from the silent nature of flames, to represent audible information, and to generate *de novo* flame images.

We use a simple setup composed of a flame from a candle whose deformation, due to an acoustic source, is recorded through a digital camera. We used the tones from an octave to create a direct mapping between the deformations of the flame and pure sounds. To encode and decode images of the flames exposed to different frequencies, we used a convolutional variational autoencoder trained on a set of 1,300 unlabeled images (100 images for each audible condition), and uses a 2-dimensional latent space vector.

This tool provides a new interactive musical instrument, which from the observation of a flame, or interaction of it with the environment – such as wind or temperature fluctuations, or different environmental gases – will result in flame shape and dynamics changes, which in turn is associated with particular sounds.

Additionally, we are able to generate *de novo* images by applying the trained deep neural network model to augment images, thus creating a deep inceptionism of fire, and use a deep convolutional variational autoencoder to realize synthetic flame shapes, including temporal sequences that resemble flickering flames.

From the materials science standpoint, we realize new materials inspired by fire by using autoencoder to generate image stacks to yield 3D geometries that are manufactured using 3D printing. This represents the first even generation of nature-inspired materials from fire, and can be a platform to be used for other natural phenomena in the quest for *de novo* architectures, geometries, and design ideas. These concepts provide a new dimension of nature-inspired design, as it yields novel image data that can be manipulated, or associated with, other forms of expression, and creates new directions in artistic and scientific research through the creative manipulation of data with structural similarities across fields. This work also underscores the fundamental importance of vibrations as a translational means to find semblances of structures across manifestations, from the invisible, to the visible, to material form.

2:45 PM DS03.02.07

Tuning Optoelectronic Properties of Semiconductors with First Principles Modeling and Machine Learning Arun Kumar Mannodi Kanakkithodi¹, Maria K. Chan², Xiaofeng Xiang³, Laura Jacoby³, Robert Biegaj³, Rishi Kumar⁴ and David P. Fenning⁴; ¹Purdue University, United States; ²Argonne National Laboratory, United States; ³University of Washington, United States; ⁴University of California, San Diego, United States

Semiconductors with desirable electronic band structure and optical absorption are sought for solar cells, electronic devices, infrared sensors and quantum computing. Compositional manipulation via alloying at cation or anion sites, or via incorporation of point defects and impurities, can help tune the properties of semiconductors in known chemical spaces. In this work, we develop AI-based frameworks for the on-demand prediction and multi-objective optimization of the phase stability, band gap, optical absorption spectra, photovoltaic efficiency, dielectric constant, defect formation energies, and impurity energy levels in two broad classes of semiconductors, namely (a) halide perovskites with the general formula ABX₃ (where A is a large organic or inorganic monovalent cation, B is a divalent cation and X is a halogen anion), and (b) group IV, III-V and II-VI semiconductors in binary, ternary and quaternary forms. These frameworks are powered by high-throughput density functional theory (DFT) computations, unique encoding of the atom-composition-structure information, and rigorous training of advanced neural network-based predictive and optimization models.

Bayesian optimization-based active learning approaches are applied to systematically improve prediction accuracies and comprehensively traverse the compositional chemical space. Multi-fidelity learning helps to bridge the gap between (high quantities of) low accuracy calculations and (lower quantities of) high-fidelity data, constituted of either accurate, expensive computations or experimental measurements collected from the published literature. High-accuracy predictions based on modest datasets are thus accomplished for (a) band gaps and formation energies at the HSE06 level of theory utilizing PBE-level data, (b) defect and impurity energy levels with experimental accuracy utilizing PBE-level data, (c) large supercell properties utilizing smaller cell calculations, and (d) properties of all alloy compositions utilizing data from end-point and selected mixed compositions. The best predictive models are combined with two different multi-objective optimization techniques, namely, state-of-the-art genetic algorithms and variational autoencoders, to determine optimal semiconductor atom-composition-structure combinations with desired stability, optoelectronic, and defect properties. Finally, AI-based recommendations are synergistically coupled with targeted synthesis and characterization, leading to successful validation and discovery of novel compositions for improved performance in solar cells.

References

1. A. Mannodi-Kanakkithodi, J. S. Park, N. Jeon, D. H. Cao, D. J. Gosztola, A. B. F. Martinson, M. K. Y. Chan, "Comprehensive Computational Study of Partial Lead Substitution in Methylammonium Lead Bromide", *Chemistry of Materials* 31 (10), 3599–3612 (2019).
2. A. Mannodi-Kanakkithodi, M. Toriyama, F. G. Sen, M. Davis, R. F. Klie, M. K. Y. Chan, "Machine learned impurity level prediction in semiconductors: the example of Cd-based chalcogenides", *npj Computational Materials* 6, 39 (2020).
3. A. Mannodi-Kanakkithodi, M. K. Y. Chan, "Computational Data-Driven Materials Discovery", *Trends in Chemistry* 3, 2, 79–82, (2021).
4. X. Xiang, L. Jacoby, A. Mannodi-Kanakkithodi, R. Biegaj, M. K. Y. Chan, "Universal Machine Learning Framework for Impurity Level Prediction in Group IV, III-V and II-VI Semiconductor", *in preparation*.
5. A. Mannodi-Kanakkithodi, R. E. Kumar, D. Fenning, M. K. Y. Chan, "Data-Driven Design of Novel Halide Perovskite Alloys", *in preparation*.

3:00 PM DS03.02.08

AI-Aided Interpretation of Electronic Transport Measurements Luca Bonaldo¹, Terry E. Stearns¹, Ilaria Siloi², Nicholas Mecholsky³ and Marco Fornari¹; ¹Central Michigan University, United States; ²University of Southern California, United States; ³Catholic University of America, United States

The solution of the inverse problem involves reconstructing a model from a set of observations; such a task is crucial to the majority of indirect experimental measurements, which use a variety of fitting procedures. Unfortunately, this approach often requires crude approximations and generates a misalignment between theory and experiments. A typical example is the effective mass of the charge carriers in a complex semiconductor.

To reconcile theory with experiments, we propose an innovative approach based on bi-directional training of an invertible neural network. Supported by specific domain knowledge, deep learning models are trained to correctly predict both the outcome from a set of model parameters and the parameters themselves. We will apply this approach to the electronic transport properties of materials to link the features of the band structure to conductivity, Seebeck coefficient, and carrier concentrations.

During the talk, we introduce m*2T, a code we developed to inspect the direct problem. The software involves the prediction of transport properties from band structure models which we use to efficiently generate meaningful data to train the invertible neural network. Results on the solution of the inverse problem will also be discussed.

3:15 PM DS03.02.06

De Novo Inverse Design of Nanoporous Materials by Machine Learning Mathieu Bauchy; University of California, Los Angeles, United States

Although simulations excel at mapping an input material to its output property, their direct application to inverse design (i.e., mapping an input property to an optimal output material) has traditionally been limited by their high computing cost and lack of differentiability—so that simulations are often replaced by surrogate machine learning models in inverse design problems. Here, taking the example of the inverse design of a porous matrix featuring targeted sorption isotherm, we introduce a computational inverse design framework that addresses these challenges. We reformulate a lattice density functional theory of sorption in terms of a convolutional neural network with fixed hard-coded weights that leverages automated end-to-end differentiation. Thanks to its differentiability, the simulation is used to directly train a deep generative model, which outputs an optimal porous matrix based on an arbitrary input sorption isotherm curve. Importantly, this pipeline leverages for the first time the power of tensor processing units (TPU)—an emerging family of

dedicated chips, which, although they are specialized in deep learning, are flexible enough for intensive scientific simulations. This approach holds promise to accelerate inverse materials design.

3:30 PM BREAK

4:00 PM DS03.02.09

Reconstructing Representative Dislocation Structures from XRD Measurements Through Machine Learning of Discrete Dislocation Dynamics Simulations [Dylan Madiseti](#)¹, Christopher Stiles^{2,1} and Jaafar El-Awady¹; ¹Johns Hopkins University, United States; ²Johns Hopkins University Applied Physics Laboratory, United States

A GPU-accelerated computational modeling method for simulating X-ray diffraction (XRD) is developed and implemented to track microstructure evolution through three-dimensional (3D) discrete dislocation dynamics (DDD). This is leveraged to generate a large repository of computational XRD images, and machine learned feature vectors for processing experimental XRD images. The physics-based model implements ray-tracing techniques, Bragg-scattering theory, alloy composition, and a virtual sensor to capture micro-Laue and Debye-Scherrer images from simulated synchrotron X-ray emission. The computational speed improvement provided by this GPU-accelerated method allows for in-situ tracking of diffraction patterns over the course of a virtual experiment, and XRD image data generation from large scale 3D DDD simulations. Implementing convolutional neural networks on this data, we demonstrate that dislocation density can be tracked through time as a function of XRD peak broadening. By determining feature importance (feature attribution) within the machine learned model, the known microstructure is attributed to spreading in Laue-spots. Spreading phenomenon observed in experimental XRD patterns is then associated by similarity analysis to a microstructure in the computational repository, providing insight into the experimental sample.

4:15 PM DS03.02.10

High-Throughput Glass Transition Temperature Computations for Polymers Using Machine Learning Based Molecular Dynamics [Christopher B. Kueneth](#), Kuan-Hsuan Shen and Rampi Ramprasad; Georgia Institute of Technology, United States

Polymers are an important class of materials that display morphological complexity and diverse inter-atomic interactions. These two and other factors have defied large-scale and long-time quantum-accurate atomic-level simulations of polymer dynamics which are required to access many properties such as the glass transition or melting temperature. Traditional simulation methods utilize parameterized classical potentials or force fields which often lack accuracy, transferability, and versatility. To overcome these issues, here, we develop general machine learning based models for the polymer dynamics of hydrocarbons that learn from reference quantum mechanical data. Once learned, these models can emulate the parent quantum calculations in accuracy, but be about a billion orders of magnitude faster. Using our models, we perform glass transition temperature calculations of a diverse set of polymers that demonstrate a pathway towards high-throughput data generation using molecular dynamics. Challenges that remain are discussed and pathways to overcome such challenges are presented.

4:30 PM DS03.02.12

Tailoring Deep Learning Neural Networks for Atomic Column and Nanoparticle Segmentation in HR-TEM Data [Matthew Helmi Leth Larsen](#), William Bang Lomholdt, Anders Siig Dreisig, Stig Helveg, Ole Winther, Thomas W. Hansen and Jakob Schiotz; Technical University of Denmark, Denmark

Identifying individual atoms in material samples is a challenging task in high-resolution transmission electron microscopy (HR-TEM) since the signal to noise ratio is often low to prevent that the electron beam causes irreversible changes in the sample. This is an area where machine learning can step in to assist the process.

Here we will report advancements on the tailoring of deep learning neural networks for fast detection of nanoparticles and atomic columns. This concept has previously been demonstrated for tracking gold atoms in HR-TEM image sequences [1] with an industry standard U-net architecture [2].

Training a network to distinguish between atomic species in multi-component material samples is possible by feeding the network a focal series of images. For example, providing three images of an MoS₂ sample at three different defocus settings allows a neural network to differentiate between atomic columns consisting of either 1 molybdenum, 2 sulphur, or 1 sulphur atom in HR-TEM images.

We have simulated HR-TEM images of bare MoS₂ and MoS₂ on graphene substrates in the (001) crystal direction. A training set of 10,000 images and a validation set of 500 images has been simulated applying microscopy parameter values randomly sampled from a specified range.

This work presents the superiority of the MSD-net [3], over the U-net architecture, in distinguishing between the described atomic columns in simulated HR-TEM images of MoS₂. Results show that the MSD-net achieves higher F1-scores overall for the validation set of data.

Next to identifying atomic columns, we display the ability of the MSD-net to segment entire nanoparticles and substrates, which is shown to assist in Fourier analyses by separating the nanoparticle from the substrate and providing a clarified image of the Fourier domain. This ultimately assists the process in determining crystal orientation and facet information in experimental images. The MSD-net is trained on a dataset consisting of unsupported Au nanoparticles and Au nanoparticles supported on CeO₂, both in the [110] zone axis, following a similar methodology as described for the MoS₂ datasets, but where the entire nanoparticle is labelled.

To improve the ability of the MSD-net in analyzing experimental images, we present a new method to include thermal vibrations in HR-TEM image simulations. This method consists of extracting a mean standard deviation of atomic positions dependent on their coordination number from a series of molecular dynamics simulations. These values are then used to perturb the atoms correctly by a simple translation of the positions. This is the frozen phonon approximation, but with vibrational amplitudes depending on the local structure obtained from molecular dynamics simulations. As a result, this includes thermal vibrational effects into the simulated images at a low computational cost.

In conclusion, the MSD-net is shown to outperform the U-net in identifying atomic columns in multi-component materials. This along with nanoparticle segmentation and the computationally cheap implementation of thermal vibrations presents promising applications in the future of HR-TEM image analysis and developing deep learning assisted tools for information extraction.

1. Madsen, Jacob, et al. "A Deep Learning Approach to Identify Local Structures in Atomic-Resolution Transmission Electron Microscopy Images." *Adv. Theory Simul.*, vol. 1, no. 8, Wiley-VCH Verlag, 2018, p. 1800037, doi:10.1002/adts.201800037.

2. Ronneberger, Olaf, et al. "U-Net: Convolutional Networks for Biomedical Image Segmentation." *Lecture Notes in Computer Science (Including*

Subseries Lecture Notes in Artificial Intelligence and Lecture Notes in Bioinformatics), vol. 9351, Springer Verlag, 2015, pp. 234–41, doi:10.1007/978-3-319-24574-4_28.

3. Pelt, Daniël M., and Sethian, James A. “A Mixed-Scale Dense Convolutional Neural Network for Image Analysis.” PNAS of the United States of America, vol. 115, 2018, pp. 254–59.

4:45 PM DS03.02.13

Machine Learning for Grain Boundary Solute Segregation [Malik Wagih](#) and Christopher Schuh; Massachusetts Institute of Technology, United States

In polycrystalline alloys, the grain boundary network has a variety of local atomic environments (site-types) that can be energetically more favorable for a solute atom to substitutionally occupy over the bulk (intra-grain) lattice. This can cause the segregation of solute atoms at the grain boundary - a well-documented phenomenon that is known to significantly impact the material properties, including, for example, mechanical, electrochemical, and magnetic properties. However, to date, there is a limited understanding of the spectrum of such atomic environments at the grain boundary, and their different affinities to solute atoms i.e. whether it promotes or prohibits solute segregation, as quantified by the segregation energy for that site-type. In this talk, we show our recently developed machine-learning framework, which can be used to predict the segregation energy of a solute atom at a grain boundary site, based solely on its unalloyed (pure solvent) local atomic environment. We also highlight the utility of the framework by using it to develop an extensive database for grain boundary solute segregation spectra for over 200 alloys.

SESSION DS03.03: Machine Learning for Targeted Material Design II

Session Chairs: Sumanta Das and Christian Hoover

Wednesday Morning, December 1, 2021

Sheraton, 5th Floor, The Fens

10:30 AM DS03.03.01

Computational Discovery and Informatics-Assisted Classification of Double Spinel Compounds [Ghanshyam Pilania](#), Vancho Kocovski and Blas P. Uberuaga; Los Alamos National Laboratory, United States

Spinel compounds represent an important class of technologically-relevant materials, used in diverse applications ranging from dielectrics, sensors and energy materials. While solid solutions combining two “single” spinels have been known for a long time, no ordered “double” spinel chemistries have been reported till date. Our recent computational investigations, based on a unique approach combining theory and experiments, indeed suggest presence of such distinctly-ordered double spinels for a wide range of cation chemistries.^[1-2] This talk will focus on applications of informatics-based tools to understand design rules within this newly-identified double spinel chemical space.^[2]

[1] Pilania, G., Kocovski, V., Valdez, J.A., Kreller, C.R. and Uberuaga, B.P., Prediction of structure and cation ordering in an ordered normal-inverse double spinel. *Communications Materials*, 1(1) 1-11 (2020).

[2] Kocovski, V., Pilania, G. and Uberuaga, B.P., High-throughput investigation of the formation of double spinels. *Journal of Materials Chemistry A*, 8(48), 25756-25767 (2020).

10:45 AM DS03.03.02

Ensemble Neural Network for Lithium Dendrite Growth [Issei Nakamura](#); Michigan Technological University, United States

Lithium dendrite formation in Li-ion batteries causes fire when the dendrite continues to grow over many charge/discharge cycles and reaches the other electrode. Our recent lattice Monte Carlo (MC) simulation was based on the diffusion-limited aggregation model which accounts for metal dendrite growth in electrolytes and suggested that ionic liquids can substantially inhibit the dendrite growth and make the dendrite surface relatively uniform. However, the height and aspect ratio of the dendrite varies nonmonotonically with the ion concentrations, the model parameters, and applied voltage. Due to this complexity of the simulation results, challenges remain to identify the properties of ionic liquids for efficient dendrite inhibition. To address this issue, we have developed ensemble neural networks (NNs) that capture the MC simulation data. Our ensemble NNs outperform normal, single NNs and can learn the severe nonmonotonicity of the height and aspect ratio of the dendrite, thus enabling significant reduction in the MC simulation time.

11:00 AM DS03.03.04

A Deep Learning Augmented Genetic Algorithm Approach for 2D Fracture Discovery and Design [Andrew Lew](#) and Markus J. Buehler; Massachusetts Institute of Technology, United States

Materials fracture is a complex multiscale process in which macroscopic behavior is inexorably linked to atomic-scale interactions. While molecular dynamics (MD) simulations can provide detailed fracture behavior, it remains computationally infeasible to probe the general problems of understanding fracture mechanisms and designing fracture behavior with this method alone. Here we present a machine learning (ML) approach consisting of a convolutional neural network to predict fracture propagation in 2D materials guided by a genetic algorithm to optimize for particular behaviors of interest. By training this ML model with fracture information from MD, we are able to replace traditional MD simulations with ML predictions and treat the fracture of larger systems, in less time, with consistency to MD baselines. Our method is transferrable to multiple 2D materials and both identifies specific novel fracture mechanisms and allows us to design material structures with controlled fracture paths.

11:15 AM DS03.03.05

Multi Reward Reinforcement Learning Based Bond Order Potential to Study Strain Assisted Phase Transitions in Phosphorene [Aditya Koneru](#)^{1,2}, Rohit Batra², Sukriti Manna^{1,2}, Troy Loeffler^{1,2}, Henry Chan^{1,2}, Harpal Singh³, Mathew J. Cherukara² and Subramanian Sankaranarayanan^{1,2}; ¹University of Illinois at Chicago, United States; ²Argonne National Laboratory, United States; ³Sentient Science Corporation, United States

2D single sheet materials, owing to their exceptional mechanical, thermal, electrical and optical properties over their bulk counterparts, are being explored at a rapid pace. Molecular simulations remain a popular technique to explore the structure and dynamics of such materials. Accessibility to accurate and fast interatomic force-fields would promote the discovery and property evaluations of such novel materials. In this work, we introduce, design and test a machine learning workflow capable of searching the high dimensional parameter space and subsequent refining of a Tersoff type Bond Order Potential (BOP). We select Phosphorene as a representative system of interest and the parameter search is performed using a multi-reward reinforcement learning (RL) agent that has been programmed with Monte Carlo Tree Search (MCTS). The training data comprising of structure, energetics, equation of state

(EOS), elastic constants and phonon dispersions was curated from Density Functional Theory (DFT) calculations for multiple phosphorene polymorphs. We demonstrate that the new class of RL trained bond order models adequately capture all the properties of the different Phosphorene polymorphs. We next perform Molecular Dynamics (MD) using parameters obtained from this approach to access the effect of strain and temperature on phase transition between black and blue phosphorene. Overall, the models are computationally cheap yet accurate and can be used to simulate dynamics and structural transformations of Phosphorene polymorphs for a wide variety of energy applications.

11:30 AM DS03.03.06

Graph Neural Networks for an Accurate and Interpretable Prediction of the Properties of Polycrystalline Materials [Minyi Dai](#), Mehmet F Demirel, Yingyu Liang and Jianian Hu; University of Wisconsin-Madison, United States

Various machine learning models have been used to predict the properties of polycrystalline materials, but none of them directly consider the physical interactions among neighboring grains despite such microscopic interactions critically determining macroscopic material properties. Here, we develop a graph neural network (GNN) model for obtaining an embedding of polycrystalline microstructure which incorporates not only the physical features of individual grains but also their interactions. The embedding is then linked to the target property using a feed-forward neural network. Using the magnetostriction of polycrystalline $Tb_{0.3}Dy_{0.7}Fe_2$ alloys as an example, we show that a single GNN model with fixed network architecture and hyperparameters allows for a low prediction error of $\sim 10\%$ over a group of remarkably different microstructures as well as quantifying the importance of each feature in each grain of a microstructure to its magnetostriction. Such microstructure-graph-based GNN model therefore enables an accurate and interpretable prediction of the properties of polycrystalline materials.

SESSION DS03.04: Machine Learning for Accelerating Simulations II

Session Chair: Mathieu Bauchy

Wednesday Afternoon, December 1, 2021

Sheraton, 5th Floor, The Fens

2:00 PM DS03.04.02

A Machine Learning Correction to DFTB and Its Effectiveness on Charge Transfer Salts [Corina A. Magdaleno](#), Lucas Cavalcanté, Makena Dettmann and Karina Masalkovaité; University of California, Davis, United States

The accurate prediction of phonon modes is important for scientific progress in fields ranging from heat and electron transport in thermoelectrics to correlated disorder in metal-organic frameworks (MOFs). Density Functional Theory (DFT) is a simulation method that is highly accurate at predicting the phonon modes, but it is computationally more expensive and requires more computational hours than simulation methods such as Density Functional Tight Binding (DFTB). Recently, the Chebyshev Interaction Model for Efficient Simulation (ChIMES) was developed as an approach to correct DFTB calculations by training a machine learning model. DFTB with ChIMES was shown to be effective at improving phonon predictions in a number of small-molecule systems. However, this method has never been applied to charge-transfer salt systems, some of the most promising hole conducting materials. In this study, training sets were created for TTF-TCNQ and TCNQ systems and the models were validated by testing each training set on both systems with DFTB. The accuracy of each training set was compared against the Inelastic Neutron Scattering (INS) spectra created using DFT.

2:15 PM DS03.04.03

A Machine Learning Approach for Longitudinal Spin Fluctuation Effects in bcc Fe at T_C and Under Earth's Core Conditions [Marian Arale Brännvall](#), Davide Gambino, Rickard Armiento and Bjorn Alling; Linköping University, Sweden

To understand the magnetism of solids at high temperature we need to study the interplay between vibrations and the magnetic degrees of freedom. The variation in magnitude of the atomic magnetic moments, the longitudinal spin fluctuations (LSF), is a degree of freedom of particular relevance in metallic magnets. The LSF energy depending on the local magnetic moment size of an atom, called the LSF energy landscape, can be calculated using density functional theory. It has been seen that, at elevated temperature, these LSF energy landscapes depend on the local environment of the atom i.e., they are influenced by both the lattice disorder caused by vibrations and the variations in the transverse orientations of neighboring moments. To simulate a magnetic material in e.g., an *ab initio* molecular dynamics simulation one needs to know how the atoms and their moments will interact with each other which, in principle, would require calculating the LSF energy landscape of each atom at every step in time. In this work we have developed a machine learning approach to predict the shapes of the energy landscapes to dramatically accelerate this process. The material used when developing this approach is bcc Fe at the Curie temperature and ambient pressure. The machine learning method used is kernel ridge regression. Two machine learning models are trained to predict the two parameters involved in determining the shape of the LSF energy landscape. As a critical test of the generality of the trained machine learning models, they are applied to predict the LSF energy landscapes of bcc Fe at temperature and pressure comparable to the conditions at the Earth's core.

Our machine learning approach is compared to other approximative methods for determining the shape of the landscapes and is shown to significantly reduce the errors. By applying the trained machine learning models in combined atomistic spin dynamics – *ab initio* molecular dynamics, the effects of LSF:s can be incorporated without having to explicitly calculate each LSF energy landscape in each time step. We perform such dynamical *ab initio* simulations for bcc Fe at both the Curie temperature and at the conditions of the Earth's core. This reveals the relevance of magnetic fluctuations on the low-density-problem of the current Earth core models.

2:30 PM DS03.04.04

Late News: Accelerated Prediction of Atomically Precise Cluster Structures Using On-the-Fly Machine Learning [Yunzhe Wang](#), Shanping Liu, Peter Lile, Sam Norwood, Alberto Hernandez, Sukriti Manna and Tim Mueller; Johns Hopkins University, United States

The chemical and structural properties of nanoclusters are of great interest in numerous applications. A systematic study of structure-property relationship necessitates the knowledge of atomically precise structures of stable clusters over a variety of sizes. However, experimental characterization of the structures of these non-crystalline materials can be challenging. Computationally searching for stable structures using *ab initio* calculations is a feasible solution, but can be computationally expensive. In this work, we present a procedure that can accelerate prediction of low-energy nanocluster structures by combining genetic algorithms with interatomic potentials actively learned on-the-fly. A pool-based genetic algorithm is implemented to efficiently sample the configuration space, and moment tensor potentials are used to rapidly relax and evaluate the energies of predicted clusters. Moment tensor potentials are regularly retrained on-the-fly on density functional theory (DFT) calculations of structures that are poorly represented by existing training data and of

low-energy pool clusters. Only DFT energies of pool clusters are reported at the end to guarantee *ab initio* level of accuracy. We demonstrate an acceleration rate of ~12 times on average, comparing our procedure with genetic algorithm using purely DFT calculations. Moreover, for aluminum clusters with 21 to 55 atoms, which we used as the benchmarking systems, our genetic algorithm search identified structures with lower energy in 25 sizes than any reported clusters in the literatures, and confirmed equivalent structures for another 8 sizes. This work demonstrates a feasible way to systematically discover stable structures for large nanoclusters and provides insights into the transferability of machine-learned interatomic potentials for nanoclusters. We believe the new procedure can greatly facilitate the discovery and design of novel nanomaterials for a wide range of applications.

SESSION DS03.05: Machine Learning for Accelerating Simulations III

Session Chair: Sumanta Das

Thursday Morning, December 2, 2021

Sheraton, 5th Floor, The Fens

10:30 AM DS03.05.01

Active Learning of Many-Body Bayesian Potentials for Large-Scale Simulations of Phase Transformations and Thermal Transport [Yu Xie](#)¹, Jonathan Vandermause¹, Senja Ramakers^{2,3}, Nakib Protik^{1,4}, Anders Johansson¹ and Boris Kozinsky^{1,5}; ¹Harvard University, United States; ²Robert Bosch GmbH, Germany; ³Ruhr-Universität Bochum, Germany; ⁴Catalan Institute of Nanoscience and Nanotechnology (ICN2), Spain; ⁵Robert Bosch LLC, United States

Machine learning interatomic potentials (MLIPs) with high efficiency and quantum accuracy are emerging as an enabling capability to simulate complex atomic level processes. To address the challenge of reliability and automated training of MLIPs, we introduced Bayesian active learning (BAL) that relies on quantified prediction uncertainty to drive an autonomous data acquisition strategy [1]. In this workflow, Bayesian MLIPs are constructed from Gaussian process (GP) based on atomic cluster expansion (ACE) descriptors. By developing a highly efficient approximation of the GP uncertainty, whose cost is independent of the training set size, we gain orders of magnitude speedup compared to inference with exact GPs.

As a demonstration, we train a MLIP for silicon carbide (SiC), a wide-gap semiconductor with diverse applications in electronics and physics. For example, point defects in SiC are promising candidates for stable controllable qubits, and an accurate description is desired of their long-time evolution. The resulting MLIP has excellent agreement with the density functional theory and outperforms previous empirical potentials in the prediction of elastic and thermal properties of pristine bulk, as well dynamics of point defects. The highly efficient active learning workflow can be extended to other systems and accelerate the discovery and understanding of materials for quantum technologies.

[1] Yu Xie et al, "Bayesian force fields from active learning for simulation of inter-dimensional transformation of stanene". npj computational materials (2021).

10:45 AM DS03.05.02

End to End Force Field Parametrization for Polymer Electrolytes Using Machine Learning [Pablo A. Leon](#) and Rafael Gómez-Bombarelli; Massachusetts Institute of Technology, United States

Solid polymer electrolytes (SPEs) are seen as promising alternatives to conventional liquid electrolytes in lithium battery systems due to their low density, mechanical compliance, and low flammability but are challenged by lower ionic conductivity. Molecular dynamics (MD) simulations can be used to guide the design of novel SPEs by allowing quantitative determination of separable anion and cation diffusions as well as local solvation environments. Classical potential MD simulations update molecular conformations by the net force on each atom due to bonds, angles and torsions as well as Coulomb and dispersion interactions. However, these classical potentials require the prior knowledge of materials- and local environment-specific parameters such as unique bond stiffnesses, which are often not well defined.

In this work, we explore the effects of anharmonic bonded interactions on polymer segmental motion and resulting ionic solvation and conductivity in polymer electrolyte systems. An in-house, neural network-based workflow, named AuTopology, was used to learn the interatomic potential parameters of distinct atomic environments for two different classical models from DFT forces as training data. The learned harmonic OPLS model and anharmonic PCFF+ model parameters were then used to equilibrate condensed-phase simulations at a variety of experimentally-relevant concentrations. These simulations were allowed to run for hundreds of nanoseconds to determine the individual anion and cation diffusivities and resulting conductivities. Using this framework and an in-house database of molecular conformations, we have been able to reproduce wB97XD3-level DFT forces from trained OPLS force fields to within 5.5 kcal/mol-Å as well as compare the condensed phase solvation and conductivities between the OPLS and PCFF+ models for PEO and carbonate systems.

11:00 AM DS03.05.03

Development of Deep and RF-MEAM Potentials to Model Physical and Thermo-Mechanical Properties of Metal-Rich Carbides [Tyler J. McGilvry-James](#)¹, Bikash Timalina¹, Andrew I. Duff², Nirmal Baishnab³, Puja Adhikari⁴, Saro San⁴, Wai-Yim Ching⁴ and Ridwan Sakidja¹; ¹Missouri State University, United States; ²STFC Daresbury Laboratory, United Kingdom; ³Iowa State University, United States; ⁴University of Missouri–Kansas City, United States

In the current study, we have developed Deep Learning Potentials as implemented in DeepMD code to model physical and thermo-mechanical properties of complex metal-rich carbides. These phases are critical to the creep properties of advanced Ni-based Superalloys. For this purpose, we utilized the results from *ab-initio* calculations following the Density Functional Theory approximations including the energy, forces, and virial database as generated from the Vienna Ab-initio Software Package. The efficiency and validity of the developed potentials were verified through a series of predictive molecular dynamics simulations of thermomechanical properties that are of interest to the development of advanced superalloys. In addition, we compared the Deep Learning Potentials to the analytical potentials of Reference-Free Modified Embedded Atomic Method (RF-MEAM) that we obtained by using a combined parametrization approach of Conjugate Gradient Minimization (CGM) and Genetic Algorithms as implemented in MEAMfit V2 code. The support from the National Energy Technology Laboratory (Grant No. FE0031554) is gratefully acknowledged. We also would like to thank NERSC for the supercomputer facility.

11:15 AM DS03.05.04

Accurate Prediction of Free Solvation Energy of Organic Molecules via Graph Attention Network and Message Passing Neural Network from Pairwise Atomistic Interactions [Ramin Ansari](#)¹, Amirata Ghorbani² and John Kieffer¹; ¹University of Michigan, United States; ²Stanford University, United States

Deep learning based methods have been widely applied to predict various kinds of molecular properties in the pharmaceutical industry with increasing success. The solvation free energy is an important index in the field of organic synthesis, medicinal chemistry, drug delivery, and biological processes. However, accurate experimental solvation free energy determination is a time-consuming process, and hence, methods to assess this quantity in the absence of physical samples are of interest. Here, we propose two novel models for the problem of free solvation energy predictions, based on the Graph Neural Network (GNN) architectures: Message Passing Neural Network (MPNN) and Graph Attention Network (GAT). GNNs are capable of summarizing the predictive information of a molecule as low-dimensional features directly from its graph structure, without reliance on extensive intra-molecular descriptors. Consequently, accurate predictions of the molecular properties can be made without time consuming experimental measurements. We show that our proposed models also outperform all quantum mechanical and molecular dynamics methods in addition to existing alternative machine learning based approaches in the task of solvation free energy prediction. The novelty of our neural network model is that we take pair-wise interaction of solute and solvent into consideration. We believe our proposed architecture can be used for pair-wise interactions such as solvent-solute, protein-ligand, and etc.

11:30 AM DS03.05.06

Late News: Using Machine Learning Empirical Potentials to Investigate Interdiffusion at Metal-Chalcogenide Alloy Interfaces Siddarth K. Achar^{1,2}, Derek Stewart² and Julian Schneider³; ¹University of Pittsburgh, United States; ²Western Digital Corporation, United States; ³Synopsys Inc., Denmark

Chalcogenide alloys are key materials for both selector and memory elements found in next generation non-volatile memory cells. Developing robust material stacks for memory devices is crucial for optimal device performance and long-term endurance. However, Joule heating and high electric fields during operation can often lead to atomic interdiffusion at interfaces that can degrade device performance over time. While first principles atomistic simulation can provide insight into the electronic structure and local atomic bonding configurations, due to computational constraints, this approach is limited to small atomic systems (<1000 atoms) and time scales (~10 ps). To evaluate long term device performance, we need an approach that can comfortably address complex atomic configurations at different temperatures and time scales.

While classical molecular dynamics is up for the task, the field has suffered from a lack of robust empirical potentials for materials beyond traditional semiconductors. Machine learning provides one promising approach to use *ab-initio* insight from density functional theory to inform the systematic development of new empirical potentials. In this work, we developed a robust set of machine learning potentials to examine the interaction between Ge-Se alloys and Ti electrodes. Previous experimental investigations have shown evidence for strong interfacial interaction between Ti and chalcogenide alloys[1-3]. The first principles training set draws from a range of linear combination of atomic orbitals (LCAO) DFT calculations on bulk crystal compounds, multilayer structures, and *ab-initio* molecular dynamic runs at different temperatures. Using this data set, we trained the empirical potentials using the moment tensor potential framework[4] implemented in QuantumATK[5]. The initial empirical potentials were also further refined by active learning which incorporates new configurations in the training dataset. The amorphous chalcogenide glasses and interface structures were intentionally not part of the training set. The machine learning empirical potentials provide accurate predictions for key material parameters in the training data (lattice constant, bulk modulus, etc). They are also able to generate reasonable atomic models for Ge-Se amorphous materials outside the training set. Long term (> 1 ns) molecular dynamic simulations[6] using these potentials shows clear evidence of interdiffusion at the Ti|Ge-Se interfaces. In this presentation, we will discuss the evolution of the composition profile over time and the impact interdiffusion will have on the electronic properties of these device structures.

[1] S. G. Alberici, R. Zonca, and B. Pahshmakov, *Applied Surface Science*, **231-232**, 821 (2004)

[2] V. A. Venugopal, G. Ottaviani, C. Bersolin, D. Erbetta, A. Modelli, *Journal of Electronic Materials*, **38**, 2063 (2009)

[3] J.-L. Battaglia, A. Kusiak, A. Saci, R. Fallica, A. Lamperti, *Applied Physics Letters*, **105**, 121903 (2014)

[4] A. V. Shapeev, *Multiscale Modeling and Simulation*, **14**, 1153 (2016).

[5] S. Smidstrup et al., *Journal of Physics: Condensed Matter*, **32**, 015901 (2020).

[6] J. Schneider et al., *Modeling Simul. Mater. Sci. Eng.* **25**, 085007 (2017).

11:45 AM DS03.05.07

Late News: (Garcia High School Student) Performance Analysis of an AI-Guided Coarse-Graining Methodology for More Efficient Protein Modeling Raaghav Malik¹, Ziji Zhang², Miriam Rafailovich², Marcia Simon², Yuefan Deng² and Peng Zhang²; ¹Columbus Academy, United States; ²Stony Brook University, The State University of New York, United States

Background: For complex biological dynamics in silico studies, conventional all-atomic (AA) simulations are far too computationally expensive for large-scale systems which take up to months or even years. In the last decade, a rise in coarse-grained (CG) modeling allows for the extension of time-scales compared to the AA model, by combining atoms in larger macromolecules and leading to significant simulation speedups. Such modeling techniques hold promise, yet the most crucial part in retaining accuracy compared to all-atom models is the parameterization of CG force fields.

Methods: We evaluate two methods for parameterizing CG models for improved accuracy: a conventional iterative Boltzmann inversion (IBI) by comparing target radial distribution functions, and the CG-Net neural network model which intelligently learns the parameters from short all-atomic trajectories. CG-Net is fed inputs as Cartesian coordinates of CG particles and serves as the potential energy function from which particle forces can be computed. Network weights represent parameters of this potential energy function, and the loss function for the discrepancy between atomistic dynamics and NN-predicted CG dynamics is minimized. The molecule studied was the protein chignolin (PDB: 1UAO) at 350K (the folding transition temperature), selected to make the training time for CG-Net manageable and the ground-truth AA simulation easier to compute. After the AA equilibrium was computed using NAMD, the molecule was coarse-grained by extracting the alpha carbon atoms. After the first guess for the CG parameters was computed using VMD's CG Builder GUI, an IBI analysis was performed to iteratively generate improved parameters. Iterations are repeated until differences in RMSD values are negligible. The full AA-ground truth serves as a basis of comparison for these models.

Results: The original AA chignolin molecule used contains 138 atoms in 10 amino acid residues, with 141 bonds, 249 angles, and 369 dihedrals built using the LAMMPS topology file. After the initial alpha-carbon coarse-grained model was defined, with 10 beads each representing approximately 14 atoms, both the nonbonded Lennard-Jones and bonded interaction parameters were computed using IBI. The bonded interaction parameters were tuned until the stiffness constants differed ~10% from those derived from the atomic-scale simulations. The CG model is simple, containing only 9 bonds and 8 angles built using a custom topology file and effectively reducing the degrees of freedom by 94-97%, but the IBI showed that the CG model is stable when used on chignolin due to bond lengths and angles having little alteration through successive iterations. RMSD and RDF values were also computed and compared to the all-atom simulations for validation of this method. This analysis was done both in vacuum and with chignolin solvated in TIP3P water.

Discussion and Future Work: The focus of this work was to conduct performance analysis of two different methods for parameterizing CG force fields, allowing us to accelerate the conventional AA model by 16-30 orders of magnitude. ML methods such as CG-Net show the potential for improving accuracy of CG models making it an effective technique to study large macromolecules. However, one limitation of CG-Net is the precision that is lost from modeling CG bead interactions instead of atomic interactions. Drawbacks of IBI include the inability to work with hybrid CG models and the failure to account for dihedral angles. Future work will be done to implement a combined CG model which utilizes both techniques for improved accuracy. Such

techniques can be applied in many ways to study a variety of materials, including human fibrinogen and the SARS-COV-2 spike glycoprotein. **Acknowledgment:** The project is supported by the Stony Brook Garcia Center for Materials Research and the Garcia High School Program.

SESSION DS03.06: Machine Learning for Accelerating Simulations IV
Session Chairs: Mathieu Bauchy and Christian Hoover
Thursday Afternoon, December 2, 2021
Sheraton, 5th Floor, The Fens

1:45 PM DS03.06.03

NequIP—E(3)-Equivariant Convolutions Enable Sample-Efficient, Scalable and Highly Accurate Machine Learning Interatomic Potentials [Simon L. Batzner](#)¹, [Albert Musaelian](#)¹, [Lixin Sun](#)¹, [Tess Smidt](#)², [Mario Geiger](#)³, [Jonathan Mailoa](#)⁴, [Mordechai Kornbluth](#)⁴, [Nicola Molinari](#)¹ and [Boris Kozinsky](#)¹; ¹Harvard University, United States; ²Lawrence Berkeley National Laboratory, United States; ³EPFL, Switzerland; ⁴Robert Bosch Research and Technology Center, United States

We present Neural Equivariant Interatomic Potentials (NequIP), an E(3)-equivariant deep learning approach for learning interatomic potentials for molecular dynamics simulations. Instead of the commonly deployed invariant convolutions over scalar features, NequIP uses E(3)-equivariant convolutions over geometric tensors, better representing the symmetries of Euclidean space. The proposed model obtains state-of-the-art accuracy on a challenging set of diverse molecules and materials while at the same exhibiting remarkable sample efficiency. Interestingly, NequIP outperforms existing, invariant models with up to three orders of magnitude fewer training data and performs better than kernel methods, even on tiny data sets, thereby challenging the widely held belief that deep neural networks require massive training sets. We show results from molecular dynamics simulations using NequIP on a series of technologically relevant bulk materials as well as the folding of small proteins. The method is implemented in a scalable and highly efficient software implementation, integrated with the molecular dynamics code LAMMPS, and can be used to simulate large time- and length-scales at high accuracy and low computational cost.

2:00 PM DS03.06.02

DICE—A Linear-Scaling N-Body Interatomic Potential from E(3)-Equivariant Convolutions [Simon L. Batzner](#), [Albert Musaelian](#), [Lixin Sun](#), [Steven B. Torrisi](#) and [Boris Kozinsky](#); Harvard University, United States

Message Passing Graph Neural Networks (MPNNs) based on pairwise interactions have emerged as the leading paradigm for modeling atomistic systems by recursively propagating information along a molecular graph. While MPNNs have consistently been demonstrated to give low generalization errors, they inherently have a low level of interpretability, are not systematically improvable, and are difficult to scale to large numbers of atoms. Here, we introduce the Deep Interatomic Cluster Expansion (DICE), an equivariant neural network that leverages many-body information in a single interaction, without the need for message passing or convolutions. The method can be systematically improved by including higher-order interactions at linear cost, has physically meaningful hyperparameters, and is embarrassingly parallel. DICE builds on a novel, learnable E(3)-equivariant many-body representation that utilizes weighted tensor products of geometric features to describe N-point correlations of atoms. The proposed many-body representation overcomes the exponential scaling of a naive cluster expansion and instead scales linearly with the number of simultaneously correlated particles. We demonstrate that the use of higher-order correlations of atoms systematically improves the accuracy. We further find that DICE gives excellent performance across a wide variety of settings, outperforming both MPNNs as well as kernel-based methods on small data sets.

2:15 PM DS03.06.04

Differentiable Sampling of Molecular Geometries with Uncertainty-Based Adversarial Attacks [Daniel Schwalbe Koda](#), [Aik Rui Tan](#) and [Rafael Gómez-Bombarelli](#); Massachusetts Institute of Technology, United States

While neural network (NN) interatomic potentials enable fast prediction of potential energy surfaces with an accuracy matching that of the electronic structure methods, they often show volatile behaviors when extrapolating outside well-learned training domains. Domains with low prediction confidence can be identified using uncertainty quantification methods. However, arriving at such uncertainty regions requires thorough exploration of the NN phase space, often using slow atomistic simulations. Here, we exploit automatic differentiation to drive atomistic systems towards high-likelihood, high-uncertainty configurations without the need for atomistic simulations. Adversarial attacks are employed on an uncertainty metric to sample informative geometries that expand training domains of the NNs. In combination with an active learning loop, this approach provides a efficient way to bootstrap and improve NN potentials, while decreasing number of calls to the ground truth method. We demonstrate this framework on sampling of kinetic barriers, collective variables in molecules, and supramolecular chemistry. This framework can also be extended to any NN potential architecture and materials system.

2:30 PM DS03.06.05

Complex Dynamics of the CO/Pt Interaction from Bayesian Active Learning Simulations [Cameron J. Owen](#), [Lixin Sun](#), [Jin Soo Lim](#), [Isabel Diersen](#) and [Boris Kozinsky](#); Harvard University, United States

Quantitative understanding and controlling interfacial reactions between the gas-phase and solid surfaces are crucial for improving numerous catalysis and energy conversion systems. For example, the adsorption of CO on Pt surfaces is important for a variety of industrial processes (e.g., water-gas-shift reaction, PEM fuel cell catalyst poisoning). CO/Pt interaction is poorly understood but known to strongly affect the metal surface structure and dynamics. An accurate and fast reactive model could provide enormous insight into the current, and future, design of such Pt-based catalysts. Density functional theoretical (DFT) methods and existing parametric interatomic potentials have long struggled with accurately describing heterogeneous interactions. Here, we employ the FLARE framework [1] to actively learn the CO/Pt interaction, using a mapped Gaussian Process (MGP) machine-learning model, with molecular dynamics used to sample configurational space. The model accurately reproduces DFT energies, forces, and stresses as well as rigorous quantitative Bayesian uncertainties. When predictive uncertainty falls outside of the accepted tolerance, additional DFT calculations are performed to augment the training set.

We then use the MGP model to conduct large-scale MD to explore the effect of CO adsorption on various Pt-surface facets and benchmark to expected outcomes as provided by experiment.

[1] J. Vandermause et al, NPJ Computational Materials 6 (2020).

8:00 AM *DS03.07.01

Four Generations of Neural Network Potentials for Materials Science Jörg Behler; University of Göttingen, Germany

A lot of progress has been made in recent years in the development of machine learning (ML) potentials for atomistic simulations [1]. Neural network potentials (NNPs), which have been introduced more than two decades ago [2], are an important class of ML potentials. While the first generation of NNPs has been restricted to small molecules with only a few degrees of freedom, the second generation extended the applicability of ML potentials to high-dimensional systems containing thousands of atoms by constructing the total energy as a sum of environment-dependent atomic energies [3]. Long-range electrostatic interactions can be included in third-generation NNPs employing environment-dependent charges [4], but only recently limitations of this locality approximation could be overcome by the introduction of fourth-generation NNPs [5], which are able to describe non-local charge transfer using a global charge equilibration step in combination with an accurate short-range term. In this talk an overview about the evolution of high-dimensional neural network potentials will be given along with typical applications in large-scale atomistic simulations.

- [1] J. Behler, *J. Chem. Phys.* **145** (2016) 170901.
- [2] T. B. Blank, S. D. Brown, A. W. Calhoun, and D. J. Doren, *J. Chem. Phys.* **103** (1995) 4129.
- [3] J. Behler and M. Parrinello, *Phys. Rev. Lett.* **98** (2007) 146401.
- [4] N. Artrith, T. Morawietz, J. Behler, *Phys. Rev. B* **83** (2011) 153101.
- [5] T. W. Ko, J. A. Finkler, S. Goedecker, J. Behler, *Nature Comm.* **12** (2021) 398.

8:30 AM DS03.07.02

Local Gaussian Process Regression for Interatomic Potentials Spencer Hill¹, Tucker Carrington¹, Sergei Manzhos² and Manabu Ihara²; ¹Queen's University, Canada; ²Tokyo Institute of Technology, Japan

Gaussian process regression (GPR) has gained increasing attention for the construction of interatomic potentials. In particular, GPR has been shown to produce spectroscopically accurate potential energy surfaces (PES) of molecules from fewer samples than neural networks (*J Chem Phys* 148 (2018) 241702). This, the absence of non-linear parameters other than a small number of hyperparameters, and the capability to compute estimates of uncertainties make GPR a promising method. GPR, however, suffers from rapidly escalating CPU cost with the number of training data. Both the cost of model training and the cost of computing the PES at points post-training increase, making calculations with more than a few tens of thousand training data not routinely feasible. The increasing cost is due to the need to calculate a matrix-vector product with the inverse of a covariance matrix \mathbf{K} . We explore a local version of GPR, LGPR, in which for each test point, a local covariance matrix \mathbf{K}' is built, equivalent to using blocks of a permuted \mathbf{K} . This approach raises the prefactor of the CPU cost but allows working with arbitrarily large training datasets. We test the approach in comparison with the classic GPR on PESs of formaldehyde and UF6 using very large test sets and property calculations and show that the size of \mathbf{K}' can be considerably reduced compared to \mathbf{K} with a small extra error.

8:45 AM DS03.07.03

Development of SNAP Machine Learned Interatomic Potentials for Materials in Extreme Environments Mary Alice Cusentino, Mitchell A. Wood and Aidan Thompson; Sandia National Laboratories, United States

Molecular dynamics (MD) is a widely used tool for studying materials at the atomistic scale. However, the accuracy of MD simulations is limited by the interatomic potential. This is especially true for modeling materials in extreme environments where the interatomic potential is typically utilized far from the equilibrium properties it was fitted to. Recently, machine learning has been used to develop interatomic potentials where the potential is trained on large datasets of quantum accurate data as opposed to fitting the potential to a physics based functional form. These types of machine learning interatomic potentials (MLIAPs) have been shown to have increased accuracy compared to traditional potentials [1]. One such MLIAP method, the spectral neighbor analysis potential (SNAP) [2] has been applied to a variety of materials with increased accuracy [2,3]. In this talk, we will discuss the development of SNAP potentials for molecular dynamics simulations of materials in extreme environments such as radiation or high pressure and temperature environments.

- [1] Zuo, et al, *J. Phys. Chem. A* 124, 731-745 (2020)
- [2] Thompson, et al. *J. Comp. Phys.* 285, 316-330 (2015)
- [3] Wood, et al. *Phys. Rev. B* 99, 184305 (2019)

SNL is managed and operated by NTESS under DOE NNSA contract DE-NA0003525

9:00 AM DS03.07.04

Machine Learning in Multiscale Mechanics of Materials Huck Beng Chew and Yue Cui; University of Illinois at Urbana-Champaign, United States

With the recent improvement of algorithms and rapid growth of computing power, machine learning is fast becoming an emerging tool for predicting and understanding material behavior across multiple length scales. With Peta-scale supercomputing resources, we are now able to generate a large number of data sets with existing deterministic material models to train the machine learning algorithms. In this technical presentation, we will discuss our recent attempts to quantify microstructural effects on material strength and fracture response at both the atomistic and the meso-scale.

The first part of the talk will discuss the utilization of machine learning to elucidate the structure-property relationship at grain boundaries of nanocrystalline metals. We now know that the strength of nanocrystalline metals is ultimately controlled by the absorption, emission, or transmission of single dislocations at the grain boundaries, which closely depend on the local atomistic stress state at the grain boundaries. Here, we develop a machine learning algorithm based on an artificial neural network (ANN) to predict the local atomistic stress (output) along [110] bicrystal symmetrical tilt Cu grain boundaries from the local atomic configuration (input). We demonstrate that successful predictions of the atomistic stress state can be achieved by ensuring

that the training set comprises of grain boundaries with both the same type and sequence of structural units. The predictive accuracy can be significantly improved by including the deformed configuration and stress state in the training dataset. This atomistic constitutive law will be used to predict the atomistic stress state from DFT calculations or HRTEM imaging, thus extending the notion of atomistic stress beyond MD domain.

The second part of this talk examines the ability of ANNs to predict the tortuous crack path in a heterogeneous microstructure, comprising of two distinct size-scales of voids which is commonplace in additively manufactured metals – the larger-scale voids represent the ~30 μm defects resulting from gas bubbles or unsintered powder in the additive manufacturing process, while the smaller ~2-10 μm background voids originate from nucleated particles or inclusions responsible for ductile fracture process in metal alloys. A small-scale yielding, modified boundary layer model with monotonic K_I -T displacement loading was used to study crack propagation through a material with local distribution of dual-scale pre-existing voids resembling AM Ti-6Al-4V. The Gurson ductile damage model was implemented to model both the background pores and the larger AM defects, and the initial porosity distribution ahead of the current crack-tip, and resulting crack propagation path was used to train an ANN. The machine learning algorithms provide critical insights into the effects of porosity distributions on the crack propagation path, supporting the notion of achieving fracture by design.

9:15 AM DS03.07.05

Late News: (Garcia High School Student) MR-Net—Multi-Representation Learning for Protein-Ligand Binding Affinity Prediction Emirhan Kurutulus¹, Bernard Essaman², Ziji Zhang², Miriam Rafailovich², Marcia Simon², Yuefan Deng² and Peng Zhang²; ¹Cagaloglu Anatolian High School, Turkey; ²Stony Brook University, The State University of New York, United States

Accurately predicting binding affinities of a given protein-ligand system fast and robustly is of high importance for drug discovery and experimental microbiology simulations. Compared with deterministic models which require heavy computational workloads, deep learning models are faster yet with great generalization capabilities, providing an efficient path for knowledge discovery in molecular scientific studies.

We present MR-Net, a state-of-the-art deep learning model on PDBbind v.2019 and v.2016 datasets for protein-ligand binding affinity prediction. The proposed architecture consists of 2 transformer modules, a fully convolutional encoder and a fully convolutional decoder. To maximize the amount of extracted features from the input, 3 different representations of a given system are used: SMILES string, point cloud and atom sequence. Only the binding pocket of the system is used for the prediction. The point cloud representation is a 4D tensor of shape (length of the feature vector, x, y, z) where each atom is represented on a grid of resolution 0.5 Angstroms where the maximum distance between each atom is 30 Angstroms. The number of features in the feature vector is determined as 32. For SMILES and sequences, transformer modules are used, whereas for the point-cloud a fully convolutional encoder is proposed. The encoder is constructed with 3D depthwise separable convolution modules where skip connections are utilized to maximize the gradient flow. The transformer modules are designed with the “deeper better than larger” principle. The embedding dimension is determined as 64 and learnt from the data with additional positional encoding. The dictionary sizes are 65 and 25 for the SMILES transformer and the sequence transformer respectively. For SMILES strings, inputs longer than 2500 characters are truncated. With average pooling and convolutions with kernel size of 3, the outputs of each module are reshaped into (1, 64, 64) and concatenated along the first dimension. Then, the resulting matrix is fed into a fully convolutional decoder consisting of 2D convolutions connected to a fully connected layer. The proposed network is trained with a custom loss function aiming to minimize the Root Mean Squared Error Loss while maximizing the Pearson’s Correlation Coefficient.

For experiments on PDBbind v.2016 and v.2019 datasets containing 16,179 and 21,382 protein-ligand complexes respectively, the core set splits are used for testing purposes while the rest is used for training. During training, each sample in the input space is rotated to all the 24 combinations possible and has been added random translation to make our model center-invariant. Our experiments showed that single-headed attention performs much better than multi-head attention because of the long input sequences; hence, both used transformers are single-headed and have 6 encoder and 6 decoder layers with feed-forward dimension of 2048. To prevent overfitting, weight decay is applied. We report 1.184 Root Mean Squared Error and 0.878 Pearson’s Correlation Coefficient on PDBbind v.2016 dataset which, to our knowledge, is above the current state-of-the-art.

Our MR-Net achieves state-of-the-art performance on both PDBbind v.2016 and v.2019 datasets, greatly reducing the need for computational resources and accurately predicting the protein-ligand binding affinity. We are also planning on more optimization approaches to further extend the capability of MR-Net. Experiments with the preprocessing pipeline of our model are to be conducted for the atomic feature descriptors and grid resolution. To learn embeddings from a larger dataset, we are working on an extended version of the Word2Vec algorithm for protein-ligand complexes.

This work is supported by the Garcia High School Program. The numerical calculations reported were partially performed at TUBITAK ULAKBIM, High Performance and Grid Computing Center.

9:30 AM DS03.07.07

Accelerated Crystal Structure Search for Multinary Phases—Introduction to SPINNER Framework and Its Application Wonseok Jeong¹, Sungwoo Kang¹, Changho Hong¹, Seungwoo Hwang¹, Younchae Yoon¹, Youngho Kang² and Seungwu Han¹; ¹Seoul National Univ, Korea (the Republic of); ²Incheon National Univ, Korea (the Republic of)

Over the years, computational materials science has greatly contributed to novel materials search, adding to the experimental search which is inherently low-throughput compared to computational search. Computational exploration of unknown materials has two key components: crystal structure generation algorithms, and energy evaluation of the generated crystal structures. The latter is critical as the energy of the crystal structure is directly related to synthesizability. Conventionally, the energy evaluation has been carried by quantum mechanical calculations, notably density functional theory (DFT). However, when it comes to ternary or higher (multinary) phases search, DFT shows its limitation, as the size of the materials space grows exponentially with the increase of the complexity and DFT is still too slow to evaluate the immense number of crystal structures that can appear during the crystal structure search. In addition, as previous researches are more focused on crystal structure search of unary and binary phases, an efficient crystal structure generation algorithm optimized on multinary phases is still lacking.

In this presentation, we introduce SPINNER, an efficient crystal structure search framework that can carry more than 10^5 energy evaluations and has optimized crystal structure generation algorithms for multinary phases. The high efficiency of the SPINNER framework is realized by adopting machine-learning (ML) based interatomic potentials for crystal energy evaluations. ML potentials can evaluate the energy and force of given atomic structures at low computational costs while maintaining an accuracy comparable to that of DFT. With the newly developed SPINNER framework, we aim to find novel military crystals which have high Li-ion conductivity and suggest some of the promising new compounds.

10:30 AM *DS03.08.01

Data-Driven Atomistic Models for the Simulation of Material Failure [James Kermode](#); University of Warwick, United Kingdom

The degradation and eventual failure of a specimen through fracture, fatigue or creep represents an extremely challenging test-case for atomistic materials modelling, since there is a simultaneous requirement for high accuracy in the anharmonic region near a crack tip or dislocation core where chemical bonds break, and for large length- and time-scales to correctly capture elastic relaxation associated with long-range stress fields. I will demonstrate how the Gaussian Approximation Potential (GAP) framework has been successfully applied to this problem using models trained on *ab initio* data for silicon [1], silicon carbide [2] and diamond [3,4], as well as considering how the approach could be further leveraged in future, for example as part of QM/ML (quantum mechanics/machine learning) multiscale schemes and/or to carry out active learning [5].

[1] A. P. Bartók, J. R. Kermode, N. Bernstein, and G. Csányi, Machine Learning a General-Purpose Interatomic Potential for Silicon, *Phys. Rev. X* **8**, 041048 (2018)

[2] H. Tunstall, J. R. Kermode and G. Sosso, *In Prep* (2021)

[3] P. Rowe, V. L. Deringer, P. Gasparotto, G. Csányi, and A. Michaelides, *An Accurate and Transferable Machine Learning Potential for Carbon*, *J. Chem. Phys.* **153**, 034702 (2020)

[4] J. Brixey and J. R. Kermode, *In Prep* (2021)

[5] Z. Li, J. R. Kermode, and A. De Vita, *Molecular Dynamics with On-the-Fly Machine Learning of Quantum-Mechanical Forces*, *Phys. Rev. Lett.* **114**, 096405 (2015)

11:00 AM DS03.08.03

Machine Learning at the Exascale for Atomistic Simulations with Improved Accuracy, Length and Time Scales [Mitchell A. Wood](#) and Aidan Thompson; Sandia National Laboratories, United States

With exascale super computers arriving in the near future, it is timely to ask whether our simulation software is capable of matching this unprecedented computing capability. While many research challenges in material physics, chemistry and biology lie just out of reach on peta-scale machines due to length and time restrictions inherent to Molecular Dynamics(MD), questions of the accuracy of our simulations will continue to linger. Simply running the same peta-scale simulations with more atoms on a larger computer (weak scaling) does not advance the accessible timescales, nor does it avoid the pitfalls of empirically developed constitutive models. This talk will overview the U.S. Department of Energy* EXAALT (EXascale Atomistics for Accuracy, Length and Time) project and our efforts to provide software tools for MD that not only scale efficiently to huge atom counts, but also enable efficient MD simulations for smaller systems too. Central to this effort are machine learned models via the Spectral Neighborhood Analysis Potential(SNAP) which demonstrate both tunable accuracy and computational cost, a highly advantageous trait for MD on exascale resources.

*This work is funded through the Exascale Computing Project (No. 17-SC-20-SC), a collaborative effort of the U.S. Department of Energy Office of Science and the National Nuclear Security Administration

11:15 AM DS03.08.04

Deep Learning Methods for Fast Prediction of Protein Vibrational Modes [Darnell Granberry](#), Kai Guo and Markus J. Buehler; MIT Lab for Atomistic and Molecular Modeling, United States

Normal mode analysis is a powerful technique for understanding the motions of chemical and biological systems, with applications in molecular design and fingerprinting. The number of operations required to compute the normal modes of such a system scales cubically with the size of the system, making such analyses computationally intractable. In order to make this technique more accessible to the broader scientific community, prior work produced a data-driven model that relied on geometric and structural properties to predict protein normal modes with high accuracy. In this work, we experimented with creating fully end-to-end models in two ways: first, we investigated multiple architectures for predicting normal modes from amino acid sequences alone, and second, we investigated graph-based architectures. Success in this project will enable faster and more sophisticated applications in functional protein design and recognition, such as screening and inhibiting novel coronavirus spike proteins.

11:30 AM DS03.08.05

Late News: Machine Learning Accelerates Atomistic Dynamics Simulations for Single-Molecule Photodynamics and Multi-Scale Modeling of Organic Solids [Patrick Reiser](#)^{1,1}, Jingbai Li², Manuel Konrad¹, Steven Lopez², Wolfgang Wenzel¹ and Pascal Friederich^{1,1}; ¹Karlsruhe Institute of Technology, Germany; ²Northeastern University, United States

In many multi-scale and reactive Molecular Dynamics (MD) simulations, *ab-initio* quantum calculations such as Density Functional Theory (DFT) or post-Hartree-Fock (post-HF) methods constitute a bottleneck in simulation workflows which prevents exact predictions for long time-scales or large system sizes due to its prohibitively expensive computation costs. In the past years, machine learning has emerged as a tool to enable fast and accurate energy predictions with so-called neural network potentials [1]. A set of neural networks trained on a sufficiently large amount of quantum data offer differentiable energy predictions at constant evaluation times. Here, we adapted this methodology to develop the Python Rapid Artificial Intelligence Ab Initio Molecular Dynamics (PyRAI²MD) software for photodynamics simulations investigating the cis-trans isomerization of trans-hexafluoro-2-butene and the 4 π -electrocyclic ring-closing of a norbornyl hexacyclodiene [2]. The active learning approach of the neural network photodynamics simulations is capable of revealing reaction pathways like the low-yielding syn-product, which was absent in the quantum chemical trajectories, and the subsequent thermal reactions within 1 ns for the norbornyl cyclohexadiene. Additionally, we integrated the machine learning model in multi-scale simulations for organic semiconductors to compute the complete distribution of energy levels in a MD simulation to support more accurate charge transport models [3]. We find that static disorder and thus the distribution of shallow traps is highly asymmetrical for many materials, impacting the widely considered Gaussian disorder models. We furthermore analyze characteristic energy level fluctuation times and compare them to typical hopping rates to evaluate the importance of dynamic disorder for charge transport.

[1] J Behler 2014. Representing potential energy surfaces by high-dimensional neural network potentials. *J. Phys.: Condens. Matter* **26** 183001.

[2] Li, J., Reiser, P., Boswell, B.R., Eberhard, A., Burns, N.Z., Friederich, P. and Lopez, S.A., 2021. Automatic discovery of photoisomerization mechanisms with nanosecond machine learning photodynamics simulations. *Chemical Science*, 12(14), pp.5302-5314.

[3] Reiser P., Konrad M., Fediai A., Léon S., Wenzel W. and Friederich P., 2021. Analyzing Dynamical Disorder for Charge Transport in Organic Semiconductors via Machine Learning. *J. Chem. Theory Comput.*, **17**, 3750–3759.

11:45 AM DS03.08.06

Late News: Characterizing Possible Failure Modes in Physics-Informed Neural Networks [Aditi Krishnapriyan](#)^{1,2}, Amir Gholami¹, Shandian Zhe³, Robert Kirby³ and Michael Mahoney^{1,2}; ¹University of California, Berkeley, United States; ²Lawrence Berkeley National Laboratory, United States; ³The University of Utah, United States

Recent work in scientific machine learning has developed so-called physics-informed neural network (PINN) models. The typical approach is to incorporate physical domain knowledge as soft constraints on an empirical loss function and use existing machine learning methodologies to train the model. We demonstrate that, while existing PINN methodologies can learn good models for relatively trivial problems, they can easily fail to learn relevant physical phenomena even for simple PDEs. In particular, we analyze several distinct situations of widespread physical interest, including learning differential equations with convection, reaction, and diffusion operators. We provide evidence that the soft regularization in PINNs, which involves differential operators, can introduce a number of subtle problems, including making the problem ill-conditioned. Importantly, we show that these possible failure modes are not due to the lack of expressivity in the NN architecture, but that the PINN's setup makes the loss landscape very hard to optimize. We then describe two promising solutions to address these failure modes. The first approach is to use curriculum regularization, where the PINN's loss term starts from a simple PDE regularization, and becomes progressively more complex as the NN gets trained. The second approach is to pose the problem as a sequence-to-sequence learning task, rather than learning to predict the entire space-time at once. Extensive testing shows that we can achieve up to 1-2 orders of magnitude lower error with these methods as compared to regular PINN training.

12:00 PM DS03.01.02

Molecular Dynamics Simulation Using Graph Neural Networks [Ravinder Bhattoo](#), Sayan Ranu and N M Anoop Krishnan; Indian Institute of Technology Delhi, India

Molecular dynamics simulations are used to realistically simulate the material properties. The interatomic potential energy function (PEF) is critical in determining the validity of the results. We use density functional theory (DFT) to parameterize the interatomic PEF. Usually, interatomic PEF is a multi-body function whose functional form is non-trivial to determine. Therefore, estimating the functional form is very critical in determining the interatomic PEF and hence the material properties. Herein, we use a graph neural network with multi-message passing to model the interatomic PEF. Further, we use the Euler-Lagrange equation to determine the acceleration of the atomic system. Finally, we train the GNN against the simulation trajectories of unary and binary Lennard Jones (LJ) systems created from traditional molecular dynamics (MD) simulations. The trained GNN is then used to do MD simulations and demonstrate energy conservation.

SESSION DS03.09: Machine Learning for Accelerating Simulations VII
Session Chairs: Mathieu Bauchy, Christian Hoover and N M Anoop Krishnan
Monday Afternoon, December 6, 2021
DS03-Virtual

4:00 PM *DS03.09.01

Automatically Interpreting Materials Characterization Data to Model Materials Properties Using Machine Learning [Jacqueline M. Cole](#)^{1,2}; ¹University of Cambridge, United Kingdom; ²ISIS Pulsed Neutron and Muon Source, United Kingdom

Data-driven materials discovery requires the automated interpretation of large volumes of materials characterization data and its onward use in materials modeling. Thereby, materials can be designed with properties that suit a given functional application. This data-science approach is enabled by a range of methods from artificial intelligence (AI): machine learning and natural language processing. This talk will show how such AI-based methods can be employed to source materials characterization data from the academic literature, automatically interpret these data, and use them to model and predict materials properties in a molecular-engineering fashion.

4:30 PM DS03.09.02

Data-Driven Design of Switchable Nanomaterials Composed of Polarizable Nanoparticles [Siva Dasetty](#), Igor Coropceanu, Jiyuan Li, Juan J. dePablo, Dmitri Talapin and Andrew Ferguson; The University of Chicago, United States

Homogeneous metallic nanoparticles form highly stable colloids because of the strong electrostatic repulsions. Coating with metal chalcogenide complexes and with changes to solvent polarity, the colloidal stability can be altered to result in the formation of highly ordered aggregates with diverse applications in energy storage, photonics and electronics. The structure of the self-assembled aggregates depends on the delicate interplay between the dispersion and the electrostatic interactions governed by the design parameters such as temperature, size-charge-dielectric constant of the nanoparticle and the dielectric strength of the solvent. To aid in the rational design of engineered materials composed of polarizable nanoparticles, we have established a computational and machine learning framework to efficiently screen the experimental design space, identify regimes leading to spontaneous and triggerable self-assembly, and extract microscopic design rules for engineered assembly.

We perform high-throughput virtual screening of the particle design space using a coarse-grained simulation model implementing an image-charge formalism that rigorously accounts for the many-body polarization interactions. We efficiently sample the design space and identify self-assembly phase boundaries using a data-driven active learning approach to optimally guide the deployment of computational resources. Our computational phase boundaries are in good agreement with experimental scattering measurements, and predict the structure of self-assembled aggregates become more ordered with decreasing nanoparticle size and increasing solvent dielectric constant. Finally, we use our computational models to design switchable materials systems composed of polarizable nanoparticles that are capable of triggered assembly and disassembly upon changes in temperature and solvent quality.

4:45 PM DS03.09.03

A Hierarchical Design on Bioinspired Structural Composites Using Reinforcement Learning [Chi Hua Yu](#)^{1,2}, Bor-Yann Tseng³, Cheng-Che Tung³, Zhenze Yang², Elena Zhao⁴, Po-Yu Chen³, Chuin-Shan Chen^{5,5} and Markus J. Buehler²; ¹National Cheng Kung University, Taiwan; ²Massachusetts Institute of Technology, United States; ³National Tsing Hua University, Taiwan; ⁴Deerfield Academy, United States; ⁵National Taiwan University, Taiwan

Here we propose a new design method using reinforcement learning to solve bioinspired composite materials in a complex system. Biological structural materials are made by a stiff matrix and a compliance glue to exhibit extraordinary mechanical properties which synthetic materials do not possess. The reason for this excellent performance is because a particular order makes them of microstructures. To imitate the exceptional material properties of biomaterials, the idea of bioinspired structural material has been proposed. However, the number of combinations of design space is usually intractable. Therefore, we offer a new design method by using reinforcement learning to solve the problem. Here we developed a hierarchical design paradigm. The hierarchical design process starts from a design space with limited combinations. After obtaining the best design of the current system size, we expanded the design system and searched for the best design with higher resolution. We searched for the best crack resistance by using the hierarchical reinforcement

learning from a lower resolution. By comparing the design results in the two design systems, the hierarchical design can effectively increase the convergence rate. We further discussed the results obtained from each hierarchical level. It can be observed that the best structure obtained from a high-resolution design space shows a significant improvement by depressing the stress concentration at the crack tip. The best composition was examined through 3D printing. The experimental results show that there is an excellent agreement with our AI design. The design framework proposed in this research can be used as an alternative method for optimization in a complex design system with various constraints. This research can be potentially applied to bionic structural design, nanoengineering, and material design in the future.

5:00 PM DS03.09.04

Machine-learned Potential Energy Model for Extensive Sampling of the Microstructure of Complex Mixed-Ion Perovskite Hsin-An Chen and Chun-Wei Pao; Academia Sinica, Taiwan

The organic-inorganic mixed-ion perovskite materials are one of the promising active materials in the photovoltaic and optoelectronic applications because of their high absorption coefficient, high power conversion efficiency, easy processing and low fabrication cost. The microstructures of the mixed ion perovskites are vital for the device performance. However, experimental characterization of the microstructures of mixed-ion perovskites is still considered to be a challenging task; furthermore, the chemical complexity in conjunction with the huge permutation degrees of freedom makes extensive samplings over the composition space using conventional ab-initio calculations intractable. In the present study, a machine learning-enabled potential model for $MA_xFA_{1-x}Pb(Br_xI_{1-x})_3$ mixed-ion perovskite was trained for extensive exploration over both the composition and permutation space to access the energetics and microstructure properties¹. Subsequent correlation analysis of low energy structures over the composition space allowed us to construct the process-structure-property (PSP) relationship of mixed ion perovskites, namely, to reveal the correlations among chemical compositions, ion mixing energies, chemical short-range orderings, atomic strains as well as the device performance. Our analysis suggest that the lattice distortion is the primary factor impacting material performance – in the high MA/Br concentration regime, strong lattice distortion induces high mixing energy, resulting in phase segregation and introducing defects such as domain boundaries. Hence, mitigating the lattice distortion to retain the single-phase solid solution phase is one necessary condition of the optimal composition of mixed-ion perovskite material. The present study therefore demonstrate the capability of machine-learned potential in evaluating the energetics and microstructures of mixed-ion perovskites, and can be readily extended to studying other chemically complex materials such as the high entropy materials.

¹Chen, H. A., Tang, P. H., Chen, G. J., Chang, C. C., & Pao, C. W. (2021). Microstructure Maps of Complex Perovskite Materials from Extensive Monte Carlo Sampling Using Machine Learning Enabled Energy Model. *The Journal of Physical Chemistry Letters*, 12(14), 3591-3599.

5:15 PM DS03.09.05

Accelerating Lattice Thermal Conductivity Calculations with Neural Network Potentials Kyeongpung Lee, Jeong Min Choi, Wonseok Jeong, Jaehoon Kim and Seungwu Han; Seoul National University, Korea (the Republic of)

Lattice thermal conductivity is of central importance in engineering field, as insulator for silicon-on-insulator devices needs sufficiently high thermal conductivity to dissipate heat effectively during operation, for example. A fast and accurate estimation of lattice thermal conductivity can be helpful to product designers. A reliable approach for the theoretical evaluation of lattice thermal conductivity exploits ab initio calculations to decide the harmonic and anharmonic factors of Boltzmann transport equation solution. However, the anharmonic effect requires exhaustive amount of ab initio calculations, which is the most time-consuming process and hence the main bottleneck of this approach.

One of the emerging alternatives is to replace the fully ab initio approach with neural network potential (NNP), which has an accuracy comparable to ab initio calculations at a significantly reduced computation time. In this study, we employed NNP to calculate harmonic and anharmonic factors to evaluate lattice thermal conductivity. Results were in good agreements with the ab initio results. Three types of datasets for NNP training were tested, where molecular dynamics trajectories outperformed the superposition of phonon modes and random displacements. We then discussed the framework to make this approach efficient and how to obtain reliable and high-precision results. We finally showed the total computation time compared to the fully ab initio approach.

5:30 PM DS03.09.06

Late News: Structured Gaussian Process Regression Models to Address Difficulties in Modeling Very High Dimensional Data with Product Kernels Eita Sasaki, Manabu Ihara and Sergei Manzhos; Tokyo Institute of Technology, Japan

Gaussian process regression has become increasingly popular in machine learning based materials research, quantum dynamics, and other applications. Advantages include the non-parametric nature of the method, and, by ricochet, ease of use with high-dimensional data, as increase in dimensionality does not lead to a rapid increase in the number of non-linear parameters (contrary for example to neural networks) except a small number of hyperparameters. However with very high-dimensional data, especially when some features are subject to uncertainty, commonly used product kernels (of the Matern family) can lead to a failure of the method. We will show how this phenomenon arises and propose possible solutions based on the use of high-dimensional model representations (HDMR). We will demonstrate the advantages of imposing HDMR structure on the entire function model or on the GPR kernel. In particular, we will show how the use of HDMR allows working with very sparse data and obtaining physical insight with an otherwise general ML method. Examples from modeling of kinetic energy densities, potential energy surfaces, and electricity demand prediction will be discussed.

5:45 PM DS03.09.07

Nanocrystalline Microstructure Modulation Based on Reinforcement Learning Hao Sun; Queen's University, Canada

Polycrystals are thermodynamically unstable; hence, their properties are path-dependent. Polycrystals prepared using different methods should exhibit different microstructures and properties. Although most polycrystalline metals are formed via solidification of the liquid phase, there are vast, continuous, thermal processing strategies available during solidification (temperature, cooling rates, etc.). Identifying the optimal approach to obtain a given microstructure—e.g., small average grain size, narrow grain size distribution, high density of coherent twin boundaries, and a high proportion of coincident-site-lattice boundaries—can be quite challenging. Using molecular dynamics simulations, we investigated the grain boundary properties and microstructures of nanocrystalline FCC and HCP metals formed using different strategies. Based on our simulation results, we circumvent conventional trial-and-error methods via reinforcement learning to find the most efficient pathway toward desirable microstructures and properties. Our work shows a path towards tailoring polycrystalline microstructures in a controllable and efficient manner.

6:30 PM DS03.10.02

A Machine-Learned Potential Energy Model for Large-Scale Atomistic Simulation of 2D Ruddlesden-Popper Perovskite Material [Svetozar Najman](#)^{1,2}, Po Yu Yang¹ and Chun-Wei Pao¹; ¹Research Center for Applied Sciences, Academia Sinica, Taiwan; ²National Tsing Hua University, Taiwan

2D organic-inorganic Ruddlesden-Popper perovskite material is a promising alternative for optoelectronic and photovoltaic applications because of its long-term stability in ambient conditions relative to its 3D perovskite counterparts. Furthermore, the band gap and exciton binding energies of 2D perovskite materials are directly correlated with the number of anionic inorganic perovskite layers, indicating tunable optoelectronic properties by adjusting the proper stoichiometric ratio of the methylammonium (MA) and butylammonium (BA) spacer cations during synthesis. However, it has been shown recently that the quantum well width distribution is not uniform for selected MA to BA cation ratio¹. Furthermore, it has been reported that 2D Ruddlesden-Popper perovskites with principle number $n > 5$ are thermodynamically unstable relative to their 3D counterparts, namely, higher 2D perovskite members would segregate into lower members and 3D like-phase². Therefore, comprehensive insights into the stability and microstructure of 2D perovskite, in particular, the distribution of quantum well width are critical for enhancing the performance of 2D perovskite materials. In this work, a machine-learned potential energy model based on the Spectral Neighbor Analysis Potential (SNAP) was trained using images obtained from ab-initio molecular dynamics simulations 2D perovskite of a variety of members. The trained potential energy model possesses high fidelity in both energies and atomic forces relative to ab initio calculations, and the potential model is stable during regular molecular dynamics simulations under canonical ensemble. The potential energy model allows us to perform a series of large-scale atomistic Monte Carlo simulations of 2D perovskite slabs containing several tens of quantum wells to examine the quantum well width distribution and their impacts on the optoelectronic properties of 2D perovskites. Furthermore, this way, it is also possible to extract the properties of an active layer in a working device for the different initial stoichiometric ratio of MA and BA cations during synthesis.

1. Quintero-Bermudez, R. et al. Compositional and orientational control in metal halide perovskites of reduced dimensionality. Nat. Mater. 17, 900–907 (2018).
2. Soe, C. M. M. et al. Structural and thermodynamic limits of layer thickness in 2D halide perovskites. Proc. Natl. Acad. Sci. 116, 58 LP – 66 (2019).

6:45 PM DS03.10.03

Quantum-Accurate Machine-Learned Potential Model for Large-Scale Atomistic Simulations of Mechanical Properties Chemically Complex Alloy [Po Yu Yang](#), [Cheng-Lun Wu](#) and [Chun-Wei Pao](#); Academia Sinica, Taiwan

The increasing demands for developing novel chemically complex alloys have imposed a significant challenge to the modeling and simulation community. The mechanical properties of these complex alloys are essential for their applications; however, the length scale required for studying the plasticity of these alloys is beyond the reach of quantum chemistry calculations. In this study, we harnessed the power of machine learning and trained a potential model for the chemically complex Ni/Co/Ti/Zr/Hf alloy system by combining the spectral neighbor analysis potential (SNAP) model and the Bayesian optimization based on a large data set of training images labeled with energies and atomic forces computed from the density functional theory (DFT). We demonstrate that the trained potential model can predict the energies and atomic forces of this chemically complex alloy with high fidelity to the DFT calculations. A series of large-scale (over 10^5 atoms) molecular dynamics simulations were performed to examine the deformation and dislocation dynamics of both nanowires and bulk structures, and the formation of amorphous, shear band-like region following dislocation pinning was observed, which is in excellent agreement with experiments. Hence, the present study demonstrates that the machine-learned SNAP model yields quantum accuracy even for complex alloy comprised of five constituents, allowing for investigating the plasticity deformation of chemically complex alloys with atomistic insights.

7:00 PM DS03.10.04

Development of Coarse-Grained Models of Carbohydrates [Parisa Farzeen](#), [Soumil Y. Joshi](#) and [Sanket Deshmukh](#); Virginia Tech, United States

Over the last few years, coarse-grained (CG) molecular dynamics (MD) has emerged as a way to accurately simulate large and complex systems in an efficient and inexpensive manner due to its lowered resolution, faster dynamics, and larger time steps. Although several CG models for proteins and soft materials are available in literature, few models for carbohydrates can be found. Carbohydrates, due to their nature, open up the possibility of a large variety of sequences, linkages and structures, which makes CG model development arduous. Replicating α and β configurations of monosaccharides separately and capturing their ring structures also remain challenging. Here, we will discuss our machine learning (ML) accelerated approach and results on the development of a CG model for monosaccharide units which captures the aforementioned intricacies in their structures. In this study we use a bottom-up approach to map CG beads onto monosaccharides, while capturing the differences in orientation of the hydroxyl groups with respect to the aromatic rings. The force-field parameters for these CG models are optimized using the artificial neural network (ANN)-assisted particle swarm optimization (PSO) method. These models have further potential to simulate larger systems consisting of oligo- and polysaccharides.

7:15 PM DS03.10.06

Machine Learned Interatomic Potentials for the Calculation of the Detonation State of Energetic Materials with Quantum Accuracy [Cong Huy Pham](#), [Nir Goldman](#) and [Laurence Fried](#); Lawrence Livermore National Laboratory, United States

In this work, we present the development and application of the Chebyshev Interaction Model for Efficient Simulations (ChIMES) to the study of hydrazoic acid (HN_3) under detonation. Computational study of HN_3 is challenging due to its ultrafast detonation, i.e. the chemical decomposition to stable products is complete in less than 10 ps, and the system evolves through multiple thermodynamics (ambient and extreme conditions) and electronic (metal and insulator) states. We show that ChIMES, a generalized many-body reactive force field machine-learned to density-functional theory molecular dynamics (DFT-MD) trajectories, is able to retain the accuracy of DFT simulation in describing structural properties and chemistry for a wide range of unreactive and decomposition conditions of liquid HN_3 while increasing orders of magnitude in computational efficiency. The techniques and recipes for MD model creation here allow for direct simulation of nanosecond shock compression experiments and calculation of the detonation properties of materials with the accuracy of Kohn-Sham DFT. This work was performed under the auspices of the U.S. Department of Energy by Lawrence Livermore National Laboratory under Contract DE-AC52-07NA27344.

7:30 PM DS03.10.07

Low-Dimensional Manifolds Underpin the Atomic Structure of Glassy Materials [Thomas J. Hardin](#)¹, [Mark Wilson](#)¹ and [Michael Shields](#)²; ¹Sandia National Laboratories, United States; ²Johns Hopkins University, United States

The atomic structure of glassy materials lacks long-range order; glassy materials do, however, possess short- and medium-range order imposed by nature's thermodynamic drive towards an energetic minimum. So, while the space of local atomic configurations that appear in a glass is in some sense "larger" than one would find in a crystalline material, that space is nonetheless constrained to a manifold by energetics, with the details of that manifold depending on the chemistry of the glass. We generated molecular dynamics samples of a silicate glass and a generic binary metallic glass, extracted the local atomic environments from each, and applied diffusion maps and an autoencoder architecture to identify the low-dimensional manifold underpinning the local structure of both exemplar materials. The resulting structural parameterizations are partially interpretable in terms of intuitive physical quantities, and enable identification of both outliers and reoccurring structural motifs. Comparison of the structural parameterizations between the covalent glass and the metallic glass illuminates the relative local structural complexity of these materials, reflecting the inflexibility of bonds in the covalent glass compared to bonds in the metallic glass. This presentation will cover our methods and analysis, and will look forward to applications of our structural parameterizations in computational statistical mechanics and as structural state variables in mesoscale and continuum models.

Sandia National Laboratories is a multimission laboratory managed and operated by National Technology and Engineering Solutions of Sandia, LLC., a wholly owned subsidiary of Honeywell International, Inc., for the U.S. Department of Energy's National Nuclear Security Administration under contract DE-NA0003525 (SAND2021-7304 A).

SESSION DS03.11: Machine Learning for Targeted Material Design III

Session Chairs: Christian Hoover and N M Anoop Krishnan

Tuesday Morning, December 7, 2021

DS03-Virtual

8:00 AM *DS03.11.01

Computational Materials Modeling with Integrated Machine Learning Michele Ceriotti; EPFL, Switzerland

When modeling materials at the atomic scale, achieving a realistic level of complexity and making quantitative predictions are usually conflicting goals. Data-driven techniques have made great strides towards enabling simulations of materials in realistic conditions with uncompromising accuracy. In this talk I will summarize the core concepts that have driven the extraordinarily fast progress of the field and discuss some of the most promising modeling techniques that combine physics-inspired and data-driven paradigms. I will focus in particular on "integrated" models that combine a prediction of the interatomic potential and that of functional properties, that open up a new dimension to the simulation of materials in realistic conditions. I will present several compelling examples ranging from water to semiconductors and from metals to molecular solids, and indicate the most pressing open challenges in the field

8:30 AM DS03.11.02

A Machine Learning-Based 3D Battery Design Method Kaito Miyamoto^{1,2}, Scott Broderick¹ and Krishna Rajan¹; ¹University at Buffalo, The State University of New York, United States; ²Toyota Research Institute of North America, United States

To power microelectronics of IoT (internet-of-things) applications, high-performance microbatteries are critically important. Given their limited size, the three-dimensional design of microbatteries is key to maximize their performance. To design the 3D microbattery architecture following the power-sources requirements of a variety of IoT devices, a computational strategy to identify the target battery architecture is vital. In this talk, we propose a 3D battery optimization system which consists of the automatic geometry generator [1] and highly accurate machine-learning (ML) based performance simulators that utilize a small number of performance data obtained from the continuum simulations. As the ML-based performance simulators evaluate the energies of the 3D battery with much smaller computational cost and with comparable accuracy, as compared with the continuum simulations, it is possible to find the best geometries from a huge number of randomly generated 3D battery geometries. We demonstrate the effectiveness of our approach by designing a set of microbatteries having higher energy than the simplest 3D battery (i.e., an interdigitated plates configuration which is characterized by the shortest ion-transport distance) without reducing the power. Compared with the simplest geometry, one of the designed geometries displayed 1.4 times higher energy at low current density and the other showed 6.5 times higher energy at high current density. The best geometry changes with the applied current, indicating that there exists a particular optimal geometry for each electronic device. This work is an important first step toward the realization of such a tailor-made 3D microbattery design.

[1] Miyamoto et al., *iScience*, 23, 101317 (2020).

8:45 AM DS03.11.03

PSP—A Toolkit for Efficient Generation of 3D Atomic-Level Polymer Models Harikrishna Sahu¹, Huan Tran¹, Kuan-Hsuan Shen¹, Joseph H. Montoya² and Ramamurthy Ramprasad¹; ¹Georgia Institute of Technology, USA, United States; ²Toyota Research Institute, United States

Typically, 3D atomic models are required for physics-based simulations of materials. Within the specific area of polymer science, an automatic engine for generating such polymer models is needed. We have developed a python toolkit named **Polymer Structure Predictor (PSP)** for suggesting a hierarchy of polymer models, ranging from oligomer/infinite polymer chains to sophisticated amorphous models[1], which can be used downstream in physics-based simulations. The only input of PSP is the simplified molecular-input line-entry system (SMILES) string of the repeat unit of a polymer. The performance of PSP was tested by comparing the generated models with the known experimental data of several polymers. The output files can be directly used with several computational software, such as VASP, ORCA, LAMMPS, and GAMESS, allowing automation for computing properties. PSP has already been used in the polymer version of computational autonomy for materials discovery (CAMD) [2], establishing extensive databases for polymer bandgap and charge injection barriers that power the Polymer Genome platform (www.polymergenome.org).

PSP is expected to benefit a wide number of academic and industrial research activities, realizing automation in polymer discovery. In the context of the emerging polymer informatics ecosystem, this toolkit will substantially reduce efforts to develop extensive databases of computed polymer properties. Besides, simpler visual models of polymeric materials would likely aid in polymer synthesis research, benefiting experimental polymer scientists.

Reference

- [1] H. Sahu, T. D. Huan, K.-H. Shen, J. H. Montoya, R. Ramprasad, PSP: A python toolkit for predicting 3D models of polymers, *in preparation*.
[2] J. H. Montoya, K. T. Winther, R. A. Flores, T. Bliigaard, J. S. Hummelshøj, M. Aykol, Autonomous intelligent agents for accelerated materials discovery, *Chem. Sci.*, **2020**, 11, 8517-8532.

9:00 AM DS03.11.04

Inverse Design of Two-Dimensional Materials with Invertible Neural Networks [Victor Fung](#)¹, Jiaxin Zhang¹, Guoxiang Hu², Panchapakesan Ganesh¹ and Bobby Sumpter¹; ¹Oak Ridge National Laboratory, United States; ²The City University of New York, United States

The ability to readily design novel materials with chosen functional properties on-demand represents a next frontier in materials discovery. However, thoroughly and efficiently sampling the entire design space in a computationally tractable manner remains a highly challenging task. To tackle this problem, we propose an inverse design framework (MatDesINNe) utilizing invertible neural networks which can map both forward and reverse processes between the design space and target property. This approach can be used to generate materials candidates for a designated property, thereby satisfying the highly sought-after goal of inverse design. We then apply this framework to the task of band gap engineering in two-dimensional materials, starting with MoS₂. We show the framework can generate novel, high fidelity, and diverse candidates with near-chemical accuracy. We extend this generative capability further to provide insights regarding metal-insulator transition, important for memristive neuromorphic applications among others, in MoS₂ which is not otherwise possible with brute force screening. This approach is general and can be directly extended to other materials and their corresponding design spaces and target properties.

9:15 AM DS03.11.05

Gaussian Process Regression Acceleration of Mechanism and Transition Rate Calculations [Hannes Jonsson](#); University of Iceland, Iceland

The task of finding the mechanism and estimating the rate of an atomic rearrangement in a material typically involves finding a minimum energy path and first order saddle point on the energy surface. When such calculations are combined with electronic structure calculations, the computational effort can be large. Furthermore, in order to carry out simulations of long time scale dynamics, all relevant saddle points on the energy rim surrounding a given initial state minimum need to be found, a significant challenge when electronic structure calculations are involved. Machine learning using Gaussian process regression can accelerate these tasks and reduce the computational effort by an order of magnitude [1,2]. An approximate energy surface is generated and most of the iterations in the path optimization and saddle point searches are carried on this faster, approximate surface, which is updated when new electronic structure calculations have been performed. By using a kernel based on pairwise distances between atoms and introducing a length scale or each type of atom pair, and working with inverse distances in a non-stationary kernel, a robust algorithm has been developed for rate calculations and long time scale simulations [3,4]. Examples of diffusion in and on the surface of solids, as well as reactions at solids surfaces will be presented as examples of such calculations where density functional theory is used to evaluate the atomic forces.

[1] 'Minimum energy path calculations with Gaussian process regression', O-P. Koistinen, E. Maras, A. Vehtari, H. Jónsson. *Nanosystems: Physics, Chemistry, Mathematics*, 7, 925 (2016).

[2] 'Nudged Elastic Band Calculations Accelerated with Gaussian Process Regression', O-P. Koistinen, F. Dagbjartsdóttir, V. Ásgeirsson, A. Vehtari, and H. Jónsson, *J. Chem. Phys.* 147, 152720 (2017).

[3] 'Nudged Elastic Band Calculations Accelerated with Gaussian Process Regression Based on Inverse Inter-atomic Distances', O-P. Koistinen, V. Ásgeirsson, A. Vehtari and H. Jónsson. *J. Chem. Theo. Comput.* 15, 6738 (2019).

[4] 'Minimum Mode Saddle Point Searches Using Gaussian Process Regression with Inverse-distance Covariance Function', O-P. Koistinen, V. Ásgeirsson, A. Vehtari and H. Jónsson. *J. Chem. Theo. Comput.* 16, 499 (2020)

9:30 AM DS03.11.06

Late News: Analogical Materials Discovery—An Unsupervised Learning Approach for Inverse Design of Disordered Perovskite Materials [Achintha A. Ihalage](#) and Yang Hao; Queen Mary University of London, United Kingdom

While compositional disorder can generate exciting properties in perovskites, it is often challenging to predict the formability of such materials using *ab initio* methods such as density functional theory (DFT). Target-driven discovery of disordered perovskite materials can be accelerated by applying experimental data powered machine learning methods. Here, we demonstrate that an unsupervised deep learning strategy can find fingerprints of disordered materials that embed perovskite formability and underlying crystal structure information by learning only from the chemical composition, manifested in $(A_{1-x}A'_x)BO_3$ and $A(B_{1-x}B'_x)O_3$ formulae. The unsupervised model learns the crystal system of disordered solid solutions at a 72% success rate even though no information on the crystal structures was originally supplied to the model. Material fingerprints extracted by the model facilitates inverse exploration of promising perovskites based on similarity investigation with known materials, identified as analogical materials discovery. Quantifying materials analogies can further provide insights on possible phase transitions and significantly reduce the computational time required by DFT in predicting the properties of disordered materials. We demonstrate analogical materials discovery can also assist in finding a plausible experimental geometry required to initialise DFT computations by modelling six novel lead-free perovskites.

9:45 AM DS03.02.11

Machine Learning Models to Predict Defect Properties in High Entropy Alloys Gaurav Arora, Anus Manzoor and [Dilpuneet S. Aidhy](#); University of Wyoming, United States

The presence of multiple elements in large proportions poses a major computational challenge to understand and predict defect properties in high entropy alloys (HEAs) using conventional atomistic methods. To overcome this challenge, we have developed a machine learning (ML) model to predict the defect properties such as vacancy formation energies, migration energies, and stacking fault energy (SFE) in HEAs. Using the support vector machine model and local nearest-neighbor information of only the binary constituents' alloys, we predict the defect energies in ternary, quaternary, and quinary alloys with high level of accuracy. Similarly, using linear regression and bond lengths, we predict SFEs in HEAs. Our scheme utilizes density functional theory and atomistic simulations database of binary alloys fed to ML models. The relative importance of various descriptors, both electronic and atomic, and the accuracy of various algorithms are discussed. The work is performed in Ni-based HEAs towards the development of high-temperature materials for extreme environments. A key benefit of this approach is that once the binary database is built and the model is trained, defect energies can be predicted with little computational expense thereby bypassing a large number of calculations that would be otherwise needed every time a new composition is discovered in the HEA phase space.

1:00 PM *DS03.12.01

AI-Enabled Nanoscale Imaging [Mathew J. Cherukara](#); Argonne National Laboratory, United States

Gaining transformative insight into dynamic materials processes at the nanoscale is extremely desirable but has largely remained elusive. Emerging characterization techniques such as coherent imaging methods (e.g. Ptychography), nano-CT and Lorentz TEM are providing an unprecedented view of materials structure and properties at the nanoscale. However, these methods that rely on algorithmic inversion of measured data are not typically suited to *in-situ* or *operando* imaging. This is because the successful inversion of raw data requires enormous online computing power which is projected to increase even more with faster detectors and next generation x-ray and electron sources (> PFLOPS). I will describe our work in applying AI to both accelerate current methods and create new imaging modalities from various X-ray and electron imaging techniques. Our AI-enabled methods are hundreds of times faster than traditional algorithms used for image reconstruction, opening up the prospect of real-time 3D imaging at the nanoscale.

1:30 PM DS03.12.02

Deep Learning Model to Predict Complex Stress and Strain Fields in Hierarchical Composites [Zhenze Yang](#), Chi Hua Yu and Markus J. Buehler; Massachusetts Institute of Technology, United States

Materials-by-design is new paradigm to develop novel high-performance materials. However, finding materials with superior properties is often computationally or experimentally intractable because of the astronomical number of possible combinations in the design space. Especially for composite materials, the heterogeneity and structural complexity really hinder us from calculating materials properties and searching for optimal designs at low costs. Fortunately, with the recent advances in artificial intelligence (AI) or machine learning (ML), new approaches and perspectives are provided to solve the puzzles. This study is proposed to leverage deep learning methods to bridge the gap between a material's microstructure – the design space – and the physical performance. Specifically, it will answer research questions about how to use AI for fast predictions on physical fields of composite materials like stress or strain directly from the input materials geometry. Using a game-theory based conditional generative adversarial networks (cGANs), an end-to-end deep learning approach are developed to give accurate predictions on not only physical fields data but also derivative global properties such as modulus and recoverability. Furthermore, the proposed approach offers extensibility by predicting complex materials behaviors regardless of component shapes, boundary conditions and geometrical hierarchy, providing new perspectives of performing physical modeling and simulations. The method outperforms some conventional numerical methods such as finite element analysis (FEA) and is able to vastly improve the efficiency of evaluating physical properties of hierarchical materials directly from the geometry of its structural makeup. In addition, the idea of geometry-to-field translation can also be applied to other areas in the sciences, such as density functional theory fields, fluid mechanical fields, or electromagnetism.

1:45 PM DS03.12.04

A Deep Learning Approach to the Inverse Problem of Modulus Identification in Elasticity [Bo Ni](#)^{1,2} and [Huajian Gao](#)³; ¹Brown University, United States; ²Massachusetts Institute of Technology, United States; ³Nanyang Technological University, Singapore

The inverse elasticity problem of identifying elastic modulus distribution based on measured displacement/strain fields plays a key role in various non-destructive evaluation (NDE) techniques used in geological exploration, quality control and medical diagnosis (e.g., elastography). Conventional methods in this field are often computationally costly and cannot meet the increasing demand for real-time and high-throughput solutions for advanced manufacturing and clinical practices. Here, we propose a deep learning (DL) approach to address this challenge. By constructing representative sampling spaces of shear modulus distribution and adopting a conditional generative adversarial net (cGAN), we demonstrate that the DL model can learn the high-dimensional mapping between strain and modulus via training over a limited portion of the sampling space. The proposed DL approach bypasses the costly iterative solver in conventional methods and can be rapidly deployed with high accuracy, making it particularly suitable for applications such as real-time elastography and high-throughput NDE techniques.

2:00 PM DS03.12.05

Predicting Properties of BCC Refractory Multicomponent Alloys Using Physics Informed Statistical Learning [Yong-Jie Hu](#)^{1,2} and [Liang Qi](#)¹; ¹Univ of Michigan, United States; ²Drexel University, United States

Body-centered cubic (bcc) refractory multicomponent alloys are of great interest due to their remarkable strength at high temperatures. Optimizing the chemical compositions of these alloys to achieve a combination of high strength and room-temperature ductility remains challenging. We first analyzed the electronic structures of crystalline defects in BCC refractory alloys. The interactions between solute atoms and crystalline defects such as vacancies, dislocations, and grain boundaries are essential in determining alloy properties. Here we present a general linear correlation between two descriptors of local electronic structures and the solute-defect interaction energies in binary alloys of body-centered-cubic (bcc) refractory metals (such as W and Ta) with transition-metal substitutional solutes. One electronic descriptor is the bimodality of the d-orbital local density of states for a matrix atom at the substitutional site, and the other is related to the hybridization strength between the valence sp- and d-bands for the same matrix atom. For a particular pair of solute-matrix elements, this linear correlation is valid independent of types of defects and the locations of substitutional sites. These results provide the possibility to apply local electronic descriptors for quantitative and efficient predictions on the solute-defect interactions and defect properties in alloys. At the second step, with these local/global electronic descriptors and a simple bond-counting model, we developed regression models to accurately and efficiently predict the unstable stacking fault energy (γ_{usf}) and surface energy (γ_{surf}) for refractory multicomponent alloys. We performed first-principles calculations with the special quasi-random structure (SQS) method to predict γ_{usf} and γ_{surf} for 106 individual binary, ternary and quaternary bcc solid-solution alloys with constituent elements among Ti, Zr, Hf, V, Nb, Ta, Mo, W, Re, and Ru. Then we developed surrogate models based on statistical regression to accurately and efficiently predict γ_{usf} and γ_{surf} for refractory multicomponent alloys in the 10-element compositional space. Building upon binary and ternary data, the surrogate models show outstanding predictive capability in the high-order multicomponent systems. The ratio between γ_{usf} and γ_{surf} can be used to populate a model of intrinsic ductility based on the Rice model of crack-tip deformation. Therefore, using the surrogate models, we performed a systematic screening of γ_{usf} , γ_{surf} , and their ratio over 112,378 alloy compositions to search for alloy candidates that may have enhanced strength-ductility synergies. Search results were also validated by additional first-principles calculations and reported experimental results.

2:15 PM *DS03.12.06

Data-Driven Insights into Materials Design [Abhishek K. Singh](#); Indian Institute of Science, India

Data driven machine learning methods in materials science are emerging as one of the promising tools for expanding the discovery domain of materials to

unravel useful knowledge. The power of these methods will be illustrated by covering three major aspects, namely, development of prediction models, establishment of hidden connections and scope of new algorithmic developments. For the first aspect, we have developed accurate prediction models for various computationally expensive physical properties such as band gap, band edges and lattice thermal conductivity. The prediction model for band gap and band edges are developed on 2D family of materials -MXene, which are very promising for a wide range of electronic to energy applications, which rely on accurate estimation of band gap and band edges. These models are developed with GW level accuracy, and hence can accelerate the screening of desired materials. For the lattice thermal conductivity prediction model, an exhaustive database of bulk materials is prepared. By employing the high-throughput approach, several ultra-low and ultra-high lattice thermal conductivity compounds are predicted. The property map is generated from the high-throughput approach and four simple features directly related to the physics of lattice thermal conductivity are proposed. For the second aspect, we have connected the otherwise independent electronic and thermal transport properties. The role of bonding attributes in establishing this relationship is unraveled by machine learning. An accurate machine learning model for thermal transport properties is proposed, where electronic transport and bonding characteristics are employed as descriptors. In the third aspect, we have proposed a new algorithm to develop highly transferable prediction models. The approach is named as guided patchwork kriging, which is applied for prediction of lattice thermal conductivity.

Ref: *Chem. Mater.* **31**, **14**, 5145 (2019), *J. Mater. Chem. A*, **8**, 8716 (2020), *Chem. Mater.* **32**, **15**, 6507 (2020)

2:45 PM DS03.06.01

Predicting Ground State and Metastable Crystal Structures Using Elemental and Phonon Mode Descriptors [Aria Mansouri Tehrani](#), Bastien Grosso, Ramon Frey and Nicola Spaldin; ETH Zurich, Switzerland

We present two methods to predict the crystal structure, given the chemical composition, by combining machine learning and high-throughput density functional theory (DFT) methods.

In our work, initially, a classification model predicts the point groups of the given stoichiometries. Based on the predicted point group, a series of high-throughput DFT calculations determine the ground state of non-centrosymmetric crystal structures. Using this framework, we also extended our analysis to predict new ferroelectric compounds. In addition to the ground state structure, identifying metastable polymorphs that might get stabilized by controlling the synthetic conditions is of great importance as they can exhibit different functionalities. Then, using the example of bismuth ferrite, we illustrate how crystal structure, decomposed into distortion modes, can be implemented as a feature to explore the energy surface leading to the identification of metastable polymorphs. Therefore, we studied BiFeO₃ as a multifunctional compound with a rich low-energy phase space. A training set is constructed by mapping the phase space based on possible distortion modes starting from the cubic perovskite structure. A machine learning model is built using the generated training set predicting new metastable phases of BiFeO₃.

SESSION DS03.13: Machine Learning for Targeted Material Design V
Session Chairs: Mathieu Bauchy, Christian Hoover and N M Anoop Krishnan
Tuesday Afternoon, December 7, 2021
DS03-Virtual

9:00 PM *DS03.13.01

Graph-Based Neural ODEs for Learning Dynamical Systems [Yizhou Sun](#), Zijie Huang and Wei Wang; University of California, Los Angeles, United States

Many real-world systems, such as moving planets, can be considered as multi agent dynamical systems, where objects interact with each other and co-evolve along with the time. Such dynamics is usually difficult to capture. Understanding and predicting the dynamics based on observed trajectories of objects become a critical research problem in many domains. In this talk, we propose to treat dynamical systems as evolving graphs, and design graph neural network (GNN)-based ODEs to approximate system dynamics via the observed signals. In particular, we provide solutions to two challenging scenarios. First, we propose to learn system dynamics from irregularly-sampled partial observations with underlying graph structure. To tackle the above challenge, we present LG-ODE, a latent ordinary differential equation generative model for modeling multi-agent dynamical system with known graph structure, which is the first Graph ODE model in this direction. Second, we propose to learn system dynamics where both node features and edges are evolving. We present a dual Graph ODE, CG-ODE, where both node and edge dynamics are modeled. Experiments on motion capture, spring system, charged particle datasets, COVID-19, and simulated social dynamical systems demonstrate the effectiveness of our approaches.

9:30 PM DS03.13.02

Development of a Realistic 3D Model of Multicrystalline Si Structure Using Image Processing and Machine Learning of Optical Images and Finite Element Stress Analysis on the Model [Kenta Yamakoshi](#)¹, Kentaro Kutsukake², Takuto Kojima¹, Hiroaki Kudo¹ and Noritaka Usami¹; ¹Nagoya University, Japan; ²RIKEN, Japan

Multicrystalline Si (mc-Si) is widely used as a material for solar cells. Mc-Si can be usually produced at a low cost by the directional solidification (DS) method. However, many crystal defects exist in mc-Si ingot and among them, especially the dislocation cluster leads to lower solar cell efficiency than that of monocrystalline Si solar cells. For the growth of multicrystalline materials, the mechanism of crystal defect generation has not yet been elucidated due to the complexity of the structure caused by the diversity of crystal orientations and grain boundaries. We aim to elucidate the universal mechanism by combining experiments, theories, simulations, and machine learning using realistic data-driven models collected from actual multicrystals. In this study, a realistic 3D mc-Si model including the dislocation cluster generation region was created by image processing and machine learning on a large amount of PL and optical images collected from actual mc-Si ingots. In addition, finite element stress analysis was performed on the model to investigate the effect of stress on dislocation cluster generation.

We used high-performance (HP) mc-Si in this research. The ingot was sliced into 729 wafers of 156 mm x 156 mm x 180μm. First, Photo Luminescence (PL) images of the sequentially numbered as-slice wafers on the top of the ingot were taken. From the PL image, the distribution of dislocation clusters in HP mc-Si ingot is obtained [1], and taking a look at this distribution, we determined the 9.18 mm×9.18 mm×3.60 mm region to be modeled, in which a dislocation cluster is generated. Then, the wafers were alkali etched and taken their optical images. By taking the optical images while changing the position of the light source, a vector reflecting the crystal orientation can be obtained for each pixel. These vectors were used to analyze crystal orientation by originally developed crystal orientation estimation model using machine learning [2], and crystal grain segmentation at the region by Mean Shift Clustering. Finally, the mc-Si model for finite element stress analysis was then created by stacking sequentially numbered sections with corrections. The model consists of 53816 nodes and 48373 hexahedral elements, and each grain is given the orientation of a representative point obtained by orientation prediction. Then, finite element stress analysis was performed on this model. From the distribution of dislocation clusters, we expect that dislocation clusters are generated during crystal growth, not in the cooling process. So the conditions for the analysis were the temperature and stress that reproduced

the inside of the ingot during crystal growth by the DS method.

As a result, finite element stress analysis was successfully performed on the realistic model which reproduces the mc-Si structure well, and we could obtain the stress tensor at each node in this model. From these tensors, various analysis results can be obtained, such as the distribution of Mises equivalent stress. From the distribution of Mises equivalent stress, it was found that the stresses were concentrated at grain boundaries and grain boundary triple points as expected. On the other hand, there is no stress concentration near the dislocation cluster generation point. Therefore, the Mises equivalent stress is not likely to contribute to dislocation cluster generation. In the future, the stress tensors obtained from the analysis results should be used to investigate the resolved shear stress at the slip plane, which has a large impact on dislocation generation and to discuss its effect on the generation of dislocation clusters.

[1] Y. Hayama *et al.*, *Solar Energy Mat. and Solar Cells* **189**, pp. 239-244 (2019).

[2] T. Kojima *et al.*, Abstr. of 68th JSAP Spring meeting, 2021, 18a-Z32-9.

9:45 PM DS03.13.03

Chemical Hardness-Driven Interpretable Machine Learning Approach for Rapid Search of Photocatalysts Ritesh Kumar; Indian Institute of Science, India

Strategies combining high-throughput (HT) and machine learning (ML) to accelerate the discovery of promising new materials have garnered immense attention in recent years. The knowledge of new guiding principles is usually scarce in such studies, essentially due to the “black-box” nature of the ML models. Therefore, we devised an intuitive method of interpreting such opaque ML models through SHapley Additive exPlanations (SHAP) values and coupling them with the HT approach for finding efficient two-dimensional (2D) water splitting photocatalysts. We developed a new database of 3099 2D materials consisting of metals of various oxidation states connected to six ligands in an octahedral geometry, termed the 2DO database. The first tier of the HT scheme screened 2DO materials with high thermodynamic and dynamic stabilities. The ML models were constructed using a combination of composition and chemical hardness-based features to gain insights into the thermodynamic and overall stabilities. Most importantly, it distinguished the target properties of the isocompositional 2DO materials differing in bond connectivities, since it combines the advantages of both elemental and structural features. The interpretable ML regression, classification, and data analysis lead to a new hypothesis that the highly stable 2DO materials follow the hard and soft acids and bases (HSAB) principle. The most stable 2DO materials were further screened based on suitable band gaps lying within the visible region and band alignments with respect to standard redox potentials using the GW method, resulting in 21 potential candidates. Moreover, HfSe₂ and ZrSe₂ were found to have high solar-to-hydrogen efficiencies reaching their theoretical limits. The proposed methodology will enable materials scientists and engineers to formulate predictive models, which will be accurate, physically interpretable, transferable, and computationally tractable.

10:00 PM DS03.13.04

Prediction of Toughness in Heterogeneous Materials Using Machine Learning A. N. S. Sadi and Zubaer M. Hossain; University of Delaware, United States

Composites or heterogeneous materials have a wide range of applications in the fields of aerospace, structural materials, biomedical, energy conversion devices, high-temperature materials, etc. But the effective properties of composites, in particular, toughness and strength are hard to predict as a function of their constituent properties. By definition, heterogeneous materials contain different shapes, sizes, compositions, and material or phase distributions at different length scales, making iterative experiments inefficient, time-consuming, and expensive to use for this purpose. In this work, the toughness of heterogeneous brittle material is investigated using a combination of continuum scale simulations and machine learning techniques. Our goal is to predict the configurations (or different structural and material parameters) of the composite that optimize its effective toughness. The continuum simulations are based on the variational phase-field modeling of fracture, and we applied the novel surfing boundary condition, which allows adequate time for the crack to propagate, enabling evaluation of the critical energy release rate or toughness. In particular, we focus on understanding the criteria for deflection vs. penetration for a number of composite configurations and identify the structural or material descriptors that define the criteria. Using the descriptors, we develop supervised machine learning models for predicting the toughness of the composite. The models are trained using data sets, collected from continuum simulations and are used to ascertain the toughness-structure correlation for a number of unexplored variants of the configurations. This talk will discuss the findings and highlight the need for applying machine learning tools to predict the toughness of a composite, for an arbitrary choice of structural and material parameters.

10:15 PM DS03.13.05

Late News: Development of Machine-Learning Force Fields for Complex Materials Systems in Energy Applications Kwangnam Kim¹, Aniruddha Dive¹, Andrew Grieder^{1,2}, Nicole Adelstein², ShinYoung Kang¹, Liwen Wan¹ and Brandon Wood¹; ¹Lawrence Livermore National Laboratory, United States; ²San Francisco State University, United States

There are increasing interests in using machine-learning (ML) interatomic potentials in molecular dynamics (MD) simulations to explore local structure and chemistry that governs key physical and chemical properties of materials for energy applications. A number of methodologies has been developed to train ML potentials (e.g., neural network potential, Gaussian approximation potential, etc.) using local atomic environments in structure data as feature inputs and energies, forces, and/or virial tensors of the structures as outputs. The training data are often collected from highly accurate ab-initio simulation and therefore the trained and validated ML potentials are capable of performing simulations with quantum-level accuracy while achieving thousands of times faster computational speed than ab-initio calculations. In this talk, we will discuss our recent development of ML interatomic potentials based on artificial neural network[1,2] to study ion transport phenomena in highly-disordered, garnet-type LLZO solid-electrolyte and establishment of local correlation between Li-ion transport kinetics and the structural and chemical features of disordered LLZO. The training data was collected from AIMD simulations at a wide range of temperatures and our developed ML potentials are able to predict energies and forces for both crystalline and amorphous LLZO with DFT level of accuracy. Our predicted elastic properties, ion diffusivities, radial distribution functions, and vibrational characteristics of atoms also show excellent agreement with those calculated by ab-initio simulations. Based on similar methodology, we will briefly discuss the development of ML force field for the LLZO/LiCoO₂ interfaces that are relevant for all-solid-state battery technologies, and illustrate how the ML force field can be applied to understand Li-ion transport at the interfaces and to probe the structural and chemical instabilities at the interfaces.

[1] A. Singraber, J. Behler, and C. Dellago, *J. Chem. Theory Comput.* **2019**, *15*, 1827–1840.

[2] A. Singraber, T. Morawietz, J. Behler, and C. Dellago, *J. Chem. Theory Comput.* **2019**, *15*, 3075–3092.

Acknowledgement:

This work was performed under the auspices of the U.S. Department of Energy by Lawrence Livermore National Laboratory under contract number DEAC52-07NA27344. Authors acknowledge funding support from the Vehicle Technologies Office, Office of Energy Efficiency and Renewable Energy, U.S. Department of Energy and computational resource support from the Innovative and Novel Computational Impact on Theory and Experiment (INCITE) program. This research used resources of the Argonne Leadership Computing Facility, which is a DOE Office of Science User Facility supported under Contract DE-AC02-06CH11357.

10:30 PM *DS03.04.01

Differentiable Simulations and Deep Learning for Materials Design [Ekin D. Cubuk](#); Google, United States

Materials informatics datasets and computational resources are growing rapidly. While machine learning offers a promising set of generic tools for extracting insight from large volumes of data, these tools are not inherently good at generalizing to new data. For this reason, tools that enable a seamless integration of physically informed priors with machine learning are crucial for building data-driven models that generalize in a useful way. I will talk about our recent work in this direction where we combine differentiable atomistic simulations with graph neural networks and meta-learning, with applications to materials modelling, optimization, and discovery.

SYMPOSIUM EN01

Materials for Sustainable Electronics

November 29 - December 8, 2021

Symposium Organizers

David Cahen, Weizmann Institute and Bar-Ilan University

David Ginley, National Renewable Energy Laboratory

Alp Sehirlioglu, Case Western Reserve University

Anke Weidenkaff, Fraunhofer Research Institution for Materials Recycling and Resource Strategies IWKS

* Invited Paper

SESSION Tutorial EN01: Materials for Sustainable Electronics

Session Chairs: David Cahen, David Ginley, Alp Sehirlioglu and Anke Weidenkaff

Monday Afternoon, November 29, 2021

Virtual

1:30 PM

Key Materials Issues for Sustainable Electronics [Anke Weidenkaff](#); Fraunhofer Research Institution for Materials Recycling and Resource Strategies IWKS, Germany

abstract coming

2:10 PM Q&A

2:25 PM

Prospects for Self Healing Systems [David Cahen](#); Weizmann Institute and Bar-Ilan University, Israel

abstract coming

3:05 PM Q&A

3:20 PM

Increasing Role of Sustainable Electronics [David S. Ginley](#); National Renewable Energy Laboratory, United States

abstract coming

3:50 PM Q&A

4:05 PM

Recycling [Alp Sehirlioglu](#)¹ and David Cahen²; ¹Case Western Reserve University, United States; ²Weizmann Institute of Science, Israel

abstract coming

4:35 PM Q&A

4:50 PM

Circular Economy for Sustainable Electronics [David S. Ginley](#); National Renewable Energy Laboratory, United States

abstract coming

5:20 PM Q&A

5:35 PM

Designing for Ultimately Sustainable Electronics Anke Weidenkaff; Fraunhofer Research Institution for Materials Recycling and Resource Strategies IWKS, Germany

abstract coming

6:05 PM Q&A

SESSION EN01.01: Sustainable Solar
Session Chair: David Cahen
Tuesday Morning, November 30, 2021
Hynes, Level 3, Room 305

10:30 AM EN01.01.01

Improved Air Processability of Organic Photovoltaics by Using a Stabilizing Antioxidant to Prevent Thermal Oxidation Marc Steinberger, Hans Joachim Egelhaaf, Andreas Distler and Christoph J. Brabec; I-Meet Institute Materials for Electronics and Energy Technology, Germany

During the production of organic solar cells, the exposure of constituting materials and resulting devices to light, heat, oxygen and water is a potential source of degradation. We show that thermo-oxidation of the active materials occurs upon annealing the active layer or upon stirring the active materials solutions in air at elevated temperatures. By comparing various blends of donor polymers with fullerene or non-fullerene acceptors, the fullerene is identified to be the most susceptible component to thermal oxidation in both film and solution, while the polymer remains unaffected. In both cases, the effect on the photovoltaic device performance consists predominantly in a decreased short-circuit current (J_{SC}), suggesting that the underlying degradation mechanism is the same in the solid state and in solution. Thermo-oxidation of the active layer during annealing of the device can be decelerated by blending nickel(II) dibutylthiocarbamate ($Ni(dtc)_2$) as antioxidant additive into the active layer. While small concentrations of additive stabilize the J_{SC} and therefore the power conversion efficiency, higher contents negatively affect device performance. Thermo-oxidation of the active materials in solution during stirring in air at elevated temperatures can be avoided for several hours by adding as little as 0.5% of $Ni(dtc)_2$. The observation that the antioxidant is consumed during stabilization of the active materials suggests a sacrificial protection mechanism.

SESSION EN01.02: Circular Economy and Sustainability
Session Chair: David Ginley
Tuesday Afternoon, November 30, 2021
Hynes, Level 3, Room 305

1:30 PM *EN01.02.01

Recycling of Rare-Earth Magnets and Lithium Batteries Without Toxic Byproducts Valery Kaplan¹, Ellen Wachtel¹, Kyoung-Tae Park² and Igor Lubomirsky¹; ¹Weizmann Institute of Science, Israel; ²Korean Institute of Industrial Technology, Korea (the Republic of)

Sustainable technological development requires recycling of materials, particularly those essential for energy generation and storage, such as the lanthanides and lithium (Li). Recycling of these metals is currently not performed on a large scale, but with growth in demand, one may foresee serious shortages already by the end of the current decade.

High energy density magnets, based on alloys of $Nd(+/-Pr +/-Dy)-Fe-B$ (Nd-alloy), are critical components of a variety of electromechanical and electronic devices. During the last decade, consumption of lanthanide (*a.k.a.* "rare earth", RE, element) has risen annually by $\approx 30\%$ (!!!), primarily due to increased production of hybrid and electric vehicles. Since a standard hybrid/electric automobile requires $\approx 5-10$ kg of RE, while ≈ 40 wt % of the Nd-alloy is lost as scrap during the manufacturing process, large-scale recycling of RE has become an urgent necessity. However, recovery of RE from manufacturing scrap, and especially from end-of-life magnets, poses a difficult technical challenge. The latter requires removing the magnets from the used device, demagnetization, crushing/milling, and applying chemical processes to separate the RE from the Fe component. Demagnetization, by heating *in vacuo*, and crushing/milling are both costly procedures and the latter may introduce unwanted contamination. Strong acids/bases and/or corrosive melts are currently employed to extract the RE metals. Both routes produce toxic waste, for which the cost of neutralization often exceeds the value of the recovered RE. *Instead*, we developed an economically and ecologically friendly RE recycling process. Pulverization (decrepitation) into ~ 45 mm particles is achieved by introducing atomic hydrogen into the used magnets, without the necessity for prior demagnetization, *via* room temperature electrolysis in a diluted NaOH solution. Separation of Fe from the RE is achieved by chlorination of the fine powder at ~ 673 K, which results in sublimation of chlorides of Fe and B, leaving pure RE chloride. Chlorine gas from non-RE sublimates is recycled, while the RE chlorides may be reduced to metal *via* moderate temperature eutectic melt electrolysis.

Although Li-batteries initially emerged as a power source for portable devices, incorporation of Li-batteries in vehicles and industrial power banks, led to an exponential growth in the demand for lithium and cobalt. While lithium production is almost exclusively oriented towards batteries, cobalt is also an essential component of high-strength alloys and magnets, with demand for batteries beginning to compete with these traditional applications. Recovery of Li and Co from spent Li-batteries poses technical challenges. In addition to the fact that opening and crushing spent batteries may result in self-ignition, current technologies aim at Co extraction only. Many of these technologies require sequential treatment with acids and bases, producing toxic waste, or involve dumping of crushed batteries into Co-smelting ovens. In both cases, lithium ends up in compounds from which it cannot be readily recovered. We have developed an economical procedure that recovers metallic Co and Ni, and Li in carbonate form. This process is based on treating crushed, spent batteries with natural gas in a rotating kiln at 973K. Following treatment, Co and Ni may be extracted with a magnetic separator and Li_2CO_3 can be leached out with water, leaving all other components, *e.g.*, compounds of Cu, Mn and Al, for further recycling. Since the proposed process does not use or produce

toxic substances, runs at relatively low temperature, yields high recovery for both Co and Li and can be run with simple equipment, it may be considered as suitable for immediate scaling-up and industrial implementation.

2:00 PM EN01.02.02

Printable and Recyclable Carbon Electronics Using Crystalline Nanocellulose Dielectrics [Nicholas Williams](#), George Bullard, Nathaniel Brooke, Michael Therien and Aaron D. Franklin; Duke University, United States

Electronic waste (e-waste) is a global concern, adding millions of tons of refuse that frequently contains environmental and biological toxins to landfills on a yearly basis. Efforts to extend the life of electronics through right to repair advocacy have thus far not been successful to curb the accumulation of e-waste. Recyclable electronics offers a promising solution to prevent this environmental disaster; however, demonstrations to date often evince recyclability or environmental compatibility through simple, single component demonstrations that focus on re-capturing conductive components. While these reports make pivotal progress towards green electronics, further investigations are required to create a truly revolutionary technology to thoroughly address the e-waste concerns—namely the accumulation of all components of an electronic device. Hence, a completely recyclable electrical device is desperately needed.

Through the use of nanocellulose as a dielectric, we report the creation of the first fully recyclable transistor device with a paper substrate, conductive graphene contacts, and a semiconducting carbon nanotubes channel. To further address environmental concerns associated with energy usage during device manufacturing, these electrical devices are printed almost entirely in a “print-in-place” fabrication procedure at room temperature with only a single toluene rinse at 80 °C. With the addition of a small concentration of table salt to the nanocellulose dielectric ink, these transistors have among the highest area specific on-currents and lowest subthreshold swings of any printed transistor (regardless of substrate) and maintain their performance over 6 months storage in air. Finally, after these devices complete their utility, they can be controllably broken down to their base components and the environmentally damaging nanomaterial inks (graphene and carbon nanotubes) can be recaptured for the later printing of new recyclable transistors with similar performance. The realization of fully recyclable electronics on a broad scale has the potential to be the watershed forestalling the environmental disaster that will inevitably result from the continued accumulation of electronic waste.

2:15 PM EN01.02.03

Microstructure Transition at the LTCC-Wafer Interface of Electronic Carrier Substrates That are Designed by SiCer Technology [Hannes Engelhardt](#)¹, Clemens Motzkus¹, Katharina Freiberg², Beate Capraro¹, Arno L. Görne¹ and Markus Rettenmayr²; ¹Fraunhofer IKTS, Germany; ²Friedrich-Schiller-Universität Jena, Germany

The combination of semiconductor technologies with micro-electro-mechanical systems (MEMS) as sensors and actuators has been developed in recent years. This technology combines a silicon wafer and a multilayer low-temperature cofired ceramic (LTCC) carrier and is named *SiCer*. Several design concepts were established and this innovative substrate technology is gaining importance in sensor integration (Stehr et al. 2019). The elaborated LTCC is adopted to the thermal properties of the silicon wafer and the bonding at the silicon-LTCC interface is the key to the versatility and robustness of the *SiCer* technology. This contribution focuses on the investigation of the microstructure transition at the bonding interface between silicon and LTCC. High resolution transmission electron microscopy investigations including a highly sensitive EDS for elemental analysis reveals phase transformations that take place during the combined bonding and sintering process of *SiCer* substrates. The observed phase evolution is discussed by means of thermodynamic considerations and conclusions on the bonding mechanism are proposed. The influence of the initial wafer surface including oxidic thin films is interpreted with regard to desirable *SiCer* substrate properties.

Stehr et al. 2019:

Stehr, Uwe; Hagelauer, Amelie; Hein, Matthias A. (2019): SiCer: Meeting the Challenges of Tomorrow's Complex Electronic Systems [From the Guest Editors' Desk]. In: *IEEE Microwave* 20 (10), S. 26–92. DOI: 10.1109/MMM.2019.2928614.

2:30 PM EN01.02.04

Towards a Sustainable Preparation of Hybrid PVDF-CoFe₂O₄ Self-Standing Films for Magnetolectric Applications—Seeking For a Substitute of N,N-Dimethylformamide [Fayna Mammeri](#)^{1,2,3}, Raphaël Hanemian^{1,2,3}, Ulises Acevedo-Salas^{4,2} and Hakeim Talleb^{4,2}; ¹Université de Paris, France; ²Centre National de la Recherche Scientifique, France; ³Labex SEAM, France; ⁴Sorbonne Université, France

Multiferroic materials have the potential for many applications such as actuators, sensors, or memory devices, thanks to their magnetolectric effect (ME). Such effect was first observed in inorganic single crystals but due to their low Curie temperature and their weak ME coupling coefficient, they were seldom integrated into devices. To overcome these limitations, the composite material strategy offers the opportunity to tune the ferromagnetic and ferroelectric properties of the two phases acting on the hybrid interface. In this context, we developed new flexible multiferroic composite materials through (i) smart tailoring of the hybrid interface between a ferroelectric and *piezoelectric* fluoropolymer, PVDF, crystallized in its β -polymorph to present suitable properties, and inorganic ferrimagnetic and *magnetostrictive* nanoparticles (NPs), cobalt ferrite (CoFe₂O₄), and (ii) effective control of NPs size [1] and surface chemistry [2].

To the best of our knowledge, up to now, there is no paper dealing with the sustainable preparation of hybrid CoFe₂O₄-PVDF films for magnetolectric applications: Dimethylformamide (DMF) is still the most used solvent to prepare these materials since it is considered the best solvent to induce the crystallization of PVDF in its β -polymorph. However, it is now well-known that solvents with high polarity tend to induce the crystallization of β -PVDF [3]. Hence, the question raised is now: new solvents are doubtless required to improve the sustainability of the synthesis of PVDF-based films but will they be as efficient as DMF to induce the crystallization of β -PVDF in presence of 13 nm CoFe₂O₄ nanoparticles?

We present here our first studies on the synthesis of CoFe₂O₄-PVDF magnetolectric thin films using less toxic solvents and their resulting properties. A comparison with the first series prepared in DMF is presented too.

[1] M. Bibani, R. Breitwieser, A. Aubert, V. Loyau, S. Mercone, S. Ammar, F. Mammeri, Beilstein J Nanotechnol. 10, 1166 (2019).

[2] C. Ben Osman, E. Barthas, P. Decorse, F. Mammeri, Colloids Surface A, 577, 405 (2019).

[3] F. Mammeri, Frontiers of Nanoscience 14, 67 (2019).

2:45 PM *EN01.02.05

Informing Availability and Recycling Potential in Metals [Elsa Olivetti](#); Massachusetts Institute of Technology, United States

As product complexity in electronics increases, our consideration of the manufacturing, end of life processes and materials supply chains required to produce these electronics must keep pace of that complexity. Metrics that only cover technical performance miss opportunities to drive towards more sustainable approaches to design and processing. This presentation will discuss work in understanding materials availability and the potential for materials

recovery to improve the sustainability of electronics. We will also describe materials market modeling work to understand limits on metals recycling policy to reduce primary mining for copper and other electronics-prevalent materials.

3:15 PM BREAK

SESSION EN01.03: Green Synthesis and Processing

Session Chair: Anke Weidenkaff

Tuesday Afternoon, November 30, 2021

Hynes, Level 3, Room 305

4:00 PM EN01.03.01

Nanoscale Grain Growth Suppression in Metal Oxide Nanoribbons at High Temperature Hyeuk Jin Han¹, Gyu Rac Lee², Yujun Xie¹, Hanhwi Jang², David Hynek¹, Eugene Cho², Ye Ji Kim², Yeon Sik Jung² and Judy Cha¹; ¹Yale University, United States; ²Korea Advanced Institute of Science and Technology, Korea (the Republic of)

Nano-grained metal oxides can significantly improve the physical and chemical properties of the metal oxides for diverse applications that utilize a large surface area, such as gas sensors and catalysts. However, the inherent thermal instability of nanoscale grains is a major challenge and hinders technological applications that are operated at elevated temperatures. Thus, controlling the temperature-stability of nano-grained structures represents both a scientifically interesting problem as well as a major technological advancement to enable widespread applications of metal oxides.

Here, we report highly effective grain growth suppression in metal oxide nanoribbons to demonstrate the high-temperature stability of nanoscale grains. By controlling the metal to oxygen ratio and the nanoscale dimension of the initial amorphous metal oxide nanoribbons, we show that the average grain size was maintained at ~ 6 nm, despite high annealing temperatures up to 900°C for 6 hours. We find that excess oxygen in the initial amorphous metal oxide nanoribbons prevents the merging of small grains during crystallization, leading to suppressed growth of the small grains. This was verified by *in situ* transmission electron microscopy experiments, during which we directly observed crystallization of the nanoribbons. As an exemplary application that exploits nanoscale grains, we demonstrate a gas sensor using grain growth suppressed tin oxide nanoribbons, which exhibited both high sensitivity and unusual long-term operation stability due to the thermodynamically stable nanoscale grains. Our findings provide a new pathway to simultaneously achieve high performance and excellent thermal stability in nano-grained metal oxides, which will be useful for various device applications.

4:15 PM EN01.03.02

Bioresorbable Primary Battery Anodes Built on Core-Double-Shell Zinc Microparticle Networks Yutao Dong and Xudong Wang; University of Wisconsin-Madison, United States

Bioresorbable electronics, which decomposed in the physiological environment after a designed period of stable function and corresponding byproducts are resorbed and vanish, have gained increasing interests in state-of-the-art biomedical implants for pre-diagnosis, monitoring and treatment of diseases, drug delivery which only requires the function for a certain period of time. Compared to other transient power supplies, such as piezoelectric nanogenerators, supercapacitors, bioresorbable batteries are promising power source with higher energy density and continuous output which typically are composed of bioresorbable material that degrade into non-toxic contents in physiological environment during and/or after discharge. State-of-the-art bioresorbable batteries are built upon Mg or Zn metal-based galvanic cells due to their good biosafety and electrochemical activity. Due to extreme high chemical activity of Mg, current Mg-based bioresorbable batteries all exhibited fluctuating voltage output and rapid output drops without a controllable lifetime, which cannot meet the requirements of an implantable power supply. Additionally, the fast degradation rate could induce localized releasing of concentrated hydroxyl ions, leading to inflammation or other harmful effects. Compared to Mg, Zn metal has moderate degradation rate which can circumvent undesirable local pH increase and minimize gaseous hydrogen evolution. Furthermore, in bioresorbable metal-based galvanic cell systems, although both the anode and cathode are needed, it is the metal anode that dissolves in the electrolyte and primarily determines battery lifetime and power output. Nevertheless, almost all current models were built on bulky foils or plates, where their degradation occurred naturally on the metal surface. Therefore, there was no control over the degradation rate, direction and sequence, and thus all showed a poor controllability on the battery output and lifetime, which further limits their practical applications. In this work, we report a bioresorbable zinc primary battery anode filament built on Zn micro-particles (MPs) coated with chitosan and Al₂O₃ nano-films. This battery filament exhibited a well-controlled dissolution direction and rate due to the mesoscale MP assembly, and the protective coatings. When discharged in 0.9% NaCl saline, single Zn MP filament with a 0.17 x 2 mm cross-section exhibited a stable voltage output of 0.55 V at a current of 0.01 mA, where the current and voltage output could be simply designed by integration of the battery filaments in parallel or in series, respectively. The operational time could be directly adjusted by the length of filament. A stable 200-hour discharging time was achieved by a 15 mm Zn MP filament. By increasing the filament cross-sectional area, higher current output can be achieved at the same discharging voltage, raising the output power. The final discharging byproducts, mostly ZnO/Zn(OH)₂, could slowly dissolve in biofluids, making this composite filament completely degradable. This complete bioresorbable primary battery showed a full level of control of output and lifetime, providing a promising solution to in vivo powering transient bioelectronics.

4:30 PM EN01.03.05

Study of Competing Effect of In-Plane and Out-of-Plane Anisotropies on the Overall Properties of Magnetic Tunnel Junction-Based Molecular Spintronics Device (MTJMSD) Properties Bishnu R. Dahal, Marzieh Savadkoobi, Eva Mutunga, Andrew Grizzle, Christopher D'Angelo and Pawan Tyagi; University of the District of Columbia, United States

Molecular spintronics is gaining attraction because molecules possess weak scattering mechanism. As a result, molecules retain spin information over a long time. Molecular Spintronics devices (MSD) are also considered crucial for futuristic quantum computing technology [1]. The major challenge of MSD is making robust and mass-producible spintronic devices at the nanoscale. To overcome this issue, we have designed a magnetic tunnel junction-based molecular spintronics device (MTJMSD). MTJMSD is fabricated by bridging paramagnetic molecules across the edges of the ferromagnetic electrodes. These molecules form dominant conducting channels over tunneling conduction between two ferromagnetic electrodes of an MTJ. MTJMSD enables the utilization of ferromagnetic electrodes with a wide range of magnetic anisotropies. Here, we are analyzing the magnetic switching mechanism, hysteresis loop (M-H Curve), and the overall magnetic properties of MTJMSD as a function of anisotropies along with constant Heisenberg couplings. In this paper, we report a theoretical Monte Carlo Simulation (MCS) study to explain the impact of anisotropies on the MTJMSD equilibrium properties. We also investigate theoretically how the nature of magnetic hysteresis changes as we apply the in-plane, out-of-plane, and in-plane and out-of-plane at the same time on the same ferromagnetic electrode. The application of anisotropy creates multiple magnetic phases of opposite magnetic spins on the same ferromagnetic electrode. When in-plane and out-of-plane anisotropies are applied on an electrode simultaneously, the magnetic moment of the electrodes

possessed its maximum value. The MTJMSD possessed its maximum value since the competing effect of anisotropies wiped out the multiple magnetic phases.

In this study, we also investigated the effect of anisotropies on the nature of the hysteresis curves generated computationally using MCS. We applied the in-plane and out-of-plane magnetic anisotropies on the same ferromagnetic electrode of an MTJ. The effect of the in-plane anisotropy transformed the regular magnetic hysteresis of MTJMSD into a "wasp-waisted" -like hysteresis curve[2]. The "wasp-waisted" -like hysteresis curve is hypothesized due to the presence of multiple magnetic phases on the ferromagnetic electrodes caused by strong magnetic anisotropy. The application of equal magnitude of in-plane and out-of-plane anisotropies brings back the M-H curve into a regular hysteresis curve but with nearly zero coercivity. The zero coercive hysteresis closely agree with the experimentally measured M-H curves under the same situations. In this paper, we will also present the overall properties of MTJMSD when the spin fluctuations option is incorporated in the MCS code.

This research is supported by National Science Foundation-CREST Award (Contract # HRD- 1914751), Department of Energy/ National Nuclear Security Agency (DE-FOA-0003945).

References

- [1] A. R. Rocha, V. M. García-suárez, S. W. Bailey, C. J. Lambert, J. Ferrer, and S. Sanvito, "Towards molecular spintronics," *Nature Materials*, vol. 4, no. 4, pp. 335-339, 2005/04/01 2005, doi: 10.1038/nmat1349.
- [2] T. M. de Lima Alves *et al.*, "Wasp-waisted behavior in magnetic hysteresis curves of CoFe₂O₄ nanopowder at a low temperature: Experimental evidence and theoretical approach," *RSC advances*, vol. 7, no. 36, pp. 22187-22196, 2017.

4:45 PM EN01.03.06

Investigation of Spin Fluctuation, Thermal Energy and Exchange Coupling Effect on Magnetic Tunnel Junction-Based Molecular Spintronic Devices (MTJMSD) Marzieh Savadkoochi, Bishnu R. Dahal, Andrew Grizzle, Christopher D'Angelo and Pawan Tyagi; University of District of Columbia, United States

Molecular spintronics is an emerging field that takes advantage of both spin properties and molecular electronics. The conjugation of spin degrees of freedom with molecular magnetic properties results in novel electronic devices with several advantages. The spin carriers carry and encode information in their spin state which allows development of efficient memory and logic devices [1]. Molecules have also unlimited passive and active magnetic properties that can be tailored with spin properties of atoms. Combination of spintronics with molecular electronics is an attractive method of making nanoscale devices with improved performance and functionality. Using organic molecules as conducting bridges between ferromagnetic electrodes has been a fascinating way of manipulating spin properties. However, the conventional techniques struggle with various challenges such as mass-productibility, durability, and reliability of fabricated devices. In this work, we have proposed, and simulated a cross-junction shaped spintronic device called magnetic tunnel junction based molecular spintronic device (MTJMSD) using Monte Carlo Simulation (MCS) to investigate spin-dependent charge transport phenomenon. MTJMSD is made of two ferromagnetic electrodes (FME) separated by a few nanometer-thick tunneling barrier. Unlike previous methods, magnetic molecules are attached on the exposed edges of the FM electrodes in the outer world [2-4].

The interaction between magnetic molecules and FM electrodes, strengths and nature of couplings, molecules and electrodes' type, thermal energy, and several other factors play important role in defining MTJMSD ultimate properties. In this work, we have computationally investigated few parameters (e.g., Heisenberg exchange coupling, electrodes' size, thermal energy, spin fluctuation) that affect MTJMSD's magnetic properties. Our results show that the magnetic couplings between molecules and FM-electrodes have a dominant role in dictating MTJMSD's magnetic moment and spin orientation.

Antiferromagnetic and ferromagnetic molecule-FME couplings forced the FM electrodes to take antiparallel and parallel spin states with respect to each other respectively at room temperature. Our results also showed that despite significant increase in time evolution of magnetic moment, stability is not achieved at higher temperatures. The electrodes' size (length and thickness) affected molecules' ability to induce magnetic properties in FM electrodes to some extent. However, the nature of coupling between FMEs is still dictated by molecules at stronger Heisenberg exchange coupling values. Spin fluctuation increased equilibrium energy and temporal evolution of magnetic moment compared to the non-spin fluctuation case. It also introduced some stripe-shaped spin orientation within electrodes. The current MCS studies complement our ongoing experimental research which investigates the effect of organometallic molecules on MTJ's hysteresis loop and saturated magnetic moments.

Acknowledgement:

This work is supported by National Science Foundation-CREST Award (Contract # HRD- 1914751), Department of Energy/ National Nuclear Security Agency (DE-FOA-0003945).

References:

1. A. R. Rocha, V. M. García-suárez, S. W. Bailey, C. J. Lambert, J. Ferrer, and S. Sanvito, "Towards molecular spintronics," *Nature Materials*, vol. 4, no. 4, pp. 335-339, 2005/04/01 2005, doi: 10.1038/nmat1349
2. P. Tyagi, C. Baker and C. D'Angelo, *Nanotechnology* **26**, 305602 (2015).
3. P. Tyagi and E. Friebe, *J. Mag. Mag. Mat.* **453**, 186-192 (2018).
4. P. Tyagi and C. Riso, *Organic Electronics* **75**, 105421 (2019).

SESSION EN01.04: Poster Session: Materials for Sustainable Electronics

Session Chair: David Ginley

Tuesday Afternoon, November 30, 2021

8:00 PM - 10:00 PM

Hynes, Level 1, Hall B

EN01.04.01

ZnO Nanobrush Electrodes for Enhanced Photoelectrochemical Water Splitting Young-Min Kim and Yun-Mo Sung; Korea Univ, Korea (the Republic of)

ZnO has been highlighted as one of the most attractive candidates for water splitting due to its high oxidation power, chemical stability, non-toxicity, and low production cost. Despite its superior intrinsic properties, there exist a few reports on photoelectrochemical (PEC) water splitting with pure and monolithic ZnO. Due to the large energy band gap (3.2 eV) ZnO can be activated only under the ultra-violet light irradiation, which seriously limits its broad applications to water splitting. Thus, to overcome this drawback most researches on PEC water splitting with ZnO have been focused on the impurity doping for energy band gap modification, the noble metal decoration for the plasmon resonance energy transfer (PRET), and the type II heterojunction

formation with other semiconductors for visible light absorption.

Here, we report the breakthrough for the water splitting of pure ZnO photoelectrodes. First, we developed the growth method of high-density and faceted ZnO micro-rod (MR) structures on a conductive substrate. Subsequently, nano-branches were grown all over the facets of ZnO MRs using a dip coating followed by hydrothermal synthesis to realize ZnO nanobrush (NB) structures. The ZnO NB electrodes (NBEs) revealed the photocurrent density of 1.687 mA/cm² at 1.23 V_{RHE} and 0.48% conversion efficiency (ABPE) at 0.81 V_{RHE}, which is as far as we know the highest conversion efficiency value among monolithic ZnO photoelectrodes. The length of nano-branches could be precisely controlled by the solvothermal reaction time. As-synthesized ZnO NBEs exhibited photocurrent density ~1.36 times higher than that of bare micro-rod electrodes (MREs). The role of nano-branches in the photocurrent density increase was verified by the open-circuit potential and Nyquist plot analyses. The extra space charge region (SCR) occurring by introducing nano-branches on the surfaces of ZnO MRs was for the first time proposed as a mechanism for the increased photocurrent density in the ZnO NB structures.

SESSION EN01.05: Green Electronics I
Session Chair: David Cahen
Monday Morning, December 6, 2021
EN01-Virtual

8:00 AM EN01.05.01

Tunable Redox-Active Materials for Sustainable Electrochemically-Mediated Separations Kai-Jher Tan and T. A. Hatton; Massachusetts Institute of Technology, United States

Separation processes are ubiquitously employed for purification purposes in chemical production, as well as potable water generation and environmental remediation. The rising intensity of global issues such as the growing world population, low water security, and worsening industrial pollution all necessitate further advancement in the discovery, development, and application of materials for separations. Electrochemical approaches are an attractive alternative due to the innate propensities of redox-active species for modular design, molecular recognition, reversible operation, and lower energetic requirements, all of which can be realized via only electrochemical stimuli without any chemical additives. The current state-of-the-art for sustainable electrochemical separation technologies was delineated in a recent review,¹ and include electrochemically-mediated techniques at its forefront. In this work, the focused design of redox-active materials for imparting specific functionalities to electrosorption processes are discussed.

Redox-active composite materials have been developed from four different classes of electroactive species in order to enable redox-mediated ion detection and removal in water, with designed controllability over their pseudocapacitance, stability, analyte selectivity, and energetics. Anion separation was achieved using an organometallic ferrocene co-polymer whose electrochemical activity in different electrolyte solutions can be manipulated based on its co-monomer.^{2,3} Through principles of hydrophobicity, the metallopolymer can be engineered to activate in the presence of hydrophilic anions instead of hydrophobic ones, for subsequent application in the stable and seven-fold selective electrochemical extraction of perchlorate over nitrate. The ferrocene macromolecule motif was also extended to the generation of zwitterionic polyelectrolytes that possess pH-sensitive electrochemical behavior in both homogeneous and heterogeneous environments.⁴ Cation separation was facilitated through the preparation of pH-dependent quinone and electronically-tunable crystalline hexacyanoferrate-based conductive electrodes, which were paired together with polymeric ferrocenes to produce asymmetric redox-active systems that could reduce the extent of anode fouling by preventing parasitic water reduction, offer optimizable separation energies, allow for the enhanced and simultaneous recovery of transition metal compounds without altering their bulk oxidation state, and enable continuous operation under flow conditions.^{2,3} Lastly, redox-active components were incorporated into a particulate scaffold instead of an electrode framework with the purpose of further improving their potential for ion separation through heightened maneuverability and phase contact provided in part by the judicious variation of material hydrophilicity.⁵ Polypyrrole and polyferrocene-containing magnetic composites were synthesized through a facile multi-step procedure, and exhibit strong adsorption capacities for both inorganic and organic contaminants.

References:

1. Tan, K.-J.; Hatton, T.A., *Sustainable Separation Engineering* **2021**, *Accepted*.
2. Tan, K.-J.; Hatton, T.A. et al., *Adv. Func. Mater.* **2020**, 30 (15), 1910363
3. Tan, K.-J.; Hatton, T.A. et al., **2021**, *Submitted*.
4. Tan, K.-J.; Hatton, T.A. et al., **2021**, *In Preparation*.
5. Tan, K.-J.; Hatton, T.A. et al., **2021**, *In Preparation*.

8:15 AM EN01.05.02

Introduction of TiO₂ as a New Potential Alternate Electron Transport Layer in Kesterite Solar Cells—Energy Band Alignment and Nanoscale Probing of CZTS/TiO₂ Heterojunction Nisika Nisika and Mukesh Kumar; Indian Institute of Technology Ropar, India

Kesterite-based Cu-Zn-Sn-S (CZTS) solar cells with layer stacking of Al/Al:ZnO/ZnO/CdS/CZTS/Mo are attracting attention in last few years, owing to less toxic and more abundant elements [1-2]. However, the current efficiency of CZTS champion solar cell is 11.01% that shows high disparity from its counterpart, Cu-In-Ga-Se (CIGS) solar cell [3]. High voltage deficit in CZTS solar cells is one of the primary cause of low efficiency. The lower performance of CZTS solar cells is mainly attributed to high open circuit voltage deficit due to increased interface recombination. Therefore, absorber-buffer interface engineering is essential and deserves more investigation to understand the charge dynamics at the interface. Here, we report wide band gap (3.8 eV) TiO₂ as a potential candidate to substitute conventional CdS buffer layer with low-band gap (2.4 eV) and toxic in nature. The surface and interface of CZTS-TiO₂ layer was investigated using X-ray photoelectron spectroscopy (XPS) and ultraviolet photoelectron spectroscopy (UPS). The result reveals favourable "spike"-like conformation at CZTS-TiO₂ interface with conduction band offset (CBO) value of 0.17 eV. The nanoscale probing of interface by Kelvin Probe Force Microscopy (KPFM) across CZTS-TiO₂ layers show a higher potential barrier for interface recombination at CZTS-TiO₂ in contrast to conventional CZTS-CdS interface. Finally, the fast decay response and lower persistent photoconductivity (PPC) of photogenerated carriers for CZTS-TiO₂ heterojunction based photodetector, further validate our results. Carrier management via interface engineering using emerging materials will help to obtain high efficiencies in CZTS solar cells.

8:30 AM EN01.05.03

Evolution of Structure, Composition and Optical Properties of ZnO Nanocrystals Films Co-Doped with Ga and In Donor-Like Impurities Brahim El Filali¹, Tetyana V. Torchynska², Georgiy Polupan³, Jorge L. Ramirez Garcia³ and Lyudmyla Shcherbyna⁴; ¹Instituto Politecnico Nacional, UPIITA, Mexico; ²Instituto Politecnico Nacional, ESFM, Mexico; ³Instituto Politecnico Nacional, ESIME, Mexico; ⁴V. Lashkaryov Institute of Semiconductor Physics at NASU, Ukraine

The impact of double donor doping on the crystal structure, morphology, film compositions, emission and electrical properties has been studied in the ZnO:Ga:In nanocrystal films. The films were deposited by ultrasonic spray pyrolysis on silicon substrates heated to 400°C. To the study of double donor doping, two groups of samples were prepared. In the first group the In content was of 1at%, but the Ga contents were varied in the range 0.5-3.0at%. In the second group the In content was of 2at% and the Ga contents were changed in the range 0.5-2.5at%. To stimulate the film crystallization, all samples were annealed at 400 °C for 4h in a nitrogen flow (5L/min).

The variation non monotonous of the crystal lattice parameters, compositions, the PL intensities, and electrical resistivity has been detected in the ZnO nanocrystal (NC) films. The high-quality NC films with the wurtzite-type crystal structure, planar morphology, bright near band edge (NBE) emission and the small intensity of defect related PL bands have been obtained. The reasons for parameter varying non monotonically and the optimal concentrations for the Ga/In double donor doping of ZnO NC films have been analyzed and discussed.

8:45 AM EN01.05.04

Pb Sequestration to Safeguard Using Halide Perovskite-Based Devices Rene D. Mendez Lopez¹, David Cahen^{1,2} and Barry Breen³; ¹Bar Ilan University, Israel; ²Weizmann Institute of Science, Israel; ³3GSolar Photovoltaics Ltd., Israel

We aim at providing functionalized encapsulation of Halide Perovskites (HaPs) to prevent Pb from reaching the environment, especially the groundwater, in case of module device damage/breakage and subsequent exposure to the elements. HaPs are widely explored in research and development, specifically for optoelectronic devices, including large-scale outdoors employment in solar cell panels, due to their outstanding properties as light-absorbing materials. The most efficient devices use a Pb-based HaP. PbI₂ and PbBr₂, together possibly with oxides/hydroxides, are the most likely decomposition products if devices are broken and the HaP is exposed to the ambient. As these Pb dihalides are soluble, albeit sparingly, in water, exposure to rain can release Pb ions that may reach the groundwater.

Such a scenario carries obvious environmental and public health risks. We show here how to mitigate and even eliminate this scenario by efficient sequestering of Pb ions. A scheme of ligands is presented for sequestration as part of an encapsulation, using commercial materials and methods, reaching, till now, 90% lead retention in a commercially viable process.

9:00 AM EN01.05.06

Opto-Electronic Properties of Al₂O₃/ZnO Multilayer Heterostructure as a Transparent Conductor Krishan Ghosh^{1,2}, Bishwajite Karmakar¹ and Ariful Haque²; ¹Missouri State University, United States; ²Texas State University, United States

Transparent conductors (TC) have great importance in day-to-day life and state of the art high-tech applications. For instance, they are used in light-emitting diodes, solar cells, transparent thin film resistors, display devices, and many others due to their good electrical conductivity and high transmittance in the visible region. However, current materials used for the TC are very costly. Current research interest is to develop low-cost TC with better electrical conductivity and high optical transmittance. The objective of this work is to tune the electrical and optical properties of low cost Al₂O₃/ZnO multilayer heterostructure on quartz substrates through anion as well as cation doping in ZnO and find out a better TC. All the heterostructures were made using pulsed laser deposition technique through varying growth parameters such as oxygen pressure, substrate temperature, and number of laser shots. The initial sample was a pristine ZnO layer, followed by a 95/5 ZnO/Al₂O₃ superlattice, then 90/10, and 80/20. To enhance electrical conductivity with minimum reduction in transmittance, the samples were annealed under forming gas (96% Ar and 4% H₂). The structure of the heterostructures was characterized via X-ray diffraction (XRD), Raman spectroscopy, photoluminescence (PL), and scanning electron microscopy. The electrical conductivity of the samples was determined via four probe electrical measurements, and the optical transmittance was determined by UV-VIS spectroscopy. XRD and Raman spectroscopy data confirm the presence of Al-doped ZnO and Al₂O₃ in the sample. The PL spectroscopy indicates the presence of oxygen as well as other point defects in the samples and specially, the number of oxygen vacancies increases with annealing. The optical measurements show that the transmittance of the superlattice oxide thin film decreases from 90 to 80 % with annealing. However, the electrical conductivity increases 4-6 order of magnitude with annealing. The resistivity decreases from 2 Ohm-cm to 6.2 E-03 Ohm-cm for the optimum sample. This multilayer heterostructure oxides can be useful for developing low-cost TC for optoelectronic applications.

9:15 AM EN01.05.07

Effect on the Ferromagnetic Property in Q-Carbon as a Function of Size Nayna Khosla¹, Jagdish Narayan¹, Kaushik Sarkar¹ and Dhananjay Kumar²; ¹North Carolina State University, United States; ²North Carolina Agricultural and Technical State University, United States

The recent discovery of Q – carbon has opened ways for the fabrication of fascinating heterostructures using the non-equilibrium technique of nanosecond pulse laser annealing. Q- carbon is reportedly the densely packed metastable state phase of carbon with about 80% sp³ content. The pure Q- carbon exhibits extraordinary hall effect and room temperature ferromagnetism whereas the Boron doped Q- carbon shows superconductivity. In Q carbon films which we have grown on sapphire, we observed that these magnetic and electrical properties can be attributed to the abundant unpaired electrons near the fermi energy level. This talk will put a light on the ferromagnetic properties as a function of size. With the increase in the size, we observe that the ferromagnetism increases up to a critical size. It is very interesting to see how does the magnetism changes with the size and what is this critical size. This will be an interesting lead in the magnetic and electron transport properties of Q- carbon which will enhance the functionalities of the fabricated devices and its application in carbon based spintronics.

SESSION EN01.06: Circular Economy and Sustainability II

Session Chair: Anke Weidenkaff

Monday Afternoon, December 6, 2021

EN01-Virtual

1:00 PM EN01.06.01

Late News: Multifunctional Coatings for Textiles Based on Functional Particles Derived from Sustainable Sources Jagadeshvaran P L and Suryasarathi Bose; Indian Institute of Science, India

Recently, there is an increased demand for the development of multifunctional materials and hence they have allured enormous interest in every other application possible. With the threat of escalating electromagnetic (EM) pollution, there is a strong need to develop materials and strategies to curb it. Textiles have been used as promising candidates for electromagnetic waves, particularly in the microwave frequency ranges, owing to their numerous advantages like flexibility, lightweight and conformability. In addition, it is beneficial in creating multiple interfaces for microwave attenuation on textiles

with functional coatings. Herein, we report for the first time, the preparation of a multifunctional coating that is based on iron titanate (FT) and multiwalled carbon nanotubes (CNT) which can shield both microwaves and UV radiations. The iron titanate used here is sourced from a sustainable precursor – the ilmenite sand, while the CNT is commercially sourced. In order to demonstrate the contribution of FT in EMI shielding, another particle was also used – this was synthesized in the same protocol as that of FT with copper ions incorporated (CuFT). On comparison, it was found that FT tends to interact with and attenuate EM radiation along with CNT – much better than CuFT. The coated fabrics show an EMI shielding effectiveness of -30 dB for a stack of four layers in the broadbands viz. X and Ku – translating to a 99.9% attenuation of the incident EM signals. Further, there is a jump in conductivity of around four orders in magnitude for the coated fabric in comparison to the neat fabric. It is worth to note that the coating confers an ability to block 99.9% of the UV radiation over the wavelength ranging 200-400 nm. Furthermore, the prepared coatings significantly improve the flame retarding properties of the neat fabric. With such remarkable properties, these coatings have the huge potential to significantly enhance the commercial value of cotton fabrics without adding much to its cost.

1:15 PM EN01.06.02

Late News: Controlling H₂ Production in Si Etching while Utilizing Advanced Chemical Concentration Ismail Kashkoush, Tyler Webber, Dennis Nemeth, Darian Waugh and Steven McKinley; NAURA-Akron, United States

Anisotropic etching of silicon is usually performed using alkaline etchants such as aqueous KOH, TMAH and other hydroxides like NaOH. A large variety of silicon structures can be fabricated in a highly controllable and reproducible manner with the strong correlation of the etch rate due to the orientation of the crystal structure, etchant concentration and temperature. Therefore, anisotropic etching of <100> silicon has been a key process in common MEMS based technologies for realizing 3-D structures. These structures include V-grooves for transistors, small holes for ink jets and diaphragms for MEMS pressure sensors. The actual reaction mechanism has not been well understood and comprehensive physical and chemical models for the process have not yet been developed. With increasing numbers of MEMS applications, interest has grown in recent years for process modelling, simulation, and software tools useful for the prediction of etched surface profiles [1-4]. Utilizing near infrared spectrometry (NIR) technology allows TMAH/KOH concentration to be controlled effectively while monitoring the silicate concentration within the bath during the silicon etching process. This technique allows for higher uniformity and longer continuous etching times without interrupting the wafer process within the tank. While maintaining the Si concentration, the system will partially drain the tank bath mixture and replenish it with fresh chemical of each component at the desired concentration [5]. This was effective to a specific number of wafers to be processed in one lot batches, however with this new application the number of wafers processed per lot has been increased two-fold. In the present study, controlling the production of the H₂ byproduct from the etching reaction with TMAH/KOH while monitoring the bath concentration increases the overall throughput. The chemical solution travels through a new application which allows the hydrogen gas to be released from the solution and transferred to the top of the tank effectively removing from the solution. The now H₂ gas removed solution then re-enters the tank, with minimal H₂ in the solution, removing the chances of any contamination blocking the Si wafer and decreasing the uniformity or etching. The results show that the number of wafers per lot have been increased via controlled chemical replenishment while mitigating the hydrogen gas by-product. With this new application the process can run higher throughput, even with long etch processing times for Si.

1. K. Peterson: Silicon as a Mechanical Material (IEEE Proceedings, San Diego, CA, 1982).
2. Alvi, P.A., et al, Int. J. Chem. Sci., 6 (3), 1168-1176 (2008).
3. K. Sato et al., Sensors and Actuators, 64, 87-93 (1988).
4. M. Sekimura: Anisotropic Etching of Surfactant-Added TMAH Solution (12th IEEE Conference on MEMS Proceedings, Orlando, FL, 1999).
5. Kashkoush, I., Rieker, J., Chen, G., & Nemeth, D. (2014). Process Control Challenges of Wet Etching Large MEMS Si Cavities. Solid State Phenomena, 219, 73–77. <https://doi.org/10.4028/www.scientific.net/ssp.219.73>

1:30 PM *EN01.06.03

Energy Efficient Computing and Memory-Storage Devices Stuart Parkin; Max Planck Institute of Microstructure Physics, Germany

Energy efficient computing and memory-storage devices are key to further increases in high performance computing that is essential to today's data centric world. We discuss, on the one hand, Magnetic Racetrack Memory[1, 2] that promises a high capacity, high performance, non-volatile, memory-storage device that could supplant magnetic disk drives and solid-state FLASH, and, on the other hand an extremely energy-efficient memcapacitor device[3] that could allow for massive neuromorphic computing systems.

- 1 Yang, S.-H., Naaman, R., Paltiel, Y., and Parkin, S.S.P.: 'Chiral spintronics', Nat. Rev. Phys., 2021, 3, pp. 328–343
- 2 Bläsing, R., Khan, A.A., Filippou, P.C., Garg, C., Hameed, F., Castrillon, J., and Parkin, S.S.P.: 'Magnetic Racetrack Memory: From Physics to the Cusp of Applications within a Decade', Proc. IEEE, 2020, 108, pp. 1303-1321
- 3 Demasius, K.-U., Kirschen, A., and Parkin, S.: 'Energy-Efficient Memcapacitor Devices for Neuromorphic Computing', Nat. Electron., 2021, accepted

2:00 PM EN01.06.04

Late News: Recyclate-Based Additive Manufacturing for Functional Materials in Green ICT Sebastian Klemen¹, Jürgen Gassmann¹ and Anke Weidenkaff^{1,2}; ¹Fraunhofer-Einrichtung für Wertstoffkreisläufe und Ressourcenstrategie IWKS Hanau, Germany; ²Technische Universität Darmstadt, Germany

The future in functional materials manufacturing has to have the challenge of resource criticality in mind. Ways to address this issue include providing resource efficient material manufacturing methods (e.g. additive manufacturing of functional materials) and reducing the use of critical materials by providing alternative materials or resources such as efficient recycling processes. While additive manufacturing has advantages to more energy demanding and waste producing methods, this method has to be adjusted for the use of sustainable printing materials and the production of functional materials for sustainable technologies such as green ICT. This would reduce not only the energy demand of ICT systems, but also increase their materials sustainability. Our activities on recyclate-based additive manufacturing is based on materials flow analysis and electronic waste recycling. The goal is a versatile process for recyclate powder production to provide sustainable printing materials for additive manufacturing of functional materials in high-tech technologies. We present our plan for the close connection of efficient recycling and powder production techniques, our technical capability at Fraunhofer IWKS and give an overview of the research questions we are working on.

2:15 PM EN01.06.05

Late News: Advancing Green Resilient Materials for Sustainable Housing Alexis Smith and Lilian P. Davila; University of California, Merced, United States

Researchers have been using different approaches to address challenges in the fabrication of sustainable building materials such as reproducibility, reliability, and using renewable materials while preserving properties. Despite these efforts, there are still fundamental limitations in the current fabrication methods of such materials. To solve those challenges, investigators have been studying recently wood-based insulating material, in combination with

ceramic binding agents, to create novel green materials for housing applications. This new material can lead to fully capable load-bearing house components (e.g. wall systems) with high-insulation high-strength properties, where burning is not required in the molding process of the sample preparation. In this study, we have investigated the properties and ecological traits of the new green material by calculating composition-dependent properties and life-cycle assessment (LCA) via physics-based modeling. Using eco-audit data and materials design software, we have conducted systematic analyses of several housing siding samples and evaluated traits including mechanical properties, price, energy, and CO₂ footprint. We evaluated the role of material composition, binder type, and the environmental impact of potential house sidings made of cedarwood, fiber cement, pine-magnesia, and flame block-oriented strand board (OSB). Results indicate the most impactful material for house sidings is Flame block OSB. The effect of resins (painting, enamel baked coating, polymer powder coating) was also evaluated and LCA results show that OSB with polymer powder coating is the least eco-friendly in the manufacturing stage. The hypothesis is that by modifying the siding's composition and binder type, the impact on the environment could be further decreased. Overall results from this study were found to be in good agreement with recent experiments reported elsewhere independently, and mechanical properties together with LCA data of the new green material are significant in determining sustainable alternatives compared to other counterparts. This research contributes to improving material discovery by the combination of design, predictive modeling, and LCA evaluation which allows researchers to determine the technical and commercial feasibility of new sustainable house components.

SESSION EN01.07: Green Electronics II
Session Chair: David Cahen
Tuesday Morning, December 7, 2021
EN01-Virtual

8:00 AM EN01.07.01

Steep-Slope Transistors with Subthreshold Swing < 10 mV/dec Using Organic Memory Devices, Threshold Switching Devices and Schottky Diodes [Jamal Aziz](#), Honggyun Kim, Shania Rehman and Deok-kee Kim; Sejong University, Korea (the Republic of)

With the rapid development of transparent integrated circuits, the requirement of transistors with lower subthreshold swing (SS) is becoming necessary. Here, we fabricate three device structures showing abrupt switching and make their series connection with conventional field effect transistors (FET) to lower the SS value. Firstly, we demonstrate an environmentally friendly, disposable, and transparent conductive bridge random access memory (CBRAM) device, composed of 99.3 vol.% nanocellulose fiber. Our CBRAM consists of silver (Ag) electrochemically active electrode and nanocellulose fiber (ca. 15 nm) based switching layer on FTO coated glass substrates. Devices with CBRAM can enable the FET with lowest SS slope by switching the metallic filament between ON and OFF. Niobium oxide (NbO₂) based threshold switching devices and zinc oxide (ZnO) based transparent and flexible Schottky diodes with electrical breakdown were also stacked with FET giving the SS < 10 mV/dec. Comparatively, the transistor plus CBRAM stack can significantly improve the SS slope with lowest leakage current compared to the other series stack, showing the great potential to boost the development of the future generation workhorse transistors.

8:15 AM EN01.07.02

Late News: Novel Stabilization Mechanism on Polar Oxide Surface [Jinho Byun](#)¹, Zhipeng Wang², Sangho Oh² and Jaekwang Lee¹; ¹Pusan National University, Korea (the Republic of); ²Sungkyunkwan University, Korea (the Republic of)

The stability of polar oxide surfaces has long been an interesting topic in surface science. Since the electrostatic potential diverges with increasing polar oxide thickness, various screening processes involve such as surface reconstruction, charge transfer, and adsorption of foreign charged species. Here, combining the density functional theory calculations and molecular dynamic simulations, we report that the vicinal surface steps can completely stabilize the polar oxide surface without introducing defects and excess charge. The evolution of steps at the vicinal surface, and resulting stabilized polar surface will be discussed and associated underlying mechanism will be introduced along with atomic-scale scanning transmission electron microscopy images.

8:30 AM EN01.07.03

Late News: On the Origin of the Dark Current and Its Relationship with the Electronic Noise Current in Organic Photodiodes [Canek Fuentes](#)^{1,2}, Wen-Fang Chou² and Bernard Kippelen²; ¹Northeastern University, United States; ²Georgia Institute of Technology, United States

Organic photodiodes (OPDs) are expected to play an important role in the development of sustainable electronics since they can be used for photovoltaic or photodetector applications and be fabricated in biodegradable substrates, such as those based on nanocellulosic materials, and be easily recycled [1]. To optimize the properties of organic semiconductors used in such devices for photodetector applications, it is critical to develop an improved understanding of the electronic noise characteristics of OPDs. In the dark, the electronic noise current of a photodetector such as an OPD determines the lowest detectable optical power [2]. Yet the physical origin of the electronic noise current and its relationship with the dark current measured in steady state is rarely studied through direct measurements and consequently remains poorly understood [2,3,4].

Using detailed temperature- and optical power-dependent studies of the electrical characteristics of OPDs, we demonstrate that grounded in thermodynamic principles, the steady-state optoelectronic properties of OPDs can be described using an equivalent circuit approach to derive the reverse saturation current, ideality factor and shunt resistance values as a function of temperature.

These detailed studies reveal that the reverse saturation current is thermally activated with a barrier height that is equal to the transport bandgap divided by the ideality factor. The value of the ideality factor is well-approximated as the inverse of the recombination order of the limiting recombination process in the dark, yielding a value between 1 and 2 for most common recombination mechanisms, such as band-to-band recombination and trap-assisted recombination, either through mid-gap states or through an exponential trap distribution (Urbach tail).

Derivation of these parameters and its thermal dependence enables an accurate description of the current density in OPDs in the dark as a function of voltage and temperature and under illumination conditions varying over nine orders of magnitude. Furthermore, thermodynamically consistent expressions for the shot and thermal noise contributions using the reverse saturation current and shunt resistance values derived experimentally, are used to estimate the white noise electronic noise current. This analysis shows that at the low measurement bandwidth values typically used to characterize OPDs, the electronic noise is limited by flicker noise even in OPDs showing electronic noise current values in the tens of femtoampere. Critically, we show that the electronic noise at low measurement bandwidth values does not scale with the steady-state dark current density, as it is often assumed in the literature.

These findings, have important implications for the accurate characterization of OPDs, but also, reveal the critical role that trap-assisted charge recombination and the width of the transport bandwidth play in determining their steady-state dark current characteristics. Although these material properties play a critical role in determining the magnitude of the white noise, our results suggest that they may play a secondary role in determining the magnitude of the electronic noise in OPDs at low measurement bandwidth values.

[1] Y. Zhou, et al. *Sci Rep* 3, 1536 (2013).

[2] C. Fuentes-Hernandez, et al., Science, 370, 698 (2020).

[3] Y. Fang, et al., Nature Photonics, 13,1 (2019).

[4] J., Kublitski, et al. Nat Commun 12, 551 (2021).

8:45 AM EN01.07.04

Late News: Tellurium Oxide as a Back-Contact Layer for Long Lasting CdTe Solar Cells Camden Kasik, Ramesh Pandey and James Sites; Colorado State University, United States

The formation of a passivating and selective back contact is necessary for constructing CdTe solar cells with an open circuit voltage greater than 1 volt. Recombination at the back surface and a large back-contact barrier are widely recognized as major problems limiting CdTe solar-cell performance. Other solar cell technologies have demonstrated the use of metal oxides to help passivate the back contact. We explore the use of tellurium oxide as a passivating buffer layer to improve device performance. In these experiments we study the effect tellurium oxide's () thickness, treatment, and process gas composition have on device performance. The large bandgap of also has implications for electron reflectors, to reduce recombination at the surface, and bifacial applications. The effects of on device performance are characterized by current-voltage and quantum-efficiency measurements, showing efficiencies and open-circuit voltages up to 17.5% and 849 mV. Admittance and capacitance voltage measurements are used to study the depletion width and carrier concentration, while time resolved photoluminescence measurements are used to explore the effects on recombination. We found cells with carrier densities up to 1×10^{15} carriers per cubic centimeter and carrier lifetimes up to 160 ns. Our results demonstrate the viability of as a buffer layer to improve passivation and performance in CdTe solar cells. An added benefit of is the ability to utilize an undoped absorber, which is crucial to reduce degradation in CdTe solar cells.

9:00 AM EN01.07.05

One-Pot Synthesis of Nitrogen-Doped Hierarchical Porous Carbon Using Combustion Waves for High-Performance Supercapacitor Electrodes Seonghyun Park, Seo Byungseok and Wonjoon Choi; Korea University, Korea (the Republic of)

Supercapacitors have attracted tremendous interests due to their long-term stability and high power density derived from fast charge/discharge rate. Among them, heteroatom-doped porous carbon materials have been extensively explored and synthesized for industrial applications. However, their complex and time-consuming synthesis routes impede scalable fabrication. Herein, we report a facile one-pot synthesis strategy of nitrogen-doped hierarchical porous carbon void shell (N-HPCVS) using combustion waves. Free-standing films were prepared by mixing recrystallized sodium chloride particles with collodion, which is a nitrocellulose solution, where the particles and the nitrocellulose could act as templates and fuel covering the precursors, respectively. When a heat source, enabled by a joule-heated nichrome wire applied to the film, the combustion wave appeared as an instant thermochemical processing and propagated along the whole film within ten seconds. Owing to the rapid combustion waves involving the functional reaction of the NaCl particles, which could manipulate the thermodynamic transition, the incomplete combustion naturally occurred, and the carbon residue around the templates remained as resulting materials. Since the nitrocellulose comprises cellulose with nitro-group, the remaining carbon spontaneously includes nitrogen dopants. Through simple rinsing with DI water, the NaCl templates were removed and N-HPCVS were finally obtained. Owing to the thermal decomposition of NaCl templates and sudden evaporation of gases during the propagation of combustion waves, the hierarchical porous structure of N-HPVCS comprising of macro and meso-/micro-pores was completed. Furthermore, the tunable physicochemical characteristics of N-HPVCS could be achieved by only optimizing initial fuel loading. Based on screening the processing conditions of combustion waves, the properly adjusted N-HPCVS30 which was prepared with 500 mg of NaCl and 30 g of collodion, exhibited outstanding specific capacitance (305 F/g at 0.5 A/g) and long-term cycling stability (116% retained after 10,000 cycles). Furthermore, the symmetric two-electrode cell employing the N-HPVCS presented remarkable power and energy density (25 kW/kg and 18.8 Wh/kg), as well as long-term cycling retention (98.25 % after 10,000 cycles). The rational fabrication strategy of N-doped hierarchical porous carbon using the combustion waves will inspire fascinating hybrid electrodes and catalysts which cannot be achieved through conventional synthesis methods.

9:15 AM EN01.07.06

Defect Formation Energies and Charge Transition Levels of Gold-Related Defects in Silicon via Semilocal and Hybrid Density Functional Theory Naheed Ferdous; University of Illinois at Urbana-Champaign, United States

Reconciling results from conventional and hybrid density functional theory is important to establish the level of accuracy achievable and best practices in first-principles simulations of defects in semiconductors. We present a case study to assess the extent to which calculations performed with (i) Perdew, Burke, and Ernzerhof (PBE) combined with systematic band edge shifts and (ii) Heyd, Scuseria, and Ernzerhof hybrid HSE06 can reproduce experimental results for gold-related defects in silicon. Substitutional $\text{Au}_{\{\text{Si}\}}$, substitutional dimers $\text{Au}_{\{\text{Si}\}}\text{-Au}_{\{\text{Si}\}}$, and tetrahedral interstitials Au_{i} are considered in detail.

SESSION EN01.08: Circular Economy and Sustainability III

Session Chair: David Ginley

Wednesday Morning, December 8, 2021

EN01-Virtual

10:30 AM EN01.08.01

Ab Initio Study of Structural, Electronic and Optical Properties of $\text{Cu}_2\text{NiSnSe}_4$ J. El Hamdaoui¹, L. M. Pérez², D. Laroze², M. EL- Yadri¹, El Mustapha Feddi¹ and Gen Long³; ¹Mohammed V University in Rabat, Morocco; ²Universidad de Tarapacá, Chile; ³Saint John's University, United States

In this manuscript, we report a recent investigation of the structural, electronic and optical properties of the new quaternary chalcogenide $\text{Cu}_2\text{NiSnSe}_4$ (CNTSe). Our calculations were done using the first principle approach. We have employed the full-potential linearized augmented plan-wave (FP-LAPW) method implemented in wien2k code. To treat the exchange and correlation effect of our numerical calculations we used the Tran-Blaha modified Becke-Johnson potential combined with the Hubbard potential U (mBJ+U). Our numerical calculations showed that CNTSe exhibit high absorption and direct bandgap. We also determined the real and imaginary parts of the dielectric function, the reflectivity, and the refraction index.

10:45 AM EN01.08.02

Synthesis and Characterization of Biomass-Derived Charge-Transfer Salts Using Asymmetric Donor Molecules with Tetrathiafulvalene

Structure Masaru Ide¹, Eiji Masai², Yuichiro Otsuka³, Masaya Nakamura³ and Hironori Ogata¹; ¹Hosei University, Japan; ²Nagaoka University of Technology, Japan; ³Forest Research and Management Organization, Japan

Lignin, which is contained in woody biomass at 20 to 30%, is a polymer with a three-dimensional network structure in which complex aromatic molecules are bonded. It was abandoned. If useful applications can be established by converting lignin into high value-added organic materials, it can be expected to greatly contribute to the formation of a recycling society. In 2006, a technology for producing 2-pyrone-4,6-dicarboxylic acid (PDC), which is an intermediate metabolite of lignin, was developed using the lignin metabolism system of the bacterial SYK-6. Focusing on the high electron acceptability of PDCs, we have developed various charge transfer salts based on PDCs and investigated their structures and electrical properties. Therefore, we have focused on tetrathiafulvalene(TTF) derivatives as electron donors, and have synthesized charge-transfer salts with PDC using these molecules by electrolytic method and clarified their various physical properties.

In this study, we expanded our research to asymmetric electron donors with the TTF molecular framework. we have synthesized the several kinds of charge-transfer salts with asymmetric TTF derivatives by taking advantage of the low crystallinity based on the asymmetry.

In this study, we report the results of systematic investigation of these crystal morphologies, crystal structures, electronic properties and magnetic properties, as well as the differences in structure and properties of charge-transfer salts with symmetric TTF derivatives.

10:50 AM *EN01.08.03

Towards Circular Economy in Electro Mobility Oliver Gutfleisch^{1,2}, Jürgen Gassmann¹, Mario Schönfeldt¹, Konrad Opelt², Eva Brouwer¹, Oliver Diehl¹, Urban Rohrmann¹, Jörg Zimmermann¹ and Anke Weidenkaff^{1,2}; ¹Fraunhofer-Einrichtung IWKS, Germany; ²Technische Universität Darmstadt, Germany

The current transformation in the mobility sector is accompanied by a change in the materials needed for the new key components. Rechargeable batteries are one imperative in electro mobility. The same holds for their usage in mobile devices, power tools and stationary energy storage devices. Equally important for electro mobility, but also for the other named devices, are the high performance permanent magnets, which are used in motors with the highest efficiency, lowest weight and volume. Every battery in a modern electric vehicle needs a magnet; the more efficient the magnet the less battery is needed, the longer the driving range. Batteries as well as motors contain valuable and resource critical metals elements such as neodymium, dysprosium, cobalt, lithium, and copper. The mining of these elements is intense in energy and chemical consumption. Furthermore, they also contain substances that would endanger our environment and health if disposed of improperly. Effective recycling of end-of life products is therefore of great relevance from both an economic and an ecologic point of view. Using the technosphere will also yield some leverage from the monopolistic supply situation for primary strategic metals.

We will highlight first in this talk the *Center for Dismantling and Recycling for Electromobility*, which is build up at Fraunhofer IWKS in Hanau. Here, the robot assisted dismantling and recycling of key components of electric vehicles like batteries, fuel cells, electric motors and power electronics are in the focus. For traction motors in electric vehicles, permanent magnets based on rare earth elements (REE) like Nd-Fe-B and Sm-Co are used due to their outstanding magnetic performance in a wide temperature range. The global demand for REE will increase drastically in the near future. To meet this demand and to secure the supply for other magnet applications several recycling techniques for permanent magnets are highlighted. The recycled magnets show a low environmental footprint and compete well with those made from primary materials in terms of magnetic properties and cost.

In a second part, we will focus on secondary properties of permanent magnets. The driving force for R&D has been the demand for superior primary magnetic properties. Now, the increasing number of applications using Nd-Fe-B permanent magnets in more severe conditions leads to extended requirements for the magnets. In fly wheel energy storages or electric motors for example, high rotational speeds are used. The resulting high forces on the magnets and can lead to a magnet failure due to the high intrinsic brittleness of Nd-Fe-B intermetallic compound. Concepts for Nd-Fe-B based magnets with high fracture strength are introduced.

11:20 AM *EN01.08.04

Achieving a Circular Economy Bill Tumas, David S. Ginley and Nancy Haegel; National Renewable Energy Laboratory, United States

Based on a definition of the MacArthur Foundation a circular economy is “Looking beyond the current take-make-waste extractive industrial model, a circular economy aims to redefine growth, focusing on positive society-wide benefits. It entails gradually decoupling economic activity from the consumption of finite resources, and designing waste out of the system. Underpinned by a transition to renewable energy sources, the circular model builds economic, natural, and social capital. It is based on three principles:

Design out waste and pollution

Keep products and materials in use

Regenerate natural systems”

NREL has initiated a comprehensive program to examine a number of supply chains from raw materials to end of life and recycling. Key observations are that you can design even complicated systems to have nearly zero environmental impact and lead to true sustainability. An important element of this is to develop materials systems that are not only reusable but are also self healing and self restoring. A true circular economy incorporated te concepts of increased use of renewable electrons for many processes and improved approaches to grid and storage utilization.

We will discuss practical examples of this approach including: approaches to solar energy conversion with earth abundant non-toxic elements, lifecycle extension of materials in PV, Wind, and energy storage. A key element of a long term strategy can be illustrated in the polymer and composites area where materials are designed for easy end of life reuse and where self-healing materials can extent initial lifetimes substantially. This is especially true as we move to the “electrification of everything”. We will discuss new approaches to materials design for longevity, self healing and ultimate recycling where these approaches are ultimately enabling for a true circular economy.

SYMPOSIUM EN02

Solid-State Batteries—Electrodes, Electrolytes and Interphases
November 30 - December 8, 2021

Symposium Organizers

Montserrat Casas-Cabanas, CIC Energigune
Fudong Han, Rensselaer Polytechnic Institute
Huilin Pan, Zhejiang University
Yuyan Shao, Pacific Northwest National Laboratory

Symposium Support

Silver

Energy Material Advances, a Science Partner Journal | AAAS

* Invited Paper

SESSION EN02.01: Computation and Modeling I
Session Chairs: Fudong Han and Yan Wang
Tuesday Morning, November 30, 2021
Hynes, Level 3, Ballroom C

10:30 AM *EN02.01.01

Modeling of the Potential Distribution and the Electrical Double Layer in Solid-State Batteries Yue Qi^{1,2}, Michael Swift^{2,3}, Harsh D. Jagad¹ and James W. Swift⁴; ¹Brown University, United States; ²Michigan State University, United States; ³US Naval Research Laboratory, United States; ⁴Northern Arizona University, United States

The electrical double layer (EDL) is a key feature of all electrochemical interfaces, controlling the kinetics and thermodynamics of both electron transfer and ion transfer reactions, and therefore the performance of solid-state batteries (SSB). Unlike in a liquid electrolyte with an EDL made of solvated ions, the EDL in a solid electrolyte is made up of charged point defects. Thus, the well-known Poisson-Boltzmann equation at electrode/liquid-electrolyte interfaces no longer holds in SSBs. This problem is even more challenging, as ion insertion and/or reaction with the electrode alters the material and thus band alignments at the electrode/solid-electrolyte interfaces.

In this talk, a density functional theory (DFT)-informed theoretical framework was established to predict the interface potential profiles. We first assumed the electrochemical potential for Li⁺ ions reached a constant at the open circuit equilibrium condition, then derived the relationship among the electrostatic potential, the lithium chemical potential, Fermi level, ionization potential, and the work function. This relationship yielded quantitative profiles of the electrostatic potential and electronic energy level alignments across the entire solid-state batteries. It was predicted the electrostatic potential inside the solid electrolyte can be either flat or sloped due to the point defect chemistry in the different solid electrolyte materials. The electrostatic potential jump at the electrode/electrolyte interface creates intrinsic barriers for Li⁺ transport across the interface. The model prediction over a range of solid-state battery systems can be used to explain multiple experimental impedance observations at solid-electrolyte/cathode interfaces. To obtain the electrostatic potential variation as a function of the distance to the interface, a more general model for the EDL at a solid-state electrochemical interface based on the Poisson-Fermi-Dirac equation was developed. The EDL structure is presented in various materials that are thermodynamically stable in contact with a lithium metal anode. The model further allows designing the optimum interlayer thicknesses to stabilize the interface without introducing additional electrostatic barriers for lithium ion transport at relevant solid-state battery interfaces.

11:00 AM EN02.01.02

Compressive Stress in Solid-State Electrolyte by Ion Implantation—A Molecular Dynamics Case Study for LLZO Harsh D. Jagad¹, Stephen J. Harris², Chunmei Ban³ and Yue Qi¹; ¹Brown University, United States; ²Lawrence Berkeley National Laboratory, United States; ³University of Colorado Boulder, United States

Cracks and Fracture in solid state electrolytes such as LLZO enables Li dendrites to penetrate in the form of dendrites. These dendrites pierce through the solid-state electrolyte and eventually cause an electrical short between the anode and the cathode. One method to slow down this process is to increase the fracture resistance of the glass / ceramic type solid electrolyte via ion exchange, where, for example, large iso-valent cation exchanges with a primary cation in the glass thus increasing the residual compressive stress, and hence increasing its toughness. This technique is used commercially, for example, to make crack-resistant glass for cell phones (Gorilla Glass) where Na⁺ ions in the glass are exchanged with larger iso-valent K⁺ ions. In this work we use quantum calculations combined with molecular dynamics modelling to explore the residual stress situation for the case when Li⁺ ions are exchanged with the larger K⁺ ions in LLZO. Increasing the fraction of Li⁺ ions exchanged increases the residual compressive stress. Unfortunately, if too many Li⁺ are exchanged, the Li⁺ conductivity is reduced. Another concern is the diffusion of K should be negligible compared to Li, thus ensuring that the compressive zone remains stable. We explore how to optimize these tradeoffs in order to make a solid-state electrolyte that has both high resistance to fracture and high Li⁺ ion conductivity.

11:15 AM EN02.01.03

Modeling of the Effects of Interface and Compressive Stress in Maintaining a Flat Li Surface During the Stripping Process Min Feng¹, Chi-Ta Yang² and Yue Qi¹; ¹Brown University, United States; ²Michigan State University, United States

The Li metal is a good candidate for the anode in the solid-state batteries due to its high specific capacity (3860 mAh/g), but the Li dendrites formed due to nonuniform Li deposition usually cause short-circuiting, impeding the commercial application of the Li metal-based solid-state batteries. The non-uniform Li deposition is the result of an uneven distribution of current density on the inhomogeneous Li surface, where Li atoms tend to deposit on the surface protrusions and further promote the dendrite growth. Since the stripping process generates vacancies when removing Li, which may accumulate as voids and lead to uneven distribution of current density and dendrite growth, understanding how vacancies evolve near the Li/solid electrolyte (SE) interface is critical to help maintain a smooth Li surface during the stripping process and contribute to a uniform Li deposition in subsequent cycling.

In this work, a density functional theory (DFT) - kinetic Monte Carlo (KMC) multiscale simulation scheme is developed to simulate the Li vacancy evolution at two representative interfaces: Li/LiF (lithiophobic) and Li/Li₂O (lithiophilic). As the compressive stress is usually applied during the battery operation, the stress induced Li creep effects are considered given the low melting point of Li. Specifically, the DFT calculations are utilized to get the optimized atomic interface structure, calculate the Li vacancy formation energy and the Li forward (towards the interface) and backward (towards the bulk) hopping barriers. The KMC simulation is then used to simulate the evolution of Li vacancies near the interface by taking various Li hopping rates based on the DFT as inputs. To incorporate the creep behavior under a mechanical bias (E_p) into the hopping events, the DFT-calculated forward (backward) hopping barrier is decreased (increased) by half of E_p , which leads to a net Li flux rate corresponding to the creep strain rate imposed by the compressive stress (σ) on a given Li foil thickness (L).

It was found that at room temperature, without the creep effects, few vacancies at the Li/LiF interface migrate to the bulk Li, while at the Li/Li₂O interface, vacancies submerge into the bulk quickly. When the creep effect is considered, although vacancies at the Li/Li₂O interface more readily travel into deeper regions in the bulk Li, a large portion of vacancies at the Li/LiF interface migrate into the bulk as well. Thus, the interfacial properties (lithiophilic or lithiophobic) determine the vacancy hopping behavior with no creep effects but have weaker impacts on the vacancy evolution under compressive stress. Over the typical range of the product of L and strain rate in Li metal batteries spanning over 6 orders of magnitude, vacancies in Li/LiF can always form a uniform distribution in the Li metal and show little dependence on $L \times$ strain rate values, suggesting the importance of applying the compressive stress during Li stripping.

11:30 AM EN02.01.04

Guiding Principles to Find Fast Li-Ion Conductors [KyuJung Jun](#)¹, Yan E. Wang², Yihan Xiao¹ and Gerbrand Ceder¹; ¹University of California, Berkeley, United States; ²Samsung Research America, United States

Solids with high lithium-ion conductivity are of great importance for the realization of solid-state batteries. So far thiophosphates have been reported to exhibit the highest lithium ionic conductivity. However, they pose several intrinsic problems such as their narrow thermodynamic window[2] and H₂S gas evolution from the oxidation of the sulfide solid electrolyte.[3] This has led to a shift of interest towards oxide superionic conductors. The discovery of novel fast Li-ion conductors within an oxide anion framework has been challenging due to the less effective screening of cation interactions by the oxygen anions.[4] Most of the work so far has been limited to the compositional and structural modification within the frameworks of the known superionic conductors such as garnet[5] or the lithium analogue of the Na-superionic conductors (NASICON).[6]

In this talk, we will discuss our recent findings on the relation between the topology of the crystal structure and fast Li-ion transport by utilizing first principles modeling based on density functional theory. We find that there are well-defined features of crystal structures that promote fast Li-ion conduction. In some cases, these crystallographic features provide a highly distorted lithium environment which reduces the barrier for Li hopping by several hundreds of meVs. Using these features we performed high-throughput ab-initio molecular dynamics on the Materials Project database to search for novel oxide superionic conductors and discover 10 novel oxide frameworks that are predicted to exhibit high ionic conductivity exceeding 0.1 mS/cm at room temperature. This study provides new insights on the structural origin of fast diffusion in oxide superionic conductors and can be applied as a general guideline to discover novel frameworks that can be designed to enable fast lithium diffusion.

References:

- [1] A. Manthiram, X. Yu, S. Wang, *Nat. Rev. Mater.* 2:16103 (2017)
- [2] W. Richards, L. Miara, Y. Wang, J. Kim, G. Ceder, *Chem. Mater.* 27:266-273 (2016)
- [3] H. Murumatsu, A. Hayashi, T. Ohtomo, S. Hama, M. Tatsumisago, *Solid State Ionics* 182:116-119 (2011)
- [4] S. Ong, Y. Mo, W. Richards, L. Miara, H. Lee, G. Ceder, *Energ. Environ. Sci.* 6:148-156 (2012)
- [5] R. Murugan, V. Thangadurai, W. Weppner, *Angew. Chem. Int. Ed.* 46:7778-7781 (2007)
- [6] H. Aono, E. Sugimoto, Y. Sadaoka, N. Imanaka, G. Adachi, *Solid State Ionics* 40:38-42 (1990)

11:45 AM EN02.01.05

Thermodynamic Modeling of Cycling-Induced Damage in Lithium-Ion Battery [Fuqian Yang](#); Univ of Kentucky, United States

One of the obstacles hindering the development of lithium-ion battery of high quality is the cycling-induced structural damage/degradation, which contributes to the capacity fade. In this work, we bring out the important role of the structural damage/degradation in the deformation analysis of active material in lithium-ion battery during charging and discharging. Following the approach in damage mechanics, we introduce a scalar state variable in thermodynamic potentials to describe the evolution of the structural damage/degradation. The scalar state variable is dependent on chemical reaction, enthalpy change, dilatation and strain energy during electrochemical cycling. A constitutive relation is developed, in which the elastic properties and the molar volume of the active material are implicit functions of the scalar state variable. Using the constitutive relation, we incorporate the lithiation-induced damage in the analysis of the lithiation-induced deflection of an electrode beam. The numerical results show the relaxation of the lithiation-bending moment induced by the lithiation-induced damage. The method developed in this work provides an approach to incorporate cycling-induced structural damage/damage in the deformation analysis of lithium-ion battery.

SESSION EN02.02: Solid Electrolytes I
Session Chairs: Fudong Han and Yue Qi
Tuesday Afternoon, November 30, 2021
Hynes, Level 3, Ballroom C

1:30 PM *EN02.02.01

Computational Materials Design for Solid-State Li and Na Ionic Conductors [Yan E. Wang](#)^{1,2}; ¹Samsung Advanced Institute of Technology, United States; ²Samsung Semiconductor, Inc., United States

Solid-state batteries have attracted tremendous academic and industrial attention as the likely successor to lithium ion batteries. The key component of solid-state batteries is the solid-state electrolytes with high ionic conductivity [1] and great interfacial stability against battery electrodes [2]. While many sulfide and halide ionic conductors are reported with high conductivity, the chemical instability in the air of these materials inhibits their practical usage in batteries. Due to their stability and non-toxicity, oxides are the preferred choice for solid-electrolyte materials, but only a handful of oxide Li-ion conductors have been experimentally discovered with high conductivity.

Computational modeling based on density-functional-theory methods has been used to accurately predict the intrinsic properties of solid electrolyte materials. Such predictive power has made computational modeling a critical tool to efficiently design and discover new materials with desired properties, such as low cost, high ionic conductivity, great phase and electrochemical stability, accelerating the development of all-solid-state batteries [3].

In this talk, I will present our new discoveries in the physical and chemical design principles for solid-state electrolyte materials using computational modeling. More specifically, I will discuss crystallographic descriptors in solid-state ionic conductors which would enable fast ionic transport. I will report our recent progress in using high-throughput screening for computational design and experimental discovery of novel lithium and sodium solid-state electrolytes.

[1] Yan Wang *et al.*, "Design principles for solid-state lithium superionic conductors," *Nat. Mater.*, 14, 1026-1031, (2015).

[2] Y. Xiao, Y. Wang, S.-H. Bo, J. C. Kim, L. Miara, G. Ceder, "Understanding interface stability in solid-state batteries", *Nature Review Materials*, 5, 105-126 (2020).

[3] G. Ceder, S. Ong, Y. Wang, "Predictive modeling and design rules for solid electrolytes." *MRS Bulletin*, 43(10), 746-751 (2018).

2:00 PM EN02.02.03

Rate-Dependent Deformation in Amorphous Sulfide Glass Electrolytes Christos E. Athanasiou¹, Xing Liu¹, Eugene Nimon², Steve Visco², Nitin P. Padture¹, Huajian Gao³ and Brian W. Sheldon¹; ¹Brown University, United States; ²Polyplus Battery Company, United States; ³Nanyang Technological University, Singapore

Amorphous sulfide electrolytes exhibit exceptionally high Li-ion conductivity near room temperature. A key concern, however, is their mechanical stability in the presence of strains in the adjacent electrode materials accompanying reversible Li storage. Detailed understanding of elastoplastic and fracture properties is lacking, mainly due to the difficulties associated with characterizing such highly moist-sensitive materials. In this talk, we will present our experimental results showing that the mechanical behavior of amorphous sulfide electrolytes is rate-dependent, i.e., they exhibit viscous characteristics when undergoing deformation. We will further demonstrate through careful instrumented indentation experiments, that the material behaves in a viscoplastic manner at short timescales of ~ 1 min. Finally, we will discuss the implications of these findings for understanding and improving the contact of the sulfide electrolytes with Li-metal anodes.

2:15 PM EN02.02.04

Temperature Dependent Anion Rotational Dynamics Correlated to Cation Transport in Cluster Ion Anti-Perovskites Sunil Mair¹, Ping-Chun Tsai^{2,1}, Yiliang Li¹, Kwangnam Kim³, Alex Chien⁴, Jeffrey Smith³, David Halat⁵, Liang Yin⁶, Duhan Zhang¹, Jue Liu⁴, Saul Lapidus⁶, Nitash Balsara⁵, Jeffrey Reimer⁵, Donald Siegel³ and Yet-Ming Chiang¹; ¹Massachusetts Institute of Technology, United States; ²National Taiwan University of Science and Technology, Taiwan; ³University of Michigan–Ann Arbor, United States; ⁴Oak Ridge National Laboratory, United States; ⁵Lawrence Berkeley National Laboratory, United States; ⁶Argonne National Laboratory, United States

As fast-ion conductors, cluster-ion anti-perovskites (APs) are attractive for potential new mechanisms of conduction whereby cation and anion motion is highly correlated [1, 2]. Cluster-ion APs, like perovskites, have a framework that accommodates diverse atomic substitutions. Furthermore, the potential for cluster-ion substitution onto one or both anion sites (A and B in X₃AB) provides additional compositional degrees of freedom. We have synthesized and characterized a series of compositions Na_{3-x}(NH₂)_xO_{1-x}(BH₄), a unique sodium ion conductor with two chemically distinct cluster anions, in order to further understand the correlation between anion rotation and cation translation. We are particularly interested in the x = 1 composition which shows a significant positive deviation from conductivity trends as predicted by a vacancy diffusion model. This presentation will discuss the synthesis and characterization of Na₂(NH₂)(BH₄) via XRD, neutron diffraction, NMR, and AIMD, aimed at understanding the temperature dependent rotational dynamics of the cluster anions and their effects on cation transport.

This work was supported as part of the Joint Center for Energy Storage Research, an Energy Innovation Hub funded by the U.S. Department of Energy, Office of Science, Basic Energy Sciences.

References:

[1] Hong Fang and Puru Jena. Li-rich antiperovskite superionic conductors based on cluster ions. *Proceedings of the National Academy of Sciences*, 2017, 114, 110461.

[2] Hong Fang and Puru Jena. Sodium Superionic Conductors Based on Clusters. *ACS Appl. Mater. Interfaces*. 2019, 11, 963-972.

2:30 PM EN02.02.05

Polymorphism in the Solid Electrolyte Na₄P₂S₆: Phase Formation through Synthetic Control and Superionic Sodium-Ion Conduction Christian Schneider¹, Tanja Scholz¹, Maxwell W. Terban¹, Zeyu Deng², Roland Eger¹, Viola Duppel¹, Igor Moudrakovski¹, Armin Schulz¹, Jürgen Nuss¹, Pieremanuele Canepa² and Bettina V. Lotsch^{1,3}; ¹Max Planck Institute for Solid State Research, Germany; ²National University of Singapore, Singapore; ³Ludwig Maximilian University, Germany

The search for fast new sodium-ion solid electrolytes remains intense to eventually realize all-solid-state sodium batteries for scalable energy storage solutions in the future. In the pursuit of extraordinary performing electrolytes, candidate materials are currently often designed from scratch while drawing on chemical intuition to improve the ionic conductivity.

For the sodium hexathiohypodiphosphate Na₄P₂S₆ a complementary strategy will be showcased, namely, how synthetic control and post-synthetic treatment impact this material's properties, even though structural differences are minute.¹ Two different synthesis methods are compared: a solid-state reaction² and a precipitation route from aqueous solution³. Combined investigations using powder X-ray diffraction (PXRD), precession electron diffraction (PED), differential scanning calorimetry (DSC), solid-state nuclear magnetic resonance spectroscopy (ssNMR), and Raman spectroscopy reveal that the solid-state synthesized material is characterized by a Na⁺ and vacancy disorder-driven enantiotropic phase transition at 160 °C (α- to β-Na₄P₂S₆), which is accompanied by a symmetry change of the P₂S₆⁴⁻ anion. Precipitated Na₄P₂S₆ already crystallizes in a β-like polymorph at room temperature, likely assisted by inter- and intralayer defects. Bond-valence and nudged elastic band (NEB) calculations are employed to identify a low energy, 2D conduction network in β-Na₄P₂S₆, suggesting facile 2D long-range Na⁺ diffusion. Electrochemical impedance spectroscopy reveals a higher ionic conductivity at room temperature in precipitated β-like Na₄P₂S₆ (2×10⁻⁶ S cm⁻¹) compared to the solid-state α polymorph (7×10⁻⁷ S cm⁻¹). The activation energy is around 0.4 eV for both materials.

Independent of the synthetic protocol, Na₄P₂S₆ exhibits another high-temperature polymorph (γ). A structural analysis spanning local and long-range length scales enables the elucidation of the complex structure. The anion and cation arrangement facilitates 3D superionic Na⁺ conduction, which we confirm with *ab initio* molecular dynamic (MD) simulations.

¹ Scholz, T.; Schneider, C.; Eger, R.; Duppel, V.; Moudrakovski, I.; Schulz, A.; Nuss, J.; Lotsch, B. V. *J. Mater. Chem. A*, **2021**, 9, 8692–8703.

² Kuhn, A.; Eger, R.; Nuss, J.; Lotsch, B. V. *Z. Anorg. Allg. Chem.*, **2014**, 640, 689–692.

³ Fincher, T.; LeBret, G.; Cleary, D. A. *J. Solid State Chem.*, **1998**, 141, 274–281.

2:45 PM EN02.02.06

Scalable LLZO Solid Electrolyte Processing for Solid-State Batteries Arno L. Göme, Juliane Hüttl, Martin Drie, Michael Arnold, Kristian Nikolowski and Mareike Wolter; Fraunhofer Institute for Ceramic Technologies and Systems (IKTS), Germany

The substitution of liquid electrolytes with solid ionic conductors is a promising strategy for a new generation of safer batteries with higher energy densities. In terms of developing components for All Solid-State Batteries, plenty of research focused on optimization of solid electrolyte properties. Garnet materials, especially doped $\text{Li}_7\text{La}_3\text{Zr}_2\text{O}_{12}$ (LLZO), are considered a very promising class of solid electrolytes due to their high lithium-ion conductivity in the range of 10^{-4} S/cm^{1,2}, as well as their compatibility with metallic lithium as anode. Recently, the combination of inorganic electrolytes with conducting polymers to form hybrid materials has also come into focus.^{3,4}

Scientific research mainly addresses material properties and characterization, but less manufacturing methods and cell assembly. Fraunhofer IKTS is investigating different scalable manufacturing processes for All Solid-State Batteries⁵ in several projects. We have developed a process chain for freestanding LLZO separator sheets with high ion conductivity, and we have started the processing of LLZO inks for rapid printing of electrolytes or as conductive additives. This talk will give an overview about the material's synthesis, slurry preparation, tape casting, lamination, and sintering, as well as ink development and printing. Some of the challenges encountered during the development will be included, too.

The properties of the obtained LLZO were evaluated using XRD, scanning electron microscopy and electrochemical methods, especially impedance spectroscopy. The morphological and electrochemical properties of the cast and sintered LLZO sheets or printed LLZO were compared to sintered pellets of the same powder.

1. Ohta, S.; Kobayashi, T.; Asaoka, T., *J. Power Sources* **2011**, 196 (6), 3342–3345.

2. Li, Y.; Han, J.-T.; Wang, C. an; Xie, H.; Goodenough, J. B., *J. Mater. Chem.* **2012**, 22 (30), 15357–15361.

3. Zhang, X.; Liu, T.; Zhang, S.; Huang, X.; Xu, B.; Lin, Y.; Xu, B.; Li, L.; Nan, C.-W.; Shen, Y., *J. Amer. Chem. Soc.* **2017**, 139 (39), 13779–13785.

4. Zhang, W.; Nie, J.; Li, F.; Wang, Z. L.; Sun, C., *Nano Energy* **2018**, 45, 413–419.

5. Hüttl, J.; Seidl, C.; Auer, H.; Nikolowski, K.; Göme, A. L.; Arnold, M.; Heubner, C.; Wolter, M.; Michaelis, A. *Energy Storage Mater.* **2021**, 40, 259–267.

3:00 PM BREAK

SESSION EN02.03: Cathodes and Interphases

Session Chairs: Fudong Han and Hui Wang

Tuesday Afternoon, November 30, 2021

Hynes, Level 3, Ballroom C

4:00 PM *EN02.03.01

Development of Materials for All-Solid-State Lithium-Sulfur Batteries Donghai Wang; The Pennsylvania State University, United States

All-solid-state Lithium-Sulfur battery technology is the most promising candidate for next-generation batteries due to its high energy density, long cycle life, and superior safety. However, it faces many challenges, such as unstable lithium/solid-state electrolyte (SSE) interface, lithium dendrite penetration, and poor sulfur utilization of the cathode, which hinder its practical application. In this talk, first, I will present a novel approach based on the use of organic-inorganic nanocomposite interphase to construct stable lithium/Li₁₀GePS₁₂ (LGPS) interface. The nanocomposite is formed in situ on Li by the electrochemical decomposition of a liquid electrolyte, thus having excellent chemical and electrochemical stability, an affinity for Li and LGPS, and limited interfacial resistance. And stable Li electrodeposition over 200 cycles for a full cell was achieved. Second, a sulfur vapor deposition (SVD) method for fabricating sulfur-carbon composite with a high sulfur content of 71.4–83.3 wt% will be present for all-solid-state lithium-sulfur batteries. By creating better interfacial contact at the carbon-sulfur interface and confining sulfur within porous carbon, the electronic transport within the sulfur cathode is improved. Enhanced discharge specific capacities, rate performance, and cycling stability of sulfur cathode were demonstrated using the SVD method compared with conventional sulfur-carbon preparation approaches. Last, I will present the development of solid-state-electrolyte with high conductivity to significantly enhance sulfur utilization to enable solid-state Li-S to achieve high energy density.

4:30 PM EN02.03.02

4 V Room-Temperature All-Solid-State Sodium Battery Enabled by a Passivating Cathode/Hydroborate Solid Electrolyte Interface Ryo Asakura^{1,2}, David Reber¹, Léo Duchêne¹, Seyedhosein Payandeh¹, Arndt Remhof¹, Hans R. Hagemann² and Corsin Battaglia¹; ¹Empa-Swiss Federal Laboratories for Materials Science and Technology, Switzerland; ²University of Geneva, Switzerland

Room-temperature operation of high-voltage all-solid-state batteries requires solid electrolytes that combine high cation conductivity (≥ 1 mS cm⁻¹), compatibility with lithium or sodium metal anodes and high-voltage cathodes, and intimate electrode/solid electrolyte interfaces. However, none of the solid electrolytes has fulfilled these material properties so far. Hydroborates, a yet underexplored class of solid electrolytes,^{1,2} are highly conductive at room temperature and compatible with lithium and sodium metal anodes. However, the cell voltage was limited up to 3 V in previous reports,^{3–6} mainly due to the limited electrochemical oxidative stability of the solid electrolytes.⁷

Here we show that a hydroborate solid electrolyte, consisting of two kinds of hydroborate anions with different oxidative stability limits, can be effectively stabilized in contact with a 4 V-class cathode.⁸ At high voltage, the less stable anions tend to form a passivating interphase layer upon electrochemical oxidation at the cathode/solid electrolyte interface, while the more stable anions remain intact in the interphase layer, maintaining cation conduction. The self-passivating interphase enables the first stable cycling of a 4 V-class hydroborate-based all-solid-state battery employing a sodium metal anode and a cobalt-free, high-voltage cathode. The cells exhibit a discharge capacity of 100 mAh g⁻¹ at C/5 and an excellent capacity (78 %) and energy (76 %) retention after >800 cycles at room temperature. Applying external pressure enables a discharge capacity of >110 mAh g⁻¹ at C/10 with a high areal capacity close to 1.0 mAh cm⁻². This work records the highest discharge cell voltage and specific energy at the active material level among all reported all-solid-state sodium batteries, demonstrating the attractive material properties and potential of hydroborates that surpass intensively investigated oxides and

sulfides as solid electrolytes for high-voltage all-solid-state batteries.

References:

1. L. Duchêne, A. Remhof, H. Hagemann, and C. Battaglia, *Energy Storage Mater.* **2020**, *25*, 782.
2. M. Brighi, F. Murgia, R. Černý, *Cell Rep. Phys. Sci.* **2020**, *1*, 100217.
3. L. Duchêne, R.-S. Kuehnel, E. Stilp, E. Cuervo Reyes, A. Remhof, H. Hagemann, C. Battaglia, *Energy Environ. Sci.* **2017**, *10*, 2609.
4. L. Duchêne, D. H. Kim, Y. B. Song, S. Jun, R. Moury, A. Remhof, H. Hagemann, Y. S. Jung, and C. Battaglia, *Energy Storage Mater.* **2020**, *26*, 543.
5. F. Murgia, M. Brighi, R. Černý, *Electrochem. Commun.* **2019**, *106*, 106534.
6. S. Kim, H. Oguchi, N. Toyama, T. Sato, S. Takagi, T. Otomo, D. Arunkumar, N. Kuwata, J. Kawamura, and S. Orimo, *Nat. Commun.* **2019**, *10*, 1081.
7. R. Asakura, L. Duchêne, R.-S. Kuehnel, A. Remhof, H. Hagemann, and C. Battaglia, *ACS Appl. Energy Mater.* **2019**, *2*, 6924.
8. R. Asakura, D. Reber, L. Duchêne, S. Payandeh, A. Remhof, H. Hagemann, and C. Battaglia, *Energy Environ. Sci.* **2020**, *13*, 5048.

SESSION EN02.04/EN09.03: Keynote Session: New Perspectives on Materials Challenges in Li Metal and Solid-State Batteries

Session Chairs: Fudong Han, Weiyang Li and Hui Wang

Tuesday Afternoon, November 30, 2021

Hynes, Level 3, Ballroom C

5:00 PM *EN02.04/EN09.03.01

Keynote: New Perspectives on Materials Challenges in Li Metal and Solid-State Batteries Y. Shirley Meng; University of California, San Diego, United States

Lithium (Li) metal has been considered as an ideal anode for high-energy rechargeable Li batteries while Li nucleation and growth at the nano scale remains mysterious as to achieving reversible stripping and deposition. A few decades of research have been dedicated to this topic and we have seen breakthroughs in novel electrolytes in the last few years, where the efficiency of lithium deposition is exceeding 99%. Here, cryogenic-transmission electron microscopy (Cryo-TEM/Cryo-FIB) was used to reveal the evolving nanostructure of Li deposits at various transient states in the nucleation and growth process, in which a disorder-order phase transition was observed as a function of current density and deposition time. More importantly, the complementary techniques such as titration gas chromatography (TGC) reveals the important insights about the phase fraction of solid electrolyte interphases (SEI) and electrochemical deposited Li (EDLi). While cryo-EM has made significant contributions to enabling lithium metal anodes for batteries, its applications in the area of solid state electrolytes, thick cathodes are still in its infancy. I hope to showcase how innovative characterization for solid state batteries can be designed to probe buried interphases. Last but not least, I will discuss a few new perspectives about how future cryogenic imaging and spectroscopic techniques can accelerate the innovation of novel energy storage materials and architectures.

SESSION EN02.05: Poster Session: Solid State Batteries

Session Chair: Fudong Han

Tuesday Afternoon, November 30, 2021

8:00 PM - 10:00 PM

Hynes, Level 1, Hall B

EN02.05.03

Flame Assisted Spray Pyrolysis of LiAlO₂ Thin-Film Electrolytes for All-Solid-State Batteries Valerie L. Muldoon, Jianan Zhang and Sili Deng; Massachusetts Institute of Technology, United States

As the demand for lithium-ion batteries with improved safety and energy density increases, all-solid-state batteries (ASSBs) have become a promising option for a wide variety of applications due to the elimination of the flammable liquid electrolyte. In particular, oxide-based solid electrolytes are advantageous because of their exceptional chemical stability against many high voltage cathode materials and lithium metal. However, oxide-based solid electrolytes generally have a lower ionic conductivity than that of liquid electrolytes and sulfide-based solid electrolytes, thereby necessitating the use of a thin, dense film to shorten the ionic diffusion path and ensure a good rate performance. Many current methods used to synthesize oxides produce aggregated powders with wide size distributions and therefore cannot be used to make thin, dense, defect-free films. Furthermore, gas-phase deposition techniques, such as atomic layer deposition, can produce high quality thin films, but are severely limited by their high cost and low production rate. We investigated using flame assisted spray pyrolysis, an inexpensive, scalable method that produces loosely agglomerated nanoparticles with controlled morphology, combined with conventional tape casting to produce thin film solid-state electrolytes. LiAlO₂ was specifically chosen as the solid-state electrolyte due to its impressive chemical stability that has recently made it a promising choice for electrode coatings in both conventional batteries and ASSBs. The morphology and ionic conductivity of the as-synthesized LiAlO₂ films as well as the cycling performance of a battery with LiAlO₂ films, a lithium metal anode, and a Li(Ni_{0.8}Co_{0.1}Mn_{0.1})O₂ cathode were characterized and discussed.

EN02.05.04

Fabrication of High-Quality Thin Solid-State Electrolyte Films Assisted by Machine Learning Yu-Ting Chen¹, Marc Duquesnoy^{2,3,4}, Darren H. S. Tan¹, Jean-Marie Doux¹, Hedi Yang¹, Grayson Deysher¹, Phillip Ridley¹, Alejandro A. Franco^{2,3,4}, Y. Shirley Meng¹ and Zheng Chen¹; ¹University of California, San Diego, United States; ²Laboratoire de Réactivité et Chimie des Solides (LRCS), Université de Picardie Jules Verne UMR CNRS 7314, France; ³Réseau sur le Stockage Electrochimique de l'Energie (RS2E), France; ⁴Alistore-ERI European Research Institute, France

Solid-state electrolytes (SSEs) are promising candidates to circumvent flammability concerns of liquid-based batteries. However, attaining high energy densities requires thinning down SSE layers remains challenging as scalable coating processes are needed. Manufacturing parameters, including binder type, binder ratio, liquid to solid ratio, and cosolvent among others, have a significant influence on the performance of SSE films. While previous studies have reported the fabrication of thin and flexible SSEs, only ionic conductivity was considered for performance evaluation, and no systematic research on the effects of manufacturing conditions on the quality of the SSE films was performed. Here, both uniformity and ionic conductivity are considered for evaluating the SSE films under the guidance of machine learning (ML). Unsupervised ML algorithms, Principal Component Analysis and *k*-

Means clustering, associated to Support Vector Machine, are employed to decipher the interdependencies between manufacturing conditions and film performance. Guided by ML models, an SSE film with a thickness of 40 μm was fabricated and used to construct a $\text{LiNi}_{0.8}\text{Co}_{0.1}\text{Mn}_{0.1}\text{O}_2 \parallel \text{Li}_6\text{PS}_5\text{Cl} \parallel \text{LiIn}$ cell, leveraging its high ionic conductivity and good uniformity to achieve stable cycling performance. This study presents a ML-assisted experimental approach as an efficient strategy to optimize SSE films, paving the way towards mass production of all-solid-state batteries.

EN02.05.05

Improved Ionic Conductivity and Battery Function in a Lithium Iodide Solid Electrolyte via Particle Size Modification [Mikaela Dunkin](#)¹, Steven King¹, Kenneth Takeuchi^{1,2}, Esther S. Takeuchi^{1,2}, Lei Wang² and Amy Marschilok^{1,2}; ¹Stony Brook University, United States; ²Brookhaven National Laboratory, United States

In high energy density batteries, solid electrolytes (SEs) are a safe and promising alternative to liquid electrolytes, but challenges such as low ionic conductivity and dendrite formation, remain. Recent work by others has determined that dendrite formation within $\text{Li}_7\text{La}_5\text{Zr}_2\text{O}_{12}$ and Li_3PS_4 SEs is due to their non-negligible electronic conductivity. Thus, research must re-focus its efforts to keep electronic conductivity low. Notably, solid LiI has negligible electronic conductivity, making LiI a good candidate for SE development. In our previous work, we utilized LiI SE with a conductive additive to create a composite SE capable of forming a Li/I_2 rechargeable battery *in situ*. Additional work demonstrated interfacial modification with either lithium or gold contacts, can effectively lower the cell impedance and improve coulombic efficiency (CE).

In this work, a LiI SE was improved by reducing particle size via processing. Several processing methods were examined; grinding (G), sonicating (C-S), and grinding with sonicating (G-S), and compared to a control (C) sample of LiI that underwent no processing. To control for LiI hydration effects, which results in increased conductivity via increased defect density, LiI monohydrate content was controlled among samples. With further processing, particle size was reduced from $5 \pm 1 \mu\text{m}$ to $2.0 \pm 0.2 \mu\text{m}$ for the C and G-S samples. Each sample was utilized with a 1:2 lithium iodide:3-hydroxypropionitrile ($\text{LiI}(\text{HPN})_2$) conductive additive, creating a 80/20 $\text{LiI}/\text{LiI}(\text{HPN})_2$ SE composites. Reducing particle size resulted in a significant increase in ionic conductivity, from 7.7×10^{-8} to $6.1 \times 10^{-7} \text{ S cm}^{-1}$, at room temperature. This improvement is attributed to an increase in the number of grain boundaries and defects, enabling better mixing with the electrolyte additive, $\text{LiI}(\text{HPN})_2$ and an overall improvement in ion transport. 3D confocal Raman spectroscopy with non-negative matrix factorization (NMF) analysis determined aggregation of HPN within the composites was lessened in the sample with smallest particle size. When utilized in a self-forming Li/I_2 battery, reduced particle size (improved conductivity) led to significantly reduced overpotential, enabling the coulombic efficiency to reach 100% in the first cycle. Additionally, the cells with G-S composite electrolyte (smallest LiI particle size) exhibited improved electrochemical function at higher cycling rates compared with the other electrolyte types. This work demonstrates the effect(s) of decreasing solid electrolyte particle size in a self-forming, self-healing, all solid-state battery.

EN02.05.06

Characterization Study on Deposited $\text{Li}_{1-x}\text{Al}_x\text{Ti}_{2-x}(\text{PO}_4)_3$ Thin Films for All-Solid-State Li-Ion Battery Applications [Marie Françoise C. Millares](#), Christopher Ajiduah, Latiika Susheel, Kevin Shah, Seichiro Higashiya, Hassaram Bakhru, Devendra Kumar and Haralabos Efstathiadis; SUNY Polytechnic Institute, United States

All solid-state Li-ion batteries hold the promise of safety, lower cost, and improvements concerning specific energy, specific power, and cycle performance compared to traditional liquid Li-ion batteries. However, there has been little work done on the fabrication of solid electrolyte via plasma vapor deposition (PVD) technique. Our goal is to deposit and characterize solid electrolyte thin film using a NASICON-like, lithium aluminum titanium, phosphate ($\text{Li}_{1-x}\text{Al}_x\text{Ti}_{2-x}(\text{PO}_4)_3$, (LATP)) solid compound and fabricate microbatteries using lithography. LATP is the interest in this study due to its high ionic conductivity of $\sim 3 \times 10^{-3} \text{ S cm}^{-1}$ and reported stability. They are deposited through RF-magnetron sputtering of a 99.9% pure single LATP target onto a thermal silicon oxide substrate. The films' structural and compositional properties were characterized using multiple techniques such as scanning electron microscopy (SEM) and X-ray diffraction while the lithium depth profile on pristine and cycled devices was measured by secondary ion mass spectroscopy (SIMS) and nuclear reaction analysis (NRA). SIMS and NRA data were combined to depict a lithium depth profile of 0.1 atomic % ^7Li in the electrolyte. SIMS and NRA will also be used to correlated the atomic % of ^7Li in the electrolyte and quantify the Li trapped in the electrodes after cycling to the battery performance.

EN02.05.07

Spatially-Resolved Operando Structural Analysis of Sulfur-Based All-Solid-State Lithium Batteries Using EDXRD [Alyssa Stavola](#), Xiao Sun, Andrea Bruck, Daxian Cao, Hongli Zhu and Joshua Gallaway; Northeastern University, United States

All solid-state lithium batteries (ASSBs) offer higher power and energy density than traditional lithium-ion batteries and are inherently safer due to solid-state electrolytes (SSEs) replacing flammable organic liquid electrolytes. Due to their high room temperature ionic conductivity and malleability allowing for good contact at the electrodes, sulfide-based SSEs are promising candidates for ASSBs. However, thiophosphate based SSEs face two main challenges for commercialization: the narrow voltage window where the electrolyte is electrochemically stable, and its reactivity with NMC and Li metal active materials. Pairing sulfide SSEs with compatible cathodes is crucial to designing high energy dense ASSBs.

An FeS_2 metal sulfide cathode offers a high theoretical capacity (894 mAh/g) and excellent compatibility with sulfide SSEs without additional interface engineering. ASSBs based on $\text{Li}_{6.6}\text{Ge}_{0.6}\text{Sb}_{0.4}\text{S}_5\text{I}$ (LGSSI) and FeS_2 exhibit an initial capacity of 715 mAh/g at C/10 and are stable for 220 cycles with a capacity retention of 84.5% at room temperature. The structural stabilities of $\text{Li}_{6.6}\text{Ge}_{0.6}\text{Sb}_{0.4}\text{S}_5\text{I}$ (LGSSI) during cycling are characterized by operando energy dispersive X-ray diffraction (EDXRD), which allows rapid collection of spatially-resolved structural data without redesigning or disassembling the sealed cells and risking contamination by air (Figure 1a). The electrochemical stability is assessed, and an operating voltage window from 0.7-2.4 V (vs. In-Li) is confirmed. Initial EDXRD of a carbon/In-Li half cell is shown in Figure 1b, with the primary reflection of LGSSI observed near a photon energy of 86 keV. During a negative potential sweep (shown in Figure 1c) LGSSI reflections located in the carbon cathode shifted to lower energy, indicating a locally higher d-spacing. This demonstrated that contact with conductive carbon caused a structural instability in the LGSSI.

Layered $\text{Li-Ni}_{1/3}\text{Mn}_{1/3}\text{Co}_{1/3}\text{O}_2$ (NMC111) is a widely used cathode material due to its high working potential (>3.6V), and high capacity of 160 mAh/g. However it is proposed that sulfide SSE decomposes where it contacts the NMC cathode particles, causing ionically insulating interfaces to form and hindering the transport of lithium ions. This decomposition of active materials causes a large capacity loss in the first cycle, and the reactivity of NMC and the SSE has prevented this battery from achieving high energy density. A 120 μm thick NMC111 cathode was paired with electrolyte $\text{Li}_6\text{PS}_5\text{Cl}$ as the SSE and operando EDXRD was utilized to determine the time-dependent lithiation gradient during the first two cycles. This structural analysis of the cathode reveals information about the current distribution and its time evolution; vital information to increasing the energy density of sulfide based ASSBs.

EN02.05.08

Nano Additives Having Low Interfacial Energy to Sulfur That Enable Stable Reactions of Sulfur Cathode in Solid-State Batteries [Jong Ho Won](#); Kookmin University, Korea (the Republic of)

With the use of energy storage devices rather than generators in larger and harsher environments, the demand for new energy storage devices with superior performance and reliability is increasing. The ideal structure proposed to meet this requirement is in the form of using lithium metal for the positive electrode, sulfur for the negative electrode, and placing a solid electrolyte between the two electrodes. The sulfur electrode has a theoretical capacity of at least five times higher than that of the conventional cathode, so it is expected to improve the performance of energy storage devices. However, the actual capacity of sulfur electrode varies depending on the state of the solid electrolyte. If a solid electrolyte with high crystallinity and high rigidity is used, the interfacial compatibility with sulfur is low, so that only a small part of the theoretical capacity of sulfur can be utilized. Therefore, for high capacity, a gel-type solid electrolyte with low crystallinity should be used to increase the interfacial properties of sulfur and electrolyte. However, in a gel-type solid electrolyte with a low crystallinity that sulfur exhibits theoretical performance, the sulfur electrode is combined with lithium and causes a shuttle effect that can't be easily controlled and reversed, just like a liquid electrolyte, and the sulfur diffuses to all parts of the battery. When lithium is removed from sulfur, sulfur with low conductivity is irregularly precipitated in the cell, seriously impeding repeated charge/discharge and stable operation. In this study, nano-additives were used to increase the stability when using a gel-type solid electrolyte and a sulfur electrode. The use of nano-additives significantly improved the performance of the sulfur electrode while maintaining the properties of the solid electrolyte. Nanoadditives have been materials with highly controlled internal structures and high surface areas, such as graphene pomegranate pockets and nitrogen-rich carbon nanotubes. For example, graphene pomegranate sacs provide conductivity to the sulfur electrode and make the sulfur stable around it because of its low interfacial energy with sulfur. In addition, when lithium is removed from the sulfur electrode, sulfur is precipitated around the graphene pomegranate bag, leading to a stable reaction. In addition, in the case of nitrogen-rich carbon nanotubes, excellent conductivity was provided by uniformly stacking structures extending in one direction, and sulfur was accommodated in a large internal space. In addition, the low interfacial energy with sulfur allowed sulfur to stay near the nanotubes with sufficient nitrogen, leading to structurally reversible reactions during charging and discharging. We accurately revealed the interfacial energy between nano-additives, sulfur electrodes, and electrolytes based on experiments, and through electrochemical tests, stability was verified through more than 3,000 charge/discharge reactions, and close to theoretical capacity were achieved. As a result, nano additives with similar surface energy to sulfur stabilize the unstable behavior of sulfur through low interfacial energy and control the irreversible reaction of sulfur in solid electrolytes.

EN02.05.09

Fast Lithium-Ion Conduction in the Perovskite-Type Solid Electrolyte [Jaejin Hwang](#) and Jaekwang Lee; Pusan National University, United States

Solid electrolytes with a fast ion conduction are crucial for all solid batteries. The perovskite type lithium lanthanum titanate (LLTO) solid electrolytes have been known as one of promising next-generation lithium-ion batteries because they provide high-energy density and superior cyclic stability. However, in spite of these advantages, their practical application is plagued by low ionic conductivity at room temperature. Here, the LLTO solid electrolyte optimized at the temperature of 1380°C are found to exhibit high lithium ion conductivity of 2.55×10^{-4} S/cm, which was more than 100 times higher than that of the solid electrolyte stabilized at 1200°C. In addition, periodic lattice shrink/expansion was observed in the LLTO optimized at 1380°C. Using the first-principles density functional theory calculations, we find that the oxygen vacancies play critical roles in expanding the lattice parameter normal to the lithium migration path, which greatly enhance lithium ion conductivity. Relevant structure reconstructions and underlying mechanism will be discussed in detail at the atomic scale.

EN02.05.10

Late News: Efforts to Increase the Ionic Conductivity of Lithium Carbonphosphonitride Thermosets [Andrew Purdy](#), Brian L. Chaloux, Megan B. Sassin, Christopher A. Klug and Daniel M. Fragiadakis; Naval Research Laboratory, United States

Lithium dicyanamide ($\text{LiN}(\text{CN})_2$) reacts with phosphorus cyanide ($\text{P}(\text{CN})_3$) in a 2:1 or greater mole ratio in any anhydrous non-protic mutual solvent to form a resin. The resin solution is used to coat metal coupons or to impregnate silica fiber paper, which are then cured at temperatures of 200-300 °C, forming adherent, ion conducting films. When fully cured, those films have a low ionic conductivity, probably due to rigid crosslinking of the thermoset. We will report our efforts to increase that ionic conductivity by introducing various additives to the system. We have explored (1) adding cations of different sizes, (2) increasing the Li concentration by adding lithium cyanide, (3) introducing $\text{RP}(\text{CN})_2$ components to reduce the crosslink density, (4) adding non-volatile, Li-coordinating organic plasticizers to increase ion mobility. The ionic conductivity and chain motions of these films were characterized by impedance and dielectric relaxation spectroscopy. Additionally, reactions in solution were followed by NMR and bulk thermoset material was analyzed by solid state NMR. We evaluated how the composition and conductivities of these materials depends on conditions of preparation.

EN02.05.11

Late News: A study on the Improvement of Atmospheric Stability of LLZTO Solid Electrolyte for All-Solid-State Batteries [Jong Woo Kim](#), Young Ah Park, Su Hyeong Kim, Jisu Na and Young Soo Yoon; Gachon University, Korea (the Republic of)

To recognize the autonomous driving of electric vehicles in real-time, large-capacity batteries should be installed in the vehicle. Liquid electrolyte-based lithium-ion batteries (LIBs) have limited battery capacity expansion due to their liquid electrolytes and have an explosion risk during driving. To resolve the LIB's limitations, solid-state electrolytes (SEs) are promising to considerable research attention. However, SEs are low ion conductivity than liquid electrolytes and make the dendrite during the working process. Garnet structure solid electrolytes were known that have high ion conductivity at room temperature, among solid electrolytes.

In this study, we studied the characteristics of the garnet structure-based Li-La-Zr-Ta-O (LLZTO) according to atmospheric exposure time after the solid-state synthesis method. LLZTO's morphology characteristic according to the synthetic environment was analyzed using the XRD (X-ray Diffraction) and SEM (Scanning electron microscopy). To analysis electrochemistry properties such as ion conductivity and activation energy, impedance analysis was performed. LLZTO's impedance data is comparing was compared the commercial LLZTO's ion conductivity. To compare the LLZTO's ionic conductivity reduction ratio according to the atmospheric exposure time, we compared synthetic LLZTO and commercial LLZTO with atmospheric exposure time. As a result, we found that the ionic conductivity reduction ratio of synthetic solid electrolytes is smaller than commercial LLZTO.

EN02.05.12

Late News: Optimization of Lithium Ceramic - Poly(vinylidene fluoride-co-hexafluoropropylene) (PVDF-HFP) Composite Separator for Lithium Metal Batteries [Lara Dienemann](#), [Lily Geller](#), Anil Saigal and Michael A. Zimmerman; Tufts University, United States

Lithium metal batteries are more energy-dense than commercial lithium-ion batteries; however, unstable and non-uniform plating and stripping at the lithium metal anode can lead to short circuiting if the structures, known as dendrites, breach the gap between anode and cathode. To mitigate this problem, inorganic-organic hybrid films have been placed at the lithium metal anode to encourage uniform deposition arguably through the robust mechanics and diffusion mechanisms of the composite. This study aims to optimize the design of these films by focusing on poly(vinylidene fluoride-co-hexafluoropropylene) (PVDF-HFP) composite films, quantifying the relationship between concentration of LiF and $\text{Li}_{6.4}\text{La}_3\text{Zr}_{1.4}\text{Ta}_{0.6}\text{O}_{12}$ (Ta-doped LLZO) ceramic fillers to mechanics and conductivity of the separator as well as to plating and stripping uniformity at the lithium metal anode after cycling. The hybrid separators demonstrate high modulus, yield stress, and ductility in uniaxial tension experiments as both pristine and swollen with electrolyte. Additionally, long term cycling validates the composite as electrochemically compatible in a lithium metal system through *postmortem* surface analysis of

the lithium metal electrodes.

EN02.05.13

Late News: (Garcia High School Student) Modeling Ion Transport and Dendrite Formation in All-Solid-State Lithium-Ion Batteries Jack Kugler¹, Aishik Dhori², Satvik Lolla³, Neha Basu⁴, Anirudh Bharadwaj⁵, Zhuolin Xia⁶ and Dilip Gersappe⁶; ¹Philips Exeter Academy, United States; ²Munster High School, United States; ³Poolesville High School, United States; ⁴BASIS Scottsdale, United States; ⁵Lynbrook High School, United States; ⁶SUNY-Stony Brook, United States

All-Solid-state Lithium-Ion batteries (ASSLIBs) are considered as more efficient and safer alternatives to traditional lithium-ion batteries with liquid electrolytes. Among the candidate solid electrolyte materials, Lithium Phosphorus Sulfide (LPS) has attracted the attention of researchers due to its high Lithium ion conductivity. However, major challenges arise due to LPS having complicated porous geometries and multiple phases with different ion transport abilities. Additionally, suppressing dendrite growth at the anode surface is needed for high energy density solid state batteries using Li metal as anode. Our goal is to identify the electrolyte that best promotes ion transport and the interface morphology that best suppresses dendrite growth.

In this study, we used the Lattice Boltzmann Method (LBM) to simulate half-cells with a Li working electrode, virtual Li counter electrode, and LPS solid electrolyte. In order to investigate the ion transport process, we tested the electrolyte with various porosities, diffusivities, and phases with different ion conductivities. In our ion-transport simulations, we simulated Li-ion transport through solid-state electrolytes by measuring flux at the electrolyte-electrode interface. The results show that flux at the electrolyte-electrode interface increases as porosity decreases or diffusivity increases. Our multiphase simulations were conducted with a single porous electrolyte with less conductive secondary phases. The simulation indicated that lower percentage of the second phase resulted in higher Li-ion flux. To investigate dendrite formation, we studied three interface morphologies: rough with no micropattern, rough with micropattern, and smooth with micropattern. For each system, we varied charge current, surface roughness, and micropattern hole size. Our results reveal that dendrite formation at the anode/electrolyte interface is favored in the rough systems and is inhibited in micropattern systems. Our study demonstrates the effects of factors on the performances of ASSLIBs in order to provide information for finding high-performing and commercially-viable candidate systems.

EN02.05.14

Highly Stable LiNi_{0.8}Mn_{0.1}Co_{0.1}O₂ with LiOH Coating in Thiophosphate-Based All-Solid-State Batteries Xiao Sun¹, Yubin Zhang², Yan Wang² and Hongli Zhu¹; ¹Northeastern University, United States; ²Worcester Polytechnic Institute, United States

Nickel-rich LiNi_{0.8}Co_{0.1}Mn_{0.1}O₂ (NMC 811) exhibits outstanding properties in high energy density and low cost, making it promising as the cathode material in all-solid-state lithium batteries (ASSLBs). In various solid-state electrolytes (SEs), thiophosphate-based electrolytes own superior ionic conductivity and processibility. However, NMC 811 suffers from severe surface electrochemical, chemical, and voltage incompatibility towards thiophosphate-based electrolytes. Diverse interface engineering has been reported to solve this issue, whereas they are typically cumbersome and expensive. Therefore, finding a coating strategy that satisfied all the requirements of cost-efficiency, stability, uniformity, scalability, and easy-achieving is necessary. In this work, we fabricated a highly stable NMC 811 coated with a ~10 nm of LiOH-based layer through a time- and cost-effective one-step sintering process. Compared with conventional coating strategies, this method made a conformally coating in the NMC 811 lithiation process without extra processes. Meanwhile, LiOH interfacial coating layer only conducts ions but not electrons resulting suppressed decomposition of sulfide electrolyte. As a result, the ASSLBs exhibited remarkable cycling stability for 600 cycles with a capacity of 130 mAh g⁻¹ on average at C/10 at a wide electrochemical window of 2.50–4.20 V (vs. Li-In) and satisfactory rate capability (119.4 mAh g⁻¹ at 1C).

EN02.05.15

High Performance Stretchable Spiral Lithium-Ion Battery Banafsheh Hekmatnia, Hamidreza Fallahtafti, Alamgir Karim and Haleh Ardebili; University of Houston, United States

Recently, there has been a great attention toward stretchable and flexible lithium-ion batteries (LIBs) that are safe, leakage-proof, low cost, and electrochemically and mechanically stable. These stretchable batteries must provide long cycle life and show high electrochemical and mechanical performance for a wide variety of applications such as wearable electronics, biomedical sensors and portable devices. Due to this accelerated demand, in this study, a thin-film stretchable lithium-ion battery has been fabricated, tested and optimized. The lithium-ion cell is fabricated in a spiral configuration with the thickness of less than 0.8 mm and provides out-of-plane stretchability. In addition, comprehensive tests including electrochemical and mechanical cycling, and electrochemical impedance spectroscopy (EIS) has been conducted to evaluate and optimize the performance of the stretchable batteries. Results show that high areal discharge capacity of 1 mAh/cm² after 100 electrochemical cycles is achieved for spiral stretchable batteries. Moreover, electrochemical performance, EIS and voltage of the stretchable batteries have been measured simultaneously in both flat and stretched states. Results reveal that the spiral battery can be stretched up to 500% without any significant change in its electrochemical performance. Furthermore, scanning electron microscopy (SEM) images of the battery confirm stable interfaces and structural integrity throughout cycling and stable specific capacity up to 200 cycles has been demonstrated. In comparison with the previous work on stretchable batteries, a significant enhancement has been achieved with respect to specific capacity, energy density, performance stability in stretched state and during long cycles.

SESSION EN02.06: Metal Anodes I
Session Chair: Fudong Han
Wednesday Morning, December 1, 2021
Hynes, Level 3, Ballroom C

10:30 AM *EN02.06.01

Interfacial Dynamics in Anode-Free Solid-State Batteries Neil P. Dasgupta; University of Michigan, United States

Solid-state batteries (SSBs) have seen a dramatic increase in research in recent years because of their ability to address safety challenges associated with flammable liquid electrolytes, and the potential to enable Li metal anodes. Recently there has been an increase in attention paid to anode-free SSB configurations, where all of the lithium inventory in the battery is supplied from the cathode. Accordingly, Li metal is plated out at the interface between a solid electrolyte and a metallic current collector. This enables a N:P ratio of 1, representing a significant increase in the theoretical energy density compared to cells with excess Li metal in the anode. The anode-free configuration results in unique physical phenomena with regards to chemo-mechanics at the interface, and also represents a valuable platform to quantify the stability and reversibility of Li plating and stripping at solid-solid interfaces.

To probe the dynamic evolution of anode-free solid-state batteries, in this talk, I will present results using a complimentary set of *in situ/operando* methodologies. First, we will explore quantify the impacts of electrochemical cycling conditions and external variables on the voltage signatures and reversibility of anode formation. Comparisons will be made between anode-free cells using state-of-the-art metal oxide and sulfide solid electrolytes. *Operando* video microscopy will be used to study the morphological evolution of the interface, including 3-dimensional analysis using focus variation microscopy. The chemical evolution of SEI formation during the initial anode formation cycle will be explored using *operando* x-ray photoelectron spectroscopy (XPS). The results of these investigations point towards unique processes that occur in anode-free SSBs, including transitions in reaction pathways between SEI formation and Li plating, as well as mechanical evolution of both the Li metal and current collector during nucleation and growth.

11:00 AM EN02.06.02

Lithium Deposition-Induced Fracture of Carbon Nanotubes. Measurement of Hydrostatic Stress in Plated Li Stephen J. Harris¹, Yongfu Tang², Sulin Zhang³, Feng Ding⁴ and Jianyu Huang^{2,5}; ¹Lawrence Berkeley National Laboratory, United States; ²Yanshan University, China; ³The Pennsylvania State University, United States; ⁴Ulsan National Institute of Science and Technology, Korea (the Republic of); ⁵Xiangtan University, China

The increasing demand for safe and dense energy storage has shifted research focus from liquid electrolyte-based Li-ion batteries towards solid-state batteries (SSBs). However, the application of SSBs is impeded by uncontrollable Li dendrite growth and short circuiting, whose mechanism remains elusive. Herein we conceptualize a scheme to visualize Li deposition in the confined space inside carbon nanotubes (CNTs) to mimic Li deposition dynamics inside solid electrolyte (SE) cracks, where the high-strength CNT walls mimic the mechanically strong SEs. We observed that the deposited Li propagates as a creeping solid in the CNTs, presenting an effective pathway for stress relaxation. When the stress-relaxation pathway is blocked, Li deposition-induced stress reaches GPa level and causes CNT fracture. Mechanics analysis suggests that interfacial lithiophilicity critically governs Li deposition dynamics and stress relaxation. Our study offers critical strategies for suppressing Li dendritic growth and constructing high energy density, electrochemically and mechanically robust SSBs.

11:15 AM EN02.06.03

Ultra-High Areal Capacity Li Electrodeposition at Metal-Solid Electrolyte Interfaces Under Minimal Stack Pressures Enabled by Interfacial Na-K Liquids Richard Park, Cole D. Fincher, Andres Badel, Michael Wang, W. C. Carter and Yet-Ming Chiang; Massachusetts Institute of Technology, United States

The need for higher energy density rechargeable batteries has generated interest in metallic electrodes paired with solid electrolytes. However, impedance growth at the Li metal-solid electrolytes interface due to void formation during cycling at practical current densities and areal capacities, e.g., greater than 0.5 mA cm⁻² and 1.5 mAh cm⁻² respectively, remains a significant barrier. Here, we show that introducing a wetting interfacial film of Na-K liquid between Li metal and Li_{6.75}La₃Zr_{1.75}Ta_{0.25}O₁₂ (LLZTO) solid electrolyte permits reversible stripping and plating of up to 150µm of Li (30 mAhcm⁻²), approximately ten times the areal capacity of today's lithium-ion batteries, at current densities above 0.5 mA cm⁻² and stack pressures below 75 kPa, all with minimal changes in cell impedance. We further show that this increase in the accessible areal capacity at high stripping current densities is due to the presence of Na-K liquid at the Li stripping interface; this performance improvement is not enabled in the absence of the Na-K liquid. This design approach holds promise for overcoming interfacial stability issues that have heretofore limited performance of solid-state metal batteries.

11:30 AM EN02.06.04

An Investigation of Chemo-Mechanical Phenomena in All-Solid-State Lithium Metal Batteries Using *In Situ* Curvature Measurements Jung Hwi Cho¹, Kunjoong Kim², Srinath Chakravarthy³, Xingcheng Xiao⁴, Jennifer L. Rupp² and Brian W. Sheldon¹; ¹Brown University, United States; ²Massachusetts Institute of Technology, United States; ³Samsung Advanced Institute of Technology, United States; ⁴General Motors, United States

Lithium metal penetration through garnet based LLZO solid electrolytes (SEs) have been identified as a critical failure process. At critical current density, LLZO SE has been known to short-circuiting, and can even result in fracturing of the SE. The combined chemo-mechanical phenomena- which can significantly affect the performance in all solid-state batteries, requires detailed investigation of several related phenomena. Characterizing the dynamical mechanical evolution that occurs in the electrode-SE is challenging. Investigation of the mechanical driving forces of lithium metal penetration through the SE is a particularly important challenge. To probe the chemo-mechanical phenomena that occur during lithium plating, this study reports in-situ curvature measurements that were designed to evaluate the stresses that evolve in LLZO during lithium plating. The experimental configuration created for this work provides data which was analyzed with a detailed Finite Element Model (FEM) to quantitatively evaluate stress evolution in the solid electrolyte. The results show that Li metal plating within a surface flaw can produce stress build-up prior to short-circuiting. The combined results from both the experiments and the FEM suggest that it is critical to minimize surface defects and flaws during manufacturing processes.

11:45 AM EN02.06.05

Measurements and Maps to Understand the Mechanical Behavior of Lithium, Sodium and Potassium Metal Cole D. Fincher¹, Yuwei Zhang², Jungho Shin², George Pharr² and Matt Pharr²; ¹Massachusetts Institute of Technology, United States; ²Texas A&M University, United States

Pure metals (i.e., Li, Na, K) are attractive battery anodes because they possess large theoretical capacities for their respective systems. However, pairing metal anodes with solid electrolytes produces a rigid interface with fundamental mechanical issues: stress buildup can lead to electrolyte fracture and metal penetration, while a lack of sufficient pressure leads to a loss of anode-electrolyte contact. The anode's mechanical properties govern both stress buildup and relaxation, but such properties (e.g., the yield stress) are highly sensitive, varying by orders of magnitude with temperature, rate, and size. In this work, we systematically survey the mechanical behavior of lithium, sodium, and potassium at bulk scales for temperatures from 0 C to 45 C and strain rates from 10⁻² to 10⁻⁴ s⁻¹, while using micro- and nano-indentation measurements to delineate the size-dependence of mechanical behavior. Temperature dependent and (separately) size dependent deformation mechanism maps emerge from these measurements, allowing the prediction of flow stress for alkali metals under a broad variety of conditions. Towards illustrating the utility of the deformation mechanism maps, we outline the implications for stress buildup within metallic protrusions at the solid-state electrolyte / anode interface. Furthermore, both deformation maps and mechanical measurements demonstrate that Na and K metal are far softer than Li metal under equivalent conditions, and may provide more conformal interfaces than Li metal during operation of fast-charging solid-state batteries. Overall, the results presented herein will provide important guidance in designing solid-state batteries with persistent interfacial contact

Wednesday Afternoon, December 1, 2021
Hynes, Level 3, Ballroom C

1:30 PM *EN02.07.01

Dynamic Operation of Solid-State Batteries [Kelsey B. Hatzell](#) and Wahid Zaman; Princeton University, United States

Garnet solid-state electrolyte $\text{Li}_7\text{La}_3\text{Zr}_2\text{O}_{12}$ (LLZO) are promising candidates for the development of all solid-state batteries, owing to their high ionic conductivity and chemical stability in contact with Lithium metal. However, insufficient interfacial contacts in LLZO-based solid-state batteries leads to high area-specific resistance (ASR), gradual void formation and dendrite-induced shorting during electrochemical cycling². By applying external pressure to symmetric / full cells, proper interfacial contact can be achieved. However, excessive stack pressure can be detrimental to Li-LLZO kinetics and stability, which affects the overall cell performance³. In this study, we systematically evaluated the combined effect of stack pressure (5-30 MPa) and temperature (25-70C) in Li stripping/plating behavior (symmetric cells). The morphological changes at Li-LLZO interfaces under pressure and temperature are complex in nature. Improper contact points lead to void formation and inhomogeneous plating, which result to rise in constriction resistance. The contact issues can be eliminated completely under extreme confinement. But stress-induced Li dissolution along grain boundaries or surface flaws of LLZO can still cause shorting. Through critical current density (CCD) and long-term Li-stripping measurements on Li/LLZO/Li cells, an optimum pressure range of 10-20 MPa is observed for stable operation at room temperature up to 0.5 mA/cm². The cell shorting scenarios at high current densities are different. At low pressure (5 MPa) cells encounter a void-induced shorting, whereas at high pressure (20 MPa), stress-induced shorting is evident. Increasing the temperature at the optimum pressure range shows a significant increment of current density (> 1.3 mA/cm²). Combined effect of pressure and temperature in full cell performance and stability was also investigated by employing composite LiFePO_4 electrodes.

2:00 PM EN02.07.02

Cooperative Role of Concentration and Electric Field for Dendritic Growth in Rechargeable Batteries [Asghar Aryanfar](#)^{1,2} and Sajed Medlej¹; ¹American University of Beirut, Lebanon; ²California Institute of Technology, United States

We develop a real-time framework for computing the concentration and electric fields in one dimensional battery cell. Subsequently we calculate the kinetics of dendritic growth using asynchronous evolution in the concentration of anions and cations and the cell voltage. Consequently, we develop a phase field model for the initiation and growth process of the dendritic microstructures which is highly dependent to the computed three variables. The main focus in the phase field model is the variation in the charge density ρ and the value of the computed electric potential V for determining the ultimate energy functional ΔG . The results are useful for determining the design strategy for controlling the microstructures particularly for the effect of the original concentration C_0 , the potential difference V_0 and the inter-electrode separation l .

2:15 PM EN02.07.03

Mechanistic Understanding of Lithium Dendrite Formation in Solid Electrolytes [Fudong Han](#); Rensselaer Polytechnic Institute, United States

The successful integration of Li metal anode with solid electrolytes seems to be a must for a high-energy-density solid-state battery. However, Li dendrites tend to form in solid electrolytes during plating and eventually lead to the short circuit of the cell. The formation of dendrites has been observed in solid electrolytes with various crystal structures from glass, glass-ceramic, poly-crystalline to single-crystalline, but the mechanism of such an unexpected dendrite growth remains elusive. In this presentation, I will introduce our recent understandings of lithium dendrite formation in solid electrolytes based on neutron depth profiling characterizations and electrochemical measurements on typical solid electrolytes. We highlight the important role of the electronic conductivity of solid electrolytes in the formation of isolating dendrites inside solid electrolytes. We will also discuss corresponding dendrite prevention strategies.

2:30 PM EN02.07.04

Structural and Mechanical Characterization of NaSICON Solid Electrolytes Upon Cycling in Molten Sodium [Ryan C. Hill](#)¹, Martha M. Gross², Amanda Peretti², Leo J. Small², Erik D. Spoeke² and Yang-Tse Cheng¹; ¹University of Kentucky, United States; ²Sandia National Laboratories, United States

The ever-growing demand for robust, long-duration energy storage has driven research into emerging technologies, such as sodium-based batteries. Solid sodium electrolytes are a key component to the successful implementation of molten sodium, solid-state, and sodium-ion batteries for large-scale and long-duration energy storage. The sodium (Na) Super Ion CONductor (NaSICON) is a promising candidate solid electrolyte, due to its high conductivity and chemical stability against molten sodium. At high current densities or after extended use, however, potential changes in the material properties of NaSICON may lead to various forms of degradation. In-situ deterioration of NaSICON stands to potentially decrease the performance, lifetime, and safety of sodium batteries. Characterizing potential degradation mechanisms is critical to widespread NaSICON utilization, but these processes have not been studied extensively. In this presentation, the microstructural, mechanical, and electrochemical properties of NaSICON before and after exposure to sodium battery environments are investigated. Structural characterization by x-ray diffraction, atomic force microscopy, and scanning electron microscopy is combined with mechanical and electrochemical measurements, such as nanoindentation and electrochemical impedance spectroscopy. We have found that critical properties, such as elastic modulus, of NaSICON are altered after exposure to electrochemical cycling. These changes, coupled with high current density, can lead to localized failure in the form of microcracking or dendrite formation and propagation. The degradation and failure of these electrolytes may be further exacerbated by the presence of microstructural ceramic defects, such as porosity, from the fabrication process. Understanding these mechanisms will be used to guide improved design and formulation of NaSICON for use in sodium batteries.

Sandia National Laboratories is a multimission laboratory managed and operated by National Technology & Engineering Solutions of Sandia, LLC, a wholly owned subsidiary of Honeywell International Inc., for the U.S. Department of Energy's National Nuclear Security Administration under contract DE-NA0003525.

2:45 PM BREAK

4:00 PM EN02.07.05

Late News: Creep and Anisotropy of Free-Standing Lithium Metal Foils in an Industrial Dry Room [Lara Dienemann](#), Anil Saigal and Michael A. Zimmerman; Tufts University, United States

Commercialization of energy-dense lithium metal batteries relies on stable and uniform plating and stripping on the lithium metal anode. In electrochemical-mechanical modeling of solid-state batteries, there is a lack of consideration of specific mechanical properties of battery-grade lithium metal. Defining these characteristics is crucial for understanding how lithium ions plate on the lithium metal anode, how plating and stripping affect

deformation of the anode and its interfacial material, and whether dendrites are suppressed. Recent experiments show that the dominant mode of deformation of lithium metal is creep. This study measures the time and temperature-dependent mechanics of two thicknesses of commercial lithium anodes inside an industrial dry room, where battery cells are manufactured at high volume. Furthermore, a directional study examines the anisotropic microstructure of 100 μm thick lithium anodes and its effect on bulk creep mechanics. It is shown that these lithium anodes undergo plastic creep as soon as a coin cell is manufactured at a pressure of 0.30 MPa, and achieving thinner lithium foils, a critical goal for solid-state lithium batteries, is correlated to anisotropy in both lithium's microstructure and mechanical properties.

4:15 PM EN02.07.06

Late News: Tracking Li Microstructure Growth in Solid-State Batteries with Lithium Anode Observed with Non-Invasive *In Situ* Three-Dimensional 7Li MRI Haoyu Liu¹, Po-Hsiu Chien¹, Ghoncheh Amouzandeh¹, Jens T. Rosenberg², Samuel C. Grant² and Yan-Yan Hu^{1,2}; ¹Florida State University, United States; ²National High Magnetic Field Lab, United States

Dendrite formation is one major cause of battery failure and associated safety hazards. The emergent solid-state batteries using lithium anodes remain victim to dendrite growth, which hinders its commercial viability. The mechanism of dendrite formation and propagation in solid electrolytes is largely different from that in liquid systems, yet the challenges in non-invasively and directly tracking the process in real-time leave the exact mechanism elusive. Herein, we demonstrate for the first time to track the kinetics of lithium dendrite growth at both the interface and bulk of different depths in Li/Li₇La₅Zr₂O₁₂ (LLZO)/Li solid cells using three-dimensional in-situ and ex-situ nuclear magnetic resonance imaging (MRI) non-invasively. We show that the accumulation of Li microstructure kicks off from the surface of LLZO before hard shorting the Li/LLZO/Li cell. More importantly, we identified Li evolution originated both from the interface and from the bulk LLZO electrolyte. The techniques developed and demonstrated herein can also be applied to other related fields in materials research.

4:30 PM EN02.07.07

Monolithically Printed All-Solid-State Lithium Metal Micro-Battery from Liquid Dispersions Ahmed Abdelaziz, Anthony S. Childress and Ahmed Busnaina; Northeastern university, United States

Recent demands for very small electronic devices generated a need for miniaturized energy-storage devices that can provide the power and energy needed for various applications such as wearable gadgets, medical devices and wireless sensor networks. Rechargeable micro-batteries have been investigated as a reliable route for achieving this target. However, in order to reach reliable performance of such micro-batteries while reducing the size and minimizing the fabrication cost, more sophisticated architectures need to be developed. Here, we introduce a novel approach to fabricate an all solid-state Li metal micro-battery based on directed fluidic assembly-based printing. This unique approach facilitated the assembly of all battery components including cathode, anode, and electrolyte at micro-scale dimensions, without the need of implementing costly fabrication techniques or utilizing complicated sacrificial templates as in the case of traditional micro-battery fabrication methods. Moreover, the porous cathode framework attained using this approach provided enough space for the polymer electrolyte to infiltrate the porous cathode leading to a cathode-supported electrolyte membrane. This drastically enhanced the battery performance through combining superior ionic transport and low interfacial resistance between the electrolyte and the cathode, as well as providing excellent electronic pathways through the cathode scaffoldings. Results shows that the as-printed LiFePO₄/Li solid state battery has an outstanding performance with discharge capacity of 157 mA h g⁻¹ at 0.1C, and a long-term cycling stability of 99.6% coulombic efficiency with a capacity retention of 89.5 % after 200 cycles. The EIS measurements also showed a lower interfacial resistance of the cathode-supported electrolyte micro-battery compared to its separated membrane counterpart. We believe that this unique approach will pave the way for mass production of high performance all solid-state micro batteries based on Li metal anodes as miniaturized energy devices.

4:45 PM EN02.07.08

Late News: Interrupted Anion Sublattice for Fast Li⁺-ion Conduction in Li₃PO₄-LiI Sawankumar V. Patel¹, Haoyu Liu¹, Erica Truong¹, Yan E. Wang², Lincoln Miara², Valentina Lacivita², Ryounghee Kim² and Yan-Yan Hu¹; ¹Florida State University, United States; ²Samsung Advanced Institute of Technology, United States

Rational design and synthesis of solid electrolytes using cost-effective precursors for fast ion conduction is an effective approach for producing solid electrolytes for mass production at a low-cost. In this study, we demonstrate how the ionic conductivity in a poor Li⁺-ion conductor-Li₃PO₄-can be tuned to a fast Li⁺-ion conductor by interrupting the PO₄³⁻ anion sublattice via diversifying the anion species. This is achieved by first introducing a highly polarizable I⁻ anion in the vicinity of PO₄³⁻ which results in a frustrated Li-anion interaction, thereby encouraging fast hopping around the interrupted anion framework. An ionic conductivity of 0.15 mS/cm at room temperature was achieved for the composition 1.4Li₃PO₄ - LiI, a 10¹⁰-fold enhancement compared with the ionic conductivity of Li₃PO₄, 10⁻¹⁴ mS/cm. Phase analysis from multinuclear solid-state NMR revealed a large fraction of amorphous phases Li_{3-y}PO₄I_y and Li₄PO₄I, in addition to the residual crystalline LiI and LiH₂O phases. The formation of Li_{3-y}PO₄I_y and Li₄PO₄I phases was determined to be the reason for achieving high Li⁺-ion conduction which was confirmed by AIMD. ⁷Li NMR relaxometry revealed fast-Li⁺-ion mobility because of the incorporation of iodide anions that resulted in the interruption of the PO₄³⁻ sublattice. ⁶Li tracer-exchange NMR showed Li₄PO₄I to be more conductive than the Li_{3-y}PO₄I_y. Overall, this study demonstrates that interruption of anion frameworks by introducing large polarizable anion in an amorphous matrix is powerful strategy to enhance Li⁺-ion conduction.

5:00 PM EN02.07.09

Late News: Unraveling the Enhanced Ion Dynamics and Structural Disorder in Li_{5.3}PS_{4.3}Cl_{1.7}-xBr_x Pengbo Wang¹, Sawankumar V. Patel¹, Haoyu Liu¹, Po-Hsiu Chien¹, Lina Gao¹, Xuyong Feng¹, Jue Liu² and Yan-Yan Hu¹; ¹Florida State University, United States; ²Oak Ridge National Laboratory, United States

Fast ion conductors with high conductivity and stability are key to realizing high-performance all-solid-state batteries for next-generation energy storage. Lithium argyrodites have demonstrated tunable conductivity via anion doping. However, Li deficiency and anion mixing coexist in previously studied halogen-doped argyrodite compounds, and both of them impact Li⁺ conduction.¹⁻³ To investigate the effects of anion mixing, we synthesized novel argyrodites Li_{5.3}PS_{4.3}Cl_{1.7-x}Br_x (0 ≤ x ≤ 1.7) with fixed Li content. The highest room-temperature conductivity around 26 mS/cm is achieved in Li_{5.3}PS_{4.3}Cl_{0.7}Br, with an exceptionally low activation energy of 0.16 eV for Li⁺ transport. To characterize the long- and short-range structural order and to discover the origin of fast Li⁺ conduction, X-ray diffraction and nuclear magnetic resonance are utilized. It shows that a diversified anion sublattice is formed via S/Cl/Br mixing at Wyckoff 4d sites. While the long-range structure is maintained, the introduction of Br⁻ in the structure displaces Cl⁻ to off-center positions from 4a/4d sites. The effects of the observed anion disorder on the mobility of Li⁺ and anions are investigated using NMR relaxometry. It reveals that Br⁻ incorporation slows down Li⁺ motion but increases PS₄³⁻ rotation, and overall leads to lower energy barriers for Li⁺ transport.

References:

1. Pengbo Wang, Haoyu Liu, Sawankumar Patel, Xuyong Feng, Po-Hsiu Chien, Yan Wang, and Yan-Yan Hu. Chemistry of Materials, 2020, 32, 9, 3833-3840.

2. Xuyong Feng, Po-Hsiu Chien, Yan Wang, Sawankumar Patel, Pengbo Wang, Haoyu Liu, Marcello Immediato-Scuotto, and Yan-Yan Hu. *Energy Storage Materials*, 30 (2020) 67–7368.

3. Sawankumar Patel, Swastika Banerjee, Haoyu Liu, Pengbo Wang, Po-Hsiu Chien, Xuyong Feng, Jue Liu, Shyue Ping Ong, Yan-Yan Hu. *Chemistry of Materials*, 2021, 33, 1435–1443.

SESSION EN02.08: Advanced Characterizations

Session Chair: Fudong Han

Thursday Morning, December 2, 2021

Hynes, Level 3, Ballroom C

10:30 AM *EN02.08.01

Multidimensional Diagnostics of Solid-State Lithium Batteries Yan Yao; University of Houston, United States

The complex origins of solid-state battery failure call for multidimensional diagnostics utilizing not one but a combination of tools that can quantify the void and dendrite formation, identify the chemical and mechanical natures of the Li dendrites and electrolyte decomposition products, and *in situ* monitor the evolution of the processes. However, there is lack of tools that connect multiple techniques with desirable length scale, resolution and sensitivity for characterizing solid-state batteries. The objective of this work is to develop an air-free vessel with an in-situ cell test platform connecting FIB-SEM tomography, ToF-SIMS, and in-SEM nanoindentation for structural, chemical, and mechanical characterizations of solid-state Li batteries. We fabricated solid-state thin-cells (less than 100 μm) and micro-cells with electrochemical performance on par with their bulk-type counterparts. Electrochemical tests with precise temperature control, external pressure, and pressure monitoring of thin solid-state cells were demonstrated with structural, chemical and mechanical characterizations. We hope the consolidated diagnostic platform presented here will allow us to effectively predict and optimize the physical and chemical changes of components within solid-state Li batteries during charge and discharge.

Acknowledgement: This work was supported by the U.S. Department of Energy's Office of Energy Efficiency and Renewable Energy (EERE) under the Vehicle Technologies Program under Contract DE-EE0008864.

11:00 AM EN02.08.03

Imaging Interfaces and Interphases in All-Solid-State Batteries at the Nanoscale Ece Deniz¹, Elliot J. Fuller², A. A. Talin² and Marina Leite¹; ¹University of California, Davis, United States; ²Sandia National Laboratories, United States

To date, a primary challenge for the further development of all-solid-state batteries is resolving and controlling the Li-ion distribution within their interfaces and interphases. Therefore, spatially determining where Li⁺ favorably accumulates upon device cycling can reveal how to mitigate the chemical reactions that lead to capacity fade. Here, we implement nanoscale-resolved secondary ion mass spectroscopy (SIMS) in an oxygen-free environment to elucidate the spatial distribution of Li⁺ ions in energy-storage devices composed by Si/LiPON/LiCoO₂ in a thin film configuration, an ideal model system with >90% capacity retention after 100 cycles and 98% of Coulombic efficiency. We acquire the ionic depth profile and 3D map of Li⁺ for both pristine and cycled devices, revealing a Li⁺ enrichment at the electrolyte layer upon cycling. This 3D tomography of Li⁺ spatial distribution indicates enrichment of Li⁺ at the LiPON electrolyte. As an independent technique to tomographical studies, we will also discuss the surface potential distribution in both in-plane and cross-section modes, from nanoscale maps acquired with environmental Kelvin-probe force microscopy (KPFM), performed under Ar and with no air exposure. Our KPFM measurements enable access to all relevant interfaces in full devices under various environmental conditions, such as temperature and humidity. The complementary imaging methods employed in our work represent a useful platform for screening Li-ions and can be extended to 3D designs and to other types of batteries, such as Na-ion devices.

SESSION EN02.09: Polymer and Composite Electrolytes

Session Chairs: Fudong Han and Wyatt Tenhaeff

Thursday Afternoon, December 2, 2021

Hynes, Level 3, Ballroom C

1:30 PM EN02.09.01

Wood-Derived Solid Electrolyte for Li-Metal Batteries—Atomic Structure and Fast Ion Transport Mechanism Qisheng Wu¹, Chunpeng Yang², Liangbing Hu² and Yue Qi¹; ¹Brown University, United States; ²University of Maryland, United States

Solid-state batteries with lithium metal anodes are attractive for next-generation energy-storage systems with high energy density and safety. But the realization of these promises largely depends on the development of superior ion conductors for the solid-state electrolyte as well as ion-conducting additives for the cathode materials. A research group led by Prof. Liangbing Hu at the University of Maryland, College Park demonstrated that molecule-engineered cellulose nanofibrils through the insertion of copper and lithium ions can be used as a high-performance solid polymer electrolyte that presents record-high ionic conductivity, wide electrochemical stability window, low activation energy, and scalability. The new system, namely Li-Cu-CNF, has the benefit of low cost since the main material sources are wood fibers. In addition, the one-dimensional structure of Li-Cu-CNF also makes it an effective ion-conducting binder for the cathode, and its effective ionic percolation allowed us to fabricate the thickest LiFePO₄ solid-state cathode ever reported, suggesting the material's potential for increasing battery energy density.

Despite the experimental discovery, the origin of the high Li-ion conductivity in the Li-Cu-CNF system remained a mystery. We have developed both quantum and atomistic models to uncover the accurate atomic structures of the Li-Cu-CNF system and the lithium-ion conduction mechanism therein. These understandings cannot be obtained by any currently available experimental techniques. We have unveiled the atomic structures of Li-Cu-CNF very quickly with input from experiments. Through comprehensive density functional theory calculations, classical molecular dynamics simulations, and x-ray absorption spectroscopy modeling, we clearly showed how copper ions connect the cellulose chains and open the channels, which are preconditions for insertion and effective transport of lithium ions in Li-Cu-CNF. More than that, we have proposed that the abundant oxygen-containing functional groups and bound water in the cellulose molecular channels lead to a lithium-ion hopping mechanism that is decoupled from the polymer segmental motion, which is the most fundamental reason that Li-Cu-CNF can deliver the highest lithium-ion conductivity among all the solid polymer electrolytes ever reported

during the last four decades. Using molecular dynamics simulations, we have pointed out that the conduction mechanism can also be generalized to cellulose-based sodium-ion and potassium-ion batteries.

Reference:

[1] Chunpeng Yang, # **Qisheng Wu**, # Weiqi Xie, #, ..., **Yue Qi**,* Liangbing Hu,*. *Nature*, in press. (#Equal contribution; *Corresponding authors)

1:45 PM EN02.09.02

Li-Salt Doped Single-Ion Conducting Polymer Electrolytes **Laura C. Loaiza**¹ and Patrik Johansson^{1,2}; ¹Chalmers University of Technology, Sweden; ²Alistore-ERI (CNRS FR 3104), France

Traditional solid polymer electrolytes (SPEs) aiming at lithium battery application are made by simply dissolving a Li-salt in a suitable polymer matrix, rendering both Li⁺ cations and anions mobile. As a result, since most of the lithium batteries chemistries involve the intercalation/deintercalation of the Li⁺ cation, concentration gradients and cell polarization develop, causing premature cell failures. Another polymer electrolyte design is to graft the anion onto the polymer backbone, whereby single-ion conductors (SICs) with the Li⁺ cation as the sole mobile species can be created. SICs both provide the safety, the mechanical stability, and the flexibility of SPEs, and circumvent the problematic issues connected with cycling, but their ionic conductivities remain low at room temperature, due to the rigidity of the polymer matrix and the dense electrostatic interactions from the attached ionic group.^{1,2} Herein we suggest and explore an intermediate and synergetic design; by using a SIC, LiPSTFSI (poly[(4-styrenesulfonyl) (trifluoromethanesulfonyl) imide]), doped with the LiTFSI salt. The aim is to improve the ion transport mechanism by both increasing the Li⁺ concentration and the flexibility of the polymer matrix – as TFSI is a plasticizing anion.^{3,4}

We have explored different doping degrees, from 1 to 90 wt%, and how they induce changes in the glass transition temperatures, the mechanical properties, and the charge carrier speciation. With a rather high doping degree, 50-70 wt% LiTFSI, we find considerable improvements in the Li⁺ dynamics and the ionic conductivity. A deeper analysis of the conduction mechanism reveals an Arrhenius behavior, with possibilities for strong trade-offs/synergies between ion transport by hopping between ionic clusters, a different speciation, an increased charge carrier concentration, and an increased free volume.

1. H. Zhang, C. Li, M. Piszcz, E. Coya, T. Rojo, L. M. Rodriguez-Martinez, M. Armand and Z. Zhou. *Chem. Soc. Rev.* **46** (3), 797–815 (2017).
2. J. Liu, P. D. Pickett, B. Park, S. P. Upadhyay, S. V. Orski and J. L. Schaefer. *Polym. Chem.* **11** (2), 461–471 (2020).
3. S. Sylla, J. Y. Sanchez and M. Armand. *Electrochim. Acta* **37** (9), 1699–1701 (1992).
4. Q. Ma, Y. Xia, W. Feng, J. Nie, Y. S. Hu, H. Li, X. Huang, L. Chen, M. Armand and Z. Zhou. *RSC Adv.* **6** (39), 32454–32461 (2016).

2:00 PM EN02.09.03

Polyborane-Based Electrolytes for Solid-State, Lithium-Ion Batteries **Fernando Villafuerte**, William Wolf, Jeongmin Kim, Quan Gan, Stephen Munoz, Julia R. Greer, Robert H. Grubbs, Thomas F. Miller, III and Simon C. Jones; California Institute of Technology, United States

Lithium-ion batteries (LIBs) are the primary candidates for advancing energy storage needs, but their function is hampered by the liquid, organic-solvent-based electrolytes that shuttle lithium cations between electrodes during charging and discharging. These electrolytes, e.g. LiPF₆ in EC:DEC, can combust if a battery's operating constraints are exceeded. Solid polymer electrolytes (SPEs) offer a promising alternative: they are more thermodynamically stable than their liquid counterparts, and are stable when in contact with Li metal, which could substantially increase a battery's capacity. Polyethylene oxide (PEO), noted for its ability to dissolve lithium salts and conduct lithium ions, has been the focus of SPE research since the 70's. Its primary drawback is the strong coordination of Li⁺ relative to loosely coordinated anions, which translates into a low cationic transference number. In addition, ionic conduction occurs only in amorphous domains of the bulk polymer matrix, which renders ionic conductivity suboptimal at ambient conditions, approaching the benchmark of 10⁻³ S/cm only at 80°C.

The persistent issues with PEO and PEO-based architectures are low ionic conductivity and transference number. Recent computational work by Savoie et al.¹ suggests that using Lewis-acidic boron moieties in the polymer backbone, as opposed to the Lewis-basic ether oxygen, can invert the solvation mechanism and increase Li⁺ cation mobility relative to that of the anion. It has been experimentally demonstrated that including boron-containing moieties in polymer electrolyte materials provides an anion trapping site which improves Li⁺ transference.^{2,3}

We present the synthesis of a novel, single-ion conducting, polymer electrolyte and its preliminary electrochemical and material characterization. The electrolyte is accessible through the modification of a simple and abundant polyolefin, polybutadiene, by the introduction of dialkylborane moieties to the backbone through hydroboration. We create an ionically conductive polymer film by first drop casting the synthesized polyborane onto stainless steel discs, and then adding butyllithium to it. This electrolyte exhibits geometry-normalized conductivities approaching 10⁻⁷ S/cm at 50°C. Further electrochemical and material characterization, in addition to molecular dynamics simulations, provide insight into the mechanism of ionic conduction in these polymer films and allow for further optimization.

1. Savoie, B. M., Webb, M. A. & Miller, T. F. Enhancing Cation Diffusion and Suppressing Anion Diffusion via Lewis-Acidic Polymer Electrolytes. *J. Phys. Chem. Lett.* **8**, 641–646 (2017).
2. Matsumi, N., Sugai, K. & Ohno, H. Ion conductive characteristics of alkylborane type and boric ester type polymer electrolytes derived from mesitylborane. *Macromolecules* **36**, 2321–2326 (2003).
3. Mizumo, T., Sakamoto, K., Matsumi, N. & Ohno, H. Simple introduction of anion trapping site to polymer electrolytes through dehydrocoupling or hydroboration reaction using 9-borabicyclo[3.3.1]nonane. *Electrochim. Acta* **50**, 3928–3933 (2005).

2:15 PM EN02.09.04

Structural Investigation of LAGP/PEO Composite for Solid-State Batteries Using Vibrational and Nuclear Magnetic Resonance Spectroscopies L. J. Deiner¹, Kalle Levon², **David Clarkson**^{3,4}, Mounesha Garaga³ and Steven G. Greenbaum^{3,4}; ¹NYC College of Technology, United States; ²NYU Tandon School of Engineering, United States; ³Hunter College-CUNY, United States; ⁴CUNY Graduate Center, United States

Solid state lithium ion batteries have the potential to meet increasingly stringent safety and power density requirements in the transportation and consumer electronics sectors. Realizing the promise of solid state lithium ion batteries will require development of composite solid electrolytes that combine the compliance and processability of polymers with the ruggedness, temperature flexibility, and ionic conductivity of ceramics. In this work, we present a simple one-pot method for preparation of a high inorganics composite comprised of lithium aluminum germanium phosphate (LAGP) and polyethylene oxide (PEO). This is the first step toward development of composite materials more readily compatible with a broad range of battery fabrication techniques. Fourier transform infrared (FTIR) analysis of the polymer/ceramic product shows perturbations in the P-O stretching region (800 cm⁻¹ to 1250 cm⁻¹) of the LAGP spectrum, consistent with specific surface interaction between the LAGP and the PEO. Solid state multinuclear magnetic resonance (⁷Li, ²⁷Al, ³¹P), which is sensitive to even small changes in short-range structure of the bulk phase, reveals little difference between LAGP and the LAGP/PEO composite, suggesting that the polymer-ceramic interaction is confined to a thin surface region. Results obtained for other composite

preparation schemes, including shear vs. impact milling and pre-treatment activation of the LAGP surface will be presented.

2:30 PM EN02.09.05

Safety Impacts of Liquid Electrolyte Inclusion in Solid State Batteries Alex Bates¹, Yuliya Preger¹, Loraine Torres Castro¹, Katharine L. Harrison¹, Stephen J. Harris² and John Hewson¹; ¹Sandia National Laboratories, United States; ²Lawrence Berkeley National Laboratory, United States

Solid-state battery (SSB) technology is racing toward commercialization due to its perceived inherent safety and high energy density, both key metrics for the electric vehicle market. To that end, high interfacial resistance between solid electrolyte (SE) and cathode is a critical challenge that must be overcome. The addition of liquid electrolyte (LE) at the SE and cathode interface has been shown to substantially reduce interfacial resistance. However, the inclusion of LE has also led to safety concerns and an emphasis on all-solid-state batteries (ASSBs). In this presentation we quantify the potential thermal consequences of various failure modes, to inform the safety-performance trade-off associated with the potential inclusion of LE in SSBs.

Thermodynamic modeling of a SSB allowing for addition of LE will be presented for the first time, alongside analysis of an ASSB and Li-ion battery (LIB). Three failure scenarios were considered; thermal runaway from external heating, internal short circuit, and catastrophic mechanical failure of the SE. Thermal runaway from external heating included cathode decomposition, LE reaction with the resulting O₂, and LE reaction with the lithiated anode. Internal short circuit considered the complete conversion of stored electrochemical energy to heat, without other reactions. Catastrophic mechanical failure allowed for thermal runaway combined with cathode-generated O₂ reacting with the Li anode through a broken SE. The volume of LE in SSB and LIB was varied, and the resulting potential heat release compared. Heat release and potential temperature rise was analyzed for different ASSB, SSB, and LIB formats of increasing energy density. The results show that the addition of small quantities of LE at the cathode in SSBs has modest safety consequences and may be a relevant pathway to commercialization. For small quantities of LE, the potential temperature rise of the typical thermal runaway reactions are small relative to the release of stored energy, highlighting the importance of the overall energy density in assessing safety. The results allow safety concerns to be integrated with interfacial resistance performance challenges to better inform SSB designs.

Sandia National Laboratories is a multimission laboratory managed and operated by National Technology and Engineering Solutions of Sandia LLC, a wholly owned subsidiary of Honeywell International Inc. for the U.S. Department of Energy's National Nuclear Security Administration under contract DE-NA0003525.

2:45 PM BREAK

SESSION EN02.10: Cell Architecture and Fabrication I

Session Chair: Fudong Han

Thursday Afternoon, December 2, 2021

Hynes, Level 3, Ballroom C

4:00 PM EN02.10.01

Low Temperature Preparation of Thin-Film Lithium Battery Cathodes Wyatt E. Tenhaeff, Zhuo Li and Fei Hu; University of Rochester, United States

Solid-state lithium thin-film batteries (TFBs) offer exceptional energy storage performance with high energy density, long cycle life, and enhanced safety. Fabrication of thin film cathodes typically involves high temperature depositions or a thermal annealing step to crystallize the thin film cathodes into the desired crystallographic phases. For example, state-of-the-art sputter deposited LiCoO₂ (LCO) must be annealed at >500°C to achieve a maximum charge storage capacity of 67 μAh cm⁻² μm⁻¹ (equivalent to 135 mAh g⁻¹). These high temperatures place significant constraints on the materials of construction and processing of solid-state thin film batteries. In this talk, our efforts to develop low temperature cathode fabrication approaches to mitigate these constraints and expand the potential applications of thin film batteries will be discussed.

The first project utilizes polymeric charge-transfer complexes. These complexes are formed through vapor phase infiltration of I₂ or ICl into poly(4-vinylpyridine) (P4VP) films prepared by initiated chemical vapor deposition (iCVD). iCVD enables room-temperature synthesis of well-defined films directly on the surface of Pt current collectors. After infiltration with I₂ or ICl, the cathodes are coated nominally with 1 mm of lithium phosphorous oxynitride (LiPON) electrolyte and an evaporated Li metal anode. Discharging at 70°C, the P4VP-I₂ and P4VP-ICl deliver capacities of 8.7 and 36.2 μAh cm⁻² μm⁻¹, respectively, with an average voltage of 2.2V and 3.15V. The cathodes appear to be irreversible under normal operating conditions, limiting their application to primary electrochemical cells. However, it has been shown that these cathodes are readily prepared on flexible, temperature sensitive substrates, as well as complex, three dimensional architectures, which should allow them to be readily integrated into wearable, low cost devices and enable additional energy-intensive applications.

In the second project, a class of lithium metal oxide cathode materials are prepared by RF magnetron sputtering and incorporated into solid state thin film batteries consisting of LiPON electrolyte and Li metal anode. Charged to 4V vs. Li/Li⁺, specific capacities in excess of 110 mAh cm⁻² mm⁻¹ have been achieved, which is 64% larger than state-of-the-art LCO cathodes. When cycled at a rate of 0.6C (100 minutes for charge/discharge), 83% of the maximum capacity is retained. Moreover, the cathodes are highly reversible with coulombic efficiencies in excess of 99.8%, resulting in greater than 94.7% capacity retention over 100 galvanostatic charge/discharge cycles. Efforts to further enhance rate performance and cycle lives will be discussed, in addition to demonstrations of these cathodes on flexible, polymeric (temperature sensitive) substrates.

4:15 PM EN02.10.02

Facile Solution Synthesis of Lithium Thiophosphate Solid Electrolyte with High Room-Temperature Ionic Conductivity Daiwei Wang, Li-Ji Jhang and Donghai Wang; The Pennsylvania State University, United States

All-solid-state lithium battery technology is one of the most promising candidates for next-generation batteries due to the high energy density, long cycle life and superior safety. To realize the technology in practical application, solid electrolyte (SE) is the key. The family of thiophosphate SEs is receiving much attention due to the high ionic conductivity at room temperature (> 1 mS cm⁻¹) which could even exceed conventional liquid electrolytes. However, most of the thiophosphate SEs were prepared through solid-state-reaction route by high-energy ball milling and post high-temperature treatment at above 300 °C which is energy consuming and not suitable for large-scale production. Here, we will demonstrate the synthesis of argyrodite-type SEs through facile solution-based method with low annealing temperature below 200 °C. The synthesized SE demonstrated a high ionic conductivity of ~ 4.01 mS cm⁻¹

¹ at room temperature and superior stability against lithium metal anode. At room temperature, Li|SE|Li symmetric cell demonstrated a high critical current density of 1 mA cm⁻² and low areal interfacial resistance of 6 ~ 7 Ω cm². The demonstration of the synthesis of argyrodite-type SEs extend the family of solution-synthesized sulfide-based SEs.

SESSION EN02.11: Solid Electrolytes II
Session Chairs: Javier Carrasco and Montserrat Casas-Cabanas
Monday Morning, December 6, 2021
EN02-Virtual

10:30 AM *EN02.11.01

Prediction of the Electrochemical Stability and Reaction Mechanisms of Solid-State Electrolytes Marnix Wagemaker, Tammo K. Schwietert and Alexandros Vasileiadis; Delft Univ of Technology, Netherlands

Solid-state batteries have significant advantages over conventional liquid batteries, providing improved safety, design freedom, and potentially reaching higher power and energy densities. One of the major obstacle in the commercial realization of solid-state batteries is the high resistance at the interfaces. Essential for overcoming this bottleneck is to achieve in-depth fundamental understanding of the crucial electrochemical processes at the interface. Conventional electrochemical stability calculations for solid electrolytes, determining the formation energy towards the energetically favourable decomposition products, often underestimate the stability window because kinetics are not included. Here we discuss a computational scheme that takes the redox-activity of the solid electrolytes into account in calculating the electrochemical stability, which in many cases appears to dictate decomposition route and thus the electrochemical stability. This methodology is applied to different chemical and structural classes of solid electrolytes, exhibiting good agreement with experimentally observed electrochemical stability. Several examples will be discussed, and compared to experimental observations. These results suggest that the electrochemical stability of solid electrolytes is not always determined by the stability of the decomposition products but often originates from the intrinsic stability of the material itself. The processes occurring outside the stability window can lead towards phase separation or solid-solution depending on the reaction mechanism of the material. These newly gained insights provide better predictions of the practical voltage ranges and structural stabilities of solid electrolytes, which may be valuable for material and interface design of solid-state batteries.

11:00 AM *EN02.11.02

How Disorder and Particle Size Affects Solid Ionic Conduction and Solid-State Batteries Wolfgang Zeier; University of Muenster, Germany

The advent of solid-state batteries has spawned a recent increase in interest in lithium conducting solid electrolytes, especially in the lithium thiophosphates. However, many open questions remain when trying to optimize electrolytes and understand solid state battery chemistries.

In this presentation, we will show how an understanding of the structure-transport properties of the lithium argyrodites Li₆PS₅X can help tailor the ionic conductivity. We show that an anion site-disorder and anionic charge inhomogeneities are important and that tailoring dis disorder leads to improvements of the conductivity.

Further, we will show that it is not only important to find fast ionic conductors, but that fast ionic conduction is paramount within solid state battery composites. Measuring the effective ionic transport in cathode composites provides an avenue to explore transport and stability limitations that in turn provide better criteria for solid state battery performance.

Lastly, we will show how tailoring particle size distributions can help create solid-state battery cells with conversion-type active materials.

11:30 AM EN02.11.03

Exploring Aliovalent Substitutions in the Lithium Halide Superionic Conductor Li_{3-x}In_{1-x}Zr_xCl₆ (0 ≤ x ≤ 0.5) Bianca Helm¹, Roman Schlem¹, Bjoern Wankmiller¹, Ananya Banik¹, Ajay Gautam², Justine Ruhl², Cheng Li³, Michael R. Hansen¹ and Wolfgang Zeier¹; ¹University of Muenster, Germany; ²Justus-Liebig-Universität Giessen, Germany; ³Oak Ridge National Laboratory, United States

Solid-state batteries enable safer energy storage than common liquid ion batteries due to the use of a solid electrolyte. To compete with liquid ion batteries the solid electrolytes need to be structurally tailored to provide comparable conductivities.^[1,2] In recent years, the ternary halides Li₃MX₆ (M = Y, Er, In; X = Cl, Br, I) have garnered the interest of researchers due to their high ionic conductivities. Iso- or aliovalent substitutions within this material class are scarce preventing a deeper understanding of structure-property relationships. In this work, we investigate the impact of Zr substitution on the structure and ionic conductivity of Li₃InCl₆ (Li_{3-x}In_{1-x}Zr_xCl₆ with 0 ≤ x ≤ 0.5) using a combination of neutron diffraction, nuclear magnetic resonance and impedance spectroscopy. Analysis of high-resolution neutron diffraction data suggests a cation site-disorder and a tetrahedrally coordinated Li⁺ site, which has not been reported in Li₃InCl₆ yet. In combination, all here-found Li⁺ positions form a three-dimensional polyhedral network enabling 3D diffusion. The Zr⁴⁺ substitution in Li₃InCl₆ induces non-uniform volume changes and increases the number of vacancies in the structure, all of which lead to an increasing ionic conductivity in this series of solid solutions. This investigation highlights the importance of understanding the solid electrolyte structure-property relationships to further improve not just the materials themselves but also for the utilization in solid-state batteries.

References.

- (1) Ohno S., Rosenbach C., Dewald G.F., Janek J., Zeier W.G. "Linking Solid Electrolyte Degradation to Charge Carrier Transport in the Thiophosphate-Based Composite Cathode toward Solid-State Lithium-Sulfur Batteries" *Adv. Funct. Mater.* 2021, 31, 2010620.
- (2) Ohno S., Koerver R., Dewald G., Rosenbach C., Titscher P., Steckermeier D., Kwade A., Janek J., Zeier W.G., "Observation of chemo-mechanical failure and influence of cut-off potentials in all-solid-state Li-S batteries" *Chem. Mater.* 2019, 31, 2930-2940.
- (3) Helm B., Schlem R., Wankmiller B., Banik A., Gautam A., Ruhl J., Li C., Hansen M.R., Zeier W.G. "Exploring Aliovalent Substitutions in the Lithium Halide Superionic Conductor Li_{3-x}In_{1-x}Zr_xCl₆ (0 < x < 0.5)" *Chem Mater.* 2021. doi.org/10.1021/acs.chemmater.1c01348.

11:45 AM EN02.11.04

Consequences of Br/S Site-Exchange on the Properties of Li₆PS₅Br Argyrodites Marcel Sadowski and Karsten Albe; Technical University of Darmstadt, Germany

Li₆PS₅Br argyrodites have been identified as promising solid electrolytes due to high ionic conductivities. Although it is known that the material can be

synthesized with anion site-disorder among Br and S the exact effect on its properties has not been clear so far. In line with experimental investigations we show in this contribution how systematic density functional theory calculations have been applied to understand the intricate interplay between the underlying Br/S site-exchange and the materials properties.

The lattice constant of Li₆PSSBr was found to depend on the degree of Br/S site-exchange and shows a minimum at 50% site-exchange. Also energetically a relationship is found and the most stable structures are obtained for the ordered material, i.e., at 0% site-exchange. At 50% the least stable structures are found and the energy difference amounts to 125 meV/f.u. on average. The assessment of the configurational entropy due to Br/S site-exchange itself and the vibrational entropy cannot explain the experimentally observed dependence between temperature and equilibrium site-exchange. We therefore conclude that a substantial part of the entropy needs to stem from the highly mobile Li ions.

Indeed, the Br/S site-exchange is key for favorable transport properties of Li₆PSSBr. In the absence of any site-exchange only local Li motion within Li "cages" around the S ions is observed. Even at 700 K such intracage jumps dominate the simulations. Temperatures of 800 K or higher are needed to initiate intercage jumps that are needed for true long range transport within reasonable simulation times. The introduction of Br/S site-exchange changes the situation drastically: At 50% site-exchange long-range transport is observed already at 500 K. In order to understand the diffusion mechanism we analyzed the individual anion exchanges. According to our simulations the main reason for improved transport properties is due to Br ions on S sites. These defects mainly cause for the generation of Li Frenkel pairs whose interstitial is rather mobile and travels among the neighboring Li cages via interstitial and interstitialcy mechanisms. The Li vacancy, on the other hand, seems to be strongly bound to the anion defect.

At last we focused on grain boundaries in Li₆PSSBr. Admittedly, their resistances to the ionic conductivity seem to be of little concern experimentally but the reasons for this circumstance have not been elucidated, yet. To this end we prepared simple tilt and twist grain boundaries and analyzed their influence on the Li diffusion. We find that again the Br/S site-exchange plays a delicate role in this context: At 0% site-exchange grain boundaries seem to improve the transport properties because they locally disrupt the strict cage ordering. At 50%, however, Li transport is slightly deteriorated compared to the bulk phase.

12:00 PM EN02.11.05

Structure-Composition-Conductivity Relationships of Glass-Ceramic Lithium Thiophosphates Electrolytes [Haoyue Guo](#), Qian Wang, Alexander Urban and Nongnuch Artrith; Columbia University, United States

Lithium thiophosphates (LPS), with the general composition (Li₂S)_x(P₂S₅)_{1-x}, are one of the most promising classes of prospective electrolyte materials in solid-state batteries (SSBs), owing to their superionic conductivity at room temperature ($>10^{-3}$ S cm⁻¹), soft mechanical properties, and low grain boundary resistance. So far, several glass-ceramic (*gc*) LPS compositions have been synthesized and characterized experimentally. The ionic conductivity of the *gc*-LPS materials is significantly influenced by the glassy phases, and the relationship between structures and conductivity remains unclear due to the limitation of experimental techniques in characterizing amorphous phases. To resolve the atomic structures of *gc*-LPS with varying compositions, we mapped the phase diagram by integrating density functional theory (DFT), artificial neural network (ANN) potentials as implemented in the atomic energy network package (anet), genetic-algorithm (GA) sampling, and *ab initio* molecular dynamics (AIMD) simulations. The thermodynamic stability and ionic conductivity of glassy/ceramic phases was correlated with the local structural motifs in the known LPS crystal structures. Structure-composition-conductivity relationships of *gc*-LPS were demonstrated. With machine learning accelerated sampling and AIMD simulations, a candidate solid-state electrolyte composition with high ionic conductivity ($>10^{-2}$ S cm⁻¹) was identified, which could provide a design strategy for optimized LPS materials with enhanced conductivity and stability.

References

[1] Haoyue Guo, Qian Wang, Alexander Urban, Nongnuch Artrith. "Structure-Composition-Conductivity Relationships of Glass-Ceramic Lithium Thiophosphates Electrolytes." in preparation.

12:15 PM EN02.11.06

Exploring the Synthesis of Alkali-Metal Anti-Perovskites [Kwangnam Kim](#)^{1,2}, Yiliang Li³, Ping-Chun Tsai^{3,4}, Fei Wang³, Seoung-Bum Son⁵, Yet-Ming Chiang³ and Donald Siegel¹; ¹University of Michigan, United States; ²Lawrence Livermore National Laboratory, United States; ³Massachusetts Institute of Technology, United States; ⁴National Taiwan University of Science and Technology, Taiwan; ⁵Argonne National Laboratory, United States

The development of solid-state batteries has been slowed by limited understanding of the features that control ion mobility in solid electrolytes (SE). In the case of anti-perovskite (AP) SE, lattice distortions have been proposed as one such controlling factor: APs that exhibit distortions of the octahedral building blocks are predicted to exhibit enhanced ionic mobility. Nevertheless, large distortions come at a cost to stability, implying a tradeoff between stability and ionic mobility. The present study combines theory and experiments to explore the synthesizability of several marginally-stable APs predicted to exhibit high mobility for Li⁺, Na⁺, and K⁺. Density functional theory calculations, in combination with the quasi-harmonic approximation, were used to predict the free energy change, $\Delta G_f(T)$, for synthesis reactions involving 36 alkali-metal-based APs, X₃AZ (X = Li, Na, or K; A = O, S, or Se; Z = F, Cl, Br, or I). A linear correlation is observed between the degree of lattice distortion and the stabilization temperature, at which $\Delta G_f(T) = 0$. Hence, APs with the highest ionic mobility generally require the highest synthesis temperatures. These data were used to guide experimental synthesis efforts of APs by estimating the temperatures above which a given AP is expected to be thermodynamically stable. Attempts were made to synthesize several AP compositions; overall, good agreement is obtained with the computational predictions. These data suggest that a compound's zero Kelvin decomposition energy is an efficient descriptor for predicting the ease and likelihood of synthesizing new SEs.

SESSION EN02.12: Solid Electrolytes III
Session Chairs: Montserrat Casas-Cabanas and Yuyan Shao
Monday Afternoon, December 6, 2021
EN02-Virtual

1:00 PM *EN02.12.01

Halide-Based Solid-State Batteries—Electrolyte, Stability, Interface and Electrode [Xueliang A. Sun](#); University of Western Ontario, Canada

All-state-state lithium batteries (ASSLBs) have gained worldwide attention because of intrinsic safety and increased energy density. Compared with other types of solid-state electrolytes including oxide-based, polymer-based and sulfide-based electrolytes, recently-developed halide-based solid-state electrolytes (SSEs) have garnered considerable attention for all-solid-state lithium batteries (ASSLBs) due to the high ionic conductivity, high oxidation voltage and good stability toward oxide cathode materials [1]. However, there are still many challenges in halide-based solid-state electrolytes for ASSLBs including controllable and mass-production synthesis, achieving high humidity tolerance and demonstrate high-performance of ASSLBs; in particular,

increased understanding of mechanisms during synthesis and tuning their properties of the electrolytes as well as interface with electrode materials[1].

In this talk, (i) I will demonstrate synthesis strategy [2-3], in particular, new and salable water-mediated synthesis method [2]. (ii) I will report a systematic study on the correlations among structural evolution, Li^+ migration properties, and humidity stability resulting of the halide-based electrolytes, along with in-situ characterization for understanding of the mechanisms [4]. (iii) Full cell battery performance will be optimized [5], and (iv) humidity ability [6]. In the end, energy densities of ASSLBs using different solid-state electrolytes in ASSLBs will be discussed [7].

References:

- X. Li, J. Liang, X. Yang, K. Adair, C. Wang, F. Zhao, X. Sun. Progress and Perspectives of Halide-based Lithium Conductors for All-Solid-State Batteries. **Energy Environ. Sci.**, 13, 1429-1461 (2020).
- X. Li, J. Liang, X. Sun, et al., H₂O-Mediated Synthesis of Superionic Halide Solid Electrolyte. **Angewandte Chemie International Edition**, 58, 16427-16432 (2019).
- X. Li, J. Liang, X. Sun, et al., Air-Stable Li₃InCl₆ Electrolyte with High Voltage Compatibility for All-Solid-State Batteries. **Energy Environ. Sci.**, 12, 2665 - 267 (2019).
- X. Li, J. Liang, X. Sun, et al., Origin of Superionic Halide Solid Electrolytes with High Humidity Tolerance, **J. Am. Chem. Soc.** 142, 7012-7022 (2020).
- C. Wang, X. Li, J. Liang, X. Sun, et al., Eliminating Interfacial Resistance in All-Inorganic Batteries by In-situ Interfacial Growth of Halide-based Electrolyte. **Nano Energy**, 2020, in press.
- X. Li, J. Liang, X. Sun, et al., Origin of Superionic Li₃Y_{1-x}In_xCl₆ Halide Solid Electrolytes with High Humidity Tolerance, **Nano Letters**, 20, 6, 4384-4392 (2020).
- J. Liang, X. Li, K. Adair, X. Sun, Metal Halide Superionic Conductor for All-Solid-State Batteries, **Acc. Chem. Res.** 54, 1023-1033(2021).

1:30 PM EN02.12.03

Development of PEO-Based Polymer-In-Salt Electrolytes for High-Voltage Lithium Metal Batteries Haiping Wu, Peiyuan Gao, Hao Jia, Ji-Guang Zhang and Wu Xu; Pacific Northwest National Laboratory, United States

Rechargeable lithium (Li) metal batteries are regarded as the next-generation power sources due to their high energy density that can potentially reach 500 Wh kg⁻¹ at cell level. The success of high energy-density Li metal batteries largely depends on the development of electrolytes because the electrolyte should be chemically and electrochemically stable on both Li metal anode and high-voltage cathode, suppress the growth of mossy/dendritic Li morphology and prevent the penetration of Li dendrites. Currently, the liquid electrolytes have achieved much progress, reaching a high Li Coulombic efficiency (CE) about 99.5% and a high voltage stability up to 4.5 V. However, the Li CE is still not high enough to ensure the long cycle life and the mossy/dendritic Li formation during repeated cycling would cause safety concerns. The solid-state inorganic electrolytes face more challenges, in either low ionic conductivity, high interfacial resistance with electrodes, poor stability with Li metal or high voltage cathode, unable to prevent Li penetration, or low mechanical strength, etc. The third approach is to use polymer or polymer composite electrolytes, which may mitigate the above issues related to liquid electrolytes and solid-state inorganic electrolytes. Polyethylene oxide (PEO) is the most widely studied polymer in polymer electrolytes and batteries. However, the conventional PEO-based electrolytes have low room-temperature ionic conductivity and low oxidative stability (< 4 V vs. Li/Li⁺), thus their applications must be set at high temperatures and limited to 4 V-class cathode materials, resulting in a low energy density of the batteries. Therefore, to develop high-voltage PEO-based electrolytes for Li metal batteries is of high significance. In this talk, we will report the efforts at PNNL to develop PEO-based polymer-in-salt electrolytes that are stable up to 4.3 V. More details will be discussed during the presentation at the meeting.

1:45 PM EN02.12.04

Ionic Conductivity Transitions in Sodium Antiperovskite Ionic Conductors Yiliang Li¹, Ping-Chun Tsai¹, Fei Wang¹, Sunil Mair¹, Duhan Zhang¹, Liang Yin², Saul Lapidus² and Yet-Ming Chiang¹; ¹Massachusetts Institute of Technology, United States; ²Argonne National Laboratory, United States

Anti-perovskites materials have recently attracted great interest as a family of solid state electrolytes with high ionic conduction.[1] Typical solid-state ionic conductors have temperature-dependent ionic conductivity following Arrhenius behavior over a substantial range of temperature, corresponding to a constant activation energy E_a . In the Na₃OCl antiperovskite, there are regimes of Arrhenius behavior separated by broad transitions, all while the structure remains cubic. Such non-Arrhenius ionic conductivity of Na₃OCl has been observed in previous literature. [2][3] However, there is no clear explanation for this non-Arrhenius transition. Differential scanning calorimetry shows thermal transitions in the vicinity of these conductivity transitions. Reitveld refinement on temperature dependent synchrotron XRD of Na₃OCl suggests changes in the B_{eq} and anisotropic U_{33} of Na around 305°C, which is consistent with the conductivity jump temperature. Meanwhile, the octahedral tilts observed at low temperature becomes much less above the transition temperature. We explain this as the activation of octahedra fluctuation[1] above the transition temperature as the time-averaged synchrotron fitted structure becomes closer to cubics. In this work, we use multiple temperature-resolved characterization methods including synchrotron XRD, transport measurements, and calorimetry, and modeling by AIMD and DFT, to understand this behavior and to gain insight into tuning antiperovskites for high ionic conductivity.

This work was supported as part of the Joint Center for Energy Storage Research, an Energy Innovation Hub funded by the U.S. Department of Energy, Office of Science, Basic Energy Sciences.

References:

1. Kim, K., & Siegel, D. J. (2019). Correlating lattice distortions, ion migration barriers, and stability in solid electrolytes. *Journal of materials chemistry A*, 7(7), 3216-3227.
2. Ahiavi, Ernest, et al. "Mechanochemical synthesis and ion transport properties of Na₃OX (X= Cl, Br, I and BH₄) antiperovskite solid electrolytes." *Journal of Power Sources* 471 (2020): 228489.
3. Wang, Yonggang, et al. "Structural manipulation approaches towards enhanced sodium ionic conductivity in Na-rich antiperovskites." *Journal of Power Sources* 293 (2015): 735-740.

2:00 PM EN02.12.05

Visualizing the Morphology Variation of CuS-Based SSBs by 3D Tomography Katherine A. Mazzio^{1,2}, Zhenggang Zhang², Kang Dong¹, Ingo Manke¹ and Philipp Adelhelm^{2,1}; ¹Helmholtz-Zentrum Berlin, Germany; ²Humboldt-Universität zu Berlin, Germany

Solid state batteries (SSBs), especially those utilizing conversion-type active materials (C-AMs), are one of the most promising future energy storage devices.¹ However, the volume variation of C-AMs upon electrochemical cycling are a great challenge for the mechanical stability of SSBs. The periodic volume variation is known to deteriorate the physical contact between the AMs and solid electrolytes (SEs), and emphasizes the necessity of achieving robust mechanical properties.² Although considerable progress already made by choice of materials, modulation of their interfaces, or even adopting new

battery concepts,³ there is still a long way to go in order to realize practical SSBs.

Obtaining a better understanding of SSBs is highly desirable, but appropriate methods are often limited by their shallow penetration depth alongside design aspects of the cells. Compared with other technologies, 3D tomography is able to penetrate solid-state samples and detect details of the bulk by virtue of utilizing high energy X-Rays, making 3D tomography a powerful technology for visualizing SSBs during operation.⁴ CuS is a well-studied conversion material with high electronic and ionic conductivity that exhibits a volume expansion of 75% after being fully lithiated. It also shows good cycling stability and is known to react with lithium in a manner that produces a macro-scale displacement of Cu in SSBs.⁵ While known to occur in standard cells, this type of displacement reaction in metal sulfides has not yet been studied in SSBs.

Herein, a model SSB with Li/ β -Li₃PS₄/μm-CuS structure was investigated by 3D tomography to study the macro-scale displacement reaction and its accompanying morphological and volume variations. We found that the applied mechanical field can seriously affect the reaction, where the reduced Cu particles and cracks clearly demonstrate growth in preferred orientations. While Cu reduction is reversible, nearly 50% of cracks are maintained within the electrodes after the 1st delithiation. This results in disruption of the ionic and electronic transport pathways, as supported by a higher transfer resistance and the observation of more “dead” materials produced in the electrodes.

References:

- (1) Randau, S.; Weber, D. A.; Kötzt, O.; Koerver, R.; Braun, P.; Weber, A.; Ivers-Tiffée, E.; Adermann, T.; Kulisch, J.; Zeier, W. G.; Richter, F. H.; Janek, J. *Nat. Energy* **2020**, 5 (3), 259–270.
- (2) Wu, X.; Billaud, J.; Jerjen, I.; Marone, F.; Ishihara, Y.; Adachi, M.; Adachi, Y.; Villevieille, C.; Kato, Y. *Adv. Energy Mater.* **2019**, 9 (34), 1–10.
- (3) Baggetto, L.; Niessen, R. A. H.; Roozehoom, F.; Notten, P. H. L. *Adv. Funct. Mater.* **2008**, 18 (7), 1057–1066.
- (4) Ning, Z.; Jolly, D. S.; Li, G.; De Meyere, R.; Pu, S. D.; Chen, Y.; Kasemchainan, J.; Ihli, J.; Gong, C.; Liu, B.; Melvin, D. L. R.; Bonnin, A.; Magdysyuk, O.; Adamson, P.; Hartley, G. O.; Monroe, C. W.; Marrow, T. J.; Bruce, P. G. *Nat. Mater.* **2021**.
- (5) Santhosha, A. L.; Nazer, N.; Koerver, R.; Randau, S.; Richter, F. H.; Weber, D. A.; Kulisch, J.; Adermann, T.; Janek, J.; Adelhelm, P. *Adv. Energy Mater.* **2020**, 10 (41), 1–9.

2:15 PM EN02.12.06

Crystal Structure and Structure-Property Relationship of New Halide Li-Ion Conductors as Solid Electrolyte for All-Solid-State Batteries Zhantao Liu¹, Jue Liu² and Hailong Chen¹; ¹Georgia Institute of Technology, United States; ²Oak Ridge National Laboratory, United States

Solid electrolyte is the key component for all-solid-state batteries. Extensive research attentions are being attracted to the design and development of high performance solid electrolytes with high ionic conductivity and low diffusion energy barriers. Recently halides with general formula Li₃MX₆ (M=metals such as Y, In and Sc; X=Cl or Br) have attracted a lot of attention from both industry and academia because the halide Li-ion conductors are potentially more all-around candidates for all-solid-state batteries than existing sulfides and oxides. They showed higher ionic conductivities than those of oxides (such as LLZO and variants) and better chemical and electrochemical stabilities than sulfides (such as LGPS and argyrodite materials). However, many detailed features in their crystal structure are yet to be clearly described and the key factors that govern the ionic conductivity are yet to be revealed. Here we report our recent findings in design, synthesis, electrochemical testing and particularly crystal structure characterizations of novel halide compounds. The long range structure and the thermodynamic stability are investigated with using ex situ and in situ synchrotron X-ray diffraction. The Li sublattice, local ordering and stacking faults are characterized with using neutron diffraction and pair distribution function analysis. The relation between these structural features and the ionic conductivity and diffusion energy barriers are revealed and discussed.

SESSION EN02.13: Interfaces and Interphases
Session Chairs: Fudong Han and Yuyan Shao
Monday Afternoon, December 6, 2021
EN02-Virtual

4:00 PM *EN02.13.01

A Solid Transformation of Energy Storage Eric D. Wachsman; University of Maryland, United States

Solid-state Li-batteries (SSLiBs) have the potential to be a transformational and intrinsically safe energy storage solution. However, their progress has been limited by high solid-solid interfacial impedance and numerous reports of Li-dendrites and a corresponding “critical current density”. By first modifying the garnet surface to enable Li-metal to wet it and then fabricating garnet-electrolytes into tailored tri-layer microstructures to form electrode supported dense thin-film (~10μm) solid-state electrolytes we have been able to overcome these limitations. The microstructurally tailored porous garnet scaffold support increases electrode/electrolyte interfacial area, overcoming the high impedance typical of planar geometry SSLiBs resulting in an area specific resistance (ASR) of only ~2 to 7 Ωcm² at room temperature. The unique garnet scaffold/electrolyte/scaffold structure further allows for charge/discharge of the Li-metal anode and cathode scaffolds by pore-filling, thus providing high depth of discharge ability without mechanical cycling fatigue seen with typical electrodes. Moreover, these scalable multilayer ceramic fabrication techniques, without need for dry rooms or vacuum equipment, provide for dramatically reduced manufacturing cost.

The fabrication of supported dense thin-film garnet electrolytes, their ability to cycle Li-metal at high current densities with no dendrite formation, and results for Li-metal anode/garnet-electrolyte based batteries with a number of different cathode chemistries will be presented.

4:30 PM *EN02.13.02

Solid State BaSeries—From Interfaces to High Energy Density Jihui Yang; University of Washington, United States

Room temperature lithium ion conductors have been intensively studied in an attempt to develop solid state batteries that can be deployed for high energy applications. In recent years, promising solid lithium ion conductors with competitive ionic conductivity to those of liquid electrolytes have been demonstrated. The integration of highly conductive solid electrolytes into the battery system is, however, still very challenging mainly due to the high impedance existing at different interfaces throughout the battery structure.

In this talk, I will highlight our recent work on the understanding of interfaces between the solid electrolytes and anode & cathode, providing new insights into enabling future all solid-state batteries. I will also show that high energy and long cycle life can be achieved in solid state batteries via optimizing the

interfacial thermodynamics.

5:00 PM EN02.13.03

Strategies to Enhance the Performance of All-Solid-State Sodium Batteries Yang Li, William Arnold, Selim Halacoglu and Hui Wang; University of Louisville, United States

All-solid-state sodium (Na) batteries (ASSSBs) attract increasing attention due to the use of high-capacity Na metal anode and solid electrolytes (SEs) with high safety. Recently, significant research achievements have been made in developing Na-ion conductors. In particular, sulfide SEs generally offer higher ionic conductivity (10^{-4} – 10^{-3} S cm⁻¹ at room temperature) and lower grain boundary resistance. However, the practical applications of sulfide-based ASSSBs are significantly hampered by the challenges originating from (1) significant reactions at SE/Na interface; (2) poor solid-solid contact between SE and electrodes. To solve these issues and enhance the electrochemical performance of sulfide-based ASSSBs, here, we design and demonstrate several strategies including elements doping in sulfide SEs and interface modifications between sulfide SEs and electrodes. As a result, long-term cycling stability was achieved due to 1) the formation of stable interface to prevent the severe interfacial reactions; 2) the creation of intimate contact between sulfide SEs and electrodes. These methods provide effective strategies to address the challenges between sulfide SEs and Na metal, enabling the successful utilization of Na metal and sulfide SEs in ASSSBs towards next-generation safe and high-energy density energy storage systems.

5:15 PM EN02.13.04

Enabling a Long Lasting Sodium All-Solid-State Battery Swastika Banerjee and Shyue Ping Ong; University of California, San Diego, United States

Sodium all solid-state batteries (Na-ASSBs) offer a combination of improved safety and lowered costs due to the use of non-flammable solid-state electrolytes (SSEs) and naturally abundant Na-based raw materials. However, a fundamentally different approach is necessary to achieve a simultaneous leap in multiple SSE properties – ionic conductivity, (electro) chemical stability and processibility. Our recent work has demonstrated long cycle performance of a Na-ASSB enabled by a new class of halide-based SSE, achieving a capacity retention of approximately 90% after 1000 cycles at a rate of 1C, representing one of the best Na-based battery performances in the literature till date. This was made possible through a joint computational and experimental exploration of novel halide-based Na SSEs. In this talk, I will discuss computational strategies based on ab initio and the machine learning interatomic potential, that has proven to be highly effective to report the discovery of moderate ionic conductivity of 6.6×10^{-5} S cm⁻¹ at ambient temperature for Na_{3-x}Y_{1-x}Zr₆Cl₆ (NYZC) several orders of magnitude higher than oxide coatings. Enhanced Na-conductivity in NYZC is attributed to abundant Na vacancies and cooperative MCl₆ rotation resulting non-Arrhenius behavior.

5:30 PM EN02.13.05

Shedding Light on the Sulfide Electrolytes/Electrode Interphases in Solid-State Batteries via Integrated Computation and Spectroscopy Chuntian Cao¹, Sizhan Liu¹, Yonghua Du¹, Nongnuch Artrith², Alexander Urban², Deyu Lu¹, Shinjae Yoo¹ and Feng Wang¹; ¹Brookhaven National Laboratory, United States; ²Columbia University, United States

Solid-state batteries (SSBs) have been recognized as promising next-generation rechargeable batteries because of their potential to push energy density limits and ensure safety. Sulfide-based solid electrolytes (SEs) are promising candidates for solid-state batteries (SSBs) because of their high ionic conductivity and good malleability. Like conventional liquid electrolytes, SE decomposes at the electrode-electrolyte interface when the potential is outside its electrochemical stability window, forming a solid-solid interphase (SSI) layer. SSI's properties and the dynamic evolution of its structure are crucial for the stability and performance of SSBs. For example, some decomposition products may have high ionic resistance, which is detrimental to the cell performance; some redox processes are reversible and participate in the electrochemical cycle with the active electrode materials. Understanding the dynamic structure of the SSI and its impact to transport properties is essential for incorporating sulfide SE into commercial batteries.

Modelling the inherent complexity and the dynamic evolution of the SSIs is very challenging with first-principles methods, such as density functional theory, because of the computational hurdle associated with the large system size (*e.g.*, more than one thousand atoms) and time scale. Herein, we develop an integrated approach that combines high-performance computing and machine learning tools with state-of-the-art synchrotron X-ray absorption spectroscopy (XAS)/electron energy-loss spectroscopy (EELS), to tackle the complex SSIs. *Ex situ* and *in situ* XAS/EELS are applied to characterize SSIs' chemical structure and dynamic evolutions upon formation and during electrochemical cycling. We focus on two types of sulfide SEs, the baseline glass/ceramic Li₂S-P₂S₅ (LPS), and the more advanced argyrodite Li₆PS₅Cl (LPSCl) which has higher ionic conductivity and is promising for commercial use. Our results reveal the reaction mechanism at the interface of sulfide-based SEs and provide a fundamental understanding of the current material limitations. This study can help identify key material parameters to optimize cell performance, thus providing a basis for the design and optimization of SEs for SSBs.

5:45 PM EN02.13.06

Rational Design of Cathode Interface for Wide Temperature All-Solid-State Batteries Sixu Deng, Changhong Wang and Xueliang A. Sun; Western University, Canada

Inorganic all-solid-state lithium-ion batteries (ASSLIBs) are considered as a promising candidate for next-generation energy storage devices that can meet the safety requirements of electric vehicles by utilizing nonflammable solid-state electrolytes (SSEs).[1, 2] However, the poor interfacial compatibility in composite cathodes (SSE/cathode/carbon/current collector) is challenging the stable delivery of electrochemical performance.[3, 4] Our research mainly focuses on the development of interfacial engineering strategies to address the challenges at the internal and external interfaces in the composite cathodes targeting high-performance ASSLIBs. [5-7] In this talk, three parts will be included. Firstly, I will review our previous studies. For example, at the SE/cathode interface, we designed a dual-functional Li₃PO₄ (LPO) modification to suppress both the side-reactions and contact loss at the SSE/cathode interface.[8] We also developed a surface-cleaning strategy to investigate the underlying degradation mechanism at SSE/cathode interface.[9] At the SSE/carbon interface, a poly(3,4-ethylenedioxythiophene) (PEDOT) modification is designed as a semiconductive additive for composite cathodes.[10] The modified ASSLIB demonstrates a competitive rate capacity, which is 10 times greater than that of the bare cathode. Secondly, I will introduce our recent work, focusing on the current collector interface. Our study found that the interfacial stability at the current collector interface is highly dependent on the temperatures. At the end of this talk, I will introduce our work on low-temperature inorganic ASSLIBs. Our study revealed that manipulating the electronic conductivity in the composite cathodes is the key factor that determines the electrochemical performance at low temperatures.

References

- [1] F. Zhao, J. Liang, C. Yu, Q. Sun, X. Li, K. Adair, C. Wang, Y. Zhao, S. Zhang, W. Li, S. Deng, R. Li, Y. Huang, H. Huang, L. Zhang, S. Zhao, S. Lu, X. Sun, *Advanced Energy Materials*, 10 (2020) 1903422.
- [2] X. Li, J. Liang, J. Luo, M. Norouzi Banis, C. Wang, W. Li, S. Deng, C. Yu, F. Zhao, Y. Hu, T.-K. Sham, L. Zhang, S. Zhao, S. Lu, H. Huang, R. Li, K.R. Adair, X. Sun, *Energy &*

Environmental Science, 2019, 12, 2665.

- [3] C. Yu, Y. Li, M. Willans, Y. Zhao, K.R. Adair, F. Zhao, W. Li, S. Deng, J. Liang, M.N. Banis, R. Li, H. Huang, L. Zhang, R. Yang, S. Lu, Y. Huang, X. Sun, Nano Energy, 2020, 69, 104396.
- [4] C. Yu, Y. Li, K.R. Adair, W. Li, K. Goubitz, Y. Zhao, M.J. Willans, M.A. Thijs, C. Wang, F. Zhao, Q. Sun, S. Deng, J. Liang, X. Li, R. Li, T.-K. Sham, H. Huang, S. Lu, S. Zhao, L. Zhang, L. van Eijck, Y. Huang, X. Sun, Nano Energy, 2020, 77, 105097.
- [5] X. Li, Z. Ren, M. Norouzi Banis, S. Deng, Y. Zhao, Q. Sun, C. Wang, X. Yang, W. Li, J. Liang, X. Li, Y. Sun, K. Adair, R. Li, Y. Hu, T.-K. Sham, H. Huang, L. Zhang, S. Lu, J. Luo, X. Sun, ACS Energy Letters, 2019, 4, 2480.
- [6] C. Wang, J. Liang, S. Hwang, X. Li, Y. Zhao, K. Adair, C. Zhao, X. Li, S. Deng, X. Lin, X. Yang, R. Li, H. Huang, L. Zhang, S. Lu, D. Su, X. Sun, Nano Energy, 2020, 72, 104686.
- [7] C. Wang, X. Li, Y. Zhao, M.N. Banis, J. Liang, X. Li, Y. Sun, K.R. Adair, Q. Sun, Y. Liu, F. Zhao, S. Deng, X. Lin, R. Li, Y. Hu, T.-K. Sham, H. Huang, L. Zhang, R. Yang, S. Lu, X. Sun, Small Methods, 2019, 3, 1900261.
- [8] S. Deng, X. Li, Z. Ren, W. Li, J. Luo, J. Liang, J. Liang, M.N. Banis, M. Li, Y. Zhao, X. Li, C. Wang, Y. Sun, Q. Sun, R. Li, Y. Hu, H. Huang, L. Zhang, S. Lu, J. Luo, X. Sun, Energy Storage Materials, 2020, 27 117.
- [9] S. Deng, Q. Sun, M. Li, K. Adair, C. Yu, J. Li, W. Li, J. Fu, X. Li, R. Li, Y. Hu, N. Chen, H. Huang, L. Zhang, S. Zhao, S. Lu, X. Sun, Energy Storage Materials, 2021, 35, 661.
- [10] S. Deng, Y. Sun, X. Li, Z. Ren, J. Liang, K. Doyle-Davis, J. Liang, W. Li, M. Norouzi Banis, Q. Sun, R. Li, Y. Hu, H. Huang, L. Zhang, S. Lu, J. Luo, X. Sun, ACS Energy Letters, 2020, 5, 1243.

SESSION EN02.14: Solid State Batteries I
Session Chairs: Fudong Han and Huilin Pan
Monday Afternoon, December 6, 2021
EN02-Virtual

6:30 PM *EN02.14.01

Stabilized Interface in Li-Ion Batteries via *In Situ* Solidification Jiaze Lu¹, Rusong Chen¹, Xiqian Yu¹ and Hong Li^{1,2}; ¹Institute of Physics, Chinese Academy of Sciences, China; ²Beijing Welion New Energy Technology Co., Ltd., China

Thermal runaway of nonaqueous Li-ion batteries starts from decomposition of the solid electrolyte interphase (SEI). Introduction of solid electrolyte has been considered as a promising solution to improve the safety and achieving high energy density. However, it is quite challenging for the construction well-conducted and thermal stable interfaces. Our previous research indicates the thermal stability between metallic lithium and inorganic solid-state electrolytes is not always under controlled. Herein, we proposed that the *in-situ* solidification strategy is a comprehensive methodology for the pathway toward practical solid state batteries. For example, the *in-situ* solidification strategy is applied to generate artificial solid electrolyte interface (SEI) between electrodes (both cathode and anode) and electrolytes. The *in-situ* built SEI not only promotes the electrochemical stability, but also shows great potential for the promotion on the thermal stability of SSBs. Thus, the *in-situ* solidification could make the thermal property of SEI well-designed and controllable, which means the thermal stability of the battery could be improved significantly.

7:00 PM *EN02.14.02

Sulfide Electrolyte for All-Solid-State Rechargeable Batteries Xiayin Yao, Hongli Wan, Gaozhan Liu and Zhihua Zhang; Ningbo Institute of Materials Technology and Engineering, Chinese Academy of Sciences, China

Sulfide electrolytes have been considered as one of the most promising ion conductors for all-solid-state lithium batteries due to the breakthrough in ionic conductivity, low particle-boundary resistance and excellent ductility.^[1] Different type sulfide electrolytes with room temperature ionic conductivity of $10^{-3} \sim 10^{-2}$ S/cm have been successfully synthesized. The electrochemical stability and compatibility with lithium can be improved with oxide or halogen doping^[2] as well as densified solid electrolyte with flat surface^[3]. Based on the high ionic conductive sulfide electrolyte powder, thin film were obtained by wet chemical surface modification method^[4] or dry film approach^[5]. The obtained $\text{Li}_{5.4}\text{PS}_{4.4}\text{Cl}_{1.6}$ sulfide electrolyte membrane possesses a high ionic conductivity of 8.4 mS cm^{-1} with a thin thickness of $30 \mu\text{m}$, which is crucial to realize high energy density all-solid-state rechargeable batteries.^[5] Compared with lithium transition metal oxide cathodes, sulfur based materials, especially transition metal sulfides, show much better interface compatibility with sulfide electrolytes. A series of transition metal sulfides or sulfur-based materials are employed as electrodes for all-solid-state rechargeable batteries, such as MoS_2 ^[6] FeS_2 ^[7], VS_4 ^[8] or sulfur^[9]. The intimate contact interface can be realized by coating sulfide electrolytes evenly on the surface of active materials, which enables the battery to withstand the large stresses/strains during repeated charging/discharging, leading to significant improvements in energy density and cycle life.^[10] Besides, in order to improve electronic conduction, highly conductive carbonaceous materials were employed as hosts for nanosized sulfur based materials to form active material/electrom additive nanocomposites. Although different reaction mechanisms, all these nanocomposites employed as cathodes in all-solid-state lithium batteries show enhanced electrochemical performances^[6, 9]. Furthermore, coating sulfide electrolyte on active material/electrom additive nanocomposites can simultaneously realize three-dimensional electronic/ionic conduction networks at the triple solid-solid contact interface^[8, 11]. For example, $10\% \text{rGO-VS}_4 @ \text{Li}_7\text{P}_3\text{S}_{11}$ nanocomposites with multi-channel continuous electronic/ionic conductive network can be prepared by a facile liquid-phase deposition reaction and further employed as an alternative material for sulfur cathode in all-solid-state room temperature lithium batteries, exhibiting improved rate capability and cycling stability.^[8] Clearly, all-solid-state lithium batteries with sulfur-based cathodes and sulfide electrolytes are promising next generation high energy density batteries. More attentions should be concerned in the dendrite formation, interfacial contact, reducing the electrolyte thickness as well as high specific areal capacity with high current density.

References:

- [1] J. Wu, L. Shen, Z. Zhang, et al., *Electrochemical Energy Reviews* 2021, 4, 101.
[2] G. Liu, D. Xie, X. Wang, et al., *Energy Storage Materials* 2019, 17, 266.
[3] G. Liu, W. Weng, Z. Zhang, et al., *Nano Letters* 2020, 20, 6660.
[4] G. Liu, J. Shi, M. Zhu, et al., *Energy Storage Materials* 2021, 38, 249.

- [5] Z. Zhang, L. Wu, D. Zhou, et al., *Nano Letters* 2021, doi:10.1021/acs.nanolett.1c01344.
 [6] Q. Zhang, Z. Ding, G. Liu, et al., *Energy Storage Materials* 2019, 23, 168.
 [7] H. Wan, G. Liu, Y. Li, et al., *ACS Nano* 2019, 13, 9551.
 [8] Q. Zhang, H. Wan, G. Liu, et al., *Nano Energy* 2019, 57, 771.
 [9] X. Yao, N. Huang, F. Han, et al., *Advanced Energy Materials* 2017, 7, 1602923.
 [10] X. Yao, D. Liu, C. Wang, et al., *Nano Letters* 2016, 16, 7148.
 [11] H. Wan, L. Cai, F. Han, et al., *Small* 2019, 15, 1905849.
 [12] J. Wu, S. Liu, F. Han, et al., *Advanced Materials* 2021, 33, 2000751.

7:30 PM EN02.14.03

Exploration of Li-Rich Inorganic Compounds with Inverse Ruddlesden-Popper-Type Structure by First-Principles DFT Calculations for Solid Electrolyte Application in All-Solid-State Batteries Randy Jalem¹, Yoshitaka Tateyama¹, Kazunori Takada¹ and Masanobu Nakayama²; ¹NIMS-GREEN, Japan; ²Nagoya Institute of Technology, Japan

The all-solid-state Li-ion battery (Li-ASSB) is expected as one of the next-generation energy conversion and storage devices that could potentially become widespread in use owing to a number of its promising features such as high energy density (with the use of Li metal/alloy as anode), high working capacity (with the use of high-voltage cathodes), and high safety in contrast to conventional batteries with organic and liquid components (i.e., organic/liquid electrolytes). These aforementioned features are closely linked to the inorganic solid electrolyte (SE) component in Li-ASSB. Thus, novel high-performance SE design and optimization has become one of the highly active areas in battery research.

Recently, electronically-inverted Li-rich perovskites have attracted great interest for SE use. In here, using density functional theory (DFT) calculations, an in-silico-generated chemical space of more than 500 inorganic compounds with an inverse Ruddlesden-Popper-type structure ($\text{Li}_4(\text{X}_{1-a}\text{X}'_a)(\text{Z}_{1-b}\text{Z}'_b)_2$, where $\text{X}, \text{X}' = \{\text{O}^{2-}, \text{S}^{2-}, \text{Se}^{2-}, \text{Te}^{2-}\}$ and $\text{Z}, \text{Z}' = \{\text{F}, \text{Cl}, \text{Br}, \text{I}\}$, $0 \leq a, b \leq 1$) was explored in order to find novel solid electrolyte candidates. Based from DFT thermodynamic convex hull results, about 167 compounds were determined to be (meta)stable, at least 20 novel compounds were found to belong to the $\text{Li}_4\text{O}(\text{Cl}_{1-b}\text{Br}_b)_2$ series and O/S/I-bearing compositions. Representative compounds were further evaluated using: i) phase diagram approach for (electro)chemical stability analysis, ii) slab modelling for surface properties and ii) DFT molecular dynamics method for characterizing Li^+ ion conductivity and transport mechanism. Computationally cheap, yet useful, material descriptors were also determined based from correlation analysis of the accumulated DFT dataset. These descriptors can be useful in future solid electrolyte design/screening, such as for thermodynamic phase stability, electronic property, and Li^+ ion conduction properties.

R.J. is thankful for the Japan Science and Technology Agency (JST) Precursory Research for Embryonic Science and Technology (PRESTO) program for the financial support. This research was also supported in part by JST through "Materials research by Information Integration" Initiative (MI2I)" and Advanced Low Carbon Technology-Specially Promoted Research for Innovative Next Generation Batteries Program (ALCA-SPRING Grant Number JPMJAL1301), JSPS KAKENHI Grant Number JP19H05815, JSPS KAKENHI Grant Number JP21K14729, and MEXT as Elements Strategy Initiative, Grant Number JPMXP0112101003, Materials Processing Science project ("Materealize"), Grant Number JPMXP0219207397 and "Program for Promoting Researches on the Supercomputer Fugaku (Fugaku Battery & Fuel Cell Project).

Reference:

Randy Jalem, Yoshitaka Tateyama, Kazunori Takada, and Masanobu Nakayama, *Chem. Mater.* 2021 (<https://doi.org/10.1021/acs.chemmater.1c00124>)

7:45 PM EN02.14.04

Mechanochemical Synthesis and Characterization of Hexagonal Li_4SnS_4 -Based Solid Electrolytes Misae Otoyama, Kentaro Kuratani and Hironori Kobayashi; National Institute of Advanced Industrial Science and Technology (AIST), Japan

Sulfide solid electrolytes (SEs) have attracted much attention because of their high ionic conductivity and deformability. However, sulfide SEs have an issue of low air-stability. They generate H_2S gas when exposed to air. Sahu *et al* reported that stability of sulfide SEs against moisture in air can be explained by hard and soft acids and bases theory.^[1] Based on the theory, Sn-based SEs such as Li_4SnS_4 show higher air-stability than argyrodite type SEs and $\text{Li}_2\text{S}-\text{P}_2\text{S}_5$ type SEs, which have P-S bonds.^[2,3] However, Li_4SnS_4 showed lower ionic conductivity of $\sim 10^{-5} \text{ S cm}^{-1}$ at 25 °C than the conventional SEs ($10^{-3}-10^{-4} \text{ S cm}^{-1}$). Kanazawa *et al* reported that the hexagonal Li_4SnS_4 prepared by mechanochemical treatment showed higher ionic conductivity than orthorhombic Li_4SnS_4 prepared by solid phase synthesis.^[3] In this study, LiI and Li_3PS_4 were added to hexagonal Li_4SnS_4 to increase ionic conductivity of Li_4SnS_4 -based SEs. Furthermore, air-stability of them was compared.

The XRD patterns of LiI-added Li_4SnS_4 showed the diffraction peaks of hexagonal Li_4SnS_4 shifted to the lower angle, suggesting that the lattice volume increased due to the Γ ion with large ionic radius. The sample with $x = 0.43$ in $x\text{LiI} \cdot (1-x)\text{Li}_4\text{SnS}_4$ showed the higher ionic conductivity of $1.6 \times 10^{-4} \text{ S cm}^{-1}$ at 25 °C than that with $x = 0$ ($4.5 \times 10^{-5} \text{ S cm}^{-1}$). Furthermore, XRD patterns of as-milled samples of $\text{LiI}-\text{Li}_4\text{SnS}_4-\text{Li}_3\text{PS}_4$ systems exhibited halo patterns, indicating that they became amorphous state due to the multicomponent. The sample of $37\text{LiI} \cdot 38\text{Li}_4\text{SnS}_4 \cdot 25\text{Li}_3\text{PS}_4$ (mol%) showed the ionic conductivity of $4.5 \times 10^{-4} \text{ S cm}^{-1}$ at 25 °C. These samples are decomposed by heat-treatment at more than 240 °C, suggesting that they are thermally metastable. The prepared Li_4SnS_4 -based SEs showed similar air-stability to hexagonal Li_4SnS_4 and generated smaller amount of H_2S gas than the argyrodite type SEs.

References

- [1] G. Sahu *et al.*, *Energy Environ. Sci.*, **7** (2014) 1053.
 [2] H. Kwak *et al.*, *J. Power Sources*, **446** (2020) 227338.
 [3] K. Kanazawa *et al.*, *Inorg. Chem.*, **57** (2018) 9925.

Acknowledgement

This work was supported by JSPS KAKENHI Grant Number JP20K22558.

8:00 PM EN02.14.05

Molecular Dynamics Study of Peculiarly High Li-Ion Conductivity in $\text{Li}\{\text{N}(\text{SO}_2\text{F})_2\}(\text{NCCH}_2\text{CH}_2\text{CN})_2$ Molecular Crystal Ryoma Sasaki^{1,2}, Makoto Moriya³, Yuki Watanabe¹, Kazunori Nishio¹, Taro Hitosugi¹ and Yoshitaka Tateyama^{1,2}; ¹Tokyo Institute of Technology, Japan; ²National Institute for Materials Science, Japan; ³Shizuoka University, Japan

All-solid-state battery (ASSB) has attracted great attention for future energy storage with safety and high-energy density. The practical application of ASSBs requires solid-state electrolytes (SSEs) which are not only highly conductive but also flexible for good interfacial contact between SSEs and electrodes. Recently, $\text{Li}\{\text{N}(\text{SO}_2\text{F})_2\}(\text{NCCH}_2\text{CH}_2\text{CN})_2$ ($\text{Li}(\text{FSA})(\text{SN})_2$) organic flexible molecular crystal has been experimentally reported as a promising SSE with high Li-ion conductivity of ca. $10^{-4} \text{ S cm}^{-1}$ at room temperature and exceptionally low activation energy (E_a) of 28 kJ mol^{-1} [K. Tanaka *et*

al., *Nano Lett.*, 2020, **20**, 8200-8204]. However, the fast conduction mechanism remains unexplained because all the Li-ions are held in the crystal framework, and the distances between the constituent Li-ions are too long for hopping. Herein, molecular dynamics (MD) simulations were performed to clarify the mechanism of the extraordinarily fast Li-ion conduction in the succinonitrile (SN)-based molecular crystal. Atomistic MD revealed that Li-ion vacancies can exist stably in Li(FSA)(SN)₂ crystal and give rise to the one-dimensional Li-ion hopping pathway contrary to the conventional scenario in which the fast conduction is attributed to the three-dimensional pathway. The calculated E_a of 34 kJ mol⁻¹ is in good agreement with the experimental value, which substantially supports the one-dimensional conduction. The low E_a is intimately connected with the motion of the SN molecules. Two SN molecules at the vacancy site change their conformation, following which one of the SN molecules creates an electronegative region, while the other one carries the adjacent Li-ion to the electronegative region by the swing motion. The insights on the behavior of organic moieties and Li-ion conduction obtained from this study enable to propose a novel design principle for the fast ion-conductive molecular crystals.

SESSION EN02.15: Solid State Batteries II
Session Chairs: Fudong Han and Huilin Pan
Monday Afternoon, December 6, 2021
EN02-Virtual

9:00 PM *EN02.15.01

Universal Liquid-Phase Synthesis of Sulfide Solid Electrolyte for All-Solid-State Batteries Yoon Seok Jung; Yonsei University, Korea (the Republic of)

For addressing the requirements of better safety and higher energy density of lithium-ion batteries targeting for the electric vehicle application, solidification of electrolytes using nonflammable superionic conductors has been rigorously investigated. Owing to their high ionic conductivities reaching maximum 10⁻² S cm⁻¹ at room temperature and the mechanically-sinterable property, sulfide solid electrolyte (SE) materials are considered as the key to the success of all-solid-state batteries. Moreover, wet-chemical syntheses and/or processes of sulfide SEs have been developed. The wet-chemical synthesis, such as using tetrahydrofuran, proceeds in a suspension, and provides opportunities in multiple aspects including particle size control and the reduction of mixing energy. For several compositions of sulfide materials, it has been shown that SEs could be fully dissolved into specific solvents, such as ethanol and methanol, and then the original SEs could be precipitated via the removal of solvent and subsequent heat treatment. This is referred to as the solution process. The solution processability of sulfide SEs offers direct SE coatings on active materials and infiltration of the conventional electrodes used for lithium-ion batteries. Both of which allow for intimate ionic contacts between active materials and SEs.

In this presentation, we report on a new universal liquid-phase synthesis of sulfide solid electrolytes, which takes the combined advantages of the wet-chemical synthesis and the solution process. It is demonstrated that SE precursors including not only conventional Li₂S, P₂S₅, and LiX but also metal sulfides are fully dissolved in a solvent, forming a homogeneous solution. Via the universal liquid-phase synthesis, promising electrochemical performances are demonstrated for Li- and Na-ion all-solid-state batteries.

References

- [1] Dae Yang Oh, A. Reum Ha, Ji Eun Lee, Sung Hoo Jung, Goojin Jeong, Woosuk Cho, Kyung Su Kim, Yoon Seok Jung, *ChemSusChem* **2020**, *13*, 146.
- [2] Yong Bae Song, Dong Hyeon Kim, Hiram Kwak, Daseul Han, Sujin Kang, Jong Hoon Lee, Seongmin Bak, Kyung-Wan Nam, Hyun-Wook Lee, Yoon Seok Jung, *Nano Lett.* **2020**, *6*, 4337.
- [2] Kern Ho Park, Dae Yang Oh, Young Eun Choi, Young Jin Nam, Lili Han, Ju-Young Kim, Huolin Xin, Feng Lin, Seung M. Oh, Yoon Seok Jung, *Adv. Mater.* **2016**, *28*, 1874.

9:30 PM EN02.15.02

Tailoring Slurries Using Cosolvents and Li Salt for Contact Engineering for All-Solid-State Batteries Kyu Tae Kim¹, Dae Yang Oh¹, Tae Young Kwon^{1,2} and Yoon Seok Jung¹; ¹Yonsei University, Korea (the Republic of); ²Hanyang University, Korea (the Republic of)

All-solid-state Li or Li-ion batteries (ASLBs) using inorganic solid electrolytes (SEs) have promising opportunities in terms of better safety and higher energy density. The cut-off score of Li⁺ conductivities of 10⁻³ S cm⁻¹ for room-temperature operable ASLBs severely narrows the SE materials to several classes of materials, including sulfides, closo-borates, and halides. Thanks to mechanical sinterability, cost, and density, sulfide SEs are highly competitive, however, they suffer from poor chemical stability when preparing wet-slurries. They are dissolved in conventional polar organic solvents and conventional polymers such as PVDF are thus not available. Furthermore, the polymeric binders impedes Li⁺ ion transport. This could be relieved by employing liquid electrolytes or gel polymer electrolyte binders but at the expense of the ASLB's thermal stability.^[1]

In this study, we reports on our recent development of dry polymer electrolyte (DPE) binders for practical ASLBs.^[2] Furthermore, the use of cosolvents and Li salt offers the engineering ability to control ionic contacts and Li⁺-conductivity, respectively. Remarkable enhancements in utilizing electrode active materials and their outstanding thermal stability, enabled by the contact and Li⁺-conductivity engineerable DPE-based binders, will be presented.

References

- [1] D. Y. Oh, Y. J. Nam, K. H. Park, S. H. Jung, K. T. Kim, A. R. Ha, Y. S. Jung, *Adv. Energy Mater.*, **2019**, *9*, 1802927.
- [2] K. T. Kim, D. Y. Oh, S. Jun, Y. B. Song, T. Y. Kwon, Y. Han, Y. S. Jung, *Adv. Energy Mater.*, **2021**, *11*, 2003766.

9:45 PM EN02.15.03

Development of New Ionic Electrolytes by Tailoring the Cation, Anion and Molecular Structure. Jenny Pringle, Faezeh Makhlooghiyazad and Colin Kang; Deakin University, Australia

Organic ionic plastic crystals (OIPCs) have shown increasing promise as solid state electrolytes for energy devices such as lithium or sodium batteries, DSSCs and fuel cells. OIPCs are crystalline phases found in many of the same organic salt families as ionic liquids but these materials have elevated melting points and exhibit various forms of disorder, which is the origin of their plastic mechanical properties. This intrinsic disorder is fundamentally responsible for the fast ion conduction of introduced target ions, such as lithium or sodium, and core to their efficient performance as solid-state electrolytes. However, how different cation, anion and molecular structures impact the phase behaviour, disorder and ion transport in the electrolytes is still not well understood.

Key to the development of plastic crystal electrolytes is expanding the range of cations and anions available, and understanding the resulting structure and dynamics. Here we discuss our development of new plastic crystal-based materials for energy applications, in particular lithium metal batteries. We also discuss our recent research into novel zwitterion-based electrolytes. Insights into the relationships between the different cations, anions and zwitterionic

structures and the physical, thermal and electrochemical properties of the resultant solid electrolytes are presented.

10:00 PM EN02.15.04

Fabrication and Characterization of Solid-State Li Batteries Using Li{N(SO₂F)₂}(NCCH₂CH₂CN)₂ Molecular Crystalline Electrolyte and LiCoO₂ Thin-Film Electrode Yuki Watanabe¹, Kenjiro Tanaka², Kazunori Nishio¹, Ryo Nakayama¹, Ryota Shimizu^{1,3}, Makoto Moriya² and Taro Hitosugi¹; ¹Tokyo Institute of Technology, Japan; ²Shizuoka University, Japan; ³Japan Science and Technology Agency, Japan

Solid-state Li batteries have the potential for the increased power density. For this aim, it is crucial to understand the structural, chemical, and mechanical properties of interfaces between electrolyte and electrode. A molecular crystalline solid electrolyte is a candidate for better mechanical contact with the electrode due to its physical flexibility [1]. Among a variety of molecular crystals, we selected Li(FSA)(SN)₂ composed of lithium bis(fluorosulfonyl)amide (FSA: Li{N(SO₂F)₂}) and succinonitrile (SN: NCCH₂CH₂CN) [2]. Although Li(FSA)(SN)₂ exhibits a high Li-ion conductivity of ~10⁻⁴ S cm⁻¹ at 30 °C, the battery operation using this electrolyte has yet been tested. In this study, we fabricated solid-state batteries using Li(FSA)(SN)₂ molecular crystals and LiCoO₂ thin-film electrodes. The cyclic voltammogram showed redox current peaks at around 3.9 V vs. Li/Li⁺, being in good agreement with the redox voltages of Co^{3+/4+} for LiCoO₂ positive electrode. When the battery was charged and discharged at the current density of 1 μA cm⁻² in 3.0–4.0 V vs. Li/Li⁺, the discharge capacity after 100 cycles maintained 90% of the 1st discharge capacity (50 mAh g⁻¹) and the Coulombic efficiency in each cycle was approximately 95%. These results indicate the high cycle stability and efficiency in solid-state Li batteries using Li(FSA)(SN)₂ molecular crystals [2].

[1] Moriya, *Sci. Technol. Adv. Mater.*, **18** (2017) 634.

[2] Tanaka, Watanabe *et al.*, *Nano Lett.*, **20** (2020) 8200.

10:05 PM EN02.15.05

Chemically-Modified Binders with Improved Mechanical Strength for Sheet-Type Electrodes of All-Solid-State Batteries Tae Young Kwon^{1,2}, Kyu Tae Kim¹, Dae Yang Oh¹, Seungwoo Jun¹, Yong Bae Song¹ and Yoon Seok Jung¹; ¹Yonsei University, Korea (the Republic of); ²Hanyang University, Korea (the Republic of)

Despite the increased demand of high-energy density lithium-ion batteries (LIBs), safety issues caused by the use of flammable organic electrolytes hinder their market expansion. In this regard, all-solid-state lithium batteries (ASLBs) using nonflammable inorganic solid electrolytes (SEs) are considered a promising alternative to conventional LIBs.^[1] In particular, high Li-ion conductivity and deformable property of sulfide SEs are important advantages for high-performance practical ASLBs. However, there has been much room for improvement of performances of ASLBs using sulfide SEs. Specifically, the chemo-mechanical issues of crack propagation occurring at electrode active materials and interfaces are attributed to the severe deterioration of the performance.^[2,3] Thus, the adhesion property of polymeric binders that provides the mechanical integrity of ASLBs is important. In this presentation, we report on our recent development of polymeric binders whose mechanical strength are improved via chemical method during slurry fabrication process. Promising electrochemical performances of ASLBs using the chemically-modified binders will be presented

References

[1] D. Y. Oh, Y. J. Nam, K. H. Park, S. H. Jung, K. T. Kim, A. R. Ha, Y. S. Jung, *Adv. Energy Mater.* **2019**, 1802927

[2] D. Y. Oh, K. T. Kim, S. H. Jung, D. H. Kim, S. Jun, S. Jeoung, H. R. Moon, Y. S. Jung, *Mater. Today*, **2021** (in press)

[3] K. T. Kim, D. Y. Oh, S. Jun, Y. B. Song, T. Y. Kwon, Y. Han, Y. S. Jung, *Adv. Energy Mater.*, **2021**, 2003766

10:10 PM EN02.15.06

Tuning Schottky Barrier Height at the Interface of Metal and Mixed Conductor Kazunori Nishio¹, Tetsuroh Shirasawa², Koji Shimizu³, Naoto Nakamura¹, Ryota Shimizu¹, Satoshi Watanabe³ and Taro Hitosugi¹; ¹Tokyo Institute of Technology, Japan; ²National Institute of Advanced Industrial Science and Technology (AIST), Japan; ³The University of Tokyo, Japan

Understanding electronic and ionic transport across interfaces is critical for designing high-performance electronic and ionic devices. However, the electronic structures at the interfaces of metals and mixed conductors, which conduct both electrons and ions, remain poorly understood. To quantitatively address the issue, we fabricated thin-film batteries using epitaxial thin films through an in-vacuo process [1]. This study reveals that a Schottky barrier is present at the interface of a Nb-doped SrTiO₃ metal (current collector) and a LiCoO₂ mixed conductor (positive electrode) and that the interfacial resistance can be tuned by inserting an electric dipole layer. Furthermore, the interfacial resistance significantly decreased by more than 5 orders of magnitude upon the insertion of a 1 nm-thick insulating LaAlO₃ layer at the interface [2]. We apply these techniques to solid-state lithium batteries and demonstrate that tuning the electronic energy band alignment by interfacial engineering is applicable to the interface of metals and mixed conductors. These results highlight the importance of designing positive electrode and current collector interfaces for solid-state lithium batteries with high power density.

[1] M. Haruta, T. Hitosugi *et al.*, *Solid State Ion.* 2016, 285, 118-121.

[2] K. Nishio, T. Hitosugi *et al.*, *ACS Appl. Mater. Interfaces* 2021, 13, 15746-15754.

10:15 PM EN02.15.08

The Synthesis of Core-Shell Particles for Lithium-Ion Batteries by Chemical Solution Deposition Dries De Sloovere^{1,2}, Fulya Ulu Okudur^{1,2}, Satish Kumar Mylavarapu^{1,2}, Marlies Van Bael^{1,2} and An Hardy^{1,2}; ¹UHasselt, Belgium; ²EnergyVille, Belgium

Lithium-ion batteries (LIBs) are the most common energy storage technology for portable electronics and electric vehicles. Their performance may be further improved by the synthesis of core-shell particles, where an active material core is coated with a shell consisting of a material with high conductivity. As such, the shell may enhance the energy and power density of batteries containing a liquid electrolyte by creating a network for electron and ion transport. The shell materials may also act as protective coatings for an improved electrochemical stability, e.g. by preventing the dissolution of transition metals, particularly manganese.

This presentation will provide an overview of our recent research on the preparation of core-shell particles for use as positive electrode materials in LIBs. The synthesis of these materials relied on chemical solution deposition (CSD) as coating technique, where the shell material is formed from a solution. By careful control of the hydrolysis and condensation of a titanium precursor dissolved in ethanol, an amorphous TiO₂ layer was formed on the surface of LiNi_{0.5}Mn_{1.5}O₄ (LNMO) particles.¹ Subsequent annealing caused the diffusion of Ti ions into the LNMO surface and the formation of a 2-4 nm thick Ti-rich spinel surface. Ti surface doping suppressed the dissolution of Ni and Mn and thereby increased LNMO's electrochemical stability and rate capability. In another instance, LNMO core particles were coated with amorphous Li₄Ti₅O₁₂ (LTO) using a solution-gel synthesis route.² In this technique, aqueous precursor solutions containing the metal ions are made and mixed in stoichiometric ratios. The LNMO particles are dispersed in the precursor mixture, after which the water is dried off and the resulting material is annealed. The amorphous LTO coating improved LNMO's rate capability and acted as a HF scavenger, increasing the electrochemical stability.

Similar coating techniques were also employed for the coating of titanium oxide layers on $\text{LiNi}_{0.6}\text{Mn}_{0.2}\text{Co}_{0.2}\text{O}_2$ (NMC-622) particles.³ NMC-622 can offer a high energy density owing to its high theoretical capacity. However, increasing the upper cut-off potential to further increase the energy density has a negative impact on its electrochemical stability. Applying a TiO_x coating on the NMC-622 surface was found to have a positive influence on the electrochemical stability of NMC-622/ $\text{Li}_4\text{Ti}_5\text{O}_{12}$ full cells. In half cells, TiO_x coated NMC-622 showcased an improved rate capability compared to the uncoated material. The rate capability of NMC-622 could also be improved by coating it with LiNbO_3 using a solution-gel coating technique. In summary, CSD routes were developed for the synthesis of core-shell materials, consisting of a core of an active material for LIBs, and a shell that provides conductivity and electrochemical stability. The CSD routes are versatile and may be extended to numerous shell and core materials, providing exciting opportunities to improve the latter's performance in various applications.

The authors acknowledge the Research Foundation Flanders (FWO Vlaanderen) for financial support under the project number S005017N (SBO XL-Lion).

- (1) Ulu Okudur, F. et al. RSC Adv. 2018, 8 (13).
- (2) Ulu Okudur, F. et al. Manuscript in preparation.
- (3) Mylavaram, S. K. et al. Submitted.

SESSION EN02.16: Computation and Modeling II
Session Chairs: Javier Carrasco and Fudong Han
Tuesday Morning, December 7, 2021
EN02-Virtual

10:30 AM *EN02.16.01

Atomistic Insights into Oxide and Oxyhalide Solid Electrolyte Materials Saiful Islam; University of Bath, United Kingdom

In the critical area of sustainable energy storage, solid-state batteries are attracting considerable attention due to their potential safety, energy-density and cycle-life benefits [1]. A complete understanding of solid electrolyte materials for lithium- and sodium-ion batteries requires greater fundamental knowledge of their structural, ion transport and interface properties. For example, the impact of aliovalent doping, defect clustering and grain boundaries on Li- and Na-ion conduction properties are often not fully understood on the atomic-scale. This talk will highlight recent studies [2-4] on ion conduction mechanisms, doping effects and grain boundary structures in oxide and oxyhalide anti-perovskite based solid electrolyte materials.

- [1] T. Famprikis et al., *Nature Mater.*, 18, 1278 (2019).
- [2] M.J. Clarke et al. *ACS Appl. Energy Mater.* 4, 5094 (2021).
- [2] J.A. Dawson et al., *Chem. Mater.*, 31, 5296 (2019)
- [3] J. A. Dawson et al., *J. Am. Chem. Soc.*, 140, 362 (2018).

11:00 AM *EN02.16.02

Understanding Bulk and Interfacial Li-Ion Transport in $\text{Li}_7\text{La}_3\text{Zr}_2\text{O}_{12}$ Garnets and Composite Solid Electrolytes Using Atomistic Simulations Javier Carrasco¹, Mauricio R. Bonilla², Fabian A. Garcia Daza³, Pierre Ranque¹, Frederic Aguesse¹ and Elena Akhmatkaya^{2,4}; ¹CIC energiGUNE, Spain; ²Basque Center for Applied Mathematics, Spain; ³The University of Manchester, United Kingdom; ⁴Basque Foundation for Science, Spain

Garnet $\text{Li}_7\text{La}_3\text{Zr}_2\text{O}_{12}$ is a promising solid electrolyte candidate for solid-state Li-ion batteries. However, sufficiently fast Li-ion mobility required for battery applications only emerges at high temperatures, upon a phase transition to cubic structure. A well-known strategy to stabilize the cubic phase at room temperature relies on aliovalent substitution; in particular, the partial replacement of Li^+ by Al^{3+} and Ga^{3+} ions. Yet, fundamental aspects regarding this aliovalent substitution remain poorly understood. Here we present some exciting examples of our most recent theoretical work in this area [1-2] and, with the aid of experiments, also expand our simulation capabilities towards understanding interfacial Li-ion transport in composite materials comprising a conductive, flexible polymer matrix embedding $\text{Li}_7\text{La}_3\text{Zr}_2\text{O}_{12}$ filler particles [3].

We first examine why, despite having the same formal charge, Ga^{3+} substitution yields higher conductivities (10^{-3} S/cm) than Al^{3+} (10^{-4} S/cm). To answer this long-standing question, we combined for the first time molecular dynamic simulations and advanced hybrid Monte Carlo sampling techniques to precisely unveil the atomistic origin of this phenomenon explicitly performing simulations at room temperature [1]. Our results show that Li^+ vacancies generated by Al^{3+} and Ga^{3+} substitution remain adjacent to Ga^{3+} and Al^{3+} ions, without contributing to the promotion of Li^+ mobility. However, while Ga^{3+} ions tend to allow limited Li^+ diffusion within their immediate surroundings, the less repulsive interactions associated with Al^{3+} ions lead to a complete blockage of neighboring Li^+ diffusion paths. This effect is magnified at lower temperatures and explains the higher conductivities observed for Ga-substituted systems.

In addition, we thoroughly compared the room temperature Li-ion diffusion in tetragonal and cubic Al-substituted $\text{Li}_7\text{La}_3\text{Zr}_2\text{O}_{12}$ [2]. Combining the conductivities of individual phases through an effective medium approximation allowed us to estimate the conductivities of cubic/tetragonal phase mixtures that are in good agreement with those reported in several experimental works. This suggests that phase coexistence (due to phase equilibrium or gradients in Al content within a sample) could have a significant impact on the conductivity of Al-substituted $\text{Li}_7\text{La}_3\text{Zr}_2\text{O}_{12}$, particularly at low Al contents.

Finally, we investigate interfacial Li-ion transport in a composite solid-state electrolyte integrating polyethylene oxide (PEO) plus lithium bis(trifluoromethanesulfonyl) imide (LiTFSI) and Ga-doped $\text{Li}_7\text{La}_3\text{Zr}_2\text{O}_{12}$ fillers [3]. Our simulations automatically produce the interfacial Li-ion distribution assumed in previous space-charge models and, for the first time, a long-range impact of the garnet surface on the Li-ion diffusivity is unveiled. Based on our calculations and tensile strength and conductivity experimental measurements, we are also able to explain a previously reported drop in conductivity at a critical filler fraction well below the theoretical percolation threshold.

Overall, by making a thorough comparison with reported experimental data, our theoretical studies and simulations advance the current understanding of Li-ion mobility in $\text{Li}_7\text{La}_3\text{Zr}_2\text{O}_{12}$ garnets and their interfaces with polymer matrices in composite electrolytes. These fundamental insights might guide future in-depth characterization experiments of these relevant energy storage materials.

References

- [1] *ACS Appl. Mater. Interfaces* **2019**, 11, 753.
- [2] *Acta Materialia* **2019**, 175, 426.

[3] *ACS Appl. Mater. Interfaces* **2021**, accepted.

11:30 AM EN02.16.03

Electric Potential Distribution and Interface Impedances in a Solid-State Battery Elliot J. Fuller¹, Evgheni Strelcov², Jamie Weaver², Michael W. Swift³, Joshua Sugar¹, Andrei Kolmakov², Nikolai Zhitenev², Jabez McClelland², Yue Qi⁴, Joseph Dura² and A. A. Talin¹; ¹Sandia National Laboratories, United States; ²National Institute of standards and technology, United States; ³U.S. Naval Research Laboratory, United States; ⁴Brown University, United States

Measuring and predicting potential distributions within solid-state batteries is key to understanding and controlling the mechanisms that limit their performance. We combine Kelvin probe force microscopy (KPFM) and neutron depth profiling (NDP) to map the contact electric potential difference and the corresponding Li distributions within operating Si-LiPON-LiCoO₂ solid-state batteries under open circuit, low current and high current conditions. We observe the largest drop in potential at the anode-electrolyte interface with a smaller drop at the cathode electrolyte interface and a shallow gradient within the bulk of the electrolyte. Cycling at high current irreversibly increases the potential drop at the electrolyte/anode interface, a change that is also observed in impedance spectra collected in situ. We deconvolve the contributions from ions, electrons, and interfaces to the measured potential distributions by correlating KPFM and NDP profiles and by comparisons with a first principles-informed energy 'band' model for ions and electrons.

11:45 AM EN02.16.05

Effect of Polymer Architecture on Microstructure, Segmental Dynamics and Ionic Conductivity in PEO-PMMA Based Solid Polymer Electrolytes Recep Bakar and Erkan Senses; Koc University, Turkey

Poly(ethylene oxide) based solid polymer electrolytes (SPEs) have been increasingly popular due to its fast segmental dynamics, high conductivity, and the ability of solving a wide range of different lithium salts. However, downsides of using PEO are its semi-crystalline nature and poor mechanical performance. The primary challenge for this electrolyte system is to increase the mechanical strength without decreasing ionic conductivity. To achieve this, one technique is to blend PEO with another polymer that can provide mechanical rigidity and eliminate crystallinity. In this sense, a high (T_g) polymer poly(methyl methacrylate) (PMMA) is commonly used. Incorporation of PMMA into PEO significantly increased the mechanical strength and efficiently decreased PEO crystallization. However, there was a major drawback: PEO segmental dynamics decreased dramatically. To overcome this, using various PEO architectures as linear and non-linear ones including stars, hyper-branched and bottlebrushes could be a promising way. Neat non-linear PEOs were reported to have less crystallization and more free volume due to branching compared to linear counterparts. Moreover, there would be fewer contact sites and interpenetration between PEO and PMMA due to topological constraints, which will suppress the decrease in PEO segmental dynamics. To these hypotheses, we used PMMA in blends with varying PEO architectures (linear, stars, hyper-branched and bottlebrushes) and then doped with lithium bis(trifluoromethane-sulfonyl)-imide (LiTFSI) salt to form novel SPEs. XRD results revealed that room temperature miscibility of these polymers can be strikingly expanded over 50 % using non-linear PEO (PEO:PMMA). Temperature modulated DSC results showed two distinct effective glass transition temperatures which could be tuned from linear to non-linear structures with increased number of branching. Broadband dielectric spectroscopy (BDS) measurements have unveiled PMMA segmental dynamics known as α relaxation have increased less for the non-linear PEO/PMMA blends in comparison to their linear counterparts because of less contact sites and interpenetration between PMMA and PEO introduced by the topological changes, suggesting that faster PEO segmental dynamics would be possible and promote ionic conductivity in these systems. The PEO/PMMA blend based electrolytes consisting of 20%wt PEO showed that the ionic conductivity for the bottlebrush PEO architecture was five times greater than the linear counterpart at around room temperature while other non-linear topologies have similar ionic conductivities when compared to linear PEO architecture. Furthermore, extending PEO content over 50wt% PEO in these linear and non-linear PEO/PMMA based solid polymer electrolytes resulted in a significant increase reaching up to 3.6×10^{-4} S/cm, as high as one order of magnitude at room temperature and three times higher at higher temperatures up to in the ionic conductivities when compared to ionic conductivities of pure PEO based electrolytes usually ranged between 10^{-5} - 10^{-4} S/cm. Thus, this study indicates promising results such that non-linear PEO/PMMA based solid polymer electrolytes with faster segmental dynamics and higher PEO content could potentially lead higher ionic conductivities required for the application standpoint of the PEO based solid polymer electrolytes. Eventually, room temperature mechanical characteristics for PEO/PMMA blends will be also discussed.

11:50 AM EN02.16.06

Computation Discovery and Design of Chloride Lithium-Ion Conductors Yunsheng Liu, Shuo Wang, Adelaide Nolan and Yifei Mo; University of Maryland, United States

All-solid-state Li-ion batteries require Li-ion conductors as solid electrolytes (SEs). Li-containing halides are emerging as a promising class of lithium-ion conductors with good electrochemical stability and other properties needed for SEs in all-solid-state batteries. Compared to oxides and sulfides, Li-ion diffusion mechanisms in Li-containing halides are less well understood, in particular regarding the effects of Li content and cation sublattices, which can be tailored for improving Li-ion conduction. Using first-principles computation, a systematic study is performed on the Li-ion conduction of known Li-containing chlorides with close-packed anion frameworks and a wide range of their doped compounds. A dozen potential chloride Li-ion conductors are predicted with increased Li-ion conductivities, and it is revealed that the Li-ion migration is greatly impacted by the cation configuration and concentrations. By analyzing a large set of materials data, it is proposed that low Li content, low cation concentration, and sparse cation distribution increase Li-ion conduction in chlorides, and these principles are demonstrated in designing new chloride Li-ion conductors. This study provides insights into the effects of the cation sublattice on Li-ion diffusion, highlights potential chloride Li superionic conductors, and proposes design principles to further develop halide Li-ion conductors.

Paper reference:

Liu, Y., Wang, S., Nolan, A. M., Ling, C., Mo, Y., Tailoring the Cation Lattice for Chloride Lithium-Ion Conductors. *Adv. Energy Mater.* 2020, 10, 2002356. <https://doi.org/10.1002/aenm.202002356>

11:55 AM EN02.16.07

Analyzing Microstructural Implications on Fast Charge Behavior of Solid-State Batteries Bairav Sabarish Vishnugopi and Partha Mukherjee; Purdue University, United States

Solid-state batteries (SSBs) that pair an inflammable solid electrolyte with a lithium metal anode can potentially improve the energy density, power density and safety of current lithium-ion batteries. Designing a composite cathode with sufficient ionic/electronic transport pathways and active interfacial area is pivotal to achieve optimal rate performance in SSBs. Electrode microstructure-coupled transport and kinetic interactions affect the evolution of internal resistive pathways, utilization of active material and the electrochemical reaction distribution within these systems. In this work, we analyze the mesoscale underpinnings of electrode microstructure on the underlying kinetic-transport mechanisms, thermo-electrochemical interplay, and the resulting influence on cell performance. Design criteria including the fraction of conductive additives and particle sizes required to achieve fast charge/discharge rates in SSBs are discussed.

12:00 PM EN02.16.09

Impact of Protonation on the Electrochemical Performance of $\text{Li}_7\text{La}_3\text{Zr}_2\text{O}_{12}$ Garnets [Rabeb Grissa](#), Seyedhosein Payandeh, Meike Heinz and Corsin Battaglia; Empa-Swiss Federal Laboratories for Materials Science and Technology, Switzerland

$\text{Li}_7\text{La}_3\text{Zr}_2\text{O}_{12}$ (LLZO) garnet ceramics are promising electrolytes for all-solid-state lithium-metal batteries with high energy density. However, these electrolytes are prone to Li^+/H^+ exchange, that is, protonation, resulting in degradation of their Li-ion conductivity. Here, we identify how common processing steps, such as surface cleaning in alcohol or acetone, trigger LLZO partial protonation¹. We deconvolute the contributions to the electrochemical impedance spectra of both the protonated LLZO phase (HLLZO) and its decomposition products forming upon annealing. While the mixed conduction of H^+/Li^+ ions in HLLZO decreases the contribution of the electrolyte to the overall impedance, it deteriorates the transport of Li^+ ions across the LLZO/Li interface. This is also the case after thermal decomposition of HLLZO, which occurs at significantly lower temperature than that for pristine LLZO. As a result, symmetric Li/LLZO/Li cells suffer from inhomogeneous lithium electrodeposition within the first three cycles when stripping and plating a capacity of 1 mAh/cm² per half-cycle at 0.1 mA/cm². We demonstrate that LLZO protonation is avoided when applying solvents with very low acidity, such as hexane. Such Li/LLZO/Li cells provide stable cycling over more than 300 h, demonstrating the importance of selecting an appropriate solvent for LLZO processing to prevent dendrites formation.

Reference:

1. Grissa, R., Payandeh, S., Heinz, M. & Battaglia, C. Impact of Protonation on the Electrochemical Performance of $\text{Li}_7\text{La}_3\text{Zr}_2\text{O}_{12}$ Garnets. *ACS Appl. Mater. Interfaces* **13**, 14700–1409 (2021).

12:03 PM EN02.16.10

Molecular Dynamics Simulations of Hydroxide Diffusion in Polymer Electrolytes Young C. Kim, Michelle D. Johannes, Brian L. Chaloux and [Megan B. Sassin](#); U.S. Naval Research Laboratory, United States

Many factors affect the conduction of ions through polyelectrolyte membranes including: water and ion content, glass transition (T_g) of the polymer, dielectric constant of the medium, and microstructure (e.g. aggregation, microphase separation). Determining the effects that chemical changes to a polymer will have on the conductivity of the resulting ion exchange materials requires characterizing and deconvoluting the many different properties that depend upon polymer chemistry. Molecular dynamics (MD) simulations can be applied to rapidly screen whether candidate changes to a polyelectrolyte's structure will have the desired effect on ion transport.

Poly(dimethylaminomethyl styrene) (pDMAMS) is a structurally simple polymer capable of hydroxide conduction after quaternization with CH₃I and OH⁻ exchange. The effects of changing ion content on OH⁻ ion diffusivity in anhydrous, quaternized pDMAMS are studied using MD simulations on linear co-polymers of 4-dimethylaminomethylstyrene (4-DMAMS) and 4-butylstyrene, selected for its similar T_g to pDMAMS. Molecular dynamics is utilized to characterize truly anhydrous systems, whereas most experimental materials would contain a non-negligible amount of tightly bound water. Increasing content of neutral 4-butylstyrene over methylated 4-DMAMS results in a tradeoff between increased polymer flexibility and decreased dielectric strength and ion content. MD simulations are performed on co-polymers with 4-butylstyrene content from 0% to 75%. At 300 K, MD simulations yield an OH⁻ self-diffusion coefficient of ~0.05 $\mu\text{m}^2/\text{s}$ in pure methylated pDMAMS (0% 4-butylstyrene). As the 4-butylstyrene content of co-polymers increases up to 50%, OH⁻ diffusivity decreases by a factor of two, but at 75% 4-butylstyrene content, the OH⁻ diffusion constant increases by a factor of two compared to that of 100% methylated pDMAMS. The glass transition temperature of the co-polymers decreases as the 4-butylstyrene content increases, from ~800 K at 0% 4-butylstyrene to ~500 K at 75%, thus providing a more mobile platform for OH⁻ at high 4-butylstyrene content. The dramatic decrease in T_g with increasing 4-butylstyrene but minimum OH⁻ diffusivity at ~50% 4-butylstyrene shows that there are competing factors affecting hydroxide conduction in these materials. Simulations of alternating and random co-polymers show that the patterning of co-polymers has little effect on the OH⁻ diffusivity. This study presents a computational framework to understand fundamental principles regarding hydroxide conduction in polymer electrolytes.

SESSION EN02.17: Anodes and Interphases
Session Chairs: Montserrat Casas-Cabanas and Fudong Han
Tuesday Afternoon, December 7, 2021
EN02-Virtual

1:00 PM *EN02.17.01

Lithiophobic-Lithophilic Gradient Interlayer Enabled Solid-State Lithium Metal Batteries Chunsheng Wang and [Hongli Wan](#); University of Maryland, United States

A low Li plating/stripping Coulombic efficiency and continuous lithium dendrite growth are two critical challenges for all-solid-state batteries. Here, we address both challenges by inserting a mix-conductive interlayer between electrolyte and Li anode. The lithiophilic side of interlayer promotes the uniform deposition of lithium, while lithiophobic layer inhibits the Li plating on electrolyte surface and prevents the lithium dendrite growth. The mixed ionic/electronic conductive interlayer enables Li anode to achieve a high Coulombic efficiency (CE) of 99.6%, which is the highest CE reported. The electrochemical performance of solid state Li/LiCoO₂ full cells was also investigated.

1:30 PM *EN02.17.02

Solid-State Batteries with High-Capacity Anodes—Interface Evolution and Chemo-Mechanics [Matthew T. McDowell](#); Georgia Institute of Technology, United States

Solid-state batteries offer the promise of improved energy density and safety characteristics compared to lithium-ion batteries, but electro-chemo-mechanical evolution and degradation of materials and interfaces can play an outsized role in limiting their performance due to the all-solid nature of these systems. Here, I will present my group's recent work using *in situ* and *operando* experiments to understand interfacial evolution and stress changes in solid-state batteries with lithium metal and alloy anodes. *Operando* X-ray tomography is used to reveal interfacial dynamics in solid-state batteries with Li metal anodes. Segmentation and detailed image analysis enable correlation of interfacial contact loss to electrochemical behavior of symmetric cells, and the loss of interfacial contact area at the Li metal interface is found to cause current constriction and cell failure. The effects of interphase formation on mechanical degradation, stress evolution, and contact area loss are also discussed. Finally, stack pressure evolution during cycling of full solid-state batteries is measured *in situ* and correlated with fundamental processes within electrode materials and the properties of composite electrode structures. Cells with alloy-based anodes are found to exhibit large (megapascal-level) changes in stack pressure during cycling in a constant volume cell casing, with stable capacity and stress changes over long-term cycling. Together, these findings show the importance of controlling chemo-mechanics and interfaces in solid-state batteries.

2:00 PM EN02.17.03

Analysis of Interphase Formation between Metal Ion Containing Solid Electrolytes and the Lithium Metal Anode in Solid-State Batteries Luise Riegger^{1,2}, Svenja-Katharina Otto^{1,2}, Sven Jovanovic³, Steffen Merz³, Marcel Sadowski⁴, Olaf Kötzi^{1,2}, Roman Schlem⁵, Sascha Harm^{6,7}, Robert Calaminus^{7,8}, Simon Burkhardt^{1,2}, Felix Richter^{1,2}, Joachim Sann^{1,2}, Wolfgang Zeier⁵, Bettina V. Lotsch^{7,6}, Karsten Albe⁴, Josef Granwehr³ and Jürgen Janek^{1,2}; ¹Justus Liebig University, Germany; ²Center for Materials Research (LaMa), Germany; ³Forschungszentrum Jülich GmbH, Germany; ⁴Technische Universität Darmstadt, Germany; ⁵University of Muenster, Germany; ⁶Ludwig-Maximilians-Universität München, Germany; ⁷Max Planck Institute for Solid State Research, Germany

Solid electrolytes (SEs) containing metal ions such as Li_3InCl_6 or Li_7SiPS_8 have gained interest for applications in solid-state batteries (SSBs) in recent years due to their high ionic conductivities. However, there are still some challenges to overcome, such as their inherent reduction instability, which impedes the application with a lithium metal anode (LMA) [1].

If the decomposition layer formed upon contact of a SE with lithium metal contains electronically conducting compounds like metals, the decomposition layer can form a mixed conducting interphase (MCI) that continues to grow until either lithium is depleted or the SE is completely reduced. As a result of the metal dispersed in the MCI, the electronic conductivity of the cell should increase, which in turn decreases the internal cell resistance and leads to short circuits [2]. However, this is not the case for all metal ion containing SEs. The resistance of a $\text{Li}|\text{Li}_3\text{InCl}_6|\text{Li}$ cell, for example, constantly increases during the decomposition. Despite the fact that indium metal is among the formed decomposition products the interphase behaves like a Solid Electrolyte Interphase with a low interphase conductivity [3]. Therefore, knowledge about the composition of the interphase between lithium metal and SEs as well as the temporal evolution of the cell resistance is crucial.

Here, we report our latest findings on the stability of a variety of metal ion containing SEs in contact with lithium metal. We further cover the kinetics of the heterogeneous solid-state reaction and the chemical composition of the resulting interphase. Impedance spectroscopy measurements were conducted to investigate the temporal evolution of the interphase resistance between the lithium metal anode and the SE. *In situ*-sputter-deposition of lithium metal onto the surface of the SE pellets and subsequent X-ray photoelectron spectroscopy measurements were performed to study the chemical composition upon contact. Multiple repetitions of these steps allow a detailed characterization and identification of the decomposition products within the forming interphase. By additionally employing time-of-flight secondary ion mass spectrometry, we were able to categorize the interphase and estimate its spatial extension. Combining the results allows a detailed distinction between possible interphases of metal ion containing electrolytes and thereby promotes the understanding of the SE stability toward LMAs.

References:

- [1] X. Li, J. Liang, X. Yang, K. Adair, C. Wang, F. Zhao, X. Sun, *Energy Environ. Sci.* (2020) 10.1039/C9EE03828K
- [2] S. Wenzel, T. Leichtweiss, D. Krüger, J. Sann, J. Janek, *Solid State Ion.* 278 (2015) 10.1016/j.ssi.2015.06.001
- [3] L. Riegger, R. Schlem, J. Sann, W. Zier, J. Janek, *Angew. Chem.* (2020) 10.1002/ange.202015238

2:15 PM EN02.17.04

Building Li Free Anodes for Solid-State Batteries Kevin Guo; Ford Motor Company, United States

Solid state batteries (SSB) offer potential advantages over traditional lithium ion batteries in energy density, safety and battery packing. Much of the prior work has focused on the development of solid electrolytes but the anodes and cathodes are also key to delivering the potential benefits of a SSB. The anode of a SSB could use several different choices of active material, such as graphite, silicon, graphite/silicon, and Li metal, which is generally considered as the ultimate choice for a SSB due to its high specific capacity. However, since in principle the cathode provides all Li needed in the battery operation, there is technically no need to put extra Li in the anode to achieve an operating cell.

Various concepts for a Li-free anode have been studied, but there are many challenges to implement this concept. Particularly when the anode only consists of current collector, inducing Li to plate and strip at the interface between LLZO and current collector has proven difficult. We start with approaches to directly reduce the interfacial resistance between LLZO and the current collector by sputtering a thin film of metal directly onto the LLZO separator. A simple test cell is used with a Li metal foil on one side of a LLZO separator which has a metal film and current collector on other side. At the beginning of performance testing, the cell requires an "initialization" by plating a small amount of Li onto the current collector. This initial charging conditions the interface between the metallized LLZO and the current collector and the quality of new interface affects the performance of cell in terms of the critical current density and cycling behavior. In this work, two type of metallization (Au or Cu) are used to explore this approach. The impact of initial Li plating for various values of current and total deposited capacity is described. In addition, the impact of operating temperature is investigated.

2:30 PM EN02.17.05

On the Cause of Pore Formation and the Limitation of Pore Annihilation at Lithium Metal/Solid electrolyte Interfaces Lisette Haarmann¹, Stefanie Frick¹, Shreyas Ramachandran², Jochen Rohrer¹ and Karsten Albe¹; ¹Technische Universität Darmstadt, Germany; ²Birla Institute of Technology & Science, India

Pore formation at the lithium metal anode (LMA) | solid electrolyte (SE) interface is a key obstacle in the path to utilizing LMAs in solid state batteries (SSB) at the industrial level.

Oftentimes it is theorized that this pore formation would occur due to an insufficient vacancy diffusion within the LMA. Recently, however, it has been shown that the interfacial work of adhesion between the LMA and the SE is a key factor in determining if vacancy agglomeration at the LMA | SE interface is thermodynamically favored. [1]

In order to computationally address the kinetics of this system at finite temperature, kinetic Monte Carlo (KMC) simulations based on a nearest neighbour bond counting approach are applied in this work. As SE, differently treated garnet $\text{Li}_7\text{La}_3\text{Zr}_2\text{O}_{12}$ (LLZO) were considered [2].

It was found that neither the formation, nor the annihilation of pores are a result of slow vacancy diffusion. The pore formation, on the one hand, is mainly influenced by the interface thermodynamics between the LMA and the SE. The pore annihilation, on the other hand, is limited by the stripping of vacancies from the pore surface.

Within the implemented setup, an analytical expression for the anodic critical current density, beyond which the interface becomes morphologically unstable, was defined. The results are in accordance with values determined experimentally by electrochemical impedance spectroscopy (EIS) measurements and reveal an order of magnitude variation depending on the interface thermodynamics. Likewise, the time until full contact loss, t_0 , strongly depends on the interaction strength between the LMA and the SE. For a given LMA|SE interaction energy, the experimentally observed square root dependence between t_0 and the applied stripping current density was reproduced [3].

The analysis of pore dissolution in a lithium metal bulk cell showed that the healing time (until a pore is completely dissolved) can be described by an

analytical model of precipitate shrinkage if the curvature of the pore surface is taken into account. Moreover, it was concluded that the transfer of vacancies into the bulk is the limiting step of pore dissolution, which is in accordance with activation barriers determined by Density Functional Theory (DFT) calculations.

Finally, a proposed method to attenuate and/or compensate pore formation at the LMA | SE interface, namely the introduction of a thin ionic liquid interlayer (IL) [4], is incorporated within the KMC model. The experimentally observed increase in the time until contact loss is reproduced and attributed to a suppression of vacancy kinetics at the interface due to an instantaneous adjustment of the IL until its maximal volume expansion is reached.

[1] Seymour, I., & Agudero, A. (2021). Suppressing Void Formation in All-Solid-State Batteries: The Role of Interfacial Adhesion on Alkali Metal Vacancy Transport. *Journal of Materials Chemistry A*

[2] Sharafi, A., Kazyak, E., Davis, A. L., Yu, S., Thompson, T., Siegel, D. J., ... & Sakamoto, J. (2017). Surface chemistry mechanism of ultra-low interfacial resistance in the solid-state electrolyte Li₇La₃Zr₂O₁₂. *Chemistry of Materials*, 29(18), 7961-7968.

[3] Krauskopf, T., Mogwitz, B., Hartmann, H., Singh, D. K., Zeier, W. G., & Janek, J. (2020). The Fast Charge Transfer Kinetics of the Lithium Metal Anode on the Garnet Type Solid Electrolyte Li_{6.25}Al_{0.25}La₃Zr₂O₁₂. *Advanced Energy Materials*, 10(27), 2000945

[4] Fuchs, T., Mogwitz, B., Otto, S. K., Passerini, S., Richter, F. H., & Janek, J. (2021). Working Principle of an Ionic Liquid Interlayer During Pressureless Lithium Stripping on Li_{6.25}Al_{0.25}La₃Zr₂O₁₂ (LLZO) Garnet Type Solid Electrolyte. *Batteries & Supercaps*.

2:35 PM EN02.17.07

Soybean Oil Derived Solid-State Electrolytes for Lithium Batteries Ashish Raj¹, Satyanarayana Panchireddy¹, Bruno Grignard², Christophe Detrembleur² and Jean-Francois Gohy¹; ¹Université Catholique de Louvain, Belgium; ²University of Liège, Belgium

The solid-state battery has drawn a huge interest with its motive to overcome the issues and challenges faced by batteries using conventional liquid electrolytes. The novel idea of using green approaches or bio-based sources for lithium batteries excites many researchers due to their eco-friendly, less carbon footprint in its synthesis and recycling at the end. In this work, we report a full bio-based solid-state electrolyte based on functionalized carbonated soybean oil (CSBO) obtained from the naturally occurring epoxidised soybean oil (ESBO) using CO₂ and biomass. CSBO shows remarkable adhesive properties as characterized by rheological measurements owing to its bigger chains bearing multifunctional cyclic carbonates. LiTFSI salt reinforced CSBO was characterized following standard electrochemical measurements exhibiting ionic conductivity to ~10⁻³ S cm⁻¹ at 100 °C and 10⁻⁵ S cm⁻¹ at room temperature. The electrochemical window for this electrolyte was obtained to be 4.8 V (vs. Li/Li⁺) and transference number up to 0.31, allowing it to be explored for high voltage cathodes. CSBO shows stable stripping and plating behaviour for longer cycles making it a good candidate for higher coulombic efficiency electrolyte batteries. We also demonstrated the galvanostatic charge-discharge of LiFePO₄ (Lithium Ferrophosphate, LFP) with CSBO electrolytes delivering the gravimetric capacity of 124 mAhg⁻¹ and 150 mAhg⁻¹ appx. at ambient room and higher temperature respectively. Therefore, our study provides a promising direction of developing bio-based solid electrolytes to facilitate progress in sustainability, cost-effective and safe manner to create a solid-state lithium-ion battery for global utilization.

2:40 PM EN02.17.08

Fabrication of LLZO Powder and Fibres and Their Application in PEO-LLZO Composite Solid Electrolytes Tor Olav O. Sunde, Laure Guironnet, Maria Teresa Guzman Gutierrez, Roberto Scipioni, Marius Sandru, Peter Molesworth, Nils Wagner and Anita H. Reksten; SINTEF Industry, Norway

The dramatic possible effects of climate change are becoming clearer day by day. Batteries are a key technology to reach the UN Sustainable Development Goals, by accelerating the shift to zero-emission transportation and providing energy storage to allow for an increased proportion of intermittent renewable energy sources. However, today's conventional lithium-ion batteries with a liquid electrolyte are steadily reaching the limit of their physiochemical energy density, while safety issues related to the flammable liquid electrolyte remain a challenge. Solid state batteries, on the other hand, offers the potential of high safety, high energy density and high power density. There are many classes of solid electrolytes, each with their own advantages and disadvantages. Hybrid composite electrolytes, with ceramic fillers in a solid polymer electrolyte, offers the potential to overcome the disadvantages related to both ceramic and polymeric electrolytes alone.

Here, we present a detailed investigation of the fabrication and performance of solid poly (ethylene oxide) (PEO) - Li_{6.25}Al_{0.25}La₃Zr₂O₁₂ (Al-doped LLZO) composite electrolytes. LLZO powder and fibres were prepared, by solid state reaction and needleless electrospinning, respectively. Both fabrication routes were chosen due to their scalability. For the powder, the effect of the calcination temperature and ball milling on the phase purity and particle size of the LLZO powder was investigated. The preparation of solutions for needleless electrospinning is more challenging than for conventional electrospinning. Here, the conductivity and viscosity to prepare spinnable solutions for needleless electrospinning was investigated, as well as the effect of the calcination temperature on the phase purity. The solid electrolytes were prepared by casting composites of the ceramic fillers in PEO with lithium bis(trifluoromethanesulfonyl)imide (LiTFSI). The effect of ceramic filler content, particle size and morphology and dopamine functionalization on the solid electrolyte performance was investigated. While there are several reports of these effects studied individually, a detailed understanding of their combined effects appears to still be lacking, which is necessary for composite electrolytes to successfully reach their potential.

SESSION EN02.18: Cell Architecture and Fabrication II

Session Chairs: Fudong Han and Yuyan Shao

Tuesday Afternoon, December 7, 2021

EN02-Virtual

4:00 PM *EN02.18.01

Towards Low-Cost Solid State Li-S Batteries Jianbin Zhou, Shen Wang, Charles Soulen and Ping Liu; University of California, San Diego, United States

Li-S batteries promise high energy density, low cost, and free of resource constraints of transition metals. Solid state Li-S also in principle circumvents the soluble sulfur species involved in its liquid electrolyte counterpart, resulting in longer cycle life. However, the volume change of both Li and S cathode, the insulating nature of S, and the tendency of Li dendrite-related cell shorting have continued to plague the technology. In this talk, we will report our recent effort towards building a long-life solid state Li-S cell. To stabilize the Li anode, we employ porous carbon as a mixed-conducting 3D host for Li metal. This reduces the effective current density acting on the electrolyte layer, increases the apparent critical current and mitigates cell shorting. To reduce the thickness and enhance the mechanical stability of the electrolyte, we use in-situ polymerization to form nanoscopic composites of sulfide-based solid electrolytes. Finally, we engineer sulfur cathodes with intrinsic electronic conductivities and limited volume changes to extend cycle life. With

advancements on all components of the cell, we will fully realize a long-life, low-cost solid state Li-S technology.

4:30 PM *EN02.18.02

Thin-Film Glassy Solid Electrolytes Enabling High Energy Density Li and Na Batteries [Steve W. Martin](#); Iowa State University, United States

Fast ion conducting glasses have long been considered as alternatives to flammable liquid electrolytes in Li and Na batteries. However, for such glassy solid electrolytes (GSEs) studied so far, they have lacked the unique combination of required electrochemical properties for use as a solid electrolyte with the equally important requirements of viscoelastic behavior to form them into thin films suitable for high ion conductivity separators. Indeed, to date, most GSEs are considered as “invert” glasses where the high viscosity promoting glass formers in the compositions, such as SiO₂, B₂O₃, or P₂O₅ are not the dominant component, but rather are the minor component and the alkali salt, such as Li₂O or Na₂O is the majority component. This has led to the general observation that such high alkali content invert glasses are rather poor glasses formers that crystallize rapidly upon heating above their glass transition temperature into the viscoelastic supercooled liquid regime. This has forced most workers in this field to consider only fully crystallized polycrystalline ceramic versions of these compositions or at most glass ceramics where the crystalline phase is dominant, > 90 v/v%. In this first ever report of thin film fast ion conducting glasses made by viscoelastic deformation processing of redrawing glass preforms, we report new compositions where we have broken this long standing paradigm of high conductivity combined with high alkali salt concentration but poor glass formability and will summarize our efforts to produce thin films of Li and Na ion conducting glasses and test in them in symmetric and asymmetric cells.

5:00 PM EN02.18.03

Safe Flexible Rechargeable Batteries with Subzero-Temperature Operation and Self-Charging Capabilities [Ying Wang](#); Louisiana State University, United States

Flexible solid-state batteries are designed to be conformal, lightweight, and can be rolled without any loss of energy. They are needed for powering wearable electronics, smart packaging, and medical devices, etc. Most of them target at room temperature applications, as the sluggish ionic transport in the solid-state electrolytes degrades even faster at lower temperature. Though organic electrolytes allow for a wide working temperature window, most organic electrolytes require expensive, tedious, and toxic synthesis processes. Recently, rechargeable batteries based on aqueous electrolytes have shown high potential attributed to their low cost and intrinsic safety. For instance, the zinc ion battery (ZIB) is attractive owing to its stable zinc anode from abundant sources, features of multivalent charge transfer, a superb theoretical capacity and low redox potential of the zinc anode. Another appealing choice is an aqueous battery using non-metal ions as charge carriers, such as NH₄⁺ with a lighter molecular weight (18 g mol⁻¹) than metal ions above and a small hydrated ionic size of 3.31 Å, leading to faster ion diffusion in the electrolyte. However, the use of aqueous electrolytes poses a challenge due to its freezing at sub-zero temperature.

In this work, concentrated hydrogel electrolytes are employed to construct flexible zinc ion batteries and ammonium ion batteries that can operate at subzero temperature with better safety and lower cost, while maintaining high energy/power and long cycling life. The quasi-solid-state electrolyte is simply synthesized via using respective salt, water, and hydrophilic polymer (e.g., biodegradable edible xanthan gum). The composition of the electrolyte is optimized to maximize the battery performance. A flexible ZIB is assembled using the hydrogel electrolyte sandwiched between a vanadate cathode and a zinc anode, while a flexible ammonium ion battery consists of the electrolyte between a vanadate cathode and a polyaniline anode. For example, the flexible ZIB exhibits a very high capacity of 239 and 83 mAh g⁻¹ under 0.2 A g⁻¹ at -20 degreeC and -40 degreeC, respectively. Additionally, chemically self-charging flexible batteries are fabricated, which are different from conventional self-charging systems relying on energy sources. Notably, the ZIB can be chemically self-charged by the oxidation reaction between the cathode and the oxygen in air. The flexible ZIB delivers a specific discharge capacity of 179 mAh g⁻¹ after the cathode is exposed to air and oxidized for 12 hours at room temperature, exhibiting a decent self-recharging ability. As such, this study sheds new light on the utilization of concentrated hydrogel electrolytes in flexible batteries with new capabilities, for developments of next-generation electrochemical energy storage technology with high safety and low cost.

5:15 PM EN02.18.04

In Situ FIB as a Method to Prepare and Characterize Solid-State-Batteries [Yevheniy Pivak](#), Christian Deen-van Rossum and Hugo H. Pérez Garza; Denssolutions, Netherlands

In situ biasing Transmission Electron Microscopy technique is a powerful tool to reveal morphological and structural changes in solid state battery samples at the nanoscale during charge and discharge cycles. It has an advantage over other methods like X-ray or Neutron Diffraction as it provides a direct observation on the dynamic evolution of crystal and electronic structures and can uncover intrinsic mechanisms behind it. The former one is especially important as it accounts for the performance of batteries.

One of the main limitations in the application of in situ biasing TEM to study solid state batteries is FIB lamella sample preparation process. It's not only complicated, but it also possess a very low success rate and as a result, very time consuming. In general, preparing a clean and electrically connected biasing sample without electrical short circuit is a challenging task. There are a lot of pitfalls when preparing FIB lamellas for electrical experiments. Often the preparation process needs to be repeated several times after unsuccessful TEM experiments due to sample's bad electrical quality. These repetitions cost additional FIB and TEM time.

In this work we would like to present a new method of preparing and preliminary characterizing solid state battery samples in a dual beam microscope - an in situ FIB. This method is based on MEMS Nano-Chips designed for biasing and heating and biasing TEM experiments. The method uses a modified SEM stub, e.g. FIB stub with electrical connections to the outside world. The stub is specifically designed to prepare the FIB lamella on the MEMS chip in one go (without breaking the vacuum). During the preparation, the sample can be biased to check for short circuits and for proper electrical connection to the sample, ensuring the good quality of the lamella. We will also discuss how the tool can be employed to do further characterization of the sample inside FIB/SEM and its correlation with the in situ TEM technique.

5:30 PM EN02.18.05

Utilizing iCVD to Polymerize Thin, Conformal Electrolytes for Alkaline Batteries [Megan B. Sassin](#), Brian L. Chaloux, Jeffrey Long, Joel Miller and Debra R. Rolison; U.S. Naval Research Laboratory, United States

Polymer electrolytes can provide several advantages over liquid electrolytes in alkaline battery architectures. Mechanically robust polymer separators such as Celgard membranes inhibit dendrite growth and can be made exceptionally thin, which increases current density by minimizing IR losses. However, preparing ionically conductive, submicron-thick polyelectrolyte films on nonplanar electrode geometries remains a challenge for solution and melt polymer processing methods.

We use free radical-initiated chemical vapor deposition (iCVD) of styrenic monomers to grow 100 nm – 1 μm thick films on a variety of metallic and insulating substrates and then convert the polymer into anion-conductive polyelectrolytes. By judicious choice of quaternization and ion-exchange conditions, the thin-film polymer survives conversion from hydrophobic insulator to high ion-exchange capacity (IEC up to 3 mEq g⁻¹) polyelectrolyte

without delamination or pinhole formation. The single-ion conductivity of bicarbonate (HCO_3^-), the equilibrium anionic species, is measured by impedance spectroscopy of the films on interdigitated electrodes as a function of relative humidity; the films exhibit modest conductivity even when equilibrated at low relative humidity.

The chemical structure of these thin films is characterized using surface overlayer enhanced ATR-IR spectroscopy and X-ray photoelectron spectroscopy to determine their similarity to previously reported iCVD-grown polymer and bulk materials polymerized using the same monomer and initiator. Solid-state magic-angle spinning ^1H and ^{13}C NMR spectroscopy performed on films grown on high surface-area substrates allows us to contrast chemical structure in the supported thin-film expression with their bulk-polymerized counterparts.

5:35 PM EN02.18.06

Lithium Vanadium Oxide Made by Co-Sputtering as a Cathode Material for Solid-State Batteries Victoria Castagna Ferrari, Nam Soo Kim, Sang Bok Lee, Gary Rubloff and David Stewart; University of Maryland, College Park, United States

Solid-state batteries (SSBs) are emerging as the next devices to substitute conventional lithium-ion batteries. Besides improved safety and reliability, the capability of thin film processing to design devices in novel form factors creates new opportunities in energy storage. Nevertheless, the most common cathode material used in thin film batteries is lithium cobalt oxide (LCO), which is only electrochemically active in a particular phase formed at 500 °C, and there are many reports of Li deficiency in the films after annealing. In pursuit of a low temperature alternative which will also address the Li deficiency, we have studied a new process to deposit lithiated vanadium oxide (LVO) thin films as a promising cathode material for application in SSBs. Vanadium oxide (V_2O_5) has a layered structure that can be preserved with the insertion of up to 2 lithium ions, giving it a higher theoretical capacity when compared to LCO. Herein, the lithium content of the cathode is controlled simultaneously with the deposition of the vanadium oxide host on a silicon wafer substrate using a co-sputtering process, where two targets – vanadium oxide (V_2O_5) and lithium oxide (Li_2O) – are run at the same time to produce the films.

The LVO co-sputtering process was studied and analyzed, including structural characterization and electrochemical evaluation using a conventional liquid cell. A SSB employing the LVO as a cathode was successfully fabricated, and presented electrochemical activity with good reversibility at different electrochemical conditions, which proves that the LVO is a good candidate as a cathode material for SSBs. The power of the V_2O_5 target was fixed at ~150 W while the Li_2O target power was varied to change the amount of lithium in the LVO films to have a desirable capacity during charge and discharge. The effect of a post-deposition annealing at 300 °C was also studied in comparison to LVO samples produced at ambient temperature. To the best of our knowledge, this is the first time that a successful co-sputtered lithiated vanadium oxide material is fabricated and tested in a SSB.

Raman spectroscopy indicates that some peaks correspond to vibrations which are found in crystalline V_2O_5 films, but it suggests that the LVO has its own characteristic peaks. A post-deposition annealing step did not dramatically alter the Raman spectrum, but the vibrational modes were better preserved after electrochemically cycling when the LVO is post-annealed at 300 °C under a nitrogen atmosphere. Surface analysis obtained from XPS confirmed a lithiated V_2O_5 composition up to 3 lithium ions per vanadium oxide. The best LVO film held ~70 % of the theoretical capacity (1 lithium per V_2O_5) as calibrated by liquid cell testing, and less when used in a SSB, but showed excellent reversibility in early cycling and a higher voltage than bulk V_2O_5 . The use of co-sputtered LVO in SSBs will still be further investigated, but the preliminary results indicate the developed LVO is an excellent candidate for a cathode material. The use of a relatively low post-annealing temperature to produce an electrochemically active material, and the possibility to apply the developed co-sputtering process with different ion species, like magnesium or sodium, reveal the potential use of this work for a broader range of solid-state devices.

5:40 PM EN02.18.07

Lithium Cyanophosphine Sol-Gels as Polyelectrolyte Matrices for Li^+ Conduction Brian L. Chaloux, Megan B. Sassin, Andrew Purdy and Albert Epshteyn; Naval Research Laboratory, United States

A primary hazard associated with lithium ion batteries is the combustibility of the liquid electrolyte, which is a key component for conduction of Li^+ between anode and cathode. Polymer electrolytes can nominally improve safety by reducing the quantity and volatility of organic species. However, their poor room-temperature conductivity (10–100× lower in plasticized PEO than in pure propylene carbonate) and propensity to pyrolyze into volatile, flammable species at sufficiently elevated temperature makes them less-than-ideal electrolytes for lithium-ion batteries.

Lithium dicyanamide – $\text{LiN}(\text{CN})_2$, itself a lithium salt explored for battery electrolytes – is shown to react with cyanophosphines (e.g. $\text{P}(\text{CN})_3$, $\text{RP}(\text{CN})_2$ where R is an aromatic moiety) in up to a 2:1 mole ratio, resulting in cross-linked sol-gel networks that fully incorporate both monomers. The high phosphorus and low hydrocarbon content of the resulting lithium cyanophosphine yields a material that is thermo-oxidatively stable, while simultaneously providing a high density of labile Li^+ (up to 5 mEq g^{-1}).

Pulsed field gradient (PFG) ^1H , ^7Li , and ^{13}C NMR spectroscopies were utilized to demonstrate that: a) Oligomerization of both dicyanamide and cyanophosphine definitively occurs prior to gelation; b) Negligible amounts of either monomer remain unreacted; and c) Lithium remains effectively coordinated by the solvent, diffusing in concert with solvent instead of the oligomeric cyanophosphine polyanions. The resulting sol-gels exhibit a Li^+ transference number near unity when used as an electrolyte between lithium foils, in accordance with NMR data showing negligible polyanion diffusivity under these conditions. Application of the measured Li^+ -solvent complex diffusion coefficients as the reaction mixture approaches gelation also allows estimation of Li^+ mobility and, by proxy, the fraction of mobile Li^+ in the system.

5:45 PM EN02.18.08

Lithium Ion Mobility in Oligomerized and Polymerized Lithium Dicyanamide Christopher A. Klug, Daniel M. Fragiadakis and Andrew Purdy; Naval Research Laboratory, United States

Lithium dicyanamide ($\text{LiN}(\text{CN})_2$) can trimerize, oligomerize, or polymerize through thermal treatment, and the product of this polymerization is dependent on both impurities and conditions of heating. We have thermally treated LiC_2N_3 containing small amounts of various additives such as halide, NaC_2N_3 , LiCN , and other materials as pressed pellets under vacuum, and characterized the products by both solution and solid state NMR, and by dielectric relaxation spectroscopy. Direct detection of ^{13}C NMR spectra for the solid products was used to the relative amounts triazine and $\text{C}\equiv\text{N}$. The relative intensities and widths of the triazine peaks reflected variations in the reaction completion. Variable temperature ^7Li NMR was particularly useful for determining the correlation times and activation energies of the lithium ion motion in these materials as a function of preparation conditions and thermal history.

5:50 PM EN02.18.09

Highly Conductive Solid-State Electrolytes Based on *closo* Borates Compounds Hiroko Kuwata, Oscar Tutusaus and Rana Mohtadi; Toyota Motor North America, Inc, United States

All solid-state batteries (ASSB) are receiving increased attention for a variety of reasons that include elimination of the volatile solvents and support of faster battery charging compared with typical liquid-type systems [1]. One of most important components in the ASSB is the solid state electrolyte. To enable fast battery charging, it is necessary that the electrolytes have high ionic conductivities. Several families of solid state electrolytes currently exist and

include sulfides, halides, oxides and boron-hydrogen salts. *Closo* borate materials are promising candidates owing to their high ionic conductivity ($> 6 \text{ mS cm}^{-1}$ in Li system [2] and $> 30 \text{ mS cm}^{-1}$ in Na system [3,4] and wide electrochemical window. Our group has demonstrated that these anions have high compatibility with active metals such as magnesium making these salts highly attractive for utilization as solid state electrolytes [4,5,6]. Herein, we will assess the potential of these solid state electrolytes and discuss our recent efforts towards understanding and improving the Li^+ and Na^+ ionic mobilities in these electrolytes.

Reference

- [1] Y. Kato, et al, *Nature Energy*, **1**, 16030 (2019).
- [2] S. Kim, et al, *Nature commun.*, **10**, 1081 (2019).
- [3] W. S. Tang, et al, *ACS Energy Lett.*, **1**, 659-664 (2016).
- [4] R. Mohtadi, et al., *Nature Reviews*, **2**, 16091 (2016).
- [5] M. Kar, et al., *Energy Environ. Sci.*, **12**, 566-571 (2019).
- [6] R. Mohtadi, et al, *Molecules* **25**, 1791 (2020).

5:53 PM EN02.18.10

Solid-Electrolyte Interphase Progressive Growth Towards the Si Interior [Yang He](#)¹, Lin Jiang² and Chongmin N. Wang³; ¹University of Science and Technology Beijing, China; ²Thermo Fisher Scientific, United States; ³Pacific Northwest National Laboratory, United States

Solid-electrolyte interphase (SEI), a layer formed on the electrode surface, is essential for electrochemical reactions in batteries and critically governs the battery stability. Active materials, especially those with extremely high energy density, such as silicon (Si), often inevitably undergo large volume swing upon ion insertion and extraction, raising a critical question as how the SEI interactively responds to and evolves with the material and consequently controls the cycling stability of the battery. Here, by integrating sensitive elemental tomography, advanced algorithm and cryogenic scanning transmission electron microscopy, we unveil, in three-dimension, a correlated structural and chemical evolution of Si and SEI. Corroborated with a chemomechanical model, we demonstrate progressive electrolyte permeation and SEI growth along the percolation channel of the nanovoids due to vacancy injection and condensation during the delithiation process. Consequently, the Si-SEI spatial configuration evolves from the classic “core-shell” structure in the first few cycles to a “plum-pudding” structure following extended cycling, featuring the engulfing of Si domains by the SEI, which leads to the disruption of electron conduction pathways and formation of dead Si, contributing to capacity loss. The spatially coupled interactive evolution model of SEI and active materials, in principle, applies to a broad class of high-capacity electrode materials, leading to a critical insight for remedying the fading of high-capacity electrodes.

5:56 PM EN02.18.11

Lithium Nitride Coating Layer Deposited Using Magnetron Sputtering on Sulfide Solid-State Electrolyte [Zhifei Li](#) and Andriy Zakutayev; National Renewable Energy Laboratory, United States

Lithium containing materials have been of great interest for coating development, due to the rapid development of lithium-ion batteries. Among these materials, lithium nitride has received much attention recently due to its high lithium-ion conductivity and low electric conductivity, which together are beneficial for coating layers at the interface between lithium metal anodes and sulfide electrolytes in solid-state lithium batteries. Previously reported lithium nitride coatings were prepared by the reaction between lithium metal and nitrogen atmosphere at elevated temperature, which makes it challenging to precisely control the thickness of the resulting lithium nitride layer. The thickness of the coating layer is important for the performance of the obtained batteries, because too thick coating introduces unnecessary interfacial impedance, and too thin coating does not improve the stability. In this study, we prepared lithium nitride via magnetron sputtering for the first time, using Li metal target in Ar/N_2 gas atmosphere, with deliberate preparation of the Li target surface to avoid oxide contamination, and careful control of the sputtering power to avoid melting of the Li target. The polycrystalline Li_3N formed on the target surface and the amorphous coating on the glass substrate were measured by x-ray diffraction and other characterization methods. The thickness of the obtained lithium nitride coating can be controlled by varying the sputtering time. We applied the resulting lithium nitride coating on the sulfide electrolyte as an interfacial layer to stabilize the sulfide electrolyte in contact with Li metal. After cell assembly protocol was systematically optimized, the obtained coated sulfide solid-state electrolyte showed a slightly increased impedance and a significantly improved cycling performance in a spring-loaded lithium metal symmetric cell. These results demonstrate the feasibility of sputtering Li_3N binary and related ternary lithium nitride coatings as interfacial layers in solid-state batteries.

SESSION EN02.19: Solid State Batteries III
Session Chairs: Fudong Han and Yuyan Shao
Wednesday Morning, December 8, 2021
EN02-Virtual

10:30 AM EN02.19.01

Overscreening and Underscreening in Solid-Electrolyte Grain Boundary Space-Charge Layers [Jacob M. Dean](#)^{1,2}, Samuel W. Coles^{1,2}, William Saunders¹, Andrew McCluskey^{3,1}, Matthew Wolf¹, Alison Walker¹ and Benjamin J. Morgan^{1,2}; ¹University of Bath, United Kingdom; ²The Faraday Institution, United Kingdom; ³Data Management and Software Centre, European Spallation Source, Denmark

Polycrystalline solids can exhibit material properties that differ significantly from those of equivalent single-crystal samples, in part, because of a spontaneous redistribution of mobile point defects into so-called space-charge regions adjacent to grain boundaries. The general analytical form of these space-charge regions is known only in the dilute limit, where defect-defect correlations can be neglected. Using kinetic Monte Carlo simulations of a three-dimensional Coulomb lattice gas, we show that grain-boundary space-charge regions in non-dilute solid electrolytes exhibit overscreening -- damped oscillatory space-charge profiles -- and underscreening -- decay lengths that are longer than the corresponding Debye length and that increase with increasing defect-defect interaction strength. Overscreening and underscreening are known phenomena in concentrated liquid electrolytes, and the observation of functionally analogous behaviour in solid electrolyte space-charge regions suggests that the same underlying physics drives behaviour in both classes of systems. We therefore expect theoretical approaches developed to study non-dilute liquid electrolytes to be equally applicable to future studies of solid electrolytes.

10:45 AM EN02.19.02

Thin and Robust LATP Solid Electrolytes with Close-to-Bulk Ionic Conductivity and Its Integration in Solid-State Architectures [Juan Carlos](#)

Gonzalez-Rosillo¹, Valerie Siller¹, Marc Nuñez Eroles¹, Raul Arenal^{2,3,4}, Juan Miguel Lopez del Amo⁵, Alex Morata¹ and Albert Tarancon^{1,6}; ¹Catalonia Institute of Energy Research, Spain; ²Instituto de Nanociencia y Materiales de Aragón, Spain; ³Universidad de Zaragoza, Spain; ⁴Fundación ARAID, Spain; ⁵CIC energiGUNE, Spain; ⁶Catalan Institution for Research and Advanced Studies, Spain

Glassy-type solid state electrolytes such as state-of-the-art LiPON avoid grain boundaries and prevent Li-dendrite propagation leading to extremely good cyclability and the commercialization of planar thin-film LiPON-based microbatteries. However, its reduced ionic conductivity (~1 μS/cm) limits its performance at high/discharge rates and the severe degradation of its electrochemical and structural properties upon their exposure to ambient conditions and high temperatures (> 300 °C) hinders scalability and manufacturability. Among the next generation solid-state electrolytes, NASICON superionic solid electrolyte $\text{Li}_{(1-x)}\text{Al}_x\text{Ti}_{(2-x)}(\text{PO}_4)_3$ (LATP) with $0.3 \leq x \leq 0.5$ remains one of the most promising solid electrolytes thanks to its good ionic conductivity (~0.5 - 1 mS•cm⁻¹) and outstanding stability in ambient air. Despite the intensive research for bulk systems, there are only very few studies of LATP in thin film form. In particular, the only successful reports of relatively high ionic conduction (~10⁻⁵ S•cm⁻¹) have been achieved through amorphous sputtered films.

In this talk, we will explore the properties of high performance LATP thin films fabricated by Large-Area Pulsed Laser Deposition. The as-deposited thin films exhibit an ionic conductivity around 0.5 μS•cm⁻¹ at room temperature (comparable to the state-of-the-art of LiPON) which increases to remarkably high values of 0.1 mS•cm⁻¹ after an additional annealing at 800 °C. We will discuss the formation of a glassy, intergranular phase connecting highly conducting LATP grains as a possible cause for the significant enhancement in ionic conductivity by two orders of magnitude. The performance of both as-deposited and annealed LATP films makes them suitable as solid electrolytes, which opens the path to a new family of stable and highly performing thin solid-electrolytes. We will discuss its integration with other battery components, with special attention to interfacial coatings matching the electrochemical window at low potentials.

11:00 AM EN02.19.03

Synthesis and Characterization of Li₃PO₄-Coated LiMn_{1.5}Ni_{0.5}O₄ Spinel as Positive Electrode for High Voltage Li-Ion Batteries Jon Serrano-Sevillano^{1,2}, Montserrat Casas-Cabanas¹ and Dany Carlier²; ¹CIC EnergiGUNE, Spain; ²Institut de Chimie de la Matière Condensée de Bordeaux, France

LiMn_{1.5}Ni_{0.5}O₄ (LNMO) spinel material, is being thoroughly studied as a cathode candidate for lithium ion battery. LNMO can crystallize either with an ordered structure (*P4₃32* space group), where the manganese and the nickel atoms are located in specific sites, or with a disordered structure (*Fd-3m* space group), where the manganese and the nickel are randomly distributed. Synthesis parameters are key to control the degree of ordering in LNMO and the electrochemical performance is highly affected by it. In particular, the disordered structure is found to have better performances, especially at high rates. The ordering can be studied using several techniques such as neutron powder diffraction (NPD), Raman or solid state magic angle spinning nuclear magnetic resonance (NMR). In particular, ⁷Li NMR spectra shows a single peak for the fully ordered structure, while a larger number of signals is found for the disordered one. In the first part of this study, we propose a signal assignment of the NMR signals using DFT calculations, which has helped to understand how each different lithium local environment modifies the Fermi contact shift.

Some of the main advantages of LNMO are that they have good performance at high rates due to their 3D structure, and their ability to store large energy density as their work at high voltage. However, cycling at high voltage has as well some drawbacks, especially in terms of structural and chemical stability. Electrolyte degradation and manganese dissolution in the electrolyte are two of the main problems this material faces. Coating the LNMO with a protective layer is regarded as an effective approach to stabilize the electrode/electrolyte interface. Li₃PO₄ was calculated to have a good compatibility [1] and it has been experimentally found to avoid chemical attacks from the electrolyte [2]. One of the main issues in the study of the coating refers to their characterization. This is often challenging and can cast doubts on their goodness. By instance, HRTEM images can only provide local information, so the combination of different techniques is required. In this work, ⁷Li and ³¹P MAS NMR is used, in combination with X-ray diffraction (XRD) and scanning and transition electron microscopies (SEM and TEM), to provide a trustworthy characterization of Li₃PO₄-coated LNMO prepared by different routes. In particular, the closeness of diamagnetic compounds (such as Li₃PO₄) to paramagnetic ones (such as LNMO) have strong influence on the NMR spectra, [3] so NMR can be a useful technique to have an overall idea on the goodness of the coating. In addition, ⁷Li MAS NMR allows to characterize as well, whether the coating process does modify the Ni/Mn distribution in the spinel phase.

Bibliography:

- [1] Xiao, Y. *et al. Joule* **2019**, 3 (5), 1252–1275.
- [2] Chong, J. *et al. Chem. - A Eur. J.* **2014**, 20 (24), 7479–7485.
- [3] Dupré, N. *et al. J. Mater. Chem.* **2008**, 18 (36), 4266–4273.

11:15 AM EN02.19.04

Understanding Metal Deposition in Solid Electrolytes Due to Mixed Ionic-Electronic Conduction Qingsong Tu¹, Tan Shi¹, Srinath Chakravarthy² and Gerbrand Ceder¹; ¹University of California, Berkeley, United States; ²Samsung Research America, United States

Among the alternatives to conventional Li-ion batteries, solid-state batteries (SSBs) have the potential for high energy density as they may enable the use of a metal anode. However, the penetration of metal filaments into a solid electrolyte (SE) and resulting shorting is an obstacle to the commercialization of metal-anode SSBs. This work utilizes continuum modeling to study the mechanism of metal deposition within the SE due to the electronic conductivity of the SE. We show that metal deposition can happen in isolated micro-size voids within the SE and we specify the conditions under which it causes failure due to SE fracture. The vulnerability to metal deposition in the SE is investigated by controllable parameters (such as the cell voltage, applied current density, and etc.), and suppression strategies of metal deposition are proposed. These findings provide a deeper understanding of the Li penetration in the SE in order to eventually overcome the challenge in solid-state batteries. In addition, our work shows that metal propagation through the electronic can be overcome with a few focused strategies.

11:30 AM EN02.19.05

In Situ Transmission Electron Microscopy Characterization of Electro-Chemo-Mechanics at Interface Between Solid Electrolyte and Lithium Anode Akihiro Kushima; University of Central Florida, United States

All-solid-state lithium battery is attracting attention as one of the promising candidates for a next generation energy storage technology. The solid electrolyte (SE) with much higher modulus than lithium is expected to prevent lithium dendrite penetrations and contributes to improved safety while increasing the energy density. However, there are many cases where lithium dendrite penetrates the solid electrolyte leading to a short circuit and premature failure of the battery. The interaction between the growing lithium dendrites and the solid electrolyte involves complex interplay of electrochemistry and mechanics. This can become even more complicated when the size-scale of the dendrites are in nano-scale, particularly at the initial state of the nucleation and growth, since the mechanical properties deviates from the bulk. Here in situ transmission electron microscopy (TEM) plays an important role in directly observing the growth behavior of the dendrites and how it is affected by the mechanical stress at the SE/Li interface. We developed a quantitative in situ TEM technique that can measure the force imposed on the lithium dendrite as it grows from the solid electrolyte.

The method was applied to evaluate the critical force that changes growth direction of the dendrite from vertical to horizontal with respect to the SE surface. Since the size of the dendrite was in nano-scale it sustained much higher stress than the bulk yield stress. Furthermore, the method successfully captured the change in the mechanical behavior of the dendrite at different growth rate indicating higher stress can be imposed to the SE at faster growth rate. In addition to the mechanical response of the dendrite growth, the crack propagation of the SE was characterized. It revealed that the lithium dendrite, during its growth process, can cause the crack to propagate in the SE from the surface defect. The in situ TEM observation clearly showed the crack growth and opening behavior, and the force associated with the process was precisely evaluated. The in situ TEM provides fundamental insights to the electro-chemo-mechanics of the lithium dendrite and solid electrolytes, and the information obtained in this work can be used as essential parameters to design all-solid-state lithium batteries with improved performance.

11:45 AM EN02.19.06

Anionic Polyelectrolyte Coating as Artificial Solid Electrolyte Interface for Zinc Anode Phonnapha Tangthum and Soorathep Kheawhom; Chulalongkorn University, Thailand

Zinc (Zn) anode has good promise for energy storage application due to its excellent intrinsic properties such as high stability, high volumetric capacity, abundance, and low cost. Its relatively high electrode potential of -0.76 V vs. standard hydrogen electrode is ideal for neutral or mildly acidic aqueous electrolytes. Further, its polarization is much lower than other multivalent metal anodes such as magnesium and aluminum. However, its significantly high self-corrosion, hydrogen evolution reaction during the charging process, dendrite growth, and nonuniform stripping/plating of the Zn over long-term cycling restrict its practical application. These issues can lead to the migration of Zn during the plating/stripping processes and even cause battery failure. Artificial solid electrolyte interface (ASEI) applied on the surface of Zn anode has been suggested as a promising approach to address these issues. ASEI regulates the initial nucleation and manipulates Zn ion distribution in the surroundings of the anode surface. Nonetheless, only a few studies have investigated ASEI prepared using anionic polyelectrolyte.

In this study, we report the observation of ASEI on a Zn-carbon composite anode, based on ultra-thin layers of carboxymethyl cellulose (CMC), which is an anionic polyelectrolyte. The Zn anode having ASEI enables reversible and dendrite-free zinc plating/stripping even at high current densities, endowed by the fast ion migration coupled with cationic modulation. The ASEI is highly permeable for Zn ions and avoids excessive Zn utilization by hindering the access of water molecules and electrons. The ASEI can effectively suppress corrosion and regulate Zn plating/stripping behavior as confirmed via electrochemical characterization. Electrochemical impedance spectroscopy studies confirm that the anode having ASEI exhibits reduced charge transfer resistance and enhanced Zn ions absorption/desorption. As confirmed by X-ray tomography, during the charging and discharging cycle, no evidence for dendrite growth and zinc migration are observed. A mechanistic investigation of the role of CMC as ASEI is presented, along with data showing that the CMC coating layer can enhance the cycling stability of the Zn anode in aqueous Zn-ion batteries. This technique can be also applied in other Zn-based batteries having aqueous electrolytes.

12:00 PM EN02.19.07

Late News: Lithiophilic Thin Films on Li₂CO₃-Free Garnet Solid Electrolytes—A Double Approach to Improve the Interface Stability with Lithium Marco Siniscalchi, Susannah Speller and Chris Grovenor; University of Oxford, United Kingdom

The interfacial impedance between lithium metal and garnet solid electrolytes (e.g. LLZO) is usually dominated by poor solid-solid contact. This can lead to current constriction spots at the interface and to the rapid growth of lithium filaments through the LLZO, eventually short-circuiting the cell at small nominal current densities. Different approaches have proven effective to decrease such interfacial impedance, for example the removal of the lithio-phobic Li₂CO₃ layer which can form on the LLZO surface during glovebox storage. Alternatively, lithio-philic thin films like amorphous Al₂O₃ can be deposited at the Li|LLZO interface. Both approaches show similar interfacial impedances before cycling, but the difference in the long-term effect on the interface stability is unclear. Also, whether lithio-philic thin films can provide a mechanical and/or electronic-insulating barrier hindering the propagation of lithium filaments, or whether their role is simply to improve the lithium wettability on the LLZO surface to avoid current constrictions, remains an open question. In this study, we deposit amorphous Al₂O₃ and LiPON thin films via magnetron sputtering on Li₂CO₃-free LLZO solid electrolytes obtained via a rapid acid treatment. We assess the performance of such thin films through potential step chronoamperometry and in-operando impedance spectroscopy, and we use scanning electron microscopy to investigate the morphological stability of the modified Li|LLZO interface. Our findings provide a better understanding of the effect of interfacial ceramic thin films on improving the cycle life of a lithium metal cell. We also assess the most useful properties of the interfacial thin films which prevent the propagation of lithium filaments through the solid electrolyte.

12:15 PM EN02.19.08

In Situ Precipitation of LATP in PEO-Matrix Composite to Form Strong Interphase-Conducting Solid Electrolyte Guangyu Wang and John Kieffer; University of Michigan—Ann Arbor, United States

A novel water based in-situ precipitation method is devised for the fabrication of polymer matrix composite solid electrolytes, achieving effective spatial dispersion of Li_{1.3}Al_{0.3}Ti_{1.7}(PO₄)₃ (LATP) nanoparticles up to particle loadings of 30 wt% (15 vol%). Amorphous LATP nanoparticles precipitate in ostensibly random locations within the poly(ethylene) oxide (PEO) matrix. The highest 20°C ionic conductivity of 3.8×10^{-4} S/cm, observed at 13 vol% LATP and EO/Li = 10, which exceeds that of the polymer matrix by 2 orders of magnitude. This result is consistent with earlier predictions based on our tri-phase model, both in composition and magnitude. Accordingly, the most highly conductive region is the interphase into which the polymer surrounding the LATP particles is transformed. Minimizing particle agglomeration permits expansion of the interphase into a larger fraction of the bulk polymer. Detailed analyses of our data provide new insights into the nature of the interphase and the transport mechanisms in these systems. (NSF-DMR 1610742)

SESSION EN02.20: On-Demand
Sunday Morning, December 5, 2021
On-Demand

8:00 AM EN02.05.02

Performance Analysis of Li-Ion Battery for Low-Temperature Space Applications Amani Alhammadi, Amarsingh Bhabu Kanagaraj and Daniel Choi; Khalifa University, United Arab Emirates

The main challenge that hinders the use of lithium (Li)-ion batteries in space applications is their low performance at low temperatures from -30 to 20 °C. Such low performance is mostly due to the low ionic conductivity and freezing of the non-solid electrolyte leading to a significant loss in the battery's capacity. In this research, the behavior of Li-ion batteries is investigated by employing electrochemical characterization techniques to study their

performance at low temperatures. The findings of this research indicate that the capacity of Li-ion batteries is decreased greatly at subzero temperature. Cyclic voltammetry profiles show that the peak separation increases with decreasing the temperature while the current decreases. The charge transfer resistance increases due to the freezing of the non-solid electrolyte, which leads to unstable Solid Electrolyte Interphase (SEI) film formation and weak permeation of electrolyte into the active material. The capacity decreases due to a significant decrease in the diffusivity of lithium ions and substantially increased charge-transfer resistance. The cell retains nearly 50% of its room-temperature capacity at 0 °C. This can be ascribed to the low diffusivity of lithium ions which affects the interface stability between the cathode and the electrolyte. Material characterization methods such as x-ray photoelectron spectroscopy (XPS) and X-ray diffractions (XRD) are used to examine the change in the material of the electrodes and the electrolyte to determine the reasons behind the performance degradation. This study contributes to the development of Li-ion batteries for low temperature and space applications by understanding the electrochemical behavior of Li-ion batteries.

8:05 AM EN02.17.06

A Spreadable Interlayer Enables Highly Stable NASICON Solid Electrolyte/Li Metal Interface Shizhao Xiong and Aleksandar Matic; Chalmers University of Technology, Sweden

The solid-state lithium metal battery (SSLMB) has been considered as a promising candidate for safe high-energy-density storage systems as it can deliver superior safety, cycling life, energy density and cell design. Despite considerable advantages, the advance of SSLMB-technology is still hindered by a highly resistive and unstable interface between the Li-metal anode and the solid electrolyte leading to decreased practical capacity and continuous side reactions [1, 2].

To achieve good interface compatibility between the solid electrolyte and Li anode, interlayers have been proposed to stabilize the interface through improved physical contact between the solid electrolyte and Li anode and increased chemical/electrochemical stability. During the past decades several years, several strategies have been considered which can be summarized as top-down approaches (magnetron sputtering, spark plasma sintering, electron-beam evaporation, pulsed laser deposition, solvent casting, spin coating), and bottom-up approaches (sol-gel derived synthesis, atomic layer deposition, chemical vapor deposition, electrochemical-assisted synthesis)[3-5]. However, most of those strategies are not capable of building an interface that can fulfil the demands of high conductivity, good physical contact, and chemical stability at the same time.

In this contribution we demonstrate an approach, based on a tailored multifunctional interlayer between the NASICON solid electrolyte ($\text{Li}_{1.5}\text{Al}_{0.5}\text{Ge}_{1.5}(\text{PO}_4)_3$, LAGP) and Li anode, that successfully addresses the interfacial issues[6]. This interlayer is designed by creating a quasi-solid-state paste in which the functionalities of LAGP nanoparticles and an ionic liquid electrolyte (IL) are combined. In the solid-state cell, the LAGP-IL interlayer separates the Li metal from bulk LAGP electrolyte and creates a chemically stable interface with low resistance ($\sim 5 \text{ Ohm cm}^2$) and efficiently prevents thermal runaway at elevated temperatures (300 °C). We show that solid-state cells designed with this interlayer can operate at high current densities, 2 mA cm^{-2} (an order of magnitude higher than that previously reported) and deliver high energy density, high-rate capability, and increased safety. The same strategy can also be applied to the SSLMB based on other classes of solid electrolytes for future energy storage technologies to meet the demand of high energy density.

Reference

- [1] J. Janek, W. G. Zeier, Nat. Energy 2016, 1, 16141.
- [2] Y. Xiao, Y. Wang, S.-H. Bo, J. C. Kim, L. J. Miara, G. Ceder, Nat. Rev. Mater. 2019, 5, 105.
- [3] S. Lobe, A. Bauer, S. Uhlenbruck, D. Fattakhova-Rohlfing, Adv. Sci. 2021, n/a, 2002044.
- [4] A. Banerjee, X. Wang, C. Fang, E. A. Wu, Y. S. Meng, Chem. Rev. 2020, 120, 6878.
- [5] Q. Liu, Y. Liu, X. Jiao, Z. Song, M. Sadd, X. Xu, A. Matic, S. Xiong, J. Song, Energy Storage Mater. 2019, 23, 105.
- [6] S. Xiong, Y. Liu, P. Jankowski, Q. Liu, F. Nitze, K. Xie, J. Song, A. Matic, Adv. Funct. Mater. 2020, 30, 2001444.

SYMPOSIUM EN03

Thermal Materials, Modeling and Technoeconomic Impacts for Thermal Management and Energy Application
November 29 - December 8, 2021

Symposium Organizers

Yee Kan Koh, National University of Singapore
Xiulin Ruan, Purdue University
Bo Sun, Tsinghua University
Yanfei Xu, University of Massachusetts Amherst

* Invited Paper

SESSION Tutorial EN03: Four-Phonon Scattering—A Critical Process Determining Thermal and Radiative Properties
Monday Afternoon, November 29, 2021
Hynes, Level 2, Room 202

1:30 PM

Four-Phonon Scattering—A Critical Process Determining Thermal and Radiative Properties [Tianli Feng](#); The University of Utah, United States

Phonon scattering plays a central role in the quantum theory of phonon linewidth, which in turn governs important properties including infrared spectra, Raman spectra, lattice thermal conductivity, thermal radiative properties, and also significantly affects other important processes such as hot electron relaxation. Since Maradudin and Fein's classic work in 1962, three-phonon scattering had been considered as the dominant intrinsic phonon scattering mechanism and has seen tremendous advances. However, the role of four-phonon scattering had been persistently unclear and so was ignored. The tremendous complexity of the formalism and computational challenges stood in the way, prohibiting the direct and quantitative treatment of four-phonon scattering. In 2016, a rigorous four-phonon scattering formalism was developed, and the prediction was realized using empirical potentials. In 2017, the method was extended using first-principles calculated force constants, and the thermal conductivities of boron arsenides (BAs), Si and diamond were predicted. The predictions for BAs were later confirmed by several independent experiments. Four-phonon scattering has since been investigated in a range of materials and established as an important intrinsic scattering mechanism for thermal transport and radiative properties. After this tutorial, the audience is expected to (1) be familiar with the background of three- and four-phonon scattering and their roles in thermal and radiative properties of materials, (2) understand the various characteristics of four-phonon scattering mechanism in different systems and scenarios, (3) understand the broad impact of four-phonon scattering on thermal transport and radiative properties in various materials, (4) be able to tell in which types of materials and scenarios will four-phonon scattering be critical, (5) be able to use the open-source code Four-Phonon together with Sheng BTE to calculate four-phonon scattering rates (linewidth) and thermal conductivities for materials.

SESSION EN03.01: Thermal Materials I
Session Chairs: Jun Liu and Zhiting Tian
Tuesday Morning, November 30, 2021
Hynes, Level 3, Room 306

10:30 AM *EN03.01.01

Relationships Between Molecular Structure and Thermal Conductivity of Epoxy Resins [David Cahill](#); University of Illinois, United States

High and low thermal conductivities in polymers are needed for new materials for thermal management. While the thermal conductivity of simple inorganic crystals can be calculated from first principles with good accuracy, a predictive understanding of the relationship between the thermal conductivity and the molecular structure of polymers is not yet established. We recently embarked on an extensive experimental study of the molecular structure/thermal-conductivity relationships within the class of materials known as epoxy thermosets, i.e., mixtures of epoxide monomers and amine hardeners. We measured 32 formulations to-date. For each formulation, we measure the thermal diffusivity using frequency domain probe beam deflection (FD-PBD), thermal effusivity by time-domain thermoreflectance (TDTR), acoustic velocity by picosecond interferometry, density by buoyancy, and for selected compositions, crystalline and liquid-crystalline order by small and wide-angle x-ray diffraction (SAXS and WAXS). We compare the results to predictions based on the model of the minimum thermal conductivity. The thermal conductivity of these 32 epoxy resins spans the range from 0.15 to 1.0 W/m-K. Thermal conductivity is enhanced by extended aromatic structures, high molecular density, and liquid crystalline and crystalline order. We have discovered a striking odd-even effect in the dependence of thermal conductivity on the molecular length of an aliphatic linker segment in epoxide monomers.

11:00 AM EN03.01.02

Amorphous-Like Ultralow Thermal Conductivity in Crystalline BaZrS₃ and Its Ruddlesden Popper Phase Ba₃Zr₂S₇ [Md Shafkat Bin Hoque](#)¹, [Boyang Zhao](#)², [Eric R. Hoglund](#)¹, [Ethan A. Scott](#)¹, [Mythili Surendran](#)², [Eric Osei Agyemang](#)³, [Kiumars Aryana](#)¹, [John A. Tomko](#)¹, [John T. Gaskins](#)¹, [Ganesh Balasubramanian](#)², [Jayakanth Ravichandran](#)² and [Patrick E. Hopkins](#)¹; ¹University of Virginia, United States; ²University of Southern California, United States; ³Lehigh University, United States

Crystalline materials with amorphous-like ultralow thermal conductivity are highly coveted for thermal barrier coating and thermoelectric applications. However, such behavior is rarely observed in high-quality, bulk crystals with simple crystal structures. In this study, we report on the amorphous-like ultralow thermal conductivity of high-purity, bulk, crystalline chalcogenide perovskite BaZrS₃ and its ruddlesden popper phase Ba₃Zr₂S₇. Extensive microstructural characterizations and first-principles calculations are performed to explain these exceptional thermal behaviors. Both BaZrS₃ and Ba₃Zr₂S₇ exhibit very high phonon scattering rates as indicated by some of the highest ever reported elastic modulus/thermal conductivity ratios. The low number density of the acoustic phonon modes, strong gruneisen parameter, and short phonon lifetimes lead to a thermal conductivity of $1.21 \pm 0.18 \text{ W m}^{-1} \text{ K}^{-1}$ in BaZrS₃. In addition, this material also exhibits an amorphous-like thermal conductivity trend which likely stems from the phonon-domain boundary scattering. The highly ordered layered crystal structure of Ba₃Zr₂S₇, on the other hand, leads to a thermal conductivity of $0.46 \pm 0.08 \text{ W m}^{-1} \text{ K}^{-1}$, nearly one third of that of the BaZrS₃. Moreover, the thermal conductivity of Ba₃Zr₂S₇ is in agreement with the diffuson-mediated thermal conductivity limit indicating the dominance of diffuson like vibrational modes. As a result, at 100 K, the thermal conductivity of Ba₃Zr₂S₇ is the lowest reported to date among bulk crystalline materials. Introduction of disorder by ion bombardment gradually reduces the thermal conductivity of BaZrS₃. This is in contrast to Ba₃Zr₂S₇ where no change in thermal conductivity is observed with irradiation doses. Our study provides conclusive evidence that highly ordered nanostructuring can lead to diffuson like lattice vibrations in already low thermal conductivity crystalline materials.

11:15 AM *EN03.01.03

Thermodynamic Modeling of Hydrogel—Applications to Water Evaporation, Atmospheric Water Harvesting and Desalination [Gang Chen](#); Massachusetts Institute of Technology, United States

Most thermodynamic modeling of hydrogels focused on predicting their final volumes in equilibrium with water, built on Flory theories for the entropy of mixing, rubber elasticity, and the Donnan equilibrium. This work will focus on water and ions in and outside hydrogels. Deficiencies and confusions in the Donnan equilibrium theory and Flory hydrogel model will be discussed and amended. It turns out that Donnan's equilibrium criteria established over 100 years ago neglected the coupling between ion concentrations and the osmotic pressure. The revised model will be employed to study thermodynamic properties of water in hydrogels including (1) the latent heat of evaporation, (2) the ability of hydrogels to retain water and to absorb water from the atmosphere, and (3) the use of hydrogels for desalination. Such thermodynamic studies will also be useful for understanding polymer electrolytes and ion transport in membranes in electrochemical systems.

11:45 AM EN03.01.04

Thermal Conductivity of Dynamic Polymer Network [Guangxin Lv](#), Christopher Evans and David Cahill; University of Illinois at Urbana-Champaign, United States

Polymers typically have low thermal conductivities, ~ 0.2 W/(m K), which limits their application in systems that must manage high heat loads. Dynamic covalent networks are a class of polymer networks studied for their self-healing and stress relaxation properties and they have potential applications as shape memory polymers, flame retardants, solid electrolytes and shockwave dissipation materials. Thermal conductivity of dynamic polymer network is measured by time-domain thermoreflectance (TDTR) and frequency domain probe beam deflection (FD-PBD). At room temperature, thermal conductivity of dynamic polymer network varies from 0.05 W/(m K) to 1.0 W/(m K) by a factor of 20. Dynamic polymer network with crystal structure can have thermal conductivity of 1.0 W/(m K). Thermal conductivity of amorphous ethylene dynamic networks, synthesized from benzene diboronic acid and alkane diols, decreases from 0.19 W/(m K) to 0.095 W/(m K) at room temperature as ethylene linker length increases from 4 to 12. Thermal conductivity of these amorphous ethylene dynamic networks also decreases from 0.29 W/(m K) to 0.095 W/(m K) by a factor of 3 as the temperature increases across glass transition temperature. Minimum thermal conductivity model (MTCM) successfully predicts thermal conductivity of dynamic polymer network with different ethylene linker length and under different temperatures.

SESSION EN03.02: Modeling Phonons
Session Chairs: Sebastian Volz and Qiye Zheng
Tuesday Afternoon, November 30, 2021
Hynes, Level 3, Room 306

1:30 PM EN03.02.02

Late News: Quantum Prediction of Ultra-Low Thermal Conductivity in Lithium Intercalation Materials [Tianli Feng](#)¹ and Sokrates T. Pantelides²; ¹The University of Utah, United States; ²Vanderbilt University, United States

Lithium-intercalated layered transition-metal oxides, Li_xTMO_2 brought about a paradigm change in rechargeable batteries in recent decades and show promise for use in memristors, a type of device for future neural computing and on-chip storage. Thermal transport properties, although being a crucial element in limiting the charging/discharging rate, package density, energy efficiency, and safety of batteries as well as the controllability and energy consumption of memristors, are poorly managed or even understood yet. Here, for the first time, we employ quantum calculations including high-order lattice anharmonicity and find that the thermal conductivity κ of Li_xTMO_2 materials is significantly lower than hitherto believed. More specifically, the theoretical upper limit of κ of LiCoO_2 is 6 W/m-K, 2–6 times lower than the prior theoretical predictions. Delithiation further reduces κ by 40–70% for LiCoO_2 and LiNbO_2 . Grain boundaries, strain, and porosity are yet additional causes of thermal-conductivity reduction, while Li-ion diffusion and electrical transport are found to have only a minor effect on phonon thermal transport. The results elucidate several long-standing issues regarding the thermal transport in lithium-intercalated materials and provide guidance toward designing high-energy-density batteries and controllable memristors.

1:45 PM EN03.02.03

Transfer Learning for Phonon and Thermal Property Predictions [Tengfei Luo](#), Zeyu Liu and Meng Jiang; University of Notre Dame, United States

Machine learning is trending to be an integral part of thermal science. In this talk, I will introduce our efforts in utilizing machine learning (ML) techniques to predict phonon and thermal properties. I will talk about the use of a new ML method, called transfer learning, to establish accurate models based on limited data for predicting phonon and thermal transport properties, such as phonon frequency gap, heat capacity, speed of sound and lattice thermal conductivity.

2:00 PM EN03.02.04

First-Principles Calculation of Nernst Effects in Complex Band Structures [Jennifer Coulter](#), Andrea Cepellotti and Boris Kozinsky; Harvard University, United States

As the need for energy-efficient devices has become more pressing, so has interest in finding ways to enhance the thermoelectric performance of materials. While the Seebeck effect has been intensely studied, the Nernst effect has been rarely investigated computationally. Recent results, such as those showing enhanced thermopower in compensated semimetals via the Nernst effect, suggest that it also has potential to provide enhancements in thermoelectric performance in the right circumstances. Additionally, established results such as those for bismuth, which shows a low-temperature peak in the Nernst coefficient, could be better understood and further engineered for potential applications.

However, these interesting and possibly useful behaviors can be difficult to interpret from experimental results alone. Using first-principles solutions of the Boltzmann transport equation as implemented in our new open-source code package, Phoebe [1], we calculate the Seebeck and Nernst coefficients to better understand the physics underlying these effects. Time permitting, we will also discuss the role of phonon drag on these coefficients at low temperatures.

[1] <https://mir-group.github.io/phoebe/>

2:15 PM EN03.02.05

Geometric Parameters to Maximize or Minimize the Thermal Conductivity of Periodic Coaxial Cylindrical Nanowires Yingru Song and [Geoffrey Wehmyer](#); Rice University, United States

The thermal conductivity (k) of semiconducting nanomaterials is determined by the geometry-dependent phonon boundary scattering mean free path (MFP). Although prior work has investigated phonon transport in periodically corrugated rectangular nanowires, the detailed relationship between geometric parameters and the MFP in recently fabricated diameter-modulated cylindrical nanowires is not known. For example, it is not clear whether enhancing the larger cylinder diameter would reduce the MFP due to the phonon backscattering effect, or enhance the MFP due to the larger average path length between phonon collisions in the larger cylinder. In addition to these fundamental questions about the phonon transport physics, understanding the thermal conductivity in modulated diameter nanowires may be important for future applications of modulated silicon nanowires as photodetectors or optomechanical sensors.

Here, we use Monte Carlo phonon ray tracing simulations to comprehensively study the effect of geometric parameters on the boundary scattering MFP in

periodic coaxial cylindrical nanowires. We find that for a fixed smaller cylinder diameter, the MFP can be maximized or minimized via geometric control of the pitch, length, and diameter ratios. Our simulations show that the phonon backscattering framework is appropriate for small-pitch nanowires and gives rise to the minimum in the dimensionless MFP, while an enhanced path-length mechanism is appropriate for long-pitch nanowires and leads to the maximum in the dimensionless MFP.

Combining our calculations with analytical phonon dispersion and bulk scattering models, we predict that the thermal conductivity of periodic silicon nanowires with a fixed smaller diameter and cylinder length ratio can be tuned by up to 34% via geometric control of the larger diameter and pitch. A stronger geometric enhancement can be observed in the thermal conductance than in the thermal conductivity. Our results provide insight into the mechanisms of thermal conductivity suppression and enhancement in periodically modulated nanowires, and can be used by experimentalists to explore phonon backscattering and path-length effects in modulated nanowires.

2:30 PM EN03.02.06

Evaluating the Roles of Temperature-Dependent Eigenvectors in Predicting Phonon Transport Properties of Anharmonic Crystals Using Normal Mode Analysis Methods Jixiong He and Jun Liu; North Carolina State University, United States

Theoretical modeling of phonon transport process in strongly anharmonic materials at a finite temperature needs to accurately capture the effects of lattice anharmonicity. The anharmonicity of potential energy surface would result in not only strong phonon scatterings but also shifts of phonon frequencies and eigenvectors. In this work, we evaluated the roles of anharmonicity-renormalized phonon eigenvectors in predicting phonon transport properties of anharmonic crystals at high temperatures, using molecular dynamics-based normal mode analysis (NMA) methods in both time domain and frequency domain. Using PbTe as a model of strongly anharmonic crystal, we analyzed the numerical challenges to extract phonon lifetimes using NMA methods when phonon eigenvectors deviate from their harmonic values at high temperatures. To solve these issues, we proposed and verified a better fitting strategy, Sum-up Spectrum Fitting Method (SSFm), than the original frequency-domain NMA method. SSFM is to project the total spectrum energy density data of all phonon modes onto an inaccurate (harmonic or quasi-harmonic) eigenvector base and then manually sum up the peaks that belong to the same phonon mode (at the same frequency). The SSFM relaxes the requirement for accurate temperature-dependent eigenvectors, making it robust for analyzing strongly anharmonic crystals at high temperatures.

2:45 PM EN03.02.07

Machine Learning Based Approach for 2D-3D Thermal Boundary Conductance Cameron Foss and Zlatan Aksamija; University of Massachusetts, United States

Two-dimensional (2D) materials have the potential to be a breakthrough platform for designing next-generation solid-state devices with enhanced performance and novel functionalities. However, the ongoing design concern of heat dissipation is further exacerbated in 2D-based systems due to their weak interlayer van der Waals (vdW) atomic bonding with surrounding three-dimensional (3D), particularly the substrate. Since the primary pathway for heat removal in 2D-devices is suspected to be across the 2D/3D interface and through the 3D substrate, the uniquely poor thermal performance of 2D/3D interfaces is a pressing issue for the development and implementation of 2D-based devices. Therefore, there have been several efforts to experimentally measure 2D/3D TBC as well as to provide explanations of the underlying physical dynamics through theoretical modeling. Simultaneously, materials informatics based on machine learning (ML) algorithms has seen tremendous success in new material discovery and application-specific material selection. However, the existing literature does not hold enough TBC data (both experimental and theoretical) to construct a diverse set of 2D/3D interface pairs which is required to reliably train ML algorithms.

In this work, we use our first-principles-driven TBC model to expand upon available data in the literature by computing the TBC for 156 unique interface pairs, including technologically relevant substrates such as HfO₂ and CaF₂. Then we employ machine learning to develop a streamlined predictive model that is computationally cheap and demonstrates strong transferability. For single-layer 2D materials our dataset includes dispersions of graphene, silicene, boron nitride, boron arsenide, black phosphorus, blue phosphorus, and 1H-MX₂ transition metal dichalcogenides (with M=Mo, W and X=S, Se, Te). For 3D materials, our dataset includes dispersions of silicon, germanium, diamond, CaF₂, titanium, AlN, GaN, 6H-SiC, Al₂O₃, SiO₂, AlO_x, HfO₂, and PMMA. We then use our 2D/3D thermal boundary conductance (TBC) model to calculate the TBC of each 2D/3D pair from the above lists. We then vary the substrate coupling strength, which is a crucial and highly sample-dependent property, resulting in a total observation pool of 5460 TBC values which are then randomized and split 70/30 for training and testing datasets. We train a range of machine learning models and find that fine tree and wide-neural network (WNN) regression algorithms perform the best out of an array of algorithms (linear, step-wise linear, gaussian process, and support vector) due to their unbiased residuals. We then train fine tree and WNN models on the dependence of TBC on the van der Waals spring coupling constant (K_a) enabling the machine learning algorithm to accurately predict the TBC vs. K_a curve for any 2D/3D interface provided the known list of material descriptors are available and within the extrema of the parameter space. Our results show that fine tree ensembles and wide neural networks can predict the 2D/3D TBC within $\pm 1.41 \text{ MW}\cdot\text{m}^{-2}\cdot\text{K}^{-1}$ and $1.046 \text{ MW}\cdot\text{m}^{-2}\cdot\text{K}^{-1}$, respectively, with a descriptor set comprised of structural data, select thermal transport properties (e.g., thermal conductivity, Debye temperature, etc.), and the vdW spring coupling constant. The reported R-squared values for either model are 0.98 (fine tree) and 0.999 (WNN). We further show that fine tree ensembles demonstrate good transferability by withholding select materials from the training pool and subsequently testing the trained models on the unseen data. In most cases, the model retains an RMSE $< 10 \text{ MW}\cdot\text{m}^{-2}\cdot\text{K}^{-1}$ and R-squared values greater than 0.65. Lastly, we use sensitivity analysis and Pearson correlation coefficients to identify the vdW spring coupling constant, amorphous flag, and resonant frequency gap as the descriptors that are most correlated with the TBC.

3:00 PM EN03.02.08

Fast Simulations of Thermal Transport in Complex Materials Using Machine Learning and Bayesian Force Fields Anders Johansson, Andrea Cepellotti and Boris Kozinsky; Harvard University, United States

Controlling thermal conductivities of materials is important for a wide range of applications, from thermoelectrics for clean energy generation to electronic devices and thermal barrier coatings. The thermal conductivity is commonly estimated using molecular dynamics simulations within the Green-Kubo formulation. This requires a force field that is both 1) an accurate estimate of the interatomic interactions and 2) fast enough to allow simulations with sufficiently large length and time scales. Traditionally, only empirical force fields have fulfilled both of these requirements, which severely limits the applicability of the method.

In this work, we employ the Gaussian Process-based FLARE force field, which automatically learns the interactions of more complex materials than empirical force fields. The resulting model can then be mapped to a low-dimensional, computationally efficient model. Through GPU-acceleration with LAMMPS and the Kokkos library, we achieve excellent performance and obtain well-converged estimates for the thermal conductivity. Furthermore, we investigate state-of-the-art sampling and spectral denoising methods for further acceleration of the simulations.

3:45 PM BREAK

SESSION EN03.03: Thermal Materials II
Session Chairs: Md Shafkat Bin Hoque and Kirill Kovnir
Tuesday Afternoon, November 30, 2021
Hynes, Level 3, Room 306

4:00 PM *EN03.03.01

Thermal Transport in Complex Structures and Across Interfaces Zhiting Tian; Cornell University, United States

Understanding thermal transport processes is essential to design materials and devices with desired thermal transport properties for thermal energy conversion and management. Despite the significant progress in thermal transport of simple inorganic crystals, our understanding of thermal transport in complex structures and across interfaces remains limited. In this talk, I will present my research group's efforts to understand thermal transport in complex structures and across interfaces, using atomic modeling and experimental characterization. I will start with our study on boron suboxides, which have unusually high thermal conductivity despite their complex structures. I will then cover phonon dynamics in 3D and 2D hybrid organic-inorganic perovskites using inelastic x-ray scattering, where we gained useful insights into their ultralow thermal conductivity and remarkably weak anisotropy in 2D hybrid. Last but not least, I will share our development of rigorous formalism for anharmonic atomistic Green's function to capture the contribution of inelastic scattering at the interfaces, direct observation of phonon Anderson localization in aperiodic superlattices, and machine-learning-assisted interface design.

4:30 PM EN03.03.02

Objective Oriented Design of Phase Change Material Composites Alison Hoe, Achutha Tamraparni, Chen Zhang, Alaa Elwany, Jonathan Felts and Patrick Shamberger; Texas A&M University, United States

While phase change material (PCM) heatsinks and energy storage modules have been shown to act as highly efficient transient energy storage components in thermal management systems, they have traditionally been limited by the rate at which heat is absorbed into the PCM. Composite thermal energy storage (TES) materials, consisting of highly thermally conductive elements and PCMs can overcome some of the challenges presented by the slow rate of heat absorption by most PCM phases. However, the application of these components is limited by a lack of coherent design guidelines. Here, we present a design framework based around the concept of phase change material (PCM) composites, where the effective thermal properties of a composite are dictated by constitutive relationships relating the composite structure to its transport properties. Under this approximation, relatively simple approximate analytical solutions or numerical solutions reveal the response of PCM composites to different transient heat loads. Furthermore, that response can be optimized, given a particular performance metric of interest (total heat absorbed, heat absorbed per unit mass, etc.).

First, we develop the concept of composite PCM volumes, and demonstrate that the defining criteria of a composite PCM is the critical length scale separating conductive elements. For systems below this length scale, the composite can be defined by effective thermal properties, which dramatically simplifies the description of the system, and computation of transient thermal response. Both numerical and experimental results illustrate that this length scale is on the order of 1 mm for many systems of interest, and thus is easily achievable by a number of manufacturing techniques.

Next, we demonstrate the role of metal volume fraction in governing transient thermal performance by considering heat transfer in both planar and cylindrical systems. Systems which are designed to optimize the total rate of heat transfer into the composite volume (or similarly, to minimize the transient temperature range at an interface) have dramatically higher volume fractions of conductive component than are generally considered. However, if the performance metric is modified to take into account the system volume and mass, the resulting optimal composite structure varies as a function of 1) the thermal boundary condition, 2) the period over which heat is absorbed, 3) material properties, and 4) composite geometry. The outcome of this task is a set of design guidelines for thermal storage composites, valid across a range of geometries, orientations, and material thermophysical properties. Such design guidelines will enable order of magnitude improvements in cooling power densities for TES composites.

Finally, the concept of objective oriented design of PCM composites is presented, and is illustrated with examples based around two design objectives for a finite volume cylindrical PCM composite: 1) Maximizing thermal buffering capacity at a given time, and 2) Maximizing the time the system can achieve a minimum thermal buffering capacity threshold. To this end, we demonstrate that there exist two design regimes where the thermal buffering capacity is either limited by the rate at which the system can absorb thermal energy, or by the total thermal capacitance of the system. We present expressions of the optimal volume fraction for each combination of design objectives, coordinate systems and boundary conditions based on appropriate analytical solutions for the melting problem.

4:45 PM *EN03.03.03

High-Temperature Thermal Transport in Ceramic Materials Renkun Chen; University of California, San Diego, United States

High temperature thermal transport processes are important for a variety of thermal energy conversion and management processes, such as concentrating solar power, thermophotovoltaic, thermoelectric, and thermal storage. While characterization and understanding of high-temperature thermal conductivity of various materials have been studied for several decades, there are still challenges associated with many materials in different forms (bulk, particles, films). In particular, complex high- and medium- entropy ceramic materials have recently emerged as an appealing class of materials due to their various unusual attributes, such as thermal and chemical stability, but their thermal conductivity mechanisms and potential applications as thermal materials are yet to be fully explored. In this work, we study thermal transport properties of both simple and complex (high- and medium- entropy) metal oxides. We use both traditional methods (such as laser flash) and new optical technique to measure thermal conductivity of these oxides in the form of bulk solids, coatings, and particles. The measured thermal conductivity is understood through intrinsic phonon scattering mechanisms from room to high temperature in bulk solids as well as extrinsic effects in coatings and particles.

5:15 PM EN03.03.04

Thermal Conductivity Prediction of Ceramic Materials at High Temperature Zherui Han and Xiulin Ruan; Purdue University, United States

Many applications such as effective thermal barrier coatings require ceramic materials to have low thermal conductivities at high temperature. In these crystals, phonons are the main heat carriers and thermal conductivity is largely determined by phonon-phonon interactions. We predict this key property of ceramic materials using first-principles calculations, where we consider recent theoretical advances: four-phonon scattering and phonon renormalization. We find these two effects to be significant at high temperatures, a condition where ceramics are expected to work. Our predictions agree well with available experimental data and our own measurements, and can guide thermal barrier coating design for high temperature applications.

5:30 PM EN03.03.05

Nanoscale Mechanisms for Increasing Thermal Boundary Conductance via Ion Irradiation Thomas W. Pfeifer¹, Ethan A. Scott², Ashutosh Giri³, John A. Tomko¹, Khalid Hattar² and Patrick E. Hopkins¹; ¹University of Virginia, United States; ²Sandia National Laboratories, United States; ³University of Rhode Island, United States

A fundamental understanding of thermal boundary conductance is critical for device cooling, and with ion bombardment as a prominent method of doping of semiconductors, the impact on TBC must be explored. We present a two-part study in which we experimentally measure the TBC across defected / pristine crystalline-crystalline interfaces, and use molecular dynamics to help explain the results.

Experimentally, we measure Gallium Nitride bombarded with varying doses of Helium, Carbon, Nitrogen, and Gallium ions, with an Aluminum capping layer deposited, and we observe a consistent increase in TBC with increasing ion dose. These measurements are performed using Time Domain Thermoreflectance (TDTR), which is a pump-probe technique that measures the change in thermoreflectance on the surface of a sample as a function of pump-probe delay time from picoseconds to nanoseconds. This change in thermoreflectance is related to both the temporal temperature decay from impulse heating driven by the sub-picosecond pump pulse and the frequency-dependent temperature rise induced from the modulated pump pulse train. Thus, TDTR is well suited to measure the thermal conductance across near surface interfaces. Our TDTR apparatus includes an 800nm 80MHz femtosecond pulsed laser, the pump is modulated at 8.4MHz, and all samples included an aluminum transducer deposited on the surface. Computationally, we explore a Silicon / Heavy Silicon system in which Frenkel defects are introduced. We note an increase in TBC when defects are added, and point to an increased level of lattice deformation (in addition to the sparse defects themselves) as leading to an increase in phonon scattering within the material near the interface. This portion of the study uses Non-Equilibrium Molecular Dynamics (NEMD) simulations using Large-scale Atomic/Molecular Massively Parallel Simulator (LAMMPS). A Stillinger Weber potential is used for the Silicon - Heavy Silicon system, and the system is initialized with pairs of void / interstitial defects present.

SESSION EN03.04: Poster Session I: Thermal Materials, Modeling and Technoeconomic Impacts for Thermal Management and Energy Application
Session Chairs: Xiangyu Li and Xiulin Ruan
Tuesday Afternoon, November 30, 2021
8:00 PM - 10:00 PM
Hynes, Level 1, Hall B

EN03.04.01

Late News: Modeling the Effect of Thermal Boundary Resistance on the Thermal Behaviors of a Lithium-Ion Battery for Energy-Storage Applications Dongcheul Lee, Byungmook Kim, Seohee Kang and Chee-Burm Shin; Ajou University, Korea (the Republic of)

Any power generation through energy harvesting or from renewable sources should be combined with a suitable energy storage system to complement the intermittency of energy sources. Lithium-ion batteries (LIBs) are by far the most popular energy storage option in the global energy storage market. Thermal management is indispensable to control the temperature of LIB within a suitable range for energy-storage applications. For a proper thermal management of LIB, it is important to establish a thermal modeling methodology which is computationally efficient. An LIB cell consists of multiple alternating layers of positive and negative electrode materials, aluminum and copper current collectors, and porous separators impregnated with electrolyte. For the thermal modeling of LIB, we need a systematic way to obtain the thermal properties of the various compartments of the cell components as well as the thermal boundary resistances of the interfaces between the cell components.

In this work, a thermal modeling methodology is presented with a special emphasis to investigate the effect of thermal boundary resistance on the thermal behaviors of an LIB cell. A 63 Ah LIB cell fabricated by LG Chem. is modeled. The density and specific heat capacities are obtained by using the volume-averaged values of the various compartments of the cell components and the effective thermal conductivities are calculated by using the values estimated based on the equivalent networks of parallel and serial thermal resistances of the cell components including the thermal boundary resistances of the interfaces between the cell components. The non-uniform distribution of the heat generation rate in an LIB cell is calculated based on the modeling results of the potential and current density distributions of the battery cell. Thermal modeling of an LIB cell is validated by the comparison between the experimental measurements and modeling results. The modeling methodology presented in this work can be used to estimate accurately the thermal behaviors of various devices used for thermoelectric and thermophotovoltaic energy conversion.

EN03.04.02

Raman Linewidth Contributions from Four-Phonon and Electron-Phonon Interactions in Graphene Zherui Han¹, Xiaolong Yang², Sean Sullivan³, Tianli Feng⁴, Li Shi³, Wu Li² and Xiulin Ruan¹; ¹Purdue University, United States; ²Shenzhen University, China; ³The University of Texas at Austin, United States; ⁴The University of Utah, United States

The Raman peak position and linewidth provide insight into phonon anharmonicity and electron-phonon interaction in materials. For monolayer graphene that has emerged as a potential electronic and optoelectronic material, prior first-principles calculations have yielded opposite temperature dependence of the linewidth compared to measurement results. Here, we explicitly consider four-phonon anharmonicity, phonon renormalization, and electron-phonon coupling, all found important to successfully explain both the G peak frequency shift and linewidths in our suspended graphene sample at a wide temperature range. Our calculation shows that the Raman linewidth can be widely tuned by varying carrier doping.

EN03.04.03

Thickness-Dependent Thermal Conductivity of Mechanically Exfoliated β -Ga₂O₃ Thin Films Yingying Zhang¹, Qun Su¹, Jie Zhu², Sandhaya Koirala¹, Steven Koester¹ and Xiaojia Wang¹; ¹University of Minnesota Twin Cities, United States; ²Dalian University of Technology, China

Beta-phase gallium oxide (β -Ga₂O₃), the most thermally stable phase of Ga₂O₃, has stimulated great interest in power electronics due to its ultra-wide bandgap (~4.9 eV) and high breakdown electric field. The relatively low thermal conductivity of β -Ga₂O₃, however, limits the device performance due to excessive temperature driven by self-heating. Recently, integrating β -Ga₂O₃ thin films on substrates with high thermal conductivities has been proposed to improve heat rejection and device reliability. In this work, we prepare high-quality single-crystal β -Ga₂O₃ thin films by mechanical exfoliation of bulk crystals and study their thermal transport properties. Both the anisotropic thermal conductivity of β -Ga₂O₃ bulk crystals and the thickness-dependent thermal conductivity of β -Ga₂O₃ thin films are measured using the time-domain thermoreflectance technique. The reduction in the thin-film thermal conductivity, compared to the bulk value, can be well explained by the size effect resulting from the enhanced phonon-boundary scattering when the film thickness decreases. This work not only provides fundamental insight into the thermal transport mechanisms for high-quality β -Ga₂O₃ thin films but also facilitates the design and optimization of β -Ga₂O₃-based electronic devices.

EN03.04.04

A Pump-Probe Thermoreflectance Technique for Measuring Specific Heat Capacity of Thin Films Milena Milich, John A. Tomko and Patrick E. Hopkins; University of Virginia, United States

From the energy sector to the pharmaceutical industry, there has been a growing need for characterization of thermal properties of materials at the nanoscale. In particular, measuring the specific heat capacity of a material is critical to quantifying heat dissipation in thermal management research as well as optimizing additive manufacturing routines and pharmaceutical development. While traditional methods for determining specific heat capacity, such as differential scanning calorimetry, rely on bulk samples for measurement, it can be both extremely expensive and time-consuming to produce bulk volumes of sample materials.

In this work, we introduce a novel pump-probe thermoreflectance technique for measuring thermal properties of thin films, on the order of nanometers thick. More specifically, we use a boxcar averager to monitor the transient temperature rise of the sample surface as it is periodically heated by the “pump” laser beam. By measuring the laser-induced heating over multiple modulation frequencies we are able to measure not only specific heat capacity, but also thermal conductivity and thermal boundary conductance. We demonstrate the application of the proposed measurement technique by measuring and analyzing standard “film on substrate” samples as well as a collection of low-temperature phase change materials.

EN03.04.05

Nickel-Infused Nanoporous Alumina as Tunable Solar Absorber Xuanjie Wang; Rensselaer Polytechnic Institute, United States

Solar energy can alleviate our dependence on traditional energy sources like coal and petroleum. In this regard, the design and performance of solar absorbers are crucial for capturing energy from sunlight. Specifically, for applications relying on solar-thermal energy conversion, it is desirable to construct solar absorbers using scalable techniques that also allow a variation in optical properties. In this study, we demonstrate the ability to tune the spectral absorptance of nickel-infused nanoporous alumina using a scalable and inexpensive fabrication procedure. With simple variations in the geometry of the nanostructures, we enable broadband absorption with a net solar absorptance of 0.96 and thermal emittance of 0.98 and spectrally-selective absorption with a net solar absorptance of 0.83 and thermal emittance of 0.22. The simple manufacturing techniques presented in this study to generate nanoengineered surfaces can lead to further advancements in solar absorbers with well-controlled and application-specific optical properties.

EN03.04.07

Effect of Temperature on the Solubility of Magnesium in Molten Salt $MgCl_2$ -KCl-NaCl and the Resulting Redox Potential and Corrosivity Kalyn M. Fuelling^{1,2}, Olivia Dale¹, Suhee Choi¹ and Michael Simpson¹; ¹The University of Utah, United States; ²University of Michigan, United States

Molten chloride salts are a promising option for heat transfer use in concentrating solar power plants due to their ability to transfer heat efficiently and remain stable at a variety of temperatures. However, these salts are corrosive and therefore break down pipes in the plant. In this study, the aim is to further investigate the solubility of magnesium in $MgCl_2$ -KCl-NaCl salt to reduce the formation of corrosive hydroxide/oxide ions. Redox potential was used to indicate the dissolution of the magnesium in the molten chloride salts at different temperatures. A previous study reported that the addition of the magnesium to the $MgCl_2$ -KCl-NaCl salt resulted in a lower redox potential than that of pure $MgCl_2$ -KCl-NaCl. This study will focus on refining the relationship between the solubility of magnesium and operating temperature. Tests were conducted at 500°C, 600°C, and 650°C. With this data correlating to temperature, concentrating solar power plants can know precisely how much magnesium needs to be added to the molten chloride salt at a certain temperature in order to adequately lower the redox potential and thus result in a less corrosive substance.

EN03.04.08

Single-Nanodiamond Luminescence Lifetime Thermometry for Transient Hotspot Quantification Dinesh Bommididi and Andrea Pickel; University of Rochester, United States

Modern electronic and data storage technologies combine shrinking feature sizes with ever-increasing operating speeds, leading to transient nanoscale hotspots that can limit device performance. Quantifying hotspots in operating devices thus requires a non-invasive thermometer with sub-100 nm spatial resolution and sub-100 ns temporal resolution. One promising approach is to optically probe the time-resolved, temperature-dependent luminescence of an individual nanoparticle placed at a specific critical location. Nitrogen vacancy (NV) centers are bright, photostable luminescent defects found in diamond nanoparticles (nanodiamonds, or NDs) that have emerged as exemplar optical sensors with wide-ranging applications, including nanoscale magnetometry, bioimaging, quantum computing, stress mapping, and thermometry. The spin state of NV centers can be coherently manipulated using resonant microwave pulses and read out via the emitted luminescence, an approach known as optically detected magnetic resonance (ODMR). The ODMR signal has well-known temperature dependence, enabling ODMR-based thermometry. However, the temporal resolution of ODMR thermometry is limited to ~10 ms. Furthermore, ODMR measurements require a microwave antenna, an experimental complication that can also interfere with device operation.

To overcome the limitations of ODMR thermometry while retaining the advantages of ND-based sensing, we utilize the temperature-dependent luminescence lifetimes of NV centers in individual NDs for thermometry. NV centers have luminescence lifetimes of ~25 ns, naturally facilitating high temporal resolution measurements. At elevated temperatures, the probability of phonon-assisted non-radiative relaxation increases, thereby decreasing the luminescence lifetime. To demonstrate single-ND luminescence lifetime thermometry, we first developed robust strategies for cross-identifying single NDs via luminescence, atomic force microscope (AFM), and scanning electron microscope (SEM) imaging, since luminescence emission intensity is not a reliable indicator for distinguishing single NDs from aggregates. We then measured the luminescence lifetimes of individual ~70 nm NDs as a function of temperature using an approach called time-correlated single photon counting (TCSPC). TCSPC relies on the repeated detection of single photons over many excitation and decay cycles, allowing us to overcome the challenge of low photon counts associated with small NDs and high temperatures. We assessed the temperature dependence, repeatability, and ND-to-ND uniformity of single-ND luminescence lifetimes. We find that single-ND lifetimes show reliable, sensitive temperature dependence that can be calibrated and employed for thermometry. We also show that AFM-based nanomanipulation can be used to position individual NDs with ~20 nm precision. The combination of high spatial and temporal resolution along with precise positioning control can enable practical applications of single-ND luminescence lifetime thermometry for transient hotspot characterization.

10:30 AM *EN03.05.01

Surface Phonon-Polaritons as Efficient Cooling Vectors [Sebastian Volz](#), Yunhui Wu, Jose Ordonez, Laurent Jalabert, Saeko Tachikawa, Roman Anufriev and Masahiro Nomura; The University of Tokyo, Japan

Surface phonon-polaritons (SPhPs), electromagnetic modes excited by optical phonons, are investigated to promote heat spreading in nanostructures. In the first stage, it will be shown that SPhPs can carry heat more efficiently than phonons in ultra-thin SiN amorphous membranes by measuring thermal conductivity as a function of temperature and thickness by using Time-Domain ThermoReflectance. The significant contribution of SPhPs is proven in the 400K-800K temperature range.

By using the 3w technique, we then show the presence of SPhPs in the 300K-400K temperature range and their quasi-ballistic contribution to thermal conduction over a distance larger than 100 microns to be compared to the few hundred 100nms of phonon mean path.

In a second stage, we show that SPhPs also impact heat conduction in silicon devices by measuring the SPhP heat flux in SiO₂/Si/SiO₂ multilayers with a gap. In this latter case, a predominant SPhP contribution is highlighted.

11:00 AM EN03.05.02

Late News: New Transport Behavior in Nanostructured Silicon—Increased In-Plane Phonon Scattering Drives Enhanced Thermal Conduction [Brendan McBennett](#)¹, Joshua Knobloch¹, Albert Beardo², Hossein Honarvar^{1,1}, Travis Frazer¹, Begoña Abad¹, Lluç Sendra², Javier Bafaluy², Juan Camacho², Jorge Nicolas Hernandez Charpak¹, Henry Kapteyn¹, Mahmoud Hussein¹, Xavier Alvarez² and Margaret Murnane¹; ¹University of Colorado Boulder, United States; ²Universitat Autònoma de Barcelona, Spain

Understanding nanoscale thermal transport is critical for nano-engineered devices such as quantum sensors, thermoelectrics, and nanoelectronics. However, despite overwhelming experimental evidence for non-diffusive heat dissipation from nanoscale heat sources, the underlying mechanisms are still not understood. In this work, we model nanoscale heat flow with both advanced mesoscopic and microscopic approaches to elucidate the fundamental physics of an unexplained and counter-intuitive behavior: *decreasing nanoscale heat source spacing actually enhances cross-plane thermal conduction* [1].

Using advanced atomic-level simulations, we obtain the microscopic information needed for a fundamental investigation of nonequilibrium phonon scattering amidst *interacting* heat sources [2]. We observe a reduction in in-plane phonon lifetimes with decreasing nanoheater spacing, as phonons from neighboring heat sources scatter downwards into the substrate. The increased scattering is accompanied by elevated cross-plane thermal conduction – a novel *channeling* phenomenon that lies beyond many of the traditional Boltzmann transport equation approximations and opens the door to nanoscale engineering of thermally anisotropic materials. We also note the striking similarities between the non-diffusive temperature profiles calculated from the atomistic data and our second, mesoscopic approach.

The kinetic-collective model (KCM) is a hydrodynamic transport model which uses finite element analysis to solve the Guyer-Krumhansl equation over large, device-relevant geometries [3]. While resistive scattering in bulk silicon is traditionally thought to obscure hydrodynamic effects, we observe good agreement between KCM and experimental data for the thermal relaxation of 1 and 2D nanoscale hot spots [4]. In the case of small, effectively isolated heaters, the temperature decay is double-exponential, with distinct time scales for interface resistance and hydrodynamic-like phonon transport. By tuning a nonlocality parameter in KCM to the limiting length scale, we can also predict the increased conduction observed experimentally for closely-packed sources. Moreover, we predict the full thermomechanical physics in ultrafast laser-based experiments, even in complex and general geometries, without the need for geometrical fit parameters, an advance beyond traditional simulations. The combined models explain the counterintuitive experimental observations of enhanced cooling for close-packed heat sources, from atomic to >micron length scales and represent a new fundamental behavior in materials, with far reaching implications for electronics and future quantum devices.

[1] Frazer et al., *Phys. Rev. Appl.* **11**, 024042 (2019)

[2] Honarvar et al., *PNAS*, accepted (2021)

[3] Beardo et al., *Phys. Rev. Appl.* **11**, 034003 (2017)

[4] Beardo, Knobloch et al., *ACS Nano* **15**, 13019 (2021)

11:15 AM EN03.05.03

The Influence of Extrinsic Lattice Defects on Thermal Transport in Single Crystal Thorium Dioxide [Cody A. Dennett](#) and David H. Hurley; Idaho National Laboratory, United States

Actinide and lanthanide fluorite oxides, UO₂, CeO₂, ThO₂, form an important class of ceramic energy materials with applications ranging from nuclear fuels to solid oxide fuel cells. Of these systems, ThO₂ (thoria), has been the least explored and offers unique features including an extremely high melting temperature and a fixed tetravalent oxidation state. Many potential application environments for thoria include high radiation fields or temperatures which either promote or directly generate lattice defects. Such defects drastically influence thermal transport, a controlling safety and performance property in many applications. To date, little experimentally-validated understanding has been generated on the role of defect formation and clustering on thermal transport in thoria due to the lack of high-quality starting material in which these effects may be explored. In this work, high-quality oriented single crystals of thoria are grown using hydrothermal synthesis and then exposed to proton irradiation to generate extrinsic lattice defects (both nanoscale point defects and extended dislocation loops). The thermal conductivity of these damaged crystals is measured direction using a spatial domain thermoreflectance (SDTR) technique and defects are quantified using optical spectroscopy and electron microscopy. Experimental values are compared with the calculation of thermal conductivity from the linearized Boltzmann transport equation for phonons taking into account the relevant scattering mechanisms. This combined experimental and computational approach provides a framework for predicting the thermal performance of this class of materials from first principles in a variety of environmental conditions.

11:30 AM EN03.05.04

Anomalous Thermoelectric Transport Phenomena from Interband Electron-Phonon Scattering [Boris Kozinsky](#)^{1,2}, Natalya Fedorova^{1,3} and Andrea Cepellotti¹; ¹Harvard University, United States; ²Bosch Research, United States; ³Luxembourg Institute of Science and Technology, Luxembourg

The Seebeck coefficient and electrical conductivity are two central quantities to be optimized simultaneously in designing thermoelectric materials, and they are determined by the dynamics of carrier scattering. We uncover a new regime where the presence of multiple electron bands with different effective masses, crossing near the Fermi level, leads to strongly energy-dependent carrier lifetimes due to intrinsic electron-phonon scattering. In this anomalous regime, electrical conductivity decreases with carrier concentration, Seebeck coefficient reverses sign even at high doping, and power factor exhibits an unusual second peak. We explain the origin and magnitude of this effect using a general simplified model as well as first-principles Boltzmann transport calculations in recently discovered half-Heusler alloys. We identify general design rules for using this paradigm to engineer enhanced performance in thermoelectric materials.

SESSION EN03.06: Thermoelectrics I
Session Chairs: Renkun Chen and Patrick Shamberger
Wednesday Afternoon, December 1, 2021
Hynes, Level 3, Room 306

1:30 PM *EN03.06.01

Engineering Grain Boundaries in Thermoelectric Materials [G. J. Snyder](#); Northwestern University, United States

Grain boundaries have a remarkable effect on the thermal and electrical transport properties of polycrystalline materials but are often ignored by prevailing physical theories. Grain boundaries and interfaces can adversely alter the properties of Solar Cells, Batteries and Thermoelectrics. To devise strategies for improving the thermoelectric performance of materials, it is essential to understand the coupled charge and thermal transport mechanisms including an interfacial Seebeck effect. The inhomogeneous nature of materials, such as that caused by grain boundaries, must be taken into account to rethink engineering strategies based on Matthiessen's rule which interprets scattering homogeneously.

Prevailing models for thermal transport treat interfaces and grain boundaries as structureless even though at the atomic scale they are better described as arrays of linear defects of various types. Allowing for this inherent structure, several fundamental characteristics of heat transport arise, such as diffraction conditions when heat carrying phonons scatter off the periodic, linear defect arrays that should be present in grain boundaries. Furthermore, a dimensionality crossover is observed in diffusive heat transport where phonons with a wavelength longer than the linear defect spacing see the interface simply as a structureless planar defect, and phonons with see the interface as a collection of independently scattering linear defects.

2:00 PM EN03.06.02

Influence of Thermoelectric Leg Shape on Power Generation Potential Under Constant Temperature and Heat Flux Boundary Conditions [Bengisu Sisik](#) and [Saniya LeBlanc](#); The George Washington University, United States

Thermoelectric devices offer the potential to convert wasted heat into electricity, and they can be used for thermal management by pumping heat. The shape of thermoelectric devices, particularly the active semiconducting material units (or thermoelectric legs) within the device, has remained largely unchanged – thus limiting our ability to customize device thermal resistances. The advent of new manufacturing techniques such as additive manufacturing enables customizable device shapes, but there is little knowledge about what shapes are desirable. In this work, we show the effect of different (non-rectangular) thermoelectric leg designs on thermoelectric device performance. Various leg shapes (rectangular prisms, rectangular prisms with interior hollows, trapezoids, hourglass, and Y-shapes) were modeled numerically to determine their thermal and electrical performance under constant temperature and heat flux boundary conditions. Two thermoelectric materials, bismuth telluride and silicon germanium, were modeled to capture low and high temperature applications, respectively. An hourglass-shaped thermoelectric leg subjected to a fixed temperature boundary condition has the best thermal and electrical performance: the hourglass-shaped leg results in more than double the electrical potential and maximum power compared to the conventional rectangular shape. Under a fixed heat flux boundary condition on the hot side, a trapezoid-shaped leg results in almost double the electrical potential and a 50% increase in the power output compared to the conventional leg shape. Varying boundary conditions, which reflect different device operating conditions, result in different performance values for the same leg shapes. These findings underscore the importance of leg geometry on electrical and thermal performance of a thermoelectric leg, as well as the importance of considering the device operating condition when selecting the best leg shape. The results are relevant as new processing techniques emerge and enable topological optimization of thermoelectric devices.

2:15 PM EN03.06.04

Synthesis, Structure and Properties of Pnictide-Based Clathrates [Kirill Kovnir](#)^{1,2}; ¹Iowa State University, United States; ²US DOE Ames Laboratory, United States

Unique class of 3D framework materials with large polyhedral cages, clathrates, is a promising platform for the development of novel thermoelectric materials due to intrinsically low thermal conductivity. Traditionally the tetrahedral clathrate frameworks are based on tetrels, group 14 elements, Si, Ge, and Sn. In this work we will present recent advances in the design, synthesis, order-disorder structural transitions, and properties of unconventional clathrates with three-dimensional frameworks comprised of oversized metal-pnictide (P, As, and Sb) polyhedral cages that encapsulate guest cations.

2:30 PM EN03.06.05

Sr₂Sb₂O₇ as a Novel Thermoelectric Material [Luisa Herring Rodriguez](#)¹ and David O. Scanlon^{1,2,3}; ¹University College London, United Kingdom; ²Diamond Light Source, United Kingdom; ³Thomas Young Centre, United Kingdom

Around 60% of primary energy consumption is wasted as heat energy, representing an untapped source of energy with huge potential to reduce our overall consumption.¹ Thermoelectric materials convert heat energy into electricity through the use of temperature gradients. The materials historically used for this purpose include bismuth chalcogenides and lead tellurides. However, issues relating to their natural abundance and toxicity, combined with the increasing demand for environmentally friendly energy sources, is driving research into novel materials with potential thermoelectric properties to replace these.

The effectiveness of a thermoelectric is measured by the dimensionless figure of merit ZT. Materials with a high ZT need to balance a high electrical conductivity and a low thermal conductivity. Oxides generally exhibit properties valuable for thermoelectric applications, including low cost, thermal and chemical stability and environmental benignity. However, their thermoelectric performance has been hindered by their high lattice thermal conductivities. Novel ternary oxides have advanced research in this field as their complex crystal structures possess lower lattice thermal conductivities than traditionally seen in oxides.

In this study, we conduct a detailed investigation into the thermoelectric properties of the ternary wide band semiconductor Sr₂Sb₂O₇, which has previously been synthesised under high temperature conditions and shown to be thermally stable.^{2,3} Our study uses the latest approach to separately calculate the different contributions to overall scattering rates, in order to more accurately predict thermal conductivity as compared to the constant relaxation time approximation (CTRA).⁴ We benchmark this approach against the CTRA and show that Sr₂Sb₂O₇ possesses a ZT greater than many existing oxide thermoelectric materials, and has the potential to perform as a high-performance n-type thermoelectric component. We go on to investigate the defect chemistry of this exciting new thermoelectric candidate to further assess its suitability.

¹ M Kanatzidis, Chem. Matter. 2010, 22, 648

² Sato et al., J. Photochem. Photobiol., A 2002, 148, 85

³ Xue et al., J. Phys. Chem. C 2008, 112, 5850

⁴ Ganose et al., Nat. Commun. 2021, 12, 2222

2:45 PM EN03.06.06

Classifying $(p \times n)$ -Type Transverse Thermoelectric Semimetals and Semiconductors [Qing Shao](#) and Matthew Grayson; Northwestern University, United States

Unlike the longitudinal 2-leg thermoelectrics, $(p \times n)$ -type transverse thermoelectrics (TTE) function with a single leg hosting orthogonal p - and n - Seebeck behavior. The anisotropic ambipolar thermoelectric behavior is originated from the anisotropic effective masses of electrons and holes, leading to opposite dominant transport types along different crystal axes despite the parallel transport of electrons and holes along both directions. Whereas doped unipolar thermoelectrics have activated conduction to a single band, these $(p \times n)$ -type materials can have activated conduction to both bands since both electrons and holes simultaneously contribute to the anisotropic conduction in all directions. As such an important concept here is that of the “partial gap”, i.e. the gap between the Fermi energy and the electron or hole band edges for the n - and p -type partial gaps, respectively. The partial gap is defined as positive for non-degenerate doping, designated n or p , and negative for degenerately doping, designated n^+ or p^+ . Consequently, we categorize intrinsic semiconductors with the label $p \times n$ given the positive electron and hole partial gaps, while the intrinsic semimetal is labelled $p^+ \times n^+$ given the heavy doping resulting in two negative partial gaps. There remain two intermediate hybrid cases, namely $p^+ \times n$ and $p \times n^+$ where one band is degenerately and the other non-degenerately doped. Theoretical analysis and simulations show that among all four types of bulk TTE materials, the semiconducting $(p \times n)$ -type TTEs have the largest transverse power factors. By comparison, the metallic transport of both electrons and holes of $(p^+ \times n^+)$ -type TTE leads to the lowest transverse power factors, though these might be the most promising TTE candidates in extreme low-temperature applications. The dependence of transverse Seebeck coefficient on electron and hole effective mass anisotropy is explored as a function of Fermi energy for different directional effective mass ratios for both electrons and holes. All categories of semiconductor, semimetal, and hybrid $(p \times n)$ -type TTE are modeled with band gap $E_g = \pm 3 k_B T$ to illustrate peak TTE performance, including Seebeck tensor terms and transverse power factors. We point out unusual scenarios in the hybrid case where, for example, the valence band can be degenerately doped, yet the Seebeck coefficient in one of the transport directions can still be n -type, dominated by activated conduction to the electron band. The introduction of this classification method will greatly help the characterization and performance enhancement of $(p \times n)$ -type TTE materials, allowing broader application of this type of emerging TTE material.

3:00 PM EN03.06.07

Uncovering Intrinsic Thermoelectric Properties of Polycrystalline SnSe [In Chung](#); Seoul National University, Korea (the Republic of)

Despite the extraordinarily high maximum thermoelectric figure of merit (ZT) ~ 2.2 - 2.8 discovered in single-crystal SnSe materials, their performance has been severely debated. Many research groups have observed paradoxically higher thermal conductivity in polycrystalline samples than the reported values for single crystals, leading to much lower ZT. Accordingly, the widely sought goal in the thermoelectric society has been to realizing polycrystalline SnSe samples with comparable to or even higher performance than the single-crystals. In this talk, I will discuss the origin of such higher thermal conductivity and poorer ZT of polycrystalline SnSe samples. Then, I will introduce our facile synthesis process to remedy this problem. Our properly prepared, hole-doped SnSe polycrystalline samples show a record-breaking peak ZT greater than ~ 3.0 at 783 K and average ZT ~ 2.0 between 300 and 783 K. Their lattice thermal conductivity is finally ultralow at ~ 0.07 W m⁻¹ K⁻¹ at 783 K, much lower than that of the single crystals.

3:15 PM BREAK

SESSION EN03.07: Modeling Phonons, Electrons and Their Interactions

Session Chairs: Tianli Feng and Zherui Han

Wednesday Afternoon, December 1, 2021

Hynes, Level 3, Room 306

4:00 PM *EN03.07.01

Advances in Understanding and Modeling Phonons [Asegun Henry](#); Massachusetts Institute of Technology, United States

From the standpoint of pure crystalline materials, phonons have been long considered a solved problem. The standard model is sometimes termed the phonon gas model (PGM), and it provides a useful physical picture for both understanding and predicting behavior of phonons in pure crystalline materials. However, a variety of studies over the last decade have highlighted the fact that when symmetry is broken, for example by compositional or structural defects (e.g., random alloys, amorphous materials and interfaces) the mode shapes can change from what is traditionally envisaged for phonons, namely plane waves. The physics of these alternative types of phonons, how they interact, and how they impact phenomena such as chemical reaction is still being explored, and this talk will review progress made on these questions by the Atomistic Simulation & Energy (ASE) research group at MIT. This talk will also review recent progress on techniques to model the interactions between atoms and phonon transport.

4:30 PM EN03.07.02

Electronic Transport Properties Beyond the Boltzmann Equation [Andrea Cepellotti](#)¹, Jennifer Coulter¹, Anders Johansson¹, Natalya Fedorova^{2,1} and Boris Kozinsky¹; ¹Harvard University, United States; ²Luxembourg Institute of Science and Technology, Luxembourg

In this talk we will present some of our efforts for characterizing materials transport properties from first-principles simulations. First, we will discuss how first-principles calculations, typically limited to semiclassical models, are unable to capture the electronic transport properties of Bi₂Se₃, a narrow-gap semiconductor. In fact, we show that transport in this material at low doping concentrations is dominated by Zener tunneling [1], a phenomenon in which carriers tunnel between the valence and the conduction band, rather than just diffusing under the action of the electric field. This transport mechanism can be described using a novel first-principles model based on the Wigner distribution. Surprisingly, we find that Zener tunneling is not limited to low-energy carriers, but occurs also between band subvalleys of energy larger than the band gap.

Next, we will introduce Phoebe [2], a software for computing thermoelectric properties by solving the electron and phonon Boltzmann equation. Phoebe can compute electron-phonon and phonon-phonon scattering properties from first-principles simulations, allowing a fully ab-initio prediction of thermoelectric properties. Additionally, we implemented an efficient mixed MPI and OpenMP parallelization and GPU acceleration, allowing us to take advantage of contemporary computing infrastructure.

[1] A. Cepellotti & B. Kozinsky, Mater. Tod. Phys. 19, 100412 (2021)

[2] <https://mir-group.github.io/phoebe/>

4:45 PM *EN03.07.03

Thermal Transport in Topological Materials [Bolin Liao](#); University of California, Santa Barbara, United States

Topological phase transitions occur when the electronic bands change their topological properties, typically featuring the closing of the bandgap. While the influence of topological phase transitions on electronic and optical properties has been extensively studied, its implication on phononic properties and thermal transport remains unexplored. In this work, we use first-principles simulations to show that certain phonon modes are significantly softened near topological phase transitions, leading to increased phonon-phonon scattering and reduced lattice thermal conductivity. We demonstrate this effect using two model systems: pressure-induced topological phase transition in $ZrTe_5$ and chemical composition induced topological phase transition in $Hg_{1-x}Cd_xTe$. We attribute the phonon softening to emergent Kohn anomalies associated with the closing of the bandgap. Our study reveals the strong connection between electronic band structures and lattice instabilities and opens up a potential direction towards controlling heat conduction in solids. This work is based on research supported by DOE under the award number DE-SC0019244 and the UC Santa Barbara NSF Quantum Foundry funded via the Q-AMASE-i program under award DMR-1906325.

5:15 PM EN03.07.04

Interplay Between Electron-Phonon Coupling and Ballistic Transport in Thin Films Ali Alkurdi, Julien Legendre and [Pierre-Olivier Chapuis](#); CNRS - INSA Lyon, France

Thermal management is essential in many electronic devices, the components of which have been scaled down to the nanometer. When the characteristic size becomes comparable to the mean free path of energy carriers, interactions with boundaries can dominate thermal transport and the quasi-ballistic heat conduction regime arises: Fourier's diffusive law is no more valid to describe thermal transport and 'temperature jumps' appear at contacts. This heat conduction regime takes place for both phonons and electrons, however these two types of energy carriers do not have the same mean free path. In addition, it is known that electron and phonon temperatures can differ under some circumstances, when they are driven out of equilibrium. In this contribution, we investigate the deviation from the diffusive regime in thin films. To this end, we solve the Boltzmann Transport Equation (BTE) both for phonons and electrons using the Discrete Ordinate Method (DOM) [1-4], in particular in the isotropic-crystal and single relaxation time approximations. A coupling term reminiscent of the two-temperature model is added in the BTE equations [5]. This method accounts for the directional and non-local aspects of the energy flux, which can be tuned by the electron-phonon coupling constant. We analyze the impact of the electric field and the geometry on the flux transport, and compare the results with diffusion-based energy/charge conservation equations. These results shed light on the relation between local energy non-equilibrium and transport properties.

Références :

- [1] A. Majumdar, J. Heat Transfer 115, pp. 7-16 (1993)
- [2] S. Volz, D. Lemonnier, J.-B. Saulnier, Microscale Thermophys. Eng. 5 (3), pp. 191-207, (2001)
- [3] Thermal transport phenomena beyond the diffusive regime, P.-O. Chapuis et al., Proceedings of MIXDES (2016)
- [4] A. Alkurdi et al., Phonon Boltzmann Transport Equation and its EPRT approximation: lessons learned and outlooks, submitted
- [5] A. Pattamatta and C.K. Madnia, Journal of Heat Transfer, 131(8), 082401 (2009)

Acknowledgements:

The support of project EFINED (H2020-FETOPEN-1-2016-2017 766853) is acknowledged. We address a special thank to D. Lemmonier (Pprime), S.Merabia (ILM), A. Varpula and M. Prunnila (VTT).

SESSION EN03.08: Poster Session II: Thermal Materials, Modeling and Technoeconomic Impacts for Thermal Management and Energy Application
Session Chairs: Xiangyu Li and Xiulin Ruan
Wednesday Afternoon, December 1, 2021
8:00 PM - 10:00 PM
Hynes, Level 1, Hall B

EN03.08.02

Tuning Network Topology and Vibrational Mode Localization to Achieve Ultralow Thermal Conductivity in Amorphous Chalcogenides [Kiumars Aryana](#)¹, Derek Stewart², John T. Gaskins¹, Joyeeta Nag², John Read², David H. Olson¹, Michael Grobis² and Patrick E. Hopkins¹; ¹University of Virginia, United States; ²Western Digital Corporation, United States

In recent years, there have been numerous efforts to synthesize materials with ultralow thermal conductivities, a crucial parameter in the development of thermoelectric materials, memory devices, and thermally protective coatings. It has been generally believed that amorphous solids possess the lowest thermal conductivity possible. The heat transport mechanisms in ultralow thermal conductivity materials are often described using formalisms originally put forth by Einstein, and later refined by others, which account for some degree of localization of the vibrational modes or strong suppression of vibrational scattering length scales. These concepts, which partially form the basis of analytical minimum thermal conductivity models, are able to successfully predict the thermal conductivity of a wide range of amorphous solids. With advances in nanofabrication, several studies have shown that, by reducing the mean free paths of the vibrational modes, the thermal conductivity of crystalline materials can be significantly lower than this aforementioned minimum limit. In amorphous materials, however, manipulating the atomic structure to reach values below the minimum limit is more complicated, as it is already in its highest disordered state. Thus, a question remains: how can the thermal conductivity of a fully dense amorphous solid be further reduced?

Here, we report on a mechanism to suppress the thermal transport in a representative amorphous chalcogenide system, silicon telluride (SiTe), by nearly an order of magnitude via systematically tailoring the cross-linking network among the atoms. As such, we experimentally demonstrate that in fully dense amorphous SiTe the thermal conductivity can be reduced to as low as $0.10 \pm 0.01 \text{ W m}^{-1} \text{ K}^{-1}$ for high tellurium content with a density nearly twice that of amorphous silicon. Using ab-initio simulations integrated with lattice dynamics, we attribute the ultralow thermal conductivity of SiTe to the suppressed contribution of extended modes of vibration, namely propagons and diffusons. This leads to a large shift in the mobility edge - a factor of five - towards lower frequency and localization of nearly 42% of the modes. This localization is the result of reductions in coordination number and a transition from over-constrained to under-constrained atomic network.

EN03.08.03

Investigating Phonon Transport in Dense 2D and 3D Random Nanoparticulates [Ongira Chowdhury](#), Rohit Kakodkar and Joseph P. Feser; University of Delaware, United States

The frequency domain perfectly matched layer method is used to study phonon scattering and localization in two and three dimensional domains of randomly embedded nanoparticles. We show the FDPML method has the capability of capturing mode-by-mode phonon transport in domains with up to 100 million atoms with the use of parallel computing. From simulations of phonon-nanoparticle scattering across a wide range of volume fractions of nanoparticles, in the Mie and Rayleigh regime, we show that the elastic mean free path scales inversely with the number density of nanoparticles, for volume fractions as high as ~23% before exhibiting dependent scattering effects which causes the mean free path to increase again. We also observe phonon localization by using the Landauer method in 2D and 3D domains of random nanoparticles, at volume fractions up to ~40%. The modal decomposition method is also used to study localized modes in 2D and the results of the two approaches are compared.

EN03.08.04

New Incoherent and Coherent Models for Metal-Metal Thermal Interface Conductance [Joseph P. Feser](#); University of Delaware, United States

Since both sides of a metal-metal interface can support high intensity of electron emission and absorption, thermal transport at metal-metal interface is dominated by electronic carriers. Metal-metal thermal interface conductances (ITC) are at least 1-2 orders of magnitude higher than for interfaces that contain at least one dielectric material, yet the current state of knowledge of thermal transport across metal-metal interfaces remains surprisingly underdeveloped, with just a single simplified model - the electron diffuse mismatch model (eDMM) in the parabolic band approximation - having been employed and compared against experimental data. Here we develop several more advanced models of electronic transmission that can handle diffuse and coherent transport, using realistic band structures derives from first principles calculations. Using a tetrahedron interpolation method, we develop an accurate full-dispersion, multiband implementation of the electronic diffuse mismatch model that is particularly useful for capturing transport in transition metals, intermetallics, and transition metal compounds (XN, XC, XB2, X=X= transition metals); even in the case of Al-Cu we show that previous apparent experimental agreement with the eDMM is less convincing when using realistic band structure, and that agreement found in previous studies on Ir-Pd, hinges on the inclusion of electron-phonon coupling corrections to the electronic heat capacity. We give eDMM predictions for ITCs of a variety of interfaces types both with and without inclusion of electron-phonon coupling corrections. We also present two coherent electron transmission frameworks: (1) an analytic approach valid for nearly free-electron metals and (2) and NEGF approach appropriate for epitaxial metal-metal interfaces.

EN03.08.05

Late News: Quantized Thermoelectric Hall Effect Induces Giant Power Factor in a Topological Semimetal [Thanh Nguyen](#)¹, Fei Han¹, Nina Andrejevic¹, Vladyslav Kozii¹, Quynh Nguyen¹, Tom Hogan², Zhiwei Ding¹, Ricardo Pablo-Pedro¹, Shreya Parjan³, Brian Skinner¹, Ahmet Alatas⁴, Ercan Alp⁴, Songxue Chi⁵, Jaime Fernandez-Baca⁵, Shengxi Huang⁶, Liang Fu¹ and Mingda Li¹; ¹Massachusetts Institute of Technology, United States; ²Quantum Design, Inc., United States; ³Wellesley College, United States; ⁴Argonne National Laboratory, United States; ⁵Oak Ridge National Laboratory, United States; ⁶The Pennsylvania State University, United States

Identifying new materials that have a large thermoelectric response would be beneficial for global energy production by converting waste heat into useful electric power. While conventional thermoelectrics have regularly faced challenges with regards to vanishing electronic entropy at lower temperatures, topological materials offer an alternative pathway to surpass them through the topological protection of electronic states. Notably, theories have proposed that topological semimetals can large to a large, non-saturating thermopower and quantized thermoelectric Hall conductivity at the quantum limit. We experimentally demonstrate these unique features in topological Weyl semimetal tantalum phosphide (TaP), showcasing an ultrahigh longitudinal thermopower and a giant power factor which are predominantly attributable to the quantized thermoelectric Hall effect. Our findings demonstrate a confluence in the pursuit of effective thermoelectrics and novel topological materials in addition to the realization of the quantum thermoelectric Hall effect towards low-temperature energy harvesting applications.

Han, F., Andrejevic, N., Nguyen, T., Kozii, V., *et al.* Quantized thermoelectric Hall effect induces giant power factor in a topological semimetal. *Nat Commun* **11**, 6167 (2020).

SESSION EN03.09: Radiative Heat Transfer I

Session Chair: Xiaojia Wang

Thursday Morning, December 2, 2021

Hynes, Level 3, Room 306

10:30 AM *EN03.09.01

Radiative Energy Transport in Hyperbolic Materials [Hakan Salihoglu](#) and [Xianfan Xu](#); Purdue Univ, United States

Hyperbolic materials (HM) have unique properties of opposite signs in the principal components of dielectric permittivity in frequency ranges called Reststrahlen bands. These properties enable a significantly greater number of propagating radiation modes inside the bulk material compared with other materials, called hyperbolic phonon polaritons. Hexagonal boron nitride (hBN) is one of the natural HMs with low loss and supports propagation of hyperbolic phonon polaritons in the Reststrahlen bands. Thermal energy can excite hyperbolic phonon polariton modes in hBN at around room temperature and above. We study contributions of hyperbolic polariton modes to energy transport inside bulk hBN. Using the fluctuation-dissipation theorem, a theoretical model is derived to compute the energy transport by the hyperbolic modes. This model employs the many-body scattering method to account for radiative interactions within the bulk, across an interface, and across a small gap between two surfaces in the near-field radiation regime. The calculation results showed that hyperbolic polaritons in the Reststrahlen bands contribute to a significant amount of energy transport inside the bulk. The model also revealed that the equivalent radiative thermal conductivity by phonon polariton increases with temperature increase and can be comparable to phonon thermal conductivity at elevated temperatures. Experimental measurements conducted over a temperature range between 300 K - 600 K agree with the result of the theoretical model. Additionally, enhancement of near-field radiation due to the bulk phonon polaritons is also illustrated. In addition to hBN, other hyperbolic materials are also being investigated. This work reveals the significance of radiative transfer as a new energy transfer mode inside the hyperbolic materials and across an interface.

11:00 AM EN03.09.02

Thermal Conductivity Switching in Polymeric Photonic Mirrors for Building Envelope Thermal Management [Daron R. Spence](#) and Shannon K. Yee; Georgia Institute of Technology, United States

Dynamic management of heat loads in building envelopes can utilize polymeric photonic mirrors as dynamic thermal switches. This work investigates both the tunable thermally radiative and thermally conductive properties of photonic mirrors as a function of fabrication parameters and humidity. In particular, a sequential sol-gel process is used to fabricate distributed Bragg reflectors (DBRs) consisting of periodic multilayers of hydrophobic Polymethyl methacrylate (PMMA) and hydrophilic Poly Vinyl Alcohol (PVA). Variable volume fractions of optically transparent titania hydrate (TiO_x) are added to the PVA, forming a hybrid material that increases the refractive index contrast between layers and is moisture sensitive. UV-vis spectroscopy is employed to quantify the dynamic optical responses from polymer swelling obstructing the periodic conditions required to achieve constructive (reflective) interference. Corresponding changes to the films thermal conductivity using a differential 3 Omega technique are also observed beyond film swelling resulting from the degree of moisture uptake that is hypothesized to be effect by the degree of titania hydrate crosslinking. The results of this work provide novel insight into the dynamic nature of polymeric photonic mirrors and suggest applications for these materials as energy saving building technologies.

11:15 AM EN03.09.03

Smart Building Envelopes—Dynamic Switching Between Solar Heating and Radiative Cooling [Po-Chun Hsu](#); Duke University, United States

Solar thermal energy has been one of the major energy sources to realize zero energy buildings for a sustainable future. The high efficiency and low cost make it particularly attractive to reduce the energy consumption for hot water and space heating. On the other hand, the radiative cooling uses the rest of the sky, i.e. the outer space, as the cold source to generate cooling that can reduce the usage of refrigeration and space cooling. Recent progress in photonics and thermal science have further pushed this field to daytime subambient cooling, which created vast opportunities for sustainability and energy. Both technologies showed rapid improvement in the past decade, which become the enablers for the next generation smart net zero energy buildings. In this talk, I will introduce our recent research progress of switchable building envelope that can change between solar heating and radiative cooling. The dual-mode switchable device can be applied to buildings at various climate zones (spatial variation) under different weather or demand (temporal variation). I will give two examples of the dynamic envelope: (i) The mechanically switchable device can produce $\sim 600 \text{ W/m}^2$ of solar heating or $\sim 100 \text{ W/m}^2$ of radiative cooling with less than one minute switching time. This high performance is the outcome of heat transport analysis and thermal interface engineering. we perform building energy simulation for all the climate zones in the U.S. The results show our dual-mode device, if widely deployed, can save 45.8% of the heating, ventilation and air conditioning (HVAC) energy, which is 2.46 times higher than cooling-only and 1.43 times higher than heating-only approaches. (ii) The electrochromic device has continuous tunability and operates without any moving part. Rational photonic modeling and electrochemical cell design were implemented to achieve synergistic multispectral (solar + mid-IR) radiative heat management. At solar heating state, the device exhibits high solar absorptivity and low thermal emissivity; whereas at cooling state, the device shows high solar reflectivity and high thermal emissivity.

11:30 AM EN03.09.04

Late News: Ultrahighly Thermally Conducting Templated-MWCNT Coatings [John Texter](#), Xiumin Ma and Rene Crombez; Eastern Michigan University, United States

Polymeric stabilizers derived from imidazolium-based ionic liquids have been developed to prepare high concentration nanocarbon dispersions in water to yield aqueous dispersions up to 17 percent in MWCNT (and dispersions 1.4 percent in SWCNT and 6.4 percent in graphene). Stable MWCNT dispersions require a stabilizer/MWCNT weight ratio of 0.2 - 0.3 for effective stabilization in water. MWCNT concentration variations demonstrate slow equilibration effects that affect stabilizer demand, which increases with concentration. Highly scalable and anisotropic templated coatings have been prepared by drawdown-bar coating these aqueous dispersions on mulberry paper and fiberglass tissue substrates. Electrical and thermal conductivities for such coatings exhibit in-plane/through-plane anisotropies of up to 200 and 2,000, respectively. Electrical conductivities measured by a four-point method and broadband dielectric spectroscopy yield high but unremarkable in-plane conductivities in the 1 - 10 S/cm range, consistent with stabilizer-resistive connectivity between MWCNT. Ultrahigh thermal diffusivities ($1,000 - 6,000 \text{ mm}^2/\text{s}$) were obtained by a Fourier-transform analysis of Xenon flash data. Heat capacities of coatings measured by modulated differential scanning calorimetry and coating densities measured gravimetrically along with such diffusivities yield thermal conductivities in the range of 0.5 - 3 kW/mK. These conductivities appear to be the largest observed for MWCNT assemblies produced outside a vacuum chamber and 500-fold higher than available commercially. The stabilizer-induced electrical resistance at MWCNT junctions appears not to impede phonon transport across such junctions significantly. This thermal transport is likely related to stabilizer binding to the MWCNT sp^2 surfaces by π -orbital overlap. But bulk phonon transport through stabilizer assemblies seems unlikely. Photoacoustic experiments to examine thermal transport by such stabilizers are proposed. However, the de facto highly efficient phonon transport between MWCNT is more likely due to stabilizer rearrangement, promoting physical contact, and near contact at connecting junctions.

11:45 AM EN03.09.05

Radiative Cooling Paints With High Figure of Merit [Xiangyu Li](#), Joseph Peoples, Peiyan Yao and Xiulin Ruan; Purdue University, United States

Cooling consumes a great portion of energy in both residential and commercial applications. Passive radiative cooling can provide cooling power without any energy consumption by directly emitting heat to deep space. Conventional air conditioners only move the heat from the inside of the space to the outdoors while consuming electricity. Hence, passive radiative cooling holds great promises for addressing the global warming effect. A recent review paper on commercial heat reflective paints shows solar reflectance around 80% to maybe 92%, but none of these paints has achieved full daytime below-ambient cooling. To achieve passive daytime radiative cooling, current state-of-the-art solutions often utilize complicated multilayer structures or a reflective metal layer, limiting their applications in many fields. Attempts have been made to achieve passive daytime radiative cooling with single-layer paints, but they often require a thick coating or show partial daytime cooling. Therefore, it is a pertinent task to develop radiative cooling paints similar to commercial paints, since they provide ease of use, low cost, scalable fabrication, and are able to take advantage of the reliability engineering in the paint industry.

Here we have demonstrated that with the right fillers under certain concentrations and a broad particle size distribution, we can achieve below-ambient cooling in paints under direct sunlight. Monte Carlo simulations show consistent results with experimental characterization, validating the strategies we adopted to achieve high radiative cooling power. One of the designs showed a solar reflectance of 98% among paints and a high sky-window emissivity of 0.95. Outdoor tests exhibited that our paints showed comparable or better cooling performance than the other state-of-the-art approaches while offering unprecedented benefits including the convenient paint form, a fraction of the cost of the other approaches, and compatibility with the commercial paint fabrication process. A system figure of merit is defined in this work to evaluate the cooling power performance of different radiative cooling systems regardless of weather conditions. Additional testings of viscosity, abrasion resistance and outdoor weathering indicate the potential of the paints as a replacement for commercial white paints. Due to the abundance of the filler materials and a similar fabrication cost with commercial paint, our cooling paints are expected to save \$0.7 to \$1.5 for a moderate 100m² apartment during a summer sunny day compared to commercial white paints.

SESSION EN03.10: Thermometry and Thermophysical Properties

Session Chair: Po-Chun Hsu

Thursday Afternoon, December 2, 2021

Hynes, Level 3, Room 306

1:30 PM *EN03.10.01

Transient Thermoreflectance Pump-Probe Imaging for 3D Heterogeneous Integrated Circuit Characterization Sami Alajlouni and Ali Shakouri; Purdue University, United States

Recent advances in integrated circuits require integration of multiple chips in the same package as well as 3D chip modules with multi-layer metallization, copper through silicon vias and more complex heterogeneous integration. Heat dissipation in such devices require careful optimization of bonding interfaces, thermal interface materials and heat sink integration. During operation, small defects or voids can create hot spots and overtime reduce the chip performance and reliability. It is advantageous if the integrity of complex ICs could be characterized during manufacturing before full packaging and powering of the device which require integration on test boards and complex electrical work load. Laser heating and transient thermoreflectance full field imaging is used to characterize heat flow in 3D ICs. While inverse problems in heat diffusion are ill-posed, transient temperature profile provide valuable information about in-plane and out-of-the-plane material and interface properties. Applications to material characterization during manufacturing will be also discussed.

2:00 PM EN03.10.02

Structured Illumination with Thermal Imaging (SI-TI)—A Dynamically Reconfigurable Optical Method for Parallelized Thermal Property Measurements Qiyue Zheng^{1,2}, Divya Chalise^{1,2}, Mingxin Jia^{1,2}, Yuqiang Zeng¹, Minxiang Zeng³, Mortaza Saeidi-Javash³, Sumanjeet Kaur¹, Tengfei Luo³, Yanliang Zhang³, Ravi Prasher^{1,2} and Chris Dames^{2,1}; ¹Lawrence Berkeley National Laboratory, United States; ²University of California, Berkeley, United States; ³University of Notre Dame, United States

The recent push for the “materials by design” paradigm requires synergistic integration of synthesis, characterization, theory, computation and data-driven approaches. Among these, techniques for efficient measurement of thermal transport are still challenging, especially for diverse materials with a range of roughness, porosity, and anisotropy. Traditional contact methods like steady-state, 3ω , and transient plane source methods suffer from relatively slow throughput, sometimes the requirement of large sample volumes, and the lack of spatially resolvable property mapping capability for parallel measurements. Non-contact pump probe laser methods (e.g., TDTR, FDTR) often need mirror smooth sample surfaces and serial rastering for property mapping which can be inefficient when applied to larger sample areas. Here, we present a new thermal characterization tool which has the potential to significantly improve the measurement throughput based on Structured Illumination with Thermal Imaging (SI-TI). SI gives convenient software control of the shape and frequency of heating light pattern, and thermoreflectance based TI enables efficient large area temperature mapping with good temperature and spatial resolutions. Experimental results will be presented showing how the SI-TI method enables: (1) paralleled measurement of multiple samples in a single field of view without any raster scanning; (2) software control of the dynamically adjustable heating pattern, which can be tuned to optimize the measurement sensitivity in different directions for anisotropic materials; and (3) can tolerate porous, rough, and/or scratched sample surfaces. This work highlights a new avenue in efficient thermal characterization for “materials by design.”

2:15 PM EN03.10.03

Thermal Conductivity Measurement of Flowing Granular Media using Modulated Photothermal Radiometry Jian Zeng, Ka Man Chung, Xintong Zhang, Sarath Reddy Adapa and Renkun Chen; University of California, San Diego, United States

Granular media such as Carbo ceramic particles and silica sands have been used as heat transfer media in heat exchangers for solar-thermal energy storage systems. However, thermal transport processes in the particulate heat exchangers are still not fully understood. In particular, it is still not clear whether and how the thermal conductivity of the particles in the near-wall region could be impacted by the particle -wall interaction. While numerous models exist, there is a lack of suitable experimental technique to probe the thermal transport processes of granular media when they are flowing in a heat exchanger. In this work, we report the instrumentation development of high-temperature thermal conductivity measurement of flowing ceramic particles within a confined channel. We use an existing technique called modulated photothermal radiometry (MPR) and first develop it for high temperature measurements (up to 800 deg. C). MPR is a non-contact technique where the surface of the sample is heated by an intensity-modulated laser and it utilizes the intrinsic thermal emission from the specimens for thermometry, which is favorable for the measurement at high temperature in harsh environment. The high-temperature MPR setup is validated by measuring bulk and thin coating materials with known thermal conductivity. We then develop the technique for measuring both stationary and flowing ceramic particles. The measurement results are compared with modeling based on the discrete element method (DEM) to understand thermal transport in both bulk and near-wall regions of flowing granular media.

2:30 PM *EN03.10.04

Magnetization Dynamics of Functional Materials Enabled by Ultrafast Optical Metrology Xiaojia Wang; Univ of Minnesota, Twin Cities, United States

As an updated version of the ultrafast pump-probe laser technique, the time-resolved magneto-optical Kerr effect (TR-MOKE) metrology can capture the magnetization dynamics of materials with superb temporal (sub-picosecond) and spatial (diffraction-limited beam spot) resolutions. With optical excitation and detection, TR-MOKE can probe spin precession at high resonance frequencies (up to a few hundreds of GHz), beyond those achievable by conventional Ferromagnetic Resonance (FMR) approaches. Thus, it is a powerful tool to reveal the rich physics of magnetization dynamics of magnetic thin films, in addition to thermal transport properties. In this talk, I will highlight several representative applications of the TR-MOKE metrology for capturing the magnetization dynamics in technologically important spintronic materials. Examples include the studies of temperature-dependent Gilbert damping, the spin-strain coupling, and the interlayer exchange coupling of materials with strong perpendicular magnetic anisotropy (PMA). The structure-property relationships of these emerging materials established by TR-MOKE open up opportunities of tailoring material properties by structural engineering for applications in spintronic and memory devices with low energy consumption, high thermal stability, and fast switching.

3:00 PM EN03.10.05

Single-Scan Quantitative Mapping of Steady Temperature Fields with Nanometer Resolution Amin Reihani, Shen Yan, Yuxuan Luan, Edgar Meyhofer and Pramod Sangi Reddy; University of Michigan, United States

Quantitative mapping of temperature fields at the nanoscale is critical in various areas of scientific research and technology, such as nanoelectronics, surface chemistry, plasmonic and quantum systems. Scanning Thermal Microscopy (SThM) techniques, developed in the past, enable temperature mapping with ~10 nm spatial resolution. The main challenge in achieving quantitative thermal imaging with SThM is a lack of knowledge of the tip-sample thermal resistance (R_{TS}) which is critical for quantifying the sample temperature. A recent advance in SThM enabled the quantification of R_{TS} in situations where the temperature field is modulated. However, such an approach is not directly applicable to situations where the device operates under conditions where it is not readily possible to modulate the temperature field. Here, we present a novel SThM measurement technique using custom-fabricated scanning thermal probes (STPs) with a sharp tip and an integrated heater/thermometer where the steady-state temperature field of the device can be quantitatively mapped in a single scan with <5 nm spatial resolution and ~50 mK temperature resolution. This is accomplished by introducing a modulated heat input to the STP and measuring the AC and DC response of the probe temperature which allows for simultaneous mapping of tip-sample thermal resistance and sample surface temperature. The advances presented here can greatly facilitate temperature mapping of a variety of microdevices under practical operating conditions.

3:15 PM EN03.10.06

Thermal Conductivity Measurement of Stationary and Flowing Molten Salt Using Modulated Photothermal Radiometry Ka Man Chung, Jian Zeng, Tianshi Feng and Renkun Chen; University of California, San Diego, United States

Molten salts are being used or studied for thermal energy conversion systems, such as concentrating solar power and nuclear power. Thermal conductivity is an important thermophysical property dictating the performance of these systems but its accurate measurement of molten salts has been challenging. The corrosive and conductive nature of these fluids makes it difficult to use traditional contact methods such as the hot wire method. Techniques that require a large volume of the fluids, such as the steady-state method, could also be prone to errors caused by natural convection. Commonly used non-contact optical thermoreflectance techniques are difficult to operate at high temperatures. Here, we report the thermal conductivity measurement of molten salts using a modulated photothermal radiometry (MPR) technique. MPR is a laser-based, non-contact, frequency domain method that has been used to measure thermophysical properties of various materials. We develop the technique for the measurement of molten salts at both stationary and flow states. Stationary molten salts, including nitrate and chloride salts, have been measured using a high-temperature MPR holder. The measurement results are compared with those obtained from a laser flash analyzer (LFA). Our results demonstrate the reliability of the MPR method to measure the thermal conductivity of stationary molten salts. We further extend the technique to perform in-operando measurements on flowing fluids and show that the intrinsic thermal conductivity can be reliably obtained under certain experimental conditions. Finally, the in-operando technique is applied to a laboratory-scale molten salt loop to demonstrate the capability of measuring flowing molten salts in real-time. Our work shows that the MPR technique is a convenient tool to provide reliable molten salt thermal conductivity data and could serve as a diagnostic tool for flowing molten salts.

3:30 PM BREAK

SESSION EN03.11: Thermal Energy Harvesting, Transport and Storage

Session Chair: Daron Spence

Thursday Afternoon, December 2, 2021

Hynes, Level 3, Room 306

4:00 PM *EN03.11.01

A Green Materials Processing Route to Graphitic Heat Spreaders on Organic Substrates Mostafa Abuseada, Yang Li and Timothy Fisher; University of California, Los Angeles, United States

This work describes a new material deposition process to synthesize graphitic layers using a custom system that employs a concentrated xenon light source (3.5 kW optical) that simulates solar irradiance. A peak heated zone of approx. 3 cm diameter ($q_{max} = 3.2 \text{ MW/m}^2$) can heat samples up to 1000°C in less than 1 sec, orders of magnitude faster than electric heaters integrated within conventional CVD systems. We have found clear signs of surface graphitization on organic samples exposed in vacuum. Recent tests on pulsed heating at ~1 Hz indicates further graphitization via a controlled heating/cooling process that avoids pyrolysis. Significant advantages of this unique approach include: (1) ultrafast heating and cooling of substrates, allowing more flexibility to tune physical and electrical properties of the graphitic layer; (2) improved graphitic growth speed because of the ultrafast response to concentrated light heating; (3) ability to build a substantial depth of graphitic layering due to the optical transparency that emerges in the upper layers that transform under pulsed heating; and (4) low cost and easy serviceability of concentrated light as compared to laser-induced graphene (LIG) systems that in theory could produce similar results. Process optimization for this problem will be important, and as such, we apply adaptive Bayesian experimental design as in prior work to maximize a heat spreading metric (a combination of thermal conductivity and layer thickness). Parameters to be optimized include: gas composition and pressure; light pulse intensity, duration, and pulse duty cycle; and substrate type. The output metric, thermal spreading capability, is captured to first order by the product of film thickness and thermal conductivity. Here, we employ an extensive set of capabilities for heat conduction testing and modeling, including a highly accurate, rapid screening approach for heat spreading.

4:30 PM EN03.11.02

Late News: Atomistic Simulations of Heat Transfer in Polymer Linked Gold Nanoparticle Networks for Autonomous Computing Xingfei Wei and Rigoberto Hernandez; Johns Hopkins University, United States

Polymer linked nanoparticle networks are important to many applications, such as advanced composite materials and nano-phononics. Developing networked materials capable of emulating neuronal networks for information processing is critical to the construction of a brain-like cognitive computing system. In this work, we elaborate heat transfer mechanisms between polymer linked gold nanoparticle (AuNP) dimers. We find the effects of different polymer types on heat flux, using 6 different polymers, *viz.* polyethylene (PE), polyacetylene (PA), poly(*p*-phenylene) (PPP), polyacene (ACE), polythiophene (PT) and poly(3,4-ethylenedioxythiophene) (PEDOT). We also uncover the effects of AuNP size on heat flux, using three different AuNP sizes: 2, 4 and 8 nm diameter. By steering the AuNPs to different distances, the heat flux is compared between a straight polymer conformation and a loose (or bended) polymer conformation. The effect of heat transfer channels on the total heat flux between AuNP dimers is revealed using 1, 2 and 3 polymer links. The discussion of AuNP facet effect is also included using different linked facets: (111)-(111), (111)-(001) and (001)-(001). Dimers made of different AuNP sizes --- *viz.* 2 nm AuNP linked 8 nm AuNP --- can have different heat fluxes towards two directions like a thermal diode. Finally, we use four simple networks constructed from 3, 4, 5 and 6 AuNPs, to mimic neuronal networks for information processing. In our models, the information is recorded by the thermal potential (temperature)—that is, the driving heat flux—in analogy to the neuronal networks where the electric potential drives the ion flux. We expect that this work can help improve our understanding of heat transfer mechanisms inside polymer linked nanoparticle networks. Our

simulations can also provide guidance for developing new materials and devices of use in brain-like computing.

4:45 PM EN03.11.03

The Potential Impact of Thermochromic Smart Windows on the Dutch Built Environment—A Simulation Study [Daniel Mann](#)^{1,2}, Cindy Yeung^{1,2}, Roberto Habets^{1,2}, Zeger Vroon^{1,2,3} and Pascal Buskens^{1,2,4}; ¹TNO, Netherlands; ²Brightlands Materials Center, Netherlands; ³Zuyd University of Applied Sciences, Netherlands; ⁴Hasselt University, Belgium

With progressing climate change and global warming, we face the challenge to reduce our energy consumption and CO₂ emission. In Europe, more than one third of the total energy consumption and CO₂ emission result from the built environment, with energy for heating and cooling of buildings as a major share. A recent study analyzing the energy and CO₂ emission savings potential, has shown that by equipping all buildings in Europe with commercially available energy-efficient glazing the total energy consumption of the building sector can be reduced by over 30% for most countries. Current energy efficient glazing systems are static and therefore best suited for either hot or cold climates. In climates that vary between hot summers and cold winters, the windows have to adapt to the environment for optimized energy efficiency. Thermochromics can be used for adaptive glazing since they can autonomously switch their solar infrared (IR) transmission depending on the glazing temperature. In a recent study we have shown that thermochromic windows are perfect for intermediate climate regions. Using building energy simulations, we demonstrated that energy savings of up to 22% could be achieved with our thermochromic smart window, outperforming commercially available energy-efficient glazing systems.

For a more detailed analysis of the performance of thermochromic smart windows in the Netherlands, we here present a study on the 4 main building types: free-standing buildings, duplex houses, terraced houses and apartments. In our labs we have developed a thermochromic coating with excellent optical properties for application in smart windows. The coating shows high visible transmission (T_{vis}) of 74% combined with a large solar modulation (ΔT_{sol}) of 10%, which as a combination is unrivaled by thermochromic VO₂ based coatings reported in literature to date.

For the building energy simulation study we modeled the annual energy consumption for heating, cooling and lighting of the 4 selected building units equipped with our smart window, where our thermochromic coated glass is combined with a commercial low-e coated glass to yield a double glass window, and compared the results to building units with uncoated double glazing.

The free-standing building with the largest floor area and all 4 outside walls in contact with the environment showed the largest benefit of the smart window on annual energy consumption. Here annual energy savings of 21.2% could be reached. With reduced floor area and either three or two outside walls being in contact with the environment, for duplex and terraced houses, respectively, the impact of the smart window on total energy consumption was lower. Here annual energy savings of 16.1% and 15.4% were achieved for the duplex and terraced house, respectively. The apartment was a more special case, since it is a one floor unit with large window surfaces on the two outside walls in contact with the environment. Here the large window surface area in relation to the total floor area leads to a big impact of the thermochromic smart window on annual energy consumption. Here annual energy savings of 29.4% could be reached in comparison to non-coated insulating glass units (IGUs).

Suggesting that natural gas was used for heating and electricity for cooling and lighting, the average cost price for gas and electricity in the Netherlands was used to calculate annual cost savings for each building type. Here annual cost savings of up to 445 € could be calculated. Due to the cheap material and processing costs a return on invest within 7 years will be possible with attributed annual cost savings of 6-7.5 €/m².

Furthermore, we have analyzed the impact on CO₂ emissions the smart window can have in the Netherlands. By extrapolating the data to the complete Dutch built environment, we could show that annual CO₂ emissions for building operations can be reduced by 46%. This means annual CO₂ emission savings of 5.8 Mt for the Dutch built environment.

5:00 PM EN03.11.05

Understanding the Thermodynamics of Metal–Organic Phase-Change Materials for Thermal Energy Storage [Ryan McGillicuddy](#), Surendra Thapa, Malia Wenny, Miguel I. Gonzalez and Jarad A. Mason; Harvard University, United States

With most of the primary energy generated in the USA being thermal in nature, developing materials that can reversibly store thermal energy is critical to more efficiently using and managing thermal energy. Metal–organic phase-change materials, which consist of meltable metal coordination complexes with organic ligands, offer an opportunity to expand the library of existing phase-change materials for thermal energy storage and further establish fundamental structure-property relationships to design energy-dense thermal energy storage materials. Herein, we study an isostructural series of divalent metal amide complexes featuring expanded hydrogen bond networks that can undergo tunable, high-enthalpy melting transitions over a wide temperature range. We investigate the influence of coordination bonds, hydrogen bonds, neutral ligands, and outer sphere anions on the phase change thermodynamics, studying how metal dependent hydrogen and coordination bond breaking across the melting transitions alters the melting thermodynamics of metal–organic phase-change materials. Importantly, despite having lower volumetric hydrogen bond densities than the structurally similar metal-salt hydrate systems, the metal–organic phase-change materials investigated here show similar volumetric energy densities to metal-salt hydrates, indicating that metal–organic phase-change materials offer alternative pathways to designing new thermal energy storage materials.

5:15 PM EN03.11.06

Carbide Precipitation Study During Tempering in Model Ferritic Alloys for Nuclear Power Plant Application [Anna Benarosch](#)^{1,2}, [Caroline Toffolon-Masclat](#)¹, [Bernard Marini](#)¹, [Estelle Meslin](#)¹, [Raphaëlle Guillou](#)¹, [Jean-Marc Joubert](#)², [Dominique Thiaudière](#)³, [Cristian Mocuta](#)³, [Zofia Trzaska](#)² and [Ivan Guillot](#)²; ¹Université Paris-Saclay, France; ²Univ. Paris Est, France; ³Synchrotron SOLEIL, France

Large components of the primary circuit of nuclear reactors, made with 16MND5 low alloy bainitic steels, operate at 300°C under a pressure of 155 bars, undergoing thermal aging and irradiation, and must retain their mechanical properties throughout the plant life. A thorough understanding of the links between microstructure and mechanical properties is therefore crucial to be able to predict their evolution under operating conditions. Carbides are known to play an important role in explaining the mechanical properties of the steels. [1–3] Their population, size and distribution, evolve mainly during temper heat treatments performed after a step of austenitisation and quenching. However, after quenching, chemical heterogeneities can appear, locally affecting the microstructure, the carbide population, hence the mechanical properties. Therefore, it is necessary to understand the impact of alloying elements on carbide populations to be able to predict the mechanical properties of these heterogeneous areas. Furthermore, understanding the impact of alloying elements on the carbide precipitation sequence can lead to an optimisation of the heat treatments, and the design of steels with enhanced mechanical properties, as well.

Amongst the three main alloying elements (Mn, Ni, Mo) of 16MND5 steels, molybdenum, and manganese to a lesser extent, contribute to define the carbide population. In this context, to isolate the contribution of each alloying element, high-purity model alloys, FeCMo, FeCMn and FeCMoMn were investigated, which compositions were chosen close to the industrial alloy.

Two tempering temperatures were explored, 650 and 700°C, for times of several seconds up to two months. The starting microstructures of the model alloys were selected to be as close as possible to the 16MND5 steel bainite, using continuous cooling transformation diagrams and the associated examinations.

The carbide crystallography and chemistry were determined by TEM and STEM/EDS on carbon extractive replicas, while their size distributions and morphologies were obtained by SEM image analysis. Their volume fraction and lattice volume were measured by *ex-situ* synchrotron X-ray diffraction. It resulted in the complete characterization of the precipitation sequences and in the quantification of the impact of Mo and Mn on these precipitation

sequences. The use of thermodynamic calculations gave valuable information on the carbides thermodynamical stability. At last, these precipitation sequences were modelled using the Prisma module from the Thermocalc suite and compared to the experimental results obtained within this study.

- [1] Y. R. Im, Y. J. Oh, B. J. Lee, J. H. Hong, and H. C. Lee, Effects of carbide precipitation on the strength and Charpy impact properties of low carbon Mn-Ni-Mo bainitic steels, *J. Nucl. Mater.*, **297** (2001) 138–148, doi: 10.1016/S0022-3115(01)00610-9.
- [2] P. Bowen, S. Druce, and J. Knott, Effects of microstructure on cleavage fracture in pressure vessel steel, *Acta Metall.*, **34** (1986) 1121–1131, .
- [3] K. J. Irvine and F. B. Pickering, The tempering characteristics of low-carbon low-alloy steels, *J. Iron Steel Inst.*, **194** (1960) 137–153, .

SESSION EN03.12: Thermal Transport Across Interfaces
Session Chairs: Qinshu Li and Bo Sun
Monday Morning, December 6, 2021
EN03-Virtual

8:00 AM *EN03.12.01

Universal Model for Predicting the Thermal Boundary Conductance of a Multilayered-Metal/Dielectric Interface [Alan McGaughey](#), Henry Aller and Jonathan A. Malen; Carnegie Mellon University, United States

A model is developed to predict how the effective thermal boundary conductance (TBC) of a metal cap/metal contact/dielectric junction varies with the contact thickness. Two-temperature model molecular dynamics (MD) simulations are applied to qualitatively recreate the experimental observation that the junction TBC increases and then saturates as the contact thickness increases. The MD simulations reveal a strong correlation between the junction TBC and the fraction of the electron-phonon coupling that occurs in the contact versus that in the cap. This correlation is then combined with insights gained from an analytical solution to the two-temperature model in the cap and contact to propose a model that predicts how TBC varies with contact thickness. The model, which contains no fitting parameters, is validated against more than one hundred experimental measurements from the literature on a variety of cap/contact/dielectric junctions. By normalizing the TBC and the contact thickness, all the experimental data collapse onto a single curve, with 92% of it lying within 10% of the model. Through physically-motivated approximations, the model reduces to a simple thermal circuit that maintains high predictive ability. Population-weighted phonon density of states extracted from the MD simulations suggest that the TBC contact thickness dependence is strongly influenced by electron-phonon coupling in the contact. The model provides guidance for streamlining the design of thermally-efficient electrical contacts.

8:30 AM EN03.12.02

Non-Equilibrium Phonon Thermal Resistance at MoS₂/Oxide and Graphene/Oxide Interfaces Weidong Zheng¹, Connor McClellan², Eric Pop^{2,2} and [Yee Kan Koh](#)¹; ¹National University of Singapore, Singapore; ²Stanford University, United States

Accurate measurements of interfacial thermal conductance (G) of two-dimensional (2D) materials are imperative for effective thermal management of 2D material devices. Despite the importance, there is a large discrepancy in the literature on G of interfaces of 2D materials. Here, we accurately measure G of oxide/MoS₂/oxide and oxide/graphene/oxide interfaces for three oxides (SiO₂, HfO₂, Al₂O₃) by differential time-domain thermoreflectance (TDTR). We find that TDTR measurements of G of these interfaces are 2-to-4 times larger than previously reported G of the similar interfaces measured by Raman thermometry. Using a simple model, we show that the observed discrepancy can be explained by an additional internal thermal resistance between non-equilibrium phonon modes in Raman thermometry measurements. Moreover, the additional internal resistance in Raman thermometry measurements also leads to a stronger temperature dependence of G of 2D materials. Our work provides important guidelines for correct interpretation and analysis of Raman measurements of heat transport across interfaces of 2D materials.

8:45 AM EN03.12.03

Thermal Interfacial Resistance of Water with Solids—A Nanoscale Investigation Using Molecular Dynamics Simulations [William Gonçalves](#) and Konstantinos Termentzidis; Université de Lyon, France

The fabrication of nano-architected materials has improved considerably over the last decade. It is now possible to synthesize series of nanoporous materials with functionalized internal surfaces. However, the impact of humidity on heat transfer at the nanoscale is not fully understood. The structural and vibrational properties of nanoconfined water differ from those of the bulk near the solid/liquid interface [1]. Thus, for materials with nanoscale features, macroscopic models such as Fourier's law or the Effective Media Approach (EMA) can not predict the effective thermal properties of solid/liquid composites [1]. In addition, experimental measurements are difficult due to humidity. During Scanning Thermal Microscopy (STM) experiments, the presence of a water meniscus at the mechanical contact between the tip and the sample creates capillary forces that impact the thermal conductance [2,3].

In this study, we simulate solid/liquid interfaces using molecular dynamics (MD) simulations. The interfacial thermal resistance (Kapitza resistance) is calculated between a film of water and various solids such as crystalline and amorphous silicon or amorphous silica with functionalized surfaces. The impact of the average temperature, the heat flux and the thickness of the water slab on the Kapitza resistance is investigated. Finally, we modified the hydrophobicity level of the silica by grafting hydrophobic molecules on the hydroxylated surface. The results of this study provide interesting insights about the nanoscale heat transfer through solid/liquid interfaces.

- [1] Isaiev, Mykola, et al. "Thermal transport enhancement of hybrid nanocomposites; impact of confined water inside nanoporous silicon." *Applied Physics Letters* 117.3 (2020): 033701.
- [2] Assy, Ali, et al. "Analysis of heat transfer in the water meniscus at the tip-sample contact in scanning thermal microscopy." *Journal of Physics D: Applied Physics* 47.44 (2014): 442001.
- [3] Assy, Ali, and Séverine Gomès. "Temperature-dependent capillary forces at nano-contacts for estimating the heat conduction through a water meniscus." *Nanotechnology* 26.35 (2015): 355401.

9:00 AM EN03.12.04

Inelastic Phonon Transport Enhanced Thermal Conductance Across Atomically Sharp Interfaces [Qinshu Li](#)¹, Fang Liu^{2,3}, Song Hu⁴, Xiaokun Gu⁴, Xinqiang Wang^{2,3} and Bo Sun^{1,5}; ¹Tsinghua University, China; ²State Key Laboratory of Artificial Microstructure and Mesoscopic Physics, School of Physics, Peking University, China; ³Collaborative Innovation Center of Quantum Matter, China; ⁴Institute of Engineering Thermophysics, School of

Mechanical Engineering, Shanghai Jiao Tong University, China; ⁵Tsinghua Shenzhen International Graduate School, and Guangdong Provincial Key Laboratory of Thermal Management Engineering & Materials, China

Understanding thermal transport across interfaces is crucial for the thermal management of electronic devices. Phonons, the dominant heat carriers across solid-solid interfaces, have been shown to transport elastically in most experiments, except for a few extreme cases where inelastic phonon transport occurs when the two materials of the interface are highly dissimilar. However, there is still limited information on when the inelastic transport will occur. Here, we measured the interface thermal conductance of atomically sharp Al/Si and Al/GaN interfaces, and found that the thermal conductance linearly increases with temperature at high temperatures, suggesting inelastic phonon transport dominates heat conduction across interfaces, though the two materials have similar Debye temperatures. Moreover, we found that when the interface roughness increased to 5-7 atomic layers, inelastic thermal transport diminishes. Our molecular dynamics calculation indicates that phonon non-equilibrium drives the inelastic phonon transport when the interface is atomically sharp. When the interface becomes rough, phonon non-equilibrium reduces, leading to a saturated thermal conductance at high temperatures. Our results provide new insights on phonon transport across interfaces and open up opportunities for reengineering their thermal conductance.

9:15 AM EN03.12.05

Determination of Interfacial Thermal Resistance Inside Thermal Interface Materials Enabling High-Throughput Computational Screening of the Material Formula Jibao Lu¹, Xiaoxin Lu¹, Rong Sun¹ and Ching-Ping Wong²; ¹Shenzhen Institute of Advanced Electronic Materials, Shenzhen Institutes of Advanced Technology Chinese Academy of Sciences, China; ²Georgia Institute of Technology, United States

Thermal interface materials (TIMs), usually composed of polymer matrix filled with thermally conductive particulate fillers, are pivotal for heat transfer between the layers in high-density electronic packaging. Numerical simulation provides a versatile tool for understanding the mechanism of thermal transport and design of TIMs; however, the insufficient efficiency and accuracy in modeling the composites with complex microscopic structures hinders its application in engineering the formula of material. Here we present a strategy of modeling the effective thermal conductivity of polymer-based composites with high efficiency and accuracy, which enables a high-throughput screening of the formula of TIMs. The efficiency of the strategy comes from an implementation of a numerical homogenization algorithm based on fast Fourier transform, in which the unit cell problem is solved by means of a polarization-based iterative scheme. The algorithm shows good precision and requires dramatically reduced computational cost compared with finite element modeling. The accuracy of the strategy originates from an accurate determination of the interfacial thermal resistance (ITR) between different components inside the TIM composites, which is achieved by combining high-throughput calculations, machine learning and experiments. As an example of application of the strategy, the ITRs for the interfaces of filler-silicone and filler-filler in the Al₂O₃/silicone composites are determined as 2.2e-08 m²K/W and 1.0e-07m²K/W, respectively. We further conduct a high-throughput computational screening of the gradation scheme for the silicone based composite TIMs filled with Al₂O₃ and AlN fillers with different size distributions, weights, and surface characteristics, and validate the results by comparing the results with experiments. The proposed strategy could be an effective tool for the smart engineering of the formula of TIMs for electronic packaging, as well as other thermally conductive composite materials.

9:30 AM EN03.12.06

Late News: Understanding Thermal Transport in Polymer-based Composites Yijie m. Zhou and Yanfei Xu; University of Massachusetts Amherst, United States

Polymer-based thermal interface materials play key roles in thermal management applications thanks to their unique combination of properties not available from any other known materials.¹⁻³ They are lightweight, corrosion-resistant, easy to process, and among others. However, common polymers are thermal insulators with low thermal conductivity on the order of 0.1 Wm⁻¹ K⁻¹.^{4,5} To achieve high thermal conductivity in polymers, highly thermally conductive fillers such as graphene and nano-diamond powder have been added into polymers.⁶⁻⁹ Although polymers are blended with highly thermally conductive fillers (e.g. silver nanoparticle ~400 Wm⁻¹ K⁻¹) at a high loading volume fraction of 70 vol%, thermal conductivity in polymer-based composites is limited to ~5 Wm⁻¹ K⁻¹.¹⁰ This is because low thermal conductivities in common polymer matrices, high thermal interface resistance between filler and polymer, and high thermal interface resistance between filler and filler.^{3,11} In this poster, we will present our current research on developing polymer-based thermal interface materials. To increase effective thermal conductivity in polymer-based composites, we strive to increase thermal conductivity in pure polymer matrices (e.g. polyethylene, polyvinyl alcohol, and epoxy) and reduce thermal interface resistances between fillers and polymers by enhancing vibrational couplings. We believe that polymer-based thermal interface materials will play a key role in many existing and unforeseen thermal management applications.

1. Qian, X.; Zhou, J.; Chen, G., Phonon-engineered extreme thermal conductivity materials. *Nat. Mater.* **2021**, 1-15.
2. Feng, C. P.; Chen, L. B.; Tian, G. L.; Wan, S. S.; Bai, L.; Bao, R. Y.; Liu, Z. Y.; Yang, M. B.; Yang, W., Multifunctional Thermal Management Materials with Excellent Heat Dissipation and Generation Capability for Future Electronics. *ACS Appl. Mater. Inter.* **2019**, *11* (20), 18739-18745.
3. Xu, Y.; Wang, X.; Hao, Q., A mini review on thermally conductive polymers and polymer-based composites. *Compos. Commun.* **2021**, *24*.
4. Choy, C., Thermal conductivity of polymers. *Polymer.* **1977**, *18* (10), 984-1004.
5. Sperling, L. H., *Introduction to physical polymer science*. John Wiley & Sons: 2005.
6. Huang, Y.; Ellingford, C.; Bowen, C.; McNally, T.; Wu, D.; Wan, C., Tailoring the electrical and thermal conductivity of multi-component and multi-phase polymer composites. *Int. Mater. Rev.* **2019**, *65* (3), 129-163.
7. Burger, N.; Laachachi, A.; Ferriol, M.; Lutz, M.; Toniazzo, V.; Ruch, D., Review of thermal conductivity in composites: Mechanisms, parameters and theory. *Prog. Polym. Sci.* **2016**, *61*, 1-28.
8. Ma, H.; Gao, B.; Wang, M.; Yuan, Z.; Shen, J.; Zhao, J.; Feng, Y., Strategies for enhancing thermal conductivity of polymer-based thermal interface materials: a review. *J. Mater. Sci.* **2020**, *56* (2), 1064-1086.
9. Han, Y.; Shi, X.; Yang, X.; Guo, Y.; Zhang, J.; Kong, J.; Gu, J., Enhanced thermal conductivities of epoxy nanocomposites via incorporating in-situ fabricated hetero-structured SiC-BNNS fillers. *Compos. Sci. Technol.* **2020**, *187*.
10. Chen, H.; Ginzburg, V. V.; Yang, J.; Liu, W.; Huang, Y.; Du, L.; Chen, B., Thermal conductivity of polymer-based composites: Fundamentals and applications. *Prog. Polym. Sci.* **2016**, *59*, 41-85.
11. Ruan, K.; Shi, X.; Guo, Y.; Gu, J., Interfacial thermal resistance in thermally conductive polymer composites: A review. *Compos. Commun.* **2020**, *22*.

9:35 AM EN03.12.07

Unraveling Ultrafast Electrical-Thermal-Structural Coupling in Electronic Devices Aditya Sood^{1,2}; ¹Stanford University, United States; ²SLAC National Accelerator Laboratory, United States

Identifying the ultimate operating limits of electronic devices requires an understanding of how atomic motions couple to changes in electronic transport -- a coupling that is often mediated by energy dissipation (i.e. Joule heating) and thermal transport. One class of electronics where this coupling has been especially challenging to understand is phase-change Mott-memory. Mott insulators (e.g. VO₂) have long been known to undergo an insulator-to-metal transition under an applied voltage. However, several aspects of this electric-field-driven transition has remained unclear, in particular, the role of Joule

heating in triggering the transition on fast timescales, and the thermal relaxations on slow timescales. We address these questions by developing a new platform for ultrafast, correlative electrical-thermal-structural characterization of phase-change electronics [1]. Following electrical excitation of VO₂, we directly probe the role of Joule heating on short timescales, distinguishing it from direct field-induced effects. We discover a new phase of this material under electrical excitation, which points towards a non-equilibrium modification of the free-energy landscape. On long timescales, we uncover a regime of thermally-bottlenecked structural relaxation, which determines the fastest turn-off speed of the device. Taken together, our approach identifies the ultimate speed and energy-efficiency limits of phase-change electronics.

[1] A. Sood et al., *Science* (2021) "Universal phase dynamics in VO₂ switches revealed by ultrafast operando diffraction", <https://arxiv.org/abs/2102.06013>

SESSION EN03.13: Thermal Materials III
Session Chairs: Xi Chen and Songrui Hou
Monday Morning, December 6, 2021
EN03-Virtual

10:30 AM EN03.13.01

Insights in the Aqueous Precursor Chemistry during the Synthesis of Thermochromic Vanadium Dioxide Ken Elen^{1,2}, Lavinia Calvi^{2,1}, Pascal Buskens^{2,3,4}, An Hardy^{2,1} and Marlies Van Bael^{2,1}; ¹Imec - Imomec, Belgium; ²UHasselt, Belgium; ³TNO, Netherlands; ⁴Brightlands Materials Center, Netherlands

Vanadium dioxide (VO₂) is a multipurpose material with notable applications in fields such as energy storage and energy-efficient smart windows. The versatility of VO₂ is related to its extensive crystallography with many polymorphic forms. VO₂ can undergo a reversible metal-insulator phase transition (MIT) at a critical temperature of 68 °C, which is accompanied by a structure transformation from a low-temperature insulator phase VO₂ (M) to a high-temperature metal phase VO₂ (R). This phase transition results in a distinct change of the infrared transmittance, rendering VO₂ suitable as a pigment for thermochromic glazing.

Various methods for the synthesis of VO₂ have been reported, including chemical vapor deposition, atomic layer deposition, pulsed laser deposition and sputtering. Wet chemical synthesis routes are widely considered as valuable alternatives for vacuum based techniques on account of their low cost, limited environmental impact and reasonably simple experimental setup. Also, the versatility of the method allows the direct synthesis of both ceramic (nano)powders as well as thin (nanostructured) films. However, many earlier wet chemical routes intermediately form V₂O₅ and require an additional, reductive anneal to obtain VO₂. This emphasizes the large challenge in the immediate formation of thermochromic VO₂ from an aqueous solution. Given the complex redox chemistry of vanadium, it is therefore essential to gain fundamental insights in the aqueous vanadium precursor chemistry and in their relation to the vanadium oxide stoichiometry and phase formation, obtained via a solution-based strategy.

Our approach starts with the formulation of stable aqueous precursor solutions containing oxovanadium(IV) complexes. To analyze and understand each step, and the associated chemical transformations, during this synthesis, various complementary spectroscopic techniques (UV-Vis, ⁵¹V-NMR, FTIR) are used to probe and identify each vanadium species during the entire synthesis sequence. The structure and stability of the final complexes that are present in the aqueous solution, and their relation to the synthesis parameters will be highlighted. Subsequently, the formation of vanadium oxide, starting from aqueous vanadium precursor solution, requires a thermally-induced transformation of the precursor gel into the oxide. As an illustration, the thermal decomposition pathway of a citrato/oxalato-oxovanadium(IV) gel, obtained by evaporation of a precursor solution, is analyzed by Simultaneous Differential Calorimetry Thermogravimetry (SDT), High temperature X-ray Diffraction (HT-XRD) and ex-situ analysis of the remaining products. The thermochromic nature of the resulting VO₂ products is demonstrated by monitoring the underlying structural phase transition with Differential Scanning Calorimetry (DSC) and UV-Vis spectroscopy.

The authors thank the European Fund for Regional Development (crossborder collaborative Interreg V program Flanders-the Netherlands, project SUNOVATE) for their financial support.

10:45 AM EN03.13.02

Solid-State Phononic Thermal Regulator and Rectifier Based on Polyethylene Nanofibers Sheng Shen; Carnegie Mellon University, United States

We have fabricated polyethylene nanofibers with high chain alignment and high degree of crystallinity. The nanofibers show an orthorhombic crystal structure with high thermal conductivity at room temperature. However, rotational disorder occurs at a high temperature close to melting temperature. The nanofibers switch to the hexagonal phase with a high-contrast and abrupt thermal conductivity change. Such a solid-state phase transition makes the polyethylene nanofiber intrinsically a thermal regulator. Measurements show a thermal switching ratio in average ~8x with maximum ~10x, which is the highest among solid-solid and solid-liquid phase transitions of all existing materials. Based on the sharp and high-contrast phase transition, an unusual dual-mode solid-state thermal rectification effect is demonstrated using a heterogeneous "irradiated-pristine" polyethylene nanofiber junction as a nanoscale thermal diode, in which heat flow can be rectified in both directions by changing the working temperature. For the nanofiber samples measured here, we observe a maximum thermal rectification factor as large as ~50 %, which only requires a small temperature bias of <10 K. The nanoscale thermal regulators and rectifiers open up new possibilities for developing advanced thermal management, energy conversion and, potentially thermophonic technologies.

11:00 AM EN03.13.03

Achieving Long-Term Condensation with Cell-Inspired Interfaces Jingcheng Ma, Zhuoyuan Zheng, Paul V. Braun, Pingfeng Wang and Nenad Miljkovic; University of Illinois at Urbana-Champaign, United States

Dropwise condensation on thin (< 100 nm) hydrophobic coatings enables exceptional condensation heat transfer. However, hydrophobic coatings can be easily delaminated by the formation of water blisters in wet environments or during steam condensation. To prevent delamination while maintaining nanoscale thickness, designing interfaces with high wet adhesion is a key challenge. In nature, cell membranes face the identical challenge where nanometer-thick lipid bilayers require exceptional adhesion in wet environments to maintain their integrity. Nature achieves high inter-layer adhesion by using a lipid interface having two non-polar surfaces, which does not rely on chemical bonding. Instead, physicochemical resistance is used to prevent biofluids from opening and delaminating the interface. Based on this nature-inspired strategy, we develop fluorine-carbon molecular chains on nanostructured surfaces to build lipid-like interfaces for nanometric fluorinated coatings. Our superhydrophobic materials show unprecedented jumping

droplet condensation stability as demonstrated from continual one-year condensation experiments. Our work presents a solution to the century-old problem of hydrophobic and superhydrophobic coating durability through bio-inspired materials design with robustness beyond what is currently available.

11:15 AM *EN03.13.04

Temperature-Adaptive Radiative Coating for All-Season Household Thermal Regulation Kechao Tang¹, Kaichen Dong¹, Jiachen Li¹, Madeleine Gordon¹, Finnegan Reichertz¹, Hyungjin Kim¹, Yoonsoo Rho¹, Qingjun Wang¹, Costas Grigoropoulos¹, Ali Javey¹, Jeff Urban², Jie Yao¹, Ronnen Levinson² and Junqiao Wu¹; ¹University of California, Berkeley, United States; ²Lawrence Berkeley National Laboratory, United States

The sky is a natural heat sink that has been extensively used for passive radiative cooling of households. Past experimental works have focused on maximizing the radiative cooling power of roof coating in hot daytime using static, cooling-optimized material properties. However, the resultant overcooling in cold night or winter times exacerbates the heating cost, especially in climates where heating dominates energy consumption. In this work, we approach the thermal regulation from an all-season perspective by developing a mechanically flexible coating that adapts its thermal emittance to different ambient temperatures. The fabricated temperature-adaptive radiative coating (TARC) optimally absorbs the solar energy and automatically switches thermal emittance from 0.20 for ambient temperatures lower than 15 °C to 0.90 for temperatures above 30 °C, driven by a photonically amplified metal-insulator transition. The TARC is simulated to outperform all existing roof coatings for energy saving in most climates, especially those with significant seasonal variations, yielding a cut in annual source energy consumption up to 3.65 GJ for a typical single-family home in the U.S.

11:45 AM EN03.13.05

Sub-Ambient Radiative Cooling Using CaCO₃ Micro-Particle Composite Without Metal Reflector Layer Hangyu Lim, Dongwoo Chae, Soomin Son and Suheol Ju; Korea University, Korea (the Republic of)

Conventional cooling systems, that is, air conditioners, should be replaced because they consume a substantial amount of energy and cause environmental pollution. In this context, radiative cooling systems, which perform cooling without consuming any energy or causing environmental pollution, are emerging as an alternative. However, most of the radiative coolers explored thus far include metals, such as silver, that are used as solar reflectors, thereby entailing problems in terms of practicality, mass production, cost, and light pollution. Herein, we propose calcium carbonate (CaCO₃) micro-particle-based radiative cooling, which utilizes the high-energy band gap of CaCO₃ for high-performance radiative cooling. As the cooler has only a single layer of a CaCO₃ composite without any metal reflector, it is mass-producible, cheap, and does not cause light pollution. To demonstrate the cooling performance of CaCO₃, optical properties and temperature changes are measured and compared with those of commercial white paint. As a result, it is demonstrated that the CaCO₃-based radiative cooler has cooling power 93.1 W/m² in calculation and can be cooled 6.52 °C and 3.38 °C under ambient temperature in daytime and nighttime respectively. Thus, it can perform as radiative cooler in entire day.

12:00 PM EN03.13.06

Enhanced Superhydrophobicity of Additively Manufactured Metallic Alloys Jin Yao Ho^{1,2}, Kazi Fazle Rabbi¹, Teck Neng Wong², Kai Choong Leong² and Nenad Miljkovic^{1,1,1}; ¹University of Illinois at Urbana-Champaign, United States; ²Nanyang Technological University, Singapore

Metal additive manufacturing (AM) has revolutionized engineering design and production of components, eliciting a wide design space for geometrical, material, and functional optimization. This wide design space has led to the development of innovative functional devices for a plethora of applications including energy, transportation, chemical and bioengineering. The new processing phenomena and requirement for use of different alloying materials in AM poses unprecedented nanostructuring challenges of AM surfaces along with opportunities for the development of novel generations of surface architectures. Here, through the understanding of the grain formation mechanisms and material compositions resulting from the AM process, we developed an ultrascaleable and cost-effective method to rationally generate nanostructures on metallic AM surfaces for enhanced droplet repellency, condensation, evaporation, and boiling heat and mass transfer. By combining a facile microdroplet impact method with high speed optical imaging, we quantify that the AM structures significantly lower droplet adhesion as compared to state-of-the-art nanostructured surface on conventional aluminum alloys. We further explored the nanostructure morphology governing the departure size and frequency of condensed droplets and developed an AM structuring strategy that categorically reduces condensate flooding and enhanced condensation heat transfer coefficient by 6X, as compared to untreated surfaces in high supersaturation environments. This work not only shows the potential of using AM structured surfaces to achieve multi-functional performance enhancement, but it also outlines design guidelines and performance optimization strategies for structuring metallic AM materials.

SESSION EN03.14: Phonon Dynamics and Thermal Transport

Session Chairs: Yee Kan Koh and Jingcheng Ma

Monday Afternoon, December 6, 2021

EN03-Virtual

1:00 PM *EN03.14.01

Phonon-Mediated Unidirectional Magnetoresistance in a Metal on an Insulator with Highly Nonequilibrium Magnons Sean Sullivan, Hwijong Lee, Annie Weathers and Li Shi; The University of Texas at Austin, United States

Heavy metal (HM)/magnet bilayers host many magnetoresistance (MR) and spin caloritronic (SC) effects. Here we show that the spin Peltier effect and electron-phonon scattering result in a much larger measured unidirectional MR of an HM on a magnetic insulator than existing theories that neglect the interplay between MR and SC effects. This spin Peltier MR and the frequency-dependent spin Seebeck effect (SSE) reveal Onsager reciprocity and offer experimental probes of elusive properties of the nonequilibrium magnons driving these effects, including the magnon-phonon thermalization length and SSE coefficient.

1:30 PM EN03.14.02

Symmetry Consequences on Phonons and Thermal Transport Rinkle Juneja and Lucas Lindsay; Oak Ridge National Laboratory, United States

Structural symmetries determine the underlying physical properties of materials and thereby govern their potential functionalities. Here, I will discuss the role of twist structural symmetry in determining vibrational and thermal transport properties of one dimensional and bulk materials. The developed twist dynamics dictate symmetry-enforced band degeneracies, non-trivial topologies, phonon interactions, and unique scattering observables. This will be demonstrated by first-principles calculations supported by inelastic neutron scattering measurements.

R.J. and L.L. acknowledge support from the U. S. Department of Energy, Office of Science, Basic Energy Sciences, Materials Sciences and Engineering Division.

1:45 PM EN03.14.03

Late News: Effects of Impurities on the Thermal and Electrical Transport Properties of Cubic Boron Arsenide Xi Chen¹, Chunhua Li², Youming Xu¹, Andrei Dolocan³, Gareth Seward¹, Ambrose Van Roekeghem⁴, Fei Tian⁵, Jie Xing¹, Shuncheng Guo¹, Ni Ni¹, Zhifeng Ren⁵, Jianshi Zhou³, Natalio Mingo⁴, David Broido² and Li Shi³; ¹University of California, United States; ²Boston College, United States; ³The University of Texas at Austin, United States; ⁴Université Grenoble Alpes, France; ⁵University of Houston, United States

Cubic boron arsenide (BAs) is a promising compound semiconductor for thermal management applications due to its high thermal conductivity, exceeding $1000 \text{ W m}^{-1} \text{ K}^{-1}$ at room temperature in high-quality samples. However, the as-grown BAs crystals usually exhibit large variations in thermal and electronic transport properties. The origin of these large variations has thus far been inconclusive. Here, we investigate the effects of impurities on the thermal and electrical properties of BAs. Time-of-flight secondary ion mass spectrometry and electron probe microanalysis measurements reveal the presence of several impurities in BAs, including Si, C, O, H, Te, Na, and I. Some of these impurities, especially Si, C, and H, could serve as shallow acceptors, leading to the p-type conducting behavior commonly measured in BAs. The thermal conductivity and hole mobility are reduced more in the samples with higher impurity concentrations due to the enhanced impurity scattering of phonons and holes, respectively. First-principles calculations are used to determine the thermal conductivity reduction induced by different impurities. The calculated results confirm the experimental trends. The substitution of O for As leads to a large bond distortion resulting from the breaking of the T_d symmetry, which yields unusually strong phonon scattering with a correspondingly large reduction in thermal conductivity. Our results offer useful insights into the impurity-sensitive transport properties of BAs.

2:00 PM EN03.14.04

Transition to Ballistic Regime of Nanoscale Heat Transport in Silicon at Room Temperature Samuel Huberman¹, Zhiwei Ding², Gang Chen², Keith Nelson² and Alexei Maznev²; ¹McGill University, Canada; ²Massachusetts Institute of Technology, United States

In the past decade, non-diffusive heat transport by phonons at room temperature at the micro/nanoscale was reported in many single crystal materials. However, the transition to the ballistic transport regime, well studied in heat pulse experiments at the liquid He temperatures, remained elusive at room temperature. Motivated by the recent experimental work at the FERMI free electron laser facility in Trieste, Italy, where the extreme ultraviolet (EUV) laser source was used to produce nanoscale transient thermal gratings (TTGs) with heat transfer distances in the tens of nanometers range, we theoretically study heat transport in silicon in the TTG geometry using the Peierls-Boltzmann phonon transport equation based on first-principles calculations of the phonon dispersion and scattering rates. We find that the transition to the ballistic regime takes place in the sub-100 nm range of TTG periods. We compare the calculations done with the relaxation time approximation and the full scattering matrix and investigate the effect of different initial heat source distributions (e.g. optical phonon excitation). The results will be compared with the experimental EUV TTG data from single crystal silicon membranes.

2:15 PM EN03.14.05

Thermal Conductivity of BAs versus Pressure Songrui Hou¹, Bo Sun², Fei Tian³, Zhifeng Ren⁴, Xi Chen¹, Chen Li^{1,1} and Richard Wilson^{1,1}; ¹University of California, Riverside, United States; ²Tsinghua University, China; ³Sun Yat-sen University, China; ⁴University of Houston, United States

Boron arsenide (BAs) has ultrahigh thermal conductivity because of its unique phonon-phonon scattering properties [1]. At ambient pressure, “bunching” of acoustic phonon branches in BAs leads to a small phase-space for three-phonon scattering [2]. Density functional theory calculations suggest three-phonon scattering rates increase at high pressures because “bunching” of acoustic phonon branches decrease [2]. To test this hypothesis, we measure the thermal conductivity of BAs vs. pressure using time-domain thermoreflectance (TDTR) with a diamond anvil cell (DAC). We observe a pressure independent thermal conductivity from 0 to 25 GPa. We explain our observations as a result of the pressure dependence of the phonon dispersion relation, three-phonon scattering rates, and mass-disorder scattering.

[1] Feng, T., Lindsay, L., & Ruan, X. *Physical Review B*, 96(16), 1–6 (2017).

[2] Ravichandran, N. K., & Broido, D. *Nature Communications*, 10(1), 1–8 (2019).

2:30 PM EN03.14.06

Late News: Magnetocaloric Composites for High Efficiency Thermal Management Christopher Kovacs¹, Timothy Haugan², Michael McLeod², Devin Grant³, Leonard Jung⁴ and Matt Rindfleisch¹; ¹Hyper Tech Research Inc., United States; ²Air Force Research Laboratory, United States; ³Central State University, United States; ⁴Purdue University, United States

Cooling with magnetocaloric materials has been pursued by numerous agencies and companies, but many of the challenges remain unsolved. Some of these challenges are excessive pressure drop across the magnetocaloric regenerator, mechanical failure from magnetostructural and thermal cycling, and material degradation due to exposure. Presented here is a continuously processable powder-in-tube (PIT) composite in which the tube is a high thermal conductivity metal, and the core is dense GdF₃. Using this PIT composite, the magnetocaloric material is not exposed to the external environment. Additionally, the metal sheathing keeps the magnetocaloric material in slight compression to prevent mechanical fatigue. The arrangement of these PIT wires into an axially aligned array results in a high effective thermal conductivity, low demagnetization factor, and low impedance regenerator, overcoming some of the most difficult challenges in proposed magnetocaloric systems.

2:45 PM EN03.14.07

Study of Magnetocaloric Properties of Shape-Dependent Nanostructured Gadolinium Oxide Dipesh Neupane¹, Arjun K. Pathak² and Sanjay R Mishra¹; ¹Univ of Memphis, United States; ²SUNY Buffalo State, United States

Conventional gas compression refrigeration technique needs to be replaced by alternative cooling technology to reduce the depletion of the ozone layer and carbon production. Nowadays, scientists give more interest in magnetocaloric materials (MCM) for refrigeration to replace the vapor compression technique. MCMs are eco-friendly, more efficient, economical, and easy to use. In general, good magnetocaloric materials should have a low Debye temperature value, phase transition near working temperature, large temperature difference (ΔT_{ad}) in the vicinity of phase transition, no thermal or magnetic hysteresis, low specific heat, high thermal conductivity, high electrical resistance, resistant to corrosion, and good mechanical properties. Additionally, eddy current heating depends on the surface morphology that is caused by fast varying magnetic fields. Thus, the morphology of materials plays an important role to control the magnetocaloric properties. Gd₂O₃ nanomaterial was reported to exhibit a large magnetocaloric entropy change at $\sim 10\text{K}$ which is suitable for liquefying helium useful for cryogenic space application. Literature shows different values of magnetic entropy change (ΔS_m) with the same Gd₂O₃ nanostructures with different morphology like -8.7 J/kg.K for nanotubes, -20 J/kg.K for the rod. Several attempts have been made to study MCE on different morphology but comparative study on different morphology is lacking.

In this present study, we investigate the magnetocaloric properties of Gd₂O₃ nanoparticles of different morphology. Single phase Gd₂O₃ nanoparticles were synthesized via the hydrothermal method and a homogeneous precipitation method followed by heat treatment in air at $1100 \text{ }^\circ\text{C}$ for 12 h. Thus

Gd₂O₃ nanoparticles of different shape viz. bulk, rod, spheres, and plate were prepared. The morphology of the samples was analyzed using SEM. The SEM images of synthesized Gd₂O₃ showed 1D nano-rods, 2D nano-plates like architecture prepared via hydrothermal method while hollow nanosphere morphology achieved with a homogeneous precipitation method. The average area of plates are 1mm², the average length of rods are ~500 nm and diameter of hollow micro sphere are ~600 nm. The phase identification and lattice parameter of the powders performed using x-ray diffraction showed presence of highly-crystalline single phase cubic crystal structure with JCPDS No.11-0604. The average crystallite size of sample were lies between 20-30 nm calculated by using Scherrer formula. The lattice parameter of the sample using profile fitting is lies between 10.810 to 10.832 Å. Magnetic measurements were performed using a SQUID magnetometer. Temperature dependence of zero-field-cooled (ZFC) curve exhibits unchanged phase. The material demonstrate typical paramagnetic behavior in the whole measured temperature 5K to 100K. The paramagnetic susceptibility follows Curie-Weiss law and the fit parameters yield a paramagnetic Curie temperature (T_c) value of ~5K for all samples. The M-H data in the temperature range of 3–30 K is used to calculate the isothermal magnetic entropy change. The M-H data shows the paramagnetic behavior. The maximum value of ΔS_m for 50 kOe field change at 5K is 11.2 Jkg⁻¹ K⁻¹ for the nanoplate sample, 9.4 Jkg⁻¹ K⁻¹ for the nano-rod and 9.2 Jkg⁻¹ K⁻¹ for the nano-sphere, and 10.7 J/kg.K for Bulk. The reason for achieving large ΔS_m could be the surface area and surface geometry of the samples. More surface area indicates more surface spins that enhanced magnetization value. These results shows the Gd₂O₃ nano plates are the promising materials for magnetic refrigeration technology compare with oxide nanoparticles at 5K. Our study suggests that the Gd₂O₃ nanostructures of various morphologies could exhibit interesting magnetocaloric properties at low temperatures.

References

1. Phan, M. H. et al, Journal of Magnetism and Magnetic Materials, 308 (2007) 325-340.
2. Hazarika, S. et. al, Applied Surface Science, 491,(2019) 779-783.

2:50 PM EN03.14.08

Advanced Experimental Technique to Measure Thermal Conductivity using Suspended Micro-Island Devices Anh Tuan Nguyen and Woochul Lee; University of Hawaii, United States

Suspended micro-island device has enabled researchers to directly measure thermoelectric properties in nanomaterials spanning from nanowires and nanotubes to 2 dimensional materials. The unique capability of this device of probing thermal conductivity at the level of single nanowire and 2D material has significantly contributed to expanding knowledge in nanoscale thermal transport. While the suspended micro-island device remains a powerful tool to measure thermoelectric properties, we further advanced experimental techniques using suspended micro-island devices in order to increase success rates in sample preparation as well as to increase accuracy in thermal conductivity measurements. We will explain the detailed structure of the newly designed suspended micro-island devices and our experimental configurations. Further, we will describe advantages and versatile usages of our experimental technique in various scenarios.

2:55 PM EN03.14.09

Thermal Conductivity Mapping of Composite Materials by Time-Domain Thermoreflectance Xiaoyang Ji, Satoshi Matsuo, Zhe Cheng, Ella Pek, Nancy Sottos and David Cahill; University of Illinois at Urbana-Champaign, United States

Time-domain thermoreflectance (TDTR) mapping technique has been applied in many fields for detecting the spatial variation of the thermal properties of materials. Here we report the TDTR mapping work with a micro-scale spatial resolution on single carbon fibers and an oxidized SiC/SiC composite. We determine the transverse thermal conductivity of a single IM7 carbon fiber to be ~1.7 W/m-K and obtain uniform thermal conductivities at different radial positions by mapping a carved step structure on the IM7 carbon fiber. Moreover, we determine both the thermal conductance of the oxide layer and the thermal conductivity of the SiC/SiC composite by mapping at different delay times, and figure out the differences between the fibers and the matrix. The effective thermal conductance of the oxide formed on the fibers (27-40 MW/m²-K) is lower than the oxide on the matrix (40-47 MW/m²-K), while the fibers have lower thermal conductivities (15 W/m-K) than the matrix (50-90 W/m-K). TDTR mapping on these two small-size composite materials allows for obtaining accurate thermal property changes that are related to the microstructure discrepancies of materials. In addition, we enable a faster data acquisition rate up to 33 μm/s by introducing heterodyne detection into the conventional TDTR setup, which allows for a 17 times higher scanning speed than the conventional TDTR mapping.

SESSION EN03.15: Thermal Conductivity and Phonon Transport
Session Chairs: Rinkle Juneja and Yijie Zhou
Monday Afternoon, December 6, 2021
EN03-Virtual

4:00 PM *EN03.15.01

Principles of Thermal Energy Transport, Storage and Conversion in Diverse Settings Jeff Urban; Lawrence Berkeley National Laboratory, United States

Thermal energy lies at the heart of any irreversible process that constitutes much of the operating world around us. Despite this, there is seldom a unifying call to fashion better thermal materials and understand their phenomenology directly; it is often treated as a secondary problem. However, as technoeconomic modeling and global impact are of increasing prominence in materials design and applied physics, I argue that thermal properties should be a primary consideration. Here, I present recent research on a variety of topics - design of phase change cooling materials, phonons in hybrid materials, water separations, thermoelectrics, hydrogen storage, personal comfort, and computing - all of which orbit around how thermal energy can be better harnessed, guided, and utilized. Some highlights will be design considerations of flexible heat exchangers, interfacial solar evaporation in brine management, thermal storage in molecular-invaded porous crystals, unusual temperature dependent plasmonic catalysis, phonon transport in soft materials, and thoughts on computing limitations.

4:30 PM EN03.15.02

Stacking Order Driven Thermal Transport in ReS₂ Yongjian Zhou and Yaguo Wang; Mechanical Engineering, Texas Materials Institute, The University of Texas at Austin, United States

ReS₂ is a rising star in the transition metal dichalcogenide family. The uniqueness of ReS₂ lies in its distorted 1T triclinic crystal structure where the additional *d* valence electrons of Re atoms form zigzag Re chains parallel to the *b*-axis, drastically reducing its symmetry. As a result, ReS₂ possesses

extremely weak interlayer bonding and anisotropic optical, thermal, and electronic properties. Unlike black phosphorus, ReS₂ is very stable in air, making it more suitable for optoelectronic applications. Recently, two stacking orders were identified in multi-layer ReS₂: AA stacking where adjacent layers sit right on top of one another with minimal displacement, and AB stacking where adjacent layers shift by one-unit cell along *a*-axis. With, Ab-initio calculations, the interlayer distance of stacking AB is determined to be 2.59 Å, smaller than that of stacking AA, 2.71 Å, which suggests the stronger interlayer interaction in stacking AB. The carrier dynamics, and both optical and vibrational properties in different stacking orders were found to be drastically distinct. In this study, we prepared ReS₂ flakes via mechanical exfoliation with both AA and AB stacking and measured their thickness dependent cross-plane thermal conductivity. We found that the stacking orders of ReS₂ are very robust. Pure stacking order (either AA or AB) can persist up to the thickness of several microns. For both stacking orders, thermal conductivity increases with sample thickness until around 2µm, indicating an extremely long phonon mean free path along cross plane direction. The thickness dependent thermal conductivity in samples with AA stacking increases much faster than those with AB stacking. Our results suggest that stacking order can be an additional degree of freedom to manipulate thermal transport in 2D materials.

4:45 PM EN03.15.03

Modeling Phase Noise with Machine Learning Potentials in Cu₂O Claire N. Saunders¹, Dennis S. Kim², Olle Hellman³ and Brent Fultz¹; ¹California Institute of Technology, United States; ²Massachusetts Institute of Technology, United States; ³Weizmann Institute of Science, Israel

Higher-order force constants of Cu₂O, cuprite, were calculated with a perturbative *ab initio* effective potential method, and used to predict thermal expansion and other temperature-dependent phonon behaviors. Inelastic neutron scattering was used to measure phonon dispersions in single crystal cuprite at 10, 300, 700, and 900 K. Low- and high-order force constants accounted for the negative thermal expansion of cuprite; however, calculations with high-order force constants were more effective in predicting the observed temperature-dependent phonon behavior. None of these calculations sufficiently accounted for an observed broad, diffuse intensity in the measured phonon spectrum. Classical molecular dynamics with machine learning interatomic potentials models will be compared with perturbative anharmonic calculations. A local dynamics model is proposed to explain this diffuse inelastic scattering, analogous to phase noise in oscillators.

5:00 PM EN03.15.04

Physics-Informed Neural Networks for Solving Multiscale Mode-Resolved Phonon Boltzmann Transport Equation Ruiyang Li¹, Eungkyu Lee² and Tengfei Luo¹; ¹University of Notre Dame, United States; ²Kyung Hee University, Korea (the Republic of)

Boltzmann transport equation (BTE) is an ideal tool to describe the multiscale phonon transport phenomena, which are critical to applications like microelectronics cooling. Numerically solving phonon BTE is extremely computationally challenging due to the high dimensionality of such problems, especially when mode-resolved properties are considered. In this work, we demonstrate the use of physics-informed neural networks (PINNs) to efficiently solve phonon BTE for multiscale thermal transport problems with the consideration of phonon dispersion and polarization. In particular, a PINN framework is devised to predict the phonon energy distribution by minimizing the residuals of governing equations and boundary conditions, without the need for any labeled training data. Moreover, geometric parameters, such as the characteristic length scale, are included as a part of the input to PINN for learning BTE solutions in a parametric setting. This enables our method to handle structures over a wide range of length scales after a single training. The effectiveness of the present scheme is demonstrated by solving a number of phonon transport problems in different spatial dimensions (from 1D to 3D). Compared to existing numerical BTE solvers, the proposed method exhibits superiority in efficiency and accuracy, showing great promises for practical applications, such as the thermal design of electronic devices.

5:15 PM EN03.15.05

Thermal Conductivity of ZrS₂ Monolayer Driven by Finite-Temperature and Anharmonic Lattice Dynamics Abhiyan Pandit and Bothina Hamad; University of Arkansas-Fayetteville, United States

Two-dimensional (2D) ZrS₂ monolayer (ML) has emerged as a promising candidate for thermoelectric (TE) device applications due to its high TE figure of merit, which is mainly contributed by its inherently low lattice thermal conductivity. This work investigates the effect of the lattice anharmonicity driven by temperature-dependent phonon dispersions on the thermal transport of ZrS₂ ML. The calculations are based on the self-consistent phonon (SCP) theory to calculate the thermodynamic parameters along with the lattice thermal conductivity. The higher-order (quartic) force constants were extracted by using an efficient compressive sensing lattice dynamics technique, which estimates the necessary data based on the emerging machine learning program as an alternative to computationally expensive density functional theory calculations. Resolve of the degeneracy and hardening of the vibrational frequencies of low-energy optical modes were predicted upon including the quartic anharmonicity. As compared to the conventional Boltzmann transport equation (BTE) approach, the lattice thermal conductivity of the optimized ZrS₂ ML unit cell within the SCP + BTE approach is found to be significantly enhanced (e.g., by 21% at 300 K). This enhancement is due to the relatively lower value of phonon linewidth contributed by the anharmonic frequency renormalization included in the SCP theory. Mainly, the conventional BTE approach neglects the temperature dependence of the phonon frequencies due to the consideration of harmonic lattice dynamics and treats the normal process of three-phonon scattering incorrectly due to the use of quasi-particle lifetimes. These limitations are addressed in this work within the SCP + BTE approach, which signifies the validity and accuracy of this approach.

5:30 PM EN03.15.06

Resonant Interaction Between Phonons and PbTe/PbSe(100) Misfit Dislocations Yang Li¹, Adrian Diaz¹, David McDowell² and Youping Chen¹; ¹University of Florida, United States; ²Georgia Institute of Technology, United States

As a consequence of a lattice mismatch between dissimilar materials, misfit dislocations are unavoidable at the phase interfaces in heterostructures when the epilayer thickness exceeds a critical thickness, regardless of the growth mechanisms and conditions. In this study, we report simulation results of the resonant interaction between long-wavelength transverse acoustic (TA) phonons and misfit dislocations at the PbTe/PbSe(100) interface, using the Concurrent Atomistic-Continuum method. It is found that TA phonons with frequency near a specific value excite the resonance behavior of the misfit dislocations, as identified by large-amplitude, out-of-phase vibration of the atoms on both sides of the slip plane of the misfit dislocations. The vibration amplitude can be up to ten times of the amplitude of the incident phonon wave. The resonant interaction leads to a low energy transmission of TA phonons.

8:00 AM *EN03.16.01

Overview of US DOE Research and Development in Concentrating Solar-Thermal Power [Avi Shultz](#); U.S. Department of Energy, United States

To meet the global threat of climate change and ensure that all Americans benefit from the transition to a clean energy economy, the DOE Solar Energy Technologies Office (SETO) works to accelerate the development and deployment of solar technologies to decarbonize the electricity system by 2035 and decarbonize the energy sector by 2050. A fully decarbonized grid will likely require large amounts of energy storage to provide energy when it is needed and increase the grid's reliability and resilience. While lithium-ion batteries have enabled rapid deployment of energy storage, most commercial applications have been limited to four hours of storage or less. Longer-duration storage can help alleviate the impact of extended periods of cloudy weather, for example, or even seasonal variations of solar energy production.

Concentrating solar-thermal power (CSP) plants use mirrors to capture the sun's energy as heat, which can be stored in a thermal energy storage (TES) system and used to produce electricity on demand, even when the sun is not shining. Commercial CSP plants with TES have demonstrated the viability of thermal storage to be responsive to grid needs, particularly for long durations of daily storage, up to 17 hours, which is not currently economically viable with lithium-ion batteries. Thermal systems can decouple the storage capacity component (e.g., molten salt stored in tanks) from the power-generating component (heat engine). This enables system designers to increase marginal storage capacity or duration—without having to build additional generating capacity—by increasing the size of the storage tank. The combination of readily scalable TES and conventional turbine technology can allow CSP to provide reliable and flexible renewable electricity production.

SETO has set a cost target of \$0.05 per kilowatt-hour electric (kWh_e) for baseload plant configurations with 12 or more hours of storage, which could enable deployment of 25 to 160 GW of U.S. CSP capacity by 2050. To reach this target, SETO is supporting the development of next-generation CSP plants that are capable of delivering heat to the power cycle at temperatures exceeding 700°C, increasing plant efficiency. Current technologies that use molten salt cannot exceed 565°C owing to thermal decomposition of the salt, which is used as a heat-transfer fluid. If successful, these third-generation (Gen3) CSP designs will enable CSP systems to utilize advanced power cycles based on supercritical carbon dioxide (sCO₂), which are much more efficient than existing steam-based cycles.

Projects in SETO's Gen3 CSP program have been investigating and designing fully integrated thermal transport systems based on three competing concepts for the heat-transfer media (HTM) organized by the phase of matter for leading HTM candidates—gas, liquid, or solid. In March 2021, SETO announced the selection of Sandia National Laboratories to develop a design based on solid particles as the HTM. Sandia will receive \$25 million to construct a 2 megawatt (MW) thermal integrated test facility to validate the proposed system.

Beyond electricity generation, solar-thermal technologies may also be able to help meet the national goal of decarbonizing the entire U.S. energy sector by 2050 by providing industrial process heat. Even with more renewable electricity available, many industrial processes will be difficult to electrify because they require high temperatures or have other challenging process characteristics. SETO aims to make solar industrial process heat cost-competitive with fossil fuels to address high-priority applications, including calcination to produce cement, thermochemical water splitting for producing solar fuels, and ammonia synthesis for producing fertilizer. The solid particle heat-transfer pathway being developed for Gen3 CSP may be particularly relevant for a number of these processes, which have solid-phase components or are mediated by solid-phase catalysts.

8:30 AM EN03.16.04

Materials Challenges Associated with 100-Gigawatt-Hour Nitrate-Salt Crushed-Rock Heat Storage [Disha Bandyopadhyay](#)^{1,2} and Charles W. Forsberg¹; ¹Massachusetts Institute of Technology, United States; ²Imperial College London, United Kingdom

We are developing a 100-GWh Crushed-Rock Ultra-large Stored Heat (CRUSH) System that couples to nuclear reactors or very large Concentrated Solar Power (CSP) heat sources. Heat storage enables nuclear or CSP plants to operate at full capacity with dispatchable electricity. The electric storage capabilities of CRUSH are similar to the Tennessee Valley Authority Raccoon Mountain pumped hydro facility that can provide 1600 MW(e) for 22 hours to address hourly to weekly storage. Heat is transferred into and out of storage using nitrate salts (<600°C). The CRUSH system capital-cost goals are \$2-4/kWh—an order of magnitude less than current heat storage systems and a factor of 50 less than batteries.

Existing solar power towers use clean nitrate salt for heat transfer and storage. Cold salt is heated by the CSP system and sent to hot nitrate storage tanks. The power block, sized for peak electricity demand, takes hot nitrate salt, produces dispatchable electricity and sends the cold salt to cold-salt storage tanks. Three advanced nuclear reactor concepts use nitrate salt in the intermediate loop and propose the same system design as CSP plants—cold salt heated with a reactor operating at base load, hot salt sent to the hot salt storage tank, hot salt from storage goes to the power block to produce variable electricity and the resultant cold salt is sent to the cold-salt storage tank. Existing CSP systems have up to several gigawatt hours of heat storage and have capital costs of \$20-30/kWh of heat stored. About half the capital cost is associated with the tanks and a third or more of the cost is associated with the nitrate salts.

With the CRUSH system, heat storage is in a crushed rock pile (200 m by 200 m with heights of 20 to 40 m) with heat transfer by hot nitrate salt that is sprayed on the crushed rock and drains to the catch pan below. Heat is recovered by spraying cold fluid onto the hot crushed rock and recovery of the hot fluid from the catch pan below. To minimize costs, nitrate salt is used for heat transfer, not heat storage. This process has similarities to heap leaching of copper ores where solutions are sprayed on top of large crushed rock piles, flow through the piles, dissolve the copper and are collected by the drain pans below. The crushed rock pile has a flat top surface with sloping sides of crushed rock. This allows free expansion and contraction of the rock pile with changing temperatures. The building over the crushed rock is similar to an aircraft hangar with a gas-tight insulation on the inside—no rock or liquid nitrate salt touches the building structure. Unlike current nitrate-salt heat storage systems with clean nitrate salt in clean tanks, the CRUSH salt is in direct contact with the crushed rock.

We are examining materials reactions between the salt, the crushed rock, heat exchangers and piping. The thermal transients will generate fines; thus, filters are required to remove larger solid particles in the liquid salt. Rock choices must be chosen to (1) withstand thermal cycling, (2) forces by 20+ meters of crushed rock height, (3) dissolution of selected components that may or may not be limited by solubility limits in nitrate salts, (4) dissolution and precipitation of rock components with temperature and (5) corrosion and fouling of heat exchangers and other components. There has been some experimental work associated with nitrate salt/crushed rock in proposed heat-storage thermocline systems with hot salt on top of cold salt in a tank filled with crushed rock. Only some crushed rocks are chemically compatible with the nitrate salts. We review the existing work, our analysis and priorities going forward. Major work, including poly-temperature flowing salt loops, will be required to qualify rock types for this service.

8:45 AM EN03.16.02

FeMnNiAlCr High Entropy Alloys with High Efficiency Native Oxide Solar Absorbers for Concentrated Solar Power Systems [Xiaoxue Gao](#), Edwin Jiang, Huan Wang, Weiyang Li, Ian Baker and Jifeng Liu; Dartmouth College, United States

As a complementary technology to photovoltaics in harvesting and converting solar energy, concentrated solar power (CSP) system offers a unique

advantage in that it stores solar energy as heat at low cost, which enables dispatchable solar electricity supply even at night. Same as other heat engine systems, the CSP system follows the Carnot's theorem: the higher the operation temperature of the system, the higher the conversion efficiency. Thus, a key component of the CSP system, the tubing material, is required to be both mechanically strong at high temperatures >873 K and resistant to the corrosion of both the working fluids inside and the oxidation in air outside at this working temperature. Currently, most of the tubing materials employed in power plants could not operate at temperature higher than 873K due to their mechanical and chemical limits. Even though the nickel or titanium-based alloy could have better performance, they would not be economic solutions to this challenge at a cost ~10x that of stainless steels. In this paper, we present FeMnNiAlCr high entropy alloys (HEAs) to address this challenge. Low-cost Fe and Mn constitute >60 at.% of the HEA composition, much more cost-effective than the nickel-based superalloys, while the tensile strength of the HEAs are comparable to Ni-based Inconel alloys at 973K [1,2]. Compared with 304 stainless steels, its yield strength is also twice as high at 973K. Therefore, our FeMnNiAlCr HEA shows promising mechanical properties to satisfy the mechanical requirements of the high temperature tubing material. The other crucial element of the CSP system is the solar selective absorber. High solar absorbance, low thermal emittance loss and stable optical-to-thermal energy conversion efficiency at 1023K for long term are essential properties of the solar selective absorber utilized in this working environment. One of the widely applied solar selective absorber coatings, Pyromark 2500, has high solar emittance loss (~80%) and would need sophisticated fabrication steps to ensure its adherence to the substrate [3]. Its conversion efficiency also degrades after operation at 1023K for just 300h. The native oxide we grown on two phase HEAs, which mostly comprises Mn₂O₃ on the surface and a dense Al₂O₃ at the oxide/HEA interface, provides a facile synergistic solution to solar absorbers. This native oxide layer has high solar absorbance of 91.4%, low thermal emittance of 27% and an optical-to-thermal energy conversion efficiency of 89.7% at 1023K for 1000x solar concentration ratio. The solar absorption is mainly contributed by manganese oxide on the surface, while the dense protective aluminum oxide at the oxide/HEA interface can be engineered to prevent excessive oxidation. Interestingly, the manganese oxide spontaneously forms surface texture upon oxidation, similar to the surface engineering of photovoltaic cells, which enhances the solar absorption while the dense and robust layer itself protects the alloy from both the corrosion of the working fluids and excessive oxidation of the air. In preliminary high-temperature corrosion studies, two-phase FeMnNiAlCr HEAs have sustained bromide molten salts for 14 days at 1023 K with <2% weight loss. Thus, the potential of synergistically addressing mechanical, optical and chemical challenges makes FeMnNiAlCr HEAs a promising cost-effective candidate for high-temperature tubing materials in future CSP systems.

[1] Baker, Ian, et al. "Recrystallization of a novel two-phase FeNiMnAlCr high entropy alloy." *Journal of Alloys and Compounds* 656 (2016): 458-464.

[2] Z. Wang, M. Wu, Z. Cai, S. Chen and I. Baker, "The microstructure and mechanical behavior of (Fe₃₆Ni₁₈Mn₃₃Al₁₃)_{100-x}Ti_x high-entropy alloys", *Intermetallics* 75, 79-87 (2016). <http://dx.doi.org/10.1016/j.intermet.2016.06.001>

[3] Ho, Clifford K., et al. "Characterization of Pyromark 2500 paint for high-temperature solar receivers." *Journal of Solar Energy Engineering* 136.1 (2014).

9:00 AM EN03.16.03

Design of Nitrate-Based Molten Salt/Nanoporous Alumina Composites with Improved Thermophysical Properties Göktürk M. Yazlak¹, Martin Steinhart², Jürgen Thiel³ and Hatice Duran¹; ¹TOBB University of Economics and Technology, Turkey; ²Universitaet Osnabrück, Germany; ³Max-Planck-Institute for Polymer Research, Germany

Selection of an appropriate heat transfer agent (HTA) and thermal energy storage (TES) material is important for minimizing the cost of the solar receiver, thermal storage and heat exchangers, and for achieving high receiver and cycle efficiencies. It has also been observed that the use of the molten salt eutectic composition as an HTA / TES fluid in many different areas is effective in increasing system efficiency. Current molten salt HTAs have high melting points (>200°C) and degrade above 600°C. The main problem with this application is that it can easily freeze in the evening or in the winter months and clog the pipeline to make working conditions difficult. For this reason, there is an urgent need for inexpensive salt melt compositions having a lower melting point and a higher thermal stability temperature. To do this, a new nanostructured eutectic molten salt was designed to achieve lower melting point (>200°C) and higher thermal conductivity. In this study, we prepared phase diagrams of molten salts and anodic alumina oxide (AAO) with different pore size (25 to 400nm). Maximum melting temperature depression was observed as $\Delta T \approx -170^\circ\text{C}$ for AAO/KNO₃ composites for 35nm pore size. Furthermore, a drastic increase on thermal conductivity (73%) was recorded for the same composite. It was observed that this increase was not systematic in AAO / KNO₃ composite structures, but it was systematic in AAO / NaNO₃ composite structure. The highest thermal conductivity increase is seen in AAO / KNO₃ composite structure with pore diameter of 35nm.

9:15 AM EN03.16.05

Transitioning Toward Robust Industry-Grade Predictive Workflows for Thermal Management Applications Kiran Sasikumar¹, Sushant Sonde² and Subramanian Sankaranarayanan³; ¹Avant-garde Materials Simulation GmbH, Germany; ²EPIR Inc., United States; ³Argonne National Laboratory, United States

Ab-initio design or engineering of systems and processes may be considered a holy grail in computational sciences, spanning across the fields of materials science, chemistry, biology, and engineering. The goal here is to integrate multiple simulation modalities, from quantum mechanical calculations to continuum finite element simulations, for a fully ab-initio prediction of device or process operation with limited experimental input. Such an ab-initio predictive workflow, a digital twin, can complement experimental investigation by narrowing the relevant design space.

Specifically, thermal management of electronics is an important aspect in the design of semiconductor devices, where certain applications require device operation in temperature extremes. Chips with electromagnetic detector arrays often have to operate at 77 K and frequently cycle back to room temperature when not in use. One of the design goals here is, thus, to optimise device geometry to minimize thermal stresses upon temperature cycling and improve operational reliability of the resulting integrated detector array.

In this contribution, we introduce the design of Modified Direct Band Interconnect (MoDiBI) detector arrays using artificial-intelligence inspired optimization heuristics integrated with a finite element thermo-mechanical model. While fully ab-initio device engineering is not a reality yet, we use this system as a template to discuss the effect changes in the material properties of device components have on the optimized device geometry. This, in turn, paints a picture on the accuracy needed in the prediction of thermo-mechanical material properties in a fully ab-initio workflow.

Further, we discuss some case studies to evaluate if current state-of-the-art in thermal property prediction from atomistic simulation is sufficient to enable a robust predictive workflow for thermo-mechanical device optimization. Finally, a perspective is provided on recipes to transition toward robust industry-grade predictive workflows for thermal management applications.

9:30 AM EN03.16.06

Extreme Durability of Grafted Polymer Film in Condensation Heat Transfer Using Initiated Chemical Vapor Deposition Abinash Tripathy¹, M. Donati¹, Cheuk Wing Edmond Lam¹, A. Milionis¹, Chander S. Sharma² and Dimos Poulikakos¹; ¹ETH Zürich, Switzerland; ²Indian Institute of Technology Ropar, India

Condensation has significant applications in various industries. Commercially condensation can be used for thermal management, power generation,

refrigeration, air conditioning, water desalination etc. Condensation can be distinguished in to two distinct modes commonly termed as filmwise condensation (FWC) and dropwise condensation (DWC). Among these DWC is the preferred mode of condensation in heat transfer applications due to the inherently higher heat transfer coefficient (almost one order of magnitude). However, condensation still manifests as FWC on most of the condenser surfaces (copper, aluminium, steel etc.) used in industry. This is because the metal surfaces are hydrophilic, and an additional hydrophobic coating is required to achieve DWC. An ideal hydrophobic coating should have high droplet shedding efficiency, mechanical durability and low thermal resistance. However, it is difficult to attain all these properties in one coating.

In this work, we report DWC with stable heat transfer performance on poly-[1H,1H,2H,2H- perfluorodecyl acrylate] (pPFDA) coating grafted on flat copper and aluminum substrates using initiated chemical vapor deposition (iCVD) technique. iCVD is environmental friendly as it is solvent-free and vapor phase process. The condensation heat transfer performance and durability of this coating is compared with 1H,1H,2H,2H-Perfluorodecyltriethoxysilane (Silane) functionalized copper and aluminium substrates.

The grafted polymer coating using iCVD was obtained in two steps. First, we coated flat copper or aluminum substrate with trichlorovinylsilane (TCVS) in a custom-made chemical vapor deposition chamber at 10 bar. Post TCVS coating, we utilized the iCVD tool (iLab Coating System, GVD Corporation) to deposit an ultra-thin layer of pPFDA (Advancing contact angle (ACA) – $127^{\circ}\pm 3^{\circ}$, contact angle hysteresis (CAH) – $10.3^{\circ}\pm 3.4^{\circ}$). The thickness of the coating was found to be ~40 nm. For silane coating, flat copper and aluminium samples were dipped in a mixture of Silane and hexane for 1 hour followed by baking it on a hot plate (ACA – $123.3^{\circ}\pm 1^{\circ}$, CAH – $21.3^{\circ}\pm 1.2^{\circ}$).

The condensation heat transfer performance of both the coatings was evaluated in a harsh condensation environment. The surfaces were mounted in a high saturation pressure chamber (1.42 bar) and exposed to superheated steam (111°C). These are extreme conditions to test the performance of the hydrophobic coatings as compared to a low saturation pressure conditions typical for industrial condensers. The superheated steam was flowing on the test substrates at 3 m/s and 9 m/s during the experiments by exerting a vapor shear on the coating. The heat transfer performance was quantified in terms of the heat transfer coefficient (HTC).

Apart from heat transfer performance, the mechano-chemical robustness of both the coatings was tested for their practical applicability with a protocol consisting of eleven different durability tests. The grafted polymer coating via iCVD outperformed the Silane coating in terms of mechano-chemical durability. Additionally, it survived exposure to superheated steam during condensation experiment and exhibited DWC with a stable HTC during the experiment. This can be attributed to the higher chemical strength of the hydrophobic coating with the substrate deposited via iCVD. Vinyl groups in TCVS are covalently bound to the surface and the reaction between the surface vinyl groups and the vinyl groups in PFDA monomer binds them chemically to the substrate. On the other hand, Silane coating is a monolayer (~2-3 nm) and hence is susceptible to deterioration in extreme environments. Consequently, the silane coating failed in the condensation chamber, and we observed FWC on the surface. These findings make iCVD coating an ideal candidate for practical applications.

9:45 AM EN03.16.07

Ragone Relationships in Thermal Batteries to Evaluate Phase Change Material Composite Design Charles M. Shoalmire¹, Alison Hoe¹, Michael Shanks², Neera Jain² and Patrick Shamberger¹; ¹Texas A&M University, United States; ²Purdue University, United States

Energy storage technologies are marked by tradeoffs in energy and power density; a Ragone plot is a standard graphical representation used to investigate the relationship between these two quantities. Absolute upper limits on energy density generally derive from intrinsic thermodynamic limits. In contrast, the power density of a substance represents kinetic limits on heat, mass, or charge transfer which limit the rate of energy storage. Viewed through this lens, the relationship between these two quantities represents how much of the potential or theoretical energy storage density must be sacrificed to achieve a particular rate of energy storage. Ragone relationships offer an approach to critically analyze the dependence of material performance on different design parameters.

Phase change materials (PCMs) are of intense interest due to their ability to passively store thermal energy in order to mitigate a transient temperature rise, or to improve the overall efficiency of a system. While PCMs possess high effective thermal capacitance, due to the latent heat of transformation, many suffer from low intrinsic thermal conductivity. To increase conductivity, PCMs can be combined with materials with higher thermal conductivities (e.g., metals, graphite, etc.) to create composite PCMs. In this case, the maximum energy density of a composite PCM volume is defined primarily by the intrinsic material properties of the PCM phase, the fraction of the composite composed of PCM phase, and the temperature rise. In contrast, the power density of a composite PCM volume is a non-trivial quantity, as it depends strongly on the many factors that affect heat transfer rate, including intrinsic material properties, operating conditions, the geometry of thermal energy storage (TES) modules, the coupling between the composite PCM volume and the design of the PCM composite itself.

In this study we develop and validate a numerical finite difference model to interrogate heat transfer from a heat transfer fluid into a planar or cylindrical volume composed of a composite PCM. From this, we extract energy density and power density Ragone relationships over the period of charging or discharging (5 to 5000 s). Here, we focus on the effects of composite structure, including the relative volume fraction of PCM and conductive components, the role of component orientation and anisotropic transport, and the interaction between different PCMs (paraffins, salt hydrates, low melting point metals) and conductive elements (aluminum, graphite). Systems which are optimized for longer timescales allow the system to approach its maximum energy storage density, as minimal mass and volume is devoted to enhancing heat transfer into the composite PCM bed. As an example, a planar module composed of aluminum and hexadecane (a paraffin wax) optimized to store energy over a period of 500 s can achieve energy densities (180 J/g; 175 J/cm³) that are approximately 70% of the intrinsic limit, corresponding to relatively low power densities (0.36 W/g, 0.35 W/cm³). In contrast, a module of the same geometry that is optimized to store energy over a period of 50 s can achieve energy densities (130 J/g; 155 J/cm³) that are approximately 50% of the intrinsic limit, corresponding to an order of magnitude larger energy storage rates (2.6 W/g, 3.1 W/cm³). [SPJ1] These results reveal the interactions between different thermophysical properties and composite design parameters, and also allow for efficient optimal design of energy storage components to meet application specific requirements.

SESSION EN03.17: Radiative Heat Transfer II

Session Chair: Yee Kan Koh

Tuesday Morning, December 7, 2021

EN03-Virtual

10:30 AM *EN03.17.01

Towards Massive Material Search Space with Machine Learning and Quantum Annealer—Application to Thermal Radiation Junichiro Shiomi; The University of Tokyo, Japan

Materials informatics (MI), developing or studying materials with an aid of informatics or machine learning, has become popular in academia and industry. Use of MI for heat transfer started later than other fields but now there are growing number of reports showing good compatibility. A general methodology

is to train a black box model that relates basic descriptors (structure, composition, etc) and figure of merit (target properties) and predict or design a material with largest FOM. At Thermal Energy Engineering Lab at University of Tokyo, together with the collaborators, we have been working on MI for heat transfer for about 6 years, starting from nanostructure design using Bayesian optimization[1, 2]. We have applied the methodology to computationally design and experimentally realize aperiodic superlattice that optimally impedes coherent thermal transport[3] and multilayer metamaterial with ultranarrow-band wavelength-selective thermal radiation[4]. While Bayesian optimization has limitation in the size of search space for global optimization, considering the complex system with many dimensions or parameters needed for further MI, the challenge now is to develop a scheme that can efficiently handle massive material search space. Quantum annealing is a powerful tool since it can quickly solve combinatorial optimization problems of the size that scales with the power of number of qubits, and number of qubits commercially available for use is increasing year by year. However, there are some practical challenges. One is that the quantum annealing can only solve the problem in form of Ising model, and this has been overcome by using factorization machine [5]. Another is that even if optimization is quick and large, it is only useful when the speed and size are well balanced with those of data generation. In that sense, radiative heat transfer problem, such as designing metamaterial for wavelength-selective thermal emitter, is most suited to go massive because calculation of electromagnetic field is light and easy to parallelize. In the talk, we will introduce these progresses in applying annealers to thermal radiation problems and discuss the capability and remaining challenges for further development.

[1] Ju, Shiga, Feng, Hou, Tsuda, Shiomi, *Physical Review X*, 7, 021024 (2017).

[2] Yamawaki, Ohnishi, Ju, Shiomi, *Science Advances*, 4, eaar4192 (2018).

[3] Hu, Iwamoto, Feng, Ju, Hu, Ohnishi, Nagai, Hirakawa, Shiomi, *Physical Review X*, 10, 021050.

[4] Sakurai, Yada, Simomura, Ju, Kashiwagi, Okada, Nagao, Tsuda, Shiomi, *ACS Central Science* 5, 319-326 (2019).

[5] Kitai, Guo, Ju, Tanaka, Tsuda, Shiomi, Tamura, *Physical Review Research*, 2, 013319 (2020).

11:00 AM EN03.17.02

Late News: Near-field Heat Transfer by Quantum Mechanics [Thomas Prevenslik](#); QED Radiations, Germany

Near-field heat radiative transfer (NFRHT) is based on the classical Fluctuation Dissipation Theorem that requires the heat produced in macroscopic bodies upon absorbing EM radiation creates temperature fluctuations that is reciprocated by temperature fluctuations producing EM radiation. But NFRHT in nanoscale gaps between hot and cold bodies is governed by quantum mechanics (QM) and not classical physics. Indeed, the Planck law precludes temperature fluctuations in nanoscale gaps upon absorbing heat. However, all known NFRHT theories are based on the difference of surface temperatures of nanoscale gaps. In effect, the Planck law requires theories of NFRHT that do not depend on temperature which means all known NFRHT theories are invalid.

One such temperature independent NFRHT theory is simple QED based on the Planck law that conserves heat by creating temperature independent EM standing or travelling waves across the evacuated nanoscale gaps. But the heat requires EM confinement across the gap to a half-wavelength having the dimension d of the gap. In simple QED, the EM confinement is provided by the momenta of the thermal kT energy of atoms participating in the heat flow between hot and cold bodies, the hot and cold momenta directed toward their respective gap surfaces because of the thermal gradient with gap surface temperatures at absolute zero, the gap surface temperatures taken at absolute zero because the Planck law requires Brownian motion to cease everywhere in the nanoscale gap. Under EM confinement by opposing thermal momenta, heat flows if the hot momentum exceeds its cold counterpart

Simple QED highlights the stark difference between QM and classical physics illustrated by the emission of bright white-light from a Joule heated single graphene layer (0.337 nm) over a nanoscale trench reported in the literature. The application of NFRHT to the nanoscale trench is difficult to implement as the Joule heat from the graphene layer into the nanoscale trench is not known. Instead, the Fourier equation was applied to the graphene layer assuming Joule heating produces electron temperatures of 2800 K giving graphene temperatures near 2000 K. But bright-white light may require higher temperatures, say up to 5000 K.

In contrast, simple QED argues the graphene remains at ambient temperature. Instead, 1.8 keV soft X-rays are produced across the graphene thickness that fluoresce down to about 200 eV, the heat of which is either lost to the surroundings or enters the trench, the latter by simple QED creating IR waves standing in the trench, the overtones of the IR producing the observed bright white-light absent high temperatures. Consistent with simple QED, the graphene does not acquire 2800 K electron temperatures evidenced by the observation of white-light at 10 K. Indeed, there is a stark difference between QM and classical physics and should be expected whenever classical physics including NFRHT is used to explain observations at the nanoscale.

11:15 AM EN03.17.03

Efficient Heat Shielding of Steel with Multilayer Nanocomposite Thin Film [Carolyn T. Long](#), Ruisong Wang, Charles Shoalmire, Dion Antao, Patrick Shamberger and Jaime C. Grunlan; Texas A&M University, United States

In an effort to protect metal substrates from extreme heat, polymer-clay multilayer thin films are studied as expendable thermal barrier coatings. Nanocomposite films with a thickness ranging from 2 to 35 μm were deposited on steel plates and exposed to the flame from a butane torch. The 35 μm coating, composed of 14 deposited bilayers of tris(hydroxymethyl)aminomethane (THAM)-buffered polyethylenimine (PEI) and vermiculite clay (VMT), decreased the maximum temperature observed on the back side of a 0.32 cm thick steel plate by over 100 $^{\circ}\text{C}$ when heated with a butane torch. Upon exposure to high temperature, the polymer and amine salt undergo pyrolysis and intumesce, subsequently forming a char and blowing gas. The char encases the nanoclay platelets, and a ceramic bubble is formed. The macro-scale bubble, in tandem with the nanocomposite coating properties, increases resistance to heat transfer into the underlying metal substrate. This heat shielding behavior occurs through radiative effects and low aggregate through-plane conductivity resulting from multilayer nanodomains and intumesced porosity (i.e., conduction through the gas as the film expands to form a ceramic bubble). These relatively thin and lightweight films could be used to protect important metal parts (in automobiles, aircraft, etc.) from fire-related damage or other types of transient high-temperature situations.

11:30 AM *EN03.17.04

Enhanced Evaporation via Nanoengineered Materials for Solar Thermal Sterilization and Desalination [Lin Zhao](#)¹, [Lenan Zhang](#)¹, [Zhenyuan Xu](#)^{1,2}, [Arny Leroy](#)¹, [Elise Strobach](#)¹, [Bikram Bhatia](#)¹, [Sungwoo Yang](#)¹, [Thomas Cooper](#)¹, [Lee Weinstein](#)¹, [Omar Labban](#)¹, [John Lienhard](#)¹, [Anish Modi](#)³, [Shireesh Kedare](#)³, [Ruzhu Wang](#)², [Gang Chen](#)¹ and [Evelyn N. Wang](#)¹; ¹Massachusetts Institute of Technology, United States; ²Shanghai Jiao Tong University, China; ³IIT Bombay, India

Enhancing evaporation processes via nanoengineered materials design offers unique opportunities for a range of energy applications. In this work, we show our ability to enhance evaporation processes and new device designs with various engineered materials sets. First, we show how we achieve a passive high-temperature solar steam generator for medical sterilization. The high performance leverages optimized ultra-transparent silica aerogel to achieve efficient thermal concentration to locally increase the heat flux and temperature. We show nearly a 2x higher energy efficiency compared to past work, and successful sterilization in field tests in Mumbai, India. Next, we show novel architectures that take advantage of thermal localization and multiple stages for

vaporization enthalpy recycling to achieve ultra-high efficiency passive solar desalination. With a ten-stage design with scalable and low-cost materials, a solar-to-vapor conversion efficiency of 385% and total production rate of 5.78 Lm⁻² h⁻¹ under one-sun illumination was achieved. We also present techno-economic analysis that highlights the balance between water production, reliability, and cost. The works presented here promises new opportunities for the development efficient solar thermal systems in energy conversion, storage, and transport, as well as water applications.

SESSION EN03.18: Thermal Management of Electronics and Batteries

Session Chair: Yanfei Xu

Tuesday Afternoon, December 7, 2021

EN03-Virtual

1:00 PM *EN03.18.01

Materials and Manufacturing: Keys to Developing Wide Bandgap Power Electronic Devices [Samuel Graham](#)^{1,2}; ¹Georgia Institute of Technology, United States; ²University of Maryland, United States

Wide bandgap electronics are currently under development due to their potential to create future power electronics. The growth of materials based on gallium nitride and more recently gallium oxide is expected to help create technological advancements that may yield a range of devices that operate with more efficiency, higher operational frequency, and smaller form factors.

In this talk, we will discuss a range of materials and device architectures that are being developed to enable efficient heat dissipation from both GaN and Ga₂O₃ devices starting at the device level. We will discuss materials integration issues that will enable lower thermal resistance device architectures to assist with thermal management strategies. This will include bonding of heterogeneous layers as well as direct growth methods. Finally, we will discuss new aspects of materials processing and properties to create a low CTE mismatch cooled power substrate for packaging power devices. At each step, we will show how considerations for materials development and methods for scalable manufacturing are necessary to help transition these advancements to applications.

1:30 PM EN03.18.02

Monolithic Integration of Copper with Electronics for High Efficiency Cooling [Tarek Gebrael](#)¹, [Jiaqi Li](#)¹, [Joseph Schaadt](#)², [Logan Horowitz](#)², [Robert Pilawa-Podgurski](#)² and [Nenad Miljkovic](#)¹; ¹University of Illinois at Urbana Champaign, United States; ²University of California, Berkeley, United States

Power densification of modern electronics is greatly shaped by emerging thermal management technologies. Heat spreaders represent a thermal routing technique implemented to reduce thermal resistance and limit temperature variations. Here, we demonstrate the monolithic integration of copper (Cu) conformal coatings directly on electronics to serve as heat spreaders and temperature stabilizers. We developed a fabrication recipe to electrically insulate the electronics with Parylene C and coat them with the Cu heat spreaders, demonstrating better proximity to heat generating elements, removal of thermal interface materials, and enhanced cooling performance compared to standard thermal components. Our results show that 8 μm thick Parylene C can handle up to 600 V, and that the Cu coatings provide device-to-ambient specific thermal resistance as low as 2.5 (cm².K)/W in quiescent air and 0.8 (cm².K)/W in quiescent water, with time constants of 110 s in air and 5.61 s in water. Our cooling technology has the potential to enable the continued miniaturization of electronics, potentially extending Moore's law and greatly reducing the energy consumption used for electronics cooling. Furthermore, by removing the need for large external heat sinks, our approach should enable the realization of very compact and highly power dense co-designed power converters.

1:45 PM EN03.18.03

Boron Nitride Nanotube Coatings for Thermal Management of Printed Silver Inks on Temperature Sensitive Substrates [Kaitlin Wagner](#)^{1,2}, [Chantal Paquet](#)², [Yadienka Martinez-Rubi](#)², [Marc Genest](#)², [Jingwen Guan](#)², [Katie Sampson](#)², [Keun Su Kim](#)², [Arnold Kell](#)², [Patrick Malenfant](#)² and [Benoit Lessard](#)¹; ¹University of Ottawa, Canada; ²National Research Council, Canada

One major challenge in printing conductive metal inks onto heat-sensitive plastic substrates is the adverse effects of high temperatures experienced during the sintering process and during operation as a result of joule heating, which leads to substrate damage and current carrying capacity limitations. To combat this issue, incorporating an electrically insulating film interposed between the substrate and the printed feature can aid in spreading heat laterally away from the substrate-feature interface without sacrificing conductive performance or rigidity of the plastic substrate. Boron nitride nanotubes (BNNTs) in particular exhibit relatively high thermal conductivity and impressive thermal stability, and therefore present a promising platform to minimize thermal degradation of the printed feature and the substrate over time.

We report on a highly transparent BNNT heat-spreading interlayer for thermal management of silver components screen-printed onto polyethylene terephthalate (PET) substrates. Printed features of varying widths are investigated to optimize the transparency and conductivity of the resulting design. Upon exposure to increasing photonic energies, the BNNT layer actively dissipates the heat through the tube network, resulting in morphological improvements in both the feature and the substrate and reducing sheet resistance by up to 200%. Thermal imaging demonstrates a reduction in localized areas of excessive heat accumulation, achieving greater uniformity in heat distribution throughout the printed feature upon applied current. In summary, the BNNT thin film provides a simple approach to shield the substrate from deformation and damage at high temperatures while simultaneously improving electrical performance of the printed features and structural integrity of the substrate.

2:00 PM *EN03.18.04

Thermal Considerations for High Density Fast Charging Lithium-Ion Batteries [Ravi Prasher](#)^{1,2}; ¹Lawrence Berkeley National Laboratory, United States; ²University of California, Berkeley, United States

Traditionally it has been assumed that battery thermal management systems should be designed to maintain the battery temperature around room temperature. That is not always true as Lithium-ion battery (LIB) R&D is pivoting towards the development of high energy density and fast charging batteries. As the energy density and charge rate increases, the optimal battery temperature can shift to be higher than room temperature. To improve the temperature uniformity and avoid excessive internal temperature rise, heat transfer inside the battery needs to be enhanced, and reducing the thermal contact resistance between the electrodes and separator can significantly increase the effective thermal conductivity of batteries. In this talk various challenges and latest developments related to heat generation, thermal transport and properties of LIBs will be discussed. The importance of heat of mixing due to ion diffusion during fast charging will be also highlighted. Finally *operando* measurement of Lithium concentration inhomogeneity and plating under fast charging conditions using thermal wave sensing will be presented.

2:30 PM EN03.18.05

Late News: High Thermal Conductivity Continuous Fiber Reinforced Alkali-Halides for Cryogenic Electrical Isolation and Mechanical Reinforcement Christopher Kovacs¹, Timothy Haugan², Michael Susner², Jacob Adams³, Emanuela Barzi⁴, Daniele Turrioni³, Devin Grant⁵ and Leonard Jung⁶; ¹Hyper Tech Research Inc., United States; ²Air Force Research Laboratory, United States; ³Massachusetts Institute of Technology, United States; ⁴Fermi National Accelerator Laboratory, United States; ⁵Central State University, United States; ⁶Purdue University, United States

A novel ceramic-ceramic fiber composite for use at cryogenic temperatures is presented in this research. Thermal properties, mechanical properties, and electrical properties are compared to more standard polymeric-ceramic fiber composites such as G-10 and CTD-101K/S-glass. It is shown that this composite can function in certain areas to reduce thermal impedance, while retaining sufficient mechanical properties and electrical isolation capability. Multiphysics simulations are used to predict improvements to applications such as cryogenic motors and magnets. Processing routes will be presented to incorporate this composite into windings.

2:45 PM EN03.18.06

Heat Transfer Between Metallic Nanofilaments and its Impact on the Electric Conductivity of Copper Nanofilament Marius K. Orłowski; Virginia Tech, United States

When a resistive random access memory (RRAM) memory crossbar array is switched repeatedly, a considerable amount of Joule heat is dissipated in the cells of the array [1,2]. A conductive nanofilament (CF) is heated in one cell by switching the cell frequently on and off and the electrical conductance of the CFs of the neighboring cells is measured. The neighboring cells have been set to a conductive low resistance state (LRS). The CF-to-CF heat transfer comprehends nanoscale heat transport from CF to the mesoscopic electrode and from mesoscopic electrode to another CF. When, under such heating conditions the electric properties of the neighboring cells are tested immediately after the heating of the heated cell has ended, we find that in most cases the neighboring cells are in high resistance state (HRS) despite having been set to an LRS state prior to the heating. Thus remote heating ruptures the CFs, i.e. erases the neighboring cells. The probing of the neighboring cell is done at voltages much smaller than the minimum set voltage. The key findings are: (i) only for robust CFs (low resistance R_{on}) formed at high compliance current $I_{cc} > 0.2\text{mA}$ we find that the probed cell remains in an LRS state just after the heating of the heated cell. In most cases, we find slightly degraded resistance R_{on} compared with the original R_{on} value. (ii) For all probed cells that have been set at $I_{cc} < 0.2\text{ mA}$ (high resistance R_{on}), we find that the probed cell is in HRS immediately after completion of the heating of cell. However, when those cells are probed again, after 2 min or longer, we find the cell does no longer persist in HRS but returns of its own accord back to the original LRS state, with R_{on} in most cases the same as the original R_{on} . Thus, during the heat dissipation period, the CF in the probed cell spontaneously recovers and restores itself to the original R_{on} value to which they have been set prior to the heating. (iii) In a few cases we managed to capture the time evolution of the spontaneous restoration of the CF to LRS demonstrating the transient, non-equilibrium behavior of the heat transfer phenomenon. The heat dissipation time constant for our devices is of the order of 15s and depends strongly on the thermal conductivity of the metal electrodes. This behavior can be explained in terms of 3D resistor network with a unit resistance $R_0 = 1/G_0$ with $G_0 = (2e^2/h) \times t$, where t is the electron tunneling probability from Cu atom to Cu atom of the CF and depends on the distance L between the two Cu atoms, thus $t \sim \exp(-2kL)$ where the wave vector k depends on the barrier height between the two Cu atoms. The truncated pyramidal resistor 3D network describes accurately the resistance of the CF as a function of the number of surface Cu atoms at the vertex of the pyramid. We demonstrate experimentally the presence of the quantum conductance nature of the filament's resistance for this kind of Cu nanofilaments. The experiments point to a tight interaction between phonons of the oscillating Cu atoms and the electron tunneling rate between the Cu atoms. Harmonic oscillator model argues that the tunneling probability t is proportional to $\exp(-K\sqrt{T})$ with a constant $K > 0$, implying that t decreases exponentially with increasing temperature and thus explains the transient effect of the heat dissipation. As shown elsewhere the local temperature T in a CF can be as high as 1500K [3]. We also show that the same heat transfer effects are substantially mitigated when the thermal conductivity of the electrodes is substantially increased. With modified electrodes replacing a 150nm thick Cu electrode by a 250nm thick and 50 nm thick Pt electrode by a Pt(50nm)/Cu(200nm) composite electrode the time dissipation constant can be reduced to less than 1 second.

M.Al-Mamun, M.Orłowski, , Electronics & Photonics 4(48), 2593-2600, 2019

M.Al-Mamun, M.Orłowski, Electronics, 9. 127, p.2-11, 2020

[3] M. Al Mamun and M. Orłowski, Scientific Reports, 11:7413, 2021

SESSION EN03.19: Thermoelectrics II

Session Chair: Bo Sun

Wednesday Morning, December 8, 2021

EN03-Virtual

8:00 AM *EN03.19.01

Generative Design of Thermoelectric Materials Kedar Hippalgaonkar^{1,2}; ¹Nanyang Technological University, Singapore; ²Institute of Materials Research and Engineering, Singapore

Machine Learning (ML) and feature engineering have had success in predicting the thermoelectric (TE) performance of inorganic materials. Generally, there are two steps: the first involves featurizing the materials into numerical inputs in machine-readable format. The second step is the use of regression models to predict their TE performance, typically the powerfactor given by $S^2\sigma$. We have used this methodology to screen for potential undiscovered materials using a known database of compounds; we found that this ML screening process self-discovers Half-Heuslers as good materials with no prior knowledge. In addition, going beyond screening, there are a wide range of unexplored inorganics, which are not in any existing databases. I will describe our use of generative models, similar to generating new images learning from existing ones, that are expected to have high TE performance¹. Finally, I will talk about our efforts at synthesizing some of these new predicted compounds and describe our progress in defining synthesizability of such new materials. ¹<https://arxiv.org/abs/2005.07609>

8:30 AM EN03.19.02

High-Throughput Characterization of Thermoelectric Cu₂P in Thin-Film Form Andrea Crovetto^{1,2}, Danny Kojda¹, Klaus Habicht¹, Thomas Unold¹ and Andriy Zakutayev²; ¹Helmholtz-Zentrum Berlin, Germany; ²National Renewable Energy Laboratory, United States

Certain metal phosphides have recently been proposed as potential thermoelectric materials [1]. In particular, the simple binary Cu₂P possesses multi-valley degeneracy in the valence band and low-frequency acoustic phonon modes. These features are expected to enhance its electrical properties and lower its thermal conductivity respectively.

As CuP₂ has not been experimentally studied as a thermoelectric material yet, we have synthesized CuP₂ thin films for rapid thermoelectric characterization on specialized chips. The films are grown by reactive sputtering of a Cu target in a PH₃-containing atmosphere under a high phosphorus chemical potential.

Thermoelectric characterization is performed on CuP₂ films with different Cu/P ratios and thermal treatments. The films are deposited on multi-purpose chips for simultaneous characterization of electrical conductivity, Seebeck coefficient, and thermal conductivity as a function of temperature. We generally find high Seebeck coefficients, low thermal conductivities, and p-type conductivity. The electrical conductivity is rather low, owing to a low hole concentration in the films without external doping. We suggest that suitable p-type dopants should be found to increase the hole concentration. If these efforts are successful, CuP₂ would be a highly attractive earth-abundant thermoelectric material.

[1] Pöhls et al., J. Mater. Chem. C 5, 12441 (2017).

8:45 AM EN03.19.04

Native Defect Chemistry and Extrinsic Dopability Limits of Binary Sn-Based Chalcogenides Ferdaushi A. Bipasha^{1,2}, Lidia C. Gomes² and Elif Ertekin¹; ¹University of Illinois at Urbana Champaign, United States; ²National Centre for Supercomputing Applications, United States

In this work, we assess the full range of n-type and p-type dopability achievable in the group IV-VI binary chalcogenides with A1B1 stoichiometry, well-known to be excellent thermoelectric materials. Despite being well-studied, they are more commonly observed as p-type thermoelectric materials while n-type performance is more rarely reported in the literature. Yet, n-type thermoelectric performance is expected to be nearly as good as (SnSe, SnTe) and even better (SnS) than p-type, which has driven recent experimental interest in realizing n-type material. Therefore, we use first-principles methods to assess the limits of dopability in three Sn-based chalcogenides, SnS, SnSe, and SnTe, and establish whether there is room for improvement in reported n-type performance. By analysis of phase stability and defect chemistry, we assess the full range of dopability ranging from maximum p-type to maximum n-type that is possible in these compounds. While SnTe is degenerately p-type in all environments, we find that SnS and SnSe exhibit windows for both p-type and n-type dopability in the proper growth environment. We consider Bi and Br as candidate n-type dopants. This reveals that n-type carrier concentrations of 5(10¹⁷) cm⁻³ and 1.3(10¹⁸) cm⁻³ for SnS and SnSe respectively are achievable, which are in good agreement with experimentally reported concentrations. The differences in the dopability across all three compounds are attributed to differences in band edge positions and the allowable ranges of chemical potentials.

SESSION EN03.20: Thermal Measurement Techniques

Session Chair: Bo Sun

Wednesday Morning, December 8, 2021

EN03-Virtual

10:30 AM *EN03.20.01

Local Study of the Evaporation Mass Flux in a Thin Liquid Film Using Thermoreflectance Experiments and Numerical Methods Xiaoman Wang, Seyed-Arman Ghaffari-Zadeh, Alan McGaughey and Jonathan A. Malen; Carnegie Mellon University, United States

Thin film evaporation is important in the design of heat pipes, desalination, lubrication, air conditioning, and medical devices. Existing theories suggest that with smaller film thickness, the local evaporation mass flux will increase due in part to an increased interfacial temperature that results from lower conduction resistance in the liquid. However, this mass flux will sharply decrease to zero as the film gets even thinner due to the increased interface forces that inhibit the escape of interfacial vapor molecules.

In this project, we present the first experimental effort to locally measure the evaporation mass flux in a liquid meniscus. The microscale lateral extent of the meniscus and sub-Kelvin liquid-vapor temperature differences (superheats) challenge conventional thermometry. Here, Frequency domain thermoreflectance (FDTR), a non-contact laser-based method with a lateral resolution of micrometers, is used. A non-monotonic experimental signal change is observed as a function of position in the thin film portion of the meniscus, where a high evaporation heat flux is expected. This experimental technique has been hitherto widely employed with micron-scale lateral resolution in thin solid films, but not when evaporation is present. To extract the evaporation heat transfer coefficient in the meniscus region from the obtained signal, we modify the analytical solution to the heat diffusion equation to account for the phase change. This modification provides a new paradigm for investigating heat flux discontinuity in thermal models. Furthermore, to account for the thickness variation in the meniscus we also analyze the data using a finite element simulation performed with ANSYS. The ANSYS simulations are first validated against the modified FDTR equation for uniform liquid thicknesses. The ANSYS model is also able to capture account for the variation in evaporative heat transfer coefficient that occurs within the region interrogated by the 3 μm laser spot. A machine learning framework that uses neural networks is then used to find the optimal combination of meniscus thickness and evaporative heat transfer coefficient distribution to match the ANSYS model to the experimental data.

11:00 AM EN03.20.02

Heat Transfer Across Au/thiol Heterojunctions with Atomic Spatial Resolution Yee Kan Koh, Hongkun Li and Yuexiang Yan; National University of Singapore, Singapore

Heat transfer across organic-inorganic heterojunctions and solid/liquid interfaces, is crucial for applications such as photothermal cancer therapy and flexible hybrid thermoelectric materials. However, fundamental knowledge of heat transport at atomic scale is still limited, due to challenges to experimentally probe heat transport with an atomic spatial resolution. In this talk, we will discuss our recent results to experimentally measure the heat transfer across the Au/thiol heterojunctions. We integrate two pump-probe techniques, the picosecond transient absorption and time-resolved Raman spectroscopy, to concurrently monitor heating and cooling of gold nanorods and bonds in the conjugated ligands, with a sub-picosecond time resolution and an atomic spatial resolution. We find that bonds in the conjugated ligands are heated almost instantaneously and reach a peak temperature within ~ 1 ps after the nanorods were heated by the laser pulse. We attribute this fast heating to direct heating of bond by the non-equilibrium electrons in gold nanorods, due to the remote coupling across the Au-thiol heterojunction. Our analysis suggests that the remote coupling could contribute substantially to heat transport across Au-thiol heterojunctions.

11:15 AM EN03.20.03

Optimization of AuGe Thin Films for High-Sensitivity Thermometry Ethan A. Scott, Sueli Skinner Ramos and Tom Harris; Sandia National Laboratories, United States

Resistive thermometer materials enable transduction of temperature to a measurable electrical signal. Detection of this signal is limited by the material's temperature coefficient of resistance (TCR), the degree to which its fractional resistance changes in response to a change in temperature. AuGe has been demonstrated to yield a high TCR at low temperatures, which lends itself towards applications in cryogenic thermometry. Here, we investigate the role of annealing temperature and film thickness on the TCR of $\text{Au}_{0.17}\text{Ge}_{0.83}$, a composition of particular interest. Temperature-dependent electrical resistance measurements spanning 10 K to 300 K provide insight into the performance of the film, demonstrating orders-of-magnitude enhancement in sensitivity over commonly used materials such as pure metallic platinum. Furthermore, we observe that a movement towards thinner films provides additional enhancement in TCR with lower required annealing temperatures.

This work was performed, in part, at the Center for Integrated Nanotechnologies, an Office of Science User Facility operated for the U.S. Department of Energy (DOE) Office of Science. A portion of this work was supported by the Laboratory Directed Research and Development program at Sandia National Laboratories. Sandia National Laboratories is a multimission laboratory managed and operated by National Technology & Engineering Solutions of Sandia, LLC, a wholly owned subsidiary of Honeywell International Inc., for the U.S. Department of Energy's National Nuclear Security Administration under contract DE-NA0003525.

11:30 AM *EN03.20.04

Non-Contact Thermal Metrologies Using SEM and Optical Microscopy [Chris Dames](#)^{1,2}; ¹University of California, Berkeley, United States; ²Lawrence Berkeley National Laboratory, United States

I will summarize several collaborative efforts to develop new non-contact methods for heating, thermometry, and thermal property measurements. The main focus will be on nanoscale techniques using SEM. The incident electron beam can serve as a point heat source, and in certain conditions the local sample temperature can also be deduced from the electrons leaving the sample. I also will briefly introduce an all-optical "structured illumination, thermal imaging" (SI-TI) technique which: can tolerate rough, porous, and/or scratched samples; enables parallel measurement of multiple samples in a single field of view; and uses software-controllable heating patterns which can be tuned to extract directional properties like the thermal conductivity tensor.

12:00 PM EN03.20.05

Aerosol Jet Printed 3 Omega Sensors for Thermal Conductivity Measurement [Nicholas Kempf](#) and Yanliang Zhang; University of Notre Dame, United States

The 3 omega (3ω) method is a trusted technique for measuring thermal conductivity – a fundamental material property of critical importance in a broad range of applications. However, traditional 3ω sensor processing requires some form of physical vapor deposition, such as metal evaporation or sputtering. Such 3ω sensor deposition techniques limit the materials and sample sizes applicable to the 3ω method. This work demonstrates an aerosol jet printing method to directly print silver 3ω sensors that yield accurate temperature-dependent measurement up to 300°C on materials with thermal conductivity ranging from 13 to 150 W/m-K. Thermal conductivity measurement with 3ω sensors conventionally sintered at 300°C agrees to independent laser flash measurement within 4% from room temperature to 150°C. Beyond 150°C, printed sensors display thermally activated tunneling effects that introduce significant errors in 3ω measurements. An unconventional rapid high-temperature sintering method is shown to eliminate the tunneling effects, producing sensors that agree within 3% of laser flash measurements from room temperature to 300°C. The rapid sintering profiles also reduced the sensor-substrate thermal boundary resistance of the printed sensors by as much as 88%. The direct printing of 3ω sensors creates opportunities for measurement of thermal transport properties in applications previously inapplicable to the 3ω method while the ultrafast sintering technique to eliminate tunneling effects and significantly reduce the sensor-substrate thermal contact resistance has implications for many types of aerosol jet printed sensors.

12:15 PM EN03.20.06

Which Material Property Should be Reconstructed from Thermal Spectroscopy Experiments? [Mojtaba Forghani](#)¹ and Nicolas Hadjicostantinou²; ¹Stanford University, United States; ²Massachusetts Institute of Technology, United States

Phonon transport properties, such as phonon relaxation-time and free path distributions, play an essential role in the study of nanoscale solid-state heat transfer. Reliable descriptions of these properties are required for modeling heat transport at the kinetic level, which becomes necessary due to the failure of Fourier-based analyses at micron/sub-micron scales. Applications of practical interest include improved heat management in nanoelectronic circuits and devices, microelectromechanical sensors, and nano-structured materials for improved thermoelectric conversion efficiency.

Theoretical approaches such as density functional theory (DFT) have been widely used to calculate phonon transport properties, but have yet to gain widespread acceptance, in part due to their inability to consistently reproduce experimental observations. An alternative class of approaches relies on extracting material constitutive information from thermal spectroscopy experiments. However, the analysis of thermal spectroscopy data remains a challenging task. One such analysis technique seeks to extract the cumulative distribution function of thermal conductivity as a function of the phonon free path, $F(\Lambda)$, from the experimentally measured thermal responses using the "effective heat conductivity" concept. This approach attempts to match the experimentally measured response to solutions of the heat conduction equation with the thermal conductivity (or thermal diffusivity) treated as an adjustable, "effective", property. Unfortunately, as it was discussed previously (see [Physical Review B 94, 155439 (2016)] and [Physical Review B 97, 195440 (2018)]), among many other approximations, this procedure implicitly assumes that heat transport is Fourier-like, which is only justified under fairly restrictive conditions of late times and large scales that are not always satisfied under experimental conditions.

In this work, we discuss some fundamental issues associated with the analysis of thermal spectroscopy experiments, such as the uniqueness of reconstructed quantities (e.g., $F(\Lambda)$), as well as their ability to reproduce the experimental results (e.g., temperature profiles). In particular, we show that approaches that are based on reconstruction of $F(\Lambda)$ (as a means to defining "effective heat conductivities") fail to guarantee a unique thermal response. This can be understood by noting that it is the relaxation-time and *not* $F(\Lambda)$ which appears as a primary material-parameter input to the Boltzmann transport equation (BTE). Specifically, we show that the same $F(\Lambda)$ can be arrived at from multiple relaxation-time functions, which, in general, will correspond to multiple thermal responses. This observation seriously questions the reliability of approaches which use $F(\Lambda)$ in the reconstruction. This implies that in the context of thermal transport at the nanoscale within the Boltzmann relaxation-time approximation framework, the "fundamental" property that should be reconstructed from the thermal spectroscopy experiments is the frequency-dependent relaxation-times function (provided group velocities are known), since it explicitly appears in the BTE as the input material property.

In response to the failure of effective heat conductivity-based methods, we developed and extensively validated (on both synthetically generated and experimentally measured data) an optimization-based methodology for directly reconstructing frequency-dependent phonon relaxation-times from thermal spectroscopy data [Physical Review B 94, 155439 (2016); Physical Review B 97, 195440 (2018); Applied Physics Letters 114, 026103 (2019)]. Extensive validation, including global optimization studies, shows that this formulation provides numerically unique solutions and is robust to the noise in the measurement.

SYMPOSIUM EN04

Silicon for Photovoltaics
November 29 - December 7, 2021

Symposium Organizers

James Bullock, The University of Melbourne
Kaining Ding, Forschungszentrum Jülich GmbH
Ivan Gordon, imec
Emily Warren, National Renewable Energy Laboratory

* Invited Paper

SESSION Tutorial EN04: The Physics and Engineering of Crystalline Silicon Photo-Voltaic Conversion, Technology and Systems
Session Chairs: Kaining Ding and Arno Smets
Monday Afternoon, November 29, 2021
Virtual

1:30 PM

The Physics and Engineering of Crystalline Silicon Photo-Voltaic Conversion, Technology and Systems Arno Smets; Delft University of Technology, Netherlands

All major future energy scenarios forecast a key role for photovoltaic solar energy. The crystalline silicon PV technology will dominate the future residential and large-scale utility PV applications. The learning objective of this comprehensive tutorial are 1) understanding the fundamental principles of photovoltaic energy conversions; 2) understanding of the physics and chemistry behind materials and interface engineering for crystalline silicon PV technology, 3) understanding of the design principles of the various silicon PV device architectures and module concepts and 4) the understanding of the role of a circular value chain of crystalline silicon photovoltaics in the energy transition towards a 100% renewable energy future.

The Fundamental Principles of Photovoltaic Energy Conversion

The key factor in getting more efficient and cheaper solar energy panels is the advance in the development of photovoltaic cells. In part 1 you will learn how photovoltaic cells convert solar energy into useable electricity. You will also discover how to tackle potential loss mechanisms in solar cells. By understanding the semiconductor physics and optics involved, you will develop in-depth knowledge of how a photovoltaic cell works under different conditions.

Materials and Interface Engineering for Crystalline Silicon PV Technology

The nature of the materials and interfaces for crystalline silicon PV will be presented. In Part 2 you will gain the latest insights how impurities, doping, crystal orientation, interstitials, and defects affect the optical and electrical performance of the novel materials and interfaces. A special focus will be on new materials, processing methods and innovative interface engineering (chemical and electrical passivation) for passivating contacts.

Introduction in to Silicon PV Device Architectures and Module Concepts

In part 3 you will be introduced to the recent advances in the development of the various crystalline silicon device architectures. You will use the design rules, to reduce the optical and electrical losses as discussed in Part 1, to understand the underlying principles of Al Back Surface Field solar cells, Partial Back Contact (PERC) solar cells, heterojunction junction solar cells (HJ/HIT), interdigitated back contact (IBC), tunnel oxide passivated contact (TOPCon), bifacial solar cells and hybrid multi-junction PV concepts. In addition, you will be introduced to the design rules to manufacture PV modules using PV cells. The various modules architectures and the recent advances will be reviewed.

The Role of Circular Value Chain of Crystalline Silicon Photovoltaics in The Energy Transition Towards a 100% Renewable Energy Future

All major future energy scenarios forecast a key role for photovoltaic solar energy. In part 4 the important role of crystalline silicon in future residential and large-scale utility PV applications will be discussed. You will be introduced to new metrics -beyond that of module efficiencies- that will be important for the successful upscaling of the PV technologies in the coming decades.

SESSION EN04.01: PV Systems, Light Management and Surface Passivation
Session Chair: Brett Kamino
Wednesday Afternoon, December 1, 2021
Hynes, Level 3, Room 305

1:30 PM *EN04.01.01

New Tools for Modeling and Metrology of Silicon Module Degradation Modes Rishi Kumar¹, Erick Martinez-Loran¹, Guillaume von Gastrow¹, Jacob Clenney², April Jeffries², Nicholas Theut², Tala Sidawi¹, Rico Meier², Mariana Bertoni² and David P. Fenning¹; ¹University of California, San Diego, United States; ²Arizona State University, United States

In this talk, I will share our recent findings regarding silicon module durability arising from tools we have developed to study potential induced degradation (PID) and the effects of moisture. PID has re-emerged as an alarming reliability issue in silicon PV. Sodium is known to be correlated with PID of the shunting type, but a quantitative description of its kinetics in PV modules has been lacking. I will describe a finite element method model of PID we have developed that relies only on parameterization of Na kinetics within the module stack. This parameterization can be directly correlated with the bill of materials. We use a series of bottom-up and top-down experimental approaches to validate the model, including a new method to measure the kinetics of mobile ion migration through dielectric layers. Ultimately, we provide a sensitivity analysis of PID rates on the bill of materials that can serve as a guide toward robust modules.

The second part of the talk will focus on moisture impacts. Moisture is implicated in many modes of performance degradation in silicon PV, but it has proved difficult to assess the water content within modules to determine its direct role in degradation reactions. We have developed a short-wave IR optical Water Reflectometry Detection (WaRD) technique to quantify moisture levels within the module. We combine this moisture measurement with correlative luminescence imaging to track water content and cell performance at millimeter resolution over 2500 hours of accelerated testing at multiple levels of humidity and temperature. The approach reveals dominant modes of power loss with distinct and rather counterintuitive moisture sensitivities in glass-glass vs. glass-backsheet packages. Metallization interrupts in fingers occur earliest in dry conditions and are delayed in backsheet modules at higher humidity, suggestive of plasticization of the backsheet. Background series resistance sharply increases in backsheet modules at high humidity, by a mechanism not seen in glass-glass modules. Overall, we dissect the losses over time to attribute the marginal power loss from each mode as a function of temperature, humidity, and package type.

These new tools for durability science should aid in understanding the progression and severity of module degradation modes, the development of targeted accelerated tests, and ultimately new technologies that extend silicon durability.

2:00 PM EN04.01.02

Late News: Circularity Impacts of Waste-Management Scenarios for Photovoltaics Acadia Hegedus¹, Silvana Ovaitt², Julien Walzberg², Heather Mirlitz^{2,3} and Teresa Barnes²; ¹Middlebury College, United States; ²National Renewable Energy Laboratory, United States; ³Colorado School of Mines, United States

Solar photovoltaic (PV) technologies are at the forefront of the clean energy transition, with at least 1 TW of PV installations projected by 2050. There will be a cumulative demand for 56 million metric tonnes of virgin material by 2050, considering future PV technology evolution and current end-of-life (EoL) management practices. 17 million metric tonnes of waste will need to be managed as PV modules have a lifetime of around 30 years. To mitigate negative impacts and ensure the increased solar energy deployment is sustainable, a circular economy (CE) for PV must be implemented. A quantitative analysis of waste-management interventions is needed to identify which actions should be taken to promote a CE for crystalline-Silicon (c-Si) PV while integrating future technology improvements and social factors. Here, we use a novel, dynamic, Python-based tool called PV ICE (PV in the Circular Economy), created by researchers at the National Renewable Energy Laboratory (NREL), to quantify the future mass flow impacts of ten waste-management interventions. The interventions and corresponding EoL pathway rates come from Walzberg et al.'s agent-based model (ABM). This ABM considered social factors to predict human behavior and decision-making surrounding PV EoL. Progressive simulations were run using PV ICE to explore the impact of improving circular EoL pathways, recycling efficiencies, and module reliability. The results suggest that a certain intervention, *Landfill ban*, can drastically reduce cumulative PV EoL waste to only 2 metric tonnes by 2050. Improving module reliability (*Improved lifetime*) is shown to have a powerful impact on maintaining installed capacity, increasing from 0.77 TW to 0.95 TW by 2050. When seeking to maintain a target capacity, lower quality modules can demand up to 16% more virgin materials and produce 200% more waste, pointing to the importance of module reliability for circularity. Further research should widen the scope of the intervention analysis to include energy and cost considerations.

2:15 PM EN04.01.03

Photonic Mirror Light Management in Bifacial Photovoltaics Bryan Cote¹, Ian M. Slauch¹, Timothy J. Silverman², Michael Deceglie² and Vivian E. Ferry¹; ¹University of Minnesota Twin Cities, United States; ²National Renewable Energy Laboratory, United States

Bifacial photovoltaics are expected to gain significant market share over the next decade due to the reduced levelized cost of energy. However, the thermal performance of bifacial modules is not yet well understood, nor have thermal management strategies been developed for this module configuration. Elevated operating temperatures in Si photovoltaics led to both diminished efficiency and accelerated module degradation.

A significant percentage of this waste heat is generated by sub-bandgap parasitic absorption within the module. Because of this, spectrally selective mirrors that act as above bandgap antireflection coatings and sub-bandgap light rejectors are a promising photon management strategy for reducing the operating temperature of monofacial photovoltaics. However, it remains an open question whether bifacial photovoltaics that possess partial sub-bandgap transparency thermally benefit from this light management strategy. Here we use rigorous finite-element simulations to study the performance benefits of spectrally-selective mirrors on bifacial modules.

The optical properties of test modules containing commercial, 20.6 % efficient bifacial PERC cells were modeled using a combination of ray-tracing, Beer's law, and transfer matrix calculations. This optical description was combined with a view-factor irradiance model with SMARTS2 integration and a finite-element model to solve for the module's temperature and power output over a typical meteorological year.

We first studied idealized mirrors, with unity above-bandgap transmittance and unity sub-bandgap reflectance, to determine the limits to performance. To mimic laboratory tests, AM1.5G irradiance was normally incident on the module's front face while irradiance on the rear face was varied. When there is no rear irradiance, applying mirrors at either the front only or the front and rear provided an approximate 4 % optical benefit, corresponding to the reflectance of an air/glass interface, as well as a 1.1 % thermal benefit, equating to 2.7 °C of module cooling. These results show that partial sub-bandgap transparency does not prohibit spectrally selective mirrors from being a promising thermal management strategy. As the rear irradiance increased, the configuration with the mirror only on the front exhibited decreasing optical and thermal benefits, due to a decreasing percentage of above-bandgap light incident on the front face and sub-bandgap light trapping of rear side incident light, respectively. With mirrors on both interfaces, the optical benefit was maintained as rear irradiance increased, and the thermal benefit increased linearly due to the linear increase in sub-bandgap irradiance rejection.

We then developed 4- and 6-layer photonic mirrors using real materials and compared performance to a traditional antireflection coating (ARC). The mirror designs were classified as thermally aware ARCs, providing 0.2 and 0.6 % more above bandgap antireflection than a traditional ARC, without the associated -0.13 % thermal penalty. Adding a rear spectrally-selective mirror improved the optical benefit when placed over high albedo ground, but also led to an increase in sub-bandgap light trapping, as observed by a small, 0.02 % thermal penalty. In addition to the studies described above, the idealized and realistic mirrors' performance were tested in single-axis tracking arrays at varying row spacings, array height, and at 12 different US cities. Each study provided insight into how varying angle of incidence distributions, rear irradiance fractions, total irradiance, and varying climate affect the optical and thermal benefits the mirrors can provide. Our results indicate that spectrally-selective mirrors enhance the energy yield of bifacial photovoltaics through a combination of improved anti-reflection and reduced operating temperature.

2:30 PM EN04.01.04

Biomimetic Broadband Antireflection Coatings for Highly Efficient Crystalline Silicon Photovoltaics Peng Jiang; University of Florida, United States

Millions of years before people began to generate functional nanostructures, biological systems were using nanometer-scale architectures to produce unique functionalities. Some nocturnal moths use hexagonal arrays of subwavelength nipples as antireflection coatings to reduce reflection from their compound eyes. Similar periodic arrays of nanopillars have also been observed on the wings of cicada to render superhydrophobic surfaces for self-cleaning functionality. Inspired by these natural nanostructures, we have developed three scalable nanofabrication technologies based on colloidal self-assembly, maskless reactive ion etching, and metal-assisted chemical etching for producing wafer-scale, self-cleaning, broadband antireflection coatings on a large variety of PV-relevant substrates, such as single-crystalline silicon, multicrystalline silicon, GaAs, GaSb, and glass. These techniques combine the simplicity and cost benefits of bottom-up self-assembly with the scalability and compatibility of standard top-down microfabrication. The resulting subwavelength-structured antireflection coatings can greatly suppress light reflection from both crystalline silicon and encapsulating glass surfaces, enhancing light absorption and ultimate conversion efficiency of the crystalline silicon solar panels. Importantly, optimal moth-eye antireflection nanostructures with tapered geometries can be easily passivated by conventional passivation technologies, resolving an outstanding challenge faced by many other black silicon approaches.

2:45 PM EN04.01.05

Effectively Transparent Contacts for Elimination of Shading Losses in Concentrator Solar Cells Stefan Tabernig¹, Anastasia Soeriyadi², Udo Roemer², Andreas Pusch², Dmitry Lamers¹, Michael Nielsen², Albert Polman¹ and Nicholas Ekins-Daukes²; ¹AMOLF, Netherlands; ²University of New South Wales, Australia

Concentrator solar cells have served as the absolute efficiency record holder for more than 25 years. Contrary to non-concentrator photovoltaics (PV), where silicon has been the flagship absorber material, concentrator PV research has been dominated by high efficiency III-V absorber layers. The main reason for this is that high Auger losses impose a comparably lower efficiency limit onto Si solar cells under concentration. Beyond the higher efficiencies of concentrator solar cells due to a logarithmic gain in open-circuit voltage, the amount of material needed per unit area scales inversely with increasing concentration. While Auger recombination might be an overall limit for efficiencies of Si concentrator solar cells, the option of saving material per unit area is becoming increasingly attractive. Considering projections of worldwide shortages for elements such as Ag, Cu, In etc, partially caused by the quickly rising demand of the Si PV industry itself, the time for concentrator Si PV might have come.

In this work we introduce a patterned and transparent polymer structure that attempts to address two problems that do not only apply to Si concentrator PV (CPV) but to CPV in general. First of all we want to solve the unsatisfying trade-off between shading losses that arise from high front metal coverage and Joule losses that increase with lower front metal coverage. Secondly, the same structure will actually allow for a decrease of the total area required to obtain a certain short-circuit current density (J_{SC}), due to lower shading losses.

The mentioned structure is a transparent polymer layer with V-shaped grooves, imprinted above the cell's metal fingers. These V-grooves redirect light away from the metal grid and onto the absorber material. This renders the contacts effectively transparent and breaks the trade-off between shading losses and Joule losses from the metal grid, thus allowing for higher concentration ratios and higher efficiency. We will demonstrate how performance of a Si solar cell with 25% front metal grid coverage and an initial short-circuit current density (J_{SC}) of 29.95 mA/cm² can be improved to a J_{SC} of 39.12 mA/cm² after adding the patterned polymer, mitigating shading losses almost completely. Optical microscope images as well as reflection data from integrating sphere measurements confirm that the contacts have become effectively transparent, showing little to no metal-grid-related features in the reflection spectrum. Furthermore, we will show that the angular performance of the V-grooves allows for shading losses to remain absent for concentrations beyond 1000 suns. Lastly, we present experimental IV-data of solar cells with V-grooves under concentration.

To conclude, the polymeric V-groove design allows for complete mitigation of shading losses, even with high metal coverage. In a concentrator system, this would allow for higher efficiencies, and especially higher power output per unit solar cell area compared to non-concentrating PV. Furthermore, lower shading losses also mean less area usage per concentrator system, as less concentration is needed to achieve the same J_{SC} . This could be beneficial as it might allow for cheaper and simpler concentration optics.

3:00 PM BREAK

4:00 PM EN04.01.06

Understanding the Role of Hydrogen Plasma Treatment and Thermal Annealing in Improving the a-Si:H/c-Si Interface Passivation Anishkumar Soman, Dhameylz Silva-Quinones, Steven Hegedus, Andrew Teplyakov and Ujjwal Das; University of Delaware, United States

The solar industry has seen rapid growth over the last few decades with installations over 600 GW contributing to over 2.2% of the global electricity¹. Silicon (Si) solar cells contribute to the bulk of the PV market, having more than 95% of the total production. The trend is for advanced high-efficiency device structures on n-type monocrystalline silicon to dominate by 2025². Current examples having commercial-scale production include tunnel-oxide passivated contact (TOPCon), Interdigitated back contact (IBC), and Heterojunction (HJ), which employs advanced improved interface passivation. In particular, Si HJ structures could be favorable due to their ease of fabrication, compatibility with thin wafers (< 100 μm), low thermal budget (< 300°C), and potential to reduce the cost per watt. The performance of these solar cells critically depends on the interface passivation quality of the amorphous silicon (a-Si:H) and crystalline silicon (c-Si) hetero-interface. It has been shown that extrinsic methods like hydrogen plasma treatment (HPT) and thermal annealing treatment (AT) strongly enhance the passivation of dangling bonds at the a-Si:H/c-Si interface³. In this work, we have investigated the underlying surface passivation mechanism of HPT and AT by analyzing the hydrogen bonding using Fourier transform Infrared spectroscopy. The hydrogen bonding environment in a-Si:H samples undergoing different treatments has been corroborated with the passivation quality in terms of effective minority carrier lifetime and implied open-circuit voltage (iV_{OC}) measured by quasi-steady-state photoconductance. Our initial results show that just AT reduces the Si-H₂ dihydrides, whereas a combination of HPT with AT improves monohydride concentration, in addition to the reduction of the dihydride

complexes, and resulted in higher minority carrier lifetime & implied V_{OC} . Temperature-dependent infrared spectroscopic analysis helps to understand the kinetics of hydrogen redistribution and effusion from the a-Si:H films due to annealing and will probe the activation energies of these processes. This will provide a complete understanding of the passivation improvement mechanism under the post-deposition extrinsic treatments. Additional characterization of the HJ structures was performed using Raman and UV-VIS-NIR spectroscopy to validate the quality of the a-Si:H films and interfaces to be used for making Silicon Heterojunction solar cells.

References:

- (1) Solar PV - Analysis - IEA <https://www.iea.org/reports/solar-pv>.
- (2) Fraunhofer Institute for Solar Energy Systems. *Photovoltaics Report*; 2020.
- (3) Soman, A.; Nsofor, U.; Das, U.; Gu, T.; Hegedus, S. Correlation between in Situ Diagnostics of the Hydrogen Plasma and the Interface Passivation Quality of Hydrogen Plasma Post-Treated a-Si:H in Silicon Heterojunction Solar Cells. *ACS Appl. Mater. Interfaces* **11**, 16181–16190.

4:15 PM EN04.03.03

Spotlight Talk—Scanning Nonlinear Dielectric Microscopic Investigation of Active Dopant Density Distribution in Black Silicon Solar Cell Yasuo Cho¹, Beniamino Iandolo² and Ole Hansen²; ¹Tohoku University, Japan; ²Technical University of Denmark, Denmark

Black silicon (Si) is a nanostructured type of Si capable of near-total absorption of light. Therefore, the use of black Si can lead to highly efficient solar cells. The performance of Si solar cells is dependent on the active dopant carrier distribution in emitters. The carrier distribution in black Si solar cells has been difficult to measure, and thus to optimize, due to the irregular, nano-scaled structure of the emitter.[1]-[5]

Thus, obtaining more information regarding active dopant density distribution in black Si solar cell requires measurements of carrier distributions on a nanoscopic scale.

One of the authors have previously succeeded in quantitatively analyzing such distributions in monocrystalline Si solar cells using scanning nonlinear dielectric microscopy (SNDM) [6]-[9].

In the present study, we investigated quantitatively the carrier distribution in a phosphorous (P) diffused black Si solar cell using SNDM. As a reference, we also measured the carrier distribution on a flat Si sample fabricated under the same P diffusion conditions. The precise carrier distributions in the emitter were visualized, which revealed the feature of carrier distribution in the emitter of black Si solar cell. Super-higher-order-SNDM was also employed to perform a quantitative analysis of the depletion layer distribution. It was found that the carrier density profile and the depletion layer thickness is less regular in the black Si than in the flat emitter, suggesting that this fluctuation may affect the power conversion efficiency of black Si solar cell. This work demonstrates that SNDM is a very useful means of investigating carrier distributions in the nano-scaled emitter of black Si solar cell.

References:

- [1] Y. Liu, T. Lai, H. Li, Y. Wang, Z. Mei, H. Liang, Z. Li, F. Zhang, W. Wang, A.Y. Kuznetsov, X. Du, *Small*, **8**, 1392 (2012).
- [2] K. Peng, Y. Xu, Y. Wu, Y. Yan, S.-T. Lee, J. Zhu, *Small*, **1**, 1062 (2005).
- [3] K. Peng, X. Wang, S.T. Lee, *Appl. Phys. Lett.*, **92**, 163103 (2008).
- [4] J. Z. Shen, B. Liu, Y. Xia, J. Liu, J. Liu, S. Zhong, C. Li, *Scr. Mater.*, **68**, 199 (2013).
- [5] C.-H. Hsu, J.-R. Wu, Y.-T. Lu, D. J. Flood, A. R. Barron, L.-C. Chen, *Materials Science in Semiconductor Processing*, **25**, 2 (2014).
- [6] K. Hirose, K. Tanahashi, H. Takato, and Y. Cho, *Appl. Phys. Lett.* **111**, 032101 (2017).
- [7] Y. Cho, S. Jonai, and A. Masuda, *Appl. Phys. Lett.*, **116**, 182107 (2020).
- [8] Y. Cho, A. Kirihara, and T. Saeki, *Rev. Sci. Instrum.* **67**, 2297 (1996).
- [9] Y. Cho, “Scanning Nonlinear Dielectric Microscopy”, Elsevier, ISBN 9780128172469 (2020).

4:20 PM EN04.03.01

Spotlight Talk—CV Analysis of c-Si Surface Passivation by H₂S Reaction Isaac K. Lam^{1,2}, Tasnim K. Mouri^{1,2}, Anishkumar Soman^{1,2}, William Shafarman^{1,2} and Ujjwal Das²; ¹University of Delaware, United States; ²Institute of Energy Conversion, United States

The desired direction for modern c-Si solar cells is to make them both thinner and higher efficiency, which makes passivation of the c-Si surface to reduce interface recombination a top priority. Traditional passivation techniques such as thermal oxidation and a-Si can cause issues in processing due to various temperature limitations [1]–[3]. Passivation of the c-Si surface using H₂S gas has been demonstrated to produce high quality passivation and has resulted in high (>2000 μs) minority carrier lifetimes [4]. It has been demonstrated that by H₂S reaction, c-Si surface dangling bonds can be reduced by bonding with S [4].

This work presents an investigation of the surface passivation mechanism by S by capacitance-voltage-frequency (C-V-f) measurements and will be compared with the surface passivation process by SiN_x and a-Si. Surface passivation quality is quantified by effective minority carrier lifetime (τ_{eff}) measured by quasi-steady-state photoconductance and the interface trap density (D_{it}) and fixed charge (Q_{fix}) are obtained from C-V-f measurements. The metal-insulator-semiconductor (MIS) structures were fabricated with the Si surface passivated by different materials for C-V-f measurements.

Lifetime and CV data are used together to characterize the passivation quality of the different treatments on two types of c-Si wafers. Both the a-Si and H₂S treatments ($\tau_{eff} \approx 1000 \mu s$ and $1700 \mu s$ for a-Si and H₂S treatment, respectively) show better passivation than the SiN_x ($\tau_{eff} \approx 14 \mu s$) with the H₂S giving the highest lifetime. Additionally, the data shows a reduction in Q_{fix} when the H₂S passivation process is used compared to the SiN_x sample, with $Q_{fix} = 7.5 \times 10^{11} \text{ cm}^{-2}$ and $2.1 \times 10^{13} \text{ cm}^{-2}$, for H₂S and SiN_x respectively.

The change in lifetime is explained by Q_{fix} and D_{it} which are functions of passivation quality. CV data allows calculation of Q_{fix} and D_{it} , which are used to fit the lifetime data using the method of Shu et al. [7][8], and further allowing for extraction of electron and hole capture cross sections (σ_n, σ_p).

In summary, two types of c-Si wafer with three different passivation treatments will be used to prepare MIS devices for CV measurement. Fixed charge calculated based on CV data shows a reduction in Q_{fix} for H₂S samples compared to the SiN_x passivated sample. Additionally, qualitative analysis of the CV curves as well as fitting of lifetime data shows a reduction in D_{it} for the H₂S samples, indicating high-quality passivation of the c-Si surface is due to low $D_{it} \approx 4.0 \times 10^{10} \text{ cm}^{-2} \text{ eV}^{-1}$ with a moderate positive Q_{fix} .

A detailed comparative study of interface passivation mechanisms by SiN_x, a-Si, and H₂S treatment will be provided in the final conference submission. Additionally, low frequency capacitance measurements, and conductance vs. AC frequency measurements will be included for all samples, which will allow for an accurate and quantitative determination of D_{it} for all samples. This in turn will yield a more robust lifetime fit to extract values for capture cross sections.

- [1] A. G. Aberle, et al., *Progress in Photovoltaics: Research and Applications*, Vol. 2, pp. 265-273, 1994.

- [2] U. K. Das, et al., *Apl. Phys. Lett.*, Vol. 92, 063504, 2008.
 [3] W. Liu, et al., *ACS Appl. Mater. Interfaces*, Vol. 7, pp. 26522-26529, 2015.
 [4] H. S. Liu, et al., *Langmuir*, Vol. 33, pp. 14580-14585, 2017.
 [5] P. A. G. O'Hare, *Pure Appl. Chem.*, Vol. 71, pp. 1243-1248, 1999.
 [6] A. Haas, *Angew. Chem. Int. Ed. Engl.*, Vol. 4, pp. 1014-1023, 1965.
 [7] Z. Shu, et al., *Prog. in Photovoltaics: Research and Applications*, Vol. 23, pp.78-93, 2013.
 [8] U. Das, et al., *Proc. 7th WCPEC*, 2018.
 [9] D. K. Schroder, John Wiley & Sons, 2006.

SESSION EN04.03: Poster Session: Silicon Photovoltaics
 Session Chair: David Fenning
 Thursday Afternoon, December 2, 2021
 8:00 PM - 10:00 PM
 Hynes, Level 1, Hall B

EN04.03.01

Spotlight Talk—CV Analysis of c-Si Surface Passivation by H₂S Reaction Isaac K. Lam^{1,2}, Tasnim K. Mouri^{1,2}, Anishkumar Soman^{1,2}, William Shafarman^{1,2} and Ujjwal Das²; ¹University of Delaware, United States; ²Institute of Energy Conversion, United States

The desired direction for modern c-Si solar cells is to make them both thinner and higher efficiency, which makes passivation of the c-Si surface to reduce interface recombination a top priority. Traditional passivation techniques such as thermal oxidation and a-Si can cause issues in processing due to various temperature limitations [1]–[3]. Passivation of the c-Si surface using H₂S gas has been demonstrated to produce high quality passivation and has resulted in high (>2000 μs) minority carrier lifetimes [4]. It has been demonstrated that by H₂S reaction, c-Si surface dangling bonds can be reduced by bonding with S [4].

This work presents an investigation of the surface passivation mechanism by S by capacitance-voltage-frequency (C-V-f) measurements and will be compared with the surface passivation process by SiN_x and a-Si. Surface passivation quality is quantified by effective minority carrier lifetime (τ_{eff}) measured by quasi-steady-state photoconductance and the interface trap density (D_{it}) and fixed charge (Q_{fix}) are obtained from C-V-f measurements. The metal-insulator-semiconductor (MIS) structures were fabricated with the Si surface passivated by different materials for C-V-f measurements.

Lifetime and CV data are used together to characterize the passivation quality of the different treatments on two types of c-Si wafers. Both the a-Si and H₂S treatments ($\tau_{eff} \approx 1000 \mu\text{s}$ and $1700 \mu\text{s}$ for a-Si and H₂S treatment, respectively) show better passivation than the SiN_x ($\tau_{eff} \approx 14 \mu\text{s}$) with the H₂S giving the highest lifetime. Additionally, the data shows a reduction in Q_{fix} when the H₂S passivation process is used compared to the SiN_x sample, with $Q_{fix} = 7.5 \times 10^{11} \text{ cm}^{-2}$ and $2.1 \times 10^{13} \text{ cm}^{-2}$, for H₂S and SiN_x, respectively.

The change in lifetime is explained by Q_{fix} and D_{it} which are functions of passivation quality. CV data allows calculation of Q_{fix} and D_{it} , which are used to fit the lifetime data using the method of Shu et al. [7][8], and further allowing for extraction of electron and hole capture cross sections (σ_n, σ_p).

In summary, two types of c-Si wafer with three different passivation treatments will be used to prepare MIS devices for CV measurement. Fixed charge calculated based on CV data shows a reduction in Q_{fix} for H₂S samples compared to the SiN_x passivated sample. Additionally, qualitative analysis of the CV curves as well as fitting of lifetime data shows a reduction in D_{it} for the H₂S samples, indicating high-quality passivation of the c-Si surface is due to low $D_{it} \approx 4.0 \times 10^{10} \text{ cm}^{-2} \text{ eV}^{-1}$ with a moderate positive Q_{fix} .

A detailed comparative study of interface passivation mechanisms by SiN_x, a-Si, and H₂S treatment will be provided in the final conference submission. Additionally, low frequency capacitance measurements, and conductance vs. AC frequency measurements will be included for all samples, which will allow for an accurate and quantitative determination of D_{it} for all samples. This in turn will yield a more robust lifetime fit to extract values for capture cross sections.

- [1] A. G. Aberle, et al., *Progress in Photovoltaics: Research and Applications*, Vol. 2, pp. 265-273, 1994.
 [2] U. K. Das, et al., *Apl. Phys. Lett.*, Vol. 92, 063504, 2008.
 [3] W. Liu, et al., *ACS Appl. Mater. Interfaces*, Vol. 7, pp. 26522-26529, 2015.
 [4] H. S. Liu, et al., *Langmuir*, Vol. 33, pp. 14580-14585, 2017.
 [5] P. A. G. O'Hare, *Pure Appl. Chem.*, Vol. 71, pp. 1243-1248, 1999.
 [6] A. Haas, *Angew. Chem. Int. Ed. Engl.*, Vol. 4, pp. 1014-1023, 1965.
 [7] Z. Shu, et al., *Prog. in Photovoltaics: Research and Applications*, Vol. 23, pp.78-93, 2013.
 [8] U. Das, et al., *Proc. 7th WCPEC*, 2018.
 [9] D. K. Schroder, John Wiley & Sons, 2006.

EN04.03.03

Spotlight Talk—Scanning Nonlinear Dielectric Microscopic Investigation of Active Dopant Density Distribution in Black Silicon Solar Cell Yasuo Cho¹, Beniamino Iandolo² and Ole Hansen²; ¹Tohoku University, Japan; ²Technical University of Denmark, Denmark

Black silicon (Si) is a nanostructured type of Si capable of near-total absorption of light. Therefore, the use of black Si can lead to highly efficient solar cells. The performance of Si solar cells is dependent on the active dopant carrier distribution in emitters. The carrier distribution in black Si solar cells has been difficult to measure, and thus to optimize, due to the irregular, nano-scaled structure of the emitter.[1]-[5]

Thus, obtaining more information regarding active dopant density distribution in black Si solar cell requires measurements of carrier distributions on a nanoscopic scale.

One of the authors have previously succeeded in quantitatively analyzing such distributions in monocrystalline Si solar cells using scanning nonlinear dielectric microscopy (SNDM) [6]-[9].

In the present study, we investigated quantitatively the carrier distribution in a phosphorous (P) diffused black Si solar cell using SNDM. As a reference, we also measured the carrier distribution on a flat Si sample fabricated under the same P diffusion conditions. The precise carrier distributions in the

emitter were visualized, which revealed the feature of carrier distribution in the emitter of black Si solar cell. Super-higher-order-SNDM was also employed to perform a quantitative analysis of the depletion layer distribution. It was found that the carrier density profile and the depletion layer thickness is less regular in the black Si than in the flat emitter, suggesting that this fluctuation may affect the power conversion efficiency of black Si solar cell. This work demonstrates that SNDM is a very useful means of investigating carrier distributions in the nano-scaled emitter of black Si solar cell.

References:

- [1] Y. Liu, T. Lai, H. Li, Y. Wang, Z. Mei, H. Liang, Z. Li, F. Zhang, W. Wang, A.Y. Kuznetsov, X. Du, *Small*, 8, 1392 (2012).
- [2] K. Peng, Y. Xu, Y. Wu, Y. Yan, S.-T. Lee, J. Zhu, *Small*, 1, 1062 (2005).
- [3] K. Peng, X. Wang, S.T. Lee, *Appl. Phys. Lett.*, 92, 163103 (2008).
- [4] J.Z. Shen, B. Liu, Y. Xia, J. Liu, J. Liu, S. Zhong, C. Li, *Scr. Mater.*, 68, 199 (2013).
- [5] C.-H. Hsu, J.-R. Wu, Y.-T. Lu, D. J. Flood, A. R. Barron, L.-C. Chen, *Materials Science in Semiconductor Processing*, 25, 2 (2014).
- [6] K. Hirose, K. Tanahashi, H. Takato, and Y. Cho, *Appl. Phys. Lett.* 111, 032101 (2017).
- [7] Y. Cho, S. Jonai, and A. Masuda, *Appl. Phys. Lett.*, 116, 182107 (2020).
- [8] Y. Cho, A. Kirihara, and T. Saeki, *Rev. Sci. Instrum.* 67, 2297 (1996).
- [9] Y. Cho, "Scanning Nonlinear Dielectric Microscopy", Elsevier, ISBN 9780128172469 (2020).

SESSION EN04.04: Passivated Contacts I
Session Chairs: James Bullock and Kaining Ding
Monday Morning, December 6, 2021
EN04-Virtual

8:00 AM *EN04.04.01

Production Application of Poly-Si Junction Passivated Contact Technology—Champion Solar Cell and Module Product Performance Xinyu Zhang, Peiting Zheng, Menglei Xu and Zhiqiu Guo; JinkoSolar Co., Ltd, China

The global power generation is in a transition toward renewable energy forms in a visible speed. Photovoltaic (PV) technology using crystalline silicon solar panels is playing a more important role, with more than 500GW global installation and relevant solutions becoming more mature. Continuous solar cell efficiency improvement is a dominating factor that accelerates PV industry in recent years, where the mainstream technology Passivated Emitter and Rear Contact (PERC) allows an average solar cell efficiency from 21% to 23%. However, further efficiency increase is limited by the significant carrier recombination loss at the metal-silicon interface regions. Hence, the passivating contacts have attracted great attention in both the research and the industry society, where polysilicon (poly-Si) tunnel junction technology using a thin silicon oxide tunneling layer and doped polysilicon carrier selective layer combination. It allows the contact interface region to achieve a significantly reduced recombination rate and increased open circuit voltage reaching 720mV. The laboratory world records for homo-junction cells, either front-rear contacted or back-contacted, utilized such passivating contact structure: the 25.8% efficiency n-type TOPCon cell from ISE Freiburg and the POLO-IBC cell from ISFH. Strong interests from the PV industrial players promote a rapid development of passivated contact technology in the manufacturing level. This work presents JinkoSolar's latest attempt of achieving over 25% efficiency for passivated contact structure solar cells using production size n-type silicon wafers.

Solar cell performance

This work presents the overall performance of solar cells from several production batches, where the average efficiency is over 24.8%. Among the batch results, the champion cell achieve a third-party certified efficiency of 25.25%, with an open circuit voltage (V_{oc}) of 715 mV and a fill factor of 84.9%. The distribution of batch cells' electrical performance indicates a strong alignment between the cell efficiency and the fill factor, where the fill factor parameters vary in a relatively large range. It well suggests that the contact quality of the passivated contact solar cells using screen printing technique is crucial, which is determined by various factors such as the screen paste composition, contact region surface morphology, poly junction thickness and doping concentration, quality of the tunneling oxide layer, etc. This work presents some specific characterization resulting aiming to explain the contacting mechanism of a high efficiency poly-Si passivated contact solar cell. In addition, several loss analysis have been performed for the champion cell.

Module performance and the field performance

Manufacturing produced passivated contact solar cells, particularly those commonly referred as n-type TOPCon cell by the PV industry, are relatively new to the market, with only limited field performance record. Thus the module reliability research for passivated contact technology is a hot research topic, major evaluation methods include a series of IEC standard tests such as temperature circle, dump heat test, potential induced degradation test, and so on. This work will present some testing and result details. In addition, this work will also present some field power generation results of passivated contact technology modules, including the analysis of performance improvement comparing to conventional PV modules.

8:30 AM EN04.04.03

Fabrication of solar cells with poly-SiO_x Carrier Selective Passivating Contacts on Ultra-Thin Thermal Tunnelling Oxide Manvika Singh¹, Aswathy Amarnath¹, Guangtao Yang¹, Arthur Weeber^{1,2}, Miro Zeman¹ and Olindo Isabella¹; ¹Delft University of Technology, Netherlands; ²TNO Energy Transition, Netherlands

Polycrystalline silicon (poly-Si) has proven to be a game-changing material in the field of high thermal budget carrier-selective passivating contacts (CSPCs) for c-Si solar cells beyond PERC architecture [1]-[4]. However, doped poly-Si exhibits a very high free carrier absorption (FCA), which has turned the attention of researchers towards wide bandgap materials, such as poly-SiO_x [5][6]. In these materials, the opto-electronic properties depend on oxygen [6][7] alloying. Such CSPCs consist of heavily doped poly-Si alloyed with oxygen and deposited on an ultra-thin SiO_x layer, prepared by thermal oxidation [8], wet-chemical process [6], UV/O₃ process [9], or low temperature plasma oxide [10]. Solar cells fabricated with such CSPCs on wet-chemical tunnelling SiO_x have exhibited illuminated efficiency of around 21% in front/back contacted (FBC) architecture [11]. In this work, building on our single-side poly-SiO_x processing, an ultra-thin SiO_x layer prepared by thermal oxidation was used as tunnelling oxide. The advantages of using this type of oxide are better uniformity on textured interfaces and better control over the oxidation rate by changing the oxygen flow rate, temperature, and time. First, we optimized the passivation of n-type and p-type doped poly-SiO_x CSPCs symmetric samples. Ultra-thin thermal oxide of around 1.5 nm was grown at 675 °C for 6 minutes. The standard thickness of the poly-SiO_x layer is around 30 nm for both polarities. An in-situ, single side, doping approach using PH₃ or B₂H₆ gas flow was used to dope the poly-SiO_x CSPCs to n-type or p-type, respectively. Double side textured n-type and double side flat p-type doped poly-SiO_x symmetric samples give an iV_{oc} of 690 mV after annealing and iV_{oc} of 710mV after hydrogenation. Single side textured FBC c-Si solar cells passivated with poly-SiO_x were fabricated on n-type FZ wafers and using the optimized n-type and p-type doped

poly-SiO_x CSPCs. These were realized by using n-type poly-SiO_x layer on the sunny side and p-type poly-SiO_x layer on the rear flat surface. All solar cells were annealed at 950 °C for 10 minutes to crystallize the poly-SiO_x layers and drive in the dopants. In this high temperature process, hydrogen effuses from c-Si bulk/SiO_x interface. So, these cells were hydrogenated by forming gas annealing (FGA) at 400 °C for 1 hour after being preliminarily capped with 100-nm thick PECVD SiN_x layer. Upon the removal of SiN_x, indium tin oxide (ITO) layers were sputtered (75-nm and 150-nm thick at front and back side, respectively) to ensure efficient lateral carrier transport of charge carriers. The front ITO layer also acts as anti-reflective coating. Screen printing was used to deposit front and rear metallic contacts. The best solar cell gave an illuminated efficiency of 21.44% ($V_{oc} = 697$ mV, $J_{sc} = 38.52$ mA/cm², FF = 79.86%, metallization fraction ~3%, illuminated area = 3.92 cm²). Moving from wet-chemical tunnelling SiO_x and evaporated metallic contacts [11] as well as further optimizing our doped poly-SiO_x layers, we could improve both the V_{oc} and the FF of our solar cells based on poly-SiO_x by an absolute 0.7%. Currently we are analysing the integration of this poly-SiO_x passivated c-Si solar cell as bottom cell in 2T perovskite/c-Si tandem configuration. The results will be presented at the conference.

- [1] G. Yang, *et al.*, Sol. Energy Mater. Sol. Cells, 2016.
- [2] F. Haase, *et al.*, Sol. Energy Mater. Sol. Cells, 2018.
- [3] F. Feldmann, *et al.*, Sol. Energy Mater. Sol. Cells, 2017.
- [4] A. Richter, *et al.*, Nat. Energy, 2021.
- [5] J. Stückelberger, *et al.*, Sol. Energy Mater. Sol. Cells, 2016.
- [6] G. Yang, *et al.*, Appl. Phys. Lett., 2018.
- [7] M. Singh, *et al.*, Sol. Energy Mater. Sol. Cells, 2020.
- [8] F. Haase, *et al.*, SiliconPV, 2018.
- [9] R. van der Vossen, *et al.*, 7th SiliconPV, 2017.
- [10] W. Lerch, *et al.*, ECS Transactions, 2012.
- [11] G. Yang, *et al.*, Prog. Photovolt. Res. Appl., 2021 (under review).

8:45 AM EN04.04.04

Structure and Electronic Properties of Mesopores in Si PV Devices with PLEO Contacts [Harvey Guthrey](#)¹, Caroline Lima de Souza^{1,2}, William Nemeth¹, Matthew Page¹, David L. Young¹, Sumit Agarwal² and Paul Stradins¹; ¹National Renewable Energy Laboratory, United States; ²Colorado School of Mines, United States

All current state-of-the-art silicon photovoltaic (PV) devices employ some flavor of passivating contact structure to minimize detrimental recombination while providing good conductivity. These properties are most often provided by a dielectric layer (SiN_x, Al₂O₃, or SiO_x) that is in contact with the crystalline silicon (c-Si) substrate. The effectiveness of these layers is heavily dependent on the nanoscale structure of both the dielectric layers and the crystalline silicon interface. As an example, the tunneling probability for charge carriers across thin SiO_x layers, a process that is critical to maintain high conductivity, is extremely sensitive to the SiO_x thickness. SiO_x with a thickness below 2 nm readily allows charge carrier tunneling, whereas it is impeded for greater thicknesses. In the latter case it has been shown that modifications to the thermal processing schedule can induce disruptions, or pinholes, in thick SiO_x layers that allow transport of charge carriers while maintaining excellent passivation. However, this requires higher temperatures processes that may inhibit widespread adoption by industry. Recently, another option has been presented that may circumvent the necessity for high temperature processing to produce pinholes, namely metal assisted chemical etching (MACE) of the SiO_x layer. MACE relies on deposition of Ag nanoparticles onto the SiO_x layers with subsequent electroless etching to form mesopores in the SiO_x layers that are analogous to the pinholes created with high temperature processing. The size and density can be controlled based on the Ag nanoparticle deposition conditions. The resulting contact structure is known as polysilicon on locally etched oxide (PLEO) contacts. The nanoscale structure of the mesopores in PLEO contacts define the device level observables such as recombination current (J_0) and junction resistance. In this work we present atomic resolution transmission electron microscopy (TEM) analysis of mesopores in PLEO contacts formed with different processing conditions to provide insight into how the nanoscale structure of the SiO_x layer influences PV device properties. Additionally, we have previously used electron beam induced current (EBIC) to probe local transport properties in Si PV devices with a SiO_x layer containing pinholes formed with high temperature processing. Using EBIC we were able to directly show the enhance charge carrier transport through the pinholes. Here we also employ EBIC to study non-uniformities in charge carrier recombination and transport associated with mesopores in PLEO contacts and compare these results with our previous work on devices with pinholes in the SiO_x formed through high temperature processes. The products of this work provide critical information that is required to both further optimize performance of Si PV devices with PLEO contacts and to drive future adoption of this technology by industry.

SESSION EN04.05: Light Management and New Absorbers

Session Chairs: Ivan Gordon and Emily Warren

Monday Morning, December 6, 2021

EN04-Virtual

10:30 AM *EN04.05.01

Black Silicon for PV—Which Technology to Choose? Xiaolong Liu, Behrad Radfar, Kexun Chen, Olli Setälä, Toni Pasanen, Ville Vähänissi and [Hele Savin](#); Aalto University, Finland

Black silicon (b-Si) surface texture that consists of nanoscale structures is well known to reduce the optical losses both in multi- and monocrystalline silicon solar cells. The enhanced surface recombination related to the increased surface area of nanostructures is no longer an issue as conformal atomic layer deposited thin films provide excellent surface passivation. [1] Furthermore, pn-junction formation and related control of dopant atoms inside nanostructures has resulted recently in totally recombination-free emitters yielding external quantum efficiencies even above unity in front-junction Si solar cells. [2] These developments have made the b-Si technology attractive for the PV industry as well.

So far only one black silicon fabrication technology has emerged as cost competitive technology to conventional texturization, that is, metal assisted chemical etching (MACE). [3] However, there are other b-Si fabrication technologies that have their benefits over MACE (e.g. extended infrared absorption) and which could find interest among PV industry, too. These include dry-etching as well as laser-based methods. All these technologies have seen lately great progress, so in this contribution we give an updated overview of b-Si fabrication methods and related achievements. Furthermore, in order to make a direct comparison of the methods easier, we present a systematic study on the properties of b-Si wafers fabricated in the same facility on sister wafers using three different fabrication methods: i) MACE ii) reactive ion etching and iii) femtosecond-laser. A special emphasis is placed on optical properties, recombination and surface passivation quality, surface morphology, silicon consumption, throughput, and patternability. Finally, the pros and

cons of each method are discussed and the future outlook is given for each technology.

- [1] P. Repo et al. IEEE Journal of Photovoltaics 3 (90-94) 2013.
- [2] K. Chen et al. APL Materials (submitted 2021).
- [3] K. Chen et al. Solar Energy Materials and Solar Cells 191 (1-8) 2019.

11:00 AM *EN04.05.02

Scalable Nano and Macro Light Management Approaches for Silicon Photovoltaics Bingtao Gao, Jacob Sindt, Wenqi Duan and Fatima Toor; The University of Iowa, United States

In this talk I will introduce low-cost and scalable light management approaches for crystalline silicon (c-Si) photovoltaic (PV) cells utilizing, (i) lithography-free inverted pyramids, (ii) electroless plated metal nanoparticles (NPs), and (iii) 3D printed light trapping films, that my team has been developing recently.

Industrial-scale passivated emitter rear contact (PERC) solar cells typically utilize upright pyramids fabricated utilizing potassium hydroxide (KOH) based alkaline etching of c-Si. ISFH's champion cell also utilizes the upright pyramid texture. While high efficiency lab-scale PERC solar cells utilize inverted pyramids because of higher antireflection (AR) relative to upright pyramids; these inverted pyramids are fabricated utilizing photolithography and an alkaline etch. Photolithography required to fabricate inverted pyramids is a slow and high cost process that is not compatible with low cost solar cell manufacturing needed for competitive solar energy generation. Hence, to-date, inverted pyramid texture has not been utilized in industrial-scale c-Si PERC cells. I will present results on a vacuum- and lithography-free wet chemical etching process that results in inverted pyramid textures on c-Si with extremely low spectrum weighted surface reflectivity (R_{ave}) of 4.4% and 10% relative improvement in power conversion efficiency (PCE) as compared to c-Si solar cells with no surface texture.

Next I will present our work on a light management structure on c-Si utilizing electroless plating of silver nanoparticles (AgNPs). With the help of a MATLAB-based analytical model on Mie theory, the size distribution of AgNPs for desired optical properties was determined, and experimental results confirmed the reduction in reflection by up to 24.8% at a wavelength of 371 nm. An atmospheric degradation study of the AgNPs was also conducted, which demonstrated that the LSPR response of unprotected AgNPs is markedly impaired after 14 days, while the LSPR response of aluminum oxide (Al₂O₃) protected AgNPs is unchanged even after 90 days. AgNPs covered with an Al₂O₃ layer on a c-Si solar cell exhibit the highest absolute gain of 19.2% in external quantum efficiency (EQE) at 700 nm and an overall 20% relative increase in PCE compared to the reference c-Si solar cell without NPs.

Finally, I will discuss our recent work on 3D-printed solar concentrators using acrylonitrile butadiene styrene (ABS) printing filament and designed using a CAD software. Post designing and printing, the concentrators underwent a layer of varnish to both smoothen the 3D-printed surface and improve the overall strength. Varnished 3D-printed structures were then spray coated with a layer of metal. The metals chosen were aluminum (Al) and chromium (Cr), due to both having low cost and high reflectivity in the visible spectrum. We obtained around 4x light concentration with the 3D-printed concentrators while reducing the weight of the concentrators to that of milled metal concentrators by two times and reducing the production cost compared to binary-optics by up to 500 times.

11:30 AM EN04.05.03

Optical and Electronic Properties of Type II Silicon Clathrate Films with Low Na Content Yinan Liu¹, Joseph Briggs¹, William K. Schenken², Lakshmi Krishna¹, Ahmad A.A. Majid¹, Thomas E. Furtak¹, Michael Walker¹, Carolyn A. Koh¹, P. Craig Taylor¹ and Reuben T. Collins¹; ¹Colorado School of Mines, United States; ²University of California, Santa Barbara, United States

Si has been widely used in nearly all aspects of semiconductor technology. However, Si in the bulk, diamond-structured form (d-Si) has an indirect bandgap and weak absorption. Exotic forms of crystalline silicon (silicon allotropes) that have been stabilized at ambient temperature and pressure include caged, open channel, and layered structures. One of the most well-known Si allotropes is Si clathrate, a cage-like, crystalline Si inclusion compound. Si clathrate has been synthesized to form either type I (Na₈Si₄₆) or type II Na_xSi₁₃₆ (0 < x < 1) phases in the presence of alkali atoms, such as Na, which sits inside the cage acting as an interstitial guest. If the Na content is low enough, which can only be achieved in type II (x << 1 in Na_xSi₁₃₆), Si clathrate can become a semiconductor with Na as a shallow, n-type, dopant. Theoretical studies have predicted type II Si clathrate to have a direct or nearly direct bandgap, near 2.0 eV, making it an exciting alternative to d-Si in optoelectronic applications. Most studies of Si clathrate have focused on powder synthesis. Compared with clathrate powder, thin-film Si clathrate is more interesting due to its potential for practical applications. Si clathrate films can be formed using a two-step process adapted from powder synthesis: formation of a Zintl precursor NaSi film and decomposition of the precursor into the clathrate phase. However, this thermal decomposition technique is very sensitive to growth parameters and the local environment, limiting controllable synthesis and complicating the characterization of film properties.

Here, we explore systematically the two-step synthesis technique in more detail by studying the key factors leading to thin, low-Na content, and high-quality films. Films have been synthesized with Na concentrations, varying from near the metal insulator transition (x ~10) values, comparable with the lowest Na content reported for powder samples. However, X-ray diffraction, Raman scattering spectroscopy, and Electron Paramagnetic Resonance measurements all provide evidence for a disordered or amorphous silicon-like phase that can dominate the surface and grain boundaries of the film. Time-of-Flight Secondary Ion Mass Spectrometry also demonstrates inhomogeneity of the ion profiles, showing regions of high Na content at the film surface and near boundaries surrounding low Na content regions, where high-quality clathrate material is located. We find that the presence of disordered Si and the inhomogeneity can significantly affect the film properties, complicating determination of the intrinsic properties of the clathrate.

Several growth and post growth techniques are studied to improve the film crystallinity and isolate the desired type II clathrate phase with low Na content. By exfoliating the film surface from the Si substrate, the high-quality clathrate structure is exposed and detected at the buried interface. Wet and dry acid etching are also applied, of which SF₆ reactive ion etching (RIE) is shown to selectively remove the disordered phase, while also decreasing the Na concentration in the films. These techniques provide promising methods of isolating high-quality clathrate material for investigation and application. Using these techniques, band edge characteristics were probed on high-quality films and surfaces using a range of measurements including absorption, photoluminescence (PL), and ellipsometry. A bandgap near 1.7 eV and an absorption coefficient about two orders of magnitude higher than diamond Si were observed. Room temperature PL is also detected in the near infrared region. An analysis of the temperature dependent PL emission confirms that Na in type II Si clathrate films can be a shallow donor with an activation energy of about 19 meV. This makes type II Si clathrate a n-type Si allotrope with exciting potential for Si based solar cells, LEDs, and sensors. This work was supported by National Science Foundation Awards 1810463.

11:45 AM EN04.05.04

Deterministic Broadband Absorption and Antireflection Using Deep Subwavelength Scalloping Arrays Ashish Prajapati¹, Jordi Llobet², Patricia C. Sousa³, Helder Fonseca³, Carlos Calaza³, João Gaspar³ and Gil Shalev¹; ¹Ben Gurion University of the Negev, Israel; ²IMB-CNM CSIC, Spain; ³International Iberian Nanotechnology Laboratory, Portugal

Light trapping and the broadband absorption of the solar radiation are significant to a plethora of absorption-based photonic devices. Specifically, efficient broadband absorption was recently demonstrated with arrays of subwavelength structures. The current study examines both numerically and experimentally light trapping driven by deep sidewall subwavelength structures (DSSS) in silicon nanopillar (NP) arrays (DSSS arrays). Particularly, the focus is on DSSS geometries that are an inherent outcome of the top-down dry etch approach used in arrays of high aspect ratio NPs due to the periodical operationality of the Bosch dry etch method. ~10% enhancement in the broadband absorption of DSSS arrays compared with NP arrays is demonstrated numerically, as well as the generation of near-IR absorptivity peaks of ~25% for DSSS arrays. Importantly, it is shown that the introduction of DSSS systematically blue-shifts the absorptivity peaks of the NP arrays and in this manner a deterministic light trapping is possible. Finally, decrements of ~40% in direct reflectivity and ~7% in diffused reflectivity in DSSS arrays realized on silicon wafers is demonstrated experimentally.

SESSION EN04.06: Perovskite-Silicon Tandems
Session Chairs: Carolin Sutter-Fella and Emily Warren
Monday Afternoon, December 6, 2021
EN04-Virtual

4:00 PM *EN04.06.01

Low-Cost, High-Efficiency, Stable Monolithic Si/Perovskite Tandem Solar Cell [Heping Shen](#); Australian National University, Australia

Increasing the power conversion efficiency of silicon (Si) photovoltaics is a key enabler for continued reductions in the cost of solar electricity. A two-terminal perovskite/Si tandem design that increases the Si cell's output in the simplest possible manner: by placing a perovskite cell directly on top of the Si bottom cell. The advantageous omission of a conventional interlayer eliminates both optical losses and processing steps and is enabled by the low contact resistivity attainable between n-type TiO₂ and Si, established here using atomic layer deposition. The fabricated proof-of-concept perovskite/Si tandems on both homojunction and passivating contact heterojunction Si cells to demonstrate the broad applicability of the interlayer-free concept. Stabilized efficiencies of 22.9 and >25% were obtained for the homojunction and passivating contact heterojunction tandems, respectively. Based on this, a clear route is provided for minimizing optical losses aided by optical simulations which result in tandem current densities of ~20 mAcm⁻² with front-side texture. In addition, electrical modeling on the Si-subcell has also been conducted in order to understand the efficiency potential of this cell under filtered light in a tandem configuration. The possibility of increasing the Si subcell efficiency by 1% absolute is offered through joint improvements to the bulk lifetime, which exceeds 4 ms, and improves surface passivation quality to saturation current densities below 10 fA cm⁻². A combination of optical modeling of the complete tandem structure alongside electrical modeling of the Si-subcell, both with state-of-the-art modeling tools, provides the first complete picture of the practical efficiency potential of over 30% for perovskite/Si tandems.

4:30 PM EN04.06.02

Ligand-Bridged Charge Extraction and Enhanced Quantum Efficiency Enable 27% Efficient n-i-p Perovskite/Silicon Tandem Solar Cells [Erkan Aydin](#)¹, [Jiang Liu](#)¹, [Esmat Ugrul](#)¹, [Randi Azmi](#)¹, [George T. Harrison](#)¹, [Yi Hou](#)², [Bin Chen](#)², [Shynggys Zhumagalı](#)¹, [Michele De Bastiani](#)¹, [Mingcong Wang](#)¹, [Waseem Raja](#)¹, [Thomas Allen](#)¹, [Atteq ur Rehman](#)¹, [Anand S. Subbiah](#)¹, [Maxime Babics](#)¹, [Aslihan H. Babayigit](#)¹, [Furkan H. Isikgor](#)¹, [Kai Wang](#)¹, [Emmanuel Van Kerschaver](#)¹, [Leonidas Tsetseris](#)³, [Edward H. Sargent](#)², [Frédéric Laquai](#)¹ and [Stefaan De Wolf](#)¹; ¹King Abdullah University of Science and Technology, Saudi Arabia; ²University of Toronto, Canada; ³National Technical University of Athens, Greece

Monolithic perovskite/silicon tandem solar cells are of interest thanks to their high power conversion efficiency (PCE) potential at affordable cost. Also, the possibility to fabricate silicon heterojunction bottom cells either in the *n-i-p* or *p-i-n* polarity provides considerable flexibility to choose the device architecture. The initial perovskite/silicon tandems were in the *n-i-p* configuration. However, as light in this architecture enters from the *p*-side, applying the typical electron and hole selective contacts of single-junction devices to the tandem configuration resulted in devices with a poor blue response, mainly due to parasitic absorption in the front-contact stack. Therefore, global tandem research refocused on the inverted structure (*p-i-n* configuration, with electron collection at the front). So far, several efficient devices have been reported in this configuration. Increasingly the PCE of *p-i-n* tandems further is constrained by parasitic absorption and recombination-active defects in the front SnO_x/C₆₀ ESL stack, prompting us to revisit the *n-i-p* structure to benefit from the expansive library of efficient hole selective layers in single-junction *n-i-p* perovskite solar cells.

In this study, we overcome the challenges of the *n-i-p* perovskite/silicon tandem solar cell platform and unveil the true potential of this architecture. We do so by developing novel electron and hole selective contacts which combine high broadband transparency with efficient charge extraction. First, we needed to develop efficient electron selective layers exhibiting high conformality on macroscale textured silicon substrates: the texture is needed to minimize light reflection. We implemented this concept by developing room temperature sputtered amorphous niobium oxide (a-NbO_x) films, combined with a C₆₀ self-assembled molecular monolayer. On the sunward side, we needed to overcome the high parasitic absorption and fast degradation challenges of spiro-OMeTAD. We developed conformal, transparent, and efficient hole selective layers (molecularly doped evaporated spiro-TTB). We combined this contact with a low-temperature atomic layer deposited vanadium oxide (VO_x) layer, which prevented sputtering damage and did not introduce significant optical losses. To enhance the stability of this contact stack, we introduced ultrathin TPBI layers between the spiro-TTB and VO_x. Combining these advancements with a two-dimensional perovskite passivation layer on the perovskite absorber, we achieved a power conversion efficiency exceeding 27%. This represents a significant advance over the best prior report in the *n-i-p* configuration of only 21.8% on similar bottom cells. The new device platform allows for translating the achievements of *n-i-p* single-junction solar cells into the context of tandems. The rich library of broadband transparent small-molecule HSLs and the possibility to utilize two-dimensional perovskite passivation strategies can now be easily implemented in tandems. From this, we expect rapid progress to be achieved in the field of perovskite/silicon tandems in the *n-i-p* configuration. We expect that our research will also propel the perovskite/perovskite tandem solar cells research which has been suffering from a lack of efficient vacuum-deposited hole selective contacts, where we offer a unique solution here.

4:45 PM EN04.06.03

Design and Optimizations of Silicon Heterojunction Solar Cells for High-Efficiency Monolithic Perovskite/c-Si Tandem Applications [Yifeng Zhao](#)¹, [Giulia Paggiaro](#)¹, [Hanchen Liu](#)¹, [Can Han](#)¹, [Paul Procel](#)¹, [Guangtao Yang](#)¹, [Arthur Weeber](#)^{1,2}, [Miro Zeman](#)¹, [Luana Mazzarella](#)¹ and [Olindo Isabella](#)¹; ¹Delft University of Technology, Netherlands; ²TNO Energy Transition, Netherlands

Silicon heterojunction (SHJ) solar cells have exhibited efficiencies well above 25% [1]. To further boost the efficiencies of c-Si-based solar cells, high-bandgap perovskite cells are stacked on top, achieving a world record efficiency of 29.52% [2]. However, as most of the high-quality perovskite films are solution-processed [3], the front surface of the bottom device should be flat. Therefore, in this work, we optimized SHJ bottom c-Si cells featuring front-side-flat and rear-side-textured morphology, which delivers high V_{OC} [4] together with excellent near-infrared response [5].

We firstly optimized plasma-enhanced chemical-vapor-deposition (PECVD) deposition conditions of (*i*)a-Si:H for both symmetrical flat <100> and textured <111> *n*-type c-Si surfaces. We observed that the optimized (*i*)a-Si:H monolayer (~ 10-nm-thick) on flat <100> surface using pure SiH₄ plasma results in limited performances ($\tau_{\text{eff}} = 1.2$ ms, i -V_{OC} = 701 mV). While an optimized hydrogen dilution ratio (DR = $f[\text{H}_2]/f[\text{SiH}_4]$) of 3 was found for textured <111> surface ($\tau_{\text{eff}} = 4.3$ ms, i -V_{OC} = 730 mV). This may be ascribed to an easier defective epitaxial growth for <100> as compared to <111> as reported previously [6]. To understand better the relations between passivation qualities and the microstructure properties (*i*)a-Si:H on flat <100> surface, we characterized layers via Fourier-transform infrared spectroscopy (FTIR) and spectroscopic ellipsometry (SE). We conclude that the monolayer that contains more H, a higher fraction of monohydrides and fewer defects (high refractive index) is beneficial for achieving a better passivation quality. To improve further the passivation quality of monolayer (*i*)a-Si:H on flat <100> surface, we investigate approaches aiming at incorporating more H without promoting detrimental epitaxial growth. Firstly, we tested hydrogen plasma treatment (HPT) [7]. With HPT, we could only slightly improve the i -V_{OC} from 701 mV to 705 mV. While with a bilayer approach [8] that features firstly a less H-containing (*i*)a-Si:H to prevent epitaxial growth and then covered by a H-rich (*i*)a-Si:H, we could double the τ_{eff} to 2.4 ms with an i -V_{OC} of 720 mV. Eventually, by combining the bilayer approach with an intermediate HPT, the best sample showed a τ_{eff} up to 8.3 ms and an i -V_{OC} of 734 mV for a total thickness of 10-nm (*i*)a-Si:H on the flat <100> surface.

For the two-terminal tandem solar cells, bottom cells with (*n*)-contact on top are preferred due to the optical advantage of the perovskite top cells with the *p-i-n* configuration. Therefore, we symmetrically deposited (*n*)-type hydrogenated nanocrystalline silicon oxide (nc-SiO_x:H) on (*i*)a-Si:H coated flat <100> surface. Surprisingly, a drop of i -V_{OC} to 689 mV was observed after depositing (*n*)nc-SiO_x:H on (*i*)a-Si:H obtained via bilayer + HPT approach. We ascribe the deteriorated passivation qualities to possible excessive H incorporation during the (*n*)nc-SiO_x:H depositions. Therefore, we chose bilayer (*i*)a-Si:H, which has lower H-content as compared to the combined approach, and we obtained improved τ_{eff} (5.8 ms) and i -V_{OC} (724 mV) in combination with doped layers.

With this method, we successfully implemented various (*n*)-contacts with either (*n*)a-Si:H, (*n*)nc-Si:H, (*n*)nc-SiO_x:H or (*n*)nc-Si:H/(*n*)nc-SiO_x:H/(*p*)nc-Si:H into solar cells, which delivered V_{OCs} range from 703 to 710 mV and FFs range from 78.8% to 81.0%. Therefore, we have building blocks ready for tandem cell fabrications. Besides, advanced optical simulations aiming at improving the matched tandem current are also being conducted.

[1] X. Ru, *et al.*, Sol. Energy Mater. Sol. Cells, 2020

[2] Oxford PV. oxfordpv.com (Accessed 21st of June, 2021)

[3] J. Jeong, *et al.*, Nature, 2021

[4] M. Taguchi, *et al.*, Prog. Photovolt. Res. Appl., 2005

[5] ZC Holman, *et al.*, IEEE J. Photovolt., 2013

[6] B. Demareux, *et al.* J. Appl. Phys., 2014

[7] M. Mews, *et al.*, Appl. Phys. Lett., 2013

[8] H. Sai, *et al.*, Appl. Phys. Lett., 2018

5:00 PM EN04.06.04

Loss Analysis for Perovskite/Si Tandem Solar Cells Masafumi Yamaguchi, Kan-Hua Lee, Ryo Ozaki, Kyotaro Nakamura, Nobuaki Kojima and Yoshio Ohshita; Toyota Tech. Inst., Japan

PV-powered vehicle application are very attractive for reducing CO₂ emission and creation of new market. Development of high-efficiency (> 30%) and low-cost solar cell modules is necessary [1]. According to our analysis [2], the 2-junction and 3-junction tandem solar cells have potential efficiencies of more than 36% and 42%, respectively. The perovskite/Si tandem solar cells are thought to be one of the most promising PV devices because of high-efficiency and low-cost potential. However, efficiencies of perovskite/Si tandem solar cells with an efficiency of 29.15% are lower compared to 37.9% with III-V 3-junction tandem solar cells and 35.9% with III-V/Si 3-junction tandem solar cells. Therefore, it is necessary to clarify and reduce several losses of perovskite/Si tandem solar cells. This paper presents high efficiency potential of perovskite/Si tandem solar cells analyzed by using our analytical procedure [3] and discusses about non-radiative recombination, optical and resistance losses in those tandem solar cells.

One of problems to attain the higher efficiency perovskite/Si tandem solar cells is to reduce non-radiative recombination loss. The open-circuit voltage V_{oc} drop compared to bandgap energy (E_g/q - V_{oc}) is dependent upon non-radiative voltage loss (V_{oc, nrad}) that is expressed by external radiative efficiency (ERE). Open-circuit voltage is expressed by

$$V_{oc} = V_{oc, rad} + (kT/q)\log(ERE), \quad (1)$$

where the second term shows non-radiative voltage loss, is radiative open-circuit voltage and 0.28V was used as $\Delta V_{oc, rad} (= E_g/q - V_{oc, rad})$ for perovskite and III-V compounds and 0.26V was used for Si in this study. The practical limiting efficiencies of perovskite/Si tandem solar cells were calculated by assuming ERE = 30%, optical loss of 5% and resistance loss of 2%.

The perovskite/Si 2-junction tandem solar cells is shown to have efficiency potential of 37.4% as a result of non-radiative recombination loss of 2.3%, optical loss of 2.7% and resistance loss of 3.1%. The perovskite/Si 3-junction tandem solar cells are thought to be very attractive because the III-V and III-V/Si 3-junction tandem solar cells have potential efficiencies of 45.9% and 42.9%, respectively. Although they still have non-radiative recombination loss of 1.9% and 1.5%, optical loss of 2.9% and 2.3% and resistance loss of 3.2% and 2.7%, respectively.

Several non-radiative recombination losses such as bulk recombination, interface recombination, resistance loss including inter-connection and so forth in tandem solar cells are discussed in this paper. In addition, practical limiting efficiency (29.4%) and several losses of crystalline Si single-junction solar cells are discussed in order to compare with those of tandem solar cells in this study.

References

[1] M. Yamaguchi *et al.*, Prog. Photovolt. (2020) <https://doi.org/10.1002/pip.3343>.

[2] M. Yamaguchi *et al.*, J. Phys. D: Appl. Phys. 51, 133002 (2018).

[3] M. Yamaguchi *et al.*, J. Mater. Res. 32, 3445 (2017).

5:05 PM EN04.06.05

Role of Amorphous Silica Interlayer in Enhancing the Performance of Perovskite/Silicon Tandem Solar Cells Gekko P. Budiutama, Sergei Manzhos and Manabu Ihara; Tokyo Institute of Technology, Japan

Tandem solar cells with perovskite top cell and Si bottom cell have attracted a lot of attention for their potential to achieve energy conversion efficiency beyond the Shockley-Queisser limit. In the *n-i-p* perovskite/c-Si variant of this tandem solar cell, recombination at the interface of c-Si and the electron transporting layer of perovskite top cell greatly affect the performance of the device. In this study, we propose the utilization of Scanning Zone Annealing (SZA), a selective heat treatment with high degree of control, to control carrier recombination at Si/TiO₂ interface for perovskite/Si tandem solar cell application. Here, we found that recombination velocity at Si/TiO₂ interface can be reduced down to 40 cm/s using SZA. We also found that the amorphous silica interlayer affected the recombination dynamics at Si/TiO₂ greatly. To understand this phenomenon, theoretical approaches to model triple layer interfaces of Si/SiO_x/TiO₂ were utilized. A combination of molecular dynamics and density functional theory calculations was employed to study the effect of amorphous silica stoichiometry and layer thickness on the electronic properties of the interfaces including band alignment, charge transport, and carrier lifetime.

5:10 PM EN04.06.06

Micrometer-Thick Solution Processed Perovskite Solar Cells on Industrial-Like Textured Si Substrates for Efficient Light Harvesting Ahmed Farag^{1,2}, Raphael Schmagel¹, Paul Fassl^{1,2}, Bianca Wattenberg³, Torsten Dippell³ and Ulrich W. Paetzold^{1,2}; ¹Institute of Microstructure Technology, Karlsruhe Institute of Technology (KIT), Germany; ²Light Technology Institute, Karlsruhe Institute of Technology (KIT), Germany; ³SINGULUS Technologies AG, Germany

In the past few years, perovskite/silicon (Si) tandem solar cells have emerged as one of the most promising candidates for next generation photovoltaics with the potential to beat the theoretical efficiency limit of single junction solar cells (~33%). Lately, a record power conversion efficiency (PCE) > 29 % has been demonstrated for two-terminal (2T) perovskite/Si tandem solar cells, which already surpasses the record PCE of single junction Si solar cells.

Yet the vast majority of high efficiency 2T perovskite/Si tandem solar cells reported to date, have been demonstrated using front-side polished Si wafers. While this approach is compatible with laboratory scale processes, it is not practical as industrial standard for Si photovoltaics due to the high costs. Industrial textured Si wafers are essential to achieve efficient light incoupling (i.e., to reduce the reflection losses) and light trapping near the band gap and typically exhibit pyramids that partly exceed 3 μm in size. However, such large textures are not compatible with the fabrication of conventional solution-processed perovskite thin films (thickness ~500 nm) on top.

In response to this challenge, we report on industrial-like textured Si wafers with a reduced pyramid size of ~1-2 μm that demonstrates (1) very low reflectance, similar to the conventional industrial textured Si wafers and (2) compatibility with thick solution-processed perovskite solar cells (PSCs) on top. To investigate the light management in PSCs fabricated over textured surfaces in depth, we replicate the Si texture by nanoimprint lithography on glass substrates and fabricate highly efficient *p-i-n* PSCs over the replicated texture.

A thick PSC absorber layer is necessary to cover all pyramid tips and prevent shunting paths. Therefore, we first developed highly-efficient *p-i-n* PSCs on a planar surface (PCE > 19 %) with a 1 μm thick double cation perovskite absorber layer (Cs_{0.17}FA_{0.83}PbI_{2.75}Br_{0.25}). Efficient charge carrier extraction is achieved by using urea additive to enhance the charge carrier diffusion length. Then, we optimized the spin-coating parameters for perovskite thin films processed over the replicated textures such that all pyramids are fully covered. In comparison to the planar PSCs, the PSCs processed over the textured substrates exhibit a voltage loss of ~50 mV. To explain the underlying reasons of the voltage loss, we investigated the perovskite crystallization dynamics over the industrial-like textured substrates by performing a full characterization scheme using XRD, EDX, EBIC, cross sectional SEM as well as the standard electrical and optical characterization means. Thereby, we present a guideline on how to minimize these voltage losses [1].

Finally, to demonstrate the optical gains that can be obtained by processing PSCs over textured surfaces, we study in detail the optical properties of the optimized thick PSCs processed over the replicated texture as well as the planar surface. While the textured stack exhibits a considerable broadband antireflection behavior, the planar stack suffers from higher reflection losses due to the thin film interference pattern (2.5 times higher reflection than the textured stack at around 570 nm). The textured stack also exhibits very efficient light incoupling even up to 70° angle of incidence as compared to the planar reference. The efficient light harvesting in our devices results in a remarkable improvement in the broadband spectral response, which leads to efficient J_{sc} amplification with one of the highest reported J_{sc}/J_{SQ} ratios [2,3].

In summary, our contribution shows that, by means of optimized pyramidal surface textures and adapted thick solution-processed PSC, we can solve a key hurdle in the fabrication of textured perovskite/Si tandem photovoltaics.

[1] A. Farag, *et al.* (in preparation)

[2] A. Farag, *et al.* (submitted)

[3] F. Gota, *et al.* (submitted)

5:25 PM EN04.06.07

Implementation and Analysis of Tunnel Junction Based on Transition Metal Oxides on Carrier Selective Contact Architecture Shikha Marwaha and Kunal Ghosh; Indian Institute of Technology Mandi, India

Till date, the photovoltaic industry is dominated by crystalline silicon (c-Si) solar cells because of their reliability, rapid cost reduction and improved efficiency. However, the thermalization losses occurring in the device limits its performance. Most common approach to surpass this limit is to use solar cells in tandem configuration with the top sub-cell having wide band gap absorber and bottom sub-cell possessing silicon as the absorber layer. Perovskite solar cells have proven to be a promising candidate to be used as a top sub-cell in tandem configuration because of their band gap tuning. Monolithic integration of silicon/perovskite devices reduces the wiring complexity and the additional fabrication steps. Most of the monolithic silicon/perovskite solar cells have been obtained either by homojunction or heterojunction silicon bottom cells. However, a tremendous amount of work shows an improved efficiency of transparent metal oxide (TMO) based carrier selective contact (CSC) silicon solar cells. The doped a-Si:H layers in the conventional SHJ solar cells are replaced by TMOs such as V₂O₅, MoO_x, TiO₂, and NiO_x. MoO_x has been proven to be an efficient substitute for p-doped aSi:H layer. The high work function (about 6.7eV) in MoO_x and higher band gap (about 3.2 eV) increases the fraction of light reaching the CSC device. The larger work function also causes an inversion in the c-Si thereby facilitating the transfer of holes from c-Si to the front end electrode. The CSC solar cell incorporating MoO_x as a hole transport layer has obtained an experimental efficiency of 22.5%. The rear side p-doped a-Si:H is also being substituted by TiO_x which introduces higher conductivity for electrons and lower conductivity for holes in CSC configuration. The highest efficiency reported for TiO_x based CSC devices is 21.6%. The monolithic tandem configuration requires optical coupling and minimized electrical losses which is obtained by adding a tunnel layer in between the top and bottom solar cells.

In this work, the performance parameters of tunnel junction (TJ) formed by TMO layers are investigated on the top of a carrier selective contact (CSC) based silicon solar cell in Sentaurus. We have employed a tunnel junction by adding TiO_x on the top of a hole transport layer, MoO_x from the silicon bottom sub-cell. The band alignment between TiO_x and MoO_x would allow transport of charge carriers by tunneling thus substituting the conventional tunnel layers. The simulations give a profound picture of the transport mechanism occurring in the device. The variations in electron affinity values and defect density of tunneling layers shows their effect on the hole collection ability of MoO_x.

6:30 PM *EN04.07.01

Superacid-Based Passivation of Silicon—New Insights into Bulk and Surface Recombination and a Route to Stability John D. Murphy¹, Sophie L. Pain¹, Marc Walker¹, Pietro Altermatt² and Nicholas E. Grant¹; ¹University of Warwick, United Kingdom; ²Trina Solar Limited, China

High quality stable surface passivation is an essential requirement for high efficiency silicon solar cells, and there are many ways of achieving this (e.g. Al₂O₃, SiN_x, their stacks and more recently TOPCON). Good surface passivation is also required for the accurate diagnosis of defect-related degradation phenomena in cells and wafers, although the stability requirement is less critical in this context. Established passivation strategies for solar cells and test structures often complicate material and degradation studies, as they can modify the bulk properties of the sample under investigation. This is because they include elevated temperature (>300 °C) steps during which recombination-active defects can form, be annihilated or even be generated. Changes in the hydrogenation state of the material also need to be considered.

Over the past five years, we have developed a range of temporary surface passivation schemes for measuring very long carrier lifetimes in silicon. Thin films are formed on wafer surfaces by treatment with bis(trifluoromethanesulfonyl)-based solutions, including superacidic and non-acidic chemicals, at room temperature. The films provide excellent surface passivation (surface recombination velocity < 1 cm/s), without modifying the bulk lifetime under investigation. Effective lifetimes in excess of 75 ms have been measured, and bulk lifetimes exceeding the currently accepted Auger limit have been extracted in some cases. As part of the talk's introduction, the latest developments in our passivation methods will be presented, building on studies we have published previously [1-4].

The main part of the talk will include new insights gained from using these temporary passivation schemes on the latest silicon materials and photovoltaic cells. One key feature of the superacid-derived approach is that it can be applied after samples have been stripped of dielectric passivation, diffusions or even metallisation. We can therefore use it to measure the true impact of a process on the material's lifetime without the modification that occurs in other passivation processes. New results to be presented will show how the activation annealing widely used for Al₂O₃ surface passivation can modify bulk lifetime, as well as chemical and field effect passivation. Our data show that the optimal activation temperature of around 460 °C occurs because recombination centres form in the bulk at higher processing temperatures. Our approach is also valuable in the study of light and elevated temperature induced degradation (LeTID), and data for some of the latest commercial Ga doped passivated emitter and rear cell (PERC) devices will be presented.

The final part of the talk will focus on the stability of superacid-derived passivation. Our standard approach is stable on the timescale of hours, which is sufficient for diagnostics but not for devices. Our standard approach involves an HF treatment to remove any native oxide layer on the sample surface, as native oxides provide very little surface passivation. Importantly, we have found that treating a thin (<1 nm) native oxide layer on the sample's surface with a superacid-based solution at room temperature can however give rise to good levels of surface passivation (surface recombination velocity < 20 cm/s), which can last for several months. Using X-ray photoelectron spectroscopy (XPS) we show that fragments of the superacid molecule (particularly fluorine) become incorporated into the treated native oxide layer. Room temperature chemically enhanced thin oxides could therefore be a promising concept for silicon-based solar cell devices.

1. N.E. Grant *et al.*, *IEEE Journal of Photovoltaics* **7**, 1574-1583 (2017).
2. A.I. Pointon *et al.*, *Solar Energy Materials & Solar Cells* **183**, 164-172 (2018).
3. A.I. Pointon *et al.*, *ACS Applied Electronic Materials* **1**, 1322-1329 (2019).
4. A.I. Pointon *et al.*, *Applied Physics Letters* **116**, 121601 (2020).

7:00 PM *EN04.07.02

Graphene Oxide Films As Passivation Material For Silicon Solar Cells Michelle Vaqueiro-Conteras; University of New South Wales, Australia

Reduction of the surface and interface recombination losses on crystalline silicon (c-Si) solar cells is at present a crucial need for the fabrication of high efficiency devices. At an industrial level, these losses account for at least 0.5% absolute efficiency decrease on passivated emitter and rear cells (PERC). In recent years many efforts have been made to reduce these recombination currents for which the concept of a passivated contact cell has aroused and gained a lot of attention. This more advanced concept of a cell, which is often referred to as carrier-selective contact cell, is meant to supply a carrier collection channel that will be able to reduce metal-semiconductor interface recombination while allowing free flow of selected charge carriers. Several approaches for the formation of selective contacts in silicon solar cells have been proposed. Amongst them there is: 1) the application of heavily doped regions under the contacts which reduce minority carrier conductivity as the result of a chemical potential introduction and low minority carrier mobility, 2) reduction of the minority carrier concentration at the surface by the application of external potential sources from materials with large fixed charges (Q_f) or a low (/high) work-functions, or 3) the formation of a heterojunction with a wide-bandgap material with the desired conductivity type (*n* or *p*). At present, the highest achieved power conversion efficiencies (PCE) on silicon devices have been achieved by the application of amorphous silicon (a-Si) passivated contact and heterojunction technology. This technology benefits from carrier selectivity provided by the combined cases 2 and 3 given by the a-Si properties, and has led to the remarkable PCE = 26.3%, with the potential to reach >27% efficiencies.

A graphite oxide monolayer, also known as graphene oxide (GO), is a carbon-based material whose properties have been investigated since its discovery and first-time fabrication over a hundred years ago. This material exhibits some remarkable properties such as high transmittance and fixed surface negative charge which makes it very appealing for optoelectronic applications. Further to this, graphene oxide optical absorption can be tuned by the degree of oxidation of the material. Thorough studies of this process have been shown experimentally, resulting in optical bandgap tuneability from 1.15 eV and up to 3.06 eV. Similar to the a-Si case, these two properties of graphene oxide are likely to provide the carrier selectivity required for a high-quality passivating contact on PV devices, with the advantage of very low temperature and low-cost fabrication.

It has already been shown that graphene oxide films on silicon can act as passivation layers achieving surface recombination velocities as low as 17.4 cm/s. In this work, we study the application of multilayered graphene oxide films as passivating contacts on passivated emitter and rear locally diffused cells (PERL). It is found that graphene oxide interlayers aid carrier collection and reduce rear recombination leading to an increase of open-circuit voltages in the excess of 5mV and short-circuit currents greater than 3.5mA. A discussion of the cell performance and recombination parameters will be discussed during the presentation.

7:30 PM EN04.07.03

Method for Extraction of Spatial External Luminescence Efficiency in Solar Cells Using Photoluminescence Measurements and Optical Modeling Tamir Yeshurun, Mor Fiegenbaum-Raz and Gideon Segev; Tel Aviv University, Israel

Continuous effort is being put towards device optimization for high efficiency solar energy conversion systems. As these devices are greatly affected by the various loss mechanisms and charge transport properties of the structures and materials, in-depth mapping of loss and charge transport mechanisms can be

key for rapid device optimization.

By combining wavelength dependent photoluminescence quantum yield (PLQY) measurements with optical modeling, we extract the depth dependent spatial external luminescence efficiency (SELE), which is defined as the probability of an electron-hole pair that is photo-generated at a certain depth to contribute to photoluminescence from the device. Since the external luminescence efficiency is related to the obtainable photovoltage from the device, extraction of the SELE profile could be used to map the contribution of different regions in the device to the photovoltage. In this contribution, we will discuss the SELE extraction method and analyze the SELE profiles of Silicon and GaAs wafers, serving as model systems.

In addition, the use of finite elements simulations of the measured structures while accounting for charge transport and photon recycling effects, allows computing of the SELE profile and attributing features in the profile to important physical quantities such as the surface recombination velocity, internal luminescence yield and the optical coupling between the device and its ambient. Analysis of SELE profiles for advanced solar cells could assist in mapping loss mechanisms and further promote high efficiency solar energy conversion devices optimization.

7:45 PM EN04.07.04

Study of Terbium-Doped AlN_xO_y: H / c-Si (p) Interfaces by Transient Surface Photovoltage Spectroscopy Jorge A. Dulanto Carbajal¹, Miguel Á. Sevillano-Bendezú¹, Rolf Grieseler^{1,2}, Jorge A. Guerra¹, Steffen Fengler³, Jan A. Töfflinger¹ and Thomas Dittrich⁴; ¹Pontificia Universidad Católica del Perú, Peru; ²Technische Universität Ilmenau, Germany; ³Helmholtz-Zentrum HEREON GmbH, Germany; ⁴Helmholtz-Zentrum Berlin für Materialien und Energie GmbH, Germany

Aluminum nitride (AlN) is a versatile material for chemical and field-effect passivation of silicon since fixed charges can be positive or negative, enabling to passivate n-type and p-type c-Si [1]. In this study, hydrogenated AlN layers (AlN:H) were deposited onto p-type c-Si by sputtering at hydrogen fluxes of 1 sccm, 3 sccm and 5 sccm and negative charges were activated on AlN through rapid thermal annealing (RTA) at 850°C. AlN also can work as a converter layer as it is suitable as a host for rare earth ions such as Terbium Ions for spectral downshift in solar cells [2].

Transient surface photovoltage (SPV) spectroscopy allows to investigate transport, generation and recombination processes as well as their relaxation times. In addition, due to its non-contact characteristic of transient SPV spectroscopy, it is possible to perform measurements where other techniques are not capable.

SPV signals associated with the transfer of electrons and holes at the AlN_xO_y: H / c-Si (p) interfaces were separated from those related to reducing the surface band bending. The distribution of negative fixed charges was high so that an accumulation regime near the silicon surface was established. At high hydrogen flux, the band bending was low due to an increase in the interface defects that compensate for the negative fixed charge. Complementary measurements with modulated SPV give additional information on defect and tail energies [3].

By measuring SPV spectra at different times, one can obtain information about the charge transfer [4], the tail energies and offset deep defects [3]. Comparing the results obtained from the tail energies and offsets, we found that charge transfer to defects was dominated by a disordered layer at the AlN_xO_y:H / c-Si interface and by deep defect states for the samples deposited at 1 and 5 sccm of hydrogen flow, respectively.

The three-variable measurements (time, photon energy/wavelength, SPV) allows for a deeper study of dominating charge separation mechanisms.

References

- [1] G. Krugel et al., Energy Procedia 55, 792-804 (2014).
- [2] K. Tucto et al., MRS Advances, vol. 2, 52, 2989-2995 (2017)
- [3] J. Dulanto et al., J. Phys.: Conf. Ser. 1841 012003 (2021)
- [4] S. Fengler et al., ACS Appl. Mater. Interfaces 12, 3140-3149 (2020)

SESSION EN04.09: Big Picture Photovoltaics
Session Chairs: Mathieu Boccard and Ivan Gordon
Tuesday Morning, December 7, 2021
EN04-Virtual

10:30 AM *EN04.09.01

Understanding Light and Elevated Temperature Induced Degradation in Fielded Arrays Ingrid Repins, Dirk Jordan, Michael Woodhouse, Joseph Karas, Alexandria McPherson and Christopher Deline; National Renewable Energy Laboratory, United States

A leveled cost of electricity (LCOE) of 3¢/w, for U.S. locations with average solar resource, has been identified as a critical threshold for wide-spread adoption of photovoltaics without subsidies. Achieving this cost goal requires improvements in all facets of the technology, from cell efficiency increases, to component cost decreases, to lower soft costs associated with installation, to reduced system performance degradation, and so forth. Maintaining long-term high performance in modules is often an under-recognized opportunity in this cost reduction because it is not fully quantified at the time of manufacture. While certain standardized tests minimize risk of early failure, information on long-term performance for new modules is largely unknown and thus does not appear in datasheets or quotes.

In this work, we explore several aspects of how light and elevated temperature degradation (LeTID) impacts long-term module performance and thus LCOE. First, we document the behavior of two commercial module types deployed at NREL starting in 2016 and 2018. ~7 kW of each module type was installed on-site at NREL, and both exhibited degradation hypothesized to be LeTID. In cooperation with the international testing and standards community, an accelerated test for LeTID was developed. This accelerated test was performed on unfielded spare modules from the degrading NREL arrays, and the presence of LeTID was confirmed. An approach for predicting long-term performance loss due to LeTID, utilizing the accelerated test results and observed defect behavior, is presented. The predictions from this approach are compared with yearly flash test data on fielded modules from the two degrading 7 kW arrays at NREL and other published results. Cost models based on the predictions indicate that LeTID has a significant and climate-dependent impact on LCOE. Areas where predictions could benefit from a deeper understanding of LeTID are identified.

Although there are significant uncertainties in the predictions, the general process demonstrated in this work is the same as that needed to develop reliability predictions more widely. The process starts with observation of degradation in the field or in accelerated tests. Next a physical model – a mathematical relationship between the stresses and the degradation – is hypothesized, and accelerated tests to probe the kinetics are performed. Long-term predictions are compared with fielded behavior and extended experiments with modest acceleration. As more information about the physical mechanism and how to measure it become available, the model may be refined. This iterative approach can supply some information for stakeholders to estimate costs associated with new products, while successively decreasing uncertainty of predictions and addressing apparent disagreement between data sets.

11:00 AM *EN04.09.02

Research Challenges in Silicon Photovoltaics [Susan Huang](#); U.S. Department of Energy Solar Energy Technologies Office, United States

The Department of Energy's Solar Energy Technologies Office (SETO) supports applied research related to photovoltaics, concentrating solar power, and systems integration with the goal of making solar energy more affordable and facilitating solar energy deployment. Over the past decade, commercial silicon cell developments have targeted efficiency losses under standard test conditions due to surface and bulk defects. The silicon photovoltaic cell industry continues to move towards new architectures to reduce losses from defects and increase efficiency. In the future, addressing performance challenges at the module-level, controlling field performance through better understanding of degradation pathways, such as potential and carrier induced degradation, and improving sustainability will become increasingly important. This talk will highlight the research funded by the SETO in silicon-based photovoltaics, how research areas have evolved as industrial capabilities and technologies change, and a few of the materials-level research problems in silicon photovoltaics that will promote future solar deployment.

11:30 AM *EN04.09.03

Photovoltatronics—Intelligent PV-Based Devices for Energy and Information Applications [Patrizio Manganiello](#), Hesam Ziar, Miro Zeman and Olindo Isabella; Delft University of Technology, Netherlands

Two of the major trends in nowadays energy sector are electrification and digitalization. Large-scale introduction of variable renewable energy sources, energy storage and power-electronics components, all based on direct current (DC), is fundamentally changing the electrical energy system of today, based on alternating current (AC). This trend leads to a complex hybrid AC/DC power system with the extensive deployment of information and communication technologies (ICT) to keep the system stable and reliable. Furthermore, the expanding urban areas are increasingly so energy intensive that the demand for local and optimal generation of clean electricity is growing as well. In this scenario, photovoltaics (PV) technology will play an essential role. However, to take full advantage of PV in the urban environment, PV technology must become intelligent and PV devices must become multi-functional.

Recently, we identified, described, and labelled a new research field that deals with intelligent PV and its application in components with multiple functionalities. We denoted this field **photovoltatronics** [1]. Photovoltatronics aims at facilitating the large-scale implementation of photovoltaic technology in urban areas by combining it with electronic and photonic devices as well as digital technologies. As a result, photovoltatronics will deliver intelligent devices that we refer to as multi-functional *PV-based intelligent energy agents* (PV-IEA), by bringing together disciplines of energy and informatics. Since photons and electrons are carriers of both energy and information, photovoltatronics is the field that designs and delivers autonomous devices for electricity generation and information communication. It introduces a pathway from harvesting energy of photons ($h\nu$) to creating bits of information (01) through the energy of photo-generated electrons (eV). Photovoltatronics will deliver solutions for electricity generation and information communication in applications such as building environment, e-mobility, sensing, and domotics. This aim is realized by combining different research areas. Five major research areas that lay the foundations for the photovoltatronics research field are: (1) modelling and multi-layer mapping for maximizing energy harvesting from ambient energy sources at a particular location; (2) design of PV-IEAs for delivering optimum electrical energy including reconfigurable electrical topologies of PV generators, (passive) cooling elements, electronics, sensor systems, and control; (3) security and flexibility of electrical energy supply by integrated storage (4) wireless transmission of electricity through a novel design of PV module electrode, and (5) light-based communication (e.g. LiFi) by integrating and controlling embedded light-generating elements such as light-emitting diodes (LEDs) and by leveraging the inherent ability of PV devices to work as receiver in light-based communication systems while still being able to generate energy from the received natural or artificial light.

Soon, these devices can become building blocks for energy and information flows in cities, as every surface in urban areas can play an important role in providing useful energy from solar radiation to urban dwellers. Multi-functional PV-IEAs will thus represent the backbone of the combined energy/information system of the future.

We review photovoltatronics research areas and introduce new directions for each area. In this process, we show that ~ 10 keV energy is at least needed for transceiving one bit of information in the energy-information chain of the photovoltatronics, while the ultimate efficiency of the chain can reach up to 33.4%. We show that the number of publications related to photovoltatronics is exponentially increasing and the publication rate of combined research areas has been doubled in the present decade and reached 3.4% as a clear sign of its emergence.

[1] H. Ziar, *et al.*, Energy Environ. Sci., 2021.

12:00 PM EN04.09.04

Late News: In-Space Research and Manufacturing of Semiconductor Materials [Divya Panchanathan](#); Axiom Space, United States

Over the past several decades, the semiconductor materials landscape has expanded from silicon-group elements to binary compounds, ternary alloys, perovskites, and 2D materials. However, each one of these materials has been created under the constraints of Earth's gravitational field. What if this force could be negated? Microgravity offers a unique environment to achieve materials innovation in ways that cannot be accomplished on Earth. Changes in fluid behavior such as the lack of buoyancy-driven convection and sedimentation in microgravity lead to beneficial characteristics in materials like semiconductor crystals, 2D materials, and photonic materials. Some demonstrated benefits of the microgravity environment include the ability to isolate and study non-gravitational phenomena, preparing defect-free crystals, diffusion dominated processing, and containerless processing of materials.

While early focus of experiments in space was on fundamental research to enable and improve space exploration, the advent of the new space age has made it possible to bring the benefits of space closer to home. The emergence of commercial space stations like Axiom Station opens new opportunities for academic and industry researchers to perform focused applied research that leads to manufacturing of advanced materials in space for electronics and energy applications. This talk will highlight: (1) the fundamental ways in which microgravity affects materials processes; (2) the use of microgravity environment an innovation platform; and (3) potential future in-space manufacturing applications.

SESSION EN04.10: Passivated Contacts II
Session Chairs: James Bullock and Kristopher Davis
Tuesday Afternoon, December 7, 2021
EN04-Virtual

1:00 PM *EN04.10.01

Improving the Rear Side of High Efficiency Rear Junction Silicon Heterojunction Solar Cells Andres Lambertz, Weiyuan Duan, Karsten Bittkau, Depeng Qiu and Kaining Ding; Forschungszentrum Juelich GmbH, Germany

The main objective of crystalline silicon photovoltaic (PV) technology development is to increase the power conversion efficiency and further reduce the production costs, aiming to reduce the levelized cost of electricity (LCOE). As one of the technologies with passivating contacts, silicon heterojunction (SHJ) solar cell technology is considered to expand its share in the PV industry in the coming years due to the high-power conversion efficiency, lean fabrication process and low temperature coefficient.

In this work, we show how to improve the rear side of silicon heterojunction (SHJ) solar cells. The improved rear side increases the cell certified efficiency of 23.55% to 24.51% on a full-size n-type wafer (total area, 244.53 cm²). The route towards the higher efficiency SHJ solar cell is proposed through a combination of experimental work accompanied by device simulation. In this study the gain in efficiency was achieved primarily by (i) adjusting the properties of the hydrogenated intrinsic amorphous silicon (a-Si:H) i-layer on the rear side of the solar cell and (ii) improving the optical properties of the back reflector of the solar cell.

All SHJ solar cells were fabricated using M2-size n-type Czochralski (CZ) crystalline silicon as-cut wafers from LONGi company textured in alkaline solution and cleaned via an ozone cleaning process. The plasma enhanced chemical vapor deposition (PECVD) process was performed in an AK 1000 system from Meyer Burger for intrinsic and doped a-Si:H layers. Afterwards, indium tin oxide (ITO) layers were sputtered from an 3% Sn-doped In₂O₃ target. Silver grids with a busbar-less design were screen printed and subsequently cured at 170 °C for 40 min. The MgF₂ and Ag layers were evaporated. For material characterization we used an ellipsometer (J. A. Woollam M-2000) and the structural characterization was performed by Fourier Transform Infrared Spectroscopy (FTIR) in a Nicolet 5700 system. To evaluate the solar cells performance, current-voltage characteristics, the external quantum efficiency, and reflectance were measured by the integrated solar cell characterization system called LOANA from pv-tools with a Wavelabs Sinus 220 light source.

The properties of the a-Si:H i-layers play multiple roles in SHJ solar cells not only as a surface passivation layer but also as a carrier transport to the electrode. To improve both, intrinsic a-Si:H bi-layers with a porous first layer (i₁) and a dense second layer (i₂) are a viable route. The silane (SiH₄)/hydrogen (H₂) flow ratio and thickness of the second intrinsic a-Si:H (i₂), were specially optimized here to reduce the vertical charge carrier transport loss but still achieving an excellent passivation quality. By using a denser and thinner second part of the intrinsic a-Si:H layer, a reduced vertical rear resistance loss was achieved. This favored vertical carrier transport and led to a higher *FF*.

To improve the optical properties of the back reflector we reduced the plasmonic absorption at the back reflector by inserting a low-refractive-index magnesium fluoride (MgF₂) before the Ag layer resulting in an increased short circuit current density (*J*_{sc}). In total, together with MgF₂ double antireflection coating and other small optimizations during cell fabrication process, ~1% absolute efficiency enhancement is finally obtained. Finally, we were able to improve the efficiency from certified 23.55% mainly due to an improvement in *FF* and *J*_{sc} improvement to 24.51%, with an *J*_{sc} of 39.52 mA/cm², an open circuit voltage (*V*_{oc}) of 741.8 mV and a *FF* of 83.61%.

1:30 PM *EN04.10.02

Selectivity and Extraction Efficiency of Solar Cell Contacts—Comparing Different Definitions and Their Experimental Quantification Michael Rienäcker¹, V. Titova^{1,2}, J. Schmidt^{1,3}, R. Peibst^{1,3} and R. Brendel^{1,3}; ¹Institute for Solar Energy Research in Hamelin (ISFH), Germany; ²Hamburg University of Applied Sciences, Germany; ³Leibniz Universität Hannover, Germany

Although carrier-selective contacts are crucial for the operation of any photovoltaic energy converter, it was only the increasing interest in non-traditional contact schemes in c-Si PV that has sparked a debate of how a metric for the ability of a contact to extract desired charge carriers versus blocking undesired ones should be defined and measured.

In the last years, several authors defined metrics for the quantification of the selectivity of contacts to solar cells. They can be classified in two categories: the first one compares the internal versus external voltage of the solar cell at open-circuit operation and the second one compares the transport coefficients for electron and hole transport through the contact. The different approaches are not identical in terms of defining the spatial boundaries of the selective contact and the processes involved in the charge carrier extraction at the contact. In the following, we present the carrier-selective contact from a thermodynamic and kinetic point of view, and compare different figures of merit for carrier-selective contacts. We present experimental investigations to access the different figures of merit by means of a three-terminal photovoltaic device.

First, we briefly summarize the thermodynamic interpretation of a solar cell in terms of a two-step conversion process with two respective conversion efficiencies: After converting sun's heat radiation into an excited electron-hole gas in the absorber, the contacts convert the chemical energy of the electron-hole gas into electrical energy. The (carrier) extraction efficiency corresponds to the efficiency of the latter and measures the contact's ability to extract charge carriers selectively. For the kinetic considerations, we discuss the spatial boundaries of the absorber, the carrier-selective membranes and the electrodes of a photovoltaic energy converter and pay special attention to the charge carrier processes occurring in the selective membrane and the electrode. We review the existing definitions of the contact selectivity metric and its measurement from the literature.

In order to examine the selectivity and the extraction efficiency, we use a three-terminal photovoltaic device with almost perfectly electron-selective and hole-selective reference contacts and a TiO_x-based electron-selective contact as model system. The perfectly selective reference contacts allow to measure the electron and hole current densities at the TiO_x-based contact separately. Therefore, it enables us to study the two different categories of selectivity metrics in the literature on a single test device by using two different methods.

For the first method – the three-terminal Suns-*V*_{oc} method – our device operates without an external current flow and provides access to the internal and external open-circuit voltage of the device as often used by several author in c-Si, organic and perovskite PV. From a TiO_x-based-contact-limited test device, we determine the extraction efficiency and selectivity coefficient of the TiO_x-based contact as function of the illumination intensity.

For the second method, we use the transport coefficients of electron and hole transport through the TiO_x-based contact to quantify the selectivity coefficient. For this purpose, we estimate the transport coefficient for holes – the recombination pre-factor *J*_{0,C} – from *J*_{sc}-*V*_{oc} characteristic between the electron-selective TiO_x-based contact and the perfectly hole-selective reference contacts. From dark *J*-*V* characteristic between the electron-selective TiO_x-based contact and the perfectly electron-selective reference contact of the three-terminal device, we determine the transport coefficient for electrons in the TiO_x-based contact – the contact resistivity. Finally, we compare the results of both methods.

2:00 PM *EN04.10.03

The Critical Role of TCO Deposition on Solar Cell Performance Monica Morales-Masis; University of Twente, Netherlands

Transparent Conducting Oxides (TCOs) are widely accepted transparent electrodes in a variety of solar cells employing passivating and selective contacts, such as silicon heterojunction (SHJ) solar cells and thin film technologies such as CIGS and perovskite solar cells¹. Among all possible ways to deposit TCOs, sputter deposition is the most employed technology, both in academia and industry. However, the high kinetic energies of the arriving species during sputtering may damage sensitive functional layers beneath, affecting interface formation, passivation and ultimately device performance. This has motivated the search for alternative sputter system designs or deposition techniques, allowing low damage growth of TCOs on the sensitive layers. Here we explore pulsed laser deposition (PLD) as an alternative low-damage physical vapor deposition technique. PLD is operated at high deposition pressures, promoting thermalization of particles, and therefore reducing the kinetic energy of ablated species. Broadband transparent and high mobility TCOs were developed using wafer-scale (4-inch) PLD with deposition rates on par with lab-scale RF sputtering². To investigate the effects of the deposition pressure,

we developed ITO with identical sheet resistance (50 Ohm/sq) at deposition pressures three orders of magnitude apart, and applied them as a front TCO in SHJ cells and as rear-contact in semitransparent perovskite cells. The role of the deposition pressure on TCO properties, absorber carrier lifetime and its link to SHJ and perovskite solar cell parameters such as series resistance and fill factor (FF) will be discussed. Strategies to mitigate damage, for each type of cell will be furthermore discussed.

References

¹M. Morales-Masis et al. *Adv. Electron. Mater.* 3 (5), 1600529, 2017.

<https://doi.org/10.1002/aelm.201600529>

²Y. Smirnov et al. *Adv. Mater. Technol.* 6 (2), 2000856, 2021. <https://doi.org/10.1002/admt.202000856>

2:30 PM EN04.10.04

The Application of Ultra-Thin MoO_x in Silicon Heterojunction Solar Cells Liqi Cao, Yifeng Zhao, Can Han, Guangtao Yang, Miro Zeman, Luana Mazzarella and Olindo Isabella; Delft University of Technology, Netherlands

Since the first inception of silicon heterojunction (SHJ) solar cells, prominent developments have been realized in both front/back-contacted (FBC) [1] and interdigitated back-contacted (IBC) [2] (world record efficiency of 26.7%) architectures. However, the conventional silicon-based doped layers, which work as carrier-selective transport layers, are not optimally transparent especially when used as window layers.

To circumvent this fundamental limitation, several transition metal oxide (TMO) layers have been investigated because of their good transparency in the wavelength range of interest and appealing electronic properties to efficiently extract charge carriers from the device [3]. MoO_x as the most promising for hole-selective transport layer (HTL) has been applied in SHJ solar cells to replace the conventional doped layer in SHJ FBC devices. Normally, the thickness of HTL is between 6 and 10 nm, while a power conversion efficiency (PCE) of 23.5% SHJ solar cell with 4-nm thick MoO_x was recently demonstrated by J. Dreón et al. [4]. The thinner the layer is, the less the optical loss is. However, still 0.5 mA/cm² was found to be lost in MoO_x [5]. According to the work by L. Mazzarella et al. [6], who applied a plasma treatment (PT) on the interface of i-a-Si:H and MoO_x to improve the electric performance, thinner MoO_x layer could be possible for application in solar cells. This is the focus of our contribution.

We used 4-in wide double-side textured n-type FZ wafers as substrate. A layer of i-a-Si:H was deposited on both sides and n-a-Si:H film was deposited on the rear side by plasma-enhanced chemical vapor deposition (PECVD). A PT was applied on the front surface before the deposition of MoO_x. A thickness series of MoO_x HTL was thermally evaporated at the pressure of 5×10⁻⁶ mbar. Tested thickness of MoO_x were 0 nm, 1 nm, 1.7 nm, 2 nm, 2.9 nm, and 4 nm. After that, indium tin oxide (ITO) was sputtered through a mask on the front and rear side with the thickness of 70 nm and 150 nm, respectively, forming five 2×2-cm² wide cells per wafer. From the light facing side, the stack of the layer is therefore ITO/MoO_x/i-a-Si:H/n-Si/(i+n)-a-Si:H/ITO. Initially, front grid and rear contact were screen printed with Ag paste followed by curing (30 min at 170 °C) and two standard SHJ solar cells [7] were fabricated as reference. After measuring our devices, we found that screen printing was rather aggressive on MoO_x-based cells with V_{oc} dropping by more than 20 mV with respect to the implied V_{oc} prior metallization. So, to isolate the performance of the thin MoO_x HTL, we used a thin Ag layer as seed for room temperature Cu-plating at the front side (~1.6% metallization fraction) and sputtered a full-cell wide 500-nm thick Ag at the rear side. Overall, thanks to our PT, thinner-than-4nm MoO_x layers in Cu-plated SHJ FBC cells delivered excellent transport (FF > 81%) in combination with good passivation (V_{oc} > 720 mV). So far, the best device was endowed with 2.9-nm thick MoO_x and exhibited η_{active} = 22.92% (V_{oc} = 722 mV, J_{sc, EQE} = 39.04 mA/cm², FF = 81.3%). The realization of other thicknesses of MoO_x in SHJ FBC solar cells is ongoing and will be presented at the conference. From preliminary passivation tests up until front/rear sputtered ITO, we expect even higher performance for thickness of MoO_x < 2 nm, which would positively translate into larger cell J_{sc}.

[1] X. Ru, et al., *Sol. Energy Mater. Sol. Cells*, 2020.

[2] K. Yoshikawa, et al., *Nat. Energy*, 2017.

[3] H. Mehmood, et al., *Renew. Energy*, 2019.

[4] J. Dreón, et al., *Nano Energy*, 2020.

[5] J. Dreón, et al., *IEEE J. Photovolt.*, 2021.

[6] L. Mazzarella, et al., *Prog. Photovolt. Res. Appl.*, 2020.

[7] Y. Zhao, et al., *Prog. Photovolt. Res. Appl.*, 2020.

2:45 PM EN04.10.05

Towards TCO-Less Bifacial Cu-Plated SHJ Solar Cells Can Han, Rudi Santbergen, Yifeng Zhao, Daragh O'Connor, Guangtao Yang, Paul Procel, Miro Zeman, Luana Mazzarella and Olindo Isabella; Delft University of Technology, Netherlands

Silicon heterojunction (SHJ) solar cells have exhibited high efficiencies in both academia and industry [1,2]. Key challenges to be addressed in the upscaling process are the cost of materials and the abundance of the utilized elements. Therefore, consumption of Ag and In, widely used in the electrodes of SHJ devices, must be reduced [3]. Cu has proven to be a good candidate for replacing Ag electrode; however, complexity in the metallization process remains to be tackled [4]. For the widely used electrochemical Cu-plating technique, separate control is generally needed for processing both sides of the wafer, which means that one side of the wafer is protected when plating the other side [5]. This step further increases the cell production costs. On the other hand, to reduce the In consumption, basic strategies include: (i) use of In-free TCOs, such as AZO; (ii) reduction of the TCO thickness (*TCO-less* option); (iii) development of TCO-free SHJ devices. For (i), challenges may lie in low carrier mobility, interface/material stability issues [6]; For (ii), proof-of-concept TCO-free SHJ cells have been demonstrated recently [7], but efforts have been partially frustrated from the passivation deterioration, and contact problems [8]. Also, it is still an open question whether TCO-free design could give optimal device performance. Moreover, a TCO layer is practically needed to act as a Cu diffusion barrier layer in Cu-plating processes. To circumvent these limitations, we focus on the *TCO-less* solution in combination with Cu-plating metallization approach.

We developed TCOs with different opto-electrical properties, which are tin-, fluorine-, and tungsten-doped indium oxides, namely, ITO, IFO, and IWO [9][10]. By utilizing a double layer anti-reflection coating formed by TCO/SiO_x layer stacks on both sides of our SHJ device structure, we performed optical simulations with varied front and back TCO/SiO_x thicknesses. Results show that bifacial solar cell architecture provides the most effective way to reduce the TCO use, and the optimal optical response appears at the point where a thin TCO layer is applied, due to a low free carrier absorption and a favorable refractive index enabling light in-coupling. Thus, we applied 25 nm-thick of different TCOs on both sides of the cell precursors fabricated using plasma-enhanced chemical vapor deposition technique. Finally, we developed single step Cu-plating process on lithography patterned openings, which could well control the metal finger growth on both sides of the wafer and largely simplify the simultaneous metallization on both sides. Champions bifacial cell was observed in the devices with IWO use on front and ITO use on the rear side of the device. After applying an additional 110 nm-thick SiO_x layers on both sides of the complete cell, the device parameters were measured to be: V_{oc} = 721 mV, J_{sc} = 39.20 mA/cm², FF = 79.57%, η = 22.50% (n side illumination); V_{oc} = 717 mV, J_{sc} = 38.72 mA/cm², FF = 79.91%, η = 22.19% (p side illumination). The bifaciality factor is 0.99. Compared to the standard

TCO utilization of 75 nm and 150 nm on front and rear side of the monofacial SHJ device, respectively, we achieved comparable cell performance with a 78% reduction in TCO use. TCO thickness-dependent contact properties for both *n*-contact and *p*-contact are still under investigation.

- [1] K. Yoshikawa, *et al.*, Sol. Energy Mater. Sol. Cells, 173, 37-42(2017)
- [2] TaiyangNews, 2nd Heterojunction report, 15-17 (2020)
- [3] E. Gervais, *et al.*, Renew. Sustain. Energy Rev., 137, 110589 (2021)
- [4] J. Yu, *et al.*, Sol. Energy Mater. Sol. Cells, 224, 110993 (2021).
- [5] H. H. Kuhnlein, SiliconPV 2021.
- [6] A. B. Morales-Vilches, *et al.*, IEEE J. Photovolt., 9, 34-39(2019)
- [7] S. Li, *et al.*, Joule, 5, 1535-1547 (2021)
- [8] M. Bivour, *et al.*, SiliconPV 2021.
- [9] C. Han, *et al.*, ACS Appl. Mater. Interfaces, 11, 45586 (2019)
- [10] C. Han, *et al.*, Sol. Energy Mater. Sol. Cells, 227, 111082 (2021)

3:00 PM EN04.10.06

Late News: Impact of Process Steps on the Performance of Heterostructure Solar Cells [Sergey M. Karabanov](#) and Mikhail Reginecich; Ryazan State Radio Engineering University, Russian Federation

The high open circuit voltage (up to 750 mV) of heterojunction solar cells provided by the excellent ability of a layer of hydrogenated amorphous silicon to passivate the surface of the silicon wafer. A number of methods for the deposition of a-Si:H layers are well known. To obtain solar cells with high parameters, it is necessary not only to get good passivation of the crystalline silicon surface, but also to create conditions for efficient charge transfer. One of the widely used methods of deposition of a-Si:H is the method of PECVD; during the formation of a-Si:H layer, various types of defects arise. Various process steps, including annealing, lead to a decrease in the number of defects.

In this work, we investigated the formation of defects and the properties of the a-Si:H layer after two-stage deposition with intermediate hydrogen plasma treatment, followed by deposition of a transparent conducting oxide, annealing of defects, and the influence of these factors on the characteristics of solar cells.

For the study, we used *n*-type monocrystalline silicon wafer with a resistivity of 1-5 Ohm * cm, with a size of 156.75 * 156.75 mm, and 180 microns thick. After the damaged layer removal, texturing and appropriate cleaning a-Si:H layers were applied to the surface of silicon wafer with the goal to obtain a *p-i-n* structure on one side and *n-i-i-n* on the other side. An ITO layer about 75 nm thick was deposited by magnetron sputtering of an In-Sn target in an argon-oxygen atmosphere. Metallization was formed as a final step and the parameters of solar cells were measured.

As a result of the studies carried out, it was found that the use of an intermediate hydrogen plasma treatment of the first layer of amorphous silicon leads to the passivation of defects with hydrogen; an increase in the number of silicon-hydrogen bonds and, as a consequence, an increase in the microstructure factor *R* from 0.4 to 0.55. This additional step in the PECVD process results in an increase in the lifetime of minority charge carriers from 2 to 5 milliseconds and an increase in the efficiency of the solar cell.

SESSION EN04.11: Bulk Lifetime Studies
Tuesday Afternoon, December 7, 2021
EN04-Virtual

4:00 PM *EN04.11.01

Gettering and Hydrogenation of Defects and Impurities in High Efficiency Silicon Solar Cells [Daniel Macdonald](#), An Yao Liu, Hang Cheong Sio, Sieu Pheng Phang, Rabin Basnet and Chang Sun; Australian National University, Australia

Impurities and defects continue to play an important role in limiting the efficiency of both laboratory and industrial silicon solar cells. In this work, we review recent progress in reducing the impact of some of the most important of these limiting defects through impurity gettering and hydrogenation steps, which occur coincidentally during device fabrication. Since the dominant defects in a material depend very strongly on the crystal growth conditions, we categorise them by the three common silicon crystal growth techniques – Czochralski-grown mono-crystalline silicon, Cast-grown silicon (including both multicrystalline and cast-mono silicon), and Float-Zone silicon.

Czochralski-grown monocrystalline silicon (Cz-Si)

The primary defects in Cz-si, whether *p*- or *n*-type, are oxygen-related. In boron-doped *p*-type silicon, the very well-known Light-Induced Degradation (LID) caused by boron-oxygen defects dominates. Although in principle it is not affected by gettering, hydrogen is widely thought to play a key role in the permanent regeneration of this defect, which is a crucial step in stabilising the high efficiency *p*-type PERC cells that now dominate the PV industry.

In *n*-type Cz-Si, which is the preferred substrate for IBC, SHJ and poly-silicon passivating contact solar cells, an important class of defects that sometimes occur during high-temperature processing are the oxygen-related ring defects. These consist of oxygen precipitates, and sometimes their associated dislocations and decorating metallic impurities. Under certain conditions, they can be partially mitigated by impurity gettering and hydrogenation steps. These ring defects can also occur in *p*-type Cz-Si wafers.

Industrial Cz-Si wafers often also contain traces of dissolved metals such as Fe, which can significantly affect the carrier lifetime, if not removed during processing by gettering. Such gettering can be achieved by phosphorus or boron diffusion, aluminium alloying, doped-poly-silicon layers, and even deposited dielectric films such as silicon nitride and aluminium oxide.

Cast-grown silicon (HP mc-Si and cast-mono Si)

Cast high-performance multicrystalline silicon (HP mc-Si), by design, contains many grain boundaries. Fortunately the recombination activity of these grain boundaries can be significantly reduced after hydrogenation, such as via fired silicon nitride films during cell metallisation. Cast-monocrystalline silicon (cast-mono Si), on the other hand, tends to be dominated by dislocation clusters. These are much more difficult to negate through hydrogenation, which reduces the achievable efficiency and yield for devices made on such wafers. Both HP mc-Si and cast-mono wafers also contain significant quantities of metallic impurities, some of which are precipitated at structural defects, whilst others remain dissolved. Under the right conditions, they can be gettered to a significant extent during phosphorus or boron diffusions, or by deposited films. This provides a convenient method to identify the metallic species present in these materials.

Float-Zone silicon (FZ-Si)

Although not used in industrial solar cells, Float-Zone silicon (FZ-Si) is often used in research laboratories, partly due to its immunity to oxygen-related LID and ring defects, and very low metallic impurity concentrations. However, due to the addition of nitrogen during crystal growth to control dislocations, they are subject to the formation of nitrogen-vacancy complexes. Once formed, these defects are highly recombination active. However they can be partly mitigated by hydrogenation.

Finally, although hydrogen is helpful in passivating some defects in silicon, it can also cause recombination-active defects when present in excess, such as the widely-researched Light and elevated-Temperature Induced Degradation (LeTID). Since these defects are caused by firing hydrogen-containing dielectric films, they can be found in all three types silicon wafer described above, whether n- or p-type.

4:30 PM *EN04.11.02

Light Induced Degradation in Silicon—A Comparison of Defects Detected in Boron-Doped Material and in Si with Other Group III

Dopants Matthew P. Halsall¹, Joyce A. De Guzman¹, Vladimir Markevich¹, Ian Hawkins¹, Jose Couthino², Jeff Binns³, Nikolay V. Abrosimov⁴, Iain F. Crowe¹ and Anthony Peaker¹; ¹The University of Manchester, United Kingdom; ²University of Alveiro, Portugal; ³GCL Solar Materials, United States; ⁴Leibniz Institute for Crystal Growth, Germany

It has been known for decades that solar cells fabricated from Czochralski-grown silicon (Cz-Si) using Boron as p-dopant display a loss of efficiency in their first few hours of operation. In order for the effect to be observed both Oxygen and Boron need to be present, giving the effects its usual name of Boron Oxygen light induced degradation or BOLID. It has been recently argued that a complex consisting of a substitutional boron atom and two oxygen atoms (B_2O_2) is a center with negative-U properties, and it is responsible for minority carrier trapping effects, persistent photoconductivity and light induced degradation of lifetime (and hence BOLID) in these materials. Depending on the position of the Fermi level, the B_2O_2 defect is either a deep donor or it can be in a few configurations with a shallow acceptor level. The $E(-/+)$ occupancy level of the defect has been found to be at $E_v + 0.32$ eV using deep level transient spectroscopy (DLTS). Transitions between the different states associated with hole/electron emission or capture by the defect have been monitored with the use of junction capacitance techniques. The presenter will review the evidence that this defect is responsible for this energy loss process in commercial cells from a combination of techniques, DLTS and optical spectroscopy.

The ability to detect the defect electrically gives scientists a vital tool to detect the presence of this defect, for Boron and, potentially, other alternative p-type dopants. The presenter will review recent work at Manchester on alternative dopants. We have detected a hole emission signal similar to that due to the B_2O_2 defect in Schottky diodes on p-type Si crystals doped with either Al, Ga, or In impurities. It appears that nearly identical hole emission signals with their maxima at about 391-392 K occur in all the DLTS spectra. The hole emission rates have been measured in these diodes in the temperature range from 360 K to 420 K with the use of the high-resolution Laplace DLTS technique. Arrhenius plots of the measured hole emission rates in Si samples doped with either B, Al, Ga, or In impurity atoms show that the emission rates and the derived values of activation energy for hole emission are very close for the differently doped samples. Finally we have carried out measurements of temperature dependencies of equilibrium occupancy and hole capture kinetics for the detected traps in samples doped with the different acceptor impurities. It is found from the analysis of the changes in magnitude of the DLTS signals with temperature that in all the samples the equilibrium occupancy function of the traps are characteristic for a defect with negative-U properties. Further, it is revealed that positions of the $E(+/-)$ occupancy level are very close in different samples, $E(+/-) \approx E_v + 0.32$ eV. We suggest that the observed negative-U defects in Cz-Si samples doped with different acceptor impurities are associated with the complexes incorporating a substitutional group-III impurity atom and two oxygen atoms (A_2O_2 , where A can be B, Al, Ga, or In). According to the model proposed transformations between the deep donor and shallow acceptor configurations of the B_2O_2 center are related to a transformation of the oxygen dimer in the vicinity of a B_s atom from a "square" to a staggered configuration. It appears that the presence of different group-III atoms in the A_2O_2 complex does not result in significant changes of the O_2 transformation processes. However, the (B_2O_2) to $(B_2O_2)^+$ reaction is enhanced compared to that for other Group III atoms probably because of local tensile strain induced in the lattice by a relatively small substitutional boron atom. It is argued that this enhancement is one of possible reasons of much more effective formation of recombination active defects, which are responsible for LID, in p-type material doped with boron compared to that in Si crystals doped with other group-III impurity atoms.

5:00 PM EN04.11.03

Excess Carrier Concentration in Silicon Device and Wafers: How Material Properties are Expected to Accelerate Light and Elevated

Temperature Degradation Alexandria N. McPherson, Joseph Karas, David L. Young and Ingrid Repins; National Renewable Energy Laboratory, United States

Predicting degradation rates under fielded conditions is important for understanding energy yield, project return on investment, and how to assign higher value to products where the degradation has been eradicated. Some processes, such as light and elevated temperature induced degradation (LeTID), and the regeneration portion of boron-oxygen light induced degradation (BO LID), are accelerated by the presence of excess carriers. It is therefore important to understand how excess carrier concentration changes as a function of conditions and materials properties both in operating solar cells, and in wafers, where these processes are often studied. In this investigation, we simulate excess carrier concentration as a function of wafer thickness and minority carrier lifetime in solar cells and wafers using SCAPS and Quokka. The same results are obtained whether one uses simulation software or analytic expressions based on the physics of p-n junctions. For wafers, there is a simple nearly linear relationship between excess carrier concentration, lifetime, and thickness. For solar cells, as lifetime increases or thickness decreases, excess carrier concentration becomes limited by rear surface recombination. Thus, LeTID may appear to progress more quickly in wafers than in cells, and the degradation rate will have a stronger dependence on minority carrier lifetime in wafers than in cells.

5:15 PM *EN04.11.04

Overview and State-of-the-Art of Degradation Phenomena in c-Si Solar Cells Giso Hahn; Univ of Konstanz, Germany

Over the last years, tremendous progress could be observed in improving the efficiency of industrial crystalline Si solar cells. The race towards higher efficiencies brings degradation phenomena occurring under working conditions of the solar cell more and more into the focus as the bulk material quality and surface passivation both play a crucial role for obtaining high efficiencies. In this presentation an overview of the known degradation phenomena on solar cell level will be given. This includes degradation of the bulk quality like the well-known boron-oxygen(BO)-related degradation under injection of charge carriers and the more recently detected LeTID (light and elevated temperature induced degradation) phenomenon as well as degradation of surface passivation quality under injection conditions in conjunction with elevated temperatures.

For BO-related degradation, the presence of H in the Si bulk allows for a regeneration of bulk material quality after degradation, which is stable under further illumination. The LeTID phenomenon seems to be triggered by the presence of H in the Si bulk, too, but here H seems to be the (direct or indirect) cause for degradation. As for BO-related degradation, a regeneration process for LeTID can be observed for longer treatment times, making it harder to cope with in cell processing. For longer treatment times, often changes in the surface passivation quality can be observed as well, at least for some dielectric layer systems. While the detailed microscopic picture of the defect formation is still unclear at least for LeTID and most surface passivation degradation phenomena, H seems to be involved for all of them in a direct or catalytic way.

For BO-related degradation a recently developed generalized model including the interactions of the BO-related defect and H in the c-Si wafer will be

discussed. For LeTID, some key findings and experiments will be presented to highlight the state-of-the-art of understanding. For degradation of surface passivation selected examples will be given and discussed. In the last decades, B-doped c-Si had highest PV market share. Currently a trend towards Ga-doped c-Si wafer material can be observed which eliminated the BO-related degradation. But LeTID seems to be observed in Ga-doped c-Si wafers, too, although with a different kinetics. Some recent findings in this field will be presented and discussed.

SESSION EQ17.08/EN04.02: Joint Session: Silicon PV Contacts and Perovskite/Silicon Tandems

Session Chair: David Fenning

Thursday Afternoon, December 2, 2021

Hynes, Level 2, Room 203

1:45 PM EQ17.08/EN04.02.01

Reactive Silver Inks as Front Electrodes for Next-Generation Silicon Solar Cells Michael W. Martinez-Szewczyk¹, April Jeffries¹, Steven DiGregorio², Owen Hildreth² and Mariana Bertoni¹; ¹Arizona State University, United States; ²Colorado School of Mines, United States

Fabrication of low-resistivity, robust front contacts for solar cell electrodes typically requires temperatures exceeding 200 °C to evaporate high-resistivity organic additives and sinter the suspended silver particles that form screen printing pastes. Novel technologies such as passivating contact, perovskite, and silicon heterojunction solar cells, along with their tandems, stand to benefit greatly from high performance metallization formed at temperatures that are compatible with each solar cell architecture [1,2,3].

Passivating contact technologies like silicon heterojunction (SHJ) cells have shown record power conversion efficiencies of 25.11% on full-size M2 monocrystalline wafers and continue to show promise as the platform for ever higher efficiencies (e.g. tandem) [4,5]. One of the main drivers of the SHJ solar cell's high efficiency is the passivating layers of a-Si that offer extremely low surface recombination velocity, <5 cm/s at room temperature [6]. The efficiencies of these cells are typically limited by their series resistance, which arises from the low conductivity of the low temperature silver paste used for front-grid metallization. While higher processing temperatures would enable lower metallization-related losses it would inevitably degrade the surface passivation quality of the SHJ cells. Therefore, metallization technologies that can offer silver-like resistivity and low contact resistance at temperatures below 150 °C have the potential to further propel passivating contact technologies.

In this presentation we will present the use of reactive silver ink (RSI) and dispense printing to fabricate solar cell front-grids that result in a low-resistivity, low-temperature metallization. When used to metallize a front-grid, the RSI results in media resistivities of 2.4-6 μΩ-cm and a cell series resistance of 0.76 Ω-cm², which is lower than commercially available screen-printed low-temperature silver paste with a media resistivity of 10 μΩ-cm and series resistance of 0.79 Ω-cm². This RSI metallization can be deposited at temperatures between 60-115 °C depending on the ink composition with a much lower silver loading than low temperature screen-printing pastes. These inks composition offer also the added benefit of being more corrosion resistant than the screen-printing paste counterparts. Using RSI allows a 55% decrease in silver consumption with improved cell efficiency when compared to the standard low-temperature silver paste metallized cell. This results in a substantial decrease in the cell metallization cost, which accounts for 30% of cell production costs [7]. Herein we will show the electrical performance of cells and modules prepared with RSI metallization, optical modeling of the dispensed RSI fingers as well as aging results under damp heat conditions.

[1] Y. Wang et al., *Solar RRL*, vol. 2(1), 1700180, 2017.

[2] S. Zhu et al., *Nano Energy*, vol. 45, 280-286, 2017.

[3] A. Moldovan., *IEEE 42nd PVSC*, 2015.

[4] X. Ru et al., *J. Solmat*, vol. 215, 110643, 2020.

[5] Hermle, M., ... & Glunz, S. W. *Appl Phys Rev* 7, 021305 (2020).

[6] Bernardini, S. & Bertoni, M. *physica status solidi (a)* 1800705-6 (2018)

[7] Louwen et al., *J. Solmat*, vol. 147, 295-314, 2016.

2:00 PM *EQ17.08/EN04.02.03

Towards Industrialization of Perovskite/Silicon Tandem Solar Cells—Advances in Metallization, Large-Area Perovskite Deposition, and Encapsulation Brett A. Kamin¹, Ton Offermans², Soo-Jin Moon¹, Arnaud Walter¹, Christophe Allebé¹, Gabriel Christmann¹, Ludovic Lauber¹, Patrick Wyss¹, Adriana Paracchino¹, Bertrand Paviet-Salomon¹, Quentin Jeangros¹, Christophe Ballif¹ and Sylvain Nicolay¹; ¹CSEM, Switzerland; ²CSEM Muttenz, Switzerland

While crystalline silicon solar cells (cSi) continue their steady march towards ever higher efficiencies, the practical physical efficiency limit for these devices looms on the horizon. In order to continue to increase module efficiency and lower overall system costs, new technologies which can surpass this limit must be realized. A tandem solar cell approach which pairs cSi with a Perovskite solar cell is the most promising current possibility to achieving this. Such an approach promises the potential of minimal additional production costs over existing cSi with a significantly higher efficiency limit. Indeed, with efficiencies of over 29% having been reported by several laboratories it is clear that this technology has great potential. However, significant work still must be done in order to assess the compatibility of this technology with industrialization and to challenge the assumption that the processing steps will incur a minimal cost increase. One central question in this vein is can we adapt existing industrial solutions for the large-scale production of Silicon/Perovskite tandems? Towards answering this question, three critical areas are examined: 1) Metallization, 2) Large-area perovskite deposition, and 3) Encapsulation.

Screen-printed Ag metallization is a standard process for commercial solar cells. However, the heat sensitive nature of perovskite solar cells makes this step challenging to adapt in tandem solar cells. Specifically, the requirement to have high conductivity and low contact resistance between the Ag fingers and the TCO appears difficult to achieve with most commercial pastes. Using optimized Ag pastes and standard screen-printing processes we demonstrate 4 cm² devices with a flat or textured front surface can be produced achieving efficiencies of 27.7% and 26.2%, respectively.

While these results are very promising, they were accomplished using spin coated layers on non-standard PV wafers. Moving towards a normal PV wafer requires a process with a very high throughput, good process control, and ultimately result in good semiconductor properties. However, the design parameters of this process are convoluted with the surface topology of the silicon wafer. As mechanically polished wafers are not realistic for commercial production, the question of surface preparation on commercial wafers becomes very important. To this end, we demonstrate a strategy of using meniscus deposited perovskite layers on top of chemically polished silicon M2 CZ bottom cells to achieve efficiencies over 22% on an area of 100cm². Such an approach should be compatible with existing industry standard wet-chemical preparation of silicon wafers. Additionally, meniscus coating of perovskite layers promises extremely high throughput potential using a technique that is already widespread commercially (albeit not in the PV world).

Finally, encapsulation of these devices is a critical step to ensuring good stability and reliability in the field. To enable adoption of this technology into existing production lines, demonstration of glass-glass encapsulation using a membrane laminator appears to be essential. It is demonstrated that by

optimizing the encapsulant materials and lamination process for lower temperature conditions allows for good encapsulation of tandem solar cells. However, a significant performance drop related to degradation of the cell during the process is observed. Through process optimization and optical refinement of the tandem stack we can minimize this performance loss and demonstrate a 4cm² device with printed metallization and glass-glass encapsulation with a stabilized efficiency of 24.8% (representing a 0.3% drop in efficiency over the unencapsulated cell).

2:30 PM EQ17.08/EN04.02.04

Detailed-Balance Efficiency Limits of Two-Terminal Perovskite/Silicon Tandem Solar Cells with Planar and Lambertian Spectral Splitters Verena Neder, [Stefan Tabernig](#) and Albert Polman; AMOLF, Netherlands

The photovoltaic conversion efficiency of two-terminal (2T) perovskite/Si tandem solar cells is strongly dependent on the degree of current matching that can be achieved between the top and bottom cell. In conventional cell designs, the distribution of light that is absorbed in the top and bottom cells is simply determined by the single or double-pass absorption in the planar sub-cells. For high-bandgap perovskites this will always lead to a current mismatch, as too small an amount of light is absorbed in the top cell. Here we show how a spectrum-splitting metasurface, placed at the perovskite/Si interface can help optimize the absorption distribution between the subcells for certain tandem cell geometries.

As a starting point we use detailed-balance calculations of the tandem cell efficiency for ideal subcells. For a 500 nm thick perovskite top cell the optimum perovskite bandgap is 1.57 eV for single-pass absorption (1.66 eV for double-pass absorption), in order to achieve optimal current matching. We then add a Lambertian-scattering metasurface at the perovskite/Si interface that reflects light in a narrow spectral band above the perovskite bandgap. This shifts the bandgap for which current matching is achieved to 1.70 eV and yields a higher efficiency, as the bandgap is closer to the ideal bandgap for perovskite/Si tandems (1.73 eV).

For wider perovskite bandgaps >1.73 eV, a spectrum splitter shows a major improvement as it strongly enhances the current in the (current-limiting) top-cell. For an idealized geometry we predict an absolute efficiency enhancement of more than 5% absolute for a top cell bandgap of 1.77 eV. Using experimental external quantum efficiency data for perovskite and Si cells this would translate to a practical efficiency gain of 2.7% (absolute) for this perovskite bandgap.

In practice, spectrum splitter metasurfaces may have small parasitic absorption. We include this in our model and find that for a top cell bandgap of 1.70 eV, a Lambertian spectral splitter with 15% parasitic loss and a reflectivity of 0.5 would still yield an efficiency gain of 2% absolute. Hydrogenated amorphous Si scatterers are ideal candidates to achieve this experimentally, as we have experimentally shown in four-terminal perovskite/Si tandem solar cells.

A subtlety in our analysis is the fact that the optimum energy at which the spectral splitter reflects light back into the top cell does not necessarily coincide with the top cell bandgap. This energy depends on which cell is current limiting, and for bandgaps around the ideal bandgap, like 1.70 eV, an onset of 20 meV above the bandgap yields the highest efficiency.

Our calculations show that a planar or Lambertian spectral splitter could be of significant benefit for two-terminal perovskite/Si tandems, especially around and above the ideal perovskite bandgap of 1.73 eV. Furthermore, we find that for non-ideal reflectivities and considering parasitic loss, significant efficiency gains can be achieved in these tandem solar cells.

SESSION EQ17.12/EN04.08: Joint Session: Contacts and Interfaces in Silicon Photovoltaics

Session Chairs: [Kaining Ding](#) and [Monica Morales-Masis](#)

Tuesday Morning, December 7, 2021

EQ17-Virtual

8:00 AM *EQ17.12/EN04.08.01

Low-Temperature Passivated Contacts for Silicon Solar Cells [Mathieu Boccard](#), Luca Antognini, Julie Dréon, Davi Febba, Julien Hurni, Vincent Paratte, Corentin Sthioul, Jonathan Thomet and Deniz Türkay; EPFL - PVlab, Switzerland

We review here the recent trends in silicon heterojunction solar cells using low-temperature passivated contacts. Beyond the archetypal amorphous silicon and indium tin oxide (ITO), several novel materials have recently demonstrated excellent performances when integrated in devices. Nanocrystalline silicon and silicon oxide alloys relax in part the trade-off between optical and electrical performances. Both n- and p-type contacts can be made with such material, with different strategies being necessary to enable excellent performance while maintaining surface passivation. Beyond silicon, several materials are investigated as more transparent alternative, including metal-oxides or nitrides. We will discuss what makes such materials attractive and what is still limiting the performance of devices incorporating them.

8:30 AM *EQ17.12/EN04.08.02

Titanium Oxide Carrier Selective Contacts for High Efficiency Crystalline Silicon Solar Cells Jesús Ibarra, Di Yan and [James Bullock](#); The University of Melbourne, Australia

Titanium oxide (TiO_x, x≈2) has been shown to be an effective passivating contact interlayer in a range of high efficiency crystalline silicon (c-Si) solar cells. It has been incorporated in a broad range of configurations; with and without passivating interlayers (i.e. silicon oxide SiO_x and amorphous silicon α-Si:H); with and without overlaying low work function electrodes (i.e. calcium, lithium fluoride / aluminium stacks LiF/Al); and in partial area and full area contact architectures. Passivating contacts incorporating TiO_x have enabled <10 fA/cm² scale recombination currents and <10 mΩcm² contact resistivities which are no inhibitor to cell efficiencies above 24%, with efficiencies above 23% already demonstrated in the laboratory. Though most of these high-efficiency structures employ TiO_x at the electron side of the cells, some studies have shown its potential tunability, which has enabled its use in hole contacts on c-Si as well, simply by varying deposition conditions and consequently changing its material properties. This talk explores the tunability of TiO_x thin films and their incorporation into passivated contacts. Interface properties, doping, thermal stability and post-metallisation stability will all be covered. Finally, remaining challenges for the incorporation of TiO_x in industrial c-Si cells will be discussed.

9:00 AM *EQ17.12/EN04.08.03

Atomic Layer Deposition of Passivating, Carrier-Selective Oxides for Silicon Photovoltaics [Kristopher O. Davis](#), Jannatul Ferdous Mousumi, Geoffrey

Gregory, Chien-Hsuan Chen, Parag Banerjee and Titel Jurca; University of Central Florida, United States

Metal oxides offer a diverse range of physical properties and can serve various roles in photovoltaic (PV) cells. The wide band gap of these materials allows them to be used on the front side of devices without adding parasitic optical absorption. There is a long track record of depositing metal oxides with atomic layer deposition (ALD), a manufacturing friendly process that results in highly conformal film growth and excellent film thickness control. This presentation will review how ALD metal oxides can be used as passivating, carrier-selective contacts for crystalline silicon (c-Si) PV cells. This begins with a breakdown of desirable characteristics for passivating contact materials, including transparency, interface defect passivation, carrier-selectivity, and carrier transport, as well as thermal stability and compatibility with high-volume manufacturing processes. Next, the performance of the more common metal oxides are surveyed and their process-structure-property relationships discussed, including how chemical interactions between layers can impact performance for better or worse. Much of this discussion will focus on aluminum oxide as a tunneling passivation layer, molybdenum oxide as a hole-selective material, and titanium oxide as an electron-selective material. Finally, remaining challenges and areas of opportunity for future research are covered.

9:30 AM EQ17.12/EN04.08.04

Polymer-Embedded Silver Microgrids by Particle-Free Reactive Inks for Flexible High-Performance Transparent Conducting Electrodes Ziyu Zhou and Paul W. Leu; University of Pittsburgh, United States

Metal microgrid-based transparent conductors enable the acceleration of wearable electronic applications development by constructing the high transparency, low sheet resistance and mechanically stable metal grid within flexible substrates. In this study, we demonstrate polymer-embedded silver microgrid structures with low porosity using a particle-free silver ink for flexible transparent electrodes. The conductive grids indicate a high transparency of 91.8% and a low sheet resistance of 0.88 Ω/sq , corresponding to a figure of merit value σ_{dc}/σ_{op} of nearly 4500 with gridlines of 10 μm width. The optimized gridline width may be fabricated down to 3.5 μm . Furthermore, the embedded structure of Ag microgrids shows 3 times lower surface roughness compared to particle-based conductive Ag inks and better mechanical as indicated by bending, folding and tape peeling test. The results demonstrate (1) a scalable approach for microgrid manufacturing, (2) microgrids with nearly the best transparent electrode performance properties, and (3) the benefit of reactive silver inks as opposed to particle-based ones. Metal microgrids may address technical and economical limitations with indium tin oxide (ITO) as well as enable the development of a various flexible and wearable optoelectronic applications.

9:45 AM EQ17.12/EN04.08.05

Selective Passivation of TiO_2 Defects via Targeted Dehydration Jessica C. Jones and Alex Martinson; Argonne National Laboratory, United States

Heterostructure interfaces are of critical importance for next generation device architectures. Defects at these interfaces significantly impact the resulting properties and ultimately device performance. Many studies focus on the growth of thin films by Atomic Layer Deposition (ALD) but neglect the unique surface chemistry and atomic structures formed at the resulting interface. This limits the device applications of heterostructures made with these types of thin films due to the limitations in crystallinity and lattice match. In an ALD-based approach we call selective interface reactions (SIRs) we target specific undesirable defect sites on a surface to achieve uniform behavior at interfaces formed on these surfaces. TiO_2 is considered the prototypical oxide surface and has been intensely studied due to its photocatalytic and optoelectronic properties. It is well established that the defects on the TiO_2 surface affect the optical and electronic properties, interfaces, and performance of resulting devices. DFT calculations are used to predict the difference in reactivity of "perfect" TiO_2 and minority atomic configurations such as step edges. We translate these differences in site reactivity to differences in thermal dehydration which is confirmed by STM. SIR is ultimately used to exploit these differences in thermal dehydration to selectively deposit material specifically on defect sites to prevent defect formation.

SYMPOSIUM EN05

Emerging Energy and Materials Sciences in Halide Perovskites
November 29 - December 8, 2021

Symposium Organizers

Maria Antonietta Loi, University of Groningen
Michael Saliba, University of Stuttgart
Feng Yan, Hong Kong Polytechnic University
Yuanyuan Zhou, Hong Kong Baptist University

Symposium Support

Bronze

Matter | Cell Press

* Invited Paper

SESSION EN05.01: Perovskite Characterization
Session Chairs: Juan Pablo Correa Baena, Maria Antonietta Loi and Mathias Rothmann

Monday Morning, November 29, 2021
Hynes, Level 3, Ballroom B

8:00 AM *EN05.01.01

The Role of Crystallographic Orientation and Heterostructures on Charge Carrier Transport in Halide Perovskite Solar Cells Juan Pablo Correa Baena; Georgia Institute of Technology, United States

Electronic defect passivation has been used as a strategy to achieve high performance perovskite solar cells. This strategy relies on interlayers that hinder carrier transfer through the bulk and across interfaces. I will discuss how different crystallographic phases of the halide perovskite affect charge carrier transport in the bulk. Charge carrier transport across interfaces will be further studied to understand whether crystalline structures or amorphous phases are able to efficiently allow transport out the device. Synchrotron-based characterization techniques, such as grazing incidence x-ray spectroscopy and x-ray fluorescence will be used to understand the structural and chemical composition of the films, whereas intensity-modulated photocurrent spectroscopy will be used to understand transport processes in the devices. As a result of these contributions, we aim at further understanding the role of interfacial layers and texture on carrier transport for efficient optoelectronic devices.

8:30 AM EN05.01.02

Quantitative Imaging of Structural Dynamics and Emerging Ferroelectricity in Inorganic Halide Perovskites Ye Zhang and Peidong Yang; University of California, Berkeley, United States

Halide perovskites are a class of semiconductor materials holding great promise for various energy conversion applications such as photovoltaics, light-emitting diodes and even electromechanical devices. Their advantages including the ease of processing, bandgap tunability, phase modification and defect tolerance are largely due to the soft and dynamical ionic lattice of halide perovskite structure. In particular, all-inorganic halide perovskites, with better thermal stability and a rich diagram of chemical/phase transformations, provide ideal platforms for the fundamental understanding of their structural dynamics as well as studying the emerging properties. A facile anion exchange chemistry is one of the examples of their dynamical lattice behaviors, which has been utilized in tuning the electronic bandgaps while the host perovskite structure still remains. In this presentation, I will first focus on a quantitative study of the anion exchange kinetics by directly visualizing the transformation process on single-particle level with spatial, temporal and spectroscopic information, enabled by the confocal photoluminescence imaging microscopy and a design of vapor-phase chemical treatment. We identified the two-step transformation for CsPbBr₃ to CsPbI₃ as: 1) initial surface reaction; 2) subsequent lattice anion diffusion. The quantitative imaging of anion exchange also revealed a diffusion-limited reaction mechanism. Another example of structural dynamics is the phase transition in CsPbI₃ between a metastable perovskite phase and a non-perovskite phase that is reversible and responsive to external stimulus such as temperature, moisture and light. The optical microscopic imaging method is also applied to study a moisture-induced phase transition kinetics where the nucleation and the propagation steps can be decoupled on individual single crystals.

I will later focus on discussing a different structural phase transition in CsGeX₃ (X=Cl, Br, I) where Ge (II) cation displacement leads to a rhombohedral distortion that introduces an inversion symmetry breaking and the emergence of ferroelectricity. Through a combination of *ab initio* theory and experiments from structural characterizations to multiscale material behaviors, we identified the role of lone pair stereochemical activity of Ge (II) in determining the ferroelectric origin and found out their spontaneous polarizations. Furthermore, characteristic ferroelectric domain patterns are imaged with both piezo-response force microscopy and nonlinear optical microscopic method. We anticipate that our discovery of this new semiconducting ferroelectric system will expand the understanding of physical phenomena related to ferroelectrics and introduce new possibilities to halide perovskites as well.

8:45 AM EN05.01.03

Defect Quantification in Lead Halide Perovskites—The Shortcut to Stability Michel De Keersmaecker, Neal R. Armstrong and Erin L. Ratcliff; The University of Arizona, United States

Since the late 1970s, operando electrochemical approaches have allowed a direct connection to the defect chemistry in semiconductor materials and the quantification of their energy levels with unprecedented limits of detection. However, the applicability of these solution-based electrochemical methods for defect quantification in metal halide perovskites has been rather limited and restricted to a few non-solvents.

Here, we demonstrate a straightforward three-electrode configuration with a "peel and stick" electrolyte for the electrochemical and spectroscopic investigation of metal halide perovskites. Our ability to effectively characterize defect energetics and densities is illustrated by controlling hole and electron injection in methylammonium lead triiodide and triple cation perovskite films using a systematic modulation of the potential. Introducing redox active probes facilitates operando mapping of the electronic structure, including probing the density of states, elucidation of surface defect reactivity, and assessment of defect passivation strategies, as electron transfer events represent charge injection and charge extraction events in operational optoelectronic platforms. Additional advantages include the ability to make chemical-electronic-physical connections, translate from macro-to nanometer length scales, and study the effect of photon flux, heat, humidity, and/or electrical bias. Finally, we illustrate the electrolyte film is optically transparent to visible and X-ray photons for simultaneous characterization of band gap and physical structure, and can be easily removed for characterization of the near-surface composition and energetics using photoelectron spectroscopies.

Overall, we establish an electrochemical approach that overcomes challenges in characterizing defects in printable electronic materials and provides opportunities for the operando characterization of thin film perovskites, organic semiconductors, quantum dots, conventional semiconductor materials, material blends and device stacks, where the removable solid electrolyte functions as the "top contact". These advanced electrochemical characterization platforms are crucial towards the search for low cost, improved and stable (opto)electronic materials to realize industry-scalable technologies in the field of photovoltaics, charge storage systems, photoelectrochemical cells, etc.

9:00 AM EN05.01.04

Manganese Doping for Enhanced Magnetic Brightening and Circular Polarization Control of Dark Excitons in Paramagnetic Layered Hybrid Metal-Halide Perovskites Timo Neumann¹, Sascha Feldmann¹ and Felix Deschler²; ¹University of Cambridge, United Kingdom; ²Technical University of Munich, Germany

Materials combining semiconductor functionalities with spin control are desired for the advancement of quantum technologies. Here, we study the magneto-optical properties of novel paramagnetic Ruddlesden-Popper hybrid perovskites Mn:(PEA)₂PbI₄ (PEA = phenethylammonium) and report magnetically brightened excitonic luminescence with strong circular polarization from the interaction with isolated Mn²⁺ ions. Using a combination of superconducting quantum interference device (SQUID) magnetometry, magneto-absorption and transient optical spectroscopy, we find that a dark exciton population is brightened by state mixing with the bright excitons in the presence of a magnetic field. Unexpectedly, the circular polarization of the dark exciton luminescence follows the Brillouin-shaped magnetization with a saturation polarization of 13% at 4 K and 6 T. From high-field transient magneto-luminescence we attribute our observations to spin-dependent exciton dynamics at early times after excitation, with first indications for a Mn-mediated

spin-flip process. Our findings demonstrate manganese doping as a powerful approach to control excitonic spin physics in Ruddlesden-Popper perovskites, which will stimulate research on this highly tuneable material platform with promise for tailored interactions between magnetic moments and excitonic states.

9:15 AM EN05.01.05

Multiple Exciton Series in Two-Dimensional Metal Halide Perovskites Arise from Lattice Deformations Giulia Folpini¹, Maurizia Palumbo², Daniele Cortecchia¹, Luca Moretti³, Giacomo Giorgi⁴, Giulio Cerullo³, Annamaria Petrozza¹ and Ajay Ram Srimath Kandada⁵; ¹Istituto Italiano di Tecnologia, Italy; ²Università degli Studi di Roma Tor Vergata, Italy; ³Politecnico di Milano, Italy; ⁴Università di Perugia, Italy; ⁵Wake Forest University, United States

In recent years, two-dimensional metal-halide perovskites (2D MHPs) have emerged as a promising class of due to their desirable characteristics, with bright and color pure emission at room temperature stemming from their high excitonic binding energy. The study of excitonic properties in 2D MHPs is not only relevant for light emitting and photovoltaic applications [1], but has garnered interest also for the unique physics of exciton-polarons in these materials, where the coexistence of multiple bright and dark states has been revealed [2-4]. Optical and electronic properties of lead-based 2D MHPs are conventionally tuned by changing halides or organic cations, but the effect of substituting the metal cation is also crucial to the development of more environmentally friendly alternatives based on tin [5-6].

Here we investigate the excitonic energetic landscape of the prototypical 2D MHP phenethylammonium tin iodide ((PEA)₂SnI₄), and compare it with its lead counterpart to clarify the role of the metal cation [7], demonstrating that the role of the organic-inorganic interactions can also be effectively manipulated by the metal cation, especially moving from the heavier lead to lighter tin. We elaborate on the origin of multiple excitonic resonances uniquely observed in the linear absorption spectrum of (PEA)₂SnI₄ at energies about 200-300 meV above the primary exciton. We investigate their origin through calculations based on density functional theory and many-body perturbation theory, which suggest that the excitonic series at these higher energies are composed of electronic transitions from a lower lying valence band. Importantly, the valence band splitting does not stem from changes in spin-orbit coupling, but it is driven by the octahedral conformations that follow small variations in the organic-inorganic interactions within the crystal lattice. We then discuss transient absorption spectroscopy results upon resonant and non-resonant exciton generation conditions to investigate the interaction between the multiple excitonic resonances: we experimentally show that the presence of the higher energy states results in a relatively slow nanosecond component in the formation dynamics of the primary exciton, in addition to the ultrafast phonon-driven hot carrier thermalization. While the presence of such slow relaxation channel for the excitons might be beneficial to many optoelectronic applications, our work suggests its possible control via systematic design of the organic cation. Moreover, our observations indicate that spin-orbit coupling does not play a primary role in the intricate yet crucial change as in the excitonic characteristics imparted by the tin substitution.

[1] *Nat. Nanotechnol.* **15**, 969–985 (2020)

[2] *Nat. Mater.* **18**, 349–356 (2019).

[3] *J. Mater. Chem. C*, 2020, **8**, 10889–10896

[4] *J. Phys. Chem. Lett.* 2020, **11**, 9, 3173–3184

[5] *Nature* **369**, 467–469 (1994)

[6] *Adv. Mater.* 2019, **31**, 1803230

[7] 10.26434/chemrxiv.14330018.v1

10:00 AM EN05.01.07

Late News: The Atomic-Scale Microstructure of Metal Halide Perovskites Elucidated via Low-Dose Scanning Transmission Electron Microscopy Mathias U. Rothmann^{1,1}, Judy S. Kim^{1,2,3}, Juliane Borchert^{4,1}, Kilian B. Lohmann¹, Colum M. O’Leary^{5,1}, Alex A. Shearer¹, Laura Clark¹, Henry Snaith¹, Michael B. Johnston¹, Peter D. Nellist¹ and Laura Herz¹; ¹University of Oxford, United Kingdom; ²Diamond Light Source, United Kingdom; ³Rosalind Franklin Institute, United Kingdom; ⁴University of Cambridge, United Kingdom; ⁵University of California, Los Angeles, United States

Understanding the atomic-scale crystallographic properties of photovoltaic semiconductor materials such as silicon, GaAs, and CdTe, has been essential in their development from interesting materials to large-scale energy conversion industries. However, studying photoactive hybrid perovskites by transmission electron microscopy (TEM) has proved particularly challenging due to the large electron energies typically employed in these studies.[1] In particular, the very close structural relationship between a number of crystallographic orientations of the pristine perovskite and lead iodide has resulted in severe ambiguity in the interpretation of EM-derived information, severely impeding the advance of atomic resolution understanding of the materials.

Here, we successfully image the archetypal CH(NH₂)₂PbI₃ (FAPbI₃) and CH₃NH₃PbI₃ (MAPbI₃) hybrid perovskites in their thin-film form with atomic resolution using a carefully developed protocol of low-dose STEM.[2] Our images enable a wide range of previously undescribed phenomena to be observed, including a remarkably highly ordered atomic arrangement of sharp grain boundaries and coherent perovskite/PbI₂ interfaces, with a striking absence of long-range disorder in the crystal. These findings explain why inter-grain interfaces are not necessarily detrimental to perovskite solar cell performance, in contrast to what is commonly observed for other polycrystalline semiconductors. Additionally, we observe aligned point defects and dislocations that we identify to be climb-dissociated, and confirm the room-temperature phase of CH(NH₂)₂PbI₃ to be cubic. We further demonstrate that degradation of the perovskite under electron irradiation leads to an initial loss of CH(NH₂)₂²⁺ ions, leaving behind a partially unoccupied, but structurally intact, perovskite lattice, explaining the unusual regenerative properties of partly degraded perovskite films. Our findings thus provide a significant shift in our atomic-level understanding of this technologically important class of lead-halide perovskites.

[1] *Adv. Mater.* 2018, **30**, 1800629

[2] *Science* 370, eabb5940 (2020)

9:45 AM BREAK

10:15 AM EN05.01.08

Observation of Spatially-Resolved Rashba States on the Surface of CH₃NH₃PbBr₃ Single Crystals Zhengjie Huang¹, Shai Vardeny², Tonghui Wang³, Zeeshan Ahmad⁴, Ashish Chanana⁵, Eric Vetter^{1,3}, Shijia Yang¹, Xiaojie Liu³, Giulia Galli^{4,6,7}, Aram Amassian³, Z. Valy Vardeny⁵ and Dali Sun^{1,1}; ¹North Carolina State University, United States; ²Los Alamos National Laboratory, United States; ³North Carolina Central University, United States; ⁴The University of Chicago, United States; ⁵University of Utah, United States; ⁶University of Chicago, United States; ⁷Argonne National Laboratory, United States

Hybrid organic-inorganic perovskites (HOIPs) are prime candidates for studying Rashba effects due to the heavy metal and halogen atoms in their crystal structure coupled with predicted inversion symmetry breaking. Nevertheless, the observation of Rashba effect in cubic

CH₃NH₃PbBr₃ single crystals that possess bulk inversion symmetry is the subject of extensive debate due to the lack of conclusive experiments and theoretical explanations. Here we provide experimental evidence that *Rashba state* in cubic CH₃NH₃PbBr₃ single crystal at room temperature occurs exclusively on the crystal surface and depends on specific surface termination that results in local symmetry breaking. We demonstrate this using a suite of spatially-resolved and depth-sensitive techniques, including circular photogalvanic effect, inverse spin Hall effect and multi-photon microscopy; and is supported by first-principle calculations. Our work resolves the existing controversy of Rashba states in three-dimensional HOIPs, and suggests using surface Rashba states in these materials for spintronic applications.

10:30 AM EN05.01.09

Structural Origins of Stability in Cubic Photoactive Metal Halide Perovskites Tiarnan A. Doherty¹, Satyawati D. Nagane¹, Dominik Kubicki¹, Young-Kwang Jung², Duncan Johnstone¹, Kyle Frohna¹, Miguel Anaya¹, Stuart Macpherson¹, Sean Collins³, Aron Walsh⁴, Paul Midgley¹ and Samuel D. Stranks¹; ¹University of Cambridge, United Kingdom; ²Yonsei University, Korea (the Republic of); ³University of Leeds, United Kingdom; ⁴Imperial College London, United Kingdom

Halide perovskite materials exhibit promising performance characteristics for low-cost optoelectronic applications. Photovoltaic devices fabricated from perovskite absorbers have reached power conversion efficiencies above 25.5 % in single-junction devices and 29.5% in tandem devices. Formamidinium (FA) lead iodide (FAPbI₃) and FA-rich perovskites are preferred for photovoltaic applications, but their widespread adoption is hindered by the rapid degradation of the desirable corner-sharing cubic (3C) phase to an undesirable wide bandgap, face-sharing, hexagonal (2H) phase under ambient conditions. Alloying FA with small amounts of Cs⁺ and methylammonium (MA) on the A site cation of the ABX₃ perovskite structure has proven a promising strategy for stabilizing photoactive perovskite phases. For example, photovoltaic devices fabricated with compositions such as Cs_{0.05}FA_{0.78}MA_{0.17}Pb(I_{0.83}Br_{0.17})₃ (triple cation) perovskites have achieved high device efficiencies with greatly enhanced reproducibility and ambient stability¹. Recently, there has also been renewed interest in methods to stabilize pure FAPbI₃ through strategies such as the incorporation of MA via treatment with methylammonium thiocyanate vapour², addition of formamidinium formate³ or methylammonium formate⁴. The mechanism of improved stability obtained from these approaches is generally explained as either originating from a tuning of the Goldschmidt tolerance factor towards the perfect cubic perovskite structure via cation mixing in the case of Triple Cation perovskites^{1,5}, by templating growth of the corner-sharing cubic structure in stabilized-FAPbI₃ perovskites^{2,4}, or by reducing intrinsic defect density³. A key tenet in all these explanations is that the final photoactive perovskite material, regardless of stabilization approach, is a cubic perovskite structure and that this is the structure that should be pursued for optimal stability and performance. Here, we reveal that contrary to conventional wisdom, this is not the case. In this talk using scanning electron diffraction (SED) we reveal the nanoscale structural origins of improved material stability in (Cs_{0.05}FA_{0.78}MA_{0.17})Pb(I_{0.83}Br_{0.17})₃ and stabilized thin films of α -FAPbI₃, two of the most promising candidates for commercial PV applications. Further, we will describe how these nanoscale stability mechanisms are related to our recent reports of performance limiting trap clusters in high-performing perovskite films⁶. Together, our talk will help answer questions such as “*What are the nanoscale origins of instability in perovskite materials and devices?*”, “*how important is phase purity for performance?*”

1. Saliba, M. *et al.* Cesium-containing triple cation perovskite solar cells: improved stability, reproducibility and high efficiency. *Energy & Environmental Science* **9**, 1989–1997 (2016).
2. Lu, H. *et al.* Vapor-assisted deposition of highly efficient, stable black-phase FAPbI₃ perovskite solar cells. *Science* **370**, (2020).
3. Jeong, J. *et al.* Pseudo-halide anion engineering for α -FAPbI₃ perovskite solar cells. *Nature* **592**, 381–385 (2021).
4. Hui, W. *et al.* Stabilizing black-phase formamidinium perovskite formation at room temperature and high humidity. *Science* **371**, 1359–1364 (2021).
5. Kim, J. Y., Lee, J.-W., Jung, H. S., Shin, H. & Park, N.-G. High-Efficiency Perovskite Solar Cells. *Chem. Rev.* **120**, 7867–7918 (2020).
6. Doherty, T. A. S. *et al.* Performance-limiting nanoscale trap clusters at grain junctions in halide perovskites. *Nature* **580**, 360–366 (2020).

10:45 AM EN05.01.10

Effects of Anion-Cation Composition on the Urbach Energy and Voc Deficit of Perovskite Solar Cells Biwas Subedi, Chongwen Li, Zhaoning Song, Maxwell M. Junda, Yanfa Yan and Nikolas J. Podraza; University of Toledo, United States

Power conversion efficiency of organic-inorganic metal halide ABX₃ (A: methylammonium-MA, formamidinium-FA, cesium-Cs; B: lead-Pb, tin-Sn; X: iodine-I, bromine-Br, chlorine-Cl) perovskite-based solar cells highly depends upon the structural and optoelectronic quality of the absorber layer. For polycrystalline perovskite films, higher material quality generally implies larger grain size, continuity of grains with reduced grain boundaries, increased carrier lifetimes and diffusion lengths, and reduced recombination, thereby increasing both the current and voltage generation in solar cells. Variation in the anion-cation composition affects the bandgap energies, absorption coefficient, and material structural quality such as crystal structure, phase stability, and grain size. In semiconductors like these perovskites, a wider exponentially decaying tailing effect in the absorption coefficient spectra below the bandgaps is indicative of the presence of lattice vibrations, defects, and impurities. The Urbach energy is the width of this exponentially decaying tail, and its value is reported for more than 60 unique perovskite compositions with bandgaps ranging from 1.2–2.3 eV. Urbach energies for pristine perovskite films are measured using the combination of photothermal deflection spectroscopy and spectroscopic ellipsometry. In mixed Sn + Pb perovskites, films with < 50% Sn increase the Urbach energy, whereas intermediate or higher Sn contents lower it. Doping small amounts of Cl and Br (< 30%) with I slightly decreases the Urbach energy, whereas Cl or Br content > 30% increases it. More importantly, a correlation between the Urbach energy of perovskite absorber and corresponding device performance, in terms of the open-circuit voltage (V_{OC}) deficit here, has been studied. V_{OC} deficit is defined as the difference between the absorber bandgap normalized to the electron charge and the measured device V_{OC}, and largely refers to the existence of imperfections in the absorber layer. Most perovskite solar cells fabricated with low Urbach energy absorbers also exhibit low V_{OC} deficit and vice versa. However, those with Cs-based inorganic or mixed Sn + Pb perovskites with very high Sn content show a large V_{OC} deficit even though the corresponding pristine absorber layers show low Urbach energy. In these cases, the absorber layers inside these solar cells degrade or transition to non-perovskite phases due to atmospheric exposure, and no longer reflect the pristine film conditions at which their Urbach energies were measured.

SESSION EN05.02: Perovskite Synthesis
Session Chairs: Letian Dou, Maria Antonietta Loi and Ana Nogueira
Monday Afternoon, November 29, 2021
Hynes, Level 3, Ballroom B

1:30 PM *EN05.02.01

“Hollow” Iodide and Bromide Perovskites—Between 2D and 3D Mercouri G. Kanatzidis; Northwestern University, United States

Hybrid halide perovskites consisting of corner-sharing metal halide octahedra and small cuboctahedral cages filled with counter cations have proven to be

prominent candidates for many high-performance optoelectronic devices. The stability limits of their three-dimensional perovskite framework are defined by the size range of the cations present in the cages of the structure. In some cases, the stability of the perovskite-type structure can be extended even when the counterions violate the size and shape requirements, as is the case in the so-called “hollow” perovskites. We can take advantage of their defect tolerance to engineer a new family of 3D highly defective “hollow” iodide and bromide perovskites with general formula $(FA)_{1-x}(en)_x(Pb)_{1-0.7x}(X)_{3-0.4x}$ (FA = formamidinium, en = ethylenediammonium, x = 0-0.44, X=Br, I). The corresponding materials were characterized by a battery of techniques, including single crystal X-ray diffraction (XRD), high resolution powder X-ray diffraction (PXRD), and solid state nuclear magnetic resonance (NMR) measurements. Pair distribution function (PDF) analysis shed light on the local structural coherence, revealing a wide distribution of Pb-Pb distances in the crystal structure, validating further that the corresponding materials are lead deficient and that en inclusion has the same structural effect as in the case of the “hollow” iodide analogs. By manipulating the number of defects, we finely tuned the optical properties of the pristine FAPbBr₃, by blue shifting the band gap from 2.20 eV to 2.60 eV for the 42% en sample. A most unexpected outcome was the fact that above 40% en incorporation the material exhibits strong broad light emission with 1% photoluminescence quantum yield that is maintained after exposure in air for more than a year. This is the first example of strong broad light emission from a 3D hybrid halide perovskite and is a clear demonstration that defect engineering can be utilized in our favour to add unusual, exotic optoelectronic properties to this versatile class of materials.

2:00 PM *EN05.02.02

Multi-Functional Conjugated Ligand Engineering for Perovskite Solar Cells and LEDs Letian Dou; Purdue University, United States

Surface passivation is an effective way to boost the efficiency and stability of perovskite devices. However, a key challenge faced by most of the passivation strategies is reducing the interface charge recombination without imposing energy barriers to charge extraction. In this talk, I will present a novel multi-functional semiconducting organic ammonium cationic interface modifier inserted between the light-harvesting perovskite film and the hole transporting layer. We show that the conjugated cations can directly extract holes from perovskite efficiently, and simultaneously reduce interface non-radiative recombination. Together with improved energy level alignment and stabilized interface in device, we demonstrate a triple-cation mixed-halide medium-bandgap perovskite solar cell with an excellent power conversion efficiency of 22.06% (improved from 19.94%), and the suppressed ion migration and halide phase segregation, which lead to a long-term operational stability over 1000 hours. Using a similar concept, we achieved high performance red LEDs with external quantum efficiency over 20%. Our strategy provides a new practical method of interface engineering in perovskite solar cells and LEDs towards improved efficiency and stability.

2:30 PM EN05.02.03

Characterization and Modeling of Solid-Vapor Reactions for MAPbI₃ Perovskite Solar Cell Processing Alexander Harding, Austin Kuba, Kevin Dobson, Ujjwal Das, Babatunde Ogunnaike and William Shafarman; University of Delaware, United States

As the stability and efficiency of perovskite solar cells improve, efforts toward developing a manufacturing process have expanded. One promising candidate for high-speed perovskite production is vapor transport deposition (VTD). A variant of this process is used by First Solar LLC for the deposition of CdTe solar modules and has assisted CdTe in becoming the market leader in thin film photovoltaics. While VTD presents a viable fabrication route for single-step or two-step perovskite deposition, an understanding of the processing fundamentals is required to design functional equipment. This information is acquired from the precursor technology: close space vapor transport (CSVT).

Previously, we presented a two-step, all-vapor, CSVT deposition process to fabricate methylammonium lead iodide (MAPbI₃) thin films.¹ The two steps of this process are 1) the deposition of a PbI₂ thin film, followed by 2) a reaction in methylammonium iodide (MAI) vapor.¹ While the PbI₂ deposition process is well-understood,^{2,3} the MAI reaction remains uncharacterized. Our preliminary work found that the consumption of PbI₂ to form MAPbI₃ could be approximated using a first-order reaction rate law, though deviations between model and experiment were notable.¹ Here, we expand upon our understanding of the MAI reaction process using controlled experimentation and mathematical modeling.

Experiments were carried out on reacted thick films of PbI₂ (600-800 nm) onto C₆₀/ITO/glass substrates. Isothermal reactions in MAI vapor were then carried out at a fixed pressure of 9 Torr for three temperatures: 110°C, 120°C, and 130°C. Reaction times were varied at each condition, and replicates were carried out to assess process reproducibility. This allowed the intermediate reaction states to be studied using variable-angle glancing incidence x-ray diffraction (GIXRD) and cross-sectional scanning electron microscopy (SEM).

GIXRD measurements were carried out on reacted samples from an incident angle of 0.3° to 3.0° in 0.1° increments and were used to determine the structure of the sample at different x-ray penetration depths. These scans showed that the principal tetragonal MAPbI₃ peak (110)/(002) at 2θ = 14.0° was present at every incident angle, while the principal PbI₂ (001) peak at 2θ = 12.6° appeared at different angles of incidence depending on the reaction temperature and time. The onset angle was measured for each sample and used to calculate an x-ray penetration depth to determine the MAPbI₃ film thickness.

Cross-sectional SEM measurements were performed on each partially-reacted sample to determine the structure as a function of film thickness. It was observed that a distinct layered structure formed during the reaction. There was good agreement between the calculated x-ray penetration depth through MAPbI₃ and the thickness of the top layer, which confirmed the layers were MAPbI₃ on top of unreacted PbI₂.

The MAI reaction was found to be consistent with a non-catalytic, heterogeneous, solid-fluid reaction model.⁴ A mathematical model will be developed based on these experimental data, and a reaction rate law will be presented at the conference. Using the three reaction temperatures, the temperature dependence of the reaction will also be presented and will account for the concentration of MAI taking part in the reaction⁵ and the temperature dependence of the Thiele modulus.⁴

The information to be presented at the conference will serve as a critical stepping-stone for the development of high-throughput, two-step perovskite vapor processes.

References

1. A. Harding et al. *RSC Adv.* 2020, **10**, 16125-16131.
2. A. Kuba et al. *2020 47th IEEE Photovoltaic Specialists Conference (PVSC)*, 1203-1206.
3. A. Harding et al. *2021 48th IEEE Photovoltaic Specialists Conference (PVSC)*.
4. C. Y. Wen. *Ind. Eng. Chem. Res.* **60**, 34-54, 1968.
5. A. Dualeh et al. *Chem. Mater.* 2014, **26**, 6160-6164.

2:45 PM EN05.02.04

Compositional Tailoring and Photophysical Features of Thick-Layers in 2D Hybrid Lead Halide Perovskites: Structure, Luminescent Properties and Stability Eugenia S. Vasileiadou¹, Xinyi Jiang¹, Ido Hadar¹, Mikael Kepenekian², Jacky Even², Bin Wang³, Qing Tu⁴, Christos Malliakas¹, Daniel Friedrich¹, Ioannis Spanopoulos¹, Justin Hoffman¹, Vinayak Dravid¹, Alexandra Navrotsky⁵ and Mercouri G. Kanatzidis¹; ¹Northwestern University, United States; ²Univ Rennes, France; ³University of California, Davis, United States; ⁴Texas A&M University, United States; ⁵Arizona State University, United States

2D hybrid lead halide perovskites are light-harvesting semiconductors with tailorable structural and photophysical features that provide a vast

compositional space to engineer new and environmental stable materials for optoelectronic applications. Herein, we actuate a comprehensive exploration of the structure-property relationships in several, newly reported series of 2D halide perovskites with thick layers ($n \geq 2$) in bulk crystal and film form. Firstly, thermochemical evaluation of the representative 2D structure types of Ruddlesden-Popper (RP) and Dion-Jacobson (DJ) perovskites is presented based on calorimetric measurements that reveal that the enthalpy of formation for the studied RP perovskites is negative while for the DJ perovskites is positive.¹ Film stability tests demonstrate consistent observations with the thermochemical findings, where RP lead iodide perovskites are both thermodynamically and environmentally stable candidates for optoelectronic applications. Synthesis and characterization of the second known example of a $n=6$ perovskite compound: $(\text{PA})_2\text{MA}_3\text{Pb}_6\text{I}_{19}$ (where PA= pentylammonium) is reported with a favorable enthalpy of formation.¹ Secondly, the methodical tailoring of the 2D perovskite structure's composition (organic and inorganic component), unveils trends in the comparison of thick-layered lead iodide and lead bromide perovskites, for the acquisition of halide perovskites with enhanced stability.² New members of $n=2$ lead bromide perovskites that belong to the Ruddlesden-Popper structure type are presented with formula: $(\text{C}_m\text{H}_{2m+1}\text{NH}_3)_2(\text{CH}_3\text{NH}_3)\text{Pb}_2\text{Br}_7$ ($m = 6-8$) incorporating long chain alkyl-monoammonium cations ($\text{C}_m\text{H}_{2m+1}\text{NH}_3$) of hexylammonium ($m=6$), heptylammonium ($m=7$) and octylammonium ($m=8$). 2D thick-layer lead bromide perovskites reveals pronounced differences with their lead iodide congeners, in terms of lattice match between the inorganic $[\text{PbX}_6]^{2+}$ perovskite layer and organic layer, carrier lifetime and film stability behavior.² Lastly, we examine the crystal chemistry of thick-layer perovskites consisting of organic molecules with bifunctional groups and investigate thoroughly the excited-state dynamics by transient absorption (TA) spectroscopy. Our work highlights the importance of the optimal synthetic design and engineering of environmentally robust, 2D lead halide perovskite materials for next-generation optoelectronic devices.

1. Vasileiadou, E. S.; Wang, B.; Spanopoulos, I.; Hadar, I.; Navrotsky, A.; Kanatzidis, M. G., Insight on the Stability of Thick Layers in 2D Ruddlesden-Popper and Dion-Jacobson Lead Iodide Perovskites. *J. Am. Chem. Soc.* **2021**, *143* (6), 2523-2536.
 2. Eugenia S. Vasileiadou, I. H., Mikael Kepenekian, Jacky Even, Qing Tu, Christos Malliakas, Daniel Friedrich, Ioannis Spanopoulos, Justin M. Hoffman, Vinayak P. Dravid, and Mercouri G. Kanatzidis, Shedding Light on the Stability and Structure-Property Relationships of Two-Dimensional Hybrid Lead Bromide Perovskites. *Chem. Mater.* **2021**, *10.1021/acs.chemmater.1c01129*.

3:30 PM *EN05.02.06

Double Perovskite Single-Crystals of $\text{Cs}_2\text{AgBiBr}_6$ —The Role of Cu Doping on the Photophysics and Crystal Structure Ana F. Nogueira; University of Campinas (UNICAMP), Brazil

The use of lead-based perovskites in photovoltaic applications has demonstrated to be a successful alternative for future energy generation, but still lead toxicity is a concern and a limitation in some countries. Lead-free double perovskites have attracted attention of the research community due to the ability of tuning their bandgap, structure and stability by selectively choosing the combination of metals. $\text{Cs}_2\text{AgBiBr}_6$ presents great ambient stability, a relatively easy synthesis route, and consists of cheap and abundant materials. However, the large and indirect band gap of this composition hinders its potential as an efficient light-harvesting material. Doping is a promising strategy to improve the optical and electronic properties of this material, even though only few works studied in details the chemistry and physics involved in $\text{Cs}_2\text{AgBiBr}_6$ doping. In this work, we work on some modifications of $\text{Cs}_2\text{AgBiBr}_6$ single crystals with various cations and realize structural investigations combined with photophysical tests to elucidate the mechanism involved in the doping. The understanding of doping allows the comprehension of $\text{Cs}_2\text{AgBiBr}_6$ chemistry, opening opportunities to obtain other promising double perovskites.

3:15 PM BREAK

4:00 PM EN05.02.07

AI-Driven Design of High Entropy Halide Perovskite Alloys Arun Kumar Mannodi Kanakkithodi¹, Maria K. Chan², Rishi Kumar³ and David P. Fenning³; ¹Purdue University, United States; ²Argonne National Laboratory, United States; ³University of California, San Diego, United States

Halide perovskites with desirable stability, electronic band structure, and optical absorption are sought for solar cells, electronic devices, infrared sensors and quantum computing. Compositional manipulation via alloying at cation or anion sites, or via incorporation of point defects and impurities, can help tune their properties. In this work, we develop AI-based frameworks for the on-demand prediction and multi-objective optimization of the phase stability, band gap, optical absorption spectra, photovoltaic efficiency, and defect formation energies for a chemical space of ABX_3 halide perovskites with several choices for A, B and X, mixing allowed at each site, and several possible crystal structures. These frameworks are powered by high-throughput density functional theory (DFT) computations, dimensionality reduction techniques applied upon unique encodings of the atom-composition-structure (ACS) information, and rigorous training of advanced neural network (NN)-based predictive and optimization models. In the current work, we restrict the atom choices to the following: A \hat{I} {FA, MA, Cs, Rb, K}, B \hat{I} {Pb, Sn, Ge, Ba, Sr, Ca}, and X \hat{I} {I, Br, Cl}; we also note that the design frameworks can easily be extended to other atom choices with the infusion of fresh data.

DFT-based geometry optimization and property estimation is performed for hundreds of perovskite alloys simulated using special quasi-random structures (SQS), with new data points sequentially selected using Bayesian active learning approaches to comprehensively traverse the compositional chemical space and iteratively improve prediction accuracies. NN regression models trained upon the DFT data enable the simultaneous prediction of all properties of any ACS combination in the perovskite chemical space, with a special focus on high entropy alloys containing fractions of 5 or 6 elements at the A or B sites. We find that with all end-point and selected mixed compositions included in the training dataset, the predictive models are successfully able to reproduce known formation energy and band gap bowing behavior in perovskite alloy compositions. Further, multi-fidelity learning helps to bridge the gap between (high quantities of) low accuracy calculations and (lower quantities of) high-fidelity data, constituted of either accurate, expensive computations or experimental measurements collected from the published literature. The best predictive models are combined with two different multi-objective optimization techniques, namely, state-of-the-art genetic algorithms and variational autoencoders, to determine optimal high entropy alloy perovskite compositions with desired stability, optoelectronic, and defect properties. Finally, AI-based recommendations are synergistically coupled with targeted synthesis and characterization, leading to successful validation and discovery of novel halide perovskite compositions for improved performance in solar cells.

References

1. A. Mannodi-Kanakkithodi, J. S. Park, N. Jeon, D. H. Cao, D. J. Gosztola, A. B. F. Martinson, M. K. Y. Chan, "Comprehensive Computational Study of Partial Lead Substitution in Methylammonium Lead Bromide", *Chemistry of Materials* **31** (10), 3599–3612 (2019).
2. A. Mannodi-Kanakkithodi, M. Toriyama, F. G. Sen, M. Davis, R. F. Klie, M. K. Y. Chan, "Machine learned impurity level prediction in semiconductors:

the example of Cd-based chalcogenides", npj Computational Materials 6, 39 (2020).

3. A. Mannodi-Kanakkithodi, J. S. Park, A. B. F. Martinson, M. K. Y. Chan, "Defect Energetics in Pseudo-Cubic Mixed Halide Lead Perovskites from First-Principles", Journal of Physical Chemistry C. 124, 31, 16729–16738 (2020).

4. A. Mannodi-Kanakkithodi, M. K. Y. Chan, "Computational Data-Driven Materials Discovery", Trends in Chemistry 3, 2, 79–82, (2021).

5. A. Mannodi-Kanakkithodi, R. E. Kumar, D. Fenning, M. K. Y. Chan, "Data-Driven Design of Novel Halide Perovskite Alloys", *in preparation*.

4:15 PM EN05.02.08

Exploration of Hybrid Perovskite Superlattice for Efficient and Structurally Stable Stand-Alone Hybrid Solar PV Material Tsz Hin Edmund Chan and Steven Hepplestone; University of Exeter, United Kingdom

Hybrid perovskite solar cells (with chemical formula ABX_3) are of great interest due to the recently measured power conversion efficiency of greater than 25% (but theoretically, 33.7%). Perovskite structures are easily customisable, with a range of options for A, B and X. This enables us to both tune the electronic band gap and the stability by varying the composition. Two promising perovskites are the $CH_3NH_3PbI_3$ (MAPI) and $CH(NH_2)_2PbBr_3$ (FAPB) structures. By varying the ratio of FA and MA and doping with Br, we can potentially tune the band gap and effective masses (and hence electronic transport).

In order to compromise for a more desirable bandgap for stand-alone PV and better structural stability, the hybrid perovskite constituents are then strategically layered into superlattice form. We explore the bulk properties and interfacial engineering to improve the material's electronic transport.

We present a theoretical investigation of the structural and electronic properties of MAPI(x)/FAPB(y) superlattice, performed using first-principles density functional theory and temperature dependent vibrational entropy correction. Our results show that dominating number of layers of FAPB over MAPI will decrease the band gap. We discuss why the formation energies of superlattice in hexagonal and cubic phases differ across temperature and contradicts from the ones of its ground-state constituents. The solutions will be suggested for experimental validation.

SESSION EN05.03: Perovskite Devices I

Session Chair: Mathias Rothmann

Tuesday Morning, November 30, 2021

Hynes, Level 3, Ballroom B

10:30 AM EN05.03.01

No Need for Tin—Perovskite/Organic Tandem Solar Cells Approaching 24% Kai O. Brinkmann¹, Tim Becker¹, Florian Zimmermann¹, Cedric Kreusel¹, Tobias Gahlmann¹, Manuel Theisen¹, Tobias Haeger¹, Selina Olthof², Manuel Günster¹, Timo Maschwitz¹, Fabian Göbelsmann¹, Christine Koch², Dirk Hertel², Pietro Caprioglio^{3,4}, Lorena Perdigon⁴, Lena Merten⁵, Alexander Hinderhofer⁵, Amran Al-Ashouri⁶, Leonie Gomell⁷, Steve Albrecht⁶, Frank Schreiber⁵, Klaus Meerholz², Dieter Neher⁴, Martin Stollerfoht⁴ and Thomas Riedl¹; ¹University of Wuppertal, Germany; ²University of Cologne, Germany; ³University of Oxford, United Kingdom; ⁴University of Potsdam, Germany; ⁵University of Tuebingen, Germany; ⁶Helmholtz-Zentrum Berlin, Germany; ⁷Max-Planck-Institute Duesseldorf, Germany

Perovskite solar cells saw a phenomenal development over the past years and for some time dwarfed all progress in the field of organic solar cells. Meanwhile, the introduction of non-fullerene acceptors unlocked skyrocketing efficiencies of up to >18% in organic solar cells recently, with an absorption spectrum extending well into the infrared.^[1] Therefore, new opportunities open up, to implement them for high efficiency tandem architectures. As perovskites and organic semiconductors share similar processing technologies they are attractive partners for the monolithic tandem integration. On top of that, low gap perovskite materials are almost exclusively based on Sn²⁺ containing structures, which still give rise to fundamental stability concerns, as the 2+ state is easily oxidized resulting in deterioration by parasitic self-doping of the active material.^[2]

Likewise, serious concerns currently exist about photo instability of most non-fullerene organic systems. Now, in surprising contrast to these almost paradigmatic concerns, we evidenced an outstanding operation stability of an organic single junction (~ 100% PCE remaining after >1000 h continuous operation) that is based on the PM6:Y6 active system (>17% efficiency), if excitons are exclusively generated on the acceptor material Y6 (which is the case in a tandem application). Hence, in stark contrast to perovskite-perovskite tandem approaches, the sub-cell limiting operation stability shifted from the low gap (Sn-) perovskite to the wide gap (1.85 eV) Br-rich perovskite cell. To this end we were also able to show, that the effect of detrimental halide segregation in high (50%) Br content perovskite solar cells strongly depends on the choice of hole transporting material, providing a possible pathway towards how those concerns might be further addressed in the future.

Despite of high promise, as of yet the efficiency of perovskite/organic tandem cells remain underwhelming at approximately 20% due to severe optical and electronic losses.^[3] By a combination of interface optimization at the wide-gap perovskite cell, a lossless and almost perfectly shunt resilient ALD grown indium oxide interconnect and the highly robust gas quenching technique utilizing n-methyl-2-pyrrolidone (NMP) as co-solvent, we are now able to demonstrate perovskite / organic tandems with efficiencies approaching 24%. As all three utilized sub processes for the building blocks are extremely reproducible, we were at the same time able to achieve an extremely narrow process variation.

Based on a realistic simulation, we foresee efficiencies of perovskite/organic tandem cells exceeding 31% in the future.

[1] Liu Q, *et al. Science Bulletin* **65**, 272-275 (2020).

[2] Lin R, *et al. Nature Energy* **4**, 864–873 (2019).

[3] Chen X, *et al. Joule* **4**, 1594-1606 (2020).

10:45 AM EN05.03.05

Origin of High Photoresponse in Anisotropic Strain-Engineered CsPbBr₃ Photodetectors Da Bin Kim and Yong S. Cho; Yonsei University, Korea (the Republic of)

Lattice-strain has been recognized as a critical attribute in determining electronic and optoelectronic properties of halide materials, on the basis of experiment and theoretical estimation. Herein, we propose a unique experimental approach to induce extra lattice-strain in flexible cesium lead bromide (CsPbBr₃) thin films by modulating the level of bending curvature of the plastic substrate to produce different magnitudes of tensile or compressive strain during the two-step solution deposition. The CsPbBr₃ thin films processed with the in situ strain of -0.83% to +0.83% were used to fabricate a self-

powered photodetector of Ag:LiF/ Phenyl-C61-butiric acid methyl ester (PCBM)/CsPbBr₃/ poly(3,4-ethylenedioxythiophene) polystyrene sulfonate (PEDOT:PSS)/ITO/PEN structure. As a result, the maximum responsivity of 121.5 mA W⁻¹ and detectivity of 2.28x10¹⁰ cmHz^{0.5}W⁻¹ were achieved at a light intensity of 0.47 mWcm⁻² for the maximum tensile strain of +0.83% without applying a bias, which were the increases by ~61 and ~55%, respectively, relative to the unstrained reference case. These improvements were attributed to the weakened orbital coupling between Pb 6s and Br 4p with longer Pb-Br bonds in the case of tensile strain, causing the down-shifts in the valence band minimum and conduction band minimum, with the promoted drift of photogenerated carriers.

11:00 AM EN05.03.06

Non Corrosive Halide Exchange to Form CsPb(Br_{1-x}Cl_x)₃ from CsPbBr₃ for Light Emission and Lasing Cedric Kreusel^{1,2}, Kai O. Brinkmann^{1,2}, Manuel Runke^{1,2}, Manuel Theisen^{1,2}, Detlef Rogalla³, Selina Olthof⁴, Frederic van gen Hassend¹, Lena Merten⁵, Alexander Hinderhofer⁵, Frank Schreiber⁵, Arne Röttger¹ and Thomas Riedl^{1,2}; ¹University of Wuppertal, Germany; ²Wuppertal Center for Smart Materials & Systems, Germany; ³Ruhr-Universität Bochum, Germany; ⁴University of Cologne, Germany; ⁵University of Tübingen, Germany

All-inorganic perovskites are particularly attractive for optoelectronic applications such as light emitting diodes and lasers, due to their excitonic properties and benefits of thermal and environmental stability in comparison to some hybrid analogues.[1] Especially for lasers all-inorganic perovskites, such as CsPbCl₃, with emission in the blue/violet wavelength region are desirable. Unfortunately, as of yet, the solution-based preparation of CsPbCl₃ is strongly complicated by the poor concomitant solubility of the two precursor salts PbCl₂ and CsCl.

Recent reports have shown the conversion of CsPbBr₃ by exposure to hydrochloric acid (HCl) as a chlorine source.[2] While the resulting CsPbCl₃ layers showed some blue emission, the HCl simultaneously caused significant etching of the exposed perovskite layers.

Here, we propose a non-corrosive and highly controllable halide exchange process for CsPbBr₃ via pulsed exposure to metal halide precursors (e.g. SnCl₄ or TiCl₄) inside an Atomic Layer Deposition (ALD) reactor. The successive conversion from CsPbBr₃ to CsPb(Br_{1-x}Cl_x)₃ (up to x = 1) with an increasing number of ALD pulses is confirmed by optical absorption and emission spectroscopy, X-ray diffraction (XRD), as well as Rutherford-Backscattering Spectrometry (RBS) and X-ray photoelectron spectroscopy (XPS). Grazing-incidence wide-angle X-ray scattering (GIWAXS) evidenced that the layers are homogeneously converted. We demonstrate that the converted films do not show any signs of etching due to the conversion process. We furthermore demonstrate that our concept can be likewise applied for CsPbBr₃ layers that have been imprinted by thermal nanoimprint, which is particularly important with regard to photonic nanostructures. In first orienting studies, optically pumped amplified spontaneous emission (ASE) at λ = 426 nm with a threshold of 1.2 mJ/cm² at room temperature could be achieved in these converted layers. This is a significant step towards all-inorganic perovskite lasers emitting in the violet/blue spectral region.

[1] Pourdavoud N., et al., *Adv. Mater.* **2019**, *31*, 1903717, DOI: 10.1002/adma.201903717

[2] J. M. Pina, et al., *Adv. Mater.* **2021**, *33*, 2006697, DOI: 10.1002/adma.202006697

SESSION EN05.04: Perovskite Properties
Session Chairs: Davide Ceratti and Maria Antonietta Loi
Tuesday Afternoon, November 30, 2021
Hynes, Level 3, Ballroom B

1:30 PM *EN05.04.08

Light-Soaking, Photo-Damage and Self-Healing in Halide Perovskites Gary Hodes¹, David Cahen¹, Philip Schulz², Jean-François Guillemeot² and Davide R. Ceratti²; ¹Weizmann Institute of Science, France; ²Centre National de la Recherche Scientifique, France

Light-soaking, photo-damage and self-healing are intriguing phenomena widely reported in halide perovskites. Yet, their origin is still not understood even if they strongly influence the stability of the material. We discussed recently which could be the chemical origin of various phenomena connected to these effects [1] revealing how the stability of the interstitial Br defects (associated with photodamage) in MAPbBr₃, FAPbBr₃, CsPbBr₃ is inversely related to the kinetic of self-healing of photodamage after intense illumination.

In this talk, I will extend the description of the effects of intense illumination to MAPbI₃ showing how this material can also self-heal from photodamage with kinetics in the order of (several) minutes. I will reveal the presence of multiple (chemical) pathways activated by intense illumination some of which cause an increase of the photoluminescence (light soaking) and some of which decreasing it (photodamage). All of these are, at least partially, reversible and proceed from what can be called the “high entropy” of the halide perovskites.

I will also show how water, even in conditions that do not cause the degradation of the material, strongly influences all the mentioned processes actually “protecting” MAPbI₃ from photodamage but also substantially impeding light-soaking. This causes the measurements performed over a short time in an inert atmosphere to provide better results because of transient light-soaking effects which, eventually, disappear over time in both humid and inert atmospheres.

The talk will conclude with a panoramic over the literature of the reported effect trying to identify any other critical experimental condition inducing variations on the photodamage and light soaking effect or the kinetics and extent of self-healing. I will also provide additional information on the activation energies involved in the mentioned processes as obtained studying the temperature dependence of these in MAPbBr₃, FAPbBr₃ and CsPbBr₃

2:00 PM EN05.04.02

Process Engineering-Based Modification for Optimal Performance of Organometallic Halide Perovskite Solar Cells Vikas Sharma¹, Neha Sepat², Suraj Prasad³ and Dinesh Kabra¹; ¹Indian Institute of Technology Bombay, India; ²Linköping University, Sweden; ³Karlstad University, Sweden

Halide perovskite semiconductors are emerging candidates for new age Photovoltaics with high power conversion efficiency in single-junction cell and tandem geometry.¹ Researcher are exploring the structural, photo-physics, and optoelectronic properties of these semiconductors.^{2,3} In this quest, we investigate the different layers of cells from the electron transport layer to the oxide protection layer, the active layer, and the hole transport layer in terms of thickness, molar concentration of precursors, doping concentration for optimal performance. The photoluminescence study of ETL-perovskite reveals that electrons extracted efficiently without quenching due to the high conductivity of tin oxide and better interface alignment with the perovskite layer. A significant change of near about 21 % between the highest and lowest power conversion efficiency was observed by a simple variation of process parameters.

Keywords: Process Engineering; Halide Perovskite; Planer Structure; Photoconversion Efficiency

Reference:

- [1] I. Mora-Seró, M. Saliba, Y. Zhou, Towards the Next Decade for Perovskite Solar Cells, *Solar RRL*, 4, 2, 1900563, 2020.
- [2] K. Zhu, M. Yang, Y. Zhou, N. P. Padture, Organo-metal halide perovskites films and methods of making the same, *US Patent*, 10,910,569, 2021.
- [3] S. Singh, Laxmi, and D. Kabra, Defects in halide perovskite semiconductors impact on photo-physics and solar cell performance, *J. Phys. D: Appl. Phys.* 53, 503003, 2020

2:15 PM EN05.04.04

Time-Series Prediction of Perovskite Film Photoluminescence Using Machine Learning Meghna Srivastava¹, Tao Gong^{1,1}, John Howard^{2,2} and Marina Leite¹; ¹University of California, Davis, United States; ²University of Maryland, United States

The commercialization of perovskite solar cells (PSC) for next-generation photovoltaic technology hinges on improvements to their long-term stability. Several environmental stressors (light, humidity, temperature, bias, and oxygen) are known to trigger degradation in PSC, which limits device lifetimes to far below those of state-of-the-art Si cells. For effective commercialization, the large parameter space of perovskite compositions and synthesis conditions must be traversed to design optimal devices. Such devices must also undergo lengthy stability testing to prove their viability. With this development process in mind, taking a standard trial-and-error materials research approach to PSC design, fabrication, and stability testing becomes untenably time consuming while demanding significant human labor costs. The field of machine learning (ML) presents an alternate strategy that can contribute to a new research paradigm: one with greater pace, rationality, and reproducibility than trial-and-error methods. Here, we first present ML as a toolkit to accelerate PSC commercialization and demonstrate a general framework for projects to follow. We establish a roadmap to guide researchers through all steps of ML model development, which include collecting the initial training data, data cleaning and pre-processing, feature engineering, model selection, and model optimization and testing.

Next, we showcase this framework in action by using ML to forecast the optical performance of perovskite thin films under dynamic environmental conditions. We track the photoluminescence (PL) signal from the films over time while controlling the relative humidity (rH) and temperature in a sealed, nitrogen-filled chamber, then use ML to predict the PL response for each film composition using rH and temperature data alone. For this time-series prediction task, we implement recurrent neural networks (RNN), a class of neural networks with a historical state or “memory.” The network forecasts dynamic PL responses using the environmental state (rH and temp) at a specific time point along with the historical state, which represents physical changes that have occurred within the film. Our optimized model generates PL forecasts over 4 hours for methylammonium lead triiodide (MAPbI₃) and triple-cation (formamidinium-methylammonium-cesium) perovskite thin films with normalized root mean square error (NRMSE) of 18% and 14%, respectively. Our network can be driven by weather forecast data, predicting future PL output with high time resolution (one point every 15 seconds) and providing insight into the optical response and stability of perovskite materials under various weather conditions. This work illustrates the potential of ML for PSC development through the example of time-series prediction of optical properties. We envision extensions of this concept to other perovskite compositional families and to other combinations of environmental stressors, including full devices under standard operating conditions and International Summit on Organic Photovoltaic Stability (ISOS) stability testing protocols.

2:30 PM EN05.04.05

Late News: Ultrafast Excited-State Localization and Charge-Carrier Mobility in Cs₂AgBiBr₆ and Cu₂AgBiI₆ Adam D. Wright^{1,2}; ¹Princeton University, United States; ²University of Oxford, United Kingdom

Building upon the success of lead halide perovskites, lead-free silver–bismuth semiconductors have become increasingly popular materials for optoelectronic applications. Of these materials, perhaps the most prominent is Cs₂AgBiBr₆, which has demonstrated a better thermodynamic stability than MAPbI₃ but whose photovoltaic power conversion efficiency lags behind [1]. One reason for this is the strong electron-phonon coupling in Cs₂AgBiBr₆, which sets a fundamental limit on the charge-carrier mobilities and hence critically affects device performance. Understanding the nature of the charge-lattice coupling in Cs₂AgBiBr₆, and its influence on charge-carrier dynamics, is thus crucial for the optimization of these materials in a variety of optoelectronic applications and to further the understanding of a wide range of related silver–bismuth–halide semiconducting materials. Of these, one particularly promising contender is Cu₂AgBiI₆, which was first reported earlier this year [2] and is notable for its direct bandgap.

In this study, I report on the evolution of photoexcited charge carriers in Cs₂AgBiBr₆ [3] and Cu₂AgBiI₆ [4]. In both materials, I observe rapid decays in terahertz photoconductivity transients that reveal an ultrafast, barrier-free localization of free carriers on the time scale of a few picoseconds to an intrinsic small polaronic state. I attribute this to the strong charge-lattice coupling in these bismuth-silver materials, while the temperature-independence of the self-trapping is indicative of low electronic dimensionality due to the electronic isolation of the distinct Ag⁺ and Bi³⁺ sites. Through a combination of temperature-dependent photoluminescence and absorption spectroscopy, I identify the electronic states occupied before and after localization, directly tracing the localization of the charge carriers with time and interpreting its influence on the charge-carrier mobility in terms of a quantitative model. Since the small polaron motion is temperature-activated, I find that their mobility still exceeds 1 cm² V⁻¹s⁻¹ in both materials, leaving open the prospect of their application in efficient photovoltaic devices.

- [1] Longo, G.; Mahesh, S.; Buizza, L. R. V.; Wright, A. D.; Ramadan, A. J.; Abdi-Jalebi, M.; Nayak, P. K.; Herz, L. M.; Snaith, H. J. Understanding the Performance-Limiting Factors of Cs₂AgBiBr₆ Double-Perovskite Solar Cells. *ACS Energy Lett.* **2020**, *5*, 2200–2207.
- [2] Sansom, H. C.; Longo, G.; Wright, A. D.; Buizza, L. R. V.; Mahesh, S.; Wenger, B.; Zanella, M.; Abdi-jalebi, M.; Pitcher, M. J.; Dyer, M. S.; Manning, T. D.; Friend, R. H.; Herz, L. M.; Snaith, H. J.; Claridge, J. B.; Rosseinsky, M. J. Highly Absorbing Lead-Free Semiconductor Cu₂AgBiI₆ for Photovoltaic Applications from the Quaternary CuI–AgI–BiI₃ Phase Space. *J. Am. Chem. Soc.* **2021**, *143*, 3983–3992.
- [3] Wright, A. D.; Buizza, L. R. V.; Savill, K. J.; Longo, G.; Snaith, H. J.; Johnston, M. B.; Herz, L. M. Ultrafast Excited-State Localization in Cs₂AgBiBr₆ Double Perovskite. *J. Phys. Chem. Lett.* **2021**, *12*, 3352–3360.
- [4] Buizza, L. R. V.; Wright, A. D.; Longo, G.; Sansom, H. C.; Xia, C. Q.; Rosseinsky, M. J.; Johnston, M. B.; Snaith, H. J.; Herz, L. M. Charge-Carrier Mobility and Localization in Semiconducting Cu₂AgBiI₆ for Photovoltaic Applications. *ACS Energy Lett.* **2021**, *6*, 1729–1739.

2:45 PM EN05.04.06

Late News: Understanding the Effects of Grain Size and Indentation Size on the Mechanical Properties of Hybrid Organic-Inorganic Perovskite Materials Omolara V. Oyelade^{1,2,3}, Oluwaseun K. Oyewole², Yusuf A. Olanrewaju¹, Richard Koech¹, Sarafadeen Adeniji¹, Dairu Sanni¹, Kingsley Orisekeh¹, Vitalis Anye¹ and Winston W. Soboyejo^{2,4}; ¹African University of Science and Technology, Nigeria; ²Worcester Polytechnic Institute, Worcester, MA 01609., United States; ³Bingham University, Nigeria; ⁴Worcester Polytechnic Institute, United States

This paper examines the effects of grain size on the mechanical properties of hybrid organic-inorganic perovskites (HOIPs). Nanoindentation measurements and statistical deconvolution techniques are used to study the Young's moduli and hardness or strengths of perovskite layers in HOIPs. The

size dependence of indentation hardness is discussed within the context of Mechanism-based Strain Gradient (MSG) plasticity theories. These are also used to obtain information on the underlying geometrically necessary and statistically stored dislocation densities. The grain size effects associated with the different annealing temperatures (between 80 and 170°C) are also characterized using Hall-Petch approaches. The implications of the results are then discussed for the microstructural design of robust perovskite solar cells on rigid and flexible substrates.

3:00 PM EN05.04.09

High Quality 2D Perovskite Thin Films Obtained Through a Simple Blade-Coating Approach Herman Duim¹, Sampson Adjokatsé¹, Gert H. Ten Brink¹, René De Kloe², Simon Kahmann^{1,3}, Bart J. Kooi¹, Giuseppe Portale¹ and Maria Antonietta Loi¹; ¹University of Groningen, Netherlands; ²Ametek BV, Netherlands; ³University of Cambridge, United Kingdom

Layered metal halide perovskites are attractive semiconductors for a range of different optoelectronic applications owing to their large structural versatility and rich photophysics. As is the case for the more conventional 3D perovskites, thin films of these materials can be deposited directly from solution, thereby holding the promise of procuring flexible and cost-effective films through large-scale fabrication techniques. However, such solution-based deposition techniques often induce large degrees of heterogeneity due to poorly controlled crystallization. While much attention is focused on the optimization of thin film microstructure and its relation to device performance in the case of 3D perovskites, the microstructure of layered perovskite thin films remains markedly underexplored.

In this talk, I will present a detailed characterization of the optical properties and microstructure of the archetypal 2D perovskite phenylethylammonium lead iodide ((PEA)₂PbI₄). Using a combination of structural characterization techniques, we demonstrate that thin films with large grains and strong texture are readily obtained through a simple and scalable blade-coating process. Moreover, we highlight the large impact that the stoichiometry of the precursor solution has on the crystallinity, morphology, and optical properties of the resulting thin films.

All in all, we illustrate the large potential for scalable fabrication of 2D perovskite films and underline some of the major hurdles to be overcome for the further development of devices based on large area layered perovskite film.

3:15 PM EN05.04.10

Thermal Properties of Large Crystalline CsPbBr₃ Perovskite Thin Films—Remarkable Behavior at Phase Transitions Tobias Haeger^{1,2}, Moritz Ketterer¹, Ralf Heiderhoff^{1,2} and Thomas Riedl^{1,2}; ¹University of Wuppertal, Germany; ²Wuppertal Center for Smart Materials & Systems, Germany

Thermal management in LEDs and lasers is important for both efficiency and lifetime. Thermal management is especially challenging in perovskite-based devices [1], due to their exceptional thermal properties, such as ultra-low thermal conductivity λ , low thermal diffusivity a , and small volumetric heat capacity c_{vol} at room-temperature [2]. These thermal properties strongly depend on temperature and structural phase transitions, which in some perovskites even occur at moderate temperatures. In this context it should be noted that for inorganic cesium-based perovskites there are only a few reports on the thermal properties at their respective phase transitions [3].

Here the thermal properties of perovskites are studied using a Scanning Thermal Microscope, which takes advantage of the 3ω -method in the frequency domain without the need of elaborate sample preparation. Furthermore, it allows the simultaneous acquisition of the thermal properties $\lambda(T)$, $a(T)$, and $c_{vol}(T)$ [4]. The thermal properties of nano crystalline and large crystalline CsPbBr₃ perovskite thin films were examined from room-temperature to 150°C, in which orthorhombic to tetragonal to cubic phase transitions occur [5]. The thermal properties of large crystalline films with layer thicknesses 110 nm, 150 nm, and 200 nm were investigated.

It could be confirmed from the $\lambda(T)$, $a(T)$, and $c_{vol}(T)$ characteristics that CsPbBr₃ thin films with small crystallites (200nm) show a second order phase transition at 88°C from orthorhombic to tetragonal and a first order transition at 132°C from tetragonal to cubic, as described in earlier works [6]. In stark contrast, for thin films with large crystals (5-10 μ m), instead of abrupt changes in $l(T)$ at the tetragonal to cubic phase transition temperature, a continuous increase was found. The onset of the increase of the thermal conductivity shifts slightly to lower temperatures with decreasing the layer thickness from 200 nm to 110 nm. In addition, we also find that the thermal diffusivity $a(T)$ significantly decreases already in the tetragonal phase in comparison to the orthorhombic phase. On the other hand, only the thin films with a thickness of 110 nm a typical signature of latent heat (pointing to a first order transition) is found in the transition from tetragonal to the cubic phase, basically associated with the freedom of rotational modes of PbBr₆ octahedra around the three principal axes, while $c_{vol}(T)$ of the thicker films (150 nm and 200 nm) indicate a 2nd order phase transition. It should be noted that the 1st order phase transition of the 110 nm thick CsPbBr₃ perovskite film was found at a lower temperature 115°C than that reported for polycrystalline films and large single crystals at 132°C.

These temperature dependent thermal properties of large crystalline CsPbBr₃ perovskite thin films are similar to that of a material that exhibits phase transitions causing the material to contract upon increasing the temperature due to either a redistribution or ordering effects. This remarkable behavior at phase transitions requires particular attention because it will significantly influence the thermal management in perovskite-based LEDs and lasers.

1. Li X. et al., Energy Technol. 2015,3,551–555
2. Haeger T. et al., J. Mater. Chem. C, 2020,8, 14289—14311
3. Haeger T. et al., J. Phys. Mater., 2020, 3, 024004
4. Haeger T. et al., J. Phys. Chem. Lett. 2019, 10, 3019
5. Zhang M. et al., CrystEngComm,2017,19,6797
6. Hirotsu S. et al., J. Phys. Soc. Jpn., 1974, 37, 1393–1398

3:30 PM EN05.04.11

Bromine in Triple Mesoscopic Hole-Conductor-Free Perovskite Solar Cells Hindia Nahdi^{1,2}, Sarah Cherif³, Frédéric Oswald⁴, Stephanie Narbey⁵, Olivier Plantevin³, Bernard Geffroy^{4,1}, Denis Tondelier¹, Yvan Bonnassieux¹ and Madjid Haddad²; ¹LPICM, CNRS, Ecole polytechnique, France; ²SEGULA Technologies, France; ³Université Paris-Saclay, France; ⁴CEA, CNRS, France; ⁵Solaronix, Switzerland

Within the challenging race for alternative energy sources, hybrid metal halide perovskite solar cells (PSCs) have undergone unprecedented progress with efficiencies reaching now 25.5% [1-3]. These remarkable performances result from the exceptional optoelectrical properties of hybrid perovskite materials. Coupled with their potential for low fabrication cost, perovskite solar cell technology is very promising. However, since hybrid halide perovskites have a highly ionic character, they can decompose under external stresses such as moisture, solvents and heating cycles [4-6]. Reducing environmental stresses imposed by moisture or oxygen for example, in order to improve the long-term stability of perovskite solar cells, is critical to the deployment of this technology.

In 2017, Grancini *et al* [7] published a structure proven to be stable for more than 10,000 hrs, measured under controlled standard conditions, by engineering an ultra-stable 2D/3D $(\text{HOOC}(\text{CH}_2)_4\text{NH}_3)_2\text{PbI}_4/\text{CH}_3\text{NH}_3\text{PbI}_3$ perovskite junction. This structure is based on a fully printable architecture made of three mesoporous layers in which the perovskite is embed.

In this communication, we investigate the effects of changing the perovskite composition in this architecture by adding and/or replacing iodine with bromine into its chemical composition to tune device, increasing the band gap of the material [8], opening the gate to potential application in water splitting ($V_{\text{OC}} > 1.23$ V at pH = 0 [9]). After characterization of their photovoltaic properties, the cells, reaching $V_{\text{OC}} \sim 1.3$ V are studied by SEM coupled to EDX, XRD, Raman, absorption and photoluminescence spectroscopies.

1. Green, M. A., Ho-Baillie, A. & Snaith, H. J. The emergence of perovskite solar cells. *Nature Photonics* **8**, 506–514 (2014).
2. Green, M. A. & Ho-Baillie, A. Perovskite Solar Cells: The Birth of a New Era in Photovoltaics. *ACS Energy Lett.* **2**, 822–830 (2017).
3. Best Research Cell Efficiencies. *NREL* <https://www.nrel.gov/pv/cell-efficiency.html> (2021).
4. Berhe, T. A. *et al.* Organometal halide perovskite solar cells: degradation and stability. *Energy Environ. Sci.* **9**, 323–356 (2016).
5. Leijtens, T. *et al.* Stability of Metal Halide Perovskite Solar Cells. *Adv. Energy Mater.* **5**, 1500963 (2015).
6. Rong, Y., Liu, L., Mei, A., Li, X. & Han, H. Beyond Efficiency: the Challenge of Stability in Mesoscopic Perovskite Solar Cells. *Adv. Energy Mater.* **5**, 1501066 (2015).
7. Grancini, G. *et al.* One-Year stable perovskite solar cells by 2D/3D interface engineering. *Nature Communications* **8**, 15684 (2017).
8. Yu, W. *et al.* Diversity of band gap and photoluminescence properties of lead halide perovskite: A halogen-dependent spectroscopic study. *Chemical Physics Letters* **699**, 93–98 (2018).
9. Walter, M. G. *et al.* Solar Water Splitting Cells. *Chem. Rev.* **110**, 6446–6473 (2010).

SESSION EN05.05: Perovskite Interfaces
Session Chairs: Letian Dou and Maria Antonietta Loi
Wednesday Morning, December 1, 2021
Hynes, Level 3, Ballroom B

10:30 AM *EN05.05.01

Instability at Interfaces—How Metal-Oxides Interact with Perovskites and Their Precursors Selina Olthof, University of Cologne, Germany

In optoelectronic devices, the function and performance depends crucially on the proper alignment of the energy level landscape throughout the device, allowing for efficient charge transport across the various interfaces. For applications containing halide perovskites as active layer it turned out that such interfaces can show rather complex behavior. Not only the energetic alignment of transport levels play a role - more importantly, the perovskite composition and formation can be significantly influenced by chemical reactions taking place at these interfaces. In order to prepare highly efficient and stable devices, it is crucial to understand and control these interactions.

In this talk, I will summarize our work on a variety of metal-oxides such as SnO_2 , MoO_3 , ZnO , TiO_2 etc. where we use photoelectron spectroscopy to analyze which components are responsible for the strong interface chemistry. For this, we investigated a variety of different perovskites (i.e. organic vs. inorganic ones, I vs. Br, etc.) as well as the individual perovskite precursors. We find that the reactivity strongly depends on the individual material combination and that different metal oxides show fundamentally different reaction/degradation pathways. Furthermore, we found that by changing the defect density of the surface we can affect the degree of thin film degradation significantly.

Overall, I will show how photoelectron spectroscopy measurements can help to probe and understand the processes going on at these various bottom contact materials which should ultimately help to improve the stability of perovskite related devices.

11:00 AM EN05.05.02

Probing the Chemistry of Perovskite Systems by XPS and GD-OES Depth-Profiling—Potentials and Limitations Pia Dally^{1,2}, Stefania Cacovich^{3,1}, Davina Messou^{1,2}, Armelle Yaiche^{4,1}, Jean Rousset^{4,1}, Arnaud Etcheberry² and Muriel Boutemy²; ¹IPVF, France; ²ILV, France; ³CNRS, France; ⁴EDF, France

Despite the outstanding rapid evolution of Perovskite based solar cells efficiencies, the main drawbacks of this technology remain their intrinsic and extrinsic stabilities. Researches nowadays are focusing on enhancing the device architecture where interfaces properties play a crucial role on the final performances and durability. In particular, it is crucial to understand the physical and chemical phenomena occurring at those interfaces, site of defects accumulation and carrier recombination, band mis-alignment or even chemical drift.

This approach is particularly challenging on perovskite solar cells because of the alternating of organic / inorganic layers, requiring a fine optimization of the analysis conditions. The present study addresses the question of the reliability of the chemical information when profiling perovskite layers by X-ray Photoelectron Spectroscopy (XPS) and Glow Discharge Optical Emission Spectroscopy (GD-OES).

XPS and GD-OES are first performed separately on a half-cell constituted of glass/FTO/c-TiO₂/m-TiO₂/triple cation Perovskites ($\text{Cs}_{0.05}(\text{MA}_{0.14}\text{FA}_{0.86})_{0.95}\text{Pb}(\text{I}_{0.84}\text{Br}_{0.16})_3$). The high sensibility of perovskite layers requires to first evaluate the stability of those layers during the transfer from the glove box where they are elaborated to the spectrometers and during analyses themselves (X-Ray, UHV and ion bombardment) to find optimal operating conditions. Especially, the perturbation generated by ion beam and plasma etching has to be accurately studied to infer possible artefacts likely leading to misinterpretation and to determine the best parameters for the abrasion sequences.

In the case of GD-OES, not only the Radio Frequency power and the plasma gas pressure are changed, but also the nature of this gas (Ar, Ar/O, Ne).

Concerning XPS, both monoatomic (Ar^+) and cluster (Ar_n^+) projectiles are tested, varying their energies and the cluster size. Finally, GD-OES and XPS show similar trends for the composition profiles. However, we observe that all the conditions employed for XPS profiling lead to a systematic reduction of lead as well as the degradation of the organic part and iodine loss, more or less pronounced. This raises the question of the bombardment effect on the perovskite surface, influencing the integrity of the collected chemical information. Craters obtained with the ion gun of the XPS spectrometer have been accurately characterized to have a better understanding on the bombardment impact on the perovskite surface and also beyond. First, AFM (Atomic Force Microscopy) and SEM (Secondary Electron Imaging) clearly evidence a remarkable change in the surface morphology between a bombarded surface by Ar^+ and Ar_n^+ , and thus a proof that analyzed surfaces during XPS sequential sputtering differ. Secondly, the perturbed depth is evaluated in the case of Ar^+ by means of PL (Photoluminescence) and optical measurements. Obtained spectra inside craters resulting from different sputtering duration (i.e. different residual perovskite thicknesses) show no peak shift nor phase segregation. This demonstrates that there is no cumulative effect of sputtering nor drastic chemical modifications.

Finally, a strategy for studying the complete device by an innovative coupling between GD-OES and XPS, very complementary, is discussed. The GD-OES, semi-quantitative technique, assures a fast depth profiling to quickly reach specific areas of interest, which makes it interesting to perform profiling on complete cells and quickly reach the perovskite layer. On the other hand, XPS allows to precisely probe the composition of the extreme surface and to have access to the atomic composition and the chemical environments. This strategy has already been satisfactorily implemented on CIGS, Si and III-V materials. Results of this coupling will be presented and discussed in the case of a perovskite absorber, showing the potential as well as the remaining obstacles that still need to be addressed.

11:15 AM EN05.05.03

Mobile Interfaces Encourage Degradation of MAPbI₃ [Rhiannon M. Kennard](#)¹, Clayton Dahlman¹, Ryan DeCrescent¹, Jon Schuller¹, Kunal Mukherjee², Ram Seshadri¹ and Michael L. Chabinye¹; ¹University of California, Santa Barbara, United States; ²Stanford University, United States

Hybrid perovskites are being commercialized using roll-to-roll processing and are attractive for flexible optoelectronics. This raises questions about how bending impacts the structure and stability of thin films. Here, we examine how mobile interfaces respond to bending in MAPbI₃, the prototypical halide perovskite. MAPbI₃ is a ferroelastic, which means that it forms domains that are contained within the features seen via SEM. We will first review distinctions between ferroelastics and ferroelectrics, and explain conditions necessary for ferroelasticity: briefly, ferroelastics have spontaneous strain, while ferroelectrics have spontaneous electric polarization. Ferroelastic domains have identical crystal structure and different crystallographic orientations, and are separated by interfaces called twin walls. Bending MAPbI₃ moves the twin walls, which changes the proportions of the ferroelastic domains. We mapped the stresses needed to move the twin walls onto the stress-strain curve of MAPbI₃. Bending MAPbI₃ films outwards causes faster degradation to the undesired PbI₂ phase: this degradation is correlated with nucleation of new ferroelastic domains that form to accommodate the applied strain, and consequently, formation of new twin walls. The enhanced degradation is attributed to twin walls containing higher concentrations of point defects, which is a well-known phenomenon in oxide ferroelastics. To prevent twin wall movement or nucleation, and thus reduce degradation, one must keep mechanical or thermal stresses below 50 MPa. The roles played by twin walls in influencing ion migration, carrier trapping, and degradation are discussed. [1]

[1] Kennard, R. M., Dahlman, C. J., DeCrescent, R. A., Schuller, J. A., Mukherjee, K., Seshadri, R., & Chabinye, M. L. Ferroelastic Hysteresis in Thin Films of Methylammonium Lead Iodide. *Chem. Mater.*, 2020, 33, 298-309.

11:30 AM EN05.05.04

Improvement of the Thermal Stability of the Inverted (p-i-n) Perovskite Solar Cell Devices Using Alumina as a Passivation Layer [Tamanna Mariam](#), Ramez H. Ahanghamejad, Zhaoning Song, Abdul Quader, Zahrah S. Almutawah, Suman Rijal, Kamala K. Subedi, Adam J. Phillips, Yanfa Yan, Randy J. Ellingson and Michael J. Heben; Wright Center for Photovoltaics Innovation and Commercialization, United States

One of the main challenges for perovskite solar cells is the lack of stability in hot and/or humid environments. In this research, we intend to improve the thermal stability of inverted(p-i-n) structured perovskite solar cell devices by depositing alumina (Al₂O₃) as a passivation layer at charge transporting layer (CTL)/absorbing layer interfaces using atomic layer deposition (ALD) technique. To do this, we use fully solution processed Poly[bis(4-phenyl) (2,5,6-trimethylphenyl) amine (PTAA) hole transport layer (HTL) and (6,6)-phenyl C61 butyric acid methyl ester (PCBM)/Bathocuproine (BCP) electron transport layer (ETL). For the absorber perovskite material, we use a triple cation and mixed halide material with composition Cs_{0.05}(FA_{0.83}MA_{0.17})_{0.95}PbI_{0.83}Br_{0.17} and 1.62 eV bandgap. We fabricated devices with and without alumina at the HTL/perovskite, perovskite/ETL and both CTL/perovskite interfaces. To investigate how the alumina affects the thermal stability, compare the device performance of the samples with the passivation layer at various interface as a function of time on a 55 °C hotplate. To avoid other potential degradation pathways, the samples are heated inside an N₂-filled glovebox. The performance was tracked by measuring the open circuit stability of the samples for 960 hours. The device with alumina at the HTL/absorber layer maintained 75% of the initial value, while the sample with the alumina at the absorber/ETL maintained 56% of the initial value. Both of these were higher than the control sample, which held 44% of the initial value. These results clearly indicate that incorporating alumina at the interfaces of the inverted perovskite solar cell can increase the thermal stability of the devices. In addition to the open circuit stability tests, we completed maximum power point (MPP) tracking on the devices held at 50 °C in a moisture-free, N₂ environment for 85 hours. The MPP tracking data also shows the improved stability of the devices with alumina compared to the control device. These measurements clearly exhibit the improved stability of the alumina passivated inverted perovskite solar cell devices in comparison with the non-passivated inverted structured devices.

11:45 AM EN05.05.05

Study of Degradation Mechanism in Halide Perovskite Solar Cells Using Impedance and Modulus Spectroscopy [Haeyeon Jun](#)^{1,2}, Denis Tondelier¹, Bernard Geoffroy^{1,3}, Jean-Eric Bourée¹, Sufal Swaraj² and Yvan Bonnassieux¹; ¹LPICM-CNRS (UMR7647), Ecole Polytechnique, IP Paris, France; ²Synchrotron SOLEIL, France; ³Université Paris-Saclay, CEA, CNRS, NIMBE, LICSEN, France

Organic inorganic hybrid halide perovskites have emerged as an innovative material with excellent optoelectronic properties, in bulk or as single crystals with low defect density with specific morphologies [1]–[3]. Perovskite solar cells (PSCs) have become a trending technology in photovoltaic research due to a rapid increase in efficiency in recent years. [4].

However, they show a degradation of their performance under operational conditions (light, bias, environmental stress, etc.). To increase their long-term stability is one of the biggest challenges for market applications. The presence of strong internal electric fields, the existence of ferroelectric domains, or the diffusion of ions/defects are suggested as possible causes for the degradation processes. Several authors suggest the existence of native vacancy defects in these materials and attribute to those defects a major role in the control of the optoelectronic properties, such as hysteresis in the photo-induced current-voltage curve, as well as in device degradation and lifetime. [5], [6]

Among various degradation mechanism in PSCs, it's important to understand the mechanism in both bulk perovskite and at the interfaces between perovskite layer and transport layers.

Electrochemical impedance spectroscopy (EIS) is a powerful technique to examine the charge carrier dynamics in perovskite solar cells. It gives insight about internal electrical processes in PSCs and distinguishes between bulk and interfacial processes [7]–[9]. Each physical parameter can be extracted in the form of resistance (R), capacitance (C) and Warburg capacitance (W) using an equivalent electrical circuit model. In addition, dielectric modulus is applied for studying the microscopic mechanism of charge transport, contribution of grains (crystals) and grain boundaries and recombination dynamics [10].

In this study, we focus on the degradation of inverted planar structure perovskite solar cells through impedance and modulus spectroscopy. Two samples with the same structure are prepared and stored in air and under dark for 30 days. EIS is measured periodically, on the first sample, without J-V measurement to prevent EIS results from being affected by electrical field that occurs during J-V measurements, while J-V characteristic is measured periodically on the second sample. From combined impedance and modulus data, we confirmed that grains and grain boundaries can be distinguished. The results of modulus spectroscopy imply that the grain size decreases and grain boundaries increases which accelerates ionic accumulation and electronic polarization at interfaces. The results of J-V measurement confirms this hypothesis. Furthermore, we prepared two types of PSCs with electron transport layer based on wet- and dry- processes in order to investigate the effect of solvent on degradation mechanism.

- [1] N. G. Park *et al.*, *MRS Bull.*, 43, 7, 527–533 (2018).
- [2] M. A. Green *et al.*, *Nat. Photonics*, 8, 7, 506–514 (2014).
- [3] J. Chen *et al.*, *J. Mater. Chem. C*, 4, 1, 11–27 (2015).
- [4] “NREL efficiency chart.” [Online]. Available: <https://www.nrel.gov/pv/cell-efficiency.html>.
- [5] F. El-Mellouhi *et al.*, 9, 18, 2648–2655 (2016).
- [6] Y. Wang *et al.*, *Science*, 365, 6454, 687–691 (2019).
- [7] A. Guerrero *et al.*, *J. Phys. Chem. C*, 120, 15, 8023–8032 (2016).
- [8] Feng *et al.*, *ACS Appl. Energy Mater.*, 3, 8, 8017–8025 (2020).
- [9] Fabregat-Santiago *et al.*, *ACS Energy Lett.*, 2, 9, 2007–2013 (2017).
- [10] T. Zangina *et al.*, *Results Phys.*, 6, 719–725 (2016).

SESSION EN05.06: Perovskite Devices II
 Session Chairs: Maria Antonietta Loi, Nitin Padture and Qiuming Yu
 Wednesday Afternoon, December 1, 2021
 Hynes, Level 3, Ballroom B

1:30 PM *EN05.06.01

Addressing the Stability and Reliability Challenges in Perovskite Solar Cells via Microstructural and Interfacial Tailoring Nitin P. Padture; Brown University, United States

Most commercial devices, including photovoltaics (PVs), have gone through a familiar research and development trajectory — increasing performance, upscaling, improving stability, and enhancing mechanical reliability — before making it to the marketplace successfully. In this context, perovskite solar cells (PSCs) are likely to be no exception, but little attention has been paid to the latter issue of mechanical reliability. In fact, enhancing the mechanical reliability of PSCs is particularly important and challenging because the low formation energies of MHPs that makes them easy to solution-process renders them inherently poor in mechanical properties: they are compliant (low Young’s modulus), soft (low hardness), and brittle (low toughness). To address this perhaps final hurdle in the path towards PSCs commercialization, several rationally designed microstructural- and interfacial-tailoring approaches are used. These include grain-coarsening, grain-boundary functionalization, and interfacial engineering. Most importantly, these approaches are designed such that they not only enhance the PSCs mechanical reliability but also increase performance and improve stability. The scientific rationales for these approaches are discussed, together with the presentation of the current results.

2:00 PM EN05.06.02

Perovskite’s Additives—A General Assessment Strategy Towards Stable p-i-n Devices Luigi Angelo Castriotta¹, Francesco Di Giacomo¹, Emanuele Calabrò¹, Reddy Sathy Harshavardhan¹, Daimiota Takhellambam¹ and Aldo Di Carlo^{1,2}; ¹CHOSE Centre for Hybrid and Organic Solar Energy, Italy; ²CNR-ISM, Italy

During the last few years research community has been interested in studying hybrid (organic-inorganic) metal halide Perovskite materials, a brilliant semiconductor as an active layer in new generation photovoltaics, due to its large absorption coefficient, excellent charge mobilities, and the capability of tuning the bandgap. An additional value to this technology is the possibility to be fabricated by low temperature (below 100°C) and solution-processable techniques, lowering the actual production cost of its Silicon counterpart. Perovskite also widens its potential application as from standard Perovskite Solar Cell to Tandem thin film application, Building Integrated Photovoltaics (BIPV), Building Applied Photovoltaics (BAPV), e-Mobility and Internet of Things (IoT). Perovskite solar technology has become a trending topic in the last decade, reaching promising efficiencies up to 25.5%. In the first decade from its photovoltaic application, researchers mainly focused on obtaining high results instead of caring about stability measurements over time using standard stress test conditions, such as thermal and light soaking stressing tests. Only in 2020, an interlaboratory effort among more than 50 researchers agreed on standardizing stability measurements for Perovskite Solar Cells, recognizing its importance to address the research in this topic in order to grab the attention of the investors, stakeholders and the rest of the population, with the final aim of lowering the CO₂ consumption as stated in the Sustainable Development Goals of the United Nations by 2030. For this reason, we conducted our work taking into account the integrated lifetime energy yield (LEY), a fundamental parameter to check the performances of a device over time. We started by studying a standard triple cation perovskite, with the presence of Methylammonium (MA), Formamidinium (FA) and Cesium (Cs) as cations, Iodide (I) and Bromide (Br) as anions, in a combination to form a narrow bandgap active material (~1.55eV) suitable for single-junction device. We then move towards wider bandgap materials (~1.63eV) more suitable for tandem application with the scope of finding a common strategy to build a robust device stable over time irrespective of the perovskite used. In order to improve the intrinsic stability of the perovskite layer, we focused on the addition of perovskite precursors first, such as the use of PbI₂ excess, the addition of FACl (both materials known for increasing the device performances), and the removal of MA cation, the most volatile material which easily degrades and it is mainly known for accelerating intrinsic degradation. We finally combine all these engineering approaches and have arrived to a stage of inserting ionic liquids, such as 1-Butyl-3-methylimidazolium tetrafluoroborate (BMIM-BF₄), and alkylamine ligands, such as Oleylamine (Oam), studying their effects at different trace amounts separately and together. Our work reveals that the excess of PbI₂, more than 4%, and the presence of FACl shows lower LEY with respect to their references, whereas the removal of MA in the perovskite crystal indeed improves LEY values, also with the presence of BMIM-BF₄ and OAm. As a final remark of our study, we upscaled the best combination of additives in the perovskite film, giving us the better LEY, for the fabrication of high efficient Perovskite Solar Module (PSM), showing exciting ISOS-T1 and ISOS-L1 test results.

2:15 PM EN05.06.03

Efficiency Enhancement Due to Nonreciprocal Photonic Management of Materials with High Radiative Efficiency Andrei Sergeev¹ and Kimberly Sablon²; ¹Army Research Laboratory, United States; ²AFC, United States

Recent progress in photovoltaic materials with high radiative efficiency, such as halide perovskites, raises a set of principle questions about optimal photonic management, limiting efficiencies of photovoltaic (PV) converters with advanced photonic management, and design of such converters. Here we propose a practical design of the single cell converter with nonreciprocal photonic management, generalize the finite time thermodynamics to electron distributions with the photon-induced chemical potential, calculate the limiting efficiency of the nonreciprocal converter with a single junction cell, and evaluate efficiency of such converters with available GaAs and halide perovskite cells.

Advanced photonic nanostructures with broken time-reversal symmetries demonstrate a strong potential to revolutionize numerous applications ranging from optical quantum-information technologies to solar energy conversion. Nonreciprocal optical structures can provide high absorptivity, $\alpha(\omega, \mathbf{n}) \approx 1$, together with near-zero emissivity, $\epsilon(\omega, \mathbf{n}) \approx 0$, in some narrow absorption cone with the axis direction \mathbf{n} and high emissivity, $\epsilon(\omega, \mathbf{n}') \approx 1$, together with

near-zero absorptivity, $\alpha(\omega, \mathbf{n}') \approx 0$, in the strongly different direction \mathbf{n}' . Due to separation of emission and absorption, nonreciprocal optical structures can drastically reduce emission from a PV converter without reduction in the light absorption. In our design, we split the absorption cone into two parts. The first part will be used for absorption of solar light. The second part of the cone is employed for re-absorption of the emission by the same PV cell. Alternatively, we can employ the design with high quality mirror dome, which reflects the emitted light back to the cell. In this design, the nonreciprocal high absorption - low emission electrodynamics should be realized just in the narrow angle directed to the narrow hole for incoming solar light. By using of cells with large number of junctions, we can also suppress the losses related to the relaxation of photocarriers and approach the Carnot efficiency with ideal PV material with negligible nonradiative recombination. Operating of the proposed PV converter with multi-junction cell at the Carnot limit requires an infinite number of external recycling processes. So, any small dissipation in the non-reciprocal photonic system significantly affects this limiting solution. This result provides straightforward resolution of the thermodynamics paradox related to optical diode. We generalize the finite time thermodynamics to nonequilibrium electron distribution functions specific for PV conversion and derive the limiting efficiency of a single-junction non-reciprocal PV converter. Nonreciprocal photonic management of PV cells with high radiative efficiency may substantially increase the photovoltaic performance. We evaluate performance of the nonreciprocal converter with high quality GaAs and halide perovskite solar cells. Our results show that the nonreciprocal management increases the conversion efficiency of these cells by $\sim 5\%$. For solar light conversion, the nonreciprocal high absorption-low emission should be realized just in very narrow angle range (9.3×10^{-3} radians) and the narrow photon energy range of 5 - 7 kB T above the bandgap. The light emitted from the cell may be reflected back by high quality mirror dome. Development of such PV converters may be expected in the nearest future.

2:30 PM EN05.06.04

Controlling Stress and Strain in Perovskite Solar Cells to Enhance Efficiency and Stability Gabriel McAndrews^{1,2}, Boyu Guo³, Aram Amassian³ and Michael McGehee^{1,2}; ¹University of Colorado Boulder, United States; ²National Renewable Energy Laboratory, United States; ³North Carolina State University, United States

Despite promising initial efficiencies of metal halide perovskite solar cells, their operational stability is hindered by degradation which limits commercial viability. Mechanical strain has recently been identified as a significant factor influencing perovskite degradation. Specifically, tensile strain in perovskites has been shown to accelerate undesirable PbI_2 formation (1, 2). Therefore, it is crucial to identify and reduce sources of residual tensile strain to enhance the stability of metal halide perovskites. Thermal annealing promotes crystallization and removes excess solvent from solution processed perovskites. High temperature crystallite attachment combined with a coefficient of thermal expansion (CTE) mismatch between the perovskite and rigid substrate, such as glass, results in in-plane biaxial tensile stress (2).

Despite the demonstrated origin of residual tensile strain and its influence on perovskite stability only a few studies have addressed potential solutions (3,4). Here, we evaluate several strategies to reduce or avoid tensile strain on their ability to enhance stability of perovskites without sacrificing optimal initial optoelectronic properties and efficiencies. First, room temperature crystallization and mechanical attachment of perovskite crystallites to the substrate avoids tensile stress from the CTE mismatch during the cooldown from the elevated anneal temperature. In fact, perovskites attached to the substrate at room temperature are under compression at operating conditions (i.e. 65C) which is hypothesized to enhance stability (1, 2). The film formation kinetics can be influenced by several factors to induce room temperature perovskite attachment. For example, certain antisolvents and quench methods rapidly remove excess solvent, decomplex solvate phases, and induce a chain reaction perovskite crystallization at room temperature. Furthermore, extended times between the quench and subsequent anneal allows for adequate time for perovskite crystallites to form and mechanically attach to the substrate.

Using room temperature perovskite attachment to avoid tensile strain from the CTE mismatch has several advantages over alternative strain mitigation strategies. Using substrates with CTEs matched with perovskites or manipulating strain post crystallization introduce additional costs and can sacrifice optimal photovoltaic performance. We present a solution to reduce tensile strain in metal halide perovskites: room temperature attachment using typical processing methods.

1. J. Zhao, Y. Deng, H. Wei, X. Zheng, Z. Yu, Y. Shao, J.E. Shield, J. Huang, Strained hybrid perovskite thin films and their impact on the intrinsic stability of perovskite solar cells. *Sci. Adv.*, **3**, (2017)
2. N. Rolston, K.A. Bush, A.D. Printz, A. Gold-Parker, Y. Ding, M.F. Toney, M.D. McGehee, R.H. Dauskardt, Engineering Stress in Perovskite Solar Cells to Improve Stability. *Adv. Ener. Mats.*, **8**, (2018)
3. D-J Xue, Y. Hou, S-C Liu, M. Wei, B. Chen, Z. Huang, Z. Li, B. Sun, A.H. Proppe, Y. Dong, M.I. Saidaminov, S.O. Kelly, J-S Hu, E.H. Sargent, Regulating strain in perovskite thin films through charge-transport layers, *Nat. Comm.*, **11**, (2020)
4. H. Wang, C. Zhu, L. Liu, S. Ma, P. Liu, J. Wu, C. Shi, Q. Du, Y. Hao, S. Xiang, H. Chen, P. Chen, Y. Bai, H. Zhou, Y. Li, Q. Chen, Interfacial Residual Stress Relaxation in Perovskite Solar Cells with Improved Stability. *Adv. Mats.*, **31**, (2019)

2:45 PM EN05.06.05

Efficient and Stable Pb-Based All-Perovskite Tandem Solar Cells Chongwen Li, Zhaoning Song and Yanfa Yan; University of Toledo, United States

Bandgap-tunability of metal halide perovskites endows them with a wide selection for assembling all-perovskite tandem solar cells to break the efficiency limit for single-junction solar cells. FAPbI_3 showing outstanding optical and electronic properties has been exclusively employed to pursue record efficiencies for single-junction perovskite solar cells, yet it has not been exploited in the fabrication of all-perovskite tandem solar cells. Here, to pair with high-quality FAPbI_3 , all-inorganic $\text{CsPbI}_x\text{Br}_{3-x}$ with superior thermal stability is introduced as the top subcell. By finely tuning the bandgap of $\text{CsPbI}_x\text{Br}_{3-x}$, we achieved an excellent current match of the two subcells. Moreover, a self-assembled polyelectrolyte was used as the surface modifier for NiO_x to reduce the non-radiative recombination at the $\text{CsPbI}_x\text{Br}_{3-x}/\text{NiO}_x$ interface, which contributes to improved hole extraction and overall device performance. More importantly, this new tandem combination based on Pb-perovskites significantly advances the operational stability, one such a tandem cell delivered an initial efficiency of $>23\%$ and remained 80% of the efficiency after >1000 hours operation under continuous one sun (AM 1.5G) illumination at 65°C . Our strategy provides an alternative pathway for realizing practical application of all-perovskite tandem solar cells.

3:00 PM BREAK

4:00 PM *EN05.06.06

Chemical (In)Stability in MA-Free Halide Perovskites – Thin Films versus Quantum Dots Qiuming Yu; Cornell University, United States

Methylammonium lead triiodide (MAPbI_3) perovskite is one of the most studied perovskites, and a power conversion efficiency (PCE) over 20% has been demonstrated for single junction solar cells. However, MAPbI_3 perovskite is not an ideal option to fabricate high performance and stable single junction perovskite solar cells mainly due to its intrinsic moisture and thermal instability. Formamidinium (FA) as another organic cation has been applied as a replacement for MA to solve the instability issues. However, FAPbI_3 suffers from phase instability under room temperature. It spontaneously transfers

from a black photoactive α -phase to a yellow photoinactive δ -phase at room temperature in a few days. To solve the phase instability problem, alkaline cation such as Cs^+ and Rb^+ cations are introduced to partially replace the large FA cation to adjust the Goldschmidt tolerance factor. We investigate the phase and device stability of FAPbI_3 perovskites by introducing both Cs^+ and Rb^+ cations in compared to Cs^+ -only with the perovskite thin films fabricated via one-step plus anti-solvent solution process. We also investigate the stability of phase and device made by spin-coating plus solid-state ligand exchange of FAPbI_3 colloid quantum dots. We find that even with incomplete incorporation, Rb^+ cation can significantly improve the device performance. We reveal the defect-mediated cation and anion migration under electric field using cross-sectional secondary electron microscopy, X-ray photoelectron spectroscopy, and time-of-flight secondary ion mass spectrometry, and identify that Rb^+ is more vulnerable compared to Cs^+ . By simply mixing the precursor solution before spin coating, we significantly reduce the defect states in both types of perovskites and improve the device stability against an electric field. The modified precursor solution provides the devices with $\text{Rb}_{0.05}\text{Cs}_{0.1}\text{FA}_{0.85}\text{PbI}_3$ and $\text{Cs}_{0.15}\text{FA}_{0.85}\text{PbI}_3$ active layers that retain 68% and 92% of their initial PCE, respectively, over 30 days under N_2 protection. Surprisingly, solar cells made with spin-coating plus solid-state ligand exchange of FAPbI_3 quantum dots display long-time stability with no device performance degradation over 30 days under N_2 protection. We conduct systematically structural, chemical, electronic, and photophysical studies to reveal that cations and anion, used in solid-state ligand exchange, can selectively passivate surface defects and suppress ion migration. The rationally controlled ligand exchange of colloid perovskite quantum dots could open a new avenue to manipulate the chemical stability of halide perovskites.

4:30 PM EN05.06.08

To Be or Not to Be? Methylammonium in Hybrid Lead Halide Perovskites for Tandem Solar Cells Moses Kodur¹, Deniz N. Cakan¹, Rishi Kumar¹, Connor Dolan¹, Yanqi Luo², Barry Lai² and David P. Fenning¹; ¹University of California, San Diego, United States; ²Argonne National Laboratory, United States

Whether methylammonium is beneficial or detrimental, necessary or superfluous for high-performing wide-bandgap perovskite compositions suitable for tandem photovoltaics has remained a contested enigma. Borrowing from advances in single-junction perovskite design, mixed cation and halide chemistries have shown improvements to both the open-circuit voltage and stability of top-cell devices, but also suffer from compositional complexity and the risk of phase separation under the wide range of operating conditions a PV cell experiences. Here, we investigate the role of methylammonium (MA) on the formation, halide incorporation, optoelectronic properties, and photovoltaic performance of perovskite thin films designed for perovskite-silicon tandems devices, exploring the >1.6 eV triple-halide compositional space (A-site: Cs/MA/FA).

We use synchrotron X-ray microscopy combined with correlative mapping of optoelectronic performance to assess the role of MA-incorporation on the microscopic chemical distribution and device performance. We see little distinction in performance between MA and MA-free triple halide perovskite compositions. In contrast, whether MA is present or not, Cl incorporation to create triple halide compositions shows distinct benefits, and we gain insights into the limits of Cl incorporation before phase segregation manifests and how MA modulates those limits. Our results suggests that MA is not critical to the high-quality wide bandgap, chlorine-incorporated perovskites and that its removal may facilitate the development of more stable perovskite solar cells.

4:45 PM EN05.06.10

Reducing Roughness and Improving Efficiency of MAPbI₃ Perovskite Solar Cells Made by High-Throughput Photonic Curing Weijie Xu and Julia Hsu; The University of Texas at Dallas, United States

For perovskite solar cells (PSCs) to be commercially viable, the slow and energy-insufficient thermal annealing step must be eliminated. Among the photo-irradiation methods proposed to replace thermal annealing, photonic curing is the fastest conversion method. Photonic curing delivers short (20 μs to 100 ms) but intense light pulses from a broadband (200-1500 nm) xenon flash lamp, making it the only method to convert perovskite under 20 ms. This processing time can be extrapolated to a roll-to-roll web speed of 40 m/min based on laboratory processing conditions.¹ However, most reported PSCs made by photonic curing under 1 second have inferior performance ($\sim 10\%$ PCE). Although SEM images show dense and pinhole-free perovskite films, AFM images indicate secondary wavy features of 500 nm-wide ridge and 80 nm-deep trenches on photonic cured perovskite films, the existence of which correlates with poor device performance. We suggest that this morphology feature is produced by volatile solvent evaporation during the fast photonic curing process. Two approaches have been made to remedy this issue: (1) adding CH_2I_2 as the third solvent in the conventional DMF-DMSO system and (2) applying a controlled air-blowing step before photonic curing to remove excess solvent further. Combining these two approaches produces photonic-cured perovskite films with a comparable film roughness and device performance. Alkyl halide additives have been reported to enhance PSC performance by modulated solvent-solute interactions and C-X (X = Cl, Br, and I) cleavage. Photonic curing can cleave CH_2I_2 , producing disassociated iodide ions to replenish iodine loss induced by photonic curing, which is confirmed by EDX. As a co-solvent, the high boiling point of CH_2I_2 can also make the solvent less volatile, reducing surface roughness in photonic cured perovskite films. Additionally, photonic-cured perovskite films have longer PL lifetimes and a higher recombination resistance compared to thermally-annealed counterparts. As a result, we demonstrate that photonic curing is a suitable method to replace thermal annealing in high-throughput PSC fabrication.

(1) Xu, W.; Dausis, T. B.; Piper, R. T.; Hsu, J. W. P. Effects of Photonic Curing Processing Conditions on MAPbI₃ Film Properties and Solar Cell Performance. *ACS Appl. Energy Mater.* **2020**, 3 (9), 8636–8645. <https://doi.org/10.1021/acsam.0c01243>.

SESSION EN05.07: Perovskite Structure and Properties
Session Chairs: Letian Dou and Mathias Rothmann
Thursday Morning, December 2, 2021
Hynes, Level 3, Ballroom B

10:30 AM EN05.07.01

Polysalt Ligands Achieve Higher Quantum Yield and Improved Colloidal Stability for CsPbBr₃ Quantum Dots Sisi Wang, Selin E. Donmez and Hedi M. Mattoussi; Florida State University, United States

Recently, Colloidal all inorganic lead halide perovskite quantum dots (PQDs) have generated much interest and activity, due to the great promise they offer for use in optoelectronic applications. However, their poor colloidal stability, which can be traced to the ionic nature of the crystal cores and the high desorption rates of the native ligands, has impeded progress in fundamental research and slowed integration of such materials in devices. Developing novel surface ligands with strong coordination to passivate surface traps and enhance fluorescence, while improving colloidal stability is needed. Here, we detail the synthesis of a new family of multifunctional polymer ligands and their use for surface engineering of the CsPbBr_3 nanocrystals. The ligand synthesis relies on the nucleophilic addition reaction between poly(isobutylene-alt-maleic anhydride), PIMA, and distinct nucleophiles. The modular

ligand stoichiometrically displays multiple ammonium and/or imidazolium salt groups for coordination onto the PQD surfaces, along with several alkyl chains with different length to promote affinity to various organic solvents. The results show that the PQDs coated with those polysalts exhibit great colloidal stability and significantly enhanced photoluminescence. The coating also allows the resulting colloids to be dispersed a wide range of solvent conditions, including ethanol and methanol, while maintaining strong fluorescence and preserving the nanocrystal integrity after ligand substitution.

10:45 AM EN05.07.04

Late News: Mechanical Reliability of Perovskite Solar Cells Reisya Ichwani, Oluwaseun K. Oyewole and Winston W. Soboyejo; Worcester Polytechnic Institute, United States

Highly efficient organic-inorganic perovskite solar cells (PSCs) consisting of multiple layers of functional materials are needed to be mechanically stable for the development of perovskite solar cells that can be deposited on rigid or flexible perovskite solar cells. In this study, we explore the possible effects of interfacial robustness on the performance of organic-inorganic PSCs. The interfacial fracture energies are determined for the interfaces in model perovskite solar cell structures. These are obtained using Brazil disk specimens that are used to study the mode-mixity dependence of the interfacial fracture toughness in bi-material interfaces. The underlying crack/microstructure interactions are investigated along with the crack-tip shielding mechanisms associated with crack growth under monotonic loading. These are elucidated via scanning electron microscopy and energy-dispersive X-ray spectroscopy studies of the crack profiles and fracture surfaces. These reveal the kinking in-and-out of interfaces that can occur between layers in PSCs. The observed crack-tip shielding models are also modeled with zone shielding fracture mechanics models. The measured interfacial toughening/fracture toughness levels are then correlated with the performance characteristics (power conversion efficiencies, short circuit currents, and open circuit voltages) of PSCs with perovskite layers that are produced using spin coating and vapor deposition techniques. The implications of the results are then used to rank the robustness of interfaces in multilayered PSCs.

SESSION EN05.08: Perovskite Stability
Session Chairs: Maria Antonietta Loi and Mathias Rothmann
Thursday Afternoon, December 2, 2021
Hynes, Level 3, Ballroom B

1:30 PM EN05.08.01

Feature Engineering to Capture Effects of Uncertainty in Machine Learning Models Forecasting the Decay of Halide Perovskite Optoelectronic Properties Wiley A. Dunlap-Shohl, Timothy Siegler, Andrew Tischhauser, Chang-En Tsai, Yuhuan Meng, Preetham Sunkari, Yu-Chia Chen, David Beck, Marina Meila and Hugh W. Hillhouse; University of Washington, United States

A promising application of machine learning in materials science is service lifetime forecasting¹ of halide perovskites, a potentially disruptive photovoltaic technology limited by degradation in ambient environments due to the action of heat, light, moisture, and oxygen. It is imperative for prospective manufacturers to know how long their products are likely to survive to provide warranties and develop sound business plans. In prior work, we have developed predictive machine learning models that can accurately forecast the service lifetime of the archetypal halide perovskite, methylammonium lead iodide (MAPbI₃), in a variety of different environmental conditions, using data available from a unique characterization tool that simultaneously measures transmittance, photoluminescence, and photoconductivity *in situ*. Early modeling efforts indicated that the material decomposition rate, detected by using the optical transmittance of perovskite films, is strongly predictive of decay in the perovskite's carrier diffusion length. The importance of environmental factors on halide perovskite degradation is well, if incompletely, understood. However, the degree to which sample-to-sample variation can affect lifetime forecasts has not been studied. It is well-known that the manner and environment in which a perovskite film is prepared can have large impacts on its photovoltaic performance, but these links are often opaque and may involve factors that are hard or impossible to measure. To understand how best to handle this inherent uncertainty, we employ a dataset consisting of over 60 perovskite degradation runs in which environmental conditions are held constant, and identify features that capture the influence of this variation on service lifetime. We observe that T80-LD, the time it takes for the diffusion length to decay to 80% of its starting value, can vary by over an order of magnitude in the same ambient conditions, making the ability to capture this variation extremely important for forecasting. In assigning decomposition rate-related features high importance, machine learning algorithms that forecast T80-LD thus uncover key links between the extent of a perovskite film's degradation and the evolution of its electronic properties: T80-LD possesses a strong inverse relation to the material decomposition rate, as calculated from *in-situ* transmittance measurements. This relationship is quite similar to the T80-LD-decomposition rate relationship observed over a dataset in which environmental conditions are deliberately varied, showing that these relatively simple models can nevertheless uncover the general patterns underlying degradation. We have recently developed a first-principles kinetic model to predict the initial degradation rate of MAPbI₃ from the ambient environmental conditions,² and we explore the performance of hybrid models that incorporate both *a priori* information about the expected degradation rate in a given environment using physics-inspired features derived from the kinetic model, and *in situ* optical and optoelectronic measurements made on each specific sample in the dataset. This approach maximizes the predictive potential of the models by encoding both contextual and sample-specific information.

References:

- (1) Stoddard, R. J.; Dunlap-Shohl, W. A.; Qiao, H.; Meng, Y.; Kau, W. F.; Hillhouse, H. W. Forecasting the Decay of Hybrid Perovskite Performance Using Optical Transmittance or Reflected Dark-Field Imaging. *ACS Energy Lett.* **2020**, *5* (3), 946–954. <https://doi.org/10.1021/acsenerylett.0c00164>.
- (2) Siegler, T. D.; Dunlap-Shohl, W. A.; Meng, Y.; Kau, W. F.; Sunkari, P. P.; Tsai, C.-E.; Armstrong, Z. J.; Chen, Y.-C.; Beck, D. A. C.; Meila, M.; Hillhouse, H. W. Water-Accelerated Photo-Oxidation of CH₃NH₃PbI₃ Perovskite: Mechanism, Rate Orders, and Rate Constants. *ChemRxiv* **2021**. <https://doi.org/10.33774/chemrxiv-2021-30ggh>.

1:45 PM EN05.08.02

Insights into the Carrier-Induced Degradation of Halide Perovskites Through Correlated Structure-Property Measurements Rebecca A. Belisle; Wellesley College, United States

The mixed-conducting nature of halide perovskites has a variety of impacts on their optoelectronic properties and device performance. Current-voltage hysteresis, reverse-bias breakdown, photo-brightening, carrier-induced degradation, and thermal stability are all examples of behaviors that have been linked to the appreciable ionic conductivity in these materials. However, despite the significance of ionic defects on perovskite performance, there remain many open questions as to the number of ionic defects in perovskite semiconductors and their effects on device performance. In this work I will present recent advances in our understanding of one phenomenon linked to ionic defects in perovskite semiconductors: carrier-induced degradation. Using correlated structure, optoelectronic property, and transport measurements we monitor the chemistry and performance of MAPb_{1-x}Br_x perovskites over extended illumination and document both reversible and irreversible changes in performance in halide perovskites. Using complimentary XRD,

photothermal deflection spectroscopy, photoluminescence, and mixed-conductivity measurements we document changes in crystal structure, bandgap, and Urbach energy, and connect those changes to variations in ionic conductivity and optoelectronic performance. In the case of mixed halides, we see a non-reversible increase in bromine concentration and corresponding increase in the photoluminescence stability with prolonged illumination, suggesting that the loss of iodine leaves behind a higher-quality and more photostable film. Overall, these advances shed light on the relationship between perovskite chemistry, ionic defect density, and photostability in this increasingly important class of semiconductors and suggest pathways towards increased device performance and stability.

2:00 PM EN05.08.03

Late News: Defect States Transformation in Perovskite During Photo-Aging and Their Passivation by Fluorinated Interface Modifier Seong Ho Cho¹, Junseop Byeon¹, Kiwan Jeong², Jiseon Hwang³, Hyunjoon Lee¹, Jihun Jang², Jieun Lee¹, Taehoon Kim¹, Kihwan Kim³, Mansoo Choi^{1,2} and Yun Seog Lee^{1,2}; ¹Seoul National University, Korea (the Republic of); ²Global Frontier Center for Multiscale Energy Systems, Korea (the Republic of); ³Korea Institute of Energy Research (KIER), Korea (the Republic of)

Stability of perovskite solar cells has advanced significantly by removing extrinsic degradation factors such as moisture and oxygen through encapsulation techniques. However, encapsulated devices often show irreversible degradation during photo-stability test. In this contribution, we investigated photo-aging mechanism by observing changes in intrinsic defects excluding extrinsic degradation factors. We fabricated perovskite solar cells with similar power conversion efficiencies of 21% but different Pb to I ratio at interface, which exhibited completely different photo-aging trend. We investigated the shift in their intrinsic properties during photo-aging in nitrogen-filled chamber. Evolutions in opto-electronic properties and elemental constituents during photo-aging were traced by various measurement, including photoluminescence spectra, UV-visible absorption spectra, X-ray fluorescence measurements, and time-of-flight secondary-ion mass spectroscopy. Relatively Pb-rich interface presented halide sublimation and strain relaxation, implying formation of new defect states near grain boundaries and interfaces. We investigated changes in Fermi level and intrinsic defect properties and energetic distribution by X-ray photoelectron spectroscopy measurements, space charge limited current measurement, and thermal admittance spectroscopy. Formation of donor-type deep-traps were shown in the perovskite after irreversible degradation.[1] We suggest balanced stoichiometry at the interface and passivation of Pb-I related defects are crucial for enhancing photo-stability.[1] We studied interfacial defect passivation using novel fluorinated organic spacers by synthesizing fluorine groups with different anchoring positions on organic spacers and compared their properties. We report an enhanced efficiency by effective defect passivation retaining over 90% of their initial power conversion efficiency during 500 hours of continuous 1-Sun illumination and outstanding hydrophobic nature without encapsulation.

[1] S. H. Cho *et al.*, *Advanced Energy Materials*, 11.17 (2021): 2100555.

2:15 PM EN05.08.04

Late News: Temperature-Induced Degradation of Triple-Cation Mixed Halide Perovskite Solar Cells Yusuf A. Olanrewaju^{1,2}, Omolara V. Oyelade^{3,2}, Richard Koech^{1,2}, Oluwaseun K. Oyewole^{2,4} and Winston W. Soboyejo^{2,5,4}; ¹African University of Science and Technology, Abuja (AUST), Km 10 Airport Road, Abuja, Nigeria, Nigeria; ²Worcester Polytechnic Institute, 100 Institute Road, Worcester, MA 01609, USA., Nigeria; ³African University of Science and Technology,(AUST) Km 10 Airport Road, Abuja, Nigeria, Nigeria; ⁴Worcester Polytechnic Institute, 100 Institute Road, Worcester, MA 01609, USA, United States; ⁵Worcester Polytechnic Institute, 60 Prescott Street, Gateway Park Life Sciences and Bioengineering Center, Worcester, MA 01609, USA., United States

The triple-cation mixed halide perovskite $\text{Cs}_{0.05}(\text{MA}_{0.17}\text{FA}_{0.83})_{0.95}\text{Pb}(\text{I}_{0.83}\text{Br}_{0.17})_3$ is one of the most promising photon absorbers that is being considered for emerging photovoltaic applications. This is due to its outstanding optoelectronic properties. However, the limited thermal stability of mixed halide perovskites is still a major challenge that may limit their applications over a wide range of temperatures that may be encountered in service. Hence, in this work, we study the temperature-dependence of the degradation of solution processed triple-cation mixed halide perovskite solar cells. These are subjected to temperatures that simulate potential service conditions. Our results show that the reductions in device power conversion efficiency originate from decreasing charge mobility and the formation of charge recombination sites at the ETL/perovskite layer interface. This is shown (using scanning electron microscopy) to be associated with the thermal-induced delamination of the layered structure. The underlying degradation of the solar cell characteristics is also shown to be associated with the formation of defects during the controlled heating of mixed halide perovskite cells. The implications of the results are then discussed for the development of perovskite solar cells with improved thermal stability.

2:30 PM EN05.08.05

Vapor-Phase Tuning of Ruddlesden-Popper Perovskites via Deliquescence/Efflorescence Lorenzo Y. Serafini; University of North Carolina at Chapel Hill, United States

Hybrid perovskites (HPs) have created intense excitement in the chemistry and materials community for a variety of reasons, not the least of which is their remarkable capacity for facile tuning of optoelectronic properties. Specifically, regarding the layered Ruddlesden-Popper perovskites this is accomplished by tuning the stoichiometric ratio of the small intercalating ion (e.g. methylammonium) to the larger organic spacer cation (usually an alkyl ammonium such as *n*-butylammonium). The inclusion of the bulkier alkylammonium cation has the effect of breaking up the regular packing of the lead halide octahedra, creating “slabs” of the traditional perovskite structure, separated from each other by the dielectric environment created by the layers of the bulky spacer cations. The size of these slabs is dictated by the stoichiometry between the two varieties of cations, and synthesis of pure single crystals of these various layered perovskites has been accomplished via solution-grown methods. Attempts to create a phase-pure thin film, containing only slabs of a certain thickness have yielded mixed results. The deliquescent properties of HPs (the uptake of vapor phase amine molecules by HPs leading to the liquefaction of the HP) have been thought of as a way to improve crystallinity of HP thin films. We show herein that this deliquescent behavior of HPs can be used as a way to exert control over the stoichiometry of HP thin films by carefully controlling the vapor-phase stoichiometry of an amine atmosphere during deliquescence. This approach may even be a way to realize the elusive goal of creating a phase-pure Ruddlesden-Popper thin film, something that has not been accomplished as yet through conventional solution processing methods.

2:45 PM EN05.08.06

Photooxidative Healing of Lead Halide Perovskite Solar Cells Katelyn P. Goetz^{1,2}, Qingzhi An¹, Yvonne J. Hofstetter¹, Tim Schramm¹, Fabian Thome³, Aymen Yangui⁴, Ivan Scheblikyn⁴, Nir Tessler⁵ and Yana Vaynzof⁶; ¹Technische Universität Dresden, Germany; ²National Institute of Standards and Technologies, United States; ³Universität Heidelberg, Germany; ⁴Lund University, Sweden; ⁵Technion-Israel Institute of Technology, Israel

Lead halide perovskites have attracted enormous interest from both the scientific and industrial communities due to their unprecedented success in optoelectronic devices. Particularly impressive is their performance as active layers in solar cells, where certified power conversion efficiencies (PCE) surpassing 25% have been demonstrated. Despite this tremendous success, several key challenges prevent their large-scale deployment and require further research. Among these challenges, the presence of hysteresis in perovskite solar cells has triggered significant efforts in developing strategies for its suppression. The fundamental origins of hysteresis, however, remain under debate. Moreover, the interplay between the presence of specific ionic defects

in the perovskite layer and the appearance of hysteresis remains largely unexplored.

Focusing on methylammonium lead triiodide (MAPbI₃) as a model system, we purposefully introduce defects into the perovskite layer by fractionally modifying the solution precursor stoichiometry.[1] We find that only overstoichiometric devices – those with excess of iodine – show significant hysteresis, as well as a greatly reduced short-circuit current (J_{SC}), thus resulting in low PCEs. While exposure to O₂ under illumination is typically associated with causing the degradation of perovskite thin films,[2] surprisingly, for the overstoichiometric perovskite layers such exposure leads to the elimination of hysteresis and the recovery of the short-current density to the expected value for high-performance perovskite solar cells.

To investigate the origin of this effect, we characterized the composition of the overstoichiometric films before and after exposure to O₂ under illumination. As expected, we find that the I/Pb ratio in the overstoichiometric films, measured by X-ray photoemission spectroscopy, is rather high (4.08±0.15) due to the excess iodine introduced during processing. After the exposure to oxygen, this ratio is reduced to 3.86±0.19, suggesting that a photooxidative process leads to the expulsion of excess iodine from the surface of the perovskite film. 2D photoluminescence mapping in the fluence and frequency domains [3] revealed that the overstoichiometric samples exhibit a large density of traps, which, upon photooxidation, are eliminated from the film, bringing it to the same electronic quality as a perfectly stoichiometric MAPbI₃ film. A similar, albeit less pronounced effect, was also observed for overstoichiometric triple cation and MA-free perovskite solar cells, suggesting that photooxidative healing can be applied to various perovskite compositions.

References:

- [1] P. Fassel et al, Energy Environ. Sci. 11, 3380 (2018).
- [2] Q. Sun et al, Adv. Energy Mater. 7 (20), 1700977 (2017).
- [3] A. Kiligaridis et al, Nat. Commun. 12, 3329 (2021).

3:00 PM EN05.08.07

Late News: Residual Stress/Strain by Phase Transition Govern Optoelectronic Properties of Halide Perovskites Muhammad N. Lintangpradipto and Osman M. Bakr; King Abdullah University of Science and Technology, Saudi Arabia

Methylammonium lead iodide has become a holy-grail of perovskite material since its inception owing to the facile fabrication (e.g., one/two-step film process, Inverse temperature crystallization) and versatile semiconductor applications (e.g., Light Emitting Diode, photovoltaic) with its superior absorption coefficient, charge mobility, and diffusion length properties. Despite extensive studies of MAPbI₃ in optoelectronic application, it possesses a significant challenge that may prove counter-productive as in seemingly inconsistent results of TDPL (Temperature-Dependent Photoluminescence) properties, particularly during phase transition. Unification explanation is essential since TDPL properties have emerged as standard to elucidate the optoelectronic's defect, charge carrier dynamics, and device performance.

In this study, we investigate three archetypal MAPbI₃ crystals (Single-crystal, Polycrystalline, Highly oriented Crystal) representing different crystal states based on optoelectronic device variation. We illustrated considerable numbers of diffraction peak trends over the temperature range and observed onset phase transition from certain orientations of crystal states and the co-existence phase of orthorhombic-tetragonal phase of MAPbI₃ at PC and HOC using TD-XRD (Temperature Dependent X-ray Diffractometer). We calculated the FWHM value based on the Gaussian model to illustrate the peak broadening trend that occurred strongly on PC and HOC states throughout the temperature range as evident of inter-domain stress by domain boundaries. We showed stress accumulation on MAPI SC and PC with (TDRS) Temperature-Dependent Raman Spectroscopy. Accessing low wavenumber of octahedral twist (SC) and C-N torsion (PC), we realized abrupt lattice rearrangement and smooth transition Raman vibration between SC and PC during temperature change.

In conclusion, we found that domain-size and density of domain boundaries from MAPbI₃ crystal states determine the degree of residual stress/strain for thermal lattice expansion and reconstruction lattice to define the phase transition of crystal. We observed that the phase transition characteristics agree with TDPL properties as the origin of MAPbI₃ distinctive characteristics as optoelectronic devices. We consider crystal states of being an essential factor to control in order to obtain consistent device properties.

3:15 PM EN05.08.08

The Importance of Proton Chemistry in Halide Perovskites Davide R. Ceratti¹, Gary Hodes², David Cahen², Philip Schulz¹ and Jean-François Guillemeot¹; ¹Centre National de la Recherche Scientifique, France; ²Weizmann Institute of Science, Israel

The widely used Methylammonium (MA⁺) and Formamidinium (FA⁺) cations are relatively acidic compounds, with the potential to dissociate in the halide perovskites, giving a proton (H⁺) and the corresponding ammine. Despite the fact that they were considered not to do so, I will bring new evidence that the dissociation does happen and that H⁺ can migrate, associate with eventual water molecules internalized in the perovskite, be absorbed by basic hole transporting layers and other related phenomena. I will also comment on the chemistry of H⁺ in solution and show how it influences the final state of a perovskite layer after the coating.

As it happens in general, in the perovskites the chemistry of protons is reversible and is characterized by chemical equilibria, which are modified by a large number of factors. I will provide indications on how temperature, illumination intensity, electronic doping of the perovskite material and the presence of other molecules pushes the acid-base equilibrium towards the dissociation or the association. The complexity of these equilibria is at the base of a series of phenomena that have been observed in halide perovskites like fast ion-migration, light-soaking and reversible damage repair (self-healing).

In this talk, I will provide proof of the migration of protons in the perovskites as obtained by exchange of H⁺ with deuterons (D⁺) and discuss their diffusion coefficient in halide perovskite single crystals. Through optical microscopy (confocal, hyperspectral, fluorescence lifetime imaging spectroscopy), I will also provide proof on how the proton chemistry influences the photoluminescence of the perovskites showing how proton deficient perovskites have better optoelectronic properties. In particular, I will analyze how the positive effects of methylamine treatment in the perovskites can be related to proton chemistry and how light might locally originate methylamine causing the effect of light soaking in the perovskites. I will also show that H⁺ acts as an oxidizer when the perovskite is put into contact with metals and its influence should be considered when depositing contacts directly on the perovskite material.

I will also analyze the chemistry of protons in the perovskite precursor solutions showing how their presence influences which particular lead complexes are actually in solution during crystallization. I will show how the electrochemical potential of the precursor solution (and therefore of the perovskite material) is partially determined by the presence of protons with consequences on the quality and quantity of defects in the perovskite materials.

To conclude, the aim of this talk is to provide the listener a wide view on proton chemistry in halide perovskites providing the theoretical tools to understand the influences that proton chemistry has on the optoelectronic properties and the stability of the perovskites. This talk will be rich in chemical knowledge but it will be adapted to an audience working on halide perovskite devices with more engineering or physics background.

3:30 PM BREAK

4:00 PM EN05.08.09

Late News: Nanostructure Strategies for Improved Perovskite Solar Cells Zhelu Hu¹, Lionel Aigouy¹, Jose Miguel Garcia-Martin², Maria Ujue González², Hung-Ju Lin¹, Mathilde SCHOENAUER¹, Laurent Billot¹, Patrick Gredin³, Michel MORTIER³, Zhuoying Chen¹ and Antonio Garcia-Martin²; ¹LPEM, ESPCI Paris, PSL Research University, CNRS, Sorbonne Universités, France; ²Instituto de Micro y Nanotecnología -CSIC, Spain; ³Chimie ParisTech, PSL Research University, CNRS, Institut de Recherche de Chimie Paris, France

Organic-inorganic hybrid perovskite solar cells have attracted much attention due to their high power conversion efficiency (>23%) and low-cost fabrication. Directions to further improve these solar cells include strategies to enhance their stability and their efficiency by modifying either the perovskite absorber layer or the electron/hole transport layer. For example, the transparent electron transport layer (ETL) can be an important tuning knob influencing the charge extraction, [1] light harvesting, [2] and stability [3] in these solar cells, or the use of up-conversion nanoparticles to get better performance in the near IR part of the visible spectrum. [4] Here we present two strategies based on nanostructuration, first a fundamental study of upconversion fluorescence enhancement effects near Au nanodisks by scanning near-field optical microscopy and second the effects of a nanocolumnar TiO₂ layer on the performance and the stability of Cs_{0.05}(FA_{0.83}MA_{0.17})_{0.95}Pb₃(I_{0.83}Br_{0.17})₃ perovskite solar cells. For the first case, the enhancement and localization of light near the metallic structures are directly visualized by using a single Er/Yb-codoped fluorescent nanocrystal glued at the end of a sharp scanning tip. [5] For the second we find that, compared to devices with planar TiO₂ ETLs, the TiO₂ nanocolumns can significantly enhance the power conversion efficiency of the perovskite solar cells by 17 % and prolong their shelf life. By analyzing the optical properties, solar cells characteristics, as well as transport/recombination properties by impedance spectroscopy, we observed light-trapping and reduced carrier recombination in solar cells associated with the use of TiO₂ nanocolumn arrays. [6]

References

- [1] S.S. Mali, et al., *Chemistry of Materials* **27**, 1541 (2015).
- [2] C. Liu, et al., *Journal of Materials Chemistry A* **5**, 15970 (2017).
- [3] M. Salado, et al., *Nano Energy* **35**, 215 (2017)
- [4] M. Bauch et al., *Plasmonics* **9**, 781 (2014)
- [5] L. Aigouy, et al., *Nanoscale* **11**, 10365 (2019)
- [6] Z. Hu, et al., *ACS Appl. Mater. Interfaces* **12**, 5979 (2020)

4:15 PM EN05.08.11

Ab Initio Material Design of Low-Band Gap Double and Vacancy Ordered Perovskites George Volonakis¹, Bruno Cucco¹, Pedesseau Laurent² and Mikael Kepenekian¹; ¹Université de Rennes 1, France; ²INSA Rennes, France

Lead-based halide perovskites have emerged as a most prominent candidate for emerging opto-electronic applications. In this talk we will briefly showcase recent efforts towards designing new Pb-free semiconductors that are alternatives to traditional halide perovskites, for which computational approaches from first-principles have been extensively successful and revealed a series of new compounds within the so-called halide double perovskites family and vacancy ordered perovskites. Among these, Cs₂BiAgBr₆ has the narrower indirect band gap of 1.9 eV, [1] and Cs₂InAgCl₆ is the only direct band gap semiconductor, yet with a large gap of 3.3 eV. [2] All of them exhibit low carrier effective masses and consequently, are prominent candidates for a range of opto-electronic applications such as photovoltaics, light-emitting devices, sensors, and photo-catalysts. [3] We will specifically outline the computational ab initio design strategy that led to the synthesis of these compounds, and particularly focus on the insights we can get from first-principles calculations in order to facilitate the synthesis, improve their opto-electronic properties and the in-silico identification of compounds with properties that are similar to the lead-halide perovskites. The newly developed concept of analogs will lead us to identify a new oxide double perovskite semiconductor, Ba₂AgIO₆, which exhibits an electronic band structure remarkably similar to that of our recently discovered halide double perovskite Cs₂AgInCl₆, but with a band gap in the visible range at 1.9 eV. [4] In the final part of our talk, we will employ this strategy to explore the phase space of vacancy-ordered double perovskite and discuss the case of Zr-based compounds as stable alternatives to Cs₂TiX₆ with X=Br,I, which exhibit lighter charge carrier effective masses.[5]

- [1] G. Volonakis et al., *Journal Physical Chemistry Letters* **7** 1254 (2016)
- [2] G. Volonakis et al., *Journal Physical Chemistry Letters* **8** 772 (2017)
- [3] G. Volonakis et al., *Journal Physical Chemistry Letters*, **8** 3917 (2017)
- [4] G. Volonakis et al., *Journal Physical Chemistry Letters*, **10** 1722 (2019)
- [5] B. Cucco et al., *Applied Physics Letters* (under review 2021)

4:30 PM EN05.08.12

Material Stability Assessment of Low Band Gap Pb-Sn Perovskites Christina Kamaraki^{1,2}, Matthew T. Klug¹ and Laura Miranda¹; ¹Oxford Photovoltaics Ltd, United Kingdom; ²University of Bath, United Kingdom

Mixed lead-tin (Pb-Sn) perovskites have excelled as leading candidates for low band gap absorber materials demonstrating efficiencies up to 21% for single junctions^{1,2} and 24.8% for all-perovskite tandem solar cells³. Although various ionic species and ratios can be combined to form low band gap perovskites, the propensity of Sn²⁺ to oxidize comprises the Achilles' heel of all of these compositions resulting in undesirable p-type doping of the material and poor optoelectronic quality⁴⁻⁷. A deep understanding of the intrinsic degradation mechanisms is imperative in order to successfully integrate these materials into perovskite multi-junctions and even though the deleterious effects of Sn oxidation have been widely explored, the composition's influence on degradation mechanisms has captured less attention.

Herein, the impact of the intrinsic stability of various low band gap compositions is investigated by monitoring changes in their structural and optoelectronic properties during either thermal or humidity stressing over time. As expected, the vulnerability of the material under humidity exposure scales with increased Sn content, while the degradation is governed by the A-cation choice under thermal stressing and absence of oxygen, with the compositions including volatile species proving to be more susceptible. Interestingly, even under humidity exposure different degradation response was observed for compositions with the same Sn content and different A-cation combination, indicating that ambient stability depends not only in Sn content but on A-site as well. Moreover, practical characterization methods which best capture this degradation at the time scales meaningful for device operation are identified. Our side-by-side degradation assessment highlights how materials composition can alter the degradation footprint and particularly how ion choice influences the speed and the mechanism of degradation, which can inform compositional selection for the practical development of all-perovskite tandems.

¹ J. Tong, Z. Song, D.H. Kim, X. Chen, C. Chen, A.F. Palmstrom, P.F. Ndione, M.O. Reese, S.P. Dunfield, O.G. Reid, J. Liu, F. Zhang, S.P. Harvey, Z. Li,

- S.T. Christensen, G. Teeter, D. Zhao, M.M. Al-Jassim, M.F.A.M. van Hest, M.C. Beard, S.E. Shaheen, J.J. Berry, Y. Yan, and K. Zhu, *Science* **364**, 475 (2019).
- ² J. Werner, T. Moot, T.A. Gossett, I.E. Gould, A.F. Palmstrom, E.J. Wolf, C.C. Boyd, M.F.A.M. van Hest, J.M. Luther, J.J. Berry, and M.D. McGehee, *ACS Energy Lett.* **5**, 1215 (2020).
- ³ R. Lin and H. Tan, *Nature Energy* (2019).
- ⁴ D. Meggiolaro, D. Ricciarelli, A.A. Alasmari, F.A.S. Alasmari, and F. De Angelis, *J. Phys. Chem. Lett.* **11**, 3546 (2020).
- ⁵ F. Hao, C.C. Stoumpos, D.H. Cao, R.P.H. Chang, and M.G. Kanatzidis, *Nature Photonics* (2014).
- ⁶ N.K. Noel, S.D. Stranks, A. Abate, C. Wehrenfennig, S. Guarnera, A.-A. Haghighirad, A. Sadhanala, G.E. Eperon, S.K. Pathak, M.B. Johnston, A. Petrozza, L.M. Herz, and H.J. Snaith, *Energy & Environmental Science* **7**, 3061 (2014).
- ⁷ M.T. Klug, R.L. Milot, J.B. Patel, T. Green, H.C. Sansom, M.D. Farrar, A.J. Ramadan, S. Martani, Z. Wang, B. Wenger, J.M. Ball, L. Langshaw, A. Petrozza, M.B. Johnston, L.M. Herz, and H.J. Snaith, *Energy Environ. Sci.* **13**, 1776 (2020).
- ⁸ L.E. Mundt, J. Tong, A.F. Palmstrom, S.P. Dunfield, K. Zhu, J.J. Berry, L.T. Schelhas, and E.L. Ratcliff, *ACS Energy Lett.* **5**, 3344 (2020).
- ⁹ T. Leijtens, R. Prasanna, A. Gold-Parker, M.F. Toney, and M.D. McGehee, *ACS Energy Letters* **2**, 2159 (2017).
- ¹⁰ T. Leijtens, R. Prasanna, K.A. Bush, G.E. Eperon, J.A. Raiford, A. Gold-Parker, E.J. Wolf, S.A. Swifter, C.C. Boyd, H.-P. Wang, M.F. Toney, S.F. Bent, and M.D. McGehee, *Sustainable Energy Fuels* **2**, 2450 (2018).

SESSION EN05.09: Poster Session I: Emerging Energy and Materials Sciences in Halide Perovskites

Session Chairs: Maria Antonietta Loi and Mathias Rothmann

Thursday Afternoon, December 2, 2021

8:00 PM - 10:00 PM

Hynes, Level 1, Hall B

EN05.09.02

Nonpareil Electrical Performance of Rb-Based Halide Perovskite at the Nanoscale Richa Lahoti^{1,2,1}, John Howard^{1,1}, MD Arafat Mahmud³, Thomas White³ and Marina Leite²; ¹University of Maryland, United States; ²University of California, Davis, United States; ³The Australian National University, Australia

A-site cation management in metal halide perovskites (MHPs) has shown to appreciably impact the stability and optoelectrical properties of the material. There has been notable investigation on MHPs at the nanoscale using atomic force microscopy (AFM) – based techniques. [1, 2] The incorporation of a small cation such as Rb⁺ cation to the A-site of the traditional perovskite has considerably alleviated shortcomings in device performance. Though these advancements are well-realized at the macroscopic level, a comprehensive study on the electrical characteristics at the nanoscale remains incomplete. At the macroscopic level, quad-cation (Cs_{0.07}Rb_{0.03}FA_{0.76}MA_{0.14}Pb(I_{0.85}Br_{0.15})₃) solar cells show reduced J-V hysteresis (90%) in comparison to dual-cation (Cs_{0.17}FA_{0.83}Pb(I_{0.83}Br_{0.17})₃) devices. We resolve their electrical performance through photovoltage [3] and photocurrent with nanoscale spatial resolution using Kelvin probe force microscopy (KPFM) and photoconductive-AFM (pc-AFM), respectively. At the nanoscale, our dark KPFM results indicate upward band bending at grain boundaries (GBs) for both chemical compositions. We note increased voltage homogeneity (34%) in quad-cation perovskite largely due to improved halide homogeneity by Rb⁺ cations. We observe a 55% faster post-illumination residual voltage decay in quad-cation perovskite. For the pc-AFM experiments, a Schottky contact is formed between the metal probe and the perovskite, which leads to the collection of holes at the probe end. From the upward band bending indicated by the KPFM results, we expect to see the presence of holes at GBs due to an electron barrier formation. We find that the photocurrent maps for quad-cation perovskite are in agreement with the expected outcome with most GBs reading a photocurrent value higher than their adjacent grains. Surprisingly, the majority of the GBs in dual-cation perovskites display photocurrent response comparable to dark current values. We conclude defect-assisted recombination at GBs in dual-cation perovskite and defect-passivation at GBs in quad-cation perovskite due to the addition of Rb⁺ cations. Further, we uncover that the defect-passivated GBs in quad-cation perovskite form a highly conductive GB network that enhances the overall photocurrent response of the material by ~50%. In addition, the photocurrent is independent of topography for both chemical compositions. Our analytical approach, which uses the combined knowledge of band bending and photocurrent response at GBs from KPFM and pc-AFM, respectively, can be used as a universal method to probe the presence and passivation of defects at GBs for any optoelectronic material. Our results underscore the beneficial characteristics, such as improved efficiency, reduced J-V hysteresis, and increased uniformity in photovoltage/current response present in quad-cation perovskite, imparted by the addition of Rb⁺ cation.[4]

[1] J.M. Howard, R. Lahoti, M. S. Leite. *Adv. Energy Mater.* **10**, 201903161 (2019) – Invited Review

[2] E. M. Tennyson, C. Gong, M. S. Leite. *ACS Energy Letters* **2**, 2761 (2017) – Invited Review

[3] E. M. Tennyson et al. *ACS Nano* **13**, 1538 (2019).

[4] R. Lahoti, et al. (2021), in preparation.

EN05.09.03

Fracture Behavior of Organic-Inorganic Halide Perovskite Thin Films for Solar Cells Zhenghong Dai and Nitin P. Padture; Brown University, United States

Organic-inorganic halide perovskites (OIHPs) has emerged as the most promising light-absorber materials in the photovoltaic community due to their near-ideal bandgaps. However, the low formation energies of OIHPs render them unstable. While significant progress has been made in improving the stability of OIHPs, perovskite solar cells (PSCs) will also need to be mechanically reliable if they are to service satisfactorily for decades. In this context, we study the fracture behavior of PSCs by measuring their cohesion energies (Gc) using double cantilever beam method and report a novel approach to strategically enhance the interfacial adhesion and performance of PSCs using self-assembled monolayers (SAMs), where we find that the perovskite solar cell stability is closely intertwined with its mechanical reliability. This work points to a new route for designing mechanically robust PSCs with long-term durability.

EN05.09.04

Double-Layered Porous Planar Electron Transport Layer for Flexible Perovskite Solar Cell and Modules Jaehoon Chung^{1,2}, Seong Sik Shin², Yanfa Yan¹ and Jangwon Seo^{3,2}; ¹The University of Toledo, United States; ²Korea Research Institute of Chemical Technology, Korea (the Republic of); ³Korea Advanced Institute of Science and Technology, Korea (the Republic of)

Planar perovskite solar cells(PSCs) using low temperature process is a promising candidate for high throughput production such as roll-to-roll process using a flexible substrate. However, the performance of the planar PSCs is still lower than that of the mesoscopic PSCs using high temperature process. Here, we report a new concept on low temperature processed porous planar electron transport layer (ETL) inspired by mesoporous structure for improving

the performance of flexible devices. The structurally and energetically designed porous planar ETL has induced the formation of high quality perovskite and a preferred band alignment, resulting in the improved charge collection efficiency in device. Through the porous planar ETL, we have achieved an efficiency of 20.7% with a certified efficiency of 19.9 % on a flexible substrate, which is the highest power conversion efficiency ever reported. In addition, for the first time, we succeed to fabricate a large area flexible module with porous planar ETL, demonstrating an efficiency of 15.5% and 12.9% on 100 cm² and 225 cm², respectively. We believe that this strategy shed a new light on the overcoming a limit of flexible devices.

EN05.09.05

Refractory Plasmonics Enabling 20% Efficient Lead-Free Perovskite Solar Cells [Nageh K. Allam](#); American University in Cairo, Egypt

Core-shell refractory plasmonic nanoparticles are used as excellent nanoantennas to improve the efficiency of lead-free perovskite solar cells (PSCs). SiO₂ is used as the shell coating due to its high refractive index and low extinction coefficient, enabling the control over the sunlight directivity. An optoelectronic model is developed using 3D finite element method (FEM) as implemented in COMSOL Multiphysics to calculate the optical and electrical parameters of plain and ZrN/SiO₂-modified PSCs. For a fair comparison, ZrN-decorated PSCs are also simulated. While the decoration with ZrN nanoparticles boosts the power conversion efficiency (PCE) of the PSC from 12.9% to 17%, the use of ZrN/SiO₂ core/shell nanoparticles shows an unprecedented enhancement in the PCE to reach 20%. The enhancement in the PCE is discussed in details.

EN05.09.07

Evaporation Properties of Formamidinium Iodide During the Preparation of Perovskite Solar Cells [Martin Kroll](#), Zongbao Zhang, Ran Ji, Marcus Pappmeyer, Yana Vaynzof and Karl Leo; TU Dresden IAPP, Germany

The fast development of metal halide perovskite solar cells over the last years has reached a level where application in commercial devices is becoming very realistic. This requires scalable deposition techniques like vacuum deposition. It is widely known that during the processing of perovskite, many factors influence the quality of the absorber layer. For solution processed perovskite layers, the research on this topic is growing, but in the case vacuum deposition, the influencing factors are still not fully known. One important factor is the quality of the vacuum in the deposition chamber. Because of material changes of the precursors, residual water, and the vacuum system power, the background pressure changes from deposition to deposition, or even over the course of the processing of a single absorber layer. Due to the different deposition properties of the organic and inorganic precursor salts, the materials are influenced differently. To ensure high reproducibility and high film quality, an increase in the control over all processing parameters is important. In this work, we investigate the influence of the background pressure during the deposition process on important factors like the material tooling and with it the stoichiometry, the crystal structure and finally the device performance. By varying the background pressure about ~ 2 orders of magnitude (~2*10⁻⁶mbar à 1*10⁻⁴mbar) a bandgap change of the produced perovskite of 60 meV was observed. Besides the stoichiometry the layer thickness is strongly influenced by the background pressure. This results in a decrease in device performance from 15.6 % to 12.6 %.

EN05.09.08

Characterizing Organic Cation Dynamics in Hybrid Halide Perovskites with Neutron Scattering [Eve Mozur](#)¹ and James R. Neilson²; ¹University of California, Santa Barbara, United States; ²Colorado State University, United States

Hybrid halide perovskites have many exciting optoelectronic properties that make them suitable for photovoltaic and lighting applications. Unlike conventional inorganic semiconductors, including silicon, cadmium telluride, and gallium arsenide, hybrid halide perovskites possess many dynamical degrees of freedom. These dynamics underly many of their optoelectronic properties, suggesting a new paradigm of dynamics-based structure property relationships. Neutron scattering and spectroscopies are ideal tools to better understand the dynamics of these materials. Here, we present several case studies that demonstrate how neutron scattering enriches our understanding of the phase behavior and functional properties of hybrid halide perovskites. We propose that these insights provide targets for engineering perovskite functional properties.

EN05.09.10

Two-Phased but Not Two-Faced—Superior Performance of Two-Phase Triple Halide Inorganic Perovskites [Deniz N. Cakan](#)¹, Moses Kodur¹, Rishi Kumar¹, Connor Dolan¹, Yanqi Luo², Tao Zhou², Zhonghou Cai², Barry Lai², Martin Holt² and David P. Fenning¹; ¹University of California, San Diego, United States; ²Argonne National Laboratory, United States

Inorganic halide perovskites are attractive for achieving the wide bandgap optimal for a high-efficiency perovskite-perovskite tandem based on today's Pb-Sn low bandgap compositions. However, they have suffered from lower photoluminescent quantum yield relative to hybrid compositions and phase instability. To improve upon metastable CsPbI₃, we explore triple-halide alloying of minor amounts of Br and Cl with I. In agreement with previous reports for hybrid analogues, we observe a chlorine solubility limit in the majority iodine-bromine all-inorganic perovskite lattice. Past this solubility limit we observe the perovskite forming a split phase of iodine-bromine-rich and bromine-chlorine-rich clusters. Interestingly, these dual-phase thin-films show superior performance, which hints at possible *synergistic* effects of this chemical heterogeneity. We leverage multi-modal synchrotron microscopy and correlative spectroscopic micro-photoluminescence (μPL) on all-inorganic triple halide perovskites CsPbX₃ (X-site: I/Br/Cl) films to elucidate mechanisms for superior performance in the face of phase segregation. The results suggest that a greater focus on harnessing the flexibility of the inorganic perovskite material system holds promise to retrace the outstanding performance and stability gains made in hybrid analogues.

EN05.09.11

Late News: What is the Origin of Optical Emission in Cs₂TiBr₆? [Emma J. Pellerin](#), Emma Burton, Caroline Jaeger, Maranda Allen, Ronald L. Grimm and Lyubov Titova; Worcester Polytechnic Institute, United States Minor Outlying Islands

Thin-film perovskite solar cells (PSCs) now rival established Si photovoltaics inefficiencies and could be less expensive with fewer resources required for processing. A major drawback of the leading PSCs is the presence of Pb in their structure, raising concerns about toxicity. Cs₂TiBr₆ is one leading candidate among Pb-free perovskites. It has a suitable bandgap to be the top absorber in tandem-junction photovoltaics at ~1.8 eV, and Cs₂TiBr₆-based PSCs have demonstrated efficiencies up to 3.3%. However, a complete view of the optical properties, carrier dynamics, and environmental stability remains incomplete.

Herein, we use time-resolved photoluminescence spectroscopy to investigate optical emission and carrier lifetime in both large-grain and thin-film Cs₂TiBr₆ under different environmental conditions. Cs₂TiBr₆ demonstrates high stability in an N₂ with photoexcited radiative lifetimes on the order of 0.5 ns, sufficient for photovoltaic consideration. We investigate the origins of several prominent emission features and their dependence on sample morphology as well as on environmental conditions.

EN05.09.12

Maximizing the Global PLQY Through Local Bandgap Variation in Mixed-Halide Perovskites [Sascha Feldmann](#)¹, Henning Sirringhaus¹, Michael

Saliba², David Beljonne³, Samuel D. Stranks¹, Achim Hartschuh⁴ and Felix Deschler⁵; ¹University of Cambridge, United Kingdom; ²Universität Stuttgart, Germany; ³Université de Mons, Belgium; ⁴Ludwig-Maximilians-Universität München, Germany; ⁵Technische Universität München, Germany

Halide perovskites have emerged as high-performance semiconductors for efficient optoelectronic devices, not least because of their bandgap tunability using mixtures of different halide ions. This makes them particularly attractive as candidates for tandem solar cells or spectrally tailored lighting. We demonstrate that spatially varying energetic disorder in the electronic states of such mixed-halide films causes local charge accumulation, creating photodoped regions, which unearths a strategy for efficient energy conversion in solar cells and light-emitting diodes at low charge densities. We combine temperature-dependent photoluminescence microscopy with computational modelling to quantify the impact of local bandgap variations from disordered halide distributions on the global photoluminescence yield in mixed-halide perovskite films. We find that fabrication temperature, surface energy, and charge recombination constants are key for describing local bandgap variations and charge carrier funneling processes that control the photoluminescence quantum efficiency. We report that further luminescence efficiency gains are possible through tailored bandgap modulation, even for materials that have already demonstrated high luminescence yields.

EN05.09.14

Synthesis, Properties and Prospects for Photovoltaics of Chalcogenide Perovskite Thin Films Ida Sadeghi, Kevin Ye and Rafael Jaramillo; Massachusetts Institute of Technology, United States

Sulfides and selenides in the perovskite and related crystal structures - chalcogenide perovskites - are an exciting family of semiconductors for solar energy conversion and optoelectronics [1]. Here, we explore materials in the Ba-Zr-S system to determine their potential for thin-film photovoltaics (PV). We demonstrate making BaZrS₃ thin films by gas-source molecular beam epitaxy (MBE) [2]. BaZrS₃ forms in the orthorhombic distorted-perovskite structure with corner-sharing ZrS₆ octahedra (space group Pnma, no. 62), and has a direct band gap of $E_g = 1.85$ eV. We present a wealth of data reporting film processing and properties, including reflection high-energy electron diffraction (RHEED), atomic-force microscopy (AFM), X-ray reflectivity and diffraction (XRR and XRD), scanning transmission electron microscopy (STEM), spectroscopic ellipsometry, Hall transport, and photoconductivity. Our single-step MBE growth process produces films that are atomically smooth, single phase, chemically homogeneous, and oxygen free. The films are brightly colored even at 20 nm thick, due to the strong optical absorption typical of chalcogenide perovskites. Films grow via two, competing epitaxial growth modes: (1) buffered epitaxy, with a self-assembled interface layer that relieves the epitaxial strain, and (2) direct epitaxy, with rotated-cube-on-cube growth that accommodates the large lattice constant mismatch between the oxide and the sulfide. The propensity for these two modes can be tuned by adjusting the H₂S gas delivery rate. We further show results making thin films of BaZr(S,Se)₃ alloys (achieved by co-flowing H₂S and H₂Se), which provide a path towards tuning the direct band gap in the range 1.3 – 1.9 eV.

We also report on time-resolved photoluminescence (TRPL) and photoconductivity (TRPC) studies of excited-state transport in BaZrS₃ and the related, Ruddlesden-Popper phase Ba₂Zr₂S₇ ($E_g = 1.25$ eV). We model the data using semiconductor physics simulations, to enable more direct determination of parameters key for photovoltaic performance (e.g. surface recombination velocity, Shockley-Read-Hall lifetime, diffusivity) than is possible with empirical data modeling. We find that chalcogenide perovskites have SRH lifetime exceeding 100 ns and ambipolar diffusion length on the order of 10 μm. If time allows, we will present further results of advanced characterization including impedance spectroscopy and X-ray absorption spectroscopy.

Our high-quality thin-film synthesis and excited-state transport measurements suggest a bright future for chalcogenide perovskites thin-film PV. We will end by briefly summarizing the state of the field, and highlighting key challenges on the road to device demonstrations and commercialization.

[1] Jaramillo, R. & Ravichandran, J. In praise and in search of highly-polarizable semiconductors: Technological promise and discovery strategies. *APL Materials* 7, 100902 (2019).

[2] Sadeghi, I., Ye, K., Xu, M., LeBeau, J. M. & Jaramillo, R. Making BaZrS₃ chalcogenide perovskite thin films by molecular beam epitaxy. arXiv:2105.10258 [cond-mat] (2021). at <<http://arxiv.org/abs/2105.10258>>

EN05.09.16

Optical Origin of External Quantum Efficiencies near Unity in Perovskite Solar Cells Kai O. Brinkmann, Tim Becker, Florian Zimmermann, Cedric Kreusel, Tobias Gahlmann, Tobias Haeger and Thomas Riedl; University of Wuppertal, Germany

Hand in hand with the outstanding progress of perovskite photovoltaics, reports of very high values of external quantum efficiency (EQE) appeared. Values of EQE up to 98 % were reported, typically peaked in the range between 400 and 500 nm. Even considering a very high internal quantum efficiencies of the perovskite close to 100%,^[1] this observation strikes as a contradiction at a first glance, as the transmittance of ITO/glass substrates typically does not exceed 90% in this wavelength range. Therefore reports of high EQE numbers (EQE is one of the standard characterization procedures for solar cells to exclude or correct spectral mismatch of light sources used for solar cell fabrication^[2]) frequently give rise to doubts or concerns about potentially erroneous EQE measurements.

Here, we discuss and explain the root cause of the high EQE by a combination of experimental data and optical simulations. We show, how the transmittance into the active material is significantly governed by its refractive index, enabling very high portions of light being coupled into the high refractive perovskite material at the given wavelength region. At the same time transmission into a low refractive material like air, gives rise to a significant reflectance.^[3]

These effects can be nicely seen in optical simulation, experimentally acquired EQE spectra, and optical absorption/reflection measurements. Finally we are able to unravel, that the maximum of the transmittance spectrum is mainly shifted by the thickness of the underlying transparent conductive oxide (TCO) layer. As an example, for our wide gap FA_{0.8}CS_{0.2}Pb(I_{0.5}Br_{0.5})₃ cells (1.85 eV) we found that an increasing ITO thickness would even increase the maximal reachable current and therefore being beneficial in a twofold purpose: reducing the sheet resistance of the bottom electrode while simultaneously increasing the in-coupling of light into the active layer.

[1] Q. Lin et al. *Nat. Photonics* **2015**, 9, 106.

[2] J. A. Christians et al. *J. Phys. Chem. Lett.* **2015**, 6, 852.

[3] K.O. Brinkmann et al. *Solar RRL* (in review)

EN05.09.17

Late News: Light Intensity Analysis of Photovoltaic Parameters for Perovskite Solar Cells Damian Glowienka^{1,2} and Yulia Galagan²; ¹Gdansk University of Technology, Poland; ²National Taiwan University, Taiwan

The number of publications on perovskite solar cells (PSC) continues to grow exponentially. Although the efficiency of PSC is exceeded 25.5%, not every research laboratory can reproduce this result or even pass the border of 20%. Unfortunately, it is not always clear which dominating mechanism is responsible for the performance drop. Here, we develop a simple method of light intensity analysis of JV parameters allowing the understanding what are

the mechanisms appearing in the solar cell and limiting device performance. The developed method is supported by the drift-diffusion model and aimed to help in the explanation of the parasitic losses from the interface or bulk recombination, series, or shunt resistance in the perovskite solar cell. This method can help not only point on the dominating of bulk or interface recombination in the devices but also determine which interface is more defective. The detailed and stepwise guidance for such a type of light intensity analysis of JV parameters is provided. The proposed method and the conclusions of this study are supported by a series of case studies, showing the effectiveness of the proposed method on real examples.

SESSION EN05.10: Advancing Perovskite Devices I
Session Chairs: Mengxia Liu, Michael Saliba and Yuanyuan Zhou
Monday Morning, December 6, 2021
EN05-Virtual

8:00 AM *EN05.10.01

Engineering Long Lived Perovskite Solar Cells—The Role of Cation Induced Temperature Destabilization [Christoph J. Brabec](#)^{1,2} and Yicheng Zhao²; ¹FAU Erlangen-Nuremberg, Germany; ²Research Center Julich, Germany

Perovskite photovoltaics based on metal halide perovskites is a most promising photovoltaic technology, but further advance demands improved device stability. Here we show the importance of perovskite composition engineering by demonstrating long-term stable perovskite solar cells. A high-throughput robotic approach is used to screen 160 mixed-cation mixed-halide perovskites based on several optical characterizations, such as UV-vis absorption and photoluminescence spectra. Such automated big data approaches allow to uniquely identify the most photo-thermal-stable perovskites under elevated temperature and 1-Sun illumination. Most interestingly, while several perovskite compositions are found to be stable against high temperatures of up to 85 C, the situation is more complex in working devices, as a stable device requires both - a stable semiconductor layer and stable interfaces. A p-type interface consisting of polymeric multilayers with variable dopant is introduced as a robust anode interface. By integrating the most stable perovskite into this structure, we achieve stable devices without encapsulation that attain nearly 100% of their initial efficiency and 98% of their peak efficiency, after 1000 hrs of continuous mpp operation at temperatures of 60-65 degrees Celsius. Nevertheless, degradation is still observable when the operation temperature is further raised towards 85 C and above, which highlights that the microscopic degradation mechanisms in perovskite devices are still not fully understood. This work introduces into the fundamentals how to accelerate the screening for stable perovskites layer and devices for operation at elevated temperatures.

8:30 AM *EN05.10.02

Efficient Perovskite Solar Cells and Light-Emitting Diodes [Jingbi You](#); Chinese Academy of Sciences, China

The champion efficiency of perovskite solar cells (PSCs) is over than 25%, and the external quantum efficiency of perovskite light-emitting diodes (PeLEDs) in green and red is over than 20%, which is great potential for practical application. In this report, I will talk about our recent progresses in PSCs and PeLEDs. 1) By rational design the composition of perovskite, we got over than 25% efficiency while using nearly pure FAPbI₃, 2) For the perovskite light-emitting diodes with blue emission, we modulated the hole transport layer to reduce the injection barrier, and got over than 16% external quantum efficiency of PeLEDs in blue.

9:00 AM EN05.10.03

Late News: Nanostructured Metal Halide Perovskite Materials for Novel Optoelectronic Devices [Zhiyong Fan](#); Hong Kong University of Science and Technology, China

Metal halide perovskite materials are regarded as highly promising materials for high performance optoelectronics due to excellent optical absorption, long carrier diffusion length, tunable composition, etc., thus have triggered broad attention for applications including solar cells, photodetectors and light-emitting diodes. Conventionally, solution processes have been utilized to fabricate perovskite materials. In our work, in order to achieve high material quality and device scalability, we have developed chemical vapor deposition process to grow ordered high density perovskite nanowire (NW) arrays in nanoengineering templates with materials including MAPbI₃, MASnI₃, CsPbI₃ and FAPbI₃. The geometrical factors of NWs, namely, periodicity, diameter and length can be precisely nanoengineered. Intriguingly, we have discovered that the chemically and mechanically robust template can effectively protect perovskite NWs against water and oxygen invasion thus the material chemical stability and phase stability are significantly better than planar perovskite films. To explore device applications of perovskite NW arrays, they have been fabricated into novel optoelectronic devices such as photodetectors and bionic eye. Meanwhile, we have also fabricated high efficiency thin film Pero LEDs on self-organized nanophotonic templates and achieved much improved external quantum efficiency (EQE) as compared to planar control device. These results will be demonstrated in this presentation. And they suggest that in addition to material optimization, device structure innovation, particularly utilization of various types of nanostructures can lead to high performance optoelectronics.

9:30 AM *EN05.10.04

Thermally Co-Evaporated Perovskites for Mini-Modules, Tandem Solar Cells Annalisa Bruno, Nripan Mathews and [Subodh Mhaisalkar](#); Nanyang Technological University, Singapore

Although perovskite solar cells (PSC's) with efficiencies of 25.5% [1] have been reported, the best-performing perovskite solar cells rely primarily on lab-scale solution-processed techniques that typically yield small-scale (~0.1 cm²) devices. Besides scaling up of these devices, demonstration of stability of these devices are also essential. [2-5]

Deposition of perovskite absorber layers by thermal co-evaporation have gathered considerable interest for silicon-perovskite tandem solar cells. The main advantages for thermal evaporation include potential compatibility with silicon solar cell processing, conformal coatings, control of deposited layer thicknesses, and possibility of multi-layer processing. We have recently demonstrated highly efficient, large area, planar PSCs with uniform MAPbI₃ perovskite active layer deposited by thermal co-evaporation of PbI₂ and MAI. The high-quality co-evaporated perovskite thin films are pinhole-free and uniform over several centimetres, showing large grain sizes, low surface roughness, and a long carrier lifetime. The high-quality perovskite thin films translates to small area PSCs (0.16 cm²) with PCE above 20% and high reproducibility. Large area PSCs with area up to 4 cm² did not show a significant drop in the PCE. Furthermore, the first thermally evaporated mini-modules with an active area larger than 20 cm² achieved the record PCE of 18.13%. [6]

Thermal stability is a critical criterion for assessing the long-term stability of perovskite solar cells. Thermally evaporated perovskites also deliver remarkable thermal stability compared with solution processed solar cells. The improved stability may be attributed to the perovskite growth process leading to a compact and almost strain-free films. This work represents an important step towards the development of high quality, stable, and reproducible large-area perovskite solar cells and mini-modules, the main requirements for the industrialization of this technology.

SESSION EN05.12: Fundamental Structure and Properties of Perovskites I
Session Chairs: Mahshid Ahmadi, Michael Saliba and Yuanyuan Zhou
Monday Afternoon, December 6, 2021
EN05-Virtual

1:00 PM *en05.04.01

Defects Activity in Wide and Narrow Bandgap Metal Halide Perovskite Semiconductors [Annamaria Petrozza](#); Istituto Italiano di Tecnologia, Italy

Metal halide perovskites (MHPs) have demonstrated huge potential to build a rich library of materials for a new disruptive optoelectronic technology. The main strength comes from the possibility of easily tune the semiconductor bandgap in order to integrate it in devices with different functionalities – in principle. In reality, this cannot be achieved yet. In fact, while defect tolerance is claimed for MHPs with a bandgap of about 1.6 eV, the model system object of intense investigations, MHPs with lower and higher bandgaps are far from this claim. They show various forms of instabilities which are mainly driven by a strong defect activity.

Here I will discuss our studies on the nature of defects and their photo-chemistry as a function of the semiconductor bandgap and chemical composition in order to identify their role in defining the semiconductor electronic properties and stability.

1:30 PM EN05.12.01

Local Structural Correlations and Low-Temperature Anharmonicity in Methylammonium Lead Tribromide [Nicholas J. Weadock](#)¹, Cameron MacKeen², Louis Waquier³, Julian Vigil⁴, Yevgeny Rakita^{5,6}, Hemamala Karunadasa⁴, Frank Bridges² and Michael Toney¹; ¹University of Colorado Boulder, United States; ²University of California, Santa Cruz, United States; ³SLAC National Accelerator Laboratory, United States; ⁴Stanford University, United States; ⁵Columbia University, United States; ⁶Weizmann Institute of Science, Israel

The hybrid metal halide perovskite (MHP) family exhibits large structural fluctuations which are believed to contribute to, or perhaps cause, their remarkable optoelectronic properties. Additionally, experimental studies including Raman spectroscopy and X-ray total scattering demonstrate that these fluctuations cause local deviations from the **average** bulk structure in the three-dimensional MHPs, such as CH₃NH₃PbBr₃ (herein MAPB). [1–3] MAPB has three well defined crystal structures; orthorhombic, tetragonal, and cubic, with phase transitions identified at 141 K and 235 K. An additional incommensurate phase bridges the orthogonal and tetragonal phases. These phase transitions proceed as an unlocking of the organic cation and rotational modes of the PbBr₆ octahedra. Several studies have characterized the dynamics of the organic cation, the PbBr₆ octahedra, and their interactions, however the dynamics of the Pb-Br bond have received less attention. [4–7]

We investigate the temperature dependence of correlated motions and anharmonicity of the Pb-Br bond with a combined extended X-ray absorption fine structure (EXAFS) and single crystal X-ray diffraction (XRD) study of MAPB. EXAFS provides a snapshot of the local environment around the probe atom, rather than the time- and space-averaged structure obtained from XRD. Fitting the EXAFS spectra to a cumulant expansion reveals that the Pb-Br bond exhibits anharmonicity even in the low-temperature orthorhombic phase. We also examine the correlated motion of the Pb and Br atoms by comparing the mean squared displacement obtained from XRD with the mean squared *relative* displacement obtained from EXAFS. [8,9] In this picture, we find that Pb and Br motions are strongly correlated along the bond direction and somewhat correlated perpendicular to the bond direction. Interestingly, the effective Pb-Br spring constant and correlation coefficients increase through the orthorhombic-tetragonal transition, a highly unusual effect likely resulting from a charge rearrangement on the Pb atom which increases the Pb-Br orbital overlap. Finally, we compare the various asymmetric Pb-Br pair distribution functions which can arise from an anharmonic potential. An in-depth understanding of anharmonicity and the phase transitions will allow designs of structurally robust MHP devices.

NJW and MFT gratefully acknowledge full support from the Center for Hybrid Organic Inorganic Semiconductors for Energy (CHOISE), an Energy Frontier Research Center funded by the Office of Basic Energy Sciences, Office of Science within the U.S. Department of Energy through contract number DE-AC36-08G028308.

References:

- [1] A. N. Beecher, et al. ACS Energy Lett. **1**, 880 (2016).
- [2] O. Yaffe, et al. Phys. Rev. Lett. **118**, 136001 (2017).
- [3] R. Comin, et al. Phys. Rev. B **94**, 094301 (2016).
- [4] Y. Guo, et al. Phys. Rev. Materials **1**, 042401 (2017).
- [5] I. P. Swainson, et al. Phys. Rev. B **92**, 100303 (2015).
- [6] A. C. Ferreira, et al. Phys. Rev. Lett. **121**, 085502 (2018).
- [7] G. Laurita, et al. Chemical Science **8**, 5628 (2017).
- [8] C. H. Booth, et al. Phys. Rev. B **52**, R15745 (1995).
- [9] W. R. Busing and H. A. Levy, Acta Cryst **17**, 2 (1964).

1:45 PM EN05.12.02

Late News: Shallow Dopants and Deep Defects in Halide Perovskites [John L. Lyons](#)¹ and Michael W. Swift²; ¹U.S. Naval Research Laboratory, United States; ²ASEE Fellow residing at the Naval Research Laboratory, United States

Chemical doping of lead halide perovskites remains challenging. One major issue is that commonly considered dopants (such as bismuth, substituting on the lead site) have high ionization energies, making them ineffective. Our recent density functional theory (DFT) calculations indicate that the deep donor behavior of bismuth (along with antimony) is due to their *p* orbitals giving rise to mid-gap states. Furthermore, the *s* orbitals of gallium dopants lie deep in the CsPbBr₃ band gap, also leading to deep defect behavior. In contrast, the group 3 elements scandium and yttrium do not give rise to such mid-gap states, and are thus shallow donors when incorporating on the Pb site. These donors are stable relative to other configurations and have modest formation energies. Analogous behavior is found in FAPbI₃ and CsPbCl₃, indicating that *n*-type conductivity could be achieved in lead halide perovskites with Y and Sc dopants [1].

A second issue is the potential for native defects (such as vacancies and interstitials) to compensate intentional dopants. Via a thorough first-principles inventory of native defects and hydrogen impurities, we determine the stability and electronic behavior of potential compensating species. We find that a number of relevant species exhibit deep levels (most notably the bromine interstitial and hydrogen interstitial) challenging the idea that “defect tolerance” in these materials is due to the shallow character of native defects [2]. Guided by the theoretical identification of these defects with DFT, growth efforts can take steps to mitigate trap-assisted non-radiative recombination to boost efficiencies of lead halide perovskites and aid in efforts at achieving controllable electrical conductivity.

[1] *Chem. Mater.* **33**, 6200 (2021).

[2] *J. Mater. Chem. A* **9**, 7491 (2021).

This work was supported by the ONR/NRL 6.1 Basic Research Program.

2:00 PM EN05.12.03

Very Fast and Very Slow Ionic Processes and Charge Accumulation in Lead Halide Perovskite Solar Cells Brian O'Regan¹, Michael McGehee², Caleb Boyd³, Joseph Luther⁴, Severin Habisreutinger⁴ and Rohit Prasanna⁵; ¹BSL, United States; ²University of Colorado Boulder, United States; ³Unternehmertum Venture Capital Partners GmbH, Germany; ⁴National Renewable Energy Laboratory, United States; ⁵Swift Solar, United States

Using JV scan speeds from 0.01 to 4000 V/sec one can find that seemingly all lead halide perovskite solar cells show considerable photocurrent JV hysteresis somewhere between the 10 ms and 10 second time scales. The JV hysteresis generally shows up as a large change in fill factor (FF) and energy efficiency, although smaller hysteresis can be found in the dark current as well. Mobile ions (vacancies) seem to be able to explain most of the JV hysteresis, although there is still argument about the maximum mobility of the ions in relation to the fastest observed hysteresis.

In many perovskite cells, the fast JV hysteresis coexists with a reversible day/night cycle in the short circuit current (Jsc) and FF. This day/night cycle varies strongly between cell types and fabrications, ranging from degradation in the dark and recovery in the light, to the complete opposite. I will discuss new measurements of the amount of excess charge stored during an 8 hour illumination cycle at the maximum power point (MPP), at short circuit, and at the MPP voltage in the dark. After an 8 hour illumination cycle, we find that measurable current continues to flow out of the cell for up to 10 hours after the light and voltage are removed. The amounts of stored charge can be large (e.g. up to 1% of the Pb ions in the absorber) without causing irreversible damage to the film. In some cells the amount of charge stored for a given illumination time is linearly related to the loss of efficiency over that time. I will discuss some experiments on the chemical nature and physical location of this charge, but, sadly, will not give a definitive answer.

2:15 PM EN05.12.04

Revealing Humidity-Dependent Mechanical Properties in Halide Perovskites Isaac Buchine¹, David Cahen^{2,1}, Sidney R. Cohen² and Irit Rosenhek Goldian²; ¹Bar-Ilan University, Israel; ²Weizmann Institute of Science, Israel

Effects of humidity on the optoelectronic properties and degradation mechanisms of ABX₃ Halide Perovskites, HaPs, where A= Methylammonium (MA), Formamidinium (FA), or Cesium (Cs), B= Pb, X=Chloride (Cl), Bromide (Br), or Iodide (I), have been investigated thoroughly. However, no studies exist on how humidity influences their *structural and mechanical integrity*, which is critical for their successful integration into future technologies. The out-of-plane mechanical properties of HaPs are known to depend strongly on the Pb-X bond, but the effect of humidity remains ill-explored. This presents a difficulty in engineering devices, containing these materials, that are meant to function over a range of ambient conditions, as well as casting doubt on the generality of fundamental behavior, measured under uncontrolled humidity conditions.

Single crystals of five different HaP, MAPbX₃ (X = Cl, Br, and I) and APbBr₃ (A = Cs and FA) were grown and used to investigate the role that the different A and X ions play for humidity-dependence of mechanical properties. A two-pronged approach employing both instrumented nanoindentation (INI), and atomic force microscopy (AFM)-based nanomechanical measurements were used to measure *in situ* changes in elastic and plastic deformation under different humidity conditions. AFM measurements included both elastic modulus determination using the contact resonance technique and hardness measurements, using the AFM to both apply load to sample and to image the indentation profile in-situ using the same diamond tip. The INI was done at slightly larger loads and inferred the indentation area by standard calibration techniques and not from the imprint image. By combining analysis between AFM and INI methods, we are able to verify the significance of these results from two independent techniques which are based on similar but distinct measurement and analysis procedures.

Our results reveal that for MAPbCl₃, MAPbBr₃, and FAPbBr₃ the elastic modulus (E) increases by 4-10% while the hardness (H) decreases by ~25% when RH (relative humidity) increases from 10% to 60% and that these changes are reversible. E is a measure of the elastic response and H is related to the plastic response. CsPbBr₃ and MAPbI₃ show negligible humidity dependence within experimental uncertainty, with the latter showing differences between shallow and deep indentations. We propose an explanation for these observations incorporating the interplay between composition, lattice structure, and absorbed H₂O.

2:30 PM EN05.12.05

Strong Spin-Dependent Interactions of Photoexcited Charge Carriers with Magnetic Transition Metal Dopants in MAPbBr₃ Jonathan Zerhoch¹, Stanislav Bodnar¹, Timo Neumann², Barbara Sergl¹, Lissa Eyre¹ and Felix Deschler¹; ¹Walter Schottky Institut, Germany; ²Cavendish Laboratory, United Kingdom

Combining the advantageous electrical and optical properties of semiconductors with magnetic characteristics gives access to extraordinary phenomena and applications. Fully inorganic dilute magnetic semiconductors (DMS) have been known for decades, which show diverse functionalities like control of magnetism by electrical fields. Typically, the material class of DMS is obtained by introducing a substantial number of magnetic ions to an otherwise non-magnetic host semiconductor.

In this work we investigate the magneto-optical properties of the heavily doped hybrid semiconductors MAPbBr₃ (CH₃NH₃PbBr₃) with circularly polarized broadband femtosecond transient absorption (CTA), from which we find strong interactions between the excited charge carriers' angular momentum and the dopants' spin.

Due to their outstanding optoelectronic properties and high defect tolerance, organo-metal halide perovskites form an ideal system for efficient magnetic doping. We prepared a selection of magnetic perovskites using simple solution processing techniques in the host MAPbBr₃ perovskite with three different magnetic ions Mn²⁺, Co²⁺, Ni²⁺. We investigated the fundamental optical, structural and magnetic properties of the perovskites with absorption and photoluminescence spectroscopy, XRD and SQUID measurements. Doping of the host lattice leads in all cases to structural changes and an increase or decrease of the bandgap of several 10 meV for Co²⁺ and Mn²⁺/Ni²⁺, respectively. We observe paramagnetic properties for all dopants and different doping concentrations.

To reveal the impact of doping on excitation dynamics, we employ the technique of CTA at cryogenic temperatures down to 4 K and magnetic fields up to 700 mT to gain a better understanding of possible ultrafast processes and coupling mechanisms between the angular momentum of photoexcited charge carriers and the d-electron spin of the dopants. Measuring CTA with different combinations of right- and left-handed circularly polarized pump ($\lambda_{ex} = 515$ nm) and probe (super-continuum white light) at variable temperatures and magnetic fields with an exceptional spectral resolution of 0.1 nm enabled us to

precisely compare the energetic shifts and ultrafast dynamics of the charge carriers. For all investigated samples we observed an energy splitting of the CTA spectra for two different circular polarizations of the pump pulse even at zero magnetic field, which is substantially larger for the doped samples. Both, lattice deformations and remanent magnetism due to high doping concentrations could lead to an energetically preferred spin alignment of the photoexcited charge carriers mediated via spin-orbit coupling. We plan to employ transient circularly polarized photoluminescence spectroscopy (CPL) to show if this spin polarization is long-lived and if it will lead to a significant degree of circularly polarized PL, which would be of high interest for future light emitting diode applications.

2:45 PM EN05.12.07

Defect Densities in Halide Perovskite Thin Films and Single Crystals Johanna Siekmann¹, Sandheep Ravishankar¹ and Thomas Kirchartz^{1,2}; ¹Forschungszentrum Jülich, Germany; ²Universität Duisburg-Essen, Germany

The majority of halide perovskite solar cells are thin film devices.^[1] This is not surprising if we look at the simplicity of making devices based on stacks of multiple thin films as opposed to making single crystal solar cells. However, single crystals seem to have some fundamental advantages relative to thin films, because their lack of grain boundaries apparently leads to defect densities that are orders of magnitude lower in single crystals as opposed to thin films.^[2] The typically stated data in support of this claim is based mostly on two methods, namely the use of the so-called trap-filled limit in the current-voltage curve of single-carrier devices^[3] and the use of capacitance-voltage measurements or related techniques^[4,5] to determine defect densities via the width of space charge regions. Both methods have in common that they measure quantities that are affected by the charge density of a defect and not by the defect density itself. An important consequence is that bulk charge densities have to compete with surface charge densities of electrodes to be visible in a measurement. Furthermore, for a charge density to be visible in any measurement, the charge density has to be high enough that its associated Debye length is at least on the order of the film thickness (or shorter). Otherwise, the charge density will be unable to affect the electrostatic potential over the available distance and in consequence will be unable to visibly affect the current or capacitance measured in a device. From these simple electrostatic arguments, one can conclude that charge densities have to exceed a certain threshold value that depends on the permittivity ϵ and thickness d of the sample. Actually, both arguments noted above lead to a detection limit that could be expressed by noting that the density of charged defects has to exceed a minimum value $N_{\min} \propto \epsilon/d^2$ that inversely depends on d^2 . By doing a meta-analysis of literature data, we note that nearly no reported defect density of a thin film done by a charge-detecting method exceeds threshold criteria for both methods that are derived analytically and verified numerically. Only few of the single crystal data exceed the threshold, suggesting that defect densities might be much lower than originally thought in many cases and further suggesting that there is no reliable trend that would support the presence of superior electronic properties in single crystals. Furthermore, we use numerical simulations to identify possible reasons that may lead to the possible misinterpretation of data as being representative of a certain defect density. We find that in particular, small variations of injection barrier heights can lead to apparent trap-filled current regimes that may cause literature data to follow the detectability limit. Finally, we also do a meta-analysis of charge carrier lifetimes and non-radiative voltage losses that does not show any indication of a trend favoring single crystals which one would expect if there was a strong trend in defect densities.

[1] National Renewable Energy Laboratory *Best Research-Cell Efficiencies* <https://www.nrel.gov/pv/assets/pdfs/cell-pv-eff-emergingpv.202001042.pdf> (NREL,2021).

[2] C. Ran, J. Xu, W. Gao, C. Huang, S. Dou, *Chemical Society Reviews* **2018**, *47*, 4581.

[3] M. A. Lampert, *Reports on Progress in Physics* **1964**, *27*, 329.

[4] Z. Ni, C. Bao, Y. Liu, Q. Jiang, W.-Q. Wu, S. Chen, X. Dai, B. Chen, B. Hartweg, Z. Yu, Z. Holman, J. Huang, *Science* **2020**, *367*, 1352.

[5] Heath, J.; Zabierowski, P., *Capacitance Spectroscopy of Thin-Film Solar Cells*. In *Advanced Characterization Techniques for Thin Film Solar Cells*, Abou-Ras, D.; Kirchartz, T.; Rau, U., Eds. Wiley-Vch: Weinheim, 2011; pp 81-105.

SESSION EN05.13: Poster Session II: Emerging Energy and Materials Sciences in Halide Perovskites

Session Chairs: Mahshid Ahmadi, Mengxia Liu and Yuanyuan Zhou

Monday Afternoon, December 6, 2021

EN05-Virtual

4:00 PM EN05.13.03

Performance Losses Due to the Diffusion of Back Contact Metals in Perovskite Solar Cells Alexander V. Bordoalvos, Biwas Subedi, Lei Chen, Marie Tumusange, Zhaoning Song, Yanfa Yan and Nikolas J. Podraza; University of Toledo, United States

Organic-inorganic metal halide ABX_3 (A: methylammonium-MA, formamidinium-FA, cesium-Cs; B: lead-Pb, tin-Sn; X: iodine-I, bromine-Br, chlorine-Cl) perovskite-based photovoltaics (PV) are of great interest in the field because they can be manufactured in a low-cost solution process, have desirable opto-electronic properties, and can produce high efficiency devices. When silver (Ag) is used as a back contact metal in perovskite solar cells, it can diffuse into the underlying charge transport and absorber layers of the device leading to optical and electrical losses. Mitigating these losses is essential to developing higher efficiency devices. Perovskite solar cells consisting of nominally soda-lime glass / tin doped indium oxide (ITO) / PEDOT:PSS / $MA_{0.3}FA_{0.7}Sn_{0.5}Pb_{0.5}I_3$ / fullerene(C_{60}) / bathocuproine (BCP) with Ag and copper (Cu) metal back contacts are examined by spectroscopic ellipsometry over the photon energy range from 0.74 to 4.0 eV. The measured ellipsometric spectra are analyzed using a parametric model based upon the complex optical properties and thicknesses for each component layer as well as interfaces between materials. In these devices, it is observed that the metals used as back contact may diffuse into and mix with the electron transport and hole blocking layers, BCP and C_{60} , to form a physically mixed layer consisting of metal, BCP, and C_{60} . To further validate these results and to identify the optical and electronic losses in the device, external quantum efficiency (EQE) simulations are compared to experimental EQE. The physically mixed layer of metal, C_{60} , and BCP near the back contact can substantially absorb back reflected photons from the metal interface, thereby reducing the potential current generation in the perovskite absorber. The presence of this physically mixed layer shows an optical loss of up to 1 mA/cm² in terms of short circuit current density. Film stacks of glass/ C_{60} /BCP or SnO_2 /Ag or Cu are also measured using spectroscopic ellipsometry to study if SnO_2 can prevent diffusion of the back contact metal and prevent optical losses. The optical and electronic losses are quantified from these spectroscopic ellipsometry and EQE measurements for cells with Ag and Cu metal contacts with and without the presence of SnO_2 . The film stacks containing SnO_2 shows that it can prevent diffusion of the back contact metal, and EQE simulations with SnO_2 show recovery of some of this optical loss arising from the formation of the physically mixed metal, BCP, and C_{60} .

4:03 PM EN05.13.05

Copper Dopant Incorporation for Bandgap Engineering of MAPbBr₃ Perovskite Thin Films with Enhanced Near-Infrared Photocurrent-Response Amr M. Elattar^{1,2}, Kosei Tsutsumi¹, Kodai Nakao¹, Hiroo Suzuki¹, Takeshi Nishikawa¹ and Yasuhiko Hayashi¹; ¹Graduate School of Natural Science and Technology, Okayama University, Japan; ²Ain Shams University, Egypt

Lead-based halide perovskite with B-site doping is an effective strategy to enhance its optoelectronic devices. Herein, we study the B-site doping of MAPbBr₃ thin films with copper (Cu²⁺). Developing doped perovskites, MA(Pb:Cu)Br₃, thin films show darkness in their color from yellowish orange color for pristine MAPbBr₃ thin film to dark brown color for Cu-doped perovskite thin film, enlarged average grain boundaries area from 0.042 μm² for pristine MAPbBr₃ to 0.71 μm² for 40% Cu-doped MAPbBr₃, and lowering in the optical bandgap from 2.32 eV for pristine MAPbBr₃ to 1.85 eV for 50% Cu-doped MAPbBr₃. The Cu ions incorporation in the perovskite crystal lattice is confirmed by the X-ray diffraction (XRD) and Energy Dispersive Spectroscopy (EDS) measurements. Surprisingly, Cu-rich new phase was observed via EDS measurement at 50% Cu-doped perovskites. This new phase was further confirmed with the appearance of a new XRD diffraction peak which neither related to crystal structure peaks of MAPbBr₃ nor initial precursor. The absorption band edge of 50% Cu-doped MAPbBr₃ is developed to the near-infrared range. The conductivity of MAPbBr₃ increases over three orders of magnitude upon doping. More interestingly, photocurrent measurements of doped perovskites show the generation of band carriers upon excitation at the near-infrared region. This work provides an insight into the importance of doping over phase modulation and tailoring the optoelectronic and electronic properties of halide perovskites for a wide range of efficient optoelectronic devices.

4:06 PM EN05.13.06

Microfluidic Processing of Ligand-Engineered NiO Nanoparticles for Low-Temperature Hole-Transporting Layers in Perovskite Solar Cells Monika Michalska¹, Maciej A. Surmiak¹, Doojin Vak², Udo Bach¹ and Jacek Jasieniak¹; ¹Monash University, Australia; ²CSIRO, Australia

Perovskite solar cells (PSCs) have recently reached over 25% in power conversion efficiency and are emerging as a promising competitor to silicon technology. The key challenge that remains in further developing of the PSCs is their scaling towards commercial fabrication. Fully printed PSCs are still a major goal for the solar industry. As perovskites are inherently temperature sensitive, a key requirement for printing of these devices are low-temperature processed layers that can form the individual components of a solar cell device. Hole transporting layers (HTLs) among the entire structure are the most problematic ones, where the conventional spiro-MeOTAD, an organic molecule, is too expensive and unstable for commercial applications. Contrarily, inorganic nanomaterials can overcome the limitations of organic HTLs. Nickel oxide (NiO) has been widely used as an HTL in PSCs, however, the processing temperatures of such films is typically >250 °C to achieve sufficient crystallinity. The only way to omit high-temperature post-deposition annealing of solution-processed NiO HTLs is by spin-coating dispersion already containing metal oxide particles. However, for highly efficient perovskite solar cells additional interface engineering also needs to be studied to facilitate the charge transfer. Interestingly, ligand engineering approaches have been comprehensively investigated on a wide range of nanoparticles, yet these research outcomes are not sufficiently applied in perovskite devices. Our motivation was to fabricate NiO nanoparticle-based HTL inks for low temperature deposition, dedicated for perovskite solar cells. To achieve this, we have synthesized fine NiO nanoparticles via heat-up approach. The as-obtained NiO NPs are dispersible in nonpolar solvents, due to oleate (OA) ligands present at their surface. However, these long alkyl chain ligands are not favourable for efficient charge transfer. For that reason, our second aim was to apply ligand modification procedures to improve the hole transfer within the device after removal of long alkyl ligands, and also, to investigate how the introduced ligands impact the charge extraction at the perovskite/HTL interface.

Two different ligand exchange routes were applied, and for the very first time, deposited as NiO HTLs. In the first procedure, a Meerwein's salt Me₃OBf₄ was used where the resulting NiO nanoparticles are stabilized by BF₄ ligands. The second procedure involved 4-hydroxybenzoic acid (HBA). To assess the performance of the synthesized and modified NiO HTLs we have fabricated PSCs of the inverted architecture. Before the deposition the NiO inks were processed through microfluidic mixer system for improved film morphology. All of the HTL films were annealed at a low temperature <150 °C to remove the residual solvent. Such processing parameters are in line with printing regime, especially on flexible substrates, which is an additional advantage of the developed materials. The fabricated devices exhibited stabilized PCEs of 17.9% and 17.1% for the ligand-exchange NiO BF₄ and NiO HBA HTLs, respectively, which were superior in comparison with control devices harnessing the native surface chemistry (OA) and a postprocessing oxygen-plasma treatment step (PCE of 16.1%). Furthermore, while all NiO HTLs exhibited good photostability factors, a significant enhancement was observed for the ligand-exchange NiO HTLs, which, for NiO-BF₄, showed a 0.2% reduction in efficiency over a 300 h testing period compared with 0.9% for the NiO-OA-based PSCs. These findings showcase the importance of ligand engineering of NiO NPs for achieving efficient hole-transporting materials and its prospects for developing low-temperature-processable and high-stability PSCs. Future work will consider the printability of these dispersions to achieve fully printed flexible inverted PSCs.

4:09 PM EN05.13.09

Low Temperature Solution-Processed Antimony Chalcogenide Films for Solar Cell Applications Yong Chan Choi; Daegu Gyeongbuk Institute of Science & Technology, Korea (the Republic of)

Despite the remarkable performance of lead perovskite (Pb perovskite) solar cells, many researchers are looking for an alternative to Pb perovskite to overcome its fatal problems, such as instability and Pb toxicity. Antimony chalcogenides (SbChI, Ch = S, Se) are recently considered as potential absorbers due to their low-toxicity and photovoltaic properties [1].

In this presentation, we introduce a versatile solution-based method for the fabrication of antimony chalcogenide films. The method consists of two steps: deposition of antimony chalcogenides Sb₂Ch₃ (step I) and its conversion to antimony chalcogenides SbChI (step II). Antimony chalcogenides were fabricated by SbCl₃-thiourea/selenourea based solution approach. Conversion to SbChI was performed by spin coating SbI₃ solution on Sb₂Ch₃ and subsequent heating. Pure phase Sb(S,Se)I films with high crystallinity were obtained at low-temperature of 150–200°C. The absorption, structure, morphology, and electronic structure were controlled by tuning S/Se molar ratio and annealing temperature. In addition, Bi-alloyed SbChI films were fabricated using BiI₃ instead of SbI₃ in step II. Our results demonstrate that two-step solution method is applicable to the fabrication of various chalcogenides.

REFERENCES

[1] Y. C. Choi and K.-W. Jung., *Nanomaterials*, 2020, **10**, 2284.

4:12 PM EN05.13.11

Spatial External Luminescence Efficiency of Perovskite Solar Cells Mor Fiegenbaum-Raz¹, Tamir Yeshurun¹, Stav Rahmany², Lioz Etgar² and Gideon Segev¹; ¹Tel Aviv University, Israel; ²The Hebrew University of Jerusalem, Israel

Lead halide perovskites have recently emerged as one of the most promising future candidates for replacing silicon-based photovoltaics. Their unique optoelectronic properties, such as tunable and direct bandgap and high absorbance coefficient, in combination with a low-cost fabrication process, make them promising candidates for the use in next-generation and tandem solar cells. Although their photocurrents are reaching the theoretical maximum, the devices' open-circuit voltage can be improved significantly. Thus, an *operando* characterization method that can map the contributions to the device's photovoltage is called for.

With the progress in device performance, surface and SRH recombination are suppressed, making radiative recombination more dominant. In this process, electron-hole pairs combine to generate photons that can be either reabsorbed elsewhere within the device or be emitted through photoluminescence. Since the photoluminescence quantum yield (PLQY) and the harvestable voltage are tightly coupled, mapping the contribution to photoluminescence

within the device can inform on the contribution to the buildup of photovoltage within it.

The spatial external luminescence efficiency (SELE) is the probability for a photon absorbed at a specific point in the device to contribute to the measured photoluminescence. The SELE can be extracted by combining wavelength-dependent PLQY measurements with detailed optical modeling. Hence, the SELE maps the contribution of different regions to the device photovoltage. In this contribution we apply SELE extraction to perovskite solar cells. This spatial information can shed light upon different loss mechanisms, quantify surface recombination at the interfaces between the different layers in the device, and discriminate between radiative and non-radiative recombination processes at the surface and in the bulk of the device.

4:15 PM EN05.13.12

The Effects of PEA Concentration on the Conversion of CsPbBr₃ to Stable 2D/3D Perovskite Mmantsae M. Diale, Sadile J. Thubane and Juvet Fru; University of Pretoria, South Africa

While the power conversion efficiencies of perovskite solar cells have exceeded 24.2% in less than a decade of extensive research, the material still suffer from instability due to moisture and high temperatures, hindering scalability and commercialisation. In this work, we have synthesized the CsPbBr₃, which is known to have poor controlled microstructures. The perovskite was a 3D hybrid organic-inorganic material, which was then treated further with different amounts of PEABr concentrations (10%, 20%, 40%, 60%, 80% and 100%) to produce a 2D materials of the form PEA₂Cs_{n-1}Pb_nBr_{3n+1}. A gradual PL shift from 540 nm (CsPbBr₃) to 507 nm (100% PEABr) can be observed, indicating a shift of the distribution of average crystal size to smaller values as the PEABr ratio increases, which in turn indicates the formation of a 2D perovskite. An efficiency exceeding 15% can now be achieved through additive-controlled nanostructure tailoring for 2D perovskites.

4:18 PM EN05.13.13

Low Energy Ion Irradiation Effect on the Optoelectronic Properties of Perovskite Films Hironori Ogata, Tomoaki Nishimura, Tomohiro Watanuki, Keitaro Kikuchi and Yuki Matsui; Hosei University, Japan

Perovskite solar cells are an important photovoltaic technology with high efficiencies exceeding 20% due to their optimal band gap, large absorption coefficient, and high charge mobilities. One of these challenges is the understanding and control of their defect structures because perovskite compounds are relatively soft ionic crystals and ions are migrating in the crystals relatively low activation energy. Several research groups have reported on the effects of proton irradiation on perovskite solar cells on perovskite compounds and solar cell characteristics. It has been reported that hardness and self-healing associated with defect formation in perovskite compounds by proton irradiation. In this study, we have investigated the effect of low energy ion irradiation to both all inorganic and organic-inorganic mixed halide perovskite films on the structure, morphology, optical, electronic properties and photovoltaic properties systematically. Several kinds of halogen ion beam irradiations on the halide perovskite thin films were systematically investigated by using a tandem type ion accelerator with changing acceleration voltages and irradiation time. Detailed experimental results will be reported on the conference.

References:

Su, T.-S. et al., Sci. Rep. 5, 16098; 10.1038/srep16098 (2015).
Kavan, L., et al. Chem. 346, 291–307 (1993).
Felix Lang et al., Advanced Mater. 28, Issue39, 8726-8731(2016).
Y. Miyazawa et al., iScience, 2, 148(2018).
Felix Lang et al., Joule 4, 1054-1069 (2020).
Olga Malinkiewicz et al., Emergent Materials, 3, 9-14(2020).

4:21 PM EN05.13.15

Late News: Sputtered Nickel Nitride Passivation for Stable Halide Perovskites Inverted Solar Cells Anat Itzhak^{1,2} and David Cahen^{1,2}; ¹Bar Ilan University, Israel; ²Weizmann Institute of Science, Israel

Stability is one of the significant barriers in commercializing halide perovskite, HaP, solar cells, PSCs. Metal oxide (MO) selective contacts have already been shown to improve the stability of PSCs substantially. However, especially the surfaces of, and thus interfaces with MOs are reactive, as they readily adsorb water and/or O₂ and form hydroxides when exposed to moist air. Adsorption of hydroxide can change the oxidation states of the MO, forming trap states at the interface with the HaPs and increase the MO reactivity and causing HaP degradation. Furthermore, the oxygen in the hydroxide groups themselves is electro-negative and can react with the methylamine in the HaP compounds, forming PbI₂. We demonstrate RF sputtering of nickel oxide (NiO_x) as a hole transport layer, followed by an ultra-thin nickel nitride passivation layer, which becomes a buffer layer at the interface between the NiO_x and the HaP, deposited on the passivated NiO_x. The thin, amorphous nickel nitride layer suppresses interfacial HaP degradation, as shown by the increased stability of PSCs with a nickel nitride layer. Using RF sputtering to deposit inorganic passivation layers is an innovative step towards a scalable procedure of stable HaP based solar cells.

4:24 PM EN05.13.16

Late News: Improving Thermal Stability of Perovskite Solar Cells by Suppressing Ion Migration Using Copolymer Grain Encapsulation Yuchen Zhou¹, Yifan Yin¹, Chang-Yong Nam² and Miriam Rafailovich¹; ¹Stony Brook University, United States; ²Brookhaven National Laboratory, United States

Thermal stability of organic-inorganic hybrid perovskites (OIHPs) remains as one of the critical challenges against the stable operation of perovskite solar cells (PSCs) in direct sunlight with elevated temperatures. Here, we show that the addition of a polystyrene-co-polyacrylonitrile (SAN) copolymer can significantly enhance thermal stability of OIHPs and improve the stability of the corresponding PSCs by suppressing the migration of organic cations in OIHP. The methylammonium lead iodide (MAPI) with SAN incorporated within the perovskite layer featured a superior thermal stability compared to pure MAPI without SAN, only displaying an average of 5–15% decrease in PCE even after continuous thermal aging for 24 h at 100 °C. The secondary ion mass spectrometry revealed that the thermal degradation of the pure MAPI was largely associated with MA⁺ out-migration. Conducting atomic force microscopy analysis further indicated that the incorporated SAN led to a suppression of ionic currents present at the grain boundaries of the perovskite film, which was understood by high immiscibility between SAN and MA⁺ components as confirmed by the experimentally estimated Flory-Huggins parameter between them. This study newly identifies a promising potential of using polymer grain encapsulation for enhancing thermal stability of OIHPs and their solar cell performance by suppressing the outdiffusion of cationic organic components.

4:27 PM EN05.13.17

Evaluation of Electron-Phonon Coupling in Halide Perovskites for Innovative Device Applications Yasuhiro Yamada¹, Yuto Kajino¹, Takumi Kimura¹, Hirofumi Mino¹, Kenichi Oto¹, Hidekatsu Suzuura² and Yoshihiko Kanemitsu³; ¹Chiba University, Japan; ²Hokkaido University, Japan; ³Kyoto University, Japan

Lead halide perovskites attract growing attention because they are promising for applications to solar cells, light-emitting diodes, and various optoelectronic devices. In recent years, we have demonstrated their unique optical properties, such as long excited-state lifetime and high photoluminescence quantum efficiency [1-7], which attribute to the excellent performance of the perovskite-based devices. In contrast, the carrier transport characteristics of this class of materials are poor compared with those of conventional semiconductors; the reported carrier mobility is below 100 cm²/Vs at room temperature, which is a two-order magnitude smaller than that of GaAs. The origin of such a low carrier mobility has been discussed in terms of polarons due to large electron-phonon interactions. Moreover, it has been pointed out that polarons are also involved in the photo-accelerated ion migration and photodegradation. Therefore, it is essential to gain a thorough understanding of the nature of polarons in halide perovskites. However, the polaron formation mechanisms and its impact on the optoelectronic properties are still under active debate.

Determination of carrier masses is the direct way to discuss the polaron effect. The magneto-reflectance measurement is one of the most powerful tools to estimate carrier mass through the observation of Landau levels and high-order exciton Rydberg states. We recently performed high-sensitivity measurements using circular dichroism of reflectance at low temperatures (1.5 K) under relatively weak magnetic fields (< 7T), where the cyclotron energy is sufficiently small compared with the LO phonon energy [8]. We successfully observed the higher-order Rydberg exciton states and Landau levels in CH₃NH₃PbX₃ [X = I, Br, and Cl], which enabled us to determine the reduced mass and the exciton binding energy accurately. For CH₃NH₃PbBr₃ and CH₃NH₃PbI₃, we estimated heavier reduced mass compared with that reported in the previous strong-field experiments, which evidences the polaron mass enhancement. The degree of mass enhancement agrees well with the prediction by the Fröhlich large polaron model. This means that the carrier mass is enhanced only by 50 % even in the case of coupling constant $\alpha = 3$ (strong coupling regime), while $\alpha < 3$ holds for lead halide perovskites. Therefore, the large polarons might not be the origin of the small carrier mobility.

To confirm this idea, we performed highly sensitive carrier transport measurements using an AC photo-Hall technique [9]. This technique enables us to estimate carrier mobilities even in highly insulating materials. We find that both electron and hole mobilities are significantly enhanced by photo-doping and exceed 300 cm²/Vs, which are comparable to the electron Hall mobilities of conventional inorganic semiconductors.

In the presentation, we will show the detailed experimental results and discuss the impact of polarons on optoelectronic properties of halide perovskites. We will also discuss the possible device application utilizing the strong electron-phonon interactions of lead halide perovskites.

Part of this work was supported by JST-CREST (JPMJCR16N3), JSPS KAKENHI (JP 19K03683, JP19H05465, JP20K03798), Canon foundation, and Chiba Iodine Resource Innovation Center.

- 1) Y. Yamada *et al.*, Appl. Phys. Express **7** (3), 032302 (2014).
- 2) Y. Yamada *et al.*, J. Am. Chem. Soc. **136** (33), 11610-11613 (2014).
- 3) Y. Yamada *et al.* J. Am. Chem. Soc. **137**, 10456-10459 (2015).
- 4) Y. Yamada, T. Yamada, Y. Kanemitsu, Bull. Chem. Soc. Japan **90** (10), 1129-1140 (2017).
- 5) Y. Yamada *et al.*, J. Phys. Chem. Lett. **8**, 5798-5803 (2017).
- 6) M. Nagai *et al.*, Phys. Rev. Lett. **121**, 145506 (2018).
- 7) K. Kojima *et al.*, APL Materials **7**, 071116 (2019).
- 8) Y. Yamada *et al.* Phys. Rev. Lett. **126**, 237401 (2021).
- 9) T. Kimura *et al.*, Appl. Phys. Express **14**, 041009 (2021).

4:30 PM EN05.13.18

Robust, Ultra-fast, Downscalable and Optically Programmable Resistive RAM with Three Dimensionally Integrated Perovskite Quantum Wire Array Swapnadeep Poddar, Yuting Zhang and Zhiyong Fan; The Hong Kong University of Science and Technology, Hong Kong

Resistive RAMs (Re-RAMs) have come to the fore as a promising candidate for next generation information and data storage because of their strikingly fast speed, prolonged data retention ability and high storage density. In a first, we developed an electrochemical metallization based Re-RAM with three-dimensionally integrated single-crystalline perovskite (methyl ammonium lead iodide) quantum wire (PQW) array rooted in a nano-engineered porous alumina membrane (PAM), as the switching medium. The PQWs grown by a vapor-solid-solid-reaction (VSSR) process was sandwiched between top silver (Ag) and bottom aluminium (Al) or gold (Au) contacts respectively. The PQW based Re-RAM demonstrated ultra-fast switching speed of 100 ps which is a record for perovskite Re-RAMs and also among the fastest for all types of Re-RAMs reported. The ultra-fast switching speed was ascribed to the engendered ionic (Ag⁺) and electronic mobility and subsequent accelerated filament formation within the body of the monocrystalline PQWs. The PQW Re-RAM demonstrated a high ON/OFF ratio of 10⁷, estimated data retention > 2 years and record high (for all perovskite Re-RAMs reported) cyclic endurance of 6 × 10⁶ cycles. The excellent retention and endurance performance was attributed to the material and electrical stability instilled by the electrically insulating PAM to the PQWs. Compared to Re-RAMs based on perovskite nanowires of larger diameter (around 250 nm), the PQWs with diameter around 10 nm, portrayed a much lower proclivity of high resistance state (HRS) degradation to low resistance state (LRS) upon multiple cycles of operation owing to the relatively less number of remnant filamentary Ag paths formed due to prolonged cyclic operations. This rendered the PQW devices to be more electrically robust and power efficient for longer cycle operations. Also, utilizing the ultra-high density (2 × 10¹¹/cm²) of the PQWs, a 14 nm lateral dimension ultra-small memory cell was constructed. Coupled with multi-bit storage, an effective device footprint area of 76.5 nm² was achieved for single bit storage. As a concept proof, an 8 × 8 Re-RAM crossbar array device was fabricated which demonstrated temporally robust alphabetic data storage, with a unique metal-semiconductor-insulator-metal (MSIM) architecture to alleviate the sneaky path problem. The MSIM scheme based on quasi-self-selecting elements, exhibited a strong potential for unhindered scalability in the future, a problem often faced with integrating external selecting diodes and transistors. The PQW Re-RAMs also responded to light stimuli, demonstrating optical programmability of the LRSs. These intriguing characteristics, in conjunction, present an attractive potency of PQW Re-RAMs as a promising technology for multifunctional non-volatile memories with broad applications in future storage and advanced computing systems.

4:33 PM EN05.13.20

The Impact of the Rashba, Dresselhaus, and Overhauser Effects on the Magneto-Optical Properties of Bulk MAPbBr₃ Perovskites Alyssa Kostadinov-Mutza¹, Efrat Lifshitz¹ and Liang Z. Tan²; ¹Technion- Israel Institute of Technology, Israel; ²Lawrence Berkeley National Laboratory, United States

Halide perovskites have been at the forefront of scientific and technological interest for a decade, triggered by the discovery of their noteworthy performance in solar cells, light sources, X/γ-ray detectors, and display devices. Furthermore, the potential for exploiting spin-properties of the halide perovskites for applications in spin-electronic and spin-optical devices has emerged, based on the materials' spin-orbit coupling, Rashba/Dresselhaus effects, optically-induced spin polarization, and relatively long spin coherence and lifetime, compared to classic semiconductors. The current work presents optical experimental evidence for an intriguing phenomenon, related to the anisotropy of Rashba/Dresselhaus effects. The study explored different luminescence processes in a single bulk crystal of MAPbBr₃, using magneto-photoluminescence spectroscopy, monitored along several different crystallographic directions. The photoluminescence spectra were dominated by dual exciton emission peaks, each exhibiting a highly non-linear response to a magnetic field with an anisotropy from -B₀ to +B₀, a strong dependence on the axis of observations (parallel or perpendicular to a crystallographic symmetry axis) and on the detected spectral region. A theoretical model, implementing a dominant anisotropy in Rashba/Dresselhaus terms, anisotropy in the Landé g-factors, and a contribution from an Overhauser effect- the hyperfine interaction, corroborated the experimental results. Even though the

Rashba/Dresselhaus effects vary from location to location on the crystal, they show reproducible features such as MPL dips at low magnetic fields, and facet-dependent MPL trends at high magnetic fields. Our work shows that these are consequences of a multi-component Rashba/Dresselhaus effect and g-factor anisotropy. The Rashba/Dresselhaus couplings likely arise from different nano-crystallinities within the bulk of halide perovskites, such as grain boundaries.

4:36 PM EN05.13.21

CW Laser Deposition Yields Smooth, Oriented Pb Halide Perovskite Films Naga Prathibha Jasti, Shay Tirosh and David Cahen; Bar Ilan University, Israel

Opto-electronic and mechanical properties of Pb Halide Perovskite (HaP) thin films, as well as ways to contact them, will be influenced strongly by morphology, and, for several physical properties, by crystallographic orientation. Thus, a method to grow smooth, well-oriented thin films in a pre-selected orientation in a scalable and potentially high-throughput way, is of interest.

We report that highly oriented, smooth HaP films, especially of methylammonium lead-bromide (MAPbBr₃) and -iodide (MAPbI₃) can be deposited by CW laser ablation. HaPs were time and again shown to be different from conventional (inorganic) semiconductors like Si, GaAs, CdTe, CIGS, both in terms of which preparation methods give high quality material and in their physical properties. While pulsed laser-based synthesis / deposition methods have been reported, our finding that a *low power continuous* laser (orders of magnitude less than the equivalent power used in pulsed laser, and significantly below that of flash deposition/annealing), can yield highly oriented, relatively smooth thin films on FTO (~ 20 nm rms) and Si (~3 nm rms) substrates of MAPbBr₃ (001) and MAPbI₃ (110), using their single crystals as targets, adds to the HaP surprises. The quality and homogeneity of the thin films were checked with XRD, AFM and Photoluminescence. The deposition is solvent-free, at room temperature and works in vacuum levels comparable to those used in laboratory physical vapor deposition (PVD). Further properties of the materials, and timer-permitting, of devices will be described.

4:39 PM EN05.13.22

Late News: Highly Stable and Red-Shifted Colloidal CsPbI₃ Perovskites Quantum Dots with Photoluminescence Quantum Yield Efficiency Almost 100% Miguel Honorato¹, Wilma Luna², Alicia Alvarado², Ramon Carriles³, Alejandro Torres⁴, Miguel Vallejo⁵, Gabriel Ramos³ and Elder De la Rosa²; ¹Universidad DE La Salle Bajío, Mexico; ²Universidad De La Salle BAjío, Mexico; ³Centro de Investigaciones en Optica, Mexico; ⁴UANL, Mexico; ⁵Universidad de Guanajuato, Mexico

Recently, inorganic perovskite quantum dots (PQDs) have attracted a lot of attention for optoelectronic and photovoltaics applications because of tunability and stability. The case of CsPbI₃ deserves special attention for solar cells and LEDs devices. The inclusion of Cs and the small size of PQDs improve stability, however absorption band is blue-shifted that represent a drawback for solar cells design and LEDs. Therefore, bigger PQDs to redshift the absorption band with better stability and high photoluminescence quantum yield (PLQY) are desired. However, bigger nanocrystals are unstable and transform into yellow phase non-perovskite that is inactive under photoexcitation. Here in this work, we report the synthesis of CsPbI₃ QDs with a PLQY ~100% at 690 nm and FWHM~3nm with a reduction lower than 10% of efficiency after 12months, synthesized by hot injection at 170°C. It is analyzed in detail the effect of precursors and temperature on the synthesis process and evaluates the spectroscopic properties such as decay time, band gap and emission. PQDs were tested to design an LED and solar cells devices showing excellent performance, and then offering good opportunities for non-linear photonics and photoelectronic devices.

4:42 PM EN05.13.25

Impact of Carbon Nanotubes Growth on the Interfacial Composition and Energetics of Organic Metal Halide Perovskites Javid Hajhemati¹, Rachele Ihly², Mengjin Yang², David Moore², Roberto Felix Duarte³, Regan Wilks³, Kai Zhu², Jeffrey Blackburn², Marcus Baer³, Joseph Berry² and Philip Schulz¹; ¹CNRS, UMR 9006, Institut Photovoltaïque d'Ile-de-France (IPVF), France; ²National Renewable Energy Laboratory, Chemical and Materials Science Center, United States; ³Helmholtz Zentrum Berlin für Materialien und Energie GmbH (HZB), Germany

Halide perovskite (HaPs) solar cells have shown outstanding progress in performance in recent years, exceeding power conversion efficiency of 25%, thus promising to be a strong competitor for the current silicon solar cell technology. Limits to this trend originate from non-radiative recombination of electrons and holes as the dominant loss processes in photovoltaics. This phenomenon originating from defect states which arise imperfection of the crystalline quality in the bulk, and particularly at the interfaces of photovoltaic devices. Remarkably, the quality of the perovskite film as the light-harvesting materials has been improved to such a high level with accordingly long carrier diffusion lengths that recombination in the bulk of perovskite layers does not significantly limit the functionality of the device. Therefore, study of the defects states at the surface and at the interfaces in the layer stack has advanced to the center of attention. [1] Here, we focus on one of these interfaces and discuss the chemical properties and energy level alignment at the interface between HaPs absorber and carbon nanotube charge transport layers.

Single-walled carbon nanotubes (SWCNT) with their unique optoelectronic properties, show a strong potential to be integrated in various architecture of perovskite solar cells.[2] SWCNTs with high charge carrier mobility improve carrier collection which in turn, enhance HaPs solar cell performance. In addition, their high optical transmission in the visible range makes them an excellent candidate for charge transport layer in HaPs solar cells. Tunable electronic properties, via changing the design of the tubes and the doping characteristics, make them suitable for both electron and hole transport layers. In the present study, we report on the electronic and chemical properties and the energy level alignment at the interface between HaPs materials, MAPbI₃ and MAPbBr₃, and SWCNTs overlayers. The SWCNT layers were grown by ultrasonic spray deposition at various thicknesses on top of the perovskite absorber. We then used synchrotron-based hard x-ray photoemission spectroscopy (HAXPES) to investigate the electronic characteristics and compositional gradient of the two systems at 2 keV and 6 keV excitation energy. HAXPES measurement provides similar features of the target layer as soft X-ray photoemission spectroscopy (XPS). However, the higher kinetic energy of the emitted electrons in HAXPES increases the information depth and therefore allows us to selectively probe the immediate interface and sub-surface region, respectively.

Our results show generally different surface and interface electronic and chemical characteristics between MAPbI₃ and MAPbBr₃ before and after SWCNTs film growth. We observe selective core level peak shifts which we attribute to the formation of new species at the interface. Furthermore, the compositional study shows the distribution of elements is different between buried and topmost perovskite layer for MAPbI₃ and MAPbBr₃ upon deposition of the SWCNT, respectively. These gradients result in deficiency and/or surplus of the perovskite components that in turn affect the landscape of interface defects and consequently the device performance.

1. Schulz, Philip, David Cahen, and Antoine Kahn. "Halide perovskites: is it all about the interfaces?." *Chemical reviews* 119.5 (2019): 3349-3417.

2. Habisreutinger, Severin N., Robin J. Nicholas, and Henry J. Snaith. "Carbon nanotubes in perovskite solar cells." *Advanced Energy Materials* 7.10 (2017): 1601839.

4:45 PM EN05.13.27

Study of Capacitive Behaviour of CuI Passivated Perovskite Solar Cells Bidisha Nath, Praveen C Ramamurthy, Debiprosad R. Mahapatra and Gopalkrishna Hegde; Indian Institute of Science, India

Methylammonium lead iodide (MAPbI₃) perovskite has shown high defect tolerance. This is well known that defects in the perovskite absorber layer hinder the power conversion efficiency (PCE) of perovskite solar cells in approaching the Shockley-Queisser limit. Understanding the effect of defects in the performance of the perovskite solar cells is a very interesting area and needs further exploration.

Different types of intrinsic defects (vacancies, substitutions, and interstitials) are possible in MAPbI₃. Sources of defects in the perovskite layer can be from impurities. Even grain boundaries are considered as sources for high defect densities in solution-processed polycrystalline MAPbI₃ perovskite films. The quality of the films depends on factors like the purity of the precursors, solvents, process parameters, crystal growth, etc. The defect levels of both point and structural defects can be the contribution of breaking and addition of bonds i.e., wrong bonds or dangling bonds.

Cuprous iodide (CuI) has attracted extensive attention in p-i-n structured perovskite solar cells as a hole transport layer because of its high transmittance, optimal band matching, and ease of processibility. CuI has been used as the passivating material to improve the film quality by reducing defects. Cu²⁺ is expected to passivate the defects because of its small size and also prevent iodine from migrating from its place. I⁻ ion may help to overcome iodine deficiency caused due to ion migration. Iodine defects are much easier to create because of their low formation energy.

Passivation of defects and imperfections is expected to cause a reduction in ion migration to achieve improved efficiency and stability. J-V performance of the devices was analysed under dark and light conditions. There is no change in the crystal structure as confirmed from the XRD analysis. High intensity of PL peaks has been obtained in the passivated film which is related to more band-to-band recombination i.e., less number of traps in the film. Since the charge carrier density is different for passivated and non-passivated perovskite film, a difference in the capacitive behaviour of the films is expected. The capacitive behaviour is related to charge transport and charge accumulation. Hence analysis of the capacitive behaviour of the devices under the dark and light has been carried out to understand the change in polarization behaviour because of the addition of passivation material.

4:48 PM EN05.13.28

Hybrid Atomic Layer Deposition (ALD) for Deposition of Halide Perovskites Jacob Vagott, Kathryn Bairley, Carlo Andrea Riccardo Perini, Andres Felipe Castro Mendez, Christian Jamison and Juan Pablo Correa Baena; Georgia Institute of Technology, United States

Perovskite solar cells (PSCs) have quickly risen in efficiency since their initial fabrication in 2009, with the current record power conversion efficiency (PCE) being over 25%. Quickly approaching the Shockley—Queisser limit of 33% for single-junction solar cells, focus on stability and scalability has become crucial. While solution deposition of the perovskite absorber layer by spin-coating has resulted in the highest efficiency devices, vapor deposition methods have shown promise and may help resolve both the stability and scalability problems that PSCs are currently facing. Atomic layer deposition (ALD), as a vapor deposition process, provides advantages such as fine thickness control, improved conformity and uniformity, and the ability to be incorporated into existing industrial processes such as roll-to-roll manufacturing. The stoichiometry of the perovskite may also be easily tuned through manipulation of the precursor doses. This work focuses on depositing perovskite through a two-step ALD/ molecular layer deposition (MLD) hybrid process, with ALD referring to the inorganic aspects of the process and MLD incorporating organic materials. The first step, which we have recently achieved, is to deposit a conformal lead iodide film which may be converted to methylammonium lead triiodide (MAPbI₃) through exposure to methylammonium iodide (MAI). For the lead precursor, Pb(tmhd)₂ was chosen due to its adequate vapor pressure at relatively low source temperatures (less than 200°C) and higher reactivity when compared to other commonly utilized lead precursors such as Pb(acac)₂. HI (aq) was chosen as the iodine precursor due to its high vapor pressure and reactivity. The precursors involved are easily accessible through commercial means and do not require any additional processing before use. The second step, which we are currently developing, involves the introduction of a third precursor within every cycle of the previous recipe, which would allow for an effective ALD/MLD process for MAPbI₃. Once we are able to deposit highly uniform perovskite thin films by ALD/MLD, this will allow us the ability to deposit 2D perovskite passivation layers which will help improve stability by decreasing defects at the perovskite/charge transport layer interface. This will increase moisture and thermal stability in the PSCs while also being a scalable process.

SESSION EN05.11/EQ17.09: Joint Session: Interfaces in Perovskite Photovoltaics

Session Chairs: Michael Saliba, Philip Schulz and Yuanyuan Zhou

Monday Afternoon, December 6, 2021

EN05-Virtual

6:30 PM *EN05.11/EQ17.09.01

Revealing 2D/3D Interface Energetics for Efficient and Stable Perovskite Solar Cells Giulia Grancini; University of Pavia, Italy

Engineering interfaces in perovskite solar cells is nowadays paramount in the optimization of multilayer perovskite device stack. This stems true for multi-dimensional (2D/3D) perovskite based solar cells, where high efficiency can be combined with promising device durability. However, the exact function of the 2D/3D interface in controlling the device behaviour and the interface physics therein are still vague.

Here I will discuss the 2D/3D functions which can simultaneously act as surface passivant, electron blocking layer, and driving efficient and selective charge extraction. In particular, I will demonstrate that the exact knowledge on the interface energetics is crucial to obtain for a smart interface engineering. As an example, I will discuss the case of thiophene-based 2D perovskite/ 3D perovskite interfaces forming a p-n junction. This leads to a reduction of the electron density at the hole transport layer interface and ultimately suppress the interfacial recombination. As a consequence, we demonstrate that photovoltaic devices with enhanced fill factor (FF) and open-circuit voltage (VOC) of 1.19V which approaches the potential internal Quasi-Fermi Level Splitting (QFLS) voltage of the perovskite absorber, nullifying the interfacial losses. We thus identify the essential parameters and energetic alignment scenario required for 2D/3D perovskite systems in order to surpass the current limitations of hybrid perovskite solar cell performances. This knowledge turns fundamental for device design, opening a new avenue for perovskite interface optimization.

[1] A. Sutanto, P. Caprioglio, N. Drigo, Y. J. Hofstetter, I. Garcia-Benito, V. I. E. Queloz, D. Neher, M. K. Nazeeruddin, M. Stollerfoht, Y. Vaynzof, G. Grancini "2D/3D Perovskite Engineering Eliminates Interfacial Recombination Losses in Hybrid Perovskite Solar Cells", *Chem* DOI:10.1016/j.chempr.2021.04.002 (2021)

I acknowledge the HY-NANO project that has received funding from the European Research Council (ERC) Starting Grant 2018 under the European Union's Horizon 2020 research and innovation programme (Grant agreement No. 802862).

7:00 PM *EN05.11/EQ17.09.02

Colored, Stable and Flexible Co-Evaporated Perovskites Solar Cells and Minimodules Jia Li, Hao Wang, Enkthur Erdeebileg, Herlina Dewi, Nripan Mathews, Subodh Mhaisalkar and Annalisa Bruno; Nanyang Technological University, Singapore

Metal-halide perovskites are one of the most promising active materials for photovoltaic and light-emitting technologies, due to their excellent optoelectronic properties and fabrication versatility. Within a decade, perovskite solar cells (PSCs) have achieved record power conversion efficiency (PCE) of 25.6% [1], for active areas smaller than 1 cm², and a constantly improving operational stability [2-5]. This rapid progress has triggered the interest in transferring the existing technology from small area devices into large-area perovskite modules, necessary for industrial development.

Recently we have demonstrated highly efficient, large-area, planar PSCs where the MAPbI₃ perovskite layer has been deposited by thermal co-evaporation of PbI₂ and MAI. The high-quality co-evaporated perovskite thin films are uniform over large areas showing low surface roughness, and a long carrier lifetime. The high-quality perovskite of the thin films translates PSCs with PCE above 20% in both n.i.p [6, 7] and p.i.n [8] configurations, and impressive thermal and environmental long-term stability [9] even without encapsulation. Furthermore, the first co-evaporated mini-modules achieved record PCEs of 18.13% and 18.4% for active areas of 20 cm² [6] and 6.4 cm² [10]

At the same time, looking forward to tandem integration and building-integrated photovoltaics we have also developed colored semi-transparent PSCs and mini-modules with transparency above 75% in near-infrared for all the range of colors realized.

These results represent a significant step towards the development of high-quality large-area perovskite solar cells and mini-modules, one of the main requirements for the commercialization of the technology.

References:

1. NREL. Best Research-Cell Efficiency Chart; U.S. Department of Energy; <https://www.nrel.gov/pv/cell-efficiency.htm>.
2. A. Kojima, K. Teshima, Y. Shirai, T. Miyasaka, *J. Am. Chem. Soc.* **2009**, *131*, 6050.
3. N. Arora, M. I. Dar, A. Hinderhofer, N. Pellet, F. Schreiber, S. M. Zakeeruddin, M. Grätzel, *Science* **2017**, *358*, 768.
4. S. Yang, S. Chen, E. Mosconi, Y. Fang, X. Xiao, C. Wang, Y. Zhou, Z. Yu, J. Zhao, Y. Gao, *Science* **2019**, *365*, 473.
5. Y. Wang, T. Wu, J. Barbaud, W. Kong, D. Cui, H. Chen, X. Yang, L. Han, *Science* **2019** *365*, 687.
6. J. Li, H. Wang, X. Y. Chin, H. A. Dewi, K. Vergeer, T. W. Goh, J. W. M. Lim, J. H. Lew, K. P. Loh, C. Soci, T. C. Sum, H. J. Bolink, N. Mathews, S. Mhaisalkar, A. Bruno, *Joule* **2020**, *4*, 1035
7. L Li, HA Dewi, W Hao, N Mathews, S Mhaisalkar, A Bruno, *Coatings*, **2022** *10*(12), 1163
8. L Li, HA Dewi, W Hao, J Zhao, N Tiwari, N Yantara, T Malinauskas, V Getautis, T J. Savenije, N Mathews, S. Mhaisalkar, A Bruno, *Adv. Funct. Mater.* **2021**.
9. HA Dewi, L Li, W Hao, N Mathews, S Mhaisalkar, A Bruno, *Adv. Funct. Mater.* **2021** 2100557,
10. L Li, HA Dewi, W Hao, L Jia Haur, N Mathews, S Mhaisalkar, A Bruno, *Solar RRL*, **2020**, *4*, 2000473

7:30 PM *EN05.11/EQ17.09.03

Efficient, Stable and Scalable All-Perovskite Tandem Solar Cells Hairen Tan; Nanjing University, China

Organic-inorganic halide perovskites have received widespread attention thanks to their strong light absorption, long carrier diffusion lengths, tunable bandgaps, and low temperature processing. Single-junction perovskite solar cells (PSCs) have achieved a boost of the power conversion efficiency (PCE) from 3.8% to 25.5% in just a decade. With the continuous growth of PCE in single-junction PSCs, exploiting of monolithic all-perovskite tandem solar cells is now an important strategy to go beyond the efficiency available in single-junction PSCs. However, their actual efficiencies today are diminished by the subpar performance of mixed lead-tin narrow-bandgap subcells. We firstly reported a strategy to reduce Sn vacancies in mixed Pb-Sn perovskites that use metallic tin to reduce the Sn⁴⁺ to Sn²⁺ via a comproportionation reaction. We increased thereby the charge carrier diffusion length in narrow-bandgap perovskites from sub-micrometer to 3 micrometers. We further reported simultaneous enhancements in the efficiency, uniformity and stability of narrow-bandgap subcells using strongly-reductive surface-anchoring zwitterionic molecules. The zwitterionic antioxidant inhibits Sn²⁺ oxidation and passivates defects at the grain surfaces in mixed lead-tin perovskite film, enabling an efficiency of 21.7% (certified 20.7%) for single-junction solar cells. We obtained a certified efficiency of 24.2% in 1-cm²-area all-perovskite tandem cells, and in-lab PCEs of 25.6% and 21.4% for 0.049 and 12 cm² devices, respectively. The encapsulated tandem devices retain 88% of their initial performance following 500 hours of operation under one-sun illumination in ambient conditions.

8:00 PM *EN05.11/EQ17.09.04

Efficient and Stable Tandem Solar Cells Enabled by Wide-Bandgap Perovskites Prepared with Anion-Engineered 2D Additives Daehan Kim¹, Hee Joon Jung², Ik Jae Park³, Vinayak Dravid², Jin Young Kim³, Kai Zhu⁴, Dong Hoe Kim^{4,5} and Byungha Shin¹; ¹Korea Advanced Institute of Science and Technology, Korea (the Republic of); ²Northwestern University, United States; ³Seoul National University, Korea (the Republic of); ⁴National Renewable Energy Laboratory, United States; ⁵Sejong University, Korea (the Republic of)

Perovskite photovoltaic technology has advanced substantially, with the present record efficiency for single-junction devices reaching > 25%. One of the most promising strategies for commercializing these devices is to apply a perovskite top cell in tandem with a Si bottom cell to reach ultrahigh efficiency beyond the Shockley-Queisser limit for single-junction devices. The ideal band gap for the tandem configuration is ~1.67 to 1.75 eV for the top cell and 1.12 eV for the bottom cell, which, fortuitously, is the Si band gap. The band gap of perovskites can be tuned by (partial) replacement of iodine anions with bromine or chlorine. However, the replacement of I with Br by more than 20%, which is necessary to enlarge the band gap to ~1.7 eV, leads to stability issues under illumination through phase separation that forms I-rich and Br-rich structures. One approach to stabilize the perovskite is to create a two-dimensional (2D) phase in which sheets of [PbX₆]²⁻ octahedra are separated by an excess number of long-chain (or aromatic) molecules that act as a passivation agent. Common long-chain or aromatic molecule-based 2D additives include n-butylammonium iodide (n-BAI) and phenethylammonium iodide (PEAI). Most of the recent studies have focused on the cation components of the 2D additives rather than focusing on the anions. We developed a 2D-3D mixed wide band gap (1.68 eV) perovskite using a mixture of thiocyanate (SCN) with the more conventional choice, iodine. Through a careful application of atomic resolution transmission electron microscopy, we demonstrated that electrical and charge transport properties as well as the physical location of 2D passivation layers can be controlled with anion engineering of the 2D additives. Moreover, we can use this approach to extend light stability and to improve device performance. For a perovskite device, we achieved a PCE of 20.7% that retained > 80% of its initial efficiency after 1000 hours of continuous illumination in working conditions. For a monolithic 2T perovskite/Si tandem solar cells, the champion 2T tandem device achieved a PCE of 26.7%. If time permits, I will also discuss our recent progress in perovskite/Cu(In,Ga)Se₂ tandem solar cells.

8:00 AM *EN05.14.04**Metastability and Durability of Perovskite Solar Cells** Anita W. Ho-Baillie; The University of Sydney, Australia

One of the challenges of perovskite solar cells is its instability. I will talk about our work on understanding intrinsic stability of perovskites and metastability of perovskite solar cells and strategies for boosting perovskite solar cells' durability against thermal extremes and humidity. Our perovskite solar cells were the first to exceed the strict requirements of International Electrotechnical Commission standards for thermal cycling damp heat and humidity freeze. Such a major breakthrough represents an important step towards commercial viability.

8:30 AM *EN05.14.01**Nanosheet-Based Interfacial Modifications for High Performance Planar Perovskite Solar Cells** Tsutomu Miyasaka; Toin University of Yokohama, Japan

Planar or semi-planar type perovskite photovoltaic (PV) cells have been developed with various carrier transport materials in normal and inverse structures. Planar structures could be cost-efficient in device manufacture compared with mesoporous ones because of simplified layered structures in which deposition of a metal oxide electron transport layer (ETL) is replaced with a hole-blocking thin surface layer covering the electrode substrate. Successful modification of the electrode surface with organic or inorganic molecular layers as hole-blocking nanosheet materials leads to enhancement of efficiency and stability of the perovskite devices. Hysteresis in current-voltage (J-V) characteristics is also suppressed as a result of well-balanced electron/hole transports being accompanied by an increase in open-circuit voltage (Voc). As an inorganic nanosheet, thin films (<10 nm) of amorphous metal oxides such as TiOx and SnOx are effective in creating a void-less compact interlayer to connect ETL and perovskite. In fabrication of CsPbI₂Br-based semi-planar photovoltaic cells, we modified the surface of SnO₂ ETL with an amorphous SnOx (<5 nm) as an interlayer for junction of CsPbI₂Br layer. Using a dopant-free polymer hole-transport layer (HTL), the CsPbI₂Br device yielded a power conversion efficiency of 17% with a high Voc reaching 1.42V.¹ A reference device without the SnOx interlayer gave a poor J-V performance with a large hysteresis and a low Voc (<1.2V), indicating the essential role of the interlayer. Another example of inorganic nanosheet is MXene, a 2D layered material comprising Ti₃C₂. We treated a colloidal solution of MXene by oxidation to form nanosheets of HO-Ti₃C₂T_x, which show semiconductivity suitable for ETL. Thin layer (<20 nm) of the oxidized MXene works as a good ETL in a planar device with efficiency over 18%.² Efficiency reaches more than 20% when HO-Ti₃C₂T_x is hybridized with SnO₂, which chemically interacts HO-Ti₃C₂T_x via oxygen bonding. Being mechanically and thermally robust, MXenes are promising nanomaterials to modify the function of heterojunction interfaces. Organic small molecules also serve as modulators to passivate the defects at the junction interface. Among various molecules, we found an organic peroxide, artemisinin (water-insoluble anti-malarial drug), works to modify the interface of SnO₂ ETL and multi-cation perovskite (Rb_{0.05}Cs_{0.05}(FA_{0.83}MA_{0.17})_{0.9}Pb(I_{0.95}Br_{0.05})₃).³ This redox-active molecule is considered to interact with the oxide surface and lead cation in passivation process. Artemisinin-based passivation was applied to the SnO₂-perovskite interface of a plastic film flexible PV device. The device showed decreased hygroscopicity due to the effect of artemisinin, leading to an increase in shelf life. Its effects of enhancing Voc improved the device efficiency up to 21.1% with Voc of 1.13V; the efficiency is the highest value ever achieved for plastic perovskite PV device. All of the above inorganic and organic passivators are chemically and thermally stable non-ionic materials and inactive against their diffusion. Such properties will guarantee structural stability of ultra-thin hole-blocking interlayers involved in defect passivation.

References:

1. Z. Guo, A. K. Jena, I. Takei, G. M. Kim, M. A. Kamarudin, Y. Sanehira, A. Ishii, Y. Numata, S. Hayase, and T. Miyasaka, *J. Am. Chem. Soc.* **2020**, *142*, 21, 9725–9734.
2. L. Yang, D. Kan, C. Dall'Agnese, Y. Dall'Agnese, B. Wang, A. K. Jena, Y. Wei, G. Chen, X. -F. Wang, Y. Gogotsi, and T. Miyasaka, *J. Mater. Chem. A*, **2021**, *9*, 5016–5025
3. L. Yang, Q. Xiong, Y. Li, P. Gao, B. Xu, H. Lin, X. Li and T. Miyasaka, *J. Mater. Chem. A*, **2021**, *9*, 1574–1582.

9:00 AM *EN05.14.02**SnPb Based Perovskites for Efficient and Stable Photovoltaic Devices** Wallace C. Choy; University of Hong Kong, China

Sn-Pb perovskites have shown their potentials in wide-bandgap photovoltaics and near-infrared photodetection applications which could become alternatives to traditional silicon and inorganic devices. To achieve efficient devices, high-quality and thick Sn-Pb perovskite films featuring well-packed, smooth, pinhole/void-free are highly desirable. Besides, understanding the crystallization kinetics and tuning the crystallization are fundamentally important to reach the Sn-Pb perovskite films, and have been limitedly explored. Herein, we propose an approach of double-side crystallization tuning through low-temperature space-restricted annealing in MA-free Sn-Pb perovskite films. By simultaneously retarding the crystallization in the top of precursor films and promoting the crystal growth of the bottom of precursor films, we achieve high-quality and block-like 1 μm thick Sn-Pb perovskite films with improved crystallinity and reduced trap density [1]. The high-quality Sn-Pb perovskite can also be fabricated on metal/ silicon substrates for promoting direct integration with CMOS electronics and realizing an efficient photodiode imaging array [2]. Meanwhile, we develop the approach of in-situ tin(II) inorganic complex anti-solvent process for particularly tuning the perovskite nucleation and crystal growing process. Interestingly, we uniquely form the quasi core-shell structure of the Pb-Sn perovskite-tin(II) complex as well as heterojunction perovskite structure at the same time for suppressing the nonradiative recombination, extending carrier lifetime, and enhancing the carrier extraction. As a result, the mixed Pb-Sn low-bandgap perovskite device achieves a high power conversion efficiency up to 19.03% with a fill factor over 0.8, which is among the highest fill factor in high-performance Pb-Sn perovskite solar cells. Remarkably, the device fail time under continuous light illumination is extended by over 18.5 folds reaching 560 h [3]. To realize the integration of Sn-Pb perovskite for tandem cell applications, we also develop a new thermionic emission-based interconnecting layer (ICL) structure with the enhanced solvent-resistance feature. Fundamentally, the thermionic emission plays a critical role in the electron transport process in the ICL, which is confirmed through both experimental and theoretical studies [4]. The works not only demonstrate the solid potential of Sn-Pb perovskite in solar cells and photodetectors but also promoting all perovskite tandem solar cells for low-cost photovoltaics.

[1] H. Liu, H.L. Zhu, W.C.H. Choy, et al, "Double-Side Crystallization Tuning to Achieve Over 1 μm Thick and Well-aligned Block-like Narrow-bandgap Perovskites for High-efficiency Near-infrared Photodetectors", *Adv. Funct. Mat.* in press.

[2] H.L. Zhu, W.C.H. Choy, et al, *ACS Nano*, **13**, 11800, 2019.

[3] C. Li, W.C.H. Choy, et al, *Adv. Energy Mater.*, **10**, 1903013, 2020.

[4] C. Li, W.C.H. Choy, et al, *Adv. Energy Mater.*, **8**, 1801954, 2018.

9:30 AM *EN05.14.03**MXenes and Other Two-Dimensional Materials for Perovskite Photovoltaics** Aldo Di Carlo^{1,2,3}; ¹ISM-CNR Institute for Structure of the Matter, National Research Council, Italy; ²University of Rome Tor Vergata, Italy; ³– National University of Science and Technology NUST-MISIS, Russian Federation

Two-dimensional (2D) materials are playing an important role in perovskite photovoltaics. Halide perovskite and 2D materials, including 2D perovskites, can be combined to enhance efficiency and stability of solar cells. Recently, a new perspective class of 2D materials - MXenes demonstrated a beneficial result for interface engineering in perovskite solar cells (PSCs) [1,2]. In general, the MXenes are metal carbides/nitrides with single or multilayer 2D structures and have general formula of $M_nX_nT_x$ ($n = 1, 2, 3$), where M represents an early transition metal, X is a carbon and/or nitrogen atom and T are surface functionalization groups (-F, -O, -OH). In this talk I will present the progresses made in the use of MXenes and other 2D materials such as Graphene, MoS₂ to improve the performance and the stability of perovskite solar cells. With a thorough multiscale experimental investigation, we point out that 2D materials can tune interfaces properties, reduce ion migration and modify the work-function of the perovskite absorber and charge transporting layers, all aspects that directly impact on the final efficiency and the stability under accelerated stress tests. The use of 2D materials allows us to reach more than 26% efficiency in a tandem graphene-perovskite/silicon cell [3] and $\approx 20\%$ on 10 cm² module, and improve the stability for light soaking stress beyond 2000 hours out of glove-box. By using 2D materials we realize a solar farm with 0.5 sqm panels obtained with single junction graphene-perovskite sub-modules with efficiency up to 16% (on a substrate area of more than 100cm²) and panel efficiency exceeding 10%

References:

- [1] Agresti, A., Pazniak, A., Pescetelli, S. et al. Titanium-carbide MXenes for work function and interface engineering in perovskite solar cells. *Nat. Mater.* 18, 1228–1234 (2019). <https://doi.org/10.1038/s41563-019-0478-1>
- [2] D. Saranin et al. Transition metal carbides (MXenes) for efficient NiO-based inverted perovskite solar cells, *Nano Energy* 82, 105771, (2021)
- [3] E. Lamanna et al, Mechanically Stacked, Two-Terminal Graphene-Based Perovskite/Silicon Tandem Solar Cell with Efficiency over 26%, *Joule* 4, 865 (2020)

SESSION EN05.15: Fundamental Structure and Properties of Perovskites II
Session Chairs: Mengxia Liu and Yuanyuan Zhou
Tuesday Morning, December 7, 2021
EN05-Virtual

10:30 AM *EN05.15.01

Structure, Defects and Performance of Perovskite Photovoltaics Joanne Etheridge¹, Wei Li², Mathias U. Rothmann³, Ye Zhu⁴, Weilin Li¹, Mengmeng Hao⁵, Weijian Chen⁶, Chenquan Yang², Yongbo Yuan⁷, Yen Yee Choo¹, Xiaoming Wen⁶, Lianzhou Wang⁵, Udo Bach¹ and Yi-Bing Cheng^{2,1}; ¹Monash University, Australia; ²Wuhan University of Technology, China; ³University of Oxford, United Kingdom; ⁴The Hong Kong Polytechnic University, Hong Kong; ⁵The University of Queensland, Australia; ⁶Swinburne University of Technology, Australia; ⁷Central South University, China

The perovskite structure is proving to be a versatile platform for creating photoactive compounds for application in solar cells, achieving excellent power conversion efficiencies, long carrier diffusion lengths and low recombination rates. However, a number of challenges remain, including current density-voltage hysteresis and structural degradation in air and light.

Many parameters impact on device properties from grain structure to the integrity of the interface between the transport and photoactive layers. Here we investigate the local crystal structure and intragrain defect structure of popular photoactive perovskite compounds and correlate these observations with device performance and properties.

We develop and apply specific strategies for pristine structure analysis using transmission electron microscopy (TEM). This includes the preparation of TEM foils using processes that mimic the preparation of the device photoadsorber (and avoids the use of ion beams) and the subsequent examination in the TEM using a total electron dose well below measured damage thresholds [1,2].

We investigate the crystal structure and associated defects in several photoactive perovskites: the mixed organic cation perovskite $MA_xFA_{1-x}PbI_3$ (with methylammonium, $MA = CH_3NH_3^+$ and formadimium, $FA = NH_2CH=NH_2^+$ and $x=0, 0.15, 0.5, 0.8, 0.9$ and 1) [3, 4], the more structurally stable pure inorganic $CsPb_{(1-x)}Br_{(2-x)}$ [5] and the mixed cation $FA_xCs_{1-x}PbI_3$.

We reveal different types of point and planar defects induced by different elemental compositions and stoichiometries and measure the corresponding changes in device performance, including charge carrier lifetime, open-circuit voltage-deficit, and current-voltage hysteresis. We identify which structural defects are benign and which may be detrimental to device performance, suggesting further avenues for improving device properties and performance.

- [1] Rothmann MU, Li W, Zhu Y, Liu A, Ku, Bach U, Etheridge J, Cheng YB; *Advanced Materials* 1800629 (2018) and manuscript in preparation (2021).
- [2] Rothmann MU, Li W, Etheridge J, Cheng YB *Advanced Energy Materials* 7 23 (2017).
- [3] Rothmann MU, Li W, Zhu Y, Bach U, Spiccia L, Etheridge J, Cheng YB *Nature Communications* 8 14547 (2017).
- [4] Li W, Rothmann MU, Zhu Y, Chen W, Yuan Y, Choo YY, Yang C, Wen X, Bach U, Cheng YB, Etheridge J *Nature Energy* 6 624–632 (2021).
- [5] Li W, Rothmann MU, Liu A, Wang Z, Zhang Y, Pascoe AR, Lu J, Jiang L, Chen Y, Huang F, Peng Y, Bao Q, Etheridge J, Bach U, Cheng YB *Advanced Energy Materials* 7 20 (2017).

11:00 AM *EN05.15.02

Computational Materials Design—Focus on Perovskites Silvana Botti; Friedrich Schiller University Jena, Germany

Perovskite materials have attracted increasing attention in different application fields thanks to their composition diversity and extraordinary variety of electronic properties. Perovskite solar devices are nowadays the fastest advancing photovoltaic technology, but a large-scale application is restrained by open challenges that still delay their market entry.

How can the design of functional materials, and in particular perovskite materials, be accelerated using supercomputers?

In this talk I will discuss how to combine first-principles calculations and machine learning to speed up the discovery of new materials.

Characterizing the electronic properties of crystalline bulk materials can however be insufficient to evaluate their suitability for applications. Interfaces are in fact at the heart of electronic devices: the ability to shape potential gradients at interfaces opens up the possibility to manipulate electrons and develop new functionalities. The design of interfaces, as well as the deep understanding and control of their properties, is still beyond the current state of the art. I

will discuss some recent progresses in this direction.

11:30 AM *EN05.15.03

Interplay Between Structural and Optoelectronic Properties of Multilayered Perovskites [Jacky Even](#)¹, Hao Zhang², Wenbin Li², Siraj Sidhik², Xiaotong Li³, Eugenia S. Vasileiadou³, Justin Hoffman³, Ioannis Spanopoulos³, Yan Qin⁴, Wei Li⁴, Claudio Quarti⁵, Boubacar Traore⁶, Pedesseau Laurent¹, Mikael Kepenekian⁶, Jean-Christophe Blancon², Mercouri G. Kanatzidis³, Aditya D. Mohite² and Claudine Katan⁶; ¹INSA Rennes, France; ²Rice University, United States; ³Northwestern University, United States; ⁴Nankai University, China; ⁵University of Mons, Belgium; ⁶ISCR (Institut des Sciences Chimiques de Rennes), France

The presentation will review recent experimental and theoretical results for 2D multilayered halide perovskites, dedicated to photovoltaic or light emission applications. The complex interplay between structural and optoelectronic properties will be emphasized, including the influence of light soaking, the ultrafast relaxation of the lattice induced by hot carriers and the localization of carriers at the layer edges.

12:00 PM EN05.15.04

Enhanced Operational Stability of Perovskite Light-Emitting Devices Through Differentiated Ion Motion Aditya Mishra and [Jason D. Slinker](#); The University of Texas at Dallas, United States

Hybrid perovskites are emerging as highly efficient materials for optoelectronic applications, however, their operational lifetime has remained a limiting factor for their continued progress. In thin-film perovskite light-emitting devices, ionic redistribution may distort the perovskite crystal structure, lowering conductivity and light emission due to the formation of vacancies and other traps. Our strategy for enhanced lifetimes involves producing differentiated ion motion within a device with a rational materials blend. The materials selectively move additive ions while restricting the transport of perovskite ions. To accomplish differentiated ion transport with optimal thin-film morphology, we combine a perovskite, a polyelectrolyte such as poly(ethylene oxide), and a salt additive such as LiPF₆. The added mobile Li⁺ and PF₆⁻ ions redistribute more favorably than the intrinsic ionic species and largely preserve the inherent structure of the perovskite film. At 0.5 wt% LiPF₆, CsPbBr₃ devices exhibit 100 h operation at high brightness in excess of 800 cd/m² under constant current driving, achieving a maximum luminance of 3260 cd/m². This performance extrapolates to a 6700 h luminance half-life from 100 cd/m², a 5.6-fold improvement over devices with no LiPF₆. For quantum dot blended devices, a 45 h half-life was obtained at 3640 cd/m², extrapolating to over 37000 h at 100 cd/m². We rationalize these findings through optical spectroscopy, impedance spectroscopy, X-ray photoelectron spectroscopy, scanning electron microscopy, and X-ray diffraction.

12:15 PM EN05.15.05

Late News: Charge Transfer Rates and Electron Trapping at Buried Interfaces of Perovskite Solar Cells [Igal Levine](#)¹, Amran Al-Ashouri¹, Artem Musiienko¹, Hannes Hempel¹, Artem Magomedov², Aida Drevilkauskaitė², Vytautas Getautis², Dorothee Menzel¹, Karsten Hinrichs³, Thomas Unold¹, Steve Albrecht^{1,4} and Thomas Dittrich¹; ¹Helmholtz-Zentrum Berlin, Germany; ²Kaunas University of Technology, Lithuania; ³Leibniz-Institut für Analytische Wissenschaften ISAS e.V., Germany; ⁴Technical University Berlin, Germany

Identification of electronic processes at charge-selective interfaces is crucial not only for the further development of high efficiency solar cells based on metal halide perovskite (HaP) absorbers but also for other materials systems in photovoltaic research, photocatalysis etc. Transient surface photovoltage (SPV) measurements provide information about dynamics of charge separation and relaxation across interfaces from the nanosecond to the second range. Passivation of different hole-selective ITO / SAM / HaP contacts (SAM: self-assembled monolayer, here: carbazole-based molecules with a phosphonic acid linker group) is studied by transient SPV, compared with radiative bulk recombination (measured by transient photoluminescence) and correlated with the performance of solar cells. It is shown that transient SPV and transient photoluminescence provide complementary information on charge transfer kinetics and trapping/de-trapping mechanisms. Hole transfer rates to the ITO and densities of traps at ITO / SAM interfaces were obtained by fitting SPV transients with a minimalistic kinetic simulation model. The hole transfer rates and the density of interface traps depended strongly on the SAM's structure, and densities of interface traps as low as 10⁹ cm⁻², in par with highly passivated c-Si surfaces, were reached for Me-4PACz, which was previously used in record perovskite/silicon tandem solar cells. The extracted hole transfer rates and densities of interface traps correlated well with corresponding fill factors and open-circuit voltages of high efficiency solar cells based on HaP absorbers. Our results show that, aside tuning of barriers for charge transfer, SAMs can efficiently passivate defect states at interfaces.

SESSION EN05.16: Fundamental Structure and Properties of Perovskites III

Session Chairs: Mengxia Liu, Michael Saliba and Yuanyuan Zhou

Tuesday Afternoon, December 7, 2021

EN05-Virtual

1:00 PM *EN05.16.01

A Matter of Mixing: Nanoscale Heterogeneity and Stability in Metal Halide Perovskite Solar Cells [Laura T. Schelhas](#)¹, Laura Mundt², Fei Zhang¹, Axel Palmstrom¹, Junwei Xu², Robert Tirawa¹, Leah Kelly², Kevin Stone², Kai Zhu¹, Michael Toney³ and Joseph Berry¹; ¹National Renewable Energy Laboratory, United States; ²SLAC National Accelerator Laboratory, United States; ³University of Colorado Boulder, United States

Halide perovskite photovoltaics (PV) are known to have a wide range of chemical compositions. The perovskite lattice is quite tunable and able to accommodate various ions of different sizes. To date, halide perovskite solar cells (PSC) yield the highest efficiency and stability when absorbers comprised of a mixture of ions are utilized. However, some compositions such as FAPbI₃ (FA = formamidinium) or the fully inorganic composition CsPbI₃ exhibit non-ideal geometric conditions, often measured using the Goldschmidt tolerance factor. When ions are too large or too small for the lattice non-perovskite δ -phases that are detrimental for PV applications are formed. Mixed compositions allow for a fine tuning of the geometric conditions and enables the formation of photoactive perovskite phases.^[1] Nevertheless, chemical heterogeneity in the film can initiate phase segregation of the material into pure phases, which as noted prefer their non-perovskite δ -phases, and consequently lead to degradation of the device performance.

Spatially resolved analyses have repeatedly revealed microscopic heterogeneity in halide perovskite thin films, including compositional heterogeneity. Evidence has been found that decomposition during operation could be triggered/facilitated by local compositional variation from the averaged mixed phase.^[2] However, characterizing the chemical heterogeneity on small length scales has proven challenging. Recently work by Barrier et al demonstrated an X-ray scattering based methods for probing this nanoscale heterogeneity in halide perovskites.^[3] In this talk, we use these methods reported by Barrier et al. to probe nanoscale heterogeneity in PSC absorber layers and couple these results to device level

stability studies to understand the role heterogeneity plays in device performance. This work relies on the hypothesis that the cubic to tetragonal phase transition width is a measure of the chemical heterogeneity in mixed halide perovskites. To measure the phase transition width from the tetragonal to the cubic phase, temperature-dependent in situ wide angle X-ray scattering is utilized. Barrier et al. report that the transition is abrupt for pure MAPbI₃ (MA = methyl ammonium), however, the transition is stretched over a larger temperature range for the mixed compositions measured in their study.

To build on this work we prepare a set of FA_{0.83}CS_{0.17}PbI₃ perovskite thin films, choosing a variation of annealing conditions. The variation in annealing time and temperature can impact the compositional heterogeneity as measured using in-situ X-ray scattering. We couple these results to device level stability studies and ex-situ scattering studies of the degraded devices to understand how heterogeneity impacts the operational stability of these materials. In this talk, we will provide a summary of the approach used to characterize the heterogeneity in these films and comment on the loss in device performance and subsequent phase segregation induced by nanoscale heterogeneity.

References:

- [1] Z. Li, M. Yang, J. S. Park, S. H. Wei, J. J. Berry, K. Zhu, *Chem. Mater.* **2016**, *28*, 284.
- [2] L. T. Schelhas, Z. Li, J. A. Christians, A. Goyal, P. Kairys, S. P. Harvey, D. H. Kim, K. H. Stone, J. M. Luther, K. Zhu, V. Stevanovic, J. J. Berry, *Energy Environ. Sci.* **2019**, *12*, 1341.
- [3] J. Barrier, A. Gold-Parker, R. E. Beal, E. Wolf, L. Waquier, R. Szostak, A. F. Nogueira, M. D. McGehee, M. F. Toney, *submitted n.d.*

1:30 PM *EN05.04.07

Water-Accelerated Photo-Oxidation of Hybrid Perovskites—Mechanism, Rate Orders and Rate Constants Timothy Siegler, Wiley A. Dunlap-Shohl and Hugh W. Hillhouse; University of Washington, United States

Understanding the chemical reactions that hybrid organic-inorganic halide perovskite (HP) semiconductors undergo in the presence of moisture, oxygen, and light are essential to the commercial development of HP solar cells and optoelectronics. Here we use optical absorbance (105 degradations were conducted over 41 unique environmental conditions) to quantify the kinetics of methylammonium lead iodide (MAPbI₃) degradation in response to combinations of moisture, oxygen, and illumination over a range of temperatures. We discover and report a new chemical reaction pathway referred to as a water-accelerated photo-oxidation (WPO) pathway [1], which is the dominant chemical degradation pathway when light, oxygen, and humidity are present. At 25 °C in 50% RH air under 1 Sun illumination, the water-accelerated photooxidation proceeds with a rate of 2×10^{-7} mol/m²s with an activation energy of E_A=0.07 eV. Commonly reported pathways based on: (i) dry photo-oxidative degradation (DPO, degradation in oxygen under illumination but without water as a reactant), (ii) humidity-driven hydrate formation (degradation with humidity with and without illumination but without oxygen), (iii) blue light exposure, and (iv) thermally driven degradation (without humidity and oxygen) are demonstrated to have rates that are respectively 50, 200, 1000, and >1000 times slower than the water-accelerated photooxidation processes. The activation energy of the DPO process is much higher at 0.62 eV, and at higher temperatures (85°C) the rate of the DPO process is roughly equivalent to the WPO process. Given the much lower activation energy and much faster rate of the WPO process, the overall rate of degradation is very sensitive to small amounts of water. Water thus behaves like catalyst. Since it is consumed in one step and later re-generated, we refer to it as an accelerant. The WPO process has significant implications for perovskite stability and encapsulation, which will be discussed. A detailed kinetic model is developed for both the WPO and DPO processes. The rate determining step for WPO is proton abstraction from water by superoxide radical that creates several different reactive oxygen species, which then react with the perovskite. However, the rate determining step for the DPO process is proton abstraction from methylammonium by superoxide radical. A detailed rate law for each process is derived from this mechanism, and the entire dataset is fit to extract rate constants for DPO and WPO processes. The presentation will focus on the kinetics of perovskite degradation and will include experiments on the broader (FA, MA, Cs)Pb(L,Br)₃ space as well as discuss how chemistry inspired features (like the rate of chemical reaction) can be used in machine learning models for perovskite degradation.

[1] Siegler, T.D., Dunlap-Shohl, W.A., Meng, Y., Kau, W.F., Sunkari, P.P., Tsai, C., Armstrong, Z.J., Chen, Y., Beck, D.A.C., Meila, M., Hillhouse, H.W., "Water-Accelerated Photo-oxidation of CH₃NH₃PbI₃ Perovskite: Mechanism, rate orders, and rate constants," *ChemRxiv* 2021, preprint online June 21 at <https://doi.org/10.33774/chemrxiv-2021-30ggh>

[2] Stoddard, R.J., Dunlap-Shohl, W.A., Qiao, H., Meng, Y., Kau, W.F., Hillhouse, H.W. "Forecasting the Decay of Hybrid Perovskite Performance Using Optical Transmittance or Reflected Dark-Field Imaging," *ACS Energy Lett.* 2020, 5, 3, 946-954

2:00 PM EN05.16.03

Measurement of Radiative Decay Rate in Hybrid Metal-Halide Perovskites Angelica Simbula¹, Riccardo Pau^{1,2}, Fang Liu¹, Luyan Wu¹, Daniela Marongiu¹, Francesco Quochi¹, Andrea Mura¹, Alessio Filippetti¹, Michele Saba¹ and Giovanni Bongiovanni¹; ¹Università di Cagliari, Italy; ²University of Groningen, Netherlands

One of the main goals for perovskite materials is to approach ideal efficiency limits in solar cells or LEDs: being the radiative decay of optical excitations unavoidable, this can be done by reducing contributions from traps and defects. Despite all the advances in device performances, the bimolecular radiative recombination rate in metal halide perovskites is still not clearly established: coefficients derived under different assumptions can take very different values, and a lively debate is going on trying to conjugate their exceptionally long excitation lifetimes with large optical absorption coefficients. Here we provide a calibrated radiometric measurement of the instantaneous photoluminescence flux emitted by thin-films of hybrid perovskites with controlled carrier density under pulsed excitation. In all the analysed samples we uncover a radiative recombination rate much lower than the bimolecular recombination coefficient, revealing the presence of non-radiative bimolecular recombination rate that can be attributed to a population of dark states, possibly large polarons. Our findings suggest that to minimize unwanted decay channels for optical excitations one should also take account of non-radiative contributions to the bimolecular decay, that is due to extrinsic effects, like trapping and defects, and can be substantially reduced with materials optimization.

2:15 PM EN05.16.04

The Role of Photon Recycling and Scattering in High Efficiency Perovskite Solar Cells Changsoon Cho^{1,2}, Yeoun-Woo Jang³, Seungmin Lee⁴, Yana Vaynzof², Mansoo Choi³, Jun Hong Noh⁴ and Karl Leo²; ¹University of Cambridge, United Kingdom; ²Technische Universität Dresden, Germany; ³Seoul National University, Korea (the Republic of); ⁴Korea University, Korea (the Republic of)

In the last decade, power conversion efficiencies (PCE) of thin-film perovskite solar cells (PSCs) have rapidly grown from 3.8% to 25%. As most of PSCs are already achieving efficient light absorption and charge collection, enhancing electroluminescence (EL) is the key for them to approach the Shockley-Queisser limit. While the classical optics restricts the EL quantum efficiency (ELQE) of thin-film optoelectronics to $1/2n^2$, which is 7.4% for perovskites ($n=2.6$), photon recycling (PR) and scattering can give a chance to overcome it by extracting photons trapped in waveguide and substrate modes. Here, we investigate the role of PR and scattering in a PSC with passivation of octylammonium (OA) bromide, having PCE of 24%. The device exhibits the high ELQE of 13.7% at 1-sun equivalent excitation, exceeding the classical limit. The primary evidence for PR is given by the self-excitation

experiment, where EL of one pixel induces photocurrents of nearby pixels through the reabsorption of photons trapped in substrate mode. Spectral analysis of the spatially resolved photoluminescence and electroluminescence prove that both PR and scattering contribute to the external radiation of PSCs. Moreover, by resolving the previous optical issues and establishing a new optical model, we quantify various optical parameters in PSCs. At open-circuit condition, 80% of out-coupled photons are shown to have undergone at least one PR or scattering event. Consequently, PR and scattering increase the ELQE of our PSC by a factor of 4.5 (3.1% to 13.7%), reducing the non-radiative voltage loss (V_{nr}) from 89 mV to 50 mV, and increasing PCE from 23.3% to 24.0%. We also discuss future strategies for further improvement in current state-of-the-art PSCs.

2:30 PM EN05.16.05

Lead Adsorbing Ionogel-Based Encapsulation for Impact-Resistant, Stable and Lead-Safe Perovskite Modules Xun Xiao and Jinsong Huang; University of North Carolina at Chapel Hill, United States

Despite the demonstrated high efficiency and low-cost prospect for perovskite solar cells, great concerns of lead toxicity and instability remain for the commercialization of this technology. Here, we report an encapsulation strategy for perovskite modules based on lead-adsorbing ionogel, which effectively prevents lead leakage even if the modules are completely damaged and help to withstand long-term stability tests. The ionogel can absorb lead up to 30% of its mass because of the lead absorbing polymer backbone and phosphate ionic liquid. The elastic ionogel layers are integrated on both metal electrodes and on top of front glass window of perovskite modules, which significantly enhances their impact resistance in simulated hail tests, and can hold the shattered broken glass. The self-healable ionogel can physically prevent the permeation of water into the perovskite layer by blocking the cracks of broken glass, and absorbs lead that might otherwise leak. With the thermal and mechanical compatibility of ionogel and commercial encapsulant, the encapsulated solar cells pass the Damp Heat and Thermal Cycling accelerated stability tests according to IEC 61215 standard. The encapsulated perovskite mini-modules with ionogel show an aperture efficiency of 18.5%. The ionogel encapsulation also reduces lead leakage to undetectable level (<1 part per billion) after the hail-damaged module is soaked in water for 24 hours. Even under extreme scenario of being rolled over by a car followed by water-soaking for 45 days, the ionogel encapsulation reduces lead leakage by three orders of magnitude. This work provides a new strategy to address lead leakage and multiple-facet device stability simultaneously for perovskite modules.

SESSION EN05.17: Poster Session III: Emerging Energy and Materials Science in Halide Perovskites
Session Chairs: Mengxia Liu and Yuanyuan Zhou
Tuesday Afternoon, December 7, 2021
EN05-Virtual

4:00 PM EN05.17.01

Impact of Doping/Photodoping and Bandgap Variation on the Efficiency of Perovskite Solar Cell Basita Das^{1,2} and Thomas Kirchartz^{1,3}; ¹Forschungszentrum Jülich GmbH, Germany; ²RWTH Aachen University, Germany; ³University of Duisburg-Essen, Germany

Creating functionality in electronic devices is often achieved by modulating carrier concentrations with doping. In photovoltaics, optimization of doping concentrations can be an important tool to reduce recombination losses e.g. in crystalline Si solar cells. In emerging photovoltaic technologies such as the halide perovskites, comparably little work is done so far on intentionally controlling carrier densities in order to maximize efficiency. Some recent publications have discussed the effect of doping on solar cell efficiency both experimentally and theoretically using similar arguments and concepts as in classical Si photovoltaics. A fairly unconventional concept was recently presented by Feldmann et al., who proposed that photo-doping by small bandgap variations leads to increased external photoluminescence (PL) quantum efficiency Q_e^{lum} which might then lead to the increase in open-circuit voltage and potentially in photovoltaic efficiency. While it is an interesting thought that stoichiometric and energetic disorder could be beneficial for efficiency, the concept is in complete opposition to earlier findings in other photovoltaic communities working on multinary compounds (e.g. Cu(In,Ga)Se₂) where extensive theoretical work on the *negative* effect of band gap inhomogeneities was developed about 15 years ago. Hence, one motivation for the current study is the reconciliation of these opposing findings that have important consequences on how to optimize devices and how to explain performance gains or losses.

Here, we provide a theoretical basis for the findings of Feldmann et al. and explain the phenomenon of photodoping as well as its relation to conventional doping. We also aim to develop models to perform a critical assessment of the role of doping on PL quantum efficiency and photovoltaic device performance. To tackle the different questions, we use two approaches. First, we develop a simple analytical model to study the effect of small lateral band gap variations and conclude that it cannot possibly be the source of photodoping and thus the substantially increased Q_e^{lum} observed by Feldmann et al. We also find that such lateral fluctuations in the bandgap of the material can have adverse effects on the device performance. We then explore the relation between doping and photodoping and describe the consequences of these two forms of modulating carrier densities on luminescence, charge transport and photovoltaic efficiency using numerical device modelling. Furthermore, we highlight how the effects of doping on device performance depend on the choice of asymmetric defect capture coefficients as well as mobility of the charge transport layers.

4:05 PM EN05.17.02

Two-Dimensional Overdamped Fluctuations of Soft Lattice in Halide Perovskites Xing He¹, Tyson Lanigan-Atkins¹, Matthew J. Krogstad², Daniel Pajeroski³, Doug L. Abernathy³, Guangyong Xu⁴, Zhijun Xu⁴, Duck Y. Chung², Mercuri G. Kanatzidis⁵, Stephan Rosenkranz², Raymond Osborn² and Olivier Delaire¹; ¹Duke University, United States; ²Argonne National Laboratory, United States; ³Oak Ridge National Laboratory, United States; ⁴National Institute of Standards and Technology, United States; ⁵Northwestern University, United States

The all-inorganic halide perovskite compounds are currently attracting interest for photovoltaic, radiation detection, and thermoelectric applications. They exhibit long lifetimes of photoexcited carriers beneficial for photovoltaics, and ultralow thermal conductivity of interest for thermoelectrics. Among the simplest members of this family, CsPbBr₃ undergoes a typical sequence of phase transitions upon cooling, from cubic to tetragonal at ~400K and from tetragonal to orthorhombic at ~360K, associated with zone-boundary lattice instabilities. We have conducted inelastic neutron scattering (INS) of phonons on single-crystals of CsPbBr₃, to probe anharmonic effects around lattice instabilities, and the origin of the ultralow thermal conductivity. Heavily overdamped Br-dominated acoustic modes were found with INS along the edges of the Brillouin zone in the tetragonal and cubic phases, forming a continuum of quasielastic scattering, which we associate to the strongly anharmonic potential energy surface against octahedral tilts. Further, we performed first-principles simulations of the anharmonic phonon self-energy that reproduce the observed overdamping. These large atomic fluctuations exhibit two-dimensional correlations of Br octahedra rotations in real-space and impact optoelectronic properties by modulating the Pb-Br derived electronic states at the edges of the bandgap. In addition, we show how other compositions of metal halide perovskites exhibit similar diffuse rods, including the double perovskite Cs₂AgBiBr₆ and CsSnBr₃ or CsPbCl₃, which indicates that anharmonic halide octahedral tilts are a common feature of the structure and its dynamics for this family of materials.

[1] T. Lanigan-Atkins*, X. He*, M. J. Krogstad, D. M. Pajeroski, D. L. Abernathy, Guangyong N. M. N. Xu, Zhijun Xu, D.-Y. Chung, M. G. Kanatzidis, S. Rosenkranz, R. Osborn and O. Delaire, "Two-dimensional overdamped fluctuations of the soft perovskite lattice in CsPbBr₃", *Nature Materials* (2021). This work was funded by the U.S. DOE, Office of Science, Basic Energy Sciences, MSE Division.

4:10 PM EN05.17.03

Strain in Metal Halide Perovskites—The Critical Role of A-Cation [Yongtao Liu](#)¹, Bobby Sumpter^{1,1}, Jong K. Keum^{1,1}, Bin Hu², Mahshid Ahmadi² and Olga Ovchinnikova^{1,1}; ¹Oak Ridge National Laboratory, United States; ²The University of Tennessee, Knoxville, United States

Adjusting A-site cation composition in metal halide perovskites (MHPs) is an important approach to modulate the static lattice strain and hence enhance the efficiency and stability of MHPs solar cells. However, an understanding of how A-site cation affects the lattice dynamic during the operation of MHPs devices is missing. In this work, we investigate the role of A-site cation in the lattice strain of MHPs upon light illumination and heating—two inevitable factors during the operation of photovoltaic devices. We reveal that A-site cation plays an important role in light-induced strain in MHPs. In particular, formamidinium (FA) cation is different compared to the other cations studied in this work, where FA-based MHP does not show light-induced strain but the other cations based MHPs show a light-induced strain. We also discovered that the MA distribution is strongly coupled with the strain distribution, and MA heterogeneity can lead to a local light-induced strain heterogeneity under illumination. We further performed density functional theory (DFT) calculations to look at the photoexcitation induced lattice change in the atomic scale and explore the underlying mechanism. We found that hydrogen bonding interactions and ionization energy of A-site cation are potential reasons responsible for the light-induced lattice strain in MHPs. These findings offer an approach to modulate the light-induced strain in MHPs, which is critical for further improving the efficiency and stability of MHP photovoltaics.

Acknowledgments: This work is conducted at the Center for Nanophase Materials Sciences, a US Department of Energy Office of Science User Facility. We also acknowledge support from StART, a UTK-ORNL science alliance program.

4:13 PM EN05.17.05

Late News: Optimization of Optoelectronic Performance and Stability of Organic-Inorganic Halide Solar Cells with Hexagonal Boron Nitride Nanosheets [Yifan Yin](#), Yuchen Zhou and Miriam Rafailovich; Stony Brook University, The State University of New York, United States

Organic-inorganic halide perovskite solar cells (PSCs) have been considered a viable member of next generation photovoltaics, which can address the scalability changes with a low-cost solution process. The energy loss in the hybrid system has been approved to be principally caused by defects/traps at grain boundaries and surfaces as well as point defects such as interstitial defects or vacancies in the perovskite compounds crystal lattice. It has been approved that halide ions migrating into charge transporting layers will be detrimental to their transport properties, especially under solar cell working conditions. Inspired by the quasi-2D-perovskite which shows a great device maintenance in photovoltaic performance, here, the hexagonal boron nitride (h-BN) was incorporated into the perovskite absorber as a cationic diffusion barrier. This low-cost, lower dimensional material can work as a growth template which leads to a larger grain size. On the other hand, the integration of h-BN enables a better device stability as the result from the efficient suppression on the ion-migration induced degradation. The h-BN/perovskites has an initial PCE of 19.7% that shows no degradation exhibit in over 72 h, whereas the PCE of pristine MAPI devices diminishes by more than 30% within the first 24 h.

4:18 PM EN05.17.06

Role of Spin-Orbit Splitting on Optical Nonlinearities in Lead Halide Perovskite Single Crystals [Takumi Yamada](#)¹, Keiichi Ohara¹, Tomoko Aharen¹, Hirokazu Tahara¹, Hideki Hirori¹, Hidekatsu Suzuura² and Yoshihiko Kanemitsu¹; ¹Kyoto University, Japan; ²Hokkaido University, Japan

Lead halide perovskite semiconductors MAPbX₃ (MA = CH₃NH₃, X = I, Br, and Cl) are attracting much attention as a new class of materials for optoelectrical device applications because of their outstanding optical properties. Recently, unique nonlinear optical responses such as large optical modulation [1], efficient higher-order harmonic generation [2–4], and strong spin-orbit coupling inducing Autler–Townes effect [5] were found in MAPbX₃ perovskites. The precise determination of nonlinear optical coefficients is important to understand their fundamental material properties and the origin of their large nonlinear optical responses.

Because of strong light scattering in their grain structures and surfaces, it is difficult to determine intrinsic nonlinear optical coefficients for polycrystalline and nanocrystals. To exclude these influences, we fabricated high-quality single crystal MAPbX₃ (X = Cl and Br) samples and clarified their third-order nonlinear optical coefficients for the wide wavelength range. The obtained spectra near the band gap can be quantitatively explained by a two-band model including the exciton effect and 4×4 Kane model. Based on this model, we successfully determined the Kane energy (23 eV) and exciton reduced mass (0.20 m₀), and found that the nonlinear optical coefficient is enhanced about twice by the exciton effect in MAPbCl₃ single crystal [6]. In addition, we studied the two-photon absorption spectra of MAPbBr₃ single crystal with circularly and linearly polarized excitation light [7]. We observed a dip structure in the linear-circular dichroism spectrum of two-photon absorption, which corresponds to the spin-orbit splitting energy according to the 8×8 Kane model. From the experimental results and a theoretical analysis of the two-photon absorption spectra, we successfully determined the spin-orbit splitting energy (0.8 eV), exciton binding energy (28 meV), and reduced exciton mass (0.089 m₀), which characterize the electronic structure of MAPbBr₃. Our results provide a direct experimental reference on the electronic structure of halide perovskites.

Part of this work was supported by JSPS KAKENHI (JP19H05465 and JP20K03798) and CREST, JST (JPMJCR16N3).

[1] H. Tahara *et al.*, *Adv. Optical Mater.* **6**, 1701366 (2018).

[2] H. Hirori *et al.*, *APL Mater.* **7**, 041107 (2019).

[3] Y. Sanari *et al.*, *Phys. Rev. B* **102**, 041125(R) (2020).

[4] K. Nakagawa *et al.*, *Phys. Rev. Materials* **5**, 016001 (2021).

[5] G. Yumoto *et al.*, *Nat. Commun.* **12**, 3026 (2021).

[6] K. Ohara *et al.*, *Phys. Rev. Materials* **3**, 111601(R) (2019).

[7] K. Ohara *et al.*, *Phys. Rev. B* **103**, L041201 (2021).

4:23 PM EN05.17.07

Late News: (Garcia High School Student) Polymeric Hole Transport Layer in Perovskite Solar Cells [Grace Kyoko Wong](#)¹, Miller Liao² and Miriam Rafailovich³; ¹St Paul's Girls' School, United Kingdom; ²Shenzhen Middle School, China; ³Stony Brook University, The State University of New York, United States

Perovskite solar cells (PSCs) have become one of the most promising types of next-generation solar cell ever since 2009 due to their excellent photovoltaic performance. Despite of decent photo conversion efficiency (PCE), PSCs with a Spiro-OMeTAD hole transport layer (HTL) have been shown to have poor device stability and noticeable current-voltage (J-V) hysteresis PV performance.

In our study, we used PTAA as a substitute for Spiro-OMeTAD and compared the PV parameters along with the device stability of both PSCs. To compare the parameters between doped PTAA and Spiro-OMeTAD PSCs, we used the regular n-i-p device with the structure of FTO/c-TiO₂/m-TiO₂/MAPbI₃/HTL/Au. Three different HTLs were prepared: pristine PTAA, Li-TFSI doped PTAA and Spiro-OMeTAD. From the cross-section SEM

results, we found the Spiro-OMeTAD layer had a thickness of around 180 nm, while the thickness of the PTAA layer with and without Li-TFSI were all around 50 nm. The data for the current density-voltage (J-V) curves of the PSCs were collected using a PV test station. The MAPbI₃ (MAPI) PSC with Spiro-OMeTAD showed typical PCE of 17.3% in reverse scan (RS) and 14.2% in forward scan (FS), while the MAPI PSC using doped PTAA as the HTL had typical PCE values of 16.6% in RS and 14.7% in FS. Although the Spiro-OMeTAD PSC showed a slightly higher PCE in RS, the sample showed a greater hysteresis in comparison to the PTAA one. Moreover, the continuous maximum power point (MPP) test in an ambient environment (humidity ~ 60%) with a Xenon solar lamp on non-encapsulated PSCs showed that the PSC using PTAA HTL presented a slightly more stable current output compared to the Spiro-OMeTAD counterpart. Using contact angle measurements, we found the typical water contact angles of 69.8° and 88.2° for Spiro-OMeTAD and PTAA layers, respectively, indicating that the PTAA was more hydrophobic than the Spiro-OMeTAD. We suggest that the higher hydrophobicity of the PTAA could contribute to better PSC stability when exposed to moisture with moderate high temperatures.

4:28 PM EN05.17.08

Fabrication and Characterization of Structurally Controlled Lead Halide Perovskite Single Crystal Thin Films for Optoelectronics Tomohiro Watanuki, Hironori Ogata, Keitaro Kikuchi and Yuki Matsui; Hosei University, Japan

Currently, the energy conversion efficiency(PCE) of perovskite solar cells (PSCs) has reached 25.5% and there is a great deal of interest in the practical application of perovskite solar cells (PSCs). Almost all reported PSCs use polycrystalline films as photoactive layers. However, since it contains many grain boundaries, it has been pointed out about the possibility of deterioration through the grain boundaries. Recently, solar cells using a perovskite single crystal thin film as a photoactive layer have been reported to improve durability and solar cell characteristics because they have a longer carrier diffusion length, a lower trap density, a higher light absorption coefficient, and a lower ion diffusion length. However, the world record for PCE has been achieved with polycrystalline thin films. It is important to develop manufacturing technology for precisely structurally controlled perovskite single crystal thin films. In this study, several kinds of lead halide perovskite single crystal thin films were prepared under various conditions by a space-limited reverse temperature crystallization method, and their structures and optoelectric properties were evaluated. .. We will report on the detailed experimental results.

4:33 PM EN05.17.09

Sub-Bandgap Photons Harvesting via Up-Conversion for Perovskite Solar Cells Roja Singh^{1,2}, Eduard Madirov^{1,3}, Dmitry Busko¹, Ihtez M. Hossain^{1,2}, Vasilii A. Konyushkin⁴, Andrey N. Nakladov⁴, Sergey Kuznetsov⁴, Amjad Farooq^{1,2,5}, Saba Gharibzadeh^{1,2}, Ulrich W. Paetzold^{1,2}, Bryce Richards^{1,2} and Andrey Turshatov¹; ¹Institute of Microstructure Technology, Karlsruhe Institute of Technology, Germany; ²Light Technology Institute, Karlsruhe Institute of Technology, Germany; ³Kazan Federal University, Russian Federation; ⁴Prokhorov General Physics Institute of the Russian Academy of Sciences, Russian Federation; ⁵Institute for Materials Science and Center for Nanointegration Duisburg-Essen (CENIDE), University of Duisburg-Essen, Germany

Spectral conversion aims to tailor the incident solar spectrum such that it is better suited for particular photovoltaic absorber material; here an organometal halide perovskite semiconductor. In our perovskite solar cells with double cation perovskite absorber (bandgap 1.57eV), 41% of the incident spectrum is wasted by sub-bandgap losses. With the target to reduce these losses in the future, we research up-conversion (UC) crystal BaF₂:Yb³⁺, Er³⁺ for the annihilation of two low-energy photons to form a high-energy photon. When tested under terrestrial sunlight representing one sun above the perovskite's bandgap and sub-bandgap illumination at 980 nm (via a laser), the BaF₂ crystal emits usable upconverted photons in the spectral range of 520 to 700 nm. In our bifacial PSC with the UC crystal beneath, these upconverted photons contribute to 0.38 mA/cm² enhancement in short-circuit current density at a laser intensity equivalent to 120 suns. We demonstrate that UC scales non-linearly with incident intensity, with an 880 suns equivalent intensity resulting in 2.09 mA/cm² enhancement in current. Our study demonstrates that UC is a potentially viable process to extend the response of PSC to a wider spectral range.

4:38 PM EN05.17.10

Late News: (Garcia High School Student) Methylammonium Chloride Assisted Growth of High Quality FAPbI₃ Justin Shnyder¹, Adin Moskowit², Shiqi Cheng³ and Miriam Rafailovich⁴; ¹Staten Island Technical High School, United States; ²Hebrew Academy of Nassau County, United States; ³Illinois Mathematics and Science Academy, United States; ⁴Stony Brook University, The State University of New York, United States

As greenhouse gas emissions rise and induce the complications associated with climate change, solar cells, devices which convert sunlight into electricity through the photovoltaic effect, are regarded as a promising solution to the issue. The use of the organic and inorganic hybrid perovskite (OIHPs) as the photoactive semiconductors for new generation of solar cells has been widely investigated due to panchromatic light absorption, high charge mobility, and low exciton binding energy, etc, which contributes to high performance perovskite solar cells (PSCs) with high photo conversion efficiency (PCE) surpassing other types of thin film solar cells and comparable to III-IV and II-IV types of solar cell devices. Among different compositions of OIHP, methylammonium lead iodide (MAPbI₃ or MAPI) is one of the most widely studied OIHP due to its overall simple processing and good moisture endurance. On the other hand, the formamidinium lead iodide perovskite (FAPbI₃ or FAPI) becomes more popular in the community due to its optimal bandgap, broader light absorption, as well as better thermal stability, etc, as compared with the MAPI perovskite. However, preparation of a high quality FAPI perovskite films with minimized surface and structural defects are more difficult than MA based perovskite, due to less favorable lattice parameters after replacing with FA cations. Previous studies have indicated that addition of methylammonium chloride (MACl) into the FAPbI₃ system can help improve the crystallinity and morphology of FAPbI₃ films. Thus, the objective of this study was to study the effects of various concentration of MACl (15, 30, and 45 mol%) addition for the fabrication of high quality FAPbI₃ films. Specifically, the FAPI with 30% MACl yielded optimal results with large and compact grains, while FAPI doped with 15% MACl and 45% MACl yielded imperfections such as rough surface with pinholes. Further analysis revealed that optimal FAPI-MACl (30%) formed grains with average size around 820 nm, more than double that of the grains on MAPI perovskite, which has an average value around 370 nm. In addition, the analysis of photovoltaic performance was also conducted. The typical reverse and forward J-V scans of the PSC based on pristine-FAPI revealed PCEs of 12.3% and 8.1% respectively. In contrast, the typical reverse and forward scans of the FAPI with 30% MACl revealed higher PCE of 16.5% and 16.4% respectively. The improved PCE with negligible hysteresis of the FA-based PSC indicates the improvement in crystallinity and quality of the perovskite films with the optimal MACl concentration. The XRD analysis further indicated that: 1) pure FAPI exhibited a dominant photo-inactive δ -phase, and 2) the addition of MACl, particularly at concentrations larger than 30%, promoted the photo-active α -phase and reduced the photo-inactive δ -phase. Lastly, UV-vis absorption spectra revealed that FAPI perovskites with or without MACl all have broader light absorption, with the onset wavelength of around 780 nm, as compared with 750 nm of MAPI perovskites. In conclusion, our results confirm that the addition of MACl as the processing additive, particularly at a concentration of 30%, produced good quality FAPbI₃ films, leading to high performance PSCs with decent PCE and low hysteresis.

4:43 PM EN05.17.11

Exploring Recombination Dynamics in Emerging Non-Fullerene Acceptor Based Organic Solar Cells Vinod K. Sangwan, Guoping Li, Liang-Wen Feng, Antonio Facchetti, Tobin J. Marks and Mark C. Hersam; Northwestern University, United States

Next-generation solar energy harvesting technologies rely on the discovery, refinement, and implementation of new organic photovoltaic materials with high quantum efficiency, excellent stability, and reliability. In recent years, organic bulk heterojunction (BHJ) solar cells based on non-fullerene acceptors

(NFAs) have emerged as potential candidates due to rapidly improving power conversion efficiencies, now exceeding 18% in single-junction cells. Improved performance of recent NFAs is attributed to wider solar spectral absorption, efficient exciton dissociation, and strong π - π interactions, leading to excellent charge transport and collection. Despite these innovations in synthetic chemistry, there remain significant losses in all steps of the photoconversion process from exciton dissociation within the BHJ to charge collection at the contacts. Especially, bimolecular recombination losses are known to dominate in BHJ cells due to non-ideal band energetics, disordered morphology of donor and acceptor domains, and poor interfaces and contacts. Electric charge- and photocurrent-based spectroscopies using impedance spectroscopy provide a direct probe to reveal these relatively slow processes not accessible to conventional ultrafast spectroscopies. Furthermore, the non-invasive nature of this measurement can quantify performance-limiting dynamical processes in fabricated devices operating at the maximum power point. In this presentation, an impedance and photocurrent spectroscopy method will be discussed to quantify bimolecular recombination rates in NFA-based organic solar cells.¹⁻⁵ Two emerging NFA-polymer BHJ systems, indacenodithienothiophene-, and Y6-based NFAs, will be used to demonstrate the effectiveness of the methodology to assess differences in cells resulting from different molecule structure and processing conditions such as thermal annealing. Extracted variation in device parameters is correlated with improved morphology and packing motifs. Overall, this in-situ analysis allows a more realistic device model that can distinguish the competing effects on functionalization in NFA molecules such as π -extension and fluorination. In this manner, the new understanding gained in these systems provides a rational strategy for further optimization of high-performance and stable organic solar cells.

References:

¹ *Journal of the American Chemical Society* **142**, 14532 (2020).

² *Adv. Eng. Mater.* **10**, 2000635 (2020).

³ *ACS Eng. Lett.* **5**, 1780 (2020).

⁴ *ACS Appl. Mater. Inter.* **11**, 14166 (2019).

⁵ *Adv. Funct. Mater.* **27**, 1703805 (2017).

4:48 PM EN05.17.13

Kinetics and Mechanism of Light-Induced Phase Separation in Mixed-Halide Perovskite Crystals Siying Peng^{1,2}, Yanming Wang^{1,3}, Michael Braun¹, Yikai Yin¹, Andrew C. Meng^{4,1}, Wanliang Tan¹, Balreen Saini¹, Kayla Severson¹, Ann Marshall¹, Katherine Sytwu¹, John Baniecki⁵, Jennifer A. Dionne¹, Wei Cai¹ and Paul McIntyre^{1,5}; ¹Stanford University, United States; ²Westlake University, China; ³Shanghai Jiao Tong University, China; ⁴University of Pennsylvania, United States; ⁵SLAC National Accelerator Laboratory, United States

Halide perovskites are a very promising class of material for optoelectronics. Employing inexpensive and scalable synthesis methods, earth-abundant semiconductors that exhibit desirable optical properties, including unity quantum yield, can be achieved. The composition of both the cation and anion (halide) sublattices of perovskite crystals can be manipulated over a wide range to engineer their light absorption and emission behavior. Halide ion phase separation is a well-known barrier for the application of mixed-halide perovskites in solar cells and LEDs, whereby the presence of large populations of photo-generated or electrically-injected carriers causes undesirable changes of the local band gap by demixing of initially homogeneous mixed halide ion compositions. Previous reports have established that illumination with above the band gap energy causes the phase separation of mixed iodide-bromide perovskites into iodide- and bromide-rich domains and is reversible in the dark, where evidence of structural changes in mixed-halide alloys has been observed by X-ray diffraction. The phase separation mechanism appears to involve a self-reinforcing demixing of Br- and I- ions driven by reducing the potential energies of photogenerated carriers that trap in regions of smaller bandgap. Subwavelength imaging has been performed to visualize the process in single crystalline and poly-crystalline organic perovskites. However, many aspects of the phase separation are not well understood, such as factors that influence the length scale, kinetics of the phase separation, and whether the mechanism involves spinodal decomposition or nucleation and growth. We investigate the mechanism of phase separation in mixed-halide CsPbI_{1-x}Br_{3-x} perovskite crystals driven by photocarrier generation and spatial redistribution during absorption of band gap light. We visualize the phase separation process and its dynamics at the nanoscale using Cryo-TEM-CL, where formation of iodide-rich regions is detected as locally red-shifted emission. An extracted length scale for the phase separation is ~ 200 to 500 nm depending upon the degree of phase separation. Using photoluminescence spectroscopy, ellipsometry, and x-ray diffraction, we demonstrate that the temporal dynamics of this phase separation can be modulated by controlling both 1) the intensity of illumination, which, when increased, promotes faster phase separation; and 2) the temperature, which, when increased has the opposite effect. Correlating the optical property modulation with structural changes via in-situ experiments reveals that both the amplitude and the length scale of this fully-reversible phase separation increase as a function of time. Combined with phase field modeling that accounts for the coupling between the electronic and chemical effects, this points to a diffusional transformation mechanism, similar to spinodal decomposition, combined with coarsening of the iodide-rich domains at longer time-scales.

4:53 PM EN05.17.14

A Novel Perovskite-Polymer Composite Piezoelectric Film—From Crystal Growth to IoT Application Asif Abdullah Khan^{1,2}, Md. Masud Rana^{1,2}, Guangguang Huang¹, Nanqin Mei¹, Resul Saritas^{1,2}, Boyu Wen^{1,2}, Steven Zhang¹, Weiguang Zhu¹, Peter Voss³, Eihab-Abdel Rahman^{1,2}, Zoya Leonenko¹, Shariful Islam³ and Dayan Ban^{1,2}; ¹University of Waterloo, Canada; ²Waterloo Institute for Nanotechnology, Canada; ³Shimco North America Inc, Canada

Developing compact, efficient, and sustainable power sources are of the urgent demand for the next generation of self-powered micro/nano devices for IoT (Internet of Things). One of the most prospective routes is to harness environmental energy by piezoelectric nanogenerator (PNG), as it is compact, flexible and has high electricity generation capabilities. In this aspect, by dispersing highly-piezoelectric nanoparticles (NPs) in a flexible polymer, creating a composite film is an attractive, yet easier approach in terms of PNG fabrication scalability, and device performance; as it can be synergistically benefitted from the incorporated highly piezoelectric NPs & flexible host polymer matrix. The quest for that, we rationally designed a novel perovskite/ PVDF composite piezoelectric film, which simultaneously benefits from a self-assembled highly ordered porous structure of PVDF, and new hybrid halide perovskite-formamidinium lead bromine iodine (FAPbBr₂I). Enhanced mechanical strain by the self-assembled highly porous PVDF, and reduced film conductivity by the FAPbBr₂I (higher relative permittivity~13) , generates a strain-induced piezo potential of 85 V (peak-to-peak), and current of up to 30 μ A (peak-to-peak) (138 g (gram) of applied load). Benefiting from the above, a high output peak power density of ~ 18 mW/cm³ (while~ 3 mW/cm³ at 7 M Ω load resistance) was obtained for the self-powered integrated wireless electronics node (SIWEN) and then extended it to the real application by realizing wireless structural health monitoring.

In order to synthesize the hybrid perovskite-polymer composite piezoelectric film, low temperature and fully solution-based growth processes were adopted. The FAPbBr₂I precursor solution was prepared via dissolving FAI (formamidinium iodide $\geq 99\%$, Sigma-Aldrich) and PbBr₂ (lead (II) bromide $\geq 98\%$, Sigma-Aldrich) of equal molar ratio (0.5:0.5) in N, N DMF (N, N-dimethylformamide $\geq 99\%$, Sigma-Aldrich) solvent, followed by stirring at 60 °C for 12 hours. The PVDF solution was dissolved in the N, N DMF with constant stirring at 50 °C for 24 h. The final concentrations of FAPbBr₂I and PVDF in the N, N DMF were kept at 20 wt. % and 10 wt. %, respectively. Intentionally, the concentration of PVDF in the final solution was diluted by perovskite precursor and the thickness of preformed films was controlled to less than 50 μ m. The aim is to decrease the inner vapor pressure during the film growth and to form the highly ordered porous structure. The optimized 20 wt. % FAPbBr₂I –PVDF solution was drop-casted on a glass substrate and stored about 1 hour for the degassing process (ambient condition). In order to obtain the composite films, an annealing process at 1200C for 2-3 hours was performed (self-assembled highly ordered porosity was confirmed by SEM-EDS mapping, and the crystallinity by the X-ray diffraction peaks). After peeling off, to align the dipoles, a high voltage electrical poling of the film (thickness ~30 μ m) was performed with an electric field of (50-120 V/ μ m) for 2-3 hours (β -phase was confirmed by FTIR spectrum analysis). Finally, the film was sandwiched between two copper/polyester substrates by using a thermal pressing

technique for the integration of PNG.

The generated output voltage and current of perovskite-polymer PNG (P-PNG) were measured at 30 Hz frequency by applying a periodic mechanical vibration from an electrodynamic shaker (ET-126-I from Labworks Inc.) and placing a 138 g (gram) metal block (stainless steel) on top of the device. The high piezo potential 85V (peak-to-peak), and current of 30 μ A (peak-to-peak), was recorded by a commercial oscilloscope. Later, to assess a real-time application, we designed a self-powered integrated wireless electronics node (SIWEN) enabled by the PNG, that can communicate with personal electronics

4:58 PM EN05.17.15

High-Sensitivity Near-UV PES for Valence Band Determination and Observation of Defect Formation In Halide Perovskites [Dorothee Menzel](#)¹, Alvaro Tejada Esteves^{1,2}, Amran Al-Ashouri¹, Igal Levine¹, Jorge A. Guerra², Bernd Rech¹, Steve Albrecht¹ and Lars Korte¹; ¹Helmholtz-Zentrum Berlin für Materialien und Energie, Germany; ²Pontificia Universidad Católica del Perú, Peru

Halide perovskites (HAPs) have attracted immense interest in the optoelectronic community over the past decade. While the power conversion efficiency of perovskite solar cells has rapidly increased during this time, fundamental material properties, such as the true arrangement of the valence bands and dispersion relation of halide perovskites or defects at/close to their surfaces are still under debate.

Here, we report on photoelectron spectroscopy investigations on a multi cation multi halide perovskite composition, which has been used for recently reported highest silicon/perovskite tandem solar cell efficiencies.^[1]

Conventionally, He-I UPS is applied to study the valence band maximum, required for understanding the electronic formation of semiconductor interfaces. He UPS suffers from a rather high noise floor and the need for correction of He-satellite lines. As we show in our study, the characteristically low density of states close to the valence band maximum^[2,3] can only be revealed by very high sensitivity PES techniques. To this end, we apply a “classical” but rarely used technique: near-UV photoemission spectroscopy in constant final mode (CFSYS) and can directly trace the density of states over a very high dynamic range of seven orders of magnitude. This is four orders of magnitude better compared to conventional He-I UPS. Additionally, with the low photon energy, the information depth is strongly enhanced to up to 10 nm and thus, the gained information is significantly less distorted by changes of material composition in the first monolayers or surface contaminations, as compared to He-I UPS.

Using a newly developed model^[4] to describe the valence band edge and exponential band tail, we can distinguish between two valence band maxima, at two different positions in k-space, in one angle-integrated spectrum. Furthermore, it becomes apparent, that the widely applied method to determine the valence band maximum (by an extrapolation of the leading valence band edge on a semi-logarithmic scale) strongly depends on the noise level and can thus not provide reliable results. Importantly, we also show that there is a fundamental caveat to such extrapolation approaches: The highest valence band maximum at the R-point of the Brillouin zone overlaps with a distinct defect band and can thus only be located by combining the analysis of experimental data with DFT calculations.

The low detection limit of CFSYS further reveals occupied gap states, i.e. defect states that will influence recombination and thereby device performance. By rescaling our data to published DFT calculations^[5], we can quantify these depending on the damage by illumination (UV, X-Rays) or storing condition (vacuum, short air exposure). To our knowledge, this is the first time that such defects are not only observed, but also quantified from photoelectron spectroscopy data. These unprecedented results show the decomposition of HAP films and creation of defect states at a sensitivity level, which can hardly be reached by any other PES technique.

[1] A. Al-Ashouri et al., *Science* 2020, 370, 1300.

[2] F. Zu et al., *J. Phys. Chem. Lett.* 2019, 10, 601.

[3] J. Endres et al., *J. Phys. Chem. Lett.* 2016, 7, 2722.

[4] J. A. Guerra et al., *J. Phys. D: Appl. Phys.* 2019, 52, 105303.

[5] Y. Zhou et al., *J. Phys. Chem. C* 2017, 121, 1455.

5:03 PM EN05.17.17

High Carrier Mobilities of Lead Halide Perovskite Single Crystals Evaluated by AC Photo-Hall Measurements [Takumi Kimura](#)¹, Kouhei Matsumori¹, Kenichi Oto¹, Yoshihiko Kanemitsu² and Yasuhiro Yamada¹; ¹Chiba University, Japan; ²Kyoto University, Japan

Lead halide perovskites have recently attracted attention as high-quality semiconductors with excellent optical properties, promising for various device applications. In contrast, the reported carrier mobilities in lead halide perovskites are relatively low compared to other high-quality inorganic semiconductors. The low mobilities have been discussed in terms of polarons, which enhance the carrier mass through electron-phonon coupling and reduce the carrier mobility. However, the impact of polarons on carrier transport of lead halide perovskite still remains unclear. To reveal the physical origin of the low carrier mobility, we need to perform the reliable Hall measurement in high-quality single crystals and evaluate their intrinsic mobility. Nevertheless, lead halide perovskite materials have very high resistivities; therefore, it is difficult to measure the Hall mobility of carriers by the conventional method.

In this study, we performed an AC Hall measurement of a CH₃NH₃PbBr₃ bulk crystal at room temperature under light irradiation [1]. We illuminated the sample by a green laser ($\lambda=555$ nm) to generate photocarriers uniformly. We can estimate the mobilities of holes and electrons independently from conductivities and Hall coefficients under different photoexcitation intensities based on two-carrier analysis [1]. The conductivities were measured by van der Pauw method. We evaluated the resistivities from the slope of I-V profiles to eliminate the photovoltaic effect. To obtain the Hall voltage in a low-current regime, we performed the Hall measurement under ac-magnetic field (0.4 T / 0.1 Hz) by a lock-in technique. We prepared undoped single crystals of CH₃NH₃PbBr₃ by the anti-solvent crystallization method [2]. The crystals were thinned to 50 μ m in order to increase the current density and generate the photocarrier more uniformly. We fabricated Au/rubrene electrodes at the four corners of the sample. The intermediate layer of rubrene between CH₃NH₃PbBr₃ and Au reduces the contact resistance.

The observed carrier mobilities were enhanced drastically with increasing photocarrier density and show the square-root dependence on photocarrier density [3]. We consider that the dependence of photocarrier density is attributable to the screening of the charged dislocations by photocarriers [4]. We obtained the hole and electron mobilities of 322 cm²/Vs and 318 cm²/Vs at the maximum photocarrier density, and these mobilities would further increase with carrier density. The mobilities obtained from this research are much higher than those reported in previous studies. The result implies that polarons do not have a large impact on the carrier mobilities, which is consistent with our recent magnetorefectance study [5]. Rather, we consider that the scattering by defects is more important in room-temperature carrier transport in lead halide perovskite. Therefore, it is significant to reduce defects, which could help deliver the full potential of this material.

Part of this work was supported by JST-CREST (JPMJCR16N3), JSPS KAKENHI (JP19K03683), Canon foundation, and Chiba Iodine Resource Innovation Center.

[1] O. Gunawan, et al., *Nature* 575, 151-155 (2019).

[2] D. Shi, et al., *Science* 347, 519-522 (2015).

[3] T. Kimura, et al., *Appl. Phys. Express* 14, 041009 (2021).

[4] H. M. Ng, et al., *Appl. Phys. Lett.* 73, 821 (1998).

[5] Y. Yamada, et al., *Phys. Rev. Lett.* 126, 237041 (2021).

5:08 PM EN05.17.18

Highly Piezoelectric Organic-Inorganic Hybrid Vacancy-Ordered Double Perovskite for Energy Harvesting Asif Abdullah Khan^{1,2}, Md. Masud Rana^{1,2}, Guangguang Huang¹, Chao Xu^{1,2}, Shuhong Xu³, Resul Saritas^{1,2}, Steven Zhang¹, Weiguang Zhu^{1,2}, Eihab-Abdel Rahman^{1,2}, Pascal Turban⁴, Soraya Ahabou-Girard⁴, Chunlei Wang³ and Dayan Ban^{1,2}; ¹University of Waterloo, Canada; ²Waterloo Institute for Nanotechnology, Canada; ³Southeast University, China; ⁴Univ Rennes, CNRS, France

To maximize the output power of PNGs, the piezoelectric charge (d_{33}) and voltage (g_{33}) coefficients of the piezoelectric materials are both important, which will determine the output current and voltage respectively. However, in the past decades, it is difficult to combine them in one material for piezoelectric energy harvesting, such as piezoelectric nanogenerators (PNGs). In this work, we firstly report a combined large d_{33} of $137 \text{ pC}\cdot\text{N}^{-1}$ and giant g_{33} of $980 \times 10^{-3} \text{ Vm}\cdot\text{N}^{-1}$ in a novel vacancy-ordered double perovskite of $\text{TMC}_2\text{M}_2\text{SnCl}_6$ (TMC is trimethyl chloromethyl ammonium). The piezoelectric origin is demonstrated as the halogen-bonding mediated synergistic movements of atom displacement in inorganic $[\text{SnCl}_6]^{2-}$ octahedrons and dipole reorientation of organic molecular TMC via a combined density functional theory (DFT) and experimental study. The piezoelectric composite films are grown via dispersing $\text{TMC}_2\text{M}_2\text{SnCl}_6$ into the polydimethylsiloxane ($\text{TMC}_2\text{M}_2\text{SnCl}_6/\text{PDMS}$). The final PNGs exhibit the highest outstanding outputs with an open-circuit voltage of 149 V (peak-to-peak), short-circuit current density of $1.54 \mu\text{A}\cdot\text{cm}^{-2}$ (peak-to-peak), and total power of 26 μW under periodically vertical compression (4.8 N). Moreover, the PNGs are used as the power source of self-powered wire-less electronics (SPWLE) and enable communication successful. Our studies not only innovatively open a door for a new green piezoelectric perovskite design but also extend its further application in energy harvesting and its SPWLE.

5:13 PM EN05.17.19

Advances in Hybrid Perovskite Film Deposition by Slot-Die Coating Method Yaneth A. Florez Velasquez, Juan P. Velasquez, Rafael A. Betancur, Daniel E. Ramírez, Juan F. Tirado, Juan F. Montoya and Franklin Jaramillo; Universidad de Antioquia, Colombia

Among the emerging photovoltaic technologies, hybrid perovskite solar cells (PSCs) provide the highest energy conversion efficiencies years (Phaometvarithorn, Chuangchote, Kumnorkaew, & Wootthikanokkhan, 2018; Tang & Yan, 2021) however, it is necessary to promote the transition from laboratory-scale to large-area manufacturing ensuring high throughput and comprising the analysis of perovskite film formation and the scalable deposition techniques, aiming to improve the perovskite thin-film stability and homogeneity (Burkitt et al., 2020; Burkitt, Searle, A. Worsley, & Watson, 2018; Patidar, Burkitt, Hooper, Richards, & Watson, 2020).

Slot-Die Coating technique has been extensively applied in industry, where a great effort is directed to stabilize the coating process (Miller, 2012; O. J. Romero, Suszynski, Scriven, & Carvalho, 2004; Oldrich Joel Romero, Scriven, & Carvalho, 2006; X. Ding, J. Liu, 2016). In this direction, a prior condition is achieving a uniform volume distribution along the slot-die head and related to the crystallization process for uniform film formation, which to the best of our knowledge this has not been studied for perovskite inks. In this paper we propose to explore the nature of the flow patterns inside the slot-die head and the influence of this study in the fabrication of hybrid perovskites films by slot-die processing.

We included an analysis of the volume uniformity inside a lab-scale slot-die head, as a function of the head angle and inlet flow, designed for the fabrication of perovskite solar cells, is accomplished. We identify issues such as poor filling of the shim apertures and a non-fully developed laminar flow inside the slot-die head for the common lab processing conditions, as the main causes of non-uniform volumetric flow and the result is nonhomogeneous films and crystallization defects of the perovskite. These results contribute to pave the way towards highly reproducible and scalable perovskite solar devices by slot-die coating.

5:18 PM EN05.09.06

Green-Synthesized Tungsten-doped Zinc Oxide as Promising Electron Transport Material for Perovskite Solar Cells Munkhtuul Gantumur¹, Md. Shahiduzzaman¹, Md. Shahinuzzaman², LiangLe Wang¹, Masahiro Nakano¹, Makoto Karakawa^{1,1,1}, Jean Michel Nunzi¹, Md. Akhtaruzzaman² and Tetsuya Taima^{1,1,1}; ¹Kanazawa University, Japan; ²The National University of Malaysia, Malaysia

Organic-inorganic hybrid halide perovskite solar cells (PSCs) have been extensively researched and achieved impressive power conversion efficiency (PCE) of 25.5% at laboratory scale. To date, several metal oxides, such as ZnO, TiO₂, and SnO₂ are used as electron transport layer (ETL) for the fabrication of efficient PSCs. Particularly, ZnO showed favorable energy level, smooth surface coverage and most importantly low-cost deposition capabilities are highly desired for efficient photovoltaic performances and their future commercialization and market adoption. However, the application of ZnO ETL to PSCs remains limited by drawbacks such as low conductivity and large amounts defects, which inevitably lead to carrier recombination. Notable efforts have been made by using doping, nanocomposites or interface engineering strategies to resolve these drawbacks to enhance the performances of PSCs. Tungsten (W) is one of the candidates for doping ZnO due to the similar ionic radius of Zn²⁺ (0.074 nm) and W⁶⁺ (0.064 nm). In this study, we introduced W-doped ZnO synthesized using Aloe Vera leaf extract as the ETL and investigated their influences in PSCs performance. Our results demonstrated a smooth and dense surface morphology of W-doped ZnO deposited on ITO-patterned substrate. Higher crystallinity was observed for Cs_{0.1}FA_{0.9}PbI₃ perovskite layer formed on W-doped ZnO because the as-prepared W-doped ZnO material started with better crystallinity. Ultimately, PSCs with W-doped ZnO ETL exhibited PCEs as high as 16.2%, which is superior to those of PSCs with pristine ZnO as the ETL (12.9%). The integrated J_{sc} values of the IPCE spectra are 20.4 and 22.5 $\text{mA}\cdot\text{cm}^{-2}$ for the pristine ZnO and W-doped ZnO based PSCs, respectively. These values are coherent with the J_{sc} values extracted from the $J-V$ curves. Hence, the present study provides a significant advance to the design of photovoltaic devices with respect to charge transport and electron-hole recombination.

SESSION EN05.18: Perovskite Composition Versatility
Session Chairs: Mengxia Liu and Yuanyuan Zhou
Tuesday Afternoon, December 7, 2021
EN05-Virtual

9:00 PM *EN05.18.01

Unraveling the Hysteretic Behavior at Double Cations-Double Halides Perovskite-Electrode Interfaces Dohyung Kim¹, Yongtao Liu², Anton V. Ievlev², Kate Higgins¹, Olga Ovchinnikova², Sergei V. Kalinin² and Mahshid Ahmadi¹; ¹University of Tennessee, Knoxville, United States; ²Oak Ridge National Laboratory, United States

Despite over a decade of research on metal halide perovskites (MHPs) in the context of photovoltaic applications, understanding the nature of electronic and ionic processes associated with current-voltage (*I-V*) hysteretic behavior has been limited. In this study, we explore the hysteretic behavior in (FAPbI₃)_{0.85}(MAPbBr₃)_{0.15} perovskite devices with lateral Cr and Au electrodes by applying first order reversal curve (FORC) bias waveform in *I-V*, Kelvin probe force microscopy (KPFM) measurements, and in-situ chemical imaging by time-resolved time-of-flight secondary ion mass spectrometry (tr-ToF-SIMS).

Previous studies suggested that *I-V* hysteresis in MHP devices is associated with various interfacial phenomena such as space charge layers, resulting from ion migration^{1,2}, interfacial charge accumulation and recombination³, and charge trapping and de-trapping at the interface⁴. Particularly, ion migration has a critical role in the hysteresis and transient phenomena in MHPs devices.^{4,5} Many intriguing properties in MHPs are highly associated with the interplay between electronic charge carriers and multiple mobile ion species. The ion migration is in fact one of the most acute issues that perovskites community faces, due to the key role it plays on device stability and performance. Although, double cations and double halides perovskites have been attracted much attention due to their high efficiencies and remarkable long-term stability in photovoltaics. More complex interplay between electronic and ionic charge carries is expected in the double cations and double halides perovskites due to the presence of multiple mobile ions.

Here, we strategically utilize the combination of time- and voltage-dependent *I-V* and KPFM, with in-situ chemical imaging by tr-ToF-SIMS measurements to identify spatial localization and nature of the involved species. To study the time dynamics, we use a bias waveform referred as FORC that allows separating bias-induced chemical effects in dark and under illumination. The FORC waveform is also applied to the KPFM measurements to clarify spatial- and time-resolved contact potential difference (CPD) in the devices. The time- and bias-dependent ion distribution is explored using tr-ToF-SIMS to directly investigate the chemical changes in operando devices. This approach supported by machine learning analysis provides the correlation between ion dynamics and the hysteresis phenomenon in *I-V* and CPD-*V* curves. Some of the key findings in this study include: i) We discovered that Br⁻ ions accumulate at the interface between (FAPbI₃)_{0.85}(MAPbBr₃)_{0.15} perovskites and drain electrode in both on- and off-fields. ii) The low mobility of MA⁺ ions result in transient behavior and contribute to the hysteretic phenomena in the *I-V* and KPFM results. iii) It was shown that Pb²⁺ ions can be reduced at the interfaces due to electrochemical reactions with the electrode in the presence of charge injection and photogenerated charge carriers. iv) The ion migration can be fully or partially reversible while the electrochemical reaction at the interface can result in non-reversible and permanent damage to the device performance and stability.

Overall, our results clearly show the important role of interfacial phenomena and highlight that appropriate interface engineering is critical for highly efficient and stable MHPs-based devices. Our study suggests that lower concentration of Br⁻ and MA⁺ ions can result in higher interfacial stability and less hysteretic behaviors in double cations and double halides perovskite devices.

This article is already submitted and currently under review.

References:

- 1 Mosconi, E. & De Angelis, F. *ACS Energy Letters* **1**, 182 (2016).
- 2 Tress, W. *The Journal of Physical Chemistry Letters* **8**, 3106-3114 (2017).
- 3 Rong, Y. *et al. Energy & Environmental Science* **10** (2017).
- 4 Snaith, H. J. *et al. The Journal of Physical Chemistry Letters* **5**, 1511 (2014).
- 5 Tress, W. *et al. Energy & Environmental Science* **8**, 995 (2015).

9:30 PM EN05.18.02

Late News: Halide Perovskite Formation Mechanism Unveiled by Synchrotron-Based *In Situ* GIWAXS Minchao Qin, Yuhao Li, Zhaotong Qin and Xinhui Lu; The Chinese University of Hong Kong, Hong Kong

Solution-processed halide perovskite solar cells (PSCs) have attracted tremendous attention due to their skyrocketing power conversion efficiency (PCE) from 3.8% to 25.5% in recent years. The rapidly rising efficiency is mainly attributed to the improved perovskite film quality, which is usually achieved through precursor engineering, compositional regulation, and optimization of the film fabrication process. However, most developments of these methods are empirical, and few efforts have been devoted to the fundamental studies of the perovskite film formation mechanism. In this work, the underlying perovskite crystallization process from the initial precursor solution to the final polycrystalline film was investigated and unveiled with the aid of synchrotron-based in situ grazing-incidence wide-angle X-ray scattering (GIWAXS) measurements. Specifically, the detailed crystallization pathways of mixed perovskites (MA_{0.17}FA_{0.83}Pb(I_{0.83}Br_{0.17})₃) during the one-step spin-coating process were monitored via state-of-the-art in situ GIWAXS. Three crystallization stages were successfully identified: the precursor solution (stage I), hexagonal δ -phase (2H) (stage II), and complex phases (stage III) including the intermediate phase, hexagonal 4H, 6H polycrystals, and perovskite α -phase. In the light of in situ GIWAXS results, we revealed the existence of an “annealing window” for the first time. The as-cast film should be timely annealed within stage II (annealing window) before the formation of complex phases, in order to obtain a high-quality perovskite film. Intriguingly, the incorporating of Cs⁺ can significantly extend the annealing window by inhibiting the formation of complex phases, thereby improving the device performance and reproducibility. This work provides insightful guidelines for manipulating the perovskite crystallization pathways towards higher performance. Furthermore, in situ GIWAXS was employed to monitor the perovskite crystallization kinetics during the two-step spin-coating process, including a first step of depositing the PbI₂ layer and a second step of converting PbI₂ into perovskites with organic salts (e.g. MAI, FAI). It was found that incorporating Cs⁺ in the first step induced an alternative pathway from δ -CsPbI₃ to perovskite α -phase, which is energetically more favorable than the conventional pathways from PbI₂. However, the new phase transition caused an imbalance between the perovskite nucleation and crystal growth, resulting in pinholes in the film. Fortunately, introducing GA⁺ in the second step can promote crystal growth and eliminate pinholes, boosting efficiencies by over 23%. This work demonstrates an unprecedented advantage of the two-step process over the one-step process, allowing precise control of the perovskite crystallization kinetics by decoupling the crystal nucleation and growth processes.

Reference:

- 1) M. Qin, K. Tse, T.-K. Lau, Y. Li, C.-J. Su, G. Yang, J. Chen, J. Zhu, U.-S. Jeng, G. Li, H. Chen, and X. Lu*, Manipulating the Mixed-Perovskite Crystallization Pathway Unveiled by In Situ GIWAXS, *Adv. Mater.* **2019**, 31, 1901284.
- 2) M. Qin, H. Xue, H. Zhang, H. Hu, K. Liu, Y. Li, Z. Qin, J. Ma, H. Zhu, K. Yan, G. Fang, G. Li, U.-S. Jeng, G. Brocks, S. Tao*, and X. Lu*, Precise Control of Perovskite Crystallization Kinetics via Sequential A-site Doping, *Adv. Mater.*, **2020**, 32, 2004630.

9:45 PM EN05.18.03

Optoelectronic Functionality of the A-Site Cation in Prototypical Lead Halide Perovskites—Combined Synchrotron-Based Core Level Spectroscopy and Computational Studies Gabriel J. Man¹, Pabitra K. Nayak², Håkan Rensmo¹ and Sergei M. Butorin¹; ¹Uppsala University, Sweden; ²Tata Institute of Fundamental Research, India

Lead halide perovskite (HaP) materials of the form ABX₃ have attracted substantial global research interest for over a decade and commercial solar cell and light-emitting diode (LED) applications are starting to appear on the market [1]. The A-site cation (A-cation) can be an organic or inorganic cation (methylammonium, formamidinium, cesium), the B-site cation is lead in the most well studied HaPs, and the X-site cation can be iodide, bromide,

chloride. In spite of the recent research interest and a history of basic research dating back to as early as the 1970's, there are fundamental questions to be answered. One concerns the optoelectronic function of the A-cation [2]. Solar cell and mechanical nano-indentation studies suggest the A-cation does not play an optoelectronic role, while time-resolved photoluminescence studies suggest it does.

Here we report our findings that are relevant for unraveling this scientific mystery, utilizing the first application of core level spectroscopy to single crystals of HaPs. In the first part of my talk, I will present a comparative study of three archetypal lead bromide perovskite (APbBr₃) compounds using Br K-edge high energy resolution fluorescence detection X-ray absorption spectroscopy (HERFD-XAS) and simulated XAS spectra. We find a nearly linear correlation between relative Goldschmidt tolerance factor, a widely used structural descriptor that is affected by the size of the A-site cation, and the energetic width of the conduction band [3]. These findings are potentially relevant for understanding the mechanism of slow hot electron cooling in HaPs. Using Br K X-ray emission spectroscopy (XES), we find relative differences in lead-bromide bond ionicity. These results are potentially relevant for understanding the origin of A-cation-related trends in device-relevant energy levels, which are crucial for designing HaP device interfaces. In the second part of my talk, I will present a study which utilizes N K-edge Resonant Photoelectron Spectroscopy (RPES) to search for electronic coupling between the organic and inorganic sub-lattices of methylammonium lead tri-iodide (MAPbI₃), the prototypical hybrid organic-inorganic HaP. We find that the occupied states are weakly coupled, but find substantial coupling in the unoccupied states via the observation of normal Auger decay upon resonant excitation [4]. I will also talk briefly about findings from a complementary computational-oriented study [5]. Our studies challenge a notion based on previous studies that the A-cation is electronically inert.

References

- [1] <https://www.perovskite-info.com/companies-list/perovskite-application-developers>
- [2] Egger, D. A. *et al.* Adv. Mater. 2018, 30 (20), 1800691. <https://doi.org/10.1002/adma.201800691>.
- [3] Man, G. J. *et al.* A-Site Cation Influence on the Conduction Band of Lead Bromide Perovskites. In Manuscript 2021.
- [4] Man, G. J. *et al.* Electronic Coupling between the Organic and Inorganic Sub-Lattices of a Hybrid Organic-Inorganic Perovskite Single Crystal. arXiv 2020. <http://arxiv.org/abs/2011.02016>
- [5] Sterling, C. M. *et al.* J. Phys. Chem. C 2021, 125 (15), 8360–8368. <https://doi.org/10.1021/acs.jpcc.1c02017>.

10:00 PM EN05.18.04

Optical Gain Performance of Lanthanide-Based Chloride Double Perovskite in the Near Infrared Daniela Marongiu¹, Fang Liu¹, Stefano Lai¹, Fabio Manna², Maria Laura Mercuri², Michele Saba¹, Francesco Quochi¹, Andrea Mura¹ and Giovanni Bongiovanni¹; ¹Università di Cagliari, Italy; ²Università degli Studi di Cagliari, Italy

Codoping chloride double perovskites of general formula Cs₂Na_xAg_{1-x}InCl₆ with Bi³⁺ and Ln³⁺ (Ln = Yb,Er) ions is attracting increasing interest owing to the potential of this class of materials as broad-band phosphors across the visible and near infrared (NIR) spectrum [1-4]. Beside the application in phosphors, it is interesting to assess the suitability of these materials as NIR gain and laser media when lanthanide concentration is raised up towards the level of 100% at.

Here, we explore the optical performance of a number of Ln-based chloride double perovskites with special emphasis on Ln optical cross-sections, excited-state lifetimes and radiative efficiencies. We compare double perovskites' optical gain figures of merit with those of a conventional Ln-doped crystal, that is, yttrium aluminium garnet (YAG).

All chloride double perovskites were synthesized as polycrystalline powders by solvent evaporation of acidic solutions of precursor salts.

Cs₂Na_{0.8}Ag_{0.2}InCl₆ doped with Yb³⁺ and Er³⁺ at ~1% at. level displayed unprecedentedly long excited-state lifetimes of ~3 ms (Yb) and ~21 ms (Er), from which radiative efficiencies for the emissions at ~1030 nm (Yb) and 1530 nm (Er) were estimated to be ~60% and ~80%, respectively. In Cs₂NaYb_{0.9}Bi_{0.1}InCl₆ and Cs₂NaYb_{0.9}Bi_{0.1}InCl₆, where Ln concentration is ~3×10²¹ at/cm³ (equivalent to YAG doping level of ~20% at.), Ln emission lifetimes exhibited only a minor decrease to ~2.5 ms (Yb) and ~12 ms (Er), demonstrating that Ln concentration quenching processes are relatively ineffective in these materials.

Absorption and emission cross-section spectra, inferred from measurements of diffuse absorbance, allowed to estimate optical gain coefficients and, consequently, derive all-optical figures of merit for end-pumped lasing. These estimates were also done for reference laser crystals, Yb:YAG and Er:YAG [5]. Owing to the largely suppressed concentration quenching, chloride double perovskites effectively emerge as interesting materials for NIR solid-state lasers.

References

- 1 - J. Luo, *et al.*, *Nature* (2018), 563, 541
- 2 - G. Zhang, *et al.*, *Dalton Trans.* (2020), 49, 15231
- 3 - H. Arfin, *et al.*, *Angew. Chem. Int. Ed.* (2020), 59, 11307
- 4 - S. Yang, *et al.*, *J. Phys. Chem. C* (2021), 125, 10431
- 5 - F. Liu, *et al.*, in preparation.

10:15 PM EN05.18.05

Chiral Lead-Free (R/S-CHEA)₄Bi₂Br_xI_{10-x} (x = 0 to 10) Semiconductors with Color Tunable Circular Dichroism Shangpu Liu¹, Gregor Kieslich², Markus W. Heindl¹, Natalie Fehn², Aras Kartouzian², Ian Sharp¹ and Felix Deschler¹; ¹Walter Schottky Institut and Physik-Department, Technische Universität München, Germany; ²Fakultät für Chemie Technische, Universität München, Germany

Hybrid organic inorganic perovskites are optoelectronic materials with tunable chemical and electronic structures. Incorporating chiral organic molecules into perovskite networks also attracts great attention due to their potential optical communication applications. Nevertheless, most reported chiral perovskite materials possess high toxic Pb, which potentially limits their practical applications. Here, we introduce chiral organic molecules R/S-1-cyclohexylethylamine (R/S-CHEA) into lead-free bismuth based materials with perovskite motif, and grow color tunable chiral lead-free (R/S-CHEA)₄Bi₂Br_xI_{10-x} (x = 0 to 10) crystals and thin films. We perform single crystal XRD measurement and DFT calculation to identify their crystal structure and electronic band structure. We further investigate their optical properties. We find the absorption peak position is shifted from 386 nm to 493 nm, while Circular Dichroism (CD) signals can be turned widely from 366 nm to 535 nm, by changing the ratios of bromide and iodide anions in (R/S-CHEA)₄Bi₂Br_xI_{10-x}. Specifically, we employ steady-state and time-resolved PL spectra measurements on (R-CHEA)₄Bi₂Br₁₀ film, which has a broad emission peak located at around 520 nm and shorter lifetime compared with that of Cs₂AgBiBr₆. Besides, temperature and fluence dependent time-resolved PL spectra are also performed to investigate the charge carrier dynamics in (R-CHEA)₄Bi₂Br₁₀. Our demonstration of color tunable chiral lead-free perovskites gives the possibility to discover high performance and nontoxic optical spintronic materials.

10:30 PM EN05.18.06

Compositional Screening of Bi and Br Incorporation to Stabilize Black γ-CsPbI₃ Films via Pulsed Laser Deposition Wiria Soltanpoor¹, Yorick A. Birkholzer¹, Vivien Kiyek¹, Martin Ledinsky² and Monica Morales-Masis¹; ¹Mesa+ Institute for Nanotechnology, University of Twente,

Netherlands; ²Institute of Physics, Academy of Science of the Czech Republic, Czechia

Halide perovskites have lured enormous attention due their unique optoelectronic properties. However, the complex stoichiometry of stable halide perovskite compounds motivates the search for volatility- and solubility-insensitive deposition methods.

Pulsed Laser Deposition (PLD) is a versatile method capable of multi-element ablation off a solid target irrespective of its chemical complexity, allowing single-source deposition of complex halide perovskite compositions [1–3]. This relaxes concerns of thin film formation such as incompatible solubility issues with solution process or different elemental volatilities in the case of co-evaporation [4]. Here we use PLD to trigger the structural instability of CsPbI₃ at room temperature by partial replacement of Pb with Bi or that of I with Br. The link between the PLD parameters and the film crystallinity and morphology was investigated proving compact, smooth and highly crystalline black orthorhombic CsPbI₃. The stoichiometric control was implemented by the precursors molar concentration in the PLD target. The correlation between different levels of Bi concentration and the crystallinity, film stoichiometry, and optoelectronic structure of CsPbI₃ was monitored using X-ray diffractometry (XRD), X-ray fluorescence (XRF), photoluminescence and photothermal deflection spectroscopy (PDS) analyses. The incorporation of Bi in the structure of CsPbI₃ resulted in improved stability of the film up to 154 hours. In a similar fashion, introducing Br to CsPbI₃ resulted in films stable over 100 days.

The stabilization of halide perovskites through adding chemical species during PLD unlocks its grave potential in growing optimal halide perovskite films and optoelectronic devices. In addition, the solvent-free nature of PLD, nearly stoichiometric transfer, scalability, and control over the chemical composition and thickness, make this technique particularly interesting for composition screening of dopants and multicomponents, as well as to fabricate and study multi-layered solar cells such as all-perovskite tandem solar cells.

[1] U. Bansode, R. Naphade, O. Game, S. Agarkar, and S. Ogale, *Hybrid Perovskite Films by a New Variant of Pulsed Excimer Laser Deposition: A Room-temperature Dry Process*, *J. Phys. Chem. C* **119**, 9177 (2015).

[2] S. Cheng, Q. Chang, Z. Wang, L. Xiao, E. E. M. Chia, and H. Sun, *Observation of Net Stimulated Emission in CsPbBr₃ Thin Films Prepared by Pulsed Laser Deposition*, *Adv. Opt. Mater.* 2100564 (2021).

[3] V. M. Kiyek, Y. A. Birkhölzer, Y. Smirnov, M. Ledinsky, Z. Remes, J. Momand, B. J. Kooi, G. Koster, G. Rijnders, and M. Morales-Masis, *Single-Source, Solvent-Free, Room Temperature Deposition of Black γ -CsSnI₃ Films*, *Adv. Mater. Interfaces* **2000162**, 1 (2020).

[4] T. Soto-Montero, W. Soltanpoor, and M. Morales-Masis, *Pressing Challenges of Halide Perovskite Thin Film Growth*, *APL Materials*.

SESSION EN05.19: Perovskite Synthesis and Characterization I
Session Chairs: Mahshid Ahmadi, Mengxia Liu, Michael Saliba and Feng Yan
Wednesday Morning, December 8, 2021
EN05-Virtual

8:00 AM *EN05.19.01

Chirality and Structure-Property Tunability within Hybrid Metal Halide Perovskites [David B. Mitzi](#); Duke University, United States

Hybrid organic-inorganic perovskite (HOIP) semiconductors based on metal halide frameworks offer unprecedented opportunity to tailor structural and materials properties using the full flexibility afforded by the associated inorganic and organic components,^{1,2} and such tunability points towards wide-ranging potential for applications including solar cells, light-emitting devices, detectors, transistors and advanced computing devices. In this talk we will focus on the role that organic cation chirality can have on HOIP structure and properties including, for example, the impact on chiroptical and electrical transport (e.g., circularly polarized absorption and chirality-induced spin selectivity³), electronic structure (e.g., spin splitting of the conduction band⁴) and thermal properties (e.g., accessing a low-melting temperature and glassy state⁵). The above examples point to the great potential of using chirality for enabling and coupling control over light, charge and spin within the important HOIP semiconductor family.

References:

[1] B. Saparov, D. B. Mitzi, *Chem. Rev.* 116, 4558 (2016).

[2] D. B. Mitzi, *Prog. Inorg. Chem.* 48, 1 (1999).

[3] H. Lu, C. Xiao, R. Song, T. Li, A. E. Maughan, A. Levin, R. Brunecky, J. J. Berry, D. B. Mitzi, V. Blum, M. C. Beard, *J. Amer. Chem. Soc.* 142, 13030 (2020).

[4] M. K. Jana, R. Song, H. Liu, D. R. Khanal, S. M. Janke, R. Zhao, C. Liu, Z. V. Vardeny, V. Blum, D. B. Mitzi, *Nature Commun.* 11, 4699 (2020).

[5] A. Singh, M. K. Jana, D. B. Mitzi, *Adv. Mater.* 33, 2005868 (2021).

8:30 AM *EN05.19.02

Novel Film Annealing Process and Durable Perovskite Solar Cells [Huanping Zhou](#); Peking University, China

Recently, solution processed hybrid perovskites show intriguing electronic and optoelectronic properties applicable in various device application, and the developing of high quality materials with improved homogeneity and less defects is crucial. In this talk, I mainly focused on the rational design and fabricate perovskite films, and the construction of efficient and stable photovoltaic devices. Two related aspects are discussed: 1) Develop liquid medium annealing process that leads to the films with high crystallinity, less defects, desired stoichiometry, and overall film homogeneity, to achieve high performance photovoltaics with certified efficiency of 24.5%; 2) Propose methods such as "redox ion pair" and "multiple non-covalent bond synergistic effect" to suppress defect pairs in a sustainable way, which greatly improved the long-term stability of perovskite solar cells for over 2000 h under the stressors, e.g. light, heat, and electricity. Corresponding degradation mechanism of hybrid perovskite films and devices under operational conditions are revealed on the molecular and atomic scales.

9:00 AM *EN05.19.03

Molecular Additives in Perovskite LEDs—From Defect Passivation to Crystallization Manipulation [Feng Gao](#); Linköping Univ, Sweden

Metal halide perovskites have shown promising optoelectronic properties suitable for light-emitting applications. The development of perovskite light-emitting diodes (PeLEDs) has progressed rapidly over the past several years, and molecular additives have played an important role in these advances. By rational design of these molecular additives, we can significantly enhance the interaction with defects sites and minimize non-radiative recombination losses. In addition, we also demonstrate that the molecular additives can manipulate the perovskite crystallization and help to enhance the radiative recombination. As such, we have been able to demonstrate perovskite LEDs with high external quantum efficiencies over 20%. We find that our devices can also work efficiently in an emitting/detector switchable mode, with tens-megahertz speed for both functions. We further demonstrate the potential of

the dual-functional diode for biomedicine diagnosis applications (as a monolithic heart pulse sensor) and for inter- and intra-chip bidirectional optical communications.

9:30 AM EN05.19.04

Large Area Defects Compensation for Highly Efficient and Stable Formamidinium-Cesium Perovskite Solar Modules Yehao Deng^{1,2} and Jinsong Huang¹; ¹University of North Carolina at Chapel Hill, United States; ²Perotech Inc., United States

After several years of rapid development of scalable printing of perovskites thin films, the obtainable film morphologies have been well optimized with desired smoothness, compactness, and full coverage on substrates, which are all indispensable for making a good solar cell. Now the next step is scalable defect controlling for further promoting the solar cell efficiency and stability. Two important issues arise:

- (1) What types of defects are detrimental to perovskite solar cells? How do they impact efficiency or stability?
- (2) How can we eliminate such defects with scalable, industry-compatible process?

This talk will discuss our recent efforts in answering these two questions. We start with formamidinium-cesium perovskite, which are known to be thermally more stable than methylamine perovskite. However, the former is found to be less photostable. We studied the light-induced degradation mechanism and found that it is the generation of iodine interstitials that capture photo-generated holes and degrade the solar cell photocurrent. We investigated the mechanism of iodine interstitial generation process and invented a defect compensation strategy by choosing a slightly AX (A is formamidinium or cesium cation and X is iodine) excessive composition to effectively suppress the process. Eventually, we improved the large area perovskite solar module's photostability with the highly-industry-compatible defect compensation strategy.

9:45 AM EN05.19.05

New Deposition Method for Pb-Free Halide Perovskite Thin Film, with Tunable Bandgap and Improved Stability Adi Kama, Anat Itzhak and David Cahen; Bar Ilan University, Israel

Pb-based halide perovskite, HaP, single-junction solar cells have improved dramatically to over 25% for small laboratory cells. Considering the toxicity of lead ions, substituting Pb with other non-toxic elements in the perovskite structure has become one of the most significant challenges associated with these materials. In this work, we replace Pb with Sn + Ge in an all-inorganic HaP for improved stability, focussing on $\text{CsSn}_x\text{Ge}_{1-x}\text{Br}_3$. We do so by using a new deposition technique for thin film formation. The choice of Br as the halide is influenced by the fact that we have (much) smaller divalent cations on the B site. Naturally, doing so leads to a larger bandgap than the corresponding iodide, with enhanced environmental stability, already aided by having inorganic Cs instead of organic cations. X-Ray Diffraction results show that $\text{CsSn}_x\text{Ge}_{1-x}\text{Br}_3$ forms a homogeneous solid solution, and up to 70% Ge, maintains the cubic structure of pure CsSnBr_3 with a shift to smaller lattice spacings with increasing Ge concentration. The optical bandgap is found to be tunable from 1.7 eV to 2.3 eV, from pure Sn to pure Ge, respectively. In N_2 atmosphere, the stability of the mixed Sn-Ge HaP is improved compared to that of the pure Sn one.

SESSION EN05.20: Perovskite Synthesis and Characterization II
Session Chairs: Mahshid Ahmadi, Mengxia Liu, Michael Saliba and Yuanyuan Zhou
Wednesday Morning, December 8, 2021
EN05-Virtual

10:30 AM *EN05.20.01

Correlating Complex Synthesis with Defect Formation in Wide Bandgap Perovskites Carolin M. Sutter-Fella; Lawrence Berkeley National Laboratory, United States

Wide bandgap mixed-halide perovskites as the top absorbers in tandem solar cells typically exhibit a larger voltage deficit in contrast to their corresponding tri-iodide-based perovskites. With this work we are tackling the challenge of directly correlating the multi-stage synthesis of bromide-containing perovskites with optoelectronic properties and consequently device performance. Our results show that the incorporation of bromide occurs via a halide homogenization process where the perovskite composition transitions from an initial bromide-rich phase to the final target stoichiometry. In situ photoluminescence measurements during synthesis reveal that bromide inclusion alters the formation dynamics. By combining experiments with first-principle calculations we suggest that the formation of $\text{FAMACsPb}(\text{I}_{1-x}\text{Br}_x)_3$ starts with the nucleation of a bromide-rich phase from solution during supersaturation followed by a retarded growth stage. The retarded growth stage is associated with a halide homogenization process that brings the composition of crystallized material to the target stoichiometry. This homogenization process not only changes the formation dynamics of mixed-halide perovskites but also promotes defect formation, which consequently leads to increased non-radiative recombination losses in the final perovskite film and thus, could explain the larger voltage deficit.

11:00 AM EN05.20.04

Emission Properties of Double Perovskites with Alloyed Bi and Ag Fang Liu¹, Daniela Marongiu¹, Angelica Simbula¹, Stefano Lai¹, Alessio Filippetti^{1,2}, Francesco Quochi¹, Andrea Mura¹, Giovanni Bongiovanni¹ and Michele Saba¹; ¹Universita di Cagliari, Italy; ²Istituto Officina dei Materiali (CNR - IOM), Italy

Lead-free halide perovskites have gained interest in competition to the lead-based counterparts which are affected by toxicity and instability over moisture. Among them, double perovskites have been developed to alternatively substitute the divalent cations Pb^{2+} in single perovskite with a combination of a monovalent and trivalent cation, forming structure as $\text{A}_2\text{BB}'\text{X}_6$.

Here we report the highly stable $\text{Cs}_2\text{Na}_{1-x}\text{Ag}_x\text{In}_{1-y}\text{Bi}_y\text{Cl}_6$ compounds, with Silver (x) and Bismuth (y) fractions ranging from 10% to 1 ppm, that exhibit efficient and stable broadband, white-light emission ideally suited for lighting applications.

Double perovskites were synthesized in small crystals by a super-saturation precipitation method followed by filtration and their photoluminescence quantum yield (PLQY) was measured. The highest PLQY was found to be very close to 100% and the optical properties of the crystals were studied by a combination of time resolved photoluminescence and differential transmission, in order to establish the nature of the light-emitting excited states. The measurements confirmed that emission is produced by self-trapped exciton states; the two key elements to achieve such outstanding emission properties are Bi, whose 6p states enhance the lifetime for electrons in the conduction band, and Ag, with 4d states at the top of the valence band allow efficient radiative recombination of excitons. A systematic study as a function of Bi and Ag content was employed to reveal the diffusion length for optical excitations, localization processes as well as the intrinsic limits for the excited state lifetime.

The results provide guidance for rational optimization of such compounds in view of the use as phosphors and active materials for LEDs and displays.

11:15 AM EN05.20.05

Late News: Unraveling the Surface States of Photovoltaic Perovskite Thin Film [Rui Wang](#)^{1,2}; ¹Westlake University, China; ²University of California, Los Angeles, United States

Semiconductor surfaces play an important role in the behavior of their electronic devices. The vulnerable lattice of metal-halide perovskite renders a fragile surface, where defect states can easily form. Very recently, most of the highly efficient perovskite optoelectronic devices have been reported to employ effective surface passivation strategies, further confirming the significance of surface states in regulating their device performance. Here, we present methodical studies towards understanding the surface states in perovskite thin films utilizing a strategy of molecular “defect indicator” that is able to interact with specific surface defects. In formamidinium (FA)-methylammonium (MA) mixed cation perovskite thin films, a nonuniform distribution of cations is uncovered with FA cations being close to the top and MA close to the bottom of the film, leading to unique surface defect energetics. Antisite FA_i was found to become a dominant deep trap on the surface of this system.

11:30 AM EN05.20.06

In Depth Study of Complex Perovskite-Solvent Interactions by *In Situ* Photoluminescence Spectroscopy [Mehmet Derya Özeren](#), [Bea Botka](#), [Áron Pekker](#) and [Katalin Kamarás](#); Wigner Research Centre for Physics, Hungary

Lead halide perovskites have undergone rapid developments in recent years to become well established semiconductors for future optoelectronic applications. These advancements are achieved through the understanding of the solution and surface chemistry of perovskites. A selection of functional molecules lead to better control of the film formation dynamics and passivation of surface and bulk defects. These molecules are capable to form coordinate bonds, known as Lewis acid/base interactions, with perovskites. Especially Lewis bases are in the centre of attention, because they have a great impact on the performance: they promote long term stability, heal surface defects and improve the morphology of the films. However, some solvents (e.g. water) which passivate perovskite defects can cause degradation upon longer exposure. This indicates a more complex interaction which needs to be explored.

Photoluminescence (PL) is a simple and effective tool that allows us to track interactions between perovskite and reactive molecules in a controlled environment. We have evaluated by in-situ PL measurements a variety of solvents that are commonly used in perovskite processing to understand photobrightening and photodegradation responses regarding the interactions between the functional groups and the surface. Establishing the mechanism behind these interactions will provide a better understanding on how the stability of perovskites can be improved.

11:45 AM EN05.20.08

Spatially Resolving the Inhomogeneous Degradation in Perovskite Solar Cells Using Electroluminescence Mapping [Zahrah S. Almutawah](#)^{1,2}, [Tamanna Mariam](#)^{1,2}, [Prabodika N. Kaluarachchi](#)^{1,2}, [Kshitiz Dolia](#)^{1,2}, [Abdul Quader](#)^{1,2}, [Zhaoning Song](#)^{1,2}, [Adam J. Phillips](#)^{1,2}, [Yanfa Yan](#)^{1,2} and [Michael J. Heben](#)^{1,2}; ¹Wright Center for Photovoltaics Innovation and Commercialization, School for Solar and Advanced Renewable Energy, Department of Physics and Astronomy, University of Toledo, United States; ²University of Toledo, United States

Electroluminescence (EL) mapping technique is a non-contact, non-destructive, fast, and simple testing method that spatially resolves the inhomogeneity in the electrical and optical properties of solar cells and detects micro-cracks or pinholes. It is an essential diagnostic tool for the quality control of commercial solar cells and modules. However, it is less commonly used for characterizing small-sized thin-film solar cells fabricated in laboratories.

Here, we assemble a fast EL imaging system with a high spatial resolution of ~1 μm/pixel to investigate the inhomogeneity and decomposition processing in a variety of perovskite solar cells (PSCs) with different absorber layer compositions and device configurations. We observe that most high-efficiency (>22%) PSCs show uniform and bright EL signals, while defective cells exhibit weak and spatially non-uniform EL intensity. Under different aging conditions (e.g., electric field, thermal stress, humid air, light soaking, etc.), PSCs with different absorber compositions exhibit different degradation behaviors. To explore the degradation mechanism in detail, we quantitatively compare the spatially-resolved and time-resolved EL images of FA/Cs-based PSCs with different Cs contents ranging from 0 to 40% aged in humid air with controlled humidity. Interestingly, we find that the perovskites with a high Cs content (>20%) exhibit more severe phase segregation and faster degradation in humid air, while the perovskites with too little Cs (< 10%) are phase-unstable and lose EL signal rapidly. The findings shed light on compositional engineering to enable uniform, efficient, and stable PSCs.

SESSION EN05.21: Advancing Perovskite Devices III

Session Chairs: [Mahshid Ahmadi](#), [Michael Saliba](#) and [Yuanyuan Zhou](#)

Wednesday Afternoon, December 8, 2021

EN05-Virtual

1:00 PM *EN05.21.01

Optical Design for High-Efficiency White Perovskite LEDs [Hin-Lap Yip](#)^{1,2}, [Ziming Chen](#)² and [Zhenchao Li](#)²; ¹City University of Hong Kong, Hong Kong; ²South China University of Technology, China

Metal halide perovskite light-emitting diodes (PeLEDs) show great potentials to be the next-generation lighting technology, with external quantum efficiencies (EQEs) exceeding 20% for infrared, red and green LEDs. However, the efficiencies of blue and white devices severely lag behind. To improve the performance of blue PeLEDs, we employed an integrated strategy combining dimensional engineering of perovskite film and recombination zone modulation in the LED device to obtain an EQE up to 5%.^[1] While further incorporating the strategy of interfacial engineering, highly efficient blue PeLEDs with EQEs over 10% have been successfully realized in our group, establishing an excellent platform for white-light emission. In our latest work, we demonstrated efficient white PeLEDs by optically coupling a blue PeLED with a red emitting perovskite nanocrystal layer in an advanced device structure, which allows to extract the trapped optical modes (waveguide and SPP modes) of blue photons in the device to the red perovskite layer via near-field effects. As a result, a white PeLEDs with EQE over 12% is achieved, which represents the state-of-the-art performance for white PeLEDs.^[2]

References:

[1] Z. Li, Z. Chen, H.-L. Yip et al. *Nat. Commun.* 2019, 10, 1027

[2] Z. Chen, Z. Li, H.-L. Yip et al. *Joule* 2021, 5, 456

1:30 PM *EN05.21.02

Surface Passivation of Metal Halide Perovskites for Optoelectronics Biwu Ma; Florida State University, United States

Metal halide perovskites have attracted tremendous attentions as new generation functional materials for applications in a variety of optoelectronic devices, such as solar cells and light emitting diodes (LEDs), owing to their exceptional optical and electronic properties, as well as low temperature solution processability. While remarkable progresses have been achieved for highly efficient perovskite solar cells (PSCs) and LEDs (PeLEDs) during the last decade, numerous issues and challenges remain, including stability, lead toxicity, large scale manufacturing, etc. To achieve high efficiency and stability simultaneously, surface passivation of perovskite thin films and nanocrystals by organic/inorganic species is one of the most effective approaches, which could not only reduce surface defects, but also protect the surface from atmospheric moisture. In this talk, I will discuss our recent efforts on the development and study of various types of surface passivation agents for halide perovskite thin films and nanocrystals, with which highly efficient and stable PSCs and PeLEDs are achieved. For instance, a low-cost industrial organic pigment, quinacridone (QA), has been investigated as surface passivation agent for PSCs by solution processing of a soluble QA derivative followed by thermal annealing to convert it into insoluble QA. Passivation with strong interactions between QA and metal halides, together with the hydrophobicity of QA coating, enabled highly efficient PSCs with remarkable stability.

2:00 PM EN05.21.04

Double N-Type Interconnection Structure of C_{60}/SnO_{2-x} for Efficient and Stable All-Perovskite Tandem Solar Cells Zhenhua Yu and Jinsong Huang; University of North Carolina at Chapel Hill, United States

The efficiencies of all-perovskite tandem devices are improving quickly. However, their complex interconnection layer (ICL) structures – with typically four or more layers deposited by different processes – limit their prospects for applications. Here, we report an ICL in all-perovskite tandem cells consisting merely of a fullerene layer and a SnO_{2-x} ($0 < x < 1$) layer. The C_{60} layer is unintentionally n-doped by iodine ions from the perovskite and thus acts as an effective electron collecting layer. The SnO_{2-x} layer, formed by the incomplete oxidation of tin ($x=1.76$), has ambipolar carrier transport property enabled by the presence of a large density of Sn^{2+} . The $C_{60}/SnO_{1.76}$ ICL forms Ohmic contacts with both wide and narrow bandgap perovskite subcells with low contact resistivity. The ICL boosts the efficiencies of small-area tandem cells (5.9 mm^2) and large-area tandem cells (1.15 cm^2) to 24.4% and 22.2%, respectively. The tandem cells remain 94% of its initial efficiency after continues 1-sun illumination for 1,000 hours. The efficiency of all-perovskite tandem solar cell is further improved to beyond 25% by increasing the carrier diffusion length of Sn-Pb NBG perovskite to $\sim 2 \mu\text{m}$ via doping modification.

2:15 PM EN05.21.05

High Carrier Mobility Hybrid Organic–Inorganic Perovskites Quantum Wells Pan P. Adhikari¹, Yao Gao², Chendi Xie¹, Letian Dou² and Jianbo Gao¹; ¹Clemson University, United States; ²Purdue University, United States

In contrast to the traditional inorganic semiconductors quantum wells, solution-processed hybrid organic–inorganic perovskites (HOIP) quantum wells, as emergent new materials, can be a vital player in optoelectronics such as solar cells, LEDs, transistors, and photodetectors. The molecular engineering of organic semiconductors, combining with the composition engineering of monolayer perovskites offer the tunability of electrical and optical property. In this report, we investigate the carrier transport dynamics of the (4Tm)2PbI₄ and (4Tm)2SnI₄, where 4Tm is a π -conjugated oligothiophene ligand of 2-(3''',4'-dimethyl-[2,2':5',2'':5''-quaterthiophen]-5-yl)ethan-1-ammonium. By using the state-of-the-art ultrafast photocurrent spectroscopy with a sub-20 ps time resolution, the (4Tm)2PbI₄ and (4Tm)2SnI₄ HOIP quantum wells demonstrate $> 10 \text{ cm}^2/\text{Vs}$ carrier mobility, and the transport dynamics can be described by a band-like transport mechanism with a rapid trapping time of 60 ps after photoexcitation. Our work demonstrate the promising applications of HOIP quantum well in high-speed photodetection and optical quantum communication.

2:30 PM en05.12.06

The Non-Innocent Role of HTMs in Perovskite Solar Cell Development—The Case of CuSCN Francesco Lamberti¹, Min Kim², Gaudenzio Meneghesso¹, Silvia Gross¹, Annamaria Petrozza³ and Teresa Gatti⁴; ¹University of Padova, Italy; ²Jeonbuk National University, Korea (the Republic of); ³Istituto Italiano di Tecnologia, Italy; ⁴Justus-Liebig-Universität Giessen, Germany

The development of novel hole transporting materials (HTMs) which can improve the stability of lead-halide perovskite solar cells (PSCs) operating in ambient conditions is a valuable strategy to address the future commercialization of this ultra-cheap photovoltaic technology. Among other HTMs, we have identified poly(3-hexylthiophene) (P3HT), a highly soluble and easy-to-process from solution semiconducting polymer, to be a good compromise for ensuring decent efficiencies to PSCs at relatively low-costs in comparison with the benchmark HTM based on the Spiro-OMeTAD small molecule. Spiro-OMeTAD indeed requires doping with LiTFSI and tert-butyl pyridine additives to be sufficiently active for hole transport and, in this regard, we have recently demonstrated an up-to-now unknown mechanism of de-doping induced by the latter additive, that we will discuss in this contribution.[1] We then looked for other possible nanomaterials to couple with P3HT for the development of even more efficient HTMs and stable PSCs. We will thus discuss here the outcomes of our most recent contribution, [2] in which we suggest that a CuSCN nanoplatelets/P3HT composite, combining hole extraction and transport properties with water oxidation activity, transforms incoming water molecules and triggers the in situ p-doping of the conjugated polymer, improving transport of photocharges. Insertion of the nanocomposite into a lead perovskite solar cell with a direct photovoltaic architecture causes stable device performance for 28 days in high-moisture conditions. Our findings demonstrate that the engineering of a hole extraction layer with water-splitting additives could be a viable strategy to reduce the impact of moisture in perovskite devices. References [1] F. Lamberti et al. Chem 2019, 5, 1; [2] M. Kim et al., T. Gatti, F. Lamberti Commun. Mater. 2021, 2, 6

SESSION EN05.22: On-Demand
Sunday Morning, December 5, 2021
On-Demand

8:00 AM EN05.08.10

Stable Ambient Processed Mixed-Cation Perovskite Solar Cells Ivy M. Asuo¹, Riad Nechache¹, Sylvain G. Cloutier² and Alain Pignolet¹; ¹INRS, Canada; ²École de Technologie Supérieure, Canada

The fabrication of stable and efficient halide perovskite solar cells under ambient conditions is a formidable challenge due to the sensitivity of halide perovskites to moisture, oxygen, and thermal stress effects ¹⁻⁴. In order to simplify the synthesis processes and consequently bring down the production cost, there is an imperative interest to develop a method for fabricating perovskite solar cells with long term stability under ambient conditions. This work presents a method for synthesizing efficient and stable mixed-cation halide perovskites by tuning their physical and microstructural properties entirely under ambient conditions. We highlight the essential contribution of lead thiocyanate additives and solvent treatment in the fabrication of

perovskite thin films and the very promising performance and stability of their solar cells made using this method^[4,5]. The developed approach leads to a significant improvement of both the morphology and the crystallinity of the films. As a result, the optimized solar cells without encapsulation retained ~80% of their initial performance after ten months of storage, resulting in a lifetime T_{80} of approximately 5000 hours (i.e., ~7 months). Our findings suggest that the efficiency and stability of the perovskite solar cells are highly dependent on the processing conditions, thin film morphology, trap density, and carrier mobility in the device before and after storage. The ability to develop these perovskite solar cells entirely under ambient conditions coupled with their high performance paves the way towards the industrial production of low-cost, efficient, and long-term stable solar cells.

References

- [1] N. Arora, M. I. Dar, A. Hinderhofer, N. Pellet, F. Schreiber, S. M. Zakeeruddin, M. Grätzel, *Science* **2017**, 358, 768.
- [2] L. K. Ono, Y. Qi, S. (Frank) Liu, *Joule* **2018**, 2, 1961.
- [3] D. Bryant, N. Aristidou, S. Pont, I. Sanchez-Molina, T. Chotchunangatchaval, S. Wheeler, J. R. Durrant, S. A. Haque, *Energy Environ. Sci.* **2016**, 9, 1655.
- [4] I. M. Asuo, D. Gedamu, N. Y. Doumon, I. Ka, A. Pignolet, S. G. Cloutier, R. Nechache, *Mater. Adv.* **2020**, 1, 1866.
- [5] I. M. Asuo, S. Bouzidi, I. Ka, F. Rosei, A. Pignolet, R. Nechache, S. G. Cloutier, *Energy Technol.* **2021**, 9, DOI: 10.1002/ente.202000791.

8:15 AM EN05.09.15

Late News: Colloidal Synthesis of Lead-Free Cs₂TiBr_{6-x}I_x and Cs₂Ti_{1-x}Sn_xI₆ Vacancy-Ordered Perovskite Nanocrystals Shanti Maria Liga¹ and Gerasimos Konstantatos^{1,2}; ¹ICFO, Spain; ²ICREA, Spain

Perovskites now play a pivotal role as an emerging class of semiconductors after their first introduction in solar cells in 2009, but their commercialization has been hindered so far by the toxicity of lead and by their instability. For this reason, in the last few years, part of the perovskite community has focused on the search for alternative elements to lead that are not a threat to the environment and that can produce a stable perovskite structure. Vacancy-ordered halide perovskites, with general formula $A_2B^{+4}X_6$, are one of the alternative structures that have been designed to replace Pb^{2+} with non-toxic tetravalent cations. Among these, cesium titanium(IV) bromide perovskite is an environmentally friendly material that has attracted attention in the last three years for its application in solar cells with power conversion efficiencies reaching 3.3% [1]. However, a solution method suitable for the preparation of thin films has not yet been developed. We present here the first colloidal synthesis of pure and mixed bromide-iodide cesium titanium perovskite nanocrystals (NCs), carried out using the hot-injection method [2]. With this method, we were able to synthesize stable solutions of mixed bromide/iodide $Cs_2TiBr_{6-x}I_x$ NCs that can be easily deposited as thin films. In our approach, titanium and cesium organic salts are dissolved in octadecene with oleic acid and a zwitterionic ligand and react at 140 °C with a mixture of trimethylsilyl bromide and trimethylsilyl iodide. The resulting perovskite NCs show the expected cubic structure, with lattice parameter increasing with the higher amount of iodide in the structure, and exhibit bandgap tunability from 2.3 eV to 1.2 eV going from a pure bromide to a pure iodide perovskite. Moreover, we have observed that the method used to quench the reaction plays a fundamental role in determining the shape of the NCs. Finally, we measured that the Cs_2TiBr_6 NC films are stable for 1 hour at 100 °C and after 4 hours of UV light irradiation in a nitrogen atmosphere. However, they decompose quickly in air. Their fast decomposition in air motivated us to look for strategies to stabilize them. Since cesium tin(IV) halide perovskites have the same crystal structure as cesium titanium(IV) halide perovskites and are stable in air, we decided to replace partially or fully the titanium with tin, using the same synthetic method developed for pure titanium vacancy-ordered perovskites. A series of new materials, namely mixed titanium-tin $Cs_2Ti_{1-x}Sn_xI_6$ vacancy-ordered perovskite nanocrystals, was synthesized and characterized. The lattice parameter slightly increases from a pure titanium to a pure tin perovskite, going from 11.5 Å to 11.7 Å, and the bandgap increases up to about 1.55 eV when replacing all the titanium with tin.

[1] Chen, M., Ju, M. G., Carl, A. D., Zong, Y., Grimm, R. L., Gu, J., ... & Pature, N. P., *Joule*, 2018, 2(3), 558-570.

[2] Liga, S. M., and Konstantatos, G., *J. Mater. Chem. C*, 2021, DOI: 10.1039/d1tc01732b.

SYMPOSIUM EN06

Sustainable Electronics—Green Chemistry, Circular Materials, End-of-Life and Eco-Design
December 1 - December 8, 2021

Symposium Organizers

Francesca Iacopi, University of Technology Sydney

Christine Luscombe, University of Washington

Federico Rosei, Université du Québec

Clara Santato, Ecole Polytechnique de Montreal

* Invited Paper

SESSION EN06.01: Electronics Energy I
Session Chair: Clara Santato

10:30 AM EN06.01.02

Low Voltage Edible Electronic Devices—Organic Transistors and Circuits Based on Natural Electrolytes Alina Sharova^{1,2} and Mario Caironi¹; ¹Istituto Italiano di Tecnologia, Italy; ²Politecnico di Milano, Italy

Edible electronics is an evolving field of research whose ultimate goal is to develop a new class of microelectronic devices that are edible. The concept of this unconventional approach implies the use of natural and food-based materials, and their electronic properties for realization of safe for ingestion devices. The unique combination of electronic functionality, low cost, and safety for both human and environment suggests broad application opportunities for smart medications and food safety monitoring.

In this framework, we explore the potential of natural edible substances, honey and chitosan, to be used as electrolytic gate dielectrics in complementary organic transistors and integrated logic circuits, namely, inverting logic gates and ring oscillators. Low voltage operation in air < 1 V and compatibility with both hole and electron transporting materials are the feature characteristics of the designed devices. In addition, a strong responsivity of the devices to relative humidity levels suggests their possible use as humidity indicators, in perspective, for moisture monitoring of dried or dehydrated food. Lastly, we realize the arrays of lightweight fully printed devices on edible flexible and conformable substrates.

10:45 AM EN06.01.03

Late News: All-Polymer Field Effect Transistors Printed on Biodegradable Substrates Fabrizio A. Viola, Elena Stucchi and Mario Caironi; Italian Institute of Technology, Italy

The growing demand of disposable electronics raises serious concerns for the corresponding increase amount of electronic waste (e-waste), with severe environmental impact. Organic and flexible electronics have been proposed long ago as a more sustainable and energy efficient technological platform with respect to established ones. Yet, such technology is inevitably leading to a drastic increase of plastic waste if common approaches for flexible substrates are followed. In this scenario, biodegradable solutions can significantly limit the environmental impact, actively contributing to eliminate the waste streams (plastic or electronic) associated with disposal of devices. However, achieving suitably scalable processes to pattern mechanically robust organic electronics onto largely available biodegradable substrates is still an open challenge. In this work, all-organic and highly flexible field-effect transistors, inkjet printed onto biodegradable and compostable substrates (such as commercial Mater-Bi and polyhydroxybutyrate - PHB - biopolymer) are demonstrated. The degradation behavior of the final system shows unaltered biodegradability level. Furthermore, the electrical characterization of the devices showed a proper current modulation, which remained almost unaltered also after intensive mechanical stresses as bending and rolling. Such mechanical stability and flexibility together with the biodegradability, make these devices great candidates for new demanding applications in the field of biomedical electronics or food packaging. These results represent a promising step toward sustainable flexible and large area electronics, combining energy and materials efficient processes with largely available biodegradable substrates.

11:00 AM EN06.01.04

Evidence of Exclusive Electronic Transport in Sepia Melanin Ink-Printed Films Manuel Reali¹, Anthony Camus¹, Mike Rozel² and Clara Santato¹; ¹Polytechnique Montréal, Canada; ²Institute of Graphic Communication and Printability, Canada

Over the last few years, the terrific technological advancements in the field of electronics paralleled by higher purchasing power, large scale urbanization and industrialization, shorter lifetime and replacing cycles, lead to the generation of unbearable amounts of Waste Electrical and Electronics Equipment (E-Waste).^{1,2} Only in 2019, 53.6 Mt of E-Waste were produced worldwide and such amount is expected to growth up to 74.7 Mt by 2030.¹ E-Waste contains toxic elements that if buried in landfill or inhaled, can seriously put in danger the health of the current and future generations.

A paradigm shift from linear to circular economy, focusing on eco-design, durability, refurbishment and recycling is needed.^{3,4} A viable route to reduce the carbon footprint of electronics is the development of Sustainable Green Organic Electronics, using ubiquitous biosourced (bioinspired), biocompatible, compostable and possibly biodegradable materials.⁵ Among the biosourced materials available in nature, eumelanin is one of the most fascinating.⁶ The synergy between electronic conjugation (alternance of single-double carbon bonds) and hydration dependent electrical response, make eumelanin a mixed protonic-electronic conductor.⁷⁻¹⁰ Furthermore, eumelanin is a quinone-based redox active biopigment, which makes it an ideal candidate for energy storage applications.¹¹ However, the poor solubility of eumelanin in the majority of organic solvents is a real setback and often limiting its range of applications. Herein, we report on a green ink formulation method to fabricate Sepia melanin films from powders extracted from *Sepia Officinalis* cuttlefish ink. Our ink-formulation leads to a reproducible, effective printing of Sepia melanin on flexible substrates (i.e. polyethylene terephthalate (PET), paper) and carbon paper. Sepia ink can be also spin-coated and/or brushed on several patterned substrates. Sepia melanin films exhibit high electrical conductivity and environmental stability. Our results open the debate whether Eumelanin features exclusive electronic transport under certain conditions. Work is in progress to study structural aggregation of Sepia particles in the ink to shed light onto the efficient charge carrier transport properties herein observed.

References:

- 1 V. Forti, C. P. Baldé, R. Kuehr and G. Bel, *The Global E-waste Monitor 2020: Quantities, Flows, and the Circular Economy Potential*, 2020.
- 2 C. P. Balde, V. Forti, V. Gray, R. Kuehr and P. Stegmann, *The Global E-waste Monitor 2017. Quantities, Flows and Resources.*, United Nation University, 2017.
- 3 H. Zhao, D. Waughray, D. M. Malone, J. Msuya, G. Ryder, P. Bakker, N. Seth, L. Yong and R. Payet, *World Econ. Forum*, 2019, 1–24.
- 4 M. Meloni, F. Souchet and D. Sturges, *Ellen MacArthur Found.*, 2018, 1–17.
- 5 S. Irimia-Vladu, M., Glowacki, E. D., Sariciftci, N. S. & Bauer, *Green Materials for Electronics*, Wiley-VCH, Weinheim, Germany, 2018.
- 6 M. Reali, P. Saini and C. Santato, *Mater. Adv.*, 2021, **2**, 15–31.
- 7 M. Reali, A. Gouda, J. Bellemare, D. Ménard, J. M. Nunzi, F. Soavi and C. Santato, *ACS Appl. Bio Mater.*, 2020, **3**, 5244–5252.
- 8 A. B. Mostert, B. J. Powell, I. R. Gentle and P. Meredith, *Appl. Phys. Lett.*, 2012, **100**, 1–3.
- 9 M. Sheliakina, A. B. Mostert and P. Meredith, *Adv. Funct. Mater.*, 2018, 1805514.
- 10 M. Reali and C. Santato, in *Handbook of Nanoengineering, Quantum Science and Nanotechnology*, ed. S. E. Lyshevski, CRC Press, 1st edn., 2019, pp. 101–113.
- 11 A. Gouda, S. R. Bobbara, M. Reali and C. Santato, *J. Phys. D. Appl. Phys.*, 2020, **53**, (4), 043003.

11:15 AM EN06.01.05

High Performance Organic Electronic Devices Based on a Green Hybrid Dielectric Mathieu Tousignant, Nicole Rice, Jukka Niskanen and Benoit Lessard; University of Ottawa, Canada

Smart packaging has become a multi billion-dollar industry that relies on the integration of flexible and inexpensive sensors within product packaging to provide critical quality assurance information such as temperature and humidity. However, these sensors need to be flexible, biodegradable, and low cost in order to be incorporated into a wide variety of packaging.¹

One way to address these issues is by using organic thin film transistors (OTFTs) which are fabricated using carbon-based active materials, can be integrated onto flexible substrates, and have found many sensing applications. The dielectric is one of the active layers within an OTFT. It facilitates charge accumulation at the organic semiconductor interface when a source-gate voltage is applied. The ideal dielectric should have low leakage currents and a high dielectric constant. Unfortunately, most polymer dielectrics that meet these requirements are not environmentally friendly.

Poly(vinyl alcohol) (PVA) is a biodegradable, water soluble, high-k dielectric polymer however it is moisture sensitive, has poor film forming properties with large leakage currents. Recently we found that the film forming capabilities could be improved through the addition of low weight percentages of cellulose nanocrystals which increase the viscosity of the solutions.² Building upon these findings, a thin layer of polycaprolactone (PCL) was deposited on top of our PVA dielectric to reduce the moisture sensitivity and leakage currents of PVA. PCL is a hydrophobic, biodegradable, low-K polymer with good insulating properties. The PCL layer was functionalized with toluene diisocyanate (TDI). The functionalized TDI-PCL can then be thermally cross-linked to the hydroxyl groups of PVA at the TDI-PCL/PVA interface. Crosslinking at the bilayer interface increased the thin film stability and facilitated orthogonal processing of the semiconducting layer. TDI-PCL/PVA metal-insulator-metal capacitors were fabricated and found to be highly stable, even after being exposed to 95% relative humidity, unlike pure PVA based devices. Finally, the TDI-PCL/PVA dielectric was used in the fabrication of single walled carbon nanotube top gate bottom contact OTFTs. The TDI-PCL/PVA dielectric showed greater average mobilities of 0.42 cm²/Vs compared to 0.032 cm²/Vs for PVA, a reduced average hysteresis, better output curve saturation, a negative threshold voltage shift and greater on/off ratios with a lower device variation. When compared against silicon dioxide the TDI-PCL/PVA dielectric had a six-fold decrease in operating voltage for both the output and transfer curves. These results demonstrate a novel method for incorporating a green bilayer dielectric in high performing OTFTs while mitigating challenges associated with thin film processing and moisture sensitivity.

1 Chen, S. *et al. J. Food Sci.* 85, 517–525 (2020)

2 Tousignant, M. N. *et al. Langmuir* 36, (2020)

11:30 AM EN06.01.06

Facile Fabrication of Multifunctional and Transient All-PVA Based Green Electronics Mete Batuhan Durukan, Melih O. Cicek, Doga Doganay, Mustafa C. Gorur, Simge Cinar and Husnu E. Unalan; Middle East Technical University, Turkey

Over the last decade, rapid progress in wearable devices including consumer electronics and healthcare monitoring devices resulted in an excessive increase in electronic waste. Hazardous content and limited recyclability of these electronic devices is a great threat to the environment. Thus, research and development on the “green” electronics with non-hazardous materials and facile, low-cost fabrication is a must. This requirement paved a way for a new emerging field; transient electronics. Transient electronics disintegrates at the end of their use or when it is required with almost zero waste. To achieve totally green electronics, rather than focusing on a single component in an electronic system, all of the components must be designed and engineered as transient. Herein, we successfully fabricated transient supercapacitors, capacitive sensors and triboelectric nanogenerators by engineering PVA based layers including the electrodes, electrolyte, insulating layer and the encapsulant. Fabricated supercapacitors achieved a specific capacitance of 1.8 F.g⁻¹ with excellent rate capability up to 1 V.s⁻¹. Capacitive sensors based on PVA showed a promising sensitivity of 0.49 kPa⁻¹ up to 44 kPa. These flexible and transient capacitive sensors were used to monitor both small and large movements in different muscle groups on human body. Fabricated single electrode triboelectric nanogenerators, on the other hand, showed an open circuit voltage and short circuit current of 18 V and 3.5 μA, respectively, charged up small sized capacitors and used as self-powered sensors.

SESSION EN06.02: Electronics Synthesis I

Session Chair: Federico Rosei

Wednesday Afternoon, December 1, 2021

Hynes, Level 3, Room 308

1:30 PM *EN06.02.01

Processing Organic Semiconductors from Green Solvents Thuc-Quyen Nguyen; University of California, Santa Barbara, United States

Organic semiconductors have potential applications in various low cost, large area, flexible, light-weight devices ranging from sensors, light-emitting diodes (LEDs), displays, transistors, solar cells, photodetectors, thermoelectrics, and ratchets. Most organic semiconductors are processed in chlorinated solvents such as chlorobenzene and chloroform. In this talk, I will discuss the design, synthesis, and applications of conjugated polyelectrolytes (CPEs), a class of organic semiconductors characterized by a conjugated backbone and pendant ionic side chains. The conjugated backbone endows CPEs with the optical and charge transport properties of organic semiconductors, while the ionic functionalities render CPEs soluble in high dielectric constant media and in particular water. CPEs have been used as charge transporting layers in OLEDs, organic solar cells, perovskite solar cells, thermoelectrics, and organic electrochemical transistors.

2:00 PM EN06.02.02

A Green Edible Electrically Conductive Paste for Fruit Ripening Detection Pietro Cataldi¹, Leonardo Lamanna¹, Claudia Bertei², Federica Arena¹, Mufeng Liu³, Dimitrios Papageorgiou², Alessandro Luzio¹ and Mario Caironi¹; ¹Istituto Italiano di Tecnologia, Italy; ²Queen Mary University of London, United Kingdom; ³The University of Manchester, United Kingdom

Ingestible electronics was introduced as a powerful tool to control physiological parameters and deliver drugs with tunable rates and in a specific intestinal tract but is limited by the use of standard rigid electronics components, the risk of retention after ingestion, and the need to collect the device after expulsion, which is made of non-degradable and long-lasting materials.^{1,2,3} Edible electronics, which bridge ingestible with green electronics, propose to shift from ingestible to digestible components, ensuring a safe administration without medical supervision and enabling the degradation of the device in the body/environment after performing a specific function.^{2,3}

Producing edible electrical conductors with green methods, degradable and conformable materials, and industrially compatible processes will enable passive eatable electronics components if coupled with already abundant edible dielectrics. Such electrodes will also permit the monitoring of the maturation of vegetables through degradable and edible devices that can measure the electrical impedance of fruits, which is currently performed via Ag/AgCl electrodes.⁴ Indeed, state-of-the-art ingestible/edible conductors are rigid metals that are not safely eatable at high amounts (g/Kg), have a high price, and are not degradable in the body/environments after performing their function.^{1,3}

We present conductive pastes made entirely of food-grade materials with a high tolerable upper intake limit (g/Kg). A matrix made with biodegradable and digestible polymers and a micrometric size eatable conductive filler constitutes the conductors. The composite pastes are the first designed specifically for edible and sustainable electronics. These conductors can reach a resistivity in the order of 100 Ω cm, are fabricated without solvents' employment, and with processes that involve a low temperature (100°C) therefore using a small amount of energy. They exhibit tunable electromechanical features and adhesion depending on the composition. The composites are compatible with green and large-scale production processes such as extrusion, direct ink writing, and injection molding and thus are ideal for an industrial scale-up. Moreover, they feature antibacterial and hydrophobic properties, avoiding food contamination and possible adverse effect upon ingestion and the variation of their properties interacting with the body/environment.

The edible conductors are assembled as a food label that can monitor the maturation of fruit through simple electrical impedance measurements.^[4] The device can monitor the impedance change on different fruits for 14 days showing reliable results compared with standard Ag electrodes used for food monitoring. ^[4] Such technology could constitute the first building block towards green and sustainable substitutes of current ingestible conductors and the monitoring of the fruit production chain from the three to the table.

References:

[1] *An ingestible bacterial-electronic system to monitor gastrointestinal health*, Mimeo M. et al., **2018**, Science, DOI: 10.1126/science.aas9315

[2] *Tattoo-Paper Transfer as a Versatile Platform for All-Printed Organic Edible Electronics*, Bonacchini G. E. et al., **2018**, DOI: <https://doi.org/10.1002/adma.201706091>

[3] *Edible Electronics: The Vision and the Challenge*, Sharova A.S. et al., **2021**, Adv. Mater. Technol., DOI: 10.1002/admt.202000757

[4] *Bio-impedance and circuit parameters: An analysis for tracking fruit ripening*, Ibba P. et al., **2020**, Postharvest Biol. Technol., <https://doi.org/10.1016/j.postharvbio.2019.110978>

2:15 PM *EN06.02.03

Biocompatible Composites or Heterojunctions for Biological Modulation Bozhi Tian; University of Chicago, United States

Biocompatible and biodegradable devices for modulation of cells and tissues have many potential impacts on medical and industrial technologies. In this talk, I will present several recent projects in this area. First, I will discuss a bottom-up synthesis to construct a soil-like material consisting of nanostructured minerals, starch granules, and liquid metals, to mimic immobile inorganic and organic materials and the mobile phases in soil. The soil-like material is biocompatible and recyclable. It possesses chemical, optical, or mechanical responsiveness to yield write-erase electrical functions. We show this soil-like material can enhance microbial metabolism and biofuel production *in vitro*. It can also enrich gut bacteria diversity under a pathological condition and rectify bacterial dysbiosis *in vivo*. Next, I will showcase a class of granules-enabled hydrogel composites, with multiple naturally occurring biopolymers and synthetic hydrogels as the key components. The composites have many tissue-like properties, such as strain-stiffening behaviors. The granules-enabled tissue-like materials have enabled the pneumatically actuated bioelectronic devices for applications such as recording the heart electrocardiogram signal *ex vivo*. Moreover, I will present a newly developed nanoporous/non-porous heterojunction for improved biointerfaces. Without any interconnects or metal modifications, the heterojunction enables efficient non-genetic pulse stimulation of isolated rat hearts *ex vivo* and sciatic nerves *in vivo* with radiant exposure similar to that used in optogenetics. At the end of my talk, I will discuss future composite or heterojunction development towards more efficient biological modulation.

2:45 PM *EN06.02.04

Recycled Critical Elements from Batteries as Catalysts for Hydrogen-Rich Gas and Biofuel Production Ange Nzihou; Université de Toulouse, France

The increase in the share of renewable energies is essential to move towards the sustainable economy. In 2020, the share of energy from renewable sources in gross final energy consumption reached 20% in the EU, while at least 32% is targeted by 2030. In this strategic vision, the European Commission intends to highlight the advantages of biofuels in terms of reducing emissions of greenhouse gases. Accordingly, new advanced biofuels are needed and should be sustainably produced from biomass and bio-feedstock. Reforming of methane is one of the potential routes to achieve this Transition. Nevertheless, it suffers from the lack of robust catalysts to take off the ground. Dry reforming of methane (DRM) converts methane (CH₄) and carbon dioxide (CO₂) into syngas (CO, H₂), that can be directly used or further converted into green hydrogen and/or olefins, alcohols, and other hydrocarbons. An energetic optimization of this process is possible, by considering complementary oxidant agents, such as H₂O and O₂. In this regard, two other reforming routes named Steam (SRM) and Bireforming (BRM) have been considered. SRM consists of the conversion of methane in the presence of steam whilst BRM transforms a mixture of CH₄, CO₂ and H₂O into syngas. This process is one that allows the direct valorization of biogas (CH₄ and CO₂) for instance. Then, the syngas can be further converted into higher rate hydrogen and/or valuable chemicals via Fischer-Tropsch (FT) synthesis. The reforming reactions require noble-supported catalysts with SiO₂, Al₂O₃, CeO₂ and ZrO₂ as most common support materials and metals (Ni, Fe, Ru, Pd, ...) as active phases. We have developed a new approach of catalysts for the reforming of methane, that overcome the main hurdles in the field namely (1) deactivation, (2) metal sintering, (3) coke deposition, (4) lack of robustness to the variation of feedstock composition resulting in the decrease of the efficiency. The catalysts we have developed are free of rare and noble metals and made of Hydroxyapatite, Ca₁₀(PO₄)₆(OH)₂ as support material, and Ni and/or Co as active phases. Hydroxyapatite is a hierarchical structure with tunable physicochemical, mechanical, and thermal properties. The phosphate (PO₄) utilized has been recycled from used Lithium-ion batteries. The results obtained show highest performance in hydrogen production from DRM, BRM and SRM, and in hydrocarbons production in FT reaction. This lecture will summarize the research carried out and the main findings in this field, towards the sustainable use and recycling of critical chemical elements from batteries for energy and biofuel production.

3:15 PM BREAK

SESSION EN06.03: Urban Mining I
Session Chair: Clara Santato
Wednesday Afternoon, December 1, 2021
Hynes, Level 3, Room 308

4:00 PM EN06.03.01

Cold-Sintering Process—Sustainable Recycling Technology for Li_{6.95}Mg_{0.15}La_{2.75}Sr_{0.25}Zr₂O₁₂ (LLZO) and Li_{1+x-y}Al_xTi_{2-x}Si_yP_{3-y}O₁₂ (LATP)-Based Solid-State Composite Electrolytes Yi-Chen Lan and Enrique D. Gomez; The Pennsylvania State University, United States

As the demand for high-performance and safe batteries increases, researchers anticipate that all-solid-state batteries are the key to satisfy the market's needs. As large-scale production becomes possible, the unprecedented number of spent batteries will trigger disposal issues. Unfortunately, little effort is

placed in recycling solid-state electrolytes. Recycling composite electrolytes is in particular complicated due to the differences in the chemical and thermal stability of each component. Herein, we propose a sustainable recycling technology, cold-sintering process, to recycle composite electrolytes, $\text{Li}_{6.95}\text{Mg}_{0.15}\text{La}_{2.75}\text{Sr}_{0.25}\text{Zr}_{12}\text{O}_{12}$ with polypropylene carbonate and lithium perchlorate (LLZO-PPC-LiClO₄), and $\text{Li}_{1+x+y}\text{Al}_x\text{Ti}_{2-x}\text{Si}_y\text{P}_{3-y}\text{O}_{12}$ with bis(trifluoromethanesulfonyl)imide salts (LATP-LiTFSI). Due to the low sintering temperature, cold-sintering process can repair mechanical defects by reintegrating ceramic, polymer, and salt materials without significantly compromising their properties. LLZO-PPC-LiClO₄ and LATP-LiTFSI demonstrate extraordinary recyclability. As reprocessed samples show a similar compactness as the pristine samples and ionic conductivities are above $10^{-4} \text{ S cm}^{-1}$ at room temperature after four-times recycling. The recycled LATP-LiTFSI is electrochemically stable in lithium titanate symmetric cells over 1300 h at 0.1 mAh cm^{-2} . This work demonstrates the first sustainable way to recycle solid-state composite electrolytes in order to move towards a circular economy.

4:15 PM EN06.03.02

Regenerating and Up-Recycling Aged Lithium-Ion Battery Cathode Materials in a Green Process Claire Zhang, Jerry Xiang and Xiaofang Yang; Princeton NuEnergy, United States

Lithium-ion batteries (LIBs) have emerged as the battery of choice for rapidly growing markets in electric vehicles (EVs) and grid electricity storage. This spurs a great demand for lithium, graphite, cobalt, and nickel that could outstrip the supply of virgin materials. Thus, there is an enormous interest in the development of new sustainable technologies for recycling and recovery of valuable materials from secondary resources, especially from used lithium-ion batteries. Compared to conventional high temperature pyrometallurgical or hydrometallurgical methods, the direct recycling of LIBs is a promising method because it can directly regenerate the cathode materials by relithiation without destroying the compounds. Additionally, direct recycling is a comparatively low-cost and less resource intensive method of recovering LIB materials.

However, complete regenerating the full capacity and long-term performance is still particularly challenging. For instance, the cathode materials are often coated with a nanometer-thick protecting layer, which is engineered to reduce the degrading effect on the cathode due to the direct contact with the electrolyte. The long-term charge-discharge cycling causes damage to the coating layer and it thus needs to be repaired in order to recover the material performance. To address this challenge, we have developed a novel process that can regenerate and upgrade cathode materials from aged lithium-ion batteries, as well as creating a new coating layer to improve the cathode materials' performance. In this presentation, we will provide a case study to show the performance improvement of recycled lithium cobalt oxide (LCO) materials by forming an alumina coating layer on the surface. By controlling the thickness and sintering temperature, this surface alumina coating can be an effective way to improve the stability and cyclability of recycled LCO cathode materials. Material characterizations by XPS, SEM, STEM, and XRD help to reveal the structure and composition of the surface Al coating layer, and provides insights of the healing and protective roles of this layer for recycled LCO particles.

4:30 PM EN06.03.03

Sustainable Gold Peeling from E-Waste via Food Waste Byproducts Teresa Cecchi; ITT MONTANI, Italy

Recovery of non-leaching gold from e-waste gold coatings was achieved using aqueous chemistry with hydrogen peroxide and friendly organic acids that are food chain byproducts. The oxidation of the base metals, also part of the edges, enables the release of gold in its original metallic state in the form of flakes subsequently separated via simple filtration. Our route avoids crushing and chemical refining steps, reduces the losses of gold, thus saving cost and time, and decreases environmental pollution. Moreover, recovered gold, characterized by scanning electron microscopy and X-ray photoelectron spectroscopy to gain insight into the structure of the flakes and their chemical composition, was used to fabricate organic field-effect transistors making use of photolithographically patterned electrodes made of the recycled gold.

SESSION EN06.04: Batteries I
Session Chair: Teresa Cecchi
Wednesday Afternoon, December 1, 2021
Hynes, Level 3, Room 308

4:45 PM EN06.04.01

Biochar-Based Composites for Hybrid Supercapacitor Applications Thomas Sadowski^{1,2}, Jules Scanley^{1,2}, Kaleb Roman^{1,2}, Monica Kiehnle-Benitez^{1,2}, Daniel Shibu^{1,2}, Rahul Singhal^{3,2} and Christine Broadbridge^{1,2}; ¹Southern Connecticut State University, United States; ²CSCU Center for Nanotechnology, United States; ³Central Connecticut State University, United States

As renewables become an increasing percentage of the global energy portfolio, finding and implementing cost-effective, environmentally friendly, and sustainable grid-scale electrical energy storage devices to maintain a continuous and reliable power supply will be critical. From this perspective, hybrid supercapacitors represent an attractive alternative to batteries, being typically fabricated from more environmentally benign and easily sourced materials coupled with a cycling lifetime that often exceeds batteries by several orders of magnitude. The performance of these devices is ultimately tied to the choice of electrode material, with carbon nanotube (CNT) - manganese dioxide (MnO₂) composites receiving focus recently due to the promise of energy storage approaching that of conventional batteries. MnO₂ is an ideal material from an environmental and sustainability standpoint due to its natural abundance, low toxicity, and simple synthesis routes; however, CNT synthesis typically requires hydrocarbons as feedstock and present potential health risks via inhalation and dermal contact. Biochar, on the other hand, represents a sustainable alternative to CNT with lower predicted health risks. The fabrication of biochar is carbon negative, and significant opportunities exist to engineer the morphology through rational choice of biomass precursor. In this study, biochar-MnO₂ composites were investigated to assess their potential in hybrid supercapacitors. Biochar was obtained from a variety of commercial sources and the initial concentrations varied to synthesize a range of composites via a hydrothermal method. The morphology and microstructure were characterized using scanning and transmission electron microscopy and x-ray diffraction. Supercapacitive performances were investigated using cyclic voltammetry, charge-discharge, and rate capability studies. The resulting characterization and performance data of biochar-MnO₂ will be presented and compared to CNT-MnO₂ of identical weight composition.

5:00 PM EN06.04.02

Effect of Multi Wall Carbon Nanotubes on Electrochemical Performances of MnO₂ Rahul Singhal¹, Bhagirath Saini², Monica Kiehnle-Benitez³, Thomas Sadowski³, Christine Broadbridge³, Jules Scanley³ and Rakesh Sharma²; ¹Central Connecticut State University, United States; ²Indian Institute of Technology Jodhpur, India; ³Southern Connecticut State University, United States

Due to the continuous depletion of the fossil fuels, scientists are looking for alternative energy sources and energy storage devices. Supercapacitors are energy storage devices with higher power density and high energy density than conventional capacitors. Manganese oxides have attracted a lot of attention because of their easy preparation, environmental friendliness, and relatively low cost. However, MnO_2 suffers from low electronic conductivity, which severely limits its fast charge/discharge behavior. This can be overcome by mixing it with electronically conductive materials such as carbon black or carbon nanotubes (CNTs). Composites of $\text{MnO}_2/\text{MWCNT}$ were prepared using different weight ratios of $\text{MWCNTs}:\text{KMnO}_4$ (1:2, 1:5, 1:10, 1:15, 1:20, 1:25). The synthesized materials were physically characterized using X-ray diffraction (XRD) and transmission electron microscopy (TEM). TEM studies confirm that MnO_2 is homogeneously entangled with MWCNT. The electrochemical performances evaluation was carried out in a 3-electrode system using $\text{MnO}_2/\text{MWCNT}$ electrode coated onto Ni mesh as working electrode, Pt foil as counter electrode and Ag/AgCl as reference electrode. An aqueous solution of 1 M Na_2SO_4 was used as electrolyte. The specific capacitance was obtained from charge discharge studies at various current densities between 0.5 A/g – 5 A/g. The specific capacitance of $\text{MWCNTs}-\text{KMnO}_4$ (1:10, 1:15, 1:25) samples were obtained as 111 F/g, 159 F/g, and 161 F/g, respectively at a current density of 1 A/g. The detailed morphological and electrochemical results will be presented.

5:15 PM EN06.04.03

Late News: Poly (3,4-ethylenedioxythiophene) (PEDOT) Modified with Carbon Nanotubes as Counter Electrode and Bipyridine Cobalt(II/III) Complexes as Redox Mediator in Solar Cells Sensitized with Membrane Protein-Pigment Complexes Stephanie Monge^{1,1}, Alexandra H. Teodor², Dariana Aguilar^{1,1}, Alexandra Tames^{1,1}, Roger Nunez³, Juan J. Montero Rodriguez¹, Jesse Bergkamp³, Ricardo Starbird^{1,1}, Barry D. Bruce^{2,2,2} and Claudia C. Villarreal^{1,1,1}; ¹Instituto Tecnológico de Costa Rica, Costa Rica; ²University of Tennessee at Knoxville, United States; ³California State University Bakersfield, United States

In nature, light is captured by different classes of membrane protein-pigment complexes. Two proteins of interest are retinal-containing proteins (RMP) and chlorophyll-pigment protein complexes (CPP) associated with photosynthesis. Bacteriorhodopsin (BR) is an example of an RMP that functions as a light-driven proton pump. Photosystem I (PSI) is one of two CPP associated with oxygenic photosynthesis that catalyzes photoactivated unidirectional electron transfer. Interestingly, although these proteins come from highly divergent prokaryotes, bR from archaeobacteria, and PSI from cyanobacteria, they form trimeric complexes that are highly thermostable, and both are exceptionally well characterized at the structural, functional, and spectroscopic level. Both complexes have been integrated into new eco-centric, photovoltaic (PV) devices built from flexible, biodegradable, renewable carbon materials. More importantly, PSI and bR stand out as some of the best performing natural light absorbers in the bio-PV devices reported. The best power conversion efficiencies have been obtained in bio-sensitized solar cell architecture, using nanostructured wide-bandgap semiconducting electrodes to assemble these proteins. The membrane protein-pigment complexes in these devices can directly donate either electron or protons upon light absorption, enabling photocatalyzed hydrogen production, electric power generation, chemical catalysis, and other redox reactions. Despite the progress in these bR- and PSI-sensitized solar cells, little attention has been devoted to the development of alternative counter electrodes and electrolytes to the commonly used Pt and I^-/I_3^- . A careful selection of the redox mediator and the electrolyte and counter electrode components is a core part of the design of low resistance, high photocurrent protein bio-PV devices. This work explores using a counter electrode of poly (3,4-ethylene dioxythiophene) (PEDOT) modified with carbon nanotubes for both PSI and bR devices. We also explore using hydroquinone/benzoquinone and aqueous-soluble bipyridine cobalt(II/III) complexes as direct redox mediators. It is a novel discovery that the same counter electrode and redox mediator system can perform well for two different biomolecules that have developed independently over millions of years to harvest solar energy in nature. Such compatibility of PSI and bR with a common mediator and counter electrode may be helpful to realize the uptake of a larger portion of the sun spectrum with these two natural light absorbers that have complementary absorption spectra. The improvement of bio-PVs design is an advancement towards more energy-efficient and green chemistry principles-based manufacturing paradigms as the biosynthesis of biomolecules like bR and PSI for PV feedstock contributes to CO_2 fixation from the atmosphere and solar energy is used multiple times across fabrication and device use.

5:30 PM EN06.04.04

Untapped Potential of Polymorph MoS_2 —Tuned Cationic Intercalation for High-Performance Symmetric Energy Storage Devices Nageh K. Allam; American University in Cairo, Egypt

Supercapacitors have been the key target as energy storage devices for modern technology that need fast charging. Although supercapacitors have large power density, modifications should be done to manufacture electrodes with high energy density, longer stability, and simple device structure. The polymorph MoS_2 has been one of the targeted materials for supercapacitor electrodes. However, it was hard to tune its phase and stability to achieve the maximum possible efficiency. Herein, we demonstrate the effect of the three main phases of MoS_2 (the stable semiconductor 2H, the metastable semiconductor 3R, and the metastable metallic 1T) on the capacitance performance. The effect of the cation intercalation on the capacitance performance was also studied in Li_2SO_4 , Na_2SO_4 , and K_2SO_4 electrolytes. The performance of the electrode containing the metallic 1T outperforms those of the 2H and 3R phases in all electrolytes, with the order $1\text{T} > 3\text{R} > 2\text{H}$. The 1T/2H phase showed a maximum performance in the K_2SO_4 electrolyte with a specific capacitance of 590 F g^{-1} at a scan rate of 5 mV s^{-1} . MoS_2 showed a good performance in both positive and negative potential windows allowing the fabrication of symmetric supercapacitor devices. The 1T MoS_2 symmetric device showed a power density of 225 W/kg with an energy density of 4.19 Wh/kg . The capacitance retention was 82% after 1000 cycles, which is an outstanding performance for the metastable 1T-containing electrode.

SESSION EN06.05: Poster Session: Sustainable Electronics—Green Chemistry, Circular Materials, End-of-Life and Eco-Design

Session Chairs: Federico Rosei and Clara Santato

Wednesday Afternoon, December 1, 2021

8:00 PM - 10:00 PM

Hynes, Level 1, Hall B

EN06.05.01

Toward a Structure-Properties Relationship Phase Diagram for Eumelanin Films Manuel Reali¹, Anthony Camus¹, Jennifer MacLeod², Alessandro Pezzella³ and Clara Santato¹; ¹Polytechnique Montréal, Canada; ²The University of Queensland, Australia; ³Università degli Studi di Napoli Federico II, Italy

The charge transfer and transport properties of bio-sourced materials are complex, due to their chemical and structural composition. Their biosynthesis generates chemical heterogeneity, e.g. macromolecules resulting from more than one building block (monomer), and physical disorder, e.g. $\pi-\pi$ stacked regions coexisting in the supramolecular structure. Chemical and physical disorder are key factors limiting the performance of organic electronics¹⁻³. Among the plethora biomaterials available in nature, eumelanin, a black-brown bio-pigment of the melanin family, is an interesting candidate for study⁴⁻⁶. It is a redox-active⁷⁻¹⁰ quinone-based bio-macromolecule featuring electronic conjugation (alternating single and double Carbon bonds), broadband

UV-Vis absorption and hydration-dependent electrical response^{11–16}. Eumelanin originates from the oxidative polymerization of 5,6-dihydroxyindole (DHI) and 5,6-dihydroxyindole-2-carboxylic acid (DHICA) monomers (building blocks). DHI and DHICA have several polymerization sites and co-exist in different redox states (fully reduced hydroquinone, semi-reduced semiquinone, and fully oxidized quinone). Therefore, eumelanin features chemical heterogeneity^{17–19}. Monomers and oligomers generate several supramolecular structures, such that eumelanin also features physical disorder²⁰. Recently, we showed that the early stages of DHI and DHICA films formation is driven by both chemical (covalent) and physical (self-assembly) interactions²¹. Particularly, self assembly of DHI is expected to deliver films featuring higher degree of pi-pi stacking with respect to DHICA, this last being a critical condition to the rational design of eumelanin-based functional devices²².

Herein, we investigate the role of oligomeric composition, relative humidity and type of solvent during DHI film processing. Preliminary results show that DHI films undergo to de-wetting^{23,24} or diffusion limited aggregation (DLA) phenomena^{25,26} depending on specific combination of solvent, relative humidity and molar mass distribution. Our investigation is a step forward to establish a phase diagram correlating film processing and structural properties of eumelanin films.

References

- 1 R. Mukherjee et al., *Soft Matter*, 2015, **11**, 8717–8740.
- 2 S. Irimia-Vladu et al., *Green Materials for Electronics*, Wiley-VCH, Germany, 2018.
- 3 S. Riera-Galindo et al., *ACS Omega*, 2018, **3**, 2329–2339.
- 4 M. D'Ischia et al., *Angew. Chemie - Int. Ed.*, 2009, **48**, 3914–3921.
- 5 G. Prota, *Pigment Cell Res.*, 2000, **13**, 283–293.
- 6 P. Meredith et al., *Pigment Cell Res.*, 2006, **19**, 572–594.
- 7 Y. J. Kim et al. *Proc. Natl. Acad. Sci.*, 2013, **110**, 20912–20917.
- 8 R. Xu et al. *ACS Omega*, 2019, **4**, 12244–12251.
- 9 A. B. Mostert et al., *Sci. Adv.*, 2018, **4**, 1–6.
- 10 A. Gouda et al., *J. Phys. D: Appl. Phys.*, 2020, **53**, 043003.
- 11 M. Ambrico et al., *Org. Electron.*, 2010, **11**, 1809–1814.
- 12 M. Sheliakina et al., *Mater. Horizons*, 2018, **5**, 256–263.
- 13 M. Sheliakina et al., *Adv. Funct. Mater.*, 2018, 1805514.
- 14 A. B. Mostert et al., *Appl. Phys. Lett.*, 2012, **100**, 1–3.
- 15 M. Reali et al., *Handbook of Nanoengineering, Quantum Science and Nanotechnology*, ed. S. E. Lyshevski, CRC Press, 2019, 101–113.
- 16 M. Reali, et al., *Mater. Adv.*, 2021, **2**, 15–31.
- 17 S. Meng et al., *Biophys. J.*, 2008, **94**, 2095–2105.
- 18 M. Arzillo et al., *Biomacromolecules*, 2012, **13**, 2379–2390.
- 19 A. Antidormi et al., *J. Phys. Chem. C*, 2018, **122**, 28368–28374.
- 20 C. T. Chen et al., *Nat. Commun.*, 2014, **5**, 1–10.
- 21 M. Reali et al., *J. Phys. Chem. C*, 2021, **125**, 3567–3576.
- 22 M. d'Ischia et al., *Angew. Chemie - Int. Ed.*, 2019, 11196–11205.
- 23 S. A. Burke et al., *J. Phys. Condens. Matter*, 2009, **42**, 1–14.
- 24 L. Xue et al., *Sci.*, 2012, **57**, 947–979.
- 25 J. S. Huang et al., *J. Chem. Phys.*, 1989, **90**, 25–29.
- 26 T. C. Halsey, *Phys. Today*, 2000, **53**, 36–41.

EN06.05.02

Regenerating and Up-Recycling Aged Lithium-Ion Battery Cathode Materials in a Novel Gas-Phase Process Jerry Xiang, Claire Zhang and Xiaofang Yang; Princeton NuEnergy, United States

Lithium-ion batteries (LIBs) have emerged as the battery of choice for rapidly growing markets in electric vehicles (EVs) and grid electricity storage. This spurs a great demand for lithium, graphite, cobalt, and nickel that could outstrip the supply of virgin materials. Thus, there is an enormous interest in the development of new sustainable technologies for recycling and recovery of valuable materials from secondary resources, especially from used lithium-ion batteries. Compared to conventional high temperature pyrometallurgical or hydrometallurgical methods, the direct recycling of LIBs is a promising method because it can directly regenerate the cathode materials by relithiation without destroying the compounds. Additionally, direct recycling is a comparatively low-cost and less resource intensive method of recovering LIB materials. However, since the aged materials are usually 5 to 10 years older than the current materials, the regenerated materials may not meet new market needs due to due to due to improvements in material properties and emerging new chemistries. In order to meet this challenge, we have developed a novel gas-phase process that can regenerate and upgrade cathode materials from aged lithium-ion batteries, as well as adding new functionality to improve the cathode materials performance. In this presentation, we will provide a case study to show the upgrading of old chemistries of cathode materials (e.g., NCM 111 and NCM 523) to newer chemistries (NCM 622 and NCM 811) After upgrading, the performance and long-term cycle performance of the high-nickel NCM cathode material are comparable to those of commercial battery materials.

This new direct battery recycling technology has the potential to create a new lithium-ion battery cathode material manufacturing process from recycled batteries as it offers systematic advantages in costs, energy efficiency, and environmental protection by reusing, recycling, and reproducing lithium-ion batteries within an optimized system.

EN06.05.03

Late News: A Novel Ion-Na Batteries—Synthesis and Characterization of Nanostructured Sodium Rhodizonate Cathodes Emilio Navarrete¹, Eduardo Cisternas¹, Fabian Dietrich¹ and Eduardo Muñoz²; ¹Universidad de la Frontera, Chile; ²Pontificia Universidad Católica de Valparaíso, Chile

Several studies have emerged that seek to solve the energy deficit that we face as a society, where energy storage plays an important role. In this regard, Ion-Sodium batteries (Ion-Na) represent an excellent alternative to the Ion-Li batteries currently on the market. These new Ion-Na batteries have adequate charge densities and at a lower cost. Taking this issue into account, there is great interest in studying the composition, structure, and morphology of cathodes as active materials to optimize this type of battery. [i],[ii].

In this study, the synthesis and characterization of sodium rhodizonate nanostructures to be used as cathode material in Sodium-ion batteries was carried out. In a first stage, a two-level factorial design was used as an exploratory stage to evaluate the statistical significance of the variables involved in the synthesis: i) temperature, ii) reaction time, iii) molar ratio of precursors and iv) addition time. The nanostructuring of the sodium rhodizonate crystals was carried out by the ultrasonic crystallization method and was characterized by X-ray Diffraction (XRD) and Scanning Electron Microscopy (SEM). The electrochemical characterization was performed using cyclic voltammetry, galvanostatic charge/discharge profiles, and cyclability. The results show that

the nanostructuring of the material causes an increase in the storage capacity of sodium ions in the sodiation/desodiation process. This shows a strong size-dependence in the Na⁺ ion intercalation process. Finally, these results will allow the generation of causal relationships that lead to the optimization of the electronic properties of alternative Na-ion batteries.

[i] Minah Lee, Jihyun Hong, Jeffrey Lopez, Yongming Sun, Dawei Feng, Kipil Lim, William C. Chueh, Michael F. Toney, Yi Cui & Zhenan Bao. *Nature Energy*, volume 2, pages 861–868 (2017).

[ii] R.-E. Dinnebier, H. Nuss, M. Jansen, Disodium rhodizonate: a powder diffraction study, *Acta Crystallographica E61* (2005) m2148–m2150.

SESSION EN06.06: Electronics Energy II
Session Chairs: Christine Luscombe and Clara Santato
Monday Afternoon, December 6, 2021
EN06-Virtual

6:30 PM *EN06.06.01

Fabrication of Transient Printing Circuits Through Low-Cost Water Sintering Techniques Xian Huang; Tianjin University, China

Transient electronics refer to emerging types that only last limited periods of time and disappear after completing their functions and generating environmentally-friendly by-products. Among many approaches that have been developed for fabricating transient circuits, printing techniques are suitable methods for mass fabricating large-area transient circuits in high printing speed. However, inks and pastes as well as the processing methods of the printed patterns remain to be developed for high-performance transient circuits with excellent electrical conductivities and mechanical robustness. This presentation will focus on our recent effort in developing transient circuits based on bioresorbable zinc nanocomposites printed on bioresorbable substrates and sintered through low-cost and high-efficient water sintering. The entire printing and sintering processes can be conducted at room temperature and in atmosphere conditions, leading to the maximum conductivity of 307664.4 S/m and the capability to withstand repeated bending for more than 8000 times. The techniques have led to the development of dissolvable consumer electronics that have the same functions as conventional devices but dissolve in the liquid environment to facilitate recycling. The materials and techniques developed in these works may reform the electronics recycling industry by reducing the cost of recycling and minimizing environmental pollution.

7:00 PM EN06.06.02

Eumelanin, from Molecular State to Film Manuel Reali¹, Anthony Camus¹, Guillaume Beaulieu¹, Jordan De Angelis², Christian Pellerin³, Alessandro Pezzella⁴ and Clara Santato¹; ¹Polytechnique Montréal, Canada; ²Università di Bologna, Italy; ³University of Montreal, Canada; ⁴University of Naples Federico II, Italy

Melanins are ubiquitous biopigments responsible of manifold functionalities in living organisms¹. Eumelanin is a hygroscopic, black-brown biomacromolecule belonging to the family of melanin biopigments. Eumelanin originates from the oxidative polymerization of (5,6)-dihydroxyindole (DHI) and (5,6)-dihydroxyindole 2-carboxyl acid (DHICA) building blocks. Different available polymerization sites and co-existing redox states, as well as distinct supramolecular arrangements, bring chemical and physical disorder to the biopigment². Eumelanin features fascinating physicochemical properties such as broadband optical absorption, free radical scavenging, metal-ion chelation and hydration dependent electrical response^{3,4}, this last mainly attributed to protonic transport. Being non-toxic, abundant, solution processable and potentially biodegradable⁵, eumelanin is a promising candidate for green electronics⁶.

Owing to its complex structural organization, the charge carrier transport properties of eumelanin, are still elusive^{7–11}. Our observations of exclusive electronic transport in dry eumelanin pellets¹² reopen the debate whether the biopigment would be a mixed protonic-electronic conductor in the hydrated state and an amorphous semiconductor in the dry state¹³. Correlating supramolecular self-assembly to fundamental optical and electrical properties of eumelanin is paramount to fill such a knowledge gap.

Herein¹⁴, we investigated the early stages of formation of DHI and DHICA films at technologically relevant surfaces. We observe that the monomers aggregate, possibly eventually polymerizing in a time scale of few hours at ambient condition. Atomic Force Microscopy (AFM) images of DHI and DHICA acquired at ambient conditions (AC) show the formation of well-defined *fern-like* structures and regular rod-shaped structures, respectively. We attribute the growth of fern-like and rod-shaped structures to diffusion limited aggregation (DLA) and Ostwald ripening processes, respectively. The increase of UV-Vis absorbance overtime for AC-DHI and AC-DHICA films suggests an improved π -electron delocalization of oligomeric structures. Fourier Transform Infrared (FTIR) and UV-Vis spectroscopy suggests that the interplay between chemical (oxidative polymerization) and physical interactions (hierarchical self-assembly) plays a key role during the early stages of film formation over time. Preliminary investigation into the electrical response of eumelanin films were also conducted.

Our results add a piece of knowledge to unravel structure-properties relationship in eumelanin, a condition *sine qua non* to design and develop eumelanin-based functional devices.

REFERENCES

- 1 M. d'Ischia et al., *Pigment Cell Melanoma Res.*, 2015, **28**, 520–544.
- 2 L. Panzella et al., *Angew. Chemie - Int. Ed.*, 2013, **52**, 1–5.
- 3 R. Micillo et al. *Sci. Rep.*, 2017, **7**, 41532.
- 4 E. Di Mauro et al., *MRS Commun.*, 2017, **7**, 141–151.
- 5 E. Di Mauro, et al., *Nat. Commun.*, 2021, **12**, 1–10.
- 6 M. Irimia-Vladu, *Chem. Soc. Rev.*, 2014, **43**, 588–610.
- 7 M. Sheliakina et al., *Adv. Funct. Mater.*, 2018, 1805514.
- 8 A. B. Mostert et al., *Proc. Natl. Acad. Sci.*, 2012, **109**, 8943–8947.
- 9 J. McGinness et al., *Science* 1974, **183**, 853–855.
- 10 J. Wünsche et al., *Chem. Mater.*, 2015, **27**, 436–442.
- 11 L. Migliaccio et al., *Front. Chem.*, 2019, **7**, 1–8.
- 12 M. Reali et al., *ACS Appl. Bio Mater.*, 2020, **3**, 5244–5252.
- 13 M. Reali et al. *Mater. Adv.*, 2021, **2**, 15–31.

7:15 PM *EN06.06.03

Green Monomers and Polymers for Green Electronics Mario LeClerc¹, David Gendron², Louis-Philippe Boivin¹ and William Dupont¹; ¹Laval University, Canada; ²Kemitec, Canada

The growth of consumer electronics has drastically changed our daily routine. For instance, those electronic products (cellphone, laptop, camera, etc.) have become essential tools in our modern reality to facilitate access to information or to maintain our social activities. However, even though new performing technologies (OLED or OPV) have now emerged, the fact remains that their lifespan is limited and the resources utilized for their manufacture are demanding on the environment.

Therefore, a change in the way we harness resources and manage electronic waste is required to minimize negative impacts on the environment. Organic electronic represent a promising alternative to the traditional inorganic electronic as it is carbon-based, printable and the optoelectronic properties can be easily tuned to match the requirements. Hence, in order to eliminate electronic waste, materials from renewable and recyclable sources are sought. In this regard, forest biomass is considered the only sustainable source of organic carbon and therefore the ideal replacement for petroleum products for the production of chemical compounds. One of the resources derived from biomass, lignocellulose, is the most abundant bio-based material on earth. Indeed, the main added-value compound obtained from the depolymerization of lignin is vanillin. Vanillin is an aromatic compound with three functional groups that can be chemically modified. The present work describes how the vanillin moiety can be expanded into several building blocks for the preparation of bio-based conjugated polymers. Moreover, our synthetic approach involved direct heteroarylation polymerization (DHAP), which avoids the generation of toxic side products usually present in the preparation of conducting polymers. At last, the optoelectronics properties of the materials and their corresponding devices' performances will be discussed.

7:45 PM *EN06.06.05

Why Soft, Solution Processing(=Low-Energy Production) of Advanced Nano- Materials is Difficult but Necessary for Sustainable Society? Masahiro Yoshimura^{1,2}; ¹National Cheng Kung University, Taiwan; ²Tokyo Institute of Technology, Japan

Modern our society has been developed with various Advanced Materials. Most of advanced materials, Metallurgical materials, Semiconductors, Ceramic materials and Plastics have been used in wide area of applications like structural, mechanical, chemical, electrical, electronic, optical, photonic, biological, medical, etc. Most of them except for bio-polymers & bio-minerals have never been produced via biological systems & processes. Thus they have been fabricated artificially and/or industrially by so-called High-Technology, where using Sophisticated Equipment & High Energetic Conditions:high temperature, high pressure, vacuum, molecule, atom, ion, plasma, etc. for their fabrications, then consumed huge amounts of resources and energies thus exhausted huge amounts of wastes: Materials, Heats and Entropy. To save this tragedy, we must consider Cascade use of Heats, and (SSP) Soft, Solution Processing (=Low-Energy Production of Advanced Materials via solution-based processing). SSP is Bio-inspired process, which means that Learn from Bio-systems then Exceed them. We have challenged to fabricate those advanced inorganic materials with desired shape/size/location,etc. directly in low energetic routes using aqueous solutions since 1989 when we could fabricate BaTiO₃ film on Ti substrate in a Ba(OH)₂ solution by Hydrothermal Electrochemical method at low temperatures of 60-200 C. We proposed in late 90's an innovative concept and technology, Soft Processing or Soft, Solution Processing, that aims low energetic (=environmentally friendly) fabrication of shaped, sized, located, and oriented inorganic materials in/from solutions(1,2). It can be regarded as Green processing, or Eco-processing by other groups. When we have activated/stimulated interfacial reactions locally and/or moved the reaction point dynamically, we can get patterned ceramic films directly in solution without any firing, masking nor etching: i.e. Direct Patterning of CdS, PbS and CaWO₄ on papers by Ink-Jet Reaction method, furthermore, we have succeeded to fabricate BaTiO₃ patterns on Ti by a laser beam scanning(3) and carbon patterns on Si by plasma using a needle electrode scanning directly in solutions. Successes in TiO₂ and CeO₂ patterns by Ink-Jet Deposition, where nano-particles are nucleated and grown successively on the surface of substrate thus become dense even below 300 C. Other nano-structured 2D/3D films could be prepared without firing. Soft Processing for various 2D: Graphene, MXene, MoS₂ have been established including the preparation of functionalized Graphene Ink via successive processes under ambient temperature and pressure conditions.(4-6)

1) MRS Bulletin,25[9],Sept. 2000, special issue for Soft Processing of Advanced Inorganic Materials ,Guest Editors:M. Yoshimura and J. Livage.

2) Yoshimura, M., *J. Mater. Sci.*,41 [5],1299-1306 (2006), 43[7]2085-2103(2008).

3) Watanabe, T.,Yoshimura,M.,et al.,*Thin Solid Film*, 515,2696-2699(2006)

4) J. Senthilnathan, M.Yoshimura et al., *J. Mater Chem A*,(2014) 2, 3332-3337 (2015)

5) Sanjeeva Rao, K and Yoshimura, M et al. *Adv. Funct. Mater.*,25,298305(2015)

6) E. Satheshkumar,Y. Gogotsi,M. Yoshimura,et al. *Sci, Repts*, 6,32049(2016), *Front. Mater.* 6,216(2019), *Microchim. Acta*, 187,33(2020)

SESSION EN06.07: Batteries II

Session Chairs: Federico Rosei and Clara Santato

Monday Afternoon, December 6, 2021

EN06-Virtual

9:00 PM EN06.07.01

Flowing Electrolyte System of Bifacial Dye-Sensitized Solar Cells Under Low-Concentrated Light Tika E. Putri, Lesley Fadza F. Chawarambwa, Pankaj Attri, Kunihiro Kamataki, Naho Itagaki, Kazunori Koga and Masaharu Shiratani; Kyushu University, Japan

DSSCs are promising for future photovoltaics due to their good price/performance ratio and ability to work at wider angles. In low light, long life, mechanical robustness, ability to operate at lower internal temperatures.^{1,2} Although DSSCs coupled with a concentrator increase the power out (Pout),³ applying a concentrator increases the device temperature to limited operation lifetime and electrolyte evaporation. Therefore, a suitable cooling system is needed to prevent temperature rise in the DSSCs coupled with a concentrator. In this study, we applied an electrolyte-flowing cooling system to prevent the temperature rise of DSSCs.

Bifacial DSSCs were fabricated with FTO/TiO₂/N719dye/electrolyte/Pt/FTO structure. Adjustable external concave mirror concentrators were placed at both sides of the DSSC. Z-100 Electrolytes flowed through DSSCs equipped with silicon pipes and hydraulic pumps as a cooling system. The photovoltaic performance and device temperature rise of cells under flowing continuously (FC) and flowing with a stopping period (FS) of electrolyte were compared with those of normal cells without the flowing system (NC).

The flowing electrolyte system with FC (161.7°C) and FS (167.8°C) have a lower temperature than NC (221.8°C) after 3 hours of operation. The open-circuit voltage (V_{oc}) decreases from around 0.75 V to 0.52 V (FC), 0.53 V (FS), and 0.36 V (NC) due to the effect of temperature rise. Short-circuit current (J_{sc}) in both flowing systems gradually is reduced due to improper transfer of electrons in the flowing electrolyte. This reduction corresponds to increases in Z1 resistance value from 9.3 Ω to 92.1 Ω (FC) and 6.5 Ω to 33.9 Ω (FS) from electrochemical impedance spectroscopy (EIS) analysis. Pout of FS and NC are almost the same, around 7.5 mW/cm² after 3 hours operation, whereas Pout of FC decreases to 1 mW/cm². In conclusion, an electrolyte-flowing cooling system with a stopping period can reduce the temperature rise and improper transfer of electrons in electrolytes caused by flow.

Yum, J., et al., *Energy Environ. Sci.* **4**, 842–857 (2011).

Mariotti, N., et al., *Green Chem.* **22**, 7168–7218 (2020).

Selvaraj, P., et al. *Sol. Energy Mater. Sol. Cells* **175**, 29–34 (2018).

9:15 PM EN06.07.03

Fractal Based EDS Design for Increased Solar Panel Dust Removal Efficiency [Asaad Alduais](#), Abdulrahman Javaid, Miswar Syed, Jhonathan P. Rojas and Mosab Alhrntomi; King Fahd University of Petroleum and Minerals, Saudi Arabia

Solar power is one of the fastest growing renewable energy technologies in the world. However, dusty weather conditions pose a threat to the solar panel's efficiency and reduce the power produced. The lack of an effective and long-term solution that successfully cleans solar panels while consuming low energy has been a challenge for the industry. Hence, the idea of a more reliable method that is more effective and cost-efficient to employ is appealing. Among the different proposed alternatives, a very promising cleaning technique involves the utilization of an Electrodynamical Screen (EDS) to actively remove the dust. The advantages of this technique include self-cleaning, high cleaning efficiency, and the eradication of manual labor, robots, and water-based cleaning techniques. An EDS consists of a transparent dielectric laminate with electrodes embedded in it. Commonly, the electrodes are arranged in a parallel configuration. In this work, we propose and analyze the employment of different electrode arrangement configurations for the EDS based on the fractal concept. This research aims to improve the EDS performance in terms of its cleaning efficiency, power consumption, and time taken. Finite element analysis results conclude that the Hilbert fractal-based electrode arrangement design performs better than the parallel design in terms of dust repulsion. Additionally, it results in low area coverage by the electrodes, ensuring an increased transparency of the EDS, hence increasing the overall irradiance absorbed by the solar panel. Specifically, as compared to the parallel design, the proposed Hilbert design reduces the power consumption and the area ratio by 25.25% and 33.83%, respectively and it also increases the maximum electric field intensity by 30%. This increase in the electric field intensity is directly associated with higher cleaning efficiency.

9:30 PM EN06.07.04

Carbon Dots Based Transparent Film for Efficient UV and High-Energy Blue Light Screening [Barun K. Barman](#)¹, Ørjan Sele Handegård^{1,2} and Tadaaki Nagao^{1,2}; ¹National Institute for Materials Science, Japan; ²Hokkaido University, Japan

On the Earth's surface, the incoming radiation comprises ~5 % of ultraviolet, visible light, 43 %, and infrared light, 52%. Exposure to high-energy UV radiation can be harmful to humans, increasing the risk of skin cancers and damage to the eyes. Not only UV light, a major part of visible light is high-energy blue light (HEBL), ranging from 400–450 nm. HEBL can also have huge negative impacts on human health. It damages our eyes and can even affect mental health. In the past decade, the dramatic evolution of electronic gadgets such as smartphones, tablets, and flat televisions that use back-lighting technology, such as compact fluorescent lamps (CFLs) and LEDs, exposes us to large amounts of harmful radiation. These devices emit HEBL and small amounts of UV. Natural blue light can regulate our sleep and wake cycles, boost alertness, modulate mood, etc., but prolonged exposure to blue light at night can disrupt circadian rhythm, and can cause many additional health issues, such as diabetes, heart disease, and depression. Most importantly it can cause permanent eye damage and age-related macular degradation, leading to vision loss. It is essential to block all UV and HEBL light with tunable filters having high visible light transparency to protect our health from these hazardous light sources. Carbon dots (CDs) are a newly discovered class of carbon-based nanomaterials that are composed only of earth-abundant, light elements such as carbon, oxygen, hydrogen, and nitrogen, which are non-toxic and completely metal-free. By utilizing the absorption and emission properties of CDs, we have developed a new hybrid film composed of carbon dots (CDs) and cellulose film combined via H-bonding. CDs encapsulated cellulose films (CDs@Cel) are highly transparent in the visible spectral region. These films efficiently absorb UV light and HEBL, simultaneously down-converting them to longer wavelengths in the visible spectrum.

References

1. Luther, U.; Dichmann, S.; Schlobe, A.; Czech, W.; Norgauer, J., UV light and skin cancer. *Med Monatsschr Pharm* **2000**, *23* (8), 261–6.
2. Johnson, J. A., Durable protection against long-wavelength UV-A radiation and blue light. *Arch Dermatol* **1992**, *128* (3), 409.
3. Barman, K. B.; Nagao, T.; Nanda, K. K., Dual roles of a transparent polymer film containing dispersed N-doped carbon dots: A high-efficiency blue light converter and UV screen. *Applied Surface Science* **2020**, *510*, 145405.

9:45 PM *EN06.07.05

Biodegradable Materials for Transient Batteries and Electronic Medicine [Lan Yin](#); Tsinghua University, China

Biodegradable devices represent a new type of electronics that is built on fully biodegradable materials and is capable of degrading in aqueous environments, which can therefore eliminate a second surgery for device retraction and minimize environmental footprints. Such devices could play important roles in many therapeutic and diagnostic processes, as well as handling electronic waste. Herein, we introduce novel materials strategies and fabrication schemes that enable fully transient batteries based on magnesium anodes that can provide energy supplies for consumer electronics and implantable devices. The battery systems can offer sufficient energy density and prolonged operational lifetime. Self-powered nerve conduit for peripheral nerve regeneration based on biodegradable galvanic cells are also achieved. Successful nerve regrowth and motor functional recovery are realized in rodent models. These works provide new insights for building energy devices for green electronics and implantable electronic medicine.

10:15 PM EN06.07.06

Transient Rechargeable Battery with a High Lithium Transference Number Cellulosic Separator [Neeru Mittal](#)¹, Alazne Ojanguren¹, Erlantz Lizundia² and Markus Niederberger¹; ¹ETH Zurich, Switzerland; ²University of the Basque Country, Spain

Transient/degradable technology is a flourishing research area aimed at designing materials, devices, or systems that undergo controlled degradation processes after a period of stable and reliable operation. Transient devices work exactly like their conventional analogs but have an extra advantage; these devices can disintegrate into the environment in a controlled fashion without leaving any toxic products behind. Transient technology is rapidly gaining ground for biomedical applications, zero waste electronics, and data-secure hardware, to name a few. To power such devices, transient batteries are required. To date, there are very few reports on transient batteries in literature, mainly due to the lack of suitable soluble materials, fabrication schemes, and battery designs that must fulfill entirely different requirements than traditional batteries.

Here, we reported the development of a fully transient lithium-ion battery (LIB) with competitive electrochemical performance. At first, we designed a degradable separator based on polyvinyl alcohol and cellulose nanocrystals that offer several unique advantages: electrolyte (organic solvent-based) uptake

up to 510%, the ionic conductivity of 3.077 mS/cm, electrochemical stability up to 5.5 V vs. Li/Li⁺, and a high transference number of 0.56. As a result, a stable lithium metal deposition and a high specific capacity of 105 mAh/g in Li/LiFePO₄ cell for over 250 cycles were achieved for the separator soaked in organic electrolyte. The toxic organic electrolyte was replaced with a biodegradable ionic liquid, providing an ionic conductivity of 0.988 mS/cm and a specific capacity of 87 mAh/g in Li/LiFePO₄ cell. Finally, the ionic liquid-separator pair was assembled into a fully transient lithium-vanadium(V) oxide (Li-V₂O₅) cell, which can be cycled over 400 times and degraded in 15 minutes once an aqueous trigger was applied. This prototype of a transient LIB represents a proof of concept to develop innovative transient energy storage systems with a long lifecycle.

SESSION EN06.08: Urban Mining II
Session Chair: Clara Santato
Tuesday Morning, December 7, 2021
EN06-Virtual

8:00 AM *EN06.08.01

Resource Recovery from Wastewater Using Bioelectrochemical Systems [Praveena Gangadharan](#); Indian Institute of Technology Palakkad, India

The rapid growth of population generates huge waste, and its management is extremely challenging. In fact, wastewater is a well-recognized valuable source of renewable resources like water, energy, nutrients, heavy metals, etc. Considering the overall depletion of renewable resources from the earth, wastewater treatment facilities need to be upgraded as renewable resource recovery facilities. Such advancement replaces the use of fossil fuels for energy source and facilitates clean water production and cradle-to-cradle waste management. In this context, the bioelectrochemical system (BES) has gained much attention as it converts organics in wastewater to electrical energy by microbial interactions on the electrode. Beyond pollutant removal, BES exhibits critical functions like recovery of water, nutrients, and heavy metals from wastewater/industrial effluents. In recent years, extensive studies on BES have grown up with more research articles from different countries making this technology truly comprehensive.

The present talk will throw light into the various applications of BES, especially energy production from organic wastewater, concentrating nutrients and recovering water from urine, water recovery by desalination, and chromium and copper recovery from industrial effluents. The presentation will also brief on the prospects of recycling/reusing e-waste for synchronized removal/recovery of heavy metals along with energy production using BES.

8:30 AM *EN06.08.02

Circular Economy in Electronics and Electronic Waste Recycling [Maria Holuszko](#)¹ and Nani Pajunen²; ¹The University of British Columbia, Canada; ²The Finnish Innovation Fund Sitra, Finland

Circular economy and the role of life-cycle analysis in the design and manufacturing of small electronic devices is the focus of this presentation. The transition towards a carbon neutral and circular economy as well as sustainability in the manufacturing of small electronic devices may be necessary and possible sooner than one could expect. There are enormous prospects in the recovery of valuable components and critical materials from e-waste as well as the promotion of eco-design and design for recyclability, all of which could be coupled with the business opportunities. According to some, if the circular economy were to be carried out extensively, it could reduce the consumption of new materials substantially - possibly by more than 50% by 2050. There are many barriers to moving from our currently-practiced cradle-to-grave economy, discussed in this presentation in the context of electrical and electronic equipment (EEE) devices as well as material design and development. This presentation provides perspective on recycling, life cycle analysis in the design process, challenges for e-waste recycling, and drivers for change in the complex industrial system.

9:00 AM EN06.08.03

Backscattered Visible Light Sensing—Towards Ecologically Aware Sensor Systems [Andreas P. Weiss](#), [Kushal Madane](#), [Christian Fragner](#), [Andreas Kröpfel](#), [Stefan Schantl](#) and [Franz P. Wenzl](#); Joanneum Research Forschungsges mbH, Austria

Today it becomes more and more apparent that the conception of the Internet of Things (IOT) in the manner of objects equipped with a multitude of electronic sensors that all communicate with one another will pose serious problems both from ecological (energy consumption, e-waste) and technical (bandwidth limitations) point of views.

Nowadays, with the rise of light-emitting diode (LED) based luminaires also functionalities beyond illumination become more and more of relevance. For example, light can take over communication tasks and thereby offload the RF-spectrum. In this so-called visible light communication (VLC) scenario, the data are encoded into intensity modulations of the light emitted by the LEDs of the luminaires. Subsequently, these modulations are recorded by a photosensitive device, for example a photodiode. Furthermore, besides its application for communication, this infrastructure (modulated LEDs and photosensitive elements), can be also applied for another promising functionality future luminaires can provide, visible light positioning (VLP), which is on the way to play a decisive role in indoor localization.

While an enormous number of research studies focus on VLC and VLP, at present another potential functionality of artificial lighting, which again takes advantage of the same infrastructure as VLC and VLP, emerges: Visible Light Sensing (VLS). VLS expands the scope of functionalities of lighting into the domains of sensing and detection. In VLS, the photosensitive element records that light emitted from the luminaire that is reflected backwards from an object. Based on this principle and by equipping the objects with tailored reflective materials that purposively modulate the spectrum and/or the intensity of the light reflected from the object, information can be conveyed. Most notably, the basic concept of VLS only necessitates to equip the object with optical structures, but does not require any active device to be placed on the object. The basic conception of VLS relies on backscattering, which, in general, is one of the most promising technologies to be added in the 6G era of wireless communication technologies. Although most discussions on backscatter communication currently focus on RF-backscatter, similarly to the complementary role of VLC and RF for communication, also visible light-based backscatter technologies have a huge potential to complement RF-based ones.

An appropriate coding strategy for exploiting the visible light spectral range in this regard is to equip surfaces with colored "codes", consisting of tailored sequences of different colors and the reflected light from this surface is detected with the help of an RGB-photodiode and further on analyzed. Appropriate machine learning algorithms can support this analysis and allow to maintain a high percentage of correct classifications even in case that the lighting conditions are changed.

Here we discuss appropriate system designs for artificial lighting sources, which allow for tunable artificial illumination (dimming and variation of color temperatures of the luminaires) while still being able to perform sensing tasks in parallel. Examples include the identification and velocity determination of indoor moving objects, the determination of the rotation direction and the rotation velocity of a robotic arm or the determination of the rotation of a human wrist by using a colored wristband. All these examples do not require any active devices to be placed on the objects. We show how the sensing tasks can be operated in parallel with tunable illumination and in parallel with communication (VLC). With this, artificial lighting, which is obligatory at least in indoor

environments, including VLC, VLP and VLS functionalities turns out as a promising technology for fulfilling one of the crucial challenges of 6G, which is to amalgamate sensing, positioning and communication, while drastically reducing energy use and e-waste.

9:15 AM *EN06.08.04

Commercially-Relevant, Cadmium-Containing Qdots as Models to Study Environmental Fate and Toxicity of TV Display Components [Audrey Moores](#), Aude Bechu, Subhasis Ghoshal, Saji George, Maureen McKeague, Niladri Basu and Ke Xu; McGill University, Canada

Cadmium-containing quantum dot nanoparticles (QDs) are integrated into electronic displays because of their ability to efficiently convert colors. There are conflicting accounts as to whether these particles present a hazard to the environment, as they have been studied either as (1) embedded QDs in display screen films or (2) as model QDs with small, hydrophilic ligands. Both approaches have limitations that we addressed by synthesizing QDs featuring the core-shell structure and the thick polymer coating present in commercial devices. These models are used to probe the effect of environmental fate, in the form of low pH conditions, aerobically and anaerobically, as well as their transformation. Toxicity with liver cells is analyzed for both pristine QDs and the ones exposed to different fate conditions. We also studied the fate of these model systems in gastrointestinal track (GIT) conditions and studied how each step leads to transformation of the QDs. GIT cells toxicity was also studied and cellular uptake explored.

9:45 AM EN06.08.05

Late News: Using the Ostrom Framework for Sustainable Social-Ecological Systems to Create Circular Economies [Carol A. Handwerker](#); Purdue University, United States

Creating circular economies requires creating resilient, sustainable, and self-managing communities of people who see circularity as vital to their livelihoods. Dr. Elinor Ostrom (2009 Nobel Laureate in Economics) laid out a framework for how people and organizations are able to develop voluntary, community-based solutions involving adaptive, self-governing systems that effectively manage "the commons," without the need for government regulations or privatization. I'll present examples where this framework of viewing products as "commons" has been applied, including creating a circular economy for hard disk drives. We will discuss how these concepts can be applied not only to other systems, but also to create a university community to train students to view materials, components, and products as parts of potential circular economies.

SESSION EN06.09: Electronics Synthesis II

Session Chair: Clara Santato

Wednesday Morning, December 8, 2021

EN06-Virtual

8:00 AM *EN06.09.01

Ecofriendly Materials for Digitally Printed Organic Light-Emitting and Electrochromic Devices [Gerardo Hernandez-Sosa](#)^{1,2}; ¹Karlsruhe Institute of Technology, Germany; ²InnovationLab, Germany

The field of *Green Electronics* strives for the sustainable fabrication and utilization of electronics via responsible use of resources and elimination of negative environmental effects. The most direct way to mitigate negative sustainability issues in most end-of-life phases would be the utilization of inherently sustainable materials and processes from the very conception of a technology. This would effectively simplify or reduce the economic, energetic and environmental burden on regulation, recycling or recovery of electronic waste.

In this contribution, we will discuss our efforts towards the fabrication of ecofriendly organic electronic devices. We will present the investigation of biodegradable electrolyte systems based on gelatin, DNA, poly(lactic-co-glycolic acid) and *Polycaprolactone* for the fabrication of light-emitting electrochemical cells (LEC) and electrochromic (EC) devices. We will present inkjet-printed LECs exhibiting maximum luminance over 12,000 Cd/m² operational lifetimes > 100 h and emission covering all the visible spectrum while containing > 90% ecofriendly materials. Furthermore, we will show EC devices which biodegradation was certified via an independently performed ISO (14855) test. These devices were integrated into a flexible inkjet-printed display demonstrating the potential of the industrial relevant printing techniques for the up-scalable fabrication of solution-processed ecofriendly electronics.

8:30 AM *EN06.09.02

One-step Conversion from Elemental Sulfur to Sulfur-Containing Functional Polymer Materials [Rongrong Hu](#); South China University of Technology, China

Sulfur-containing polymers have attracted increasing attention, owing to their fascinating properties such as metal coordination ability, high refractive indices, self-healing capability, optoelectronic property, and so on. However, the rapid development of sulfur-containing polymer materials are hindered by the lack of economic monomers and efficient synthetic approaches. On the other hand, the utilization of elemental sulfur is a global concern considering its large surplus from petroleum industry and the safety/environmental problems caused during its storage, which is an idea source for the preparation of sulfur-containing polymers with the challenges of the poor solubility of sulfur in organic solvents and its toxicity to transition metal catalysts.

In this talk, a series of elemental sulfur-based multicomponent polymerizations (MCPs) will be introduced to directly convert elemental sulfur to sulfur-containing polymers such as polythioamides, polythioureas, polycarbamothioates, and polythiophenes with well-defined structures, good solubility, high yields, and high molecular weights in one step. These MCPs can generally proceed smoothly with catalyst-free condition, at mild temperature such as room temperature, in air atmosphere, which also usually enjoy high atom economy and wide monomer scope, enabling facile construction of sulfur-containing polymer with great structural diversity. With the cost-effective monomers, mild conditions, and no harmful smelly side product released, several MCPs are proved to be scalable.

Besides the high refractive indices, potential high dielectric constants and semiconducting property for the potential application in sustainable electronics, these sulfur-containing polymers can also be applied in gold recovery from the abundantly discarded electronic wastes. They can extract trace amount of Au³⁺ selectively, rapidly, and efficiently from aqueous solution in the practical condition with strong acidity and other metal ion interferences, directly affording elemental gold with high purity through in situ reduction or simple pyrolysis.

These sulfur-based MCPs are economic, efficient, and convenient tools for the direct conversion from sulfur at mild condition to profitable sulfur-containing functional polymers, which could make use of both abundantly existing sulfur waste and trace amount of gold residue in electronic wastes, and accelerate the development of sulfur-containing polymers with diversified structures and functionalities, demonstrating their great potential in resource

utilization and sustainable electronics.

9:00 AM *EN06.09.03

***In Vivo* Polymerization of Conjugated Oligomers for Self-Organized Electronics in Plants and Animals** [Eleni Stavrinidou](#); Linköping University, Sweden

Leveraging the biocatalytic machinery of living organisms for fabricating functional bioelectronic interfaces in-vivo not only enables seamless integration of microdevices into the tissue but also a greener solution for advanced microfabrication. Previously we have demonstrated that plants can polymerize conjugated oligomers in-vivo forming conductors within their structure. We showed that the polymerization is enzymatically catalyzed by endogenous peroxidases and we developed a series of conjugated oligomers that can be enzymatically polymerized in physiological conditions. The conjugated polymers integrate within the plant cell wall structure adding electronic functionality into the plant that is then explored for energy storage. Recently we have extended this concept into an animal model system. We demonstrate that Hydra, an invertebrate animal can polymerize intracellularly conjugated oligomers in cells that expresses peroxidase activity. The conjugated polymer forms electronically conducting and electrochemically active domains in the μm range integrated within the hydra tissue. Our work paves the way for self-organized electronics in plant and animal tissue for modulating biological functions and in-vivo bio-fabrication of hybrid functional materials and devices.

SESSION EN06.10: Electronics Energy III

Session Chair: Clara Santato

Wednesday Morning, December 8, 2021

EN06-Virtual

10:30 AM *EN06.10.01

Next Generation, Low Embodied Semiconductors for Local Power and Light Sensing [Paul Meredith](#), Ardan Armin, Greg Burwell, Oskar Sandberg and Wei Li; Swansea University, United Kingdom

Next generation semiconductors such as the perovskites and organics can be sourced from earth abundant elements and processed from solution or via low temperature vapour deposition. This means they have intrinsically low embodied manufacturing energy and much reduced environmental footprints relative to more traditional semiconductor systems. In addition, organic semiconductors in particular (and in a more limited sense the perovskites) can be tuned at the molecular level to provide a vast palette of different materials with engineered electro-optical properties such as optical gap, absorption coefficient, electron affinity and ionization potential, etc. These 'unique selling points' are increasingly recognized as essentials for creating more sustainable electronic and optoelectronic technologies, including in areas such as the internet of things (power sources and sensors), wearable and bioelectronic healthcare, and mobile, local clean energy generation.

In my talk I will specifically focus on the development of bespoke, spectrally tuned photovoltaics and photodetector systems. I will discuss the latest advances in perovskite and organic semiconductor PV in relation to (for example) indoor local power generation including considerations such as materials design, thermodynamics, spectral matching and the constraints of the crucial transparent conductive electrode. I will also outline recent results and latest thinking on the development of organic and perovskite semiconductor photodetectors – both greyscale and color sensitive, and show how it may be possible to engineer so called 'illuminant independent' full color imaging photodetectors of the sort required for true machine / artificial vision.

11:00 AM *EN06.10.02

Natural Materials Selection for High Performance and Low Energy Fabrication Avenues for Electronics [Mihai Irimia-Vladu](#); Johannes Kepler Universität Linz, Austria

Through its appealing avenues of processing the component devices at room temperature and from low-cost precursor materials, organic electronics has a tremendous potential for the development of products able to achieve the goals of production sustainability as well as environmental and human friendliness for electronics. In an effort to stave off the e-waste growth, the presenter and his research group went further down the path opened by organic electronics research and investigated a large number of biomaterials as substrates, dielectrics, semiconductors and smoothening layers for the fabrication of organic field effect transistors, integrated circuits and organic solar cells. The seminar presentation will focus on the highlights of our recent research, especially with respect to materials investigated, devices fabricated and the immense potential for follow up research:

-Flexible natural and biodegradable substrates with high resistance to solvent exposure and temperature stability

-Natural dielectrics

-Bio-origin, H-bonded semiconductors in the families of indigos, anthraquinones and acridones

-Bio-degradation protocols for organic semiconductors

The potential of follow-up research in the bioelectronics field is immense, with large area electronics fabrication, biomedical implants, bio-sensing and smart labeling, representing only the tip of the iceberg of many more immediate possibilities of high interest for our group. Natural and nature-inspired materials have the unrivalled capability to create "safe-first" electronic markets for human and environment, with minimal or even neutral carbon footprint.

SYMPOSIUM EN07

Mechano-Thermal and Electrical Coupling in Emerging Energy Materials

November 30 - December 8, 2021

Symposium Organizers
Shangchao Lin, Shanghai Jiao Tong University
Shengjie Ling, ShanghaiTech University
Seunghwa Ryu, KAIST

* Invited Paper

SESSION EN07.01: Mechano-Thermal and Electrical Coupling in Emerging Energy Materials I
Session Chair: Jingjie Yeo
Tuesday Morning, November 30, 2021
Sheraton, 3rd Floor, Hampton

10:30 AM *EN07.01.01

Modulating Polyelectrolyte Mechanical Properties with Electric Fields Meredith N. Silberstein¹, Prathamesh Raiter¹, Hongyi Cai¹, Zhongtong Wang¹ and Yuval Vidavsky²; ¹Cornell University, United States; ²Soreq NRC, Israel

Multifunctionality in polymers facilitates their application in emerging energy technologies. Electrical fields are a preferred stimulus because of the speed and ease of application to bulk polymers. While a wide range of electrically triggered actuators have been developed, and electrically controlled adhesion between gels has been demonstrated, modification of bulk mechanical properties via electrical stimuli remains elusive. Such a function could be particularly useful in electrochemical devices such as batteries and low temperature fuel cells that rely on polymer membranes to conduct ions while maintaining mechanical integrity. Fields vary temporarily and tend to deviate locally, for example from dendrite growth, and an electric field adaptive polymer could help avoid short circuits that lead to device failure. Polymers with covalently incorporated ionic charge should be well suited to achieving this goal since the mechanical properties depend on electrostatic interactions and these charges are intrinsically susceptible to electric fields. I will present our work investigating whether electric fields can modulate the mechanical properties of polyelectrolytes and our efforts to understand potential governing mechanisms. I will focus primarily on our molecular dynamics (MD) simulations. These simulations reveal the importance of polymer chain architecture and show how chain orientation and ion clustering relates to bulk mechanical properties. I will also share some of our theoretical, synthetic, and experimental work that builds from these MD simulations towards a physical realization of the idea.

11:00 AM EN07.01.02

Electrochemical Energy Harvester Driven by Eye-Blinking as a Power Supply to the Smart Contact Lenses Erfan Pourshaban, Mohit Karkhanis, Adwait Deshpande, Aishwaryadev Banerjee, Chayanjit Ghosh, Hanseup Kim and Carlos Mastrangelo; University of Utah, United States

Biomedical implantable and wearable electronic devices are promising tools to improve human wellness by real-time monitoring health indicators and curing disease more effectively. The development of smart contact lenses is of great importance mainly due to their wide range of applications, from vision correction to drug delivery. Accordingly, there are numerous research studies taking place to commercialize smart contact lenses. One of the main roadblocking issues toward its commercialization is the power supply and management for the microelectronics, which should be mounted on the device. Batteries, photovoltaics, and wireless power transfer are the most well-known strategies to supply power to smart contact lenses. However, all of these techniques suffer from several drawbacks. For instance, radio power scavenging either requires large antennas or the ranging distance is lower than 10 cm. Besides, batteries need periodic charging, which is a cumbersome practice for a contact lens user. On the other hand, mechanical to electrical energy conversion can supply power to the smart contact lenses by natural human eye blinking that is an environmentally independent source of energy. Triboelectricity based on contact electrification and electrostatic induction, piezoelectricity based on applying stress to a non-centrosymmetric crystal structure, and electrostatic generator based on capacitance gradient are among the most famous mechanisms to convert mechanical energy to electricity. However, herein, we demonstrate the performance of our recent mechanical to electrical energy harvester operating based on electrochemical reactions and charge transfer. A 300nm SiO₂ was thermally grown on a 5×5 mm² p-type silicon piece, followed by the spin coating of 2 μm Cytop as a hydrophobic layer. A 5×1 mm² of the SiO₂/Cytop stack was photolithographically patterned and etched utilizing CF₄ and oxygen gases with the flow rate of 50 and 5 sccm, respectively. A silver paste was used as the bottom contact of the device. Employing a linear actuator, the device has a back-and-forth motion (speed = 20 mm.s⁻¹) on a moisturizing eye drop in contact with a metal foil. In the present study, we have experimentally measured the electrical output of the sliding electrochemical electrifier using three metal foils, including copper (Cu), aluminum (Al), and gold (Au). The voltage outputs were directly detected at the Siglent oscilloscope with the input impedance of 1 MΩ. The current outputs were detected using the SR570 low noise amplifier. Results demonstrate the maximum voltage of 80, 200, 620 mV while using Cu, Au, and Al metals, respectively. The corresponding maximum currents are 17.5, 8, and 80 μA. Accordingly, we used a 4.7 μF capacitor to experimentally measure the energy and power output of the electrochemical sliding energy harvester. 15 nJ (0.075 μW.cm⁻²), 94 nJ (0.47 μW.cm⁻²), and 0.9 μJ (3.6 μW.cm⁻²) are the energy (power density) output of the device while using Cu, Au, and Al metals. The electrical output was recorded when the eye drop touches the device's contact (silver paste). The ascending voltage and energy outputs of the harvester is clearly following the electrochemical potentials of the metals. Physically speaking, the electrochemical reactions between the moisturizing eye drop and metals' surface resulting in redox reactions. Hence, the liquid either loses or gains electrons which will be dragged and transferred to the silver paste using the frequent sliding motion. This phenomenon can be optimized and used to supply power to the smart contact lenses through a natural eye blinking.

11:15 AM EN07.01.03

Manipulating and Understanding Barocaloric Effects in Metal–Organic Materials Jinyoung Seo¹, Ryan McGillicuddy¹, Adam Slavney¹, Selena Zhang¹, Andrey A. Yakovenko², Shao-Liang Zheng¹ and Jarad A. Mason¹; ¹Harvard University, United States; ²Argonne National Laboratory, United States

Barocaloric materials—which exhibit pressure-induced thermal changes—can be used to drive solid-state cooling cycles that offer an environmentally friendly alternative to vapor compression refrigeration. The development of efficient, scalable barocaloric cooling will benefit from a class of materials featuring a phase transition mechanism that provides large entropy changes, minimal hysteresis, high sensitivity to hydrostatic pressure, and chemical tunability. Here, we describe a mechanism for realizing a new class of materials that feature colossal and tunable barocaloric effects. This mechanism is

based on conformational order–disorder transitions of long-chain organic molecules—confined in space—that give rise to large changes in volume and entropy. Additionally, we demonstrate how the synthetic tunability of this system can be leveraged to control structural and chemical factors that influence the thermodynamics and kinetics of pressure-induced phase transitions. Through these efforts, we report a library of materials that feature a combination of colossal entropy changes, high barocaloric coefficients, and ultralow hysteresis. Further, the excellent processability of these materials, in combination with their unique mechanical properties, offers particularly simple strategies for harnessing barocaloric effects in prototype cooling devices across length scales. This work provides new insights into barocaloric effects of metal–organic materials, with a particular emphasis on understanding and manipulating thermodynamics and kinetics of pressure-induced phase transitions.

SESSION EN07.02: Mechano-Thermal and Electrical Coupling in Emerging Energy Materials II

Session Chair: Jingjie Yeo

Tuesday Afternoon, November 30, 2021

Sheraton, 3rd Floor, Hampton

1:30 PM *EN07.02.01

Modelling Biobased Materials—From Quantum Chemistry to Large-Scale Simulations Anna Bachs-Herrera¹, Isaac Vidal-Daza², Daniel York¹, Tristan Stephan-Jones¹, Jingjie Yeo³ and Francisco Martin-Martinez¹; ¹Swansea University, United Kingdom; ²Universidad de Granada, Spain; ³Cornell University, United States

The ability to valorise waste is a cornerstone of circular economy. Developing materials from waste biomass requires fundamental understanding of biomass degradation and biobased materials structure-property relationships. In this talk, we will provide an overview of ongoing work and future perspectives on multiscale modelling and simulations of biomass and biobased functional materials, including lignin, nanocellulose, chitin, biocrude oils, and carbon nanoparticles. By coupling modelling and simulations to hydrothermal processing (HTP) experiments we develop fit-for-purpose biobased materials with applications in energy harvesting and storage, infrastructure and precision agriculture, among others. We apply Density Functional Theory (DFT), Molecular Dynamics (MD) simulations, and coarse-grained (CG) modelling to simulate materials behaviour from the nanoscale to the mesoscale. We simulate chemical reactivity, electron transport, mechanical properties, and degradation mechanisms.

2:00 PM EN07.02.02

In-Plane Thermo-Mechanical Property of 2D Hybrid Organic-Inorganic Perovskites Doyun Kim¹, Eugenia S. Vasileiadou², Ioannis Spanopoulos², Mercouri G. Kanatzidis² and Qing Tu¹; ¹Texas A&M University, United States; ²Northwestern University, United States

2D hybrid organic-inorganic perovskites (HOIPs) are low-cost, high-performance semiconductor materials with great potential demonstrated in various fields, including photovoltaics, light-emitting diodes, lasers, and field-effect transistors. During device fabrication and device operation, 2D HOIPs will go through various temperature statuses. Because of the hybrid organic and inorganic nature, the temperature fluctuation will cause a significant influence on the mechanical behavior of 2D HOIPs, which is vital for material processing and device durability, but is largely unknown. Here we measured the in-plane elastic modulus E of a prototypical 2D HOIP, $(C_4H_9-NH_3)_2(CH_3NH_3)_2Pb_3I_{10}$ as a function of temperature across a range of technological interest (*i.e.*, -15 °C to 65 °C) by AFM stretching suspended 2D HOIP nanosheets. Compared to the values at room temperature, E varies by more than 20% and exhibits a non-monotonic temperature dependence, which does not follow the general anharmonic expectation of the thermo-mechanical behavior for materials, where a higher temperature usually leads to weaker bonds and lower E . The observed abnormal trend can be explained by temperature-induced melting and stacking of the organic spacer molecules, which modulates the interlayer interactions of the 2D HOIPs at the van der Waals interface. Our results reveal the critical role of the organic layers in determining the mechanical behaviors of 2D HOIPs, unlike the negligible influence of the organic cations on the mechanical properties of their 3D counterparts, and provides indispensable insights into the processing and device applications of 2D HOIPs involving temperature fluctuations

2:15 PM EN07.02.03

Topographically-Modified Triboelectric Nanogenerator by Controllable Phase Separation of Polymer Blend Films Kuan Cheng, Haleh Ardebili, Hadi Ghasemi and Alamgir Karim; University of Houston, United States

Conventional methods to harvest and supply energy can hardly satisfy the rapid expansion of the Internet of Things (IoT). As an emerging solution, flexible triboelectric nanogenerators (TENGs) have been invented and developed for over a decade to scavenge mechanical energy from the ambient environment. The operation of TENGs mostly depends on contact electrification, which exists between any two materials with electrostatic charge potential difference which makes it a portable solution to energy generation on demand in the future. Much research has focused in recent years on enhancing the output power of TENGs to its maximum limit. To optimize the performance of TENGs, choosing the desirable material pair with high work function difference, increasing contact surface area between materials, and designing an efficient device structure are deemed to be the three most dominant tasks. Even though many strategies have been applied to enhance contact electrification, for instance, adding nanoparticles or nanofiller, plasma treatment, soft lithography, dry-etch, etc., most of them are still restricted by the materials selection, cost of chemical processing, and loss of mechanical properties. Herein, we present a robust and unique route to fabricate a surface-modified triboelectric nanogenerator to harvest wind energy, realized by the phase separation of polymer blend films. Among many nature and organic matter, polyvinylidene difluoride (PVDF) has been experimentally proven as excellent dielectric materials in TENGs and other energy harvesting technologies, owing to its good formability and flexibility, large dipole moment, and low acoustic impedance. Our proposed approach is based on the increase of surface roughness in nanoscale derived from the controlled phase separation of PVDF containing blend film. This strategy is aimed to enhance the performance of PVDF films in TENGs by regulating the contact surface area and the mechanical energy induced by relative friction force. The topographically designed films, along with metal electrodes, fixed on a supporting device is seamlessly assembled by additive manufacturing (3D printing). The fabrication of future TENG devices followed our proposed methods will be cost effective, and target high power density output in the competition for power via next-generation flexible devices and electronics.

We acknowledge Kostas Research Institute(KRI) At Northeastern University Grant #555033-78055 for the support of the work.

2:30 PM EN07.02.04

Understanding the Metal-Insulator Transition in Transition Metal Oxides Jonathan Paras and Antoine Allanore; Massachusetts Institute of Technology, United States

Developing a stronger understanding of the metal-insulator transition in transition metal oxides (TMOs) is key for modulating the performance of TMO devices. Two TMO materials (NbO_2 and VO_2) exhibit metal-insulator transitions whose thermodynamics have proven difficult to describe using conventional electronic structure calculation methods. We develop a formalism that links electronic transport properties to the state electronic entropy and apply this formalism to calculate the change in the electronic entropy of transition. Our electronic entropy calculations agree with estimates of the vibrational entropy and calorimetrically measured totals. Further, these calculations suggest a method for quantifying the effect of doping on the transition entropy, thereby enabling the engineering of the metal-insulator transition as a function of chemistry. For systems where the thermodynamics of the transition are well understood, our formalism provides estimates of the electronic transport properties, including Seebeck coefficient and resistivity.

2:45 PM EN07.02.05

Electro-Chemo-Mechanical Coupling—A Novel Approach to Micro Actuation Evgeniy Makagon¹, Ellen Wachtel¹, Lothar Houben¹, Sidney R. Cohen¹, Yuanyuan Li², Junying Li², Anatoly Frenkel² and Igor Lubomirsky¹; ¹Weizmann Inst of Science, Israel; ²Stony Brook University, United States

The chemo-mechanical effect in solids refers to dimensional change due to change in stoichiometry. Dimensional change due to electrochemically-induced compositional change has been termed the electro-chemo-mechanical (ECM) effect. The mechanical instability inherent in this effect is clearly deleterious for batteries or fuel cells, but, as recently suggested, has potential for use in actuation[1]. The structure of an actuator device that operates on the ECM principle comprises a micrometer thick solid electrolyte (SE) sandwiched between two ECM-active, working body (WB) layers. An electrochemical reaction must occur in these layers, causing them to alternately expand or contract. In order to facilitate the ECM response, the WB layers should have mixed ionic and electronic conductivity and a large chemical expansion coefficient.

We have constructed a 2mm diameter thin film membrane ECM actuator device comprising 20mol% Gd doped CeO_2 (20GDC) as the SE and $[\text{TiO}_2 \delta]20\text{GDC}$ or $[\text{V}_2\text{O}_5 \delta]20\text{GDC}$ composites as the WBs[2]. Selected area electron diffraction measurements showed the composite to be nanocrystalline, a morphology that promotes interfacial oxygen ion diffusion. Synchrotron X-ray absorption (XAS) measurements detected a mixture of $\text{Ce}^{3+}/\text{Ce}^{4+}$ ($\sim[0.4]/[0.6]$) and $\text{Ti}^{3+}/\text{Ti}^{4+}$ ($\sim[0.1]/[0.9]$) oxidation states in the WB. XAS measurements under bias showed changes in the short-range order of Ti and V oxides supporting the presence of a redox reaction. The deformation of the ECM actuator was observed to be in the bending regime producing large vertical displacements ($\sim 3 \mu\text{m}$) and $\sim 4 \text{ MPa}$ stress. The stress/voltage ratio yields a pseudo piezoelectric stress coefficient of $e_{31}=1.26 \text{ C/m}^2$, comparable to common lead-free piezoelectrics such as lithium niobate, lithium tantalate and alkali niobates.

SESSION EN07.03: Poster Session: Mechano-Thermal and Electrical Coupling in Emerging Energy Materials

Session Chair: Jingjie Yeo

Tuesday Afternoon, November 30, 2021

8:00 PM - 10:00 PM

Hynes, Level 1, Hall B

EN07.03.01

Late News: Ultrafast Spectroscopy of Hot Electrons and Chemical Potential Shifts in Al During Conditions of Strong Non-Equilibrium William Riffe, Md. Rafiqul Islam and John A. Tomko; University of Virginia, United States

Metals remain the prototypical test-bed for understanding ultrafast energy transfer amongst non-equilibrium carrier populations, such as electron-phonon scattering rates, due to their dynamics being well-described by the two-temperature model (TTM). The majority of experimental studies in this area of research have devoted their efforts to pump-probe measurements of gold films due to its relatively simple electronic band structure and corresponding optical response. Aluminum, on the other hand, has received significantly less attention, despite a number of works demonstrating interesting and unique processes such as preferential phonon scattering times and non-thermal phonon populations that greatly affect the ultrafast dynamics. Additionally, the understanding of ultrafast energy processes in Al is more relevant than ever, particularly at low temperatures, due to its applicability in quantum sciences. In this work, we perform a series of wavelength-resolved ultrafast thermometry measurements to directly monitor the dynamics of both the lattice and hot electrons near the interband transition threshold of Aluminum thin films. By monitoring the ITT energy as a function of both incident fluence and pump-probe time delay, we extract changes in the Fermi energy, and thus electronic chemical potential, based on varying electron temperatures. Further, by relating the wavelength-dependent response, an accurate model of the electron temperature of Aluminum upon ultrafast heating is extracted, allowing for measure of an average electron-phonon coupling factor.

SESSION EN07.04: Mechano-Thermal and Electrical Coupling in Emerging Energy Materials III

Session Chairs: Shengjie Ling and Seunghwa Ryu

Monday Morning, December 6, 2021

EN07-Virtual

8:00 AM *EN07.04.01

Engineering of Carbon and Silk Materials Toward Flexible Electronics Yingying Zhang; Tsinghua University, China

Flexible and wearable electronics are attracting wide attention due to their potential applications in wearable human health monitoring and care systems. It is of great importance to explore low cost and scalable preparation approaches for high performance flexible and wearable electronics. Carbon materials have combined superiorities such as good electrical conductivity, intrinsic and structural flexibility, light weight, high chemical and thermal stability, ease to be chemically functionalized, as well as potential mass-production, enabling them to be promising candidate materials for flexible and wearable electronics. In the last several years, based on the unique properties of nanocarbon materials, we have been working on the rational design and controlled fabrication of flexible electronics based on carbon nanotubes, graphene, silk and their hybrid materials and explored their applications in human health monitoring and human-machine interfaces. For examples, we have used carbon materials, including carbon nanotubes, graphene, and natural mass derived carbon as the key materials and develop a series of flexible wearable sensors (strain sensors, pressure sensors, temperature sensors, airflow sensors, sweat monitoring patch etc.), wires and flexible energy devices. The hierarchical structures of the carbon materials plays important roles in achieving flexible devices with desired performance. We have also explored the application of silk in flexible sensors by developing a carbonization strategy of silk

nanofibers and fabric and by combing nanocarbons with natural silk materials. High performance strain/pressure/temperature sensors, E-skin, silk/graphene E-tattoos, and silk based conductive wires have been developed. We also developed new technique for the 3D printing of nanocarbon-silk-based smart fibers/textiles. Based on the above, the applications of the obtained electronics in human health monitoring (such as pulse, breath, and temperature and environmental risks), human motion tracking, and human-machine interfaces have been demonstrated. These strategy provide new approaches for the low-cost production of high performance flexible and wearable electronics, which may promote the development of next generation smart electronics.

8:30 AM EN07.04.02

Electro Curing of Oriented Bismaleimide Between Aligned Carbon Nanotubes for High Mechanical and Thermal Performances Lin Qiu; University Of Science and Technology Beijing, China

Aligned assembly of carbon nanotubes (CNTs) is the key for high mechanical, electrical and thermal properties for CNT fibers. To overcome the weak van der Waals interactions between the CNTs, thermosetting polymers can be introduced into the fibers because efficient strengthening can be realized after a thermal curing. Here a better curing strategy, namely electro curing, is applied to bismaleimid (BMI)-impregnated CNT fibers to improve the inter-tube thermal transport. As the electric current is conducting along the CNT surface and induces the strongest Joule heating right there, the aromatic BMI resins can be cured into an oriented structure. Under the optimal curing current whose Joule heating is strong without inducing the BMI degradation, the fiber's intrinsic thermal conductivity can be improved from 30 to 177 W m⁻¹K⁻¹, and the apparent conductivity can be up to 374 W m⁻¹K⁻¹ at a sample length of 12 mm. The effect of thermal radiation is also semi-quantitatively studied by estimating the real surface area that radiates heat in the 3 ω method.

9:00 AM EN07.04.03

Molecular Dynamics Simulations of the Structure-Thermal-Mechanics Relationship of Polyvinyl Alcohol and Its Composite Materials Junbo Zhou^{1,2} and Zhao Qin¹; ¹Syracuse University, United States; ²Shanghai Starriver Bilingual School, China

Plastic, though once is considered a miracle material with its durability and malleability, now poses a significant environmental problem by creating hazardous wastes, because of its massive application to single-use products and difficulty in degradation in nature. Our team aims to create a substitute of plastic with better mechanical strength, low cost, and biodegradability for fields like agriculture, packaging, and more. Polyvinyl alcohol (PVA) is a water-soluble synthetic polymer that can be used to make non-toxic bags/films which break down over time. Its production keeps increasing and it has been used in food and drug packaging, as well as biomedical fields including cartilage replacements and contact lenses. Its massive use can effectively reduce land and ocean pollution. However, it lacks thermal stability and is easy to absorb water from a humid environment. We are thus motivated to investigate the large-scale molecular structures of PVA and reveal its structure-thermal-mechanics relationship by using molecular dynamics simulation. We obtain the folded PVA structure from a fully extended state and unfold it in steered molecular dynamics to reveal its nanomechanics, as well as how it interfaces to other biomolecules. We find that the PVA structure folded at room temperature is stabilized by the randomly formed hydrogen bonds between hydroxyl groups but there is a lack of ordered structure, making the structure easy to unfold by temperature fluctuation and interaction with water molecules. A smaller amount of crystallinity and less energy dissipation is found by comparing to the PVA sheet-like structures folded through the annealing process. We study the hybrid mixture of PVA and collagen and investigate how the PVA structure and mechanics are stabilized by forming the interface with collagen. Our study provides insights into mixing PVA to collagen to construct a biodegradable composite material with higher thermal and humidity, enabling its durability in use but still friendly to the environment.

9:15 AM EN07.04.04

A Micromechanical Study of Creep Fracture of FeCoNiCrMn at High Temperature Chi Hua Yu^{1,2}, Wei-Tang Huang¹, Chang-Wei Huang³, Yu-Chieh Lo⁴ and Shian-Ching Cheng⁵; ¹National Cheng Kung University, Taiwan; ²Massachusetts Institute of Technology, United States; ³Chung Yuan Christian University, Taiwan; ⁴National Yang Ming Chiao Tung University, Taiwan; ⁵National Central University, Taiwan

High entropy alloys have attracted extensive attention due to the complex formation from several metal elements and their extraordinary performances, such as lightweight, high ductility in extreme working temperatures. In this study, we studied the intergranular creep fracture of FeCoNiCrMn by exploiting micromechanical modeling. We considered a dislocation-based crystal plasticity model for grain interior and a cohesive zone model for grain boundary sliding and separation. We developed an integrated computational framework to simulate the mechanical properties of FeCoNiCrMn by implementing user-defined material (UMAT) for grain interiors and user-defined element (UEL) for grain boundaries in commercial finite element software Abaqus. We first performed a parametrical study to examine the robustness of the model. The simulation results agree well with the experimental research. Furthermore, we discussed the effects of strain rate, grain boundary separation, and grain boundary viscosity on the mechanical behaviors. We found that the stress concentration occurs at the grain boundaries with a larger disorientation angle, making the grain boundary prone to separate from alleviating this severe strain inhomogeneous. Finally, the competition mechanisms of creep fracture for FeCoNiCrMn were studied. The simulation result suggested that the creep fracture is dominated by grain boundary separation, consistent with the experimental observation. Thus, our model can be applied to study grain interior and grain boundary mechanical behavior at high temperature for different high entropy alloys with great potential in automobile, aerospace, and high-performance alloy design.

SESSION EN07.05: Mechano-Thermal and Electrical Coupling in Emerging Energy Materials IV

Session Chairs: Shangchao Lin and Jingjie Yeo

Monday Afternoon, December 6, 2021

EN07-Virtual

9:00 PM *EN07.05.01

Biaxial Strain and Electron-Phonon Coupling Effects on Thermal Transport Properties of GaN Bingyang Cao; Tsinghua University, China

GaN-based electronic devices has been widely applied in energy, information and vehicle areas. Strain inevitably exists in practical GaN based devices due to the mismatch of lattice structure and thermal expansion brought by heteroepitaxial growth and band engineering with strain, and significantly influence phonon thermal properties of GaN. In this work, phonon properties and thermal conductivity of GaN including contribution from electron-phonon coupling (EPC) as well as the effects of in-plane biaxial strain are systematically investigated using the first principle calculation method and phonon Boltzmann transport equation. Thermal conductivity of free GaN is 263 and 257 W/mK for in-plane and cross-plane directions, respectively, which is consistent better with the maximum experimental values in literature than previous theoretical reports, and shows a nearly negligible anisotropy of thermal conductivity. Under strain state, thermal conductivity changes remarkably both in absolute values and anisotropy. For instance, under +5% tensile strain state, average thermal conductivity at room temperature decreases by 63% while it increases by 53% under -5% compressive strain state, which is mostly attributed to the

changes of phonon relaxation time. Besides, anisotropy of thermal conductivity changes under different strain states, which may result from the weakening effect from strain induced piezoelectric polarization. EPC is also calculated from first principles, and it decreases the lattice thermal conductivity significantly. Specifically, the decrease shows significant dependence on strain state, which is due to the relative changes between phonon-phonon and electron-phonon scattering rates, as well as the absolute value of lattice thermal conductivity without including EPC. Under compressive strain state, decreases of lattice thermal conductivity are 15% and 18% for in-plane and cross-plane conditions, respectively, comparable with those under free state. However, the decreases become very small under tensile strain state, especially for cross-plane condition, which results from the decreased electron-phonon scattering rates and increased phonon anharmonicity.

9:30 PM *EN07.05.02

Liquid Thermocells with High Thermopowers for Low-Grade Heat Harvesting Yang Han¹, Jian Zhang¹, Run Hu² and Dongyan Xu¹; ¹The Chinese University of Hong Kong, Hong Kong; ²Huazhong University of Science & Technology, China

Low-grade heat is abundant in the ambient environment and provides a sustainable energy source for health monitoring devices and wireless sensor network. Liquid thermocells offer a promising solution for converting the widespread low-grade heat directly into electricity due to the advantages of relatively high thermopower, low cost, and high flexibility. Recently, we developed a polarized ternary electrolyte that switches from n-type to p-type when the hot electrode temperature is heated above the gelation temperature of methylcellulose. The ternary electrolyte achieves ultrahigh thermopowers of -8.18 mV K^{-1} for n-type and 9.62 mV K^{-1} for p-type. The polarization switching can be attributed to the strong hydrophobic interaction between methylcellulose and I_3^- ions, while the giant thermopowers mainly come from the thermogalvanic effect of the I^-/I_3^- redox couple enhanced synergistically by methylcellulose and potassium chloride. With the developed electrolyte, a single p-type liquid thermocell gives rise to an open-circuit voltage of 134 mV and a maximum power of 80.47 mW under a temperature difference of 15°C , corresponding to a normalized maximum power density of $0.36 \text{ mW m}^{-2} \text{ K}^{-2}$, which is far superior to other reported I^-/I_3^- -based liquid thermocells. Our work demonstrates a cost-effective, high-thermopower polarized electrolyte for low-grade heat harvesting.

10:00 PM *EN07.05.03

Strain-Engineering the Thermal and Electronic Properties of 2D Semiconducting Materials Yong-Wei Zhang¹, Zhun-Yong Ong¹, Gang Zhang¹, Zhi-Gen Yu¹ and Kah-Wee Ang^{2,3}; ¹Institute of High Performance Computing, Singapore; ²National University of Singapore, Singapore; ³Institute of Materials Research and Engineering, Singapore

Two-dimensional (2D) semiconducting materials, such as phosphorene, MoS_2 , InSe, et al. have attracted a great deal of interest due to their unusual structures and fascinating physical properties promising for many novel applications. Since these 2D materials are able to sustain a large tensile strain, which can cause significant changes in electronic and thermal properties, strain engineering is an effective approach to tune their physical properties, which can greatly widen their applications. To do so, however, it is both important and necessary to understand and further tune these properties by applying strain.

In this talk, we report our research work on the strain engineering of 2D semiconducting materials to tune their electronic and/or thermal properties by using computational study. Using first-principles calculations and the non-equilibrium Green's function method, we investigate ballistic thermal transport in 2D monolayer phosphorene. A significant crystallographic orientation dependence of thermal conductance is observed. Furthermore, we find that the thermal conductance anisotropy with the orientation can be tuned by applying strain. In particular, the zigzag-oriented thermal conductance is enhanced when a zigzag-oriented strain is applied but decreases when an armchair-oriented strain is applied; whereas the armchair-oriented thermal conductance always decreases when either a zigzag- or an armchair-oriented strain is applied. The present work suggests that the remarkable thermal transport anisotropy and its strain-modulated effect in single-layer phosphorene may be used for thermal management in phosphorene-based electronics and optoelectronic devices. Next, using first-principles calculations, we design a 2D transition metal compound, Ni-MoS₂, to investigate its HER catalytic performance. We reveal that with strain engineering, the bandgap can be reduced and a semiconductor-to-metal transition can be induced, which lead to an enhancement in the charge transfer and HER performance. Moreover, together with strain engineering, the thermoneutral condition can be achieved at the S vacancy concentration of only $\sim 2.5\%$, which is in strong contrast to $\sim 12.5\%$ required for MoS₂. Finally, we report our work of using 2D InSe to fabricate a flexible and ultrasensitive three-terminal strain sensor. The strain sensor shows a prominent enhancement of sensitivity through gating effect. We also demonstrated InSe based flexible transistor and Boolean inverter circuit, which achieves a high mobility and an on/off current ratio. This work highlights the potential of using InSe as a common material platform for next generation flexible electronics and strain sensors applications.

10:30 PM EN07.05.04

Strain Engineering for Tailored Thermoelectric Performance in Metal Halide Perovskites from First-Principle Calculations Shangchao Lin¹, Lifu Yan² and Lingling Zhao²; ¹Shanghai Jiao Tong University, China; ²Southeast University, China

Emerging metal halide perovskites have attracted attentions in thermoelectric energy conversions due to their ultralow thermal conductivity and excellent carrier transport properties. Using first-principle calculations, we find that halogen mixing (alloy) in $\text{CsPb}(\text{I}_{1-x}\text{Br}_x)_3$ not only leads to suppressed thermal conductivity, but also anisotropic carrier transport due to symmetry-breaking induced residue strains. External strain engineering strategies could tailor various thermoelectric properties, including carrier effective mass, carrier lifetime, and lattice thermal conductivity, in a more controllable manner to achieve the optimal thermoelectric figure of merit (ZT). Anisotropic ZT values predicted for $\text{CsPb}(\text{I}_{1-x}\text{Br}_x)_3$ upon uniaxial or biaxial loading show a wide range of variations from 20% to 400% compared to the unstrained cases with an enhanced ZT up to ~ 1.5 at 300 K. In addition, they could be used to reduce the optimal carrier concentration to achieve the maximum ZT by an order of magnitude compared to the unstrained cases, providing a new avenue to tackle the challenge in heavily-doping perovskites.

SESSION EN07.06: Mechano-Thermal and Electrical Coupling in Emerging Energy Materials V

Session Chairs: Shangchao Lin and Seunghwa Ryu

Tuesday Morning, December 7, 2021

EN07-Virtual

8:00 AM *EN07.06.01

Energy-Conversion Efficiency of Twisted-Filament Artificial Muscles Zhiping Xu; Tsinghua University, China

Artificial muscles are materials or devices producing work or motion under external stimuli. Recently, twisted-filament artificial muscles (TFAMs) have

been demonstrated to meet the demands of miniaturization and multi-functionality in smart systems. TFAMs share a two-step process in triggering rotation or contraction: volumetric expansion and tension-torsion coupling. Various actuating mechanisms such as thermal expansion, electrochemical cues, solvents absorption were proposed. To understand the performance of TFAMs, we simulate the actuating processes by numerical simulations using the discrete elastic model (DER). Theoretical analysis is also conducted for models with a symmetric cross section in supplementary to the simulation results, revealing the basic principles that direct the actuating performance. We estimate the energy conversion efficiency as a function of the material properties and microstructural characteristics, which identifies the upper limits for realistic artificial muscles. We conclude that artificial muscles of twisted-microfilaments still have much space to improve in terms of the energy-conversion efficiency and work capacity.

8:30 AM *EN07.06.02

Tailoring Piezoelectric Polymer Nanofibers for Energy Harvesting Miso Kim; Sungkyunkwan University, Korea (the Republic of)

Piezoelectric polymer nanofibers have emerged as a competitive platform for shape-adaptive energy harvesting and sensing applications because of mechanical flexibility, lightweight, and relatively low-temperature processing. However, a key challenge has been the relatively low piezoelectric coefficients of these organic piezoelectric materials when compared to their inorganic counterparts. Here, we summarize a collection of advances that push the boundaries to achieve a drastic enhancement of mechanical energy harvesting performance by tailoring both material and structural properties of electrospun piezoelectric polymer fibers at multi-scales. Engineering structural morphology of piezoelectric materials from molecular to device scales will be discussed as a route to achieving improvement in the key figures of merit for energy harvesting and sensing, along with our unfolding new understanding of the underlying physics.

9:00 AM EN07.06.03

Neural Network-Assisted Optimization of Segmented Thermoelectric Power Generators Using Active Learning Based on Genetic Optimization Algorithm Wabi Demek and Seunghwa Ryu; KAIST, Korea (the Republic of)

Because the best performing temperature range of thermoelectric (TE) materials differ from each other, segmented TE legs stacked with multiple TE materials has been studied as a mean to improve the performance of thermoelectric generators (TEGs). However, due to the inherent nonlinearity that limits the application of conventional optimization approaches, the optimal segmented TEGs (STEGs) had to be sought heuristically. In this study, we propose a systematic approach enabling the efficient exploration and exploitation of vast design space of STEG by leveraging the fast inference of deep learning. First, we train a neural network (NN) model using dataset generated from FEM simulations for a single TE leg stacked with 4 segments out of 18 TE materials by varying segment lengths and external load. We then conduct a genetic optimization algorithm (GOA) using our trained NN model to search for high-performing design candidates. The performance of the new candidates are computed with FEM, which is used to update the neural network by active transfer learning technique. After iteratively performing the procedure, we are able to fine-tune the TE legs with optimal efficiency, optimal power, as well as a given combination of both. Furthermore, we discuss the physical origin of the optimal performing STEGs.

9:30 AM *EN07.06.04

Thermoelectric Efficiency Theory for Temperature-Dependent Thermoelectric Properties Byungki Ryu, Jaywan Chung and SuDong Park; Korea Electrotechnology Research Institute, Korea (the Republic of)

Thermoelectric effects refer to the direct energy conversion between thermal and electrical energies. When a temperature difference is applied on a thermoelectric element, a thermoelectric generator module can generate electrical power with induced electrical voltage and current while the thermoelectric heat current flows with Fourier (diffusion) and Peltier heat.

Traditionally, thermoelectric efficiency is estimated using a simple metric called a dimensionless figure of merit, expressed as $zT = (\alpha^2/\rho\kappa)T$, where α , ρ , κ , and T are the Seebeck coefficient, electrical resistivity, thermal conductivity, and temperature, respectively. In the constant property model (CPM), in which thermoelectric properties are constant, the maximum thermoelectric efficiency η_{\max} is simply given as $\eta_{\max} = (T_h - T_c)/T_h \times [(1+zT_m)^{0.5} - 1]/[(1+zT_m)^{0.5} + T_c/T_h]$, where T_h and T_c are hot- and cold-side temperatures, respectively, and T_m is $(T_h + T_c)/2$ [1]. With a monotonic nature of zT_m in efficiency, it has been widely used to guide thermoelectric material discovery.

However, as the thermoelectric conversion module works under a non-zero temperature difference ($T_h - T_c > 0$), the crucial assumption of CPM that thermoelectric properties are constant no longer holds. Some studies have attempted to find a suitable efficiency metric for wide temperature applications [1–7]. However, many recent studies have shown that discrepancies between the CPM and efficiency are unavoidable [8–14]. Although a few cumulative approaches have been investigated to correct thermoelectric heat current equations [12,13], the accuracy of efficiency prediction remains questionable. In addition, a counterintuitive example between ZT and efficiency highlights the need for a highly accurate efficiency evaluation method [14]. This type of non-negligible mismatch becomes an obstacle for further material optimization and device design for higher efficiency.

In this work, we develop the general efficiency theory of thermoelectric conversion with temperature-dependent thermoelectric properties to overcome the limitation of zT . We derive thermoelectric equations for power conversion and heat transfer, where the thermoelectric differential equation is successfully transformed into the T integral equation. By introducing two additional indices in addition to the proper definitions for device parameters, we formulate heat current equations at boundaries. As a result, we derive an efficiency equation determined by three thermoelectric degrees of freedom (DOFs): Z_{gen} , τ , and β , where the existence of non-zero τ and β well explains the origin of the discrepancy between CPM and efficiency. Our thorough data-driven investigation on approximately 300 published materials confirms that our method is sufficiently accurate. Furthermore, we find that efficiency is a monotonic function of each DOF, which indicates the potential use of a DOF as a figure of merit. Finally, with suitable temperature approximation, we derive highly accurate approximate analytical expressions for thermoelectric module performance that can be easily applied to segmented leg design and p/n-leg pair module performance estimation even with interfacial contact resistance.

[1] A.F. Ioffe, Semiconductor Thermoelements and Thermoelectric Cooling (1957).

[2] J.M. Borrego, IEEE Trans Aerospace 2, 4 (1964).

[3] G. Min et al., J. Phys. D 37, 1301 (2004).

[4] G.J. Snyder and A.H. Snyder, EES 10, 2280 (2017).

[6] B. Ryu, Bulletin of the American Physical Society 64, R47.00007 (2019).

[7] P. Ponnusamy et al., Appl. Energy 262, 114587 (2020).

[8] B. Sherman et al., JAP 31, 1 (1960).

[9] B. Ryu et al., ArXiv:1810.11148 (2018).

[10] B. Ryu et al., ArXiv:1910.11132 (2019).

[11] P. Ponnusamy et al., Müller, Entropy 22, 1128 (2020).

[12] A.A. Efremov and A.S. Pushkarsky, Energy Conversion 11, 101 (1971).

[13] H.S. Kim et al., PNAS 112, 8205 (2015).

[14] B. Ryu et al., APL 116, 193903 (2020).

10:30 AM *EN07.07.01

Trapping of Ionic Defects and Long-Lived Electret States in Methylammonium Lead Halides—Insights from Classical Molecular

Dynamics Alessandro Mattoni and Claudia Caddeo; Istituto Officina dei Materiali - IOM Materials Foundry Consiglio Nazionale delle Ricerche - National Research Council, Italy

Hybrid organic-inorganic perovskites have attracted enormous attention for low-cost solution-processable photovoltaics. In addition to the excellent defects-tolerant optoelectronic properties of the metal halide inorganic lattice, hybrid perovskites have peculiar properties associated to the hybrid organic/inorganic and covalent/ionic nature, giving rise to phenomena coupling electronic properties and ionic dynamics, of relevance for sensing, thermoelectricity, spintronics and many others.

We start discussing the ability of classical interatomic force-fields[1], to reproduce the main structural and thermodynamical properties of 3D and 2D hybrid perovskites[2] and we review a selection of properties associated to ionic dynamics: the dielectric response and macroscopic polarization[3]; the ultra-high and anisotropic mobility of ionic defects[4]; the interaction of defects with extended defects[5,6] and their relevance for hysteresis and memory effects. In particular we report evidence of the formation of long-lived electret states associated to the interaction of defects and ferroelastic domains in the tetragonal phase[7].

[1] A. Mattoni, A. Filippetti, and C. Caddeo, "Modeling hybrid perovskites by molecular dynamics," *J. Phys. Condens. Matter*, vol. 29, no. 4, p. 043001, Feb. 2017. 10.1088/1361-648X/29/4/043001

[2] Giri, A.; Chen, A. Z.; Mattoni, A.; Aryana, K.; Zhang, D.; Hu, X.; Lee, S.-H.; Choi, J. J.; Hopkins, P. E. Ultralow Thermal Conductivity of Two-Dimensional Metal Halide Perovskites. *Nano Lett.* 2020, 20 (5), 3331–3337 10.1021/acs.nanolett.0c00214

[3] A. Mattoni and C. Caddeo, "Dielectric function of hybrid perovskites at finite temperature investigated by classical molecular dynamics," *J. Chem. Phys.*, vol. 152, no. 10, p. 104705, Mar. 2020. 10.1063/1.5133064

[4] P. Delugas, C. Caddeo, A. Filippetti, and A. Mattoni, "Thermally Activated Point Defect Diffusion in Methylammonium Lead Trihalide: Anisotropic and Ultrahigh Mobility of Iodine," *J. Phys. Chem. Lett.*, vol. 7, no. 13, 2016. 10.1021/acs.jpcclett.6b00963

[5] C. Caddeo, A. Filippetti, and A. Mattoni, "The dominant role of surfaces in the hysteretic behavior of hybrid perovskites," *Nano Energy*, vol. 67, p. 104162, Jan. 2020. 10.1016/j.nanoen.2019.104162

[6] N. Phung *et al.*, "The Role of Grain Boundaries on Ionic Defect Migration in Metal Halide Perovskites," *Adv. Energy Mater.*, vol. 1903735, p. 1903735, Apr. 2020. 10.1002/aenm.201903735

[7] A.G. Lehmann *et al.*, "Long-lived electrets and lack of ferroelectricity in methylammonium lead bromide $\text{CH}_3\text{NH}_3\text{PbBr}_3$ ferroelastic single crystals," *Phys. Chem. Chem. Phys.* vol. 23, p. 3233–3245. 2021 <https://doi.org/10.1039/D0CP05918H>.

11:00 AM EN07.07.02

Late News: Enhancing Thermophotovoltaic Performance Using Graphene-BN-InSb Heterostructures Rongqian Wang, Jincheng Lu and Jian-Hua Jiang; Soochow University, China

Near-field Thermophotovoltaic (NTPV) cells have attracted a wide range of research interest due to their enhanced performances compared to far-field counterparts. However, most of the existing studies are focused on the regime where the thermal emitter has very high temperature, e.g., higher than 1000 K, corresponding to solar radiations or heat radiations from a secondary emitter which receives the solar energy. Besides, due to the considerable frequency mismatch between the thermal emitter and the PV cell, the near-field effect becomes ineffective and the performance of the NTPV systems is significantly reduced.

In our previous paper [1], We focus on the situation where the temperature of the thermal emitter is in the range of common industrial waste heat, i.e., 400 K ~ 800 K. To convert such mid infrared thermal radiation into electricity and to make the photon tunneling efficient, we propose to use graphene-h-BN heterostructures as the emitter and the graphene-covered InSb p-n junction as the TPV cell. We show that the optimal output electrical power can reach 76000 Watts per square meters and the best efficiency is achieved with 33% of the Carnot efficiency. These results show that the performances of near-field thermophotovoltaic systems can be comparable with or even superior to the state-of-the-art thermoelectric devices. The significant improvement of the thermophotovoltaic performance is understood as due to the resonant coupling between the emitter and the p-n junction, where the surface plasmons in graphene and surface-phonon polaritons in boron nitride play crucial roles.

It is remarked that our findings are consistent with the study in Ref. [2], where the synergy between near-field thermal radiation and inelastic thermoelectricity is shown to have considerably improved performance even in the linear-transport regime. Apart from this, our work is also based on the previous studies where the near-field effects are shown to improve the heat radiation flux by orders of magnitude via infrared hyperbolic metamaterials [3-4].

Reference papers:

[1] Rongqian Wang, Jincheng Lu and J.-H. Jiang, Enhancing Thermophotovoltaic Performance using Graphene-BN-InSb Near-Field Heterostructures, *Phys. Rev. Applied* 12, 044038 (2019).

[2] Jian-Hua Jiang and Yoseph Imry, Near-field three-terminal thermoelectric heat engine, *Phys. Rev. B* 97, 125422 (2018).

[3] Bo Zhao and Zhuomin Zhang, Enhanced photon tunneling by surface plasmon polaritons in graphene/h-BN heterostructures, *J. Heat Transfer* 139, 022701 (2015).

[4] Bo Zhao, Brahim Guizal, Zhuomin Zhang, Shanhu Fan, and Mauro Antezza, Near-field heat transfer between graphene/hBN multilayers, *Phys. Rev. B* 95, 245437 (2017).

11:15 AM EN07.07.03

Organic Inorganic Hybrid Thermoelectric Generator Using Low Cost Non-Toxic Materials Y.M.D.C.Y. Bandara¹, L.K. Narangamma¹, Ajith DeSilva² and T. M. W. J. Bandara¹; ¹University of Peradeniya, Sri Lanka; ²University of West Georgia, United States

The search of alternative energy resources, the development of novel technologies and devices to fight against the use of fossil fuel is indeed a subject of interest worldwide. Thermoelectricity which transforms heat energy directly into electricity, can be utilized to convert waste heat into electricity. The

thermoelectric generators that consist of an array of *p-n* junctions made of two different thermoelectric materials (TEMs) that create a potential difference as the result of a temperature difference across the junction. Widely used and the best known TEMs are hazardous in nature such as Bi₂Te₃ and Sb₂Te₃, therefore, there is a need for a search of new non-toxic TEMs. In this study, thermal, electrical as well as thermoelectric properties of organic polymer of polyaniline (PANI) and inorganic ceramic material of Zinc oxide (ZnO) are investigated. The study is extended to fabricate a novel organic/inorganic *p-n* junction as a hybrid thermoelectric generator using PANI and ZnO, whereas organic *p* and inorganic *n* type material respectively using compressed pellets of HCl doped PANI and Al doped ZnO. Electrical conductivity, thermal conductivity and Seebeck coefficient were investigated, and the figure of merits was calculated for PANI, ZnO and Al-doped ZnO. Fourier-transform infrared and XRD spectra confirmed the synthesis of PANI, ZnO and Al-doped ZnO. The pellets of PANI, ZnO and Al-doped ZnO exhibited electrical conductivities of 63.6 (90 °C), 313 (100 °C) and 356 S m⁻¹ (100 °C) respectively. The thermal conductivities of respective pellets are 7.38 (90 °C), 23.8 (100 °C), 14.0 W m⁻¹ K⁻¹ (100 °C) respectively. PANI showed a positive Seebeck coefficient (confirming the *p*-type nature) of 34.6 μV K⁻¹ at 90 °C. ZnO and Al-doped ZnO showed negative Seebeck coefficients (confirming the *n*-type nature) of -165 μV K⁻¹ and -225 μV K⁻¹ respectively at 100 °C. The PANI/ZnO junction generator exhibited a voltage of 21.9 mV for a temperature difference of 78 °C across the junction.

11:20 AM EN07.07.04

Frequency, Temperature, Voltage Tunability and Optical Constant Measurement of VO₂/V_{1-x}W_xO₂ Thermochromic Films for Device Applications Golali Naziripour¹, Jin Cheng Zhao², Guru Subramanyam², Eunsung Shin², Andrew Sarangan², Chin-Cheng Chiang¹ and Zhihong Chen¹; ¹Purdue University, United States; ²University of Dayton, United States

Vanadium dioxide (VO₂) and W-doped Vanadium dioxide (VO_{2-x}) are known to be reliable thermochromic materials for their insulating/metal transition temperature, which can be controlled by the doping concentration level (x), in VO₂/V_{1-x}W_xO₂. In this paper, the deposition of various thicknesses VO₂ and W doped V_{1-x}O₂ films on R plane substrate, with two different techniques including (a) pulse laser deposition (PLD) and (b) by reactive electron beam deposition was described.

Various parameters including resistance, refractive index, extinction coefficient, as a function of temperature from 25 to 80 degree C and wavelength ranging from 500 to 3000nm using direct TR, are set up in addition to conventional ellipsometry.

Comparison between reflectance and transmission of spectra obtained from doped and un-doped vanadium shows that below the IMT temperature or in the insulating state, the doped VO₂ is more reflective and less transitive. The real and imaginary parts show that the doped materials produce a loss in the results, which has been confirmed by n and k and RT at various temperature and frequencies, a lower doping level and higher oxygen concentration is needed

Moreover, the influence of temperature and doping on direct and indirect optical has been reported and various phases have been identified by comparing the transition temperature for direct and indirect bandgap data at room and elevated temperature. Comparison of various batches synthesized at different temperatures shows intermediate phases including VO₂(B) and V₂O₅ shows at a lower temperature less than 500 degree C, single phase is produced by heating the film at elevated temperature and adjusting oxygen pressure. Finally, We are able to adjust various parameters to make the film more suitable for practical applications including frequency detector and memory devices for NIR frequencies.

11:25 AM *EN07.07.05

Mechanical and Thermal Effects of Low Dimensional Materials on Nanocomposites Arun K. Nair; University of Arkansas, United States

Nanocomposites have tremendous application in many industries due to their superior mechanical, and unique thermal properties. In automobile industry this class of composites are used for door panels, engine cover, tire, and for improving gas mileage. In energy and aerospace sector, it is used to make windmill blades and aircraft components. Low dimensional materials-based nanocomposites are also gaining interest in the scientific community. For all broad applications possible in industry, the quest for composites with superior mechanical and thermal properties are common factors. Low dimensional materials are prime candidates to achieve these properties. This talk focuses on the mechanical and thermal properties of low dimensional materials in nanocomposites and investigates different types, shape, and bonding characteristics of low dimensional materials on metallic substrates.

We use different computational methods to predict the thermal stability of low dimensional materials on nickel and copper substrates. We then studied the mechanical and interface properties of low dimensional materials-based nanocomposites and investigated the use of low dimensional materials as a fiber in nanocomposites. The result of these studies show that the mechanical properties of a metal matrix can be improved with the addition of these low dimensional materials and provide an insight into the design of metal-based nanocomposites.

SESSION EN07.08: Mechano-Thermal and Electrical Coupling in Emerging Energy Materials VII
Session Chairs: Shangchao Lin and Jingjie Yeo
Tuesday Afternoon, December 7, 2021
EN07-Virtual

9:00 PM *EN07.08.01

Fundamental Study on Phonon Modulation Nuo Yang; Huazhong Univ of S&T, China

Recently, with the rapid development of smart society, our demand for new functional materials and hardware is urgent. Thermal functional materials play an important role in thermal management, energy storage and energy conversion. Phonons are lattice vibrational waves, which are the main energy carriers in dielectric solids. After electronic engineering and photonic engineering, the research progress of phonon engineering has attracted much attention.

Phonon engineering is the discipline of designing and controlling phonon transport and conversion by using phonon devices with micro/nano structure, which plays a leading role in the design of thermal functional materials. The research objects of phonon engineering include lattice wave quantum transport, thermoelectric conversion, phonon devices and so on. The progress of nanotechnology has also promoted the development of phonon engineering, so there is an urgent need to understand the mechanism of phonon regulation and transport.

Professor Nuo YANG and the Nano Heat Group [1] focus on the fundamental and applied research of heat transfer, thermal control and energy conversion in micro/nano scale. The report will introduce the research progress of the Nano Heat Group in the following aspects: nanoscale heat conduction [2-6], thermal control [7-12], thermoelectric conversion [13-15], etc.

References

- [1] <http://nanoheat.energy.hust.edu.cn/>
- [2] Wan, et.al Nano Lett. 19, 3387 (2019)

- [3] Deng, et.al *Materials Today Phys.* 16 (2021) 100305
- [4] An, et.al *Nano Lett.* 17, 5805 (2017)
- [5] Xiao, et.al *ES Mater. Manuf.*, (2019), 5, 2
- [6] Zhang, et.al arXiv:1905.09183
- [7] Deng, et.al *Nano Energy* 82 (2021) 105749
- [8] Wan, et.al *Materials Today Physics* 20 (2021) 100445
- [9] Ma, et.al *Materials Today Phys.* 8(2019) 56
- [10] Yu, et.al *Chin. Phys. Lett.* 38, (2021) 014401 Express
- [11] Ma, et.al *Phys. Rev. B* 98 (2018), 245420
- [12] Yang, et.al *Phys. Rev. B* 103, 155305 (2021)
- [13] Mi, et.al *Nano Lett.* 15, 5229, (2015)
- [14] Ding, et.al *J Mat Chem A*, 7(2019), 2114
- [15] Ji, et.al *Materials Today Physics* 19 (2021) 100430

9:30 PM *EN07.08.02

Interfacial Thermal Resistance Between Two-Dimensional Materials and Their Dielectric Substrate Xiangfan Xu; Tongji University, China

Interfacial thermal resistance (ITR) plays an important role in thermal dissipation across different materials and it has been widely investigated in recent years. An example is the integrated electronic circles in which heat dissipating issue has recently become the bottleneck. With further miniaturization of electronics, the accumulated waste heat has increased the operating temperature to a high value where thermal management and heat dissipation become crucial for the performance of devices^[1]. The severe thermal management problem has prevented the operating frequency from going beyond several GHz when the dissipated waste heat exceeds 100 Wcm⁻². This work is separated into two parts: (a) Chemical vapor deposition (CVD) method was utilized to fabricate monolayer transition metal dichalcogenides (TMDCs) depositing directly onto SiO₂/Si substrate; we demonstrated that the interfacial thermal conductance of TMDCs/oxide was significantly promoted by introducing a phonon vibration bridge at the interface of TMDCs/oxide^[2-5]. (b) We introduced an additional electron-phonon coupling channel in the thermal transport across graphene-dielectric interfaces and the scanning thermal microscopy technique measurement of graphene electronic devices gave direct evidence of an enhanced heat dissipation by tuning the surface carries concentration^[6].

References:

- [1] X. Xu *et al. Adv. Mat.* **30**, 1705544 (2018); *Adv. Funct. Mater.* **30**, 1904704 (2020)
- [2] J. Guo *et al. J. Phys. D: Appl. Phys.* **52**, 385306 (2019)
- [3] D. Liu *et al. Nat. Comm.* **10**, 1188 (2019)
- [4] X. Li *et al. J. Phys. D: Appl. Phys.* **50**, 104002 (2017)
- [5] D. Liu *et al. Adv. Electron. Mater.* **6**, 2000059 (2020)
- [6] Zhang *et al. ES Energy & Environ.* **8**, 42-47 (2020)

10:00 PM *EN07.08.03

Coherent Phonon Transport in Nanostructures Jie Chen; Tongji University, China

The particle nature of phonons has been widely studied in the past, and the control of thermal transport is mainly focused on the *incoherent scattering mechanisms* via various approaches, such as defect, roughness, isotope and etc. Thanks to the advances in the synthesis technology of nanostructures with ultra-fine features, the study on the wave nature of phonons, namely the coherent phonons, is receiving increasing attention recently. In this talk, I shall first discuss the physical mechanism for storing monochromatic and coherent phonons in a host-guest system built by carbon schwarzite structure. Interestingly, the coherent phonons stored in this phonon nanocapacitor can also be released separately via uniaxial strain. Then, I will demonstrate that a phononic rectifier, which has asymmetric thermal transport in two directions, with large rectification efficiency can be realized based on such host-guest system. Finally, I will discuss how to achieve total-reflection and total-transmission of individual phonons in the periodic nanostructures. Our study reveals that the control of coherent phonons offers a new path to regulate the thermal and phonon transport in nanostructures.

10:30 PM *EN07.08.04

Illusion Thermotics-Enabled Thermal Metamaterials Run Hu; Huazhong University of Science and Technology, China

Thermal metamaterials have attracted increasing attentions in recent years as they can be used to manipulate heat almost at will by resorting to specific-designed anisotropic thermal properties beyond natural materials. Most thermal metamaterials are designed by the prevailing transformation thermotics, an extended version of transformation optics in the thermal field. However, the traditional transformed thermal metamaterials only work well without heat sources. To cope with it, we develop the illusion thermotics techniques and proposed some new thermal functionalities such as thermal camouflage, thermal printing, and so on. Both the transformation thermotics and topology optimization were used to achieve illusion thermotics. In this talk, I will introduce the illusion thermotics and the state-of-the-art progress of thermal metamaterials.

SESSION EN07.09: Mechano-Thermal and Electrical Coupling in Emerging Energy Materials VIII

Session Chairs: Shangchao Lin and Shengjie Ling

Wednesday Morning, December 8, 2021

EN07-Virtual

8:00 AM *EN07.09.01

Colossal Barocaloric Effects—A Delicate Tuning of Heat by Pressure Bing Li; Shenyang National Laboratory for Materials Science, Institute of Metal Research, Chinese Academy of Sciences, China

Colossal barocaloric effects (CBCEs) have been discovered in a class of disordered solids called plastic crystals as the cooling effects of pressure-induced phase transitions [1]. CBCEs are characteristic of huge entropy changes up to several hundred joules per kilogram per kelvin under a small pressure change, which are attributed to the combination of extensive molecular orientational disorder, giant compressibility, and highly anharmonic lattice dynamics of these materials [1,2].

Following this physical scenario, a diversity of colossal barocaloric materials have been found, which exhibit very distinct performances including thermal conductivity, thermal hysteresis, critical pressure, transition temperature spans under pressure, and so forth. In particular, NH_4SCN has been identified as the first system with inverse CBCEs [3]. A compromise would be made based on the systematical considerations of these factors and practically promising colossal barocaloric materials can be expected. In this regard, our efforts will be reported in detail.

In addition to refrigeration, the application of colossal barocaloric materials in thermal energy storage has been exploited as well. Compared to the conventional phase-change materials, pressure is an extra dimension and enhances the controllability of heat. In the presentation, the concept of barocaloric thermal batteries will be demonstrated.

References:

- 1) B. Li et al., *Nature* **567**, 506-511 (2019).
- 2) F. B. Li et al., *Nat. Commun.* **11**, 4190 (2020).
- 3) Zhe Zhang et al., arXiv:2103.04348.

8:30 AM EN07.09.03

Late News: The Synergy of Electronic and Geometry Structure Leads to Ultra-Low Thermal Conductivity—A Comparison of Graphene-Like Compounds [Linfeng Yu](#) and Guangzhao Qin; Hunan University, China

The design of new systems with specific technical interests through structural properties and bonding promotes the vigorous development of materials informatics. Here, we propose the concept of component reconstruction, which based on combination the structural and bonding characteristics of initial materials. With this strategy, we developed a new two-dimensional graphene-like compound, named as $g\text{-B}_3\text{N}_5$, which has light atomic mass but counter-intuitive ultra-low thermal conductivity of 21.08 W/mK. The ultra-low thermal conductivity is attributed to the component reconstruction of $g\text{-BN}$ and nitrogene, which will lead to a synergy of electronics and geometry on thermal transport. Thus, the dominant acoustic branches are strongly softened, and simultaneously the scattering absorption and Umklapp process are suppressed, resulting in low thermal conductivity. Furthermore, based on the component reconstruction strategy, we also constructed $g\text{-B}_3\text{P}_5$ and $g\text{-B}_3\text{As}_5$ with ultra-low thermal conductivity of 2.50 and 1.85 W/mK, respectively. The ultra-low thermal conductivity materials with lightweight atomic mass cater to the need for lightweight development of momentum machinery, such as aerospace vehicles, high-speed rail, and automobiles.

8:45 AM EN07.09.04

Atomistic Simulation of Ferroelectric Domain Growth in BaTiO_3 by Applied Electric Field: Effects of Vacancies [Takahiro Tsuzuki](#)¹, [Shuji Ogata](#)¹, [Ryo Kobayashi](#)¹, [Masayuki Uranagase](#)¹, [Seiya Shimoi](#)¹, [Saki Tsujimoto](#)¹, [Frank Wendler](#)² and [Dilshod Durdiev](#)²; ¹Nagoya Institute of Technology, Japan; ²Friedrich-Alexander University of Erlangen-Nürnberg, Germany

BaTiO_3 (BT) is a well-known ferroelectric and piezoelectric material, widely used in various devices as, e.g., capacitor for electric circuit, stress sensor, and actuator. However, little is known about the atomistic dynamics of ferroelectric domain growth. Depending on the production procedure (e.g., solidification from melt), doping (e.g., La), and oxygen gas pressure, various point defects are expected to form in BT. The oxygen vacancies (V_{O}) exist at a relatively low oxygen pressure. As for the barium vacancy (V_{Ba}) or titanium vacancy (V_{Ti}) that exist in oxygen-rich BT, the experiment and DFT calculations predicted that such negatively charged monovacancies may combine with positively charged V_{O} to form the divacancy $V_{\text{Ba}}\text{-}V_{\text{O}}$ or $V_{\text{Ti}}\text{-}V_{\text{O}}$. In this study, we comprehensively analyze the effects of mono- and di-vacancies on the domain growth of BT by using the MD simulation with the core-shell inter-atomic potential. We consider not only the monovacancies V_{Ba} , V_{Ti} , and V_{O} but also the divacancies of 1st- and 2nd-neighbor $V_{\text{Ba}}\text{-}V_{\text{O}}$ and $V_{\text{Ti}}\text{-}V_{\text{O}}$. We also compare the domain growth speed between the parallel and perpendicular directions to the applied electric field. We found the following: (1) One kind of monovacancy, $V_{\text{O}1}$, located on the TiO plane perpendicular to the applied electric field direction, acts to hinder the polarization inversion induced by the applied electric field. The monopole electric field produced by $V_{\text{O}1}$ either hinders or assists the local polarization inversion in accordance with the local intensity of the total electric field. (2) The 1st-neighbor divacancies $V_{\text{Ba}}\text{-}V_{\text{O}}$ and $V_{\text{Ti}}\text{-}V_{\text{O}}$, as compared to the 2nd-neighbor divacancies, asymmetrically affect the domain growth with respect to the applied electric field, determining the hysteresis behavior of applied electric field vs. polarization. The domain grows even at a small electric field when the directions of the applied electric field and the divacancy dipole are mutually the same. (3) The domain growth speed towards the applied electric field direction is about 2 orders of magnitude higher than that towards the perpendicular direction.

8:50 AM EN07.09.05

Inverse Domain-Size Dependence of Piezoelectricity in Ferroelectric Crystals [Bo Wang](#)¹, [Fei Li](#)² and [Long-Qing Chen](#)¹; ¹The Pennsylvania State University, United States; ²Xi'an Jiaotong University, China

Piezoelectricity of ferroelectric crystals has been widely utilized in electromechanical devices such as sensors and actuators. It is broadly believed that the smaller the ferroelectric domain size, the higher the piezoelectricity, arising from the commonly assumed larger contributions from the domain walls. Here we theoretically analyze the domain-size dependence of piezoelectric coefficients of prototypical ferroelectric crystals, guided by phase-field simulations. We reveal that the inverse domain-size effect, i.e., the larger the domain size, the higher the piezoelectricity, is just as common. The nature of the domain-size dependence of piezoelectricity is shown to be determined by the propensity of polarization rotation inside the domains instead of the domain wall contributions. We establish a simple, unified analytical model for predicting the domain-size dependence of piezoelectricity, which is valid regardless of the crystalline symmetry, the materials chemistry, and the domain structures of a ferroelectric crystal, and thus can serve as a guiding tool for optimizing piezoelectricity of ferroelectric materials beyond the “nanodomain” engineering. The same strategy can be extended to understand the microstructural size effect of multiple-physical coupling properties in ferroic material systems to achieve a combination of seemingly conflicting properties.

9:05 AM EN07.09.07

Large Non-Classical Electrostriction in Aliovalent and Isovalent Doped Ceria [Maxim Varenik](#), [Ellen Wachtel](#), [Elad Gaver](#) and [Igor Lubomirsky](#); Weizmann Institute of Science, Israel

The majority of commonly used electrostrictive ceramics are based on lead manganese niobate. These ceramics display large electrostriction strain coefficients $\approx 10^{-16} \text{ m}^2/\text{V}^2$ at frequencies up to a few kHz; however they suffer from two major drawbacks: large dielectric constants (>10000), which require high driving currents, and incompatibility with thin-film Si-microfabrication techniques. We have recently reported that aliovalent doped ceria exhibits electrostriction coefficients >100 -fold larger than estimated on the basis of Newnham's scaling law for classical electrostrictors, despite ceria's large Young's modulus ($\sim 200 \text{ GPa}$) and low dielectric constant (~ 30). This “non-classical” behavior has been attributed to the formation of highly polarizable, elastic dipoles reorienting under external electric field.

For 10mol% Sm- or Gd-doped ceria, the measured longitudinal electrostriction strain coefficient, $|M|$, reaches $10^{-16} \text{ m}^2/\text{V}^2$; however, relaxation to $< 10^{-$

$10^{-18} \text{ m}^2/\text{V}^2$ is observed at frequencies $> 1 \text{ Hz}$, well below the technologically important frequency range $100\text{Hz}-100 \text{ kHz}$. The introduction of aliovalent lanthanide dopants with smaller radii than that of Gd, such as Lu or Yb, succeeds in increasing $|M|$ at 100Hz to $\gg 10^{-17} \text{ m}^2/\text{V}^2$. Nevertheless, aliovalent dopants with radii smaller than that of Lu do not continue the trend.

We have found that partially reduced, $10 \text{ mol}\%$ Zr^{4+} -doped ceria displays $|M| \approx 10^{-16} \text{ m}^2/\text{V}^2$ throughout the $0.1-150 \text{ Hz}$ frequency range. However, practical application of these ceramics may be hindered by the relatively large, room-temperature electrical conductivity (10^{-10} S/m), a result of the formation of Ce^{3+} which can promote electron hopping. Formation of Ce^{3+} also raises the dielectric constant to $\gg 200$, as measured by impedance spectroscopy.

Suppression of Ce^{3+} by co-doping with $0.5 \text{ mol}\%$ Yb produces a dramatically reduced electrostriction strain coefficient (at $f = 0.1-150\text{Hz}$), $\sim 4 \times 10^{-18} \text{ m}^2/\text{V}^2$. If the Yb concentration is raised to $10 \text{ mol}\%$, $|M|$ increases to $\sim 2 \times 10^{-17} \text{ m}^2/\text{V}^2$ but is sharply lowered to $2 \times 10^{-18} \text{ m}^2/\text{V}^2$ at $15 \text{ mol}\%$ Yb. Co-doping with a large radius, aliovalent lanthanide, e.g. $0.5-10 \text{ mol}\%$ La, returns the measured high frequency $|M|$ to $4 \times 10^{-18} \text{ m}^2/\text{V}^2$.

Taken together, these results suggest that elastic dipoles induced in ceria ceramics by small aliovalent dopants, give stronger electrostrictive response at high frequencies ($>10 \text{ Hz}$) than the larger aliovalent dopants. For the case of isovalent doping with Zr of reduced ceria, the presence of Ce^{3+} seems to be essential for large $|M|$. Noting that Ce^{3+} is almost as large as La^{3+} , we may conclude that the elastic dipoles operating in Zr-doped, reduced ceria are fundamentally different from those observed for aliovalent doping. Our results imply that by systematically adjusting the composition of ceria-based solid solutions, the potential exists for development of technologically useful electrostrictive materials which are, at the same time, fully compatible with Si-microfabrication.

SESSION EN07.10: Mechano-Thermal and Electrical Coupling in Emerging Energy Materials IX
Session Chairs: Shangchao Lin and Seunghwa Ryu
Wednesday Morning, December 8, 2021
EN07-Virtual

10:30 AM *EN07.10.01

Nanoslot Patterns to Tune the Phonon Transport within Thin Films [Qing Hao](#); University of Arizona, United States

Nanoporous thin films with periodic circular pores have been extensively studied for their potential applications such as thermoelectrics, heat waveguides, thermal cloaks, thermal diodes, and heat imaging [1]. Fundamentally, it is acknowledged that diffusive phonon scattering by pore edges, as classical phonon size effects, is the major mechanism for the observed thermal conductivity reduction. Despite some earlier debates, phononic effects due to coherent phonon transport within a periodic structure are found to be only critical at cryogenic temperatures [2-4].

Based on classical phonon size effects, new nanoporous patterns have been pursued to better tune the thermal conductivity of thin films [5, 6]. As one new pattern, periodic nanoslots can be employed to effectively tune the in-film phonon transport. When phonons travel ballistically through the narrow neck between adjacent nanoslots, a ballistic thermal resistance is introduced to lower the thermal conductivity. As a result, the lattice thermal conductivity can be largely reduced along the direction perpendicular to nanoslot rows, while keeping a much higher thermal conductivity along the direction parallel to nanoslots. The in-plane thermal anisotropy can be further enhanced with offset nanoslot patterns [7], which can largely benefit the thermal management of thin-film devices.

In analytical modeling, an accurate characteristic length can be derived for nanoslot patterns to predict the thermoelectric properties of such films [8, 9], whereas an accurate characteristic length is hard to be found for thin films with periodic circular pores [1]. For representative nanoslot patterns, the thermoelectric properties can be predicted and compared with nanostructured bulk Si [7, 8]. The predicted thermal conductivities agree well with the experimental data on some nanoslot-patterned Si thin films. A bulk-like specific heat is also measured for these thin films, indicating negligible phononic effects to change the phonon dispersion.

In nanoslot-patterned thin films, the in-plane thermal resistance is a strong function of the neck width between nanoslots. By measuring a series of samples with varied neck widths, inverse phonon transport analysis can be used to reconstruct the in-plane phonon MFP distribution down to $\sim 10 \text{ nm}$ [9, 10]. In this aspect, pump probe measurements using nanofabricated heating patterns [11-12] are not suitable for suspended thin films because phonon modes and scattering can be remarkably affected with deposited metal patterns [13]. In practice, nanoporous patterns can also be used to achieve two-dimension thermal cloaking or thermal camouflaging [7]. This new application will also be discussed.

References:

1. Xiao et al., *ES Materials & Manufacturing*, 2019, 5, 2-18.
2. Hao et al., *Scientific reports*, 2018, 8, 1-9.
3. Maire et al., *Science Advances*, 2017, 3, e1700027.
4. Lee et al., *Nature Communications*, 2017, 8, 14054.
5. Romano et al., *Applied Physics Letters*, 2014, 105, 033116.
6. Romano et al., *Applied Physics Letters*, 2017, 110, 093104.
7. Xiao et al., *International Journal of Heat and Mass Transfer*, 2021, 170, 120944.
8. Hao et al., *Physical Review Applied*, 2020, 13, 064020.
9. Hao et al., *Materials Today Physics*, 2019, 10, 100126.
10. Anufriev et al., *Physical Review B*, 2020, 101, 115301.
11. Hu et al., *Nature nanotechnology*, 2015, 10, 701-706.
12. Zeng et al., *Scientific reports*, 2015, 5, 17131.
13. Anufriev et al., *Nanoscale*, 2017, 9, 15083-15088.

11:00 AM EN07.10.02

Electrical and Mechanical Properties of Thermally Drawn Multimaterial Fibers [Xiaoting Jia](#); Virginia Tech, United States

Recent advancement in the thermal drawing of multimaterial fibers have enabled unique material properties and functions in a scalable manner. Here we present the electrical and mechanical properties of thermally drawn multimaterial fibers which make the fibers advantageous for biomedical and wearable applications. First, we demonstrate that thermal drawing promotes unidirectional alignment of carbon nanofibers (CNFs) in a polymer composite. The resultant CNF-composite shows a significant increase in the electrical conductivity by two orders of magnitude compared to that before thermal drawing. Therefore, these highly conductive fiber electrodes can enable miniaturized devices for neural recording in the brain. Next, I will introduce the thermal drawing of other polymer composites such as carbon black in thermoplastic elastomers (TPEs). The scalable fabrication of conductive elastomers can be used for strain sensors in ropes or smart textiles. The electrical and mechanical performance of these fibers will be presented. Finally, thermally drawn piezoelectric fibers will be presented which consist of PVDF-TrFE as the sensing layer and two carbon-loaded polymer layers as the electrodes. The

piezoelectric performance of these fibers will be discussed. These results show that thermal drawing provides a unique platform for producing flexible and miniaturized multifunctional devices with unique electrical and mechanical properties.

11:30 AM EN07.10.04

Hierarchical Micro-Nano Patterned Modified PDMS Triboelectric Nanogenerator Enhanced by Carbon Based Nanofillers Mina Shanbedi, Haleh Ardebili, Hadi Ghasemi and Alamgir Karim; University of Houston, United States

Triboelectric nanogenerators (TENGs) have received recent interest for converting unconventional mechanical energy to electricity, particularly as a sustainable form of energy generation from sources such as wind and friction. Energy conversion in TENGs is based on the triboelectrification and electrostatic induction effects. In this regard, Polydimethylsiloxane (PDMS) elastomer has been widely used as a good triboelectric active layer in TENG owing to its high electronegativity as ranked in the triboelectric series of different materials. The casting process is simple for PDMS having comparatively low surface energy, and more importantly, their formability is superior to many other counterparts in polymers. The TENGs based on PDMS exhibit a relatively high energy conversion efficiency, however, its output electrical characteristics still need more development. One critical key device parameter to enhancing the output performance of TENG is increasing the contact area between triboelectric active material layers. Patterning the surface, and changing the shape and density of patterns on the surface, is assumed to be an effective strategy for this purpose. However, the origin of the output enhancement by patterning and the role of surface roughness on the charge generation aspects needs further investigation. We present research on what makes the shape of the patterns more effective by their contribution to enhancing surface roughness and contacting area, and thereby higher efficiency, with mechanical pressure and sliding contact. On the other hand, increasing the triboelectric polymer conductivity significantly enhances the current density by facilitating the charge transfer from the contact surface towards electrodes. Many nanoparticles have been used to enhance charge transfer in TENGs owing to having high conductivity. In this research, we investigate this proposed hypothesis to relate pattern size and roughness to the output performance of aluminum/polydimethylsiloxane (Al/PDMS) TENG, modified by carbon-based nanoparticles including carbon nanotube (CNT), reduced graphene oxide (r-GO) and carbon black (CB). The uniform and periodic nanoscale morphology of optical discs (CD and DVD) were replicated onto PDMS films. The procedure is followed by a sequential development of hierarchical low amplitude patterns made by oxygen plasma and ultraviolet ozone wrinkling method, to create a hierarchical pattern as a superposition on the optical disc pattern. The patterning procedure is repeated after replacing PDMS with a nanocomposite of PDMS and polytetrafluoroethylene (PTFE) to take advantage of both the molding capability of PDMS and the higher triboelectric affinity of PTFE. Our hierarchical topographic designed TENG led to a considerably higher current and voltage output, due to the efficient shape and roughness compared to CD and DVD patterns alone, useful to rationally design TENGs with high efficiency for capturing energy from unconventional sources.

We acknowledge DoD Grant #555033-78055 (Contract: Kostas Research Institute (KRI) at Northeastern University) for support of the work.

SESSION EN07.11: Mechano-Thermal and Electrical Coupling in Emerging Energy Materials X
Session Chairs: Shangchao Lin and Jingjie Yeo
Wednesday Afternoon, December 8, 2021
EN07-Virtual

9:00 PM *EN07.11.01

Analyzing Thermal Transport in Strained MAPbI₃ Crystals Jin Yang, Yuan Zhou and Wee-Liat Ong; Zhejiang University, China

The thermal conductivity of pseudo-cubic MAPbI₃ was studied using classical molecular dynamics and found to be invariant under compressive strains below 3%. Such invariance contrasts with the rapid thermal conductivity increase seen in other solids with a similar Young modulus value. Larger compressive strains increase the thermal conductivity as observed in most solids.

Hybrid halide perovskites have attracted a lot of interest due to their excellent energy conversion efficiency. The need for improving its thermoelectric performance in thermoelectrics as well as enhancing its thermal stability in photovoltaic cells has spurred thermal transport investigations. As temperature will unavoidably increase during operation, stress will be induced on a piece of mounted perovskite, changing its properties. Additionally, further enhancement to its solar conversion efficiency by applying structural compression was recently reported. It is, therefore, quintessential to understand how straining a perovskite crystal will affect its thermal transport.

The full phonon dispersion and the respective phonon lifetimes under various pressures were calculated. Stable acoustics phonon branches are obtained at these pressures. The vibration modes in these branches are participated by atoms mainly from the inorganic framework. These modes contribute about 40% to the thermal conductivity in MAPbI₃ at pressures between 0 to 1 GPa, but more than 60% at 30 GPa. The almost invariant thermal conductivity contribution at the lower pressure range arises from the canceling effect between the changes in the heat capacity, group velocity, and lifetime of these acoustic phonons. On the other hand, the increase in both the phonon group velocities and lifetimes are responsible for the larger thermal conductivity contribution at higher pressure.

9:30 PM *EN07.11.02

Performance Regulation of Heat Transfer in Semiconductors Guangzhao Qin; Hunan University, China

High-performance thermal management is of great significance to the operational stability of integrated chip and electronic devices, where the heat transfer performance of the core semiconductors plays a key role. In this talk, I would like to introduce our recent work on the performance regulation of heat transfer focusing on few typical semiconductors, such as gallium nitride, boron nitride, boron arsenide, silicene, *etc.* Based on a concise strategy of accelerating evaluation of converged lattice thermal conductivity, the regulation effects of lots of manners, such as temperature controlling, strain engineering, applying external field, alloying, *etc.* have been systematically investigated. The fundamental mechanism is revealed based on the deep analysis of the electronic structures. The performance regulation of heat transfer and the underlying mechanism would be helpful on future studies of thermal and electrical coupling in emerging energy materials.

10:00 PM EN07.11.03

Thermal Characteristics of a Cylindrical Battery Module Based on Lateral Thermoelectric Cooling Hengyun Zhang; Shanghai University of Engineering Science, China

The threats of oil depletion, automotive emission and global warming are on the horizon for many years. Clean and environmentally friendly, electric vehicles have the advantages of energy conservation and emission reduction, which greatly alleviates the dependence on traditional energy sources and are expected to usher in new transportation era in the near future [1, 2]. As the power source of electric vehicles, the lithium-ion battery features salient

advantages such as high energy density, high discharge voltage, minimal self-discharge rate and long cycle life, and so on [3, 4]. However, the safety and efficiency of lithium-ion batteries are closely related to their operating temperature. When the batteries work under high load, the battery module and pack produce large amount of heat due to the associated electrochemical exothermic reaction, resulting in the unfavorable rise of battery temperature in the battery. This would lead to the decline in battery capacity, or even cause the battery thermal runaway [5-7]. An effective battery thermal management system (BTMS) is then required to maintain the battery thermal environment, thereby preventing potential operating risks. Existing battery thermal management techniques include air cooling [8-9], liquid cooling [10, 11], phase change material (PCM) cooling [12] and a combination of these cooling methods [13]. Nonetheless, all the above techniques would fail to work if the climatic temperature is close to the battery threshold temperature around 40-50 °C, especially in hot summer days.

Thermoelectric cooling has attracted attention for thermal management of batteries in a module or pack. Thermoelectric cooling is an advanced cooling technique taking advantage of the Peltier effect. Compact in size and silent in operation, the TEC is able to provide sub-ambient cooling as well as heating in cold winter days, which is a potential technique for thermal management of battery module for electric vehicles. In this paper, the thermal characteristics of thermoelectric cooler (TEC) for thermal control of cylindrical battery module is investigated both experimentally and theoretically.

The battery module under investigation consisted of 18650 test batteries in 3x5 matrix embedded in the composite paraffin wax for accelerated heat dissipation. In the experimental test, the transient and steady-state thermal performances were examined based on the thermoelectric cooling in comparison with the natural convection and liquid cooling conditions. Either one lateral side or two lateral sides of the battery module were attached with the thermoelectric cooler to minimize the temperature of the battery module. In comparison, the thermoelectric cooling reduced the battery temperature and prolonged the working time significantly. The optimal current was experimentally obtained to be about 6.0-6.5A based on the highest cooling power or lowest battery temperature. One-dimensional steady-state thermal resistance network is also developed for the battery module with TEC. The theoretical analysis agrees with the optimal current range obtained from the experimental measurements. Further analysis shows that the optimal current is affected markedly by the hot-side thermal resistance, but little by the cold-side thermal resistance. The two-side TEC cooling is also compared with the one-side TEC cooling. The two-side TEC cooling has a better thermal performance, but with an additional liquid cooled heat sink, which may add complexity to system setup. The cooling performance can be further enhanced such as by increasing the pair of TEC arms. Increasing the number of TEC thermoelectric arms has a favorable effect in both minimizing the maximum temperature and increase the coefficient of performance (COP) of the TEC module. Detailed results will be given in the final presentation.

10:30 PM *EN07.11.04

Characterization of Acoustic Deformation Potential of Mg_3Sb_2 by Femtosecond Spectroscopy [Liang Guo](#); Southern University of Science and Technology, China

As a promising thermoelectric material, Mg_3Sb_2 has kindled intense research interest in recent years. Since acoustic phonons are the main heat carriers and thermoelectric materials in applications are usually doped at high carrier concentration, coupling of acoustic phonons and carriers determines the thermoelectric performance to a large extent. In this work, acoustic deformation potential coupling constant, the key parameter for quantifying acoustic phonon-carrier interaction, of Mg_3Sb_2 is measured through coherent phonon detection by femtosecond spectroscopy. Agreement between experiment and first-principles calculation results is achieved in terms of acoustic deformation potential quantification. The information about acoustic deformation potential extracted in this work could guide the study on thermal and electrical transport of Mg_3Sb_2 and the performance optimization of this thermoelectric material.

SYMPOSIUM EN08

Low-Dimensional Halide Perovskites—From Fundamentals to Applications
November 30 - December 8, 2021

Symposium Organizers

Giulia Grancini, University of Pavia
Aditya Mohite, Rice University
Yana Vaynzof, Technical University Dresden
Elizabeth von Hauff, Vrije University

* Invited Paper

SESSION EN08.01: Structure-Function Relations in Low Dimensional Perovskites I
Session Chair: Lioz Etgar
Tuesday Morning, November 30, 2021
Hynes, Level 3, Room 310

10:30 AM *EN08.01.01

Dynamics of Multicomponent Halide Perovskites Probed by *In Situ* Experiments Using Synchrotron Light [Ana F. Nogueira](#); University of Campinas (UNICAMP), Brazil

Multicomponent perovskite solar cells have reached the recent efficiency breakthrough of 25.5%, higher than silicon polycrystalline photovoltaics. Such fantastic result was only possible due to a precise control and engineering of the morphology, interfaces and the use of multiple cations in perovskite A-site. For tandem perovskite solar cells, a mixture of different anions, as Br and I is also desired to adjust the band gap. Such cocktail of different cations and anions influences the formation of intermediates, new phases, favours halide homogenization, etc; so that at the end, the efficiency of the device is closely related to not only the optical quality of the film (e.g. crystallinity), but morphology and composition.

In this presentation, we will summarize important results using *in situ* experiments to probe perovskite formation (2D and 3D), stability and composition. We employed time-resolved grazing incidence wide angle x-ray scattering (GIWAXS), small angle x-ray scattering (SAXS) and high-resolution XRD taken at the Brazilian Synchrotron National Laboratory.

In situ GIWAXS experiments allowed us to understand the influence of the relative humidity and time to drop the antisolvent during the preparation of perovskite films and get important information about final composition and morphology [1]. It is well known that a 2D layer on the top of a 3D bulk perovskite improves stability and performance. *In situ* GIWAXS revealed us that during thermal annealing the 2D layer transforms itself into a disorder layer, improving hole transfer and stability [2]. This technique was also employed to identify the first intermediates formed during the degradation of different Cs and Br perovskite compositions under ambient conditions [3].

In situ SAXS is another powerful technique to follow the first stages of the 2D perovskite's formation. Our results suggest that the formation of the individual slabs in $\text{BA}_2\text{FAPbI}_3\text{PbI}_4$ is quite fast (within the first 10 s) and, then, these slabs self-assemble into bulk crystallites during the next 40 minutes [4].

Another topic of interest is the photoinduced phase segregation in FAc-based perovskite films. We investigated this phenomenon by photoluminescence (PL) studies and *in situ* high-resolution XRD (dark and under illumination). We found out that cubic-tetragonal transition is able to stabilize the samples with higher Br and Cs content, however this is not true for the films with 17% Br. Thus, other mechanisms must be operating and ruling phase segregation [5].

[1] R. Szostak, S. Sanchez, P. E. Marchezi, A. Marques, J. C. Silva, M. S. Holanda, H. C. N. Tolentino, A. Hagfeldt, A. F. Nogueira, "Revealing the perovskite film formation using the gas quenching method by *in situ* GIWAXS: morphology, properties and device performance", *Advanced Functional Materials*, 31, 2007473 (2021)

[2] A. Souto, R. Szostak, N. Drigo, V. Queiroz, P. E. Marchezi, J. C. Germino, H. N. Tolentino, M. Nazeeruddin, A. F. Nogueira, G. Grancini "In Situ Analysis Reveals the Role of 2D Perovskite in Preventing Thermal-Induced Degradation in 2D/3D Perovskite Interfaces", *Nano Letters*, 20(5) 3992-3998 (2020)

[3] P. E. Marchezi, E. M. Therézio, R. Szostak, H. C. Loureiro, K. Bruening, A. Gold-Parker, M. A. Melo Jr., C. J. Tassone, H. C. N. Tolentino, M. F. Toney, A. F. Nogueira, "Degradation mechanisms in mixed-cation and mixed-halide $\text{Cs}_x\text{FA}_{1-x}\text{Pb}(\text{Br}_y\text{I}_{1-y})_3$ perovskite films under ambient conditions" *J. Mater. Chem. A*, 9, 9302-9312 (2020)

[4] R. F. Moral, L. G. Bonato, J. C. Germino, W. X. Oliveira, R. Kamat, J. Xu, C. Tassone, D. D. Stranks, M. F. Toney, A. F. Nogueira, "Synthesis of Polycrystalline Ruddlesden-Popper Organic Lead Halides and Their Growth Dynamics", *Chemistry of Materials*, 31 (22) (2019), 9472-9479

11:00 AM EN08.01.02

Integrating Emissive 0D Perovskites into a 3D Perovskite Matrix for Efficient and Stable Single-Layer Electroluminescent Devices Aditya Mishra, Jason D. Slinker, Riya Bose and Anton Malko; The University of Texas at Dallas, United States

Zero-dimensional (0D) inorganic perovskites have emerged as promising candidates over their higher dimensional (3D, 2D) analogs by showing superior photoluminescence quantum yield (PLQY) and significant physicochemical stability under ambient conditions. In previous efforts, the inclusion of the 0D phase into a 3D perovskite matrix improved photoluminescence (PL) characteristics by passivating surface defects. Nonetheless, the 0D phase itself is generally non-luminescent, limiting its applicability. Given this, we designed a novel solvent engineering method to incorporate highly emissive 0D perovskite nanocrystals (NCs) into a 3D perovskite composite film (CsPbBr_3 , a polyelectrolyte and Li salt) to form the emissive layer in single-layer perovskite light-emitting electrochemical cells. An optimized 3D-0D composite achieved a maximum luminance of 11200 cd m^{-2} , an external quantum efficiency of 8.2%, a current efficiency of 33 cd/A , and a power efficiency of 31 lm/W . Constant current driving of the 3D-0D composite exhibited 150 h operation at over 400 cd m^{-2} brightness. Extrapolating this to a 100 cd m^{-2} initial luminance, a luminance half-life of over 37000 h is obtained, among the highest for perovskite devices to date. The inclusion of 0D NCs increases photoluminescence lifetime by surface passivation, suppresses non-radiative losses, induces thin-film smoothness, produces smaller crystallites for efficient charge confinement.

11:15 AM EN08.01.03

Shedding Light on the Stability and Structure-Property Relationships of 2D Hybrid Lead Bromide Perovskites Eugenia S. Vasilejadou¹, Ido Hadar¹, Mikael Kepenekian², Jacky Even², Qing Tu³, Christos Malliakas¹, Daniel Friedrich¹, Ioannis Spanopoulos¹, Justin Hoffman¹, Vinayak Dravid¹ and Mercouri G. Kanatzidis¹; ¹Northwestern University, United States; ²Univ Rennes, France; ³Texas A&M University, United States

2D thick-layer lead bromide perovskites remain an unfathomed phase space with the lack of systematic studies to establish the structure, photophysical properties and stability behavior of this family of 2D halide perovskites. Herein, we present new members of $n=2$ lead bromide perovskites ($\text{C}_m\text{H}_{2m+1}\text{NH}_3$)₂(CH_3NH_3)₂Pb₂Br₇ ($m = 6-8$) that belong to the Ruddlesden-Popper structure type, incorporating long chain alkyl-monoammonium cations ($\text{C}_m\text{H}_{2m+1}\text{NH}_3$) of hexylammonium ($m=6$), heptylammonium ($m=7$) and octylammonium ($m=8$). A universal solution synthetic methodology for bulk, thick-layer lead bromide perovskites is presented with all structures solved single crystal X-ray diffraction. The studied bilayer lead bromide perovskites demonstrate a decrease in the lattice rigidity and lattice match of the inorganic perovskite layer - organic layer, as the monoammonium chain length increases. In comparison to their iodide analogues, the bilayer lead bromide compounds exhibit elongation of their stacking axis despite the smaller dimensions of the $[\text{PbBr}_6]^{4-}$ lattice with a reduced calculated internal lattice strain, inferring a greater lattice match between the inorganic $[\text{PbBr}_6]^{4-}$ perovskite layer and organic layer. The titled compounds exhibit narrow-band green emission near 2.5 eV. Time-resolved photoluminescence (PL) displays longer carrier lifetimes compared to their iodide analogues, where electronic structure calculations indicate that the increase of the monoammonium chain length and thus, lattice softness enhances non-radiative recombinations. A complete set of air, light and heat stability tests on unencapsulated thin films of ($\text{C}_m\text{H}_{2m+1}\text{NH}_3$)₂(CH_3NH_3)₂Pb₂Br₇ ($m = 4, 6-8$) and MAPbBr₃ show they are stable in ambient air for at least 5 months. Extraordinarily, 3D MAPbBr₃ films prove to be more stable than films of 2D lead bromide perovskites, in contrast to MAPbI₃ which is less stable than the 2D lead iodide perovskites.

11:30 AM EN08.01.04

Composition Engineering of 2D Ruddlesden-Popper Perovskites Susana Ramos Terrón¹, Cristóbal Verdugo Escamilla², Luis Camacho Delgado¹ and Gustavo de Miguel Rojas¹; ¹University of Córdoba, Spain; ²CSIC-University of Granada, Spain

The partial incorporation of large organic cations into the octahedral sites of 3D perovskites has been widely investigated but few works have reported their addition in 2D Ruddlesden-Popper (RP) perovskites. Here, the gradual substitution of the methylammonium (MA) cation in thin films of 2D RP perovskites $(\text{BA})_2(\text{MA})_2\text{Pb}_3\text{I}_{10}$ ($\text{BA} = n$ -butylammonium) by guanidinium (Gua), dimethylammonium (DA), ethylammonium (EA), rubidium (Rb), propylammonium (PA), cesium (Cs) or formamidinium (FA) to synthesize mixed A-cation $(\text{BA})_2(\text{MA}_{1-x}\text{A}_x)_2\text{Pb}_3\text{I}_{10}$ perovskites has been studied. The limit

in the percentage of the A-site cation at which it is homogeneously incorporated in all n phases without destabilizing the overall structure is determined. It is found that the structural changes in the 2D RP perovskites may lead to modifications of the optoelectronic properties as larger bandgap (EA), blue-shift of the PL peak position (above the threshold), strong quenching of the PL (Cs) or reduced concentration of trap states (Gua and EA). Solar devices fabricated with the different mixed A-cation 2D RP display an enhanced performance for those perovskites containing low percentages of Gua or EA cations. This characterization is very valuable to correlate the size and shape of the A-cation with the changes of the properties of the material.

SESSION EN08.02: Application of Low Dimensional Perovskites in Optoelectronics

Session Chair: Ana Nogueira

Tuesday Afternoon, November 30, 2021

Hynes, Level 3, Room 310

1:30 PM *EN08.02.01

Printable Optoelectronics Based on Perovskites and Organic-Perovskite Composites [Thomas D. Anthopoulos](#); King Abdullah University of Science and Technology, Saudi Arabia

Metal-halide perovskites offer numerous opportunities for use in large-area optoelectronics due to their strong optical absorption, long charge carrier diffusion lengths, low trap densities and processing versatility. However, full exploitation of these important attributes for the development of large-area opto/electronics remains challenging. In this presentation I will present and discuss results from our recent efforts to utilize perovskite semiconductors for a variety of applications. Particular emphasis will be placed on our recent work that aims to combine organic with perovskite semiconducting materials to produce prototype devices with unusual microstructural characteristics and advanced functionalities. Devices to be discussed include nanogap photodiodes, phototransistors, transistor memories, memtransistors, and light-emitting devices.

2:00 PM EN08.02.02

Deposition Scheme for Low-Dimensional Hybrid Perovskite Thin Films with Functional Molecules [Niara E. Wright](#) and Adrienne Stiff-Roberts; Duke University, United States

The applications of two-dimensional (2D) hybrid organic-inorganic perovskites (HOIPs) have broadened as functional molecules are explored and incorporated into this emerging material.¹ However, obtaining quality films of HOIPs with functional molecules remains a challenge.¹ One group successfully engineered and incorporated new conjugated functional molecules that changed the band alignment, but only created small crystals, not contiguous films.² Mitzi et al. created layered perovskites with functional molecules via single source thermal ablation, however film thickness was difficult to control and the risk of organic cation damage remained.³ Solution processing is challenged by finding a single solvent for both the inorganic and organic precursor materials. Two-step solution-processing partially avoids the single solvent criterion, but solvent choice is still a critical challenge and a limiting factor for synthesis of 2D HOIPs with functional molecules.⁴

Herein, a deposition technique is presented that better accommodates organic cation deposition to address the challenge of consistently producing controlled, quality thin films of HOIPs with functional molecules. Resonant-infrared, matrix-assisted pulsed laser evaporation (RIR-MAPLE) is a modified pulsed laser deposition technique that uses a frozen target solution with precursor materials. The laser energy is resonantly absorbed by the matrix solvent (monoethylene glycol), the sublimation of which ejects the inorganic and organic precursor materials onto the substrate, making this method gentle on the organic precursor unlike physical vapor deposition. RIR-MAPLE has been used previously to successfully deposit high quality thin films of oligothiophene-based HOIPs.⁵ This demonstration was enabled by an extremely low solution concentration (22 mM) of the organic and inorganic precursors in a single target solution (known as simultaneous deposition scheme). However, this simultaneous deposition scheme may not suffice for other large, functional molecules for which a low concentration target solution is not adequate to address solvent incompatibility between the organic and inorganic precursors.

Therefore, this work investigates an alternative deposition scheme to demonstrate a potential benefit of RIR-MAPLE: the ability to completely separate the inorganic and organic precursor target solutions. In this sequential deposition scheme, the frozen inorganic and organic precursor solutions are spatially separated within the target. Each precursor is deposited alternately according to the laser raster pattern on a time-scale less than that needed for full substrate coverage. The RIR-MAPLE sequential deposition scheme has been demonstrated for polymer-nanomaterial composites.^{6,7} In this work, film characterization (including X-ray diffraction, energy dispersive spectroscopy, photoluminescence, UV-vis absorbance spectroscopy, scanning electron microscopy, and atomic force microscopy) will be used to compare film quality resulting from simultaneous and sequential deposition schemes. Specifically, thin films of $(C_8H_{12}N)_2PbI_4$ are investigated, instead of oligothiophenes, to confirm film quality because phenethylammonium-based HOIPs have been well characterized by other deposition techniques. The conclusive demonstration of high-quality 2D HOIPs by the RIR-MAPLE sequential deposition scheme will expand eligible functional molecules by circumventing the well-known solubility and vapor deposition challenges.

REFERENCES

1. Saparov, B. & Mitzi, D. B. *Chemical Reviews* **116**, 4558–4596 (2016).
2. Gao, Y. *et al. Nat. Chem.* **11**, 1151–1157 (2019).
3. Mitzi, D. B., Chondroudis, K. & Kagan, C. R. *Inorg. Chem.* **38**, 6246–6256 (1999).
4. Liang, K., Mitzi, D. B. & Prikas, M. T. *Chem. Mater.* **10**, 403–411 (1998).
5. Dunlap-Shohl, W. A. *et al. Mater. Horizons* **6**, 1707–1716 (2019).
6. Ajnsztajn, A. *et al. Crystals* **10**, 152 (2020).
7. Ge, W., *et al. Appl. Phys. Lett.* **104**, 223901 (2014).

2:15 PM EN08.02.03

Light-Induced Enhancement of Organo-Metal Halide Perovskite Lithium-Ion Batteries [Angus Mathieson](#) and Michael De Volder; University of Cambridge, United Kingdom

Increases in the global energy demand necessitate the development of new approaches to energy conversion and storage. In particular, the utilisation of solar energy could provide a basis of evolving technologies capable of meeting modern and future demands.

By combining the photovoltaic and newfound electrochemical properties of organo-metal hybrid perovskite materials in a single device, a novel

photobattery technology is proposed [1]. Utilising the photovoltaic performance of perovskite materials in combination with the intercalation and conversion mechanisms available to Lithium ion species [2], a device with the ability both to convert light to electrochemical energy and store it is demonstrated. The motivation for such a device will be discussed, with its inherent impact in areas such as off-grid energy solutions and the internet of things. The fabrication techniques are described and characterisation techniques common to both photovoltaic and electrochemical disciplines, with their recent results are discussed. Modifications are made to conventional electrochemical coin cells and pouch cells, in order to facilitate optical access to the electrode material. Using *in-operando* x-ray diffraction and optical probing, the fundamental mechanisms of charge storage and ion conversion are investigated both in the presence of light, to replicate a light-charging cycle and in the absence of light.

[1] *Nano Lett.* 2018, 18, 3, 1856-1862

[2] *Mater. Adv.*, 2021, 2, 3370-3377

2:30 PM EN08.02.04

Room-Temperature Amplified Spontaneous Emission and Lasing of Sequentially Thermally Evaporated CsPbCl₃ Perovskite Thin Films Manuel Runkel^{1,2}, Tobias Haeger^{1,2}, Huiyue Ping¹, Johannes Bahr¹, Lena Merten³, Selina Olthof⁴, Detlef Rogalla⁵, Alexander Hinderhofer³, Ralf Heiderhoff^{1,2}, Frank Schreiber³, Klaus Meerholz⁴ and Thomas Riedl^{1,2}; ¹University of Wuppertal, Germany; ²Wuppertal Center for Smart Materials & Systems, Germany; ³University of Tübingen, Germany; ⁴University of Cologne, Germany; ⁵Ruhr University Bochum, Germany

Inorganic cesium-lead-halide perovskites are of interest for optoelectronic applications such as solar cells, LEDs and lasers, since they not only exhibit excellent optical properties, but are also more thermally stable [1]. However, inorganic perovskites frequently come with serious processing challenges and high-quality thin films (no pinholes, high photoluminescence quantum yield) are difficult to achieve. Amplified spontaneous emission (ASE) in thin films of these materials, which is an important prerequisite for lasing, can often only be reached at cryogenic temperatures. The blue to ultraviolet spectral range, which would be reached by CsPbCl₃, is a particular challenge in this regard. Solution-based deposition of CsPbCl₃ is extremely hampered by the poor concomitant solubility of the precursor salts PbCl₂ and CsCl.

Within this study, the preparation of wide-gap CsPbCl₃ perovskite thin films is presented by the use of thermal evaporation of the individual salts. Specifically, a stack of alternating layers of PbCl₂ and CsCl is designed, that leads to some kind of self-limiting formation of the desired 3D - CsPbCl₃ perovskite at the interfaces of the superlattice. We analysed the formation of CsPbCl₃ by photoelectron spectroscopy and X-ray diffraction as well as grazing incidence wide angle x-ray scattering (GIWAXS), to unravel the appearance of the various phases (0D-Cs₄PbCl₆, 2D-CsPb₂Cl₅, 3D-CsPbCl₃). The insights gained from these studies allowed us to optimize the superlattice architecture.

The resulting CsPbCl₃ shows an intense photoluminescence at 413 nm with a narrow line width of 10 nm (FWHM), which agrees with reports of CsPbCl₃ single crystals [2]. Most notably, we were able to optimize the CsPbCl₃ thin film to support amplified spontaneous emission in the deep blue spectral region at 427 nm (line width 2.2nm) under pulsed optical excitation (355nm, 300 ps) above a threshold energy density of 190 μJ/cm² at room-temperature (RT). This is the first report of CsPbCl₃ thin films showing ASE at RT. The integration of this active material in a resonator to achieve the first thin film CsPbCl₃ lasers at RT will be presented.

1. Pourdavoud N., et al., *Adv. Mater.* 2019, 31, 1903717, DOI: 10.1002/adma.201903717

2. Gui P., et al., *Small* 2019, 15, 1902618, DOI: 10.1002/smll.201902618

2:45 PM EN08.02.05

Lead-Free Halide Light-Emitting Diodes with External Quantum Efficiency Exceeding 7 Percent Using Vacuum Thermal Evaporation Process Gijun Seo¹, Hyecheol Jung¹, Tielyr D. Creason², Vishal Yeddu¹, Matthew Bamidele¹, Elena Echeverria¹, Ji-Hoon Lee³, Dave N. McLroy¹, Bayram Saparov² and Do Young Kim¹; ¹Oklahoma State University, United States; ²The University of Oklahoma, United States; ³Korea National University of Transportation, Korea (the Republic of)

Perovskite-based visible light-emitting diodes (LEDs) with blue, green, and red emissions have successfully been demonstrated with high external quantum efficiencies (EQEs) and bright luminance for next-generation display and solid-state lighting applications. In spite of the high performances of perovskite-based visible LEDs, however, their applications will be limited due to the toxicity of lead-based halide perovskites. While there have currently been many reports about lead-free metal halide emitters to solve this toxicity issue, most lead-free halide LEDs show still significantly low performance, resulting in below 1 %.

In this work, lead-free halide LEDs are fabricated using non-toxic and earth-abundant CsCu₂I₃ with a strong yellow emission at a peak wavelength of 568 nm. CsCu₂I₃-based host-dopant emitters are formed by vacuum thermal evaporation (VTE) film co-deposition process instead of the commonly-used solution-based film deposition process. Using the VTE process, extremely thin (30 nm) host-dopant emitters have successfully been formed with the CsCu₂I₃ dopant and various organic host molecules. A bright yellow emission with a photoluminescence quantum yield value of 84.8% is achieved in the 0.5% CsCu₂I₃-doped halide emitter film due to the successful spatial localization of charge carriers and excitons using an organic host with appropriate energy levels to CsCu₂I₃. With the further enhancement in charge balance using the co-host system, a record-breaking lead-free halide LED has been fabricated with an EQE of 7.4%. The lead-free halide LEDs are also highly stable in the device operation with LT70 of 20 hours at 100 cd/m².

3:00 PM BREAK

SESSION EN08.03: Novel Directions for Low Dimensional Perovskites

Session Chair: Laura Herz

Tuesday Afternoon, November 30, 2021

Hynes, Level 3, Room 310

4:00 PM *EN08.03.01

Low Dimensional Perovskite and Their Applications in Photovoltaic Cells, Nanostructures and Semitransparency Lioz Etgar; Hebrew University of Jerusalem, Israel

Recent discoveries have revealed a breakthrough in the field using inorganic-organic hybrid layers called perovskites as the light harvester in the solar cell. The inorganic-organic arrangement is self-assembled as alternate layers, being a simple, low cost procedure. These organic-inorganic hybrids promise

several benefits not delivered by the separate constituents. In this lecture I will discuss new directions in low dimensional perovskite and their applications in solar cells.

In low dimensional systems, stability of excitons in quantum wells is greatly enhanced due to the confined effect and the coulomb interaction. The exciton binding energy of the typical 2D organic-inorganic perovskites is up to 300 meV and their self-assembled films exhibit bright photoluminescence at room temperature.

In this work we will show the dimensionality in the perovskite structure. The 2D perovskite structure should provide stable perovskite structure compare to the 3D structure. The additional long organic cation, which is added to the perovskite structure (in the 2D structure), is expected to provide hydrophobicity, which will enhance the resistivity of the perovskite to humidity. We will demonstrate the use of 2D perovskite using unique barrier molecules in high efficiency solar cells.

Moreover, we will show a highly efficient semitransparent perovskite solar cell. The semitransparency was achieved through an inkjet printing of “holes” in the perovskite film. The “holes” in the perovskite allows to control the semitransparency of the solar cell.

Organic-inorganic halide perovskite is used mainly in its “bulk” form in the solar cell. Confined perovskite nanostructures could be a promising candidate for efficient optoelectronic devices, taking advantage of the superior bulk properties of organo-metal halide perovskite, as well as the nanoscale properties. In this talk, I will present our recent progress related to the synthesis and characterization of perovskite NPs- i.e. Inorganic and hybrid organic-inorganic NPs. New nanostructures such as: NRs and NWs will be presented and the introduction of other cations such as Rb will be shown.

4:30 PM EN08.03.02

Challenges and Opportunities for Bismuth-Based Low-Dimension Halide Perovskites Mikael Kepenekian¹, Boubacar Traore¹, Claudine Katan¹, Jacky Even², Matthieu Manceau³, Nicolas Mercier⁴, Xiaotong Li⁵ and Mercouri G. Kanatzidis⁵; ¹Univ of Rennes, France; ²INSA Rennes, France; ³Univ. Grenoble Alpes, France; ⁴Université d'Angers, France; ⁵Northwestern University, United States

The impressive flexibility exhibited by halide perovskites [1] offers many opportunities for chemists to design application driven materials [2,3]. Among the challenges still to be overcome is the replacement of toxic lead in materials for optoelectronic devices. If bismuth seems to be an ideal candidate owing to its low toxicity and natural abundance, the performances of 3-dimensional (3D) Bi-based materials in solar cells remain far from their Pb-based competition [4]. However, the low-dimension side of the family (2D and 1D) still holds promises.

Here, we focus on 2D and 1D Bi-based halide perovskites thanks to joint experimental characterization and computational investigations. By highlighting, among others, the key aspects of connectivity between octahedra, we will describe the challenges of designing efficient lead-free materials, as well as the opportunities offered by this not yet fully explored territory [5,6].

- [1] B. Saparov, D. B. Mitzi, *Chem. Rev.* **2016**, *116*, 4558.
- [2] L. Pedesseau, M.K. *et al.*, *ACS Nano* **2016**, *10*, 9776.
- [3] C. Katan, N. Mercier, J. Even, *Chem. Rev.* **2019**, *119*, 3140.
- [4] Z. Jin *et al.*, *J. Mater. Chem. A* **2020**, *8*, 1616.
- [5] N. Louvain, N. Mercier, F. Boucher, *Inorg. Chem.* **2009**, *48*, 879.
- [6] E. S. Vasileiadou, M.K. *et al.*, *Chem. Mater.*, *in press*.
- [6] N. Mercier, M.K. *et al.*, *manuscript in preparation*.

4:45 PM EN08.03.03

Between Chemical Exfoliation and Direct Nucleation—Understanding the Formation Process of 2D Lead Bromide Perovskites at the Nanoscale Jakob Dahl^{1,2,2}, Samuel Niblett¹, Xingzhi Wang^{1,2}, Emory Chan², David Limmer¹ and A. Paul Alivisatos^{1,2}; ¹University of California, Berkeley, United States; ²Lawrence Berkeley National Laboratory, United States

2D materials have captured the imagination of the materials science community, yet the chemical processes leading up to the formation of these materials are often difficult to probe. Working with colloidal nanomaterials allows us to use wet-chemical control and fast in-situ techniques to understand the reactions occurring during synthesis. In this study, we demonstrate that 2D perovskites can form through two processes at the nanoscale: Either from a layer-by-layer chemical exfoliation process from lead bromide nanocrystals or through direct nucleation from precursors. We study these processes in detail through in-situ spectroscopy in a stopped flow chamber. Chemical exfoliation appears to leave entire layers of the lead bromide nanocrystal intact – stopped flow experiments show little lateral confinement of the 2D exciton peak at short time scales, and the level of confinement is correlated to the size of the initially synthesized lead bromide nanocrystals. Direct nucleation leads to initial exciton peaks that are about 200 meV higher in energy compared to bulk values. The ratio of organic amine to lead controls which formation pathway dominates, as well as the size at which lead bromide nanocrystals exfoliate into 2D perovskite nanoflakes. We demonstrate qualitative agreement with simulations of a kinetic nanocrystal growth model with a single layer exfoliation step. Isotropic absorption, measurable lateral confinement and observations of growth kinetics make in-situ experiments of colloidal nanomaterials an ideal platform for understanding the complicated processes of nucleation, growth and phase transformation of 2D perovskites and 2D materials more generally. Deeper understanding of the formation processes, especially in their initial stages, will be important for ongoing development of synthetic procedures in this field.

5:00 PM EN08.03.04

Effect of Co-Solvents on the Crystallization and Phase Distribution of Quasi-2D Perovskites Alessandro Caiazzo¹, Kunal Datta¹, Junke Jiang¹, Maria C. Gélvez-Rueda², Junyu Li¹, Shuxia Tao¹, Ferdinand C. Grozema², Martijn Wienk¹ and Rene Janssen¹; ¹Eindhoven University of Technology, Netherlands; ²TU Delft, Netherlands

Quasi-2D perovskites (q2D PVKs) are promising candidates for stable and highly efficient solar cells. On top of the superior environmental stability compared to their 3D counterparts, q2D PVKs possess tunable optoelectronic properties, as it is possible to change the number of inorganic layers (*n*) sandwiched between the organic spacers to tune bandgap and exciton binding energy. However, centering the phase distribution on a specific *n*-value is challenging. Together with a variety of processing techniques, solvent engineering has previously been used in the literature to tune both phase purity and device efficiency. Nevertheless, no reports have investigated the effect of co-solvents on the crystallization mechanism and the reasons behind the changes in phase distribution.

To fill this gap, we first investigated the kinetics of film formation of BA₂MA₃Pb₄I₁₃ processed from DMF/co-solvent mixtures (DMSO and NMP) via in-situ absorption measurements conducted during room-temperature spin coating or thermal annealing. By combining these results with photoluminescence (PL) spectroscopy and angle-dependent grazing-incidence wide-angle X-ray scattering (GIWAXS), we concluded that the crystallization starts as a 3D-like perovskite from the liquid-air interface, both when the q2D PVK forms during spin coating (low amounts of DMSO or NMP in the solvent mixture) and during annealing (high amounts). The structure of the 3D-like perovskite on the top of the film, however, is impacted by the crystallization at the bottom, as suggested by the redshift of the absorption onset.

In agreement with previous reports, we observed a 2D-3D gradient in the film, with q2D PVKs formed mostly at the bottom of the film and 3D-like PVKs at the top. Even though the crystallization mechanism is the same when using DMSO and NMP as co-solvents, the phase distribution at the bottom of the film is different. More specifically, for the 4:1 DMF/NMP ratio, the distribution shifts toward small n -values, mainly $n = 2$. On the contrary, when using DMSO as a co-solvent with the same volumetric ratio, a broader phase distribution appears. During the crystallization, as described before, a 3D-like layer is initially formed on the top of the film, while underneath a wet film consisting of perovskite precursors has yet to crystallize. The interactions of the co-solvents with the precursors in the wet film are important in shifting the resulting phase distribution, as they influence the availability of MAI or BAI molecules to participate in the crystallization process. We investigated the ternary interactions between BAI or MAI, PbI_2 , and the solvents with FT-IR and DFT. By analyzing the S=O and C=O stretching peaks, we observed that NMP interacts more strongly with MAI- PbI_2 than with BAI- PbI_2 , indicating that BAI is less bound to the ternary complex, compared to MAI, and thus more available to participate in the formation of quasi-2D perovskite phases. This explains the phase distribution shifted to smaller n -values when using NMP. The same analysis showed that DMSO, instead, interacts similarly in ternary complexes with both MAI and BAI, agreeing with a broader phase distribution.

Overall, we propose a crystallization mechanism for $\text{BA}_2\text{MA}_3\text{Pb}_4\text{I}_{13}$ in a DMF/co-solvent mixture where 3D-like perovskites crystallize first at the liquid-air interface. While the crystallization proceeds, the phase distribution in the underlying perovskite layer is influenced by the availability of MAI and BAI molecules, which is in turn influenced by the co-solvent's choice. This conclusion confirms the importance of the co-solvents (or additives) in the challenging formation of phase-pure quasi-2D perovskites. By carefully tuning the DMF/co-solvent ratio, we finally fabricated a more phase-pure q2D PVK with device efficiencies up to 11%, a low degree of 2D-3D vertical gradient, and a narrow phase distribution.

SESSION EN08.04: Photophysics of Low Dimensional Perovskites I

Session Chair: Lioz Etgar

Wednesday Morning, December 1, 2021

Hynes, Level 3, Room 310

10:30 AM *EN08.04.01

Electronic Confinement Effects in Nominally Bulk and Nanocrystalline Metal Halide Perovskite Thin Films [Laura Herz](#); University of Oxford, United Kingdom

In this presentation, we discuss how the electronic landscape of metal halide perovskites may be modified under two scenarios, first, through intrinsic quantum confinement effects found to occur in a nominally bulk semiconducting perovskite [1], and second, in thin films of nanocrystals within the weak electronic confinement regime [2].

We have recently reported the surprising presence of above-bandgap oscillatory features in the absorption spectra of formamidinium lead triiodide thin films [1]. We attribute these discrete features to intrinsically occurring quantum confinement effects, for which the related energies change with temperature according to the inverse square of the intrinsic lattice parameter, and with peak index in a quadratic manner. By determining the threshold film thickness at which the amplitude of the peaks is appreciably decreased, and through ab initio simulations of the absorption features, we estimate the length scale of confinement to be 10–20 nm. Such absorption peaks present a new and intriguing quantum electronic phenomenon in a nominally bulk semiconductor, offering intrinsic nanoscale optoelectronic properties without necessitating cumbersome additional processing steps. We discuss two potential explanations for the formation of such quantum well or superlattice structures, the inclusion of thin electronic barrier layers of hexagonal delta phase, or the presence of ferroelectric domains.

We further discuss the vibrational and electronic transport properties of thin films comprising metal-halide perovskites nanocrystals (NCs) which offer an effective approach for processing films from inks for low-cost, high-performance device fabrication. We disentangle the effects of surface ligands, morphology, and boundaries on charge-carrier transport in thin films fabricated with these high-quality NCs [2]. We employ terahertz (THz) spectroscopy to optically probe the photoconductivity of CsPbBr_3 NC films. The vibrational and optoelectronic properties of the NCs are compared with those of the corresponding bulk polycrystalline perovskite and significant deviations are found. Charge-carrier mobilities and recombination rates are demonstrated to vary significantly with the NC size. Such dependences derive from the localized nature of charge carriers within NCs, with local mobilities dominating over interparticle transport. It is further shown that the colloiddally synthesized NCs have distinct vibrational properties with respect to the bulk perovskite, exhibiting blue-shifted optical phonon modes with enhanced THz absorption strength that also manifest as strong modulations in the THz photoconductivity spectra. Such fundamental insights into NC versus bulk properties will guide the optimization of nanocrystalline perovskite thin films for optoelectronic applications.

[1] Intrinsic quantum confinement in formamidinium lead triiodide perovskite,

A. D. Wright, G. Volonakis, J. Borchert, C. L. Davies, F. Giustino, M. B. Johnston, and L. M. Herz, Nature Materials 19, 1201–1206 (2020).

[2] CsPbBr_3 nanocrystal films: Deviations from bulk vibrational and optoelectronic properties,

S. G. Motti, F. Krieg, A. J. Ramadan, J. B. Patel, H. J. Snaith, M. V. Kovalenko, M. B. Johnston, and L. M. Herz, Advanced Functional Materials 30, 1909904 (2020).

11:00 AM EN08.04.03

Charge Screening Behavior of 2D Hybrid Organic-Inorganic Perovskites Mohammed Shyikh¹, Eugenia S. Vasileiadou², Ioannis Spanopoulos², Doyun Kim¹, Mercouri G. Kanatzidis² and [Qing Tu](#)¹; ¹Texas A&M University, United States; ²Northwestern University, United States

2D hybrid organic-inorganic perovskites (HOIPs) are low-cost, high-performance semiconductor materials with great potential demonstrated in various fields, including photovoltaics, light-emitting diodes, lasers, and field-effect transistors. In these applications, it is common for 2D HOIPs to encounter charged species, including defects, molecular dopants, interfacial dipoles, and excitons, which could modulate the carrier transport properties inside the functional materials. How the 2D HOIPs will re-arrange the internal charges to screen the Coulombic interaction and how this charge screening behavior is related to the structure and composition of the 2D HOIPs are vital for the device design and optimization and yet largely remain unknown. Here we report a systematic study of the charge screening length of prototypical 2D HOIPs with a general formula of $(\text{C}_4\text{H}_9\text{-NH}_3)_2(\text{CH}_3\text{NH}_3)_{n-1}\text{Pb}_n\text{I}_{3n+1}$ ($n = 1$ to 5) by measuring the work function of 2D HOIP flakes on a charged dielectric surface SiO_2 using kelvin probe force microscopy. The work functions of the 2D

HOIP nanoflakes monotonically change as the flake thickness increases, showing a progressive screening of the influence from the SiO₂ surface charges. The screening length is short, less than 20 nm, which decreases monotonically with respect to the n number, i.e., the thickness of the inorganic slab within each repeating unit. 2D HOIP with n = 5 exhibits the shortest screening length, which could completely shield the electrostatic interaction with only 2 repeating units. The screening lengths of 2D HOIPs are much larger than, comparable to, and shorter than those of graphene, MoS₂, and h-BN, respectively. While the inorganic framework dominates the charge screening behavior, the organic spacer molecules can affect the charge screening by modulating the interlayer charge coupling through the van der Waals interfaces. Our results can provide valuable insights from the charge screening perspectives into the carrier dynamics and device design involving 2D HOIPs.

11:15 AM EN08.04.04

Solvent Polarity of Antisolvent Influences the Surface Chemistry and Optoelectronic Properties of Purified Lead Halide Perovskite Nanocrystals. Junzhi Ye¹, Zhenchao Li², Dominik Kubicki¹, Yunwei Zhang¹, Linjie Dai¹, Clara O. Martinez³, Manuel A. Scheel⁴, Zahra Andaji-Garmaroudi¹, Yi-Teng Huang¹, Zewei Li¹, Ziming Chen², Peter Müller-Buschbaum⁴, Hin-Lap Yip², Samuel D. Stranks¹, Neil Greenham¹, Richard H. Friend¹, Lakshminarayana Polavarapu³, Akshay Rao¹ and Robert Hoyer⁵; ¹University of Cambridge, United Kingdom; ²State Key Laboratory of Luminescent Materials and Devices, China; ³Universidade de Vigo, Spain; ⁴Technische Universitaat Munchen, Germany; ⁵Imperial College London, United Kingdom

Lead-halide perovskite colloidal nanocrystals (LHP NCs) have emerged over the past decade as leading candidates for next-generation, efficient light-emitting diodes (LEDs). Owing to their high photoluminescence quantum yields (PLQYs), LHPs efficiently convert injected charge-carriers to light and vice versa. In the synthesis of high-quality LHP NCs, the purification process is a critical step that influences the final PLQY, transport properties and polydispersity of the NCs. Despite the important role of the antisolvent in the purification process, a detailed understanding of how the antisolvent influences the surface chemistry of the NCs is missing in the field. Here, we address this knowledge gap, using CsPbBr₃I_{3-x} NCs as the model system. We find that as the polarity of the antisolvent increased (from methyl acetate through to butanol), there was an increased blue-shift in the photoluminescence (PL) peak of the NCs, along with a decrease in PLQY. Through transmission electron microscopy and X-ray photoemission spectroscopy measurements, we identify the change of PL spectra to be due to solvent-induced iodide removal, which leads to a change in halide composition and band-gap. By using detailed nuclear magnetic resonance (NMR) measurements, along with density functional theory calculations, the mechanism we propose is that the oleic acid and oleylamine ligands undergo an amide condensation reaction at the surface of NCs in the presence of the polar antisolvent during purification. The conversion of amine to amide lead to ligand and surface halide detachment. Solvent polarity plays an important role in this reaction, in which solvents with higher polarity tend to remove more surface ligands and halides. This leads to higher surface halide vacancy densities, resulting in decreases in the PLQY. Furthermore, washing with high polarity solvent would cause an inhomogeneous distribution of surface halides, and reduces electroluminescence spectral stability of LED devices. Our work shows that maintaining high-PLQY NCs with low defect density requires the use of low-polarity antisolvents during

11:30 AM EN08.04.05

Broad Tunability of Carrier Effective Masses in Two-Dimensional Halide Perovskites Herman Duim¹, Mateusz Dyksik^{2,3}, Xiangzhou Zhu⁴, Zhuo Yang⁵, Masaki Gen⁵, Yoshimitsu Kohama⁵, Sampson Adjokatsé¹, Duncan K. Maude², Maria Antonietta Loi¹, David Egger⁴, Michael Baranowski³ and Paulina Plochcka^{2,3}; ¹University of Groningen, Netherlands; ²Laboratoire National des Champs Magnétiques Intenses, France; ³Wroclaw University of Science and Technology, Poland; ⁴Technical University of Munich, Germany; ⁵The University of Tokyo, Japan

The effective mass of charge carriers is a crucial parameter for the design of any optoelectronic device, as it is directly linked to key material characteristics such as the carrier mobility, exciton binding energy, and diffusion length. Consequently, a precise determination of its value is of paramount importance for the in-depth understanding of any semiconductor. The estimated values of the effective mass of 2D halide perovskites currently span a broad range, providing a source of uncertainty in this promising material system.

Using high magnetic fields up to 65 T we were able to observe multiple interband Landau level transitions in the absorption spectra of (PEA)₂SnI₄ and (PEA)₂PbI₄, providing us with a direct measure for the reduced effective mass of charge carriers in these systems. The determined reduced effective masses are found to be very close to or even lower than that of their 3D analogues, which is atypical in the presence of quantum confinement effects. We highlight how the distortion imposed by the organic spacers, and orbital hybridization effects by the metal cation, govern the effective mass in 2D halide perovskites. Combining the experimental results with electronic band-structure calculations, we propose a scaling diagram for the effective mass value versus the distortion of the octahedra imposed by the organic cations. As a result, we postulate that the effective mass in these systems can be easily tailored over a wide range by appropriate selection of organic spacers and metal ions.

SESSION EN08.05: Photophysics and Applications of Low Dimensional Perovskites

Session Chair: Ana Nogueira

Wednesday Afternoon, December 1, 2021

Hynes, Level 3, Room 310

1:30 PM EN08.05.01

Green Synthesis of Dual-Color CsPbBr₃ Quantum Dots and poly(methyl methacrylate)-CsPbBr₃ Films with Deflection-Endurable Photoluminescence Fuqian Yang; Univ of Kentucky, United States

Perovskite nanocrystals have attracted great interest due to tunable optoelectronic characteristics and potential applications in photonics, energy storage, lighting and display. To date, most synthesis methods have involved organic solvent, such as N,N-dimethylformamide and dimethyl sulfoxide, which poses a potential threat to the environment, health and security. In this work, we develop an environmental-friendly and cost-efficient method to synthesize CsPbBr₃ powders at room temperature with water. Using ultrasonication and centrifugation, we obtain CsPbBr₃ nanocrystals with green (~522 nm) and blue (~493 nm) emissions from the powders. The photoluminescence quantum yield of the blue-emitting nanocrystals is 80%, much larger than 61.4% of the CsPbBr₃ nanocrystals made by an anti-solvent method. We prepare polymer composite films with PMMA and the green-emitting CsPbBr₃ nanocrystal on a polyethylene terephthalate plate. The composite films exhibit deflection-endurable photoluminescence, i.e. there is no observable change in the PL characteristics for local radius of curvature up to 10.07 mm. The method developed in this work provides a unique approach to produce halide perovskite nanocrystals without harmful organic solvents in precursor solutions.

This work is supported by the NSF through the grant CMMI-1854554 and CBET- 2018411.

1:45 PM EN08.05.02

Direct Optical Lithography of CsPbX₃ Nanocrystals via Photoinduced Ligand Cleavage with Post-Patterning Chemical Modification and Electronic Coupling [Jia-Ahn Pan](#), Justin C. Ondry and Dmitri Talapin; University of Chicago, United States

Microscale patterning of solution-processed nanomaterials is important for integration in functional devices. Colloidal lead halide perovskite (LHP) nanocrystals (NCs) can be particularly challenging to pattern due to their incompatibility with polar solvents and lability of surface ligands. Here, we introduce a direct photo-patterning approach for LHP NCs through the binding and subsequent cleavage of a photosensitive oxime sulfonate ester. The photosensitizer binds to the NCs through its sulfonate group and is cleaved at the N-O bond during photo-irradiation with 405 nm light. This bond cleavage decreases the solubility of the NCs which allows patterns to emerge upon development with toluene. Post-patterning ligand exchange results in photoluminescence quantum yields up to 76%, while anion exchange provides tunability in the emission color. The patterned NC films also show photoconductive behavior, proving that good electrical contact between the NCs can be established.

2:00 PM EN08.05.03

Chlorinated Interface Modifier for Improving the Microstructural and Electronic Properties of Inorganic Lead-Free Cesium Bismuth Iodide Perovskite [Vincent O. Eze](#), Lucas Braga Carani and Okenwa Okoli; Florida State University, United States

Recently, inorganic lead-free metal halide perovskites have gained attention as promising optoelectronic materials for various applications due to their nontoxicity, environmental moisture, and thermal stability. In particular, the lead-free cesium bismuth halide perovskites with the general formula $A_xB_yX_z$; $z = x + 3y$, where A=Cesium (Cs), B=Bismuth (Bi), X=Iodide (I), Bromide (Br) have generated enormous interest among the perovskite research community as emerging materials for optoelectronic applications. Among the Bi-based perovskites, the CsBi₃I₁₀ perovskite (where x=1, y=3, and z=10) has the lowest bandgap of about 1.77 eV with a broad light absorption spectrum that is beneficial for solar cell, broad photodetection, and mechanoluminescence pressure sensing application. However, studies focused on understanding the microstructural and electronics properties of solution-processed CsBi₃I₁₀ perovskite is still lacking. Moreover, it is still challenging to prepare uniform, compact, and void-free CsBi₃I₁₀ perovskites. Herein, we systematically study the microstructural, optical, charge transport, defect density, and electronic properties of CsBi₃I₁₀ perovskite with and without the incorporation of the chlorinated interface modifier. The experimental results show that the interface modifier led to enhanced light absorption, crystallinity, and microstructural features. Furthermore, this work explores the underlying mechanism for such enhancement and assesses the influence of chlorinated interface modifiers for improving the performance of a self-powered photodetector for mechanoluminescence pressure sensing applications.

2:15 PM *EN08.09.01

The 2D Halide Perovskites [Mercuri G. Kanatzidis](#); Northwestern University, United States

Two-dimensional (2D) halide perovskites have emerged as outstanding semiconducting materials thanks to their superior stability and structural diversity. However, the ever-growing field of optoelectronic device research using 2D perovskites requires systematic understanding of the effects of the spacer on the structure, properties, and device performance. So far, many studies are based on trial-and-error tests of random spacers with limited ability to predict the resulting structure of these synthetic experiments, hindering the discovery of novel 2D materials to be incorporated into high-performance devices. In this presentation, we provide guidelines on successfully choosing spacers and incorporating them into crystalline materials and optoelectronic devices. Useful insights are emerging on what kind of spacer cations can stabilize 2D perovskites thanks to an extensive collection of spacer cations, which have been shown to stabilize 2D perovskites. There will be emphasis on the effects of the spacer on the structure and optical properties.

2:45 PM BREAK

SESSION EN08.06: Processes in Low Dimensional Perovskites
Wednesday Afternoon, December 1, 2021
Hynes, Level 3, Room 310

4:00 PM EN08.06.01

Surface Defect States Act as Excitonic Quenching Layers in 2D Perovskites Thin Films [Giulia Folpini](#), Jetsabel M. Figueroa Tapia, Daniele Cortecchia, Mirko Prato and Annamaria Petrozza; Istituto Italiano di Tecnologia, Italy

The optoelectronic properties of two-dimensional metal halide perovskites (2D MHPs), such as large exciton binding energies, narrow excitonic emission and small Stokes shifts, make them excellent candidates for light emitting applications. However, the purely 2D MHPs, characterized by large organic cations (e.g. phenethylammonium PEA, butylammonium BA, naphthylammonium NMA), are outperformed in LED and lasing devices by other low-dimensionality systems such as fully inorganic nanoparticles or multidimensional perovskites based on a mixture of smaller and bulkier organic cations. Importantly, an unexpected limitation comes from 2D MHPs poor luminescence efficiency: to rationalize this, different mechanisms have been proposed involving recombination on defects and grain boundaries, competing multi-exciton processes, poorer charge transport qualities and effects on luminescence of exciton-phonon coupling. [1-4]. However, the lower radiative recombination efficiencies of 2D MHPs compared to 3D counterparts is not yet fully understood.

In this work, we investigate exciton transport properties in the prototypical 2D MHP phenethylammonium lead iodide ((PEA)₂PbI₄) to identify the effect of surface states on the excitonic luminescence, and assess their role in photoluminescence (PL) quenching compared to bulk defects. More specifically, we investigate exciton transport in polycrystalline thin films, establishing an exciton diffusion length of 150 nm in good agreement with values reported in other 2D MHPs [5, 6]. By comparing the radiative lifetime and luminescence efficiencies in films of varying thicknesses [7], we identify the role of the surface as a quencher of excitonic radiative recombination. In films thicker than the diffusion length, where most excitons recombine before interacting with the surface, the PL lifetime is comparable to that of single crystals, indicating a limited role of grain boundaries as non-radiative recombination centers. In thinner films however, a significant quenching of radiative lifetime is observed. The quenching role of surface defects is further confirmed by comparison with (PEA)₂PbI₄ nanoparticles, where no quenching is observed despite their characteristically smaller spatial scale. Finally, we relate surface defectivity to the presence of undercoordinated lead atoms, and explore how ad-hoc passivating strategies may be exploited to reduce exciton quenching at the film surface.

[1] Adv. Funct. Mater. 2020, 30, 1907979

[2] Nat. Mater. 17, 550–556 (2018)

[3] Science 355, 1288–1292 (2017)

[4] ACS Nano 2016, 10, 11, 9776–9786

[5] J. Phys. Chem. Lett. 2021, 12, 4003–4011

[6] Nat Commun 11, 2035 (2020)

[7] J. Phys. Chem. B 2009, 113, 9104–9109

4:15 PM EN08.06.02

Exciton and Lattice Dynamics of One-Dimensional Halide Perovskite Nanowires Mengyu Gao and Peidong Yang; University of California, Berkeley, United States

Many electronic and structural properties of halide perovskite evade conventional categorization. In the talk, we will present two synthetic platforms consisting of atomically-defined one-dimensional halide perovskite nanowires, where we will address the lingering scientific questions of the intriguing optical and structural behaviors of halide perovskite nanostructures.

In the first synthetic platform, we synthesized uniform colloiddally stable nanowires with fixed diameter but varied aspect ratios. Using this system, we revealed the scaling laws of photoluminescence quantum yield and radiative lifetime with respect to the aspect ratio of nanocrystals. The scaling laws derived herein are not only a phenomenological observation but proved a powerful tool disentangling the carrier dynamics of microscopic systems in a quantitative and interpretable manner. The investigation of our model system and theoretical formulation bring to light the dimensionality, as a hidden constraint on carrier dynamics, and identify the diffusion length as an important parameter that distinguishes nanoscale and macroscale carrier behaviors. In the second synthetic platform, we successfully encapsulated single-unit-cell thick halide perovskite nanowires inside single-walled carbon nanotubes. State-of-art transmission electron microscope coupled with a fast electron detection camera was employed to observe the transient structure dynamics of the atomically-thin halide perovskite nanowires. We found that due to the protection of carbon nanotubes, the notoriously beam-sensitive perovskite nanostructure behaved “resiliently” to the electron beam so that their lattice is dynamic but maintain a degree of integrity throughout the acquisition. Overall, with the atomic-level synthetic control we created two types of 1D halide perovskite nanowires, and due to their structural and morphological uniqueness, new photophysics and structure dynamics were explored. We will demonstrate in the talk how to use these systems and their interesting properties to articulate the explanatory gaps in the field of low dimensional halide perovskite.

4:30 PM EN08.06.03

Strongly Anharmonic Octahedral Tilting in 2D Hybrid Halide Perovskites Matan Menahem¹, Zhenbang Dai², Sigalit Aharon¹, Rituraj Sharma¹, Maor Asher¹, Yael Diskin-Posner¹, Roman Korobko¹, Andrew M. Rappe² and Omer Yaffe¹; ¹Weizmann Institute of Science, Israel; ²University of Pennsylvania, United States

Two-dimensional hybrid halide perovskites (2D HHPs) intrigue material scientists from both the scientific and technological points of views. They exhibit pronounced and easily tunable excitonic properties, which are strongly coupled to thermal fluctuations. The structure of 2D HHPs is closely related to that of their extensively studied 3D counterparts, in which the electronic properties are strongly influenced by anharmonic lattice dynamics.

In this presentation, I will show a study[1] of the structural dynamics of the prototypical 2D HHP (CH₃(CH₂)₃NH₃)₂PbI₄ (BAPF) by comparing it to its 3D counterpart CH₃NH₃PbI₃ (MAPI) and aromatic counterpart (C₆H₅-(CH₂)₂NH₃)₂PbI₄. We use single-crystal x-ray diffraction and temperature dependent Raman scattering to show that stronger intermolecular interactions between the organic molecules force the structure to a lower symmetry with more harmonic thermal fluctuations. Moreover, we use polarization-orientation Raman scattering and density-functional-perturbation-theory to relate the low-temperature thermal fluctuations of MAPI and BAPF, showing strong similarities between the structural dynamics of the materials. Finally, we uncover the mechanism of the order-disorder phase transition in BAPF which preserves the crystal symmetry due to a skewed double-well potential, biased by the hydrogen bonding between the organic amine and the inorganic scaffold. The phase transition involves unlocking of an anharmonic octahedral tilting motion which increases the anharmonicity of the lattice dynamics and decreases other phonons' lifetime.

These anharmonic fluctuations are important for technological applications and novel designs of materials and devices since they induce charge carrier localization and affect the optoelectronic performance.

[1] M. Menahem et al., ACS Nano, *In Press*. DOI: 10.1021/acsnano.1c02022

SESSION EN08.07: Emissive Properties of Low Dimensional Perovskites

Session Chair: Letian Dou

Thursday Morning, December 2, 2021

Hynes, Level 3, Room 310

10:30 AM *EN08.07.01

Metal Halide Ruddlesden-Popper Phases for Efficient Blue-Emitting Light Emitting Diodes Maria Antonietta Loi; University of Groningen, Netherlands

Ruddlesden-Popper (RP) perovskite phases of nominal composition PEA₂(Cs_{0.75}MA_{0.25})Pb₂Br₇ with and without the addition of the isopropylammonium additive, are demonstrated to emit in the wavelength range around 480 nm and 500 nm, respectively. The sample with isopropylammonium when deposited on a PEDOT-PSS coated substrate displays an exceptional PL QY as high as 64%. Cross correlation of the optical and structural investigations indicate that the RP phase is composed of domains of n=3 phases surrounded by higher dimensionality phases, which allow the efficient transport of charge carriers towards the low dimensional domains. Interestingly, the funneling of the photoexcitations towards the low dimensional phases is blocked in samples using the isopropylammonium additive, mostly due to the random orientation of very small crystalline domains. All the features of this new RP phase allowed us to fabricate LEDs emitting at an average wavelength of 483 nm, with FWHM of the electroluminescence of 25 nm and an external quantum efficiency up to 6%.

These results demonstrate that there is an opportunity to achieve high efficiency LEDs also in the blue spectra range by engineering RP phases.

11:00 AM EN08.07.02

Growth Controls Phonon-Coupled Emission in 2D Perovskite Films Rhiannon M. Kennard¹, Clayton Dahlman¹, Juil (Jay) Chung¹, Ben Cotts², Alexander Mikhailovsky¹, Lingling Mao¹, Ryan DeCrescent¹, Kevin Stone², Naveen Venkatesan¹, Yahya Mohtashami¹, Sepanta Assadi¹, Alberto Salles², Jon Schuller¹, Ram Seshadri¹ and Michael L. Chabinye¹; ¹University of California, Santa Barbara, United States; ²Stanford University, United States

2D/3D perovskites are attractive for a variety of applications due to their enhanced stability over their 3D perovskite-based counterparts. However, improvements to 2D/3D perovskite-based devices are hampered by missing knowledge about the 2D perovskite itself. In particular, greater understanding

is needed about how processing and composition engineering affect film structure and optoelectronic properties. Because charge generation in 2D perovskites is primarily excitonic, understanding excitonic emission and its link(s) to film processing is crucial for improving 2D/3D perovskite-based devices.

Here, we show that film processing can turn on or off exciton emission that is phonon-coupled. We made thin films of (EA)₄Pb₃Br₁₀, where EA is ethylammonium. The films are found to be phase-pure; this phase-purity is attributed to using a single A/A'-site cation in the Ruddlesden-Popper n=3 structure, which prohibits crystallization of off-target phases. Composition engineering can thus be used to select for specific Ruddlesden-Popper phases in films. Thin films and bulk crystals (EA)₄Pb₃Br₁₀ have three emission features: a narrow feature at higher energy, and two features at lower energy. Temperature dependent luminescence measurements reveal that the lower-energy features are phonon-coupled, and are perhaps either phonon replicas or self-trapped excitons. Notably, the intensity of the broad, lowest-energy emission feature depends on film casting kinetics. This intensity dependence is attributed to the presence/absence of film strain imparted by the casting. These results provide an additional knob with which to change the proportions of different types of exciton emission in films. We anticipate that the results here will lead to new 2D/3D perovskite heterostructures with better control over composition and excitonic transitions. [1]

[1] Kennard, R.M.; Dahlman, C.J.; Chung, J.; Cotts, B.; Mikhailovsky, A.A.; Mao, L.; DeCrescent, R.A.; Stone, K.H.; Venkatesan, N.R.; Mohtashami, Y.; Assadi, S.; Salleo, A.; Schuller, J.A.; Seshadri, S.; Chabiny, M.L. Under Review, 2021.

11:15 AM EN08.07.03

Color Tunable Quasi 2D Blue Perovskite Light-Emitting Diode Utilizing Double Side Amido Ligand Masoud Alahbakhshi¹, Aditya Mishra¹, Grigori Verkhogliadov^{2,3}, Ross Haroldson¹, Qing Gu¹, Jason D. Slinker¹ and Anvar Zakhidov^{1,2,3}; ¹The University of Texas at Dallas, United States; ²TMO University, Russian Federation; ³The university of Texas at Dallas, United States

Metal halide perovskite, as an emerging semiconductor, provides a unique opportunity for high-definition display and solid-state lighting. Rapid and breakthrough improvements have been achieved in green, red, and near-infrared perovskite light-emitting diodes (PeLEDs). However, blue PeLEDs are still far behind with much lower performance. Herein, we introduce a new dual ligand strategy of 2D/3D perovskite thin film preparation by using the appropriate ratio of Ethane-1,2-diammonium bromide (EDBr) and Phenethyl ammonium bromide (PEABr). The steady-state photoluminescence spectra demonstrate that double side amido terminals EDBr ligand can suppress efficiently the small n domains and non-radiative recombination, leads to strong energy transfer to larger n domains. Based on such films, a sky blue PeLED at 485 nm with about 730 cd/m² brightness and low turn-on voltage (2.8V) was achieved.

11:30 AM EN08.07.04

Exciton Diffusion in Two-Dimensional Hybrid Perovskites Jonas D. Ziegler¹, Jonas Zipfel^{1,2}, Barbara Meisinger¹, Matan Menahem³, Xiangzhou Zhu⁴, Takashi Taniguchi⁵, Kenji Watanabe⁵, Omer Yaffe³, David Egger⁴ and Alexey Chernikov^{1,6}; ¹University of Regensburg, Germany; ²Molecular Foundry, Lawrence Berkeley National Laboratory, United States; ³Weizmann Institute of Science, Israel; ⁴Technical University of Munich, Germany; ⁵National Institute for Materials Science, Japan; ⁶Dresden University of Technology, Germany

Two-dimensional hybrid perovskites have attracted renewed interest of the condensed matter community due to their intriguing electronic and vibrational properties. They offer excellent platforms to study fundamental many-body physics with promising opportunities for optoelectronic applications. Composed by self-assembly from nanometer-thin sheets of inorganic molecules separated by organic spacers, layered perovskites represent natural, two-dimensional quantum wells. An important consequence of the reduced dimensionality together with weak dielectric screening is the formation of tightly bound electron-hole complexes, commonly known as excitons. In these systems, the excitons are exceptionally robust and, most importantly, couple strongly to light. Following photon absorption, they not only serve as the main energy carriers in the crystal, but also determine the conversion of that energy back to light. Motivated by these properties, a wealth of recent research activities emerged, aimed at the study of *exciton transport* in two-dimensional hybrid perovskites.

A central question in this context is how the excitons move as a function of temperature. In close analogy to *electrons*, temperature-dependent transport is considered key to understand the physics of the *excitonic* mobility. Here, we present the results of our study of exciton propagation in two-dimensional hybrid perovskites, performed from liquid helium up to room temperature conditions [1]. The exciton diffusion is directly monitored by optical means using spatially- and time-resolved photoluminescence microscopy. To avoid material degradation under illumination, the samples are fully encapsulated between thin layers of hexagonal boron nitride. At all studied temperatures our measurements demonstrate that the excitons are highly mobile during their nanosecond lifetimes. The extracted diffusion coefficients range from 1 up to 30 cm²/s and the corresponding diffusion lengths are as high as 1 micrometer. Two distinct regimes of exciton transport are identified. For all temperatures above 50 K, the excitons propagation follows the conventional diffusion law. Moreover, the extracted diffusion coefficient is either constant or decreases with increasing temperature. This behavior is a characteristic hallmark of free exciton propagation, that is one of our key results. In the temperature regime below 50 K, however, the diffusion is anomalous. First, the exciton cloud expands rapidly after the excitation and then the expansion slows down over time. At liquid helium temperature, the exciton distribution even shrinks again after 100 ps. This observation corresponds to an effectively negative diffusion coefficient that subsequently converges towards zero at longer timescales. Our findings are discussed in the context of an effective mass model from first-principles calculations and temperature-dependent collision broadening based on spectral linewidth analysis. Further considered is the potential impact of non-equilibrium dynamics and exciton localization. Finally, we demonstrate the apparent applicability of a semi-classical diffusion model and provide an outlook towards understanding exciton transport in two-dimensional halide perovskites.

[1] J. D. Ziegler et al., Nano Lett. 20, 6674 (2020), DOI:10.1021/acs.nanolett.0c02472

SESSION EN08.08: Application of Low Dimensional Perovskites in Optoelectronics
Session Chair: Maria Antonietta Loi
Thursday Afternoon, December 2, 2021
Hynes, Level 3, Room 310

1:30 PM *EN08.08.01

Two-Dimensional Organic-Perovskite Hybrid Materials and Heterostructures Letian Dou, Purdue University, United States

Two-dimensional halide perovskites are exciting new semiconductors that show great promising in low cost and high-performance optoelectronics devices

including solar cells, LEDs, photodetectors, transistors, *etc.* In the first part of this talk, I will present a molecular approach to the synthesis of high-quality organic-inorganic hybrid perovskite quantum wells through incorporating widely tunable organic semiconducting building blocks as the surface capping ligands. By introducing sterically tailored groups into the molecular motif, the strong self-aggregation of the conjugated organic molecules can be suppressed, and single crystalline organic-perovskite hybrid quantum wells and superlattices can be easily obtained via one-step solution-processing. Energy transfer and charge transfer between adjacent organic and inorganic layers are extremely fast and efficient, owing to the atomically-flat interface and ultra-small interlayer distance. Furthermore, this conjugated ligand design greatly enhances materials chemical stability and suppresses halide anion migration. Based on this, we demonstrate for the first time an epitaxial halide perovskite heterostructure with near atomically-sharp interface. Finally, we demonstrate stable and efficient LEDs and FETs using the novel 2D hybrid materials.

2:00 PM EN08.08.02

Synergetic Molecular Treatment for Efficient and Stable Quasi 2D Perovskite LEDs Miguel Anaya, Linsong Cui, Kyle Frohna and Samuel D. Stranks; University of Cambridge, United Kingdom

Metal-halide perovskites have emerged over the past years as a versatile class of semiconductors for high-performance optoelectronic devices.[1] However, despite their unique properties, this family of perovskites has been observed to display strong instability, especially when electrostimulated, limiting their definitive integration in real-world light-emitting devices.[2-4]

In this talk, we will present a detailed photophysical characterisation of quasi 2D green-emitting halide perovskite films in which different passivation strategies are employed to improve both their optical and electrical properties. We will introduce a new powerful technique with which we can evaluate the performance of perovskite-based LEDs at the nanoscale by hyperspectral wide-field imaging. We show how to obtain maps at the diffraction limit scale for their External Quantum Efficiency (EQE), luminance, and luminous efficacy. Our observations reveal the degradation pathways of this emerging class of LEDs, induced by microscale heterogeneities that hamper the ultimate device performance. The lessons learned from our multimodal microscopy approach allow us to identify a novel dual molecular treatment that selectively 1) optimises the thin film quality (e.g. suppression of pinholes while maximising light outcoupling) and 2) enhances the intrinsic optoelectronic quality of the quasi 2D perovskite (e.g. PLQE, IQE). This methodology results in bright (>14,000 cd/m²) and efficient (>20% EQE) green LEDs with operational lifetimes surpassing 100 h. Our work represents a step forward in diagnosing the in-operando properties of low dimensional perovskite-based devices at the nanoscale and opens avenues to identify strategies for stable and efficient LEDs with spatially maximised performance.[5]

[1] Stranks, S. D. and Snaith, H. J. Metal-halide perovskites for photovoltaic and light-emitting devices. *Nat. Nanotechnol.* 2015, 10, 391.

[2] Anaya, M.; et al. Best practices for measuring emerging light-emitting diode technologies. *Nature Photonics*, 2019, 12, 818.

[3] Hoye, R. L. Z.; Lai, M.-L.; Anaya, M. et al. Identifying and Reducing Interfacial Losses to Enhance Color-Pure Electroluminescence in Blue-Emitting Perovskite Nanoplatelet Light-Emitting Diodes. *ACS Energy Lett.* 2019, 5, 1181-1188.

[4] Ji, K.; Anaya, M.; Abfalterer, A.; Stranks, S. Halide Perovskite Light Emitting Diode Technologies. *Adv. Opt. Mater.* 2021, 2002128.

[5] Anaya, M.; Cui, L.; Frohna, K.; Stranks, S. D. et al. to be submitted.

2:15 PM EN08.08.03

Defective and Double Perovskites—*Ab Initio* Excitonic Properties in Lower-Dimensional Inorganic Halides Christopher Savory; University College London, United Kingdom

While 3-dimensional inorganic and hybrid halide perovskites have rightly seen great success in photovoltaics and LEDs, lower dimensional perovskites and perovskite-like materials, whether layered or ordered defect 'OD', have also shown similarly promising optoelectronic properties. The onset of self-trapped excitonic behaviour that has also been observed and associated with reduction in structural or electronic dimensionality make this class of materials highly promising as light emitters.¹ In the stable, wholly inorganic low-D perovskites, such strong excitonic behaviour has been seen in the 'OD' perovskite-like Cs₂M^(IV)X₆ compounds,² as well as at room temperature in the 2D ordered-defect pnictide-based perovskites of the Cs₃M^(III)₂X₉ family,³ and also resulting in high quantum efficiency in the highly promising Cs₂M^(I)M^(III)X₆ double perovskites,⁴ which while 3-dimensional in structure, can demonstrate a 'OD'-like electronic structure due to the substitution of the perovskite 'B' site;⁵ all of these materials maintain the added benefit of moving away from toxic Pb.

Nevertheless, a reliable theoretical description of the physical origin of these phenomena across the range of different structures available to lower-dimensional perovskites is lacking due to the inability of standard 'independent particle' methods such as Density Functional Theory (DFT) to describe excitons. In this study, we select example compounds from each of the aforementioned materials families and use *ab-initio* calculations to establish their electronic, optical and excitonic properties: Cs₂M^(IV)X₆ (M^(IV) = Zr, Sn; X = Cl, Br), Cs₃M^(III)₂X₉ (M^(III) = Bi, X = Br) and Cs₂M^(I)M^(III)X₆ (M^(I) = Ag, Na; M^(III) = Bi, In; X = Cl, Br). We initially establish a comparison in the electronic structures predicted through accurate standard *ab-initio* methods, such as hybrid DFT, and higher level many-body perturbation methods (QSGW) available within the open-source code Questaal.⁶ Then, where standard DFT fails, we calculate the excitonic spectrum, within the Bethe-Salpeter Equation, of each material to establish a consistent understanding of the excitonic properties and establish the influence of both structure and composition. We also computationally examine the dynamic and thermodynamic stability of these materials to confirm whether the advantage of stability attributed in both lower-dimensional and inorganic perovskites is maintained. In performing this survey across a range of inorganic perovskite-like structures, we hope to establish the structure-property relationships that can potentially provide insight into the behaviour of current inorganic or hybrid inorganic-organic low-dimensional perovskites and also guide future syntheses of lead-free, efficient light emitters.

(1) Smith, M. D.; Karunadasa, H. I. *Acc. Chem. Res.* 2018, 51, 619.

(2) Abfalterer, A.; Shamsi, J.; Kubicki, D.J.; Savory, C.N.; Xiao, J., *et al. ACS Materials Letters*, 2020, 2, 1633-1652

(3) McCall, K.M.; Stoumpos, C.C.; Kostina, S.S.; Kanatzidis, M.G.; Wessels, B.W. *Chem. Mater.* 2017, 29, 4129-4145

(4) Luo, J.; Wang, X.; Li, S.; Liu, J.; Guo, Y. *et al. Nature*, 2018, 563, 541

(5) Xiao, Z.; Meng, W.; Wang, J.; Mitzi, D.B.; Yan, Y. *Mater. Horiz.*, 2017, 4, 206-216

(6) Pashov, D.; Acharya, S.; Lambrecht, W.R.L.; Jackson, J.; Belashchenko, K.D.; Chantis, A.; Jamet, F.; van Schilfegaarde, M. *Comp. Phys. Commun.*, 2020, 249, 107065

2:45 PM BREAK

Thursday Afternoon, December 2, 2021
Hynes, Level 3, Room 310

4:00 PM EN08.09.02

Synthesis of Lead-Free Cs₃Bi₂Br₉ NCs with Enhanced Photocatalytic Activity in the Degradation of Organic Pollutants in an Aqueous Environment Alexander G. Aragon, Xiao Ma and Scott Geyer; Wake Forest University, United States

Over the past decade, metal halide perovskites, with a particular focus on traditional structures such as CsPbX₃ (X = Br, Cl, I) have garnered much interest as potential photocatalysts for many reactions such as solar fuel production (CO₂ reduction, HER), and in the degradation of organic pollutants. The fully ionic nature of these materials, however, has resulted in major challenges for their practical use. More stable perovskite alternative structures such as Cs₃B₂X₉ (B = Sb³⁺, Bi³⁺; X = Br, Cl, I) have shown great promise as novel photocatalysts and have not been heavily studied yet, especially at the 0D structural level in the form of NCs. Thus, this study was aimed at investigating the photocatalytic capabilities of Cs₃Bi₂Br₉ NCs synthesized by hot injection method. As synthesized Cs₃Bi₂Br₉ NCs with an observed optical bandgap of 2.85 eV were applied to the photocatalytic degradation of Rhodamine G (RhG) dye in an aqueous environment. For comparison, CsPbBr₃ NCs synthesized by hot injection method and P25 TiO₂ (Sigma) were also tested. The degradation of RhG follows pseudo-zeroth order kinetics with Cs₃Bi₂Br₉ NCs reaching catalytic efficiencies near 90%. Furthermore, the observed stability of the Cs₃Bi₂Br₉ NCs is much greater than the CsPbBr₃ NCs in that near zero catalytic efficiency was observed for CsPbBr₃. This is due to the degradation of CsPbBr₃ NCs in water occurring at a much faster rate than RhG degradation. Despite this, it was observed that as synthesized Cs₃Bi₂Br₉ NCs do degrade over time and thus the overall stability of the system must be improved for practical use. Current efforts to enhance the stability of the system include overcoating via ALD in order to passivate the surface and protect the perovskite layer, with an overall goal of producing a suitable water stable photocatalyst with high efficiency for wastewater purification.

4:15 PM EN08.09.03

Colloidal Synthesis of Metal Halide Layered Double Perovskite Nanocrystals with Composition Engineering and Structural Transformation Tong Cai, Wenwu Shi, Hanjun Yang and Ou Chen; Brown University, United States

Lead halide perovskites have been well explored in various optoelectronic applications due to their unique properties. While issues like toxicity and instabilities hinder their further use, which aroused great interest for the development of alternative lead-free perovskites. Recently, a new family of layered double perovskites (LDPs) with a chemical formula of Cs₄M(II)M(III)₂X₁₂ provide a new route to solve these problems by combining two main strategies including composition substitution and dimensionality reduction. On the one hand, Pb²⁺ cations are substituted by a combination of M(II) and M(III) cations with the enlarged composition tuning space. On the other hand, the layered structure consists of one layer of [M(II)X₆]⁴⁻ octahedra sandwiched by two layers of [M(III)X₆]³⁻ octahedra in between two adjacent vacancy layers. However, accessibilities to this class of perovskite-type nanomaterials remain inadequate, hindering their practical implementations in various applications. Here, we report the colloidal synthesis of several types of LDP NCs using a modified hot-injection method, such as Cs₄CuSb₂Cl₁₂, Cs₄MnBi₂Cl₁₂, Cs₄CdBi₂Cl₁₂ and Cs₄CdSb₂Cl₁₂ LDP NCs. The resulting LDP NCs show unique optical, electronic and magnetic properties with different crystal structures, inspiring to build the composition-structure-property relations between various LDP NCs. Therefore, a series of Cs₄Cu_xAg_{2-2x}Sb₂Cl₁₂, Cs₄Cd_{1-x}Mn_xBi₂Cl₁₂, and Cs₄Cd_{1-x}Cu_xSb₂Cl₁₂ perovskite-type NCs (0 ≤ x ≤ 1) are synthesized to investigate the composition-induced crystal structural transformation, and thus, the evolution of electronic bandgap, magnetic ordering and charge carrier dynamics. These transformation processes are explored by experimental observations and further confirmed by theoretical DFT calculations on the band structures, charge density differences and electron localization function. Photo-generated charge carrier dynamics of the LDP NCs are investigated using ultrafast spectroscopic techniques. Taking advantage of both the unique electronic structures and solution processability, we demonstrate that the LDP NCs can be solution-processed as high-speed photodetectors with ultrafast photo-response and narrow bandwidth. We anticipate that our study will prompt future research to design and fabricate novel and high-performance lead-free perovskite-type NCs for a range of photovoltaic applications in the future.

SESSION EN08.10: Alternatives to Lead in Low Dimensional Perovskites
Session Chair: Giulia Grancini
Monday Morning, December 6, 2021
EN08-Virtual

8:00 AM *EN08.10.01

Lead-Based Perovskites: How Toxic are These and What are the Prospects of Alternatives Like Cs₂AgBiBr₆ Huygen J. Jöbsis¹, María C. Gélvez-Rueda², Reiny Sangster³, Valentine M. Caselli⁴, Sven Askes², Erik C. Garnett², Charlotte M. Gommers³, Bruno Ehrler², Ferdinand C. Grozema⁴, Freddy T. Rabouw¹, Tom Savenije⁴ and Eline M. Hutter¹; ¹University of Utrecht, Netherlands; ²AMOLF, Netherlands; ³Wageningen University & Research, Netherlands; ⁴Delft University of Technology, Netherlands

Cs₂AgBiBr₆ (CABB) has been proposed as a less toxic and more stable alternative to lead halide perovskites. However, low charge carrier collection efficiencies remain an obstacle for the incorporation of this material in optoelectronic applications. In this talk, I will elaborate on the dynamics of charge transport, localization and recombination in CABB thin films, studied using time-resolved photoconductivity and transient absorption/reflectance measurements. Temperature-dependent photoconductivity measurements indicate band-like charge transport of free charges, similar to lead-based perovskites.¹ We find that replacement of Bi with Sb shifts the absorption onset, while preserving the charge transport mechanism. However, as charges lose mobility within tens of nanoseconds, diffusion lengths remain relatively short in these lead-free materials. While mobile charges have a nanosecond-lifetime, we observe microsecond-long lifetimes in transient absorption measurements.³ This suggests that the conductivity loss in CABB films is due to a combined effect of carrier recombination and localization. Moreover, we find that the charge carrier diffusion length is similar to the sample thickness, suggesting that charge localization occurs at the materials surface. Therefore, improving surface quality could be a strategy to optimize performance of CABB-based optoelectronic devices. In parallel to investigating CABB, we performed a toxicity study of methylammonium lead iodide perovskites on *A. Thaliana* plants, and found that the iodide was actually much more toxic than the lead.² Altogether, these results stress the importance of further understanding which perovskites are most harmful to the environment, while optimizing the optoelectronic quality of materials with the lowest toxicity.

(1) Hutter, E. M.; Gélvez-Rueda, M. C.; Bartsaghi, D.; Grozema, F. C.; Savenije, T. J. Band-Like Charge Transport in Cs₂AgBiBr₆ and Mixed Antimony-Bismuth Cs₂AgBi_{1-x}Sb_xBr₆ Halide Double Perovskites. *ACS Omega* 2018, 3 (9), 11655–11662. <https://doi.org/10.1021/acsomega.8b01705>.

(2) Hutter, E. M.; Sangster, R.; Testerink, C.; Ehrler, B.; Gommers, C. M. M. Metal Halide Perovskite Toxicity Effects on Plants Are Caused by Iodide Ions. *arXiv:2012.06219* 2020.

(3) Jöbsis, H. J.; Caselli, V. M.; Askes, S. H. C.; Garnett, E. C.; Savenije, T. J.; Rabouw, F. T.; Hutter, E. M. Recombination and Localization : Unfolding

the Pathways behind Conductivity Losses in Cs₂AgBiBr₆ Thin Films. *arXiv:2107.01852* 2021.

8:30 AM *EN08.10.02

Lead-Free Metal Halide Nanocrystals Combining High Photoluminescence Quantum Yield with Picosecond Radiative Lifetime Osman M. Bakr; King Abdullah University of Science and Technology, Saudi Arabia

Lead halide compounds, including lead halide perovskite nanocrystals (NCs), have attracted the interest of researchers in optoelectronics and photonics due to their high photoluminescence quantum yields (PLQYs) coupled with relatively short PL lifetimes (on the order of a few nanoseconds). However, lead-free metal halides of high PLQY, including double perovskites and their doped NCs, typically possess long PL lifetimes (up to microseconds), due to the nature of their excitons, which limits their application space. Here, I introduce CsMnBr₃ NCs, which are lead-free and combine a high PLQY with an exceptionally short radiative lifetime (on the order of picoseconds). We find that the octahedral coordination of Mn²⁺ in CsMnBr₃ induces a red emission centered at ~643 nm with a PLQY of ~54% and a fast radiative decay rate. Femtosecond transient absorption and transient PL spectroscopies reveal the existence of a low-lying excited state of Mn²⁺ that relaxes to the ground state within ~600 ps by emitting light at ~643 nm. At greater excitation energies, higher excited states of Mn²⁺ relax within a sub-nanosecond timescale to this low-lying excited state. A similarly positioned PL peak with a short picosecond-scale PL lifetime and a PLQY of ~6.7% was also detected in bulk CsMnBr₃ single crystals – a relatively high quantum yield for a bulk material. Our experimental results and density functional theory modelling show that the crystal structure and the strong coupling among Mn²⁺ ions govern those luminescence properties of CsMnBr₃ NCs and single crystals. These findings pave the way for new lead-free materials that combine high PLQY and ultrafast luminescence.

9:00 AM EN08.10.04

Layer Number Dependent Ferroelasticity in 2D Ruddlesden-Popper Organic-Inorganic Hybrid Perovskites Xun Xiao and Jinsong Huang; University of North Carolina at Chapel Hill, United States

Ferroelasticity represents material domains possessing spontaneous strain that can be switched by external stress. Three-dimensional perovskites like methylammonium lead iodide are determined to be ferroelastic. Layered perovskites have been applied in optoelectronic devices with outstanding performance. However, the understanding of lattice strain and ferroelasticity in layered perovskites is still lacking. Here, using the in-situ observation of switching domains in layered perovskite single crystals under external strain, we discover the evidence of ferroelasticity in layered perovskites with layer number more than one, while the perovskites with single octahedra layer do not show ferroelasticity. Density functional theory calculation shows that ferroelasticity in layered perovskites originates from the distortion of inorganic octahedra resulting from the rotation of aspherical methylammonium cations. The absence of methylammonium cations in single layer perovskite accounts for the lack of ferroelasticity. These ferroelastic domains do not induce non-radiative recombination or reduce the photoluminescence quantum yield.

9:15 AM EN08.10.05

Expanding the 0D Rb₇M₃X₁₆ (M=Sb, Bi; X=Br, I) Family—Dual-Band Luminescence in Rb₇Sb₃Br₁₆ Kyle M. McCall^{1,2}, Bogdan M. Benin^{1,2}, Michael Woerle¹, Thomas Vonderach¹, Detlef Guenther¹ and Maksym V. Kovalenko^{1,2}; ¹ETH Zurich, Switzerland; ²Empa—Swiss Federal Laboratories for Materials Science and Technology, Switzerland

Low-dimensional metal halides have been the focus of intense investigations in recent years following the success of the three-dimensional (3D) hybrid lead halide perovskites as optoelectronic materials for solar cells, semiconductor radiation detectors, and narrow emitters. In particular, the light emission of zero-dimensional (0D) metal halides have found utility in a variety of applications (including X-ray scintillation and remote thermometry) that are complementary to those of the 3D halide perovskites, thanks to their unusual properties including intrinsic broadband emission and highly temperature-dependent lifetimes. Inorganic, lead-free compositions are especially sought after thanks to their enhanced stability and reduced toxicity. Here, we flesh out the family of fully inorganic, 0D pnictogen halides based on the Rb₇M₃X₁₆ (M=Sb, Bi; X=Br, I) stoichiometry by solvothermal and solid-state synthesis of the heavier halides, namely Rb₇Sb₃Br₁₆, Rb₇Bi₃Br₁₆, and Rb₇Bi₃I₁₆. The title compound exhibits a 0D structure comprised of two isolated units: [SbBr₆]³⁻ octahedra and edge-sharing bioctahedra [Sb₂Br₁₀]⁴⁻ dimers which order into layers along the *c*-axis. The compound is air-stable and exhibits weak orange-red photoluminescence (PL) at room temperature, but intriguingly at low temperatures has two distinct emission bands with different excitation characteristics. Temperature-dependent PL and PL excitation spectra reveal that these bands correspond to these two motifs, and that there is a crossover near 150 K where the high-energy emission quenches as the units begin to interact.

We are also able to obtain Rb₇Bi₃Br₁₆ and Rb₇Bi₃I₁₆ which both crystallize in orthorhombic symmetry, with Rb₇Bi₃Br₁₆ presenting weak low-temperature luminescence while Rb₇Bi₃I₁₆ is non-luminescent. These trends in PL intensity with changing composition can be directly linked to the lone pair activity, which is maximized in the Sb analogues with lighter halides, yielding insight into how to design optically emissive materials. This work expands the library of emissive inorganic metal halides and provides further evidence for the efficacy of low-dimensional Sb-X luminescent centers based on octahedral and edge-sharing [Sb₂X₁₀]⁴⁻ dimers.

SESSION EN08.11: Structure-Function Relations in Low Dimensional Perovskites II

Session Chairs: Eline Hutter and Christian May

Monday Morning, December 6, 2021

EN08-Virtual

10:30 AM *EN08.11.01

0D and 2D Perovskites for Light Emission Applications Edward H. Sargent; University of Toronto, Canada

I will review advances in perovskite LEDs, focusing on the use of quantum wells and quantum dots.

11:00 AM *EN08.11.02

Superlattices from Lead Halide Perovskite Nanocrystals Maksym V. Kovalenko^{1,2}; ¹ETH Zurich, Switzerland; ²Empa—Swiss Federal Laboratories for Materials Science and Technology, Switzerland

Lead halide perovskite nanocrystals (LHP NCs, NCs, A=Cs⁺, FA⁺, FA=formamidinium; X=Cl, Br, I) exhibit spectrally narrow (<100 meV) fluorescence, tunable over the entire visible spectral region of 400-800 nm [1,2]. Owing to their high oscillator strength, slow dephasing (long coherence times of up to

80 ps), minimal inhomogeneous broadening of emission lines, and a bright triplet exciton character with orthogonal dipole orientation [2], these NCs make for a highly versatile platform for creating controlled, aggregated states exhibiting collective phenomena. Long-range ordered superlattices (SLs) with the simple cubic packing of cubic perovskite NCs exhibit sharp red-shifted lines in their emission spectra and superfluorescence (a fast collective emission resulting from coherent multi-NCs excited states) [4]. We now present perovskite-type ABO₃ binary and ternary NC SLs by a shape-directed co-assembly of CsPbBr₃ nanocubes (occupying B- and/or O-sites) with spherical dielectric Fe₃O₄ or NaGdF₄ NCs (A-sites) and truncated-cuboid PbS NCs (B-site) [5]. Such ABO₃ SLs, as well as other newly obtained SL structures (binary NaCl- and AlB₂-types, columnar assemblies with disks, *etc.*), exhibit a high degree of orientational ordering of CsPbBr₃ nanocubes. These mesostructures exhibit superfluorescence as well, characterized, at high excitation density, by emission pulses with ultrafast (22 ps) radiative decay and Burnham-Chiao ringing behavior with a strongly accelerated build-up time.

- [1] M. V. Kovalenko *et al.* *Science* **2017**, *358*, 745-750
- [2] Q.A. Akkerman *et al.* *Nature Materials* **2018**, *17*, 394–405
- [3] M. A. Becker *et al.* *Nature* **2018**, *553*, 189-193
- [4] G. Rainò *et al.* *Nature* **2018**, *563*, 671–675
- [5] I. Cherniukh *et al.* *Nature* **2021**, *593*, 535–542

11:30 AM EN08.11.03

Broad Band Emission from Excitons in Layered Ruddlesden-Popper Hybrid Perovskites with Tailored Layer-Phase Composition [Anna Stadlbauer](#)¹, Lissa Eyre¹, Miguel Anaya², Samuel D. Stranks² and Felix Deschler¹; ¹Walter Schottky Institut - Technical University Munich, Germany; ²University of Cambridge, United Kingdom

Lighting applications require cheap and sustainable materials for broadband white-light emission generation. Recently, layered hybrid perovskites have been proposed as a potential material system, in which broad emission from self-trapped excitons was reported, among varying optical properties and unfortunately with low stability [1], [2].

Here, we report the generation of broad spectra from free, bright excitons by producing thin films of layered Ruddlesden-Popper lead iodide perovskites with tailored composition of multiple phases with varying layer number.

We investigate structure and photophysics of our hybrid perovskite films with selected linear and aromatic monoammonium cations [3], and a range of small cations (Cs, FA, MA). The chosen materials were produced by optimizing fabrication parameters, which were reported to influence the optical and structural properties [3]. We find best performance from the Cs containing compositions.

The resulting optimized materials are optically investigated with time resolved photoluminescence spectroscopy and transient absorption spectroscopy both at room temperature and at cryogenic temperatures. Furthermore, we characterize photoluminescence quantum efficiency. A detailed structural analysis with X-ray diffraction spectroscopy, atomic force microscopy and scanning electron microscope is performed to correlate structural and optical properties.

For the materials which show the broadest emission spectrum and best optoelectronic performance, we fabricate LEDs and use them as the emitter layer in combination with a blue LED for broadband white light emission.

Our findings have promise as a new approach for using Ruddlesden-Popper lead iodide perovskites in the broader application of white LEDs, which could result in lower cost and more efficient lighting.

- [1] M. Bidikoudi, E. Fresta, and R. D. Costa, "White perovskite based lighting devices," *Chem. Commun.*, vol. 54, no. 59, pp. 8150–8169, 2018, doi: 10.1039/c8cc03166e.
- [2] S. Kahmann, E. K. Tekelenburg, H. Duim, M. E. Kamminga, and M. A. Loi, "Extrinsic nature of the broad photoluminescence in lead iodide-based Ruddlesden–Popper perovskites," *Nat. Commun.*, vol. 11, no. 1, pp. 1–8, 2020, doi: 10.1038/s41467-020-15970-x.
- [3] X. Li, J. M. Hoffman, and M. G. Kanatzidis, "The 2D halide perovskite rulebook: How the spacer influences everything from the structure to optoelectronic device efficiency," *Chem. Rev.*, vol. 121, no. 4, pp. 2230–2291, 2021, doi: 10.1021/acs.chemrev.0c01006.

11:45 AM EN08.11.04

Estimation of Emission Properties of 2D Halide Perovskites Using DFT and Machine Learning [Hiromitsu Takaba](#), Kouta Miura, Yasuo Suzuki and Masaya Miyagawa; Kogakuin Univ, Japan

Recently, 2-dimension (2D) organic-inorganic halide perovskites have become one of the key materials in emission diode. The electronic structure and structural stability of these materials show a significant dependence on chemical composition. Therefore the emission properties and durability of the halide perovskite can be tuned by changing the combination of composition. In this study, using density functional theory (DFT) and molecular dynamics, we theoretically investigated a crystal structure and electronic structure of the partially substituted cubic (A)₂PbX₃ (A = butylammonium (BA), octylammonium (OA), X = halide). Our calculation results indicate that a bandgap is associated with Pb-X distance in the lattice, although the contribution of A-site ions is little. The relation of bandgap with Pb-X length is further confirmed and refined by expanding the investigated composition based on the 2D perovskite database reported by Marchenko *et al.* [*Chem. Mater.* (2020) 32, 7383]. It is found that the structural parameter of Pb-X simply explains the bandgap for different compositions. The relationship of bandgap and emission peaks in photoluminescence (PL) is further investigated with machine learning. Finally, PL emission peaks are predicted for the database and some of them are compared with the experiments for validation. This model explained the trend of the Stokes shift in 2D halide perovskite. The broadness of emission peaks, which may be related to the A site species, is also discussed.

12:00 PM EN08.11.05

Late News: Strongly Luminescent Hybrid Lead Halides with a Symmetric, Triamine Chromophore [Imra Tajuddin](#), Eugenia S. Vasileiadou, Michael C. De Siena, Ioannis Spanopoulos and Mercouri G. Kanatzidis; Northwestern University, United States

Hybrid lead halide perovskites and their lower dimensional related-structures are rising materials with extensive applications in photovoltaics and light-emitting diodes (LEDs), in part due to their luminescent properties. Herein, we present a family of low-dimensional lead halides with strong photoluminescence, incorporating into their structure the symmetric, triamine chromophore: 1,3,4-tris(1,3,5-tris(4-aminophenyl)benzene, symbolized as T. A zero-dimensional (0D) lead bromide structure is synthesized with the formula: (T)₇Pb₃Br₂₇.DMF. The novel 0D material contains the triamine molecules with isolated [PbBr₆]⁴⁻ octahedra and (DMF) molecules dispersed throughout.

The distance of the terminal amino-tail of the triamine to the nearest bromine atom is 3.652 Å. As a result of the extended conjugation of the triamine chromophore, (T)₇Pb₃Br₂₇.DMF displays cation-π interactions, with π-π interactions of 3.498 Å distance between the closest aromatic rings of the

adjacent triamine molecules. The DMF molecules are orientated adjacent to the lead bromide octahedra with an average distance of 3.05 Å of the oxygen atom with the nearest bromine atoms.

The (T)7Pb3Br27.DMF compound exhibits high distortion levels of the [PbBr6]4- octahedra, with an average bond length of 3.01 Å, an average bond angle variance of 46.696 deg.2 and an average bond length distortion index of 0.02676. The measured UV absorption spectra of the triamine itself shows two features, one with an absorption edge at 2.85 eV and another absorption edge at 2.58 eV. The (T)7Pb3Br27.DMF compound also displays two features in its absorption spectra with absorption edges at 2.95 eV and 2.00 eV. The studied compounds demonstrate vibrant, strong photoluminescence emission. The triamine chromophore exhibits blueish-white emission with a broad emission peak centered at 428 nm along with a shoulder at 370 nm. The (T)7Pb3Br27.DMF compound demonstrates strong and narrow blue emission at 368 nm with a lifetime of 5 ms due to self-trapped excitons. Additionally, the lead chloride and lead iodide analogues incorporating the triamine molecule have been synthesized. Our work proposes a synthetic strategy in designing hybrid lead halide compounds with symmetric chromophore molecules that exhibit strong photoluminescent emission.

12:15 PM EN08.11.06

Coherent Control of Asymmetric Spintronic Terahertz Emission from Two-Dimensional Hybrid Metal Halides Kankan Cong¹, Eric Vetter^{2,2}, Liang Yan^{3,2}, Yi Li^{4,1}, Qi Zhang¹, Yuzan Xiong^{4,4}, Hongwei Qu^{4,4}, Richard Schaller¹, Axel Hoffmann^{5,1}, Alexander Kemper², Yongxin Yao⁶, Jigang Wang⁶, Wei You^{3,2}, Haidan Wen¹, Wei Zhang⁴ and Dali Sun^{2,2}; ¹Argonne National Laboratory, United States; ²North Carolina State University, United States; ³University of North Carolina at Chapel Hill, United States; ⁴Oakland University, United States; ⁵University of Illinois at Urbana-Champaign, United States; ⁶Iowa State University, United States

Next-generation terahertz (THz) sources demand light-weight, low-cost, defect-tolerant, and robust components with synergistic, tunable capabilities. However, a paucity of materials systems simultaneously possessing these desirable attributes and functionalities has made device realization difficult. Here we report the observation of asymmetric spintronic-THz radiation in **Two-Dimensional Hybrid Metal Halides (2D-HMH)** interfaced with a ferromagnetic metal, produced by ultrafast spin current under femtosecond laser excitation. The generated THz radiation exhibits an asymmetric intensity toward forward and backward emission direction whose directionality can be mutually controlled by the direction of applied magnetic field and linear polarization of the laser pulse. Our work demonstrates the capability for the coherent control of THz emission from 2D-HMHs, enabling their promising applications on the ultrafast timescale as solution-processed material candidates for future THz emitters.

SESSION EN08.12: Physico-Chemical Properties of Emissive Low Dimensional Perovskite

Session Chairs: Christian May and Aditya Mohite

Tuesday Morning, December 7, 2021

EN08-Virtual

8:00 AM *EN08.12.01

Optically Resonant Halide Perovskite Nanostructures—From Light Control to Lasing Applications Sergey Makarov; ITMO University, Russian Federation

Nanophotonics and meta-optics based on optically resonant all-dielectric structures is a rapidly developing research area driven by its potential applications for low-loss efficient metadevices. Recently, the study of halide perovskites has attracted enormous attention due to their exceptional optical and electrical properties. As a result, this family of materials can provide a prospective platform for modern nanophotonics [1] and meta-optics [2], allowing us to overcome many obstacles associated with the use of conventional semiconductor materials. Here, we overview the recent progress in the field of halide perovskite nanophotonics starting from single-particle light-emitting nanoantennas [3,4], nanolasers [5], microlasers [6,7], and to the large-scale designs working for surface coloration, anti-reflection, and optical information encoding [8-9].

References:

- [1] Makarov, S., Furasova, A., Tiguntseva, E., Hemmetter, A., Berestennikov, A., Pushkarev, A., Zakhidov, A. and Kivshar, Y., 2019. Halide-Perovskite Resonant Nanophotonics. *Advanced optical materials*, 7(1), p.1800784.
- [2] Berestennikov, A.S., Voroshilov, P.M., Makarov, S.V. and Kivshar, Y.S., 2019. Active meta-optics and nanophotonics with halide perovskites. *Applied Physics Reviews*, 6(3), p.031307.
- [3] Tiguntseva, E.Y., Zograf, G.P., Komissarenko, F.E., Zuev, D.A., Zakhidov, A.A., Makarov, S.V. and Kivshar, Y.S., 2018. Light-emitting halide perovskite nanoantennas. *Nano letters*, 18(2), pp.1185-1190.
- [4] Tiguntseva, E.Y., Baranov, D.G., Pushkarev, A.P., Munkhbat, B., Komissarenko, F., Franckevicius, M., Zakhidov, A.A., Shegai, T., Kivshar, Y.S. and Makarov, S.V., 2018. Tunable hybrid Fano resonances in halide perovskite nanoparticles. *Nano letters*, 18(9), pp.5522-5529.
- [5] Tiguntseva, E., Koshelev, K., Furasova, A., Tonkaev, P., Mikhailovskii, V., Ushakova, E.V., Baranov, D.G., Shegai, T., Zakhidov, A.A., Kivshar, Y. and Makarov, S.V., 2020. Room-Temperature Lasing from Mie-Resonant Non-Plasmonic Nanoparticles. *ACS Nano* 13 (4), 4140-4147.
- [6] Zhizhchenko, A., Syubaev, S., Berestennikov, A., Yulin, A.V., Porfirev, A., Pushkarev, A., Shishkin, I., Golokhvast, K., Bogdanov, A.A., Zakhidov, A.A. and Kuchmizhak, A.A., 2019. Single-mode lasing from imprinted halide-perovskite microdisks. *ACS nano*, 13(4), pp.4140-4147.
- [7] Trofimov, P., Pushkarev, A.P., Sinev, I.S., Fedorov, V.V., Bruyère, S., Bolshakov, A., Mukhin, I.S. and Makarov, S.V., 2020. Perovskite-Gallium Phosphide Platform for Reconfigurable Visible-Light Nanophotonic Chip. *ACS nano*, 14(7), pp.8126-8134.
- [8] Zhizhchenko, A.Y., Tonkaev, P., Gets, D., Larin, A., Zuev, D., Starikov, S., Pustovalov, E.V., Zakharenko, A.M., Kulinich, S.A., Juodkazis, S. and Kuchmizhak, A.A., 2020. Light-Emitting Nanophotonic Designs Enabled by Ultrafast Laser Processing of Halide Perovskites. *Small*, 16(19), p.2000410.
- [9] Zhizhchenko, A.Y., Cherepakhin, A.B., Masharin, M.A., Pushkarev, A.P., Kulinich, S.A., Porfirev, A.P., Kuchmizhak, A.A. and Makarov, S.V., 2021. Direct Imprinting of Laser Field on Halide Perovskite Single Crystal for Advanced Photonic Applications. *Laser & Photonics Reviews*, p.2100094.

8:30 AM *EN08.12.02

Nanocrystal Heterostructures Involving Halide Perovskites and Other Materials Liberato Manna; Istituto Italiano di Tecnologia, Italy

Halide perovskite semiconductors can merge the highly efficient operational principles of conventional inorganic semiconductors with the low temperature solution processability of emerging organic and hybrid materials, offering a promising route towards cheaply generating electricity as well as light.

Following a surge of interest in this class of materials, research on the corresponding halide perovskite nanocrystals (NCs) as well as gathered momentum in the last years.¹ A hot area of research in this field is the fabrication of nano-heterostructures in which the perovskite is one of the domains, which will be briefly reviewed, including work from our group. Another class of materials that has been recently investigated by us is that of metal chalcogenides. These

materials offer a broad solid-state chemistry and they been investigated for applications in solar energy conversion, thermoelectrics, hard radiation detection, and superconductivity. Among them, lead chalcogenides have been rarely studied in the past. We have recently reported the synthesis of a series of lead chalcogenides, by means of colloidal approaches, delivering phases and compositions that had not been previously identified in the bulk.² These materials present indirect band gaps, they emit in the NIR region of the spectrum at cryogenic temperatures and have unique crystal structures. We will also show our recent results on the synthesis and advanced characterization of heterostructured nanocrystals in which one domain is a lead chalcogenide and the other domain is a cesium lead halide perovskite.³ The two domains are separated by a flat, atomically defined, epitaxial interface. In these materials, the photogenerated carriers are separated at their interface, and as such they might be promising in applications ranging from catalysis to photovoltaics. The talk will also discuss on how the presence of the halide perovskite domain dictates the phase and chemical composition of the metal halide domain.

References

1. Q. Akkerman et al. "Genesis, challenges and opportunities for colloidal lead halide perovskite nanocrystals", *Nat. Mater.* 2018, 17, 394.
2. S. Toso et al. "Nanocrystals of Lead Chalcogenides: A Series of Kinetically Trapped Metastable Nanostructures", *J. Am. Chem. Soc.* 2020, 142, 22, 10198.
3. S. Toso et al. "Nanocrystals of Lead Chalcogenides: A Series of Kinetically Trapped Metastable Nanostructures", *J. Am. Chem. Soc.* 2021, 143, 3, 1435.

9:00 AM EN08.12.04

Low Barrier for Exciton Self-Trapping Enables High Photoluminescence Quantum Yield in Cs₃Cu₂I₅ [Young-Kwang Jung](#)¹ and Aron Walsh^{1,2}; ¹Yonsei University, Korea (the Republic of); ²Imperial College London, United Kingdom

Low-dimensional metal halides have attracted interest from researchers in the field of optoelectronics due to their high photoluminescence quantum yield (PLQY) [1-2]. The fact that these metal halides exhibit a high bulk PLQY, without preparing them in nanocrystal form, makes them an interesting class of optoelectronic materials. One characteristic feature is a large Stokes shift - the difference between absorbed and emitted light wavelength - which is usually attributed to the formation of self-trapped excitons (STEs). STE indicates the state where a photoexcited electron-hole pair is stabilized and trapped at a lattice site. This phenomenon is the result of strong electron-phonon coupling and can be enhanced by a soft crystal host [3]. Although low-dimensional metal halides shows the high PLQY of > 90% via STE emission, the emission processes happening within low-dimensional metal halides is poorly understood at the moment. Indeed, (i) why self-trapping occurs so efficiently; (ii) how self-trapped exciton emission competes against intrinsic band-to-band transitions are not known.

Here, we performed first-principles density-functional theory (DFT) calculations to explain why this class of materials exhibit such a high PLQY. We selected Cs₃Cu₂I₅ as the model system for this work as the material is a well-known example of STE emission [4]. Optical properties originate from its intrinsic bulk electronic structure (e.g. high-frequency dielectric function and absorption coefficient) will be firstly assess. Then explicit modelling of STE formation will be carried out to calculate the STE emission energy and self-trapping barrier in Cs₃Cu₂I₅. Based on these quantities, we will evaluate the rates of band-to-band recombination and STE emission, and consequently, we predict the quantum yield of blue emission as a function of the excited carrier concentration.

[1] X. Li, X. Gao, X. Zhang, X. Shen, M. Lu, J. Wu, Z. Shi, V. L. Colvin, J. Hu, X. Bai, W. W. Yu, and Y. Zhang, *Adv. Sci.* **8**, 2003334 (2021)

[2] M. Li and Z. Xia, *Chem. Soc. Rev.* **50**, 2626 (2021)

[3] S. Li, J. Luo, J. Liu, and J. Tang, *J. Phys. Chem. Lett.* **10**, 1999 (2019).

[4] T. Jun, K. Sim, S. Imura, M. Sasase, H. Kamioka, J. Kim, and H. Hosono, *Adv. Mater.* **30**, 1804547 (2018).

9:15 AM EN08.12.05

Transport in 2D Layered Lead-Halide Perovskite Films [Doaa Shamalia](#) and Nir Tessler; Technion, Israel

Organic-inorganic hybrid perovskites emerged as a very promising material for many applications such as photovoltaics, LEDs, and transistors. These materials have the composition of ABX₃ where A is a small organic cation such as MA⁺, FA⁺, B is Pb²⁺ or Sn²⁺ and X is a halide anion such as I⁻, Br⁻ and Cl⁻. Partial substitution of organic cations in the 3D structure with hydrophobic organic cations can lead to the formation of lower-dimensional perovskites. This led to methods of forming 2D/3D bilayered perovskite, whereby a single-step fabrication process a phase separation is driven by self-assembly is obtained forming an upper 2D layer that serves as a capping layer and a bottom 3D layer. In our research, we present the influence of the deposition method, the stoichiometry of the precursors' solution, and the surface energy of the substrate on the quality of the perovskite layers in terms of grain size and crystallinity as well as on the composition of the 2D/3D structure in terms of n=1,2,... This film optimization allowed us to fabricate field-effect transistors that are based on layered perovskite and use the transistor as a tool to evaluate the material's properties. We'll describe the performance of the transistors in terms of device J-V characteristics as well as extraction of residual doping and mobility, as a function of the processing methods. These parameters would assist in designing efficient and stable photovoltaic devices.

9:30 AM EN08.12.06

Dominance of Ion-Migration in Controlling the Hysteresis in Perovskite Solar Cells [Spandankumar H. Ranpariya](#) and Dhirendra K. Sinha; Indian Institute of Information Technology Vadodra, India

In recent years, the organic-inorganic hybrid lead-halide perovskite solar cells (PSCs) have attracted attention due to the record-breaking rise in power conversion efficiency (PCE) from 3.8% in 2009 to 25.5% in 2021. This attractiveness is mainly due to its high optical absorption coefficient with sharp absorption onset, long charge-carrier lifetime, tunable band-gap, and low-cost fabrication. However, the correctness of the reported efficiencies is suspected due to hysteresis in the current density (*J*) versus voltage (*V*) characteristics. In literature, there are mainly two physical reasons widely debated for hysteresis in *J-V* characteristics. The first is the ion migration from the perovskite layer towards the interfaces forming vacancies and thus creating trapping centers for the charge-carriers. The second one is trap-assisted recombination via the defect states, which trap the charge-carriers at the grain boundaries and the interface of charge-transporting layers. In this work, the underlying interest is to comprehend the hysteresis behavior by deriving the hysteresis index (HI) from the simulated power density-voltage characteristic. The value of HI reflects the extent of hysteresis observed in the current-voltage characteristics. We consider a perovskite solar cell in a *p-i-n* structure with CH₃NH₃PbI₃ as an active layer. The Spiro and TiO₂ are taken as a hole- and electron- transporting layers, respectively. We utilized a one-dimensional drift-diffusion equation to simulate the current density vs. voltage characteristics by varying the active layer thickness from 100 nm to 500 nm. In addition, the interfacial thickness between the active layer and electron (hole) transporting layers were also varied from 10 nm to 80 nm keeping the active layer thickness intact. The value of HI is observed to be increasing from 0.1 to 0.6 with increasing the thickness of the active layer. It is also observed to be saturated in devices whose active layer thickness is beyond 400 nm. On the other hand, the value of HI was observed to be nearly constant, i.e., roughly 0.5, with a wide variation of interfacial thickness. The observations indicate that the value of HI is dependent on the variation in the active layer thickness, thereby indicating the role of ion-migration is dominant in controlling the hysteresis.

SESSION EN08.13: Photophysics of Low Dimensional Perovskites II
Session Chairs: Giulia Grancini and Sergey Makarov
Tuesday Morning, December 7, 2021
EN08-Virtual

10:30 AM *EN08.13.01

Carrier Cooling in Low-Dimensional Perovskites [Artem Bakulin](#); Imperial College London, United Kingdom

The rapid relaxation of above-gap 'hot' carriers in absorber layer materials currently places a limit on the open-circuit voltage achievable in perovskite photovoltaic devices. The dimensions and dimensionality of perovskite materials is expected to affect carrier cooling on account of changing coupling between electronic states as well as coupling electronic system to lattice phonon energy levels. Here, ultrafast pump-push-probe spectroscopy is used to compare hot carrier cooling dynamics in 3D perovskites, 8 and 5 nm cuboidal nanocrystals, 3.5 nm nanoplatelets and bulk 2D perovskites prepared using different techniques. Carrier cooling rates are shown to be similar to bulk materials in all but 2D-confined perovskite nanosystems. Surprisingly, cooling rates are observed to increase in such systems, while hot phonon bottleneck phenomena become much less pronounced. This work offers further insight into fundamental physical processes occurring in nanoscale materials and aid in the design of future solar cell absorber systems.

11:00 AM *EN08.13.02

What Do Dephasing Dynamics Teach Us About Exciton Polarons in Hybrid Ruddlesden-Popper Metal Halides? [Ajay Ram Srimath Kandada](#)¹ and [Carlos Silva](#)²; ¹Wake Forest University, United States; ²Georgia Institute of Technology, United States

It is common in the context of hybrid metal halide perovskites and its derivatives to use temperature dependence of photoluminescence linewidths to estimate electron-phonon coupling parameters. However, due to comparable contributions from homogeneous and inhomogeneous mechanisms to the spectral broadening, linear spectroscopies like photoluminescence are incapable of isolating the pure dephasing rates and thus are not representative of the system-bath interactions. In these circumstances, nonlinear coherent optical spectroscopy offers insights into the nature of many-body interactions that are entirely inaccessible to temperature-dependent linear spectroscopies. When applied to Ruddlesden-Popper metal halides, these techniques have indeed enabled us to quantify the elastic scattering effects on the exciton dephasing rates. Here, we will discuss the mechanistic nature of exciton-phonon, exciton-exciton and phonon-phonon interactions in prototypical Ruddlesden-Popper metal halides based on such experimental observations. We will discuss our perspective on how the coherent lineshapes of Ruddlesden-Popper metal halides can be effectively rationalized within an exciton polaron framework. We will also discuss the critical role of the metal cation in the observed coherent exciton dynamics.

11:30 AM EN08.13.03

Room-Temperature Continuous-Wave Lasing from 2D Layered Organic-Inorganic Hybrid Perovskites Embedded Microcavities [Hongbo Zhang](#), [Yuzhong Hu](#), [Ting Yu](#) and [Hong Jin Fan](#); Nanyang Technological University, Singapore

Two dimensional (2D) layered lead halide perovskites with large exciton binding energies, efficient radiative recombination, and outstanding environmental stability are regarded as supreme candidates for realizing highly compact and ultralow threshold lasers. However, continuous-wave (CW) pumped lasing of 2D Lead halide perovskites, as the precondition for the electrically pumped lasing, is still challenging. Here, the phenylethylammonium lead iodide [(PEA)₂PbI₄] thin flakes, exfoliated from the solution-processed millimeter-sized single crystal, were utilized as gain media to construct a vertical-cavity surface-emitting laser (VCSEL), which presents the robust single-mode CW lasing operation with an ultra-low threshold of 5.7 W cm⁻² at room temperature, attributed to strong optical confinement in the high-Q cavity. Moreover, the multi-mode emission has been synchronously discussed through experiments and simulations. This work opens up a new window for developing novel 2D VCSELs based on the layered lead halide perovskites.

11:45 AM EN08.13.04

Anisotropic Charge Carrier Dynamics in Layered Hybrid Perovskites Probed by Oblique Incidence Ultrafast Terahertz Spectroscopy [Kyle Virgil](#), [William Goddard](#), [Geoffrey Blake](#) and [Harry A. Atwater](#); California Institute of Technology, United States

Understanding the transport properties of layered perovskite optoelectronics requires the characterization of carrier dynamics both in the plane of and transverse to the layer structure. We explore carrier transport using polarization-dependent terahertz (THz) conductivity measurements in layered (2D) hybrid perovskites. We have synthesized ~300 nm thick films of n = 1 butylammonium and phenethylammonium lead iodide layered perovskite semiconductors, with layers oriented parallel to sapphire substrates and with crystalline domain sizes of approximately 1 micron diameter. In the measurements, around 110 femtosecond pump pulses from a Ti:sapphire laser source were converted to THz radiation with picosecond pulse duration via an electro-optic crystal. Transmission measurements at normal incidence yielded values of complex transmission coefficients which enable determination of the complex dielectric function in the 0.3 - 2 THz range, corresponding to the in-plane complex conductivities of these materials. We will also discuss results of non-normally incident transmission measurements varying s and p THz polarization to probe the differences in ligand-mediated out-of-plane transport between these layered perovskites, as well as results of density functional theory calculations. This work expands on the utility of oblique incidence terahertz experiments which are rarely implemented for complex parameter extraction in uniaxial thin films. Furthermore, these results underscore the potential for THz spectroscopy to probe fundamental charge transport phenomena in complex photovoltaic materials with layered structures.

12:00 PM EN08.13.06

Controlling Halide Anion Diffusion in Perovskite Heterojunction with the Dimension of Vacuum Evaporated Perovskites [Sang-Hyun Chin](#), [Lorenzo Mardegan](#), [Francisco Palazon](#), [Michele Sessolo](#) and [Henk J. Bolink](#); University of Valencia, Spain

Halide perovskite has been investigated intensively as an attractive candidate for some optoelectronic applications such as solar cells, light-emitting diodes, lasers and photodetectors. Especially, the sharp and easily changeable emission with halide anion exchange make this material group even more attractive for the light-emitting applications. Among this material group, inorganic 3D CsPbX₃ (X: Cl, Br, I) semiconductors produce 0D Cs₄PbX₆ insulators in specific conditions. This can be easily done with vacuum co-evaporation with excess CsX. In this regard, we investigate the anion diffusion and emission property of the halide perovskite. These heterojunctions are electrically excited between two electrodes as the light-emitting electrochemical cells (LECs), as a proof-of-concept application. With this simplified structure, the optoelectronic property can be explored without the effects from any charge transport layer. Herein we demonstrate different behavior of anion diffusion depending on the dimension of vacuum co-evaporated cesium lead chloride.

12:15 PM EN08.13.07

Evaluation of Structure and Optoelectrical Properties of Copper Halide Perovskite Films Yuki Matsui, Keitaro Kikuchi, Tomohiro Watanuki and Hironori Ogata; Hosei university, Japan

In recent years, lead halide perovskite solar cells (PSCs) have been attracting attention as the next generation of solar cells because they can be fabricated by the solution process and their high energy conversion efficiency. On the other hand, the lead halide perovskite compounds that constitute PSCs have problems of instability and toxicity under various conditions. In recent years, researches on solar cells using a copper halide perovskite compounds as a photoactive layer in which Pb is replaced with Cu, which has low toxicity, have been reported. It has been reported that copper halide perovskite compounds have a high absorption coefficient and high charge mobility depending on the compound. However, a solar cell using them has a conversion efficiency of about 2%, and it has been pointed out that further improvement including selection of the compound is necessary.

We have systematically investigated the effects of cation and halide ion types of copper halide perovskite compound films on the stability, morphology and optical properties under various conditions. In this presentation, we will report the detailed experimental results on the electronic characteristics of these thin films and the characteristics of solar cells.

In order to solve these problems, research has been conducted on perovskite compounds in which the Pb at the B site is replaced by Cu, which is less toxic. The Cu-based perovskites have been reported to have high absorption coefficient and charge mobility depending on the compound. However, the conversion efficiency of solar cells using Cu-based perovskite compounds as the photoactive layer is only about 2%, indicating the need for further improvement, including the selection of compounds.

In this study, we prepared thin films of $(\text{C}_6\text{H}_5\text{CH}_2\text{NH}_3)_2\text{CuX}_4$ by changing the X site of the perovskite layer and investigated the application of the compound. The optical band gap energies obtained from the optical absorption spectra are 2.03 eV for $(\text{C}_6\text{H}_5\text{CH}_2\text{NH}_3)_2\text{Cu Br}_4$ and 2.05 eV for $(\text{C}_6\text{H}_5\text{CH}_2\text{NH}_3)_2\text{Cu Cl}_4$. Both compounds were found to be highly stable in air. The detailed physical properties of the films will be reported in the day.

SESSION EN08.14: Heterostructures, Properties and Applications of Low Dimensional Perovskites
Session Chairs: Giulia Grancini and Shuxia Tao
Tuesday Afternoon, December 7, 2021
EN08-Virtual

1:00 PM *EN08.14.01

Luminescence from Low-Dimensional Perovskites—From Photophysics to Devices Samuel D. Stranks; University of Cambridge, United Kingdom

Halide perovskites have opened up a new world of semiconductors that can be processed crudely yet exhibit exceptional optoelectronic performance. Their performance has continued to improve not just in photovoltaic configurations, but also in light-emitting diodes (LEDs) and quantum technologies. While the bulk majority of work over the last decade has focused on 3D halide perovskite materials, there is a vast family of perovskites of different dimensions, for example 2D and quasi-2D layered structures in both bulk and nanostructured forms, which can show modular, tunable and high-quality performance.

Here I will present recent progress on synthesis, understanding and device development of several low-dimensional halide perovskite systems. First, I will show results using local time-resolved luminescence measurements to track exciton diffusion in low-dimensional 2D halide perovskite flakes, revealing how the local energy landscape can drive long-range exciton diffusion on the order of hundreds of nanometres. I will show how we can controllably monitor the growth of 2D/3D lead-tin bulk films, and control energy transfer between the different species in the subsequently tailored films. Finally, I will demonstrate the use of low-dimensional perovskites in efficient light emission systems towards white light applications, including in LED device configurations.

1:30 PM EN08.14.04

A Study on the Phase Formation Behavior of 2D Layered Perovskites and Low-Dimensional Hybrids Containing Oligothiophene

Derivatives Wouter Van Gompel¹, Paul-Henry Denis¹, Martijn Mertens¹, Kristof Van Hecke², Laurence Lutsen^{3,1} and Dirk Vanderzande^{1,3}; ¹Universiteit Hasselt, Belgium; ²Ghent University, Belgium; ³imec, Belgium

2D layered hybrid perovskites are receiving increased attention as active materials for use in various optoelectronic applications, including solar cells, light-emitting diodes, photodetectors, and transistors. Understanding the phase formation behavior of these materials is crucial for their use in optoelectronic devices since different crystal phases possess different optical and electronic properties. The design rules to obtain the desired 2D layered perovskite crystal phase have not been fully determined yet.

For this study, we explored the formation of 2D layered perovskites and low-dimensional hybrids containing oligothiophene derivatives in the organic layer. On the one hand, we varied the number of thiophene rings in the oligothiophene. On the other hand, we varied the halide that is used. We studied the formation of the hybrids in thin films as well as through crystal growth methods.

For the series of lead iodide hybrids, we show that the use of two different processing methods (spin-coating or drop-casting) leads to the formation of two different crystal phases for bithiophene, terthiophene, and quaterthiophene propylammonium cations. One of these phases corresponds to the typical 2D layered perovskite, while the other phase has optical properties corresponding to a dimensionality intermediate between typical 2D and 1D hybrids.

For the bithiophene propylammonium cation, we varied the halide that is used. The crystal structure and phase behavior of the 2D layered perovskites were studied in detail. It is suggested that *via* halide substitution from iodide to bromide to chloride, the molecular degrees of freedom of the bithiophene cations are reduced by spatial confinement due to a smaller inorganic framework. In this way, the formation of lower-dimensional hybrids besides the targeted 2D layered perovskite is limited.

1:45 PM EN08.14.06

Plasmonic Nanocavity Enhanced Luminescence of 2D Ruddlesden Popper Perovskite Thin Film Yashika Gupta, Anuj K. Singh, Abhay A. VS and Anshuman Kumar; Indian Institute of Technology Bombay, India

2D Ruddlesden Popper perovskites are considered potential candidates for next generation optoelectronic devices due to their favourable properties like large excitonic binding energy, superior stability and structural tunability as compared to 3D perovskites^{1,2}. The strong quantum and dielectric effects

arising due to the layered structure of these materials offer easy modulation of band-gap in the entire visible spectra, establishing great prospects in laser and light emitting applications. While the quantum confinement effects are stronger in lower dimensional Ruddlesden Popper perovskites resulting in narrow emission linewidth, these perovskites suffer from low intrinsic photoluminescence quantum yield (PLQY), which is found to be less than 1% for completely 2D perovskite thin films³, thus hampering their optoelectronic performance. Since PL intensity has direct correlation with their emission characteristics, it is important to engineer the device to compensate for the low PLQY of perovskite emitter layer. In this work, we demonstrate a significant fluorescence enhancement can be obtained using a plasmonic nanocavity. Optical simulations based on Lumerical FDTD show a strong near field enhancement coupled with radiative decay enhancement due to Purcell factor results in around **5-fold enhancement in PL intensity** for a 2D BA2PbI4 perovskite thin film sandwiched between a metal layer and nanoparticle cavity.

References:

1. X. Gao, X. Zhang, W. Yin, H. Wang, Y. Hu, Q. Zhang, Z. Shi, V. L. Colvin, W. W. Yu, and Y. Zhang, "Ruddlesden–Popper perovskites: synthesis and optical properties for optoelectronic applications", *Adv. Sci.* 6, (2019) 1900941.
2. T. C. Sum, M. Righetto, and S. S. Lim, "Quo vadis, perovskite emitters?", *J. Chem. Phys.* 152, (2020) 130901.
3. D. N. Congreve, M. C. Weidman, M. Seitz, W. Paritmongkol, N. S Dahod, and W. A Tisdale, "Tunable light emitting diodes utilizing quantum-confined layered perovskite emitters", *ACS Photonics* 4, (2017) 476.

2:00 PM EN08.14.07

Chirality-Induced Pseudo-Magnetization in 2D Chiral Hybrid Perovskites Eric Vetter¹, Liang Yan², Yuzan Xiong^{3,3}, Steven S.-L. Zhang⁴, Zhizhi Zhang⁵, Yi Li⁵, Hongwei Qu³, Manoj Jana⁶, David B. Mitzi⁶, Valentine Novosad⁵, Axel Hoffmann^{5,7}, Wei Zhang³, Wei You^{2,1} and Dali Sun^{1,1}; ¹North Carolina State University, United States; ²University of North Carolina at Chapel Hill, United States; ³Oakland University, United States; ⁴Case Western Reserve University, United States; ⁵Argonne National Laboratory, United States; ⁶Duke University, United States; ⁷University of Illinois at Urbana-Champaign, United States

The ability to generate and manipulate spin information underpins the field of spintronics, which utilizes the electron's spin degree of freedom to transfer and process information. Identifying new 2D magnetic materials empowers the direct control of spin information through the manipulation of magnetization at a low-dimensional limit. However, the Mermin–Wagner restriction induced by thermal fluctuations presents a significant barrier to this pursuit. Here, we report the observation of chirality-induced pseudo-magnetization native to a non-magnetic 2D chiral hybrid organic-inorganic perovskite (chiral-HOIP) identified by spin Hall magnetoresistance measurements. We find pronounced magnetoresistance signals persisting up to room temperature despite the lack of any magnetic elements in the hybrid structures, as well as tunable magnetic hysteretic behaviors controlled by injected spin currents. Our work paves the way for utilizing solution-processed 2D chiral hybrid perovskites in room temperature spintronic applications.

2:15 PM EN08.14.03

Lead-Free Halometallates—The Next Generation of Hybrid Photovoltaic Absorber Materials Harsh Bhatia, Bob Schroeder and Robert G. Palgrave; University College London, United Kingdom

Photovoltaics (PV) play a very key role in achieving the target of world's economic powers to achieve low or zero carbon emission based economy. The present PV market is dominated by silicon based solar cells, however, the high cost of materials have led the scientific community to look for the alternative ways to harness the sunlight. In the recent years, hybrid perovskites have emerged as a possible solar cell technology to achieve the power conversion efficiency in excess of 20%. Despite the very high efficiency due to the strong absorption coefficient, defect tolerance, and high ambipolar carrier mobility, the hybrid perovskite materials suffer from the problems of device stability, and high content of lead (Pb) which makes the commercialization of these materials a gigantic task.

In the present work we have focused on to develop highly tunable lead-free halometallates for use in hybrid solar cells.¹ The materials developed in this work can be best described as the materials between OPV and perovskites. In the present work we have used the conjugated organic molecules rather than the ammonium ions as the organic component to mimic the perovskite packing.² This design principle enables us to avoid lead (Pb) as the metal component in the molecule while the 3-D packing of the molecular system is maintained. The 3-D packing of the organic components lead to high charge transport properties and strong absorption in the visible region. Moreover, the inorganic post-transition metal iodides (BiI₃, SbI₃ and SnI₂)³ have been chosen to coordinate with the organic part due to the presence of filled metal *s* states and large spin-orbit coupling which leads to small band gaps and high carrier mobility. Such inorganic-organic coordinated system lead to high tunability of optical, electronic and structural properties which can lead to efficient PV absorber materials.

References:

1. Liu, J.; Guan, Y.; Jiao, C.; Lin, M.; Huang, C.; Dai, W. *Dalton Trans.* **2015**, *44*, 5957-5960.
2. Travis, W.; Knapp, C. E.; Savory, C. N.; Ganose, A. M.; Kafourou, P.; Song, X.; Sharif, Z.; Cockcroft, J. K.; Scanlon, D. O.; Bronstein, H.; Palgrave, R. G. *Inorg. Chem.* **2016**, *55*, 3393-3400.
3. Cheetham, A. K.; Rao, C. N. R.; Feller, R. K. *Chem. Commun.* **2006**, *46*, 4780-4795.

SESSION EN08.15: Optical, Electrical, and Mechanical Properties of Low Dimensional Perovskites

Session Chair: Ajay Ram Srimath Kandada

Tuesday Afternoon, December 7, 2021

EN08-Virtual

4:00 PM EN08.15.01

In Situ Ultrafast and Nanoscale Evolution of Carrier Drift Dynamics in CsPbI₃ Nanocrystal Film Kanishka Kobbekaduwa¹, Qian Zhao², Chendi Xie¹, Joseph Luther², Matthew C. Beard² and Jianbo Gao¹; ¹Clemson University, United States; ²National Renewable Energy Laboratory, United States

For solution-processing perovskite nanocrystal photonics and optoelectronics, it remains a challenge to uncover the carrier drift dynamics with an intrinsic phonon-scattering mechanism in *in-situ* devices, and within an ultrafast timescale, since the classic time-resolved photoluminescence and transient absorption spectroscopies mainly capture the carrier diffusion dynamics prior to the defect scattering mechanism. Here, we use ultrafast photocurrent spectroscopy to observe *in-situ* the band-like transport prior to carrier trapping in a CsPbI₃ nanocrystal array. We attribute transport to the longitudinal optical phonon scattering, while the coupling between phonon and carriers is predominant among classic polar semiconductors and similar perovskites. At room temperature, the carriers preserve band-like transport for more than 70 nm long range drift length and a mobility of more than 14 cm²/Vs.

4:15 PM EN08.15.02

Ferroelectric and Charge Transport Properties in Strain-Engineered Two-Dimensional Lead Iodide Perovskites Dohyung Kim¹, Bogdan Dryzhakov¹, Yongtao Liu², Anton V. Ievlev², Olga Ovchinnikova², Bin Hu¹, Sergei V. Kalinin² and Mahshid Ahmadi¹; ¹University of Tennessee, Knoxville, United States; ²Oak Ridge National Laboratory, United States

Transitions from three-dimensional (3D) hybrid organic-inorganic perovskite (HOIP) structures to lower dimensions including 2D and quasi 2D structures opened new range of functional properties in these materials systems. Yet, the performance of solar cells made from 2D HOIP is below 3D compositions due to the higher band gap energy, low carrier concentration and anisotropy in charge transport. Controlling ferroelectricity in 2D HOIPs is considered as a powerful strategy to drive the spatial separation of photogenerated charge carriers to improve the photovoltaic action in this class of HOIPs. In this study, we reveal the strain-dependent ferroelectricity and charge carrier properties in strain-engineered 2D 4,4-difluoropiperidinium (DFPD) lead iodide or (4,4-DFPD, C₅H₁₀F₂N)₂PbI₄ perovskite utilizing advanced scanning probe microscopy (SPM) techniques¹. We demonstrate crystallization- and strain-dependent thin films with different thickness prepared by drop-casting, spin-coating, and vacuum-poling treatment¹. Band-excitation piezo-response force microscopy (BE-PFM) and contact mode Kelvin probe force microscopy (cKPFM) reveal ferroelectric domains and switchable dynamics with significantly low switching voltages in the low strain film. Photoluminescence (PL) spectroscopy shows strain-dependent optical properties and non-centrosymmetric structure with strong second harmonic generation (SHG) peaks in in the low strain film. In addition, KPFM results demonstrate a higher surface potential in the low strain films while the photovoltage and local current are the highest on the high strain film. Our study demonstrates the critical role of strain engineering on electromechanical and charge carrier dynamics in 2D HOIPs, being important for development of 2D HOIP devices. Additionally, we will present the underlying physical mechanisms of light-ferroelectricity interaction in 2D MHPs². X-ray diffraction (XRD) patterns exhibit significant change in preferential orientation of individual lattice planes under external stimuli. Particularly, the reduced intensity of the (1 1 1) lattice plane under illumination leads to transitioning from a ferroelectric to paraelectric phase. The instability of organic cations is also observed under illumination by time-of-flight secondary ion mass spectrometry (ToF-SIMS). The combination of lattice variation and chemical changes under illumination clearly contribute to the origin of light-ferroelectricity interaction in 2D (4,4-DFPD, C₅H₁₀F₂N)₂PbI₄.

References:

1 Kim, D. *et al.* Ferroelectric and Charge Transport Properties in Strain-Engineered Two-Dimensional Lead Iodide Perovskites. *Chemistry of Materials* **33**, 4077-4088, doi:10.1021/acs.chemmater.1c00679 (2021).

2 Kim, D., Ievlev, A. V., Ovchinnikova, O. O., Kalinin, S. V. & Ahmadi, M. Light-Ferroelectricity Interaction in Two-Dimensional Lead Iodide Perovskites. *Submitted (under review)* (2021).

4:30 PM EN08.15.03

Mechanical Buckling in Thin Layer Perovskite Nanobelts of CsPbBr₃ Composition Yehonadav Bekenstein; Technion - Israel Institute of Technology, Israel

Flexible semiconductor materials, where structural fluctuations and transformation are tolerable and have low impact on electronic properties, focus interest for future applications. Two dimensional and thin layer lead halide perovskites are hailed for their unconventional optoelectronic features. We report a surprising structural deformation that appears in thin layer colloidal nanobelts upon their adsorption on hydrophobic carbon substrates. We show that the variations in microstructure we detect, are mechanical buckling of the nanobelts. These are determined using transmission electron microscopy (TEM), including selected orientation dark field imaging (SODFI) and tilting experiments. Atomic force near-field microscopy (SNOM-AFM) was used to correlate structure properties with 10nm resolution. By employing plate buckling theory to the data, we approximate adhesion forces between the buckled nanobelt and the substrate. The effect of the buckled perovskite crystal lattice on optoelectronic and other physical properties is still being unveiled. However, the forces and the capillary action leading to the buckling of metal-halide perovskites at the nanoscale, are critical for the design of future devices and heterostructures based on Nano-perovskites. If time permits we will show also preliminary results of spontaneous self-healing/annealing of structural defect in perovskite nanocrystals.

4:45 PM EN08.15.04

Strong Circular Dichroism in the Low-Dimensional Hybrid Perovskite DMAPbI₃ from Chiral Amino Acid Incorporation Markus W. Heindl¹, Natalie Fehn¹, Shangpu Liu¹, Lissa Eyre¹, Maged Abdelsamie², Tim Kodalle², Gregor Kieslich¹, Ian Sharp¹, Aras Kartouzian¹, Carolin M. Sutter-Fella² and Felix Deschler¹; ¹Technische Universität München, Germany; ²Lawrence Berkeley National Laboratory, United States

Chirality in semiconductor materials enables a number of powerful applications, reaching from consumer electronics and 3D displays to drug screening and encryption [1-3]. Recently, chiral hybrid perovskites have emerged as a promising class of materials for optoelectronic applications based on their ability to preferably absorb and emit one type of circularly polarized light. However, so far, the chiral organics used to introduce chirality into lead halide perovskites almost exclusively consist of a small group of commercially available, primary amines [1].

A textbook example for chiral molecules are the naturally occurring amino acids. These represent a diverse group of organic compounds whose application for industrial production is highly desirable as they are non-toxic, biodegradable and are available in large quantities at relatively low cost. In this work, we now introduce the chiral small organic 3-aminobutyric acid into the 1D perovskite dimethylammonium lead iodide (DMAPbI₃) using a simple spin-coating based approach. We find that the resulting material displays strong circular dichroism up to 400 mdeg ($g_{\text{abs}} = 17.5 \times 10^{-3}$) in the blue spectral region that is tunable in strength by adjusting the amount of amino acid introduced. We resolve the detailed structural origin of the chirality from XRD experiments of the crystal structure. We employ transient optical spectroscopy to investigate the dynamics of excited state polarization and recombination.

Our findings expand the pool of chiral hybrid materials and provide fresh impulses for future maximization of chiral effects in hybrid perovskite materials.

[1] G. Long, R. Sabatini, M. I. Saidaminov, G. Lakhwani, A. Rasmita, X. Liu, E. H. Sargent, W. Gao Chiral-perovskite optoelectronics. *Nat. Rev. Mater.* **5**, 423-439 (2020).

[2] B. Thaom, X. Gao, K. Pan, J. Deng Chiral Helical Polymer/Perovskite Hybrid Nanofibers with Intense Circularly Polarized Luminescence. *ACS Nano* **15**, 7463-7471 (2021).

[3] C. Chen, L. Gao, W. Gao, C. Ge, X. Du, Z. Li, Y. Yang, G. Niu, J. Tang Circularly polarized light detection using chiral hybrid perovskite *Nat. Comm.* **10**, 1927 (2019).

5:00 PM EN08.15.05

Equilibrium Between Bright Excitons and Polaron Plasma in 2D and 3D Metal-Halide Perovskites Angelica Simbula¹, Riccardo Pau^{1,2}, Fang Liu¹, Stefano Lai¹, Daniela Marongiu¹, Francesco Quochi¹, Michele Saba¹, Andrea Mura¹ and Giovanni Bongiovanni¹; ¹Università di Cagliari, Italy; ²University

of Groningen, Netherlands

One of the main reasons for the success of perovskite photovoltaics is the presence of free carriers as majority optical excitations in 3D materials at room temperature. To get efficient solar cells, stability and duration improving can be achieved thanks to variations in materials composition, including the use of layered 2D perovskites. However, the current understanding is that in 2D perovskites or at cryogenic temperatures insulating bound excitons form, which need to be split are not beneficial to photoconversion. Here we present a tandem spectroscopy technique, applied to several 3D and 2D hybrid perovskite thin films, that combines ultrafast time-resolved photoluminescence and differential transmission (pump and probe). Our results demonstrate a chemical equilibrium between a majority of non-emitting large polarons and a minority phase of bright excitons, even in 2D perovskites and at low temperatures. The presence of a conductive polaron plasma foresees novel mechanisms for LEDs and lasers, as well as new perspectives for 2D perovskites in photovoltaics.

SESSION EN08.16: Electronic and Optical Properties of Low Dimensional Perovskites
Session Chairs: Jean-Christophe Blancon and Giulia Grancini
Wednesday Morning, December 8, 2021
EN08-Virtual

8:00 AM *EN08.16.01

Defect Self-Healing in 2D and 2D-3D Lead Halide Perovskites [David Cahen](#)^{1,2}, Gary Hodes¹ and Sigalit Aharon¹; ¹Weizmann Institute, Israel; ²Bar-Ilan University, Israel

Experiments show low to ultra-low densities of optoelectronically active, static, defects in Lead Halide Perovskites, HaPs. We first present a simple logic argument that this must be because of an active reaction to damage, rather than to tolerance to damage. For 3D HaPs we and others presented evidence for self-healing,* a process that, in inanimate matter, is explained by equilibrium thermodynamics. Indeed, we argued that the main cause for such healing and the resulting low (static) defect densities is the small free energy of reaction that just stabilizes the materials against decomposition.* Here we will show the effect of kinetics, by reporting and discussing results of studying *single crystals* of 2D and 2D-3D HaPs, and compare these to those obtained on 3D single crystals, in terms of their recovery from photodamage.

* cf. Rakita et al., *Mater. Hor.* (2019); Ceratti et al., *Mater. Hor.* (2021); *Adv. Mater.* (2018); Kumar et al., *MRS Bull* (2020)

8:30 AM *EN08.16.02

Materials Engineering of Halide Perovskites—A Computational Materials Science Point of View [Shuxia Tao](#); Eindhoven University of Technology, Netherlands

Metal halide perovskites have attracted enormous attention in the scientific community in recent years. This attention has been drawn by breakthroughs in perovskite optoelectronics, mainly in photovoltaics and LEDs. Although there has been great progress in their use in optoelectronics, fundamentally understanding this class of materials is still challenging, in particular the interplay of several physical and chemical processes. Many fundamental questions are left unanswered, such as what makes them unique/excellent semiconductors; how to tune their optoelectronic properties; why some compositions are more stable than others; the consequence of their chemical instability on their optoelectronic properties; and how to stabilize them.

My research group focuses on addressing such questions using computer simulations, combining DFT calculations and MD simulations to go from the atomistic scale to molecular scale. In this talk, I will highlight our recent progress on improving the stability of this class of materials by composition engineering, the use of additives, ect. I will also give an outlook of our materials engineering strategies for going from 3D systems to systems with lower dimensions.

9:00 AM EN08.16.03

Structural Dynamics of the 2D-on-3D Pb Halide Perovskite Interface Revealed by Ultra-Low Fluence STEM [Sujit Kumar](#)^{1,2}, Lothar Houben², Katya Rechav² and David Cahen^{1,2}; ¹Bar-Ilan University, Israel; ²Weizmann Inst. of Science, Israel

To minimize surface reactivity, defects and the possibility of water and O₂ absorption of/by 3D metal Halide Perovskites (HaPs), covering them with an ultra-thin layer of hydrophobic 2D HaP has been reported to be beneficial. At the same time the stability of a 2D-on-3D HaP composite has been questioned, especially based on results from GI-XRD and PL studies. The question of what is happening on an atomic scale is a vexing one, if higher stability is the goal. It is also a fascinating one because of the dynamic nature of the lattices, which, for 3D HaPs at times seems to approach, from the literature, “*panta rhei*” i.e., everything flows. We studied the 2D-on-3D HaP composite by TEM-based methods, using FIB-prepared cross-sections of films; the films were prepared by a new controlled gas-phase cation exchange process of the top layer of a spin-coated 3D MAPbI₃ film and characterized by GI-XRD and PL. The 2D HaP was the n=1 Ruddlesden-Popper (F)PEA₂PbI₄, where PEA = phenyl-ethylamine and F-PEA, its mono-fluorinated derivative. All through the study we strove to minimize electron and ion fluences, often below what could be deduced from fluences reported in other works. The results allow us to follow the effects of beam damage and thus to determine conditions of measurement before that stage. We used 4D-STEM and scanning nanobeam electron diffraction (NBED), on relatively fresh and aged (all in inert atmosphere) samples. We find direct evidence for the 2D n=1 phase appearing inside the 3D matrix and also for the formation of quasi-2D phases near the interface with the carbon coat. The results imply 2D/3D perovskite heterointerface lattice rearrangements involving migration of not only (the smaller) MA⁺, but also of (the larger) FPEA⁺ cation. As PEA was found too labile for controlled measurements F-PEA was used to be able to get clear “before” and “after” results and measure actual structural evolution under the beam, which primarily shows the loss of long-range periodicity as well structural rearrangements, leading to quasi-2D phase formation. Our results complement extensive empirical and semi-empirical data to engineer stable 2D-on-3D composites and define conditions for atomic resolution studies of real 2D/3D samples in device-relevant configurations.

9:15 AM EN08.16.04

Post-Synthetic Transformation of Zero-Dimensional Perovskite Nanocrystals [Hanjun Yang](#), Tong Cai, Lacie Dube, Katie Hills-Kimball and Ou Chen; Brown University, United States

The synthesis of perovskite nanocrystals (NCs) and the control of their composition and morphology is critical to tuning their optical and electronic properties. Beyond direct synthesis methods, in recent years the indirect synthesis of perovskite NCs based on the post-synthetic transformation reactions

of zero-dimensional perovskite NCs has been developed to fine-tune the nucleation and growth of NCs. Herein, we report two examples of the transformation reaction of 0D perovskite NCs to obtain perovskite NCs with uniform morphology, and well-defined crystal structure. Firstly we present the synthesis of ultra-thin CsPbBr₃ NWs through the reaction between PbBr₂ and Cs₄PbBr₆ 0D perovskite NCs. The synthesized CsPbBr₃ NWs averaged 2.5 nm in width and tens of micrometers in length, and show blue photoluminescence (PL) with a quantum yield of 15%. We tentatively attribute the formation mechanism of CsPbBr₃ NWs to the formation of the PbBr₂-ligand intermediates, whose structure and growth can be controlled by the length of organic ligands. We further expand this reaction scheme to the synthesis of CsPbI₃ NCs with a low-dimensional morphology. Secondly, we present a versatile synthesis technique of bismuth-based perovskites based on the Cs₃BiX₆ (X = Cl, Br) NCs. Both Cs₂AgBiX₆ double perovskite nanocubes and Cs₃MBi₂Cl₁₂ (M = Cl, Br) layered double perovskite NCs were obtained in this manner. Furthermore, we found the intermediates during the transformation of Cs₃BiCl₆ to Cs₂AgBiCl₆ double perovskite NCs showed a red-shifted PL at 770 nm with enhanced PL intensity, which was tentatively attributed to the passivation of Cs cation in the Cs₂(Cs_{1-x}Ag_x)BiCl₆ NC and the large lattice deformation leading to the formation of self-trapped exciton with large trapping energy. Our works provide methods to tune the morphology and composition of perovskite NCs and give insights into the chemical activity of 0D perovskite NCs.

9:30 AM EN08.16.05

Accessing Oriented, Phase-Pure Ruddlesden-Popper Perovskite Films Through Additive-Assisted Processing Shripathi Ramakrishnan, Hao Li, Yuanze Xu, Dongyoon Shin and Qiuming Yu; Cornell University, United States

Low-dimensional Ruddlesden-Popper (RP) perovskites have steadily risen to prominence as stable and efficient photovoltaic materials for solar cell applications due to enhanced structure stability and reduced moisture intrusion in comparison to standard 3D perovskites. However, thin-films processed from stoichiometric 2D precursor solutions tend to possess polydisperse distribution of different number of inorganic layers with the organic dielectric layers behaving as charge transport inhibitors with large binding energies, crippling device performance. Precise processing and composition engineering is necessary to accurately control nucleation and crystallization events to fabricate 2D RP perovskite films of high phase purity devoid of 3D mixtures. Perpendicular crystallographic growth is equally desirable to achieve fluent charge transport along charge collection direction.

In this work, we fabricated 2D RP perovskites (PEA)₂(MA)₄Pb₅I₁₆ (Nominal *n*-value = 5) using anti-solvent and hot-casting methods with different combinations of processing additives to improve the vertical orientation and reduce polydispersity of low *n* 2D RP phases and 3D phase. The critical influence of drip-time on phase-distribution and crystal growth was revealed during the application of toluene as anti-solvent with methylammonium chloride (MACl, MACl/MAI = 0.5 mol ratio) as additive. Earlier drip times during spin-coating resulted in greater density of 2D and 3D-like phases, while later times yielded a narrow distribution of vertically oriented polydisperse high *n*-value 2D phases (*n* = 3, 4, and 5) and no 3D phase, confirmed by UV-Vis absorption spectral and XRD study of thin films and EQE measurements of devices. Fine-tuning the anti-solvent discharge time and phase control afforded inverted solar cells of ITO/PEDOT:PSS/(PEA)₂(MA)₄Pb₅I₁₆/PC₆₁BM/BCP/Ag with PCEs up to 8.51%.

Hot-casting was found to yield RP perovskite films (MACl/MAI = 0.5 mol ratio) with dramatically increased crystallinity and “perfect” perpendicular orientation compared to anti-solvent method. Substrate temperature was found to have a strong impact on the phase distribution and orientation, with sub-optimal heating resulting in high degree of polydispersity and poor crystallinity. Hot-cast films exhibited higher PCE values up to 10.7% owing to improved FF and *V*_{oc} whilst maintaining an identical EQE profile to anti-solvent treated devices having pure 2D phases.

Thin-films of (PEA)₂(MA)₄Pb₅I₁₆ with different concentrations of MACl and NH₄Cl additives were fabricated to understand whether the absence of 3D-character was due to the crystallisation rate, presence of excess [MA⁺] or Cl⁻. It was found that NH₄Cl additive induced drastically enhanced crystal growth along [111] and [202] planes and formed smooth films with low pinhole density upon hot-casting compared to the MACl additive. However, thin films prepared with NH₄Cl additive displayed a broader distribution of 2D phases with *n* ranging from 1 to 5 and 3D character. Furthermore, devices with the thin films prepared by adding NH₄Cl additive exhibited lower PCEs of 6.1% upon hot-casting, despite favourable orientation, thus demonstrating the benefit of phase purity with large *n* values. These results will be augmented with Transient Absorption Spectroscopy (TAS) to probe the energy transfer mechanism of graded structure of the polydisperse perovskite and Grazing-Incidence Wide Angle Scattering (GIWAXS) to underpin the time-resolved structural evolution of 2D RP perovskites and quantify individual phases.

This mechanisms on orientational control and fine-tuning the phase distribution of 2D RP phases via adding additives and controlling nucleation and crystallization kinetics as well as how these effects are reflected by photophysical properties of solar cells will be discussed.

SESSION EN08.17: Optoelectronic Applications of Low Dimensional Perovskites

Session Chairs: Giulia Grancini and Sujit Kumar

Wednesday Morning, December 8, 2021

EN08-Virtual

10:30 AM *EN08.17.01

Hybrid Perovskite Quantum Dots for High Efficiency Solar Cells Lianzhou Wang; University of Queensland, Australia

Perovskite quantum dots (QDs) have the advantages of quantum confinement effect, defect-tolerant nature, and the capability of developing lightweight and flexible films, thus attracting much recent research for a variety of functional device developments including QD solar cells and LEDs. Here we report our recent progress on a novel surface ligand engineering strategy in designing new hybrid perovskite QDs, which leads to not only fundamental understanding on the optoelectronic working mechanism of the QDs, but also remarkably improve the optoelectronic quality of the perovskite QDs. The new classes of perovskite quantum dots have been used as building blocks in Quantum Dot Solar Cells with a certified record efficiency of 16.6% with excellent long-term operation stability. By using QDs as light absorbing materials, the QD based photocatalysts also exhibited good performance in photocatalytic gaseous hydrogen production.

11:00 AM *EN08.17.02

Understanding the Synthesis, Structure and Physics of Hybrid 2D Perovskites for Efficient Optoelectronics Jean-Christophe Blancon; Rice University, United States

Organic-inorganic two-dimensional halide perovskites (2DPKs) are soft semiconductors formed by combining organic and inorganic moieties, which self-assemble in solution to form highly ordered periodic stacks. They exhibit a large compositional and structural phase space, which has led to novel and emergent physical properties offering potential for applications in optoelectronics, energy conversion, photonics, spintronics, and quantum devices. To achieve this paradigm, there is a need to understand both the fundamental physics and the growth of both 2DPK crystals and thin films used for integration in devices. In this presentation, I will describe three exciting results.

First we overcome a long-standing challenge in 2D perovskites of realizing phase pure thin-films. Briefly, we demonstrate a scalable approach involving dissolution of single-phase crystalline powders with homogeneous perovskite layer thickness in desired solvents, to fabricate 2D perovskite thin-films with

high phase purity. In-situ characterizations reveal the presence of sub-micron-sized seeds in solution that preserve the memory of the dissolved single-crystals, and dictates nucleation and growth of grains with identical layer thickness of the perovskite layers in thin-films. Photovoltaic devices fabricated with such films yield an efficiency of 17.1% and 1.20V open-circuit voltage, while preserving 97.5% of their peak-performance after 800 hours under illumination without any external thermal management.

Second, we report sunlight-activated anisotropic lattice contraction in 2DPKs, which is reversible and strongly dependent on both the nature of the interlayer organics and the details of the structure. Our theory suggests that light-generated charge accumulation results in the build-up of a bulk compressive strain, which induces a continuous lattice contraction over minutes. In-situ structural measurements on photovoltaic devices directly correlate the light-induced lattice contraction to an increase in the photovoltaic efficiency of Dion-Jacobson 2DPK solar cells from 15.6% to 18.3%. We found that compressive strain enhances inter-layer electronic interactions in 2DPKs leading to three-fold increase in carrier mobility and conductivity in 2DPK thin films.

Third, we employed ultrafast electron diffraction (UED) to capture at the picosecond time scale how light generated hot carriers dissipate their energy to the lattice and affect the 2DPK structure. The carrier cooling dynamic in 2DPKs yields a fast lattice re-ordering that is distinct from 3DPKs, followed by classic slow thermal dissipation of carriers excess energy to the lattice. The former process suggests the light-induced activation of an incipient phase transition, toward a hypothetical undistorted phase due charge-lattice interactions. The effect of anisotropy and the nature of the bulky organic cations were also confirmed to play a role in tailoring carrier-phonon interactions.

11:30 AM EN08.17.03

SnPb Perovskite Solar Cell Exceeding 18% Efficiency with a 1-cm² Cell Fabricated Using a One-Step Meniscus Coating Method at a Speed of over 5 m/min Shunsuke Shimo¹, Shigehiko Mori¹, Haruhi Oooka¹, Akio Amano¹, Gaurav Kapil², Shuzi Hayase² and Kenji Todor¹, ¹Toshiba Corporation, Japan; ²The University of Electro-Communications, Japan

Perovskite solar cells (PSCs) are one of the most promising candidates for the next generation of solar cells because they have high power conversion efficiency (PCE) exceeding 20% and they can be manufactured by a high-productivity fabrication process involving low-temperature processing and a roll-to-roll coating method. To meet the growing demand for renewable energy generation, it is necessary to mass-produce solar cells with high PCE at low cost. The PCE limit of MAPbI₃ (MA: methylammonium), which is a typical perovskite material, is 31% based on the Shockley-Queisser (S-Q) limit due to its band gap of 1.55 eV. It is thought that the maximum theoretical PCE of a material can be achieved at a band gap of around 1.1-1.4 eV and that a SnPb iodide perovskite compound is a suitable candidate for realizing the maximum PCE value of 33% based on its S-Q limit. In addition, SnPb PSCs are relatively environmentally friendly because they require far less Pb compared with Pb-based PSCs. Studies of SnPb PSCs have been increasing and PCEs exceeding 20% have been reported recently [1]. However, many of these SnPb PSCs are millimeter-scale cells fabricated using spin-coating method. Thus, it is necessary to find a way to manufacture SnPb PSCs with larger areas in a more highly productive manner.

To realize large-area coating, we have been developing the "meniscus coating method" [2,3], which is capable of producing uniform layers with low variations in thickness over a large area. By using this coating method in MAPbI₃-based PSCs, we have achieved a PCE of 14.1% in a polymer film module with an active area of 703 cm², and 16.1% with an active area of 781 cm² in a glass-based module [4]. Accordingly, we expect to realize high-productivity fabrication of SnPb PSCs by utilizing a roll-to-roll process and applying the meniscus coating method.

In this study, we developed the meniscus coating method for a SnPb perovskite layer. This coating realizes high productivity via the 1-step process at a speed of over 5 m/min. In addition, by employing the equimolar constitution of Sn and Pb (Sn:Pb = 1:1), a band gap of around 1.2 eV was realized in the SnPb perovskite layer. We also examined the surface passivation of the SnPb perovskite layer and found a PCE of 18.3% in a 1-cm² cell of the SnPb PSC having an inverted structure (ITO/hole transport layer/SnPb perovskite layer/PCBM/BSP/Ag).

Acknowledgments

This work was supported by the New Energy and Industrial Technology Development Organization (NEDO) project "Development of Technologies to Promote Photovoltaic Power Generation as a Main Power Source."

References

[1] Jiupeng Cao and Feng Yan, Recent progress in tin-based perovskite solar cells, *Energy Environ. Sci.* 14, 3 (2021), 1286-1325.

<https://doi.org/10.1039/D0EE04007J>

[2] H. Oooka, Y. Shinjo, T. Sawabe, T. Sugizaki, A. Amano, T. Ono, K. Sugi, I. Takasu, Y. Mizuno, J. Yoshida, S. Enomoto, A. Hirao, and I. Amemiya, High-Brightness Large-Area White OLED Fabricated by Meniscus Printing Process. Society for information display, International symposium (2012). <https://doi.org/10.1889/1.3500459>

[3] S. Mori, H. Oooka, H. Nakao, T. Gotanda, Y. Nakano, H. Jung, A. Iida, R. Hayase, N. Shida, M. Saito, K. Todor, T. Asakura, A. Matsui, and M. Hosoya, Organic photovoltaic module development with inverted device structure. Proceedings of MRS Meetings mrsf14-1737-u17-02 (2015). <https://doi.org/10.1557/opl.2015.540>

[4] Kenji Todor, Hiroyuki Miyauchi, Toshiba Review, vol.76, No.3, 17-20 (2021).

11:45 AM EN08.17.04

Simultaneous 2D/3D Heterostructure Passivation of Interface and Grain-Boundary for Highly Efficient Inverted Methylammonium-Free Perovskite Photovoltaics Saba Gharibzadeh^{1,1}, Paul Fassl^{1,1}, Intezar M. Hossain^{1,1}, Pascal Rohrbeck², Markus Frericks^{3,1}, Moritz Schmidt¹, The Duong⁴, Motiur Rahman Khan¹, Tobias Abzieher¹, Bahram Abdollahi Nejad^{1,1}, Fabian Schackmar^{1,1}, Osbel Almora⁵, Thomas Feeney¹, Roja Singh^{1,1}, Ulrich Lemmer¹, Jan P. Hofmann³, Stefan Weber^{2,2} and Ulrich W. Paetzold^{1,1}; ¹Karlsruhe Institute of Technology, Germany; ²Max Planck Institute for Polymer Research, Germany; ³Technical University of Darmstadt, Germany; ⁴The Australian National University, Australia; ⁵Universitat Jaume I, Spain

While power conversion efficiencies of perovskite solar cells using the standard (n-i-p) mesoporous and planar architecture have surpassed 24% some time ago, inverted (p-i-n) planar PSCs lag behind considerably. Severe non-radiative interfacial recombination at the perovskite/electron transport layer and at the grain boundaries still limits their open-circuit voltage (V_{OC}) and fill factor (FF) as compared to their n-i-p counterparts. Particularly for next generation monolithic perovskite/Si tandem photovoltaics, which commonly apply a p-i-n perovskite top solar cell, these recombination processes introduce a conceptual hurdle.

To address this challenge, we introduce a novel dual 2D/3D perovskite heterostructure passivation approach by adding phenethylammonium chloride (PEACl) to our methylammonium-free double cation p-i-n perovskite solar cell. Using PEACl:PbCl₂ as the additive and PEACl for surface treatment, our approach simultaneously passivates recombination centers at the grain boundaries in the bulk of the perovskite film and recombination centers at the perovskite/C₆₀ interface, respectively. The dual 2D/3D heterostructure passivation results in one of the highest reported PCEs for p-i-n PSCs of 22.7% with a remarkable V_{OC} and FF of 1.162 V ($E_g = 1.57$ eV) and 83.2%, respectively. Furthermore, a remarkable stabilized efficiency of 22.3% is demonstrated (5 min at maximum power point tracking), one of the highest reported for MA-free p-i-n PSCs.

Our study researches the advanced use of dual passivation as a key mechanism to manage the detrimental defects both in the grain boundaries and at the perovskite/ETL interface to achieve highly efficient p-i-n PSCs. By means of time resolved photoluminescence and photoluminescence quantum yield, we show that the charge carrier lifetime and quasi-Fermi level splitting are significantly enhanced compared to reference devices. We attribute the improvements to the formation of a 2D Ruddlesden Popper perovskite phase at the film surface and GBs, which leads to efficient chemical passivation of GB and surface defects as well as additional electronic passivation at the perovskite/C₆₀ interface. At the same time, the activation energy for ion migration is significantly increased, resulting in enhanced stability of the PSCs under light, humidity, and thermal stress.

12:00 PM EN08.17.05

Efficient and Stable Two-Dimensional Ruddlesden–Popper Tin Perovskite Solar Cells via Anion Engineering Hao Li, Shripathi Ramakrishnan, Yuanze Xu, Tony L. Xu and Qiuming Yu; Cornell University, United States

Two-dimensional (2D) Ruddlesden–Popper (RP) phase hybrid perovskites have since received a lot of attention as one of the most promising materials for making long-term, stable, high-performance perovskite solar cells (PSCs). The presence of big ammonium cations, such as butylammonium (BA) and phenylethylammonium (PEA), in a 2D or mixed 2D and three-dimensional (3D) structure has recently been shown to limit moisture infiltration at the boundaries of Sn-based perovskites, resulting in exceptional high film and device stability.¹ However, even when synthesized with stoichiometric concentrations of precursors, solution processed 2D tin perovskites still exhibit a mixed 2D phase with varying number of inorganic frameworks that is a signal for spreading of the quantum well (QW) width, inhibiting charge transport, increasing interfacial charge accumulation and affecting final device performance.^{2,3} Therefore, it is highly desired to control the QW width into an extremely small distribution and optimize the charge-transport characteristic. In this study, we fabricated 2D RP phase tin perovskite PEA₂FA_{n-1}Sn_nI_{3n+1} thin films with targeted $n = 5$, because of their suitable bandgaps for solar cells, using phenylethylammonium acetate (PEAAc) instead of commonly used PEAI. It is highly expected that compounds with a uniformly distributed intermediate phase in precursors will result in narrower distributed QW width and higher film and device stability due to the strong coordination effect between Ac⁻ group and Sn²⁺. The precursor solution prepared from PEAAc has a narrower size distribution and better stability than the solution prepared from PEAI, ensuring the uniform and narrower distribution of QW width and better stability of the thin films prepared via one-step plus anti-solvent solution process. Fourier transform infrared (FTIR) spectra reveal the coordination interaction between Ac⁻ group and Sn²⁺ via the C=O bond vibration shift in the thin film. In addition, X-ray diffraction (XRD) patterns and UV-vis absorption spectra demonstrate that the films have reduced the amount of small n number of 2D perovskites, which is preferred for device charge transport. The orientation of 2D perovskites and QW distribution are studied by grazing incidence wide-angle X-ray scattering (GIWAXS) and femtosecond transient absorption (TA) measurements. In comparison to standard organic spacers PEAI, the photovoltaic performance for the devices made under optimal conditions using PEAAc has a best power conversion efficiency (PCE) of over 9% with no hysteresis using a device structure of ITO/PEDOT:PSS/2D tin perovskite/ICBA/Ag. This is among the highest efficiency for 2D tin perovskite solar cells. This work demonstrates that anion in large organic spacers could play a critical role in forming a narrower distribution of QW, enhancing phase and device stability, and improving device performance. Therefore, anion engineering has the potential to aid in the further development of solar cells, photodetectors, and LEDs utilizing 2D perovskites.

References

1. Tsai, H. et al. High-efficiency two-dimensional Ruddlesden-Popper perovskite solar cells. *Nature* 2016, 536 (7616), 312-6.
2. Gabriella A T. et al. Tuning cesium–guanidinium in formamidinium tin triiodide perovskites with an ethylene diammonium additive for efficient and stable lead-free perovskite solar cells. *Mater. Adv.*, 2020, 1, 3507-3517.
3. Gabriella A T. et al. Impact of cesium on the phase and device stability of triple cation Pb–Sn double halide perovskite films and solar cells. *J. Mater. Chem. A*, 2018, 6, 17426-17436.

12:15 PM EN08.17.06

Ion-Assisted Ligand Exchange for Enhanced Electronic Coupling in FAPbI₃ Perovskite Quantum Dot Solar Cells Yuanze Xu, Hao Li, Shripathi Ramakrishnan and Qiuming Yu; Cornell University, United States

Colloidal lead halide perovskite quantum dot (QD) has emerged as a promising material for next generation optoelectronic devices due to its unique properties, such as quantum confinement effect, high photoluminescence quantum yield, defect tolerance, and multiexciton generation. For photovoltaic applications, native insulating ligands on QD surfaces need to be removed to achieve strong electronic coupling of adjacent QDs. Unlike metal chalcogenide QDs, the ionic crystalline structure of perovskite is susceptible to decomposition under polar solvents and harsh ligand exchange conditions. Therefore, fundamental insights are needed to establish a mild ligand exchange method to gently modify surface ligand density without causing decomposition. Among the choices of solvents, methyl acetate (MeOAc) strikes to have the moderate polarity to remove surface ligands without decomposing the QDs. However, how inter-QD coupling can be improved during ligand exchange has not been well understood and developed. Here, we report an ion-assisted ligand exchange strategy that enhances the electronic coupling and prevents defect formation in FAPbI₃ QD films for perovskite QD solar cells. We synthesized FAPbI₃ QDs with hot injection method, followed by a series of purification steps. An average QD size of 12 nm with narrow size distribution was measured from TEM images. UV-Vis absorption spectra of QD solutions show an absorption edge of 775 nm and photoluminescence emission spectra show a peak at 785 nm. Iterative spin coating steps were applied to stack QD films to reach ~300 nm thickness. To conduct the solid-state ligand exchange, spin coated QD films after each spin coating step were dipped into MeOAc solutions, in which acetate salts with different cations (FA⁺, GA⁺, PEA⁺, Pb²⁺) were added to manipulate ligand exchange capability and suppress defect formation. Acetate, with a higher affinity to Pb²⁺ than oleate, can accelerate the removal of oleate. In addition, it can fill the X-site vacancy and therefore prevent the migration of iodide ions. The cations can fill the vacancies cause by removal of oleylammonium (A-site) and Pb-oleate complex (B-site). The ligand exchange reaction rates with different acetate salts were estimated from the intensity change of the vibrational mode in FTIR spectra and compared. SEM images show that the packing of QDs become more compact after ligand exchange while smooth film surfaces are retained. A slight redshift was observed from photoluminescence emission spectra, verifying successful inter-QD coupling. XRD confirms that no phase transitions happened during ligand exchange, indicating the preservation of nanocrystalline structure. The coupled film exhibits a long PL lifetime because of suppressed trap formation. We fabricated QD solar cells with the structure of ITO/PEDOT:PSS/FAPbI₃ QD/PCBM/BCP/Ag. Consequently, all the acetate salts contributed to a significant improvement of J_{SC}, and fill factors were maintained above 75%. The improved J_{SC} was attributed to a net reduction of insulating ligands due to stronger ligand exchange effect of acetate. Except FAOAc–MeOAc, all other acetate salts MeOAc treatments led to increased V_{OC} because of suppressed trap formation. Charge carrier mobilities were measured with electron-/hole-only devices. Light intensity dependent J–V measurements were conducted to investigate the charge recombination mechanisms. This work demonstrates a more reliable solid-state ligand exchange strategy, which enhances the electronic coupling and prevents defect formation in FAPbI₃ QD films, and sheds light on the roles of ions in solid-state ligand exchange.

1:00 PM EN08.18.01

Photoinduced Iodide Repulsion and Halides-Demixing in Layered Perovskites [Yongtao Liu](#)¹, Miaosheng Wang², Anton V. Ievlev¹, Mahshid Ahmadi², Bin Hu² and Olga Ovchinnikova¹; ¹Oak Ridge National Laboratory, United States; ²The University of Tennessee, Knoxville, United States

Mixing halides in metal halide perovskites (MHPs) is an effective approach to adjust MHPs bandgap for applications in tandem solar cells. However, mixed-halide (MH-) MHPs undergo light-induced-phase-segregation (LIPS) under continuous illumination. Therefore, understanding the mechanism of LIPS is necessary for developing stable MH-MHPs. In this work, we investigated LIPS in layered (L)-MHPs, unveiling that spacer cation plays a crucial effect on LIPS. Our chemical characterization of LIPS in L-MHPs revealed an iodide-repulsion effect and consequently the formation of pure-Br-phase or extremely Br-rich phase in the illuminated region, where iodide repulsion is dependent on light intensity and chemical environment (e.g., oxygen penetration into MHPs affect iodide repulsion process). By further probing chemical changes in a MAPb(Br_{0.5}I_{0.5})₃ film under illumination, we observed, in addition to the formation of I-rich and Br-rich domains (that is a generally believed mechanism of LIPS), LIPS also leads to a significant vertical chemical redistribution, which is critical to charge carrier transport and extraction in MHPs devices. Moreover, we discovered that LIPS is more significant in the bulk of the MHP film, which is probably due to a large population of photogenerated charge carriers in the bulk. Overall, by directly characterizing chemical changes due to LIPS, we revealed the chemical changes associated with LIPS in MHPs, which is the key for understanding LIPS mechanism and developing stable mixed-halides MHPs. Our studies about the role of spacer cation in LIPS and extrinsic ion penetration also offers insight into improving the stability of MHPs.

Acknowledgments: This work is conducted at the Center for Nanophase Materials Sciences, a US Department of Energy Office of Science User Facility.

1:15 PM EN08.18.04

Thermodynamically Stable Colloidal Solids—Interface Energetics from Particle Size Distributions [Andrew Nelson](#) and Lawrence Friedman; National Institute of Standards and Technology, United States

The thermodynamics of interfaces, encapsulated in the parameter of the work of interface formation, dictate the stability and evolution of suspensions, gels, emulsions, and many other dispersed systems. In particular, it is one of the main axes along which workers engineer the properties, especially size and shape, of colloidal nanoparticles. A widespread assumption is that such colloidal solutions are never thermodynamically stable: they will tend to aggregate, ripen, or coarsen, limiting their performance and long-term usefulness. This need not be the case, however, and truly stable solid colloidal systems have been contemplated or even proposed for many decades. We build on this work using the framework of classical nucleation theory for colloidal solids, from which a simple expression for the size distribution depending on the concentration of the particle components and the interface energy can be obtained. The need for a statistical-mechanical model describing the particle degrees of freedom hints that colloidal solutions could serve as tests of this contentious part of nucleation theory. Conversely, an experimentally measurable size distribution corresponds directly to a size-dependent interface energy, and thus thermodynamically stable colloids are probes of solid-solution interactions at nanoscopic dimensions. We invert this relation to examine previous data sets from colloidal nanoparticles, and suggest that, from the apparent dependence of interface energy on size, the mechanism of colloid stabilization may be more complex than one of those already proposed, e.g. interface bending energy or dielectric charging. We conclude with a note of caution, however, that so far it remains to be demonstrated conclusively that the systems considered in our work are really thermodynamically stable with a definite place in a multicomponent phase diagram.

1:30 PM EN08.18.05

Imaging Organic Cations Interfacial Passivation of Inverted Perovskite Solar Cells [Stefania Cacovich](#)¹, Guillaume Vidon², Laxman Gouda³, Matteo Degani³, Jean Rousset⁴, Jean-Baptiste Puel⁴, Marie Legrand⁴, Jean-François Guillemoles¹, Daniel Ory⁴ and Giulia Grancini²; ¹CNRS IPVF UMR 9006, France; ²IPVF (Institut Photovoltaïque d'Île-de-France), France; ³University of Pavia, Italy; ⁴Électricité de France (EDF), R&D, France

Inverted perovskite solar cells passivated *via* organic cations exhibit superior power conversion efficiency compared to unpassivated ones. These record efficiencies have been reached thanks to the use of large organic cations to passivate the interface between the perovskite absorber and the transport layers. However, the passivation mechanism of 2D perovskites on top of the 3D bulk absorber layer is still under intense debate in the community. In particular, issues regarding the complete coverage of the passivating layer, the full formation of a 2D layer on top of the 3D bulk perovskite and the possible effects on carrier extractions still need to be clarified. Here, we study the optoelectronic properties and chemical structure of interface doped perovskite solar cells where large cations, namely Cl-PEAI and F-PEAI, were incorporated at both front and rear interfaces of the absorber. The effect of the cation addition led to an increase of all the main PV characteristic, reaching PCE values up to 23.7%. We combined steady-state and time-resolved multidimensional photoluminescence imaging techniques to probe the main optoelectronic and transport properties of such devices. We thus obtained quantitative maps for physical parameters such as Quasi Fermi Level Splitting (QFLS), Urbach Energy and surface recombination rate, which proved a homogenous passivation by Cl-PEAI and F-PEAI cations over the 3D surface. Moreover, we identified interfacial passivation as the main mechanism leading to a clear improvement of the Voc which increases from 1.10 to 1.16 eV on full devices, whereas the addition of the cations on bare perovskite thin films resulted into an increase of the QFLS in the range of 0.01 -0.02 eV. Complementary Raman analyses proved that passivation effect and deeper interaction of delocalised [π - electron from the F-PEAI and Cl-PEAI with the Pb-I perovskite octahedral are cause for the enhanced thermal fluctuation and formation of large polaron in the perovskite lattice. These passivation effect induces structural deformation which are the main responsible phenomena for the observed delayed carrier recombination and increased photovoltaic performance. By linking optical and electrical measurements we highlight the benefits of this passivation method in maximising all the main photovoltaic characteristics and in approaching inverted perovskite solar cell theoretical limit.

1:45 PM EN08.18.06

Structural Control and Evaluation of Bismuth-Based Mixed Perovskite Films for Optoelectronic Applications [Keitaro Kikuchi](#), Yuki Matsui, Tomohiro Watanuki and Hironori Ogata; Hosei University, Japan

In recent years, lead halide perovskite solar cells, which have been attracting attention as next-generation solar cells, have an energy conversion efficiency of over 25% and are expected to be practical use in the near future. However, the lead halide perovskite compounds contains lead, which is harmful to the human body and the environment, and is an issue for practical use.

Many studies have been reported on solar cells using perovskite compounds based on tin, germanium, bismuth, etc., which are less toxic than lead. Among them, research on solar cells using bismuth halide perovskite(Ca₃Bi₂I₆) has been actively conducted and it has been reported that the energy conversion efficiency(PCE) is 3.20 %.

In this study, for the purpose of developing high-quality films applicable to optoelectronic applications with adjusted band gap energy in A₃Bi₂X₆ compound semiconductors, we fabricated mixed bismuth halide perovskite films with various chemical compositions. Crystal morphology, crystal structure and

physical properties were evaluated using SEM, powder XRD measurement, and light absorption spectrum measurements. In this presentation, we will report these detailed results and the characteristics of solar cells using mixed bismuth halide perovskites.

2:00 PM EN08.18.07

White-Light Emitting Ruddlesden-Popper Perovskites Ashanti Bergonzoni¹, Sébastien Pillet², Kamel Boukheddaden³, Aymen Yanguï⁴, Pedesseau Laurent¹, Boubacar Traore⁵, Claudine Katan⁵ and Jacky Even¹; ¹INSA, iFOTON - CNRS, France; ²CRMM (Cristallographie, Résonance Magnétique et Modélisation) laboratory - CNRS, France; ³University Paris Saclay, France; ⁴Lund University, Sweden; ⁵ISCR (Institut des Sciences Chimiques de Rennes), France

Recently, owing to their excellent optoelectronic properties combined with an enhanced material stability, two-dimensional (2D) organic halide perovskites have emerged as an attractive alternative to 3D perovskites for photovoltaics^{1,2}. More, their ability to emit white-light at room temperature with a good color rendering projected this family of materials into the spotlight of potential future low-cost white LED components³. However, the underlying physical mechanisms behind these emissive properties are not fully understood. Herein we propose to investigate the origin of the broad-band emission observed at different temperatures in a series of $(\text{C}_6\text{H}_5\text{NH}_3)_2\text{PbX}_4$ 2D Ruddlesden Popper perovskites (X= Br or I)^{4,5} by coupling advanced structural measurements with an atomistic approach based on the density functional theory (DFT). Indeed, as the temperature is decreased, phase transitions between undistorted and distorted structures were observed for the two compounds of the series by means of temperature dependent X-ray diffraction. While this crystallographic phase transition goes along with a measured polarization-electric field hysteresis for the bromide compound, apparition of satellite incommensurate reflections was instead obtained for the Iodine one. We believe that these satellite reflections might also be connected to a low temperature ferroelectric ordering. In order to set a clear interplay between the structural distortions and the observed optoelectronic properties, theoretical studies intend to provide insights of the electronic band structures and polarization characteristics for these compounds.

(1) Tsai, H.; Nie, W.; Blancon, J.-C.; Stoumpos, C. C.; Asadpour, R.; Harutyunyan, B.; Neukirch, A. J.; Verduzco, R.; Crochet, J. J.; Tretiak, S.; Pedesseau, L.; Even, J.; Alam, M. A.; Gupta, G.; Lou, J.; Ajayan, P. M.; Bedzyk, M. J.; Kanatzidis, M. G.; Mohite, A. D. High-Efficiency Two-Dimensional Ruddlesden-Popper Perovskite Solar Cells. *Nature* **2016**, *536* (7616), 312–316. <https://doi.org/10.1038/nature18306>.

(2) Katan, C.; Mercier, N.; Even, J. Quantum and Dielectric Confinement Effects in Lower-Dimensional Hybrid Perovskite Semiconductors. *Chem. Rev.* **2019**, *119* (5), 3140–3192. <https://doi.org/10.1021/acs.chemrev.8b00417>.

(3) Dohner, E. R.; Jaffe, A.; Bradshaw, L. R.; Karunadasa, H. I. Intrinsic White-Light Emission from Layered Hybrid Perovskites. *J. Am. Chem. Soc.* **2014**, *136* (38), 13154–13157. <https://doi.org/10.1021/ja507086b>.

(4) Yanguï, A.; Garrot, D.; Laurent, J. S.; Lusson, A.; Bouchez, G.; Deleporte, E.; Pillet, S.; Bendeif, E. E.; Castro, M.; Triki, S.; Abid, Y.; Boukheddaden, K. Optical Investigation of Broadband White-Light Emission in Self-Assembled Organic-Inorganic Perovskite $(\text{C}_6\text{H}_{11}\text{NH}_3)_2\text{PbBr}_4$. *J. Phys. Chem. C* **2015**, *119* (41), 23638–23647. <https://doi.org/10.1021/acs.jpcc.5b06211>.

(5) Yanguï, A.; Pillet, S.; Mlayah, A.; Lusson, A.; Bouchez, G.; Triki, S.; Abid, Y.; Boukheddaden, K. Structural Phase Transition Causing Anomalous Photoluminescence Behavior in Perovskite $(\text{C}_6\text{H}_{11}\text{NH}_3)_2[\text{PbI}_4]$. *J. Chem. Phys.* **2015**, *143* (22), 224201. <https://doi.org/10.1063/1.4936776>.

2:15 PM EN08.18.08

2D Phase Purity Determines Charge Transfer Yield at 3D/2D Lead Halide Perovskite Heterojunctions Robert J. Westbrook^{1,2}, Weidong Xu¹, Xinxing Liang¹, Thomas Webb³, Tracey M. Clarke² and Saif A. Haque¹; ¹Imperial College London, United Kingdom; ²University College London, United Kingdom; ³University of Surrey, United Kingdom

Targeted functionalisation of 3D perovskite with a 2D passivation layer via R-NH₃I treatment has emerged as an effective strategy for enhancing both the efficiency [1,2] and chemical stability [3] of ABX₃ perovskite solar cells, but the underlying mechanisms behind these improvements remain unclear. Here, we correlate the chemical evolution of the 3D/2D charge transport layer (CTL) interface with the injection yield to the CTL through a mixture of surface sensitive structural and time-resolved optical techniques.

We assign a passivation mechanism where R-NH₃I reacts with excess PbI₂ in the MAPbI₃ film and unsaturated PbI₆ octahedra to form $(\text{R-NH}_3)_2(\text{MA})_{1-n}\text{Pb}_n\text{I}_{3n+1}$. Crucially, we show that precise control of the 2D $(\text{R-NH}_3)_2(\text{MA})_{1-n}\text{Pb}_n\text{I}_{3n+1}$ layer underpins performance improvements: $n = 1$ yields over a two-fold improvement in hole injection to the HTL; $n > 1$ deteriorates hole injection. Ultrafast transient absorption spectroscopy suggests that this n -dependence is rooted in the fact that fast ($< 6\text{ns}$) hole injection does not occur between the 3D perovskite and 2D layer. Finally, we correlate these improvements in hole transfer with a 30% enhancement in device efficiency. [4] These results help explain contemporary empirical findings in the field and set out an important design rule for the further optimisation of multidimensional perovskite optoelectronics.

[1] Cho *et al*, *Energy Environ. Sci.*, 2018, **11**, 952–959.

[2] Jung *et al*, *Nature*, 2019, **567**, 511–515.

[3] Grancini *et al*, *Nat. Commun.*, 2017, **8**, 15684.

[4] Westbrook *et al*, *J. Phys. Chem. Lett.* 2021, **12**, 13, 3312.

SESSION EN08.19: On-Demand
Sunday Morning, December 5, 2021
On-Demand

8:00 AM EN08.04.02

Dark and Bright Excitons in Halide Perovskite Nanoplatelets Moritz Gramlich¹, Michael W. Swift², Carola Lampe¹, John L. Lyons², Markus Döblinger¹, Alexander Efros², Peter Sercel³ and Alexander S. Urban¹; ¹Ludwig-Maximilians-Universität München, Germany; ²U.S. Naval Research Laboratory, United States; ³California Institute of Technology, United States

Halide perovskite nanocrystals have emerged as excellent light sources for light-emitting devices and lasers due to quantum yields approaching unity and an emission wavelength tunable throughout the visible range. As recently shown, it is the only material currently known that could possess a lowest-lying bright exciton state, greatly enhancing radiative efficiency. This last feature, known as bright-dark exciton inversion, is induced through the Rashba effect, resulting from breaking the nanocrystal inversion symmetry. Nanoplatelets, colloidal semiconductor quantum wells, have additional advantages for light emission, as their radiative rates and outcoupling efficiencies are strongly enhanced through quantum confinement and dielectric confinement effects. Here, we investigate the excitonic fine structure of thickness tunable halide perovskite nanoplatelets by merging time- and temperature-resolved photoluminescence spectroscopy with an effective mass model. We find a thickness-dependent bright-dark exciton splitting reaching up to 33 meV, the

largest ever reported value. Additionally, we find that the bright exciton is further split by up to 16 meV for the in-plane and out-of-plane polarized states. Due to these immense splitting energies, the radiative properties of the nanoplatelets will also be affected at room temperature. The experimental results obtained in this paper are in excellent agreement with the novel theory, which takes quantum confinement and dielectric confinement anisotropy into account. Notably, the model we develop can be directly applied to any semiconductor nanoplatelet and generalized for any nanostructure.

SYMPOSIUM EN09

Metal Sulfides for High Performance Electrochemical Batteries
November 30 - December 6, 2021

Symposium Organizers

Yoon Seok Jung, Yonsei University
Hui Wang, University of Louisville
Wolfgang Zeier, University of Muenster
Hongli Zhu, Northeastern University

* Invited Paper

SESSION EN09.01: Metal Sulfides in Batteries I
Session Chairs: Hui Wang and Hongli Zhu
Tuesday Morning, November 30, 2021
Hynes, Level 3, Room 309

10:30 AM *EN09.01.01

Ionic Transport, Stability and Interfacial Reactivity of Metal Sulfides Solid Electrolytes Gerbrand Ceder; University of California, Berkeley, United States

In this presentation I will give an overview of the mechanism by which Li ions achieve fast ion conductivity in sulfides and contrast it to oxide solid electrolytes. While screening of the electrostatic interaction through the large sulfur ion is very effective in providing a flat energy landscape for lithium, oxygen anions do not provide effective screening, rationalizing why sulfides and oxides require different structure types and compositions to achieve high ionic conductivity. I will also discuss claimed mechanisms for high conductivity such as paddle wheels etc. Finally, I will review the limitations on the anodic and cathodic stability of sulfide-based conductors and discuss their breakdown products.

11:00 AM EN09.01.02

Preparation and Defect Control of Transition Metal Sulfides for Lithium Sulfur Batteries via Chemical and Electrochemical Synthesis Approaches Amy Marschillok^{1,2}, Esther S. Takeuchi^{1,2}, Lei Wang² and Kenneth Takeuchi^{1,2}; ¹Stony Brook University, United States; ²Brookhaven National Laboratory, United States

Transition metal sulfides are appealing for next generation electrochemical energy storage as they can serve multiple roles as sulfur-equivalent electroactive materials and species promoting effective polysulfide trapping. Chemically and electrochemically based synthesis approaches providing control of sulfide composition and defect structure will be described in this presentation. Materials to mesoscale characterization and correlation with electrochemical function will also be reviewed.

SESSION EN09.02: Metal Sulfides in Batteries II
Session Chairs: Hui Wang and Hongli Zhu
Tuesday Afternoon, November 30, 2021
Hynes, Level 3, Room 309

1:30 PM *EN09.02.01

Understanding the Role of Electronic and Interfacial Properties During Li Plating and Stripping Yue Qi; Brown University, United States

The key challenge for the Li-metal electrode is to maintain the smooth surface at the microscopic scale during cycling. The same crystalline structure of Li₂O and Li₂S but different chemistry serve as model systems for the fundamental understanding of the difference of oxides and sulfides during Li stripping and plating processes. To simulate the vacancy formation and accumulation at the Li-metal surface, a combined density functional theory (DFT)

and kinetic Monte Carlo (KMC) simulation was developed. It was found that the lithiophilic interface repels vacancies into the bulk Li, so Li atoms can quickly fill the Li vacancies near the interface and maintain a smooth Li surface. In contrast, the lithiophobic interface traps Li vacancies toward the interface, and the accumulated Li vacancies form voids and roughen the surface. While Li/Li₂O interface adhesion is larger than the Li/Li₂S interface, it is predicted that it is easier to maintain a smooth Li surface during delithiation at Li/Li₂O interface. During lithiation plating, it was found the bandgap, tunneling barriers, and electron localization on internal defects, such as pores and crack surfaces and grain boundaries play a more important role for Li-dendrite nucleation and growth. A combined DFT and phase-field method was developed to demonstrate these effects. Several oxides (cubic Li₇La₃Zr₂O₁₂ (c-LLZO), Li_{1.17}Al_{0.17}Ti_{1.83}(PO₄)₃ (LATP), and Li₂PO₂N) and sulfide (β-Li₃PS₄) solid electrolytes and interlayer materials (LiF, Li₂O, and Li₂S) were compared. All of them showed smaller bandgaps on the surface and grain boundaries than the corresponding bulk materials. While LLZO showed the most significant excess electrons on the surface and grain boundaries, β-Li₃PS₄ showed no such behavior. This is consistent with the observed trend and morphology of Li dendrite growth in different solid electrolyte materials.

2:00 PM *EN09.02.02

Development of Thiophosphate Solid-State Electrolytes for All-Solid-State Lithium Metal Batteries [Donghai Wang](#); The Pennsylvania State University, United States

The family of thiophosphate solid-state electrolytes (SSEs) is one of the most promising candidates for future all-solid-state lithium metal batteries due to their high ionic conductivity (>1 mS cm⁻¹), even exceeding conventional liquid electrolytes. However, high-ionic-conductive solid electrolytes such as Li₁₀GePS₁₂ are not stable against lithium metal, leading to fast failure of the cell. This talk will first present the synthesis of a new Li₂S-P₂S₅-Li₃N-Al₂S₃ glass-ceramic SSE system through a solid-state reaction approach. The synthesized SSE demonstrated a high ionic conductivity of ~ 5.19 mS cm⁻¹ at room temperature and superior stability against lithium metal anode. And stable Li electrodeposition over 1000 h was achieved at a high current rate of 0.6 mA cm⁻² and a high areal capacity of 0.6 mAh cm⁻². Second, a solution synthesis of argyrodite-type SSEs with low annealing temperatures below 200 °C will be present. The synthesized SSE demonstrated a high ionic conductivity of ~ 4.01 mS cm⁻¹ at room temperature and superior stability against lithium metal anode. At room temperature, Li|SSE|Li symmetric cell demonstrated a high critical current density of 1 mA cm⁻² and low areal interfacial resistance of 6 ~ 7 Ω cm². Last, I will present the use of highly conductive SSEs in fabrications of all-solid-state Li-S batteries to achieve high utilization of sulfur and high energy density.

2:30 PM *EN09.02.03

Ultra Stable Sodium-Sulfur Electrochemistry Enabled by Phosphorus-Based Complexation [Weiyang Li](#); Dartmouth College, United States

Beyond the current lithium ion technologies, sodium-sulfur batteries stand out because of the high theoretical specific energy attributed to the multi-electron redox reaction, which overcomes the capacity limitation of intercalation-based chemistry. Major challenges in realizing the full potential of a sodium-sulfur battery are associated with the formation of undesirable intermediates and irreversible precipitation of solid products. This work presents a new series of sodium phosphorothioate complexes that offer superior battery performance across a wide temperature range from -60°C to ambient temperature, showing great promise for enabling next-generation high energy and low cost energy storage systems. The complexes are designed by taking advantage of the chemical affinity of phosphorus with both sulfur and sodium. The complex structures and the electrochemical reaction mechanisms are revealed through coupled experimental characterization and theoretical calculations. The desirable electrochemical properties are attributed to the ability of the complexes to prevent the formation of undesirable precipitates over a fairly wide range of voltages.

3:00 PM EN09.02.04

In Situ TEM Investigation of the Effects of Sodium on the Thermal Stability of TiS₂ Nanowires [Rose H. Pham](#)¹, [Rory Weeks](#)², [Edwin Miller](#)², [Partha Mukherjee](#)³, [Luisa L. Whittaker-Brooks](#)² and [Beth Gupton](#)¹; ¹University of Kentucky, United States; ²The University of Utah, United States; ³Purdue University, United States

Understanding the thermal stability of nanowires is of key importance for the performance and longevity of nanowire-containing devices, particularly where resistive heating may occur. With growing interest in sodium-ion batteries (NIBs) as a more economical and lower environmental impact alternative to lithium-ion batteries (LIBs), and layered transition-metal dichalcogenides (TMDs) as energy storage materials, it is important to determine both the advantages and limitations of replacing lithium-ion conductors with their sodium analogs. Here, we report an *in situ* heating study to investigate the thermal stability of sodium-intercalated titanium (IV) sulfide (TiS₂) nanowires, performed in the transmission electron microscope (TEM). Both sodiated (Na_xTiS₂) and non-sodiated nanowires were studied using a specialized heating holder, heating between room temperature and 700 °C. Control areas were also investigated to distinguish between heating and electron-beam effects. We observed chemical, morphological, and crystalline changes with increased temperature, solely in the sodiated-TiS₂ samples, demonstrating that sodiation profoundly affects the thermal stability of TiS₂ nanowires.

3:15 PM EN09.02.05

Stable Sodium Alloy Anodes for All-Solid-State Sodium-Sulfur Batteries [Li-Ji Jhang](#), [Daiwei Wang](#) and [Donghai Wang](#); The Pennsylvania State University, United States

Sodium-Sulfur (Na-S) batteries are considered a promising candidate for stationary energy storage techniques due to their low cost, long cycle life, and high energy density. For example, Na/β'-alumina/S battery has already been developed as stationary energy storage systems. However, the requirement of high temperature (>300 °C) to maintain the molten state of Na anode and S cathode causes extra power consumption and potential safety issues, restricting its broader applications. All-solid-state Na-S batteries operating at a lower temperature (e.g., < 100 °C) have attracted significant attention because of potentially improved safety features while maintaining long cycling life due to no generation of soluble polysulfide. One of the main challenges in developing such all-solid-state Na-S batteries operating at lower temperatures is its poor interfacial stability between Na metal anode and solid electrolyte, resulting in increased impedance, dendrite formation/penetration, and poor cycling life. Herein, we investigated Na alloy anodes and their applications in Na-S batteries. The alloy anode materials (e.g., Na-Sn and Na-Sb alloys) were synthesized by a high-energy ball-milling procedure. Electrochemical performance of the alloy anodes was evaluated, including comparing overpotential and critical current densities in Na-alloy symmetric cells, studying effects of different mass loading and N/P ratios in Na-S batteries. It is found that Na-Sb alloy is a more stable alloy anode with low overpotentials at a wide range of current densities. By pairing with TiS₂ cathode, Na-Sb alloy anode exhibits stable cycle life than Na-Sn alloy anode. All-solid-state Na-S battery cells were also fabricated with high mass loading of the sulfur cathode. The all-solid-state Na-S battery cell can deliver a high initial discharge capacity and maintain a specific capacity above 1000 mAh/g after long-term cycling operating at 60 °C. This finding shows a promising stable Na alloy anode for all-solid-state Na metal batteries to achieve long cycle life at a lower temperature for practical applications in stationary energy storage.

3:30 PM EN09.02.07

Covalent Sulfur Confined in Tunable Mesoporous Hollow Carbon Spheres Enabling High-Rate and Long-Cycling Room-Temperature Sodium-Sulfur Batteries [Jianmin Luo](#)¹, [Wenkui Zhang](#)², [Xinyong Tao](#)², [Weiyang Li](#)¹ and [Yiwen Zhang](#)¹; ¹Dartmouth College, United States; ²Zhejiang University of Technology, China

Although room temperature sodium-sulfur (Na-S) batteries have attracted huge attention due to its promise for large-scale applications, severe shuttle effect of polysulfide and the sluggish reaction kinetics of non-conductive sulfur in sulfur cathodes, as well as dendritic Na growth in Na metal anodes are the main challenges of this technology. **Notably, most of the previous published works usually devote to solving the issues related to sulfur cathode or sodium metal anode separately. There are rare works of simultaneously enhancing the electrochemical performance of both cathode and anode with two-in-one materials.** Herein, high-rate and long-cycling room-temperature Na-S batteries are achieved by employing covalent sulfur confined in mesoporous hollow carbon spheres (S@MHCS) as stable sulfur cathodes and solid additives for metallic sodium anode **in a carbonate electrolyte** to overcome the above obstacles simultaneously. As the cathode, MHCS can not only provide sufficient electrical contact and accessible Na⁺ diffusion to the encapsulated sulfur copolymers for fast kinetics and high capacity, but effectively confine formed short-chain sodium polysulfides for prolonged cycle life. Additionally, the direct addition of the S@MHCS into bulk Na contributes to the homogenous Na plating by inducing Na nucleation and growth within the inner cavity of carbon spheres, and minimizes volume change during cycling, enabling extremely stable Na metal anodes at a ultrahigh current density (**up to 40 mA/cm²**) along with an ultrahigh capacity (**up to 40 mAh/cm²**). As a result, a Na-S full cell constructed with S@MHCS exhibits excellent rate capability and outstanding cycling performance.

SESSION EN09.04: Poster Session: Metal Sulfides in Batteries
Session Chairs: Hui Wang and Hongli Zhu
Tuesday Afternoon, November 30, 2021
8:00 PM - 10:00 PM
Hynes, Level 1, Hall B

EN09.04.01

Three-Dimensional Interconnected Binder-Free Mn–Ni–S Nanosheets for High-Performance Asymmetric Energy Storage Devices with Exceptional Cyclic Stability [Nageh K. Allam](#); American University in Cairo, Egypt

A facile one-step method was demonstrated for the electrodeposition of manganese–nickel sulfide (Mn–Ni–S) 3D interconnected sheets on nickel foam substrates. The as-synthesized materials were characterized using field-emission scanning electron microscopy (FESEM), X-ray diffraction (XRD), energy-dispersive X-ray spectroscopy (EDS), and X-ray photoelectron spectroscopy (XPS) techniques. Upon their use as supercapacitor electrodes, the electrodeposited Mn–Ni–S showed exceptionally high specific capacitance (2849 and 1986 F/g at 1 and 5 A/g, respectively) and an excellent rate capability. Using Fe₃O₄-GR as the negative electrode and the Mn–Ni–S 3D interconnected sheets as the positive electrode to assemble an asymmetric supercapacitor device revealed high power density (800 W kg⁻¹) and energy density (40.44 Wh kg⁻¹) with 90% capacitance retention and a Columbic efficiency of 100% after 11 000 cycles, indicating the high potential of the fabricated materials for practical energy storage devices.

EN09.04.02

Understanding Solid-State Synthesis of Sodium Chalcogenide Superionic Conductors Selim Halacoglu¹, Yang Li¹, Sabina Chertmanova¹, Yan Chen², Badri Narayanan¹ and [Hui Wang](#)¹; ¹University of Louisville, United States; ²Oak Ridge National Laboratory, United States

Sulfide-based superionic sodium (Na) conductors show promising applications as solid electrolytes (SEs) in solid-state Na batteries to achieve the high energy dense, safe, and economic features. For solid-state ionic conductors, the synthesis process strongly influences their crystal structures/phase purity, and thus affect their ionically conductive properties. In situ neutron diffraction (ND) is a powerful tool to track the structural changes during solid-state synthesis process. Among sulfide-based SEs, Na₃SbS₄ family conductors have attractive intense attentions due to their high ionic conductivity (10⁻⁴–10⁻³ S cm⁻¹) at room temperature and impressive chemical stability in ambient environment. In this work, we performed in situ neutron diffraction on pristine Na₃SbS₄ without and with doping (i.e. Se) to track the phase change and structural evolution during the synthesis and heat treatment (heating or cooling). The solid-state reaction mechanism during the synthesis process was revealed. In addition, the doping effects on the solid-state reactions, lattice parameters and structure stability were studied. This work presents a detailed structural study using in situ NDs for the synthesis of sulfide-based Na conductors, which provide useful information for the design and synthesis of new solid-state conductors.

SESSION EN09.05: Metal Sulfides in Batteries III
Session Chairs: Karsten Albe and Hui Wang
Monday Morning, December 6, 2021
EN09-Virtual

8:00 AM *EN09.05.01

Air-Stable Sulfide-Based Electrolytes and Interfaces for All-Solid-State Li Batteries [Xueliang A. Sun](#); University of Western Ontario, Canada

All-solid-state Lithium metal batteries (ASSLMBs) cannot only maximize the energy density, but also show improved safety compared with the conventional liquid electrolyte-based Li-ion batteries. Solid-state electrolytes (SSEs), as the most important component in the ASSLMBs, can determine the electrochemical performance. High ionic conductivity is one of the most basic requirements for an excellent SSE. Sulfide-based SSEs exhibit ultrahigh ionic conductivity (> 10⁻² S cm⁻¹ at room temperature) that can be comparable to the liquid electrolytes, making this kind of SSEs popular and promising. However, air sensitivity and Li metal incompatibility are two major obstacles, which are together with the problematic cathode interface, hindering the development of sulfide SSEs for practical ASSLMBs.^{1,2} In our work, we employed the strategy of element substitution to design F-substituted Li₆PS₅Cl, Sn-substituted Li₆PS₅I, and Sn-substituted Li₃PS₄ as high-performance Li-metal compatible sulfide SSEs.⁴⁻⁶ Using these element doping SSEs can derive functional interphases that contain LiF, LiI, and Li-Sn alloy, respectively. These interfacial contents were demonstrated as important to achieve stable Li plating/stripping. Importantly, we found that replacing P with Sn could significantly improve the air stability and ionic conductivity at the same time. The high reaction energy between the Sn-substituted PS₄ tetrahedra and moisture was regarded as the main reason for the improved air stability, while the expanded unit cell and increased Li⁺ concentration led to superior ionic conductivity. Our modifications on various common-used sulfide SSEs with multi-function elements provide more choices of sulfide SSEs for practical ASSLMBs. At the cathode side,⁷⁻¹¹ we used interface modification (coating strategy) to improve the interfacial Li⁺ transport and

chemical inertness. The electrode and electrochemical performance will be discussed.¹²

References

1. C. Wang, J. Liang, Y. Zhao, M. Zheng, X. Li, X. Sun*, *Energy Environ. Sci.*, 2021, doi:10.1039/d1ee00551k.
2. C. Yu, F. Zhao, X. Sun*, et al. Recent Development of lithium argyrodite solid-state electrolytes for solid-state batteries: synthesis, structure, stability and dynamics. *Nano Energy*, 2021, **83**, 105858.
3. Y. Zhao, F. Zhao, X. Sun*, et al. Atomic/molecular layer deposition for energy storage and conversion. *Chem. Soc. Rev.*, 2021, **50**, 3889-3956.
4. F. Zhao, X. Sun*, et al. Ultrastable anode interface achieved by fluorinating electrolytes for all-solid-state Li metal batteries, *ACS Energy Lett.* 2020, **5**, 1035-1043
5. F. Zhao, X. Sun*, et al. A Versatile Sn-Substituted Argyrodite Sulfide Electrolyte for All-Solid-State Li Metal Batteries, *Adv. Energy Mater.* 2020, **10**, 1903422.
6. F. Zhao, X. Sun*, et al. An Air-Stable and Li-Metal-Compatible Glass-Ceramic Electrolyte enabling High-Performance All-Solid-State Li-Metal Batteries. *Adv. Mater.* 2021, **33**, 2006577.
7. F. Zhao, X. Sun*, et al. Tuning bifunctional interface for advanced sulfide-based all-solid-state batteries. *Energy Storage Mater.* 2020, **33**, 139-146.
8. C. Wang, F. Zhao, X. Sun* et al. Manipulating Interfacial Nanostructure to Achieve High-Performance All-Solid-State Lithium-Ion Batteries, *Small Methods*, 2019, **3**, 1900261.
9. S. Deng, X. Sun*, et al. Dual-functional interfaces for highly stable Ni-rich layered cathodes in sulfide all-solid-state batteries *Energy Storage Mater.* 2020, **27**, 117-123.
10. S. Deng, X. Sun*, et al. Eliminating the Detrimental Effects of Conductive Agents in Sulfide-Based Solid-State Batteries, *ACS Energy Lett.* 2020, **5**, 1243-1251.
11. C. Wang, X. Sun* et al. *Adv. Energy Mater.*, 2021, 2100210. doi:10.1002/aenm.202100210.
12. X. Yang, X. Sun*, et al., Recent Advances and Perspectives on Thin Electrolytes for High-Energy-Density Solid-State Lithium Batteries. *Energy & Environmental Science*, 2020, doi.org/10.1039/D0EE02714F.

8:30 AM *EN09.05.02

Structural and Ion Conduction Properties of Sulfide-Based Solid Electrolyte Materials [Saiful Islam](#); University of Bath, United Kingdom

It is clear that a deeper understanding of metal sulfide materials for solid state batteries requires greater insights into their underlying structure-property relationships. This talk will highlight recent studies in two related areas: (i) Na₃PS₄ is one of the most promising Na-ion conductors, and our studies indicate a new high temperature polymorph showing fast-ion conduction associated with rotational motion of the thiophosphate poly-anions; (ii) nanoscale effects on sulfide-based lithium-ion conductors are investigated with the results indicating enhancement in ion conductivity due to changes in local structure and ion diffusion pathways. A combination of materials modelling and experimental methods has helped us gain new insights into sulfide materials, which are valuable in developing strategies to optimize their solid electrolyte properties.

T. Famprikis et al., *J. Am. Chem. Soc.*, **142**, 18422 (2020); *ACS Mater. Lett.*, **1**, 641 (2019); *Nature Mater.*, **18**, 1278 (2019).

9:00 AM *EN09.05.03

With a Little Help from ³¹P: Localized Hopping and Long-Range Li⁺ Transport in Argyrodite-Type Li₆PS₅I and Related Compounds [Katharina Hogrefe](#) and H. Martin R. Wilkening; Graz University of Technology, Austria

Site-disordered thiophosphates of the formula Li₆PS₅X (X = Br, Cl) are considered as the most promising solid electrolytes for all-solid-state lithium batteries with respect to their superior Li⁺ diffusion properties [1]. Also for Li₆PS₅I, with its ordered anion and cation sublattice, ⁷Li (and ³¹P) nuclear magnetic resonance (NMR) measurements suggest rapid localized Li⁺ exchange processes. However, the missing site disorder of Li₆PS₅I does only result in poor long-range ion transport as verified by conductivity spectroscopy [1]. Here, we compare results from ³¹P spin-lock NMR measurements with recent results from 1/T_{1ρ} ⁷Li NMR experiments [1] to shed light on the pronounced bimodal diffusion behaviour seen in Li₆PS₅I. The observation of ³¹P via spin-lock NMR offers a another perspective to look at ion diffusion within solids. The influence of rotational jump processes of the PS₄³⁻ poly-anions on Li⁺ dynamics (and *vice versa*) is discussed as well [2,3]. In conclusion, site disorder in the Li₆PS₅X family is the key property to understand the extraordinarily high Li⁺ self-diffusivities seen by NMR for the samples with X = Br, Cl [4]. In addition, we will discuss the influence of nanostructuring on Li diffusion in high-energy ball milled Li₆PS₅I [5] and Li₁₀GeP₂S₁₂ (LGPS). In structurally disordered Li₆PS₅I an increase in ion conductivity by 2 orders of magnitude is observed. Hence, Li₆PS₅I turned out to be a suitable model system to study the influence of local disorder by both broadband conductivity spectroscopy and NMR relaxation techniques [5].

References

- [1] I. Hanghofer, M. Brinek, S. L. Eisbacher, B. Bitschnau, M. Volck, V. Hennige, I. Hanzu, D. Rettenwander, H. M. R. Wilkening, *Phys. Chem. Chem. Phys.* **21** (2019) 8489.
- [2] I. Hanghofer, B. Gadermaier, and H. M. R. Wilkening, *Chem. Mater.* **31** (2019) 4591.
- [3] M. Brinek, C. Hiebl, K. Hogrefe, I. Hanghofer, and H. M. R. Wilkening, *J. Phys. Chem. C* **124** (2020) 22934.
- [4] M. Gombotz, K. Hogrefe, R. Zettl, B. Gadermaier, and H. M. R. Wilkening, *Phil. Trans. A*, 2021, in press.
- [5] M. Brinek, C. Hiebl, H. M. R. Wilkening, *Chem. Mater.* **32** (2020) 4754.

9:30 AM EN09.05.04

Deconvoluting Structural and Dynamic Contributions to the Activation Barrier in Solid State Electrolytes [Paul Till](#)¹, Matthias Agne² and Wolfgang Zeier¹; ¹University of Münster, Germany; ²Research-Center Jülich, Germany

Highly conductive solid electrolytes are necessary to build well performing All Solid-State Batteries with high energy densities.^{1,2} However, the discovery and optimization of suitable solid electrolyte materials has been limited, in part due to the lack of a fundamental understanding of the connection between the crystal structure, lattice dynamics and the diffusion process.³ Many of the established connections have been investigated through one-dimensional solid-solution type substitution experiments, where one atom is exchanged for another and corresponding changes in ionic transport are monitored.⁴ However, the simultaneous alterations of the crystal structure and lattice dynamics in these substitution series makes it extremely challenging to discern different influences on the transport properties. Herein we utilize a two-dimensional solid solution approach to show that the correlation of structure-based metrics with ionic transport can be misleading, whereas dynamical descriptors (e.g. bond strengths) may be more pertinent to the activation barrier in some fast ionic conductors. Specifically, we use the model Na₃P_{1-x}Sb_xS_{4-y}Se_y system, comprised of the four substitution series Na₃P_{1-x}Sb_xS₄, Na₃P_{1-x}Sb_xSe₄, Na₃PS_{4-y}Se_y and Na₃SbS_{4-y}Se_y, to systematically decouple static and dynamic contributions to the activation barrier. This study indicates that lattice dynamical properties cannot be overlooked in assessing trends of the activation barrier in solid electrolyte substitution series.

- (1) Culver, S. P.; Koerver, R.; Krauskopf, T.; Zeier, W. G., Designing Ionic Conductors: The Interplay between Structural Phenomena and Interfaces in Thiophosphate-Based Solid-State Batteries. *Chem. Mater.* **2018**, *30* (13), 4179–4192. <https://doi.org/10.1021/acs.chemmater.8b01293>.
- (2) Janek, J.; Zeier, W. G., A Solid Future for Battery Development. *Nat. Energy* **2016**, *1* (16141). <https://doi.org/10.1038/nenergy.2016.141>.
- (3) Ohno, S.; Banik, A.; Dewald, G. F.; Kraft, M. A.; Krauskopf, T.; Minafra, N.; Till, P.; Weiss, M.; Zeier, W. G., Materials Design of Ionic Conductors for Solid State Batteries. *Prog. Energy* **2020**, *2*, 022001. <https://doi.org/10.1088/2516-1083/ab73dd>.
- (4) Krauskopf, T.; Pompe, C.; Kraft, M. A.; Zeier, W. G., Influence of Lattice Dynamics on Na⁺ Transport in the Solid Electrolyte Na₃PS_{4-x}Se_x. *Chem. Mater.* **2017**, *29*, 8859–8869.
- (5) Schlem, R.; Ghidui, M.; Culver, S. P.; Hansen, A. L.; Zeier, W. G., Changing the Static and Dynamic Lattice Effects for the Improvement of the Ionic Transport Properties within the Argyrodite Li₆PS_{5-x}Se_xI. *ACS Appl. Energy Mater.* **2020**, *3* (1), 9–18. <https://doi.org/10.1021/acs.aem.9b01794>.
- (6) Bachman, J. C.; Muy, S.; Grimaud, A.; Chang, H.-H.; Pour, N.; Lux, S. F.; Paschos, O.; Maglia, F.; Lupart, S.; Lamp, P.; Giordano, L.; Shao-Horn, Y., Inorganic Solid-State Electrolytes for Lithium Batteries: Mechanisms and Properties Governing Ion Conduction. *Chem. Rev.* **2015**, *116* (1), 140–162. [doi:10.1021/acs.chemrev.5b00563](https://doi.org/10.1021/acs.chemrev.5b00563).

9:45 AM EN09.05.02

High Capacity Retention in Lithium Batteries Utilizing Nano Iron Sulfide Particles Noah B. Schorr, Igor Kolesnichenko, Laura Merrill, Katharine L. Harrison and Timothy N. Lambert; Sandia National Laboratories, United States

The high theoretical specific capacity of 893 mAh/g and energy density of 1273 Wh/kg of FeS₂ make it an attractive choice to pair with a lithium anode for next generation batteries. Development and implementation of secondary FeS₂/Li batteries has been hampered for a variety of reasons including soluble polysulfide formation which causes capacity loss and cell death. Another factor has been a lack of suitable electrolyte for cycling both the FeS₂ cathode and Li anode, with high coulombic efficiency. This talk will focus on the synthesis of FeS₂ nanoparticles, choice of a suitable electrolyte, and cycling protocol to enabling stable cycling of a FeS₂/Li cell. By cycling the nano FeS₂ in a concentrated bisalt electrolyte with a charging voltage cutoff of 2.4 V we have achieved 80 cycles (at the time of this submission) with an average discharge capacity of 421 mAh/g, well above 80% capacity retention under this condition. Using Cu/Li cells we show the plating/stripping of Li in the bisalt electrolyte has an average coulombic efficiency of 98.8% over 50 cycles and 99.1% for the last 40 cycles. Furthermore, we show that the high performance cycling of the cathode and anode is attributed not only to use of a bisalt electrolyte, but also by ensuring a submicron domain size of the FeS₂ particles to mitigate polysulfide generation.

This work was supported by the Laboratory Directed Research and Development program at Sandia National Laboratories, a multi-mission laboratory managed and operated by National Technology and Engineering Solutions of Sandia, LLC., a wholly owned subsidiary of Honeywell International, Inc., for the U.S. Department of Energy's National Nuclear Security Administration under contract DE-NA-0003525. The views expressed herein do not necessarily represent the views of the U.S. Department of Energy or the United States Government.

SESSION EN09.06: Metal Sulfides in Batteries IV
Session Chairs: Yang Li and Hui Wang
Monday Morning, December 6, 2021
EN09-Virtual

10:30 AM *EN09.06.02

Phase Control and Microstructure Engineering in Thiophosphate Solid Electrolytes Bettina V. Lotsch^{1,2}; ¹Max Planck Institute, Germany; ²University of Munich (LMU), Germany

Solid electrolytes (SEs) are at the heart of all-solid-state batteries (ASSBs), which promise higher energy density along with safer operation compared to commercial Li ion batteries. As the ASSB technology matures, research in the field needs to respond to questions pertaining to the upscaling of solid electrolytes, their stability, and the integration of the individual components into ASSBs with extended cycle life. As a consequence, new research areas have been emerging lately, including interfacial engineering and microstructure design, and questions such as the role of stack pressure on battery performance increasingly enter the focus of ASSB design.

This presentation will discuss the development and optimization of lithium^{1,2} and sodium³ thiophosphate SEs based on three complementary approaches, which address both the atomistic level and microstructure of SEs:

(i) We highlight the importance of phase engineering and hybridization in thiophosphate solid electrolytes, exemplified by the discovery of two new polymorphs of Na₄P₂S₆ and the formation of composite thiophosphate SEs.⁴ Our results showcase how synthetic control and post-synthetic treatment of solid electrolytes can significantly impact the materials properties, even though structural differences may be minute or even hidden by the glassy ceramic character of many thiophosphates.⁵

(ii) The development of solution processing routes for the thiophosphate Li₇SiPS₈ is demonstrated, revealing that aprotic solvents with donor numbers smaller than 15 kcalmol⁻¹ are suitable for wet processing, since both crystal structure of the SE and high ionic conductivities (> 1 mScm⁻¹) are retained.⁶

(iii) Finally, we pinpoint the role of moderate pressure on the microstructure of SEs and demonstrate its complex impact on the Li ion conductivity of LGPS-type SEs.

Taken together, our findings reinforce the notion that a holistic picture of a SE – including its atomistic structure, defect- and disorder-related phenomena, as well as its microstructure – is needed to understand and accurately predict its function in a realistic ASSB environment.

Literature:

- [1] A. Kuhn, O. Gerbig, C. Zhu, F. Falkenberg, J. Maier, B.V. Lotsch, *Phys. Chem. Chem. Phys.* **2014**, *16*, 14669–14674.
 [2] A. Kuhn, J. Köhler, B.V. Lotsch, *Phys. Chem. Chem. Phys.* **2013**, *15*, 11620–11622.
 [3] S. Harm, A.-K. Hatz, C. Schneider, C. Hofer, C. Hoch, B.V. Lotsch, *Front. Chem.* **2020**, *8*:90.
 [4] T. Scholz, C. Schneider, R. Eger, V. Duppel, I. Moudrakovski, A. Schulz, J. Nuss, B.V. Lotsch, *J. Mater. Chem. A* **2021**, *9*, 8692–8703.
 [5] S. Harm, A. Hatz, I. Moudrakovski, R. Eger, A. Kuhn, C. Hoch, B. V. Lotsch, *Chem. Mater.* **2019**, *31*, 1280–1288.
 [6] A.-K. Hatz, R. Calaminus, J. Feijoo, F. Treber, J. Blahusch, T. Lenz, M. Reichel, K. Karaghiosoff, N. M. Vargas-Barbosa, B. V. Lotsch, *submitted*.

11:00 AM *EN09.06.03

Fast Sodium Diffusion and Anharmonic Phonons Olivier Delaire¹, Mayanak K. Gupta^{1,2}, Jingxuan Ding¹, Naresh Osti³, Doug L. Abernathy³, William Arnold⁴, Hui Wang⁴ and Zachary Hood⁵; ¹Duke University, United States; ²Bhabha Atomic Research Centre, India; ³Oak Ridge National Laboratory, United States; ⁴University of Louisville, United States; ⁵Argonne National Laboratory, United States

Solid electrolytes (SEs) exhibit complex atomic dynamics, featuring simultaneous facile hopping of mobile species and soft lattice dynamics of the host lattice. Importantly, fast diffusion involves large-amplitude motions on strongly anharmonic potential energy surfaces, and such anharmonic effects need to be assessed when investigating phonons and their coupling with the stochastic hopping underlying the diffusion process. Phonons describe the atomic dynamics in crystalline materials and provide a basis to encode possible minimum energy pathways for ion migration. Identifying and controlling the pertinent phonon modes coupled most strongly with ionic conductivity could pave the way for discovering and designing new SEs via phonon engineering. This talk will report on investigations of phonons in Na₃PX₄ and Na₃SbX₄ (X=S, Se), highlighting strong anharmonic effects and their coupling to fast Na diffusion, using a combination of neutron scattering, ab-initio molecular dynamics (AIMD) and machine-learning accelerated MD. We identify specific anharmonic soft-modes that strongly couple with the Na diffusion process, and show how these modes enable Na-ions to hop along the minimum energy pathways. Further, our quasi-elastic neutron scattering (QENS) measurements, supplemented with large-scale molecular dynamics simulation, provide the Na diffusion constant and the diffusion characteristics. These results offer detailed microscopic insights into the dynamic mechanism of fast Na diffusion and provide an avenue to search for further Na solid electrolytes.

11:30 AM EN09.06.04

Don't Trust Fool's When Looking for Gold—Iron Sulfide as Cathode Material for Mg-Batteries Michael Wilhelm, Veronika Brune, Fabian Hartl and Sanjay Mathur; University of Cologne, Germany

The big market of energy storage systems is mainly dominated by the widely available and conventional lithium-ion batteries (LiBs). Low earth-abundance of lithium and the use of not sustainable cathode materials, like lithium cobalt oxide's, are currently bottlenecks of the commercially available LiBs. In quest of new cathode materials, metal sulfide getting more and more attention to be next-generation cathode materials. Nevertheless, achieving high capacity and good cycling stability are remaining challenges. Especially, pyrite (FeS₂), also known as fool's gold, is a promising candidate to overcome the issues of availability (iron = 5.6 %; sulfur = 0.035 %) and specific capacity (894 mAh g⁻¹). Moreover, by changing the battery setup from lithium to magnesium the energy storage technology can be even more sustainable (Li = 0.002 %; Mg = 2.4 %). Crucial to achieving good energy storage performance of the metal sulfides is the size and shape of the particles in the electrode which affects the thermodynamic properties. Different analogs of iron sulfides (FeS, Fe₃S₄, and Fe₇S₈) were investigated as cathode material in combination with a magnesium metal anode and characterized by XPS, SEM, and Raman spectroscopy. The influences of the particle size and additives were studied, and demonstrators were successfully manufactured. Additionally, the effect of carbon additives, like CNF and rGO, on the performance of the battery was investigated.

11:45 AM EN09.06.05

Redox Mediated Li-S Flow Battery for Grid-Scale Energy Storage Applications Melissa Meyerson and Leo J. Small; Sandia National Laboratories, United States

There is a need for safe, reliable, and inexpensive batteries with high capacity for grid storage applications. The high capacity (1675 mAh/g) and low cost (~0.1 \$/kg) of sulfur make Li-S batteries an excellent candidate for this; however, S has poor electrical conductivity and the proximity of Li to the cathode in conventional batteries can present a safety hazard at grid scale. We address these problems by designing a highly scalable, membrane free redox-mediated Li-S flow battery. Benefits of this design include: 1) The presence of soluble redox mediators enable the reduction/oxidation of the S without the need for conductive carbon additives. 2) The physical separation of the Li anode from the cathode reduces the risk of short circuiting and propagating battery fires. 3) The use of electrolyte additives enables stable Li plating on the anode which improves the cell efficiency, extends the cycle life, and removes the need for expensive solid state separators. We chose decamethyl ferrocene (DmFc, 2.86 V vs Li/Li⁺) and cobaltocene (CoCp₂, 2.06 V vs Li/Li⁺) as redox mediators for their proximity to the redox potential of the Li-S reaction. During cycling, these mediators help chemically oxidize or reduce the S without the need for electrical contact between the S and the electrode. Instead, the soluble mediators are electrochemically oxidized or reduced at the electrode. In order to address the non-uniform deposition of Li on Li metal anodes, we presoaked the Li metal in a LiI solution to form a more stable solid electrolyte interphase (SEI) and used LiNO₃ in the electrolyte to improve the stability of the Li deposition. To examine the Li surface chemistry and explain the cycling performance, we conducted pre- and post-cycling characterization of the system. Characterization with x-ray photoelectron spectroscopy and energy dispersive x-ray spectroscopy revealed the presence of uniformly dispersed LiI in the SEI on the Li before cycling, which improves the uniformity of Li deposition on the anode. Scanning electron microscopy revealed globular, rather than filament-like, Li deposition, which is attributed to the presence of LiNO₃ in the electrolyte and explains the high coulombic efficiency and cycle life. UV-vis spectroscopy revealed a decrease in the amount of polysulfides present in the electrolyte between 50 and 200 cycles, indicating that the observed capacity loss is likely due to the loss of available sulfur. The combination of the redox mediators and additives enabled our cells to cycle stably for 200 cycles with an average coulombic efficiency of 99.0% and a voltage efficiency of 82.0%.

Sandia National Laboratories is a multi-mission laboratory managed and operated by National Technology and Engineering Solutions of Sandia, LLC., a wholly owned subsidiary of Honeywell International, Inc., for the U.S. Department of Energy's National Nuclear Security Administration under contract DE-NA0003525.

SESSION EN09.07: Metal Sulfides in Batteries V

Session Chair: Hongli Zhu

Monday Afternoon, December 6, 2021

EN09-Virtual

1:00 PM *EN09.07.01

Computation Guided Design of All-Around Solid Electrolytes for Solid-State Batteries Yifei Mo; University of Maryland, United States

All-solid-state batteries using ceramic solid electrolyte is promising next-generation battery technology. To enable a high-performance solid-state battery, the solid electrolytes need to exhibit high ionic conductivity, wide electrochemical window, interfacial compatibility with anode and cathode, multiple mechanical properties, and air/moisture stability. However, no single solid electrolyte material can satisfy all these desired attributes. For example, sulfides have the highest ionic conductivity but exhibit narrow electrochemical windows and notoriously poor air stability, whereas oxides generally exhibit better

stability but lower ionic conductivity. In order to develop all-around solid electrolytes, our first-principles computation will provide guiding principles and design strategies for improving ionic conductivity, electrochemical window, air stability in solid electrolyte materials. We will also show new solid electrolyte materials systems discovered and designed by computation through an accelerated fashion.

1:30 PM *EN09.07.02

Interplay of Structural Disorder, Site-Disorder and Ionic Conductivity of Superionic Conductors—Insights from Atomistic Computer Simulations Marcel Sadowski and Karsten Albe; TU Darmstadt, Germany

Glassy, glass-ceramic, and crystalline lithium thiophosphates have attracted interest in their use as solid electrolytes in all-solid-state batteries. Despite similar structural motifs, including PS_4^{3-} , $P_2S_6^{4-}$, and $P_2S_7^{4-}$ polyhedra, these materials exhibit a wide range of possible compositions, crystal and amorphous structures, as well as ionic conductivities. Calculations based on density functional theory can be a helpful tool for understanding diffusion pathways and Li^+ ionic conductivity and interface stabilities.

In this contribution I will first discuss recent results on the defect chemistry and conductivity of the solid electrolyte $Li_4P_2S_6$ as well as its interfacial instability with respect to Li. Then, molecular dynamics simulations of crystalline and amorphous Li_4PS_4I will be shown, which unravel the diffusion mechanism and can be explained by a rate-equation model based on superbasins. Finally, results on the Lithium argyrodites of the type Li_6PS_3X ($X = Cl, Br, I$) are presented, where the influence of S_2 -/Br- site-disorder was studied. The simulations reveal that local “Li cages” trap Li ions in the ordered material. At higher degrees of site-disorder the cage structures dissolve and long-range low energy pathways are established. The analysis of pair distribution functions (PDF) and Li-density maps elucidates the correlation between structural disorder and ionic conductivity.

[1] C Dietrich, M Sadowski, S Sicolo, DA Weber, SJ Sedlmaier, KS Weldert, et al, Chemistry of Materials 2016, 28, 8764-8773

[2] M Sadowski, S Sicolo, K Albe, Solid State Ionics 2018, 319, 53-60

[3] S. Sicolo, C. Kalcher, S. Sedlmaier, J. Janek, K. Albe, Solid State Ionics, 2018, 319, 83-91

[4] A Gautam, M Sadowski, N Prinz, H Eickhoff, et al., Chemistry of Materials, 2019, 31, 10178-10185

[5] M Sadowski, K. Albe, J. Power Sources 2020, 478, 229041

[6] M. Sadowski, K. Albe, Phil. Trans. A, 2021

2:00 PM *EN09.07.03

Discovery of New Compounds as Li-Ion and Na-Ion Conductors for All-Solid-State-Batteries Hailong Chen; Georgia Institute of Technology, United States

High performance solid state ionic conductors are much desired as the solid electrolyte for all-solid-state-batteries. The solid electrolyte materials are required to have high room temperature ionic conductivity, low electronic conductivity, good chemical and electrochemical stabilities, and good mechanical properties, and low cost. With these expectations, in recent years we have design and discovered a number of new compounds with promising Li-ion and Na-ion conduction properties, including oxide, sulfide and halide compounds. In this MRS conference we will report some of our recent findings, including sulfide Li-ion conductors with argyrodite structure, halides with layered structures, and Na-ion conductors with modified cubic structures. These compounds all show very high room temperature ionic conductivities and good performance in the cycling test of all solid state batteries. High resolution synchrotron X-ray and neutron scattering techniques, solid state NMR and electron microscopy were complementarily used to reveal the structure-property relationships in these compounds. The impacts of synthesis condition, chemical composition and processing to the ionic conductivity and battery performances will be discussed.

2:30 PM EN09.07.04

Lithiation Mechanism and Structure-Performance Properties of SnS and SnS₂ Anode Active Materials for Lithium-Ion Batteries Damian M. Cupid¹, Albina Glibo^{1,2}, Nicolas Eshraghi¹, Hans Flandorfer² and Marcus Jahn¹; ¹AIT Austrian Institute of Technology GmbH, Austria; ²University of Vienna, Austria

Metal chalcogenides such as SnS₂ and SnS are promising anode materials for lithium-ion batteries as their theoretical reversible capacities (644 mAh/g for SnS₂ and 755 mAh/g for SnS) are significantly higher than that of graphite (372 mAh/g). SnS₂ exhibits a layered, hexagonal CdI₂-type crystal structure, in which each Sn⁴⁺ ion is octahedrally coordinated by S ions with S–Sn–S stacking across the crystallographic *c*-direction. On the other hand, α-SnS can be considered as a “pseudo-2D” orthorhombic structure in which each Sn²⁺ ion is coordinated to three S ions within the layer. The complete lithiation of SnS takes place via successive conversion and alloying reactions. In the conversion reaction, an electrochemically inactive but ionically conductive Li₂S matrix is formed, which buffers the volume change of Sn (~ 300% for formation of Li₁₇Sn₄) during the alloying reaction. On the other hand, due to the higher +4 oxidation state of the Sn ions in SnS₂ as well as the presence of vacant interstitial sites in the crystal lattice, the lithiation of SnS₂ starts with the intercalation of lithium ions into the octahedral sites between the S–Sn–S layers. This is followed by the conversion and alloying reactions as for SnS.

In the literature, the electrochemical performance properties of SnS₂ and SnS have been investigated separately from each other, so that there is a lack of comparative data for SnS and SnS₂ anodes with comparable particle morphologies and subjected to the same electrochemical test conditions. Therefore, the motivation of this work is to establish the structure–processing–property relations of SnS₂ and SnS anode active materials with similar particle morphologies, understand the fundamental lithiation mechanisms of both, and elucidate their degradation mechanisms under long-term cycling. In all our experiments, a single, commercially available SnS₂ powder with ~ 10 μm particle size was used as the starting material.

In the first step, XRD, SEM and laser diffraction were performed on the pristine SnS₂ micro-powder to characterize its crystal structure, particle morphology and particle size distribution. Differential thermal analysis, thermogravimetric analysis and heat-treatment experiments in flowing argon followed by XRD with Rietveld refinement of the measured diffraction patterns were conducted to understand the phase transformation kinetics of pristine SnS₂ to SnS. Based on these results, phase pure SnS was synthesized from pristine SnS₂ by subjecting it to heat treatments at T > 700°C in Argon atmosphere.

To produce the anode active materials, pristine SnS₂ and SnS synthesized by the thermal decomposition of SnS₂ were subjected to high-energy ball-milling in ZrO₂ bowls at 200 rpm in an argon atmosphere. This processing yields SnS₂ and SnS nanoparticles with similar morphologies. The anode active materials were subjected to electrochemical testing including galvanostatic cycling, cyclic-voltammetry, impedance spectroscopy, galvanostatic titration and in-situ dilatometry to quantify their structure–performance properties. Furthermore, ex-situ XRD was performed on electrodes at different states of charge to characterize the discharge reaction mechanism, and SEM and XRD were performed on electrodes after 100 discharge/charge cycles to assess the change in structure of the active anode materials after cycling.

Our results show that although the theoretic reversible capacity of SnS is larger than that of SnS₂, SnS₂ performs better during long term cycling. This is attributed to the intercalation of lithium into the SnS₂ crystal structure before the conversion mechanism. This crucial step generates a finer distribution of Li₂S, which is better suited to buffer the volume changes of the Sn particles during successive lithiation/de-lithiation steps.

2:45 PM EN09.07.05

Novel Metal/Sulfur High-Loading Cathodes in Low-Electrolyte Lithium-Sulfur Batteries Sheng-Heng Chung and Cun-Sheng Cheng; National Cheng Kung University, Taiwan

The lithium-sulfur battery is a promising candidate for next-generation electrical energy storage. The inexpensive, naturally abundant, and environmentally benign sulfur cathode offers an order of magnitude higher theoretical charge-storage capacity ($1,672 \text{ mAh g}^{-1}$) than the those of currently used insertion-compound cathodes. However, as a new energy-storage battery system, the lithium-sulfur battery cathodes suffer both material and electrochemical challenges. The sulfur cathode and its end-discharge sulfide products are both good insulators. The high cathode resistance causes a low and irreversible electrochemical utilization of the cell. The conversion between sulfur and sulfides generates liquid polysulfides, which readily diffuse out of the cathode and migrate in the cell. The irreversible migration of polysulfides within the cells results in the fast capacity fade and poor discharge/charge efficiency. Moreover, the low electrochemical utilization and stability challenge the design and fabrication of a high-performance sulfur cathode with a necessary high amount of sulfur and a desired low amount of electrolyte in a cell. The inappropriate cathode design impacts the sulfur cathode electrochemistry, which impedes the development of sulfur cathodes with high energy density and the commercialization of the lithium-sulfur technology.

In our presentation, we present innovations on metal-sulfur nanocomposite possessing a conductive metal nanoshell coated on sulfur particles to improve the conductivity of sulfur cathode, the stabilization of polysulfides, and the reaction kinetics of lithium-sulfur batteries. We adopt the electroless-nickel plating method to synthesize the nickel/sulfur nanocomposite features a multi-functional nickel nanoshell. The metallic coating provides the metal/sulfur nanocomposite with high conductivity. Moreover, nickel has the high polysulfide trapping capability and strong electrocatalytic capability. As a result of these critical advantages in sulfur cathode, the metal/sulfur nanocomposite exhibits excellent lithium-sulfur battery performance, showing high electrochemical utilization and kinetics with high discharge capacity of above $1,000 \text{ mAh g}^{-1}$ and excellent rate capability of $C/20$ - $C/2$ rates with stable cyclability for 200 cycles. These improved electrochemical performances are realized by the high-loading cathode with a high sulfur content of 74 wt% and a high sulfur loading of 14 mg cm^{-2} in a lean-electrolyte lithium-sulfur battery with a low electrolyte-to-sulfur ratio of $7 \mu\text{L mg}^{-1}$. The simultaneous improvement in the outstanding material and electrochemical characteristics results in high areal and gravimetric capacities along with a high energy density of 28 mWh cm^{-2} . In conclusion, the superior material design and electrochemical characteristics obtained by our nickel/sulfur nanocomposite as the high-loading sulfur cathode in a lean-electrolyte lithium-sulfur cells make its advanced cathode designs for the development of high-energy-density lithium-sulfur batteries.

SESSION EN09.08: Metal Sulfides in Batteries VI

Session Chair: Hui Wang

Monday Afternoon, December 6, 2021

EN09-Virtual

4:00 PM *EN09.08.02

Metal-Sulfur Batteries with Stabilized Sulfur Cathodes and Metal Anodes [Arumugam Manthiram](#); The University of Texas at Austin, United States

Metal-sulfur batteries offer tremendous advantages compared to lithium-ion batteries in terms of cost and energy density as sulfur is abundant, inexpensive, and environmentally benign, and both sulfur cathode and metal anodes offer much higher capacities. However, the practical viability of metal-sulfur batteries is hampered by the low energy density and poor cycle life in practical cells. These challenges originate from the poor electronic and ionic conduction in sulfur and its discharged products, polysulfide shuttle, and poor cyclability of metal anodes. To overcome some of these difficulties, generally a large amount of conductive carbon and liquid electrolyte are added to the cell; they enhance the cycle life, but drastically lower the practical energy density and make the metal-sulfur batteries uncompetitive with lithium-ion batteries. On the other hand, it is challenging to manufacture and handle thin lithium-metal or sodium-metal foils, drastically increasing their cost.

To overcome the above challenges, this presentation will first focus on anode-free cells, in which lithium sulfide (Li_2S) cathode is paired with an anode current collector without any free lithium at the anode. The anode-free cells eliminate the handling and manufacturing issues associated with thin lithium-metal foils, increase the cell energy density, and suppress self-discharge before deploying the cells as the cells are assembled in the discharged state similar to the currently used lithium-ion cells. To stabilize lithium-metal plating and stripping, a small amount of additive is incorporated into the Li_2S cathode. The presentation will first present the effect of the incorporation of a small amount of tellurium as a case study. Being in the same group as sulfur in the periodic table, but with a metalloid behavior, tellurium substitutes into polysulfides to form polytellurosulfides, which migrate to the anode and get reduced to form Li_2TeS_3 as a thin, lithium-ion conducting solid-electrolyte interphase (SEI) layer on the plated lithium metal. This enables a uniform deposition of lithium and mitigates the severe electrolyte decomposition, enabling the assembly of cells with less amount of electrolyte. As a result, remarkable improvement in cyclability and capacity is achieved in energy-dense, anode-free full cells and lean-electrolyte pouch cells with high sulfur loading. The mechanisms involved in the drastic improvement in the performance is elucidated with in-depth characterization methodologies, such as time-of-flight secondary ion spectrometry (TOF-SIMS), x-ray photoelectron spectroscopy (XPS), nuclear magnetic resonance (NMR) spectroscopy, *etc.* The speciation with TOF-SIMS is particularly valuable to delineate the dynamics involved in lithium plating and stripping as well as to understand the chemistry involved.

The presentation will then focus on the incorporation of other additives to engineer the behavior of dissolved polysulfides in order to stabilize both the sulfur cathode and lithium-metal plating and stripping. The role of additives on the electrochemical performances will be illustrated with pouch cells fabricated with high sulfur loading and low electrolyte/sulfur ratio to be practically viable. Then, the presentation will transition to employ some of the understanding gained with lithium-sulfur batteries to sodium-sulfur batteries. Long-life, dendrite free sodium-sulfur cells will be presented, including pouch cell performances, with appropriate engineering of the cell chemistry.

4:30 PM *EN09.08.03

Design of Stable Cathodes for Solid State Li-S Batteries [Ping Liu](#); University of California, San Diego, United States

Solid state Li-S battery promises high energy density and low cost. Multiple challenges remain for the sulfur cathode. S is insulating and experiences large volume changes during cycling. In this talk, we will report our recent effort in developing polymer-S composite materials to address these challenges. The first class of material is based on sulfurized polyacrylonitrile (SPAN). SPAN contains ~45% of S and demonstrates excellent cycling stability due to small volume change. Its capacity is limited to ~600 mAh/g with a discharge voltage of 1.8 V. In order to further improve materials energy density, we have investigated polymer-S materials with higher S content. SPAN has an approximate formula of C_3NS . The carbon content can be reduced to a unit formula of CNS in poly (SCN). The material can be synthesized with free radical oxidation of SCN salts. The material demonstrates an average voltage of 2.1 V with a capacity of 700 mAh/g, thus a much higher energy density than SPAN. Further optimization of materials morphology and cell fabrication will pave the way towards a long-life solid state Li-S battery.

5:00 PM *EN09.08.04**Highly Ion-conductive, Ultrathin, and Robust Sulfide Solid Electrolyte Membrane** Daxian Cao, Qiang Li, Xiao Sun and Hongli Zhu; Northeastern University, United States

Sulfide solid-state electrolytes (SEs) featured with nonflammability and superior ionic conductivity ($>10^{-3}$ S cm⁻¹) enable all-solid-state lithium batteries (ASLBs) to deliver safer and more reliable energy storage. However, current sulfides-based ASLBs exhibit far below expected energy densities at the cell level (<50 Wh kg⁻¹, <100 Wh L⁻¹), due to the employment of SE membranes with extreme high thickness (>500 μm), large weight (>150 mg cm⁻²), and high areal resistance (>100 Ω cm²). The binder-assisted solution method is a promising strategy to fabricate a thin and robust sulfide SE membrane. However, the high sensitivity to polar solvents and natural brittleness of sulfide SE challenge the fabrication of thin, light-weight SE membranes with no sacrifice in ionic conductivity. To successfully fabricate a thin SE membrane with high ionic conductivity and mechanical strength, a critical step is to select a binder satisfying the following requirements: 1) excellent solubility and stability in the nonpolar solvent; 2) high stability with sulfide SE; 3) high thermal stability; 4) high binding strength. This work will report an advanced binder and a freestanding SE membrane with an ultralow thickness of 47 μm, ultralow areal resistance of 5.10 Ω cm², and superior ionic conductivity of 1.08 mS cm⁻¹, and the ultrahigh ion conductance of 190.11 mS. The ASLB utilizing this advanced SE membrane delivered cell-level high gravimetric and volumetric energy densities of 175 Wh kg⁻¹ and 675 Wh L⁻¹, individually.

SESSION EN09.09: Metal Sulfides in Batteries VII

Session Chair: Yoon Seok Jung

Monday Afternoon, December 6, 2021

EN09-Virtual

6:30 PM *EN09.09.01**Superionic Lithium Argyrodite Sulfide Electrolytes with Enhanced Air-Stability** Yongheum Lee^{1,2}, Jiwon Jeong^{1,3}, Hun-Gi Jung^{1,2}, Seungho Yu^{1,2} and Kyung Yoon Chung^{1,2}; ¹Korea Institute of Science and Technology, Korea (the Republic of); ²KIST School, Korea University of Science and Technology, Korea (the Republic of); ³Korea University, Korea (the Republic of)

Under the carbon reduction policy, the use of internal combustion engines and fossil fuels has been reduced and electric vehicles and renewable energy have begun to be widely distributed. Batteries are drawing attention as a means of using electric vehicles as electricity and storing renewable energy. However, due to the limitations of the capacity and stability of existing lithium-ion batteries, research is underway on next-generation batteries that can replace the above-mentioned applications.

One of the next-generation batteries that has close performance with existing lithium-ion batteries is sulfide based All Solid State Batteries (ASSBs). In general, the higher the ionic conductivity of used solid electrolytes, the greater the capacity. Sulfide solid electrolyte has relatively higher ionic conductivity than other solid electrolytes. In addition, sulfide solid electrolytes have soft property, making it easy to manufacture batteries with smooth inter-material contacts. It reduce internal resistance of batteries and improves batter performance. For this reason, many developments are underway for sulfide solid electrolytes with high ionic conductivity and soft properties. However, sulfide solid electrolyte is reactive because materials used in sulfide solid electrolyte is P₂S₅ precursor and P-S bond is relatively weak. Therefore the phosphorus in sulfide solid electrolyte react with water, making the electrolyte vulnerable to moisture. Recent studies have been developing chemically stable and high ionic conductive solid electrolytes by replacing or doping the solid electrolyte.

In this study, argyrodite structure sulfide solid electrolyte is synthesized using mechanical milling method. In addition, to improve moisture-weak properties and ionic conductivity, argyrodite sulfide solid electrolytes with other composition are synthesized using antimony and halogen elements. The electrochemical analysis was performed using synthesized solid electrolytes.

7:00 PM *EN09.09.02**Analyzing the Internal Resistance of a Sulfide-Based Solid-State Battery** Wonsung Choi, Hyeokjo Gwon, Jun Hwan Ku, Heung Chan Lee, Gabin Yoon and Dongmin Im; Samsung Advanced Institute of Technology, Korea (the Republic of)

The expectations on the solid-state batteries are growing fast. The employment of solid electrolyte instead of liquid not only provides a much better safety, but also enables the use of lithium metal anode, leading to a higher cell energy density [1]. Although it is widely accepted that Li dendrite can penetrate through the solid electrolyte layer causing internal short circuits [2], we have demonstrated that lithium metal anode can be successfully cycled with a proper design of the interfacial layer on the solid electrolyte [3].

High internal resistance is one of the remaining challenges that has to be addressed in the development of solid-state batteries. The ionic conductivity of some sulfide-based solid electrolytes (1 ~ 10 mS/cm) is comparable to that of liquid electrolytes with counting the cation transference number near unity. Nevertheless, the internal resistance of solid-state batteries is considered high due mainly to the interfacial behaviors between solid phases [4, 5]. The charge transfer resistances at the both electrodes and the bulk and grain boundary resistances of the electrolyte are the factors that contribute to the overall cell impedance.

In this work, the internal resistance of a sulfide-based solid-state battery is analyzed component by component. For example, the bulk resistance and the grain boundary resistance for the electrolyte inside the cathode are extracted separately with an AC method employing a transmission line model [6]. In addition, the influences of cell design and process will be discussed.

References

- [1] Y. Su et al., *Energy Environ. Sci.*, 2020, **13**, 908-916.
- [2] E. Kazyak et al., *Matter*, 2020, **2**, 1025-1048.
- [3] Y.-G. Lee et al., *Nat. Energy*, 2020, **5**, 299-308.
- [4] Y. Xiao et al., *Joule*, 2019, **3**, 1252-1275.
- [5] C. Yu et al., *Nat. Commun.*, 2017, **8**, 1086.

7:30 PM *EN09.09.03**High Donor Electrolyte Designs for Lithium-Sulfur Batteries with Lean Electrolyte Conditions** Jang Wook Choi; Seoul National University, Korea (the Republic of)

Li-S batteries have witnessed considerable progress in the past decades, mainly in terms of cycle life. The shuttling process, the main capacity fading mechanism, was addressed by a variety of approaches targeting all of sulfur cathode, separator, and electrolyte. Nevertheless, the main progress was based

on ether-based electrolytes with compatibility with Li metal counter electrode. To achieve more competitive energy density, electrolyte amount should be minimized thus satisfying the necessity of lean electrolyte conditions. In this talk, I will introduce recent progress in my lab in identifying high donor electrolytes. High solubility of polysulfides results directly in boosting the volumetric energy density. I will also discuss how to secure the compatibility with Li metal anode so that high donor electrolytes can be adopted in practically viable conditions.

8:00 PM EN09.09.05

New Halide Na⁺ Conductors Using Earth Abundant Elements for All-Solid-State Na⁺ Batteries [Hiram Kwak](#)¹, Jeyne Lyoo², Juhyoun Park¹, Yoonjae Han¹, Seung-Tae Hong² and Yoon Seok Jung¹; ¹Yonsei University, Korea (the Republic of); ²Daegu Gyeongbuk Institute of Science and Technology, Korea (the Republic of)

The application of lithium-ion batteries (LIBs) has been expanded from portable electronic devices to battery-driven electric vehicles and grid-scale energy storage systems. Accordingly, considerations about safety and cost issues have become a top priority. Specifically, the safety concerns originating from the use of flammable organic liquid electrolytes and the cost issues related to Li are serious obstacles. In this regard, the replacement of flammable liquid electrolytes with inorganic Na⁺ superionic conductors are considered as an ideal solution. Among various materials for Na⁺-conducting solid electrolytes (SEs), sulfide materials have drawn significant attraction with their high ionic conductivities and mechanical deformability, which enables scalable cold-pressing-based fabrication protocols. Unfortunately, due to the intrinsically narrow electrochemical windows, the sulfide SE materials undergo severe side reactions. They do not exhibit sufficient stability with the 3 V-class oxide cathode materials, such as NaCrO₂.

Recently, through the reinvestigations on halide SEs, Asano and coworkers reported that trigonal Li₃YCl₆ and monoclinic Li₃YBr₆ showed high Li⁺ conductivities of 0.51 and 1.7 mS cm⁻¹, respectively. More importantly, halide SEs, especially chloride compounds, exhibit the combined advantages of sulfide and oxide SEs: deformability and excellent (electro)chemical oxidation stability. Despite these advances in Li⁺-conducting halide SEs, reports on Na⁺-conducting halide SEs have been scarce.

In this presentation, our recent results on the development of new Na⁺-conducting halide SE, Na₂ZrCl₆, and their application to all-solid-state batteries will be presented.

SESSION EN09.10: Metal Sulfides in Batteries VIII

Session Chair: Daxian Cao

Monday Afternoon, December 6, 2021

EN09-Virtual

9:00 PM *EN09.10.01

Transition Metal Sulfides for High-Energy-Density Lithium Metal Battery Cathodes [Liping Wang](#)¹ and Hong Li^{2,3}; ¹University of Electronic Science and Technology of China, China; ²Institute of Physics, Chinese Academy of Sciences, China; ³Tianmulake Institute for Energy Storage, China

Li-free cathodes (e.g. FeS_x, FeF_x) demonstrate high operational voltages and high specific capacities, offering high energy densities for rechargeable lithium metal batteries. However, they suffer from severe capacity decay. Here, in this work, we synthesized a series of transition metal sulfides (M = Ti, V, Cr, Mn, Fe, Co, Ni, and Cu). We find that FeS_x demonstrates the best cycling stability and rate performances. Its electrochemical reaction mechanism is correspondingly revealed. Pouch cell using FeS_x as cathodes demonstrates a specific energy density of higher than 350 Wh kg⁻¹. This study reveals that Li-free cathodes will receive broad attentions, especially with the mature of Li metal and electrolyte.

9:30 PM *EN09.10.02

Design Strategies for the Development of Efficient Metal-S Batteries [Aninda J. Bhattacharyya](#); Indian Institute of Science, India

An important strategy for beyond Li-ion rechargeable battery chemistries has been to use cheaper earth-abundant and sustainable electroactive materials. In this line of thought, sulfur is an important example as it is available in considerable abundance and is non-toxic. Sulfur delivers a high theoretical capacity of 1672 mAh g⁻¹, nearly one order higher compared to the best of the intercalation cathodes (IOCs) used in Li/Na-ion batteries. Metal sulfur-based batteries function based on conversion reactions with the possibility of two exchangeable Li-ions per S-atom as compared to approximately one Li-ion/formula unit of IOC. The underlying electrochemistry in a liquid electrolyte-based metal-S battery poses several challenges. The formation of intermediate polysulfides during the reversible conversion of elemental S₈ to metal-sulfide is a major challenge. The majority of the published work focuses on the design of suitable conducting matrices targeted towards high S-loading and efficient entrapment of polysulfides. The initial part of the lecture will discuss a few of our contributions from this perspective for Li/Na/Mg-S batteries. Our work highlights the critical role of materials design and *in operando* studies for the development of highly stable metal-S batteries (Gomes et al. *ACS Sustainable Chem. Eng.* 2020; Bhardwaj et al *ACS Appl. Materials Interfaces. Eng.* 2020; *ACS Appl. Energy Mater.* 2018). The studies reveal several interesting fundamental insights related to the mechanism of storage which eventually has a strong bearing on the metal-sulfur battery performance. For the success of metal-sulfur batteries at the commercial level, drastic new and alternate strategies are necessary. The subsequent part of the talk focuses on this aspect and discusses alternative configurations of metal-sulfur batteries. An important example in this regard is our recent demonstration of a Li-metal free sulfur battery employing a lithiated anatase TiO₂ anode and free-standing Li₂S-carbon cathode (Bhardwaj et al, 2021).

10:00 PM EN09.10.03

A Development of Low-Electrolyte Lithium-Sulfur Cells with High-Loading Sulfur Cathodes [Sheng-Heng Chung](#) and Yin-Ju Yen; National Cheng Kung University, Taiwan

The increasing demand for advanced rechargeable batteries featuring a high energy density and high electrochemical efficiency has driven the development of new electrode materials with a higher charge-storage capacity than those of traditional intercalation cathodes. In this regard, the conversion lithium-sulfur battery is the most promising inexpensive, high-capacity novel rechargeable battery system because of the low cost, wide availability, low environmental impact, and high energy density of sulfur. However, the fast progress in the lithium-sulfur technology has encountered the inability to develop a high-loading sulfur cathode with a promising electrochemical performance in a lean-electrolyte lithium-sulfur battery. A result of the insulating nature of solid active materials and the diffusion problem of the liquid active materials, the lithium-sulfur literature usually reports performance of devices by utilizing a sulfur loading and sulfur content of less than 4 mg cm⁻² and 60 wt%, respectively, in a cell using an excess amount of liquid electrolyte with a high electrolyte-to-sulfur ratio of over 11–20 μL mg⁻¹. Unfortunately, this might result in a challenge in the development and investigation of the lean-electrolyte lithium-sulfur cell with high-loading sulfur cathode and with high electrochemical utilization of sulfur.

In our presentation, we present the development of a lean-electrolyte lithium-sulfur with low electrolyte-to-sulfur ratios of 4–7 $\mu\text{L mg}^{-1}$. In the lean-electrolyte lithium-sulfur, a high-loading sulfur cathode with a high sulfur content of 68 wt% and a high sulfur loading of 8.64 mg cm^{-2} demonstrates high electrochemical utilization, excellent reaction kinetics, and stable cyclability. The cells exhibit discharge capacities of 630–870 mAh g^{-1} and 580–631 mAh g^{-1} at C/10 and C/5 cycling rates for 200 cycles. The corresponding energy density values attain 11–16 mWh cm^{-2} . Moreover, we investigate the possible failure mechanism of a lean-electrolyte lithium-sulfur cell with a high-loading sulfur cathode. Our study indicates that the consumption of electrolyte during cycling leads to the slow ion diffusion and the deposition of insulating solid active material on the electrode, which causes the decreased Coulombic efficiency and irreversible capacity loss. Therefore, it would be necessary studies of the lithium-sulfur battery cathode at a slow rate for a long cycle life to guarantee the electrochemical stability and with the Coulombic efficiency to ensure the cyclability and the electrochemical efficiency during long cycles.

In conclusion, our cathode and cell design exhibit an outstanding cathode performance featuring high energy density and long cyclability with a high amount of sulfur at a lean electrolyte condition. Moreover, we explore the challenges that might be encountered by other high-loading cathodes under research at a low electrolyte-to-sulfur ratio, and propose the possible analytical tools and solutions to address the issues found.

10:05 PM EN09.10.04

Ni-Rich Layered Oxide Cathodes Using Mixed Catholytes of Sulfide and Halide for All-Solid-State Batteries Jong Seok Kim, Yoonjae Han and Yoon Seok Jung; Yonsei University, Korea (the Republic of)

Owing to the high energy density, lithium-ion batteries (LIBs) have expanded their applications from mobile electronic devices to electric vehicles and energy storage systems. In terms of high energy density and safety, all-solid-state lithium batteries (ASLBs) are promising next-generation batteries. Ni-rich layered lithium metal oxides, LiMO_2 ($M = \text{Co, Ni, Mn, Al}$), and inorganic solid electrolytes are considered as the crucial components for high-performance ASLBs. Especially, sulfide SEs (e.g., $\text{Li}_{10}\text{GeP}_2\text{S}_{12}$, $\text{Li}_{5.5}\text{PS}_4\text{Cl}_{1.5}$) that exhibit the maximum Li^+ conductivity of $10^{-2} \text{ S cm}^{-1}$ and mechanical deformability that enables simple cold-pressing-based fabrication of ASLBs, are expected to achieve commercialization of ASLBs. However, sulfide SEs suffer from serious interfacial degradation between LiMO_2 and SEs, which originates from their low electrochemical oxidation stability ($< 3 \text{ V vs. Li/Li}^+$). Specifically, the high reactivity of Ni^{4+} of LiMO_2 induces high interfacial resistances of cathodes. Despite unsatisfactory ionic conductivity (max. $10^{-3} \text{ S cm}^{-1}$), halide SEs have been newly emerging due to their excellent electrochemical oxidation stability ($> 4 \text{ V vs. Li/Li}^+$) and thus good compatibility with LiMO_2 ^{[1][2]}.

In this work, we propose a multi-use of sulfide and halide SEs to compromise their drawbacks for the application to LiMO_2 cathodes in ASLBs. The partial replacement of catholytes with Li_3YCl_6 in $\text{LiNi}_{0.88}\text{Co}_{0.11}\text{Al}_{0.01}\text{O}_2$ electrodes using $\text{Li}_6\text{PS}_5\text{Cl}$, which leads to the improved electrochemical performances, will be presented.

References

[1] Y. Han, S.H. Jung, H. Kwak, S. Jun, H.H. Kwak, J.H. Lee, S.T. Hong, Y.S. Jun *Adv. Energy Mater.* **2021**, *11*, 2003190

[2] H. Kwak, D. Han, J. Lyoo, J. Park, S.H. Jung, Y. Han, G. Kwon, H. Kim, S.-T. Hong, K.-W. Nam, Y.S. Jung *Adv. Energy Mater.* **2021**, *11*, 2100126

10:10 PM EN09.10.05

Stable and High Energy All-Solid-State Lithium Metal Battery by Li Metal Modification Haechannara Lim¹, Seunggoo Jun¹, Yong Bae Song¹, HongYeol Bae², Jin-Hong Kim² and Yoon Seok Jung¹; ¹Yonsei University, Korea (the Republic of); ²RIST, Korea (the Republic of)

Electrification of vehicles boosted research regarding Li ion batteries (LIBs) with higher energy. However, energy density of conventional LIBs has approached its theoretical limit. Applying alternative electrode such as Li metal anode is one promising strategy. Unfortunately, it is hindered by internal short circuit and severe reaction with liquid electrolyte. All-solid-state Li metal batteries (ASLMBs) using non-flammable inorganic solid electrolytes have thus emerged to resolve the problems related with liquid electrolytes and the safety concerns as well. Especially, sulfide solid electrolytes have been one of the most promising candidates thanks to their high ionic conductivities comparable to that of liquid electrolyte ($\sim 2.0 \times 10^{-2} \text{ S cm}^{-1}$) and mechanically ductile property. However, sulfide SEs also do not fully stabilize Li metal anodes. They are reductively decomposed to form byproducts, such as Li_2S and Li_3P , in contact with Li metal. Moreover, cycling upon high current density leads to the void formation which promotes the dendritic Li growth, which calls for the need to pressurize the ASLMBs. Thus far, in most previous reports, ASLMB cells have been tested using thick Li metal foils ($\sim 1 \text{ mm}$). Herein, we report on our recent results of ASLMB cells employing thin ($\sim 20 \text{ }\mu\text{m}$) Li metal anodes that are prepared by scalable electroplating process. Furthermore, cycling performances affected by the application of protective layers will be presented.

10:15 PM EN09.10.07

Origin of Polysulfide Shuttling in Li-FeS₂ Batteries Aliya S. Lapp¹, Grace Whang², Austin Bhandarkar¹, Bruce S. Dunn² and A. A. Talin¹; ¹Sandia National Laboratories, United States; ²University of California, Los Angeles, United States

FeS_2 is a promising conversion cathode material, due to its earth abundance, low toxicity, and high energy density. Despite these advantages, commercialization of rechargeable Li- FeS_2 batteries has been inhibited by rapid capacity fade. One factor believed to play a critical role in the origin of this capacity fade is polysulfide shuttling. However, mechanistic understanding of polysulfide shuttling in Li- FeS_2 batteries is lacking. Herein, we use in-situ UV-vis spectroscopy to study the formation and shuttling of polysulfides in Li- FeS_2 batteries. We find two key results. First, both our chemical and electrochemical lithiation studies show that polysulfides form during the initial lithiation step. This surprising finding is in contrast with the previously proposed mechanism for Li- FeS_2 batteries. Second, polysulfide shuttling decreases by a factor of 2–4x when an ionic liquid electrolyte is used in place of a conventional organic electrolyte. Furthermore, we show that careful choice of the electrolyte anion can lead to nearly complete polysulfide mitigation. Overall, our results provide important insights for understanding and thus prevention of polysulfide shuttling in Li- FeS_2 batteries.

SESSION EN09.11: On-Demand
Sunday Morning, December 5, 2021
On-Demand

8:00 AM EN09.02.06

Bimetallic Co–W–S Chalcogenides Confined in N, S-Codoped Porous Carbon Matrix Derived from Metal-Organic Frameworks for Highly Stable Electrochemical Energy Storage Devices Nageh K. Allam; American University in Cairo, Egypt

Transition-metal dichalcogenides are gaining much interest in the energy storage sector due to the two-dimensional (2D) nature and conductivity of the materials. However, single transition-metal dichalcogenides are not stable, preventing their practical use in real devices. Herein, we demonstrate the

synthesis of binary metal dichalcogenides (Co–W–S) via carbonization of zeolitic imidazolate framework (ZIF-67), a subclass of metal-organic frameworks, encapsulated with phosphotungstic acid (PTA@ZIF-67). The morphology and surface functional groups of the as-synthesized Co–W–S composite are characterized via field-emission scanning electron microscopy (FESEM), high-resolution transmission electron microscopy (HRTEM), and Fourier transform infrared (FTIR) spectroscopy. Furthermore, the crystal structure and elemental composition of the fabricated Co–W–S composite are elucidated by X-ray diffraction (XRD) and X-ray photoelectron spectroscopy (XPS) analyses. Upon testing its electrochemical performance as a supercapacitor electrode, the fabricated Co–W–S@N, S-codoped porous carbon (N, S-PC) shows exceptional specific capacitance (1929 F g^{-1} at 5 mV s^{-1}). Furthermore, the constructed asymmetric supercapacitor device using Co–W–S@N, S-PC, and activated carbon as positive and negative poles, respectively, displays superior energy density and power density of 32.9 Wh kg^{-1} and 700.2 W kg^{-1} , respectively, with high Columbic efficiency over 10 000 charge/discharge cycles at 10 A g^{-1} .

SYMPOSIUM EN10

Advanced Materials for Thermal Energy Management and Harvesting
November 30 - December 8, 2021

Symposium Organizers

Youngsuk Nam, Korea Advanced Institute of Science and Technology
Yuan Yang, Columbia University
Mona Zebarjadi, University of Virginia
Yangying Zhu, University of California, Santa Barbara

* Invited Paper

SESSION EN10:14: Thermoelectrics III
Session Chair: Bolin Liao
Monday Afternoon, December 6, 2021
EN10-Virtual

4:00 PM EN10.14.02

Role of Spin Interactions in Thermoelectric Properties of Fe-Rich Magnetic FeTe Md Mobarak Hossain Polash and Daryoosh Vashaee; North Carolina State University, United States

The anomalous thermoelectric transport properties of iron-telluride (FeTe) near magneto-structural transition temperature ($\sim 70\text{K}$) have been reported earlier with little insight. The coexistence of magnetism and quantum effects can be the probable origin of these anomalies, requiring detailed investigations of the magnetic, galvanomagnetic, and thermoelectric transport properties. The magnetic susceptibility shows a bicollinear stripe type spin ordering in the antiferromagnetic domain and short-range ferromagnetic ordering at the beginning of the paramagnetic domain. The galvanomagnetic properties reveal a multicarrier transport impacted by spin fluctuations. Further, phonon- and magnon-drag contributions are evaluated related to the origin of the anomalous thermoelectric properties. The small entropy contribution from the magnonic heat capacity supports the phonon-drag as the origin of a thermopower peak at $\sim 50\text{K}$, while the field-dependent reduction of the thermopower is associated with the field-dependent modification of the spin-phonon interaction. The field-dependent change of the paramagnetic thermopower is attributed to the spin-fluctuation suppression or the paramagnons. The sharp drop in thermal conductivity above $\sim 70\text{K}$ is related to the structural change modifying the phonon modes. The knowledge gained from studying the spin and quantum effects on transport properties of FeTe is instrumental for designing high-performance spin-driven thermoelectrics.

4:15 PM EN10.14.03

Characterization of Intra- and Inter-Valley Scattering in Thermoelectric Materials—A First-Principles Investigation Vahid Askarpour and Jesse Maassen; Dalhousie University, Canada

A major goal of thermoelectric (TE) research is to find or develop materials with improved efficiencies. One strategy towards higher-performance TEs is band convergence, which seeks to align multiple electronic valleys within a narrow energy range. This approach can boost the power factor, a component of TE efficiency, compared to a single valley by simultaneously increasing the Seebeck coefficient and the electrical conductivity – two competing quantities. While band convergence has been demonstrated experimentally and is the source of many theoretical studies, rigorous scattering calculations indicate that the benefits of this strategy depend sensitively on the strength of inter-valley collision processes. Unlike intra-valley scattering with both initial and final states residing within the same valley, inter-valley processes scatter carriers from one valley to another. The latter can increase significantly when aligning multiple valleys, and potentially offset the gains from band convergence.

In this talk, we present results of a first-principles investigation to characterize, and to understand what controls, intra- and inter-valley electron-phonon scattering in TE materials. For this study we selected six materials, including three lead chalcogenides (PbS, PbSe, PbTe) and three half-Heuslers (ScNiBi, ScPbSb, ZrNiSn), which possess multiple equivalent conduction valleys. Density functional theory (DFT) was utilized to rigorously compute the electron-

phonon scattering and TE characteristics. The intra- and inter-valley scattering rates are analyzed by separating the contributions originating from the electron dispersion and from the electron-phonon coupling, and by elucidating what controls each component. We find that increasing the energy of the zone-edge phonons is effective at reducing inter-valley scattering and enhancing the power factor by >50%. Finally, since DFT electron-phonon calculations can be very demanding, we propose a simple approach to estimate the inter-valley coupling strength, which is found to agree qualitatively with the rigorous results. These findings provide insights into what controls the scattering characteristics to help to guide our search and design of new TE materials with reduced inter-valley scattering and enhanced power factors.

This research was supported by NSERC (Discovery Grant No. RGPIN-2016-04881) with computational resources provided by Compute Canada.

4:30 PM EN10.14.04

Grain Size Dependence of Thermoelectric and Thermomagnetic Transport in the Weyl Semimetal NbP Eleanor Scott¹, Katherine Schlaak¹, Chenguang Fu², Satya N. Guin³, Safa Khodabakhsh¹, Ashley Paz y Puente¹, Claudia Felser³ and Sarah J. Watzman¹; ¹University of Cincinnati, United States; ²Zhejiang University, China; ³Max Planck Institute for Chemical Physics of Solids, Germany

Weyl semimetals combine both topological and semimetallic effects in their transport of fermions through both bulk and surface states, making them excellent candidates for transverse thermoelectric transport via the Nernst effect. The Nernst effect is a transverse thermoelectric effect in which an applied magnetic field and perpendicular temperature gradient produce a mutually perpendicular voltage. The applied field creates a skew force separating charge carriers. Contributions from both polarities of charge carriers add together, so two-carrier systems such as NbP and other Weyl semimetals are advantageous. Single crystalline NbP has shown an unprecedentedly large Nernst thermopower, exceeding 800 $\mu\text{V K}^{-1}$ at 109 K and 9 T [1]. Bulk polycrystalline NbP maintains a large Nernst thermopower, although its magnitude is decreased by approximately a factor of 8 under similar circumstances [2]. Here, we explore both transverse and longitudinal thermoelectric and thermomagnetic transport as a function of grain size in bulk polycrystalline samples of NbP, where different annealing times result in different grain sizes. The polycrystalline samples show a significantly larger Seebeck coefficient in comparison to results in single-crystalline NbP, however this decreases with increasing grain size. The Nernst thermopower is much smaller when compared to single-crystalline NbP, however the Nernst effect is still very pronounced in polycrystalline NbP, even as the Nernst thermopower decreases with increasing grain size. Polycrystalline NbP also exhibits a large isothermal magneto-Seebeck effect, which was rigorously not the case in isothermal measurements of single-crystalline NbP. The polycrystalline samples' deviation in transport from results on single-crystalline NbP are hypothesized to be due to increasing the number of grains and thus interfaces of the topological material, which can then cause topological states to potentially dominate transport. The field dependence of electrical resistivity, thermal conductivity, and the Hall effect in each sample have also been determined. Chemical analysis has been completed using ICP-OES in order to determine the effect of annealing on composition and ensure it remained consistent for each sample. Via microstructural characterization and thermoelectric transport measurements, we can begin to determine the effects of grain size on transport in Weyl semimetals.

[1] S. J. Watzman et al. Phys. Rev. B 97(16), 161404(R) (2018).

[2] C. Fu et al. Energy Environ. Sci. 11(10), 2813-2830 (2018).

4:45 PM EN10.14.05

In Situ Performance of a Nanostructured Bulk Thermoelectric Generator in the Core of a Nuclear Reactor Nicholas Kempf¹, Mortaza Saeidi-Javash¹, Haowei Xu², Ju Li² and Yanliang Zhang¹; ¹University of Notre Dame, United States; ²Massachusetts Institute of Technology, United States

Thermoelectric devices placed in the core of a nuclear reactor can generate electricity from thermal energy to enable self-powered sensors for in-situ monitoring of critical parameters of the nuclear fuel assembly, increasing power plant safety. The in-situ performance of a Thermoelectric Generator (TEG) has never been tested in the extreme environment of a nuclear reactor core. A TEG made from state-of-the-art nanostructured bulk half-Heusler materials was inserted into the core of a nuclear reactor and irradiated for 30 days to an exposure of 153 megawatt-days. The TEG electrical resistance, voltage, and power output were measured continuously while it generated electricity using radiation as a heat source. Despite a sharp drop in TEG power when operating at relatively lower temperature, the TEG showed a 1900% increase in power output due to in-situ annealing and a significant recovery of both the Seebeck coefficient and electrical conductivity when operating at increased temperature and reactor power. Atomic scale modeling indicates the irradiation provided sufficient energy to induce a partial phase transformation, converting the semiconducting half-Heusler structure into a metallic phase stable at low temperatures. However, with sufficient thermal energy, the structure reverts to the original non-irradiated phase and thermoelectric properties quickly recover. The same materials comprising the TEG were separately irradiated with alpha particles and scanning thermal microscopy was used to determine the influence of irradiation dose on thermal conductivity and Seebeck coefficient while microstructural characterization of the irradiated materials confirmed predictions from atomic scale modeling. These results indicate the thermoelectric materials experienced thermally activated healing during which irradiation-induced defects were annihilated and the material microstructure partially recovered along with the thermoelectric properties. These results suggest that with proper control over the TEG operating temperatures, the nanostructured half-Heusler TEG could produce power and operate indefinitely in the core of a nuclear reactor. This work creates opportunities for solid-state power generation utilizing high-efficiency nanostructured thermoelectric materials in the harsh environment of a nuclear reactor.

5:00 PM EN10.14.06

Grain Size Dependence of Thermoelectric and Thermomagnetic Transport in the Triple Point Topological Metal MoP Abhishek Saini¹, Chenguang Fu^{2,3}, Safa Khodabakhsh¹, Ashley Paz y Puente¹, Claudia Felser³ and Sarah J. Watzman¹; ¹University of Cincinnati, United States; ²Zhejiang University, China; ³Max Planck Institute for Chemical Physics of Solids, Germany

MoP (Molybdenum Phosphide) is a topological metal which has been shown to host a triply degenerate point in its electronic structure and a pair of Weyl points in its bulk electronic structure [1]. Its complex band structure makes it unique for electrical and thermal transport, with single-crystalline MoP previously demonstrating an extremely high electrical conductivity and the potential for hydrodynamic charge flow [2]. In this work, both longitudinal thermoelectric (Seebeck effect) and transverse thermomagnetic (Nernst effect) phenomena are investigated for the first time in polycrystalline samples of MoP over a range of temperatures (2 K – 400 K) and externally applied magnetic fields (-9 T to +9 T). Temperature and magnetic field dependent measurements of thermal conductivity, electrical resistivity, and the Hall effect are also investigated. This study is extended to grain-size dependence of the aforementioned physical properties by annealing different samples for varying amounts of time to promote grain growth, with average grain size confirmed via SEM.

Compared to single-crystalline MoP [2], thermal conductivity is found to be approximately 2 orders of magnitude smaller while electrical resistivity is 1-2 orders higher in polycrystalline MoP. The Seebeck coefficient is small, due to a very high carrier density as is the case with most metals, with a maximum value of $\sim 4 \mu\text{V K}^{-1}$ at 380 K. A small magneto-Seebeck effect is seen at temperatures below 200 K with the magnitude of the Seebeck coefficient decreasing in a magnetic field. At temperatures below 100 K, thermal conductivity has also been found to decrease in a magnetic field, with the effect most pronounced at the peak of thermal conductivity in the temperature range of 28-35 K. The magnetoresistance effect is large and increases with decreasing temperatures, showing a similar trend in comparison to single-crystalline MoP [2]. Moreover, a minimal Nernst effect is detected. Furthermore, the effect of grain size is clearly visible in these measured transport properties. Thermal conductivity increases significantly with increasing grain size, while the

electrical resistivity reduced marginally with larger grain size. The magnitude of the Seebeck coefficient also increased in larger grain-sized samples. These changes can be attributed to the reduced number of grain boundaries in the material due to annealing and hence lesser obstruction to charge flow.

[1] B. Q. Lv et al. *Nature* **546**, 627–631 (2017).

[2] N. Kumar et al. *Nat. Commun.* **10**, 2475 (2019).

5:15 PM EN10.14.07

Measurements of Thermal Conductivity of Porous Media by Time-Domain Thermoreflectance (TDTR) Using Transferred Metal Films [Husam Walwil](#)¹, Yunshan Zhao^{2,1}, John Thong^{1,3} and Yee Kan Koh¹; ¹National University of Singapore, Singapore; ²Nanjing Normal University of China, China; ³Singapore Institute of Technology, Singapore

Thermal transport in porous structures is yet to be fully understood. For example, the influence of the microstructure's heterogeneities in porous electrodes of Li ion batteries remain poorly addressed, in part due to challenges in accurate thermal measurement of porous samples. In this talk, we introduce an approach based on time-domain thermoreflectance (TDTR) to accurately measure the thermal conductivity of porous materials, by transferring a metal film to bridge the micro-pores to provide a continuous, flat, and smooth surface for TDTR measurements. We demonstrate our approach by measuring the cross-plane thermal conductivity (k_{PnC}) of a wide range of microscale SiO₂ phononic crystals, with pore diameters of 1 – 3.5 μm and porosity of 13 – 50 %. To achieve accurate TDTR measurements, we ensure that the metal transducer films are sufficiently stiff and thus establish good thermal contact with the necks of the phononic crystals. The good agreement between our k_{PnC} measurements and calculations of effective medium theory validates our approach. We also introduce a guideline that allows the design of the film transfer process onto the porous materials. This approach could be conveniently employed in future studies of heat transport in a wide range of porous materials.

5:30 PM EN10.14.08

Ultra-Sensitive Thermometry Enables Direct Measurements of Reversible Heat Absorption in Li-Ion Batteries [Zhe Cheng](#) and David Cahill; University of Illinois at Urbana-Champaign, United States

The control of temperature in lithium-ion batteries (LIBs) is critically important for the performance, reliability, and safety of LIBs. To design proper thermal management strategies, a greater understanding of thermal effects in LIBs is needed. The reversible heat in LIBs due to entropy change is fundamentally important to understand the chemical reactions in LIBs. However, the reversible heat has not been directly measured previously due to the limited temperature resolution of applied thermometry. We develop an ultra-sensitive thermometry with a noise floor of 32 $\mu\text{K}/\sqrt{\text{Hz}}$ and a noise equivalent temperature resolution of $\pm 10 \mu\text{K}$, which is several orders of magnitude higher than previous temperature measurements applied on LIBs in the literature. We observe the reversible heat absorption of a LIR2032 coin cell during charging with negligible irreversible heat generations at a charging rate of C/200. The entropy changes of the cell obtained from the directly measured reversible heat agree excellently with the entropy changes obtained by measuring temperature dependent open circuit voltage (OCV). This is the first verification of the way to obtain entropy changes by measuring temperature dependent OCV which is widely used in the literature, while the changes in mechanical stress with temperature could also possibly change OCV. Our work enables a new regime of studying thermal effects in batteries at charging rates orders of magnitude lower than previous works, and significantly contributes to fundamental understanding of the entropy changes of the chemical reactions in LIBs.

SESSION EN10.01: Phase Change
Session Chairs: Yuan Yang and Yangying Zhu
Tuesday Morning, November 30, 2021
Hynes, Level 3, Room 311

10:30 AM EN10.01.01

Using Frost to Promote Cassie Ice on Hydrophilic Pillars [Hyunggon Park](#)¹, Farzad Ahmadi² and Jonathan Boreyko¹; ¹Virginia Tech, United States; ²University of California, Santa Barbara, United States

Nanostructured superhydrophobic coatings can trap air pockets underneath ice and frost, greatly reducing their adhesion strength to the surface, but these coatings readily degrade in real-life conditions. Here, we develop a novel approach to trapping air pockets between ice and hydrophilic aluminum micropillars that does not require any hydrophobic coatings or nanostructures. First, frost was preferentially grown atop the micropillars by a two-step process: condensation primarily grew on top of the micropillars due to their sharp corners and elevation over the non-condensable gas barrier; as this upper condensate froze, it evaporated any underlying condensate due to the hygroscopic nature of ice. Second, Cassie ice was formed by virtue of the impacting droplets freezing atop the frost-tipped micropillars before impalement could occur. A scaling model reveals that the dynamic pressure of an impacting droplet causes the water to wick inside the frost much faster than the time scale to impale between the pillars. Our findings suggest that frost-tipped structures can suspend freezing droplets in the Cassie state.

10:45 AM EN10.01.02

Bridging-Droplet Thermal Diodes [Mojtaba Edalatpour](#) and Jonathan Boreyko; Virginia Tech, United States

Solid-state thermal diodes are bottlenecked by poor diodicity while phase-change thermal diodes are constrained by either a gravitational dependence, a 1D configuration, or poor durability. Here, we invent a novel bridging-droplet thermal diode which bypasses all of these existing shortcomings. Our diode consists of two opposing copper plates separated by a micrometric-thick insulating gasket; one plate contains a superhydrophilic wick structure while the other contains a smooth hydrophobic coating. In the forward mode of operation, liquid water evaporates from the heated wicked plate and vapor condenses onto the hydrophobic plate. The large contact angle of the dropwise condensate enables droplet bridging across the gap to replenish the wicked evaporator, sustaining the phase-change heat transfer. Conversely, in the reverse mode, our diode is an excellent thermal insulator as the heat source is now on the back face of the hydrophobic plate. A lumped resistance thermal model is developed to quantify the overall heat transfer coefficient across our thermal diode. Results show that the overall heat transfer ratio (i.e. diodicity) can be boosted considerably through careful design of the wick structure and gasket thickness.

11:00 AM *EN10.01.03

Learning Hidden Physics from Reduced-Order Modeling of Bubble Dynamics in Boiling Heat Transfer Arif Rokoni¹, Lige Zhang¹, Tejaswi Soori¹, Han Hu² and [Ying Sun](#)¹; ¹Drexel University, United States; ²University of Arkansas, United States

Boiling heat transfer is a highly effective but stochastic process where the working fluid undergoes vigorous liquid to vapor transition. Physics-based modeling of bubble dynamics during boiling is challenging due to the drastic changes in system parameters, such as nucleation, bubble morphology, temperature, pressure, and velocity. The vast amount of data from both experiments and numerical simulations have led to the use of artificial intelligence (AI)/deep learning (DL) to gain valuable physical understanding of complex phenomena occurring during natural and industrial processes, including reduced order modeling, turbulence closure model, flow control, and extraction of governing equations. Real-time analysis of bubble statistics in pool boiling is challenging at high heat fluxes where vigorous bubble coalescence is observed. Unsupervised deep learning approaches, such as principal component analysis (PCA), clustering, and autoencoders, have the advantage of minimal human intervention unlike supervised learning. The PCA is a versatile data-analysis tool to determine low-dimensional representations of high-dimensional images by extracting dominant variations and patterns in the raw data without any supervision. In nuclear reactors and other boiling heat transfer applications, early forecasting of the boiling crisis can aid in mitigating catastrophic damage of the heater surface. To predict the future states of the boiling phenomena, long short-term memory (LSTM) neural network is a very efficient tool to estimate time-series variations in the input data, such as bubble dynamics.

In the present study, PCA is used to extract hidden physics from boiling heat transfer processes using in-house pool boiling experimental images of the bubble dynamics. The principal component (PC) representations are made in the new low-dimensional coordinate system by determining the dominant correlations within the high-dimensional data. The first few dominating principal components are used to reconstruct the instantaneous bubble shape and size, which drastically reduces the dimensions of boiling images. The results show that the dominant frequency of the first PC increases with heat flux in the discrete bubble regime until it reaches a peak and then decreases with heat flux in the bubble interference and coalescence regime where the former is associated with the increase in bubble nucleation sites and the latter is associated with the bubble coalescence during pool boiling. Image segmentation is also performed to capture bubble statistics, such as size and numbers to verify the findings of PCA analysis. The temporal variations of the PCs are then used as training data for long short-term memory (LSTM) which predicts the future variations of the PCs. Future predictions of PCs are used to reconstruct the bubble images demonstrating the capability of deep learning (DL) model to predict bubble dynamics. Both steady state and transient pool boiling cases are studied using PCA-LSTM DL algorithm and trained DL model can predict bubble dynamics well.

11:30 AM EN10.01.04

Design of a Multiscale Ceramic Heat Exchanger for High-Temperature, High-Pressure Applications Chad Wilson¹, Xiangyu Li¹, Evelyn N. Wang¹, Olivia Brandt², Rodrigo Orta Guerra², Rodney W. Trice² and Jeffrey P. Youngblood²; ¹Massachusetts Institute of Technology, United States; ²Purdue University, United States

By operating in a high-temperature, high-pressure environment, the efficiency of a thermodynamic cycle can be significantly improved. However, extreme operating conditions require material and design innovations on the classic heat exchanger component. Previous work has attempted to develop heat exchangers for extreme environments by employing superalloy materials in traditional architectures, leading to costly fabrication and limited power density improvement. In this work, we present the design of a multiscale silicon carbide heat exchanger capable of operating in extreme conditions (1300 °C, 250 bar). Enabled by ceramic co-extrusion and geometrically optimized for both high thermal performance and mechanical strength during steady state operation, our heat exchanger offers a scalable and effective solution to address traditional material limitations while offering promising efficiency and performance improvements compared to current state-of-the-art heat exchangers.

SESSION EN10.02: Thermoelectrics I
Session Chairs: Joseph Heremans and Kornelius Nielsch
Tuesday Afternoon, November 30, 2021
Hynes, Level 3, Room 311

1:30 PM EN10.02.01

Re₄Si₇-Based Transverse Thermoelectric Generator with No Hot-Side Contacts Michael R. Scudder¹, Bin He¹, Yaxian Wang¹, Aksah Rai², David Cahill², Wolfgang Windl¹, Joseph Heremans^{1,1,1} and Joshua E. Goldberger¹; ¹The Ohio State University, United States; ²University of Illinois at Urbana-Champaign, United States

Making diffusion-resistant and thermally stable electrical and thermal contacts to the hot side of a thermocouple-based thermoelectric generator (TEG) is a major technological challenge. Such contacts are not needed in transverse thermoelectric devices, in which a thermal gradient in a single material with two cold end contacts induces a perpendicular voltage. Furthermore, the contact resistances of multi-thermocouple (thermopile) generators contribute irreversible losses, to the extent that the device figure of merit ZT of such a thermopile-based TEG is often much lower than the materials ZT of the n-type and p-type legs. In a transverse TEG, only two voltage contacts are needed, reducing the irreversible losses in the contacts and bringing ZT much closer to the material transverse thermoelectric figure of merit, $zxy^{-1}T$. Until now material $zxyT$ values have always been too low for practical applications. When cut at a particular angle, single-crystals of Re₄Si₇ have a $zxyT$ of 0.7 ± 0.15 at 980 K. A combination of thermal and electronic measurements of multiple single crystals with different doping levels, density functional theory calculations, and analytical models establish that these large $zxy^{-1}T$ values come from anisotropic thermopowers that arise from thermal population of the highly anisotropic valence band and isotropic conduction band. A transverse Re₄Si₇ TEG was constructed with no contacts on the hot side, and the ZT derived from measurements of its thermal efficiency near 600 K fits the values of $zxy^{-1}T$ well. This proves experimentally that contact losses are minimized in this geometry as well. Hopefully, thus, transverse TEGs open a new approach to circumventing two of the major technological problems that stand in the way of making practical TEGs.

1:45 PM EN10.02.02

Exploring the Effects of Counter Ion Chemistry in Doped Thermoelectric Carbon Nanotube Networks Tucker L. Murrey¹, Taylor Aubry², Jeffrey Blackburn² and Andrew Ferguson²; ¹University of California, Davis, United States; ²National Renewable Energy Laboratory, United States

Semiconducting single walled carbon nanotubes (s-SWCNTs) have demonstrated promising performance in low temperature thermoelectric thin films. Like polymer-based organic electronic materials, charge carrier density and in-turn thermoelectric properties, can be tuned using molecular charge-transfer dopants. In this work, we build upon previous demonstrations of p-type doping by employing a series of novel molecular dopants based on dodecaborane (DDB) clusters. The unique chemical and electronic structure of these DDB clusters, compared to oxidants like triethyloxonium hexachloroantimonate (OA) and 2,3,5,6-tetrafluoro-7,7,8,8-tetracyanoquinodimethane (F₄TCNQ), increases the spatial separation between the negative DDB counter ion and the hole carriers injected into the nanotubes. Thereby increasing the mobility of the charge carriers and yielding an increase in the thermopower (Seebeck coefficient) for a given electrical conductivity. This enhanced transport ultimately increases the thermoelectric power factor to surpass the previous best-in-class for enriched s-SWCNT thin film networks.

2:00 PM EN10.02.03

Hybrid Ionic-Electronic Thermoelectric Converters to Harvest Heat from Temperature Gradient and Temperature Fluctuation [Jianyong Ouyang](#); National University of Singapore, Singapore

Although great progress has been made in thermoelectric conversion, the performance of thermoelectric generators is still not good enough for large-scale practical application. The conventional thermoelectric generators utilize heat only from the temperature gradient through the Seebeck effect. Apart from the temperature gradient, the temperature related to waste heat always fluctuates. Here, I will report our work on developing hybrid ionic-electronic thermoelectric converters that can harvest generate electricity from both temperature gradient and temperature fluctuation. As a result, they can generate output power at least 4 times of the conventional thermoelectric generators.

2:15 PM EN10.02.04

Towards Tellurium-Free Thermoelectric Modules for Power Generation from Low-Grade Heat Pingjun Ying¹, Ran He¹, Jun Mao², Qihao Zhang¹, Heiko Reith¹, Jiehe Sui³, Zhifeng Ren², Gabi Schiering^{1,4} and [Kornelius Nielsch](#)^{1,5,5}; ¹IFW Dresden, Germany; ²University of Houston, United States; ³National Key Laboratory for Precision Hot Processing of Metals, China; ⁴University of Bielefeld, Germany; ⁵Technische Universität Dresden, Germany

Thermoelectric technology converts heat into electricity directly and is a promising source of clean electricity. Commercial thermoelectric modules have relied on Bi₂Te₃-based compounds because of their unparalleled thermoelectric properties at temperatures associated with low-grade heat up to 550 K. However, the scarcity of elemental Te greatly limits the applicability of such modules. Here we report the performance of thermoelectric modules assembled from Bi₂Te₃-substitute compounds, including p-type MgAgSb and n-type Mg₃(Sb,Bi)₂, by using a simple, versatile, and thus scalable processing routine. For a temperature difference of 250 K, whereas a single-stage module displayed a conversion efficiency of 6.5 %, a module using segmented n-type legs displayed a record efficiency of 7.0 % that is comparable to the state-of-the-art Bi₂Te₃-based thermoelectric modules. Our work demonstrates the feasibility and scalability of high-performance thermoelectric modules based on sustainable elements for recovering low-grade heat.

Reference: P. Ying et al., *Nature Communications* **12**, 1121 (2021)

2:30 PM EN10.02.05

Silicon—A Revenant Thermoelectric Material for Micropower Applications Mark Lee¹, [Ruchika Dhawan](#)¹, Hari P. Panthi¹ and Hal Edwards²; ¹The University of Texas at Dallas, United States; ²Texas Instruments, United States

The development of miniature (~ 0.1 cm² area) silicon integrated circuit (IC) sensors and networking devices for internet-of-things (IoT) and biomedical electronics has spurred the question of how to make such devices energy autonomous, i.e., how to reliably and sustainably energize such devices when they are embedded in remote environments that are often dark, have no access to wall plug power, and are not routinely accessible for battery replacement. Recently, interest has developed in small microelectronic thermoelectric generators (μ TEGs) as one method to give IoT and biomedical devices energy autonomy wherever a reliable thermal gradient exists. Most current research on TE technology concentrates on developing new materials having a high TE figure-of-merit $ZT = (S^2\sigma/\kappa)T$, where S , σ , and κ are the material's thermopower, electrical conductivity, and thermal conductivity, and T is the mean operating temperature. Doped Si is known to have a poor $ZT \sim 0.01$ due to its high κ . The focus on complex materials having high $ZT \sim 1$ is because a TEG's ideal thermodynamic efficiency increases with the ZT of the materials used to form the thermopile. However, high ZT materials can be expensive to synthesize, often contain toxic or non-earth-abundant elements, and are generally incompatible with Si IC processing, all of which can substantially increase the cost of integration with standard IC devices.

We report on small area ($\ll 1$ mm²) μ TEGs using doped Si and Si_{0.97}Ge_{0.03} as the TE material, all fabricated on a standard industrial Si IC process line following the same protocols and process flows used to make commercial IC devices. These μ TEGs can generate specific power densities (per unit area for heat flow per square of temperature difference, ΔT) greater than 80 μ Wcm⁻²K⁻², which is comparable to or better than most existing bulk TEGs using high ZT materials. Moreover, these small area Si μ TEGs can generate voltages exceeding 1.5 V with several μ A of current using commonly encountered ΔT s ~ 20 to 25 °C. This voltage and current level is sufficient to properly energize some existing commercially available IoT ICs using only a warm copper rod as the energy source. Because these μ TEGs can be directly integrated on-chip in the same process flow with the circuits they support, they provide one solution to energy autonomy at extremely low marginal cost.

These Si-based μ TEGs build on an alternative approach to μ TEG device design that emphasizes application of device physics and circuit engineering principles to optimize a μ TEG's generated power per unit area at any given ΔT , rather than narrowly focusing on thermodynamic efficiency. This strategy exploits the ability of industrial Si processing to fabricate thermopiles consisting of a very large number of TE elements in a small area, thereby producing a high total power and voltage density despite relatively low efficiency per TE element. Modern Si processing is also very good at controlling parasitic thermal and electrical resistances, thus minimizing extrinsic degradation of overall TEG performance. Experimental results on power and voltage generation as well as Peltier cooling will be presented. Physics-based models for optimizing performance will also be discussed at both the material level (e.g., effects of dopant concentration and small percentage Ge alloying) and the device design level (e.g., effects of parasitic electrical and thermal resistances and proper design of thermopile packing fraction).

2:45 PM EN10.02.06

High-Throughput Printing and Doping Engineering of High-Performance and Flexible Thermoelectric Devices Using Colloidal Nanocrystal Inks [Yanliang Zhang](#); University of Notre Dame, United States

The flexible thermoelectric generator (f-TEG) is a very promising technology for energy harvesting to enable self-powered wireless sensors and wearable devices, an area of exponential growth. Here, we present high-throughput and scalable additive manufacturing methods to fabricate f-TEGs using colloidal nanocrystals, and rapid screening and optimization of doping to achieve unprecedented thermoelectric performances. Flexible TE films with gradient doping concentrations were printed using a high-throughput aerosol jet printing method. A scanning probe method is applied to quickly identify the optimal doping concentrations. Highly scalable extrusion printing (or screen printing) method is applied to print relatively thick films to achieve high thermoelectric efficiency and enable practical device applications. Along with the nanoparticle ink printing, we developed innovative interface engineering and sintering method in order to improve the density and charge carrier mobility of the printed films.

The p-type and n-type printed films demonstrate peak ZTs of 1 and 0.8 near room temperature along with superior flexibility, which is among the highest reported ZT values in flexible thermoelectric materials. A flexible thermoelectric device fabricated using the printed films produces a high power density above 19 mW/cm² with 80 K temperature difference between the hot side and cold side. The high-throughput and scalable printing methods can efficient and low-cost manufacturing process to transform high-efficiency colloidal nanocrystals into high-performance and flexible TEG devices for broad range of applications.

3:00 PM *EN10.02.07

Engineering Thermal Conductivity in Thermoelectric Materials G. J. Snyder and [Ramya Gurunathan](#); Northwestern University, United States

Reducing phonon or lattice thermal conductivity is one of the most straightforward ways to improve thermoelectric performance of a material. Introducing phonon scattering easily lowers lattice thermal conductivity but in order to improve thermoelectric performance it must reduce electron mobility to much a lesser extent. While this has been quantified for some point defect scattering examples, it is rarely considered for other scattering mechanisms.

Interfaces such as grain boundaries and precipitates are well known to reduce thermal conductivity but their effect on mobility is poorly studied both experimentally and theoretically. Dirty high-angle grain boundaries are known to dramatically reduce mobility in Mg₂Si and Mg₃Sb₂ making some samples unusable as thermoelectrics while clean, low angle grain boundaries can be as good as single crystals. There are many ways to engineer various types of clean, epitaxy-like interfaces in bulk materials.

It has recently become apparent that the low thermal conductivity in PbTe that enables $zT \sim 2$ is largely due to the lattice softening correlated to defects that produce internal strain rather than directly scattering phonons. New revelations about heat transport further indicate that heat is transported diffusively and not even by phonons in many good thermoelectric materials. The detailed understanding of nanoscale microstructure will usher in a new era of nanostructured thermoelectric materials.

3:30 PM BREAK

SESSION EN10.03: Radiation
Session Chairs: Po-Chun Hsu and Ying Sun
Tuesday Afternoon, November 30, 2021
Hynes, Level 3, Room 311

4:00 PM EN10.03.01

Designing Porous Polymers for Passive Daytime Radiative Cooling [Yuan Yang](#); Columbia University, United States

Cooling plays an important role in the human society. It consumes significant amount of electricity and generates 8% of CO₂ by human activities. Passive Daytime Radiative Cooling (PDRC) is an electricity-free method for cooling terrestrial entities, which has potential to remarkably reduce electricity consumption. In PDRC, a surface has a solar reflectance of nearly 1 to avoid solar heating, and high emittance close to 1 in the long wavelength infrared (LWIR) transparent window of the atmosphere (wavelength $\lambda = 8-13$ mm) for radiating heat to the cold sky. This allows the surface to passively achieve sub-ambient cooling. In the talk I will present our recent studies on developing porous polymers with excellent PDRC performance. The high density of nano/micropores in polymer leads to efficient light scattering at the interface between the polymer and air, which effectively enhance solar reflectance and thermal emittance. High solar reflectance above 0.96 and high thermal emittance of 0.97 are achieved simultaneously. This talk will emphasize on 1) How to achieve high performance by simple and environmental benign aqueous processing, and 2) Modeling to understand optimal pore distribution in porous radiative cooling polymers.

4:15 PM EN10.03.02

Quantification of the Radiative Contribution to Transient Thermal Grating Decay [Alexei Maznev](#), Sean Robertson, Michael Short and Keith Nelson; Massachusetts Institute of Technology, United States

Thermal conductivity measurements at elevated temperatures are complicated by the contribution of radiative heat transport. Accounting for the radiative contribution is difficult as it often depends on the configuration of the measurement apparatus and the dimensions of the sample. Furthermore, the Radiation Transfer Equation (RTE), which is essentially the Boltzmann transport equation for photons, is difficult to solve even for simple geometries. The laser-induced transient thermal grating (TTG) technique has an advantage in that heat transport takes place entirely within the sample, with no other parts of the apparatus involved, and the simplicity of the sinusoidal spatial temperature profile makes the heat transfer problem amenable to analytical treatment.

In this report, we present a rigorous analysis of the thermal grating decay in a non-scattering absorbing medium in the presence of both radiative transport which is described by the RTE and non-radiative (intrinsic) transport described by the conventional heat diffusion equation. We provide an analytical solution to the coupled equations and quantify the radiative contribution to the effective thermal conductivity. We analyze the limiting cases of diffusive and ballistic radiative transport and show that the radiative contribution is maximized in the intermediate case when the absorption length of thermal radiation is comparable to the heat transfer distance, namely, at $a/L \sim 1/4$, where a is the absorption length and L is the TTG period. We present calculations for specific materials focusing on molten salts that have been proposed as thermal energy transport and storage media. We also calculate the upper bound for the radiative contribution, which does not require the knowledge of the absorption coefficient.

We find that while the radiative contribution to the effective thermal conductivity may be significant for L in the millimeter or centimeter range, in a typical transient grating measurement with $L \leq 20$ μm it will be in most cases negligible. Thus the TTG technique yields the intrinsic thermal conductivity unaffected by radiative transport. In addition to this practical conclusion, our analysis provides a Fourier-domain Green's function that can be used to calculate the temperature field in the presence of radiative transport for an arbitrary initial temperature distribution or an arbitrary distribution of heat sources in an unbounded medium.

4:30 PM EN10.03.03

A High-Performance Solar-Thermal Regulation Through Switchable Transmittance Window [Xuanjie Wang](#) and Shankar Narayanan; Rensselaer Polytechnic Institute, United States

With industrialization and population growth, the rise in energy consumption has become a critical global issue. A significant portion of the energy in buildings is due to heating, ventilation, and air conditioning (HVAC). The major source of the consumption is the heat transfer to building envelopes. Recently, smart windows have been investigated extensively to reduce energy consumption while maintaining thermal comfort for indoor environment. Smart windows are glazed units coated with special materials to have dynamic control on the transmittance of solar irradiation into buildings under different ambient environments. In our study, a high-performance solar-thermal regulation is achieved through switchable transmittance window. Specifically, the surface turns reflective (lessen the cooling demand) and absorbing (lessen the heating demand) under different modes. The difference of solar transmittance ($\Delta\tau$) is 0.59, accordingly. The device level testing shows a good ability of large range thermal regulation under the illuminance of 1 sun.

4:45 PM *EN10.03.04

Nanophotonic Control of Thermal Emission: From Broadband Directionality to Radiative Cooling [Aaswath Raman](#); University of California, Los Angeles, United States

Thermally generated light is a fundamental feature of nature. Its ubiquity makes its control and harnessing both of intrinsic scientific interest and of great importance for energy and heat transfer applications. In this talk, we will discuss our results in nanophotonic approaches to controlling thermal emission, particularly using epsilon-near-zero (ENZ) materials. We will introduce gradient epsilon-near-zero materials that can support leaky electromagnetic modes that couple to free-space waves at fixed angles of incidence over a broad bandwidth. We will then present experimental demonstrations of broadband directional thermal emitters using a range of oxides, designed to operate over long-wave infrared wavelengths. We will furthermore demonstrate implementations of gradient ENZ using doped semiconductors that allow for arbitrary control of spectral bandwidths and directional response as a function of doping gradient, highlighting a new degree of freedom enabled by configuring ENZ response spatially in a layered photonic structure. Finally, we will also illustrate the benefits of directional and spectral control of thermal emission in the context of radiative cooling applications.

SESSION EN10.04: Poster Session: Advanced Materials for Thermal Energy Management and Harvesting
Session Chairs: Mona Zebarjadi and Yangying Zhu
Tuesday Afternoon, November 30, 2021
8:00 PM - 10:00 PM
Hynes, Level 1, Hall B

EN10.04.03

Y₂Ti₂O₅S₂ - A Quasi-layered Oxysulphide for Thermoelectric Applications [Katarina Brlec](#) and David O. Scanlon; University College London, United Kingdom

One of the many pathways to decreasing the impact of climate change is to increase the efficiency of current fossil fuel based systems. Even the best internal combustion engines suffer from thermal losses where up to 70% of energy is lost as exhaust heat. These losses can be offset to an extent by thermoelectric devices which convert waste heat into useful electrical energy via the Seebeck effect. The efficiency of thermoelectric materials is typically evaluated using the figure of merit (ZT), with some of the best performing materials reaching ZTs of over 2 at low temperatures.[1] However, current state-of-the-art thermoelectric materials contain rare or toxic materials, making them commercially unappealing.

The quest for high ZT materials at low temperatures is complicated by the interdependence of the properties that determine ZT, so maximising the factor is challenging. High Seebeck coefficient and low lattice thermal conductivity favour good thermoelectric performance. Generally, anions of differing mass also help to scatter phonons which decreases the lattice thermal conductivity meaning that mixed anion materials are particularly good candidates for the discovery of novel thermoelectrics.

Y₂Ti₂O₅S₂ has been studied as a potential battery anode, with both experimental and computational studies agreeing on the presence of fast Li-ion diffusion through the material.[2,3] The unique cation deficient Ruddlesden-Poppler structure opening type I Wadsley-Roth intercalation windows in the distorted perovskite-like TiOSS layer was found to govern the diffusion of species. The relative stability to Li, Na, K and Mg intercalation also points to the dopability of the material, which is important for thermoelectric purposes.

In this study we use hybrid density functional theory to computationally predict the thermoelectric properties of Y₂Ti₂O₅S₂. Analysis of the electronic conductivity and Seebeck coefficient using the state-of-the-art AMSET code, which factors in realistic scattering processes, demonstrates that Y₂Ti₂O₅S₂ shows promise for low temperature thermoelectric applications.

[1] L. D. Zhao, S. H. Lo, Y. Zhang, H. Sun, G. Tan, C. Uher, C. Wolverton, V. P. Dravid and M. G. Kanatzidis, *Nature*, **2014**, 508, 373–377.

[2] K. McColl and F. Corà, *J. Mater. Chem. A*, **2021**, 9, 7068–7084.

[3] G. Hyett, O. J. Rutt, Z. A. Gál, S. G. Denis, M. A. Hayward and S. J. Clarke, *J. Am. Chem. Soc.*, **2004**, 126, 1980–1991.

EN10.04.04

A Novel Class of Rigid and Structured Capillary Materials by Femto-Laser Etching for Passive Devices—Towards the Water-Energy Nexus [Matteo Alberghini](#)^{1,2}, Matteo Morciano^{1,2}, Paolo Sirianni³, Eliodoro Chivavazzo¹, Luciano Scaltrito^{1,3}, Matteo Fasano^{1,2} and Pietro Asinari^{1,4}; ¹Politecnico di Torino, Italy; ²Clean Water Center, Italy; ³Microla Optoelectronics, Italy; ⁴Istituto Italiano di Ricerca Metrologica, Italy

Passive devices based on water absorption and evaporation offer a robust, cost-effective, off-grid and sustainable alternative for a wide variety of applications, ranging from personal thermal management to water treatment, filtration and sustainable cooling technologies. These devices do not require high quality energy inputs and, due to the absence of moving mechanical parts, require low maintenance, are cost-effective and usually made from off-the-shelf materials. Moreover, they are optimal for off-grid installations and, in general, promote the sustainable transition to the water-energy nexus. These devices generally exploit porous capillary media to overcome small hydraulic heads and supply the working fluids throughout the system without the need for active mechanical or electrical components. Clearly, maximizing the capillary properties of the porous materials used is crucial to enhance their overall performance: poor capillary properties leads to dry-out and would significantly limit the maximum achievable device size. Thus, neglecting the capillary properties of the porous materials employed would significantly hinder the productivity and scalability of the proposed technology.

This work proposes a paradigm shift in the design of passive devices by replacing the traditional porous materials with a rigid layer, etched with optimized grooves. The concept was tested on aluminum sheets, which were machined by femto-laser to promote wicking on an otherwise flat surface. The technique guarantees an optimal control of the resulting geometrical parameters of the channel, which, through its interplay with the material surface chemistry, allows fine-tuning of the resulting capillary properties. The wicking properties of the obtained sample were compared with those of other engineered porous layers, used as components of passive devices previously reported in the literature. The experimental results were interpreted by a novel theoretical model for mass transfer in open microchannels, which was then used to estimate the effects of the geometry and hydrophilicity of the grooves on their resulting capillary action. Finally, the perspective application of the proposed material in passive desalination devices was investigated both theoretically and experimentally. First, the validated capillary model was coupled with a lumped-parameters heat and mass transfer model for vapor transport in hydrophobic membranes, aiming to evaluate how the capillary properties of porous materials affect the optimal size and maximum productivity of such devices. Then, the salt-rejection capabilities and the durability of the proposed material were evaluated.

The developed theoretical model might serve as a tool to investigate the combined effects of capillary and geometric properties and working conditions on the design constraints of a passive devices component and identify its optimal configuration. Furthermore, the experimental investigation demonstrates the potential of the proposed material for novel components of passive devices for the energy and water sector, paving the way to a new class of rigid materials capable of significant scalability and, thus, their range of use.

EN10.04.05

Scalable and Robust Silica Aerogel Materials from Ambient Pressure Drying Massimiliano Di Luigi and Shenqiang Ren; University at Buffalo, United States

Aerogels constitute one of the best thermal insulating materials, typically featuring remarkably low values of thermal conductivity due to their extremely high porosity above 95% comprised mostly of mesopores with an average size of approximately 10 nm, as well as considerably high values of specific surface area (> 500 m²/g), all properties that result in an outstanding option for applications related to energy saving purposes. However, two of their main disadvantages are associated to (a) a relatively high cost at industrial level, and (b) their brittleness and lack of good mechanical properties as a consequence. By leveraging the benefits of ion-exchange sodium silicate solution as silica source, as well as the use of surfactants, we report an ambient pressure drying silica aerogel nanocomposite material that yields superior thermal insulation and mechanical properties. Such combination of components and process parameters provide an exceptionally overall low-cost alternative for the production of aerogel-based, eco-friendly solutions that are suitable for energy efficient applications.

EN10.04.06

Heterogeneous Nucleation of Gallium with Lattice-Matched Cubic Carbides and Nitrides Phases Sourav Chakravarty¹, Darin Sharar² and Patrick Shamberger¹; ¹Texas A&M University, United States; ²CCDC Army Research Laboratory, United States

Latent thermal energy systems (LTES) store/discharge energy at nearly constant temperatures using melting/solidification of phase change materials (PCMs). However, energy barriers associated with the nucleation of a solid can cause the liquid state to remain in a metastable state below the equilibrium melting temperature, requiring additional undercooling to initiate solidification. Thus, the existence of undercooling tends to reduce reversibility and overall efficiency of LTES, and to introducing an element of stochastic variability in the solidification process that makes accurate prediction of the state of the system challenging. Among PCMs, metallic PCMs are of particular interest because of their high volumetric energy density and ability to rapidly absorb heat, which is critical in thermal management of electronics, optical, and photovoltaic systems. Gallium is a low melting metal ($T_{\text{fusion}} = 30\text{ }^{\circ}\text{C}$) with a high volumetric energy density (400 MJ/m³) and high thermal conductivity (29.4 W/m²C), making it an ideal candidate for room temperature thermal management applications, where rapid absorption of heat is a key performance indicator. However, the application of Ga as a PCM is severely limited due to the large degree of undercooling, which can exceed 60 °C in small volumes (10 ml) as measured by DSC in aluminum containers at relatively rapid cooling rates (10 °C/min). Here, we exploit epitaxial relationships to identify several cubic carbide and nitride phases that reduce the undercooling of Ga. Among these, HfC and ZrN result in maximum reduction undercooling, with undercooling in the range of <20° C and <10° C for volumes of 10 ml. The observed relationship between lattice mismatch and measured undercooling conform to the relationship predicted by heterogeneous nucleation theory. Thus, this study supports parallel efforts in other classes of materials systems (organic compounds, inorganic salts and salt hydrates), which suggest that epitaxial relationships offer an efficient and valid approach for identify candidate nucleation agents, and predicting the activity of those phases across a broad class of phase change material systems. Among other applications, Ga and Ga based eutectics are of interest for thermal management in electronics packaging and photovoltaics. The carbides and nitrides used in this work are commonly used as coatings and diffusion barriers, thereby suggesting the usage of these carbides and nitrides as thin film barriers to protect the underlying components in addition to serving as nucleation agents for Ga.

EN10.04.08

Engineering Antiphase Boundaries in Fe₂VAl Towards Cost-Effective, High Performance Thermoelectrics Cory T. Cline, Weiling Dong, Ian Baker and Jifeng Liu; Dartmouth College, United States

The Heusler alloy Fe₂VAl shows great promise as an ecofriendly and low cost replacement to conventional low temperature (250-500 K) thermoelectric materials. Current thermoelectrics use toxic and expensive elements like Te and Sb, whereas Fe₂VAl offers a larger power factor at a lower cost and is non-toxic. Fe₂VAl also allows for mechanical robustness leading to formable thermoelectric modules than can wrap a concave surface rather than typical flat modules that are commercially made for cold temperature applications. The key issue with Fe₂VAl is it's a relatively large thermal conductivity compared to its semiconductor competitors. The aim of this project is to examine multiple routes to reduce thermal conductivity by enhancing phonon scattering by:

1. Partial lattice substitutions/doping with heavier atomic mass elements (1D phonon scattering sites)
2. Microstructural engineering through anneal/quench treatments (3D phonon scattering)

Arc-melted Fe₂VAl alloy shows a thermal conductivity around 10 W/m²K measured at 300 K. Replacing some of the V with Sn or Ti has been shown to reduce the thermal conductivity by 20% and produce a good n-type or p-type material, respectively. Thermal conductivity, Seebeck coefficient and electrical conductivity have been measured for the dopant additions of 1-5 at.% for Sn, Ti, W, Ta, Ge and Si. Ge shows the most notable performance improvement with both a reduction in thermal conductivity and an enhancement in the Seebeck coefficient. However, Sn additions produce very similar performance improvements with the added benefit of better ductility.

Using water-quench treatments, we have also seen a significant drop in thermal conductivity in Ge-doped Fe₂VAl. X-ray diffraction (XRD) showed that annealing at 1273 K for 48 h produces an ordered L₂₁ phase. Differential scanning calorimetry + XRD have shown that a stable B2-phase is achievable if the material is held above 1393 K for 2 h. Once the material achieves the B2 phase, where the V and Al atoms are random in the lattice, the material is water-quenched to preserve the B2 phase as the bulk phase. Dark-field transmission electron microscopy using superlattice reflections showed the presence of numerous thermal anti-phase boundaries (APBs). The room temperature thermal conductivity of Fe₂VAl_{0.9}Ge_{0.1} annealed at 1273 K for 48 h is 9.3 W/m²K whereas the thermal conductivity of the same alloy annealed at 1393 K for 2 h and water-quenched is 4.5 W/m²K mainly due the presence of APBs in the material. Various anneals have been used to produce changes in the density of the APB domains and the resulting effect on both the thermal and electrical conductivity has been determined. Overall, through a combination of partial lattice doping and microstructural phase engineering, the zT of the Fe₂VAl Heusler alloy has been increased from 0.07 to 0.18 at 300 K.

EN10.04.09

Late News: Synergetic Enhancement of Thermoelectric Performance in Coated Grain Nanocomposite by Wave-Like Phonon Scattering and Carrier Filtering Junphil Hwang¹, Minju Lee¹, Jungwon Kim², Sujin Kim¹, Woochul Kim³ and Sung-Jin Kim¹; ¹Ewha Womans University, Korea (the Republic of); ²KIST, Korea (the Republic of); ³Yonsei Univ, Korea (the Republic of)

Thermoelectric energy conversion has a lot of attention because of its simple and convenient energy conversion of heat to electricity. In this work, thermoelectric nanocomposite with coating layer at the grain boundary was synthesized using chemical synthesis. Coated grain nanostructure has significant advantages for thermoelectricity because of energy filtering and effective coherent phonon scattering by coated grain boundary. Our newly developed phonon scattering model has proved phonon scattering by coated grain boundary is caused by interference of wave-like phonons. The coherent phonon scattering in coated grain boundaries is more powerful than particle-like phonon scattering by other kinds of impurities. The chemical synthesis strategy for coating process is conducted by cation exchange reaction of SnTe powder considering HSAB theory, thermodynamic factors. The thermoelectric figure of merit (zT) was 1.90 at 923 K for the CdTe/SnTe and 1.68 at 823 K for the eco-friendly CuInTe₂/SnTe nanocomposite.

EN10.04.11

Exploiting Bi-Modulated Magnetic Field and Drive Current Modulation to Achieve High-Sensitivity Hall Measurements on Thermoelectric Samples Gabor Parada¹, Ferenc Korsos¹, Christophe Defranoux¹, Jan-Willem G. Bos², Eric Don³, Jake Bowers⁴ and Mustafa Togay⁴; ¹Semilab Semiconductor Physics Laboratory Co. Ltd., Hungary; ²Heriot-Watt University, United Kingdom; ³Semimetrix Ltd, United Kingdom; ⁴Loughborough University, United Kingdom

Hall mobility measurements of samples with high carrier density is challenging due to the low Hall voltage. Although an increase of the drive current enhances the Hall voltage, over a certain level, Joule heating at the contacts results in unreliable measurements, due to changes in the resistivity around the contact and/or the generation of thermoelectric voltage at the contacts. Localised heating may even damage the sample.

Therefore, suppressing measurement noise is essential to obtain valid Hall mobility results from low resistivity samples, which can be achieved using modulation methods, varying periodically either the magnetic field or the drive current during the Hall measurement.

The Parallel dipole line (PDL) AC Hall measurement technique is a very practical way to realize pure harmonic magnetic field modulation in a very compact design using rotating permanent magnets. The frequency selective “lock-in” evaluation of the resulting sinusoidal Hall voltages significantly reduces measurement noise and makes it possible to determine the Hall-mobility in highly conductive materials, up to a certain limit.

However, in metals or in thermoelectric materials featuring very high free carrier density (over $1 \times 10^{21} \text{ cm}^{-3}$) the signal-to-noise ratio is still not sufficient to get a valid result.

In this work, we combine magnetic field modulation with alternating polarity drive current, i.e. using a simultaneous two-parameter modulation at very different frequencies to gain further noise reduction.

The reliability of the bi-modulated PDL Hall method was investigated by comparing the results with the standard AC field PDL Hall measurement from several moderately conductive materials. Hall mobility results from Si and SiAs samples using the two methods were within 1% and were in good agreement to typical values in the literature.

Then, Sn doped NbCoSb thermoelectric samples were tested, featuring very high carrier density, above the specification of the standard PDL Hall measurement.

While the standard PDL Hall measurement provided inconsistent and highly fluctuating results depending on the drive current as well, the bi-modulated method resulted in very stable Hall voltage reading and repeatable mobility values. The Hall mobility values measured from the highly conductive samples ($1-3 \times 10^{21} \text{ cm}^{-3}$ carrier density) are in the $2-11 \text{ cm}^2/\text{V}\cdot\text{s}^{-1}$ range in good agreement with results of material simulations.

Analysing the frequency dependence of the AC drive current using a series of resistors defined the applicability range of the drive current modulation which turned to be limited by the “RC” time constant of the sample resistance (R) and the cable capacitances (C). Since higher resistance samples can be tested reliably without alternating the drive current, these tests confirmed the applicability of bi-modulated PDL Hall method for the high carrier density range in interest.

In conclusion, the combination of the AC magnetic field and alternating drive current in PDL Hall systems provides an astonishing Hall voltage sensitivity which results in accurate Hall mobility results even in thermoelectric samples featuring carrier concentration above $1 \times 10^{21} \text{ cm}^{-3}$.

SESSION EN10.05: Measurement

Session Chairs: David Cahill and Patrick Hopkins

Wednesday Morning, December 1, 2021

Hynes, Level 3, Room 311

10:30 AM EN10.05.01

Measuring the Gradients in Thermal Properties Due to Ion Bombardment Thomas W. Pfeifer¹, Ethan A. Scott², Khalid Hattar², John A. Tomko¹, Patrick E. Hopkins¹, Kenny Huynh³, Michael Liao³ and Mark Goorsky³; ¹University of Virginia, United States; ²Sandia National Laboratories, United States; ³University of California, Los Angeles, United States

The thermal properties of semiconductors following exposure to ion irradiation are of great interest as pertaining to the cooling of electronic devices, however the spatially-varying structural and compositional changes inherent to ion bombardment often make measurement difficult. We present an advance to the Time Domain Thermoreflectance (TDTR) technique, and a study in which we demonstrate the measurement of Silicon bombarded with Krypton ions, throughout the stopping region. We also use Transmission Electron Microscopy (TEM) to validate our findings and further explore the structural effects of bombardment.

TDTR is a pump-probe technique that measures the change in thermoreflectance on the surface of a sample as a function of pump-probe delay time from picoseconds to nanoseconds. This change in thermoreflectance is related to both the temporal temperature decay from impulse heating driven by the sub-picosecond pump pulse and the frequency-dependent temperature rise induced from the modulated pump pulse train. The thermal decay response is then fitted to a multi-layer model in order to extract the thermal properties of interest. Ordinarily, TDTR is well-suited to the measure thermal properties even beneath the surface of the sample, which in our case, allows for the measure of properties within the ion-stopping region. We modify the traditional analysis by discretizing a layer and instead fitting for a function of thermal conductivity. This allows the measure of the depth-dependent thermal conductivity due to ion bombardment, and we find a thermal conductivity profile with an excellent match to the predicted and observed damage profiles from SRIM and TEM. This is beneficial for thermal characterization of materials, and as a tool for profiling bombardment-induced damage.

Our technique, in combination with TEM, is able to show a measured thermal conductivity of as low as $2.34 \text{ W/m}\cdot\text{K}$ for regions of defected crystalline silicon containing 5-15nm amorphous pockets. We explain this measured thermal conductivity as being a product of both porosity / nanocomposite interface scattering effects, and greatly reduced thermal conductivity of the crystalline regions as a product of purely structural disorder. We also note that the measure of the thermal conductivity of the defected crystalline regions between the amorphous pockets is among the lowest ever measured.

10:45 AM *EN10.05.02

Thermal Conductivity, Li Stoichiometry and Three-Dimensional Thermometry of Solid Electrolytes for Li-Ion Batteries David Cahill; University

of Illinois, United States

Thermal management in Li-ion batteries is critical for their safety, reliability, and performance. I will discuss three aspects of our current work on the physical properties of solid electrolytes (SEs) for solid-state batteries. 1) Measurements of the thermal conductivity of air and moisture sensitive halide and sulfide SEs are enabled by depositing the Al transducer film for time-domain thermoreflectance (TDTR) measurements with a compact sputter deposition chamber mounted inside a glove box. Thermal conductivities of halide and sulfide SEs are in the range $0.45\text{--}0.70\text{ W m}^{-1}\text{ K}^{-1}$, a factor of 2-3 smaller than the thermal conductivities of oxide SEs. The thermal conductivity has a glass-like temperature dependence that presumably arises from the strong atomic scale disorder that is necessary for high ionic conductivities. 2) Characterization of the Li composition of solid-electrolytes and electrodes is a ubiquitous challenge in battery research because analytical techniques based on core-level excitations are not applicable to Li. We recently implemented nuclear reaction analysis using a 1.8 MeV proton beam and spectrometry of 4-8 MeV alpha particles that are generated by the ${}^7\text{Li}(p,\alpha){}^4\text{He}$ reaction. This ion-beam analysis technique achieves a Li composition accuracy of a few percent across a depth of several microns with a depth resolution of 100 nm. 3) While knowledge of boundary conditions and thermal properties of materials is sufficient to calculate the temperature field within a battery, direct measurements of temperature fields in three-dimensions would be valuable in situations where the heat sources and thermal properties are not well known. As a first step in this direction, we have characterized the temperature dependence of the nuclear magnetic resonance linewidths of ${}^7\text{Li}$ in common solid electrolytes. The linewidth has a strong temperature dependence when the hopping rate of the ${}^7\text{Li}$ ion overlaps with the natural linewidth created by dipolar coupling and may provide an approach for 3D thermometry by magnetic resonance imaging.

11:15 AM *EN10.05.03

Ultrafast Infrared Pump-probe Measurements for Time Domain Measurements of Electron, Phonon and Polariton (Plasmon and Phonon) Relaxation [Patrick E. Hopkins](#); University of Virginia, United States

The fundamental interactions among photons, electrons and phonons at interfaces dictate heat transport in a wide array of materials and interfaces used in energy conversion and storage technologies. Characterization of these electron and phonon thermal properties are commonly studied with pump-probe methods. In standard implementations of these techniques, visible light laser sources are used to excite and probe electronic transitions on the surface of samples, and thus relate the temporal decay of these electronic states to temperature and resulting material properties. At these photon energies, the nature of the probe response is electronic, in that electronic interband transitions dominate the optical response.

In this presentation, we demonstrate the use of sub-picosecond infrared laser pulses as a means of more direct resolving the thermal response of nonequilibrium carriers. The low energy nature of these laser pulses with respect to electronic interband transition energies in metals and semiconductors allows for direct probing of free electron responses in metals and semiconductors and resonating with coupled nonequilibrium polaritonic carriers in non-metals. We will show the ability to: i) probe the purely free electron response in Au and recover the predicted thermal electron-phonon coupling factor; ii) probe the time domain relaxation of phonons in semiconductors based on optical interactions with optical phonon modes; and iii) monitor the ultrafast thermal decay of coupled plasmon-polariton modes in doped CdO and phonon-polariton modes in hexagonal boron nitride.

Tomko, J.A., Runnerstrom, E.L., Wang, Y.-S., Chu, W., Nolen, J.R., Olson, D.H., Kelley, K.P., Cleri, A., Nordlander, J., Caldwell, J.D., Prezhdo, O.V., Maria, J.-P., Hopkins, P.E., "Long-lived modulation of plasmonic absorption by ballistic thermal injection," *Nature Nanotechnology* **16**, 47-51 (2021).

Tomko, J.A., Kumar, S., Sundararaman, R., Hopkins, P.E., "Temperature dependent electron-phonon coupling of Au resolved via lattice dynamics measured with sub-picosecond infrared pulses," *Journal of Applied Physics* **118**, 193104 (2021).

11:45 AM EN10.05.04

Thermally Conductive Carbon Fiber-Phase Change Material Composite for Thermal Runaway Prevention [Jose A. Martinez](#) and [Randall M. Erb](#); Northeastern University, United States

The increasing prevalence and efficiency of electric vehicles have continuously driven the need for high-energy-density lithium-ion battery packs. Within these battery packs, the exothermic reactions of the cell cause an increase in temperature and thus require efficient thermal management systems to prevent thermal runaway events and catastrophic failure. Current solutions include polymer PCMs, which absorb heat as they melt. Their low thermal conductivity limits the heat transfer rate through the PCM, making them inefficient for thermal runaway scenarios. We tackle this problem by incorporating aligned carbon fibers into a polymer PCM. Our material shows a five times increase in through-plane thermal conductivity and more efficient thermal energy absorption. We demonstrate this through thermal characterization, computational modeling, and simulated thermal runaway on a benchtop scale testbed.

SESSION EN10.06: Heat Conduction
Session Chair: Bolin Liao
Wednesday Afternoon, December 1, 2021
Hynes, Level 3, Room 311

1:30 PM *EN10.06.01

Progress in Measuring, Modeling and Manipulating Thermal Boundary Conductance [Pamela M. Norris](#), [LeighAnne Larkin](#), [Nam Q. Le](#), [Carlos Polanco](#), [Justin Smoyer](#) and [Jingjie Zhang](#); University of Virginia, United States

The ability to predict, understand, and control thermal transport in materials and at interfaces remains a critical challenge and goal of nanoscale thermal transport research. In nanostructures where phonons are the primary thermal energy carriers, interfaces between dissimilar materials represent the dominant thermal resistance. An increased understanding of phonon-mediated transport across interfaces is critically needed, so that nanostructured devices can be more effectively designed and implemented.

Over the past several decades, the nanoscale heat transfer community has identified and investigated many factors that influence phonon transport across solid-solid interfaces. Experimental data, simulation results and theoretical analysis have all elucidated the collective effects of vibrational spectra, harmonic and anharmonic processes, defects, and mixing on the ability to transport heat across a solid-solid interface. As the community continues to study these phenomena many challenges arise. In the regime of simulations, it is difficult to develop a computational model that captures all the properties of a physical material and the interactions between materials. From the standpoint of the experimentalist, there is no perfect system or set of systems that allows factors influencing thermal transport to be decoupled. In all areas of thermal transport research, the challenge is either decoupling or understanding the

interplay of complex effects that manifest differently in various materials and experimental/computational environments.

At the Nanoscale Energy Transport Laboratory at the University of Virginia, our research efforts combine computational and experimental techniques to model, measure, and predict phonon dynamics, and the resulting thermal properties, for a wide range of technologically relevant systems. We have approached this problem experimentally, measuring nanoscale systems with time-domain thermoreflectance (TDTR), and computationally, tracking atomic thermal motion in non-equilibrium molecular dynamics (NEMD) simulations, and investigating quantum mechanical effects using the non-equilibrium Green's functions (NEGF) approach. This work is complicated by the wide spectra of phonon mean free paths, ranging from a single atomic spacing to the size of the material system.

Here we review approaches for measuring, modeling and manipulating thermal boundary conductance across solid-solid interfaces in hopes of developing avenues to control the heat transport at the atomistic length scale. For example, we have demonstrated that insertion of a layer with intermediate vibrational properties of the two contacts joining at an interface can enhance the interfacial thermal conduction under certain conditions. By utilizing an exponentially mass-graded interface, even further increases in enhancement are possible, attributed to the strength of anharmonicity in addition to matching of vibrational spectra. The ultimate goal is to drive the discussion of thermal management from a design afterthought down to intentional design at the nanoscale where the heat is generated, completing the journey from TIM to transistor.

2:00 PM EN10.06.02

Observation of Solid-State Bidirectional Thermal Conductivity Switching in Antiferroelectric Lead Zirconate (PbZrO₃) [Kiumars Aryana](#)¹, John A. Tomko¹, Ran Gao², Md Shafkat Bin Hoque¹, Thomas W. Pfeifer¹, Alejandro Salanova¹, David H. Olson¹, Jeffery Braun¹, Eric R. Hoglund¹, Joyeeta Nag³, John Read³, Michael Grobis³, Elizabeth Opila¹, Lane W. Martin², Jon Ihlefeld¹ and Patrick E. Hopkins¹; ¹University of Virginia, United States; ²University of California, Berkeley, United States; ³Western Digital Corporation, United States

Thermal regulators that enable controlling temperature on demand is a key component in the development of solid-state thermal circuits. A highly efficient thermal regulator should operate near or above room temperature and offer a quick and large on/off switching ratio. Switching the thermal conductivity of a material can be achieved upon repeatable transformations in the electronic or phononic structure. However, reliable high-performance thermal regulators are still missing from the literature. A promising class of material candidates for dynamic thermal conductivity switching that have recently received considerable attention due to their fast, repeatable, and well-integrated trigger mechanism are ferroelectric perovskites such as lead zirconate titanate PbZr_{1-x}Ti_xO₃ (PZT_x) and lead titanate PbTiO₃ (PTO). Despite the large focus on investigating the thermal conductivity of PZT and PTO with varying conditions, their antiferroelectric end-member, lead zirconate PbZrO₃ (PZO), has received much less attention. In this material, a sufficient electric field will transition the antiferroelectric phase to a ferroelectric phase where there is a volume expansion, reduction in the unit cell size from 8 formula units to 6, and the possibility of altering the populations of ferroelastic domains. Furthermore, there are ferroelastic domains within antiferroelectric PZO and they too may impact phonon scattering rates. In addition to AFE to FE phase transition, PZO undergoes another phase transition upon heating where the lattice structure goes from 8 formula units to 1, and is expected to reduce the phonon scattering rate and lead to higher thermal conductivities. In this study, we experimentally demonstrate how thermal conductivity of antiferroelectric PbZrO₃ can be bidirectionally switched by -10% and +15% upon applying electric field and thermal excitation, respectively. Our approach takes advantage of two separate phase transformation mechanisms in PbZrO₃ that influence the phonon scattering rate in different manners. This is the first experimental realization of a fast (<1 second) and high-performance thermal regulator with a net switching ratio of 25% from 1.2 to 1.5 W/mK.

2:15 PM EN10.06.03

Nanoscale Si Fishbone Structures For Manipulating Heat Transport Using Phononic Resonators for Thermoelectric Applications [James Lees](#), Ben Durham, Christopher Reardon, Martha Anderson-Taylor, Philip J. Hasnip, Thomas Krauss and Sarah Thompson; University of York, United Kingdom

Thermoelectric devices have significant potential for energy management, but current materials struggle with efficiency, usually captured using the Figure of Merit (zT):

$$zT = S^2 \sigma T / \kappa$$

where S is Seebeck coefficient, T is Temperature, κ is thermal conductivity and σ is electrical conductivity. The goal is to create a material with a low κ but a high σ . In Silicon (Si) the electrical energy is carried by electrons (or holes) but the thermal energy is mostly carried by phonons. This means that it is possible in principle to affect only phonons and so decrease κ without affecting σ .

There has been much work on modifying the κ value of semiconductors by increasing the phonon scattering, but this tends to also increase scattering of the charge carriers.[1] In this work we take a different approach in which metamaterials are designed to exhibit resonances which lie within the range of thermal phonons. These resonant phonons are predicted to hybridise with the thermal phonons causing standing waves, decreasing their group velocity and hence κ , these structures are known as nanophononic metamaterials (NPM).[2] Molecular dynamics simulations of Si NPMs suggest that the κ value may be reduced by up to two orders of magnitude in comparison to Si membranes, where the effect is largest for NPMs with high aspect-ratio nanoresonators.

The majority of previous attempts to experimentally test these predictions have relied on the growth of nanopillars of Si where it is difficult to control the critical model parameters such as aspect ratio and density of the pillars. Here, we present an all-planar design similar to the work of J.Marie et al[3] in which these parameters can be individually varied. In this work, the thermal transport properties are spatially resolved using Scanning Thermal Microscopy (S_{Th}M) which enables the correlation of the thermal properties with the geometry.

For this new device a freestanding Si membrane is constructed and patterned using E-beam lithography to produce a series of lateral resonant nanostructures off a central shaft which leaves the top surface of the shaft exposed for direct measurement using S_{Th}M. These naturally resonant nanostructures can be individually controlled across a number of the critical model parameters such as length and width (thus aspect ratio) as well as position, number of and spacing between the structures. This enables direct measurement of the impact of the various parameters on the resultant κ . The Si nanostructures have been fabricated at a variety of sizes to a minimum width of 115 nm and a maximum length of 30 μ m. Workable structures up to a maximum aspect ratio of 26:1 have been tested.

S_{Th}M, in both air and vacuum, is used to take simultaneous localised topography and thermal measurements across the device with a spatial resolution of 100 nm. Two methods were used to measure the local κ of the structures enabling correlation between the dimensions and the thermal properties. In the first method, the S_{Th}M tip becomes a heat source, whose measured temperature is a function of the local κ . In the second method, an external temperature gradient of up to 2.8mK/ μ m across the sample was established using a fabricated micro heater; the S_{Th}M tip is used to measure the variations in the temperature gradient along the shaft correlated with dimensional variations. Using this gradient

changes of as low as ~10% can be determined. The κ values were extracted using COMSOL to model the thermal profiles which enabled the effects of the sample topography to be accounted for.

[1] Wang S, et al. Grain boundary scattering effects on mobilities in p-type polycrystalline SnSe. *J. Mater. Chem. C*, 2017,5, 10191-10200

[2] Honarvar, H.; and Hussein, M.I. Two orders of magnitude reduction in silicon membrane thermal conductivity by resonance hybridizations. *Phys. Rev. B*, 2018, 97, 195413

[3] Maire J, et al. Thermal conductivity reduction in silicon fishbone nanowires. *Scientific Reports*. 2018 Dec 1;8(1):4452

2:30 PM EN10.06.04

Discovery of the Novel Sustainable n-Type Thermoelectrics Zn₂NX (X = Cl, Br, I) by Anion Mutation of ZnO Kieran B. Spooner^{1,2} and David O. Scanlon^{1,2,3}; ¹University College London, United Kingdom; ²Thomas Young Centre, United Kingdom; ³Diamond Light Source, United Kingdom

Thermoelectrics transform heat into electricity and vice versa, making them valuable tools for the generation and recycling of clean, renewable energy. While progress has been made increasing the efficiency of thermoelectrics, measured by the dimensionless figure of merit, ZT, the best systems often contain rare or toxic elements, such as PbTe and Bi₂Te₃, which reduces their sustainability. Furthermore, ZTs of n-type thermoelectrics have lagged behind those of their p-type counterparts. Conductive oxides have shown promise as potential thermoelectrics¹ due to their strong electrical conductivity and high temperature stability, particularly ZnO, which has reached a ZT of 0.65 at 1000 K.² As they are often hindered by their high thermal conductivity, nanostructuring has been extensively tested for overcoming this problem,³ but limits the electrical conductivity as well as the thermal conductivity, reducing the potential ZT increases.

Here we use hybrid density functional theory (DFT) to screen the anion mutated ZnO derivatives Zn₂NX (X = Cl, Br, I)⁴ for thermoelectric properties. We analyse their thermal and electronic transport beyond the constant relaxation time approximation (CRT) using Phono3py⁵ and AMSET⁶ respectively. We show that anion mutation is a highly effective means to reduce the lattice thermal conductivity, and analyse the combined effect of the various other changes this makes to the materials, comparing to each other, ZnO and thermoelectric materials in general. We then use these insights to assess the potential of the anion mutation method.

[1] Spooner, K. B. *et al.*, *Submitted*. 2021.

[2] Ohtaki, M. *et al.*, *J. Electron. Mater.* 2009, 38, 1234.

[3] Spooner, K. B. *et al.*, *J. Mater. Chem A* 2020, 8, 11948.

[4] Liu, X. *et al.*, *J. Solid State Chem.* 2013, 203, 31.

[5] Togo, A., Tanaka, I., *Phys. Rev. B* 2015, 91, 094306.

[6] Ganose, A. M. *et al.*, *Nat. Commun.* 2021, 12, 2222.

2:45 PM BREAK

SESSION EN10.07: Thermal Materials
Session Chairs: Po-Chun Hsu and Yangying Zhu
Wednesday Afternoon, December 1, 2021
Hynes, Level 3, Room 311

4:00 PM EN10.07.01

Hydrogel-Based Materials with Fast Kinetics for Water-Harvesting and Thermal Management of Electronics Jian Zeng, Ka Man Chung, Xintong Zhang and Renkun Chen; University of California, San Diego, United States

Efficient harnessing and management of thermal energy attracts widespread interest in the context of water-energy nexus. Recently, hydrogels have shown great promises for water-based heat and mass transfer processes such as thermally driven water harvesting, desalination and thermal management of electronics due to the high capacity of water adsorption by hydrogel (could store water up to > 100 times of dry gel mass) and high osmotic pressure for salt rejection. Despite extensive studies on the high adsorption capacity, much less efforts have been paid to improve the kinetics of the heat and mass transfer processes, which are important performance metrics such as the water production yield in water harvesting from air, water flux in desalination and thermal conductance of electronic cooling. In this talk, we present the structural engineering of hydrogels for significantly enhanced kinetics. The general strategy is based on thin polyelectrolyte hydrogel coating on the surface of a metal scaffold with large effective surface area. Due to small thickness of the hydrogel coating and high thermal conductivity of the metallic scaffold, the heat and mass transfer rate are significantly improved, leading to high adsorption/desorption kinetics. As an example, porous aluminum foam was coated with ~ 100 μm thick hydrogel to provide 10-fold increase in the surface area, leading to a short adsorption time constant of < 15 mins and short desorption time constant of 10 mins. In an optimized adsorption/desorption cycle, we can obtain water yield > 20 $\text{kg}_{\text{water}} \text{kg}_{\text{gel}}^{-1} \text{day}^{-1}$ and > 10 $\text{kg}_{\text{water}} \text{m}^{-2} \text{day}^{-1}$ by using the thermo-responsive polyelectrolyte hydrogel. We also apply an aluminum fin heat sink coated with thin hydrogel for passive evaporative cooling of electronics. Taking advantage of the high latent heat of water during evaporation, small thermal resistance across the thin gel and high adsorption capacity of gel, we achieve high thermal conductance ~ 200 $\text{W m}^{-2} \text{K}^{-1}$, high cooling power of > 1.5 kW m^{-2} and long operational time of ~ 6 hours in the peak-hours. The gel can also be fully regenerated during the off-peak hours at night. Our studies show the potential of structural engineering of hydrogel-based materials to enhance heat and mass transfer kinetics.

4:15 PM EN10.07.02

The Orbital Chemistry of High Valence Band Convergence and Low-Dimensional Topology in PbTe Madison Brod and G. J. Snyder; Northwestern University, United States

PbTe, one of the most highly performing thermoelectric materials, and similar GeTe- and SnTe- based alloys have been used in the power sources for NASA space missions for several decades. The exceptional thermoelectric performance of PbTe and its alloys is partially attributed to the high valley degeneracy of its valence band edges, which leads to an enhanced thermoelectric quality factor, and hence, maximum attainable efficiency. The high valley degeneracy of the valence bands is due to the convergence of multiple valence band maxima at low-symmetry points in the first Brillouin zone. In fact, prior studies using first-principles calculations suggest that as the valence band edges become more highly converged, the valence band Fermi surface undergoes a topological transition from a valence band edge described by a 3D density of states to a thread-like Fermi surface described by a 2D density of states. Transport modeling with the Boltzmann transport equation (BTE) predicts significant gains in thermoelectric performance upon this transition to

lower-dimensional bands in bulk 3D materials. In the work presented here, we study the chemical origins of this favorable valence band behavior in PbTe by considering both numerical and analytical solutions to a tight-binding model with nearest and next-nearest neighbors. The tight-binding method offers the advantages of extremely short computational times and of employing a chemically intuitive basis comprised of recognizable atomic orbitals. We develop simple atomic orbital pictures and molecular orbital energy level diagrams for high symmetry k -points in the Brillouin zone to describe a tight-binding wavefunction corresponding to the valence band edge in PbTe. Furthermore, we find that in a theoretical tight-binding electronic structure of a model IV-VI rock salt compound where four different valence band extrema are effectively converged, a 1D Fermi surface can be obtained. Using the BTE, we predict further gains in thermoelectric performance from this 1D Fermi surface topology relative to the 2D and 3D cases. We use the results of this analysis to predict and to understand potential alloying strategies to further optimize the electronic structure of PbTe and its analogues. This work can be directly extended to the other IV-VI rock salt compounds (IV = Ge, Sn, Pb; VI = S, Se, Te), and the orbital chemistry framework applied here can be more generally applied to new materials systems in order to guide the understanding and discovery of materials with optimal electronic structures for thermoelectric performance.

4:30 PM EN10.07.03

Programming Exothermic Phase Change Material Crystallization and Downstream Thermoresponsive Processes in Hydrogels Thomas B. Schroeder and Joanna Aizenberg; Harvard University, United States

The on-demand exothermic crystallization of stably supercooled phase change materials, which have long been used in the context of hand warmers and heat pads, shows promise as a component of engineered energy transduction cascades. These processes amplify a small nucleation trigger to release large quantities of thermal energy that can be used to activate downstream processes that respond to changes in temperature.

Our group has developed a strategy for controlling the spatiotemporal evolution of crystal growth and heat release in metastable phase change materials. In this work, we synthesize polymer networks from acrylamide monomers in supersaturated aqueous solutions of sodium acetate using ultraviolet light and a photoinitiator. Photomasks are used to create metastable hydrogels with patterned domains that remain unpolymerized. Upon nucleation with seed crystals of sodium acetate trihydrate, long needle-like crystals grow through unpolymerized regions; the growth front in these areas is up to seven times faster than in polymerized domains, where a polycrystalline composite forms. Crystal growth is accompanied by a wavelike temperature profile with a peak at the solid/liquid interface. In one set of conditions, the peak temperature during fast crystallization through unpolymerized solutions was 45 °C, whereas the slower crystal growth process through a polymer network peaked at 30 °C. These profiles are well-described by a one-dimensional analytical model; the discrepancy between peak temperatures can be fully explained by the velocity difference.

We demonstrate the utility of this technique by using it to pattern thermoresponsive processes, which can be induced to proceed in a wavelike fashion following the peak temperatures of the crystal growth fronts. We use the temperature difference between polymerized and unpolymerized regions to selectively activate processes that proceed at threshold temperatures above 30 °C, such as wax melting or hydrogel contraction, within predefined areas to form complex patterns such as text.

4:45 PM EN10.07.04

Can Dynamic Covalent Networks Be Used as Thermal Conductivity Switches? Joshua M. Rinehart, John R. Reynolds and Shannon K. Yee; Georgia Institute of Technology, United States

The ability to dynamically control heat flow in materials (i.e. thermal conductivity switches) would enable the development of more efficient energy systems, ranging from controlling heat flow in computer chips to allowing phase change materials to be more efficient in buildings. However, developing polymer systems that exhibit dynamic thermal conductivity changes remains a challenge due to the difficulty in using external stimulus to significantly alter a polymer's ability to conduct heat. It has been previously shown that a mixture of polymers that interact via hydrogen bonding can form a network with a drastic increase in thermal conductivity compared to their pure components. One potential mechanism is to reversibly switch the strength of interactions between chains by using dynamic covalent crosslinks. It has been hypothesized that Diels-Alder reactions are one such way to dynamically control crosslinking and thereby the utilization of the Diels-Alder reaction could result in dynamic thermal switching. In this work, a series of precursor uncrosslinked statistical copolymers with varying mole fractions of furan functional groups were synthesized via RAFT polymerization. The precursor polymers were crosslinked using a reversible Diels-Alder cycloaddition to form dynamic covalent networks of varying crosslink densities. Two separate crosslinkers were used to investigate how the molecular weight and length of the crosslinker influence the thermal and mechanical properties of the network. It was found that the thermal conductivity was largely unaffected by the extent of crosslinking and the structure of the crosslinker counter to previous motivating studies. Additionally, the elastic modulus was measured and gives insight into why thermal conductivity did not significantly change. For this system, the Diels-Alder reaction was also found to be slow in the solid-state, possibly further limiting its utility as a thermal conductivity switch due to slow switching speeds.

5:00 PM EN10.07.05

Chemically Tuning Non-Parabolic Electronic Structures in Rock-Salt IV-VI Compounds Michael Toriyama, Madison Brod and G. J. Snyder; Northwestern University, United States

Non-parabolic electronic structures oftentimes reinforce the thermoelectric performance of a material, due to a larger effective valley degeneracy. While materials with inverted bands sometimes exhibit high valley degeneracy, for example rock-salt SnSe, the beneficial feature is not guaranteed for all materials with such unique inverted electronic structure topology. We survey the electronic structures of rock-salt IV-VI compounds, which demonstrates that band inversion is a necessary, but not sufficient, condition for high valley degeneracy in inverted band compounds. Using a combination of $k \cdot p$ theory, tight binding theory, and Density Functional Theory calculations, we show that the degree to which the bands are inverted is a chemically-tunable parameter that is partly responsible for inducing multiple carrier pockets in IV-VI compounds.

5:15 PM EN10.07.06

Thermal Evolution of Internal Strain in Doped PbTe James P. Male¹, Riley Hanus^{1,2}, G. J. Snyder¹ and Raphael P. Hermann²; ¹Northwestern University, United States; ²Oak Ridge National Laboratory, United States

Recent improvements in the efficiency of heat-to-electricity energy conversion in lead chalcogenide thermoelectrics involve reducing the thermal conductivity by incorporating large amounts of internal strain. The extent to which typical lead chalcogenide processing techniques (such as doping, ball milling, and densification) increase internal strain and dislocation density must be quantified to improve materials design. In this study, neutron powder diffraction is leveraged to evaluate the internal strain introduced by ball milling in doped and undoped powders. Doping with Na and/or Eu increases internal strain beyond ball milling alone with the greatest increase from combining the two dopants. Strain recovery occurs in each powder above 400 K but can be suppressed by co-doping – indicating a strong dopant-dislocation interaction in this system. Therefore, high temperature processing of PbTe powders should be avoided if high internal strain is desired. Low temperature densification and/or rapid pressing techniques may be key to maintaining

internal strain in the final pressed pellet. This work provides key guidance for defect engineering to maximize internal strain and thermoelectric performance in PbTe thermoelectrics.

SESSION EN10.08: Water
Session Chairs: Lenan Zhang and Yangying Zhu
Thursday Morning, December 2, 2021
Hynes, Level 3, Room 311

10:30 AM EN10.08.02

Atmospheric Water Harvesting Using Organic-Inorganic Hybrids and Isoenthalpic Thermodynamic Cycle Vincenzo Gentile¹, Michael Bozlar^{2,3}, Marco Simonetti¹ and Forrest Meggers³; ¹Politecnico di Torino, Italy; ²The University of Texas at Arlington, United States; ³Princeton University, United States

Over the last five years, atmospheric water harvesting has gained significant interest as a promising alternative to address the growing water scarcity problems across the globe. In this work, we synthesized a hygroscopic, organic-inorganic hybrid material and combined it with an efficient thermodynamics cycle to convert atmospheric water vapor to liquid water. We demonstrate the potential of the novel hygroscopic materials under extreme (arid) climate conditions: ambient temperature higher than 30°C and dew point lower than 5°C. The hybrid hydrogel material is obtained through the crosslinking reaction of polyelectrolytes with counter ions. We used sodium alginate and calcium alginate as the precursors to form the hygroscopic material into any desired geometries (spherical particles, rectangular structure, etc). The water vapor capture and subsequent release and conversion to liquid water is achieved through a co-located heat/mass transfer. During the water uptake step (adsorption), the stream of humid air flows through the sorbent, and the water vapor is stored in the hydrogel through a combination of endothermic and exothermic reactions. During the regeneration step, the air flow running through the device is inverted to allow a stream of hot air to contact the hydrogel. The hot air combined with high relative humidity allows for high dew points operations, such that spontaneous water condensation can take place at ambient temperatures. In addition, our experiments show that our setup can operate under dry climate conditions (ambient dew points lower than 5°C), and only use solar thermal energy to drive the regeneration cycle (water release). Finally, we demonstrate that the whole process can be scaled-up to enable the production of liter-scale freshwater on a day-night cycle.

10:45 AM EN10.08.03

High Performance Solar Evaporator with Salt Rejecting Capability Xiangyu Li, Lenan Zhang, Yang Zhong, Amy Leroy and Evelyn N. Wang; Massachusetts Institute of Technology, United States

Thermally localized solar evaporation provides a sustainable solution to address the water-energy nexus, which is promising for the applications in vapor generation, seawater desalination, wastewater treatment, and medical sterilization. However, salt accumulation has been identified as one of main practical challenges, which induces undesired fouling and reduces device lifetime. Here, we develop a novel confined water layer structure enabling a simultaneously highly efficient and salt rejecting solar evaporation. With high-fidelity modeling and experimental characterization of salt transport, we optimize the fluidic flow in the confined water layer. With the optimized flow field, our design is capable of salt transport without sacrificing energy efficiency. In addition, we further applied our design to the contactless solar evaporator and report a record-high efficiency. The fundamental understanding of salt transport shown in this work paves a new avenue toward the high-performance and reliable solar evaporation with low-cost and high material flexibility.

11:00 AM EN10.08.04

Modeling the Adsorption Kinetics of Salt-Embedded Hygroscopic Hydrogels Lenan Zhang, Carlos D. Diaz, Zhengmao Lu, Jeffrey C. Grossman and Evelyn N. Wang; Massachusetts Institute of Technology, United States

Water adsorption has attracted particular attention owing to its broad applications in atmospheric water harvesting, energy storage, and thermal management. Hygroscopic hydrogel has been recognized as a promising material due to the large total uptake, fast kinetics, and low material cost. Although high-performance water adsorption with hydrogel has been experimentally demonstrated by several recent works, the fundamental understanding of the adsorption kinetics remains elusive because of the complex transport mechanics inside the hydrogel. In this work, we develop a two-concentration model to predict the adsorption kinetics of hydrogel, where two coupled diffusion equations are introduced to describe the vapor and liquid transport, respectively. Taking the CaCl₂ embedded hydrogel as an example, we calculated the adsorption kinetics at various relative humidity and showed good agreement with experiments. More importantly, we show that liquid transport, driven by the gradient of water chemical potential, plays a significant role in the rapid kinetics of hydrogel. Liquid transport induces the redistribution of water in the polymer matrix the therefore leads to the volumetric expansion of the hydrogel. With a parametric study, we identified the key parameters responsible to the kinetics of adsorption, where an optimal initial porosity is predicted. Furthermore, the kinetics can be largely engineered by changing the elastic modulus of the hydrogel. This work provides the first modeling framework for the adsorption kinetics of hydrogel, which can serve as a design guideline in applications of the atmospheric water harvesting, energy conversion, and thermal management.

11:15 AM *EN10.08.05

A Few Recipes to Move the Leidenfrost Point David Quéré^{1,2}; ¹ESPCI, France; ²École Polytechnique, France

The levitation of water drops can be triggered by augmenting the temperature of the solid on which they sit. Above a threshold (typically 200°C on regular solids), water detaches from its substrate, owing to the presence of a continuous vapor film, which makes the liquid extremely mobile. We discuss how to decrease and increase the Leidenfrost point (LFP), which can be exploited in different applications: on the one hand, a smaller LFP allows us to make water mobile with a much smaller quantity of energy; on the other hand, a larger LFP makes it possible to maintain heat exchange at high temperature, a valuable property for heat pipes.

SESSION EN10.09: Thermoelectrics II
Session Chair: Lenan Zhang

1:30 PM EN10.09.01

Understanding the Defect Chemistry of the Mixed-Anion Thermoelectric, LaZnOP [Maud Einhorn](#), Benjamin A. Williamson and David O. Scanlon; University College London, United Kingdom

The ever increasing societal demand for clean energy, coupled with the impending global climate emergency has driven an influx of research into renewable energy. To attempt to mitigate the most catastrophic effects of climate change, it has been proposed that greenhouse gas emissions must be reduced by 20%, alongside a significant increase in the energy efficiency of existing processes. Wasted thermal energy is generated by processes across the energy sector, transportation, and the human body itself. Thermoelectric devices, can be used to convert thermal energy into a clean source of electricity, generating no emissions and without the need for moving parts. Importantly, these materials can provide a route to significantly increase the overall energy efficiency of existing process across a range of sectors via waste-heat harvesting.^[1]

The effectiveness of a thermoelectric material is measured using the dimensionless figure of merit ZT , with the world record set at 2.6 for single-crystal SnSe along the through-plane direction.^[2] Realising reasonable conversion efficiencies generally requires high electrical conductivity and low thermal conductivity, with the maximum ZT of a material often limited by the strong correlation between these properties. The parameters that contribute to the overall ZT of a material are also highly dependent on the concentration of charge carriers in the system, and therefore it is important to gain a comprehensive understanding of the defect chemistry of thermoelectric materials to maximise efficiency.

In this study, we predict the maximum theoretical ZT of LaZnOP, a mixed-anion compound which has promising thermoelectric properties, using density functional theory. The performance of oxide thermoelectrics generally lagging behind the efficiencies achieved by chalcogenide-based materials such as Bi₂Te₃, with poor carrier mobilities and high intrinsic thermal conductivities hampering progress.^[3] Mixed-anion materials have been looked to in an attempt to tackle these issues, with the more complex crystal structures reducing the lattice component of thermal conductivity. Many high-mobility mixed-anion compounds have also been reported on recently. The charge transport properties will be calculated using state-of-the-art methods based on hybrid-density functional theory, employing the AMSET approach to calculate electron-scattering rates going beyond the constant relaxation time approximation.^[4]

We show that LaZnOP has the potential to be an extremely promising earth-abundant thermoelectric material, with a ZT exceeding that of most oxide materials, provided it is dopable to 10^{19} - 10^{20} carriers cm^{-3} .^[5] Electronic-structure and band-alignment calculations suggest p-type dopability, according to the doping limit rules, and predict high hole mobilities. A full study of the defect chemistry of LaZnOP was also performed using hybrid-DFT, to assess the doping potential of LaZnOP, and guide future synthesis.

1. L. E. Bell, Cooling, heating, generating power, and recovering waste heat with thermoelectric systems. *Science* **321**, 1457–1461 (2008)
2. L-D, Zhao, S-H. Lo, Y. Zhang, H. Sun, G. Tan, C. Uher, C. Wolverton, V. P. Dravid and M. G. Kanatzidis, Ultralow thermal conductivity and high thermoelectric figure of merit in SnSe crystals. *Nature* **508**, 373-377 (2014)
3. G. Tan, L-D. Zhao, and M. G. Kanatzidis, Rationally designing high-performance bulk thermoelectric materials, *Chemical Reviews* **116**, 12123–12149 (2016)
4. Ganose, A. M.; Park, J.; Faghaninia, A.; Woods-Robinson, R.; Persson, K. A.; Jain, A. Efficient Calculation of Carrier Scattering Rates from First Principles. *arXiv:2008.09734 [cond-mat, physics:physics]* (2020)
5. Einhorn, M.; Williamson, B. A. D.; Scanlon, D. O. Computational prediction of the thermoelectric performance of LaZnOPn (Pn = P, As) *J. Mater. Chem. A*, **8**, 7914–7924 (2020)

1:45 PM EN10.09.03

Photonic Flash Sintering of High-Performance and Flexible Silver Selenide Thermoelectric Films [Mortaza Saeidi-Javash](#), Minxiang Zeng and Yanliang Zhang; University of Notre Dame, United States

Flexible thermoelectric generators have the ability to harvest thermal energy from a variety of heat sources (e.g. human skin) and directly convert it into electricity to work as a sustainable power source for sensors and wearable devices. Due to the limited thermoelectric (TE) performance of conducting polymers and rigidity of inorganic materials (e.g., Bi₂Te₃ and Sb₂Te₃), it remains a challenge to prepare low-cost, highly flexible, and high-performance TE materials. An efficient thermoelectric generator is composed of materials with a high thermoelectric power factor $S^2\sigma$ (S is the Seebeck coefficient and σ is the electrical conductivity), and low thermal conductivity κ . Herein, we fabricated n-type silver selenide films on flexible porous nylon membrane using vacuum-assisted filtration, followed by photonic flash (i.e., intense pulsed light) sintering. In contrast to conventional thermal sintering, rapid and versatile photonic sintering using intense pulsed light offers great advantages as it can sinter the silver selenide films at elevated temperatures without overheating/damaging the underneath polymeric substrate. Moreover, silver selenide shows an excellent absorptivity throughout the ultraviolet-vis (UV-vis) spectra with perfect overlap with the wavelength range of the emitted light during flash sintering. Silver selenide with exceptional thermoelectric power factor of $\sim 2200 \mu\text{W/mK}^2$ can be achieved within an extremely short sintering period of 2 ms. The flexible silver selenide materials with high thermoelectric performance near ambient temperatures can be considered an ideal candidate for low-grade waste-heat-recovery applications. This work introduced a promising pathway to realize high-performance and flexible TE devices with a broad range of applications in harvesting and managing thermal energy.

2:00 PM EN10.09.04

Full Experimental Seebeck Tensor Characterization for (p × n)-Type Transverse Thermoelectrics [Juncen Li](#), Matthew Grayson and Mercouri G. Kanatzidis; Northwestern University, United States

(p × n)-Type transverse thermoelectrics were proposed as a potential thermoelectric material for Peltier cooling at cryogenic temperature and integrated thermoelectric devices. In transverse thermoelectric materials, highly anisotropic ambipolar conduction gives rise to an off-diagonal Seebeck coefficient, generating a voltage drop perpendicular to an applied temperature gradient [1]. Some anisotropic thermoelectric materials are found to have an ambipolar Seebeck effect, with a negative Seebeck coefficient along one direction and positive orthogonal Seebeck, hence the name (p × n)-type. However, standard experiments only measured Seebeck coefficients along specific crystal axes, which is, in principle, insufficient to map the full Seebeck tensor of a low symmetry crystal. And due to the lack of Onsager symmetry, the Seebeck tensor, unlike transport coefficients like electrical conductivity, can have up to 9 independent components for the lowest symmetry case (triclinic) [2]. It is also advantageous to use a single sample to measure all Seebeck components since multiple samples might have slightly different doping [3]. Here, we report results for an all-in-one measurement set-up for measuring the full Seebeck

tensor on one sample with custom-made apparatus. Experiments on pre-characterized isotropic material confirm this apparatus can accurately determine the 9 Seebeck components. Anisotropic van der Pauw measurement can also be integrated into the apparatus to measure the full in-plane anisotropic resistivity tensor on the same sample, hence giving the anisotropic in-plane power factor [4]. Results of Seebeck tensor measurements in known anisotropic materials such as bismuth single crystals will also be presented.

The apparatus is an insulated aluminum sandwich-structure with contacts and thermocouples built in. First, two aluminum plates ($25 \times 25 \times 4 \text{ mm}^3$) are machined with aligned thru-holes and tapped holes for the respective plates. Second, grooves for contacts and thermocouples are laser cut on the inner surface of machined aluminum blocks with accurate positioning. Then, the aluminum plates are anodized to create an electrically insulated surface. After that, indium contacts and thermocouples are placed into the grooves. Finally, samples ($8 \times 8 \times 2 \text{ mm}^3$) are sandwiched between the two aluminum plates, with thermal epoxy/paste to ensure good thermal contact. A temperature gradient along 3 orthogonal directions can be achieved by placing the sandwiched blocks between the heater and heat sink in different orientations. The temperature gradients are measured by the built-in thermocouples while voltages along different directions are measured by the electrical contacts, thus giving the full Seebeck tensor. We used pre-characterized isotropic thermoelectric material PbTe as a reference sample to test the accuracy of the method. The diagonal Seebeck coefficients agree with results from the standard measurement method within 10%, and the error introduced in the 6 off-diagonal terms are smaller than 5% of the diagonal values.

References

- 1) Zhou, C. *et al*, *Phys. Rev. Lett.*, 110, 227701 (2013); Tang, Y. *et al*, *J. Electron. Mater.*, 44, 2095–2104 (2015); Shao, Q. *et al*, *MRS Advances*, 4, 491–497(2019).
- 2) R. E. Newnham, *Properties of Materials: Anisotropy, Symmetry, Structure*, (OUP Oxford, United Kingdom, 2005), pp. 234-240.
- 3) J.-J. Gu *et al*, *Phys. Rev. B*, 71.11, 113201 (2005); K.A. Borup *et al*, *Energy Environ. Sci.*, 8, 423(2015).
- 4) Peng, L. *et al*, *Phys. Rev. Lett.*, 120.8, 086801(2018).

2:15 PM EN10.09.05

Thermoelectric Properties and Scattering Mechanisms in Lead Ruthenate Derivatives Sepideh AkhbariFar, Werner Lutze and Ian L. Pegg; The Catholic University of America, United States

We synthesized several derivatives of lead ruthenate pyrochlore ($\text{Pb}_{(2-x)}\text{Ru}_{(2-x)}\text{O}_{(6.5 \pm x)}$) by varying the Pb/Ru ratio, thereby introducing changes of lattice site occupancy, vacancies and valences. Reducing the number of Pb^{2+} ions create more vacancies in the $\text{A}_2\text{O}'$ sublattice and change the properties of the already existing oxygen vacancies, which are occupied by Pb $6s^2$ electron lone pairs in pure lead ruthenate ($\text{Pb}_2\text{Ru}_2\text{O}_{6.5}$). Less than two Pb^{2+} ions mean less electrons for the vacancies. Decreasing the concentration of Ru^{4+} affects electrical conductivity, which is mainly governed by the RuO_6 backbone structure of ruthenate pyrochlores. We applied solid state synthesis and measured the thermoelectric properties of the ceramic compounds between 298 and 573 K. All compounds were isomorphic, like pure $\text{Pb}_2\text{Ru}_2\text{O}_{6.5}$. We analyzed our results for underlying scattering mechanisms of electrical (σ) and thermal conductivity (κ), the Seebeck coefficients (S) in terms of carrier concentrations, using existing quantum physical models. All ceramics were p -type and showed metal-like electrical conductivity and glass-like thermal conductivity. Therefore, the same scattering mechanisms were seen for all pyrochlores. Electrical conductivity $\sigma(T)$ and electronic thermal conductivity $\kappa_e(T)$ were governed by 'electron impurity scattering'. The 3-phonon resistive process (Umklapp scattering) controlled the lattice thermal conductivity $\kappa_l(T)$, which supports the electron-impurity scattering mechanism. In all compounds, the Seebeck coefficients were inversely proportional to the carrier concentration.

2:30 PM EN10.09.06

Modelling Thermoelectric Properties in a Multicomponent Alloy Space Ramya Gurunathan¹, Suchismita Sarker², Logan Ward³, James Saal⁴, Apurva Mehta² and G. J. Snyder¹; ¹Northwestern University, United States; ²SLAC National Accelerator Laboratory, United States; ³Argonne National Laboratory, United States; ⁴Citrine Informatics, United States

Alloy systems with multiple principal elements are considered attractive for thermoelectric materials because the mass and strain fluctuations introduced into the lattice can effectively scatter phonons and suppress the lattice thermal conductivity. However, both charge carriers and heat-carrying phonons are known to experience scattering due to alloying effects. We apply analytic transport models, based on perturbation and effective medium theories, to predict how alloy scattering will affect the thermal and electronic transport across the full compositional range of several pseudo-ternary and pseudo-quaternary alloy systems. For carrier mobility, the work of Makowski and Glicksman[1] provides a straightforward expression for alloy effects in a binary system, however, an extension to higher-order systems has not been presented. We develop a multicomponent extension to the alloy mobility model by applying computational thermodynamics techniques used to calculate excess Gibbs energy, namely the Redlich-Kister polynomial and Muggianu model. In the case of thermal transport, a recent reformulation of the Klemens alloy model[2] provides a straightforward route to compute the thermal conductivity of multicomponent alloys. From our calculations, we find that the thermal conductivity is lowest along the binary system with the largest mass contrast such that adding additional alloying elements is not necessarily beneficial from the standpoint of alloy scattering.

The alloy scattering analytic methods will predict smooth variations of transport properties with increasing disorder. However, through experiment, we can occasionally observe discontinuous changes in properties, resulting from abrupt transitions due to electronic band convergence or phase separation. In order to retain these experimental insights, we combine the physical models described above with the statistical Gaussian Process Regression (GPR) method. In this physics-informed GPR, the transport models are used to specify the prior means of the Gaussian process. Bayesian inference is then used to simultaneously update the prediction mean and variance using all the available experimental data. As a result, we can acquire both predicted values and their associated uncertainties, informed both by the physics-based functional form of alloy scattering and the full corpus of experimental data available.

References:

- [1] Makowski, L., Glicksman, M. Disorder Scattering in Solid Solutions of III-V Semiconducting Compounds. *J. Phys. Chem. Solids*. 34, 487-492, (1973)
- [2] Gurunathan, R., Hanus, R., *et al*. Analytical Models of Phonon—Point-Defect Scattering. *Physical Review Applied*. 13 (034011) (2020)

2:45 PM BREAK

Thursday Afternoon, December 2, 2021
Hynes, Level 3, Room 311

4:00 PM *EN10.10.01

Thermal Batteries as a Solution to the Grid Storage Problem Asegun Henry; Massachusetts Institute of Technology, United States

Energy storage is arguably the most important single technology we have to develop in order to mitigate climate change. We have to store an overabundance of renewable energy, when the weather is favorable, and discharge it back to grid when there is demand. Commercially available technologies are unable to meet the future needs of the grid, and the most critical property is the cost per unit energy (CPE). Towards solving this problem, the Atomistic Simulation & Energy (ASE) group at MIT is developing an extremely low-cost (< \$10/kWh) technology termed thermal batteries. This talk will review how the technology works and progress to date.

4:30 PM EN10.10.02

Energy-Efficient Adaptive Personal Thermal Management Po-Chun Hsu; Duke University, United States

Energy-Efficient Adaptive Personal Thermal Management

Thermal homeostasis is one of the most vital factors for humans. Small deviations from thermal comfort zones can reduce work productivity, while sudden or large changes in thermal environments can lead to serious health issues such as cardiovascular diseases, influenza, and stroke. The indispensable nature of thermal comfort leads to enormous energy consumption for indoor temperature control, which constitutes 15% of the total US energy consumption and is responsible for considerable amounts of carbon footprint and climate change. To mitigate the issue and find the balance between thermal comfort and energy-efficient, personal thermal management has been demonstrated to be a powerful solution. By developing new wearable technologies with thermal engineering functionalities, we can provide the optimal local thermal environment to the users rather than the entire building. As our environments and physiological conditions change frequently, there is a pressing need to develop dynamic personal thermal management techniques that can essentially act as artificial thermoregulation. Nevertheless, the limited portable power source has again become a harsh constriction. There is still room to improve in terms of wearability, tunability, and energy efficiency.

In this talk, I will introduce our recent research progress of wearable varied emittance (WeaVE) devices that modulate the human body radiative heat transfer to accomplish thermoregulation with ultralow energy consumption. Compared with active generating/pumping heat, WeaVE devices are non-volatile and do not consume energy to maintain heating/cooling. I will explain three different versions of WeaVE devices, each of which with different application scenarios. (i) Electrochromic WeaVE vary the emissivity with only 0.5 V and are stretchable to fit the human body contour. (ii) Sweat-actuated WeaVE combines radiative and convective heat transfer to achieve large-range autonomous thermoregulation. (iii) Mechanical triple-mode WeaVE can vary between transmittance, emittance, and reflectance modes to expand from human skin to other objects with various emissivities.

4:45 PM EN10.10.03

Nano-to-Microsphere Polycrystalline Opals Using Slope Self-Assembly for Advanced Thermal Management Carlos D. Diaz, Rishabh M. Shetty, Samantha Cheung, Geoffrey Vaartstra, Ashwin Gopinath and Evelyn N. Wang; Massachusetts Institute of Technology, United States

Inverse opals have attracted significant interest over the last decade as a templated microporous architecture with great potential for high-performance phase-change heat transfer devices. However, commonly used fabrication methods for the initial opal template yield structures with limited permeability due to small achievable feature sizes and the presence of defects in the crystalline array, hindering the use and performance of inverse opals in thermo-fluidic applications. In this work, we show how slope self-assembly method is a promising approach for phase-change thermal management. We developed a model, which was validated by experiments, to achieve high throughput and controllable opal self-assembly method with the potential of overcoming limitations in previous fabrication methods. We demonstrated the ability to fabricate millimeter-scale polycrystalline opal monolayers with sphere sizes ranging from 500 nm up to 10 μm , while centimeter-scale opals, comparable with wafer-scale state-of-the-art demonstrations, were also possible with some sparse sphere stacking or small uncovered areas. Due to the large achievable pore sizes, which exceed by an order of magnitude the sizes possible with the vertical deposition method, these structures have the potential to yield inverse opals capable of withstanding heat fluxes up to two orders of magnitude higher than those made with other fabrication methods. In addition, due to the simplicity, high throughput, and large range of achievable feature sizes of the method, these structures can also be used in a broad range of applications such as molecule printing and high-performance electrochemical systems.

SESSION EN10.11: Thermal Management II
Session Chairs: Samuel Graham and Junichiro Shiomi
Monday Morning, December 6, 2021
EN10-Virtual

8:00 AM *EN10.11.01

New Insight and Route for Developing Isotropic Heat Spreader with Small Thermal Boundary Resistance Junichiro Shiomi; The University of Tokyo, Japan

The topic of developing high-performance heat spreader has been around for a long time and there has been great advancement thanks to the community, but the demand for better heat spreader is getting larger than ever for thermal management of high-speed telecommunication and electric vehicles. In those application of important for sustainability and resilience, the large heat flux generated during the operation would overly elevate the temperature of devices, which can degrade the device and limit the performance. What is required is to effectively spread the condensed heat in three-dimensions using materials with (effectively) isotropically high thermal conductivity. In this talk, we will introduce two approaches; copper-diamond composite and graphite-copper composite. In both cases, the key is to bond materials with small thermal boundary resistance or large thermal boundary conductance (TBC).

As for the copper-diamond composite, an unconventional approach applying self-assembled monolayer (SAM) prior to the high-temperature sintering of copper/diamond composite was utilized to enhance the TBC between copper and diamond. The enhancement was first systematically confirmed on a model interface system consisting of deposited-copper-layer/SAM/diamond-substrate by detailed SAM morphology characterization and TBC measurements. TBC significantly depends on the SAM coverage and ordering, and the formation of high-quality SAM promoted the TBC. There, by systematically varying the end groups of SAM and the kind of substrate, some interesting insight was found. Although, TBC is typically positively correlated with interfacial adhesion at an interface, the experiments showed that a weak van der Waals interface can give a higher TBC than a strong covalently bonded

interface. This occurs in a system with highly mismatched vibrational frequencies (copper/diamond) modified by SAM. Further analyses revealed that this is attributed to the trade-off between the bridging (of vibrational spectra) and binding effects [1]. Then, applying the knowledge to the copper diamond composite, the diamond particles were simultaneously functionalized by SAM with the condition giving the highest TBC in the model system and sintered together with the copper to fabricate isotropically high thermal conductivity composite [2].

For the graphite-copper composite, although graphite is a promising candidate owing to its high basal-plane thermal conductivity, its application has been restricted by its low c-axis thermal conductivity. Here, this issue is resolved by transforming graphite into an isotropic thermal conductor by building a structure that can effectively route heat in all three dimensions. We developed a double-decker structure with differently oriented graphite layers to realize high heat dissipation from a local heat source. The critical issue of bonding the graphite layers was overcome by a high-temperature process using copper as the binding layer. As a result, graphite/copper composite efficiently dissipates heat nearly isotropically and performs even better than the above copper-diamond composite [3]. The detailed experimental analysis and demonstration of the heat transfer will be presented at the talk.

[1] B. Xu, S. Hu, S.-W. Hung, C. Shao, H. Chandra, F.-R. Chen, T. Kodama, J. Shiomi, "Weaker bonding can give larger thermal conductance at highly mismatched interfaces", *Science Advances* 7, eabf8197 (2021).

[2] B. Xu, S.-W. Hung, S. Hu, C. Shao, R. Guo, J. Choi, T. Kodama, F.-R. Chen, J. Shiomi, "Scalable monolayer-functionalized nanointerface for thermal conductivity enhancement in copper/diamond composite", *Carbon*, 175, 299-306 (2021).

[3] B. Xu, et al, (submitted).

8:30 AM *EN10.11.04

Dynamic Droplet Events on Heat Transfer Surfaces [Ryan Enright](#); Nokia Bell Labs., United States

Dynamic droplet events on heat transfer surfaces give rise to interesting and surprising behaviours that are relevant to advancing our understanding of thermal energy transfer across interfaces. Here, we discuss two particularly interesting cases; jumping droplet condensation on superhydrophobic surfaces and the impact of a volatile droplet on a superheated wetting surface.

In the first part of this talk we address the heat transfer performance of superhydrophobic surfaces limited by the low individual droplet growth rates associated with extreme droplet apparent advancing contact angles ($\theta_{app} \rightarrow 180^\circ$) and the fundamental size limits of coalescence-induced droplet jumping. Our detailed condensation heat transfer modelling coupled with numerical simulations of binary ($N = 2$) and coordinated ($N > 2$) droplet coalescence, show that biphilic surfaces with smooth, low surface energy spots on a superhydrophobic background exhibit an unprecedented 10X higher jumping droplet condensation heat transfer coefficient when compared to homogenous superhydrophobic surfaces. Model predicted design optimization of the biphilic surface is validated against condensation experiments. Our findings clarify the role of droplet jumping dynamics and distribution densities by revealing optimum design guidelines for biphilic surface development for maximum condensation heat flux. Contrary to current understanding, we observe that spot wettability should not be optimized towards minimizing droplet nucleation energy barrier, rather it should minimize droplet adhesion while maximizing individual droplet growth rate.

We then describe the crucial impact thermal capillary waves and ambient gas rarefaction have on enhancing/limiting the jumping speeds of coalescing nanodroplets on low adhesion surfaces. By using high-fidelity non-equilibrium molecular dynamics simulations in conjunction with well-resolved volume-of-fluid continuum calculations, we are able to quantify the different dissipation mechanisms that govern nanodroplet jumping at length scales that are currently difficult to access experimentally. We find that interfacial thermal capillary waves contribute to a large statistical spread of nanodroplet jumping speeds. As the gas surrounding these liquid droplets is no longer in thermodynamic equilibrium, we also show how the reduced external drag leads to increased jumping speeds. This work demonstrates that, in the viscous-dominated regime, the Ohnesorge number and viscosity ratio between the two phases alone are not sufficient, but that the thermal fluctuation number (Th) and the Knudsen Number (Kn) are both needed to recover the relevant molecular physics at nanoscales. Our results and analysis suggest that these dimensionless parameters would be relevant for many other free-surface flow processes and applications that operate at the nanoscale.

In the second part of this talk, we present preliminary results on the Leidenfrost (critical heat flux) limit for dynamic droplet interactions with superheated surfaces. We identify a scientifically and practically relevant wetting behaviour in the Leidenfrost transition regime. We provide experimental observation of an inverted phase fingering instability demonstrating fractal-like wetting structures at the Leidenfrost transition indicating a rich interplay of fluid flow undergoing a change of phase and surface forces that is not currently well understood.

9:00 AM *EN10.11.02

Thermal Management Strategies to Enable Ga₂O₃ and AlGa_N-Based Electronics [Samuel Graham](#)^{1,2}, Mark Goorsky³, Asif Khan⁴ and James Speck⁵; ¹Georgia Institute of Technology, United States; ²University of Maryland, United States; ³University of California, Los Angeles, United States; ⁴University of South Carolina, United States; ⁵University of California, Santa Barbara, United States

Ultrawide bandgap semiconductors made from high Al content AlGa_N alloys and Ga₂O₃ have promise for future rf electronics and power switches. One of the key issues that arises from using these ternary alloys is the intrinsic low thermal conductivity of AlGa_N and Ga₂O₃ and the low thermal boundary conductance at contacts with these alloys. This requires careful design of the device architecture and layout in order to yield effective heat dissipation pathways for AlGa_N systems. In this talk, we will present modeling results which demonstrated specific regimes where cooling from the backside or top side of the ultrawide bandgap devices provide the most efficient pathway for heat dissipation. We will also present modeling and experimental results that demonstrate the effectiveness of the integration of high thermal conductivity dielectrics on the heat dissipation efficiency in these devices. Limitations on the integration of these layers through direct growth or bonding will be discussed. Finally, the impact of the reaction between metal contacts and UWBG materials like Ga₂O₃ will be discussed and its role on thermal transport from the devices analyzed through device modeling.

9:30 AM *EN10.11.03

Co-Designing Electronics with Direct Monolithic Integration of Metals for More Sustainable Thermal Management [Nenad Milijkovic](#); University of Illinois at Urbana-Champaign, United States

Power densification of electronics is greatly shaped by their co-design with emerging thermal management technologies. Heat spreaders represent a thermal routing technique implemented to reduce thermal resistance and limit electronic device temperature fluctuation. Here, we demonstrate the co-design of electronic systems through the monolithic integration of copper (Cu) directly on electronic devices to serve as heat spreaders and temperature stabilizers. We developed a fabrication recipe to electrically insulate the electronics with Parylene C and conformally coat them with Cu, demonstrating greater proximity to heat generating elements, elimination of thermal interface materials, and unprecedented cooling performance compared to existing cooling technologies. Our sustainable cooling method with 8 μm thick Parylene C can handle up to 600 V, providing exceptionally low device-to-ambient specific thermal resistances approaching 2.5 (cm²K)/W in quiescent air and 0.8 (cm²K)/W in quiescent water, with time constants of 110 s in air and 5.61 s

in water. Our cooling technology has the potential to enable the continued realization of very compact and highly power dense electronics and reduction in the cooling energy consumption.

SESSION EN10.12: Thermal Management and Radiation
Session Chair: Yangying Zhu
Monday Morning, December 6, 2021
EN10-Virtual

10:30 AM EN10.12.01

Organopolysilazane Polymer as High Emissive Coating for Passive Daytime Radiative Cooling Applications Udayan Banik, Hosni Meddeb, Maximilian Götz-Köhler, Ashutosh Agrawal, Nies Reininghaus, Kai Gehrke, Oleg Sergeev, Jonas Stührenberg, Maciej Sznajder, Martin Vehse and Carsten Agert; German Aerospace Center, Germany

Passive Daytime Radiative cooling (PDRC) technology has the potential to significantly reduce our energy dependency for cooling buildings. It is an emerging, innovative green technology which uses the deep space as a cold sink to emit excess heat from an object through earth's atmosphere mitigating the heat island effect in urban areas. Achieving an efficient PDRC cooler requires high emission through the spectral range (8-13 μm) where the atmosphere is transparent, while reflecting the incoming solar spectra^[1,2]. IR emissive polymers present a simple yet promising approach that enables controlling emission through molecular bonding^[3]. However, relatively thick polymer coatings (20-200 μm) are required to achieve sufficient high emissivity. To realize high cooling performance, an emitter with low absorption of the downward heat radiation from the atmosphere is desired. Aforementioned spectral selectivity on the other hand, generally requires complex nano-engineered structures to achieve restricted emission in the spectral range of 8-13 μm . We have recently demonstrated for the first time a PDRC structure based on a spectrally selective organopolysilazane planar emitter which is simple to manufacture^[4].

Organopolysilazane are silicon-based polymers where alternating silicon and nitrogen atoms form the backbone of the polymeric structure along with methyl and vinyl group attached to it. Polysilazane (PSZ) barrier coatings have been studied widely for their chemical resistance, stability, corrosion protection properties and easy applicability. The exceptional high transmissivity in the UV-Vis region and flexibility of polysilazane based coatings enable versatile application of these coatings^[5,6]. We present here the optical properties and cooling performance of a simple dual layer spectrally selective PDRC structure with PSZ coating as a thermal emitter on a thin film silver reflector. Due to the high transparency of the polymer coating the structure allows for 97% reflection of the solar spectrum. We demonstrate the characteristic bond vibrations from the functional groups of the polymeric structure which coincides very well with the atmospheric transmittance window of 8-13 μm resulting in the high emissivity of 0.9 in the 8-13 μm wavelength range. The structure with a 5 μm thin coating can cool down to 6.8°C below ambient owing to a cooling power of 93.7 W/m². Based on long term outdoor performance tests and degradation tests under different environment, the changes in optical response and reliability of the PDRC structure was evaluated. We believe that polysilazane emitter coatings due to its simplicity and tenability will open new research possibilities for PDRC applications.

References-

- [1] A. P. Raman, M. A. Anoma, L. Zhu, E. Rephaeli, S. Fan, *Nature* **2014**, *515*, 540.
- [2] D. Zhao, A. Aili, Y. Zhai, S. Xu, G. Tan, X. Yin, R. Yang, *Applied Physics Reviews* **2019**, *6*, 21306.
- [3] A. Aili, Z. Y. Wei, Y. Z. Chen, D. L. Zhao, R. G. Yang, X. B. Yin, *Materials Today Physics* **2019**, *10*, 100127.
- [4] U. Banik, A. Agrawal, H. Meddeb, O. Sergeev, N. Reininghaus, M. Götz-Köhler, K. Gehrke, J. Stührenberg, M. Vehse, M. Sznajder, C. Agert, *ACS applied materials & interfaces* **2021**, *13*, 24130.
- [5] U. Banik, K. Sasaki, N. Reininghaus, K. Gehrke, M. Vehse, M. Sznajder, T. Sproewitz, C. Agert, *Solar Energy Materials and Solar Cells* **2020**, *209*, 110456.
- [6] U. Banik, N. Reininghaus, P. Seefeldt, M. Sznajder, K. Gehrke, M. Vehse, P. Spietz, T. Sproewitz, C. Agert, *2019 European Space Power Conference (ESPC) 2019*.

10:45 AM EN10.12.02

Improve Effective Thermal Conductivity in N-Type Copper-Nickel Alloy for Active Cooling Application Shuai Li¹, Sabbir Akhanda¹, Kyle Synder² and Mona Zebarjadi¹; ¹University of Virginia, United States; ²CCAM - Commonwealth Center for Advanced Manufacturing, United States

The conventional thermoelectric (TE) cooling modules are optimized for refrigeration to pump heat from the cold end to a heat sink. To achieve the best energy conversion efficiency, it requires a combination of a large thermoelectric power factor and low thermal conductivity to reach a high figure of merit. Whereas active cooling aims at draining heat from the heat source to a heat sink, which makes the low thermal conductivity of the commercial TE cooling disadvantageous. The metallic thermoelectric modules, on the contrary, combine large thermoelectric power factor and large thermal conductivity, allowing a more efficient drain of heat via both active Peltier cooling and passive cooling than the passive or the TE refrigeration ones. The fact that the active Peltier cooling can be adjusted by applying current to the modules also provides a more controllable way of heat management. In this study, we show that a Cu-Ni alloy with both a high power factor and a reasonable thermal conductivity can be synthesized with cheap industrial level ingredients and via the simple ball-mill and hot-press process in the lab. A power factor of 42 $\mu\text{W}/(\text{cm}^1\text{K}^2)$ can be reached at room temperature with the proper Cu-Ni composition and annealing process, which is surpassed the state-of-art study on Cu-Ni thermoelectric materials synthesized with expensive high purity elements. The effective thermal conductivity of the Cu-Ni alloy with proper composition can surpass the passive thermal conductivity of pure copper at raised temperature (>400K). The deposition parameters of Directed Energy Deposition (DED) have been optimized for the specific Cu-Ni composition. Dense samples with properties comparable with samples from the laboratory have been made and characterized. Our study shows the potential of Cu-Ni alloys as an active cooling material and the compatibility of Cu-Ni Alloy with additive manufacturing, which enables the TE active cooling modules to adopt the optimal geometry to minimize the interfacial thermal resistance between the heat source and the heat sink, as well as scale down for the heat management of integrated circuits.

11:00 AM EN10.12.03

Broadband Light Absorber with Au-Coated Hierarchical Nanoturf Structures for Solar-Thermal Conversion Jong Uk Kim, Seung Ji Kang, Seok Joon Kwon and Tae-il Kim; Sungkyunkwan University, Korea (the Republic of)

Although much attention has been paid to the development of photothermal materials and designs that can convert solar irradiation into exploitable thermal energy, it remains some obstacles such as limited light absorbing band and narrow incident angle. This study proposes a black gold-coated hierarchical nanoturf (Au/h-nanoturf) membrane incorporated with randomly distributed high aspect ratio (AR) nanostructures and micro-through holes. Thanks to structural advantages, this large area membrane exhibited good absorption of the broadband solar light

spectrum. The h-nanoturf is further combined with a microcone array to enhance solar absorption extended to the near-infrared range as well as the omnidirectional incident direction of the light. The fundamental mechanism of the strong omnidirectional broadband absorption performance of the h-nanoturf was thoroughly analyzed with computational electrostatics simulations. Consequently, we employed the Au/3D h-nanoturf with microscale hole (μ -hole) membrane to fabricate an advanced solar-vapor generator.

11:15 AM EN10.12.04

Radiative Heat Transfer Between Superconducting Films Raul Esquivel-Sirvent, Shunashi Castillo-López, Giuseppe Pirruccio and Carlos Villarreal; Universidad Nacional Autónoma de México, México

We present a theoretical study of the near-field radiative heat transfer between high- T_c superconducting thin films made of optimally doped $\text{YBa}_2\text{Cu}_3\text{O}_{7-\delta}$. The critical temperature for these ceramics is $T_c = 93$ K. We show that thin films significantly enhance the radiative heat transfer by efficiently coupling each interface's optical modes. The heat transfer between thin films turns out to be up to one order of magnitude higher than that for bulk plates in normal and superconducting states. The change of the optical response above and below T_c also plays an important role since the superconducting phase transition leads to an abrupt suppression of the total heat flux. A detailed study of the different modes and the heat transfer is also presented, showing that for these materials, the infrared damping of the dielectric function determines to a significant extent the role in the magnitude of the heat flux.

11:30 AM EN10.12.05

Large Change of Thermal Conductivity Induced by Temperature and Light in Azobenzene-Based Mesophases Noa Varela-Dominguez¹, Carlos López-Bueno¹, Alejandro López-Moreno^{1,2}, Gustavo Rama¹, María Giménez-López¹ and Francisco Rivadulla¹; ¹Centro Singular de Investigación en Química Biológica e Materiais Moleculares (CiQUS), Universidade de Santiago de Compostela, Spain; ²IMDEA Nanociencia, Spain

Achieving an efficient management of the heat dissipated in a variety of devices, is important for their proper functioning, and to prevent their uncontrolled failure. Research in the field of thermal regulation has mainly focused on the development of complex fluids through the dispersion of nanoparticles in different solvents (Kebllinski et al., *Materials Today*, 8, 36, 2005) and on the manufacture of 'defective' solid materials, in which the thermal conductivity is limited by the introduction of impurities or interfaces at the atomic scale. However, these materials have several drawbacks: in the case of nanofluids, the high concentrations of dispersed particles needed to achieve a substantial change in thermal conductivity often result in rheological problems, preventing their application; in the case of 'defective' solids, the artificial impurities cannot be modified once the material has been manufactured, so that the modulation of thermal conductivity by an external stimulus is impossible. Thus, the development of efficient and tunable thermal regulators is one of the challenges in materials science.

'Soft matter' thermal devices based on liquids, gels or mesophases, are promising candidates in this direction. Shin et al. reported a reversible threefold change in the thermal conductivity of an azobenzene polymer induced by light (Shin et al., *PNAS*, 116, 8629, 2019).

Here we report the synthesis and thermal conductivity of 4,4'-dialkyl-3-methylazobenzene derivatives, with different alkyl chain lengths (between 3 and 10 carbon atoms). These systems show a rich thermal phase diagram, with different crystalline, anisotropic mesophases, and isotropic liquid configurations, as a function of temperature. The reversible changes in the alignment of the alkyl chains along these phases results in reversible variations of the thermal conductivity up to 26%. Moreover, the conformational transition between trans and cis azobenzene groups under UV-Vis illumination leads to reversible crystal-to-liquid transition, changing the thermal conductivity up to 40%.

We discuss the effect of chain length and temperature on the kinetics of the transformation, and on the stability of the different phases formed.

The large variety of light-responsive chemical groups, combined with the powerful strategies developed by organic and polymer chemists over the last decades, suggest that this could be a successful approach to develop effective thermal switches.

11:45 AM *EN10.12.06

Thermodynamics of Light Management in Near-Field Thermophotovoltaics Georgia T. Papadakis¹ and Shanhui Fan²; ¹ICFO – Institute of Photonic Sciences, United States; ²Stanford University, United States

We analyze near-field thermophotovoltaic systems in terms of their open-circuit voltage (V_{oc}). Unlike previous numerical results with fluctuational electrostatics, we introduce a simple analytic model that captures the physics of near-field thermophotovoltaic systems and predicts their performance metrics in terms of both current and voltage. We show that (i) operating in the near-field naturally enhances radiative recombination, and that (ii) owing to photon recycling and minimal radiation leakage, near-field thermophotovoltaic systems can be much thinner compared to typical PV cells, thus reducing non-radiative losses. Combination of these effects leads to values of V_{oc} that can approach the radiative limit.

SESSION EN10.13: Simulation and Machine Learning

Session Chair: Yuan Yang

Monday Afternoon, December 6, 2021

EN10-Virtual

1:00 PM EN10.13.01

Discovery of Materials for Thermionic Energy Conversion by High-Throughput Density Functional Theory and Machine Learning Peter Schindler^{1,2}, Evan Antoniuk¹, Gowoon Cheon¹, Yanbing Zhu¹ and Evan Reed¹; ¹Stanford University, United States; ²University of Vienna, Austria

The work function is the key surface property that determines how much energy is required for an electron to escape the surface of a material. This property is crucial for thermionic energy conversion, band alignment in heterostructures, and electron emission devices. The discovery of thermally stable, ultra-low work function materials (less than 1.5 eV) would allow thermionic conversion of heat (>1500 °C) directly to electricity with efficiencies exceeding 30% (typical thermionic and thermoelectric converters have efficiencies around 10%). In recent years, data-driven approaches based on high-throughput *ab-initio* calculations have emerged as a new paradigm to facilitate the search through vast chemical spaces for new materials with tuned properties or novel behavior. The rapid increase in available computational data structured in open source material databases such as Materials Project, AFLOW, and NOMAD has opened an avenue towards material discovery using data-mining and statistically driven machine learning approaches. However, most big material databases largely lack to report surface properties like the work function as each bulk material typically has dozens of distinct low-index crystalline surfaces and terminations. Here, we report a high-throughput workflow using density functional theory (DFT) to calculate the work functions of 29,270 surfaces (23,603 slab calculations) that we created from 2,492 bulk materials, including up to ternary compounds. On the low tail end of the work function distribution, we discover 162 surfaces with an ultra-low (<2.5 eV) work function. Based on this database we develop a physics-based

approach to featurize surfaces and use supervised machine learning to predict the work function. We find that physical choice of features improves prediction performance far more than choice of model. Our random forest model achieves a mean absolute test error of 0.19 eV when predicting the work function, which is more than 4 times better than the baseline and comparable to the accuracy of DFT. This surrogate model enables rapid predictions of the work function ($\sim 10^5$ faster than DFT) across a vast chemical space and facilitates the discovery of material surfaces with extremely low work functions for energy conversion and electronic applications.

1:15 PM EN10.13.02

Study of Thermoelectric Performance of Polymer Nanocomposites by Applying Generalized Effective Medium Theory Shivani Shisodia¹, Abdelhak H. Sahraoui¹, Dharmendra P. Singh¹, Benoit Escome² and Michael Depriester¹; ¹Université du Littoral Côte d'Opale, France; ²Université du Littoral Côte d'Opale, France

Thermoelectric (TE) materials grabbed much interest in various applications such as cooling, power generation, sensors, aircraft, etc. due to their ability to convert waste thermal energy into electric energy¹⁻³. The interdependency among thermal conductivity, electrical conductivity, and Seebeck coefficient acts as a barrier to enhance thermoelectric performance. However, thanks to nanotechnology, it is possible to break this interdependency by employing interface phonon scattering approach to enhance the TE efficiency. Introducing lattice mismatch concept at nanoscale can decrease the lattice thermal conductivity more effectively than electrical conductivity⁴. Also, Seebeck coefficient can increase due to the quantum confinement effect at nanoscale, without decreasing the electrical conductivity⁵.

The current work is the continuation of our previous work based on the synthesis and characterization of poly (3,4-ethylene dioxythiophene): polystyrene sulfonate (PEDOT: PSS) filled with different wt. fractions (0.001-0.05) of inorganic graphene oxide-titanium dioxide (GO-TiO₂). Here, we succeed to break the interdependency of thermoelectric parameters by enhancing electrical conductivity and Seebeck coefficient whilst deducing thermal conductivity as a function of filler wt. fraction.

The present work is more focused on in-depth analysis of the obtained experimental results by using theoretical predictions. Firstly, the electrical conductivities, the thermal conductivities, and the Seebeck coefficients of aforementioned composites were measured experimentally. Secondly, the experimentally obtained results were fitted by using Effective medium theory (EMT) and Generalized effective medium theory (GEMT) based on Landauer and Sonntag's equations. The obtained best-fit parameters demonstrate the individual TE properties of the matrix and the filler.

EMT and GEMT have been directly applied to understand the evolution of electrical and thermal conductivities of the composites as a function of filler wt. fraction. However, for the Seebeck coefficient, we have utilized the Sonntag's extended model for degenerate semiconductors where the heat flux was replaced by the entropy flux. Therefore, the ratio of thermal conductivity to Seebeck coefficient is considered as a transport parameter and has been utilized to understand the evolution as a function of filler wt. fraction instead of Seebeck coefficient alone. The obtained best-fit parameters for the matrix and the filler were found to be in good agreement with the literature.

Keywords: Thermoelectricity, thermal conductivity, Electrical conductivity, Seebeck coefficient, Generalized effective medium theory.

Bibliography:

1. Samson, D., Otterpohl, T., Kluge, M., Schmid, U. & Becker, Th. Aircraft-Specific Thermoelectric Generator Module. *J. Electron. Mater.* 39, 2092–2095 (2010).
2. Kim, S., Park, S., Kim, S. & Rhi, S.-H. A Thermoelectric Generator Using Engine Coolant for Light-Duty Internal Combustion Engine-Powered Vehicles. *J. Electron. Mater.* 40, 812–816 (2011).
3. LeBlanc, S. Thermoelectric generators: Linking material properties and systems engineering for waste heat recovery applications. *Sustain. Mater. Technol.* 1–2, 26–35 (2014).
4. Ahmad, K., Wan, C. & Zong, P. Thermoelectric properties of BiSbTe/graphene nanocomposites. *J. Mater. Sci. Mater. Electron.* 30, 11923–11930 (2019).
5. Tavkhelidze, A. Large enhancement of the thermoelectric figure of merit in a ridged quantum well. *Nanotechnology* 20, 405401 (2009).

1:30 PM *EN10.13.03

Machine Vision and Learning Models for Materials Design Youngjoon Suh, Chuanning Zhao, Ramin Bostanabad and Yoonjin Won; University of California, Irvine, United States

Advances in thermal and energy sciences bring transformational efficiency enhancements in energy, water, manufacturing processes, and electronics cooling by fundamentally manipulating energy processes across multiple length and time scales. Herein, the energy processes are naturally complex, and create dynamic changes in thermofluidic features, which are represented as bubbles or droplets. Furthermore, the improvements in the energy process critically depend on our ability to design and realize materials with optimal properties, adding another level of complexity. Unveiling energy processes integrated with materials design can be possible by collecting interpretable and rich physical descriptors from bubbles or droplets. These challenges for extracting physics from complex, dynamic, and fast-moving objects may be addressed using revolutionary intelligent machine vision. Therefore, one of my research interests is to build a data-driven framework based on live images by converging the recent advancements in artificial intelligence (AI)-enabled machine vision, data processing, and deep learning models, to push the boundaries of knowledge about thermofluidic physics.

In this talk, I will discuss AI-enabled innovations, data-centric thinking, and opportunities, by showcasing a few examples. 1) I will first introduce the modular framework that can produce high-throughput fast data acquisition, streamline automatic data processing, and create a spatiotemporal thermal mapping at extreme resolutions. 2) I will explore input space (e.g., material or surface parameters) by generating imaging data on dynamic bubble/droplet topologies along with heat transfer data where the experimental design and heat transfer performance will be fully connected with physical descriptions. Therefore, the rational design of material or surface parameters can engineer solid-liquid-vapor contact lines that result in favorable phase change curves. 3) Then, I will discuss avenues to design functional thermal architectures that are widely employed as high-surface conduits for thermofluidic applications.

2:00 PM EN10.04.10

Late News: Spark Plasma Sintering of SrVO_{3-δ} and Mixed Perovskites for Thermal Energy Management Liam E. Fisher, Xiaochuan Tang and Kaka Ma; Colorado State University, United States

Previous density functional theory work suggested that SrVO_{3-δ} is a promising candidate as electron emissive material for thermionic energy conversion because of the predicted ultralow work function (1.86eV). Additionally, A- and B-site doping in ABO₃ perovskites can increase power factors and decrease thermal conductivity compared to traditional oxide perovskites for thermoelectric energy conversion. To experimentally explore the potential of using SrVO_{3-δ} and its mixed perovskites for thermal energy management via thermionic or thermoelectric conversion, bulk polycrystalline SrVO_{3-δ} samples were synthesized via spark plasma sintering. The effects of Ba- and Ti- doping on the microstructure, electrical conductivity, and thermal stability of SrVO_{3-δ} were investigated. Results revealed that the microstructure consists of predominant SrVO_{3-δ} phase with minor SrTiO_{3-δ} phase, with grain size of approximately 15 μm. The thermionic emission behavior tested in an Ar plasma will be discussed as well.

6:30 PM EN10.15.01

Improvement of Thermoelectric Power Generation Performance in Silicide-Based Thermoelectric Modules Using Higher Manganese Silicide

MnSi_γ Naoto Fukutani¹, Masakuni Okamoto¹, Yosuke Kurosaki¹, Shin Yabuuchi¹, Tomohisa Takamatsu², Yuzuru Miyazaki² and Jun Hayakawa¹; ¹Hitachi Ltd, Japan; ²Tohoku University, Japan

A lot of energy is lost as waste heat in the process of producing and consuming electricity. Utilizing a vast amount of heat energy is essential for realizing a sustainable society. Thermoelectric conversion technology is one of the solutions for utilizing waste heat effectively because it enables a direct conversion of heat into electricity without any moving parts. The higher manganese silicide of MnSi_γ is a promising thermoelectric material composed of less-toxic elements with a material figure of merit *ZT* reaching up to 1.0. We have previously reported that it is possible to reduce the thermal conductivity and improve *ZT* by co-doing Re and Ge to the matrix of MnSi_γ. In this study, silicide thermoelectric modules using p-type (MnRe)(SiGe)_γ were prepared and its power generation characteristics were evaluated.

An alloy powder of p-type (MnRe)(SiGe)_γ was prepared by a mechanical alloying method, and then sintered using a spark plasma sintering method. For the n type, a Mg₂Si-based material, which was developed by Yasunaga Co., was used. To join the p-type, n-type elements and Cu electrodes, the modules were sintered at 550 – 750°C with a pressure of 10 MPa.

We investigated the dependence of thermoelectric properties on the Re and Ge amount in (MnRe)(SiGe)_γ. The ratio between sublattices of MnSi_γ, *γ*, was clarified to be reduced with increasing Re and Ge amount. Both Seebeck coefficient and electrical resistivity decreased, and the power factor increased, owing to the generated carriers by the reduced *γ*. On the other hand, the lattice thermal conductivity decreased with increasing Re and Ge amount due to the mass-difference and strain-field-difference phonon scattering. As a result, *ZT* increased up to 0.70 at 500°C when the substitution amount of Re was 0.10 and that of Ge was 0.03. The power generation characteristics of the 1-pair and 9-pair thermoelectric modules composed of (MnRe)(SiGe)_γ and Mg₂Si were evaluated by changing the elements heights *h* = 1.0, 2.0, 3.0, 3.5 mm when the hot side and cold side are 500°C and 20°C, respectively. The output power density increased as the element height decreased and showed the similar tendency as the results of the power generation characteristic simulation. As the element height decreased, the temperature difference applied to the element decreased and the open voltage also decreased, but the electrical resistance value also decreased significantly. As a result, output power density took the maximum value with respect to the element height. The maximum output power density of 14.3 kW/m² at 500°C was obtained when *h* = 2.0 mm. On the other hand, module resistance analysis revealed that interfacial resistance was present in about 20 – 30% of the total due to non-uniform bonding between the thermoelectric elements and the electrode. To improve the binding condition, sintering temperature of the modules were varied in the temperature range of 550 – 750°C. As increasing sintering temperatures, the module resistance decreased due to the improvement of the bonding between the elements and electrode. At high sintering temperatures above 650°C, although the module resistance decreased, the open voltages of the modules decreased due to the diffusion of Cu from the electrode to the elements, and the output power also decreased. As a result, maximum output power density of 17 kW/m² was obtained at the sintering temperature of 600°C, which is the highest level in the reported thermoelectric module using MnSi_γ and Mg₂Si. The power generation simulation suggests that the maximum output power increases up to 22 kW/m² if the interfacial resistance in the module were completely removed.

This study is based on results obtained from the Future Pioneering Program “Research and Development of Thermal Management and Technology” commissioned by the New Energy and Industrial Technology Development Organization (NEDO). This work is also supported by TherMAT.

6:45 PM EN10.15.02

High-Resolution Elemental and Strain Study of High Entropy Thermoelectric Materials Yong Yu^{1,2}, Stephen Pennycook¹, Bosman Michel¹ and Jiaqing He²; ¹National University of Singapore, Singapore; ²Southern University of Science and Technology, China

Thermoelectric materials directly convert thermal energy to electrical energy and *vice versa*. To improve the energy conversion efficiency, accurate characterization of the atomic structure is critical, as this defines the charge- and phonon-transport. Scanning transmission electron microscopy (STEM) is widely used for defect characterization in thermoelectric materials, as structural defects and lattice strain often play a critical role in phonon scattering. However, the recently emerging high entropy thermoelectric materials are challenging objects for this characterization due to their very small strain and atomic-scale elemental mixture.

Here we show that these challenges can be solved by careful sample preparation, microscope fine-tuning, and the application of new experimental methods. Three STEM-based techniques are applied: atomic resolution energy-dispersive X-ray spectroscopy (EDS), geometric phase analysis (GPA), and nanobeam diffraction analysis (NBED) to understand the elemental positions and subtle lattice distortion, which are important for understanding the structure-property relationship.

Our high entropy material has a composition of Pb_{0.89}Sb_{0.012}Sn_{0.1}Se_{0.5}Te_{0.25}S_{0.25} and was compared to the low entropy PbSe control material. The atomic positions of Pb, Sn, Te, Se were found by atomic resolution EDS mapping. Pb and Sn occupy the ‘Na’ position, while Te and Se occupy the ‘Cl’ position of the NaCl crystal structure, demonstrating that the elements were mixed homogeneously at the atomic level.[1]

GPA can quantify the local strain distribution. However, weak strain fields require careful attention since the inevitable sample drift and scan noise will induce artifacts. To optimize this, we first wait a long time to minimize the sample drift, then we adopt fast scanning and take a stack of 30 frames, and finally, we use the ‘Smart Align’ software plugin to align the stacks together. This can simultaneously reduce the artifacts from sample drift and from scan noise, to give a strain analysis with 0.3% accuracy. With this, we find that the strain distribution in our high entropy alloy is much wider than that of low entropy alloy. The histogram shows that the statistical distribution in the high entropy alloy is much wider along with the normal <002> and shear <220> directions than in the low entropy alloy. This is important information, as the normal and shear strains are directly linked to the lattice thermal conductivity.[1]

As GPA requires atomic resolution images, the observational area cannot be very large and NBED is used to overcome this shortage. We use a 4 nm parallel probe to scan a much larger area of 400 nm by 400 nm to obtain a series of electron diffraction patterns. With careful analysis, we are able to map the strain with an accuracy of 0.06%. The results of NBED indeed confirm that the strain distribution of the high entropy alloy is much wider than the low entropy alloy. However, the absolute values in the strain field by NBED are lower than what was obtained with GPA. This shows the strength of GPA at a very small scale: in this high entropy alloy, the local strain varies in areas smaller than 2 nm and the strain measured with NBED only gives an average of the probed 4 nm area. In the case of our high entropy alloy, a full picture of the strain fields will therefore only be obtained by a combination of the GPA and NBED results.[1]

The authors acknowledge support from the Singapore Ministry of Education (MOE), AcRF Tier 1 (R-284-000-179-133) grant.

Reference:

[1] B. Jiang, Y. Yu, J. Cui, X. Liu, L. Xie, J. Liao, Q. Zhang, Y. Huang, S. Ning, B. Jia, B. Zhu, S. Bai, L. Chen, S. J. Pennycook, J. He, High-entropy-stabilized chalcogenides with high thermoelectric performance. **Science** (80-.). 371, 830–834 (2021).

7:00 PM EN10.15.03

Improvement of Thermoelectric Performance via Hierarchical Defect Engineering Using Nanoparticles as Building Blocks Mari Takahashi¹, Kimihiro Numano¹, Wei Zhou¹, Masanobu Miyata¹, Michihiro Ohta² and Shinya Maenosono¹; ¹Japan Advanced Institute of Science and Technology, Japan; ²National Institute of Advanced Industrial Science and Technology (AIST), Japan

Sustainable development goals (SDGs) have recently been considered across the world. Keeping requirements of sustainable and clean energy in mind, energy harvesting is one of the important technologies, since this technology can convert waste heat into electricity. The thermoelectric (TE) figure of merit ZT is expressed by $\sigma S^2 T / \kappa$, where σ is electrical conductivity, S is Seebeck coefficient, T is absolute temperature and κ is thermal conductivity. For the practical applications, TE materials with $ZT > 1$ have been desired. On the other hand, over 80% of the waste heat generated in industry is in the ranges of 373–575 K.¹⁾ Therefore, sustainable TE materials consisting of earth abundant and relatively non-toxic elements whose ZT value is higher than 1 at such low temperature range have been desired for many years.

There are several methods to improve ZT of TE materials. Among them, the fabrication of TE materials by sintering chemically-synthesized nanoparticles (NPs) has attracted much attention, mainly because κ can be significantly reduced through phonon scattering at the interfaces of well-defined nanograins. Comparing to the conventional ball milling technique, the use of chemical-synthesis of NPs as building blocks has several advantages.^{2,3)} For example, the fabrication time required to obtain a pellet is shorter; the size of well-defined nanograins in the pellet can be easily controlled; various kinds of nanoinclusions can be introduced in the material just by mixing two or more different types of NPs; mesoscale defects can be created by controlling the size of domain of nanoinclusions; atomic defects can readily introduced in NPs. In other words, it offers unprecedented opportunities for the hierarchical defect engineering.

Previously, we synthesized Zn doped Cu_2SnS_3 NPs (Zn-CTS) with changing Zn content. The results showed that the pellet fabricated by either $\text{Cu}_2\text{Sn}_{0.85}\text{Zn}_{0.15}\text{S}_3$ or $\text{Cu}_2\text{Sn}_{0.95}\text{Zn}_{0.05}\text{S}_3$ NPs showed relatively high ZT value of 0.37 at 670 K than that of pristine CTS fabricated by the conventional method.⁴⁾ Basically, Zn incorporation causes hole doping, and thus, as Zn content increased, σ of Zn-CTS increased. However, when the material became metallic, κ increased according to the Wiedemann–Franz law. In order to decrease carrier thermal conductivity κ_{car} , $\text{Cu}_2\text{Sn}_{0.9}\text{Zn}_{0.1}\text{S}_3$ NPs, which has the lower κ , were mixed with $\text{Cu}_2\text{Sn}_{0.85}\text{Zn}_{0.15}\text{S}_3$ NPs, which has the higher σ , in the ratio of 1:9. Owing to the sea-island structure composed of $\text{Cu}_2\text{Sn}_{0.9}\text{Zn}_{0.1}\text{S}_3$ NPs (island) and $\text{Cu}_2\text{Sn}_{0.85}\text{Zn}_{0.15}\text{S}_3$ (sea), the pellet could maintain high σ while κ showed lower value than that of pure $\text{Cu}_2\text{Sn}_{0.85}\text{Zn}_{0.15}\text{S}_3$ because of the efficient phonon scattering at the interfaces between sea and islands. As a result, the highest ZT value of 0.64 was achieved at 670K.⁵⁾

As this example shows, there is plenty of room for improvement of ZT by the hierarchical defect engineering using NPs as building blocks. In this talk, we will show you our recent results about the hierarchical defect engineering for discussion.

References:

1) S. O. J. Long *et al.*, *Chem. Mater.*, **30**, 456 (2018); 2) S. Fei *et al.*, *AIP Adv.*, **10**, 075021 (2020); 3) A. O. Moghaddam *et al.*, *Iran J. Mater. Sci. Eng.*, **16**, 20 (2019); 4) W. Zhou *et al.*, *Appl. Phys. Lett.*, **111**, 263105 (2017).; 5) W. Zhou *et al.*, *ACS Appl. Nano Mater.*, **1**, 4819 (2018).

7:15 PM EN10.15.04

Ultra-Light-Mass Band Engineering in N-Type Mg_3Bi_2 -Based Materials Ryosuke Yamamura, Yuriko Kaneko, Tsutomu Kanno and Hiromasa Tamaki; Panasonic Corporation, Japan

N-type Mg_3Sb_2 -based compounds, discovered by our group in 2016, are one of the potential candidates for low-cost and high-performance thermoelectric materials comparable to the commercial Bi_2Te_3 [1]. A Bi-rich side of N-type Mg_3Sb_2 - Mg_3Bi_2 solid solution has recently attracted attention by its excellent low-temperature thermoelectric performance [2]. One possible, yet controversial, mechanism is the band convergence between the six-valley carrier pocket (CB_1 band) and the single-valley band at Γ -point (Γ band) with increasing the Mg_3Bi_2 content [3, 4]. This motivates us to perform DFT-based modelling of electronic structure and thermoelectric properties for Mg_3Sb_2 - Mg_3Bi_2 solid solution.

Our analysis reveals that the band convergence does not occur even for Mg_3Bi_2 end, but ultra-light Γ band slightly above the CB_1 minima enhances its power factor. We find that, by increasing Bi content, the band effective mass of the Kane-type Γ band becomes one order of magnitude lighter than that of the parabolic CB_1 band, where the energy gap is nearly closed. Despite the single-valley and not converged character, the contribution of the ultra-light Γ band to the transport properties is as significant as the six-valley CB_1 band, leading to the enhanced power factor greater than $30 \mu\text{W}/\text{cmK}^2$ for Mg_3Bi_2 end. In this talk, we also compare our computational modeling with experimental results. Discovery of the ultralight Γ band in Mg_3Bi_2 -based materials will open the possibility of ultra-light-mass band engineering to design high-performance thermoelectric materials.

[1]. H. Tamaki, H.K. Sato, and T. Kanno, *Adv. Mater* **28**, 10182 (2016).

[2]. Zhijia Han, Zhigang Gui, Y. B. Zhu, Peng Qin, Bo-Ping Zhang, Wenqing Zhang, Li Huang, and Weishu Liu, *Research*, **2020**, 1672051 (2020).

[3]. K. Imasato, S. D. Kang, G. J. Snyder, *Energy Environ. Sci.* **12**, 965 (2019).

[4]. J. Zhang and B.B. Iversen, *J. Appl. Phys.* **126**, 085104 (2019).

7:30 PM EN10.15.05

Double Charge Polarity Conversion by Sb Doping in Layered SnSe with Switchable Substitution Sites Xinyi He¹, Chihiro Yamamoto¹, Takayoshi Katase¹, Keisuke Ide¹, Hidenori Hiramatsu^{1,2}, Hideo Hosono² and Toshio Kamiya^{1,2}; ¹Laboratory for Materials and Structures, Tokyo Institute of Technology, Japan; ²Materials Research Center for Element Strategy, Tokyo Institute of Technology, Japan

Due to the current growing energy issues, the importance of thermoelectric energy conversion has been increasing. Recently, tin selenide (SnSe) with a layered crystal structure has extensively been studied as it exhibits a high figure-of-merit $ZT > 2$ [1]. However, SnSe has a serious issue; i.e., the carrier polarity control is still difficult, which is critical to realize p-n homojunction devices. Pure SnSe is a native p-type semiconductor, and p-type conductivity is enhanced by impurity doping, e.g., by alkali ion-doping [2]. Bi and halogen ions have been employed for electron doping at the Sn and the Se sites, respectively [3–5]. However, the maximum carrier concentration has been limited to 10^{17} cm^{-3} because of the low activation efficiency (less than 0.1%) of the Bi^{3+} donor. Antimony ion (Sb^{3+}) doping at Sn²⁺ site is expected to produce n-type SnSe, and the Sb-doped SnSe is reported to show high thermoelectric efficiency with $ZT = 1.1$ even in practical polycrystalline form. However, there are contradicting reports on the charge polarity (n-type or p-type); i.e., some papers report n-type and the others p-type [6–8].

In this work, we have discovered an unusual phenomenon, the double inversion of the charge polarity, in $(\text{Sn}_{1-x}\text{Sb}_x)\text{Se}$ by varying only the Sb concentration (x), and elucidated the doping mechanism. Pure SnSe shows p-type conduction, while $(\text{Sn}_{1-x}\text{Sb}_x)\text{Se}$ shows n-type conduction for $0.005 < x < 0.05$, and finally re-inverts to p-type conduction for $x > 0.05$. The substitution sites of Sb distributes for the Sn sites and the Se sites, and the major substitution site

switches from the Se (Sb_{Se}) to the Sn site (Sb_{Sn}) with increasing x . This means the charge state of Sb changes from -3 to +3 with increasing x . We explain the mechanism of the double polarity inversion from the band alignment and the first-principles calculations; pure SnSe shows p-type conduction due to the formation of Sn vacancy, and $(\text{Sn}_{1-x}\text{Sb}_x)\text{Se}$ exhibits the apparent n-type behavior due to conduction through additional Sb_{Se} impurity band, and then finally re-inverts to weak p-type, where the Fermi level approaches the midgap level located between the additional Sb_{Se} band and conduction band minimum. The clarification of Sb doping mechanism would give a crucial guide to develop more sophisticated doping route for SnSe and high-performance energy-related devices.

References

[1] L.-D. Zhao et al., *Nature* 508, 373-377, (2014). [2] T.-R. Wei et al., *J. Am. Chem. Soc.* 138, 8875-8882 (2016). [3] A. T. Duong et al., *Nat. Commun.* 7, 13713 (2016). [4] Q. Zhang et al., *Adv. Energy Mater.* 5, 1500360 (2015). [5] S. Li et al., *Adv. Sci.* 5, 1800598 (2018). [6] J. Umeda, *J. Phys. Soc. Jpn.* 16, 124-125 (1961). [7] S. Patel et al., *J. Appl. Phys.* 124, 215103 (2018). [8] X.-L. Shi et al., *Adv. Energy Mater.* 8, 1800775 (2018).

7:35 PM EN10.15.06

Wearable Flexible Thermoelectric Generator System for Self-Powered Temperature Sensor Jeong Hun Kim, Jong-Pil Im, Yeriaron Kim and Seung Eon Moon; Electronics and Telecommunications Research Institute, Korea (the Republic of)

Thermoelectric power generators that can produce electrical energy from the temperature difference between the two ends are attracting attention as a next-generation clean power generation system because they can be applied to various places where heat sources exist and do not generate by-products during the power generation process. Recently, results of operating application systems such as simple acceleration sensors or electrocardiograms by attaching them to the human body have been published. As such, thermoelectric generators are easy to apply with a small volume of independent power source. It is also receiving attention as a power source for wearable devices that can be monitored at all times.

In this study, a flexible thermoelectric element capable of uniform contact with human arm was fabricated through a printing process-based thermoelectric element manufacturing method that applied a BiTe-based inorganic material and a flexible silver electrode on the sacrificial layer. In particular, by using Polyurethane foam as a polymer filler material to support the structure and lowering the thermal conductivity, it was possible to confirm more than twice the power compared to the case of using Poly(dimethylsiloxane) (PDMS). In addition, on a curved surface with a radius of curvature of 4 cm, the output was 5 times higher than that of a flat metal substrate, and through this, a method for effectively collecting heat from the human body was presented.

In the case of a cooling unit to maintain a temperature difference, a fin-type heatsink that is generally used has a relatively large volume and uses a hard material, so it is difficult to apply it to a flexible thermoelectric device. To solve this, UV curability hydrogel that can absorb water was used as a flexible and stretchable heat sink. Effective cooling properties were obtained from the evaporation of water contained in the hydrogel heatsink, and as a result of testing the performance of the manufactured thermoelectric generator system in the form of a band that can be worn on the human body, the power generation amount of more than $30 \mu\text{W}/\text{cm}^2$ under the convection condition of 1.5 m/s was able to confirm. It was confirmed that the capacitor could be charged and the temperature sensor could be driven. As an eco-friendly independent power system technology, it is expected that it can contribute as an energy device for various wearable applications that require continuous measurement and communication, such as an attachable biometric sensor.

7:40 PM EN10.15.07

Prediction of High Thermoelectric Performance in the Low-Dimensional Metal Halide $\text{Cs}_3\text{Cu}_2\text{I}_5$ Young-Kwang Jung¹ and Aron Walsh^{1,2}; ¹Yonsei University, Korea (the Republic of); ²Imperial College London, United Kingdom

Metal halides have been intensively studied for their optoelectronic applications e.g. solar cells and light emitting devices. Recently, their potential as thermoelectric materials has emerged where unique vibrational properties of metal halides -- such as localised phonons and ultra-low lattice thermal conductivity -- plays important roles. Up to date, the highest thermoelectric figure of merit ZT reported among metal halides is ~0.15, which is well short of the champion ZT of 2.6 achieved in SnSe. $\text{Cs}_3\text{Cu}_2\text{I}_5$ is an alternative metal halide with a low-dimensional crystal structure where $[\text{Cu}_2\text{I}_5]^{3-}$ clusters are surrounded and isolated by Cs^+ cations and there is no direct connectivity between neighboring anionic clusters [1]. Its unique optoelectronic properties related with the low-dimensional structure have been studied, but its charge and heat transport properties have not been identified yet.

In this study, we assess the thermoelectric potential of $\text{Cs}_3\text{Cu}_2\text{I}_5$ combining state-of-art first-principles simulation techniques. Thermal transport properties were calculated using anharmonic lattice dynamics [2] where an ultra-low conductivity for the perfect crystal that is found. By employing an *ab initio* description of carrier scattering [3], we further investigate electron transport properties of the material. Efficient electron transport throughout the crystal is confirmed, which is attributed to an unexpectedly low effective mass for the electron in the low dimensional structure. As a result of imbalanced electron and heat transport, $\text{Cs}_3\text{Cu}_2\text{I}_5$ is predicted as an ideal thermoelectric semiconductor that exhibits the characteristics of "phonon-glass electron-crystal" with an accessible ZT of greater than 2 [4].

[1] T. Jun, K. Sim, S. Iimura, M. Sasase, H. Kamioka, J. Kim, and H. Hosono, *Adv. Mater.* 30, 1804547 (2018).

[2] A. Togo, L. Chaput, and I. Tanaka, *Phys. Rev. B* 91, 094306 (2015)

[3] A. M. Ganose, J. Park, A. Faghaninia, R. Woods-Robinson, K. A. Persson, and A. Jain, *Nat. Commun.* 12, 2222 (2021)

[4] Y.-K. Jung, I. T. Han, Y. C. Kim, and A. Walsh, *npj Comput. Mater.* 7, 51 (2021)

7:45 PM EN10.15.08

Large Phonon Drag Thermopower Enhancement by Epitaxial Strain and Phonon Leaking in $\text{LaAlO}_3 / \text{LaNiO}_3 /$

LaAlO_3 Heterostructure Masatoshi Kimura, Xinyi He, Takayoshi Katase, Keisuke Ide, Hidenori Hiramatsu, Hideo Hosono and Toshio Kamiya; Tokyo Institute of Technology, Japan

Phonon drag thermopower (S_g) has received great attention because total S is enhanced compared to the conventional carrier-diffusion thermopower (S_d) by $S = S_d + S_g$, and thus the energy conversion efficiency is enhanced [1]. S_g is expressed as $S_g = (m^* v_x l_x) / (\tau_e e T)$ in the non-degenerated regime [2]. Therefore, the conventional approach to observe S_g is to utilize ballistic phonon with long mean free paths (l_x) in high quality semiconductors [3] or large electron effective mass (m^*) in strongly correlated electron systems [4]. However, S_g is observed only in limited materials at low temperatures and its peak value is small. Here, we report an unusually large S_g enhancement in the thin-film heterostructure of a strongly correlated electron oxide LaNiO_3 (LNO). We investigated the effects of layer thickness and surface termination on S of LNO epitaxial films grown on LaAlO_3 (LAO) substrates with the in-plane lattice mismatch of -1.5%. The 50 - 3 unit cells (u.c.) thick LNO epitaxial films with step & terrace surfaces were grown by pulsed laser deposition on (001) LAO single crystal. LAO-capped LNO films were fabricated by first depositing a 3 u.c. LNO film, followed by growing a 10 u.c. LAO capping layer. The LNO film grows coherently with strain up to thickness 50 u.c. on the LAO substrate. The pseudo-cubic lattice parameters for out-of-plane (c) and in-plane (a) are 3.88 Å and 3.78 Å, respectively. The c/a is 1.026, indicating the in-plane compressive strain in the LNO films. For the LAO-capped 3 u.c. LNO film, the tri-layer structure of LAO/LNO/LAO grows coherently with strain. By reducing the LNO layer thickness, the film showed the metal-insulator transition at a critical thickness of 5 u.c. On the other hand, the surface termination by 10 u.c. LAO capping layer changed the 3 u.c. LNO film

more conductive again, which shows a metal-insulator transition at $T = 77$ K.

The phonon-drag S_g is not observed in the bulk LNO, whereas it appeared at $T = 25$ -33 K for the LNO epitaxial films with compressive strain by the LAO substrate. By reducing LNO layer thickness down to 3 u.c. and subsequent LAO surface termination, S was enhanced 10 times from that of bulk LNO due to the large phonon drag S_g , and the S_g contribution to the total S spreads in much wider temperature range, reaching up to 220 K. We clarified that the S_g enhancement originates from a coupling of lattice vibrational phonons to the Ni 3d-electrons whose effective mass becomes larger in the strained ultra-thin LNO film and also from the strong electron-phonon scattering enhanced by the phonon leakage from the LAO substrate and the capping layer. The present results demonstrate a new approach to manipulate both electronic and phononic properties in atomic-scale controlled transition metal oxide (TMO) heterostructures for high-performance thermoelectrics.

References

- 1) J. Zhou *et al.*, *Proc. Natl. Acad. Sci. USA* **112**, 14777 (2015).
- 2) C. Herring, *Phys. Rev.* **96**, 1163 (1954).
- 3) B. L. Gallagher *et al.*, *J. Phys.: Condens. Matter* **2**, 755 (1990).
- 4) A. Bienten *et al.*, *EPL* **80**, 17008 (2007).

7:50 PM EN10.15.09

Enhanced Thermoelectric Response in Sb₂Te₃ Thin Film by Incorporation of Size-Selected Gold Nanoparticles [Abhishek Ghosh](#) and Bodh Raj Mehta; Indian Institute of Technology, India

Enhancement in the thermoelectric (TE) properties through carrier filtering in polycrystalline Sb₂Te₃ thin film is realized by incorporating size-selected Au nanoparticles grown by an integrated gas-phase synthesis method. Crystalline Singlet nanoparticles of Au having a narrow size distribution are embedded between two Sb₂Te₃ layers. Thermoelectric properties have been investigated by varying the concentration of nanoparticles, which reveal a significant increase in the Seebeck coefficient and power factor with a slight deterioration in electrical conductivity. Samples containing non-size selected Au particles with broad size distribution are also synthesized to understand the effect of non-uniformity in size distribution on TE properties and compared with the samples containing size-selected particles. In addition, scanning probe techniques were employed to understand the nature of the interface formed between Sb₂Te₃ and Au nanoparticles which reveals the formation of a Schottky barrier in the interface. The study provides an opportunity to manipulate the TE properties in Sb₂Te₃ thin films by constructing a metal-semiconductor heterostructure by controlling the concentration and randomness to achieve a high TE performance.

SESSION EN10.16: Phase Change and Measurement I
Session Chair: TieJun Zhang
Tuesday Morning, December 7, 2021
EN10-Virtual

10:30 AM *EN10.16.01

Capillary-Driven Condensation for Enhanced Energy Efficiency Samuel Cruz, Yajing Zhao, Kyle Wilke, Hyeongyun Cha, Daniel J. Preston and [Evelyn N. Wang](#); Massachusetts Institute of Technology, United States

Significant interests in enhancing the efficiency of condenser designs and reducing water consumption have emerged for thermoelectric power plants. While substantial efforts have focused on methods to enhance heat transfer performance in condensers, ongoing challenges remain including maintaining robust non-wetting behavior for enhanced heat transfer enhancement during dropwise condensation. In our work, we present a new mode of condensation termed capillary-driven condensation. In this approach, a porous hydrophobic membrane atop a wicking structure on the condensing surface helps generate a capillary pressure gradient to drive liquid transport through the wick to an exit port for condensate removal. The wick both sets the thickness of the condensate-wick layer and increases its effective thermal conductivity, reducing the overall thermal resistance. Meanwhile, the hydrophobic porous membrane helps generate the capillary driving pressure via its microscale pores to transport the condensing fluid out of the wick and significantly increase the heat transfer performance. With well-controlled microfabricated structures, i.e., a silicon nitride membrane suspended on a micropillar wick, we show a successful proof-of-concept. The wick fills completely upon nucleation, and small droplets on top of the membrane are continually absorbed into the wick through the membrane pores. The visualizations suggest promising heat transfer enhancements and are corroborated by our developed models. Simultaneously, we have been pursuing scalable approaches to achieve capillary-driven condenser designs, including diffusion-bonded, hydrophobized hierarchical copper meshes, and electro-spun membrane covered metal wicks. This work suggests a promising path for incorporating capillary-based condenser designs to enhance the efficiency of power plants, thermal management strategies, and water desalination systems, among others.

11:00 AM *EN10.16.02

Monitoring and Quantifying Condensation Frosting on Lubricant-Impregnated Surface [Doris Vollmer](#), Lukas Hauer, Katharina Hegner and William S. Wong; Max Planck Institute for Polymer Research, Germany

Despite the widespread occurrence of frost, understanding and controlling condensation-frosting still poses several challenges. Control of condensation-frosting is relevant for a range of industries: In the energy, transportation or telecommunication sectors, frost constitutes serious hazards when it forms on critical components of machines and devices, causing them to fail.

Amongst anti-frosting and anti-icing surfaces, slippery lubricant-impregnated porous surfaces (SLIPS) are discussed due to frosting-retardant and ultra-low ice adhesion properties [1]. However, the understanding of its formation and growth – particularly on SLIPS – remains elusive. The reasons are multi-fold: Insights into frosting are hampered by poor optical contrast between water, frost and lubricant and by the non-equilibrium nature of frost formation, that involves multiple time and length scales.

To reach better insight, we have developed a novel setup that enables the *in-situ* monitoring of lubricant reorganization, condensation and freezing of water drops using Laser Scanning Confocal Microscopy. Such a setup discriminates between condensation and freezing of water, reorganization of lubricant accompanied by growth of dendrites. In particular, our setup provides spatially and temporally resolved data of the formation and growth of frost, accompanied by quantifiable lubricant reorganization.

As model system, we utilize surfaces with micro- and nanostructures. The coatings are lubricated with silicone oil. Condensation frosting starts with

nucleation and growth of water droplets. The condensation and continued growth of droplets on lubricant impregnated surfaces is largely influenced by the structure geometry and wetting property of the lubricated solid surface [2].

Lowering the temperature results in droplet freezing and frost formation. Frosting results in lubricant depletion in the array. Although detrimental at first sight, we note that frost induced lubricant depletion is reversible when the frost is melted in situ. We determined the suction pressure induced by frost dendrites, which wicks lubricant into the frost structure [3].

Formation of frost dendrites result in a particularly harsh depletion mechanism. Notably lubricant depletion can be prevented. Therefore, the interstitial spacing of the lubricant impregnated surface needs to be kept lower than that found in frost dendrites (≥ 100 nm). To prove this concept, we used densely packed nanoparticles. The nano-interstices are kept between 10 to 50 nm. The capillary pressure keeping lubricants in the nano-interstices exceeds the capillary suction pressure by frost dendrites. We term this the design concept “*capillary-balancing*”. Notably, the facile and scalable coating shows passive anti-icing [4].

[1] Kreder, M.J., Alvarenga, J., Kim, P. & Aizenberg, J. Design of anti-icing surfaces: smooth, textured or slippery? *Nat. Rev. Mater.* **1**, 15003 (2016).

[2] T. Kajiya, F. Schellenberger, P. Papadopoulos, D. Vollmer and H.-J. Butt: 3D imaging of water-drop condensation on hydrophobic and hydrophilic lubricant-impregnated surfaces, *Scientific Reports*, 2016, 6, 23687.

[3] L. Hauer, W.S.Y. Wong, V. Donadei, K.I. Hegner, L. Kondic, D. Vollmer: How frost forms and grows on lubricated micro- and nanostructured surfaces, *ACS Nano*, 2021, 15, 4658.

[4] W.S.Y. Wong, K.I. Hegner, V. Donadei, L. Hauer, A. Naga and D. Vollmer: Capillary balancing: designing frost-resistant lubricant-infused surfaces, *Nano Lett*, 2020, 20, 8508.

11:30 AM EN10.16.03

Hierarchical Microtube Structures for Pool Boiling Heat Transfer Enhancement Yongsup Song, Carlos D. Diaz, Hyeongyun Cha, Lenan Zhang, Yajing Zhao and Evelyn N. Wang; Massachusetts Institute of Technology, United States

Boiling is an essential process in a variety of applications such as power plants, water purification, and steam generation. The boiling performance can be described by two major parameters: heat transfer coefficient (HTC) and critical heat flux (CHF), which dictate the efficiency and operational heat flux limit during the nucleate boiling, respectively. The previous study has shown that simultaneous enhancements of HTC and CHF values can be achieved with hemi-wicking surfaces consist of micropillar and microtube structures. There has been a trade-off, however, between the two parameters associated with the competition between nucleation site density and complete utilization of capillary wicking. In this work, we mitigate the trade-off by incorporating nanostructures on top of microtube and micropillar structures and demonstrate the extreme pool boiling performance for both HTC and CHF. Specifically, we controlled vapor nucleation for HTC enhancement with surface structures in millimeter, micrometer, and nanometer scales by the separation of microtube clusters, microtube cavities, and nanostructures, respectively. At the same time, the augmented capillary wicking on hierarchical structures achieved significant CHF enhancement. The visualization of bubble dynamics with a high-speed camera supports our findings that HTC and CHF enhancements can be achieved by multi-scale control of vapor nucleation on hemi-wicking surfaces. The extreme boiling performance achieved in this work is not only promising for various boiling applications but also providing important implications for fundamental aspects of boiling heat transfer mechanisms.

11:45 AM EN10.16.04

Real-Time Manipulation of Liquid Droplets on SLIPS Using Photo-Responsive Surfactants Xichen Liang¹, Lei Zhao², Serena Seshadri^{2,1}, Sophia Bailey², Michael Haggmark¹, Farzad Ahmadi², Michael Gordon¹, Javier Read de Alaniz², Paolo Luzzatto-Fegiz² and Yangying Zhu²; ¹University of California, Santa Barbara, United States; ²UCSB, United States

Fast and programmable transport of liquid droplets on a solid substrate is desirable in microfluidic devices, condensation in power plants, microchips cooling, and even water collection in the space. Past research has focused on designing substrates with asymmetric structures or surface modifications where droplets behaviors are passively controlled, or by applying external stimuli such as electrowetting where patterning of intricate electrodes is required. In this work, we demonstrate tunable and programmable droplet motion on a slippery liquid-infused porous surface (SLIPS) using light and photo-responsive surfactants. When illuminated by the light of appropriate wavelengths, these surfactants can reversibly change interfacial tensions in a multi-phase fluid system, which generates Marangoni flow that drives droplet motions. Experimental results demonstrate that a 70 μ L static droplet can move 9 mm in one minute upon irradiation of a UV laser and the merging time of two droplets can be manipulated by adjusting light projection positions. We also model the photo-Marangoni flow inside the droplet and calculate the net driving force. The method demonstrated in this study serves as a simple and exciting new approach for dynamic manipulation of droplets for microfluidic, thermal and water harvesting devices.

12:00 PM EN10.16.05

Bulk Lubricant Infusion in Soft Substrates Enhances Condensate Removal Cheuk Wing Edmond Lam¹, Chander S. Sharma², A. Milionis¹, Abhinav Naga³, Gabriel Rodriguez¹, Marco F. Del Ponte¹, Valentina Negri¹, Hopf Raoul¹, Maria D'Acunzi³, Doris Vollmer³, Hans-Jürgen Butt³ and Dimos Poulikakos¹; ¹ETH Zürich, Switzerland; ²Indian Institute of Technology Ropar, India; ³Max Planck Institute for Polymer Research, Germany

Heterogeneous condensation on soft substrates benefits from higher nucleation density. However, compared to rigid substrates, condensate droplets on such surfaces suffer from viscoelastic dissipation at the three-phase contact line as they slide, inhibiting their removal. These droplets manifest as thermal resistance to condensation heat transfer between the cooled substrate and the ambient vapour. The presence of these pinned droplets also limits the available area for fresh nucleation sites as well, thus lowering overall heat transfer efficiency.

In this work, we explore the effects of infusing a lubricant into the bulk of polydimethylsiloxane (PDMS, Sylgard 184) on the material properties relevant to wetting phenomena. By varying the proportion of the base, curing agent and the lubricant, we identify the resulting amount of uncrosslinked chains by a swelling-and-deswelling process and their molecular distribution with gel permeation chromatography (GPC). Elasticity of the different substrates is measured with micro-indentation tests which we correlate with measured wetting ridge heights at the contact line. Viscoelastic dissipation at the contact line is characterised by measuring droplet sliding velocities. Cloaking of the water droplets is studied with laser scanning confocal microscopy followed by a transient measurement of the resulting change in droplet surface tension. We conclude the study with microscale observation of condensation for nucleation densities and droplet growth rate, and a dew collection experiment for overall performance improvement in condensate removal. We correlate the measured condensation characteristics with the material properties of the substrate.

We find that 5 wt. % of bulk lubricant infusion, despite resulting in a substrate of lower bulk elasticity, significantly reduces viscoelastic dissipation at the contact line as indicated by an increase in droplet sliding velocity. Additionally, the nucleation density is more than doubled compared to PDMS substrates without bulk lubricant infusion. We also observe that further increase above 5 wt. % bulk lubricant concentration has an insignificant effect on the

condensation dynamics over the substrate. Moreover, there is a small reduction in droplet growth rate for lubricated substrates. This reduction can be attributed to the cloaking of droplets by uncrosslinked chains due to the presence of a lubricant layer on the substrate top surface. Overall, these factors combine to result in an increase of ~40% in dew water collection for lubricated substrates compared to non-lubricated ones.

12:15 PM EN10.16.06

Understanding the Temperature Dependence of Carrier Mobility Alex M. Ganose^{1,2}, Junsoo Park¹ and Anubhav Jain¹; ¹Lawrence Berkeley National Laboratory, United States; ²Imperial College London, United Kingdom

The temperature dependence of experimental mobility is commonly used as a predictor of the dominant scattering mechanism in thermoelectric materials. Knowledge of the dominant scattering mechanism is employed to fit models of charge transport including deformation potentials and effective masses, and to obtain estimates of the optimal doping concentration and temperatures that maximise thermoelectric performance. However, if the scattering mechanism is determined incorrectly, this can lead to wildly inaccurate predictions of materials properties and optimal conditions, frustrating efforts to optimise devices. By reviewing the temperature dependence of 24,000 mobility calculations, I demonstrate that the temperature-dependence of mobility is not a reliable indicator of the dominant scattering mechanism. Furthermore, I reveal that many materials long considered to be dominated by deformation-potential scattering are instead controlled by polar optical phonons. I conclude with the pitfalls of predicting the major scattering type based on the experimental mobility trend alone.

SESSION EN10.17: Conduction Measurement
Session Chairs: Yuan Yang and Mona Zebarjadi
Tuesday Afternoon, December 7, 2021
EN10-Virtual

1:00 PM EN10.17.01

Soft Anharmonic Phonons and Ultralow Thermal Conductivity in $Mg_3(Sb, Bi)_2$ Jingxuan Ding¹, Tyson Lanigan-Atkins¹, Mario R. Calderon Cueva², Arnab Banerjee^{3,4}, Doug L. Abernathy⁴, Ayman Said⁵, Alexandra Zevalkink² and Olivier Delaire^{1,1,1}; ¹Duke University, United States; ²Michigan State University, United States; ³Purdue University, United States; ⁴Oak Ridge National Laboratory, United States; ⁵Argonne National Laboratory, United States

Thermoelectric materials enable direct conversion of waste heat into electrical energy. The conversion efficiency is inversely proportional to the thermal conductivity, which is generally dominated by phonons in semiconductors. Zintl compounds AMg_2X_2 ($A=Mg, Ca, Yb$; $X=Sb, Bi$) constitute a class of new thermoelectric compounds with excellent thermoelectric performance in n-type $Mg_3(Sb, Bi)_2$ alloys, with zT values up to 1.6 reported so far. Mg_3Sb_2 exhibits very low lattice thermal conductivity (~1-1.5 W/m/K at 300K), comparable with PbTe and Bi_2Te_3 with only half of their mass densities. Meanwhile, contrary to common mass-trend expectations, replacing Mg with heavier Ca or Yb yields a threefold increase in k_L in $CaMg_2X_2$ or $YbMg_2X_2$. We report on neutron scattering and first-principles studies of the lattice dynamics of AMg_2X_2 . Inelastic neutron scattering measurements found a large phonon softening and flattening of low-energy transverse acoustic phonons in Mg_3Sb_2 and Mg_3Bi_2 compared to $CaMg_2X_2$ or $YbMg_2X_2$. Combined with simulations, we highlight the importance of a specific soft Mg-X chemical bond that suppresses phonon group velocities and drastically enlarges the scattering phase-space, enabling the threefold suppression in thermal conductivity. These results provide key insights for manipulating phonon scattering without the traditional reliance on heavy elements and disorder.

Reference: Ding, J., Lanigan-Atkins, T., Calderón-Cueva, M., Banerjee, A., Abernathy, D. L., Said, A., Zevalkink, A., Delaire, O. (2021). Soft anharmonic phonons and ultralow thermal conductivity in $Mg_3(Sb, Bi)_2$ thermoelectrics. *Science Advances*, 7(21), eabg1449.

1:15 PM EN10.17.02

Probing Local Vibrational Modes at Crystal Defects in 3D and 2D Systems by Space- and Angle-Resolved Vibrational Spectroscopy Xingxu Yan, Chaitanya A. Gadre, Toshihiro Aoki, Ruqian Wu and Xiaoqing Pan; University of California, Irvine, United States

Imperfections such as stacking faults and interfaces are recognized as critical factors in modifying thermal properties and heat transport in crystal materials by scattering phonon and changing vibrational structure. They play an even more decisive role when the material's dimension is reduced to the nanoscale. Although diverse modelling tools have been deployed to understand the interaction between heat and imperfections in solids, the effect of crystal defects on thermal conductivity is being treated without considering the local change of phonon dispersion relation. In contrast, some studies have predicted the existence of extra vibrational modes due to dislocations or interfaces [1, 2]. However, the experimental evidence of those local modes is fundamentally elusive from either thermal conductivity measurements or conventional vibrational spectroscopies such as Raman and inelastic neutron scattering spectroscopies due to their inefficient spatial resolution [3]. Recently, the energy resolution of monochromated electron energy-loss spectroscopy (EELS) has been dramatically improved to a few millielectronvolts, which opens a new era of probing nanoscale feature of vibrational modes in materials using the aberration-corrected scanning transmission electron microscope (STEM) [3]. By balancing spatial, energy, and momentum resolutions, we can obtain a powerful space- and angle-resolved vibrational EELS method [4]. Here we show three cases to demonstrate how to utilize this emerging tool to reveal the local vibrational modes at (1) a stacking fault in cubic silicon carbide, (2) an interface in a Si-Ge heterojunction, and (3) an interface in a two-dimensional (2D) MoS_2 - WSe_2 lateral heterojunction.

Stacking faults are common imperfections in SiC, and remarkably affect the bulk thermal conductivity. We acquired the angle-resolved vibrational spectra from both the stacking-fault-containing region and defect-free region. At the defect, the acoustic phonons at X point of the first Brillouin zone undergo an energy red shift of 3.8 meV and major intensity modulations. These striking features arise from the symmetry breaking and variation of interatomic force constants and are assigned to the local defect phonon modes. Both the reduced phonon energy and flattened dispersion curves of defect phonon modes help understand the defect-induced reduction of thermal conductivity [4]. In the second case, we employed a similar strategy to probe the interface phonon modes at a Si-Ge epitaxial interface, which is believed to facilitate the heat transport across interface [2]. The interfacial vibrational EEL spectrum contains extra vibrational signals at 48 meV (11.6 THz), which are absent in the phonon structure of either Si or Ge [5]. The exotic vibrational feature is also unveiled at the interface of monolayer MoS_2 - WSe_2 heterojunctions [6]. Our work opens the door to investigating phonon propagation around crystal defects and provides guidance to the engineering of desired heat management for semiconductors and power electronic devices [7].

References:

- [1] M. D. Li *et al.* Nano Lett. **17** (2017), p. 1587–1594.
- [2] Y. Chalopin and S. Volz, Appl. Phys. Lett. **103** (2013), 051602.

[3] O. L. Krivanek *et al.*, *Nature* **514** (2014), p. 209–212.

[4] X. X. Yan *et al.*, *Nature* **589**, (2021), p. 65–69.

[5] Z. Cheng, R. Y. Li, X. X. Yan *et al.*, arXiv:2105.14415 (2021).

[6] X. Z. Tian, X. X. Yan, G. Varnavides *et al.*, arXiv:2104.08978 (2021).

[7] This work was supported by the Department of Energy, Office of Basic Energy Sciences, Division of Materials Sciences and Engineering (DE-SC0014430). The authors acknowledge the use of facilities and instrumentation at the UC Irvine Materials Research Institute (IMRI) supported in part by the National Science Foundation through the Materials Research Science and Engineering Center program (DMR-2011967).

1:30 PM EN10.17.03

Direct Measurement of Electrocaloric Temperature Changes in Ferroelectric Relaxor Polymers for Thermal Management Applications Yusra Hambal¹, Vladimir Shvartsman¹, Qiming Zhang² and Doru C. Lupascu¹; ¹University of Duisburg-Essen, Essen, Germany; ²The Pennsylvania State University, United States

Alternative concepts of electric mobility, miniaturization in the electronics industry and the quest for environmentally friendly air-conditioning and refrigeration technology have opened many doors for advancements in the area of new materials for thermal management. The electrocaloric effect can be an alternative technology in this regard. The electrocaloric effect is a phenomenon observed in dielectric materials, as they undergo an adiabatic temperature change or an isothermal entropy change upon the application/removal of an electric field. Ferroelectric relaxor polymers are attractive, as they show slim hysteresis loops close to room temperature, which is favorable for the electrocaloric performance.

In the present work, we measure the electrocaloric temperature change in Polyvinylidene fluoride – trifluoroethylene – chlorofluoroethylene P(VDF-TrFE-CFE). The solution casting method was employed to prepare free-standing polymer films of P(VDF-TrFE-CFE). The free-standing polymer films are about 20 μm thick. The sputter coating technique was used to deposit silver electrodes onto the free-standing film. The dielectric permittivity curves measured against temperature show typical broad frequency dependent maxima which is typical for relaxors. The $P - E$ hysteresis loops were measured as a function of temperature. A slim hysteresis loop is observed confirming the relaxor behavior of P(VDF-TrFE-CFE). The direct electrocaloric effect was measured as a function of temperature and electric field using a custom-designed quasi-adiabatic calorimeter. A maximum electrocaloric temperature change of ~ 2 K is observed in 20 μm thick P(VDF-TrFE-CFE) films.

1:45 PM EN10.17.04

Passive Solar Desalination Systems Using Membranes Farzad Ahmadi and Yangying Zhu; University of California, Santa Barbara, United States

Over two-third of the world's population will lack sufficient access to fresh water by 2025. As water scarcity increases, desalination plants are on the rise as over 98% of the earth's water is brackish and sea. The current large-scale desalination plants mainly utilize thermal evaporation or reverse osmosis to increase the supply of fresh water. However, these techniques are energy-intensive and require large infrastructures. Along this line of thought, solar desalination systems could be great candidate choice as a reliable device. Despite the great attempt to increase the evaporation efficiency of the solar desalination devices, the condensation part of the system is not yet optimized which limits the overall solar-to-water conversion efficiency. Here, we are presenting a passive, reliable, and highly efficient solar desalination system that does not require any energy consumption except one sun power. Our device consists of two parallel porous membranes which are mounted closely together that make our device efficient due to the minimal vapor diffusion resistance. Unlike other methods that use capillary force to transport the sea water, we are using hydrostatic pressure to flow the sea water into our device which is subsequently getting preheated using heat recycling. This study provides insights into improving the overall efficiency of solar desalination devices. Using scaling analysis, the evaporation and condensation flux has been modelled.

2:00 PM EN10.17.05

Robust Silane Self-Assembled Monolayer Coatings on Plasma-Engineered Copper Surfaces Promoting Dropwise Condensation Ruisong Wang, Jiahui Guo and Dion Antao; Texas A&M University, United States

Vapor condensation is prevalent in various industrial and heat/mass transfer applications, such as power generation and conversion, water harvesting/desalination, and electronics thermal management. Dropwise condensation has been demonstrated to have better heat transfer performance due to faster condensate removal (*i.e.*, droplets shedding), as compared to the traditional filmwise mode, which occurs on typical metal oxide condenser surfaces. The key to enhanced condensation is thin (< 100 nm) coatings with low contact angle hysteresis. Thin low surface energy coatings (*e.g.*, self-assembled monolayers or SAMs) have been utilized to promote dropwise condensation especially on copper surfaces for over half a century. However, all thin coatings (polymer or SAM) degrade within a few hours during condensation of water vapor, and specifically trichlorosilane SAMs fail within 30 mins on metal surfaces. After coating failure/degradation, water vapor condensation transitions from the dropwise mode to the filmwise mode. In this work, we significantly enhance the durability of silane SAMs on copper surfaces *via* plasma modification of the substrate, and the preferential dropwise condensation mode is maintained for hundreds of hours when condensing water vapor. Low surface energy silane SAM coatings deposited on our plasma modified copper substrates demonstrate a low contact angle hysteresis ($\approx 20^\circ$), and better bonding between the silane SAM and the copper substrate is achieved for substrates at different roughness levels. Additionally, we elucidated the degradation mechanism of silane SAMs on copper during water vapor condensation and revealed the required surface chemistry to develop robust silane SAM coatings on copper surfaces. Various nano-to-microscale surface analysis techniques are utilized to characterize the coating, surface and interface properties. This work sheds light on the degradation mechanisms of low surface energy monolayer coatings on copper during water vapor condensation, and provides durable solutions for industrial applications with enhanced heat transfer performance.

2:15 PM EN10.17.06

Tuning the Ferroelectric Response in Blend Film of P(VDF-TrFE) by Direct Measurements via ThermoReflectance Atul S. Tripathi¹, Layla Farhat^{1,2}, Mathieu Bardoux¹, Stéphane Longuemart¹, Ziad Herro² and Abdelhak H. Sahraoui¹; ¹Université du Littoral Côte d'Opale, France; ²Université Libanaise, Fanar, Liban, Lebanon

The exploitation of electrocaloric effect (ECE) is an emerging field of research because it provides an energy-efficient and environment-friendly alternative to conventional cooling devices for a broad range of applications, such as on-chip and temperature regulation for sensors and electronic devices. Although ECE has been observed in a variety of ferroelectric ceramics, crystal and polymer and performance were not satisfactory. Recently, a ferroelectric thin film based on P(VDF-TrFE) has been demonstrated a high EC effect. Compared to ferroelectric ceramics, P(VDF-TrFE) has the advantage of low density, good toughness, high electrostriction rate, and environmental protection too. Currently, a number of the existing methods have been developed to characterize the electrocaloric effect in the Direct and Indirect methods. Direct methods, measure the change in EC temperature or heat exchanged in the material in the presence or removal of the electric field. However, the indirect method is based on Maxwell's equation that allows obtaining the variation of entropy and variation of temperature. Detect the temperature variation in the thin film is difficult due to the rapid dissipation of heat in the substrate. In addition mass of the assembly (substrate +measuring device) is greater than that of the thin layer alone, and makes the heat variation is undetectable by direct and indirect method. Therefore, we need to study this material using instruments offering high resolution.

Thermoreflectance is a photothermal technique whose high frequency of operation makes it possible to probe the material on small thicknesses. This method has a function based on temperature dependant reflectivity of a surface which is probed using the intensity variation of a reflected laser beam. In this work, blend film of copolymer P (VDF-TrFE) and relaxor Ter polymer P (VDF-TrFE-CFE) in a different ratio. After optimization, the copolymer crystallinity was improved due to the coupling that was observed from the characterization. This optimized crystalline thin film was further characterized by recently developed direct measurement via thermoreflectance where the pump laser beam was replaced by an alternating electric field that is applied across our electrocaloric material to induce the electrocaloric effect (ECE). To apply this method, variation of ΔT as a function of applied field and frequency was studied in optimized blend film and achieved the $\Delta T(K) > 2$ at room temperature.

SESSION EN10.18: Phase Change and Measurement II
Session Chairs: Youngsuk Nam and Yangying Zhu
Tuesday Afternoon, December 7, 2021
EN10-Virtual

6:30 PM EN10.18.01

Raising Dielectric Permittivity Mitigates Dopant-Induced Disorder in Conjugated Polymers Meenakshi Upadhyaya, Michael Lu-Díaz, Subhayan Samanta, Muhammad Abdullah, Kevin Kittilstved, Dhandapani Venkataraman and Zlatan Aksamija; University of Massachusetts Amherst, United States

Conjugated polymers need to be doped to increase charge carrier density and reach the electrical conductivity necessary for electronic and energy applications. While doping increases carrier density, Coulomb interactions between the dopant molecules and the localized carriers are poorly screened in organic semiconductors because of their low dielectric permittivity and thus causes an increase in energetic disorder as evident in the broadening and a heavy tail effect in the electronic density-of-states (DOS). We relate the dopant-induced energetic disorder to a reduction in the Seebeck coefficient while deep traps in the heavy tail cause a collapse in the conductivity. We show that increasing the dielectric permittivity (ϵ) of the polymer mitigates dopant-carrier Coulomb interactions resulting in a simultaneous increase in conductivity and Seebeck coefficient. We simulated electron hopping between localized sites with a modified Gaussian disorder model and included electrostatic interactions between carriers and clustered dopants. We iteratively solved the non-linear Pauli's master equation to compute time-averaged occupational probabilities of the sites from which relevant transport quantities are calculated. Increasing ϵ from 3 to 12 nearly restores the intrinsic DOS, resulting in a large increase in the power factor. We validated this prediction experimentally in iodine-doped P3HT and P3HT blended with barium titanate nanoparticles. The addition of 2% w/w barium titanate nanoparticles increased conductivity and Seebeck across a broad range of doping, resulting in a four-fold increase in power factor. Beyond improving the thermoelectric performance, we note that most of the improvement we observed in the power factor comes from increases in the conductivity, particularly at low to medium doping concentrations, which is broadly useful in organic electronics. Our method of incorporating additives with a high dielectric constant precludes the need for synthetic modifications and thus can be applied to a wide range of polymers. The vapor doping method followed in our study avoids interfacial effects on the DOS that can arise from modulation doping using field-effect transistors and also wide angle X-ray scattering (WAXS) studies show that the overall film morphology is essentially maintained during the measurement over a wide range of carrier concentration. This synergetic computational and experimental study shows a clear path forward to mitigate dopant-induced energetic disorder and develop high-performance organic electronic materials with improved charge transport through dielectric screening.

6:45 PM EN10.18.02

Negative Thermal Expansion and Ultra-Low Thermal Conductivity of ZrW_2O_8 Sora-At Tanusilp¹, Masaya Kumagai^{1,2}, Yuji Ohishi³, Hideki Furusawa⁴, Motoomi Suwabe⁴ and Ken Kurosaki^{1,5}; ¹Institute for Integrated Radiation and Nuclear Science, Kyoto University, Japan; ²SAKURA Research Center, SAKURA internet Inc., Japan; ³Osaka University, Japan; ⁴Furuuchi Chemical Corporation, Japan; ⁵University of Fukui, Japan

For decades, ZrW_2O_8 has been known as a negative coefficient of thermal expansion (CTE) material. The negative CTE is probably due to its unique crystal structure. ZrW_2O_8 has been therefore considered as a promising candidate for thermal management applications, which can be applied to use as a CTE compensating component for controlling thermal expansion of various composites such as ceramics, polymers, and metals. On the other hand, thermal properties other than the CTE of ZrW_2O_8 , such as thermal conductivity, are almost unknown. Here, we synthesized a highly dense bulk sample (%T.D. > 95%) of ZrW_2O_8 from a very fine powder (~31 nm) using a spark plasma sintering (SPS) technique. It was revealed that ZrW_2O_8 exhibited the lowest level of thermal conductivity among various oxides in a wide temperature range from 300 to 823 K. Furthermore, we investigated various physical properties related to such low thermal conductivity through the anharmonicity such as peculiar CTE, elastic constant, and Grüneisen parameter. Owing to its extremely low thermal conductivity, ZrW_2O_8 can be used as a thermal barrier material, which generally operates at high temperatures.

7:00 PM EN10.18.03

Oxide-Free Copper Nanoparticle Incorporated Gallium-Based Liquid Metal Alloy for High-Performance Thermal Interface Materials Seokkan Ki^{1,2}, Jaehwan Shim^{1,2}, Seungtae Oh¹, Seungeol Ryu³, Jaechoon Kim³ and Youngsuk Nam²; ¹Kyung Hee University, Korea (the Republic of); ²Korea Advanced Institute of Science and Technology, Korea (the Republic of); ³Samsung Electronics Co., Ltd, Korea (the Republic of)

Thermal interface materials (TIMs) with high thermal conductivity, surface wettability, and fluidic characteristics are crucial for the thermal management of high-power electronics. Gallium-based liquid metal alloys (LMAs) have been investigated as TIM due to their relatively high thermal conductivity (~23 $Wm^{-1}K^{-1}$), low melting point (<10°C), and low processing temperature. To further increase the thermal conductivity of LMA, a few studies tried to incorporate metallic fillers into the liquid metal matrix. However, these attempts have been limited due to the oxidation of the LMA matrix, which leads to severe solidification of the fabricated composite at a high volume fraction of fillers. In this work, we incorporate copper nanoparticles (Cu NPs) into the eutectic gallium-indium-tin (GaInSn) LMA using an oxide-free ultrasonication-assisted particle internalization method. Developed GaInSn/Cu NPs composite provides over 180% enhancement of thermal conductivity (~65 $Wm^{-1}K^{-1}$) with only 4% volume fraction of fillers. The obtained thermal conductivity is higher than those of the previously-reported Ga-based composites at over 20% volume fraction of fillers. In the liquid metal droplet impacting test, the GaInSn/Cu NPs shows almost identical spreading diameter compared to the untreated GaInSn, which represents the maintained fluidity of the composite. Experimentally measured thermal property is demonstrated based on the nanoparticle clustering phenomenon, in which we microscopically visualize the formation of the copper clusters within the liquid metal matrix to calculate the prediction model. The calculated effective thermal conductivity is well-matched to the experimental data, indicating that the nanoparticle clusters provide additional heat pathways. In terms of surface wetting characteristics, the LMA shows a high-quality interface with silicon substrate due to the formation of ~10nm of Ga_2O_3 adhesion layer confirmed through X-ray photoelectron spectroscopy (XPS). In the heat dissipation performance test, GaInSn/Cu NPs presents over 20% lower hot-spot temperature compared to the one obtained with the thermal grease at high (>150 Wcm^{-2}) heat flux regime and also provides thermal stability over 230 cycles of acceleration test at high-temperature exposure (~100°C), suggesting applicability for high-power density semiconductor packaging applications.

7:15 PM EN10.18.04

Power Generation via Droplet Impact on Superhydrophobic PMN-PT Pyroelectric Surfaces Jeonghoon Han¹, Seungtae Oh², Hee Jae Hwang², Dukhyun Choi², Choongyeop Lee² and Youngsuk Nam¹; ¹Korea Advanced Institute of Science and Technology, Korea (the Republic of); ²Kyung Hee University, Korea (the Republic of)

Single crystalline pyroelectric materials offers new opportunities for efficient thermal energy harvesting utilizing temperature fluctuation. Recent works have demonstrated the pyroelectric generators utilizing various thermal energy such as body heat and latent heat of fluids. However, the sustainable and high performance pyroelectric thermal harvesting has not been realized yet. In this work, we introduce the pyroelectric generator utilizing the rapid temperature fluctuation during a droplet impact. The thin single-crystalline PMN-PT of 100 μm thickness was incorporated to the generator in order to improve the pyroelectric coefficient with reducing the thermal mass. To further enhance the temperature fluctuation during the drop impact, the top surface of the pyroelectric generator was coated by the silanized titanium oxide nanoparticles. Then a 14 μl water drop of 293K was impacted on the developed pyroelectric generator by varying the surface temperature from 313K to 353K. Based on the measured pyroelectric current and voltage values, the pyroelectric current prediction model was developed utilizing the correlation of the maximum spreading diameter during drop impact. The developed model accurately predicted the pyroelectric electricity generation under a wide range of experimental conditions. The maximum pyroelectric current and power density were measured to be 66 μA and 19.2 $\mu\text{W}/\text{cm}^2$, which surpasses previous pyroelectric thermal harvesting results. We believe this work will help to develop efficient pyroelectric thermal energy harvesters.

7:30 PM EN10.18.05

Erythritol Impregnated within Surface-Roughened Hydrophilic Metal Foam for Medium-Temperature Solar-Thermal Energy Harvesting Xiaoxiang Li; Shanghai Jiao Tong University, China

Erythritol (ET) has received increasing research attention for medium-temperature phase change solar-thermal energy storage. However, ET suffers from serious supercooling, low thermal conductivity, poor solar absorption, and leakage after melting, which lead to low solar-thermal energy harvesting and releasing efficiency. Herein, we simultaneously overcome these inherent shortcomings by impregnating ET within the surface-roughened hydrophilic copper foam, which is prepared by subsequent oxidization of commercial copper foam and thermal reduction under hydrogen and using stably dispersed crumpled graphene particles as the solar-thermal converter. Such oxidization-reduction-treated copper foam not only provides numerous heterogeneous nucleation sites and lowers the nucleation energy barrier for forming ET crystals during the solidification process, but also facilitates rapid charging and discharging along with three-dimensional heat conductive networks, and confines the melted ET. Compared with neat ET, the copper foam-templated composites have reduced the supercooling degree by $\sim 60^\circ\text{C}$ and improved thermal conductivity by more than 5 times, which in turn lead to a large latent-heat releasing percentage of 85.8% and a high heat-extraction efficiency of 94.2%. We demonstrate that such composites can be used for high-efficiency, medium-temperature, form-stable, direct solar-thermal energy harvesting, and the harvested heat can be readily converted into electricity to power small devices.

7:45 PM EN10.18.06

Reduced Graphene Oxide-Coated Micropillar Structure of Different Aspect Ratio for Boiling Heat Transfer Maroosol Yun¹, Geehong Choi², Donghwi Lee³ and Hyung Hee Cho¹; ¹Department of Mechanical engineering, Yonsei University, Korea (the Republic of); ²Hyundai steel, Korea (the Republic of); ³University of Wisconsin–Madison, United States

Boiling heat transfer is a promising approach for an ever-growing need for higher cooling capacities. To heighten the operating limit of boiling heat transfer, critical heat flux (CHF) should be enhanced. CHF is the maximum heat flux of fully developed nucleate boiling, just before vapor film covers heated surfaces, which results in an abrupt increase of wall temperature. To delay CHF, supplying sufficient working fluid to the heated surface should be ensured, thus research into CHF enhancement had explored various surface modification techniques including nanoparticle coated surface. In general, nanoparticle coatings are known to enhance CHF and heat transfer coefficient (HTC) by efficiently dissipate heat into the working fluid and promoting bubble nucleation by providing porous nucleation sites. And graphene materials could be fitting candidates since they exhibit superb thermal conductivity and graphene platelet could form porous layers on the substrates which promote bubble nucleation. However, gathering an excessive amount of graphene platelet onto the surface could discourage liquid supply due to its hydrophobic nature. This overcrowding graphene problem could be modulated by combining graphene deposition with an appropriately micro-structured surface since the particle deposition takes place at the microlayer region. Here, we propose reduced graphene oxide (rGO)-coated micropillar structure with varying aspect ratios to promote nucleate boiling and save liquid supply paths. The rGO-coated micropillar surfaces were prepared by deep reactive ion etching (DRIE) and following nanofluid boiling step with rGO solution of 0.0005 wt%. Micropillar structures of different aspect ratios (m5, m10, m20) fabricated by DRIE are 4 μm in diameter and 5, 10, 20 μm in height, respectively. Fabricated surfaces were evaluated by a pool boiling setup with deionized (DI) water as a working fluid. The temperature of DI water was maintained at the saturated temperature at atmospheric pressure. The results showed that rGO coated surface shows smoother and faster ONB by providing suitable cavities which promote bubble nucleation for lower wall superheat. And wall superheat was lessened for all rGO-coated cases owing to the high thermal conductivity of rGO particles. For the morphologies of the rGO coating, porous rGO coating embraced the lateral side of micropillar when the aspect ratios of the micropillar arrays were relatively lower (m5, m10), which might result in blockage of water supply, while the rGO layer coated over the tip of the micropillar when the aspect ratio of the micropillar was sufficiently high (m20). This difference came from the location of the microlayer varies with the aspect ratio of the micropillar arrays during the fully developed nucleate boiling regime. Presented surfaces of plain, rGO-coated m5, m10, and m20 recorded 89 W/cm^2 , 174 W/cm^2 , 177 W/cm^2 , and 256 W/cm^2 in CHF, respectively. The maximum heat transfer coefficients were recorded as 20.4 $\text{kW}/\text{m}^2\text{K}$, 50.9 $\text{kW}/\text{m}^2\text{K}$, 45.9 $\text{kW}/\text{m}^2\text{K}$, and 74.3 $\text{kW}/\text{m}^2\text{K}$, respectively. The significant improvement on CHF and HTC in the rGO-coated m20 case indicates that rGO coatings on the m20 were mainly placed over the tip, saving spaces between micropillars and emphasizes the importance of ensuring flow paths to enhance the nucleate boiling. This study will be helpful for enhancing boiling heat transfer for the usage in the field needing extreme cooling capacities such as data storage center, heat exchanger, and fusion reactor.

8:00 PM EN10.18.08

The Effect of Al Doping on Nanoscale Thermal Transport in Swift Heavy Ion Irradiated Polycrystalline $\beta\text{-Si}_3\text{N}_4$ Azat Abdullaev¹, Mostafa Valadkhani², Arno Janse van Vuuren³, Jacques O'Connell³, Ruslan Rymzhanov⁴, Anel Ibrayeva^{4,5}, Mehdi V. Allaei², Vladimir Skuratov⁴ and Zhandos Utegulov¹; ¹Nazarbayev University, Kazakhstan; ²University of Tehran, Iran (the Islamic Republic of); ³Nelson Mandela University, South Africa; ⁴Joint Institute for Nuclear Research, Russian Federation; ⁵Nur-Sultan Branch of Institute of Nuclear Physics, Kazakhstan

Comprehensive understanding on radiation resistance of nuclear fuels and cladding materials during normal reactor operation is very important for the construction of a new generation of safe and energy-efficient nuclear reactors. Particularly, the control of radiation-induced heat transport is a critical issue for nuclear reactor system design and validation.

Swift heavy ion (SHI) irradiation simulates nuclear fission products in terms of the structural damage caused to materials in the actual nuclear reactors [1]. At high energies, typical of SHIs, where the ion penetration depth is of the order of several microns, the projectile energy is deposited in the target through

an inelastic process through which electronic energy loss dominates on nanoscale depths, leading to intense localized *thermal spikes* causing displacement of lattice atoms along nanoscale-thick ion tracks along the ion path in insulating materials [2].

It is well known that nitride ceramics demonstrate a high level of resistance to SHI radiation and no visible tracks have been observed in most ceramics except silicon nitride. This material is considered to be a promising material as inert matrix fuel host and therefore it is vital to understand the parameters of latent track formation and structural change. Several works have shown that the doping of materials and thermal conductivity play an important role in the formation of these tracks [3,4]. Therefore, the main goal of this study is to determine the impact of Al doping on thermal conductivity degradation due to the related nano-structural damage.

We used polycrystalline β - Si_3N_4 ceramic samples with different level of Al doped concentration ranging from 0.05 to 3%. The SHI irradiation was performed at the IC-100 FLNR JINR cyclotron facility in Dubna, Russia where the samples were irradiated by Bi, Xe, Kr and Ar ions at room temperature and fluences ranging from 10^{12} to 10^{14} ions/cm². For structural analysis the samples were analyzed in both TEM and STEM modes and complimented with diffraction analysis using a JEOL ARM-200F TEM operating at 200 kV. Cross-plane thermal conductivity measurements were done using picosecond time domain thermoreflectance (TDTR) technique at different modulation frequencies to enable thermal probing at nanoscale depths. Both TEM analysis and thermal conductivity measurements revealed that the high concentration of Al doping lowers the resistance of β - Si_3N_4 to ion track formation resulting in amorphization and substantial decay in thermal conductivity. Depth-resolved TDTR measurements were used to validate models based on semi-analytical Klemens phonon transport and non-equilibrium molecular dynamics to analyze SHI-induced nanoscale damage.

References

- [1] G.S. Was, Challenges to the use of ion irradiation for emulating reactor irradiation, *J. Mater. Res.* 30 (2015). <https://doi.org/10.1557/jmr.2015.73>.
- [2] V.A. Skuratov, J. O'Connell, N.S. Kirilkin, J. Neethling, On the threshold of damage formation in aluminum oxide via electronic excitations, *Nucl. Instruments Methods Phys. Res. Sect. B Beam Interact. with Mater. Atoms.* 326 (2014). <https://doi.org/10.1016/j.nimb.2013.10.037>.
- [3] A. Janse Van Vuuren, V. Skuratov, A. Ibrayeva, M. Zdorovets, Microstructural effects of Al doping on Si_3N_4 irradiated with swift heavy ions, in: *Acta Phys. Pol. A*, 2019. <https://doi.org/10.12693/APhysPolA.136.241>.
- [4] M. Toulemonde, W. Assmann, C. Dufour, A. Meftah, C. Trautmann, Nanometric transformation of the matter by short and intense electronic excitation: Experimental data versus inelastic thermal spike model, *Nucl. Instruments Methods Phys. Res. Sect. B Beam Interact. with Mater. Atoms.* 277 (2012) 28–39. <https://doi.org/10.1016/j.nimb.2011.12.045>.

SESSION EN10.19: Phase Change and Water
Session Chairs: Youngsuk Nam and Yangying Zhu
Wednesday Morning, December 8, 2021
EN10-Virtual

8:00 AM *EN10.19.01

Innovative Surface Engineering for Transformative, Hybrid Energy Management and Exploitation (THEME) Zuankai Wang; City University of Hong Kong, China

The progress of human civilization is highly dependent on the capability to harness and deploy energy and water. On one hand, owing to carrying plenty of kinetic and electrostatic energies, water is at the heart of many energy conversion and harvesting devices. On the other hand, the large latent heat of water also endows it as a ubiquitous flowing currency in energy transfer (heat transfer) devices. The close intertwining among water, energy, and heat becomes pronounced with the penetration of miniaturized devices in every corner of our society. Despite inherent coupling and diversity in varying energy processes, there lies in a common need, i.e., achieving high energy efficiency while low water consumption.

This simple need, however, encounters several challenges. First, the miniaturization of electrical devices driven by the Moore's Law poses increased heat flux and difficulty in energy supply, especially for implantable application. Second, scientifically, harnessing the synergy between water, energy and heat to improve energy efficiency calls for the heterogeneous integration of different materials, interfaces, and systems, which poses the daunting complexities in formulating a basic framework, rational design, and scalable fabrication. Third, technically, recent breakthroughs have demonstrated the power of designing surfaces to mediate water transport for efficient thermal cooling and energy harvesting for sustained power supply, however, conventional approaches for surface design are handled separately, which are complicated and inefficient. Without proper design, surfaces are also susceptible to structural and functional instability and compromise overall performances.

Leveraging the dual nature of both water and surfaces as well as drawing inspirations from nature's power in managing the flow of water, energy, heat through the elegant control of surface properties, in this talk, I will discuss an innovative surface engineering-based approach for transformative, hybrid energy management and exploitation (THEME) that results in synergistic effects and novel functionalities that go beyond conventional designs. Examples include how to efficiently promote phase change heat transfer such as condensation, boiling, in particular cooling down large-scale hot surfaces by several hundreds of degrees, how to achieve energy-free cooling and how to efficiently harvest water energy from moisture, encapsulated water and flowing water.

8:30 AM *EN10.19.02

Nanostructured Passive Cooling Based on Evaporation and Radiation Jia Zhu; Nanjing University, China

Nanostructures with carefully tailored properties can be used to manipulate the flow of light, heat and water, to enable high performing passive cooling through evaporation and radiation. I will present our recent progress.

The first example is cooling photovoltaic device through evaporative cooling. We demonstrate a monolithic tandem solar electricity-water generator that synergistically produces electricity and clean water by utilizing the full spectrum of solar irradiance. This design possesses two components: a top infrared-transparent photovoltaic device using above-band-gap photons, and a bottom solar water purifier using the below-band-gap photons. A well-designed water-proof thermal interconnecting layer (WTIL) makes these two components work synergistically: the bottom purifier serves as an evaporative cooler of the top solar cell to increase its efficiency, whereas the thermalization energy of the top cell is reutilized by the bottom purifier for producing more clean water. We experimentally demonstrate that a prototype hybrid tandem solar device with WTIL can generate electricity with a power output of 204 W m⁻² and purify water at a rate of 0.80 kg m⁻² h⁻¹ under 1-sun illumination.

The second example is about passive cooling. Radiative cooling which sends heat to space through atmospheric transparency window without any energy consumption, is attracting significant attention. For radiative cooling to achieve high cooling performance, it is ideal to have a selective emitter, with an emissivity dominant in the atmospheric transparency window. However, so far scalable production of radiative cooling materials with selective emissivity

has not been realized. Here we will present a hierarchical design for a selective thermal emitter to achieve high performing all-day radiative cooling. Moreover, it is revealed that this hierarchically designed selective thermal emitter shows significant advantage if being applied to alleviate Global Warming or to regulate temperature of the Earth-like planet.

9:00 AM *EN10.19.03

Enhancing Light-Heat-Fluid Transport via Nanofabrication and Micro-3D Printing for Solar Energy-Water Nexus TieJun Zhang; Khalifa University of Science and Technology, United Arab Emirates

Harvesting natural energy and water resources from the earth and beyond is essential for the mankind. Solar energy-water nexus is of paramount importance to achieve sustainable development goals of our world, where effective transport at the light-matter and fluid-solid interfaces is the key. In this talk, I will present recent advances in enhancing interfacial transport by tailoring optical and wetting properties of materials and structures via micro-3D printing and nanofabrication. A new class of spectrally selective nanocomposite solar absorbers is proposed to harness sunlight and minimize thermal emission. Functionalized micro and nanoporous membranes are applied to enhance liquid propagation and vapor generation, meanwhile new physical insights are obtained from infrared imaging and magnetic resonance analyzer. Latest development of micro-3D printing technologies enables the digital fabrication of biomimetic structures for high-performance transport devices in various energy and water applications. These innovations pave the way for accelerating the knowledge discovery of light-heat-fluid transport and developing cost-effective solutions to real-world grand challenges.

9:30 AM *EN10.19.04

Device and Material Innovation for Energy-Neutral Sunlight-Assisted Atmospheric Water Harvesting Dimos Poulikakos, T. Schutzius, I. Haechler, H. Park, G. Schnoering, Cheuk Wing Edmond Lam, M. Donati and A. Milionis; ETH Zurich, Switzerland

Two-thirds of humanity live under conditions where the net fresh water withdrawal is more than twice the natural water availability for at least 1 month per year, and half a billion people suffer from this water stress throughout the entire year. Atmospheric water vapor is ubiquitous and represents a promising alternative to address global clean water scarcity. Sustainably harvesting this resource requires energy neutrality, continuous production, and facility of use. In this talk I will discuss promising approaches from my research group addressing the above challenges, Refs. (1-3), involving the development of innovative materials and systems. These utilize radiative cooling to the outer space with optimized radiation shielding (1), or sorption intermittency guided by the time scales of the designed materials, combined with solar energy (2), to harvest atmospheric water efficiently and continuously (over 24 hours), beyond the capabilities of the state-of-the-art solar energy driven water harvesting systems. Water removal from such systems without expending additional energy is also addressed. This is enabled with a fully passive superhydrophobic condensate harvester, working with a coalescence-induced water removal mechanism from a novel sprayable superhydrophobic coating (3).

1. I. Haechler, H. Park, G. Schnoering, T. Gulich, M. Rohner, A. Tripathy, A. Milionis, T. M. Schutzius and D. Poulikakos, Exploiting radiative cooling for uninterrupted 24-hour water harvesting from the atmosphere, *Science Advances*, in press.

2. H. Park, I. Haechler, G. Schnoering, M. D. Ponte, T. M. Schutzius, D. Poulikakos, Enhanced atmospheric water harvesting with sunlight activated sorption ratcheting, in review.

3. Matteo Donati et al., *Advanced Materials Interfaces*, vol. 8: no. 1, pp. 2001176 2020. DOI: 10.1002/admi.202001176.

SYMPOSIUM EN11

Electrocatalytic Materials to Sustainably Convert Atmospheric C, H, O and N into Fuels and Chemicals
November 30 - December 7, 2021

Symposium Organizers

Chong Liu, University of California, Los Angeles
Samira Siahrostami, University of Calgary
Wilson Smith, National Renewable Energy Laboratory
Haotian Wang, Rice University

* Invited Paper

SESSION EN11.01: CO₂ Reduction I
Session Chairs: Wilson Smith and Haotian Wang
Tuesday Morning, November 30, 2021
Hynes, Level 3, Room 312

10:30 AM EN11.01.01

Transient Effects Caused by Gas Depletion During Carbon Dioxide Electroreduction Alvaro Moreno Soto^{1,2}, Jack R. Lake¹ and Kripa K. Varanasi¹; ¹Massachusetts Institute of Technology, United States; ²Universidad Carlos III de Madrid, Spain

The novel use of CO₂ electroreduction to produce carbon-based components that do not contribute to the Greenhouse effect has encouraged the vision of carbon dioxide as a renewable feedstock with the goal to reach net zero emissions into the atmosphere.

The variety of useful products that may be obtained from such an electrochemical process strongly depends on the material of selection as electrocatalyst. In this research, we have focused on the 'coinage' metals, i.e. copper, silver and gold, due to their accessibility and the vast literature available. Whereas gold and silver are very selective to carbon monoxide, copper produces wide variety of components, covering liquids (such as methanol, formate and ethanol) and gases (such as carbon monoxide, methane and ethylene). However, one aspect that has not been yet addressed in detail and which heavily affects the chemical reaction efficiency is the CO₂ availability to the working electrode. In this aspect, the performance of any chemical reaction is significantly affected by the concentration of reactant gas in the proximity of the reacting site. Therefore, the overall chemical reaction efficiency strongly depends on the mass transfer capabilities of the system. A means of measuring the performance of the carbon dioxide electroreduction process is by comparing the total amount of generated carbon-based products and the amount of produced hydrogen. Hydrogen is originated at the parallel side-reaction occurring at the same time than CO₂ electroreduction. Its formation implies then that not all the current invested in the system is dedicated to consume carbon dioxide. Even though H₂ co-evolution is unavoidable with current techniques, other novel technologies (such as the gas diffusion electrode) are being developed to optimize the partial current exclusively dedicated to reduce CO₂. Here, mass transfer capabilities play a major role: the reaction consumes CO₂ in areas close to the electrode surface and originates a gas depletion environment that needs to be compensated. Therefore, in quiescent electrochemical cells, gas depletion drastically affects the overall chemical efficiency, especially in the long run.

In this research, we present a detailed description of the mass transport limitations originated by diffusion alone compensating for gas depletion in the vicinity of the electrode. This investigation is particularly important and relevant for the cases in which a reaction is maintained over long periods of time, as it would be the case for industrial scale CO₂ electroreduction. More specifically, this work focuses on the evolution of gas depletion over time as the reaction consumes the available CO₂ and provides an indirect accurate means of measuring that evolving gas concentration by pH. Indeed, the level of pH near the electrode's surface is based on two major contributions: the decrease in the CO₂ concentration due to gas depletion and the generation of ions during chemical reaction. We develop a mathematical model that accounts for the evolution of the gas concentration in areas surrounding the electrode and refer it to the experimentally-measured pH.

Finally, we conclude that CO₂ depletion is the cause of the strong decay in the chemical efficiency of a continuous chemical reaction. Pulsed electrochemistry is then proposed as an alternative method to compensate for such an effect. In this scenario, a certain current is cycled on and off periodically, allowing the electrodes to react for a certain period of time, letting the system rest afterwards. This way, gas diffusion through the liquid electrolyte is able to partially compensate for the consumed CO₂ in the vicinity of the electrode. The overall chemical efficiency can be then maintained over longer periods of time. However, the total production is compromised. A discussion over the preferability of efficiency over production rate is then debated at the end and open to discussion.

10:45 AM EN11.01.02

Characterizing Degradation Mechanisms in Gas Diffusion Electrodes for the Electrochemical Reduction of Carbon Dioxide [Emiliana Cofell](#)¹, Uzoma Nwabara¹, Saket Bhargava¹, Danielle Henckel², Zachary Park¹ and Paul Kenis¹; ¹University of Illinois at Urbana-Champaign, United States; ²National Renewable Energy Laboratory, United States

The electrochemical reduction of CO₂ offers the dual benefits of recycling CO₂, thereby mitigating emissions, and producing intermediates for valuable fuels and chemicals such as CO, formic acid, ethylene, and ethanol in a carbon-neutral manner.^{1,2} Previous research has focused on the application of gas diffusion electrodes (GDEs) in CO₂ reduction systems, which has enabled the conversion of CO₂ into products at a high rate.^{3,4} Despite these GDEs requiring a lifetime of at least 3000 hours for economic feasibility, their durability has not been studied widely.^{4,5} In fact, many GDEs studied to date show declining performance over time, the causes of which have not been determined. Progress in this area, in particular with respect to understanding GDE degradation mechanisms, will be crucial for further development of CO₂ reduction technology.

This presentation will discuss post-testing changes in GDE cathode surface morphology and composition as a function of electrolyte composition and applied current density/potential. We investigated these changes *via* a variety of surface and bulk characterization techniques (SEM, EDS, Micro-CT, XRD). This approach identified degradation mechanisms including carbonate deposit formation, surface passivation, and catalyst layer restructuring, leading to loss of catalyst availability. In particular, we determined that a highly alkaline electrolyte, although beneficial for achieving high current densities and efficiency for CO production, causes the rapid formation of carbonate deposits on the GDE surface due to high local pH at the reaction interface.⁷ The extent of carbonate deposit formation depends heavily on electrolyte cation identity and concentration. We also explored the impact of potential cycling on the catalyst layer, noting significant restructuring and loss of catalyst layer when more positive potentials are repeatedly applied to the cathode. By using a combination of materials characterization techniques and electrochemical methods, we are able to image the evolution of the GDE surface, determine which conditions lead to loss of catalyst surface area, and better understand how to develop long-lasting electrodes for electrochemical reduction of CO₂ to value-added chemicals.

References:

- Lee, M.-Y., Park, K. T. Lee, W., Lim H., Kwon, Y., Kang, S., *Crit Rev Env Sci Tec* **50**, 789-815 (2019).
- Endrodi, B., Bencsik, G., Darvas, F., Jones, R., Rajeshwar, K., Janaky, C., *PECS* **62**, 133-154 (2017).
- Weng, L.-C., Bell, A., Weber, A., *Phys. Chem. Chem. Phys.* **20**, 16973-16984 (2018).
- Cofell, E., Nwabara, O., Negro, E., Verma, S., Kenis, P. J. A., *Chemsuschem* **13**, 855-875 (2020).
- Verma, S., Kim, B., Jhong, H., Ma, S. C. & Kenis, P. J. A. *Chemsuschem* **9**, 1972-1979 (2016).
- Kim, B., Hillman, F., Ariyoshi, M., Fujikawa, S. & Kenis, P. J. A. *J Power Sources* **312**, 192-198 (2016)
- Cofell, E., Nwabara, O., Bhargava, S., Henckel, D., Kenis, P. J. A., *ACS Appl. Matter. Interfaces* **13**, 15132-15142 (2021).

11:00 AM EN11.01.03

Revealing Chemical Processes in CO₂ Reduction with Local pH Imaging Confocal Microscopy [Characterization of Gas Diffusion Electrodes](#) [Annette Boehme](#), Alex Welch and Harry A. Atwater; California Institute of Technology, United States

Carbon dioxide reduction in a gas diffusion electrode is a complex chemical process with potential for achieving electrocatalytic product synthesis with high throughput and selectivity. Spatially and time-resolved chemical measurements have the potential to elucidate the kinetic and transport processes in this complex environment. To this end, we report results of *operando* local pH measurements with confocal fluorescence microscopy around an operating CO₂ reduction gas diffusion electrode that enable understanding about CO₂ reduction electrocatalysis. Because the pH varies on the micrometer-scale close to the surface of an electrode, measuring the bulk pH does not provide a sufficiently detailed picture to understand the local reaction conditions. In our first experiments we have compiled three-dimensional pH maps with micron-scale resolution that are indicative of CO₂ flow through the inhomogeneous morphology of a porous gas diffusion electrode permeated by a periodic array of cracks in the microporous layer. These maps provide clear evidence for inhomogeneous CO₂ diffusion in the microporous layer, such that CO₂ diffuses faster through cracks and larger pores in the electrode. As CO₂ travels through a gas diffusion electrode and dissolves in the electrolyte, it lowers the local pH due to carbonate reactions. Therefore, the local pH can provide valuable information about the diffusion of CO₂ through different electrode morphologies. However, when an electrical current is applied, the pH around a

gas diffusion electrode increases because CO₂ reduction reaction and the hydrogen evolution reaction both consume protons. The interplay between these two effects is crucial to understand and tailor the reaction microenvironment around the working electrode surface. We use the two-color fluorescent pH sensitive dye 8-Aminopyrene-1,3,6-trisulfonic-acid-trisodium-salt (APTS) that is sensitive between pH 11.5 and 14 to spatially resolve the pH close to the surface of an operating gas diffusion electrode. The dye is dissolved with a concentration of 125 μM in 2 M KOH electrolyte and excited by a laser at 458 nm under a confocal microscope. The fluorescence of the dye is collected separately for two wavelength intervals from 480-550 nm and 551-754 nm and the ratio of the emission collected from the two excitations is a measure for the pH. The confocal microscope allows to excite the dye at different heights in z above and in cracks in porous gas diffusion electrodes. Through movement of the stage in x- and y-direction and taking measurements consecutively, we can map the pH time-resolved in all three spatial dimensions. With this setup, we performed time-dependent measurements without any applied current to investigate how the CO₂ flux through different gas diffusion electrode substrates made of porous PTFE and carbon paper influences the pH. We found that CO₂ dissolves faster through gas diffusion electrodes made of PTFE due to its larger pore size. We also investigated how the CO₂ permeates through different cracks 10s of microns wide in the carbon paper support and found that the pH first changes locally within the crack relative to the planar electrode surface. Additionally, cracks promote faster CO₂ transport through the electrode. To investigate if this is advantageous for CO₂ reduction, we will report results of experiments with current densities in the 0-30 mA/cm² range. Further, we will discuss the local pH at the electrode surfaces for different gas diffusion electrode structures with the goal to identify ideal gas diffusion electrode designs. For this, we will present three-dimensional pH maps with different applied current densities for PTFE working electrode supports with different pore sizes. We expect that these results will provide valuable insights into the interplay between local pH and CO₂ reduction mechanisms for differently structured gas diffusion electrodes.

11:15 AM *EN11.01.04

Modifying the Electrolyte in CO₂ Electroreduction with Additives to Influence Product Selectivity [Elizabeth J. Biddinger](#); City College of New York, United States

CO₂ electroreduction offers the opportunity to convert a waste and greenhouse gas into valuable products using renewable electricity. CO₂ electroreduction on copper results in a plethora of carbonaceous products unselectively and generates hydrogen. Methods for tuning the selectivity include controlling the reduction potential, modifying the catalyst morphology, adjusting the electrolyte pH, changing the reactor design, and altering the electrolyte composition. By including additives in the electrolyte, the CO₂ solubility, pH, conductivity and interactions at the electrode interface can be modified, resulting in changes to the product selectivity in CO₂ electroreduction. Salts and ionic liquids, added at low concentrations to aqueous bicarbonate electrolytes, can be promising modifications to the electrolyte while still maintaining the favorable buffering ability that bicarbonates bring. The hydrophilicity of the anion plays a significant role in the product selectivity on copper. For example, when the highly hydrophilic dicyanamide ([DCA]⁻) – based additives are used, CO₂ electroreduction is effectively shutoff and hydrogen evolution is enhanced. In contrast, highly hydrophobic bis(trifluoromethylsulfonyl)imide ([NTF₂]⁻) – based additives lower hydrogen evolution activity and increase formate production. XPS, EQCM and FTIR suggest that the surface coverage of the additives significantly influences CO₂ electroreduction.

SESSION EN11.02: CO₂ Reduction II
Session Chairs: Wilson Smith and Haotian Wang
Tuesday Afternoon, November 30, 2021
Hynes, Level 3, Room 312

1:30 PM EN11.02.01

Exploring How Collective Ionic Assembly Influences Electrochemical Carbon Dioxide Upgrading [Matthew A. Gebbie](#) and Beichen Liu; University of Wisconsin–Madison, United States

Electrochemical reduction of CO₂ to CO, CH₄, and other value-added products provides compelling opportunities to realize the sustainable production of commodity chemicals. While increasingly demonstrated in lab-scale systems, a critical roadblock slowing the development of industrial processes is a poor understanding of how molecular assembly at electrode-electrolyte interfaces contributes to catalytic activity. Recently, ionic liquids have emerged as promising CO₂ reduction electrolytes, since low overpotentials and enhanced product selectivity has been observed for several classes of ionic liquids. However, the mechanisms of ionic liquid-mediated catalysis remain subject to ongoing discussion. Here, we present our research on tuning the collective assembly of ionic liquids to understand mechanisms of ionic liquid-mediated CO₂ reduction at silver, copper, and carbon surfaces. By changing ion structures, concentrations, and solvent environments, we reveal unexpected scaling relationships between structure, concentration, and reactivity. Notably, our findings point to collective assembly as a key factor underpinning structure-reactivity relationships for CO₂ electro-reduction. To highlight the impact of this concept, we will show how our findings help resolve mechanistic puzzles in the ionic liquids electrocatalysis community and suggest new strategies for controlling the performance of sustainable CO₂ electrochemical upgrading.

1:45 PM EN11.02.02

Microenvironment Created by Nanoparticle Ligands for Selective CO₂ Electroreduction [Sunmoon Yu](#), Dohyung Kim and Peidong Yang; University of California, Berkeley, United States

Local reaction environments where catalysts operate have been considered as critical as intrinsic active site nature of the catalysts in governing overall catalytic performance. For instance, enzymes are known to attain superior catalytic specificity and activity by creating optimal local reaction environments around their active sites using amino acid side chains. However, creating such ideal microenvironment for synthetic catalysts has been a grand challenge. Recently, we have found that nanoparticle surface ligands (e.g., alkylphosphonic acid), inevitably introduced for colloidal nanoparticle synthesis, in fact can actively create favorable microenvironment under electrochemical bias for selective CO₂-to-CO electroconversion. This microenvironment, so-called nanoparticle/ordered-ligand interlayer (NOLI), is composed of a metal (e.g., silver) nanoparticle and a structurally ordered ligand layer in a detached state. The interlayer created between the nanoparticle surface and the ordered-ligand layer encompasses dehydrated cations, associated with the ligand layer in the vicinity, exhibiting pseudocapacitive characteristics. This microenvironment offers unique active site centers through enhanced electrostatic interactions between the NOLI constituents and adsorbed CO₂ molecules, significantly enhancing catalytic turnover. In this talk, I will present how this catalytic interlayer can be created and its catalytic effect for selective CO₂ electroreduction. We also show the generality of the NOLI catalyst design, which is demonstrated across several transition metal nanoparticles, ultimately achieving up to 99% selectivity towards CO at low overpotentials. Furthermore, the NOLI catalyst is translated to a gas-diffusion environment, retaining nearly unit CO selectivity up to high current densities in neutral media (e.g., 98.1% at 400 mA/cm² in 1 M KHCO₃). In addition, I will also present our recent spectroscopic results that give insights into how initial nanoparticle assembly on a support, found necessary for the formation of the structurally ordered ligand layer and thus the NOLI, can enhance intermolecular ligand interactions and

promote collective behavior of the ligands. I will conclude by giving a broad perspective on new opportunities in harnessing nanoparticle ligand interactions for developing advanced electrocatalysts.

2:00 PM EN11.02.03

Direct and Continuous Generation of Pure Liquid Fuels via Electrocatalytic Carbon Dioxide Reduction in Solid Electrolytes Peng Zhu and Haotian Wang; Rice University, United States

With continuously decreased price of renewable electricity, it becomes increasingly attractive to utilize electrical energy for the production of fundamental chemical feedstocks or fuels. Electrochemical CO₂ reduction reaction (CO₂RR) provides a green and sustainable “bottom-up” pathway to generate basic chemical feedstocks ranging from C₁ to C₃ products. Liquid fuels from CO₂RR, such as formic acid, methanol, acetic acid, ethanol, and propanol, are of particular interest due to their high energy densities and ease of storage and distribution. However, this route is still retarded by the following two long-standing challenges in the field: there is still a lack of highly selective, active, and stable catalysts for CO₂RR to produce target liquid fuels, especially for high-value products beyond formic acid; another challenge is that the liquid fuels generated from CO₂RR electrolysis are always in a mixture with conventional liquid electrolyte, which subsequently necessitates energy- and cost-intensive downstream separation processes to recover pure liquid fuels. Through integrating rational designs in both catalyst and reactor, here we demonstrate a direct and continuous generation of high-purity and high-concentrated liquid fuels via electrochemical CO₂/CO reduction. By designing a novel porous solid electrolyte (PSE) layer between cathode and anode, other than traditional liquid electrolyte, efficient ionic transport was successfully maintained while no impurity ions (e.g. K⁺, Na⁺, HCO₃⁻, OH⁻...) were mixed into generated liquid fuel. When employed in this novel PSE reactor, we successfully demonstrated directly producing pure formic acid solutions from CO₂RR on Bi-based catalysts with nearly 100 % purity. Through flexible tuning of the carrier gas stream, we also achieved an ultra-high concentration up to nearly 100 wt.%. Meanwhile, by tuning the edge-to-surface ratio of Cu nanocube catalyst, we demonstrated an unprecedented acetate performance in neutral pH with an ultrahigh relative purity of up to 98% and concentrations up to 2 wt.%, with excellent stability of over 150 h continuous operation.

2:15 PM *EN11.02.04

Engineering Atomically Dispersed Single Metal Active Sites for CO₂ Electroreduction Gang Wu; SUNY Buffalo, United States

Atomically dispersed and nitrogen coordinated single metal sites (MN_x; M=Ni, Co, and Fe) embedded in carbon support have exhibited exceptional catalytic activity and selectivity for the electrochemical CO₂ reduction reaction (CO₂RR) to CO. However, the understanding of the intrinsic and morphological factors contributing to the catalytic properties of MN_x sites is still lacking. Using a Fe-N-C model catalyst derived from the ZIF-8, we deconvoluted three key morphological and structural elements of FeN₄ sites, including particle sizes of catalysts, Fe content, and Fe-N bond structures. Their monotonous effects on the CO₂RR were comprehensively elucidated. Engineering the particle size and Fe doping is critical to control extrinsic morphological factors of FeN₄ sites for optimal porosity, electrochemically active surface areas, and the graphitization of the carbon support. In contrast, the intrinsic activity of FeN₄ sites was only tunable by varying thermal activation temperatures during the formation of FeN₄ sites, which impacted the length of the Fe-N bonds and the local strains. The structural evolution of Fe-N bonds was characterized at the atomic level. First-principles calculations further elucidated the origin of intrinsic activity improvement associated with the optimal local strain on the Fe-N bond. The obtained understanding can further apply to the design of other singles (e.g., Ni) and dual metal sites (Ni-Fe) catalysts

2:45 PM *EN11.02.05

Towards Electrifying Chemical Manufacturing Through Enhanced Electrode Durability, Process Intensification and Co-Conversion Paul Kenis; University of Illinois at Urbana-Champaign, United States

Today, the chemical industry manufactures most chemicals and fuels using energy-intensive thermal / catalytic processes that are responsible for a significant fraction of anthropogenic CO₂ emissions. Impending climate change necessitates a drastic reduction of greenhouse gas emissions over the next few decades. Electrifying manufacturing of some intermediates or products holds promise to significantly reduce the carbon footprint of the chemical industry. While techno-economic (TEA) and life-cycle (LCA) analyses of the electrochemical reduction of CO₂ to products such as CO, formic acid, ethylene, and ethanol indicate their promise, these also highlight the challenge to compete in terms of cost with present-day chemical conversion processes operated at scale [1].

This contribution will elaborate on three approaches to bring economically feasible, (close to) carbon-neutral electrified chemical manufacturing (electrolysis) closer. First, while active and selective catalysts now exist for electroreduction of CO₂ to products such as CO, formic acid, ethanol, and ethylene, the electrode technology enabling electrolysis over 1000s of hours is still lacking. This presentation will summarize the range of encountered electrode degradation mechanisms [2], elaborate on accelerated durability CO₂ electrolysis testing methods, and present a few approaches to mitigate electrode degradation.

Second, the electroreduction of CO₂ is highly dependent on the exact operating conditions of the process. This presentation will summarize system design rules that enhance CO₂ electrolysis performance (Faradaic efficiency, energy efficiency, conversion efficiency) through fine-tuning of a combination of parameters [3]: (i) Electrolyte composition and pH; (ii) Electrolyte flowrate; (iii) CO₂ feed flowrate; (iv) Catalyst loading; and (v) The use of magnetic fields to enhance mass transfer.

Third, this presentation will elaborate on how performing desired chemical conversions on both electrodes will drastically reduce the energy required to drive these electrolysis processes individually. We found, for example, that co-conversion of CO₂ (reduction at the cathode) with organic waste molecules (oxidation at the anode) reduced the overall energy consumption by 40-50%. [4] Identifying suitable anode catalysts and electrodes for selective organic oxidations will be a major materials research challenge for the next decade. Co-conversion electrolysis process technology could be the starting point for a new generation of chemical manufacturing technology that is significantly more energy efficient than the traditional thermochemical processes, while also able to use renewable feedstocks, such as CO₂, water, biomass adducts, or organic waste streams.

3:15 PM BREAK

SESSION EN11.03: Mechanism Studies
Session Chairs: Wilson Smith and Haotian Wang
Tuesday Afternoon, November 30, 2021
Hynes, Level 3, Room 312

4:00 PM EN11.03.01

The Influence of Magnetic Moment on Chemical Activity for Design of 3D Electrochemical Systems [Chloe Groome](#), [Huong Ngo](#), [Jie Li](#), [Ruqian Wu](#) and [Regina Ragan](#); University of California, Irvine, United States

We present results elucidating the role of magnetic moment on catalytic activation energy barriers with a first principles approach. While many structure-activity relationships have been uncovered, further insight is still needed to design new catalysts from the large elemental design space on high surface area supports with performance comparable to platinum group metals. Specifically, single atom transition metal catalysts on graphene defect moieties with different magnetic moments, but similar charge transfer, are found to exhibit differing degrees of asymmetry of spin states near the Fermi energy. The effect of spin-dependent chemical pathways for transition metal SAC supported on graphene defects has been examined only recently. Previously, chemical reactions undergoing spin crossing have been considered to be spin forbidden or too slow to be practical. However, transition metal SAC have been demonstrated to facilitate spin crossing at points of minimal energy difference (<0.1 eV), allowing reactions such as CO oxidation to proceed along pathways with lower energy barriers. We utilize a first principles approach to examine how the spin state of the SAC and reactants can affect catalytic energy barriers of V, Fe, Mo, and Ta on two different graphene defects with differing magnetic moments. Single vacancy and pyridinic N-doped single vacancy defect moieties were investigated since they have similar charge transfer to metal adatoms but differing magnetic moments. Climbing image-nudged elastic band (CI-NEB) calculations of activation energy barriers of CO oxidation on all transition metal SAC in relaxed geometries on both defect moieties show all barrier energies on N-doped single vacancy defects were 0.8 eV or less. These low activation energy barriers suggest that the CO oxidation reaction would proceed at room temperature with pyridinic N-dopants present in the defect environment. Due to the similar charge transfer calculated for both defect moieties, changes in activation barrier energy values were correlated with differences in the spin state of the frontier orbitals. Spin polarized projected density of states calculations demonstrate relatively lower activation energy barriers for systems with higher spin state asymmetry near the Fermi energy; CO oxidation on Ta and V SAC have decreases in activation barrier energies of 27% and 44%, respectively. This motivated additional NEB calculations to compare the activation barrier energies of spin-constrained reaction pathways having differing spin states. By constraining the magnetic moment of the CO oxidation reaction to be either 0 (singlet), 1 (doublet), or 3 (quartet) states, the energy barriers of the doublet and quartet spin states were found to be quite similar with less than 0.05 eV of difference. However, both magnetic states had significantly lower energy barriers compared to the non-magnetic spin state, over 0.5 eV of difference. Since mainly the frontier orbital affects bonding, magnetic moment alone does not explain differences in chemical activity. We will present results suggesting that the magnetic moment of frontier orbitals could play a significant role in enhancing catalytic performance, as well as more traditionally understood mechanisms such as charge transfer and the proximity of frontier d-orbitals to the Fermi level. Computational design of materials is used to define processing conditions for three-dimensional porous graphene structures. Fabrication and characterization of macroscopic graphene structures with high surface area and architectures to facilitate mass transport will also be presented.

4:15 PM EN11.03.02

Potential of Zero Charge Measurement by Second Harmonic Generation [Pengtao Xu](#) and [Jin Suntivich](#); Cornell University, United States

The rational design of high-performance electrochemical systems requires a fundamental understanding of the electrode-electrolyte interface. One of the key parameters essential for this understanding is the potential of zero charge (U_{pzc}). We present a methodology for characterizing this parameter. Our approach is based on electric-field induced second-harmonic generation (EFISH), a nonlinear optical method specific to the solid-liquid interface. We will discuss the physics behind this effect and how a potential-dependent EFISH experiment can reveal the electric field inside the electrochemical double layer and consequently U_{pzc} . We will further compare the results to the values obtained from other experimental approaches and discuss the implication from the work function analysis. Our work demonstrates EFISH as a facile method for measuring U_{pzc} and studying how the interfacial electric field influences electrocatalysis.

4:30 PM EN11.03.03

The Presence and Role of the Intermediary CO Reservoir During the Electroreduction of CO₂ at the Cu Surface [Sheena Louisia](#), [Dohyung Kim](#) and [Peidong Yang](#); University of California, Berkeley, United States

The optimization of the electrochemical reduction of CO₂ to value-added products using Cu catalysts requires tailoring past the surface. Although often overlooked in heterogeneous catalysis, the microenvironment confined near the surface has been recognized as a necessary component of catalytic performance. Despite its importance, this regime still remains understudied due to a lack of suitable characterization techniques. A better understanding of the microenvironment formed near the catalyst surface is especially relevant to multistep reactions like the electroconversion of CO₂ to multicarbon (C₂₊) products during which its formation is likely inherent to the reaction pathway. In this work, we report on-stream substitution of reactant isotope (OSRI), a new method that uses the subsequent introduction CO₂ isotopes and mathematical modeling to shed a new light on the unique microenvironment formed near Cu surfaces during CO₂ electrolysis. This method reveals the presence of an intermediary CO reservoir concentrated near the Cu surface during the reaction that influences C₂₊ formation. Applied to a Cu nanoparticle (NP) ensemble and Cu foil, the OSRI method indicates that more than a monolayer of CO intermediates is necessary to facilitate CO₂-to-C₂₊ conversion. Specifically, the intrinsic C₂₊ activity only increased after reaching a density of ~100 CO molecules per surface Cu atom. The Cu NP ensemble is found to satisfy this criterion at a lower overpotential than the Cu foil thus making it a better candidate for efficient C₂₊ production. Furthermore, given the same reservoir size, the ensemble's intrinsically higher C-C coupling ability is highlighted by the 4-fold higher C₂₊ turnover it achieves at a more positive potential. Applicable to any Cu surfaces, this method offers a novel approach to distinguish the contribution of the microenvironment from the Cu surface's intrinsic C-C coupling ability. OSRI provides new insights on how the presence of CO intermediates in the microenvironment impacts C₂₊ formation during the electroreduction of CO₂ on Cu surfaces and thus, highlights an additional dimension to consider when pushing future CO₂ reducing-catalysts designs beyond the surface.

4:45 PM *EN11.03.04

Regulating Surface Oxide Activity for Decarbonizing Chemicals and Fuels [Yang Shao-Horn](#); Massachusetts Institute of Technology, United States

We will discuss how to tune oxide electronic structure and design oxide surfaces to control the kinetics of key reactions central to making of chemicals and fuels using electrons from renewables ([Kuznetsov et al. Joule 2018](#) and [Hwang et al. Science 2017](#)). Increasing metal-oxygen covalency (smaller energy gap between metal d and O 2p states) enhances activity for oxygen evolution upon water splitting but beyond an optimal value reduces oxide stability. Exploiting this concept to examine a series of oxides not only sets record catalytic activity but also establishes a new reaction mechanism for the most active oxides, where both metal and oxygen sites can catalyze oxygen evolution ([Grimaud et al. Nature Chemistry 2017](#)) and deprotonation from oxide surface can be rate-limiting ([Hong et al. EES 2017](#)) – contrary to long-standing belief. Tuning metal-covalency and activating surface oxygen sites points to a new direction to increase oxide activity and stability ([Kuznetsov et al., JPCC 2018](#)). Such concepts have been applied in the design of oxide surfaces to enhance the catalytic activity of NO oxidation to NO₂ ([Nature Catalysis 2021](#)) and suppress the dehydrogenation of electrolytes to enhance the lifetime of high-energy Li-ion batteries ([Giordano et al. JPCL 2017](#), and [Zhang et al., EES 2020](#)).

[Kuznetsov, D. A.](#), [B. Han](#), [Y. Yu](#), [R. R. Rao](#), [J. Hwang](#), [Y. Román-Leshkov](#), and [Y. Shao-Horn](#), Tuning Redox Transitions via Inductive Effect in Metal Oxides and Complexes, and Implications in Oxygen Electrocatalysis, *Joule*, **2**, 1–20 February 2018.

Hwang, J., R.R. Rao, L. Giordano, Y. Katayama, Y. Yu, and Y. Shao-Horn, Perovskites in Catalysis and Electrocatalysis, *Science*, **358**, 751-756 November 2017.

Hong, W., K.A. Stoerzinger, Y.-L. Lee, L. Giordano, A.J.L. Grimaud, A.M. Johnson, J. Hwang, E. Crumlin, W. Yang, Y. Shao-Horn, Charge-transfer-energy-dependent oxygen evolution reaction mechanisms for perovskite oxides, *Energy & Environmental Science*, **10**, 2190-2200 October 2017.

Giordano, L., P. Karayalali, Y. Yu, Y. Katayama, F. Maglia, S. Lux, and Y. Shao-Horn, Chemical Reactivity Descriptor for the Oxide-Electrolyte Interface in Li-Ion Batteries, *Journal of Physical Chemistry Letters*, **8**, 3881-3887 August 2017.

Grimaud, A., O. Diaz-morales, B.H. Han, W. T. Hong, Y.L. Lee, L. Giordano, K. A. Stoerzinger, M.T.M. Koper, Y. Shao-Horn, Activating lattice oxygen redox reactions in metal oxides to catalyze oxygen evolution, *Nature Chemistry*, **9**, 457-465 May 2017.

Kuznetsov, D.A., J. Peng, L. Giordano, Y. Román-Leshkov and Y. Shao-Horn, Bismuth Substituted Strontium Cobalt Perovskites for Catalyzing Oxygen Evolution, *Journal of Physical Chemistry C*, **124**, 6652-6570, February 2020.

Y. Zhang, Y. Katayama, R. Tatara, L. Giordano, Y. Yu, D. Fraggedakis, J. Sun, F. Maglia, R. Jung, M.Z. Bazant and Y. Shao-Horn, Revealing Electrolyte Oxidation via Carbonate Dehydrogenation on Ni-based Oxides in Li-ion Batteries by in situ Fourier Transform Infrared Spectroscopy, *Energy and Environmental Science*, **13**, 183-199, January 2020.

J. Hwang, R.R. Rao, L. Giordano, K. Akkiraju, X.R. Wang, E. Crumlin and Y. Shao-Horn, Regulating oxygen activity of perovskites to promote NO_x oxidation, *Nature Catalysis*, *in press* 2021.

SESSION EN11.04: Poster Session: Electrocatalytic Materials to Sustainably Convert Atmospheric C, H, O and N into Fuels and Chemicals

Session Chairs: Chong Liu and Haotian Wang

Tuesday Afternoon, November 30, 2021

8:00 PM - 10:00 PM

Hynes, Level 1, Hall B

EN11.04.01

The Study of TiO₂ Polymorphs for Solar Fuels Production Francesca S. Freyria¹, Nicola Blangetti¹, Sandra Doria^{2,3}, Simelys Hernandez¹, Mariangela Di Donato^{2,3}, Sergio Brovelli⁴, Maela Manzoni⁵, Serena Esposito¹ and Barbara Bonelli¹; ¹Politecnico di Torino, Italy; ²LENS - European Laboratory for Non-Linear Spectroscopy, Italy; ³Italian National Research Council (CNR), Italy; ⁴Università degli Studi di Milano-Bicocca, Italy; ⁵University of Torino, Italy

During this century, climate change and energy demand have been becoming one of the major global concerns for the human beings. Taking inspiration from nature, the production of fuels and chemicals through CO₂ conversion or water splitting under the solar light can counteract these challenges.¹ So far, although TiO₂ is one of the most studied and applied photocatalysts due to low toxicity and cost and high biocompatibility and stability, some scientific questions are still unresolved. Several physico-chemical aspects can affect its photocatalytic performance, such as particles morphology, crystalline phases, band gap and specific surface area. Among these, by applying different sol-gel synthesis methods,² we study how the presence of polymorphs and Ti⁴⁺/Ti³⁺ defects can play a role in the photocatalytic efficiency for solar fuels production when they act alone or coupled with quantum dots (QDs).³ TiO₂ mainly exists in three different crystalline polymorphs: anatase and rutile (tetragonal structure) and brookite (orthorhombic structure), where the latter two phases have a direct band gap whereas the former phase shows an indirect band gap, with an average value from 3.0 eV up to 3.4 eV. The photogenerated electrons and holes show different behavior among the polymorphs due to different electron-trap depths and possible defects, which influence the final photocatalytic performance.⁴ Moreover, to absorb a wider part of the solar spectrum and to fast deliver photons to the photocatalytic centers, copper-based QDs at different wavelength emissions in the visible and NIR range are chosen as harvesting antennas. To control the presence of the polymorphs and the coupling with QDs, we change the titanium precursors and the type of template, by also adopting a greener template-free procedure in mild calcination conditions. The photocatalysts are characterized by means of X-ray powder diffraction (XRPD), quantitative phase analysis as obtained by Rietveld refinement, diffuse reflectance (DR) UV-Vis spectroscopy, N₂ adsorption/desorption at -196 °C, electrophoretic mobility in water (ζ-potential), X-rays photoelectron spectroscopy (XPS) and electron microscopy. Charge transfer and recombination processes are characterized using transient absorption spectroscopy. The photocatalytic behavior of these nanostructures is assessed under simulated sunlight at 1 Sun (i.e. 100 mW/cm² of intensity).

(1) Freyria, F. S. . In *Nanostructured Catalysts for Environmental Applications*; Eds.; Springer International Publishing, 2021; pp 214–248.

(2) Freyria, F. S.; Blangetti, N.; Esposito, S.; Nasi, R.; Armandi, M.; Annelio, V.; Bonelli, B. *ChemistryOpen* 2020, 903–912.

(3) Li, L.; Pandey, A.; Werder, D. J.; Khanal, B. P.; Pietryga, J. M.; Klimov, V. I. *J. Am. Chem. Soc.* 2011, **133** (5), 1176–1179.

(4) Vequizo, J. J. M.; Matsunaga, H.; Ishiku, T.; Kamimura, S.; Ohno, T.; Yamakata, A. *ACS Catal.* 2017, **7** (4), 2644–2651.

EN11.04.02

Strong Photoreductant Consisting of a Two-Dimensional Electride Electron Donor and a Pt(II) Complex Photoredox Catalyst Seunga Heo¹, Yu Sung Chun¹, Joonho Bang², Ho Seong Hwang³, Eun Jin Cho³, Sung Wng Kim² and Youngmin You¹; ¹Ewha Womans University, Korea (the Republic of); ²Sungkyunkwan University, Korea (the Republic of); ³Chung-Ang University, Korea (the Republic of)

Inorganic electrifieds are solid-state sources of solvated electrons which serve as powerful reducing agents in organic transformations. Since electrons in electrifieds are strongly confined within the interstitial sites, their effective detrapping is the key to harnessing the strong reducing power of solvated electrons. Recent studies have revealed that two-dimensional (2D) electrifieds, such as [Ca₂N]⁺e⁻, exhibit superior electron-donating ability beyond the conventional [Ca₂₄Al₂₈O₆₄]⁴⁺4e⁻ electrified, because of extremely high densities of anionic electrons that are delocalized over the interlayer space between the cationic layers. However, the inherent instability of [Ca₂N]⁺e⁻ in organic solvents retards utilization of their superior electron-donating ability.

To overcome this limitation, we propose a strategy that uniquely combines a photoredox catalyst molecule and a chemically stable 2D electrified.

[Gd₂C]²⁺2e⁻ was chosen because it exhibits high robustness against air and moisture. The notable stability was ascribed to anionic electrons being weakly localized at the Gd sites between layers of [Gd₂C]²⁺. In addition, [Gd₂C]²⁺ has a rigid layer framework with strong covalent bonding between the Gd and C atoms. [Gd₂C]²⁺2e⁻ slowly decomposed in 2,2,2-trifluoroethanol (TFE) to release solvated electrons. The effective diffusion length of the solvated electrons should remain small due to the slow alcoholysis. To utilize the released solvated electrons, we added Pt(II) complexes of cyclometalating ligands, including 2-phenylpyridinate (Ptpy), 2-(4,6-difluorophenyl)pyridinate (Ptdfpy), and 2-(3-methoxyphenyl)pyridinate (PtOMe), into the [Gd₂C]²⁺2e⁻ suspension. The planar and electron-rich Pt(II) complex adsorbed onto the surface of the [Gd₂C]²⁺2e⁻ electrified, and rapidly accepted one electron at a rate of 10⁷ s⁻¹ upon photoexcitation, which is greater than the diffusion rate in TFE (~10⁵ s⁻¹). The one-electron-reduced Pt complexes were electrochemically stable enough to deliver the electron to benzyl bromide substrates in the bulk with very negative reduction potentials (*E*_{red}, -2.20 ~ -2.46 V vs standard calomel electrode (SCE)). This electron transfer recovered the neutral Pt(II) complexes. Therefore, the cycle enabled photogated electron transport from the stable

[Gd₂C]²⁺2e⁻ electride to substrates. The key benefit of this reducing system was the suppression of undesirable charge recombination. The charge recombination by back electron transfer was prohibited due to the irreversible disruption of the [Gd₂C]²⁺2e⁻ electride after the electron ejection. The desirable properties collectively served as the photoredox catalysis principle for the reductive generation of the benzyl radical from benzyl bromide, which is the key intermediate of dehalogenation or homocoupled products. We examined the photoinduced reducing ability of the combined [Gd₂C]²⁺2e⁻/Pt complex system for a variety of benzyl bromides. Our optimized reaction conditions included deaerated CH₃CN:TFE (3:1, v/v) containing 0.25 M substrate, [Gd₂C]²⁺2e⁻ (4e⁻ mmol), and Ptdfppy (2 mol %), which was photoirradiated at a wavelength of 365 nm (4 W) at room temperature for 18 h. The conditions yielded dehalogenated and homocoupled products in yields as high as 98%. These results successfully demonstrated the effectiveness of our photoreducing system. We expect that our strategy will stimulate renewed research interest in the synthetic applications of stable yet unreactive 2D electrides.

EN11.04.03

Effect of Substrate-Induced Lattice Strain on the Electrochemical Properties of Pulsed Laser Deposited Nickel Oxide Thin Film Jacob Som¹, Jonghyun Choi², Nikhil R. Mucha¹, Panupong Jaipan¹, Svitlana Fialkova¹, Kwadwo Mensah-Darkwa³, Ram K. Gupta² and Dhananjay Kumar¹; ¹North Carolina Agricultural & Technical State University, United States; ²Pittsburg State University, United States; ³Kwame Nkrumah University of Science and Technology, Ghana

For decades, the vast ignition of non-renewable energy sources represents an extreme risk to the world by discharging gases that cause air contamination and global warming. Using a facile pulsed laser deposition process, nickel oxide (NiO) thin films has been deposited on strontium titanate, lanthanum aluminate, and sapphire substrates. The substrate–film lattice mismatch and how it influences the electrochemical properties of NiO thin film electrocatalyst have been studied. X-ray diffraction measurements were carried out to confirm the phases and determine interfacial lattice strain. AFM measurements were used to analyze the surface topography of the catalyst and determine the surface roughness of the film. The electrochemical analysis was performed in one molar potassium hydroxide solution. It was observed that the electrocatalytic activities of the NiO thin films exhibit a strong sensitivity to strain; the NiO thin film samples with the smallest strain recorded the lowest overpotential for the half-cell hydrogen evolution reaction. Additionally, the charge storage capacity of the NiO electrocatalyst has been explored and might be a function of surface roughness. The electrochemical properties and simple synthesis make these NiO-based catalyst thin films helpful in incorporating as high-surface-area electrodes for water electrolysis.

EN11.04.04

Self-Assembled Monolayer Modulated Ag Catalysts—Enhanced Catalysis of CO₂RR to CO Zhengyang Yang, Fanglin Che and Zhiyong Gu; University of Massachusetts Lowell, United States

The self-assembled monolayer (SAM) has been widely applied to modulate surface science for heterogeneous catalysis. In particular, 4-Mercaptobenzonitrile (4-MBN) SAM features a highly delocalized electron environment along with the benzene-nitrile head group, and its tail group – sulfur strongly bonds to the metal surface, i.e., Ag. Thus, 4-MBN SAM becomes a promising stable modifier to fine-tune the catalytic activity and selectivity of metal surfaces for the chemical process involving electron-transfer step, i.e., electrocatalysis. The electro-reduction reaction of CO₂ to CO (CO₂RR-to-CO) over Ag provides a sustainable approach to utilize renewable energy and generate value-added chemicals. However, there are major limitations of CO₂RR-to-CO over Ag: (1) low stability of Ag surface-active sites under high overpotentials due to the surface reconstruction; (2) high energy requirement of the potential rate-limiting step (RDS) – initial CO₂ activation.

To address the above challenges, we hypothesize that a highly ordered 4-MBN SAM will stabilize the Ag surface-active sites via strong thiol-metal chemisorption and promote initial CO₂ activation via the enhanced electron transfer between OCOH[•] and 4-MBN SAM. To examine our hypothesis, we first applied DFT calculations to investigate the stabilities of 4-MBN SAMs modulated Ag catalysts. The DFT results show that 4-MBN SAM strongly bonds to Ag surfaces, with the adsorption energies of ~2 eV at a low 4-MBN surface coverage (< ¼ monolayer). With an increase of the 4-MBN surface coverage over ¼ monolayer, 4-MBN SAMs stabilize active and less thermo-favored surfaces (i.e., Ag100 and Ag211), and will potentially inhibit the surface reconstruction and stabilize Ag surface active sites. In addition, we examined the potential RDS of CO₂RR-to-CO (i.e., CO₂+H⁺→OCO[•]) over 4-MBN modulated Ag catalysts. Interestingly, at a high surface coverage of 4-MBN (> ¼ monolayer), the adsorption of OCOH[•] is more favorable over the organic active sites – nitrogen of 4-MBN, and the stabilized OCOH[•] intermediate results in lower reaction energies of CO₂+H⁺→OCO[•], as compared to the pristine Ag scenario. This improvement can be explained via a high ET region at the high surface coverages of 4-MBN, which greatly strengthens the electronic interaction between the nitrogen of 4-MBN and the carbon of OCOH[•]. In summary, our work provides a systematic understanding of the physical and chemical properties of 4-MBN modulated Ag catalyst and its potential catalytic performance of CO₂RR-to-CO at the atomic scale. This work also guides a new strategy for the (electro)catalyst design with improved stability and activity via the SAMs modification as compared to the conventional metal catalysts.

EN11.04.05

From Rusting to Solar Power Plants—A Successful Nano-Patterning of Stainless Steel 316L for Visible-Light-Induced Photoelectrocatalytic Water Splitting Nageh K. Allam; American University in Cairo, Egypt

A novel propitious nanoporous anodized stainless steel 316L (NASS316L) photoanode was developed for water splitting. The anodization could successfully produce a uniform nanoporous (~ 90 nm in pore diameter) array (~ 2.0 μm thick) of NASS316L with a high pore density. Several techniques, including FESEM, EDX, XRD, XPS, ICP-OES, and UV–vis-NIR spectrophotometry, were employed to characterize the catalyst and to assess and interpret its activity toward water splitting. Surprisingly, the NASS316L retained almost the same composition of the bare stainless steel 316L, which recommended a symmetric dealloying mechanism during anodization. It also possessed a narrow band gap energy (1.77 eV) and a unique photoelectrocatalytic activity (~ 4.1 mA cm⁻² at 0.65 V versus Ag/AgCl, 4-fold to that of α-Fe₂O₃) toward water splitting. The onset potential (–0.85 V) in the photocurrent–voltage curve of the NASS316L catalyst demonstrated a negative shift in its Fermi level when compared to α-Fe₂O₃. The high (23% at 0.2 V vs Ag/AgCl) incident-photon-to-current conversion efficiency and the robust durability revealed from the in situ analysis of the produced H₂ gas continued recommending the peerless inexpensive and abundant NASS316L catalyst for potential visible-induced solar applications.

EN11.04.06

Electrochemical Methane Conversion with IrO₂(110) Catalysts Jaehyun Lee, Jiwoo Yang, Jiwon Sul and Jun Hyuk Moon; Sogang University, Korea (the Republic of)

Liquid phase CH₄ oxidation under mild conditions is a promising field for energy-efficient conversion. Although highly active electrochemical catalysts have achieved methane-alcohol conversion at room temperature and pressure, high alcohol production remains a challenge. We have confirmed the sustainable electrochemical conversion of methane to alcohol using IrO₂ catalyst. IrO₂ has an activation energy for C-H bond of 9.5 kJ/mol, which is very low compared to conventional metal oxide catalysts. It is a catalyst known to facilitate methane activation reaction due to strong interaction between Ir_{ox} sites and methane molecules. Nevertheless, IrO₂ has not yet been reported as an electrochemical catalyst for methane oxidation. The surface phase of IrO₂ is determined by the sintering temperature, and we selectively fabricated the IrO₂ (110) surface, which is the most effective surface for CH₄

activation. Higher methane oxidation activity was confirmed compared to previously reported studies, and 216.9% higher alcohol production was achieved at room temperature and pressure, and the mechanism of alcohol formation by oxidation of methane by active oxygen in the catalyst was confirmed.

EN11.04.08

First-Principles Studies of Doped SnO₂ for Photocatalytic Applications [Yeongrok Jin](#) and Jaekwang Lee; Pusan National University, Korea (the Republic of)

SnO₂ has been identified as one of the promising and suitable oxide-based photocatalytic semiconductors. However, the large bandgap limits its application in the visible region. Doping is an efficient way of optimizing the materials properties and improving the photocatalytic performance. Here, using the first-principles density functional theory calculations, we considered the substitutional and interstitial doping of SnO₂ with Fe and Cr atoms. We find that Fe atoms tend to occupy interstitial sites while Cr atoms prefer to occupy substitutional sites with the different amount of oxygen vacancies. Bandgap narrowing, O-K edge electron energy loss spectra due to the oxygen vacancy, and resulting enhanced photocatalytic behavior of visible light will be discussed and associated underlying mechanism will be introduced along with scanning transmitted electron microscopy measurements.

EN11.04.09

Spontaneously Formed Cu_{S_x} Catalysts for Electrochemical Reduction of Industrial CO₂ Gases [Jinwook Lim](#), Wan Jae Dong, Jae Yong Park, Dae Myung Hong and Jong-Lam Lee; Pohang University of Science and Technology (POSTECH), Pohang, Korea (the Republic of)

The development of selective and stable catalysts for electrochemical CO₂ reduction reaction (CO₂RR) in CO₂-purged electrolyte that contains sulfur is essential for practical application because CO₂ gas emitted from industry inevitably contains hundreds ppm-level of H₂S gas. Despite many researchers have been demonstrated selective and stable catalysts for electrochemical reduction of pure CO₂ gas, the conversion of industrial CO₂ gas has been limited. Here, we demonstrated the copper sulfide (CuS_x) catalysts which were spontaneously formed by dipping the Cu foil into laboratory-prepared industrial CO₂-purged in 0.1 M KHCO₃ electrolyte. Since the industrial CO₂ contains H₂S gas, sulfur species dissolved in the electrolyte can easily react with Cu foil. As the concentration of dissolved sulfur species increased, the reaction between Cu foil and sulfur enhanced. As a result, the average size and surface density of CuS_x increased to 133.2<!--[if gte msEquation 12]><m:Math><i style='mso-bidi-font-style:normal'><m:r>±</m:r></m:Math><![endif]--><!--[if gte vml 1]><v:shapetype id="_x0000_t75" coordsize="21600,21600" o:spt="75" o:preferrelative="t" path="m@4@51@4@11@9@11@9@5xe" filled="f" stroked="f"><v:stroke joinstyle="miter"><v:formulas><v:f eqn="if lineDrawn pixelLineWidth 0"/><v:f eqn="sum @0 1 0"/><v:f eqn="sum 0 0 @1"/><v:f eqn="prod @2 1 2"/><v:f eqn="prod @3 21600 pixelWidth"/><v:f eqn="prod @3 21600 pixelHeight"/><v:f eqn="sum @0 0 1"/><v:f eqn="prod @6 1 2"/><v:f eqn="prod @7 21600 pixelWidth"/><v:f eqn="sum @8 21600 0"/><v:f eqn="prod @7 21600 pixelHeight"/><v:f eqn="sum @10 21600 0"/><v:formulas><v:path o:extrusionok="f" gradientshapeok="t" o:connecttype="rect"/><o:lock v:ext="edit" aspectratio="t"/></v:shapetype><v:shape id="_x0000_i1025" type="#_x0000_t75" style='width:9pt; height:14.25pt'><v:imagedata src="file:///C:/Users/JW/AppData/Local/Temp/msohtmlclip1/01/clip_image001.png" o:title="" chromakey="white"/></v:shape><![endif]-->33.1 nm and 86.2<!--[if gte msEquation 12]><m:Math><i style='mso-bidi-font-style:normal'><m:r>±</m:r></m:Math><![endif]--><!--[if gte vml 1]><v:shapetype id="_x0000_i1025" type="#_x0000_t75" style='width:9pt; height:14.25pt'><v:imagedata src="file:///C:/Users/JW/AppData/Local/Temp/msohtmlclip1/01/clip_image001.png" o:title="" chromakey="white"/></v:shape><![endif]-->3.3%, respectively. Due to the larger amount of sulfur content and the enlarged electrochemical surface area of CuS_x, the faradaic efficiency of formate was improved from 22.7 to 72.0% at -0.6 V_{RHE}. Additionally, CuS_x catalysts showed excellent stability for reducing the industrial CO₂ to formate. Change in faradaic efficiency was hardly observed even after long-term (72 h) operation. This study experimentally demonstrated that spontaneously formed CuS_x catalysts are efficient and stable for reducing the industrial CO₂ gas to formate.

EN11.04.11

Electrochemical Control of Multiscale Morphology in Dendritic Copper Foams [Hamed Mehrabi](#)¹, Johanna Nelson Weker² and Robert H. Coridan¹; ¹University of Arkansas, United States; ²Stanford University, United States

Structured copper substrates have gained scientific attraction as electrodes for catalysis, especially for CO₂ reduction (CO₂RR). Dendritic copper foams offer many of the functional aspects considered to be beneficial for activity and selectivity for CO₂RR, including three-dimensional structure, high surface areas, and a large density of grain boundaries. The typical fabrication method for dendritic copper foams is via high-rate cathodic electrodeposition in acidic solutions of Cu²⁺ ions. The competing hydrogen evolution introduces large voids to the foam structure because of bubbles evolving from the surface, which can add to the hierarchical structure of the electrode, but also provides ready-made bubble nucleation sites for hydrogen evolution during CO₂RR. Here, we consider how to fabricate copper foams with intentional control over these bubble nucleation sites. Namely, we explore high-rate Cu electrodeposition in lactate-stabilized, alkaline copper solutions and its effects on the hierarchical structure on multiple length scales. We will show the control that the electrochemical growth conditions exert on the nanoscale, microscale, and macroscale structure of the Cu foams. The electrochemical nature of the Cu-lactate complex and the significant reduction of hydrogen evolution during deposition result in copper dendrites that are significantly denser and more fine-grained than Cu foams derived from acidic solutions, as indicated by tomographic studies of synchrotron-based, transmission x-ray microscopy computed tomography reconstructions. We will also demonstrate that this morphological control has consequences for both the electrocatalytic and mass transport behavior for the Cu electrocatalysts in both hydrogen evolution and in selectivity in CO₂RR reactions.

EN11.04.13

Enhanced Photoelectrochemical Performance of Ca₂Fe₂O₅ Photocathodes via Two-Step Annealing [Joon-Soo Yoon](#), [Joo-Won Lee](#) and [Yun-Mo Sung](#); Korea Univ, Korea (the Republic of)

Recently, ternary oxide semiconductors have received increasing attention as a promising photocathode material for photoelectrochemical (PEC) water splitting. There exists large room to tune their electronic structures which can directly affect PEC properties. However, developing a ternary oxide photoelectrode showing improved PEC performance still remains at a challenging stage. Here, we report the success in the synthesis of high-density Ca₂Fe₂O₅ (CFO) nanorods on a NiO/FTO layer that is an effective hole transport layer (HTL) using a wet chemical approach. Also, we propose a two-step annealing strategy to further increase the PEC efficiency of Ca₂Fe₂O₅ (CFO) photocathode. It was elucidated that two-step annealing was beneficial to their PEC properties in various aspects such as morphologies, chemical states, optical properties, and impedances. In addition, the NiO buffer layer further enhanced their charge transport properties. Enhanced PEC performance was observed by LSV and IPCE measurements. CFO on NiO HTL fabricated via two-step annealing demonstrates a photocurrent density of up to -313.7 μA/cm², which is 76 % higher than that of CFO without HTL fabricated via single-step annealing. The mechanism that the annealing process modifies material characteristics and affects the PEC performance was discussed in detail.

10:30 AM EN11.05.01

Ag^{II}-Mediated Electrocatalytic Ambient CH₄ Functionalization Inspired by HSAB Theory [Danlei Xiang](#)¹, Jesus A. Iniguez¹, Jiao Deng¹, Xun Guan¹ and Chong Liu^{1,2}; ¹University of California, Los Angeles, United States; ²California NanoSystems Institute, United States

Developing an efficient chemical transformation pathway of ambient CH₄ functionalization is an ongoing challenge and the key resides on the discovery of new catalytic systems. The hard-soft acid-base (HSAB) theory suggests that high-valent transition metals, as soft class (b) Lewis acids based on Pearson's classification, are suitable candidates for CH₄ activation due to methyl moiety's relatively low value of chemical hardness. While most of class (b) transition metals have been studied, divalent silver (Ag^{II}), possibly due to its reactive nature, is the only class (b) high-valent transition metal center that is yet reported to exhibit reactivities towards CH₄ activation. Inspired by such notion, here we report that electrochemically generated Ag^{II} metalloradical readily functionalizes CH₄ into methyl bisulfate (CH₃OSO₃H) at ambient conditions in 98% H₂SO₄. Mechanistic investigation experimentally unveils a low activation energy of 13.1 kcal mol⁻¹, a high pseudo-first-order rate constant of CH₄ activation up to 2.8 × 10³ h⁻¹ at room temperature and a CH₄ pressure of 85 psi, and two competing reaction pathways preferable towards CH₄ activation over solvent oxidation. Reaction kinetic data suggest a Faradaic efficiency exceeding 99% beyond 180 psi CH₄ at room temperature for potential chemical production from widely distributed natural gas resources with minimal infrastructure reliance.

10:45 AM EN11.05.02

Molybdenum Chalcogenides as Electrocatalysts for Energy Conversion [Jessica Ortiz Rodriguez](#)¹ and Joseph Perryman^{1,2}; ¹University of California, Davis, United States; ²Stanford University, United States

The successful use of electrolysis processes at an industrial scale, such as aluminum electrorefining, brine electrolysis, and water splitting, has increased the interest of using electrochemistry to promote other promising reactions, including hydrogen evolution, CO₂ reduction, and ammonia synthesis. To design electrocatalysts which selectively produce fuel from aqueous media, the tuning of local surface coordination and electronic structure becomes imperative. In this work, we tune the surface electronic structure by changing chalcogen composition in different molybdenum chalcogenides systems to understand proton adsorption interactions. The molybdenum chalcogenides evaluated were synthesized successfully via high-temperature microwave-assisted and template-controlled approaches. Their ability to stabilize proton adsorption was studied under relevant conditions for hydrogen production in acidic media. Electrochemical characterization showed that increasing the electronegativity of the chalcogen increases the hydrogen adsorption strength due to the higher relative basicity of the chalcogen. The results presented here provide guidelines to improve proton adsorption in metal chalcogenide systems and increase selectivity in various electrochemical reactions.

11:00 AM EN11.05.04

A Microbial-Material Hybrid System for Photocatalytic Nitrogen Fixation with High Quantum Efficiency [Xun Guan](#)¹, Sevcian Ersan¹, Xiangchen Hu², Timothy Atallah¹, Yongchao Xie¹, Shengtao Lv¹, Bocheng Cao¹, Jingwen Sun¹, Ke Wu¹, Xiangfeng Duan¹, Justin Caram¹, Yi Yu², Junyoung Park¹ and Chong Liu¹; ¹University of California, Los Angeles, United States; ²ShanghaiTech University, China

Nitrogen in biological molecules ultimately comes from the reduction of dinitrogen. Interfacing biological catalysts with inorganic materials is constructive towards efficient and customizable chemical production at ambient temperature and pressure. Here, we demonstrate a microbial-material hybrid system with an appreciable internal quantum efficiency of (19.8 ± 2.6)% for photocatalytic nitrogen fixation. This hybrid system consists of nitrogen-fixing microbes and semiconductor quantum dots with a unique interfacial charge transfer behavior at the microbial-material interface. Metabolomics and proteomics studies reveal a metabolism favoring nitrogen accumulation, pertinent to our observed efficiency of nitrogen fixation.

11:15 AM *EN11.05.05

Rate and Mechanism of Electrochemical Formation of Surface-Bound Hydrogen Ding-Yuan Kuo, Xinyao Lu, Bintao Hu, Hector Abruna and [Jin Suntivich](#); Cornell University, United States

The formation of a surface-bound hydrogen atom from one proton and one electron plays an enabling role in renewable hydrogen production. Quantifying the surface-bound hydrogen kinetics, however, requires decoupling the delicate interplay of numerous processes. In this work, we describe a cyclic-voltammetry method for measuring the rate constant for the formation of surface-bound hydrogen atoms ("hydrogen electro-adsorption"). We find that the hydrogen electro-adsorption on platinum single crystals is ~100x faster in acid than in base. Reaction-order analysis suggests that the electro-adsorption occurs as a proton-coupled electron transfer (PCET) reaction in acid, whereas in base, the electro-adsorption requires the interfacial water reorganization. This work demonstrates a methodology for quantifying the interfacial PCET kinetics and reveals the hydrogen electro-adsorption kinetics as the reason why the hydrogen evolution electrocatalysis on platinum is faster in acid than in base.

11:45 AM EN11.05.06

Late News: Epitaxial Growth of Flower-like MoS₂ on One-Dimensional Nickel Titanate Nanofibers as a Sweet Spot for Efficient Photoreduction of Carbon Dioxide Haritham Khan, Hazina Charles and [Caroline S. Lee](#); Hanyang University, Korea (the Republic of)

The ever-increasing human demand for energy and constant depletion of fossil fuels have sparked a global crisis with urgent attention. Global warming has also become an increasingly serious environmental concern due to its excessive emission of carbon dioxide and similar greenhouse gases. Currently, the conversion of CO₂ into renewable energy in the presence of sunlight is considered to be a viable technique to reduce global warming. Photocatalytic reduction of CO₂ has recently attracted substantial interest, but the activity, stability, and stability of products were severely determined by the efficiencies of light-harvesting, charge migration, and surface reactions. The rational design and preparation of dissimilar dimensional materials (1D/2D) have been therefore extensively investigated as heterogeneous photocatalysts. 1D materials possess distinct advantages of efficient electron transport and optical excitation while suffering from the drawback of low surface area. Meanwhile, 2D materials show a large surface area but tend to agglomerate. Interfacial engineering is a promising technique to take full advantage of the unique dimensionality-dependent advantage while mitigating the disadvantage during sustainable energy applications.

Herein, a highly synergized NiTiO₃/MoS₂ (1D/2D) heterostructure was synthesized using a two-step process. In the first step, NiTiO₃ nanofibers were synthesized through electrospinning which was later combined with 2D flower-like MoS₂ through a hydrothermal process. The morphologies and optical properties of as-synthesized photocatalysts were analyzed by a series of characterizations. The selective growth of highly reactive 1T along honeycomb-

like 2H phases were also observed through XPS and TEM analysis. The hybrid NiTiO₃/MoS₂ exhibited a red-shift to the visible light region with an enhanced absorption capacity. At the optimum loading of 2wt.% MoS₂, NiTiO₃/MoS₂ exhibited the highest CO₂ reduction producing CO and CH₄ gases of 130 μmolg⁻¹h⁻¹ and 55 μmolg⁻¹h⁻¹ which are 3.8 (34 μmolg⁻¹h⁻¹) and 3.6 (15 μmolg⁻¹h⁻¹)-fold higher than those of pristine NiTiO₃ nanofibers respectively, with overall CO₂ selectivity of 84%. The enhanced photoreduction performance could be attributed to the enhanced light absorption, higher surface area and coexistence of 1T and 2H phases of MoS₂ in the hybrid structures. Moreover, the significantly accelerated charge separation and reduced recombination of charge carriers on account of the strong electronic coupling is verified through photoluminescence and EIS analysis. This work contributes to the development of efficient and stable photocatalytic materials which could also be used further in water splitting, H₂ evolution, and other photocatalytic activities as an efficient photocatalyst.

SESSION EN11.06: Electro-Bio Systems
Session Chairs: Chong Liu and Wilson Smith
Wednesday Afternoon, December 1, 2021
Hynes, Level 3, Room 312

1:30 PM *EN11.06.01

Employing Synthetic Biology to Design Microbial Electrocatalysts for Nitrogen Reduction [Shelley Minteer](#); University of Utah, United States

Ammonia is one of the most widely produced chemical in the world. Most ammonia (over 66%) is now produced through the Haber–Bosch process, consuming approximately 5% of the global natural gas production and contributes to over 3% of global carbon dioxide emissions. In an effort to develop an electrochemical alternative, we have engineered cyanobacterium to perform nitrogen fixation under ambient conditions without consuming natural gas, in stark contrast to the Haber-Bosch process that requires extreme temperatures and pressures to the same end. To realize the heterologous expression of nitrogenase, we transformed the cyanobacterium *S. elongatus* PCC 7942 with the minimal nitrogen fixation (*nif*) gene cluster. Biosynthesis of Mo-nitrogenase generally requires a large number of *nif* genes. However, the transformation and transcription of such a larger set of gene cluster into the cyanobacterium is challenging. In this work, a minimal *nif* cluster with reduced genetic complexity was chosen to accomplish the transformation of the cyanobacterium *S. elongatus* PCC 7942. The cyanobacterium *S. elongatus* PCC 7942 was transformed with *nif* genes and it was shown to be able to express active nitrogenase. The engineered *S. elongatus* PCC 7942 was immobilized on an electrode to accelerate the microbial conversion of nitrogen into ammonium using electrochemical driving forces. Methyl viologen (MV) was added as an electron mediator to shuttle electrons from the electrode to the enzyme active center, since MV can go through the cell membrane and deliver continuous electrons to nitrogenase. In this talk, we will compare and contrast this strategy to other bioelectrocatalytic strategies for nitrogen reduction.

2:00 PM *EN11.06.02

Powering Catalysis in Microorganisms Using Electrochemistry and Synthetic Biology [Caroline Ajo-Franklin](#); Rice University, United States

Microorganisms precisely control biological processes, including biosynthesis and cell growth, by regulating the redox state of different biomolecules. These processes can be modulated by electrochemically coupling intracellular biomolecules to an external electrode, but current approaches afford only limited control and specificity. Here we describe using electrical current to reduce specific biomolecules, allowing control of biosynthesis and cell growth in two industrially relevant microorganisms, *Escherichia coli* and *Lactobacillus plantarum*. To enable electrochemical control of *E. coli*, we used synthetic biology to introduce a heterologous electron transfer pathway. *E. coli* expressing *mtrCAB* from *Shewanella oneidensis* MR-1 consumed electrons directly from a cathode when fumarate or nitrate, both intracellular electron acceptors, were present. The fumarate-triggered current consumption occurred only when fumarate reductase was present, indicating all the electrons passed through this enzyme. Moreover, *MtrCAB*-expressing *E. coli* used current to stoichiometrically produce ammonia. Thus, our work introduces a modular genetic tool to reduce a specific intracellular redox molecule with an electrode, opening the possibility of electronically controlling biological processes such as biosynthesis and growth in any microorganism. Complementing this approach, we discovered that *L. plantarum*, a lactic acid bacteria used industrially to produce fermented foods, can uptake electrons. This electron uptake occurs under anaerobic conditions when a terminal electron acceptor and its corresponding oxidoreductase are present. Unlike other anaerobic respiratory modes in *L. plantarum*, this current consumption does not require addition of co-factors such as heme or riboflavin. Electron uptake promotes cell growth and acidification of the media, both processes essential for food fermentation. We find that the *L. plantarum* metabolism is shifted towards ATP producing pathways in the presence of both a cathode and a suitable electron acceptor. This surprising discovery opens the possibility of using electrical current to drive industrial production of fermented foods using lactic acid bacteria.

2:30 PM *EN11.06.03

Sustainable Bioelectrochemical Conversion of CO₂ and N₂ to High Value Materials [Peidong Yang](#) and [Stefano Cestellos-Blanco](#); University of California, Berkeley, United States

Climate change is a pressing global dilemma driven by the combustion of hydrocarbon fuels to CO₂, a potent greenhouse gas. CO₂ reduction has been the focus of intensive research with the goal of closing the carbon loop. A promising avenue to CO₂ conversion encompasses the materials-biology nexus. Microorganisms evolved over millions of years to fix CO₂, H₂O and N₂ with high selectivity and low substrate activation while self-regenerating. We have designed light-active nanomaterials that pair biocompatibly with these microorganisms in order to harness their biocatalytic activity. We demonstrate that by controlling the microenvironment in a silicon nanowire – bacteria ensemble, we can boost the solar-driven turnover rate of CO₂ reduction. Furthermore, adaptation of whole-cell autotrophic biocatalysts to a cytotoxic environment increases their ability to process CO₂. In addition to optimizing the CO₂ conversion rate by improving the material-biology interface and biocatalyst robustness, we establish synergistic co-cultures with guidable dynamics and outputs. We firstly present an integrated process for the production of 3D-printable biopolymer from CO₂. An autotrophic bacteria-mediated process converts CO₂ to acetate which is then directly used as the primary carbon source for biopolymer production by secondary bacteria without any processing of the culture medium between microbial production steps. We also showcase a consortium involving acetogenic *Sporomusa ovata* and diazotrophic *Rhodospseudomonas palustris* for tandem CO₂ and N₂ fixation to tunable value-added products. Co-culture dynamics and products can be directed by substrate availability and electrochemical inputs. Finally, we illustrate an electrochemically catalyzed abiotic pathway for sugar generation from CO₂. The sugars are employed as an *Escherichia coli* feedstock for the production of value-added materials.

3:00 PM BREAK

SESSION EN11.07: Fuel Cells and Hydrogen Peroxide
Session Chairs: Chong Liu and Samira Siahrostami
Wednesday Afternoon, December 1, 2021
Hynes, Level 3, Room 312

4:00 PM *EN11.07.01

Surface and Interface Engineering for High Performing Catalysis Yu Huang; University of California, Los Angeles, United States

The rising demands in providing energy, food, and water for the rapid-growing world population while addressing climate change and environmental pollution requires dramatic acceleration in technical innovations. Green and sustainable production of renewable energy is critical in solving the imminent challenges. Electrocatalysis plays a central role in diverse energy technologies that are of increasing importance for applications in mobile electronics, electric vehicles, as well as renewable energy industry. Despite considerable progresses, many electrocatalytic systems are still plagued by insufficient catalytic efficiency, poor stability or high cost of the precious metal catalysts used. In this talk I will share our research centred around pushing the limits of novel catalysts based on the understanding of the fundamental physical and chemical processes at the catalytic surfaces which can vastly improve the efficiency of diverse electrocatalytic systems, leading to a sustainable and energy efficient society. In particular, I will discuss our efforts in promoting the mass activity and enhancing the stability of Pt-based cathode catalysts for hydrogen fuel cell applications.

4:30 PM EN11.07.02

Iron Quantum Dots Electro-Assembled on Nanocarbons as Electrocatalyst for the Oxygen Reduction Reaction in Terrestrial and Space Applications Armando Pena-Duarte¹, Timothy D. Hall², Santosh Vijapur², E J. Taylor² and Carlos R. Cabrera-Martinez¹; ¹University of Puerto Rico, United States; ²Faraday Technology Inc, United States

Highly dispersed iron-based quantum dots (QDs) onto nanocarbons were successfully electrodeposited by the Rotating Disk Slurry Electrodeposition (RoDSE) technique. Our findings through chemical physics characterization revealed that the continuous electron pathway interaction between the interface metal-carbon was controlled.

The rotating ring-disk electrode (RRDE) and the prototype generation unit (PGU) of *in-situ* H₂O₂ generation in fuel cell experiments revealed a high activity for the oxygen reduction reaction (ORR) via two-electron pathway. These results establish the Fe/C catalyst at a competitive level for space and terrestrial new materials carriers, specifically for the *in-situ* H₂O₂ production. Transmission electron microscopy (TEM) analysis reveals the well-dispersed Fe-based quantum dots with a particle size of 4 nm. The structural and chemical-physical characterization through induced coupled plasma-optical emission spectroscopy (ICP-OES), transmission scanning electron microscopy (STEM), X-ray diffraction (XRD), Raman spectroscopy, X-ray photoelectron spectroscopy (XPS), and X-ray absorption spectroscopy (XAS); reveals that, under atmospheric conditions, our quantum dots system is a Fe^{2+/3+}/Fe³⁺ combination. The QDs oxidation state tunability was showed by the applied potential.

The obtention of H₂O₂ under the compatibility conditions of the drinking water resources available in the International Space Station (ISS) enhances the applicability of this iron- and carbon-based materials for *in-situ* H₂O₂ production in future space scenarios. Terrestrial and space abundance of iron and carbon, combined with its low toxicity and high stability, consolidates this present work to be further extended for the large-scale production of Fe-based nanoparticles for several applications.

Our approach is to switch the nanocarbon source and metal-carbon configurations, to control the two-electrons route in the ORR kinetics for fuel cells in space technologies. This consolidates our present work as a large-scale production process of highly active Fe nanoparticles for *in situ* H₂O₂ generation.

Likewise, the origin of the current transients, generated during the RoDSE technique, are associated with the Fe/C and H₂O/H⁺ couple interactions through electrocatalytic amplification. The enhanced current transients open the possibility to design a fluidized bed reactor-like, to study the electrochemical amplification reactions where the electrocatalyst is used as a label to obtain higher yields. Accurately, large-scale production of treasured gases for human space missions via electrochemical amplification of the HER and OER, to produce large quantities of gases such as H₂ and O₂, represents a fascinating research field.

References:

1. Peña-Duarte, A.; Vijapur, S. H.; Hall, T. D.; Hayes, K. L.; Larios-Rodríguez, E.; Pilar-Albaladejo, J. D.; Santiago, M. E. B.; Snyder, S.; Taylor, J.; Cabrera, C. R., Iron Quantum Dots Electro-Assembling on Vulcan XC-72R: Hydrogen Peroxide Generation for Space Applications. *ACS Applied Materials & Interfaces* **2021**.
2. Nelson, G. J.; Vijapur, S. H.; Hall, T. D.; Brown, B. R.; Peña-Duarte, A.; Cabrera, C. R., Electrochemistry for Space Life Support. *Electrochemical Society Interface* **2020**, *29* (1), 47-52.

4:45 PM EN11.07.03

Experimental Sabatier Plot for Predictive Design of Active and Stable Pt-alloy Oxygen Reduction Reaction Catalysts Jin Huang¹, Xiangfeng Duan^{1,1}, William Goddard², Alessandro Fortunelli³, Qingying Jia⁴ and Yu Huang^{1,1}; ¹University of California, Los Angeles, United States; ²California Institute of Technology, United States; ³Consiglio Nazionale delle Ricerche, Italy; ⁴Northeastern University, United States

The broad dissemination of proton-exchange membrane fuel cells (PEMFCs) is largely limited by the high cost of platinum (Pt)-based catalysts that are used to accelerate the sluggish oxygen reduction reaction (ORR) at the cathode. While the theoretical descriptor, ΔE_{O} (oxygen binding energy to the catalyst surface), has been widely adopted for predicting the activity, its experimental analogue has met very limited success and the durability of the resulting catalysts is yet difficult to predict. To date, the developments of highly active and stable Pt-alloy nanocatalysts have largely relied on anecdotal discoveries. Therefore, it is essential to develop experimentally tangible descriptors that capture key parameters for efficient and rapid catalyst design. Herein, by combining theoretical modeling and experimental observations, we developed a binary experimental descriptor that directly reflects the calculated ΔE_{O} on Pt-alloy catalyst surface, leading to an experimental Sabatier plot that can be used to comprehensively predict both the catalytic activity and stability of a wide range of Pt-alloy ORR catalysts. Furthermore, based on the established Sabatier plot, we demonstrated the design of a PtNiCo catalyst that simultaneously delivers a superior activity and robust stability, approaching the peak of the Sabatier plot.

5:00 PM EN11.07.04

Direct Electrosynthesis of Pure Aqueous H₂O₂ Solutions with High Production Rates Based on Carbon Catalysts in a Solid Electrolyte Reactor Yang Xia and Haotian Wang; Rice University, United States

Hydrogen peroxide (H₂O₂) is a crucial chemical with a wide range of applications in civil and industrial fields. It is currently produced from the industrial energy- and waste-intensive anthraquinone process. Its centralized feature also makes it rely heavily on the storage and transportation of H₂O₂, which is unstable and hazardous. Electrocatalytic oxygen reduction reaction (ORR) to H₂O₂ provides an alternative to realize green and delocalized production, with the only inputs from renewable electricity, water and air. However, this route still faces two challenges: 1) lack of catalysts which selectively drive the 2e⁻ ORR towards H₂O₂ (instead of H₂O); 2) generated H₂O₂ are typically in mix with solutes in traditional electrolyzers, which necessitates complicated separation processes to recover pure H₂O₂ solutions for applications.

To make the electrochemical route more reliable in the future scaling-up, we reported a direct and continuous production of pure H₂O₂ solutions for the first time, through rational design of both catalyst and reactor. Here, we report a direct electrosynthesis strategy that delivers separate water (H₂O) and oxygen (O₂) streams to an anode and cathode separated by a porous solid electrolyte, wherein the electrochemically generated H⁺ and HO₂⁻ recombine to form pure aqueous H₂O₂ solutions with different concentrations. By optimizing a functionalized carbon black catalyst, we achieved over 90% selectivity for pure H₂O₂ at current densities up to 200 mA cm⁻², which represents a H₂O₂ productivity of 3.4 millimoles per square centimeter per hour.

To further improve the activity and lower the overpotential at high current densities for industrial-level applications, we introduced boron-doped carbon catalyst which can achieve better activity under industrial-relevant current densities (saving over 200 mV overpotential at up to 300 mA cm⁻²) compared to the state-of-the-art oxidized carbon catalyst while maintaining a high selectivity (up to 90%). By incorporating the boron-doped carbon catalyst into our solid electrolyte cell setup, we achieved high partial H₂O₂ current densities (400 mA cm⁻²) with high selectivity (up to 95%), which represents a H₂O₂ productivity of 7.36 millimoles per square centimeter per hour. The setup can also undergo 200-hour stability test without degradation, making it a good candidate to be further improved in the aspect of potential scaling-up for electrochemical H₂O₂ production in industrial level with long-lasting performance.

5:15 PM EN11.07.05

Understanding the Role of P in Achieving Selective Catalysis for CO₂ Reduction and H₂O₂ Generation by Oxygen Reduction Scott Geyer; Wake Forest University, United States

Development of efficient, selective and cost-effective electrocatalysts is central to the efficient production of sustainable fuels and industrial feedstocks. While significant progress has been made in the hydrogen evolution reaction (HER) for water splitting, the direct synthesis of industrial fuels and feedstocks by the CO₂ reduction reaction (CO₂RR) still presents significant challenges related to the limited number of metals that maintain selectivity over many reaction steps while sufficiently inhibiting competing HER. In this presentation we will show our success in promoting CO₂RR over HER as well as H₂O₂ over H₂O in the oxygen reduction reaction (ORR) using metal-phosphorus nanocrystalline catalysts based. Taken together, these three examples show the promise of controlled stoichiometric control in promoting desirable catalytic properties.

Recently (Nature Communications 2019) we demonstrated that CO₂ reduction on AgP₂ NCs shows a 3-fold reduction in Faradaic CO overpotential compared to Ag NCs. The reduced overpotential is consistent with the free-energies of the intermediates calculated with density functional theory in which the calculated free energy for COOH* is roughly three times lower for both the AgP₂ (111) and AgP₂ (211) surfaces compared to Ag (111). Operando X-ray absorption spectroscopy (XAS) gave insight into the role of P in stabilizing positive Ag partial oxidation states under reductive potentials, where at -0.8 V vs. RHE (corresponding to the peak in selectivity for CO₂-to-CO), the Ag oxidation state in AgP₂ NCs is +1.08 and stable for 2 h. In comparison, Ag₂O and Ag₂O are reduced to Ag⁰ in less than 50 s at -0.8 V vs. RHE. Consistent with experiment, Bader charge analysis of COOH* on Ag and AgP₂ also shows a higher Ag oxidation state of AgP₂ versus metallic Ag. Notably, the decrease in overpotential was observed for a system that still maintained selectivity for CO₂RR over HER, despite the presence of P atoms on the surface. Free energy calculations for H* on Ag and P suggest Ag remains inactive for HER and that for the Ag(211) surface P over-binds H, consequently limiting HER.

Pushing towards selective C₂ product formation requires efficient C-C bond formation at sufficiently low overpotentials to avoid methane formation. Current work demonstrates a 280 mV reduction in ethylene overpotential on Cu₃P compared to Cu nanocrystals, with C₂H₄ selectivity reaching 68%. Encouragingly, HER is again limited. The mechanism behind the observed increase in C₂H₄ selectivity is partially revealed by density functional theory and in situ FTIR, which suggests the reduction in the barrier for formation of CHO* creates a low overpotential regime in which a CO* and CHO* rich surface facilitates the bimolecular C-C bond formation reaction.

The role of P in templating metal atoms to control selectivity is demonstrated in the selective H₂O₂ ORR by PtP₂ NCs (Nature Communications 2020). For Pt-based oxygen reduction, the selectivity for the 2 e⁻ H₂O₂ pathway versus the 4 e⁻ H₂O pathway depends critically on the comparative strength of the Pt-OOH and the O-OH bonds. On pure Pt, strong bridge binding of OOH* decreases the chance of desorption and weakens the OOH bond which increases reactivity in the subsequent 4 e⁻ pathway steps. PtP₂ increases the Pt separation and destabilizes the OOH* bridge bond based on DFT calculated bond distances. The result is a dramatic change in selectivity toward H₂O₂ which reaches 98%. Atomic layer deposition of Al₂O₃ prevents NC aggregation and enables application in a polymer electrolyte membrane fuel cell (PEMFC) with a maximum r(H₂O₂) of 2.26 mmol h⁻¹ cm⁻² and a current efficiency of 78.8% even at a high current density of 150 mA cm⁻². Catalyst stability enables an accumulated neutral H₂O₂ concentration in 600 mL of 3.0 wt% (pH = 6.6).

5:30 PM EN11.07.06

H₂O₂ Production using Polymeric Organic Semiconducting Electrocatalysts J. Tyler Mefford, Ana De La Fuente Duran, Allen Yu-Lun Liang, Stephen D. Kang, William C. Chueh, Alberto Salleo and Alexander Giovannitti; Stanford University, United States

Decarbonization of the chemical industry requires transitioning from thermochemical transformations towards electrochemical pathways that use “green” electricity generated from renewables. These electrochemical processes focus on converting abundant natural chemical resources, such as the atmospheric gases O₂, N₂, CO₂, and H₂O, into fuels and valuable commodity chemicals, such as H₂, H₂O₂, NH₃, and multi-carbon products. But these processes are kinetically unfavorable and require the use of electrocatalysts for reasonable efficiencies. An ideal electrocatalyst should be (1) highly active and selective for generation of the desired end product with near 100% Faradaic efficiency at low overpotentials, (2) able to transport electrons (or holes), ions, and molecules to/from the catalytic site, and (3) affordable—meaning that they should only contain elements with reasonably high abundance and use synthetic methods that can scale to meet global demand. Unfortunately, simultaneously achieving all three desired qualities is difficult and often multi-component electrodes are necessary—for example Pt is highly active and selective for the full 4 e⁻ reduction of O₂ to H₂O in fuel cell electrodes but requires the incorporation of carbon black additives to minimize Pt content and reduce costs. Additionally, Pt is not ionically conductive and requires Nafion polymeric

binders to efficiently transport ions to the reaction sites.¹ Inspired by nature's design of enzymatic catalytic sites, we set out to synthesize organic electrocatalytic structures that, in principle, may achieve all three desired qualities.²

In this talk, we will describe the development of electrocatalysts based on n-type (electron conducting) organic semiconducting (OSC) polymers and their applications towards the production of H₂O₂ from O₂. These polymeric OSC's are mixed ionic-electronic conductors with redox active polaronic states formed through electrochemical ion insertion reactions. Rational design of the chemical structure of the OSC polymer backbone can be used to tune the energy (reduction potential) of these polaronic states and the adsorption strength of reactive intermediates to optimize selectivity and catalytic activity. Simultaneously, the attachment of a mixture of polar and non-polar side-chains to the backbone modifies the hydrophilicity of the polymer to tune the ionic and molecular transport properties through the bulk of the electrode. This approach enables full utilization of electrochemically active redox sites while simultaneously ensuring robust mechanical and chemical stability.³ *Operando* UV-Vis spectroelectrochemistry and transport measurements performed during active electrochemical oxygen reduction in electrolytes at various pH's yield insights into the nature of the reaction site and mechanism of the reaction, providing chemical design principles for future development of this emerging class of electrocatalysts.

1. F. Barbir, *PEM Fuel Cells: Theory and Practice, 2nd Edition* (Elsevier, 2012).
2. R. Morris Bullock *et al. Science* **369**, eabc3183 (2020)
3. A. Giovannitti *et al. Nat. Commun.* **7**:13066 (2016)

5:45 PM EN11.07.07

A Highly Active and Selective Redox Active 2D Metal Organic Framework Catalyst for Electrosynthesis of Hydrogen Peroxide in Neutral Media R. Dominic Ross, Hongyuan Sheng and Song Jin; University of Wisconsin-Madison, United States

Hydrogen peroxide (H₂O₂) is a widely produced green oxidant with applications in paper bleaching, chemical synthesis, and disinfection. H₂O₂ could be electrochemically produced safely and on-demand by using a catalyst selective for the two-electron oxygen reduction reaction (2e⁻ ORR) as opposed to the four-electron (4e⁻) pathway, though development of such catalysts has been hindered by lack of systematic design principles. Recently, well-defined crystalline two-dimensional conductive metal organic frameworks (2D-MOFs) with a square planar metal-nitrogen (M-N₄) motif have shown selective 2e⁻ ORR but the origins of the catalytic activity and selectivity remain unclear. Here, we demonstrate that one such 2D-MOF, Ni-HAB (HAB = hexaaminobenzene), has high selectivity compared to other similar 2D-MOFs with M-N₄ motifs. Bulk electrolysis experiments prove the practical efficacy of Ni-HAB as a 2e⁻ ORR catalyst in buffered near-neutral electrolyte and reveal a strong dependence on operating potential. *Operando* X-ray absorption spectroscopy reveals highly stable metal coordination sites and charging of the organic linkers that occurs during ORR that directly competes with the production of H₂O₂. These results confirm the dominant active site during ORR in these MOF catalysts and reveal a unique interplay between the material's catalytic and redox properties that can guide the future design of similar MOFs for enhanced catalytic activity.

SESSION EN11.08: Water Splitting
Session Chairs: Chong Liu and Samira Siahrostami
Thursday Morning, December 2, 2021
Hynes, Level 3, Room 312

10:30 AM EN11.08.01

Oxygen Evolution Reaction Over Catalytic Single-Site Co in Well-Defined Brookite TiO₂ Nanorod Surface Chang Liu¹, Sen Zhang¹, William Goddard² and Jin Qian³; ¹University of Virginia, United States; ²California Institute of Technology, United States; ³Lawrence Berkeley National Laboratory, United States

Oxygen evolution reaction (OER) is an essential reaction and often a limiting step in many electrochemical devices that hold great potential for clean energy conversion and fuel transformation. The two paramount questions remain unclear in OER heterogeneous catalyst design: (1) how to identify and construct well-defined catalytic centers for efficient OER catalysis, and (2) how to delineate unambiguously the atomistic mechanism and kinetics for OER and competitive reactions at this center. In this work, we developed a new synthesis for the single-site cobalt (Co) doped TiO₂ nanorods with well-defined catalytic surface (210). This material was systematically studied with a suite of *operando* probes under electrochemical conditions and exhibited a record-high intrinsic activity for the OER reported to date. Moreover, based on grand canonical quantum mechanics (GCQM) calculations on well-defined single-site Co atomic structure, we establish a full description of reaction kinetics for the Co-TiO₂ as a function of applied potential, revealing an adsorbate evolution mechanism for the OER. The computationally predicted Tafel slope and TOFs also exhibit unprecedentedly good agreement with experiment. Moreover, we demonstrated a methodological advance for the study of OER by combining the atomic-precision synthesis of nanocrystals and GCQM calculations. With the accuracy of GCQM calculations validated here, it can potentially allow us to perform high-accuracy *in-silico* design of rational catalyst and subsequently maximize its benefit through controlled synthesis of nanocatalysts.

10:45 AM EN11.08.02

Leveraging the Inductive Effect to Promote Oxygen Evolution on Oxides and Metal-Hydroxide-Organic Frameworks Jiayu Peng, Shuai Yuan, Bin Cai, Livia Giordano, Yuriy Román-Leshkov and Yang Shao-Horn; Massachusetts Institute of Technology, United States

Late transition metal oxides are reported to be the most active non-precious catalysts for oxygen evolution reaction (OER),^[1] but the most active oxides based on Ni or Co^[2] still have turnover frequencies per metal site at least one order of magnitude lower than that of oxygen-evolving complex (OEC) in biological systems.^[3] The OEC contains an intricate manganese-calcium-oxo cluster, and its unparalleled OER activity can be attributed to the unique characteristics of Mn centers regulated by Ca²⁺ cations.^[4,5] Such electronic structure tuning can be generalized as the inductive effect.^[6] Specifically, substituting metal oxides and complexes using foreign metals with higher electronegativity can effectively increase their redox potentials and promote their activity. We have recently employed this concept to design bismuth-substituted strontium cobaltite, where the strongly electronegative Bi³⁺ ions give rise to Co centers with record intrinsic OER activity in alkaline solutions.^[7]

Unfortunately, metal substitution in oxides exhibits a much smaller tunability of electronic structures than that found in metal-oxo clusters. For instance, Ca²⁺ substitution of Mn⁴⁺ in synthetic [CaMn₃O₄] clusters can tune the Mn^{3+/4+} redox potential by ~1 V,^[4,5] whereas negligible changes of ~0.02 V are typically observed for oxides.^[6] To tackle this limitation, we have designed metal-hydroxide-organic frameworks (MHOFs) that combine the great tunability of enzymatic systems with known oxide-based chemistries. A series of MHOFs were constructed by transforming layered hydroxides into 2D sheets composed of metal-octahedra chains cross-linked with neighboring chains using organic linkers. MHOFs can act as a tunable platform for OER,

where the nature of π - π interactions between adjacent stacked linkers and the transition metals in the layered metal hydroxides dictate stability and activity, respectively. Substituting MHOF nanosheets with more electron-withdrawing cations increased their OER activity, where Fe-substituted Ni-based MHOFs exhibited three orders of magnitude enhancement in activity per metal site, rivaling those of state-of-the-art OER catalysts. This enhancement was correlated with the MHOF-based modulation of Ni redox potentials and the optimized binding of reaction intermediates. These results represent a step forward towards designing active metal centers with ligand fields akin to those in homogenous/enzymatic systems, where MHOFs can act as a versatile platform to design catalysts with unparalleled tunability.

References:

- [1] J. Hwang, R. R. Rao, L. Giordano, Y. Katayama, Y. Yu, Y. Shao-Horn, *Science* 2017, 358, 751.
- [2] C. Wei, R. R. Rao, J. Peng, B. Huang, I. E. L. Stephens, M. Risch, Z. J. Xu, Y. Shao-Horn, *Adv. Mater.* 2019, 31, 1806296.
- [3] W. T. Hong, M. Risch, K. A. Stoerzinger, A. Grimaud, J. Suntivich, Y. Shao-Horn, *Energy Environ. Sci.* 2015, 8, 1404.
- [4] E. Y. Tsui, R. Tran, J. Yano, T. Agapie, *Nat. Chem.* 2013, 5, 293.
- [5] E. Y. Tsui, T. Agapie, *Proc. Natl. Acad. Sci.* 2013, 110, 10084.
- [6] D. A. Kuznetsov, B. Han, Y. Yu, R. R. Rao, J. Hwang, Y. Román-Leshkov, Y. Shao-Horn, *Joule* 2018, 2, 225.
- [7] D. A. Kuznetsov, J. Peng, L. Giordano, Y. Román-Leshkov, Y. Shao-Horn, *J. Phys. Chem. C* 2020, 124, 6562.

11:00 AM EN11.08.04

Tuning Confined Water Structure and Hydrogen Evolution/Reduction Through Water-in-Solvent Yirui Zhang, Botao Huang, Graham Leverick and Yang Shao-Horn; Massachusetts Institute of Technology, United States

The production of molecular hydrogen by catalyzing water splitting is central to achieving the decarbonization of sustainable fuels and chemical transformations. While the hydrogen evolution reaction (HER) and hydrogen oxidation reaction (HOR) have been studied on a variety of electrode materials and pH, the mechanisms at play in the electrochemical double-layer and the roles of water structure are poorly understood. Especially changes in water structure have gained interest because of its direct implications on many of its properties, such as diffusion, dielectric function and H-bond dynamics. In this work, we achieved to confine water in organic solvents, and tune the water structure and hydrogen-bonding networks by changing the water concentration and organic solvents. Fourier-transform infrared spectroscopy (FTIR) and nuclear magnetic resonance (NMR) reveals the change of water structure confined in organics, and the HER/HOR kinetics are altered accordingly. We further perform surface-enhanced infrared absorption spectroscopy (SEIRAS) measurements to probe the water structure change during the reactions, and understand the role of water structure, and more specifically confined water, in reaction kinetics. This work highlights immense opportunities to control the water activity and HER/HOR kinetics by tuning interfacial structures of water and solvents. The understanding in controlling water activity would also be impactful across other reactions crucial to improving decarbonizing efforts in energy storage such as CO₂ reduction and aqueous batteries.

11:15 AM *EN11.08.05

Decoupling Mass Transport Effects from Intrinsic Kinetics on the Study of Electrocatalytic Materials Carlos G. Morales-Guio; University of California, Los Angeles, United States

Understanding the underlying mechanisms for the electrocatalytic transformation of CO₂ to fuels and chemicals, the electrochemical oxidation of methane to methanol or the electrocatalytic transformation of nitrogen to ammonia is a significant challenge for the scientific community. In our group, we have recently discovered that the H-type and gas diffusion electrode cells broadly used for the study of electrocatalytic transformations suffer from ill-defined mass and heat transfer characteristics obscuring the results obtained in kinetic studies and thus complicating further development of the field. The complexity of electrocatalytic reactions is due to the coupling between reaction and diffusion and requires a profound understanding of processes occurring at multiple scales. In this work, a novel electrochemical cell is presented with well-defined mass transport properties where the hydrodynamics of the cell can be controlled from Reynolds numbers from 200 to 20,000 while the dimensionless mass transfer coefficient, the Sherwood number, is varied over an order of magnitude. Using this advanced electrochemical cell, we show that the product distribution obtained on a flat polycrystalline electrode for the electrocatalytic reduction of CO₂ varies widely under different mass transport regimes. Under the same applied potential, low Sherwood numbers favor the generation of >2 electrons reduction products such as ethylene and alcohols while high Sherwood numbers favor the production of hydrogen, carbon monoxide and formate. We also show that changes in the hydrodynamics of the cell can be used to change the selectivity of transition metal oxides for the electrocatalytic oxidation of methane to methanol. We show for the first time that various transition metal oxides are indeed selective for the transformation of methane to methanol under optimized conditions of applied potential and mass transfer. Through the study of these systems at different temperatures it is possible to decouple thermal from electron transfer steps in the electrochemical activation and oxidation of methane and extract intrinsic kinetics for this process. Understanding the coupling between reaction and diffusion should facilitate the study of electrocatalytic materials and the scale-up of electrocatalytic reactors in the near future.

SESSION EN11.09: Photoelectrocatalysis

Session Chair: Chong Liu

Thursday Afternoon, December 2, 2021

Hynes, Level 3, Room 312

1:30 PM EN11.09.01

Microfluidic System for Solar Energy Conversion Based on Metal-Doped Carbon Nitride Ewelina M. Kuna, Izabela Stefanowicz-Pieta and Martin Jonsson-Niedziolka; Institute of Physical Chemistry Polish Academy of Science, Poland

In recent years, a growing emphasis has been put on developing clean energy technologies and processes based on renewable energy sources. Solar power is the key to a clean energy future.¹ Artificial systems that mimic natural photosynthesis can be used to convert the Sun's energy to chemical or electrical energy. However, the effective conversion of light into a usable form of energy is mainly limited due to non-efficient charge separation and poor light-harvesting architecture.^{2,3} This issue might be overcome by the proper selection of photoactive materials and the suitable engineering of photoreactors. Consequently, the challenge of developing successful solar-driven technology starts from understanding the nature of the performed chemical processes and the design of devices which can be implemented with photo-catalytic technologies. Following this trend, we have decided to examine how one of the most promising materials for alcohol photo/electrooxidation, metal-doped carbon nitrides (g-C₃N₄), can be applied to microfluidic fuel cells.⁴ Our research indicates that among various materials, Ni-doped g-C₃N₄ exhibits outstanding catalytic activity towards methanol photo/electrooxidation upon batch reaction conditions.⁵ Therefore, this stable and efficient catalytic reaction system has been transferred towards continuous flow technology *via* adopting a

microfluidic system.

- [1] G. Ciamician, *Science*, 1912, 36 (926), 385.
- [2] V. Balzani, G. Bergamini, P. Ceroni, *Angew. Chem.*, 2015, 54, 11320.
- [3] C. C. Chua, D. M. Bassani, *Photochem. Photobiol. Sci.*, 2008, 7, 521.
- [4] E. Kuna, D. Mrdenovic, M. Jonsson-Niedziolka, P. Pieta, I.S. Pieta, *Nanoscale Adv.*, 2021, 3, 1342.
- [5] I.S. Pieta, P. Pieta, R. Nowakowski, M. Holdynski, M. Pisarek, A. Kaminska, M.B. Gawande, R. Zboril, *Appl. Catal. B.*, 2019, 244, 272.

1:45 PM EN11.09.02

Semiconductor/Bacteriorhodopsin Junctions for Enhanced Photoelectrochemical Water Splitting Nageh K. Allam; American University in Cairo, Egypt

In recent years, considerable efforts have been made to improve the performance of photoactive nanostructured materials for water splitting applications. Herein, we report on the assembly and use of a bacteriorhodopsin (bR)/TiO₂ nanotube array hybrid electrode system. Photoanode materials composed of ~7 μm long self-ordered and vertically oriented nanotube array of titanium dioxide films were fabricated via the anodization of Ti foil in formamide electrolytes containing NH₄F at room temperature followed by sensitization of the electrodes with bR. The stability of bR on the TiO₂ surface was found to depend on the pretreatment process of the TiO₂ films. Our results demonstrate the opportunity to fabricate fairly stable bR/TiO₂ hybrid electrodes that can be used as photoanodes for photoelectrochemical water splitting. Under AM 1.5 illumination (100 mW/cm²), the hybrid electrodes achieved a photocurrent density of 0.65 mA/cm² which is a ~50% increase over that measured for pure TiO₂ nanotubes (0.43 mA/cm²) fabricated and tested under the same conditions. In the presence of a redox electrolyte, the photocurrent increased to 0.87 mA/cm². To the best of our knowledge, this is the first report on the use of bR/TiO₂ hybrid electrodes in photoelectrochemical water oxidation cells. We believe the proton pumping property of bR can be used in a variety of applications, especially those related to third generation photovoltaic cells.

2:00 PM EN11.09.04

In Situ Magnetic Alignment of a Slurry of Tandem Semiconductor Microwires Using a Ni Catalyst Saumya Gulati^{1,2} and Joshua Spurgeon^{1,2}; ¹University of Louisville, United States; ²Conn center for renewable energy research, United States

There has been a vast improvement in photovoltaic (PV) technology in the last couple of decades; however, solar PV technology has a lot of drawbacks, including that it is intermittent, broadly dispersed, and non-transportable. Hence, cost-effective solar energy storage is critical for widespread implementation of solar energy as the primary energy source. Slurries of semiconductor particles individually capable of unassisted light-driven water-splitting are modeled to have a promising path to low-cost solar hydrogen generation, but they have had poor efficiencies. Tandem microparticle systems are a clear direction to pursue to increase the efficiency. However, light absorption must be carefully managed in a tandem to prevent current mismatch in the subcells, which presents a possible challenge for tandem microwire particles suspended in a liquid. In this work, a Ni-catalyzed Si/TiO₂ tandem microwire slurry was used as a stand-in for an ideal bandgap combination to demonstrate proof-of-concept alignment of unassisted water-splitting microwires with an external magnetic field. The Ni hydrogen evolution catalyst was selectively photodeposited at the exposed Si microwire core to serve as the cathode site as well as a handle for magnetic orientation. The frequency distribution of the suspended microwire orientation angles was determined as a function of magnetic field strength under dispersion with and without uplifting microbubbles. After magnetizing the Ni bulb, tandem microwires could be highly aligned in water under a magnetic field despite active dispersion from bubbling or convection.

2:15 PM *EN11.09.05

Understanding Water Oxidation Mechanisms on Heterogeneous Catalysts with Atomically Defined Active Centers Dunwei Wang; Boston College, United States

Water oxidation is an important first step toward artificial photosynthesis. A key challenge in this field is the lack of clarity on how water is oxidized. As a result, a durable but highly active heterogeneous catalyst that is also low-cost has not been found. Important questions on why certain catalysts are more active than others also remain unanswered. This problem has been difficult to solve because, at least in part, there is a lack of clarity on the structure of the active sites. The fact that the catalyst structure also evolves during the catalytic reaction further exacerbates the situation. Here we present a new catalyst platform that has the potential to address this issue. Starting from molecular catalysts whose structure is well resolved, we synthesize heterogeneous catalysts that preserve the active site structure. The resulting material is a dinuclear catalyst that is highly active but also durable. More importantly, it provides an opportunity to test the various hypotheses concerning water oxidation mechanisms.

3:00 PM BREAK

SESSION EN11.10: Nitrogen Reduction
Session Chair: Chong Liu
Thursday Afternoon, December 2, 2021
Hynes, Level 3, Room 312

4:00 PM EN11.10.03

Engineering PdCu Bimetals for Enhanced Electrochemical Nitrate Reduction to Nitrogen and Ammonia Jeonghoon Lim, Seung Woo Lee and Marta Hatzell; Georgia Institute of Technology, United States

Nitrate (NO₃⁻) pollution of groundwater is an arising issue due to the high input of nitrogen-rich agriculture fertilizers. Furthermore, nitrite (NO₂⁻), which is the product of NO₃⁻ reduction, is also a major threat to human health such as methemoglobinemia ("blue baby syndrome") and cancer. Electrochemical conversion of harmful nitrate has attracted attention to produce benign dinitrogen (N₂) and ammonia (NH₃) as a means of transforming waste into fertilizers. Designing structure of PdCu bimetallic nanoparticles is important for developing highly efficient and selective electrocatalysts. Here, we engineered the atomic structure of PdCu and controlled Cu surface coverage on Pd nanocube nanoparticles for enhancing the NO₃⁻ conversion rate and steer the selectivity of N₂/NH₃. Highly ordered structure of PdCu nanoparticles showed high nitrate reduction activity, excellent dinitrogen selectivity and robust stability in a neutral electrolyte compared to disordered PdCu nanoparticles. We also develop Pd nanocube nanoparticles and introduce Cu metals on

the surface by underpotential deposition (UPD) method. The decorated Cu metals catalyze the reduction of NO_3^- to NO_2^- and the Pd (100) enhances the activity and selectivity of NO_2^- to N_2 . Rotating disk electrode (RDE) and H-cell tests were conducted for $\text{NO}_3^-/\text{NO}_2^-$ reduction activity and the selectivity of PdCu bimetal electrocatalysts were examined by UV-vis and *in-situ* mass spectrometry. This study demonstrates that designing nanostructure of PdCu is an efficient approach to facilitate the nitrate reduction process and control the selectivity of N_2/NH_3 as reducing environmental issues associated with removing NO_3^- and NO_2^- from water.

4:15 PM EN11.10.04

Oxide-Derived Silver Nanocatalysts with Tunable Selectivity in Electrocatalytic Nitrate Reduction Jaeryul Park, Hengzhou Liu, Yifu Chen, Wenzhen Li and Luke T. Roling; Iowa State University, United States

Nitrate contamination in groundwater due to agricultural runoff is one of the most significant modern environmental challenges, with substantial implications on wildlife and human health. The electrochemical reduction of nitrate has demonstrated promise for its elimination; however, developing methods for improving selectivity to desired products is paramount toward its effectiveness. Nitrogen gas (N_2) is benign and a desirable target for wastewater remediation, though maintaining its production at sufficient activity and current efficiency has been elusive.

This presentation describes our recent computational and experimental work¹ in developing transition metal nitrate reduction catalysts. Our experimental results, combining rigorous electrochemistry with online gas chromatography, have found that Ag electrocatalysts demonstrate a unique activity and selectivity for nitrate to nitrite not found on other transition metal catalysts. In particular, an oxide-derived (OD-)Ag catalyst demonstrated up to 98% nitrate-to-nitrite selectivity with 95% faradaic efficiency. The product selectivity can be tuned simply by changing the electrode potential to more reducing conditions, yielding ammonia with faradaic efficiency of 89%. Alternatively, the nitrite generated by the electrocatalytic process can be efficiently and selectively reduced to N_2 in a separate (nonelectrochemical) catalytic process on Pd/C to yield a clean two-step process for nitrate reduction.

Density functional theory (DFT) calculations on model surfaces show that the undercoordinated nature of the OD-Ag catalysts is particularly advantageous for nitrate reduction relative to traditional Ag nanoparticles. The Ag-based catalysts have difficulty in directly activating N-O bonds, instead relying on proton-mediated pathways to perform N-O bond dissociation. The unique selectivity arises from the relative ease of nitrate vs. nitrite reduction along these proton-mediated pathways, with the undercoordinated nature of OD-Ag aiding the electrocatalytic performance due to the preferential adsorption of nitrate. In contrast, Cu-based catalysts demonstrate poorer selectivity to nitrate due to their ability to directly activate N-O through non-electrochemical routes. Together, these results open the possibility of electrochemical nitrate remediation to close the nitrogen cycle (by forming N_2) and/or the potential use of nitrite as a platform for the generation of other N-containing compounds (e.g., ammonia, hydroxylamine) when treating concentrated nitrate sources.

¹H Liu, J Park, Y Chen, Y Qiu, Y Cheng, K Srivastava, S Gu, B H Shanks, L T Roling, W Li, *ACS Catalysis* (accepted), <https://doi.org/10.1021/acscatal.1c01525>

SESSION EN11.11: CO₂ Reduction III
Session Chairs: Wilson Smith and Haotian Wang
Monday Morning, December 6, 2021
EN11-Virtual

8:00 AM EN11.11.01

Water and Solute Activities Regulate CO₂ Reduction at High Current Densities Nathan T. Nesbitt¹ and Wilson Smith^{1,2,2}; ¹National Renewable Energy Laboratory, United States; ²University of Colorado Boulder, United States

High current density electrochemical CO₂ reduction (CO₂R) (~1 A cm⁻²) can create concentrated hydroxide at the cathode, causing the activity coefficient of water and hydroxide to deviate from the "dilute solution approximation." Also, for CO₂ reduction to CO, as the ratio of CO₂ to CO changes along the gas flow channel at a gas-diffusion electrode the reaction equilibrium potential will shift. Here I discuss the implications of these effects for CO₂R energy efficiency and product selectivity based on Nernstian analysis. Promising reactor designs are suggested, accordingly.

8:15 AM EN11.11.02

Single Site M-N₄-C Electrocatalysts for the CO₂ Reduction Reaction Peter Bogdanoff¹, Stephen Paul², Yi-Lin Kao¹, Iris Herrmann-Geppert³, Roel van de Krol¹ and Ulrike I. Kramm²; ¹Helmholtz-Zentrum-Berlin, Germany; ²TU-Darmstadt, Germany; ³HS-Mittweida, Germany

The influences of various transition metal ions (Ni, Fe, Co, Cu, Mn, Zn, and Sn) in metal- and nitrogen-doped carbon (M-N-C) are systematically investigated for the electrochemical reduction of water and CO₂ (CO₂RR). By careful pyrolysis of carbon-supported porphyrins at low loading predominately M-N₄-centers embedded in a carbon matrix are achieved, while avoiding significant amounts of undesired metal- and nitrogen byproducts. The catalysts were electrochemically investigated in a Gas Diffusion Electrode (GDE) arrangement coupled in-line to a mass spectrometer, allowing the almost simultaneous detection of product selectivity, Faraday efficiencies and current densities in linear sweep voltage (LSV) experiments. Among these catalysts, Fe- and Ni-based samples have shown remarkable high Faraday efficiencies of > 90% for the formation of CO even at current densities exceeding 175 mA cm⁻² in pH 7.5 carbonate buffer. The comparison of measurements with different gas supply (Ar vs CO₂) underlines that this is achieved by an almost completely suppressed hydrogen evolution in the presence of CO₂, as theoretically expected for single site centers like MeN₄. The Fe-N-C and the Cu-N-C catalyst show a change in reaction mechanism for potentials more negative than -1.5V/NHE accompanied by a steep increase of the formation of CH₄, H₂ (and C₂H₄ on Cu-N-C) whereas CO formation is partially suppressed. *Post mortem* XPS analysis of Cu-N-C reveals that Cu²⁺ of the Cu-N₄ centers is partially reduced to Cu⁰ in that potential range, which led us assume that also in M-N-C catalysts Cu⁰ structures are involved in the formation of hydrocarbons. While Zn-N-C and Mn-N-C in our study generally show only little CO₂RR activity, Sn-N-C produces as main product formate with an FE of about 40% and production rates of about 20 μmol h⁻¹ cm⁻² at potentials smaller than -1.5V/NHE. Our work allows new insights into the potential dependent behavior of M-N-C catalysts and reveals the high selectivity of MN₄ centers for the CO₂RR.

8:30 AM EN11.11.04

Late News: Conductive Metal Organic Frameworks with Molecularly Defined M-O₄ Active Sites as Highly Active Biomass Valorization Electrocatalysts Yuxuan Zhang and Nikolay Kornienko; Université de Montréal, Canada

The electrochemical oxidation of biomass platform 5-hydroxymethyl furfural (HMF) to 2,5-furandicarboxylic acid (FDCA), is an important reaction in the

emerging area of renewably powered biomass valorization. To this end, the efficiency of catalytic systems still needs to be improved to render these systems economically competitive. In the electrochemical HMF oxidation reaction (HMFOR), the utilization of well-defined active sites is critical for fundamental insights into their function and subsequently rationally turning them to maximize catalytic activity. However, heterogeneous catalysis of HMF conversion often feature poorly defined catalytic surfaces, hampering the community's complete understanding of the reaction mechanism. To the end, we report the use of reticular chemistry to design a conductive metal organic framework-based electrocatalytic model system with well-defined M-O₄ active sites for HMFOR. The activity of MOFs bearing Ni-O₄ (Ni-CAT) and Co-O₄ (Co-CAT) active sites were analyzed with electrochemical and operando spectroscopic techniques to elucidate the reaction mechanism occurring on the surface. Electrochemical experiments reveal that Co-CAT has an earlier onset potential for enabling HMFOR, relative to other known catalysts thus far, while the Ni-CAT shows faster kinetics for the conversion of HMF to FDCA.

Also, Ni-CAT exhibits efficient charge transfer properties and intrinsically high kinetic towards HMFOR. It achieved FDCA yields of 98.7% yield with 86.8% faradic efficiency at 1.42 V vs RHE.

Infrared spectroscopy captures the surface-bound aldehyde group as the key intermediate in the catalytic cycle, which forms once M(II/III) oxidation occurs. This work illustrates the advantage of utilizing molecularly defined active sites coupled with operando spectroscopy to provide fundamental insights into a variety of electrosynthetic reactions and pave the way for future catalyst design.

8:45 AM EN11.11.05

Tandem Architectures for High-Rate CO₂ Electrolysis Toward Multicarbon [Chubai Chen](#); University of California, Berkeley, United States

CO₂ electrolysis is a promising technique for CO₂ recycling and utilization offering carbon-neutral chemical feedstocks for downstream applications. Electrocatalyst development for CO₂ reduction reaction (CO₂RR) toward single carbon products has achieved enormous progress. However, copper has been found the only metal that can efficiently catalyze CO₂ to higher-value and energy concentrated multicarbon products (e.g., ethylene, ethanol, acetate). Therefore, how to tune the selectivity and boost productivity towards multicarbon based on Cu catalysts becomes a central question in CO₂RR. Here, we highlight that tandem electrocatalysis can be a promising approach towards this target. With tandem strategy, a chemically complicated pathway can be decoupled into individual steps within via multicomponent catalyst design. As a demonstration, we show that a Cu-Ag tandem catalyst on a GDE can enhance the multicarbon production rate from CO₂ through CO₂ reduction to CO on Ag and subsequent carbon coupling on Cu. With added Ag, the multicarbon partial current over a Cu surface increases by 4-fold at -0.70 V vs RHE in 1M KOH. Corresponding CO reduction experiments have been conducted to show that no mutual interference between these two metals can be observed at the catalytic level. More interestingly, the intrinsic C₂H₄ and C₂H₅OH turnover frequency in the tandem platform are significantly higher than Cu alone under either pure CO₂ or CO atmosphere. Such results highlight the unexpected superiority of the tandem strategy for CO₂RR in a flow cell, which offers the opportunity to enhance the efficiency of C-C bonding on a Cu surface beyond conventional CORR during high-rate electrolysis. Considering that the tandem strategy is an independent approach and can be further conjugated with catalyst surface engineering, we aim to optimize the Cu-Ag nanostructure and further boost the catalyst performance. Meanwhile, *operando* spectroscopy can be a powerful method to explore the microenvironment tunability and structure-catalysis relationship.

9:00 AM *EN11.11.06

Shape-Controlled Nanocrystals to Unlock Selectivity Pathways in the Electrochemical CO₂ Reduction Reaction [Raffaella Buonsanti](#); Ecole Polytechnique Federale de Lausanne, Switzerland

In the electrochemical CO₂ reduction reaction (CO₂RR) selectivity still remains an important issue.

In this talk, I will showcase a few examples which highlight how shape-controlled nanocrystals can contribute to address this challenge. First of all, I will discuss how size control of Cu nanocubes (Cu_{cu}) and Cu octahedra (Cu_{oh}) has revealed the importance of facet-ratio to maximize the selectivity towards ethylene and methane, respectively. Second, I will present our recent computational-experimental efforts towards using well-defined NCs to elucidate selectivity rules at the hydrocarbons/alcohols branching nodes in the CO₂RR pathway. The formation of ethanol via *CH_x-*CO coupling or *CO-*CO coupling is an open debate in the literature. As a platform to address this question, we have used CH₄ favoring (i.e. *CH_x populated) Cu_{oh} and C₂H₄ favoring (i.e. *CO-*CO populated) Cu_{cu} under enhanced *CO coverage induced by the presence of Ag NCs. The selective promotion of ethanol in the Cu_{oh} provided evidence for *CH_x-*CO coupling being the preferred pathway. Having learned this, we have also explored the size-dependent edge/face ratio of the Cu_{cu} to interrogate the reactivity of the high index (711) copper surface. The results of this last study indicate the propensity of (711) step sites towards ethanol production.

SESSION EN11.12: CO₂ Reduction IV
Session Chairs: Wilson Smith and Haotian Wang
Monday Morning, December 6, 2021
EN11-Virtual

10:30 AM EN11.12.03

Scalable Cu/Metal-Oxide-Based Catalysts for the Sustainable and Tunable CO₂ Electroreduction to Value-Added Products [Simelys Hernandez](#), Hilmar Guzman, Federica Zammillo, Daniela Roldan and Micaela Castellino; Politecnico di Torino, Italy

The electrocatalytic (EC) CO₂ reduction (CO₂R) driven by renewable energy can be exploited for the future energy transition, for the carbon storage into valuable products like syngas (H₂/CO mixtures), organic acids (formic acid) and chemicals/fuels (C₁₊ alcohols).^{1,2} A big challenge for the industrialization of this technology is to find low-cost electrocatalyst, efficient reactors and process conditions. In our lab, we are exploiting the current knowledge of the thermocatalytic CO₂ hydrogenation to develop noble-metal-free CO₂R electrocatalysts.³ Our results open a promising path for the prospective implementation of metal-oxides nanostructures for the CO₂ conversion to the chemicals and fuels of the future.

We have developed novel structures of Cu/Zn/Al-based catalysts, which produce methanol and CO from the CO₂ thermocatalytic (TC) hydrogenation (at H₂ pressure (P) of 30 bar and temperature (T) > 200 °C) and are able to generate H₂, CO and other C₁ to C₃ liquid products like alcohols, during the electrochemical CO₂R in a gas-diffusion-electrode (GDE) system at ambient T,P. We have also developed B,N-doped Cu oxide catalysts, inducing the formation and stabilization of Cu⁺¹/Cu⁰ interfaces and promoting the dimerization of the *CO intermediate. Incorporating both B and N heteroatoms led to greater selectivity for reducing CO₂ to products of interest: that is, a total FE of 64% to CO₂ reduction products with 49% of liquid products (i.e. 77% selectivity towards formate and alcohols) at a relevant current density of 23 mA cm⁻². The catalysts and electrodes have been prepared by scalable techniques (i.e. co-precipitation and spray-coating) and characterized ex-situ by different physico-chemical methods like X-ray diffraction, BET, porosimetry, field-emission scanning electron microscopy (FESEM), X-ray photoelectron spectroscopy (XPS) among others. A correlation has been found between their activity and selectivity with respect to their porosity and superficial Cu states. The physical and chemical properties of these Cu-based

materials can be manipulated to tune the performance of the electrochemical reaction. In addition, the electrochemical reactor configuration (GDE vs. CO₂ dissolved in liquid electrolyte) also play an important role in the final selectivity and productivity.⁴ These interesting results could help find a suitable electrocatalytic systems for the future implementation of this technology at industrial level.

References:

- 1 H. Guzmán, M. A. Farkhondehfal, K. Rodulfo Tolod, N. Russo and S. Hernández, in *Solar Hydrogen Production Processes, Systems and Technologies*, Elsevier Inc., 2019, p. 560.
- 2 H. Guzmán, N. Russo and S. Hernández, *Green Chem.*, 2021, **23**, 1896–1920.
- 3 H. Guzmán, F. Salomone, E. Batuecas, T. Tommasi, N. Russo, S. Bensaid and S. Hernández, *Chem. Eng. J.*, 2020, 127973.
- 4 H. Guzmán, F. Zammillo, D. Roldán, C. Galletti, N. Russo and S. Hernández, *Catalysts*, 2021, **11**, 482.

Acknowledgements: This work has received financial support by the EU H2020 Project SunCOChem grant agreement: 862192 and Eni SpA: R&D Program Energy Transition (Cattura e Utilizzo CO₂).

10:45 AM EN11.12.04

Late News: Improved Electrochemical Conversion of CO₂ to Multicarbon Products by Using Molecular Doping [Huali Wu](#), Kun Qi, Philippe Miele and Damien Voiry; Institute of European Membrane, France

CO₂ conversion has been proposed as a potential way to close the carbon cycle and generate chemical fuels. The electrocatalytic reduction of carbon dioxide, powered by renewable electricity, to produce valuable fuels and feedstocks provides a sustainable and carbon-neutral approach to the storage of energy produced by intermittent renewable sources.

The development of such a technology is currently hampered by the lack of catalysts, which can drive the reaction at industrially relevant current densities with high efficiency and selectivity. Examples of strategies for optimizing the CO₂RR performance include alloying, surface doping, ligand modification, and interface engineering. Our investigations focus on exploring the role of functionalization on the catalytic activity of Cu towards the conversion of CO₂ to hydrocarbon products.

We developed a method to modify the surface of bimetallic silver-copper (Ag-Cu) catalyst with aromatic heterocycles such as thiadiazole and triazole derivatives. By combining operando Raman and X-ray absorption spectroscopy with electrocatalytic measurements and analysis of the reaction products, we identified that the electron withdrawing nature of functional groups orients the reaction pathway towards the production of C₂₊ species such as ethanol and ethylene and enhances the reaction rates on the surface of the catalyst. As a result, we achieve a maximum Faradaic efficiency for the formation of C₂₊ of ~80% and full-cell energy efficiency of 20.3% with a specific current density of 261.4 mA cm⁻² for C₂₊, using functionalized Ag-Cu electrodes, compared to only 33.8% and 70.6 mA cm⁻² for the pristine Ag-Cu electrodes. We anticipate that our strategy can further be extended in order to improve the selectivity of the reaction towards the production of specific multicarbon molecules.

11:00 AM *EN11.12.05

Designing Efficient Zero-Gap Carbon Monoxide Electrolyzer [Jiao Feng](#) and Sean Overa; University of Delaware, United States

Carbon monoxide electroreduction is a rapidly developing field for the production of valuable commodity chemicals. When coupled with CO₂ capture and electrochemical conversion, it can be used as a clean CO₂ negative process for the production of a variety of products. Carbon monoxide reduction has the distinct advantage over direct electrochemical CO₂ reduction to multi-carbon products (C₂₊) in that it does not suffer from carbonate formation, allowing for higher single pass conversion and electrolyte stability. This work focuses on the design and production of a zero gap membrane electrode assembly carbon monoxide electrolyzer, which operates at low cell potentials (< 2.5 V), and industrially relevant current densities (> 200 mA/cm²) for the production of acetate and ethylene. Acetate and ethylene are valuable target products due to their high value and market potential. Zero gap electrolyzers place the cathode and anode in direct contact with a conductive polymer membrane, whereas conventionally carbon monoxide electrolyzers have relied on a three-compartment design where the cathode is in contact with a liquid electrolyte layer.

By utilizing the zero-gap design, liquid products can be collected in either cathode or anode chamber. To enhance product selectivity, we choose suitable electrocatalysts for both cathode and anode to maximize the selectivity towards carboxylates. By utilizing a suitable combination of electrocatalysts, we have successfully improved the product selectivity towards acetate substantially. The system was also found to have improved current densities and cell voltages when compared to conventional three-compartment carbon monoxide electroreduction systems. Increased residence time of the anolyte by recirculation also allowed for the production of highly concentrated acetate streams with >90% purity relative to other liquid CO reduction products.

11:30 AM *EN11.12.06

CO₂ to Low-Carbon Fuels via Electrochemical Routes [Edward H. Sargent](#); University of Toronto, Canada

I will review progress in CO₂ to ethanol, and to n-propanol, in electrochemical CO₂RR and CORR systems.

SESSION EN11.13: Catalyst and Electrode Engineering
Session Chairs: Wilson Smith and Haotian Wang
Monday Afternoon, December 6, 2021
EN11-Virtual

1:00 PM EN11.13.01

Partial Oxidation of Ethylene to Valuable Chemicals with Hydrogen Co-Production [Yanwei Lum](#)^{1,2} and Edward H. Sargent¹; ¹University of Toronto, Canada; ²National University of Singapore, Singapore

There is significant interest in developing efficient electrochemical processes for commodity chemical manufacturing, all directly powered by renewable electricity. Here we report a one-step electrochemical route at ambient temperature and pressure in aqueous media for the selective anodic partial oxidation of ethylene to ethylene glycol with co-production of hydrogen at the cathode^[1]. Tuning of the catalyst OH binding energy was hypothesized to be crucial for facilitating the transfer of OH to *C₂H₄OH to form ethylene glycol. Computational studies suggested that a gold-doped palladium catalyst could perform this step efficiently, and experimentally we found it to exhibit an approximate 80% Faradaic efficiency to ethylene glycol, retaining its performance for 100 hours of continuous operation. I will also describe our efforts in developing an electrochemical system for the electrosynthesis of ethylene oxide from ethylene using a chloride mediator^[2]. A 2 step integrated system involving CO₂-to-ethylene conversion and subsequent conversion to ethylene oxide was also demonstrated. In summary, these findings represent a significant advance in the development of selective anodic partial oxidation

reactions in aqueous media under mild conditions.

References

[1] [Lum, Y.*](#); Huang, J. E.* and Sargent, E. H et al. Tuning OH binding energy enables selective electrochemical oxidation of ethylene to ethylene glycol. *Nature Catalysis* 2020, 3 (1), 14–22.

[1] Leow, W.*; [Lum, Y.*](#) and Sargent, E.H et al. Chloride-mediated selective electrosynthesis of ethylene and propylene oxides at high current density. *Science* 2020, 368 (6496), 1228-1233.

1:15 PM EN11.13.02

Bifunctional Nickel and Copper Electrocatalysts for CO₂ Reduction and the Oxygen Evolution Reaction [Hanqing Pan](#) and Chris Barile; University of Nevada, Reno, United States

In this study, a bifunctional electrocatalyst for CO₂ reduction and the O₂ evolution reaction (OER) was constructed from the electrodeposition of cuprous oxide (Cu₂O) and Ni on a carbon substrate. Different Ni thicknesses on Cu₂O were achieved by varying the time of chronopotentiometric deposition of Ni. Electrochemical CO₂ reduction was carried out at -0.89 V and -1.89 V vs. RHE, and it was found that formate and CO were the two major products. Cu₂O modified with a Ni overlayer with a thickness of ~700 nm resulted in the highest formate Faradaic efficiency of 18%, and Cu₂O resulted in highest CO Faradaic efficiency of 7.9%. The enhanced Faradaic efficiency for formate is attributed to the synergistic effect between Ni and Cu₂O due to maximized amounts of exposed bimetallic sites that facilitate CO₂ reduction. The electrocatalyst also produces ~9 times more current density than previous studies using Ni-Cu₂O electrocatalysts for the OER. The ability of the Ni-Cu₂O thin films to catalyze both the OER and CO₂ reduction allows them to be incorporated in the first demonstration of a two-electrode CO₂ conversion device with a bifunctional catalyst.

1:30 PM EN11.13.04

Nanostructured Fe-Based Materials for Electrocatalytic Energy Conversion Christopher Simon and [Roland Marschall](#); University of Bayreuth, Germany

Electrocatalytic water splitting can be regarded as promising method to store electrical energy in form of hydrogen as a sustainable green energy carrier. However, water splitting typically suffers from the sluggish reaction kinetics of the oxygen evolution half reaction (OER). By employing electrocatalysts, the required overpotential of the OER can be decreased significantly.

In recent years, earth-abundant spinel ferrites have emerged as auspicious materials for applications in photoelectrochemistry and electrocatalysis. Spinel-type first-row transition metal oxides (TMOs) or their composite compounds containing nickel, manganese, iron, or cobalt are attractive materials for the electrocatalytic oxygen evolution reaction in alkaline media. However, Mn-based electrocatalysts often lack due to stability issues, and the use of cobalt is further discussed critically due to its toxicity hazards and limited availability. Therefore, low cost and high abundant bimetallic NiFe spinel oxide with the elemental composition NiFe₂O₄ has gained attention in the field of alkaline water electrolysis, combining remarkable stability in alkaline media with excellent redox properties.[1,2]

We developed a fast microwave-assisted synthesis yielding phase-pure spinel ferrite nanoparticles of e.g. MgFe₂O₄, CoFe₂O₄, NiFe₂O₄ and ZnFe₂O₄ at temperatures as low as 170-200 °C.[3-6] The crystallite size can be tailored by post-synthetic heat treatment, however the materials are already (partly) crystalline as-prepared, with specific surface areas of around 200 m²/g and good colloidal stability. Photocatalytic and electrocatalytic experiments will be presented, as well as the conversion of some spinel oxides into sulfides, e.g. pendladites.[7] A new direct microwave synthesis for nickel-iron sulfides for electrocatalytic CO₂ reduction will also be presented.[8]

[1] M. Gong, H. Dai, *Nano Res.* 2015, 8, 23

[2] L. Gong et al., *Adv. Sustain. Syst.* 2021, 5, 2000136.

[3] K. Kirchberg et al., *J. Phys. Chem. C* 121 (2017) 27126

[4] C. Simon et al., in revision

[5] P. Dolcet et al., *Inorg. Chem. Front.* 6 (2019) 1527

[6] A. Bloesser et al., *ACS Appl. Nano Mater.* 3 (2020) 11587

[7] D. Tetzlaff et al., *Faraday Discussions* 215 (2019) 216

[8] C. Simon et al., in revision

1:45 PM EN11.13.05

Late News: Zirconium Phosphate Supported Electrocatalysts for the Oxygen-Evolution Reaction [Jorge L. Colón](#)¹, Mario V. Ramos-Garcés², Joel Sanchez³, Kárlery La Luz-Rivera¹, Andrea R. Cortés-Ortiz¹, Victoria M. Figueroa¹, Yannelly A. Serrano-Rosario¹, Isabel Barraza-Alvarez⁴, Yanyu Wu⁵, Dino Villagran⁶ and Thomas Jaramillo³; ¹University of Puerto Rico, United States; ²The Pennsylvania State University, United States; ³Stanford University, United States; ⁴University of California at Santa Barbara, United States; ⁵University of Houston, United States; ⁶The University of Texas at El Paso, United States

We are studying new applications of layered zirconium phosphate (ZrP) inorganic nanomaterials. The θ phase of ZrP can be directly ion-exchanged with large metal complexes, producing intercalated phases useful for artificial photosynthesis schemes for water splitting, amperometric biosensors, and drug delivery applications. Recently, we have demonstrated improved electrocatalytic activity of ZrP nanomaterials loaded with metal ions suitable for the oxygen evolution reaction (OER) of water splitting.

Adsorbing Co and Ni catalysts on the ZrP nanoparticles surface proved to improved OER activity compared to intercalated catalysts. A comparison between adsorbed Co or Ni catalysts and those catalysts on exfoliated ZrP nanoplatelets proved that those on exfoliated nanoplatelets were more active, with diminished overpotentials and reduced Tafel plot slopes as well as higher mass activities. More recently, comparison between Co and Ni catalyst on ZrP particles with different morphologies (hexagonal platelets, rods, cubes, and spheres) revealed that the more active Co catalysts are those on hexagonal ZrP platelets, whereas the best Ni catalysts are those on ZrP spheres. We are exploring the OER activities of mixed-metal catalysts and porphyrins, as well as operando synchrotron X-ray absorption spectroscopy studies to elucidate the nature of the active catalysts.

2:00 PM *EN11.13.06

Integrating Materials Design and Operando Spectroscopy for the Development of Next Electrocatalytic Systems [Nikolay Kornienko](#); University of Montreal, Canada

Electrochemical conversion of abundant feedstocks to fuels and value-added chemicals is rapidly gaining significance as a promising method to harness renewable electricity. Specific reactions within this context that my research group is focused on are the reduction of CO₂ and oxidation of biomass platforms to fuels and value-added chemicals. Because the design of new catalytic systems is inherently linked to a precise understanding of how these

reactions proceed on heterogeneous surfaces, we put considerable efforts in developing methodology for *operando* probing with vibrational spectroscopy. In all, I show how using these experiments provide the key mechanistic information on surface reaction mechanisms that enhance our understanding of functional hybrid interfaces and how the research provide avenues for future materials design within the context of electrosynthesis of fuels and chemicals.

2:30 PM EN11.13.07

Tuning Catalyst-Ionomer Coverage and Interactions Towards Selective and High Current Density CO₂ Reduction [Oyinkansola Romiluyi](#)^{1,2}, Nemanja Danilovic², Alexis T. Bell¹ and Adam Z. Weber²; ¹University of California, Berkeley, United States; ²Lawrence Berkeley National Laboratory, United States

CO₂ electrolyzers operating at high current densities and product selectivities are essential for the commercialization of electrochemical CO₂ reduction (CO₂R) systems to chemicals and fuels. An electrolyzer based on a membrane-electrode assembly (MEA) enables the achievement of these desired criteria. A critical component of an MEA is its catalyst layers, which are composed of catalyst nanoparticles and an ionomer. The latter component provides a pathway for ion transport from the catalyst to the ion-conducting membrane.

The materials design parameters that characterize these ionomer-based catalyst-layers are the ionomer-to-catalyst ratio (I:Cat), catalyst loading, and catalyst-layer thickness. In this study, we systematically analyze the effects of these parameters on the activity and product selectivity of a Ag cathode CO₂R MEA. An optimum I:Cat ratio of 3 is rationalized based on electrochemically-active surface area (ECSA) and ionomer coverage/distribution arguments, where the extent of this coverage and the resulting ionomer-catalyst interaction significantly impacts the total current density and CO selectivity. Coverage regimes range from a patchy/sparse ionomer distribution at low I:Cat ratios (i.e., I:Cat < 3) suffering from poor ECSA and ionic pathway to excessive coverages at high I:Cat ratios (i.e., I:Cat > 3) suffering from poor electronic contact and CO₂ utilization. The effect of decreasing the catalyst loading and/or catalyst-layer thickness changes mainly the CO₂R product selectivity (in agreement with previous modeling work) and the CO FE is shown to be highly sensitive to this metric. By changing these catalyst-layer design parameters, our results demonstrate that the MEA architecture can behave similarly to traditional cells in their ability to highly tune CO₂R selectivity with their electrode/electrolyte interfaces.

The crucial insights gained from the reported trends are compounded to yield an efficient Ag CO₂R MEA cell that operates at current densities of 200 mA cm⁻² to 1000 mA cm⁻², CO faradaic efficiencies of 78 to 91%, and an area-specific resistance under 1 Ω cm². These findings can be applied to a broad range of CO₂R MEA-based devices, including CO₂-to-CO tandem devices and flexible manufacturing systems where changing the aforementioned catalyst-layer properties can effectively tune the outlet CO:H₂ ratio for various syngas applications. The scientific and experimental design learnings from our Ag-cathode MEA studies are subsequently applied to a Cu-cathode MEA, which has farther reaching and impactful applications due to its ability to produce value-added chemical precursors such as ethylene and ethanol.

Acknowledgements

The authors gratefully acknowledge Lawrence Berkeley National Laboratory's Laboratory Directed Research and Development (LDRD) Grant for funding. This material is also based upon work performed by the Joint Center for Artificial Photosynthesis, a DOE Energy Innovation Hub, supported through the Office of Science of the U.S. Department of Energy under Award Number DE-SC0004993.

2:45 PM EN11.04.10

Quasi-Graphitic Carbon Shell-Induced Cu Confinement Promotes Electrocatalytic CO₂ Reduction Toward C₂₊ Products [Ji Yong Kim](#)¹, Deokgi Hong¹, Gun-Do Lee¹, Dae-Hyun Nam² and Young-Chang Joo¹; ¹Seoul National University, Korea (the Republic of); ²Daegu Gyeongbuk Institute of Science and Technology, Korea (the Republic of)

The electrochemical CO₂ reduction reaction (CO₂RR), which converts CO₂ to value-added chemical products with high energy density, is a promising solution for fossil fuel-induced energy and environmental issues because it can help realize a sustainable energy cycle. A commercially feasible CO₂RR requires the development of an electrocatalyst that can steer the reaction pathway toward specific products on a multidimensional scale by controlling the binding energy of the reaction intermediates to design a reaction configuration. This enables economic earnings to be achieved by renewable energy conversion-induced electrochemical reactions in terms of energy efficiency, current density and stability.

For steady electroconversion to value-added chemical products with high efficiency, electrocatalyst reconstruction during electrochemical reactions is a critical issue in catalyst design strategies. Here, we report a reconstruction-immunized catalyst system in which Cu nanoparticles are protected by a quasi-graphitic C shell. This C shell epitaxially grew on Cu with quasi-graphitic bonding via a gas-solid reaction governed by the CO (g) - CO₂ (g) - C (s) equilibrium. The quasi-graphitic C shell-coated Cu was stable during the CO₂ reduction reaction and provided a platform for rational material design. C₂₊ product selectivity could be additionally improved by doping *p*-block elements. These elements modulated the electronic structure of the Cu surface and its binding properties, which can affect the intermediate binding and CO dimerization barrier. B-modified Cu attained a 68.1% Faradaic efficiency for C₂H₄ at -0.55 V (vs RHE) and a C₂H₄ cathodic power conversion efficiency of 44.0%. In the case of N-modified Cu, an improved C₂₊ selectivity of 82.3% at a partial current density of 329.2 mA/cm² was acquired. Quasi-graphitic C shells, which enable surface stabilization and inner element doping, can realize stable CO₂-to-C₂H₄ conversion over 180 hours and allow practical application of electrocatalysts for renewable energy conversion.

SESSION EN11.14: Mechanism Studies
Session Chairs: Wilson Smith and Haotian Wang
Monday Afternoon, December 6, 2021
EN11-Virtual

4:00 PM *EN11.14.01

Advanced Electrocatalytic Processes from a Theoretical Perspective [Núria López](#); The Barcelona Institute of Science and Technology, Spain

In the present talk I will illustrate the main challenges in the modeling of advanced electrocatalytic processes. To start with the changes induced by the rearrangement of the initial catalytic material under reaction conditions will be analyzed for oxygen-derived copper systems. In a second step the role of cations at the interface and how they affect adsorption and reactivity will be investigated. In the final part, the need for advanced fast screening reaction profiles for C3 and longer chain molecules will be presented.

4:30 PM EN11.14.02

Evaluation of Catalytic Activity and Durability of Pt/Carbon-Sphere Catalyst in Acidic Environment [Takahiro Saida](#), Yuto Nohara and Takahiro

Maruyama; Meijo University, Japan

Polymer electrolyte fuel cell (PEFC) is expected to be the next generation power source, but its high cost and low service life are inhibited the wide-spread commercialization. In particular, the platinum utilization and the durability of the carbon supported platinum (Pt/C) used as cathode catalyst are big problems for PEFC. To improve the catalyst activity and durability, many researchers have developed the new catalyst nanoparticle. However, the development of catalyst support is not enough in comparison with the catalyst nanoparticles. In general, the activated carbon, which has a high surface area, is employed as the catalyst support to realize the high dispersion supporting of catalyst nanoparticles. However, the activated carbon leads to the low platinum utilization by its high substance diffusion resistance attributed to the complex pore structure. And the functional groups on the surface conduce to the carbon corrosion. Graphitized carbon is well known as one of the high corrosion tolerance carbon materials. But it is hard to disperse catalyst nanoparticles highly due to the low surface area of the graphitized carbon. When developing the new catalyst support, it is necessary to consider the balance between the catalytic activity and the carbon-corrosion tolerance.

We developed the carbon-sphere composing with the reduced graphene oxide (rGO) wall and SiO₂ core as a new familiar of carbon materials [1]. The carbon-sphere is expected to have low substance diffusion resistance due to its simple pore structure compared to conventional carbon. Previous reports indicate that the rGO trends to disperse the platinum nanoparticles highly [2-8]. Thence, the carbon-sphere developed by our group can be expected to balance the catalytic activity and the carbon corrosion tolerance. In this study, the carbon-sphere supported platinum (Pt/CS) was synthesized and evaluated the oxygen reduction reaction (ORR) activity and durability.

Carbon sphere was prepared as previously reported. [1] Pt/CS was synthesized by an impregnation method. Morphology, crystalline structure and electronic state of Pt/Carbon-sphere were observed SEM, XRD, and XPS. The electrochemical measurement was conducted by the rotating disk electrode (RDE) method.

The morphology of Pt/CS was maintained to the uniform sphere shape. The presence of Pt was confirmed by XRD, SEM and XPS. The platinum particle size on CS was around 5 nm. The ORR activity of Pt/CS was higher than that of a commercial catalyst (TEC10E50E, TANAKA KIKINZOKU KOUGYOU). After the durability test, the activity of Pt/CS remained about 50% of the initial state, although a commercial catalyst showed almost no activity. We concluded that Pt/CS could balance the catalytic activity and the carbon corrosion tolerance.

[1] T. Saida, T. Kogiso, T. Maruyama, *Chem. Lett.*, **45**, 330-332, (2016).

[2] P. Kundu, C. Nethravathi, P. A. Deshpande, M. Rajamathi, G. Madras, and N. Ravishanker, *Chem. Mater.*, **23**, 2772-2780 (2011).

[3] J. Sato, K. Higurashi, K. Fukuda, W. Sugimoto, *Electrochemistry*, **79**, 337-339 (2011).

[4] Y. Li, Y. Li, E. Zhu, T. McLouth, C.-Y. Chiu, X. Huang, Y. Huang, *J. Am. Chem. Soc.*, **134**, 12326-12329 (2012).

[5] K. Cheng, D. He, T. Peng, H. Lv, M. Pan, S. Mu, *Electrochim. Acta*, **132**, 356-363 (2014).

[6] D. Higgins, M. A. Hoque, M. H. Seo, R. Wang, F. Hassan, J.-Y. Choi, M. Pritzker, A. Yu, J. Zhang, Z. Chen, *Adv. Funct. Mater.*, **4**, 4325-4336 (2014).

[7] P. Zhang, W. Tu, R. Wang, S. Cai, J. Wu, Q. Yan, H. Pan, H. Zhang, H. Tang, *Int. J. Electrochem. Sci.*, **11**, 10763-10778 (2016).

[8] P. Mardle, O. Fernihough, S. Du, *Coatings*, **8**, 48-9 (2018).

4:45 PM EN11.14.03

In Silico Design of Niobium Based MXenes for Acidic Electrocatalysis Ebrahim Ghasemy, Kulbir K. Ghuman and Ana Tavares; Institut National de la Recherche Scientifique, Canada

MXenes, as the newest family of 2-dimensional materials, can pave the way toward passing the obstacles against developing novel energy materials. However, among different MXene compositions, negligible attention has been paid to Nb-based MXenes in electrocatalysis, where, Niobium possesses a high number of empty orbitals, providing more opportunities for properties engineering. In addition, various synthesis methods in exfoliating the Nb-based MAX phase can lead to the formation of different terminating groups, each of which can result in different catalytic properties. Up to now, no works have been devoted to perusing the role of terminating groups in varying the MXenes' electrocatalytic properties. Moreover, exploiting computational methods can facilitate the properties engineering of MXenes significantly, by which, the synthesis process can be optimized as a function of each catalytic reaction. In the presented work, by employing DFT calculations, the acidic and basic stability of Nb-based MXenes, terminated by F, S, Cl, FS, FCl, ClS groups, will be deciphered. Furthermore, the effect of each terminating groups on electronic properties and activity of the Nb₂C MXene will be revealed. Therefore, considering the descriptors of the electrocatalytic reactions, the suitability of each Nb₂C MXene in electrocatalysis will be studied.

5:00 PM EN11.14.04

Evaluating the Stability and Catalytic Reactivity of Binary and Ternary Molybdenum Chalcogenides Joseph Perryman; University of California, Davis, United States

The development of precisely tailored catalyst materials is predicated on a fundamental understanding of their composition-structure-function relationships. In this work, rapid microwave-assisted synthetic methods were employed to generate dimensionally controlled binary and ternary chalcogenide materials wherein compositional and structural variations modulated charge transport dynamics, interfacial reaction kinetics, as well as bulk and surface energetics. Through an interplay of synthetic materials chemistry, synchrotron X-ray spectroscopy analysis of electronic and atomistic structure, CO₂ reduction and hydrogen evolution electrocatalysis, as well as computational modeling, material design principles are established and the evolution of electrochemical reactivity is evaluated in order to gain fundamental insights into energy conversion and storage. Of note, catalytic performance metrics for the Chevrel-Phase M_yMo₆X₈ (M = alkali, alkaline, transition or post transition metal; y = 0-4; X = S, Se, Te) and Pseudo-Chevrel-Phase M₂Mo₆X₆ (M = alkali metal; X = S, Se, Te) composition spaces indicate that proton reduction overpotentials decrease significantly over M-X bridging sites with increased ionic character. Selective conversion of aqueous CO₂ to methanol and formate is also observed at mild applied potentials over metal-promoted Mo₆S₈ cluster frameworks, which is explored via electrochemistry as well as X-ray absorption spectroscopy in order to correlate frontier electronic structure with interfacial reactivity. Lastly, to further advance the discovery of new materials, we integrate a new feature regression machine learning methodology for extracting stability and synthesizability metrics for the expansive M_yMo₆X₈ composition space in order to expand the library of functional materials with applications in energy conversion, energy storage, and electronic devices.

5:15 PM EN11.14.05

Extensive Benchmarking of Nonempirical DFT+U Calculations for Band Gap Predictions and Photocatalytic Materials Discovery Nicole Hall¹, Wayne Zhao¹, Yihuang Xiong¹, Iurii Timrov² and Ismaila Dabo¹; ¹The Pennsylvania State University, United States; ²École Polytechnique Fédérale de Lausanne, Switzerland

Molecular hydrogen is a sustainable energy carrier of primary interest to draw down carbon dioxide emissions and accelerate the transition to renewable modes of energy production for transportation, commercial, and residential applications. Photocatalytic materials use solar energy to split water and generate hydrogen, emitting oxygen as the only byproduct, but many of the known water-splitting photoactive semiconductors have limited solar-to-hydrogen conversion efficiency. We present a high-throughput screening protocol that was collaboratively developed to discover water-splitting

photocatalysts [1] and yielded 7 newly predicted photoactive materials from an initial set of 70,150 candidate materials from the *Materials Project* database [2]. We also provide a comparison of the computational and experimental data to test the validity of computational predictions using a Hubbard-corrected density-functional theory (DFT+*U*) approach, in which the *U* parameters are obtained self-consistently from density-functional perturbation theory to impose the piecewise linearity of the total energy with respect to the occupations of a subset of electronic states in the system (typically, of *d* or *f* character) [3]. By systematically comparing DFT+*U* results obtained using nonorthogonalized and orthogonalized atomic orbitals as Hubbard projectors for a representative set of 20 compounds containing transition-metal or p-block (group III-IV) elements, including oxides, nitrides, sulfides, oxynitrides, and oxysulfides, we find that the predicted band gaps are extremely sensitive to the type of projector functions and that the orthogonalized projectors give the most accurate band gaps. These results demonstrate that DFT+*U* may serve as a useful method for high-throughput workflows that require reliable band gap predictions at moderate computational cost.

[1] Xiong, Y.; Campbell, *et al.*, Optimizing accuracy and efficacy in data-driven materials discovery for the solar production of hydrogen, *Energy Environ. Sci.*, 2021, **14**, 2335-2348.

[2] Jain, A.; Ong, S.; Hautier, G.; Chen, W.; Richards, W.; Dacek, S.; Cholia, S.; Gunter, D.; Skinner, D.; Ceder, G.; *et al.*, The Materials Project: A materials genome approach to accelerating materials innovation, *APL Mater.*, 2013, **1**, 011002.

[3] Kirchner-Hall, N.; Zhao, W.; Xiong, Y.; Timrov, I.; Dabo, I., Extensive benchmarking of DFT+*U* calculations for predicting band gaps, *Appl. Sci.*, 2021, **11**, 2395.

5:30 PM EN11.14.06

Development of Three-Dimensional Boron-Doped Diamond Electrodes for (Photo)Electrochemical Reduction of CO₂ and Water Treatment in Water-Based Electrolytes Petr Ashcheulov, Simona Baluchova, Andrew Taylor, Marina Davydova, Joris More-Chevalier and Vincent Mortet; FZU – Institute of Physics of the Czech Academy of Sciences, Czechia

Electrochemical methods are currently seen as a promising approach to convert CO₂ into a variety of value-added chemical products such as formic acid, formaldehyde and carbon monoxide [1]. In addition, the electrochemical approach is commonly utilized for the removal of various contaminants/pollutants from wastewater [2]. However, for these processes to be efficient and economically viable, inexpensive and chemically robust electrodes with long operation life-time in harsh electrochemical conditions are required.

Recently, electrochemical reduction of CO₂ from the seawater and water-based electrolytes into various chemical products using boron-doped diamond (BDD) polycrystalline electrode has been reported [3]. In general, BDD electrodes are known for their superior chemical and mechanical characteristics, and such electrodes can be fabricated using chemical vapor deposition (CVD) techniques in a variety of forms (e.g. planar, porous) on different substrates and at different temperatures [4,5].

In this work, we fabricate nanocrystalline boron-doped diamond BDD electrodes of planar and porous (3D) geometries using the CVD method. Additionally, photoelectrodes based on Si solar cell absorber and BDD electrodes were constructed. We examine fabricated BDD electrodes for the (photo)electrochemical of CO₂ from the water-based electrolytes. Furthermore, fabricated BDD electrodes were utilized for the (photo)electrochemical treatment/degradation of organic pollutants (i.e. phenol) in water-based electrolytes.

This work has been supported by the Grant Agency of the Czech Republic (GACR) contract 19-09784Y.

[1] A. Goepfert *et al.*, *Chem. Soc. Rev.* (2014) 43, 7995-8048.

[2] I. Sirés *et al.*, *Environ Sci Pollut Res* (2014) 21: 8336.

[3] K. Nakata *et al.*, *Angew. Chem. Int. Ed.* (2014) 53, 871 –874.

[4] P. Ashcheulov *et al.*, *Appl. Mater. Today* (2020) 19, 100633

[5] Z. Vlckova Zivcova *et al.*, *Diam. Relat. Mater.* (2018) 87, 61-69

5:45 PM EN11.14.07

Late News: C-N Triple Bond Cleavage via Trans-Membrane Hydrogenation Yuxuan Zhang and Nikolay Kornienko; University of Montreal, Canada

The renewable energy-driven valorization of excess feedstocks into commodity chemicals and societally useful products constitutes a longstanding push in energy and sustainability research. To this end, this work pushes to expand the scope of green electrosynthesis by innovating a new approach to convert acetonitrile, industrially generated in excess and burned off, to in-demand ammonia and acetaldehyde products. Success here was enabled through the use of a Pd-membrane based reactor which abstracted hydrogen atoms from water, which subsequently diffused through to a separate organic compartment in which they carried out the hydrogenation reaction. In this geometry, the reaction proceeded at 5.2 mA/cm² partial current density and 60% Faradaic efficiency towards ammonia generation. Further, the transmembrane hydrogenation approach gave rise to an onset potential of 0.2V_{Ag/AgCl}, surpassing previous state-of-the-art systems by 0.7V. A customized infrared spectroelectrochemical setup was built up to probe the mechanism of the reaction, which was shown to proceed through an imine hydrolysis-like pathway, with the hydrogenation of the NH_x species that remained to be the rate-limiting steps in the process. This work establishes a new route in electrochemical nitrile hydrogenation and general opens up promising avenues in green electrosynthesis.

5:50 PM EN11.14.08

Late News: Mechanism of Electrosynthesis of Amides by Coupling CO₂ Reduction Reaction with Ammonia Junnan Li; Université de Montréal, Canada

CO₂ electroreduction reaction (CO₂RR) is a promising method to produce fuels or useful chemicals in a clean and sustainable way. Electricity can be derived from the conversion of other clean energy sources, such as solar or wind, and the extra electricity can be converted into chemical fuels and stored in the form of chemical bonds. The consumption of CO₂ can also release greenhouse effect, thus this reaction has the potential to solve energy crisis and environmental problems. Various products (carbon monoxide, methanol, methane, ethanol, ethylene, n-propanol) can be produced by CO₂RR, but products with heteroatoms like acetamide or urea are more valuable than these products. Recently, nitrogen source (such as N₂ or ammonia) was added into CO₂RR system and products with C-N bonds was obtained, but the mechanism of the formation of C-N bonds is still unclear. Herein, we combine electrochemical method with in-situ spectroscopy to reveal the intermediate of the reaction, and propose the possible reaction pathways. Cu or CuO nanoparticles (NPs) commercial powder was used as electrocatalyst. CO₂ and NH₄OH was used as the precursor, acetamide and formamide was observed as the final products with heteroatom. Electrolysis experiment shows that formamide is preferential to be formed on Cu catalyst, while CuO is more likely to produce acetamide. The faradaic efficiency (FE) is maximum for the formation of acetamide at -1.8V, which is 0.63%. While for Cu, the formation of formamide reach maximum (3.78% FE) at -2.0V. As the formation of acetamide and acetate share the same intermediate, the production of formamide and formate may also undergo the same reaction pathway at the initial stage of the reaction. In-situ infrared (IR) spectroscopy was conducted to prove this speculation.

5:55 PM EN11.04.07

III-V Core/Oxide Shell Nanowires for Light-Driven Water Splitting [Thomas Dursap](#)¹, Philippe Regreny¹, Cristina Tapia Garcia², Mariam Fadel², Céline Chevalier³, Nicolas Chauvin³, Michel Gendry¹, Alexandre Danescu¹, Matthieu Koepf², Vincent Artero², Matthieu Bugnet⁴ and José Penuelas¹; ¹Univ Lyon, CNRS, INSA Lyon, ECL, UCBL, CPE Lyon, INL, UMR 5270, France; ²Univ Grenoble Alpes, CNRS, CEA, IRIG, Laboratoire de Chimie et Biologie des Métaux, France; ³Univ Lyon, INSA Lyon, ECL, CNRS, UCBL, CPE Lyon, INL, UMR 5270, France; ⁴Univ Lyon, CNRS, INSA Lyon, UCBL, MATEIS, UMR 5510, France

Photoelectrochemical cells (PEC) are one of the most promising approaches for the production of alternative energy carrier in the global effort to diminish the usage of fossil fuels¹. In this context, III-V nanowires (NW) based photoelectrodes² are particularly attractive thanks to their high surface/volume ratio and their efficient charge separation and collection. However III-V NWs suffer from corrosion in aqueous electrolyte that prevents their utilization for long period. In order to avoid the surface degradation of the III-V NW under working conditions, a particular attention has to be given to their surfaces. We proposed to grow an oxide shell transparent to visible light and compatible with the carrier transfer from the III-V semiconductor to the electrolyte to increase the viability of these photoelectrodes.

GaP and GaAs NWs were grown by molecular beam epitaxy (MBE) using the vapor-liquid-solid (VLS) mechanism on silicon substrate and a TiO₂ shell was deposited by atomic layer deposition (ALD). The morphology, interface, and structure of the NWs were studied by scanning transmission electron microscopy and electron energy loss spectroscopy before and after the measurements of their photoelectrochemical activity after combination with suitable hydrogen or oxygen evolution catalysis.⁷

1 N. Armaroli *et al*, *Angew. Chem.* **46**, (2007), 52

2 M. G. Kibria *et al*, *Nat. Commun.* **5** (2014), 3825

3 J. Kamimura *et al*, *Semicond. Sci. Technol.* **31** (2016), 074001

4 K. T. Fountaine *et al*, *ACS Photonics* **3** (2016), 1826

5 L. Gao *et al*, *Adv. Funct. Mater.* **26** (2016), 679

6 N. Kornienko *et al*, *ACS Nano* **10** (2016), 5525

7 This work was done as part of the ANR BEEP project (ANR-18-CE05-0017)

SESSION EN11.15: Fuel Cells and Hydrogen Peroxide

Session Chairs: Chong Liu and Samira Siahrostami

Tuesday Morning, December 7, 2021

EN11-Virtual

8:00 AM EN11.15.04

Insight Into the Synergy Between Metal Transition Phosphide and the Carbonaceous Based Support for High Current Density Hydrogen Production [Maria Isabel D. Garcia](#)¹, Sebastian Murcia¹, Mohammad Qamar² and Joan Ramon Morante¹; ¹Institut de la Recerca de la Energia de Catalunya, Spain; ²King Fahd University of Petroleum & Minerals, Saudi Arabia

There are needs for finding anodic and cathodic electrocatalysts having high efficiencies and durability based on abundant, environmentally friendly materials and low-cost materials. Among the electrode materials fulfilling these requirements, iron phosphide has engaged interest in the last years as electrocatalyst in the cathode. It is composed of two elements highly abundant in the Earth's crust and the synthesis routes are making this catalyst simpler and cheaper. Nevertheless, aside of these performances, support's microstructure is also critical in determining the catalytic activity, selectivity and overall energy efficiency of the supported catalytic nanoassemblies. In this work, ultrathin interconnected carbon nanosheets (CN) are prepared and used as robust support for dispersion of iron phosphide (FeP) nanoparticles, and the resulting catalytic system is evaluated as a low-cost electrocatalyst for hydrogen evolution reaction (HER). A different approach consists of the direct deposition of FeP on the carbonaceous substrate composed by carbon microfibers. Firstly, intermediate iron species are deposited and then, they are converted to FeP by in situ PH₃ generation at 300-400 °C. In both cases, high coverage of the substrate is achieved as observed by SEM. The electrochemical current density-overvoltage curves for HER will be evaluated in both acidic and alkaline electrolytes. The differences between both approaches in terms of reference overpotentials at different low, medium and high current density values and stability tests under cathodic conditions will be addressed. Electrodes under the most outperformed conditions have been tested in a flow cell using a cation exchange membranes (CEM) or anion exchange membranes (AEM) to evaluate the feasibility of the cathodes for HER in continuous operation and the obtained data will be discussed according to the employed support material characteristics.

8:15 AM EN11.15.05

Bimetallic Transition Metal Material as Robust Anode for Oxygen Evolution Reaction [Maria Isabel D. Garcia](#)¹, Guillem Montaña¹, Marc Botifoll², Andreu Cabot¹, Jordi Arbiol² and Joan Ramon Morante¹; ¹Institut de la Recerca de la Energia de Catalunya, Spain; ²Institut Català de Nanociència i Nanotecnologia (ICN2), Spain

Catalytic materials employed in both half-reactions of the water splitting must have high electrocatalytic activity and low Tafel slope for lowering the applied voltage to the electrochemical cell and long-term stability for the durability of the device vanishing the degradation mechanisms. Additionally, these catalyst materials must be composed by Earth-abundant elements and the synthetic route should be cheap and scalable for industrial production. In general, OER required higher overpotentials than HER, then mostly contributing to the required applied voltage in practical devices. Although Ir/Ru oxides have demonstrated good performance for OER, there is a need for research in cost-effective materials that could compete with the precious metal-based catalysts for OER in order to reduce electrode fabrication costs. Cobalt and iron elements have been reported as electrocatalysts active centers enhancing OER. In this work, we investigate the use of CoFeP nanoparticles to obtain ultra-disperse CoFeP particles supported on metallic foam. It allows achieving high current densities with lower overpotentials as the prepared electrode are showing a low Tafel slope. Under operando conditions for OER in alkaline media, chemical species are found to be different from the ones present in the freshly prepared electrode due to the reactivity of the electrocatalytic material under anodic conditions. Nonetheless, after few initial minutes, the electrodes were stable for long-time tests under anodic currents. A deep analysis is performed for identifying the electrochemically active species for OER in alkaline media by XPS, TPR and IR spectroscopy and their functional role discussed taking into account the initial composition of the freshly prepared catalyst.

8:30 AM *EN11.15.07

Designing Electrocatalytic Devices Across Multiple Length Scales from Atom to 3D Integration [Yi Cui](#)^{1,2}; ¹Stanford University, United States; ²SLAC National Accelerator Laboratory, United States

Some of the most important electrocatalytic reactions related to clean energy often involves gas reactants or products, including CO₂, H₂, O₂, N₂ mixed with liquid electrolyte and solid catalysts. The efficient electrocatalytic systems need to consider multiple length design from the atomic scale to 3D electrode integration. Here I will present key results from my lab, including: 1) Atomic design and understanding of catalysts for improving catalytic reaction selectivity and throughput; 2) Tuning the activity of catalysts by lithium ion interaction; 3) A novel concept of self-selective catalyst (SELF-CAT) to rapidly identify the proper catalyst for a certain chemical reaction by having the target reaction itself select its own catalyst. 4) 3D electrochemical concept to optimize the electron and mass transport involving three-phase reactions.

SESSION EN11.16: Photoelectrocatalysis and Electro-Biosystems
Session Chairs: Chong Liu and Samira Siahrostami
Tuesday Morning, December 7, 2021
EN11-Virtual

10:30 AM EN11.16.02

Core-Shell Dendritic Superstructural Catalysts by Design for Highly Efficient and Stable Electrochemical Oxygen Evolution Reaction Yifei Liu and Donglei Fan; The University of Texas at Austin, United States

Efficient, stable, and low-cost oxygen evolution reaction (OER) catalysts are in great demand for the practical application of electrochemical water splitting for energy conversion and storage. This work reports a rationally designed and innovatively fabricated three-dimensional (3D) core-shell dendritically porous OER catalyst that exhibits outstanding and highly reproducible performance. The porous superstructure provides not only substantially enhanced loading capacity of electrochemical catalysts but also easy access of electrolyte to active catalysts. With a facile and designed sulfurization process followed by anodization, core-shell (FeCoNi)OOH@dendritic foam can be obtained and exhibits a remarkably low overpotential of 204.4 mV at a current density of 10 mA cm⁻², which are among the best of the reported FeCoNi OER catalysts. Such value is also highly reproducible and stable with over 18-hour operation time. This excellent performance could be attributed to the synergism of trimetal chemistry, the unique structure with metal/metal sulfide as the conductive core and (oxy)hydroxide catalysts as the active shell, and the enhanced superstructural surface area. This work points towards a synergistic way based on rational design and innovative fabrication for creating scalable, stable, low-cost, and high-performance OER catalysts.

10:45 AM EN11.16.03

Late News: Microfluidic Photoelectrochemical CO₂ Based Reduction Using Perovskite Oxides and Their Nanocomposites José C. Zárate¹, Srinivas Godavarthi², Luis A. Ortíz¹, Jesús A. Díaz¹, Goldie Oza¹ and Clifford Kubiak³; ¹CIDETEQ, Mexico; ²UJAT, Mexico; ³University of California, San Diego, United States

CO₂ emissions have contributed largely to climate change (over 60%), negatively impacting the environment through its increase due to anthropogenic activities; its close relation to the energetic crisis, as a decrease in the supply of energy resources (oil shortage) and its economic impact, forces the search of sustainable and integral solutions. Transforming CO₂ (a very inert molecule with no direct use in the market) to value-added products (renewable fuels and other material precursors) is no easy task, as its reduction is thermodynamically and kinetically unfavored. Taking into consideration costs, mild reaction conditions, energetic requirements, and sustainability of the reaction system to be designed, photoelectrocatalytic (PEC) systems seem to be the pathway to follow towards environmentally-friendly reduction of CO₂; and microfluidic designs offer quite the advantages (lower energetic consumption, higher active surface equaling higher yields, and easier flow dynamics). Therefore a microfluidic PEC device for CO₂-based reduction using SrTiO₃ based nanocomposites is proposed. As photocathodes, nanomaterials are a good choice as larger active surfaces mean greater catalytic activities, and perovskite oxides (SrTiO₃ NPs) are desired in novel PEC systems for their great stability, energy conversion, and low costs. Coupling with g-C₃N₄ NSs in order to generate a heterostructure enhances CO₂ adsorption, and light absorption resulting in greater energetic conversion towards value-added products. The resulting hydrothermally synthesized composite (20% g-C₃N₄/SrTiO₃) has already shown enhanced photoelectrochemical activity, as well as adequate band gap (2.85 eV) and enhanced band alignment (E_{CB} -1.63 V vs. NHE) minimizing possible hydrogen evolution, and maximizing possible CO₂ reduction yield.

11:00 AM EN11.16.04

Late News: Linker Modulated Peroxide Electrosynthesis Using Metal-Organic Nanosheets Kirankumar Kuruvinashetti and Nikolay Kornienko; University of Montreal, Canada

Electrochemical oxygen reduction to peroxide has garnered significant interest as a green alternative to the conventional anthraquinone production process. Electrochemical synthesis offers potentially economical and environmentally friendly route to peroxide (H₂O₂) synthesis. The significant challenge in electrochemical oxygen reduction reaction is to have selectivity for peroxide production vs oxygen reduction to water by modulating the binding strength of intermediates. Herein linker modulated Ni-based metal-organic nanosheets (Ni-MONs) catalysts were investigated as catalysts for peroxide synthesis. The electronic structure of the Ni active sites was tuned by constructing analogous Ni-MONs with electron-withdrawing groups - fluorine (Ni-F-MON) and electron-donating groups such as (hydroxyl, amine) (Ni-OH-MON, Ni-Amine-MON) grafted onto their linkers. The electronic structure of the Ni active sites of the MONs was investigated through a series of electrochemical experiments and X-ray photoelectron spectroscopy measurements. Amongst the Ni-MONs studied, the Ni-MONs with an electron-donating group -hydroxyl and amine have demonstrated higher activity and selectivity. In a gas diffusion electrode set up with Ni-Amine-MON partial current density of 21.7 mAcm⁻² were obtained. Subsequently the system is scaled up to obtain the higher partial current density. Our interpretation is that modifying the Ni electronic structure modulates the binding energy to the *OOH intermediate and is thus the determining factor for H₂O₂ vs. H₂O selectivity in this system and electron-donating groups (hydroxyl and amine) linkers regulated the Ni catalytic activity. This study puts forward design principles towards attaining higher selectivity of electrosynthesis of H₂O₂ through rational modulation of catalytic sites.

11:15 AM *EN11.16.05

CO₂ Photoreduction Using Porous Amorphous Catalysts Giulia Schukraft¹, Ravi Shankar¹, Robert Woodward² and Camille Petit¹; ¹Imperial College London, United Kingdom; ²University of Vienna, Austria

Reshaping our energy portfolio considering the sustainability of global energy resources is central to the European Energy Roadmap 2050. Hence, researchers need to identify efficient routes towards solar fuels production. Unlike H₂ evolution, CO₂ photoreduction has been poorly studied. Given the

scope for CO₂ utilisation in a carbon-constrained future, there is an exciting opportunity to devote targeted research towards CO₂ photoreduction. Photocatalysis is one route towards CO₂ reduction. Yet, the design of a cost-effective, sustainable, efficient and robust photocatalyst remains a highly challenging task.

To date, the majority of studies on CO₂ reduction photocatalyst focuses on crystalline and non-porous materials, with TiO₂ remaining the 40-year old benchmark in the field. Yet, porous amorphous materials can present interesting photocatalytic features. The high surface area allows one to favour access to catalytic sites, tune the strength of adsorption/desorption of reactants/products and possibly control electronic transfer mechanisms. Scaling up amorphous materials synthesis can be easier than for crystalline materials.

Herein, we will discuss our recent work towards the development of CO₂ photoreduction catalysts that present both a porous and an amorphous character. We will highlight in particular our studies on boron nitride and hypercrosslinked polymers, two types of materials that do not involve any rare-earth metals. For both types, we show that the selective conversion of CO₂ into CO is possible under both UV and visible light. Using analytical and spectroscopic tools, we are starting to understand the mechanisms of reaction of these materials.

11:45 AM *EN11.16.06

Photoelectrocatalytic Biofilms for Solar Energy Conversion—A Sustainable Alternative to Bioenergy? Jenny Zhang; University of Cambridge, United Kingdom

Biohybrid systems for solar energy conversion have the potential to combine the strengths of artificial and natural regimes to overcome their respective limitations and deliver efficient electricity and chemical generation. Already, efficient biohybrid approaches exist that couple synthetic 'light' reactions to microbial 'dark' reactions for chemical synthesis. Could photosynthetic microbial 'light' reactions also be coupled to other dark reactions for alternative biohybrid regimes? In this talk, I will show our recent efforts to electrochemically wire into the photosynthetic electron transfer chain in vivo, thereby applying photosynthetic microorganisms as living photoelectrocatalysts. First, we investigate how electron flux from the photosynthetic pathway can be streamlined via exogenous mediators, then we use 3D-printing to design bespoke electrode interfaces that can address the complex needs of the biofilm-electrode interface to optimise photocurrent output. Overall, we will show how this is a more efficient and sustainable means of utilising photosynthetic materials compared to classical bioenergy conversion.

SESSION EN11.17: Nitrogen Reduction
Session Chairs: Chong Liu and Samira Siahrostami
Tuesday Afternoon, December 7, 2021
EN11-Virtual

1:00 PM EN11.17.01

Design of Cu-Ni Based Alloys for Electrochemical Ammonia Production Parastoo Agharezaei and Kulbir K. Ghuman; Institut National de la Recherche Scientifique, Canada

Ammonia is highly used in the fertilizer industry, causing 1% of total GHG emissions. The design of proficient and low-cost catalysts is highly challenging for CO_x-free ammonia production. Alloying non-noble with noble metals is a good approach to obtain elevated catalytic activity. Ni-based materials are known to have a great potential to improve the catalytic activity by tuning the d-band center of Cu and enhance the adsorption energies of intermediate compounds. However, today's development in understanding this reaction remains inexplicable by the lack of a clear image of how catalyst structure can be altered to enhance its properties. This research provides further information on catalytic properties of Cu/Ni alloys for Nitrate reduction reaction (NO₃⁻RR). Using Density Functional Theory (DFT), different compositions of Cu/Ni alloys are modeled. In order to further understand the NO₃⁻RR mechanism, the energy path of the reaction along with the active sites, adsorption energies of reactants and intermediate compounds are investigated and compared in pure Cu and Cu/Ni alloys. This research paves the way for further development and design of economical bimetallic catalysts for NO₃⁻RR.

1:15 PM EN11.17.02

Cobalt doped BiOCl Nano-Coins for Efficient N₂ Photo-Fixation Under UV-Visible Light without Sacrificial Reagent Mohammadjavad Mohebinia and Jiming Bao; University of Houston, United States

Photocatalytic ammonia production is an ideal solution to mitigate carbon dioxide emission in two different ways; firstly, by obsoleting the old Haber-Bosch-based factories and secondly, by storing clean hydrogen fuel in the form of ammonia. However, there is a long way to achieve these goals due to the inertness of nitrogen molecules and rapid recombination of the charge carriers in the photocatalyst nanoparticles. In this work, we have proposed a novel method to modify BiOCl nano-coins by cobalt doping for the photocatalytic nitrogen reduction reaction. The modified BiOCl nano-coins showed a notable photocatalytic NH₃ generation rate in pure water. The strong OER catalytic performance of nano-coins and boosted electron/hole separation efficiency, due to separation of NRR and OER active sites, allowed 4.6 times improvement of ammonia evolution rate. Thus, this study provides a blueprint for the development of new and practical photocatalysts for solar fuel production.

1:30 PM EN11.17.04

Highly Selective Ion Pumping for Product Specific Electrocatalysis Alon Herman, Eran Weil, Itamar Eyal and Gideon Segev; Tel Aviv University, Israel

Highly selective electrocatalysis is one of the key challenges impeding sustainable chemical and fuel production. However, the product distribution of CO₂ and N₂ reduction systems is extremely sensitive to the physical and chemical environment at which the reaction takes place. Thus, control of the electrolyte ionic content at the vicinity of the electrodes can enhance their selectivity towards the desired products. In this contribution we show that ion pumps based on a ratcheting mechanism can drive ions selectively. The integration of ratchet based ion pumps (RBIPs) with electrochemical devices may provide a necessary step for product specific electrocatalysis.

Flashing ratchets are devices that utilize temporal modulation of a spatially asymmetric electric field to drive a non-zero time averaged current. Electronic flashing ratchets have been demonstrated experimentally by pumping electrons through organic semiconductors. We have recently demonstrated experimentally first-of-their-kind ratchet-based ion pumps. RBIPs were fabricated by coating the two surfaces of nano-porous alumina wafers with gold forming nano-porous capacitors. The electric field within the nano-pores is modulated by oscillating the capacitors voltage. Thus, when immersed in solution, ions within the pores experience a modulating electric field resulting in ratchet based ion pumping.

An important hallmark of ratchets is the ability to invert the direction of particle flow with a change in the input signal frequency. The current inversion frequency, which is the input signal frequency at which the particle flux changes its direction, is determined by the potential distribution and particles transport properties. As a result, for a given ratchet, there can be a frequency at which particles with the same charge but different diffusion coefficients are transported in opposite directions resulting in particle sorting. This effect was used to sort gold nanoparticles and micron scale colloidal particles according to size and shape. In this talk we will show how this effect can be used to selectively pump ions in different directions according to their diffusion coefficients. Selective ion pumping may allow tuning the electrolyte content at the vicinity of the electrodes performing the electrochemical reaction independent of their potential thus providing another degree of freedom for the electrochemical process.

1:45 PM *EN11.17.06

Prospects and Challenges for Photoinduced Dinitrogen Fixation [Marta Hatzell](#); Georgia Institute of Technology, United States

Reports of photocatalytic nitrogen fixation on various environmental and synthetic photocatalyst have surfaced for decades. Demonstrations have occurred in both the gas and aqueous phase, and with various reactants (oxygen, nitrogen, water, hydrogen). Nearly all experimental observations suggest that photocatalytic nitrogen fixation is possible at ambient temperature and pressure, and that nitrogen is converted to ammonia through a direct reduction process. This is impactful as it promotes the possibility for ammonia based fertilizer production from environmentally abundant materials using only the sun as a source of energy. This is in contrast with state of the art methods for ammonia production, which are energy and carbon intensive. Despite this promise, there is lack of molecular-scale understanding on how this reaction proceeds, with the reaction pathway and active sites still largely misunderstood.

Given the growing interest in this field, it is critical to begin to demystify how this reaction proceeds through conducting fundamental studies aimed at observing molecular level processes. Thus the main goal of this presentation will be to outline what molecular-scale processes which may allow for nitrogen fixation to proceed on titania. We will provide an overview of a new reaction pathway which was observed through the use of advanced spectroscopy (XPS, IR Spectroscopy, EPR), and electroanalytical testing. Furthermore, we will highlight the role catalyst design may play in enabling aerobic nitrogen fixation. Finally, we will end on discussing the economic and systems related challenges which must be overcome to transition toward a real technology.

2:15 PM EN11.17.07

High-Throughput Electrochemical Characterization of Multi-Element Catalysts [Olga A. Krysiak](#), [Lars Banko](#), [Alfred Ludwig](#) and [Wolfgang Schuhmann](#); Ruhr University Bochum, Germany

Electrochemical processes play an essential role in energy conversion reactions inevitable for the mitigation of climate change. To make these processes at the same time efficient, cost-effective and as climate-neutral as possible new catalysts are needed. One of the approaches in catalyst discovery is combining multiple chemical elements. Adjusting the configuration (i.e., which elements) and composition (i.e., the ratio of elements) allows tailoring the final material's properties. There are about 50 chemical elements that are available for the development of novel and sustainable catalysts (i.e. elements, which are abundant, non-radioactive, and non-toxic). If, for example, five of these potentially plausible elements are combined, there are more than 2 million possible combinations, and this is without considering different ratios of the elements. The various combinations lead to diverse electrochemical properties, making the material disparately suitable for a given reaction. Therefore, the challenge is to find a material from the large number of possible combinations that meets the given electrochemical requirements particularly well. This is like looking for a needle in a haystack, and testing many catalysts usually requires serious investment in time and money. Considering the number of possible compositions of new catalysts, which activity cannot be predicted, finding and synthesizing new materials needs to be coupled with high-throughput characterization to accelerate the discovery process. Speeding up the characterization process should not be accomplished by lowering the quality of measurements but by automatization and unsupervised operation.

Electrochemical characterization needs a three-electrode cell under potentiostatic control. In high-throughput processes, this is successfully realized with the use of a scanning droplet cell (SDC). The set-up consists of a positioning system, an electrochemical probe head and an electrolyte-delivery system controlled by the software. The electrolyte is replaced using a pump to the probe head after each measurement providing a fresh solution for reliable measurements. Reference electrode and counter electrode are built into the probe head. The working electrode is created on the sample by the tip, and its surface area is defined by the tip opening size and can be as small as 0.8 mm².

High-throughput screening of materials libraries by means of SDC was successfully used to discover novel complex solid solution electrocatalysts, e.g. (TiNi)-Cu-Hf-Pd-Zr, in an unconventional search space.[1] Introducing unusual elements allows the discovery of catalytic activity for hitherto unknown compositions. Moreover, it was shown that material libraries with very similar composition spreads could show different activity vs composition trends for different reactions. A combination of high-throughput experimentation with theoretical prediction led to identifying the optimal composition of Ag-Ir-Pd-Pt-Ru complex solid solution electrocatalyst.[2] Unsupervised machine learning together with high-throughput experimentation applied to the Rh-Ir-Pd-Pt-Ru system, revealed that electrochemical activity is governed by the complex interplay of chemical and structural factors.[3] Results obtained from high-throughput experimentation are crucial input data for future data-driven materials discoveries and will be shown in this contribution.

1. O.A. Krysiak,[#] S. Schumacher,[#] A. Savan, W. Schuhmann, A. Ludwig, C. Andronesco, accepted in Nano Research

2. T.A.A. Batchelor,[#] T. Löffler,[#] B. Xiao,[#] O. A. Krysiak, V. Strotkötter, J.K. Pedersen, C.M. Clausen, A. Savan, Y. Li, W. Schuhmann, J. Rossmeisl, A. Ludwig, *Angew. Chem. Int. Ed.* **2021**, 60, 1 – 7

3. L. Banko,[#] O.A. Krysiak,[#] B. Xiao, T. Löffler, A. Savan, J.K. Pedersen, J. Rossmeisl, W. Schuhmann, A. Ludwig, arXiv:2106.08776

2:18 PM EN11.17.09

Late News: Unlocking the CO₂ Electrolysis to Multicarbon Products via Supersaturation Strategy [Kun Qi](#), [Yang Zhang](#), [Huali Wu](#) and [Damien Voiry](#); Institut Européen des Membranes, France

The fast-increasing atmospheric carbon dioxide (CO₂) concentration is a critical challenge for human society. In the quest for developing techniques for carbon neutrality and CO₂ utilization, electrochemical reduction offers a potential route for the conversion of CO₂ into value-added chemicals and fuels is of interest to close the carbon cycle. While active and selective catalysts for CO₂ reduction to the C₁ product have been developed and shown economic output potentials over the past few years, the formation of multi-carbon (C₂₊) products at industry-relevant rates remain challenging.

Among the transition metals, copper-based catalysts are the only candidates able to generate C₂₊ products at significant rates. However, the use of copper is still hampered by poor selectivity towards high-value and high-energy-density multicarbon chemicals with 3 or more carbons (C₃₊). Besides, the most restrictive parameter for CO₂ mass transport resides in its aqueous solubility, which plagues the electrocatalytic performance of the catalysts. From a mechanical point of view, during the CO₂RR, the *CO intermediate has been identified as a key intermediate involved in the C-C coupling to produce multicarbon hydrocarbons and oxygenates. The moderate coverage of *CO on the surface of the catalyst was also found to be beneficial for the CO₂RR into C₃₊ products.

Herein, we report a co-deposition method using CO₂ as a surfactant for the growth of Cu-Alloy catalyst on the electrode. The use of CO₂ during the deposition protects the alloy and avoids the aggregation of Ag on the catalyst surface. Our *operando* Raman measurements revealed that the peculiar alloy structure of the catalyst gets rapidly covered with *CO on the bridge and atop sites, which translates in a record-high selectivity for the 2-propanol (C₃H₈O)

of 57.61 % at a partial current density of 59.33 mA cm⁻². We finally report retentions of both the Faradaic efficiency and the current density for C₃₊ of 98.3 % and 97.5 %, respectively for 200 hours.

SYMPOSIUM EN12

Advanced Materials and Chemistries for Low-Cost and Sustainable Batteries
November 29 - December 8, 2021

Symposium Organizers

Dominic Bresser, Karlsruhe Institute of Technology
Seok Woo Lee, Nanyang Technological University
Weiyang Li, Dartmouth College
Xiaolin Li, Pacific Northwest National Laboratory

* Invited Paper

SESSION Tutorial EN12: Emerging Tools for Battery Technologies—Cost, Materials and Performance Analysis and Prediction
Session Chairs: Weiyang Li, Giuliana Materzanini and Stefano Passerini
Monday Morning, November 29, 2021
Virtual

8:30 AM

A Cost and Resource Analysis of Lithium/Sodium-Ion Batteries [Stefano Passerini](#); Karlsruhe Institute of Technology, Germany

In this tutorial, I will review the use a Battery Performance and Cost model to undertake a cost analysis of the materials for sodium-ion and lithium-ion cells, as well as complete batteries, and determine the effect of exchanging lithium with sodium, as well as the effect of replacing the material used for the anode current collector foil, on the cost. Moreover, I will compare the calculated production costs of exemplary sodium-ion and lithium-ion batteries and highlight the most relevant parameters for optimization. Finally, the major raw materials for lithium-ion cathodes will be examined in terms of potential supply risks because supply issues may lead to increased costs. Through the use of a scenario-based supply and demand analysis, the risks to the supply of lithium and cobalt will be assessed, and implications for battery research will be discussed.

10:00 AM BREAK

10:15 AM

Ab Initio Techniques in Li-Ion Battery Materials—Addressing Ionic Diffusion [Giuliana Materzanini](#); Université Catholique de Louvain, Belgium

In the last two decades, Li-ion batteries have proven to offer some of the best performance among the existing electrochemical energy storage technologies, striving to firm variable renewable generation and mass-market full electrification. A Li-ion battery cell exploits the redox activities of the anode and cathode to generate electricity outside the cell while reversibly intercalating Li ions between the two electrodes through an ionic conducting electrolyte. The difference in electrochemical potential between the electrodes is the thermodynamical driving force of the cell, while its rate capability is governed by the kinetics of the ion transport in the electrodes and in the electrolyte. Ab initio techniques, relying on the knowledge of the physical laws without the need of experimental inputs, provide insight onto the materials' electronic and structural properties, and shed light onto the dynamical processes that underlie the battery performance. Calculation of intercalation potentials, prediction of electrochemical, chemical and phase stabilities, study of dissolution and diffusion phenomena in the electrolytes and electrodes, and characterization of mechanical properties are a few examples of the various applications of the state-of-the-art ab initio approaches for the modelling of battery materials. In this tutorial, we provide an overview of the ab initio methods to study ionic diffusion in battery materials. First, we discuss the simulation approaches to probe the dynamic evolution of a system of atoms via the quantum mechanical potential, namely the Born-Oppenheimer and the Car-Parrinello first-principles molecular dynamics (FPMD) techniques. Thus, the extraction of the diffusion coefficients from the sampled trajectories according to the Green-Kubo relation is described, together with the role of ionic correlations in these systems (tracer/charge diffusion coefficient), and the use of the Nernst-Einstein equation to compute the ionic conductivity from the diffusion. To conclude, we present few benchmark cases from the recent literature and we discuss intrinsic limitations together with recently proposed solutions, as the use of ab initio molecular dynamics in conjunction with machine learning, to give reliable ambient temperature diffusion coefficients that can be directly compared with the experiments.

SESSION EN12.01: Metal Batteries I
Session Chairs: Dominic Bresser and Weiyang Li

Tuesday Morning, November 30, 2021
Hynes, Level 3, Ballroom A

10:30 AM *EN12.01.01

Microstructural Design Principles for Achieving Stable Electrochemical Interfaces for Metal Anodes [David Mitlin](#); The University of Texas at Austin, United States

Lithium metal battery systems (LMBs) are being sought as an ultimate replacement to LIBs, potentially increasing the cell energy by over fifty percent due to the high capacity and low voltage of the metal anode. Analogous improvement in energy is possible with sodium metal batteries (NMBs) and with potassium metal batteries (KMBs), where existing ion insertion anodes can be replaced by plating/stripping metal. However, in all three cases safety and performance are compromised by an unstable solid electrolyte interphase (SEI) that consumes metal ions and electrolyte, and ultimately leads to dendrites. This presentation provides a series of case studies derived from the group's LMB, NMB and KMB research on the microstructural design principles that provide for long-term cycling and fast-charge stability of metal anodes. The approaches may be categorized as the following: a) design of plating/stripping supports and templates with tuned geometry and functionality; b) design of secondary interlayers placed between the metal anode and the separator; and c) design of multifunctional hybrid separators to replace the conventional polymer separators employed with LIBs. It is demonstrated that despite appearing distinct, the efficacy of each in enabling electrochemical stability originates from three fundamental features that are directly interrelated. The wetting behavior of the electrolyte on the anode must be optimized, the wetting/stripping behavior of the metal anode on the current collector must be controlled, and a geometrically and chemically modified SEI must be established. Simultaneously achieving all three leads to stable plating/stripping, while missing even one leads to rapid dendrite growth. Cryogenic FIB cross sections and cryo-TEM are combined to yield new insight regarding film wetting behavior and early dendrite formation in optimized versus baseline specimens, analyzing growth in several representative electrolytes.

11:00 AM EN12.01.02

Iterative Solvent Molecule Tuning for High-Performance Lithium Metal Battery Electrolytes [Zhiao Yu](#), Jian Qin, Yi Cui and Zhenan Bao; Stanford University, United States

Electrolyte engineering has enabled improved cycling of Li metal batteries and anode-free cells at low current densities; however, fast ionic conduction and high-rate capability are desirable yet less-studied. Meanwhile, the understanding of tuning ionic transport in advanced electrolytes is still lacking. Herein, we iteratively design and synthesize a family of fluorinated-1,2-diethoxyethanes (fluorinated-DEEs) as electrolyte solvents. The position and amount of fluorine atoms functionalized on the DEE were found to significantly impact Li cyclability, oxidative stability, and ionic conduction. The partially-fluorinated, locally-polar $-\text{CHF}_2$ is identified as the optimal group rather than fully-fluorinated $-\text{CF}_3$ in common designs. Paired with 1.2M LiFSI, these developed single-salt-single-solvent electrolytes simultaneously enable high conductivity, low and stable overpotential, >99.5% Li || Cu efficiency (up to 99.9%), and fast activation (Li || Cu efficiency >99.3% within two cycles). Combined with high-voltage stability, these electrolytes achieve ~200 cycles in thin-Li || high-loading-NMC811 full batteries and >140 cycles in fast-cycling Cu || microparticle-LFP pouch cells under realistic testing conditions, which stand among the state-of-the-art. The correlation of Li ion-solvent coordination, solvation environments, and battery performance is investigated. Our electrolyte design and systematic study point out the path towards practical Li metal batteries.

11:15 AM EN12.01.03

Ultra-Low Temperature Li Metal Batteries Enabled by Highly Resilient Solid-Electrolyte Interphase [Yiwen Zhang](#) and Weiyang Li; Dartmouth College, United States

One of the key challenges in the development of energy storage devices is the ability to operate efficiently under extremely cold environments (i.e. below -20 °C), especially for batteries in temperature-sensitive applications such as portable electronic devices, transportation, and stationary energy storage. As reported, at low temperature, the increased internal resistance and sluggish ion diffusion in batteries lead to declined charge-delivering capability, which deteriorates cell performance and eventually terminates the power output. Although lithium (Li) metal battery (LMB) with ether electrolyte is considered promising in overcoming these issues due to the low viscosity of ether solvent and its distinctive electrode structure, the low-temperature performance of LMBs remains unsatisfactory. A series of problems are observed upon the anode-electrolyte interphase, including aggravated side reactions, abnormal Li deposition, and dramatically increased solid-electrolyte interphase (SEI) resistance. Thus, building a stable SEI layer on the Li metal anode is critical for the development of low-temperature LMBs.

Here, we demonstrate a dioxolane (DOL)-based electrolyte with dimethyl sulfoxide (DMSO) as the low-temperature additive, which helps to construct a robust SEI layer that possesses uniform structure and good composition consistency even under extremely cold condition. In this electrolyte, DOL works as the primary electrolyte component that defines the basic electrochemical properties, while DMSO further tunes the SEI composition to boost the low-temperature performance. To elucidate the modified microstructure and chemical composition of the SEI film, cryogenic transmission electron microscopy, X-ray photoelectron spectroscopy, and energy-dispersive X-ray spectroscopy are conducted to make a comprehensive investigation. Moreover, a series of electrochemical tests are conducted under extremely cold environments, and results demonstrate that the adjusted SEI is resilient to the stripping and plating cycles of Li metal at temperatures as low as -80 °C. Full cells with lithium iron phosphate as the cathode material are assembled and good electrochemical performance is achieved at -40 °C at 0.2 C. The solvation structure of DMSO added electrolyte is also investigated to fundamentally understand how it affects the SEI formation. Our work establishes fundamental insights into the low-temperature electrolyte additives and paves the road to the further applications of LMBs in harsh environments.

11:30 AM EN12.01.04

Accelerating the Electrochemical Kinetics of Sulfur Intermediates in Lithium-Sulfur Batteries [Fang Liu](#)¹, Geng Sun², Bruce S. Dunn², Philippe Sautet² and Yunfeng Lu²; ¹Stanford University, United States; ²University of California, Los Angeles, United States

The sluggish electrochemical kinetics of sulfur species has impeded the wide adoption of lithium-sulfur battery, which is one of the most promising candidates for next-generation energy storage system. Here, we present the electronic and geometric structures of all possible sulfur species and construct an electronic energy diagram to unveil their reaction pathways in batteries, as well as the molecular origin of their sluggish kinetics. By decoupling the contradictory requirements of accelerating charging and discharging processes, we select two pseudocapacitive oxides to enable the efficient transport of electron/Li⁺ to and from sulfur intermediates respectively. After incorporating pseudocapacitive oxides, the electrochemical kinetics of sulfur cathode is significantly accelerated by a factor of 5 times and 1.8 times, respectively. This strategy, which couples a fast-electrochemical reaction with a spontaneous chemical reaction to bypass a slow-electrochemical reaction pathway, offers a solution to accelerate an electrochemical reaction, providing new perspectives for the development of high-energy battery systems.

SESSION EN12.02: Metal Batteries II & Na-Ion Batteries
Session Chairs: Dominic Bresser and Xiaolin Li
Tuesday Afternoon, November 30, 2021
Sheraton, 2nd Floor, Grand Ballroom

1:30 PM *EN12.02.01

Rational Design of Multivalent Metal Batteries—Enolization Cathode and Nonporous Separator Yan Yao; University of Houston, United States

Batteries based on multivalent metals have the potential to meet the future needs of large-scale energy storage. However, the complexity of multivalent metal-ion chemistries has led to technical challenges. Mg^{2+} interacts strongly with electrolyte solutions and cathode materials, leading to sluggish ion dissociation and diffusion, and consequently low power. With better understanding of electrolyte-electrode interactions and recognizing the strong influence of electrolyte solutions on cathode storage mechanism, fast Mg^{2+} storage could be realized by combining a highly performing single salt electrolyte and heterogeneous enolization redox chemistry in a Mg battery that delivers a specific power nearly two orders of magnitude higher than that of state-of-the-art Mg batteries. In a separate work, we studied zinc plating/stripping behavior in the presence of porous and nonporous separators. We find that adoption of porous separators results in directional metal penetration upon plating and “dead zinc” formation upon stripping. Using a nonporous separator, zinc plating/stripping was limited beneath the separator. The uniform ion flux generated by intermolecular solvent channels leads to a dense and uniform metal deposition morphology and reversible stripping. These results emphasize the microstructure of separators can serve to stabilize metal and provide guidelines for developing novel separators for long-cycle-life aqueous zinc batteries.

2:00 PM EN12.02.02

Bifunctional Surfactants as Electrolyte Additives for High Performance Sodium Metal Anodes Jianmin Luo, Weiyang Li and Yiwen Zhang; Dartmouth College, United States

Sodium (Na) based batteries are the promising alternative to Li-ion batteries due to the similar physical and chemical properties between Na and Li, as well as the natural abundance and therefore low cost of Na resources. Among all possible anodes for Na batteries, Na metal anode exhibits exceptional advantages because of its high theoretical capacity (1166 mAh/g) and low redox potential (-2.71 V vs. SHE). However, highly reactive Na metal anodes suffer from rapid electrode degradation and short-circuit related safety issues caused by the formation of unstable and fragile solid electrolyte interphase (SEI) and dendritic Na growth. Herein, we present a bifunctional and inexpensive electrolyte additive, hexadecyl trimethylammonium bromide (CTAB) that provides a synergistic effect to stabilize Na metal anode from CTA^+ cation and Br^- anion. Previous study on Li metal anode indicated that cationic surfactant used as an electrolyte additive could suppress Li dendrites growth by the role of lithiophobic surfactant cations, whereas the anions are ineffective on the anode protection. However, in this work, **we discovered that the cation CTA^+ and anion Br^- can work synergistically to enhance the stability and electrochemical performance of Na metal anode.** Specifically, sodiophobic CTA^+ can be absorbed onto the Na protuberant areas of the Na metal surface by electrostatic forces, which promotes preferential deposition of Na to surrounding regions by sodiophobic repulsion mechanism, thereby enabling uniform Na plating. More promisingly, Br^- anions can facilitate the formation of a stable NaBr-rich SEI layer, which has been confirmed by the cryogenic transmission electron microscopy (Cryo-TEM). The NaBr-rich SEI layer exhibit low energy barrier for Na^+ transport, which restrain the propensity of dendrite nucleation. We show that with the addition of 5 mM CTAB in the electrolyte, a superior electrochemical performance of Na metal anode with high areal capacity (**up to 30 mAh/cm²**) and high current density (**up to 8 mA/cm²**) can be achieved over long-term cycling for **800 h**. As a proof of concept, the constructed Na-S full cell delivers high performance with a **high cathode loading of 4 mg/cm²**.

2:15 PM EN12.02.04

Low-Temperature Liquid Metals for Next-Generation High-Energy-Density Energy Storage Applications Driven by Interfacial Chemistry Study Xuelin Guo and Guihua Yu; The University of Texas at Austin, United States

Rapidly developing technologies call for sustaining, safe, and cost-efficient rechargeable energy storage devices for portable electronics and electrical vehicles beyond traditional lithium-ion batteries. Alkali metal batteries allowing high battery voltages and high electrode capacities are intensively studied aiming to fulfill this increasing need of efficient energy storage, whereas the dendrite issue as well as interfacial issues are threatening the battery safety, limiting the battery performance, and therefore being hindered in commercialization. Low-temperature liquid metals including mainly fusible alloys are considered as promising alternatives of alkali metals as anode materials thanks to their dendrite-free or self-healing features, as well as superior mechanical and electrochemical properties. Beside the dendrite-free feature, liquid metals could also promise coherent electron and ion conduction at the interfaces in a battery. As another one of the competitive high-energy-density battery components, the solid-state electrolytes have been suffering from the poor interfacial contact, which could potentially be solved by the conformal liquid metal electrodes. Since multiple species of elements can be obtained in a liquid alloy, the interfacial charge selection behavior with various interfaces is an interesting and crucial designing principle that needs further study for deeper understandings. With deeper understanding of the interfacial behaviors and rational designs of battery, liquid metals can promise a bright future for next-generation high-energy-density and safe energy storage applications.

2:30 PM EN12.02.05

Gel Polymer Electrolytes Based on Cross-Linked Poly(ethylene glycol) Diacrylate for Calcium-Ion Conduction Shreyas Pathreker, Saeid Biria, Francielli S. Genier, Fu-Hao Chen, Hansheng Li, Cameron Burdin, Paul A. Chando, Nannan Ding and Ian Hosein; Syracuse University, United States

Calcium batteries are promising alternatives to lithium batteries owing to their high energy density, comparable redox potential, and Earth abundance. However, to meet practical demands in high-performance applications, suitable electrolytes are required, which, for Calcium batteries remains a challenge. Here, we report the synthesis and characterization of poly(ethylene glycol) diacrylate (PEGDA)-based gel electrolytes using calcium salts in a mixture of ethylene carbonate (EC) and propylene carbonate (PC) solvents. We report room-temperature conductivity between 10^{-5} and 10^{-4} S/cm, an electrochemical stability window of ~3.8 V, full dissociation of the salt, and minimal coordination with the PEGDA backbone. Cycling of symmetric Ca metal cells using this gel electrolyte proceeds but with increasing overpotentials, which can be attributed to interfacial impedance between the electrolyte and calcium surface, which inhibits charge transfer. Calcium may still be plated and stripped yielding high-purity deposits and no indication of significant electrolyte breakdown, indicating that high overpotentials are associated with an electrically insulating, yet ion-permeable solid electrolyte interface (SEI). This work provides a contribution to the study and understanding of polymer gel materials toward their improvement and application as electrolytes for calcium batteries¹.

1. Biria, Saeid, Shreyas Pathreker, Francielli S. Genier, Fu-Hao Chen, Hansheng Li, Cameron V. Burdin, and Ian D. Hosein. "Gel Polymer Electrolytes Based on Cross-Linked Poly (ethylene glycol) Diacrylate for Calcium-Ion Conduction." *ACS Omega* (2021).

2:45 PM EN12.02.06

Interfacial Chemistry of Nanoscale Sodium-Ion Solid State Batteries Fabricated by Atomic Layer Deposition Ramsay B. Nuwayhid, Alexander C.

Kozen, David Stewart, Gary Rubloff and Keith Gregorczyk; University of Maryland, United States

Lithium-ion batteries (LIBs) dominate today's renewable energy storage market, however increasing energy storage demands will require use of more abundant materials in order to keep cost under control. Sodium-ion batteries (SIBs) are considered a promising route given its vast abundance but they suffer worse reactivity issues than LIBs. Developing all solid state Na ion batteries (SSBs) is not only needed to ensure device safety but may be enabling for market entry. We propose, building on our architecture-based approach successful in solid-state LIBs¹, to solve the problems mentioned above. This approach uses nanoscale area enhanced topographies (i.e. nanopores, trenches, pillars, etc) to dramatically improve both energy and power density (areal and volumetric). Here we present initial steps toward expanding this concept into solid state Na systems.

We recently developed an atomic layer deposition (ALD) process for sodium phosphorus oxynitride (NaPON), analogous to the well-known lithium phosphorus oxynitride (LiPON) solid-state electrolyte (SSE). ALD NaPON exhibited an ionic conductivity of 2.5×10^{-6} S/cm at 80 °C, comparable to those of ALD fabricated Li⁺ conductors and high enough to use in 3D Na-SSBs.² In this presentation, we will report on the underlying materials chemistry and challenges of fabricating the first thin-film nanoscale Na-SSB using an evaporated Na metal anode and an ALD V₂O₅ (30 nm) cathode, and offer direct comparisons to the analogous lithium-based devices.

V₂O₅ was chosen as the cathode material due to its success in thin-film LIBs and its capability to reversibly intercalate Na⁺ up to a capacity of 235 mAh/g. Initial electrochemical analysis was conducted with NaPON-coated V₂O₅ vs. Na metal in liquid electrolyte cells. The observed redox chemistry suggests that V₂O₅ is sodiated to Na₂V₂O₅ during the NaPON ALD deposition. However, when NaPON-coated V₂O₅ is used with a liquid electrolyte, NaPON acts as a stable solid electrolyte interphase layer, extending cycling lifetime and reducing interfacial resistance. All solid-state device (Na/NaPON/V₂O₅) electrochemical characterization suggests further sodiation of the V₂O₅ cathode during the Na metal evaporation to a fully sodiated Na₃V₂O₅ state. We use TEM, ToF-SIMS, and XPS analysis to infer the underlying processing phenomena and the subsequent electrochemical effects on the Na-SSB. Unlike their sodium analogues, V₂O₅ remains un lithiated during ALD LiPON deposition and subsequent Li evaporation.¹ This finding highlights the nontrivial contrast between a Na/NaPON/V₂O₅ SSB to a Li/LiPON/V₂O₅ SSB, assembled identically except for the Li and LiPON (i.e. same deposition techniques).

1. Pearse, A.; Schmitt, T.; Sahadeo, E.; Stewart, D. M.; Kozen, A.; Gerasopoulos, K.; Talin, A. A.; Lee, S. B.; Rubloff, G. W.; Gregorczyk, K. E., Three-Dimensional Solid-State Lithium-Ion Batteries Fabricated by Conformal Vapor-Phase Chemistry. *ACS Nano* **2018**, *12* (5), 4286-4294.
2. Nuwayhid, R. B.; Jarry, A.; Rubloff, G. W.; Gregorczyk, K. E., Atomic Layer Deposition of Sodium Phosphorus Oxynitride: A Conformal Solid-State Sodium-Ion Conductor. *ACS Applied Materials & Interfaces* **2020**, *12* (19), 21641-21650.

3:00 PM EN12.02.07

Computational Investigation on the Role of Al Doping on Na₂Mn₃O₇ Cathodes for Enhanced Na-Ion Storage Yong-Seok Choi^{1,2}, Begoña Silván^{3,2}, Nuria Tapia-Ruiz^{3,2} and David O. Scanlon^{1,2,4}, ¹University College London, United Kingdom; ²Faraday Institution, United Kingdom; ³Lancaster University, United Kingdom; ⁴Diamond Light Source Ltd., United Kingdom

Owing to its low-cost advantage, Na-ion batteries (NIBs) have been widely studied as a promising candidate competitive with conventional Li-ion batteries (LIBs) for large-scale applications. Nevertheless, the current energy-normalized cost of NIBs (0.14\$/Wh⁻¹) is more expensive than that of LIBs (0.11\$/Wh⁻¹) and the development of high-capacity electrodes for NIBs are essential for future energy storage system. Of electrodes discovered to date, layered Na-Mn-O cathodes have attracted much attention due to its high specific capacity and operating voltage.² These materials commonly accommodate Na ions by the redox reactions between Mn³⁺ and Mn⁴⁺, allowing large theoretical capacity (e.g. 244 mAhg⁻¹ for Na₂MnO₂). However, the Mn³⁺/Mn⁴⁺ redox reaction necessarily accompanies with the Jahn-Teller distortion³ that lowers the capacity retention, which hinders the use of Na-Mn-O based cathodes.

One effective way to avoid the Jahn-Teller effect is to change the chemical composition; recent studies reported that Na₂Mn₃O₇ layered oxides can accommodate Na⁺ ions without the Mn³⁺/Mn⁴⁺ redox reaction and display improved cyclability.⁴ In addition, introducing Al dopants is also known to be effective in soothing the Jahn-Teller effect.⁵ In this context, the addition of Al dopants on Na₂Mn₃O₇ may enable the further enhancement in cathode performance. Still, the effect of Al dopants on Na₂Mn₃O₇ is yet to be elucidated. In this study, using density functional theory calculations, we performed a comparative study between pristine Na₂Mn₃O₇ and Al-doped Na_{2.4}Al_{0.4}Mn_{2.6}O₇ to analyse the effect of Al dopants on the cathode performance. Calculations suggest that the substitution of Al for Mn makes Na⁺ ions to be inserted in various sites other than those in Na₂Mn₃O₇, resulting in smooth voltage profiles with improved capacity. Furthermore, owing to relatively high electronegativity of Al, the addition of Al dopants alters anionic redox reactions and associated structural changes of Na₂Mn₃O₇ upon charge. Based on above findings, we also discuss potential strategies for finding dopants that enable high performance sodium manganese oxide cathodes.

References

- ¹ J. W. Choi and D. Aurbach, *Nat. Rev. Mater.*, 2016, **1**, 1-16.
- ² K. Lu, Z. Hu, Z. Xiang, J. Ma, B. Song, J. Zhang, and H. Ma, *Angew. Chem.*, 2016, **128**, 10604-10608.
- ³ C. Stock, L. Chapon, O. Adamopoulos, A. Lappas, M. Giot, J. Taylor, M. Green, C. Brown, and P. Radaelli, *Phys. Rev. Lett.*, 2009, **103**, 077202.
- ⁴ B. Song, M. Tang, E. Hu, et al., *Chem. Mater.*, 2019, **31**, 3756-3765.
- ⁵ W.-L. Pang, X.-H. Zhang, J.-Z. Guo, et al., *J. Power Sources*, 2017, **356**, 80-88.

3:15 PM *EN12.02.08

The Perspective of Multivalent Batteries Robert Dominko^{1,2,3}, Tjasa Pavcnik¹, Alen Vizintin¹, Sara Drvarič Talian¹ and Jan Bitenc¹; ¹NIC, Slovenia; ²University Ljubljana, Slovenia; ³Alistore ERI, France

Magnesium, calcium and aluminum are promising elements for future low-cost batteries due to the attractive energy density of metals and possible application of metal anodes in battery cells. All three elements are highly abundant in the earth's crust with homogenous distribution on the globe. They are considered sustainable elements for batteries used in renewal energy storage, contributing to the decrease of cell cost.

Besides the above-mentioned benefits, there are several challenges connected with stripping and deposition of the metals, with the appropriate electrolyte formulation compatible with the metal anode and potential cathode materials, with current collectors, the housing of the cell and with the choice of appropriate cathode materials. A combination of multivalent anodes with classical insertion cathodes typically results in low electrochemical activity, while much better activity can be obtained with cathodes that allow coordination redox reaction or conversion redox reaction. Among those, the highest applicability can be obtained with redox-active polymers and sulfur-based cathodes.

In this presentation, an overview of recent achievements in our group in the field of multivalent batteries will be discussed with a focus on the proper selection of battery components in order to achieve electrochemical properties attractive for commercialization.

Acknowledgement: This work is supported HONDA R&D Europe and by the Slovenian Research Agency (research core funding No. P2-0393 and

research project Z2-1864).

References:

- J. Bitenc, K. Pirnat, T. Bančič, M. Gaberšček, B. Genorio, A. Randon-Vitanova and R. Dominko, Anthraquinone-Based Polymer as Cathode in Rechargeable Magnesium Batteries, *ChemSusChem*, 2015, 8, 4128–4132.
- A. Vizintin, J. Bitenc, A. Kopač Lautar, K. Pirnat, J. Grdadolnik, J. Stare, A. Radon-Vitanova and R. Dominko, Probing electrochemical reactions in organic cathode materials via in operando infrared spectroscopy, *Nat. Commun.*, 2018, 9, 661.
- Jan Bitenc, Alen Vizintin, Joze Grdadolnik, Robert Dominko, Tracking electrochemical reactions inside organic electrodes by operando IR spectroscopy *Energy Storage Materials* 21 (2019) 347–353
- A. Robba, A. Vizintin, J. Bitenc, G. Mali, I. Arčon, M. Kavčič, M. Zitnik, K. Bučar, G. Aquilanti, C. Martineau-Corcoc, A. Randon-Vitanova, R. Dominko, *Chem. Mater.*, 2018, 29, 9555-9564.
- J. Bitenc, N. Lindahl, A. Vizintin, M. Abdelhami, R. Dominko, P. Johansson, Concept and electrochemical mechanism of an Al metal anode - organic cathode battery. *Energy storage materials*, Jan. 2020, vol. 24, str. 379-383
- J. Bitenc, A. Scafuri, K. Pirnat, M. Lozinskec, I. Jerman, J. Grdadolnik, B. Fraisse, R. Berthelot, L. Stievano, R. Dominko, Electrochemical performance and mechanism of calcium metal-organic battery. *Batteries & supercaps*, ISSN 2566-6223, [in press] 2020, 14 str.

3:45 PM BREAK

SESSION EN12.03: Poster Session I: Advanced Materials and Chemistries for Low-Cost and Sustainable Batteries
Session Chairs: Seok Woo Lee and Xiaolin Li
Tuesday Afternoon, November 30, 2021
8:00 PM - 10:00 PM
Hynes, Level 1, Hall B

EN12.03.01

A Liquid Metal as a Self-Healing Electrocatalyst to Surpass Shuttle Effect in Lithium Sulfur Batteries Saisaban Fahad and Akihiro Kushima;
University of Central Florida, United States

Lithium sulfur batteries (LSBs) are a promising next generation energy storage technology due to their high theoretical capacity, low cost, and environmental friendliness surpassing that of current lithium ion batteries (LIBs). However, the LSB still has challenges that restricts its practical applications. A major obstacle that limits its performance is the dissolution of long-chain lithium polysulfides into the electrolyte which results in loss of active material and capacity fade during the charge/discharge cycles. Here, we developed a novel sulfur composite with a liquid metal (LM) and graphene oxide dispensed on carbon cloth electrode to achieve a long cycling of lithium sulfur batteries. The liquid nature of the metal results in many advantages. It provides a strong encapsulation of the sulfur particles, which inhibits the polysulfide shuttle effect. In addition, it prevents the detachment of the sulfur particles from the current collector albeit large volume changes and cracking of the sulfur during lithiation and delithiation, maintaining the electron conduction paths. This innovative composite resulted in a high discharge capacity, an outstanding capacity retention over 300 cycles at 0.2 C, and a high coulombic efficiency. Our results demonstrate an effective method to surpass the polysulfide shuttle effect and pave a new way towards practical applications of lithium sulfur batteries by using multifunctional liquid metal composites.

EN12.03.02

Local and Bulk Probe of $K_xV_yMn_{8-y}O_{16}$ Electrochemistry in Li Batteries Diana M. Lutz¹, Mikaela Dunkin¹, Killian Tallman¹, Lei Wang², Shize Yang², Bingjie Zhang¹, Ping Liu², David Bock², Yimei Zhu^{2,1}, Amy Marschilok^{1,2}, Esther S. Takeuchi^{1,2} and Kenneth Takeuchi^{1,2}; ¹Stony Brook University, United States; ²Brookhaven National Laboratory, United States

Manganese oxides have been highly studied as cathode materials for Li-ion batteries (LIBs) due to their low cost, environmentally benign nature, high theoretical capacity, and unique morphologies that allow for facile ion intercalation. Demonstrated here, V-substituted α -MnO₂ was successfully synthesized with no crystalline or amorphous impurities, as evidenced by X-ray diffraction (XRD) and Raman spectroscopy. TEM revealed a morphological evolution from nanorods to nanoplatelets as V-substitution increased, while electron-energy loss spectroscopy (EELS) confirmed uniform distribution of vanadium within the materials. Rietveld refinement of synchrotron XRD described an increase in bond lengths and larger range of bond angles with increasing V-substitution, indicating structural distortion. X-ray absorption spectroscopy (XAS) of the pristine materials revealed the V valence to be above 4+ and the Mn valence to decrease as V content increases. Upon electrochemical lithiation, increasing amounts of V were found to preserve the Mn-Mn relationship at higher depths of discharge, which relates to enhanced structural stability. Electrochemical testing showed the 10% V-substituted sample delivered the highest capacity and capacity retention after 50 cycles and had the lowest polarization resistance according to pulse test results. This enhanced electrochemistry is related to the high level of V-substitution and the nanoplatelet morphology of the 10% V-substituted material. DFT calculations predicted that the high stability of highly oxidized V ions upon lithiation is essential to ensure the structural stability and polarization-resistance by enhancing the stability of the K⁺-centered 2 by 2 tunnel and promoting symmetric structural changes, which likely lead to the observed enhancement in structural stability.

EN12.03.03

Lithium Trivanadate ($Li_{1.1}V_3O_8$) Utilization in Thick Porous Electrodes with High Rate Capacity Upon Extended Cycling Elucidated via Operando Energy Dispersive X-ray Diffraction Alison McCarthy¹, Karthik Malyilvahanan², Mikaela Dunkin¹, Steven King¹, Calvin D. Quilty¹, Lisa House¹, Jason Kuang¹, Kenneth Takeuchi^{1,3}, Esther S. Takeuchi^{1,3}, Alan West², Lei Wang³ and Amy Marschilok^{1,3}; ¹Stony Brook University, United States; ²Columbia University, United States; ³Brookhaven National Laboratory, United States

New energy storage systems require developments in electrode design and architectures to enable high energy density along with high power and fast charge rates. A balance between active material loading and full utilization of the electrode needs to be made when considering conventional battery electrode fabrication techniques such as slurry-cast electrodes and dense pelletized electrodes. In this work, thick porous electrode fabrication techniques have been developed to obtain a higher active mass loading in an architecture which also enables ion and electron transport. Synchrotron-based operando energy dispersive X-ray diffraction (EDXRD) was used to examine the homogeneity of the phase distribution in a thick porous electrode (TPE) of lithiated LVO over extended high rate cycling. Three locations were probed, while cycling at a fast rate of 1C, revealing a homogeneous phase transition across the thickness of the electrode at the 1st and 95th cycles. Continuum modelling results agreed with the EDXRD results, indicating

homogenous lithiation across the electrode upon discharge at 1C and ascribed decreasing accessible active material to be the cause of capacity fade between the 1st and 95th cycles. The model was supported by the observation of significant particle fracture by *ex situ* SEM, consistent with loss of electrical contact. The absence of the beta phase peaks in the EDXRD over extended cycling are consistent with electrochemical accessibility of only part of the active material. Overall, through combining *operando* EDXRD, continuum modeling, and *ex situ* measurements we gained a deeper understanding of lithium vanadate transport properties and the capacity loss mechanism under high rate extended cycling within a thick highly porous electrode architecture.

EN12.03.04

Impact of Charge Voltage on Factors Influencing Capacity Fade—An *Operando* X-Ray Study of Li/NMC622 Batteries During Extended Cycling Calvin D. Quilty¹, Garrett Wheeler², Lei Wang², Alison McCarthy¹, Shan Yan², Killian Tallman¹, Steven Ehrlich², Lu Ma², David Bock², Esther S. Takeuchi^{1,2}, Kenneth Takeuchi^{1,2} and Amy Marschilok^{1,2}; ¹Stony Brook University, United States; ²Brookhaven National Laboratory, United States

Ni-rich NMC, such as NMC622, is an attractive Li-ion battery cathode material due to its balance of energy density, thermal stability, and reversibility. However, a compromise must be struck between higher energy density associated with a more positive upper voltage limit, and better reversibility at lower voltage limits. Improved understanding of structural transformations occurring as a function of voltage window, and their associated impacts on capacity fading, are critically needed to rationalize electrochemical behavior. Through *operando* X-ray characterization of cells cycled at 3-4.3 V and 3-4.7 V both before and after extensive cycling, this study presents an in-depth investigation into the effects of voltage window on the structural transformations of NMC622 over extended cycling. The utilization of this *operando* methodology over many cycles enables the collection of data on the structural transformations that can cause capacity fade as the fade occurs in real time. Cycling at 3-4.7 V, initially led to a higher delivered capacity along with greater lithium extraction and greater structural distortion. However, charging at this higher potential led to significantly more capacity fade along with reduced lithium (de)insertion, increased structural distortion, and significant particle cracking. This study provides important insights into the mechanisms of capacity fade in NMC622/Li-ion batteries, which will enable the design of NMC622 electrodes that deliver both higher capacities and exhibit better capacity retention.

EN12.03.05

Development of Low and No-Cobalt Cathode Materials for Lithium-Ion Batteries Au Nguyen and Donghai Wang; The Pennsylvania State University, United States

High-nickel layered cathode LiNi_xCo_yMn_{1-(x+y)}O₂ material is the center of attention for high energy density cathode materials and sustainable resources. In this work, cathode material with low or no cobalt (0 <= y <= 0.06) was synthesized successfully by the co-precipitation method followed by the lithiation process. The resulted materials have spherical and uniform size distribution morphology. Coatings and dopings (such as transition metal doping and Li containing glass material coating) on these materials were studied to show a significant improvement in cycling stability. The post-cycling TEM and SEM characterization indicate that the doping and coating can reduce the reconstruction layer of the layer structured, high-Ni and low-Co cathode materials and maintain the spherical morphology in contrast to bare control materials. The procedure for synthesizing single-crystals cathode using these precursors was also explored and promising potential for a long-cycling low-Cobalt material.

EN12.03.06

Functional Lithium-Ion Affinity Polymer Binder for Fast-Charging Lithium-Ion Batteries Pei Shi, Yuming Zhao and Donghai Wang; The Pennsylvania State University, United States

The fast charging of lithium-ion batteries (LIBs) is vital for the broad adoption of electric vehicles. However, the poor ionic conductivity of the electrolyte, low electronic conductivity of thick graphite anode electrodes, and increased impedances at electrode/electrolyte interphases upon cycling is the critical barrier to achieving the fast-charging performance of LIBs. The polymer binder of battery electrodes is used to ensure their mechanical integrity. It significantly influences the Li⁺ transport and charge transfer in the electrode materials, particularly for ultrathick electrodes. Herein, a new Li⁺ affinity polymer material is proposed as a binder for graphite anode with a practical level of areal capacity (4 mAh cm⁻²). The functional polymer binder can not only deliver higher ionic conductivity than conventional graphite binder, but it also can facilitate Li⁺ transport in anode by creating additional ion transport pathways through surface conduction when the Li-ion transport rate is limited to a liquid electrolyte at extreme fast charging conditions. As a result, the LiNi_{0.8}Co_{0.1}Mn_{0.1}O₂ || graphite full cell with a high mass loading (3.5 mAh cm⁻²) and high charging rate (6 C) can stably operate over 100 cycles.

EN12.03.07

Electrode Design Considerations for High Capacity Magnetite Anodes Genesis Renders¹, Krysten Minnici², Yo Han Kwon², Lisa House³, Kenneth Takeuchi^{1,3}, Esther S. Takeuchi^{1,3}, Elsa Reichmanis⁴ and Amy Marschilok^{1,3}; ¹Stony Brook University, United States; ²Georgia Institute of Technology, United States; ³Brookhaven National Laboratory, United States; ⁴Lehigh University, United States

Current electrodes for lithium ion technology rely on graphite-based anodes that have a relatively low theoretical capacity (372 mAh g⁻¹). Alternative materials such as transition metal oxides provide higher specific capacities due to multiple electron transfers. Particularly appealing is magnetite, Fe₃O₄, as it is a low cost, earth abundant and environmentally friendly material with the potential to deliver 924 mAh/g. Despite significant research on the design and synthesis of electrode active materials, the design and composition of the electrodes has also been shown to affect the function of the battery including the rate capability and capacity retention. Herein, is the exploration of electrode factors and binders that aid in electron and ion transport of magnetite (Fe₃O₄) based anodes. Water-soluble polymers in conjunction with polyethylene glycol (PEG) are studied to determine the role of carboxylate functionalities on overall function. Overall, this study compares a series of electrode designs to identify materials that can be manipulated to assist overall electrochemical performance of composite Li-ion battery anodes.

EN12.03.08

Investigating the Effects of Doping Layered Lithium Nickel Oxide Lavan Ganeshkumar^{1,2,3}, Christopher Savory^{1,2}, Maud Einhorn^{1,2} and David O. Scanlon^{1,4,3}; ¹University College London, United Kingdom; ²Thomas Young Centre, United Kingdom; ³The Faraday Institution, United Kingdom; ⁴Diamond Light Source, United Kingdom

Lithium ion batteries have long been established as the leading technology for energy storage devices due to their high energy density and longevity¹. Common cathode materials for these batteries are layered oxides. LiCoO₂ (LCO) is a popular layered oxide which is commonly used within the electronic industry. Yet, due to increasing environmental impacts tied with the price of the cobalt, there has been a substantial push for cobalt-free cathode materials, especially for the automotive application².

The isostructural compound LiNiO₂ (LNO) has been identified as the ideal replacement for LCO. This is principally due to LNO's comparably high theoretical capacity, however, the material is affected by mechanical and thermodynamical instabilities. Recent work has demonstrated that substitution strategies can cater for the instabilities whilst also minimising the reduction in capacity^{3,4}. In this study, density functional theory calculations have been

carried out in order to fully understand the doped structure with the aim to find a stable nickel-rich cathode with a high theoretical capacity. Experimentally it has been reported that the ground state structure of LNO has the $R3m$ space group. However, computational calculations have demonstrated that it is in fact the $P2_1/c$ structure⁵. Using the true ground state structure, point defects will be investigated in these cathode materials in order to fully understand the doped structure.

References

- [1] J. Peres, C. Delmas, A. Rougier, M. Broussely, F. Pertion, P. Biensan and P. Willmann, *Journal of Physics and Chemistry of Solids*, 1996, **57**, 1057-1060.
- [2] P. Zehetmaier, A. Cornélis, F. Zoller, B. Böller, A. Wisnet, M. Döblinger, D. Böhm, T. Bein and D. Fattakhova-Rohlfing, *Chemistry of Materials*, 2019, **31**, 8685-8694.
- [3] U. Kim, D. Jun, K. Park, Q. Zhang, P. Kaghazchi, D. Aurbach, D. Major, G. Goobes, M. Dixit, N. Leifer, C. Wang, P. Yan, D. Ahn, K. Kim, C. Yoon and Y. Sun, *Energy & Environmental Science*, 2018, **11**, 1271-1279.
- [4] H. Ryu, G. Park, C. Yoon and Y. Sun, *Journal of Materials Chemistry A*, 2019, **7**, 18580-18588.
- [5] S. Siculo, M. Mock, M. Bianchini, K. Albe, *Chem. Mater.* 2020, **32**, 10096–10103.

EN12.03.09

A Comparative Study of Electrolytes for Next Generation High Power Li-Ion Batteries Based on LNMO/LTO Chemistry Sidsel Hanetho¹, Peter Molesworth¹, Kaushik Jayasayee¹ and Nils Wagner^{1,2}; ¹SINTEF Industry, Norway; ²Norwegian University of Science and Technology, Norway

The application of secondary batteries for electric propulsion, personal consumer electronics as well as power tools has grown immensely over the last decade and battery chemistries can be tailor made to meet the requirements of the application. Super high charge rates and cycle-life can be achieved employing zero strain anodes based on LTO ($\text{Li}_4\text{Ti}_5\text{O}_{12}$). With a (de)intercalation potential of 1.55V vs. Li/Li^+ , LTO based batteries are inherently safer as lithium plating at high charge rates is omitted.

However, the high operation potential and the rather low specific capacity of LTO (~170 mAh/g) comes with the cost of a reduced cell potential and hence gravimetric and volumetric energy density. Pairing LTO based anodes with high capacity cathodes such as NCA ($\text{LiNi}_{0.8}\text{Co}_{0.15}\text{Al}_{0.05}\text{O}_2$) or NMC 811 ($\text{LiNi}_{0.8}\text{Mn}_{0.1}\text{Co}_{0.1}\text{O}_2$) increases the energy content of such a battery concept. Yet, these materials rely on cobalt, which is not viable from an ethical nor sustainable perspective. A more pronounced effect with respect to the energy density as well as sustainability is apparent when pairing LTO anodes with high voltage materials such as LNMO ($\text{LiNi}_{0.5}\text{Mn}_{1.5}\text{O}_4$). This spinel cathode has a rather moderate capacity of 147 mAh/g, but an almost 1 V higher intercalation potential compared to layered oxides. This combination could in principle increase the gravimetric energy density of LTO based cells by up to 30% compared to a NMC442/LTO cell. Unfortunately, the LiPF_6 containing carbonate-based electrolytes are deemed inapplicable at these potentials, and a cobalt free LTO based battery with increased energy is contingent on a high voltage electrolyte that allows for high cycling stability.

This study screens the cyclability of LNMO/LTO full cells with alternative electrolytes aiming for a high voltage tolerable solution with adequate properties such as conductivity, safety, and operational temperature. Alternative solvents such as sulfones, nitriles and fluorocarbonates and combinations thereof, as well as different high voltage additives, are screened and characterised in this study. The results are benchmarked against a state-of-the-art electrolyte based on LiPF_6 in EC/EMC.

EN12.03.10

Revisiting Polyethyleneimine as the Basis for Solid Polymer Electrolytes (SPEs) for Next Generation Li-Ion Batteries Peter Molesworth, Wilhelm R. Glomm, Marius Sandru, Roberto Scipioni, Le T. Truong and Nils Wagner; SINTEF Industry, Norway

Replacement of liquid electrolytes in Li-ion batteries with all solid systems based upon polymers (SPEs), ceramics or composites will enable Li-ion batteries to achieve enhanced safety characteristics by reducing the flammability, removing solvents and providing resistance to lithium metal dendrite formation. To achieve this safety goal, it is critical that these replacements function without plasticiser, or the need for even small amounts of solvent additives. However, the potential benefits of SPEs are tempered by reduced Li^+ conductivity when contrasted to conventional liquid systems, and the need to run at elevated temperature to ensure the highest possible conductivity.

Much effort has been directed at the replacement of polyethylene oxide (PEO) which, despite significant effort cannot be easily used above 4 V. PEO is vulnerable to oxidation and degradation caused by Li salts and electrode by-products under operating conditions. Replacement for PEO has involved the study of many systems including polyesters, polycarbonates and poly nitriles, with more exotic systems looking at co-polymers and composite SPEs. Polyethyleneimine (PEI), is the nitrogen bearing analogue of PEO, and contains NH which allows for Li salts anion sequestration via H-bonding.

Theoretically, it should be weakly Li co-ordinating and strongly anion-coordinating, thus promoting Li^+ transport. However, early studies have shown low conductivity for PEI systems, thought in part to be due to high crystallinity.

This study will look at the preparation of novel, plasticiser free polyethyleneimine (PEI) co-polymers designed with the aim of reducing crystallinity in the SPE. The route from monomer to SPE, and subsequent testing and benchmarking against PEO systems will be shown. Performance data from studies using a flexible cell solution, that allows simultaneous, *in operando* measurement of SPE thickness under electrochemical characterisation, at a range of temperatures will be shown. This method allows for accurate determination of SPE conductivity and Li^+ transference number at different temperatures.

EN12.03.11

Plasmon-Enhanced Lithium–O₂ Batteries Kyunghye Chae, Filipe Marques Mota and Dong Ha Kim; Ewha Womans University, Korea (the Republic of)

Rechargeable lithium–oxygen batteries have high theoretical energy density (~3600 Wh kg⁻¹). During operation, oxygen undergoes a reduction reaction (ORR) to generate the discharge product of Li_2O_2 , which is decomposed during the recharge process with oxygen evolution (OER).¹ However, this recharging process is primarily disturbed by the large overpotential attributed to the sluggish OER kinetics. Very recently, photo-assisted $\text{Li}-\text{O}_2$ batteries with semiconductor-containing cathodes have gained attention as a promising approach for enhanced energy storage.² Plasmonic materials (such as Au, Ag, Cu, Pd, and Al) have unique properties interacting with light, known as surface plasmon resonance (SPR).³ Under light illumination, plasmonic effects such as near-field enhancement, FRET, local heat, and hot carriers have found increasing application in catalysis. In this study, we demonstrate plasmonic effect in the $\text{Li}-\text{O}_2$ battery system by incorporating gold nanoparticles on the Ketjen Black (KB) cathode with different amounts and sizes. Upon light irradiation, during discharge, the presence of plasmonic Au NPs induce a morphology change to thin and small Li_2O_2 particles, which can be easily decomposed during the charging process. Most importantly, during both discharging and charging processes, the hot carrier from plasmonic Au NPs help to form and decompose the Li_2O_2 with decreasing charge voltage. As a result, the cell with Au NP/KB shows a significant increase in the round-trip efficiency from 75.2 to 80.2%. Our approach, further supported by a meticulous analysis of the near-field enhancement and local heat effects, is the first report individually showcasing the promise of plasmonic metal nanostructures in high-energy storage.

References

- [1] Y.-C. Lu, B. M. Gallant, D. G. Kwabi, J. R. Harding, R. R. Mitchell, M. S. Whittingham, Y. Shao-Horn, *Energy Environ. Sci.* 2013, **6**, 750.

- [2] P. Tan, X. Xiao, Y. Dai, C. Cheng, M. Ni, Photo-assisted non-aqueous lithium-oxygen batteries: progress and prospects, *Renew. Sustain. Energy Rev.* 2020, 127, 109877.
- [3] S. V. Boriskina, H. Ghasemi, G. Chen, *Chem. Rev.* 2016, 116(24), 14982-15034.

EN12.03.12

3D Network of Sepia Melanin and N,S-Doped Graphitic Carbon Quantum Dots for Sustainable Electrochemical Capacitors [Abdelaziz M. Gouda](#); Ecole Polytechnique Montreal, Canada

Organic electrode materials operating in aqueous electrolytes offer the opportunity to avoid toxic, critical and expensive materials but often feature limited cyclability. In this work, we report on a 3D network composite material, based on natural melanin (sepia melanin, extracted from the ink sac of cuttlefish) and nitrogen and sulfur doped graphitic carbon quantum dots (N,S GCQDs). N,S GCQDs not only improve the conductivity of the formed composite but also provide functional groups and active sites, and add faradaic activity for better electrode wettability and electrochemical performance. We also investigated the effect of various undoped and doped CQDs, synthesized from acetic acid and sucrose, on the electrochemical performance of sepia melanin, a quinone macromolecule. The sepia/N,S GCQD (8:2 W/W) composite shows optimum areal capacitance (ca. 180 mF/cm²) that is about 2 times higher than sepia alone (ca. 77 mF/cm²) with enhanced charge transfer resistance (1 ohm for sepia/N,S GCQDs compared to 10 ohms for sepia) evaluated through electrochemical impedance spectroscopy. Sepia/N,S GCQD symmetric supercapacitor in 0.5 M Na₂SO₄ aqueous electrolyte features promising capacitance retention ca. 92% after 10 000 cycles at 5 A g⁻¹, 100% coulombic efficiency, 11 μW h cm⁻² and 102 mW cm⁻² maximum energy and power densities. This work aims at easy preparation of stable and potentially biodegradable supercapacitor electrode materials from green resources for applications in environmentally benign electrochemical energy storage devices.

EN12.03.14

Highly Stable Energy Storage Devices Based on Electrospun Mesoporous Mn-V-O@C Nanofibers [Nageh K. Allam](#); American University in Cairo, Egypt

Supercapacitors (SCs) are being considered the next-generation power storage devices due to their many favorable properties. In this regard, mesoporous nanostructures are excellent supercapacitor electrodes as they enjoy a large number of active sites and high surface area promising the utilization of the full capacitance of the active materials. In this study, we report on the assembly of electrospun, binder-free mesoporous Mn_{0.56}V_{0.42}O@C fibrous electrodes. The morphological and structural analyses of the fabricated Mn_{0.56}V_{0.42}O@C electrodes were investigated using field emission scanning electron microscopy (FESEM), high-resolution transmission electron microscopy (HRTEM), and glancing angle X-ray diffraction (GAXRD). The X-ray photoelectron spectroscopy (XPS) and GAXRD confirm the formation of Mn_{0.56}V_{0.42}O nanofibers and their successful bonding to carbon during crystal growth. Those fibrous composite electrodes showed excellent specific capacitance of 668.5 F g⁻¹ at 1 A g⁻¹. The highly obtained capacitance is attributed to the multiple oxidation states of the Mn-V oxides, the binder-free electrodes, surface roughness, and the mesoporous nature of the fabricated nanofibers. The asymmetric supercapacitor composed of the mesoporous Mn_{0.56}V_{0.42}O@C nanofibers as the positive electrode and graphene hydrogel as the negative electrode possesses ultrahigh energy density of 37.77 W h kg⁻¹ and a power density of 900 W kg⁻¹ with superior Coulombic efficiency over 13000 charge/discharge cycles.

EN12.03.15

Late News: Electrodeposition for Low-Cost, Water-Based Li-Ion Battery Electrode Manufacturing [Kevin Sylvester](#); PPG Industries, United States

The state-of-the-art manufacture of lithium ion battery (LIB) cathodes is slot-die coating of a high viscosity slurry consisting of active materials, conductive additives, and a polymeric binder in N-methyl-2-pyrrolidone (NMP). The operation of slot-die is costly due to the 2-coat/2-cure electrode processing and the use of NMP solvent, which is an expensive consumable with serious health concerns. An alternative approach is the use of waterborne binder systems applied to metal foils using electrocoat. Electrocoat is a process widely recognized to be a high-throughput, low cost, coating application method that allows simultaneous coating of both sides of metal. This presentation will demonstrate the development of novel binders to enable electrodeposited lithium-ion battery electrode coating system. The novel binders were designed for flexibility, ionic mobility, and compatibility with high-energy density active materials and formulated to result in stable water-based cathode coating systems. Furthermore, electrodeposition process parameters were explored and validated in proof-of-concept, semi-continuous lab scale testing. Compared to the conventional NMP based coatings with slot-die process, the electrocoat process is environmentally friendly and capable of reducing the cell costs by at least 20% while improving battery performance.

EN12.03.16

Late News: Ni Coated Iron Fluoride Cathode for Lithium-Ion Batteries [Hyeong Cheol Roh](#), Young Ah Park, Ji Hyeok Choi, Jisu Na, Jeong Hye Jo and Young Soo Yoon; Gachon University, Korea (the Republic of)

Iron fluoride (FeF₃·0.33H₂O) is a candidate for Lithium Ion Battery (LIB) due to great theoretical capacity and low cost. However, the poor electric conductivity hinders its application to LIB. The electric conductivity of cathode part is factor that influence to battery performance such as capacity and cycle stability. Thus, conductive materials are essential for improve electric conductivity. Generally, composite with carbon material for example Carbon Black (CB) and Multi-Wall Carbon Nano-Tubes (MWCNTs) are applied [1]. Nevertheless, poor cycle stability is an obstacle to become the dominant cathode material in the LIB market. Herein, we suggest that electro-less Nickel plating on FeF₃·0.33H₂O powder for improving electric conductivity. We carried out X-Ray Diffraction pattern analysis (XRD), Scanning Electron Microscopy (SEM), Transmission Electron Microscopy (TEM) and Energy Dispersion Spectroscopy (EDS) for material characteristics. Also, we carried out Four-point probe, charge-discharge test and Electrochemical Impedance Spectroscopy (EIS) for electrochemical properties. Ni layer which is coating on iron fluoride powder layer with thicknesses of 10 nm~ 20 nm is observed by SEM and TEM. Respectively, Ni-coated FeF₃·0.33H₂O powder show 150% increased electric conductivity than FeF₃·0.33H₂O powder. Also, It shows good capacity up to 150 mAhg⁻¹ at 0.2C (cut-off voltage 1.0V) and capacity retention ~80% after 50 cycles.

Reference

- [1] Liu, Li, et al., *Journal of Power Sources* 238 (2013), 501-515.

EN12.03.17

Enhanced Mobility of Ions in Polymer Electrolytes with the Addition of Inorganic Nanofibers [Mounesha Garaga](#)¹, [Sahana Bhattacharyya](#)^{1,2}, [Domènec Paterno](#)³, [Sophia Suarez](#)^{3,2} and [Steven G. Greenbaum](#)^{1,2}; ¹Hunter College-CUNY, United States; ²CUNY Graduate Center, United States; ³Brooklyn College, CUNY, United States

Polymer electrolytes have received increasing attention in battery materials research and development. Their performance can be improved with addition of ionic liquids (ILs), which increases the ionic conductivity and provides enhanced safety. In a recent study, self-healing capability that reduces lithium dendrite formation at the electrolyte/electrolyte interface has been reported, for example, in PVDF-HFP-ILs electrolyte containing Al₂O₃ nanofibers. [1] In

this work, a series of PVDF-HFP-ILs with different ratios of Al₂O₃ nanofiber content were prepared through solution cast technique. The dynamics of ions confined within polymer-Al₂O₃ matrix were explored by impedance and pulsed field gradient NMR spectroscopy. The distribution of Al₂O₃ nanofibers in the polymer network was probed through SEM-EDX analysis. Lastly, the local environment of ions and their interaction with polymer and Al₂O₃ nanofibers were established through a detailed solid-state NMR analyses detecting ¹H, ²⁷Al, ¹³C, ¹⁹F, ⁷Li nuclei including 2D ¹³C(¹H) HETCOR experiments. In addition to mechanical reinforcement, enhancement of ionic conductivity was observed with the addition of Al₂O₃ nanofibers.

1. T. Chen, W. Kong, Z. Zhang, L. Wang, Y. Hu, G. Zhu, R. Chen, L. Ma, W. Yan, Y. Wang, J. Liu, and Z. Jin, *Nano Energy* **54**, 17 (2018).

EN12.03.18

Late News: Engineering One Dimensional Organic Material for Ultra-High Rate Pseudocapacitive Energy Storage [Mingyu Jung](#) and [Hoseok Park](#); Sungkyunkwan University, Korea (the Republic of)

Among the electrochemical energy storage devices, batteries have attracted tremendous attention of scientific society due to its amazing feature of high power, good cycle life, tunable energy density. The development of active and safe organic materials for electrochemical storage devices is another area of interest for electrochemical energy storage system, which can be contained low cost, natural abundance, possibly green compounds (i.e., C, H, O, N or S), and simple synthesis. [1] Until now, many organic materials have been investigated but only conducting polymers are used for energy storage system and others restricted due to their electrical conductivity issue and material loading. Herein, we attempted new material and engineering strategies to resolve the key issues facing the electrochemical energy storage system. Our material with new synthesis approach is able to offer optimistic electrochemical performance and reach unmatched ultra-high rate pseudocapacitive performance.

References

Jouhara, A., Dupré, N., Gaillot, A. C., Guyomard, D., Dolhem, F., & Poizot, P, *Nat. Commun.* 2018, 9(1), 4401.

SESSION EN12.04: Battery Sustainability
Session Chairs: Weiyang Li and Xiaolin Li
Wednesday Morning, December 1, 2021
Hynes, Level 3, Ballroom A

10:30 AM *EN12.04.01

Sustainability in 3D—Distributing Local Electrochemistry by Wiring Transport Functions in Architected Electrodes [Debra R. Rolison](#), Brandon J. Hopkins, Jeffrey Long, Jesse S. Ko, Christopher N. Chervin, Megan B. Sassin, Ryan H. Deblock and Joseph F. Parker; U.S. Naval Research Laboratory, United States

A sustainable, carbon-neutral future will be an aspiration, not a reality, without cost-effective energy storage. Batteries will be a critical technology in the suite of choices for energy storage, especially for electrification of vehicles. But shouldn't batteries themselves be sustainable? We evaluated the supply risk of elements versus their abundance in the earth's upper crust [1]. A supply risk of 1 or less and an abundance above 0.003 wt% includes such battery-relevant elements as Ni, Zn, S, Mn, Ti, Fe, and Al. Our team has focused on rechargeable zinc-based batteries whose aqueous electrolytes impart a safer battery chemistry over lithium-based batteries as well as competitive gravimetric and volumetric energy at the system-level. Designing electrodes as architectures in which the entire volume of the electrode is electron- and ion-wired in 3D distributes the available electrified interface thereby lowering local current density. Formulating zinc as a sponge creates an alkaline anode that cannot form zinc dendrites. Similarly, formulating layered MnOx as a nanometric coating throughout a carbon nanofoam improves the rate performance of zinc-ion cathodes.

[1] B.J. Hopkins, C.N. Chervin, M.B. Sassin, J.W. Long, D.R. Rolison, J.F. Parker, *Sustain. Energy Fuels* **2020**, 4, 3363–3369.

[2] J.S. Ko, M.B. Sassin, D.R. Rolison, J.W. Long, *Sustain. Energy Fuels* **2018**, 2, 626–636.

11:00 AM EN12.04.02

Securing Li Resource for Sustainable Battery Technology Development [Chong Liu](#); University of Chicago, United States

The demand for lithium has grown tremendously over the past decades due to Li-ion battery development for electric vehicles, portable electronics, and stationary energy storage. Electrochemical intercalation is a new platform method for separation. It allows selective Li extraction from complex aqueous systems such as brines and seawater. However, the high concentration of Na poses a great challenge to compete (co-intercalate) with Li during extraction. In this talk, I will present the host electrode materials' structural response upon co-intercalation of Li and Na which have big ionic radius differences. I will also discuss strategies to promote Li intercalation during co-intercalation from both aspects of materials design and electrochemical methods development.

11:15 AM EN12.04.03

Redox-Active Polymers Designed for the Circular Economy of Energy Storage Devices Siew Ting Melissa Tan, Alberto Salleo and [Alexander Giovannitti](#); Stanford University, United States

Electrochemical energy storage is a keystone to support the rapid transition to a low carbon emission future for grid storage and transportation. While research on electrochemical energy storage devices has mostly dealt with performance improvements (energy density and power density), little attention has been paid to designing devices that can be recycled with low-cost and low environmental impact. Thus, next-generation energy storage devices should also address the integration of recyclability into the device design. In this talk, we present the development of recyclable energy storage devices based on solution processible redox-active conjugated polymers [1]. The high electronic and ionic charge transport in these polymers enables the operation of single-phase electrodes in aqueous electrolytes with C rates >100 with excellent electrochemical stability when charged to 1.2 V. Finally, we demonstrate the recyclability of these devices, achieving >85% capacity retention in each recycling step and recycled devices twice. Our work provides a new direction for developing recyclable devices for sustainable energy storage technologies.

[1] D. Moia, A. Giovannitti, A. A. Szumska, I. P. Maria, E. Rezasoltani, M. Sachs, M. Schnurr, P. R. F. Barnes, I. McCulloch, J. Nelson, *Energy Environ. Sci.* **2019**, 12, 1349.

11:30 AM EN12.04.04

Hard Carbon Derived from Avocado Peels as a High-Performance Anode Material for Sodium-Ion Batteries [Francielli S. Genier](#)¹, Shreyas Pathreker¹, Robson Schuarca¹, Mohammad Islam² and Ian Hosein¹; ¹Syracuse University, United States; ²State University of New York at Oswego, United States

Sodium-ion conduction is a promising alternative to lithium-ion batteries (LIB). The advantages of sodium include higher natural abundance, similar physicochemical properties to lithium, and lower cost of battery active materials. However, a simple technology transference from LIB to sodium-ion batteries (SIB) is impeded by differences in intercalation mechanisms. Particularly, graphite, an established anode material in LIBs, is unsuitable to SIBs because the interlayer distance between its graphene sheets is too small for effective Na⁺ insertion. For this reason, some of the preferred anode materials for SIBs are disordered carbons with larger interlayer spacing, such as hard carbons. Hard carbons (HCs) also have the advantage of being predominately produced by the carbonization of biomass and residues, which contributes positively to the environmental and economic impact of SIBs. However, the method of HC production often includes chemical activation steps and high carbonization temperatures. In this work, we produced HC from avocado peels by simply water washing and relatively mild temperatures of carbonization (900 and 1100 °C). We chose avocados due to the considerable waste generated and its constant increase in consumption. Avocados generate waste from their peels, seeds, and parts of the pulp, which can amount to a total of up to 30% of its weight in solid waste. Efficient ways to process and repurpose this waste are especially relevant due to the continuous market growth of avocados. In 2019, they were the 8th most consumed fruit or vegetable in the USA, partially due to lifestyle trends and potential health benefits. To the best of our knowledge, the possibility of producing HC from avocado peels for energy storage has never been explored. HC produced by avocado peels was characterized regarding its crystalline properties (XRD), surface area and porosity (BET and BJH analysis), morphology and atomic composition (SEM-EDX), and degree of graphitization (Raman spectroscopy). The material characterization revealed the conversion of the avocado peels in carbon powders with a carbon content of > 92 at. %, graphene interlayer distances of 3.95 Å (superior to the required for Na⁺ intercalation), pore size of approximately 4.8 nm, and degree of graphitization of 0.96. After confirming the suitability of the produced HC as anode materials, electrochemical characterization was carried out with coin cells containing HC anodes and sodium metal discs as cathodes. Our samples demonstrated reversible intercalation and deintercalation of sodium ions and excellent cycling performance, namely, a reversible capacity of 352.55 mAh/g at 0.05 A/g, rate capability up to 86 mAh/g at 3.5 A/g, capacity retention of >90%, and 99.9% Coulombic efficiencies after 500 cycles. This study shows for the first time avocado peels as a sustainable source to produce hard carbon that can provide excellent anode performance in sodium-ion batteries.

11:45 AM EN12.04.05

Critical Sustainability Evaluation of Multi-doped SnO₂ as Anode Material for Li-Ion Batteries and In-Depth Insights into the Synergistic Impact of the Dopants [Adele Birozzi](#)^{1,2}, [Jakob Asenbauer](#)^{1,2}, [Sebastián P. Bautista](#)^{1,2}, [Marcel Weil](#)^{1,2}, [Thomas E. Ashton](#)³, [Alexandra R. Groves](#)³, [Jawwad Darr](#)³ and [Dominic Bresser](#)^{1,2}; ¹Helmholtz Institute Ulm, Germany; ²Karlsruhe Institute of Technology, Germany; ³University College London, United Kingdom

Tin oxide-based materials have been intensively investigated as alternative anodes for lithium-ion batteries due to their high specific capacity, non-toxicity, and ease of handling.^[1] However, the initial formation of Li₂O upon lithiation is essentially irreversible, which has a severe effect on the first cycle Coulombic efficiency and the reversibly achievable capacity upon cycling.^[2] It has been shown that the incorporation of transition metal dopants can address this issue, as it enables the reversible formation of Li₂O. The choice of the dopant, however, plays a critical role for the long-term cycling stability, rate capability, and eventual energy density of the resulting lithium-ion cells.^[3] Herein, we show that the incorporation of specific combinations of different dopants allows for further tailoring the electrochemical properties. We also demonstrate the production of such materials using a scalable continuous hydrothermal flow method. The performance of the best performing composition was further improved by applying a carbonaceous coating. The electrochemical investigation of the coated anode material was conducted in half-cells and in high-energy full-cells using high-voltage LiNi_{0.5}Mn_{1.5}O₄ as active material for the cathode^[4] – in addition to the realization of some large-scale battery cells to power a remotely controlled model car. Following these first scale-up activities, we conducted a preliminary life cycle assessment to compare the sustainability and suitability of such materials with the state of the art. Simultaneously to these rather application-oriented research, we performed also an in-depth investigation of the synergistic impact of the different dopants via ex situ synchrotron X-ray absorption spectroscopy to elucidate the de-/lithiation mechanism at the atomic scale. This comprehensive and extensive analysis provides additional insights into the potential application of (multi-doped) SnO₂ for lithium-ion batteries.

References

- [1] F. Zoller, D. Böhm, T. Bein, D. Fattakhova Rohlfing, *ChemSusChem* **2019**, *12*, 4140.
- [2] D. Bresser, S. Passerini, B. Scrosati, *Energy Environ. Sci.* **2016**, *9*, 3348.
- [3] Y. Ma, Y. Ma, G. Giuli, T. Diemant, R. J. Behm, D. Geiger, U. Kaiser, U. Ulissi, S. Passerini, D. Bresser, *Sustain. Energy Fuels* **2018**, *2*, 2601.
- [4] A. Birozzi, J. Asenbauer, T. E. Ashton, A. R. Groves, D. Geiger, U. Kaiser, J. A. Darr, D. Bresser, *Batter. Supercaps* **2020**, *3* (3), 284–292.

SESSION EN12.05: Li-Ion Batteries I
Session Chair: Dominic Bresser
Wednesday Afternoon, December 1, 2021
Hynes, Level 3, Ballroom A

1:30 PM EN12.05.02

Bio-Inspired Vascularized Electrodes for Fast-Charging Batteries Designed by Deep Learning [Po-Chun Hsu](#); Duke University, United States

Vascular structures are ubiquitous in nature. Examples such as roots, blood vessels, and lung alveoli are the outcomes of millions of years of evolution to balance between surface area and mass transport. For lithium-ion batteries, it is anticipated that creating vascular channels in the electrodes also enhances the kinetics by ensuring the fresh electrolyte supply to achieve fast charging. Ideally, such optimal vasculature can help to fully utilize the electrode uniformly and to minimize overpotential. However, it is challenging to find the right parameters out of the immense parameter hyperspace. Herein, we use artificial neural network (ANN) to accelerate the computation of possible structures with high accuracy. An inverse searching library is compiled to find the top-ranked vascular structures under different industrial fabrication criteria. The prototype delivers a customized package containing optimal geometric parameters, and their uncertainty and sensitivity analysis. Finally, the full-vascularized cell shows a 75% improvement of charging capacity than the traditional homogeneous cell under 3.2C current density. This research provides an innovative methodology to solve the fast-charging problem in batteries and broaden the applicability of data-driven deep learning to different scientific or engineering areas.

1:45 PM EN12.05.03

Surface-Stabilized Cobalt-Free and Manganese-Rich Cathodes and Bio-Derived Binders for Sustainable Lithium-Ion Batteries Markus Binder^{1,2}, Annika R. Schür^{1,2}, Matthias Kuenzel^{1,2}, Vidur Kumar^{1,2}, Arefeh Kazzazi^{1,2}, Stefano Passerini^{1,2} and Dominic Bresser^{1,2}; ¹Helmholtz Institute Ulm, Germany; ²Karlsruhe Institute of Technology, Germany

Lithium-ion batteries have enabled the continuous transition from gasoline-powered to electric vehicles and several “traditional” car-makers have (very) recently announced their “exit” from combustion engines in the near future. The impressive success of this technology, however, raises also an increasing awareness of sustainability issues – not least with regard to critical elements such as cobalt, commonly comprised in the positive electrode active material, and the use of toxic and harmful solvents for the (positive) electrode preparation.^{11–31} Cobalt-free and manganese-rich $\text{LiNi}_{0.5}\text{Mn}_{1.5}\text{O}_4$ (LNMO) would provide a viable solution to overcome these issues, especially in combination with the utilization of water-soluble, bio-derived polymers as binders, but the pronounced water-sensitivity and high de-/lithiation potential of LNMO are still hampering the commercial breakthrough.^{13–51} Apparently, the key towards overcoming these issues relies on the stabilization of the LNMO|water and LNMO|electrolyte interface. Herein, we will report a comprehensive overview of our activities in this field, covering (i) an in-depth understanding of the processes occurring at the interface with the LNMO particles, (ii) the development of suitable active material and electrode treatments prior to the cell assembly, (iii) the optimization of the electrolyte composition to achieve stable interphases for both the anode and the cathode, as well as (iv) the tailored design of suitable binder compositions that allow for suitable mechanical properties and stable long-term cycling of commercially relevant sized electrodes – in half-cells and high-performance full-cells. We will show that only the combination of these complementary approaches appears capable of overcoming the present challenges and, thus, enabling the commercial application of LNMO-based cathodes in (more) sustainable lithium-ion batteries.

References

- [1] E. A. Olivetti, G. Ceder, G. G. Gaustad, X. Fu, *Joule* **2017**, *1*, 229.
- [2] C. Vaalma, D. Buchholz, M. Weil, S. Passerini, *Nature Reviews Materials* **2018**, *3*, 18013.
- [3] D. Bresser, D. Buchholz, A. Moretti, A. Varzi, S. Passerini, *Energy Environ. Sci.* **2018**, *11*, 3096.
- [4] B. Aktekin, M. J. Lacey, T. Nordh, R. Younesi, C. Tengstedt, W. Zipprich, D. Brandell, K. Edström, *The Journal of Physical Chemistry C* **2018**, *122*, 11234.
- [5] M. Wentker, M. Greenwood, J. Leker, *Energies* **2019**, *12*, 504.

2:00 PM EN12.05.04

Quantifying the Role of Reaction Inhomogeneity on Optimizing Capacity and Reducing Lithium Plating in Conventional and Architected Electrodes During Fast Charging Aleksandar Mijailovic¹, Guanyi Wang², Yejing Li³, Jian Yang², Wenquan Lu³, Qingliu Wu² and Brian W. Sheldon¹; ¹Brown University, United States; ²Western Michigan University, United States; ³Argonne National Laboratory, United States

Non-uniform lithium intercalation in porous electrodes during charging reduces the capacity of lithium ion batteries at fast charge rates. Recent work highlights the importance of the thermodynamics of cathode materials in dictating charging capacity at high rates. The analogous thermodynamic behavior of negative electrodes and its relationship to Li plating have not been investigated at high charge rates. In this study, we use finite element analysis and simplified numerical and analytical models to study conventional and architected electrode structures (i.e., layered with varied porosity, patterned with secondary channels, etc.) at high charge rates. While some of these strategies can increase capacity at a given rate, the benefits in reducing lithium plating are generally more striking. For example, layered designs can reduce the overpotential that drives plating even though these structures do not substantially increase capacity. Our modeling results are compared to and validated by experiments. Further, we demonstrate that reaction inhomogeneity is substantially affected by staging behavior in the equilibrium potential in ways that can contribute to Li plating events at high charge rates. The overall results of this study provide guidance for designing both electrode architectures and optimized charging protocols for fast charging applications.

2:15 PM EN12.05.05

Porous Electrode Architecture Design towards High-Performance Lithium-Ion Batteries Xiao Zhang¹, Zhengyu Ju¹, Zeyu Hui², Lei Wang³, Steven King⁴, Amy Marschilok⁴, Kenneth Takeuchi⁴, Esther S. Takeuchi⁴, Alan West² and Guihua Yu¹; ¹The University of Texas at Austin, United States; ²Columbia University, United States; ³Brookhaven National Laboratory, United States; ⁴Stony Brook University, The State University of New York, United States

Developing lithium-ion battery electrodes with high energy and power is essential to meet the ever-growing portable electronics and electric vehicle markets, which calls for achieving high utilization of the active material in thick electrode designs and elevating the overall energy density. In this talk, I will present our recent research progress on high-performance electrode architecture design and the impacts of structural parameters on the underlying kinetics. A low-tortuosity design could provide faster ion transport across electrode thickness, enabling thick electrode composed of graphene oxide (GO) supported magnetite (Fe_3O_4) nanoparticles with excellent rate capability, achieving areal capacity of 3.6 mAh cm^{-2} under 10 mA cm^{-2} . In addition, further fine tuning of the lamellar thickness and the pore size in low-tortuosity architecture shows significant impact on the electrochemical kinetics in thick $\text{LiNi}_{1/3}\text{Mn}_{1/3}\text{Co}_{1/3}\text{O}_2$ (NCM111) electrodes, where a better capacity retention with increasing C-rates (70% retention under 2.5 C) is found in electrodes with thinner lamellar thickness ($\sim 5 \mu\text{m}$) and relatively large pore size ($\sim 20 \mu\text{m}$) compared to those with thicker lamellar walls. Providing similar low-tortuosity morphology, this could be ascribed to faster diffusion into thin lamellar walls as opposed to their thick counterparts. Our research reveals more insights into structure-affected electrochemistry and highlights more delicate designs in low-tortuosity electrode architectures.

2:30 PM EN12.05.06

Decreasing LIB Separator Cost of Manufacturing with Facile One-Step Method Alexander Manly and Wyatt E. Tenhaeff; University of Rochester, United States

Microporous separators are critical components in lithium ion batteries (LIBs). Most battery separators serve two key functions: to physically separate the electrodes to avoid electrical shorting, and to allow the transport of ions. Conventional separators are fabricated from low cost, commodity thermoplastics, such as polyethylene and polypropylene, but make up 20% of the total material cost of a cell due to complex, energy-intensive manufacturing process. Moreover, conventional separators are considered passive components, providing adequate electrolyte uptake and ohmic resistance but contributing little other functionality to the cell. Thus, developing low cost, multifunctional separators is a potential strategy to reduce battery costs, while addressing cell cycle/calendar life.

In this presentation, we will introduce a novel separator fabrication process, where microporous separators are coated directly onto electrode foils in a facile, one-step additive process. This process promises to reduce energy consumption and manufacturing steps, and microporous poly(1,4-butanediol diacrylate) (pBDDA) separators fabricated using this approach possess superior performance metrics compared to commercial separators. These separators have a porous morphology with an average pore diameter of $40 \mu\text{m}$, and a porosity of 38%. In a lab setting, the fabricated separators have a thickness between $40\text{--}50 \mu\text{m}$. We have demonstrated that pBDDA separators hold 30% more electrolyte by mass when compared to Celgard 2500, and have an effective ionic conductivity of 3.32 mS/cm – a 66% improvement over the same commercial benchmark. When incorporated into an electrochemical cell, the capacity retention of pBDDA separators is on par with Celgard over long-term cycling, showing the material is stable and effective during use.

In addition to simplifying separator manufacturing and cell fabrication, our approach provides for facile incorporation of novel polymer chemistries without additional processing steps. For example, novel copolymer compositions have been designed to scavenge HF contamination that is intrinsic to LiPF₆-based liquid electrolytes. These functional separators mitigate the buildup of HF in the electrolytes, thereby suppressing Mn²⁺ dissolution in LiMnO₂ cathodes and improving capacity retention and lifetime of the lithium ion cells.

2:45 PM EN12.05.08

Flame Spray Synthesis of Single Crystal Nickel-Rich Cathode Materials of Lithium-Ion Batteries Jianan Zhang, Valerie L. Muldoon and Sili Deng; Massachusetts Institute of Technology, United States

Cathode material plays a dominant role in determining the capacity and cost of lithium-ion batteries (LIBs). Reducing the cost and improving the performance of cathode materials is critical for further advancing the application of LIBs in areas such as electric vehicles and grid energy storage. One type of the most promising cathode materials is nickel-rich metal oxides including Li(Ni_{0.6}Co_{0.2}Mn_{0.2})O₂ (NCM622) and Li(Ni_{0.8}Co_{0.1}Mn_{0.1})O₂ (NCM811) due to their high capacity and low cobalt content, especially considering the high price and toxicity of cobalt. Nevertheless, current nickel-rich cathode materials are experiencing challenges such as a fast capacity fading and low thermal stability, which are the result of structural degradation, microcracks, and side reactions related to the polycrystalline structure. An efficient way to solve those issues is using single crystal cathodes (SCC) that have better thermal stability and lower capacity fading because of improved structural stability and mechanical strength. However, current synthesis methods of SCC are facing various challenges, inhibiting their application for large-scale low-cost production of high-performance SCC. For instance, the coprecipitation method needs long-time preparation of precursor, whereas the solid-state molten salt method usually introduces impurity phase due to non-uniform mixing and post-treatment. Therefore, a flame spray synthesis (FSS) method is proposed for SCC materials with following features: (1) all needed metal elements are dissolved in the form of salt in precursor solution to guarantee homogeneous mixing and avoid extra steps of solid-state mixing; (2) the droplet-to-particle route allows easy control of the size of particles by adjusting spray properties; (3) the high temperature operating condition allows fast decomposition of raw material. In the current work, nickel-rich NCM811 cathode materials were synthesized with an FSS setup that has two heating sections, with a low-temperature section for evaporation control and a flame section for fast decomposition of precursor. The as-prepared sample was then post-annealed to produce the single crystal material. To obtain materials with optimized performance, we are investigating a wide range of parameters including the precursor concentration, amount of additives, operating temperature and residence time in each heating section, and post-anneal temperature and time. Our current coin cell tests showed that single crystal NCM811 synthesized with FSS had an improved cycling performance when compared with polycrystalline NCM811. We believe that FSS is promising in advancing the production and application of single crystal cathode materials because of its features such as fast production, homogenous mixing, and high scalable potential.

3:00 PM BREAK

SESSION EN12.06: Poster Session II: Advanced Materials and Chemistries for Low-Cost and Sustainable Batteries

Session Chairs: Dominic Bresser and Xiaolin Li

Wednesday Afternoon, December 1, 2021

8:00 PM - 10:00 PM

Hynes, Level 1, Hall B

EN12.06.01

Impact of Sodium Vanadium Oxide (NaV3O8, NVO) Material Synthesis Conditions on Charge Storage Mechanism in Zn-Ion Aqueous Batteries Christopher Tang¹, Gurpreet Singh¹, Lisa Housel², Sung Joo Kim², Calvin D. Quilty¹, Yimei Zhu^{2,1}, Lei Wang², Kenneth Takeuchi^{1,2}, Esther S. Takeuchi^{1,2} and Amy Marschikok^{1,2}; ¹Stony Brook University, United States; ²Brookhaven National Laboratory, United States

The use of zinc negative electrodes and aqueous electrolytes is an appealing modality for low cost scalable batteries. Further, transition metal oxides are viable options for cathode materials in these systems. Specifically, the electrochemical charge storage of sodium vanadate (NaV₃O₈ or NVO) cathodes in aqueous Zn-ion batteries has been demonstrated and is hypothesized to be influenced by the inclusion of structural water for facilitating ion transfer in the material. Materials properties considered important (morphology, crystallite and particle size, surface area) are systematically studied herein through investigation of two NVO materials, NaV₃O₈ · 0.34H₂O [NVO(300)] and NaV₃O₈ · 0.05H₂O [NVO(500)], with different water content, acicular morphologies with different size and surface area achieved via post-synthesis heat treatment. The electrochemistry of the two materials was evaluated in aqueous Zn-ion cells with 2 M ZnSO₄ electrolyte using cyclic voltammetry, galvanostatic cycling, and rate capability testing. The thinner NVO(300) nanobelts demonstrate greater specific capacities and higher effective diffusion coefficients relative to the thicker NVO(500) nanorods. Notably however, while cells containing NVO(500) deliver lower specific capacity, they demonstrate enhanced capacity retention with cycling. The structural changes accompanying oxidation and reduction are elucidated via ex situ X-ray diffraction, transmission electron microscopy, and operando V K-edge X-ray absorption spectroscopy (XAS), where NVO material properties are shown to influence the ion insertion. Operando XAS verified that electron transfer corresponds directly to change in vanadium oxidation state, affirming vanadium redox as the governing electrochemical process.

EN12.06.02

A Bioinspired Vanadium Compound as a Robust Scaffold for Next-Generation Flow Batteries Patrick J. Cappillino¹, Shyam K. Pahari¹, Jennifer Bolibok¹, Benjoe R. Visayas¹, Tugba Ceren Gokoglan², Maricris L. Mayes¹ and Ertan Agar²; ¹University of Massachusetts Dartmouth, United States; ²University of Massachusetts Lowell, United States

Modern electrical grids, especially those comprising energy from intermittent, renewable sources, such as wind and solar, require storage.¹ Nonaqueous redox flow batteries (NRFB) are a promising technology to meet this growing need.² Compared to their aqueous counterparts, they have the potential to approach the energy density of lithium-ion batteries, while maintaining the advantages of flow systems, including decoupled scaling of power and energy ratings and thermal stability.

Despite their promise, fundamental technical obstacles have limited the application of NRFB so far. These include low solubility and poor stability of active-materials as well as poor electrochemical performance. To address these issues, we have developed an active-material known as vanadium bis-hydroxyiminodiacetate (VBH), which is based on a family of molecules that is naturally occurring and produced biologically.³ Biosynthesis of this molecule evolved in mushrooms of the *Amanita* genus, to bind vanadium selectively and with the highest stability ever reported, using a unique, tetradentate, bis-carboxylato-η²-hydroxyimino- motif.⁴ Ligand-substitution is suppressed, shutting down a major mechanism of decomposition. In this way, natural selection serves as a toolkit for molecular design, elucidating a scaffold for optimized NRFB active materials.

In this presentation we provide an overview of some key challenges in NRFB development, along with our recent efforts at addressing them, and some strategies we are pursuing to make further in-roads. We will show that our bioinspired active-material exhibits excellent chemical stability during long durations of electrochemical cycling to high states-of-charge.⁵ Further, we will demonstrate that the thermodynamics of the electrolyte can be tuned to greatly enhance the solubility of the active-material.⁶ Finally, we will report our recent progress on a modular synthetic scheme, whereby the VBH scaffold can be covalently modified to tune its electronics and steric properties.

1. P. Albertus et al., *Joule*, 2020, 4, 21-32.
2. R. M. Darling et al, *Energy Environ. Sci.*, 2014, 7, 3459-3477.
3. H. Huang et al., *J. Mater. Chem. A*, 2017, 5, 11586-11591.
4. R. E. Berry et al., *Angew Chem Int Ed Engl*, 1999, 38, 795-797.
5. Gokoglan et al., *J. Electrochem. Soc.*, 2019, 166, A1745-A1751.
6. Pahari et al., *RSC Adv*, 2021, 11, 5432-5443.

EN12.06.03

A Molecular Dynamics Study of the Effect of Coordination Behavior in Polymer Electrolytes for Sodium-Ion Conduction [Francielli S. Genier](#) and Ian Hosein; Syracuse University, United States

The establishment of sustainable energy sources highly depends on efficient storage devices to guarantee a consistent power supply. The growing demand for lithium-ion batteries (LIBs) for this purpose combined with concerns about lithium availability has motivated the search for viable storage alternatives. Sodium-ion conduction is a suitable candidate due to sodium's abundance in the earth's crust and similar monovalent storage mechanism as Li⁺. In recent years, the development of components specifically for sodium-ion batteries (SIBs) have inspired much research interest, but fundamental inquiries on ion transport remain unanswered. Notably, solid polymer electrolyte (SPE) studies remain almost solely concentrated on Li-ions, even though revolutionary storage devices could result from the combination of sodium's natural availability with the possibility of higher energy density in solid-state devices. The challenges associated with SPEs, such as low ionic conductivities, could be further addressed by characterizing the ion-transport properties of the polymer host and the strength of the salt-polymer interactions. In this work, we used atomistic molecular dynamic simulations of sodium SPEs to observe the influence of oxygen density in polymer chains on the resulting electrolyte's diffusivity, coordination, and cation-anion interactions. For this purpose, we characterize sodium-ion transport in two polymer hosts, namely, polyethylene oxide (PEO) and poly(tetrahydrofuran) (PTHF) that contain two and four carbons in their repeating units, respectively. Sodium perchlorate was added to the systems in a concentration of EO/Na (EO = ethylene oxide) or BO/Na (BO = butylene oxide) equal to 15. The simulation boxes were created using the software Medea 3.1 from Materials Design, and the molecular dynamics package LAMMPS was used in the equilibration and production runs, with the universal forcefield PCFF+. To mitigate the limitations of our non-polarizable model, we multiplied the charges of Na, Cl, and O by 0.75 to reproduce transport properties without overestimation. Production runs were carried out in NPT at 353 K (80 °C), 1 atm, with timestep of 1 fs, for 100 ns. The radial distribution function (RDF) between Na-O from the polymers PEO and PTHF was calculated to investigate the local solvation environment, which confirmed the stronger coordination of sodium cations with PEO's polymer backbone, while, in PTHF, the lower oxygen density in its chains resulted in weaker coordination. The differences in oxygen density in the polymer chain also influence the hopping mechanism in each electrolyte. In PTHF, interchain hopping was more prevalent, while in PEO, intrachain hopping happened more often due to the stronger coordination with the polymer chains. Additionally, sodium cations showed a higher probability of coordinating with 2-3 oxygens from PEO while in PTHF, Na⁺ coordinated with only one polymer oxygen. Consequently, the Na⁺ decomplexation could easily be achieved in the PTHF electrolytes. This caused the faster motion of Na⁺ in PTHF, as demonstrated by the sodium ion self-diffusivity 2.3x higher in PTHF than in PEO. However, significant ion cluster formation was seen in the PTHF system. In PTHF, only 8.11% of ions were fully isolated from each other, mostly because Na⁺ was free to form larger clusters with ClO₄⁻. In PEO, 32.2% of all ions were dissociated due to a greater dispute of coordination between PEO oxygens and perchlorate ones. The significant presence of clusters in the PTHF electrolyte could potentially result in the transport of Na⁺ ions in the opposite direction from where cations should move during battery cycling, which could be verified by lower transference numbers experimentally. This work's findings elucidate the fundamental influences and correlations of polymer ether content on ion transport, which can inform on novel syntheses to improve future sodium polymer electrolytes.

EN12.06.04

Investigating Ion Transport in Aqueous Electrolytes for Aluminum-Ion Batteries [Allen Zheng](#)^{1,2}, Glenn R. Pastel³, Mounesha Garaga¹, Michael Ding³, Kang Xu³ and Steven G. Greenbaum^{1,2}; ¹Hunter College-CUNY, United States; ²CUNY Graduate Center, United States; ³U.S. Army Research Laboratory, United States

Among the candidates competing with lithium ion battery technology for large-scale energy storage applications are aluminum-based systems, which have significant cost and safety advantages. In this work, we investigate aqueous electrolytes containing aluminum trifluoromethanesulfonate (AlTF₃) ranging in concentration from 0.1M to 3.6M. Cation, anion, and water molecular self-diffusion coefficients were determined by pulsed field gradient nuclear magnetic resonance (NMR) measurements of the ²⁷Al, ¹⁹F, and ¹H nuclei, respectively. A special high-gradient probe was used for the ²⁷Al measurements due to short relaxation times associated with nuclear quadrupole interactions characteristic of this spin-5/2 nucleus. Together with ionic conductivity measurements, the NMR results yield information on the degree of salt dissociation and Al ion transference at all concentrations.

EN12.06.05

A Strategy to Decrease the Viscosity of Ionic Liquids for Electrochemical Applications—A Broadband NMR Relaxometry Study Sophia Suarez^{1,2}, Frederik Philippi³, [Tawhid Pranto](#)^{1,2}, Daniel Rauber⁴, Christopher Kay⁴, Tom Welton³ and Steven G. Greenbaum^{5,2}; ¹Brooklyn College of CUNY, United States; ²CUNY Graduate Center, United States; ³Imperial College London, United Kingdom; ⁴Universität des Saarlandes, Germany; ⁵Hunter College-CUNY, United States

Ionic liquids (ILs) have become ubiquitous due to their many attractive characteristics including their task specific tunability. In their application as electrolytes, low viscosity is a necessity to allow fast ion dynamics. One of the ways in which low viscosity can be achieved is by using large asymmetric ions with high conformational flexibility. Towards this, large cations such as 1-butyl-3-methylimidazolium (BMIM⁺) with relatively short and flexible alkyl chains have been successful. Additionally, the use of large weakly interacting anions such as bis(trifluoromethanesulfonyl)imide (TFSI⁻) have found similar success. In this study, we performed ¹H and ¹⁹F NMR Fast Field Cycling (FFC) broadband relaxometry measurements on four ILs comprised of the BMIM⁺ cation combined with the tetracyanoborate (BCN₄⁻), acetyl(trifluoromethylsulfonyl)imide (TfAc⁻), (methylsulfonyl) 2,2,2-trifluoroacetyl amide (MsNTFA⁻), and bis(trifluoromethanesulfonyl) methane (TFSM⁻) anions. The objective of the study is to determine how the anion's conformational flexibility affects the dynamics of both ions.

Variable temperature ¹H relaxation dispersion (*R*₁) results followed the anion order: MsNTFA⁻ > TfAc⁻ > TFSM⁻ > B(CN)₄⁻. These results demonstrate that the MsNTFA⁻ and B(CN)₄⁻ anions provide the least and most favorable environments, respectively, for the cation's transport. This result is also

supported by solution viscosity (η), ionic conductivity (σ) and cation self-diffusion coefficient (D) measurements.

EN12.06.10

Silicon/Germanium Nanostructures via Photonic Curing—A Facile Approach to Synthesize Nanomaterials in Large Scale Najma Khatoon, Binod Subedi and Douglas B. Chrisey; Tulane University, United States

Silicon/Germanium (Si/Ge) nanostructures are promising materials for energy storage applications due to their high energy density (both volumetric and gravimetric), large lithiation capacity, low toxicity, and high thermal stability. The challenge to utilize these tremendous properties of Si/Ge nanostructures for desired applications is controlled growth over large scale. Here, we report a unique approach to achieve controlled synthesis of Si/Ge nanostructures. We have used a novel photonic curing technique, which uses an intense pulsed light with a broad spectrum (220–1500 nm), to instantaneously prepare these nanoparticles. Unlike conventional methods like rapid thermal annealing where there is enough time to relax to the preferred equilibrium state, quenching during photonic curing occurs much more rapidly (milliseconds), allowing the trapping of metastable states to form unique nanostructures. Si/Ge precursors were spray coated on glass and processed with PulseForge. At capacitor bank voltage of 600V, 10 pulses of light with 8 J/cm² fluence each (total fluence of 80 J/cm²) were used to produce Si/Ge nanoparticles (20 nm – 60 nm). Scanning Electron Microscopy (SEM) and Energy Dispersive Spectroscopy (EDS) showed presence of Si/Ge nanostructure resulting from instantaneous photonic curing process. 3-Aminopropyltrimethoxysilane was used to improve attachment of the Si/Ge precursors on the substrate, and it was observed through EDS analysis that it increased the carbon content in the synthesized nanomaterial. The present work shows that photonic curing route for Si/Ge nanostructures can be promising way for low-cost large scale-controlled synthesis of energy efficient Si/Ge nanostructures.

SESSION EN12.07: Beyond Li-Ion I
Session Chairs: Dominic Bresser and Weiyang Li
Thursday Morning, December 2, 2021
Hynes, Level 3, Ballroom A

10:30 AM EN12.07.02

Late News: Metal-Free Organic Batteries with a Sustainable Design and Enhanced Performance Jakob Asenbauer^{1,2}, Kai Shi^{1,2}, Cleber Marchiori³, Moyses Araujo^{3,4}, Rodrigo Carvalho⁴, Daniel Brandell⁴, Stéphanie Pouget⁵, Lionel Picard⁵, Simon Jestin⁶, Marie Völlmer⁶, Sylvie Bayle⁷ and Dominic Bresser^{1,2}; ¹Helmholtz Institute Ulm, Germany; ²Karlsruhe Institute of Technology, Germany; ³Karlstad University, Sweden; ⁴Uppsala University, Sweden; ⁵University Grenoble Alpes, France; ⁶CANOE – Platform for Composites and Advanced Materials, France; ⁷Bernard Dumas, France

Organic batteries are composed of abundant elements (i.e. C, H, O, N and S) and can be produced through eco-friendly procedures. Thereby they provide the possibility for electrochemical energy storage with a –compared to conventional inorganic batteries – smaller environmental footprint and lower cost.^{1–3} Despite an increased interest in the scientific community within the last years, there are still unresolved issues with organic battery materials that need to be addressed before commercialization. First, the electric conductivity of organic materials is frequently very low. Thus, large amounts of conductive carbon need to be added and the achievable areal mass loading is too low for practical applications. Second, the processing of the electrode should be without the usage of hazardous solvents and binders to be in line with the general goal of sustainability. And third, the understanding of the reaction mechanism of organic active materials upon cycling is so far still limited, but essential to rationally improve the materials. Herein, we present an in-depth analysis of the (de-)lithiation mechanism of tetra-lithium perylene-3,4,9,10-tetracarboxylate (PTCLi₄) as an exemplary organic active material. Furthermore, we replaced the metallic current collector foil with a carbon current collector (CCC), made of ex cellulose carbon fibers, i.e. from cheap and renewable sources. This in combination with an environmentally friendly aqueous processing allowed us to produce metal-free organic electrodes with good electrochemical performance, a high active material content (80 wt%), an excellent cycling stability (>10,000 cycles), and a very high areal mass loading (>50 mg cm⁻²).

References

1. Poizot, P., Dolhem, F. & Gaubicher, J. Progress in all-organic rechargeable batteries using cationic and anionic configurations: Toward low-cost and greener storage solutions? *Curr. Opin. Electrochem.* **9**, 70–80 (2018).
2. Esser, B. *et al.* A perspective on organic electrode materials and technologies for next generation batteries. *J. Power Sources* **482**, 228814 (2021).
3. Lu, Y. & Chen, J. Prospects of organic electrode materials for practical lithium batteries. *Nat. Rev. Chem.* **4**, 127–142 (2020).

10:45 AM EN12.07.03

Predicting Topotactic Ion-Insertion Reactions in Manganese Oxides for Low-Cost Aqueous Battery Cathodes Evan Z. Carlson¹, William C. Chueh¹, J. Tyler Mefford¹ and Michal Bajdich²; ¹Stanford University, United States; ²SLAC National Laboratory, United States

To eliminate power sector emissions, low-cost energy storage of weekly to seasonal duration must accompany renewable generation. Recent analysis suggests that long-duration energy storage systems must cost less than \$20/kWh to facilitate the transition.¹ These storage systems must simultaneously be safe, energy-dense, and have long cycle/calendar life to ensure market adoption. One intriguing approach to satisfy all of these criteria is the development of aqueous batteries with electrodes made from cheap, energy-dense materials. Manganese oxides, which are earth-abundant, water-stable, and have rich ion-insertion chemistry, are attractive candidates for aqueous battery cathodes. However, rational design of these batteries demands a better understanding of their ion intercalation mechanisms and the relationships between voltage, electrolyte composition and electrode structure.

In this talk, we will discuss our efforts to predict insertion voltages of protons and alkali ions (H⁺, Li⁺, Na⁺, K⁺) into manganese oxides using first-principles DFT calculations. Despite the success of the SCAN functional in predicting the polymorphic structure of manganese oxides grown during chemical synthesis,² we will show that a DFT+U approach is required for accurate computation of manganese oxide energetics. We will discuss our computed energy referencing scheme that captures the appropriate physics of the manganese oxide system (e.g. magnetic structure, 3d electron energies, zero point energies and entropies) and ensures reasonable predictive accuracy while avoiding overfitting. In doing so, we will highlight some of the tradeoffs associated with this computational approach. We will also analyze how the computed Pourbaix diagrams predict electrode thermodynamic behavior for a specific alkali ion and manganese oxide polymorph. Emphasis will be placed on the implications for the design of aqueous batteries with different alkali intercalant ions. Finally, we will compare our computational results to our own experiments and suggest promising strategies for improved aqueous battery cathodes.

1) Sepulveda, N.A. *et al.* *Nat Energy* **6**, 506–516 (2021)

11:00 AM EN12.07.04

Reversible Charging of Redox-Active Conjugated Polymers Beyond the Polaronic State in Aqueous Electrolytes Alexander Giovannitti¹, Anna Szumska², Iuliana P. Maria³, Davide Moia⁴ and Jenny Nelson²; ¹Stanford University, United States; ²Imperial College London, United Kingdom; ³University of Oxford, United Kingdom; ⁴Max Planck Institute for Solid State Research, Germany

Redox-active conjugated polymers are an interesting class of materials for electrochemical devices since their properties can be tuned by chemical design to enable redox activity in various electrolytes. In our presentation, we will introduce design rules for the development of conjugated polymers with high electronic and ionic charge transport properties to enable fast charging of single-phase electrodes in aqueous electrolytes [1,2]. While the choice of the polymer backbone is important for achieving electrochemical stability of the charged polymer states, it is found that the tuning of the local environment of the polymers is equally important. The tuning of the local environment of the materials is achieved by attaching hydrophilic (polar) side chains to the polymer backbone to enable fast ion transport, swelling, and reversible phase changes. Electrodes fabricated with these polymers can utilize more than 70 % of the available redox-active state in the bulk of the polymer while maintaining high electrochemical stability during continuous cycling. Our work shows the importance of chemical design strategies for achieving high electrochemical stability for conjugated polymers in aqueous electrolytes.

[1] A. Giovannitti, C. B. Nielsen, D.-T. Sbircea, S. Inal, M. Donahue, M. R. Niazi, D. A. Hanifi, A. Amassian, G. G. Malliaras, J. Rivnay, I. McCulloch, *Nat. Commun.* **2016**, *7*, 13066.

[2] D. Moia, A. Giovannitti, A. A. Szumska, I. P. Maria, E. Rezasoltani, M. Sachs, M. Schnurr, P. R. F. Barnes, I. McCulloch, J. Nelson, *Energy Environ. Sci.* **2019**, *12*, 1349.

11:15 AM EN12.07.05

High Energy Density Redox-Mediated Flow Batteries Using Bio-Inspired Electrolytes Tugba Ceren Gokoglan¹, Shyam K. Pahari², Joseph M. Egitto¹, Sundar Rajan Aravamuthan¹, Patrick J. Cappillino² and Ertan Agar^{1,1}; ¹University of Massachusetts Lowell, United States; ²University of Massachusetts Dartmouth, United States

Redox flow batteries (RFBs) are considered as a prime candidate for addressing the intermittency problem in renewable energy sources, due to their unique architecture that allows for unparalleled scalability and flexibility required for grid integration. [1]. Among several types of RFBs under development, non-aqueous redox flow batteries (NRFBs) have the potential to approach the energy density of lithium-ion batteries, while maintaining the advantages of flow systems, including ability to decouple power and energy ratings, and thermal stability [2]. Regardless of the active materials used, NRFBs suffer from low energy densities because the energy density is primarily dependent on the electrolyte concentration used [3]. The solubility values of redox active materials in non-aqueous organic solvents are relatively lower compared to aqueous systems, which negatively affects the energy density of the flow cell [4]. One promising approach for drastically improving the energy density of NRFBs is the utilization of solid charge storage materials, which are reversibly oxidized/reduced in the electrolyte tanks upon interaction with the redox active species dissolved in electrolyte [5].

Herein, we aim to demonstrate a redox-mediated flow battery using a highly stable bio-inspired electrolyte and a suitable solid storage material to provide evidence that the addition of a compatible solid material greatly improves the energy density. To accomplish this objective, a highly stable bio-inspired electrolyte, vanadium(IV/V)bis-hydroxyiminodiacetate (VBH) [6], is selected as the redox active material. Implementing VBH as a high-stability testbed (i.e., no interference from side reactions) would allow the detailed analysis required for the elucidation of the indirect redox mediation reactions between the solid storage and redox active materials. For the solid storage material, cobalt hexacyanoferrate (CoHCF), a Prussian blue analog, is selected based on its formal potential, which overlaps well with the formal potential of VBH. After sufficient evidence of improvement in the capacity is established, the solid charge storage material is optimized to further improve the energy density. Optimization of the critical parameters such as the amount of solid storage material, the operating current density, and the electrolyte flow rate is presented. The performance characteristics of the RFBs with and without solid charge storage materials present are reported and compared using a suite of electrochemical methods, including charge/discharge cycling.

References:

[1] G. L. Soloveichik, *Chem. Rev.*, 2015, **115** (20), 11533-11558.

[2] K. Gong, Q. Fang, S. Gu, S. F. Y. Li, Y. Yan, *Energy Environ. Sci.*, 2015, **8** (12), 3515-3530.

[3] S. Gentil, D. Reynard, H. H. Girault, *Curr. Opin. Electrochem.* 2020, **21**, 7-13.

[4] Y. Cao, J. -J. Chen, M. A. Barteau, *J. Energy Chem.* 2020, **50**, 115-124.

[5] R. Yan and Q. Wang, *Adv. Mater.*, 2018, **30**, 1802406.

[6] H. Huang, R. Howland, E. Agar, M. Nourani, J. A. Golen, P. J. Cappillino, *J. Mater. Chem. A.*, 2017, **5**, 11586-11591.

SESSION EN12.08: Beyond Li-Ion II

Session Chair: Dominic Bresser

Thursday Afternoon, December 2, 2021

Hynes, Level 3, Ballroom A

1:30 PM EN12.08.01

Alloys for Magnesium Batteries—From Bulk Electrode to Surface Protection Clément Pechberty^{1,2}, Lorenzo Stievano^{1,2} and Romain Berthelot^{1,2}; ¹ICGM, CNRS, Univ Montpellier, France; ²Reseau sur le Stockage Electrochimique de l'Energie (RS2E), France

In the context of looking beyond the lithium-ion technology, magnesium batteries appear as promising candidates. Indeed, magnesium is abundant and less reactive than alkali metals, and its low redox potential opens the way to high energy density batteries. However, two major roadblocks slow down the development of magnesium batteries: the strong passivation of the magnesium surface with classical electrolytes and the lack of suitable positive electrode materials.

Alloy-type materials that can react electrochemically with magnesium have been widely evaluated as negative electrode materials, with very high corresponding capacities as well as a good behavior with classical electrolytes. However, their application as bulk electrode materials replacing magnesium metal lowers significantly the total energy density, in some cases below a critical threshold where the system becomes not competitive.

In the ongoing revival of lithium-metal batteries, the protection of lithium metal by alloy-type materials has been proposed. Such coating strongly influences the evolution of the electrode-electrolyte interface and induces long lifespan, with especially less polarization and less dendrite formation.

The purpose of our work is to adapt such coating strategy to protect the magnesium surface, thus enabling the use of classical electrolytes based on the

Mg(TFSI)₂ salt. Here, we aim to show our attempts to deposit a thin layer of a p-block element on the surface of a magnesium electrode, through chemical reduction of metallic salt in solution, or via solid-solid and liquid-solid reactions. Coating are characterized by combining X-ray diffraction and electronic microscopy with surface-scale techniques such as X-ray photoemission spectroscopy. The positive impact of the coating is checked by evaluating the behavior of unprotected and protected electrodes in full cells, first with standard Chevrel phase Mo₆S₈, and then with more promising sulfur-based composites as high energy density systems are targeted. In comparison with bare magnesium electrodes, lower capacity decay and long battery lifespan is observed. These preliminary works are very promising and pave the way to the development of magnesium-metal batteries with very simple electrolytes.

1:45 PM EN12.08.02

Late News: Picoliter-Sized Zn-Air Batteries for Releasable Microscopic Sensors and Colloidal Robots [Ge Zhang](#), Michael Strano, Volodymyr Koman, Jingfan Yang, Yuwen Zeng, Matthias Kuehne, Albert T. Liu, Sungyun Yang and Allan M. Brooks; Massachusetts Institute of Technology, United States

The recent interest in microscopic autonomous systems, such as microrobots, colloidal state machines and *smart dust* has created a need for microscale energy storage and harvesting. However, the incompatibility of material properties used at the macroscale with micro-fabrication techniques creates significant challenges to realizing microscale energy systems. Herein, we use photolithography to create picoliter (10⁻¹² L) devices that scavenge ambient air for Zn oxidation, achieving the highest recorded energy densities of 760 to 1070 Wh L⁻¹ at a scale less than 100 μm in lateral size. We have elucidated the critical role of phosphate buffered electrolyte in achieving such high energy densities. Zinc phosphate precipitates contributed to a higher discharge voltage in phosphate buffered saline compared to other neutral electrolytes. More than 10,000 devices per wafer can be released into solution as functional colloids with in-built power supplies. Within a volume of only 2 pL, these batteries can deliver open circuit voltages of 1.16 V with total energies ranging from 5.5 ± 0.3 to 7.7 ± 1.0 μJ and maximal power around 2.7 nW. Such systems can power a memristor providing access to two-state memory, as well as bimorph actuators for colloidal robotic applications. The high energy density, tiny size and simple configuration promise the mass fabrication and adoption of such picoliter Zn-air batteries for micron-scale, colloidal robotics with autonomous functions.

2:00 PM EN12.08.03

Bioinspired, Tree-Root-Like Interfacial Designs for Structural Batteries with Enhanced Mechanical Properties [Tianwei Jin](#) and Yuan Yang; Columbia University, United States

In the past decades, lots of efforts are made by researchers to promote the development of structural lithium ion batteries, which endow energy storage ability to structural parts for vehicle lightweighting. However, the two strategies people normally use nowadays still have major challenges. One method is introducing thick or heavy packaging and mechanically supporting parts to or inside cells, which intrinsically decreases the energy densities of these energy storage devices. The other one is replacing conventional cell parts like electrodes and electrolytes with materials which have strong mechanical properties but poor electrochemical cycling stability, which sacrifice cycling performance of batteries.

By finite element analysis, we find that the reason of unsatisfying flexural behavior of conventional lithium ion batteries is the sliding of separator and electrode layers relative to each other, and it will greatly increase if we can suppress this sliding. The reason is that if layers are bonded together, all components will participate in the resistance of bending rather than slide relatively, which inspires us with a new idea to improve the mechanical behavior of batteries.

Here we propose a bioinspired and scalable interfacial design to make cell parts of lithium ion batteries robust by applying suitable and strong “binders” to each interface inside. With a thin coating layer of porous PVDF-HFP, which is previously shown without detriment to cycling performance, electrodes can be bonded with PVDF-coated separators tightly by hot pressing. With these techniques, all components in cells can contribute to the overall mechanical strength with more efficient load transfer, which dramatically enhances the flexural modulus of pouch cells from 0.28 to 3.1 GPa. On the other side, on account of the chemical simplicity of this strategy, the structural battery in this work can deliver a comparable specific capacity of 148.6 mAh g⁻¹ with conventional cells and show 95.5% capacity retention after 500 cycles. Moreover, the specific energy only decreases by 3%, which is the smallest reduction reported so far in structural batteries. A prototype of “electric wings” is also demonstrated, which allows an aircraft model to fly steadily. This work comes up with a new and straightforward way to design structural batteries, with both mechanical performance and energy density satisfied, and the method can be easily transferred to large-scale production in industry.

In addition, we apply finite element analysis to conduct simulations to compare the contribution of materials' intrinsic mechanical properties and interfacial adhesion strength in flexural behaviors of batteries, which provides a valuable insight into feasible structural batteries with balanced mechanical and electrochemical properties.

2:15 PM EN12.08.04

Bio-Inspired Quinone Macromolecules Grafted on O, N, S, P Codoped Carbon Paper for High Energy Density Electrochemical Capacitors [Abdelaziz M. Gouda](#); Ecole Polytechnique Montreal, Canada

Developing sustainable biosourced electrode materials for energy storage applications is an urgent need, to keep pace with the ongoing increase in energy demand combined with the rapid use of electric vehicles and portable electric devices. Growing environmental concerns have spurred investments in renewable but intermittent energies. The need to switch to environmentally friendly, widely available, organic materials is confronted by the low conductivity and stability of most candidates and the difficulties of creating an efficient, metal-free current collector. In this work, we present a sustainable high energy density supercapacitors based on bio-sourced materials grafted on surface treated carbon paper electrode. An acidic and thermal treatment is used to induce O, N, S, and P surface doping and increase the surface area of the carbon paper. This doping improves wettability, conductivity (through the formation of graphene quantum dots), and adds faradaic activity improving the capacitance of the bare electrode. Additional deposition of sepia melanin and catechin (a tannin) with high specific capacitance and energy density shows very promising results for supercapacitors. Up to 2850 mF/cm² (228 F/g) capacitance, with 100% retention after 5 000 cycles at 20 A/g, 100% coulombic efficiency, 0.87 and 1.01 mW h/cm² (69.71, 81.25 W h/kg) and 277.15 and 158.10 mW/cm² (22.20 and 12.66 kW/kg) energy and power densities for sepia melanin and catechin, respectively, were achieved for symmetric supercapacitor devices in 0.5 M Na₂SO₄ (pH 5) electrolyte. This work provides a general guidance to design high-performance supercapacitor electrodes based on bio-sourced and potentially biodegradable materials

2:30 PM EN12.08.05

Relaxometry and Diffusometry Investigation of Deep Eutectic Solvents Based on Choline Chloride [Carla C. Fraenza](#) and Steven G. Greenbaum; Hunter College of CUNY, United States

The development of the new generation of electrolytes for energy storage, which simultaneously enable substantial improvements in energy and power density, safety and reductions of environmental impacts and cost, is a big challenge at the present time. Deep eutectic solvents (DESs), which sometimes are considered a sub-class of ionic liquids due to their similar properties, have shown to be promising as electrolytes.^{1,2} These solvents are defined as a mixture of two or more species, typically a hydrogen bond donor (HBD) species and a hydrogen bond acceptor (HBA) species which may be solid or liquid, and that at a particular composition present a melting point depression usually being liquids at room temperature. Among their most relevant

properties, they have low volatility, low flammability and wide electrochemical and thermal stability windows. Unlike typical ionic liquids, DESs can be inexpensive, readily synthesized, and can often be prepared from biodegradable, and nontoxic constituents. In this work, the molecular rotational and translational dynamics of three different DESs based on choline chloride (ChCl) were studied using the fast field-cycling nuclear magnetic resonance relaxometry (FFC-NMR) and pulsed-field gradient (PFG) NMR techniques. Specifically, ChCl was chosen as the HBA at concentrations between 5 and 33mol% and glycerol, ethylene glycol (EG) or phenol were used as the HBDs. It was observed that the translational and rotational motions of all species became slower with increasing ChCl concentration for EG and phenol as the HBDs, but the opposite trend was observed for glycerol. Moreover, the PFG-NMR diffusion measurements identified a slow exchange process between the hydroxyl (OH) groups of choline and the HBDs.

1. Smith, E. L.; Abbott, A. P.; Ryder, K. S. Deep Eutectic Solvents (DESs) and Their Applications. *Chemical Reviews* 2014, 114, 11060–11082.
2. Tome, L. I. N.; Baiao, V.; da Silva, W.; Brett, C. M. A. Deep eutectic solvents for the production and application of new materials. *Applied Materials Today* 2018, 10, 30–50.

2:45 PM EN12.08.06

Using Classical Molecular Dynamics to Investigate the Lithium Transport Mechanisms in Various Solvent–Lithium-Salt Systems in Lithium-Oxygen Batteries Emily J. Crabb¹, Graham Leverick¹, Ryan Stephens², Yang Shao-Horn¹ and Jeffrey C. Grossman¹; ¹Massachusetts Institute of Technology, United States; ²Shell International Exploration & Production Inc., United States

Lithium-oxygen batteries have higher energy densities than traditional lithium-ion batteries. However, they are not yet commercially viable due to poor efficiency, high charging voltages, and low cycle lifetimes. These issues could be addressed with a deeper fundamental understanding of the atomistic behavior of these batteries, especially how different factors impact lithium transport behavior. We have used classical MD simulations to examine lithium transport behavior in ten different solvents. We have validated our classical force fields by experimentally measuring the densities, viscosities, and ionic conductivities of our solvent–LiTFSI systems for comparison. However, our classical MD simulations have allowed us to go beyond these measurements and investigate properties that can be more difficult to access experimentally, such as the residence time of solvent molecules in the lithium solvation shell.

3:00 PM EN12.08.07

Toward VBH Based High Energy Density Flow Batteries—A Computational and Experimental Approach Shyam K. Pahari¹, Benjoe R. Visayas¹, Jennifer Woehl¹, Tugba Ceren Gokoglan², Maricris L. Mayes¹, Ertan Agar² and Patrick J. Cappillino¹; ¹University of Massachusetts Dartmouth, United States; ²University of Massachusetts Lowell, United States

In last few decades, mounting concerns about the sustainability of fossil fuel-based energy and ever-increasing energy demand around the globe has led to the exploration of clean and renewable energy sources.^{1,2} As a result, incorporation of renewable energy sources such as wind and solar into the electrical grid is taking place rapidly.³ However, the inherent intermittency of these sources results in demand-supply imbalance which impedes efficiency.⁴ One of the ways to tackle this problem is assuring reliability by integrating energy storage systems into the grid.⁵ Redox flow batteries (RFBs) are a promising technology for grid level energy storage with a potential to match the performance of state-of-the-art Li-ion batteries with numerous additional advantages including decoupled power and energy rating⁶, a wide range of working temperatures and a good safety profile.

Despite the numerous benefits of RFBs, the technology is still at its infancy and widescale implementation of them is hindered due to following three fundamental issues namely poor stability (cycling and calendar life), low energy density resulting from poor solubility of active material, and poor performance. In our previous study, we bio-mimicked an octa-coordinated dianionic vanadium complex, vanadium-bis-hydroxyiminodiacetate (VBH), from a naturally occurring biomolecule, amavadin, as a redox active molecule for flow battery application and established its extraordinary stability during exhaustive cycling.^{7,8,9} Herein, we utilize the VBH scaffold to tune thermodynamic parameters including solvation free energy and lattice enthalpy by designing molecules with varying counter cations and provide the clear pathway to further solubilize the VBH based active materials. In particular, we present evidences that increasing alkyl chain length of quaternary ammonium counter-cations, despite less favorable solvation energy, increases the solubility by facilitating the weakening of the crystal lattice. We further report electrochemical cycling of this material at moderate concentration in both symmetric and full-cells, in conjunction with an anthraquinone neryolyte.

References

1. Höök, M., & Tang, X. (2013). Depletion of fossil fuels and anthropogenic climate change—A review. *Energy Policy*, 52, 797-809.
2. IEA (2015). *Energy Statistics of OECD Countries 2015*. OECD Publishing, Paris, https://doi.org/10.1787/energy_stats_oecd-2015-en.
3. IEA (2021). *Renewable Energy Market Update 2021*, IEA, Paris <https://www.iea.org/reports/renewable-energy-market-update-2021>
4. Yang, Z., Zhang, J., Kintner-Meyer, M. C. W., Lu, X., Choi, D., Lemmon, J. P., & Liu, J. (2011). Electrochemical Energy Storage for Green Grid. *Chemical Reviews*, 111(5), 3577–3613.
5. *Grid energy storage*, US Department of Energy (2013)
6. Dunn, B., Kamath, H., & Tarascon, J.-M. (2011). Electrical Energy Storage for the Grid: A Battery of Choices. *Science*, 334(6058), 928–935.
7. Huang, H., Howland, R., Agar, E., Nourani, M., Golen, J. A., & Cappillino, P. J. (2017). Bioinspired, high-stability, nonaqueous redox flow battery electrolytes. *Journal of Materials Chemistry A*, 5(23), 11586–11591.
8. Gokoglan, T. C., Pahari, S. K., Hamel, A., Howland, R., Cappillino, P. J., & Agar, E. (2019). Operando Spectroelectrochemical Characterization of a Highly Stable Bioinspired Redox Flow Battery Active Material. *Journal of The Electrochemical Society*, 166(10), A1745–A1751.
9. Pahari, S. K., Gokoglan, T. C., Visayas, B. R. B., Woehl, J., Golen, J. A., Howland, R., Mayes, M. L., Agar, E., & Cappillino, P. J. (2021). Designing high energy density flow batteries by tuning active-material thermodynamics. *RSC Advances*, 11(10), 5432–5443.

3:15 PM EN12.08.08

Neural Equivariant Interatomic Potentials for Large-Scale Electrolyte Simulations Nicola Molinari, Albert Musaelian, Juan Felipe Gomez, Robert D. Newman, Simon L. Batzner and Boris Kozinsky; Harvard University, United States

Electrolytes control battery recharge time and efficiency, anode/cathode stability, and ultimately safety, thus their optimization is crucial for the design of modern energy storage devices. In this work, we focus on ionic liquid-based electrolytes. This promising class of electrolytes possesses superior chemical stability compared to standard organic solvents, however, poor and anomalous transport properties are hindering their applicability [1]. Unfortunately, classical energy models struggle to provide the level of accuracy needed to reliably predict and investigate ionic conductivity.

Here we study the applicability to such systems of state-of-the-art equivariant graph neural networks (NequIP [2]). Ionic liquid-based electrolytes provide a unique challenge due to their strong ionic interactions and liquid nature. Additionally, substantially diverse inter-atomic environments are expected as a function of lithium-salt doping [3], raising the question of model transferability. Our promising results show that we can circumnavigate the ad-hoc and system-dependent tweaks to the classical energy models (for instance charge rescaling or polarizability), while retaining computational speed and near-DFT accuracy for large-scale ionic transport molecular dynamics investigations.

- [1] N Molinari, JP Mailloa, N Craig, J Christensen, and B Kozinsky. Transport anomalies emerging from strong correlation in ionic liquid electrolytes. (2019)
- [2] S Bätzner, TE Smidt, L Sun, JP Mailloa, M Kornbluth, N Molinari, and B Kozinsky. SE(3)-Equivariant Graph Neural Networks for Data-Efficient and Accurate Interatomic Potentials. (2021)
- [3] N Molinari, JP Mailloa, and B Kozinsky. General trend of a negative Li effective charge in ionic liquid electrolytes. (2019)

3:30 PM BREAK

4:00 PM EN12.08.09

Late News: Mutually Exclusive MXene and Graphene Oxide Multilayer Composites in Lithium-Sulfur Battery Sanghee Nam, Il-Kwon Oh and Manmatha Mahato; Korea Advanced Institute of Science and Technology, Korea (the Republic of)

The shuttle effect of soluble lithium polysulfide (LiPS), which results in the gravest capacity degradation, is one of the critical issues to hinder the commercialization of lithium-sulfur batteries (LSBs). Here, we report mutually exclusive $Ti_3C_2T_x$ MXene and graphene oxide multilayer composite to suppress the shuttle effect by both physical inhibition of micro/mesoporous and chemical absorption of surface functional groups. The abundant surface functional groups of GO and MXene attract the positively charged lithium ion (Li^+) and eject the negatively charged polysulfides (S_n^{2-}) through electrostatic affinity and repulsion. A simple approach using vacuum filtration was utilized to encapsulate elemental sulfur (S_8) between GO and MXene film (GSM), playing role in a permselective separator and functionalized current collector, respectively. The functionally antagonistic GSM is directly utilized as cathode for LSBs and exhibits a specific capacity of $1,425 \text{ mAh g}^{-1}$ at 0.1C in the initial cycle. The abundant functional groups, which can chemisorb the LiPSs, result in a high cyclic retention of approximately 85.1% after 500 cycles. Furthermore, we demonstrate a flexible LSB with a PEO-LiTFSI electrolyte based on the flexibility of the exceptionally thin GSM due to the 2D nanomaterials, MXene and graphene oxide.

4:15 PM EN12.08.10

Aqueous Electrolytes for Aluminum-Carbon Rechargeable Batteries Jasmin Smajic, Bashir E. Hasanov, Amira Alazmi, Abdelhamid Emwas, Nimer Wehbe, Alessandro Genovese, Abdulrahman Ellabban and Pedro Costa; KAUST, Saudi Arabia

By virtue of their chemical and mechanical resiliency, carbon cathodes have shown excellent electrochemical behavior in aluminum batteries. Oppositely, this was possible only with expensive ionic liquid electrolytes, whose biodegradability, corrosivity and moisture sensitivity is an issue. By contrast, their use in Al systems operating in the aqueous electrolytes has scarcely been explored and the reported results were consistently poor. In this work, we assemble an Al-C battery with an aqueous electrolyte (aluminum trifluoromethanesulfonate) and study the electrode-electrolyte interactions. On the anode side, we find that both the electrode pretreatment and the electrolyte concentration play essential roles in solid-electrolyte interface (SEI) formation. While on the cathode side, we find pore size and hydrophilicity as important parameters in enabling superior performances. Consequently, employing a hydrophilic reduced graphene oxide (rGO) as the active cathode material enables an aqueous Al-C battery with a high energy density (136 Wh kg^{-1} per cathode mass) and one of the best capacity retentions reported (>60% across a range of current densities and constant Coulombic efficiency close to unit). Furthermore, our rGO cathode more than doubles the benchmark for life cycles (to +200 cycles) and can be charged rapidly (<5 minutes). To explain this response, we propose a charge storage mechanism wherein the $[Al(H_2O)_6]^{3+}$ ions do not get desolvated when inserted into the cathode. The guest Al ions (surface adsorbed or intercalated) act as proton donors and may get anchored on the oxygen moieties of the rGO, further promoting the formation of an electrochemical double layer. A mixed charge-storage regime follows that stabilizes the carbon cathode and enables unprecedented response.

SESSION EN12.09: Na & Mg Batteries
 Session Chair: Dominic Bresser
 Monday Morning, December 6, 2021
 EN12-Virtual

8:00 AM *EN12.09.01

Towards Low-Cost and Sustainable Na-Ion Batteries Using Vanadium Phosphate Positive Electrode Materials Laurence Croguennec¹, Long H.B. Nguyen^{1,2}, Chloé Pablos^{1,2}, Emmanuel Petit¹, François Rabuel², Grégory Gachot², Paula Sanz Camacho¹, Antonella Iadecola³, Jacob Olchowka¹, Mathieu Morcrette², Dany Carlier¹ and Christian Masquelier²; ¹ICMCB, CNRS, Bordeaux Univ., Bordeaux INP, France; ²LRCS, Picardie Jules Verne Univ., France; ³RS2E, Réseau Français sur le Stockage Electrochimique de l'Energie, FR CNRS 3459, France

Polyanionic materials are intensively studied as promising positive electrode materials for Na-ion batteries thanks to high stability and fast ionic mobility within their structural framework.¹⁻³ Among those polyanionic materials, $Na_3V_2(PO_4)_2F_3$ and $Na_3(VO)_2(PO_4)_2F$ are the two most attractive ones due to their high voltage for two Na^+ ions extraction and their high theoretical energy densities of $\sim 500 \text{ mAh.g}^{-1}$. These two compositions are indeed the two end members of a family of compounds described with the general formula $Na_3V_2(PO_4)_2F_{3-y}O_y$ where $0 \leq y \leq 2$. We will first discuss the stability of these active compounds in aqueous media, and at different states of charge and discharge.⁴ Then, we will compare the performance of optimized carbon-coated stoichiometric $Na_3V_2(PO_4)_2F_3$ in a large panel of cycling conditions, at different rates and temperatures.⁵⁻⁶ Finally, we will show how cationic and anionic substitution have been widely explored with the target to reversibly de-intercalate and re-intercalate the third Na^+ ion from/in the structure.

Acknowledgements: This study is performed in the frame of the French RS2E and European Alistore-ERI networks on battery research. The authors thank Région Nouvelle Aquitaine, the French National Research Agency (STORE-EX Labex Project ANR-10-LABX-76-01) and the European Union's Horizon 2020 research and innovation program under grant agreement No 875629 (NAIMA) for their financial support.

References

- Masquelier et al., Chem. Rev. 2013, 113, 6552
- Hasa et al., J. Power Sources 2021, 482, 228872
- Singh et al., J. Mater. Chem. A 2021, 9, 281
- Nguyen et al., Energy Storage Mater. 2019, 20, 324
- Broux et al., Small Methods 2018, 1800215
- Nguyen et al., J. Phys. Chem. C 2020, 124, 23511

8:30 AM *EN12.05.01

Towards Cobalt Free and Manganese Rich Cathode Materials for Lithium-Ion Batteries Peter Axmann, Marilena Mancini, Nicola Jobst and Margret Wohlfahrt-Mehrens; ZSW, Zentrum für Sonnenenergie, und Wasserstoffforschung, Germany

Lithium ion batteries are the state of the art electrochemical storage systems in many mobile applications. The further development of high-performance, cost-efficient and sustainable energy storage systems continues to be a key technology both for the full transition from combustion engines to full electric vehicles and for the intermediate storage of renewable energies. The rapidly increasing market for lithium-ion batteries in the transport and energy sectors is leading to a rapidly growing need for materials for these cells, whose supply security and environmental compatibility must be ensured – especially for critical raw materials such as cobalt, which is a component in state of the art cathode materials. The high costs of cobalt have led to the development of nickel rich layered materials with reduced cobalt content and the next generation of cathode material will contain less than 5 percent cobalt by weight (NCM811).

The development of cobalt free, manganese rich cathode materials with reduced nickel content such as $\text{LiNi}_{0.5}\text{Mn}_{1.5}\text{O}_4$ (LNMO) or $\text{Li}_{1+x}\text{Ni}_{0.5}\text{Mn}_{1.5}\text{O}_4$ ($0 < x < 1$) can contribute significantly to further reduction of cost, high electrochemical performance and higher safety compared to lithium ion batteries with nickel-rich layered oxides. The lithium-nickel-manganese oxide compounds can be tailored with respect to composition and crystal structure in order to reach high capacities up to 250 mAh g^{-1} [1-3] The presentation will give an overview on synthesis routes and electrochemical performance of LNMO and a series of $\text{Li}_{1+x}\text{Ni}_{0.5}\text{Mn}_{1.5}\text{O}_4$ ($0 < x < 1$) cathode materials. Strategies to increase the electrochemical performance and the long life stability include i) development of tailored crystallite and particle design, ii) a profound understanding of the reaction mechanisms during lithium insertion and extraction, iii) the analysis of underlying ageing mechanisms in half and full cells, iv) development of protective surface coatings and v) the optimization of electrode/electrolyte interfaces. We will present full cell data with LNMO and $\text{Li}_{1+x}\text{Ni}_{0.5}\text{Mn}_{1.5}\text{O}_4$ ($0 < x < 1$) cathode materials using various electrolytes and will discuss strategies for further optimization.

1 P. Axmann, G. Gabrielli, M. Wohlfahrt-Mehrens, J. Power Sources 301, 2016, 151-159

2 G. Gabrielli, M. Marinaro, M. Mancini, P. Axmann, M. Wohlfahrt-Mehrens, J. Power Sources 351, 2017, 35-44

3 M. Mancini, P. Axmann, G. Gabrielli, M. Kinyanjui, U. Kaiser, M. Wohlfahrt-Mehrens, ChemSusChem 9, 2016, 1-8

9:00 AM EN12.09.03

A Water-Soluble Lignosulfonate Binder for Hard Carbon Anodes in Sodium-Ion Batteries Ritambhara Gond¹, Habtom D. Asfaw¹, Omid Hosseinaei², Kristina Edstrom¹, Reza Younesi¹ and Andrew Naylor¹; ¹Uppsala University, Sweden; ²RISE Research Institutes of Sweden, Sweden

Sodium-ion batteries (SIBs) have rapidly gained interest for their potential usage in large-scale grid energy storage, due to the higher abundance of sodium over lithium [1-2]. Inspired by electrodes common in lithium-ion batteries (LIBs), analogous materials are often considered in the development of SIBs [3]. However, while graphite anodes ($\sim 360 \text{ mA h g}^{-1}$) are most frequently used for LIBs, it is hard carbon ($\sim 300 \text{ mA h g}^{-1}$) which are one of the most promising for SIBs. The electrode binder, which connects particles of the electrode to one another as well as to the current collector, is regularly found to be polyvinylidene fluoride (PVDF). To improve sustainability of batteries, PVDF should be replaced with non-fluorinated, environmentally friendly binders. Lignin is an abundant natural polymer, and Kraft lignin, a by-product from pulp mills, has previously been reported as an inexpensive and environmentally-friendly NMP (*N*-methyl pyrrolidone)-soluble binder for LIBs [4].

Here, sodium lignosulfonate, a sulfonated lignin derivative, is introduced as a non-toxic, *water-soluble* binder for hard carbon electrodes. Its electrochemical performance in half- and full-cells against Prussian White is compared with other water-soluble binders, sodium carboxymethyl cellulose (CMC) and sodium alginate, as well as the NMP-soluble lignin. Furthermore, the impact of the lignosulfonate and CMC binders on the composition of the solid electrolyte interphase (SEI) layer is determined by X-ray photoelectron spectroscopy (XPS).

[1] Larcher, D. & Tarascon, J. M. Towards greener and more sustainable batteries for electrical energy storage. Nat. Chem. 7, 19–29 (2015).

[2] Yabuuchi, N., Kubota, K., Dahbi, M. & Komaba, S. Research development on sodium-ion batteries. Chem. Rev. 114, 11636–11682 (2014).

[3] Luo, W., Shen, F., Bommier, C., Zhu, H., Ji, X. & Hu, L. Na-Ion Battery Anodes: Materials and Electrochemistry. Acc. Chem. Res. 49, 231–240 (2016).

[4] Domínguez-Robles, J., Sánchez, R. Dfiaz-Carrasco, P., Espinosa, E., García-Domínguez, M. T. & Rodríguez, A. Isolation and characterization of lignins from wheat straw: Application as binder in lithium batteries. Int. J. Biol. Macromol. 104, 909–918 (2017).

9:15 AM EN12.09.04

Mg²⁺ Intercalation into Nanostructured H₂V₃O₈—A Post-Mortem Study Yuri Surace, Martina Romio, Damian M. Cupid and Marcus Jahn; AIT - Austrian Institute of Technology GmbH, Austria

Magnesium-ion batteries (MIBs) have received great attention in recent years as an alternative battery chemistry to Li-ion technologies thanks to the intrinsic advantages of Mg over Li. Mg has a significantly larger volumetric capacity (3832 mAh cm^{-3} vs 2061 mAh cm^{-3} for Li), higher natural abundance and lower cost than Li [1]; Mg also has a relatively low standard redox potential (-2.37 V vs. SHE [1]). Furthermore, due to the divalent nature of the Mg²⁺ cation, for the same amount of ions stored in a host material (usually the cathode), the specific capacity is doubled in comparison with a monovalent cation. Thanks to these key advantages MIBs can theoretically achieve higher energy densities at a lower cost than LIBs [2] making MIBs a very attractive battery technology. However, one of the main fundamental challenges in MIBs is the slow Mg²⁺ ion solid state diffusion into the cathode active material's lattice. This is generally attributed to the high charge/radius ratio of the Mg²⁺ ion, which results in strong interactions between the anions and cations of the host structures [3]. As consequence, cathode materials for MIBs usually show very poor electrochemical performance (low specific capacities, high overpotentials and poor rate capability).

Vanadium-based oxides cathodes have been the object of intense study over the past few years due to their relatively high potential of 2.5 V vs Mg²⁺/Mg, and the possibility to explore multiple oxidation states of vanadium, i.e. V⁵⁺/V⁴⁺ and V⁴⁺/V³⁺, resulting in higher theoretically achievable specific capacities [4]. Within this family, the H₂V₃O₈ (HVO) phase shows promising structural and morphological characteristics which could favour Mg²⁺ intercalation. Specifically, H₂V₃O₈ has a relatively large interlayer distance of 8.4 \AA and can crystallize in a nanowire morphology. However, H₂V₃O₈ has only recently been tested in a MIB for the first time, showing a specific capacity of around 80 mAh g^{-1} at room temperature, even though its theoretical specific capacity is 190 mAh g^{-1} , for the intercalation of 1 eq. of Mg²⁺ [5].

In our study, a post-mortem analysis of HVO electrodes upon charge and discharge at specific cycle numbers was carried out to investigate the intercalation mechanism of Mg²⁺ into HVO. For the first time, we demonstrate the electrochemical performance of HVO in TFSI-based electrolytes with a specific capacity approaching 200 mAh g^{-1} at room temperature. Furthermore, by combining bulk and surface characterization techniques, changes in the HVO crystal structure, morphology and surface chemistry were analysed in-depth. Depending on the cycle number, Mg²⁺ intercalation upon discharge resulted in a 0.5% to 4% change in the unit cell parameters compared to the pristine electrode. The intercalation caused a change in the V⁵⁺/V⁴⁺ ratio, with a

lower ratio (i.e. higher amount of V^{4+}) associated with cycle numbers showing the highest capacity values. However, Mg^{2+} ions could not be completely extracted upon charge, resulting in lattice parameters which do not return to their original values. Although the nanostructured morphology of HVO did not change over cycling, surface roughening of the nanowires was observed at high cycles numbers, indicating formation of a TFSI-containing surface layer. Evidence of V dissolution could also be confirmed, resulting in capacity fading after about 35 cycles.

- [1] C. Kuang, W. Zeng, and Y. Li, *J. Nanosci. Nanotechnol.*, vol. 19, no. 1, pp. 12–25, 2019.
- [2] Y. Tian *et al.*, *Chem. Rev.*, vol. 121, no. 3, pp. 1623–1669, Feb. 2021.
- [3] E. Levi, YGofer, and D. Aurbach, *Chem. Mater.*, vol. 22, no. 3, pp. 860–868, 2010.
- [4] H. Tang *et al.*, *Electrochem. Energy Rev.*, vol. 1, no. 2, pp. 169–199, Jun. 2018.
- [5] M. Rastgoo-Deylami, M. S. Chae, and S.-T. Hong, *Chem. Mater.*, vol. 30, no. 21, pp. 7464–7472, Nov. 2018.

9:30 AM EN12.09.05

The Critical Role of Electrolyte Selection in Sodium Oxygen Batteries Nagore Ortiz-Vitoriano^{1,2}; ¹CIC Energigune, Spain; ²Ikerbasque, Spain

Research into new energy storage technologies, for both portable and stationary applications, has become imperative in order to meet present and future energy requirements. Recently, rechargeable sodium oxygen batteries are receiving a great deal of interest as possible alternatives to lithium ion batteries, because of their potentially higher gravimetric energy densities (1605 or 1108 Wh/kg based on Na_2O_2 or NaO_2 discharge products, respectively)¹.

In order to facilitate the advancement of this technology, the development of targeted approaches to dealing with the technology's unique chemistry are required. The vast majority of the work reported on sodium oxygen batteries has been devoted to the development of suitable air cathodes² (primarily focused on carbon), catalysts, and - to a lesser extent - redox mediators, neglecting electrolytes despite their importance. Electrolytes, consisting of a salt and a non-aqueous solvent, are a key component of any optimized system. The parameters affecting electrolyte physiochemistry (solvent-salt structure and dynamics) are, therefore, critical to battery performance, lifetime and safety. The composition of the electrolyte (solvent and salt) has been identified as key parameter which controls the crystal growth during the discharge process, and subsequently the dissolution of discharge products during charge. Glyme-based solvents have been widely - but arbitrarily - used, and to date no clear correlation between solvent/electrolyte properties and battery performance have been outlined.

In this work, we will discuss and clarify the relationship between glyme chain length and cell chemistry and performance. We will, moreover, demonstrate how solvent selection helps define cell chemistry and performance, by linking salt-solvent interactions to solvation energies - and subsequently to sodium battery electrolyte properties - through the combination of both experimental and computational methodologies. In addition, we will unravel how careful combination of different solvents such as ionic liquids can modify the speciation and solvation of the discharge products, so as to obtain the desired deposition mechanism and crystal growth.

References

- ¹ I. Landa-Medrano, C. Li, N. Ortiz-Vitoriano, I. Ruiz de Larramendi, J. Carrasco and T. Rojo *J. Phys. Chem. Lett.* **2016**, 7(7), 1161–1166.
- ² M. Enterría, C. Botas, J.L. Gómez-Urbano, B. Acebedo, J.M. López del Amo, D. Carriazo, T. Rojo, and N. Ortiz-Vitoriano. *J Mater. Chem. A* **2018**, 6 (42), 20778–20787.

9:45 AM EN12.09.06

Lower Temperature, Lower Cost Molten Sodium Batteries Martha M. Gross, Stephen J. Percival, Rose Lee, Amanda Peretti, Erik D. Spoecker and Leo J. Small; Sandia National Laboratories, United States

Molten sodium batteries are a grid-scale energy storage technology with over 500 MW/4 GWh deployed worldwide that utilize inexpensive sodium and sulfur or aluminum-containing materials. Despite their legacy of reliably and safely providing large capacity energy storage for decades, they do not enjoy widespread popularity as an alternative to grid-scale lithium-ion batteries. This can largely be attributed to the high temperatures necessary to operate these systems (270 – 350 °C), which greatly increases the capital cost to install them (\$600-700/kWh) despite their use of low-cost active materials. Lowering the temperature to near the melting temperature of sodium (97.8°C) can create dramatic savings by reducing the cost of inactive materials such as the insulation, wiring, and seals, while increasing battery longevity by slowing aging of all system components. Traditional battery chemistries such as sulfur/polysulfides and nickel/nickel chloride, while effective for high temperatures, simply do not work at low temperatures (< 150 °C) as materials solidify. To lower the temperature by nearly 200 °C, complete re-engineering of the cathode is necessary. Here we describe the development of a low temperature catholyte utilizing low-cost and earth-abundant materials to create a high performance, low temperature molten sodium battery. This was achieved by first identifying redox-active molten salts composed of sodium iodide and a metal halide salt that are liquid at 100 °C. The effect of sodium iodide content and choice of metal halide salt on battery voltage and power performance was studied to identify compositions capable of near-commercially relevant levels of power and energy density. The long-term cyclability of catholyte compositions was evaluated in batteries at 110 °C, with some catholyte compositions capable of cycling in some cases for up to 8 months. Electrochemical performance was weighed against constraints in molten salt cost to create a low-cost, high performance catholyte.

Sandia National Laboratories is a multi-mission laboratory managed and operated by National Technology & Engineering Solutions of Sandia, LLC, a wholly owned subsidiary of Honeywell International Inc., for the U.S. Department of Energy's National Nuclear Security Administration under contract DE-NA0003525.

SESSION EN12.10: Zn Batteries
Session Chairs: Dominic Bresser and Weiyang Li
Monday Morning, December 6, 2021
EN12-Virtual

10:30 AM *EN12.10.01

An In-Depth Assessment of Zinc-Ion Diffusion in Solid-State Hosts Arumugam Manthiram; The University of Texas at Austin, United States

As the energy-storage market is accelerating and expanding globally with lithium-ion batteries, cost and sustainability of the technology for electric vehicles and grid-storage are becoming a serious concern. This has prompted immense interest on battery chemistries based on earth-abundant, low-cost materials. In this regard, batteries based on multivalent ions, such as magnesium, calcium, zinc, aluminum, *etc.* have generated much interest, as they occur at much higher terrestrial concentrations, diminishing the issues associated with sustainability and supply chain. Also, multivalent ions can theoretically store more charge than monovalent lithium or sodium, although with a lower operating voltage. However, multivalent-ion batteries are faced with a few scientific and technological challenges.

First, nonaqueous multivalent-ion batteries suffer from a lack of appropriate electrolytes, which makes a true assessment of their performance difficult. Second, except for zinc, the lack of appropriate anode/electrolyte combinations also makes the reversible plating and stripping of the multivalent metallic anodes challenging. Without proper assessment of the electrochemical cells, it will be hard to understand the true behavior of the cathode. Therefore, this presentation will focus first on the use of chemical insertion/extraction reactions of multivalent ions with appropriate reagents to assess the potential of various hosts.

Among the various multivalent-ion batteries, much of the fundamental research has focused on aqueous zinc-ion batteries, and attractive performances have been reported with high capacity and rates with oxide-based cathodes. Despite the apparent success with zinc-ion batteries in aqueous electrolytes, the concept of multivalent-ion batteries remains elusive, as witnessed by a lack of sensible progress in other multivalent-ion chemistries, such as magnesium-ion and aluminum-ion batteries. This mismatch points to a fundamental gap in the knowledge surrounding aqueous zinc-ion batteries, especially the hidden role of protons originating from aqueous electrolyte or from any water present in the cathode.

To delineate the actual solid-state diffusion behavior of zinc ions, the presentation will provide a series of studies to assess the relative extent of zinc-ion versus proton insertion in common solid-state hosts. The use of a microwave-assisted insertion technique for chemical insertion of zinc ions into hosts and elevated-temperature electrochemical zinc-ion insertion will be discussed. Our results indicate that in general and as expected, the diffusion of zinc ions in oxidic hosts is an energy-demanding process that prohibits its efficient utilization in rechargeable batteries. On the contrary, the inclusion of aqueous electrolytes allows the introduction of charge-compensating protons that can readily diffuse into the solid-state hosts, with the release of an equivalent amount of zinc ions into the electrolyte. Therefore, the utilization of aqueous electrolytes with zinc anode is conceptually similar to other systems in which protons are the actual working ions.

Overall, our study reveals that attempts to insert zinc ions strictly in non-aqueous electrolytes are accompanied by severe thermodynamic and kinetic limitations, often encountering significant host-guest electrostatic repulsions due to the higher charge on Zn^{2+} and subsequent capacity loss. This issue can be suppressed by employing more covalent chalcogenide-based hosts, but at the cost of lower cell capacity and voltage. Even in the chalcogenides, zinc-ion diffusion tends to be slow compared to that in other rechargeable batteries. Given the slow native diffusivity of multivalent ions in solid-state hosts, it appears that the possibility of multivalent-ion batteries hinges on the development of alternative cathode architectures that do not rely on the long-range solid-state diffusion of guest ions.

11:00 AM EN12.10.04

Stabilizing Nanostructured α -Ni(OH)₂ for High Energy Density Rechargeable Nickel–Zinc Batteries Samuel W. Kimmel^{1,2}, Ryan H. Deblock², Christopher N. Chervin², Jeffrey Long², Joseph F. Parker², Brandon J. Hopkins², Debra R. Rolison² and Christopher Rhodes¹; ¹Texas State University, United States; ²U.S. Naval Research Laboratory, United States

Rechargeable aqueous Ni–Zn batteries can provide an energy-dense, safer alternative to Li-ion batteries for a wide range of applications including electric vehicles, portable electronic devices, and grid-level energy storage. We investigate approaches to obtain high-capacity cathodes that can support the performance of dendrite-suppressing Zn sponge anodes pioneered at the U.S. Naval Research Laboratory. We substitute metal ions (aluminum, cobalt, manganese, or zinc) into α -Ni(OH)₂, a phase that stores greater than one-electron per Ni, but requires stabilization to avoid transformation to the lower capacity β -phase. We use a microwave-assisted process that expresses α -Ni(OH)₂ in a high surface-area nanosheet morphology, and show that this morphology is retained for all metal-ion substituents.¹ The substituents do, however, influence aggregate growth, interlayer spacing, and Raman vibrational frequencies. The metal-ion-substituted materials are fabricated into powder-composite cathodes and tested versus zinc sponge anodes in alkaline electrolyte. We find that of the substituents evaluated, only Al³⁺-substitution favorably increases the discharge capacity, discharge voltage, and oxygen evolution reaction onset voltage and improves the cycling stability of the α -phase. The enhanced electrochemical performance and phase stability of Al³⁺-substituted α -Ni(OH)₂ nanosheets correlate to the presence of interlayer ordered nitrates and changes to the environment of intralayer Ni. The rational selection of substituents and rethinking the electronic wiring within the cathode structure provide a pathway to realize energy dense, safe, rechargeable Ni–Zn batteries.

References

1. Kimmel, S.W.; Hopkins, B.J.; Chervin, C.N.; Skeelee, N. L.; Ko, J.S.; DeBlock, R.H.; Long, J.W.; Parker, J.F.; Hudak, B.M.; Stroud, R.M.; Rolison, D.R.; Rhodes, C.P. Capacity and Phase Stability of Metal-Substituted α -Ni(OH)₂ Nanosheets in Aqueous Ni–Zn Batteries. *Materials Advances* **2021**, *2*, 3060–3074.

11:15 AM EN12.10.05

Achieving Stable Molybdenum Oxide Cathodes for Aqueous Zinc-Ion Batteries in Water-in-Salt Electrolyte Lei Wang^{1,2}, Amy Marschilok^{2,2,1}, Shan Yan^{1,2}, Calvin D. Quilty^{2,2}, Jason Kuang^{2,2}, Mikaela Dunkin^{2,2}, Steven Ehrlich¹, Lu Ma¹, Kenneth Takeuchi^{2,2,1} and Esther S. Takeuchi^{2,2,1}; ¹Brookhaven National Laboratory, United States; ²Stony Brook University, The State University of New York, United States

A layered MoO₃ material with large interlayer spacing represents a promising cathode for aqueous rechargeable Zn-ion batteries (ARZIBs), but the implementation of this material is limited due to the intrinsically low conductivity and poor structural stability. A 30 m ZnCl₂ water-in-salt electrolyte (WISE) was introduced to a MoO₃ nanobelt cathode for the first time, significantly increasing the stability of MoO₃ cathodes compared to those in 3 M ZnSO₄ and 3 M ZnCl₂ electrolyte. The Zn/MoO₃ cell in WISE unambiguously demonstrated significantly improved rate performance delivering 349, 253, and 222 mAh/g at 100, 500, and 1000 mA/g, denoting a 2x, and 12x capacity increase of those achieved in 3 M electrolytes at 500 and 1000 mA/g, respectively. A capacity retention rate of 73% was achieved after (dis)charging at 100 mA/g for 100 cycles, and no obvious capacity fading was observed at higher current densities of 500 mA/g and 2A/g. A compilation of structural and morphological characterization was systematically performed to provide insight into the mechanisms of the improved performance in ZnCl₂ WISE for the MoO₃ cathode materials. Specifically, our data collectively suggested that the drastic fading in 3M electrolytes can be attributed to the parasitic surface deposits on Zn originated from Mo dissolution and H₂ formation due to Zn corrosion and hydrogen evolution reaction (HER), which were significantly suppressed in the ZnCl₂ WISE. The direct visualization of these side reactions was achieved for the first time in the Zn–MoO₃ system, using an in situ optoelectrochemical measurement.

11:30 AM EN12.10.06

Li₁₀GeP₂O₁₂ Electrolyte for All-Solid-State Batteries [Giuliana Materzanini](#)^{1,2,3}, Leonid Kahle^{3,4}, Aris Marcolongo^{3,4} and Nicola Marzari^{2,3}; ¹Université Catholique de Louvain, Belgium; ²École Polytechnique Fédérale de Lausanne, Switzerland; ³National Centre for Computation Design and Discovery of Novel Materials, Switzerland; ⁴IBM RSM Zurich Research Laboratory, Switzerland

All-solid-state battery technologies point toward a sustainable energy future, aiming to replace the amenable liquid organic electrolytes currently used with safer solid-state inorganic electrolytes. Oxides generally show better electrochemical properties but weaker ionic conductivity when compared to their sulfide counterparts. Here we use first-principles molecular dynamics simulations to extensively simulate LGPO, the oxide analogue of LGPS, one among the best conducting solid-state electrolytes. From canonical simulations we predict that a hypothetical tetragonal phase mirroring that of LGPS would be highly conductive. We thus explore the dynamical stability of this phase and of an existing orthorhombic phase of LGPO via isobaric-isothermal simulations, while extracting from the trajectories the relevant elastic moduli.

SESSION EN12.11: Beyond Li-Ion III
Session Chairs: Weiyang Li and Xiaolin Li
Monday Afternoon, December 6, 2021
EN12-Virtual

1:00 PM *EN12.11.01

Metal-H₂ Batteries for Large Scale Stationary Energy Storage [Yi Cui](#)^{1,2}; ¹Stanford University, United States; ²SLAC National Accelerator Laboratory, United States

Grid scale stationary energy storage is critical for integration of renewable electricity such as solar and wind into electric grid, and also enable the new opportunity for resilient and smart grid. The cost, life and temperature range of batteries need to be significantly improved for this purpose. My lab we developed a breakthrough metal-H₂ battery chemistry to meet the needs of grid scale storage, in which hydrogen gas electrodes is anodes and transition metal oxides are cathodes. This battery chemistry is low-cost, with long life over 30,000 cycles and 30 years. It can be operated in a wide range of temperature of -40 to +60 °C and is maintenance-free. The fast charging/discharge up to 10min is possible in this chemistry. The spinout company EnerVenue has realized very exciting commercial prototypes based on this technology. The metal-H₂ battery affords an ideal storage solution to integrate solar and wind electricity into the grid.

1:30 PM *EN12.11.02

New Anode Materials for Sustainable Sodium-Ion Batteries [Marca M. Doeff](#); Lawrence Berkeley National Laboratory, United States

Sodium-ion batteries (NIBs) are the closest of the “Beyond Lithium-Ion” batteries to commercialization. Their benefits include reduced cost and potentially better safety compared to lithium-ion analogs as well as sustainability, due to the greater earth abundance of sodium compared to lithium. Layered titanate anodes are proposed as alternatives to the more commonly used hard carbons, and have advantages such as greater density and higher first cycle coulombic efficiencies. For this talk, we will discuss several examples of this materials.

2:00 PM EN12.11.03

Investigation of Olivine Structured Phosphate as Potential Cathode Material for Magnesium-Ion Batteries [Martina Romio](#)¹, Damian M. Cupid¹, Yuri Surace¹, Marcus Jahn¹ and Isaac Abrahams²; ¹Austrian Institute of Technology (AIT), Austria; ²Queen Mary University of London, United Kingdom

Batteries based on the magnesium-ion chemistry are considered as promising alternatives to lithium ion technologies due to the high theoretical volumetric capacity (3833 mAhcm⁻³ for the Mg-anode), low toxicity and natural abundance of magnesium, as well as the di-valent character of the Mg²⁺ cations. Furthermore, since magnesium deposition takes place without dendrite formation on the Mg-metal anode surface, the Mg-cell is expected to be considerably safer than comparable cells based on Li metal.¹

Despite these positive attributes, the development of Mg secondary batteries is hindered by the slow solid-state diffusion of Mg²⁺ ions into the cathode lattice, which lead to relatively low practical capacities, irreversible capacity losses and poor cyclic stability. In this work, this issue is explored by synthesising and characterising a phosphate-based system with olivine-related structure to investigate its suitability as cathode materials for Mg-ion batteries, with phosphates building-blocks chosen due to their open three-dimensional framework, structural stability and safety under oxidizing conditions.² Therefore, in this work the novel olivine-related (Mg_{0.5}Ni_{0.5})₃(PO₄)₂ compound was synthesised by the solid-state method and investigated as a potential electrode active material.

(Mg_{0.5}Ni_{0.5})₃(PO₄)₂ was subjected to a comprehensive physico-chemical characterization in order to optimize the synthesis conditions, determine the phase purities and assess the particle morphologies. Furthermore, the reaction mechanisms and electrochemical behaviour of the orthophosphate-based material with monovalent Li⁺ and divalent Mg²⁺ ions were investigated using post-mortem analysis (XRD, FTIR and XPS) in order to establish the nature of the charge storage reaction mechanisms.

In addition to the challenges associated with the development of novel electrode materials, it is well known that Mg-based electrolytes, which consist of ionic salts (*i.e.* Mg(ClO₄)₂) dissolved in aprotic organic solvents (*i.e.* acetonitrile), form passivating layers on the surface of the Mg metal anode, leading to poor performance of the overall cell. In order to address this problem, activated carbon was used as the counter electrode to replace the metallic magnesium. Our results show that (Mg_{0.5}Ni_{0.5})₃(PO₄)₂ has a first cycle discharge capacity of 90 mAhg⁻¹ when a 0.5 M Mg(ClO₄)₂ in acetonitrile solution is used as the electrolyte. Post mortem XRD, FTIR and XPS analysis of the electrode after cycling suggest that a conversion reaction takes place during discharge due to the extrusion of Ni²⁺ cations from the host material lattice. In a similar fashion, Cu-Ni alloys and amorphous Li₃PO₄ form during the electrochemical reaction between (Mg_{0.5}Ni_{0.5})₃(PO₄)₂ and lithium metal using a LiPF₆-based electrolyte, achieving a practical capacity of 600 mAhg⁻¹. Based on the electrochemical data, it is possible to conclude that the conversion reaction of (Mg_{0.5}Ni_{0.5})₃(PO₄)₂ with Mg metal as the counter electrode should occur as observed for lithium, if an electrolyte is found which does not passivate the Mg surface. However, since the Mg-electrode is passivated, our findings show that the use of a carbon-based counter electrode significantly improves the practical capacity of (Mg_{0.5}Ni_{0.5})₃(PO₄)₂ when a Mg-electrolyte is used.

References

1. H. D. Yoo, I. Shterenberg, Y. Gofer, G. Gershinsky, N. Pour, D. Aurbach, *Energy Environ. Sci.*, **2013**, 6, 2265–2279;
2. P. Canepa, G. Sai Gautam, D. C. Hannah, R. Malik, M. Liu, K. G. Gallagher, K. A. Persson, G. Ceder, *Chem. Rev.*, **2017**, 117, 4287–4341.

2:15 PM EN12.11.04

Late News: The Economically Sustainable Hydrothermal Synthesis of Dextrosil-Viologen as a Robust Anolyte in Aqueous Redox Flow Batteries Dawei Feng, Patrick Sullivan and Xiuliang Lyu; University of Wisconsin--Madison, United States

Aqueous organic redox flow batteries (RFBs) are promising for grid-scale energy storage, but identifying stable and inexpensive organic redox couples suitable for practical applications has been challenging. Here we report a new, inexpensive, and robust anolyte, Dextrosil-Viologen (Dex-Vi), that demonstrates a record overall RFB performance for viologen redox species in neutral aqueous media, including reduced anion-exchange membrane permeability, increased volumetric capacity capability, and improved chemical stability. At 0.1 M, the first redox state of Dex-Vi demonstrates no distinguishable capacity decay over two weeks of cycling (1,200+ cycles) when paired with BTMAP-Fc catholyte in an anolyte-limiting cell configuration. Even at a high concentration of 1.5 M in a practical capacity-balanced RFB, Dex-Vi demonstrates extremely stable cycling performance for one-electron utilization as well as flowable and soluble behavior when it is doubly reduced. Furthermore, by rationalizing a high-yield hydrothermal synthetic approach that has never been applied to viologen RFB molecules along with a low-cost precursor, the predicted mass production cost of Dex-Vi is below \$10/kAh. These results not only establish a new benchmark organic anolyte promising for practical RFB applications but also shows that the properties of organic redox species for RFB can be enhanced with minute performance tradeoffs through rationalized structural and synthetic design.

2:30 PM EN12.11.05

Effect of Fluorination and Li-Excess on the Li Migration Barrier in Mn-Based Cathode Materials Zinab Jadidi¹, Tina Chen¹, Penghao Xiao², Alexander Urban³ and Gerbrand Ceder¹; ¹University of California, Berkeley, United States; ²Lawrence Livermore National Laboratory, United States; ³Columbia University, United States

Disordered rock-salt Li-rich transition metal (TM) oxides, especially those based on Mn, are exciting prospective high-energy-density cathode materials for the next generation of LIBs due to their potential to replace Co-based cathodes [1]. Recently it has been shown that F substitution can reduce oxygen redox by lowering the average anion valence and increasing the amount of redox-active TM [2] as well as improve energy density, average voltage, and rate performance [3]. The substituting F tends to be incorporated in Li-rich environments due to its preference to bond with Li rather than TM [2]. We have investigated how both F substitution and Li excess affect the migration energy for Li diffusion in various local atomic configurations using first-principles calculations in combination with the nudged elastic band (NEB) method [4]. We use orthorhombic-LiMnO₂ as a model case to investigate the effects of F substitution and Li excess. Based on our results, we demonstrate that F has only a small effect on Li migration barriers while Li excess has a strong positive effect and actually decreases Li migration barriers. Hence, we do not expect any detrimental impact on Li transport when fluorination is used as a design strategy to increase the TM redox [4].

[1] Lee, J., Kitchaev, D. A., Kwon, D. H., Lee, C. W., Papp, J. K., Liu, Y. S., ... & Guo, J. (2018). Reversible Mn 2+/Mn 4+ double redox in lithium-excess cathode materials. *Nature*, 556(7700), 185.

[2] Kitchaev, D. A., Lun, Z., Richards, W. D., Ji, H., Clément, R. J., Balasubramanian, M., ... & McCloskey, B. D. (2018). Design principles for high transition metal capacity in disordered rocksalt Li-ion cathodes. *Energy & Environmental Science*, 11(8), 2159-2171 [2].

[3] Lee, J., Papp, J. K., Clément, R. J., Sallis, S., Kwon, D. H., Shi, T., ... & Ceder, G. (2017). Mitigating oxygen loss to improve the cycling performance of high capacity cation-disordered cathode materials. *Nature communications*, 8(1), 981 [3].

[4] Jadidi, Z., Chen, T., Xiao, P., Urban, A., & Ceder, G. (2020). Effect of fluorination and Li-excess on the Li migration barrier in Mn-based cathode materials. *Journal of Materials Chemistry A*, 8(38), 19965-19974.

2:45 PM EN12.11.06

Low Temperature Molten Sodium Batteries for Long-Duration Energy Storage Erik D. Spoecker, Martha M. Gross, Melissa L. Meyerson, Leo J. Small and Stephen J. Percival; Sandia National Laboratories, United States

The importance of long-duration energy storage (LDES) in the emerging sustainable, carbon-free global energy infrastructure continues to become increasingly clear. While several different types of storage are likely needed to meet growing LDES demands, new or adapted battery technologies are expected to play key roles in the future LDES technology space. Here, we describe how emerging low temperature, high voltage molten sodium batteries offer promise as one of these batteries. LDES can refer to storage from several different perspectives and application sets: 1) long discharge duration (e.g., >6-10 hours), 2) long storage duration between charge and discharge, or 3) long battery lifetime (>10-15 years). We will describe here the structure and chemistry of a developing low temperature (near 100°C) molten sodium-halide battery and discuss why it may be especially well-suited for LDES applications. These batteries comprise a molten sodium anode, a fully inorganic, molten sodium iodide-based metal halide salt catholyte, and an efficient solid state sodium ion-conducting separator. The specific composition of the molten salt catholyte and the engineering of the solid-state separator allow for the operation of these batteries at the low temperature of 110°C with a stable cycling voltage of 3.65V. We will discuss recent extended battery cycling behavior and the stability of battery performance during extended "frozen" storage experiments. Connecting our findings to LDES applications including extended discharge duration, extended storage duration, and long-lifetime storage, we outline the potential impact of low temperature molten sodium batteries to the rapidly evolving LDES technical landscape.

Sandia National Laboratories is a multimission laboratory managed and operated by National Technology & Engineering Solutions of Sandia, LLC, a wholly owned subsidiary of Honeywell International Inc., for the U.S. Department of Energy's National Nuclear Security Administration under contract DE-NA0003525.

SESSION EN12.12: Beyond Li-Ion IV
Session Chairs: Weiyang Li and Xiaolin Li
Monday Afternoon, December 6, 2021
EN12-Virtual

4:00 PM *EN12.12.01

Reversible Ketone Hydrogenation and Dehydrogenation for Aqueous Organic Redox Flow Batteries Wei Wang; Pacific Northwest National Laboratory, United States

Aqueous soluble organic (ASO) redox-active materials have recently shown great promise as alternatives to transition metal ions to be employed as energy-

bearing active materials in redox flow batteries for large-scale energy storage because of their structural tunability, cost-effectiveness, availability, and safety features. Development so far however has been limited to a small palette of organics that are aqueous soluble and tend to display the necessary redox reversibility within the water stability window. There is however noticeably much larger number of organic molecules that exhibit some degree of irreversible redox activities. In this presentation, we show how the molecular engineering of fluorenone enables the alcohol electro-oxidation needed for reversible ketone hydrogenation and dehydrogenation at room temperature without the use of a catalyst. Flow batteries based on these fluorenone derivative analytes operate efficiently and exhibit stable long-term cycling at ambient and mildly increased temperatures in a non-demanding environment. These results suggest the potential for identifying other atypical organic redox molecules for energy storage.

Reference: Feng et al., *Science* 372, 836–840 (2021)

4:30 PM EN12.12.02

A Low-Cost Flexible Full Ammonium-Ion Battery Enabled by a Novel Concentrated Hydrogel Electrolyte Ying Wang and Shelton Kuchena; Louisiana State University, United States

Nonmetal ammonium (NH_4^+) ions have recently been explored as effective charge carriers in battery systems due to their abundance, light weight, small hydration shells in water. The research concerning the use of redox chemistry in ammonium ion batteries, particularly in flexible ammonium ion batteries, is still in its infancy. For the first time, we report a flexible full ammonium ion battery (AIB) composed of a concentrated hydrogel electrolyte sandwiched between nanosized hydrated ammonium vanadate cathode and polyaniline (PANI) anode, for enhanced performance. The hydrogel electrolyte is simply synthesized by using ammonium sulfate, xanthan gum and water. As a reference, the AIB based on the liquid aqueous electrolyte is prepared first, which exhibits a capacity of 121 mAh g^{-1} and a capacity retention of 95% after 400 cycles at a specific current of 0.1 A g^{-1} . The simple synthesis of the hydrogel electrolyte allows us to facilitate tune and optimize the salt contents in the electrolyte, to maximize the ionic conductivity, transport kinetics, mechanical characteristics, and consequently the battery performance. It is found that the flexible battery based on the hydrogel electrolyte prepared from 3 M ammonium sulfate solution shows the best electrochemical performance, i.e., a capacity of 60 mAh g^{-1} while maintaining a capacity retention of 88% after 250 cycles at a specific current of 0.1 A g^{-1} , which are better than the few results reported for flexible AIBs in literature. Moreover, the flexible AIB retains excellent electrochemical performance when bent by 90 and 180 degrees, demonstrating remarkable mechanical strength and flexibility. Therefore, this study sheds new light on the utilization of concentrated hydrogel electrolyte in the AIB chemistry, for future developments of new electrochemical energy storage technology with high safety and low cost.

4:45 PM EN12.12.03

Copper Oxide Cathodes for Rechargeable Alkaline Zinc Batteries Noah B. Schorr¹, David J. Arnot¹, Andrea M. Bruck², Joshua Gallaway² and Timothy N. Lambert¹; ¹Sandia National Laboratories, United States; ²Northeastern University, United States

Relegated to the annals of history, Zn/CuO batteries have long thought to be solely a primary battery system. Surpassed by Zn/MnO₂ in both the commercialization as a primary cell and focus on fundamental investigations into generating secondary versions of the battery, very little research has been performed on CuO alkaline cells. However we have recently demonstrated that by including a bismuth additive into the CuO cathode formulation, Zn/CuO cells are capable of cycling over 100 times at $> 124 \text{ Wh/L}$, with capacities from 674 mAh/g (cycle 1) to 362 mAh/g (cycle 150).¹ To mitigate the capacity losses of long-term cycling CuO cells, we demonstrate two limited depth of discharge (DOD) strategies capable of cycling at 202 mAh/g for over 250 cycles or for $\sim 40 \text{ mAh/cm}^2$ and unprecedented energy densities of $\sim 260 \text{ Wh/L}$ for up to 80 cycles. Using a suite of electrochemical and spectroscopic techniques, including rotating ring disk electrochemistry, impedance, and energy dispersive x-ray diffraction the role of the bismuth additive in enabling the CuO cycling is elucidated. This work serves as a steppingstone for the development of low-cost, safe, and energy dense secondary batteries based on often overlooked conversion chemistries.

This work was Supported by the Laboratory Directed Research and Development program at Sandia National Laboratories, a multi-mission laboratory managed and operated by National Technology and Engineering Solutions of Sandia, LLC., a wholly owned subsidiary of Honeywell International, Inc., for the U.S. Department of Energy's National Nuclear Security Administration under contract DE-NA-0003525. The views expressed herein do not necessarily represent the views of the U.S. Department of Energy or the United States Government.

Ref 1 Schorr, N.B.; Arnot, D.J.; Bruck, A.M.; Duay, J.; Kelly, M. Habing, R.L.; Ricketts, L.S.; Vigil, J.A.; Gallaway, J.W.; Lambert, T.N. *ACS Applied Energy Materials*, 2021, Accepted

5:00 PM EN12.12.04

Prototypical Study of Double-Layered Cathodes for Aqueous Rechargeable Static Zn-I₂ Batteries Dun Lin and Yat Li; University of California, Santa Cruz, United States

Aqueous rechargeable zinc-iodine batteries (ZIBs) are promising candidates for grid energy storage because they are safe and low-cost and have high energy density. However, the shuttling of highly soluble triiodide ions severely limits the device's Coulombic efficiency. Herein, we demonstrate for the first time a double-layered cathode configuration with a conductive layer (CL) coupled with an adsorptive layer (AL) for ZIBs. This unique cathode structure enables the formation and reduction of adsorbed I₃⁻ ions at the CL/AL interface, successfully suppressing triiodide ion shuttling. A prototypical ZIB using a carbon cloth as the CL and a polypyrrole layer as the AL simultaneously achieves outstanding Coulombic efficiency (up to 95.6%) and voltage efficiency (up to 91.3%) in the aqueous ZnI₂ electrolyte even at high-rate intermittent charging/discharging, without the need of ion selective membranes. These findings provide new insights to the design and fabrication of ZIBs and other batteries based on conversion reactions.

5:15 PM *EN12.12.05

Developing Ionogel Electrolytes for Solid-State Batteries Ryan H. DeBlock¹ and Bruce S. Dunn²; ¹U.S. Naval Research Laboratory, United States; ²University of California, Los Angeles, United States

Ionogels are pseudo-solid state electrolytes in which an ionic liquid electrolyte is confined in an organic or inorganic matrix. One well established ionogel synthesis route is based on sol-gel chemistry where silica precursors dissolved in an ionic liquid electrolyte (ILE) undergo hydrolysis and condensation polymerization. By using an ionic liquid as the solvent, no evaporation occurs and the resulting material is a macroscopically rigid, nonporous material in which the ionic liquid is trapped by capillary forces in the nanometer sized pores in the silica network. Using this approach, it is possible to develop pseudo-solid state materials that possess the electrochemical, thermal and chemical properties of the ionic liquid. Moreover, sol-gel synthesis enables the precursor sol to penetrate porous electrodes before solidifying, a feature which is especially attractive for solid-state batteries.

In this presentation, we review our recent work on synthesizing Li-ion and Na-ion conducting ionogels and their incorporation in solid-state battery structures. We developed Li-ion conducting ionogels based on using an ILE comprised of 0.5M LiTFSI in [BMIM] [TFSI] that exhibited conductivity and

electrochemical properties comparable to those of the parent ILE. These pseudo-solid state materials were also incorporated in '2.5D' batteries comprised of a LiFePO₄ cathode array with a lithium anode. More recently we have focused on Na-ion conducting ionogels. One approach was based on using an ionic liquid electrolyte consisting of 0.5M NaFSI in [PYR14][TFSI]. The resulting material exhibited good ionic conductivity (0.7 mS cm⁻¹) and a nearly 5V electrochemical stability window. Sodium-ion solid-state batteries with excellent reversibility were demonstrated using this Na-ion conducting ionogel in conjunction with two Na-ion intercalation materials which served as positive and negative electrodes. We have also begun to investigate the synthesis and properties of ionogels that incorporate glyme-based electrolytes as such electrolytes have shown excellent stability in contact with sodium metal. We have successfully developed tetraglyme-based ionogels and incorporated them in sodium metal batteries using Na₃(VO)₂(PO₄)₂F as the cathode. Capacities in excess of 400 Wh kg⁻¹ were achieved at 0.5C. In summary, the ability to design the ion transport properties of ionogels coupled with their thermal and electrochemical stability makes these materials a very promising direction for use in solid-state energy storage devices.

SESSION EN12.13: Beyond Li-Ion V
Session Chairs: Seok Woo Lee and Xiaolin Li
Monday Afternoon, December 6, 2021
EN12-Virtual

9:00 PM *EN12.13.01

Potassium-Insertable Graphite and PBA Electrodes Tomooki Hosaka^{1,2}, Daisuke Igarashi¹, Kei Kubota^{1,2}, Ryoichi Tatara^{1,2} and Shinichi Komaba^{1,2}; ¹Tokyo University of Science, Japan; ²Kyoto University, Japan

K-ion battery (KIB) has recently attracted much attention as a potential high-voltage and high-power battery due to low standard electrode potential of K⁺/K and fast ionic diffusion of K⁺ ion in electrolyte solutions, respectively [1]. In 2015, our group reported graphite negative electrode, which delivered a reversible capacity of more than 250 mAh g⁻¹ with excellent reversibility and rate performance [2]. We also confirmed that a K-graphite intercalation compound of KC₈ was electrochemically formed with several stage transformations [3]. Furthermore, a Prussian blue analog (PBA) of K₂Mn[Fe(CN)₆] (KMnHCF) showed highly reversible potassium insertion/extraction and ca. 4 V vs. K⁺/K operation to realize a 4 V-class graphite // K₂Mn[Fe(CN)₆] full cell [4]. The cycle performance of the full cells drastically improved using the proper electrolytes, such as KPF₆-KN(SO₂F)₂ binary salt electrolytes [5]. In contrast, the bulk properties that affect the electrochemical properties of graphite and PBA have not been fully understood. Thus, we investigated the predominant bulk properties affecting the potassium insertion reaction into graphite and PBA electrodes.

Potassium insertion properties of several types of graphite were investigated, and we found that the crystallinity significantly affects the reversibility of K⁺ ion intercalation. Although the high reversible capacity and Coulombic efficiency of graphite electrodes in K cells were achieved during initial cycles regardless of the crystallinity, high crystallinity graphite demonstrated less potential-hysteresis and superior capacity retention to low crystallinity graphite. Operando XRD measurement confirmed a similar staging process of K-GICs for both graphite samples. However, high crystallinity graphite was transformed into higher crystallinity K-GIC as well as higher reversibility of potassium de-/intercalation than low crystallinity graphite. A turbostratic disorder in low crystallinity graphite led to the redox-potential split and lower crystalline K-GIC and potassium-extracted graphite. Thus, we concluded that high crystallinity is important for applying graphite to long-life potassium-ion batteries.

In addition to the graphite electrodes, we investigated the K⁺ insertion reaction into KMnHCF. Although the particle size and the number of [Fe(CN)₆]⁴⁻ anion vacancies may affect the electrochemical performance of PBAs, the difficulty of independently controlling the particle size and number of anion vacancies has hindered understanding the impact of each factor [6]. We successfully synthesized KMnHCFs through a precipitation route, and the particle size and number of the anion vacancies were varied by employing a proper chelate agent and Na/K ionic exchange route. When nearly stoichiometric KMnHCF was synthesized and tested, smaller particle sizes were important for achieving superior electrochemical performance in capacity and rate capability. However, even in larger particles, introducing a suitable number of anion vacancies enabled KMnHCF to exhibit comparable electrode performance, which would be due to the enhancement of K⁺ ion diffusion. From these results, we will present future insight into electrochemical potassium insertion chemistry.

References:

- [1] T. Hosaka, S. Komaba *et al.*, *Chem. Rev.*, 2020, **120**, 6358–6466.
- [2] S. Komaba, K. Kubota *et al.*, *Electrochem. Commun.*, 2015, **60**, 172-175.
- [3] K. Kubota, S. Komaba *et al.*, *Chem. Rec.*, 2018, **18**, 459-479.
- [4] X. Bie, S. Komaba *et al.*, *J. Mater. Chem. A*, 2017, **5**, 4325-4330.
- [5] T. Hosaka, S. Komaba *et al.*, *ACS Appl. Mater. Interfaces*, 2020, **12**, 34873-34881.
- [6] T. Hosaka, S. Komaba, *ChemSusChem*, 2021, **14**, 1166-1175.

9:30 PM *EN12.13.02

Aqueous Battery for Large-Scale Energy Storage—Towards Both High Energy Density and Superior Safety Chunyi Zhi; City Univ of Hong Kong, Hong Kong

Development of energy storage system in the past year focus on improvement of energy density. While the progress is remarkable, safety problems of lithium ion batteries (LIB) have been intensively exposed. On one hand, LIB is not intrinsically safe with very active anode, flammable electrolyte and oxygen-releasing cathode; on the other hand, many application scenarios actually don't require very high energy density.

We work on aqueous electrolyte batteries to achieve both high energy density and superior safety performance. We show how to activate the desired reversible I⁰/I⁺ redox at a potential of 0.99 V vs. SHE by electrolyte tailoring via F⁻, Cl⁻ ions-containing salts. The electronegative F⁻ and Cl⁻ ions can stabilize the I⁺ during charging. In an aqueous Zn ion battery based on an optimized ZnCl₂ + KCl electrolyte with abundant Cl⁻, I-terminated halogenated Ti₃C₂ MXene cathode delivers two well-defined discharge plateaus at 1.65 V and 1.30 V, superior to all reported aqueous I₂-metal (Zn, Fe, Cu) counterparts. Together with the 108% capacity enhancement, the high voltage output results in a significant 231% energy density enhancement. In addition, we also develop various approaches to stabilize the Zn anode. We accurately quantifying the hydrogen evolution in Zn metal battery by *in-situ* battery-gas chromatography-mass analysis. Then, we propose a vapor-solid method for an highly electronically insulating (0.11 mS×cm⁻¹) but high Zn²⁺ ion conductive (80.2 mS×cm⁻¹) ZnF₂ solid ion conductor with high Zn²⁺ transfer number (0.65) to isolate Zn metal from liquid electrolyte, which can not only prohibit over 99.2 % parasitic hydrogen evolution reaction during cycling but also guide uniform Zn electrodeposition. Meanwhile, Zn@ZnF₂/Zn@ZnF₂ symmetric cell exhibits excellent stability over 2500 h (over 6250 cycles) with 1 mAh×cm⁻² of Zn reversibly cycled at 5 mA×cm⁻², and stable cycling under ultrahigh current density and areal capacity (10 mA×cm⁻², 10 mAh×cm⁻²) over 590 h (285 cycles), which far outperforms all reported Zn metal anode in aqueous system. In light of the superior Zn@ZnF₂ anode, the practical-level aqueous Zn@ZnF₂/MnO₂ batteries (~3.2 mAh×cm⁻²) shows remarkable cycling stability over 1000 cycles with 93.63 % capacity retained at ~100 % coulombic efficiency.

10:00 PM EN12.13.04

Stabilizing Zn Anodes Through Trace Functional Polymer Additives in Low-Cost Dilute Aqueous Electrolytes Huilin Pan; Zhejiang University, China

Recently, a variety of approaches have been proposed to address the key challenges of Zn anodes for Zn batteries, i.e., Zn dendrites, low reversibility, hydrogen generations and limited cycle life. Fundamentally, the electrolyte and electrode-electrolyte interface play a vital role in the electrochemical performance of Zn anodes. Nevertheless, the principles of stabilizing the Zn anode interface are not well developed so far.

In this talk, we will systematically discuss the fundamental principles of developing high-performance Zn anodes in low-cost dilute aqueous electrolytes with a trace amount of functional polymer additives. The correlation between the reaction kinetics and the stability of Zn anodes and polarity of the polymer additive in dilute 1 M ZnSO₄ aqueous electrolytes was revealed. The polymer additive tailors the electrochemical performance by rearranging the “Zn²⁺-H₂O-SO₄²⁻-polymer” bonding network and the space charge region of Zn anodes. PAM polymer with moderate polarity exhibits synergic enhancement as the “smoother” and “thruster” for the diffusion of Zn²⁺ towards the Zn anodes, showing uniform Zn deposition with minimal impact on reaction kinetics in both half and full cells. This work significantly provides useful insight on designing low-cost and high-performance aqueous electrolytes through functional electrolyte additives.

Reference:

1. Y. Jin, K.S. Han, Y. Shao, M.L. Sushko, J. Xiao, H. Pan, J. Liu, *Advanced Functional Materials* 2020, 30, 2003932.
2. M. Yan, H. Ni, H. Pan, *Rechargeable Mild Aqueous Zinc Batteries for Grid Storage*. *Advanced Energy and Sustainability Research* 2020, 1, 2000026.
3. M. Yan, C. Xu, Y. Sun, H. Pan, H. Li, *Nano Energy* 2021, 82, 105739.
4. M. Yan, H. Pan et al., Tailoring the stability and kinetics of Zn anodes through trace organic polymer additives in dilute aqueous electrolytes, under review.

10:15 PM *EN12.09.02

Development of Layered Oxides Cathodes and Phosphorus Anode for High-Energy and Low-Cost Sodium-Ion Batteries Guiliang Xu and Khalil Amine; Argonne National Laboratory, United States

Considering the natural abundance and low cost of sodium resources, sodium ion batteries (SIBs) have received much attention for large scale electrochemical energy storage. However, rational electrode materials design and good mechanistic understanding are required to enable advanced SIBs with high energy density. On the cathode side, P2 type and O3 type layered oxides are promising cathode materials due to their high specific capacity. However, they both suffer from rapid capacity degradation during high-voltage operation, and yet the mechanism remained poorly understood. On the anode side, phosphorus delivers the highest theoretical capacity (ca. 2600 mAh/g) among various anode materials, but undergo huge volume changes during sodiation/de-sodiation and severe capacity degradation. In this work, we will present our mechanistic understanding on the degradation of layered oxide cathodes during high-voltage charge and how intergrowth structure can mitigate these problem. We will also introduce our strategies to stabilize and improve the rate performance of high-capacity phosphorus anode through structure design and Sb doping. We expect our findings could promote the development of high-energy and low-cost SIBs based on layered oxides cathode and phosphorus anode chemistry.

SESSION EN12.14: Li-Ion Batteries II
Session Chairs: Dominic Bresser and Seok Woo Lee
Tuesday Morning, December 7, 2021
EN12-Virtual

8:00 AM *EN12.14.01

Digitalization of Lithium-Ion Battery Manufacturing—From Physics-Based Modeling to Artificial Intelligence and Augmented Reality Alejandro A. Franco^{1,2}; ¹Universite de Picardie Jules Verne, France; ²Institut Universitaire de France, France

The needed massive deployment of lithium ion batteries (LIBs), in particular to satisfy the demand from the Electric Vehicle (EV) sector, encourage battery manufacturers to multiply the number of giga-factories to reduce the cost of production. Such a production consists of a complex process involving multiple steps, such as the slurry preparation, its coating, drying, calendaring, electrolyte infiltration and formation. The choice of the manufacturing parameters along the process strongly impacts the overall LIB cell performance. However, the optimization of the manufacturing parameters to obtain the desired characteristics of LIB cells is currently based on a forward "trial and error" approach. This approach is inefficient in terms of time and cost due to the infinite number of possibilities for adjusting the manufacturing parameters. The integration of digitalization into giga-factories such as Artificial Intelligence (AI) and multiscale modeling is essential to accelerate the manufacturing process optimization and significantly raise the work efficiency of scientists, engineers and production line operators. Here I present our efforts in developing a digital twin of battery manufacturing within the context of the ERC-funded ARTISTIC project [1,2], supported on a combination of physical and AI/machine learning models trained with data arising from in house high throughput characterizations. This digital twin allows simulating the different steps along the manufacturing process, predicting in three dimensions the resulting electrode properties and evaluating the associated electrochemical performance upon battery cell cycling. The predictive capabilities of this digital twin are illustrated with results for different electrode materials (graphite, Silicon/graphite, NMC, LFP) and formulations, paving the way towards manufacturing digital optimization. I also present the online free services that the project is offering, such as a tool for battery manufacturing simulation from an internet browser and a tool for stochastic generation and meshing of lithium ion battery electrodes and separators [3]. Finally, I conclude with our recent work by us (extending our work published in Ref. [4]) on the implementation of our computational models in novel Augmented Reality interfaces to assist the battery manufacturing work.

References

- [1] <https://www.erc-artistic.eu/>
- [2] <https://www.erc-artistic.eu/scientific-production/publications>
- [3] <https://www.erc-artistic.eu/computational-portal>
- [4] Franco, A.A., Chotard, J.N., Loup Escande, E., Yin, Y., Zhao, R., Rucci, A., Ngandjong, A.C., Herbulot, S., Beye, B., Ciger, J. and Lelong, R., 2020. Entering the Augmented Era: Immersive and Interactive Virtual Reality for Battery Education and Research. *Batteries & Supercaps*, 3(11), pp.1147-1164.

8:30 AM *EN12.14.02

Molecular Modeling of Electrolytes for Lithium and Divalent Batteries [Oleg Borodin](#); U.S. Army Research Laboratory, United States

A molecular scale insight into ion transport and compatibility with electrodes is important for understanding deficiencies of the currently used aqueous and non-aqueous electrolytes. In this presentation I will summarize recent progress made towards improving molecular scale understanding of the structure and electrochemistry for a wide range of aqueous and non-aqueous electrolytes for lithium and divalent batteries. Accurate molecular dynamics (MD) simulations of these electrolytes using polarizable force field will be used to establish a correlation between the ion transport mechanisms, electrolyte structure and transference number. Reactive modeling will focus on the competitive solvent and salt reduction and oxidation at the passivated electrochemical interfaces using Born Oppenheimer Molecular Dynamics (BOMD) simulations using DFT functionals. These BOMD simulations included critical factors needed to realistically represent electrolyte reactivity at electrodes such as explicit description of the substrate – electrolyte interactions; accurate representation of electrolyte structure, ion pairing and aggregation near an electrode.

9:00 AM *EN12.14.03

Organic Electroactive Materials For The Lithium Metal Polymer Technology [Joel Gaubicher](#) and Philippe Poizot; CNRS Nantes Université, France

Lithium metal polymer (LMP⁰) solid-state batteries based on the use of dry PEO-based electrolytes have been developed since the early 2000's by the Bollore's group and its subsidiary BlueSolutions company. The reliability of this technology which derives from polymer electrolyte (SPE) membrane Li batteries proposed by M. Armand in the late 70's^{[1],[2]} has been demonstrated in different applications with the first practical deployment in the world in full electric vehicles in 2011. This technology is now widely utilized not only in multiple e-mobility scenarios but also in stationary storage applications all over the world (Europe, North America, Asia and Africa). Like many other electrochemical storage technologies, the search for efficient, cheaper but also earth-abundant insertion electroactive materials remains an ongoing challenge to mitigate environmental issues. In this respect, the potential interest of electroactive organic materials to build eco-friendlier batteries has been the subject of intense research^[3]. However, little is known about their behavior when implemented in the LMP⁰ technology. We therefore embarked in the investigation of the electrochemical and physicochemical behaviors of neutral molecule and salt compounds as positive electrode material of LMP⁰ cells.

[1]Armand, M.B.; Chabagno, J.M.; Duclot, M. *Second International Meeting on Solid Electrolytes Extended Abstracts*; St Andrews, Scotland, 1978.

[2] Armand, M.B.; Chabagno, J.M.; Duclot, M. *Fast Ion Transport in Solids*; Vashishta, P., Mundy, J.N., Shenoy, J.K., Eds.; North Holland Publishers: Amsterdam, The Netherlands, 1979; p. 131

[3]Poizot, P.; Gaubicher, J.; Renault, S.; Dubois, L.; Liang, Y.; Yao, Y. *Chem. Rev.* 2020, 120, 6490.

9:30 AM EN12.14.04

Structured Electrodes for Improved Performance of Lithium-Ion Batteries [Chuan Cheng](#)¹, Ross Drummond², Stephen Duncan² and Patrick Grant²; ¹University of Warwick, United Kingdom; ²University of Oxford, United Kingdom

Electrode structures of commercial lithium-ion cells are isotropic at the macro-scale, comprising a homogenous mixture of constituents including active materials, carbon conductive additives, polymeric binders, and randomly distributed inter-connected porosity. Due to restricted ion mobility in the tortuous pore channels and anisotropic electric-field distribution when in operation, the Li-ion concentration and activation overpotential are inevitably inhomogeneous through the electrode thickness, especially at fast charge-discharge rates when the concentration and overpotential gradients become steeper. As a result, the electrochemically active material is inhomogeneously utilized and the reaction rate is spatially varying, which have detrimental effects on battery performance and lifetime, local capacity degradation, overheating and stress concentration. This is an electrode-scale problem, regardless of the specific electrode materials.

We design, manufacture and assess the performance of carefully controlled heterogeneous, graded electrode structures with the aim of promoting greater uniformity in overpotential distribution, and reaction rates across the electrode thickness. We investigate the arising polarization, and impedance behavior, as well as side reactions such as SEI formation. We demonstrate that micro-scale composition-graded electrodes provide enhanced capacity retention at fast charge-discharge rates to mitigate the long-lasting challenge of energy-power trade-off of lithium-ion batteries, and reduce battery degradation rate in both half-cell and full-cell lithium-ion batteries.

References

- C. Cheng, R. Drummond, S. R. Duncan, and P. S. Grant, *J. Power Sources* **413**, 59 (2019)
C. Cheng, R. Drummond, S. R. Duncan, and P. S. Grant, *J. Power Sources* **448**, 227376 (2020)

9:45 AM EN12.14.05

In Silico Discovery of Organic Lithium-Ion Positive Electrodes Driven by Artificial Intelligence [Rodrigo Carvalho](#)^{1,1}, Cleber Marchiori², Daniel Brandelli¹ and Moyses Araujo^{2,1}; ¹Uppsala University, Sweden; ²Karlstad University, Sweden

Electrical energy storage (EES) devices have staged important technological revolutions in the past years, with special attention given to Li-ion batteries (LIBs). However, novel socioeconomical paradigms¹ have urged for environmentally friendly and sustainable alternatives regarding these technologies. In this context, organic materials have attracted attention as potential candidates to pave the way toward the achievement of truly green batteries. They offer several advantages like cost efficiency, sustainability, synthesis from renewable or feedstock and tunable properties.² Nonetheless, hindrances related to cyclability and energy density need to be solved before the achievement of such alternative technologies. In this study, we report the development of a novel Artificial Intelligence (AI) methodology to accelerate the discovery of organic electroactive materials, with special focus given to LIBs positive electrodes. This framework has rendered an AI-*kernel* that enabled us to tap into the almost limitless organic library in a fast and accurate fashion. Requiring only the molecular SMILES representation as input, the *kernel* is divided in three levels, each composed by an independent learning scheme. The **first level** is based on Graph Neural Networks (GNN) and is responsible to identify if a given molecule is redox stable. The **second level** predicts the oxidation and reduction potentials (P_{Ox} and P_{Red}) of the redox-stable molecules by using a combination of Natural Language Processing (NLP) to analyze the SMILES and Recurrent Neural Networks (RNN). Finally, the **third level** is composed by a least squares multi-regression model that connects the molecular redox potentials (P_{Ox} and P_{Red}) predicted in the previous level to the battery open circuit voltage (OCV) (V vs. Li/Li⁺). To fuel the AI, two different databases have been developed: a small set of predicted molecular crystals following an interplay between DFT and an evolutionary algorithm^{3,4}; and a larger set of more than 30000 unique molecules with redox properties extracted from DFT. We demonstrate the AI-*kernel* efficiency by performing a high-throughput screening in 20 million molecules following a $capacity (mAh/g) \rightarrow OCV (V vs Li/Li^+) selection$ to find suitable electrode candidates. As the final part of this screening, new DFT calculations were performed for the selected molecules with a two-fold goal: to validate the AI-*kernel* performance and to further filter the candidates list. This process led to the discovery of about 500 promising molecules for cathode compounds, with some exhibiting theoretical energy densities superior to 2000 Wh/kg. Moreover, the AI-*kernel* accurately identified common molecular characteristics

that lead to such higher-voltage electrodes and pointed out an interesting donor-accepter-like effect that may drive the future design of cathode-active materials.

References:

- 1 P. T. Brown and K. Caldeira, *Nature*, 2017, **552**, 45–50.
- 2 S. E. Burkhardt, J. Bois, J. M. Tarascon, R. G. Hennig and H. D. Abruña, *Chemistry of Materials*, 2013, **25**, 132–141.
- 3 R. P. Carvalho, C. F. N. Marchiori, D. Brandell and C. M. Araujo, *ChemSusChem*, 2020, **13**, 2402–2409.
- 4 R. P. Carvalho, C. F. N. Marchiori, V.-A. Oltean, S. Renault, T. Willhammar, C. Pay Gómez, C. M. Araujo and D. Brandell, *Materials Advances*, 2021, **2**, 1024–1034.

SESSION EN12.15: Beyond Li-Ion VI
Session Chairs: Dominic Bresser and Weiyang Li
Tuesday Morning, December 7, 2021
EN12-Virtual

10:30 AM *EN12.17.01

K-Ion Batteries—Progress and Outlook Mauro Pasta; University of Oxford, United Kingdom

Potassium-ion batteries (KIBs) are emerging as a promising complementary technology to lithium-ion batteries due to their potential low cost and high rate capability¹.

In my talk, I will discuss the progress we have made in understanding the crystal structure-electrochemistry relationship in Prussian Blue Analogue cathodes², the electro-chemo-mechanical properties of red phosphorous (RP) upon alloying with potassium³ and its application in RP-graphite composite anodes⁴ and, lastly, in identifying and characterising electrolytes and interfaces compatible with both electrodes.

I will then discuss the critical research challenges that need to be addressed for KIBs to become a viable technology.

References

- 1 S. Dhir, S. Wheeler, I. Capone and M. Pasta, *Chem*, 2020, **6**, 2442–2460.
- 2 M. Fiore, S. Wheeler, K. Hurlbutt, I. Capone, J. Fawdon, R. Ruffo and M. Pasta, *Chemistry of Materials*, 2020, **32**, 7653–7661.
- 3 I. Capone and J. Aspinall, *Matter*, 2020, 1–17.
- 4 I. Capone, J. Aspinall, H. J. Lee, A. Xiao, J. Ihli and M. Pasta, *ChemRxiv*, 2020.

11:00 AM *EN12.15.02

Mechanistic Investigations of Manganese and Vanadium Oxide Electrochemistry in Aqueous Zinc Batteries Esther S. Takeuchi^{1,2}, Amy Marschilok^{1,2} and Kenneth Takeuchi^{1,2}; ¹Stony Brook University, United States; ²Brookhaven National Laboratory, United States

Implementation of intermittent renewable energy sources derived from wind and solar power motivates development of safe, sustainable, low cost energy storage devices, specifically batteries based on aqueous electrolytes. As a negative electrode material, Zn has a high theoretical capacity (820 mAh/g), low redox potential (-0.76 V vs. SHE), and low toxicity such that aqueous electrolyte zinc based batteries may prove to be a desirable alternative for Li-ion batteries for some applications. Recent studies on aqueous Zn ion batteries using mildly acidic electrolytes have demonstrated the possibility of zinc anodes with high cycle life. Several classes of cathode materials have been explored as possible candidates including metal-inserted vanadates and manganese oxides.

Vanadium based materials are appealing for aqueous electrochemical energy storage due to the multiple accessible redox states for the vanadium center. Layered vanadates, supported by cation pillars, are of interest for Zn-ion batteries as the vanadium redox center allows for high capacity and the layered structure promotes facile ion transfer. In particular, sodium vanadium oxides (NVO) show promise as cathode materials for Zn-ion aqueous batteries. Manganese oxides are also of interest due to their low cost and low environmental impact. Manganese oxide structural chemistry is synthetically rich and a number of polymorphs have been considered. Tunnel-type materials such as α -MnO₂ are particularly noteworthy owing to their facile synthesis and high energy density. Despite its appealing electrochemistry, however, the exact reaction mechanism of α -MnO₂ in zinc batteries has remained unclear where zinc insertion, proton insertion, and/or structural changes have been proposed.

Understanding the key parameters that govern the charge storage mechanisms of the Zn aqueous systems remains a critical challenge in order to advance these systems to next generation products. Thus, investigations that probe mechanisms can provide a pathway for ultimately controlling electrochemical outcomes. This presentation will discuss the influence of material properties on the electrochemistry of NVO in Zn-ion aqueous cells and operando studies clarifying the dominant redox mechanism of α -MnO₂ in zinc batteries.

11:30 AM EN12.15.03

Cu/Ni/Co Ordered Mesoporous Oxides as High-Performance Cathode Catalysts for Li-O₂ Batteries Tatiana Priamushko¹, Nicolas Eshraghi², Jürgen Kahr², Marcus Jahn² and Freddy Kleitz¹; ¹University of Vienna, Austria; ²AIT Austrian Institute of Technology GmbH, Austria

In recent years, rechargeable lithium-oxygen (Li-O₂) batteries have been studied as a future battery system mainly due to their ultrahigh theoretical capacity, low cost, and environmental friendliness. However, the further development of Li-O₂ batteries into commercial applications is hindered by issues such as low energy efficiency, short cycle life, parasitic reactions, and poor rate capability. These issues are mainly the result of the voltage hysteresis and high overpotential in the cathode side. The voltage hysteresis during cycling is large, giving rise to low energy efficiencies and high overpotentials, which in turn, cause significant electrode and electrolyte decomposition. Thus, it is necessary to develop high-performance catalysts for the cathode to address the challenges raised by the overpotential and to boost the performance of Li-O₂ batteries. Three groups of positive-electrode catalysts for Li-O₂ batteries were studied by researchers: carbon materials, noble metal-based materials, and transition metal-based materials.

Considering that the cathodic process is a complicated redox reaction taking place in the triple-phase of gas, liquid, and solid, the structural design of cathode electrodes is critical to achieving high-performance Li-O₂ batteries. Indeed, the catalysts used in cathodes generally have a high surface area to provide transport pathways for oxygen, lithium ions, and electrons and thus increase the reaction sites for the Oxygen reduction reaction (ORR). Among the transition metal-based materials, Co₃O₄ can reduce the charge overpotential and improve the cycling performance of Li-O₂ batteries. Co₃O₄ crystallizes in the spinel structure (Co^{II}Co^{III}₂O₄), with edge-sharing CoO₆ octahedra (Co³⁺ centered) interconnected by corner-sharing

CoO₄ tetrahedra (Co²⁺ centered), this structure can accommodate vacancies and lattice defects, that potentially act as active sites to promote electrochemical reactions. Cu/Ni substitution of Co in the structure would ensure a more sustainable material development as well as the improved electrical conductivity of the material to increase the electron supply to reaction sites. Furthermore, using ordered mesoporous Co-based oxides is beneficial due to their high surface area.

In this context, a series of ordered mesoporous Cu/Ni/Co oxides are prepared via nanocasting with varied Cu/Ni ratios to establish their impact on the electrochemical performance of the catalysts. The performance of non-aqueous Li-O₂ batteries is directly determined by the reversible formation mechanism of the discharge products, being either Li₂O₂ or LiOH [1]. Therefore, the nature and evolution of the discharge products, in different voltage steps for the first discharge cycle was investigated by *ex situ* XRD tests. These tests show the formation of LiOH as a discharge product in presence of mesoporous Cu/Ni/Co oxides in the cathode. A lower overpotential was observed both in ORR and oxygen evolution reaction (OER) with a discharge capacity in the range of 4000-6000 mAh/g_{carbon} based on different Cu/Ni ratios. During discharge, O₂ reduction was detected along with the LiOH formation with a voltage plateau at 2.8V (≈ 0.1V discharge overpotential). During charge, O₂ evolution was detected along with LiOH decomposition up to 3.55 V, and at higher voltages, products from parasitic reactions can be detected. These results show promising properties of the mesoporous Cu/Ni/Co oxides as catalysts that can effectively promote the OER at a low overpotential. This lower overpotential is a key step in the development of reversible Li-O₂, particularly in LiOH-based Li-O₂ due to the increased stability of LiOH over other discharge products.

[1] Li Z. et al. Understanding the electrochemical formation and decomposition of Li₂O₂ and LiOH with operando X-ray diffraction. *Chemistry of Materials*. 2017, 29, 1577-1586.

11:45 AM EN12.15.06

Bottom-Up Mechanochemical Synthesis of Tin (Sn) Nanoparticles for Sodium-Ion Batteries Katherine A. Mazzi^{1,2}, Baris Akduman² and Philipp Adelhelm^{2,1}; ¹Helmholtz-Zentrum Berlin, Germany; ²Humboldt-Universität zu Berlin, Germany

Sodium-ion batteries (NIBs) are attractive alternatives to lithium-ion batteries (LIBs) due to the high earth abundance and low cost of Na, the cathodes do not require cobalt, and their device architectures can be similar to those of LIBs, thereby streamlining production. One challenge associated with the development of NIBs is that the cost reduction must make up for the lower energy densities relative to LIBs, and as a result there is a strong drive towards development of alloying anodes for NIBs due to their high storage capacity and favorable redox potentials. Sn nanoparticles appear as an attractive option to increase the capacity of NIB anodes. This is because of a desirable redox potential of around 0.2 V vs. Na⁺/Na combined with a very high theoretical capacity of 847 mAh/g and high rate capability.^{1,2} Nanosizing can further help prevent cracking and pulverization of the electrodes arising from volume expansion during alloying. The combination of chemical and mechanical resilience during electrochemical cycling ultimately enhances both the maximum capacity and lifetime of devices employing these materials.

Bottom-up synthesis methods rely on chemical pathways utilizing different precursor materials and chemical reducing agents for the production of nanomaterials. These methods have been successfully employed at the lab scale for the production of nanomaterials with good control over their dimensions, dispersity, morphology, and composition, but are severely lacking in the ability to scale up to industrial levels. Mechanochemistry is a technique that has been widely used on the industrial scale for the production of materials for battery anodes, but almost exclusively via top-down approaches relying on comminution of bulk materials that does not allow for control over the resulting morphology or composition. In this work we demonstrate a new method for the bottom-up mechanochemical synthesis of Sn nanoparticles with controlled dimensions for use in NIBs. The synthesis itself is entirely solid-state, employing only a metal halide precursor and a reducing agent during ball milling, and does not necessitate any capping agents for size control or solvents until the workup of the synthesized materials. The sizes of the particles are controlled by adjusting the milling time, and the influence of particle size on the electrochemical performance was investigated in proof of concept NIBs. The milling time does not have a direct relationship with the particle size because once the particles grow for long enough, they will begin to experience comminution and not continuously grow. The product from the shortest milling time demonstrated capacities of 475 mAh/g at 0.1C alongside the highest current rates in the series, which can be attributed to the fast diffusion of Na⁺ in the nano-sized particles. The samples milled the longest showed the highest capacity of 594 mAh/g at 0.1C. Rate capability studies demonstrated stable CE values close to 100%, indicating high reversibility and structural resilience. Overall these results demonstrate proof of concept for Sn nanoparticles in NIBs synthesized via a new scalable synthesis method based on solid-state bottom-up mechanochemistry.

References:

(1) Palaniselvam, T.; Goktas, M.; Anothumakkool, B.; Sun, Y.; Schmich, R.; Zhao, L.; Han, B.; Winter, M.; Adelhelm, P. *Adv. Funct. Mater.* **2019**, 29 (18), 1900790.

(2) Palaniselvam, T.; Babu, B.; Moon, H.; Hasa, I.; Santhosha, A. L.; Goktas, M.; Sun, Y.; Zhao, L.; Han, B.; Passerini, S.; Balducci, A.; Adelhelm, P. *Batter. Supercaps* **2021**, 4 (1), 173–182.

SESSION EN12.16: Electrolyte and Interface
Session Chairs: Weiyang Li and Xiaolin Li
Tuesday Afternoon, December 7, 2021
EN12-Virtual

1:00 PM *EN12.16.01

Sodium Batteries—From Small to Large-Scale Stationary Energy Storage Stefano Passerini; Karlsruhe Institute of Technology, Germany

The European Strategic Energy Technology Plan established the transformation to climate neutrality by 2050 since energy production is responsible for 75% of the greenhouse gas emission in the EU.¹ For this transformation, the use of renewable energy sources and clean energy carriers should be drastically increased. In parallel, the mobility should implement sustainable and smart technologies in transportation. In this scenario, energy storage devices, especially batteries, are a key technology towards a low-carbon energy system, as large-scale stationary energy storage and electric vehicle applications. Lithium-ion batteries (LIBs) are excellent candidates due to their high energy and high-power density. In fact, LIBs dominate the market for portable electronics and electric vehicles. However, the demand of LIBs is increasing, and the future supply of the raw materials (cobalt and lithium) makes uncertain their feasibility for massive renewables' energy storage.² Therefore, there is an urgent need to develop alternative energy storage devices that meet the cost, raw material availability and good performance requirements.

In this context, Sodium-ion batteries (SIBs) have been postulated as potential low-cost energy storage devices for large-scale stationary applications and light electromobility due to the almost infinite and widely distributed sodium resources and a 30% cost reduction respect with LIBs.^{3,4} In fact, SIBs employing non-aqueous liquid electrolyte are rather close to commercialization.^{5,6} Among cathode chemistries, different positive materials have been selected, being the main used one layered oxides while as negative electrode Hard Carbon (HC) is considered the anode of choice.⁷

With regards to large-scale stationary energy storage, sodium-based battery systems appear to be promising even for seasonal/annual storage systems. In particular, Na-seawater batteries, making use of multiple electrolytes, i.e., seawater as the catholyte (as well as the cathode material), a solid electrolyte physically separating the two electrode compartments, and a non-aqueous anolyte, appear very promising.⁸ Because natural seawater is also the active material in the open-structured cathode, the Na seawater battery can be supplied infinitely with Na⁺ cations, which are transferred to the anode side during charging. The generated sodium can be stored inside (for daily/weekly storage) and/or outside (for seasonal/annual storage) the cell. The process can be reversed during discharge, delivering electricity on demand.

As additional benefits, Na-seawater batteries upon charge produce desalinated water (for industrial and residential uses), and chlorine (for bleach, disinfectant, and polymer chemistries) while during discharge generates NaOH, which can be used for CO₂ capture.

References

- 1) https://setis.ec.europa.eu/implementing-set-plan-2020-report-2020-11-23_en
- 2) C. Vaalma, D. Buchholz, M. Weil, S. Passerini, *Nature Rev. Mat.* 3, 18013 (2018).
- 3) M. A. Muñoz-Márquez, D. Saurel, J.L. Gómez-Cámer, M. Casas-Cabanas, E. Castillo-Martínez, T. Rojo. *Adv. Energy Mater.* 7, 1700463 (2017).
- 4) I. Hasa, S. Mariyappan, D. Saurel, P. Adelhelm, A.Y. Kuposov, C. Masquelier, L. Croguennec, M. Casas-Cabanas, *J. Power Sources* 482, 228872 (2021).
- 5) https://www.greencarreports.com/news/1098434_faradion-electric-bike-prototype-powered-by-sodium-ion-batteries
- 6) X.H. Rong, Y.X. Lu, X.G. Qi, Q. Zhou, W.H. Kong, K. Tang, L.Q. Chem, Y.-H. Hu, *Energy Storage Sci. Technol.* 9, 515 (2020).
- 7) H. Moon, M. Zarrabeitia, E. Frank, O. Böse, M. Enterría, D. Saurel, I. Hasa, S. Passerini, *Batteries & Supercaps* 4, 960 (2021).
- 8) Y. Kim *et al.*, Sodium Biphenyl as Anolyte for Sodium-Seawater Batteries, *Adv. Funct. Mater.* 2001249 (2020)

1:30 PM *EN12.16.02

Interface Design of All-Solid-State Batteries Xueliang A. Sun; University of Western Ontario, Canada

The state-of-the-art rechargeable Lithium-ion batteries (LIBs) use liquid electrolytes and are the major choice for current EVs and portable electronic applications. However, these LIBs still suffer from many issues related to safety, lifespan and energy density. Accordingly, solid-state lithium batteries (SSLBs) have recently emerged as a promising alternative energy storage device due to their ability to overcome the intrinsic disadvantages of liquid-electrolyte LIBs and possess a greater volumetric energy density due to the use of solid-state electrolytes (SSEs). However, the interfacial issues between SSEs and electrodes (both cathode and anode) have a significant impact on the stability and lifetime of SSLBs [1-3]. The origin of these interfacial phenomena is the unstable contact and chemical reactions between electrodes and electrolytes to form an interlayer with extremely low electronic and/or ionic conductivities, which restricts the performance of the SSLBs. An artificial, uniform and ultrathin interfacial layer is critical to address these challenges [2, 3]. Atomic layer deposition (ALD) and molecular layer deposition (MLD) are unique coating techniques that can realize excellent coverage and conformal deposition with precisely controllable at the nanoscale level due to its self-limiting nature, which are ideal for addressing the challenges of interface in SSLBs [2, 3]. In addition, design of SEI in SSLBs is very important for obtaining high performance of SSLBs.

In this talk, we will report to address the interfacial challenges in SSLBs via two strategies: (i) develop ALD/MLD to rationally design novel coatings for sulfide-based interface design [4-7]; and (ii) SEI design of solid-state Li-S batteries [8-10]. The goal is to prevent capacity degradation of SSLBs caused by high interfacial resistance and chemical/electrochemical reactions between electrodes and electrolytes.

2:00 PM EN12.16.03

Protective Li⁺ Conducting Polymer Coatings for Lithium-Metal Anode Yumi Kim, Amaresh Pandian, Anthony Fong, Maxwell Giammona and Younghye Na; IBM Almaden Research Center, United States

Lithium (Li) anode has been actively investigated in the battery R&D in order to achieve advanced batteries with higher energy density. Among various studies, Li protection strategies have been a crucial topic of interest since the evolution of a thick solid electrolyte interface (SEI) layer on the reactive lithium metal anode and dendrite growth caused by irregular lithium deposition result in poor cyclic performance and low coulombic efficiency of lithium-metal batteries. In this study, to reduce the undesirable side reactions on the surface of metallic Li anode, Li⁺ conducting polymer coatings have been investigated for the application of a lithium-halide battery. The Li anode protected by a crosslinked PEG-POSS polymer coating demonstrated enhanced specific capacity, rate performance, and cyclability compared to the battery with bare Li anode. In addition, we confirmed that Li deposits with a round shaped-granular morphology are uniformly formed underneath the polymer layer, which indicates that this polymer layer is successfully functioning as a Li⁺ conducting protective layer on the lithium anode. Detailed experimental data and the working mechanism for the performance enhancement will be addressed in the presentation.

2:15 PM EN12.16.04

A System-Level Approach to Li Metal/Iron Fluoride Batteries Enabled by Optimal Electrolyte Choice Bryan R. Wygant, Laura Merrill, Timothy N. Lambert and Katharine L. Harrison; Sandia National Laboratories, United States

Moving beyond Li-ion/intercalation cathode batteries to Li and other alkali metal batteries paired with high capacity metal fluoride conversion cathodes like FeF_x (x = 2 or 3) represents a promising route to high capacity secondary batteries. Fe is considerably more earth abundant and environmentally friendly than elements like Co, and Fe-based conversion cathodes have significantly higher capacities than intercalation cathodes like FePO₄. However, the pairing of a Li metal anode with an FeF_x cathode presents new challenges for battery design. While studies on Li have long emphasized the importance of a protective solid-electrolyte interphase (SEI) on anode performance, recent work has shown that the cathode-electrolyte interphase (CEI) is likewise important to FeF_x cathode performance. Therefore, it is important to find an electrolyte that is compatible with, and creates a protective layer on, both the Li metal anode and the FeF_x cathode.

Here, we present a series of electrolytes optimized for either Li metal or FeF₃ and identify an electrolyte that enables a system-level solution for a Li metal/FeF₃ full cell battery. We show that while an electrolyte with high Li(T)FSI concentration results in high coulombic efficiency (CE) at the Li anode, it produces a poorly performing organic-rich CEI on the FeF₃ surface. Conversely, the FeF₃ cathode shows excellent performance in a pyrrolidinium-based ionic liquid electrolyte, but the Li anode appears to exhibit parasitic side reactions and very poor CE. Bridging the gap between these two results, we will report on our work that demonstrates using an electrolyte that forms an inorganic-rich CEI and a Li₂O-rich SEI, stabilizing the cathode and the anode, respectively leads to high overall coulombic efficiencies. Using this electrolyte, we demonstrate a coin cell-scale full cell battery that retains 80% of its post-formation cycle capacity over 50 cycles. Additional characterization including STEM, XPS, and other techniques is also presented. These initial results using well-studied Li metal provide a launching point for the further development of such system-level approaches, as well as the investigation of Na metal as an anode. While more reactive and possessing a lower theoretical capacity than Li, Na is more earth-abundant and its system-level compatibility with conversion cathodes is of great interest.

This work was supported by the Laboratory Directed Research and Development program at Sandia National Laboratories, a multi-mission laboratory managed and operated by National Technology and Engineering Solutions of Sandia, LLC., a wholly owned subsidiary of Honeywell International, Inc., for the U.S. Department of Energy's National Nuclear Security Administration under contract DE-NA-0003525. The views expressed herein do not necessarily represent the views of the U.S. Department of Energy or the United States Government.

2:30 PM EN12.16.05

Cryogenic TEM Characterization of and Control Over the Native Oxide Interphase on Calcium Electrodeposits Scott A. McClary, Daniel Long, Alan Landers, Paul Kotula, Katherine Jungjohann and Kevin Zavadil; Sandia National Laboratories, United States

Calcium anodes are attractive for use in beyond lithium-ion batteries due to their high theoretical energy densities (1337 mAh g⁻¹, 2073 mAh mL⁻¹), high natural abundance, and reported low propensity for dendrite formation [1, 2]. To achieve high (> 99.9%) coulombic efficiencies (CE), calcium anodes require a robust solid-electrolyte interphase (SEI) that suppresses parasitic reduction of electrolyte components while permitting cationic transport at appreciable rates. While high CEs for long cycling life have not yet been achieved in calcium-based electrolyte systems, the Ca(BH₄)₂-THF system (≤ 99% CE) can serve as a model for identifying surface components responsible for protective and transport functions. Several research groups have explored the native SEIs that form on Ca(BH₄)₂-THF electrodeposits. Wang et al. used X-ray diffraction and chemical digestion (i.e. bulk techniques) to suggest that CaH₂ is the primary surface interphase component [3], while Jie et al. used X-ray photoelectron spectroscopy (i.e. a surface-sensitive technique) to identify CaCO₃ and CaO as interphase constituents [4]. These contrasting experimental results, coupled with reports of significant nonuniformity during plating and stripping of calcium [5, 6], underscore a critical need to clarify the chemical identity of the species in calcium interphases and to spatially map their chemistry and microstructure.

In this contribution, we present detailed characterization of interphases of calcium electrodeposits generated from high concentration Ca(BH₄)₂-THF electrolytes. Central to our work is the use of cryogenic transmission electron microscopy (cryo-TEM), which enables analysis of calcium deposits with the liquid electrolyte vitrified in place, thereby preserving the native interphase generated upon electrodeposition. By applying techniques such as electron energy loss spectroscopy (EELS) mapping, selected-area diffraction (SAD), and high-resolution transmission electron microscopy (HRTEM) imaging to cryogenic samples, we demonstrate that the native interphase is a nanometric calcium oxide with a heterogeneous distribution of secondary phases, including borates. Furthermore, we find that CaH₂ exists as segregates in the bulk calcium deposit rather than at the surface. Further cryo-TEM studies, supplemented with electrochemical measurements, elucidate the protective function of the evolving oxide interphase during open-circuit holds. Finally, we leverage our findings to manipulate the heterogeneity and chemistry of the oxide interphase; by employing mixed solvents and mixed anions, the cationic transport properties are significantly enhanced.

Our results are a critical step towards the design and realization of an ideal solid-electrolyte interphase for high-efficiency rechargeable calcium metal batteries.

This work was performed, in part, at the Center for Integrated Nanotechnologies (CINT), an Office of Science User Facility operated for the U.S. Department of Energy (DOE) Office of Science. Sandia National Laboratories is a multimission laboratory managed and operated by National Technology & Engineering Solutions of Sandia, LLC, a wholly owned subsidiary of Honeywell International, Inc., for the U.S. DOE's National Nuclear Security Administration under contract DE-NA-0003525. The views expressed in the article do not necessarily represent the views of the U.S. DOE or the United States Government.

References:

- [1] M. E. Arroyo-de Dompablo et al. *Chem. Rev.* **2020**, 120(14), 6331-6357.
- [2] B. Ji et al. *Adv. Mater.* **2020**, 33(2), 2005501.
- [3] D. Wang et al. *Nat. Mater.* **2018**, 17(1), 16-20.
- [4] Y. Jie et al. *Angew. Chem. Int. Ed.* **2020**, 59(21), 12689-12693.
- [5] A. M. Melemed and B. M. Gallant. *J. Electrochem. Soc.* **2020**, 167(14), 140543.
- [6] S. D. Pu et al. *ACS Energy Letters* **2020**, 5(7), 2283-2290.

2:45 PM EN12.16.06

Facile Protection Layer Suppressing Surface Contamination of Cobalt-Free Cathodes for Lithium-Ion Batteries Ju-Myung Kim, Yaobin Xu, Mark Engelhard, Jiangtao Hu, Hyung-Seok Lim, Hao Jia, Bethany Matthews, Chongmin N. Wang and Wu Xu; Pacific Northwest National Laboratory, United States

In recent years, tremendous researches have been conducted to achieve high-energy-density lithium (Li)-ion batteries. Among various candidates, cobalt (Co)-free/nickel (Ni)-rich layered cathode materials are considered as one of the promising candidates that can provide practical battery use and cost reduction. However, the Co-free/Ni-rich layered cathode materials have a highly reactive surface that can easily lead to inevitable contaminations in air by forming residual Li compounds such as LiOH and Li₂CO₃ which cause capacity decay and poor cell performance. Here, we demonstrate the effectiveness of a thin polyimide/polyvinyl pyrrolidone (PI/PVP, as referred to as PP) layer to protect LiNi_{0.96}Mg_{0.02}Ti_{0.02}O₂ (NMT) cathode particles under storage in an atmosphere with ~30% humidity for two weeks. Compared to the fresh bare NMT, the stored bare NMT shows visible contaminated surface, Li consumption and decreased lattice O due to exposure to limited moisture and CO₂ in the air. On the other hand, the PP coated NMT (PP@NMT) has practically the same surface and structure before and after exposure to air. In the cycling performance test using a conventional LiPF₆/carbonate electrolyte at the current density of C/3 (1C = 1.5 mA cm⁻²) under 25 °C, the graphite (Gr)-based Li-ion battery of Gr||NMT system with stored bare NMT shows a continuous capacity decay, resulting in the capacity retention of merely 49.5% after 100 cycles, while the Gr||NMT cell with stored PP@NMT has the capacity retention of 84.7% after 100 cycles. In addition, after cycling, not only the stored bare NMT cathode material has more cracks inside the particle with NiF byproducts and structural degradation than stored PP@NMT but also the Gr anode paired with stored bare NMT has more generation of byproducts on the surface than Gr anode paired with PP@NMT. Furthermore, an advanced localized high-concentration electrolyte can enable the cell with stored PP@NMT cathode to achieve capacity retention of 89% over 400 cycles at 25 °C. This work offers a promising facile approach to protection of Co-free/Ni-rich layered cathodes for practical applications.

6:30 PM *EN12.15.01

Nanocellulose Batteries [Liangbing Hu](#); University of Maryland, United States

I will start by giving an overview of our work on assembly and functionalization strategies of nanocellulose aimed at specific properties, with an eye toward high impact applications including energy, electronics, building materials. Examples include transparent nanopaper for optoelectronics (as a replacement of plastics), super strong and tough wood (replacement of steel, *Nature* 2018), and radiative cooling wood (*Science*, 2019). I will then focus on our work on applying nanocellulose/wood as building blocks for advanced energy devices, including flexible, thick battery electrodes with nanocellulose binder, three-dimensional carbon derived from wood for advanced batteries (replacement of metal current collectors for beyond Li-ion batteries), and all solid-state Li metal batteries using nanocellulose ion conductors (*Nature*, 2021).

7:00 PM *EN12.17.02

Enhanced Stability and Rate Performance of Sodium Batteries by Tuning SEI Formation Through Ionic Liquid Chemistry and Controlled Formation Cycles Maria Forsyth^{1,2}, Patrick C. Howlett^{1,2}, Jun (Jenny) Sun¹, Shammi Ferdousi¹, Dmitrii Rakov^{1,2} and Fangfang Chen^{1,2}; ¹Deakin University, Australia; ²ARC Centre of Excellence for Electromaterials Science, Australia

Lithium ion batteries are ubiquitous in our society with uses extending from personal electronics to EVs and stationary storage. However, due to the environmental and ethical issues of raw materials (i.e., lithium, high purity graphite and cobalt) and increasing demands for lower cost and high safety, emerging battery technologies such as those based on sodium chemistries are becoming more attractive. Sodium metal provides the opportunity for higher energy density devices while the possibility of carbonising waste biomass to produce hard carbons for Na ion batteries offers a more sustainable energy solution. Ionic liquid electrolytes have been investigated for over two decades as a safe alternative to traditional organic solvents, in particular for higher energy density, metal anodes. IL electrolytes based on fluorosulfonimide (FSI) anions have particularly favourable properties with respect to enhanced ion transport, high sodium salt solubility and the stable SEI formation. Even within this family of IL electrolytes, the salt concentration, IL cation chemistry and molecular additives have a dramatic effect on the electrochemical performance of both Na metal and carbon anodes. Using solid state NMR, SEM and XPS, we show that this is related to the SEI composition on the anode surface. The effect of anode pre-conditioning on cycling stability is also discussed. MD simulations provide some insights into the influence of chemistry and preconditioning on stability. Finally, we also demonstrate significant stability enhancement at high rate and high capacity cycling of Na metal when a phosphonium IL cation is present in contrast to the pyrrolidinium IL cation.

7:30 PM *EN12.17.03

Hexacyanometallates for Rechargeable Batteries [Hyun-Wook Lee](#); Ulsan National Institute of Science and Technology, Korea (the Republic of)

Hexacyanometallates have gained great attention due to their interesting properties originating from their flexibility in synthetic methods, allowing a large degree of chemical tunability. Hexacyanometallates can be prepared by bottom-up assembly of molecular precursors via the formation of continuous chemical bonding between transition metal ions and ligand molecules. These cyanide ligands can enable the long-range charge transport with abundant CN triple bonds that can provide free electrons for electrical conduction. Due to such flexibility in their design and resultant properties, they can have a wide variety of applications including energy storage, harvesting, catalysis, and magnetic applications. In this talk, I will introduce diverse applications of hexacyanometallates for electrode, coating, and redox mediator materials. First, a new Cr-based negolyte coordinated with strong-field ligands will be introduced. The complex of $[\text{Cr}(\text{CN})_6]^{4-}$ prefers low-spin states, facilitating a stable and fast redox reaction, capable of mitigating strong Jahn–Teller effects, thereby facilitating low redox potential, high stability, and rapid kinetics. The prototype full-cell configuration features a high-energy density of 11.4 Wh L^{-1} and a stable lifetime of 250 cycles. Second, manganese hexacyanometallates (MnHCMn) shows a monoclinic crystal structure composed of nonlinear Mn–N≡C–Mn bonds and containing eight large interstitial sites occupied by Na^+ ions. The experiments demonstrate a high specific capacity of 210 mAh g^{-1} and excellent capacity retention at high rates. Here, we discover a novel mechanism wherein small lattice distortions allow for the unprecedented storage of 50% more sodium cations than in the undistorted case. These results represent a step forward in the development of high-performance redox flow and sodium-ion batteries.

8:00 PM EN12.17.04

Chloroaluminate Ionic Liquid Electrolytes for Safe and High-Performance Sodium and Potassium Metal Batteries [Hao Sun](#); Shanghai Jiao Tong University, China

Rechargeable sodium and potassium metal batteries are considered to be important to various energy applications in modern society. The pursuit of higher energy density should ideally come with high safety, a goal difficult for electrolytes based on organic solvents. Room temperature ionic liquids have been widely explored as promising candidates due to their non-flammable nature¹. Among them, ionic liquids comprised of AlCl_3 and 1-ethyl-3-methylimidazolium chloride are a classical chloroaluminate based electrolyte system with many desired properties including non-flammability, non-volatility, low viscosity, high conductivity, and high thermal stability and chemical inertness². However, it remains challenging to realize ideal battery performances on the basis of chloroaluminate ionic liquids, due to the severe corrosion of chloroaluminate based compounds to alkali metal.

Here we report chloroaluminate ionic liquid electrolytes comprised of aluminium chloride/1-methyl-3-ethylimidazolium chloride/sodium chloride ionic liquid spiked with important additives, e.g., ethylaluminum dichloride and 1-ethyl-3-methylimidazolium bis(fluorosulfonyl)imide. This leads to the first chloroaluminate ionic liquid electrolyte for rechargeable sodium metal battery³. The obtained batteries reached voltages up to ~ 4 V, high Coulombic efficiency (up to 99.9%), and high energy and power density of ~ 420 Wh kg^{-1} and ~ 1766 W kg^{-1} , respectively. More than 90% of the original capacity can be retained after 700 cycles. In addition, stable and high-energy-density potassium metal batteries were obtained on the basis of chloroaluminate ionic liquid electrolyte⁴, which could stably work at high temperature up to 60 °C. These results provide a new approach to advanced alkali metal batteries with high energy/high power densities, long cycle life and high safety⁵.

References

1. Yang, Q. *et al.* Ionic liquids and derived materials for lithium and sodium batteries. *Chem. Soc. Rev.* 2018, 47, 2020–2064.
2. Pickup, P. G. & Osteryoung, R. A. Charging and discharging rate studies of polypyrrole films in AlCl_3 : 1-methyl-(3-ethyl)-imidazolium chloride molten salts and in CH_3CN . *J. Electroanal. Chem. Interfacial Electrochem.* 1985, 195, 271–288.
3. Sun, H., Zhu, G., Xu, X., Liao M., Li, Y., Angell, M., Gu, M., Zhu, Y., Hung, W., Li, J., Kuang, Y., Meng, Y., Lin, M., Peng, H., Dai, H. A safe and non-flammable sodium metal battery based on an ionic liquid electrolyte. *Nat. Commun.* 2019, 10, 3302.
4. Sun, H., Liang, P., Zhu, G., Hung, W., Li, Y., Tai, H., Huang, C., Li, J., Meng, Y., Angell, M., Wang, C., Dai, H. A high-performance potassium metal battery using safe ionic liquid electrolyte. *PNAS.* 2020, 117, 27847–27853.
5. Sun, H., Zhu, G., Zhu, Y., Lin, M., Chen, H., Li, Y., Hung, W., Zhou, B., Wang, X., Bai, Y., Gu, M., Huang, C., Tai, H., Xu, X., Angell, M., Shyue, J., Dai, H. High safety and high energy density lithium metal batteries in a novel ionic liquid electrolyte. *Adv. Mater.* 2020, 2001741.

8:15 PM EN12.17.05**Correlations Between Structural Disorder, Covalent Bonding and Oxygen Redox Chemistry in Lithium-Rich Layered Oxide Electrodes** Byunghoon Kim; Seoul National University, Korea (the Republic of)

The oxygen redox is expected to offer a new route to attain an unprecedentedly high energy density for lithium-rich layered oxides, thus regarded as an alternative cathode chemistry beyond the high-nickel layered materials. However, the complexity from the dynamic changes in the structure, e.g. cation migrations/disorders and local oxygen bond alternations, and the corresponding redox activity change prohibits the full understanding of this class of materials, making it difficult to achieve the highly reversible oxygen redox. Herein, we present a consistent theoretical framework for the triptych of structural disorder, subsequent oxygen bonding rearrangement and redox chemistry, encompassing a wide range of layered oxides both in Charge-Transfer and Mott-Hubbard systems. It is unraveled that cation disorders stabilize oxygen redox by promoting strong oxygen-oxygen and/or metal-oxygen π hybridization, which hinges on the occupancy of oxygen non-bonding states and metal-oxygen covalency. On the other hand, anion disorders compensate for the electron deficiency of oxygen network without significantly regulating bonding arrangements. More importantly, we address how the formation of short covalent bonds affects electrochemical and structural reversibility, and report oxygen dimers that freely move in the structure as a key catalyst of the poor structural resilience. Our findings rationalize long-reported phenomenological correlations between structural disorders and oxygen redox, and offer a fundamental basis for optimizing the reversibility of oxygen redox taking into account of inevitable formation of structural disorders.

SESSION EN12.18: Poster Session III: Advanced Materials and Chemistries for Low-Cost and Sustainable Batteries

Session Chair: Seok Woo Lee

Tuesday Afternoon, December 7, 2021

EN12-Virtual

9:00 PM EN12.18.02**An Aqueous Battery with a Tear Electrolyte for Flexible Smart Contact Lenses** Jeonghun Yun, Moobum Kim and Seok Woo Lee; Nanyang Technological University, Singapore

As the demand for healthcare increases, various types of wearable devices have been developed for monitoring physiological information and biomarkers. Among these, smart contact lenses are attracting attention due to their huge applications ranging from health monitoring to digital entertainment. Inserting batteries inside contact lenses is still a challenge due to the need for miniaturization and the high safety requirements of placing batteries in the ocular system. Conventional batteries are not suitable to contact lenses because it can cause serious damage to the eyes if they break due to the release of toxic substances. We introduced a safe aqueous battery that utilizes tears as an electrolyte and supplies electric power to a microprocessor. Prussian blue analogues (PBAs), known as biocompatible host materials for Na- or K- ions, have been used as cathode and anode materials for electrochemical cell operation in the tears solution containing low concentrations of ions. The ultraviolet (UV) polymerized hydrogel was utilized as an ion-permeable separator as well as soft contact lens with embedding the electrodes which consist of carbon nanotubes and PBA. The battery embedded in the contact lens showed a discharge capacity of 155 μ Ah at potentials between 0.2 V and 0.9 V in an artificial tears solution. Bending tests and cytotoxicity tests while charging and discharging the battery were conducted to verify the mechanical stability and biocompatibility of the battery, respectively. For practical application, stable charge and discharge cycles of the battery in commercial contact lens cleaning solutions have demonstrated. The battery can supply high enough power to operate the low-power static random access memory. It could supply electric power to smart contact lenses without worrying about damage to eyes due to leakage of harmful substances from mechanical failure of the battery.

Acknowledgment

The content of this abstract has been published in J. Yun et al., Nano Lett., Vol 21, page 1659–1665.

9:05 PM EN12.18.03**2D-Layered Coordination Polymer of Nickel Dithioamide as a Precursor of Bifunctional Catalyst for Metal-Air Batteries** Ihsan B. Rachman¹, Ridwan P. Putra¹, Hideyuki Horino² and Izabela Rzeznicka¹; ¹Shibaura Institute of Technology, Japan; ²Tohoku University, Japan

Two-dimensional (2D) layered materials have been an important part of rechargeable battery research and development. Graphite and inorganic layered compounds such as transition metal dichalcogenides found application in low-capacity Li-ion batteries as electrode components. On the other hand, the commercialization of high-capacity rechargeable batteries such as metal-air batteries for electric vehicles is hampered by poor kinetics of oxygen redox chemistry. In order to efficiently harvest the energy density of metal-air batteries (theoretical specific energy of Li-O₂ is 13 kWh/kg [1]), a bifunctional catalyst is needed to catalyze oxygen reduction reaction (ORR) and oxygen evolution reaction (OER). Here, we propose to use an organic 2D-layered coordination polymer of transition metals (Ni, Fe, Cu) as a precursor of a highly efficient bifunctional catalyst [2, 3]. In this presentation, we will introduce our work on Ni(II) dithioamide (dto) coordination polymer and discuss OER and ORR electrochemistry in alkaline solutions on a nanocomposite derived from Ni(dto). Ni(dto) forms a coordination polymer with a layered structure composed of sheets of four Ni(II) atoms in planar configuration with five dto ligands. The interlayer distance is 3.6 Å [4]. Electrochemical cycling of Ni(dto), dispersed in a carbon matrix, in the potential range of 0.4 to 1.6 V vs. RHE, resulted in the formation of g-NiOOH which was found active towards OER and ORR in 1 M KOH solutions. The nanocomposite showed an enhanced ORR activity with the onset potential of 0.78 V and the half-wave potential of 0.72 V vs. RHE in O₂-saturated 1 M KOH solutions. The overpotential, h , for OER on NiOOH/C was 390 mV at $I = 12 \text{ mA/cm}^2$ [5]. At the same current density, the h_{OER} for Fe-doped NiOOH was 308 mV. Fe doping was found to improve OER kinetics. In this presentation, we will discuss the effect of Fe doping on OER and ORR performance with the help of *in-situ* Raman spectroscopy.

References:

- [1] M. A. Rahman, X. Wang and C. Wen, *J. Electrochem.Soc.*, **160**, A1759 (2013).
- [2] R.P. Putra, H. Horino, I.I. Rzeznicka, *Catalysts*, **10**, 233 (2020).
- [3] R.P. Putra, Y. Samejima, S. Nakabayashi, H. Horino, I.I. Rzeznicka *Catal. Today* (2020).
- [4] M. Abboudi, A. Mosset, J. Galy, *Inorg. Chem.*, **24**, 209 (1985).
- [5] R. P. Putra, I. Rachman, H. Horino and I. Rzeznicka, *Catal. Today*, under review (2021).

9:10 PM EN12.18.04

Interpretation of Low Temperature Behavior of Highly Concentrated Aqueous Electrolyte Based Supercapacitor Jaeil Park¹, Jongyoon Kim¹, Myung-Han Yoon¹, Dong Wook Lee² and Seung Joon Yoo¹; ¹Gwangju Institute of Science and Technology, Korea (the Republic of); ²Hongik University, Korea (the Republic of)

Water-in-Salt Electrolyte (WiSE) which is highly concentrated aqueous solution is a promising electrolyte for energy storage devices such as battery and supercapacitor. WiSE shows three surprising features; a) very stable SEI formation during the first few charging/discharging cycles; b) more than 3 V electrochemical stability window; c) fast ion transfer in a highly viscous solution. Despite such superior electrochemical properties, however, there exist no research suggesting a theoretical boundary between dilute solution and WiSE. In this research, we propose a new approach to understand WiSE based on an eutectic mixture. Although potassium acetate (KOAc) WiSE is an aqueous solution, liquid state was observed at sub-zero temperature. As salt is added in water, the number of strongly bound water molecules to a point charge is increased in the solution. This non-freezing water renders aqueous solution difficult to crystallize. Eventually the freezing temperature (T_f) of the aqueous solution dropped to below $-60\text{ }^\circ\text{C}$ near the critical point. After the lowest or critical point is reached, T_f increases again. Therefore, we suggest that before the critical point, the solution is sufficiently dilute where colligative properties are observed, and after the critical point, the solution is called WiSE. Finally, we demonstrated the sub-zero operation of WiSE based supercapacitor. The capacitance of a symmetric cell using activated carbon electrodes is measured approximately 50 F/g at $-20\text{ }^\circ\text{C}$.

9:15 PM EN12.18.05

Atomic-Scale Observation of Multiphase Evolution During Zinc-Ion Insertion in Vanadium Oxide Pilgyu Byeon, Youngjae Hong and Sung-Yoon Chung; Korea Advanced Institute of Science and Technology, Korea (the Republic of)

An initial crystalline phase transforms into another phases as cations are electrochemically inserted into its lattice. Precise identification of phase evolution at an atomic level during transformation is thus the very first step to comprehensively understand the cation insertion behavior. By using atomic-column-resolved scanning transmission electron microscopy, we directly visualize the simultaneous intercalation of both H_2O and Zn during discharge of Zn into V_2O_5 with an aqueous electrolyte. In particular, when further Zn insertion proceeds, multiple intermediate phases, which are not identified by a macroscopic powder diffraction method, are clearly imaged, showing structurally topotactic correlation between the phases. These findings suggest that smooth multiphase evolution with a low transition barrier is significantly related to the high reversible capacity of oxide cathodes for aqueous rechargeable cells.

9:20 PM EN12.18.06

Electrolyte Design for High Voltage and Safe Sodium Ion Batteries Yan Jin, Phung M. Le, Thanh D. Vo and Ji-Guang Zhang; Pacific Northwest National Laboratory, United States

Sodium (Na) ion battery (NIB) is an attractive alternative solution for stationary energy storage and electrical vehicles because of its low cost and abundant availability. Although rapid progress has been made on electrode materials, the stable electrolyte that is compatible with both cathode and anode is still limited, which hinders large-scale application of NIBs. Here, we report a low flammable electrolyte for highly reversible and high voltage sodium ion batteries. The high capacity retention ($>80\%$ for 300 cycles) and high columbic efficiency can be achieved for high voltage (4.2 V) full cells because of the stable interphases on both cathode and anode sides. These interphase layers can minimize undesirable reactions between the electrode and the electrolyte, and block the dissolution of transition metals from cathode. The interphase analysis, including XPS, TEM and EIS, has been used to identify the correlation between electrochemical performance and electrolyte properties. The insights obtained in this work can be used to guide the further development of stable electrolyte to enable safe and long cycle life of rechargeable batteries.

9:25 PM EN12.18.07

Enhanced Thermal Stability of LiPF₆-Based Carbonate Electrolyte in Li-ion Battery at Elevated Temperatures Mal-Soon Lee, Kee Sung Han, Sujong Chae, Vijayakumar Murugesan and Karl T. Mueller; Pacific Northwest National Laboratory, United States

Electrolytes play a crucial role in lithium-ion batteries (LIBs) by strongly affecting longevity and safety. Lithium hexafluorophosphate (LiPF₆) salt in carbonate-based solvents has been widely used as an electrolyte in commercial LIBs for over three decades. However, its insufficient thermal stability limits the cycle-life of LIBs. Studies have shown that the PF₆⁻ decomposition at elevated temperature is initiated by the reaction: $\text{LiPF}_6 \rightarrow \text{LiF} + \text{PF}_5$. Nevertheless, the underlying process that triggers thermal decomposition of PF₆⁻ at elevated temperatures is still unknown and impedes our ability to design optimal electrolytes. We report that the presence of urea (2 wt %) suppresses the decomposition reaction in 1 M LiPF₆ dissolved in propylene carbonate (PC) at elevated temperatures. A combined study of nuclear magnetic resonance (NMR) and ab initio molecular dynamics (AIMD) simulations elucidate the structure and dynamic properties of the LiPF₆/PC electrolytes in the absence and presence of urea additive, which are correlated with the stability of the electrolyte at elevated temperatures. Spin-lattice (T_1) relaxation time measurement and pulsed-field gradient (PFG) NMR reveal that (i) rotational motion of PF₆⁻ and PC changes from small-angle libration to reorientation with elevated temperatures, and (ii) the hopping motion of Li⁺ at elevated temperature ($\geq 80\text{ }^\circ\text{C}$) seen in the electrolyte is suppressed when urea additive is present. The latter is inferred due to preferential solvation with urea leading to capture of Li⁺ within a solvation cage. To attain atomic understanding of the observations, we performed AIMD simulations at room temperature and $100\text{ }^\circ\text{C}$ with and without urea. AIMD simulation at $100\text{ }^\circ\text{C}$ reveals an elongated P-F bond and a shortened Li⁺-F when PF₆ binds to Li⁺ which are not seen at room temperature, which may prompt the PF₆⁻ decomposition. In the presence of urea, a shorter Li⁺-O_{urea} bond length is observed relative to Li⁺-F_{PF6} and Li⁺-O_{PC} bond lengths, indicating a stronger interaction of urea with Li⁺ than PF₆ and PC. Based on these observations, we infer that thermally activated dynamics of PF₆⁻ accelerate the first decomposition reaction to form LiF and PF₅. In this presentation, we will discuss the correlation between macroscopic thermal stability and molecular level ion/solvent dynamics of the LiPF₆-based carbonate electrolytes.

9:30 PM EN12.18.08

Understanding Electrochemical Processes in Molten Salt Catholytes for Low-Temperature Molten Sodium Batteries Leo J. Small, Rose Lee, Stephen J. Percival, Martha M. Gross, Amanda Peretti, Melissa L. Meyerson and Erik D. Spoecker; Sandia National Laboratories, United States

Molten sodium batteries offer a promising technology for grid scale energy storage. Typical molten sodium battery chemistries such as Na-S and Na-NiCl₂ (ZEBRA) require temperatures near $300\text{ }^\circ\text{C}$ and $200\text{ }^\circ\text{C}$, respectively, to operate. Driving operating temperatures down to near $100\text{ }^\circ\text{C}$ would decrease operating costs, minimize materials aging effects, and minimize system-level materials costs through use of polymeric seals, thinner wires, and less insulation. To enable battery operation at such low temperatures, we have developed a suite of redox-active molten salt catholytes based on metal halide-sodium iodide chemistries that melt at $<100\text{ }^\circ\text{C}$. While each metal halide-sodium iodide system provides a unique phase stability, conductivity, and redox potential, they all share the same underlying I⁻/I₃⁻ redox used to store energy in the molten sodium battery. Nevertheless, each system shows distinct electrochemical performance. We couple idealized electrochemical measurements in a three-electrode cell with electrochemical modeling to better understand the electrochemical reactions and chemical equilibrium present during the deceptively simple oxidation of iodide. This modeling effort provides insights as to the factors which limit electrochemical performance, enabling targeted improvements to catholyte composition that significantly improve overall electrochemical kinetics. Leveraging this understanding, we identify cost-competitive metal halide-sodium iodide catholyte compositions for use in

a molten sodium battery.

Sandia National Laboratories is a multi-mission laboratory managed and operated by National Technology and Engineering Solutions of Sandia, LLC., a wholly owned subsidiary of Honeywell International, Inc., for the U.S. Department of Energy's National Nuclear Security Administration under contract DE-NA0003525.

9:35 PM EN12.18.09

Highly Porous Aramid Nanofiber Separators for Suppression of Li Dendrite Formations in Li Metal Batteries Arum Jung¹, Nayeon Kim², Jeong Gon Son² and Bongjun Yeom¹; ¹Hanyang University, Korea (the Republic of); ²Korea Institute of Science and Technology, Korea (the Republic of)

Lithium metals for anode of secondary batteries are drawing great attentions due to high theoretical capacity, high potential, and low density for next-generation high-energy storage systems. However, dendritic growth of lithium (Li) metal during repetitive charge and discharge cycles can cause severe problems such as low lifespan and risks of explosions raised from short circuits. In this study, we synthesized highly porous aramid nanofiber film (PANF) separators by sequential solvent-substitution methods to suppress Li dendritic growth. Porosities and pore sizes of PANF were controlled by self-assembly processes of aramid nanofibers during solvent-substitutions. Highly porous nanostructures enabled to improve wettability to electrolytes and ionic conductivities for PANF. Symmetric cell tests showed stable cycle operations up to 3000 cycles at current density of 50 mA/cm² with cycling capacity of 1 mAh/cm², that could be attributed to effective suppressions of Li dendrite formations. For the full cell tests with LiFePO₄ (LFP) cathodes, PANF samples showed higher capacity than commercialized separator samples from 1 C to 30 C rates. The PANF separators are expected to one of most promising candidates for advanced separators for the Li metal batteries.

9:40 PM EN12.18.11

Intrinsic Defect Study on High-voltage Spinel LiMn_{1.5}Ni_{0.5}O₄ Cathode Material for Li-ion Batteries Jiayi Cen^{1,2,3}, Bonan Zhu^{1,2,3} and David O. Scanlon^{1,2,3}; ¹University College London, United Kingdom; ²The Faraday Institution, United Kingdom; ³Thomas Young Centre, United Kingdom

High-voltage spinel LiMn_{1.5}Ni_{0.5}O₄ (LMNO) is an attractive cobalt-free cathode material which can deliver high energy density (650 Wh kg⁻¹) due to its high operating voltage ~4.7 V (vs Li⁺/Li) arising from the Ni²⁺/Ni⁴⁺ couple.¹ The spinel framework offers a 3D diffusion channel for Li⁺, leading to high ionic conductivity. Another unique characteristic of the material arises from the potential to tune performance through harnessing cation disorder.² Introducing cation disorder during synthesis inevitably brings additional complexity (e.g. oxygen vacancies), making it challenging to rationalise the most significant factors towards designing LMNO with optimum electrochemical performance.³⁻⁵

In this study we used quantum chemistry techniques^{6,7} to predict the defect landscapes of LMNO under various synthesis conditions. Analysis of the formation energy of all intrinsic defects in the ordered phase P4₃32 LMNO using the supercell approach, can provide logical explanations for experimental observations and reveal insights on the charge compensation mechanisms and changes to local cation-ordering associated with those defects, which cannot be obtained easily through experiments and characterisations.

References

- [1] G. Liang, V. K. Peterson, K. W. See, Z. Guo and W. K. Pang, *J. Mater. Chem. A*, 2020, **8**, 15373–15398.
- [2] J. H. Kim, S. T. Myung, C. S. Yoon, S. G. Kang and Y. K. Sun, *Chem. Mater.*, 2004, **16**, 906–914.
- [3] B. Aktekin, M. Valvo, R. I. Smith, M. H. Sörby, F. Lodi Marzano, W. Zipprich, D. Brandell, K. Edström and W. R. Brant, *ACS Appl. Energy Mater.*, 2019, **2**, 3323–3335.
- [4] Y. Chen, Y. Sun and X. Huang, *Comput. Mater. Sci.*, 2016, **115**, 109–116.
- [5] B. Aktekin, F. Massel, M. Ahmadi, M. Valvo, M. Hahlin, W. Zipprich, F. Marzano, L. Duda, R. Younesi, K. Edström and D. Brandell, *ACS Appl. Energy Mater.*, 2020, **3**, 6001–6013.
- [6] C. Freysoldt, B. Grabowski, T. Hickel, J. Neugebauer, G. Kresse, A. Janotti and C. G. Van de Walle, *Rev. Mod. Phys.*, 2014, **86**, 253–305.
- [7] S. Kim, S. N. Hood, J. S. Park, L. D. Whalley and A. Walsh, *J. Phys.: Energy*, 2020, **2**, 036001.

9:45 PM EN12.18.12

Improvement of Charge/Discharge Characteristics with Surface Structure Controlled Bismuth Anode Materials by Electrodeposition for Magnesium-Ion Batteries Takeyasu Saito, Natsuki Narumoto and Naoki Okamoto; Osaka Prefecture University, Japan

The magnesium ion secondary battery (MIB) has attracted much attention because magnesium (Mg) metal has high theoretical capacity (3,755 mAh/cm³), high electrochemical stability, and high abundance in the earth. However, developing anode and cathode materials with superior capacity for conventional electrolytes has required considerable study. Bismuth (Bi) has high capacity as an anode and also resists oxidation in Mg-containing electrolyte, so is a promising candidate material. However, experimental studies suggest that the available capacity has not yet reached the theoretical limit, and that the cycle life is short. This is due to sluggish diffusion of Mg²⁺ into the anode material and the slow interfacial charge transfer. We aimed to improve the electrochemical properties by atomizing the internal and surface structure of the Bi anode and enhancing the diffusion of Mg²⁺. In this study, we prepared Bi films by an electrodeposition method, in which the structure of the Bi electrodes could be controlled by changing electrodeposition conditions. We also evaluated the electrochemical properties of Bi anode materials deposited with different deposition times and current densities, to elucidate the relationships between the structure of the Bi anode and its capacity and cycle life.

We prepared an electrolytic bath by dissolving H₂SO₄, Na₂SO₄ and polyethylene glycol in pure water, and subsequently added H₂SO₄ to the electrolytic bath to control the pH at 1.2. Before electrodeposition, we removed organic species and native oxide from the Cu foil surface with NaOH and HCl. We employed a Cu plate with an exposed foil area of 2 × 2 cm² and a carbon plate as the cathode and anode, respectively. The Bi electrodeposition was carried out, while changing the deposition time and current density (from 10 to 50 mA/cm²). The film thickness was controlled by the deposition time (from 1.5 to 3.0 μm), and was calculated based on the weight increase under the assumption that the film was uniform. The surface morphology and crystal structure of the Bi films were evaluated by scanning electron microscopy (SEM) and X-ray diffraction (XRD), respectively. In addition, the characteristics were compared before and after discharge/charge. The cycle characteristics of the Bi anodes were studied in PhMgCl/THF electrolyte. The bipolar half-cells were assembled with Mg plate as the anode and Bi electrode as the cathode. We established representative galvanostatic charge/discharge profiles of the Bi electrodes, at a current density of 50 mA/g within 0–0.6 V, versus Mg²⁺/Mg. We evaluated the cyclic stability of the Bi electrodes under the same conditions until the 50th cycle. The elemental composition and chemical bonding state of the Bi films after charge/discharge were evaluated by energy dispersive X-ray spectroscopy (EDS) and X-ray photoelectron spectroscopy (XPS).

The cycling performance of Bi films with thicknesses of 1.5, 2.0, and 3.0 μm until the 50th cycle. Each film showed a capacity of about 300 mAh/g at the early stage of cycling, which is the maximum capacity. The capacities were about 1.5 times those of the Bi anodes which Niu et al. prepared by powder metallurgy. The cycle performance differed among Bi films differing in thickness, and the 1.5-μm Bi film maintained the maximum capacity until the 25th cycle. Thus, film thickness had an impact on the cycle performance. The surface morphology of Bi films with different thicknesses before and after the charge/discharge reaction shows agglomerates involving a large number of particles with increasing film thickness, which consists of particles from 1 to 3

µm. after charging/discharging, and also consists of Mg dendrites with thicknesses of 2 and 3 µm. The localized formation of Mg dendrites on the Bi surface could explain the decreased cycle performance of the Bi films prepared in this study.

9:50 PM EN12.18.13

Late News: Multi-Principal Metal Chalcogenides as the Air Electrode with CNT-Zn Modified Anode for Rechargeable Zinc-Air Battery Chetna Madan and Aditi Halder; IIT Mandi, India

Metal-air batteries happen to be more viable and sustainable energy storage systems due to high safety, low cost and less environmental repercussions. Li-air battery despite of having the highest theoretical energy density lags behind Zn-air battery in terms of resource availability and operation safety. Also, the electrode potential of such metals like Li, Na, Al is very negative, thus making them more susceptible to anodic corrosion in aqueous environment by evolution of hydrogen, further compromising the safety of the battery. Zinc being the most promising candidate for metal-air batteries is extensively being studied to improve the short-comings of by-product saturation and precipitation, dendritic growth during Zn plating and hydrogen evolution. In this work, conductive substrate modified with carbon nanotube is deposited with zinc to be utilized for the improvement of life-cycle and durability of the anode for zinc-air battery. To construct a flexible rechargeable battery, CNT can provide larger surface area for Zn deposition and improves its performance by allowing better flow of electrolyte as well as prohibits the dendritic growth by anchoring strongly. On the other hand, multi-principal 2-D metal chalcogenides have been used a bifunctional oxygen electrocatalyst for the cathode of ZAB giving maximum charge-discharge cyclic stability and constant discharge voltage (close to 1.65 V). These high-entropy materials comprising of quasi-equimolar quinary or higher principal metals, provide numerous combinations of surface structure and therefore, adsorption sites and electronic environments. The tunable properties influence the catalytic behavior through charge transfer, adsorption, etc. The high-entropy metal sulfides, as in this study, stabilized by configurational entropy are ideal to explore the structure-property relationship.

SESSION EN12.19: Poster Session IV: Advanced Materials and Chemistries for Low-Cost and Sustainable Batteries

Session Chair: Seok Woo Lee

Wednesday Morning, December 8, 2021

EN12-Virtual

10:30 AM EN12.19.03

A Critical Evaluation of the Separate Contribution of Carbon Fiber and Carbon Nanotubes Activated for Pseudocapacitance of Composite Electrodes Camila A. Escanio, Erica F. Antunes, Evaldo J. Corat and Vladimir J. Trava-Airoldi; National Institute of Space Research, Brazil

Carbon-containing materials are a promising alternative to develop novel technologies applicable in supercapacitors and energy storage devices. Among these materials, Carbon Fibers (CF) are base electrodes of wide use in electrochemical cells mainly because of their good flexibility and high mechanical resistance. Carbon nanotubes (CNT) films have high electrical conductivity, high resistance to acid electrolytes, and high specific surface area. This work aims to develop CNT/CF electrodes and study the electrochemical behavior of both separated materials, CF and CNT, and in the composite. A viscose fabric pyrolysis produced the CF, using a temperature ramp-up to 850 °C at a 5 °C/min heating rate. The CNT was deposited over two different substrates: the CF and silica fabric. The latter was used to evaluate only the contribution of the CNT since the silica fiber presents no electrochemical response. Thermal Assisted Chemical Vapor Deposition (TA-CVD) at atmospheric pressure was the CNT film growth technique. The precursors for floating catalyst growth were the mixture of 84% camphor and 16% ferrocene, in which 12.5 g was dissolved in 50 mL of n-hexane. It was evaporated while inserted dropwise in a chamber at a temperature of 220 °C. An argon gas flow (200 sccm) carried this vapor into the reactor at 850 °C. The process lasted for 15 minutes, promoting the CNT growth. To increase the CNT samples' hydrophilicity, we performed a surface activation process using steam and CO₂ simultaneously. The electrochemical behavior of the CF, CNT, and CNT/CF samples was measured using a three-electrode cell setup with an Ag/AgCl saturated reference electrode and a platinum grid counter electrode. The electrolyte was an aqueous sulfuric acid solution of 1.0 M. Electrochemical characterization of the samples involved electrochemical impedance spectroscopy (EIS) technique, cyclic voltammetry (CV), and galvanostatic charge and discharge (GCD) routines. In addition, the samples were morphologically and structurally characterized by scanning electron microscopy (SEM), and Raman spectroscopy, respectively. The results got by electrochemical measurements showed a distinct behavior for the samples. The FC acts as a double-layer electrochemical capacitor (EDLC) while CNT exhibited typical Faradaic behavior. The CNT/FC composite showed an intermediate behavior between EDLC and battery, characterized as a supercapacitor. Electrochemical purification to remove electrochemically available iron residues shows that the Faradaic behavior was because of these residues. The combination of FC and CNT properties provides a composite with high specific capacitance (150F/g) and high conductivity and presents a prospective application as supercapacitors and energy storage devices.

10:35 AM EN12.19.04

Copper Sulfide—A Conversion Cathode Material for Mg-Batteries Michael Wilhelm, Veronika Brune, Khan Lê and Sanjay Mathur; University of Cologne, Germany

Magnesium secondary batteries have been regarded as promising candidates for large-scale storage systems with high safety, high energy density, and low production costs. Magnesium batteries profit from the use of a metal anode due to the dendrite-free deposition of magnesium ions. In addition to the challenge of finding suitable liquid or solid-state electrolytes, the hunt for viable cathode materials is a key success factor for battery fabrication. Copper sulfide can be reversibly converted into magnesium sulfide and delivers high capacity (560 mAh g⁻¹). Interestingly, the charged and discharged products (CuS/Cu₂S and Cu) are electrically conductive, which is profitable for the positive electrode. Copper (0.01 %) and sulfur (0.05 %) as well as magnesium (2.4 %) are highly earth-abundant and are therefore sustainable raw materials.

Conventional battery cell production makes use of common current collectors like Al and Cu foil, which is on the one hand side non-active material and on the other side not feasible because of undesirable side reactions with sulfur and the electrolyte. This makes the battery heavier and less efficient. Therefore, we designed electrospun cathode material of copper sulfide and carbon nanofibers with flexible network architecture and promising properties as the positive electrode for magnesium batteries. These copper sulfide loaded fibers have been analyzed using XPS, SEM, and Raman spectroscopy. The advantages of the composite material are large surface area, high porosity, large liquid permeability, and good electrical conductivity, making these prepared fibers ideal candidates for application as electrode material in Mg-based secondary batteries for large-scalable, sustainable, and low-cost energy storage devices.

10:40 AM EN12.19.07

Temperature-Dependent Structural Analysis of NaFePO₄ Using Neutron Powder Diffraction Elizabeth Brown and Hillary Smith; Swarthmore College, United States

Olivine NaFePO₄ is a promising cathode material for Na-ion batteries, but aspects of the phase diagram for Na_xFePO₄ (0<x<1) remain poorly understood. Reports using x-ray diffraction have found the NaFePO₄ phase diagram to be quite distinct from LiFePO₄ with both a solid solution forming at x>2/3 and an intermediate ordered phase at x=2/3. The larger differential in unit cell size for Na_xFePO₄ with x=1 and x=0 compared to LiFePO₄ is thought to allow for more structural relaxation in the sodium material. In this work, the phase diagram of Na_xFePO₄ is investigated for x=0, x=2/3, and x=1 using neutron powder diffraction. We find new insight into the lattice volume expansion as a function of temperature for the intermediate phase. Our measurements extend to higher temperatures than previously reported and the reversibility of high-temperature structural transformations are examined.

10:45 AM EN12.19.08

SiOC Functionalized Transition Metal Monochalcogenides as Electrodes for Beyond Lithium-Ion Batteries Shakir Bin Mujib and Gurpreet Singh; Kansas State University, United States

The development of feasible, scalable, and environmentally safe electrode materials that provide stable cycling performance is critical for the success of beyond lithium-ion batteries. With respect to the sodium- and potassium-ion battery anodes fabricated using transition metal monochalcogenides such as germanium and tin sulfides and tellurides show poor cycle stability and fast capacity degradation, due to low electronic conductivity and dissolution of chemical species in the electrolyte. Herein we report chemical functionalization of monochalcogenide nanosheets with polymer-derived silicon oxycarbide (SiOC) with the aim to preserve the electrodes from dissolution in the organic electrolyte, without compromising its role in charge/discharge processes. The high performances of electrodes are attributed to the high electric conductivity and structural stability of the SiOC fibers with unique structure, which not only buffers the volume change of monochalcogenides with the internal space but also acts as high-efficient transport pathways for ions and electrons. Our results suggest that monochalcogenides-SiOC composite electrode are effective in bringing improved cycle stability over neat monochalcogenides.

10:50 AM EN12.19.09

Study of Gallium-Based Liquid Alloys as Electrodes for Na-Ion Batteries Ronan Le Ruyet, Florent Mohimont, Andrew Naylor and Reza Younesi; Uppsala University, Sweden

Gallium has always been an intriguing metal, especially because of its low melting temperature (30°C). This melting temperature can even be lower when alloying Gallium with elements such as Indium and Tin. The Ga₈₆In₁₄, Ga₉₂Sn₈ and Ga₇₇In₁₅Sn₈ alloys have melting temperatures of 16 °C, 25 °C and 11 °C, respectively. These alloys are extensively studied to design stretchable and self-healing electronic circuits.¹ In the recent years, they have been also studied in the field of Li-ion batteries as self-healing electrode materials with prolonged cycle-life.² Indeed, after delithiation, the liquid alloys recover their initial shape due to the transition from the solid lithiated phases back to the pure liquid delithiated phase. However, as they are being tested in Li-ion batteries, almost no study has been performed for their use in beyond Li-based technologies such as Na-ion batteries.

In this presentation, our results on using Gallium, Ga₈₆In₁₄, Ga₉₂Sn₈ and Ga₇₇In₁₅Sn₈ as electrodes in Na-ion batteries will be presented.³ The electrochemical reactions of these compounds with Na were carefully studied. Electrochemical measurements were coupled with ex-situ PXRD and SEM analyses to have a complete overview of the involved reactions, their potentials, their capacities and the self-healing properties of the alloys. Finally, the possible applications of these liquid alloys in Na-ion batteries will be discussed.

References

1. Tang, S.-Y., Tabor, C., Kalantar-Zadeh, K. & Dickey, M. D. Gallium Liquid Metal: The Devil's Elixir. *Annu. Rev. Mater. Res.* 51 (2021).
2. Guo, X., Zhang, L., Ding, Y., Goodenough, J. B. & Yu, G. Room-temperature liquid metal and alloy systems for energy storage applications. *Energy Environ. Sci.* 12 (2019).
3. Le Ruyet, R., Mohimont, F., Naylor A. & Younesi, R. Gallium-based liquid alloys as electrodes for Na-ion batteries. In preparation.

10:55 AM EN12.19.10

Enhancing VO²⁺/VO₂⁺ Kinetics and Inhibiting Chlorine Evolution in Mixed Acid All-Vanadium Redox Flow Batteries Using C₇₆ Fullerene Farah El Diwany, Basant A. Ali, Ehab N. Elsayy and Nageh K. Allam; The American University in Cairo, Egypt

The growing energy demand met by fossil fuels for decades, leading to pollution and global warming. Therefore, the shift to clean and renewable energy sources is a must to achieve carbon neutrality. However, the alternating nature of wind and solar energy necessitates the development of energy storage technologies for frequency balancing and grid stability. Batteries are thought to be the optimal solution. Among all types of batteries, all-vanadium redox flow batteries (VRFBs) have independent modularity of energy and power ratings, flexible design, and provide large-scale energy storage at a reasonable cost. However, the energy efficiency of VRFBs is still not satisfactory for widespread applications.

Commercial VRFBs use graphitized carbon-based electrodes due to their high chemical and electrochemical stability and conductivity. However, their electrochemical activity towards vanadium ions is poor. For improved electrochemical activity, the thermal treatment and its role in introducing the necessary surface functional groups and the increase of the electrode wettability were thoroughly investigated. However, to further reduce polarization losses, interest in carbon nanostructures, such as graphene¹, reduced graphene oxide², carbon nanotubes³, carbon nanowalls⁴, carbon nanofibers⁵, and carbon nanoplatelets⁶, is growing owing to their excellent conductivity, stability, and large surface area.

The fullerene family has not yet been explored in the VRFBs application. Fullerenes have a very unique cage-like structure with high surface area and conductivity, which would allow fast electron transfer. The electronic cloud surrounding the fullerene molecule could also enhance the adsorption of ions onto its surface. In this work, we, therefore, report, for the first time, the electrochemical activity of fullerene C₇₆ towards VO²⁺/VO₂⁺ redox reaction in G1 and G3 VRFBs. C₇₆ showed superior electrocatalytic activity in both versions of VRFBs, as evaluated by cyclic voltammetry (CV) and electrochemical impedance spectroscopy (EIS), while also inhibited the chlorine evolution in G3 VRFB when compared to thermally treated carbon cloth (TCC) electrode. It is noteworthy to point out that treatment is, thus, unnecessary and undesirable in G3 VRFBs.⁷

References

- 1 Z. González, C. Flox, C. Blanco, M. Granda, J. R. Morante, R. Menéndez and R. Santamaría, *J. Power Sources*, 2017, **338**, 155–162.
- 2 M. Jing, C. Zhang, X. Qi, Y. Yang, J. Liu, X. Fan, C. Yan, and D. Fang, *Int. J. Hydrogen Energy*, 2020, **45**, 916–923.
- 3 G. Wei, C. Jia, J. Liu, and C. Yan, *J. Power Sources*, 2012, **220**, 185–192.
- 4 Z. González, S. Vizireanu, G. Dinescu, C. Blanco and R. Santamaría, *Nano Energy*, 2012, **1**, 833–839.
- 5 G. Wei, X. Fan, J. Liu, and C. Yan, *J. Power Sources*, 2014, **270**, 634–645.
- 6 P. Han, H. Wang, Z. Liu, X. Chen, W. Ma, J. Yao, Y. Zhu, and G. Cui, *Carbon N. Y.*, 2011, **49**, 693–700.
- 7 F. A. El Diwany, B. A. Ali, E. N. El Sawy and N. K. Allam, *Chem. Commun.*, 2020, **56**, 7569–7572.

11:00 AM EN12.19.11

Catalyzing the Vanadium Redox Reactions While Inhibiting the Parasitic Ones of the Mixed-Acid All-Vanadium Redox Flow Batteries Using

Tungsten Oxide/Fullerene Nanocomposites Farah El Diwany, Nageh K. Allam and Ehab N. Elsayy; The American University in Cairo, Egypt

The penetration of clean and renewable wind and solar energies is expected to reach up to 75% of the total electrical energy by 2050. However, the electrical grid becomes unstable when the power from renewable energy sources exceeds 20% of the total generated power. Developing efficient energy storage systems is crucial for such a transition since they are required to store surplus electricity and balance supply and demand. Among all energy storage systems, vanadium redox flow batteries (VRFBs) are thought to be an optimal solution for long-term energy storage (~30 years) due to the decoupling of power and energy densities, fast response, and long cycle life, and low annualized cost.¹ However, their relatively high system capital cost, primarily due to the cell stack needs to be reduced. Increasing the kinetics of both half-cell reactions can reduce the size of the stack and, consequently, the cost. Even though carbon-based electrodes have good chemical and electrochemical stability and good conductivity, with no treatment they suffer from sluggish kinetics due to the lack of oxygen functional groups and hydrophilicity.^{2,3} Therefore, different electrocatalysts were incorporated with the carbon-based electrodes, specifically carbon nanostructures^{4,5} and metal oxides^{6,7}, to enhance the kinetics at both electrodes to increase the kinetics at the VRFB electrodes.

Herein, novel hydrated tungsten oxide (HWO) nanoparticles were synthesized *via* facile hydrothermal methods and deposited on carbon cloth electrodes for both half-cell reactions. The superior electrocatalytic activity was observed for the V^{2+}/V^{3+} reaction, in addition to suppressed HER. As for the VO^{2+}/VO_2^+ reaction, the incorporation of C_{76} was necessary to enhance the conductivity and kinetics, while the HWO inhibited chlorine evolution. Experiments were also done in the mixed acid electrolyte (H_2SO_4/HCl) to imitate the 3rd Generation (G3) VRFB for more practicality and to study the effect of HWO on the chlorine evolution parasitic reaction.

References

- 1 2020 Grid Energy Storage Technology Cost and Performance Assessment | Department of Energy, <https://www.energy.gov/energy-storage-grand-challenge/downloads/2020-grid-energy-storage-technology-cost-and-performance>, (accessed 22 June 2021).
- 2 Y. Gao, H. Wang, Q. Ma, A. Wu, W. Zhang, C. Zhang, Z. Chen, X. X. Zeng, X. Wu and Y. Wu, *Carbon N. Y.*, 2019, **148**, 9–15.
- 3 R. Wang and Y. Li, *J. Power Sources*, 2019, **421**, 139–146.
- 4 Z. González, C. Flox, C. Blanco, M. Granda, J. R. Morante, R. Menéndez and R. Santamaría, *J. Power Sources*, 2017, **338**, 155–162.
- 5 D. O. Opar, R. Nankya, J. Lee and H. Jung, *Electrochim. Acta*, 2020, **330**, 135276.
- 6 M. G. Hosseini, S. Mousavihashemi, S. Murcia-López, C. Flox, T. Andreu and J. R. Morante, *Carbon N. Y.*, 2018, **136**, 444–453.
- 7 M. Faraji, R. Khalilzadeh Soltanahmadi, S. Seyfi, B. Mostafavi Bavani, and H. Mohammadzadeh Aydishah, *J. Solid State Electrochem.*, 2020, **24**, 2315–2324.

11:05 AM EN12.19.12

Flexible and Freestanding Carbon Nanotube and Niobium Pentoxide Composite for Sodium Electrochemical Energy Storage with Intercalation Pseudocapacitance Carla G. Real¹, Gurpreet Singh² and Hudson Zanin¹; ¹UNICAMP, Brazil; ²Kansas State University, United States

Sodium ion-based devices have been intensively investigated as a promising alternative to lithium-ion devices for large scale energy storage due to their similar electrochemical properties and sodium low-cost thanks to its abundance resources. However, many challenges remain sodium ion devices to become commercially competitive as lithium-ion devices. One of them concerns the ionic size of sodium, larger than that of lithium, resulting in slower electrochemical kinetics and significant restrictions in the intercalation process reducing performance and device lifetime. Despite these drawbacks, extensive efforts are focused on the rational design of nanostructured and novel electrodes to improve the Na^+ transport kinetics. Niobium pentoxide is promising as it presents electrochemical stability and rapid ion transport throughout the a–b plane, suitable for a wide array of electrochemical energy applications. This work reports the preparation of a flexible and freestanding film of multiwalled carbon nanotube decorated with Nb_2O_5 nanoparticles through vacuum filtration and investigate the effect of Nb_2O_5 as sodium-ion symmetric supercapacitor (SIC) and anode battery (SIB). In both cases, the results show a pseudocapacitance contribution. In a SIB half-cell configuration, the electrode delivers a reversible sodium-ion storage capacity of ~ 163 mA h g⁻¹ at 25 mA g⁻¹ and present a retention of capacity of ~ 68 mA h g⁻¹ after 100 cycles at 25 mA g⁻¹. The SIC full cell shows a long cycling stability after 10,000 cycles and delivers a high energy density of 64.11 W h kg⁻¹ with a power density of 74.98 W kg⁻¹. Even with a power density of 14,766 W kg⁻¹, it delivers a high energy density of 55 W h kg⁻¹.

11:10 AM EN12.19.13

Sn Nanoparticles and Nitrogen-Doped Activated Carbon Nanofiber Composite as Anode for Sodium-Ion Batteries Carla G. Real¹, Gurpreet Singh² and Hudson Zanin¹; ¹UNICAMP, Brazil; ²Kansas State University, United States

Sodium ion batteries have attracted attention because sodium is an abundant metal in the Earth's crust, which facilitates its obtaining and processing and, consequently, offers sustainability and low cost. Although sodium-ion batteries have a similar function to lithium-ion batteries, due to the greater atomic radius of sodium, they have poor diffusion and restrictions of the intercalation process in the interstices of the electrode. To address these deficiencies, Sn a promising anode candidate to construct viable, stable, and low-cost sodium-ion batteries for energy storage systems because it alloys high theoretical capacities, high conductivity and safe reaction potential. In this work, we related a Sn-based anode material by synthesizing a composite of Sn nanoparticles on nitrogen-doped carbon nanofibers via electrospinning technique for sodium ion batteries. The composite shows a high reversible capacity of ~1100 mA g⁻¹ at 25 mA g⁻¹. Even with a current density of 1 A g⁻¹, the material delivers a capacity of ~120 mA g⁻¹. Results show a long cycling stability within 0 to 2.5 V potential window.

11:15 AM EN12.19.14

An *Ab Initio* Based Thermodynamic Modeling of the Si-Li System Including Charged Defects And Stress Charbel Jose El Khoury, Maylise Nastar and Fabien Bruneval; Université Paris-Saclay, CEA, France

Si-Li batteries are promising in many ways, e.g. they have high theoretical specific capacity (4200 mAh/g). However, the volume expansion upon lithiation may lead to high internal strain/stresses and fracture phenomena. We associate this phenomenon to the fact that an electrochemical insertion of Li leads to multi-phase particles with significant changes in specific volumes of phases. We introduce a thermodynamic formulation of the phase transformation including the role of charged lattice point defects, the internal stress/strain field, and the deviation from perfect stoichiometry of the compounds.

From our *ab initio* calculations, we obtain: the formation energies (Ef) of Si-Li compounds; the Ef of defects (both charged and neutral vacancies/interstitials) in pure and lithiated Si; the dielectric constants (needed for charged defect); and the elastic constants of Si and several compounds. The DFT calculations are performed with PBE and HSE06 functionals. The hybrid functional HSE06 allows us to reproduce the semi-conductor nature of the solid solution Si(Li) and the Li-poor compounds, by providing a closer-to-reality band gap and therefore, permitting us to investigate realistic properties of the charged point defects. From the formation energies of the Si-Li compounds, the neutral and charged defects in Si and its lithiated compounds, the phonon frequencies and the elastic constants, we compute the free Gibbs energies of the particle with respect to the composition, temperature, and the particle size. The increment of the Gibbs free energy with the number of Li yields the open circuit voltage (OCV).

Our results are in good agreement with measured OCV at high temperature (415°C), with respect to the off-stoichiometric composition of the stable compounds [1]. From the investigation of the metastable Si-Li phases that are only formed under electrochemical insertion of Li, we simulate the charging-discharging OCV cycles.

References:

[1] C.J. Wen and R.A. Huggins, *Journal of Solid State Chemistry* 37, 271 (1981).

11:20 AM EN12.19.15

Bi-Functional Use of Natural Graphite in High Voltage Battery Electrodes Habtom D. Asfaw¹, Tove Ericson¹, Antonia Kotronia¹, Filip Kozłowski² and Maria Hahlin¹; ¹Uppsala University, Sweden; ²Leading Edge Materials, Sweden

New electrolytes with enhanced anodic stability have enabled electrochemical synthesis of anion-intercalated graphite (or p-doped graphite) compounds at voltages > 4.5 V vs Li⁺/Li. The p-doped GICs form the basis of an emerging battery concept called dual-ion battery (DIB) in which both cations and anions from the electrolyte participate in the energy storage process. With the current state-of-the-art electrolytes and electrode materials, DIBs have been demonstrated to offer specific energy densities close to 200 Wh kg⁻¹, and are potentially attractive for stationary applications. In this contribution, we will explore the design of hybrid DIB cells based on composite electrodes consisting of high voltage positive active materials such as LNMO and natural graphite, which doubles as a conductive additive and an anion intercalation host. Since it contributes (~100-120 mAh g⁻¹) to the overall capacity, natural graphite can be used in much higher proportions without affecting the specific capacity of the composite electrode, while enhancing the rate capability by virtue of its metallic conductivity. The ratios of both active materials are varied to achieve optimal combinations.

Similar to ordinary DIBs, this battery concept is, however, affected by challenges associated with instability of electrolytes within the high operating voltage required for anion intercalation (typically ranging from 4.5 to 5.2 V Li⁺/Li), corrosion of Al current collector and graphite exfoliation. Highly concentrated-salt electrolytes and ionic liquids are often used as they have wider kinetic stability windows than conventional battery electrolytes. These limitations give rise to poor coulombic efficiency (typically < 90 %), aggravated self-discharge and poor capacity retention over extended cycles. Efforts are geared towards understanding and mitigating the parasitic reactions by creating stable cathode-electrolyte interface (CEI) layer and generating passivated Al current collectors with the help of various electrolyte additives (salt additives and co-solvents). Using a range of surface and bulk characterizations tools, and operando gas pressure measurements we strive to understand the nature and resilience of the CEI layer forming at different states-of-charge in such electrodes. In addition, works on the design of new current collectors with improved anodic stability will be introduced.

11:25 AM EN12.19.16

Design of a Deep Eutectic Solvent Electrolyte for Sodium-Ion Batteries with Increased Durability Dries De Sloovere^{1,2}, Danny E. P. Vanpoucke¹, Andreas Paulus^{1,2}, Bjorn Joos^{1,2}, Lavinia Calvi¹, Thomas Vranken^{1,2}, Gunter Reekmans¹, Peter Adriaensens¹, Nicolas Eshraghi^{3,4}, Abdelfattah Mahmoud³, Frédéric Boschini³, Mohammadhosein Safari^{1,2}, Marlies Van Bael^{1,2} and An Hardy^{1,2}; ¹UHasselt, Institute for Materials Research (IMO-Imomec) and imec, Division Imomec, Belgium; ²EnergyVille, Belgium; ³University of Liège, Belgium; ⁴AIT Austrian Institute of Technology GmbH, Austria

In the large-scale storage of renewable energy, sustainability and cost-effectiveness are of utmost importance. Lithium-ion batteries (LIBs) are a common energy storage technology for portable electronics and electric vehicles. However, reserves of lithium are limited and therefore, the increasing use of LIBs on larger scales could result in a significantly higher price in future. Next to lithium, sodium is the smallest and lightest alkali metal and therefore, sodium-ion batteries (SIBs) are a potential alternative technology to LIBs. Sodium is the 6th most abundant element in the Earth's crust and is widely available, which positively influences the sustainability of SIBs.

Conventional liquid electrolytes for SIBs consist of a sodium salt dissolved in (an) organic solvent(s). However, the latter cause a safety hazard because of their high flammability. At temperatures of 55 °C or higher, the solubility of the solid electrolyte interphase (SEI) components derived from such electrolytes is higher than at ambient temperature. This can have a negative influence on the electrochemical performance. Ionic liquids can be used as alternatives for organic solvents. They consist entirely out of ions, are liquid in a wide temperature range, are non-flammable, and offer a high electrochemical stability. They have a high conductivity and can also dissolve high amounts of salt. However, their main drawback is their high cost. Deep eutectic solvents (DESs) are mixtures of Lewis/Brønsted acids and bases. The melting point of a DES is below that of the individual components. Their use as electrolyte in batteries may offer substantial benefits over conventional electrolytes and ionic liquids. They can significantly improve safety because they have a low vapor pressure and can be non-flammable, and they can be cost-effective. Thus far, DESs have not yet been reported as electrolytes for SIBs. In LIBs, however, a DES (LiTFSI dissolved in *N*-methyl acetamide (NMA)) allowed stable electrochemical cycling of full cells, even at 60 °C.¹ The low solubility of sodium salts (compared to lithium salts) and sodium's milder Lewis acidity imply that it is more difficult to create a DES based on a sodium salt than a similar DES based on a lithium salt. In the example described above, changing LiTFSI to NaTFSI might not lead to the formation of a DES at all, or will at least have a large impact on the physico- and electrochemical properties.

In this presentation, we will report non-flammable DESs, based on the dissolution of NaTFSI in NMA, that can be used as electrolyte in SIBs. Increasing the NaTFSI concentration increased the DESs' reductive and oxidative stability. First-principles modelling revealed that the increased anodic stability was related to the strong ionic interactions between NMA molecules and TFSI⁻ with Na⁺. The hydrogen bonds between individual NMA molecules are progressively disrupted with increasing NaTFSI concentration. When cycled at 55 °C, (Na₃V₂(PO₄)₂F₃)/(Na_{2+x}Ti₄O₉/C) full cells showed an improved electrochemical stability when a DES was used in comparison to when a conventional electrolyte was used, with 74.8% capacity retention after 1000 cycles at 1 C and 97.0% capacity retention after 250 cycles at 0.2 C. This shows that DESs can be viable electrolytes for SIBs, as they can offer a high durability and safety.

The authors acknowledge the Research Foundation Flanders (FWO Vlaanderen) for financial support under the project number G053519N. This work is further supported by Hasselt University and Research Foundation Flanders via the Hercules project AUHL/15/2 - GOH3816N). The computational resources and services used in this work were provided by the VSC (Flemish Supercomputer Center), funded by Research Foundation Flanders and the Flemish Government – department EWI.

(1) Boisset, A. et al. *Phys. Chem. Chem. Phys.* 2013, 15, 20054–20063.

11:30 AM EN12.19.17

A Combined First Principles and Grand Canonical Monte Carlo Approach to Understand Sodium (De)-Intercalation in O3 and P2 Type Na_xRhO₂ Systems Madhulika Mazumder, Abhiroop Lahiri and Swapan Pati; JNCASR (Jawaharlal Nehru Centre for Advanced Scientific Research), India

The demand for generating clean and sustainable sources of energy has led to a huge leap in the research of efficient, high-performance electrochemical systems for energy storage and harvesting. In terms of resource availability, manufacturing expense and safety, Na ion batteries (SIBs) are now evolving as contenders for the highly successful Lithium ion battery (LIB) technology.

Layered oxide materials are promising candidates for cathode systems, because of their high capacities arising from fast ionic conduction. However, there still exist pitfalls of irreversible structural transition during electrochemical cycles, the most prominent one being the gliding of (MO)_n layers, O3 to P3 phase or P2 to O2 phase, which eventually leads to degradation and capacity loss.

The Na_xMO_2 (M=3d transition metal) class of compounds, with 3d transition elements have been extensively researched on as cathodes. The 4d transition series is relatively newer, and sodium (de)-intercalation has been proved to occur in Nb, Mo and Rh systems^[1,2]. As reported by Delmas *et al*^[3], NaRhO_2 can be synthesised in O3 and P2 type structures with Na ions occupying octahedral and trigonal prismatic sites respectively. It is interesting to note that these systems preserve the O3 type stacking upto a high temperature (300°C). Thus, a nearly reversible (de)-intercalation of Na in the $0.33 < x < 1$ composition range, makes it a superior cathodic system. In this work, we have theoretically studied the electrochemistry in O3 and P2 type NaRhO_2 , using Density Functional Theory for detailed insights into the electronic structures of the intermediates Na_xRhO_2 . We have also delineated the Minimum Energy Pathways for Na diffusion with low activation barriers of ~210meV and compared it with previously reported Na_xMO_2 systems. In addition to this, we have employed a Cluster Expansion (CE) technique followed by Grand Canonical Monte Carlo (GCMC) simulations, to reproduce the trends in the voltage profiles of O3 and P2 systems, as a function of composition x . The computed voltage profile from MC simulations corroborate well with the experimental observation^[3], with voltage steps at $-x=0.3$ and $x=0.5$. This cumulative approach involving First Principles theory and stochastic simulations provides a clear understanding of the (de)-intercalation mechanism, from the associated Na/vacancy orderings within the voltage window of 2.4V to 4.2V.

References :

1. Chang, S. O.; Park, H.-H.; Maazaz, A.; Delmas, C. Sur l'Obtention des Oxydes Lamellaires LiNbO_2 et NaNbO_2 par Voie Chimique et Electrochimique. Preparation par Desintercalation des Solutions Solides Correspondantes. C.R. Acad.Sc.Paris, Serie II (1989), 308, 475–478.
2. Delmas, C.; Fouassier, C.; Hagemuller, P. "Structural Classification and Properties of the Layered Oxides". Physica B+C (1980), 99 (1–4), 81–85.
3. Verger, L., Guignard, M., Delmas, C. "Sodium Electrochemical Deintercalation and Intercalation in O3 – NaRhO_2 and P2 – Na_xRhO_2 Layered Oxides" Inorg. Chem. (2019), 58, 2543–2549 .
4. Lee, E., Iddir, H., Benedek, R., "Rapidly convergent cluster expansion and application to lithium ion battery materials", Phys. Rev. B 95, 085134 (2017).

SESSION EN12.20: On-Demand
Sunday Morning, December 5, 2021
On-Demand

8:00 AM EN12.02.03

Electrolyte-Mediated Interfacial Dynamics in Na-S Battery [Susmita Sarkar](#)¹, Rachel Carter², Corey Love² and Partha Mukherjee¹; ¹Purdue University, United States; ²U. S. Naval Research Laboratory, United States

Polysulfide shuttling is an inevitable trait of metal-sulfur (S)-based batteries. Such shuttling behavior is directly related to the amount of soluble intermediate polysulfide species and is primarily affected by electrolyte constituents. While the sulfur electrode suffers from lower accessible capacity due to the loss of active S species, sodium (Na) metal is also plagued by severe plating/stripping and dendrite growth, leading to cyclable Na loss. However, it is still poorly understood whether Na or S electrode has the most deleterious consequences for overall Na-S chemistry in specific electrolyte combinations. Given the influence of electrolyte in dictating the intermediate reaction steps, electrode-electrolyte interphase formation, and effectiveness of ionic transport, this work carefully investigates the effects of single and multi-solvent electrolyte on the electrochemical signatures of S electrode. Additionally, this work probes the aging process of Na metal, altered by different types of electrolyte-specific morphological evolution, manifesting a dramatic drop-off in cell performance. This complex electrochemical interaction in both the electrodes is further compounded by the limiting ionic transport at low-operating temperatures. Current work explores the electrolyte-mediated changes in decoupled cathode-anode cell signature and impedances and performances using a three-electrode cell configuration in different temperature conditions. By correlating the electrolyte-specific structural-compositional evolution and operational specifications of both the metal and sulfur electrodes, this work aims to lay the ground for thermally versatile and high-performance Na-S batteries.

SYMPOSIUM EN13

Climate Change Mitigation Technologies
November 30 - December 8, 2021

Symposium Organizers

Radu Custelcean, Oak Ridge National Laboratory
Klaus Lackner, Arizona State University
Mihrimah Ozkan, University of California, Riverside
Susan Rempe, Sandia National Laboratories

Symposium Support

Platinum
Sandia National Laboratories

Gold
IBM Research

Bronze
Joule | Cell Press
Chem Catalysis | Cell Press

* Invited Paper

SESSION EN13.01: Climate Change Mitigation Technologies I
Session Chair: Phillip Milner
Tuesday Morning, November 30, 2021
Hynes, Level 3, Room 313

10:30 AM *EN13.01.01

Global Thermostat Direct Air Capture Technology Miles A. Sakwa-Novak, Eric Ping, Ron Chance and Peter Eisenberger; Global Thermostat, United States

Direct air capture of CO₂, or DAC, is gaining increasing attention as an important technology with significant potential as a climate change mitigation approach. DAC is a feasible technology, whose primary barrier to deployment in support of the climate is cost. Since 2010, Global Thermostat (GT) has been developing a technology platform for DAC addressing the primary cost drivers of the process. In this contribution, we discuss the primary elements of the GT DAC technology platform and their relation to reducing the cost of DAC.

The core challenges that GT has identified as critical to enabling low-cost DAC are i) efficient air processing, ii) selective and stable CO₂ binding, iii) energy efficient sorbent regeneration, iv) efficient use of plant capital, and v) design for continuous improvement. Innovations in materials design and engineering spanning several decades of length scale are key to addressing these challenges. GT's technology platform is based on structured honeycomb monolith air contactors, similar to those used in automobile catalytic converters or stationary deNO_x emissions abatement cartridges. Porosity is engineered into these high surface area, low pressure-drop contactors through existing industrial manufacturing techniques. Quasi-solid amine-based CO₂ sorbents are utilized in targeted porosity domains of the monolith contactors. These materials are employed in a rapid temperature swing process employing direct contact phase change heat transfer with saturated steam condensing on the monolith channel surface to regenerate the bound CO₂ within the pore structure. Process performance is strongly linked to fundamental material-process phenomena such as adsorption rates, desorption rates, degradative mechanisms and the condensation / evaporation of steam.

The unique properties of these materials, and their interactions with the various environments imposed by the DAC process, present both opportunities and challenges in their successful deployment. In this talk we will discuss progress in both of these areas as well as an outlook on their potential.

11:00 AM EN13.01.02

Turning up the Pressure on Carbon Dioxide—Towards the Commercial Application of a Green Solvent Kristoffer K. Kortsens, Joachim Christopher Lentz, Vincenzo Taresco and Steven M. Howdle; University of Nottingham, United Kingdom

Current industrial polymer particle production processes often use water as the main solvent, generally resulting in contamination of that water through the use of volatile organic compounds and chlorofluorocarbons¹. This results in contaminated wastewater streams, with negative consequences for the environment, oceans, and availability of drinking water. Additionally, water must be removed from the final product in costly and energy intensive drying processes, further increasing the negative environmental impact². As environmental impact becomes a more pressing concern, there is an increasing interest in sustainable solvents that have the potential to alleviate water contamination issues, reduce energy costs and reduce the impact on the environment³. Supercritical carbon dioxide (scCO₂) is a promising alternative solvent, combining considerable environmental advantages⁴ with desirable solvation and diffusivity properties of SCFs². It is a cheap, non-flammable and environmentally friendly solvent⁴, with an easily attainable critical point ($T_c = 31.1\text{ }^\circ\text{C}$ and $P_c = 73.8\text{ bar}$)². When returning to atmospheric conditions, CO₂ reverts to the gas phase providing a solvent free polymer product, without the need for energy and cost intensive drying processes and allowing the solvent to be reused.

A large hurdle in the development and wider adoption of scCO₂ as a polymerization medium is the lack of a reliable and accessible monitoring method. While the tracking of an ongoing polymerization reaction in traditional solvents can be achieved with a wide range of techniques⁵, reactions in scCO₂ are more complicated to monitor due to the elevated pressure contained in a sealed system. Our recent publication⁶ shows a versatile and reliable on-line sampling system for polymerization reactions in supercritical fluids, unlocking the potential of this sustainable solvent. By withdrawing a small volume of a high-pressure reaction mixture and expanding it in a controlled volume before capturing it in a suitable solvent, reliable kinetic data were obtained for a range of polymerizations and reactions in scCO₂. The facile applicability of this monitoring method resulted in additional insights into the unique conditions found in scCO₂ and their effect on polymerization systems. It was discovered that the tunable density of scCO₂ could be exploited to control the particle size of dispersion polymerizations, further expanding on the usefulness of this green solvent.

The kinetic information gained from this research, was exploited for precise dosing control during multistage polymerizations allowing for controlled tapering between successive polymer feeds and predictable layering of core-shell polymer particles.

The combination of kinetic monitoring, solubility control, and sequential monomer addition has finally unlocked the potential to synthesize commercially desirable polymer particles in this green and sustainable solvent for a wide array of applications such as 3D printing, plastic additives, metal oxide templating and medical devices.

1. Lovell, P. A.; El-Aasser, M. S., *Emulsion Polymerization and Emulsion Polymers*. Wiley: 1997

2. Kendall, J., et al., Polymerizations in supercritical carbon dioxide. In *Chem. Rev.*, 1999; Vol. 99, pp 543-563

3. Millner, A.; Ollivier, H., Beliefs, Politics, and Environmental Policy. *Review of Environmental Economics and Policy* 2016, 10 (2), 226-244

4. Krishna Mohan, S., Green solvents for polymerization of methyl methacrylate to poly(methyl methacrylate). In *Green Solvents I: Properties and Applications in Chemistry*, 2012; pp 251-298

5. Haven, J. J.; Junkers, T., Online Monitoring of Polymerizations: Current Status. *European Journal of Organic Chemistry*, 2017, 6474-6482
6. Kortsen, K., et al., On-line polymerisation monitoring in scCO₂: a reliable and inexpensive sampling method in high pressure applications. *The Journal of Supercritical Fluids*, 2020, 105047

11:15 AM EN13.01.03

Capacitive Deionization for Direct Air Capture of CO₂—An Implementation of the Alkalinity Concentration Swing [Andrew Bergman](#), Anatoly Rinberg, Daniel Schrag and Michael Aziz; Harvard University, United States

The Alkalinity Concentration Swing (ACS) is a new process for direct air capture of carbon dioxide, driven by concentrating an alkaline solution that has been exposed to the atmosphere and loaded with dissolved inorganic carbon (DIC). We theoretically and experimentally evaluate driving the ACS through capacitive deionization (CDI), a method of removing anions and cations from solution by applying a voltage across two electrodes. When voltage is applied, anions electrosorb to the positive electrode and cations to the negative electrode. When the voltage is switched off or reversed, ions are released, driving the ACS through concentration of ions in solution. Upon concentration, the DIC per unit alkalinity decreases and the partial pressure of CO₂ increases, allowing for extraction and compression. We find that higher concentration factors result in proportionally higher outgassing pressure, and higher initial alkalinity concentrations at the same concentration factor outgas a higher concentration of CO₂.

CDI has been deployed industrially in municipal wastewater treatment and brackish water desalination facilities. CDI operates best in brackish water conditions, enabling high concentration factors and access to higher efficiency ACS regimes, without the need for high pressure systems. CDI also enables selectivity of bicarbonate ions, through use of ion exchange membranes and enhanced porous carbon electrode ion selectivity, allowing for an increase in ACS efficiency.

11:30 AM EN13.01.04

Accelerated Discovery of Novel Solvents for CO₂ Capture [Benjamin Wunsch](#)¹, Stacey Gifford¹, Theodore van Kessel¹, Flaviu Cipcigan², James McDonagh², Dmitry Zubarev³, Alexander Harrison² and Stamatia Zavitsanou²; ¹IBM T.J. Watson Research Center, United States; ²IBM Research - UK, United Kingdom; ³IBM Research - Almaden, United States

Today, we capture less than 1% of all emitted carbon dioxide, but in 2018, the Intergovernmental Panel on Climate Change (IPCC) reported that limiting atmospheric warming to less than 2 degrees Celsius will require both capture of carbon emissions from point sources such as power and industrial plants as well as the removal of existing atmospheric carbon dioxide. Amine solvents have gained the most traction in large-scale CCUS implementation, but limitations include high energy penalties associated with regeneration, cost, toxic degradation products, and corrosiveness. Improvements in stability, binding capacity, kinetics, and vapor-liquid equilibria have been achieved by blending different primary, secondary, and tertiary amines, but accelerating their discovery with machine learning and AI has seen limited exploration.

We have built a parallelized assay platform for rapid testing and measurement of capacity, kinetics, and thermodynamics of CO₂ binding to binary and tertiary blends of standard primary, secondary, and tertiary amines. Our platform replicates gas sparging of CO₂ through liquid solvents and leverages NDIR sensors to measure CO₂ absorption from complex mixtures of simulated flue gas. We also measure other physical parameters such as pKa, viscosity, and stability. With these data sets, we leverage machine learning to capture properties of novel blends and rank performance of these mixtures. New blends are tested and validated, and these data are delivered back to the model to improve its predictive capabilities with the end goal of generating new materials and solvent blends with improved performance for carbon capture.

11:45 AM EN13.01.05

Greenhouse Gas Capture in Metal-Organic Frameworks—Carbon Dioxide and Beyond Mary Zick, Tristan Pitt, Ronald Jerozal and [Phillip Milner](#); Cornell University, United States

Rising atmospheric levels of the greenhouse gases carbon dioxide, nitrous oxide, and hydrofluorocarbons are contributing to global climate change. Therefore, new strategies for capturing greenhouse gas for subsequent sequestration or conversion into value-added products are needed to minimize global climate change over the next century. A promising strategy is to develop new reactivity-based separations of greenhouse gases, which will enable higher selectivities than traditional separations. Herein, we will discuss new separation strategies for greenhouse gas capture using metal-organic frameworks, which are crystalline well-defined porous materials with highly tunable pore environments. We will discuss carbon dioxide capture in frameworks bearing extra-framework and metal-bound hydroxide sites, which reversibly react with carbon dioxide to yield (bi)carbonates. In addition, we will discuss the interaction of nitrous oxide with redox-active metal centers in frameworks. Last, we will explore how hydrogen- and halogen-bonding interactions can be leveraged to capture fluorinated gases such as fluoroform and sulfur hexafluoride.

SESSION EN13.02: Climate Change Mitigation Technologies II

Session Chairs: Mert Atilhan and Thomas George

Tuesday Afternoon, November 30, 2021

Hynes, Level 3, Room 313

1:30 PM *EN13.02.01

AI for Accelerated Discovery of Materials for Carbon Capture [Stacey Gifford](#); IBM Research, United States

In 2018, the IPCC reported that limiting atmospheric warming to less than 2 °C will require both capture and storage of anthropomorphic carbon dioxide (CO₂) emissions. Despite estimates that we will need to capture upwards of 10 GtCO₂ per year by 2050, today we capture less than 1% of all emitted CO₂. Dramatic reductions in the cost of carbon capture processes are needed to drive adoption at scale. IBM Research is building AI-driven tools to accelerate the discovery of materials with improved performance for carbon capture, utilization, and storage including solvents, solid sorbents, and membranes. We have also developed automated synthesis platforms for production of carbon capture materials and novel catalysts for carbon dioxide conversion. Finally, we have created a digital rock platform coupled with high-precision microfluidics to accurately simulate CO₂ fluid flow at pore scales relevant for geological storage.

2:00 PM *EN13.02.02

Clean Energy and Decarbonization Research, Development and Demonstration at Oak Ridge National Laboratory [Xin Sun](#); Oak Ridge National

Laboratory, United States

This talk provides the overview of Oak Ridge National Laboratory's (ORNL) transformational science and technologies towards the clean and decarbonized energy future with capabilities spanning the entire spectrum from clean energy generation to distribution, at-scale storage, and end-use. Being the largest DOE Office of Science Laboratory, ORNL is well-recognized for its energy efficiency research portfolio with the most comprehensive user facilities and capabilities in fundamental science and applied energy space among all the DOE national laboratories. We are accelerating decarbonization in the US with a three-pronged approach on integrated energy systems: 1.) Achieve deeper energy savings through enhanced energy efficiency efforts across all spectrums of the energy service sectors, i.e., buildings, industry, and transportation; 2.) Accelerate net-carbon neutrality by capturing and converting CO₂ into valuable materials, fuels, and feedstocks for downstream utilizations; and 3.) Enable bi-directional electron flows between the grid and end users with at-scale energy storage and transactive controls to enable a sustainable, resilient, and secure energy infrastructure. Exemplary ORNL RD&D advancements in all the areas above will be presented and future opportunities and challenges in the integrated energy systems approach will be discussed.

2:30 PM EN13.02.03

Reverse Osmosis for Direct Air Capture of CO₂—An Implementation of the Alkalinity Concentration Swing Anatoly Rinberg, Andrew Bergman, Daniel Schrag and Michael Aziz; Harvard University, United States

The Alkalinity Concentration Swing (ACS) is a new process for direct air capture of carbon dioxide, driven by concentrating an alkaline solution that has been exposed to the atmosphere and loaded with dissolved inorganic carbon. We theoretically and experimentally evaluate driving the ACS through reverse osmosis (RO), a membrane-based separation process in which pressure is applied against a solvent-filled solution to create a concentrated and a dilute stream. RO is the most widely used desalination approach - producing approximately 100 million cubic meters of purified water per day - allowing for technological advances to be leveraged for ACS deployment. Upon concentration, the partial pressure of CO₂ increases, allowing for extraction and compression of gaseous CO₂. We find that higher concentration factors result in proportionally higher outgassing pressure, and higher initial alkalinity concentrations at the same concentration factor outgas a higher concentration of CO₂. Theoretical projections suggest the ACS poses certain challenges, such as high water and land requirements, but it also confers advantages over incumbent technologies, especially in terms of simplicity of material requirements and possibility of reaching low energy costs through tuning operation parameters.

2:45 PM EN13.02.05

An Integrated Materials Approach to Ultraporous and Ultrasensitive Polymer Membranes for Carbon Capture: Breaking Through the Upper Bound Marius Sandru¹, Eugenia M. Sandru¹, Liyuan Deng² and Richard Spontak³; ¹SINTEF Industry, Norway; ²Norwegian University of Science and Technology, Norway; ³North Carolina State University, United States

While a wide range of carbon-capture efforts are being developed around the world to help mitigate the adverse effects of global climate change, advances in membrane technologies that combine greatly improved CO₂ separation efficacy with low cost, facile fabrication, upscaling and implementation, and mechanical robustness are still needed. In this study, we introduce an integrated membrane strategy wherein a high-permeability thin film is chemically functionalized with a highly CO₂-philic open, brush-like surface layer. This nanofabrication scheme is based on a low-diffusivity, high-solubility mechanism that relies on enrichment of CO₂ in the surface layer naturally hydrated by the water vapor present in all targeted gas streams, followed by fast CO₂ transport through a supported thin film of a highly permeable polymer. Since this design employs commercial polymer thin films that are already available for gas separations, these new membranes can immediately be produced, upscaled and put into field operation after surface functionalization, achieved by controllably growing short, controlled amine-modified chains from the polymer surface. Spectroscopic methods confirm the existence of the amine surface layer, which also serves to enhance surface roughness and, thus, separation area. Integrated multilayer membranes prepared in this fashion are not diffusion-limited and, in some cases, are able to retain much of their inherently high CO₂ permeability while their CO₂ selectivity is increased in some cases by over ~150x, far exceeding the Robeson upper bound that traditionally reflects the trade-off between gas permeability and selectivity.

3:00 PM EN13.02.06

Development of Metal-Organic Framework (MOF) Materials as Room-Temperature Chemoresistors for Greenhouse Gas Monitoring Ignasi Fort-Grandas^{1,1}, Ariana Neyra-Perez¹, Alex Rodriguez-Iglesias¹, Arnald Grabulosa^{1,1}, Mauricio Moreno^{1,1}, Anton Vidal-Ferran^{1,1,2}, Paolo Pellegrino^{1,1}, Daniel Sainz^{1,1} and Albert Romano-Rodriguez^{1,1}; ¹Universitat de Barcelona, Spain; ²Catalan Institution of Research and Advanced Studies (ICREA), Spain

The reduction in emission of greenhouse gases (GHGs) is an important step towards mitigating the human impact on the climate change. Technically capturing CO₂, for example, is addressed by different emerging and established technologies. To effectively monitor the actual result of such a removal of this or other greenhouse gases, specifically adapted gas measuring systems are required.

At present, to monitor the environment, each National surveillance agency uses highly sensitive, selective, complex, bulky and expensive systems, which can only be used as reference measuring units installed in few specific, mostly fixed, key locations. For a more detailed monitoring and for the development of climate change models, a more distributed control of the GHGs emission is required and can be achieved through large numbers of deployed and connected gas sensing systems, thanks to the advent of Internet of Things (IoT). The required devices need to be sensitive, selective and low energy consuming, usually with a lower level of accuracy and precision than the reference instruments. Current commercial sensors do not fulfill all the requirements together and novel improved functional nanomaterials and sensors are needed.

The goal of this work is to show the actual stage of development of advanced miniaturised gas sensing devices for their use in monitoring of GHGs emissions. These devices are based on metal-organic framework (MOF) materials, that present a high degree of porosity and a reasonable conductivity, which allows their resistance to be measured.

The synthesis of the MOFs uses triphenylene-derived ligands, namely hexahydroxytriphenylene (HHTP) or hexaiminotriphenylene (HITP), and different metal centers. The synthesis route is described in detail elsewhere [1] for Cu and Ni metals. In this work, we have extended the synthesis to Mg, Zn and Co. In this way, 2D arrangements of metal-ligand, giving rise to hexagonal structures with a center pore, are formed. Vertical arrangement of such 2D structures occur through p-p stacking, giving rise to nanostructures whose dimensions vary between 100 and 300 nm in any direction. X-ray diffraction spectra prove the crystalline nature of such nanostructures.

The MOFs have been dispersed in ultrapure water, sonicated for 10 minutes, and one drop (0.5 ml) of the solution has been dispersed on a glass chip with interdigitated Ti/Au electrodes (IDE). Next, the chips have been dry heated in a furnace at 80°C for 10 minutes. The remaining material contacted the IDE and allowed current to flow between the IDE. The sample was then mounted and bonded to a TO8 holder and this was introduced in a gas measuring system, whose volume was only 8.6 ml. Through Mass-flow controllers, different gases and their mixtures were allowed to flow into the chamber at a rate of 50 sccm while the resistance of the MOF material was simultaneously measured.

Due to the porous nature of these samples and to the charge transfer between the flowing background synthetic dry air gas and the MOF, the resistance changes over time as a result of the continuous adsorption of components of the gas. Strategies for reversing this situation and bringing back the sample to its initial resistance value consist in either controlled heating or vacuum treating the sample. By adding 500 ppm of CO₂ to the synthetic air, a sizeable increase in the resistance was observed, while after removal of the CO₂ from the atmosphere, an incomplete recovery of to its baseline was attained. This response to CO₂ has been observed for different metal core and ligands, proving that these materials are potential candidates for innovative CO₂ gas

sensors.

In this work a systematic study of the effect of the metal cores, of the ligands and of the measuring history and recovery methods will be presented with the aim of bringing forward these innovative and low power consuming gas sensor devices for greenhouse gas detection.

[1] M.G. Campbell et al, JACS 137, 13780 (2015)

3:15 PM EN13.02.07

Redox-Mediated Bipolar Membrane Electrodialysis for Direct Air Capture of Carbon Dioxide Thomas Y. George, Clifton Wang, Daniel Schrag and Michael Aziz; Harvard University, United States

Complementing the rapid decarbonization of energy technology, CO₂ removal will be necessary to offset some continued emissions and avoid the most harmful climate outcomes. Direct air capture (DAC), separating atmospheric CO₂ for subsequent storage with physical or chemical methods, is one CO₂ removal approach. Many DAC technologies use a solid or solvent-based sorbent to reversibly bind CO₂, and CO₂ release is driven by heating. New electrochemical methods offer opportunities because they interface readily with sources of inexpensive carbon-free electricity and may operate at very high efficiency. A central challenge for these methods is minimizing the voltage required by the electrochemical process, which is determined by ohmic resistance of the reactor components and the voltage required for electrochemical reactions.

We propose a new DAC cycle utilizing a redox-mediated bipolar membrane electrodialysis (RM-BPMED) reactor that dramatically decreases the energy required compared to other reactors of this type. RM-BPMED is used for electrochemical salt splitting (*e.g.*, NaCl) to create a strong base (*e.g.*, NaOH) and a strong acid (*e.g.*, HCl). The base is used to absorb CO₂ from ambient air; the acid is then used to extract the CO₂ by recombining with the base, essentially reversing the salt splitting process. The research presented here demonstrates the RM-BPMED reactor, which is the centerpiece of our DAC approach.

The iron (II/III) hexacyanide redox couple affords facile redox kinetics on carbon electrodes, replacing the hydrogen and oxygen evolution reactions at the anode and cathode of traditional BPMED processes to decrease the required cell voltage. In addition to the redox mediators, RM-BPMED relies on ion exchange membranes that direct the ion transport for salt splitting. The ion exchange membranes must minimize leakage of species via unwanted crossover mechanisms while enabling high ionic conductivity. Some particular advantages of this method for DAC are that the acid and base products need not be pure and the salt splitting need not reach complete desalination. This allows additional supporting salt in all electrolytes flowing through the reactor, including the product streams. We present a design process informed by a fundamental understanding of membrane phenomena: the water content of ion exchange membranes determines the available transport pathways. The effects of electrolyte composition and membrane chemistry on water content and conductivity are elucidated to design a membrane-electrolyte system for RM-BPMED. A model of this strategy of electrochemical reactor engineering predicts RM-BPMED energy use below 100 kJ/mol CO₂ removed, as well as salt splitting at up to 100 mA/cm² current density. We will report on experiments that are under way to test the model.

3:30 PM BREAK

SESSION EN13.03: Climate Change Mitigation Technologies III

Session Chair: Yunchao Xie

Wednesday Morning, December 1, 2021

Hynes, Level 3, Room 313

10:30 AM EN13.03.01

Mining Materials Literature for Rediscovery of Methane Storage and Separation in Porous Carbon Yunchao Xie, Chi Zhang, Dawei Li, Ming Xin and Jian Lin; University of Missouri-Columbia, United States

Porous carbon (PC) has been widely regarded as one of the most promising absorbents for methane storage. Studies show that its uptake capacity and selectivity highly depend on textural structures. Although much effort has been made, unveiling their detailed structure-performance relationship remains a challenge. Here, we propose an innovative study where, with the assistance of machine learning, the hidden relationship of the textural structures of PC with the methane uptake and separation can be derived from existing data in material literature. Machine learning models were trained by the data, including specific surface area, micropore volume, mesopore volume, temperature, and pressure as the input variables and methane uptake as the output variable for prediction. Among the tested models, the multilayer perceptron (MLP) shows the highest accuracy in predicting the methane uptake. In addition, the model enables to automatically construct a uptake performance map in terms of micropore volume and mesopore volume. The obtained MLP model was also extended to explore the CO₂/CH₄ selectivity by retraining it with the data collected from literature of PC for the CO₂ uptake. The constructed 2D selectivity map shows that the high selectivity can be achieved in the low CH₄ uptake region.

10:45 AM EN13.03.02

Late News: Monitoring the Carbon Paths in the Dry Reforming of Methane Over Ni/Ce-M-Cu-O (M: La, Sm) Catalyst Aseel Hussien^{1,1}, Constantinos M. Damaskinos², Dalaver Anjum^{1,1}, Maryam T. A. Khaleel^{1,1}, Michalis A. Vasiliades², Angelos Efstathiou² and Kyriaki Polychronopoulou^{1,1}; ¹Khalifa University of Science and Technology, United Arab Emirates; ²University of Cyprus, Cyprus

Dry reforming of methane (DRM) reaction ($\text{CH}_4 + \text{CO}_2 \leftrightarrow 2\text{CO} + 2\text{H}_2$) produces synthesis gas (CO/H₂) which can be used for the production of high value-added chemicals and fuels via Fischer-Tropsch (FT) process. Despite the benefits and significance of DRM, this process has not been industrialized yet due to the absence of a stable and coke resistance catalyst. Ni-based catalysts are economically feasible, yet they suffer mainly from coke deposition and deactivation through CH₄ decomposition and CO disproportionation routes. On the other hand, supports, especially ceria-based ones, play an important role in tackling the coking challenge. In supported catalysts, both active metal and support can be engineered to inhibit carbon formation. *The approach followed in this particular work is (a) tuning the support's basicity and lattice oxygen mobility via ceria doping with rare-earth metals (La³⁺, Sm³⁺, and Pr³⁺) and (b) inducing in situ alloying of the Ni active metal with Cu species (originated from the support).*

This work's originality and significance to the field is reflected in presenting the role of trivalent M= La³⁺ and Sm³⁺ used in the ternary type of reducible support Ce-M-Cu-O composition as a carrier of Ni nanoparticles on the carbon paths in the DRM reaction. In addition, transient kinetics and isotopic experiments were designed to investigate the crucial coking factors for the DRM reaction over La vs. Sm co-dopants. The experiments studied (a) the

carbon formation and their relative contribution of CH₄ decomposition and CO disproportionation reaction in the coking network, (b) the amount of inactive carbon accumulation on the catalyst surface after DRM, and (c) the extent of participation of support's labile oxygen in the removal of carbon from the catalyst surface via oxidation to CO.

Due to the complexity of the catalyst composition, many analytical techniques were employed to get an insight into the catalysts' intrinsic properties and structure and relate these to catalytic performance. Powder XRD, HAADF-STEM, SAED, EELS, elemental mapping, Raman, CO₂-TPD, H₂-TPR, and H₂-TPD were employed. The La³⁺- and Sm³⁺-doped ceria supported Ni catalysts presented tuned intrinsic properties, such as redox behavior and oxygen vacant sites concentration, and surface basicity. Also, La³⁺-doped support composition favored the formation of NiCu alloy nanoparticles and enhanced lattice oxygen mobility, which in turn appears to favor reduction in carbon deposition and enhanced carbon removal rates under DRM via mainly the participation of lattice oxygen.

A systematic transient kinetic study of CH₄ and CO decomposition reactions (main carbon deposition routes in DRM) by measuring initial rates of carbon deposition and the following dynamics of it, over the La³⁺- and Sm³⁺-doped ceria-supported Ni catalysts, along with advanced experimentation in measuring both the rates of carbon oxidation by lattice oxygen of support and by oxygen from the CO₂ activation route under DRM were conducted. Ni nanoparticles (23 nm) supported on the La³⁺-doped ceria exhibited ~3 times higher rates of carbon oxidation to CO by lattice oxygen and ~13 times lower rates of carbon accumulation than Ni (18 nm) supported on Sm³⁺-doped ceria. The oxygen vacant sites and surface basic sites were found to correlate with carbon deposition.

We strongly believe that this type of transient and isotopic work paves the way to fundamentally understand the role of dopants introduced in the ceria lattice and used as a carrier of Ni (or other metal) nanoparticles towards an efficient design of carbon-resistant doped ceria-supported Ni catalysts.

11:00 AM EN13.03.03

Atmospheric- and Low-Level Methane Abatement via Copper Zeolites [Rebecca Brenneis](#)¹, Eric P. Johnson², Wenbo Shi¹ and Desiree Plata¹; ¹Massachusetts Institute of Technology, United States; ²Yale University, United States

Climate action scenarios that limit changes in global temperature to less than 4°C require methane controls in addition to carbon dioxide mitigation, yet few methane abatement technologies exist. Importantly, restoration of atmospheric methane from current levels 1.85 ppmv to pre-industrial concentrations of 0.76 ppmv would save 16% of global climate forcing within decades. Here, we describe the use of a biomimetic copper zeolite capable of converting atmospheric and low-level methane at relatively low temperatures (e.g., 200-300°C) in simulated air. Depending on the duty cycle, 40%, over 60%, or complete conversion could be achieved (a two-step process at 450°C activation and 200°C reaction, or a short and long-activation at isothermal 310°C conditions, respectively). Conversion rate increased over a range of methane concentrations (0.0002 to 2% methane), indicating promise of this technology to abate methane from any sub-flammable stream. Finally, uncompromised catalyst turnover over 300 hours (12 days) in simulated air was demonstrated under isothermal reaction conditions (310°C). Taken together, this work illustrates the promise of using low-cost, Earth-abundant materials innovations to mitigate methane at the diffuse and dilute sources that drive growth of this important greenhouse gas, and ultimately slow the pace of climate change.

11:15 AM EN13.03.04

Development of Composite Dual Functional Catalysts and Mechanistic Insights for CO₂ Methanation Reaction [Ayesha A. Alkhoori](#)^{1,2}, Constantinos Damaskinos³, Aasif Dabbawala¹, Dalaver Anjum^{1,2}, Angelos Efstathiou³, Nikolaos Charisiou⁴, Maria Goula⁴ and Kyriaki Polychronopoulou^{1,2}; ¹Khalifa University of Science and Technology, United Arab Emirates; ²Center of Catalysis and Separation, United Arab Emirates; ³University of Cyprus, Cyprus; ⁴University of Western Macedonia, Greece

Carbon dioxide mitigation is a great challenge for the twenty-first century. The increasing atmospheric CO₂ concentration peaked near 420 ppm on May 2021 at NOAA's Mauna Loa Atmospheric Baseline Observatory. Controlling CO₂ emissions can be achieved by capturing and converting it into value-added chemicals via dual function materials (DFM) for in-situ methanation. In this study, different Ni-based catalysts with composite supports i.e., Ni/nCeO₂/mAl₂O₃ (n = different wt.%, m = different porosities) were synthesized. A set of state-of-the-art techniques were utilized to unveil the physicochemical properties of the catalysts such as Raman, temperature programmed reduction/desorption techniques, XPS, and high-resolution imaging using HRTEM-EELS and HAADF. A key to the rational design of highly efficient catalyst is understanding the reaction mechanism of CO₂ hydrogenation via *Operando* SSITKA-DRIFTS technique. The current results show three types of CO-s correspond to linear type CO-s adsorbed on top surface defects, top hollow and 3-fold hollow nickel sites. Moreover, the catalytic results indicate that the CO₂ methanation in the 200–500°C temperature region has an optimum performance at 20 wt.% CeO₂ loading and medium alumina porosity at 300°C. However, when 450°C < T < 300°C CO production takes over, implying the predominance of RWGS side reaction. Finally, the synthetic methods towards formation of adjacent [Ni]–[Ce] sites or highly dispersed active metal entities was found to boost the catalytic activity.

SESSION EN13.04: Climate Change Mitigation Technologies IV

Session Chairs: Mathieu Bauchy and Stephanie Ribet

Wednesday Afternoon, December 1, 2021

Hynes, Level 3, Room 313

1:30 PM EN13.04.01

Combating Global Warming—Modeling Enhanced Rock Weathering of Silicates Using Density Functional Theory [Pratik P. Dholabhai](#) and Brian Luan; Rochester Institute of Technology, United States

Negative emissions technologies target the removal of CO₂ from the atmosphere as a way of combating global warming. Enhanced rock weathering (ERW) is a vital negative emissions technology that, applied globally, could remove gigatonnes of CO₂ per year from the atmosphere. In ERW, silicate minerals exposed to the atmosphere trap CO₂ via mineral carbonation as thermodynamically stable carbonates. The present challenge is that the most reactive naturally-occurring silicates are not abundant. In order to design novel materials for ERW, a fundamental understanding of their structure and reactivity is necessitated at the nanoscale. To this end, we have employed density functional theory to predict the atomic scale structure of (100), (010), and (001) surfaces of wollastonite (CaSiO₃) and study the thermodynamics of their interaction with CO₂. Based on surface energy calculations, (001) and (010) surfaces of wollastonite exhibit similar stabilities, whereas (100) surface is found to be least stable. Utilizing stable surface models, molecular and dissociative adsorption of CO₂ at various surface sites has been explored. A common trend emerges, wherein the CO₂ molecule demonstrates proclivity to bond with surface layer calcium atoms. We will shed light on the electronic charge transfer between the adsorbate and the substrate and discuss the

fundamental aspects of these interactions. Results from this work will be exploited to study the reaction kinetics of CO₂ adsorption and dissociation on silicates using *ab initio* molecular dynamics. Overall, we will elucidate the fundamental mechanisms that govern the interaction between CO₂ and wollastonite. Such fundamental understanding will be imperative to guide large-scale synthesis of novel silicates for ERW.

1:45 PM EN13.04.02

Late News: Decoupling the Chemical and Mechanical Strain Effect on Steering the CO₂ Activation Over CeO₂-Based Oxides—An Experimental and DFT Approach Kyriaki Polychronopoulou, Shaima AlBedwawi, Sara AlKhoori, Seba Alareeqi, Nirpendra Singh and Lourdes Vega; Khalifa University of Science and Technology, United Arab Emirates

Doped ceria-based oxides are widely used as supports and stand-alone catalysts in reactions where CO₂ is involved. Thus, it is important to understand how to tailor their CO₂ adsorptive behavior. In this work, steering the CO₂ activation behavior of Ce-La-Cu-O ternary oxide surfaces through the combined effect of chemical and mechanical strain was thoroughly examined using both experimental and *ab initio* modeling approaches. Chemical strain is originated from the doping of CeO₂ with aliovalent metal cations (La³⁺ or La³⁺/Cu²⁺), whereas mechanical strain is originated from post synthetic ball milling able to impose mechanical forces on the oxide. Ce-La-O (111), Ce-Cu-O (111) and CeO₂ (111) surfaces were used as reference surfaces due to the complexity of the solid composition under investigation. Experimentally, microwave-reflux prepared Ce-La-Cu-O ternary oxide was imposed into mechanical forces to tune the structure, defects and CO₂ surface adsorptive properties. The purpose was to decouple the combined effect of the chemical strain (ϵ_c), and mechanical strain (ϵ_M), on the modification of the Ce-La-Cu-O surface reactivity towards CO₂ activation. During the *ab initio* calculations, the stability (energy of formation, $E_{\text{O}_v}^f$) of different configurations of oxygen vacant sites (O_v) was assessed under biaxial tensile ($\epsilon > 0$) and compressive ($\epsilon < 0$) strain, whereas the CO₂-philicity of the surface was assessed at different levels of imposed mechanical strain. $E_{\text{O}_v}^f$ values were found to decrease with increasing tensile strain. Ce-La-Cu-O (111) surface exhibited the lowest $E_{\text{O}_v}^f$ values for the single subsurface sites, implying that O_v may occur spontaneously upon Cu addition. The structural, textural, redox and basic properties of the surface were used as descriptors to unveil the mechanical strain impact. The mobility of the surface and bulk oxygen ions in the lattice contributing to the O_v population was measured using ¹⁶O/¹⁸O transient isothermal isotopic exchange (TIE) experiments; the maximum rate in ¹⁶O/¹⁸O formation, $R_{\text{max}}(^{16}\text{O}/^{18}\text{O})$ was 13.1 and 8.5 $\mu\text{mol g}^{-1}\text{s}^{-1}$ for the pristine (chemically strained) and dry ball-milled (chemically and mechanically strained) oxide, respectively. The CO₂ activation pathway (redox vs. associative) was experimentally probed using *in situ* DRIFTS. It was demonstrated that mechanical strain increases up to 6 times the CO₂ adsorption sites, though reduces their thermal stability. This result supports a mechanical actuation of the 'carbonate' bound species; the latter is in agreement with the DFT calculated C-O bond lengths and O-C-O angles. *Ab initio* studies shed light on the CO₂ adsorption energy (E_{ads}) suggesting a covalent bonding which is enhanced in the presence of doping and under tensile strain. Bader charge analysis probed the adsorbate/surface charge distribution and illustrated that CO₂ interacts with dual sites (acidic and basic ones) on the surface leading to the formation of bidentate carbonate species. Density of States (DOS) studies gave an insight on the electronic structure of the Ce-La-Cu-O (111) surface, and revealed the band gap (E_g) engineering which takes place in the clean and reduced surface, with a significant E_g drop in the presence of double O_v and compressive strain; a finding with design implications in covalent type of interactions. This study opens new possibilities to manipulate the CO₂ activation for a portfolio of heterogeneous reactions.

2:00 PM EN13.04.03

Novel, Smaller Contactor for Markedly Reducing the Total Cost of the Direct Air Capture of CO₂ Mansour Masoudi and Ed Tegeler; Emissol LLC, United States

Perhaps the greatest obstacle to commercialization of the Direct Air Capture (DAC) of CO₂ is the DAC cost. Aiming to reduce the cost of DAC, a novel honeycomb contactor has been developed, designed, tested and demonstrated, showing its strong potentials to markedly lower the DAC cost through reducing the amount of needed sorbent, the largest contributor to the total DAC cost [National Academy of Science, 2019*]. Utilizing a novel approach to configure the channel internal flow in the sorbent-coated contactor, the channels develop a strong and stable secondary flow in the form of one or more pairs of Dean vortices, accelerating transport of CO₂ to the channel walls coated with a solid sorbent (Polyethylenimine/ PEI). In essence, the diffusion-dominated CO₂ transport to the sorbent, dominant in standard, mainstream honeycomb contactors, is practically replaced with the far-stronger convective transport, increasing the net CO₂ transport per unit surface area per unit time. Both modeling investigation and experiments were utilized in this study. The high fidelity model and extensive experiments focused on examining the impact of novel flow patterns on CO₂ adsorption to the sorbent-coated walls and its desorption from the sorbent. Model contactors coated with PEI adsorbent were subjected to CO₂ adsorption and desorption tests and compared with a standard (baseline) DAC contactor, so to evaluate the impact of novel channel configuration on CO₂ transport to/from the adsorbent. Good agreement was observed between the modeling prediction and the test data. The novel contactor well outperforms the standard contactors, displaying Sherwood number as high as 7.5, i.e., 2.5 times higher than that in standard ones, accelerating the rate of CO₂ adsorption/ desorption per channel unit surface area, enabling more efficient use of the contactor volume and its sorbent for CO₂ capture. Results indicate that the novel DAC contactor (i) Enables reducing the sorbent use by 37%. Considering that sorbent CapEx forms more than 80% of the total DAC cost [National Academy of Science, 2019 *], it reduces the total DAC cost by about 30%. (ii) Enables reducing the overall volume (downsizing) of DAC contactors by up to about 40%.

Acknowledgment: This R&D project was funded by the US Department of Energy.

* National Academy of Science, Engineering and Medicine. "Negative Emissions Technologies and Reliable Sequestration: A Research Agenda." National Academies Press. (2019).

2:15 PM EN13.04.04

Turning CO₂ Into Cementitious Binders by Mineralization Mathieu Bauchy and Gaurav Sant; University of California, Los Angeles, United States

CO₂ is usually considered as an environmental burden. Here, we reimagine CO₂ as a resource for the production of a concrete-like construction material, that is, a value-added product. We present a new carbon immobilization process based on a 3D-printable portlandite-based cementitious binder that permits CO₂ uptake by mineralization. This carbonation process is fast, inexpensive, and robust. Carbonation leads to an increase in the strength of the binder and, hence, increases its value. This process could facilitate the beneficial use of CO₂ as a key ingredient for durable construction materials, thereby resolving the apparent opposition between the needs for new infrastructure and enhanced sustainability.

2:30 PM EN13.04.05

Algae and Concrete Composites—Structural Materials as a CO₂ Sink Marcos M. Hernandez, Ashley D. Atencio, Cesar R. Gonzalez Esquer, Babetta L. Marrone and Joseph Dumont; Los Alamos National Laboratory, United States

Concrete is the second most consumed material in the world only behind water, comprising a majority of construction materials.[1] As a result, global

cement production is responsible for about 8 percent of the world's carbon emissions. Biomass from algae offers serious advantages such as carbon and nitrogen capture as well as a superior growth per area than other conventional plant crops. [2] Algae production may play an important role in CO₂ mitigation through the integration in existing technologies. In this work, we use algae to reduce the use of cement or replace it as a component in concrete. Samples were prepared similarly to concrete and characterized using a wide range of mechanical, chemical and spectroscopic techniques. Through this study, we evaluate the use of algae in construction materials to mitigate the CO₂ emissions, reduce concrete use, lower construction costs, and utilize biomass.

1. Gagg, C.R., Cement and concrete as an engineering material: An historic appraisal and case study analysis. *Engineering Failure Analysis*, 2014. 40: p. 114-140.
2. Moreira, D. and J.C. Pires, Atmospheric CO₂ capture by algae: negative carbon dioxide emission path. *Bioresource technology*, 2016. 215: p. 371-379.

2:45 PM EN13.04.06

Humidity Sensing Behavior of Microporous Titano/Vanadosilicate Thin Films—Effect of Film Preparation and Stability Ramona Davoudnezhad, Ibrahim Cam and Burcu Akata Kurc; Middle East Technical University, Turkey

The growing demand for environmental control for a variety of chemical molecules has led to considerable interest in the research devoted to the development of new materials for sensor devices. Since humidity is a very common component in our environment, measurements and/or control of humidity are important not only for human comfort but also for a broad spectrum of industries and technologies. The constructive design of a good humidity sensor is a rather complicated topic, because high performance humidity sensors claim many requirements, including linear response, high sensitivity, fast response time, chemical and physical stability, wide operating humidity range, and low cost. Zeolites and zeo-type materials are known for their well-defined porous structure, moisture holding capacity, and ionic conduction properties. Therefore, a study is done to investigate humidity sensing Titano/Vanadosilicate thin films. Two different zeo-type materials with different types of quantum wires in their structures (i.e., -Ti-O-Ti-O-Ti- and -V-O-V-O-V- in the structures of ETS-10 and AM-6, respectively) were prepared and the humidity sensors by using these types of films were fabricated for the first time. Microporous Titano/Vanadosilicate Films were prepared by two different methods. Humidity sensing properties of these films prepared by the secondary growth method were shown to be tailored according to the desired range of humidity for sensing applications. The impedance modulus change is more than four orders of magnitude in the range from 8% to 97% at 100 Hz. High stability and low hysteresis were also observed. Complex impedance spectra, the corresponding equivalent circuit under different relative humidity was analyzed to explore the humidity sensing mechanism of these films. The project leading to these results has received funding from the Scientific and Technological Research Council of Turkey (TÜBİTAK), under grant agreement 118M631.

3:00 PM BREAK

4:00 PM EN13.04.07

The Phosphate Elimination and Recovery Lightweight (PEARL) Membrane—A Sustainable Environmental Remediation Approach Stephanie Ribet, Benjamin Shindel, Roberto dos Reis, Vikas Nandwana and Vinayak Dravid; Northwestern University, United States

Anthropogenic hypereutrophication, namely the release of excess nutrients into natural bodies of water from human activity, introduces a variety of economic, ecological, and public health problems around the globe. As with other environmental problems, this challenge is projected to grow in coming years, as it is inextricably linked to climate change and rising temperatures due to increased levels of CO₂.

To bridge the gap between the laboratory-scale nature of promising nanostructure solutions and the practical benchmarks for deploying an environmental remediation tool, we have developed a nanocomposite membrane. Here, an economical, readily available, porous substrate is dip coated using scalable, water-based processes with a slurry of nanostructures with affinity for specific adsorption of pollutants. Our Phosphate Elimination and Recovery Lightweight (PEARL) membrane can selectively sequester up to 99% of phosphate ions from polluted waters at environmentally relevant concentrations. [1] Moreover, mild tuning of pH promotes at will adsorption and desorption of nutrients, leading to phosphate recovery and reuse of the PEARL membrane.

This work builds on our prior report of the OHM sponge, made with the same platform approach, which is a nanocomposite material that can be used to repeatedly remove oil from water. [2] These two distinct examples suggest that the tailored nanostructure membrane approach is potentially a versatile platform that can be tuned to remediate other contaminants with the same core principles. In this presentation, we discuss the PEARL membrane's effective and selective performance. Moreover, we use correlative microscopy and spectroscopy techniques to interrogate the complex microstructure of the PEARL membrane and its binding efficacy, further suggesting how this approach can be applied to other pollutants.

[1] S. Ribet, et al. *PNAS*. 118, 23 (2021).

[2] V. Nandwana, S. Ribet, et al. *Ind. Eng. Chem. Res.* 59, 10945-10954 (2020).

4:15 PM EN13.04.08

Spectroscopic Monitoring of Dissolved Carbon Dioxide for CCUS Richa Sharma¹, T.S.S. Ramakrishnan¹, Quincy K. Elias¹, Susan Rempe² and Gauri Joshi³; ¹Schlumberger Doll Research, United States; ²Sandia National Laboratories, United States; ³Schlumberger, India

Decarbonization of the energy industry is an environment driven requirement. A sustained expansion and deployment of large-scale carbon capture, utilization and storage (CCUS), is needed to address this challenge, at least partly. Effectiveness of CCUS is contingent upon developing miscibility through partitioning into water or hydrocarbon. Our work is motivated by the need to reliably monitor dissolved CO₂ under conditions of high temperature and pressure. We propose a new Raman spectroscopy-based sensor system for translating molecular interactions into molar concentrations. We propose the utility and feasibility of field deployment of our sensing system in aquifer and hydrocarbon reservoir CO₂ injection projects.

4:30 PM EN13.04.09

Solar Thermochemical Reduction of Carbon Dioxide into Liquid Fuels Xueqian Li, Magel Su, Manar Shoshani, Harry A. Atwater and Theodor Agapie; California Institute of Technology, United States

Traditionally, industrial thermocatalytic processes for reducing carbon dioxide (CO₂) require high temperatures (>300 °C), high pressures (>150 bar), and several recycling steps that consume up to 2% of the world's energy supply annually. Solar-driven processes under moderate pressures (<5 bar) present a sustainable alternative to synthesis of fuels, chemicals and materials while also alleviating rising atmospheric concentrations of CO₂. Normally, heat loss from thermal radiation would prevent a solar-heated thermochemical system from reaching the operating temperatures required for industrially relevant

reactions such as the Fischer-Tropsch, Sabatier, and Haber-Bosch reactions under illumination of unconcentrated solar irradiation (1 kW m^{-2}). To reach temperatures $>90 \text{ }^\circ\text{C}$ under ambient sunlight, the spectral absorptivity and emissivity profiles of the reactor components must be redesigned such that absorption of the active catalyst region is high within the solar wavelength regime ($0.3 - 2 \text{ }\mu\text{m}$) and reflectivity is high in the infrared blackbody regime ($4 - 25 \text{ }\mu\text{m}$). Here, we report the design of a planar solar thermocatalytic reactor that incorporates a selective light absorber and allows for both flexibility and scalability of the desired reaction. The proposed solar thermocatalytic reactor has 4 layers from bottom-to-top: a broadband reflector, a solar thermocatalytic reaction chamber, a selective absorber layer, and a thermally insulating layer. We will discuss options for selective absorber layers using semiconductor layers for high absorption in the solar wavelength regime and optically transparent conductors for high reflectivity in the infrared blackbody wavelength regime. Thermocatalysis results will be reported for a model reaction converting ethylene into higher olefins via solar activated homogeneous catalysts.

4:45 PM EN13.04.10

Late News: Revealing Molecular Mechanisms in Hierarchical Nanoporous Carbon via Nuclear Magnetic Resonance Haiyan Mao¹, Jing Tang², Bing Wu¹, David Halat¹, Yi Cui² and Jeffrey Reimer¹; ¹University of California, Berkeley, United States; ²Stanford University, United States

Hierarchical nanoporous carbons (HNC) have been proven to be an effective adsorbent for the adsorption of volatile organic compounds (VOCs) and CO_2 , although questions remain regarding the hierarchical structure regulation, the adsorption mechanisms of adsorbate uptake, and interactions within the HNC. We synthesize HNC from wood, using a microwave-induced heating method incorporating K_2CO_3 activation. HNC exhibit Murray's Law multi-scale structures, prompting a molecular scale study of adsorbate adsorption via nuclear magnetic resonance (NMR). NMR chemical shifts are consistent with ring current effects from the adsorbent. Our NMR technique provides a convenient way to quantitate the adsorption of adsorbate in HNC. VOCs vapor adsorption results show NMR chemical shift changes with time, suggesting initial adsorption into mesopores, followed by diffusion into micropores. Schroeder's Paradox is demonstrated by differences in observed shifts for adsorbed liquid vis-à-vis vapor phase in these HNC. These HNC show high CO_2 adsorption capacity, portending applications to carbon capture.

SESSION EN13.05: Climate Change Mitigation Technologies V
Session Chair: Mihrimah Ozkan
Monday Morning, December 6, 2021
EN13-Virtual

8:00 AM *EN13.05.01

A New Strategy of Negative Carbon Emissions by Nanomembranes for Ubiquitous CO_2 Capture Shigenori Fujikawa^{1,1}, Roman Selyanchyn^{1,1}, Miho Ariyoshi^{1,2} and Toyoki Kunitake^{2,1}; ¹Kyushu University, Japan; ²Nanomembrane Technologies Inc., Japan

Climate change caused by emissions of greenhouse gases into the atmosphere is a most important issue for our society. The anthropogenic nature of climate change necessitates the development of novel technological solutions in order to reverse the current CO_2 trajectory. Direct capture of the carbon dioxide (CO_2) from the air (direct air capture, DAC) is one among a variety of negative emission technologies that are expected to keep global warming below $1.5 \text{ }^\circ\text{C}$, as recommended by the Intergovernmental Panel for Climate Change (IPCC).

Current DAC technologies are mainly based on sorbent-based systems where CO_2 is trapped in the solution or on the surface of the porous solids covered with compounds with high CO_2 affinity. These processes are currently rather expensive, although the cost is expected to go down as the technologies are developed and deployed at scale.

CO_2 capture by permselective membranes is advantageous because of its smaller and simpler set-up. Unfortunately, its efficiency is less than satisfactory for the practical operation of the DAC. Among polymeric membrane materials, rubbery poly(dimethylsiloxane) (PDMS) is known to display high CO_2 permeance and ultimate thinning of PDMS membranes is a promising and straightforward way to prepare high CO_2 flux membranes.

We developed defect-free, free-standing nanomembranes of PDMS and discussed the membrane thickness's effect on the gas permeance by using precisely defined nanometer-thick PDMS membranes systematically. Throughout the efforts on ultimate thinning of PDMS membranes, our achieved CO_2 permeance reaches almost 40,000 GPU (the highest one ever reported) and reasonable CO_2/N_2 selectivity at the thickness of 34 nm without a gas leak from pinholes. This value is much higher than those reported by other groups in the past (less than several thousand). Furthermore, the separation is achieved even at a CO_2 concentration of 1,000 ppm in N_2 , which has never been investigated under such ultra-diluted concentration conditions in past reports. The advantages of extremely efficient separation of CO_2 found in our result demonstrate the feasibility of direct air capture by a membrane, which has never been considered before.

8:30 AM *EN13.05.02

Carbfix: CO_2 Mineral Storage Edda S. Aradottir¹, Sandra Snaebjornsdottir¹, Bergur Sigfusson¹, Thomas Ratouis¹, Kari Helgason¹, Chiara Marieni², Martin Voigt³, Eric Oelkers² and Sigurdur R. Gislason³; ¹Carbfix, Iceland; ²CNRS, France; ³University of Iceland, Iceland

Carbon capture and storage (CCS) plays a fundamental role in achieving the goals of the Paris agreement to limit global warming to $1.5-2^\circ\text{C}$, with estimated 115 Gt CO_2 needed to be captured and safely stored by 2060 [1]. Most ongoing CCS projects inject pure CO_2 into sedimentary basins, such as saline aquifers or depleted oil or gas reservoirs where an impermeable cap rock prevents it from migrating to the surface.

Carbfix has since 2007 developed a safe and low-cost alternative in collaboration between industry and academia: By injecting dissolved CO_2 into reactive rock formations, such as mafic or ultra-mafic rocks, carbon mineralisation is promoted for CO_2 mineral storage [2]. The acidic CO_2 -charged fluid releases metals from the bedrock which combine with the injected CO_2 and rapidly form stable carbonate minerals [3]. By mineralising the injected CO_2 , it is permanently fixed and there is a negligible risk of it returning to the atmosphere.

Carbfix has since 2014 captured and injected over 70,000 tonnes of CO_2 at its flagship operation at Hellisheidi geothermal plant in SW-Iceland and is preparing for scale-up to maximise its potential impact. Emphasis is currently being placed on making this technology more cost effective and exploring its limits in terms of potential sites and injection methods, including injection of CO_2 captured directly from the atmosphere, and injection of seawater dissolved CO_2 . Furthermore, Carbfix is working on its largest project currently under development aiming on transporting CO_2 captured from European industries to Iceland, where up to 3 Mt/ CO_2 will be injected annually for permanent storage.

Mineral CO_2 storage offers a vast storage potential and unlocks large regions in the world where CCS has until now not been considered possible: The storage capacity of the Columbia River Basalts in USA alone has been estimated to be on the order of 10-100 Gt CO_2 [4]. The largest potential lies offshore within the sub-marine basaltic crust, but suitable formations are also widespread onshore, and are found in every continent [5].

[1] IEA (2020). *Special Report on Carbon Capture Utilisation and Storage. Energy Technology Perspectives*, 169.

[2] *Snæbjörnsdóttir et al. (2020). Carbon dioxide storage through mineral carbonation, Nature Reviews Earth & Environment.*

[3] *Matter, J.M., Stute, M., Snæbjörnsdóttir, S.Ó., Oelkers, E.H., Gislason, S.R., Aradóttir, E.S., et al. (2016). Rapid carbon mineralization for permanent disposal of anthropogenic carbon dioxide emissions. Science, 352, 1312-1314.*

[4] *Blondes, M.S., Merrill, M.D., Anderson, S.T., and DeVera, C.A., 2019, Carbon dioxide mineralization feasibility in the United States: U.S. Geological Survey Scientific Investigations Report 2018–5079, 29 p., <https://doi.org/10.3133/sir20185079>.*

[5] <https://www.carbfix.com/atlas>

9:00 AM *EN13.05.03

National Academies of Sciences, Engineering and Medicine—Advisors to the Nation on Climate Change Mitigation Technologies [Alton D. Romig](#); National Academy of Engineering, United States

The National Academies have done more than 1000 consensus studies and more than 1000 workshops related to climate change, the first being done in 1936. All of these reports are downloadable at the National Academies Press website (<https://www.nap.edu/>). A multitude of areas has been explored from urban sustainability to adaptation to sea level rise to decarbonization of the grid and transportation to geoengineering. Approximately 10% of the studies and workshops have specific relevance to technologies for mitigating the effects of climate change. This presentation will focus on the approximately 150 consensus reports and 110 workshops with proceedings that have been done on climate change over the past 5 years. Approximately half of the studies and workshops are relevant to climate change mitigation technologies. Specific recent reports will be reviewed with a focus on mitigation technologies for decarbonizing the grid, decarbonizing transportation including light to heavy ground vehicles and air vehicles, carbon capture and storage, mitigation of sea level rise and management of flooding, and the controversial topic of geoengineering.

9:30 AM *EN13.05.04

Direct Air Capture of CO₂ and Its Role in Mitigating Global Warming [Carlos Jimenez Haertel](#); Climeworks AG, Switzerland

In recent years, Direct Air Capture (DAC) has established itself as a promising approach to atmospheric Carbon Dioxide Removal (CDR), also referred to as Negative Emissions. In fact, DAC is seen today as critical to the 1.5°C target of the Paris Climate Agreement. Numerous studies have shown negative emissions to be necessary in order to stabilize atmospheric CO₂ at the required levels towards the middle of the century. Although DAC has higher specific cost per tonne of CO₂ than nature-based solutions - such as afforestation or soil carbon - it can scale faster and can guarantee permanence of the CO₂ removed. Due to the huge amounts of excess CO₂ in the atmosphere, CDR technologies will have to reach annual capacities at the gigaton scale over the next two to three decades in order to become climate relevant.

The presentation will give an overview of DAC and, in particular, the modular low-temperature technology developed by Climeworks.

In Climeworks' systems, ambient air is ingested by a so-called collector container during a cyclic ad-/desorption process. In the adsorption step, the CO₂ molecules are bound to a special sorbent material inside the collector. Subsequently, the sorbent material is regenerated by thermal energy. The concentrated CO₂ collected during this desorption step can then be used in different ways. For carbon removal, it is typically sent underground, where it is permanently stored in aquifers, rock formations, or depleted oil and gas reservoirs. Captured CO₂ can also be used as feedstock e.g. for the food and beverage industry or for agricultural use. Another upcoming use case is 'Power-to-X', in which hydrocarbons are produced from atmospheric CO₂, water, and renewable energy. Currently, Climeworks has 14 DAC plants of different size in operation across Europe, collecting tens of thousands of hours of real-life operational experience every year. Climeworks anticipates strongly increasing demand for carbon-removal services in the future and expects further significant cost reductions as industrial mass production of components for DAC systems gears up.

Potential co-benefits of DAC in relation to the Sustainable Development Goals (SDGs) of the UN are also briefly touched upon in the talk, which concludes with suggestions for policy approaches needed to ensure climate-relevant scale is reached in time.

SESSION EN13.06: Climate Change Mitigation Technologies VI

Session Chair: Andre Guerra

Monday Morning, December 6, 2021

EN13-Virtual

10:30 AM *EN13.06.01

New Generation Bipolar Membranes for CO₂ Reduction [Selmiye Alkan Gürsel](#)^{1,2}, [Begum Yazar Kaplan](#)², [Ahmet Can Kirişoğlu](#)¹, [Mohammad Alinezhadfar](#)¹ and [Alp Yürüm](#)²; ¹Sabancı University Faculty of Engineering and Natural Sciences, Turkey; ²Sabancı University Nanotechnology Research and Application Center (SUNUM), Turkey

Fossil fuels have been used extensively to meet the energy demand; however, their spacious use has caused to various environmental problems, particularly Greenhouse Effects because of significant carbon dioxide (CO₂) emissions. In this regard, energy efficiency and renewables are curial, yet additional technologies offering in minimal, or zero emissions of CO₂ are needed to achieve net-zero emissions. Immense efforts are being devoted to reducing CO₂ emissions in this respect. Approaches to capture CO₂ from air for permanent geological storage, power generation or fuel production and transformation are very remarkable. In addition, CO₂ reduction into valuable product, in combination with renewable energy, is another considerable approach. Transforming CO₂ by chemical reduction both eliminates the main greenhouse gas, and also converts it into useful materials. Since CO₂ is a highly stable molecule, its reduction reaction is challenging. CO₂ electrolysis is a promising technology to convert CO₂ into valuable chemicals. Membranes with high mechanical strenght, stability and durability at high density load are needed for CO₂ electrolyzers. In this study, new generation membranes for electrochemical CO₂ conversion by an electrolyzer have been developed. Bipolar membranes, exhibiting both proton and anion exchange functionalities for minimizing crossover and reducing activation energy, have been fabricated by radiation-induced grafting and electrospinning techniques. Radiation-induced grafting, a well-known method for the introduction of functional groups into a commodity polymer for design of the polymer architecture, has been proposed as an alternative method for the synthesis of novel bipolar membranes. Radiation-induced grafting offers the advantages such as simplicity and control over process without residues of initiators and catalyst as well. Electrospinning, frequently used technique to produce nanomaterials especially in the field of energy, is a promising technique for creating nanostructured materials, provides enhancement of the triple phase interface where electrochemical reactions occurred at active catalyst site. Electrospinning is a facile technique for single-step fabrication of bipolar membranes with 3D dual-fiber interface. This technique also offers advantages compared to conventional film casting or other membrane fabrication techniques due to low contact resistance, easy scale-up, easy thickness control, flexibility, and high mechanical strength. Besides, these membranes can be easily converted into dense and non-porous membrane with hot-pressing and welding steps. Herein, bipolar membranes have been fabricated with direct

physical attachment of pre-fabricated anion-exchange membrane and cation-exchange membranes and also by radiation induced grafting by means of a special and scalable grafting reactor. Optimization of radiation grafting, and electrospinning parameters have been performed to obtain high conductivity uniform membrane layers. Moreover, the membranes have been characterized ex-situ and in situ for physical and electrochemical properties and it was determined that membranes possessed promising mechanical strength and stability, and also low crossover to ensure high performance for CO₂ reduction.

11:00 AM *EN13.06.02

Role of Negative Emissions and Carbon Recycling Technologies in the Transitions of Japan's Energy Systems Toward Net-Zero Emissions
Goal Etsushi Kato; Institute of Applied Energy, Japan

Transformation of energy systems toward net-zero emissions is required globally under the Paris Agreement of the United Nations Framework of Convention of Climate Change (UNFCCC). In Japan, an updated goal was announced to achieve carbon neutrality by 2050 in October 2020. And the ambitious 2030 target (46 to 50% emissions reduction from 2013 levels) is announced in April 2021. Formulating policy recommendations of RD&D strategies to achieve the goal requires quantitative analysis on cost-effective supply-demand structure in energy systems using comprehensive energy systems models. In the circumstance of the national net-zero emissions goal, considerations are required to include innovative technologies that remove CO₂ from the atmosphere to compensate CO₂ emissions from difficult-to-decarbonized sectors, such as heavy industry and heavy-duty transportation, and also unavoidable non-CO₂ GHG emissions from the agricultural sector. However, it is relatively scarce and imperative to clearly analyze their role and RD&D needs using national energy system models containing detailed energy supply-demand technologies representations.

In this study, transitions of Japan's energy systems toward the net-zero emissions goal by 2050 are analyzed using a bottom-up energy system model, TIMES-Japan. The implication of the role of NETs and their sensitivity in Japan's energy systems are assessed with two NETs systems; bioenergy with carbon capture and storage (BECCS) in the power sector and direct air carbon capture and storage (DACCS). We also investigate the role of carbon recycling technologies using direct air capture (DAC) for the production of synthesized liquid fuel and synthesized methane. To achieve the net-zero emissions cost-effectively, both the earlier deployment of BECCS with domestic biomass and the support of the DAC in the later period are required.

Synthesized fuel productions using DAC are also effective to achieve net-zero emissions particularly in the case with limited geological CO₂ storage capacity development.

11:30 AM *EN13.06.03

Fueling the Future Kuo-Wei Huang; King Abdullah University of Science and Technology, Saudi Arabia

In 2018, the estimated world population of 7.53 billion people consumed 14.31 Gtoe of energy (at an average rate of 19.0 TW). Globally, burning of carbon-based fossil fuels supplies over 81% of the energy demand, and hence the prospering industrial societies are responsible for the observed increase in carbon dioxide levels from preindustrial 280 ppm to over 410 ppm now. To reduce the environmental footprint of modern societies and address the limitations of fossil recourses, the projected increase in global energy demand must go along with the implementation of low carbon energy production and carrier systems. In this presentation, the current energy status and future options will be discussed. It will then be concluded with the introduction of some of our research efforts in utilizing formic acid as a hydrogen/energy carrier.

References

- [1] Eppinger, J.; Huang, K.-W. "Formic Acid as a Hydrogen Energy Carrier" *ACS Energy Lett.* **2017**, *2*, 188-195.
- [2] Chatterjee, S.; Dutta, I.; Lum, Y.; Lai, Z.; Huang, K.-W. "Enabling Storage and Utilization of Low-Carbon Electricity: Power to Formic Acid" *Energy Environ. Sci.* **2021**, *14*, 1194-1246.
- [3] Chatterjee, S.; Huang, K.-W. "Unrealistic Energy and Materials Requirement for Direct Air Capture in Deep Mitigation Pathways" *Nat. Comm.* **2020**, 3287.
- [4] *IEA World Energy Outlook 2019*
- [5] House, K. Z.; Harvey, C. F.; Aziz, M. J.; Schrag, D. P. "The Energy Penalty of Post-combustion CO₂ Capture & Storage and Its Implications for Retrofitting the U.S. Installed Base" *Energy Environ. Sci.* **2009**, *2*, 193-205.
- [6] Dowell, N. M.; Fennell, P. S.; Shah, N.; Maitland, G. C. "The Role of CO₂ Capture and Utilization in Mitigating Climate Change" *Nat. Clim. Chang.* **2017**, *7*, 243-249.

12:00 PM EN13.06.04

Gas Hydrate Thermal and Interfacial Properties for Natural Gas Capture and Storage via Novel Atomistic-Molecular Dynamics Simulations Samuel Mathews, Phillip Servio and Alejandro Rey; McGill University, Canada

Gas hydrates are inclusion compounds comprising a backbone of water molecules that encloses guest molecules in separate cages. Each volume of hydrate contains 160 volume equivalents of gas. Initially, large scale gas hydrate research was centered around the flow assurance problems they cause in the extraction and transportation of petroleum and its derivatives. Eventually, interest grew in the usage of hydrates in gas capture and storage, including hydrocarbons, hydrogen, and direct air greenhouse gas capture, as well as separation processes, such as the removal of environmentally harmful constituents of flue gasses. Naturally occurring gas hydrates are also studied to satisfy global energy demand: estimates put the total energetic capacity of hydrate reserves at twice that of other fossil fuel reserves combined. As global temperatures rise, these hydrate reserves risk releasing methane gas into the atmosphere, accelerating global warming. Their potential use in the removal of carbon from the atmosphere, carbon capture and storage, and for energy exploitation makes gas hydrates a prime candidate for climate change mitigation research.

Density functional theory (DFT) is a first-principles computational method that calculates that atomic energies and forces for a given atomic configuration by solving the Schrodinger equation in a numerically efficient manner. By manipulating the atomic coordinates, thermal properties can be determined across a wide range of conditions when pairing DFT with phonon theory. Molecular dynamics (MD) is a simulation method that treats larger systems at more realistic conditions than DFT by integrating Newton's equations of motions for atoms, but it requires empirical parameters and forcefields. MD can calculate time dependent behaviors while DFT cannot. DFT and MD can therefore be used together to provide accurate descriptions of many behaviors. This work used DFT as implemented in the Vienna ab Initio Simulation Package (VASP) with phonon theory as implemented in Phonopy to calculate the heat capacity, thermal expansion coefficient, and Grüneisen parameter of gas hydrate systems. This work will use MD as implemented in the Large-scale Atomic/Molecular Massively Parallel Simulator (LAMMPS) to calculate the interfacial tension of natural gas hydrate systems.

The constant volume and constant pressure heat capacity, the thermal expansion coefficient, and the Grüneisen parameter of ice and carbon dioxide, ethane, methane, and empty sl gas hydrates were calculated using DFT and phonon theory from 0 to 300 Kelvin. DFT replicated experimental constant pressure heat capacity measurements accurately at low temperatures for all systems. Guest molecules contributed to the heat capacity by an amount slightly larger than their ideal gas heat capacity. Thermal expansion was overestimated in all cases, as was the Grüneisen parameter.

The MD study of interfacial work remains ongoing. Previous work from this group studied the growth rate, interfacial tension, and work of formation in methane hydrate systems. The interfacial energy of natural gas hydrate systems is expected to be inversely proportional to temperature. This behavior has

previously been observed in water and gas mixtures, and in methane hydrate systems. Different nucleation types will also be studied. In terms of increasing work of formation, it is expected that film-shaped heterogeneous nucleation will be first and thus lowest, followed by cap- and then lens-shaped, helping determine which type is most favorable. The same order would be valid for decreasing nucleation rate as a function of nucleation type at given conditions. This information will yield data to determine which conditions favor or hinder hydrate formation in carbon capture and storage, removing methane from the atmosphere, and avoiding methane release into the atmosphere. The predictions and computational platform contribute tools and new understanding to the energy-environmental nexus.

12:15 PM EN13.06.05

The Rheology of Methane and Carbon Dioxide Hydrates at Extreme High Pressures for the Development of Climate Change Mitigating Technologies [Andre Guerra](#), Phillip Servio, Alejandro Rey and Milan Maric; McGill University, Canada

Gas hydrates are inclusion type compounds, in which gas molecules are trapped inside the solid phase of water. In the transition from liquid to solid phase, water molecules form a lattice structure that arises from hydrogen bonds between adjacent molecules. If the phase transition occurs at high enough pressures and in the presence of dissolved gas species in liquid water, the gas molecules can become trapped in "cages" as the solid lattice structure forms. Gas hydrates have been an active research topic due to their occurrence in the oil and gas industry. As a result, much of the body of knowledge focuses on water-in-oil emulsion gas hydrate systems. Recently, however, technologies that take advantage of gas hydrate properties have sparked new research motivation. Gas hydrates are stable, cage structures trap specific types and sizes of gas molecules, and one unit volume of gas hydrate can contain up to 180 times the unit volume of gas as required under standard conditions. These properties make gas hydrates good candidates in the development of new climate change mitigation technologies such as post-combustion carbon capture from flue gas, natural gas transport and storage, or the desalination of seawater. Most of these technologies require flow systems and do not involve oil-based systems. Based on these facts, the need for the characterization and elucidation of the shear rheology of gas hydrate systems from pure water systems is apparent. This study explores pure water hydrate systems of methane and carbon dioxide at extreme high pressures (0 to 30 MPa). The viscosity of the system was measured at a constant 400 s^{-1} shear rate and at temperatures between 0 and 10°C using a double-gap measurement geometry in an Anton Paar MCR302 high-pressure rheometer. The effect of temperature on the viscosity of methane hydrate systems was one order of magnitude larger than the pressure effect on viscosity in most of the pressure range: from about 0.01 mPa·s/C to 0.001 mPa·s/MPa. This difference was especially prevalent at lower temperatures. The pressure effect on the viscosity of carbon dioxide hydrate systems was up to one order of magnitude larger than that of the methane hydrate system, likely as there was more gas present in solution due to carbon dioxide's higher solubility in water. During hydrate formation, a liquid-to-slurry phase transition occurred characterized by a progressive increase in viscosity up to a maximum value where the greatest amount of hydrate crystals was present. The time to reach maximum viscosity in methane hydrate systems was found to decrease by at least a factor of two as pressure increased from 10 to 15 MPa. For instance, it decreased from about 20 to 10 minutes at 2°C. Further increases in pressure had diminishing reductions in the time required and the fastest time to reach maximum viscosity was 1.35 minutes at 30 MPa and 0°C. Several systems with high driving forces for hydrate formation did not form gas hydrates within the 24-hour maximum experimental timeframe. The driving forces present in these systems were up to 4.1 MPa and 2.07 MPa for the methane and carbon dioxide systems, respectively. The key system limitations to the formation of hydrates were categorized as either arising from kinetic, mass diffusion, and/or heat of crystallization effects and were used to rationalize the main features of the experimental data. The presented data and analysis are a significant contribution to the currently sparse characterization of high pressure-low temperature shear rheology of these energy materials, which is crucial to the design and development of climate change mitigation technologies.

SESSION EN13.07: Climate Change Mitigation Technologies VII
Session Chairs: K. John Holmes and Mihrimah Ozkan
Monday Afternoon, December 6, 2021
EN13-Virtual

1:00 PM *EN13.07.01

The Role of Carbon Capture in Meeting Net-Zero Carbon Goals [Jennifer Wilcox](#); U.S. Department of Energy, United States

President Biden has laid out a bold and ambitious goal of achieving net-zero carbon emissions in the U.S. by 2050. The pathway to that target includes cutting total greenhouse gas emissions in half by 2030 and eliminating them entirely from the Nation's electricity sector by 2035. Research, development, demonstration, and deployment (RDD&D) will be required to achieve the president's objectives, including investments in both point source carbon capture and carbon dioxide removal approaches that target the accumulated pool of carbon in the atmosphere. Both will be required to achieve net-zero carbon emissions in time and they will require increased deployment on an accelerated timeline in order to move down the cost curve. These efforts, combined with effective policy, will improve the economic viability of the implementation of these critical approaches.

Deployment of these technologies at the scale required will necessitate the use of resources including land, water, and low-carbon energy, while ensuring the secure and reliable storage of carbon dioxide (CO₂) on a timescale that impacts climate. Therefore, CCS and CDR deployment must be implemented strategically in terms of regional goals and requirements.

The Office of Fossil Energy and Carbon Management and the National Energy Technology Laboratory will play an important role in the transition to net-zero carbon emissions by reducing the environmental impacts of fossil energy production and use. This includes helping decarbonize other hard-to-abate industrial sectors through investments in approaches like CCS, direct air capture, and technologies to produce low-carbon products and fuel - including hydrogen.

1:30 PM *EN13.07.02

Scaling Deep Decarbonization Technologies [K. John Holmes](#); National Academies of Sciences, Engineering, and Medicine, United States

This is an unprecedented opportunity to address climate change in the United States. Moving to net-zero greenhouse gas emissions by 2050 requires greatly scaling up decarbonization technologies that do not emit carbon dioxide and the continued development, demonstration, and deployment of technologies that remove carbon dioxide directly from the atmosphere. It also requires eliminating or greatly reducing emissions of other greenhouse gases, including methane, nitrous oxide, and fluorinated gases. Eliminating energy sector carbon dioxide emissions, the most important greenhouse gas within the largest emissions sector, is required for approaching net-zero emissions. Optimistically, the United States' large renewable resource base coupled with decreasing costs for electrification technologies can catalyze rapid progress over the first decade of this energy system transition. The United States also has an extremely rich base of scientists, engineers, social scientists, policy makers, and support within civic society to make progress on the other technological solutions. However, the country also faces rapidly emerging impacts from climate change that will not abate without decades of effort. In order to be successful, deep decarbonization cannot occur without broad support within society and therefore must be done in a way that not only accomplishes the

net-zero emissions goal but does so in a manner that meets wider societal goals and aspirations.

This talk addresses technology, societal, and policy issues for scaling deep decarbonization technologies. It is based on two recent activities at the National Academy of Sciences, Engineering, and Medicine (NAEM), a 2018 workshop that resulted in the proceedings *Deployment of Deep Decarbonization Technologies* and a consensus study that produced *Accelerating Decarbonization of the U.S. Energy System in 2021*. There is widespread consensus on the implementation of no-regrets, deployment-ready technologies aimed at decarbonizing electricity and electrifying end uses that make significant progress towards achieving mid-century decarbonization while preserving optionality. However, to accomplish these elements of decarbonization, existing solar and wind electricity generation technologies must be deployed by greater than four times their current highest annual rates. Electrification of vehicle sales and other end uses will require similar increases in technology deployment rates as renewable electricity. The increased challenge for decarbonization technologies involves addressing hard-to-decarbonize sectors such as heavy industry and air, rail, and shipping. This involves expanding the innovation toolkit. Examples include research, development, and demonstration for clean-firm electricity resources, long-duration energy storage, net-zero carbon fuels, electrolysis to make fuels from renewable power, low-carbon process heat solutions, and more efficient carbon dioxide capture technologies. It also involves development and deployment of negative emissions technologies that will compete as mitigation options. All of these strategies not only face the question of whether they can provide effective decarbonization options, they also face similar scaling issues as with decarbonizing electricity and electrifying end uses.

Reaching net-zero emissions is a transformation of society that will occur over decades, not years. Consideration of the societal aspects of decarbonization involves developing a social compact around the need to decarbonize and benefits that will accrue from it. Policy elements encompass the roles of federal, sub-national, economic, and regulatory approaches. Because political fortunes and societal opinions will change over this timeframe, consensus-building scientific institutions including the National Academies to facilitate the independent technical and policy advice needed.

2:00 PM *EN13.07.03

U.S. Department of Energy's Fossil Energy and Carbon Management R&D Program—Carbon Dioxide Removal Overview [Andrew Jones](#); DOE/NETL, United States

The U.S. Department of Energy's Fossil Energy and Carbon Management (DOE-FECM) R&D Program is supporting the development of transformational cost-effective carbon dioxide (CO₂) capture technologies throughout the power-generation and industrial sectors as well as carbon dioxide reduction (CDR) technologies. Since 2001, DOE-FECM's Carbon Capture Program has been identifying and advancing technologies with the goal of decreasing the cost and improving the efficiency of carbon capture. Technologies developed to date have primarily focused on the capture of CO₂ directly from large point sources, such as industrial sources and fossil fuel power plant flue gas streams. The Carbon Capture Program is leveraging this past research in materials, equipment and process development for both current and transformational CDR technologies, such as direct air capture (DAC) and bioenergy with carbon capture and storage (BECCS), while evaluating the opportunities in direct ocean capture and enhanced weathering. More research is needed to develop efficient processes and components utilizing the transformational materials to lower the cost of these systems. At the same time, DOE-FECM aims to better understand system costs, performance, as well as business case options for the existing technologies, to better focus its research and development program. Accelerating the development and deployment of these climate-critical technologies will support the U.S. goal to achieve a carbon pollution-free electricity sector by 2035 and zero-carbon economy by 2050.

2:30 PM *EN13.07.04

Diminishing the Gigaton Carbon Giant Through Hybrid Material Strategies for Capture and Conversion [Michelle Kidder](#)¹, [Luke L. Daemen](#)¹, [Yong Joo](#)² and [Alissa Park](#)³; ¹Oak Ridge National Laboratory, United States; ²Cornell University, United States; ³Columbia University, United States

Energy generated from fossil fuels dominate the global use portfolio which now has reached an all-time high emission of approximately 40 GtCO₂. Undoubtedly this has had consequential impacts on our climate and environment, and sadly emissions are expected to rise. This has brought the urgent need to remove carbon from the atmosphere to reverse the rising atmospheric CO₂ concentrations with effective carbon negative technologies. However, many strategies to capture or convert carbon dioxide have been met with challenges with standalone materials. Hence, we have developed hybrid materials that employ a polymer with intrinsic microporosity (PIM) which has superior CO₂ selectivity with tunable functional and structural characteristics to enhance its effectiveness for both capture and conversion pathways. Here we show the development of hybrid PIM materials for both (1) direct air capture (DAC) and (2) utilization processes. Our first example is of a hybrid fiber mat composed of a silica bound polyethyleneimine (PEI) nanoparticle core (NOHM) encapsulated with a PIM sheath for DAC applications. NOHMs have demonstrated CO₂ sorbent qualities such as low volatility and high selectivity, however their viscosity and water retention have impeded their effectiveness for DAC. PIM encapsulation of NOHMs allows for selective rejection water and other air pollutants to reduce the parasitic energy consumption effects of significant mass transport limitations, yet maintain high gas permeability and selectivity. Secondly, we will present our catalytic PIM for the simultaneous capture and conversion of CO₂ to chemicals. Initial experiments show that this hybrid catalyst can overcome high temperature and pressure conditions normally needed for catalytic CO₂ reduction. From these initial findings of hybrid PIM materials, we learn key material properties such as stability, capacity, and recyclability that will help to provide insight into the technical feasibility of large scale applications needed for DAC and CO₂ conversion.

SESSION EN13.08: Climate Change Mitigation Technologies VIII

Session Chair: Sue Carter

Monday Afternoon, December 6, 2021

EN13-Virtual

4:00 PM *EN13.08.01

Power-Generating Greenhouses for Supplying the World's Energy, Water and Food Needs [Sue Carter](#); University of California, Santa Cruz, United States

The increase in world population and quality of life over the next few decades is anticipated to increase the demand for food, water and energy by nearly 50%. Supplying these necessary life resources will become even more challenging with the increases in drought and temperatures brought on by climate change, as we have seen this year with the devastation of agricultural communities in the western United States. However, the same agricultural lands that are being destroyed by drought can also be part of the solution if they can be utilized more effectively. For example, covering less than 10% of the world's agricultural lands with power-generating greenhouses would, in theory, be able to meet the increased global demands for fresh water, healthy food and clean renewable electricity due to the potential for an order of magnitude reduction of water consumption and increase in crop yields that carefully

designed greenhouses can provide. This promise has spawned the new field of agrivoltaics, namely the co-location of PV with agriculture, as a climate change mitigation technology.

In this talk, I will give an overview of agrivoltaic technologies and critical economic, technology, and social challenges that exist for their wide-scale deployment. I will then discuss the basic science behind the agrivoltaics created by our laboratory at UCSC, in collaboration with Soliculture, consisting of luminescent photovoltaic (PV) panels that enhance the wavelenths of light that plants need while utilizing the wavelenths that plants do not need for renewable power generation, all while providing wavelength selective shading to reduce water consumption and overheating without negatively impacting crop yields. I will discuss the technology advances in moving this technology from small prototypes in the laboratory to full 1 meter by 2 meter agrivoltaic panels that can fit into standard greenhouse frames, including the challenges of demonstrating 20 years lifetimes and maintaining a competitive price with standard ground-mounted Si PV technology. In addition, I'll share our stories and results over the last 5 years of installing these greenhouses over acres of agricultural lands in Canada and California and working with farmers to measure the impact of the panels on crop yields. Having shown the promise, I'll end with potential pitfalls that agrivoltaics will still need to address to become widely deployed solutions for climate change mitigation.

4:30 PM *EN13.08.02

Cement as a Negative Emissions Technology Paul S. Fennell, Mark Sceats and Justin Driver; Imperial College London, United Kingdom

Cement fulfils many important roles within society today. However, its production is highly CO₂ intensive. We will consider a number of potential methods to incorporate the combination of biogenic material (including Municipal Solid Waste, but also considering waste woods, etc) within a cement plant which includes Carbon Capture and Storage. This will include the integration of a novel direct separation reactor within the cement production process. We will show that it is possible to produce significant net negative emissions from the production of cement, not including the subsequent uptake of CO₂ by the cement as it remains in place. We will consider the impact of different methods to cure the cement, including technologies such as those proposed by CarbonCure, and how these overall can add up with CCS, fuel selection and clinker substitution, to produce traceable net negative emissions from an industry that currently emits around 7 % of global CO₂.

5:00 PM *EN13.08.03

Contributions of Fellows and Senior Members of the National Academy of Inventors (NAI) Towards Climate Change Mitigation Technologies Kalliat T. Valsaraj^{1,2} and Paul Sandberg²; ¹Louisiana State University, United States; ²National Academy of Inventors, United States

Since the dawn of the industrial era, anthropogenic factors have contributed to an acceleration of climate change that is well documented in the literature. The human-induced factors presently overwhelm natural fluctuations and, global efforts to combat the effects of the same are underway. To this extent, several climate change mitigation technologies have been proposed on a global scale and reports published by the National Academies of Sciences, Engineering and Medicine (NASEM). Apart from the global efforts, it is also clear that regional efforts have to be undertaken to limit the adverse effects. Fellows and Senior Members of the National Academy of Inventors (NAI) have been at the forefront of developing and commercializing several related technologies. This relates to the overall mission of NAI in promoting innovation and technology commercialization for the benefit of humankind. This invited talk will summarize some of the technologies that are presently being considered for combating climate mitigation challenges in various parts of the world.

5:30 PM *EN13.08.04

Recent Advancement of Synthetic Oxygen Carriers for the Chemical Looping Combustion Technology Nader Mahinpey, Amr Abdalla and Mohammed Mohamedali; University of Calgary, Canada

The continuously rising concentrations of CO₂ in the atmosphere have led to significant negative impacts on the environment, which has propelled research efforts to replace fossil fuel-based energy with clean energy sources. Chemical looping combustion (CLC) has emerged in recent years as a promising technology for CO₂ capture in power plants and other CO₂ intensive industries. One of the main components of CLC is the oxygen carrier (OC) that is circulated between air and fuel reactors. The evolution of effective OCs with the desired properties for CLC application is deemed to be very significant for the commercialization of CLC. The research in this field is rapidly growing to tackle the major materials and operational challenges to advance the knowledge toward an industrial scale CLC application. This study provides a review of the advancements accomplished over the past five years in the progress of synthetic single oxide-based OCs. A summary of key performance indicators used to evaluate OCs is presented in this study to enable a systematic assessment of the OCs properties and performance. A focused and critical literature review over the last 5 years (2016-2021) on the OCs development was summarized. Moreover, the role of supports, synthesis protocols, promoters and other aspects affecting the OCs performance in CLC were outlined. This talk summarizes the main challenges, research needs and opportunities for future progress to highlight the potential pathways to develop synthetic single oxide OCs in an environmentally friendly, and cost-effective manner.

SESSION EN13.09: Climate Change Mitigation Technologies IX
Session Chairs: Ken Caldeira and Radu Custelcean
Monday Afternoon, December 6, 2021
EN13-Virtual

6:30 PM EN13.09.01

Stability Limits and Mechanical Behaviors of Methane Gas Hydrates for Use in Greenhouse Gas Mitigation Technologies Xiaodan Zhu, Alejandro Rey and Phillip Servio; McGill University, Canada

With the increasing crises of the global warming phenomenon, greenhouse gas mitigation technologies are essential to maintain the world's sustainability. Carbon dioxide (CO₂) sequestration is an inevitable component during this development. It aims to capture and store the CO₂ gases in the atmosphere to mitigate or reverse global warming. However, the selection of places to store the CO₂ gases is always a challenging process. The CO₂ storage in soil and ocean leads the sites to become acidic and threatens human life. To avoid potential problems like these, gas hydrates are potential material for CO₂ sequestration due to their excellent storage capacity.

Gas hydrates are guest-host crystalline materials formed by water cages and host gases such as methane and carbon dioxide. Regarding this structural feature, 1 m³ gas hydrate can contain approximately 160 m³ gases.

The CO₂ sequestration process is based on SI methane gas hydrates; methane is replaced by carbon dioxide. During this process, the pressures and temperatures surrounding the gas hydrates change, making the hydrate structure unstable. Jendi et al. reported that material properties of gas hydrates associated with structural stabilities change along with pressures and temperatures. Jia, J. et al. demonstrated the role of the guest molecules (methane and carbon dioxide) on the gas hydrates' stability. However, although the performance of the gas hydrates under different pressures and temperatures was demonstrated, little attention has been paid to the description and characterization of their stability limits.

This contribution will present the pressure stability limits of monocystal defect-free methane gas hydrates, using accurate density functional theory (DFT) to simulate the hydrate's performance under varying pressure. The effects of pressure on the geometric and atomic bonding feature of this guest-host crystal are presented and analyzed using various atomic angle and bond length distribution functions. Important gaps or forbidden zones are identified and related to potential stability mechanisms as pressure increases. Locations of concentrated distortions in the crystal lattice are identified. Comprehensive characterization of the elastic properties with pressure is presented and related to the crystal geometry changes. Validation and accuracy are determined using available simulations, theory, and experiments. Taken together, these results contribute to understand the methane gas hydrate stability under a great range of pressures and provide a comprehensive prediction on the hydrate's performance during CO₂ sequestration.

6:45 PM EN13.09.02

Direct Air Capture of CO₂ with Aqueous Amino Acids/Peptides and Crystalline Guanidines Radu Custelcean; Oak Ridge National Laboratory, United States

Negative emission technologies, including direct air capture (DAC) of carbon dioxide, are now considered essential for mitigating climate change, but existing DAC processes tend to have excessively high energy requirements, mostly associated with solvent/sorbent regeneration. Recently, we have developed a promising approach to DAC that combines atmospheric CO₂ absorption by aqueous amino acids or peptide (e.g., glycine, glycyglycine) with (bi)carbonate crystallization by simple guanidine compounds. In this phase-changing system, the amino acid/peptide and the guanidine compounds work in synergy, and the cyclic CO₂ capacity can be maximized by matching the basicity of the two components. The resulting DAC process has a significantly lower regeneration energy compared to state-of-the-art solvent-based DAC technologies.

This research was sponsored by the U.S. Department of Energy, Office of Science, Basic Energy Sciences, Chemical Sciences, Geosciences, and Biosciences Division.

7:00 PM EN13.09.03

Development of the Membranes for the CO₂ Separation from Air Based on the CO₂ Selective NbOFFIVE-1-Ni Metal-Organic Framework Roman Selyanchyn and Shigenori Fujikawa; Kyushu University, Japan

The membrane-based gas separation proved to be energy efficient in industrial processes and is also studied for the post- and pre-combustion CO₂ separation from N₂ and H₂ respectively. Meanwhile, direct capture of CO₂ from air represents a tougher challenge for the membrane approach due to the significantly lower concentration and very low driving force needed for gas transport. Advances in the membranes design, membrane processes, combination with CO₂ conversion are important to enable the energy competitive CO₂ extraction from low concentrated environmental mixes.

Metal-organic frameworks (MOFs) are novel microporous and tunable materials that suggested for separation processes, due to ability to precisely design the internal pores' size or chemical affinity via reticular chemistry. NbOFFIVE-1-Ni is among the recently discovered MOFs that demonstrated a peculiar CO₂ sorption property. Namely, in addition to its relevant sorption capacity of ~2.2 mmol CO₂ per gram of MOF, the sorption to full capacity undergoes at very low partial pressures. This causes the material to be filled with CO₂ when exposed to concentrations as low as 400 ppm. This property of NbOFFIVE-1-Ni and several other similar ultramicroporous materials suggested their use as solid sorbents in DAC application. However, the complexity of solid adsorption-based capture, tough requirements for the material regeneration (ultra-low vacuum), and even cost and scale make this approach impractical. To utilize the unique properties of NbOFFIVE-1-Ni we speculate that instead of solid adsorption it is possible to design the membranes and use the material in form of nanofillers in the mixed matrix architecture. It is known that fillers can improve membrane performance by increasing selectivity, permeability, or even both properties.

Here we report the fabrication, structure, and gas transport properties of mixed matrix membranes (MMM) composed of the fluorinated MOF (NbOFFIVE-1-Ni) and CO₂ selective polyether-polyamide block copolymer (Pebax-1657). The performance of MMM with different amounts of fillers (10-40 wt%) for CO₂, N₂, O₂, and H₂ gas permeation was studied with particular focus on the mixed CO₂/N₂ formulations (with concentrations as low as 1000 ppm CO₂). For better performance, MMMs should have well-dispersed fillers in matrix polymer without interfacial gaps or blocking interfaces between them. As such, the hypothesis of this study was that if NbOFFIVE-1-Ni material is optimally incorporated in the polymer it could provide better CO₂ separation from the matrices with low concentration.

It was found that the particles of as-synthesized NbOFFIVE-1-Ni MOFs have very large sizes, not suitable for uniform membranes fabrication. Therefore, planetary ball milling was used to reduce particle sizes reaching well below the sub-100 nm size range. The presence of ultramicroporous fillers of smaller size in Pebax-1567 made a significant impact on gas transport. In particular, the increased CO₂/N₂ selectivity (from ~60 in polymer to >100 in MMMs) was observed with the increase of filler loading. These results suggest the manifestation of the ultra-CO₂-selective nature of the NbOFFIVE-1-Ni. The highest CO₂/N₂ selectivity and CO₂ permeability of MMMs was observed when a 1000 ppm CO₂ mixture was used as a feed gas. The performance of MMMs at higher temperatures (40-60 °C) allowed us to achieve even better separation results matching the sorption performance of MOF in similar conditions and significantly overcoming the performance of pure polymer used as a matrix.

While the improvement in selectivity is important for the efficient membrane-based CO₂ capture processes, especially for the post-combustion and direct air capture, further efforts on the particle size reduction and mixed matrix membrane thinning for effective utilization of the excellent molecular sieving properties of NbOFFIVE-1-Ni are necessary. These experiments are underway, and results will be also reported.

7:15 PM EN13.09.04

Upcycling of Waste Materials for Sustainable and Scalable Energy Storage Cengiz S. Ozkan; University of California, Riverside, United States

Great many tons of waste glass and plastics end up in landfills without proper recycling, which aggravates the burden of waste disposal. Plastic pollution is especially harmful to the Earth's ecosystem, and impacts the quality of life all around. Plastics and glass are used on a massive scale in various sectors of industry, including the automobile, textile, and packaging industries. The conversion from waste glass or plastics to favorable materials is of great significance for sustainable strategies. In this talk, I will describe recent advancements in upcycling polyethylene terephthalate (PET) waste and glass waste bottles into active electrode materials of nanocarbon fibers and nanostructured silicon particles, respectively. Compared to other quartz sources obtained via pre-leaching processes that apply toxic acids and require high energy-consuming annealing, an interconnected silicon network is directly derived from

waste glass bottles via magnesiothermic reduction. In the case of PET waste plastic, materials are first dissolved in a mixture of trifluoroacetic acid and dichloromethane, followed by carbonization under an argon/hydrogen atmosphere. Nanocarbon electrodes derived from waste PET have been successfully employed in electric double layer supercapacitors. Glass bottles are directly utilized for magnesiothermic reduction without pre-leaching and annealing, which offers a more environmentally-benign, energy-saving and efficient route to prepare silica source materials. Their abundance in silica without any loss due to the non-etching process result in high silicon yield towards fabricating Li-ion battery anodes with excellent electrochemical performance with a capacity of over 1400 mAh/g at C/2 after 400 cycles. Both conversion processes for waste glass and plastics are highly scalable with environmental and economic advantages, and our methodologies could provide the means for achieving a circular economy involving the upcycling of sustainable waste materials integrated to manufacturing of scalable energy storage technologies.

7:30 PM *EN13.09.06

Climate Change Mitigation Technologies Ken Caldeira^{1,2}; ¹Carnegie Institution for Science, United States; ²Breakthrough Energy, United States

Climate change is one of the central challenges facing the world today. One of the basic ways to reduce risks from climate change is to reduce emissions of the greenhouse gases that are causing our planet to warm. In climate change jargon, efforts to reduce emissions have come to be known as “climate change mitigation”.

The three main ways to reduce greenhouse gas emissions are to: (1) reduce consumption; (2) reduce amount of energy used per unit consumption (efficiency); and (3) reduce the amount of net greenhouse gas emissions per unit energy used (carbon-emission-free energy).

Most national governments are working hard to increase abilities of populations to consume, so most mitigation efforts center on improving efficiency and powering systems with carbon-emission-free energy.

Efficiency can be improved through a change in systems (e.g., a shift from manufacturing to service sector) or through a change in devices (e.g., a more efficient engine).

There are only a small number of possible energy carriers and a finite number of technologies that could in principle convert energy from one carrier to another at scale without releasing greenhouse gases into the atmosphere. These include wind, solar, hydropower, nuclear and perhaps power from the oceans. Fossil fuels and bioenergy could perhaps be made carbon neutral through some combination of flue gas and direct air carbon capture and storage. While some non-emitting technologies are cost competitive with fossil-fuel alternatives in some settings, at today’s costs, near-zero emission energy systems have higher direct costs today than would a CO₂-emitting system with similar characteristics. Therefore, substantial effort is being invested in lowering the “Green Premium” that must be paid to avoid greenhouse gas emissions.

This talk will present a taxonomy of mitigation technologies and approaches, with attention given to areas in which materials science might hopefully contribute to addressing important societal needs.

SESSION EN13.10: Climate Change Mitigation Technologies X

Session Chair: Ronaldo Giro

Monday Afternoon, December 6, 2021

EN13-Virtual

9:00 PM EN13.10.01

Accelerate Polymer Membrane Discovery for CO₂ Separation with Graph-Based Generative Model and Molecular Dynamics

Simulation Hsianghan Hsu¹, Akihiro Kishimoto¹, Ronaldo Giro², Mathias Steiner², Seiji Takeda¹ and Lisa Hamada¹; ¹IBM Research-Tokyo, Japan; ²IBM Research - Brazil, Brazil

Polymer membranes are potent materials for exhaust gas separation in energy production and transportation. Separating off carbon dioxide (CO₂) from flue gases could help to mitigate climate change which is mainly driven by greenhouse gas emissions. Due to the trade-off between a membrane’s CO₂ permeability and its selectivity with regards to CO₂ and nitrogen (N₂), and because of the harsh operation conditions, only very few polymers are actually used at industrial scale. In this study, consider the complexity of the process conditions and complicated interaction when flue gases permeate the membrane, we develop a simplified end-to-end framework and target to homopolymer type membranes first. Powered by the less data hungry artificial intelligence algorithms and physical validation, a similar trend compared to the literature values is observed. The results and challenges which include small number of the dataset, molecule generation efficiency, and validation with molecular dynamics (MD) are discussed.

The dataset is mostly acquired from the review article [1] and then converted to their corresponding SMILES. The target is to find membrane materials perform superior to Robeson’s 2008 upper bound. Within the selected 150 samples none of them perform over the boundary. With the small data size, we tested the performance of three linear models (Lasso, Ridge and elastic net) and three non-linear models (random forest, kernel ridge and support vector machine). By performing grid search the best hyperparameter sets are configured automatically. For the linear models, we selected important features based on the Lasso penalty available in the scikit-learn library. For the non-linear models, we performed a combination of greedy search with local search that attempts to bypass the local optimum of the R² score. This benefits to the final CV scores improve at least 0.1 and finally random forest is used for doing structure generation. In the generation step, our strategy is to involve prescribed sub-structures embed in those samples close to the boundary rather than decided by exhaustive generation algorithm. The newly generated SMILES are clustered by Murcko scaffolds first and those predicted over the boundary are selected for MD validation.

The newly generated structures lack of clear identification for the atom charge and bond type information. The purpose of the MD validation is to efficiently observe the trend rather than to reproduce the literature values. An automation process is developed to convert generated SMILES to polymer slabs with MD input format. Since most experimental observations are performed at constant temperature and pressure, we realize the permeability calculation with an isothermal-isobaric (NPT) based methodology in which constant pressure difference is kept during the gas injection. According to the benchmark results under available options, polymer slabs with 800 heavy atoms per chain, 6 nm in thickness, and DREDDING force field are selected. The benchmark results shows that the CO₂ permeability is in the same order between predicted and calculated values. Instead, the selectivity is less comparable to the original values which is because that N₂ permeability usually 10 to 40-fold smaller and a long enough simulation time (ex: 100 ns) is necessary.

The overall fitting results we have obtained are encouraging, considering the limitations of the training dataset and the membrane formation method. The automated process allows to put innovation on structure generation and MD methodology. Based on the results obtained, we are now analyzing the newly generated structures with highest predicted CO₂ permeability. The inclusion of additional physical parameters such as adsorption energy, free volume, and gyration radius in the optimization could help further improve our material discovery results for polymer separation membranes.

9:15 PM EN13.10.02

Effect of Pore Expander on Pluronic Block Copolymer-Alumina Co-Assembly Geok Leng Zoey Z. Seah^{1,2}, Adam K. Usadi³, Jonathan McConnachie³ and Kwan Tan¹; ¹Nanyang Technological University, Singapore; ²KAIST, Korea (the Republic of); ³ExxonMobil Research and Engineering Company, United States

Co-assembly of a structure-directing block copolymer and aluminium tri-sec-butoxide derived sols enables formation of highly ordered mesoporous alumina structures that are appealing for various applications such as carbon capture, separation and catalyst supports. We found that the addition of trimethylbenzene further induced an order-disorder-order mesophase transition in the F127- Al_2O_3 system. Thermal annealing resulted in the formation of micro- and mesoporous alumina structures with enhanced carbon dioxide adsorption capacity.

9:30 PM EN13.10.03

Automated AI-Driven Screening of Nanoporous Materials for Enhanced Carbon Dioxide Adsorption Rodrigo Neumann¹, Fausto Martelli², Binquan Luan³, Ronaldo Giro¹, Tonia Elengikal³, Nicholas Yankey³, Anshul Gupta³, Guojing Cong⁴, Mathias Steiner¹, Tom Peters⁵, Amir Farmahini⁶, Joseph Manning⁶, Conor Cleeton⁶, Flor Siperstein⁶, Lev Sarkisov⁶ and Breannan O Conchuir²; ¹IBM Research Brazil, Brazil; ²IBM Research Europe, United Kingdom; ³IBM T.J. Watson Research Center, United States; ⁴Oak Ridge National Laboratory, United States; ⁵University of Connecticut, United States; ⁶The University of Manchester, United Kingdom

Millions of crystalline nanoporous materials have been identified for carbon capture, making the task of measuring the adsorption performance of each individual nanopore using computer simulations wholly unfeasible. Furthermore, experimentally synthesising and calculating the adsorption properties of each sample is even more impractical. A screening framework is thus required to identify a smaller number of promising candidates for further investigation. In this presentation, we introduce our work which deploys several distinct mathematical techniques to efficiently characterize nanopore structures, leading to a rapid high throughput nanopore screening mechanism.

Our automated cloud-based materials screening tool is composed of two distinct parts. Firstly, several computational geometric and topological descriptors are determined for each individual nanopore, allowing us to immediately discount samples with unfavourable structural properties. Next, Grand Canonical Monte Carlo (GCMC) simulations are deployed to calculate the target adsorption figures of merit. The computed results can be ingested into machine learning algorithms to produce a surrogate model to the original simulations, thus accelerating the estimation of desired adsorption properties of the candidate nanoporous materials.

9:45 PM EN13.10.04

Evaluating Classical Molecular Dynamics Methods for the Validation of Carbon Dioxide Separation Performance in Polymer Membranes Ronaldo Giro¹, Hsianghan Hsu², Akihiro Kishimoto², Seiji Takeda² and Mathias Steiner¹; ¹IBM Research - Brazil, Brazil; ²IBM Research - Japan, Japan

Climate change is mainly due to CO₂ emissions occurring in energy production and transportation. A set of technologies are being developed to separate and sequester CO₂ from point sources. Among these are liquid and solid adsorbents as well as membranes and hydrates. Polymer membranes show certain advantages with regards to their storage and disposal properties, they allow for passive operation, have high tolerance to SO_x and NO_x content and can be integrated within an existing power plant steam cycle (post combustion application).

Candidate materials for application in polymer separation membranes must fulfill two key requirements: high CO₂ permeability and high CO₂/N₂ selectivity. Many candidate materials exist today or can be computationally designed; however, the time and cost of experimental lab validation is the principal limitation in materials discovery applications. In this contribution, we investigate the potential of Classical Molecular Dynamics (CMD) simulations as a time- and cost-efficient validation option for suited polymer candidates.

CMD simulations have been employed successfully for calculating permeation in glassy polymers [1], however, significant uncertainties with this approach remain. We have reviewed a set of available CMD methodologies and analyzed their strengths and weaknesses in application to the polymer membrane use case. Specifically, we have investigated effects related to number of atoms, membrane thickness and area, size of polymeric chain and membrane composition, respectively, on both CO₂ permeability and selectivity. We show quantitative results for representative polymers that lead to the conclusion that Constant Pressure Difference Molecular Dynamics (CPDMD) [2,3] is the most appropriate methodology.

References:

- [1] H. Frentrup et al. In Silico Determination of Gas Permeabilities by Non-Equilibrium Molecular Dynamics: CO₂ and He through PIM-1, *Membranes* 5, 99-119 (2015).
- [2] X. Kong and J. Liu, An Atomistic Simulation Study on POC/PIM Mixed-Matrix Membranes for Gas Separation, *J. Phys. Chem. C* 123, 15113-15121 (2019).
- [3] J. LKiu and J. Jiang, Molecular Design of Microporous Polymer Membranes for the Upgrading of Natural Gas, *J. Phys. Chem. C* 123, 6607-6615 (2019).

10:00 PM EN13.10.05

Simulating Fluid Flow at Pore Scale with Carbon Dioxide in Digital Rock Jaione Tirapu Aziproz¹, Rodrigo Neumann¹, Ronaldo Giro¹, Adolfo Emmanuel Correa Lopez¹, Ricardo Luis Ohta¹, Abel Cabral Arruda¹, Matheus Esteves Ferreira¹, Ademir Ferreira Silva¹, Benjamin Wunsch² and Mathias Steiner¹; ¹IBM Research-Brazil, Brazil; ²IBM T.J. Watson Research Center, United States

Carbon dioxide capture and storage technologies will be required to reduce emissions into the atmosphere and limit global warming in the coming decades. Geo-sequestration involving the injection of CO₂ directly into the pore space in sedimentary rocks, saline formations or abandoned oil fields may present a permanent storage solution. More scientific research is needed to understand and optimize CO₂ injection process and long-term storage at the pore scale of these underground geological formations.

In our research, we model the rock pore space as a network of capillaries with spatially varying radii and the flow rate in each capillary is modelled as laminar flow. The capillary network representation is extracted from high-resolution X-ray microtomography images of suitable rocks [1]. This fine-grained capillary network representation allows for both single- and two-phase flow simulations with a high level of geometric accuracy at microscale. The two-phase flow simulations employ a time-dependent interface tracking approach for simulating displacement experiments that results in a system of differential-algebraic equations. Solving these time-dependent equations on the high-resolution three-dimensional geometrical representation of the rock sample obtained from the X-ray microtomography remains very time and computationally intensive. Alternatively, analysis is carried out on the aggregate

results of multiple two-phase flow simulations, each applied to a different simplified capillary network model of the rock sample. These simplified network models are generated algorithmically and allow for a higher level of control on the number of capillaries and their properties. The resulting networks are optimized to match the physical properties of permeability and porosity of the original sample at a significantly lower computational cost.

In this work we present results from the accuracy benchmark of the single-phase flow simulations against other known network methods from the literature and with respect to measurements of permeability performed at lab scale in the same rock samples. We then apply the methodology described to simulate two-phase flow on capillary network representations of porous sandstone rock samples extracted from the geometric boundaries of the connected pore space from x-ray microscale computer tomography data. In order to understand the physics of carbon dioxide trapping at the pore scale, we simulate two-phase fluid flow scenarios under varying conditions of temperature, pressure and fluid properties, and present our findings in optimizing parameters that maximize fluid saturation of the rock.

[1] Neumann, R.F., Barsi-Andreetta, M., Lucas-Oliveira, E. et al. High accuracy capillary network representation in digital rock reveals permeability scaling functions. *Sci Rep* 11, 11370 (2021). <https://doi.org/10.1038/s41598-021-90090-0>

10:15 PM EN13.10.06

Rapid Thermal Swing Adsorption Gas Separation for Carbon Capture Emanuele Piccoli^{1,2}, Patrick Ruch¹ and Bruno Michel¹; ¹IBM Research - Zurich, Switzerland; ²EMPA, Switzerland

The large column inventory enforced by the long regeneration times prevented the use of thermal swing adsorption for gas separation. But with shorter regeneration times the technology would have a good potential due to the low operation cost enabled by the use of low grade waste heat. The key to shorter regeneration times is a **rapid thermal swing adsorption (RTSA) process**. This process has been developed in adsorption heat pumps that offer a clean technology for cooling or heating utilizing waste or renewable heat as driving energy. RTSA constitutes a similar step improvement as the rapid pressure swing process that reduced the investment cost for many gas purification and separation processes including oxygen separators used in treating COVID patients. A crucial component to reduce cycling times is the use of hierarchically structured sorbents. As part of the development of better adsorption heat pumps we have devised an inexpensive and scalable magnetic alignment route for the fabrication of adsorptive coatings with vertically open channels and thermal bridges improves mass transport more than threefold [1]. This combined with methods to improve thermal transport accelerate the thermal swing process strongly reducing column inventory and cost.

A novel controlled fast temperature jump setup (TJS) accurately measures temperatures and sorption processes based on chamber pressure as function of time following temperature steps. The sorption material is mounted as beads or layers onto aluminum carriers that are temperature controlled with high performance microchannel heat exchangers. The TJS allows fast acquisition of cycled mass, thermal resistance and mass transport resistance to screen and optimize material and process libraries. Measurements were carried out as function of wide choice of sorbent materials, gas type (CO₂, N₂, H₂O) including mixtures, gas pressure, cycling time, temperature gradient, layer thickness, and layer structuring. A selection parameter was defined that contains exchanged mass per cycle, adsorption and desorption speed as well as layer thickness: Parameters that maximize the performance of an RTSA gas separation process.

The maximum achievable specific exchanged mass per cycle could be determined by gravimetric method through Dynamic Vapor Sorption experiments. All adsorbents were tested in both mono and multicomponent gases showing that maximum CO₂ adsorption capacity alone does not sufficiently represent the potential of a material, as residuals of adsorbed water in the pore can significantly decrease the cycling capacity. The same methods, as well as full adsorption isotherms, were applied to the adsorber coating materials (including binders, surfactants and thermally conductive materials) to provide a benchmark for the evaluation of the enhanced coatings tested with different cycle times.

According to the results obtained with the TJS experiments, the initial coating formulation and process was improved aiming to increase the active mass use and the CO₂ cycled per unit area, and to decrease the adsorption and regeneration times. As a result, a protocol ensuring good adsorbent adhesion, good thermal contact and fast kinetics was obtained.

It was demonstrated that a proper integration strategy of pore formation by magnetically aligned emulsions is as significant as the choice of the adsorbent material itself, leading improvement factors between 2 and 10. The material screening and integration tailoring methods proposed proved to quickly highlight the most promising direction on which to build on scale-up and further research activities. We thus can quickly select best materials and structuring processes to establish RTSA as a viable alternative to other carbon capture processes.

[1] J. Ammann, P. Ruch, B. Michel, and A. R. Studart, High-Power Adsorption Heat Pumps Using Magnetically Aligned Zeolite Structures, *ACS Appl. Mater. Interfaces* 2019, 11, 27, 24037–24046.

10:30 PM EN13.10.07

Novel Gas Hydrate Systems with Plasma-Functionalized Graphene Nanoflakes for Emerging Methane Storage and Transport Technologies Adam McElligott, Jean-Luc Meunier and Phillip Servio; McGill University, Canada

Natural gas is composed primarily of methane, a potent greenhouse gas, and is a quickly-growing non-renewable energy source worldwide. To mitigate pipeline emissions, transport has moved towards using pressure vessels with liquefied (LNG) or compressed (CNG) natural gas. Gas hydrates are crystalline compounds formed when a gas is enclosed in and stabilizes a lattice of hydrogen-bonded water molecules. They require less severe conditions for formation: lower pressures than CNG and higher temperatures than LNG. Also, 1 L of methane hydrate is estimated to store 160 L of gas. Due to the high storage capacities and reduced transportation costs, gas hydrate technologies are now being developed for natural gas transport and storage applications. Methane hydrate technologies could also be used for direct air capture of methane from pipeline leaks and could equally extend to removing atmospheric carbon dioxide using CO₂ hydrates, which have the same structure as their methane counterparts.

The study of materials that assist in the formation of hydrate structures has focused on kinetic promoters that induce the nucleation of stable gas hydrate crystals and enhance hydrate growth rates as well as gas storage capacities through higher cage occupancy. Improved gas dissolution in water at the liquid-vapor-hydrate equilibrium point has also been examined. Recently, this class of promoters has expanded to include graphene nanoflakes (GNFs) which have already been shown to increase the yields of many hydrate compounds. They are made through a plasma decomposition process wherein critical carbon clusters form homogeneously from carbon vapors. GNFs are hydrophobic as they consist of sheets of carbon atoms, so they agglomerate in and settle out of aqueous solutions. Stability improvement methods have included the addition of surfactants, though this reduces the system purity, and chemical additions on the graphene surface. Recent advancements have allowed for the GNF surface to be functionalized with oxygen-containing groups. Here, the CH₄/N₂ feed used initially to form hydrophobic GNFs is changed to air, and the oxygen forms an active species and interacts with the GNF surface. Through covalent bonding with these oxygenated functionalities (such as carboxyl, hydroxyl, and ether oxide groups), a stable nanofluid of aqueous GNFs was achieved. These hydrophilic GNFs, called O-GNFs, have in-plane dimensions of roughly 100 x 100 nm² and are between 5 and 20 atomic layers thick. The atomic composition of their surface is approximately 14.2% oxygen.

The growth rates of methane hydrates were measured in the presence of plasma-functionalized GNFs at 2 °C and 4646 kPa, a 1500 kPa driving force. Improving growth rates furthers the efficacy of hydrate technologies by increasing gas capture rates. Enhancement occurred due to improved mass transfer resulting from high GNF specific surface area and additional gas-liquid interfacial area. Enhancement by O-GNFs rose linearly and rapidly at low concentrations, peaking at 1 ppm at nearly quadruple the growth rate (288% enhancement); the most significant enhancement of a hydrate system currently demonstrated. At 5 ppm, enhancement dropped to 215% due to limitations on the mean free path of the nanoparticles. At 10 ppm, enhancement rose again

to 247% due to further increases in surface area.

The dissolution rates of methane in hydrophilic GNF nanofluids at 2 °C and 3146 kPa (three-phase equilibrium) were also measured. These rates improved with loading and were at most 44% faster at concentrations of 5 ppm. Mean free path limitations may have restricted further dissolution rate enhancements beyond this point. The maximum dissolution rate for the specific system may also have been achieved. The amount of methane dissolved in the solution did not change with any GNF loading. This finding indicates that GNFs do not affect system thermodynamics: these additives may not affect how much gas can be stored in the hydrate.

SESSION EN13.11: Climate Change Mitigation Technologies XI

Session Chair: Susan Rempe

Wednesday Morning, December 8, 2021

EN13-Virtual

8:00 AM EN13.11.02

Ultra-Thin and Robust Liquid Membrane for CO₂ Capture from Gas Mixtures [Susan Rempe](#)¹, [Ying-Bing Jiang](#)², [Yongqian Gao](#)³, [Ron Chiang](#)³ and [Chris Beamis](#)³; ¹Sandia National Laboratories, United States; ²The University of New Mexico, United States; ³Memzyme, LLC, United States

Current carbon dioxide membranes suffer from limited flux and selectivity while conventional absorption-based CO₂ sequestration are associated with high temperatures and high costs, calling for alternative CO₂ separation approaches. Here, we describe an ultra-thin and robust liquid membrane that enables both high flux and high selectivity for CO₂ separation and capture at ambient temperatures and low costs. The membrane comprises 18-nm thick arrays of 8 nm diameter hydrophilic pores that stabilize water by capillary condensation and precisely accommodate the metalloenzyme carbonic anhydrase (CA). CA catalyzes the rapid interconversion of CO₂ and water into carbonic acid, promoting uptake and release of CO₂. By minimizing diffusional constraints, stabilizing and concentrating CA within the nanopore array to a concentration 10x greater than achievable in solution, our thin, liquid membrane separates CO₂ at the highest combined flux and selectivity yet reported for ambient condition operation.

8:15 AM *EN13.11.03

The Value of Negative Emissions Technologies for Mid-Century Transitions to a Net-Zero Economy [Chris Greig](#)¹ and [Sam Uden](#)²; ¹Princeton University, United States; ²Conservation Strategy, LLC, United States

Negative emissions technologies (NETs) are often viewed as a 'risky backstop' technology for climate change mitigation. This view stems from IAM-based assessments of NETs which require very large-scale deployment of NETs in the second half of the century, to compensate for a mid-century emissions overshoot. In this presentation, we challenge this limited view of NETs. Taking Princeton's recent report, Net-zero America as a case study, we show the crucial role that negative emissions technologies plays in the economy-wide transitions to net-zero emissions by 2050 for the United States. The second part of the presentation proposes a fresh take on the value of NETs, and explores NETs via a bottom-up analysis. A decision-making framework is offered to determine the circumstances under which NETs could provide *value* as a mitigation option at jurisdictional scales. This framework is then applied to localized case studies to highlight how NETs could overcome socio-technical obstacles and/or unlock a variety of environmental and social co-benefits as part of the technology portfolio for achieving time-bound mitigation goals. Overall, the presentation aims to cut through what we see as a noisy discourse on NETs, which is wrapped-up in concerns that are dependent on scenario modeling, and offer a plain evaluation of NETs as a potential climate change mitigation option.

8:45 AM EN13.11.04

Synthesis of Hybrid Carbon Materials for CO₂ Capture [Bashir E. Hasanov](#)¹, [Amira Alazmi](#)^{2,1} and [Pedro Costa](#)¹; ¹King Abdullah University of Science and Technology, Saudi Arabia; ²University of Hafr Albatin, Saudi Arabia

The continuous use of fossil fuels, along with other urban human activities, are behind an excessive emission of greenhouse gases. The intergovernmental panel on climate change (IPCC) stated that global greenhouse gas emissions must be reduced by 50-80 per cent by 2050 to mitigate climate change¹. From the list of greenhouse gases, carbon dioxide (CO₂) has been considered a key contributor to the current state-of-affairs². Therefore, there is a pressing demand for carbon capture and storage (CCS) technologies that allow for the capture and storage of CO₂ produced from fossil fuels. Solid porous adsorbent materials are the most competitive and promising candidates for CCS technologies, offering a high uptake capacity and tailored selectivity towards specific gases³⁻⁵. Among these materials, biomass and microporous carbons have come into prominence due to a set of desirable characteristics such as high availability of source precursors, ease of preparation, low-cost production, highly developed porous structure, moderate adsorption heat and the possibility to induce an abundance of functional groups.

In this communication, we report a porous carbon-carbon powdered mixture designed to perform CO₂ capture. The hybrid powder is constituted by KOH activated hydrothermally carbonised palm date seeds (HTC-PDS) and reduced graphene oxide (rGO). Previous work with the KOH activated HTC-PDS component showed interesting results for CO₂ uptake⁶. In the present case, we mixed HTC-PDS with rGO in different ratios before activating the powder with alkaline KOH. The oxygen functional groups (remainders in the rGO) could assist in optimising the CO₂ heat of adsorption in the hybrid material, enhancing the selectivity compared to the activated biochar. The approach was also designed to test if, beyond the porous development, the structure of the graphite building units in the two carbon components could be controlled and influence the adsorption of the greenhouse gas. The structural analysis, by Raman and X-ray diffraction, confirms the development of a more ordered structure. The optimised activated mixture had a specific surface area of 845 m²/g, with 92% of the total surface area being microporous. The CO₂ adsorption capacity (at 1 bar, 273 K) was 3.40 mmol/g.

References

1. Nakicenovic, N. et al., Cambridge University Press, 2000
2. Raza, A. et al., Petroleum, 2019, 5(4), 335-340
3. Olivares-Marín, M. et al., Greenhouse Gases: Science and Technology, 2012, 2(1), 20-35.
4. Espinal, L. et al., Environmental Science & Technology, 2013, 47(21), 11960-11975
5. Pardakhti, M. et al., ACS Applied Materials & Interfaces, 2019, 11(38), 34533-34559
6. Alazmi, A. et al., Activated carbon from palm date seeds for CO₂ capture, submitted

SYMPOSIUM EN14

Advanced Materials for Hydrogen and Fuel Cell Technologies
November 30 - December 8, 2021

Symposium Organizers

Ming Dao, Massachusetts Institute of Technology
Huyen Dinh, National Renewable Energy Laboratory
Christopher San Marchi, Sandia National Labs
T. Venkatesh, Stony Brook University, The State University of New York

* Invited Paper

SESSION EN14.01: Hydrogen Production I
Session Chairs: Ming Dao and T. Venkatesh
Tuesday Morning, November 30, 2021
Hynes, Level 3, Room 300

10:30 AM *EN14.01.01

Redox-Active Metal Oxide Materials for Thermochemical Cycles—Key Thermodynamic Principles Ellen B. Stechel, Alberto de la Calle, Ivan Ermanoski and James E. Miller; Arizona State University, United States

High-temperature endothermic reduction of redox-active metal oxides, which can exchange oxygen between the solid and the gas phase at achievable conditions (where what is achievable remains an open question for the field), converts thermal energy to stored chemical energy. A subsequent re-oxidation step either recovers the stored energy as heat or utilizes it to drive other chemical reactions. If the re-oxidation step restores the material to its original state so that the two steps can repeat indefinitely, the sequence of reactions constitutes a thermochemical cycle. Two related processes (reversibly re-oxidizing with oxygen or affecting bond breaking by re-oxidizing with CO₂ and/or water) are somewhat analogous; the production of energized carriers (H₂ and/or CO) is significantly more constrained by thermodynamics and hence subject to greater challenges to objectives for high efficiency and low cost. Nonetheless, both chemistries have been of increasing interest due to their potential for high utilization of the sunlight in high direct normal irradiance (DNI) regions and economic competitiveness for clean energy, and most recently as a role in achieving negative emissions and closing the carbon cycle.

This presentation will discuss new revelations in the thermodynamics of the redox-active metal oxide and the operating conditions of a cycle. We will show recent progress towards developing high-performing materials and cycles for thermochemical energy storage and CO₂/H₂O splitting.

11:00 AM EN14.01.02

A Tale of Two Surface Terminations—Microscopic Insights into the Interaction of BiVO₄ with Water in Photoelectrochemical Applications Wennie Wang¹, Adam M. Hilbrands², Chenyu Zhou³, Emily Chen¹, Marco Favaro⁴, David Starr⁴, Kyoung-Shin Choi², Mingzhao Liu³ and Giulia Galli^{1,1,5}; ¹The University of Chicago, United States; ²University of Wisconsin–Madison, United States; ³Brookhaven National Laboratory, United States; ⁴Helmholtz-Zentrum Berlin, Germany; ⁵Argonne National Laboratory, United States

Extracting hydrogen fuel from water splitting will require identifying and optimizing materials for the oxygen evolution reaction, as it is a major bottleneck in water splitting reactions. Photoelectrochemical cells have been at the forefront of technologies with the potential to realize a hydrogen economy at scale, and transition metal oxides in particular have garnered significant interest as photoelectrodes. Bismuth vanadate (BiVO₄) is one such oxide with numerous advantageous optoelectronic properties that make it amenable as a photoanode for oxygen evolution. However, progress towards achieving the optimal photocurrent densities and performance of BiVO₄ as a photoanode has not been systematic, thus necessitating the need to mechanistically understand its material properties, especially at the surface/interface.

Here, we present a combined experimental and computational study aimed at an atomic-level understanding of the BiVO₄ (010) surface with water. Our previous work [1] demonstrated that the surface composition plays a critical role in the photoelectrochemical performance and identified that the relevant surface is actually Bi-rich, not a 1:1 Bi:V ratio as previously thought. Building on this understanding, we performed first-principles calculations with Quantum ESPRESSO (<https://www.quantum-espresso.org/>) and Qbox (<http://qboxcode.org/>), and used resonant PES and XPS to elucidate the microscopic interactions between the BiVO₄ surface and water while varying the surface termination. In this presentation, we will compare and contrast the changes in surface energetics between different surface terminations of the BiVO₄ (010) surface upon immersion in water and discuss ways in which this could impact photoelectrochemical performance.

[1] D. Lee, W. Wang, C. Zhou, X. Tong, M. Liu, G. Galli, K.-S. Choi. "The impact of surface composition on the interfacial energetics and photoelectrochemical properties of BiVO₄ ." *Nature Energy*. **6**, 287 (2021).

This work was supported in part by NSF CHE-1764399 and resources at CFN BNL through the DOE, DE-SC0012704.

11:15 AM EN14.01.03

Fractal Exfoliation—Mechanisms of Rapid Hydrogen Generation From Liquid-Metal-Activated Aluminum Water Reactions and Their Practical Implications Peter Godart and Douglas P. Hart; Massachusetts Institute of Technology, United States

Aluminum is a promising energy carrier due to its abundance, low cost, and ability to react with water to produce hydrogen gas at a high volumetric energy density (up to 36.3 MJ/L Al). Ordinarily, aluminum's passivating oxide layer that rapidly forms upon exposure to oxygen prevents its reaction with water; however, in recent years, numerous promising approaches to disrupting this oxide layer have been developed that utilize a variety of room-temperature-liquid metal alloys containing some combination of gallium, indium, and tin, for example. In this work, an activating alloy composed of eutectic gallium and indium ($e\text{Ga}_{0.8}\text{In}_{0.2}$) was studied due to its ability to activate bulk aluminum particles at added mass ratios below 5%. Prior research had shown that surface-treating bulk aluminum pellets (>5 mm in diameter) with this alloy results in complete penetration of the liquid metal along the aluminum grain boundary network, enabling near-unity theoretical hydrogen yield fractions in subsequent reactions with water. Despite the efficacy of this approach for producing hydrogen, however, numerous questions remain about the nature of the underlying reaction mechanism, in particular what happens to the $e\text{GaIn}$ throughout the reaction.

In this work, experimental techniques were developed to carry out the aluminum-water reaction at arbitrarily slow reaction rates via controlled exposure to water vapor at room temperature. By starting and stopping the reaction at various stages in the absence of liquid water, standard SEM-EDS and XRD techniques could be used to study the reaction mechanism in significantly greater detail than before. The results of these experiments show that the aluminum-water reaction occurs in two primary stages: (1) rapid disintegration of the bulk aluminum along its grain boundaries via a fractal-like exfoliation process, and (2) the subsequent reaction of water at unoxidized sites on the freshly exposed aluminum grain surfaces. The phase of the activating $e\text{GaIn}$ was also tracked and imaged at various stages of the reaction for the first time, showing ultimately that during the bulk disintegration process, reactions between gallium and ambient water and oxygen lead to the dealloying of the initial $e\text{GaIn}$, leaving behind micron-scale solid indium spheres. Given the high cost of the $e\text{GaIn}$ relative to the input aluminum, their recovery is important for many practical applications. The operational implications of these results are discussed, and methods for recovering the activating metals are proposed.

11:30 AM EN14.01.04

Modulating Interfacial Charge Density of $\text{NiP}_2\text{-FeP}_2$ via Coupling with Metallic Cu for Accelerating Alkaline Hydrogen Evolution Ashwani Kumar and Hyoyoung Lee; Sungkyunkwan University, Korea (the Republic of)

Developing efficient earth-abundant electrocatalysts to replace high-cost Pt for alkaline hydrogen evolution reaction (HER) is crucial for sustainable hydrogen production. However, an additional sluggish water dissociation step associated with alkaline HER poses a major bottleneck for real applications. Recently, developing heterostructures catalysts with an electronegative atom (P, N, O, and S) acting as a base to trap the H^* has emerged as a paramount strategy to boost HER activity. However, the alkaline HER activity of most of the heterostructure-based catalysts cannot surpass the commercial Pt, due to inadequate H^* adsorption energy (ΔG_{H^*}) and high kinetic barrier for water dissociation, mainly determined by the electronic structure and localized charge-density at the interface-region.

Herein, density functional theory (DFT) predictions reveal that the electronic structure and localized charge density at the heterointerface of $\text{NiP}_2\text{-FeP}_2$ heterostructure can be significantly modulated upon coupling with metallic Cu, resulting in optimized proton adsorption energy and reduced barrier for water dissociation, synergistically boosting alkaline HER. Motivated by theoretical predictions, we developed a facile strategy to fabricate interface-rich $\text{NiP}_2\text{-FeP}_2$ coupled with Cu nanowires (Cu_{NW}) grown on Cu foam ($\text{NiP}_2\text{-FeP}_2/\text{Cu}_{\text{NW}}/\text{Cu}_f$). Benefiting from the superior intrinsic activity, conductivity, and copious active sites, the obtained catalyst exhibited exceptional alkaline HER activity requiring a low overpotential of 23.6 mV at -10 mA/cm^2 , surpassing the state-of-the-art Pt. Additionally, a full electrolyzer required a cell voltage of 1.42/1.4 V at 10 mA/cm^2 in alkaline water/seawater with promising stability. This work highlights the importance of optimizing HER kinetics and offers a novel strategy for designing advanced electrocatalysts for various catalytic reactions (CO_2RR , ORR, OER, NRR, and so on).

11:45 AM EN14.01.05

Stabilizing OOH^* Intermediate via Pre-Adsorbed Surface Oxygen of Single Ru Atom-Bimetallic Alloy for Ultralow Overpotential Oxygen Generation Jinsun Lee, Ashwani Kumar and Hyoyoung Lee; Sungkyunkwan University, Korea (the Republic of)

Designing an efficient oxygen evolution reaction (OER) electrocatalysts based on single-atom catalysts is a highly promising option for cost-effective alkaline water electrolyzers. The main bottleneck in the practical water electrolysis system is the sluggish oxygen evolution reaction (OER) due to multiple proton/electron-coupled steps. Current technologies involve noble metal (Ir, Ru) or earth-abundant hydroxides/oxides as anodes; however, the scarcity and semiconducting nature, respectively, of these materials limit their activity. Unfortunately, earth-abundant metallic alloys have not been employed for OER. Recent work showed that single-atom catalysts (SACs) possess peculiar electronic features and near-unity atom economy, yet poor intrinsic activity and stability hinder their practical applications.

Overall, the instability of the OOH^* intermediate and the high energy barrier for the rate-determining step (RDS) (O^* to OOH^*) on pure bimetallic alloy surfaces represent serious challenges and must be overcome for replacing Ir/Ru as anode materials based on an atomic level of understanding.

In this work, we introduce a simple approach to stabilize OOH^* intermediates on a surface oxygen-rich CoFe_2/G alloy with homogeneously anchored Ru single atom (0.1 at. % of Ru) sites to boost the intrinsic activity via a facile micelle incorporated sol-gel and carbothermal reduction method. State-of-the-art characterizations including XANES, EXAFS, AC-TEM, and XPS supported by theoretical calculations confirmed the anchoring of isolated Ru atoms into the surface oxygen-rich CoFe_2 alloy. Remarkably, the resulting $\text{Ru}_{\text{SA}}\text{CoFe}_2/\text{G}$ delivered excellent OER activity with an overpotential as low as 180 mV at a current density of 10 mA cm^{-2} and a reasonable Tafel slope of 51 mV dec^{-1} in a 1 M KOH aqueous solution. These results surpassed reported literature and state-of-the-art Ru-based electrocatalysts (RuO_2 and 5% Ru/C). Density functional theory (DFT) calculations revealed that the pre-adsorbed oxygens on $\text{Ru}_{\text{SA}}\text{CoFe}_2$ (110) efficiently stabilized the OOH^* intermediates and the isolated Ru sites further dramatically reduced the Gibbs free energy for the RDS (O^* to OOH^*), thereby accelerating the OER process in alkaline medium. To meet the industrial standards of alkaline water electrolysis, we constructed a $\text{Ni}_4\text{Mo}(-) // \text{Ru}_{\text{SA}}\text{CoFe}_2/\text{G}(+) // \text{alkaline electrolyzer}$ demanding a very low cell voltage of 1.48 V at a current density of 10 mA cm^{-2} , which was much lower than those values for a commercial Pt/C-RuO₂ couple (1.65 V at 10 mA cm^{-2}).

1:30 PM EN14.02.01

Composite and Structured Electrodes for High-Performance Water Photooxidation Maxime Dufond¹, Sandra Haschke², Chiara Cozzi³, Giuseppe Barillaro³, Gabriel Loget⁴, Julien Bachmann² and Lionel Santinacci¹; ¹CNRS - Aix-Marseille Univ., France; ²Friedrich-Alexander-Universität Erlangen-Nürnberg, Germany; ³Università di Pisa, Italy; ⁴CNRS - University of Rennes 1, France

Among numerous semiconductors that can be used for water photosplitting, Si is highly interesting because it absorbs light in the visible range and its electronic structure is suitable to drive water photooxidation [1]. However, Si corrodes strongly in KOH and it is highly reflective. The concept, presented, here, consists of successively depositing a protective layer and a catalyst onto the Si surface to extend the lifetime and the efficiency of the photoelectrode. To further improve the performances, various surface structuring methods are used to enhance the light absorption, enlarge the active area, and improve the charge collection. Various electrochemical structuring methods have been used to fabricate three different surface geometries: macropores (SiMP) [2], nanospikes (SiNS) [3], and micropillars (SiPillars) [4]. Those different morphologies show a large active area and a low reflectivity. Atomic Layer Deposition (ALD) is a well-adapted method to coat such tortuous surfaces. Thus, it has been applied to grow thin protective oxide layers (TiO₂ or Fe₂O₃) onto Si and SiMP, SiNS and SiPillars. To enhance the photocurrent and to lower the overvoltage corresponding to water photooxidation, metallic Ni has been deposited onto TiO₂-covered Si through a two-step process: (i) conformal ALD of NiO from Ni(CpEt)₂ and O₃ and (ii) the reduction to Ni by annealing under H₂ atmosphere. Ultra-low loads of IrO₂ have been deposited on Fe₂O₃-covered Si and ultra-thin TiO₂ capping allows for stabilizing the catalyst in an alkaline medium.

A detailed electrochemical study has been performed to assess the stability of the composite electrodes and to measure the water photooxidation performances. The TiO₂ dissolution at open circuit potential under a low illumination mechanism is identified. It proceeds through the insertion of H into the TiO₂ [5].

The efficiency of such multilayered and structured photoelectrodes is drastically improved using significantly fewer catalysts and the photoanodes exhibit long-term stability. The SiNSs covered by Fe₂O₃ and IrO₂ show, indeed, a photocurrent improved by a factor. It demonstrates that the appropriate combination of materials on the surface exhibiting the optimized geometry leads to high-performance photoanodes.

- [1] K. Sun, S. Shen, Y. Liang, P. E. Burrows, S. S. Mao, D. Wang, *Chem. Rev.* *114*, 8662 (2014).
[2] L. Santinacci, M. W. Diouf, M. K. S. Barr, B. Fabre, L. Joanny, F. Gouttefangeas, G. Loget, *ACS Appl. Mater. Interfaces*, *8*, 24810 (2016).
[3] G. Loget, A. Vacher, B. Fabre, F. Gouttefangeas, L. Joanny, V. Dorcet, *Mater. Chem. Frontiers*, *1*, 1881 (2017).
[4] F. J. Harding, S. Surdo, B. Delalat, C. Cozzi, R. Elnathan, S. Gronthos, N. H. Voelcker, G. Barillaro, *ACS Appl. Mater. Interfaces*, *8*, 29197 (2016)
[5] M. E. Dufond, J.-N. Chazalviel, L. Santinacci, *J. Electrochem. Soc.* *168*, 031509 (2021)

1:45 PM EN14.02.03

Enhanced Photoelectrochemical Water Splitting via Engineered Surface Defects of BiPO₄ Nanorod Photoanodes Nageh K. Allam; American University in Cairo, Egypt

Herein, we report on the defect engineering of BiPO₄ nanorods (NRs) via a facile room-temperature template-free co-precipitation method, followed by hydrogen treatment. The hydrogen treatment temperature determined the type of induced defects in the fabricated BiPO₄ NRs and consequently their photocatalytic performance. Upon varying the annealing temperature, the x-ray diffraction (XRD) analysis showed phase transformation and x-ray photoelectron spectroscopy (XPS) analysis revealed variation in the oxygen vacancy content. At moderate treatment temperatures (200-300°C), shallow defects were predominant, which extended the optical activity of the material to the visible region and increased the photocurrent 3 times when compared to that of bare BiPO₄ NRs. However, treatment at higher temperatures completely altered the crystalline structure, destructed the morphology of the BiPO₄ NRs, and severely affected the photoelectrochemical performance.

2:00 PM EN14.02.05

Optimization of Functionally Graded Titanium Oxides Through Soft Chemistry Larissa S. Chaperman, Fayna Mammeri and Souad Ammar; Université de Paris, France

Within the current context of energy crisis and climate changes, the search for versatile, clean and sustainable energy sources is vital to reduce our dependency on fossil fuels. As such, photoelectrochemical (PEC) water-splitting arises as an ideal route for the obtention of hydrogen: by using sunlight as power input, it is possible to obtain a high-energy, carbon-free fuel.

In this work, we propose the elaboration of functionally graded photoanodes based on titanium oxides through a simple and fast soft chemistry route. The resulting photoanode presents an external mixed-phase TiO₂ layer that transitions to titanium suboxides (including Magnéli phases) allowing prompt charge separation and transport of the photogenerated electrons towards the metallic Ti support for current collection.

Two main factors enable the superior performance of the photoanode: an increased light absorption (due to the synergy between anatase and rutile domains in intimate contact at the outmost layer, and to Ti³⁺ species present at the oxygen deficient subjacent layers) and a more effective charge separation and transport (facilitated by the alignment of the bandgaps within the specific regions and by the increased conductivity of the titanium suboxides). [1, 2] Such unique features are achieved by using chelating agents to direct the formation of the different TiO₂ phases, and subsequently enable the pore generation and localized reduction of TiO₂ during the calcination step. We explored variety of experimental conditions in order to optimize our process and to determine the influence of each parameter on the resulting material.

The obtained photocurrent densities (ranging from 0.25 to 0.80 mA cm⁻² at 0 and 1.2V vs. Ag/AgCl respectively, in 0.5 mol L⁻¹ Na₂SO₄) are comparable or superior to doped, sensitized and/or nanostructured anatase photoanodes [3, 4], while not requiring the use of toxic components and while undergoing a much simpler, cheaper and environmentally benign productive process. As such, we envision a great potential for the development and up-scaling of adaptable, cheap and robust devices for hydrogen generation through water-splitting.

- [1] G. Li, L. Chen, M. E. Graham, and K. A. Gray, *Journal of Molecular Catalysis A: Chemical*, vol. 275, no. 1–2, 2007.
[2] S. Jayashree and M. Ashokkumar, *Catalysts*, vol. 8, no. 12, p. 601, 2018.
[3] H. Eidsvåg, S. Bentouba, P. Vajeeston, S. Yohi, and D. Velauthapillai, *Molecules*, vol. 26, no. 6, 2021.
[4] K. Arifin, R. M. Yunus, L. J. Minggu, and M. B. Kassim, *International Journal of Hydrogen Energy*, vol. 46, no. 7, 2021.

2:15 PM EN14.02.06

Non-Noble Metal MoS₂-CNO Heterostructure for Highly Efficient Electrocatalytic Hydrogen Evolution Reactions Jae-Jin Shim, Muhammed Shafi

Parasseeri and Mostafa Saad Sayed Mohamed; Yeungnam University, Korea (the Republic of)

Electrochemical water splitting is one of the most efficient techniques to produce hydrogen, which provides clean and sustainable energy. Developing an efficient catalyst for hydrogen evolution reaction (HER) based on 2D molybdenum disulfide is a challenge because of restacking of MoS₂ layers that leads to insufficient access to active sites. In this study, the drawbacks of 1T MoS₂ catalyst were overcome by employing carbon nano-onion (CNO). The unique CNO-MoS₂ heterostructure formed by growing few-layered 2D 1T MoS₂ on the CNO core facilitated smooth and barrier-free charge-transfer through the heterojunction formation. This heterostructure not only mitigates restacking but also maintains the structural stability, providing a long-term high performance catalyst. This CNO-MoS₂ exhibited an excellent HER performance with an overpotential of 53 mV vs. RHE and Tafel slope of 40.8 mV dec⁻¹ for over 25 h, showing it one of the best HER catalysts next to platinum. This study highlights a new highly stable highly performing non-noble metal catalyst for electrochemical water splitting applications.

2:30 PM EN14.02.07

Surface Engineering to Improve Hydrogen-Evolving Electrode Performance Jack R. Lake¹, Alvaro Moreno Soto^{1,2} and Kripa K. Varanasi¹; ¹Massachusetts Institute of Technology, United States; ²Universidad Carlos III de Madrid, Spain

Gas evolution at electrochemical electrodes is important for many industrial applications. Perhaps the largest activities where electrochemical bubble generation is critical are the chlor-alkali (chlorine gas production) and Hall-Héroult (electrochemical aluminum smelting) processes. Significant effort goes towards mitigating the “anode effect” of the Hall-Héroult process, where carbon dioxide gas inactivates the carbon anode, causing catastrophic increases in overpotential. Similar inefficiencies and problems are caused during water electrolysis when bubbles adhere to or flood electrodes. The limiting effects of bubbles no doubt limits the adoption of traditional, low-temperature electrochemical methods for hydrogen generation from renewable electricity, leaving natural gas reforming as the dominant form of hydrogen production in the US currently. In this way, both understanding and mitigating the negative impacts that bubbles have on electrode performance offers a unique path to enable low-temperature alkaline water electrolyzers to become a commercially viable route of hydrogen production from renewable electricity.

A key disadvantage for alkaline electrolyzers is that while their porous electrodes can increase the active area of the catalyst, the nature of the catalyst material, like nickel-foams, causes the evolved bubbles to stick, inactivating the catalyst surface and causing significant ohmic and activation losses. The extent to which these bubbles can restrict electrochemical performance is significant. For example, even for the well-established chlor-alkali process, the attachment of bubbles to electrode surfaces accounts for approximately 20% of the overpotential at industrially relevant current densities.

These problems motivate this work as we investigate the way that bubble inefficiencies manifest themselves for different types of electrode configurations for hydrogen-evolving electrodes. While previous research has characterized the impacts of electrochemical bubbles, approaches to mitigate bubbles are limited and typically focus on novel cell design, rather than the design of the electrode itself. Here, we will focus on how different architectures of the electrodes affect the performance of the electrode while systematically studying the differences that arise from a bubble perspective. In general, many approaches for improving the performance of non-gas evolving electrodes are currently used in gas-evolving systems as well. However, we will show that the inherent tradeoffs between traditional methods for improving electrode performance, and those that should be adopted for gas-evolving electrodes are distinct. As a result, we provide a novel framework for designing hydrogen-evolving electrochemical electrodes. Furthermore, implementations of the novel electrode motifs based on this new design perspective are also envisioned to improve the performance of water electrolyzer systems.

2:45 PM EN14.02.09

Dense Hydrogen Separative Membrane Fabricated by Atomic Layer Deposition Badie Clemence¹, Christophe Charmette², Martin Drobek², Anne Julbe², Jean-Manuel Decams³, Mikhael Bechelany² and Lionel Santinacci¹; ¹Aix-Marseille Université, France; ²Université de Montpellier, France; ³Annealsys, France

To provide affordable H₂ with high purity for energy applications, new strategies as H₂-selective membranes gained in interest. This technology presents interesting benefits as it is cost-effective and have a reasonable environmental impact. In addition, a large variety of materials is available, thus, the composition of the membrane can be adapted to the working temperature. This study focuses on the fabrication of dense membranes able to operate at the high temperatures required in industrial processes (400-800°C). The specificity of the present approach is to fabricate new nanocomposite devices that combine the stability of a ceramic matrix, titanium nitride, with the catalytic effect of palladium nanoparticles used as nanofillers. Both TiN films and Pd nanoparticles are deposited onto a hetero-porous alumina tubular membranes by Atomic Layer Deposition (ALD). The composite membrane is optimized to reach the highest H₂-selectivity and permeation (flow), by finely tuning the thickness and the chemical composition of the TiN/Pd coating. ALD is an original technique in this field, but it is well adapted because it allows for coating nanostructured substrates with an excellent control of the thickness and composition.

The fabrication of the membrane follows two steps. First, the TiN deposit must fill the alumina porosity. The coating forms a dense layer on the nanoporosity at the inner part and penetrates into the macroporosity of the outer part, covering the alumina grains. Afterwards, the Pd nanoparticles are deposited. The selectivity and the permeation of the TiN-Pd membrane are assessed using H₂ and N₂. The increase of the temperature up to 400°C allows for achieving an encouraging dihydrogen ideal selectivity and permeance of 35 and 258 GPU (Gas Per Unit), respectively. Moreover, these values increase during the measurement: the selectivity and the permeance rises up to 109 and 7018 GPU, respectively, after 4.5 h at 400°C. These performances are promising as a similar pure Pd membrane presents an ideal selectivity of 23 and a permeance of 991 GPU at 188°C [1]. The investigation of the thermal evolution and the stability of the present membrane is then required. Complementary results will therefore be presented. In another hand, a Pd-based membranes issue is their poisoning in presence of CO and sulfides gases that are present in industrial processes. The ALD of both TiN and Pd can be optimized to encapsulate the Pd nanoparticles within the TiN matrix. This could be a future route to take up the poisoning obstacle and to improve the performances.

[1] Weber et al., Hydrogen selective palladium-alumina composite membranes prepared by Atomic Layer Deposition, *J. Membr. Sci.* **2020**, 596, 117701.

EN14.03.03

Nucleation and Growth of Electrodeposited Cu₂O on FTO Substrates Akhilender J. Singh, Garima Aggarwal, Balasubramaniam Kavaipatti and [Sushobhita Chawla](#); Indian Institute of Technology, Bombay, India

Nucleation and growth mechanism studies of functional oxide films are essential to gain an understanding and thereby control their morphologies. Towards this, we study the effect of solution pH and deposition potential on the nucleation and growth (NG) of the technologically important material Cu₂O as a thin film on the FTO substrates. The Cu₂O films electrodeposited at a low potential value of -20 mV (vs. Hg/HgO) at pH 9 exhibit a slow layer-by-layer NG mode where the 2-D instantaneous nucleation (IN-2D) is identified as the primary contributor. The NG mechanism, however, switches to 3-D diffusion-controlled instantaneous and progressive (IN-3D_{diff} & PN-3D_{diff}) mode at the moderate potential value of -100 mV. Further raising the potential to -180 mV results in a complex process involving multiple contributions from IN-3D_{diff} & PN-3D_{diff} which would result in an island type morphology. In contrast, the films deposited at pH 12 show a minimal contribution from the 2-D type NG mechanism even at low potential values. At a low potential of -170 mV, the major contribution comes from the diffusion-controlled 3-D type progressive (PN-3D_{diff}) NG process. An additional contribution; the charge transfer controlled instantaneous (PN-3D_{ct}) NG process runs in parallel with previous processes when films are subjected to a moderate potential of -210 mV. At high potentials, however, the situation becomes similar to pH 9 having multiple contributions from both charge transfer and diffusion controlled IN and PN processes. The modeling of experimental data reveals that electrodeposition in a low pH, as well as low potential, is preferable to obtain a layer-by-layer deposition of Cu₂O thin films whereas a 3-D island type NG occurs at high potentials. These results pave the pathway to tailor the morphology of other technologically important metal oxides in a similar fashion.

EN14.03.04

Multiple Synergistic Effects of Zr-Alloying on the Phase Stability and Photostability of Black Niobium Oxide Nanotubes as Efficient Photoelectrodes for Solar Hydrogen Production [Nageh K. Allam](#); American University in Cairo, Egypt

Niobium oxides exist in a plethora of metastable, stoichiometric, nonstoichiometric, and mixed phases, rendering the Nb-O systems very complicated and hard to study. These structures significantly differ in their catalytic activity, electrical conductivity, and photoresponse. Herein, we demonstrate the ability to selectively fabricate pure T-Nb₂O₅ *via* the addition of small amount of Zr as a phase stabilizer. Moreover, we were able to tune the photoactivity of the material *via* hydrogen annealing. The photoactivity and stability of the fabricated black Zr-doped Nb₂O₅ nanotubes were correlated with the nature of induced defects upon hydrogen annealing and Zr doping. The H₂-treated nanotubes showed extraordinary and remarkable stability and photoactivity upon their use for solar water splitting. This was accompanied by a noticeable reduction in the bandgap energy from 3.23 eV to 2.5 eV, which is mainly correlated with the introduced oxygen vacancies within the lattice with a remarkable conductivity. Most importantly, the black-defective nanotubes exhibited a photocatalytic activity that is ~ 65 times that of the air-annealed counterparts. The optimized photoanodes attained a hydrogen production rate of ~ 496 μmol h⁻¹ cm⁻² in 1 M KOH, revealing increased charge carriers transport and separation. The Mott-Schottky and valence band XPS analyses confirmed the increased charge carriers' concentration and the appropriate band positions of the fabricated black nanotubes relative to the redox potentials of the water.

EN14.03.05

Structural Engineering of Ti-Mn Bimetallic Phosphide Nanotubes for Efficient Photoelectrochemical Water Splitting [Nageh K. Allam](#); American University in Cairo, Egypt

Designing next-generation advanced electrode materials by engineering their structural and compositional features can provide a feasible strategy to enhance the electrochemical performance of energy conversion devices. In this study, the rational pathway to design and fabricate nanotube arrays of titanium manganese phosphide *via* etching of titanium-manganese alloy followed by plasma phosphidation in PH₃ environment is presented and discussed. The structural and elemental analyses of the air-annealed electrodes before plasma treatment confirmed the presence of different binary oxides; TiO₂, MnO, and Mn₂O₃. However, the XPS fitting showed the presence of Ti³⁺ and higher ratio of MnO when annealed in hydrogen atmosphere. The presence of composite oxides resulted in a band gap reduction, which increased the light harvesting capability of the material. This synergetic effect resulted also in a shift in the open-circuit voltage (V_{OC}) and almost 10-fold increase in the photocurrent density compared to the performance of the nanotubes annealed in air. Mott-Schottky analysis showed a four-orders of magnitude enhancement in the carrier density for the electrodes annealed in Hydrogen and treated in PH₃-plasma compared to those annealed in O₂ or air, ascribed to the creation of Ti³⁺ defects and phosphidation. Our study thus paves the way to a new approach for creating high-performance hybrid electrodes for PEC water splitting.

EN14.03.06

Novel Bi-Based Photocatalysts with Unprecedented Visible Light-Driven Hydrogen Production Rate—Experimental and DFT Insights [Nageh K. Allam](#); American University in Cairo, Egypt

Green and efficient energy technologies are a key point where nanoscience could make a difference in the paradigm shift from fossil fuels to renewable sources. One attractive possibility is the utilization of solar energy to obtain electricity or chemical fuel based on the ability of semiconductor nanomaterials to function as photocatalysts promoting various oxidation and reduction reactions under sunlight. We report on a novel class of Bi-based photocatalysts for hydrogen production *via* water splitting. A screening DFT investigation was performed on the Bi₂(MO₄)₃ (M = Cr, Mo, and W) systems. The Bi₂(CrO₄)₃ system exhibits the smallest band gap energy, the highest dielectric constant, and the highest absorption in visible region among the other counterpart materials. Consequently, Bi₂(CrO₄)₃ nanoparticles were synthesized *via* a simple one-pot method at room temperature and characterized by XRD, XPS, DRS, FE-SEM, HR-TEM, and Raman spectroscopy. The as-prepared yellow Bi₂(CrO₄)₃ nanoparticles exhibited a direct band gap energy of 2.45 eV. The photoactivity of the as-prepared Bi₂(CrO₄)₃ nanoparticles was tested toward the photocatalytic hydrogen production, where reasonable rates of 522.44, 174.15, and 88.24 μmol/g/h were achieved under UV, AM 1.5, and visible irradiations, respectively in the absence of any hole scavengers. Those rates are higher than those reported for Bi-based photocatalysts.

EN14.03.07

10-Fold Enhancement in Light-Driven Water Splitting Using Niobium Oxynitride Microcone Array Films [Nageh K. Allam](#); American University in Cairo, Egypt

We demonstrate, for the first time, the synthesis of highly ordered niobium oxynitride microcones as an attractive class of materials for visible-light-driven water splitting. As revealed by the ultraviolet photoelectron spectroscopy (UPS), photoelectrochemical and transient photocurrent measurements, the microcones showed enhanced performance (~1000% compared to mesoporous niobium oxide) as photoanodes for water splitting with remarkable stability and visible light activity.

EN14.03.08

Computational Fluid Dynamic Modeling of Methane-Hydrogen Mixture Transportation in Pipelines [Kun Tan](#), Devinder Mahajan and T. A.

Replacing fossil fuels and natural gas with alternative fuels like hydrogen is an important step towards the goal of reaching a carbon neutral economy. As an important intermediate step towards utilizing pure hydrogen, blending hydrogen in an existing natural gas network is a practical choice for reducing carbon emissions in the near future. A computational fluid dynamic (CFD) model is developed to quantify frictional losses and energy efficiency of transport of methane/hydrogen blends across straight pipe sections. The CFD model developed in the present study is first validated by verifying that the results obtained in the present study (for pressure drops, numerical friction number (f_N), and energy specific toll (EST) agree well with those obtained in an earlier study when identical boundary conditions and model parameters such as Redlich-Kwong equation of state, $k-\epsilon$ turbulence model and pipe wall roughness, are invoked. Furthermore, additional CFD models are developed to assess the effects of other factors such as 1) hydrogen concentration, 2) pipe surface roughness of common pipe materials, and 3) pipe diameter on the dynamics of blended gas flows. The principal conclusions from the present study are as follows: (i) High hydrogen concentration in the gas blends (i.e., greater than 25% and 50%) require higher energy for transporting the blended gases in the pipelines. (ii) Polyethylene (PE) or PE coated pipes, with smoother walls, are 33-40% more energy efficient in transporting gas blends than uncoated stainless steel pipes, which are 17-31% more energy efficient than the uncoated cast iron pipes. (iii) Due to relatively fewer gas interactions with wall surfaces which result in frictional losses, than in the case of smaller diameter pipes, it requires lesser energy to transport blended gases in larger diameter pipes. The CFD model and the simulation results provide valuable operational guidelines for transitioning natural gas networks to transport greener blends of methane and hydrogen.

EN14.03.09

Enhancing Photovoltage of Metal-Insulator-Semiconductor (MIS) Photoanode by Coordination Polymer via Chemical Deposition Ponart Aroonratsameruang¹, Gabriel Loget² and Pichaya Pattanasattayavong¹; ¹Vidyasirimedhi Institute of Science and Technology, Thailand; ²Université de Rennes 1, CNRS, France

One of the remaining challenges for the development of efficient photoelectrochemical water splitting systems is related to the photoanode, which requires a high-performance light absorber with an excellent catalyst to drive oxygen evolution reaction that needs high potential [1]. The metal-insulator-semiconductor (MIS) architecture employing Si as the photoanode is an attractive system due to the wide light absorption range of Si (E_g 1.1 eV) and high OER catalytic activity of metal [2]. For the latter, metal nanoparticles can be dispersed on the semiconductor surface via electrodeposition in Si MIS photoanodes [3]. Furthermore, surrounding the metal nanoparticles and the uncoated Si with a higher-work-function material leads to significant improvement of photovoltage due to the pinch-off effect [3]. Up to this point, the surrounding layer is generally the oxidized phase of the base metal, such as its oxide or oxyhydroxide, and the fabrication techniques used to introduce the surrounding layer are limited to a few choices, i.e., electrodeposition, photodeposition, or annealing methods [4]. Copper(I) thiocyanate (CuSCN) is a coordination polymer which can be prepared by a simple chemical deposition through conversion of Cu [5]. Because Cu and CuSCN have work functions of 4.5-4.9 [6] and 5.4 eV [7], respectively, the Cu/CuSCN junction on n-Si is expected to develop the pinch-off region and increase the performance. In this talk, we aim to highlight two key developments of Cu-based MIS Si photoanodes prepared by facile methods. Firstly, we employed electrodeposition to coat 30-nm Cu nanoparticles on n-Si, resulting in a photoanode with a low OER onset potential of 1.37 V vs reversible hydrogen electrode (RHE). Secondly, we added CuSCN on the n-Si/SiO₂/Cu photoanode via a chemical deposition in an aqueous bath containing ammonium thiocyanate. The presence of CuSCN on n-Si/SiO₂/Cu was confirmed by X-ray photoelectron spectroscopy and scanning electron microscopy. The optimal n-Si/SiO₂/Cu/CuSCN with a short CuSCN deposition time showed a 100-mV improvement in the onset potential relative to the unmodified n-Si/SiO₂/Cu. Based on open-circuit-potential measurements, the CuSCN-modified photoanode exhibited a high photovoltage of 460 mV. We believe that the findings can provide a new strategy for further surface modification of PEC devices to achieve low-cost solar harvesting technology.

[1] Walter, M. G.; Warren, E. L.; McKone, J. R.; Boettcher, S. W.; Mi, Q.; Santori, E. A.; Lewis, N. S. Solar Water Splitting Cells. *Chem. Rev.* **2010**, *110* (11), 6446–6473.

[2] Aroonratsameruang, P.; Pattanasattayavong, P.; Dorcet, V.; Mériade, C.; Ababou-Girard, S.; Fryars, S.; Loget, G. Structure–Property Relationships in Redox-Derivatized Metal–Insulator–Semiconductor (MIS) Photoanodes. *J. Phys. Chem. C* **2020**, *124* (47), 25907–25916.

[3] Laskowski, F. A. L.; Oener, S. Z.; Nellist, M. R.; Gordon, A. M.; Bain, D. C.; Fehrs, J. L.; Boettcher, S. W. Nanoscale Semiconductor/Catalyst Interfaces in Photoelectrochemistry. *Nat. Mater.* **2020**, *19* (1), 69–76.

[4] Lee, S. A.; Choi, S.; Kim, C.; Yang, J. W.; Kim, S. Y.; Jang, H. W. Si-Based Water Oxidation Photoanodes Conjugated with Earth-Abundant Transition Metal-Based Catalysts. *ACS Mater. Lett.* **2020**, *2* (1), 107–126.

[5] Xu, J.; Xue, D. Fabrication of Upended Taper-Shaped Cuprous Thiocyanate Arrays on a Copper Surface at Room Temperature. *J. Phys. Chem. B* **2006**, *110* (23), 11232–11236.

[6] Gartland, P. O.; Berge, S.; Slagsvold, B. J. Photoelectric Work Function of a Copper Single Crystal for the (100), (110), (111), and (112) Faces. *Phys. Rev. Lett.* **1972**, *28* (12), 738–739.

[7] Worakajit, P.; Hamada, F.; Sahu, D.; Kidkhunthod, P.; Sudyoadsuk, T.; Promarak, V.; Harding, D. J.; Packwood, D. M.; Saeki, A.; Pattanasattayavong, P. Elucidating the Coordination of Diethyl Sulfide Molecules in Copper(I) Thiocyanate (CuSCN) Thin Films and Improving Hole Transport by Antisolvent Treatment. *Adv. Funct. Mater.* **2020**, *30* (36), 2002355.

EN14.03.10

HR-TEM Study of U Hydrides Mayerling Martinez^{1,2}, Miroslav Cieslar², Peter Minarik², Oleksandra Koloskova², Evgeniya Tereshina-Chitrova², Milan Dopita², Lukas Horak², Thomas Gouder³ and Ladislav Havela²; ¹CRISMAT/Normandie University/CNRS, France; ²Charles University, Czechia; ³European Commission Joint Research Centre, Germany

U as interesting hydrogen storage medium forms with hydrogen the hydride UH₃, which has two allotropic cubic phases, known as α - and β -UH₃. While the transient phase α -UH₃ (*bcc* lattice of U filled with H) can be stabilized by alloying of Zr, other alloyed hydrides appear as nanocrystalline β -UH₃ phase (more complicated cubic with two different U positions), the grain size of which can be as small as 2-3 nm. Conventional XRD analysis, based on several very wide diffraction peaks, does not give in such case sufficient information e.g. about possible segregation of alloying elements. That is why methods like total scattering with PDF analysis have been applied [1].

Another method applied is Transmission Electron Microscopy, which allows structural characterization at the atomic level. The TEM study became even more important in the thin film research, in which it proved feasible to synthesize the hydride films by reactive sputter deposition of metals in H₂ containing Ar working gas [2,3]. Such synthesis requires typically low temperatures, which allow H to be embedded into the deposited material. Also this synthesis yields very small grain size, which is often accompanied by a pronounced texture. The information from glancing angle XRD is also in such situation limited.

Here we present results of High-Resolution TEM study both on the bulk alloyed UH₃ and on various U-H films. While crushed fine powder can be used as TEM sample in the former case, the films require the focused ion beam lift-out technique, which allows to obtain cross-sectional thin lamellae giving information on film thickness, individual interfaces to the substrate or possible capping layer, as well as on U phases in the main layer. In particular, despite of nanometer grain size it allows to distinguish well the β -UH₃ type phase from the UH₂ phase, which does not exist as a bulk phase but can be prepared in

the thin film form [4]. The study helped to exclude any possible segregation of Mo as alloying element and proved that spurious UO_2 remains on a very low level. The analysis is based on structural analyses using STEM and HR-TEM with subsequent Fourier analysis. The TEM micrographs were compared with simulated images using the JEMS software.

The work was supported by the Czech Science Foundation under the grant No. 21-09766S.

[1] L. Havela et al., MRS Advances 1 (2016) 2987.

[2] L. Havela et al., Journal of Electron Spectroscopy and Related Phenomena 239 (2020) 146904.

[3] E. Tereshina-Chitrova et al., Materials Chemistry and Physics 260 (2021) 124069.

[4] L. Havela et al., Inorg. Chem. 57 (2018) 14727.

EN14.03.11

Experimental Investigation of Surface Resistivity of Yttrium Stabilized Zirconium as a Thin Film Matthew Melfi, Vincent De Castro and Mehmet A. Sahiner; Seton Hall Univ, United States

Solid Oxide Fuel Cells are devices that use electrochemical reactions to convert chemical energy from fuel to electricity. Solid Oxide Fuel Cells typically have three different layers, an anode, electrolyte, a cathode layer. In comparison with coal power plants, a Solid Oxide Fuel Cell, produces a higher electrical conversion efficiency. In the last couple of years, the electrical efficiency has increased from 40 to 60%. Solid Oxide Fuel Cells are modular in nature making the power output even greater. When combined with another form of energy the efficiency increases even more. However, Solid Oxide Fuel Cells typically operate at high temperatures (800-1000 degrees Celsius) which hinders the usability. At this high operating temperature, the materials that can be used are also limited. When lowering the operating temperature, the ohmic resistance increases. There are two ways to prevent this increase is to either to change the material used for the electrolyte layer or to make the electrolyte layer into a thin film. Typical Solid Oxide Fuel Cells use Yttrium Stabilized Zirconium as the electrolyte layer. In this research, the electrolyte layer will be a thin film of various concentrations, 1-10%, of the Yttrium Stabilized Zirconium. This layer is produced from a fine dimple grain structure allowing high flow of oxygen mobility. This mobility increases ionic conductivity and decreases the ohmic resistance. The goal of this research is to optimize the experimental film deposition parameters that will lead to minimum surface resistivity. These thin films are produced by the Pulsed Laser Deposition method. This method of production has shown to produce a specific thin film thickness with repetition. With this method there are numerous parameters that can be adjusted. The pressure, frequency, laser energy, etc. The Yttrium Stabilized Zirconium is deposited onto Polished Zirconium, Sapphire, and Silicon. The differences of substrates were used to compare the different characteristics of Yttrium Stabilized Zirconium layer on different materials. An ellipsometer will be used to ensure the thickness of the Yttrium Stabilized Zirconium layer. These thin films will be characterized through electrical measurements such as 4-point probe resistivity measurements as well as Scanning Electron Microscopy, for the structural characterization.

EN14.03.12

BaZr_{0.80}Y_{0.20}O_{3-d} - SrCe_{0.95}Yb_{0.05}O_{3-d} Heterostructures for Proton Conducting Membranes Taner Ozdal, Gaye Ozdemir, Gulhan Cakmak, Berke Piskin and Fatih Piskin; Mugla Sıtkı Kocman University, Turkey

Separation membranes allow purification of hydrogen from gas mixtures produced by various methods, such as the reformation of natural gas, coal gasification, or the gasification of municipal waste. Hydrogen separated in this way may be used in fuel cells to generate electricity or may be fed directly to the natural gas grid to temporarily storage. It is likely that the current network of natural gas will soon be transformed into a "gas" grid where hydrogen would be an essential ingredient. All these require the use of efficient separation membranes, which would make the easy availability of hydrogen possible as is currently the case for natural gas. Thus, the separation membranes would have a much wider scope than normally anticipated and therefore there would be a need for separation membranes that are more efficient and in particular of low cost.

The current study concentrates on proton conducting oxides that can operate at temperatures higher than 450 °C and applicable to the steam reformation of natural gas including the water-gas shift reactions. Proton conducting oxides used for this purpose are quite attractive due to their high hydrogen selectivity and superior tolerance to possible toxic gases (e.g. CO, H₂S, etc.) that may be present in the gas mixtures.

The current study adopts a membrane design methodology based on combinatorial material science. This approach makes use of a magnetron sputtering system whereby a material library of thin-film membranes is produced in a single experiment. The library is then screened by four-probe resistivity and electrochemical impedance measurements so as to identify the compositions that are highly reactive with hydrogen. A map of reactive index prepared in this way is used to determine candidates for hydrogen separation. The membranes are then fabricated in the form of discs and tested for hydrogen permeability. In the current study, BaZr_{0.80}Y_{0.20}O₃-SrCe_{0.95}Yb_{0.05}O₃ heterostructures are investigated using the above methodology.

This work was supported by TUBITAK (The Scientific and Technological Research Council of Turkey) with project Number 119M065, which the authors gratefully acknowledge.

EN14.03.14

Bimetallic Nitrides on 3D Porous Nickel Foam as a Bifunctional Binder Free Electrode for Electrochemical Water Splitting Yamini Kumaran, Haralabos Efstathiadis and Iulian Gherasoiu; State University of New York Polytechnic Institute, United States

The rising need for renewable energy storage and conversion serves as the cause to explore suitable approaches to produce hydrogen. Among the different methods, electrochemical water splitting can produce hydrogen at low cost and high efficiency with non-noble metal catalysts, that can be used to accelerate the reaction. Until now, Pt/C and IrO₂ are found to be the best-known catalyst with very low overpotentials for hydrogen and oxygen evolution reaction, respectively. Yet, these are very costly and impractical for large scale industrial use. Hence, design and fabrication of low cost and highly efficient electrode is of utmost importance to produce hydrogen and oxygen with low overpotential thereby increasing the efficiency of overall water splitting. Transition metal oxides, nitrides and sulfides have been widely explored as catalysts for both HER and OER. Transition metal nitrides are found to have good electronic conductivity and superior corrosion resistance. In particular, Mo₂N exhibits high electrochemical stability and good activity towards HER in which the presence of nitrogen in the metal lattice increases proton adsorption. From the volcano plot which shows the activity of HER as a function of M-H bond strength it can be inferred that a nitride material combining Nickel which binds H weakly, along with molybdenum which binds H strongly, will have an activity as that of Pt. Further, VN has been reported to have good performance towards oxygen evolution reaction owing to its high density of states and good chemical stability. In this work, we introduce and study bimetallic nitrides (MoVN) on 3D porous Nickel foam for catalyzing water splitting reactions. Compared to electrodes with planar surfaces, the Nickel foam offers the advantage of a much larger reactive surface per unit of volume and weight, having the potential to increase the generation rate of H₂ and O₂ of the electrolysis cell. Further, the structural characterizations such as XRD, SEM is performed for the mirror samples. The performance of the electrode is tested in N₂/O₂ saturated 1M KOH solution. Hence, we report the synthesis of novel MoVN on Nickel foam using RF Magnetron co-sputtering as an efficient, bifunctional, binder free electrode for overall water splitting.

References

- [1] H. Sun, X. Xu, Y. Song, W. Zhou, and Z. Shao, "Designing High-Valence Metal Sites for Electrochemical Water Splitting," *Adv. Funct. Mater.*, vol. 31, no. 16, pp. 1–44, 2021, doi: 10.1002/adfm.202009779.
- [2] B. Cao, G. M. Veith, J. C. Neufeind, R. R. Adzic, and P. G. Khalifah, "Mixed close-packed cobalt molybdenum nitrides as non-noble metal electrocatalysts for the hydrogen evolution reaction," *J. Am. Chem. Soc.*, vol. 135, no. 51, pp. 19186–19192, 2013, doi: 10.1021/ja4081056.
- [3] W. F. Chen, J. T. Muckerman, and E. Fujita, "Recent developments in transition metal carbides and nitrides as hydrogen evolution electrocatalysts," *Chem. Commun.*, vol. 49, no. 79, pp. 8896–8909, 2013, doi: 10.1039/c3cc44076a.
- [4] R. Adalati, A. Kumar, Y. Kumar, and R. Chandra, "A High-Performing Asymmetric Supercapacitor of Molybdenum Nitride and Vanadium Nitride Thin Films as Binder-Free Electrode Grown through Reactive Sputtering," *Energy Technol.*, vol. 8, no. 10, 2020, doi: 10.1002/ente.202000466.
- [5] B. Wei *et al.*, "Bimetallic vanadium-molybdenum nitrides using magnetron co-sputtering as alkaline hydrogen evolution catalyst," *Electrochemistry Communications*, vol. 93, pp. 166–170, 2018, doi: 10.1016/j.elecom.2018.07.012.

EN14.03.15

The Effect of Strontium Doping on Hydrogen Production of $\text{La}_{1-x}\text{Sr}_x\text{Mn}_{0.6}\text{Al}_{0.4}\text{O}_3$ ($x=0.2, 0.4$ and 0.6) Perovskite Oxides via Thermochemical Water Splitting Seyfettin Berk Sanli, Ihsan E. Yigiter, Gulhan Cakmak, Fatih Piskin and Berke Piskin; Mugla Sitki Kocman University, Turkey

Hydrogen has a very important place for green-energy applications. In this context, thermochemical methods based on solar energy come to the fore in hydrogen production. It is possible to produce hydrogen without the need for purification via the two-step thermochemical water splitting (TWS) method. TWS uses metal oxides as redox materials allowing to produce of pure hydrogen at lower temperatures as compared to thermolysis. Therefore, the thermodynamics and kinetics of redox reactions are one of the important factors that determine hydrogen production efficiency and influenced by the structural properties of active materials used in these reactions. For this purpose, perovskite-oxides draw attention to be able to use in TWS reactions due to providing higher structural stability with allowing compositional diversity.

We focused on the structural properties in terms of morphology and surface area, investigating the compositional dependence of $\text{La}_{1-x}\text{Sr}_x\text{Mn}_{0.6}\text{Al}_{0.4}\text{O}_3$ ($x=0.2, 0.4$ and 0.6) perovskite oxides to provide higher hydrogen production by TWS.

In this study, $\text{La}_{0.6}\text{Sr}_{0.4}\text{Mn}_{0.6}\text{Al}_{0.4}\text{O}_3$ (LSMA6464), $\text{La}_{0.5}\text{Sr}_{0.5}\text{Mn}_{0.6}\text{Al}_{0.4}\text{O}_3$ (LSMA5564), and $\text{La}_{0.4}\text{Sr}_{0.6}\text{Mn}_{0.6}\text{Fe}_{0.4}\text{O}_3$ (LSMA4664) were synthesized by Pechini method. As a precursor, $\text{La}(\text{NO}_3)_3 \cdot 6\text{H}_2\text{O}$, $\text{Sr}(\text{NO}_3)_2$, $\text{Mn}(\text{NO}_3)_2 \cdot 4\text{H}_2\text{O}$, and $\text{Al}(\text{NO}_3)_3 \cdot 9\text{H}_2\text{O}$ were used. After pre-calcination at 250 °C for 2 hrs, calcination was carried out at 1300 °C for 6 hrs to obtain desired crystal structure. The crystal structure of perovskite-oxide materials was analyzed by an X-Ray Diffractometer (XRD, Bruker D8 Advance) using Cu-K α radiation. It was determined that synthesized LSMA6464, LSMA5564, and LSMA4664 perovskite oxides have a cubic structure. The morphology of LSMA6464, LSMA5564, and LSMA4664 was observed by scanning electron microscopy (SEM) and average particle size, as ca. 0.1 μm . BET analysis results confirmed that the increased A-site dopant, Sr, ratio decreased the surface area as 35 m^2/g , 28 m^2/g and 25 m^2/g for LSMA6464, LSMA5564, and LSMA4664, respectively. Correlated with the structural effect of Sr, two-step water splitting results show that increases in the amount of Sr dopant, causes less hydrogen production for LSMA6464, LSMA5564, and LSMA4664 perovskite oxides as 257 $\mu\text{mol/g}$, 170 $\mu\text{mol/g}$ and 115 $\mu\text{mol/g}$, respectively.

ACKNOWLEDGMENTS: This work was supported by TÜBİTAK (The Scientific and Technological Research Council of Turkey) (Project Number 119M420), which the authors gratefully acknowledge.

SESSION EN14.04: Fuel Cells I
Session Chairs: Ming Dao and T. Venkatesh
Wednesday Morning, December 1, 2021
Hynes, Level 3, Room 300

10:30 AM EN14.04.01

Overcome the Dilemma between Low Loading and High Power Density for PEMFCs Using Ultrathin 1D PtCo Nanowire Catalyst Jin Huang¹, Bosi Peng^{1,1}, Qingying Jia², Xiangfeng Duan¹ and Yu Huang¹; ¹University of California, Los Angeles, United States; ²Northeastern University, United States

Platinum (Pt) group metals (PGMs) remain the best catalyst choice to speed up the sluggish oxygen reduction reactions (ORR) at the cathode of proton-exchange membrane fuel cells (PEMFCs). However, the requirement of a large amount of PGM catalysts has prevented the widespread adoption of PEMFCs. To address this challenge, it is central to achieve low PGM loading PEMFCs with high performance. However, using low PGM loading inevitably compromises the performance at the high current density region. To overcome this dilemma, we demonstrate an ultralow Pt loading and high-performance membrane electrode assembly (MEA) using ultrathin platinum-cobalt nanowires (PtCoNWs) as the cathode catalysts. The PtCoNWs showed an exceptional high electrochemically active surface area (ECSA) and exhibited a record-high mass activity (MA), far surpassing the Department of Energy (DOE) 2020 beginning of life (BOL) target (0.44 A/mg_{PGM}). In addition, PtCoNWs displayed an ultrahigh total Pt utilization, surpassing all state-of-the-art Pt-alloy catalyst performance in MEA. *In-situ* XAS studies suggest that the high atomic ordering core of the PtCoNWs contributes to the high ORR activity and stability of PtCoNWs in PEMFCs.

10:45 AM EN14.04.03

Nickel, Cobalt and Copper Electrodeposition on Vulcan XC-72R Via the Rotating Disk Slurry Electrodeposition (RoDSE) Technique for the Oxygen Evolution Reaction (OER) and Oxygen Reduction Reaction (ORR) in Alkaline Medium Joesene Soto-Perez¹, Carlos R. Cabrera-Martinez¹, Armando Pena-Duarte² and Pedro Trinidad¹; ¹University of Puerto Rico, Río Piedras, United States; ²University of Puerto Rico at Río Piedras, United States

Since the start of fuel cell research, electrocatalysts based on Pt have shown remarkable ORR performances. However, the high cost and low abundance of Pt limits their practical applications in the vehicle industry. The combination of Pt with first-row transition metals lowers the cost and enhances the electrocatalyst activity in the cathode compartment where the Oxygen reduction reaction (ORR) occurs. Additionally, when using an alkaline medium, the ORR is enhanced, metal oxides are more stable and non-noble metal could be used. In this study, we synthesized first-row transition metal catalysts (M= Ni, Co and Cu)—with the Rotating disk slurry electrodeposition (RoDSE) technique—supported on Vulcan XC-72R. We were able to electrodeposit Ni and Co on Vulcan XC-72R using an electrochemical potential of -0.75V vs. RHE and -0.80V vs. RHE to electrodeposit Cu on Vulcan XC-72R applying the RoDSE methodology in 0.1M KClO₄. These M/Vulcan XC-72R catalysts were modified with a Pt precursor via spontaneous galvanic displacement (SGD) and we obtained Pt-M/Vulcan XC-72R to catalyze the ORR in an alkaline medium. First, we tested the M/Vulcan XC-72R for the oxygen evolution

reaction (OER) and Ni/Vulcan XC-72R provided the lowest overpotential with 450 mV vs. RHE at 10 mA/cm²_{disk} in 0.1M KOH. We also performed oxygen polarization to characterize the electrochemical activity towards oxygen reduction in an alkaline medium. Our results indicated that under controlled temperature (25.0°C), a mass loading of 100 mg/cm² on a glassy carbon rotating electrode and at 1,600 rpm the electrocatalysts revealed good performance. The PtNi-Vulcan XC-72R, PtCo-Vulcan XC-72R and PtCu-Vulcan XC-72R catalysts obtained half-wave potentials ($E_{1/2}$) of 0.88 V, 0.88 V and 0.82 vs. RHE, respectively, under an oxygen atmosphere in 0.1M KOH, compared with commercial Pt/Vulcan XC-72R $E_{1/2} = 0.83$ V. The particle sizes of the catalysts were obtained using the X-ray diffraction (XRD) diffractograms of the nanoparticles and the Scherrer equation analysis, suggesting sizes between 2-10 nm. Upcoming studies will focus on evaluating the durability of the catalysts under electrochemical cycling and the electronic properties of the samples using X-ray Absorption Spectroscopy (XAS) techniques to determine their atomic states and coordination environments. This work was supported by the National Science Foundation NSFPREM: Center for Interfacial Electrochemistry of Energy Materials (CiE2M) grant number DMR-1827622.

11:00 AM EN14.04.04

Quantifying the Relationship Between Microstructure and Performance Improvements in Ni-infiltrated NiYSZ Anodes [Jillian Rix](#), Hector Grande, Uday Pal, Srikanth Gopalan and Soumendra Basu; Boston University, United States

Infiltrated nickel nanocatalysts have been shown to improve the performance of NiYSZ fuel cell anodes, especially at low temperatures, by decreasing feature size and increasing triple phase boundary (TPB) density. However, estimating infiltrated TPB density by microstructural characterization and relating deposited nanocatalyst morphology to performance improvements is difficult because of the complexity of the deposited nanoparticle and scaffold microstructure. In this study, performance improvements in Ni-infiltrated NiYSZ anode symmetric cells are quantified by electrochemical impedance spectroscopy (EIS) and distribution of relaxation times (DRT) analysis, and the microstructure characterized by focused ion beam/scanning electron microscopy (FIB/SEM) analysis and cross-sectional SEM. A relationship between infiltrated microstructure and performance improvements is discussed.

11:15 AM EN14.04.05

Laser-Fabricated Tantalum-Based Nanomaterials as Bifunctional Catalysts for Direct Peroxide-Peroxide Fuel Cells [Nathalie Herlin-Boime](#)¹, [Xiaoyong Mo](#)² and [Edmund Tse](#)²; ¹CEA Saclay, France; ²City University of Hong Kong, China

Efficient and durable electrocatalysts are instrumental to enabling next-generation fuel cell technologies. At present, costly precious metals are used as state-of-the-art catalysts. In this report, cost-effective tantalum-based alternatives are synthesized via a green and scalable laser pyrolysis method as bifunctional catalysts for direct peroxide-peroxide fuel cells. By varying the laser power, reactor parameters, and ammonia flow rate, five Ta/N/O nanomaterials are prepared containing Ta₂O₅, Ta₄N₅, Ta₃N₅, and TaN in tunable ratios. Electrochemical studies in neutral and alkaline conditions demonstrate that Ta₄N₅ is the active component for H₂O₂ oxidation and reduction. Kinetic isotope effect (KIE) studies show that protons are involved at or before the rate-determining step (RDS). Long-term stability studies indicate that Ta₃N₅ grants Ta/N/O nanomaterials their enhanced longevity during electrocatalytic operations. Taken together, Ta/N/O can act as active and robust electrocatalysts for H₂O₂ reduction and oxidation. Laser pyrolysis is envisioned to produce refractory metal nanomaterials with boosted corrosion resistance for energy catalysis.

SESSION EN14.05: Hydrogen Storage I
Session Chairs: Ming Dao and T. Venkatesh
Wednesday Afternoon, December 1, 2021
Hynes, Level 3, Room 300

1:30 PM EN14.05.01

Self-Assembling Amine-Borane Adducts to Nanostructure Ammonia Borane as Precursor of Nanostructured Boron Nitride for Hydrogen Storage [Kevin Turani-I-Belloto](#), [Johan Alauzun](#) and [Umit Bilge Demirci](#); University of Montpellier, France

Ammonia borane NH₃BH₃ (AB), a remarkable hydrogen storage material carrying 19.6 wt% of hydrogen, owns attractive properties [1]. It (in thermolytic conditions) has been understandably much investigated within the past two decades leading to destabilization strategies in order to decrease the onset dehydrogenation temperature (<100°C). Nanosizing AB is an attractive approach to make it suitable for solid-state hydrogen storage. The destabilization of the borane (i.e. modified thermal stability and reactivity) has been anticipated via changed atomic charges of the NH₃BH₃ molecule, perturbed intermolecular N-H-B network and lowered activation energy. The nanoconfinement of AB has then shown new pathway to dehydrogenation properties. With this knowledge, it was demonstrated that different porous structures so called scaffolds can be used to improve dehydrogenation properties of AB, such as silica (ex. SBA-15) [2], MOF (ex. Mg-MOF-74) [2] or polymers (ex. PMMA) [2]. In regards to efficiency, sustainability and disruption, AB has been nanosized without scaffold. Inspired from the nanosized AB using cetyltrimethylammonium bromide (CTAB) as surfactant [3], and obtained via an anti-precipitation method in solution, we used amine-borane adducts to produce nanosized AB particles (60 to 200nm). Adducts are the keys for shaping. Different adducts R-NH₂-BH₃ with R a carbonaceous group have been successfully synthesized and characterized. We have produced adducts such as tetradecylamineborane (C₁₆H₃₃NH₂BH₃AB) and biphenylamineborane (C₁₂H₁₁NH₂BH₃). The self-assembling properties of adducts have allowed nanostructuring of AB in solution; spherical, lamellar and polyhedral shapes have been observed. We accordingly synthesized nanoparticles of AB without a scaffold, which opens new perspectives for elaborating from these nanostructured new C-doped B-N-based materials. Recent computational works support that such materials would be the most attractive solutions for reversible H₂ storage at ambient conditions [4]. However, there is to our knowledge a lack of experimental evidence yet. The present project aims at confirming the potential of high reversible H₂ storage in the field of B-based ceramics.

[1] Demirci, U.B., Ammonia borane, a material with exceptional properties for chemical hydrogen storage. International Journal of Hydrogen Energy, 2017, 42(15): p. 9978-10013.

[2] Turani-i-belloto, K., et al, Nanosized ammonia borane for solid-state hydrogen storage: Outcomes, limitations, challenges and opportunities, international journal of hydrogen energy, 2021, 46: p.7351-7370

[3] Valero-Pedraza, M.-J., et al, ammoniaborane nanospheres for hydrogen storage, ACS Appl. Nano Mater., 2019, 2, 1129-1138

[4] Lale, A., et al., Boron nitride for hydrogen storage. ChemPlusChem, 2018, 83: p. 893-903.

1:45 PM EN14.05.02

Nickel Hydride Performed Under Cold Ar/H₂ Plasma Treatment—Material Processing and Mechanism [Marie-Charlotte Dragassi](#)^{1,2}, [Alicia Oussaidi](#)¹, [Souad Ammar-Merah](#)¹, [Michaël Redolfi](#)² and [Laurent Royon](#)¹; ¹Université de Paris, France; ²Université Sorbonne Paris Nord, France

Solid hydrogen storage is a technological obstacle for the hydrogen economy broadening. Various materials and methods have been studied under the scope of the industrial purpose such as complex metal hydrides made by the Sievert's method. Lanthanum-Nickel hydride, LaNi₅ had been chosen for its high volumetric (117kgH₂/m³) and gravimetric (1,5wt.%) hydrogen capacity. Notwithstanding, this technique requires expensive high purity materials (99,99%) and the process is performed at high temperature (300K) and high pressure (2bar). To overcome these drawbacks, we decided to go through the hydroxide-plasma path. It consists in synthesising by soft chemistry the hydroxide of the selected metal and reducing it under hydrogen plasma. For this study we chose Nickel as the matrix carrier. Three soft chemistry protocols were chosen : (i) coprecipitation and water washing, (ii) polyol and water washing (iii) polyol and ethanol washing. By coprecipitation, the obtained nanopowder is of a controlled dense structure and composition, while by polyol the composition is sensitive to ambient CO₂ pollution and washing. Polyol-made nanoparticles have a non-dense lamellar structure sensitive to washing : water can enter between the layers and leads to delamination. It leads to low mechanical strength. For the hydrogen plasma treatment, the main goal was to study the kinetic of the reduction and the composition evolution of the plasma by mass spectrometry. For both nano-nickel hydroxide made by coprecipitation and made by polyol and washed with water, the mechanism followed was : Ni(OH)₂>NiO>Ni (solid solution). Under plasma, the phase change lasted 1-2h. But for the nano-nickel hydroxide made by polyol and washed by ethanol, the mechanism was rather different : Ni(OH)₂>Ni₂H>Ni (solid solution). This shows that nano-nickel hydroxide can be reduced under plasma up to the unstable nickel-hydrogen solid solution. Further work around plasma parameters must be done to overcome this last step of hydration.

Acknowledgements :

This research was partly supported by Segula Technologies and the French National Research Agency. The authors would like to thank Mr Haddad (Segula technologies) for the fruitful discussions.

2:00 PM EN14.05.04

Uranium and U-Alloys in Hydrogen Storage and Magnetism of the U Hydrides [Ladislav Havela](#)¹, Dominik Legut², Jindrich Kolorenc³, Volodymyr Buturlim¹, Oleksandra Koloskova¹, Evgeniya Tereshina-Chitrova¹ and Thomas Gouder⁴; ¹Charles University, Czechia; ²VSB - Technical University of Ostrava, Czechia; ³Institute of Physics, Academy of Science of the Czech Republic, Czechia; ⁴European Commission Joint Research Centre, Germany

Violent reaction of Uranium metal hydrogen can be detrimental for mechanical integrity of devices containing this actinide element. The product of such reaction, UH₃, appears usually as a very fine powder, which burns spontaneously if exposed to air. This was a prohibitive feature in considerations of U for hydrogen storage in stationary applications. (Automotive applications were never considered due to the high mass of U). On the other hand, there are some pros. U absorbs H at very low pressures, working essentially as a getter, and all H is released above $T = 450$ °C. Eventually U started to be used as tritium storage medium in prospective nuclear fusion devices.

Our aim is to explore modifications of U hydrides by small substitutions of U by transition metals, which turned out possible using U-T alloys (T = Mo, Zr, V, Nb...) as precursors. It turned out that surface reactivity can be suppressed, H₂ pressure needed for hydrogenation increases and such hydrides adopt the form of brittle but monolithic pieces stable in air, while maintaining the H sorption capacity. It allowed a comfortable study of basic characteristics (magnetic, electrical resistivity, heat capacity), the results of which can be confronted with ab-initio calculations. The effort revealed a bit surprising fact that UH₃ is not simply the U metal expanded by 60% due to H absorption, but the polar character of U-H bonds is more important for the bulk properties than the overlap of 5f wave functions between nearest neighbours. UH₃ is ferromagnetic below $T \approx 165$ K, and one of striking features observed is the enhancement of the Curie temperature for any kind of dopant up to the concentration of 15 at.% [1].

For spectroscopic studies by XPS, UPS, BIS, XMCD, and XAS, we developed the technique of synthesis of U-H films by reactive sputter deposition. The films exhibit a similar properties as bulk U hydrides, but their composition and microstructure can be varied in a broader range, not being constrained by equilibrium thermodynamics. In a certain regime a di-hydride with CaF₂ structure type, not known before and analogous to rare earth dihydrides, could be obtained [2]. The sputter deposition technology opens a possibility for manufacturing sandwich devices, combining ferromagnetism of U hydrides with paramagnetism (and superconductivity) of U-T alloys on a nanoscopic scale, which can give, due to strong spin-orbit coupling, functionalities relevant in spintronics. The spectroscopies applied [3] confirm the effect of polar bonds, based on a charge transfer towards H and strong 6d-1s hybridization, which leaves behind the 5f states, responsible for magnetism. The reduction of the 5f-6d hybridization allows for pronounced magnetic properties of all hydrides studied (UH₂, α - and β -UH₃).

This work was supported by the Czech Science Foundation under the grant No. 21-09766S.

[1] O. Koloskova et al., J. Alloys Comp. 856 (2021) 157406.

[2] L. Havela et al., Inorg. Chem. 57 (2018) 14727.

[3] L. Havela et al., J. Electron Spectroscopy and Related Phenomena 239 (2020) 146904.

SESSION EN14.06: Hydrogen Compatibility of Materials I

Session Chair: William Curtin

Thursday Morning, December 2, 2021

Hynes, Level 3, Room 300

10:30 AM *EN14.06.01

Limiting Ingress While Maximizing Desorption—Exploring New Hydrogen Solutions for Pipeline Steels [Cem Tasan](#), Jinwoo Kim, Xiahui Yao, Ju Li and Bilge Yildiz; Massachusetts Institute of Technology, United States

Regulating hydrogen transport in structural metals is one of the key challenges for hydrogen related technologies. Here, we will discuss two new technologies that aim to regulate hydrogen ingress and hydrogen desorption. The former is a novel hydrogen barrier coating with multilayer composite structures of metal and oxide. This structure provides (i) enhanced resistance to delamination, (ii) formation of extended space-charge zones at oxide/metal interface that improves H-permeation barrier performance, and (iii) strong micro-cracking resistance and the self-healing potential to retain hydrogen barrier performance even after mechanical damaging. The latter method aims for recovering steels from hydrogen embrittlement at room temperature by accelerated electrochemical desorption of hydrogen. We confirmed that the method can effectively help several commercial steels to recover from the hydrogen damage, by comparing the mechanical behavior of H-precharged specimens after uncontrolled desorption and controlled electrochemical desorption experiments. Several case studies in different steels will be introduced in this presentation to discuss the influence of trapping sites on the effectiveness of this recovery approach.

11:00 AM EN14.06.02

Microstructural Engineering of Mn-Alloyed Duplex Steels and Accelerated Test Method Development to Achieve Low Cost, High Performance Solutions for Hydrogen Storage and Delivery [Yuran Kong](#)¹, Pawan Kathayat¹, Lawrence Cho¹, Kip O. Findley¹, John G. Speer¹, Brian Kagay², Christopher San Marchi² and Joseph Allen Ronevich²; ¹Colorado School of Mines, United States; ²Sandia National Laboratories, United States

Two major obstacles to the broader use of hydrogen energy technologies include (1) cost and reliability of hydrogen storage and delivery infrastructure; and (2) cost and complexity of evaluating materials in hydrogen environments. In particular, the ferrous alloys known to have high resistance to hydrogen embrittlement, e.g., high Ni-containing austenitic stainless steels, are relatively expensive. The current study aims at designing Mn-alloyed ferrite-austenite steels as economical materials for hydrogen service, as an alternative to high Ni stainless steels. The alloy design was guided by a literature review on the effects of alloying on austenite stacking fault energy (SFE), which is established to be correlated with the mechanical stability of austenite and hydrogen embrittlement resistance. The composition of a high Mn duplex steel was designed considering SFE and equilibrium volume fraction of austenite in duplex microstructures, obtained through thermodynamic calculations. Moreover, various thermomechanical processing routes are being explored to obtain desirable combinations of austenite stability, volume fraction, and deformation mechanisms and to enhance fracture toughness of the high Mn duplex steel in hydrogen at given or higher strength levels. In addition to reducing the cost of alloys, the present study also focuses on develop and validate a cheaper and easily accessible method to test alloys in hydrogen environments. Electrochemical hydrogen charging methods are being developed in parallel utilizing a 255 duplex stainless steel. The electrochemical charging method is intended to be a surrogate for testing in gaseous hydrogen at a pressure of approximately 103 MPa. The hydrogen embrittlement characteristics of the 255 duplex stainless steel were evaluated as a function of the hydrogen environment (electrochemical variables compared to testing in high-pressure gaseous hydrogen) and the geometry of circumferentially notched tensile specimens.

11:15 AM EN14.06.03

Hydrogen Detection and Discrimination Using ZnO Nanostructures Ionut Nicolae, Razvan Mihalcea, Bogdan Calin, Cristian Viespe and [Aurelian Marcu](#); NILPRP, Romania

Hydrogen technologies are a very promising option among the green energy sources. However, safety precaution have to be taking care while using, handling and storing it and sensors are a key issue in the present technological development. All existing sensors are known to have specific issues and gas discrimination and ambient factors influences are among the most frequent issues.

Surface Acoustic Wave (SAW) sensing is one of the development directions using acoustic waves propagating over a piezoelectric surface and are basing their functionality on the mechanical properties change of an 'active layer' material, which the wave is passing through in the presence of the detected gas. Nanostructure or nanostructured materials present a series of enhanced properties compared with the bulk materials, due to their high surface-to-volume ration, but their specific parameters need to be controled for optimizing sensor performances. For SAW sensor fabrication we use ZnO material as a versatile wide bang-gap semiconductor, which is having a good absorption of hydrogen isotopes and various other gases. We use Pulsed Laser Deposition (PLD) - Vapour-Liquid-Solid (VLS) techniques to grow ZnO single crystal [0001] nanowires on sensor surface as an active layer.

By controlling experimental ZnO growing parameters we are able to control VLS grow elementary processes and respectively nanostructure morphology, optimizing the sensor sensibility. By monitoring sensor response to various propagation frequencies we are able to distinguish several (known) gases presence. Some correlations between experimental parameters and sensor response are presented as well as sensor performances on hydrogen isotopes and few other gases detection.

SESSION EN14.07: Hydrogen Compatibility of Materials II

Session Chairs: Ming Dao and Cem Tasan

Thursday Afternoon, December 2, 2021

Sheraton, 2nd Floor, Grand Ballroom

1:30 PM *EN14.07.01

Hydrogen Embrittlement in Steels and High Entropy Alloys [William A. Curtin](#) and Xiao Zhou; Ecole Polytechnique Federale Lausanne, Switzerland, Switzerland

The urgent need for clean energy coupled with the exceptional promise of hydrogen (H) as a clean fuel is driving development of new metals resistant to hydrogen embrittlement. Experiments on new fcc high entropy alloys (HEAs) present a paradox, absorbing more H than Ni or austenitic 304 stainless steel (SS304) but more-resistant to embrittlement. Here, a new theory of embrittlement in fcc metals is presented based on the role of H in driving an intrinsic ductile-to-brittle transition at a crack tip. The theory quantitatively predicts a hydrogen concentration at which a transition to embrittlement occurs, and good agreement with experiments is found for the alloys SS304, SS316L, CoCrNi, CoNiV, CoCrFeNi and CoCrFeMnNi. The theory rationalizes why CoNiV is the most-resistant alloy and why SS316L is more resistant than the HEAs CoCrFeNi and CoCrFeMnNi. The theory opens a path for computationally-guided discovery of new embrittlement-resistant alloys.

2:00 PM EN14.07.02

Microstructural Basis of Mechanical Behavior of Hydrogen Resistant Austenitic Steels Po-Cheng Kung, Hoon Lee, Quinten Yurek, Jessica A. Krogstad and [James F. Stubbins](#); University of Illinois at Urbana-Champaign, United States

The development of hydrogen-resistant steels depends directly on the understanding of the role of alloy composition and microstructure on mechanical behavior. In this work, we describe the progress toward developing elevated strength, cost-effective alloys through the employment of nano-level strengthening features including short range order (SRO). The intent is to develop microstructures that are sufficiently strong, compared to the current generation stainless steels, that they could be used in hydrogen handling applications with reduced section sizes, and thus reduced cost. The alloy development effort derives from features of the 21-6-9 (Nitronic 40) alloy which has been the focus of multiple hydrogen effects studies over the years. The appeal comes from the relatively high strength, depending on the processing, and the use of Mn in place of some level of Ni. A series of developmental alloys in which the Ni/Mn ration is varied across a wide range are also analyzed. From a microstructural standpoint, the Ni/Mn balance can affect several critical materials parameters including alloy phase stability during deformation, stacking fault energy and the tendency for slip-induced twinning. This work covers the connection between the compositional and microstructural differences in these alloys and the associated mechanical behavior. In particular, the study includes the evolution of microstructure during deformation in both hydrogen charged and uncharged specimens to understand the dislocation-strengthening particle/SRO. Interactions, the tendency to transform from cross-slip to planar slip based, and the tendency for twinning, all of which influence performance in hydrogen atmospheres.

4:00 PM EN14.08.01

Effect of Various Rare Earth Doped Ceria Barrier Layers in Reversible Solid Oxide Cell Technology Ayesha Akter and Srikanth Gopalan; Boston University, United States

Renewable energy from wind turbine or photovoltaic cells will be abundant in future. We have a need for a clean, efficient system that can act as both energy conversion and storage device. A reversible solid oxide cell (RSOC) is such kind of a device that can convert electricity to fuel during the electrolysis mode by conversion of steam to hydrogen and using that hydrogen later as fuel to generate electricity during the fuel cell mode. Hydrogen is always a fuel of interest due to environmental considerations, increasing oil price and limited supply of fossil fuel. However, when operating in the SOEC mode, pressure builds up in the electrolyte-oxygen electrode interface due to the accumulation of molecular oxygen in the pores near the interface. As a result, the oxygen electrode particularly, suffers delamination in the SOEC mode causing serious performance degradation and failure of the system. To mitigate delamination of the oxygen electrode, the Ruddlesden-Popper structure based mixed ionic electronic conductors (MIEC) in the rare earth nickelate family are an attractive option. However, rare earth nickelates have the tendency to react with the YSZ electrolyte and form undesirable phases. To prevent this, a barrier layer is used between the oxygen electrode and electrolyte to prevent any kind of chemical interaction between the oxygen electrode and the electrolyte. In this work, various rare earth doped ceria have been evaluated as barrier layers and their effect on electrochemical polarization has been systematically studied. Symmetrical cells with various doped ceria barrier layers and nickelate-doped ceria composite electrode have been screen printed and EIS data has been obtained at varying temperatures and oxygen partial pressures. DRT analysis of the impedance spectra has provided insights into the reaction mechanism, and identify the rate limiting steps.

4:15 PM EN14.08.02

Comparison of Chromium Removal via Electrochemical Cleaning Technique between Predominantly Electronically Conducting versus Mixed Ionic/Electronic Conducting Solid Oxide Fuel Cell Cathode Materials Michelle A. Sugimoto, Zhikuan Zhu, Ayesha Akter, Srikanth Gopalan, Soumendra Basu and Uday Pal; Boston University, United States

Chromium poisoning remains a major obstacle to wide-spread solid oxide fuel cell (SOFC) employment. A mitigation strategy, electrochemical cleaning, has been proposed in which the Cr deposition reaction is reversed by applying a mild electrolytic current. The method has been shown to reverse chromium deposition and performance loss on cells with $(\text{La}_{0.8}\text{Sr}_{0.2})_{0.9}\text{MnO}_{3.8}$ (LSM) air electrodes. Here we demonstrate the applicability of electrochemical cleaning using more Cr-tolerant electrode materials: $\text{La}_{0.6}\text{Sr}_{0.4}\text{Co}_{0.2}\text{Fe}_{0.8}\text{O}_{3.8}$ (LSCF) and $\text{Nd}_2\text{NiO}_{4+8}$ (NNO). Three cells with LSM, LSCF, and NNO cathodes were exposed to accelerated poisoning conditions followed by electrochemical cleaning, i.e., mild electrolytic bias and increased fuel humidity. Performance recovery due to electrochemical cleaning is recorded using current-voltage and EIS measurements. Three additional cells were exposed to the same poisoning condition, but not cleaning for post-test Cr content comparison. Cell cross-sections were analyzed using energy dispersive x-ray spectroscopy (EDS). Cells that were poisoned and cleaned compared to their respective baseline poisoned cell demonstrate a decrease in overall Cr content. Whereas, the location of Cr deposition during poisoning is different between LSM and LSCF or LNO air electrodes. Due to the mixed ionic/electronic conductivity of LSCF and NNO electrodes, the effect of Cr deposition on cell performance is less pronounced compared to LSM. Therefore, when using more Cr-tolerant air electrode materials, electrochemical cleaning is effective in Cr removal and performance recovery and is required at a lower frequency compared to cells with primarily electronically conductive air electrodes.

4:30 PM EN14.08.03

Theory of the Electrostatic Surface Potential and Non-Equilibrium Thermodynamics at the Mixed Ionic Electronic Conductor (MIEC)-Gas Interface Nicholas Williams, Ieuan D. Seymour and Stephen Skinner; Imperial College London, United Kingdom

The catalytic and transport properties of mixed ionic-electronic conducting (MIEC) electrodes for solid oxide fuel cells (SOFCs) are well documented and utilised, yet poorly understood. In the current study, a novel kinetic framework for the electrochemical behaviour of hydrogen at the MIEC-gas interface will be discussed for three parallel treatments: as an ideal gas, as an adsorbate on the electrode surface and as a charge carrier dissolved in the oxide lattice. This model gives a physically meaningful reason for the enhancement in electrochemical activity of a MIEC electrode as the steam pressure is increased in both fuel cell and electrolysis modes, and is ubiquitous for any electrochemical system where the electric double layer is described as a Heaviside step function.

The process of charge transfer at the MIEC electrode/gas interface comprises of ambipolar exchange of ions and electronic species. The result of such a process causes charge separation and an associated dipole moment at the electrode surface. By applying an overpotential η to the MIEC electrode, an electrostatic surface potential shift away from equilibrium may be established where an effective double layer is formed between the electrode surface and the adsorbed species. Although no net charge transfer occurs, this surface potential shift modifies the surface chemistry and is the driving force for the ambipolar exchange of ions and electronic species.

Density Functional Theory (DFT) calculations were used to study the electrostatic potential at the ceria [111] surface, where we were able to calculate the dipole moment and adsorption energy as a function of hydroxyl coverage. The theory of the electrostatic potential at the MIEC-gas interface was then applied to predict the surface electrochemical properties as a function of local overpotential. [1]

Finally, we extend this model to show the effects of non-equilibrium thermodynamics on the bulk defect concentration and adsorbate induced electrostatic surface potential in MIEC electrodes. This methodology is used to model the current-overpotential characteristics of water electrolysis mechanism at 2 phase and 3 phase boundaries present in cermet electrodes. The mechanistic understanding gained from this model is widely applicable to a range of MIEC systems and provides a basis upon which the operating conditions can be tailored.

[1] Williams, N.J., Seymour, I.D., Leah, R.T., Mukerjee, S., Selby, M. and Skinner, S.J., 2021. Theory of the electrostatic surface potential and intrinsic dipole moments at the mixed ionic electronic conductor (MIEC)-gas interface. doi.org/10.1039/D1CP01639C

4:45 PM EN14.08.04

Oxygen and Sulfur Reduction Activities of Mesoporous N- & Fe,N-Carbon Electrocatalysts Correlate with Atomic-Scale Compositions and Structures Shona M. Becwar¹, Ziyang Wei², Rongli Liu², Xiangfeng Duan², Philippe Sautet² and Brad Chmelka¹; ¹University of California, Santa Barbara, United States; ²University of California, Los Angeles, United States

Mesoporous N- and Fe,N-carbons exhibit high and stable activities for oxygen and sulfur reduction that are comparable to or surpass those of standard Pt-activated-carbon electrocatalysts. Favorable properties include high nitrogen contents (>15 atom%), high fractions of N moieties at surface sites, 3-nm mesopores to promote diffusion, and electron conductivity to surface N environments where the reduction reactions occur. The types, quantities, and distributions of N-heteroatom environments, especially those at surface sites, are shown to strongly influence macroscopic reduction activities. N- and Fe,N-mesoporous carbons synthesized using difference mesopore templates (e.g., salt versus silica) are explored to understand the atomic level differences that correlate with increased reduction activity, and how they can be optimized. Compared to 20 wt% Pt supported on activated carbon, the salt-templated mesoporous Fe,N exhibits the highest reduction activity, exceeding even that of the commercial Pt-carbon catalyst.

While inclusion of N-heteroatoms improves carbon-based electrocatalyst reduction activity,¹ the atomic-level origins of such properties have remained elusive. Nevertheless, two-dimensional ¹³C-¹⁵N NMR spectra resolve signals from four distinct types of N-heteroatom environments: pyrrolic, graphitic, edge/isolated pyridinic, and pyrazinic/pyridinic moieties, the quantities of which vary by porogen and account for different O₂ reduction activities.^{2,3} Chemical shift assignments are corroborated by DFT, with points corresponding to different structural motifs overlaying the spectrum. Importantly, ¹⁵N-¹H NMR spectra enable surface N species to be selectively distinguished from interior moieties via interactions with adsorbed water. These analyses establish that certain types of N-carbon moieties are more important to electrocatalytic performance than others. The incorporation of non-precious transition metals (e.g., Fe) significantly increases electrocatalytic activity, which have been challenging to explain.^{4,5} Nevertheless, ⁵⁷Fe Mössbauer spectroscopy and solid-state ¹⁵N NMR and spin-lattice relaxation-time analyses resolve signals from ¹⁵N species that are proximate to paramagnetic Fe-heteroatoms, from which ¹⁵N-Fe distances are estimated. XRD, XPS, XRF, Raman spectroscopy, STEM, and EXAFS are used to characterize the materials and corroborate the hypotheses. Understanding the roles of Fe and N-carbon moieties in electrocatalytic reduction yields new design criteria for syntheses of high performance non-precious-metal electrocatalysts with diverse fuel cell and battery applications.

(1) Gong, et al., *Science* **2009**, 323, 760.

(2) Becwar, et al., submitted.

(3) Wei, et al., *J. Phys. Chem. C* **2021**, in press.

(4) Kim, et al., *ACS Appl. Mater. Interfaces* **2018**, 10, 25337.

(5) Al-Zoubi, et al., *J. Am. Chem. Soc.* **2020**, 142, 5477.

SESSION EN14.09: Hydrogen Compatibility of Materials III
Session Chairs: Christopher San Marchi and T. Venkatesh
Monday Morning, December 6, 2021
EN14-Virtual

8:00 AM *EN14.09.01

U.S. Department of Energy Hydrogen and Fuel Cell Technologies Office Overview [Neha Rustagi](#); U.S. Department of Energy, United States

The U.S. Department of Energy's (DOE) Hydrogen and Fuel Cell Technologies Office (HFTO) funds research, development, and demonstration (RD&D) activities to enable decarbonization across sectors. HFTO's R&DD portfolio includes hydrogen production, infrastructure, storage, fuel cells, and a wide range of end-uses for hydrogen, including industrial processes (e.g. steelmaking, data centers), energy storage, hydrogen blending with natural gas, and transportation. The Office's materials R&D activities are conducted largely through national laboratory consortia within the DOE's Energy Materials Network. These consortia include: H-Mat, focused on materials compatibly with hydrogen; HyMARC, focused on materials-based storage of hydrogen; HydroGEN, focused on advanced water splitting materials; and ElectroCat, focused on platinum group metal (PGM)-free catalysts for fuel cells. The current presentation will provide an overview of the HFTO RD&D portfolio and EMN consortia, including recent accomplishments and future priorities.

8:30 AM EN14.09.02

Evaluation of Tensile Behaviour of Structural Steels in High Pressure Gaseous Hydrogen Using Tubular Specimen [Thorsten Michler](#), Fabien Ebling, Ken Wackermann and Heiner Oesterlin; Fraunhofer Institut für Werkstoffmechani, Germany

Quasi-static tensile properties are the base for any component design. Often, wall thickness are set based on such data. A cost effective test method to acquire the required data for high pressure hydrogen applications is tensile testing using tubular specimen, where the hydrogen pressure is applied to the inner cavity of the specimen. Several structural steels were tested with this method and this study compares the results of tubular specimens with those of conventional specimens tested in a high pressure hydrogen autoclave. Commonalities and differences will be presented and discussed by means of FEM analysis and hydrogen failure modes.

8:45 AM *EN14.09.03

Decompression Failure Mechanisms in Hydrogen-Exposed Rubbers—Insights from *In Situ* 3D Tomography Using Synchrotron Source [Sylvie Castagnet](#)^{1,2,3}, [Azdine Nait-Ali](#)^{1,3}, [Mahak Fazal](#)^{1,3}, [David Mellier](#)¹, [Guillaume Benoit](#)¹, [Yannick Pannier](#)¹, [Mario Scheel](#)⁴ and [Timm Weitkamp](#)²; ¹Prime Institute (CNRS-ENSMA-Univ. Poitiers), France; ²Fédération de Recherche CNRS Hydrogène (FR2044 FRH2), France; ³LABEX Interactifs (ANR-11-LABX-0017-01), France; ⁴Soleil Synchrotron, France

Exposure of rubber materials to diffusive gases at high pressure and subsequent decompression may lead to cavitation and cracking depending on the exposure conditions. This phenomenon has been studied for different gas polymer systems in the past, but the interest in hydrogen as an alternative energy carrier and the application of rubber materials in Fuel Cell Vehicles and equipment for storage and transportation of hydrogen makes it important to study the compatibility of these materials with hydrogen. The relatively high pressures in use, combined with the safety measures required for the usage of hydrogen itself pose serious challenges in terms of material and design. In particular, the safety risk associated with hydrogen leakage makes specific demands on the rubber materials used as seals in terms of durability.

Decompression failure can be addressed at two different scales. At the macroscopic scale of the component, the main challenge is to capture the statistics of cavity fields (known to depend on the mechanical loading, decompression conditions and material properties), the gradients and the full diffuso-mechanical couplings, in order to model the residual mechanical and permeation properties. The question of a Representative Volume Element over which to develop modelling is a key one.

At the cavity scale, the existence of full diffuso-mechanical couplings is a key issue too: the expansion and deflation of the cavity depends on the balance between the external hydrostatic pressure and the internal pressure (which depends itself on the volume of the cavity and the gas content inside it, possibly varied by the gas flux at the cavity wall) but also on the intrinsic properties of the rubber at large strains at the cavity wall, and on the global gas content field. The type of mechanisms responsible for cavitation is another issue, for soft matters in general, regardless of the specific decompression failure

context.

The experimental works reported here aim at better understanding of the mechanisms of cavity growth, some possible interaction effects at variable range, with a free surface or between close cavities. The work was based on a very recent 3D time-resolved quantification of the kinetics and morphology of the damage, from an in-situ X-ray tomography experiment initially developed on a laboratory source (spatial resolution 16 μ m, temporal 100s) and extended under a synchrotron environment on the Anatomix beamline at SOLEIL synchrotron (France).

The gain in spatial (3 μ m) and temporal (4s) resolution made it possible to access the very first stages of growth, to properly quantify anisotropy and to detect residual damage. These different elements showed the existence of a first rapid spherical growth regime which then evolved into an anisotropic regime which reflected an underlying mechanism of cracking. The correlation with the intrinsic fracture properties of the rubber are considered more in-depth.

Then, the evolution of this damage during successive pressure cycles was investigated, raising the question of non-trivial cumulated effects.

Results mainly concern a series of unfilled EPDM, with low variable degrees of cross-link density. However, this microstructural parameter alone did not appear discriminating.

9:15 AM EN14.09.04

Morphological Changes and Their Effects on Material Properties in Natural Gas Medium Density Polyethylene Pipe in Low Pressure

Hydrogen [Kevin Simmons](#)¹, [Lisa Fring](#)¹, [Wenbin Kuang](#)¹, [Yongsoo Shin](#)¹, [Rakish Shrestha](#)² and [Christopher San Marchi](#)²; ¹Pacific Northwest National Laboratory, United States; ²Sandia National Laboratories, United States

As the energy sector decarbonizes, hydrogen is being considered as a medium to store and convey renewable energy, for example in the natural gas networks. Therefore, the interactions of hydrogen with structural materials in existing energy infrastructure is needed. Medium density polyethylene (MDPE) pipelines are commonly used in distribution gas networks to deliver natural gas from the transmission system to the end user. The open literature contains limited information on the effects of hydrogen (either pure or blended into natural gas) on these commonly used materials. In this research, the morphological changes, transport and mechanical properties associated with exposure to hydrogen were evaluated. Test specimens of PE2708 medium density polyethylene pipe were saturated with hydrogen at pressures ranging from 0.7 to 3.4 MPa for up to 72 hours, prior to evaluating morphological changes in the polymer, equilibrium hydrogen content, hydrogen diffusivity, nano-indentation properties, and burst behavior. In addition, fatigue life tests were conducted in-situ in the presence of low-pressure gaseous hydrogen. The material shows a decrease in the degree of crystallinity by up to 6% using X-ray diffraction and differential scanning calorimetry after exposure. The reduction in the diffusion coefficient was observed using thermal desorption spectroscopy, and nano indentation testing revealed up to a 30% decrease in hardness and modulus immediately following hydrogen exposure. Burst pressures test results were not significantly reduced. The fatigue life, however, was greater in hydrogen than in air. The implication of these property changes on the structural behavior of MDPE pipelines in hydrogen service are discussed.

9:30 AM EN14.09.05

Advanced Imaging to Study Hydrogen Compatibility of Polymers for Hydrogen Infrastructure [Wenbin Kuang](#)¹, [Kevin Simmons](#)¹, [Yongsoo Shin](#)¹, [Bruce Arey](#)¹, [Alice Dohnalkova](#)¹ and [Nalini Menon](#)²; ¹Pacific Northwest National Laboratory, United States; ²Sandia National Laboratories, United States

The U.S. Department of Energy Hydrogen and Fuel Cell Technologies Office launched the H2@Scale program to improve the durability and reliability of materials for hydrogen infrastructure to facilitate widespread utilization of hydrogen. Pacific Northwest National Laboratory leads a multi-lab effort to understand the mechanisms of hydrogen-polymer interactions with the goal of developing polymers with improved resistance to hydrogen degradation. Model nitrile butadiene and ethylene propylene diene rubber compounds were formulated collaboratively with Kyushu University to investigate how each constituent responds to high-pressure hydrogen exposure in such complex systems. Advanced imaging techniques offer unique advantages to visually study possible changes in polymer morphology associated with hydrogen effects at different length scales. X-ray computed tomography research revealed formation of more voids in plasticized systems after static exposure to 90 MPa hydrogen than unplasticized. Surface damage and plasticizer migration at the submicron level were captured by helium ion microscope. Transmission electron microscopy combined with energy dispersive spectroscopy highlighted hydrogen-induced voids formation around accelerator particles along with sulfur coalescing.

9:45 AM EN14.09.06

Atomistic Modeling of Elastomer Performance During Exposure to High-Pressure Hydrogen [Matthew P. Brownell](#), [Amalie L. Frischknecht](#) and [Mark Wilson](#); Sandia National Laboratories, United States

Elastomeric rubber materials serve a vital role as gas barriers in the hydrogen storage and transport infrastructure. With applications including O-rings and hose-liners, these components are exposed to pressurized hydrogen at a range of temperatures, cycling rates, and pressure extremes. High-pressure hydrogen exposure often rapidly leads to cavitation, a hydrogen-induced failure mode following several (de)pressurization cycles. This type of failure is readily visible, occurring as a material rupture during decompression and is due to the oversaturated gas traversing the polymer matrix towards the outside of the rubber. Computational modeling in the Hydrogen Materials Compatibility Program (H-Mat), co-led by Sandia National Laboratories and Pacific Northwest National Laboratory, employs multi-scale materials simulation efforts to build a predictive understanding of cavitation damage. We aim to motivate material formulations that are less sensitive to hydrogen-induced failure. Here, we will discuss the use of atomistic molecular dynamics simulations to predictively assess compositional variations and resulting performance metrics of the commonly used elastomer, ethylene propylene diene monomer (EPDM). We perform systematic studies as a function of increasing crosslink density, which show indications of improved bulk material response to the depressurization of gas at higher crosslink density. However, this performance improvement comes with a tradeoff; microscopic analysis indicates an increase in free volume at higher crosslink density, a necessity for gas localization and the initiation of cavitation. We will also discuss the mobility of hydrogen through the polymer matrix leading up to gas localization. Our diffusion results reveal that the hydrogen molecules can be divided into two classes, one with high mobility and one with low mobility in which the hydrogen gas diffusion is impeded by atomic structural features of the polymer.

Sandia National Laboratories is a multitechnology laboratory managed and operated by National Technology & Engineering Solutions of Sandia, LLC, a wholly owned subsidiary of Honeywell International Inc., for the U.S. Department of Energy's National Nuclear Security Administration under contract DE-NA0003525. SAND2021-7350 A

10:30 AM *EN14.10.01

Cost Effective Alloy Design for Hydrogen Resistant Austenitic Steels—Understanding the Impact of Short Range Order Through Integrated Computational and Experimental Approaches Jessica A. Krogstad¹, Petros Sofronis¹, Tianyu Su¹, Po-Cheng Kung¹, Quinten Yurek¹, Hoon Lee¹, Huan Yan¹, Zahra Hosseinsarani¹, Mohsen Dadfarnia², Elif Ertekin¹, Kathryn Huff¹, Brian Somerday¹ and James F. Stubbins¹; ¹University of Illinois at Urbana-Champaign, United States; ²Seattle University, United States

Development of robust, cost effective, reliable and safe hydrogen applications requires a new generation of low cost, high strength austenitic steels. In this talk we will review recent collaborative efforts to achieve this goal by intimately coupling experiments with modeling and simulation to establish how the intrinsic chemical composition, in concert with hydrogen, governs microstructural evolution and ultimately leads to fracture initiation and failure. Classical metrics of embrittlement (e.g. stacking fault energy and others) have proven to be insufficient on their own to explain failure and thus guide the design of optimum alloy composition. Several commercial and novel austenitic steels have been characterized via high-resolution electron microscopy to reveal ubiquitous short range ordering (SRO) behavior, where SRO is defined as any local deviation from a random solid solution. Direct feedback between these experimental observations and our constitutive modeling framework suggests that such SRO domains significantly modify the mobility of nearby dislocations, while atomistic simulations reveal that not only should such domains be expected but that the SRO domains may also impact the distribution of hydrogen within the lattice. In addition to these observations, we will present preliminary observations for our novel low-nickel austenitic alloys, which have been developed to suppress other known features associated with hydrogen embrittlement (phase transformation, twinning, etc) so as to explicitly explore the relationship between the observed SRO domains, slip localization and ultimately the failure modes of austenitic steels in the presence (and absence) of hydrogen.

11:00 AM *EN14.10.02

Effect of Hydrogen on Tensile Properties of Stainless Steels at Cryogenic Temperatures Daniel R. Merkel¹, Ethan K. Nickerson¹, Robert J. Seffens¹, Kevin Simmons¹, Christopher San Marchi², Brian Kagay² and Joseph Allen Ronevich²; ¹Pacific Northwest National Laboratory, United States; ²Sandia National Laboratories, United States

Safe and efficient hydrogen storage and distribution are key challenges to realizing hydrogen as an alternative energy carrier. To this end, cryogenic liquid and cryo-compressed gaseous hydrogen are considered high energy density alternatives to ambient temperature gaseous hydrogen. However, these alternatives have significant material demands: extreme temperature (20 K) and pressure (700 bar) as well as the insidious effects of hydrogen. Austenitic stainless steels are widely used for cryogenic pressure vessels owing to relatively high ductility even at 4 K. However, the influence of hydrogen on mechanical properties at cryogenic temperatures has rarely been studied. In this research, the tensile properties of 304L and Nitronic 50 (XM-19) stainless steel alloys with internal hydrogen were evaluated at 20 K, 77 K, and 113 K. Test specimens were saturated with internal hydrogen through thermal precharging at 573 K in 138 MPa H₂. In both 304L and Nitronic 50, reduced temperature increased strength properties and reduced elongation. The presence of hydrogen increased strength in both alloys but reduced ductility, as measured by reduction of area. Magnetic evaluation of the uniformly strained region of the 304L test specimens suggest that hydrogen mitigates the strain-induced transformation to α' -martensite in 304L, whereas the Nitronic 50 alloy remains stable with regard to transformation to α' -martensite. The effects of temperature and hydrogen were also explored in gas tungsten arc-welded 304L.

11:30 AM EN14.10.03

An Fe-Ni-Cr-H Interatomic Potential and Predictions of Hydrogen-Affected Stacking Fault Energies in Austenitic Stainless Steels Xiaowang Zhou¹, Chris Nowak¹, Skelton Richard Samuel¹, Michael E. Foster¹, Joseph Allen Ronevich¹, Christopher San Marchi¹ and Ryan B. Sills²; ¹Sandia National Laboratories, United States; ²Rutgers, The State University of New Jersey, United States

While Fe-Ni-Cr austenitic stainless steels exhibit relatively good resistance to hydrogen embrittlement, they still suffer from significant degradation of ductility, fatigue and fracture properties in gaseous hydrogen environments. Experimental studies in the literature suggest that hydrogen reduces stacking fault energy in austenitic stainless steels. This phenomenon causes a large separation of partial dislocations and lower propensity for cross-slip. Whereas lower stacking fault energy does not correlate well with loss of ductility in the absence of hydrogen, when hydrogen is present lower stacking fault energy trends toward greater loss of ductility. Calculations of stacking fault energy are challenging for austenitic stainless steels. One main issue is that in alloys, stacking fault energy is not a single value but rather varies depending on local composition. Herein, we first report an Fe-Ni-Cr-H quaternary interatomic potential and then use this potential to perform time-averaged molecular dynamics simulations to calculate stacking fault energies for tens of thousands of realizations of local compositions for selected stainless steels alloys with and without internal hydrogen. From statistical analyses, our results suggest that hydrogen reduces stacking fault energy, which likely impacts deformation mechanisms of Fe-Ni-Cr austenitic stainless steels when exposed to hydrogen environments. We then perform validation MD simulation tests to show that hydrogen indeed statistically increases the stacking fault widths due to statistically reduced stacking fault energies.

Acknowledgement- SNL is managed and operated by NTESS under DOE NNSA contract DE-NA0003525.

11:45 AM EN14.10.04

Molecular Dynamics of Hydrogen Cottrell Atmosphere Formation in Aluminum—Influence of Non-Dilute Concentration at the Dislocation Core Chris Nowak¹, Catalin Spataru¹, Kevin Chu², Xiaowang Zhou¹ and Ryan B. Sills³; ¹Sandia National Laboratories, United States; ²Georgia Institute of Technology, United States; ³Rutgers, The State University of New Jersey, United States

Cottrell atmosphere formation occurs when solute atoms segregate to dislocations and is one of the most basic processes by which solutes alter mechanical properties of materials.

Hydrogen Cottrell atmospheres can contribute to hydrogen embrittlement. Using molecular dynamics simulations we study the formation of hydrogen Cottrell atmospheres around edge dislocations in aluminum. By pinning dislocations to one position and using coarse-graining techniques, we can resolve the time-dependent changes in the hydrogen concentration field. Comparing to previous Cottrell atmosphere formation and thermodynamics theories, we observe a surprising reduction in peak atmosphere concentration at the dislocation core. This was found to arise from a repulsive, concentration-dependent H-H interaction at the dislocation core that is absent in the bulk far away from dislocation. Since the essential physics of Cottrell atmosphere formation is accurately represented in molecular dynamics, our results provide important inputs to improve Cottrell atmosphere theories. Based on our findings, we propose next steps to study the interaction between dislocations and their associated hydrogen Cottrell atmosphere.

12:00 PM EN14.10.05

Hydrogen Effects on Short Range Order in Austenitic Steels—Cluster Expansion and Monte Carlo Investigation Tianyu Su, Brian Somerday, Petros Sofronis, Jessica A. Krogstad and Elif Ertekin; University of Illinois at Urbana-Champaign, United States

Hydrogen embrittlement, a process whereby metals suffer the loss of ductility in hydrogen environments, limits the choice of austenitic stainless steels that can be used for reliable hydrogen applications. Although several possible mechanisms for hydrogen embrittlement have been put forward, there is still no clear consensus on the precise ways that hydrogen affects microstructural evolution and leads to failure. In this work, we consider how alloy composition and hydrogen affect the presence or absence of short range order (SRO) in austenitic steels, and how these changes to SRO may ultimately affect microstructure evolution. We present a computational assessment of alloy chemistry, SRO, and hydrogen effects using first-principles calculation and cluster expansion-Monte Carlo (CE-MC) simulation in Fe-Cr-Ni binary and ternary alloys. The degree of SRO present in typical binary and ternary austenitic steels of varying Fe-Ni-Cr composition is estimated from the Warren-Cowley short range order parameters. The composition and temperature dependence of SRO agrees with experimental and other computational works. We then demonstrate the effects of interstitial H on SRO in these alloys using a multicomponent multisublattice CE-MC method. The model results indicate that introducing H modifies the SRO preference of typical Fe-Ni-Cr alloys. In particular, we observe a strong tendency to form Cr and H rich domains. It is broadly presupposed that SRO may cause localized slip since planar glide is frequently reported in alloys known to exhibit SRO. As embrittlement is often accompanied by a transition from homogeneous to localized slip, the interaction between chemistry, SRO, and hydrogen may play a role in the slip localization that takes place during embrittlement of austenitic alloys.

12:15 PM EN14.10.06

Study of Hydrogen Permeation Using Molecular Dynamics Guang Cheng¹, Xiaoli Wang¹, Shulei Han¹, Kaiyuan Chen¹, Yang Zhang¹ and Venkatesh T. A.²; ¹Beijing University of Chemical Technology, China; ²Stony Brook University, The State University of New York, United States

We utilized molecular dynamics to study the hydrogen permeation in metallic materials such as pipeline steels, stainless steel, welding zones, and amorphous coatings. First, the nano/micro-structures and element distribution were obtained through experimental characterization. Then, the corresponding molecular dynamics models were established to represent the actual material structures within a small scale (i.e., 100 nm-1 μ m). Then, we investigated the effects of crystal defects, crystal structures, grain boundaries, interfaces, and surface roughness on hydrogen permeation. The correlation between pressure, temperature, and hydrogen permeation was also studied. The current study aims to understand the metallic materials compatibility used in pipelines and storage vessels. Meanwhile, the current investigation helps establish a method to accelerate hydrogen permeation to simulate the long-time service in hydrogen transporting and storage for mechanical properties tests. Finally, we would like to seek the possible approach to design materials with specific nano- and micro-structures for hydrogen barrier purposes considering different hydrogen pressure.

SESSION EN14.11: Hydrogen Compatibility of Materials V
Session Chairs: Christopher San Marchi and T. Venkatesh
Monday Afternoon, December 6, 2021
EN14-Virtual

1:00 PM *EN14.11.01

Investigating the Microstructural Origins of Hydrogen Effects on Deformation and Fracture Coleman Alleman, Brian Kagay and Christopher San Marchi; Sandia National Laboratories, United States

The mechanisms of hydrogen-assisted fracture in stainless steels are superficially described in the literature. Here, we attempt to produce causal and quantitative evidence of hydrogen-affected deformation and fracture. We analyze oligocrystalline microstructures to isolate deformation mechanisms in physical samples and create computationally equivalent microstructures to simulate the experimentally-observed responses.

This talk focuses on the development of a framework to simulate stress-strain responses of these microstructures, consisting of a tool to assign a best-fit crystal orientation on a regular 2D grid, an application to simulate grain growth in a 3D volume with boundary conditions imposed by a 2D domain, and a crystal plasticity model to simulate mechanical response.

Sandia National Laboratories is a multi-mission laboratory managed and operated by National Technology and Engineering Solutions of Sandia, LLC., a wholly owned subsidiary of Honeywell International, Inc., for the U.S. Department of Energy's National Nuclear Security Administration under contract DE-NA0003525.

1:30 PM EN14.11.02

Hydrogen Interaction and Storage in Transition Metal Carbides Christopher Weinberger¹, Xiaochuan Tang¹, Salehin Rofiques¹ and Gregory Thompson²; ¹Colorado State University, United States; ²The University of Alabama, United States

The interaction between transition metal carbides and hydrogen is an important topic for both hydrogen trapping and hydrogen storage. There are reports that hydrogen can be trapped in carbide precipitates in steel, increasing their tolerance to hydrogen-induced delayed fracture. This trapping could result from hydrogen interaction with the surface or in the bulk. There is also evidence that hydrogen can be stored in transition metal carbides, notably TiC_{0.6}. This raises important questions regarding hydrogen interaction and storage in transition metal carbides and its dependence on chemistry. In this talk, we examine how hydrogen binds to carbide precipitate interfaces and in the bulk using a combination of density functional theory and elastic models as a function of chemistry, both the transition element and carbon concentration. Our results reveal that metal-rich transition metal group IVB carbides are superior at trapping and storing hydrogen in the bulk while trapping at coherent interfaces is a function of both lattice mismatch and elastic constants of the carbide precipitates.

1:45 PM *EN14.11.03

A Data-Driven Roadmap Towards Pareto Optimal Hydrogen Storage Alloys Matthew Witman¹, Sanliang Ling², Gustav Ek³, Anis Bouzidi⁴, Jorge Montero⁴, Jeffery Chames¹, Sapan Agarwal¹, Justin Wong¹, Gavin Walker², David Grant², Mark D. Allendorf¹, Claudia Zlotea⁴, Martin Sahlberg³ and Vitalie Stavila¹; ¹Sandia National Laboratories, United States; ²The University of Nottingham, United Kingdom; ³Uppsala University, Sweden; ⁴Institut de Chimie et des Matériaux Paris-Est, France

After decades of research and success stories, an elusive question remains: have the truly "optimal" hydrogen storage alloys escaped discovery? The traditional approach to novel materials discovery has typically relied on researchers' significant domain expertise and trial-and-error experimentation in order to narrow down the vast space of possible materials. A recent paradigm involves the use of machine/statistical learning (ML) techniques to form surrogate models that screen materials' performance properties with many orders of magnitude greater efficiency and significantly cut the time and material costs of experimental search and validation. Focusing on materials-based hydrogen storage, we demonstrate that explainable machine learning

techniques can be used to elucidate simple, first-order design rules for predicting metal hydride thermodynamics. Trained purely on experimental data, the model does not rely directly on crystal structure and permits predictions on materials that otherwise lack well defined, computationally tractable unit cell representations. These developments are critical in order to apply these models to screen a novel chemical space of 672 high entropy alloys (HEAs), where we discover that we can finely tune the thermodynamic stability across many orders of magnitude within this set of materials. Afterwards we identify and experimentally validate two novel HEA compositions whose hydrides were significantly destabilized (up to 70x increase in equilibrium pressure) compared to the benchmark HEA hydride, thereby releasing hydrogen at much milder conditions. Exploring an even more comprehensive space of nearly 21,000 proposed HEA compositions, we are now using these ML models to optimize the competing objectives of thermodynamic stability, maximal volumetric/gravimetric capacity, and minimal cost (i.e., finding Pareto optimal materials). Our workflow takes seconds to predict the 138 Pareto optimal candidates, and a handful are currently undergoing laboratory validation within our international collaboration group. Assuming 1 month per HEA is required for synthesis and characterization, random sequential selection within this search space would consume an expected 17 years of experimental time before measuring the first Pareto material by chance.

2:15 PM *EN14.11.04

A Rational Strategy for Linking the Properties of Hydrogen Carriers with the Needs of Energy Storage Use Cases Mark Bowden, Ba Tran, Kriston Brooks and Tom Autrey; Pacific Northwest National Laboratory, United States

The successful deployment of hydrogen carriers requires careful consideration of chemical properties, engineering factors, and economic realities. The carrier effort in PNNL focuses on identifying and addressing the research needs of potential use cases that will benefit from large scale stable energy storage. The properties of the carriers must be matched to the needs of the use cases, which cover a wide range of scales, storage duration, and delivery rates. Hydrogen storage for stationary back-up or load-levelling applications poses different challenges from uses where the carrier must be transported over large distances between storage and release. We have determined the requirements of a range of representative use cases and used these to calculate operational performance parameters along with the thermodynamic, kinetic, and physiochemical properties of ideal carriers. We will discuss an example of a hydrogen storage system based on using ethanol to power a neighborhood microgrid. The lessons learned from the experimental research and associated engineering analysis are leading us to improved carrier systems for this and other applications.

2:45 PM EN14.11.05

Influence of Hydrogen on Kinetics of Dislocation Motion During Low Cycle Fatigue of 316L Stainless Steel Dayane M. Oliveira¹, Christopher San Marchi² and Jeffery C. Gibeling¹; ¹University of California, Davis, United States; ²Sandia National Laboratories, United States

The current work applies a framework of thermally activated dislocation motion to obtain fundamental information about the effect of hydrogen on the mechanisms of cyclic deformation in strain hardened 316L stainless steel, a common alloy used for hydrogen service. As-received and hydrogen-precharged specimens were deformed in plastic strain controlled low cycle fatigue tests at amplitudes ranging from 0.3% to 0.6% plastic strain, and a series of plastic strain rate change experiments were performed periodically at the peak tension stress. These tests represent constant temperature and dislocation structure experiments from which changes in operational activation area could be determined as the microstructure evolved. Specifically, operational activation areas were determined from the difference in stress associated with the logarithmic difference in plastic strain rate and then plotted as a function of the cumulative plastic strain. Both material conditions experienced a rapid increase in operational activation area during the first few cycles at all plastic strain amplitudes, followed by a region of steady state that coincides with the reduced rate of softening observed throughout most of the fatigue lifetime. The values of operational activation area were larger in the as-received than in the hydrogen-precharged condition, ranging from 100 to 150 b² and from 60 to 90 b², respectively. After the specimens had been cycled to one-half of the expected lifetime, additional tests were conducted at various plastic strain values around stable hysteresis loops to reveal information about the character of deformation and obstacles to dislocation activity in this stainless steel. Plots of the inverse of the normalized operational activation area as a function of the flow stress, also known as Haasen plots, were used as a first step in inferring the dominant deformation mechanism. The results indicated the presence of an athermal stress associated with the interactions between dislocations and the dominant glide obstacles for both material conditions, and the magnitude of this stress is reduced in presence of hydrogen. Although the operational activation areas are weakly dependent on the plastic strain amplitude for as-received and hydrogen-precharged specimens, the nature of the dominant obstacle to dislocation motion tends to be slightly more thermal than forest dislocations in the high amplitude regime. Values of operational activation area at this stage of fatigue life ranged from 100 to 300 b² and from 70 to 200 b² in the as-received and hydrogen-precharged conditions, respectively. Transmission electron microscopy was used to directly observe the differences in dislocation arrangements with and without hydrogen at half-life.

SESSION EN14.12: Hydrogen Storage II
Session Chairs: Christopher San Marchi and T. Venkatesh
Monday Afternoon, December 6, 2021
EN14-Virtual

4:00 PM *EN14.12.01

Predicting Hydrogen Storage in MOFs via Machine Learning Alauddin Ahmed and Donald Siegel; University of Michigan, United States

The H₂ capacities of a diverse set of 918,734 metal-organic frameworks (MOFs) sourced from 19 databases is predicted via machine learning (ML). Using only 7 structural features as input, ML identifies more than 8,000 MOFs with the potential to exceed the capacities of state-of-the-art materials. The identified MOFs are predominantly hypothetical compounds having low densities (<0.31 g/cm³) in combination with high surface areas (>5,300 m²/g), void fractions (~0.90), and pore volumes (>3.3 cm³/g). The relative importance of the input features are characterized, and dependencies on the ML algorithm and training set size are quantified. The most important features for predicting H₂ uptake are pore volume (for gravimetric capacity) and void fraction (for volumetric capacity). The ML models are available on the web (<https://sorberent-ml.hymarc.org>), allowing for rapid and accurate predictions of the hydrogen capacities of MOFs from limited structural data; the simplest models require only a single crystallographic feature. DOI: 10.1016/j.patter.2021.100291

4:30 PM EN14.12.02

Reversible Hydrogen Storage by Metastable Hydrides in Functionalized Porous Hosts Mark D. Allendorf¹, Vitalie Stavila¹, Sichi Li², Jonathan Snider¹, Joseph Reynolds III¹, Farid El Gabaly¹, Joshua Sugar¹, Brennan Dizdar³, Eric Majzoub³, Hendrik Schlomberg⁴, Bettina V. Lotsch⁴, Jeff Urban⁵ and Brandon Wood²; ¹Sandia National Laboratories, United States; ²Lawrence Livermore National Laboratory, United States; ³University of Missouri–St. Louis, United States; ⁴Max Planck Institute for Solid State Research, Germany; ⁵Lawrence Berkeley National Laboratory, United States

Metal hydrides continue to be of interest for materials-based hydrogen storage. However, most research has focused on hydrides that are too stable, i.e. their enthalpy of H₂ desorption is too high for the residual heat of a PEM fuel cell to drive the release. In contrast, metastable hydrides, for which H₂ release is exothermic, have received less attention. Compounds such as alane (AlH₃) are so thermodynamically unstable that direct rehydrogenation following hydrogen release is thought to be impossible.¹ Multistep chemistry involving Lewis acid-base intermediates (e.g. alane-ether complexes) can be used but is impractical for many applications, including on-board vehicular storage. This is unfortunate because AlH₃ and another metastable hydride, LiAlH₄, have attractive gravimetric capacities (10.1 wt% and 8.0 wt%, respectively). Here we show that these hydrides can be thermodynamically stabilized by nanoconfinement using two types of porous hosts: nitrogen-functionalized porous carbon (LiAlH₄@NCMK-3) and bipyridine-functionalized Covalent Triazine Framework (AlH₃@CTF-bipyridine). LiAlH₄@NCMK-3 desorbs 100% of its hydrogen by 240 °C and >80% can be regenerated at <100 MPa H₂, bypassing the Li₃AlH₆ intermediate of bulk.² Even more surprisingly, AlH₃@CTF-bipyridine is reversible at 60 °C under 700 bar hydrogen, 36 times lower than the experimentally measured H₂ plateau pressure of bulk aluminum. DFT calculations and EPR spectroscopy support a radical-based mechanism via AlH₃ binding to bipyridine, resulting in single-electron transfer to form AlH₂(AlH₃)_n clusters.³ Together, our results reopen the case in favor of these high-capacity metastable hydrides for H₂ storage. They also suggest potential for using them in batteries, supercapacitors, and heterogeneous catalysis.

1. J. Graetz, J. Wegrzyn, J. J. Reilly, *J. Am. Chem. Soc.* **2008**, *130*, 17790.

2. Y. Cho, S. Li, J. L. Snider, M. A. T. Marple, N. A. Strange, J. D. Sugar, F. El Gabaly, A. Schneemann, S. Kang, M. Kang, H. Park, J. Park, L. F. Wan, H. E. Mason, M. D. Allendorf, B. C. Wood, E. S. Cho, V. Stavila *ACS Nano*, 2021 doi.org/10.1021/acsnano.1c02079.

3. V. Stavila, S. Li, C. Dun, M. A. T. Marple, H. E. Mason, J. L. Snider¹, J. E. Reynolds III, F. El Gabaly, J. D. Sugar, C. D. Spataru, X. Zhou, B. Dizdar, E. H. Majzoub, R. Chatterjee, J. Yano, H. Schlomberg, B. V. Lotsch, J. J. Urban, B. C. Wood, M. D. Allendorf, submitted.

4:45 PM EN14.12.03

Interface Pinning Causes the Hysteresis of the Hydride Transformation in Binary Metal Hydrides Nicholas J. Weadock^{1,2}, Peter Voorhees³ and Brent Fultz¹; ¹California Institute of Technology, United States; ²University of Colorado at Boulder, United States; ³Northwestern University, United States

The absorption and desorption of hydrogen by hydride forming metals is well known to exhibit hysteresis, in which the partial pressure of hydrogen absorption is greater than desorption. We will demonstrate, by combined theoretical and experimental work, that a continuous barrier to interface motion is the origin of hysteresis. Hysteresis and elastic energies determined from high precision pressure composition isotherm and *in-situ* X-ray diffraction measurements on palladium hydride are found to be inconsistent with previous theories. Our experiments show that in bulk samples the hysteresis is present even in a partially transformed system, thus a stress-induced jump in volume fraction of hydride cannot be responsible for the hysteresis. Furthermore, we characterize the absorption and desorption kinetics stepwise and find that the equilibration time is constant within the two-phase region of the palladium-hydrogen phase diagram, indicating that there exists a persistent energy barrier.

Acknowledgement: Support from the EFree Center, an EFRC funded by the U.S. DOE, OBES Award DE-SC0001057

5:00 PM EN14.12.04

First-Principles Elucidation of Initial Dehydrogenation Pathways in Mg(BH₄)₂ Liwen Wan¹, Tom Autrey² and Brandon Wood¹; ¹Lawrence Livermore National Laboratory, United States; ²Pacific Northwest National Laboratory, United States

Hydrogen is a promising technology for long-term energy storage and realization of zero CO₂ emission. However, utilizing hydrogen as a fuel presents practical challenges due to its low volumetric energy density and therefore requires development of advanced storage medium. Complex magnesium borohydride, Mg(BH₄)₂, possesses one of the highest gravimetric (14.8 wt.%) and volumetric (112 g/L) hydrogen storage density. Yet practical challenges remain due to kinetic limitations to realize full reversibility for de- and re-hydrogenations. Early theoretical work based on density functional theory predicts hydrogen desorption temperature between 20 and 75°C via reaction Mg(BH₄)₂ → MgB₂ + 4H₂, however, in experiments, hydrogen release have only been observed above 200°C. It is speculated that this discrepancy is originated from the formation of various B_xH_y intermediates that act as a thermodynamic sink or a kinetic barrier during hydrogen desorption. In this work, we use first-principles methods to explore initial dehydrogenation, from BH₄ to B₃H_x, in bulk γ-Mg(BH₄)₂ and to identify the preferred reaction pathways for the formation of key B₂H_x and B₃H_x intermediates that limit the overall kinetics of BH₄ to B₃H_x transformation. Our results not only provide valuable thermodynamic and kinetic information regarding each of the elemental reaction steps during BH₄ to B₃H_x conversion, but also shed light on the long-standing contradiction between previous theoretical prediction and experimental observation about the existence of B₃H₈ intermediate.

This work was supported by the Hydrogen Materials Advanced Research Consortium (HyMARC), established as part of the Energy Materials Network by the U.S. Department of Energy, Office of Energy Efficiency and Renewable Energy, Fuel Cell Technologies Office and was performed under the auspices of the U.S. Department of Energy by Lawrence Livermore National Laboratory under Contract DE-AC52-07NA27344.

5:15 PM *EN14.12.05

Advanced Computational Modeling of Metal Hydrides for Vehicular and Stationary Hydrogen Storage Applications Brandon Wood, Tae Wook Heo, ShinYoung Kang, Liwen Wan, Nathan Keilbart, James Chapman, Sichi Li and Kyoung E. Kweon; Lawrence Livermore National Laboratory, United States

More efficient, compact storage of hydrogen represents a critical need for fuel cell vehicles and long-duration energy storage. Metal hydrides are promising materials to replace high-pressure tanks, offering high volumetric capacities at relatively low hydrogen pressures. However, these materials often suffer from kinetic limitations that incur undesirable energy cost under operation. Within the DOE Hydrogen Materials—Advanced Research Consortium (HyMARC), we are using multiscale models to model kinetic processes in hydrogen storage materials and identify key limitations for targeted engineering. This talk will present an overview of the materials modeling strategy within HyMARC, which incorporates and integrates atomistic simulations of complex interface chemistry, effective-medium approaches for transport and mechanical stresses, and continuum methods for microstructure evolution. Our aim is to go beyond thermodynamic models to understand harder-to-simulate kinetic processes under nonequilibrium cycling conditions. We will show how modeling coupled with high-fidelity experimental characterization has been employed to elucidate chemical reaction pathways at interfaces and to understand the formation and evolution of new solid phases. We will also present recent progress towards elucidating the interaction of hydrogen with native oxide films, which form on metal surfaces and play a key role in determining the activation temperatures and pressures for many metal hydrides. To this end, multiscale simulations and experiments are being combined with machine learning and graph-theoretic algorithms to simulate hydrogen transport through these polycrystalline and amorphous surface films. The talk will also review our recent efforts to improve kinetic predictions of hydrogen storage materials by incorporating additional physics into the simulations, which better approximates realistic operating conditions. Finally, we will discuss how modeling-derived understanding is being used within HyMARC to guide new improvement strategies, including nanoconfinement and compositional modification. Examples will be drawn from multiple materials systems, including complex light metal hydrides for vehicles and TiFe alloys for stationary energy storage.

This work was performed under the auspices of the U.S. Department of Energy by Lawrence Livermore National Laboratory under Contract DE-AC52-07NA27344.

SESSION EN14.13: Fuel Cells III
Session Chairs: Yanling Ma and Deborah Myers
Tuesday Morning, December 7, 2021
EN14-Virtual

8:00 AM *EN14.13.01

Iron-Based Proton Exchange Membrane Fuel Cell Cathode Catalysts Deborah Myers, Magali Ferrandon, Jaehyung Park, A. Jeremy Kropf and Evan Wegener; Argonne National Laboratory, United States

The sluggish kinetics of oxygen electrocatalysis and the resulting high overpotentials necessary to achieve useful current densities limit the performance and efficiency of proton exchange membrane fuel cells (PEMFCs).⁽¹⁾ The best catalysts for the oxygen reduction reactions are based on platinum, leading to limitations in the cost effective implementation of this technology.^(2,3) The development of alternative catalysts, with comparable or higher activity and durability to the platinum and derived from earth-abundant materials has thus been an active research area for decades.

Incredible progress has been made over the past decade in increasing both the ORR activity and durability of PGM-free PEMFC cathode catalysts.⁽⁴⁾ The class of catalysts demonstrating the highest ORR activities are those typically denoted as "Fe-N-C" and synthesized by heat treating iron salts and zinc-based zeolitic imidazolate frameworks (ZIFs) and/or phenanthroline, as carbon and nitrogen sources, or by heat treating iron-substituted ZIFs. For this class of PGM-free materials, it has been determined that variables such as the metal and carbon-nitrogen macrocycle content, as well as the temperature and atmosphere in which the composites are heat treated are important in determining the activity and activity stability of the resulting catalysts.^(5,6) Changing these variables and testing their effect on the resulting catalyst properties is a time-consuming process and only a limited portion of the composite composition and temperature space have been explored for this broad class of materials.

This presentation will describe the development and application of high-throughput methodology to accelerate exploration of the effects of composition and synthesis parameters on the activity of iron-carbon-nitrogen acidic electrolyte ORR electrocatalysts. The structural characterization of the materials using X-ray absorption spectroscopy (XAS) and correlation of the atomic structure with ORR activity will be described, as will the high-throughput testing and optimization of the electrode composition using a 25-electrode array fuel cell hardware.⁽⁷⁾

References

1. H. Yang, X. Han, A.I. Douka, L. Huang, L. Gong, C. Xia, H.S. Park, and B.Y. Xia, *Adv. Func. Mater.*, 31 (2021) 2007602.
2. B. Pivovar, *Nature Catalysis*, 2 (2019) 562.
3. S. Thompson and D. Papageorgopoulos, *Nature Catalysis*, 2 (2019) 558.
4. L. Osmieri, J. Park, D.A. Cullen, P. Zelenay, D.J. Myers, and K.C. Neyerlin, *Curr. Opin. Electrochem.*, 25 (2021) 100627.
5. E. Proietti, F. Jaouen, M. Lefevre, N. Larouche, J. Tian, J. Herranz, and J.-P. Dodelet, *Nature Comm.* 2 (2011) 1.
6. A. Zitolo, V. Goellner, V. Armel, M.-T. Sougrati, T. Mineva, L. Stievano, E. Fonda, and F. Jaouen, *Nature Materials*, 14 (2015) 937.
7. J. Park and D.J. Myers, *J. Power Sources*, 480 (2020) 228801.

This work was supported by the U.S. Department of Energy (DOE), Energy Efficiency and Renewable Energy, Hydrogen and Fuel Cell Technologies Office (HFTO) under the auspices of the Electrocatalysis Consortium (ElectroCat 2.0). This work utilized the resources of the Advanced Photon Source, a U.S. DOE Office of Science user facility operated by Argonne National Laboratory for DOE Office and was authored by Argonne, a U.S. Department of Energy (DOE) Office of Science laboratory operated for DOE by UChicago Argonne, LLC under contract no. DE-AC02-06CH11357.

8:30 AM EN14.13.02

Surface Engineering of Platinum-Based Nanomaterials for Highly Efficient and Durable Oxygen Reduction Reaction Electrocatalysts Yanling Ma; Shanghai Jiao Tong University, China

The essence of the electrocatalytic reactions is a heterogeneous reaction process that occurs on the surface of a solid-phase catalyst, including the adsorption, diffusion and dissociation of reactants, electron transfer and the absorption and desorption of the intermediate/reaction products. The surface physical and chemical properties of the catalyst such as geometric morphology, atomic arrangement, element composition, hydrophilicity, etc. are closely related to the adsorption behavior of active species and play a critical role in determining the catalytic activity, selectivity and stability. Moreover, the surface structure of the catalyst is also affected by the chemical environment in which it is located, and then offer significant insights in catalyst design strategies.

Based on the relationship among design, surface structure, environment and activity in catalysis, here we focus on the cathodic oxygen reduction reaction in fuel cells and takes the design and synthesis of platinum-based nanocatalysts as the research object. Starting from the surface design and engineering of nanostructured catalysts, our work studies the effect of 1. surface diffusion behavior under different reaction environments, 2. surface atomic arrangement, 3. exposed crystal planes, and 4. surface charge and the corresponding structure-activity relationship. It aims to combine the influence of the chemical reaction environment on the surface structure of the catalyst and the influence of the surface structure of the catalyst on the catalytic performance to pave the way for the development of highly-efficient and stable platinum-based oxygen reduction catalysts.

[1]. Y. Ma, A. N. Kuhn, W. Gao, T. Al-Zoubi, H. Du, X. Pan, H. Yang*, *Nano Energy* 79, 105465 (2021).

[2.] Y. Ma, F. Li, X. Ren, W. Chen, C. Li, P. Tao, C. Song, W. Shang, R. Huang*, B. Lv*, H. Zhu*, T. Deng, J. Wu*, *ACS Applied Materials & Interfaces* 10, 15322 (2018).

[3.] Y. Ma, W. Gao, H. Shan, W. Chen, W. Shang, P. Tao, C. Song, C. Addiego, T. Deng, X. Pan*, J. Wu*, *Advanced Materials* 29, 1703460 (2017).

8:45 AM EN14.13.03

Characterization of CeO_x-Decorated Pd/C Catalysts Synthesized by Controlled Surface Reactions for Hydrogen Oxidation in Anion Exchange Membrane Fuel Cells Richard Andres Ortiz Godoy¹, Ramesh Kumar Singh², Elena Davydova², Ana C. Alba-Rubio³, Dario Dekel² and Jasna Jankovic¹; ¹University of Connecticut, United States; ²Technion-Israel Institute of Technology, Israel; ³The University of Toledo, United States

The high cost and difficult task to eliminate platinum (Pt) catalyst in Proton Exchange Membrane Fuel Cells (PEM-FCs) are some of the main obstacles that thwart the wide adoption of fuel cells. For this reason, Anion Exchange Membrane Fuel Cell (AEM-FC) has been suggested as an alternative to the PEM-FC technology in which non-Pt metals may be employed. However, the common slow kinetics at the anode experienced during Hydrogen Oxidation Reaction (HOR) has been one of the challenges preventing the achievement of high-power density in the Pt-free AEM-FC. Here, our objective is to improve the efficiency of HOR catalysts by depositing various ratios of CeO_x/Pd catalysts onto carbon support using the Controlled Surface Reactions (CSR) process. It is expected that a homogenous distribution of CeO_x preferentially attached to Pd nanoparticles (NPs) can produce highly active CeO_x -Pd/C catalysts for HOR. In the present study, we offer a comprehensive characterization approach for the synthesized highly active catalyst and correlate the obtained structural/compositional parameters to its performance. The characterization of the catalysts was carried out using Inductively Coupled Plasma-Atomic Emission Spectroscopy (ICP-AES), X-ray Diffraction (XRD), High-Resolution Transmission Electron Microscopy (HR-TEM), Scanning Transmission Electron Microscopy (STEM) - Energy Dispersive Spectroscopy (EDS), Electron Energy Loss Spectroscopy (EELS), and X-ray Photoelectron Spectroscopy (XPS) to confirm the bulk composition, phases present, morphology, elemental mapping, local oxidation state and surface chemical states, respectively. The HRTEM micrographs indicated that Pd NPs were uniformly distributed on the carbon support with only some minor agglomeration. Additionally, the achieved high interfacial contact between CeO_x and Pd acquired on single Pd NPs was, for the first time, segmented and calculated using High-resolution STEM-EDS maps and Image J processing program by measuring the overlap intensities between Pd and Ce in the NPs. The intimate contact between CeO_x and Pd and the increase in their interfacial contact area with the addition of CeO_x in these NPs was observed. This interfacial contact area is higher than other previously reported for Pd- CeO_x catalysts system synthesized by other methods, suggesting that the CSR method can provide a more selective deposition of CeO_x on Pd. EELS was used to determine that the primary oxidation state of our oxide was in the form of CeO_2 and Ce^{4+} was predominantly present in the CeO_x . However, the presence of Ce^{3+} cannot be ruled out, especially near the surface of the NPs. The study also found that the already mentioned interfacial contact area was directly correlated to the electrochemical performance reflected on the HOR activity of the CeO_x -Pd/C catalysts. Additionally, to track the morphological, compositional, and structural changes at the nanoscale we used postmortem Identical location transmission electron microscopy (IL-TEM), to reveal the degradation mechanisms governing this new CeO_x -Pd/C catalyst material following Accelerated Stress Tests in a three-electrode electrochemical cell. The preliminary results have shown that CeO_x can act as a promising anchoring mechanism that prevents the mobility, agglomeration, and detachment of Pd at a considerably high degree when compared to samples without CeO_x .

9:00 AM EN14.13.04

Cathodic Nanocatalyst Development for Alkaline Fuel Cell Applications [Merissa Schneider-Coppolino](#), Audrey Taylor and Byron D. Gates; Simon Fraser University, Canada

Alkaline fuel cells are a versatile, low-emission alternative energy source for use in transportation, as well as for portable and stationary power applications. These systems use chemical energy from the electrochemical conversion of hydrogen and oxygen gas to produce electrical energy, with only water and heat as by-products. They operate through two interdependent redox reactions within the cell consisting of oxidation of the hydrogen fuel at the anode and reduction of the oxygen at the cathode. One of the most significant barriers that fuel cells face is the sluggish nature of the oxygen reduction and its dependence on platinum, a rare and costly metal, as a catalyst for the reaction. Through the development and optimization of structures and materials, the amount of catalyst can be decreased without sacrificing performance and enabling an increase in the commercial viability of the device.

An alternative cathode material is palladium, which possesses similar chemical properties to platinum but is available in a greater abundance. Additionally, palladium has exhibited improved electrochemical properties in alkaline fuel cells. It has been shown that the activity of palladium-based catalysts can be further increased when alloyed with ancillary metals such as nickel. The incorporation of nickel, a more abundant transition metal, improves the properties of the catalyst and decreases the amount of palladium needed while increasing its utilization. This creates a more cost-effective solution to preparing catalysts. Furthermore, the use of nanoparticles as the basis for the cathode catalyst allows for a high surface area for the oxygen reduction reaction to take place. Nanoparticles allow for a more efficient use of the catalyst materials and, consequently, decreases the amount of metal required and the overall cost of the catalyst.

This study assesses the viability of palladium nickel nanocatalysts as an alternative cathode material for alkaline-based fuel cells. These nanoparticles are synthesized using a water-in-oil microemulsion method and characterized using a series of electron microscopy and electrochemical techniques. By adjusting the ratio of metal salt precursors, a series of nanocatalysts were prepared with various compositions of palladium and nickel. The analysis of these nanocatalysts included assessing the relationship between their composition, structure, and function to determine an optimal ratio of the palladium and nickel within these materials for increasing their catalytic performance. Initial tests demonstrate a promising activity of these nanocatalysts, although further studies will be needed to assess the durability and to better understand the stability of these catalysts.

9:15 AM EN14.13.05

Understanding the Role of Disorder in Materials Used in Catalysis and Fuel Cells Applications [Kulbir K. Ghuman](#); Institut national de la recherche scientifique, Canada

The functionality of materials used for energy applications is critically determined by the physical properties of small active regions such as surfaces, interfaces, and grain boundaries. Although small, these regions in materials if well utilized can provide sustainable solutions to alleviate the energy crisis of today's world. In particular, the capability to manipulate disorder in materials, whether due to zero-dimensional defects (such as vacancies, dopants) or three-dimensional defects (such as pores, cracks, etc.), can bring innovation in designing sustainable technologies. Among various tools, computational materials science plays a significant role in understanding and manipulating disorder in energy materials. Hence, in this talk, I will provide a brief overview of our recent work on understanding and manipulating disorder in oxides such as TiO_2 and Ytria stabilized ZrO_2 for enhancing their performance. I will mainly focus on modeling of realistic materials with structural defects and disorder for next-generation solid oxide fuel cells electrolytes and sustainable heterogeneous catalysis. [1]

[1] Madrid, J. C. M., Ghuman, K. K. *Disorder in Energy Materials and Strategies to Model it*. Advances in Physics: X., 6:1 (2021).

9:30 AM EN14.13.06

Synthesis and Characterization of Platinum on Carbon Nanoparticles Selectively Coated with Titanium Nitride (TiN) by Atomic Layer Deposition (ALD) [Richard Andres Ortiz Godoy](#)¹, [Saidjafarzoda Ilhom](#)¹, [Mor Kattan](#)², [Necmi Biyikli](#)¹, [Yair Ein-Eli](#)² and [Jasna Jankovic](#)¹; ¹University of Connecticut, United States; ²Technion - Israel Institute of Technology, Israel

The growing demand for clean and efficient energy sources has been a direct result of the serious effect on the climate and the environment associated with high emissions of pollutants that are mainly produced from fossil fuel-based energy generators. Currently, a green technology like Proton Exchange Membrane Fuel Cell (PEMFC) can produce zero-emissions energy power by primarily using the electrochemical reactions of hydrogen and oxygen to generate electrical energy. Additionally, due to their high activity, Platinum (Pt)/Platinum alloy nanoparticles distributed on a carbon (C) catalyst support

are considered the most efficient catalyst materials use in this technology. However, the main drawbacks from this technology are (i) the scarcity of Pt, making it very expensive for widespread fuel cell application and commercialization, as well as the fact that (ii) carbon support can be prone to corrosion and degradation when operating even at the most typical PEMFC conditions. This carbon corrosion can induce the loss of Pt nanoparticles (NPs) active surface area when Pt detaches from the carbon support or agglomerates into larger Pt NPs, which can lead to premature performance losses in a PEMFC. In this work, we propose a novel approach to prevent carbon corrosion by selectively depositing a corrosion-resistant layer (approximately 1.5 nm thickness) of titanium nitride (TiN) only on the surface of the carbon support while the Pt NPs catalyst centers are left uncoated and accessible for reagents reactions (oxygen O and H⁺ protons). TiN was used as the coating material because of its attractive properties, such as its electronic conductivity, which is enough to enable the free movement of electrons from the current collector toward the catalytic centers. TiN would also act as an anchoring mechanism of Pt NPs, preventing their mobility on the carbon support and subsequent agglomeration. The deposition of TiN layers is carried out at 150°C with a Hollow-Cathode Plasma-Assisted Atomic Layer Deposition (HCPA-ALD) while using Tetrakis(dimethylamino)titanium (IV) (TDMAT) as the metal precursor in Ar/N₂ plasma, from which nitrogen was used as co-reactant. Before HCPA-ALD, to prevent TiN from depositing on top of the Pt NPs, the surface of Pt NPs is selectively coated with a thin film of oleylamine (OAm), a polymer that would only absorb onto Pt NPs, which is later removed from the catalyst and TiN system (after the HCPA-ALD process is finished), by heat treatment at 185°C. Here we will mainly focus on the TiN deposition process and the subsequent Transmission Electron Microscopy (TEM) characterization performed on these nanoparticles, which allows us to prove the successful formation of homogenous coatings and architecture characteristics of these nanoparticles after oleylamine application and TiN deposition. Electrochemical characterization, including Cyclic Voltammetry (CV) and Oxygen Reduction Reaction (ORR), were performed in a Rotating Disc Electrode (RDE) to further confirm the activity and effectiveness of our designed catalyst. Our preliminary results have shown that highly conformal TiN can be successfully grown onto Pt/C nanoparticles (as powders) by using HCPA-ALD with a custom-made agitator mechanism. The second phase of this research will be focused on inspecting the degradation mechanisms this novel catalyst system experiences after potential cycling in a Membrane Electrode Assembly (MEA).

9:45 AM EN14.13.07

Nanoporous Surface Modification of 316L Support Materials by Electrochemical Dealloying Seyfettin Berk Sanli and [Fatih Piskin](#); Mugla Sitki Kocman University, Turkey

316L porous stainless steel (PSS) is a very suitable support material for particularly thin film Pd-based membranes due to its high thermal, oxidation resistance and having a thermal expansion coefficient similar to Pd. However, commercially available PSS have often very large surface pores that affect the final thickness of the membrane that could be deposited on it. The size of pores at the commercial PSS surface can be as large as 30 μm or more. That's why the membrane thickness deposited on the PSS can reach several tens of microns in order to create a porous-free membrane. Several studies focus on applying an interlayer between PSS and thin film membrane so as to reduce the size of pores at the PSS surface and thus reduce the thickness of the membrane. However, it is often not easy to control the size of surface pores and keep their size under a threshold. In addition, a non-homogeneous application of the interlayer to be formed on the PSS surface can cause formation of large pores that might be overlooked. The deposition of a thin film membrane on such an interlayer typically causes the formation of pin-holes at the thin film membranes. The presence of pin-holes in the membrane results in a reduction in hydrogen selectivity, even though fully dense metallic membranes principally offer infinite hydrogen selectivity. That's why modification of PSS surface has to be employed in a controlled manner and should be reproducible.

The current study concentrates on surface modification of PSS as a support material in order to enable thin film (<1μm) deposition on PSS. In this respect, 316L foil was used as a model system to determine the application parameters for the formation of a nanoporous Ni surface layer on the PSS. 316L foils were initially electroplated by Ni-Cu alloys using plating solutions with different Ni:Cu ratios. Subsequently, the Ni-Cu surface layers on 316L foils were subjected to an electrochemical dealloying process in order to dissolve Cu back into the plating solution and remain nano-porous Ni surface layer. In the study, different electroplating solutions were employed to determine the suitable alloy composition that yielded the desired pore size (<100nm) in the Ni surface layer formed after the de-alloying process.

This work was supported by TUBITAK (The Scientific and Technological Research Council of Turkey) with project Number 119M636, which the authors gratefully acknowledge.

SESSION EN14.14: Fuel Cells IV
Session Chairs: Veronika Brune and K. C. Neyerlin
Tuesday Morning, December 7, 2021
EN14-Virtual

10:30 AM EN14.14.02

Approach of Metal-Sulfides for Hydrogen and Fuel Cell Technologie by Molecular Building Blocks [Veronika Brune](#), Wilhelm Michael, Khan Lê and Sanjay Mathur; University of Cologne, Germany

The unique physical properties of 2D van der Waals materials have attracted great attention to fulfill the demands of future nanoelectronics for sustainable developments and have recently attracted significant attention for addressing the current worldwide challenges of environmental pollution and energy shortage. The ultrahigh surface area in combination with and extraordinary physiochemical, electronic and optical properties offer the application in hydrogen and fuel cell technologies. The huge number of active sides of 2D van der Waals materials as well as their suitable band gap offer their application as photocatalyst. The lacking control of large-scale material synthesis corresponding to specific requirements in commercial material formation processes is still challenging, which motivated us to develop a unique synthetic approach to layered 2D materials MS₂ (M= Mo^{IV}, W^{IV}, Ti^{IV}, Sn^{IV}), MS (M=Sn^{II}, Ge^{II}). A uniform synthesis route of molecular building blocks for controlled formation of stable precursor classes [M(SeTn(Me)EtS)_x] (M = Mo^{IV}, W^{IV}, Ti^{IV}, x = 2; M = Ge^{II}, Sn^{II}, x = 1) was developed. Following a simple synthetic protocol, the reaction of tridentate SNS donor ligand with suitable metal compounds resulted in (air)stable molecular precursors, which enabled the targeted formation of homogeneous crystalline 2D MoS₂, WS₂, TiS₂, SnS₂, SnS by thermal decomposition experiments as well as in wet chemical syntheses via microwave assisted decomposition resulting in SnS and SnS₂ particles.

These molecular building blocks provide an extraordinary synthetic approach to materials for hydrogen economy.

10:45 AM EN14.14.03

Physicochemical Properties and Low Relative Humidity Fuel Cell Performance of Pt/ECSTM Catalysts Richard Andres Ortiz Godoy¹, Michael Dzara², Alexey Serov³, Madeleine Odgaard⁴, Barr Zulevi³, Svitlana Pylypenko² and Jasna Jankovic¹; ¹University of Connecticut, United States; ²Colorado

School of Mines, United States; ³Pajarito Powder, LLC, United States; ⁴IRD Fuel Cells, Denmark

Fuel cells are one of the most advantageous solutions for clean energy applications due to their near-zero-emission, high efficiency, low maintenance cost, and high energy density. However, the development of highly efficient and reliable versions of the current Polymer Electrolyte Membrane Fuel Cells (PEMFCs), mature enough to result in an increased application in the transportation and energy generation sectors, have been subjected to considerable scientific and industrial level effort. In general, PEMFCs produce electricity through the electrochemical reaction of hydrogen and oxygen (or air) taking place in the Membrane Electrode Assembly (MEA) by converting the chemical energy of the hydrogen oxidation and oxygen reduction into electrical energy with water as a byproduct. However, high performances (at scale) in oxygen reduction reaction (ORR) catalysts are a challenge that must be tackled to allow an increase in the energy generation of this technology. For this reason, tunability of the materials at the core of this technology is necessary to meet the demands of not only a specific application but also operating conditions. Here, we study commercially available ORR catalysts based on platinum nanoparticles (Pt-NPs) supported on nitrogen-functionalized carbon (Engineered Carbon Supports™, ECSTM) produced by Pajarito Powder, LLC at scale. The ORR performance of three MEAs made with different Pt/ECS catalysts, by IRD Fuel Cells, LLC was studied under low relative humidity conditions. At low Pt loading, 0.1 mg_{Pt} cm⁻², they displayed competitive performance, achieving current densities between 1.8 and 1.3 Acm⁻² at 0.6 V. A comprehensive study of the physicochemical properties and structure of these Pt/ECS catalysts and their Pt-free equivalent ECSTM carbon support materials was also performed by using several characterization techniques, such: X-ray diffraction, Raman spectroscopy, and Transmission Electron Microscopy (TEM) to investigate structural and morphological properties, X-ray Photoelectron Spectroscopy (XPS) to determine the surface composition and chemical properties, Thermogravimetric Analysis (TGA) to evaluate thermal oxidation properties, and nitrogen sorption (Brunauer-Emmett-Teller (BET) and Barrett-Joyner-Halenda (BJH)) to determine the surface area and porosity, of these catalyst materials. This detailed study allowed us to conclude that the best performing catalyst in the conditions used in this work has the highest surface area and the highest concentration of surface dopants (nitrogen and oxygen). However, it is worth mentioning that catalysts supported on low surface area carbon with a high graphitic degree, exhibited competitive performance that can be used in applications where corrosion-resistant carbon is needed. We can also conclude that based on the highly competitive MEA performance for the three Pt/ECS catalysts these carbon supports, developed by Pajarito Powder LLC with engineered morphology and composition through the VariPore™ synthetic technology, can result in tunable properties suitable for a targeted application. These commercially available materials can be adapted through modification of the versatile synthesis platform to tune the physicochemical properties of carbons for other applications and conditions.

11:00 AM EN14.14.04

Development of LSC Based Amorphous/Nanocrystalline Composite Cathodes for Intermediate Temperature Solid Oxide Fuel Cells Ramin Babazadeh Dizaj and [Tayfur Ozturk](#); Middle East Technical University, Turkey

There is a considerable interest in lowering the operating temperature of solid oxide fuel cells. In this respect, (La,Sr)CoO₃-(La,Sr)2CoO₄ dual phase oxides have attracted much attention as cathode materials due to their enhanced oxygen reduction reaction kinetics[1,2]. Moreover there is much interest to develop these cathodes in amorphous state which not only leads to significantly improved cathode performance, but also are associated with a strong resistance to Sr segregation making them as a suitable choice for IT-SOFCs[3]. In the current study so as to further improve the stability, a third oxide was introduced into the system. Over 20 cathodes compositions, all based on (La,Sr)CoO₃-(La,Sr)2CoO₄- (Gd,Ce)O₂ ternary system, were sputter deposited in combinatorial geometry. A target operating temperature of 550°C was selected and the full cell performances were measured in each cell so as to identify the best cathode composition. Scenarios how to best keep the amorphous structure at elevated temperatures and with prolonged use are discussed.

[1] ZÇ Torunoglu, D Sari, O Demircan, YE Kalay, T Ozturk, Y Kuru One pot synthesis of (La, Sr) CoO₃/(La, Sr) 2CoO₄ for IT-SOFCs cathodes, International Journal of Hydrogen Energy 43 (40), 18642-18649

[2] D Sari, F Piskin, ZC Torunoglu, B Yasar, YE Kalay, T Ozturk Combinatorial development of nanocrystalline/amorphous (La, Sr) CoO₃-(La, Sr) 2CoO₄ composite cathodes for IT-SOFCs, Solid State Ionics 326, 124-130

[3] D Sari, B Yasar, F Piskin, YE Kalay, T Ozturk Segregation Resistant Nanocrystalline/Amorphous (La, Sr) CoO₃-(La, Sr) 2CoO₄ Composite Cathodes for IT-SOFCs Journal of The Electrochemical Society 166 (15), F1157

11:15 AM EN14.14.05

YSZ Mixed Grain Boundary Modeling—Understanding Its Structure, Yttrium Segregation and Its Effect on Oxygen-Ion Self-Diffusion Jose C. [Madrid Madrid](#) and Kulbir K. Ghuman; Institut National de la Recherche Scientifique, Canada

SOFC technology currently suffers from material interaction, insulating phase formation, and thermal stresses as it operates at high temperatures, which results in rapid degradation, low reliability, and high cost for commercialization. One of the approaches to reduce the operating temperature of SOFCs is the use of thin-film electrolytes to reduce the ohmic losses experienced at a reduced temperature while offering high thermal stability. That been said, the nanoscale thin films are generally polycrystalline and contain a high density of Grain Boundaries (GBs), which can substantially affect the ion diffusion in electrolytes. Experimentally, the atomistic structure of GBs can be analyzed and observe via high-resolution scanning STEM, but unfortunately, it does not provide sufficient information about the atomic-level structure of these boundaries. Molecular Dynamics (MD) simulations have been used for studying Grain Boundaries' atomic structure and oxygen-ions transport across YSZ electrolyte over the last decades. However, high symmetry GBs have been commonly targeted even though most boundaries found in polycrystalline samples are a mix of twisted and tilted denominations- commonly named "mixed" GBs. A mixed grain boundary (GB) was modeled at the atomic level using MD in this work. The structure was built from a TEM image of an 8YSZ thin film sample using the amorphization and recrystallization (A&R) technique. Oxygen-ion self-diffusion was studied for a range of temperatures between 700 K and 2300 K and Y₂O₃ concentration between 4-14 mol%. It was found that Y₂O₃ does not segregate toward the GB core for one of the grain orientations. On the contrary, Y³⁺ prefers to accumulate in this particular grain after the A&R process. As a result, it allows a better distribution of oxygen vacancies inside the grain interior what leads to obtain a higher oxygen-ion self-diffusion for this region.

11:30 AM EN14.14.06

Triple-Conducting Electrodes for Intermediate-Temperature Fuel Cells and Electrolysis Cells [Meagan C. Papac](#)¹, [Jake Huang](#)², [Ryan O'Hayre](#)² and [Andriy Zakutayev](#)³; ¹National Institute of Standards and Technology, United States; ²Colorado School of Mines, United States; ³National Renewable Energy Laboratory, United States

Performance of intermediate-temperature fuel cells and electrolysis cells is often limited by the high polarization resistance and low electrocatalytic activity of the positive electrode (i.e., positrode). Mixed ionic-electronic conducting electrode materials have been developed to improve device performance and, recently, triple ionic-electronic conducting oxides (TIEC) have provided a pathway for further improvement. Transport of each charge carrier in these materials depends on defect concentrations, which are moderated by cation concentrations and by operating conditions. Thus, it is important to understand mixed-species transport in single-phase TIEC materials, including discovery and design principles of TIECs, and high-priority areas for further TIEC materials development.¹

Here, we describe a combinatorial experimental approach to investigate a family of TIEC materials, Ba(Co,Fe,Zr,Y)O₃ (BCFZY), which is of interest for

electrocatalytic applications in intermediate-temperature fuel cells and electrolyzers. Layered, half fuel-cell devices were deposited by pulsed laser deposition. An electrolyte layer ($\text{BaZr}_{0.8}\text{Y}_{0.2}\text{O}_{3-\delta}$) was topped with compositionally graded arrays of BCFZY thin film microelectrodes to investigate the effects of chemical composition on performance. An automated benchtop instrument was developed to measure spatially resolved impedance of these films at temperatures up to 500°C under localized dry or humidified gases (air or nitrogen).² Performance of the BCFZY thin films was evaluated as a function of temperature and gas atmosphere.³ Distribution of relaxation times analysis was applied to disentangle individual fuel cell processes with distinct time constants in the frequency-dependent impedance spectra. The dependence of the polarization resistance of each of these processes on chemical composition, temperature, and gas atmosphere are reported.

The BCFZY impedance spectra show that a low-frequency process dominates under humid N_2 , while the limiting process under dry air depends on the chemical composition of the electrode material. Total polarization resistance is low in Co-rich materials under both gas atmospheres. Low total polarization resistance is also observed in Y-rich materials under the humid N_2 atmosphere, suggesting a substantial proton-related impedance contribution at low frequencies in BCFZY. These results demonstrate a high-throughput experimental approach to studying triple-conducting materials as positive electrodes for intermediate-temperature electrolyzers and fuel cells.

Funding provided in part by the Office of Energy Efficiency and Renewable Energy (EERE) Hydrogen and Fuel Cell Technologies Office (HFTO), as a part of HydroGEN Energy Materials Network (EMN) consortium.

¹ M.C. Papac, V. Stevanović, A. Zakutayev, and R. O'Hayre, *Nat. Mater.* **20**, 301 (2021).

² M.C. Papac, K.R. Talley, R. O'Hayre, and A. Zakutayev, *Rev. Sci. Instrum.* **92**, 065105 (2021).

³ M.C. Papac, J. Huang, A. Zakutayev, and R. O'Hayre, (in preparation).

11:45 AM EN14.14.07

Effects of Binary Oxide Additives on SOFC Cathodes- An EIS Study Anna F. Staerz¹, Han Gil Seo¹, Dino Klotz^{1,2}, Clement Nicollet³ and Harry Tuller¹; ¹Massachusetts Institute of Technology, United States; ²Kyushu University, Japan; ³Institut des Matériaux Jean Rouxel (IMN), CNRS, France

It was previously found that the Smith acidity scale is a powerful descriptor for predicting how binary oxide additives influence the oxygen surface exchange kinetics of the mixed ionic-electronic conductor $\text{Pr}_{0.1}\text{Ce}_{0.9}\text{O}_{2-x}$ (PCO10). By infiltrating various binary oxides, ranging from strongly basic (Li_2O) to acidic (SiO_2) onto the surface of PCO10, basic additives reportedly result in surface electron accumulation leading to enhanced oxygen exchange while acidic materials yield surface electron depletion, deactivating the surface. [1,2] These findings are extended by examining the impact of the relative acidity of additives on the polarization resistance of screen printed porous PCO10 electrodes applied symmetrically to YSZ single-crystal wafers by Electrochemical Impedance Spectroscopy (EIS). Chromia, an acidic oxide, is a common poison for cathodes that originates from the metal interconnects used in SOFC stacks. To validate the detrimental effects of chromia, each layer of PCO was infiltrated with a Cr concentration of 230 ppm. This value was selected based on the results of Menzler et al. on a SOFC stack after 3000 h of operation, who found a Cr-deposition amount of $0.8 \mu\text{g}/\text{cm}^2$ on a cell cathode of similar morphology. [3] For comparison, the effect of an equivalent mass of lithia (1270 ppm), a basic oxide, was also examined. The area-specific resistance (ASR, Ωcm^2) increased over four-fold upon infiltration with chromia, from approximately 124 to $532 \Omega\text{cm}^2$ when measured at 450°C and in 0.1 atm O_2 , while the ASR of the cell infiltrated with the lithia was lower than the pure cell. The semicircles in the Nyquist plot, are distorted as a result of several overlapping processes. Here, the distribution of relaxation times (DRT) method enables a clearer differentiation between electrochemical processes, e.g. low frequencies processes (LF) such as gas diffusion, surface oxygen exchange and high frequency (HF) processes such as charge transfer processes across electrolyte-cathode interfaces. [4,5] At 450°C , the HF region remains largely unchanged by surface infiltration, while in the LF there are significant differences between samples. Upon chrome infiltration a new LF frequency peak forms, while after Li infiltration the peaks in the LF region largely disappear. By using a systematic temperature study under varying oxygen concentrations, the different peaks in the DRT will be attributed to specific electrochemical processes, allowing for more precise understanding of how the binary oxides influence the cathode reactivity.

[1] C. Nicollet, C. Toparli, G.F. Harrington, T. Defferriere, B. Yildiz, H.L. Tuller, Acidity of surface-infiltrated binary oxides as a sensitive descriptor of oxygen exchange kinetics in mixed conducting oxides, *Nat. Catal.* (2020). <https://doi.org/10.1038/s41929-020-00520-x>.

[2] D.W. Smith, An acidity scale for binary oxides, *J. Chem. Educ.* **64** (1987) 480–481. <https://doi.org/10.1021/ed064p480>.

[3] N.H. Menzler, F. Tietz, M. Bram, Izaak C. Vinke, L.G.J. (Bert) de Haart, Degradation Phenomena in SOFCs with metallic interconnects, in: P. Singh, N.P. Bansal (Eds.), *Adv. Solid Oxide Fuel Cells IV*, The American Ceramic Society, 2008: pp. 93–104.

[4] T.H. Wan, M. Saccoccio, C. Chen, F. Ciucci, Influence of the Discretization Methods on the Distribution of Relaxation Times Deconvolution: Implementing Radial Basis Functions with DRTtools, *Electrochim. Acta.* **184** (2015) 483–499. <https://doi.org/10.1016/j.electacta.2015.09.097>.

[5] Y. Niu, Y. Zhou, W. Lv, Y. Chen, Y. Zhang, W. Zhang, Z. Luo, N. Kane, Y. Ding, L. Soule, Y. Liu, W. He, M. Liu, Enhancing Oxygen Reduction Activity and Cr Tolerance of Solid Oxide Fuel Cell Cathodes by a Multiphase Catalyst Coating, *Adv. Funct. Mater.* **2100034** (2021) 1–11. <https://doi.org/10.1002/adfm.202100034>.

SESSION EN14.15: Poster Session II: Materials for Hydrogen Technologies

Session Chair: Christopher San Marchi

Tuesday Afternoon, December 7, 2021

EN14-Virtual

1:00 PM EN14.15.01

Understanding Hydrogen Diffusivity in Amorphous Titania—Bridging Quantum and Classical Descriptions with Graph Theory James Chapman, Kyoung E. Kweon and Nir Goldman; Lawrence Livermore National Laboratory, United States

Understanding hydrogen transport is vital to a multitude of application spaces, including energy storage and corrosion mitigation. However, knowledge of the physical diffusion pathways of hydrogen is limited, with a serious gap existing with regards to how hydrogen transport is affected by the host material's underlying atomic structure and defects. For the case of polycrystalline materials, answering this question is non-trivial, as diffusion can occur through many structurally unique environments: (1) bulk regions (2) grain boundaries, (3) surfaces, etc. In this work we have chosen to study hydrogen diffusion through titania due to its importance in corrosion mitigation and energy storage. In particular, we aim to understand diffusion through titania grain boundaries, approximated by using amorphous phases due to similarities in their short-range atomic order. Density functional theory was used to generate these amorphous configurations via ab initio molecular dynamics. A spectrum of hydrogen binding energies was then calculated using a multitude of oxygen sites with varying coordination number. Classical molecular dynamics were then performed on larger amorphous systems using a machine learning force field. A graph-based order parameter was then used to characterize the classically derived amorphous phase space which was correlated with oxygen

coordination number. Our results qualitatively indicate that hydrogen diffusivity can be tailored to either inhibit or induce diffusion based on the specific local oxygen environments present in the amorphous phase.

1:05 PM EN14.15.02

Titanium Carbide MXenes with Specific Terminations as Platinum Supports Haeji Hong¹, Filipe Marques Mota¹, Nur Aqlili Riana binti Che Mohamad¹, Won Il Cho² and Dong Ha Kim¹; ¹Ewha Womans University, Korea (the Republic of); ²Korea Institute of Science and Technology, Korea (the Republic of)

MXenes possess attractive hydrophilicity, high conductivity, and durability for application in electrocatalysis. Tailored Ti₃C₂ has been actively employed as active support candidates in Pt-loaded catalytic systems to drive the hydrogen evolution reaction (HER). It is noted that the effect of diverse surface functional groups, which may play an important role to optimize the interaction with loaded Pt nanoparticles, has not been deeply investigated to date. 3D wrinkled Ti₃C₂(OH)_x and Ti₃C₂O_x were prepared after the alkali-induced process. 3D MXene with high concentration of -F groups (Ti₃C₂F_x) were prepared by mixing with HF. The incorporation of different functional groups was confirmed by FT-IR spectroscopy. Collected XRD patterns of the MXene powders revealed that NaOH-based and subsequent treatments did not induce the formation of distinct phases. It can be clearly observed that all MXene have same structure even after subsequent treatments from evidenced by SEM and TEM images. Moreover, there is no substantial change in defect ratio. Specific electrochemical properties were obtained due to different termination groups on the surface of Ti₃C₂. In this work we direct our attention to the effect of these surface terminations on the resulting interactions with Pt to improve the electrocatalytic activity of Pt-loaded Ti₃C₂ materials toward HER.

1:10 PM EN14.15.03

Relation Between *d*-Orbital States and Oxygen Evolution Electrocatalysis in Perovskite Oxides Tae Gyu Yun and Sung-Yoon Chung; Korea institute of science and technology, Korea (the Republic of)

Numerous studies on oxide electrocatalysts for an efficient oxygen evolution reaction have been conducted to compare their catalytic performance and suggest new compositions. However, two significant constraints have been overlooked: One is the difference in electrical conductivity between catalysts and the other is the strong crystallographic surface orientation dependence of the catalysis in a crystal. Consequently, unless a comprehensive comparison of the oxygen-evolution catalytic activity between samples is made on a crystallographically identical surface with sufficient electron conduction, misleading interpretations on the catalytic performance and mechanism may be unavoidable. To overcome these limitations, we utilize both metallic (001) LaNiO₃ epitaxial thin films together with metal dopants and semiconducting (001) LaCoO₃ epitaxial thin films supported with a conductive interlayer. We identify that Fe, Cr, and Al are beneficial to enhance the catalysis in LaNiO₃ although their perovskite counterparts, LaFeO₃, LaCrO₃, and LaAlO₃, with a large bandgap, are inactive. Furthermore, semiconducting LaCoO₃ is found to have more than one order higher activity than metallic LaNiO₃, in contrast to previous reports. Showing the importance of facilitating electron conduction, our work highlights the impact of the near-Fermi-level *d*-orbital states on the oxygen-evolution catalysis performance in perovskite oxides.

1:15 PM EN14.15.07

Atomically-Dispersed Iridium on Haematite Photoanodes for Solar Water Splitting—Catalyst or Spectator? Qian Guo¹, Magdalena Titirici² and Ana Sobrido¹; ¹Queen Mary University of London, United Kingdom; ²Imperial College London, United Kingdom

Oxide semiconductors have been widely studied as photoanodes for solar water splitting to generate clean hydrogen as they are in principle inexpensive and stable [1]. To improve their solar-to-hydrogen efficiency, integration of photoanodes with suitable cocatalysts is an attractive strategy to lower reaction barriers thus boosting the photoelectrochemical water splitting ability [2-4]. Very recently, atomically-dispersed catalysts have gained significant attention for integration with semiconductors for solar-to-fuel conversion, due to their high atom utilization, superior catalytic activity, tunable physicochemical properties, and clear active sites [5, 6]. For example, atomically-dispersed iridium catalysts with superior oxygen evolution catalytic performance, have been demonstrated working efficiently on oxide semiconductors for solar water splitting [7, 8]. As the interest in atomically-dispersed catalysts on photoanodes is just rising since 2010, although the phenomenological advantages of pairing atomically-dispersed catalysts with semiconductors are now widely confirmed, the precise role of such cocatalysts, *i.e.* acting as a catalyst or playing a non-catalytic role on photoanodes, which is essential for future efficient photoanode design, are far from understood.

Haematite (α -Fe₂O₃) has long been targeted as a promising oxide semiconductor for solar water splitting in the photoelectrochemical (PEC) configuration due to its natural abundance, narrow bandgap to capture visible light, and excellent chemical stability. With the advances in improving the fundamental deficiencies of haematite over the past few decades, haematite is currently the leading performer among oxide photoanodes. Also, haematite serves as a prototype oxide photoanode in many ways. Therefore, in this research, atomically-dispersed iridium catalyst with excellent oxygen evolution catalytic activity was firstly synthesized followed by loading on hematite photoanodes. The photoelectrochemical measurements have shown a remarkable cathodic shift of the turn-on voltage and a significant increase in photocurrent. The detailed mechanism through which the atomically-dispersed iridium catalyst enhanced the photoelectrochemical performance of hematite was thoroughly investigated by in-situ transient absorption spectroscopy, in-situ Raman spectroscopy, and in-situ extended X-ray absorption fine structure analysis along with density-functional theory calculations. By doing this, we hope to unravel the mechanisms involved in the higher activity of atomically-dispersed iridium on hematite for the first time, and hence, to provide a guide to employ such cocatalysts for integrated solar-to-fuel conversion.

References

- [1] Sivula, K., van de Krol, R. *Nat Rev Mater* 1, 15010 (2016).
- [2] Montoya, J., Seitz, L., Chakhranont, P. et al. *Nature Mater* 16, 70–81 (2017).
- [3] Nellist, M. R., Laskowski, F. A. L., Lin, F., Mills, T. J. & Boettcher, S. W. *Acc. Chem. Res.* 49, 733-740 (2016).
- [4] Kuang, Y., Yamada, T. & Domen, K. *Joule* 1, 290-305 (2017).
- [5] Yang, X.-F., Wang, A. Q., Zhang, T. et al. *Acc. Chem. Res.* 46, 1740-1748, (2013).
- [6] Zhang, B. Sun, L. *Chem Soc Rev* 48, 2216-2264, (2019).
- [7] Cui, C., Heggen, M., Zabka, W.D. et al. *Nat Commun* 8, 1341 (2017).
- [8] Li, W., Sheehan, S. W., Wang, D. W. et al. *Angew.Chem.* 54, 11428-11432, (2015).
- [9] Kay, A., Cesar, I. & Grätzel, M. J. *Am. Chem. Soc.* 128, 15714–15721 (2006).

1:20 PM EN14.15.09

Liquid Metal Dealloying Toward Nanoporous Mo-Based Intermetallic Compounds for Efficient Hydrogen Production Ruirui Song^{1,1}, Jiuhui Han¹, Masayuki Okugawa², Takeshi Wada¹, Jing Jiang¹, Daixiu Wei¹ and Hidemi Kato¹; ¹Tohoku University, Japan; ²Osaka University, Japan

Dealloyed 3D nanoporous materials with bicontinuous open porous structure, large specific surface area, high electric conductivity, and superior catalytic activity are ideal monolithic electrodes for electrochemical devices. Molybdenum-based intermetallic compounds have been considered as promising low-

cost alternatives to noble platinum for the electrocatalytic hydrogen production, but they have rarely been developed into nanoporous structures due to the challenges in controlling the composition and chemical order during low-temperature chemical dealloying. Here, we report the direct fabrication of nanoporous Mo-based intermetallic compounds of Co_7Mo_6 and Fe_7Mo_6 by a liquid metal dealloying method at elevated temperatures. An unexpected derivation of the characteristic length of dealloyed nanoporous structures from the conventional linear trend in “ligament diameter *versus* inverse homologous temperature ($1/T_H = T_m/T_{\text{dealloy}}$)” is discovered, suggesting a unique intermetallic effect on the pore formation. Assisted by molecular dynamics simulation, this intermetallic effect is explained by the suppressed surface diffusivity of the ordered μ phases that retards the thermal coarsening. As a result, the nanoporous Co_7Mo_6 with a fine structure and correspondingly large surface area delivers excellent activity toward the electrochemical hydrogen production, together with high durability. This study sheds light on a previously unexplored intermetallic effect in dealloying and would promote the development of advanced nanoporous electrocatalysts for energy applications.

1:25 PM EN14.15.10

Crystalline PEDOT:PSS-Platinum Nanoparticle Composites for Volumetric Electrochemical Catalyst Da-Young Lee, Hye-Min Shin and Myung-Han Yoon; Gwangju Institute of Science and Technology, Korea (the Republic of)

Recently, poly(3,4-ethylenedioxythiophene):poly(styrene sulfonate) (PEDOT:PSS) is a widely used as an active component for water-related electrochemical catalysis and photocatalysis due to its decent electrical conductivity, high optical transparency, and good mechanical flexibility. Nonetheless, its hygroscopic nature, intrinsic inhomogeneity, and poor catalytic activity have limited its broad impact on electrochemical catalyst research. In this research we developed the PEDOT:PSS-platinum nanocomposite electrode by electroplating platinum nanoparticles within the crystalline PEDOT:PSS nanofibrillar matrix and demonstrated its electrochemical catalytic function for hydrogen evolution reaction. We systematically investigated optical, structural, electrical, and electrochemical properties of crystalline PEDOT:PSS-platinum nanoparticle composites. The resultant nanocomposite electrode showed the uniform impregnation of platinum nanoparticles into the whole volume of PEDOT:PSS films, leading to the volumetric electrochemical catalyst with high aqueous stability, high reactant permeability, large electrochemically active surface area ($20 \text{ m}^2/\text{g}_{\text{pt}}$) and enhanced catalytic activity for HER (overpotential of 54.7 mV at $10 \text{ mA}/\text{cm}^2$) compared to that of Pt nanoparticle-tethered electrode without PEDOT:PSS.

1:30 PM EN14.15.11

Effects of Replacing La with Y in A_2B_7 -type $\text{La}_{6-x}\text{Y}_x\text{Ni}_{19.5}\text{MnAl}_{0.5}$ Materials on Hydrogen Storage Properties Emil H. Jensen¹, Chiara Milanese² and Sabrina Sartori¹; ¹University of Oslo, Norway; ²University of Pavia, Italy

In recent years A_2B_7 -type RE-Mg-Ni hydrogen storage alloys have been investigated to replace the conventional AB_5 -type negative electrodes due to the higher storage capacity ($\sim 400 \text{ mAh/g}$ vs a theoretical capacity of 372 mAh/g for AB_5). Due to the high Mg vapour pressure, the exact composition of these A_2B_7 materials is challenging to control during production. At the same time, Mg is easily volatilized into ultra-fine powder particles, thus becoming a safety hazard. As a result, new production techniques have been developed. However, these are either expensive or complicated to reproduce [1]. Thus another option is to produce Mg free compositions. By replacing the Mg element with Y, a similar capacity (392.9 mAh/g) is found for $\text{LaY}_2\text{Ni}_{10}\text{Mn}_{0.5}$ [2]. Controlled studies into how Y is affecting the electrochemical capacity, stability and phase composition have been performed by Liu et al. [3] and Zhao et al. [4]. However, the effects on the gas storage properties are not well understood. In the current study, the effects of replacing La with Y on the thermodynamic and kinetic properties of $\text{La}_{6-x}\text{Y}_x\text{Ni}_{19.5}\text{MnAl}_{0.5}$ ($x = 3, 4, 5$) are presented.

1. Yan, H.; Xiong, W.; Wang, L.; Li, B.; Li, J.; Zhao, X. Investigations on AB_3 -, A_2B_7 - and A_5B_9 -type La Y Ni system hydrogen storage alloys. *Int. J. Hydrog. Energy*, **2017**, Vol 42, 2257-2264. doi:10.1016/j.ijhydene.2016.09.049

2. Xiong, W.; Yan, H.; Wang, L.; Verbetsky, V.; Zhao, X.; Mitrokhin, S.; Li, B.; Li, J.; Wang, Y. Characteristics of A_2B_7 -type La Y Ni-based hydrogen storage alloys modified by partially substituting Ni with Mn. *Int. J. Hydrog. Energy*, **2017**, Vol 42, 10131-10141. doi:10.1016/j.ijhydene.2017.01.080

3. Liu, Y.; Yuan, H.; Guo, M.; Jiang, L. Effect of Y element on cyclic stability of A_2B_7 -type La-Y-Ni-based hydrogen storage alloy. *Int. J. Hydrog. Energy*, **2019**, Vol 44, 22064-22073. doi:10.1016/j.ijhydene.2019.06.081

4. Zhao, L.; Luo, Y.; Deng, A.; Jiang, W. Hydrogen Storage and Electrochemical Properties of the Mg-free A_2B_7 -type $\text{La}_{1-x}\text{Y}_x\text{Ni}_{3.25}\text{Mn}_{0.15}\text{Al}_{0.1}$ Alloys with Superlattice Structure. *Chemical Journal of Chinese Universities*, **2018**, Vol 39, 1993-2002. doi:10.7503/cjcu20180169

1:35 PM EN14.15.12

Statistical Analysis and Machine Learning Performed on a Large Electrocatalyst Dataset Generated by High-Throughput Experimentation Lars Banko, Olga A. Krysiak, Wolfgang Schuhmann and Alfred Ludwig; Ruhr-Universität Bochum, Germany

High-throughput experimentation (HTE) generates large, comprehensive datasets with reasonable efforts. In combination with efficient electrocatalytic screening, the corresponding datasets produced by HTE have a huge potential to generate improved understanding of the governing principles that drive electrocatalytic activity in compositionally complex alloys. The challenge is to identify viable combinations of elements and their mixing ratios out of millions of possible combinations and discover new electrocatalysts with advanced properties.

In this contribution, the electrochemical activity data of > 40 sputtered composition spread materials libraries are analyzed using statistical methods and machine learning. The dataset spans > 15000 different chemical compositions distributed in > 15 compositionally complex material systems from combinations of > 25 chemical elements. Electrochemical characterization was performed using a scanning droplet cell. The electrochemical dataset contains $> 20\,000$ linear sweep voltammograms measured by the scanning droplet cell and covers relevant potential ranges for the hydrogen evolution reaction, the oxygen reduction reaction and the oxygen evolution reaction.

The results of statistical analysis and preliminary predictive machine learning models highlight the value of large experimental datasets generated by HTE for the data-driven development of high-performance catalysts.

1:40 PM EN14.15.14

Hydrogen Production using $\text{LaNi}_x\text{Co}_{1-x}\text{O}_3$ Perovskite Catalyst by Steam Reforming of Bio-Oil Model Compounds Piyush P. Singh, Neelkanth Nirmalkar and Tarak Mondal; Indian Institute of Technology Ropar, India

Now a days agriculture waste are very challenging as most of the residues burn, which deteriorate the environment directly. The conversion of agricultural waste into energy has twin benefits for society - utilization of waste and sustainable energy production. In this regard, catalytic steam reforming (SR) of bio-oil produces hydrogen, which is a clean and green source of energy having heating value 2.5 times to the petroleum products. In recent years, perovskite oxides have drawn tremendous attention for green hydrogen production due to their excellent catalytic properties. Reported study suggests that the presence of oxygen vacancies of A atoms and ability to break carbon-carbon and carbon-hydrogen bonds of B-site atom make it suitable for steam reforming processes. Here, we report a series of $\text{LaNi}_x\text{Co}_{1-x}\text{O}_3$ perovskite catalysts for the SR of a mixture of bio-oil model oxygenates to produce green hydrogen. The effect of variation of reaction temperature, Ni and Co species composition, steam to carbon molar ratio (SCMR), and weight hourly space-time (WHST) on gaseous products yield and bio-oil conversion were evaluated using fixed catalytic bed reactor unit. The $\text{LaNi}_{0.5}\text{Co}_{0.5}\text{O}_3$ exhibited the best

catalytic activity (83% hydrogen yield and 95% conversion) towards hydrogen production among all other combinations of $\text{LaNi}_x\text{Co}_{1-x}\text{O}_3$ catalysts. The catalyst deactivation study revealed that the deactivation was primarily due to two types of coke (amorphous and carbon nanotubes) deposition validate by the thermogravimetric analysis.

1:45 PM EN14.15.15

Transition Metal Chalcogenides as Electrocatalysts for Efficient Sea Water Splitting Rajarshi Kar¹, Jahangir Masud², Harish Singh¹, Umanga De Silva¹ and Manashi Nath¹; ¹Missouri University of Science & Technology, United States; ²University of North Dakota, United States

Designing a catalyst with high efficiency toward oxygen evolution reactions (OERs) through sea water splitting is a promising factor in recent times for hydrogen production from renewable sources which can consequently contribute towards energy sustainability. Seawater electrolysis possess a challenge of suppressing chlorine evolution reaction (CER), which leads to the undesirable formation of chlorine gas, while enhancing OER. In the current investigation, Nickel Telluride based electrocatalyst was synthesized through electrodeposition process directly on gold-coated glass substrate. When employed as an OER catalyst, the nickel telluride electrode exhibits a current density of 10 mA/cm² at an OER overpotential of 180 mV with superior stability in a highly alkaline electrolyte which replicates original unfiltered seawater. More importantly, it was observed that nickel telluride did not lead to generation of Cl₂ through CER in simulated seawater electrolyte. To comprehend the admirable OER activity of the Nickel Telluride electrode, a Tafel plot was derived from the LSV curves. The Tafel slope was found to be 56 mV dec⁻¹, which surpass the revolutionary RuO₂ catalyst at 114.4 mV dec⁻¹, indicating superior kinetic performance of nickel telluride. The long term OER stability of the nickel telluride electrocatalyst in artificial seawater was confirmed through surface-sensitive analytical approaches such as XPS. The stability was reestablished through high resolution surface imaging techniques such as SEM and TEM, which confirms that the catalyst surface did not undergo any deterioration, or compositional change. The oxygen and hydrogen gas evolution for Nickel Telluride catalyst was collected over an electrode surface area of 0.5 cm² at a working potential of 0.6 V over a duration of 2 hours. The ratio between the hydrogen and oxygen gas evolved was 1.82:1 which is very close to the 2:1 ratio for electrocatalytic full water electrolysis. Nickel telluride was hence identified as an ideal catalyst to promote OER through seawater electrolysis with low overpotential and high stability while suppressing generation of toxic chlorine gas.

1:50 PM EN14.15.18

Visible Light-Induced Electrochemical Performance of CdS@WS₂ as an Oxygen Evolution Photoelectrode in Water Splitting Muthuraja A. V and Praveen Meduri; IIT Hyderabad, India

Photoelectrochemical water splitting (PEC) is a compelling approach to convert solar energy to chemical energy by liberating hydrogen, making it a possible solution to the worldwide energy crisis by eliminating all carbon dioxide emissions. In practice, no single electrode material can meet all PEC water splitting requirements. The major challenges for PEC are electron-hole pair recombination, stability, and reduced absorption of visible light. Transition Metal dichalcogenides (TMD) based heterostructures are being envisioned as novel electrode materials because of their exceptional electrical, chemical, mechanical, and thermal stability which include high electron mobility, highly exposed active sites, layer dependent bandgap, and higher ionic conductivity, etc. TMDs have higher electro conductivity resulting in significant enhancement of the electrochemical performance in PEC. Further, it also exhibits desirable electrochemical behavior through its oxygen evolution reaction (OER) and hydrogen evolution reaction (HER) as a photoelectrode for water splitting. However, due to poor absorbance and significant reflection at the grain boundaries, the light-harvesting ability of bulk or nanosized TMD materials is often limited. The charge carriers produced by light illumination will also reach the surface faster than bulk materials in the semiconductor, because of the lesser transport distance.

In the present work, heterostructures consisting of Tungsten disulfide (WS₂) and cadmium sulfide (CdS) were synthesized using a hydrothermal method and Successive Ionic Layer Adsorption Reaction (SILAR) deposition method. The presence of these nanostructures was confirmed by XRD, Raman, UV-Visible spectroscopy, SEM, TEM, and PL spectroscopy. The morphological study clearly indicates a homogeneous distribution of CdS nanospheres on WS₂ nanostructures, indicating close contact between them which helps in efficient charge separation and migration. Further, the continuous nature of the heterostructures of the two materials is not limited to any visible discrete entities. The porosity of the pristine WS₂ nanostructures allows CdS nanospheres to deposit inside the pores along with the entire thickness of the nanosphere, and hence, the highly homogeneous nature of the heterostructures is obtained as indicated by the physical characterization. Due to this unique structure, the obtained heterostructures showed excellent performance as photoanode. The CdS@WS₂ photoanode demonstrated a photocurrent density of 0.15 mA cm⁻² at 1.23 V vs. RHE, which is over 20 times higher than that of the pure pristine materials. Further, CdS@WS₂ heterostructures, as compared to pure materials, have demonstrated longer emission-decay-life times and dramatically quenched the emission of fluorescence compared to pristine materials. In CdS@WS₂ heterostructures, the absorption edge of the WS₂ nanostructures also exhibits a considerable increase in light absorption in the total visible spectrum. This results in enhanced charge separation with proper band alignment leading to improvements in electrochemical performance of CdS@WS₂ photoelectrodes. Further, the low onset potential further eliminates the need for voltage bias in practical applications.

References:

[1] Peng, W.; Li, Y.; Zhang, F.; Zhang, G.; Fan, X. Roles of Two-Dimensional Transition Metal Dichalcogenides as Cocatalysts in Photocatalytic Hydrogen Evolution and Environmental Remediation. *Ind. Eng. Chem. Res.* 2017, 56, 4611-4626 <https://doi.org/10.1021/acs.iecr.7b00371>.

[2] Faraji, M.; Yousefi, M.; Yousefzadeh, S.; Zirak, M.; Naseri, N.; Hwa, T. Two-Dimensional Materials in Semiconductor Photoelectrocatalytic Systems for Water Splitting. *Energy. Environ. Sci.* 2019, 12, 59-95. <https://doi.org/10.1039/c8ee00886h>.

1:55 PM EN14.15.19

Ultrathin Palladium Nanowire-Based Chemiresistive Sensors on Paper Substrates for Room-Temperature Detection of Hydrogen Abhishek Kumar, Thomas Thundat and Mark T. Swihart; University at Buffalo SUNY, United States

Hydrogen (H₂) is often seen as a cleaner alternative to conventional fossil fuels with zero carbon emission. Its usage, however, is limited by its lower explosion limit (4%) and high permeability through many materials that make storage and handling of H₂ a challenging task. Hence, the development of low-cost, fast, and sensitive H₂ detection technologies is of paramount importance to the development of the future hydrogen-based economy. The United States Department of Energy (US-DOE) has set a target for the cost of H₂ sensors for fuel-cell-powered vehicles to be <\$15 including the cost of electronics. Paper is an inexpensive, flexible, porous, adaptable, environmentally-friendly, and degradable material that has huge potential for the development of sustainable electronics. We report an ultra-low-cost paper-based sensor for room-temperature detection of hydrogen (H₂) using ultrathin palladium nanowires (PdNWs) and prepared by a simple drop-casting method. To gain insight into the sensing mechanism of ultrathin PdNWs, we compare the performance of polycrystalline PdNWs to that of single-crystalline PdNWs. The polycrystalline PdNWs showed a response (fractional resistance change) of 4.3% to 1% H₂ with response and recovery times of 4.9 s and 10.6 s, respectively. Similarly, the single-crystalline PdNWs showed an 8% response to 1% H₂ with slightly slower response and recovery times of 9.3 s and 13.0 s, respectively. The polycrystalline PdNWs show excellent

selectivity to H₂ with a limit of detection of 10 ppm of H₂ in air and good stability under repeated exposure to H₂ and after extended storage in air. We attribute the fast response and recovery times of the ultrathin polycrystalline PdNW-based sensors to synergistic effects of their ultrathin (< 5 nm) diameter, strain-coupled grain boundaries, and the porous paper substrate that facilitates rapid transport to exposed PdNWs. This paper-based sensor, using only ~100 µg Pd per device on a substrate of negligible cost, is one of the fastest chemiresistive H₂ sensors and could be orders of magnitude less expensive than the current state-of-the-art H₂ sensing solutions.

2:00 PM EN14.15.20

PLD and O₂ Annealing Synthesis of La_{n+1}Ni_nO_{3n+1} Epitaxial Films for SOFC Cathode Material Shohei Hisatomi¹, Yuki Goto¹, Tomoaki Oga¹, Kenta Kaneko¹, Kazuki Watanabe¹, Satoru Kaneko^{2,1}, Mamoru Yoshimoto¹ and Akifumi Matsuda¹; ¹Tokyo Institute of Technology, Japan; ²Kanagawa Institute of Industrial Science and Technology, Japan

There is a strong requirement to establish a hydrogen energy system with the aim of realizing the sustainable society. Highly efficient solid oxide fuel cells (SOFCs) are capable of supplying both heat and electricity without precious catalytic metals, utilizing various fuels such as natural gas, ammonia, and biogas. SOFCs are expected to operate at low temperatures. Reduction of the operation temperature by couple of hundred degrees from conventional >800°C would expand options of surrounding materials and structures, that contributes to improved performances and cost-effective development of the systems. Thus, it has been of importance to improve conductivity of cathode materials to advance the low-temperature operation efficiency. Meanwhile, lanthanum nickelates La_{n+1}Ni_nO_{3n+1} (*n*=1, 2, and 3) with layered perovskite structures, such as La₂NiO₄, have been developed and their mixed oxygen-ion/electron conductivity has been researched as an expected property for the cathode application in SOFCs [1–3]. Although, the electronic transport properties of the higher order (*n*≥2) phases still require further study to understand its correlation with their structures. It is also of significance to find an effect of impurity doping on modification of the structure and electronic properties. In this study, La₄Ni₃O₁₀ (*n*=3) thin films were epitaxially developed on single crystal substrates, and the effect of tetravalent doping on their structure and properties was investigated.

The pure and (Hf⁴⁺, Sn⁴⁺) co-doped lanthanum nickelate thin films were grown on single crystal NdGaO₃ (110) substrates by pulsed laser deposition (PLD) method using a KrF excimer laser (λ=248 nm) and sintered targets of pure and co-doped La₄Ni₃O₁₀ (0.625 at% for each dopant). The fluence and repetition of the laser beam were *E*~1.0 J/cm² and *f*=3 Hz, respectively. Deposition ambience was 10 Pa O₂-flow (base pressure ~3×10⁻⁶ Pa), and the substrate temperature was kept at 700°C. The grown lanthanum nickelate thin films were subsequently heat treated in atmospheric O₂-flow at 950°C for 10 hours.

The epitaxy of (Hf⁴⁺, Sn⁴⁺) co-doped La₄Ni₃O₁₀ (001) thin films on NdGaO₃ (110) substrates were obtained after the deposition, that XRD analyses using monochromated CuKα1-ray demonstrated {001} diffraction peaks in 2θ/ω-scan and planar four-fold symmetry in φ-scan detecting {208} diffractions. The co-doped epitaxial La₄Ni₃O₁₀ (001) thin film revealed resistivity of ρ=8.9×10⁻² Ωcm at room-temperature, measured by four-probe DC method. Further development of La_{n+1}Ni_nO_{3n+1} crystal phases other than the case of *n*=3 was available by modification of the O₂ pressure and deposition rate during the thin film growth. Further detailed structural analyses, physical properties including electric conductivity at raised temperature, and comparative study with pure films will also be presented.

[1] S. Yoo et al., RSC Advances, 2 (2012) 4648–4655.

[2] R. Sayers et al., Solid State Ionics, 192 (2011) 531–534.

[3] Y. Gong et al., JOM, 71 (2019) 3848–3858.

SESSION EN14.16: Hydrogen Production III
Session Chair: Christopher San Marchi
Tuesday Afternoon, December 7, 2021
EN14-Virtual

4:00 PM EN14.16.01

Theoretical Insight into Absolute Surface and Interface Energies and Optoelectronic Properties of 2D Vertical Singularities for III-V/Si Heterostructure Applications Pedesseau Laurent, Ida Lucci, Lipin Chen, Jacky Even and Charles Cornet; FOTON Institute - INSA Rennes, France

Solar water splitting converting the solar energy into green hydrogen fuel is one significant milestone on the road to a sustainable energy future and has driven many researches in the past years [1]. III-V/Si heterostructure combining the good optical properties of III-V semiconductors with the low cost of Si substrates is considered as an attractive solution for efficient water splitting reactions [2-4].

Here, we first show that surface and interface energies play a central role during the epitaxy of III-V semiconductors on Si. We then demonstrate that the presence of 2D vertical singularities (antiphase boundaries) drastically modify the electronic properties of the heterostructure, yielding very promising photo-electro-chemical (PEC) device performances. The strong absorption of light by the bulk materials is the first requirement for the proper operation of the PEC. Next, it is also essential to efficiently extract and collect the carriers. Therefore, the atomistic studies based on the density functional theory have been dedicated to three different aspects: i) the optoelectronic properties of bulk materials, ii) the study of surface stability to understand III-V/Si heteroepitaxy, and iii) the study of interfaces and 2D vertical singularities used to collect charge carriers.

References:

[1] A. J. Bard and M. A. Fox, “Artificial photosynthesis: solar splitting of water to hydrogen and oxygen”, Accounts of Chemical Research, 28(3), 1995.

[2] I. Lucci et al., “A Stress-Free and Textured GaP Template on Silicon for Solar Water Splitting”, Advanced Functional Materials, 28(30):1801585, 2018.

[3] M. Alqahtani et al., “Photoelectrochemical water oxidation of GaP1– xSbx with a direct band gap of 1.65 eV for full spectrum solar energy harvesting”, Sustainable Energy & Fuels 3, 2019.

[4] I. Lucci et al., “Universal description of III-V/Si epitaxial growth processes” Physical Review Materials 2 (6), 060401, 2018

4:15 PM EN14.16.02

Semiconducting Polymers as Promising Materials for Photoelectrochemical Water Splitting Han-Hee Cho¹, Liang Yao², Dan Zhang¹, Jun-Ho Yum¹ and Kevin Sivula¹; ¹EPFL, Swaziland; ²Max Planck Institute for Solid State Research, Germany

Direct solar-driven water splitting into hydrogen (H₂) and oxygen (O₂) has emerged as a leading approach to reduce our dependence on fossil fuels as hydrogen can be converted into electrical energy using a fuel cell or transformed into chemical feedstocks. However, the identification of ideal light harvesting semiconductors that meet performance and cost requirements for industrialization still remains a main obstacle. Organic photoelectrochemical cells (OPECs) in which pi-conjugated organic semiconductors (OSs) are coupled with co-catalysts have recently attracted great attention as alternative photoelectrodes for solar water reduction (yielding hydrogen) and oxidation (yielding oxygen), considering unique features of OSs such as precisely

tunable optoelectrical properties and solution-processability at low temperature. Nevertheless, the conversion efficiency and stability of OPECs (both photocathode and photoanode) for the solar water splitting have remained particularly poor. Herein, we present high-performance and robust organic photoelectrochemical cells by employing a bulk heterojunction (BHJ) blend of semiconducting polymers as a photoactive layer. Our in-depth study using sacrificial agents for photoreduction and photooxidation unveils critical parameters that significantly affect the performance and operational stability of OPECs: (i) rational selection of semiconducting polymer donor and acceptor to generate free charges efficiently and ensure chemical stability upon illumination, (ii) large surface roughness of interlayers to improve interfacial adhesion, and (iii) mitigation of charge accumulation at the interfaces. By leveraging these insights, our optimized polymer BHJ photocathode and photoanode where the polymer BHJ layers are coupled with hydrogen and oxygen evolution catalysts, respectively, show outstanding performance and unprecedented robustness compared to previous OPECs, demonstrating a new benchmark of OPECs for solar fuel production. In particular, the polymer BHJ photocathode and photoanode exhibit initial 1 Sun photocurrent density values up to 8.7 mA cm⁻² at 0 V vs RHE and 2.3 mA cm⁻² at 1.23 V vs RHE for solar water reduction and oxidation with 100% Faradaic efficiency, respectively, which can rival the performance of their inorganic counterparts. More importantly, further engineering of charge transport layer to establish stability of polymer BHJ photocathodes in wide range of pH leads to the first demonstration of an organic tandem photoelectrochemical cell for complete solar water splitting in the same electrolyte in the absence of a membrane, which is a considerable advance in the field of OPECs. Consequently, our work coupled with the facile solution processability of the semiconducting polymers establishes the use of polymer BHJs as a promising path towards efficient, scalable, and economical photoelectrochemical cells for overall solar water splitting.

References

Han-Hee Cho *et al.* *Nat. Catal.* **2021**, 4, 431–438
Liang Yao *et al.* *J. Am. Chem. Soc.* **2020**, 142, 17, 7795–7802

4:30 PM EN14.16.03

Enhanced Water Splitting Performance of MoS₂ and PdSe₂ Using Heterostructuring Edward A. Baker, Joe Pitfield and Steven Hepplestone; University of Exeter, United Kingdom

Two dimensional materials, such as the transition metal dichalcogenides (TMDCs) are a good candidate for water splitting catalysts [1,2], as they often have larger band gaps than their bulk counterparts. However, this had to be balanced by the thin layers having a small absorption cross section and difficulties in mounting on a suitable substrate. PdSe₂ is being suggested as a potential water splitting candidate [3]. However its bulk band gap is too small for water splitting [4]. We propose to use this structure as a surface coating to a second TMDC with a larger band gap such as MoS₂ and use this as an example of how such heterostructures could function.

Using density functional theory, implemented in the Vienna Ab-initio Simulation Package, we have investigated the surfaces of TMDC monolayers MoS₂ and PdSe₂, and a Hetero-bilayer of the two, for their potential application as photocatalytic water splitters. The different functional groups involved in the Hydrogen and Oxygen evolution reactions have been added to the monolayers and the hetero-bilayer to determine their energetics. In addition to this, we have looked at how stable these materials are, to both adsorptions and substitutions, in both air and water environments.

References:

[1] Qing Tang and De En Jiang. *ACS Catalysis*, 6(8):4953–4961, Aug 2016.
[2] B. Amin, et al. *Phys. Rev. B*, 92:075439, Aug 2015.
[3] C. Long, et al. *ACS Appl. Energy Mater.*, 2, 1, 513-520, 2019.
[4] G. Zhang, et al. *Appl. Phys. Lett.*, 114, 253102, June 2019.

4:45 PM EN14.16.04

Optical and Scanning Electrochemical Microscopy for Facile Localized Photoelectrochemical Measurement Bhavana Gupta and Wojciech Nogala; Polish Academy of Science, Poland

For conducting localized photoelectrochemical analysis of photoanode, several *in-situ* electrochemical techniques have emerged. Scanning electrochemical microscopy (SECM) is one of the methods by which localized properties of the surface are analyzed with the help of a microelectrode probe. We present here a highly resolved photoelectrochemical property of α -Fe₂O₃ surface through a new and more straightforward approach in SECM set-up. Optical microscope objective is used to illuminate a localized surface from the bottom of the sample and a micro-electrode probe scan the sample from the top. The surface generation and tip collection mode of SECM is used to detect locally products of photoelectrochemical reaction at the sample. Recorded faradaic current is directly correlated to the oxygen evolution quantitatively on the surface of photoanode as the influence of light in terms of oxygen flux. Both qualitative and quantitative information of oxygen evolution will open new gateways in the field of photoelectrochemistry to understand the influence of dopants and hole scavengers by an easy and conventional approach.

5:00 PM EN14.16.05

Surface Engineering and Controlled Growth of 2D-3D In₂S₃ and ZnO Photocatalytic Heterojunction for PEC Water Splitting by Chemical Vapor Deposition Narinder Kaur and Bodh Raj Mehta; Indian Institute of Technology, India

Surface modifications and substrate effect growth of photoanode for heterojunction ZnO/In₂S₃ are achieved in this paper. 2D nanolayers of In₂S₃ and 3D ZnO have been synthesized using a two-step process physical vapor deposition (PVD) for ZnO, followed by chemical vapor deposition (CVD) for 2D layers of In₂S₃ for PEC application. Enhanced photocurrent density in heterojunction ZnO/In₂S₃ is reported due to uniformity in film growth, increased surface area, and efficient electron-hole separation at the heterojunction interface. A photocurrent density of 2.4 mAcm⁻² is produced for ZnO/In₂S₃ heterojunction, which is 2.5 and 1.4 times higher than pristine ZnO and In₂S₃ at 1.23V (vs. RHE). Transient photocurrent density plots at different wavelengths confirm that the enhancement in photoelectrical response of the interface at lower energy (2.4 eV) compared to ZnO (3.1 eV) is due to absorption in the In₂S₃ layers with energy 2.3 eV. The present approach can be extended to other heterojunctions with 2D materials having different optical and electronic properties.

5:15 PM EN14.16.06

Mitigating Voltage Losses in Scaling-up Photoelectrochemical Water Splitting Devices Keisuke Obata, Babu Radhakrishnan, Ciler Özen and Fatwa F. Abdi; Helmholtz-Zentrum Berlin, Germany

Significant progress has been reported in solar water splitting, with solar-to-hydrogen (STH) efficiency as high as 30% already demonstrated. However, two major challenges remain. First, these high-efficiency devices (> 15%) have only been achieved using expensive and non-scalable III-V semiconductors. Low-cost metal-oxide based devices, mainly using BiVO₄ as the absorber, have only achieved STH efficiency of < 10%. Due to stability limitations, many of these metal-oxide based devices are operated in near-neutral pH electrolytes, which poses an additional mass transport challenge. Second, the majority of the demonstrated devices are still at the laboratory scale. Reports on large-area devices are limited, and they typically show much lower efficiencies. This is best illustrated in a recent review:^[1] even when III-V semiconductor-based devices are considered, there is no report of devices

with a semiconductor absorber area larger than 10 cm² and STH efficiency > 10%. In this talk, we will discuss the scale-up of our photoelectrochemical water splitting devices based on a complex metal oxide absorber. Factors other than the semiconductor itself are found to be responsible for a total voltage loss of > 500 mV and therefore limit the overall performance of the large-area device.^[2] We use a combination of multiphase multiphysics simulations (2-D and 3-D finite element analysis models) and validation experiments (e.g., in-situ pH fluorescence, particle image velocimetry, shadowgraphy) to quantify and breakdown the different loss mechanisms (substrate and electrolyte Ohmic loss, concentration overpotentials, product crossover, bubble-related losses) while scaling-up photoelectrochemical water splitting devices.^[3-6] Based on these insights, electrochemical engineering strategies to overcome the scale-up related losses are offered.

References

1. J. H. Kim et al., *Chem. Soc. Rev.* 48, 2019, 1908
2. I. Y. Ahmet et al., *Sust. Energy Fuels* 3, 2019, 2366
3. F. F. Abdi et al. *Sust. Energy Fuels* 4, 2020, 2734
4. K. Obata et al. *Energy Environ. Sci.* 13, 2020, 5104
5. K. Obata et al. *Cell Rep. Phys. Sci.* 2, 2021, 100358
6. K. Obata & F. F. Abdi, *Sust. Energy Fuels*, 2021. DOI: 10.1039/D1SE00679G

5:30 PM EN14.16.08

High-Throughput Experimentation and Artificial Intelligence for the Discovery of New Energy Materials Lars Banko, Olga A. Krysiak, Wolfgang Schuhmann and Alfred Ludwig; Ruhr-Universität Bochum, Germany

High entropy alloys (HEA) comprising four or more constituent elements, are an interesting new class of materials with tunable chemical composition providing the basis for catalytic or electrocatalytic activity towards many reactions. The high electrocatalytic activity of HEA is related to an abundance of active sites, resulting from the statistical distribution of the elements on the surface. With noble metal prices on the rise, noble-metal-free HEA have the potential to decrease the cost for electrocatalysts in various energy conversions technologies.

The challenge involved with both, the experimental and computational exploration of HEA, lies in the enormous number of possible combinations of chemical elements and their mixing ratios, leading to a huge option space for the development of new catalysts. With millions of possible element combinations and roughly 10⁴ possible mixing ratios for each material system, fundamentally new research strategies are required.

In this contribution, a high-throughput experimentation strategy is reported, enabling rapid synthesis and screening of possible HEA catalysts materials for water splitting and fuel cells. Combinatorial co-deposition using magnetron sputtering is applied to cover substantial parts of the total composition space of quinary HEA material systems in materials libraries. Electrochemical high-throughput screening is applied to map the electrocatalytic activity over the chemical compositions.

It is demonstrated that within a HEA material system, the electrochemical activity can be increased significantly (e.g. by a factor of 10 as demonstrated in this contribution) by adjusting the mixing ratios of individual elements. The large electrochemical datasets generated by this approach enable the use of artificial intelligence methods (e.g. supervised and unsupervised) for the optimization of chemical composition and synthesis parameters with an enormous potential for understanding the driving forces of electrocatalytic activity and predicting advanced materials.

SESSION EN14.17: Hydrogen Production IV
Session Chairs: Huyen Dinh, Sophia Haussener and T. Venkatesh
Wednesday Morning, December 8, 2021
EN14-Virtual

8:00 AM *EN14.17.01

Material and Component Requirements for (Scaled) Photo-Electrochemical Hydrogen Processing Utilizing Concentrated Irradiation Sophia Haussener; Ecole Polytechnique Federale de Lausanne, Switzerland, Switzerland

Photoelectrochemical (PEC) approaches for the processing of solar fuels and materials are interesting, provided they can be efficiently, stably, scalably, and sustainably implemented. One way to increase the economic and sustainable competitiveness is the utilization of concentrated irradiation [1]. This pathway also allows for the thermal integration of the photoabsorbing and electrocatalytically active components, benefiting the performance as a whole [2]. Scaling of such a thermally integrated photo-electrochemical system keeps the interesting thermal dynamics while also indicating that co-generation of hydrogen and heat increase overall system efficiency [3].

I will discuss material challenges for PEC devices in terms of efficiency and longevity at the laboratory scale, specifically focusing on the unique challenges related to the utilization of concentrated radiation and thermal integration. Additionally, the transition from the laboratory scale (at ~100W power) to the demonstration scale (at ~10kW power) requires tackling alternative challenges related to different approaches for component integration and the design of a complete system, including the incorporation of fitting auxiliary components. I will discuss these integrational challenges at the larger scale, while also discussing requirements for the complete solar processing plant design, both informed by our recent large-scale outdoor and on-sun demonstration activities.

References

- [1] M. Dumortier, S. Tembhurne, S. Haussener, *Energy Environ. Sci.*, 8:3614–3628, 2015.
- [2] S. Tembhurne, F. Nandjou, S. Haussener, *Nature Energy*, 10.1038/s41560-019-0373-7, 2019.
- [3] I. Holmes-Gentle, S. Tembhurne, C. Suter, S. Haussener, *Int. Jou. of Hydrogen Energy*, 10.1016/j.ijhydene.2020.12.151, 2020.

8:30 AM EN14.17.02

High-Performance BiVO₄ Photoanode Fabricated via Sputtering on Patterned FTO Sucheol Ju, Nakhun Kim and Heon Lee; Korea University, Korea (the Republic of)

Bismuth vanadate (BiVO₄) is a promising photoanode material; however, its efficiency significantly changes depending on the atomic ratio of Bi/V, and

there is no suitable method for synthesizing large-area photoanodes. In this study, an efficient BiVO₄ photoanode was fabricated via sputtering, by manipulating the molar ratio of Bi/V with V solution annealing. V solution annealing not only adjusted the atomic ratio of Bi/V but also increased the number of O vacancies, thereby improving the charge-separation and charge-transport efficiencies. Consequently, the photocurrent density of the sputtered photoanode with V solution annealing (BVO-V) was 1.86 mA/cm², which is 23 times higher than that of the sputtered photoanode annealed under air conditions (BVO-A, 81.0 μA/cm²). Furthermore, microcone-patterned fluorine-doped SnO₂ was fabricated to increase the active area and reduce the high reflectance, owing to the dense deposition because of the sputtering. Thus, the photocurrent density of the MC-BVO was 3.11 mA/cm², which is approximately 67% higher than that of BVO-V (1.86 mA/cm²).

8:45 AM EN14.17.03

Parallel Water Photo-Oxidation Pathways in Hematite Photoanodes for Solar Water Splitting Anton Tsyganok¹, Paulino Monroy-Castillero², Yifat Piekner¹, Arik Yochelis² and Avner Rothschild¹; ¹Technion, Israel; ²Ben-Gurion University of the Negev, Israel

Hematite is considered as a promising candidate for photoanodes for water photo-oxidation for direct conversion of solar energy to hydrogen in photoelectrochemical (PEC) water splitting. The water photo-oxidation reaction on hematite surface attracts a lot of scientific interest. Different studies highlight the importance of surface states in the oxygen evolution reaction (OER) mechanism and attribute them various roles in the charge transfer and recombination processes that affect both the photocurrent and the photovoltage. In this work we report a study on the surface states by using time dependent cathodic discharge measurements (CDM) of preconditioned hematite photoanodes that were polarized under illumination and potential sufficient to drive oxygen evolution. We show that upon turning the light off, some of the charged (oxidized) surface states discharge spontaneously while others remain meta-stable in their charged state. When the potential is swept cathodically, in a suitable range and rate, double-peak cathodic discharge wave is observed. The magnitude and the shape of the discharge wave depends on the elapsed time between turning the light off and the cathodic sweep. Specifically, we show that the relative heights of the observed cathodic discharge peaks reverse after sufficient time interval. This observation indicates that the cathodic discharge mechanism involves parallel pathways with different relaxation times rather than a single pathway with consequent serial steps, suggesting parallel reaction pathways for the OER on the surface of hematite photoanodes. This conclusion is corroborated by a microkinetic model that is analytically solved for serial and parallel reaction mechanisms. Furthermore, the model predicts the evolution of the two reaction pathways as a function of time and applied potential.

9:00 AM EN14.17.04

Solution-Based Nickel Oxide Passivation on Silicon Photoanode by Light Irradiation Pre-Treatment Hye-Min Shin, Da-Young Lee and Myung-Han Yoon; Gwangju Institute of Science and Technology, Korea (the Republic of)

Photoelectrochemical cells (PEC) have drawn much attention due to their eco-friendly capability of light-to-hydrogen energy conversion. Silicon, a promising candidate for photoelectrode due to its low bandgap and high efficiency in photo water-oxidation, shows low stability during the alkaline-based photoelectrochemical reaction, which spurred the research on materials and deposition methods for thin passivation layer on silicon. Herein, we report on the formation of an efficient passivation layer on silicon photoanode using solution-processed nickel oxide in combination with light irradiation pretreatment. While the thickness of nickel oxide film and the condition for light irradiation pretreatment are systematically varied, the resultant passivation layer is characterized optically, morphologically, and electrochemically. The light irradiation pre-treatment used an excimer lamp ultra violet with a wavelength of 172 nm and was carried out under varying temperature conditions for 1 h at N₂ atmosphere. Thickness of film fabricated through light irradiation pre-treatment are about 50% thinner than that of conventional annealed films and film has a flat roughness. The nickel oxide film fabricated with light irradiation pre-treatment showed higher PEC efficiency with narrow band gap (3.41 eV), higher saturation current (36 mA/cm²), and more left shifted overpotential (-0.3 V from on-set of conventional thermal annealing processing film) than those prepared by the conventional thermal annealing process.

9:15 AM EN14.17.05

First-Principles Study of the Effect of Transition Metal Dopants on Enhancing the Carriers' Concentration in Hematite Photoanodes Hoda E. El Gibally, Nageh K. Allam and Mostafa Youssef; American University in Cairo, Egypt

Hematite's intrinsic properties qualifies it to be one of the most effective photoanodes for photoelectrochemical water splitting (PEC). On the other hand, there are several limiting factors for hematite photoanodes that prohibit them from reaching their maximum theoretical efficiencies. One of the most important negatively affecting factors is the low conductivity in hematite, which results in fast recombination rates and hence the loss of the carriers required to perform the PEC process, which eventually results in low hydrogen production rates. Adding dopants to hematite was proven to be one of the best treatments for the low conductivity issue, since donor dopants can generate sufficient electrons to enhance the conductivity and the overall PEC performance. However, in many cases the desired enhancement in conductivity cannot be attained due to compensators for the donors other than electrons such as iron vacancies and other negatively charged defects. In this research, we investigate the effect of substitutional and interstitial defects resulting from the addition of 1% dopants in hematite to determine the optimal set of dopants that can result in a 1:1 dopant-to-electron ratio while maintaining accessible thermodynamic conditions for hematite sample preparation. The investigated dopants include the whole 3d transition metals, in addition to Zr, Nb and Mo from the 4d transition metals and Hf, Ta and W from the 5d transition metals. The formation energies of the dopant defects are calculated using density function theory simulations with Hubbard U corrections and the results are used to plot Kröger Vink diagrams (KVD) which allow us to determine the donors which results in 1% electrons at reasonably accessible oxygen partial pressures. Furthermore, the diagrams are utilized to highlight the dominant dopant defects, which compensate for the electrons and hence provide an insight about their dominant oxidation state in hematite. A further utility of our computations is investigating the possibility of finding a co-doping scenario that can enhance both electrons and holes simultaneously. Our results suggest that 1% doping with W, Ta, and Nb can achieve a 1:1 electron-to-dopant ratio at the atmospheric pressure. Similarly, 1% Ti, Hf, Zr, and Mo can achieve the same effect but at an oxygen partial pressure two orders of magnitude less than the atmospheric pressure. We also propose a W-Zn doped hematite as an optimal dopant strategy to balance enhancing both electrons and holes at a reasonable oxygen partial pressure. We believe that our computational results can narrow down the search space for performing experiments to test the optimal compositions for doped hematite with the goal of enhancing the hydrogen production rates from PEC.

9:30 AM EN14.17.07

Wasted Photons—Photogeneration Yield and Charge Carrier Collection Efficiency of Hematite Photoanodes for Water Splitting Yifat Piekner¹, David S. Ellis², Daniel A. Grave^{2,3}, Anton Tsyganok² and Avner Rothschild^{2,1}; ¹Technion-Israel Institute of Technology, Israel; ²Technion-Israel Institute of Technology, Israel; ³Ben-Gurion University of the Negev, Israel

Hematite (α-Fe₂O₃) is considered as a leading photoanode candidate, primarily due to its bandgap applicability to the solar spectrum. Its photocurrent is estimated to potentially reach 12.6 mA cm⁻², assuming every photon with above band gap energy is absorbed and produces hole-electron pair that contributes to the water splitting reaction. Since hematite's spatial collection efficiency is commonly perceived as the main cause preventing its photocurrent from reaching this value, extensive efforts were made to overcome this challenge by nanostructuring or light trapping routes. However, the

record photocurrent reported for hematite photoanodes reaches about 50% of the theoretical limit. This suggests that optical transitions that do not produce mobile charge carriers contribute to light absorption but not to photocurrent generation, and hence fundamentally limits hematite's performance. The photogeneration yield spectrum, defined as the wavelength-dependent ratio between the absorption that ultimately contributes to the photocurrent and the overall absorption, is elemental fundamental material property that provides a more realistic estimation of the maximum photoconversion efficiency of hematite photoanodes. A general method, that applies to thin and thick films, to extract the photogeneration yield spectrum and the spatial collection efficiency from optical and photoelectrochemical external quantum efficiency (EQE) measurements using minimal *a priori* assumptions regarding the charge carrier collection efficiency will be presented in this talk. Analyzing a 30 nm thick Sn-doped hematite film shows that the photogeneration yield drops from ~60% at short wavelengths (300-400 nm) to ~20-30% at long wavelengths (~550-600 nm), indicating that ~50% of the photons in the solar spectrum between 300 and 600 nm are lost for non-contributing absorption. This explains the difficulty in reaching high photocurrent in hematite photoanodes, even with optimal nanostructured morphologies and ultrathin films with high charge carrier separation and collection efficiency.

SESSION EN14.18: Hydrogen Production V
Session Chairs: Huyen Dinh and T. Venkatesh
Wednesday Morning, December 8, 2021
EN14-Virtual

10:30 AM *EN14.18.01

Anode Catalyst Layer Durability in Low Temperature Electrolysis Shaun Alia¹, Kimberly S. Reeves², Elliot Padgett¹, Haoran Yu², Deborah Myers³ and David A. Cullen²; ¹National Renewable Energy Laboratory, United States; ²Oak Ridge National Laboratory, United States; ³Argonne National Laboratory, United States

Hydrogen has unique advantages as an energy carrier, with a high energy density and abilities for long term storage and conversion between electricity and chemical bonds. Although hydrogen currently has a significant role in transportation and agriculture, its use in energy consumption overall has been limited, particularly in the case of electrochemical water splitting. With decreasing electricity prices, electrolysis cost reductions can be achieved and allow for an opportunity for greater use. (1) While load-following renewable power sources can reduce feedstock cost, further cost reductions can be achieved by reducing the platinum group metal (PGM) content. (2) Efforts are needed to understand and mitigate electrolyzer degradation, particularly when accounting for lower PGM loadings and intermittent operation.

In this presentation, studies related to anode catalyst durability will be discussed and include the impact of individual stressors, observed degradation mechanisms, and the development of catalyst-specific accelerated stress tests. First, whether through simulated load-following profiles or accelerated cycling, significant performance losses were found as a result of cycling between open circuit and operating potentials. (3) Losses were further aggravated by using a thinner anode catalyst layer or reducing loading, an increase in cycling frequency, and an increase in cell operating voltage. Performance losses primarily appeared through kinetics and were accompanied by anode catalyst dissolution, migration, catalyst layer changes, and interfacial tearing. Second, how components are integrated into membrane electrode assemblies had a significant impact on catalyst layer properties and electrolyzer durability. (4, 5) Properties were modified by varying ink and spray variables during the deposition of the anode catalyst layer and several trends were found with regards to how catalyst-ionomer integration and catalyst layer uniformity affected performance non-idealities and how losses grew during extended operation.

Finally, membrane thickness and ohmic losses were deconvoluted from catalyst layer durability experiments, allowing for a transition from potential-driven parametric observations to current-driven stress tests for advanced materials and coating processes. (5, 6) Through the screening of available catalysts, increased performance losses were found with materials that incorporated less stable elements or contained sub-stoichiometric oxides, particularly when accounting for PGM thrifting and intermittent or start-stop operation. Perspectives on anode catalyst development thrusts and future needs will be also discussed. Specifically, increasing utilization beyond the catalyst layer/membrane interface is needed to better understand the role of catalyst advancements in mitigating electrolyzer performance losses during operation.

[1] B. Pivovar, N. Rustagi and S. Satyapal, *The Electrochemical Society Interface*, 27, 47 (2018).

[2] K. Ayers, N. Danilovic, R. Ouimet, M. Carmo, B. Pivovar and M. Bornstein, *Annual Review of Chemical and Biomolecular Engineering*, 10, 219 (2019).

[3] S. M. Alia, S. Stariha and R. L. Borup, *J. Electrochem. Soc.*, 166, F1164 (2019).

[4] S.M. Alia, K.S. Reeves, J.S. Baxter, D.A. Cullen, *J. Electrochem. Soc.*, 167, 144512 (2020).

[5] Electron microscopy was performed at the Center for Nanophase Materials Sciences, which is a DOE Office of Science User Facility.

[6] S.M. Alia, H2@Scale: Experimental Characterization of Durability of Advanced Electrolyzer Concepts in Dynamic Loading, https://www.hydrogen.energy.gov/pdfs/review19/ta022_alia_2019_o.pdf, 2019.

11:00 AM EN14.18.04

Going Beyond the Average Value—Depth-Specific Ion Conduction and Stiffness Behavior Across Ionomer Thin Films and Bulk Membranes Shudipto K. Dishari; University of Nebraska–Lincoln, United States

To improve the performance of electrochemical devices (like fuel cells, electrolyzers, batteries), it is critical to deeply understand very thin ionomeric materials. Ionomers in thin films experience multiple interfaces to which they interact very differently. It is thus of high interest to see how a specific property changes across the thickness of a sub-micron thick ionomer film, and how far the interfacial effects propagate deep down inside it. Techniques, like neutron reflectometry and X-ray computed tomography can offer information about mass or density distribution of water and ionomer across ionomer films. However, ion conduction and mechanical properties, the two most critical performance parameters of ionomers, are still reported as an average value for an entire sample. Understanding the need, we have developed an innovative, simple, and every-day-usable strategy using fluorescence confocal microscopy to explore depth-specific ion conduction and stiffness behavior within ionomer bulk membranes and thin films. Ionomer samples were stained with suitable functional dyes first, and then placed under a confocal microscope. A number of xy-plane images were taken and z-stacked to obtain the distribution of relevant properties across the material. The technique revealed a unique distribution of ion conduction and stiffness environment across a

range of fluorocarbon and hydrocarbon-based ionomer thin films from substrate to air interfaces and identified the critical parameters governing such distributed behavior.

11:15 AM EN14.18.05

Laser-Generated Iridium Nanoparticles Deposited on Nanoscaled Boron-Doped Silicon as Cost-Efficient Electrocatalyst for PEM Water

Electrolysis Sven Reichenberger¹, Jasmin Beverungen¹, Norbert Kazamer², Martin Underberg³, Florian J. Wirkert², Jeffrey Roth⁴, Ulrich Rost⁴, Michael Brodmann², Stephan Barcikowski¹ and **Tim Huelser**³; ¹University of Duisburg-Essen, Germany; ²Westphalian University of Applied Sciences, Germany; ³IUTA e.V., Germany; ⁴Propuls GmbH, Germany

One of the most promising ways of meeting the high demand for clean and renewable energy is the synthesis of green hydrogen via electrocatalytic water splitting. Nevertheless, green hydrogen production is currently challenged in industry-scale deployment mainly due to high material and stack costs. The present research aims to address this topic by minimizing the amount of iridium by optimization of the electrode design. Here, an Ir-decorated boron-doped Si nanoparticulate electrocatalyst is being developed and integrated into a scalable proton exchange membrane water electrolyzer by coating it to a porous titanium transport layer in an argon atmosphere.

The B-doped silicon powder was synthesized by thermal decomposition of the gaseous precursors SiH₄ and B₂H₆, while the B/Si - ratio was chosen to be 4%. Laser-generated Ir nanoparticles were subsequently deposited onto the Si@B support in an aqueous suspension.

A homogeneous catalyst distribution on the substrate was noticed by SEM, while TEM analysis reveals a high degree of crystallinity within the particles. Furthermore, it was found that electrostatically-stabilized iridium nanoparticles (~8 nm), gained from surfactant-free laser synthesis with gram-scale productivities and quantitatively were successfully adsorbed to conductive boron-doped silicon nanoparticles (100 – 300 nm) from kg-scale gas-phase synthesis under sufficiently optimized pH condition.

The activity of an Ir_{10wt%}@Si(B) catalyst for oxygen evolution reaction as well as the prepared anode layer on the Ti-substrate (Ir_{10wt%}@Si(B) +Ti-Layer) showed comparable activity in the range from 0.4 V to 1.3 V which was competitive with the activity of a pure Ir-black catalyst indicating a high Ir-accessibility and catalyst layer conductivity of the anode layer.

For validation of the catalyst's activity, a PEM electrolyzer test stack based on hydraulic compression of single cells will be developed. The stack will be suitable for simultaneous operation of 5 single test cells with 25 cm² active area each. The test system will be automated for an unattended long-term operation, during which conditions like temperature and pressure can be controlled and monitored.

11:30 AM EN14.18.06

Electrochemical and Structural Behavior of Nickel Polysulfides for Anion Exchange Membrane Water Splitting Lu Xia^{1,2}, Meital Shviro¹ and

Werner Lehnert^{1,2}; ¹Forschungszentrum Jülich, Germany; ²RWTH Aachen University, Germany

Anion exchange membrane (AEM) water electrolyzers, with economically feasible and resource-rich transition metal (TMs)-based catalysts, are promising for large-scale hydrogen production. However, compared to noble-metal catalysts, the low activity and stability of these TMs catalysts are one of the main challenges.^[1] Recently, TMs chalcogenides, like sulfides/polysulfide, have been widely used as catalysts for oxygen evolution reaction (OER) and exhibit remarkably high activity due to higher conductivity and more exposed active sites than TMs oxides.^[3-4] However, the electrochemical behavior, microstructural and phase composition changes of these chalcogenides in the OER processes need further investigation.

In this work, a scalable electrochemical method was used to activate an S-rich Nickel polysulfide nanocube microstructure prepared by a one-step hydrothermal method to obtain a Nickel-rich polysulfide/(oxy)hydroxide heterostructure. The activated Ni polysulfides show higher activity (370 mV@50 mA cm⁻²) than that of Ni/NiO (>460 mV) and Ni(OH)₂ (>470 mV), and stability (> 60 h) for the oxygen evolution reaction compared to commercial Ni/NiO and synthesized Ni(oxy)hydroxides. Moreover, the results of single-cell tests show that cells based on Ni polysulfides (1450 mA cm⁻²) have 650 mA cm⁻² higher current density than cells based on Ni/NiO (800 mA cm⁻²) in polarization performance at 2.0 V, and nearly no degradation after 80 h@1000 mA cm⁻². This work provides a strategy for better utilization of TMs-based polysulfides by in-situ electrochemical approach, and their actual stability under high current density.

[1] Buttler, A.; Spliethoff, H., Current status of water electrolysis for energy storage, grid balancing and sector coupling via power-to-gas and power-to-liquids: A review. *Renewable and Sustainable Energy Reviews* **2018**, *82*, 2440-2454.

[2] Carmo, M.; Fritz, D. L.; Mergel, J.; Stolten, D., A comprehensive review on PEM water electrolysis. *International Journal of Hydrogen Energy* **2013**, *38* (12), 4901-4934.

[3] Zhou, W.; Wu, X.-J.; Cao, X.; Huang, X.; Tan, C.; Tian, J.; Liu, H.; Wang, J.; Zhang, H., Ni₃S₂ nanorods/Ni foam composite electrode with low overpotential for electrocatalytic oxygen evolution. *Energy & Environmental Science* **2013**, *6* (10).

[4] Mabayoje, O.; Shoola, A.; Wygant, B. R.; Mullins, C. B., The Role of Anions in Metal Chalcogenide Oxygen Evolution Catalysis: Electrodeposited Thin Films of Nickel Sulfide as "Pre-catalysts". *ACS Energy Letters* **2016**, *1* (1), 195-201.

SESSION EN14.19: Hydrogen Production VI
Session Chairs: Andrea Ambrosini and Dong Ding
Wednesday Afternoon, December 8, 2021
EN14-Virtual

1:00 PM *EN14.19.01

Is Proton Conducting Solid Oxide Electrolysis Cell (p-SOEC) Ready for Scalable Electrochemical Hydrogen Production? A Overview of Research Advancement of p-SOEC at Idaho National Laboratory Dong Ding; Idaho National Laboratory, United States

The proton-conducting solid oxide electrolysis cells (p-SOEC) is an emerging and attractive technology for hydrogen production via water electrolysis at intermediate temperatures (400-600°C). Compared to its counterpart, oxygen-ion conducting SOEC (o-SOEC) that normally operated at >750°C, reduced operating temperatures can significantly improve the cell/stack durability, minimize stack sealing problems, enable the use of less expensive materials (e.g., ferritic stainless steels for interconnect), and improve response to rapid start-up and repeat thermal cycling needs. Furthermore, p-SOEC can overcome the problems that the o-SOEC encounter, including the mixture of hydrogen and steam, severe delamination of electrodes at high current densities, and partial oxidation of the Ni-based electrode. While these remarkable merits exist, there are still tremendous research efforts needed to address challenges related to electrolyte and electrode materials in p-SOEC. They include poor sinterability, unproven chemical stability and electronic leakage of electrolyte, as well as limited availability of oxygen electrode materials. It raises concerns about whether the technology could move forward for scale up and commercialization. At Idaho National Laboratory, the extensive effort is placed on these topics by both independent research and close collaboration with the universities and industry. Significant advancement is achieved by integrating the materials and microstructure R&D into cell fabrication and manufacturing, implying a

prosperous future of p-SOEC.

1:30 PM EN14.19.02

Development of Triple-Conducting PrNi_xCo_{1-x}O_{3-δ} Electrode for Proton-Conducting Solid Oxide Electrolysis Cells Hanping Ding, Wei Tang, Wenjuan Bian, Clarita Regalado Vera, Wanhua Wang and Dong Ding; Idaho National Laboratory, United States

High-temperature electrolysis by proton-conducting solid oxide electrolysis cells (p-SOECs) is a highly efficient technology to produce hydrogen at intermediate temperatures (400–600°C). The robust and stable performance is very critical to evaluate the technical feasibility of this ceramic electrolyzer in the realistic operation, particularly high steam condition. The praseodymium cobaltite-based perovskite PrNi_xCo_{1-x}O_{3-δ} (PNC) has been discovered to show triple conduction behavior which is utilized as steam electrode for water splitting reaction. The excellent initial performance and nature of high chemical stability make this electrode with great potential to be a benchmarking material for p-SOECs. To systematically evaluate the electrode properties on more aspects, a series of composition optimization study have been carried out to understand structure-property relationship, chemical/performance stability in high steam condition, and interfacial stability. In addition, the origin of the triple conduction has also been investigated to give more guidance on tuning conductivity and material composition.

1:45 PM EN14.19.04

Computational Defect and Thermodynamic Modeling of Redox Behavior of Complex Oxides for Solar Thermochemical Hydrogen (STCH) Production Anuj Goyal¹, Michael Sanders², Ryan O'Hayre² and Stephan Lany¹; ¹National Renewable Energy Laboratory, United States; ²Colorado School of Mines, United States

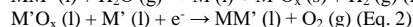
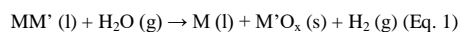
The two-step metal oxide water-splitting cycle is one of the most viable approach for Solar Thermochemical Hydrogen (STCH) production. Challenges exist in finding suitable oxides that can satisfy thermodynamics of the STCH redox cycle under viable range of temperatures and partial pressures. Recently, novel quaternary oxides Sr_{1-x}Ce_xMnO₃ (SCM) and Ce_xSr_{2-x}MnO₄ (CSM) (where x from 0.05 to 0.25) are demonstrated to exhibit promising STCH performance. However, a defect model establishing how changing Ce/Sr composition can be used to tune the STCH redox behavior of SCM/CSM systems is still missing. In this study, we investigate the atomic, electronic and defect structure of these strongly correlated oxides using first principles supercell calculations employing different levels of theory (DFT+U, SCAN+U, Hybrid-DFT). We find that O vacancy formation energy is highly sensitive to the choice of level of theory, and strongly depend on the fraction of Mn⁴⁺/Mn³⁺ in the system, ratio of which changes with Ce concentration (x) as well as with the extent of reduction or oxygen off-stoichiometry. Here, we present a defect model that incorporate dependence of Ce/Sr composition and oxygen off-stoichiometry on the O vacancy formation energy, followed by the thermodynamic modeling to quantitatively predict the redox behavior of these complex quaternary oxides. This study help develop new general approaches for modeling defects in complex oxides beyond the dilute limit and at high temperatures, which is still a critical scientific challenge for the entire computational community.

2:00 PM EN14.19.05

Liquid Metal Alloys for Hybrid Thermo-Electro-Chemical Water Splitting Cycles Andrea Ambrosini, Laura A. Achola, Matthew Witman, Margaret E. Gordon and Anthony McDaniel; Sandia National Laboratories, United States

As the world pursues the goal of lowering carbon emissions to meet the challenges of global climate change, the utilization of hydrogen in transportation, energy storage, and commodity chemical production is becoming increasingly widespread. Water-splitting using renewable energy sources such as electricity from PV or wind, or heat from concentrating solar, is a green method of hydrogen production. However, widespread adoption of these renewable, carbon-free technologies is hindered by materials challenges, low efficiencies, and high costs.

In this talk, a novel route to hydrogen production via a hybrid thermo- electro-chemical route utilizing a liquid metal solution (LMS) as the water splitting medium will be introduced. In the first step of this process, steam is thermochemically reduced by the LMS producing hydrogen and a metal oxide (Eq. 1), while in the second step, the metal oxide is electrochemically reduced back to metal and oxygen is evolved (Eq. 2):



In this reaction, MM' is an alloy consisting of two metals, one that is inert to steam (M) and remains as solution and one which is redox-active (M') and is oxidized during the water-splitting process. The reaction can be driven using heat and electricity from concentrating solar or nuclear power. Alternatively, the electrical input may be provided by wind or PV. The LMS process has the potential to produce hydrogen via water splitting at temperatures much lower than current CSP-driven thermochemical processes and at applied potentials lower than conventional high-temperature electrolysis.

A number of possible binary LMS compositions were identified using machine learning. Several candidates were downselected and tested for hydrogen production in a custom-built flow reactor. The metal alloys were characterized pre- and post-reaction to analyze changes microstructure, grain size, and metal oxide particle growth. The results of these analyses will be presented.

2:15 PM EN14.19.06

Redox Defect Thermochemistry of FeAl₂O₄ Hercynite in Water-Splitting from First Principles Methods Samantha Millican¹, Jacob M. Clary¹, Charles B. Musgrave¹ and Stephan Lany²; ¹University of Colorado Boulder, United States; ²National Renewable Energy Laboratory, United States

Solar thermochemical hydrogen (STCH) production is a promising route to produce fuels from sunlight via high-temperature water splitting. However, efficient and technologically viable implementations of this process only allow a narrow window of thermodynamic boundary conditions that can be used to cycle the system, thus limiting the design space for suitable metal oxide redox mediators. An oxygen defect redox mechanism can contribute a favorable reduction entropy to expand this window, and computational evaluation of materials with high oxygen defect entropies could play a pivotal role in guiding the discovery and design of suitable oxides. This study employs first-principles calculations to investigate the redox mediating defect mechanism of the STCH candidate material, hercynite (FeAl₂O₄). We compare the results from density functional theory (DFT) with beyond-DFT approaches, including hybrid functionals and the random phase approximation, which are among the most advanced methods currently feasible for supercell defect calculations. Using the predicted total energies, we perform thermodynamic modeling of FeAl₂O₄ reduction and oxidation via free energy minimization that incorporates ideal gas, configurational, and vibrational entropy contributions evaluated within the quasi-harmonic approximation. Special attention is devoted to understanding interactions among co-existing defects, such as the association of pairs and complexes of O vacancies and cation antisite defects, as well as the effect of mutually compensating defect charges. Our results corroborate the notion that the details of defect interactions can be decisive for the viability of hydrogen production within the desirable STCH process window.

2:30 PM EN14.19.07

Ca and Co-Doped LaMnO₃ Perovskite for Two-Step Thermochemical Water Splitting Seyfettin Berk Sanli, Ihsan E. Yigiter, Fatih Piskin, Berke Piskin and Gulhan Cakmak; Mugla Sitki Kocman University, Turkey

Increasing interest in sustainable energy sources and climate change has encouraged research in the production of H₂ from H₂O. One of the significant methods being explored for the generation of H₂ is the thermochemical splitting of H₂O and by using oxide materials.

Perovskite oxides have been suggested as promising substances for solar thermochemical separation of H₂O and have been widely studied recently. We have carried out a systematic experimental production study of doped Ca and Co-doped perovskites within the compositions of La_{1-x}CaxMn_{1-y}CoyO₃ (Ca=0.2-0.8, Co=0.2-0.8).

In the study, LCM_x perovskite oxides were synthesised by a solution-based method (Pechini, 19673). For this purpose, nitrated salts of the elements La, Ca, Mn and Co, suitable proportions for the prescribed composition, were used. Deionized water and citric acid in appropriate proportions were added to the structure. The solution was stirred by heating at 120 °C with ethylene glycol addition. After gelation, the system was dried, and the obtained powders were ground.

Powders were calcined at three different temperatures. The phase analysis of the powders were performed by using X-ray diffraction (Rigaku SmartLab X) using monochromated Cu K α radiation at 40 kV and 200 mA. The structures are refined using the Maud programme to identify their crystal structure. BET surface area was evaluated by N₂ adsorption at 77 K in a constant volume adsorption apparatus (Quantachrome Autosorb 1C-MS). The Powders obtained were examined morphologically using SEM (JEOL JSM-7600F). The effect of the composition and applied temperatures on the surface area and particle size was investigated.

The studies started by determining the synthesis parameters for each LCM_x oxide composition. For this purpose LCMC4664 composition was selected and synthesized under four different conditions (1. citric acid addition, 2. citric acid addition and pH ~8, 3. Citric acid and ethylene glycol addition, 4. Citric acid and ethylene glycol addition and pH ~8. All systems are calcined at 900 °C-1300 °C. The X-ray diffraction results show that the main diffraction peaks are characteristic of the typical cubic perovskite structure. However, with the addition, the structure turns into an orthorhombic structure. The change in lattice parameters were also obtained with Rietveld refinement of the sample. The Bragg peaks of LCMC perovskites doped on both the A and B sites were noticeably shifted due to the distinct ionic radii of the introduced metal ions

LCMC4664 compositions synthesized with different parameters and also characterized by SEM, EDS and BET to compare their grain structure, morphology, chemical composition and surface area. Within all synthesis parameters TM: CA: EG 1: 1,5: 1,5 pH = 8,00 gives the lowest surface area.

Among the synthesis conditions, the highest surface area is achieved was for synthesis condition for TM: Ca 1: 1.5 pH \leq 1.00 (0.66m² / g).

The thermochemical H₂O splitting performances of the samples were evaluated in a laboratory-scale reactor (and the O₂ and H₂ produced during the thermochemical process were monitored using a mass spectrometer (MS). We compared the thermochemical performances of the A-site doped and B site doped perovskites. The extents of oxygen vacancies generated by the prepared samples in high-temperature thermal reduction processes were investigated by measuring O₂ production, which in turn will determine the maximum solar fuel production.

In the second step, H₂O splitting tests were conducted and H₂ production was immediately detected after the aspiration of H₂O vapour into the system.

The thermochemical performance of LCMC systems are discussed with respect to their BET surface area, which is directly related to the solid-gas reaction during the thermochemical catalytic process.

Acknowledgements

This work was supported by TÜBİTAK (The Scientific and Technological Research Council of Turkey) (Project Number 119M420), which the authors gratefully acknowledge.

SESSION EN14.20: Hydrogen Production VII
Session Chairs: Shannon Boettcher and Lamya Tabassum
Wednesday Afternoon, December 8, 2021
EN14-Virtual

4:00 PM *EN14.20.01

Alkaline and Bipolar Membrane Electrolyzers Shannon W. Boettcher, Grace Lindquist and Haokun Chen; Univ of Oregon, United States

Commercialized membrane electrolyzers use acidic proton exchange membranes (PEMs). These systems offer high performance but require the use of expensive precious-metal catalysts such as IrO₂ and Pt that are nominally stable under the locally acidic conditions of the ionomer. Here I will discuss our efforts to study and develop alternative electrolysis platforms.

First, I will discuss alkaline exchange membrane (AEM) electrolyzers that, in principle, offer the performance of commercialized proton-exchange-membrane electrolyzers with the ability to use earth-abundant catalysts and inexpensive bipolar plate materials. I will present progress in building high-performance AEM electrolyzers and studying fundamental aspects of their operation and degradation. To date, our best systems operate at 1 A cm⁻² in pure water feed at < 1.9 V at a moderate temperature of 69 °C. These devices, however, degrade rapidly (~ 1 mV/h) compared to PEM electrolyzers. I will discuss our work assessing chemical changes to the anode and cathode catalyst and ionomer that is correlated with this performance loss, as well as strategies to mitigate degradation modes.

Second, I will introduce the use of bipolar membranes (BPMs) in electrolysis-type devices. BPMs consist of an AEM and PEM laminated together. Under the appropriate bias, they conduct ionic current by dissociating water into protons and hydroxide at the AEM/CEM junction. Commercially, BPMs are used in electro dialysis, but generally are used at low current densities below 100 mA cm⁻² to avoid large losses in driving water dissociation. I will present our fundamental studies on how to accelerate water dissociation in BPMs (*Science*, 2020) and how that has enabled BPMs operating at > 3 A cm⁻² and with improved efficiency. BPMs limit crossover and enable operation of a cathode and anode in different pH conditions and are thus seeing substantial interest for CO₂ electrolysis, advanced electro dialysis systems, and water electrolysis; applications that I will highlight.

4:30 PM EN14.20.02

Covalent 0D–2D Heterostructuring of Co₉S₈–MoS₂ for Enhanced Hydrogen Evolution in All pH Electrolytes Minkyung Kim¹, Mohsin A. Anjum², Min Choi¹, Sun Hee Choi³, Noejung Park¹ and Jae Sung Lee¹; ¹Ulsan National Institute of Science and Technology, Korea (the Republic of); ²Pakistan Institute of Nuclear Science and Technology, Pakistan; ³Pohang University of Science and Technology, Korea (the Republic of)

Ultrasmall Co₉S₈ nanoparticles are introduced on the basal plane of MoS₂ to fabricate a covalent 0D–2D heterostructure that enhances the hydrogen evolution reaction (HER) activity of electrochemical water splitting. In the heterostructure, separate phases of Co₉S₈ and MoS₂ are formed, but they are connected by Co–S–Mo type covalent bonds. The charge redistribution from Co to Mo occurring at the interface enhances the electron-doped

characteristics of MoS₂ to generate electron-rich Mo atoms. Besides, reductive annealing during the synthesis forms S defects that activates adjacent Mo atoms for further enhanced HER activity as elucidated by the density functional theory (DFT) calculation. Eventually, the covalent Co₉S₈-MoS₂ heterostructure shows amplified HER activity as well as stability in all pH electrolytes. The synergistic effect is pronounced when the heterostructure is coupled with a porous Ni foam (NF) support to form Co₉S₈-MoS₂/NF that displays superior performance to those of the state-of-the-art non-noble metal electrocatalysts, and even outperforms a commercial Pt/C catalyst in a practically meaningful, high current density region in alkaline (>170 mA cm⁻²) and neutral (>60 mA cm⁻²) media. The high HER performance and stability of Co₉S₈-MoS₂ heterostructure make it a promising pH universal alternative to expensive Pt-based electrocatalysts for practical water electrolyzer.

4:45 PM EN14.20.03

Nanoporous Gold Obtained by Dealloying AuFe₂ Precursor—A Promising Low-Cost Electrocatalyst for Hydrogen Evolution Reaction Deepthi Raj¹, Federico Scaglione¹, Gianluca Fiore¹, Federica Celegato² and Paola Rizzi¹; ¹Università di Torino, Italy; ²Istituto Nazionale di Ricerca Metrologica (INRIM), Italy

As an efficient and sustainable alternative to fossil fuels Hydrogen gas (H₂) has emerged to be of great importance for the future of energy generation and storage. However, H₂ production from the electrocatalytic hydrogen evolution reaction (HER) still remains a challenge. Although platinum and its alloys have been the benchmark electrocatalysts for HER, the scarcity, substandard stability and expensiveness limit their usage making it crucial to develop economical electrocatalysts with elevated activity and stability. In this quest, nanoporous metals, built of 3D scaffolds of bi-continuous ligament-pore structure, have shown growing inclination because of their large surface area to volume ratio and enhanced catalytic properties. This work focusses on Nanoporous Gold (NPG) as a promising candidate with its noble nature, high conductivity and large surface area. Instead of common precursors constituting various alloying metals and high Au concentration, a metastable supersaturated solid solution of AuFe₂ was selected – with cheap and abundant Fe and minimum possible Au concentration according to the parting limit. Long and homogeneous melt-spun ribbons were obtained by rapid solidification of the arc-melted precursor. The as-quenched ribbon was dealloyed chemically in 1 M HNO₃ and 1 M HCl at 70 °C for different durations. The structural and compositional investigation was accomplished using XRD, SEM and EDS techniques. The as-dealloyed samples possessed nanoporosity both on surface and cross-section with high Au content. One of these samples was tested as an electrocatalyst for HER in 0.5 M H₂SO₄. Low onset potential of -4 mV; low overpotential of -0.38 V at a current density of -5 mA/cm²; small Tafel slope of 47 mV/dec; and high exchange current density of 0.12 mA/cm² have been obtained. Thus, the NPG sample demonstrates excellent electrocatalytic activity considering that an overall low-cost, fast and simple synthetic route combined with the cost-effective precursor were employed for the fabrication.

5:00 PM EN14.20.04

Selenium-Doped Copper Oxide Nanoarrays for Enhanced Oxygen Evolution Reaction (OER) Lamya Tabassum and Steven Suib; University of Connecticut, United States

Global energy demand is projected to increase by 50% by 2050. Existing fossil fuels can meet this energy demand only until the end of this century. Fossil fuels are also a major source of greenhouse gas emissions. Therefore, it is one of the biggest challenges to find a sustainable, clean, and efficient energy source. Ongoing research efforts have led to the invention of promising energy storage technologies like alkaline water splitting, metal-air batteries, and fuel cells.¹ The oxygen evolution reaction (OER) is the critical anodic reaction in the aforementioned devices. OER is a four-electron process with sluggish reaction kinetics, thus the overall efficiency of these systems is low. RuO₂ and IrO₂ catalysts are considered the benchmark for OER in both acidic and alkaline media.^{2,3} However these noble metal-based catalysts are costly and suffer from disadvantages such as instability (oxidized to RuO₄ and IrO₃) under high anodic potential and dissolution into the electrolyte solution.^{4,5} Transition metal-based catalysts are cheap and abundant. Fe, Co, Ni, Mo, and W transition metal-based catalysts have been well explored in the past decade for OER and show promising results.⁶⁻⁷ However, copper oxide-based catalysts are less explored for OER due to their poor conductivity, inappropriate crystal structure, and narrow bandgap.⁸ Doping is an effective strategy to improve the conductivity and thus the electrocatalytic activity of the material. For example, doping sulfur into Cu₂O has been reported to significantly lower the onset potential for OER.⁹ In this work, we have doped Se into CuO nanoarrays for OER application. We have observed that upon doping Se into CuO nanoarray structures, the overpotential for OER can be lowered significantly. Comprehensive characterization and electrochemical performance of the Se doped CuO nanoarray for OER will be presented.

References:

- (1) Suen, N. T.; Hung, S. F.; Quan, Q.; Zhang, N.; Xu, Y. J.; Chen, H. M. *Chemical Society Reviews*. Royal Society of Chemistry January 21, 2017, pp 337–365.
- (2) An, L.; Feng, J.; Zhang, Y.; Wang, R.; Liu, H.; Wang, G. C.; Cheng, F.; Xi, P. *Adv. Funct. Mater.* **2019**, 29 (1), 1805298.
- (3) Frydendal, R.; Paoli, E. A.; Knudsen, B. P.; Wickman, B.; Malacrida, P.; Stephens, I. E. L.; Chorkendorff, I. *ChemElectroChem* **2014**, 1 (12), 2075–2081.
- (4) Kötz, R.; Lewerenz, H. J.; Stucki, S. *J. Electrochem. Soc.* **1983**, 130 (4), 825–829.
- (5) Antolini, E. *ACS Catalysis*. American Chemical Society May 2, 2014, pp 1426–1440.
- (6) Tian, T.; Huang, L.; Ai, L.; Jiang, J. *J. Mater. Chem. A* **2017**, 5 (39), 20985–20992.
- (7) Zhou, T.; Du, Y.; Wang, D.; Yin, S.; Tu, W.; Chen, Z.; Borgna, A.; Xu, R. *ACS Catal.* **2017**, 7 (9), 6000–6007.
- (8) Kumar, B.; Saha, S.; Ojha, K.; Ganguli, A. K. *Mater. Res. Bull.* **2015**, 64, 283–287.
- (9) Zhang, X.; Cui, X.; Sun, Y.; Qi, K.; Jin, Z.; Wei, S.; Li, W.; Zhang, L.; Zheng, W. *ACS Appl. Mater. Interfaces* **2018**, 10 (1), 745–752.

Related symposia

Symposium EN14-Advanced Materials for Hydrogen and Fuel Cell Technologies

5:15 PM EN14.20.05

Key Material Parameter Estimation for High-Performance Polymer Electrolyte Electrochemical Cell Evaluated by Current-Voltage Temperature Dependence Daichi Matsui^{1,2}, Katsushi Fujii², Satoshi Wada² and Atsushi Ogura^{1,3}; ¹Meiji University, Japan; ²RIKEN Center of Advanced Photonics, Japan; ³Meiji University MREL, Japan

High-performance water electrolysis is an important device for green hydrogen production. Polymer electrolyte electrochemical cell (PEEC) is considered a suitable device for renewable energy storage due to the toughness of the fluctuated energy sources.

We focused on PEEC as a device to convert electricity into hydrogen in this report. The evaluated PEEC has an electrode area of 12.5 cm² with IrO₂ as the cathode catalyst and Pt as the anode catalyst. The operating temperature of this device was varied from 30 to 70°C in order to evaluate the current-voltage characteristics. The results were compared with a chemical reaction-based device model [1,2].

The threshold voltage and the slope of the polarization curve of the current-voltage characteristics were changed with the operating temperature. The threshold voltage decreased and the slope of the polarization curve increased with increasing operating temperature. There were clarified that the activation energy of the electrochemical reaction mainly affects to change of the threshold voltage, and the resistance of the solid polymer membrane mainly affects the change of the slope of the polarization curve from the device model analysis. The other chemical parameters did not significantly affect the PEEC current-voltage temperature dependence. The results show that the reduction of activation energy of the electrochemical reaction and the suppression of

ohmic resistance of the solid polymer membrane were important parameters to improve the performance of PEEC. The PEEC performances were evaluated quantitatively by the current-voltage temperature dependence using the device model. The results of these quantitative evaluations give guide the material designs for the high-performance PEEC.

[1] B. Lee et al., Int. J. Electrochem. Science, 8 (2013) 235.

[2] V. Liso et al., Mdpi. J. Energies, 11 (2018) 3273.

SESSION EN14.21: On-Demand
Sunday Morning, December 5, 2021
On-Demand

8:00 AM EN14.04.02

High Stability PtAu Thin-Film Catalyst for Oxygen Reduction Reaction Xianxian Xie, Ivan Khalakhan, Mykhailo Vorokhta and Iva Matolínová; Charles University, Czechia

Oxygen reduction reaction is a key reaction for proton exchange membrane fuel cells (PEMFCs), which is the perspective of renewable energy for many practical applications. Platinum is the most efficient element for oxygen reduction reaction on the cathode side. However, Pt-based cathode catalysts are undergoing severe degradation due to the high potential changes. Therefore, we introduce a small amount of Au into Pt, form bimetallic PtAu alloy thin film catalyst by magnetron co-sputtering technique, resulting in a significant stability improvement in oxygen reduction reaction. Moreover, the PtAu alloy thin film catalysts show similar electrochemical activity with the identical Pt-loading, indicates its applicability for industrial PEMFCs. The stability of thin film catalysts is studied in half-cell rotating disk electrode (RDE). The morphology, structure and composition of thin film layer are characterized by scanning electron microscopy (SEM), X-ray diffraction (XRD), and X-ray photoelectron spectroscopy (XPS).

8:15 AM EN14.07.03

Characterization of Silicon Carbide Coatings for Hydrogen Permeation Barriers Michael Drory¹, Sean M. Lam², Dale Hitchcock¹, Timothy Krentz¹, Garrett Pataky² and Marian S. Kennedy²; ¹Savannah River National Laboratory, United States; ²Clemson University, United States

Silicon carbide (SiC) thin films are of interest for hydrogen permeation barriers in fusion reactors. Stainless steels such as 316L are sought for nuclear applications (for example, fission reactor and tritium process components) because of wide availability and low cost, however they are susceptible to tritium uptake that may affect tritium accountancy and release to the cooling system and environment. We examine SiC coated 316L by magnetron sputtering, followed by deuterium permeation testing at elevated temperature and pressure. Permeation was measured in a concentration-driven gas-phase experimental setup. The Arrhenius permeation behavior was derived by varying temperature and pressure gradients in a stepwise fashion. As seen in other studies, more than an order of magnitude reduction in deuterium permeation is found for thin SiC coatings compared with uncoated 316L. The emphasis here is to characterize the SiC coating and 316L substrate interface to elucidate any effects of microstructure on permeation resistance.

SYMPOSIUM EN15

Materials Research Opportunities for Energy Efficient Computing
November 30 - December 8, 2021

Symposium Organizers

Asif Khan, Georgia Institute of Technology
Iuliana Radu, imec

Subhash L. Shinde, ND Energy, University of Notre Dame
Hui Jae Yoo, Intel Corporation

* Invited Paper

SESSION EN15.01: Materials Research Opportunities for Energy Efficiency Computing
Session Chairs: Subhash L. Shinde and Hui Jae Yoo
Tuesday Afternoon, November 30, 2021
Sheraton, 3rd Floor, Clarendon

1:30 PM *EN15.01.01

New Compute Trajectories for Energy-Efficient Computer Victor V. Zhimov; Semiconductor Research Corp, United States

Computing and, more generally, Information and Communication Technologies (ICT) is the social-economic growth engine of modern world. Rapid advances in computing have provided increased performance and enhanced features in each new generation of products in nearly every market segment, whether it be servers, PCs, communications, mobile, automotive, entertainment, among others.

The use of the information and communication technologies continues to grow without bounds dominated by the exponential creation of data that must be moved, stored, computed, communicated, secured and converted to end user information. Ever-rising energy demands for computing versus global energy production are creating new risk, therefore new computing paradigms need to be discovered that would result in dramatically improved energy efficiency of computing.

How to get 10^6 more semiconductor energy efficiency? Inventing the next hardware/software computing paradigm is a tall order, to be sure. However, it is achievable if the right questions are asked and right resources are put in place. These steps are outlined in the Decadal Plan for Semiconductors (<https://www.src.org/about/decadal-plan/>) which is currently being proposed to government and the ICT industry.

2:00 PM EN15.01.02

Downscaling Effects on Resistivity of Topological Semi-Metal MoP Nanowires Hyeuk Jin Han, James L. Hart and Judy Cha; Yale University, United States

The increasing resistance of Cu interconnects is a major challenge in the continued downscaling of integrated circuits beyond the 5-nm technology node. Topological semi-metals that exhibit high conductivity and mobility are promising material candidates for low-resistance interconnects to potentially replace current Cu interconnects. Particularly, nanoscale topological semi-metals might outperform their bulk counterparts as interconnects as the contributions of the topologically protected surface states to the overall transport signals will be enhanced at the nanoscale. Recently, molybdenum phosphide (MoP) was discovered as a triple-point topological semi-metal with excellent transport properties of bulk resistivity of $8.2 \mu\Omega\cdot\text{cm}$ and a high carrier density of $1.1 \times 10^{23} \text{ cm}^{-3}$ at room temperature (N. Kumar, et al., Nat Commun (2019) 10, 2475). Due to the topological protection predicted to suppress electron scattering at the surface, MoP may preserve its low resistivity values at the nanoscale, which may rival the line resistance of current Cu interconnects.

Here, we report the synthesis and transport properties of MoP nanowires, which were synthesized by reacting MoO₃ nanostructures with phosphorous precursors (H. J. Han et al., APL Materials (2020), 8(1), 011103). We observe that the initial diameter of the MoO₃ nanowires critically determines the crystalline quality of the converted MoP nanowires, from porous flakes to poly-crystalline nanowires, and finally to single-crystalline nanowires. This size-dependent crystallinity is attributed to the suppression of nucleation at the nanoscale. While the resistivity values of the polycrystalline MoP nanowires were measured to be higher than the reported resistivity of MoP bulk single crystals due to the presence of nanoscale grains, we observe that the resistivity values approach that of the bulk with decreasing diameter of MoP nanowires. Importantly, we demonstrate that the line resistance versus the total cross-sectional area of MoP nanowires is comparable to, or even better than, those of effective Cu and barrier-less Ru interconnects, suggesting MoP is an attractive solution to the current scaling challenge of Cu interconnects. In this talk, we will also discuss the role of topological surface states in the transport properties of MoP nanowires.

2:15 PM EN15.01.03

Microstructure and Electro-Optic Response of Thick Epitaxial BaTiO₃ Films Integrated on Silicon (001) by Molecular Beam Epitaxy Marc Reynaud¹, Went Li¹, Agham Posadas¹, Alex Demkov¹, Zuoming Dong¹, Daniel Wasserman¹ and Albina Borisevich²; ¹The University of Texas, United States; ²Oak Ridge National Laboratory, United States

Recent advances in epitaxial oxide deposition enabled fabrication of thick films of ferroelectric perovskite BaTiO₃ capable of providing a robust electro-optic (EO) response via the Pockels effect. This created a plethora of potential applications in silicon photonics ranging from optical interconnect to optical neuromorphic and quantum computing. However, the EO response being a tensor property, is very sensitive to crystal microstructure. And microstructure control is therefore key to building functional EO devices such as phase shifters and modulators. We report a microstructure analysis along with the deposition process of thick EO-active films integrated on Si(001) by molecular beam epitaxy, showing how the crystal orientation changes as a function of thickness. In addition to x-ray diffraction, we have performed cross-sectional high-angle annular dark-field scanning transmission electron microscopy (HAADF-STEM) imaging to analyze in detail the crystalline structure of the BTO films. Geometric phase analysis (GPA) was performed on the STEM images to extract information regarding the orientation of the BTO crystal as a function of layer position. Phase field simulations were used to help interpret the GPA. In addition to GPA, sliding fast Fourier transformations (FFT) of the film were performed that showed similar results and good agreement with GPA. The electro-optic properties of the film have been measured in free space as well as using Si waveguides, deposited atop the film, and correlate well with the microstructural analysis and demonstrate the potential of Si-integrated BaTiO₃ for silicon photonics. The work at Austin is supported by the Air Force Office of Scientific Research under grant FA9550-18-1-0053.

2:30 PM EN15.01.04

Manufacturable Process for Thick Epitaxial BaTiO₃ Films Integrated on Silicon for Electro-Optic Modulators Agham Posadas¹, Hyoju Park¹, Marc Reynaud¹, Wei Cao², Goran Mashanovich², Jamie Warner¹ and Alex Demkov¹; ¹The University of Texas at Austin, United States; ²University of Southampton, United Kingdom

We report on a process for fabricating thick epitaxial BaTiO₃ films on silicon that is compatible with large scale production and capable of producing optical quality material of sufficient thickness for use in silicon photonics and neuromorphic computing elements. Thick BaTiO₃ films ranging from 120 nm to 1 mm were grown by off-axis rf magnetron sputtering on SrTiO₃-templated silicon-on-insulator substrates. The films microstructure was characterized in detail by x-ray diffraction and cross-section scanning transmission electron microscopy. The films are of high quality, rivaling those grown by molecular beam epitaxy in crystalline quality, but can be grown ten times faster while maintaining process repeatability. Extraction of lattice parameters from geometric phase analysis of atomic resolution scanning transmission electron microscopy images revealed how the in-plane and out-of-plane lattice spacings of sputtered BaTiO₃ changes as a function of layer position within a thick film. Our results indicate that, compared to molecular beam epitaxy, sputtered films retain their c-axis orientation for larger thicknesses. Electro-optic measurements using a transmission setup of a sputtered BaTiO₃ film grown using the optimized conditions yields an effective Pockels coefficient as large as 165 pm/V. A Si₃N₄ waveguide Mach-Zehnder modulator fabricated on such films exhibits phase shifting with an equivalent Pockels coefficient of 157 pm/V. These results demonstrate that the off-axis sputtering process is a manufacturable solution for making thick BaTiO₃ films that can be used for fabricating high efficiency and compact electro-optic modulators integrated on silicon.

2:45 PM EN15.01.05

Measuring Ionic Mobility in Oxide Thin Films by Dynamic I-V Analysis—Impact of Interfaces Dmitri Kalayev¹, Baoming Wang¹, Takashi Ando², John Rozen², Frances M. Ross¹ and Harry Tuller¹; ¹Massachusetts Institute of Technology, United States; ²IBM Thomas J. Watson Research Center, United States

Ionic transport in solids, e.g. nonstoichiometric oxides, is key to the design and control of non-volatile RAM devices considered for use in neuromorphic hardware. While significant progress has been achieved in the development of neuromorphic devices based on Resistive and ElectroChemical RAM, their performance is limited in part by knowledge of ionic transport phenomena that control conductance changes in filamentary regions and/or at oxide interfaces. We study ionic mobility in oxide materials, e.g. doped ceria, by applying our previously developed Dynamic *I-V* Analysis technique¹ capable of measuring oxygen vacancy mobility dependence on temperature, thermal history and oxygen non-stoichiometry. Here we show that interface resistance, that might arise either at the contact between the oxide under study and its electrodes or between grain boundaries created during pulsed laser deposition, varies significantly. While the interfacial contributions to overall device resistance is sometimes negligibly small, in many cases they become significantly larger than the bulk value. We show that the interface resistance has a direct impact on the effectiveness of the measurement of ionic transport in the oxides of interest. Electrical impedance spectroscopy supported with XRD and electron microscopy are applied to determine the interfacial resistance, and its origins, in oxide thin films, that impacts the oxygen defect transport and impedes characterization. We will present possible ways to mitigate the interfacial resistance, by tuning the PLD parameters and by carefully choosing the electrodes and the supporting substrates materials in the test devices. Finally, we will report near room temperature values for ionic mobility in crossbar devices with optimized ceria layers.

[1] D. Kalaev, T. Defferriere, C. Nicolle, T. Kadosh, H. L. Tuller, *Dynamic current-voltage analysis of oxygen vacancy mobility in praseodymium doped ceria over wide temperature limits*, Adv. Funct. Mater. 30(11), 2020, 1907402.

3:00 PM EN15.01.06

High Sensitivity SIMS Analysis of Oxygen Movement in Silicon Oxide ReRAM Devices—Materials Challenges for Energy Efficient Memristive Devices Horatio Cox¹, Mark Buckwell¹, Wing H. Ng¹, Daniel J. Mannion¹, Adnan Mehonic¹, Paul Shearing¹, Sarah Fearn² and Anthony Kenyon¹; ¹University College London, United Kingdom; ²Imperial College London, United Kingdom

Resistance modulation in oxide-based intrinsic ReRAM devices is a promising technology for energy efficient computing based on neural network multiply-accumulate (MAC) accelerators or neuromorphic engineering. Such modulation is driven by oxygen movement in metal-oxide-metal (MIM) stacks under electric fields. However, the sensitivity of existing analysis techniques at the nanometre scale is too limited to systematically examine complex interactions, oxygen exchange, formation of novel layers, and the role of ambient conditions. Given that the movement and storage of oxygen across the MIM stack to a large extent determines the energy efficiency of resistance modulation, the cycling endurance of devices and the stability of resistance states, it is critical to the development of novel energy efficient devices that such effects are characterised and understood. Here we report the measurement of oxygen movement in silicon oxide-based ReRAM devices using a novel Secondary Ion Mass Spectrometry (SIMS) normalisation technique that allows the measurement of ionic movement with unparalleled sensitivity

Our technique allows us for the first time to observe the movement of ¹⁶O across electrically biased silicon oxide (SiO_x) ReRAM stacks, measuring bulk concentration changes in a continuous profile with unprecedented sensitivity. This reveals nanoscale details of the reversible field-driven exchange of oxygen across the ReRAM stack. We present modelling of the electric fields in ReRAM devices which, for the first time, uses real measurements of both interface roughness and electrode porosity. This supports our findings and helps to explain how and where oxygen from ambient moisture enters devices during operation.

3:15 PM BREAK

3:45 PM *EN15.01.07

Using Magnetic Domain Walls and Skyrmions for Cognitive Computing Jean Anne C. Incorvia¹, Matthew Marinella², Sam Liu¹, Can Cui¹, Priyamvada Jadaun¹, Christopher Bennett², Tianyao Xiao², Joseph Friedman³, David Paydarfar¹, Thomas Leonard¹, Mahshid Alandari¹, Suyogya Karki¹, Vivian Rogers¹ and Otiotoaleke Akinola¹; ¹University of Texas at Austin, United States; ²Sandia National Laboratories, United States; ³The University of Texas at Dallas, United States

Over the past decades, tremendous effort has gone into designing and building computers to accomplish tasks outside the reach of humans. But, despite the revolution in computing that has occurred, there are still tasks where humans easily outperform computers. The efficiency and adaptiveness of the mammalian brain enables many immersive tasks, such as language understanding, coherent processing of multiple senses to make a decision, object perception, and consciousness.

The field of cognitive computing is inspired by continually emerging understanding of advanced brain behavior that enables efficient and real-time learning, reaction, and cognition. To achieve true brain-like computing, we need to understand 1) the advanced cognitive features of the brain to accomplish tasks and 2) how to translate those features to nanoengineered materials and devices that are 3) compatible with circuits and systems to perform actual tasks.

In particular, there are rich dynamical behaviors in magnetic materials that are bio-mimetic and highly applicable to cognitive computing. Here, we will present our recent results on understanding and leveraging the materials properties of magnetic domain walls (DWs), skyrmions, and magnetic tunnel junctions (MTJs) for energy efficient cognitive computing.

We will show that DW motion in a magnetic track can be engineered to have highly linear position vs. time behavior as it is moved along the track via either spin transfer torque or spin orbit torque, acting as an artificial synapse. We show the DW-MTJ synapse can have the necessary characteristics for energy efficient backpropagation on-chip learning: linear weight updates, controllability, and symmetry. Therefore, it can tolerate the relatively lower change in total resistance compared to other nonvolatile device types. We will show the stochasticity of the DW position is helpful for high accuracy of MNIST and Fashion-MNIST image recognition [1].

We will then show a brain-inspired “edgy-relaxed” behavior seen in biological neurons can be implemented inherently in the DW-MTJ device when it acts as an artificial neuron. When a neuron is activated often (edgy), a depolarizing shift causes the cell to be at a lower threshold for generating additional action potentials. Conversely, a neuron that is not activated often (relaxed) requires a higher threshold. This is a biological behavior that has heretofore never been used in neural networks. As in the mammalian system, edgy-relaxed neuron function should be beneficial when performing repetitive tasks. We will show that the edgy-relaxed behavior in DW-MTJ neurons improves the classification accuracy of ordered datasets, and that the materials properties can be engineered such that the classification accuracy is not lost for completely random datasets [2]. The degree of edgy-relaxed behavior can be dynamically tuned, an exciting result for task-adaptable computation: based on the expected ordering of a dataset, the magnetic neuron behavior can then be adjusted to most efficiently complete the task.

While DW dynamics are one useful materials property for cognitive computing, magnetic skyrmions can offer additional dynamics including coupled and

multi-modal oscillatory behavior. We will show results on designing a coupled skyrmions neuron. By having multiple inputs that can change the resonant behavior of the skyrmion system, we show it can be dynamically modulated based on context and environment. We will show this can implement cognitive features including context awareness (processing different types of inputs differently), neuromodulation (simultaneously processing different information), feature binding (combining information to construct a coherent perception), and bursting (neurons respond as a group to a coherent input) [3].

References:

- [1] S. Liu, *et al. Applied Physics Letters* 118, 202405 (2021).
- [2] S. Liu, *et al. IEEE Magnetics Letters* 12, 4500805 (2021).
- [3] P. Jadaun, *et al. ArXiv*: 2010.15748.

SESSION EN15.02: New Materials, Approaches I
Session Chairs: Iuliana Radu and Subhash L. Shinde
Monday Morning, December 6, 2021
EN15-Virtual

10:30 AM *EN15.02.01

***Ab Initio* Investigations of Novel 2D Materials as Next-Generation Field-Effect Transistors** Mathieu Luisier¹, Cedric Klinkert¹, Aron Szabo¹, Christian Sieger¹, Davide Campi² and Nicola Marzari²; ¹ETH Zurich, Switzerland; ²EPFL, Switzerland

Since the first experimental demonstration of a monolayer MoS₂ transistor in 2011, transition metal dichalcogenides (TMDs) have received a wide attention from the scientific community as potential replacement for Silicon FinFETs at the end of the semiconductor roadmap. As graphene, TMDs exhibit excellent electrostatic properties due to their 2-D nature, but contrary to it, they are characterized by large band gaps, while keeping decent phonon-limited mobilities up to 100³ cm²/Vs. However, so far, no TMD-based transistor has been shown to outperform the Si technology. While this limitation can be partly attributed to technology challenges, e.g. high contact resistances, poor crystal quality, or absence of native oxide, the TMD bandstructure also explains this behavior: electrons/holes are not fast enough to allow for large ON-state currents.

A recent theoretical study based on density functional theory (DFT) predicted the existence of more than 1,800 2-D materials. Among them components with the same advantages as TMDs, but with better transport properties can be found. We selected 100 monolayers out of this database according to their band gap and effective masses, combined DFT and quantum transport to simulate their “I-V” characteristics in a single-gate configuration, and identified 13 candidates with both *n*- and *p*-type ON-state currents exceeding 3,000 μA/μm at a gate length of 15 nm. Such 2-D materials could reach the same performance level as Si FinFETs, if they can be exfoliated and patterned into transistors.

In this talk, the *ab initio* simulation approach that was developed to investigate devices made of 2-D materials will be briefly reviewed before presenting a summary of the performance of the 100 2-D transistors that were examined.

11:00 AM *EN15.02.02

Thin and Ultra-Thin Antiferroelectric Thin Films—From Fundamental Science to Applications Nazanin Bassiri-Gharb; Georgia Institute of Technology, United States

Discovered in the last century, antiferroelectric materials offer exceptional energy storage capacity with high efficiencies, giant electrocaloric effect and large electrostriction. Additionally, antiferroelectrics are impervious to stray electromagnetic fields, substantially fatigue resistant, not depoled by temperature or electric field, and often radiation hard. The wide range of functionalities, accompanied by the limited vulnerability to adverse environmental effects (radiation, temperature, stray electromagnetic fields) makes these material an exciting venue to design a new generation of micro- and nano-scale electronic devices. Applications range from micro/nano-actuators, to tunable dielectrics for next-generation filters, miniaturized solid state cooling, ultra-high power capacitors or negative capacitors, adaptive pyroelectric sensors, multi-state memory devices, nanoscale opto-magneto-electric couplers, and actively tunable metamaterials.

Among antiferroelectrics, zirconia-based materials have received special attention. The perovskite-structured PbZrO₃ occupies a prominent role as the first discovered antiferroelectric and an end member in the lead zirconate titanate solid solution (PZT, of eminent technological importance for many electromechanical sensor, actuator and acoustic transducer transducers). Ultra-thin films of fluorite-structured ZrO₂ have similarly received substantial attention over the last decade, as CMOS compatible antiferroelectrics with functional characteristics exhibited in films of thickness down to a few nanometers. In both material systems, experimental and theoretical studies have moved beyond the original Kittel theory of antiferroelectricity. Literature reports have indicated the presence of cycloid polarization vectors and incommensurate polarization modulations (in amplitude and direction) in chemically modified PbZrO₃. Similarly, the antiferroelectric characteristics of zirconia have been attributed to possible paraelectric to ferroelectric phase transitions, rather than field-induced realignment of antiparallel dipoles in adjacent unit cells.

Here, we discuss some of the recent advances in the science of antiferroelectric materials, as well as properties of thin and ultra-thin lead zirconate and zirconia thin films. Specifically, we will address the size reduction effect on the properties of these materials, particularly with respect to the stability of the ferroelectric phase and its origin.

11:30 AM EN15.02.03

New Materials for Three Dimensional Ferroelectric Microelectronics Susan E. Trolier-McKinstry; The Pennsylvania State University, United States

In the last decade, there have been major changes in the families of ferroelectric materials available for integration with CMOS electronics. These new materials, including Hf_{1-x}Zr_xO₂, Al_{1-x}Sc_xN, Al_{1-x}B_xN and Zn_{1-x}Mg_xO, offer the possibility of new functionalities. Whereas the hafnia-based materials show excellent scalability, the wurtzite-structured compounds couple large polarizations (~ 100 microC/cm²) with excellent temperature stability of the polarization. In addition, the deposition temperatures are quite low (<400°C), opening up the possibility of straightforward integration in the back-end-of-the-line, including the possibility of 3D scaling. This talk will discuss the possibility of exploiting the 3rd dimension in microelectronics, enabling 3D *non-von Neumann computer architectures exploiting ferroelectrics for local memory, logic in memory, digital/analog computation, and neuromorphic functionality*. This approach circumvents the end of Moore’s law in 2D scaling, while simultaneously overcoming the “von Neumann bottleneck” in moving instructions and data between separate logic and memory circuits. The talk will cover the relevant materials, their deposition conditions, and what is known about the wake-up, fatigue, and retention processes.

SESSION EN15.03: New Materials, Approaches II
Session Chairs: Iuliana Radu and Subhash L. Shinde
Monday Afternoon, December 6, 2021
EN15-Virtual

6:30 PM EN15.03.01

Critical Role of Synthesis Temperature on Small Polaron Carrier Concentrations in Hematite—A First-Principles Study Mingpeng Chen¹, Tyler Smart^{1,2}, Yat Li¹ and Yuan Ping¹; ¹University of California, Santa Cruz, United States; ²Lawrence Livermore National Laboratory, United States

Achieving highly efficient energy conversion with transition metal oxides necessitates overcoming conductivity limitations due to the formation of small polarons. Detailed understanding of defects, dopants, and carriers can help to devise strategies for achieving higher carrier concentrations, therefore improving conduction and conversion efficiency. This work uses first-principles calculations to investigate carrier concentrations in prominent polaronic oxide, hematite, by resolving interactions between charged defects and carriers in order to reliably predict free carrier concentrations. This work addresses that both O vacancies and Fe interstitials can be primary donors in undoped hematite depending on the synthesis condition, although O vacancies possess a high ionization energy compared to kT. Furthermore, from calculations of a plethora of n-type dopants (group IV, group V, group XIV, and group XV elements), we identify dopants which are most successful at raising carrier concentrations in hematite such as Ti, Ge, Sb, and Nb. We reveal the critical role of synthesis temperature on tuning the carrier concentration of both intrinsic and doped hematite. Our theoretical analysis provides insights and general design principles for the engineering of more conductive polaronic oxides.

6:45 PM EN15.03.02

Effect of Device Geometry on Electrically-Stimulated Insulator-to-Metal Transition in Vanadium Dioxide Thin-Films Sumaiya Kabir, Shruti Nirantar, Mahta Monshipouri, Sumeet Walia, Sharath Sriram and Madhu Bhaskaran; RMIT University, Australia

Vanadium dioxide is a multifaceted phase change material that undergoes insulator-to-metal transition triggered by multiple stimuli, including temperature, light, and electricity. Among all the excitations, the electrically-driven insulator-to-metal transition is of particular advantage as it provides a higher degree of control over the scalability and fast-switching speed. However, there is limited understanding of parameters that control electrically-stimulated insulator-to-metal transition, especially device structure and channel width. In this work, we present a metal-insulator-metal structure to investigate three electrode arrangements: offset, no offset, and overlapping. We experimentally determine that the overlapping configuration of the device needs the least amount of voltage for switching among the three electrode arrangements, which is also supported by simulation results. In contrast, insulator-to-metal transition in vanadium dioxide is independent of the extent of overlap between top and bottom electrodes and channel width. These findings are integral to designing and controlling the functional domains of vanadium dioxide for energy-efficient, addressable, and scalable micro/nano-scale devices and sensor applications.

7:00 PM EN15.03.03

Differences in van der Waals Epitaxial Growth of Sb₂Te₃ Films by Sputtering and Pulsed Laser Deposition Jing Ning¹, Jose C. Martinez¹, Jamo Momand², Heng Zhang², Subodh Tiwari³, Fuyuki Shimojo⁴, Aiichiro Nakano³, Rajiv Kalia³, Priya Vashishta³, Paulo Branicio³, Bart J. Kooi² and Robert Simpson¹; ¹Singapore University of Technology and Design, Singapore; ²Zernike Institute for Advanced Materials, University of Groningen, Netherlands; ³University of Southern California, United States; ⁴Kumamoto University, Japan

High quality van der Waals chalcogenides are important for energy-efficient phase change data storage, thermoelectrics, and spintronics. Here, we combine the statistical design of experiments and density functional theory to illustrate how out-of-equilibrium epitaxial deposition methods can develop the crystal quality of Sb₂Te₃. We found the factors influencing the crystal quality were different for RF sputtering and Pulsed laser deposition (PLD) methods. A thin polycrystalline Sb₂Te₃ seed layer most significantly improves the crystal quality for PLD grown films. However, the temperature is more significant in sputtered films. This difference is very intriguing as both methods are out-of-thermal-equilibrium plasma-based methods. Time-dependent density functional theory molecular dynamics was performed to study the effect of excitation energy on the crystal quality. The PLD plasma is substantially higher in energy than the RF plasma, this increases the adatom diffusion length of deposited atoms as bonding states at the top of the valence band are depopulated. Thus, the electron excitation dominates the adatom diffusivity in PLD. On the contrary, the adatom diffusivity is determined by the thermal temperature in RF sputtering. These results provide a reasonable explanation for the wide-ranging observation of Sb₂Te₃ and superlattice crystal qualities in the literature. They also show how high-quality crystals of Sb₂Te₃, superlattices, and related materials, can be grown using different deposition methods.

SESSION EN15.04: Memory and In-Memory I
Session Chairs: Asif Khan and Iuliana Radu
Tuesday Morning, December 7, 2021
EN15-Virtual

8:00 AM *EN15.04.01

Memory Integration into 3D Integrated Circuits H.S. Philip Wong and Wei-Chen Chen; Stanford University, United States

The integrated circuit (IC) was invented more than 60 years ago. We have witnessed how semiconductor technology has become vitally important to our everyday life, from servers, to PCs, and smartphones. Semiconductor technology plays a truly vital role for humanity, not only in terms of economic development, but also in the way we live, the way we work, and the way we enjoy life. Today, this vital role is manifested in the use of high-performance computing to find a cure for COVID-19, and the computing and communication technologies that enabled work from home, online teaching and learning, and online purchase and delivery of goods and services. Future electronic systems will continue to rely on, and increasingly benefit from, the advances in semiconductor technology as they have had for more than five decades.

Three dimensional integration is one of the major technology directions for integrated circuits. I will give an overview of the new materials and device

technologies that may need to be developed to realize monolithic 3D integration with multiple logic transistor and memory device layers. I will speculate on how they will be integrated into future electronic systems and what future technologies need to be invented to realize energy-efficient 3D ICs.

8:30 AM *EN15.04.02

Achieving High Performance Resistive Switching Using Ionic Thin Films Judith L. MacManus-Driscoll, [Ming Xiao](#), Chao Yun, Mahmoud Eishenawy, Thomas Sun, Matthew Wells and Markus Hellenbrand; University of Cambridge, United Kingdom

Resistive switching (RS) materials, often called memristors, are promising candidates for next-generation non-volatile memory and neuromorphic computing applications. Positive attributes include simplicity, compatibility with conventional semiconductor processes, and the potential for 3D and scaling. For memory applications, achieving all optimized properties *together* of very long retention, fast switching time, endurance, uniformity, and scaling is challenging. In this talk, we revisit the challenge of achieving simultaneous performance optimization and show how tuning the transport properties in the ionic material is important to this end. We demonstrate pronounced resistive switching at low voltages (SET voltage of <1.2 V without high-voltage electroforming), strong endurance (no change in resistance states after >1E6 cycles), uniformity, stable switching, and fast switching speed.

9:00 AM *EN15.04.03

Ferroelectric Doped Hafnium Oxide—From Switching Kinetics to Neuromorphic Elements [Uwe Schroeder](#)^{1,2}; ¹NaMLab gGmbH, Germany; ²Technische Universität Dresden, Germany

Fluorite-structured ferroelectrics have outstanding potential for commercial applications due to their scalability, CMOS compatibility, and ease of fabrication. These advantages make ferroelectric HfO₂ very attractive for non-volatile memory solutions such as ferroelectric random-access memories (FRAM), ferroelectric field-effect transistors (FeFET), and ferroelectric tunnel junctions (FTJ). Significant efforts have been made for the physical understanding and technological exploitation of ferroelectric HfO₂. Due to the wide range of conditions under which ferroelectricity can occur in HfO₂ thin films, the scientific community has improved and optimized the ferroelectric properties using various approaches. As a result, progress in thin-film technology for ferroelectric devices is advancing rapidly.

Neuromorphic devices represent one of the most promising examples of overcoming today's computers' energy efficiency and processing speed limitations. While traditional neuromorphic circuits are based on CMOS transistors and capacitors, recently emerging nano-electronic devices appear to be promising candidates for building the fundamental neuromorphic elements: Neurons and Synapses. Unlike digital memories, this requires gradual switching to many different levels. Moreover, neuromorphic systems realized by spiking neural networks also make use of the timing between spikes. As a result, two basic functions are required: synaptic functions based on the time-dependent plasticity of spikes and neural functions that integrate input signals and generate spikes.

Before discussing the device function, a detailed characterization of the switching kinetics in doped HfO₂ films is necessary, which will be performed on ferroelectric capacitors and FeFET structures.

Different models of polarization switching are investigated and evaluated against the existing literature. Especially, nucleation-limited switching (NLS) and inhomogeneous field mechanism (IFM) data are compared with experiments for ferroelectric capacitor structures. We conclude that models are not necessarily mutually exclusive but rather provide a diverse perspective on the switching phenomenon based on thermodynamic, kinetic, statistical, microscopic, and/or macroscopic viewpoints. In the next step, a small number of grains within the gate stack of a nanoscale FeFET structure with the channel length of 30 nm are characterized, and a detailed analysis of the switching behavior of these individual grains is possible. Again, nucleation-limited switching is observed with a distribution of coercive fields for different individual grains. Multiple excitation pulses, each insufficient for polarization reversal, induce an accumulative effect that eventually leads to ferroelectric switching.

Using this knowledge, hafnium oxide-based FeFETs can be used to realize both artificial neurons and synapses for spiking neural networks. Accumulative switching can be exploited to mimic the integrate-and-fire activity of biological neurons, which, together with FeFET-based synapses, could enable the construction of basic computational blocks of brain-inspired neural networks.

9:30 AM EN15.04.04

Artificial Synapse Based on a Space Charge Modulated Double-Oxide Memcapacitor Pei-En Lin, [Jia-He Yang](#), Cheng-Han Lu and Jen-Sue Chen; Department of Materials Science and Engineering, National Cheng Kung University, Taiwan

Memristor-based devices have been widely investigated to resemble biological synapses used in neuromorphic computation applications, such as big data processing, pattern recognition, and learning tasks. While the memristors have been widely reported, other types of memelements remain underexplored. Capacitive neural networks provide an alternative physical embodiment of neural networks and can lower the power consumption of the circuit because the signal is expressed as voltage rather than current. Therefore, memcapacitors should be the superior candidates for neuromorphic computation. In this work, we design a novel bilayer WO_x/ZrO_x stack which is well-performed in capacitive switching characteristics. Furthermore, the stack unveils a broad range of capacitance states when stimulating with voltage pulses of various amplitudes and frequencies.

The WO_x/ZrO_x stack is sandwiched between Ta (top electrode) and Pt (bottom electrode) to form a memcapacitor. In addition to the capacitive switching performance, the Ta/WO_x/ZrO_x/Pt device also exhibits resistive switching characteristics under voltage sweeping operation. The memresistance and memcapacitance characteristics in the presented Ta/WO_x/ZrO_x/Pt stack are ascribed to the carrier trapping-and-detraping processes by the interaction of injected carriers and defects, which is associated with the space-charge limited conduction (SCLC) depending on the different biasing conditions. In order to confirm the connection between resistive-capacitive switching and SCLC mechanism, we controlled the thickness of WO_x with different sputtering time to observe the relationship between the current density and the thickness in WO_x. When the thickness of WO_x decreases, the current density and the capacitance increase in following with the formula of SCLC mechanism, indicating that the space charge is mainly confined in the WO_x layer and dominates the continuing resistance and capacitance variation.

Finally, the biological synapses have been successfully mimicked by emulating several synaptic functions, such as potentiation and depression, paired-pulse facilitation, short-/long-term memory, and learning-relearning behavior. This result can be integrated into the implementation of neuromorphic computing, which can provide a better guarantee for its large-scale application.

SESSION EN15.05: Memory and In-Memory II
Session Chairs: Asif Khan and Iuliana Radu
Tuesday Morning, December 7, 2021
EN15-Virtual

10:30 AM *EN15.05.01

Devices for Efficient Analog In-Memory Neural Computing at the Edge [Matthew Marinella](#), Sapan Agarwal, Christopher Bennett, Tianyao Xiao, Donald A. Robinson, Elliot J. Fuller and A. A. Talin; Sandia National Laboratories, United States

Deep learning has gained significant interest over the past decade due to unmatched pattern recognition capabilities. However, due to the high computational load, it has been challenging to use deep neural networks (DNNs) and deep convolutional neural nets (CNNs) in applications with significant size, weight, and power (SWaP) constraints. This is further complicated by challenging environments like temperature extremes and radiation encountered by embedded or edge computing systems, such as smart sensors and autonomous system controllers. In-memory computing (IMC) based on analog matrix operations has emerged as a promising hardware architecture with the potential to achieve a power-normalized performance of 100 TOPS/W (tera-operations per second per watt), which is more than 20 times that possible with today's best digital systems. However, analog IMC accelerators are not yet mainstream, due in part to the challenges involved with using nonvolatile memory devices in an analog capacity. Unlike digital computing, analog IMC closely links the final output of an algorithm to physical properties of the device and materials. Device properties such as noise, static and dynamic linearity, state drift, and even interconnect properties directly affect the neural network classification accuracy. Device research must now consider the system and algorithm in context, in order to ultimately execute neural algorithms with acceptable accuracy. With this challenge comes the opportunity to investigate both mature and emerging nonvolatile memory devices and materials for efficient, accurate inference (recognition) and training in analog IMC architectures. We have found that charge trapping semiconductor-oxide-nitride-oxide-semiconductor (SONOS) devices similar to those used in flash memory are well suited for accurate, energy-efficient CNN inference in edge systems. In fact, using SONOS, is possible to achieve inference accuracies on par with digital systems on state of the art deep CNNs such as resnet50 with more than an order of magnitude energy efficiency improvement. As a digital memory, SONOS is mature, but adapting this device technology for analog computing requires addressing new challenges to maintain accuracy and reliability in edge systems. Emerging devices including electrochemical memory (ECRAM) and magnetic domain walls offer exciting possibilities for both ultra-efficient training and inference at the edge, but these devices are less mature and have materials and device research challenges that need to be addressed before utilization in edge computing systems. This talk discusses recent progress and remaining challenges as we work to enable efficient analog in-memory neural computing at the edge.

SNL is managed and operated by NTESS under DOE NNSA contract DE-NA0003525

11:00 AM *EN15.05.02

Exploiting Polarization for Energy Efficient Devices [Chris G. Van de Walle](#); University of California, Santa Barbara, United States

Spontaneous polarization and ferroelectricity can be exploited to enhance the performance of electronic devices. Materials with spontaneous polarization can give rise to large bound charges at heterointerfaces. If the resulting two-dimensional carrier gas can be modulated, it can be used in devices such as high electron-mobility transistors. Fixed charges can be exploited in tunnel field-effect transistors or in tunnel junctions. Accurate prediction of spontaneous and piezoelectric polarization is therefore critical for understanding and designing heterostructures. We have developed a rigorous first-principles formalism for addressing polarization in wurtzite-structure semiconductors [1], and have applied the methodology to a number of other systems: (1) II-IV-nitride semiconductors, which can be integrated with III-nitrides for additional design flexibility [2]; (2) rocksalt-wurtzite interfaces, such as ScN/GaN, which exhibit a giant polarization discontinuity [3]; and (3) polar/nonpolar II-VI heterostructures that can also give rise to huge sheet carrier densities [4].

Polarization is also at the core of ferroelectric transistors. The recent finding that adding Sc to AlN not only enhances the piezoelectricity but gives rise to ferroelectricity has generated great interest for novel applications within the family of nitride semiconductors. The behavior of the alloy is surprising, given that the ground-state structure of ScN is rocksalt, which is centrosymmetric. However, when adding modest amounts of ScN to AlN, the alloys retain the wurtzite structure. One might expect the alloy properties to be interpolated between wurtzite AlN and a metastable wurtzite ScN phase. However, when ScN is constrained to a hexagonal unit cell, it is not stable in the wurtzite structure, but rather assumes a layered hexagonal structure. We have found that the enhanced piezoelectric polarization in ScAlN alloys actually arises because of the nonpolar nature of hexagonal ScN. The addition of Sc brings the alloy closer to the centrosymmetric structure, which constitutes the "saddle point" for switching of the polarization. I will present detailed first-principles results for polarization, piezoelectric coefficients, and switching barriers.

Work performed in collaboration with N. L. Adamski, C. E. Dreyer, S. Mu, H. Wang, and D. Wickramaratne, and supported by AFOSR.

[1] C. E. Dreyer, A. Janotti, C. G. Van de Walle, and D. Vanderbilt, *Phys. Rev. X* 6, 021038 (2016).

[2] N. L. Adamski, D. Wickramaratne, and C. G. Van de Walle, *J. Mater. Chem. C* 8, 7890 (2020).

[3] N. L. Adamski, C. E. Dreyer, and C. G. Van de Walle, *Appl. Phys. Lett.* 115, 232103 (2019).

[4] N. L. Adamski, C. E. Dreyer, and C. G. Van de Walle, *Phys. Rev. B* 102, 201301 (2020) (R).

11:30 AM EN15.05.03

Imaging Oxygen Transport in Oxide-Based ReRAM Devices [Baoming Wang](#)¹, Kevin May¹, Teodor Todorov², Takashi Ando², Dmitri Kalaev¹, Harry Tuller¹, Bilge Yildiz¹, John Rozen² and Frances M. Ross¹; ¹Massachusetts Institute of Technology, United States; ²IBM T.J. Watson Research Center, United States

Resistive switching (RS) has been studied in detail over the last decade due to its importance for the fabrication of electronic devices. By combining fast switching, long retention, and high-density stacking, resistive switching random access memory (ReRAM) has the potential to meet the high demand for ultra-high-density and low-cost future data storage and logic circuits. While significant progress has been achieved in the development of devices based on ReRAM, performance, including inherent stochasticity, is limited by our knowledge of ionic transport phenomena that control conductance changes in filamentary regions and at oxide interfaces. To guide the design of ReRAM devices, we applied scanning transmission electron microscopy techniques to image oxygen transport in ReRAM devices based on oxides (HfO_{2-x}) during operation in situ, allowing us to correlate electrical characteristics and compositional/structural changes in the layers and interfaces in state-of-the-art ReRAM devices. We have achieved electrical switching behavior in various electron-transparent cross-section lamellar devices and find that electrical performance of the devices in situ, both forming and cycling, can be made to replicate the behavior of complete devices. We measured oxygen elemental redistribution during operation in situ and obtained evidence for the buildup of inhomogeneous fields within HfO_{2-x} layers during device operation. Our ongoing work involves locating oxygen vacancy filaments or oxide interface layers and atomic imaging of oxygen vacancy transport during in situ operation. We are combining advanced imaging techniques including energy filtered imaging, 4D-STEM and DPC (differential phase contrast), and correlating scanning electron microscopy (SEM) and transmission electron microscopy to achieve this goal. Correlation of different microscopy modes helps to locate and measure filaments within complete devices; 4D-STEM and DPC can be employed to map the electrical field change during switching thus characterizing the filament or interface; and EELS and integrated DPC are capable of imaging the oxygen atoms directly.

8:00 AM *EN15.06.01

Memory Device Options for Energy Efficient Synapses in Brain-Inspired Neuromorphic Systems [Daniele Ielmini](#); Politecnico di Milano, Italy

The human brain can execute complicated tasks with a power consumption of about the same as an electric bulb. Neuromorphic computing aims at replicating the same connectivity and the same energy efficiency of the human brain by integrated circuits. In the neuromorphic hardware, synapses play a key role as they control the energy consumption, the computing functionality, the inter-neuron connectivity and the scalability of the circuit. While several memory technologies have been considered as artificial synapses, there is increasing evidence that synaptic materials must display a unique set of properties that cannot be met by conventional and emerging memory devices.

In this talk, I will present novel synaptic devices based on nanoscale memristive materials. First, I will discuss a volatile resistive switching memory (RRAM) with Ag top electrode, capable of tunable retention times for spatio-temporal sensing and computing. Second, I will present a random nanowire network, where nanowire synapses connect and disconnect under dynamic stimuli enabling cognitive behavior based on heterosynaptic plasticity and reservoir computing. Third, I will discuss artificial synapses consisting of 2D semiconductors, such as MoS₂, displaying outstanding weight-update linearity and low current. Finally, the prospects of synaptic materials will be finally discussed in terms of functionality, cost, scalability, CMOS integration and energy efficiency.

8:30 AM *EN15.06.02

Energy Efficiency Neuromorphic Computing with Oscillatory Neural Networks [Aida Todri-Sanial](#), Corentin Delacour, Stefania Carapezzi, Madeleine Abernot, Gabriele Boschetto and Thierry Gil; LIRMM, University of Montpellier, CNRS, France

Current classical computers are playing a critical role in advanced research such as in biology, climate analysis, economics, genomics, finance, etc. In many aspects, computing fuels the advances of our modern society. Yet, recent developments in artificial intelligence (AI) and machine learning will require even more powerful computing systems such as exascale computations per second due to an ever-increasing amount of data. But classical computing systems are hindered by the von-Neumann communication bottleneck, the physical separation between processor and memory. This offers the opportunity to explore a novel computing paradigm where the brain can serve as a computational model of how to deal with large amounts of (often fuzzy) information while being extremely dense, error-resilient and power efficient.

In this talk, a novel and alternative neuromorphic computing paradigm based on oscillating neural networks (ONN) will be presented. Energy efficient relaxation oscillators based on phase-change VO₂ material for oscillating neurons and tunable 2D TMD MoS₂ memristors for synapses are the building blocks of ONN architecture [1-3]. Inspired by neural oscillations or brain waves, in ONN, the information is encoded in the phase of coupled oscillators. The talk will cover aspects from materials, devices, circuits to ONN architecture design and hardware implementation and demonstration on AI tasks. This work is conducted in the framework of the EU H2020 NEURONN project, www.neuronn.eu.

[1] A. Todri-Sanial, S. Carapezzi, C. Delacour, M. Abernot, T. Gil, E. Corti, et al., "How Frequency Injection Locking Can Train Oscillatory Neural Networks to Compute in Phase," preprint, hal-lirmm.ccsd.cnrs.fr/lirmm-03164135, 2021.

[2] S. Carapezzi, C. Delacour, G. Boschetto, E. Corti, M. Abernot, A. Nejim, et al., "Multi-Scale Modeling and Simulation Flow for Oscillatory Neural Networks for Edge Computing," 19th IEEE Interregional NEWCAS Conference, 2021.

[3] C. Delacour, S. Carapezzi, M. Abernot, G. Boschetto, Nadine Azemard, et al., Oscillatory Neural Networks for Edge AI Computing, *IEEE Computer Society Annual Symposium on VLSI (ISVLSI 2021)*, Jul 2021, Tampa, United States.

9:00 AM *EN15.06.03

Two-Dimensional Materials for Neuromorphic Computing [Tania Roy](#); University of Central Florida, United States

Two-dimensional materials (2D) have gained significant attention in neuromorphic applications due to their low power consumption, high endurance, high retention and high linearity in weight update. A synaptic device for neural computing needs to demonstrate high endurance with low cycle-to-cycle (C-C) variability for efficient training. However, low C-C variability in conductance weight update for a substantially high number of cycles has not been demonstrated yet. We report MoS₂ based synapses with Ti/Au electrodes that exhibit ultra-low variability in SET voltage with a low reset power of 2-10 nW for over 115 cycles. Additionally, these devices show almost no variability in conductance weight update for over 100 pulsed cycles for multiple (10) devices. These devices outperform conventional Si-based memristors, indicating the viability of 2D materials for reliable implementation of neural networks.

Optoelectronic synapses are devices that behave like photodetectors with analog memory. In neuromorphic computing, these devices have the potential to perform imaging and object identification using the same device. We first demonstrate that the strong photogeneration efficiency of methylammonium lead bromide perovskite quantum dots (PQDs) can be exploited by growing PQDs from the lattice of a single layer graphene by a defect-mediated process. The rationale for designing this hybrid superstructure stems from the ability of PQDs to absorb light and generate charge carriers. The charges generated are transferred to graphene, which transports the carriers across the active layer of the device. Through the implementation of this thin superstructure in a phototransistor geometry, we produce a photoresponsivity of $1.4 \times 10^8 \text{ AW}^{-1}$ at 430 nm and a specific detectivity (D^*) of 4.72×10^{15} Jones, which is by far the best responsivity and detectivity across similar devices reported to date. This is promising for the development of highly efficient optoelectronic materials for high-speed communications, sensing, ultra-sensitive cameras and high-resolution imaging and displays. The graphene-PQD superstructure behaves as an optoelectronic synapse with low energy consumption of 36.75 pJ/spike that mimics crucial characteristics of its biological equivalent, with unique optical potentiation and electrical habituation function.

We also utilized the persistent photoconductivity of 2D MoS₂ layers to demonstrate an optoelectronic synapse. A CVD-grown monolayer MoS₂ FET exhibits substantial enhancement in drain current when illuminated with a laser of 450 nm wavelength as well as a negative shift in its threshold voltage due to the generation of photocarriers. The device undergoes optical potentiation and electrical depression. The device is "optically" potentiated by applying light pulses with ON/OFF interval of 5 s for each at 450 nm wavelength – measured at a constant drain bias of 1.0 V with $V_G = -2$ V. Also, it is "electrically" depressed by applying 50 electrical pulses with ON/OFF interval of 1 s and 9 s, respectively – measured at a drain bias of -100 mV with $V_G = -2$ V. These results confirm the active and simultaneous tunability of conductance essential for the electrical/optical training of optoelectronic synapse in neural network applications. The negative voltage pulses applied at the drain de-traps the holes from the SiO₂/MoS₂ interface, thus gradually depress the device to its initial low conductance state. By engineering the gate electrode, we observe synaptic behavior at infrared wavelengths.

9:30 AM EN15.06.04

Synaptic Functionalities in P(VDF-TrFE) Coupled Zinc-Tin Oxide Hybrid Ferroelectric Transistors for Neuromorphic Computing Ching-Kang Sheng, Kuan-Ting Chen, Yun-Huei Tseng and Jen-Sue Chen; National Cheng Kung University, Taiwan

In order to expedite data processing speed, numerous synaptic devices have been investigated for their potential implementation in neuromorphic hardware systems. In comparison with the two-terminal memristors, the concurrent learning process in three-terminal transistors can be easily designed and more advantageous because the crosstalk noise can be avoided without additional transistors (i.e. 1T1R) in the circuits. Among the synaptic transistors, the ferroelectric field effect transistors (FeFETs) have attracted much attention for their strong polarization, nonvolatile properties and lower power consumption.

Poly(vinylidene fluoride-trifluoroethylene) (P(VDF-TrFE)) is a commonly applied polymer ferroelectric material for its spontaneous polarization. It had been applied to transition metal dichalcogenide (TMD) transistors and served as synaptic devices. However, the synaptic characteristics of P(VDF-TrFE) incorporated amorphous oxide semiconductor FeFET has not been studied yet. In this work, we fabricate an organic/inorganic FeFET based on Zinc-Tin Oxide (ZTO) semiconductor channel and encapsulated by the P(VDF-TrFE) layer to investigate the charge transport characteristics modulated via the ferroelectric effects.

With P(VDF-TrFE) coated on the ZTO channel layer, a net upward dipole alignment in P(VDF-TrFE) attracts holes from the ZTO, which enables more electrons to accumulate in the effective channel. Therefore, the P(VDF-TrFE) encapsulated ZTO FET shows higher IDS than that without P(VDF-TrFE). Based on the band diagram analysis, the band bending of ZTO reflects the influence and reversal of dipole alignment, which is attributed to the accumulated electrons in the channel. In addition, the conductance, acted as weight, gets updated more easily and retains longer in the P(VDF-TrFE) coupled ZTO. Accordingly, the synaptic performance can be mimicked by stimulation on the gate terminal. We demonstrate paired-pulse facilitation (PPF), potentiation/depression cycle (P/D cycle) and spike timing dependent plasticity (STDP) of asymmetric Hebbian learning in this FeFET device. The transition from short-term memory to long-term memory is achieved via increasing the pulse number, amplitude, frequency, and duration time. The experimental results manifest that this ferroelectric coupled ZTO synaptic device has great potential for neuromorphic computing hardware systems owing to its successful emulation in functionality of the human brain.

SESSION EN15.07: New Materials
Session Chairs: Asif Khan and Subhash L. Shinde
Wednesday Morning, December 8, 2021
EN15-Virtual

10:30 AM EN15.07.01

Harnessing Anharmonicity and Electron Correlations for Energy Efficient Computing Panchapakesan Ganesh; Oak Ridge National Laboratory, United States

Metal oxide-based Resistive Random-Access Memory (RRAM) exhibits multiple resistance states, arising from the activation/deactivation of a conductive filament (CF) formed by oxygen vacancies inside a switching layer – due to an underlying metal-insulator transition (MIT). In a crossbar device architecture, you have a highly dense information-storage&computing system, that you want to be reliable, fast switching and utilizing low-power. This can enable emulating ‘brain like’ neuromorphic computing with co-located memory and compute. Similarly, ferroelectric materials – such as Hafnia – are promising candidates for synaptic weight elements in neural network hardware because of their nonvolatile multilevel memory effects. But conventional RRAM materials require high forming potentials and show high variability (device-to-device or cycle-to-cycle) and are plagued by less reliability as well as the voltage-time dilemma, similar to ferroelectric synapses. To address these challenges, we are working to answer the following open questions: what material characteristics we need when choosing a memristor material? What factors triggers a state-change (e.g. MIT, or ferroelectric-switching) in these materials? What determines the dynamics of the switching mechanism?

Using a combination of high-throughput phase-field and machine-learning methods [1] we discovered that harnessing electron-electron correlations in binary oxides can be advantageous for improved performance of RRAM devices. Using a combination of various correlated electronic structure methods, we further uncovered the underlying factors that control the MIT in non-stoichiometric correlated binary oxides – such as VO₂ [2,3]. We subsequently demonstrated how many of the correlated perovskite metals that undergo MIT are negative charge-transfer metals, with the magnitude of ligand-hole being the key to controlling MIT[4]. These works provides a fundamental understanding of the role of electron correlations in resistive switching materials. For ferroelectric-based synapses, we explored the recently discovered layered-thiophosphate family of materials [5]. We discovered [6] presence of strong anharmonic coupling in these materials between the ferroelectric polar-mode and a Raman active symmetric-mode, even down to the single-layer limit, that could allow optical or mechanical control of ferroelectric switching, potentially alleviating the voltage-time dilemma in conventional ferroelectrics.

[1]” High-throughput phase-field simulations and machine learning of resistive switching in resistive random-access memory”, npj Computational Materials volume 6, Article number: 198 (2020), Kena Zhang, Jianjun Wang, Yuhui Huang, Long-Qing Chen, P. Ganesh* & Ye Cao.

[2]” Doping a bad metal: Origin of suppression of the metal-insulator transition in nonstoichiometric VO₂”, Phys. Rev. B 101, 155129, (2020), P. Ganesh*, Frank Lechermann, Ilkka Kylänpää, Jaron T. Krogel, Paul R. C. Kent, and Olle Heinonen

[3]”Metal-insulator transition tuned by oxygen vacancy migration across TiO₂/VO₂ interface”, Scientific Reports, 10, 1854 (2020), Qiyang Lu, Changhee Sohn, Guoxiang Hu, XiangGao, Matthew F. Chisholm, Ilkka Kylänpää, Jaron T. Krogel, Paul R. C. Kent, Olle Heinonen, P. Ganesh* and Ho Nyung Lee

[4]”Origin of Metal-Insulator Transitions in Correlated Perovskite Metals”, **arXiv:2103.09809**, M. Chandler Bennett, Guoxiang Hu, Guangming Wang, Olle Heinonen, Paul R. C. Kent, Jaron T. Krogel, P. Ganesh*.

[5]”Tunable quadruple-well ferroelectric van der Waals crystals”, Nature Materials, 19, 43 (2020), John A. Brehm, Sabine M. Neumayer, Lei Tao, Andrew O’Hara, Marius Chyasnachichus, Michael A. Susner, Michael A. McGuire, Sergei V. Kalinin, Stephen Jesse, P. Ganesh*, Sokrates T. Pantelides, Petro Maksymovych and Nina Balke

[6]”Origin and stabilization of ferrielectricity in CuInP₂Se₆”, **arXiv:2106.08783**, Nikhil Sivasdas, Peter Doak, P. Ganesh*

10:45 AM EN15.07.02

Magnetic Antiskyrmions in Tetragonal Inverse Heusler Materials Rana Saha¹, Abhay Srivastava¹, Jagannath Jena¹, Ankit Sharma¹, Tianping Ma¹, Börge Göbel¹, Claudia Felser² and Stuart Parkin¹; ¹Max Planck Institute of Microstructure Physics, Germany; ²Max Planck Institute for Chemical Physics of Solids, Germany

One of the major topics in spintronics today is the study of steady-state and dynamical properties of non-collinear spin textures with various topologies¹. One of the most important of these are skyrmions that are magnetic nano-objects with chiral magnetic boundaries, which are potential information carriers for future dense and energy-efficient racetrack memory devices². Recently, a novel chiral spin texture, magnetic antiskyrmion that has distinct topological features from that of Bloch and Néel skyrmions, was discovered in tetragonal inverse Heusler compounds³⁻⁴. Antiskyrmions have boundaries that have a complex structure consisting of successive left-hand Bloch, left-hand Néel, right-hand Bloch, and right-hand Néel wall segments. This complex structure results from an anisotropic Dzyaloshinskii-Moriya exchange interaction set by the symmetry of the underlying lattice. This causes the magnetic structure of the antiskyrmion to be aligned with the crystal lattice that leads to enormous stability of antiskyrmions over a wide range of temperature, magnetic field, and thickness of the lamella in which they are formed. This magnetic texture is of great current interest both for its topological characteristics and potential spintronic applications. Therefore, it is of significant importance to understand the physical properties of these nanoscopic spin textures. In this presentation, I will describe some recent *in-situ* investigations on the nucleation, stability, and manipulation of antiskyrmions using Lorentz transmission electron microscopy (LTEM) and magnetic force microscopy (MFM). By employing these two techniques, we showed the thickness-independent intrinsic stability of antiskyrmions, robust tunability of the size of antiskyrmions, and stabilization of elliptical Bloch skyrmions in the antiskyrmions system due to long-range dipole-dipole interactions⁵⁻⁷. From these studies, we have developed a significant fundamental understanding of these fascinating chiral magnetic nano-objects, which are potential for spintronic applications.

References:

1. Nagaosa, N. et al., Topological properties and dynamics of magnetic skyrmions. *Nat. Nanotechnol.* 8, 899 (2013).
2. Parkin, S. S. P. et al., Memory on the racetrack. *Nat. Nanotechnol.* 10, 195 (2015).
3. Nayak, A. K., et al., Magnetic antiskyrmions above room temperature in tetragonal Heusler materials. *Nature* 548, 561 (2017).
4. Jena, J., et al., Observation of magnetic antiskyrmions in the low magnetization ferrimagnet $\text{Mn}_2\text{Rh}_{0.95}\text{Ir}_{0.05}\text{Sn}$. *Nano Lett.* 20, 59 (2019).
5. Jena, J., et al., Elliptical Bloch skyrmion chiral twins in an antiskyrmion system. *Nat. Commun.* 11, 1115 (2020).
6. Ma, T., et al., Tunable magnetic antiskyrmion size and helical period from nanometers to micrometers in a D_{2d} Heusler compound. *Adv. Mater.* 32, 2002043 (2020).
7. Saha, R., et al., Intrinsic stability of magnetic anti-skyrmions in the tetragonal inverse Heusler compound $\text{Mn}_{1.4}\text{Pt}_{0.9}\text{Pd}_{0.1}\text{Sn}$. *Nat. Commun.* 10, 5305 (2019).

SESSION EN15.08: Neuromorphic Computing II
 Session Chairs: Subhash L. Shinde and Hui Jae Yoo
 Wednesday Afternoon, December 8, 2021
 EN15-Virtual

9:00 PM *EN15.08.01

Materials Discovery for Energy-Efficient Neuromorphic Computing—A Co-Design Approach [Christian Mailhot](#); Sandia National Laboratories, United States

The report of the *Basic Research Needs for Microelectronics* workshop (2018)[1] documents that “as Moore’s Law nears its end, a fundamental rethinking of the science behind the materials, devices, synthesis and fabrication technologies, architectures, and algorithms is needed to enable continued advances in computing, communication, and sensing technologies.” These advances must be conceived and developed collectively and concurrently, using an interdisciplinary co-design framework, where each scientific discipline informs and engages the others, with multi-directional information flow, to achieve orders of magnitude improvements in system-level performance. This presentation will identify opportunities for transformative advances in microelectronics that uniquely result from a co-design approach. In addition, we will explore whether modern artificial-intelligence (AI) methods may accelerate co-design. Finally, the application of the co-design approach to analog computing via ion-tunable electronic materials will be presented[2]. This application builds on the emerging science of ion-tunable materials, complex networks of devices, and evolutionary algorithmic discovery to create a revolutionary neuromorphic computing platform with extreme energy efficiency, application-driven on-demand architectural flexibility, the ability to tolerate errors and self-repair against radiation damage, programmable complex dynamics, and dramatic algorithmic speedups[3].

[1] DOE SC *BRN for Microelectronics* Report (2018): <https://doi.org/10.2172/1545772>.

2 E. J. Fuller, S. T. Keene, A. Melianas, Z. Wang, S. Agarwal, Y. Li, Y. Tuchman, C. D. James, M. J. Marinella, J. J. Yang, A. Salleo, A. A. Talin, *Science* 364, 570-574, (2019).

3 E. J. Fuller, Y. Li, C. Bennet, S. T. Keene, A. Melianas, S. Agarwal, M. J. Marinella, A. Salleo, A. A. Talin, *IBM Journal of Research and Development* 63, 9: 1-9: 9, (2019)

[1] DOE SC *BRN for Microelectronics* Report (2018): <https://doi.org/10.2172/1545772>.

[2] E. J. Fuller, S. T. Keene, A. Melianas, Z. Wang, S. Agarwal, Y. Li, Y. Tuchman, C. D. James, M. J. Marinella, J. J. Yang, A. Salleo, A. A. Talin, *Science* 364, 570-574, (2019).

[3] E. J. Fuller, Y. Li, C. Bennet, S. T. Keene, A. Melianas, S. Agarwal, M. J. Marinella, A. Salleo & A. A. Talin, *IBM Journal of Research and Development* 63, 9: 1-9: 9, (2019)

9:30 PM EN15.08.02

Late News: Investigation of Ionic Programming Dynamics of Metal-Oxide Based Electrochemical Memory for Energy-Efficient Neuromorphic Computing [Da Gil Ryu](#)¹, Yanho Jeong¹, Hyunjoon Lee¹, Seong Ho Cho¹, Gawon Lee¹, Sangbum Kim¹, Seyoung Kim² and Yun Seog Lee¹; ¹Seoul National University, Korea (the Republic of); ²Pohang University of Science and Technology, Korea (the Republic of)

Crossbar arrays of synaptic devices is a key platform for neuromorphic computing architectures. To achieve time and energy efficiency compared to the von Neumann architecture, it is essential to develop synaptic devices with optimal characteristics. Among various candidates, metal-oxide based electrochemical random-access memory (ECRAM) is considered as a promising analog synaptic device due to its excellent programming characteristics and CMOS-compatibility. However, the switching mechanisms of metal-oxide ECRAM is unclear, impeding improvements of the synaptic characteristics and device performance.

In this contribution, we elucidated the mechanism of operation of metal-oxide ECRAM devices. We fabricated devices with a planar structure with a channel of tungsten oxide and an electrolyte of hafnia. Tungsten oxide thin films with different conductivities were obtained by controlling the oxygen flow rate during reactive sputtering, and their off-stoichiometry x was obtained from XPS analysis. It was confirmed that oxygen acts as a dopant that x is proportional to conductivity. Hafnia thin films with different ionic conductivity were deposited by controlling deposition temperature during ALD, and their ionic conductivity was confirmed by EIS measurement. The electrical characteristics of the device were analyzed through gate voltage sweep, transmission line measurement, voltage bias programming, and voltage pulse programming. In conclusion, we show that the metal-oxide ECRAM devices work through an electrochemical mechanism. We modeled that programming dynamics are determined from these two factors: field-driven migration occurs in the electrolyte, and diffusion of ions occurs within the channel, resulting in conductance change¹. Furthermore, we devised a vertical three-dimensional metal-oxide ECRAM structure to achieve high-density integration as well as high energy-efficiency.

[1] Y Jeong et al., *Advanced Electronic Materials.*, 2100185 (2021)

9:45 PM EN15.08.03

Low Power, Multistate, Fast Phase-Change Artificial Synapse Based on Transient-Amorphous-State-Mediated Plasticity Shao Xiang Go¹, Qiang Wang¹, Tae Hoon Lee², Stephen R. Elliott², Natasa Bajalovic¹ and Desmond K. Loke¹; ¹Singapore University of Technology and Design, Singapore; ²University of Cambridge, United Kingdom

The human brain is capable of parallel information processing while consuming low energy. Motivated by the efficiency of the brain, CMOS-based architectures are being developed for image classification and machine learning. However, the volatility, design complexity and high bias voltages for CMOS architectures complicate the path to achieve the interconnectivity, information density and energy efficiency of the brain. Here we describe a phase-change material (PCM) memory operating with a different phenomenon from existing PCMs. The PCM switches at low voltage and energy, display multiple distinct nonvolatile conductance states within a small voltage range, and achieves excellent distribution of conductance states when implemented in neural network simulations. Fast crystallization pulses were also achieved enabling the integration of neuromorphic functionality in high-density electronic systems. Thermal simulations reveal the transient-amorphous-state-assisted change in synaptic weight. Our findings pave a way towards power-efficient artificial intelligence (AI) operations that could mimic the functionalities of a human brain.

SYMPOSIUM EQ01

Quantum Optical Materials and Devices Based on Impurity Systems
November 30 - December 8, 2021

Symposium Organizers

Igor Aharonovich, University of Technology-Sydney
Abram Falk, IBM T.J. Watson Research Center
Shengxi Huang, The Pennsylvania State University
Xuedan Ma, Argonne National Laboratory

* Invited Paper

SESSION EQ01.01: Defects and Color Centers—Properties I
Session Chairs: Song Jin and Richard Layfield
Tuesday Morning, November 30, 2021
Hynes, Level 1, Room 105

10:30 AM *EQ01.01.01

Near-Infrared Wavelength Quantum Emitters Peter Udvarhelyi¹, Song Li¹, Gergo Thiering¹, András Csóré², Viktor Ivády^{1,3} and Adam Gal^{1,2}; ¹Wigner Research Centre for Physics, Hungary; ²Budapest University of Technology and Economics, Hungary; ³Linköping University, Sweden

The quest of near-infrared (NIR) solid-state quantum emitters is one of main driving forces in the crossing of computational and experimental materials science and quantum optics (e.g., Ref. [1]). Solid-state quantum emitters in the wavelength region of 1.1-1.6 micrometers have a minimum absorption in living cells, thus would be ideal *in vivo* probes or biomarkers when they operate at room temperature. Furthermore, coherent emission from the single photon sources in the telecom bands at 1.3-1.6 micrometers could be directly applied for building metropolitan quantum networks through the existing infrastructure of optical fibers. Here we show the latest results about identification and characterization of NIR quantum emitters in diverse systems. We recently identified in a bioinert material, silicon carbide (SiC), room-temperature quantum emitters with high readout contrast associated with divacancy in stacking faults. Furthermore, we carried out in-depth analysis of the fine electronic structure of vanadium defect in SiC which is a promising telecom O-band quantum emitter. Here we mention that the scalability and deterministic creation of quantum emitters are still very challenging issues in SiC, and in general, in threedimensional materials. In twodimensional materials, techniques exist to generate atomic defects on demand. We proposed defects in hexagonal boron nitride (hBN) that can act as quantum bits that have been realized in experiments. However, deterministic creation of those defects is still

not in reach. Very recently, activation of single defect spin in tungsten disulfide (WS_2) has been demonstrated at atomistic precision [2] which is a single carbon atom substituting sulfur atom. We show that the carbon defect spin can be initialized, optically readout and coherently manipulated with NIR emission. This result constitutes a scalable quantum bit in a twodimensional material that can be activated at atomistic precision. This work was supported by the Ministry of Innovation and Technology and the National Research, Development and Innovation Office of Hungary (NKFIH) within the Quantum Information National Laboratory of Hungary, the National Quantum Technology Program (NKFIH Grant no. 2017-1.2.1-NKP-2017-00001). A.G. acknowledges the National Excellence Program (NKFIH Grant no. KKP129866), the EU QuantERA project “Nanospin” (NKFIH Grant no. 127902) as well as the support of the European Commission within the Quantum Technology Flagship Project ASTERIQS (Grant no. 820394).

[1] Gang Zhang, Yuan Cheng, Jyh-Pin Chou, and Adam Gali, *Applied Physics Reviews* 7, 031308 (2020)

[2] Katherine A. Cochran, Jun-Ho Lee, Christoph Kastl, Jonah B. Haber, Tianyi Zhang, Azimkhan Kozhakhmetov, Joshua A. Robinson, Mauricio Terrones, Jascha Repp, Jeffrey B. Neaton, Alexander Weber-Bargioni, Bruno Schuler, arXiv:2008.12196

11:00 AM *EQ01.01.02

Designing Quantum Interfaces to Emitters at the Nanoscale Prineha Narang; Harvard University, United States

The potential impact of active quantum emitters (impurity-based color centers) on creating quantum information systems in the near-term is evident^{1,2}. Yet, design and control of robust quantum interfaces to these impurity systems at the nanoscale has remained challenging. In this talk, I will present promising physical mechanisms and device architectures for coupling emitters to other qubit platforms *via* dipole-, phonon-, and magnon-mediated interactions. I will present our latest work on coupling magnons to emitters as a natural step towards magnon-mediated efficient manipulation of spin-qubit states with applications in sensing and quantum information science. I will start with a scheme that uses magnetic nanoparticles that sustain antenna-like magnon resonances as nanomagnonic cavities for microwave magnetic fields. Here, in recent work we have shown that nanomagnonic cavities can modify the local magnetic environment of spin emitters in the microwave domain, facilitate the magnetic drive of spin transitions, and allow for strong coupling of these emitters with single magnons³. Next, I will discuss how the magnetic fields of nanomagnonic cavities that change spatially on the length scales of single molecular or defect emitters, coupled with descriptions of spin emitters beyond the point-dipole approximation, enables selection rule-breaking of orbital-spin transitions⁴. Such nanomagnonic cavities could pave the way towards magnon-based quantum networks and magnon-mediated quantum gates. Taking this further, I will present some of our recent work in capturing non-Markovian dynamics in open quantum systems (OQSs) built on the ensemble of Lindblad's trajectories approach^{5,6}. In the outlook, I will discuss new approaches from quantum chemistry for OQSs that could guide the controllable coupling of active quantum emitters and create robust quantum interfaces to the nanoscale.

¹ Awschalom, D. et al. Development of Quantum Interconnects (QuICs) for Next-Generation Information Technologies. *PRX Quantum* 2, 017002 (2021).

² Head-Marsden, K., Flick, J., Ciccarino, C. J. & Narang, P. Quantum Information and Algorithms for Correlated Quantum Matter. *Chem. Rev.* (2020) doi:10.1021/acs.chemrev.0c00620.

³ Neuman, T., Wang, D. S. & Narang, P. Nanomagnonic Cavities for Strong Spin-Magnon Coupling and Magnon-Mediated Spin-Spin Interactions. *Phys. Rev. Lett.* 125, 247702 (2020).

⁴ Wang, D. S., Neuman, T. & Narang, P. Spin Emitters beyond the Point Dipole Approximation in Nanomagnonic Cavities. *J. Phys. Chem. C* 125, 6222–6228 (2021).

⁵ Head-Marsden, K., Krastanov, S., Mazziotti, D. A. & Narang, P. Capturing non-Markovian dynamics on near-term quantum computers. *Phys. Rev. Research* 3, (2021).

⁶ Krastanov, S. et al. Unboxing Quantum Black Box Models: Learning Non-Markovian Dynamics. arXiv [quant-ph] (2020).

11:30 AM EQ01.01.03

Investigation of Stark Shift and Charge Noise on a Centrosymmetric Diamond Defect Lorenzo De Santis^{1,2}, Matthew Trusheim¹, Kevin Chen¹ and Dirk Englund¹; ¹Massachusetts Institute of Technology, United States; ²Delft University of Technology, Netherlands

Color centers in diamond are among the best performing optically accessible qubits in the solid state. Group IV-vacancy centers in particular can provide highly coherent and stable optical interfaces, a property which is attributed to their inversion symmetry. In this work we investigate the effect of an external electric field on the optical transition of a single tin-vacancy (SnV) center. Our study reveals a vanishingly small permanent electric dipole as well as a suppressed polarizability of the emitter, more than 4 orders of magnitude lower than for an NV center, demonstrating the inversion symmetry protection of a Group IV-vacancy defect in diamond from charge noise. Additionally, we show that by modulating the SnV electric-field-induced dipole we can use the emitter's linewidth as a nanoscale probe to quantify electric field noise at its location. To gain further insight on the effect of the electric field noise, we also probe the optical transition at different timescales. This allows to resolve the individual spectral jumps of the transition, and to measure the homogeneous linewidth of the emitter without spectral diffusion effects.

SESSION EQ01.02: Defects and Color Centers—Properties II

Session Chairs: Shengxi Huang and Prineha Narang

Tuesday Afternoon, November 30, 2021

Hynes, Level 1, Room 105

2:00 PM EQ01.02.02

Defect Polaritons from First Principles Derek Wang¹, Susanne Yelin¹ and Johannes Flick²; ¹Harvard University, United States; ²Flatiron Institute, United States

Precise control over the electronic and optical properties of defect centers in solid-state materials is necessary for their applications as quantum sensors, transducers, memories, and emitters. In this study, we demonstrate, from first principles, how to tune these properties via the formation of defect polaritons. Specifically, we investigate three defect types—CH, CB-CB, and CB-VN—in monolayer hexagonal boron nitride (hBN). The lowest-lying electronic excitation of these systems is coupled to an optical cavity where we explore the strong light-matter coupling regime. For all defect systems, we show that the polaritonic splitting that shifts the absorption energy of the lower polariton is much higher than can be expected from a Jaynes-Cummings interaction. In addition, we find that the absorption intensity of the lower polariton increases by several orders of magnitude, suggesting a possible route toward overcoming phonon-limited single-photon emission from defect centers. Finally, we find that initially localized electronic transition densities can become delocalized across the entire material under strong light-matter coupling. These findings are a result of an effective continuum of electronic transitions near the lowest-lying electronic transition for both pristine hBN and hBN with defect centers that dramatically enhances the strength of the light-matter interaction. We expect our findings to spur experimental investigations of strong light-matter coupling between defect centers and cavity photons for

applications in quantum technologies.

2:15 PM EQ01.02.03

Telecom Quantum Emitters in Atomically-Thin Molybdenum Ditelluride (MoTe₂) [Huan Zhao](#), Michael Pettes, Yu Zheng and Han Htoon; Los Alamos National Laboratory, United States

Recently, as atomically-thin transition-metal dichalcogenides (TMDCs) have advanced to the forefront of quantum information science research, quantum emitters (QEs) have been demonstrated in these materials. However, QEs discovered to date in 2D materials have their operating wavelength confined to the visible spectral range and the technologically important near-infrared (NIR) regime still remains an unconquered territory. Bringing 2D TMDCs into the research of NIR quantum photonics is highly motivated by the potential of creating on-demand telecom-compatible quantum light sources and the possibility of coupling the unique valley pseudo-spin qubits to photons propagating in optical fibers.

Meeting this challenge head on, here we report the first deterministic creation of QEs capable of high purity single photon emission at wavelengths covering entire NIR emission band from 1080 nm to 1550 nm. We achieved this by coupling mono and multi-layer molybdenum ditelluride (MoTe₂) to strain inducing nano-pillar arrays. Our Hanbury Brown and Twiss experiment yielded near-complete photon antibunching ($g^2(0) < 0.1$), unambiguously proving the single-photon nature of the emitters. Polarization-resolved magneto-optical spectroscopies further revealed that while valley symmetry, which is essential for the valley pseudo spin based quantum information processing, is preserved in some QEs, the strain induced anisotropic exchange interaction mixed valley states in other QEs to display cross-linearly polarized doublets with ~ 1 meV splitting at zero magnetic field. The valley symmetry in these QEs is restored under 8T magnetic field. These findings together point to the exciting potential of accessing valley pseudo-spin through telecom single photons.

Overall our experiment extends the quantum optics research of 2D TMDCs into the technologically important telecom regime for the first time, and establishes layered MoTe₂ as a new platform for quantum communication and transduction research. In contrast to telecom quantum emitters of other material systems such as self-assembled quantum dots and single wall carbon nanotubes, our QEs offer unique opportunities in providing access to valley pseudo-spin degree of freedom and facile integration into quantum-photonics, electronic, and sensing platforms via the layer-by-layer-assembly approach.

2:30 PM EQ01.02.04

Circulating Current and Orbital Stray Fields from a Spin-Defect in Non-Centrosymmetric Two-Dimensional Systems [Adonai R. Cruz](#)¹ and Michael E. Flatté^{2,1}; ¹Eindhoven University of Technology, Netherlands; ²The University of Iowa, United States

Single spin states associated with point defects in solid-state systems are promising candidates for the realization of qubits and novel quantum spintronic devices with applications in communication, sensing, and information processing [1]. Isolated magnetic defects embedded in two-dimensional electron gases (2DEG) with spin-orbit coupling (SOC) can be electrically and optically addressed [2] and coherently manipulated.

We present a theory of circulating current induced by spin-defect in a two-dimensional electron gas (2DEG) with Bychkov-Rashba (α) and linear Dresselhaus (β) spin-orbit couplings [1,2]. We show that the spatial anisotropy dependency on the ratio of the strengths of the spin-orbit fields (α/β) offers a possibility to locally tune spin-orbit induced features of the defect such as the dissipationless circulating current associated with its ground state. The orbital contribution to the magnetization density is sensitive to the spin-orbit ratio, changing sign with respect to the spin magnetization and being null at $\alpha=\beta$. The spatial structure of the stray field associated with the current is calculated for different 2D systems and provides a direct way to measure the host spin-orbit fields and the defect spin orientation through nanoscale magnetometry techniques such as NV-centers in diamonds [3].

* This project has received funding from the European Union's Horizon 2020 research and innovation program under the Marie Skłodowska-Curie grant agreement No 721394 and support from US DOE BES Award No. DE-SC0016379.

[1] G. Wolfowicz, et.al. *Nat. Rev. Mater.*, 1-20 (2021).

[2] R. C. Myers, et.al., *Nat. Mater.* **7** (3), 203-208 (2008).

[3] Bychkov, Y. A. and Rashba, E. L., *J. Phys. C* **17**, 6039 (1984).

[4] Dresselhaus, G., *Phys. Rev.* **100**, 580 (1955).

[5] Casola, F. et. al. *Nat. Rev. Mater.* **3** (1), 17088 (2018).

2:45 PM EQ01.02.05

Room Temperature Coherence of Silicon Vacancy Ensembles in Isotopically Purified 4H-SiC [Ignas Lekavicius](#)¹, Rachael Myers-Ward¹, Daniel J. Pennachio¹, Jenifer R. Hajzus¹, D K. Gaskill^{1,2}, Andrew Purdy¹, Andrew L. Yeats¹, Peter G. Brereton³, Evan R. Glaser¹, Thomas L. Reinecke¹ and Samuel G. Carter¹; ¹U.S. Naval Research Laboratory, United States; ²University of Maryland, United States; ³U.S. Naval Academy, United States

Due to the industrial maturity of the host crystal, defects in silicon carbide (SiC) have drawn considerable attention for quantum information and sensing applications. In particular, silicon vacancies in SiC have demonstrated impressive ground state spin properties such as optical spin initialization and readout. This has generated significant interest in room temperature sensing applications, which up until recently have been dominated by nitrogen vacancies in diamond. A key parameter in numerous sensing applications is the inhomogeneous dephasing time T_2^* , which thus far has been limited to a few 100ns in silicon vacancy ensembles. As the nuclear spin bath of the SiC is predicted to be the dominant source of dephasing, we perform isotopic purification of the host crystal leading to an order of magnitude improvement in T_2^* . Furthermore, the S=3/2 ground state quartet of the V_{Si} allows for a novel choice of basis with increased coherence due to a suppression of strain induced dephasing. A combination of these techniques leads to a nearly 2 order of magnitude improvement in the T_2^* of the defect ensemble even at high defect densities.

SESSION EQ01.03: Defects and Color Centers: Creation and Integration
Session Chairs: Adam Gali and Shengxi Huang
Wednesday Morning, December 1, 2021
Hynes, Level 1, Room 105

10:30 AM EQ01.03.01

Ultra-Fast Laser Fabrication of NV Centres in Diamond [Andrew R. Kirkpatrick](#), Benjamin Griffiths, Guangzhao Chen, Patrick Salter, Martin Booth and Jason Smith; The University of Oxford, United Kingdom

The nitrogen-vacancy (NV) defect centre in diamond is a promising candidate in spin-photon applications such as quantum computing and sensing. The centre's spin-dependant fluorescence transitions allow for a purely optical initialisation and readout of the electron spin states, providing a powerful interface to control a solid state qubit. However, the technological application of the NV centre requires its integration into optical and electronic components requiring a highly accurate and high yield fabrication method.

Ultra-fast laser fabrication has demonstrated the ability to produce coherent NV centres with high accuracy and yield. Vacancies are produced through an initial high energy 300fs seed pulse in a process which drives electrons into the conduction band using multi-photon ionisation. The electrons form a plasma which is able to redeposit its energy into the lattice. Following this initial seed the processed site can be exposed to a low energy ultra-fast pulse train which allows the vacancy to migrate through the lattice without causing additional damage. The formation of an NV centre can be monitored using a confocal fluorescence microscope to observe the centre's 627-800 nm fluorescence window. Fluorescent traces taken during laser annealing is shown to be used to monitor the creation of NV centres, whilst providing some information on their singularity and orientation. Additionally, we explore the effects of laser pulse parameters, such as pulse energy and width, on these traces.

Within, we use present an experimental and theoretical study of the laser fabrication process. Density Functional Theory (DFT) is used to investigate the interactions between the NV centre and the carbon self-interstitial involved in laser writing and report on simulations which suggest that the intermittent fluorescence spiking is caused by the NV's emission being suppressed by interactions between the two defects. In particular, we investigate simulated strain and electronic interactions between the two defects and the effect of these interactions on the NV centre's band structure and the specific excitation pathway that leads to NV emission.

Electronic interactions between configurations of the NV centre and <100>-split interstitial were simulated by generating all symmetrically unique second and third near neighbour ensembles of the two defects. Some configurations of the <100>-split interstitial and the NV centre demonstrate hybridisation between the defects in these bands. Out of the 48 total configurations simulated, 8 lead to reconstruction and 15 resulted in hybridisation. In such cases hybridisation occurs between one of the degenerate π -orbitals of the <100>-split interstitial and the e-manifold of the NV centre in the ground state, which is involved in fluorescence. This electronic hybridisation may lead to the creation of non-radiative pathways for fluorescence, which would quench the NV emission since the decay through these pathways is typically much faster than the lifetime of the NV centre excited state. Additionally it is demonstrated through a simple Monte-Carlo simulation that the migration of interstitials, around an NV centre, that can suppress fluorescence can lead to similar photon traces to those that are experimentally observed.

10:45 AM EQ01.03.02

Tunable and Transferable Diamond Membranes for Integrated Quantum Technologies Xinghan Guo¹, Nazar Deegan^{1,2}, Jonathan C. Karsch¹, Zixi Li¹, Tianle Liu¹, Robert Shreiner¹, Amy Butcher¹, David Awschalom^{1,2,1}, F. Joseph P. Heremans^{1,2} and Alexander A. High^{1,2}; ¹The University of Chicago, United States; ²Argonne National Laboratory, United States

Color centers in diamond are widely explored as qubits in quantum networking and sensing due to their exceptional quantum coherence and straightforward optical interface. The further evolution of these quantum technologies will require the integration of diamond – i.e. the quantum state host – into complex device heterostructures, akin to the multi-material heterostructures widely utilized in CMOS technology. However, the material properties of diamond create fundamental difficulties for effective and efficient device integration. Despite recent progress developed to address this material challenge, a fully realized process to reproducibly generate and transfer single-crystal diamond thin films hosting coherent color centers remains outstanding. Here we demonstrate the robust and tunable synthesis of uniform diamond membranes with sufficient quality for advanced quantum technologies. These nanoscale-thick membranes are created based on the "smart cut" technique combined with isotopically (¹²C) purified overgrowth. The membranes have tunable thicknesses (demonstrated 50 nm to 250 nm) and can be deterministically transferred to other substrates via a "dry transfer" technique involving polydimethylsiloxane/polycarbonate (PDMS/PC) stamps. Moreover, the finished membranes have bilaterally atomically flat surfaces ($R_q \leq 0.3$ nm) and bulk-diamond-like crystallinity. Furthermore, color centers are able to be synthesized via both implantation and incorporation during growth. Within 110 nm-thick membranes, individual germanium-vacancy (GeV⁻) centers exhibit stable photoluminescence at 5.4 K, with average optical transition linewidths as low as 125 MHz. The room temperature spin coherence of individual nitrogen-vacancy (NV⁻) centers shows Ramsey spin dephasing times (T_2^*) and Hahn-echo times (T_2) as long as 100 μ s and 300 μ s, respectively. This membrane platform provides a straightforward and deterministic method to integrate diamond into device heterostructures for next-generation quantum technologies and has the potential to supplant bulk diamond in many other quantum applications.

*This work was primarily supported by the U.S. Department of Energy, Office of Science, Basic Energy Sciences, Materials Sciences and Engineering Division with support from the U.S. Department of Energy, Office of Science, National Quantum Information Science Research Centers. A. H. was partially supported by the University of Chicago Materials Research Science and Engineering Center, which is funded by the National Science Foundation under award number DMR-2011854. This work made use of the Pritzker Nanofabrication Facility part of the Pritzker School of Molecular Engineering at the University of Chicago, which receives support from Soft and Hybrid Nanotechnology Experimental (SHyNE) Resource (NSF ECCS-2025633), a node of the National Science Foundation's National Nanotechnology Coordinated Infrastructure. This work also made use of the shared facilities at the University of Chicago Materials Research Science and Engineering Center, supported by the National Science Foundation under award number DMR-2011854. Funding was provided by the Boeing Company and the University of Chicago Joint Task Force Initiative. J. K. and A. B. acknowledge support from the NSF Graduate Research Fellowship under grant no. DGE-1746045.

11:00 AM EQ01.03.03

Ion Implantation and *In Situ* Optical Characterization for Deterministic Creation of Single Defects Vignesh Chandrasekan¹, Michael Titze², Anthony R. Flores², Edward Bielejec² and Han Htoon¹; ¹Los Alamos National Laboratory, United States; ²Sandia National Laboratories, United States

Ideal quantum photonic chip requires single photon emitters, processors and detectors integrated into a single chip where the single photon sources must have higher degree of brightness, purity and indistinguishability [1]. This requires a precise location of emitting sources in pre-determined positions coupled to nano-photonic structures & nano-electronic devices. Defects in solid state host matrices are promising single photon sources considering their on-demand emission, scalability and room temperature operation [2]. Recently, silicon vacancy point defects in wide band gap material like SiC were demonstrated using focused ion beam (FIB) implantation [3,4]. However, the conversion yield of creating those single vacancy defects using FIB is less than 10%. In order to achieve fully deterministic creation of these single defects in SiC, we integrated our ion implantation system with an in-situ micro-photoluminescence setup sensitive enough for single defect optical characterization. By getting a feedback on the creation of defect in real time through checking the photoluminescence on the irradiated spot, while the sample is still inside the implantation chamber without annealing, we successfully fill an array of single defects following a loop of irradiation maintained at a lower dose level. Considering the nanometer spatial resolution and the versatile energy range of our FIB system, we believe that we can extend our capabilities to other lower dimensional materials and reproduce the precise defect creation onto nano-photonic structures & nano-electronic devices.

- [1] Senellart, P., Solomon, G. & White, A. High-performance semiconductor quantum-dot single-photon sources. *Nature Nanotech* **12**, 1026–1039 (2017)
- [2] Aharonovich, I., Englund, D. & Toth, M. Solid-state single-photon emitters. *Nature Photon* **10**, 631–641 (2016)
- [3] Pavunny, S.P., Yeats, A.L., Banks, H.B. et al. Arrays of Si vacancies in 4H-SiC produced by focused Li ion beam implantation. *Sci Rep* **11**, 3561 (2021)
- [4] Wang, J., Zhang, X., Zhou, Y., et al. Scalable Fabrication of Single Silicon Vacancy Defect Arrays in Silicon Carbide Using Focused Ion Beam. *ACS Photonics* **4**, 1054 (2017)

11:15 AM EQ01.03.04

Late News: Surface Dynamics in p-InAs and n-GaAs Probed with Scanning Ultrafast Electron Microscopy Christopher Perez^{1,2}, Scott Ellis^{2,2}, J Michael², David Chandler², A. A. Talin² and Suhas Kumar²; ¹Stanford University, United States; ²Sandia National Laboratories, United States

Understanding the spatio-temporal carrier dynamics in semiconductors, especially III-V materials, is critical for improving electronic and optical devices. Here, we develop a new technique, scanning ultrafast electron microscopy (SUEM), that resolves transient carrier densities and surface-sensitive potentials with 15 ps temporal and 100 nm spatial resolution. SUEM is used to quantify the surface defect density and the recombination of surface trap states in III-V semiconductors, n-GaAs and p-InAs: two parameters which often limit electro-optical device performance. The high temporal resolution probing of transient carrier densities reveals photosaturation at high laser fluences (0.2 and 8 $\mu\text{J}/\text{cm}^2$, for p-InAs and n-GaAs, respectively) due to surface band flattening. Surprisingly, our SUEM signal is more sensitive to the local surface potential and the potential in the vacuum at short distances above the surface as opposed to the conduction band electron density itself. Our novel interpretation of SUEM contrast mechanisms opens doors for the carrier dynamics involved in the practical design of defect-driven microelectronic devices.

SESSION EQ01.04: Quantum Dots and Molecular Systems

Session Chairs: Adonai Cruz and Shengxi Huang

Wednesday Afternoon, December 1, 2021

Hynes, Level 1, Room 105

1:30 PM *EQ01.04.01

Photogenerated Molecular Quartet States as Defect Center Surrogates Michael R. Wasielewski; Northwestern University, United States

Photogenerated molecular spin systems hold great promise for applications in quantum information science because they can be prepared in well-defined spin states at modest temperatures, often exhibit long coherence times, and their properties can be tuned by chemical synthesis. We will discuss molecular spin systems composed of organic chromophores such as porphyrins and perylene diimides (PDIs) covalently linked to stable organic radicals. Following photoexcitation of the chromophore, femtosecond optical spectroscopy shows that the exchange interaction between the electrons on the chromophore and the unpaired electron spin of the radical results in quartet state formation in $>10^{11} \text{ s}^{-1}$. The linkers between the chromophores and the radicals are used to control the spin-spin exchange interaction between the chromophore and the stable radical. Time-resolved pulsed electron paramagnetic resonance experiments show that the resulting quartet state is strongly spin-polarized, having spin lattice relaxation times $> 100 \mu\text{s}$ and relatively long coherence times of $\sim 2\text{--}4 \mu\text{s}$ at temperatures as high as 80 K. Using microwave pulses to manipulate the quartet spin sublevel populations is accompanied by chromophore optical changes. These systems function in a manner analogous to defect centers in solids, such as NV centers, because they can be optically pumped to a highly spin-polarized state, manipulated using microwave pulses, and read out by monitoring optical changes making them viable for quantum information studies.

2:00 PM *EQ01.04.02

Incorporation of Pnictogen Atoms into Dysprosium Single-Molecule Magnets Fu-Sheng Guo¹, Mian He¹, Richard Layfield¹, Sean R. Giblin², Akseli Mansikkamäki³ and Ming-Liang Tong⁴; ¹University of Sussex, United Kingdom; ²University of Cardiff, United Kingdom; ³University of Oulu, Finland; ⁴Sun-Yat Sen University, China

Single-molecule magnets are compounds of transition metals or lanthanides that display slow relaxation of magnetization in the absence of a static magnetic field. SMMs may also show magnetic hysteresis and, hence, magnetic bistability, which has led to proposals that SMMs could be used in magnetic information storage. Significantly, the properties of SMM originate from within individual molecules with dimension of less than 1 nm rather than from cooperative interactions across much larger magnetic domains.

The problem with SMMs is that their magnetic bistability is typically only observed with liquid helium cooling. Recently, we reported the first SMM to function above the boiling point of liquid nitrogen. Molecules of this SMM consist of a single dysprosium atom sandwiched between two organic (i.e. cyclopentadienyl) rings, a structural arrangement that creates excellent conditions for addressing the electronic structure of the lanthanide.

In this presentation, new results describing the impact of incorporating phosphorus and arsenic atoms into the cyclopentadienyl rings on the SMM properties will be described.

2:30 PM EQ01.04.03

Near Atomistic Mesoscale Tomography of PbSe Quantum Dot Superlattices Xiaolei Chu¹, Alex Abelson², Caroline Qian², Davis Unruh¹, Chase Hansen¹, Matthew Law² and Adam J. Moule¹; ¹University of California, Davis, United States; ²University of California, Irvine, United States

Three-dimensional epitaxially fused quantum dots superlattices are theoretically predicted to exhibit band-like charge transport behavior while still retaining tunable semiconductor properties, making them promising candidates for future energy materials. Realization of the predicted emergent electronic properties has remained due in part to defective interdot epitaxial connections. These defects include edge dislocation, screw dislocations and stacking fault that contribute to the tilting and rotational misalignment between the atomic lattices of neighboring connected dots. Existing imaging techniques such as Scanning Transmission Electron Microscopy allow for direct observation of local attachment in atomic scale and characterizing two-vector-based local atomic orientations with the help of scanning diffraction techniques like the 4D-STEM. However, it is still not fully understood enough on how a collective of these geometric frustration in the atomic scale will affect the structural regularity of the local or even long-range superlattice structure variations, hence, preventing our access to defect-free superlattice attachment, especially for a three-dimensional film. Here, we present the combination of using full-tilt HAADF Electron Tomography with Geometric phase analysis in 3D to characterize and understand structural features spanning two orders (0.1 ~ 10 nm)

of magnitude in spatial length scale throughout a multi-layer superlattice film. We apply 3D windowed diffraction calculations based on the tomogram to extract phase information of desired lattice planes, with which allow us to obtain in 3D the local atomic lattice orientations, vectorial displacement field, local strain tensor field and dislocation lines that propagate in-between particles. With this vast amount of information of atomic structural details, quantitative analysis can be conducted on thousands of quantum dot pairs to understand the relation between atomic dislocations and QD orientational misalignment as well as how these geometric frustrations are reflected in strain field. The insights we gained from this particular QD SL material promises a step toward minimizing structural fault in the oriental attachment and hence further approaching the goal of charge delocalization. We also believe that the analytical method we present here provides a novel way of comprehensively understanding structural variations with multi-dimensional quantifications, which we expect, to become increasing important in the rise of complex materials.

SESSION EQ01.05: Poster Session: Quantum Dots and Molecular Systems
Wednesday Afternoon, December 1, 2021
8:00 PM - 10:00 PM
Hynes, Level 1, Hall B

EQ01.05.01

Novel Methods in Data Analysis of Tomographic Reconstructions Applied to PbSe Quantum Dot Materials [Ethan M. Field](#)¹, Xiaolei Chu¹, Caroline Qian², Alex Abelson², Matthew Law² and Adam J. Moule¹; ¹University of California, Davis, United States; ²University of California, Irvine, United States

Colloidal quantum dot (CQD) superlattices with semiconductor properties promise many exciting properties for organic opto-electronic devices including the delocalization of electronic bands with tunable properties. The scaling up of these devices would allow low-cost high-throughput methods to make organic photovoltaics and other opto-electronic devices but this is only possible through higher quality processing methods that achieve these delocalized band structures. Current characterization methods like transmission electron microscopy (TEM) and grazing-incident small angle x-ray scattering (GISAXS) do not probe the exact the structure of the superlattice in three dimensions. We have applied novel data analysis techniques to tomographic reconstruction data from STEM images to determine the center of mass of each quantum dot, the number of necks each of the PbSe quantum dots has to its nearest neighbors, the thickness of the necking, the in-plane and out-of-plane misorientation angles, and local strain measurements in the CQD superlattice. This presentation will highlight data used and its applications in improving the superlattice structure to achieve next-generation opto-electronic properties.

SESSION EQ01.06: Defects and Color Centers I
Session Chairs: Nazar Deegan and Aleksandra Radenovic
Monday Morning, December 6, 2021
EQ01-Virtual

10:30 AM *EQ01.06.01

Single Rare-Earth Ions in Solid-State Hosts—A Platform for Quantum Networks [Andrei Faraon](#), Andrei Ruskuc and Chun Ju Wu; California Institute of Technology, United States

Optically addressable spins in solids are an area of intense research interest in quantum information science with applications in quantum networks, computing and sensing. Due to recent advances in nanophotonic cavity design and fabrication, detection and control of single rare-earth ions via their highly coherent 4f-4f optical transitions have recently been demonstrated. We focus on the 171 isotope of Yb doped into a YVO4 crystal due to low electric and magnetic field noise sensitivity facilitated by no 1st-order DC stark shift combined with optical and spin clock transitions. In this talk I will introduce this platform by characterizing the optical and spin transitions. Subsequently, we leverage the high-fidelity control and long coherence times to explore the interaction of single ¹⁷¹Yb ions with a small local ensemble of vanadium lattice spins. We propose using collective modes of this ensemble as a secondary quantum register, a key resource for building quantum repeaters.

11:00 AM *EQ01.06.02

Electronic Structure and Coherence Properties of Spin Defects in Semiconductors from First Principles [Giulia Galli](#)^{1,2}; ¹University of Chicago, United States; ²Argonne National Laboratory, United States

We discuss recent progress in investigating the electronic structure [1] and coherence properties [2] of spin defects in three- and two-dimensional materials using first principles electronic structure calculations (DFT and many body perturbation theory), and spin Hamiltonians [3]. In particular we will present results for defects in diamond, SiC, and MoS₂.

Supported by AFOSR and DOE-BES (MICCoM)

- [1] H. Ma, M. Govoni and G. Galli, *npj. Comput. Mat.*, 6 (85), (2020); H. Ma, N. Sheng, M. Govoni and G. Galli *J. Chem. Theory Comput.*, 17, 2116-2125 (2021). Yu Jin et al. 2021 arXiv:2106.08608
[2] M. Onizhuk and G. Galli, *Appl. Phys. Lett.*, 118, 154003 (2021); M. Onizhuk et al. *PRX Quantum*, 2, 010311 (2021). A. Bourassa et al., *Nat. Mat.* 2020.
[3] K. Ghosh, H. Ma, V. Gavini and G. Galli, *Phys. Rev. Mat.* 3, 043801 (2019).

11:30 AM EQ01.06.03

Room-Temperature Optically Detected Magnetic Resonance of Single Defects in Hexagonal Boron Nitride [Hannah Stern](#)¹, John Jarman¹, Qiushi Gu¹, Simone Eizaguirre Barker¹, Noah Mendelson², Dipankar Chugh³, Sam Schott¹, H. Hoe Tan³, Henning Sirringhaus¹, Igor Aharonovich² and Mete Atatüre¹; ¹University of Cambridge, United Kingdom; ²University of Technology Sydney, Australia; ³The Australian National University, Australia

Optically addressable spins in materials are important platforms for quantum technologies, such as repeaters and sensors [1]. Identification of such systems

in two-dimensional (2d) layered materials offers advantages over their bulk counterparts, as their reduced dimensionality enables more feasible on-chip integration into devices.

Hexagonal boron nitride (hBN) is a two-dimensional van der Waals crystal that was recently shown to host a plethora of defects that display photoluminescence (PL) spectra ranging from 580 nm to 800 nm. Here, we show that previously identified [2] carbon-related single defects in 2d hexagonal boron nitride (hBN) show ODMR at room temperature [3].

We show that single-defect ODMR contrast is up to 100x stronger than that of hBN ensembles and displays a magnetic-field dependence with positive or negative sign per defect. By measuring hundreds of defects we can identify a yield of spin active defects of ~5%. Further, the ODMR lineshape comprises a doublet resonance, indicating a $S=1$ state with low but finite zero-field splitting. Our results offer a promising route towards realising a room-temperature spin-photon quantum interface in hexagonal boron nitride.

[1] Awschalom, D. D., Hanson, R., Wrachtrup, J. & Zhou, B. B. Quantum technologies with optically interfaced solid-state spins. *Nat. Photonics*. **12**, 516–527 (2018).

[2] Mendelson, N., Chugh, D., Reimers, J.R. *et al.* Identifying carbon as the source of visible single-photon emission from hexagonal boron nitride. *Nat. Mater.* **20**, 321–328 (2021).

[3] Stern, H.L., Jarman, J., Gu, Q., Barker, S.E., Mendelson, N., Chugh, D., Schott, S., Tan, H.H., Siringhaus, H., Aharonovich, I., Atature, M. Room-temperature optically detected magnetic resonance of single defects in hexagonal boron nitride. *Under review, arXiv preprint: 2103.16494* (2021).

11:45 AM EQ01.06.04

A New Paradigm for Quantum Optical Networks—Highly Uniform Single Photon Source Arrays Jiefei Zhang¹, Qi Huang¹, Swarnabha Chattaraj¹, Lucas Jordao¹, Siyuan Lu² and Anupam Madhukar¹; ¹University of Southern California, United States; ²IBM T.J. Watson Research Center, United States

The realization of integrated quantum optical circuits (QOCs) to enable single and high dimensional entangled photons for quantum communication, robust quantum teleportation and quantum sensing with quantum limited resolution has been a long-sought goal in the field of quantum information processing (QIP). All these applications explore the effect of quantum interference and entanglement between different on-demand single photon sources (SPSs) in a scalable architecture. The lack of a starting ordered array of SPSs so far has stood as a major obstacle to realizing compact quantum information technologies.

In this talk I will present our proposition and continued work on demonstration of such a starting platform of SPS arrays based on a unique class of spatially-ordered arrays of surface-curvature driven mesa-top single quantum dots (MTSQDs) [1-3]. These AlGaAs/InGaAs MTSQDs exhibit spectral uniformity as low as 1.8nm across 5×8 arrays including clusters of 6 as-grown QDs having emission energy within 250 μ eV (within on-chip electrical tuning range) and single photon purity > 99.5%. For the usage of this unique class of ordered spectrally uniform MTSQD SPSs to create interconnection between different SPSs for quantum circuits or networks via monolithic or hybrid integration, we also demonstrate planarization of the MTSQDs without compromising their spectral uniformity and single photon emission characteristics [3]. The highly pure single photons from such planarized MTSQD are also indistinguishable with as-measured indistinguishability of 0.5 ± 0.12 at 18.5k (without Purcell effect), limited by the spectral diffusion and phonon induced dephasing at this elevated based temperature of 18.5K of our cryostat at hand. Potential unity indistinguishability can be reached at low temperatures ~4K. Such planarized MTSQDs can have single photon emission from 700-1300nm using our AlGaAs/InGaAs material system that can be further extended to 1550nm using Phosphorus based material system to cover the full range of wavelength needed for quantum communication, teleportation, and sensing in space.

Such planarized ordered array of highly spectrally uniform SPSs generating highly pure and indistinguishable photons offers the long-sought platform for on-chip deterministic integration with light manipulating structure using either hybrid, conventional 2D PhC or dielectric metastructures [4,5] to realize QOCs generating needed multiphoton entangled states for the aforementioned applications. Work on integration of MTSQD with light manipulating units and study of photon interference/entanglement is undergoing.

The work is supported by the US Army Research Office (W911NF1910025) and the Air Force Office of Scientific Research (FA9550-17-1-0353).

[1] Jiefei Zhang et al., *Jour. App. Phys.* **120**, 243103 (2016)

[2] Jiefei Zhang, et al., *App. Phys. Lett* **114**, 071102 (2019)

[3] J. Zhang, et al., *APL photonics* **5**, 116106 (2020)

[4] S. Chattaraj and A. Madhukar, *Jour. Opt. Soc. America B.* **33**, 2414 (2016).

[5] S. Chattaraj, et al., *IEEE Jour. Quant. Elec.* **56**, 1 (2019).

12:00 PM EQ01.06.05

Late News: Toward Scalable Telecom Single-Photon Emitters for Quantum Photonics Alex Kaloyeros, Natasha Tabassum and Spyros Gallis; SUNY Polytechnic Institute, CNSE, United States

Single-photon emitters (SPEs) associated with point-defects and ions in semiconductors are currently considered a significant resource for the solid-state implementation of quantum repeaters and fiber-based long-distance quantum networks, and interconnecting quantum computers. Specifically, non-classical single-photon light sources emitting in the near-infrared region of the electromagnetic spectrum around 1.5 μ m, falling in the lowest loss wavelength range of fiber optics networks, are critical chip-scale building components for the development of fiber-based quantum networks. The realization of scalable on-chip quantum devices, such as single-photon sources and quantum memories, requires novel nanostructured materials that must be compatible and can be integrated with existing electronic circuits, waveguide architectures, and current chip-scale and silicon process technology. We present nanophotonic structures composed of arrays of silicon carbide (SiC) nanowires (NWs) based on a novel and fab-compatible nanofabrication process. Furthermore, these NW-based structures enable the positioning of erbium (Er³⁺) ions with an accuracy of 10 nm, an improvement on the current state-of-the-art ion implantation processes, and are pivotal in engineering the Er³⁺-induced 1.54 μ m emission. An approximately 22-fold increase of the room-temperature Er³⁺ PL emission is observed in these optical nanostructures compared to their thin-film analog at saturation, while using 20 times lower pumping power. These nanostructures demonstrate broadband and efficient excitation characteristics for Er³⁺, with an absorption cross-section ($\sim 2 \times 10^{-18}$ cm²) two-order larger than typical benchmark values for direct absorption in rare-earth-doped quantum materials. Additionally, we have explored the modeling foundations for plasmonic cavity engineering of the Er³⁺ emission to significantly enhance its spontaneous emission rate. Finally, we benchmark and optimize our state-of-the-art near-infrared single-photon detector system to study single-photon behavior from these Er:SiC NW telecom nanophotonic structures.

12:15 PM EQ01.06.06

Indistinguishable Single Photons from a Tin-Vacancy Center in Diamond Johannes Goerlitz¹, Robert Morsch¹, Dennis Herrmann¹, Philipp Fuchs¹,

Benjamin Kambs¹, Pierre-Olivier Colard², Matthew Markham² and Christoph Becher¹; ¹Saarland University, Germany; ²Element Six Global Innovation Centre, United Kingdom

For various applications in the field of quantum information processing stationary qubits are required, providing long-lived spin coherence and suitable level schemes for coherent control and optical read out. In addition, transferring the spin information to indistinguishable single photons is necessary e.g. to distribute entanglement in quantum networks. Similarly, quantum computing with linear optics (LOQC) inherently relies on bright light-matter interfaces that provide single indistinguishable photons.

Color centers in diamond, more specifically the group-IV-vacancy centers, have emerged as promising candidates among solid state qubits. They exhibit favorable features such as individually addressable spins with long coherence times and bright emission of single, close to transform limited photons. While for silicon-vacancy centers (SiV) long spin coherence times are only achieved at milliKelvin temperatures, recent experiments have shown that the negatively charged tin-vacancy center (SnV) [1] overcomes this drawback. Its large ground state orbital splitting results in the suppression of phonon induced dephasing processes of the spin states, allowing long spin coherence times at significantly higher temperatures (>1K) [2]. Among its good spectral qualities such as bright single photon emission and transform limited linewidths [3,4] the indistinguishability of the emitted single photons remains a missing cornerstone to be demonstrated.

By means of Hong-Ou-Mandel interferometry we here investigate the indistinguishability of single photons consecutively emitted by an off-resonantly excited single SnV-center. We find high Hong-Ou-Mandel visibilities, being a direct measure for high indistinguishability of the single photons. We compare the experimental results with the predictions of a theoretical model [5] and extract the magnitude of spectral diffusion potentially affecting single photon indistinguishability in the present system. Furthermore we estimate the timescale of spectral diffusion by repeating the experiment with various delays between emissions of the interfering photons.

[1] Iwasaki T. et al., Phys. Rev. Lett. 119, 253601 (2017).

[2] Debroux R. et al., arXiv:2106.00723 (2021).

[3] Trusheim M. E. et al., Phys. Rev. Lett. 124, 023602 (2020).

[4] Görlitz J. et al., New J. Phys. 22, 013048 (2020).

[5] Kambs B. and Becher C., New J. Phys. 20, 115003 (2018).

<!--[if !supportLineBreakNewLine]-->

<!--[endif]-->

SESSION EQ01.07: Defects and Color Centers II
Session Chairs: Andrei Faraon and Giulia Galli
Monday Afternoon, December 6, 2021
EQ01-Virtual

4:00 PM EQ01.07.01

Emergence of Entanglement Between Single Photon Emitters by Dielectric Mie Resonant Metastructure-Based Optical Circuits Swarnabha Chatteraj¹, Jiefei Zhang¹, Siyuan Lu² and Anupam Madhukar¹; ¹University of Southern California, United States; ²IBM Thomas J. Watson Research Center, United States

On-chip quantum optical circuits (QOCs) comprising ordered single photon sources (SPSs) coupled to network of light manipulating elements (LMEs) that allow manipulation of the emitted photons in a single or few photon regime to enable on-chip photon interference and photon mediated emitter-emitter entanglement is a major goal for scalable quantum information processing (QIP). The path to realization of such QOCs is recently enabled by the new class of spectrally uniform on-chip integrable mesa top single quantum dot (MTSQD) [1-3] single photon sources that provide a platform for indistinguishable photon emission with >99% purity from ordered and spectrally uniform QDs that are also integrable in the monolithic or hybrid integration techniques for codesign with LMEs to interconnect different SPSs. The LMEs must provide the needed light manipulating functions of (1) enhancement of emission rate of the emitters, (2) enhanced emission directionality (3) on-chip propagation, (4) splitting and (5) recombining of single photons to enable efficient extraction of photon, photon interference and photon mediated emitter-emitter coupling in a horizontal architecture for quantum entanglement.

The conventional approach to implementation of such LMEs has been photonic crystal and ridge waveguides-based cavities and waveguides that demand mode-matching between components and hinders scalable implementation of all the above functions. In contrast, we have recently introduced [4,5] the approach of Mie resonance of subwavelength scale dielectric building blocks (DBBs) that exploits a single collective mode of the entire circuit to provide all the five above mentioned functions- thus eliminating mode mismatch between the components. We have demonstrated via finite element method-based simulations of the EM fields [4] that such Mie resonance based DBB metastructures can provide simultaneously a Purcell enhancement ~5-10, emission directionality resulting in 50% photon coupling to the Mie mode, and at the same time propagation, splitting and combining using the same collective magnetic dipole mode of the DBB array- thus enabling realization of quantum optical circuits without any impedance mismatch.

Importantly, the Mie mode of such MTSQD-DBB quantum optical circuits allow coupling between distant emitters- spontaneously resulting in emitter-emitter entanglement over large on-chip distance, critical for applications in quantum metrology, sensing and computation. We present theoretical work to understand the emergence of emitter-emitter entanglement of a system of two MTSQDs coupled via the collective magnetic dipole mode of a DBB based back-to-back nanoantenna waveguide unit [4]. We show a ~1.7 times faster decay rate of the coupled emitter system compared to single emitter- a signature of super radiance. Owing to the lossless propagating nature of the Mie mode, the super-radiant state can be formed over large ~10-100 μm on-chip distances. The emergence of such super radiant states has been explored by employing Von-Neumann Lindblad approach to account for the coherent and incoherent processes involved in the general Hilbert space involving multiple excitons and photons. Further, using the same approach, emergence of a positive degree of entanglement between the distant emitters is shown starting from a purely product state. Spontaneous creation of entanglement between distant on-chip emitters in such MTSQD-DBB integrated optical circuits provides a way to realize architectures for quantum metrology and computation. Further work on optical studies on such DBB based light manipulating structure is ongoing.

We acknowledge support by ARO Grant (W911NF-19-1-0025) and AFOSR Grant (FA9550-17-01-0353).

1. J.Zhang et al, J.Appl.Phys.120,243103(2016)

2. J.Zhang et. al, App. Phys. Lett. 114, 071102(2019)

3. J.Zhang, et. al, APL photonics 5, 116106 (2020)

4. S.Chatteraj, et. al, IEEE J.Quant.Elec. 56, 1, 1(2019)

5. S.Chatteraj, et. al, J.Opt.Soc.Am.B. 33, 12(2016)

4:15 PM EQ01.07.02

Optical Vortex Manipulation for Topological Quantum Computation Chengyun Hua, Gábor Halász, Eugene Dumitrescu, Matthew Brahlek and Benjamin Lawrie; Oak Ridge National Laboratory, United States

Topological quantum computation based on Majorana bound states may enable new paths to fault-tolerant quantum computing. Several recent experiments have suggested that the vortex cores of topological superconductors, such as iron-based superconductors, may host Majorana bound states at zero energy. However, quantum computation with these zero-energy vortex bound states requires a precise and fast manipulation of individual vortices which is difficult to do in a scalable manner. To address this issue, we propose a control scheme based on local heating via, for example, scanning optical microscopy to braid vortex-bound Majorana zero modes in a two-dimensional topological superconductor. First, we derive the conditions required for transporting a single vortex between two defects in the superconducting material by trapping it with a hot spot generated by local optical heating. Equipped with critical conditions for the vortex motion, we then establish the ideal material properties for vortex braiding and describe how transition errors resulting from finite speed and/or temperature can be minimized. Our work paves the way toward optical or microscopic control of zero-energy vortex bound states in two-dimensional topological superconductors. *This work has been conducted by UT-Battelle, LLC, under contract DE-AC05-00OR22725 with the US Department of Energy (DOE). The US government retains and the publisher, by accepting the article for publication, acknowledges that the US government retains a nonexclusive, paid-up, irrevocable, worldwide license to publish or reproduce the published form of this manuscript, or allow others to do so, for US government purposes. DOE will provide public access to these results of federally sponsored research in accordance with the DOE Public Access Plan (<http://energy.gov/downloads/doe-public-access-plan>).

4:30 PM *EQ01.07.03

Coherence Properties of Quantum Emitters in hBN Mehran Kianinia, Simon J. White, Milos Toth and Igor Aharonovich; University of Technology Sydney, Australia

Solid state quantum light sources are emerging as promising candidates for many applications in quantum technologies [1-3]. Among these sources, optically active point defects in hexagonal boron nitride (hBN) are attracting considerable attention due to their extreme brightness, and high Debye Waller factor which means the majority of the photons are emitted into the zero phonon line (ZPL). While final defect assignments are still under debate, a number of recent experiments and theoretical papers hint at carbon related defects adjacent to a vacancy site in the hBN lattice [4,5]. In addition, numerous recent studies have shown that several defects in hBN exhibit spin dependent optical transitions, and exhibit optically detected magnetic resonance (ODMR), which is vital for their employment as solid state qubits and quantum sensors at the nano-scale [6,7].

For practical quantum photonic applications, where photon interference and generations of indistinguishable photons are required, it is important to characterize the coherent properties of the emitted photons. Specifically, studies of dephasing mechanisms, coherence and line broadening effects underpin the applicability of quantum emitters for photon interference experiments. Previous studies of hBN quantum emitters have revealed the emissions in hBN are broadly affected by spectral diffusion. Preliminary resonant excitation experiments showed that observation of Fourier Transform limited lines is possible, but rather rare, as compared to other solid state emitters, such as diamond [28,29]. Some of the challenges stemmed from the fact that the level structure of the emitters is still poorly understood, and environmental effects in layered materials are strongly sample-dependent.

In this presentation, we will report on spectroscopy of hBN defects at cryogenic temperature to study dephasing mechanism of quantum emitters in details. Importantly, our work focuses predominantly on coherent excitation (i.e. the excitation laser is on-resonance with the hBN emission). First we characterize the significant dephasing and spectral broadening mechanisms in an hBN single photon emitter under resonant excitation. We find that the resonant linewidth, even at cryogenic temperature, is dominated by phonon broadening and results in linewidths of ~ 1 GHz. We also see that degenerate electronic states and strain do not play a significant role in phonon dephasing. We further showed that spectral diffusion can be minimized by employing excitation powers well below saturation. Overall, the brightness of the emitters exemplify that emission rate in excess of 200 MHz with bandwidth of less than 1 GHz [8]. Next we employed a weak non-resonant laser at a wavelength between 500 nm and 532 nm, in addition to the resonant laser that drives the system coherently to stabilise the optical transition of single defects in hBN. The secondary laser acts as an additional excitation pathway and re-initializes the system into its bright state. The two laser repumping scheme enables the observation of brighter resonant fluorescence [9]. We provide an in-depth analysis of the photodynamics of the system, and discuss its applicability for an improved coherence. Our results provide an important analysis and required modification for future experiments on two photon interference with quantum emitters in hBN.

[1] I. Aharonovich, et al., Nat. Photonics 10, 631-641, (2016).

[2] A. W. Elshaari, et al., Nat. Photonics, (2020).

[3] M. Atatüre, et al., Nature Reviews Materials 3, 38-51, (2018).

[4] N. Mendelson, et al, Nature Materials 20, 321-328, (2021).

[5] C. Jara, et al, The Journal of Physical Chemistry A 125, 1325-1335, (2021).

[6] A. Gottscholl, et al., Nature Mater. 19, 540-545, (2020).

[7] N. Chejanovsky, et al., Nature Materials, (2021).

[8] S. J. White, et al., <https://arxiv.org/abs/2105.11687> (2021).

[9] S. J. U. White, et al., Physical Review Applied 14, 044017, (2020).

5:00 PM *EQ01.07.04

Electrical Manipulation of Quantum Light Sources in 2D Hexagonal Boron Nitride Jieun Lee; Seoul National University, Korea (the Republic of)

Single photon emitters are fundamental resources of quantum optics and quantum information technologies. Recently, the emergence of single photon emission in atomically thin materials such as hexagonal boron nitride (h-BN) has triggered tremendous interests in 2D material based single photon sources. For full exploitation of 2D single photon emitters for quantum technologies, however, the ability to control each atomic defect individually is critical. In this talk, we introduce methods to generate and manipulate single photon sources in 2D h-BN crystals using local crystalline geometries and electrical controls. First, we show the role of strain for the creation and orientation of the single photon emitters in h-BN. Second, we demonstrate that the photon energy of single photon sources in h-BN can be controlled using an electric field by fabricating 2D van der Waals heterostructures composed of h-BN and graphene layers. A diverse trail of Stark shifts is observed, providing information on crystallographic ground states of defect structures. Lastly, we will discuss the electrical switching of the quantum emitters enabled by the Fermi level tuning of graphene electrodes.

5:30 PM EQ01.07.05

First-Principles Predictions of Out-of-Plane Group IV and V Dimers as High-Symmetry High-Spin Defects in Hexagonal Boron Nitride Jooyong Bhang¹, He Ma^{2,2}, Donggyu Yim¹, Giulia Galli^{2,2,3} and Hosung Seo¹; ¹Ajou University, Korea (the Republic of); ²The University of Chicago, United States; ³Argonne National Laboratory, United States

Hexagonal boron nitride (h-BN) has been recently found to host a variety of quantum point defects, which are promising candidates as single-photon sources for solid-state quantum nanophotonics applications. Most recently, optically addressable spin qubits in h-BN have been the focus of intensive

research due to their unique potential in quantum computing, communication, and sensing. However, the number of high-symmetry high-spin defects that are desirable for developing innovative spin qubits in h-BN is highly limited. Here, we combine density functional theory (DFT) and quantum embedding theories (QET) to show that out-of-plane $X_N Y_i$ dimer defects ($X, Y=C, N, P, Si$) form a new class of stable C_{3v} spin-triplet defects in h-BN. We find that the dimer defects have a robust 3A_2 ground state and 3E excited state, both of which are isolated from the h-BN bulk states. We show that 1E and 1A shelving states exist and they are positioned between the 3E and 3A_2 states for all the dimer defects considered in this study. To support future experimental identification of the $X_N Y_i$ dimer defects, we provide an extensive characterization of the defects in terms of their spin and optical properties. We predict that the zero-phonon line of the spin-triplet $X_N Y_i$ defects lies between the infrared (~ 1.0 eV) and the visible (~ 1.8 eV) range. We compute the zero-field splitting of the dimers' spin to range from 1.79 GHz ($Si_N P_i^0$) to 29.5 GHz ($C_N N_i^0$). Our results broaden the palette of high-spin defect candidates that would be useful for the development of spin-based quantum technologies in two-dimensional hexagonal boron nitride.

5:45 PM BREAK

SESSION EQ01.08: Defects and Color Centers III
Session Chair: Edward Bielejec
Tuesday Morning, December 7, 2021
EQ01-Virtual

10:30 AM *EQ01.08.01

Deterministic Creation of Optically Active Defects in Hexagonal Boron Nitride [Aleksandra Radenovic](#); Ecole Polytechnique Federale Lausanne, Switzerland

One of the *grand challenges* in imaging defects in 2D materials is a lack of spatial structures to resolve, which complicates the interpretation of the resolution in our system. In addition, there is still very little control over the type of defects. One approach taken in diffraction-limited PL imaging exploited the strain imposed by nanopillar arrays that were spaced at least 6 microns apart. To be able to characterize better the existing SMLM setup, we will use variable spacing arrays. Currently, to induce defects, we still treat pristine exfoliated material with Oxygen, Nitrogen or Hydrogen plasma typically, obtaining defects at a random location. To address the main challenge of engineering defects deterministically at various densities, Focus ion beam (FIB), namely electrically discharged, Xe^+ of several kV that will be focused on the sample, allowing the creation of the defects in a predefined location. Given the spatial limitations linked to the substrate charging and instrument drift, achieving sub 100 nm spacing of the defects still presents a challenge.

11:00 AM *EQ01.08.02

Novel Quantum Nanostructures of Diamond Related Materials by Nanosecond Laser Annealing [Jagdish Narayan](#); North Carolina State University, United States

We present laser synthesis and processing of novel quantum nanostructures of diamond related materials. With our recent breakthrough in nonequilibrium laser processing, we have shown that amorphous carbon layers can be converted into phase-pure graphene, diamond or Q-carbon (new allotrope of carbon) by increasing the undercooling before melt quenching. Carbon layers can be converted into graphene, graphene oxide or reduced graphene oxide. Parallel results are obtained for the conversion of amorphous BN into phase-pure h-BN, c-BN or Q-BN. We will focus here on nanodiamonds, epitaxial thin films, and nanoneedles, which can be grown epitaxially by domain matching epitaxy. Through epitaxial growth, nanodiamonds are grown with a controlled orientation, such as $\langle 111 \rangle$ on $\langle 0001 \rangle$ sapphire. These nanodiamonds and nanoneedles can be doped with single NV or SiV centers, in addition to higher concentrations in macrodiamonds and thin films. Pure (undoped) Q-carbon is ferromagnetic, and it becomes superconducting upon doping with boron with record BCS transition temperature of over 57K so far. We discuss the properties and applications of these graphene, diamond and Q-carbon related nanostructures with a wafer-scale integration in nanosensing, quantum computing and quantum communication.

11:30 AM *EQ01.08.03

Engineering and Device Integration of Optically Addressable Spin Defects [Nazar Deleghan](#)^{1,2}, [Xinghan Guo](#)², [Sean Sullivan](#)^{1,2}, [Jonathan C. Karsch](#)², [Martin Holt](#)¹, [Stephan Hruszkewycz](#)¹, [Alexander A. High](#)², [David Awschalom](#)² and [F. Joseph P. Heremans](#)^{1,2}; ¹Argonne National Laboratory, United States; ²The University of Chicago, United States

Optically addressable point-defects in wide band-gap semiconductors are a versatile platform for quantum information science (QIS). Such qubits are intrinsically sensitive to their local crystalline, charge, and nuclear environments. These variations directly affect the coherence, charge stability, and the optical transition frequency of the defects, limiting their use as scalable platforms for nanoscale sensing and quantum communication. Interestingly, with recent advances in host growth, nanofabrication, and defect synthesis, these environments can be engineered via control of crystal structure, isotopic purity, and host dimensionality. Herein, we will present work on the optimization of these defect systems via isotopically controlled synthesis and localization of various defect systems in silicon carbide and diamond. An emphasis will be placed on exploring how advanced, synchrotron-based characterization techniques provide a direct means to better understand the local crystal environment surrounding the defects and offers a pathway for improving the defect-based quantum technologies. Finally, recent advances in synthesizing low-dimensionality (nano-scale particles and membranes) defect hosts for deterministic integration with other classical or quantum systems will be presented.

12:00 PM EQ01.08.04

Late News: Tuning Color Centers at a Twisted Interface of Hexagonal Boron Nitride [Cong Su](#)^{1,1,2}, [Fang Zhang](#)¹, [Salman Kahn](#)¹, [Brian Shevitski](#)¹, [Jingwei Jiang](#)¹, [Chunhui Dai](#)², [Alex Ungar](#)¹, [Ji-Hoon Park](#)³, [Kenji Watanabe](#)⁴, [Takashi Taniguchi](#)⁴, [Jing Kong](#)⁵, [Zikang Tang](#)⁵, [Wenqing Zhang](#)⁶, [Feng Wang](#)¹, [Michael Crommie](#)¹, [Steven Louie](#)¹, [Shaul Aloni](#)² and [Alex Zettl](#)¹; ¹University of California, Berkeley, United States; ²Lawrence Berkeley National Laboratory, United States; ³Massachusetts Institute of Technology, United States; ⁴National Institute for Materials Science, Japan; ⁵University of Macau, China; ⁶Southern University of Science and Technology, China

Color center is a promising platform for quantum technologies, but their application is hindered by the typically random defect distribution and complex mesoscopic environment. Employing cathodoluminescence, we here demonstrate that an ultraviolet-emitting single photon emitter can be readily activated and controlled on-demand at the twisted interface of two hexagonal boron nitride flakes. The brightness of the color center can be enhanced by two orders of magnitude by altering the twist angle. Additionally, a brightness modulation of nearly 100% of this color center is achieved by an external voltage. Our *ab-initio* GW and GW-BSE calculations suggest that the emission is correlated to nitrogen vacancies and that a twist-induced moiré potential facilitates

electron-hole recombination. This mechanism is further exploited to draw nanoscale color center patterns using electron beams.

12:15 PM EQ01.08.05

Towards a Two-Dimensional Single Spin-Photon Interface at Room Temperature [Simone Eizagirre Barker](#)¹, Hannah Stern¹, John Jarman¹, Qiushi Gu¹, Noah Mendelson², Dipankar Chugh³, H. Hoe Tan³, Igor Aharonovich² and Mete Atature¹; ¹University of Cambridge, United Kingdom; ²University of Technology Sydney, Australia; ³Australia National University, Australia

Colour centres in two-dimensional hexagonal boron nitride (hBN) have emerged as a promising platform for quantum photonic applications, as they emit single photons at room temperature and can be readily integrated into nanoscale devices thanks to their reduced dimensionality. Recently, we showed the first demonstration of optically-detected magnetic resonance (ODMR) from single spin defects in a van der Waals material at room temperature,¹ with ODMR contrasts of up to 30%, demonstrating the potential of hBN for applications in quantum information and quantum networks. Interestingly, single defects with similar spectral properties can show negative, positive or no ODMR contrast, indicating rich photo- and spin dynamics in the material. Integration of these colour centres into devices such as cavities to enhance emission or improve collection efficiencies will lead to a stronger platform to investigate and exploit their fundamental physics, and to evaluate their potential as solid-state qubits or nanoscale quantum sensors. In this contribution, we present our latest results towards integrating these individually optically addressable spin defects into tunable devices to enable a room-temperature single spin-photon interface in a two-dimensional material.

¹ H. L. Stern, J. Jarman, Q. Gu, S. Eizagirre Barker, N. Mendelson, D. Chugh, S. Schott, H. H. Tan, H. Siringhaus, I. Aharonovich, M. Atature *Room-temperature optically detected magnetic resonance of single defects in hexagonal boron nitride* (2021) arxiv:2103.16494

SESSION EQ01.09: Defects and Color Centers IV
Session Chair: Jagdish Narayan
Tuesday Afternoon, December 7, 2021
EQ01-Virtual

1:00 PM *EQ01.09.01

Scalable Semiconductor Quantum Systems [Jelena Vuckovic](#); Stanford University, United States

At the core of most quantum technologies is the development of homogeneous, long lived qubits with excellent optical interfaces, and the development of high efficiency and robust optical interconnects for such qubits. To overcome inhomogeneities in semiconductor spin qubits and in their connections, we have been relying on fast photonics inverse design and on optimization (Floquet engineering) of the qubits themselves. We illustrate this approach to scalable semiconductor quantum systems with our results on quantum photonics based on diamond and silicon carbide.

1:30 PM *EQ01.09.02

Focused Ion Beam Implantation for the Fabrication of Single Defect Centers in Wide Bandgap Substrates Using *In Situ* Counting and Photoluminescence [Edward Bielejec](#); Sandia National Laboratories, United States

We will present an overview of Sandia's focused ion beam (FIB) implantation capability as it pertains to the fabrication of single defect center-based devices via direct write nanofabrication in a wide range of devices and substrates. Sandia's Ion Beam Laboratory (IBL) has seven main accelerators including three high energy (250 keV to ~50 MeV) FIB systems with micron-scale resolution and three low energy (2 keV to 200 keV) FIB systems with nanometer scale resolution. In this talk we will highlight both the A&D nanoImplanter and the Raith Velion. These are both multi-species kV energy level FIB systems with a minimum spot size of <10 nm with both mass resolution using an ExB filter and single ion implantation using fast blanking. The combination of high spatial resolution, variable energy and the ability to implant a wide range of elements from the periodic table makes these versatile machines for a range of topics from device modification including the deterministic seeding of TaOx memristor devices, detector testing using high resolution ion beam induced charge collection (IBIC) to probe the structure of defect cascades, device fabrication including deterministic single donor devices for quantum computing research, to the formation of individual defect centers in wide bandgap substrates including diamond, SiC, hBN, etc.... Here we concentrate on FIB implantation to create defect centers in diamond making use of in-situ counting to reduce the error associated with the Poisson distribute and in SiC using a newly developed in-situ photoluminescence (PL) setup to create near deterministic array formation.

Using in-situ diamond detectors combined with FIB implantation we have demonstrated the fabrication of SiV arrays with a factor of two reduction in the error for single defect center formation as compared to standard timed implantation. This allows us to develop an improved understanding of the defect center activation under high temperature annealing. In the same accelerator we have demonstrated in-situ PL that allows for the near deterministic formation of Vsi arrays in SiC via an implant, measure PL and repeat process.

This work was performed, in part, at the Center for Integrated Nanotechnologies, an Office of Science User Facility operated for the U.S. Department of Energy (DOE) Office of Science. Sandia National Laboratories is a multi-mission laboratory managed and operated by National Technology and Engineering Solutions of Sandia, LLC., a wholly owned subsidiary of Honeywell International, Inc., for the U.S. Department of Energy's National Nuclear Security Administration under contract DE-NA-0003525.

2:00 PM EQ01.09.03

***In Situ* Ion Counting for Deterministic Placement of Single Photon Emitters** [Michael Titze](#), Heejun Byeon, Jacob D. Henshaw, Anthony R. Flores, Tom Harris, Andrew Mounce and Edward Bielejec; Sandia National Laboratories, United States

Single photon emitters (SPE) in wide bandgap semiconductors play a crucial role quantum sensing, computing, and communication. For utilization of SPEs for these quantum applications, it is crucial to locally place a precise number of ions in the host semiconductor for the highest possible yield of devices. Various techniques have been proposed for the deterministic creation of SPEs, including vacancy generation through pulsed laser, electron irradiation, and localized annealing by laser heating. However, none of these techniques can introduce non-naturally occurring impurity-type emitters, which are especially suitable for deterministic SPE creation, enabling near background free SPEs. Vacancy-centers in diamond have attracted great interest for the use in quantum information science.

The silicon vacancy center (SiV) in diamond is an ideal candidate for the use as a SPE in quantum communication because of its potential for high photon emission rate, small phonon sideband emission, large Debye-Waller factor, and microwave-controllable electronic spin. Creation of SiV through a

combination of ion implantation and high-temperature annealing is routinely realized, but to enable fabrication of large-scale devices a high confidence in the number of created SiV, implying control over the number of implanted Si ions, is required. Typical ion implantation experiments rely on measurement of the beam current and timing the ion beam implantation to obtain implantation of a specific number of ions. Since the number of ions implanted by an ion beam is determined by Poisson statistics, the uncertainty on the number of ions is large when only a few ions are required.

In this presentation, we present an in-situ ion counting experiment which can reduce the uncertainty in the number of implanted Si ions, which is especially important for small total number of implanted ions. We show that for implantation of 30 ions, required to generate on average a single SiV, the uncertainty on the number of ions per implantation is reduced to 1/4th the uncertainty in a timed implantation. We determine the number of SiV per implantation spot through using Hanbury Brown Twiss interferometry and find that the yield is approximately 3% for both timed and counted implantation techniques, demonstrating our ability to count implanted Si ions. The activation rate of 3% for implanted Si ion to SiV conversion prevents us from fully realizing the potential for counting implants, as the yield is dominated by the Poisson statistics of activation. However, in future work, implementing our counted implant technique combined with defects with high activation rates, will bring us closer to truly deterministic SPE placement.

Sandia National Laboratories is a multi-mission laboratory managed and operated by the National Technology and Engineering Solutions of Sandia, LLC, a wholly owned subsidiary of Honeywell International, Inc., for the DOE's National Nuclear Security Administration under Contract No. DE-NA0003525. This work was funded by the Laboratory Directed Research and Development Program and performed, in part, at the Center for Integrated Nanotechnologies, an Office of Science User Facility operated for the U.S. Department of Energy (DOE) Office of Science.

2:15 PM EQ01.09.04

Synthesis and Characterization of Quantum Optical Materials at Gigapascal Pressures Peter Pauzuskie and Chaman Gupta; University of Washington, United States

Developing novel methods for the synthesis, processing, and characterization of quantum optical materials for quantum sensing and communication applications remains an outstanding challenge. This talk will present recent results in designing and creating quantum defects in insulators and wide-gap diamond semiconductors using extreme (GPa) pressures and temperature (>1800K) within a diamond anvil cell (DAC). Molecular dopants including tetraethyl orthosilicate (TEOS) and hexamethylenetetramine (HMT) can be chemically doped within amorphous carbon aerogels to create the negatively charged silicon split-vacancy (SiV) as well as both neutral and negatively-charged nitrogen-vacancy (NV) point defects. Pressure-dependent optical spectroscopy of the SiV center correlates well with computational predictions based on *ab initio* / DFT quantum cluster calculations. Recently the use of lithium fluoride (LiF) as a pressure transmitting medium has enabled the recovery of novel quantum optical materials for *ex-situ* characterization at cryogenic temperatures via time-correlated single photon counting. High-pressure has also been used to tune the crystal field energies of lanthanide point defects within insulating ceramic materials that have recently demonstrated the first experimental measurements of solid-state laser refrigeration at GPa pressures.

2:30 PM EQ01.09.05

Late News: Scanning Ultrafast Electron Microscopy Reveals Photovoltage Dynamics at a Deeply Buried p-Si/SiO₂ Interface Scott Ellis¹, Norm Bartelt¹, Francois Leonard¹, Kimberlee Collins¹, Elliot J. Fuller¹, David R. Hughart¹, Diana Garland¹, Matthew Marinella¹, Christopher Perez^{2,1}, Suhas Kumar¹, J Michael¹, David Chandler¹, Bolin Liao³ and A. A. Talin¹; ¹Sandia National Laboratories, United States; ²Stanford University, United States; ³University of California, Santa Barbara, United States

The understanding and design of carrier dynamics and their interactions with defects at a buried insulator/semiconductor interface is essential for achieving optimum performance in modern electronics. We report on the use of scanning ultrafast electron microscopy (SUEM) as a non-contact and non-destructive technique to remotely probe the sub-nanosecond dynamics of excited carriers at a silicon surface buried below a 1 μm thermal silicon oxide. Our measurements illustrate a novel SUEM contrast mechanism, whereby optical modulation of the space-charge field in the semiconductor modulates the electric field in the thick oxide, thus affecting its secondary electron yield. By analyzing the SUEM contrast temporally, spatially and as a function of laser fluence we demonstrate the diffusion mediated capture of excited carriers by interfacial traps.

SESSION EQ01.10: Defects and Color Centers V
Session Chairs: Vladimir Dyakonov and Abram Falk
Wednesday Morning, December 8, 2021
EQ01-Virtual

8:00 AM *EQ01.10.01

Spin Defects in hBN as Promising Temperature, Pressure and Magnetic Field Sensors Vladimir Dyakonov; University of Wuerzburg, Germany

Van der Waals materials have emerged over the last decade as the new playground for quantum photonics devices. Among them, hexagonal boron nitride (hBN) is an interesting candidate, mainly because of its crystallographic compatibility with many different 2D materials, but also because of its ability to host optically active spin defects. We have recently reported [1] the optically detected magnetic resonance (ODMR) of spin-triplet negatively charged boron vacancies (V_B^-) in hBN and determined their spin-Hamiltonian parameters. Furthermore, we demonstrated the coherent control of V_B^- at room temperature and determined the relevant spin-relaxation times. In this respect, sensors based on such color centers embedded in an intercalated hBN layer may be particularly attractive, since the distance between the sensor and the object to be sensed can be quite small. The influence of external stimuli (magnetic field, temperature and pressure) on this spin defect will be also discussed.[2]

[1] A. Gottscholl et al., Nat. Mater. 19, 540–545 (2020)

[2] A. Gottscholl et al., Nat. Commun. (accepted) (2021)

8:30 AM *EQ01.10.02

Dipolar Interactions Between Quantum Emitters in van der Waals Heterostructures Ajit Srivastava; Emory University, United States

Atomically thin transitional metal dichalcogenides (TMDs), have recently come to the forefront of research in materials physics. This is largely due to the ease with which they can be combined into artificially engineered heterostructures that exhibit emergent electronic and optical properties. Optical excitations in semiconducting TMDs, viz., excitons, can be localized in potential wells resulting in quantum emitters. Unlike their monolayer counterparts, excitons in heterobilayers, such as MoSe₂/WSe₂, feature a permanent electric dipole which can be used to tune their emission energy electrically. Moreover, the few-body interaction between dipolar quantum emitters can be exploited for quantum nonlinearity. Furthermore, many-exciton dipolar interactions result in effective magnetic fields of ~ 6 Tesla. Thus, dipolar quantum emitters are a promising platform to study quantum optical phenomena

and to realize strongly interacting phases of optical excitations in 2D materials.

9:00 AM *EQ01.10.03

Thermodynamics of Carbon Defects in Hexagonal Boron Nitride Audrius Alkauskas^{1,2}; ¹Center for Physical Sciences and Technology (FTMC), Lithuania; ²Kaunas University of Technology, Lithuania

Single-photon emitters (SPEs) in hexagonal boron nitride, emitting in the 1.6-2.1 eV spectral region, have attracted a lot of experimental and theoretical activity since their discovery [1]. Many defects have been proposed to explain the observed emission. However, the jury is still out regarding the chemical origin of these emitters. Despite intense theoretical investigations, no single defect seems to describe the experiments in a consistent manner. In a recent work [2], it was confirmed that the presence of carbon increases the concentration of SPEs. However, it remains unclear whether carbon participates in the structure of the SPEs directly or helps create SPEs indirectly.

In this work I discuss a first-principles computational study of the thermodynamics of carbon defects in hexagonal boron nitride (hBN). The defects considered are carbon monomers, dimers, trimers and larger carbon clusters, as well as complexes of carbon with vacancies, antisites, and substitutional oxygen. Our calculations show that monomers (C_B , C_N), dimers, trimers, as well as C_N - O_N pairs are the most prevalent species under most of growth conditions. In comparison to these defects, complexes of carbon with vacancies and antisites occur at much smaller concentrations ($< 10^{14} \text{ cm}^{-3}$). Taking into account the emission wavelength of these defects, our results show that carbon trimers are the only carbon-related defects that can likely explain the results of Ref. [2]. This finding is in agreement with recent calculations that showed that optical lineshapes of trimer defects are in very good agreement with experimental spectra [3], affirming the potential role of carbon trimers in single-photon emission in hexagonal boron nitride.

The work has been performed with M. Maciaszek and L. Razinkovas.

[1] T. T. Tran *et al.*, Nature Nanotechnology 11, 37 (2016)

[2] N. Mendelson *et al.*, Nature Materials 20, 321 (2020)

[3] C. Jara *et al.*, Journal of Physical Chemistry A 125, 1325 (2021)

9:30 AM EQ01.10.04

Chemically Enhanced NV Centers in CVD Diamond for Quantum Technologies Sayali Vispute; Blue Wave Semiconductors, Inc., United States

Quantum technologies are attracting attention worldwide due to their projected benefits over existing technologies. Modern devices such as computers, communication devices, and sensors could benefit from quantum technologies because quantum devices will have the ability to collect data at a precise accuracy and a record-breaking speed. One of the quantum technologies is the NV center in CVD diamond. In this technology, NV centers, or nitrogen vacancy centers, occur when two carbon atoms are removed from a diamond and replaced with a single nitrogen atom that has a vacancy next to it. When a sufficiently high energy photon (a green light (532nm)) is directed on diamond with an NV center, the diamond re-emits a red light (665nm), and the strength of the re-emitted red light depends on the spin of the NV center. The spin of the NV center can be altered by exciting a microwave at a specific frequency, resulting in the strength of the red light emitted by the diamond to change. The ability to measure the change of strength of the light re-emitted by NV centers is often used in supercomputers, radars, and other quantum technologies. NV centers can also be used for a single photon emitter. Most importantly, NV centers can be formed in lab grown CVD diamonds by generating a plasma in a Microwave Chemical Vapor Deposition (microwave CVD). Hydrogen, nitrogen, and methane gases can be flowed into the microwave CVD and nitrogen can be introduced into the growing diamond structures to create the NV centers. Using this method, we have grown CVD diamond films with varying concentrations of NV centers. The effect of various process parameters such as deposition power, gas ratios, substrate temperatures, and growth pressure have been studied on NV center formation, density, quality, and in-situ doping of nitrogen. Quantum structures have been characterized using Raman spectroscopy, X-ray diffraction, and scanning electron microscopy. In-situ laser reflectivity was also implemented to investigate growth characteristics of CVD diamond layers. In this paper, we will discuss the dependence of process conditions and characterization of NV centers and highlight potential applications and sensor development.

SESSION EQ01.11: On-Demand
Sunday Morning, December 5, 2021
On-Demand

SYMPOSIUM EQ02

Heterostructures of Various Dimensional Materials
November 29 - December 8, 2021

Symposium Organizers

Jeehwan Kim, Massachusetts Institute of Technology
Kysang Lee, University of Virginia
Xiuling Li, University of Illinois at Urbana-Champaign
Feng Miao, Nanjing University

* Invited Paper

SESSION Tutorial EQ02: Heterostructures of Various Dimensional Materials—From Epitaxy to Device Applications

Session Chairs: Jeehwan Kim and Xiuling Li

Monday Morning, November 29, 2021

Hynes, Level 2, Room 200

8:30 AM

Remote Epitaxy—Growth of 3D Materials on 2D Materials [Jeehwan Kim](#); Massachusetts Institute of Technology, United States

The instructor will discuss about new epitaxy lift-off technique so called remote epitaxy that can produce freestanding semiconductor membranes. Discussion will include 1) Remote epitaxy mechanism 2) High yield peeling mechanism 3) Reusability of the substrates 4) Economic aspect of remote epitaxy 5) Heterointegration of 3D materials with 2D materials for advanced heterostructuring.

10:00 AM BREAK

10:30 AM

van der Waals Epitaxy—Epitaxial Growth of 2D and 3D Materials [Xinqiang Wang](#); Peking University, China

The instructor will provide the overview regarding the epitaxial growth of Nitride-based semiconductor materials by MOVPE including GaN and h-BN, and design device structures for opto-electronic devices. In addition, Instructor will cover the fabrication of nanostructures and materials characterization. The epitaxial growth of 3D and 2D materials and characterization of them is the basis of fabrication of heterointegration system for various device applications.

12:00 PM BREAK

1:30 PM

Heterostructures Built on Three-Dimensional (3D) Semiconductor [Zhenqiang \(Jack\) Ma](#); University of Wisconsin–Madison, United States

Heterostructures built on three-dimensional (3D) semiconductor materials are rooted from the theory conceived by Nobel Laureate Hebert Kroemer in 1957. Since then, the four classes, namely, GaAs-, InP-, Si/Ge-, and III-nitrides-based heterostructures, have revolutionized the electronics and optoelectronics that set the foundation of today's communications, lighting, sensing, infotainment, etc. These heterostructures were universally formed by epitaxy techniques uniquely governed and enabled by the stringent requirements of lattice matching. Limited by this requirement, realizing heterostructures between lattice-mismatched semiconductors has been a decades-long obstacle, although the materials space to explore and the number of heterostructures that can be made are vast compared to its lattice-matched counterparts. In this tutorial, lattice-mismatched heterostructures, i.e., heterogeneous heterostructures, or arbitrary heterostructures, formed via semiconductor grafting based on a quantum tunneling gluing approach are described. The tutorial will include the history of attempts on forming lattice-mismatched heterostructures, physical principles of bypassing the lattice constraints, fabrication methods and scalability, and a set of application examples that are selected from about 18 pairs of heterostructures formed between Si, Ge, GeSn, GaAs, InGaAs, AlGaAs, GaN, AlGaN, SiC, GaN, Diamond, β -Ga₂O₃, and CsPbBr₃.

2:30 PM

van der Waals Heterostructures [Deep M. Jariwala](#)¹ and [Xiangfeng Duan](#)²; ¹University of Pennsylvania, United States; ²University of California, Los Angeles, United States

The isolation of a growing number of two-dimensional (2D) van der Waals (vdW) materials has inspired worldwide efforts to integrate distinct 2D materials into vdW heterostructures. Over the past decade a tremendous amount of research activity has occurred in assembling disparate 2D materials into “all-2D” van der Waals heterostructures and thereby making outstanding progress on fundamental studies at 2D/2D interfaces. However, practical applications of 2D and other low-dimensional materials will require a broader integration strategy. Namely integration of 2D materials with other self-passivated, quantum-confined or molecular materials will be necessary. In this regard significant progress has been achieved in recent years, which involve successful integration of 2D materials with organic small molecules, quantum-dots, nanocrystals, semiconducting polymers, inorganic nanowires as well as carbon-nanotubes. These studies have produced interesting results both in terms of basic science as well as device applications including in photodetectors, logic, memory and light emitting devices. In addition, 2D van der Waals layers have also provided a rich and interesting avenue in terms of hetero-integration with three-dimensional (3D) and bulk materials including 3D semiconductors, piezoelectrics, ferroelectrics and magnets. The 2D/3D combinations are particularly favorable and attractive in terms of vertical integration on Silicon CMOS and enabling “More than Moore” approaches including memory, electronic-photonics integration etc. for semiconductor chips. In this tutorial, I will provide an overview of the progress on the above described heterostructures and their devices focusing on the unique advantages and capabilities that each materials combination provides. I will end with a broad and forward-looking perspective on future investigation and development opportunities in mixed-dimensional heterostructures and their applications for the research community.

3:30 PM BREAK

4:00 PM

Van der Waals Integration beyond 2D Materials: Probing and Pushing the Limit of Emerging Electronic Materials [Xiangfeng Duan](#); University of California, Los Angeles, United States

The heterogeneous integration of dissimilar materials is a long pursuit of material science community and has defined the material foundation for modern electronics and optoelectronics. The typical material integration approaches usually involve strong chemical bonds and aggressive synthetic conditions and are often limited to materials with strict structure match and processing compatibility. Alternatively, *van der Waals* integration, in which freestanding building blocks are physically assembled together through weak *van der Waals* interactions, offers a bond-free material integration strategy without lattice and processing limitations. In this tutorial, I will discuss the fundamental forces involved in *van der Waals* integration and generalize this approach for

flexible integration of highly disparate materials to produce artificial heterostructures with minimum interfacial disorder and to enable high-performing devices.

I will start with a brief introduction of some early background on using this approach for damage-free dielectric integration to enable high speed transistors from atomically thin graphene and 2D semiconductors, and then focus my most of my discussion on our recent efforts in exploring this approach for low-energy metal integration to enable high performance contacts for delicate materials. In particular, I will highlight our recent advancement in exploiting the *van der Waals* integration approach for seamless integration of conventional metal thin film electrodes with the 2D semiconductors to create nearly ideal metal-semiconductor junctions essentially free of interface states and Fermi level pinning, for the first time the experimental achieving Schottky-Mott limit that has been difficult to achieve in Schottky diodes, and realizing the 2D diode approaching the intrinsic exciton physics limit. Next, we further extends this approach for damage-free integration of metal contacts on delicate halide perovskite thin films, realizing high performance *van der Waals* contacts with an atomically clean contacting interface and greatly reduced contact resistance, for the first time allowing systematic electrical transport studies of halide perovskites down to cryogenic temperatures and establishing technical foundation towards unraveling the complex transport behavior and exploring new physics in this unique class of “soft-lattice” materials. These advancements highlight the unique merit of the bond-free *van der Waals* integration approach in creating pinning-free heterostructure interfaces. I will conclude with a brief perspective on these strategies for creating diverse artificial heterostructures as a versatile material platform with electronic structure by design to unlock new physical limits and enable a new generation of devices with unprecedented performance or unique functions, as illustrated in our recent effort including a new class of high-order *vdW* superlattices integrating highly distinct atomic crystals and molecular layers, solution processable *vdW* thin electronics, hybrid vertical transistors and low voltage memristors, programmable devices from 2D/superionic solid *vdW* heterostructures sensitive pressure sensors and electronic skins, highly reliable molecular tunneling transistors.

SESSION EQ02.01: Epitaxy of Mixed Dimensional Structures I
Session Chairs: Jeehwan Kim and Kyusang Lee
Tuesday Morning, November 30, 2021
Hynes, Level 2, Room 200

10:30 AM *EQ02.01.01

Defect-Seeded Lateral Epitaxy and Exfoliation on Graphene-Terminated Surfaces [Jason K. Kawasaki](#); University of Wisconsin, United States

We exploit defects in a 2D barrier layer to drive the seeded lateral epitaxy of atomically smooth, exfoliable, single-crystalline membranes [1]. This growth mode offers many of the advantages of the recently discovered remote epitaxy, including novel strain relaxation pathways and the ability to exfoliate free-standing membranes [2], plus additional advantages of (1) tolerance for imperfect graphene/substrate interfaces and (2) the ability to engineer the growth by patterning the 2D graphene layer. We show that GaSb films grow on graphene-terminated GaSb (001) via a seeded lateral epitaxy mechanism, in which pinhole defects in the graphene serve as selective nucleation sites, followed by lateral epitaxy and coalescence into a continuous film. Importantly, the small size of the pinholes permits exfoliation of a continuous, free-standing GaSb membrane. By combining molecular beam epitaxy with in-situ electron diffraction and photoemission, plus ex-situ atomic force microscopy and Raman spectroscopy, we track the graphene defect generation and GaSb growth evolution a few monolayers at a time. Our discovery provides a highly tunable method to engineer single-crystalline 3D materials on precisely tuned 2D barriers.

[1] S. Manzo, et. al., arXiv:2106.00721 (2021).

[2] D. Du, et. al., Nature Communications 12, 2494 (2021).

11:00 AM EQ02.01.02

Wafer-Scale Remote Epitaxy of III-V Semiconductors and Applications [Hyunseok Kim](#), Kuangye Lu, Sangho Lee, Ki Seok Kim, Sanghoon Bae and Jeehwan Kim; Massachusetts Institute of Technology, United States

In conventional epitaxy of single-crystalline semiconductor materials, it is challenging to separate the grown layer with the substrate due to the strong bonding at the interface. Remote epitaxy is a recently discovered method to grow single-crystalline thin films on graphene, wherein the grown film can be exfoliated at the graphene interface to form freestanding membranes.

Here, we present our recent development on remote epitaxy of III-V semiconductors. We show that directly growing 2D materials on III-V substrates as a remote epitaxy template is an ideal pathway that can eliminate transfer process-related defects and can realize wafer-scale process of remote epitaxy and substrate reuse. We present the strategies to grow 2D materials on the surface of III-V materials, which is much more challenging than thermally robust substrates such as SiO₂/Si or sapphire. The nucleation of III-V on 2D material-coated III-V platforms via remote interaction is investigated both experimentally and theoretically. Lastly, we show advanced remote epitaxial platforms and optoelectronic applications enabled by remote epitaxy, and the capability to recycle the III-V substrates for repeated remote epitaxy and production of freestanding III-V thin films.

11:15 AM EQ02.01.03

Remote Epitaxy of InP on Amorphous 2D Materials for Low-Cost High-Performance Photonics [Kuangye Lu](#)¹, Hyunseok Kim¹, Sangho Lee¹, Ki Seok Kim¹, Sanghoon Bae² and Jeehwan Kim¹; ¹Massachusetts Institute of Technology, United States; ²Washington University in St. Louis, United States

Indium phosphide (InP) is a III-V semiconductor that offers outstanding photonic properties that outperforms silicon, but the cost of InP wafers is extremely expensive. Although reusing original wafers can effectively minimize the cost of wafers, current techniques for wafer recycling of InP add significant costs in fabrication, nullifying the cost savings by reusing the wafers. Besides, unlike other III-V materials such as gallium arsenide (GaAs), commonly used epitaxial lift-off method for wafer recycling is not well studied for InP due to lack of latticed matched sacrificial layers, which makes reusing InP wafers more difficult. Remote epitaxy is a newly discovered method that enables single-crystal growth of III-V semiconductor thin films and easy exfoliation of the grown film, thus promising for a new cost-effective pathway of reusing InP wafers. However, previous methods of transferring 2D materials onto InP wafers, which use polymethyl methacrylate (PMMA) or metal stressor layers to transfer 2D materials grown on foreign substrates like copper or silicon carbide, introduce defects and damages on the 2D layer and/or substrates during the transfer process. Remote epitaxial films grown on the damaged 2D layer/substrate suffer from lower crystal quality and imperfect exfoliation, which undermines wafer reusability and device performance.

Here we report the MBE growth of amorphous boron nitride (a-BN) on InP wafers at low temperature that enabled improved quality of remote epitaxial films and their perfect exfoliation. We show fully covered a-BN on InP substrates despite phosphides' low decomposition temperatures. The surface of a-BN coated InP substrate remains smooth with a RMS roughness of around 3Å. We also demonstrate 100% coverage of single-crystalline InP thin films

grown on a-BN, with the film's quality significantly improved compared to the case of transferred 2D materials. In addition, roughness of the substrate's surface remains the same after exfoliation of grown InP film, and the growth and exfoliation were successfully repeated multiple times, proving the feasibility for InP wafer recycling. Through this low temperature MBE growth approach and remote epitaxy, we successfully demonstrate large-scale flexible thin film exfoliation and recycling of InP substrates, which will lead to new opportunities in InP thin film-based photonics and novel heterostructures with significantly reduced cost.

11:30 AM EQ02.01.04

Spontaneous Incommensurate van der Waals Heteroepitaxy Hesham El-Sherif^{1,2}, Stephen Jovanovic¹, John Preston¹ and Nabil Bassim¹; ¹McMaster University, Canada; ²Harvard University (Starting Fall 2021), United States

High-quality single-crystalline thin films are a significant factor for achieving substantial electrical and optical properties of various dimensional materials. Heterogeneous integration of these films may be achieved by in-situ fabrication or lift-off technologies from compliant substrates with remote and van der Waals epitaxy growth of semiconductors.[1] However, the quality of transferred semiconductor films depends on the quality and real-size of manually transferred two-dimensional (2D) materials, limiting the size of direct large-area single-crystal films.

In this presentation, a one-step growth method will be introduced to fabricate thin films that are incommensurate to their substrate through a *spontaneous van der Waals-like epitaxy*. [2] In this low-temperature growth, a buffer layer of chalcogenide is spontaneously attached to the interface with a weak chemical interaction between a surface-reconstructed substrate and a 3D film. An epitaxial relationship between the substrate and film is maintained across this interfacial layer. Moreover, no mismatch dislocations are observed at the interface, which allows high-quality single-crystal thin film growth. This unique interface complexion allows for the lift-off of films, such as CdTe and InSb, without first transferring a 2D material onto their growth substrate for remoting epitaxy.

The presentation will focus on the fundamental interface understanding of cadmium telluride (CdTe) on a sapphire, fabricated via pulsed laser deposition at approximately 300 °C. [2, 3] A monolayer of chalcogenide (tellurium) at the interface is examined by various spectroscopic scanning transmission electron microscopy (STEM) techniques, including low-loss and core loss electron energy-loss spectroscopy (EELS) to reveal both the bonding and chemical composition at the interface. The CdTe film is investigated at the bulk-scale using 3D x-ray diffraction measurements and the atomic-scale using STEM imaging of the interfacial and CdTe film regions. The strain at the CdTe-sapphire interface is examined using both geometric phase analysis (GPA) and the STEM-moiré analysis. Microscopic investigations provide evidence that strain-free CdTe films grow with high quality on the Tellurium-terminated sapphire surface. The relatively low growth temperature maintains the top-most sapphire layer to the single aluminum reconstruction, as confirmed by core-loss EELS. Tellurium is more kinetically favorable to nucleate above oxygen sites in sapphire than Cadmium at these growth and interface conditions. This is followed by the CdTe film with its first tellurium layer oriented toward the pseudomorphic tellurium layer on the sapphire forming van der Waal-like bonds. This interface complexion allows for a unique incommensurate van der Waals heteroepitaxy growth.

Finally, the presentation will show the realization of a monolayer *Tellurene*, a 2D form of tellurium with a 3-atom thick, if more tellurium is deposited at the film/substrate interface. The growth progress of this interface complexion could lead to the fabrication of various dimensional (3D/2D/3D) high-quality heterostructures via one-step growth using a pulsed laser deposition system.

References

- [1] S-H Bae et al., Nature Nanotechnology 15 (2020), p. 272.
- [2] SM Jovanovic et al., Small 16 (2020), p. e2004437.
- [3] H El-Sherif et al., Microsc microanal 26 (2020), p. 1.

11:45 AM EQ02.01.05

Integration of MoS₂ Monolayers onto III-V Nanowires into 1D/2D Heterostructures Akshay Balgarkashi¹, Valerio Piazza¹, Jakub Jasinski², Riccardo Frisenda³, Michael Baranowski², Alessandro Surrente², Andres Castellanos-Gomez³, Paulina Plochocka⁴ and Anna Fontcuberta i Morral^{1,1}; ¹École Polytechnique Fédérale de Lausanne, Switzerland; ²Wroclaw University of Science and Technology, Poland; ³Instituto de Ciencia de Materiales de Madrid, Spain; ⁴CNRS-UGA-UPS-INSA, France

Transition metal dichalcogenides (TMDs) are 2D semiconductors characterized by unique features such as layer-dependent direct/indirect band gap transition, high spin-orbit coupling and strain modulation [1]. Depending on the number of layers, their band gap can vary within the visible/near-infrared range making TMDs suitable for a wide variety of optoelectronic applications [2]. In particular, the possibility to induce the local emission of photons by applying strain is highly beneficial for the design of quantum emitters [3]. In this context, the combination with 1D nanostructures offers an elegant solution as the dimensionality mismatch between ultrathin TMDs and nanowires results in a localized strain [4]. For these reasons, the integration of MoS₂ with compound semiconductor nanowires in the form of a heterostructure is expected to widen the functionalities of the ensemble. Selective area epitaxy (SAE) can be used to grow ordered arrays of III-V nanowires. Due to the small footprint, nanowires with very low defect density can be grown on a large number of substrates [5]. Additionally, III-V nanowires can act as natural waveguides increasing the directionality of the photon emission [6]. In this work, we report on the fabrication of heterostructures formed by exfoliated mono- and bi-layers MoS₂ and GaAs nanowires (NWs) and preliminary optical characterization of the ensemble. Self-catalysed vertical GaAs NWs were grown by SAE on Si (111) substrate, with a diameter of 150nm and height of 400nm. The exfoliated flakes were transferred on the NWs using an all-dry viscoelastic stamping method. Atomic force microscopy (AFM) was used to get feedback on the integration. AFM analysis indicates that the monolayer is stable on top of the NWs in most of locations, although a non-zero possibility of piercing events exists. Raman analysis evidenced a small shift of the in-plane (E_{2g}) mode at low temperature. Photoluminescence (PL) spectra on bare MoS₂ showed the existence of A exciton and trion peaks as well as a large band peaked around 1.7 eV, attributed to sulfur vacancies [7]. PL analysis on MoS₂/GaAs NWs highlights an enhanced intensity of the same peaks. PL micromapping was used to visualize the increase in emission intensity within the array. The defect peak centered around 1.7 eV shows a non-uniform intensity enhancement whereas the direct bandgap emission from MoS₂ is uniformly enhanced across the nanowire array.

References

- [1] Manzeli et al., Nat.Rev.Mater. 2, (2017)
- [2] Mak et al., Nat.Photonics. 10, (2016)
- [3] Branny et al., Nat.Comm. 8 (2017)
- [4] Mukherjee et al., Nat. Commun. 11, 5502 (2020)
- [5] Glas et al., Phys. Rev. B 74, 121302(4) (2006)
- [6] Frederiksen et al., ACS Photonics 4, (2017)
- [7] S. Tongay et al., Sci. Rep., 3, (2013)

SESSION EQ02.02: Epitaxy of Mixed Dimensional Structures II
Session Chairs: Xiuling Li and Rachael Myers-Ward
Tuesday Afternoon, November 30, 2021
Hynes, Level 2, Room 200

1:30 PM *EQ02.02.01

SiC Stackable Electronics Using Remote Epitaxy Rachael Myers-Ward¹, Daniel J. Pennachio¹, Jeehwan Kim², Kuan Qiao², Yeengin Kim², Matthew T. Dejarld¹, Shojan P. Pavunny¹, Jenifer R. Hajzus¹ and D K. Gaskill¹; ¹Naval Research Laboratory, United States; ²Massachusetts Institute of Technology, United States

Remote epitaxy (RE) is a novel growth process performed on graphene covered substrates where adatom registry is guided by the partially-screened electrostatic fields from the underlying substrate rather than interactions with the graphene lattice. The graphene acts as a spacer, allowing the ease of epitaxial layer removal and transfer to desired substrates. This RE technique has the possibility of impacting many research areas including SiC and GaN SMART power, integration of opto- and electronic devices, HEMT performance, flexible electronics and quantum sciences.

In this work, we focus on the RE of SiC, which is directly grown on epitaxial graphene (EG) on SiC(0001) using a chemical vapor deposition (CVD) reactor. The graphene is grown via the Si sublimation of SiC. Both on-axis (6H-SiC) and off-axis (4H-SiC cut 4° off-axis towards the [11-20]) substrates were investigated where the ability to maintain this graphene at elevated growth temperatures in a SiC CVD environment is crucial for the success of remote epitaxy. Following epitaxial graphene growth, SiC growth was performed and the growth parameters were modified to reduce SiC polytype conversion and other extended defects. Films were characterized using scanning electron microscopy, transmission electron microscopy and electron backscattering detection. To evaluate the ability to grow SiC remote epitaxially, a Ni metal stressor technique was used to exfoliate the layers and demonstrate exfoliation yields up to 50 – 70 %.

This work was supported by the U.S. Office of Naval Research.

2:00 PM DISCUSSION TIME

2:30 PM EQ02.02.03

Nanopatterned Graphene Based Universal Epitaxy Platform for Single-Crystalline Membrane Transfer Sangho Lee¹, Yanming Zhang², Hyunseok Kim¹, Sanghoon Bae¹, Kuangye Lu¹, Jiho Shin¹, Ki Seok Kim¹, Yunfeng Shi² and Jeehwan Kim¹; ¹Massachusetts Institute of Technology, United States; ²Rensselaer Polytechnic Institute, United States

Remote epitaxy – an emerging growth method of single-crystalline membranes copied from underlying substrates through atomically thin graphene interlayer – has greatly expanded the material spectrum by efficiently producing costly thin films or heterogeneously integrating unique nanosystems. It was recently demonstrated that slippery graphene promotes a strain relaxation of epitaxial film on its surface, which also allows the heteroepitaxy of lattice-mismatched systems with reduced defect density. Despite such benefits, remote epitaxy has its fundamental limitations in non-polar materials because the ionicity of materials strongly governs a distant atomic interaction between the substrate and epitaxial layer. Thermally or chemically weak materials that are incompatible with graphene transfer or growth on them also restrict their remote epitaxy. Here, we introduce periodic openings in graphene to induce a lateral overgrowth of thin films, where an opening acts as a favorable nucleation site allowing the epitaxy to occur regardless of polarity and process compatibility of materials. Nanostructured graphene interlayer enables a facile exfoliation of epitaxial films from substrate as well as a spontaneous relaxation of misfit strain during heteroepitaxy depending on its structural parameters such as period and size of openings. Engineered graphene is, thus, expected to provide a universal epitaxy platform that can accommodate the growth, release, and transfer of a wider variety of high-quality membranes.

2:45 PM EQ02.02.04

Remote Epitaxy of GaN Membranes Towards Commercialization Kyusang Lee^{1,2}; ¹University of Virginia, United States; ²Future Semiconductor Business, United States

GaN has been widely used for various applications including power electronics, RF devices and optoelectronic applications. Recently, remote epitaxy technology has been introduced, a substrate below 2D materials also plays a role to intervene in the epitaxial growth process, leaving room to realize a novel epitaxial growth process. Potential fluctuation—the difference between potential energy maxima and minima along the surface of the substrate—is influenced by this remote interaction; the fluctuation is predominant over the vdW force, due to the atomic thickness of 2D materials. The remote interactions can be controlled by modulation of polarities of 2D materials and epitaxy materials. Polar-material-based heterostructure, such as GaAs, InP, GaP, and GaN with their substrate sandwiching 2D materials, enables the semiconductor film to be exfoliated from the underlying substrates through the 2D materials. This process is expected to open a novel avenue for the field of non-silicon electronics and photonics, where the ability to re-use graphene-coated substrates allows savings on the high cost of non-silicon substrates.

3:00 PM EQ02.02.05

Ultrathin 2D/3D Heterostructures Kate Reidy, Joachim D. Thomsen, Baoming Wang, Aubrey Penn and Frances M. Ross; Massachusetts Institute of Technology, United States

One of the frontiers of mixed dimensional heterostructure design lies in the ability to grow thin epitaxial films of conventional three-dimensional (3D) metals or semiconductors on two-dimensional (2D) materials. The structure and alignment at this 2D/3D interface affects properties, such as electron transport, contact resistance, and photo-current, of devices that utilize 2D materials.¹ Moreover, integration of 2D/3D heterostructures can result in unique (opto-)electronic, magnetic, thermal, or mechanical properties of the combined heterostructure not present in individual components.^{2,3}

Here, we report the direct epitaxial growth of ultrathin titanium/gold (Ti/Au) heterostructures on suspended 2D materials. The Ti/Au system is important due to Ti's continued use as an adhesion layer across a variety of applications in micro- and nano- electronics. Moreover, ultrathin (<1nm) Ti/Au layers exhibit improved thermal stability, plasmonic response, and superconducting transition temperature compared to thicker (>2nm) layers. We perform epitaxial metal growth on suspended 2D materials substrates in ultra-high vacuum (UHV) and monitor the structure evolution during annealing using *in-situ* transmission electron microscopy (TEM). We find that ultrathin (<1nm) epitaxial Ti nanoislands can be grown on graphene at high temperatures. The

island geometry exhibits a large dependence on the layer number of the 2D material, and on thin 2D layers the Ti is extremely thin and compliant to the substrate. Subsequent Au deposition without breaking vacuum shows 100% selectivity on these ultra-thin Ti layers, and the Au completely wets the surface instead of forming conventional Volmer-Weber islands. In contrast, the Au forms islands when the Ti layer is exposed to oxygen at 10^{-6} Torr before Au deposition. Moreover, we observe greatly improved thermal stability against dewetting of the Ti/Au layer up to 1000°C. Electron energy loss spectroscopy (EELS) evidence that the thin Au capping layer prevents the Ti from oxidation. We discuss the potential of these Ti layers as a general strategy for creating ultrathin bottom-up 2D/3D heterostructures through epitaxially anchoring other metallic or semiconducting layers on 2D materials, and consider routes towards post-oxidation of the layers to form thin oxide/2D interfaces. This opens up a new set of possibilities for the heterointegration of 2D materials and thin epitaxial 3D films, adding to the toolbox of multidimensional heterostructure growth and design.

References

1. Jariwala, D., Marks, T. J. & Hersam, M. C. Mixed-dimensional van der Waals heterostructures. *Nat. Mater.* **16**, 170–181 (2017).
2. Kim, Y. *et al.* Remote epitaxy through graphene enables two-dimensional material-based layer transfer. *Nature* **544**, 340–343 (2017).
3. Reidy, K. *et al.* Direct imaging and electronic structure modulation of moiré superlattices at the 2D/3D interface. *Nat. Commun.* **12**, 1290 (2021).

3:15 PM EQ02.02.06

Selective Area Growth of III-V Semiconductor Heterostructure Quantum Devices with *In Situ* Shadow-Wall Assisted Superconductor

Patterning Aranya Goswami¹, Hao Wu², Connor P. Dempsey¹, Po Zhang², Sergey Frolov² and Chris Palmstrom¹, ¹University of California, Santa Barbara, United States; ²University of Pittsburgh, United States

Semiconductor-superconductor hybrid structures offer an attractive platform to explore interesting low temperature transport phenomenon. In particular, one dimensional semiconducting nanowires with spin orbit coupling proximitized by a s-wave superconductor has been proposed to host Majorana Fermions, relevant for topological quantum computing. Selective area growth offers a scalable route to growing and fabricating complex networks of such semiconductor superconductor nanostructures. However selective area grown in-plane semiconductor nanowires often suffer from a high density of defects due to lattice and symmetry mismatch between the nanowire material and the substrate. This leads to poor electrical characteristics such as low electron mobility and low coherence lengths. Heterostructures can potentially solve this problem by incorporating buffer layers to reduce lattice mismatch and using capping layers to reduce surface scattering. Further, a clean interface between the superconductor and the semiconductor is crucial for inducing a hard proximitized superconducting gap in the nanowire. Since post-growth superconductor etching can often introduce defects in the semiconducting nanowire, an in-situ selective superconductor deposition can prove to be extremely useful in this respect.

In this talk, we discuss selective area growth of III-V nanowires on InP(001) substrates using chemical beam epitaxy. Specifically, we grow InP/InGaAs/InP quantum wells in in-plane nanowire geometry with lattice matched ($\text{In}_{0.53}\text{Ga}_{0.47}\text{As}$) and strained ($\text{In}_{0.75}\text{Ga}_{0.25}\text{As}$) channels that are 20nm thick. Cross-sectional scanning transmission electron microscope (STEM) imaging of the grown nanowires shows abrupt defect-free interfaces. In addition, we show growth of InAs nanowires with graded InGaAs buffers. Effects of InGaAs buffer on growth morphology are studied using high resolution cross-sectional STEM analysis. To grow superconductor islands on the in-plane nanowires, we fabricate high aspect ratio SiO_2 shadow walls positioned within 200nm of the nanowires. Together with angled low-temperature deposition, this enables in-situ growth of superconductor islands on the in-plane nanowires at predetermined positions, while maintaining the pristine nature of the interface - as confirmed by the proximity induced superconductivity in the nanowire. Superconductor-normal-superconductor junctions with sub 100nm normal junction lengths are achieved with tin as the superconductor on InAs nanowires. By incorporating different shapes of shadow walls, positioned close to the nanowire trench, we show that various semiconductor-superconductor hybrid geometries can be directly grown without breaking vacuum. Finally, we discuss magneto-transport measurements on these hybrid nanostructures.

3:30 PM BREAK

SESSION EQ02.03: Physics and Devices of Mixed Dimensional Heterostructures I

Session Chairs: Sanghoon Bae and Jason Kawasaki

Tuesday Afternoon, November 30, 2021

Hynes, Level 2, Room 200

4:00 PM *EQ02.03.01

Mixed Dimensional Heterostructures Enabled by Freestanding 3D Materials and 2D Materials [Sanghoon Bae](#); Washington University in Saint Louis, United States

Next-generation electronics will expect new functionalities such as high performance, low power consumption, lightweight, flexibility, conformality, and self-power. In this regard, demand for new heterostructures has been getting high. In this talk, I will discuss how we can produce freestanding 3D materials and 2D materials that are stepping stones to realize new heterostructures. As they are a new form of heterostructures, new architectures for functional devices and physical phenomenon can be realized. For freestanding 3D materials, we have studied single crystalline growth on graphene-coated substrates. As graphene has lattice transparency, single-crystalline materials were successfully grown. Because the interface between grown single crystals and graphene-coated substrates has substantially small binding energy, the grown single-crystalline materials can be exfoliated to produce freestanding 3D materials. For freestanding 2D materials, we have conceived a unique idea that selectively separates monolayer 2D materials from multilayers, named layer-resolved splitting, thereby multiple monolayer 2D materials are harvested from multilayer 2D materials. With such approaches, 2D and 3D mixed dimensional heterostructures have been developed for new physical coupling phenomena and new device architectures.

Reference

- [1] Sang-Hoon Bae, *et al* Nature Nanotechnology, 15, 272–276 (2020)
- [2] Sang-Hoon Bae, *et al* Nature Materials, 18, 550–560, (2019)
- [3] Jaewoo Shim, Sang-Hoon Bae *et al* Science, 362, 6415, 665–670, (2018)

4:30 PM EQ02.03.03

Mixed-Dimensional 1D/2D van der Waals Heterojunction Diodes and Transistors in the Atomic Limit [Jakub P. Jadwiszczak](#)¹, Jeffrey D. Sherman¹, David Lynall¹, Boyan Penkov¹, Erik Young¹, Alice Castan², Marija Drndić² and Kenneth Shepard¹; ¹Columbia University, United States; ²University of Pennsylvania, United States

Mixed-dimensional heterojunctions (MDHJs) are an emerging class of nanoscale devices whose electrical and optical properties reflect the nature of their

constituent materials. The prospect of mixed-dimensional van der Waals transistor architectures (1D/2D or 2D/3D) may offer substantial advantages in both the ease of fabrication and performance of the realized devices. For example, bulk p - n junctions usually need diffusion or implant-anneal sequences to achieve the necessary doping profiles, while these steps may be bypassed entirely by using synthetic van der Waals MDHJs.

In this work, we demonstrate ultra-downscaled MDHJ diodes and transistors based on the van der Waals heterojunction formed between monolayer n -type MoS₂ and an individual p -type single-walled semiconducting carbon nanotube (SWCNT). We fabricate these heterojunctions using a non-deterministic wet transfer process where chemical vapor deposition (CVD)-grown monolayer MoS₂ flakes are deposited directly on top of individual CVD-grown semiconducting SWCNTs. We demonstrate that the rectification ratio of the formed individual MDHJs can be tuned by several orders of magnitude by back-gating through the SiO₂ substrate, while the transfer characteristics of the individual junctions demonstrate anti-ambipolar behavior previously observed in ensemble CNT/MoS₂ junctions.

Moreover, we utilize the MDHJ diode to fabricate atomic-scale p -type junction field-effect transistors, where the voltage applied to the MoS₂ gate can modulate the conductance through the underlying SWCNT transistor channel. Our experimental results match well with technology computer-aided-design (TCAD) device modelling, where the transistor functionality is found to be dominated by band-to-band tunneling (BTBT) across the heterojunction forming the JFET gate region. In addition, we find that in extreme bias limits, the high breakdown voltages inherent to this mixed-dimensional van der Waals interface can push the device into unusual operating regions, where the polarity of the transistor drive current can be controlled by the gate voltage magnitude.

SESSION EQ02.04: Poster Session I
Session Chairs: Hyeonseok Kim and Jiho Shin
Tuesday Afternoon, November 30, 2021
8:00 PM - 10:00 PM
Hynes, Level 1, Hall B

EQ02.04.01

Heterogeneous Integration of 2D MoS₂ on Silicon Nanoparticle in a Core-Shell Architecture for Photonic Applications Yea-Shine Lee¹, Tatsuki Hinamoto², Sina Abedini Dereshgi¹, Matthew Cheng¹, Jennifer DiStefano^{1,1}, M. Arslan Shehzad^{1,1}, Roberto dos Reis^{1,1}, Hiroshi Sugimoto², Koray Aydin¹, Minoru Fujii² and Vinayak Dravid^{1,1,1}; ¹Northwestern University, United States; ²Kobe University, Japan

The high exciton binding energy and mechanical flexibility of transition metal dichalcogenides (TMDs) make them attractive for next-generation photonics. However, because of their atomically thin nature, there is a challenge in obtaining sufficient absorption and emission of the incoming electromagnetic (EM) field. Plasmonic core-shell structures of TMD-encapsulated nanoparticles have demonstrated significantly improved light-matter interactions, highlighting this architecture for applications in nanophotonic and optoelectronic devices. Recently, a high index silicon dielectric nanoparticle in the core-shell architecture has been theoretically predicted to further reduce losses and enhance resonance of the near-EM fields. The resonance coupling of the magnetic dipole mode of the silicon core and exciton transitions in the TMD may thereby enable longer exciton lifetimes, yielding enhanced energy transfer and absorption/emission of the field. However, to date, this architecture has not been experimentally demonstrated.

Here, we experimentally realize this proof-of-concept of advanced Si@MoS₂ heterogeneous architecture, encapsulated via chemical vapor deposition. The size of the silicon nanoparticles, which have diameter 175±25 nm, is comparable to the wavelength of the EM field, putting this hybrid system in the Mie scattering regime. Structural and chemical analyses confirm the presence of Mo and S in the shell and Si in the core. In the core-shell architecture, we observe an enhanced photonic response relative to the bare Si nanoparticles and planar MoS₂. This distinct behavior can be explained by a displacement current loop circulating inside the dielectric Si core which leaks out to the shell and enhances the near-EM field. Here, the Si core acts as an antenna to effectively excite the TMD shell emitter. Moreover, there are two major factors that control the degree of coupling response: the core diameter and shell thickness. Tuning the size of the core has enabled us to optimize the optical resonance. Dark-field single-particle optical scattering measurements confirm the energy coupling between the core and the shell measured through Rabi splitting of the magnetic dipole resonance mode of the nanoparticle. We believe Si@MoS₂ is a technological-relevant material system and can assist to understand novel optical responses and the principles underlying these phenomena.

This work is primarily supported by the National Science Foundation (NSF) under Grant No. DMR-1929356. We made use of the EPIC and KECK II facility of Northwestern University's NUANCE Center, which has received support from the SHyNE Resource (NSF ECCS-2025633), the IIN, and Northwestern's MRSEC program (NSF DMR-1720139).

EQ02.04.02

Tradeoffs Between Translational and Orientational Order in 2D Superlattices of Polygonal Nanocrystals with Differing Edge Count Justin Ondry^{1,2}, Layne B. Frechette¹, Phillip L. Geissler¹ and A. Paul Alivisatos^{1,2,3}; ¹University of California, Berkeley, United States; ²Kavli Energy NanoScience Institute, United States; ³Lawrence Berkeley National Laboratory, United States

The goal of this work is to identify factors which modulate translational and orientational order in 2D self-assembled superlattices using polygon shaped nanocrystal building blocks. Using a combination of transmission electron microscopy, electron diffraction, and hard particle Monte Carlo simulations, we quantify the translational and orientational order in 2D superlattices of hexagonal prism shaped CdSe/CdS nanocrystals and cube shaped CsPbBr₃ nanocrystals. Superlattices derived from cube shaped nanocrystals display less translational order compared to hexagonal prism shaped nanocrystals both experimentally and in simulations. To first order, this effect can be understood based on geometric considerations inherent to the combined rotational and translational symmetries of different polygonal shapes and their superlattice geometries. Cubes form a simple cubic lattice in which entire rows of nanocrystals can slide past each-other with little energy penalty whereas hexagons interlock in a hexagonal tiling, leading to a structure which is robust to nanocrystal translations. Nanocrystal shape also modulates the degree of orientational order, and in this case, cube assemblies display a narrower orientation distribution than hexagonal prism assemblies. An intuitive explanation for this arises when the influence of organic ligands surrounding the polygonal inorganic core is considered. A hexagonal prism displays a more "spherical" interaction potential compared to cubes explaining the observation to first order. The results presented here outline an intuitive framework for identifying nanocrystal superlattice structures which favor translationally versus orientationally ordered self-assembled superlattices.

EQ02.04.04

Cathodoluminescence Mapping of hBN on III-V Nanomembranes Claire Blaga, Akshay Balgarkashi, Valerio Piazza, Nicolas Tappy, Jin Jiang, Mitali

Hexagonal boron nitride (hBN) is a Van der Waals material with a 2D atomic structure similar to graphene, whose unique optical properties have raised significant interest; its wide direct band gap and robust excitons enable intense emission in the deep UV region. Additionally, the crystallographic defects in hBN form states within the band gap which can be engineered for efficient, high-brightness, quantum emission in the UV to IR range, even at room temperature [1,2]. Although extensively studied, the origin of the complex emission spectrum of hBN is still debated and mostly unknown. In this context, cathodoluminescence (CL) mapping is a powerful tool. By resolving the optical emission down to the nanoscale upon electron beam exposure, CL allows to access the optoelectronic phenomena occurring in specific locations. However, when dealing with ultrathin materials, high electron beam energies are not efficient probes as only a small fraction of the electron energy is transferred to hBN [3]. On the other hand, the use of low beam energies negatively impacts the spatial resolution.

This work explores the use of CL mapping with beam energies from below 1keV to 10keV to investigate the optoelectronic properties of hBN integrated onto different substrates. Thin flakes (3-50 nm) of hBN are exfoliated via the standard tape method and transferred on sapphire and horizontal GaAs nanomembranes (NMs) using an all-dry viscoelastic stamping method. Samples with different flake thicknesses were also fabricated to explore thickness dependent properties. Depositing the flakes onto sapphire or nanostructures allows to take advantage of the underlying substrate to increase the light emission, thus enabling the access to the optical fingerprint of the material.

GaAs NMs are grown on (111)B GaAs substrates by selective area epitaxy. These NMs present a slab morphology, whose dimensions can be tuned by modifying the growth parameters. In this study, nanostructure arrays with different heights, widths and pitches were explored. The NMs' morphology and aspect ratio are expected to dictate the strain induced on the hBN crystals as well as the contact area between membrane and hBN. Spectrally integrated CL maps evidenced that the presence of the membranes underneath the flake has an impact on the emission intensity in the whole photon energy range investigated. In particular, the emission bands at 320nm and 400nm, attributed to C/O impurities and N vacancies respectively, appear brighter in areas where there is a nanomembrane below the flake when compared to what is observed in the off-nanomembrane position. This effect is more pronounced with thicker flakes, where the light emission is more intense. Another notable variable is the topology imposed on the flake during its deposition onto the substrate. The flake can be conformal to the structures or suspended on top of them, mainly depending on the NM morphology. The results highlight how a suspended flake exhibits a stronger emission between membranes and lower emission on top of the membrane as compared to a flake conforming to the substrate. Monte Carlo simulations suggest that the topology has an impact on the interaction with backscattered electrons and therefore on the emission intensity.

References:

1. Choi, S. et al. *ACS Appl. Mater. Interfaces* **8**, 29642–29648 (2016).
2. Koperski, M. et al. *Opt. Commun.* **411**, 158–165 (2018).
3. Negri, M. et al. *Nano Lett.* **20**, 567–576 (2020).

EQ02.04.05

Ultrafast Synthesis of High Entropy Oxide Nanoparticles by Flame Spray Pyrolysis Abhijit H. Phakatkar, Tolou Shokuhfar and Reza Shahbazian-Yassar; University of Illinois at Chicago, United States

The synthesis of high entropy oxide (HEO) nanoparticles (NPs) possesses many challenges in terms of process complexity and cost, scalability, producing nanoparticle morphology, and rapid synthesis. Herein, we report the synthesis of novel single-phase solid solution $(\text{Mn, Fe, Ni, Cu, Zn})_3(\text{O})_4$ quinary HEO NPs produced by flame spray pyrolysis (FSP) route. The aberration-corrected scanning transmission electron microscopy (STEM) technique is utilized to investigate the spinel crystal structure of synthesized HEO NPs and energy dispersive X-ray spectroscopy analysis confirmed the high entropy configuration of five metal elements in their oxide form within a single HEO nanoparticle. STEM analysis shows the synthesized HEO NPs are single phase solid solution spinel-structured with the lattice constant of 8.39 Å. Selected area electron diffraction, X-ray diffraction and Raman spectroscopy analysis results are in accordance with STEM results providing the key attributes of spinel crystal structure of HEO NPs. XRD results also indicate the presence of lattice distortions in the synthesized HEO NPs. Raman spectroscopy modes A_{1g} , F_{2g} and A_{1g}^* corresponding to divalent metal cation – oxygen (M^{2+} -O) stretching vibrations indicates the evidence of spinel crystal structure fingerprints. X-ray photoelectron spectroscopy results provide the insightful understanding of chemical oxidation states of individual elements and their possible cation occupancy sites in the spinel-structured HEO NPs.

EQ02.04.07

3D Discrete Dislocation Mechanics in Heterogeneous Materials and Structures—Theoretical Solutions and Advanced Finite Element Simulations Using Adaptive Remeshing Aurélien J. Vattré and Vincent Chiaruttini; ONERA, France

The remarkable versatility of the finite element method is used to model the three-dimensional discrete dislocation dynamics in heterogeneous materials and structures. The present approach is based on the finite element strategy using advanced and flexible adaptive remeshing strategies for fine mesh resolution of complex curved dislocation loops. The numerical framework is capable of computing the stress fields and the driving forces acting on arbitrarily-shaped dislocations with a high degree of accuracy and with significant precision, as compared to novel theoretical elastic solutions for dislocation loops in the context of anisotropic hetero-elasticity theory.

The first part of the presentation continues beyond the theoretical contributions in the research area by treated dislocation loops in heterostructures formed by elastically anisotropic crystals using the Stroh formalism combining with bi-periodic Fourier-transform and dual variable and position techniques. The non-singular stress fields and driving forces are also used to investigate the comparison with the numerical finite element analysis of complex dislocation configurations. The fundamental Peach-Koehler force that governs the motion of the discrete dislocation loops is therefore captured by the numerical driving force calculation based on dissipative energy considerations. Because the numerical results show excellent agreement with analytical solutions in terms of non-singular stresses and forces, the finite element approach with adaptive remeshing techniques is used to explore more sophisticated microstructural situations, thus offering more realistic boundary-value description of dislocation loops in heterogeneous materials and structures.

SESSION EQ02.05: Physics and Devices of Mixed Dimensional Heterostructures II
Session Chairs: Xiuling Li and Mona Zebarjadi
Wednesday Morning, December 1, 2021
Hynes, Level 2, Room 200

10:30 AM *EQ02.05.01

Thermionic and Thermoelectric Transport in Mixed Phase and Mixed Dimensional Samples Mona Zebarjadi, Md. Golam Rosul and Tianhui Zhu; University of Virginia, United States

Solid-state thermionic structures made out of 3-5 layers of van der Waals heterostructures sandwiched between metallic electrodes have shown promising thermal to electrical energy conversion efficiencies theoretically. Here, I discuss our detailed theoretical studying of these structures using first-principles calculations combined with Green's function method. We study the effect of the number of layers, the energy barrier, and the asymmetry of the contacts on the performance of transition metal dichalcogenide (TMD)-based thermionic converters. We show that the key is to make low-energy, low-resistance metallic contacts and we identify copper as the optimum metal to make ohmic low-resistance contact to MoSe₂. Experimental demonstration of these structures involves a simple but mixed dimensional structure. I will next discuss the thermoelectric transport in mixed-phase 1T-2H MBE grown NbSe₂ samples and will discuss the thermal, electrical and thermoelectric transport properties of these mixed phased samples.

11:00 AM EQ02.05.02

Localization and Modulation of Excitonic Emission in MoS₂ with Mixed-Dimensional Ferroelectric Heterostructures Joonseok Kim and Lincoln Lauhon; Northwestern University, United States

Semiconducting two-dimensional (2D) materials possess intriguing optoelectronic properties deriving from a strong light-matter interaction and large exciton binding energies, which create opportunities for novel room-temperature optoelectronics such as excitonic computing with optical interconnects. It is therefore of great interest to engineer and modulate excitonic behaviors. The most widely used approaches to modulate excitons in semiconducting 2D materials are tuning the dielectric environment,[1] applying strain,[2] and applying external fields.[3] Here we describe a platform to modulate exciton emission in monolayer MoS₂ by integrating dielectric Coulomb engineering, local strain, and ferroelectric doping. Mixed-dimensional heterostructures consisting of monolayer MoS₂, P(VDF-TrFE) copolymer, and hBN were fabricated by transferring 1L-MoS₂ flakes on sub- μm P(VDF-TrFE) islands on hBN substrates. Raman and photoluminescence (PL) maps were correlated with atomic force microscopy topography to determine how local strain, dielectric contrast, and ferroelectric doping for the MoS₂ layer induced by P(VDF-TrFE) islands influence exciton emission. Notable differences in Raman and PL spectra were observed between MoS₂ on flat hBN, thinner islands, and thicker islands. The Raman E mode is redshifted on thicker islands, consistent with tensile strain generated by the topography. In addition, the PL A exciton intensity is enhanced, which could be associated with a strain-induced funneling effect that would reduce the band gap. However, the MoS₂-A exciton emission energy is increased on P(VDF-TrFE) islands, which likely arises from the decrease in exciton binding energy due to the strong dielectric screening of the P(VDF-TrFE) ($\epsilon_r \approx 10$). Effects of dielectric environment and local strain on excitonic dynamics were further examined by analyzing the A and B exciton intensity ratio; a high A-to-B intensity ratio is a sign of low nonradiative recombination and is desirable for excitonic device applications. Regions of increased A/B ratio (up to 2x) correlate well with the P(VDF-TrFE) island locations. Moreover, the B intensity showed a negative correlation with height, suggesting that enhanced substrate screening combined with higher strain from the morphology enhances the intravalley scattering from the B exciton state to the A exciton state. The A and B exciton energy difference map demonstrates that, in contact with P(VDF-TrFE), the spin-orbit coupling-induced valence band splitting is reduced, which could lead to an increased intravalley scattering rate. Finally, the ferroelectric P(VDF-TrFE) islands were poled by applying a bias to the Si substrate with respect to conductive AFM tip. The MoS₂ A-to-B intensity ratio increases by a factor of two on negatively poled islands, whereas positive poling does not substantially change the intensity ratio. The correlation of Raman, PL, and topography maps revealed that the substrate dielectric screening, local strain, and ferroelectric doping provide a means to localized and modulate excitonic emission in monolayer MoS₂.

[1] Raja et al., *Nat. Commun.* **2017**, *8*, 15251.

[2] Castellanos-Gomez et al., *Nano Lett.* **2013**, *13*, 5361.

[3] Mak et al., *Nat. Mater.* **2012**, *12*, 207.

11:15 AM EQ02.05.03

Combining Colloidal Synthesis and Assembly with Epitaxial Growth to Fuse Colloidal Nanocrystals into Tunable 0D-2D Quantum Dot-in-Matrix Superlattices Justin Ondry^{1,2}, John Philbin¹, Michael Lostica¹, Eran Rabani¹ and A. Paul Alivisatos^{1,2,3}; ¹University of California, Berkeley, United States; ²Kavli Energy NanoScience Institute, United States; ³Lawrence Berkeley National Laboratory, United States

In this talk we will discuss a new approach for preparing 0D-2D quantum dot-in-matrix heterostructures. We combine colloidal nanocrystal synthesis, self-assembly, and solution phase epitaxial growth techniques to develop a general approach for preparing single dot thick atomically attached quantum dot (QD) superlattices. These materials exhibit high quality translational and crystallographic orientational order along with state-of-the-art uniformity in the attachment thickness. Colloidal synthesis of well-faceted hexagonal prism shaped core/shell QDs, followed by liquid subphase self-assembly and immobilization of superlattices on a substrate creates a highly ordered structure for subsequent attachment. Importantly the nanocrystals are arranged such that they share a mutual crystallographic alignment. To attach the nanocrystals, we use a solution phase method to epitaxially grow additional semiconductor material in the voids between the particles resulting in a QD-in-matrix structure. The photoluminescence emission of the QD-in-matrix structure retains characteristic 0D electronic confinement. Finally, annealing of the resulting structures removes inhomogeneities in the QD-QD inorganic bridges, which atomistic electronic structure calculations demonstrate would otherwise lead to Anderson-type localization. The piece-wise nature of this methodology allows one to independently tune the size and material of the QD core, shell, QD-QD distance, and the matrix material. These four parameters can be tuned to control many properties depending on the specific applications (*e.g.* degree of quantum confinement, quantum coupling, band alignments, *etc.*). Further we can transform the QD superlattice to additional materials as demonstrated herein with a CdSe/CdS to HgSe/HgS conversion.

11:30 AM EQ02.05.04

Magnetic Properties of PrVO₃ Thin Films Wilfrid Prellier; CRISMAT Laboratory, France

Transition metal oxides often having a perovskite structure form a wide and technologically important class of compounds. In these systems, ferroelectric, ferromagnetic, ferroelastic, or even orbital and charge orderings can develop and eventually coexist. These orderings can be tuned by external electric, magnetic, or stress field, and the cross-couplings between them enable important multifunctional properties, such as piezoelectricity, magneto-electricity, or magneto-elasticity. Here, will present the effect of thickness on PrVO₃ thin films where a "dead layer" is found, and I will particularly focus on the change on the structural and magnetic properties with different substrates.

Financial support from ANR and Region Normandie (INCOX project) are acknowledged.

11:45 AM EQ02.05.05

Creating 2D Metal-Based Heterostructures—The Story of Epitaxial Graphene Nanoparticles Timothy Bowen, Alexander Vera, Maxwell Wetherington, Shalini Kumari and Joshua A. Robinson; The Pennsylvania State University, United States

It is possible to synthesize two-dimensional (2D), atomically thin metals using confinement heteroepitaxy (CHet), in which plasma treated epitaxial graphene (EG) is intercalated by a metal precursor such as Ga or In at near-atmospheric conditions. The resultant quasi-freestanding epitaxial graphene (QFEG)/2D metal heterostructure ideally provides a high-quality graphene substrate, enabling the scalable synthesis of vertical heterostructures with additional 2D materials, such as MoS₂, which are expected to exhibit extraordinary optical and sensing properties. However, this is limited by the surface

quality of the QFEG which directly impacts the adlayer nucleation, grain size, and performance.

We demonstrate that the traditional route of CHet leads to particulates on the surface following metal intercalation that can heavily impact the ability to create heterostructures with TMDs or TI adlayers. Through the growth of monolayer EG with small regions of buffer layer (BL), we show that intercalation occurs through the BL regions while maintaining high surface quality QFEG with pristine 2D metal underneath. Through use of atomic force microscopy (AFM), Raman, and x-ray photoelectron spectroscopy (XPS), we demonstrate that the 2D metal forms over the entire surface, leaving behind an atomically smooth graphene surface for subsequent growth of high quality 2D materials on these heterostructures.

SESSION EQ02.06: Physics and Devices of Mixed Dimensional Heterostructures III

Session Chairs: Jiwoong Park and Jian Shi

Wednesday Afternoon, December 1, 2021

Hynes, Level 2, Room 200

1:30 PM *EQ02.06.01

New 2D with Atomically Thin Crystals [Jiwoong Park](#); University of Chicago, United States

Two dimensional (2D) electron transport has been one of the most important topics in science and technology for decades. It was originally studied in 3D semiconductors and then continued in 2D van der Waals (vdW) crystals. In this talk, I will start with the large-scale processes for generating 2D crystalline semiconductor films and superlattices that could be used to fabricate atomically thin integrated circuits. Then we will discuss more recent directions, where we use these 2D materials to realize non-electronic 2D transport phenomena, for example, observed from phonons, photons, and mass. These new approaches could empower the development of 2D phononics, 2D photonics, and 2D mechanics.

2:00 PM EQ02.06.03

Nanoscale TERS Characterization of the Junction Boundary in MoS₂-WS₂ Heteromonolayer Crystals Sourav Garg¹, [Andrey Kravets](#)², J. Pierce Fix³, Connor Flanery³, Audrey Sulkanen⁴, Minyuan Wang⁴, Gang-Yu Liu⁴, Nicholas Borys³ and Patrick Kung¹; ¹The University of Alabama, United States; ²Horiba Scientific, United States; ³Montana State University, United States; ⁴University of California, Davis, United States

We report the nanoscale characterization of the heterojunction in MoS₂-WS₂ hetero-monolayers by means of Tip Enhanced Raman Scattering (TERS). We demonstrate that a red-shifted PL in WS₂ adjacent to the MoS₂ core, observed in as-grown samples on sapphire substrates with confocal Raman/PL microscopy, is associated with a heterojunction boundary that shows significant alloying and a varying width from about 25 nm (pixel size limited) to few hundreds of nanometers even within the same crystal. In TERS spectra collected with resonant 638 nm excitation, we observed significant increase in the intensity of the 200 cm⁻¹ and 215 cm⁻¹ peaks over the heterojunction boundary as well as a shift of the 433 cm⁻¹ peak in the WS₂ shell to 444 cm⁻¹. TERS signal of the same area collected with 785 nm laser showed no significant peaks in the 140-240 cm⁻¹ range, while the 444 cm⁻¹ peak was preserved, being slightly shifted to 442 cm⁻¹. The spectral position of this latter Raman peak as well as the presence of the resonant peaks in 140-240 cm⁻¹ range proved to be related to the degree of alloying in Mo_xW_(1-x)S₂ compounds. Based on the specifics of the gap-mode TERS response, we discuss the in-plane vs. out-of-plane nature of the composition-specific Raman peaks. TERS imaging proved to be a valuable characterization technique enabling cross-correlation of the nanoscale structural composition of 2D heterostructures with useful observables like the surface potential, topography and other physical properties probed by scanning probe microscopy.

2:15 PM EQ02.06.04

High-Responsivity and Fast Response MoS₂/Ge van der Waals Heterojunction Broadband Phototransistor [Youngseo Park](#)¹, Aujin Hwang¹, Yeongseok Shim¹, Geonwook Yoo² and Junseok Heo¹; ¹Ajou University, Korea (the Republic of); ²Soongsil University, Korea (the Republic of)

Broadband photodetection and imaging have been of significant interest because different information is obtained depending on the wavelength. Especially, short-wave infrared (SWIR) has definite advantages such as a high visibility in adverse weathers and at night. Moreover, compared to mid- or far-wave infrared for thermal imaging, SWIR allows a lower dark current at room temperature due to a larger photon energy. On the other hand, visible light (VIS) provides color information, which can utilize identifying of traffic lights. Therefore, demand for broadband photodetection ranging from VIS to SWIR is increasing in many further applications, including autonomous vehicles. For broadband detection, photodetector of various structures has been proposed such as photodiode and field-effect phototransistor. Photodiode such as MoS₂/BP heterojunction shows high photoresponse without photocurrent gain, whereas field-effect phototransistor such as Si QDs/graphene FET shows high responsivity with slow photoresponse speed due to trapping photogenerated carriers.

In this paper, we have proposed and investigated n-MoS₂/p-Ge/n-Ge van der Waals heterojunction phototransistor for broadband photodetection with photocurrent gain and fast photoresponse speed. Transition metal dichalcogenides (TMDs) can easily form van der Waals heterojunction (vdWH) despite lattice mismatch. To achieve broadband detection, heterostructure was composed of large-bandgap MoS₂ and small-bandgap Ge. Moreover, n-MoS₂/p-Ge/n-Ge phototransistor forms high potential barrier in the conduction band of heterojunction, which blocks the transport of the electrons from n-MoS₂ to n-Ge. With illumination, photogenerated holes are accumulated in p-Ge, which lower potential barrier in the conduction band and thus a large number of electrons pass through the heterojunction. Hence, this device exhibits high photocurrent in spite of weak illumination. Photoresponse characteristics of fabricated MoS₂/Ge vdWH phototransistor were measured with floating base. In I_C - V_{CE} curves under VIS (466 nm) and SWIR (1550 nm) illuminations of 10 mW/cm², broadband photodetection was clearly observed, caused by VIS detection in large-bandgap MoS₂ and SWIR detection of small-bandgap Ge. From measured results, responsivity (R), external quantum efficiency (EQE), and detectivity (D^*) were calculated. As V_{CE} increases, R and EQE linearly increase regardless of the wavelength because higher V_{CE} lower potential barrier in heterojunction. Under VIS (SWIR) illumination, R and EQE are the maximum measured values of ~ 7.4 (~ 4.7) A/W and ~ 1969 (~ 376) % at $V_{CE} = 4$ V, respectively. MoS₂/Ge vdWH phototransistor shows high photocurrent gain regardless of wavelength because photogenerated holes are accumulated in base and then potential barrier is lowered. Despite higher R with increasing V_{CE} , D^* is constant with value of $\sim 4 \times 10^7$ ($\sim 2 \times 10^7$) Jones at 466 (1550) nm illumination due to high noise caused by the high dark current.

Transient characteristics were measured under VIS and SWIR laser modulations with frequency of 20 Hz. From these results, rise times (t_{rise}) and fall times (t_{fall}) were extracted and shown fast response speed with 202.3 (88.1) μ s and 214.9 (232.8) μ s of t_{rise} (t_{fall}), respectively. This results show that the fabricated device has a fast enough photoresponse speed to be used as VIS/SWIR broadband image sensor.

Demand of VIS/SWIR broadband image sensors is increasing, which require photocurrent gain and fast photoresponse speed. In this work, we propose and fabricate n-MoS₂/p-Ge/n-Ge vdWH phototransistor. The proposed device absorbs VIS in MoS₂ with large bandgap and SWIR in Ge with small bandgap, enabling broadband photodetection. Moreover, vdWH phototransistor not only have photocurrent gain, but also have fast photoresponse speed at the same

time. We will confirm the possibility with the broadband image sensor with additional imaging measurements later.

SESSION EQ02.07: Large-Scale 2D Materials and Ultra-Thin 3D Membranes I

Session Chairs: Hyunseok Kim and Kyusang Lee

Wednesday Afternoon, December 1, 2021

Hynes, Level 2, Room 200

4:00 PM EQ02.07.01

Robotic Four-Dimensional Pixel Assembly of van der Waals Solids Andrew Ye¹, Andrew Mannix², Suk Hyun Sung³, Ariana Ray⁴, Fauzia Mujid¹, Chibeom Park¹, Myungjae Lee¹, Jong-Hoon Kang¹, David A. Muller⁴, Robert Hovden³ and Jiwoong Park¹; ¹University of Chicago, United States; ²Stanford University, United States; ³University of Michigan–Ann Arbor, United States; ⁴Cornell University, United States

Van der Waals (vdW) solids can be engineered with atomically-precise vertical composition through the assembly of layered 2D materials (2DMs). To date, most structures that have been constructed to study their interesting phenomena have been produced using an artisanal method of assembling micromechanically-exfoliated flakes. However, further engineering and application of vdW solids requires a scalable and rapid production method to precisely design and control composition and structure over all three spatial dimensions (x , y , z) and interlayer rotation (θ). Here, we demonstrate such an approach, *Robotic 4D Pixel Assembly*, for rapidly manufacturing designer vdW solids with unprecedented speed, area, patternability, and angle control. We utilize the robotic assembly of prepatterned pixels made from atomically-thin 2DM components. Wafer-scale 2DM films are grown, patterned through a clean, contact-free process, and assembled together with engineered adhesive stamps actuated by a high vacuum robot. Our technique led to the fabrication of vdW solids of up to 80 individual layers, consisting of $100\ \mu\text{m}^2$ to $1\ \text{mm}^2$ areas with pre-designed patterned shapes, laterally/vertically programmed composition, and controlled interlayer angle. This enables us to create efficient optical spectroscopy assays of vdW solids, where we can study the layer dependent evolution of optical properties. Furthermore, our approach allows for the fabrication of twisted N -layer assemblies, where we observe atomic reconstruction of twisted 4-layer WS_2 at unexpectedly high interlayer twist angles of $\geq 4^\circ$. Our vdW solids manufacturing enables rapid construction of atomically-resolved quantum materials and will help realize the full potential of vdW heterostructures as a platform for novel physics and advanced electronic technologies.

4:15 PM EQ02.07.02

Facile Chemical Route for Freestanding Complex Oxides—From the Preparation of $\text{Sr}_3\text{Al}_2\text{O}_6$ Sacrificial Layer to the Final Oxide Properties Pol Sallés Perramon¹, Ivan Caño¹, Roger Guzman², Wu Zhou², Florencio Sánchez¹ and Mariona Coll¹; ¹ICMAB-CSIC, Spain; ²University of Chinese Academy of Sciences, China

Complex oxides are of great interest for their rich variety of chemical and physical properties including magnetism, ferroelectricity, multiferroicity, catalytic behavior and superconductivity. Up to date, the preparation of crystalline complex oxide thin films has been mainly limited on substrates that can stand high temperature thermal treatments and on single crystal substrates when epitaxial growth is pursued.

These requirements dramatically limit their applicability excluding the possibility to prepare many artificial multilayered architectures to investigate emergent phenomena that arise in thin films and at their interfaces, as well as fabrication of flexible devices.

In the last few years, it has been proved successful the use of water-soluble $\text{Sr}_3\text{Al}_2\text{O}_6$ (SAO) as sacrificial layer to detach perovskite complex oxides from the growing substrate and freely manipulate them. In these cases, *in-situ* and high vacuum physical deposition techniques such as Pulsed Layer Deposition (PLD) and Molecular Beam Epitaxy (MBE) have been used.

Herein, our goal is to achieve this SAO sacrificial layer for freestanding complex oxides through the use of cost-effective chemical deposition techniques with atomic precision such as Chemical Solution Deposition (CSD) and Atomic Layer Deposition (ALD).

First, we have developed a solution-based procedure to prepare high quality textured SAO films. The relation between precursor chemistry, thermal decomposition and epitaxial growth has been thoroughly investigated by means of X-Ray Diffraction, Atomic Force Microscopy and Transmission Electron Microscopy, between others. [1]

Then, we have investigated the viability of SAO to transfer a wide variety of oxide membranes ranging from binary oxides to ternary oxides (ferrites, manganites). These oxides have been deposited on SAO by different deposition techniques (CSD, ALD and PLD), and the effect of these deposition techniques on the oxide membrane quality has been compared. The influence of air exposure on SAO degradation to subsequently transfer epitaxy has been carefully studied by means of Reflection High-Energy Electron Diffraction (RHEED) and identified an effective approach to overcome it. Finally, we studied the transfer of oxide membranes to several flexible and rigid supports (PET, PDMS, silicon wafer, ...). As a case example, we have studied the fabrication of CoFe_2O_4 membranes. The changes in epitaxy and magnetic properties throughout the transfer process are monitored by means of XRD and SQUID magnetometry obtaining crystalline and magnetic CoFe_2O_4 membranes. [2]

In short, this work introduces a chemical-based route to prepare freestanding complex oxides tackling the challenges related to this procedure. These results prove that chemical deposition could become an alternative to high vacuum physical deposition techniques, providing simplicity and cost saving to the process, and therefore making the freestanding complex oxides a step closer to large-scale production.

[1] P. Sallés, M. Coll *et al.*, *Adv Mater Interfaces*, **2021**, 8, 2001643,

[2] P. Sallés, F. Sánchez, M. Coll *et al.*, in preparation.

4:30 PM EQ02.07.03

Diffusion-Driven Mechanical Exfoliation of Rare-Earth Iron Garnet Nanosheets Karthik Srinivasan, Andrew Schwarz, Jason C. Myers, Nicholas C. Seaton and Bethanie J. Stadler; University of Minnesota, United States

Rare-earth iron garnet thin films have advanced the development of on-chip non-reciprocal photonic and prototype spintronic devices due to their large Faraday rotations and spin diffusion lengths, respectively. However, non-epitaxial garnets deposited using pulsed laser deposition (PLD) or sputtering require an annealing temperature of 800°C or greater, and epitaxial garnet films are limited to lattice-matched substrates that are not foundry compatible. Here, a modified rapid thermal annealing process enabled mechanical exfoliation of high-gyrotropy cerium-doped terbium iron garnet ($\text{Ce}_{0.25}\text{Tb}_{2.75}\text{Fe}_{4.75}\text{O}_{12}$) from a silicon substrate without the need for an intermediary graphene layer, such as used in remote-epitaxy. Exfoliation is enabled by vacancy diffusion that followed a Nabarro-Herring model where strain was varied using different thicknesses for the garnet films. An increase in the tension between the film and the substrate resulted in a diffusion of vacancies away from the substrate. The diffusivities calculated by fitting the model to the strain rate-stress data identify iron and terbium as the rate-determining lattice diffusants. Furthermore, cross-section energy dispersive X-ray

spectroscopy shows an accumulation of cations to form an amorphous Fe-Tb-Si-O interlayer at the substrate, leaving behind vacancies that create an exfoliation plane ~30nm into the film. This distance is comparable to the cation diffusion length, verifying the model. Magnetic and optical measurements from the exfoliated nanosheets reveal a saturation magnetization of 18 emu cc⁻¹ and a Faraday rotation of -2900°cm⁻¹ at 1550 nm, both of which are comparable to bulk values. Exfoliation through controlled creep-diffusion will open non-traditional pathways for incorporating garnets with other crystalline wafer platforms and protect devices from the high-temperature processes often used in crystallizing garnet films.

4:45 PM EQ02.07.05

Epitaxial Crystallization of Amorphous Complex Oxides in Complex Geometries Rui Liu¹, Peng Zuo¹, Samuel Marks¹, Peiyu Quan¹, Donald Savage¹, Hua Zhou², Susan Babcock¹ and Paul Evans¹; ¹University of Wisconsin–Madison, United States; ²Argonne National Laboratory, United States

Crystallization from an amorphous precursor via solid phase epitaxy (SPE) enables a wide range of opportunities in the formation of oxide materials in new geometries. The use of low deposition temperatures to form the amorphous precursor reduces diffusion and phase separation during deposition and thus allows the formation of chemically and structurally uniform starting materials. Kinetic phenomena arising during crystallization of oxide materials in the form of 3D nanostructures via SPE pose challenging synthesis and characterization problems. A key challenge is to achieve nanoscale control of epitaxial crystallization. Selecting the locations of the initial step of crystallization and simultaneously maintaining a low rate of nucleation away from epitaxial interfaces are particularly important. In order to probe the propagation of the crystallization transformation, the location of crystallization sites in a study of SrTiO₃ (STO) SPE were set by forming micron-scale Si₃N₄ (SN) features on SrTiO₃ 001 single-crystal substrates using optical lithography. Amorphous STO was deposited on the patterned substrates at room temperature using radio-frequency sputtering and crystallized by heating to temperatures at which crystallization occurred from seeds while the rate of homogeneous nucleation remained low. A further challenge is to understand the microscopic mechanism that leads to crystallization at amorphous/crystal interface in nanoscale complex geometries. An *in situ* synchrotron hard x-ray nanodiffraction instrument at the Advanced Photon Source enabled this process to be studied using nanobeam diffraction and reflectivity probes during amorphous deposition and epitaxial crystallization. The results indicated that amorphous STO selectively crystallized on STO seed and laterally crystallized over the SN patterns before encountering separately nucleated crystals. Three-dimensional SPE of STO provides opportunities to create a wide range of other perovskite oxides in nanoscale geometries. The results will be discussed in terms of the competition between crystal/amorphous interface motion and homogeneous nucleation, the stress-induced from the density difference between the amorphous and the crystalline films, and the consequences of small deviations from the desired STO stoichiometry.

5:00 PM EQ02.07.06

Strain-Induced Lateral Heterostructures in Patterned Semiconductor Nanomembranes Mapped by X-Ray Nano-Diffraction Imaging Abdullah Gok¹, Xiaowei Wang¹, Shelley Scott², Abhishek Bhat², Hanfei Yan³, Ajith Pattammattel³, Evgeny Nazaretski³, Yong S. Chu³, Zicong Huang⁴, Richard M. Osgood Jr.⁴, Max G. Lagally² and Roberto Paiella¹; ¹Boston University, United States; ²University of Wisconsin–Madison, United States; ³Brookhaven National Laboratory, United States; ⁴Columbia University, United States

Semiconductor heterostructures have been used extensively in the development of electronic and optoelectronic devices such as transistors, lasers, LEDs, and photodetectors. Traditionally, these composite materials are synthesized by heteroepitaxy, where films of different compositions are grown on top of one another through various atomic deposition techniques. This approach is well established in micro and optoelectronics, where it provides a powerful tool to shape the energy band profile in order to promote and enhance desired device functionalities.

Here we report a new method, based on strain engineering, for the controlled introduction of variations in bandgap energy with lateral position in thin films. External stress is applied on a semiconductor nanomembrane stacked with an array of dielectric pillars, in order to create a non-uniform strain distribution commensurate with the sample thickness variations (with the largest strain accumulating in the thinnest regions between the pillars and vice versa). In typical group-IV and III-V semiconductors, in-plane biaxial tensile strain has the effect of decreasing the fundamental energy bandgap, while at the same time lifting the degeneracy of the heavy-hole and light-hole valence-band maxima. The end result is therefore a controlled bandgap modulation – i.e., the formation of a sample that effectively behaves like a lateral (in-plane) heterostructure, but consisting of a single semiconductor material with uniform chemical composition.

Specifically, we employ 90-nm-thick Ge nanomembranes coated with a square-periodic array of cylindrical amorphous-Si pillars having micron-scale lateral dimensions and 300-nm height. The nanomembranes are transferred and bonded on a flexible film of polyimide, which is then mounted on a gas pressure cell that allows introducing biaxial tensile strain in the Ge crystal in a highly controllable fashion. The resulting strain profiles are mapped using Bragg diffraction with a hard x-ray probe featuring nanoscale spatial resolution. A clear lateral strain modulation is observed in the measurements, with the strain going through a well-defined minimum at the location of each amorphous-Si pillar. The strain difference between coated and uncoated nanomembrane regions is also found to increase with increasing gas pressure, in agreement with finite-element simulations. The measured strain maps are finally used to compute the Ge-nanomembrane energy band lineup, showing the formation of pronounced energy barriers in both conduction and valence bands.

Compared with traditional heterostructures grown by epitaxial techniques, these strain-engineered samples are not limited in the choice of compatible materials by any restriction imposed by lattice-matching requirements. Furthermore, their energy band lineups can be patterned in nearly arbitrary shapes using nanolithography to control the thickness profile, and can be tuned actively by varying the applied stress. As a result, these structures are attractive for a wide range of device applications (including lasers, LEDs, solar cells, and thermoelectrics) that require complex heterostructure lineups with multiple bandgap energies.

SESSION EQ02.08: Nanostructures of Low Dimensional Materials I

Session Chairs: Hyesung Park and Mona Zebbarjadi

Thursday Morning, December 2, 2021

Hynes, Level 2, Room 200

10:30 AM EQ02.08.01

Nanofabrication Through Molding Enables a Versatile Toolbox Naijia Liu and Jan Schroers; Yale University, United States

The fast development of nanotechnologies in the past decades desires various nanomaterials that span wide ranges of sizes, geometry, materials choice, crystal structures, and elemental distributions. However, the availability of these nanomaterials is usually leashed by the ability of specific nanofabrication methods in at least one of these aspects.

First applied for polymers and BMGs, nanomolding refers to a top-down fabrication method by which a formable or moldable material is shaped using a

mold of nanoscale dimensions. Recently, thermomechanical nanomolding (TMNM) has been developed for general crystalline materials, indicating potentially a very versatile method for large scale nanofabrication.

In this work, with carefully designed scaling experiments, we revealed the principle behind TMNM to be a diffusional atomic transport that happens at the very interface between material and mold. By controlling processing temperature and length scale, we are able to tune TMNM between this interface-diffusion principle and a dislocation-slip dominated regime. Such a transiting mechanism results in a highly versatile toolbox, enabling fully controlled nanofabrication over sizes, geometry, materials choice, and crystal structures. Specifically, the element dependence of diffusivity allows controlled growth down to single elements/components of the feedstock, indicating controllable elemental distributions. And by utilizing TMNM, we have successfully demonstrated the fabrication of heterostructure nanowires with fully controlled elemental layer sequences.

We will discuss the transiting mechanism behind TMNM and the versatile toolbox by utilizing this mechanism including controlled fabrication of heterostructures. The possibility of forming new phases through kinetical control of elements in TMNM will also be discussed.

10:45 AM EQ02.08.02

Perpendicularly Standing Two-Dimensional Fused Aromatic Network Structure Seok-Jin Kim^{1,1}, Tea-Hoon Kim², Ishfaq Ahmad³, Hyuk-Jun Noh³, Sun-Min Jung³, Yoon-Kwang Im³, Javeed Mahmood³, Youn-Sang Bae² and Jong-Beom Baek³; ¹King Abdullah University of Science and Technology, Saudi Arabia; ²Yonsei University, Korea (the Republic of); ³Ulsan National Institute of Science and Technology, Korea (the Republic of)

Two-dimensional (2D) fused aromatic networks (FANs) have a planar structure, in which flat building blocks are horizontally connected to form optimized, layered π - π stacking. Three-dimensional (3D) FAN structures, in which building blocks are divergently linked in the space, provide the maximum accessible internal surface area with permanent porosity. As sorbent materials, the confined layered stacking pattern of FANs restricts segmental motion, and the available surface area is partially blocked by adjacent layers, resulting in weak uptake capacity and kinetics. To understand the relationship between structure and performance, here, a new type of pyrazine-linked FAN structure, with vertically standing building blocks connected along the 2D direction, was designed and synthesized to minimize layer-to-layer interactions and to maximize segmental freedom. In comparison studies with flat 2D and porous 3D FANs, the vertically standing FAN (V2D-Pz) displayed intermediate performance for gas storage and separation. For example, the results for the adsorption and separation of CH_4/N_2 fell in between those of the flat 2D and porous 3D FANs. However, the standing V2D-Pz had a more structurally accessible adsorption area and higher segmental freedom, and it exhibited the highest iodine uptake capacity ($\sim 4.2 \text{ g g}^{-1}$) and capture rate ($1.51 \text{ mmol g}^{-1} \text{ h}^{-1}$).

11:00 AM EQ02.08.03

Bulk Grain-Boundary Materials from Nanocrystals Yasutaka Nagaoka and Ou Chen; Brown University, United States

Grain-boundary engineering is essential to unleash the potential of materials. While a number of methods have been used to tune up grain-boundary conditions such as hammering, plasma-assisted sintering, deposition, etc, it still remains challenging to achieve precise grain boundary engineering at the nanoscale because these methods rely almost exclusively on top-down approaches. Meanwhile, recent theoretical studies have made a striking advance in the understanding of structure-properties relationships over nanoscale grain-boundary conditions and novel materials' design strategies, thus, a methodology to make a tailored grain-boundary condition in real experiments is wanted for experimental demonstration. Herein, we introduce a new grain-boundary engineering method, "the nanocrystal coining method". With this method, various grain-boundary factors such as grain-boundary shape and size are readily tuned at least one-nanometer precision. The produced materials possess a centimeter-scale size and freestanding nature, which is ideal for many applications. Other advantages include a wide range of available components and no restriction of substrates. In this presentation, we will discuss the nanocrystal coining method in the greater details

The nanocrystal coining method uses chemically synthesized colloidal metal nanocrystals as the starting materials. We treated the nanocrystals using a surface treatment, thorough washing and drying process, and a pressure process with a piston-cylinder pressure die. The resulting materials (which we call "nanocrystal coins") showed several strikingly improved properties owing to the nanoscale grain-boundary condition and the high material density. The nanocrystal coins successfully emerged metallic properties in the appearance and conductivity while the crystal domains of the original nanocrystal building blocks remained unchanged. In addition, nanoindentation measurements confirmed the superior mechanical hardness of the nanocrystal coins due to the Hall-Petch effect. Taking further advantage of this method, we created the first example of a single-component bulk metallic glass from amorphous palladium nanoparticles. The MD simulation supported the mechanisms of the nanocrystal coining method including preservation of grain-boundary condition, low-pressure sintering, and densification under pressure. Our methods will help researchers to finely iterate structure-properties relationships whose functionality crucially depends on the crystal-domain configuration, such as superhard materials, thermoelectric generators, and functional electrodes.

11:15 AM EQ02.08.04

Generation of 3D-Heterostructures by Mechanochemical Disassembly and Re-ordering of Metal Chalcogenides Viktor Balema¹, Ihor Z. Hlova¹, Prashant Singh¹, Oleksandr Dolotko^{1,2}, Serhiy Z. Malynych³, Scott L. Carnahan⁴, Arjun K. Pathak⁵, Duane D. Johnson¹, Aaron J. Rossini^{1,4} and Roman V. Gamernyk⁶; ¹Ames Laboratory of US DOE, United States; ²Karlsruher Institut für Technologie, Germany; ³Hetman Petro Sahaidachnyi National Army Academy, Ukraine; ⁴Iowa State University of Science and Technology, United States; ⁵SUNY, Buffalo State, NY, United States; ⁶Ivan Franko National University of Lviv, Ukraine

Three-dimensional (3D) heterostructures with incommensurate arrangements of well-defined building blocks are created using an unconventional synthetic approach comprising of mechanically facilitated disassembly and reordering of layered transition-metal dichalcogenides, MX_2 [1,2], and non-layered rare-earth metal monochalcogenides, REX [2], where $\text{M} = \text{Ta}$ or Nb , $\text{RE} = \text{Sm}$ or La , and $\text{X} = \text{S}$ or Se . The discovered solid-state processes are driven by mechanochemical transformations directed by quantum interaction between chemically and structurally dissimilar solids toward atomic-scale ordering.

Remarkably, in the case of a pair of layered MoS_2 and HfS_2 compounds [1], the experimentally observed 3D-heterostructuring is energetically favorable over the formation of homogeneous multi-principle element dichalcogenides that had been observed in related dichalcogenide systems including MoS_2 , WS_2 , and TaS_2 materials [3].

Density-functional theory calculations reveal critical details about charge transfer between structural elements of the explored heterostructures and validate experimental results. High-temperature annealing improves crystallinity of 3D-heterostructures without altering their internal atomic arrangements, which resembles respective behaviors of molecular solids and polymers.

Powder X-ray diffraction, scanning transmission electron microscopy, ⁷⁷Se solid-state nuclear magnetic resonance, optical spectroscopy and electronic transport measurements unambiguously confirm the course of mechanochemical reactions and the identities of the created materials. The resulting 3D-heterostructures show broad range of electron transport behaviors varying from metallic conductivity to indirect band gap semiconductivity.

Results of this joint experimental and theoretical study open new avenues for generating unexplored metal-dichalcogenide heteroassemblies with incommensurate structures and tunable physical properties.

References:

- I. Z. Hlova et al. *Nanoscale Adv.* (2021), Ahead of Print.
O. Dolotko et al. *Nat. Commun.* (2020), 11(1), 3005
I. Z. Hlova et al. *Chem. Commun.* (2018), 54(89), 12574

11:30 AM EQ02.08.05

Color Tuning of Electrochromic TiO₂ Nanofibrous Layers with Embedded Metal and Metal Oxide Nanoparticle for Smart Colored Windows Cavit Eyogge, Arturo Susarrey Arce and Han Gardeniers; University of Twente, Netherlands

Co-axial electrospinning was applied for the structuring of non-woven webs of TiO₂ nanofibers loaded with Ag, Au, and CuO nanoparticles (NPs). The composite layers were tested in an electrochromic half-cell assembly. A clear correlation between NP composition and electrochromic effect in the nanofibrous composite is observed: TiO₂ loaded with Ag reveals a black/brown color, Au shows a dark blue color, and CuO a dark green color. For electrochromic applications, the Au/TiO₂ layer is the most promising choice, with a remarkable color modulation time of 6 s, transmittance modulation of 40%, coloration efficiency of 20 cm²/C and an areal capacitance of 300 F/cm², and cyclic stability of over 1000 cycles. Electrochemical impedance spectra of the best performing sample, Au/TiO₂ fibers, was also analysed to understand the effects of additive NPs within the fibrous network. In this study, we offer an unexplored path for the rational design of TiO₂-based nanofibrous layers with unprecedented color switching and optical efficiency gained by the fibrous layer. We foresee co-axial electrospinning as an alternative nanofabrication technique applied in smart colored windows.

11:45 AM EQ02.08.06

Two-Dimensional Xene Heterostructures on Ag(111) by Molecular Beam Epitaxy Daya Sagar Dhungana¹, Carlo Grazianetti¹, Christian Martella¹, Simona Achilli², Guido Fratesi² and Alessandro Molle¹; ¹CNR-IMM Agrate Brianza Unit, Italy; ²Università degli Studi di Milano, Italy

The past decade witnessed several developments on 2D graphene analogs, also known as Xenenes, and several milestones have been achieved on material synthesis and their application prototypes¹. If the synthesis of new Xenenes and their application prototypes are widely studied, piling up one Xene layer over another Xene layer to realize a Xene heterostructure to the date remains a challenging issue owing to interlayer mismatch, intermixing, etc.. Indeed, even if two different Xenenes can be grown on the same substrate, composing heterostructure and superlattice geometry has remained quite puzzling. Making Xene heterostructure in this framework therefore will provide substantial technological throughputs for various applications, for instance nanoelectronics, optoelectronics, plasmonic and energy.

In this work, we first introduce the Xene heterostructure² concept and present two heterostructures based on two well-established configurations: silicene-on-Ag(111)³ and stanene-on-Ag(111)⁴. We will further demonstrate Xene superlattices taking advantage of underneath Xene layer as a suitable template for another reciprocal Xene layer. Furthermore, the insights into co-deposition techniques where our results show it is possible to achieve both the heterostructure sequence by engineering the growth kinetics will be discussed in detail with various *in situ* and *ex situ* probes. Moving beyond monolayer silicene-stanene configuration, we will also present layer-by-layer growth of multilayer 4x4 Silicene on the same reciprocal stanene-on-Ag(111) template. In the end, Density Functional Theory calculations were carried out taking experimental data as starting input models in order to have deeper insights into structural stability and electronic structure.

The work is performed within the ERC-COG 2017 Grant No. 772261 "XFab".

- [1] L. Tao, E. Cinquanta, D. Chiappe, C. Grazianetti, M. Fanciulli, M. Dubey, A. Molle, D. Akinwande, *Nat. Nanotechnol.* **2015**, *10*, 227.
[2] D. S. Dhungana, C. Grazianetti, C. Martella, S. Achilli, G. Fratesi, A. Molle, *Adv. Funct. Mater.* **2021**, 2102797.
<https://doi.org/10.1002/adfm.202102797>
[3] P. Vogt, P. De Padova, C. Quaresima, J. Avila, E. Frantzeskakis, M. C. Asensio, A. Resta, B. Ealet, G. Le Lay, *Phys. Rev. Lett.* **2012**, *108*, 155501.
[4] J. Yuhara, Y. Fujii, K. Nishino, N. Isobe, M. Nakatake, L. Xian, A. Rubio, G. Le Lay, *2D Mater.* **2018**, *5*, 025002.

12:00 PM EQ02.08.07

Nanorafts—Clay Nanosheets Decorated with Magnetic Nanoparticles Paulo H. Michels Brito¹, Barbara Pacakova¹, Leander Michels¹, Ville Liljestrom¹, Sergio Toma², Daniel Wagner³, Kenneth Knudsen⁴, Koiti Araki², Josef Breu³ and Jon O. Fossum¹; ¹Norwegian University of Science and Technology, Norway; ²University of São Paulo, Brazil; ³Universität Bayreuth, Germany; ⁴Institute for Energy Technology – IFE, Norway

Emerging field of 2D materials shifts nowadays towards preparation of metamaterials, combining efficiently functionality of 2D layers themselves with additional components such as nanocrystals, forming together multifunctional 2D material with complex properties². It has been shown that combination of 2D sheets with nanoparticles does not bring together just individual properties of both components³, but also affect behaviour of 2D sheets themselves⁴. Functionalized 2D nanosheets can serve as basic building blocks for fabrication of larger structures targeting metamaterial with desired properties, for example via self-assembly, hence implementation of additional functionality directly into the 2D nanosheets is of high importance.

We present here an efficient approach of decorating 2D nanosheets in liquid phase with magnetic nanoparticles, based on functionalized iron oxide nanoparticles and high-aspect ratio sheets of insulating transparent synthetic clay, sodium fluorohectorite. Efficiency of the process is confirmed by several complementary characterization methods, including TGA, X-ray diffraction (SAXS/WAXS), spectroscopy (FTIR, UV-VIS). Particle layout on nanosheets is determined by microscopy techniques (SEM and AFM). Options of tuning particle density on nanosheets and particle geometrical arrangement in a view of possible applications will be discussed.

1. *Chem Rev.* 2015, 115(7): 2483–2531.
2. *Chem. Rev.* 2017, 117 (9): 6225–6331.
3. *Nano Lett.* 2012, 12(2): 617–621.
4. *Progress in Materials Science* 2017, 90: 75–127.

SESSION EQ02.09: Heterostructures of Various Dimensional Materials

Session Chairs: Jong-Hyun Ahn and Jian Shi

Thursday Afternoon, December 2, 2021

Hynes, Level 2, Room 200

1:45 PM *EQ02.09.01

Monolithic integration of MoS₂ with III-V Compound Semiconductors for Micro-LED Display Applications Jong-Hyun Ahn; Yonsei University, Korea (the Republic of)

Heterogeneous integration of transition-metal chalcogenides on III-V compound semiconductors provides development opportunities for a variety of new optoelectronic devices. In this talk, we present a novel method for heterogeneous integration of MoS₂ on III-V compound semiconductors. A thin film of MoS₂ was directly synthesized on a GaN-based epitaxial wafer through the MOCVD technique and fabricated as the TFT array. Subsequently, the MoS₂ TFT was monolithically integrated with micro-LED devices to produce an active matrix micro-LED display. This strategy represents a promising route to attain heterogeneous integration, which is essential for high-performance optoelectronic systems that can incorporate the established semiconductor technology and emerging 2D materials.

2:15 PM EQ02.09.02

Hydrogen Doping as a Method to Create Novel 2D-3D Metal-Oxide Heterostructures and Gradient Electronic Phases Qi Wang, Zhen Zhang and Shiram Ramanathan; Purdue University, United States

Perovskite nickelates undergo room temperature colossal electronic phase transitions which could modulate the electronic conductivity up to 8-10 orders of magnitude by hydrogen doping. This creates an unprecedented opportunity to fabricate 2D localization of electronic phases by atomic scale displacement of hydrogen in the lattice. One way to accomplish this is by locally storing hydrogen in metal gates such as palladium (Pd) that can be injected into the near surface perovskite lattice by an external electric field. Here we developed an asymmetric two-terminal device fabricated using SmNiO₃ (SNO) thin film which forms multiple heterostructures within each device. The two-terminal device, with one electrode comprising Pd and the other electrode gold (Au), enables a gradient in hydrogen doping which allows to create arbitrary electronic phases. We will describe the band structure physics of such novel electronic heterostructures that can form 2D electron puddles which can subsequently be distributed spatially by electric fields. The current-voltage characteristics show remarkable transitions in mechanisms depending on the local distribution of hydrogen proximal to the electrodes. We will discuss the response of such 2D-3D heterostructures to electric stimuli and the use in emerging neuromorphic computing architectures.

2:30 PM EQ02.09.04

Late News: Bias-Modulated UV and NIR Colour Discrimination Using MoS₂/ZnO (2D/3D) Heterostructure Based Photodetector Device Kishan L. Kumawat, Pius Augustine, Deependra Kumar Singh, K K Nanda and Krupanidhi S B; Indian institute of Science Bengaluru, India

Despite significant progress in the spectral discrimination properties of photodetectors (PDs), most of the conventional technologies use optical filters which results in expensive circuitry as well as high incident energy loss. 2D/3D integration of an MoS₂/ZnO heterostructure-based PD has been demonstrated which exhibits a bias-dependent switchable spectral response, in a manner different from the traditional PDs. Low band gap MoS₂ thin film has been vertically stacked on top of a high band gap ZnO film that allows selective charge transport from each layer by modulating the applied bias, resulting in a fine discrimination between ultraviolet (UV) and near infrared (NIR) light. Under lower applied bias, a dominant photoresponse in the UV region by the ZnO film is observed, whereas an enhanced response in the NIR region is obtained at higher bias which is attributed to the generation of charge carriers in the MoS₂ film. The device predominantly exhibits UV photoresponse at 1.0 V with responsivity of 4.56 AW⁻¹ (400 nm) and that in the NIR region at 8.0 V with responsivity of 6.04 x 10³ AW⁻¹ (900 nm). The excellent figures of merit of the device attest the high quality of the device. Thus, this approach paves a way for fabricating optical filter-free, low cost and energy-efficient imaging systems.

2:45 PM *EQ02.09.05

Heterostructures from 2D Materials and Phase Transition VO₂ Jian Shi; Rensselaer Polytechnic Institute, United States

Heterostructures based on 2D materials have been found to harbor a plethora of intriguing physical phenomena whose presence is largely due to the availability of a vast 2D materials space and a plenty of degrees of freedom (e.g. twist angle, lattice mismatch) in structural design. Introducing 2D/3D heterostructures would further expand the design space for discovering new physics and developing novel devices. In this talk, I will present the design and development of heterostructures based on 2D materials and a 3D phase transition oxide. The relevant heterostructures in this talk include MoS₂/VO₂ and hBN/VO₂. In these heterostructures, the phase transition oxide imposes controllable mechanical and electronic boundary conditions to the 2D materials allowing the discovery of flexo-photovoltaic effect in MoS₂ and reconfigurable transport behavior in hBN/VO₂. Further, the weak 2D-3D interface coupling has been harnessed to control the phase transition dynamics of VO₂. The demonstration of functional behaviors at 2D/3D interface suggests the promises of using 2D/3D heterostructures for designing new electronic and optoelectronic devices.

SESSION EQ02.10: Epitaxy of Mixed Dimensional Structures III

Session Chairs: Jeehwan Kim and Kyusang Lee

Monday Morning, December 6, 2021

EQ02-Virtual

8:00 AM *EQ02.10.01

Remote Epitaxy of Micrometer-Sized Semiconductors for Fabricating Flexible and Transferable Optoelectronic Devices Young Joon Hong; Sejong University, Korea (the Republic of)

Solid-state electronics are currently under development toward the technological paradigm shift from miniaturization to deformable form factor.[1] However, typical semiconductors, including Si, III-V, metal-oxides, etc., are not intrinsically soft because of mechanical properties of bulk crystalline with brittleness and rigidity. An innovative way to fabricate flexible electronics is to make the device overlayer away from the rigid substrate and to assemble the devices on the other soft substrate in a form of spatially separate chip arrays. However, to separate the overlayer from the mother substrate, high energy irradiation (e.g., laser lift-off) and the use of corrosive etchants should have been unavoidable before emergence of non-covalent epitaxy (i.e., van der

Waals and remote epitaxy).[2] The remote epitaxy is to grow epitaxial overlayer remotely from wafer across a gap made of two-dimensional (2d) atomic layer.[3] The technique has no restriction to obtain in use of poly-domain graphene for growing single crystalline overlayer, which is distinct from the van der Waals epitaxy whose overlayer follows the surface crystal structure of 2d layer. In this talk, we focus to present and discuss how the remote epitaxy of micro- or nano-sized epitaxial architectures is applied to fabricate deformable and transferable devices. First, the epitaxy regime (i.e., covalent, remote, and van der Waals epitaxy) is discussed in terms of attracting force from wafer and graphene and role of graphene. We introduce the random nucleation-based remote epitaxy of ZnO and GaN micrometer-sized rod, which the spatially isolated geometry can be devised to fabricate the flexible light-emitting diodes (LEDs).[4] We also present the white LEDs fabricated by the remote epitaxy of GaN *p-n* junction microrods.[5] To increase the versatility of the remote epitaxy, it is necessary to control the position and size of rod structures. Thus, the methods of site-selective remote epitaxy are presented.[6, 7] The density-functional theory simulation and atomic-resolution transmission electron microscopic analysis results are also accompanied to discuss the mechanism of remote epitaxy.

[1] D. H. Kim *et al.*, *Adv. Mater.* 22(19), 2108 (2010).

[2] K. Chung, C.-H. Lee, G.-C. Yi, *Science* 330(6004) 655 (2010).

[3] Y. Kim, S. S. Cruz, K. Lee *et al.*, *Nature* 544, 340 (2017).

[4] J. Jeong, Q. Wang, J. Cha *et al.*, *Sci. Adv.* 6(23) eaaz5180 (2020).

[5] J. Jeong *et al.*, *Nano Energy* 86, 106075 (2021).

[6] J. Jeong *et al.*, *ACS Appl. Nano Mater.* 3(9), 8920 (2020).

[7] D. K. Jin *et al.*, *APL Mater.* 9(5), 051102 (2021).

8:30 AM *EQ02.10.02

Remote Epitaxy and Heterostructuring Complex-Oxide Membranes Hyunseong Kum¹, Chang-Beom Eom² and Jeehwan Kim³; ¹Yonsei University, Korea (the Republic of); ²University of Wisconsin–Madison, United States; ³Massachusetts Institute of Technology, United States

Complex-oxide materials exhibit a plethora of physical properties desirable for next-generation electronics, photonics, and quantum devices. These properties may be present in bulk form or at a heterointerface, and may be created or enhanced by application of strain. However, to date, only epitaxial methods have been used to create various heterostructures with varying strain states. Unfortunately, epitaxial methods have strict limitations, requiring closely lattice mismatched and similar crystalline structure, which prevent unrestricted manipulation, integration, and utilization of these materials. Thus, the design space for heteroepitaxial systems are severely limited. Additionally, the range of strain that can be imparted by epitaxy is fixed by pseudomorphic conditions. Finally, epitaxial growth conditions, which typically occurs at high temperatures, preclude integration of materials that are less stable in such environments. This has been a consistent bottleneck preventing universal integration of dissimilar materials to date.

To alleviate these restrictions, we present methods to produce freestanding complex-oxide membranes allowing artificial creation of complex-oxide heterostructures with vastly different crystalline structure, lattice, and orientation, such as perovskite, spinel, and garnet films. The first lift-off method, remote epitaxy, allows epitaxial seeding of the substrate through monolayers of graphene, which can then be easily exfoliated due to the van der Waals nature of graphene. However, some complex-oxide materials, such as piezoelectric PMN-PT, are grown by sputtering, which damages the graphene due to the harsh plasma ambient. For these materials, we found that by choosing a substrate with a specific lattice misfit, the epitaxial layer can be precisely separated from the substrate using a high stress Ni layer.

We also demonstrate artificial heterostructures by stacking exfoliated complex-oxide membranes manually, observing the mechanical and physical interaction between the stacked membranes. We hope such demonstration of artificial 3D-3D and 2D-3D heterostructures will allow to significantly expand the possible permutations of materials and allow experimental realization of structures not possible by epitaxial means alone.

9:00 AM *EQ02.10.03

Atomic Structure of Nitride/Graphene/Sapphire Interface and Mechanism of Remote Epitaxy Peng Gao¹, Zhiqiang Liu², Tongbo Wei² and Zhongfan Liu¹; ¹Peking University, China; ²Institute of Semiconductors, Chinese Academy of Sciences, China

Wide-bandgap semiconductors, especially group-III nitrides (III-Ns), have excellent performance to be applied into optoelectronic and electronic devices in full-color range. In industry, as the most used epitaxial substrate, sapphire however, has large thermal and crystal mismatch with these nitrides and induces large compressive strains and density of dislocations, seriously troubling the device performance.

Recently, with the assistance of two-dimensional (2D) materials, such as graphene, remote epitaxy (or called quasi-van der Waals epitaxy) has given new choice to semiconductor films epitaxy. The weak van der Waals force in the nitride/graphene/sapphire sandwich structure alleviates the lattice and thermal mismatch, tunes nucleation behavior, reduces growth time, and/or achieves damage-free transfer for high-power and flexible devices. But still, owing to the lack of atomic resolution characterizations, the role of graphene acts in this process is still not clear. Meanwhile, the 2D materials transfer process which formal study mostly focused on can hardly be used into industry. Herein, we share some study about the atomic structure of nitride/graphene/sapphire interface and the mechanism of remote epitaxy, in which the graphene/sapphire substrates are 10*2-inch batch synthesized by chemical vapor deposition (CVD) method, offering opportunity for the usage in industry.

Firstly, we study the surface of the graphene covered sapphire. Instead of van der Waals interaction, the grown graphene is C-O-Al bonded with sapphire unexpectedly^[1]. Compared with transferred sample, the grown graphene is stronger pasted on sapphire with larger lateral force, and the structure relaxation behavior of sapphire near the surface is suppressed compared with that of the bare surface.

Upon the graphene/sapphire substrate, we grow GaN film with metal organic CVD (MOCVD) method. After this process, the sapphire surface transforms into a high Al-O ending surface, significantly different from the case before MOCVD. We also find that the whole nitride film achieves low compressive strain as well as low density of dislocations. Based on the high-quality nitride films, we further fabricate high In composition InGaN alloy. The strain relaxed nitride film creates suitable environment for up to 32% In element doping. The as-fabricated light emitting device (LED) shows a 563 nm electroluminescence emission, corresponding to yellow light.

[1] Dou *et al.*, *Nature Communications* 10, 5013 (2019)

9:30 AM EQ02.10.04

In Situ X-Ray Studies of Growth of SrTiO₃ (001) on Graphene by Molecular Beam Epitaxy Xi Yan, Hui Cao, Yan LI, Hawoong Hong, Hua Zhou and Dillon D. Fong; Argonne National Laboratory, United States

Remote epitaxy is novel synthesis technique that allows the fabrication of ultrathin, flexible, and highly unique heterostructures that cannot be created by other methods. The technique was recently applied to construct freestanding, complex oxide membranes [1]. By inserting graphene between the film and substrate during thin film growth, the van der Waals interactions between graphene and other materials are strong enough to enable epitaxial growth but weak enough to allow the rapid release the thin film. The technique may eventually be exploited to create novel, single crystal heterostructures, as each film can be “stacked” atop another, regardless of degradation due to misfit strain or incompatibilities due to high temperature reactions. However, details

regarding how remote epitaxy actually occurs remains unknown as this requires an *in situ* investigation of the remote epitaxy process. Here we conduct *in situ* synchrotron X-ray measurements during growth by molecular beam epitaxy (MBE) to observe epitaxial synthesis through graphene layers. COBRA (COherent Bragg Rod Analysis) is used to reconstruct the electron density profiles of the epitaxial system after the growth of each monolayer. Subtle changes of the graphene layers during heating and in different oxygen pressures were captured, providing crucial details in understanding the remote epitaxy technique.

[1] Hyun S. Kum et al., Nature **578**, 75 (2020).

Work supported by the Department of Energy, Office of Science, Basic Energy Sciences under contract no. DE-AC02-06CH11357.

SESSION EQ02.11: Epitaxy of Mixed Dimensional Structures IV
Session Chairs: Young Joon Hong and Suresh Sundaram
Monday Morning, December 6, 2021
EQ02-Virtual

10:30 AM *EQ02.11.01

Wafer-Scale van der Waals Epitaxy of III-Nitride Devices on h-BN—An Overview of 2D/3D Epitaxy, Device Fabrication, Mechanical Release-Transfer Methods and Device Performances [Abdallah Ougazzaden](#)^{1,2}, Suresh Sundaram¹, Phuong Vuong², Soufiane Karrakchou¹, Adama Mballo², Rajat Gujrati¹, Ashutosh Srivastava¹, Gilles Patriarche³, Paul Voss¹ and Jean-Paul Salvestrini^{1,2}; ¹Georgia Institute of Technology-Lorraine, France; ²CNRS, IRL 2958 Georgia Tech, France; ³CNRS, Centre de Nanosciences et de Nanotechnologies, France

Van der Waals (vdW) epitaxy of 3D device structures on 2D layers is particularly interesting for III-nitrides and has attracted intensive investigation. Dislocations and defects seen in typical nitride 3D epitaxy could be avoided when grown on a 2D layer, because strain due to large lattice and thermal mismatches relaxes elastically during 3D growth. The technique is also very convenient for heterogenous integration. With simple sticky holders (tapes, PDMS, metallic films...), the III-N heterostructures can be mechanically detached over a large area from its substrates and the membrane transferred to arbitrary carriers, at minimum of time and low cost. Hexagonal boron nitride (hBN) is an excellent choice of 2-D material. It exhibits good stability at high temperature, excellent compatibility with III-nitride growth conditions and growth systems (MOCVD, MBE, CVD...) and can be grown on different types of substrates, with sapphire our substrate of choice.

We have demonstrated a range of devices using 2D/3D vdW epitaxy: LEDs, solar cells, sensors and HEMTs. In this talk we overview our results in epitaxy and materials characterization, device fabrication, mechanical lift-off and transfer, and pre- and post-transfer device characterization. Different mechanical liftoff and transfer approaches will be compared in term of material quality, crack generation and flexibility. Going beyond wafer-scale epitaxy, we will also present selective area vdW epitaxy and self-lift off and transfer techniques that can further simplify and lower the cost of heterogenous integration because of innovative epitaxy and process fabrication that use commercial systems.

11:00 AM *EQ02.11.02

One-Dimensional van der Waals Materials [Alexander A. Balandin](#); University of California, Riverside, United States

The unique electrical and thermal properties of graphene stimulated the search for other two-dimensional (2d) atomic crystals with unusual properties. A number of 2D materials belong to the family of transition metal chalcogenides that contains weak van der Waals bonding between structural units. Until recently, most research utilized dichalcogenides such as MoS₂, TaS₂ and others, distinguished by 2D layers. Another class of transition metal chalcogenides – the trichalcogenides – has quasi-1D crystalline structures. In this presentation, I review our results, which show that the mechanical and chemical exfoliation approaches developed for 2D materials can be extended to a relevant class of quasi-1D van der Waals materials such as TaSe₃, ZrTe₃ and others. Electrical measurements established that the bundles of quasi-1D atomic chains have a breakdown current density approaching 100 MA/cm² [1, 2]. The atomic chain single crystal nature of TaSe₃ results in low surface roughness and the absence of grain boundaries. These features potentially can enable the downscaling of these wires to lateral dimensions in the few-nm range. The polymer composites with low loadings of quasi-1D TaSe₃ fillers reveal excellent electromagnetic interference shielding in the X-band GHz and extremely high frequency sub-THz frequency ranges, while remaining DC electrically insulating [3, 4]. The unique electromagnetic shielding characteristics of these films are attributed to effective coupling of the electromagnetic waves to the high-aspect-ratio electrically conductive TaSe₃ atomic-thread bundles even when the filler concentration is below the electrical percolation threshold. These novel films are promising for high-frequency communication technologies, which require electromagnetic shielding films that are flexible, lightweight, corrosion resistant, inexpensive, and electrically insulating.

This work was supported, in part, by the NSF DMREF program via a project DMR-1921958 Collaborative Research: Data Driven Discovery of Synthesis Pathways and Distinguishing Electronic Phenomena of 1D van der Waals Bonded Solids. The author acknowledges the Vannevar Bush Faculty Fellowship (VBFF) with the funding for the project One-Dimensional Quantum Materials.

[1] M.A. Stolyarov, et al., Nanoscale, 8, 15774 (2016); [2] A. Geremew, et al., IEEE Electron Device Lett., 39, 735 (2018); [3] Z. Barani, et al., Adv. Mater., 33, 2007286 (2021); [4] Z. Barani, et al., ACS Appl. Mater. Interfaces, 13, 21527 (2021).

11:30 AM EQ02.11.03

MOVPE Epitaxy of Group III Nitrides via Few-Layer Graphene on GaN/Sapphire Templates [Kazimieras Badokas](#)¹, Arunas Kadys¹, Dominykas Augulis¹, Juras Mickevicius¹, Ilja Ignatjev², Martynas Skapas², Giedrius Juska¹ and Tadas Malinauskas¹; ¹Vilnius University, Lithuania; ²Center for Physical Sciences and Technology, Lithuania

Integration of group III nitrides and two-dimensional buffer layers, such as graphene, has been considered as a new material system for the next-generation optoelectronic devices. However, the growth of high-quality semiconductor membranes on the slippery van der Waals surface remains challenging. Harsh metalorganic vapor phase epitaxy (MOVPE) environment and graphene transfer technique have a great impact on the successful realization of remote epitaxy.

In this work, one-step and multi-step MOVPE growth approaches were realized to fabricate GaN layers on GaN/sapphire templates covered with graphene. While the one-step approach led to the disappearance of graphene Raman fingerprints, the multi-step growth protocol resulted in the successful formation of GaN films on GaN/sapphire templates. The quality of grown layers was investigated using atomic force microscopy, X-Ray diffraction and

photoluminescence techniques. Transmission electron microscopy analysis revealed a clean GaN/graphene/GaN interface.

The seeding effect of the substrate was previously shown to take place for up to two layers of graphene. The use of bilayer graphene could be favorable as it provides an aperture-free interlayer. To investigate the effect of the number of graphene layers and their transfer technique, seeds of GaN and InN were formed. Single transfer of bilayer graphene proved to be better suited for the realization of remote epitaxy rather than double transfer of monolayer.

11:45 AM EQ02.11.04

Metallic-Dielectric Multilayers as Substrates of van der Waals Epitaxy Xuejing Wang¹, Yeonhoo Kim¹, J. K. Baldwin¹, Andrew C. Jones¹, Jeeyoon Jeong² and Jinkyong Yoo¹; ¹Los Alamos National Laboratory, United States; ²Kangwon National University, Korea (the Republic of)

Van der Waals (vdW) epitaxy has been studied as a promising materials preparation method which can overcome materials compatibility. Atomically thin two-dimensional (2D) materials serve as substrates of other low-dimensional and three-dimensional (3D) materials growth to provide surface dangling bonds-free surface, a prerequisite of vdW epitaxy. However, direct utilization of a 2D material as a substrate brings the issue of poor nucleation efficiency due to small number of nucleation sites where dangling bonds used to be. The nucleation efficiency issue has been resolved by dipole engineering method, which was developed by the presenter's team. The dipole engineering technique is based on increase in surface energy of a 2D material by transfer of the 2D material on a bulk or a thin film on which polarization is formed along the out-of-plane direction. To induce the required out-of-plane dipole moment, applying electrical bias or transfer of a 2D material onto a ferroelectric material has been utilized. However, the demonstrated techniques of dipole engineering have not been suitable for recycling the substrates due to changes of the substrates' characteristics under vdW epitaxy conditions. In the presentation, we will discuss a robust and recyclable dipole engineering based on refractory metallic-dielectric multilayers in which inherent out-of-plane dipole moments are formed. We transferred monolayer graphene onto the multilayer substrate. Then, crystalline germanium growth via chemical vapor deposition was successfully demonstrated.

12:00 PM EQ02.11.05

Remote Epitaxy of III-V Materials Using Hydride Vapor Phase Epitaxy Dennice M. Roberts¹, Elisabeth McClure¹, Hyunseok Kim², Kevin Schulte¹, Aaron Ptak¹, Jeehwan Kim² and John Simon¹; ¹National Renewable Energy Laboratory, United States; ²Massachusetts Institute of Technology, United States

The promise of remote epitaxy, in which epitaxial registry of a film can be maintained through two-dimensional layers, has emerged from an advanced understanding of the interactions between two dimensional materials and bulk semiconductors.[1] A promising application of this technology is to facilitate substrate reuse in epitaxial III-V systems, which could significantly reduce material cost and improve commercial viability of this high-efficiency photovoltaic technology. In this process the weak van der Waals bonds between the 2D layer and the III-V substrate make separation of epitaxially-grown layers simple and leaves a smooth substrate that can be reused for cost reduction.

Here we present a study of growth of GaAs on AlGaAs through a low dimensional carbon interlayer via hydride vapor phase epitaxy (HVPE). We investigate the effect of various GaAs nucleation conditions such as V/III ratio, temperature and growth rate on film roughness, crystallinity, and degree of epitaxial alignment. We demonstrate growth of single crystal GaAs layer on top of the low dimensional carbon that follow the crystal orientation of the substrate. Surface roughness measured via AFM found that lower V/III ratios result in smoother III-V films grown on the low dimensional carbon, with a lowest RMS of ~60 nm obtained at a V/III ratio of 5. Growth temperatures are optimized at 650 °C, as temperatures below 550 °C show non-crystalline growth and higher temperature samples display very rough surfaces.

Additionally, we investigate HVPE growth on various forms of low-dimensional carbon including transferred graphene, CVD-grown graphene, and MOCVD-growth amorphous carbon and find the latter to be most well suited for III-V growth as this method results in cleaner interface and potential for direct, large-area coverage. We also identify techniques to mitigate surface degradation in carbon layers as a function of both exposure time and growth environment by analyzing surface changes via x-ray reflectivity. We show growth of heteroepitaxial III-V solar cells on carbon interlayers and preliminary cell results, which are currently limited to 4% efficiency under one sun.

[1] Y. Kim, S. Cruz, K. Lee, B. Alawode, C. Choi, Y. Song, J. Johnsen *et al.* Remote epitaxy through graphene enables two-dimensional material-based layer transfer. *Nature* **544** 340-343 (2017).

12:15 PM EQ02.11.06

Toward Large Terraces Underneath Monolayer Graphene Grown by 4H-SiC (0001) Sublimation Haitham Hrich¹, Matthieu Moret¹, Olivier Briot¹, Matthieu Paillet¹, Jean-Manuel Decams², Sylvie Contreras¹ and Périne Landois¹; ¹Laboratoire Charles Coulomb, UMR 5221, France; ²Annealsys, France

Our group has recently optimized a reproducible and controlled growth process of a monolayer graphene on silicon carbide (SiC, (0001)) at low Argon (Ar) pressure (10mbar). We highlight that such process is compatible with electronic applications hence no transfer is needed. The graphene samples obtained using this process have a mobility up to 2000 cm²V⁻¹ s⁻¹, at room temperature, which corresponds to the state of the art on similar substrates. One way to enhance the graphene's mobility is to reduce SiC steps density. These steps with different surface energies have different step velocities and therefore the steps are preferable to be bunched together aiming to minimize the total surface energy during the thermal treatment. This step bunching often occurs during epitaxial growth of graphene on SiC. The height and width of the steps depend on various factors, such as, polytype of SiC, miscut angle and growth conditions. First of all, the miscut angles in our SiC substrates have been measured using a combined optical alignment and X-ray diffraction method. This method, which is unusual for SiC substrates, allowed us to reveal cut-off angles inferior to 0.07° for our SiC wafers. This result led us to not take into account the effect of the miscut angle in our process and mainly focus on the growth parameters. In this study, we have investigated both the etching of 4H-SiC (0001) by H₂ (dihydrogen) and the occurrence of GSB (giant step bunching) in Ar-H₂ mix gases system at low pressure. The steps width after our classical process, under Ar environment, is typically lower than 2 μm. The first results showed that the surface of the SiC samples annealed under Ar-H₂ environment has a homogeneous distribution of well-aligned steps with terraces width up to 20 μm. A clear effect of H₂ on steps formation is evidenced. However, the samples obtained had no graphene on top. Adding an isotherm of 900 s at 1500°C, and stopping the H₂ right after, led to the growth of graphene on large steps, with an average steps width of 11 μm. Both optical microscopy and atomic force microscope were used to characterize the surface morphology and steps width. The presence of graphene was investigated using Raman maps. The number of graphene layers were estimated using the ratio of the integrated intensity of the G band of graphene on the integrated intensity of the G band of a highly oriented pyrolytic graphite (HOPG) used as reference (A_{G-G}/A_{G-HOPG}). Raman maps demonstrate that our samples are mostly covered with 1LG (up to 70% of the surface).

1:00 PM EQ02.12.01

Interfacial Properties of a NbSe₂/ZnO Heterostructure to Form Ohmic Contact Yeonhoo Kim¹, Roxanne Tutchton¹, Ren Liu², Sergiy Krylyuk³, Jianxin Zhu¹, Albert Davydov³, Young Joon Hong⁴ and Jinkyong Yoo¹; ¹Los Alamos National Laboratory, United States; ²University of California, San Diego, United States; ³National Institute of Standards and Technology, United States; ⁴Sejong University, Korea (the Republic of)

Metal/semiconductor interfaces are essential to build devices for fabrication of electrical contacts. However, Schottky-Mott physics, a fundamental principle governing metal/semiconductor interfaces, is not applicable to metal/semiconductor interface in devices due to Fermi level pinning, affected by processings. Two-dimensional (2D) materials as contacts for semiconductor devices have attracted great attention due to minimizing Fermi level pinning. Schottky-Mott physics has widely employed to design 2D material-based electrodes and to elucidate the contact behavior. Nevertheless, the interface between 2D and three-dimensional (3D) semiconducting materials cannot be fully understood by Schottky-Mott physics. Charge transfer and interlayer coupling have been reported in various 2D/3D heterostructure. The phenomena also affect metal/semiconductor interface. In the presentation, we performed an integrated study of theoretical prediction and experimental observation of the electrical properties of the heterostructure composed of metallic NbSe₂ and semiconducting ZnO. The density function theory (DFT) calculations predicted that charge transfer between ZnO and NbSe₂ lowers barrier height at the heterojunction and conductive surface states of ZnO provides conduction channel in the ZnO/NbSe₂ heterostructures. Crystalline ZnO/NbSe₂ heterostructures were prepared by hydrothermal method. The surface characteristics of NbSe₂ were investigated by X-ray photoelectron spectroscopy. Electrical characterizations of the ZnO/NbSe₂ heterostructures showed Ohmic-like behavior as predicted by the DFT calculations, opposed to the prediction based on Schottky-Mott model.

1:15 PM EQ02.12.03

Composition and Strain Dependence of Phase Separation and Sn Surface Segregation in Ge/Ge_{1-x}Sn_x Co-Axial Heterostructures Michael Braun¹, John Lentz¹, Ishaq Bishnoi¹, Andrew C. Meng² and Paul McIntyre¹; ¹Stanford University, United States; ²University of Pennsylvania, United States

There has been significant interest in germanium-tin (GeSn) as a promising silicon-compatible group IV direct bandgap material for electronics and photonics. However, the maximum tin solubility in bulk GeSn solid solutions is only ~1 at% tin compared to the >10 at% tin compositions required for a direct bandgap material.¹ The metastability of high tin content GeSn limits the thermal processing window for film deposition and post-growth annealing of epitaxial layers.^{2,3} Previous reports on annealing results of strained germanium-tin epitaxial layers have shown undesirable surface segregation of tin. We report X-ray photoelectron spectroscopy results from *in-situ* and *ex-situ* annealing of core/shell Ge/Ge_{1-x}Sn_x nanowire assemblies. Previously, we have shown the elastic compliance of small diameter Ge core nanowires in the core/shell structure produce largely strain-free Ge_{1-x}Sn_x epilayers.⁴ Utilizing the variable strain control of this geometry, we investigate the annealing characteristics of the GeSn surface and native oxide for tin contents in the range of 2 at% - 12 at% in both air-exposed and oxide-free nanowires. For oxidized samples, we show the presence of a tin-rich oxide that exhibits a composition dependent temperature for thermal decomposition via *in-situ* annealing. By varying the shell thickness, we control the compressive strain in the shell enabling examination of phase separation behavior of the oxide-free, as-grown GeSn surface via *ex-situ* rapid thermal annealing and air-free transfer. Additionally, we have examined the annealing effects on bulk tin distribution and local surface structure via photoluminescence, X-ray diffraction, and high resolution transmission electron microscopy.

¹M. Seifner, A. Dijkstra, J. Bernardi, A. Steiger-Thirfield, M. Sistani, A. Lugstein, J. Haverkort, S. Barth, "Epitaxial Ge_{0.81}Sn_{0.19} Nanowires for Nanoscale Mid-Infrared Emitters," *ACS Nano* **13**, 7 (2019), 8047-8054.

²S. Wu, L. Zhang, B. Son, Q. Chen, H. Zhou, C. Tan, "Insights into the Origins of Guided Microtrenches and Microholes/rings from Sn Segregation in Germanium-Tin Epilayers," *J. Phys. Chem. C* **124** (2020), 20035-20045.

³W. Wang, L. Li, Q. Zhou, J. Pan, Z. Zhang, E. Tok, Y. Yeo, "Tin surface segregation, desorption, and island formation during post-growth annealing of strained epitaxial Ge_{1-x}Sn_x layer on Ge(001) substrate," *Applied Surface Science* **321** (2014), 240-244.

⁴A. Meng, M. Braun, Y. Wang, C. Fenrich, M. Xue, D. Diercks, B. Gorman, M. Richard, A. Marshall, W. Cai, J. Harris, P. McIntyre, "Coupling of coherent misfit strain and composition distributions in core-shell Ge/Ge_{1-x}Sn_x nanowire light emitters," *Materials Today Nano* **5** (2019), 100026.

1:30 PM EQ02.12.04

Hetero-Structures of Perovskite and 2D Materials Gokul M. A and Atikur Rahman; IISER Pune, India

Perovskite materials and 2D materials are 2 promising materials for future optoelectronic applications. Perovskite materials are having great optoelectronic properties such as high PL quantum yield, great absorption coefficient, easy synthesis at relatively low temperatures, tunable bandgap, high carrier mobilities to name a few. These properties make them shine in device applications like photovoltaics and LEDs. 2D materials on the other hand offer an arsenal of materials with interesting optoelectronic properties. Their bandgap range from metallic to insulator. With emerging properties in the monolayer regime, which sets them apart from their bulk counterparts, they offer a rich field of study. Here in this work, we focus on synthesizing these materials and making heterostructures out of these two classes of materials. We then explore their optoelectronic properties.

1:45 PM EQ02.12.06

Late News: Enhanced Photodetector with Low Dark Current Based on 2D n-MoS₂ Functionalized by p-MnO Quantum Dots Yusin Pak, Somak Mitra, Bin Xin and Man S. Roqan; King Abdullah University of Science and Technology, Saudi Arabia

Incorporating a heterojunction architecture into photodetectors can significantly improve the photodetection characteristics. To construct a heterojunction with the nanostructured compound semiconductor materials (CSMs), a two-dimensional (2D) platform material for stably transferring photogenerated signals into circuitry is essential. In this work, p-type manganese oxide quantum dots (MnO QDs) with zero-dimension (0D) are synthesized through femtosecond laser ablation in liquid (FLAL). An exfoliated 2D molybdenum disulfide (2D-MoS₂) is used for the counterpart platform of the heterojunction. The ablated MnO QDs with a mean diameter of 4.9 nm were uniformly spray-coated onto the 2D-MoS₂. The p-n junction device based on p-MnO QDs functionalized 2D n-MoS₂ shows a reduced dark current and an increased photocurrent compared to that of pristine 2D-MoS₂ devices due to the p-n heterojunction effect. This report will greatly contribute to developing low-cost and high-performance optoelectronic devices based on heterojunctions between other TMDCs and nanostructured CSMs.

2:00 PM EQ02.12.07

Selective Synthesis of Tunable TMD-COF Heterostructures [Lucas K. Beagle](#)^{1,2}, Ly D. Tran^{1,2}, Luke A. Baldwin¹ and Nicholas Glavin¹; ¹Air Force Research Laboratory, United States; ²UES, Inc., United States

Chemical and biological sensing using 2-D nanomaterials has been an area of intense investigation including inorganic materials that exhibit high sensitivity, however it has been limited as a field due to the lack of selectivity among analytes. While 2D inorganic materials, such as transition metal dichalcogenides (TMD), can readily decipher between donor/acceptor groups, strategies to incorporate selectivity in these devices is often challenging. Organic 2D materials known as covalent organic frameworks (COF) are large porous and repeated organic frameworks which have been shown to act as selectivity agents due to functionalization and porosity. This research focuses on the association of COFs with 2-D nanomaterials using top-down microwave-assisted activation of TMDs and deposition of COF nanoparticles. Several known TMD and COF species have been examined to understand the fundamental surface interactions between 2-D nanomaterials and few layer COFs, while Kinetics and mechanistic studies were used to determine the manner of association of the inorganic and organic substrates. Photoluminescence studies demonstrate a microwave power dependent electronic coupling of the inorganic and organic materials for a fully tunable interaction.

2:15 PM EQ02.06.02

Terahertz Dynamics of Correlated Quasiparticles in Moiré Superlattices [Chenyi Xia](#)¹, Jun Xiao¹, Fang Liu¹, Leo Yu¹, Christian Heide¹, Yuki Kobayashi¹, Burak Guzelurk², Eric Ma¹, Tony F. Heinz¹, Xiaoyang Zhu³ and Aaron Lindenberg¹; ¹Stanford University, United States; ²Argonne National Laboratory, United States; ³Columbia University, United States

Emerging twisted heterostructures based on 2D layered materials have opened a unique platform to explore exotic correlation physics and engineer Coulomb interactions in the atomically thin limit. The tunable Moiré potentials, arising from interlayer couplings, result in the emergence of various novel orderings such as Mott insulating phases, unconventional superconductivity, and Moiré excitonic phases. In particular, transition metal dichalcogenide heterostructures allow for optically-excited electrons and holes to reside in different monolayers and for trapping in the tens-of-meV Moiré potential, which is quite favorable for developing valleytronics, exciton condensation, and programmable quantum emitter arrays. Further progress along this direction requires a precise understanding of the formation of these Moiré excitons, and how such formation can be engineered by Moiré potentials and electron correlations.

Here we use ultrafast terahertz emission spectroscopy to probe interlayer charge transfer and other quasiparticle dynamics in several types of Moiré superlattices based on the transition metal dichalcogenides. With ultrafast visible and near-infrared laser pumping of these distinct Moiré superlattices, we observed nontrivial variations in the THz emission dynamics and spectroscopy as a function of twist angle. Experiments indicate such changes are closely associated with varying Moiré patterns and momentum mismatch conditions. Our findings advance our microscopic understanding of the formation, dissociation and manipulation of excitonic correlations in twisted heterostructures.

SESSION EQ02.13: Poster Session II
Session Chairs: Hyunseong Kum and Feng Miao
Monday Afternoon, December 6, 2021
EQ02-Virtual

9:00 PM EQ02.13.01

Synthesis of Epitaxial Pentasodium Trioxoundecafluoro-Trititanate with Plate-Like Morphology on Fluorine-Doped Tin Oxide Coated Glass Substrates [Crispin M. Mbulanga](#)¹, Rudolph Erasmus², Olivier Jaco¹, Christian Chinedu Ahia³, Edson Meyer³ and Johannes R. Botha¹; ¹Nelson Mandela University, South Africa; ²University of the Witwatersrand, Johannesburg, South Africa; ³University of Fort Hare, South Africa

A route for synthesis of epitaxial pentasodium trioxoundecafluoro-trititanate ($\text{Na}_5(\text{Ti}_3\text{O}_3\text{F}_{11})$) with plate-like morphology on fluorine-doped tin oxide coated glass substrates (FTO-glass) through the hydrothermal bath method is described and discussed, followed by the presentation of a systematic study of the physical properties of the samples. The samples are textured with a small amount of micron sized crystals existing among predominantly plate like structures of $\text{Na}_5(\text{Ti}_3\text{O}_3\text{F}_{11})$. These structures are attached to the F:SnO₂ (FTO) layer due to their nucleation and growth on the substrate surface during the hydrothermal process. The preferred orientation of the crystal planes of $\text{Na}_5(\text{Ti}_3\text{O}_3\text{F}_{11})$ plates are with the (331), (222) and (440) parallel to the substrate. Additionally, an epitaxial relationship between the fluorine doped SnO₂ layer and plate-like ($\text{Na}_5(\text{Ti}_3\text{O}_3\text{F}_{11})$) exists: an alignment of planes along (111). Last of all, a set of unidentified vibrational Raman modes recorded from $\text{Na}_5(\text{Ti}_3\text{O}_3\text{F}_{11})$ plates grown on fluorine-doped tin oxide is presented. It is found that in the temperature ranging from 27 to -193 °C, $\text{Na}_5(\text{Ti}_3\text{O}_3\text{F}_{11})$ vibrational Raman modes peak at: 118.1 cm⁻¹, 150.9 cm⁻¹, 191.0 cm⁻¹, 237.4 cm⁻¹, 439.5 cm⁻¹, 527.1 cm⁻¹, 642.8 cm⁻¹, 687.9 cm⁻¹, 742.6 cm⁻¹ and 943.5 cm⁻¹. Raman shifts at 527.1 cm⁻¹, 687.9 cm⁻¹, 439.5 cm⁻¹, and 943.5 cm⁻¹ are assigned to A_g, B_{1g}, B_{2g}, and B_{3g} modes, respectively.

9:05 PM EQ02.13.02

Factors Affecting the Magnetic Properties and Reversal Process of Magnetic Nanowires [Yicong Chen](#) and Bethanie J. Stadler; University of Minnesota Twin Cities, United States

Magnetic nanowires (MNWs) are increasingly important for applications in memory, biolabels, and nanowarming of cryopreserved organs. Object Oriented Micromagnetic Framework (OOMMF) was used to visualize moments inside MNWs. The magnetic properties of MNWs, such as coercivity, remanence, and reversal mechanism were investigated as a function of nanowire shape. Experimental measurements of magnetic nanowires (MNW) often reveal features that are difficult to explain due to statistical shearing of features and interaction fields in large arrays. Measurements of individual nanowires can be used to remove interaction field effects, and other measurements such as first-order reversal curves (FORC) and the projection method often attempt to statistically separate bulk effects. For nickel MNWs with fixed length of 3 μm, the coercivity and the remanence are negatively correlated to the diameter of the wire. This is in consistent with the theory that expresses the coercivity field of the infinite long cylinder as: $h_{ci}=1.08D_0^2/D^2$, $D_0=2A^{0.5}/M_s$, where h_{ci} is the reduced coercivity field of the cylinder with high aspect ratio, D_0 is the fundamental unit length defined by the exchange constant A and saturation magnetization M_s of the material (Ni in this case) used to make MNWs.

When the diameter is increased to 200 nm, in addition to a continued reduction in coercivity and remanence, a 'wasp waist' appeared in the hysteresis loop. The reversal can be divided into three different parts showing three types of magnetic moment behaviors in the MNW. In the first part, since there is a large area for curling in 200nm-diameter nanowires, the magnetic moments at the tips of the MNW fall from pointing along z-axis to aligning in the xy-plane and in the form of vortex. Next, when the external field is further reduced, the outer shell of moments turns from in-plane to the negative z-axis. Finally, the axial core of the MNW switches to the negative z-axis and the wire is fully saturated in the negative z-direction. Interestingly, at H_c ($M=0$), the two vortex walls converged in the center of the MNW, and a three-dimensional vortex(hedgehog) was observed.

Next, with all other parameters unchanged, flat-tipped cylinders were replaced with ellipsoids so that the tips of wire had infinitesimally small areas where vortex was no longer supported. With this shape, the coercivity of the nanowires significantly increased to $H_c = 180, 160, 50, 11$ mT from 140, 90, 30, 5 mT for the MNWs with 30, 50, 100, 200nm diameters, respectively. This increase in coercivity occurs because the field to nucleate a vortex at the tips is lower than to nucleate vortex in the center of the wire which is the case for ellipsoidal MNWs. For these ellipsoids, increasingly negative applied fields cause the vortex to expand to include the coherent curling of the whole nanowire.

In conclusion, the coercivity of the nanowire depends on the geometry of the wire in two ways. First, with the length of the wire fixed, the coercivity is reduced by increasing the diameter of the wire. Second, when the tip of the wire is engineered so that the nanowires are ellipsoidal rather than cylindrical, the coercivity is increased and the moment switching begins at the center of the wire instead of the end.

9:10 PM EQ02.13.03

Freestanding Relaxor Ferroelectric BCZT Membranes via Epitaxial Lift-Off [Huandong Chen](#), Yang Liu, Mythili Surendran, Harish Kumarasubramanian and Jayakanth Ravichandran; University of Southern California, United States

($\text{Ba}_{0.85}\text{Ca}_{0.15}$) ($\text{Zr}_{0.1}\text{Ti}_{0.9}$) O_3 (referred as BCZT), a solid solution of BaTiO_3 , is a novel lead-free ferroelectric relaxor that possesses a high dielectric constant, large piezoelectric coefficient as well strong electro-optic coupling. High quality BCZT thin films have been successfully synthesized by various techniques, including the epitaxial growth using pulsed laser deposition (PLD) recently by our group. However, the requirement of lattice matching to substrates and the extremely high material growth temperature (up to 800°C) are extensively limiting the practical applications in Si-based electronics integrations, as well as the emerging flexible or stretchable devices that usually use polymer as supporting substrates. Here, we report the synthesis and transfer of freestanding defect-free ferroelectric BCZT membranes via epitaxial lift off from growth substrates using LSMO as sacrificial layer. Ferroelectric and piezoelectric properties of transferred film are comparable to the as-grown epitaxial BCZT film. Furthermore, 10×10 SRO/BCZT/SRO capacitor array were fabricated using wet chemical etching method and further transferred onto alien substrate as a demonstration of potential device application. Our work paves the way of integrating single-crystalline relaxor ferroelectric oxides for on-chip electronic or energy storage applications.

9:15 PM EQ02.13.04

Quasi-2D Polyamides Reinforced with 1D Nanotubes and Nanofibers for Novel Desalination Membranes [Rodolfo Cruz-Silva](#), Hiroyuki Matsuda, Aaron Morelos-Gomez, Juan-Luis Fajardo-Diaz, Kazunori Fujisawa, Hiroyuki Muramatsu, Kenji Takeuchi, Takuya Hayashi and Morinobu Endo; Shinshu University, Japan

Crosslinked polyamides are a diverse and important group of polymers with many applications in the membrane and desalination fields. These polymers are usually synthesized by interfacial polymerization and supported over a porous polymer support that provide mechanical stability. In the last years, considerable effort has been put to make thinner and stronger polyamide films that can have higher water permeability yet mechanical robustness. The combination of thin films with one-dimensional (1D) reinforcing structures is an effective path to combine the functionality of the film with the structural stability provided by the 1D material. Indeed, this type of structures are so efficient that have resulted from evolution in many living creatures, and can be seen, for example, in insect wings and plant leaves. However, taking this design to the nanoscale poses great challenges. Ultrathin polymer films, sometimes referred as quasi two-dimensional (2D) materials, often show processing problems such as dewetting, phase separation, and creeping, among others. Nevertheless, the study of these materials has recently gained momentum. Here, we used tempo-oxidized cellulose nanofibers (CNFs) and double walled carbon nanotubes (DWCNTs) to synthesize thin and ultrathin (<30 nm) crosslinked -piperazine and phenylenediamine based polyamides films by interfacial polymerization. Tempo-oxidized CNFs are high-modulus water-dispersible colloids. They are biodegradable and its synthesis is environmentally friendly. On the other hand, DWCNTs are a superhigh modulus material that might have interesting transport properties due to their hydrophobic hollow core. We carried out liquid-liquid interfacial polymerizations to prepare sheet like quasi 2D polymer sheets reinforced with CNF, DWCNT and their combination. The mechanism of the interfacial polymerization in presence of the nanomaterials was also studied by using different methodologies to add the monomers. We use several techniques such as quartz-crystal microbalance, transmission and scanning electron microscopy to study how hydrophobic and hydrophilic 1D materials can be efficiently incorporated into interfacially synthesized polymer films. The location of the 1D materials across the films was also studied by X-ray photoelectron spectroscopy. The chemical interactions responsible for wetting, interfacial adhesion, and phase separation between the monomers and the 1D materials were studied at the atomic level through classical molecular dynamics. Understanding the incorporation of 1D materials and quasi 2D polymer films and the behavior of the resulting nanocomposite films is important to design new ultrathin nanocomposite polymers that might have applications for the next generation of separation membranes.

9:20 PM EQ02.13.05

Effect of Crystal Structure and Niobium Doping on $\text{TiO}_2/\text{SrTiO}_3$ Heterostructured Nanorod Arrays [Takaki Kimura](#), Kan Hachiya and Takashi Sagawa; Kyoto University, Japan

$\text{TiO}_2/\text{SrTiO}_3$ heterostructured nanorod arrays have been attracted much attention in photovoltaic and/or photoelectrochemical (PEC) applications such as dye-sensitized solar cells (DSSCs) and PEC cells due to its unique feature of oriented 1D structure and heterostructure. In this context, we designed anatase $\text{TiO}_2/\text{SrTiO}_3$ heterostructured nanorod arrays grown on transparent conductive fluorine-doped tin oxide (FTO) substrate and the comparison of the characteristic properties with those of typical rutile $\text{TiO}_2/\text{SrTiO}_3$ heterostructured nanorod arrays. Furthermore, novel niobium doped $\text{TiO}_2/\text{SrTiO}_3$ heterostructured nanorod arrays were also synthesized to investigate the compensation for the low conductivity of TiO_2 and SrTiO_3 themselves.

$\text{TiO}_2/\text{SrTiO}_3$ heterostructured nanorod arrays were synthesized by two-step hydrothermal reaction. Oriented 1D structure is formed by the growth of anatase or rutile TiO_2 nanorod arrays on FTO substrate directly during the first hydrothermal reaction, and $\text{TiO}_2/\text{SrTiO}_3$ heterostructure is constructed by a dissolution-precipitation process on TiO_2 nanorod arrays through the second hydrothermal reaction by changing the reaction conditions such as reaction temperature, reaction time, the initial concentration of the starting materials, and basicity of the reaction mixture. As the typical method, the obtained crystal structure of TiO_2 nanorod arrays is mainly rutile phase, which is the most stable phase among the natural phases of TiO_2 . Formation of rutile phase of TiO_2 sometimes restricts the formation of SrTiO_3 due to the higher chemical stability of the rutile TiO_2 . The morphologies and chemical components of $\text{TiO}_2/\text{SrTiO}_3$ heterostructured nanorod arrays were characterized by the measurements of X-ray diffraction (XRD), scanning electron microscopy (SEM), transmission electron microscopy (TEM), energy dispersive X-ray (EDX) spectroscopy, X-ray photoelectron spectroscopy (XPS), and ultraviolet-visible (UV-vis) spectroscopy. The amount of strontium captured in anatase TiO_2 lattice was larger than that of strontium captured in rutile TiO_2 lattice. The extent of the increment of the average diameter of the nanorod before and after the second hydrothermal reaction was also different between the two crystal phases of TiO_2 . It is suggested that better dissolution of anatase TiO_2 resulted in the larger amount of participation of SrTiO_3 and increase of the nanorod diameter effectively.

Niobium doping to $\text{TiO}_2/\text{SrTiO}_3$ heterostructured nanorod arrays was conducted by the Sr^{2+} insertion into the Nb-doped TiO_2 nanorod arrays. The existence of niobium was confirmed by XPS and scanning transmission electron microscopy (STEM) measurements. We will report the further regulation and optimization for formation of Nb-doped $\text{TiO}_2/\text{SrTiO}_3$ heterostructured nanorod arrays by changing the preparation conditions and crystal structures of TiO_2 in terms of the improvement of the conductivity.

9:25 PM EQ02.13.06

Nonlinear Optical Properties of Doped SiGe/Si/SiO₂ Core/Shell Quantum Dot Under Applied Electric Field Mohamed Kria¹, Varsha Yadav², V. Prasad², Kamal Lakkaal¹, J. El Hamdaoui¹, A. El Aouami¹, L. M. Pérez³, El Mustapha Feddi¹ and Gen Long⁴; ¹Mohammed V University in Rabat, Morocco; ²University of Delhi, India; ³Universidad de Tarapacá, Chile; ⁴Saint John's University, United States

This work reports a theoretical study of the nonlinear optical and electronic properties in oblate core/shell quantum dots SiGe in the presence of a donor impurity under electric and magnetic field. Our computations were carried out within the effective mass approximations. For the numerical solution of the resulting 3D partial differential equation (PDE) via finite element method. A detailed study of the donor binding energies as a function of the external electric and magnetic fields, the dipole matrix elements for impurity related inter-level optical transitions as a function of the electric and magnetic fields and impurity position, the absorption coefficient, second (SHG) and third harmonic generation (THG). Our results show that the electric and magnetic fields have significant influences on the ground binding energies and the absorption coefficient, second (SHG) and third harmonic generation (THG). The effect caused by electric and magnetic fields and on-center of shell donor impurities, ostensibly enrich the nonlinear and electronic properties of the system.

9:30 PM EQ02.13.07

Effect of Growth Temperature on Alignment of GaN Growth Islands on Graphene/r-Plane Sapphire Substrate Kazuki Niwa, Masami Nonogaki, Yukito Kato, Yasuhiro Fukunishi, Takahiro Maruyama and Shigeeya Naritsuka; Meijo University, Japan

The state-of-the-art epitaxial growth technique of group III nitride semiconductors can offer a wide range of the applications, such as light emitting diodes, laser diodes, and high-frequency power devices. Devices usually fabricated on the polar c-plane GaN. Therefore, the optical devices fabricated on the plane show inferior performances from the Stark effect. On the other hand, a-plane GaN, which is non-polar plane, will have advantage on the production of superior optical devices. A-plane GaN is usually grown on an r-plane sapphire, although the density of threading-dislocations is still very high.

Remotepitaxy [1] is newly proposed growth method, where growth is performed on graphene-coated substrate. The technique is expected to mitigate the lattice mismatch and the thermal stress produced from the difference between the growth layer and the substrate. A high-quality a-plane GaN crystal is expected to be grown by the method. The grown layer can also be peeled off from the substrate and suitable to make flexible devices. In addition, the reuse of the substrate is possible, which may lead to the sustainable development goals. In this study, we attempt a hetero remotepitaxy to grow a-plane GaN on graphene/r-plane sapphire. The effect of growth temperature on the crystal alignment of GaN is especially focused on to study.

Single-layer graphene was synthesized on an r-plane sapphire substrate using low-pressure CVD [2]. GaN layer was grown using a radio frequency molecular beam epitaxy directly on the graphene-covered sapphire substrate using hetero remotepitaxy. The nitrogen flow rate, RF plasma power, Ga equivalent pressure, and growth time were fixed at 2.0 sccm, 450 W, 4.0×10^{-7} torr, and 10 min while the substrate temperature was changed between 630 and 700 °C. The shape of GaN growth islands was investigated using atomic force microscopy.

C-plane GaN islands with hexagonal shape were observed on the sample grown at 630 °C. On the other hand, c-plane GaN islands decreased with the growth temperature and disappeared on the sample grown at 675 °C, and a-plane GaN islands generated instead of them. The crystal orientation of the a-plane GaN islands was found to be aligned to a certain direction from their rectangular shapes. Surprisingly, two-dimensional nuclei of GaN also started to generate on the sample grown at 700 °C. A thin GaN layer was also successfully grown whose thickness was as thin as 20nm in the condition. Namely, the hetero remotepitaxy was succeeded above 675 °C because the crystal orientation of the rectangular a-plane islands aligned to a certain direction. On the other hand, the hexagonal c-plane islands didn't align at 630 °C. One of the possible reasons of the success is the change of the gap between graphene and the substrate. The gap may be shortened by the removal of some atoms, such as oxygen or hydrogen, from the surface of the sapphire during the thermal treatment. In conclusion, the growth temperature was found as a very important parameter for a-plane GaN remotepitaxy, and even two-dimensional nucleation was successfully obtained at 700 °C.

[1] Y. Kim et al., Nature 544, 340 (2017). [2] Y. Ueda et al., Appl. Phys. Lett. 115, 013103 (2019).

Acknowledgements: This work was supported in part by JSPS KAKENHI Grant Numbers 25000011, 15H03558, 26105002, and 2660089.

9:35 PM EQ02.13.08

WITHDRAWN 12/7/2021 EQ02.13.08 Late News: Structural and Electrical Properties of CNT/Cu Heterostructure—Future Electrical Wires Shivani Dhall¹ and S.k Tripathi²; ¹DAV College, Jalandhar, India; ²Panjab University, India

The structural and electrical properties of carbon nanotubes (CNTs) and Copper (Cu) based nanostructure is presented keeping in mind their applications today and in the near future. CNTs are emerging as the most promising conducting wires in interconnection technology due to their higher electrical conductivity and extraordinary current-carrying capacity. Increased portability, versatility and ubiquity of electronics devices are a result of their progressive miniaturization, requiring current flow through narrow channels. Nowadays, devices operate close to the maximum current-carrying-capacity of conductors (such as copper and gold), leading to decreased lifetime and performance, creating demand for new conductors with higher ampacity. Therefore, researchers exploring electrical properties of CNTs/Cu composites by changing the concentrations of Cu content and vice versa. CNTs/Cu composites shows high conductivity and ampacity, making it uniquely suited for applications in microscale electronics and inverters.

9:40 PM EQ02.13.09

Effects of Graphene Layers in MoS₂/Graphene Heterostructure Ensemble Prepared by Dry Transfer Method for Optoelectronic Devices Sanju Gupta; University of Central Florida, United States

Two-dimensional layered materials that harvest or transduce light energy are of paramount interest. In this context, two-dimensional transition metal dichalcogenides such as molybdenum disulfide (MoS₂) are attractive for harnessing optoelectronics. In this work, we report the integration of MoS₂ with a strong electron accepting graphene yielding novel MoS₂ (1-2L)/graphene (1-2L) heterostructure ensemble by facile and efficient dry transfer method. We also found additional hetero-interfaces due to folded flakes such as MoS₂/MoS₂/graphene and MoS₂/MoS₂/Au hetero-interfaces. We characterized the heterointerfaces using correlated micro-Raman spectroscopy, photoluminescence (PL) spectroscopy, atomic force microscopy, Kelvin probe microscopy and conducting AFM, tip-enhanced Raman spectroscopy (TERS), and tip-enhanced photoluminescence (TEPL) techniques to gain insights into the structural quality, hetero-interfaces, and excitonic effects to elucidate the role of a number of graphene layers which are crucial in modulating the light emission. We studied the charge transfer in these vertical heterostructures unraveling the interlayer electronic coupling. We demonstrate strong evidence that the excitonic properties of MoS₂ are most effective for two layers of graphene layers underneath leading to a significant enhancement of the PL response as compared to MoS₂ supported on one-layer graphene and directly on the gold-coated substrate. We observed a marginal increase in work function with increasing MoS₂ layer as anticipated and for heterointerfaces which are indicative of electron injection. We measured C-AFM without light (dark) and with light in view of photoconducting properties of heterointerfaces and found a rectifying behavior with an apparent increase in current by almost twice for MoS₂/graphene heterostructures in contrast to MoS₂/Au which shows ohmic behavior. Our findings signify the importance of substrate engineering when constructing 2D multilayered architectures for harvesting or storing light energy. This work is financially supported in parts by NSF and NSF-MRI Grants.

9:45 PM EQ02.13.10

Late News: Controlling Exciton Transport in 1D PbI₂—2D MoSe₂ van der Waals Heterostructure Naechul Shin; Inha University, Korea (the Republic of)

Van der Waals (vdW) heterostructures composed of two-dimensional (2D) semiconducting material stacks have garnered significant attention owing to their unique optoelectronic properties compared with their single constituent counterparts. Especially, heterostructure devices composed of 2D semiconductors of which the interfacial exciton transport is controllable hold great potential in photonic and optoelectronic applications. Here, we report vdW heterostructures made of PbI₂ and MoSe₂ and demonstrate that the local exciton distribution can be controlled by modulating the vdW interface between them. PbI₂ vdW layers are prepared in one-dimensional (1D) morphologies with discrete stacking orientations and transferred onto the 2D MoSe₂ layers grown via the chemical vapor deposition (CVD) method. Specifically, the vapor-liquid-solid (VLS) method was employed to grow 1D PbI₂ vdW nanostructures in two different layer stacking orientations (*i.e.*, [001] and [010]) and layer stackings (perpendicular vs. parallel to the wire axis). Upon the transfer onto MoSe₂, we confirm that the exciton transfer between the two materials is strongly dependent on the interlayer configurations (*i.e.*, layer-to-layer vs. edge-to-layer). Strong exciton binding energy of PbI₂ enables the transport of excitons along with the PbI₂ domain via waveguide effect and localized radiative recombination according to the interface with the MoSe₂ domain. Our results provide important insights into the engineering of vdW heterostructure interfaces and develop a new design rule of ultrathin optoelectronic devices.

9:50 PM BREAK

SESSION EQ02.14: Physics and Devices of Mixed Dimensional Heterostructures V
Session Chairs: Berangere Hyot and Joshua Robinson
Tuesday Morning, December 7, 2021
EQ02-Virtual

8:00 AM *EQ02.14.01

From 3D to 2D—Understanding the Extraordinary Properties of "Traditional Materials" at the Atomic Limit Joshua A. Robinson; The Pennsylvania State University, United States

The last decade has seen an exponential growth in the science and technology of two-dimensional materials. Beyond graphene, there is a huge variety of layered materials that range in properties from insulating to superconducting that can be grown over large scales for a variety of electronic devices and quantum technologies, such as topological quantum computing, quantum sensing, and neuromorphic computing. Over the last few years, we have focused on understanding what happens to traditional bulk metals (Ga, In, Ag, Au, etc.) when they are reduced to only a few atoms thick. In this talk, I will discuss recent breakthroughs in the realization of unique 2D forms of these traditional 3D metals. I will discuss a novel synthesis method, dubbed confinement heteroepitaxy (CHet), that utilizes graphene to enable the creation of atomically thin metals, enabling a new platform for creating artificial quantum lattices consisting of 2D and 3D materials, with atomically sharp interfaces and designed properties. By shrinking these traditional metals to atomically thin structures, we find that their properties are completely different than their bulk counterparts, lending themselves to unique quantum and optical applications not possible before.

References

Nature Materials 15, 1166–1171
Nature Materials 19 (6), 637–643
Advanced Funct. Materials, 2005977
Nano Letters 20 (11), 8312–8318
Nanoscale 11(33), 15440–15447

8:30 AM *EQ02.14.02

Mixed-Dimensional van der Waals Heterostructures and Device Applications Berangere Hyot, Colin Paillet, Stéphane Cadot, Julien David-Viffantzeff, Ligaud Clotilde and Lucie Le Van Jodin; CEA, France

Scientists around the globe are investigating how to integrate distinct 2D materials into van der Waals (vdW) heterostructures. Given that any passivated, dangling bond-free surface will interact with another via vdW forces, the vdW heterostructure concept can be extended to include the integration of 2D materials with non-2D materials. Such combinations of materials would yield vdW heterostructures showing a variety of structural and electronic properties that opening up new avenues for innovative device designs. This presentation will focus on three types of mixed-dimensional vdW heterostructures. We successfully employed graphene/QDs (2D/0D) and graphene/MoS₂ (2D/2D) in their low dimensional heterostructures to form photodetector devices. Those devices showed novel functional behaviors, which are discussed based on electrical/optical characterizations and possible physical mechanisms. The third mixed-dimensional, 2D/3D, vdW heterostructure will be discussed on the basis on the growth study of (In)GaN on graphene for the preparation of relaxed templates for micro-display applications.

9:00 AM EQ02.14.03

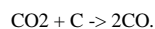
Stability of Graphene Growth on Insulating Substrates in View of Absorption Energy Evaluated by Molecular Dynamics Satoru Kaneko^{1,2,3}, Takashi Tokumashi⁴, Manabu Yasui², Masahito Kurouchi², Akifumi Matsuda³, Mamoru Yoshimoto³, Sumanta Sahoo¹, Kripasindhu Sardar¹, Jyh-Ming Ting¹ and Masahiro Yoshimura¹; ¹National Cheng Kung University, Taiwan; ²KISTEC, Japan; ³Tokyo Institute of Technology, Japan; ⁴Tohoku University, Japan

Graphene with "superclean" surface is prepared via selective etching in carbon dioxide (CO₂) gas. Gentle etchant carbon dioxide selectively eliminate intrinsic contamination such as amorphous carbon during a post annealing process[1]. Is the etching process required as a post annealing?

We used CO₂ as an atmospheric gas during carbon film deposition. Carbon films were prepared in carbon dioxide atmosphere by pulsed laser deposition (PLD) on insulating substrates; strontium titanate (SrTiO₃), sapphire(Al₂O₃) and silicon (Si) substrates. Target was a highly oriented pyrolytic graphite (HOPG), and slower Q-switched YAG was used for PLD system[2].

Graphene grew only on the STO substrate, and showed clean surface image observed by atomic force microscopy (AFM)[2]. CO₂ is a colorless and stable

gas, but CO₂ can be a gentle oxidant with reaction with carbon as,



As the same as “super-clean” surface prepared via selective etching in CO₂ atmosphere, assumed carbon cluster etched by CO₂ and only graphitic materials reach the substrates. Stability of those cluster on the substrate surface was evaluated by absorption energy between the cluster and substrate surface.

In order to estimate an absorption energy of graphitic materials on insulating substrates, a carbon atom, six membered ring (6-ring), and 6 six membered rings (nano graphene) were placed on SrTiO₃, silicon and sapphire substrates, and the absorption energy was estimated by using the density functional theory (DFT) with a semi-core pseudopotential. The generalized gradient approximation (GGA) method was used to obtain the electron density. The energy difference for self-consistent field was set at 1.0×10^{-6} Ha. Crystal structure of each substrates was optimized with periodic condition, and supercell consisting of slab and vacuum layer was used to optimize the top layer of substrate. After optimal surface was prepared on each substrates, supercell with graphitic cluster and slab was optimized, and total energy was estimated on supercell combined cluster and substrate (E_{tot_combined}).

Absorption energy was evaluated to be

$$E_{\text{tot_sub}} + E_{\text{tot_cluster}} - E_{\text{tot_combined}},$$

where E_{tot_sub} and E_{tot_cluster} were total energy of subs and graphitic cluster, respectively.

The absorption energy of graphene on SrTiO₃(001) and Si(001) were estimated to be 570 and 550 kJ/mol, respectively. Although graphene grew on SrTiO₃ substrate while DLC related materials on Si(001), there was not much difference in absorption energy between SrTiO₃ and Si substrates. However form of six-ring on each substrates was remarkably different after optimal combined structure. After optimizing combined structure of six ring placed on Si(001), the six ring did not lie on silicon substrate but it stood up vertically on the substrate while a six ring flatly lied on SrTiO₃ substrate. Actually on the silicon substrate, AFM image revealed the growth of nano balls on the surface while graphene grew with “layer by layer growth” on SrTiO₃ substrate. Cluster generated from target HOPG can be etched and graphitic materials reached to the substrate. However film growth was affected by stability of the cluster placed on substrates because graphene grow from graphitic materials such as nano-graphene and six membered ring. Evaluation of variety of combination of carbon materials and substrates is in progress.

[1] J. Zhang et al., *Angew. Chem. Int. Ed.* **58**, 14446 (2019).

[2] S. Kaneko et al., *Jpn. J. Appl. Phys.* **40**, 4870 (2001).

[3] S. Kaneko et al., *ACS Omega* **2**, 1523 (2017).

9:15 AM EQ02.14.04

Tunable Vertical Schottky Barrier in Hexagonal Boron Nitride Inserted Monolayer Tellurene-Metal Interfaces Sanchali Mitra, Arnab Kabiraj and Santanu Mahapatra; Indian Institute of Science Bangalore, India

Vertically stacked 2D materials heterostructures show potential applications in next-generation nano-electronic devices due to atomic-scale thickness, ultrafast charge transfer, scaling flexibility and precise tuning of atomic band alignment. Tellurene, a recent addition to 2D materials family, has shown promising aspects in nano-devices due to its favorable properties like good ambient stability, high carrier mobility, excellent light absorption, and exceptional thermoelectric performance.^{1,2} Atomistic understanding of the electronic properties of tellurene-metal interface is crucial to promote optimal device performance. Pristine monolayer (ML) β tellurene is semiconducting in nature and possesses an indirect bandgap of about 1.27 eV.³ When monolayer tellurene is interfaced with metals, the bandgap of tellurene completely disappears and it becomes metallic from semiconducting.⁴ This phenomena occurs for all metals that are commonly used as electrode materials, restricting the use of tellurene in vertical Schottky barrier devices. In a recent work, we have shown that inserting single layer of graphene between tellurene and metal can preserve the semiconducting nature of tellurene and hence useful to form Schottky barriers.⁵

In this work, utilizing density functional theory (DFT) we have evaluated the effect of inserting monolayer hBN between tellurene and metal. Using four metals (Au, Pd, Ru, Ti) we have shown that inserted hBN layer can also screen the metallization of tellurene and create vertical Schottky barrier. DFT calculations have been carried out using Vienna ab-initio simulation package (VASP) with Projector Augmented Wave (PAW) method and GGA-PBE exchange correlation functional. To create such heterostructures, first the tellurene-hBN interface is formed by aligning the supercells of the two and applying mean strain of 1.1% in both the surfaces. The tellurene-hBN structure is then interfaced with six layers of <111> cleaved surfaces of Au, Pd and <0001> cleaved surfaces of Ru, Ti. The applied strain on Au, Pd, Ru and Ti are 0.34, 3.45, 3.53 and 1.18% respectively. The surface area of the relaxed tellurene-hBN-metal heterostructures $22.6 \times 8.6 \text{ \AA}^2$, $8.5 \times 23 \text{ \AA}^2$, $25.7 \times 4.5 \text{ \AA}^2$ and $8.67 \times 22.96 \text{ \AA}^2$, respectively. From the projected band structure of tellurene, we found that the band structure of tellurene remains preserved in all the heterostructures, only the energy bands are shifted with respect to Fermi level creating vertical Schottky barriers between tellurene and hBN-metal interface. From Bader charge analysis we found that in Au and Pd-based heterostructures, the charge in tellurene layer is less than that of pristine tellurene, implying depletion of charge. As a result, the valence bands of tellurene shift towards the Fermi level. In case of Ru and Ti, charge accumulation takes place in tellurene layer resulting in shifting of conduction bands towards the Fermi level. However, for Pd and Ti, the shifted bands touch the Fermi level, generating Ohmic contact. For Au, p-type Schottky barrier is formed with a height of about 0.2 eV, while for Ru the barrier is n-type with a height of 0.32 eV. In graphene inserted structures, only p-type Schottky barriers are formed for all these metals, the barrier heights change depending on the metal work-function. However, using hBN we can tune the barrier height as well as the type of contact only by changing the electrode materials. This study provides quantum-mechanical insights into the realization of high-performance vertical Schottky devices using monolayer tellurene based heterostructures.

References:

1. Sang, D. K. et al. *Nanomater. (Basel, Switzerland)* **9**, (2019).
2. Wang, Y. et al. *Nat. Electron.* **1**, 228–236 (2018).
3. Wu, B. et al. *Mater. Res. Express* **4**, 95902 (2017).
4. Yan, J. et al. *J. Mater. Chem. C* **6**, 6153–6163 (2018).
5. Mitra, S. et al. *J. Phys. Chem. C* **125**, 12975–12982 (2021).

9:30 AM EQ02.14.05

Assembly of Close-Packed Ferroelectric Polymer Nanowires via Interface-Epitaxy with ReS₂ Kun Wang, Dawei Li, Shuo Sun, Zahra Ahmadi, Jeffrey Shield, Stephen Ducharme and Xia Hong; University of Nebraska - Lincoln, United States

Ferroelectric polymers such as poly(vinylidene-fluoride-trifluoroethylene) (P(VDF-TrFE)) are promising material candidates for developing flexible wearable nanoelectronics and optoelectronics. For polarization-enabled device functionalities, large-scale fabrication of polymer thin films with high crystallinity and well-controlled polarization direction is highly desirable and remains a central challenge. The widely exploited Langmuir-Blodgett (LB), spin-coating, and electrospinning methods only yield polymorphous or polycrystalline films with compromised net polarization. In this work, we report a highly scalable approach for fabricating P(VDF-TrFE) thin films with high crystalline order and out-of-plane polarization via interface-epitaxy with 1T'-ReS₂ [1]. We deposited 1 - 9 monolayer P(VDF-TrFE) thin films on mechanically exfoliated ReS₂ flakes using the LB technique. Upon controlled thermal annealing, the as-grown LB films crystallize into close-packed (010)-oriented nanowire (P-NW) structure with radii of 10 or 25 nm. The P-NWs are well aligned along the direction perpendicular to the *b*-axis of the interfacial ReS₂ layer. High-resolution transmission electron microscopy studies show that the P-NWs are single crystalline in (001)-orientation and form an epitaxial van der Waals heterointerface with the underlying ReS₂. Piezo-response force microscopy studies confirm the uniform out-of-plane polarization direction of the P-NW films, and reveal nonvolatile polarization switching performance with coercive voltages as low as 0.1 V. Reversing the polarization of the P-NWs can induce a conductance switching ratio of >10⁸ in a bilayer ReS₂ channel, which is among the highest values reported on P(VDF-TrFE)-gated 2D FETs. We also carried out in-situ atomic force microscopy to image the P-NW formation process. Our study points to an easily scalable approach for achieving wafer-size production of continuous P-NW films and high performance nonvolatile ReS₂ transistors. This work was primarily supported by DOE Award No. DE-SC0016153.

[1] Li *et al.*, *Adv. Mater.* DOI: 10.1002/adma.202100214 (2021).

9:45 AM EQ02.14.06

Inter-Valley and Inter-Electronic Transitions in MoS₂-WS₂ Heterostructures [Sungjoon Kim](#)¹, Rousan Debbarma² and Vikas Berry¹; ¹University of Illinois at Chicago, United States; ²Lund University, Sweden

Van der Waals heterostructures allow the integration of functionalities from different nanomaterials to achieve advanced, superimposed properties. Here, mixed MoS₂-WS₂ heterostructure grains were grown using atmospheric pressure chemical vapor deposition technique, and their optoelectronic properties were investigated. The field effect transistors fabricated from the heterostructure grains exhibited high photoresponsivity, which was influenced by the gating potential, as well as the measurement temperature. During the gating potential sweep from -5 V to +55 V, the light to dark source drain current ratio ($I_{\text{light}}/I_{\text{dark}}$) increased from 3 to 16 and from 2 to 7 at 60 K and 120 K, respectively. Such phenomena can be leveraged to realize novel optoelectronic and memory applications.

SESSION EQ02.15: Physics and Devices of Mixed Dimensional Heterostructures VI

Session Chairs: Hyunseong Kum and Stephanie Tomasulo

Tuesday Morning, December 7, 2021

EQ02-Virtual

10:30 AM *EQ02.15.01

Freestanding Crystalline Oxide Membranes [Harold Y. Hwang](#)^{1,2}; ¹Stanford University, United States; ²SLAC National Accelerator Laboratory, United States

The ability to create and manipulate materials in two-dimensional (2D) form has repeatedly had transformative impact on science and technology. In parallel with the exfoliation and stacking of intrinsically layered crystals, the atomic-scale thin film growth of complex materials has enabled the creation of artificial 2D heterostructures with novel functionality and emergent phenomena, as seen in perovskite oxides. We present a general method to create freestanding complex oxide membranes and heterostructures with millimeter-scale lateral dimensions and nanometer-scale thickness, using an epitaxial water-soluble buffer layer [1-3]. This facilitates many new opportunities we are beginning to explore, including the topological melting transition of 2D crystalline order [4], the application of extreme tensile strain and strain gradients [5-7], and integration with other materials families and synthesis techniques [8,9].

[1] D. Lu *et al.*, *Nat. Mater.* **15**, 1255 (2016).

[2] Z. Y. Chen *et al.*, *Phys. Rev. Mater. (RC)* **3**, 060801 (2019).

[3] P. Singh *et al.*, *ACS Appl. Electron. Mater.* **1**, 1269 (2019).

[4] S. S. Hong *et al.*, *Sci. Adv.* **3**, eaao5173 (2017).

[5] S. S. Hong *et al.*, *Science* **368**, 71-76 (2020).

[6] R. J. Xu *et al.*, *Nat. Commun.* **11**, 3141 (2020).

[7] V. Harbola *et al.*, *Nano Letters* DOI: 10.1021/acs.nanolett.0c04787 (2021).

[8] D. Lu *et al.*, *Nano Letters* **19**, 3999 (2019).

[9] D. F. Li *et al.*, *Nano Letters* DOI: 10.1021/acs.nanolett.1c01194 (2021).

11:00 AM *EQ02.15.02

Molecular Beam Epitaxy and Dislocation Dynamics of Metamorphic InAsSb for Long-Wavelength Infrared Applications [Stephanie Tomasulo](#)¹, Chaffra A. Affouda², Jill A. Nolde¹, Mark E. Twigg¹, Michael K. Yakes² and Edward H. Aifer¹; ¹U.S. Naval Research Laboratory, United States; ²Formerly U.S. Naval Research Laboratory, United States

Long-wavelength infrared (IR) III-V based devices have long been of interest for potential applications such as chemical sensing and large format IR imaging. Within the III-V family, only the InAs_{1-x}Sb_x bulk alloy in composition range 0.45 ≤ *x* ≤ 0.8, offers the required bandgap energy (*E_g*) from 100 to 125 meV at an operating temperature of 80K and below [1]. Over this composition range however, the InAs_{1-x}Sb_x lattice constant varies from 6.24 to 6.39 Å, where the lack of conventional substrates has restricted progress on the growth and study of this material system. To overcome this limitation, we employ a metamorphic step-graded InAs_{1-x}Sb_x buffer on GaSb, enabling the study of low-*E_g* InAs_{1-x}Sb_x as a function of growth conditions. Using this method, we investigated the effect of substrate temperature (*T_{sub}*) and group V to group III flux ratio (beam equivalent pressure, V/III) on Sb incorporation of the lowest-*E_g* cap layer [2]. We also used x-ray reciprocal space mapping (RSM) to examine the effect of growth conditions on strain and dislocation dynamics. Following these growth studies, we employed the metamorphic InAs_{1-x}Sb_x in an InAs/InAsSb superlattice designed with a cutoff wavelength of 9 μm which leads to improved absorption compared with the lattice-matched counterpart.

We first grew several InAs_{1-x}Sb_x step-graded structures in which the Sb/(As+Sb) flux ratio was varied from 0.05 to 0.50 in 0.05 increments, under various *T_{sub}* and V/III. Nomarski imaging revealed smoother surfaces under a V/III=10, the highest ratio we attempted. At this higher V/III, we observed

the cross-hatch morphology expected for metamorphic materials and found that the cross-hatch spacing changes, implying a change in dislocation dynamics, with T_{sub} . We also used photoluminescence (PL) to measure the Sb-content in the cap layer as well as compare intensities between samples. We found the highest Sb-incorporation to occur when $T_{sub}=415$ C and $V/III=10$, while the most intense samples used $T_{sub}=415-430$ C and $V/III=10$ [2].

We also identified the Sb composition in each layer using RSM along [110] with (004) and (115) reflections. This allowed comparison of Sb-content as a function of $Sb/(As+Sb)$ for various T_{sub} and V/III . The results suggest that V/III has little effect on Sb incorporation, in direct conflict with our previous PL results [2]. To understand the discrepancy between PL and RSM, we measured (004) RSM of the same three samples with the x-ray beam incident along [1-10], revealing extremely different strain relaxation compared to the [110] case. Asymmetric strain relaxation has been observed in other III-V graded buffer systems and has been explained by different dislocation formation energies and glide velocities along each direction resulting from the core structure of the dislocation being terminated with either a group-III or a group-V element [3]. Transmission electron microscopy is ongoing to further understand the dislocation dynamics in these samples.

Ultimately, we used the lessons learned above to investigate the effect of substrate lattice-constant on strain-balanced InAs/InAsSb superlattices designed for 9 μ m cutoff wavelength. Theoretically, by using a larger substrate lattice-constant the superlattice design results in larger electron-hole wavefunction overlap, ultimately increasing photon absorption. Our experimental results confirm this theory, even in the presence of increased threading dislocations.

[1] I. Vurgaftman et al. *JAP* **89**, 5815-5875 (2001).

[2] Tomasulo et al. *J. Vac. Sci. and Technol. B* **36**, 02D108 (2018).

[3] France et al. *J. Appl. Phys.* **107**, 103530 (2010); Gelczuk et al., *J. Cryst. Growth* **310**, 3014 (2008).

[4] Affouda, Tomasulo et al., *Appl. Phys. Lett.* **110**, 181107 (2017).

11:30 AM EQ02.15.03

Large Enhancement of Photoresponse Through Dielectric Engineering in Silicon-MoS₂ Heterostructure Vrinda Narayanan P and Atikur Rahman; IISER Pune, India

p-n junctions are at the heart of today's semiconductor industry and are the basic building blocks of numerous electronic and optoelectronic devices. Properties of conventional semiconductor p-n junctions are well defined by the type of materials and doping during fabrication and is difficult to tune them afterwards. Van der Waals materials have made it possible to realize atomic thickness p-n junctions. Due to the reduced screening in the out of plane direction, 2D materials and their heterostructures with other dimensional materials offer a unique platform with greatly tunable optoelectronic properties. In this study, we demonstrate how engineering the surrounding dielectric environment would help a p-n junction to improve the photoresponse to a great extent. A silicon-monolayer MoS₂ heterostructure was fabricated as a model system and the effects of surrounding dielectric environment on the electrical transport and photoresponse of the heterostructure was studied. We report nearly three order magnitude enhancement of photoresponse in the presence of higher dielectric environment. With increasing dielectric constant of the surrounding environment, band gap reduces in two dimensional materials changing the band alignment of the heterostructure, photogenerated carriers become easily separable and scattering of charge carriers reduces due to the screening of long range coulomb impurities contributing towards the photoresponse enhancement. Our findings lay a general pathway of improving the efficiency of 2D materials based photodetectors through dielectric engineering.

SESSION EQ02.16: Nanostructures of Low Dimensional Materials II

Session Chairs: Sanghoon Bae and Feng Miao

Wednesday Morning, December 8, 2021

EQ02-Virtual

8:00 AM EQ02.16.01

High Quality Heteroepitaxial Diamond by Using Step-Flow Growth on Misorientated Sapphire Substrate Seong-Woo Kim¹, Ryota Takaya² and Makoto Kasu²; ¹Adamant Namiki Precision Jewel, Japan; ²Saga University, Japan

Diamond semiconductors, owing to their wide bandgap of 5.47 eV and superior properties compared to SiC and GaN, can be used to develop high-power devices. However, the inch-scaled diamond wafer is essential. Recently, we have demonstrated high-quality one-inch heteroepitaxial diamond wafer (Kenzan Diamond®) with X-ray rocking curve (XRC) FWHM of 113.4 arcsec, 234.0 arcsec for (004) and (311) diffractions and threading dislocation density of 1.4×10^7 cm⁻² [1]. On the Kenzan Diamond, we have demonstrated field-effect transistors (FETs) with the highest available output power density of 345 MW/cm² [2]. So far, the Kenzan Diamonds were grown on Ir buffer layer/ just-oriented (11-20) sapphire substrate.

In this study, we performed diamond heteroepitaxial growth on Ir buffer layer/ misorientated (11-20) sapphire substrate. The heteroepitaxial diamond layer shows XRC FWHM of 98.35 for (004) and 175.3 arcsec for (311) diffractions. These values are the lowest and show the highest quality in heteroepitaxial diamonds. These results revealed that step-flow growth occurs on the misorientated surface and the misorientated layer structure releases the internal stress caused by the differences in coefficient of thermal expansion among diamond, Ir, and sapphire layers.

[1] S.-W. Kim et al., *Appl. Phys. Lett.* **117**, 202102 (2020).

[2] N. C. Saha et al., *IEEE Electron Device Lett.* **41**, 1066 (2020).

8:15 AM EQ02.16.02

Intercalation-Induced Swelling Mechanisms of 2D-Organoclay Revealed by Molecular Dynamics Simulation Masaya Miyagawa, Fumiya Hirose, Hayato Higuchi and Hiromitsu Takaba; Kogakuin University, Japan

Since the first half of the 20th century, intercalation property of two-dimensional materials has been investigated energetically. Layered clay minerals such as montmorillonite are the well-known example, and intercalation of alkylammonium ion by exchange of the interlayer cation has been known to absorb hazardous molecules such as aromatic hydrocarbons. However, ideal functionalization has yet been achieved despite of abundance of the clay minerals. One of the biggest problems is difficulty in observation of the nanostructure of the interlayer space, whose height is merely around 1 nm. It is true that the gallery height is able to be measured by X-ray diffraction, but detail morphology of the intercalated molecules is not revealed easily by experiment. In this point of view, molecular dynamic (MD) simulation is a powerful tool to investigate the nanostructure of the organoclay and its intercalation property because the MD simulation directly visualized the nanostructure. Thus, in the present study, we performed the molecular dynamics simulation on montmorillonite modified by octadecyltrimethylammonium ion (Mont-C₁₈) and the adsorption of anthracene (Ph₃) by using molecular dynamics simulation.

The gallery height of Mont-C₁₈ obtained by the MD simulation is 11 Å, which is consistent with that reported experimentally. C₁₈ ions are oriented horizontally and formed so-called pseudotrimeric layer. The intercalation of Ph₃ induces vertical orientation of the C₁₈ ions, which was revealed by atom distribution analyses, and the value of the gallery height is increased linearly along with the number of the intercalated Ph₃ molecule. Corresponding to the orientation change of the C₁₈ ions, the Ph₃ molecules are oriented vertically against the Mont layer. By stepwise intercalation simulations, detail population changes of the Ph₃ molecules are revealed based on the molecular axis. Atom distribution and orientation angle analyses reveals the detail swelling mechanisms of Mont-C₁₈: The intercalated anthracene molecules push out the C₁₈ ions, resulting in the orientation changes from the horizontal to the vertical. The Ph₃ molecules are correspondingly localized on the Mont layer with its molecular axis vertical. The latter result is consistent with that suggested experimentally, where weak interaction of the H atoms of the Ph₃ molecule with the Mont layer may be significant. Thus, it is found that the interlayer of the Mont-C₁₈ is highly inhomogeneous in the presence of the Ph₃ molecules even though the gallery height is only 11-21.6 Å, depending on the number of the intercalated Ph₃ molecules. In addition, the orientation of the Ph₃ molecules is parallel to each other as the number is increased. Because excimer emission is observed in this nanocomposite experimentally, it is strongly suggested that the localization of the Ph₃ molecules on the Mont layer is the key for the characteristic photophysical behavior. We also concluded that the continuous increase in the gallery height originates from soft response of the C₁₈ ions to the intercalation. In other words, the swelling of the interlayer is ascribed not to the volume of the Ph₃ molecules but to the orientation changes in the C₁₈ ions. Summarizing the above results, it is concluded that Å-order inhomogeneity is introduced in interlayer by the intercalation of the Ph₃ molecules, which is significant to utilize the two-dimensional nanospace for ideal materials design.

8:30 AM EQ02.16.03

Al₂O_{3-x}/IZO Heterostructure Transparent Resistive Switching Memory Jaemin Park, Daihong Huh, Soomin Son, Wonjoong Kim and Heon Lee; Korea University, Korea (the Republic of)

In this work, we fabricated the different number of IZO interlayer into Al₂O_{3-x} based transparent resistive switching memory on a transparent ITO deposited substrate at room temperature. Al₂O₃/IZO heterostructure transparent memory has sufficiently high transmittance in the visible region. Also, Al₂O_{3-x}/IZO heterostructure transparent memory has improvement results in lower electroforming voltages as the number of IZO interlayer was increased, as compared to ITO/pure Al₂O_{3-x}/IZO transparent memory. At this time, the transparent memory with 2-IZO interlayer showed a reduction in forming voltage of more than 37% compared to ITO/pure Al₂O_{3-x}/IZO memory. The fabricated transparent memory exhibit typical bipolar resistive switching behavior regardless of the number of IZO interlayer. Additionally, a flexible Al₂O_{3-x}/IZO heterostructure memory was fabricated using the same process on ITO coated PET. The fabricated flexible transparent memory also maintained resistive switching characteristics and stable switching properties during bending.

8:45 AM EQ02.16.04

Collective Modes of a Superconducting Heterostructure Jonathan Curtis, Nicholas Poniatowski, Prineha Narang and Amir Yacoby; Harvard University, United States

In this work we theoretically analyze the collective modes of a heterostructure built from materials with different pairing symmetries. In particular, we focus on the regime where the bulk superconductor has a higher transition temperature and conventional s-wave pairing, while the proximitized system has a lower-temperature transition into an unconventional pairing phase. We argue that, even when both pairing symmetries are topologically trivial, there ought to be signatures of the unconventional pairing in the collective mode spectrum of the joint heterostructure. We conclude by discussing relevant experimental probes and how they relate to the intrinsic pairing interactions in the materials.

9:00 AM EQ02.16.05

Modulation Doping in 2D Materials Yiping Wang and Kenneth Burch; Boston College, United States

2d materials offer great advantages as building blocks for the next generation of technological devices, due to their high-quality, versatility, and the ability to create heterostructures of countless combinations, each exhibiting unique properties. Despite great strides made in device fabrication over the past two decades, some aspects are still missing from the 2d material toolbox, for example being able to heavily charge dope 2d materials locally and cleanly. The ability to dope 2d materials uniformly and non-destructively is highly desirable for both exploring material properties and developing state-of-the-art nanoscale devices. In this work, we characterize the ability of the layered Mott insulator alpha-ruthenium(III) chloride (αrucl) to strongly hole dope graphene. We present that αrucl not only yields a large charge transfer in carbon-based heterostructures, but also that it does so cleanly and uniformly with quantifiable homogeneity. We also find that while the charge transfer is robust for any thickness of αrucl down to the monolayer limit, and can extend out of plane to multi-layer graphene and through insulating spacer layers.

9:15 AM EQ02.16.06

Looking at Structural Heterogeneity with Scanning Nano-Structure Electron Microscopy (SNEM) Yevgeny Rakita^{1,2}, James L. Hart², Partha Pratim Das³, Stavros Nicolopoulos³, Sina Shahrezaei⁴, Suveen N. Mathaudhu⁴, Mitra Taheri² and Simon J. Billinge^{1,5}; ¹Columbia University, United States; ²Johns Hopkins University, United States; ³NanoMegas, Belgium; ⁴University of California, Riverside, United States; ⁵Brookhaven National Laboratory, United States

In recent years, Electron Diffraction, and especially the 4D-STEM [1] is growingly becoming a routine part of structural characterizations of materials at the nano-scale. Its un-matched spatial resolution (down to sub-nm) enables the exploration of local variations within a sample, which alternatively is averaged over the entire irradiated sampled area, when explored, for example, by x-rays. As often shown in electron-microscope, samples are often heterogeneous, and consequently their local properties, which then reflect on the average behavior of the material, composite, or device. Besides morphology and composition, the local structural order can vary, especially in evolving systems. In this study, we explore how far we can take electron diffraction when the interest is in the evolution of materials.

We challenge ourselves with mapping the local structure in a composite of crystalline Ni and amorphous Zr-Cu-Ni-Al Bulk Metallic Glass (BMG) was fused into a composite via hot-rolling [2]. Using a fast camera looking through a fluorescence screen on which diffraction patterns are observed, we use scanning precession electron diffraction to captured 4D-STEM data with 3 nm step size from a FIB-fabricated Ni/BMG/Ni laminate. Using an automated data reduction and analysis pipelines, including distortion correction, auto-masking, azimuthal-integration, Fourier-transformation, and least-square function fitting, to get electron Pair Distribution Function (ePDF) and a set of structurally-meaningful features, which we generalize as Quantities of Interest (QoI). Since we use both the 2D diffraction patterns and the 1D-ePDF's, we generalize the concept of mapping structurally-significant QoI's derived from a spatially-correlated diffraction pattern as scanning nano-structure electron microscopy (SNEM).

We use SNEM to generate QoI-based maps of, for example, the virtual-dark-field (VDF) from the 2D diffraction patterns, and the peak position, peak-width, and the goodness of fit to a structural model from the reduced ePDF's. We find clear variations in structural features across the Ni/BMG interface, as well as within the BMG itself, which indicate the presence of nano-crystalline inclusions with higher structural correlation length, and evidence for variations in the degree of clustering of alike atoms (e.g., Zr-Zr) in the BMG, which indicate a varying short-range chemical order. We could also follow

trends in compositional variations using the average interatomic bond-distance (as also verified with atomic fraction EELS maps) extract the distribution of atomic pairs, exposed the BMG/Ni inter-diffusion front, and estimate the effective local structure of the nano-crystalline inclusion within the BMG as an FCC structure.

Combining these results with atomic composition EELS maps, we learn that nano-crystalline inclusions within the BMG are located in Cu-deficient regions. We also learn that the formation of Ni/BMG composite via hot-rolling, which is often found to be challenging due to the excessive formation of nano-crystallites at the Ni/BMG interface has succeeded due to the metallic Ni being amorphized instead of [BMG--Ni] crystallites being formed. These results are an example of the richness SNEM can provide, and with the assistance of automated (and in the future - automated) pipelines, bring us closer to exposing (and potentially controlling) the history of heterogeneity in evolving systems.

[1] Xiaoke Mu, Andrey Mazilkin, Christian Sprau, Alexander Colsmann, Christian Kübel, (2019). *Microscopy*. **3554**, 301

[2] Sina Shahrezaei, Douglas C. Hofmann, Suveen N. Mathaudhu (2019). *JOM*. **71**, 2

9:30 AM EQ02.16.07

Late News: SrVO₃ as a Bottom Electrode for the Heterogeneous Integration of Ferroelectric BaTiO₃ on SrTiO₃ Asrafal Haque, Sandeep Vura, Pavan Nukala, Shankar Kumar Selvaraja and Srinivasan Raghavan; Indian Institute of Science, India

SrVO₃ (SVO) is a conductive perovskite oxide with an electrical conductivity of 31 μohm.cm and optical transparency (70 %) in the visible region [1]. Its lattice constant $a = 3.8420 \text{ \AA}$ is conducive to integrating perovskite oxides on STO substrates for electro-optic applications. The growth window in pulsed laser deposition (PLD) (10^{-6} mbar and below) of SVO is relatively narrow to obtain the desired electrical and optical characteristics [2]. However, the integration of ferroelectric oxides like BaTiO₃ (BTO) requires a high deposition pressure of 5×10^{-3} mbar and above [3].

To epitaxially integrate BTO on STO via SVO layer, a dual pressure growth scheme is developed to obtain switchable out-of-plane polarized BTO film in tandem. Our XRD measurements and in-situ RHEED measurements confirm the epitaxial nature of the BTO on SVO/STO. The spotty RHEED pattern of the BTO surface indicates BTO grows on SVO via a Volmer-Weber growth mode. Both BTO and SVO films exhibit a sub-nanometer roughness. The SVO film resistivity (Vander-paw method) is 23.2 μohm.cm, comparable to that of MBE-grown films. The BTO integrated via SVO/STO has a good crystal quality, as seen from symmetric ω -scan FWHM of 0.31° . The lattice parameters extracted from out-of-plane ($00l$) and in-plane ($h0l$) RSM scans confirm the out-of-plane orientation of the BTO film. The piezo force microscopy measurements show the switchable nature of polarization in the BTO film. A large tetragonality ($c/a-1$ %) of >2 % (vs. 1 % for a single crystal BTO) is observed in our BTO films and is dependent on deposition conditions. The underlying mechanism will be discussed in detail at the conference.

References

1. M. Mirjole et al., *Adv. Func. Mater.* **29**, 1904238 (2019).
2. M. Mirjole et al., *Adv. Func. Mater.* **29**, 1808432 (2019).
3. J. Lyu et al., *Applied Mat. Interface*, **10**, 25529-25535, (2018).
4. Jarrett et al., *Adv. Mat.*, **25**, 3578-3582, (2013).

9:45 AM EQ02.16.08

Aligned Carbon Nanotube Arrays-Based Transistors Operating in Terahertz Regime Donglai Zhong¹, Huiwen Shi^{1,1}, Li Ding¹, Jie Han¹, Zhiyong Zhang^{1,2} and Lianmao Peng^{1,1,2}; ¹Peking University, China; ²Frontiers Science Center for Nano-optoelectronics, China

Advances in telecommunication technology has led to demand for faster operating frequencies and wider usable frequency ranges. The development of 5G and 6G communication technologies will, in particular, require devices capable of operating at frequencies beyond 90 GHz and up to 300 GHz. Currently, the two semiconductor technologies most used for RF devices are silicon complementary metal-oxide-semiconductor (CMOS) field-effect transistors (FETs) and transistors based on III-V compound semiconductors (primarily GaAs). Silicon transistors are capable of high levels of integration at low cost, but they suffer from poor linearity and noise performance at frequencies above 20 GHz. Devices based on III-V compounds can be used to build systems operating at frequencies beyond 20 GHz, but cannot be integrated directly with digital system in the same chip.

High-semiconducting-purity CNT arrays with suitable choice of array density and tube diameter should allow compatible fabrication of ultra-scaled digital CMOS FETs and high-performance RF transistors on the same substrate. Therefore, CNT FETs should make a better platform for SoC applications than silicon and III-V compound semiconductors-based technologies.

The performance of CNT transistors has been improved due to the developments in material preparation and device fabrication. FETs with the current gain cut-off frequency (f_T) and the power gain cut-off frequency (f_{MAX}) both over 100 GHz have been demonstrated, far behind theoretical predictions, because of lack of well-aligned semiconducting CNT arrays. Ideally, the CNT material for RF FETs is arrays with density ranged from 100 to 200 CNTs μm^{-1} , high semiconducting purity and as a high carrier mobility as possible. The most promising RF FETs have been built using arrays prepared through the floating evaporative self-assembly (FESA) method based on solution-derived CNTs, but their speeds are still limited by the relatively low density (<70 CNTs μm^{-1}) and low mobility ($230 \text{ cm}^2\text{V}^{-1}\text{s}^{-1}$).

Here, we report aligned CNT arrays that offer high density (120 CNTs μm^{-1}), high semiconducting purity (at least 99.99%), carrier mobility (up to $1580 \text{ cm}^2 \text{ V}^{-1} \text{ s}^{-1}$) and a saturation velocity of up to $3.0 \times 10^7 \text{ cm s}^{-1}$. We use a double-dispersion sorting and a binary liquid interface-confined self-assembly (BLIS) procedure, which allows for assembly of aligned arrays on both insulating or semiconducting substrates, such as silicon, glass and quartz. These processes for RF FETs are designed to be fully compatible with the fabrication digital CMOS CNT FETs, for SoC applications. FETs based on these CNT arrays exhibit high driving current, transconductance and f_T/f_{MAX} on both quartz and Si/SiO₂ substrates. In particular, FETs with a 50 nm gate length on Si/SiO₂ offer high d.c. performance with on-state current of 1.92 mA/ μm and peak transconductance of 1.40 mS/ μm at a bias of -0.9 V, and show high a.c. performance with f_T/f_{MAX} of 540 GHz and 306 GHz, respectively, and we show that f_T can be pushed beyond 1 THz when scaled to gate lengths of sub-28 nm. RF amplifiers made using 50 nm length FETs with multi-finger structure exhibit high power gain (23.2 dB) and inherent linearity (31.2 dBm OIP3) in frequencies of at least up to the K band (18 GHz).

SESSION EQ02.17: Large-Scale 2D and Ultra-Thin 3D Membranes II

Session Chairs: Jeehwan Kim and Kyusang Lee

Wednesday Morning, December 8, 2021

EQ02-Virtual

10:30 AM EQ02.17.01

Phase Dependence of Spin Pumping Effect for CoFeB/Sb₂Te₃ Bilayers Misako Morota, Yuta Saito and Noriyuki Uchida; National Institute of

Sb₂Te₃ is well known as a phase-change and thermoelectric material and has recently attracted significant attention as a topological insulator (TI). TIs possess non-trivial electronic structures originating from the strong spin-orbit interaction, resulting in unusual properties, such as the presence of helical spin currents on the surface and formation of the Dirac cone. These properties are expected to enhance spin pumping. However, the effects of atomic ordering in TI films on spin relaxation have not yet been investigated. In this work, the spin-pumping effect in CoFeB/Sb₂Te₃ bilayers was studied using ferromagnetic resonance (FMR) at 300 K for crystalline and amorphous Sb₂Te₃. FMR signal width enhancement was observed for the highly oriented crystalline Sb₂Te₃ film at thicknesses less than 7 nm compared with the amorphous counterpart. In contrast, the FMR signal widths of the amorphous sample and Pt reference were independent of the layer thickness. In particular, the enhancement of the linewidth was most remarkable at 4-nm thickness for the crystalline Sb₂Te₃ samples; this feature was not observed for amorphous Sb₂Te₃ samples. The significant increase in linewidth suggests more efficient spin injection from the ferromagnetic CoFeB layer into crystalline Sb₂Te₃ than into amorphous Sb₂Te₃. Furthermore, the stark contrast between the spin dynamics of the amorphous and crystalline Sb₂Te₃ films supports the idea that the topological phase protected by crystallographic symmetry plays a key role in spin pumping. Additionally, for the effective magnetization of Sb₂Te₃ samples, a change of the magnetic anisotropy direction depending on Sb₂Te₃ thickness was observed, implying the possibility of interactions between topological surface state in crystalline Sb₂Te₃ and ferromagnetic CoFeB films. These findings enhance understanding of the spin pumping effect between topological insulators and ferromagnetic materials and strongly suggest that it is possible to modulate the amount of injected spin by controlling the crystal structure, which provides a new perspective on spin conduction control using phase-change phenomena in conventional spintronics research. This could enable the realization of spintronic devices based on phase-change topological materials.[1]

[1] M.Morota et al., Phys. Status Solidi Rapid Res. Lett. (2021) DOI: 10.1002/pssr.202100247

10:45 AM EQ02.17.02

Precipitation of Multilayer Graphene with Smooth and Large Domain on C-Plane Sapphire Using Crystallized Ni Catalyst Shigeya Naritsuka, Asato Nakashima, Tomoaki Murahashi, Tatsuya Kashio and Takahiro Maruyama; Meijo University, Japan

Graphene is one of the promising materials for realizing a wide range of applications from its unique electrical, mechanical, and chemical characteristics. We have studied a direct precipitation method of graphene to improve its productivity with avoiding the transfer process. The direct precipitation method is promising, although the characteristics of the precipitated graphene are still inferior to those of the CVD-grown graphene. To improve the quality, high temperature growth is attractive but the grain boundary of the catalyst brings another problem. It is because the carbon atoms easily diffuse through the boundaries of the catalyst even at low temperature, and severely deteriorates the precipitated graphene. Therefore, the crystallization of the catalyst without grains is an important issue in the study of graphene growth. The crystallization is beneficial to obtain a large graphene domain too because the superior crystallinity of the catalyst is good for aligning the orientation of the graphene islands and, subsequently, an ideal stitching of the graphene islands are expected. In this presentation, the crystallization of the Ni catalyst is firstly studied on the sapphire substrate. Then, the crystallized Ni catalyst is used to directly precipitate multilayer graphene.

A 100 nm-thick Ni (111) layer was grown on a c-plane sapphire by MBE. Then, 300 nm-thick Ni layer was deposited using electron-beam deposition. The samples were annealed at 1000°C for 30min to crystallize it under hydrogen at atmospheric pressure. Then, the temperature was cooled down at a rate of 3°C/min. After the formation of the Ni crystallized catalyst, the sample was coated by nanodiamond, and heated at 900°C for 30min in a vacuum (10⁻⁴–10⁻³ Pa) using an infrared lamp apparatus. Then, the temperature was cooled down at a rate of 3°C/min. The catalyst was removed using a diluted FeCl₃ solution to directly observe the graphene on the substrate.

Almost whole surface of the sample was successfully crystallized by using the MBE layer as a seed, and a perfectly smooth and flat surface was obtained on it. It is useful to deposit an additional Ni amorphous layer on the MBE-grown layer because the amorphous layer is effective to suppress the dewetting of the Ni layer even at a high temperature.

An extremely flat surface with several growth islands was obtained on the precipitated multilayer graphene. The in-plane X-ray diffraction spectra shows an excellent crystallinity of the graphene from its quite narrow FWHM of 0.25°, which is the smallest FWHM yet reported for a graphene layer. The graphene [11] orientation was precisely aligned to the sapphire [1-100] axis. The Raman spectra indicates the precipitated graphene is multilayer. The Raman D/G mapping measurement with no associated increase also shows that their islands were smoothly connected without forming defects. In addition, no wrinkle was observed on the surface, which possibly came from the effective release of the contraction stress with gently slipping the layer with sandwiching both sides.

Acknowledgements: This work was supported in part by JSPS KAKENHI Grant Numbers 25000011, 15H03558, 26105002, and 2660089.

11:00 AM EQ02.17.04

Wafer-Scale MoS₂/Graphene Heterostructures Synthesized by MOVPE and Their Application Anh Tuan Hoang¹, Ajit K. Katiyar¹, Heechang Shin¹, Neeraj Mishra^{2,3}, Steven Forti^{2,3}, Camilla Coletti^{2,3} and Jong-Hyun Ahn¹; ¹School of Electrical & Electronic Engineering, Korea (the Republic of); ²Istituto Italiano di Tecnologia, Italy; ³Istituto Italiano di Tecnologia Piazza San Silvestro, Italy

Two-dimensional van der Waals heterostructures have attracted increasing interest, owing to the combined benefits of their constituents. These hybrid nanostructures can be realized via epitaxial growth, which offers the prospect of achieving ultraclean interfaces with strong electronic and optical coupling between layers. Here, the epitaxial growth of a continuous molybdenum disulfide (MoS₂) film on large-area graphene, which was directly grown on a sapphire substrate, is reported. Interestingly, the grain size of MoS₂ grown on graphene increases, whereas that of MoS₂ grown on SiO₂ decreases with an increasing amount of hydrogen in the chemical vapor deposition reactor. In addition, to achieve the same quality, MoS₂ grown on graphene requires a much lower growth temperature (400 °C) than that grown on SiO₂ (580 °C). The MoS₂/graphene heterostructure that was epitaxially grown on a transparent platform was investigated to explore its photosensing properties and was found to exhibit inverse photoresponse with highly uniform photoresponsivity in the photodetector pixels fabricated across a full wafer. The MoS₂/graphene heterostructure exhibited ultrahigh photoresponsivity (4.3 × 10⁴ A W⁻¹) upon exposure to visible light of a wide range of wavelengths, confirming the growth of a high-quality MoS₂/graphene heterostructure with a clean interface.

11:15 AM EQ02.17.06

Utilizing 2D Layer Transfer Technique to Fabricate Ultra-Thin Solid-State Battery Celesta S. Chang¹, Hyunseong Kum¹, Sangwook Han², Hanseul Choi², Daniele Vivona¹, Yang Shao-Horn¹, Yun Seog Lee² and Jeehwan Kim¹; ¹Massachusetts Institute of Technology, United States; ²Seoul National University, Korea (the Republic of)

Remote epitaxy, via so-called 2D material-based layer transfer (2DLT) has enabled a wide range of materials to be successfully grown as thin, free-standing layers that can be readily integrated into devices. Such method can be applied in the area of electrochemistry, where we can improve and overcome the limitations that liquid-based Li ion batteries have suffered over the past several decades. While liquid electrolytes have been mainstream owing to its high ionic conductivity and good wetting property with electrode surfaces, its fundamental limitations are set by low thermal, electrochemical stability, low energy density, and poor safety due to dendritic formation.

In particular, formation of Li dendrites penetrating through liquid electrolytes are identified as the main cause for explosions via thermal runaway, which also reduces the lifecycle of the battery. To solve this issue, solid-state batteries have been proposed as an alternative to conventional lithium batteries, which promise significantly reduced possibility of dendrite formations without sacrificing any other properties. However, high-performance thin single-crystalline solid-state electrolytes (SSE) have not yet been demonstrated since Li-containing ionic compound wafers are not commercially available in a single-crystalline form, as well as the difficulty to fabricate thin film SSE single-crystals, necessary for compact design of batteries with high volumetric energy and power density.

Here, we will demonstrate the use of graphene coated substrates for remote epitaxy of LiLaTiO₃ (LLTO) as the electrolyte for solid-state battery applications. We show comparable performance of our ultra-thin film battery to conventional lithium batteries and discuss overall improvements we are able to achieve.

11:30 AM EQ02.17.07

Viscoelastic Bandgaps in Multilayers of Inorganic-Organic Nanolayer Interfaces Rajan Khadka, Ganapati Ramanath and Pawel Koblinski; Rensselaer Polytechnic Institute, United States

Molecular nanolayers (MNLs) at inorganic interfaces are known to lead to unusual enhancements in interfacial fracture energy, thermal and electrical transport. Here, we demonstrate viscoelastic damping bandgaps in multilayered interfaces of MNL-bonded Au nanolayers. Molecular dynamics simulations of Au/octane dithiol/Au multilayers reveal high-damping-loss frequency bands in the $33 \leq \nu \leq 77$ GHz and $278 \leq \nu \leq 833$ GHz regions separated by a low-loss bandgap. The high-damping-losses are up to 31-fold higher than that in individual components in the bulk forms, and the low-losses range from ~40% to 120% of the bulk values. The viscoelastic bandgap scales with the Au-MNL interfacial bonding strength and density, and MNL coverage indicating that it is an interface effect. These findings suggest a variety of possibilities for accessing and tuning novel dynamic mechanical responses in nanocomposites, devices and systems with significant inorganic-organic interface fractions for applications.

11:45 AM EQ02.17.08

Quantum Transport in 3D Patterned SnTe Shuhang Pan, Stephen Albright, Frederick Walker and Charles Ahn; Yale University, United States

SnTe is one of the first materials in the class of topological crystalline insulators (TCIs) to be predicted and studied. In this work, we synthesize thin SnTe films (10 to 30 nm thick) patterned with a regular array of square holes on a SrTiO₃ substrate and compare quantum transport with that measured in unpatterned thin films. The weak localization/antilocalization (WL/WAL) in films is revealed by fitting the magnetoconductivity measurements with the Hikami-Larkin-Nagaoka (HLN) equation. The results show a mixture of WL and WAL in both films, indicating a partial electron spin-momentum locked state. The presence of square holes in the SnTe films suppresses conventional conduction at higher temperature, leading to a stronger WAL effect, and limits the coherence length to the hole size at low temperatures.

SESSION EQ02.18: On-Demand
Sunday Morning, December 5, 2021
On-Demand

8:00 AM EQ02.04.06

Anisotropic Interlayer Exciton in GeSe/SnS van der Waals Heterostructure Nikhilesh Maity; Indian Institute of Science, India

The observation of interlayer excitons (ILE), where the electron and hole are confined in different layers, in van der Waals (vdW) type II heterostructures has ignited a new interest in investigating the optical properties of these 2D semiconducting materials. Herein, using GW and Bethe-Salpeter equation simulations, we demonstrate the generation of linearly polarized, anisotropic intra- and interlayer excitonic bound states in the transition metal monochalcogenide (TMC) GeSe/SnS vdW heterostructure. The puckered structure of TMC results in the directional anisotropy in the band structure and in the excitonic bound state. Upon the application of compressive/tensile biaxial strain, a dramatic variation in excitonic energies, the indirect-to-direct semiconductor transition, and the red/blue shift of the optical absorption spectrum are observed. The variations in excitonic energies and optical band gap have been attributed to the change in effective dielectric constant and band dispersion upon the application of biaxial strain. The generation and control over the interlayer excitonic energies will find applications in optoelectronics and optical quantum computers and as a gain medium in lasers.

8:05 AM EQ02.09.03

MOVPE Growth of h-BN on Patterned Sapphire Substrates and Its Application on Selective Area Growth of GaN Based LEDs Structures Suresh Sundaram^{1,2,1}, Soufiane Karrakhou^{1,2}, Adama Mballo², Phuong Vuong², Yacine Halfaya², Gilles Patriarche³, Tarik Moudakir⁴, Paul L. Voss^{1,2}, Jean Paul Salvestrini^{1,2,1} and Abdallah Ougazzaden^{1,2}; ¹Georgia Institute of Technology-Lorraine, France; ²CNRS, IRL 2958, GT- CNRS, France; ³Universite Paris-Saclay, France; ⁴Institut Lafayette, France

We report MOVPE growth of h-BN on sapphire substrates pre-patterned with SiO₂ and SiN with the goal of investigating the possibility of new kinds of selective area growth. We see that after h-BN growth, the GaN-based device structures grow selectively on sapphire but not on SiO₂ and SiN. This result is surprising because BN is not anticipated to exhibit strong selectivity on dielectric patterns.

To understand how this happens, 20 nm thick h-BN layers were grown separately on dielectric patterned sapphire substrates. On sapphire, the h-BN formed the typical semi-hexagonal wrinkles which is evidence of growth of high quality single crystalline 2D h-BN layers. On SiO₂, localized SIMS measurements confirmed the deposition of BN, so as expected there is not selective area growth of BN. Additional cross sectional TEM studies confirm that the h-BN on the sapphire substrates is highly oriented and layered whereas the BN on the dielectric patterns are nanocrystalline and randomly aligned. Given the lack of crystalline order on the surface of the SiO₂ and SiN regions, the presence of disordered BN there is not surprising.

We have performed several experiments growing functional GaN-based LED structures after h-BN growth during the same growth run, and the selective growth of the GaN-based structures on the h-BN/sapphire is reliable. TEM measurements show that homogeneous, single crystalline GaN based device structure growth occurred only in regions where layered h-BN is deposited, and little to no GaN growth occurred on the randomly-oriented BN on SiO₂. SEM and cathodoluminescence studies confirm that the GaN regions are separated from each other by the dielectric patterns. We conclude from further structural and optical characterisations that the degree of order in BN deposits controls the selectivity of III-Nitride device structures. It seems that the

structure of the BN surface rather than its chemical composition determines whether or not GaN-based materials can grow. Compared to unpatterned areas, fewer GaN dislocations were found in patterned areas, and Spontaneous delamination of III-nitride device structures on h-BN, a problem with full wafer device structures on h-BN, was avoided. The results allow for localized device liftoff and transfer from h-BN since the devices are completely physically isolated from each other. The possibility of pixel by pixel selective transfer opens up heterogeneous integration possibilities needed for realization of novel device architectures and device isolation and device passivation.

8:20 AM EQ02.03.02

Effect of Aluminum Diffusion into 2D hBN on the Mechanical Release of III-N Heterostructures [Phuong Vuong](#)¹, Suresh Sundaram², Adama Mballo¹, Gilles Patriarche³, Soufiane Karrakchou², Tarik Moudakir⁴, Simon Gautier⁴, Paul Voss², Jean-Paul Salvestrini² and Abdallah Ougazzaden²; ¹CNRS, IRL 2958 Georgia Tech, France; ²Georgia Institute of Technology, France; ³CNRS, Centre de Nanosciences et de Nanotechnologies, France; ⁴Institut Lafayette, France

Hexagonal boron nitride (h-BN) is a two dimensional wide-bandgap semiconductor, which can be used as a release layer for mechanical lift-off of as-grown III-nitride heterostructures and their processed devices such as LEDs and HEMTs. However, it has been challenging to control the strain in this layered material which results in spontaneous delamination during epitaxial growth or front-end processing of these devices, mainly for large surface areas. Here, we report a unique approach of controlling the adhesion of this layered material, which can result in either desired lift-off from layered h-BN or mechanically inseparable robust h-BN layers. We found that the growth conditions of an AlN buffer layer on top of h-BN plays an important role for controlling the adhesion of the subsequent device structure grown on h-BN. AlN layer grown above a certain temperature leads to the Al diffusion into h-BN, which enhances the surface and interface dangling bonds, and anchors the layered h-BN. The effect of the Al concentration into h-BN layers on the mechanical lift-off is verified by studying carefully BAlN alloys with different Al content. It has been observed that above a certain Al content, the layered BAlN sample cannot be lifted-off, supporting our investigation. In addition, we provide the flexible approach on the control of the lift-off process by variation of the thickness of h-BN. Furthermore, we illustrate the potential of this investigation by controlling the mechanical lift-off of two types of device structures (LED and HEMT). These results extend the control of the adhesion of 2D/3D materials, opening the route to large-scale fabrication of III-N devices grown on h-BN, and bringing them close to industrial applications.

SYMPOSIUM EQ03

Spin-Based Sensing at the Nanoscale and Hyperpolarization with NV-Diamond and Beyond
December 6 - December 7, 2021

Symposium Organizers

Carlo Bradac, Trent University
Peter Knittel, Fraunhofer Institute for Applied Solid State Physics
Norikazu Mizuochi, Kyoto University
Elke Neu-Ruffing, Technische Universität Kaiserslautern

Symposium Support

Silver
Qnami

* Invited Paper

SESSION EQ03.07: General Session I
Session Chairs: Carlo Bradac and Peter Knittel
Monday Afternoon, December 6, 2021
EQ03-Virtual

1:00 PM *EQ03.07.01

Nanoscale Magnetic Resonance Enabled by Diamond Color Centers [Fedor Jelezko](#); Ulm University, Germany

Single nitrogen-vacancy (NV) color centers in diamond currently have sufficient sensitivity for detecting single external nuclear spins and resolve their position within a few angstroms. The ability to bring the sensor close to biomolecules by implantation of single NV centers and attachment of proteins to the surface of diamond enabled the first proof of principle demonstration of label-free detection of the signal from a single protein. Single-molecule nuclear magnetic resonance experiments open the way towards unraveling dynamics and structure of single biomolecules. However, for that purpose, NV magnetometers must reach spectral resolutions comparable to that of conventional solution state NMR. New techniques for this purpose will be discussed. We will also show first experiments towards hyperpolarisation of extrnuclear spins using shallow NV centers..

1:30 PM *EQ03.07.02

Quantum Sensing with Optically Hyperpolarized Nuclei [Ashok Ajoy](#); University of California, Berkeley, United States

We report on new experiments that demonstrate the potential of hyperpolarized nuclear spins to serve as sensitive magnetometers and sensors of their local environment. This methodology leverages two important features, (1) the ability of sensor nuclei to be hyperpolarized to >3% levels through optical pumping, and (2) their ability to be put into long-lived “Floquet prethermal” states that can be rendered highly sensitive to external magnetic fields. We demonstrate this with ^{13}C nuclei in diamond that are optically hyperpolarized through interactions with lattice Nitrogen-Vacancy (NV) centers. We leverage the exquisite transverse spin lifetimes possible in ^{13}C nuclei under RF driving, wherein we observe lifetimes in excess of $T_2^* = 90\text{s}$ at room temperature (see Fig. 1). These long-lived states constitute an extension of >60,000 over conventional FID decay times $T_2^* \sim 1.5\text{ms}$ in this system. Simultaneously, hyperpolarization and continuous spin readout enable significant gains in signal to noise, and forms the key basis for ultimately making these nuclei serve as quantum sensors. These experiments suggest interesting new opportunities for high-field spin sensors possible via hyperpolarized, low-gamma, nuclei.

2:00 PM *EQ03.07.03

Cryogenic Quantum Sensing and the Low Temperature Photo-Physics of Diamond NV Centers [Patrick Maletinsky](#); University of Basel, Switzerland

Quantum two-level systems offer attractive opportunities for sensing and imaging at the nanoscale. Since its inception [1], this idea has advanced from proof of concept [2] to a mature quantum technology [3], with broad applications in condensed matter physics, materials science and engineering, and a demonstrated economic impact [4].

In this talk, I will present our activities in quantum sensing of mesoscopic, solid-state systems using scanning Nitrogen-Vacancy (NV) centre magnetometry in cryogenic environments. I will on one hand discuss engineering challenges we addressed in photonic engineering of all-diamond scanning probes for quantum sensing [5], and on the other hand highlight recent achievements in nanoscale imaging of two-dimensional, “van der Waals” magnetic systems [6][7].

In the second part of my talk, I will focus on recent studies we conducted in systematically addressing the photo-physics of individual NV centres under cryogenic conditions [8], with the goal to further advancing sensing performance of NV centres at cryogenic temperatures. We observed significant variations of optical spin readout and initialisation efficiencies with magnetic field, that we connect to excited state level anti-crossing in the NVs orbital excited state. The understanding and control of these features is key for NV magnetometry in that it enabled improvements of magnetic field sensitivities by up to an order of magnitude over established baseline values at cryogenic temperatures

I will conclude with an outlook on how these insights could be used to offer fundamentally new sensing modalities and how we will further push our single spin magnetometer developments into the range of extreme environmental conditions, such as high magnetic fields, or millikelvin temperatures.

[1] B. Chernobrod and G. Berman, J. of Applied Physics 97, 014903 (2004)

[2] G. Balasubramanian et al., Nature 455, 644 (2008)

[3] P. Appel et al., Review of Scientific Instruments 87, 063703 (2016)

[4] www.qnami.ch

[5] N. Hedrich et al. Phys. Rev. Applied 14, 064007 (2020)

[6] M. Gibertini et al., Nature Nanotechnology 14, 408 (2019)

[7] L. Thiel et al., Science 364, 973 (2019)

[8] J. Happacher et al., arXiv:2105.08075 (2021)

2:30 PM EQ03.07.04

Late News: Optical Hyperpolarization of ^{13}C Nuclear Spins in Diamond at a Low Magnetic Field [Kavtanyuk Vladimir](#)¹, [Jeong Hyun Shim](#)¹, [Sangwon Oh](#)¹ and [Keunhong Jeong](#)²; ¹Korea Research Institute of Standards and Science, Korea (the Republic of); ²Korea Military Academy, Korea (the Republic of)

Hyperpolarization of nuclear spins by Dynamic Nuclear Polarization (DNP) is significantly higher compare to the thermal polarization. As the result, many Nuclear Magnetic Resonance (NMR) and Magnetic Resonance Imaging (MRI) applications become possible. Optical DNP requires high-power laser irradiation for polarizing electron spins of negatively charged nitrogen vacancy (NV^-) centres and a microwave irradiation for inducing the polarization transfer to ^{13}C nuclear spins. The initial goal of our research is hyperpolarization of diamond powder and investigating ways to improve the polarization. However here we present our DNP measurements obtained on bulk diamonds at a low magnetic field of 18 mT. We have obtained triple DNP profile, ^{13}C polarization by multi-MW frequencies, dependences of ^{13}C polarization over different parameters and NV^- concentrations. This data will be helpful for maximizing the ^{13}C polarization in diamond powder.

2:35 PM BREAK

SESSION EQ03.08: Magnetometry
Session Chairs: Peter Knittel and Elke Neu-Ruffing
Monday Afternoon, December 6, 2021
EQ03-Virtual

4:00 PM *EQ03.08.01

Some Recent Developments in Sensing with Nitrogen-Vacancy Centers in Diamond [Dmitry Budker](#)^{1,2}; ¹Helmholtz Institute, Johannes Gutenberg University, Germany; ²University of California, Berkeley, United States

We will discuss some recent results on zero-field and microwave-free magnetometry, nuclear-spin polarization and readout, demonstration of robust rotation sensing, and dual-modality magnetic imaging/magneto-optical Kerr effect.

4:30 PM *EQ03.08.02

Surface Modification of Diamond for Sensing and Imaging Applications [Anke Krueger](#); Julius-Maximilians-Universität Würzburg, Germany

The surface of diamond plays a crucial role in the control of its electronic properties. Not only the electron affinity and thus the ability to emit electrons into the surrounding media depends on the actual surface termination, but also the interaction with components from the environment such as serum proteins etc. It is thus of great importance to develop methods for the functionalization of the surface in a highly controlled manner that include the termination itself but also the grafting of more complex units for dedicated purposes.

Here we report on different methods for the selective establishment of different oxygenated surface groups as well as an efficient fluorination using wetchemical methods. The influence on the materials properties will be discussed. Additionally, methods for the grafting of protein repelling moieties based on zwitterionic motifs are discussed as an essential tool for bioapplications. Besides, diamond nanoparticles functionalized with organic fluoroionophores for sensing applications will be presented.

This research has received funding from the European Commission's Horizon 2020 program under contract 665085 (DIACAT) and the Volkswagen Foundation under contract 88393.

5:00 PM EQ03.08.03

Nitrogen Vacancy Magnetic Microscopy of Spin Textures in Magnetic Nanomaterials Adam Erickson, Wai Kiat Chin, Rupak Timalisina and [Abdelghani Laraoui](#); University of Nebraska-Lincoln, United States

Magnetic microscopy based on nitrogen vacancy (NV) centers in diamond has become a multifunctional tool to study condensed matter phenomena at the nanoscale [1]. Unlike current magnetic imaging techniques, the NV microscopy platform works at a wide range of temperatures, frequencies, magnetic fields, and it does not perturb the target magnetic sample. We present recent results where NV microscopy is used in both far field and near field (scanning probe) geometries to map spin textures and magnetic excitation (spin-wave) modes in transition metal magnetic nanostructures. Understanding their static and dynamic spin textures can help in exploiting their useful properties such as high surface-to-volume ratio and tailorable surface chemistry for applications in biosensing, catalysis, spintronics, and ultra-high-density magnetic recording. At sizes below 10 nm, surface and edge effects play a major role in determining their magnetic moment and also effect significantly their spin-wave modes. Accurate measurements of spin textures of individual magnetic nanostructures would therefore shed light on their critical properties for tailored applications. Here we report ongoing experiments using NV magnetic microscopy to measure the static and dynamic magnetic properties of individual Co, FeCo (size range 4-15 nm), and CoFeB (size range 20-100 nm) nanostructures. Histograms of important parameters such as magnetization saturation, magnetic domain size, magnetic anisotropy, spin relaxation, and dynamic magnetic excitation modes are extracted and correlated with morphology data taken by atomic force microscopy, scanning electron microscopy, and transmission electron microscopy. We acknowledge support from NSF-DMR award #1809800 and NSF-EPSCoR RII Track-1: Emergent Quantum Materials and Technologies (EQUATE), Award OIA-2044049.

[1] F. Casola, T. van der Sar, and A. Yacoby, Nat. Rev. Mat. 3, 17088 (2018).

5:15 PM EQ03.08.04

Current-Induced Switching of Thin-Film α -Fe₂O₃ Devices Imaged Using a Scanning Single-Spin Microscope [Qiaochu Guo](#)¹, Yang Cheng², Pengxiang Zhang³, Isaiah Gray¹, Fengyuan Yang², Luqiao Liu³, Katja Nowack¹ and Gregory Fuchs¹; ¹Cornell University, United States; ²The Ohio State University, United States; ³Massachusetts Institute of Technology, United States

Antiferromagnetic (AF) materials are interesting for future generation memory and logic applications due to their sub-picosecond spin dynamics and potential for high density. α -Fe₂O₃ is an AF insulator with canted spin-order that leads to a weak magnetic moment oriented perpendicular to the Néel vector at room temperature. Recent studies have shown that the magnetic order of α -Fe₂O₃ can be manipulated using applied currents and read out using spin Hall magnetoresistance. The origin of current-induced switching is still under debate – with spin-orbit torque or thermomagnetoelastic effects due to Joule heating as the two leading mechanisms. To better understand the magnetism of α -Fe₂O₃ and how it is manipulated, here we report magnetic imaging of α -Fe₂O₃ thin film devices with a diamond nitrogen-vacancy (NV) center scanning microscope. We image at 110 nm above a 60 nm thick α -Fe₂O₃ thin film capped with 6 nm of Pt patterned into a Hall cross. The local magnetic texture switches after passing a current pulse through the Pt layer. The difference images between the magnetic field images before and after the current pulse show the switched regions and their switching directions. Our results show that the amount of switching depends on the current pulse duration and the current amplitude. Pulses shorter than 1 μ s do not generate switching even with current density up to 8×10^{12} A/m². This indicates that spin-orbit torque may not be the most important mechanism for the current-induced switching. Meanwhile, we also observe switching outside the current path, where there is no spin-orbit torque. These results suggest that Joule heating from the current and/or heat-induced strain is sufficient to produce magnetic switching. The images also indicate that the current-induced switching can be reversed by an orthogonal current pulse. In addition, we perform autocorrelation analysis of the magnetic images to identify preferred directions of Néel order, which provides more information about the spin domains in thin-film α -Fe₂O₃. The high resolution, high sensitivity magnetic images obtained with scanning NV microscopy provides a means to further investigate the magnetization and switching dynamics of thin film AF insulators.

5:30 PM EQ03.08.05

Quantitative Imaging of Antiferromagnetic Spin Cycloidal Textures on Strain Engineered BiFeO₃ Thin Films with a Scanning Nitrogen-Vacancy Magnetometer Hai Zhong¹, Johanna Fischer², Angela Haykal³, Aurore Finco³, Alexander Stark¹, Felipe Favaro de Oliveira¹, Patrick Maletinsky¹, Mathieu Munsch¹, Stéphane Fusil², Vincent Jacques³, Vincent Garcia² and [Peter Rickhaus](#)¹; ¹Qnami AG, Switzerland; ²Unité Mixte de Physique, CNRS, Thales, Université Paris Saclay, France; ³Laboratoire Charles Coulomb, CNRS, Université de Montpellier, France

Antiferromagnetic thin films attract significant interest for future low-power spintronic devices [1]. Multiferroics, such as bismuth ferrite BiFeO₃, in which antiferromagnetism and ferroelectricity coexist at room temperature, appears as a unique platform for spintronic [2] and magnonic devices [3]. The nanoscale structure of its ferroelectric domains has been widely investigated with piezoresponse force microscopy (PFM), revealing unique domain structures and domain wall functionalities [4]. However, the nanoscale magnetic textures present in BiFeO₃ and their potential for spin-based technology remain concealed. In this report, we present two different antiferromagnetic spin textures in multiferroic BiFeO₃ thin films with different epitaxial strains, using a commercial non-invasive scanning Nitrogen-Vacancy (NV) magnetometer based on a single NV defect in diamond, with a calibrated NV flying height of ~60 nm and a proven DC field sensitivity of ~1 μ T/√Hz. Two BiFeO₃ samples were grown on DyScO₃ (110) and SmScO₃ (110) substrates (later mentioned as BFO/DSO and BFO/SSO, respectively) using pulsed laser deposition. The striped ferroelectric domains in both samples are first observed by the in-plane PFM. The scanning NV magnetometry (SNVM) confirms the existence of the spin cycloid texture, with zig-zag wiggling angles of 90° and 127°, and propagation wavelength of λ_{DSO} =64 nm and λ_{SSO} =103 nm, respectively. At the local scale, the combination of PFM and SNVM allows to identify the relative orientation of the ferroelectric polarization and cycloid propagation directions on both sides of a domain wall. For the BFO/DSO sample, the 90-degree in-plane rotation of the ferroelectric polarization imprints the 90-degree in-plane rotation of the cycloidal propagation direction along $k_1=[-1\ 1\ 0]$, corresponding to the type-I cycloid. On the contrary, in the BFO/SSO sample, the propagation vectors are found to be along $k_1=[-2\ 1\ 1]$ and $k_2=[1\ -2\ 1]$ directions in the neighbouring domains separated by the 71° domain wall. It is worth to mention that in the previous report [5], BFO/SSO, prepared in another growth chamber, showed G-type antiferromagnetic textures, compared to the observed type-II cycloid here. Our results here shed the light on future potential for reconfigurable nanoscale spin textures on multiferroic systems by strain engineering.

- [1] Baltz V., *et al.* (2018) Antiferromagnetic spintronics. *Rev. Mod. Phys.* **90**, 015005.
 [2] Heron J. *et al.* (2014). Deterministic switching of ferromagnetism at room temperature using an electric field. *Nature* **516**, 370–373.
 [3] Rovillain P., *et al.* (2010). Electric-field control of spin waves at room temperature in multiferroic BiFeO₃. *Nat. Mater.* **9**, 975–979
 [4] Balke N., *et al.* (2011). Enhanced electric conductivity at ferroelectric vortex cores in BiFeO₃. *Nat. Phys.* **8**, 81–88.
 [5] A. Haykal, *et al.*, (2020). Antiferromagnetic textures in BiFeO₃ controlled by strain and electric field. *Nat. Commun.* **11**, 1704.

5:45 PM BREAK

SESSION EQ03.09: Bioapplications II
 Session Chair: Norikazu Mizuochi
 Tuesday Morning, December 7, 2021
 EQ03-Virtual

8:00 AM *EQ03.09.01

Nanoscale Free Radical Detection in Living Cells Using Diamond Magnetometry Linyan Nie¹, Anggrek C. Nusantara¹, Mayeul S. Chipaux² and Romana Schirhagl¹; ¹Groningen University, Netherlands; ²EPF Lausanne, Switzerland

Free radicals play a key role in many biological processes including cell communication, immune responses, metabolism or cell development. But they are also involved whenever something is wrong in a cell and are thus important in many diseases including cardiovascular diseases, cancer or bacterial and viral infection. Unfortunately, they are very reactive and short lived and thus difficult to detect for the state of the art. We have used diamond magnetometry to achieve this. We make use of nanodiamonds which we bring into cells. We then use of NV centers in diamonds to perform relaxometry measurements. These are sensitive to spin noise (in this case from radicals) and deliver signals that are equivalent to T1 in conventional MRI but from nanoscale voxels. Using this method, we are able to quantify free radical generation with nanoscale resolution in the nanomole range¹. In our recent work we were able to detect free radical generation in single mitochondria (the energy factories of the cell) in isolated form as well as in their cellular environment².

1 Perona Martiinez, F., Nusantara, A.C., Chipaux, M., Padamati, S.K. and Schirhagl, R., 2020. Nanodiamond Relaxometry-Based Detection of Free-Radical Species When Produced in Chemical Reactions in Biologically Relevant Conditions. *ACS Sensors*.

2 Nie, L., Nusantara, A.C., Damle, V.G., Sharmin, R., Evans, E.P.P., Hemelaar, S.R., van der Laan, K.J., Li, R., Martinez, F.P., Vedelaar, T. and Chipaux, M., Schirhagl, R., 2021. Quantum monitoring of cellular metabolic activities in single mitochondria. *Science Advances*, 7(21), p.eabf0573.

8:30 AM EQ03.09.02

Magnetocardiography of Mammalian Animals Using Nitrogen-Vacancy Centers in Diamond Keigo Arai^{1,2}, Akihiro Kuwahata³, Daisuke Nishitani¹, Ikuya Fujisaki¹, Ryoma Matsuki¹, Yuki Nishio¹, Zonghao Xin⁴, Xinyu Cao⁴, Yuji Hatano¹, Shinobu Onoda⁵, Chikara Shinei⁶, Masashi Miyakawa⁶, Takashi Taniguchi⁶, Masatoshi Yamazaki^{7,4}, Tokuyuki Teraji⁶, Takeshi Ohshima⁵, Mutsuko Hatano^{1,5}, Masaki Sekino⁴ and Takayuki Iwasaki¹; ¹Tokyo Institute of Technology, Japan; ²JST PRESTO, Japan; ³Tohoku University, Japan; ⁴The University of Tokyo, Japan; ⁵National Institutes for Quantum and Radiological Science and Technology, Japan; ⁶National Institute for Materials Science, Japan; ⁷Nagano Hospital, Japan

Magnetocardiography (MCG) is a contactless technique that remotely measures the stray magnetic fields produced by cardiac currents in the heart. The spatial resolution of MCG deteriorates significantly as the standoff distance between the target and the sensor increases. Commercialized MCG devices usually provide centimeter-scale spatial resolution. As an alternative approach, nitrogen-vacancy (NV) centres in diamond have gained interest as a magnetometer for biological experiments [1,2]. In this talk, I will present MCG of mammalian animals using an ensemble of NV centers [3]. A millimeter proximity from the sensor to heart surface enhances the cardiac magnetic field to greater than nanoteslas and allows the mapping of these signals with intra-cardiac resolution. I will also discuss the possibility of further improvement in sensitivity and resolution as well as applying this technique to studying the origin and progression of myriad cardiac arrhythmias including flutter, fibrillation, and tachycardia.

This work is supported by the MEXT Quantum Leap Flagship Program (MEXT Q LEAP), Grant Numbers JPMXS0118067395 and JPMXS0118068379, and JST PRESTO, Grant Number JPMJPR20B1.

[1] D. LeSage *et al.*, Optical magnetic imaging of living cells, *Nature* 496, 486-489 (2013).

[2] J. Barry *et al.*, Optical magnetic detection of single neuron action potentials using quantum defects in diamond, *PNAS* 113 14133 (2016).

[3] K. Arai *et al.*, Millimetre-scale magnetocardiography of living rats, *arXiv2105.11676* (2021).

8:45 AM *EQ03.09.03

NV-Based Hyperpolarization and High-Resolution Detection of Molecules on the Nanoscale Ilai Schwartz; NVision Imaging Technologies GmbH, Germany

Nitrogen vacancy (NV) centers in diamond have been used as ultrasensitive sensors for performing nuclear magnetic resonance (NMR) spectroscopy of molecules external to the diamond at nanometer to micrometer length scales. However, the spectral linewidth is typically limited to the kHz level on the nanoscale, both by the NV sensor coherence time and by rapid molecular diffusion of the nuclei through the detection volume. In addition, NV centers offers promising opportunities for nanoscale hyperpolarization by combining dynamic nuclear polarization methods with optical hyperpolarization. We have previously shown that hyperpolarized signals could enable high spectral resolution on the nanoscale, not limited by molecular diffusion rates.

In this talk we will detail the schemes and challenges for nanoscale polarization using NV centers and show how these could be overcome. We will demonstrate the first unambiguous signal of NMR detection from NV-hyperpolarized external molecules and discuss the potential outlook and future applications.

9:15 AM EQ03.09.04

Room Temperature Hyperpolarization of Polycrystalline Samples with Optically Polarized Triplet Electrons—NV Centers versus Pentacene Koichiro Miyanishi^{1,1}, Takuya F. Segawa^{2,3}, Kazuyuki Takeda³, Izuru Ohki⁴, Shinobu Onoda^{5,6}, Takeshi Ohshima^{5,6}, Hiroshi Abe^{5,6}, Hideaki Takashima³, Shigeiki Takeuchi³, Alexander I. Shames⁷, Kohki Morita³, Yu Wang³, Frederick T. So^{3,5}, Daiki Terada^{3,5}, Ryuji Igarashi^{5,6,8}, Akinori

Kagawa^{1,8,1}, Masahiro Kitagawa^{1,1}, Norikazu Mizuochi³, Masahiro Shirakawa^{3,5} and Makoto Negoro⁵; ¹Osaka University, Japan; ²ETH Zürich, Switzerland; ³Kyoto University, Japan; ⁴Institute for Chemical Research, Japan; ⁵Institute for Quantum Life Science, National Institutes for Quantum and Radiological Science and Technology, Japan; ⁶Takasaki Advanced Radiation Research Institute, National Institutes for Quantum and Radiological Science and Technology, Japan; ⁷Ben-Gurion University of the Negev, Israel; ⁸JST, PREST, Japan

Dynamic nuclear polarization (DNP), a technique to transfer spin polarization from electrons to nuclei, has been studied since its early discovery [1] and has opened the way for high sensitive nuclear magnetic resonance (NMR) spectroscopy and magnetic resonance imaging. In "conventional" DNP, which uses thermally-polarized unpaired electrons as the source of polarization, the DNP enhancement factor is limited to γ_e/γ_n , where $\gamma_{e(n)}$ are the gyromagnetic ratios of the electron (nuclear) spins. In DNP using the paramagnetic electrons in thermal equilibrium, experiments need to be performed at cryogenic temperature to increase the electron-spin polarization as much as possible. Conversely, the spins of optically created electrons in the triplet state can have much higher polarization than their thermal equilibrium value, DNP using the triplet state, referred to as triplet DNP, can lead to nuclear hyperpolarization beyond the limit of the conventional DNP using thermal electron polarization. Furthermore, experiments can be carried out at room temperature, by irradiating the sample with laser light. Recently, DNP of an ensemble of ¹³C nuclear spins using negatively charged nitrogen-vacancy (NV⁻) color centers in a bulk diamond single crystal has been demonstrated at room temperature and the ¹³C polarization of 6 % has been achieved via the combination of the thermal mixing and the solid effect [2]. DNP using NV⁻ in powdered microdiamonds has been reported by Ajoy *et al.*, who took advantage of the reduced width of the anisotropic electron spin resonance powder pattern of the NV⁻ centers at the magnetic field of ca. 30 mT [3]. However, triplet DNP is much older and achieved a ¹H polarization of 34 % at room temperature and a magnetic field of 0.4 T using pentacene in *p*-terphenyl crystal [4]. Even though triplet DNP in both systems, NV⁻ centers and pentacene, relies on the transfer of spin polarization from optically hyperpolarized triplet electrons to nuclei, there are important differences. While the NV⁻ center has an electronic triplet ground state and is therefore paramagnetic, pentacene has an electronic singlet ground state, is diamagnetic, and only becomes paramagnetic through optical excitation into a triplet state. On the other hand, the zero-field splitting parameter *D* for pentacene is only half as large as in NV⁻ centers, which is an advantage when disordered powder is used as a sample. In this work, we compare triplet-DNP of NV⁻ centers in diamond and pentacene doped in [carboxyl-¹³C] benzoic acid (PBA) in polycrystalline samples at room temperature [5]. In the DNP experiments, the integrated solid effect (ISE) was used to transfer the polarization from electrons to nuclei. The ISE employs microwave irradiation and external magnetic-field sweep, so that the Hartmann-Hahn matching is implemented between the electron spins in the rotating frame and the nuclear spins in the laboratory frame. We study the behavior of the ¹³C polarization buildup in terms of the polarization efficiency of the transfer from the electron to nuclei, exchange rate, and the ¹³C spin diffusion. As a result, we obtained the ¹³C polarization of 0.01 % in the microdiamonds, and of 0.12 % in PBA at room temperature in a magnetic field of 0.4 T by using the integrated solid effect and the obtained exchange rate was 0.87 % for microdiamonds and 3.5 % for PBA. The ¹³C polarization enhancements for the diamond and the PBA were 300 and 3600 compared to the thermal NMR polarization. Besides the initial polarization transfer from the triplet electron to the nuclei, we also shed light on the process of nuclear spin-diffusion, which distributes the hyperpolarization within the sample.

References

- [1] A. W. Overhauser, *Phys. Rev.*, **92**, 411 (1953).
- [2] J. P. King *et al.*, *Nat. Commun.*, **6**, 8965, (2015).
- [3] A. Ajoy *et al.*, *Sci. Adv.*, **4**, 5, (2018).
- [4] K. Tateishi *et al.*, *Proc. Natl. Acad. Sci. U. S. A.*, **111**, 7527 (2014).
- [5] K. Miyaniishi *et al.*, *Magn. Reson.*, **2**, 1 (2021)

9:30 AM EQ03.09.05

Label-Free Phase Change Detection of Lipid Bilayers Using Nanoscale Diamond Magnetometry Hitoshi Ishiwata^{1,2}, Hiroshi C. Watanabe^{1,3}, Shinya Hanashima⁴, Takayuki Iwasaki² and Mutsuko Hatano²; ¹PRESTO, Japan; ²Tokyo Institute of Technology, Japan; ³Quantum Computing Center, Keio University, Japan; ⁴Osaka University, Japan

The cell membrane is a nanoscale 2D fluid crystalline assembly with sub-compartment domains that are critical for cellular functions, including transport of molecules, communications, and metabolic properties with its external medium [1]. These domains are distinguished by different phases of lipid membranes, and the fluidity of the lipid bilayer, described by the 2D translational diffusion of lipid molecules [2], determines the most fundamental property of lipids in different phases and therefore domains. Nanoscale NMR and correlation spectroscopy using a NV center has emerged as a quantum measurement platform that allows for label-free diffusion measurement with nuclear spin from a small detection volume of $\sim (6 \text{ nm})^3$ [3]. In this study, we investigate nanoscale phase change detection of lipid bilayers utilizing ensemble-averaged nuclear spin detection from small volume $\sim (6 \text{ nm})^3$, which is determined by the depth of the NV center. Analysis of nanoscale NMR signal confirms thickness of lipid bilayer to be $6.2 \text{ nm} \pm 3.4 \text{ nm}$ with proton density of 65 proton/nm³ on top of diamond sample. The result of the correlation spectroscopy was compared with the 2D molecular diffusion model constructed by Monte Carlo simulation combined with results from molecular dynamics (MD) simulation. There is a change in diffusion constant from $1.5 \pm 0.25 \text{ nm}^2/\mu\text{sec}$ to $3.0 \pm 0.5 \text{ nm}^2/\mu\text{sec}$ when the temperature changes from 26.5 °C to 36.0 °C [4]. Our results demonstrate that label-free detection of changes in translational diffusion of lipid molecules is possible using nanoscale diamond magnetometry. Direct observation of changes in the diffusion constant paves the way for the label-free identification of domains that are formed in the cell membrane to understand the relationship between cell membrane dynamics and cell function [5].

This study was supported by JST PRESTO Grant number JPMJPR17G1 and in part by the MEXT Quantum Leap Flagship Program (MEXT Q-LEAP) Grant Number JPMXS0118067395.

- [1] G. van Meer, A. I. P. M. de Kroon, *J Cell Sci.* **2011**, 124, 5-8.
- [2] G. van Meer, D. R. Voelker, G. W. Feigenson, *Nat. Rev. Mol. Cell Biol.* **2008**, 9, 112-124.
- [3] T. Staudacher, N. Raatz, S. Pezzagna, J. Meijer, F. Reinhard, C. A. Meriles, J. Wrachtrup, *Nat. Comm.* **2015**, 6, 8527.
- [4] H. Ishiwata, H. C. Watanabe, S. Hanashima, T. Iwasaki, M. Hatano, *Advanced Quantum Technology* **2021**, 4, 2000106.
- [5] M. A. Pavel, E. N. Petersen, H. Wang, R. A. Lerner, S. B. Hansen, *Proc. Natl. Acad. Sci. USA.* **2020**, 117, 13757-13766.

9:45 AM EQ03.09.06

Imaging of Weight Distribution Using a Hybrid System Based on Piezoactive Magnetic Material and Diamond Quantum Sensor Ryota Kitagawa¹, Shunsuke Nagata¹, Soki Urashita¹, Keigo Arai^{1,2}, Kosuke Mizuno¹, Hitoshi Ishiwata^{1,2}, Yota Takamura¹, Takayuki Iwasaki¹, Shigeki Nakagawa¹ and Mutsuko Hatano¹; ¹Tokyo Institute of Technology, Japan; ²Japan Science and Technology Agency, Japan

Imaging of weight introduces a new modality for the study of biological systems. Existing techniques either have high weight sensitivity but can measure only a single cell or offer a large field of view with limited weight sensitivity[1,2]. Thus, a key challenge in weight imaging is to provide a capability to measure various biological systems extending over multiple length scales from single cells to biological tissues. Such a high dynamic range in length scale can be realized by a hybrid sensor based on piezoactive magnetic material[3] and nitrogen-vacancy (NV) centers in diamond[4]. In the hybrid sensor, due

to the inverse magnetostrictive effect, weight is converted into the rotation of magnetization and domain wall motion in piezoactive magnetic material. This rotation and domain wall motion induce a change in the stray magnetic field, which can be detected by NV centers via optically-detected magnetic resonance (ODMR). For the realization of the hybrid sensor, accurate imaging of weight distribution is essential. Here, we demonstrate weight imaging using a hybrid system composed of piezoactive magnetic material and the NV center and calibrated weight.

We fabricated a hybrid sensor by gluing a piezoactive magnetic material of a SmFe_2 thin film, deposited on an ultra-thin glass substrate, and NV centers in a diamond film deposited on a type-Ib diamond (111) substrate. We applied weight onto the system in an area of 3.1 mm^2 by putting on a rivet with a total weight of 9 g. As a comparison, we performed the measurement without applying weight. Imaging of the magnetic field distribution was performed by continuous-wave ODMR while applying a bias magnetic field of $\sim 2 \text{ mT}$ to break the degeneracy of the NV center spin levels.

We observed a different response between the stressed and unstressed areas. The change of the magnetic field was more significant in the stressed area. On the other hand, the shape of the magnetic field distribution that is thought to originate from the magnetic domain did not change. These results imply that the rotation of the magnetization was dominant compared to domain wall motion. We can understand the weight response of SmFe_2 by a simple single domain model, including magnetization, intrinsic magnetic anisotropy, and strain-induced anisotropy. The observed magnetic field difference of about $\pm 15 \mu\text{T}$ is comparable with the value estimated by the single domain model. We established essential techniques for constructing the hybrid system through imaging weight response of piezo active magnetic material by NV center.

This study was supported in part by MEXT Q-LEAP JPMXS0118067395.

[1] G. Popescu *et al.*, *Lab Chip* **14**, 646 (2014).

[2] D. Martín *et al.*, *Nature* **550**, 500 (2017).

[3] Y. Takamura *et al.*, *Solid. State. Electron.* **128**, 194 (2017).

[4] J. Cai *et al.*, *Nat. Commun.* **5**, 1 (2014).

SESSION EQ03.10: NMR
Session Chair: Peter Knittel
Tuesday Morning, December 7, 2021
EQ03-Virtual

10:30 AM *EQ03.10.01

The Case Against Entanglement Advantages in Quantum Sensing Liam McGuinness; The Australian National University, Australia

In this talk I will outline reasoning as to why we should not expect entanglement to improve the performance of quantum sensors. I will consider the specific sensing example of estimating the frequency of an unknown field, and provide additional arguments for general sensing. The talk will also discuss published literature and why the experimental evidence is in agreement with this talk's central thesis.

11:00 AM EQ03.10.02

Remote Nuclear Magnetic Resonance Detected by Low-Frequency Quantum Sensing David Herbschleb¹, Izuru Ohki¹, Kohki Morita¹, Yoshiharu Yoshii², Hiromitsu Kato³, Toshiharu Makino³, Satoshi Yamasaki⁴ and Norikazu Mizuochi¹; ¹Kyoto University, Japan; ²Sumida Corporation, Japan; ³National Institute of Advanced Industrial Science and Technology (AIST), Japan; ⁴Kanazawa University, Japan

Quantum sensing has a bright future for many applications given its potential for high sensitivity and resolution. Sensing with nitrogen-vacancy (NV) centres is a much explored option given its room-temperature operation, making it a feasible choice for biology applications. One example is measuring nuclear magnetic resonance (NMR) spectra of molecules. Given the potential for arbitrary resolution [1,2], Fourier-based algorithms have been implemented for measuring such NMR signals [3]. However, these are limited for use at high frequencies (over $\sim 1 \text{ kHz}$) given the usage of dynamical decoupling sequences. On the other hand, low-frequency signals are important for chemical structure analysis [4] and for searching new particles beyond the standard model [5]. Here, we demonstrate a technique to measure low-frequency fields which sensitivity is frequency independent. Moreover, we apply it to measure low-frequency NMR signals with a remote NMR system, giving a line width for the free nuclear precession of water of 1.6 Hz.

[1] J. M. Boss *et al.*, *Science* **356**, 837–840 (2017).

[2] S. Schmitt *et al.*, *Science* **356**, 832–837 (2017).

[3] D. R. Glenn *et al.*, *Nature* **555**, 351–354 (2018).

[4] D. A. Barskiy *et al.*, *Nat. Commun.* **10**, 3002 (2019).

[5] T. Wu *et al.*, *Phys. Rev. Lett.* **122**, 191302 (2019).

The authors acknowledge the financial support from JST OPERA (No. JPMJOP1841), KAKENHI (No. 21H04653) and the Collaborative Research Program of ICR, Kyoto University (2021-114).

11:15 AM EQ03.10.03

Detection of Nuclear Quadrupolar Resonance of a Nanoscale 2D Material by Optimized Nitrogen Vacancy Ensembles in Diamond Jacob D. Henshaw^{1,2}, Pauli Kehayias¹, Maziar Ziabari^{2,3}, Takashi Taniguchi⁴, Kenji Watanabe⁴, Erin Morissette⁵, Jia Li⁵, Edward Bielejec¹, Michael Lilly^{1,2} and Andrew Mounce^{1,2}; ¹Sandia National Laboratories, United States; ²Center for Integrated Nanotechnologies, United States; ³The University of New Mexico, United States; ⁴National Institute for Materials Science, Japan; ⁵Brown University, United States

Nuclear magnetic resonance (NMR) and nuclear quadrupole resonance (NQR) of bulk quantum materials has provided significant insight into magnetic phenomena such as quantum phase criticality, magnetism, and superconductivity. With the emergence of nanoscale 2-D materials with magnetic phenomena, traditional, inductively detected NMR is not sufficiently sensitive to detect the small nuclear density in these materials. The nitrogen-vacancy center in diamond (NV) has shown great promise in bringing the spectroscopic capabilities of NQR to the nanoscale and has been demonstrated utilizing single NV spins to detect 11B NQR in a monolayer of hBN¹. Single NV spins provide 30nm resolution but can be unstable and maybe less sensitive to NMR than NV ensembles. However, NV NMR detection of 2D materials has yet to be demonstrated with NV ensembles. Furthermore, the optimal NV layer for NMR detection will require an optimized depth calibration which trades off sample-NV standoff (closer to the diamond surface) and higher activation/better spin properties (further from diamond surface).

In this work, we prepare a range of near-surface NV ensembles, determine their depths by 19F NMR, determine their NMR sensitivities, and use our most sensitive NV ensemble for detection of 11B NQR in hBN exfoliated onto the diamond surface. To prepare our near surface NV ensembles, we implant

approximately 100ppm nitrogen at energies from 1.5 to 7 keV and activate NVs by ultra-high vacuum annealing. By applying fomblin oil on the surface of these diamonds and detecting 19F NMR signal intensity, we find effective NV ensemble depths to be from 3 nm to 12 nm. The 19F NMR signal intensity also serves as an experimental determination of the nuclear spin sensitivity for our NV ensembles, and we find that our 3 keV (7.5 nm deep) NV ensemble is the most sensitive to 19F on the diamond surface. We then exfoliated 100nm thick flakes of hBN onto the surface of these diamonds and measure the NQR signal intensity of 11B by both CPMGXY8-N and correlation spectroscopy. The intensity of 11B NQR spectra are also found to be optimal for the 3keV NV implant, reenforcing the results of our 19F signal optimization. As a next step, with our optimized NV ensemble, we will measure the spatial dependence of the NQR frequency on our hBN flakes to determine the spatial variations of strain and electric fields.

Sandia National Laboratories is a multi-mission laboratory managed and operated by the National Technology and Engineering Solutions of Sandia, LLC, a wholly owned subsidiary of Honeywell International, Inc., for the DOE's National Nuclear Security Administration under Contract No. DE-NA0003525. This work was funded by the Laboratory Directed Research and Development Program and performed, in part, at the Center for Integrated Nanotechnologies, an Office of Science User Facility operated for the U.S. Department of Energy (DOE) Office of Science.

1. Lovchinsky, I. *et al.* Magnetic resonance spectroscopy of an atomically thin material using a single-spin qubit. *Science* (80-.). **355**, 503–507 (2017).

11:30 AM *EQ03.10.04

High-Resolution NV-NMR Spectroscopy at the Micron-Scale Ronald Walsworth and [Nithya Arunkumar](#); University of Maryland, United States

Nitrogen-vacancy (NV) quantum defects in diamond can detect nuclear magnetic resonance (NMR) signals with high-spectral resolution from micron-scale sample volumes. However, a key challenge for NV-NMR spectroscopy is detecting samples at millimolar molecular concentrations to enable analysis of complex micron-scale systems such as individual cells. Here we describe methods to increase NV-NMR concentration sensitivity by several orders of magnitude using hyperpolarization of target proton spins and a quantum memory readout. To date, these methods have allowed micron-scale NMR spectroscopy of small-molecule sample concentrations as low as 1 millimolar in picoliter volumes, with further sensitivity improvements expected.

SYMPOSIUM EQ04

Machine Learning on Experimental Data for Emergent Quantum Materials
November 29 - December 8, 2021

Symposium Organizers

Maciej Haranczyk, IMDEA Materials Institute
Mingda Li, Massachusetts Institute of Technology
Christopher Rycroft, Harvard University
Tess Smidt, Massachusetts Institute of Technology

* Invited Paper

SESSION Tutorial EQ04: Symmetry-Aware Neural Networks for the Material Sciences
Monday Morning, November 29, 2021
Hynes, Level 2, Room 205

8:30 AM

Euclidean Symmetry in Machine Learning for Materials Science [Tess Smidt](#); Lawrence Berkeley National Laboratory, United States

Understanding symmetry's role in the physical sciences is critical for choosing an appropriate machine learning method. For example, coordinates used to describe positions of atoms in a material are traditionally a challenging data type to use for machine learning -- coordinates and coordinate systems are sensitive to the symmetries of 3D space: 3D rotations, translations, and inversion. One of the motivations for incorporating symmetry into machine learning models on 3D data is that it eliminates the need for data augmentation -- the 500-fold increase in brute-force training necessary for a model to learn 3D patterns in arbitrary orientations. Additionally, many features of physical systems are consequences of symmetry -- geometric tensor properties, point groups, and space groups, degeneracy, phase transitions, atomic orbitals, etc. By incorporating symmetry into a model by construction (rather than by training), these consequences arise naturally in the behavior of the model (even in untrained models). There are two general types of symmetry-aware models: invariant and equivariant. Invariant models get rid of coordinate systems by only dealing with quantities that are invariant to the choice of coordinate system (scalars), while equivariant models preserve how quantities predictably change under coordinate transformations. While invariant models are the most prevalent symmetry-aware models because they are mathematically simpler, equivariant models more faithfully represent the complexity of physical interactions. In this tutorial we will discuss how symmetry emerges when representing physical systems and strategies for accommodating these symmetries when building machine learning algorithms. As an example, we will give an overview of some of the properties of Euclidean neural networks, a general neural network framework that fully treats the equivariance of physical systems and naturally handles 3D geometry and operates on the scalar, vector, and tensor fields that characterize them. Later lectures will dive into how these and related methods are implemented and

applied to real-world materials challenges.

9:30 AM

Group Theory, Irreducible Representations, and Tensor Products and How to Use them in e3nn to Build Euclidean Neural Networks [Mario Geiger](#); EPFL, Switzerland

In this tutorial we will introduce useful concepts group theory for creating symmetry invariant and equivariant algorithms for materials: representation of groups and the vector spaces they act on, including irreducible representations, and how to interact and combine group representations, e.g. tensor products.

We will connect this theory to practical examples in material science, for example we will give examples of tensor properties of materials and how to express them in terms of Cartesian tensors and irreducible representations.

Euclidean neural networks use these group theoretic principles to achieve global and local equivariance to 3D rotations, translations, and inversion at every layer. We will go through concrete coding examples for how to build these models using e3nn: a modular open-source PyTorch framework for Euclidean Neural Networks (<https://e3nn.org>). In e3nn, the group theoretic tools discussed above are implemented as practical PyTorch modules. We will cover the Irreps class and operations such as TensorProduct. We will also touch upon topics such as nonlinearities and how these differ from traditional neural networks. The e3nn package will continue to be used throughout the morning and afternoon tutorials to demonstrate core concepts in using invariant and equivariant algorithms for practical materials applications.

10:30 AM BREAK

11:00 AM

Analyzing geometry and structure of atomic configurations with equivariant and invariant functions Thomas J. Hardin¹ and [Martin Uhrin](#)²; ¹Sandia National Laboratories, United States; ²EPFL, Switzerland

Some of the most challenging aspects of applying machine learning to atomic configurations have to do with interfacing atomic configurations (point clouds and species labels) with machine learning methods in a way that 1) respects geometric symmetry, 2) is flexible with respect to the number of atoms in a configuration, and 3) respects indistinguishability of atoms. e3nn handles each of these issues naturally, making it an ideal framework for machine learning on atomic configurations.

In this hands-on lecture we will use e3nn to 1) demonstrate how to project atomic environments onto basis function expansions (using the SphericalTensor and FourierTensor objects in e3nn), 2) use those expansions to calculate invariant representations of the atomic configurations, and 3) show how to use optimization techniques and the automatic differentiation capabilities of e3nn to recover geometry from these representations.

12:00 PM BREAK

1:30 PM

Molecular dynamics with NequIP [Simon L. Batzner](#); Harvard University, United States

Machine-Learning Interatomic Potentials have over the past decade emerged as a powerful tool for increasing time- and length-scales of molecular dynamics simulations while retaining the high accuracy of the reference calculations they were trained on. Recently, the NequIP potential, an equivariant neural network-based interatomic potential has been demonstrated to obtain an unprecedented level of accuracy and sample efficiency, allowing ML Interatomic Potentials to be trained with up to 1000x fewer training data than competing methods.

In this tutorial, we will demonstrate how to train and subsequently deploy NequIP interatomic potentials in molecular dynamics simulations. We will outline best practices for data set selection and training of the NequIP model as well as how to successfully run efficient simulations. We will give an introduction to the NequIP software code and detail how to work with its interface to the LAMMPS molecular dynamics software suite, a highly efficient code for large-scale molecular dynamics simulations, enabling the efficient and accurate study of a diverse range of materials.

2:30 PM BREAK

3:00 PM

Predicting Electron Densities with e3nn [Josh Rackers](#); Sandia National Laboratories, United States

One of the fundamental challenges of atomic-scale science for the 21st century is the ability to simulate large molecules with quantum mechanical accuracy. What makes this problem so challenging is the poor scaling of solving the equations of quantum mechanics on a classical computer. Even the most efficient quantum chemistry programs, such as Density Functional Theory (DFT), scale with the cube of the system size. This makes accurate simulations of large molecules with these methods fundamentally impossible.

One proposed method of breaking this “quantum scaling limit” is to use machine learning (ML) to learn quantum mechanics. In this tutorial, we will demonstrate how Euclidean Neural Networks in general, and e3nn in particular, are well-suited for this task. As an instructive example, we will show how to predict the electron density of clusters of water molecules and examine how that model can transfer to larger systems.

4:00 PM

Predicting Phonon Properties of Crystal Structures [Zhantao Chen](#); Massachusetts Institute of Technology, United States

Phonon density of states (DoS) is a key determinant of many properties of crystalline solids. However, acquisition of phonon DoS is experimentally nontrivial due to limited inelastic scattering facility resources, and at the same time computationally expensive for complex materials, particularly disordered systems. These challenges further lead to a scarcity of phonon DoS data to perform data-driven studies.

e3nn enables efficient and direct prediction of phonon DoS using easily accessible input information about atomic structures, specifically atom types, masses, and positions. By directly incorporating crystallographic and 3D spatial symmetry constraints, e3nn can achieve good performance even when trained on a modest phonon DoS dataset of ~1000 examples. In this lecture, we will demonstrate how to predict phonon DoS from crystal structures using e3nn, as well as introduce the natural extension of predicting the DoS of alloy materials.

SESSION EQ04.01: Machine Learning for Spectroscopy
Session Chair: Mingda Li
Tuesday Morning, November 30, 2021
Hynes, Level 2, Room 205

10:30 AM *EQ04.01.02

Time-Resolved RIXS Technique and Applications in Nonequilibrium Quantum Materials [Yao Wang](#); Clemson University, United States

Quantum material has become a new research frontier and is widely believed to be the cornerstone of the next technological revolution. To initiate revolutionary innovations, the precise control of the electronic properties in quantum materials is on demand. The ultrafast laser pump becomes a promising control approach due to the rich degrees of freedom and the extra time axis. However, it also places an urgent requirement for the ultrafast identification of the materials' property.

In this talk, I will briefly introduce the new ultrafast pump-probe technique, time-resolved resonant inelastic x-ray scattering, from a theoretical and computational perspective. Then I will use two typical classes of quantum materials, the topological material and correlated magnets, as examples to sketch the novel applications. As a nonlinear pump-probe technique, its intermediate state selectivity provides a clean characterization of topological edge states. Its sensitivity to multiple excitations and the broad momentum coverage gives a unique opportunity to Floquet-engineer spin excitations in correlated materials.

11:00 AM *EQ04.01.03

Using Complete, Symmetry Invariant Representations of Atomic Environments to Predict New Ionic Liquids from Experimental Data [Martin Uhrin](#); EPFL, Switzerland

The ultimate goal of any atomistic design process, be it for materials or molecules, is to start with one or more target properties and predict atomic geometries that are statistically likely to possess these properties. In this talk, I will discuss how to construct complete, symmetry invariant descriptions of atomic environments that can be inverted to recover the original environment. Using this representation I will show that it is possible to build a model that can predict the conductivity of ionic liquids, an important potential electrolyte for future battery technologies. By training on a dataset of experimental results the model learns how to attribute contributions to the overall conductivity to fragments of the anion and cation. This allows us to virtually screen thousands of anion/cation combinations to pinpoint those with high conductivities. Furthermore, it opens the door to designing entirely new molecules by combining fragments to achieve properties that go beyond those that are possible using current ionic liquids.

11:30 AM *EQ04.01.04

Unravel the Frequency-dependent Phonon Transport with Scientific Machine Learning [Zhantao Chen](#); Massachusetts Institute of Technology, United States

Phonon transport at the nanoscale intimately relates to various crucial applications in the modern society. However, our understandings about frequency-dependent transport mechanisms, especially across an interface, are scarce due to the fundamental gap between observables and computables. In this talk, we introduce a framework that combines the scientific machine learning and the Boltzmann transport equation (BTE) to unravel microscopic phonon transport information inside heterostructures from the ultrafast electron diffraction (UED). We show that the time- and momentum-resolved diffraction patterns can be reliably interpreted by our approach to reconstruct frequency-dependent properties such as transmission coefficients and relaxation times, as well as other general properties like material-air emissivities, from which real-time and real-space phonon dynamics can be further recovered. We validate our approach through several numerical scenarios and apply it to analyze experiment measurements of an Au/Si heterostructure. Our work opens a new avenue to reveal phonon transport mechanisms across interfaces at the nanoscale.

SESSION EQ04.02: Unsupervised Learning and Data Mining for Materials Discovery

Session Chair: Tess Smidt
Tuesday Afternoon, November 30, 2021
Hynes, Level 2, Room 205

1:30 PM *EQ04.02.01

Unsupervised Machine Learning and Band Topology [Robert-Jan Slager](#); University of Cambridge, United Kingdom

The study of topological band structures is an active area of research in condensed matter physics and beyond. Here, we combine recent progress in this field with developments in machine learning, another rising topic of interest. Specifically, we introduce an unsupervised machine learning approach that searches for and retrieves paths of adiabatic deformations between Hamiltonians, thereby clustering them according to their topological properties. The algorithm is general, as it does not rely on a specific parametrization of the Hamiltonian and is readily applicable to any symmetry class. We demonstrate the approach using several different models in both one and two spatial dimensions and for different symmetry classes with and without crystalline symmetries. Accordingly, it is also shown how trivial and topological phases can be diagnosed upon comparing with a generally designated set of trivial atomic insulators.

2:00 PM *EQ04.02.02

Machine Learning Discovery of New Superhard Ternary and High-Entropy Borides [Cheng-Chien Chen](#); University of Alabama at Birmingham, United States

Superhard materials exhibit a Vickers hardness $H > 40$ GPa, and they have extensive industrial and technological applications. Due to the huge search space of possible element combinations, it is challenging to explore new superhard ternary or quaternary materials. Here, I will first discuss machine

learning (ML) discovery of new superhard B-C-N and B-N-O compounds. The ML results are validated by evolutionary structure prediction and density functional theory (DFT). In particular, the proposed BC₁₀N has a low formation energy and a high hardness $H \sim 86$ GPa only next to diamond. I will next discuss the calculations of entropy formation ability (EFA) using both DFT and ML approaches for 5-metal hexagonal high-entropy borides. The results indicate that EFA serves as a good descriptor for the synthesizability of high-entropy materials, some of which have superior mechanical properties promising for extreme-environment applications.

2:30 PM EQ04.02.03

Machine Learning the Relationship Between Debye and Superconducting Transition Temperatures [Adam D. Smith](#)¹, Sumner B. Harris^{1,2}, Renato P. Camata¹ and Cheng-Chien Chen¹; ¹University of Alabama at Birmingham, United States; ²Oak Ridge National Laboratory, United States

Recently a relationship between the Debye temperature and the superconducting transition temperature T_c of conventional superconductors has been proposed. The relationship indicates that the maximum T_c for phonon-mediated BCS superconductors is at most $\sim 0.1 \times$ Debye temperature. In order to verify this bound and develop tools for predicting the Debye temperature we've trained machine learning models on over 10000 compounds with just chemical formula and crystal symmetry group as features. By examining over 9000 known superconducting compounds in the NIMS SuperCon database, our predictions show that conventional superconductors in the database follow the previously proposed bound of T_c versus Debye temperature. We will also use density-functional theory calculations to examine compounds very close and very far away from this bound, and discuss possible strategies of increasing T_c by manipulating the electron-phonon coupling in these systems.

SESSION EQ04.03: Emerging Tools of Machine Learning for Materials Science I
Session Chairs: Maciej Haraczuk and David Tennant
Wednesday Morning, December 8, 2021
EQ04-Virtual

8:00 AM *EQ04.03.01

Data Integration for Accelerated Materials Design via Preference Learning [Koji Tsuda](#); The University of Tokyo, Japan

Machine learning applications in materials science are often hampered by shortage of experimental data. Integration with external datasets from past experiments is a viable way to solve the problem. But complex calibration is often necessary to use the data obtained under different conditions. In this paper, we present a novel calibration-free strategy to enhance the performance of Bayesian optimization with preference learning. The entire learning process is solely based on pairwise comparison of quantities (i.e., higher or lower) in the same dataset, and experimental design can be done without comparing quantities in different datasets. We demonstrate that Bayesian optimization is significantly enhanced via data integration for organic molecules and inorganic solid-state materials. Our method increases the chance that public datasets are reused and may encourage data sharing in various fields of physics.

8:30 AM EQ04.03.02

Automated Processing and Characterisation of EELS Spectral Images with Machine Learning [Abel Brokkelkamp](#)¹, Isabel Postmes¹, Jaco ter Hoeve^{2,3}, Sabrya van Heijst¹, Louis Maduro¹, Juan Rojo^{2,3} and Sonia Conesa-Boj¹; ¹TU Delft, Netherlands; ²Vrije Universiteit Amsterdam, Netherlands; ³Nikhef, Netherlands

Spectral images obtained with Electron Energy-Loss Spectroscopy (EELS) are two-dimensional sets of spectra where each pixel provide information on a localised region of the analysed sample. Each of these spectra contain a plethora of information related to the physical and electronic properties of the material. Exploiting this information requires reliable access to the low-loss region where the zero-loss peak (ZLP) overwhelms the inelastic scattering contributions of the specimen. Here we present a novel approach to process and analyse EEL spectral images in an automated manner based on machine learning. By clustering the constituent spectra into groups associated to sample regions with similar profiles using unsupervised learning, we can then subtract the ZLP in a model-independent manner using deep neural networks. The resulting processed spectral images can then be used to identify spatially-resolved local electronic properties such as the bandgap (and determine whether it is a direct or indirect bandgap) and the optical dielectric function across the sample. Furthermore, we correlate them to the thickness and other structural properties of the sample. In addition, our approach also allows us to identify interesting features in the low-loss region and determine how these features vary in the different regions of the sample. This strategy has been performed on both Tungsten Disulfide and Indium Selenide nanostructures obtaining results that are in agreement with the literature. Our novel method can be extended into higher-dimensional datasets in a straightforward manner and is implemented into a new release of the open source python package EELSfitter.

8:45 AM *EQ04.03.03

From Density Functional Theory to Machine Learning for Accurate Prediction of Materials Properties [Silvana Botti](#); Friedrich Schiller University Jena, Germany

I will discuss different approaches to improve the accuracy of materials property predictions, combining density-functional theory calculations, different machine learning methods and experimental datasets.

I will present different examples of applications and discuss their performance for the determination of thermodynamic stability, geometry optimization and evaluation of the electronic band gap.

9:15 AM EQ04.03.04

Unsupervised Machine Learning for Spatio-Temporal Characterization of Ultrafast Electron Microscopy Datasets [Arun Baskaran](#), Faran Zhou, Thomas Gage, Haihua Liu, Ilke Arslan, Haidan Wen and Maria K. Chan; Argonne National Laboratory, United States

Advancements in microscopy techniques have made materials investigations at nanometer-picosecond (nm-ps) spatio-temporal resolutions possible. This work details the use of a machine learning based approach to extract quantitative information, in terms of optical flow, pertaining to the motion of contrast bands as captured by an ultrafast electron microscope (UEM). UEM is an emerging technique that uses pulsed electron beams to image structural dynamics at nm-ps resolutions. This spatio-temporal characteristic of a UEM dataset is one of the main challenges encountered during its analysis. Classical image processing techniques for optical flow, such as functions that are part of the OpenCV library, are parametric and hence require manual supervision. In this

work, a U-net type convolutional neural network (CNN) is designed to take a pair of UEM images at different times as input and generate the optical flow at each pixel as output. A custom loss function is defined, consisting of a photometric loss term and a gradient loss term. The loss is regularized with the output from an adversarial model which is simultaneously trained to distinguish between image pairs with and without spatial displacement of objects. In order to overcome the lack of ground truth data for optical flow, the model is trained in an unsupervised manner. The performance of an OpenCV function for dense optical flow is chosen to be the baseline, and the optimal values for the parameters are selected through a grid search on candidate values. The model proposed in the current work outperforms the baseline method on the photometric loss metric. We detail the approach to study the effect of experiment variables, such as temperature, on the phonon dynamics of 2D semiconductor materials.

9:30 AM *EQ04.03.05

Progress Towards Leveraging Natural Language Processing for Collecting Experimental Data and Data Mining [Anubhav Jain](#); Lawrence Berkeley National Laboratory, United States

Today, experimental data sets for various applications are almost exclusively curated manually because data is scattered throughout the research literature. In this talk, I will present progress towards using natural language processing (NLP) algorithms to automatically collect and organize data on a research topic. Such methods are particularly valuable in fields like quantum materials where simulation is difficult or time consuming, necessitating efficient use of experimental data where it is available. In particular, I will present our work on detecting named entities within research texts and connecting these entities into organized data sets. For example, we have collected data pertaining to how various materials are doped by applying NLP to a large corpus of published abstracts and full texts, and connected doping information with applications. Finally, I will discuss how such methods might be applied to a variety of quantum materials applications and how such methods may complement other sources of data such as theory and simulation.

SESSION EQ04.04: Emerging Tools of Machine Learning for Materials Science II
Session Chair: Christopher Rycroft
Wednesday Morning, December 8, 2021
EQ04-Virtual

10:30 AM *EQ04.04.01

Application of Machine Learning to Neutron Scattering from Magnets [David A. Tennant](#)¹ and Anjana Samarakoon²; ¹Oak Ridge National Laboratory, United States; ²Argonne National Laboratory, United States

Inelastic and diffuse neutron scattering hold crucial information on the underlying physical states of materials and models that describe them. The difficulty of handling the large amounts of data and simulations involved as well as challenges of experiment planning and interpretation can be addressed using machine learning. We have been applying these approaches to topological flat band materials of importance as hosts to fractional quasiparticles with anyonic statistics as well as competing disordered phases. Complex behavior due to subtle competing interactions prove to be vital and machine learning provides an effective approach to handling the myriad of phases and behaviors involved. I show outcomes of our machine learning based experiments on quantum and classical spin liquids.

11:00 AM EQ04.04.02

Prediction of Localized Plasmon Resonances in Complex Nanoparticle Assemblies Using Autoencoder Networks [Kevin Roccapriore](#)¹, Maxim A. Ziatdinov¹, Shin-Hum Cho², Delia Milliron³, Jordan Hachtel¹ and Sergei V. Kalinin¹; ¹Oak Ridge National Laboratory, United States; ²Samsung Semiconductor R&D, Korea (the Republic of); ³The University of Texas at Austin, United States

Designing nanostructures with desired optical properties is critical to the field of nanophotonics. Traditionally, numerical methods and theoretical predictions are used to inform on design parameters of nanophotonic elements. On the other hand, having knowledge of the structure-property relationships of a given system provides another data-driven approach to design nanostructures. To pave the way towards stochastic design of nanoplasmonic structures, we establish the correlative relationship between local nanoparticle geometries and their plasmonic responses. By using an encoder-decoder neural networks within the framework of PyTorch, we demonstrate the predictions of spectra from local geometries in the *im2spec* network, as well as the predictions of local geometry from spectral inputs in the *spec2im* network [1].

By utilizing scanning electron transmission electron microscopy (STEM), we acquire an electron energy loss (EEL) spectrum image and its associated acquired high angle annular dark field (HAADF) image of a self-assembled monolayer of fluorine and tin doped indium oxide nanocrystal arrays [2]. While the particles mainly undergo self-assembly, many defects and irregularities are observed within and nearby the arrays – for example, missing particles, small clusters of particles, etc. With the knowledge that the plasmonic behavior at a position in space depends primarily on local geometry at that position, subimage-spectrum pairs are generated at each spatial pixel that are used to teach the network the correlative relationship between them. The network encodes the images (spectra) to a low-dimensional feature space consisting of a small number of latent variables, then decodes the latent variables back into spectra (images). The reduced descriptions contained in the so-called latent space can yield a surprising insight into the generative mechanisms of complicated plasmonic responses in nanoparticle arrays [3].

Equipped with the knowledge of correlative structure property relationships gained by the autoencoder networks, we predict the plasmonic response given an unseen nanoparticle geometry. Conversely, we predict nanoparticle geometry given a plasmonic spectrum. This method ultimately enhances the design capabilities for plasmonic systems, and may even permit a route to solving the inverse design challenge in nanophotonics.

[1] S. V. Kalinin *et al.*, *Adv. Optical Mater.* **2021**, 2001808.

[2] S. H. Cho *et al.*, *J. Chem. Mater.* **2019** *31*, 2661.

[3] K. M. Roccapriore *et al.*, *Small* **2021** *17*, 2100181.

This effort (ML and STEM) is based upon work supported by the U.S. Department of Energy (DOE), Office of Science, Basic Energy Sciences (BES), Materials Sciences and Engineering Division (K.M.R., S.V.K.) and was performed and partially supported (J.A.H., M.Z.) at the Oak Ridge National Laboratory's Center for Nanophase Materials Sciences (CNMS), a U.S. Department of Energy, Office of Science User Facility. S.H.C acknowledges (NSF, CHE-19052631609656, CBET-1704634, NASCENT, an NSF ERC EEC-1160494, and CDCM, an NSF MRSEC DMR-1720595), the Welch Foundation (F-1848), and the Fulbright Program (IIE-15151071).

11:15 AM EQ04.04.03

Mapping Polarization from STEM and STM Images [Ayana Ghosh](#)¹, Christopher Nelson¹, Mark Oxley¹, Xiaohang Zhang², Maxim A. Ziatdinov¹, Ichiro

Takeuchi² and Sergei V. Kalinin¹; ¹Oak Ridge National Laboratory, United States; ²University of Maryland, United States

Scanning transmission electron microscopy (STEM) has become an important tool for studying atomic structures of complex materials with picometer precision and the associated order parameter fields. The latter includes polarization that is classically quantified by preprocessing images to remove noise and instrumental distortions, finding positions of all the observed atomic columns corresponding and calculating atomic displacements. This process is not only highly time consuming and laborious but also may lead to systematic errors in the polarization values.

In this work, we have proposed an alternate approach of utilizing deep convolution neural networks (DCNNs) for *direct* polarization mapping from STEM data. The DCNN is trained on the manually-labeled part of the image and is subsequently applied to other images. The training data is constructed using image patches (parts of original images cropped for a specific window size) generated with and without information about atomic positions. The patches are used as the (local) feature set and the corresponding polarization values become the target set. We show that this framework allows predicting polarization maps *without* atom-finding and compare the results with those obtained using the traditional approach.

We have demonstrated the workflow for STEM images with different Sm dopant concentrations in BiFeO₃, such that the explored feature space encompasses both ferroelectric and weakly-ferroelectric systems. We further intend to apply this technique to Scanning Tunneling Microscopy (STM/S) datasets of quantum materials to study other functionalities such as superconducting gap or the intensity of selected quasiparticle interference spots.

This effort (STEM) is based upon work supported by the U.S. Department of Energy (DOE), Office of Science, Basic Energy Sciences (BES), Materials Sciences and Engineering Division (S.V.K., C.T.N.) and was performed and partially supported (M.Z.) at Oak Ridge National Laboratory's Center for Nanophase Materials Sciences (CNMS), a U.S. DOE, Office of Science User Facility. This effort (ML) is based upon work supported by the U.S. DOE, Office of Science, Office of Basic Energy Sciences Data, Artificial Intelligence and Machine Learning at DOE Scientific User Facilities (A.G.). The work at the University of Maryland was supported in part by the National Institute of Standards and Technology Cooperative Agreement 70NANB17H301 and the Center for Spintronic Materials in Advanced Information Technologies (SMART) one of the centers in nCORE, a Semiconductor Research Corporation (SRC) program sponsored by NSF and NIST.

11:30 AM *EQ04.04.04

Detection of Topological Materials with Machine Learning [Nikolas H. Claussen](#)¹, Bogdan A. Bernevig² and Nicolas Regnault^{2,3}; ¹University of California, Santa Barbara, United States; ²Princeton University, United States; ³Ecole Normal Supérieure, France

Topological insulators and topological semimetals are solid-state systems which display unique macroscopic quantum effects due to the topology of their electronic wavefunction, such as protected edge or surface modes and quantized response functions, and have potential applications in quantum technology. Recently introduced theoretical methods have allowed for their large-scale discovery: databases compiled using ab initio calculations (density functional theory) now contain tens of thousands of topological materials. This makes the application of modern machine learning methods possible. Using gradient boosted trees, we show how to construct a machine learning model which can predict the topology of a given existent material with an accuracy of 90%. Such predictions are orders of magnitude faster and less expensive than actual ab initio calculations. We use machine learning models to probe how different material properties affect topological features. Notably, we observe that topology is mostly determined by the "coarse-grained" chemical composition and crystal symmetry and depends little on the particular positions of atoms in the crystal lattice. We identify the sources of our model's errors, discuss approaches to overcome them and create a simplified human-readable classification tree. In this talk, we will put a particular emphasis on methodological questions concerning machine learning as well as lessons learned and pitfalls encountered during the research process, in the hope that others looking to apply machine learning to material science may profit.

12:00 PM *EQ04.04.05

Forward and Inverse Design of Spectral Emissivity Using Machine Learning Models Mahmoud Elzouka, Charles Yang, Minok Park, Alok Singh, Adrian Albert, Vassilia Zorba, Ravi Prasher and [Sean Lubner](#); Lawrence Berkeley National Lab, United States

A system's spectral emissivity determines how it will radiatively exchange energy with its environment and other interacting systems. This governs many natural phenomena and technologies such as optical sensors, energy harvesting and conversion, targeted drug delivery, sooty combustion, and global warming. Calculating radiative properties from known geometry and designs can be computationally expensive, and trying to invert the problem to come up with designs specific to desired radiative properties is even more challenging (typically one-to-many and nonlinear). In this talk, I will first discuss a machine-learning-based method for both the forward and inverse problem for dielectric and metallic particles. Our decision-tree-based model is able to provide explicit design rules for inverse problems. Furthermore, we can use the same trained model for both the forward and the inverse problem, which greatly simplifies the computation. Second, I will discuss our more recent work using generative models and latent space sampling to prescribe how to nanotexture a surface of a single material in order to produce a variety of desired optical properties through plasmon resonance and photon wave interference effects. These designs are experimentally realized by rapid laser machining of different substrates. Our methodologies show the promise of augmenting optical system optimizations by providing interpretable and actionable learned models for rapidly finding approximate solutions to the inverse design problem.

SESSION EQ04.05: Emerging Tools of Machine Learning for Materials Science III

Session Chair: Mingda Li

Wednesday Afternoon, December 8, 2021

EQ04-Virtual

1:00 PM *EQ04.01.01

Real-Time Physics-Constrained Machine Learning in Multimodal Spectroscopy [Joshua Agar](#); Lehigh University, United States

Machine learning (ML) has been all the rage in materials science in the past 5 years. While there have been promises of transformative acceleration of analysis capabilities, new insights, and even closed-loop control, it has yet to live up to the hype. The core challenge is that while ML models are fast to deploy they require arduous training of ensembles of models, hyperparameter tuning, and validation. In turn, ML ends up taking nearly the same or many times more person-hours as standard analysis protocols. While many ML efforts have focused on unraveling hidden insight in data, ML can also be a powerful tool to accelerate conventional analysis pipelines. There has been a boon in multimodal spectroscopy techniques that collect data with increasing volume, velocity, veracity, and variety. The use of these techniques has become limited not by their capability, but the time required to manage and process this data. Additionally, this imposes challenges to the experimentalist who cannot conduct even cursory on-the-fly analysis to guide subsequent experiments.

Here, we show how the confluence and codesign of physics-informed machine learning models and edge computing hardware can enable real-time streaming processing of band-excitation piezoresponse force switching spectroscopy without distributing computing. We acquire frequency-dependent cantilever resonance responses during ferroelectric switching at a frequency of 1 kHz. We use initial data to train a 1D-convolutional autoencoder model with a latent space that defines the amplitude, phase, quality factor, and resonance frequency. By constraining the decoder to be the empirical function of a simple harmonic oscillator, we can train the model fully unsupervised by minimizing the mean squared reconstruction loss. Training this model from scratch takes less than 5 minutes on 3M examples on a Graphical Processing Unit (GPU, Google Collab Free-Tier). Once trained, the model can fit the resonance curves; however, the necessary throughput of 1 kHz is only achievable through batching as GPU initialization takes ~1 ms. To avoid latencies associated with data movement, we deployed the model on a field-programmable gate array (FPGA). To do this, we pruned and quantized the model to fit the FPGA resources. Using a package hls4ml, we converted our model from TensorFlow to high-level synthesis (HLS). The HLS can then be compiled using vivadoHLS and was ultimately deployed on a Xilinx KU060 coprocessor in a Labview PXI chassis. By deploying this model on an FPGA, we could achieve streaming inference with latencies of $<2 \mu\text{s}$, orders of magnitude faster than is required. Furthermore, because the fits are conducted more holistically, the fits are more robust to initialization and noise. We will also discuss how a similar methodology can be applied to fit piezoelectric hysteresis loops. The ability to conduct empirical fitting with sub-ms latency provides a pathway toward real-time control of dynamics processing in materials at beyond-human response times. We will provide additional insight into other characterization modalities, for example 4-dimensional transmission electron microscopy, where a similar methodologies can be applied.

SYMPOSIUM EQ05

Plasmonics, Nanophotonics and Metaphotonics—Design, Materials and Applications
November 29 - December 8, 2021

Symposium Organizers

Viktorii Babicheva, University of New Mexico
Ho Wai (Howard) Lee, University of California, Irvine
Yu-Jung Lu, National Taiwan University
Giulia Tagliabue, École Polytechnique Fédérale de Lausanne

* Invited Paper

SESSION Tutorial EQ05: Optical Metasurfaces—Materials, Designs, and Advanced Device Applications
Monday Morning, November 29, 2021
Hynes, Level 2, Room 210

8:30 AM

High Performance Metasurface Flat Optics—From Components to Systems [Federico Capasso](#); Harvard University, United States

Metasurfaces are leading to the emergence of new optical components that circumvent the limitations of standard refractive and diffractive one by enabling dispersion engineering, which also leads to entirely new functionalities based on the local control of phase amplitude and polarization. Dispersion engineering has led to the demonstration of metalenses with correction of monochromatic aberrations and to achromatic metalenses and hybrid refractive/diffractive doublets across the visible spectrum. The planarity of flat optics will lead to the unification of semiconductor manufacturing and lens-making; recent industrial advances in this direction will be discussed. Polarization optics, polarimeters and polarization sensitive cameras without moving parts and conventional birefringent optics will be presented. Metasurfaces also offer fresh opportunities for structuring light as well as the dark. I will discuss spin to total orbital angular momentum (OAM) converters and OAM lasing, as well as flat devices that enable light's spin and OAM to evolve, simultaneously, from one state to another along the propagation direction. Finally, the demonstration of 2D phase and polarization singularities and the unique applications that they will open will be discussed.

10:00 AM BREAK

10:30 AM

Nonlinear Optical Metasurfaces—From Enhanced Light-Matter-Interaction to Functional Elements [Thomas Zentgraf](#); Universität Paderborn, Germany

For efficient nonlinear processes, the engineering of the nonlinear optical properties of media becomes an important task. The most well-known technique for spatially engineering nonlinear optical properties is the quasi-phase matching scheme for second-order processes like second harmonic generation. However, the widely used technique of periodic polling of natural crystals only provides a binary state for the nonlinear material polarization, which is equivalent to a discrete phase change of π of the nonlinear polarization. The continuous tailoring of the phase of the nonlinear susceptibility would greatly enhance flexibility in the design and reduce parasitic effects. In this tutorial, we will discuss nonlinear metamaterials with a continuously controllable phase of the local effective nonlinear polarizability. We will focus on plasmonic metasurfaces with various designs for the meta-atom geometry together with

different polarization states of the light. In particular for circular polarization states, the controllable nonlinearity phase results from the phase accumulation due to the polarization change along the polarization path on the Poincaré Sphere (the so-called Pancharatnam-Berry phase) and depends therefore only on the spatial geometry of the metasurface. By using a fixed orientation of the meta-atom, the nonlinear phase can be spatially arbitrarily tailored over the entire range from 0 to 2π . In contrast to the quasi-phase matching scheme, the continuous phase engineering of the effective nonlinear polarizability enables complete control of the propagation of harmonic generation signals, and therefore, it seamlessly combines the generation and manipulation of the harmonic waves for highly compact nonlinear nanophotonic devices. We will discuss the concepts of enhancing nonlinear processes with simultaneous phase engineering for the manipulation of second- and third-harmonic generation from metasurfaces and the restrictions with respect to symmetry and geometry of meta-atoms. Nonlinear metamaterials have fundamental significance in nonlinear optics and for tailored nonlinearities, as they provide a further degree of freedom in the design of nonlinear materials.

12:00 PM BREAK

1:30 PM

Electrically Tunable Metamaterials and Metasurfaces for Control of Absorption, Emission and Scattering [Harry A. Atwater](#); California Institute of Technology, United States

Progress in understanding resonant subwavelength optical structures has fueled a worldwide explosion of interest in both fundamental processes and nanophotonic devices for imaging, sensing, solar energy conversion and thermal radiation control. For most nanophotonic materials, the optical properties are encoded and fixed permanently into the nanoscale structure at the time of fabrication. Achieving electronic tunability of the optical properties is an emerging opportunity to bring metamaterials and metasurfaces to life as dynamic objects composed of tunable nanoscale resonators and antennas. Gated field effect tuning of the carrier density in conducting oxides and two-dimensional materials enables the optical dispersion of individual structures to be altered from dielectric to plasmonic, yielding active nano-antenna arrays with electrically tunable absorption, radiative emission and scattering properties.

3:00 PM BREAK

SESSION EQ05.01: Metasurfaces and Metamaterials I
Session Chairs: Ho Wai (Howard) Lee and Benjamin Vest
Monday Morning, November 29, 2021
Hynes, Level 2, Room 208

8:00 AM *EQ05.01.01

Van der Waals Active Metasurfaces and Heterostructures for Phase Modulation and Polarization Conversion [Harry A. Atwater](#); California Institute of Technology, United States

A grand challenge for nanophotonics is the realization of tunable metasurfaces enabling active control of the key constitutive properties of light – amplitude, phase, wavevector and polarization. Active metasurfaces that enable dynamic modulation of reflection amplitude, phase and polarization have been recently explored using several active materials and modulation phenomena, including carrier index in plasmonic ENZ structures, reorientation of liquid crystal molecules, electrooptic effects in quantum well heterostructures and index change in phase change materials. The rapid advances in understanding of exciton resonances in layered van der Waals materials has now stimulated thinking about active metasurfaces that exploit excitonic modulation phenomena to enable ‘van der Waals active metasurfaces’. As one example, I will describe recent advances in electrically reconfigurable polarization conversion across the telecommunication wavelength range in van der Waals layered materials, integrated in a Fabry-Pérot cavity. The large electrical tunability of the excitonic birefringence in tri-layer black phosphorus enables spectrally broadband polarization conversion over nearly half the Poincaré sphere. We observe both linear to circular and cross-polarization conversion with voltage, demonstrating dynamic access to polarization diversity. As a second example, we discuss the observed large gate tunability of the complex refractive index in monolayer MoSe₂ by Fermi level modulation near the A and B excitonic resonances for temperatures between 4 K to 150 K. By tuning the charge density, we observe both temperature and carrier dependent epsilon-near-zero response in the permittivity and transition from metallic to dielectric near the A exciton energy, and directly observe active phase modulation in monolayer MoSe₂ gated heterostructures, whose voltage dependence is consistent with our complex index measurements. These results have broad implications for the use of monolayer transition metal dichalcogenides in active metasurfaces, and I also will give a general outlook for the wide range of possibilities for active van der Waals metasurfaces.

8:30 AM *EQ05.01.02

Directional Metasurface Light Emitters and Image Sensors [Roberto Paiella](#); Boston University, United States

Plasmonic and dielectric metasurfaces have been widely investigated as a means to tailor the wavefronts of externally incident light for passive device applications. At the same time, their direct integration within active optoelectronic devices such as light emitters and photodetectors is far less established. In this work, we report the design and development of plasmonic metasurfaces that can promote directional light emission and angle-sensitive photodetection from a nearby active material. These results are significant for the continued miniaturization and large-scale integration of optoelectronic devices and related systems, and as a way to create new functionalities and enable novel applications. Specifically, the use of metasurface directional photodetectors for image sensing and processing will also be presented, including the demonstration of lensless compound-eye vision and optical spatial filtering for edge detection.

9:00 AM EQ05.01.03

Optomechanical Self-Stability of Freestanding Photonic Metasurfaces [Avinash Kumar](#), Daniel Kindem and Ognjen Ilic; University of Minnesota, United States

Nanostructured photonic surfaces are a promising platform for shaping the radiation pressure of light for optical manipulation beyond the limits of conventional approaches. Here, we present a framework for self-stabilizing optical manipulation of freestanding metasurfaces in three dimensions [1]. Our framework reveals that the challenging problem of self-stabilization against translational and rotational perturbations in three dimensions can be transformed to a simpler scattering analysis of the metasurface unit cell in two dimensions. We derive universal analytical stiffness coefficients applicable to arbitrary three-dimensional radial metasurfaces and radial beam intensity profiles. These derivations are confirmed with ray tracing simulations, eigenvalue analysis of the Jacobian, and numerical solutions of the full nonlinear equations of motion.

The implications of this reduced problem dimensionality are twofold. First, the framework is universally applicable to arbitrary embedded element profiles and/or radial beam variations. Second, our formalism enables efficient design of optomechanical metasurfaces as well as light beam configurations. We present examples of non-conventional phase-gradient profiles and beam intensity variations with substantial (e.g., order-of-magnitude) improvement in longitudinal propulsion force while maintaining self-stability.

These results facilitate the discovery of macroscale photonic objects for stable manipulation in collimated, but otherwise unfocused light beams. This ability to manipulate macroscopic objects is in stark contrast with traditional methods of optical tweezing which rely on focused laser beams and external feedback. Such use of metasurfaces for mechanical stabilization could open up new perspectives for long-range manipulation of macroscopic objects, with potential for terrestrial and space applications.

[1] Kumar, Kindem, Ilic, <https://arxiv.org/abs/2106.11278>.

9:15 AM EQ05.01.04

Ultrafast Broadband Dichroism by Transient Optical Symmetry Breaking in Plasmonic Metasurfaces Margherita Maiuri¹, Andrea Schirato^{1,2}, Andrea Toma², Remo Proietti Zaccaria², Paolo Laporta¹, Peter Nordlander³, Giulio Cerullo¹, Alessandro Alabastri³ and Giuseppe Della Valle²; ¹Politecnico di Milano, Italy; ²Istituto Italiano di Tecnologia, Italy; ³Rice University, United States

Ultrafast nanophotonics aims at the development of nanodevices for light modulation with unprecedented speed [1]. A promising approach exploits the optical nonlinearity of nanostructured materials to modulate their effective permittivity by exploiting intense ultrashort optical pulses [2]. In plasmonic nanostructures such pulses trigger a delayed third-order nonlinear response ruled by internal relaxation of the metallic nanosystems, thus allowing all-optical light modulation. Currently, challenge in ultrafast pulse manipulation remains the feasibility of all-optical modulation of light over a broad bandwidth, with a full recovery over sub-picosecond timescale. Among different kinds of all-optical functionalities, ultrafast polarization switching has recently attracted a huge interest for advanced applications in photonics and beyond [3,4].

Here we combine quantitative numerical model with polarization-resolved pump-probe spectroscopy to predict and observe that photoinduced spatio-temporal transients can break the symmetry of a plasmonic metasurface, even if composed of highly symmetric metaatoms. Symmetry breaking generates a broadband dichroic response with ultrafast recovery of the isotropic configuration well before the complete relaxation of the nanostructure [5].

The plasmonic metasurface used is made of symmetric gold nanocrosses, with polarization independent static transmittance with a broad dip around 800 nm, due to the degenerate longitudinal plasmonic resonances of the nanocross two arms. Such a degeneracy can be broken by the resonant absorption of a pump pulse with linear polarization along the direction of one of the arms. Photoabsorption creates a highly inhomogeneous near field. This asymmetric absorption pattern in each metaatom locally affects the electronic population of gold, inducing a non-uniform out of equilibrium hot-carriers distribution which anisotropically modifies the metal permittivity. The fingerprint of the ultrafast pump-induced symmetry breaking is a transient transmission anisotropy, which can be revealed in a polarization-resolved pump-probe experiment.

The quantitative numerical model describes the ultrafast spatial transients in terms of spatial and temporal variables linked by a set of three coupled equations, referred to as the Inhomogeneous Three-Temperature Model (I3TM). The I3TM extends the popular 3TM [6], by including the spatial dependence of these variables.

We employ finite-element method numerical analysis in the frequency domain to calculate the transmission spectrum of the metasurface for a linear polarization parallel and orthogonal to the pump, for a set of permittivity configurations obtained by sampling the gold permittivity distribution at different pump-probe delays. Such spatio-temporal electronic transients at the nanoscale translate into an anisotropic local permittivity distribution, and subsequent ultrafast dichroic optical response of the metasurface, dominated by non-thermal hot-electrons dynamics. This modulation is broadband and returns to the isotropic configuration within few hundreds of fs. Thus, the main contribution to this phenomenon arises from non-thermal carriers while thermalized carriers contribute less. This is remarkable given that the electronic temperature relaxation takes place on a much longer time scale, far beyond the symmetry breaking window.

Our results pave the way to all-optical control of light at TeraHz speed, focused on ultrafast polarization management.

[1] A. V. Kildishev, et al, *Science* **339**, 1289 (2013).

[2] N. Yu, F. Capasso, *Nature Materials* **13**, 139 (2014).

[3] Y. Yang, et al. *Nature Photonics* **11**, 390-396 (2017).

[4] L. H. Nicholls, et al. *Nature Photonics* **11**, 628-633 (2017).

[5] A. Schirato, M. Maiuri et al. **14** 723-727 *Nature Photonics* (2020).

[6] C. K. Sun, et al. *Phys. Rev. B* **50**, 15337 (1994).

9:30 AM EQ05.01.05

Termination Dependent Optical Chirality in Gyroid Optical Metamaterials Bryan Cote, William Lenart, Chris Ellison and Vivian E. Ferry; University of Minnesota Twin Cities, United States

The ability to selectively interact with one circular polarization of light has wide ranging applications, including stereoscopic displays, document security, photonic circuits, biological detection, and others. Unfortunately, most molecular chiral materials only possess a weak circular dichroism (CD) response. Top-down fabricated pseudo-chiral metasurfaces have exhibited significantly stronger interactions with circularly polarized light (CPL), however it is often difficult and cost prohibitive to fabricate these lithographically patterned metasurfaces over large areas. In this presentation, we explore the effects of surface termination on the CD response of self-assembled, 3-D network-structure, optical metamaterials.

The gyroid is a triply periodic, minimal surface that contains screw axes in the [100], [110], and [111] directions and can be fabricated via block copolymer self-assembly. The single gyroid has been well described as a photonic crystal, where it has been shown to support both polarization dependent and complete photonic bandgaps. More recently, linear and circular dichroism have been detected in metal infilled gyroid optical metamaterials. In these structures both the bulk and surface structures affect the resulting optical properties; Dolan et al. recently showed that linear dichroism in a [110] oriented gyroid metamaterial arises from the anisotropic surface termination.

Here we use finite-element time-domain simulations to show that termination dependent resonances also play a dominant role in the CD response of [100], [110], and [111] oriented, silver infilled gyroid metamaterials. Films consisting of 4-unit cell thick gyroids with sharp interfaces and a unit cell size of 65 nm support CD resonances in the visible and near infrared on the order of 10 %, with large *g*-factors of 0.2. [100] oriented gyroids possess a termination dependent differential transmission of left- and right- CPL that repeats every quarter unit cell. Differential reflectance consists of strong, redshifted resonances that also occur every quarter unit cell, but alternate in handedness. These redshifted resonances arise from an antenna effect on the surface, where nearly touching nanostructures concentrate the incident electric fields by more than 100-fold. Varying the volume fraction of the silver infill results in different termination dependent CD responses, but the common theme of strong, redshifted resonances every quarter unit cell remains.

In the [110] direction, single gyroid metamaterials display both termination independent and termination dependent CD. The termination dependent resonance is observed in differential reflection and arises from a similar antenna effect. However, in contrast to the [100] direction, the surface terminated resonances of the two enantiomeric single gyroids are shifted by a quarter unit cell. Because of this, we find that [110] oriented double gyroids, which are

achiral in the bulk, can also exhibit either a strong positive or negative CD response depending on the termination exposed. Lastly, while [111] oriented gyroid metamaterials cannot generate the antenna structures discussed above, they do support a variety of hexagonally packed, triangular metasurfaces that repeat every third of a unit cell. Depending on termination selected, [111] oriented gyroid metamaterials can either selectively resonate at the top or bottom surface or support metasurface resonances at both surfaces simultaneously. In conclusion, chiral gyroid metamaterials support strong, termination dependent CD responses in each of the high-symmetry directions. This presentation will explore the mechanism of this termination dependent resonant response.

9:45 AM EQ05.01.06

Engineering Spectrally Narrowband Emission from Active, Coupled-Mode, Thermal Metasurfaces Arun Nagpal¹, Ming Zhou², Ognjen Ilic³, Zongfu Yu² and Harry A. Atwater¹; ¹California Institute of Technology, United States; ²University of Wisconsin–Madison, United States; ³University of Minnesota, United States

Optical metasurfaces that provide spectral and spatio-temporal control of thermal radiation, particularly that in the near-to-mid infrared temperature regime, have promising applications in chemical fingerprinting, infrared imaging, and in thermophotovoltaics. Here we demonstrate a narrowband thermal emitter platform that is tunable via the application of a gate voltage. The emitter consists of a 1D photonic crystal supporting a guided mode resonance that couples to a localized surface plasmon mode of a proximitized graphene ribbon array. We show a narrowband resonance at 7 μ m which can be tuned into high and low emissivity states. The on/off ratio between the high emissivity and low emissivity modes of operation is over 60, and the Q-factor of the resonant on-state is greater than 5000. We investigate the performance of the device under realistic material conditions, and excitation schemes. Furthermore, the resonant absorption characteristic is well-modeled by a coupled-modes theory. Using this theory, we predict the response of the emitter over a large range of geometric parameters, in both the near-field coupled and the far-field coupled regime.

SESSION EQ05.02: Plasmonic Applications I
Session Chairs: Souvik Biswas and Ho Wai (Howard) Lee
Monday Morning, November 29, 2021
Hynes, Level 2, Room 208

10:30 AM EQ05.02.02

Real-time Monitoring of Dissolved Carbon Monoxide in Non-Equilibrium State with Surface-Enhanced Raman Spectroscopy Junwon Min, Youngwook Lim, Taewook Kang and Dongchoul Kim; Sogang Univ, Korea (the Republic of)

The dissolved gas concentration in a reactor has significant importance in the chemical and biological processing industries as mass transfer from the injected gas to an aqueous solution must occur for the gas to be usable. As the solubility of the gas in the solution is low and there are no probes for measuring dissolved gas concentration, a volumetric mass transfer coefficient is selected as a criterion of design for bio-chemical reactors. However, it is difficult to accurately predict the non-equilibrium state dissolved gas distribution using only the volumetric mass transfer coefficient. In this study, we predict a local concentration of dissolved carbon monoxide based on surface enhanced Raman spectroscopy and a distribution of the concentration in the reactor in a real time using computational fluid dynamics and machine learning. Through these techniques, biological C1 conversion reaction will be monitored in real-time without offline sampling.

Acknowledgement: This work was supported by a National Research Foundation of Korea (NRF) under grant(No. 2020R1A2C2010986);C1 Gas Refinery Program through the National Research Foundation of Korea (NRF) under grant(No. 2018M3D3A1A01055759).

SESSION EQ05.03: Plasmonic Applications II
Session Chairs: Souvik Biswas and Benjamin Vest
Monday Afternoon, November 29, 2021
Hynes, Level 2, Room 208

1:45 PM EQ05.03.02

Optical Properties of Electrically Interconnected Plasmonic Nanostructures with Sub-10 nm Nanogaps by Atomic Layer Deposition Brian Willis¹, Chengwu Zhang¹, John Grasso¹, Donal Sheets¹, Jason Tresback² and Jason Hancock¹; ¹University of Connecticut, United States; ²Harvard University, United States

Plasmonic nanostructures facilitate the interaction of light and matter with applications in photodetection, photocatalysis, biochemical sensing, photoelectrochemistry, and energy harvesting. In particular, the overlap of plasmon resonances with the solar spectrum makes them well suited for renewable energy technologies. A central concept in plasmonics is the strong electric field enhancement when plasmons are squeezed into nanogaps between adjacent particles. Field enhancement is directly related to physical processes including hot carrier generation. Electric fields can be enhanced by using high quality plasmonic materials such as Cu, Ag, and Au and engineering nanogaps with dimensions approaching 1 nm. Tuning plasmonic resonances to match lattice diffraction modes can further boost electric fields. Additional enhancements are possible by adding electric functions to plasmonic devices, but few studies have successfully integrated electrical interconnects with plasmonic nanostructures, and scalable fabrication of arrays with sub-10 nm nanogaps is challenging due to limits on conventional lithography. In this paper, we present a study of the optical properties of large arrays of interconnected plasmonic nanostructures with sub-10 nm nanogaps for strong field enhancements.

We use a nanofabrication approach based on selective area atomic layer deposition to modify lithographically defined nanostructures to create large arrays of plasmonic dimers with nanogaps 1-5 nm. Our plasmonic dimers are nanorod shaped with dipolar resonances tuned at 800 nm. Copper is deposited selectively on palladium coated gold nanorods and the optical resonances are monitored as nanogaps are narrowed to less than 5 nm. Palladium is used as a seed layer to promote copper growth, while gold provides high quality plasmonic resonances. Compared with pure gold, the addition of palladium increases the FWHM from 86 nm to 158 nm due to the inferior plasmonic properties of palladium. However, after copper growth to create Cu/Pd/Au layered nanorods, resonances improve and FWHM decreases to 141 nm. At early stages of deposition, plasmon resonances blue shift, which is unexpected.

Control experiments show that blue shifts are due to heat-induced rounding of features during the first cycles of growth. Single particle resolution AFM and high-resolution SEM data confirm feature rounding and reduced nanorod aspect ratios. Further deposition leads to red shifts due to narrowing of nanogaps between nanorods, as well reduction of FWHM from the improved plasmonic properties of Cu. Overall, resonance shifts are less than expected due to competing effects from deposition and heat induced shape changes.

Results for interconnected plasmonic devices are qualitatively similar to plasmonic dimers, but with more attenuation of the optical resonances. We investigate a dipole-line configuration where arrays of nanorods are interconnected and linear features are used as counter electrodes. Again, there are dominant blue shifts during the first few deposition cycles due to heat induced shape changes of the interconnected rods, but compared with control experiments, deposition adds more broadening. Continued deposition to reduce nanogaps to less than 10 nm causes expected red shifts and sharpening of the resonances, but compared to unconnected plasmonic dimers, the optical resonances are significantly broadened. Analysis of high-resolution SEM images shows that the electrical contacts contribute to reshaping of the dipole antennas more extensively than for unconnected devices. The reduced aspect ratios from reshaping leads to broader resonances. Strategies to improve the quality of resonances will be discussed. In this paper, we also discuss surface lattice resonances in the extended arrays, which can be used to reduce FWHM and increase local electric field intensity for hot carrier devices.

2:00 PM EQ05.03.04

Fabrication of Chain-Like Gold Nanoparticle Clusters and Their Application in Enhanced *In Vivo* Photoacoustic Microscopy Molecular Imaging of Eye Disease in Live Rabbits Wei Qian¹, Van Phuc Phuc², Alan McLean², Raoul Kopelman², Xueding Wang² and Yannis Paulus²; ¹IMRA America, Inc., United States; ²University of Michigan–Ann Arbor, United States

Plasmonic metal nanoparticles have emerged as particularly attractive exogenous contrast agents for a wide variety of biomedical imaging techniques because their unique properties, including intense light absorption/scattering induced by the localized surface plasmon resonance (SPR), excellent biocompatibility, and lack of toxicity, hold great potential to improve these imaging techniques for detecting early-stage diseases with high sensitivity and specificity.

In this presentation, we first describe a facile and green method of fabricating chain-like gold nanoparticle (CGNP) clusters with narrow gap distances and a red-shifted longitudinal SPR that is tunable from 590 nm to 710 nm. These CGNP clusters are fabricated via self-assembly of gold NP monomers generated by a method of pulsed laser ablation (PLA) of the bulk target in deionized water. These PLA-generated gold NP monomers have unique capping agent-free surface and high purity, which allow precision surface engineering with different types of ligands in order to self-assemble them into highly linear nanochains [1,2].

In the second part of this presentation, the application of CGNP clusters as contrast agents for enhanced in-vivo photoacoustic microscopy (PAM) molecular imaging of eye diseases, named choroidal neovascularization, in live rabbits is explained. The synthesized CGNP clusters show excellent biocompatibility and photostability. These CGNP clusters are conjugated with linear arginine–glycine–aspartate (RGD) peptides (CGNP clusters- RGD) for molecular imaging. After intravenous injection of CGNP clusters-RGD, they bind to CNV in rabbit eyes, resulting in a selective PAM imaging of CNV only at 650 nm due to minimal tissue absorption at that wavelength. In addition, from the comparison of PAM signals before and after intravenous injection of CGNP clusters-RGD, it has been observed that CGNP clusters provide up to a 17-fold increase in PAM signal at 650 nm [3].

References

- [1] W. Qian, M. Murakami, Y. Ichikawa, Y. Che, J. Phys. Chem. C., 115, 23293-23298, (2011).
- [2] A. McLean, M. Kanetidis, T. Gogineni, R. Ukani, R. McLean, A. Cooke, I. Avinor, B. Liu, P. Argyrakis, W. Qian, R. Kopelman, Chemistry of Materials, 33, 2913-2928. (2021).
- [3] V. P. Nguyen, W. Qian, Y. Li, B. Liu, M. Aaberg, J. Henry, W. Zhang, X. Wang, Y. M. Paulus, Nature Communications, 12:34 (2021).

2:15 PM EQ05.03.05

Plasmonic Metal Nanoparticles Supported on Oxide Aerogels for Decontamination of Toxic Organophosphorus Compounds Travis G. Novak¹, Wesley O. Gordon², Alex Balboa², Ashley M. Pennington¹, Debra R. Rolison¹ and Paul A. DeSario¹; ¹U.S. Naval Research Laboratory, United States; ²U.S. Army Combat Capabilities Development Command Chemical Biological Center, United States

Toxic organophosphorus pesticides and chemical warfare agents (CWAs) create health hazards for both civilian and military personnel, necessitating the design of materials that offer protection against the target molecules. Traditionally, activated carbon is used in this role, but high-surface area carbons typically only adsorb CWAs; the intact molecules persist on the material surface. Materials that adsorb and then degrade CWAs into nontoxic products are a desirable alternative as they negate the risk of re-exposure and lessen disposal burdens for spent materials. Oxide aerogels decorated with metal nanoparticles (NPs) provide ideal platforms to achieve this degradative sorption. Oxide aerogels provide a high surface area, mesoporous network that is stable under ambient conditions, while the addition of metal NPs offers additional chemical pathways and improved kinetics for CWA degradation. In this talk we compare the activity of metal NP-decorated oxide aerogels (Au/TiO₂, Cu/TiO₂, and Cu/CeO₂) for degradation of CWA simulants (DMMP), as well as live agents such as sarin, under a wide variety of environmental conditions. Generally, oxide aerogels adsorb these molecules intact under dark and dry conditions, but drive hydrolysis under humid and aerobic conditions and initiate photooxidative degradation upon excitation of the semiconducting bandgap with broadband light. Metal NP-decorated aerogels expand these capabilities by providing highly reactive basic OH sites at the interface between metal NP and networked oxide NPs to achieve rapid degradation under dark conditions. This arrangement further accelerates degradation under illumination by leveraging plasmonic absorption of visible light. Our results reveal oxide aerogel-supported metal NPs to be promising materials for decontamination of organophosphorus compounds under a wide variety of environmental conditions.

SESSION EQ05.04: Nanophotonic Devices
Session Chairs: Ho Wai (Howard) Lee and Benjamin Vest
Monday Afternoon, November 29, 2021
Hynes, Level 2, Room 208

4:00 PM EQ05.04.01

ZnS:Mn-QD-Based Electroemissive Layer for Non-Toxic LED Applications Antonio Valerio Longo¹, Baptiste Notebaert¹, Alexandre Chevillot¹, Mériem Gaceur², Riccardo Messina³, Alan Durnez³, Téo Baptiste³, Christophe Dupuis³, Ali Madouri³, Nicolas Battaglini¹ and Souad Ammar¹; ¹Université de Paris, France; ²ACTINOVA, France; ³Université Paris-Saclay, France

Quantum dots (QD) form an emerging class of photo- and electroluminescent materials. Their narrow and tunable emission spectrum offers the benefits of a broad excitation-energy range with an environmentally stable, narrow emission. QD-based LED is a strongly active research field. In the typical device structure, the QD electroluminescent layer is stacked within hybrid heterostructures. Holes and electrons, injected from opposite sides through the application of a DC voltage, recombine radiatively in the QD layer, leading to light emission [1]. These devices suffer from a major drawback: the materials (their energy configuration and refraction index) of the stacked layers should be carefully chosen so as to optimize the energy-band diagram of the system for efficient electron-hole recombination in the photoactive layer [2] and minimize internal light reflection.

A further way exists to obtain emission of light from an electroluminescent QD layer, without any charge injection. It consists in sandwiching such a layer between two transparent dielectric layers and applying an alternate voltage. The presence of an electric field inside the photoactive region induces a relative shift between the energy levels of nanoparticles at different positions. This allows, above a threshold field, the creation of electron-hole pairs and their transport within the active layer. The recombination of an electron/hole pair on the same QD is at the origin of the observed light emission [3].

Previous QD-based devices present several limitations: the use of toxic Cd-based QD [3,4,5], the necessity of a complex multilayer structure [4,5] or the necessity of a combination of QD and bulk layers to obtain light emission [6].

We present a device overcoming all these limitations. Our device is based on an active layer of spin-cast non-toxic Mn-doped ZnS nanoparticles, sandwiched between two dielectric layers. By exploiting one-pot surfactant-free microwave-assisted polyol synthesis, we obtain high-crystalline nanoparticles, with enhanced phosphorescence emission due to Mn ions [7] at the solid state, which can be closely packed in the emitting layer, allowing an emission mechanism due to local charge creation and transport with only three layers. This new synthesis route paves the way to far less expensive paths for the active layer deposition such as spin coating or inkjet printing.

More specifically, our device is based on a glass substrate covered with a conductive and transparent thin layer of Indium Tin Oxide (ITO), followed by a dielectric layer deposited by Atomic Layer Deposition (ALD), a spin-cast ZnS:Mn nanoparticle film, and a second dielectric layer. Finally, metallic contacts are deposited by thermal evaporation.

Our device is characterized structurally by means of Scanning Electron Microscopy, showing an active layer with a very compact granular structure. We observe electroluminescence from the device only above a voltage threshold, coherently with previous observations. A direct comparison between electroluminescence and the photoluminescence spectra clearly shows that the observed luminescence corresponds to the emission coming from the transition taking place in Mn ions.

Monte Carlo simulations allow to show that the excitation mechanism cannot be linked to any impact triggering. Moreover, an effective-medium description of the active layer, along with a capacitance measurement on the device, allowed us to highlight a high packing of the QD inside the active layer. Moreover, the calculated potential fall per QD is compatible with an interpretation of light emission in terms of field-induced charge transfer and recombination.

References

- [1] X. Dai et al., Nature **515**, 96 (2014)
- [2] V. Wood et al., ACS Nano **3**, 3851 (2009)
- [3] V. Wood et al., Nano Lett. **11**, 2927 (2011)
- [4] Z. Yang et al., Mat. Today **24**, 69 (2019)
- [5] Y. Shirasaki et al., Nat. Photonics **7**, 20 (2013)
- [6] V. Wood et al., Nano Lett. **9**, 2367 (2009)
- [7] D. Bera et al. Materials **3**, 2260 (2010)

4:15 PM EQ05.04.02

Infrared Resonant Nano-Antennas for the Detection of Benzene Traces at ppb Levels Javier Nunez¹, Arjen Boersma¹, Julien Grand², Svetlana Mintova² and Beniamino Sciacca^{2,3,4}; ¹TNO, Netherlands; ²CNRS, France; ³Aix-Marseille Université, France; ⁴CINaM, France

The detection of volatile organic compounds (VOCs) at trace levels (ppb to ppm) is of extreme importance in the field of environmental monitoring for health related matters. The classical method for such measurements is gas chromatography, which is time consuming, expensive, and not portable. Spectroscopic techniques in the mid infrared (3–20 μm) are able to detect directly the unique fingerprints of molecular transitions, therefore offering a valid alternative in terms of versatility and selectivity. The target substance with an active IR vibration can be detected from the unique fingerprint of its vibrational transitions, without the need for an intermediate transducer, or any prior knowledge. However, light-matter interaction is extremely weak in the IR, due to the small absorption cross-section ($\propto a^3/\lambda$), with a being the molecule characteristic size. Long optical paths are needed to boost the signal to noise ratio for applications where detection at ppb levels is required. To keep a small footprint, it has been proposed to coat mid-IR waveguides or optical fibers with materials able to adsorb species of interest, thereby locally increasing the concentration. However, this approach often lacks sensitivity that is required in many applications. One example is the monitoring of benzene at ppb or sub ppb levels, that remains challenging even if a separate pre-concentration step is employed.

Surface-enhanced infrared absorption (SEIRA) has proven effective in detecting solid state monolayers via coupling resonant nano-antennas to vibrational transition of target molecules (Neubrech et al. Chem. Rev. 2017). However, for this to work, the target molecules have to be very close to the antenna surface, where the field enhancement is the highest. For low concentrated gases the probability of a molecule transiting within the strong field enhancement region can be very low, hampering the use of SEIRA for the detection of low concentrated volatile compounds.

In this talk we will present a hybrid system composed of a plasmonic nano-antenna array (gold nanorods) coupled with nanosized zeolite (Awala et al. Nat. Mat. 2015) coating for detection of volatile organic compounds in the near field of the resonators, enabling to extend the SEIRA toward the detection of gases at very low concentrations. We will show that the concerted action of the FAU zeolite coating and the resonant nano-antennas enables us to attain performance equivalent to a ≈ 120 m long optical path, and led to the detection record traces of benzene (25 ppb) within 10 min (Nunez et al. Adv. Func. Mat., 2021). To the best of our knowledge this sets a record for benzene detection using IR spectroscopy without external pre-concentration steps, and represent a great enhancement with respect to the low ppm range detection limit reported in the literature by using IR spectroscopy or IR tunable lasers. Then, we will show detailed characterisation of the system properties (SEM, EDX, optical), compare to numerical simulations (FDTD) and assess performance as a function of IR light polarisation. Finally, we will show that we can discriminate benzene from other VOCs such as toluene. This approach may ultimately allow the fabrication of a compact system for rapid detection of pharmaceutical and biocompounds with high sensitivity and high selectivity.

4:30 PM EQ05.04.03

Simulation and Fabrication of a Photonic Force Sensor Based on Silicon Nanopillars Elena Lopez-Aymerich^{1,1}, Daniel Navarro-Urrios^{1,1}, Mauricio Moreno^{1,1}, Sergi Hernández^{1,1}, Maria Dimaki², Florencia Serras¹, Winnie E. Svendsen² and Albert Romano-Rodríguez^{1,1}; ¹Universitat de Barcelona, Spain; ²Technical University of Denmark, Denmark

During the last decades photonic crystals (PC) have been widely studied. Most of these studies have been focused on the theoretical behaviour of these structures among almost all their configurations. Nevertheless, their experimental performance has been discussed but in a narrower number of configurations mostly focusing on the 1D and 2D structures based on a holed slab. In this work, we want to present both simulation and nanofabrication

results of 2D PC based on silicon nanopillars on silicon-on-insulator (SOI) substrates. The use of this reverse configuration has been scarcely studied and brought to a successful experimental performance. The addition of waveguides (WG) and cavities within the structure will allow light control through it. The potential application of these structures will be the development of a force sensor, which will measure horizontal forces. This system will operate in the Near Infrared (NIR) wavelength range.

The design of the structures has been carried out using the MEEP Python library what uses the Finite-Difference Time-Domain (FDTD) method to solve Maxwell's Equations over time and using eigenmode and eigenfrequencies solver. The determination of the best configurations has been done with a thorough study of the band diagrams of the structures both in 2D and 3D and their Transmission-Reflection spectra. Both strategies have shown good agreement between them and with literature. These simulations have shown the opening of a photonic bandgap (PBG) between 1.3 and 1.9 μm for Transversal Magnetic (TM) polarised light. These results have been obtained for a triangular structure using pillars of 100nm radius and 500nm interpillar distance. The introduction of a WG shrinking de radii of one line of pillars has given rise to the introduction of a mode within the PBG raising from the bottom bands. Finally, the insertion of cavities within the WG has promoted the apparition of resonance peaks.

The nanofabrication of these structures has been carried out inside an advanced clean-room facility. A multi-step process has been studied and optimised for the successful fabrication of nanopillars with radii from 100nm down to 60nm. SOI substrates have been used to ensure the vertical confinement of light. The fabrication process uses an electron beam lithography (EBL) exposure, followed by a lift-off, and ending with an anisotropic dry etch of the silicon layer. The EBL process consists of the deposit of 180nm CSAR-P6200.09 photoresist, followed by a 20nm-thick layer of thermally-evaporated aluminium to ensure the correct discharge of the sample during the exposure. A JEOL JBX-9500FSZ e-beam writer, using a 100kV electron beam, is used for the exposure. The thermal aluminium layer is removed using TMAH, while the photoresist is developed using AR 600-546 developer. The lift-off process is carried out using Remover 1165 after the e-beam deposition of 20nm of aluminium. In this manner, the remaining photoresist will be removed leaving only the aluminium that was directly in contact with the substrate. This aluminium will work as a mask material during the etching step. The latest consists of a reactive ion etching (RIE) process which uses a combination of SF₆:C₄F₈ chemistries resulting in an anisotropic etch of the uncoated silicon and giving rise to the nanopillars.

Discussion about the similarities and differences between the simulated and the fabricated structures will be carried out and, if different, proposals of improvement in the nanofabrication process will be brought up.

4:45 PM EQ05.04.04

Scalable III-V Nanowire Networks for IR Photodetection [Nicholas P. Morgan](#), Valerio Piazza, Didem Dede, Martin Friedl, Stéphane Nilsson, Lucas Güniat, Jean-Baptiste Leran and Anna Fontcuberta i Morral; Ecole Polytechnique Federale de Lausanne, Switzerland

InGaAs is an ideal material for photodetection at telecommunications wavelengths thanks to its direct bandgap, which is tunable by changing the relative In and Ga content. However, InGaAs devices typically require InP substrates, which are costly and difficult to process. Moreover, the In content of the InGaAs layer is limited by the requirement for lattice matching.[1] Nanowires (NWs) are a promising platform for heteroepitaxy of InAs and InGaAs on more common substrates like Si and GaAs thanks to their inherent strain relaxation. NWs also offer several performance advantages over bulk devices.[2] As an example, their thin, anisotropic geometry enables polarization-dependent absorption and fast carrier collection, making them suitable for multiplexed applications.[3] NWs also benefit from a significant reduction in the amount of scarce materials, such as In, required to make a device, and strain relaxation mechanisms allow a greater degree of freedom over their chemical composition. NWs are most often grown vertically, perpendicular to the substrate, such as by the vapor-liquid-solid or vapor-solid techniques. However, vertical NWs are difficult to incorporate into devices, usually requiring transfer of a single NW to a secondary substrate, a process that is not scalable. A horizontal configuration is therefore preferred for many applications. Recently, horizontal networks of high-quality In(Ga)As NWs have been demonstrated by growing them on top of GaAs nanomembrane buffers using selective-area epitaxy on III-V substrates.[4,5]

In this work we investigate the growth of horizontal In(Ga)As NWs on two different crystal orientations of GaAs substrates by molecular beam epitaxy. For growth on (111)B substrates, we demonstrate InGaAs NWs positioned atop high aspect ratio GaAs nanomembranes and describe how such NWs might be used for advanced photodetector architectures. We also show that the In content of these NWs can be tuned by controlling growth conditions, but pure InAs NWs are not achievable.[6] Next, we demonstrate In(Ga)As NWs grown on (100) substrates. The NWs grow conformally on low-aspect-ratio GaAs nanomembranes, whose morphologies are dominated by either {111} or {110} facets, depending on their alignment on the substrate. We demonstrate the ability to control the In content of the InGaAs NWs with basic growth parameters and characterize the homogeneity of the alloy composition as a function of the NW geometry. We also show that pure InAs can be achieved with just a narrow intermixed region near the interface. Finally, we present preliminary electrical characterization from basic four-point photoconductive devices based on NWs grown under different conditions. The charge transport properties are largely determined by the crystal quality. Correspondingly, the presence of a surface passivation layer has a significant influence on the overall photoresponse. We compare NWs with and without a passivating shell and characterize the photoconductive response for both single NWs and ensembles in an array. Insights from these preliminary results will guide design choices for future photodetector devices based on these NWs.

¹ R. LaPierre et al., *J. Phys. D: Appl. Phys.* **50** (2017)

² C. L. Tan et al., *Nanophotonics*. **7** (2018)

³ A. Dorodnyy et al., *IEEE J. Sel. Top. Quant. Electr.* **24** (2018)

⁴ M. Friedl et al., *Nano Lett.* **18** (2018)

⁵ F. Krizek et al., *Phys. Rev. Mat.* **2** (2018)

⁶ M. Friedl et al., *Nano Lett.* **20** (2020)

Funding from Swiss National Science Foundation, NCCR QSIT

5:00 PM EQ05.04.05

Electron Beam Induced Current Measurements of Single Nanowire Solar Cells—Development of Nanowire Tandem Junction Photovoltaics [Lukas Hrachowina](#), Enriqué Barrigon and Magnus T. Borgström; Lund University, Sweden

Within one hour, the sun supplies our planet with energy sufficient for humanity's yearly energy consumption¹. Nanowire solar cells are a sustainable complementary technology to silicon solar cells, as they have the potential to reach the efficiencies of world-record III-V solar cells while only using about 10 % of the material². Although nanowire solar cells have demonstrated high efficiencies³⁻⁶ and proven to have benefits compared to their bulk counterparts such as superior radiation tolerance⁷ the next step in nanowire solar cell technology – a tandem-junction solar cell that combines different band gaps within the same nanowire – has been elusive up to now.

Here, we report on single nanowire tandem junction solar cells based on both InP/GaInP and InAsP/InP. These lattice mismatched combinations of materials are accessible because of elastic relaxation at the lateral free surface of nanowires⁸. The development of the nanowire tandem junction photovoltaics was supported by a setup that combines a nanoprobe system with electron beam induced current (EBIC) measurements and a light emitting diode (LED) inside a scanning electron microscope⁹. By the use of the nanoprobe system we show voltage addition of the two sub-cells. We are able to

study both sub-junctions independently with EBIC, by either using a light bias from the LED setup to saturate the bottom-junction, or by using a voltage bias to saturate the top-junction. We believe that this type of characterization will be helpful to further optimize the efficiency of nanowire tandem junction solar cells, and to develop nanowire multi junction solar cells using more materials similar to the six-junction solar cell which has the record efficiency of 47.1 %¹⁰.

1. Morton, O. *Nature* **2006**, 443, (7107), 19-22.
2. Anttu, N. *Acs Photonics* **2015**, 2, (3), 446-453.
3. Wallentin, J.; Anttu, N.; Asoli, D.; Huffman, M.; Åberg, I.; Magnusson, M. H.; Siefert, G.; Fuss-Kailuweit, P.; Dimroth, F.; Witzigmann, B.; Xu, H. Q.; Samuelson, L.; Deppert, K.; Borgström, M. T. *Science* **2013**, 339, (6123), 1057-60.
4. van Dam, D.; van Hoof, N. J.; Cui, Y.; van Veldhoven, P. J.; Bakkers, E. P. A. M.; Gomez Rivas, J.; Haverkort, J. E. *ACS Nano* **2016**, 10, (12), 11414-11419.
5. Åberg, I.; Vescovi, G.; Asoli, D.; Naseem, U.; Gilboy, J. P.; Sundvall, C.; Dahlgren, A.; Svensson, K. E.; Anttu, N.; Björk, M. T.; Samuelson, L. *IEEE Journal of Photovoltaics* **2016**, 6, (1), 185-190.
6. Hrachowina, L.; Zhang, Y.; Saxena, A.; Siefert, G.; Barrigón, E.; Borgström, M. T. In *Development and Characterization of a bottom-up InP Nanowire Solar Cell with 16.7% Efficiency*, 2020 47th IEEE Photovoltaic Specialists Conference (PVSC), 15 June-21 Aug. 2020, 2020; pp 1754-1756.
7. Espinet-Gonzalez, P.; Barrigón, E.; Otnes, G.; Vescovi, G.; Mann, C.; France, R. M.; Welch, A. J.; Hunt, M. S.; Walker, D.; Kelzenberg, M. D.; Åberg, I.; Borgström, M. T.; Samuelson, L.; Atwater, H. A. *ACS Nano* **2019**, 13, (11), 12860-12869.
8. Glas, F. *Physical Review B* **2006**, 74, (12).
9. Barrigón, E.; Hrachowina, L.; Borgström, M. T. *Nano Energy* **2020**, 78, 105191.
10. Geisz, J. F.; France, R. M.; Schulte, K. L.; Steiner, M. A.; Norman, A. G.; Guthrey, H. L.; Young, M. R.; Song, T.; Moriarty, T. *Nature Energy* **2020**, 5, (4), 326-335.

5:15 PM EQ05.04.06

Late News: CuFeS₂—An Intermediate Band Semiconductor with Unique Optical Properties Yuan Yao, Anuj Bhargava and Richard Robinson; Cornell University, United States

Size-dependent changes in the electronic band structure is one of the key features of nanoparticles in the quantum confinement region.

CuFeS₂ nanoparticles have a strong absorption feature in the visible region that has, controversially, been described as neither an excitonic transition nor a free carrier plasmon oscillation. Instead, the absorption feature in CuFeS₂ nanoparticles has been attributed to quasi-static optical resonances from inter-band transitions between the valence, intermediate, and conduction bands. Previous work has reported conflicting accounts of the existence of this absorption band, the size-dependent optical properties, and the cation oxidation states in this CuFeS₂.

In this work we answer these outstanding questions and determine the origin of the plasmonic behavior in CuFeS₂ by characterizing the nucleation and growth stages of the reaction through a series of *ex-situ* and *in-situ* probes (e.g., x-ray absorption spectroscopy (XAS) and x-ray emission spectroscopy (XES)), and by characterizing a size-series of nanoparticles through experiment and theoretical calculations and models. We found that CuFeS₂ nanoparticle growth is initiated by Cu_{2-x}S seeds formation and then gradual Fe cation addition. Moreover, the growth of the quasi-static resonance feature during synthesis is driven by the band structure modification from Fe²⁺ incorporation into the nanocrystals. As opposed to the pure Cu¹⁺/Fe³⁺ predicted by DFT studies, a mixed oxidation state of Cu¹⁺/Cu²⁺ and Fe²⁺/Fe³⁺ is observed, indicating that the chalcopyrite phase (CuFeS₂) encompasses a range of oxidation states depending on the synthesis conditions. Moreover, by examining a size-series of particles we find the quasi-static optical resonance redshifts while the absorption edge blueshifts as the particle size decreases. Through density functional theory (DFT) and tight binding modeling, we elucidate the size dependence of the band structure, especially focusing on the change in the intermediate band. Using a Lorentzian oscillator optical model to simulate the absorption spectrum with inputs from the DFT calculated band structure and band shifts from the tight-binding model, we find the size-dependent shifts of the optical resonance peak position in CuFeS₂ is due to a tri-band quantum confinement effect that results in both the valence band to intermediate band and intermediate band to conduction band bandgap expansion that accompanies a decrease in particle size. Moreover, the linear optical Lorentzian model predicts the optical resonance peak is tunable across the visible range by partially filling the intermediate band, lowering the conduction band, or expanding the intermediate band.

Overall, in this study, we provide fundamental understandings about the origin of the visible quasi-static resonance in CuFeS₂ nanoparticles, and elucidate the correlation between the absorption feature shift and the band structure. These results are relevant to other quantum-confined intermediate band systems, which have potential use in optical applications as well as photovoltaic devices.

SESSION EQ05.05/EQ08.01: Keynote Session
Session Chairs: Viktoriia Babicheva and Ho Wai (Howard) Lee
Tuesday Morning, November 30, 2021
Hynes, Level 2, Room 210

10:30 AM *EQ05.05/EQ08.01.01

Meta-Optics for Image Processing Jason G. Valentine; Vanderbilt University, United States

Image processing has become a critical technology in a variety of science and engineering disciplines. While most image processing is performed digitally, optical analog processing has the advantages of being low-power and high-speed though it requires a large volume. Meta-optics provide the advantage of thin form factor optics while also allowing complex transfer functions to be employed. In this talk, I will discuss the use of meta-optics for applications in image processing. Specifically, I will discuss meta-optic pre-filters including edge filters as well as filters for identifying higher level spatial features. These meta-optics are designed in conjunction with the digital system and I will discuss how co-design can make the hybrid optical / digital system more tolerant to deterministic and stochastic noise. These analog optical operations can be used to replace, or augment, digital processes for increasing speed while reducing power consumption.

SESSION EQ05.06: Metasurfaces and Metamaterials II
Session Chairs: Jason Valentine and Benjamin Vest

11:15 AM EQ05.06.02

Spatial Multiplexing Method for Multiwavelength Metalens Sangwon Baek, Jae Yong Park and Jong-Lam Lee; Pohang University of Science and Technology, Korea (the Republic of)

Bulk optics have been used for various optical instruments such as microscope or camera, but it has limitations in size and thickness because of accumulation of various lenses. Metalenses are an emerging field as one of the next-generation optical technology for miniaturization of optical system. Subwavelength thick nanostructures on metalens control the amplitude, phase, absorption, emission, and transmittance of incident light. Focal length can be control by adjusting phase shift from 0 to 2π according to the change of shape, size, and period of nanostructures. Many kinds of metalens such as GaN nanopillar, Si nanodisk, or TiO₂ nanofin have been studied recently, but chromatic aberration correction problem remains as the limitation in metalenses. Some researches such as group delay dispersion have been conducted to correct chromatic aberration, low focusing efficiency ($\sim 10\%$) is unresolved limitation.

In this work, we suggested a new method to design achromatic metalens for 400, 600 and 800 nm wavelengths focusing. Spatial multiplexing method can correct chromatic aberration very simply. First, three metalenses are designed for each wavelengths. In the next step, meta-atoms of each metalenses are interleaved in one metalens. The coupling between three kinds of meta-atoms is small, therefore we can expect three wavelength focusing in one metalens. We used finite-difference time-domain (FDTD) simulation to investigate field distribution and focusing efficiency of each metalenses. By using this method, we demonstrated achromatic metalens with numerical aperture of 0.89, which focus light at 400, 600, and 800 nm to same focal spot. Focusing efficiency of achromatic metalens for 400, 600 and 800 nm are 38, 44 and 54 %, respectively. This design method can attend significant role to demonstrate desired achromatic metalens.

11:30 AM EQ05.06.03

A Layered Metallo-Dielectric Metasurface Inducing Stimulated Electron-Photon Interactions Matthias Liebtrau¹, Kelly W. Mauser¹, Marco van der Heijden², Pieter Kruit² and Albert Polman¹; ¹AMOLF, Netherlands; ²Delft University of Technology, Netherlands

Laser-driven optical near-fields mediate stimulated emission and absorption of photons by free electrons [1,2], providing unique control over the electron wave front in both space and time [3-5]. Besides a large field amplitude, efficient energy exchange in this process requires a match between the phase velocity of the optical field and the electron velocity – a condition that can be only fulfilled in the presence of matter [6,7]. Here, we explore how optical near fields can be tailored to efficiently manipulate slow non-relativistic electrons at the nanoscale. We design a thin-film metallo-dielectric metasurface perforated by a hexagonal array of circular holes, ensuring transparency to electrons while enabling diffractive coupling of resonant lattice modes to an external light field. The layer periodicity is optimized such that the normal component of the optical field inside the holes is dominated by a single Fourier component at a spatial frequency ω/v , determined by the electron velocity v and the optical pump frequency ω .

Experiments are performed in a scanning electron microscope (SEM) at a design electron energy of 5 keV. The metasurface is illuminated by a ns-pulsed near-infrared pump laser synchronized with sub-ns electron pulses that are generated by an ultrafast electrostatic beam blaster. To measure the energy distribution of electrons transmitted through the hole array, we use an electrostatic retarding field analyzer (RFA) with an energy resolution on the order of 0.1 eV. The employed Schottky field emission source provides an intrinsic electron energy spread as low as $\Delta E < 0.9$ eV, allowing us to fully resolve discrete electron energy-gain and -loss sidebands that are evenly spaced at multiple integers of the pump photon energy of 1.2 eV. The strength of the electron-near-field coupling can be quantified by the total width of the measured electron energy distribution, with its complex shape revealing the intriguing quantum nature of the electron-near-field interaction process. We show spatially resolved measurements of the electron-near-field interaction strength across the hole array and discuss how in-plane variations can be controlled to tailor the temporal and transverse phase profile of the incident electron beam.

Our work combines concepts of nanophotonics with a growing research field on coherent electron wave front shaping, while demonstrating SEM as a versatile and robust platform to study new quantum optical phenomena at the nanoscale. For the future, we plan to gain deeper insights into the wave/particle duality of free electrons by probing the emission of coherent cathodoluminescence and correlating it with the temporal shape and spatial phase profile of pre-defined electron quantum states.

References

- [1] B. Barwick et al., *Nature* **462**, 902-906 (2009).
- [2] A. Feist et al., *Nature* **521**, 200-203 (2015).
- [3] K. E. Priebe, et al., *Nat. Photonics* **11**, 793-797 (2017).
- [4] Y. Morimoto and P. Baum, *Nat. Phys.* **14**, 252-256 (2018).
- [5] G.M. Vanacore et al., *Nat. Commun.* **9**, 2694 (2018).
- [6] F.J. Garcia de Abajo and M. Kociak, *N. J. Phys.* **10**, 073035 (2008).
- [7] S.T. Park et al., *N. J. Phys.* **12**, 123028 (2010).

11:45 AM EQ05.06.04

Novel Silicon Bipodal Cylinders with Controlled Resonances and Their Use as Beam Steering Metasurfaces Samar Fawzy and Nageh K. Allam; American University in Cairo, Egypt

Metasurfaces have paved the way for high-performance wavefront shaping and beam steering applications. Phase-gradient metasurfaces (PGM) are of high importance owing to the powerful and relatively systematic tool they offer for manipulating electromagnetic wavefronts and achieving various functionalities. Herein, we numerically present a novel unit cell known as bipodal Cylinders (BPC), made of Silicon (Si) and placed on a Silicon dioxide (SiO₂) substrate to be compatible with CMOS fabrication techniques and to avoid field leakage into a high index substrate. Owing to its geometrical structure, the BPC structure provides a promising unit cell for electromagnetic wave manipulation. We show that BPC offers a way to shift the electric dipole mode to a frequency higher than that of the magnetic dipole mode. We investigate the effect of varying different geometrical parameters on the performance of such unit cell. Building on that, a metasurface is then presented that can achieve efficient electromagnetic beam steering with high transmission of 0.84 and steering angle of 15.2°; with very good agreement with the theoretically predicted angle covering the whole phase range from 0 to 2π .

12:00 PM EQ05.06.05

Late News: Strain-Tunable Fano Resonators Based on an Integration of Bragg Reflectors and Metasurfaces Sravya Nuguri¹, Ben Cerjan², Vince Einck¹, Daniel Shreiber³, Naomi Halas², Mark Griep³ and James Watkins¹; ¹University of Massachusetts Amherst, United States; ²Rice University, United States

States; ³U.S. Army Research Laboratory, United States

Fano resonance arises via interference between discrete and continuum bands. It undergoes a dramatic change in line shape shifts with any small perturbations in the system, thus proving its potential application in active tuning for display and sensors applications. Here, we explore and demonstrate the generation of Fano resonance from the coupling of symmetric or asymmetric-shaped Metasurfaces with Bragg reflectors. We have utilized a scalable route of soft-nanoimprinting lithography for the generation of Metasurfaces and incorporated layer-by-layer assembly of slide-ring-based materials to offer desirable elasticity and strain-tunable optical properties in the integrated device. Furthermore, we study the active tuning of the device by stretching the array in the x- and y-axis and the reflector in z-direction which allows for wide color tuning ability with narrow bandwidth in the colorimetric response. Our experimental findings agree well with simulations depicting high feature fidelity of Metasurfaces. By stretching the resulting device over 40% strain we demonstrate the mechano-chromic sensing abilities in a span of wavelengths.

SESSION EQ05.07: Lasing and Radiation Engineering I
Session Chairs: Alexandra Boltasseva and Jeremy Munday
Tuesday Afternoon, November 30, 2021
Hynes, Level 2, Room 210

1:30 PM *EQ05.07.01

Tunable, Multi-Wavelength Plasmonic Nanoscale Lasing [Teri W. Odom](#); Northwestern University, United States

Nanoscale laser designs have seen major advances over the last decade, with breakthroughs in cavity architectures and gain materials. Plasmonic lasers based on nanoparticle lattices are of special interest because the cavity structure can be tuned at the unit-cell level, which then affects the type of near-field optical feedback contributing to lasing action. Moreover, depending on whether the gain materials are molecular or nanoparticulate in nature, new optical modes can contribute to the amplification process. This talk will describe different classes of plasmonic nanoparticle lasers that can produce reversible and switchable lasing. We will focus on both static and dynamic approaches to achieve tunable color and polarization at multiple, different wavelengths. Finally, we will discuss prospects for white-light lasing.

2:00 PM EQ05.07.02

Fluorescent Nanodiamond – Hyaluronate Conjugates for Molecular Imaging [Hyehyeon Han](#) and Sei Kwang Hahn; POSTECH, United States

Despite wide investigation on molecular imaging contrast agents, there are still strong unmet medical needs to enhance their signal-to background ratio, brightness, photostability, and biocompatibility with multimodal imaging capability. Here, we assessed the feasibility of fluorescent nanodiamonds (FNDs) as carbon based photostable and biocompatible materials for molecular imaging applications. Because FNDs have negatively charged nitrogen vacancy (NV) centers, they can emit bright red light. FNDs were conjugated to hyaluronate (HA) for the target-specific molecular imaging. HA is a biocompatible, biodegradable, and linear polysaccharide with abundant HA receptors in the liver, enabling the liver targeted molecular imaging. *In vitro* cell viability test revealed the biocompatibility of HA-FND conjugates and the competitive cellular uptake test confirmed their target-specific intracellular delivery to HepG2 cells with HA receptors. In addition, *in vivo* fluorescence lifetime (FLT) assessment revealed the imaging capability of FNDs and HA-FND conjugates. After that, we could confirm the statistically significant liver-targeted delivery of HA-FND conjugates by *in vivo* imaging system (IVIS) analysis and *ex vivo* biodistribution tests in various organs. The renal clearance test and histological analysis corroborated *in vivo* biocompatibility and safety of HA-FND conjugates. All these results demonstrated the feasibility of HA-FND conjugates for further molecular imaging applications.

2:15 PM EQ05.07.03

Light Emission by Thermalized Ensemble of Emitters Coupled to a Resonator [Benjamin Vest](#), Aurelian Loirette--Pelous, Elise Bailly, Jean-Paul Hugonin and Jean-Jacques Greffet; Institut d'Optique Graduate School, France

Optical nanoantennas have become ubiquitous tools to enhance the spontaneous emission of atoms, molecules and quantum dots. In order to design practical sources with high power, it is necessary to move from a single emitter to an *ensemble of emitters*.

We can therefore use layers of emitters distributed on top of planar arrays of antennas of metallic or dielectric nanostructures to build light-emitting **metasurfaces**. They are designed to control the phase and amplitude of the electromagnetic modes in the plane. They can be engineered to emit light in specific directions and for specific wavelengths and polarization. However, metasurface designs rules that have been established over the years are still based on the understanding that optical antennas operate through the Purcell effect. Models based on this paradigm fail to fully explain spectral and spatial features observed in many experiments, such as the emergence of spatial coherence or spectral modifications of emitters.

In a first part, we start by discussing the differences between emission by a single emitter and emission by a thermalized assembly of quantum emitters to show that a statistical framework is required to understand their interactions with optical antennas. We then introduce a model of **light emission by thermalized ensembles of emitters**, based on fluctuational electrodynamics and the fluctuation-dissipation theorem [1]. A **generalized form of the Kirchhoff's law**, can be derived and extended to photoluminescence and electroluminescence. Light emission by the structure can be connected to the local absorptivity rate within the structure [2].

In a second part, we use our modeling procedure in the context of two experimental and theoretical studies of light emitting systems. Firstly, we focus on the properties of light emitted by a patterned ensemble of quantum dots consisting in a lamellar grating on top of a slab. This system exhibits spatial and spectral features, such as bright, directional and polarized emission. Our model accurately reproduces and predicts all features of the system's photoluminescence. It also addresses modification of the optical properties of the resonator by the pumping process, allowing to explore regimes of intense pumping of the emitters.

Secondly we use our approach to explore the **origin of spatial coherence in light-emitting structures**. We consider a system consisting in layers of molecular dyes deposited on top of a silver metallic layer. We start by introducing a general coherence-absorption relation that connects the coherence of the fields at two positions in the system to the power absorbed by the system when illuminated by two sources [3]. This relation shows the degree of spatial coherence can be deduced from experimental measurements or numerical codes simulating absorption in the layers. We find that surface waves and delocalized modes play a major role in building the spatial coherence. Our model is a key asset in the design of directional light sources based on photoluminescence.

Our approach of light emitting systems involving ensembles of emitters provides simple and efficient design tools relying on the determination of absorptivity of the structure. It accounts for the interplay between the electromagnetic properties of the emitter (resonances, antenna effect...) and the matter excitations which are included in the model through the imaginary part of the permittivity of the material and the subsystem's temperature and chemical potential.

References :

- [1] Light emission by a thermalized ensemble of emitters coupled to a resonant structure, L. Wojszwyk, H. Monin, J.J. Greffet, *Adv. Optical Mater.* 20, 1801697 (2019)
- [2] Light emission by nonequilibrium bodies: local Kirchhoff law, J.J. Greffet, P. Bouchon, G. Brucoli, F. Marquier, *Phys.Rev.X* 8, 021008 (2018).
- [3] General relation between spatial coherence and absorption, D. Tihon, S. Withington, E. Bailly, B. Vest, and J.-J. Greffet, *Opt. Express* 29, 425-440 (2021)

2:30 PM DISCUSSION TIME

2:45 PM EQ05.07.06

Dynamic Control of Epsilon-Near-Zero Resonance in Optical Fiber Jingyi Yang^{1,2}, Khant Minn², Aleksei Anopchenko^{1,2} and Ho Wai (Howard) Lee^{1,2}; ¹University of California, Irvine, United States; ²Baylor University, United States

Optical fiber is a well-established waveguide that has been utilized in a variety of applications such as data communications, spectroscopy, imaging, remote sensing, surgeries, and seismic activity monitoring, etc. However, the optical properties of an optical fiber (for instance, mode intensity and propagation loss) are fixed after drawing fabrication due to the static property of the dielectric glasses. Therefore, integrating active materials and nanostructures into optical fibers is promising for enhancing processing and transmission capabilities and novel functionalities. Zero-index materials have been extensively studied recently due to their unique and extreme optical properties [1]. Ultrathin transparent conducting oxide (TCO) epsilon-near-zero (ENZ) layer with the real part of permittivity approaches zero can support ENZ mode with enhanced and highly confined optical field [2]. Furthermore, the ENZ properties of TCO can be dynamically tuned by nonlinear optical pulse excitation [3-4].

In this work, we demonstrated the excitation of hybrid ENZ mode in a side-polished optical fiber deposited with an ultrathin layer of aluminum-doped zinc oxide (AZO). The 40-nm-thick AZO layer on the side of the fiber, fabricated by the atomic layer deposition technique, has ENZ properties at a near-infrared wavelength of ~1550 nm. The confined ENZ mode in the AZO thin film is excited due to the evanescent field coupling between the fundamental mode of the fiber and the ENZ mode supported by the AZO layer. Transmission measurement shows a resonance at a wavelength of 1600 nm with resonant strength of 6 dB in an ~1cm long AZO-coated side-polished optical fiber, which agrees with full-wave electromagnetic simulation and phase-matching condition. We further demonstrated that the highly confined ENZ mode could be used for developing efficient tunable in-fiber devices such as ultrafast optical modulators and switches. Due to the giant nonlinearity at ENZ frequency, the mode propagating in the ENZ optical fiber can be dynamically manipulated by femtosecond laser excitation. Our preliminary results show that the modulation strength of ~9.6 dB/mm can be achieved by modulating the hybridized ENZ resonance under femtosecond laser pulse excitation with an intensity of 200 GW/cm². The dynamic control of hybridized ENZ-optical fiber mode offers a compact and efficient method of manipulating the ENZ property and functionality in the optical fiber, which can find potential applications for ultrafast optical switches, polarization controllers, and other active optical fiber devices.

This work was supported by the Air Force Office of Scientific Research (Award number: FA9550-21-1-02204).

References

- 1. Liberal, I.; Engheta, N. *Nature Photonics*, 11(3), 149 (2017).
- 2. Campione, Salvatore, Igal Brener, and Francois Marquier. *Physical Review B* 91.12, 121408 (2015).
- 3. Alam, M. Z.; Schulz, S. A.; Upham, J.; De Leon, I.; Boyd, R. W. *Nature Photonics*, 12, (2), 79 (2018).
- 4. Kinsey, N., DeVault, C., Kim, J., Ferrera, M., Shalaev, V. M., & Boltasseva, A. *Optica*, 2, (7), 616-622 (2015).

SESSION EQ05.08: Advanced Nanophotonic Design I
Session Chairs: Souvik Biswas and Ho Wai (Howard) Lee
Tuesday Afternoon, November 30, 2021
Hynes, Level 2, Room 210

4:00 PM *EQ05.08.01

Advancing Photonic Design with Machine Learning Alexandra Boltasseva^{1,2} and Vladimir Shalaev^{1,2}; ¹Purdue University, United States; ²The Quantum Science Center, United States

Discovering unconventional optical designs via machine-learning promises to advance on-chip circuitry, imaging, sensing, energy, and quantum information technology. In this talk, photonic design approaches and emerging material platforms will be discussed showcasing machine-learning-assisted topology optimization for optical metasurface designs for applications in thermophotovoltaics, reflective optics and more.

4:30 PM EQ05.08.03

Infrared Optoelectronic and Magneto-Optic Properties in Gd-Doped CdO Angela Cleri, Noel C. Giebink and Jon-Paul Maria; The Pennsylvania State University, United States

CdO is one of the most promising low-loss infrared (IR) plasmonic materials to date. Incorporation of a donor dopant such as Y, In, or F has demonstrated tunable carrier concentration between 10¹⁹-10²¹ cm⁻³, corresponding to mid-IR plasmonic modal frequencies. In addition, high-power impulse magnetron sputtering (HiPIMS) consistently produces epitaxial films with high mobilities between 300-500 cm²/V-s, minimizing optical losses. We have shown how manipulating donor and acceptor defect chemistry through controlling deposition and post-processing conditions enables one to engineer epsilon-near-zero (ENZ) modes spanning a broad range of the mid- to near-IR (1650-5325 cm⁻¹).

While we have largely explored light confinement in CdO via electron oscillations, we now aim to further manipulate light through magnetism by Gd doping to create a dilute magnetic semiconductor. In this presentation, we show the excellent structural and morphological properties of Gd-doped CdO

across a broad doping range, enabling fine permittivity control with ENZ behavior spanning the mid- to near-IR. Further, we will explore the effect of the ENZ condition on magneto-optic properties.

4:45 PM EQ05.08.04

Bottom-Up Monocrystalline Split Ring Resonators for Enhanced Absorption at Optical Frequency [Ibtissem Bouanane](#)^{1,2}, Judikaël Le Rouzo¹, Olivier Margeat³, Anna Capitaine³, Beniamino Sciacca³, Gerard Berginc² and Ludovic Escoubas¹; ¹Aix Marseille Université, Université de Toulon, CNRS, UMR 7334 – IM2NP, France; ²THALES LAS, France; ³Aix Marseille Université, Université de Toulon, CNRS, UMR 7325 – CINaM, France

The opportunity to employ sub-wavelength nanostructures to tune light-matter interaction has triggered tremendous interest in the last decade, thanks to the plethora of optical properties that can be achieved in metamaterials or metasurfaces, that are often not seen in nature. Among those examples, split-ring resonators can display optically-induced magnetic responses with unique possibilities to enhance absorption in the visible and near IR. Tuning the geometric parameters of the nanorings enables for control of the absorption band at optical frequencies, with implication in multiple fields, from thermal solar, to photovoltaic (selective absorbers, anti-reflections coatings, etc.) and optoelectronics (optical coatings, sensitive photodetectors, optical stealth, etc.) [1] [2].

However, whereas design strategies are well established, experimental techniques to fabricate such materials at a large scale and low cost are still in their infancy; they mainly rely on e-beam lithography for the fabrication of small area, high-resolution metasurfaces, or on nanoimprint lithography for larger area. In both cases, several fabrication steps have to be undertaken, including etching steps and metal evaporation steps, that are not easily scalable. In addition, the materials obtained are typically polycrystalline, with negative impact on their optical quality.

The objective of the research is to provide a first proof of concept of tunable silver circular split-rings entirely made by scalable bottom-up approaches, showing enhancement of absorption at optical frequencies.

First, FDTD simulations were performed to realize a parametric study of silver nanoring design in order to optimize its geometric parameters for absorption enhancement (inner, outer diameters, thickness, split-ring gap, array periodicity). This showed full control on resonance peaks and absorbance enhancement in the visible and near IR.

Next, we will show the realization of circular silver split-ring arrays on a large area via bottom-up techniques. Silver single-crystalline nanocubes (synthesized in solution via the polyol process) are self-assembled with high yield (>90%) in PDMS templates previously nanostructured with a pre-defined split-ring motif. Epitaxial nanowelding techniques at low temperature (Sciacca et al. *Advanced Materials*, 2017) are then employed to connect the individual nanocubes together to obtain a continuous quasi-monocrystalline material. We will show electron microscopy characterization at different steps of the fabrication process to show the high crystalline quality and support our claims.

Finally, we will show measurements of the macroscopic (5 mm²) optical properties of the split-ring arrays, and compare to those calculated via FDTD simulations.

Our work shows for the first time the realization of a high optical quality metasurfaces at a large scale fully obtained with bottom-up techniques.

[1] T. P. Otanicar, et al., Filtering light with nanoparticles: a review of optically selective particles and applications. *Adv. Opt. Photonics*, vol. 8, no. 3, pp. 541–585 (2016)

[2] A. F. Koenderink et al., Nanophotonics: Shrinking light-based technology. *Science* 348 (2015)

SESSION EQ05.09: Poster Session I
Session Chair: Ho Wai (Howard) Lee
Tuesday Afternoon, November 30, 2021
8:00 PM - 10:00 PM
Hynes, Level 1, Hall B

EQ05.09.01

Novel Core-Shell Plasmonic Nanoparticles for Hydrogen Sensing [Stephen F. Bartolucci](#), David J. Sconyers, Rosemary L. Calabro and Joshua Maurer; U.S. Army DEVCOM Armaments Center, United States

Noble metal nanoparticles exhibit localized surface plasmon resonance (LSPR) when interacting with light. This property has led to the study of these particles for numerous applications, such as catalysis, biosensing, gas detection, and chemical sensing. One commonly used material in hydrogen sensing is palladium, which can dissociate hydrogen gas and form a hydride, resulting in a shift of the LSPR absorption. The kinetics of hydrogen absorption reaction and desorption in palladium are relatively fast, which is useful for gas sensing in hydrogen economy applications. However, some applications require long-term detection of total hydrogen levels, where fast desorption is not desired. Core-shell nanoparticles consisting of a noble metal core and a shell material, such as a transition metal oxide, could provide a material system for hydrogen detection with a more permanent plasmonic shift during exposure to hydrogen. In this work, we show the synthesis of various noble metal core-shell nanoparticles, including gold-copper (I) oxide and gold-palladium, with spherical and spiked structures and evaluate their ability to detect hydrogen in colloidal suspensions. In addition, we will discuss electrochemical methods to synthesize core-shell nanoparticles and spectroelectrochemistry to characterize the nanoparticles during growth.

EQ05.09.03

Chemical Engineering of Plasmonic Modes in Disordered Cu-Sn Network Metamaterials [Jelena E. Wohlwend](#), Henning Galinski, Alla Sologubenko, Max Doebeli and Ralph Spolenak; ETH Zürich, Switzerland

Design and fabrication of large-area metamaterials is an ongoing challenge for the material science and technological communities. In the present work, we propose a scalable and low-footprint strategy to design large-area, frequency-selective Cu-Sn disordered network metamaterials that exhibit nearly perfect absorption in a given spectral range. These nano-modulated structures exhibit a broadband spectral response, similar to connected wire mesh metamaterials.

We demonstrate that chemical engineering applied to the thin film materials allows the production of nano-modulated networks and allows tuning the

absorption frequencies of the disordered meta-networks to a particular spectral region spanning the near-infrared - UV diapason.

Our approach relies on the establishment of disordered networks of a particular morphology by employing chemical etching to co-sputtered Cu-Sn-Al thin films with the purpose to remove aluminum from the film volume. As a result, the films adopt a particular topological and phase configuration that yield characteristic absorption signals. Moreover, tuning the initial composition of the Cu-Sn-Al thin film during the film production enables the control over the phase state and the spatial modulation period of the porous network which in turn defines the particular set of the plasmon absorption frequencies activated in the system.

Experimental verification of the plasmonic response of the produced networks is carried out in our work by employing electron energy loss spectroscopy (EELS) in the low-loss region. We resolve highly confined gap surface-plasmon (GSP) modes activated at the surfaces of the porous structures due to the near periodic nano-sized topology of the network.

EQ05.09.05

Late News: Plasmonic Enhancement of Strontium Titanate by Galvanic Replacement of Exsolved Ni Nanoparticles with Au [Kevin Gregor Both](#), Xiaolan Kang, Vilde M. Reinertsen, Thomas Aarholt, Truls Norby, Øystein Prytz and Athanasios Chatzitakis; University of Oslo, Norway

Photocatalysis can be regarded as part of the push towards renewable and greener energy production. Water splitting is a suitable example, where the ideal semiconductor has a bandgap of 1.9 – 2.3 eV. However, semiconductors with such a bandgap are usually unstable during photocatalytic water splitting [1]. Extending the absorption spectrum of a catalyst with larger band gaps can be achieved utilizing localized surface plasmon resonance (LSPR). The ability to tune the dominant frequency of the metal particles by changing their geometry and size makes LSPR even more intriguing [1]. The plasmon absorption peak energies of certain metal nanoparticles (NPs) are in the range of visible light, potentially allowing their energy to drive chemical reactions with sunlight or contribute to photovoltaic applications [2]. The plasmonic metal NPs can utilize the energy directly and act as photocatalysts, they can be used in an antenna-reactor setup with catalytically active metallic NPs, or they can transfer the energy to the semiconductor surrounding them [1-3]. The chemical and physical properties of these metal NPs, as well as of the substrate define the type of energy transfer and consequently chemical reaction possible.

In this work NPs of nickel (Ni), copper (Cu), and ruthenium (Ru) were created within strontium titanate (STO) by exsolution in a hydrogen/argon mix (HArmix, 5%) at elevated temperatures (600 °C to 900 °C). Subsequently, the exsolved Ni was replaced by gold (Au) to different degrees by galvanic replacement. The versatility of the technique was demonstrated by using A-site excess and A-site deficient STO, as well as galvanic replacement by platinum (Pt). While Ni, Ru, and Pt are only weakly plasmonically active, their catalytic properties may be used in an antenna-reactor setup. Thin films and powders were synthesized by pulsed laser deposition and solid state reactions methods, respectively. Particles of pure Au, ladybug-like Au decorated Ni particles on STO, and flower-like Au decorated Ni particles on STO, as well as potential antenna-reactor setups, were obtained. The main difference between the ladybug-like and flower-like samples was the size of the Au particles decorating the Ni. In general, shorter galvanic replacement times led to spherical NPs, while prolonged ones yielded (bimetallic) NPs with complex geometries.

Scanning Transmission Electron microscopy (STEM) and energy dispersive X-ray dispersion (EDX) were utilized to determine the structure and chemical environment of the particles. STEM and Electron Energy Loss Spectrometry (EELS) in the low electron energy loss regime were employed to study the plasmonic response on the nm-length scale, directly observing “hot-spots” in the electric field. The STEM-EELS/EDX experiments were performed with a monochromated 300 kV STEM probe with Zero-Loss Peak (ZLP) full-width at half maximum of 110 meV on a FEI Titan G2. The Au nanoparticles exhibited peaks in the EELS spectra between 1.50 and 2.40 eV. While the 2.40 eV peak is well known for Au nanoparticles, a Finite Difference Time Domain (FDTD) approach was used to investigate them further, determining that peaks towards 1.50 eV originate in parts of the particles near STO or with complex geometries. Geometries and the chemical environment of the particles can be used to explain the splitting and shifting of the peaks. Moreover, the PEC performance of samples with partially or fully galvanically replaced Ni NPs by Au, showed a clear improvement compared to samples without NPs.

The Research Council of Norway is acknowledged for the support to the Norwegian Center for Transmission Electron Microscopy (NORTEM, no 197405/F50), the NANO2021 researcher project FUNCTION (no. 287729) and FRINATEK project PH2ON (288320).

[1] N. Wu, *Nanoscale* 10(6), (2018), 2679-2696.

[2] Zhang, Q. et al., *J. Materiomics* 3(1), (2017), 33-50

[3] Zhou, L. et al. *Nat. Energy*, 5, (2020), 61-70

EQ05.09.06

Late News: Tuning the Plasmonic Properties by Alloying—Insights from a DFT Approach [Matej Bubaš](#) and Jordi S. Parramon; Ruder Boskovic Institute, Croatia

Changing the composition of alloy nanostructures can be a way of tuning their plasmonic properties. Rational tuning for a desired purpose requires a method that provides both prediction and the fundamental understanding of the predicted properties. We present an approach based on density functional theory (DFT) calculations coupled with electrodynamics simulations that meets the aforementioned requirements. Our results show the importance of the chosen exchange-correlation functional on the quality of prediction for bulk alloys that becomes critical in the case of nanostructures. Furthermore, we show the value that the fundamental insights provided by DFT have by explaining the causes for predicted low energy interband transitions as an emergent property of alloying. Lastly, we compare our approach to other state-of-the-art methods for computing hot carrier energy distribution and study the possibility of tuning the hot carrier distribution by alloying.

EQ05.09.07

Late News: Simulating Surface Plasmons on Ni and Au Nanoparticles Embedded on a SrTiO₃-Surface Made by Exsolution Followed by Galvanic Replacement [Vilde M. Reinertsen](#), Kevin Gregor Both, Øystein Prytz and Athanasios Chatzitakis; University of Oslo, Norway

Local Surface Plasmon Resonances (LSPR) on metal nanoparticles have been found to enhance photocatalysis with the largest enhancement by noble metals. They turn out to have properties which results in a strong LSPR response [1]. However, the catalytic properties of the noble metals are poor due to low adsorption of reactant molecules on their surface [1]. A solution to this issue is to use the LSPR in the noble metal to enhance the photocatalytic abilities of a supporting semiconductor. The semiconductor can be enhanced through different mechanisms including local electromagnetic field enhancement, resonant energy transfer and the generation of hot carriers from LSPR decay [2]. In this contribution, we investigate the latter possibility by calculating the absorption in Ni and Au nanoparticles (NPs) embedded on a SrTiO₃ (STO) surface. The hot carrier injection is especially interesting since it enables light absorption below the band gap of STO ($E_g^{STO} = 3.25$ eV).

The simulations were performed using the finite difference time domain method. The simulated geometries were modeled after the structure of Ni-doped STO thin-films grown by pulsed laser deposition, where subsequent exsolution gave socketed Ni NPs on the surface of the thin-films [3]. Some samples were afterwards treated to galvanically replace the Ni with Au [4]. To investigate the thin-film samples computationally, we compared the plasmonic

response of Au and Ni spherical NPs ($5 \text{ nm} \leq \text{radius} \leq 15 \text{ nm}$) embedded on the surface of STO in the energy range below the band gap of STO. The simulations confirmed that the Au NPs have a larger absorption cross section (σ_{abs}) than Ni NPs as expected [5] and validated the galvanic replacement as a method to increase the plasmonic effect in the thin-film samples. In addition, we found that, for both materials, the σ_{abs} increased when the NPs were embedded deeper into the substrate. The increase is probably due to the high refractive index of STO compared to vacuum which redshifts the LSPR peak away from interband transitions at 2.4 eV for Au and 4.7 eV for Ni [6,7]. The redshift therefore works to decrease damping. The σ_{abs} per geometrical cross section (σ_{geo}) peak height seems to increase linearly with the redshift in energy. For Au, a LSPR energy at 2.05 eV gives an σ_{abs} peak height equal to the σ_{geo} and at 1.9 eV σ_{abs} is almost $7\sigma_{\text{geo}}$. For Ni, most of the absorption spectra have the largest σ_{abs} around the interband transitions at 4.7 eV and a smaller peak around 2.5 eV, with a few exceptions. The exceptions have both a large size and are deeply embedded in STO which are two things that redshift the LSPR energy. However, the smaller LSPR peaks, which lie below the band gap of STO, seem to follow the same linear trend as for Au. We observe that with a LSPR energy of 2.55 eV the σ_{abs} peak height is equal to the σ_{geo} and at 2.4 eV σ_{abs} is around $1.4\sigma_{\text{geo}}$. If we look at the σ_{abs} per volume, the linear trend is not as clear. The smaller particles have a larger σ_{abs} per volume compared to the larger ones, but the absorption still increases with redshift in LSPR energy. In conclusion, we have calculated the absorption in Ni and Au NPs embedded on a STO surface, as a first insight into hot electron injection as a way to enhance the photocatalytic abilities of STO. We found that the embedding of the particles deeper into the semiconductor increased their σ_{abs} , and that the $\sigma_{\text{abs}}/\sigma_{\text{geo}}$ peak height is linearly proportional to the redshift in LSPR energy. These results are a starting point to assess this attempt to photocatalytically enhance STO.

- [1] K. Sytwu, M. Vadai, and J. A. Dionne, *Adv. Phys.-X* **4**, UNSP 1619480 (2019).
- [2] N. Wu, *Nanoscale* **10**, 2679 (2018).
- [3] D. Neagu *et al.*, *Nat. Commun.* **6**, 8120 (2015).
- [4] K. G. Both *et al.*, (unpublished).
- [5] U. Kreibig and M. Vollmer, *Optical Properties of Metal Clusters*, 1st ed. (Springer, Berlin, 2013).
- [6] P. E. Hopkins, *J. Heat Transf.* **4** (n.d.).
- [7] T. Pakizeh, *J. Phys. Chem. C* **115**, 21826 (2011).

EQ05.09.10

Spectral Robustness of Single Ultrabright Fluorescent Silica Nanoparticles [Mahshid Iraniparast](#), Berney Peng and Igor Sokolov; Tufts University, United States

We present a study of possible variations of fluorescence spectrum between individual ultrabright silica nanoparticles (SiNPs) at the level of single nanoparticles. The extremely high fluorescence brightness of these particles has been created by encapsulating fluorescent dye molecules inside the nanoporous silica matrix of nanoparticles. A specific environment around the dye molecules allows attaining a very high concentration of the dye molecules without quenching of fluorescence. Different dyes can be mixed within each nanoparticle, thereby creating a platform for fluorescent sensors. The ultrabright nature of these particles allows doing measurements using single nanoparticles. For a quantitative study, it is paramount to demonstrate that the fluorescence spectra collected from individual nanoparticles are substantially similar. Encapsulation of multiple dyes within the same particle exhibits Förster Resonance Energy Transfer (FRET), which may cause differences in fluorescence spectra because of the random location of the encapsulated dye molecules inside each particle.

In this study, direct measurements and simulations were performed to study the possible variation in the fluorescence spectra of individual SiNPs. A confocal fluorescent microscope attached with a single-photon camera was used for the direct measurements. These results were compared to the simulation of fluorescent spectra, which took into account the multiple random positioning of dye molecules inside each particle.

Overall, the direct measurements and simulation were in very good agreement with each other and showed that the spectral variation between single SiNPs was rather small. We can conclude that individual ultrabright SiNPs can be used in a variety of applications as taggants and sensors, including multiplexed biomedical imaging, flow cytometry, and ratiometric fluorescence sensors.

SESSION EQ05.10: Active Control
 Session Chairs: Souvik Biswas and Jeremy Munday
 Wednesday Morning, December 1, 2021
 Hynes, Level 2, Room 210

11:00 AM EQ05.10.02

Dynamic, Electro-Optically Controlled Wavefront Shaping via High Quality Factor Silicon-on-Lithium Niobate Metasurfaces [Elissa Klopfer](#)¹, Sahil Dagli¹, David R. Barton², Mark Lawrence³ and Jennifer A. Dionne¹; ¹Stanford University, United States; ²Harvard University, United States; ³Washington University in St. Louis, United States

Dynamic control of wavefront shaping is essential for optical technologies spanning communication, computation, and sensing. Reconfigurable metasurface devices are especially important for lightweight and compact applications, including LidAR, LiFi, and AR/VR systems. However, achieving reconfigurable devices that demonstrate efficient modulation remains an outstanding challenge, due in part to the low electro-optic coefficient of most materials and weak light-matter interactions afforded by traditional metasurfaces. Current reconfigurable metasurface designs optimize for phase contrast and thus generally operate close to absorption peaks, leading to low efficiencies and poor contrast between diffraction orders. Here we present fully reconfigurable, high-efficiency wavefront shaping, exemplified by both high reflection efficiency and a large dynamic tuning range, achieved via high-Q silicon-on-lithium niobate metasurfaces. Our metasurface consists of subwavelength nanobars of silicon, 500 nm wide and 220 nm tall, atop 100 nm thick lithium niobate. Periodic perturbations to the constituent nanobars allow guided modes to couple to free space, with strongly enhanced electromagnetic fields localized in the lithium niobate. These guided mode resonances achieve Q factors exceeding 30,000, enabling strong electromagnetic field confinement without compromising the metasurface transfer function; these high-Q resonances can make the constituent nanoantennas more sensitive to subtle changes in refractive index. Using full-field simulations, we show how applying a voltage across individual nanoantennas shifts the spectral position of the high-Q resonance, modifying the antenna phase and amplitude, and achieving nearly a full 2π phase variation with reflectance above 91%. With the ability to individually address metasurface elements through transparent conducting oxide contacts on each antenna, we construct phase gradient transfer functions defined by the applied field, rather than varying the size, spacing, or geometry of the constituent nanoantennas. By changing the nanoantenna biasing configuration, we show a single metasurface can be tuned to switch between multiple transfer functions and steer light to different angles with high diffraction efficiency. We demonstrate how an applied field can modulate the metasurface to act as reflective beamsplitting or beamsteering devices, depending on the biasing conditions, with varying angles and efficiencies as high as 85%. Near-continuous beam-steering can be achieved by modifying the

bias across each antenna; for example, voltages of +14.5, 0, and -14.5 steer to 31 degrees, while applied voltages of +18.6, +2.7, -2.7, and -18.6 and +21.1, +5, 0, -5, and -21.1 steer to 23 degrees and 18 degrees, respectively. Our presentation will discuss not only the design but also fabrication and characterization en route to a versatile metasurface platform that can reconfigurably achieve a variety of transfer functions.

11:15 AM EQ05.10.03

Reflective Optical Limiters Based on Tunable Frequency-Selective Surfaces Modulated by Vanadium Dioxide [Chenghao Wan](#)¹, Zhen Zhang², Jad Salman¹, Jonathan King¹, Yuzhe Xiao¹, Zhaoning Yu¹, Alireza Shahsafi¹, Raymond Wambold¹, Shriram Ramanathan² and Mikhail A. Kats¹; ¹University of Wisconsin--Madison, United States; ²Purdue University, United States

Optical limiters are optical devices that utilize optical nonlinearities to achieve decreasing transmittance versus increasing incident optical intensity, which is useful for protecting sensitive detectors or human eyes against high-intensity illumination. Most optical limiters utilize nonlinear absorption to absorb the light when the incident intensity increases significantly. However, such absorptive designs may be suboptimal because the absorption of high-power light may result in damage to the limiter via melting, sputtering, or ablation. Therefore, a more-ideal solution is to make optical limiters that are reflective (i.e., they reflect excess light) rather than absorptive. There have been limited efforts to realize reflective optical limiters, and existing designs have limitations in terms of spectral and angular bandwidth, speed, etc.

In our talk, we will present our design of an ultrathin, broadband reflective optical limiter based on dynamically tunable resonant transmission through metal aperture antennas using thin-film vanadium dioxide (VO₂), an electron-correlated material that features a dramatic change in optical properties across its insulator-metal phase transition (IMT). Specifically, we incorporated gold (Au) frequency-selective surfaces (FSSs), which are metallic arrays of aperture antennas that feature resonant transmission, onto VO₂ thin films on transparent substrates (here, GaAs). The FSS-VO₂ optical limiter can feature high resonant transmission when the VO₂ is in the insulating phase (open state of the device), but reflects light when the resonant transmission is detuned or extinguished by the IMT of VO₂ (limiting state of the device).

We designed and optimized the FSS-VO₂ structure using finite-difference time-domain (FDTD) simulation (implemented in Lumerical FDTD), primarily targeting three figures of merit: a) high open-state transmittance, b) low limiting-state transmittance, and c) low limiting-state absorption. Via varying the FSS geometries, our optimized design can feature a broad open-state transmission band (FWHM > 2 μm) centered at any desired wavelength in the infrared from ~2 to 11 μm and essentially zero transmittance (~0.008) for all wavelengths in the limiting state. Because of the deep-subwavelength thickness and symmetry of the FSS structure, our design works for a large angular bandwidth (up to angle of incidence of 50°) for any polarization.

We used e-beam lithography to fabricate a design that has an open-state transmission band centered at ~10 μm. We measured the transmittance spectrum of the fabricated device for both states using a Fourier-transform infrared (FTIR) microscope, and the results agreed well with our simulations. The limiting performance of the fabricated device was characterized using our intensity-dependent transmission measurement setup with a continuous-wave CO₂ laser operating at λ = 10.6 μm. Note that we needed to preset the device at a higher temperature using a heat stage because the CO₂ laser we used could not provide sufficient power to photothermally trigger the IMT of VO₂ from the room temperature. Our experiments showed that the device was able to feature limiting performance for different incident-intensity ranges by varying the preset temperature. Moreover, the experimental results were well captured by our opto-thermal simulation (implemented in COMSOL Multiphysics) which also provided us insight to the limiting performance of our design regarding the limiting threshold and the device speed. We also used this opto-thermal simulation to explore opportunities for unidirectional limiting (i.e., nonlinear optical isolators).

11:30 AM EQ05.10.04

Photonic Crystal Fabry-Perot Cavities in Thin-Film Lithium Niobate for Tunable On-Chip Photonics [David R. Barton](#), Jeffrey Holzgrafe, Di Zhu, Hana Warner, Neil Sinclair and Marko Loncar; Harvard University, United States

Photonic crystal cavities are ideal for enhancing weak light-matter interactions by simultaneously increasing the residence time of an optical mode while shrinking its mode volume. In addition, these structures can act as high extinction and narrow-band filters due to the optical bandgap formed. This can be used for on-chip filtering and dispersion engineering, both of which are necessary components in integrated photonic circuits. Lithium Niobate has emerged as a strong candidate for integrated photonics due to the ability to fabricate low-loss waveguides and high-quality factor ring resonators on a chip. In addition, its non-centrosymmetric structure allows for second order nonlinear optical effects like three-wave mixing phenomena and the electro-optic effect. Lithium Niobate's strong electro-optic effect is particularly useful, as it allows for tunability and optical modulation at microwave frequencies. Combining photonic crystals in integrated lithium niobate photonics is of great interest for optical technologies spanning nonlinear classical and quantum photonics.

Here, we explore Fabry-Perot cavities integrated in a Lithium Niobate on Insulator platform for tunable on-chip photonics. The mirrors are formed by photonic crystal sections on either side of low-loss waveguides. To reduce unwanted scattering losses, we utilize a "nanofin"-type geometry with alternating regions of wide and thin waveguide sections. We design our devices on uncladded 300 nm and 600 nm Lithium Niobate with underlying silicon dioxide. For 300 nm Lithium Niobate devices, a waveguide width of 1 micron, photonic crystal period of 480 nm, and alternating photonic crystal waveguide widths of 1600 nm and 400 nm forms an optical band gap near 1525 nm. We experimentally demonstrate bandgaps exceeding 80 nm in bandwidth at telecom frequencies and extinction exceeding 50 dB with a photonic crystal less than 30 microns long. By designing mirror segments with tapered sections to reduce impedance mismatch, we further demonstrate Fabry-Perot cavities with quality factors exceeding 150,000. We have also designed and tested devices on 600 nm Lithium Niobate with quality factors exceeding 75,000 in strongly overcoupled cavities, suggesting that much higher quality factors are achievable without sacrificing on transmission efficiency. We characterize the potential loss mechanisms by varying the cavity length and observe linear increases in the quality factor with cavity length, suggesting that mirror reflectivity is the dominant limiting factor in our devices, rather than scattering from waveguide or mirror imperfections. Future designs suggest that quality factors approaching 1 million are possible in devices with mode volumes smaller than typical ring resonator structures.

Coupled with Lithium Niobate's strong electro-optic effect ($r_{33} \sim 30$ pm/V), the high-Q nature of these devices lend themselves strongly to tunable nanophotonics and nonlinear photonics. We envision these devices in a variety of integrated optical technologies, including optical sensing and detectors, microwave-frequency modulation, and integrated quantum photonics.

11:45 AM EQ05.10.06

Tunable Photonics Enabled by Defect Engineering of Vanadium Dioxide via Ion Implantation [Chenghao Wan](#)¹, Martin Hafermann², Tae Joon Park³, Zhen Zhang³, Jura Rensberg², Shriram Ramanathan³, Carsten Ronning² and Mikhail A. Kats¹; ¹University of Wisconsin--Madison, United States; ²Friedrich-Schiller-Universität Jena, Germany; ³Purdue University, United States

Vanadium dioxide (VO₂) has been widely investigated for tunable and reconfigurable photonic devices because it features dramatic changes in its optical

properties across its insulator-metal phase transition (IMT) at ~ 68 °C. As a strongly correlated material, the IMT temperature of VO₂ is determined by the stability of the electron hybridization, which is sensitive to the strain environment in the thin film, providing opportunities for engineering of the IMT. Most existing methods for modulating the IMT temperature of VO₂ either use different substrate materials or orientations to result in different strain environments in the film, or introduce dopants via physical or chemical processes during growth. Therefore, such methods need to be developed particularly depending on the choice of synthesis method, and the IMT characteristics are predetermined during the growth and fixed in the post-growth films.

In our talk, we present a method to modulate the IMT characteristics (e.g., the IMT temperature, or the temperature range of the IMT, which we refer to as IMT width) by introducing defects into VO₂ films via a post-VO₂-growth ion-implantation process. Our method is applicable for VO₂ films synthesized using different methods, and we demonstrated that such modulation in the VO₂ properties can be achieved even after a nanostructured device has been patterned on top of the VO₂ film.

Under irradiation by high-energy ions (Ar ions in our experiments), vacancies of V and O result from the collision cascade between the impinging ions and atoms of V and O, resulting in changes in IMT characteristics due to the induced changes in the strain and stoichiometry of the VO₂. In our experiments, we used 75-keV Ar ions to irradiate a ~ 100 -nm VO₂ film grown on a sapphire substrate. We irradiated different areas of the film with different ion fluences ranging from 1×10^{13} to 2×10^{14} cm⁻². The IMT temperature and width of all the irradiated regions were characterized using temperature-dependent Fourier-transform infrared (FTIR) reflectance measurements. We also quantitatively extracted the temperature-dependent refractive index throughout the IMT for all irradiated regions using a combination of ellipsometry analysis and effective-medium calculation.

Based on our experiments, we conclude that the IMT characteristics of VO₂ can be grouped into distinct behaviors with respect to irradiation fluences: When irradiated by ion fluences of $< 6 \times 10^{13}$ cm⁻², the IMT temperature can be continuously lowered by up to ~ 20 °C with no substantial changes either in the IMT width or in the refractive-index contrast between the insulating and metallic phases. In contrast, for the higher irradiation fluences, though the IMT temperature can be further reduced, it is accompanied by a broadened IMT width and less refractive-index contrast.

The low-irradiation-fluence modulation is generally favorable for reconfigurable photonic designs because it can simply tune the IMT temperature (i.e., device triggering threshold) without trading off the optical contrast between device states. As a demonstration, we fabricated an optical limiter that incorporated gold aperture antennas onto a VO₂ thin film. The device featured a high transparency window centered at $\lambda \sim 4$ μ m when the VO₂ is in the insulating phase and low transmittance for all wavelengths when the VO₂ is triggered to the metallic phase at 68 °C. By irradiating this device with an ion fluence of 6×10^{13} cm⁻², we reduced the switching temperature to 52 °C.

SESSION EQ05.11: Fundamental of Plasmonics and Metaphotonics I
Session Chairs: Artur Davoyan and Luca Sortino
Wednesday Afternoon, December 1, 2021
Hynes, Level 2, Room 210

1:30 PM *EQ05.11.01

Quantum Photonics Empowered by Plasmonics and Machine Learning [Vladimir Shalaev](#) and Alexandra Boltasseva; Purdue University, United States

We will discuss some recent ideas and developments on how plasmonics and machine learning can be employed to dramatically speed up quantum process to make them immune to decoherence and how they can significantly improve the performance of quantum photonics devices and systems.

2:00 PM EQ05.11.02

Nonlocal and Quantum Effects in Graphene Plasmonic Devices Operating at Short Wave Infrared Wavelengths over Large Scale Areas [Joel Siegel](#), Jonathan Dwyer, Anjali Suresh, Nathaniel Saffron, Margaret Fortman, Chenghao Wan, Jonathan Choi, Wei Wei, Vivek Saraswat, Wyatt Behn, Mikhail A. Kats, Michael Arnold, Padma Gopalan and Victor Brar; University of Wisconsin--Madison, United States

Graphene plasmonic resonances have been broadly studied in the terahertz and mid-infrared (MIR) ranges because of their electrical tunability and large confinement factors, which can enable exploration of extreme light-matter interactions, among other optoelectrical applications. Plasmonic resonances occur in graphene when it is patterned into nanostructures (e.g. ribbons) which confine the graphene plasmons and enables coupling to free-space radiation. But an upper frequency limit (MIR) is set by the limits of electron beam lithography, which can make graphene nanostructures as small as 15 nm. In this talk, I will show that nonlocal and quantum effects become significant for graphene nanostructures less than 15 nm. Those changes blue-shift the frequencies of the graphene plasmons, pushing their operational range from the MIR into the short-wave infrared (SWIR). These effects are realized in centimeter-scale arrays of graphene ribbons as narrow as 12 nm created using a novel, bottom-up block copolymer lithography method that allowed for the creation of plasmonic cavities with resonant wavelengths as short as 2.2 μ m. The confinement factors of these cavities can reach 135, which, while exceedingly large, is less than what has been theoretically predicted – a result of strong nonlocality. The combined SWIR response and large confinement factors observed in these graphene nanoribbon arrays – combined with the scalable fabrication method used to create them – makes these nanostructures an attractive platform to explore next-generation optoelectrical devices and strongly enhanced spontaneous emission in the SWIR.

2:15 PM EQ05.11.04

A Fluctuational Electrodynamics Approach for Radiative Transfer Modeling of Nanocomposites with Particles of Arbitrary Shape [Francisco V. Ramirez](#)^{1,2}, Gurunatha Kargal Laxminarayana², Ivan P. Parkin² and Ioannis Papakonstantinou²; ¹Universidad Adolfo Ibanez, Chile; ²University College London, United Kingdom

Composites lie at the core of nanophotonics. Many devices in fields such as photosensing, photochemistry and thermophotonics are based on disordered nanomaterials with arbitrary shaped and randomly distributed structures, where their dispersion, filling fraction and size need to be finely tuned to achieve optimal performance. Although simulations are critical in this task, predicting the optical response of these materials is challenging, given the random orientation and anisotropic morphology of the structures involved. The radiative transfer equation (RTE), while being specifically formulated to describe light transport in random scattering media, becomes computationally expensive to solve when the structures are non-spherical.

In this talk, I will discuss our newly developed universal theory of average light scattering of randomly oriented scatterers (particles or collections of particles), and a practical method for radiative transfer simulations of composite with scatterers of arbitrary morphology. First, I will introduce our

fluctuational-electrodynamics-based theory to compute the average absorption cross section, scattering cross section, and asymmetry parameter of randomly oriented scatterers of arbitrary shape. The three parameters can be directly integrated into traditional RTE solvers, enabling computationally inexpensive radiative transfer simulations. The accuracy of this modeling framework is demonstrated against optical measurements of polymer composites with metal-oxide crystals of irregular morphology.

As I will discuss by the end of this talk, the modeling framework could provide a better understanding of the interrelation between nanoscale electromagnetic interactions and the macroscopic response of disordered nanomaterials, such as the effects of agglomeration of plasmonic nanostars in optical absorption, or the impact of multiple scattering in the light trapping of heterostructured photocatalysts.

3:45 PM EQ05.11.06

Sunlight-Powered Reverse Water Gas Shift Reaction Using a Titania Supported Plasmonic Au Nanocatalyst: Distinguishing between Photothermal and Non-Thermal Contributions Pau Martínez Molina¹, Nicole Meulendijks¹, Man Xu^{1,2}, Marcel A. Verheijen^{3,4}, Tim den Hartog^{1,5}, Francesc Sastre¹ and Pascal Buskens^{1,6}; ¹TNO, Netherlands; ²Delft University of Technology, Netherlands; ³Eurofins Material Science Netherlands B.V., Netherlands; ⁴Technische Universiteit Eindhoven, Netherlands; ⁵Zuyd University of Applied Sciences, Netherlands; ⁶Hasselt University, Belgium

Plasmon catalysis is an interesting technology concept for powering chemical processes with sunlight. It makes use of the localized surface plasmon resonance (LSPR) of catalytically active metallic nanoparticles. Upon illumination, a coherent electron oscillation occurs in these nanoparticles, which rapidly dephases and generates hot electrons. These can then either be transferred into an electron accepting orbital of an adsorbed molecule, or thermalize due to electron-electron and electron-phonon scattering leading to an increased temperature of the catalyst. Both from a fundamental and application perspective, differentiating between the non-thermal and photothermal contribution is essential.

Recently, we reported the sunlight powered conversion of carbon dioxide and green hydrogen to methane and water – the so-called Sabatier reaction – using alumina supported Ru nanocatalysts [1,2]. Here, we report the sunlight powered conversion of carbon dioxide and green hydrogen to carbon monoxide and water – the so-called reverse water gas shift (rWGS) reaction – using a titania supported plasmonic Au nanocatalyst. The rWGS reaction is endothermic ($\Delta H_{298K} = 41.2 \text{ kJ mol}^{-1}$) and limited by equilibrium. In the conventional thermal rWGS process, catalysed by *e.g.* Cu, Rh or Pt, temperatures above 800°C are applied to produce CO with an acceptable selectivity (about 80%). In our study, we demonstrate that CO can be formed with high selectivity using only sunlight and without external heating of the reactor. Using mildly concentrated artificial sunlight (1.44 W cm⁻² equals 14.4 suns) we realized a selectivity of 98% and a CO production rate of 429 mmol g_{Au}⁻¹ h⁻¹. Temperature measurements performed with a thermocouple positioned in contact with the bottom side of the catalyst bed indicated a catalyst temperature of 140°C. We expected the top layer of the catalyst bed to have a higher temperature since it is directly exposed to light. Using a simple theoretical model based on Kirchhoff's law and Stefan-Boltzmann's law for macro scale objects, we estimated that the collective temperature at the top surface of the catalyst reached 300°C upon illumination with 14 suns. We furthermore demonstrated that the relationship between the reaction rate and the light intensity is exponential, which points to a strong photothermal component contributing to this reaction.

In reference reactions performed in dark with the same catalyst methane was formed in large quantities, while upon illumination CO was formed with a selectivity of 98% and CH₄ formation was largely suppressed. We propose the promotion of H₂O and CO desorption through charge transfer of plasmon generated charges to explain this difference.

In conclusion, we have demonstrated that plasmon catalysis can be applied to convert the greenhouse gas CO₂ into the valuable chemical intermediate CO using sunlight as sustainable energy source. Further studies on quantification of photothermal and non-thermal contributors and other aspects involving the reaction mechanism as subject of research in our labs.

[1] R. Grote, R. Habets, J. Rohlfs, F. Sastre, N. Meulendijks, M. Xu, M. A. Verheijen, K. Elen, A. Hardy, M. K. Van Bael, T. den Hartog, Pascal Buskens, Collective photothermal effect of Al₂O₃ supported spheroidal plasmonic Ru nanoparticle catalysts in the sunlight powered Sabatier reaction. *ChemCatChem* **2020**, *12*, 5618-5622.

[2] Francesc Sastre Calabuig, Nicole Meulendijks, Jessica Rodríguez-Fernández, Jorgen Sweelssen, Caroline Versluis, Ken Elen, Marlies K. van Bael, Tim den Hartog, Marcel A. Verheijen, Pascal Buskens, "Sunlight Fueled, Room Temperature Conversion of CO₂ and H₂ to CH₄ with an Anisometric Plasmonic Ru Nanocatalyst", *ACS Omega* **2019**, *4*, 7369-7377.

2:45 PM BREAK

4:00 PM EQ05.11.07

Exploiting Thermoplasmonics in Dynamic Self-Assembly of Gold Nanoparticles Joscha Kruse¹, Stefan Merkens², Andrey Chuvilin² and Marek Grzelczak^{3,1}; ¹Donostia International Physics Center, Spain; ²CIC nanoGUNE, Spain; ³Centro de Física de Materiales, Spain

The development of dynamic self-assembly (nano)systems is still a young research area (1) with promising future applications due to the ability of actively rearranging building blocks on the nanoscale. An in-depth investigation of the assembly and disassembly processes is of great importance to gain insights into the intermediate assembly states. Here we show the detailed picture of temperature-driven reversible clustering of gold nanoparticles (gold nanospheres(2) and gold nanorods).

Using in-situ UV-VIS spectroscopy, we revealed the emergence of hysteresis during the cyclic temperature changes. By varying nanoparticles diameter and their surface charge as well as the rate of applied stimulus we were able to describe qualitatively the contribution of thermodynamic and kinetic hysteresis.

A particularly intriguing case is the reversible clustering of gold nanorods. They adapt to transient mutual configurations, such as tip-to-tip or side-to-side, enriching the hysteretic response. In addition, the large absorption cross-section of gold nanorods in the infrared spectral range allowed us for taking advantage of their efficient light to heat conversion. Therefore by introducing light as stimulus, instead of an external heating source, we were able to control locally the change of temperature which in turn altered the colloidal stability of the nanorods.

Then, we designed a more sophisticated colloidal system and integrated feedback loops, leading to oscillatory and self-sustained clustering under continuous energy flux. We found that the presence of hysteresis in reversible aggregation is the prime condition to invoke oscillatory clustering otherwise the system adapts to its equilibrium steady state without oscillations.

We foresee that the presented experimental framework offers an exciting playground to study the nature of meta-stable assemblies, and enables possible applications in spatiotemporal catalysis, thermo-mechanical nanotransducers, smart windows, among others.

REFERENCES

- (1) Grzelczak, M.; Liz-Marzán, L. M.; Klajn, R. Stimuli-responsive self-assembly of nanoparticles. *Chem. Soc. Rev.* DOI: 10.1039/C8CS00787J.
- (2) Kruse, J.; Merkens, S.; Chuvilin, A.; Grzelczak, M. Kinetic and Thermodynamic Hysteresis in Clustering of Gold Nanoparticles: Implications for Nanotransducers and Information Storage in Dynamic Systems. *ACS Appl. Nano Mater.* **2020**, *3* (9), 9520–9527. DOI: 10.1021/acsnm.0c02249.

4:15 PM EQ05.11.08

Understanding the Chemical Mechanism Behind Photo-Induced Enhanced Raman Spectroscopy Junzhi Ye^{1,2}, Rakesh Arul^{1,2,2}, Michel K. Nieuwoudt², Junzhe Dong², Wei Gao² and Cather Simpson²; ¹University of Cambridge, United Kingdom; ²The University of Auckland, New Zealand

Photo-Induced Enhanced Raman Spectroscopy (PIERS) is a new surface enhanced Raman spectroscopy (SERS) modality with an order-of-magnitude Raman signal enhancement of adsorbed analytes over that of typical SERS substrates. Despite the impressive PIERS enhancement factors and explosion in recent demonstrations of its utility, the detailed enhancement mechanism remains undetermined. Using a range of optical and X-ray spectroscopies, supported by density functional theory calculations, we elucidate the chemical and atomic-scale mechanism behind the PIERS enhancement. Stable PIERS substrates with enhancement factors of 106 were fabricated using self-organized hexagonal arrays of TiO₂ nanotubes that were defect-engineered via annealing in inert atmospheres, and silver nanoparticles were deposited by magnetron sputtering and subsequent thermal dewetting. We identified the key source of the enhancement of PIERS vs. SERS in these structures as an increase in the Raman polarizability of the adsorbed probe molecule upon photo-induced charge transfer. A balance between crystallinity, which enhances charge transfer due to higher electron mobility in anatase-rutile heterostructures but decreases visible light absorption, and oxygen vacancy defects, which increase visible light absorption and photo-induced electron transfers, was critical to achieve high PIERS enhancements.

SESSION EQ05.12: 2D Photonics/Nonlinear Optics

Session Chair: Benjamin Vest

Wednesday Afternoon, December 1, 2021

Hynes, Level 2, Room 210

4:45 PM EQ05.12.01

Broadband Electro-Optic Polarization Conversion with Atomically Thin Black Phosphorus Souvik Biswas¹, Meir Y. Grajower¹, Kenji Watanabe², Takashi Taniguchi² and Harry A. Atwater¹; ¹California Institute of Technology, United States; ²National Institute for Materials Science, Japan

On-demand polarization control of light plays a critical role in a variety of classical and quantum optics-based applications such as holography, imaging, dichroism sensing and polarization encoding of qubits. We demonstrate electrically reconfigurable, high dynamic range, broadband polarization conversion with atomically thin van der Waals heterostructures, using tri-layer black phosphorus (BP) integrated in a Fabry-Pérot cavity, at telecom wavelengths. Here, we leverage the exciton-dominated near-unity birefringence in naturally stacked three atomic layers of BP (~1398 nm) which enables a broadband operation window of the entire telecom E, S and C bands (1360-1580 nm). The inherent optical anisotropy of BP, further enhanced by integration into a Fabry-Pérot resonant cavity, allows generation of polarization states over the entire Poincaré sphere via spectral and input azimuthal angle tuning. Furthermore, the extreme polarizability of the exciton to an external electric field provides near-complete suppression of its dipole oscillator strength, enabling active control of the polarization state across nearly half the Poincaré sphere. Specifically, both linear to circular and linear cross-polarization conversion schemes, among numerous other trajectories, were achieved (for example at ~1444 nm) via electrical doping (up to $\sim 7 \times 10^{12}/\text{cm}^2$) demonstrating superior control over the reflected ellipticity and azimuthal angles. Our findings highlight the potential of BP in future chip-based polarization-sensitive electro-optic platforms such as spatial light modulators, variable phase retarders, and sensors.

5:00 PM EQ05.12.02

All-Dielectric Nanophotonics for Enhanced Light-Matter Interaction in 2D Semiconductors Luca Sortino^{1,2}, Panaiot Zotev², Sandro Mignuzzi³, Stefan A. Maier^{1,3}, Riccardo Sapienza³ and Alexander Tartakovskii²; ¹Ludwig-Maximilians-University Munich (LMU), Germany; ²University of Sheffield, United Kingdom; ³Imperial College London, United Kingdom

High refractive index dielectrics are emerging as a novel platform to shape and control light at the nanoscale by engineering electric and magnetic Mie-resonances in sub-wavelength nanostructures. Between two-dimensional (2D) semiconductors, the family of transition metal dichalcogenides (TMDs) exhibits exceptional optical properties, such as tightly bound excitons and single-photon emitting centers, and unique mechanical properties leading to favorable integration in current nano-photonics architectures. In our work, we integrated single and double layer TMDs WSe₂ with Mie-resonant gallium phosphide (GaP) dimer nano-antennas and demonstrate the enhancement of the light-matter interaction of 2D excitons and native single-photon emitters. At room temperature, we observe an enhancement of the PL up to 10⁴, compared to WSe₂ on planar GaP, and show this is a result of increased absorption, enhanced spontaneous emission rate, and emission redirection [1]. Moreover, the nano-structures displace the semiconducting layers in the out-of-plane direction, allowing the tuning of the local WSe₂ bandstructure via strain [2]. At cryogenic temperatures, the strain-induced potential acts as a trap for photo-generated excitons, leading to the nano-scale positioning of bright single-photon emitters in monolayer WSe₂ [3]. We compare the optical properties of quantum emitters on GaP nano-antennas to those positioned on non-resonant SiO₂ nano-pillars. In agreement with our numerical simulations, we observe more than two orders of magnitude enhancement in the collected PL intensity of nano-antenna coupled SPEs, further exhibiting long PL lifetimes - up to 200 ns - and ultra-low PL saturation thresholds. We show this is related to an increased quantum efficiency of the single-photon emission when the TMD layer is coupled to the nano-antenna near-field. We report quantum efficiency with values up to > 80% on GaP nano-antennas, compared to an average of 4% when positioned on SiO₂ nano-pillars. Our results highlight Mie resonances in dielectric nanostructures as a novel nanophotonic platform to engineer light-matter interaction in two-dimensional materials and single-photon emitters.

[1] Sortino, L. et al. Enhanced light-matter interaction in an atomically thin semiconductor coupled with dielectric nano-antennas. Nat. Commun. 10, 5119 (2019)

[2] Sortino, L. et al. Dielectric nano-antennas for strain engineering in atomically thin two-dimensional semiconductors. ACS Photonics 7, 2413–2422 (2020)

[3] Sortino, L. et al. Bright single photon emitters with enhanced quantum efficiency in a two-dimensional semiconductor coupled with dielectric nano-antennas. arXiv: 2103.16986 (2021)

5:15 PM EQ05.12.03

Light-Matter Coupling in Scalable van der Waals Superlattices Pawan Kumar¹, Jason Lynch¹, Baokun Song¹, Haonan Ling², Francisco Barrera¹, Huiqin Zhang¹, Surendra Anantharaman¹, Jagrit Digani², Haoyue Zhu³, Tanushree H. Choudhury³, Clifford McAleese⁴, Xiaochen Wang⁴, Ben R. Conran⁴, Oliver Whear⁴, Michael J. Motala⁵, Michael Snure⁵, Christopher Muratore⁶, Joan M. Redwing³, Nicholas Glavin⁵, Eric A. Stach¹, Artur Davoyan² and Deep M. Jariwala¹; ¹University of Pennsylvania, United States; ²University of California, United States; ³The Pennsylvania State University, United States; ⁴Aixtron Ltd., United Kingdom; ⁵Air Force Research Laboratory, United States; ⁶University of Dayton, United States

The ability to arbitrarily stack two-dimensional (2D) crystals have led to new opportunities to design and assemble artificial lattices without the constraints of epitaxy. However, these opportunities are limited by difficulties in controlling the thickness of exfoliated van der Waals (vdW) layers, which prevents the realization of repeat units with high fidelity. Recently, the development of metal-organic chemical vapor deposition (MOCVD) synthesis has allowed the creation of uniform, wafer-scale samples with thickness control. This allows the production of stacks of disparate 2D layers with multiple repeating units, which permits the engineering of electronic and optical dispersions in these heterostructures. We have engineered the optical dispersion in a superlattice structure by alternating layers of 2D chalcogenides and dielectric insulators. We demonstrate 94% narrowband absorption in <6 nm active layer excitonic absorber medium at room temperature through the design of the unit cell parameters. This is accompanied by an enhancement in the photoluminescence of square-centimeter-sized samples. The TMDC-insulators also show evidence of strong light-matter coupling and exciton-polariton formation with a Rabi splitting up to 190 meV. These results demonstrate that it is possible to engineer optical properties in 2D heterostructures and suggest approaches to create a broad class of scalable, designer optical metamaterials from atomically thin layers.

5:30 PM EQ05.12.04

Weyl Semimetal Thin-Films for Nonlinear and Ultrafast Nanophotonics Benjamin Tilmann¹, Amilcar Bedoya-Pinto², Gustavo Grinblat³, Yi Li⁴, Stuart Parkin² and Stefan A. Maier^{1,5}; ¹Ludwig-Maximilians-Universität, Germany; ²Max Planck Institute of Microstructure Physics, Germany; ³Universidad de Buenos Aires, Argentina; ⁴Southern University of Science and Technology, China; ⁵Imperial College London, United Kingdom

Weyl semimetals are a class of materials with unique properties as a result of a single touching point of valence and conduction band and a linear electronic dispersion, where the electrons behave as quasi-massless fermions, comparable to the Dirac cone in graphene. This leads to the formation of Fermi arcs and topologically protected edge states on the surface of Weyl semimetals and gives them a generally high electron mobility, a large magnetoresistance and effects such as the Adler-Bell-Jackiw anomaly. Furthermore, the Weyl semimetal family of transition metal monophosphides, were shown to have outstanding optical properties. Among others, the glass coefficient of TaAs in the near-infrared was measured to be the highest reported so far [1] and the second-order nonlinear coefficient has been measured to be two magnitudes larger than the one for GaAs [2]. These properties make Weyl semimetals promising candidates for optical applications, however, most previous works were limited to bulk crystals that are naturally limited in terms of flexibility and device applications.

In this work, we perform first steps towards nanophotonics with Weyl semimetals by characterizing the linear and nonlinear optical response of recently realized epitaxially grown NbP thin films [3,4]. By spectral ellipsometry, we determined the linear refractive index and extinction coefficient with good agreement to theoretical predictions and thereby confirm the semimetallic character of the material. Despite the strong absorption over the visible spectrum, we show strong third-harmonic generation that reaches a maximum efficiency of 10⁻⁵ % when exciting in the near-infrared. Comparing this to the signal detected from a bulk crystal of the same material, the nonlinear response of the thin film is stronger by more than a factor two. Furthermore, we performed non-degenerate pump-probe spectroscopy with 10 fs temporal resolution. We observe that the ultrafast optical response of the bulk NbP crystal is dominated by electronic absorption processes and subsequent scattering dynamics in the Weyl cone, in good agreement with previous studies on comparable materials. On the other hand, the NbP thin film shows a probe wavelength independent response that is dominated by the nonlinear optical Kerr effect and an ultrafast modulation depth of close to 1%, again a factor of two stronger than the bulk crystal. Undergoing a complete relaxation within less than 50 fs, the NbP film would allow all-optical switching with a full-width half-maximum bandwidth of 10-20 THz. We ascribe the boosted nonlinear performance to the reduced volume that contains only 10-20 unit cells of the material and therefore limits the absorption and electron-electron interactions. In conclusion, our results show that the epitaxially grown NbP thin films inherit the intrinsic optical properties of the bulk crystal but significantly reduce the absorption due to the reduced dimensionality, which further boosts the nonlinear optical interactions. Together with the fact that thin films enable common top-down nanofabrication techniques, this paves the way for various promising applications of Weyl semimetals in the field of nanophotonics.

REFERENCES:

- [1] G. B. Osterhoudt *et al.*, "Colossal mid-infrared bulk photovoltaic effect in a type-I Weyl semimetal," *Nat. Mater.*, vol. 18, no. 5, pp. 471-475, May 2019.
- [2] L. Wu *et al.*, "Giant anisotropic nonlinear optical response in transition metal monophosphide Weyl semimetals," *Nat. Phys.*, vol. 13, no. 4, pp. 350-355, Apr. 2017.
- [3] A. Bedoya-Pinto *et al.*, "Realization of Epitaxial NbP and TaP Weyl Semimetal Thin Films," *ACS Nano*, vol. 14, no. 4, pp. 4405-4413, Apr. 2020.
- [4] A. Bedoya-Pinto *et al.*, "Large Fermi-Energy Shift and Suppression of Trivial Surface States in NbP Weyl Semimetal Thin Films," *Adv. Mater.*, vol. 33, no. 21, p. 2008634, May 2021.

5:45 PM EQ05.12.05

Third-Harmonic Generation Reveals Strong Sub-Wavelength Optical Confinement in Photonic Gap Antennas Coupled to Epsilon-Near-Zero Thin Films Felix Thouin, David Myers, Ashutosh Patri, Bill Baloukas, Ludvik Martinu and Stephane Kena-Cohen; Polytechnique Montréal, United States

Squeezing light down to sub-wavelength scales allows the emergence of a host of fascinating phenomena in non-linear and quantum optics. These find applications in photonics and quantum information processing to name a few. While such a feat has been realized using conventional plasmonic nanoantennas, the losses inherent to these systems limit the scope of applications by lowering their damage threshold and damping quantum coherences. To this end, epsilon near-zero (ENZ) thin films, with their vanishing real permittivity and relatively low imaginary permittivity, are attractive candidates to tightly confine light with little losses. These have been used in the past in conjunction with plasmonic nanoantennas to reach high levels of confinement. We sought to integrate these materials in dielectric nanoantennas to achieve comparable levels of confinement while maintaining losses low.

We achieved sub-wavelength light confinement with photonic gap antennas (PGAs) consisting of a thin film of indium tin oxide (ITO), an ENZ material, embedded in an amorphous silicon nanopillar. PGAs of various sizes were fabricated with a multilayer deposition process followed by pseudo-Bosch photolithography. The antennas' scattering spectrum was measured using dark field scattering spectroscopy and the resonant character of the light confinement was assessed through third harmonic generation. We interpreted these results in the framework of coupled mode theory and show that the resonances responsible for the light confinement arise from the hybridization of the silicon pillar modes with the epsilon near-zero mode of the ITO thin film. This work opens up the possibility for high efficiency non-linear photonics with high damage thresholds, as well as strong light-matter interaction for the generation of quantum light and ultrastrong light-matter interaction.

6:00 PM EQ05.12.06

Developing ITO Nanolayers for ENZ-Enhanced Nonlinear Responses Wesley Britton and Luca Dal Negro; Boston University, United States

The engineered material dispersion of the thin-film transparent conductive oxide indium tin oxide (ITO) has been proven to exhibit extremely large epsilon-near-zero (ENZ) and low index-driven nonlinear responses. This has enabled the rapid development of compact and integrated CMOS-compatible

devices that perform efficient nonlinear operations such as sub-picosecond all optical modulation, ultra-fast pulse shaping through frequency translation, and optical time reversal. Recent theoretical studies indicate that both bound electrons in the lattice and hot electron contributions significantly drive the nonlinear response of ITO materials. These results strongly motivate the optimization of material structure beyond dispersion engineering to boost nonlinear enhancement using material lattice contributions. Specifically, crystallographic texture describes the tendency for the grains of a polycrystalline films to avoid random distributions in favor of preferred orientations and can profoundly affect the nonlinear optical material properties. We show how modified growth and post-deposition conditions can dramatically modify ITO crystallographic texture and impact the nonlinear properties of ITO films characterized using Z-scan and four-wave mixing experiments.

6:15 PM EQ05.12.07

Evaluation of 2D Transition Metal Carbides and Carbonitrides (MXenes) for SERS Substrates Kateryna Shevchuk, Asia Sarycheva and Yury Gogotsi; A.J. Drexel Nanomaterials Institute, United States

Two-dimensional transition metal carbides and carbonitrides are promising plasmonic materials for surface-enhanced Raman spectroscopy (SERS), allowing sensitive detection of analyte molecules. Their high electronic conductivity and rich surface chemistries enable both SERS electromagnetic and chemical enhancements. We have synthesized seven most common MXenes – Nb₂C, Mo₂C, Ti₂C, V₂C, Ti₃C₂, Mo₂TiC₂, and Ti₃CN with the transversal plasmon resonances ranging from the visible region to NIR. We were able to detect the 10⁻⁷ M concentrations of Rhodamine 6G dye on MXene substrates, reaching the enhancement factors of 10⁵-10⁶. The results were compared to the commercially available substrates and showed advantageous performance of Ti₃C₂ compared to gold nanoparticles. We tested the best performing MXene with a variety of dyes, suggesting the versatility of MXene SERS substrates. Due to high charge carrier densities and tunable surface chemistries, MXenes show potential for SERS sensors that are inexpensive, easy to fabricate, and optimize for specific applications.

SESSION EQ05.13: Poster Session II
Session Chair: Souvik Biswas
Wednesday Afternoon, December 1, 2021
8:00 PM - 10:00 PM
Hynes, Level 1, Hall B

EQ05.13.02

Improved Performance of Polymeric One-Dimensional Photonic Crystals via High-n Additive Samuel Wallaert, Ali Masud, Hadi Ghasemi and Alamgir Karim; University of Houston, United States

Interest in flexible photonic layers made of polymeric materials is growing as they can find applications to create reflective surfaces for IR reflection, UV reflection, etc. for applications such as thermal management since they can have tunable heat dissipation or shielding properties. One-dimensional photonic crystals, specifically Distributed Bragg Reflectors (DBR) made of alternating high and low refractive index polymeric materials, have attracted research attention for the past few decades in this regard. However, very few materials exhibit the optical properties to function as polymeric DBRs. Major problems encompassing polymer-based DBRs include the low refractive index of the polymer, incompatible optical properties of the polymer, and casting of uniform thickness of alternating layers without damaging the underlying layers. Herein, we explore creating a DBR with high reflective properties developed by applying an additive directly to the high refractive index polymeric material to increase the refractive index difference of the two alternating layers from 0.2 to 0.5. Such enhancements helped us achieve 100% better reflective properties for near and far-infrared regions of the electromagnetic spectrum, with broader reflection bands requiring only half the number of layers than most common DBRs used in the literature. We hope such findings would make polymeric DBR materials useful for defense vehicles and clothing for shielding purposes and heat dissipation as they are flexible and readily integrate into many surfaces.

We acknowledge DoD Grant #W911QY2190015 for support of this project.

EQ05.13.03

Wafer-Scale Synthesis and Optical Characterization of InP Nanowire Arrays for Solar Cells Lukas Hrachowina¹, Nicklas Anttu^{2,3} and Magnus T. Borgström¹; ¹Lund University, Sweden; ²Åbo Akademi University, Finland; ³Aalto University, Finland

Nanowire solar cells have the potential to reach the same efficiencies as the world record III-V solar cells by the use of a fraction of the material^{1,2}. For solar energy harvesting, large area nanowire solar cells have to be processed but so far high efficiency nanowire solar cells have been demonstrated only on small areas less than 1 mm^{2,3,5}.

In this work, we demonstrate the synthesis of epitaxial, photovoltaic InP nanowire arrays on a 2" wafer. We used talbot displacement lithography and placed black plastic stripes on the phase shift mask to block the UV light in order to define five array areas with different nanowire diameters on the same wafer by sequentially varying the exposure dose. We use a photoluminescence (PL) mapper to characterize the sample with both steady-state and time-resolved PL maps. Subsequently, we compare it to a reference wafer that was exposed homogeneously. Furthermore, by the use of a white light source inside the PL mapper instead of the laser diode used for PL, we measure reflectance (R) maps. We created a database for modeled R(λ ,D,L) for varying λ , D, and L at a fixed period of 500 nm for the hexagonal array of nanowires⁶. Then, we simultaneously extract the diameter and length of the nanowires from the several thousand experimentally measured R spectra over the full wafer, using the modeled R database. The extracted knowledge of large-scale nanowire synthesis will be crucial for the upscaling of nanowire based solar cells, and the demonstrated wafer-scale characterization methods will be central for quality control during manufacturing.

1. Wallentin, J.; Anttu, N.; Asoli, D.; Huffman, M.; Åberg, I.; Magnusson, M. H.; Siefert, G.; Fuss-Kailuweit, P.; Dimroth, F.; Witzigmann, B.; Xu, H. Q.; Samuelson, L.; Deppert, K.; Borgström, M. T. *Science* **2013**, 339, (6123), 1057-60.
2. Anttu, N. *Acs Photonics* **2015**, 2, (3), 446-453.
3. van Dam, D.; van Hoof, N. J.; Cui, Y.; van Veldhoven, P. J.; Bakkers, E. P. A. M.; Gomez Rivas, J.; Haverkort, J. E. *ACS Nano* **2016**, 10, (12), 11414-11419.
4. Åberg, I.; Vescovi, G.; Asoli, D.; Naseem, U.; Gilboy, J. P.; Sundvall, C.; Dahlgren, A.; Svensson, K. E.; Anttu, N.; Björk, M. T.; Samuelson, L. *IEEE Journal of Photovoltaics* **2016**, 6, (1), 185-190.
5. Hrachowina, L.; Zhang, Y.; Saxena, A.; Siefert, G.; Barrigon, E.; Borgström, M. T. In *Development and Characterization of a bottom-up InP Nanowire Solar Cell with 16.7% Efficiency*, 2020 47th IEEE Photovoltaic Specialists Conference (PVSC), 15 June-21 Aug. 2020, 2020; pp 1754-1756.

EQ05.13.07

Transparent Luminescent Solar Concentrator with Quantum Dots and Hexarhenium Cluster Enhanced by Energy Transfer Jun Choi and Sung-Jin Kim; Ewha Womans University, Korea (the Republic of)

A luminescent solar concentrator (LSC) photovoltaic (PV) system is a solar light harvesting device that absorb the sunlight by large LSC panel and concentrate photoluminescent light on PV cell placed at the edge of LSC panel to convert it into electricity. The nano-sized inorganic-organic cluster complex (dMDAEMA)₂[Re₆S₈(NCS)₆] (refers as RMC, where dMDAEMA is 2-dimethyl amino ethyl methacrylate) is a good candidate for LSC luminophore due to largely downshifted broad photoluminescence suitable to PV cell. However, the low quantum yield (QY) of RMC limit the performance of LSC. Here, Zn doped CuGaS/ZnS core-shell quantum dots (ZQD) as a Stokes shift engineered donor with high QY was used to improved performance of LSC. These two metal chalcogenide luminophores, RMC and ZQD, are chemically suitable to be dispersed in amphiphilic polymer matrix making clear waveguide with low reabsorption and optically well matched emission resulting high power conversion efficiency (PCE) and optical efficiency (η_{opt}). We achieved maximum η_{opt} of 3.47 % and PCE of 1.26 %, while maintaining high transparency of over 80 % in visible wavelength range. This dual-dye LSC system exhibits reabsorption free and increased emission by isolation of dyes in polymer matrix and energy transfer from ZQD to RMC. This LSC system suggests as a promising candidate for up-scaling building-integrated PVs (BIPV) for use in windows.

EQ05.13.08

Late News: X-Ray Radioluminescent Crystalline Colloidal Arrays—Fine-Tuning Color Characteristics via X-Ray Induced Sequential Förster Resonance Energy Transfer (FRET) and a Photonic Bandgap Haley W. Jones, Iurii Bandera, Eric Zhang and Stephen H. Foulger; Clemson University, United States

Photonic crystals describe a class of periodic dielectric materials that exhibit a photonic bandgap (i.e., rejection wavelength) corresponding to specific wavelengths of light where propagation through the crystal is forbidden. In the past few decades, particular interest has focused on photonic crystals composed of crystalline colloidal arrays (CCAs), which exhibit iridescent structural colors similar to that of the precious opal. These biomimetic colloids are composed of closed-packed, electrically charged particles that self-assemble into three-dimensional periodic arrays due to their repulsive Coulombic interactions. While a CCA does not exhibit a complete photonic bandgap due to a low refractive index contrast, a CCA possesses a rejection wavelength in the visible regime that can be described by Bragg's equation ($\lambda = 2n_c d_{hkl} \sin(\theta)$). The CCA's rejection wavelength (λ) can be shifted across the full visible spectrum by changing the interplanar spacing (d_{hkl}), changing the refractive index (n_c), or a combination of the two parameters.

X-ray radioluminescent CCAs with highly tunable emission colors are synthesized using an emulsion polymerization procedure. An anthracene methyl methacrylate derivative (AMMA) is copolymerized within a poly(styrene-co-propargyl acrylate) (PS-PA) basis to generate an x-ray radioluminescent PS-PA-PAMMA CCA (87 nm), emitter 1 (**E**₁). Due to the electrostatic repulsive forces between the colloidal nanoparticles, **E**₁ spontaneously self-assembles into an FCC structure. **E**₁ possesses a rejection wavelength in the visible regime that can be shifted across the visible spectrum by a change in the interplanar spacing, which is achieved by the addition or removal of deionized water. Typical anthracene radioluminescence spanning 400 – 515 nm, with a maximum at 420 nm, is detected when there is no rejection wavelength interference. However, a decrease in spontaneous emission at the rejection wavelength is observed when the rejection wavelength is shifted within **E**₁'s radioluminescence. The radioluminescence decrease corresponding to the rejection wavelength can be shifted across the entire radioluminescence of **E**₁. In this way, the CCA's radioluminescence can be manipulated by photonic means. Furthermore, the CCA's color characteristics can be adjusted across the visible spectrum by x-ray induced sequential Förster Resonance Energy Transfer (FRET). Energy transfer is achieved by copolymerizing one or two additional organic fluorophores that form FRET pairs with AMMA and each other. A naphthalimide methyl methacrylate derivative (NMMA) that absorbs in the blue region where AMMA emits is incorporated within **E**₁ to generate a PS-PA-PAMMA-PNMA CCA (125 nm), emitter 2 (**E**₂). **E**₂ emits in the green region of the visible spectrum, with a maximum at 535 nm, when pumped with an x-ray source. Additionally, a rhodamine B methyl methacrylate derivative (RMMA) that absorbs in the green region where NMMA emits is incorporated within **E**₂ to generate a PS-PA-PAMMA-PNMA-PRMMA CCA (122 nm), emitter 3 (**E**₃). **E**₃ emits in the red region of the visible spectrum, with a maximum at 630 nm, when pumped with an x-ray source. In this way, x-ray induced FRET or x-ray induced sequential FRET is achieved, respectively. Furthermore, the rejection wavelength of **E**₂ and **E**₃ can be coupled with their radioluminescence to fine-tune the color characteristics of the liquid systems.

EQ05.13.10

A Universal Synthesis Strategy for Chiral Inorganic Nanostructures via Self-Assembled Templates of Achiral Block Copolymers and Racemic Mixtures Minju Kim and Dong Ha Kim; Ewha Womans University, Korea (the Republic of)

Chiral inorganic nanostructures have attracted growing attention due to their potential applications and technological prospects. Even though various strategies have been developed for fabricating chiral inorganic nanostructures, the complex processes and expense of chiral biomolecules and their derivatives remain formidable challenges to realize mass production and large-area fabrication with simple and cost-effective processes. Here, we suggest a generalized protocol for the fabrication of chiral inorganic nanostructures including Au, Ag, Pd, and TiO₂ nanostructures based on achiral templates consisting of block copolymer inverse micelles and racemic mixtures. Self-assembly of poly(styrene-*b*-4-vinyl pyridine) (PS-*b*-P4VP) diblock copolymer inverse micelles containing inorganic precursors and DL alanine additives is shown to exhibit chiral properties in a specific environment in solution, a prerequisite element for the evolution of chirality. Notably, we found the pyridine groups of P4VP interacted more favorably with D-alanine than with L-alanine via hydrogen bonding in non-polar solvents, leading to the chirality transfer from D-alanine to the D-alanine-bonded P4VP micellar cores. In-situ synthesis of nanoparticles (NPs) in the micellar core by a mild reducing agent enabled strong electronic interaction between induced chiral micellar cores and in-situ formed NPs. Therefore, we achieve outstanding chiroptical properties with high anisotropy factors of 8×10^4 although chiral reagents and scaffolds were not involved in any step. Our design concept pinpoints forwarding steps to construct an extended library of viable chiral inorganic nanostructures, ensuring a substantial development in the field of chiroptics.

10:30 AM *EQ05.14.01

Nanophotonics for Advanced Space Exploration [Artur Davoyan](#); University of California, Los Angeles, United States

At present deep space exploration is limited by transit time and overall mission costs. Conventional spacecraft make use of chemical or electric engines, which have fundamental limitations on the possible speed one can achieve. Light driven propulsion offers a conceptually different approach to space travel. In this talk I will overview our work on solar and laser driven propulsion for space exploration.

First, I will survey our work on laser driven propulsion. I will outline key requirements and challenges associated with Breakthrough Starshot mission. I will then discuss implications of utilizing smaller and more affordable systems for near-term space exploration. I will show that with relatively moderate laser powers (~1 MW) conceptually new regimes for spacecraft maneuvering and orbiting on interplanetary and Earth orbital missions emerge. Next I will discuss nanophotonic designs that optimize the tradeoff between mass, reflectance and a need for a radiative cooling. I will also summarize challenges and opportunities of laser driven propulsion for space exploration.

Next, I will examine an alternative approach for deep space missions with the use of solar sailing. I will demonstrate that lightweight solar sails are potentially capable of reaching >30 AU/year velocities (i.e., more than 8 times faster than the Voyager – fastest space probe ever built), and can pave the way to fast and scalable exploration of the solar system and beyond. I will then survey material challenges associated with solar sailing and discuss the way nanophotonics can advance solar sail missions. Lastly, I will survey our ongoing experimental effort.

11:00 AM EQ05.14.02

Hydrogel-Encapsulated Crystalline Colloidal Arrays—Coupling the Radioluminescence of an Organic Scintillator with a Rejection Wavelength [Sarah Mell](#), Haley W. Jones, Iurii Bandera and Stephen H. Foulger; Clemson University, United States

A crystalline colloidal array (CCA) is a photonic crystal made of self-assembled colloidal nanoparticles, in which a periodic dielectric structure prohibits the propagation of a particular wavelength of light throughout the material. The blocked wavelength is known as the rejection wavelength, or stopband, of the material. Iridescence is observed in CCAs because of the rejection wavelength located within the visible light spectrum, causing the liquid system to resemble a precious opal. CCAs utilize the long-range electrostatic repulsive interactions between the colloidal particles to induce self-assembly into a crystal-like structure. Bragg's equation can be used to estimate the observed rejection wavelength based on the angle of incident light, interplanar spacing, and refractive index of the material. This dependence on interplanar spacing indicates that the rejection wavelength can be manipulated by adjusting the particle spacing. Incorporating a scintillator into the CCA results in the system exhibiting the typical emission of the scintillator, given that the rejection wavelength does not overlap the range of emission. If the rejection wavelength is located within the emission range of the scintillator, the light at that wavelength is prohibited from propagating and the signal can be blocked. In this work, an emulsion copolymerization was used to synthesize monodisperse, polystyrene-based radioluminescent terpolymer nanoparticles that self-assembled into a face-centered cubic (fcc) structure. Anthracene is an organic scintillator that emits blue light when excited with an x-ray source. During the copolymerization, anthracene was covalently incorporated into a poly(styrene-co-propargyl acrylate) (PS-PA) basis in the form of anthracene-9-ylmethylmethacrylate (AMMA) to form a poly(styrene-co-propargyl acrylate-co-anthracene-9-ylmethylmethacrylate) (PS-PA-PAMMA) liquid CCA. Because liquid CCAs are susceptible to ionic impurities and mechanical stress, the CCA was encapsulated in a hydrogel network. The hydrogel network was photopolymerized in situ with the CCA by mixing the CCA with poly(ethylene glycol) methacrylate (PEGMA), poly(ethylene glycol) dimethacrylate (PEGDMA), and diethoxyacetophenone (DEAP) and exposing the mixture to ultraviolet light. Encapsulating the liquid CCA in a hydrogel network stabilized the crystalline structure and created a more mechanically robust film which was preserved by storing in deionized (DI) water. The hydrogel-encapsulated CCAs exhibited similar rejection wavelength and emission properties to the liquid CCAs. Multiple methods can be used to shift the rejection wavelength of the CCAs. Diluting the liquid CCA with DI water increased the interparticle spacing, red-shifting the rejection wavelength. The rejection wavelength of the hydrogel-encapsulated CCA was tuned by swelling and drying the film. When excited with an x-ray source, the encapsulated CCA exhibited the radioluminescence characteristic of anthracene with a maximum emission at 425 nm. The radioluminescence of the hydrogel-encapsulated CCA decreased when the rejection wavelength was shifted to overlap the characteristic emission. The overall emission of the system can be controlled by coupling the rejection wavelength of the CCA with the emission of the scintillator.

11:15 AM EQ05.14.03

III-Nitride Photonic Crystal Membrane Cavity with Substrate Isolation [Ganapathi Subramania](#)¹, Keshab Sapkota¹, Nicholas Karl¹, George Wang¹, Igal Brener¹, Zachary Meinelt² and Daniel Feezell²; ¹Sandia National Laboratories, United States; ²The University of New Mexico, United States

On-chip nanophotonics devices such as those possible on Silicon or GaAs for near-infrared frequencies have been challenging to achieve in the visible frequency regime. III-Nitride based materials have excellent material properties for visible frequency nanophotonics such as broad gain regime (e.g., for lasing) and large refractive index for waveguiding visible light. Surface emitting lasers have been demonstrated from photonic crystal (PhC) nanowire arrays [1,2]. Nevertheless, fabricating devices such as cavities, modulators and lasers that can be integrated for on-chip photonics requires light transport to be confined to a submicron sized active layer. This can be done with a low refractive index optical cladding layer separating the active layer from the high refractive index substrate layer. This is achieved in a relatively straightforward manner in Si by using low index SiO₂ buffer layer (silicon-on-insulator) or in GaAs by oxidizing an AlGaAs buffer layer to a low index AlGa_xO_{1-x} layer. Such options are not available for III-nitrides making on-chip integrated photonics in the visible. One approach that can address this challenge is by creating a nanoporous layer of GaN with a reduced effective index between the active region and the substrate. Nanoporous GaN layer produced by electrochemical etching have been used as a low refractive index layer to fabricate a distributed Bragg reflector (DBR) mirror [3] that can be utilized for VCSELS. We will describe fabrication of membrane type PhC cavities using nanoporous GaN as cladding from the high refractive index substrate. We will describe the effects of the porosity on the PhC cavity quality factor and cavity emission wavelength.

Sandia National Laboratories is managed and operated by NTESS under DOE NNSA contract DE-NA0003525.

[1] Wright, J. B.; Liu, S.; Wang, G. T.; Li, Q.; Benz, A.; Koleske, D. D.; Lu, P.; Xu, H.; Lester, L.; Luk, T. S.; Brener, I.; Subramania, G., Multi-Colour Nanowire Photonic Crystal Laser Pixels. *Sci. Rep.* **2013**, 3, 2982.

[2] Anderson, P. D., Koleske, D. D., Povinelli, M. L. & Subramania, G. Improving emission uniformity and linearizing band dispersion in nanowire arrays using quasi-aperiodicity. *Optical Materials Express* **7**, 3634 (2017).

[3] Mishkat-Ul-Masabih, S.; Luk, T. S.; Rishinaramangalam, A.; Monavarian, M.; Nami, M.; Feezell, D., Nanoporous distributed Bragg reflectors on free-standing nonpolar m-plane GaN. *Applied Physics Letters* **2018**, 112 (4), 041109.

11:30 AM EQ05.14.05

Lattice Coupled Anapole Excitations in Photocatalytic Semiconductor Nanodisks for Improved Solar Light Harvesting [Ludwig Hüttenhofer](#)¹, Andreas Tittl¹, Lucca Kühner¹, Emiliano Cortés¹, Ian Sharp² and Stefan A. Maier^{1,3}; ¹Nanoinstitut Ludwig-Maximilians-Universität, Germany; ²Walter-Schottky-Institut Technische Universität, Germany; ³Imperial College London, United Kingdom

Efficient solar energy conversion requires broadband visible light harvesting which is not provided by most semiconductor photocatalysts. The engineering of Mie-Resonances in nanostructures of these materials offers a route for trapping light and expansion of the absorption throughout the visible spectrum. Anapole excitations and associated absorption engineering in dielectric nanoresonators are therefore the key tool of our research due to the intricate combination of nonradiating modes and strong electromagnetic field confinement in the underlying material. We present our studies on engineered nanoantennas composed of photocatalytic dielectrics and demonstrate increased light-harvesting capabilities in otherwise weakly absorptive spectral regions.

We employ anapole excitations in single nanodisks of oxygen-vacancy-rich TiO_{2-x} , a prominent photocatalyst that provides a powerful platform for exploring concepts in absorption enhancement. The arising photocatalytic effect is monitored on the single particle level using the well-established silver reduction reaction on TiO_2 . With the freedom of changing the optical properties of TiO_2 through tuning the abundance of oxygen vacancies, we discuss the interplay between cavity damping and the anapole-assisted field confinement for absorption enhancement.

On the route towards upscaling, collective anapole-anapole interactions are investigated in rectangular arrays of nanodisks of GaP, as a high refractive index of the resonator material emerges as favourable. Our experimental findings show that maximum visible light extinction by the array and maximum absorption in the GaP are not achieved by the densest packing of resonators. Counterintuitively, increasing the array periodicities such that collective effects spectrally overlap with the anapole excitation of a single particle leads to an absorption enhancement of up to 300% compared to a single disk. An analysis of coupling in one- and two-dimensional arrays with polarization-dependent measurements and numerical simulations allows us to discriminate between coupling interactions parallel and perpendicular to the polarization axis and evaluate their strengths.

Based on our findings we fabricate large-scale nanoimprinted photoelectrodes that make use of the investigated photonic effects, allowing for the generation of quantifiable catalytic yields. We share our latest results of wavelength dependent photoelectrochemistry on these electrodes and demonstrate a photocurrent enhancement by a factor of 5.7 compared to a planar film under hydrogen evolution reaction conditions.

Our results provide a fundamental understanding of tailored light absorption in coupled anapole resonators and reveal important design guidelines for advanced metasurface approaches in a wide range of energy conversion applications.

SESSION EQ05.15: Advanced Nanophotonic Design III
Session Chairs: Artur Davoyan and Benjamin Vest
Thursday Afternoon, December 2, 2021
Hynes, Level 2, Room 210

1:30 PM EQ05.15.01

Scalable, Nanometer-Precise Engineering of Light-Matter Interactions with Deterministically Patterned Colloidal Plasmonic Structures Weikun Zhu, Peter Satterthwaite, Patricia Jastrzebska-Perfect and Farnaz Niroui; Massachusetts Institute of Technology, United States

Tailoring light-matter interactions with precise yet scalable fabrication of hybrid structures, only few nanometers in size, is essential to advance nano-optics and plasmonics. Conventional top-down fabrication techniques though lack the resolution necessary to achieve such dimensions. Alternatively, colloidal nanoparticles, with controlled size, shape, composition, and crystallinity, can reach unprecedented resolutions while also enabling unique functionalities. However, their current integration suffers from stochastic processing and assembly into passive structures, lacking the positional accuracy and structural complexity essential for functional devices and systems. In this work, we present a fabrication platform in which bottom-up directed assembly is combined with dry-phase transfer printing to achieve deterministic, large-area, and high-throughput patterning of colloidal metallic nanoparticles onto arbitrary surfaces with single particle resolution. This approach provides a versatile platform for colloidal particle integration into next-generation optoelectronic devices. Utilizing gold nanocubes as an example, we discuss fabrication of scalable nanopatch antenna arrays with deterministic and easily tailorable optical response on-demand. By further integrating these structures with molecular emitters, we present controlled enhancements leveraging precise engineering of light-matter interactions towards realizing functional building blocks for diverse quantum optical technologies.

1:45 PM EQ05.15.02

Microcavity Enhanced Raman Spectroscopy of Fullerene C_{60} Bucky Balls Vinayaka H. Damle, Miri Sinwani, Hagit Aviv and Yaakov Tischler; Bar Ilan University, Israel

Raman spectroscopy is a widely used characterization technique in material science. It is a non-destructive tool with relatively simple instrumentation, and provides intrinsic qualitative information of analytes by probing their vibrational modes. In many cases, Raman enhancement is essential for detecting low-intensity signals in high-noise environments, spectrally unresolved features, and hidden modes. Here we present optical and Raman spectroscopic characterization of fullerene C_{60} in a gold microcavity. The fabrication of single-layered gold mirrors is facile, low cost and direct but was proven to give considerably significant enhancement. The findings of this work demonstrate the cavity resonance as a powerful tool in obtaining tunability over individual peak for selective enhancement in the tuned spectral range. The PL of the material within the cavity has demonstrated a red shift assumed to be caused by the low-energy transitions. These transitions are induced by virtual low-energy states generated by the cavity. We further observe that adopting this principle enables resolution of active Raman modes that until now were unobserved. Finally, we assigned the new experimentally observed modes to the corresponding motions calculated by DFT.

2:00 PM EQ05.15.03

Low Energy Band Gap Opening in Polymer-Wrapped/Metallic Single-Walled Carbon Nanotube Hybrid Assemblies via Symmetry Breaking Francesco Mastrocinque, George Bullard, Nicholas X. Williams, Aaron D. Franklin and Michael Therien; Duke University, United States

There is an incontrovertible need for low dimension materials that can provide reliable, high performance microelectronics. Single-walled carbon nanotubes (SWNTs) are one-dimensional materials that are ideal for microelectronic applications due in part to their unique optical and electronic attributes. SWNTs possess superior charge carrier mobilities when compared to conventional microelectronic materials such as Si and GaAs, and their π -conduction pathways are impervious to electromigration which is an increasing source of failure as device size decreases. Nanotube based technologies are hindered by the current standards of production, which yield heterogeneous distributions of SWNT diameters or chiralities. These irregular compositions of electronic structures often preclude their inclusion in practical applications such as field-effect transistors (FETs) or optical sensors. To isolate

homogeneous SWNT samples with unique electronic structure, the aqueous two-phase (ATP) separation method gives access to electronically sorted SWNT chiralities that were previously inaccessible. We have adapted and optimized the ATP purification method to isolate a highly enriched (11,11) metallic SWNTs (m-SWNTs). Additionally, we have developed novel compositions of matter that have unique electronic and structural characteristics: SWNTs that are helically wrapped in a single chain fashion by chiral semiconducting polymers. These assemblies provide robust organic and aqueous solvent soluble superstructures featuring exceptional electronic and morphological homogeneity.

Disruption of the highly symmetric electronic structure of (11,11) m-SWNTs through polymer wrapping shifts the allowed wave vectors away from the K and K' Dirac points in reciprocal space, resulting in a metallic to semiconducting phase transition in these m-SWNT assemblies. We have recently demonstrated metal to semiconductor phase transitions in polymer-wrapped m-SWNTs through a number of optical and potentiometric methods in both aqueous solution and the solid state. Results indicate that symmetry breaking of the SWNT electronic structure is accomplished through chiral single-chain helical polymer wrapping at a fixed pitch length that give rise to newly allowed low energy electronic transitions. These noncovalently wrapped polymer/m-SWNT hybrid assemblies do not introduce chemical defects and therefore are practical for applications leveraging electronically homogeneous nanotubes that require high reproducibility, or for devices where band gap magnitudes are tuned on the fly through modulation of electrical or optical fields. These new low energy band gap polymer/m-SWNT compositions provide a new means to manipulate optical and electro-optical function in hybrid nanoscale assemblies.

2:15 PM DISCUSSION TIME

2:30 PM EQ05.15.05

All-Dielectric Photonic Gap Antennas for Extreme Confinement of Light Ashutosh Patri¹, Kevin G. Cognee² and Stephane Kena-Cohen¹; ¹Polytechnique Montreal, Canada; ²The City College of New York, United States

The use of optical antennas has been the subject of an increasing number of scientific studies as they can improve the efficiency of a wide range of near-field optical technologies, including light transmission and reception, spectroscopy, sensing, and imaging. Antennas are designed primarily to facilitate efficient energy transfer between a localized source and free space while serving as impedance matching elements. In this regard, most previous studies have focused on antennas made of metals since their surface plasmon polaritons can effectively confine light within deep subwavelength boundaries to enhance the coupling between the source and the antenna. However, plasmonic antennas suffer from ohmic losses, which can lead to considerable heat generation, resulting in melting or irreversible structural alteration of the antenna and thermochemical destruction of the nearby matter. An alternative way to mitigate ohmic losses is to make antennas from dielectrics instead of metals. Indeed, all-dielectric antennas have several advantages over plasmonic antennas, including excellent photostability, low heating, and high radiative quantum efficiency. Unfortunately, the relatively weak spatial confinement offered by the volumetric modes in conventional dielectric antennas makes it difficult to achieve efficient coupling between the source and the antenna itself.

We present here an all-dielectric multilayer antenna configuration that supports strongly confined modes while maintaining unity antenna quantum efficiency. Our antenna design consists of a high-index pillar structure with a transverse gap filled with low-index material. The index contrast between the gap material and the pillar material allows for strong localization of the field within the gap. We provide a detailed explanation of the operation principle of such Photonic Gap Antennas (PGAs) based on Fabry-Perot-like resonances of horizontal slot-waveguides with symmetrically and asymmetrically placed gap layer. We calculate the mode volumes of the PGA based on quasinormal mode theory and obtain mode volumes in the range of $10^{-4} \lambda_0^3$ that are on par with plasmonic antennas. We demonstrate that, when acting as a transmitter, the PGA can improve the spontaneous emission rate of a point dipole by ~1300 times that of its emission rate in free space. Reciprocally, when acting as a receiver, the PGA can lead to a near-field intensity enhancement by a factor of ~3000 with comparison to the intensity of the incident plane wave. Moreover, we show that the PGA can operate over a broad spectral bandwidth ($\Delta\lambda \approx 300$ nm at $\lambda = 1.25$ μm), while providing unidirectional out-of-plane radiation.

2:45 PM EQ05.15.07

Bottom-Up Synthesis of Hybrid Dielectric/Metal Nanowires for Low-Loss Plasmonics Corban G. Murphey and James Cahoon; University of North Carolina at Chapel Hill, United States

Confining and guiding light on a deep sub-wavelength scale is a key goal in nanophotonics. Plasmonic materials are used in this respect, but are often limited by large Ohmic absorption losses, resulting in undesirable heating effects and short propagation distances in waveguides. Dielectric materials, on the other hand, have substantially lower losses than metals, but do not confine light on the same sub-wavelength scale. However, by combining these two classes of materials into a single nanostructure, it should be possible to achieve simultaneous low-loss and deep sub-wavelength modes by confining plasmonic resonances in a low-loss dielectric. Here, we show that a simple geometry – a silicon (Si) nanowire (NW) with a uniform gold (Au) shell – can confine NIR light in a NW just 210 nm in diameter. Furthermore, the hybrid dielectric environment produces two unique effects: the high-index Si core allows for the Au plasmon resonances to exist in a much smaller structure and at a substantially lower energy than they would normally occur, and the Si core's Mie resonances blueshift and adopt a Fano lineshape due to coupling with the plasmons. Core diameter and shell thickness are easily tunable and can dramatically shift the positions of the hybrid plasmonic resonances. We combine bottom-up vapor-liquid-solid SiNW growth with metal sputtering to synthesize a vertically aligned, hybrid Si/Au NW – a structure that is not accessible by more conventional lithographic or solution-phase techniques. To measure optical properties, we employ a custom-built supercontinuum laser microscope for single-NW extinction measurements. The tunability of the materials and optical properties of this structure make it an exciting candidate for a range of photonic applications, from sensing to optical computing.

3:00 PM EQ05.15.08

Circularly Polarized Light-Assisted Chiral Superstructure Assemblies on Substrate Ji-Young Kim, Connor McGlothlin, Minjeong Cha, Emine S. Turali-Emre and Nicholas Kotov; University of Michigan, United States

Self-assembly of geometrically complex structures has been accomplished in dispersions but not on the surfaces, which is needed for further studies and applications of their intriguing electromagnetic/optical properties. Their successful assembly can be accomplished using intrinsic chirality of the nanostructure and/or exerting local chiral bias. That could be translated to a variety of technologies, from medicinal chemistry to advanced manufacturing. Here, we show that the strong optical activity of plasmonic materials under circularly polarized light (CPL) affords photon-to-matter chirality transfer, fabricating centimeter-scale chiral 3D superstructures. Illuminating CPL on substrate immersed in silver salt solutions induces the formation of nanoparticles (NPs) with 15–20 nm in diameter and subsequent asymmetric deposition/assembly to construct chiral superstructures on the substrate. Circular dichroism (CD) spectra vividly showed opposite polarity after exposure to photons with left- and right circular polarization. The wavelength of the light source determined the size of the final superstructure as well as their surface plasmon resonance (SPR) and CD band wavelength. Electron microscopy images for its intermediate growth stages showed vivid handedness of the rotational assemblies of NPs. The experimental evolution of CD peaks in different growth stages correlated well with those calculated for assembled nanostructure models with complex geometry, as established by the prediction of deposition/assembly pattern by electromagnetic simulations. The chiral patterns were fabricated on polydimethylsiloxane (PDMS) stamp by CPL exposure time to demonstrate the simplicity and universality of these photosynthetic routes to direct construction of metallic 3D chiral metamaterials

on arbitrary substrates with controlled chirality. These simple and versatile architected metamaterials can be used for extensive applications, including but not limited to photonic, optoelectronic, and electromechanical devices as well as enantioselective catalytic and sensing systems.

3:15 PM EQ05.15.10

Solving Integral Equations in Free-Space with Inverse-Designed Ultrathin Optical Metagratings [Andrea Cordaro](#)^{1,2}, Brian Edwards³, Vahid Nikkhah³, Andrea Alu⁴, Nader Engheta³ and Albert Polman^{1,2}; ¹AMOLF, Netherlands; ²University of Amsterdam, Netherlands; ³University of Pennsylvania, United States; ⁴City University of New York, United States

The physical speed and power consumption of conventional microelectronics processors are reaching their limits, and consequently, novel paradigms and approaches for computing and information processing are desired. One such approach, which has gained significant renewed interest recently, is analog optical computing capable of processing large amounts of data with high speed and low energy consumption. Moreover, the tremendous recent advances in the field of metamaterials and metasurfaces have yielded the possibility of shaping optical fields in extreme ways over subwavelength thicknesses. This, in turn, has unlocked new opportunities for all-optical computing strategies and opened entirely new avenues in the field of analog signal processing and computing with waves.

Here, we demonstrate, theoretically and experimentally, a Si-metagrating-based optical platform that combines a tailored scattering matrix design and a feedback system to enable the solution of Fredholm integral equations of the second kind from the far-field

$$g(u) = I_{in}(u) + \int_a^b K(u,v) g(v) dv, \quad (1)$$

where $g(u)$ is the unknown solution of the integral equation, $K(u,v)$ is a function of two variables that acts as the kernel of the integral operator, and $I_{in}(u)$ is an arbitrary input function. This problem can be discretized by sampling the variables u and v over N points in the interval $[a,b]$ to form two vectors, \underline{u} and \underline{v} , and recast into a matrix equation

$$\underline{g} = \underline{I}_{in} + K \underline{g} \quad (2)$$

where $\underline{g} = g(u)$, $\underline{I}_{in} = I_{in}(u)$ and $K = K(u,v) * (a-b)/N$ where u and v are evaluated as N discrete points. The solution \underline{g} can be thought of as the result of the Neumann series $\underline{g} = \sum_n (K)^n \underline{I}_{in} = (I_N - K)^{-1} \underline{I}_{in}$ where I_N is the $N \times N$ identity matrix. Next, it is possible to think of the N mathematical sampling points as N discrete physical modes, and thus \underline{g} is a vector representing the complex amplitude of these modes on a given plane with a chosen direction. The integral operator can then be represented by a scattering matrix that performs matrix-vector multiplication between these sets of modes and can be mapped onto the reflective part of the scattering matrix of a Si metagrating. Finally, a semi-transparent mirror feeds the signal back into the system mimicking an analog Neumann series.

By means of the adjoint method, it is possible to inverse-design the unit cell of the Si metagrating (not including the mirror) in order to achieve a prescribed S -matrix. The unit cell is embedded in a SiO_2 superstrate. The design wavelength is $\lambda = 706$ nm while the unit cell is 825 nm wide and 400 nm deep. Next, we include a semitransparent mirror, and hence the feedback system, in the simulation and check how that results in the inversion of the designed S -matrix. From the transmission block of the S -matrix of the entire stack (metagrating, SiO_2 spacer, and semitransparent mirror) it is possible to read out the analog solution provided by the structure. At the conference, we will present the comparison between the metasurface-based analog solution and the ideal solution demonstrating good agreement for all the inputs, both in terms of the real and imaginary parts.

To demonstrate these concepts experimentally, the metasurface was fabricated with e-beam lithography on Si-on-sapphire substrate. Next, the sample was planarized with a layer of SiO_2 solgel and an extra layer of sputtered SiO_2 . Finally, 15 nm of Au were evaporated on the sample using an organic adhesion monolayer. At each step, the transmission spectrum of the sample was measured and shows a good match with the simulated spectrum. At the conference, we will show the agreement between optical measurements and simulations for the ideal structure that solves the integral equation.

Finally, future applications of these concepts could include TMDs two-dimensional materials to explore to dynamically tune the encoded mathematical operation, paving the way for all-optical reconfigurable computing circuitry solving problems of further enhanced complexity.

3:30 PM BREAK

4:00 PM EQ05.15.11

Directing Quantum Dot Emission with Resonant Mie-like Nanocylinders for Luminescent Solar Concentrators [Tom Veeken](#), Kyra Orbons and Albert Polman; AMOLF, Netherlands

Building-integrated photovoltaics (BIPV) has received much attention recently to minimize the use of land for PV systems, decrease the overall system and installation costs due to its multifunctional use, and make PV systems more aesthetically appealing. The luminescent solar concentrator (LSC) is such a building-integrated photovoltaic device, consisting of a glass or plastic waveguide with embedded luminophores and integrated solar cells along the edges or in a matrix. Therefore, the LSC can directly be used as a (vertical) facade or roof and offers more aesthetic options due to its semi-transparent and/or colored surface.

Even though the LSC concentrates sunlight in the waveguide and guides it to solar cells smaller than the top surface area, it cannot surpass the detailed balance limit for a single-junction solar cell. In short, the LSC remains at 1-sun illumination intensity, and the potential V_{OC} increase due to increased J_{SC} (concentration factor) is offset by the coincident increase in the J_0 . Thus, the power conversion efficiency (PCE) of the LSC is limited to the typical 34%, while the world record remains at 7.1%, indicating both the poor performance of LSCs so far, but also the significant potential gain. One of the main loss mechanisms in an LSC is the emission of photons through the escape-cone, accounting for about 25% of all lost photons. This is a direct consequence of isotropic luminophore emission and the escape-cone angle of a glass/plastic waveguide in air.

In this work, we use anisotropic luminophore emission to decrease the escape-cone losses in an LSC. We do so by embedding CdSe-CdZnS core-shell nanoplatelets, the luminophores, into high-index TiO_2 nanocylinders that exhibit Mie-like resonances. An array of TiO_2 cylinders is then incorporated into the waveguide. The shape and size of the cylinders are optimized such that sunlight with energy higher than the luminophore bandgap is resonantly absorbed in the out-of-plane direction, while the Stokes-shifted luminophore emission is resonantly directed in-plane. We use FDTD simulations to find the optimal nanostructure and identify the Mie-like modes that are excited by the incoming sunlight and couple to the luminophore emission. The simulations predict that the escape cone losses are reduced from 25% to 12%.

Arrays of TiO_2 nanocylinders were fabricated on top of a glass substrate. First, a multilayer stack of TiO_2 , CdSe-CdZnS core-shell nanoplatelets, and TiO_2 was created. Using e-beam lithography and subsequent lift-off, we created a chromium hard-mask for reactive ion etching of the multilayer. After removal of the chromium, we obtained an array of TiO_2 cylinders with 450 nm diameter, 120 nm height, and 1800 nm pitch, with an embedded nanoplatelet layer of 30 nm thick. SEM images and spatially resolved photoluminescence measurements show that the luminophores are only located inside the cylinders as designed.

To demonstrate the directional emission, we measure the luminophore emission in a Fourier-microscopy setup. To emulate the incorporation of the cylinder array inside the waveguide, we used an immersion-oil objective, which also enables the collection of luminophore emission under grazing angles. Besides the use in LSCs, directional luminophore emission has potential applications in LEDs and up- and down-conversion for photovoltaics.

4:15 PM EQ05.15.12

Near-Field Light Concentration with Silicon Light Funnel Arrays [Ashish Prajapati](#) and Gil Shalev; Ben Gurion University of the Negev, Israel

Silicon light funnels are three-dimensional subwavelength structures in the shape of inverted cones with respect to the incoming illumination. Light funnel (LF) arrays can serve as efficient absorbing layers on account of their light trapping capabilities, which are associated with the presence of high density complex Mie modes. Specifically, light funnel arrays exhibit broadband absorption enhancement of the solar spectrum. In the current study, we numerically explore the optical coupling between surface light funnel arrays and the underlying substrates. We show that the absorption in the LF array-substrate complex is higher than the absorption in LF arrays of the same height (~10% increase). This, we suggest, implies that a LF array serves as an efficient surface element that imparts additional momentum components to the impinging illumination, and hence optically excites the substrate by near-field light concentration, excitation of traveling guided modes in the substrate, and mode hybridization.

SESSION EQ05.16: Fundamental of Plasmonics and Metaphotonics II
Session Chairs: Stephanie Reich and Giulia Tagliabue
Monday Morning, December 6, 2021
EQ05-Virtual

8:00 AM *EQ05.16.01

Recent Advances in Mie-Resonant Metaphotonics [Yuri Kivshar](#); Australian National University, Australia

Future photonic technologies underpinning high-performance communications, ultrafast computations and compact biosensing will rely on densely packed reconfigurable optical circuitry based on nanophotonics. For many years, plasmonics was considered as the only available platform for subwavelength optics, but the recently emerged field of Mie-resonant metaphotonics provides more practical alternatives for nanoscale optics by employing resonances in high-index dielectric nanoparticles and their structures such as metasurfaces. This talk aims to discuss recent advances and future emerging directions in the physics of dielectric Mie-resonant nanostructures with high quality factors (Q factors) for efficient spatial and temporal control of light by employing multipolar Mie resonances and bound states in the continuum (BIC), with applications of these concepts to nonlinear optics, active photonics, and topological lasers.

In particular, we discuss the physics of photonic BICs and their applications to metadevices, including enhancement of nonlinear response, light-matter interaction, and development of active nanophotonic devices. We discuss how BIC-empowered dielectric metastructures can be used to generate efficiently high-order optical harmonics from bulk and to boost the intrinsic nonlinearity of transition metal dichalcogenide (TMDC) flakes. We explore TMDC resonators composed of structured dielectric arrays and individual nanoparticles for strong light-matter coupling phenomena. We discuss the extension of metasurface functionalities for biosensing applications in biomarker detection and quantum information processing with entangled photons. Finally, we demonstrate how tunability of BICs in the momentum space can be used to realize a novel type of efficient lasing based on a finite-size cavity with a small footprint.

In addition, we introduce a novel platform for plasmonic metasurfaces empowered by optical BICs, for engineering high-Q optical resonances. Our plasmonic metasurfaces are composed of arrays of vertically oriented pillar meta-molecules covered by a thin layer of gold. We suggest and realize experimentally anisotropic plasmonic metasurfaces supporting high-Q resonances governed by quasi-BIC collective resonant modes. With this platform, we demonstrate several other effects including novel plasmonic metasurfaces for full Stokes polarization perfect absorption in the mid-infrared. In this latter case, the metasurface unit cell consists of coupled anisotropic meta-atoms forming a diatomic metamolecule. The designed plasmonic metastructures provide a strong field enhancement by at least one order of magnitude higher than conventional perfect absorbers.

8:30 AM EQ05.16.02

Experimental Demonstration of Magnetic Purcell Enhancement by Magnetic Resonance of Silicon Nanospheres [Hiroshi Sugimoto](#) and Minoru Fujii; Kobe University, Japan

Optical nanoantennas play a central role for enhanced light-matter interactions in modern nanophotonics. Integration of a quantum emitter into a nanoantenna that is capable of increasing local density of optical states (LDOS) results in the enhanced spontaneous emission rate through the Purcell effect. In the past decade, the main focus of the Purcell enhancement has been placed on the manipulation of an electric dipole transition, and less attention has been paid to that of the magnetic dipole and higher order optical transitions. Dielectric nanoantennas have been suggested for manipulating spontaneous emission of a magnetic dipole through the magnetic Purcell effect. However, the experimentally observed enhancement of magnetic dipole emission has been marginal and much smaller than the theoretical prediction. In this work,[1] we develop a composite system, that is, a Si nanosphere decorated with Eu^{3+} complexes, in which magnetic dipole emission of Eu^{3+} is efficiently coupled to the magnetic Mie modes of the nanosphere. By means of single particle spectroscopy, we systematically investigate the light scattering and photoluminescence spectra of the coupled system with diameters of Si nanospheres from 130 to 245 nm. We demonstrate that by tuning the magnetic quadrupole Mie resonance to the $^5\text{D}_0$ - $^7\text{F}_1$ magnetic dipole transition of Eu^{3+} , the branching ratio between the magnetic and electric dipole transitions is enhanced up to 7 times. We also show the magnetic Purcell enhancement in an ensemble of Si nanospheres with size distribution. The observed magnetic Purcell enhancement driven by colloidal Mie resonators offers an opportunity not only to develop novel fluorophores with enhanced magnetic dipole emission, but also to control the excited state of the matter in photochemistry.

[1] H. Sugimoto, M. Fujii ACS Photonics, in press (2021) DOI:10.1021/acsp Photonics.1c00375

8:45 AM EQ05.16.03

Modeling Multi-Level Phase Change Photonics Devices [Yunzheng Wang](#)¹, Jing Ning¹, Bosman Michel² and Robert Simpson¹; ¹Singapore University of Technology and Design, Singapore; ²National University of Singapore, Singapore

Chalcogenide phase change materials (PCMs) have shown many exciting and interesting characteristics, such as non-volatile structure transition, up to trillions of reversible cycles[1], high stability, and large optical and electric differences between their two distinct structure phases. These make them not only been used in existing electric storage[2], but also a potential candidate for reprogrammable photonics devices, micro-electromechanical systems, and tunable radio frequency devices.

An accurate model to describe the PCM switching behavior is necessary for designing programmable photonic devices. The optical properties of PCMs are determined by their crystal microstructures and phase transitions which depend on the heating and quenching conditions. To understand the evolution of a PCM photonics device's optical response during switching, and the conditions that can lead to multi-level optical devices, it is important to know not only the initial and final states, but also how the optical constants evolve during nucleation, crystal growth, and melt-quenching. Therefore, a model that

accurately predicts the optical properties during and after phase transition will be a key enabler of successful photonic device designs, and in particular, phase change multi-level devices.

The existing models, such as the JMAK method and density functional theory, can not satisfy the need of modeling a PCM device in accuracy, cost, time consumption and device size. However, semi-empirical methods can have a good compromise between accuracy, scaling, and performance. Recently, Meyer et al developed a multiphysics model based on phase field method to describe the optical properties of a phase change metasurface perfect absorber but no experiments was conducted to verify the multiphysics model[3].

Herein, we developed an accurate multiphysics framework based on the Gillespie cellular automata (GCA) method to quantitatively simulate the evolution of PCM crystal microstructures and optical response of PCM photonics devices. The multiphysics framework self-consistently combines the nanosecond non-isothermal laser heating, non-linear and probabilistic GCA, effective medium theory and the Fresnel Equations together. To prove the accuracy, the framework was applied to a programmable thin-film optical stack, and laser switching experiments and transmission electron microscopy were performed. Comparison between simulation and experimental results shows that the model can accurately predict not only the final optical state, the crystallographic microstructure evolution and the transient optical response, but also multilevel optical reflectivity and transmissivity which corresponds to partial crystallization of the PCM film. Therefore, we foresee the model will be widely applied to optimizing the interconnection weights in all-optical neural network schemes, controllable metamaterial phase arrays, and displays. For this reason, the code is publicly available at the GitHub website[4], and we encourage others to use it.

1. Kim, W., et al. *ALD-based confined PCM with a metallic liner toward unlimited endurance*. in *2016 IEEE International Electron Devices Meeting (IEDM)*, 2016.

2. Hoddeson, L. and P. Garrett, *The discovery of Ovshinsky switching and phase-change memory*. *Physics Today*, 2018. **71**(6): p. 44-51.

3. Meyer, S., Z.Y. Tan, and D.N. Chigrin, *Multiphysics simulations of adaptive metasurfaces at the meta-atom length scale*. *Nanophotonics*, 2020. **9**(3): p. 675-681.

4. Wang, Y., et al. *Multiphysics GCA codes*. 2021; Available from: https://github.com/YunzhengWang/multiphysics_GCA.

9:00 AM EQ05.16.04

Plasmon-Induced Electric Effects in Various Materials—Theory and Experiment David Keene¹, Paula Fortuna¹, Maxim Durach² and Natalia Nogoinova¹; ¹Norfolk State University, United States; ²Georgia Southern University, United States

Significant photoinduced electric effects observed in nanostructured metal systems are clearly associated with plasmonic excitations. In order to better understand the origin and be able to predict the effect in various materials and geometries, we perform theoretical calculations for the effective "plasmonic pressure" and "plasmonic striction" ("gradient") forces based on the electro-magnetic hydrodynamic momentum loss approach (EHML) in various plasmonic materials, including gold, silver, aluminum and TiN. We show that the wavelength dependence for the pressure force is expected to be weak for most of the optical and near infra-red range with a rapid increase toward the short wavelengths. The opposite (a decrease with decreasing wavelength) is predicted for the striction force. A direct comparison of experimental data to the theoretical calculations offers new insight into the nature of the plasmon drag effect and promises a conclusive answer to which of the proposed forces has a larger impact on the magnitude of the plasmon drag effect. It is the hope of the authors that this more complete understanding of the phenomenon will contribute to the design on devices that will more efficiently utilize the plasmon drag effect for a myriad of applications from environmental sensors to opto-electric interfaces.

9:15 AM EQ05.16.05

Modification of Plasmonic Responses of Doped Semiconductor Nanoparticles by Electron Beam Irradiation Kevin Roccapriore¹, Andrew R. Lupini¹, Shin-Hum Cho², Delia Milliron³ and Sergei V. Kalinin¹; ¹Oak Ridge National Laboratory, United States; ²Samsung Semiconductor R&D, Korea (the Republic of); ³The University of Texas at Austin, United States

Nanoparticles can exhibit exotic physics, display quantum phenomena, and offer opportunities in multiple disciplines and applications. Plasmonics is one field in which nanoparticles has made a large impact, for example in biosensing, the pharmaceutical industry, and quantum optics. Particles are typically chemically synthesized and can be tailored to meet specific plasmon resonance requirements based on the chemical recipe. Resonances of nanoparticles can extend from the near infrared (NIR) to the ultraviolet (UV) spectral regions and can even be spectrally tunable based on the level of incorporated dopants [1]. However, once synthesized, the plasmon response cannot be dynamically modified. Here we report use of the electron beam in a scanning transmission electron microscope (STEM) to modify plasmon resonances of doped semiconductor nanocrystals in both space and energy.

Using the framework of a self-assembled system of nanoparticles, we direct the electron beam at higher-than-normal operating currents in order to intentionally modify individual nanoparticles. Previous work related to the use of an electron beam for modification of structures has shown precise cutting and welding of metallic silicon nanowires [2], positioning of atoms and dopants within two dimensional materials [3], and sculpting 1D nanowires in 2D materials [4], however, here we focus on the application to nanoparticle plasmonics, and attempt to understand the mechanisms responsible for modification.

We demonstrate that near atomic-resolution sculpting of nanoparticles is possible by selectively removing atomic columns with a converged electron beam in nanoparticles whose thicknesses range from 10-15 nm. Entire particles can also be removed from the array, allowing for plasmonic hotspots to effectively be patterned by the electron beam. The modification to the plasmonic response occurs in both space and energy domains and we explore these modifications on-the-fly with electron energy loss spectroscopy (EELS). Not surprisingly, the altered geometry supports additional localized plasmons, e.g., creation of a hole within a nanoparticle allows for existence of edge plasmons on the edge of the hole. We also observe spectral shifting of plasmon resonances upon electron irradiation in different conditions, and attribute this to element-specific removal of atoms from core-loss EELS measurements. The ability to adjust the particle response on the fly significantly increases the design possibilities for nanostructure development and is key for nanophotonic design.

[1] S. H. Cho *et al.*, *J. Chem. Mater.* **2019** *31*, 2661.

[2] S. Xu *et al.* *Small* **2005** *1*, 1221.

[3] O. Dyck *et al.* *Nat. Rev. Mat.* **2019** *4*, 497.

[4] J. Lin *et al.* *Nat. Nanotechnol.* **2014** *9*, 436-442

This effort is based upon work supported by the U.S. Department of Energy (DOE), Office of Science, Basic Energy Sciences (BES), Materials Sciences and Engineering Division (K.M.R., A.R.L. S.V.K.). S.H.C acknowledges (NSF, CHE-19052631609656, CBET-1704634, NASCENT, an NSF ERC EEC-1160494, and CDCM, an NSF MRSEC DMR-1720595), the Welch Foundation (F-1848), and the Fulbright Program (IIE-15151071).

9:30 AM EQ05.16.06

Electric and Magnetic Dipole Emission of Dense and Diluted Emitter Arrangements in Plasmonic Structures John N. Munga¹, MD Afzalur Rab¹, Maxim Durach² and Natalia Nogoinova¹; ¹Norfolk State University, United States; ²Georgia Southern University, United States

Control and enhancement of spontaneous emission of magnetic and electric dipole transitions can be achieved by use of plasmonic structures. In our work,

we study modification in the emission spectra, polarization and radiation patterns of Eu^{3+} ions in very close vicinity of plasmonic films, gratings and cavities. We compare effects observed in dense and diluted arrangements of emitters, and show that on the contrary to theoretical predictions, reduced quenching is observed in monolayers of closely packed EuTTA molecules. Significant enhancement of p-polarized emission is observed at certain angles in gratings for both dense and dilute Eu systems, which is ascribed to decoupling of surface plasmon polaritons excited by the emitters with a different efficiency for electric and magnetic emitters. Effects are considered theoretically based on the Green's function approach. The effects of roughness of metal and mutual emitter coherence of emitters are discussed.

9:45 AM EQ05.16.07

Plasmonic Electrodes with Nanoantenna Lattice Resonances Dominic Bosomtwi¹, Marek Osinski¹ and Viktoriiia Babicheva²; ¹The University of New Mexico, United States; ²University of New Mexico, United States

We report on the design of plasmonic nanostructures that enhance the hot-electron generation and can be used as nanoelectrodes. The advantage of the nanostructure is brought about by the periodic arrangement of nanoantennas and the excitation of collective resonances [1,2]. These collective multipole resonances result in a significant field enhancement in the proximity to nanoantenna and, therefore, a more efficient generation of hot electrons. We analyze the case when hot electrons are injected into the aqueous environment and the nanoantennas have a high aspect ratio supporting multipole resonances along the antenna. We show that by selecting structure dimensions and periodic arrangement comparable to the wavelength of Rayleigh anomalies, one can achieve a significant enhancement in the localized electromagnetic field and enhanced hot-electron generation.

D.B. acknowledges the support from grant N00014-18-1-2739 (the Navy HBCU-MI program) and grant N00014-19-1-2117 (the office of Naval Research). V.E.B. acknowledges the support from The University of New Mexico Research Allocations Committee, award RAC 2022, for the computational resources.

References:

- [1] D. Bosomtwi, M. Osinski, and V. E. Babicheva, "Mode Coupling and Rabi Splitting in Transdimensional Photonic Lattices," 2020 IEEE 20th International Conference on Nanotechnology, 107-110 (2020).
- [2] D. Bosomtwi, M. Osinski, and V. E. Babicheva, "Lattice Effect for Enhanced Hot-Electron Generation in Nanoelectrodes," under consideration (2021).

SESSION EQ05.17: Plasmonic Applications III
Session Chairs: Viktoriiia Babicheva and Yu-Jung Lu
Monday Morning, December 6, 2021
EQ05-Virtual

10:30 AM *EQ05.17.01

Driving Energetically Unfavorable Hydrogenation Dynamics with Plasmonics—From the Single Particle to the Reactor Scale Jennifer A. Dionne, Katherine Sytwu, Daniel Angell, Briley Bourgeois and Dayne Swearer; Stanford University, United States

Nanoparticle phase transformations and their transient states underlie many technologies in energy storage, memory, and catalysis. However, modifying these intermediate states requires bridging the length-scale gap between the atomic-scale structural features (such as atomic coordination number and surface strain) that influence dynamics and the macroscale extrinsic parameters (e.g. temperature, chemical environment) that can be controlled. Optical excitation of localized surface plasmon resonances (LSPRs) offers a solution for overcoming this size mismatch. Here, we use in situ environmental transmission electron microscopy coupled with optical illumination to demonstrate how LSPRs enable spatially-modified phase transformation dynamics in nanoparticles. As a model reaction, we study the gas-phase photocatalytic dehydrogenation of a variety of Au-Pd systems, including Au-Pd crossed-bar systems, and AgPd bimetallic nanoparticles, where [Ag,Au] acts as a plasmonic light absorber and Pd serves as the catalyst. Under controlled hydrogen pressures, temperatures, and illumination conditions, we study the kinetics of the hydrogen absorption and desorption reactions triggered by the optical excitation of plasmons. We find that plasmons control photochemistry in four ways. First, plasmons modify the rate of distinct reaction steps differently, increasing the overall rate more than ten-fold. Secondly, plasmons open new reaction pathways that are not observed without illumination. Third, reaction nucleation occurs at electromagnetic hot-spots – even when those hot-spots do not occur in the preferred nucleation site. Finally, through atomic-resolution imaging, we show how plasmons modify sub-surface hydrogen within the first few atomic layers of the nanoparticle. We link our single particle results to reactor-scale nanoparticle performance in reactive hydrogen environments, showing how catalyst sub-surface hydrogenation impacts not only product yield but also product-selectivity.

11:00 AM *EQ05.17.02

Plasmonic Nanoparticle Supercrystals Niclas S. Mueller¹, Florian Schulz², Emanuel Pfitzner¹, Bruno Vieira³, Yu Okamura¹, Sabrina Juergensen¹, Georgy Gordeev¹, Patryk Kusch¹, Joachim Heberle¹, Eduardo B. Barros³, Holger Lange² and Stephanie Reich¹; ¹Freie Universitaet Berlin, Germany; ²Universitaet Hamburg, Germany; ³Universidade Federal do Ceara, Brazil

Most materials interact weakly with light, which is why we treat light as an external perturbation. There has been growing interest in systems where light-matter interaction is much stronger so that it becomes comparable to other characteristic energies of the system. In the regime of ultrastrong and deep strong coupling the coupling energy approaches the bare excitation energy of a material. This regime leads to exotic effects like the population of the ground state with virtual photons, phase transitions, and a breakdown of the Purcell effect. Here we discuss how extreme light-matter coupling is systematically achieved in materials. We introduce densely packed supercrystals of gold nanoparticles that have coupling energies corresponding to the visible spectral range.[1,2] We present measurements of their plasmon-polaritons, confirm the breakdown of the Purcell effect as an example of the effects predicted for deep strong coupling, and show how to use such materials as enhancing agents in surface-enhanced vibrational spectroscopy.[1-4] We discuss a universal model to treat light-matter coupling in systems of different dimension and the strongest light-matter coupling we can reasonably expect to achieve in materials.

[1] Niclas S. Mueller, Yu Okamura, Bruno G. M. Vieira, Sabrina Juergensen, Holger Lange, Eduardo B. Barros, Florian Schulz, and Stephanie Reich, Deep strong light-matter coupling in plasmonic nanoparticle crystals. *Nature* **583**, 780 (2020).

[2] F. Schulz, O. Pavelka, F. Lehmkuehler, F. Westermeyer, Y. Okamura, N.S. Mueller, S. Reich, and H. Lange. Structural order in plasmonic superlattices. *Nat. Comm.* **11**, 3821 (2020).

[3] Niclas S. Mueller, Emanuel P tznner, Yu Okamura, Georgy Gordeev, Patryk Kusch, Holger Lange, Joachim Heberle, Florian Schulz, and Stephanie

Reich. Surface-enhanced raman scattering and surface-enhanced infrared absorption by plasmon polaritons in three-dimensional nanoparticle supercrystals. ACS Nano **15**, 5523 (2021).

[4] Eduardo B. Barros, Niclas S. Mueller, and Stephanie Reich, Plasmon-Polaritons in Nanoparticle Supercrystals: Microscopic Quantum Theory Beyond the Dipole Approximation. Phys Rev B, in print (2021).

11:30 AM EQ05.17.04

Late News: Optical Measurement of the Limits of Pseudoelasticity in Gold Nanocrystals K. Anika Harkins, Jonas Boettner and [Lindsey Hanson](#); Trinity College, United States

Pseudoelasticity in metal nanocrystals allows for shape recovery from strains much larger than their bulk counterparts. This fascinating property could be used to engineer self-healing or reconfigurable materials, but to take full advantage of its possibilities a deeper understanding of its mechanism and limitations is needed. For instance, it is unknown whether room-temperature pseudoelasticity can occur in all metal nanocrystals without the introduction of plastic damage. Here we report the use of non-hydrostatic compression of gold nanocrystals in a diamond anvil cell to a range of maximum pressures, up to 11.4 GPa. Optical absorbance spectroscopy of the localized surface plasmon resonance is used to non-invasively monitor changes in particle shape and crystallinity, as indicated by the plasmon resonance peak position and intensity, respectively. We find that while complete shape recovery occurs following compression to all pressures tested, irreversible crystalline defects are only introduced above a threshold of approximately 2.5 GPa. In this way, we establish the capacity of gold nanocrystals to undergo complete pseudoelastic shape recovery following compression under moderate loads, as well as the onset of limited pseudoelastic behavior at higher loads. This work lays a foundation for future all-optical investigations of the limits of pseudoelastic deformation in a wide variety of metal nanocrystals.

11:45 AM EQ05.17.05

Late News: X-Ray Investigations into the Role of Reduction Kinetics in the Atomic Distributions of Bimetallic Alloy Nanocrystals Hannah M. Johnson, Acacia M. Dasher and [Liane M. Moreau](#); Washington State University, United States

The favorable optical and catalytic properties of bimetallic noble metal nanocrystals have been directly attributed to the atomic-scale arrangement of metal atoms. In AgAu nanocrystals, for example, CO oxidation efficacy has been directly attributed to the presence of Ag-Au bonds. Despite the mechanistic hypotheses that atomic scale structure affects observed phenomena, atomic distributions within bimetallic nanocrystals are rarely investigated in tandem with synthetic advances, and often alloy structure is assumed to be homogeneous based on species miscibility alone. While thermodynamic models have suggested that Ag/Au phase segregation is favored under certain nanoscale conditions, the effects of kinetics on atomic distributions within nanoparticle alloys have not been systematically explored. Based on differences in redox behavior between noble metal species, we hypothesize that altering parameters that affect atomic reduction within bimetallic systems will lead to differences in atomic incorporation and distribution within bimetallic nanocrystals.

Herein, a systematic investigation of the effects of reduction parameters on AgAu alloy atomic-scale distributions will be discussed. In particular, the Ag:Au solution ratio, concentration of reducing agent to metal atoms and volume of reductant added have been varied, and the resulting morphology, composition and atomic coordination environments mapped accordingly using X-ray focused approaches. Electron microscopy and small angle X-ray scattering trace differences in particle morphology, X-ray fluorescence determines composition, UV-vis spectroscopy shows changes in the position of the local surface plasmon resonance peak and X-ray absorption spectroscopy reveals differences in atomic coordination environment. Together, these techniques reveal that indeed the parameters that affect reduction kinetics can alter alloy distributions within nanoparticles, even when nanoparticle composition remains constant. Other notable results include trends in Ag underincorporation and the proposal of synthetic methodology that can be employed to encourage the formation of homogeneous alloys. Results have substantial impact on the use of bimetallic noble metal nanoparticles for plasmonic sensors and as substrates for heterogeneous catalysis.

12:00 PM EQ05.17.06

Plasmon Enhanced Photodetection in NbN Superconducting Photodetectors Jingwei Yang^{1,2}, Tzu-Yu Peng^{1,2}, Jia-Wern Chen², Hao-Chen Yeh¹, Chi-Te Liang^{1,1} and Yu-Jung Lu^{1,1,2}; ¹National Taiwan University, Taiwan; ²Academia Sinica, Taiwan

The growth of highly metallic transition metal nitride films has received considerable attention using methods such as RF sputtering, atomic layer deposition, pulsed laser deposition, and molecular-beam epitaxy. Especially, niobium nitride (NbN) is known for its superconducting properties with relatively high superconducting T_c which is crucial for superconducting nanowire single-photon detectors. However, the wavelength sensitive detection with high detectivity remains unexplored. In this work, we demonstrate a plasmon enhanced photodetection in NbN superconducting photodetectors. We deposited niobium nitride (NbN) thin film by radio-frequency (RF) magnetron sputtering on MgO (100) substrate at 800 °C with high crystalline quality. Since the superconductivity of the NbN film can be varied with the argon/nitrogen flow rate, target, RF power, growth temperature, and growth substrate during sputtering. Thus, we optimize the metallicity and superconductivity (with $T_c \sim 16$ K) of NbN films by adjusting the argon/nitrogen flow rate. To increase the photodetectivity, we design an Ag nanocube nanoresonator with a strong gap-plasmon resonance in the visible range to further enhance the photoresponsivity by engineering the optical response for the superconducting devices. This is due to the superconducting states are broken down by a localizing strong electromagnetic field. To design the plasmonic nanostructures, we calculated the electromagnetic field distribution of Ag nanocube/Al₂O₃/NbN structure by finite-difference time-domain (FDTD). We observed a strong plasmonic resonance field which tightly confined in the Al₂O₃ layer between the Ag nanocube and NbN film at a resonant wavelength of 532 nm. We will discuss the detailed working mechanism and the potential application of plasmon-enhanced photodetection in NbN superconducting photodetectors.

SESSION EQ05.18: Fundamental of Plasmonics and Metaphotonics III

Session Chairs: Jennifer Dionne and Giulia Tagliabue

Monday Afternoon, December 6, 2021

EQ05-Virtual

1:00 PM *EQ05.18.01

How Photonic Metadevices Can Perform Mathematical Operations and Analog Computation with Waves Dimitrios Tzarouchis¹, Mario Junior Mencagli², Brian Edwards¹ and [Nader Engheta](#)¹; ¹University of Pennsylvania, United States; ²University of North Carolina at Charlotte, United States

In this talk, we will present an overview of our ongoing work on exploring the theoretical foundations of networks of photonic structures that can perform mathematical operations and analog computation with waves/signals. These structures may include metadevices such as couplers, which can be waveguide-

based or material-based couplers, and reconfigurable multipliers that provide phase shifting and amplification/attenuation of signals. We will discuss some of the mathematical operations such networks of metadevices can perform, including matrix-vector multiplication, equation solving and matrix inversion and related capabilities. Moreover, we will discuss the possibility of generalized inversion (also known as pseudoinversion or Moore-Penrose inversion) of matrices that can be singular and rectangular, leading to possible applications of such metadevices for gradient descent computation. We will discuss our theoretical findings and their physical insights, and we will also mention possible future research directions and applications.

1:30 PM EQ05.18.02

Electron Beam Spectroscopy of a Plasmonic Vertical Split Ring Resonator [Isobel C. Bicket](#)^{1,1}, Edson P. Bellido¹, Sophie Meuret², Toon Coenen^{3,4}, Albert Polman³ and Gianluigi Botton^{1,5}; ¹McMaster University, Canada; ²CEMES-CNRS, France; ³AMOLF, Netherlands; ⁴Delmic BV, Netherlands; ⁵Canadian Light Source, Canada

A swift electron beam can interact with localized surface plasmon resonance (LSPR) near-fields to excite an LSPR, which may then decay and emit a photon into the far-field [1,2]. The initial excitation process is detected in electron energy loss spectroscopy (EELS); the decay and photon emission is detected using cathodoluminescence (CL). The two techniques together provide a powerful combination for studying both the near- and far-field properties of LSPRs.

We use EELS and CL to study a vertical split ring resonator (VSRR), a popular nanostructure for left-handed metamaterial design and an interesting option for dichroic spectroscopy platforms [3]. The VSRR supports an LSPR mode with an electric and magnetic dipole, both in-plane and relatively strongly excited using light [4]. The ~300 nm long gold VSRRs were fabricated using a double-step electron beam lithography process, then characterized using EELS in a monochromated FEI Titan scanning transmission electron microscope, with an energy resolution of ~60 meV. We acquired polarization-resolved CL spectroscopy data in an FEI XL-30 field emission scanning electron microscope equipped with a parabolic mirror, polarization filters, and IR and visible spectrometers. Using six acquisitions with different polarization filter settings, we derive the full polarization state of the emitted light [5,6] from the VSRR LSPRs. Our experimental data is supported by simulations using the MNPBEM toolbox [7] and custom Python data processing code [8,9]. In EELS we identify the magnetic dipolar mode at a free-space wavelength of approximately 1800 nm, and a series of higher order modes in the visible region of the spectrum [10]. We isolate this dipolar mode in our CL acquisition and derive the emission polarization as a function of electron beam location. The CL signal is strongest when the electron beam is located near the tips of the VSRR, overlapping closely with EELS intensity hotspots for this mode. When the electron beam is located far from either of the symmetry axes in the VSRR, we detect a non-negligible amount of circular polarization in the emission.

At higher energies, there are a series of coupled electric dipoles on the rims of the VSRR pillars. These coupled dipoles form bonding and anti-bonding longitudinal and transverse pairs, with corresponding different linear polarization states. Although these modes are heavily intermixed in a small spectral region, they respond to different polarization states and will produce different near-field distributions under photonic excitation, as we determined from the spatially unique EELS and CL maps at different energies. The dependence of the polarization state on the electron beam location reveals that, reciprocally, the near-fields in different locations may respond strongly to different incident polarizations. With regards to assessing the viability of a nanostructure for dichroic spectroscopies, this relationship could be very fruitful.

Acknowledgements

Experimental EELS work was performed in the Canadian Centre for Electron Microscopy, supported by the Natural Sciences and Engineering Research Council of Canada (ICB, EPB, GAB). Experimental CL work was performed at AMOLF, part of the research program of the Netherlands Organization for Scientific Research and funded by the European Research Council (ICB, SM, TC, AP).

References

- [1] Nelayah *et al.*, *Nat. Phys.*, **3**, 5, 2007.
- [2] García de Abajo, *Rev. Mod. Phys.*, **82**, 1, 2010.
- [3] García-Etxarri & Dionne, *Phys. Rev. B*, **87**, 23, 2013.
- [4] Gay-Balmaz & Martin, *J. Appl. Phys.*, **92**, 5, 2002.
- [5] Coenen & Polman, *Opt. Express*, **20**, 7, 2012.
- [6] C. I. Osorio *et al.*, *ACS Photonics*, **3**, 1, 2016.
- [7] Hohenester, *Comput. Phys. Commun.*, **185**, 3, 2014.
- [8] Bicket (2020), [Python 3], <https://github.com/icbicket/CLFields>. DOI: 10.5281/zenodo.3739563.
- [9] Bicket (2020), [Python 3], <https://github.com/icbicket/SpectrumImageAnalysisPy>. DOI: 10.5281/zenodo.807763.
- [10] Bicket *et al.*, *Microscopy*, **67**, suppl_1, 2018.

1:45 PM EQ05.18.03

Vivid Colour Generation from Disordered Plasmonic Networks with Material Insensitivity [Changxu Liu](#)¹, Peng Mao^{2,3}, Fengqi Song⁴, Min Han⁴, Richard Palmer⁵, Shuang Zhang^{2,3} and Stefan A. Maier^{1,6}; ¹Ludwig-Maximilians-Universitaet Muenchen, Germany; ²University of Birmingham, United Kingdom; ³The University of Hong Kong, Hong Kong; ⁴Nanjing University, China; ⁵Swansea University, United Kingdom; ⁶Imperial College London, United Kingdom

Disordered nanostructures are ubiquitous in Nature, usually generating white or black colours due to their broadband optical response and robustness to perturbations. By manipulating the optical environment, we are able to tune the disordered plasmonic networks from broadband absorption to band-limited reflection through deterministic control of the coupling to an external cavity, producing rainbow-like colours at will [1]. Counterintuitively, fabrication imperfections (intrinsic disorder) can be harnessed as a beneficial factor to improve the purity of structural colours. More surprisingly, the disorder can disentangle optical responses and material prosperities (refractive indices), in sharp contrast with the traditional belief that optical responses vary with the material. With the assist of random scattering inside disordered structures, the same colour is achieved by metallic nanostructures composed of different noble metals including gold, silver, palladium and platinum [2]. Not limited to fundamental physics, the proposed platform may inspire novel applications ranging from Raman spectroscopy, nonlinear optics, photocatalysis.

[1] P. Mao, C. Liu, F. Song, M. Han, S.A. Maier, S. Zhang, "Manipulating disordered plasmonic systems by external cavity with transition from broadband absorption to reconfigurable reflection", *Nature Communications* 11, 1538 (2020).

[2] P. Mao, C. Liu, Y. Niu, F. Song, R. E. Palmer, M. Han, S. A. Maier, S. Zhang, "Disorder-Induced Material-Insensitive Optical Response in Plasmonic Nanostructures: Vibrant Structural Colors from Noble Metals", *Advanced Materials*, 202007623 (2021).

2:00 PM EQ05.18.04

Observation of Hyperbolic Polariton Vortices [Mingsong Wang](#)¹, Guangwei Hu^{1,2} and Andrea Alu^{1,3,4}; ¹CUNY Advanced Science Research Center,

United States; ²National University of Singapore, Singapore; ³Graduate Center of the City University of New York, United States; ⁴City College of the City University of New York, United States

Light can hybridize with low-dimensional materials, forming half-light-half-matter quasiparticles known as polaritons, featuring deeply subwavelength field confinement and broadband responses from terahertz to visible and infrared range. Among them, hyperbolic phonon polaritons (HP²) in natural materials, especially anisotropic van der Waals (vdW) crystals, are uniquely interesting. Their hyperbolicity originates from the drastic difference in atom interaction strength between in-plane covalent bondings and out-of-plane vdW bondings, and it can support large momentum for enhanced light-matter interactions. Based on these features, directional propagation and dispersion engineering of HP² have been demonstrated in hexagonal boron nitride (hBN) and α -MoO₃, facilitating super-resolution focusing and imaging, canalization, molecular sensing, reconfigurability, and other polariton applications. However, current state-of-the-art discoveries in HP² have been mostly based on studying the amplitude of polaritons, while other degrees of freedom, such as nontrivial geometric phase, remain largely unexplored. Surface plasmon polaritons (SPPs), a counterpart of phonon polaritons in the visible and near-infrared range, have gained more controllability over their phases, as additional degrees of freedom. In particular, a plasmonic vortex featuring orbital angular momentum (OAM) with spiral phases has been shown to support a large number of states in Hilbert space, thus offering the potential to increase the capacity of optical communication networks. Plasmonic OAMs can also couple to the spin of excitation, inducing spin-orbit interactions, enabling spin-controlled plasmonic applications such as unidirectional propagation, spin-locked optical vortex generation, and chiral information detection. However, plasmonic materials act as conductors in the mid-infrared (mid-IR) range, and graphene, which supports infrared plasmons, has a limited light-matter interaction efficiency due to its atomic thickness. Herein, we report mid-IR deep-subwavelength HP²Vs with high tunability in pristine hBN flakes. Our system is composed of a substrate gold disk with Archimedean spiral shapes to launch HP² in hBN. Via scattering-type scanning near-field microscopy (s-SNOM), HP²Vs are observed in real space, and the spin-orbit interaction and high tunability of HP²V are accordingly demonstrated. Our results facilitate effective optical spin-orbit interaction, super-resolution sensing and imaging, enhanced light-matter interaction, and particle manipulation in the mid-IR regime.

2:15 PM EQ05.18.05

Magnetic Dipole Emission and Effect of Gap Plasmons in Metal-Dielectric-Metal Structures MD Afzalur Rab¹, John N. Munga¹, Natalia Noginova¹ and Maxim Durach²; ¹Norfolk State University, United States; ²Georgia Southern University, United States

Gap plasmons allow strong optical field confinement, and has many promising applications in plasmonic circuitry, nonlinear optics, sensing etc. In this work, we study both flat and profile modulated three layers sandwich-like structures made of external plasmonic metal layers and a dielectric layer. The excitation of gap plasmons at specific thicknesses of the intermediate layer is predicted with COMSOL simulations. Introducing Eu³⁺ emitters into the dielectric layer, we show that such structures can provide strong control on magnetic and electric dipole emissions and radiation patterns. The experimental structure is fabricated using thermal evaporation of metal and spin coating of dielectric layer. A clear conformity between experimental observations and theoretical predictions is observed.

SESSION EQ05.19: Metasurfaces and Metamaterials III
Session Chairs: Viktoriia Babicheva and Yu-Jung Lu
Monday Afternoon, December 6, 2021
EQ05-Virtual

4:00 PM *EQ05.19.01

Flat Optics for Dynamic Wavefront Manipulation Mark L. Brongersma; Stanford University, United States

Since the development of diffractive optical elements in the 1970s, major research efforts have focused on replacing bulky optical components by thinner, planar counterparts. More recently, dynamic flat optics has been gaining importance and new opportunities are emerging for dynamic wavefront manipulation. I will discuss efforts to realize electrically-tunable flat optics based on metasurfaces that employ nanomechanics, electrochemistry, free-carrier dispersion, phase change materials, and atomically-thin semiconductors.

4:30 PM EQ05.19.02

Defect Engineered Molybdenum Sulfide Nanosheets as Catalysts for Dye-Sensitized Solar Cells Kit Sze, Tyrome Fowlkes, Chiedozie Ogueri, Alexander Nanor, Solomon Tadesse, Saroj Pramanik and Yucheng Lan; Morgan State University, United States

Molybdenum sulfide (MoS₂) shows strong optical absorptions in UV-vis electromagnetic spectrum and high photo-corrosion tolerance, being an excellent photovoltaic and photocatalytic material. Here MoS₂ nanosheets were prepared and defect engineered to tune optical properties. Their microstructures were characterized by diffractions, electron microscopies, and optical methods. The defected nanosheets were then fabricated as electrode catalysts in I³/I⁻ based dye-sensitized solar cells (DSSCs). The defects in MoS₂ nanosheets enhanced the photoelectric conversion efficiencies of the DSSCs. The work is partially supported by DOE grant DE-FE0031906.

4:45 PM EQ05.19.03

WITHDRAWN 12/6/2021 EQ05.19.03 Shape-Effect on Quantum Confinement in Alloy Quantum Dots as Applied to Photovoltaics Nicholas Ulizio and Zubaer M. Hossain; University of Delaware, United States

Alloy quantum dots (aQD) represent a new class of nano-materials whose electron confinement is determined not exclusively by size, but also by composition field. While homogeneous quantum dots have been more widely explored for applications in photonics, optoelectronics, and photovoltaics, aQDs remain less investigated. The differences in both size and composition field across differently shaped aQDs lead to differences in material properties. These variations in material properties present compelling potential applications, specifically in the field of energy generation and photovoltaics. This is primarily because of the complexity in characterizing nonuniform fields and establishing the correlation between inhomogeneity and confinement. In order to effectively analyze the varied electron confinement of these materials, we employ a combination of density functional theory based quantum simulations, and finite element analysis based k.p calculations to determine the electron energy levels for a number of uniform and nonuniform physical variables. As a part of the analysis, composition maps were constructed for each of the four different aQD shapes, namely, the steep cone, normal cone, hut, and dome. Each of these composition's maps was fitted with an analytical function that was then used to analyze the quantum confinement and general electronic properties of the aQDs. Results show that a generic expression for all four of the aQDs exists such that modification of this equation allows each of the disparate aQDs to be modeled.

The steep cone shaped aQD with a 15° sidewall angle corresponds to a composition map where spatial decay occurs from the tip of the cone to the bottom. The normal cone shaped aQD exhibits a similar behaviour, but the sidewall angle is instead 30°, and the fitting function is modified to a product of a quadratic and a linear function. For the hut shaped aQD, the composition map takes the shape of a “hut” where decay occurs from the top edges towards the bottom edges in a non-linear fashion. For the final shape, the dome, spatial decay emanates from the top tip of the dome. The dome is fitted by two sidewalls per side that have angles of 11° and 30° respectively.

For each of the quantum dot shapes above, composition maps obtained are independent of size to determine the singular effects of the compositional variation. Our results suggest that inhomogeneity in composition field has a consequential role in controlling the confinement energy levels, with the highest ground state confinement in the steep cone shape, and the lowest in the hut shape. Thus, the shape of aQDs can play a critical role in tailoring effective electronic behavior. Furthermore, a larger alloy quantum dot can behave electronically like a smaller quantum dot, if the composition field is inhomogeneous. By engineering quantum dots with certain composition maps, the photon absorption properties of the respective quantum dot can thus be tailored substantially. In particular, the most apparent application of this is to solar cells and spintronics; engineering the properties of the quantum dot allows us to increase the absorption efficiency of the photovoltaic cell, which directly leads to greater potential for green energy generation.

5:00 PM EQ05.19.04

Late News: Edge Effect on Light Distribution in Solid State Light Emitting Device Kishore Natarajan, Adam Samuel and [Yue Kuo](#); Texas A&M University, United States

A novel Solid State Incandescent Light Emitting Device (SSI-LED) that was fabricated from the MOS capacitor with the high-k gate dielectric was invented and investigated by Kuo's group (1). Upon the application of a gate voltage to the device, light emission is observed. The principle behind the light emission is the thermal excitation of nano-sized conductive paths, i.e., nanoresistors, formed after the breakdown of the dielectric layer (2). Previously, the light emission from nanoresistors across the gate electrode area was assumed to be uniform (3). However, some experimental results (4,5) showed that the density of nanoresistors near the edge of the gate was larger than that away from the edge. In this paper, authors utilize the Finite Element method to explore the reason behind the formation of the denser nanoresistors at the circumferential edge of the gate electrode. The current density distribution, which is the foundation behind the generation of the large number of nanoresistors from the dielectric breakdown process, has been simulated using the COMSOL Multiphysics software package and the results are depicted using MATLAB and Python codes. The area circumferential to the gate electrode has a larger density of nanoresistors than the rest of the area due to the accumulation of larger amount of charge carriers before the dielectric breakdown. Possible factors contributing to the uneven distribution of the nanoresistors, such as the dielectric and substrate properties, have been investigated. The substrate-to-gate electrode area ratio has been identified as the key factor in determining the width of the periphery area with the high density of nanoresistors.

1. Y. Kuo and C.-C. Lin, *Appl. Phys. Letts.*, **102**(3), 031117 (2013).
2. Y. Kuo and C.-C. Lin, *Solid State Electronics*, **89**, 120 (2013).
3. A. Shukla and Y. Kuo, *ECS Trans.*, **97**, 69-77 (2020)
4. C.-C. Lin and Y. Kuo, *ECS J. Solid State Sci. Technol.*, **3**, Q182-Q189 (2014).
5. Y. Kuo and C. C. Lin, *ECS Solid State Lett.*, **2**, 59-62 (2013).

5:15 PM EQ05.02.03

Poly(3-hexylthiophene)s with Terminal N-Heterocyclic Carbenes as Robust and Conductive Ligands to Stabilize of Gold Nanoparticles [Franziska Lissel](#)^{1,2}; ¹Leibniz Institute for Polymer Research, Germany; ²Dresden University of Technology, Germany

Gold nanoparticles (Au NPs) have unique surface plasmonic resonances (SPR) and promise a broad variety of optical applications in sensors and imaging, and combining them with organic components can give electronically functional hybrid materials [1]. In general, protecting surface ligands are required to stabilize the Au NPs and prevent their irreversible aggregation. The ligands carry one or more functional anchor groups with a high affinity for gold. Thiols are the most ubiquitously used anchor group, yet the thermal instability and comparably low conductance of the S–Au contact limit the applications of the resulting Au NPs. N-heterocyclic carbenes (NHCs) have been receiving much interest in surface chemistry as an high-performing alternative to sulfur-based ligands: The NHC–Au linkage shows excellent stability under conditions that destroy the S–Au bond (e.g. high temperature, variable pH, and electrochemical redox), and is furthermore highly conductive.

We use NHC anchors as robust and conductive anchors to bind charge-conducting conjugated polymers (CPs) to Au NPs to obtain electronically functional hybrid materials.

Three different Br-NHC-Au-X (X=Br, Cl) complexes with were synthesized in multiple steps. The complexation saturates and stabilizes the NHC, the bromo function on the benzimidazole ring can be used to further functionalize the complexes. 2-Bromo-3-hexyl-5-iodo-thiophene was converted to a Grignard monomer with isopropyl-magnesium chloride, and used for a chain-growth Kumada polymerization starting from the active aryl bromide on the NHC complexes. Using a Ni-bipyridyl complex as intermediate catalyst, P3HTs functionalized with the NHC-Au-X were prepared. The Mn values are in the range of 10k, the head-to-tail regioregularity was visible in ¹H NMR. ¹H MNR and MALDI MS were used to confirm the terminal NHC units, but also showed unmodified chains due to the tendency of the Ni catalyst to dissociate from the initiators into the reaction solution and initiate the polymerization without functional group.

Direct reduction with NaBH₄ directly gave Au NPs with P3HT as surface ligands. For these P3HT-NHC@ Au NPs, TEM images showed spherical particles with average diameters of 3.2, 2.5, and 6.5 nm, respectively. The presence of the NHC on the surface was confirmed by XPS. The P3HT-NHC@ Au NPs have a remarkable thermal stability up to 24 h in 100 °C toluene solutions, while Au NPs stabilized by sulfur-based PEG fully degrade under the same conditions. Also, continuous CV scans revealed only a slight decay of peak current after 50 cycles, indicating the good electrochemical stability of P3HT-NHC@ Au NPs.

To investigate the conductive linker, electrochromism (EC) experiments were carried out. P3HT is electrochromically active, and one can assume that binding the polymer to Au NPs via a conductive NHC anchor group will increase the electrochromic response speed, allowing to estimate the organic/inorganic electron transfer of P3HT-NHC@ Au NPs. We found that blending 10% of P3HT-NHC@ Au NP into a P3HT-NHC-Au films improves the responsive speed significantly, from 1.21/1.05 s for neat P3HT-NHC-Au to 0.79/0.52 s for the blend.

This is consistent with DFT calculations (B3LYP/6-31g(d,p) for H, C and S; B3LYP/lan12dz for Au) on a simple model compound (NHC linking tetrathiophene to a single Au⁰ atom): The electron cloud was found to be delocalized over the gold atom and the NHC in the HOMO orbit, suggesting an efficient electron transfer between Au NP and the conjugated P3HT polymer.

- [1] Steiner, Lissel, Fery, Lauth, Scheele: *Angew. Chem. Int. Ed.* **2021**, 60 (3), 1152.
[2] Sun, Zhang, Simon, Steiner, Schubert, Du, Qiao, Fery, Lissel: *Angew. Chem. Int. Ed.* **2021**, 60 (8), 3912.

5:30 PM BREAK

SESSION EQ05.20: Poster Session III
Session Chairs: Viktoriia Babicheva and Yu-Jung Lu
Monday Afternoon, December 6, 2021
EQ05-Virtual

9:00 PM EQ05.20.01

Detection of DNA Bases and Monitoring ssDNA Hybridization by Noble Metal Nanoparticles Decorated Graphene Nanosheets as Ultrasensitive G-SERS Platforms Sanju Gupta; University of Central Florida, United States

Surface- and graphene-enhanced Raman spectroscopy (SERS and G-SERS) are attractive analytical techniques for the detection of chemical and biological molecules at a single-molecule level registering their chemical fingerprints. Graphene-mediated or G-SERS boosted this phenomenon producing signal enhancement from both electromagnetic (EM) and chemical (CE) mechanisms. Graphene oxide (GO) nanosheets coated with silver; Ag (30 nm) and gold; Au (40 nm) nanoparticles were developed smart array of platforms for direct detection and differentiation of DNA bases: Adenine (A), Cytosine (C), Guanine (G), Thymine (T) as well as environmental relevant β -carotene (β -C) and malachite green (MG) biomolecules. The size and interparticle gap of metal nanoparticles were controlled via dispersion and loading on GO to achieve optimal enhancement factors. These substrates were characterized by electron microscopy, atomic force microscopy, and Raman spectroscopy. The Raman spectra consisted of discrete bands characteristic of (A: 732.8 cm^{-1} ; C: 792 cm^{-1} ; G: 658 cm^{-1} ; T: 796 cm^{-1} ; β -C: 1416 cm^{-1} ; MG: 1174 cm^{-1}), which represent molecular normal modes of vibration and serve as a fingerprint of three-dimensional structure, intramolecular interaction and steady-state dynamics of biomolecule ensemble. The GO-decorated nanoparticles are capable of sensitive biomolecular detection over a broad concentration range of 100nM-100mM with the limit of detection (LOD) noted at <1ppm for A, C, G, T, β -C, and MG. Moreover, the experimental results illustrated five to six-order magnitude signal enhancement in the following order: GO/Ag30>GO/Au40>Ag30>Au40>GO. Moreover, ssDNA probe and complementary strand target DNA were monitored simultaneously during hybridization on the same substrates assigned confidently to base, local structure, and global conformation of dsDNA. The experimental findings suggest (1) a strong GO-nanoparticle coupling leads to interfacial hybridization (charge transfer), polarization, and molecular orientation, and (2) it will help to design ultrasensitive G-SERS platforms covering a range of inorganic nanoparticles and nanostructured organic surfaces for a wealth of biomedicine and environmental applications.

9:05 PM EQ05.20.02

Combined Theoretical and Experimental Study Of Optoelectronic Properties in Transition Metal Nitrides Muhammad U. Javed^{1,2}; ¹National Taiwan University, Taiwan; ²Academia Sinica, Taiwan

We Investigated electronic structure and optical properties of transition metal nitrides i.e. TiN, HfN, ZrN, and their composition, TiZrN and TiHfN by using density functional theory and experimental techniques. These metallic materials are envisaged as alternative plasmonic materials in preference with comparison to conventional noble metals from optical to the infrared wavelength range. Band structures and density of states are calculated in addition with bulk plasma frequency, absorption-extinction coefficients using ab initio procedure. Evaluation of calculation along experimental results for frequency dependent dielectric functions contributed by their interband and intraband transitions depicted optical losses in these refractory materials. Aforementioned materials with optimized thin films were deposited on suitable substrates of MgO and Si. These stoichiometric thin films were characterized to measure real and imaginary part of dielectric function by spectroscopic ellipsometry (SE). From quantitative analysis of measured and calculated quality factors for localized surface plasmon resonance (Q_{LSPR}) and surface plasmon polaritons (Q_{SPP}) it is confirmed that HfN, TiN, TiZrN, TiHfN and ZrN possess excellent mechanical, chemical, and optical properties to be used as an alternative plasmonic material of gold in the visible and near-infrared spectral regions respectively. The photonic energy absorbed by these material is far less than gold (Au) at optical frequency, calculated and demonstrated as concrete evidence in absorption spectrum.

9:10 PM EQ05.20.03

Efficiency Increasing of Photodetectors Based on Two-Dimensional Semiconductors Using Ordered Plasmonic Elements Arseniy M. Buryakov¹, Sergey Lavrov², Andrey Guskov², Artur Avdizhiyan², Rinat Galiev¹, Anastasiya Gorbatova² and Elena Mishina²; ¹V.G. Mokerov Institute of Ultra High Frequency Semiconductor Electronics of RAS, Russian Federation; ²RTU MIREA, Russian Federation

The necessity of increasing the optical radiation absorption in two-dimensional semiconductors significantly slows down the possibility of their technological implementation in modern photovoltaic and photosensor applications. In an unmodified transition metal dichalcogenides monolayer, the optical absorption in the visible range does not exceed 7%, which is extremely low for generating a sufficiently high photoelectric effect. There are several approaches, among which the most effective is the use of low-dimensional plasmonic metallic elements. Such structures make it possible to generate local amplification of optical radiation near their surface, leading to a significant increase in absorption in adjacent semiconductor structures. Here we demonstrate a successful approach for increasing absorption in two-dimensional transition metal dichalcogenides films using ordered matrices of plasmonic elements of various shapes. The monatomic layer WS_2 was used as an active element. To achieve the highest efficiency of photodetectors, theoretical modeling of the plasmonic structures was made. Using this simulation, the optimal parameters of silver nanostructures were determined. Based on the obtained results, a series of experimental photodetectors was made. It was found that the created plasmon detectors have an almost tenfold increase in photosensitivity in comparison with conventional structures. It is shown that such an approach makes it possible to develop polarization-sensitive and spectrally selective optical devices. Moreover, their performance characteristics can be changed in a wide range by varying the geometric parameters of the plasmonic structures.

This work was supported by the Russian Science Foundation No. 19-72-10165. E.D. M. acknowledges the support of the Ministry of Education and Science of the Russian Federation (state task No. FSFZ-0706-2020-0022).

9:15 PM EQ05.20.04

Differential Enhancement of 2D Raman Band Intensity of Decoupled Multilayer Graphene Mediated by Surface Plasmons from Ag Nanoparticles Suchithra P¹, S Walia¹, U Mogera^{1,2} and Giridhar U. Kulkarni^{1,2}; ¹Centre for Nano and Soft Matter Sciences, India; ²Jawaharlal Nehru

Centre for Advanced Scientific Research (JNCASR), India

The coupling physics of localised surface plasmons of metal nanoparticles and phonons of graphene has attracted a great interest in the last few years. Surface-Enhanced Raman Scattering (SERS) is an effective method to probe this effect, where the intensity of the graphene Raman peaks are enhanced by the near field plasmonic effect originating from metal nanoparticles. In this work, we have examined the plasmonic property of the interface of a twisted multilayer graphene system and Ag nanoparticles (~ 100 nm). The twisted graphene produced in the laboratory has been established to possess decoupled layers leading to strong 2D bands [1]. The presence of plasmonic interface is found to cause relative enhancement of the 2D band intensity, the extent of enhancement varying with the nature of the substrate. Further, we have studied the particle size and laser energy dependence on this differential enhancement.

[1] Mogera, U., Dhanya, R., Pujar, R., Narayana, C., & Kulkarni, G. U. (2015). Highly decoupled graphene multilayers: turbostraticity at its best. *The journal of physical chemistry letters*, 6(21), 4437-4443.

9:20 PM EQ05.20.07

Plasmonic Photothermal Effects of Cotton Fabrics Densely Modified with Metal Nanocrystals Nobuko Fukuda, Muneyasu Suzuki, Kouji Suemori and Konami Izumi; National Institute of Advanced Industrial Science and Technology, Japan

Localized surface plasmon resonance (LSPR) brings about some interaction between metal nanostructures and the surrounding materials. Generation of hot electrons through LSPR allows a lot of applications such as photothermal manipulation of materials surrounding the metal nanostructures as well as promoting photovoltaics and photocatalysis.[1-5] Fabric is very familiar with us in our daily life. We focus on it as an attractive substrate to densely modify metal nanostructures with the viewpoint of the large surface area, chemical resistant property, and flexible workability. In this study, we prepared a gold nanostructure-modified fabric in such a way of dyeing and investigated the photothermal effect on the fabric.

Immersion of tetrachloroauric ions-adsorbed cotton fabric in a heated aqueous solution of sodium citrate gave dark purple color. The coloration is due to strong plasmonic absorption through densely formation of isolated gold nanostructures on the cotton fabric. The X-ray diffraction pattern of the gold nanostructure-modified cotton fabric (Au-cotton) shows peaks assigned as Au(111) and (200) as well as cellulose. The Au-cotton has an absorption band in visible light region with a peak around 550 nm. Irradiation of visible light to the Au-cotton causes the temperature rise at the surface. The largest temperature rise per unit given photon number occurs by irradiation at 550 nm. The rising rate to the light power at 550 nm was estimated to be ca. 0.5 K/mW between 293 and 343 K. The results of the dependence of the temperature rise on the irradiation wavelength suggest that the temperature rise comes from generation of hot electrons based on LSPR.

We demonstrate an interaction between the gold nanocrystals and the surrounding material as an example of the photothermal effect. The Au-cotton soaked with paraffin was placed on a glass plate at room temperature and irradiated with visible light. The paraffin in the Au-cotton melted and seeped out onto the glass surface attributed to the temperature rise of the Au-cotton based on LSPR. When the light irradiation was stopped, the paraffin solidified. Consequently, the Au-cotton adhered to the glass surface.

[1] A. Furube, S. Hashimoto, NPG Asia Mater. 2017, 9, e454.

[2] G. Liu, K. Du, J. Xu, G. Chen, M. Gu, C. Yang, K. Wnag, H. Jakobsen, J. Mater. Chem. A 2017, 5, 4233-4253.

[3] J. Li, S. K. Cushing, F. Meng, T. R. Senty, A. D. Bristow, N. Wu, Nat. Photonics 2015, 9, 601-608.

[4] H. Tang, C.-J. Chen, Z. Huang, J. Bright, G. Meng, R.-S. Liu, N. Wu, J. Chem. Phys. 2020, 152, 220901.

[5] T. E. Tesema, B. Kafle, T. G. Habteyes, J. Phys. Chem. C 2019, 123, 8469-8483.

9:25 PM EQ05.20.10

Bio-Inspired Porphyrin Hybrids for Enhanced Solar Harvesting Jou Lin, Zicheng Deng, Mengyao Lyu and Donglu Shi; University of Cincinnati, United States

One of the key requirements in solar harvesting is to have strong absorptions in the NIR region as the solar spectra provide nearly 50% of the infrared irradiation. In some particular photonic material applications, transparent thin films are desirable especially in dye-sensitized solar cells, therefore requiring high average visible transmittance (AVT). We have developed and synthesized transparent photonic thin films based on a bio-inspired porphyrin compound chlorophyllin that typically exhibits two peaks respectively near 400 nm (blue-violet) and 700 nm (NIR) with a high AVT above 90%. To further enhance NIR absorptions, a unique porphyrin hybrid is developed with systematic additions of another porphyrin compound phthalocyanine with much stronger NIR absorptions. Phthalocyanine has more pronounced UV and NIR absorptions, but a narrower "optical window" as compared to that of chlorophyllin. We have found that congruent mixtures between chlorophyllin and phthalocyanine can result in broader NIR absorptions while maintaining the optical window between 400 and 650 nm. This will provide an ideal spectrum for a highly transparent but strongly UV/NIR absorbing characteristic. We report the optical properties of the porphyrin hybrids based on UV-vis and Raman spectroscopy. Also discussed is the operating mechanism underlying the thermal-photonic behaviors associated with the hybrid structures.

9:30 PM EQ05.20.11

Utilization of Co-Reduction Method in Fabrication of Au@Ag@Pt Multi-Shell Nanoparticles with a Granular Surface Anh T. Dao¹, Yuta Takeuchi², Hu-jun Lee², Ryo Teranishi², Hitoshi Kasai¹ and Kenji Kaneko²; ¹Tohoku University, Japan; ²Kyushu University, Japan

Noble metallic nanoparticles (NPs) become a great scientific and industrial interest due to their unique physicochemical properties, and play important roles for a number of catalytic applications, such as oxidation and reduction reactions, environmental catalyzes, fuel cells and energy storage. Among these, platinum NPs (Pt NPs) have been receiving large attention because they are the most efficient and common catalyst for both anodes and cathodes in fuel cells. Multi-metallic Pt-based NPs were reported for enhancement of catalytic properties in comparison to monometallic Pt NPs, while reducing the Pt consumption [1]. Although possessing such potentials, the synthetic techniques for multi-metallic NPs have not yet achieved the controllability over the NPs morphology and structure, unless going through complex reaction conditions. In this study, Au@Ag@Pt core@multi-shell NPs were synthesized in one-pot by facile co-reduction method, a combination of galvanic replacement reaction (GRR) and a co-reducing agent, to obtain a well-defined nanostructure with enhanced surface area of Pt towards catalytic applications. The as-synthesized NPs were found to have Au core covered by Ag-Pt double-shell, which contained a degree of hollows with the inner surface composed of both Ag and Pt, while the outer surface composed of granular Pt. The shell-formation mechanism will also be discussed in aspect of competition role between GRR and co-reduction reactions, under the influence of unique charge transfer effect from Au core to Ag middle shell [2]. The NPs were characterized with UV-Vis, DLS, and especially high-end electron microscopic techniques, including ADF-STEM and EDS elemental mapping. Through understanding the complexity of the reaction mechanism, one can expect to design and fabricate various types of trimetallic nanoparticles with intricate structures, thus further expanding their nanotechnology and applications.

[Acknowledgements] This work was performed under the Cooperative Research Program of "Network Joint Research Center for Materials and Devices", and partially supported by JSPS KAKENHI JP19K15388 to A.T.N.D and JP18K18953 to K.K.

[References] [1] Y. Li et al. J. Mater. Chem. A 3 (2015) 368; [2] Anh T.N. Dao et al. Appl. Phys. Lett. 99 (2011) 073107.

9:35 PM EQ05.20.12

Structural Colors in Plasmonic Hafnium Nitride Metasurfaces Zong-Yi Chiao¹, Yu-Chia Chen¹, Jia-Wern Chen¹, Yu-Hung Hsieh¹, Yu-Cheng Chu², Jingwei Yang², Tzu-Yu Peng², Li-Chien T. Chang² and Yu-Jung Lu^{1,2}; ¹Academia Sinica, Taiwan; ²National Taiwan University, Taiwan

Most common plasmonic materials such as silver, gold, and aluminum have been proven to have excellent localized surface plasmon resonance (LSPR). However, the research for hafnium nitride (HfN) plasmonic nanostructures, one of the alternative plasmonic materials with high chemical stability, high melting point ($T \sim 3583$ K), still remains unexplored. In this work, we experimentally demonstrated a full-color plasmonic color filter based on HfN metasurfaces with a high melting point. By tuning the LSPR the optical response can be controlled. Thus, we demonstrated full-color imprinted color pixel including red, green, blue, and black in the subwavelength scale. By using finite-difference time-domain (FDTD) simulation, the LSPR can be tuned by the designed HfN nanodisk structure with a diameter varied from 80 nm to 640 nm. The key reason to achieve full-color plasmonic resonance is the HfN has a high bulk plasmon frequency around 3.1 eV ($\lambda_p = 400$ nm). This result provides evidence that refractory plasmonic HfN metasurface is applicable in the full-visible spectrum, thus can pave the way in the thermostable optoelectronic applications.

10:00 PM BREAK

SESSION EQ05.21: Metasurfaces and Metamaterials IV
 Session Chair: Yu-Jung Lu
 Tuesday Morning, December 7, 2021
 EQ05-Virtual

8:00 AM *EQ05.21.02

From Structured Light to Structured Dark with Metasurfaces Federico Capasso; Harvard University, United States

Recent advances by my group on structuring the wavefront of light and on new optical singularities are presented. Metasurfaces suffer from limited performance and efficiency when multiple functions with large deflection angles are required because the non-local interactions due to optical coupling between nanostructures are not fully considered. Supercell metasurfaces can achieve multiple independent optical functions at arbitrary large deflection angles with high efficiency. In one implementation the incident laser was simultaneously diffracted into Gaussian, helical and Bessel beams over a large angular range. A compact wavelength-tunable external cavity laser with arbitrary beam control capabilities – including beam shaping operations and the generation of freeform holograms has also been demonstrated utilizing supercell metasurfaces.

The majority of structured light work has been concerned with shaping the wavefront in the plane transverse to the propagation direction. Multiple degrees of freedom, such as spin and optical angular momentum, can be controlled simultaneously along the optical path with a single metasurface by sculpting the incident waveform into an ensemble of co-propagating modes with different longitudinal wavevectors which beat along the direction of propagation, thereby modulating the resulting envelope at-will via multimode interference. Note that replicating this behavior with bulk polarization optics or SLMs is inherently cumbersome (if not impossible) as the former can only modify incident polarization globally whereas the latter operates on one incident polarization at a time. Two classes of metasurfaces have been realized for structuring light along the propagation direction: namely: polarization-switchable plates that couple any pair of orthogonal polarizations to two vortices in which the magnitude and/or sense of vorticity vary with propagation, and multifunctional plates that can structure both spin and orbital angular momentum, independently, along the optical path while operating on incident light of any polarization. Compact and integrated devices of this kind can be exploited in light-matter interaction and imaging and may facilitate new applications that are not accessible with other wavefront shaping tools.

Optical phase singularities are zeros of a scalar light field. The most systematically studied class of singular fields is vortices: beams with helical wavefronts and a linear (1D) singularity along the optical axis. Beyond these common and stable 1D topologies, a broader family of zero-dimensional (point) and two-dimensional (sheet) singularities can be engineered. Sheet singularities are realized by maximizing the field phase gradient at the desired positions. Furthermore, by applying an analogous procedure to the full vectorial electric field, one can engineer paraxial transverse polarization singularity sheets. As validation, the experimental realization of phase and polarization singularity sheets with heart-shaped cross-sections using metasurfaces has been realized. Singularity engineering of the “dark” enables new degrees of freedom for light-matter interaction and can inspire similar field topologies beyond optics, from electron beams to acoustics.

Contributions by Christina Spägle, Michele Tamagnone, Ahmed H. Dorrah, Soon Wei Daniel Lim, Joon-Suh Park, Maryna L. Meretska, Dmitry Kazakov, Marcus Ossianer, Marco Piccardo, Noah A. Rubin, and Aun Zaidi are gratefully acknowledged.

8:30 AM *EQ05.21.03

High-Performance Metasurfaces for Wavefront Engineering Amir Hassanfiroozi, Chia-Hsiang Lin, Zhao-Ting Lin and Pin Chieh Wu; National Cheng Kung University, Taiwan

Metasurfaces have attracted a lot of attention because of their great capability to manipulate the attributes of an electromagnetic wave in demand. Thus, nanophotonic metasurfaces provide great flexibility in light management that highly benefits the development of low-profile optical systems. However, metasurfaces severely suffer from high optical losses that highly limit their optical performance. In addition, optical modulation in metasurface unit elements relies on strong resonances at a sub-wavelength resolution. It leads to a significant amplitude variation when a broad phase shift range is obtained. Such amplitude-phase covarying response can further degrade the optical performance of metasurfaces. In this talk, I will present two strategies to realize high-performance metasurfaces. Firstly, I will present a design method that enables a significant enhancement of the optical efficiency in a hybrid plasmonic metasurface. By integrating a solid nano-structure with its inverse complementary, we realized a plasmonic metasurface with a circular cross-polarization conversion efficiency higher than 50% in transmission at near-infrared wavelengths. Such high optical performance metasurface is achieved by simultaneously exciting the electric, magnetic, and toroidal multipolar modes, which satisfies the generalized Kerker condition and improves the transmission efficiency. We further demonstrate a couple of metasurface-based components such as beam deflector and flat focusing lens with record operating efficiency based on the proposed metasurface. Secondly, I will report an unsupervised genetic-type tree search algorithm in a virtual space wherein an automatic inverse design of metasurfaces is achieved with low computational complexity. With the developed method, we design and characterize beam deflection/steering metasurfaces, which are capable of deflecting normally incident light into target directions with minimal sidelobes; other functions of metasurfaces could also be achieved by revising the learning criterion in the virtual space. Due to the co-optimization of amplitude and phase shift, the inversely-designed metasurface possesses higher optical directivity than the forward-designed metasurface.

9:00 AM EQ05.21.04

Efficiency Enhancement of Spin Hall Effect of Light Using Metamaterials Minkyung Kim and Junsuk Rho; Pohang University of Science and Technology, Korea (the Republic of)

Spin Hall effect of light (SHEL) refers to a transverse and spin-dependent displacement of light at a planar optical interface. The SHEL is a universal phenomenon that can be readily observed in any interface, but has been neglected mostly due to the subwavelength scale of the shift. Therefore, enhancement of the shift up to wavelength scale and even beyond has been the main trend. However, the enhancement of the shift generally entails degradation of efficiency below 1%. To overcome the limitation, the simultaneous enhancement of the shift and efficiency under horizontal polarization was proposed and demonstrated in the microwave regime by using anisotropic impedance mismatching [1]. Here, we present our second proposal to achieve the large SHEL with high efficiency [2]. In contrast to the first approach, both the shift and efficiency is enhanced under arbitrarily polarized source due to the degenerate reflection coefficients [3]. The principle is a total reflection, in which both s- and p-polarized light is reflected at a denser-to-sparsier interface with unity amplitudes. The simultaneous enhancement of the shift and efficiency is demonstrated experimentally using a near-zero-index metamaterial in the microwave regime. The large SHEL with near-unity efficiency under an arbitrarily polarized source will enable highly efficient and versatile devices with spin-selective functionalities. Furthermore, we extend the recent attempts to achieve the large and efficient SHEL, which have been limited only to the microwave, to the optical regime [4]. The large SHEL with high efficiency can be also realized in the near-infrared wavelength by using an all-dielectric metasurface. A capability of metasurfaces to modulate complex transmission coefficients can be used to design a system that supports the large SHEL with high efficiency. Our recent progress in demonstrating the SHEL using Stokes polarimetry measurement will be introduced.

References

- [1] M. Kim *et al.* Spin Hall effect of light with near-unity efficiency in the microwave. *Laser & Photonics Reviews* **15**, 2000393 (2021)
- [2] M. Kim *et al.* Total reflection-induced efficiency enhancement of spin Hall effect of light. *ACS Photonics* (In review)
- [3] M. Kim *et al.* Spin Hall effect under arbitrarily polarized or unpolarized light. *Laser & Photonics Reviews* **15**, 2100138 (2021)
- [4] M. Kim *et al.* Spin Hall effect of light with high efficiency in optical wavelengths using an all-dielectric metasurface (In preparation)

9:15 AM EQ05.21.05

Near Infrared Absorption and Photocurrent Enhancement by Coupled Toroidal Dipole Modes in Silicon Metasurfaces Hiroaki Hasebe¹, Hiroshi Sugimoto^{1,2} and Minoru Fujii¹; ¹Kobe University, Japan; ²JST PRESTO, Japan

High index dielectric nanostructures have unique optical responses driven by the Mie resonance, offering a variety of functionalities for directional nanoantennas, metalenses, etc. Recently, in addition to the electric and magnetic multipole resonances, toroidal multipole resonances have attracted much attention as a third multipole family. The lowest-order toroidal dipole (TD) mode is composed of a current loop along a meridian of a torus, which leads to strong confinement of an electromagnetic field in a dielectric nanostructure [1]. The enhanced electromagnetic field associated with the TD resonance has been exploited for the enhancement of nonlinear optical responses, [2] photocatalytic activities, [3] etc.

We have studied a low aspect ratio circular silicon (Si) nanodisk, e. g., ~500 nm in diameter and ~50 nm in thickness, as a nanoantenna supporting the TD mode, and showed that a metasurface composed of the two-dimensional hexagonal array supports high quality (Q) factor TD resonances arising from coupling of the TD modes of individual nanodisks. [4] The high-Q coupled TD resonance results in narrow-band absorption enhancement in the wavelength range, where Si is almost transparent. This suggests that the Si metasurface supporting the coupled TD resonance enhances responsivity of a Si photodetector in a specific narrow wavelength range depending on the structural parameters.

In this work, we produce a Si nanodisk array metasurface having a coupled TD resonances and demonstrate that the resonant absorption results in the enhancement of the photocurrent in the near infrared range, especially in the wavelength range below the bulk Si band gap. First, we explore the structural parameters of the metasurface by the FDTD simulations, and show that at maximum ~120-fold enhancement of the absorption compared to that of a flat Si film with the same thickness is possible. We reveal from the multipole decomposition that the strong absorption enhancement is due to TD modes having an enhanced electric field within a Si nanodisk (intra-nanodisk TD mode) and between Si nanodisks (inter-nanodisk TD mode). Finally, we fabricate Si nanodisk metasurfaces and demonstrate narrow-band enhancement of the absorption and photocurrent due to coupled TD resonances.

- [1] A. Miroshnichenko *et al.*, *Nature Communications*, **6**, 8069 (2015)
- [2] G. Grinblat *et al.*, *Nano Letter*, **16**, 7, 4635 (2016)
- [3] L. Hüttenhofer *et al.*, *ACS Nano*, **14**, 2, 2456 (2020)
- [4] H. Hasebe *et al.*, *Advanced Optical Materials*, **20**, 2001148(2020)

SESSION EQ05.22: Plasmonic Sensing

Session Chairs: Federico Capasso, Giulia Tagliabue and Pin Chieh Wu
Tuesday Morning, December 7, 2021
EQ05-Virtual

10:30 AM EQ05.22.02

Single-Base-Resolved and Millisecond SERS Sensing of DNA Oligonucleotides Using Gold Nanoparticle Dimers in Aqueous Suspension Nozomi Hagiwara, Keiko Esashika and Toshiharu Saiki; Keio University, Japan

Solid-state nanopore technologies have shown a great progress for developing single-molecule DNA sequencing, in which single-stranded DNA molecules passing through a nanoscale ion channel are observed by detecting current blocking signals. At present, nanopore ionic current detection enables discrimination of four bases (adenine, thymine, cytosine, and guanine) included in DNA, but it is much more challenging to identify chemically modified bases for epigenetic sequencing. Optical DNA sequencing based on surface-enhanced Raman scattering (SERS) is promising as an alternative method for spectroscopic identification of DNA bases. SERS utilizes extremely high field enhancement in a sub-nanometer volume (hot spot) of metal nanostructures to provide single-base spatial resolution and sensitivity. In this study, we develop a method to spontaneously form Au nanoparticle (AuNP) dimers, which sandwiches a single DNA oligonucleotide within a gap of less than 1 nm. SERS measurement of single AuNP dimers in aqueous suspension demonstrates single-base resolution obtained within a 10-ms measurement period.

We formed oligonucleotide sandwich AuNP dimers in aqueous suspension by using colloidal AuNPs with a diameter of 60 nm and oligonucleotides containing adenine (A) and cytosine (C) bases with a sequence of CCCCCCCCCCACCACCCCCCCCCC (12C1A12C; 25 mers length). The adsorption of oligonucleotides on AuNP surface and the formation of AuNP dimer was promoted by protonation of oligonucleotides, addition of salt, and incubation at elevated temperature. The conditions are carefully examined and optimized for enhancing the dimerization efficiency and for maximizing the probability

to find the oligonucleotide in the dimer gap, which should be minimized to obtain pronounced SERS activity and single-base resolution. The absorption spectrum of AuNP dimers, which were reproduced from the second band (dimer band) of gel electrophoresis separation after incubation and addition of BSPP into the AuNP dimer suspension, exhibits a large red shift of the longitudinal mode of AuNP dimer, demonstrating a strong coupling of AuNPs due to an interparticle gap smaller than 1 nm.

We performed micro-Raman measurements for oligonucleotide sandwich AuNP dimers under Brownian motion in aqueous suspension. The dimer suspension was diluted such that single dimer spectroscopy could be conducted. The measurement time was set to 100 ms while the dwell time of dimer in the observation volume was approximately 40 ms. By considering the fact that the AuNP dimer experiences rotational diffusion, the effective measurement time should be less than 10 ms. Among a number of Raman spectra obtained from single dimers, some exhibited a characteristic peak purely from adenine (734 cm^{-1}) while others purely from cytosine (800 cm^{-1}). Because we observed nucleotides containing both adenine and cytosine, the SERS signal should in principle always be a mixture of adenine and cytosine even at a single nucleotide observation. The fact that we obtained the SERS signal of purely adenine is clear evidence that the measurement achieved single-base (sub-nanometer) resolution. A similar result was obtained for oligonucleotides containing guanine (G) and cytosine (C) bases.

10:45 AM EQ05.22.03

Implantable Sensors Based on Gold Nanoparticles for Continuous Long-Term Concentration Monitoring in the Body Katja Buder¹, Katharina Kafer^{1,2}, Felix Schlapp¹, Hüseyin Uzun¹, Sirin Celiksoy¹, Bastian Flietel¹, Axel Heimann³, Thies Schroeder¹, Oliver Kempfski³ and Carsten Sönnichsen¹; ¹Johannes Gutenberg-University of Mainz, Germany; ²Max Planck Graduate Center, Germany; ³University Medical Center of the Johannes Gutenberg-University, Germany

Implantable sensors continuously monitor biomarkers in bodily fluids, facilitating chronic disease observation, supporting personalized drug therapy, and enhancing the patient's comfort. Nevertheless, there are two major issues limiting long-term application: Firstly, the sensor must be well integrated into the host tissue to prevent encapsulation, and thus impediment of analyte transport [1]. Secondly, the sensor-element for external signal transduction must be robust against degradation and exhibit a long signal lifetime [2].

To overcome both issues, we have developed an implant based on plasmonic gold nanoparticle sensors embedded in a macroporous polymeric hydrogel [3]. While the hydrogel's macropores allow tissue and capillary ingrowth, the nanoparticles' plasmonic signal exhibits a potentially unlimited lifetime. The nano-sensors are coated with aptamer and show a change of their resonance wavelength upon binding the antibiotic drug kanamycin. We implant our sensor-system subcutaneously in the abdominal skin of live hairless rats and measure the plasmon spectrum with a self-built spectral imaging setup non-invasively through the skin.

Upon administering the drug kanamycin in the rat's tail vein, we can observe a concentration-dependent change of the plasmon signal verifying the drug's presence in the tissue surrounding the implant. Control experiments, where we inject analyte-free saline solution, show no such signal change. The shift of the resonance wavelength is consistent with values we expected from theoretical calculations. Finally, histological sections of the working implants confirm that they are well integrated into the host tissue.

Our sensor design is not restricted to a specific analyte and allows many possible applications due to the versatile functionalization options of gold nanoparticles. The potentially unlimited lifetime of the plasmon signal enables long-term application and is advantageous over e.g. fluorescence-based systems, which are subject to photobleaching. Additionally, the macroporous polymeric hydrogel matrix is well-integratable into the host tissue, preventing encapsulation, facilitating analyte transport, and hence further boosting the service life of the implant.

Taking all these points into account, we believe that our implant paves a realistic way towards a universal sensor-platform for continuous monitoring of biomarkers.

[1] Anderson, J. M.; Rodriguez, A.; Chang, D. T. Foreign body reaction to biomaterials. *Semin. Immunol.* **2008**, *20* (2), 86–100.

[2] Vaddiraju, S.; Burgess, D. J.; Tomazos, I.; Jain, F. C.; Papadimitrakopoulos, F. Technologies for continuous glucose monitoring: Current problems and future promises. *J. Diabetes Sci. Technol.* **2010**, *4* (6), 1540–1562.

[3] Kafer, K.; Krüger, K.; Schlapp, F.; Uzun, H.; Celiksoy, S.; Flietel, B.; Heimann, A.; Schroeder, T.; Kempfski, O.; Sönnichsen, C. Implantable sensors based on gold nanoparticles for continuous long-term concentration monitoring in the body. *Nano Lett.* **2021**, *21* (7), 3325–3330.

11:00 AM EQ05.22.04

Surface Plasmon Resonance Sensing in Electropolymerized Molecular Imprinted Polymers (E-MIPS) with *In Situ* and *In Operando* Parametrization. Rigoberto C. Advincula^{1,2,3}; ¹Case Western Reserve University, United States; ²The University of Tennessee, Knoxville, United States; ³Oak Ridge National Laboratory, United States

Plasmonics and metamaterials have a common thread of enhanced phenomena and shape/composition independent dielectric and light behavior. A common application of plasmonic materials in sensing where the "enhanced light" can be used to further the use in detecting low levels of analyte and combined with a waveguide or guided layer detection. This is especially useful when combined with spectroscopic and imaging methods for characterizing the potential for artificial intelligence and machine learning (AI/ML) paradigm. This work will report on the use of plasmon, localized surface plasmon resonance LSPR and SPR waveguiding methods to demonstrate high sensitivity and selectivity for the detection of chemical and biological analytes at a very low level of concentrations. Using electrochemically molecularly imprinted polymers enabling tuning of the dielectric parameters based on the oxidation state of the polymer to facilitate the MIP process and evaluate the figures of merit of a sensor device. The main sensitivity is achieved by the plasmonic enhancement and relationship with multilayer films and dielectric behavior closer to a guided wave platform. Thus there is a high possibility of combining in-situ and in-operando measurements methods that can be relevant for future AI/ML applications.

11:15 AM EQ05.22.05

Polymer-Supported Composite Sensor Particles for Surface-Enhanced Raman Scattering Sensing Nikunj Kumar Visaveliya; The City College of New York, United States

Surface-enhanced Raman scattering (SERS) spectroscopy is a very powerful analytical technique for the detection of various analytes in various mediums. For concentrating the electromagnetic waves (laser light), plasmon resonance is a minimum requirement for realizing the SERS effect. Therefore, various types of SERS substrates based on plasmonic metallic were developed since its discovery four decades ago. It is also required that SERS substrates are equipped with a roughened metallic surface with some nanoscale gaps and junctions that create hotspots. SERS techniques enabled the detection at the ultimate limit, *i.e.*, detection of a single molecule. Though solid substrates have potential, the mobile substrate (solution dispersion of nanoparticles) is very promising because of its small size, movability, high surface area, and ability to deal with light efficiently. In this regard, smaller-sized metal nanoparticles with hotspots are very useful. However, smaller-sized metal nanoparticles are good for one-time use as it is difficult to wash and regenerate the nanoparticles because of their very small size and the possibility of uncontrolled aggregation and oxidation. To avoid such concern and also for regeneration and sequential SERS sensing purpose, polymer-based metal composite particles are very promising. Polymer-supported sensor particles (as substrate) are versatile due to the fascinating characteristics of the polymers such as swellability, porosity, transparency, metal loading ability, and high

surface area. Microfluidics is a promising technique for the fabrication of polymer-supported sensor particles of nanoscale and microscale with uniformity. For nanoscale sensor particles, the metal nanoparticles can be incorporated and anchored at the surface of polymer nanoparticles electrostatically, and a ligand-free metal layer can be deposited by a metal-catalyzed metal enforcement process. Here, the development of the polymer-metal composite particles at nanometer and micrometer length scales, and their applications as sensor particles for SERS sensing are presented. Microfluidic techniques were utilized for the generation of uniform sensor particles with the precise distribution of metal nanoparticles in the interior and at the surface. Furthermore, metal-catalyzed metal enforcement approaches initiated for achieving a ligand-free metal surface for direct analyte interactions, and experimental demonstration of sequential SERS analysis of multiple analytes through microfluidics has been established.

11:30 AM EQ05.22.06

Gold Nanoparticle Incorporated Oxide Thin Films for Gas Sensing at High Temperature Jeffrey Wuenschell^{1,2}, Youngseok Jee^{1,2}, Michael Buric¹ and Benjamin Chorpene¹; ¹U.S. Department of Energy National Energy Technology Laboratory, United States; ²Leidos, United States

Many applications of high economic value within the energy sector operate at high temperature or under chemically harsh environments, posing a challenge for *in-situ* operation with traditional sensor technology. Oxide thin films as sensing layers for conductive sensors or on the optical fiber platform provide one solution to this problem, as these thin films have the ability to operate at high temperature under a wide range of chemical conditions. The optical fiber platform in particular offers scalable, spatially distributed sensing, with off-the-shelf silica fiber providing stability up to 800 °C under oxidizing and reducing conditions. The incorporation of tailored plasmonic nanoparticles offers an additional response in the visible spectrum which may be utilized to provide enhanced cross-sensitivity discrimination under multi-variate sensing conditions. Gold nanoparticles, for example, have been shown to be stable at high temperature when incorporated within an oxide matrix. However, the plasmonic response can be impacted by the complex interaction between free carriers and atomic vacancies (which may be mobile at elevated temperature).

Computational modeling and experimental results demonstrate the impact of defect chemistry on the high temperature sensing response of the following two model oxides on the optical fiber platform: 1) La-doped SrTiO₃, an n-type doped system for sensing reducing gas streams; and 2) Fe-doped SrTiO₃, a p-type doped system for sensing oxidizing gas streams. On optical fiber and planar substrates, the interaction between the free-carrier (Drude) response of the oxide film in the NIR and the plasmonic response in the visible spectrum is demonstrated. The dynamics of the combined electronic-ionic-plasmonic physics are also modeled and used as a tool to guide the development of sensing layers with improved sensing response time and reduced drift at extreme temperatures.

11:45 AM EQ05.11.05

Smart-Integration of Organic Light-Emitting Transistors in a Multifunctional System for Plasmonic Sensing Mario Prosa¹, Emilia Benvenuti¹, David Kallwei², Paola Pellacani³, Michael Toerker⁴, Margherita Bolognesi¹, Laura Lopez-Sanchez³, Franco Marabelli⁵ and Stefano Toffanin¹; ¹CNR-ISMN, Italy; ²CSEM Center MuttENZ, Switzerland; ³Plasmore s.r.l., Italy; ⁴Fraunhofer FEP, Germany; ⁵University of Pavia, Italy

The integration of multiple devices in a single functional unit is boosting the advent of a series of compact optical sensors for rapid and on-site analysis. In this context, the huge potential of plasmonic-based sensors has been affected by the strict constraints of the detection scheme. The resulting need for laboratory equipment, such as laser sources and expensive prism-based optics, therefore ends up in not-portable systems.

Here, an ultra-compact plasmonic sensor is demonstrated through the smart integration of an organic light-emitting transistor (OLET), an organic photodiode (OPD), and a nanostructured plasmonic grating (NPG). The direct integration of the OPD onto the planar structure of the OLET enabled unprecedented proximity of the light source and light detecting areas, which allowed the exploitation of the angle-dependent sensing characteristics of the NPG.

The most effective 3D layout of integration, including the optimal size and relative positioning of the three elements (i.e. OLET, OPD, and NPG), was unraveled by an advanced simulation tool, which also predicted the signal variation of the sensor under different conditions. Accordingly, the effectiveness of the new plasmonic-based detection scheme was demonstrated by the dependence of the OPD photocurrent on the surrounding environment of the NPG. In particular, a variation of the OPD photocurrent of about 10⁻⁹ A was recorded when exposing the NPG from water to alcoholic solutions at different concentrations.

A miniaturized plasmonic sensor with a total size of 0.1 cm³ was therefore obtained through the smart integration of cost-effective, versatile, and nanometer-thick optoelectronic and plasmonic components.

SESSION EQ05.23: Metasurfaces and Metamaterials V

Session Chairs: Ortwin Hess and Giulia Tagliabue

Tuesday Afternoon, December 7, 2021

EQ05-Virtual

1:00 PM *EQ05.23.01

Polaritonic Metasurfaces [Andrea Alu](#); City University of New York, United States

In this talk, we discuss our recent progress in the area of polaritonics, and in particular on the role of polaritons in molding the optical wavefront over engineered ultrathin surfaces. We discuss the opportunities of these concepts to manipulate the propagation of light strongly coupled with matter. We will discuss the role that polaritons can have in inducing giant nonlinear responses in metasurfaces, and we unveil the emergence of topological transitions at photonic magic angles enabled by the strong coupling between two polaritonic bilayers with a twist angle between them. We will also discuss other exotic opportunities enabled by lower symmetry materials, such as monoclinic crystals or tailored metasurfaces. During the talk, we discuss the unusual phenomena supported by these structures, and their opportunities for nano-imaging and information transport.

1:30 PM *EQ05.23.02

Metasurfaces for Orbital Angular Momentum Holography and Fiber Optical Imaging [Stefan A. Maier](#); Ludwig-Maximilians-Universität München, Germany

Metasurfaces allow the manipulation of the amplitude, phase, and polarization of light on an ultrathin platform, and have started to be explored also in the context of digitizing optical holograms. To increase the bandwidth of a metasurface hologram, essential for high-capacity holographic memory devices, different properties of light including polarisation, wavelength, and incident angles have been exploited for holographic multiplexing; however, the bandwidth of a metasurface hologram has remained too low for any practical use.

We present the design of a complex-amplitude metasurface hologram for ultrahigh-dimensional OAM-multiplexing holography in momentum space. To realise a complex-amplitude Fourier hologram, we have introduced an OAM diffuser array with a random phase function, capable of scaling down the amplitude variation in a typical Fourier image as well as eliminating the coherence of holographic image channels. We will demonstrate first realizations of holograms based on this concept.

The second part of the talk will focus on demonstration of metasurfaces on fiber end facets for optical trapping and achromatic focusing with record bandwidth over the whole telecom range.

2:00 PM *EQ05.23.03

Frontiers in Nanophotonics—Enabling Technology for Next-Generation Biosensors [Hatice Altug](#); École Polytechnique Fédérale de Lausanne, Switzerland

Biosensors play an essential role in numerous healthcare applications ranging from diagnosis of life-threatening conditions to the management of infectious diseases for preventing pandemics. Unfortunately, current biosensors are lacking precision, bulky, and costly, as well as they require long detection times, sophisticated infrastructure and trained personnel, which limit their use. In our laboratory, we address these challenges by developing next-generation nanophotonic biosensors, bioimaging, and spectroscopy technologies. We exploit nanophotonics using plasmonic and dielectric metasurfaces for achieving high sensitivity, integration and multiplexing. We integrate our sensors with microfluidics for efficient sample manipulation and automation. We use smart data science tools to improve sensor performance. In this talk, I will present some of our recent effort towards developing ultra-compact, portable, rapid, and low-cost nanophotonic biosensor and their use for early disease diagnostics [1-4].

Our lab has been developing various point-of-care (PoC) biosensors with plasmonic nanohole arrays (NHAs) supporting extraordinary optical transmission (EOT) [5-7]. Recently, we showed that gold nanoparticle (Au-NP) bindings on NHAs can dramatically enhanced the sensitivity and enable digital counting of even individual binding events [1]. The detection principle is based on local suppression of the EOT signal. Although the sizes of NPs are subwavelength, their plasmonic interaction with NHAs allows for high-contrast imaging of surface-bound NPs in a bright field optical reader over large field-of-views and eliminates the need for bulky and expensive spectrometry instrumentation. In a follow-up work, we used this new principle to develop a portable PoC device to assist sepsis diagnosis [2]. The optical is made of off-the-shelf optical components and comprises an LED, a simple sample holder, and a CMOS camera. We tested the portable reader in a hospital setting with patient samples and showed detection of two inflammatory biomarkers related to sepsis diagnosis, procalcitonin and C-reactive protein with limit-of-detection down to few tens of pg/mL directly in blood serum. Our sensor provided performance equivalent to gold-standard immunoassay based laboratory tests. Moreover, our results revealed that our sensor can perform rapid tests in less than 15 minutes.

Concurrently, we use low-loss dielectric metasurfaces and exploit their high-Q resonance modes with accessible near-field enhancements for sensing. In one work, we combined silicon-based metasurfaces supporting BIC modes in NIR spectrum with hyperspectral imaging and demonstrated detection limits at the levels of ~ 3 IgG molecules/ μm^2 [3]. Recently, we introduced a single-wavelength imaging-based dielectric biosensor for achieving superior sensitivity based on reconstructed spectral shift without requiring wavelength scanning and spectrometers [4]. Here, we employed diatomic metasurfaces and combined them with advanced data processing techniques for aided imaging. Our method acquires large-area intensity images of the metasurface in real-time by using a single wavelength illumination and processes them optimally by a linear estimation algorithm to reconstruct spectral shift data at high accuracy. We integrated the metasurfaces with microfluidics in a microarray format and performed in-flow detection of breast cancer extracellular vesicles (EV), which are important biomarkers for diagnostics. Our optofluidic sensor has enabled real-time quantification of EV bindings from solution at concentrations as low as ~ 200 femtomolar.

References:

- [1] Belushkin et al. ACS Nano (2019)
- [2] Belushkin et al. Small (2020)
- [3] Yesilkoy et al. Nature Photonics (2019)
- [4] Jahani et al. Nature Communications (2021)
- [5] Cetin et al. Light Science and Applications (2014)
- [6] Coskun et al. Scientific Reports (2014)
- [7] Yesilkoy et al. Light Science and Applications (2018)

2:30 PM EQ05.23.04

Terahertz Transverse Magnetism in Metasurface-Assisted Hybrid Plasmonic Gratings [Subhajit Karmakar](#)¹, Ravendra K. Varshney¹ and Dibakar Roy Chowdhury²; ¹Indian Institute of Technology Delhi, India; ²Ecole Centrale School of Engineering - Mahindra University, India

Plasmonic wire has drawn immense scientific interests since the inception of artificial chiral media [1], which supports dominant electric mode upon applied electric polarization parallel to its axis and does not usually induce non-axial circulating current (i.e., dominant transverse magnetic modes) in it [2 – 6]. To induce transverse magnetic moment (circulating current distribution) in conducting systems, resonator geometry must be suitably tuned to manipulate its charge distribution along a loop (e.g., split- or closed ring, spherical particles, solenoid, toroid, etc.) [2 – 5]. Moreover, plasmonic systems possess inherent ohmic and radiative losses which eventually degrades system performance in large extent. As a result, plasmonic systems like metal wires, nonmagnetic plasmonic gratings were barely used to tailor its magnetic characteristics. Motivated from this viewpoint to excite magnetic resonances in a sole plasmonic wire, a mechanism was proposed recently in periodically arranged electromagnetically coupled plasmonic cut wires with applied polarization along its length [7]. By tuning length of one cut-wire (implying asymmetry), one can effectively transform physical functionality of other wire from being ‘electric’ to ‘magnetic’ in nature at terahertz (THz) regime by interplaying with near-field coupling and lattice coupling. We may highlight, as of earlier literature [1 – 5], realization of artificial transverse magnetism had only been possible by combining or coupling of at least two coupled wires; whereas nature of a single wire (be it isolated or coupled) always remains electric in nature, unlike our case where we break this convention. Moreover, the behavior of continuous wire (constituting grating) would be significantly different than periodically oriented subwavelength cut wires. Thus, we investigated the coupling between a continuous wire (grating) and a cut-wire (dipole) to tune the nature of grating element from electric to magnetic. Hybridization between grating and metasurface responses leads to generation of magnetic Fano and nonradiative anapole modes (i.e., low loss characteristics), makes this hybrid (combination of subwavelength grating (guided mode) and cut-wire dipole (diffractive, metamaterial mode)) plasmonic device useful for prospective THz magnetic applications like realization of femtosecond opto-magnetism, magnetic cloaking, magnetic storage, spin rectification, magnetic imaging, etc.

References

- [1] J. C. Bose, “On the rotation of plane of polarisation of electric wave by a twisted structure,” Proc. R. Soc. Lond. **63146**–152 (1898).
- [2] D. R. Smith, W. J. Padilla, D. C. Vier, S. C. Nemat-Nasser, and S. Schultz, “Composite Medium with Simultaneously Negative Permeability and

Permittivity," Phys. Rev. Lett. **84**, 4184 (2000).

[3] S. Karmakar, D. Kumar, R. K. Varshney, and D. Roy Chowdhury, "Lattice induced plasmon hybridization in metamaterials," Opt. Lett. **45** (13), 3386-3389 (2020).

[4] S. Karmakar, S. Banerjee, D. Kumar, G. Kamble, R. K. Varshney, and D. Roy Chowdhury, "Deep Subwavelength Coupling Induced Fano Resonances in Symmetric Terahertz Metamaterials," Phys. Status solidi RRL **13**, 1900310 (2019).

[5] G. T. Papadakis, D. Fleischman, A. Davoyan, P. Yeh, and H. A. Atwater, "Optical magnetism in planar metamaterial heterostructures," Nat. Commun. **9**, 296 (2018).

[6] S. Karmakar, D. Kumar, R. K. Varshney, and D. Roy Chowdhury, "Strong terahertz matter interaction induced ultrasensitive sensing in Fano cavity based stacked metamaterials," J. Phys. D, **53** (41), 415101 (2020).

[7] S. Karmakar, D. Kumar, B. P. Pal, R. K. Varshney, and D. Roy Chowdhury, "Magnetic wire: transverse magnetism in a one-dimensional plasmonic system," Opt. Lett. **46** (6), 1365-1368 (2021).

2:45 PM EQ05.23.05

Energy-Resolved Plasmonic Chemistry in Individual Nanoreactors Eitan Oksenberg¹, Ilan Shlesinger¹, Angelos Xomalis², Andrea Baldi³, Jeremy J. Baumberg², Femius Koenderink¹ and Erik C. Garnett¹; ¹AMOLF Amsterdam, Netherlands; ²University of Cambridge, United Kingdom; ³Vrije Universiteit Amsterdam, Netherlands

Plasmonic resonances can concentrate light into exceptionally small volumes, approaching the molecular scale. Such extreme light confinement provides an advantageous pathway to probe molecules at the surface of plasmonic nanostructures with highly sensitive spectroscopies. Beyond the chemical information available through surface-enhanced Raman scattering (SERS), unavoidable losses associated with metals, which are usually seen as a nuisance, encode invaluable information on energy transfer to the adsorbed molecules through the resonance linewidth. We target the sharp gap resonances of gold nanocubes deposited on a gold mirror coated with a thin dielectric layer (NCoMs) and measure a thousand single nanocavities with resonances spanning the orange to red spectral range. We closely monitor changes in linewidth and peak energy of the nanocavities and combine these observations with SERS spectra to monitor, in an energy-resolved manner, energy transfer and plasmon-driven chemical reactions at their surface. Using methylene blue (MB) as a model system, we show how this approach can be used to measure the absorption spectrum of molecules following their adsorption onto a metal surface and reveal a rich plasmon-driven reactivity landscape. We show that within different energy windows distinct reaction pathways dominant: near-field driven desorption at ~1.7 eV and direct charge-transfer driven N-demethylation at ~1.9 eV.

SESSION EQ05.24: Quantum Photonics/Advanced Nanophotonic Design

Session Chairs: Ho Wai (Howard) Lee and Yu-Jung Lu

Tuesday Afternoon, December 7, 2021

EQ05-Virtual

4:00 PM *EQ05.24.01

Nanoplasmonics as Enabler of Room-Temperature Quantum Nanophotonics Ortwin Hess^{1,2}; ¹Trinity College Dublin, The University of Dublin, Ireland; ²Imperial College London, United Kingdom

Quantum technologies harness quantum effects usually in small and pure arrangements such as through cold atoms or superconducting systems. From the start, photonic quantum effects have played a central role, too, but most photonic solutions and systems based on light-matter interaction also require cryogenic environments. Strong coupling of light and matter at the single emitter level is a fundamental quantum resource offering deterministic energy exchange between single photons and a two-level system, and the possibility to achieve single-photon nonlinearities via the anharmonicity of the Jaynes-Cummings ladder. Until recently, however, the conditions for achieving strong-coupling were most commonly met at cryogenic temperatures such that decoherence processes are suppressed. As a major step forward, we have recently demonstrated room-temperature strong coupling of single molecules [1] and single quantum dots [2] to ultra-confined light fields in plasmonic resonators at ambient conditions. The fact that strong-coupling conditions may be reached at room temperature is of immense interest because it represents a clear route to a practical implementation and use of quantum behaviour in nanophotonic systems and its application in bio-sensing [3].

Here we discuss the principles of room-temperature single-emitter strong coupling in nanoplasmonics and illuminate perspectives for quantum nanophotonics [4]. We will highlight the physics associated with recently demonstrated room-temperature strong coupling of single molecules in a plasmonic nano-cavity [1] and near-field generated strong coupling of single quantum dots [2] and single quantum emitter Dicke enhancement [5] paving the road towards single-photon quantum nonlinearities. We will also explain near-field enhanced single-photon emission in near-zero index materials and multipartite dynamic quantum entanglement [6].

ACKNOWLEDGEMENTS

This work was supported by the Science Foundation Ireland (SFI) through grant 18/RP/6236.

REFERENCES

- [1] R. Chikkaraddy, B. de Nijs, F. Benz, S. J. Barrow, O. A. Scherman, E. Rosta, A. Demetriadou, P. Fox, O. Hess, and J. J. Baumberg, *Single-Molecule Strong Coupling at Room Temperature in Plasmonic Nanocavities*, Nature **535**, 127 (2016).
- [2] H. Groß, J. M. Hamm, T. Tufarelli, O. Hess, and B. Hecht, *Near-Field Strong Coupling of Single Quantum Dots*, Science Advances **4**, eaar4906 (2018).
- [3] N. Kongsuwan, X. Xiong, P. Bai, J.-B. You, C. E. Png, L. Wu, and O. Hess, *Quantum Plasmonic Immunoassay Sensing*, Nano Lett. **19**, 5853 (2019).
- [4] X. Xiong, N. Kongsuwan, Y. Lai, C. E. Png, L. Wu, and O. Hess, *Room-Temperature Plexcitonic Strong Coupling: Ultrafast Dynamics for Quantum Applications*, Appl. Phys. Lett. **118**, 130501 (2021).
- [5] T. Tufarelli, D. Friedrich, H. Groß, J. Hamm, O. Hess, and B. Hecht, *Single Quantum Emitter Dicke Enhancement*, ArXiv:2010.12585 [Cond-Mat, Physics:Quant-Ph] (2021).
- [6] F. Bello, N. Kongsuwan, J. F. Donegan, and O. Hess, *Controlled Cavity-Free, Single-Photon Emission and Bipartite Entanglement of Near-Field-Excited Quantum Emitters*, Nano Lett. **20**, 5830 (2020).

4:30 PM EQ05.24.02

Photonic Materials by Design—The Role of Chemical Bonding Matthias Wuttig; RWTH Aachen University, Germany

Controlling a state of material between its crystalline and glassy phase has fostered many real-world applications including photonic switches and phase

change materials. Nevertheless, design rules for crystallization and vitrification kinetics as well as the contrast of the corresponding optical properties still lack predictive power. Here, we identify stoichiometry trends for these processes in phase change materials, i.e. along the GeTe-GeSe, GeTe-SnTe, and GeTe-Sb₂Te₃ pseudo-binary lines employing a pump-probe laser setup and calorimetry. We discover a clear stoichiometry dependence of optical properties and crystallization speed along a line connecting regions characterized by two fundamental bonding types, metallic and covalent bonding. Increasing covalency slows down crystallization by six orders of magnitude and promotes vitrification. The stoichiometry dependence is correlated with material properties, such as the optical properties of the crystalline phase and a bond indicator, the number of electrons shared between adjacent atoms. A quantum-chemical map explains these trends and provides a blueprint to design crystallization kinetics and property contrast.

4:45 PM EQ05.24.03

Engineering the Size, Morphology and Ordering of Metal Nanoparticles on Nano-Dimpled Surfaces Gavin Farmer, Brianna Western, Yan Jiang, A.J. Syllaios, Chris Littler and Usha Philipose; University of North Texas, United States

We present a fabrication technology to produce highly ordered metal nanoparticle arrays on large surface areas of a chosen substrate. The nanoparticles were formed on a nano-dimpled aluminum template which allows for highly ordered nanoparticle distributions and also allows for their direct transfer to a substrate of choice using a polymer lift-off. The influence of several experimental parameters on the nanoparticle ordering was studied. By controlling the dimple size and the thickness of the deposited metal film, it was possible to influence the size of the nanoparticles and its spacing within the array. Post-deposition, the metal film was annealed and the annealing temperature as well as the rate of rise in temperature during the annealing process were factors that influenced the ordering of the metal nanoparticles.

The nano-dimpled alumina substrate was prepared by a two-step anodization method. Three different deposition voltages (40 V, 60 V, and 70 V) were used to study the effects of voltage on pore diameter and the spacing between the metal nanoparticles. It was observed that the pore diameter scales approximately linearly with voltage in agreement with results reported in previous works. By controlling the pore diameters, it was possible to tune the diameters and interpore distance of the metal NP's. Large pore sizes yielded metal nanoparticles with large diameters and smaller interpore distance. Constant DC voltages of 40, 60, and 70 volts resulted in pore diameters of 60 ± 10 nm, 100 ± 10 nm, and 120 ± 10 nm respectively.

Following fabrication of an ordered nano-dimpled surface, different metals (gold, silver and indium) were evaporated onto the dimpled surface to form a thin film. The thickness of the metal was varied from 8 nm to 12 nm and its effect on nanoparticle size and morphology was studied. Subsequent annealing of the metal film at different temperatures with varying rates of temperature rise enabled a study of the metal film thickness and annealing parameters on the morphology and ordering of the metal nanoparticles. The inter-particle distance was found to be inversely proportional to the thickness of the metal film. Moreover, rapid thermal annealing resulted in less uniform nanoparticles whereas slow anneal provided much more spherical nanoparticles with hexagonal close-packed ordering. The annealing temperature did not strongly influence the size and morphology of the nanoparticles, but the duration of the annealing process had a greater effect on the result. For gold nanoparticles, the optimum annealing process was a slow anneal at a temperature of about 300 C. Results of fabricating ordered arrays of indium and silver nanoparticles will be presented in this talk.

5:00 PM EQ05.24.04

A Neural Network-Based Approach for Emulating Light-Matter Interactions in Nanostructured, Disordered Photoelectrodes Robert H. Coridan; University of Arkansas, United States

Photoelectrochemical (PEC) solar energy conversion applications rely on chemical reactions driven by photogenerated minority carriers (electrons or holes) at a semiconductor-liquid junction. The optical, electronic, and chemical transport processes characteristic of these PEC reactions occur on independent and generally disparate length scales. Fabricating electrodes with hierarchical structure can optimize the performance for each of these processes simultaneously. Disordered materials with dielectric contrast on the length scales of the wavelength of light can trap light in localized modes. The simplicity of the fabrication alone makes this approach a particularly attractive one for engineering light trapping into scalable photoelectrode structures. One significant issue is that disordered materials can only be defined by ensemble or statistical parameters (pore diameter, scatterer diameter, relative volume fractions) rather than as precise structures, which results in a real, physical variance intrinsic to the ensemble structure. Simulations of the properties of a given ensemble (local light absorption, for example) require a large number of examples for generating statistically accurate measurements for those properties. In this talk, we will describe our recent efforts to use neural network emulation to explore the absorption properties of defects in a simplified, disordered photonic glass. This system provides an apt model for developing mathematical representations for electrode structure (input) and finite element simulation data (output) to interface with machine learning algorithms. It also provides an opportunity to develop appropriate error metrics for quantifying the accuracy of prediction and improve the training of a neural network emulator. We will outline the practical application of these models and show how algorithmic predictions can be used to identify the most efficient ensemble configuration for a given semiconductor photoelectrode.

5:15 PM EQ05.24.05

Semimetal Composite Nanostructures Induced Synergistic Photon Management and Band Gap Engineering of Two-Dimensional MoS₂ Xiaoxue Gao¹, Sidan Fu¹, Xiaobai Yu¹, Haozhe Wang², Tao Fang¹, Jing Kong² and Jifeng Liu¹; ¹Dartmouth College, United States; ²Massachusetts Institute of Technology, United States

Photon management techniques are widely applied in solar cells and photodetectors to improve device efficiencies by light absorption enhancement. Conventional photon management strategies like dielectric nanophotonic structures in thin film photonics are limited by complicated fabrication process, incompatibility with Si foundry, high cost of materials, and narrow resonant bandwidth. Surface-textured transparent conducting oxide (TCO) thin films, typically composed of heavily doped wide bandgap semiconductor oxides like indium tin oxide (ITO) [1], are widely developed to overcome the above challenges. However, their sub-micron surface textures tend to weaken the photon management effect on thin absorber with thickness $< 1 \mu\text{m}$. These facts leave the development of photon management strategies for two-dimensional (2D) absorbers such as graphene and molybdenum disulfide (MoS₂) an open challenge for the current optics and materials research societies. In this paper, we report two semimetal composite nanostructures designed for 2D MoS₂: pseudo-periodic Sn nanodots and SnOx ($x < 1$) core-shell nanoneedle structures. 2D MoS₂ shows up to 15x enhancement in absorption at $\lambda = 700\text{-}1000$ nm under pseudo periodic Sn nanodots and 20-30x enhancement with 11% absorption in MoS₂ at $\lambda = 700\text{-}900$ nm under SnOx ($x < 1$) nanoneedles. Both cover broad optical bands from visible to near infrared (NIR) light regimes and are self-assembled from physical vapor deposition without sophisticated nanolithography. The enhanced absorption has been verified by notable increase in Raman scattering and Photo luminescence intensities as a result of field enhancement under photon management. One mechanism of light absorption increase is the ultrahigh permittivity of Sn [2]. Same as Si which is the key element for almost all the current electronic and photonic devices, Sn is a group IV semimetal in the chemical periodic table. Compared with other conventional high-index dielectric materials (typically $\epsilon = 10\text{-}15$), it has an ultra large dielectric constant of $\epsilon > 50$ at $\lambda = 500\text{-}3000$ nm to induce strong near field enhancement in the nearby lower index regions according to the boundary condition of Maxwell's equations. Thus, Sn as a type of semimetal itself, could serve as a novel material system beyond plasmonic metals and high index dielectrics for optical interactions. The other unique feature of increased light absorption is that it covers a broadband which even achieve long wavelengths beyond intrinsic inter-band transition in 2D MoS₂. This interesting behavior could be explained by local strain induced band gap engineering. Band gap engineering techniques are developed for photoelectronic devices operated at long wavelengths. These devices require especially small bandgap semiconductors. Conventional technique of tuning the stoichiometry of different elements inside a material system would need advanced material processing method like molecule beam epitaxy (MBE) and could only boost the

absorption at a specific wavelength. Our self-assembled nanostructures effectively decrease the band gap of 2D MoS₂ by introducing local tensile strain to the material which enable the broadband long wavelength light absorption improvement. Thus, our semimetal composite nanostructures synergistically address the photon management and band gap engineering challenges of 2D MoS₂ photonic devices at long wavelength. Besides, the preparation of self-assembled Sn composite nanostructures would not require sophisticated nanolithography which would potentially hinder large-scale manufacture. The compatibility with Si also makes it favorable for current semiconductor foundries. Therefore, our semimetal composite nanostructures would potentially be a good feature on future 2D photonic devices.

[1] Tak, Yoon-Heung, et al. *Thin Solid Films* 411.1 (2002): 12-16.

[2] Fu, Sidan, et al. *ACS Photonics* 6.1 (2018): 50-58.

5:30 PM EQ05.24.06

Unconventional Metals and Dielectrics for Photonic Devices Peifen Lyu, Tao Gong and Marina Leite; University of California, Davis, United States

The employment of metal thin films and nanostructures in photonic devices has widespread applications in displays, lasers, sensors, electro-optical modulation and photovoltaics. By far, intense research has focused on conventional metals (e.g., Au, Ag and Cu) because of their low optical losses, paramount to achieving excellent plasmonic responses [1]. Yet, these metals are neither CMOS-compatible nor earth-abundant, which constrains their usage in advanced optical devices. Therefore, research for other potential candidates such as non-conventional metals/alloys is called for. Magnesium (Mg), which dissolves in water, is the eighth most abundant material on the earth's crust with confirmed biocompatibility, and has not been explored to its full potential in photonics. By investigating its etching properties with the control of thin film deposition method (radio frequency sputtering, RFS, and electron-beam evaporation, EBE), temperature (10 – 60 °C) and structural dimension, we demonstrate the promise of utilizing Mg for achieving optical tuning [2]. We fabricate scalable, transmissive color filters formed by triple-stack Mg/MgO/Mg thin films based on Fabry-Perot resonance, which feature tunable optical transmission to any color within the sRGB gamut [3]. Additionally, we fabricate tunable reflective color filters consisting of two stacked metal-insulator-metal layers (top: Mg-MgO-Mg, and bottom: Ag/Al₂O₃/Ag). After immersion in water, dynamic color tuning is successfully achieved (e.g., vivid yellow to pink), conditioned on etching time and temperature. Therefore, the transient properties of Mg-based photonics hold great promise for use in biodegradable color display, data encryption, and anticounterfeiting. Furthermore, we also exploit the modulation of optical properties of other unconventional metals such as Nickel (Ni), Cobalt (Co) and Platinum (Pt) and their alloy systems. Specifically, we implement the dewetting process of thin films to obtain large-area arrays of nanostructures. We characterize their optical behavior by *in-situ* spectroscopic ellipsometry. We establish a platform for engineering these metallic materials with *on-demand* optical responses. Research into these unconventional metals (e.g., Mg, Ni, Co and Pt) and their nanostructures opens up a new opportunity for game-changing nanophotonic components.

[1] T. Gong, P. Lyu et al, *Advanced Optical Materials* **2020**, 8(23), 2001082

[2] T. G. Farinha et al, *ACS Photonics* **2019** 6 (2), 272-278

[3] T. G. Farinha, T. Gong, P. Lyu et al, *Optical Materials Express* **2021**, 11(5), 1555-1565

5:45 PM EQ0515.04

Ultrafast Free-Carrier Dynamics in Epsilon-Near-Zero Conducting Oxide Thin Films Sudip Gurung^{1,2,3}, Subhajit Bej^{2,3,4}, Francesco Tonelli⁵, Zhenhuan Yi², Aleksei Anopchenko^{1,3}, Alessandro Ciattoni⁵, Andrea Marini⁶ and Ho Wai (Howard) Lee^{1,2,3}; ¹University of California, Irvine, United States; ²The Institute for Quantum Science and Engineering, Texas A&M University, United States; ³Department of Physics and Baylor Research and Innovation Collaborative (BRIC), Baylor University, United States; ⁴Photonics Laboratory, Physics Unit, Tampere University, Finland; ⁵CNR-SPIN, c/o Dip.to di Scienze Fisiche e Chimiche, Italy; ⁶Department of Physical and Chemical Sciences, University of L'Aquila, Italy

Understanding the ultrafast temporal dynamics of free carriers in epsilon-near-zero (ENZ) materials is important for zero-index nonlinear photonic applications [1]. Unique and fascinating features of ultrathin ENZ materials such as strong field intensity enhancement (FIE) along with high inherent nonlinearity and sub-picosecond temporal response have enabled enhanced high harmonic generation [2] and sub-picosecond optical switching [3]. However, the origin of such giant optical nonlinearity in epsilon-near-zero (ENZ) materials is still not well understood. Additionally, there is a lack of theoretical models that can accurately describe the temporal dynamics of hot electrons, especially in the strong nonlinear optical regime. In this work, we observe abnormal temporal dynamic of hot electrons in ENZ thin films under different pump fluences and excitation angles using a degenerate pump-probe spectroscopy technique. An strong intensity- and angle-dependence (for a TM polarized pump) on the relaxation time of the hot electrons are experimentally observed for the first time. Furthermore, a novel hydrodynamic model [4] has been used to validate the experimental results theoretically.

Two different ENZ materials (ITO with a thickness of 305 nm and AZO with a thickness of 205 nm) are fabricated using magnetron sputtering and atomic layer deposition respectively. The optical properties of the thin films are measured with spectroscopic ellipsometry, showing that the ENZ wavelength is 1190 nm for ITO and 1480 nm for AZO. The ultrafast temporal response of free carriers is measured with linearly polarized femtosecond laser pulses (pulse duration ~70 fs, repetition rate 1 kHz, peak wavelength (λ_p) tunable between 1100-1600 nm). Experiments are performed for normal and oblique incidences of TE/ TM polarized light pulses with different pump intensities and peak wavelengths ($\lambda_p = \lambda_{ENZ}$, $\lambda_p > \lambda_{ENZ}$, and $\lambda_p < \lambda_{ENZ}$). The temporal dynamics of the free carriers are evaluated by the relaxation time of carriers upon fitting the normalized change in probe transmission using the two-temperature model [5] and compared with the theoretical value predicted with the hydrodynamic model. Our results suggest that free carriers' relaxation time are highly dependent on the pump intensity as well as the excitation angles and wavelengths. We believe that our findings on understanding the tunability of the ultrafast free carrier dynamics of ENZ materials will be significant for efficient nonlinear zero-index photonic applications in the strong nonlinear optical regime.

SESSION EQ05.25: Plasmonic Applications IV

Session Chairs: Andrea Alu and Yu-Jung Lu

Tuesday Afternoon, December 7, 2021

EQ05-Virtual

9:00 PM *EQ05.25.01

Flexible Plasmonics Using Aluminum and Copper Epitaxial Films on Mica Le Thi Quynh¹, Chang-Wei Cheng¹, Chiao-Tzu Huang², Soniya S. Raja¹, Ragini Mishra¹, Meng-Ju Yu³, Yu-Jung Lu³ and Shang-Jr Gwo^{1,1,3}; ¹National Tsing-Hua University, Taiwan; ²National Chiao-Tung University, Taiwan; ³Academia Sinica, Taiwan

Gold and silver are the most commonly used plasmonic materials because of their excellent optical properties in the visible and near-infrared spectral ranges. However, realization of wide-spread plasmonic applications requires additional material advantages, such as low cost, material stability, device scalability, spectral tunability, as well as device integration with existing semiconductor technologies. In this work, we demonstrate growth of atomically smooth aluminum (Al), copper (Cu), gold (Au), and silver (Ag) epitaxial films on two-dimensional (2D) layered muscovite (mica) substrates via van der Waals (vdW) heteroepitaxy with controllable film thickness from a few to hundreds of nanometers. In our approach, the mica thin sheet act as a flexible and transparent substrate with an atomically flat surface for vdW heteroepitaxy, which allows for large-area formation of atomically smooth, single-crystalline, and ultrathin plasmonic materials without the conventional issue of film dewetting. The metal thin films grown on mica allow us to design and fabricate well-controlled Al and Cu plasmonic nanostructures (the focus of this work) with tunable localized surface plasmon resonance (LSPR) and propagating surface plasmon polariton (SPP) properties from visible to the near-infrared spectral region. Furthermore, we show that the plasmonic responses of Al and Cu nanostructures fabricated on mica substrates remain unchanged under large substrate bending conditions. Based on these results, we expect that the metal-on-mica vdW epitaxy platform can lead to transformative plasmonic device applications (“flexible plasmonics”) based on novel bendable functionalities.

9:30 PM EQ05.25.02

Gram-Scale and High-Throughput Synthesis of Noble Metal Nanoparticles Using Polymerizable Deep Eutectic Solvent Yoon Hyuck Kim and Jae-Seung Lee; Korea University, Korea (the Republic of)

Deep eutectic solvents (DESs) as a new generation of low-melting-point solvents have been used for syntheses of noble metal nanoparticles owing to their unique properties, such as structure-directing abilities, strong solvating power, wide reaction temperature range, non-volatility, and high thermal stability. Despite these advantages, to the best of our knowledge, the high-throughput and large-scale productions of noble metal nanoparticles using DESs have been rarely reported to date. In this work, we present the gram-scale synthesis of various noble metal nanoparticles with controlled shapes and sizes using a polymerizable DES. Acrylamide (AAm) is used to play a role as a hydrogen bond donor in DES and monomer. Importantly, the synthesis of noble metal nanoparticles and the polymerization of AAm take place simultaneously, resulting in the stabilization of highly concentrated nanoparticles in a polyacrylamide (pAAm) solid matrix. In addition, the overall synthesis of the nanoparticles in the polymerizable DES takes only 20 min in one-pot, and can be easily extended to carry out multiple reactions in a high-throughput manner. The intense optical properties of the nanoparticles are investigated, demonstrating the localized surface plasmon resonance of noble metal nanostructures. The molecular weights of the pAAms are investigated using gel permeability chromatography, indicating the roles of the reagents participating in the synthesis reactions. Moreover, alloy nanoparticles are also synthesized in the polymerizable DES. Importantly, we demonstrate that the production of the noble metal nanoparticles using the polymerizable DES could be as large as a few grams, demonstrating that our method could be truly practical for various applications, such as molecular diagnostics and therapeutics. As an example of applications that utilize a large number of nanoparticles, we demonstrate a concept of transparent displays using the synthesized nanoparticles on a round glass plate with a diameter of 10 cm.

9:45 PM EQ05.25.07

Real-Space Imaging of Strongly-Coupled Plasmon-Phonon Modes in Mid-Infrared Antennas Maureen Joel Lagos^{1,2}, Philip E. Batson³, Zihan Lyu¹ and Ulrich Hohenester⁴; ¹McMaster University, Canada; ²Canadian Centre for Electron Microscopy, Canada; ³Rutgers, The State University of New Jersey, United States; ⁴University of Graz, Austria

Strong plasmon-phonon (pl-ph) coupling can modify the energy landscape of mid-infrared antennas, thus providing opportunities to alter the energy states of infrared (IR) polaritons beyond the standard tunability approaches. Optical probes have dominated strong-coupling studies, but they offer limited spatial resolution. Nowadays, atom-wide monochromatic electron beams formed in transmission electron microscopes allow us probing and mapping IR excitations (e.g. plasmon, phonon polaritons) with better spatial sensitivity [1,2]. Here, we present a spectroscopical study of strong pl-ph coupling in mid-IR antennas using spatially-resolved electron energy loss spectroscopy (EELS). We imaged the spatial distribution of strongly-coupled ph-pl modes, revealing unique spatial behavior of polaritonic hybrid modes in mid-IR antennas [3].

We fabricated mid-IR double-antennas with extreme aspect ratio (up to 40) by joining a single rod-like Al plasmonic antenna and a rod-like *a*-SiO₂ phononic antenna, side by side. We adjusted the length of the double-antenna in such a way that the plasmon response of the Al antenna lies within the upper Reststrahlen band (RB) of the SiO₂. Optimal coupling conditions are achieved for antennas of 3 μm in length. The spatially-resolved EELS work was conducted using a transmission electron microscope equipped with an aberration corrector and monochromator that produces a ~ 2 Å electron probe with an energy resolution of ~ 9 meV.

The EELS spectra of the Al/SiO₂ antennas show double-peak resonances as a result of the pl-ph coupling. Each peak in the double-peak resonance is associated with the formation of one hybrid pl-ph mode. We determined the dispersion relationship associated with the polaritonic modes and found Rabi splittings as large as 26 meV within the RB. Our simulations indicate the appearance of only two coupled pl-ph modes, despite the large variety phonon polariton modes involved in the coupling. We measured the coupling constant of the pl-ph interaction ($g = 18$ meV), indicating that the coupling is in the strong-regime. Despite the modest quality-factor antennas built using low-cost materials, the fabricated Al/SiO₂ antennas equals performance of platforms of different geometries that capitalize on novel materials [4]. Our work suggests that geometry plays a relevant role in the development of strong-coupling hybrid platforms, likely due to the large variety of phonon polariton modes that participate in the coupling.

We mapped out the scattering associated with the strongly-coupled pl-ph modes and found that its spatial distribution is akin to the distribution of dipole optical modes in rod-like antennas. The maps of both coupled modes share several similarities along the double-antenna main axis, however minor variations can be noticed in the transverse direction, likely due to their unique charge configurations. Spatially-resolved EELS measurements across SiO₂/Al interfaces revealed a drastic scattering variation within sub 10 nm distances due to the charge symmetry of each pl-ph mode.

In summary, we have built and probed a double-antenna composed by one plasmonic Al antenna attached to a phononic SiO₂ antenna. We found evidence of strong coupling between plasmon and phonon polaritons, as revealed by the energy split in the dispersion curve. We have imaged strongly-coupled pl-ph modes bringing important physical insights into the local density of electromagnetic states. Our results suggest that geometry plays an important role in the design of hybrid strong-coupling platforms.

Acknowledgement:

For financial support, M.J.L. acknowledges NSERC under a discovery grant, and P.E.B. acknowledges support of U.S. DOE (# DE-SC0005132).

References:

- [1] O. Krivanek, *et al*, *Nature* 514 (2014) 209.
- [2] M. J. Lagos, *et al*, *Nature* 543 (2017) 529.
- [3] M. J. Lagos, *et al*, *ACS Photonics* 8 (2021) 1293.
- [4] L. Tizei, *et al*, *Nano Letters* 20 (2020) 2973.

8:00 AM *EQ05.26.01

Magic-Angle Lasers in Nanostructured Moiré Superlattice Ren-Min Ma; Peking University, China

Conventional laser cavities require discontinuity of material property or disorder to localize a light field for feedback. Recently, an emerging class of materials, i.e. twisted van der Waals materials have been explored for the applications in electronics and photonics. Here, we propose and develop magic-angle lasers where the localization is realized in a periodic twisted photonic graphene superlattices [1]. We reveal that the confinement mechanism of magic angle lasers does not rely on a full band gap but on the mode coupling between twisted two layers of photonic graphene lattice. Without any fine tuning in structure parameters, a simple twist can result in nanocavities with strong field confinement and high quality factor. Furthermore, the emissions of magic-angle lasers allow direct imaging of the wavefunctions of magic-angle states. Our work provides a robust platform to construct high quality nanocavities for nanolasers, nanoLEDs, nonlinear optics and cavity quantum electrodynamics at the nanoscale.

Reference:

[1] X. R. Mao, Z. K. Shao, H. Y. Luan, S. L. Wang & R. M. Ma. Magic-angle lasers in nanostructured moiré superlattice. *Nature Nanotechnology*, <https://doi.org/10.1038/s41565-021-00956-7>, 2021.

8:30 AM EQ05.26.02

Room Temperature Single-Mode Lasing from Metal Halide Perovskite Nanodisk Arrays Chi-Ching Liu^{1,2} and Yun-Chong Chang^{1,2}; ¹Academia Sinica, Taiwan; ²National Taiwan University, Taiwan

Lead halide perovskites have become promising materials for future lasers and optoelectronic devices. However, the conventional solution-based fabrication process greatly limits the possibility to include precision nanostructures that can further enhance the performance. In this study, we implement thermal evaporation to adapt conventional nanolithography technique, which allow us to construct MAPbI₃ perovskite nanodisk arrays. Optical pumped single-mode lasing centered at 785 nm is observed at room temperature. The Q-factors is estimated to be larger than 1500. The lasing peaks corresponds to the lattice mode and can be tuned for at least 20 nm by varying the periodicity of the nanodisk arrays. Results in this study can be extended to obtain perovskite nanolasers with tunable lasing wavelength.

8:45 AM EQ05.26.03

Photoinduced Schottky Barrier Width Modulation and Charge Transfer in Zinc-Tin Oxide and Gold Nanoparticles Hybrid Structure for Multilevel Visible Light Memory Li-Chung Shih¹, Ya-Shan Lin¹, Yen-Cheng Mi¹, Jen-Sue Chen¹, Yen-Hsun Su¹, Jih-Jen Wu¹ and Chao-Cheng Kaun²; ¹National Cheng Kung University, Taiwan; ²Academia Sinica, Taiwan

In recent year, high responsivity and low-cost phototransistors have become prospective for various applications, such as optical communication, imaging, and wearable electronics. While the semiconductor materials will dominate the transistor performances, there have been several studies to develop thin film transistors using zinc-tin oxide (ZTO) due to its high electron mobility and on/off ratio. In addition, ZTO have shown the potential for optoelectronic applications owing to their significant photocurrent arising from generation of electron-hole pairs under UV light illumination. When using the visible light sources, photoexcited electrons can be generated in ZTO via the ionization of neutral oxygen vacancies (V_o) to positively charged oxygen vacancies (V_o^{2+}) and the photoexcited electrons under illumination of visible light of wavelength less than 450 nm. However, it will be difficult to get significant light response of ZTO at wavelengths of greater than 500 nm because the neutral oxygen vacancies are mostly locating at deep levels (>2.5 eV) within the bandgap.

In order to expand the light responding spectrum of ZTO, in this work, we report a hybrid device by embedding gold nanoparticles (Au NPs) in the zinc-tin oxide (ZTO) thin film transistor. Integrating with plasmonic metals provides a promising approach for visible light photodetectors and photocatalysis since the photocurrent can be enhanced by hot electrons generated by local surface plasmon resonance (LSPR). Au NPs may act as the charge trapping/detrapping media to further control the electron concentration in ZTO via gate bias modulation. As a result, the responsivity and sensitivity of ZTO/Au NPs phototransistor depend on the gate bias under illumination and the wavelength of the light. Compared to the same lighting condition without applying negative gate bias, the responsivity and the sensitivity of ZTO/Au NPs hybrid device can be greatly increased by 5 and 200 folds, respectively, with the application of negative gate bias under 405 nm light illumination. Similar enhancement effects are also observed under illumination using 520 nm and 635 nm light, which is partially attributed to LSPR effect of Au NPs. The key factor to generate the higher photocurrent with applying negative gate bias is that the charged oxygen vacancies (V_o^{2+}) will accumulate at the ZTO/Au NPs interface, and thus form a build-in electric field to induce the electrons to tunnel from Au NPs into ZTO.

A superb memory retention performance upon light/bias operation can be achieved in ZTO/Au NPs hybrid phototransistor since the electrons tunneling from Au NPs are excessive as compared to the charged oxygen vacancies (V_o^{2+}) in the ZTO channel. As a result, the recombination process is minimized, and the current is retained. Multiple memory state can be achieved by repeated programming operation and the memory states can be erased by applying positive gate bias which trigger the recombination/trapping of photocarriers. Therefore, this novel ZTO/Au NPs hybrid phototransistor exhibits broad spectrum photoresponse and multi-level photo-memory performance that highlights the promises for optical communication and computation technologies.

9:00 AM DISCUSSION TIME

9:15 AM EQ05.26.05

Electrical Tuning of Dynamic Organic Polymer Plasmonic Nanoantennas Akchheta Karkj, Giancarlo Cincotti, Shangzhi Chen, Chuanfei Wang, Mats Fahlman and Magnus P. Jonsson; Linköping University, Sweden

Light-matter interactions with conventional metal nanostructures can be limiting as it is unduly challenging to modify their static properties after fabrication. To circumvent this issue and open up avenues to dynamically control light at the nanoscale, research is shifting towards dynamic plasmonic systems with switchable states. Our recent study showed for the first time that nanodisks of the highly conducting polymer, poly(3,4-ethylenedioxythiophene:sulfate) (PEDOT:Sulf), can function as dynamic nano-optical antennas with plasmonic resonances that are tunable via gas- or liquid-induced chemical redox reactions. Here, we take the next crucial step and present the first electrically tunable conducting polymer nano-optical antennas. In addition to switching the antennas on and off, we demonstrate gradual tuning of the plasmonic resonances by careful electrical modulation of the mobile polaronic charge carrier density. The concept can facilitate many future applications such as smart windows with tunable plasmon-induced heating or ultrathin optical components with tunable focal lengths and beam steering. Moreover, tailoring of the polymer antenna geometry enabled a significant blue-shift of the resonance peak from a previously reported lower limit of ~ 1800 nm to ~ 1270 nm, opening up the possibility to use such nano-

optical antennas for applications in the visible to near-infrared ranges.

9:30 AM EQ05.26.06

Focus-Tunable 2D Lens by Carrier Control Seong Chan Jun; Yonsei Univ, Korea (the Republic of)

Owing to the tremendous demands for high-resolution thin lenses, ultrathin flat lenses, which are different from conventional lenses, have been extensively investigated with various applications in telescopes, aerospace technology, holograms, and glasses-free 3D displays. However, such ultrathin flat lenses need some characteristics such as thickness and tunable focal length to satisfy the requirement of various applications. So, realize these characteristics of ultra-thin flat lenses, diffractive optical elements or metasurfaces are being used. In particular, Fresnel zone plates which is comprised of a set of concentric rings using diffraction to focus light can be designed as thin, low-volume for applications in various fields. In this study, ultrathin flat lenses based on Fresnel zone plates using graphene have demonstrated high focusing efficiency and broadband performance. Unlike in most other 2D material, graphene which has a very thin thickness of per layer is intrinsically an ideal conductor with zero energy bandgap. How the transmittance change when a DC voltage is applied to ultrathin flat lens by experiments and COMSOL simulations. The result indicates that the transmittance is the lowest at 0 V and increases as the magnitude of the voltage bias is increased in either direction. Furthermore, as the voltage bias increases, the carrier density increases at the edge of the pattern leading to the shift in Fermi level which results in the difference in absorption of the incident light and thus the reduction of the Fresnel zone plate ring width. Our ultrathin flat lens is able to modify the focal length while achieving high transmission efficiency and nanoscale thickness. This study will be the cornerstone of the development of ultra-thin variable focus displays in the future, and it will be able to develop into a hologram display, reducing weight and increasing efficiency of glasses-free 3D displays and multi-focusing display for vehicles.

9:45 AM EQ05.26.07

Plasmonic Upconversion Lasing from Single-Crystal Lead-Free Perovskite Nanowire Chih-Ang Lin¹, Jung-Chan Lee^{1,2}, Yu-Cheng Chu^{1,2}, Li-Chien T. Chang^{1,2}, Yu-Hung Hsieh^{1,3}, Ming-Yen Lu³, Chih-Wei Chu¹, Tzung-Fang Guo⁴ and Yu-Jung Lu^{1,2}; ¹Academia Sinica, Taiwan; ²National Taiwan University, Taiwan; ³National Tsing Hua University, Taiwan; ⁴National Cheng Kung University, Taiwan

Lead halide perovskite materials have been proven to be promising candidates for laser application owing to their extraordinary optical properties. However, the environmental pollution risk of lead-based devices has become a challenge. Thus, searching for non-toxic, lead-free perovskite materials is essential. Here, we report a plasmonic upconversion laser from a lead-free halide perovskite CsSnBr₃ nanowire which synthesized at room temperature. The length of CsSnBr₃ nanowires ranging from 5 to 10 μm, and the width is from 100 nm to 1 μm. We characterized the spontaneous emission rate using time-resolved photoluminescence (PL) and PL measurements and observed an emission centered at 675 nm from the CsSnBr₃ nanowire. However, we only observed spontaneous emission from CsSnBr₃ nanowires due to their low PL quantum yield. Hence, we designed a plasmonic nanocavity to enhance the two-photon absorption rate and photon emission rate to reach the lasing action. The plasmonic upconversion nanolaser consists of a nanowire on a sputtered plasmonic hafnium nitride film with a thin Al₂O₃ capping layer by using atomic-layer-deposition. We will discuss the potential applications of lead-free halide perovskite CsSnBr₃ nanowire lasing such as nonlinear optics, optical communication, information processing, and sensing.

SESSION EQ05.27: Low Dimensional Photonics
Session Chairs: Ren-Min Ma and Pin Chieh Wu
Wednesday Morning, December 8, 2021
EQ05-Virtual

10:30 AM EQ05.27.01

Late News: 2D Semiconductors as Highly Tunable Optoelectronic Building Blocks Tony F. Heinz^{1,2}; ¹Stanford University, United States; ²SLAC National Accelerator Laboratory, United States

2D semiconductors in the transition metal dichalcogenide family (MoS₂, MoSe₂, MoTe₂, WS₂, WSe₂) have attracted much recent attention because of their direct-gap character at monolayer thickness and the pronounced role of excitons in these systems. In addition, the possibility of combining them in vertical stacks creates a wide range of new properties, such as the emergence of interlayer excitons. In this paper, we will highlight some the distinctive ways in which these robust building blocks for optoelectronic devices can be tuned, often in ways not available or practical in bulk materials. In particular, large and spatially localized strain fields can be used to modify the gaps and to localize excitation. Also, the external dielectric environment can modify the electrical and optical gaps of these materials at monolayer thickness. Finally, in monolayers and especially in heterostructures, electrical gating can be used to tune the material properties both through doping and the Stark effect. We will give an overview of these distinctive properties and how they might be harnessed in a device context.

11:00 AM EQ05.27.02

Direct Observation of Photoinduced Charge Transfer in Intermediate Coupling of MoS₂ Monolayer Min-Wen Yu^{1,2}, Satoshi Ishii², Shisheng Li², Ji-Ren Ku¹, Jhen-Hong Yang¹, Kuan-Lin Su¹, Takaaki Taniguchi², Tadaaki Nagao² and Kuo-Ping Chen¹; ¹National Chiao Tung University, Taiwan; ²National Institute for Materials Science, Japan

In exciton-polariton coupling, the understanding of electronic energy exchange in Rabi splitting is crucial. The favorite structures that have been adopted to study such coupling are “nanoparticle-on-mirror”. Integrating with transition metal dichalcogenide (TMDC) monolayers can realize large Rabi splitting. However, such a hybrid system has a significant localized electric field in out-of-plane that cannot satisfy the couple with in-plane exciton dipole of TMDC. Here, we propose one-dimensional plasmonic nanogrooves integrated with MoS₂ monolayers. The strongly localized fields are parallel with MoS₂ exciton orientation can address the aforementioned issue. As a result, a significant Rabi splitting (65 meV) in the intermediate coupling regime is demonstrated. In addition, Kelvin probe force microscopy is used to image charge transportation in the hybrid system. We directly observed the surface potential change on the proposed system via photo-excitation caused by the charge rearrangement. Furthermore, the giant photoluminescence enhancement can be attributed to the parallel exciton-polariton interactions. Our findings can provide great potential for improving the performance of plasmonic-TMD heterodevices in the field of photoconversion.

11:15 AM EQ05.27.03

Near-Field Probing of Image Polaritons in van der Waals Crystals Sergey Menabde¹, Jacob T. Heiden¹, Jongtae Ahn², Sergejs Boroviks³, Kenji Watanabe⁴, Takashi Taniguchi⁴, N. Asger Mortensen³, Do Kyung Hwang² and Min Seok Jang¹; ¹Korea Advanced Institute of Science and Technology, Korea (the Republic of); ²Korea Institute of Science and Technology, Korea (the Republic of); ³University of Southern Denmark, Denmark; ⁴National

Polaritonic modes in van der Waals crystals provide an unexcelled degree of field confinement and a superior capability for light manipulation at nanoscale. Very recently, a new class of polaritonic modes has been spotlighted as a superior platform for low-dimensional nanophotonics: the image polaritons, supported by a polaritonic material in proximity to a metal when the polaritonic mode couples with its mirror image.

We use scanning scattering-type near-field optical microscope (s-SNOM) to study the hyperbolic image phonon-polaritons (HIP) in hexagonal boron nitride (hBN) on gold. In our experiments, atomically flat gold crystals are used as a substrate, eliminating any roughness-mediated scattering of HIP. In such system, HIP dispersion properties can be accurately measured by the near-field mapping of their interference fringes. We use the polariton propagation length in optical cycles as a figure of merit (FOM).

We observe the first-order HIP mode with FOM of 6.5, independently of hBN thickness, while its wavelength varies from 192 nm in a 30 nm-thick hBN slab to 565 nm in an 88 nm-thick slab, all measured at 1480 cm^{-1} in the upper reststrahlen band. In agreement with theory, measured FOM is 1.8 times larger than that of hyperbolic phonon-polaritons in the same hBN on a typically used SiO_2 substrate. At the same time, HIP possess an impressively 3.9 times shorter wavelength. While the hBN used in our experiments has isotope composition of $^{10}\text{B}/^{11}\text{B} \approx 82/18$, we note that FOM of the HIP in the isotopically pure hBN with $^{10}\text{B} = 98.7\%$ is expected to be as high as 19.

Our results are even more interesting in a context of the recent work by Menabde *et al.* reporting on the experimental observation of significantly improved FOM of the mid-infrared image (also called acoustic) graphene plasmons. Near-field probing has revealed image plasmon mode that is twice as compressed and has 1.4 times higher FOM compared to graphene surface plasmons under similar conditions. Importantly, these results have been obtained with a large-area, chemically grown graphene, suggesting that image graphene plasmons are less sensitive to loss in graphene. This can be explained by the field distribution of the image plasmons which is mostly confined within the dielectric spacer, in contrast to the surface graphene plasmons localized at the graphene plane.

Summarizing, the direct near-field probing of image polaritons in van der Waals materials clearly demonstrates their superiority over pristine polaritonic modes in terms of both FOM and field confinement, promising the ultra-compact photonic devices where the wave phenomena and the exceptionally strong light-matter interaction can be put to work together.

11:30 AM EQ05.27.04

Ultrafast Exciton Dynamics in Millimeter-Scale, Continuous, Janus WSeS Monolayer Ching-Wen Chan¹, Chih-Wen Yang², I-Hung Ho³, Hyeoung Ahn³, Vincent Tung² and Yu-Jung Lu^{1,4}; ¹Research Center for Applied Sciences, Academia Sinica, Taiwan; ²King Abdullah University of Science and Technology, Saudi Arabia; ³National Yang Ming Chiao Tung University, Taiwan; ⁴National Taiwan University, Taiwan

The exciton dynamics in layered transition metal dichalcogenides (TMDCs) have spurred immense interest for next generation optoelectronics. Many works regarding this topic have been reported on either mechanically exfoliated TMDCs or monolayer flakes made via the chemical vapor deposition (CVD). Meanwhile, the exciton dynamics in Janus TMDCs monolayer with structural symmetry-breaking remains unexplored in any scalable fashion. Here, we report the ultrafast exciton dynamics in millimeter-scale Janus WSeS monolayer grown by chemical vapor deposition with H_2 plasma strip method. We performed PL measurement, Raman mapping, and steady-state absorption measurement to study the optical properties of the Janus WSeS monolayer. The ultrafast carrier dynamics of A/ B /C excitons were studied by using pump-probe transient absorption spectroscopy with a broadband white-light probe beam. The transient absorption pump-probe spectra of Janus WSeS varying with pump fluences and time delay will be discussed. We find that the relaxation of A exciton in Janus WSeS follows a triple-exponential decay process of approximately 1.1 ps, 14.4 ps, and 52.4 ps, respectively. We compare the carrier dynamics in Janus WSeS monolayer to the symmetric WSe₂ and WS₂ monolayers. We conclude that the short exciton lifetime in the Janus structure is due to the built-in dipole moment. The findings provide fundamental insight into the optical properties of 2D materials. We will discuss the practical applications in the field of 2D optoelectronics and ultrafast 2D photonics.

11:45 AM EQ05.10.01

Late News: Electrically Switchable Plasmonic Nanoantennas—Active Metasurfaces for Beam Steering and Metalensing Harald Giessen, Julian Karst and Mario Hentschel; University of Stuttgart, Germany

Metasurfaces based on plasmonic materials have revolutionized nanooptics [1]. The ability to shape beams with surfaces that are only a few hundred nanometers high has added tremendous design freedoms and functionalities to optics. In principle, plasmonic metasurfaces are the ultimate spatial light modulators that include amplitude and phase control on a deep subwavelength scale. The combination of propagation phase with geometrical phase allows for a full 2π phaseshift for each individual spatial element.

The forefront of metasurface research is geared towards active metasurfaces. These devices allow for changing their functional properties. Examples include beam steering with varying angles, bifocal and zoom lensing, and, ultimately, switchable spatial light modulation.

Several approaches have been brought forward: Liquid crystals or polymers have been combined with plasmonic nanoantennas or high-index dielectric resonators, and an electric field can switch the refractive index next to the nanoantennas, hence shifting the resonance wavelength. Phase-change materials such as GST have been used in hybrid or high-index Mie resonator fashion to create metasurfaces in the infrared. Typically, materials of the GST family are switched by heat, as they can shift their refractive index drastically, depending on whether they are in the amorphous or crystalline state, which can be switched depending on heating and cooling parameters [2]. Another approach uses materials such as ITO which can shift its refractive index in the infrared depending on its charge carrier density. In combination with a perfect absorber geometry, this results in electrical switchable functionalities such as beam steering for LIDAR applications. Other possibilities include metal-to-insulator transition materials such as Mg or VO_2 , which can be switched by proton incorporation or heating [3].

All of the previous approaches have their individual benefits and drawbacks. Hybrid approaches often suffer from the fact that the plasmonic resonances are shifted only spectrally, hence influencing other wavelengths. This holds true also for several of the GST approaches. Perfect absorber geometries that can in principle give the full 2π phaseshift and can be electrically switched commonly work in reflection geometries with very low reflectances, hence making applications such as LIDAR difficult. Nanoantennas that can switch plasmonic resonances on or off have switching speed issues, as incorporation of protons from the hydrogen gas phase often requires palladium as molecule splitting catalyst and hence results in switching times of seconds [4]. Here, we present a completely different and novel approach to the above problem: We present electrically switchable nanoantennas whose plasmon resonance can be switched on and off electrically and individually. We demonstrate video-rate switching times, hence overcoming the previous speed issues.

In order to validate our concept, we combine our electrically switchable plasmonic nanoantennas in functional metasurfaces. In one implementation, we demonstrate beam steering. In another example, we demonstrate a flat metalens whose focusing ability can be switched on and off electrically. Our system can be operated in transmission as well as in reflection geometry.

Our approach represents the breakthrough that will ultimately enable spatial light modulators with densities higher than 1000 lp/mm. This is the crucial element to make possible high-angle variable beam steering, electrically addressable zoom metalenses, and, ultimately, wide-angle holographic videos. These devices are key to enable compact augmented and virtual reality devices.

- [2] Y. Wang, M.L. Brongersma, et al., *Nature Nanotechnology* 16, 667 (2021).
 [3] F. Neubrech, X.Y. Duan, and N. Liu, *Science Advances* 6, eabc2709 (2020).
 [4] F. Sterl, H. Giessen et al., *Nano Lett.* 15, 7949 (2015).

12:15 PM EQ05.27.05

High-Momentum 2D Exciton-Polaritons in Monolayer Semiconductors [Itai Epstein](#)¹ and Frank Koppens²; ¹Tel Aviv University, Israel; ²ICFO–The Institute of Photonic Sciences, Spain

Highly-confined or large-momentum polaritons are usually associated with transverse-magnetic (TM) surface modes residing at the interface between two bulk materials. Commonly, the condition for the existence of such a mode is that one of the materials exhibits a permittivity whose real part is negative, while the other is a dielectric. For example, electron in metals give rise to the existence surface-plasmon-polariton (SPP) at a metal/dielectric interface, and optical phonons give rise to the surface-phonon-polariton in polar dielectrics. Both exhibit a negative real part of the permittivity in a certain spectral range, and the response holds also for 2D monolayers with the same properties [1, 2]. In that aspect, up until recently, monolayer TMDs have been known to exhibit a positive real part of their permittivities and thus in principle, should not support such a polaritonic mode.

In this work [3], we predict the existence of a highly-confined exciton-polariton mode, which propagates in-plane and confined to the monolayer in the out-of-plane direction. It belongs to the same family of polaritons mentioned above, only here the oscillations of the impinging TM electromagnetic light field couples with collective oscillations of the TMD excitons, and indeed exhibits the known signature of negative real part of its permittivity. The latter is attainable by encapsulating the monolayer TMD with hBN and cooling down to cryogenic temperatures. We show that owing to the resonant nature of the excitonic optical response in TMDs, the formation of the 2DEP and its detection strongly depend on achieving extremely narrow excitonic linewidths.

From experimental data, we extract the temperature-dependent real part of the permittivity, for an hBN-encapsulated WS₂ monolayer, obtained from reflection measurements, and find that it can sustain increasingly negative values with decreasing temperature. We analyze the 2DEP properties under these conditions at the lowest temperature and compare them to those of SPPs at the same spectral range. We find that the 2DEP exhibits over two orders of magnitude larger wavelength confinement.

Such highly-confined polaritons in the visible spectrum can pave the way to new light-matter interaction possibilities, based on 2D-materials, and compete with current SPP-based applications.

References

- [1] Basov D.N. et al, *Science* 354-95(2016).
 [2] Low T. et al, *Nat. Mater.* 16 182–94(2017).
 [3] I. Epstein et al, "*Highly Confined In-plane Propagating Exciton-Polaritons on Monolayer Semiconductors*", *2D Materials* 7, 035031 (2020).

SESSION EQ05.28: Nonlinear Optics/Nanophotonic Devices
 Session Chairs: Igal Brener and Ho Wai (Howard) Lee
 Wednesday Afternoon, December 8, 2021
 EQ05-Virtual

1:00 PM *EQ05.28.02

Surface Nonlinear Optics with Two-Dimensional Materials [Andrea Marini](#); University of L'Aquila, Italy

Optical nonlinearity in photonic materials enables a large number of applications such as frequency conversion, all-optical signal processing, and non-classical sources of light. The speed of solid-state electronic devices, determined by the temporal dynamics of charge carriers, could potentially reach unprecedented petahertz frequencies through direct manipulation by optical fields, consisting in a million-fold increase from state-of-the-art technology. In graphene, charge carrier manipulation is facilitated by exceptionally strong coupling to optical fields, from which stems an important back-action of photoexcited carriers. Here we report the instantaneous response of graphene to ultrafast optical fields, elucidating the role of hot carriers on sub-100 fs timescales. The observed nonlinear response and its dependence on interaction time and field polarization reveal the back-action of hot carriers over timescales commensurate with the optical field. An intuitive picture is given for the carrier trajectories in response to the optical-field polarization state. We note that the peculiar interplay between optical fields and charge carriers in graphene may also apply to surface states in topological insulators with similar Dirac cone dispersion relations. Furthermore, we report harmonic generation and saturable absorption in graphene, discussing free-carrier generation and their ultrafast temporal dynamics in the atomically thin material. We further discuss the nonlinear optical properties of transition metal dichalcogenides, illustrating cavity-enhanced second-harmonic generation and parametric down-conversion and demonstrating that phase-matching free operation can be achieved in photonic micro-cavities embedding two-dimensional semiconductors as nonlinear optical media. Our results are promising for the development of integrated optical parametric oscillators and micro-sources of entangled photons.

1:30 PM EQ05.28.03

Third-Order Nonlinear Optical Response of Embedded Arrays of Plasmonic Gold Nanoparticles Synthesized by MeV Ion Implantation José-Miguel Zárate-Reyes¹, Oswaldo Sánchez-Dena², Erick Flores-Romero^{3,1}, Jorge-Alberto Peralta-Angeles¹, Jorge-Alejandro Reyes-Esqueda¹ and [Juan-Carlos Cheang-Wong](#)¹; ¹Instituto de Física, Universidad Nacional Autónoma de México, Mexico; ²Instituto de Ingeniería y Tecnología, Universidad Autónoma de Ciudad Juárez, Mexico; ³CONACYT, Instituto de Física, Universidad Nacional Autónoma de México, Mexico

Arrays of plasmonic gold nanoparticles, embedded in fused silica plates, were prepared by implanting 2 MeV Au⁺ ions through a silica particle lithographic mask. The nonlinear optical response of these periodic arrays was experimentally investigated using the z-scan technique at 532 nm with 26 ps pulses from a Nd:YAG laser. The open-aperture z-scan measurements were performed following different linear polarization angles for the incident light beam. A strong saturable absorption and a very clear nonlinear dichroic behavior were determined, the latter indicated by a sinusoidal modulation of the nonlinear absorption coefficient β (up to about 20% of its absolute value) as a function of the polarization angle. This result gives clear evidence of the formation of ordered arrays of embedded Au nanoparticles, corresponding to a honeycomb lattice symmetry with a modulation period of 30°.

1:45 PM EQ05.28.04

Simulating Diffuse, Glossy and Specular Albedo Materials for Enhanced Bifacial Solar Module Output Shweta Pal and Rebecca Saive; University of Twente, Netherlands

Simulating diffuse, glossy and specular albedo materials for enhanced bifacial solar module output.

An effective way of improving photovoltaic (PV) yield while keeping the costs low is by using bifacial modules. As opposed to conventional monofacial modules, bifacial modules produce electricity by accepting solar irradiance from the front and the rear side. A crucial element in enhancing the bifacial output is the ground reflectance, *i.e.*, albedo. The module output strongly depends on the angle and wavelength of the incident irradiance and many nanophotonic light management strategies are particularly sensitive to these parameters [1, 2, 3, 4, 5]. Thus, understanding the spectral and angular albedo of the ground-reflector becomes important for the accurate understanding of albedo-dependent module output. Various sophisticated models [6, 7, 8, 9] help in calculating the bifacial output due to albedo but often use wavelength and/or angle averaged albedo.

To overcome this, we developed an albedo-centric reverse ray-tracing algorithm that can simulate short-circuit current density of a bifacial module under the influence of albedo materials with complex spectral and angular reflectance. The software can model a wide range of reflectors, *i.e.*, diffuse, glossy [10], specular, and a combination of the three. It can also accommodate custom reflectors like metamaterials or free-space luminescent solar concentrators [11]. The algorithm also accepts any spectral and angular irradiance and tailored PV modules, while accounting for self-shading.

Our study shows that under AM1.5G illumination at 85° relative to the horizontal, a diffuse reflector outperforms a specular reflector for any value of module height and tilt. A diffuse reflector also proves to be more robust to the changes in module orientation and consequently, self-shading. Such an approach can help in the fundamental understanding of the influence surface properties of a reflector on a solar module. It can facilitate in assessing the performance of currently existing natural and artificial reflectors and inspire ideas to devise novel albedo materials for higher bifacial output. Furthermore, when combined with the open-circuit voltage and local spectro-angular irradiance [12] measurements, the above methodology can assist in selecting the best module-albedo pair and their optimal configuration.

References

- [1] R. Saive, T. C. R. Russell, and H. A. Atwater, IEEE 7th World Conference on Photovoltaic Energy Conversion (WCPEC), Waikoloa Village, HI, USA, 2018.
- [2] M. Brennan, A. Abramase, R. Andrews and J. Pearce, Solar Energy Materials & Solar Cells, vol. 124, pp. 111-116, 2014.
- [3] T. C. R. Russell, R. Saive and H. A. Atwater, 44th IEEE Photovoltaic Specialist Conference (PVSC), Washington, D.C., USA, 2017.
- [4] N. Tavakoli and Esther Alarcon-Llado, Optics Express, vol. 27, pp. A909-A923, 2019.
- [5] R. Saive, Progress in Photovoltaics: Research and Applications, pp. 1-13, 2021.
- [6] A. Asgharzadeh, M. A. Anoma, A. Hoffman, C. Chaudhari, S. Bapat, R. Perkins, D. Cohen, G. M. Kimball, D. Riley and F. Toor, IEEE 46th Photovoltaic Specialists Conference (PVSC), Chicago, IL, USA, 2019.
- [7] C. E. Valdivia, C. T. Li, A. Russell, J. E. Haysom, R. Li, D. Lekx, M. M. Sepeher, D. Henes, K. Hinzer and H. P. Schriemer, IEEE 44th Photovoltaic Specialist Conference (PVSC), Washington, DC, 2017.
- [8] M. R. Vogt, T. Gewohn, C. Schinke and R. Brendel, EUPVSEC 2018, 2018.
- [9] T. O. Fartaria and Manuel Collares Pereira, Solar Energy, vol. 91, pp. 93-101, 2013.
- [10] B. Walter, S. Marschner, H. Li and K. Torrance, Proceedings of the Eurographics Symposium on Rendering Techniques, Grenoble, France, 2007.
- [11] G. Heres, L. Einhaus and R. Saive, IEEE Photovoltaic Specialists Conference (PVSC), online, 2021.
- [12] S. Pal, A. Reinders and R. Saive, IEEE Journal of Photovoltaics, vol. 10, no. 6, pp. 1803-1815, 2020.

2:00 PM EQ05.28.05

Two-Dimensional Fluorescence Mapping (2DFM) for the Non-Destructive Analysis of Band-Gap and Defect States in Inorganic and Organic Semiconductors Carole C. Perry, Daniel J. Oliver and Victor V. Volkov; Nottingham Trent University, United Kingdom

We report a novel approach to analyze bandgap and defect states within semiconductors by fluorescence spectroscopy using a plate reader conventionally used for the study of biological samples in solution. We use two-dimensional fluorescence mapping (2DFM) to deconvolve spectral signatures that would be superimposed in 1D-spectral space; for example, the 570nm emission peak in ZnO whose emissive state is of a different physical nature depending upon the excitation wavelength used. The broad applicability of the technique is shown for a library of widely studied inorganic semiconductors CdS, CdSe, ZnS, ZnSe, ZnO (analytical standard and nanorods) & TiO₂. Anthracene is also included as a representative example of an organic semiconductor. The 2DFM approach is able to identify spectral features from the bandgap, defects and trace impurities. The technique has applicability in both academic and industrial settings for semiconductor studies and quality control (QC) applications.

2:15 PM EQ05.28.06

Au Nanoparticles Embedded in ZnO Microstructures for Optical Security Applications Daniel J. Oliver, Victor V. Volkov and Carole C. Perry; Nottingham Trent University, United Kingdom

Composites of ZnO-Au are promising materials for use in optical security applications due to multiple aspects of the materials fabrication process impacting its spectral fingerprint. We report a one-pot strategy to synthesize ZnO-Au hetero-structures using a peptide chimera with sequence GLHVMHKVAYSSGAPMPPF (ZA2). The novel ZA2 chimera combines most of a ZnO binding sequence, G-12 (GLHVMHKVAPPR) and a gold binding sequence, A3 (AYSSGAPMPPF) that has been extensively studied in the literature. The one-pot peptide mediated synthesis was performed in the presence and absence of HAuCl₄ to separately determine the impact of the peptide and gold inclusions on the structural and electronic properties of the ZnO component. Using a combination of optical spectroscopy and electron microscopy we show that both spherical and non-spherical gold nano-inclusions were successfully embedded within the ZnO forming Ohmic contacts. Simulation of the plasmon resonance of nanoscale gold inclusions in ZnO using Mie theory and finite difference time-domain (FDTD) numerical approaches report on collective plasmon phenomena from embedded inclusions suggesting an inter-inclusion spacing of 10 nm or less and informs on the tuneable spectral nature of these materials. Spectra calculated using the FDTD approach show the synthetic approach described here has the potential to generate a library of materials with varying spectral features that could be used for identification purposes.

2:30 PM *EQ05.08.02

Enhancing Classical and Quantum Effects with Epsilon-Near-Zero (ENZ) Materials Jeremy N. Munday; University of California, Davis, United States

Materials whose dielectric functions approach zero have many unique properties ranging from enhanced non-linear behavior to suppression of quantum electromagnetic fluctuations. Beyond these interesting physical phenomena, epsilon-near-zero (ENZ) concepts can be applied to devices to exploit these effects. In this talk, I will discuss our recent work on the development of devices that take advantage of these effects to create super-absorbing optical films for novel photodetectors and hydrogen sensors, modified thermal emission, and quantum effects that can be exploited using ENZ materials. Two examples

of the later are the suppression of spontaneous emission and modifications to the Casimir force, a force that is purely quantum in nature and is related to the electromagnetic boundary conditions placed on vacuum fluctuations. We will conclude with an outlook for this emerging area of research.

SESSION EQ05.29: Lasing and Radiation Engineering II
Session Chairs: Viktoriia Babicheva and Anatoly Zayats
Wednesday Afternoon, December 8, 2021
EQ05-Virtual

4:00 PM *EQ05.29.01

Emission Control with Dielectric Metasurfaces [Igal Brener](#); Sandia National Laboratories, United States

The spontaneous emission rates of emitters can be manipulated by tailoring the optical density of states of its local environment. Traditionally, this has been achieved through interaction of emitters with different types of photonic cavities. Using the same principles, metasurfaces and other types of nanostructured media have been used to control spontaneous emission of single and ensembles of quantum emitters. In this talk I will give an overview of the control and manipulation of spontaneous emission from different types of emitters (dopants in carbon nanotubes, excitons in two dimensional materials and epitaxial/colloidal quantum dots) using dielectric metasurfaces. Finally, I will describe how semiconductor metasurfaces can be used to control the directionality of spontaneous emission at ultrafast time-scales.

4:30 PM EQ05.29.02

Exciton-Polariton Lasing from a Bound State in the Continuum [Fabrizio Riminucci](#)¹, Vincenzo Ardizzone², Monica Lorenzon¹, Luca Francaviglia¹, Camille Stavarakas¹, Stefano Cabrini¹ and Daniele Sanvitto²; ¹Molecular Foundry, Lawrence Berkeley National Laboratory, United States; ²CNR Nanotec, Italy

The achievement of thresholdless lasing is a long-sought goal for many applications. Yet, the inherent working principle behind lasers hinders its realization, due to the necessity to reach population inversion. An interesting strategy to overcome this limitation is based on exciton-polaritons. These hybrid light-matter excitations can undergo a phase transition to a coherent state, known as Bose-Einstein condensate, eliminating the requirement for population inversion.

In order to undergo this phase transition that leads to the emission of laser-like light, exciton-polaritons need to live long enough to macroscopically occupy a single quantum state. Up to now they have been mainly studied in vertical microcavities but their lifetime is usually limited by the quality of the mirrors and deep etching processes.

In this work we show exciton-polariton lasing from a bound state in the continuum (BIC), obtained via shallow patterning of a GaAs/AlGaAs slab. The extremely long lifetime of the BIC, alongside the high-quality post-processed cavity, allowed us to achieve an ultra-low lasing threshold in state-of-the-art polariton lasers. We focus on the impact of the nanofabrication processing over the polariton lasing from a BIC, leading to low threshold polariton condensation, and we characterize its emission in both real and reciprocal space.

In conclusion, this work unveils new possibilities of energy efficient coherent light sources to be used in future integrated photonic devices. Our new approach to achieve exciton-polariton lasing shows several advantages over the more classical vertical microcavities, since no mirrors are required and the etching needed to manipulate the photonic mode is only a few tens of nanometers. Aside from the interesting technological advantage, bosonic condensation in symmetry-protected photonic eigenmodes could also bring new topological properties onto macroscopic quantum states, which could give new insights on the spatial properties of BIC states.

4:45 PM EQ05.29.03

Controlling the Effective Bandgap of Epsilon-Near-Zero (ENZ) Nanoparticles Coupled to Quantum Emitters [Tao Gong](#)^{1,1}, Inigo Liberal², Miguel Camacho³, Benjamin Spreng¹, Nader Engheta⁴ and Jeremy N. Munday¹; ¹University of California, Davis, United States; ²Public University of Navarre, Spain; ³University of Seville, Spain; ⁴University of Pennsylvania, United States

Epsilon-near-zero (ENZ) materials have drawn significant research interest in recent years, owing to their unique electromagnetic/optical properties at the frequencies of vanishing real part of permittivity. Effects include negligible phase advances, strong spatial coherence, and enormous field enhancement at the interfaces with dielectric materials. They have found extensive applications in supercoupling, nanocircuit boards, ultrafast optical nonlinearity, perfect optical absorption, etc. In addition, ENZ materials have also been successfully exploited to modulate the spontaneous emission intensity, including the spectrum and directionality, of quantum emitters (QEs). Here we propose the concept of electromagnetic “bandgaps” for nanoparticles comprising an ENZ material. Depending on the frequency, the spontaneous emission of a QE in close proximity to a nanoparticle can be either substantially enhanced (as a result of the coupling into surface plasmon or dielectric resonances) or significantly suppressed (due to the lack of modes available for excitation around the ENZ frequency). Our theoretical results show an enhancement factor of ~38000 for the total emitted power at the surface plasmon resonance frequency and of ~0.002 for the radiatively emitted power around the ENZ frequency from a QE placed in close proximity of a low-loss ENZ sphere with a diameter of 600 nm, compared with that placed in free space. Even for realistic ENZ materials (e.g. ITO), enhancements of ~1610 and suppressions of ~0.13 are predicted. The effective bandgap of the nanoparticles can therefore be probed by tracking the radiated power from the emitter. Our research provides an alternative perspective to explore the correlation between plasmonic resonances, ENZ behavior, and spontaneous emission dynamics of quantum emitters.

5:00 PM EQ05.15.09

Neural Network Based Inverse Design of Organic Light-Emitting Diode Structures [Sanmun Kim](#)¹, Jeongmin Shin¹, Jaeho Lee², Chanhung Park¹, Songju Lee¹, Juho Park¹, Dongjin Seo^{1,3}, Sehong Park², Chan Y. Park³ and Min Seok Jang¹; ¹Korea Advanced Institute of Science and Technology, Korea (the Republic of); ²LG Display Co., Ltd., Korea (the Republic of); ³KC-ML2, Korea (the Republic of)

Organic light-emitting diodes (OLED) are widely used light-emitting diodes that utilize the light emission from an electron-hole annihilation inside an organic material. In an OLED device, the multiple reflections and the light interference inside a layered structure cause its optical characteristics to depend heavily on the device shape. Also, it leads to an angle dependence of the emission spectra while narrowing down the emission spectra. In this manner, an optimization process is required for any OLED device for the maximization of light extraction efficiency and color gamut. Some classical approaches have been made to optimize the structure but the results are hardly global optima since the global optimization requires heavy computation.

In the meantime, it has been reported that the neural network works as an excellent platform for calculating optical response of photonic devices, and tackling photonic inverse design problems^{1,2}. In the field of OLED, machine learning techniques have also been performed to facilitate material screening processes³. However, no approach has been made to address the link between the device design parameters and the light extraction efficiency (LEE) of a

given OLED device for the purpose of the inverse design and optical performance optimization.

In this work, we present a neural network that receives the layer thicknesses and refractive indices as the inputs and predicts the LEE response of a given OLED structure. The network is trained with a dataset containing 260,000 structure parameter-LEE pairs which were obtained from the in-house Chance-Prock-Silbey (CPS) model⁴. The neural network was able to complete the spectrum predictions with 4×10^6 faster rate than the rigorous electromagnetic simulation based on CPS formulation depending on the degree of parallelization with RMSE of 1.86×10^{-3} . Two different routes were taken for the inverse design of LEE responses. One was the inverse neural network built by joining additional layers to the pre-trained forward neural network and the other was the neural network assisted genetic algorithm (NNGA) which uses the forward network as the platform for LEE prediction. NNGA showed superior performances in the inverse design of both existing and non-existing LEEs whereas the inverse neural network was unmatched in terms of the computation speed. The NNGA also successfully solves two representative OLED optimization problems: maximizing LEE and minimizing angle-dependent white color variation. Considering that both problems possess large design spaces that are difficult to be addressed by conventional numerical approaches employing rigorous electromagnetic simulations, the neural network-based methodology presented in this work provides a promising platform for tackling computation-heavy optimization tasks with one-time computation cost. Furthermore, different aspects of the neural network including its one-to-many mapping behaviour, extrapolability, and comparison between the inverse design methods were investigated extensively.

Acknowledgements

This work was supported by LG Display

References

- [1] Kiarashinejad, Y, et al., Deep learning approach based on dimensionality reduction for designing electromagnetic nanostructures. *Npj Comput Mater* 2020, 6 (1).
- [2] Ma, W., et al, Deep-Learning-Enabled On-Demand Design of Chiral Metamaterials. *ACS Nano* 2018, 12 (6), 6326-6334.
- [3] Gomez-Bombarelli, R., et al. A., Design of efficient molecular organic light-emitting diodes by a high-throughput virtual screening and experimental approach. *Nat Mater* 2016, 15 (10).
- [4] Chance, R. R., et al., Molecular Fluorescence and Energy Transfer Near Interfaces. In *Advances in Chemical Physics*, 1978; pp 1-65.

5:15 PM EQ05.14.04

Fast and Rigorous Electromagnetic Simulation of Dipole Emission in a Periodically Corrugated Light-Emitting Diode Structure Based on Diffraction Tracking Chanhyung Park, Jeongmin Shin, Sanmun Kim, Juho Park and Min Seok Jang; KAIST, Korea (the Republic of)

Organic light-emitting diodes (OLED) have become one of the major light sources for display use due to high color accuracy and luminosity. The external light efficiency of conventional OLEDs ranges around 20% while the internal quantum efficiency approaches ~100%, which is sufficiently low. The discrepancy arises from the total internal reflection and a relatively large refraction index of emission layers. It has been reported that the external light efficiency of an OLED can be improved by introducing a periodically corrugated layer boundary [1, 2], but the effect has not been analyzed quantitatively. Electromagnetic analysis of a dipole layer in a periodically corrugated LED has been done previously [3], but the approach used in that work cannot deal with the emission from a single dipole, which is crucial for analyzing a periodically corrugated dipole layer. In this work, we demonstrate how the emission from a single dipole in a periodically corrugated LED structure can be calculated by diffraction tracking. We decomposed the light emission of a point dipole source into plane waves, and tracked each wave to calculate light emission. We tracked the diffraction and polarization conversion at a periodically corrugated layer boundary. Diffraction efficiency was calculated by rigorous coupled-wave analysis method (RCWA) [4]. We have confirmed that the results from our calculation model agree well with the simulation values from finite-difference time-domain method (FDTD) in terms of far-field image and light extraction efficiency (LEE) while alleviating the computational load by a significant amount. We even showed that the results from our calculation model agree well with FDTD methods at two-dimensional periodically corrugated layer boundary. We also implemented direct calculation of incoherent dipole layer in a periodically corrugated OLED, which makes our method more time efficient.

The advantages of our method become clear during the OLED structure optimization process. The diffraction coefficients obtained from the RCWA calculation depends only on the shape of the corrugation, hence the calculation for different dipole vertical/horizontal position, dipole orientation and different emission layer thicknesses can be completed with minimal computation. Also, the analysis involving multiple dipoles can be calculated in parallel, facilitating the optimization task even more.

References

1. Zhang, Xu-Lin, et al, *Optics Letters*, Vol. 36, Issue 19, pp. 3915-3917 (2011)
2. Jeon, Sohee, et al, *Nanoscale* 6.5 (2014): 2642-2648.
3. Delbeke, Danaë, et al, *Journal of the Optical Society of America A* Vol. 19, Issue 5, pp. 871-880 (2002)
4. J.P.Hugonin, et al, *arXiv:2101.00901*

SESSION EQ05.30: On-Demand
Sunday Morning, December 5, 2021
On-Demand

8:00 AM EQ05.13.05

Spin-Valley Locking Edge States Through Staggered Chiral Photonic Crystals Yeseul Kim, Minkyung Kim and Junsuk Rho; Pohang University of Science and Technology, Korea (the Republic of)

Topological photonics mimic the topological condensed matter physics to transport the photons efficiently and robustly. In this poster presentation, we present spin-valley locking of edge states through staggered chiral photonic crystals in the two-dimensional honeycomb lattice. We demonstrate the bulk band dispersion with a bandgap in the spin-valley locked edge states and by using a coupled dipole method. And the spin-valley locking characteristics can be observed when the staggered chirality breaks the inversion symmetry.

References

- Kim, M., Kim, Y., & Rho, J. (2020). Spin-valley locked topological edge states in a staggered chiral photonic crystal. *New Journal of Physics*, 22(11), 113022.

SYMPOSIUM EQ06

Innovative Fabrication and Processing Methods for Organic and Hybrid Electronics
November 30 - December 6, 2021

Symposium Organizers

Paddy K. L. Chan, University of Hong Kong
Oana Jurchescu, Wake Forest University
Ioannis Kymissis, Columbia University
Brendan O'Connor, North Carolina State University

* Invited Paper

SESSION EQ06.01: Molecular Assembly and Charge Transport
Session Chair: Oana Jurchescu
Tuesday Morning, November 30, 2021
Hynes, Level 2, Room 209

10:30 AM *EQ06.01.01

Self-Assembled Soluble Organic Semiconductors John Anthony; University of Kentucky, United States

Solubilization of organic semiconductors is critical to enable a wide variety of deposition technologies. However, the selection and location of solubilizing groups must be made with great care, to avoid disrupting critical intermolecular interactions. This talk will address weak, non-covalent interactions that can be used as supramolecular synthons to induce or enhance crystallization in organic thin films. I will also describe current efforts to harness computation and machine learning to enhance the design of high-mobility organic semiconductors.

11:00 AM EQ06.01.02

Controlling Structure-Property Relationships of Organic Semiconductor Thin Films Using Tunable, Highly-Ordered Self-Assembled Monolayers Ashley Conley, Joshua Choi and Gaurav Giri; University of Virginia, United States

Organic semiconductors are competitive with conventional amorphous silicon due to their solution processability at room temperature, which allows for the inexpensive, high-throughput fabrication of lightweight, flexible optoelectronic and electronic devices. Organic semiconductors are applicable in optoelectronic devices such as organic light emitting diodes, organic solar cells, and organic field effect transistors. An inherent disadvantage of organic semiconductors is their propensity to adopt multiple molecular packing motifs, a phenomenon called polymorphism, which can yield highly-contrasting charge transport capabilities and optoelectronic characteristics. More specifically, singlet fission, a photophysical process whereby one exciton is converted into two, has a significant dependence on molecular packing. However, controlling the molecular packing of organic semiconductors is difficult because the underlying crystal structure is dictated by weak Van der Waals forces, and thus, variability in the molecular packing arises from even minute changes in processing conditions.

In this study, the molecular packing of TIPS-pentacene (a small molecule organic semiconductor) was finely-tuned using highly-ordered, tunable self-assembled monolayers. TIPS-pentacene thin films were deposited from solution using solution shearing and subsequently relaxed on top of five ordered self-assembled monolayers. Through this method, various interface-stabilized polymorphs of TIPS-pentacene were isolated. Grazing incidence X-ray diffraction was used to characterize the distinct crystal structures, revealing repeatable and controllable, precise structural changes spanning less than 2 percent shift from bulk crystal structure. Photoluminescence spectroscopy and UV-Vis spectroscopy were used to discern structure-property relationships. We discovered changes in the bandgap transition energies as well as relative changes to the steady-state photoluminescence, suggesting that these interface-stabilized polymorphs have significant differences in intermolecular interactions.

Singlet fission is an exciting area of study that could result in the breaking of the Shockley-Queisser limit and be the basis for next generation solar cells, and are strongly influenced by intermolecular interactions. Singlet fission rates as a function of polymorph have been studied by other researchers; however, the polymorphs had significantly different crystal structures. Here, the finely-tuned interface-stabilized polymorphs puts us in a unique position to obtain a deeper understanding of the sensitivity of singlet fission on crystal structure by experimental means through the systematic structural changes. In conclusion, this work provides a novel method to control and explore structure-property relationships through the fine tuning of the molecular packing of small molecule organic semiconductors using highly-ordered, tunable self-assembled monolayers.

11:15 AM EQ06.01.03

Remarkable In-Plane Alignment Enabled by Unique Thermomechanical and Packing Behavior of the Conjugated Polymer PBnDT-FTAZ Harry Schrickx¹, Somayeh Kashani¹, Lauren Buck¹, Jeromy Rech², Wei You², Lee Richter³, Harald Ade¹ and Brendan T. O'Connor¹; ¹North Carolina State University, United States; ²University of North Carolina at Chapel Hill, United States; ³National Institute of Standards and Technology, United States

In-plane alignment of conjugated polymers leads to anisotropic optoelectronic properties that can be exploited for multiple applications, including polarization sensitive photodetectors, light emitting devices, and thin film transistors. For example, intramolecular charge transport along the polymer backbone is typically favored, and thus promoting alignment can improve charge mobility. Given that the primary optical transition dipole moment is oriented along the polymer backbone, the greater alignment leads to increased polarized light sensitivity in detectors or polarized light emission in OLEDs. Seeing as performance metrics improve as the degree of alignment increases, maximizing in-plane alignment is highly desirable. A popular strategy for aligning conjugated polymers is straining the film on an elastomer, however the degree of alignment achieved is often modest. To maximize the degree of anisotropy, we leverage the unique thermomechanical behavior and molecular structure exhibited in PBnDT-FTAZ by applying a combination of strain and post-strain thermal anneal. The annealing process leads to optical dichroic ratios surpassing 30, the highest known reported dichroism in conjugated polymers indicative of the remarkable alignment achieved.

To better understand the mechanism behind this striking film alignment, we conducted a detailed structural analysis. In-situ UV-Visible spectroscopy reveals the change in absorption anisotropy when the films are annealed past a temperature associated with aggregate relaxation. In addition, the formation of strong vibronic features observed under parallel polarized light and a shift in the absorption spectra indicate a transition to improved packing order. In-situ GIWAXS scans further confirm the increased packing order, as sharp peaks form through annealing and subsequent cooling of the film. These scans unearth a unique packing arrangement, as two populations of crystalline order appear with distinct out-of-plane tilts in the lamellar stacking direction. The dramatic shift in film morphology with thermally annealing is further uncovered with AFM scans, which show the formation of distinct plateau-like domains. Finally, we report how the molecular structure of PBnDT-FTAZ lends itself to the reported packing behavior. Through this work, we uncover how molecular structure and thermomechanics drive packing behavior, which can guide conjugated polymer design to realize films with exceptional in-plane polymer alignment.

11:30 AM EQ06.01.04

Enhancement of Electrical Conductivity in Conjugated Polymers by Post-Processing Side Chain Removal James Ponder, Shawn A. Gregory, Amalie Atassi, John R. Reynolds and Shannon K. Yee; Georgia Institute of Technology, United States

The processability and electronic properties of electroactive conjugated polymers (CPs) have become increasingly important due to the utility of these materials in numerous redox and solid-state devices. While the π -conjugated backbone structure is considered primarily responsible for imparting the core optoelectronic and electrochemical functionality of the material, solubilizing chains - appended to the backbone for processability - also play a significant role in tuning the morphological, redox, and electronic properties. To solubilize CP backbones, the side chains must be relatively long and are typically branched to induce many degrees of conformational freedom. Such side chains reduce the relative fraction of active material in the film, potentially obstructing π - π intermolecular interactions leading to increased localization of charge carriers, and compromise many of the desirable properties of the material (such as electrical conductivity). To reduce the deleterious effects of side chains, we report that post-processing side chain removal, exemplified here via ester hydrolysis, significantly increases the electrical conductivity of chemically doped CP films with a corresponding decrease in Seebeck coefficient. Using a variety of methods, we demonstrate that this change is not due to an increase in degree of doping, but an increase in charge carrier density and reduction in charge localization. Application of this method to high-performance ProDOT/EDOT copolymer structures yield significantly higher average conductivities, even outperforming any currently reported oligoether/glycol-based CP system. Finally, further structural modification yields a highly soluble material that can be processed from a wide range of solvents with an optimized conductivity of > 800 S/cm in thick films after post-processing side chain removal.

11:45 AM EQ06.01.05

Efficient Electronic Transport Through the Insulator-Rich Phase in PEDOT:PSS Blends Scott T. Keene¹, Wesley Michaels², Armantas Melianas², Tyler J. Quill², Elliot J. Fuller³, Alexander Giovannitti², Iain McCulloch^{4,5}, Christopher J. Tassone⁶, A. A. Talin³, Jian Qin², Alessandro Troisi⁷ and Alberto Salleo²; ¹University of Cambridge, United Kingdom; ²Stanford University, United States; ³Sandia National Laboratories, United States; ⁴University of Oxford, United Kingdom; ⁵King Abdullah University of Science and Technology, Saudi Arabia; ⁶SLAC National Accelerator Laboratory, United States; ⁷University of Liverpool, United Kingdom

Conductive polymers rely on side-chains¹ or blending² to improve solubility and processability to fabricate thin films showing efficient electronic charge transport. One such blend, poly(ethylene dioxythiophene):poly(styrene sulfonate) (PEDOT:PSS), has become the most widely utilized conducting polymer because of its ease of processing, air stability, transparency, high electronic conductivity,³ and more recently for its mixed ionic and electronic conduction.⁴ However, the role of the PSS, which makes up 71% of the blend by weight, on the high conductivity is still unknown.⁵ Like other conducting polymers, PEDOT:PSS phase segregates, leading to a semi-ordered, semiconductor-rich component (PEDOT-rich grains) which are surrounded by a less conductive insulator-rich matrix (PSS-rich matrix).⁶ Here, we investigate the fundamental electronic charge transport through the insulator-rich phase to provide a more wholistic understanding of transport in PEDOT:PSS. We decrease the concentration of the conductor, PEDOT, by adding excess PSS and observe an exponential dependence of conductivity on PEDOT weight fraction. Surprisingly, a PEDOT:PSS blend consisting of < 3% PEDOT by weight displays a moderate mobility comparable to polyaniline. Using electrical characterization combined with molecular dynamics simulated microstructures, we show that inter-grain electronic transport through PSS-rich regions occurs via highly efficient tunneling between neighboring PEDOT chains. The results demonstrate the importance of the sidechain or blending polymer on efficient electronic transport and provides a framework for the molecular design of new conducting polymer systems.

[1] Meyer, D. L. *et al. The Journal of Physical Chemistry C* **123**, 20071-20083 (2019).

[2] Abbaszadeh, D. *et al. Nature Materials* **15**, 628-633 (2016).

[3] Worfolk, B. J. *et al. Proc Natl Acad Sci U S A* **112**, 14138-14143 (2015).

[4] Rivnay, J. *et al. Nature Reviews Materials* **3**, 17086 (2018).

[5] Gueye, M. N. *et al. Progress in Materials Science* **108**, 100616 (2020).

[6] Nardes, A. M. *et al. Advanced Materials* **19**, 1196-1200 (2007).

SESSION EQ06.02: Devices and Characterization

Session Chair: John Anthony

Tuesday Afternoon, November 30, 2021

Hynes, Level 2, Room 209

1:30 PM *EQ06.02.01

Formation, Growth and Applications of Microcrystalline Organic Semiconductors Barry P. Rand; Princeton University, United States

Even though record organic semiconductor mobilities are reported for organic semiconductor single crystals, making thin film crystals remains challenging. We will present our efforts to understand crystal formation, and growth (epitaxy) of pinhole free films of numerous organic semiconductors with grains with dimensions of 100s of microns. We will explain how materials that undergo a transition from amorphous to crystalline correlate well with thermal properties. Homoepitaxial studies uncover evidence of point and line defect formation in these films, indicating that homoepitaxy is not always strain-free, but films always remain remarkably smooth (rms roughness never exceeds 5 nm). Transistors made out of large-grained films of rubrene display charge carrier mobility of up to $3.5 \text{ cm}^2 \text{ V}^{-1} \text{ s}^{-1}$, very close to single crystal values, highlighting their potential for practical application. Finally, we will show efforts in achieving heteroepitaxial growth of a different molecular material on top of a crystalline organic template.

2:00 PM EQ06.02.02

High Performance Molecular Rectifiers Based on Mixed Self-Assembled Monolayers Ryan Sullivan, John T. Morningstar, Mark E. Welker and Oana D. Jurchescu; Wake Forest University, United States

The chemical composition and degree of order in self-assembled monolayers (SAMs) is critically important to the properties of molecular electronic devices. We report on the synthesis and electrical response of a series of molecular rectifiers based on benzalkylsilanes in the form of SAMs anchored to a silicon substrate and tested with an Eutectic Gallium-Indium (EGaIn) top electrode. Mixed SAMs were formed via the co-absorption method by incorporating controlled amounts of different aliphatic silane-based additives into the film of the host SAM. The impact on the current-voltage characteristics, breakdown voltages, and static contact angle measurements provided insights into the degree of order and uniformity of the mixed SAM films. We discovered that despite a reduced degree of order introduced within the SAMs, small amounts of (3-aminopropyl)triethoxysilane (APTES) enhanced the current rectification of several materials, whereas, the other additives (such as n-propyltriethoxysilane) decreased the current rectification. We attribute this behavior to the APTES molecules acting as a dopant, thus allowing more efficient charge transport under forward bias. On the contrary, under reverse bias, the shorter dopant molecules do not make intimate contact with the top electrode, decreasing the effective surface area and overall conductance of the monolayer. The most significant improvement was measured in (E)-1-(4-carbomethoxy-phenyl)-N-(3-(triethoxysilyl)propyl)methanimine, where a three-fold increase in the rectification was found when mixed with APTES at an optimized 2:1 ratio, yielding an average rectification ratio of 4500, one of the highest reported values to date for molecular diodes on silicon.

2:15 PM EQ06.02.03

Quantifying Polaron Density in Molecularly Doped Semiconducting Polymers Adam J. Moule¹, Tucker L. Murrey¹, Goktug J. Gonen¹, Meghna Jha¹, Michael Berteau-Rainville², Nikolay Shevchenko¹, Jan Saska¹, Raja Ghosh³, Alberto Salleo⁴, Mark Mascal¹, Ingo Salzmann² and Frank Spano³; ¹University of California, Davis, United States; ²Concordia University, Canada; ³Temple University, United States; ⁴Stanford University, United States

Sequential solution doping is a processing technique that allows a conjugated polymer film to be doped from a solution that will not dissolve the polymer. We present here a method to predict the film doping level in cm^{-3} from the solution concentration used to dope the film. We show using four polymers and three newly synthesized molecular dopants that the doping level can be modeled using a simple Langmuir isotherm and fit to a single equilibrium coefficient. Analysis of the free energy derived from K_{eq} yields a consistent thermodynamic model for molecular doping in polymers. We show that 50-75% of the polymer sites can be doped from solution. We compare Fermi level filling and electrochemical models for ionization efficiency of the dopant. In addition, analysis of the UV/vis/NIR and mid-IR spectra allows analysis of both the polaron sites and the neutral sites as a function of doping level. We show distinct differences between the spectral changes for polymers that when neutral formed H-aggregates rather than J-aggregates for both the neutral sites and the resulting polaron sites. Taken together we demonstrate a consistent and quantitative model for molecular doping that can be applied across different polymer and dopants.

2:30 PM EQ06.02.04

Polaron and Bipolaron Characteristics in Doped Conjugated Polymers Joel H. Bobile and Chad Risko; University of Kentucky, United States

Molecular doping is a powerful method to tune the electronic properties of solution-processed semiconductors based on π -conjugated polymers (CP), enabling high performance thermoelectric devices and thin film transistors. Despite the importance of doping, it is still challenging to predict how a given dopant will influence charge-carrier transport in semiconducting polymers. An accurate description of charge transport in these materials necessitates a good understanding of how polaron and bipolaron characteristics are affected by dopant counterions. We use first-principles calculations based on density functional theory (DFT) and time-dependent Density Functional theory (TD-DFT) with an optimally-tuned hybrid functional to determine various polaron characteristics in CP's with and without dopant counterion present. We find that the coulomb interaction between the polaron and the dopant counterion dictates the polaron size and is the dominant contribution to the polaron binding energy, exceeding polarization and nuclei reorganization. Both polaron size and binding energy play an important role in charge transport. We also find that the location of the induced charge along the polymer chain follows the counterion. As such bipolaron, which leads to faster charge transport, become more stable than polarons when the distance between dopant counterions is sufficiently reduced.

2:45 PM EQ06.02.05

The SLoT Model—A Language for Quantifying Fundamental Charge Transport Parameters in Chemically Doped Semiconducting Polymers. Shawn A. Gregory, Riley Hanus and Shannon K. Yee; Georgia Institute of Technology, United States

In this talk, I will present on the semi-localized transport (SLoT) model and demonstrate its ability to quantitatively compare fundamental charge transport parameters in semiconducting polymer-dopant-processing systems (see Gregory, Hanus, *et al.*, *Nat. Mater.* (2021)). The SLoT model spans the spectrum and captures both localized (hopping-like) and delocalized (metal-like) contributions to the observable electronic and thermoelectric properties by bridging the mathematical and physical formalisms from both polaronic transport models and the Boltzmann transport equations. Using the SLoT model, we can quantify fundamental transport parameters, such as the carrier ratio (carrier density) needed to exceed the transport edge, to what extent does localization (and its activation energy) decrease with increasing carrier density, and what is the hypothetical maximum electrical conductivity in the absence of localization. Although the SLoT model currently lacks chemical and structural predictive ability, the SLoT model provides quantitative transport parameters for each system that can be related to chemical and structural features; this enables a deeper understanding for why one system obtains different transport properties compared to another and could eventually lead to predictive ability. Lastly, I will compare the chemical, structural, and charge transport properties among several systems, which will illustrate the benefit to quantifying charge transport and developing structure-property relationships with the SLoT model.

SESSION EQ06.03: Flexible and Stretchable Devices I

Session Chair: Barry Rand
Tuesday Afternoon, November 30, 2021
Hynes, Level 2, Room 209

4:00 PM *EQ06.03.01

The Role of Device and Semiconductor Fabrication in Measurement Development [Emily G. Bittle](#); National Institute of Standards and Technology, United States

Enhancements or tailoring of organic device performance using unique physical effects requires benchmarking measurements that can be used across labs. Specific unique physical processes, such as singlet fission or dynamic disorder, are difficult to probe directly using standard electrical measurements. To develop new metrics that reflect unique physical processes, devices with researcher-defined properties are required to show reproducibility and reliability. Controlling device and semiconductor properties through fabrication is therefore extremely important. In this talk I will cover how we use controlled fabrication to develop measurements to look into device and semiconductor physics in working organic semiconductor transistors and light emitting diodes, including dynamic disorder, contact resistance, and singlet fission/triplet fusion.

4:30 PM EQ06.03.02

Spectroscopic Characterization and Electronic Transport in Conjugated Polymers Undergoing Post-Processing Side Chain Removal [Amalie Atassi](#), James Ponder, Shawn A. Gregory, Natalie Stingelin and Shannon K. Yee; Georgia Institute of Technology, United States

Conjugated polymers are an increasingly important materials class for organic electronics mainly because of their immense chemical versatility. Generally, side-chains are introduced to induce straight-forward processability, *e.g.*, from solution. However, these chemical modifications also tend to affect local assembly and, in turn, specific optoelectronic properties such as charge transport. As a consequence, sample-to-sample variation can be significant. Here, we report an alternative pathway frequently used in the semiconducting small molecule area: side chain removal through post-processing hydrolysis. We selected a series of poly(dioxy thiophenes) as a model system and employed spectroscopic techniques utilizing X-ray, ultraviolet, and visible sources in combination with thermoelectric measurements to quantify the effects of side-chain removal on the extent of doping and charge transport properties. We find that cleaving the side chains does substantially alter the carrier density and increase the electrical conductivity. Additionally, through tuning of the repeat unit structure, different temperature dependencies in the electrical conductivity are found. Since X-ray photoelectron spectroscopy (XPS) suggests that tuning the repeat unit structure also affects core-level electron interactions, we will discuss the observed differences in the temperature-resolved electrical conductivity and extent of doping with the use of the semi-localized transport model. Moreover, by comparing the side-chain-cleaved systems to materials with complex, insulating side chains, we argue that the former polymers may provide a route towards semiconducting plastics of high processing reliability and a high conjugated backbone fraction.

4:45 PM EQ06.03.03

Nonlinear Impedance Spectroscopy to Characterize Hole Transport and Recombination Dynamics in Organic Semiconductor Devices [Robin Rice](#); University of Vermont, United States

Impedance Spectroscopy (IS) is an increasingly common technique to characterize both solid state and electrochemical systems including solar cells and light emitting diodes (LEDs). However, IS relies on a system response being linear with its input such that a time invariant impedance can be defined. This is usually achieved by a small amplitude input. However, doing so suppresses responses of the nonlinear processes which are of considerable interest to those designing and optimizing these devices, such as charge carrier recombination and space charge effects. This investigation employs the recently developed nonlinear extension to IS (NLIS) based in Fourier analysis of the measured harmonic current such that a nonlinear definition of higher harmonic admittance (inverse impedance) is established. By relating Fourier coefficients of the measured current with derivatives of the voltage specific transfer function we may extract valuable physical parameters of the system in question. Benchmark tests of this technique on systems of known transfer functions will be presented specifically measuring hole mobility from space charge and the diode ideality factor from recombination limited current regimes. Finally, NLIS is used to characterise 2-(7-(4-N,N-Bis(4-methylphenyl)aminophenyl)-2,1,3-benzothiadiazol-4-yl)methylenepropanedinitrile (DTDCPB), a promising novel intramolecular charge transfer (CT) organic semiconductor (OSC). The first known report of DTDCPB hole mobility is presented.

5:00 PM EQ06.03.04

Can Vitrification Lead to Polymer:Dopant Glasses with High Electrical Conductivities and Low Thermal Transport? [Hongmo Li](#)¹, Olivier Bardagot², Stephen Barlow¹, Alejandro Vega-Flick¹, Juan Jose Alvarado-Gil³, Renaud Demadrille², Seth Marder¹ and Natalie Stingelin¹; ¹Georgia Institute of Technology, United States; ²Univ. Grenoble Alpes, CEA, CNRS, IRIG, SyMMES, France; ³Cinvestav Merida, Mexico

Here, we demonstrate that we can use vitrification at eutectic compositions as a tool to produce homogeneously intermixed, doped organic semiconductors with high electrical conductivity from solution. Doped organic semiconductors have found broad use as interlayers for organic light-emitting diodes (OLED), photovoltaic cells (OPV) and photodetectors. Doping, often, is achieved via addition of another species, an oxidizing or reducing agent – *i.e.*, a dopant. However, many semiconducting polymer:dopant systems are not highly miscible, leading in many cases to undesirable phase separation and, thus, inhomogeneous film formation. As a consequence, polymer films are commonly doped via sequential doping methodologies, to achieve more homogenous dopant dispersion and, in turn, higher electrical conductivity. By using vitrification at eutectic compositions, we simplify the procedure towards homogeneously intermixed, high-conductivity polymer:dopant blends. We show that the highest electrical conductivities are found in the most vitrified regime, attributed to enhanced charge-carrier densities at these compositions as deduced from the spin densities measured in electron paramagnetic resonance. The question that remains is whether this eutectic vitrification also assists in keeping the thermal transport in such polymer:dopant blends low. For this purpose, we present thermal transient grating measurement data. Our work, thus, starts to provide a window towards a generally applicable structure/processing/property relationships to electron and charge transport in multicomponent macromolecular matter.

5:15 PM EQ06.03.05

Simulation-Guided Design of Organic Transistors for Cost-Effective, Scalable Electronics [Matthew Waldrip](#)¹, Yue Yu¹, Hamna Haneef¹, Iain McCulloch² and Oana D. Jurchescu¹; ¹Wake Forest University, United States; ²University of Oxford, United Kingdom

Interest in organic electronics is driven in large part by the applications they can address, yet a complete set of device fabrication design rules is still absent for the devices intended to fulfill those roles. Progress is assisted by general guidelines such as minimizing the Schottky barrier at injection interfaces or reducing defect states in the semiconductor layer, but improvements are achieved mainly through experimental trial-and-error, which is time, cost, and material intensive, and yields incremental results most of the time. Here we use physically-based numerical simulations to explore a vast parameter space with high throughput in order to generate rules for material processing and device design, with the goal of optimizing charge mobility and injection. We

then use these predictions to evaluate a “window” of device design where certain parameters can be relaxed in favor of cost effectiveness, but without a penalty in device performance. Examples include the contact interface and the quality/purity of the semiconductor, which we show can be compensated through adjustment of another parameter. We investigated the impact of the trap density of states (t-DOS) and the injection barrier on the charge carrier mobility in organic field-effect transistors (OFETs) for both high- and low-capacitance dielectric devices, in co-planar and staggered architectures. The simulations revealed that lowering the dielectric capacitance results in a device that is more permissive to an injection barrier, but that is also more sensitive to changes in the t-DOS; the reverse is true for increasing the dielectric capacitance. Additionally, the staggered architecture outperforms the co-planar structure when an injection barrier is present. These trends outlined a processing window for staggered-structure devices, wherein by tuning the dielectric capacitance one can raise the tolerance of traps or poor contacts. To test these predictions and take advantage of this processing window, we fabricated and characterized a variety of OFETs. We tuned the injection barrier via self-assembled monolayers (SAMs) while the trap density of states (t-DOS) was modified by altering the semiconductor film microstructure through processing and purity by synthesis method. Beginning with the case of OFETs with high-work function (SAM-treated) contacts and typical semiconductor processing, mobility changed very little with dielectric capacitance, in accordance with simulation: the high-capacitance devices (ca. 4 nF/cm²) had mobilities of 1.5 ± 0.1 cm²/Vs (average obtained on over 100 devices), while the low-capacitance devices (1.7 nF/cm²) had mobilities of 1.6 ± 0.3 cm²/Vs. In the low-capacitance devices, a nominal 0.4 eV injection barrier was introduced and devices still retained 80% of the average mobility value. (This is compared with a decrease in mobility of over 50% in the high-capacitance devices.) We then took advantage of the high capacitance window to fabricate OFETs with a low sensitivity to traps: mobilities varied by less than 15% even when the characteristic density of traps increased by over 40%. In summary, we have shown that the low-capacitance design window relaxes the requirement for a high contact work function, allowing the selection of more cost-effective and scalable materials, while the high-capacitance devices grant more lenient requirements for the quality of the semiconductor film.

SESSION EQ06.04: Poster Session—Processing and Devices I
Session Chairs: Oana Jurchescu and Ioannis Kyriassis
Tuesday Afternoon, November 30, 2021
8:00 PM - 10:00 PM
Hynes, Level 1, Hall B

EQ06.04.02

Tuning the Peierls Bandgap in Planar, One-Dimensional Photonic Crystal OLEDs David Allemeier and Matthew S. White; University of Vermont, United States

Asymmetric optical properties of mirror electrodes in stacked microcavity OLED photonic crystals induces a Peierls bandgap in each photonic band. Here we explore the influence of the anode and cathode thicknesses on the bandgap and the bandwidth of the two sub-bands that result from the asymmetry. In the context of our device geometry, the silver anodes are shown to primarily control the Peierls bandgap and the aluminum cathodes are shown to tune the bandwidth of the upper and lower sub-bands. These effects are explained conceptually, modeled computationally, and resolved experimentally in the electroluminescence spectra.

EQ06.04.03

Late News: The Role of Molecular Aspect Ratio in the Roughness Evolution of Organic Thin-Film Crystal Growth Jordan Dull¹, Holly Johnson¹, Maria Clara Otani¹, Frank Schreiber² and Barry P. Rand¹; ¹Princeton University, United States; ²University of Tübingen, Germany

The roughness of a series of crystalline organic thin films are measured as a function of film thickness. From these data, the growth exponent of each material is extracted and plotted against the molecular aspect ratio. We find that more three dimensional molecules (low aspect ratio) tend to remain smooth as film thickness increases, in contrast to planar or rod-like molecules (high aspect ratio) which quickly roughen. This suggests that the average Ehrlich-Schwoebel barrier at a molecular step edge for low aspect ratio molecules is smaller than it is for high aspect ratio molecules. These results point to the use of low aspect ratio molecules in crystalline organic electronics because of their ability to remain smooth as thickness is tuned.

EQ06.04.04

Late News: Synthesis of an Organometallic Aluminum Compound for Monolayer Doping of Silicon Wafers Alex J. Taylor, Santosh Kurinec and Scott Williams; Rochester Institute of Technology, United States

Synthesis of an aluminum complex containing a functional mordant group will be presented. The functional vinyl group is designed to coordinate with silicon radicals on the surface of an etched silicon wafer. This process is called monolayer doping. FTIR, Raman, and NMR spectroscopy were used to analyze the different organometallic dopant compounds. A dried derivative of aluminum isopropoxide was found to have FTIR and Raman Peaks of 1612 and 3116(1/cm), which are indicative of the presence of a vinyl group. NMR spectroscopy shows peaks around 6.4ppm which is also indicative of a vinyl group on the compound. Tris(2,4-pentanedione) aluminum(III) was synthesized with aluminum chloride and acetylacetone in an aqueous solution. The reaction between the dopant and the silicon radicals creates a uniform layer of dopant-wafer bonds on the wafers surface. Silicon wafers have been successfully doping using this method. The doped wafer is washed and dried to remove any non bonded dopant from the surface of the wafer. A 70nm capping oxide is applied to the wafer using Plasma Enhanced Chemical Vapor Deposition (PECVD). The wafer is then heated to 1100 degrees Celsius for a variable amount of time between 10 to 40 seconds using Rapid Thermal Annealing (RTA). This drives the dopant into the lattice of silicon wafer and turns the wafer into a p-type semiconductor wafer. Resmap sheet resistance analysis of doped wafers has shown that there is an inverse relationship between annealing time and surface resistance.

EQ06.04.05

Late News: Seed-Induced Crystallization of Molecular Thin Films via Physical Vapor Deposition for Versatile Optoelectronic Applications Kwang-Won Park, Raaghesh Vijayan and Trisha L. Andrew; University of Massachusetts Amherst, United States

Growth of molecular semiconductor thin films with better ordering and uniformity is crucial for devising organic optoelectronics with better performance. A highly ordered and crystalline organic semiconductor thin film can be an ideal active layer owing to its charge transport ability. However, luminescence materials become less efficient when fabricated into solid films, which is known as aggregation-caused quenching. Thus, the luminescent materials are often doped in host materials or remained amorphous to suppress the aggregate formation, even though crystalline films have higher charged carrier mobilities. To address this issue, luminescent molecular rotors have been suggested, that exhibits aggregation-induced emission behavior, which is opposite to the aggregation-caused quenching effect. Nevertheless, for some organic molecules, it is challenging to form crystalline thin films upon substrates, and

their unique optoelectronic properties can be ignored.

Here, we investigate the thin films of 5,11-diphenylindeno[1,2-*b*]fluorene-6,12-dione (**Dp-IFD**) prepared by physical vapor deposition. Because pristine **Dp-IFD** thin films barely crystallize even after thermal treatment and have poor optical as well as electrical properties, **Dp-IFD** thin films have not been exploited to date. However, we discovered that crystalline **Dp-IFD** thin films can be readily achieved by sequential deposition of coronene seed layer and **Dp-IFD** molecules without breaking vacuum. Current atomic force microscope (c-AFM) measurement and space charge limited current (SCLC) devices showed that crystalline **Dp-IFD** can support 4 orders of magnitude higher electron mobility. Crystalline **Dp-IFD** thin films also exhibited brighter fluorescence emission with longer lifetime than their amorphous counterparts. Furthermore, we demonstrated versatile applications of the **Dp-IFD** thin films, such as organic solar cells (OSCs) and light emitting diodes (OLEDs), owing to its veiled superior optoelectronic properties.

EQ06.04.06

Late News: Self-Assembly of Block Copolymers for the Formation of Electronic Devices Using DNA Origami Dulashani Ruwanthika Ranasinghe Weerakkodige, John N. Harb, Robert C. Davis and Adam T. Woolley; Brigham Young University, United States

DNA origami is a powerful method to create structurally versatile, highly addressable, and distinct nanoscale objects to facilitate the field of electronics. Controlled placement of DNA origami is essential to build functional devices like biochips, electronic circuits, sensors, and optical or photonic devices. Block copolymer (BCP) self-assembly can be utilized for next-generation lithography for the advanced nanopatterning of surfaces. Here we present a method of using a BCP as a mask to create a patterned surface, rendering it capable of selective attachment of DNA origami that will eventually become the base of the electronic device. We use a polystyrene (PS) co-poly(methylmethacrylate) (PMMA) block copolymer, PS(S-b-MMA), which has cylindrical nanodomains of PMMA. These cylindrical nanodomains can be oriented normal to the surface with controlled interfacial interactions. Exposure to UV radiation then degrades the PMMA and crosslinks the PS matrix, resulting in a nanoporous film on silicon surfaces after sonicating with acetic acid and oxygen plasma etching. We investigated the process window for forming ordered arrays of nanoscale polymer cylindrical domains perpendicular to the thin films, including the effect of substrate surface treatment, spinning conditions, annealing conditions, and film thickness. The cylindrical nanodomains that are perpendicular to the film surface have ~15 nm diameter. We will use the etched PS-PMMA thin films as a mask for gold deposition. DNA origami modified with thiol groups can then be used to attach to these surface-patterned gold islands selectively. The ability to position DNA origami in a controllable manner will facilitate the integration of DNA-based materials into nanoelectronic and sensor devices where we will deposit electrically conductive metallic or/and semiconducting materials. The electronic characterization will be performed to reveal the ability to use these devices in the future. This work will contribute to the field of using organic BCP and hybrid materials contribution for future electronic and sensor devices.

EQ06.04.07

Electrodeposition of Silver Nanowire-Based Transparent Conductive Flexible Electrode for Organic Light-Emitting Diodes Sy H. Pham^{1,2}, Anthony Ferri², Antonio D. Costa², Rachel Desfeux² and Philippe E. Leclere¹; ¹University of Mons, Belgium; ²Université d'Artois, France

The transparent conductive electrode (TCE) based on a silver nanowire network (AgNW) has demonstrated high optical transparency, low sheet resistance and shows a range of potential applications in flexible electronics. However, the number of junctions and the junction resistance are the parameters governing the conductivity of the electrode and eventually limiting the applications of AgNW networks if left as it. In this work, the electroplating method was employed to decorate an Ag thin layer on AgNW-junctions to improve the contact resistance of the network. As a result, the AgNW-TCE on flexible PET substrate exhibits a sheet resistance as low as 10 Ohm/sq associated with a transmittance larger than 90% measured at $\lambda = 550$ nm by optimizing the experimental conditions. The contribution of the decorated-AgNWs network on the electric behavior of the electrode was also highlighted at the nanoscale using the conductive Atomic Force Microscopy (c-AFM). The obtained results allow us to propose a feasible process for the preparation of TCE using flexible displays, organic light-emitting diodes, and thin-film solar cells

EQ06.04.08

Functional Polymer Semiconductors from a Universal Approach for Human-Integrated Electronics Nan Li, Yahao Dai, Yang Li and Sihong Wang; The University of Chicago, United States

Polymer semiconductors based on π -conjugated structures have shown distinct promise for the development of human-integrated electronics, owing to their solution processability for large-area fabrication, mechanical softness and even stretchability, as well as low cost. However, among the wide range of functional properties required for this application domain (including, but not limited to, biochemical sensing, chemotherapeutic property, bio/immune-compatibility, micro-patternability, stimuli-responsiveness), a number of them face synthetic challenges to be imparted onto conjugated polymers and thus combined with efficient charge-transport property. Here, we develop a "click-to-polymer" (CLIP) synthesis strategy for conjugated polymers, which enables the use of a click reaction for the facile and versatile attachment of diverse types of functional units to a pre-synthesized conjugated-polymer precursor. This can be utilized to realize both bulk and surface functionalization in/on the deposited thin films. Through demonstrating the applicability on four types of functional groups that each carry distinct emerging properties, for instance, ion conduction and immune-modulation, we show that functionalized polymers from this CLIP method can still retain good charge-carrier mobility above 0.1 square centimeters per volt per second. On the other hand, the surface functionalization does not cause any influence on the mobility. We take two of the realized polymers to showcase the capability of imparting new functions to conjugated polymers: photo-patternable property and biochemical sensing function, both of which advance the state of the art of realizing these two types of functions on conjugated polymers. In the future, we expect the expanded use of this synthesis approach will largely enrich the functional properties from conjugated polymers and facilitate the electronic-biological interfacing. (Under revision)

EQ06.04.10

Thermodynamic Study of Nucleation and Growth Process During Preparation of Manganese-Cobalt Oxide Supercapacitor Electrodes by Photonic Curing Najma Khatoun, Madhu Gaire and Douglas B. Chrisey; Tulane University, United States

Metal oxide-based nanomaterials are an important class of materials because of their unique physical and chemical properties. Various techniques are being used to synthesize metal oxide-based nanomaterials. Gaire *et al.*² reported binder free manganese-cobalt oxide supercapacitor electrodes with ultra-long cycle life. In this work, we employed photonic curing using PulseForge 1300 (NovaCentrix, Austin, TX) to synthesize manganese-cobalt (Mn-Co) mixed oxide nanostructures and monitored the process of nucleation and growth during the synthesis process. A mixture of Mn and Co organometallic precursor was deposited on Pt-Si substrate using an air-spray, and processed using PulseForge in ambient conditions. To study the effect of processing conditions on nucleation and growth of nanostructures, processing parameters, such as power and number of pulses were varied while overall pulse fluence was kept constant. We varied power from 400 V to 700 V and number of pulses from 1 to 7 to achieve constant overall fluence of 16 J/cm² for each sample. A simulating tool for photonic curing based on transient 1-D heat conduction model (SimPulse) is used to simulate the temperature dependent thermal and material properties. SimPulse provided real time thermodynamic profile of Mn-Co mixed precursors as a function of thickness of the films. Our results give an insight into the nucleation and growth process of thin films as a function of energy per pulse and shows that by varying the fluence per pulse and number of pulses, nucleation, and growth changes. At high-energy fluence per pulse, the first pulse causes photodecomposition of the organometallic

precursor, and subsequent pulses result nucleation and growth, and high-temperature chemical reactions to form crystalline non-equilibrium states of metal oxides within a porous film. We observed that pulse design plays a crucial role in the nucleation and growth of nanostructures, even when overall fluence is kept constant. Our study shows that photonic curing can be utilized as a technique to tune the properties of the nanostructures by controlling nucleation and growth. It provides better understanding of nanometric control of complex materials for next generation energy applications.

2. Gaire, Madhu, et al. "Ultra-long cycle life and binder-free manganese-cobalt oxide supercapacitor electrodes through photonic nanostructuring." *RSC Advances* 10.66 (2020): 40234-40243.

EQ06.04.11

Multisource Vacuum Deposition of Methylammonium-Free Perovskite Solar Cells Yu-Hsien Chiang, Miguel Anaya and Samuel D. Stranks; University of Cambridge, United Kingdom

Organic-inorganic halide perovskites of the form ABX_3 have shown outstanding properties for solar cells. The popular compositions consist of mixtures of A-site cations methylammonium (MA), formamidinium (FA) and cesium, and X-site iodide and bromide ions, and are produced by solution processing. It is an open question whether solution processing could produce sufficient spatial performance uniformity for photovoltaic modules or compatibility with multilayered tandem solar cell deposition. In addition, the volatile MA cation presents long-term thermal stability issues. Here, we report the multisource vacuum deposition of $FA_{0.7}Cs_{0.3}Pb(I_{0.9}Br_{0.1})_3$ perovskite thin films with high-quality morphological, structural, and optoelectronic properties. We find that the controlled addition of excess PbI_2 during the deposition is critical for achieving high performance and stability of the absorber material, and we fabricate *p-i-n* solar cells with a power conversion efficiency of 20.7%. Also, the operational stability test shows ~95% of its initial efficiency after 100 hours. We also reveal the sensitivity of the deposition process to a range of parameters, including the type of substrate, annealing temperature, evaporation rates, and source purity, providing a guide for further evaporation efforts. Our results demonstrate the enormous promise for MA-free perovskite solar cells employing industry-scalable multisource evaporation processes.

EQ06.04.12

Rapid Photonic Sintering of Printed Inks to Control Thermal Effects in FHE Substrate Materials Charles Trudeau¹, Bilge Nazli Altay², Patrick Beaupré¹, Sylvain G. Cloutier² and Martin Bolduc³; ¹INO, Canada; ²École de Technologie Supérieure, Canada; ³UQTR, Canada

Additive manufacturing has been evolving towards flexible substrates for the fabrication of printable and flexible hybrid electronic (FHE) devices and circuits. Generally flexible thin polymer or paper-based, these emerging substrates suffer from their heat sensitivity and/or low glass-transition temperatures. Photonic and laser sintering has shown great promise in maintaining the integrity of the substrates without structural degradation due to shrinkage, charring or decomposition. The rapid sintering process arises from microseconds to milliseconds at high temperatures onto printed functional ink traces, in order to reduce the thermal diffusion occurring into the thermally sensitive substrate materials. The minimum sheet resistance value of the conductive traces is then obtained after the proper sintering process. These results are supported by numerical models using finite element methods of the optical wavelength induced thermal dynamics in materials.

In this paper, flash lamp [1] and laser sintering [2] techniques show optimized sheet resistance values for inkjet and screen printing silver and copper inks from 0.2 Ω /sq on PET to 4 Ω /sq on SBS paper obtained at very high speed and spatial precision in comparison with conventional oven annealing. In addition, both these techniques provide a greater control over the electronic properties of the resulting conducting ink traces, while providing a more energy-efficient process within rapid processing times. The simulation results suggest that carefully controlling the heating rates within the ink volume is critical to avoid structural surface defects and achieve optimal sheet resistance values for the sintered functional inks. The research is presented in a perspective of a technology applications development for next generation of FHE sensors and interconnectors.

[1] B.N. Altay, V.S. Turkani, A.P. Pekarovicova, P.D. Fleming, M.Z. Atashbar, M. Bolduc, S.G. Cloutier, "One-step photonic curing of screen-printed conductive Ni flake electrodes for flexible electronics", *Scientific Reports* 11 (2021) 3393.

[2] M. Bolduc, C. Trudeau, P. Beaupré, S.G. Cloutier and P. Galameau, "Thermal Dynamic Effects using Pulse-Shaping Laser Sintering of Printed Silver Inks", *Scientific Report* 8 (2018) 1418.

EQ06.04.14

Complete Haze and Transparent Film by Embedding Air-Gaps for Elimination of Angular Color Shift in Organic Light-Emitting Diodes Wonseok Cho¹, Jae Yong Park¹, Sangwon Baek¹, Kihyon Hong² and Jong-Lam Lee¹; ¹Pohang University of Science and Technology, Korea (the Republic of); ²Chungnam National University, Korea (the Republic of)

Top-emitting organic light-emitting diodes (TOLEDs) are preferred over bottom-emitting structures in terms of high aperture ratio and switching circuit integration. The device structure of typical TOLEDs consists of a metallic electrode on the top and another on the bottom, with organic layers sandwiched between them. Such electrodes induce a Fabry-Perot resonance, which is called the microcavity effect; it gives high device efficiency and high color purity. However, in most TOLEDs show viewing angle (ν) dependence of luminance spectrum; the emission peak tends to be blue-shifted with increasing ν . This phenomenon occurs strongly in white-color displays, which are achieved by combining red, green, and blue (RGB) sub-pixels: this is called white angular dependency (WAD). It distorts the color gamut as ν increases, thus should be eliminated from TOLED displays.

Several methods have been introduced to reduce WAD in TOLEDs. One is to detune the thickness of the microcavity structure. However, tuning the thickness of active layers requires multiple masking processes, and reduces device efficiency. Another approach is to apply a light-scattering layer on top of the TOLEDs without otherwise changing device structure. The light that passes through the scattering layer spreads in random directions, and lights emitted at different angles are merged, so averaged light is extracted regardless of ν , resulting in suppressed WAD. The light-scattering layers can be achieved by producing nanostructures on the film, but it could be easily damaged and scratched by external mechanical stimuli, resulting in degraded optical properties.

By embedding a high refractive index (RI) nanoparticles in polymer film could be a solution to get a robust property of the scattering film. In fact, there was a trade-off relation between haze and total transparency. Namely, the haze increases with the density of nanoparticle, but total transparency decreases, and vice versa. Such problems could be solved by employing a scattering center with RI = 1.0, air-gap embedding polymer film. The air-gap with RI=1.0 could act as not only a scattering center due to the difference of RIs between the air-gap and its surrounding polymer, but also optically transparent one. Here, we design the optimal size and distribution of air-gap to suppress WAD in RGB TOLEDs, and demonstrate the air-gap embedded hazy film (AEHF). To design the air-gap, rigorous coupled-wave analysis (RCWA) was systematically calculated with respect to the various geometries of the air-gap such as size and period. Based on the simulation results, we demonstrated the AEHF by coating the viscous resin, poly(dimethylsiloxane) (PDMS), on the patterned polymer substrate. By using patterns with a high aspect ratio (AR) during the coating procedure, the geometries of embedded air-gap were increased compared with using patterns with low AR. From the several experimental data, the geometries of the air-gap which were embedded between high AR patterns were similar to the simulation results, realizing a high haze of ~100% while retaining a high average total transmittance of 88%. Consequently, the hazy film is utilized in TOLEDs and the WAD can be dramatically reduced about > 90 % in the RGB wavelength.

EQ06.04.15

Variations in Surface Morphology and Thin Film Properties of Thermally Damaged Top-Emission Organic Light-Emitting Diodes [Changmin Lee](#), Wonho Lee, Geon Woo Jeong, Dong Hyun Kim, Dong Hyun Choi, Tae Wook Kim, Hyung Ju Chae, Amjad Islam, Sung Tae Shin and Seung Yoon Ryu; Korea University, Korea (the Republic of)

In the past few years, several properties of organic layers used for thermally damaged top-emission organic light-emitting diodes (TEOLEDs) have been investigated. However, the surface morphology of organic layers has not been fully explored yet. In this work, surface morphology of stacked layers and cathode used for thermally damaged TEOLEDs are evaluated. Thermal damage is caused by the exposure temperature obtained from the Cu deposition on TEOLEDs, which affects device performance. Because of the low glass transition temperature (T_g), the phosphorescent host material 4,4'-bis(N-carbazolyl)-1,1'-biphenyl (CBP) is rapidly degraded to a large extent, changing its surface morphology, optical and geometrical properties. A severe morphological change due to thermal damage occurred in the excitons blocking layer, tris(4-carbazoyl-9-ylphenyl)amine (TCTA), even below its T_g , owing to the intense variation in the refractive index. Therefore, both the optical and surface morphological properties of TCTA were affected under thermal damage, whereas only the surface morphological properties of the hole-transport layer, N,N'-di(1-naphthyl)-N,N'-diphenyl-(1,1'-biphenyl)-4,4'-diamine (NPB), were changed. However, the optical properties of the thick NPB remain constant despite a lower T_g than that of TCTA. Unexpectedly, increasing temperature has an effect on the hole-transport layer (NPB), the excitons blocking layer (TCTA) and the overall electroluminescence spectra and micro-cavity without affecting device performance much. The surface morphology of upper electrode (Mg:Ag) was cracked due to the difference between the thermal expansion coefficients. Moreover, electrical property of cathode was also affected by thermal damage with increasing its sheet resistance. The wrinkle structure from the full-stacked organic layer was observed, which greatly affected to the micro-cavity and optical properties. Hence, this study reveals that besides T_g , the surface morphologies and thicknesses of the organic layers are also important factors in the annealing process and play a vital role in causing thermal damage to TEOLEDs. To avoid film morphological changes, these findings highlight the need of adopting thermally stable materials in TEOLED devices.

EQ06.04.16

Late News: Highly Bendable Piezoelectric Sensor Fibers via Thermal Drawing Method [Seungmin Lee](#), Quang V. DUONG, Namhun HER, Nhi T. LAM and Seung Tae CHOI; Chung-Ang University, Korea (the Republic of)

Fiber rather than other structures and morphologies such as films or membranes is a promising path for wearable electronic systems, because this long and flexible fiber can be weaved or knitted easily, seamlessly into multifunctional fabrics. Among various fiber-based sensors, piezoelectric fibers, based on poly(vinylidene fluoride) (PVDF) and poly(vinylidene fluoride-trifluoroethylene) (P(VDF-TrFE)), are especially attractive, since they are sensitive and reliable, and show high durability in a compact structure. Recently a novel fabrication technique, named thermal drawing (TD) technique, has been frequently performed to fabricate piezoelectric fibers. TD of multimerals having different flowability at drawing temperature requires amorphous cladding such as polycarbonate (PC) or poly(ether-sulfone) (PES), of which melting temperature is higher than the other materials, to stabilize the TD process. However, these claddings greatly reduce the mechanical flexibility of fibers at room temperature, and it is difficult to selectively remove them for additional treatments such as electrode interconnection.

In this study, we propose a highly amorphous P(VDF-HFP) copolymer as the cladding material for piezoelectric sensor fibers, of which melting temperature and yield strain are known to be 122 °C and about 18%, respectively. Preform fabrication must be preceded to draw fiber through the TD process. P(VDF-TrFE) film is sandwiched between two electrically conductive composite sheets made of carbon black (CB) and polypropylene (PP), and the piezoelectric device is cladded in P(VDF-HFP) copolymer. Incompatibility of flow characteristics at drawing temperature among P(VDF-HFP), P(VDF-TrFE), and CB/PP composite requires optimization of preform geometry and TD parameters. The preform is transformed into a fiber of length more than 50 m via the TD process. The drawn fiber is stored at 140 °C for 12 hours to increase the crystallinity of the P(VDF-TrFE) polymer. The high solubility of P(VDF-HFP) to polar solvents such as acetone facilitates electrical interconnection through selective etching. The drawn piezoelectric fiber can be directly poled through the two CB/PP electrodes with the electric field of 40 MV/m for 45 minutes. The fabricated piezoelectric fiber produces about 5 V (V_{pp}) under 5% tensile strain and 0.5 V (V_{pp}) under bending deformation with a radius of curvature of 10 mm. Furthermore, the piezoelectric fiber can withstand large bending deformation of 1 mm radius of curvature without any severe degradation in the output voltage.

EQ06.04.18

Late News: Effect of Solvents on the Performance of Solution-Processed Organic Light-Emitting Diodes [Taesoo Lee](#)¹, Jaehoon Kim², Changhee Lee³ and Jeonghun Kwak¹; ¹Seoul National University, Korea (the Republic of); ²Los Alamos, Korea (the Republic of); ³Samsung Display, Korea (the Republic of)

The solution-processed organic light-emitting diode (s-OLED) is being actively studied for its advantages such as low-cost fabrication and large area application, but the efficiency and stability of s-OLEDs are still lag behind those of the evaporated devices (e-OLEDs). Many articles point out the film aggregation and pinholes as the main reason for the inferior properties of s-OLEDs, but here we highlight the chemical influence of solvents on the organic materials composing the emissive layer (EML). The investigation on the device performance of s-OLEDs is conducted with two different solvents dissolving CBP:Ir(ppy)₃—chloroform (CF) and tetrahydrofuran (THF). Comparing the device performance of s-OLEDs with e-OLEDs, the CF-based device exhibits remarkably degraded properties whereas THF-based device shows less deviation from e-OLEDs. With the Fourier-transform infrared spectroscopy (FTIR) measurement, we analyze the device degradation of CF-based devices in detail. The FTIR results strongly imply that the residual CF solvent can accelerate the chemical degradation of the emissive layer, changing the bond length and force constant of CBP:Ir(ppy)₃ film. Although further researches are required to perfectly unveil the mechanisms of CF-related degradation, our work will provide useful insights into realizing the commercialization of s-OLEDs.

EQ06.04.19

Morphological and Electrochemical Properties of Vanadium Pentoxide Thin Films Deposited by Ultrasonic Spray Deposition Method Yusuf Tutel¹, Mete Batuhan Durukan^{1,1}, Seyma Koc¹, [Serkan Koylan](#)¹, Huseyin Cakmak², Yusuf Kocak², Farzaneh Hekmat^{1,1}, Emrah Ozsenoy^{2,2}, Ekmel Ozbay^{2,2}, Levent K. Toppare³ and Husnu E. Unalan^{1,1}; ¹Middle East Technical University (METU), Turkey; ²Bilkent University, Turkey; ³Middle East Technical University(METU), Turkey

In the past decades, metal oxide semiconductors have received significant attention due to their unprecedented properties to be used in applications like electronics, optoelectronics, electrochemistry, sensors, and catalysis. Among them, vanadium pentoxide (V₂O₅) shows promising thermal, chemical and electrochromic properties as it is the most stable phase within other vanadium-oxides with an oxidation state of 5. Electronic applications of V₂O₅ films necessitate deposition of thin, homogeneous and crack-free layers thus they show low resistance and high carrier diffusion lengths. To date, various methods were used to deposit V₂O₅ thin films such as thermal evaporation, chemical vapor deposition, sputtering, sol-gel process and spray pyrolysis. Ultrasonic spray deposition (USD) method is another technique that allows the deposition of thin films over large areas. Moreover, this method is significant candidate to deposit thin films due to its good properties such as high material utilization, relatively low-cost processing and non-vacuum

requirement. Besides, it allows repeatable build-up of high-purity thin films. In this work, V_2O_5 thin films were deposited onto pre-heated fluorine-doped tin oxide/glass substrates using USD method. The effect of post deposition annealing temperature on the structural, morphological, optical and electrochromic properties of V_2O_5 thin films have been systematically investigated. Upon annealing over 450 °C, all films showed crystalline morphology while as-deposited films were in amorphous nature. XPS analyses demonstrated the oxidation state of vanadium ions of all deposited films following post deposition annealing was +5. Films have shown visible transmittance with optical band gap values in the range of 2.57 to 2.66 eV as a function of annealing temperatures. Deposited V_2O_5 thin films were also electrochemically tested. Cyclic voltammetry (CV) results with a fast scan rate of 100 mV/s showed that the color of the electrodes was initially yellow and then turned into blue and green at the reduced state for the annealed films. CV results proved the multichromic nature of V_2O_5 thin films. The cycling performance of the V_2O_5 thin films was assessed by assembling an asymmetric cell, which showed promising cyclic stability up to 1000 cycles. Results provided herein indicated that USD method is highly suitable for the deposition of functional V_2O_5 thin films over large areas.

SESSION EQ06.05: Flexible and Stretchable Devices II

Session Chair: Emily Bittle

Wednesday Morning, December 1, 2021

Hynes, Level 2, Room 209

10:30 AM *EQ06.05.01

Semiconducting—Insulating Polymer Blends Targeted for Flexible Optoelectronic Applications [Natalie Stingelin](#); Georgia Institute of Technology, United States

In recent years, immense efforts in the flexible electronics field have led to unprecedented progress and to devices of ever increasing performance. Despite these advances, new opportunities are sought in order to widen the applications of organic-based technologies and expand their functionalities and features. For this purpose, use of multicomponent systems seems an interesting approach in view of, *e.g.*, increasing the mechanical flexibility and stability of organic electronic products as well as introducing other features such as self-encapsulation. One specific strategy is based on blending polymeric *insulators* with organic semiconductors; which has led to a desired improvement of the mechanical properties of organic devices, producing in certain scenarios robust and stable architectures. Here we discuss the working principle of semiconductor:insulator blends, examining the different approaches that have recently been reported in literature. We illustrate how organic field-effect transistors (OFET)s and organic solar cells (OPV)s can be fabricated with such systems without detrimental effects on the resulting device characteristics even at high contents of the insulator. Furthermore, we review the various properties that can be enhanced and/or manipulated by blending including air stability, mechanical toughness, H- vs. J-aggregation, *etc.*

11:00 AM EQ06.05.02

3D Printed Flexible Polymer Light Emitting Diode Displays [Ruitao Su](#)¹, Sung Hyun Park² and Michael C. McAlpine¹; ¹University of Minnesota, United States; ²Korea Institute of Industrial Technology, Korea (the Republic of)

Additively manufacturing light emitting diode (LED) arrays entirely on 3D printers will enable a new and unprecedented capability to create large scale displays in a freeform manner, untethering the process from highly specialized microelectronic fabrication facilities. Fully 3D printing optoelectronics further allows for a high adaptability to varying device form factors and fabrication scales. However, current material systems and printing methods for optoelectronics present several issues to fully 3D printed LED arrays. First, the fabrication of electrodes and encapsulation layers composed of metal-oxides or solid-state metals requires sputtering or vapor deposition processes that are not compatible with 3D printing platforms. Second, active layers that are printed by solution deposition possess a high degree of layer nonuniformity as a result of the directional mass transport within the printed droplets driven by the capillary flow. Lastly, creating repeatable and stable polymer-metal junctions between the emissive layer and cathode at room temperature has proven to be challenging on 3D printers, which should also set the stage for mechanically and electrically interfacing the cathode arrays with spatially structured interconnecting wires.

Here we report a novel device configuration and a multimodal 3D printing methodology that leads to fully printed, encapsulated and highly flexible organic LED (OLED) displays. To solve the previous printability issue for electrodes and encapsulation materials, we select inks that are in the states of solution, liquid, paste and resin. While the electrodes are extrusion printed with metallic nanoparticles and a eutectic liquid metal, the active layer is spray printed with a semiconducting polymer, poly(2-methoxy-5-(3',7'-dimethyloctyloxy)-1,4-phenylenevinylene) (MDMO-PPV). Compared to extrusion printed devices, OLEDs with spray printed active layers demonstrated an improved irradiance and lifetime, attributable to the reduced barrier to charge transport, along with tunable electrical characteristics via the layer thickness. Further, by leveraging the yield-stress behavior of the oxide shell that wraps the liquid metal droplets, we implement a mechanical compression process to reconfigure the morphology of the cathode array and yield an improved contact area for the polymer-metal junction. The repeatable reconfiguration process creates a spatially uniform liquid metal array to be interfaced with the extrusion printed top interconnects. Finally, the device was encapsulated with polydimethylsiloxane (PDMS) that is cast into an extrusion printed silicone holder to form a flexible and transparent top layer. This novel device structure and 3D printing approach lead to a proof-of-concept demonstration of a flexible 8x8 OLED display with a 100% pixel working rate.

11:15 AM EQ06.05.03

Solution Processed Stretchable Organic Field Effect Transistor Touch Sensors Employing EHD Printed Ag NWs Electrodes and a Porous Elastomer Gate Dielectric [Runqiao Song](#), Ping Ren, Yuxuan Liu, Yong Zhu, Jingyan Dong and Brendan T. O'Connor; North Carolina State University, United States

Stretchable touch sensors are attractive for a number of applications including wearable electronics and soft-robotics. In flexible and stretchable devices, all materials including conductors, semiconductors, and insulators must all be effectively integrated to avoid mechanical failure during repeated loading. While there have been a number of touch sensors demonstrated, they often lack mechanical stability necessary for long term application. Here, we introduce an all-solution processed stretchable touch sensor array that employs embedded Ag NW electrodes and a porous elastomer dielectric with stable operation under a strain range of over 50% and a large pressure sensitivity. Ag nanowires (NWs) are chosen as the electrodes as they provide high electrical conductivity and mechanical durability. However, achieving high pattern resolution can be a challenge. We demonstrate an effective processing strategy of printing Ag NWs through electrohydrodynamic (EHD) jet printing to achieve precise and complex patterns. The EHD printed Ag NWs were then embedded in a thin polyimide (PI) substrate providing physically stable electrodes. The Styrene-ethylene-butylene-styrene (SEBS) gate dielectric is printed on the PI substrate followed by polymer semiconductor film and finally the Ag NW source/drain electrodes. Touch sensing was introduced into the devices by forming a nano-porous SEBS layer employing a breath figure method. Through introducing the porous SEBS the transistors become effective

touch sensors. We demonstrate that the porous structure can be tuned to vary pressure sensitivity and operating range. We then transform the ultraflexible touch sensors to stretchable touch sensors through employing a kirigami cut pattern to the PI substrate through laser ablation. One strength of this approach that the EHD can be used to pattern the electrodes to compliment the kirigami cut pattern. The resulting transistors show consistent performance during hundreds of cycles of bending or stretching. In addition, the porous SEBS touch sensors can sense a wide range of pressure from 80 Pa to 19 kPa. In summary, in this talk we highlight the novel EHD Ag NW printing process, the formation of nano-porous SEBS thin films, and kirigami cut design and processing to achieve physically robust stretchable touch sensors. Using our unique processing methods, we are able to demonstrate an ultra-thin flexible pressure sensing transistor array. The combination of EHD printing and porous SEBS dielectric hold great potential for achieving high performance touch sensors with excellent sensitivity and mechanical robustness.

11:30 AM EQ06.05.04

Comparison of the Mechanical Properties of a Conjugated Polymer Deposited Using Scalable, Roll-to-Roll Compatible Deposition Processes Alexander Chen; University of California, San Diego, United States

One reason why semiconducting (π -conjugated) polymers are amenable to the manufacture of large-area devices is because they are solution processable, making them compatible with ink-based printing or roll-to-roll deposition processes. However, the majority of literature on the mechanical properties of conjugated polymers deposit films by spin coating, a non-continuous, non-scalable process. Different deposition processes inherently have different processing conditions (and likewise, there exists a semi-infinite permutation of processing parameters) that affect the physical properties of the resulting polymer film. These morphological characteristics in turn affect the mechanical and electronic properties of the conjugated polymer film. It is currently unclear how different scalable deposition processes affect the mechanical properties, electronic properties, and morphologies of conjugated polymer films. In this talk, we compare poly(3-heptylthiophene) (P3HpT) films deposited by three roll-to-roll deposition processes – interfacial spreading (i.e., “floating film-transfer method”), solution shearing (i.e., “blade coating”), and spray coating – to those produced by spin coating. We find that the deposition process significantly affects the mechanical and electronic properties of the resulting films. We attribute these differences to changes in the amorphous and crystalline morphologies of the P3HpT films, which holds significant implications for considering how conjugated polymer films are deposited for different applications.

11:45 AM EQ06.05.05

Solid-Phase Deposition—Conformal Coverage of Light Trapping Surfaces with Stretchable Semiconducting Polymers for Photovoltaic Applications Guillermo Esparza and Darren J. Lipomi; University of California, San Diego, United States

Light trapping with textured surfaces is an important technique in photovoltaics used to increase the optical path length without increasing the thickness of the absorber. However, the use of texture limits the application of this strategy in organic and tandem silicon/perovskite photovoltaics, among others. This limitation arises because, while there are a variety of methods available for forming thin films of electronic polymers, very few of them can form thin and conformal coatings on surfaces bearing relief structures on the micron scale. Of the methods that are capable of conformal coverage of such topography, most are applicable only to coatings that can be polymerized in situ—for example, by chemical vapor deposition—and are, thus, not amenable to polymers with complex molecular structures, such as π -conjugated (semiconducting) polymers. This presentation describes a method termed solid-phase deposition (SPD). The SPD process is a variant of water transfer printing whereby a thin film of a semiconducting polymer is suspended on water and taken up by a substrate bearing micron-scale relief structures (in this case, random pyramids such as those used for light management in silicon photovoltaics). Under ambient conditions, solid films that are sufficiently compliant (thin, ductile, or of low modulus) can coat these surfaces readily. Stiffer films comprising higher modulus polymers can be made amenable to the process by the application of heat or solvent vapor. We successfully formed coatings from films of poly(3-alkylthiophenes) spanning the range from glassy (alkyl = butyl) to rubbery (alkyl = heptyl), along with the low-bandgap polymers DPP-DTT and PTB7-Th, on textured silicon and indium tin oxide (ITO) surfaces.

SESSION EQ06.06: Device Applications

Session Chair: Natalie Stingelin

Wednesday Afternoon, December 1, 2021

Hynes, Level 2, Room 209

1:30 PM *EQ06.06.01

Printed and Biodegradable Sensors for Real-Time Monitoring of Soil and Plant Conditions Gregory L. Whiting¹, Eloise Bihar¹, Elliot Strand¹, Madhur Atreya¹, Anupam Gopalakrishnan¹, Yongkun Sui¹, Charlotte Bellerjeau¹, Vaidehi Salway¹, Robert McLeod¹, Jason Neff¹, Ana Claudia Arias², Payton Goodrich², Carol Baumbauer², Raj Khosla³, Subash Dahal³ and Wub Yilma³; ¹University of Colorado Boulder, United States; ²University of California, Berkeley, United States; ³Kansas State University, United States

Understanding soil and plant properties in real-time and at high-spatial resolution is critical for optimizing agricultural input use, and for evaluating soil and plant health. Obtaining such information in real-time and at high spatiotemporal resolution can be a challenge due to limited functionality and high costs when large numbers of devices are used, thereby limiting management approaches and potentially leading to excess input and energy use. As such novel instrumentation that can directly sample soil at high spatial density (10s-100s of meters) is needed to capture current conditions and enable optimized management strategies.

In this report three device types for monitoring soil and plant properties will be described. 1) Capacitive moisture and potentiometric nitrate sensors fabricated from biodegradable materials (conductors, substrates, encapsulants, etc.). The use of transient biodegradable materials enables large numbers of devices to be widely distributed in a field without the need for maintenance or collection. 2) Fuse-like microbial activity sensors based on biodegradable materials that enable in-situ determination of the activity of microbes in soils which is important for understanding soil health. 3) Ion selective organic electrochemical transistors (OECTs) for determining the concentration of target ions of interest directly in whole plant sap. In all of these cases the sensors are fabricated using printing techniques, primarily screen and ink-jet printing, as additive manufacturing approaches readily enable creation of large numbers of devices, are compatible with a wide range of materials, and assists integration into complete measurement systems.

2:00 PM EQ06.06.02

Printed Organic Photovoltaic Modules on Transferable Ultra-Thin Substrates as Additive Power Sources Mayuran Saravanapavanantham, Jeremiah Mwaura and Vladimir Bulović; Massachusetts Institute of Technology, United States

Thin-film photovoltaics with functional components on the order of a few microns, present an avenue towards realizing additive power onto any surface of interest without excessive addition in weight and topography. To date, demonstrations of such ultra-thin photovoltaics have been limited to small-scale devices on glass substrates, fabricated through vacuum deposition or with only some of the device layers solution-processed. Furthermore, such ultra-thin devices show limited mechanical integrity for everyday human handling. The solution-processability of such device architectures presents an avenue for integration into rapid manufacturing processes and their translation from lab-scale demonstrations into consumer ready technologies. In this work we demonstrate ultra-thin organic photovoltaic (OPV) modules produced fully through scalable solution-based processes (slot-die coating and screen printing). We further demonstrate integration onto light-weight (<15 g/m²) and high-strength (5kN/m tensile strength) composite fabrics, resulting in large-area (> 10cm x 10cm) prototypes of durable fabric-PVs capable of withstanding over 500 roll-up cycles. Such processing presents a path towards realizing solar technologies with sufficient mechanical integrity for applications requiring ultra-lightweight form-factors including tents, sails, drones, micro-robots and wearables.

2:15 PM EQ06.06.04

High Density, High Performance, Low Leakage Internal Ion-Gated Organic Electrochemical Transistors (IGTs) [Claudia Cea](#), Richard Yao, Zifang Zhao, Jennifer Gelinas and Dion Khodagholy; Columbia University, United States

Organic material-based conformable electronics are optimal candidates for components of bioelectronic circuits due to their inherent flexibility and soft nature. We have shown that internally ion-gated organic electrochemical transistors (IGTs) operate by leveraging ion reservoirs inside their channels to dramatically improve the operation speed and integration capacity of this ion driven transistor. In order to establish IGTs as versatile building blocks of bioelectronics, it is critical to establish fabrication strategies to enable IGT-based high-density integrated circuits for creation of electronic components such as operational amplifiers, multiplexers and logic gates. Here, we report a fabrication process that enables creation of IGTs with channel length of < 500nm, that have high transconductance (> 10 mS) and high speed (< 1 μ s). This vertical fabrication strategy allows effective isolation of adjacent transistors, minimizing potential for cross-talk and gate current leakage. Furthermore, it is possible to encapsulate the circuit using long-term implantable grade (polyethylene C) material. Furthermore, we developed a micron-scale perforation strategy to ensure intact hydration paths for transistor channels while maintaining a low leakage current. We used these transistors to develop high density (IGTs)-based digital logics, voltage amplifiers, operational amplifiers and multiplexers. Overall, the high speed and transconductance of IGTs along their ability to be densely fabricated with minimal crosstalk facilitates their applicability to a broad range of flexible and conformable electronics.

2:30 PM EQ06.06.05

Click Chemistry Derived Polymer Ceramic Nanocomposites with Modified Interface and Improved Breakdown for Energy Storage Applications [Binod Subedi](#), Christopher Keller, Madhu Gaire, Joshua Shipman, Scott Grayson and Douglas B. Chrisey; Tulane University, United States

Tailoring the structure of interface between polymer and ceramic nanoparticles is considered as one of the key approaches to achieve high energy density in next generation dielectric capacitors. To achieve high energy density, we have attached surface engineered barium titanate nanoparticles (~100 nm) to polymer by forming covalent bonds between the nanoparticles and polymer matrix. Nanoparticles used for this work are surface engineered by using a three-step process. The first step of hydroxylation attaches -OH groups which are the reactive sites for the second step of silane treatment. The third step of monomer grafting ensures the formation of covalent bond between the nanoparticles and monomers and provides higher mobility to reactive terminations on nanoparticle surface. Thiol-ene matrix is prepared by a radical mediated process from a mixture of monomers Pentaerythritoltetrakis (3-mercaptopropionate), 2,4,6 Triallyloxy-1,3,5- triazine and 1,3- Diisopropenylbenzene. The monomers and nanoparticles undergo *click reactions* without the need of photo-initiator when the mixture is processed with an intense pulsed light from a xenon flash lamp. We compare two different routes of surface engineering: an alkene-ended silane (3- Acryloxypropyl trimethoxysilane) treatment followed by thiol monomer grafting, and a thiol ended silane (3 Mercaptopropyl trimethoxysilane) treatment followed by alkene monomer grafting. Nanocomposites with significantly higher electrical breakdown (~5 MV/cm) are prepared which implies an improved interface with reduced defects. The as prepared nanocomposites show energy density as high as 26 J/cm³ while the dielectric loss is maintained below 0.2. The results from this study show that interface can be improved by increasing the surface density and mobility of the reactive terminations on nanoparticle surface. Photonic curing process utilized in this work is a roll-to-roll amenable, rapid, and high-throughput method. The ability to tailor the interface to obtain desired properties while preparing nanocomposites in large scale using a cost-effective method provides an easy route to an industrial scale method for the preparation of high-energy density nanocomposites.

SESSION EQ06.07: Novel Processing and Performance I
Session Chair: Brendan O'Connor
Wednesday Afternoon, December 1, 2021
Hynes, Level 2, Room 209

4:00 PM *EQ06.07.01

Functionalized Polymer Dielectrics for Low-Operating Voltage Organic Field-Effect Transistors John Barron, Jaewon Lee, Payal Bhattacharya and [Suchismita Guha](#); University of Missouri–Columbia, United States

The design of appropriate dielectrics plays a crucial role in the performance of organic field-effect transistors (FETs). Along with the active semiconductor layer, the dielectric-semiconductor interface dictates charge transport properties in FETs. Polymer ferroelectric dielectrics with their high dielectric constants are attractive for low-operating voltage FETs. Another route for enhancing the dielectric constant of polymer dielectrics is via the incorporation of semiconducting and insulating nanoparticles. Amongst magnetic nanoparticles, cobalt ferrite (CoFe₂O₄ or CFO) has received a lot of interest in sensing and biomedical applications. Its insulating property is attractive in polymer gate dielectrics. CFO magnetic nanocrystals, soluble in organic solvents, were synthesized by a thermal decomposition method and coated with polymers such as poly(vinyl alcohol) (PVA). Improved performance of organic FETs (both small molecule and polymer) using CFO incorporated non-ferroelectric dielectrics are observed. In particular, the threshold voltage and the subthreshold swing are lowered in pentacene and other organic FETs using CFO incorporated cross-linked poly(4-vinyl phenol) (PVP) dielectric. The application of an external magnetic field allows for another parameter to tune the device performance. We will further discuss a nonlinear optical probe for investigating carrier transport in such FETs.

This work was supported by National Science Foundation under Grant No. ECCS-1707588

4:30 PM EQ06.07.02

Photonic Band Structure in One-Dimensional Crystals of Stacked Microcavity OLEDs [Matthew S. White](#)¹, David Allemeier¹, Benjamin Isenhardt¹,

Ekraj Dahal¹, Yuki Tsuda² and Tsukasa Yoshida²; ¹University of Vermont, United States; ²Yamagata University, Japan

A microcavity OLED, consisting of a conventional OLED stack with two metallic mirror electrodes, shows narrow-band emission centered around specific peak resonant wavelengths. These cavity modes are analogous to the energy states found in any resonator system, including musical instrument strings and 1-dimensional quantum square wells. The first three cavity modes are directly pumped by varying the thickness of the microcavity structure. The impact of the location of the dipole emitter within the microcavity on outcoupling efficiency and polarization is explored. The microcavity OLED is then used as a unit cell in a planar, 1-dimensional photonic crystal. Stacking N microcavities splits the resonant modes into N discrete states; a photonic band centered at the single microcavity state. Devices are fabricated by thermal evaporation with in-vacuo shadow mask transfers to enable parallel-connected unit cells. The photonic density of states is controlled by varying the thickness of the semitransparent metal mirror electrodes. A photonic Peierls bandgap is tuned by varying only alternate mirror thicknesses. Device parameters, including N , the thickness of the semi-transparent metal electrodes, and dipole emission position are correlated to emission properties such as peak wavelength, FWHM, and Q-factor for each of the photonic states. The experimental results are guided by a predictive computational modelling tool, which is critically important for the complex-architecture devices.

4:45 PM EQ06.07.03

Effect of Emulsified Polymer Particle Thin-Film Deposition on LED Device Performance Buang Zhang and Adrienne Stiff-Roberts; Duke University, United States

Film morphology plays a major role in polymer LED device performance. As an example, blue LEDs fabricated using polyfluorene (PFO) have shown an increase in luminance efficiency with the presence of minimal crystalline domains of a specific phase.[1] Previous work has demonstrated that PFO deposition via resonant infrared, matrix-assisted pulsed laser evaporation (RIR-MAPLE) promotes this crystalline β -phase formation in PFO while maintaining device-quality film surfaces.[2] RIR-MAPLE is a unique variation of pulsed laser deposition featuring an Er:YAG laser (peak wavelength of 2.94 microns) that is resonantly absorbed by the hydroxyl bond vibrational mode.[3] Therefore, PFO deposition occurs by formation of a frozen "oil-in-water" emulsion target in which the polymer is dissolved in primary solvent trichlorobenzene (TCB), and dispersed within the water matrix that resonantly absorbs the incident laser energy. Phenol is added as a secondary solvent to lower the emulsion vapor pressure, and minimal surfactant is added to help emulsion formation. The resonant laser absorption sublimates the water-ice matrix and transfers intact emulsified polymer particles directly from the complex emulsion to the substrate without degradation. Therefore, the morphology of the complex emulsion determines the film morphology. [2,4] In this work, the impact of the complex emulsion morphology on LED device performance is investigated.

Given that the complex emulsion target used in RIR-MAPLE contains multiple components (polymer, primary solvent, secondary solvent, surfactant, and water), the existing two-phase emulsion theory cannot predict accurately the resultant morphology. Empirical studies of RIR-MAPLE deposition have shown that an emulsion recipe with a concentration of 0.83 mg/ml PFO in water yields device-quality, pinhole-free films containing around 6% crystalline β -phase.[2] Two different emulsion recipes that maintain this specific polymer concentration in water but change the total water content in the emulsion were developed. The emulsion recipe with high water content contains 5mg/mL PFO in TCB with emulsion ratio of 1:0.5:6 (TCB:phenol:water), and low water content recipe has 2.5 mg/mL PFO in TCB with emulsion ratio of 1:0.25:3 (TCB:phenol:water). Despite having a drastic difference in emulsified particle size (dynamic light scattering), two outcoming films showed similar surface roughness and morphology determined by atomic force microscopy.[4] Further, cryo-transmission electron microscopy images of the frozen emulsions showed that the observed difference in particle sizes resulted from large agglomerations of emulsified particles occurred in the low water content emulsion.[4] While these differences in emulsion morphology did not impact the overall film morphology, it is not known how these features could impact LED performance. It is anticipated that the networked emulsified particles of the low-water content emulsions will yield better LED performance due to better charge injection.

Therefore, this work will investigate the impact of PFO complex emulsion morphology, as determined by the overall water content, on LED performance for active region films deposited by RIR-MAPLE. The LEDs will be fabricated using the following device heterostructure: ITO/PEDOT:PSS/PFO/LiF/Al. LED device characterization will include current density vs. voltage, luminous flux, and electroluminescence spectra. This work will reveal the relationship between polymer emulsion morphology and PFO LED device performance, thereby providing a guide for future RIR-MAPLE-deposited PFO devices. This work is supported by the National Science Foundation under Grant No. NSF CMMI-1727572.

Reference:

- [1] Peet, J. et al., Adv. Mat., 20(10), p 3938, 2008
- [2] Ferguson, S; et. al., J. Electron. Mat, vol. 48(5), 2019
- [3] A. D. Stiff-Roberts and W. Ge, App. Phy. Review, vol. 4, pp. 041303, 2017
- [4] S. Ferguson, et. al., Electronic Materials Conference, Ann Arbor, MI, June 2019

5:00 PM EQ06.07.04

Multifunctional Flexible Electronics Manufactured by Ultrafast Corona-Enabled Electrostatic Printing Zijian Weng and Ying Zhong; University of South Florida, United States

Flexible electronics have attracted a significant attention in the recent years due to their high demands in a variety of fields such as medical field, sports field, cosmetic field and so on. A number of manufacturing technologies have been developed to fabricate the flexible electronics based on different functional materials. However, there are quite a few challenges in current techniques such as high costs, time consuming and difficult scale-up process, making it hard to produce a large amount of high-quality flexible electronics. Here we reported a novel Corona-enabled Electrostatic Printing (CEP) technology to manufacture flexible electronics in an ultrafast manner of which the printing time can be down to 100 ms. A detail mechanism study is shown in this paper to demonstrate the printing principle of CEP by using simulations and experimental studies. With the help of CEP, a variety of functional material such as graphene, PEDOT: PSS and CNT were able to be fast printed to fabricate flexible multifunctional sensors that can detect strain, temperature and humidity signals. And CEP could also be integrated with roll-to-roll (R2R) process for ultra-fast mass production. The binder-free feature of CEP enables a fast, simple and pure printing process, producing high quality flexible electronics such as graphene-based sensors that possess high sensitivity and acoustic signal detection capabilities.

5:15 PM EQ06.07.05

Blue Light Emission from a p-i-n POPy₂ Large Band Gap Homo Junction Diode Hannah L. Smith¹, Jordan T. Dull¹, Swagat Mohapatra², Stephen Barlow², Seth Marder², Barry P. Rand¹ and Antoine Kahn¹; ¹Princeton University, United States; ²Georgia Institute of Technology, United States

p-Doping organic semiconductors with high ionization energy (IE) remains challenging, as these materials require dopants with correspondingly high electron affinity (EA). Recently, an organic molecular p-type dopant, hexacyano-trimethylene-cyclopropane (CN6-CP) was synthesized and shown to have an EA of 5.87 eV measured by cyclic voltammetry (CV), almost 300 meV higher than other known high EA molecular dopants. In this work, we measure the EA of CN6-CP using inverse photoelectron spectroscopy (IPES) and confirm a high value of 5.88 eV in condensed phase. We then use CN6-CP to

dope phenyldi(pyren-2-yl)phosphine oxide (POPy₂), a wide energy gap (3.6 eV), large IE (5.87 eV), organic semiconductor and demonstrate a more than two order of magnitude increase in film conductivity. Using CN6-CP and (pentamethylcyclopentadienyl)(1,3,5-trimethylbenzene)ruthenium (RuCp**Mes*)₂, a highly reducing n-dopant capable of n-doping a low EA (2.2 eV) material such as POPy₂, we build a rectifying p-i-n homojunction with a 2.9 eV built-in potential. We demonstrate blue emission from this p-i-n structure, indicating both hole and electron injection into this large gap diode through the n- and p-doped regions.

SESSION EQ06.08: Novel Processing and Performance II

Session Chair: Ioannis Kymissis

Thursday Morning, December 2, 2021

Hynes, Level 2, Room 209

10:30 AM *EQ06.08.01

Vacuum Deposition and Stencil Lithography for Flexible Organic Transistors and Complementary Circuits Hagen Klauk and Ute Zschieschang; Max Planck Institute for Solid State Research, Germany

Organic thin-film transistors (TFTs) are being developed for flexible electronics applications, such as rollable or bendable active-matrix displays and conformable sensor arrays. The deposition and patterning of the various transistor components (gate electrode, gate dielectric, source/drain contacts, organic-semiconductor layer) can be accomplished using a wide range of methods, which are often categorized into vacuum-based and solution-based approaches. All of these have real or perceived advantages and drawbacks, which are often related to the anticipated costs of large-scale commercial manufacturing. A lot about these can be learned by analyzing the present-day commercial manufacturing of active-matrix organic light-emitting diode (AMOLED) displays for mobile phones and television sets. All of the OLED and TFT components in these displays are deposited by vacuum-based methods, while patterning is accomplished by optical lithography (TFT stack, anodes, interconnects) or stencil lithography (OLED semiconductors and cathodes). The only process steps involving the use of liquid organic solvents are those in which the surface is coated with polyimide (to create the flexible substrate) or photoresist (in preparation for optical lithography). By keeping the use of organic solvents, which are often toxic, carcinogenic and environmentally harmful, to an absolute minimum, the costs of proper solvent management and disposal and thus the total manufacturing costs are kept as low as possible. The commercial manufacturing of organic TFTs based on small-molecule semiconductors can potentially be even less expensive, since these TFTs can be fabricated entirely without organic solvents, simply by depositing and patterning all materials in vacuum directly on the flexible substrate. Following this general proposition, organic TFTs as well as unipolar and complementary circuits with good static and dynamic performance can successfully be fabricated on a variety of flexible substrates, including plastics and paper.

11:00 AM EQ06.08.02

Continuous and High-Speed Printing of Semiconducting Polymer Line Arrays by Meniscus Oscillation Self-Assembly (MOSA) Jeong Jae Wie¹, Jisoo Jeon¹, Alvin T. Tan² and John Hart²; ¹Inha University, Korea (the Republic of); ²Massachusetts Institute of Technology, United States

Evaporative self-assembly of semiconducting polymers has been studied extensively in order to attain a facile and low-cost means of preparing hierarchical micrometer and nanometer-scale features. Yet, solvent evaporation is often a time consuming kinetic process that limits any potential for practical applications toward organic and printed electronics. In this presentation, we introduce a novel high-throughput and continuous printing technique for semiconducting polymer via a modified doctor blading technique with oscillatory meniscus motion, termed meniscus-oscillated self-assembly (MOSA). The oscillatory meniscus motion of the roller regulates a periodicity of the stick-slip phenomenon between the roller and polymer solution that can continuously output semiconducting polymer line arrays. These printed lines demonstrate highly defined boundaries and drastically enhanced crystallinity via shear-induced crystallization. This novel continuous printing technique has the capacity to pave a new path forward for practical applications in printed electronics.

11:15 AM EQ06.08.03

Rapid, High-Resolution, Large-Area Patterning of Semiconducting Polymers Using Projection Photothermal Lithography Tucker L. Murrey¹, Alice S. Ferguson^{1,2}, Meghna Jha¹, Justin T. Mulvey^{1,3}, Sarah E. Dolan¹, Daniel Tiffany-Appleton¹ and Adam J. Moule¹; ¹University of California, Davis, United States; ²Princeton University, United States; ³University of California Irvine, United States

Semiconducting Polymers (SPs) have received widespread attention due to their promising qualities like superior absorbance/emission, easy chemical tunability, low-temperature solution processing, lightweight and flexible substrates, and low environmental toxicity. A significant obstacle for the industrial development of SPs is the lack of a patterning technology that is inexpensive, rapid and viable and capable of producing sub-micron features. Photomask lithography is impossible because the SPs cannot withstand the processing steps. The Moule group recently developed a new photopatterning concept that enables micropatterning of SPs. We present a novel solution based optical patterning method that is compatible with any non-cross linked SP, termed Projection Photothermal Lithography (PPL). We have built a lab scale PPL microscope and demonstrated rapid (~ 4cm²hr⁻¹), large single exposure area (0.21 mm²), sub- μ m patterns can be obtained optically. Selective polymer domains are removed as a photo-induced temperature gradient enables selective dissolution. We estimate the commercial patterning throughput of (~ 5 m²hr⁻¹) can be obtained through optimization of optical components.

11:30 AM EQ06.08.04

Universal Electrode for Ambipolar Charge Injection in Organic Electronic Devices Tanmoy Sarkar and Gitti L. Frey; Technion--Israel Institute of Technology, Israel

Ambipolar transistors, i.e. transistors with symmetrical n- and p-type performances, open new venues for the design and integration of high-density, efficient and versatile circuits for advanced technologies. Their performance requires two processes: efficient injection of holes and electrons from the metal electrodes into the semiconductor; and transport of both carriers through the semiconductor. Organic semiconductors (OSC) support ambipolar transport, but charge injection is strongly asymmetric due to inherent misalignment of the electrode work function with both conducting levels of the OSC. Here we will introduce a new electrode concept capable of efficiently injecting both type of charge carriers into OSCs. The electrode has a mosaic-like structure composed of islands of two metals with high and low work functions, in this case Al and Au, respectively. Under suitable applied bias the Au (Al) domains in direct contact with the OSC allow efficient hole (electron) injection into the HOMO (LUMO) level. Implementing this electrode as both source and drain in organic field effect transistors (OFET) lead to fully balanced ambipolar performance while maintaining high ON/OFF ratios. We then used the ambipolar OFETs to significantly simplify circuit design and fabrication of digital and analogue elements, i.e. digital inverter and an analogue phase shifter, composed of one type of transistor only. Finally, we demonstrate that a single ambipolar OFET can replace several unipolar transistors to fabricate

digital transmission gate circuits that utilize one transistor only. The new electrode design concept can include other metal combinations and compositions to balance ambipolar injection, and the use of the mosaic electrodes can be extended to other electronic devices that require ambipolar charge injection such as light emitting transistors, memory devices etc.

11:45 AM EQ06.08.05

TCO-Based Scribing Mechanism for High-Throughput Perovskite Module Manufacturing [Austin Flick](#) and Reinhold H. Dauskardt; Stanford University, United States

Small area (~0.1 cm²) hybrid organolead-halide perovskite solar cells have recently approached efficiencies near that of single crystalline silicon cells. Scalable methods such as slot-die coating and spray coating offer the possibility of high quality large-area perovskite deposition at these performance levels; however, resistive losses across the transparent front electrode highlight the need for alternative architectures and designs. A variety of alternative designs are explored—gridline, module, and hybrid designs—to mitigate front electrode resistive losses, employing laser-scribing to achieve both controlled gridline deposition and monolithically integrated series interconnections. We have developed a laser scribing mechanism to achieve gridline patterning and removal of the electrodes and active material utilizing a single wavelength (1064nm) pulsed laser at ultrafast processing speeds (>1m/s). This process coupled with improved module design enables high throughput device and module development.

Our work first develops the primary scribing mechanism employed: TCO-based lift-off. We demonstrate the unique characteristics of this scribing method as it interacts exclusively with the front electrode transparent conducting oxide (TCO) material to perform all the necessary scribes between both the gridline and module architectures. With a single wavelength source, controlled removal of either the front electrode or active layers is achieved to perform each scribe step: front electrode patterning (gridline patterning, module P1), creating the series interconnection channel (module P2), and rear electrode patterning (module P3). The unique lift-off mechanism results in particularly improved P2 performance via reduced contact resistance and increased short-circuit current and fill factor compared to traditional P2 ablation mechanisms that often require ultra-short laser pulses to avoid residual thermal damage to the perovskite layer. By avoiding interactions with the perovskite entirely, the TCO-based lift-off mechanism is compatible with lower cost, longer pulse duration laser systems and is capable of complete device and module patterning on a single system.

Following the development of a uniquely broadly applicable laser-scribing mechanism, gridline, module, and hybrid designs are considered for large-area perovskite photovoltaic applications. Resistive losses of each of the dominant components (front electrode, gridlines, scribed interconnections) are evaluated against geometric design considerations to find the optimal device and module geometries. Reductions in resistive and geometric losses motivate the selection of an optimal architecture, though alternative designs are considered for potential compatibility with projected processing challenges.

SESSION EQ06.09: Processing and Applications I

Session Chair: Brendan O'Connor

Thursday Afternoon, December 2, 2021

Hynes, Level 2, Room 209

1:30 PM EQ06.09.01

Photonic-Induced Conversion of Semiconductor-Based Inks and Its Use for Flexible Hybrid Electronic Sensor Integration Jaime Benavides-Guerrero¹, Luis Felipe Gerlein¹, Arjun Wadhwa¹, Debika Banerjee¹, Martin Bolduc² and [Sylvain G. Cloutier](#)¹; ¹Ecole de Technologie Supérieure, Canada; ²Université du Québec à Trois-Rivières, Canada

In this work, we present our recent progress on the photonic-induced conversion of new semiconducting ink materials and their use for the fabrication of new hybrid opto-electronic sensor platforms. First, we will present the manufacturing-ready photonic curing process and its key advantages for high-speed treatment of large surfaces compared with standard laser-induced conversion. Most importantly, simulations will be used to demonstrate how photonic sintering can achieve high-temperature conversion of the functional inks without compromising the structural integrity of low-temperature substrates. Then, we will illustrate how slurries of silicon-based particles can also be sintered by photonic curing. Altogether, we will describe how we used a thorough understanding of the chemistry combined with a cutting-edge photonic curing expertise to enable novel sensor designs and their integration in fully-autonomous flexible hybrid electronic sensor platforms. Most importantly, we will show how we modified the chemistry of a sol-gel TiO₂ precursor in order to generate high concentrations of oxygen vacancies and describe how this modified chemistry can allow a conversion from amorphous to anatase and rutile polymorphs at room temperature and in ambient environment using low-power photonic irradiation [1]. As a result, unique multi-morphic film architectures are achieved using digital additive manufacturing strategies coupled with both low-power laser irradiation and photonic curing [2]. In turn, these unique metal-oxide film structures enable new printable devices architectures for a wide range of applications from biomedical to energy harvesting. We will show a few concrete examples in this presentation [4-5].

[1] J. Benavides *et al.*, ACS Applied Energy Materials **1**, 3607 (2018)

[2] L. F. Gerlein *et al.*, Advanced Engineering Materials **22**, 1901014 (2020)

[3] D. Banerjee *et al.*, Scientific Reports **9**, 17994 (2019)

[4] D. Banerjee *et al.*, Engineering Research Express **2**, 035021 (2020)

[5] C. Trudeau *et al.*, Flexible Electronics **4**, 2136 (2020)

1:45 PM EQ06.09.02

Effect of the Dipole Position on the Emission Characteristics in Microcavity Organic Light Emitting Diodes [Ekraj Dahal](#), David Allemeier and Matthew S. White; University of Vermont, United States

Organic light emitting diodes (OLED) employing two planar metallic electrodes encasing the organic layers form a microcavity etalon. This structure allows a control on the output emission characteristic of the light source resulting in a significant narrowing of the emission bandwidth and angular dispersion of light. We investigate the emission spectra using a single organic emitter molecule, by engineering the position of the dipole emitter in the microcavity structure. The position of the dipole was varied by varying the relative thickness of the electron transport layer ETL and hole transport layer HTL in fixed total thickness and fixed optical pathlength device structures. The output characteristic of a microcavity OLED is affected by its optical path length. Here we test this hypothesis that a fixed optical pathlength generates the same optical characteristics even with the changing dipole position. Varying the thickness of the ETL and HTL layers without changing the total optical pathlength of the device in principle generates the same output characteristic of light. We find that fixing the optical pathlength in the cavity functionally fixes the peak emission wavelength, but the dipole position

within the cavity has strong impact on the efficiency of outcoupling of light and on the polarization.

2:00 PM EQ06.09.03

Controlling Catalyst-Support Interactions via Modifying Metal-Organic Frameworks Won Ho Choi and Kyung Min Choi; Sookmyung Women's University, United States

The development of support materials is one of the most critical challenges in a wide range of fields including energy, the environment, and catalysis. This is because support materials can endow guest materials with new properties. In catalysis, the catalyst-support interaction influences the catalytic performance, so it is urgently required to create a high-affinitive sites in porous supporting media. Among the promising candidate support materials, highly porous and crystalline metal-organic frameworks (MOFs) have received considerable attention. Although many MOFs have been successfully utilized as supports, their metal sites have weak affinity for the guest material due to blockage by organic linkers. We hypothesized that the affinity could be increased by tearing the MOFs into smaller pieces based on this intrinsic limitation. Accordingly, we developed a new pathway for producing metal-organic fragments by tearing MOFs via hydrogen plasma bombardment. The hydrogen plasma exposed more metal nodes and created more delocalized electrons, resulting in high-affinity sites within the metal-organic fragments. Furthermore, metal-organic polyhedra (MOP), are distinct from MOFs, have opened up a possibility for controlling catalyst-support interactions. Here, we focus on the opportunity to use the pore structure without the hindrance to electron transfer by using MOP. As a result of this strategy, the metal-organic fragments and MOP were successfully applied as highly affinitive support.

2:15 PM EQ06.09.04

Simultaneous Control of Crystallinity and Molecular Alignment in Semiconducting Polymer Films Through Tailored Thermal Annealing Alessandro Luzio¹, Jaime Martin^{2,3,4} and Mario Caironi¹; ¹IT CNST, Italy; ²Universidade da Coruña, Spain; ³University of the Basque Country UPV/EHU, Spain; ⁴Kerbasque Basque Foundation for Science, Spain

Semiconducting polymers with satisfactory charge transport properties are demanded to meet the requirements for a vast range of applications in the field of flexible and printed electronics.¹ However, their effective integration into electronic devices is still hampered by a partial understanding of the interplay between microstructure and transport. Starting from 2009, the investigation of innovative donor-acceptor copolymers led to evidences of efficient transport in apparently poorly ordered films,² subverting the old perception of long-range crystallinity as the key for transport efficiency. Lately, evidences for well interconnected and efficient charge percolation pathways within otherwise disordered films was consistently reported in high mobility polymer field-effect transistors (FETs);³ this is made possible by polymers inherent anisotropy, enabling long-range alignment of molecular backbones within thin films microstructure and improved unidirectional film interconnectivity along the same direction. Accordingly, strong transport anisotropy is realized, where transport is maximized in the direction of backbone alignment and improved interconnectivity.⁴ Nevertheless, a substantial gap remains to be filled between emerging models for transport, mostly accounting for short range interactions, and the actual charge transport mechanism occurring within the multi-phase percolation paths of aligned FET channels.

Here we report on a post-processing methodology enabling control on those microstructural features that are critical for polymer transport, i.e. molecular alignment, degree of interconnectivity and crystalline structure. We show that a systematic lamellar thickening and improved molecular alignment can be induced upon the accurate choice of thermal post-processing temperatures, tailored to the actual thermal transitions of solution processed thin films. In fact, annealing at a temperature at which only the smaller crystals melt but the larger ones are maintained, allows for the thickening of non-molten crystals and the epitaxial growth of the molten fraction of molecules on the non-molten surface, thereby guiding molecular alignment of newly formed crystals.⁵ We show that our post-processing strategy represents an effective tool for charge percolation optimization, up to the demonstration of ideal, single crystal-like FETs characteristics and drastically reduced thermal barriers to transport. Validation tests were carried out on two paradigmatic *n*-type molecular systems: a diketopyrrolopyrrole-based copolymer, where electrons delocalization within crystalline domains can take place, and a series of naphthalene-diimide bithiophene copolymers, conversely characterized by a strong intra-chain charge localization at any aggregation state. Such a diverse investigation allows for a better understanding of the effect of critical chemical features for a polymeric semiconductor, like electronic structure, molecular conformation and solubilizing side chains, on charge percolation efficiency within aligned films, paving the way toward a more efficient design of polymeric semiconductors for printed electronics applications.

1 Mario Caironi and Yong-Young Noh, *Large area and flexible electronics*. (John Wiley & Sons, 2015); Ana Claudia Arias, et al. *Chemical Reviews* **110** (1), 3-24 (2010).

2 He Yan, et al. *Nature* **457** (7230), 679-686 (2009); Rodrigo Noriega, et al. *Nature materials* **12** (11), 1038-1044 (2013).

3 Brian J Eckstein, et al. *Advanced Functional Materials* **31** (15), 2009359 (2021); Sam Schott, et al. *Advanced Materials* **27** (45), 7356-7364 (2015); Alessandro Luzio, et al. *Scientific reports* **3** (1), 1-6 (2013); Nicola Martino, et al. *ACS nano* **8** (6), 5968-5978 (2014).

4 Sadir G Bucella, et al. *Nature communications* **6** (1), 1-10 (2015); Edward J. W. Crossland, et al. *Advanced Materials* **24** (6), 839-844 (2012).

5 A. Luzio, et al., *Nat Comm* **10** (1), 1-13 (2019).

2:30 PM EQ06.09.05

Structures and Mechanisms of Self-Doping N-Type Organic Semiconductors from Aqueous Solutions Lewis M. Cowen and Bob Schroeder; University College London, United Kingdom

N-type dopants for organic semiconductors with reasonable ambient stability have been difficult to develop. In addition to this, dopant and organic semiconductor pairs often exhibit morphological incompatibilities. One promising, yet relatively unexplored, tactic for avoiding morphological disruption to the semiconductor after doping is to covalently bind a doping functionality to the conjugated section. Quaternary ammonium hydroxide groups have previously been bound to rylene diimides and high n-type conductivities (≈ 0.5 S/cm) and thermoelectric power factors were observed after film-formation and annealing.^{1,2} It is likely that the active dopant is a tertiary amine,³ however multiple routes of quaternary ammonium hydroxide decomposition have been shown to lead to tertiary amine products.⁴ Any chemical transformations, such as quaternary ammonium breakdown, can have a significant effect on the morphology of the doped film and complicates any investigation into the doping mechanism.

A water-soluble and air stable naphthalene diimide molecular semiconductor, called NDI-OH, has been synthesised which is covalently bound to a quaternary ammonium hydroxide group. When thin-films were formed by drop-casting absorption features consistent with doping were observed. The chemical structure of the dopant precursor was determined for the first-time using NMR and mass spectrometry. It was seen that the ammonium hydroxide precursor is a product of ring-opening hydrolysis on the imide functionality of the naphthalene diimide. After treatment at high temperature it was found that the reverse hydrolysis reaction also took place. The dynamic nature of this ring-opening reaction was found to have a significant effect on the chemical composition of the doped films.

A steady increase in electrical conductivity was observed with increasing temperatures of drop-casting in NDI-OH thin-films. Spectroscopic structural analysis of the conducting films revealed changes to both the quaternary ammonium moiety and the NDI ring-system at higher drop-casting temperatures. These structural changes lead to large differences in film morphology, doping efficiency and therefore conductivity in films prepared at different

temperatures. Film morphology was probed using a combination of atomic force microscopy and X-ray scattering. A combination of EPR and UV-vis absorption spectroscopy was also used to determine the amount and type of charge carriers generated. The results presented show that the functionality of this promising group of water-soluble conducting organics must be carefully tuned by considering at least two different chemical transformations. The extent and direction of the dynamic hydrolysis reaction plays a role in the film morphology while the breakdown of the quaternary ammonium group contributes to the generation of the active dopant.

References:

- 1) Reilly, T. H.; Hains, A. W.; Chen, H.-Y.; Gregg, B. A., A Self-Doping, *Advanced Energy Materials* 2012, 2 (4), 455-460.
- 2) Russ, B.; Robb, M. J.; Brunetti, F. G.; Miller, P. L.; Perry, E. E.; Patel, S. N.; Ho, V.; Chang, W. B.; Urban, J. J.; Chabinyc, M. L.; Hawker, C. J.; Segalman, R. A., 2014, 26 (21), 3473-3477.
- 3) Russ, B.; Robb, M. J.; Popere, B. C.; Perry, E. E.; Mai, C.-K.; Fronk, S. L.; Patel, S. N.; Mates, T. E.; Bazan, G. C.; Urban, J. J.; Chabinyc, M. L.; Hawker, C. J.; Segalman, R. A., *Chemical Science* 2016, 7 (3), 1914-1919.
- 4) Edson, J. B.; Macomber, C. S.; Pivovar, B. S.; Boncella, J. M., *Journal of Membrane Science* 2012, 399-400, 49-59.

SESSION EQ06.10: Structure Property Relationships

Session Chair: Paddy K. L. Chan

Monday Morning, December 6, 2021

EQ06-Virtual

8:00 AM *EQ06.10.01

Tracing Channel Potentials in Organic Transistors—Theory, Experiments and Applications Chuan Liu; Sun Yat-sen University, China

Detection and understanding of unipolar and ambipolar charge accumulation and transport is the key to understand intrinsic performance of organic field effect transistor (OFET). However, it is difficult to determine the motion of the carrier with regular electrical tests. In this paper, the generalized gated four probe (G-GFP) technique [1] is extended to employ to investigate both few-mono-layer organic small molecular semiconductors and ambipolar polymer semiconductors in transistors.

For the p-type semiconductor, we fabricated monolayer semiconductor C8-BTBT films by shearing method and investigate the impacts of film thickness, contact metal, dielectric materials, and etc. by systematically monitoring the channel potentials. For the ambipolar transistors, we fabricated diketopyrrolopyrrole thieno [3,2-b] thiophene copolymer (DPPT-TT) and studied the motion of carriers in the ambipolar regimes. For both types of OFETs, the evolution of local potential is monitored in the channel to establish a clear quantitative image of the accumulation and transmission of carriers during device operation. Both simulation and experimental results confirm that G-GFP is a suitable and feasible method to extract the carrier mobility and to reveal the key limiting factors that induce the non-ideal effects in OFETs.[2] Also, the ambipolar device with G-GFP structure can work as a single OFET inverter [3], which shows that G-GFP can be used as an effective tool for bipolar transistor analysis and help to realize logic functions.

[1] C. Liu et al, *Adv. Funct. Mater.* 2019, 1901700

[2] T. Yang et al, *Adv. Funct. Mater.* 2019, 1903889

[3] C. Liu et al, *Adv. Electron. Mater.* 2021, 2001134

8:30 AM *EQ06.10.02

Organic Doping at Ultra-Low Concentrations Raj Kishen Radha Krishnan¹, Drona Dahal¹, Paudel Pushpa¹ and Bjorn Lussem^{1,2}; ¹Kent State University, United States; ²Universität Bremen, Germany

Organic Doping is widely used for tuning the Fermi level of organic semiconductors. The precise control in the charge carrier density facilitated by doping allows to maximize the efficiency of organic optoelectronic devices [Walzer, K. et al., *Chem. Rev.* **107**, 1233–1271 (2007)]. However, doping concentrations used in most studies are high (in the wt.% range), which limits the doping process itself resulting to a low doping efficiency [Tietze *et al.*, *Adv. Funct. Mater.* **25**, 2701–2707 (2015)]. In addition, these high doping concentrations can lead to large off-currents when used to dope the channel of Organic Field-Effect Transistors [Liu et al., *ACS Applied Materials & Interfaces* **12**, 49857 (2020)].

In this presentation, we discuss the design of a rotating shutter system that is capable of controlling doping concentrations in vacuum processed films down to the 100 ppm level [R. K. Radha Krishnan *et al. Adv. Opt. Mat.* in press (2021)]. The increased control over the doping concentration is used to study doping at ultra-low concentrations in C₆₀ Metal – Oxide - Semiconductor (MOS) junctions. A small-signal drift-diffusion model is presented and used to determine the doping efficiency and activation energy of the doping process. With the help of a statistical model [Tietze *et al.*, *Phys. Rev. B* **86**, 035320 (2012)] the observed trends are fitted and design rules for future dopant/matrix combinations with higher doping efficiency are proposed.

Based on the results of the MOS study, C₆₀ OFETs doped at the 100ppm level are designed that operate at ultra-low voltages of 800mV only and retain an on/off ratio of up to 10⁷ despite doping. The devices have low subthreshold swing in the range of 80 mV/dec and a transconductance of up to 8 mS/mm. To demonstrate that our results can be generalized, we will discuss the effect of ultra-low doping not only on the archetypical n-type semiconductor C₆₀, but study doping of the high-performance p-type organic semiconductor, dinaphtho[2,3-b:2',3'-f]thieno[3,2-b]thiophene) DNNT as well. Here, doping enables a balanced ambipolar device characteristic with average electron and hole mobilities of approx. . Hole and electron injecting contacts are used to study the mechanism of majority and minority charge carrier generation inside the doped films.

Overall, it will be argued that doping is a key technology for organic field-effect transistors [Lüssem, B. *et al.*, *Chem. Rev.* **116**, 13714–13751 (2016)], and allows not only to reach high performance, but to realize new device structures and to study mechanisms of charge carrier generation in organic semiconductors as well. The use of ultra-low doping concentration broadens the potential use of doping in OFETs, which will help to move the field further towards larger scale integration.

9:00 AM EQ06.10.03

Reduction of Persistent Photoconductivity Effect of Zinc Oxide Ultraviolet Photoconductors by Polymer-Assisted Deposition Method with Deep Ultraviolet Photoactivation Jun-Gyu Choi, Won-June Lee and Myung-Han Yoon; Gwangju Institutes of Science and Technology, Korea (the Republic of)

In this study, we developed zinc oxide (ZnO) based ultraviolet (UV) photoconductor devices with low persistent photoconductivity (PPC) effect by introducing polymer-assisted sol-gel precursor with deep-UV (DUV) photoactivation. The influence of DUV photoactivation on polymer-oxide complexes was investigated by comprehensive characterization analyses. Unlike poor current recovery of conventional oxide photoconductors with ohmic-contact, the

ZnO films cast with polymer-mixed precursor solution exhibited much improved PPC effects with full current recovery, especially for the films irradiated by DUV followed by thermal annealing. The polycrystalline ZnO films in the photoconductor of reduced PPC effect exhibited larger grain sizes as well as fewer defect sites deriving poor recombination of photo-excited carriers. UV photoconductors based on PEI-involved ZnO films under DUV photoactivation showed excellent device performance represented by large photocurrent (~4 μ A), rapid response/recovery time (21 s and 40 s), and enhanced on-off current ratio (~ 3.7) in combination with the reduced PPC effect.

9:15 AM EQ06.10.04

Interfacial Control of Organic Semiconductor/Electrode Contact Characters Using Additive-Metal Interaction for Top-Contact Organic Transistor Giheon Choi^{1,2}, Seungtaek Oh^{1,2}, Jungyoon Seo^{1,2} and Hwasung Lee^{1,2}; ¹Hanyang University, Korea (the Republic of); ²BK21 FOUR ERICA-ACE Center, Hanyang University, Korea (the Republic of)

One of the important factors to improve the performance of organic field-effect transistors (OFETs) is an effective charge carrier injection from the metal electrode to organic semiconducting layer, and thus various studies have been conducted so far to improve this. In this study, the organic semiconducting layer was formed by blending the thiol SAM materials with PBTTT-C14 solution to control the nature of the charge carrier injection in the top-contact bottom gate (TCBG) structure of the OFETs, for which a spontaneously generated SAM was produced through annealing process on the electrodes. This result is simple and applicable on the TCBG-structured OFETs, which is impossible to be applied with SAM treatment until now. The field-effect mobility of PBTTT-C14 FETs blended with 1-dodecanethiol was improved from 0.025 to 0.063 cm^2/Vs as compared to that without blending, and the threshold voltage was shifted from 15 to 0 V, which is closed to an ideal onset operation of the device.

9:30 AM EQ06.10.06

Understanding Marangoni Flow-Driven Solidification of Polymer Semiconducting Films on an Aqueous Substrate Seungtaek Oh^{1,2}, Giheon Choi^{1,2}, Jungyoon Seo^{1,2} and Hwasung Lee^{1,2}; ¹Hanyang University, Korea (the Republic of); ²BK21 FOUR ERICA-ACE Center, Hanyang University, Korea (the Republic of)

Here, in the context of the polymer film on an aqueous transfer process, the value of spreading coefficient (S) plays an important role in spreading the polymer solution droplet on the base media. A high S is key to improving the polymer film uniformity and crystalline structure, which affect the organic field-effect transistor (OFET) device performance. In addition, the films floating on the base media were transferred either upward (UST) or downward (BST) to differ their solidified orientations. The differences between the UST and BST cases confirmed that the solvent in the polymer solution droplet was rapidly extracted at the interface with the base media and was slowly evaporated near the air interface with the polymer solution. The results induce rapid solidification with poor structural properties at the base media interface and slow solidification with good structural properties at the air interface. The surface properties of the polymer semiconducting films were advantageous in the vicinity of the air/polymer solution interfaces for use as a channel active layer, resulting in good OFET device performances for the UST case.

SESSION EQ06.11: Materials and Devices
Session Chair: Brendan O'Connor
Monday Morning, December 6, 2021
EQ06-Virtual

10:30 AM *EQ06.11.01

Organic Dyes Derived from Molecules in Cacao Beans for Use in Lighting Applications Christine Luscombe^{1,2}; ¹University of Washington, United States; ²Okinawa Institute of Science and Technology, Japan

LEDs are the foundation of lighting and display products surrounding us. While they have obtained great success in the commercial market, related research and development activities remain highly active aiming to enhance factors such as energy efficiency, stability, and environmental sustainability. Currently, commercial LED products are comprised of two key components: an indium gallium nitride e LED backlight with emission centered at 450 nm to cover the blue region of the visible spectrum, and powder inorganic phosphors on top converting blue light into longer wavelengths (e.g., green and red) to tune the emission of the device. A drawback of inorganic phosphors is that scattering of the emission from the micron-sized phosphor powders leads to substantial backscattering and subsequent absorption of the emission into the LED chip, and reabsorption losses in the phosphor itself, both of which reduce the overall light output of the final LED device. Organic dyes possess environmental advantages over inorganic phosphors because they are pi-conjugated molecules made from abundant elements (C, H, N, O, etc.) and are potentially bio-sourced. In this talk, I will present dyes that have been developed from theobromine, derived from cacao beans. When blended within an industrial polymer, poly(styrene-butadiene-styrene) (SBS), their enhanced solubility enables the formation of highly transparent films, crucial for reducing scattering loss in LEDs. Furthermore, resultant dye-SBS films achieved photoluminescence quantum yields (PLQYs) of around 90% under ambient conditions. Taking advantage of their transparency and solution processability, we fabricated a waveguide with this theobromine-dye-SBS composite, which was subsequently assembled into an edge-lit LED device of no glare and enhanced aesthetics.

11:00 AM *EQ06.11.02

Designing Functional Polymers for Organic Electronic Devices Michael L. Chabinyc; University of California, Santa Barbara, United States

Polymers are essential materials for wearable electronic systems and soft robotics as active and passive materials. We will discuss our recent work on polymer architectures that lead to control of electronic and mechanical responses of organic electronic devices. First, we will discuss how single ion conducting polymers, known as polymeric ionic liquids (PILs), can be used as electrolytes in organic electrochemical transistors. PILs provide a unique method to control the current voltage characteristics of electrolyte-gated transistors. By appropriate molecular design of the PIL, the operation of polymer transistors can be switched from conduction at an electrical double layer to conduction in the bulk by infiltration of counter ions. The behavior of transistors with PIL gates reveals the differences in the electrical conductivity of semiconducting polymers at the surface and in the bulk at high charge carrier concentrations. Second, we will discuss how polymers with a bottlebrush architecture can be used to form super-soft elastomers useful for pressure sensors. The low mechanical modulus of bottlebrush elastomers, which is comparable to that of hydrogels, allows for the formation of capacitive pressure sensors with sensitivity comparable to human touch. These studies reveal the importance of molecular design on the development of new organic electronic devices.

11:30 AM EQ06.11.03

Enhancing the Performance of State-of-the-Art Photo Cells Using Universal Hole Extraction Structure [Hela Fadool](#)¹, Young-Jun Yu², Jung-Il Jin², Dong Hoon Choi² and Nir Tessler¹; ¹Technion, Israel; ²Korea University, Korea (the Republic of)

Organic sensors, photodiodes, and solar cells have attracted much interest in recent years for their unique properties such as flexibility, lightweight, and the low cost and ease of their fabrication processes. While not destined to replace silicon-based technology, organic-based devices provide a promising technology for wearables, windows, as well as lightweight constructions that cannot hold the current massive photovoltaic (PV) modules.

A previous work done by our group[1] presents a device engineering approach to enhance the OPVs' performance using modulation-doping of the hole transport layer (HTL). A planer heterojunction device was investigated using two well-studied materials 1,1-bis [(di-4-tolylamino) phenyl] cyclohexane (TAPC) as a hole transporting material, C₇₀ as the accepting material, and P-type dopants, C₆₀F₄₈. The dopants were induced in a δ -doped layer of 10 nm width within the TAPC layer. The presence of the doped layer within the device induces an internal electric field at the junction leading to enhanced charge separation efficiency, reaching 50% enhancement in the current at the maximum power point and 30% at 0.8V_{oc}.

To extend the applicability of the design to solution-processed cells and make it universal to (almost) any donor-acceptor pair, we developed a strategy based on a cross-linkable high band-gap polymer matrix[2] where the donor material of choice can be blended at ~20w% to serve as the charge transporting/extracting level.[3] Being insoluble it can be considered as part of the substrate and the flexibility in choosing the transport material makes it universal.

We will first describe the general properties of the enhanced charge-extraction structure utilizing Poly (vinyl carbazole) bearing cinnamate pendants (PVK-cin [50%]) as the x-linkable matrix, Poly[bis(4-phenyl) (2,4,6-trimethylphenyl) amine (PTAA) as the transport/extraction material, and C₆₀F₄₈ doped PTAA as the δ -doped layer. Next, we describe the properties of a complete cell that is based on PBDB-T-2F (PM6) and Y6 (BTP-4F) as the donor-acceptor pair, respectively. [4, 5] To place the experimental results in perspective, we conduct a detailed device simulation and compare the experimentally measured enhancement to the maximum theoretical prediction.

References:

- [1] H. Shekhar and N. Tessler, "15% enhancement of the photocurrent at the maximum power point of a thin-film solar cell," *Sustain. Energ. Fuels*, 10.1039/D0SE00836B vol. 4, no. 11, pp. 5618-5627, 2020.
- [2] O. Solomeshch, V. Medvedev, P. R. Mackie, D. Cupertino, A. Razin, and N. Tessler, "Electronic formulations - Photopatterning of luminescent conjugated polymers," *Advanced Functional Materials*, vol. 16, no. 16, pp. 2095-2102, 2006.
- [3] Y.-J. Yu *et al.*, "p-type doping in organic light-emitting diodes based on fluorinated C60," *Journal of Applied Physics*, vol. 104, no. 12, p. 124505, 2008.
- [4] K. Li *et al.*, "Ternary Blended Fullerene-Free Polymer Solar Cells with 16.5% Efficiency Enabled with a Higher-LUMO-Level Acceptor to Improve Film Morphology," *Advanced Energy Materials*, vol. 0, no. 0, p. 1901728, 2019.
- [5] T. H. Lee *et al.*, "Efficient Exciton Diffusion in Organic Bilayer Heterojunctions with Nonfullerene Small Molecular Acceptors," *ACS Energy Letters*, vol. 5, no. 5, pp. 1628-1635, 2020.

11:45 AM EQ06.11.04

Doping and Extraction of Small Molecules in Semiconducting Polymer Films—Insights from Studies of Fluorescent Chemical Sensors [Graham A. Turnbull](#), Iain A. Campbell, Edward B. Ogugu and Ross N. Gillanders; University of St Andrews, United Kingdom

The presence of extrinsic dopant molecules can have a strong impact on the photophysical or electronic properties of organic semiconductor thin film devices. For example, Extrinsic dopant molecules present at low/ medium density can greatly enhance charge transport in p-i-n OLEDs, or provide recombination sites in the emissive layer. Dopants can act as charge traps, or exciton quenchers for study of transport phenomena in organic thin films. The presence of extrinsic analyte molecules in thin film chemical sensors can either modify the properties of photoluminescence (for example through fluorescence quenching) or electrical conduction. In device studies and applications, the dopants are conventionally introduced via co-deposition with the host material; whereas in chemical sensors, the analyte molecules are absorbed from either the surrounding vapour or solution phase after the film is formed.

In this paper we present study of the process of introduction and removal of small molecules into/from thin films of semiconducting polymers. We use photoluminescence quenching chemical sensors as a model system that can provide a platform for more general study of molecule transport in polymer films. We will describe a combined approach of experiments and simulations to explore molecular doping from the vapour and solution phases; The transport of sorbed molecules under the influence of diffusion and binding processes; and the retention and thermal desorption of the dopant.

We use a computational rate equation approach to model the binding and 1-dimensional diffusion of extrinsic molecules and estimate their populations within the film. We couple Fick's laws of diffusion to chemical binding rate equations for arbitrary analyte diffusion constants and binding rates. We relate the extrinsic dopant molecule populations within the film to the film luminescence and study the influence of the molecular interaction constants on the time-dynamics of fluorescence quenching in the film. We calculate the transport of dopant molecules through the thin film when driven by a positive or negative diffusion gradient at the film surface, observe a strong asymmetry in the fluorescence quenching signal between the in-diffusion dynamics of the dopants and the desorption of stored dopants from the film.

We compare the computational study with experiments of the sorption and transport of nitroaromatic molecules in thin films of the commercial semiconducting polymer Merck Super Yellow and non-conjugated polymers AFLAS and poly(bisphenol A-co-epichlorohydrin). We study the doping of dinitrotoluene over a range of concentrations in the polymers when introduced from acetonitrile solution and from the vapour phase. Measurements of the retention of the dopant at room temperature and at elevated temperatures are made using a combination of absorption and photoluminescence spectroscopy. Combined with the computational model these experiments provide insight to the process and time dynamics of introducing extrinsic molecular dopants in thin polymer films, their distribution and long-term stability.

12:00 PM EQ06.11.05

Strategies for the Mitigation of Ion Migration in Hybrid Perovskite Field-Effect Transistors [Amita Ummadisingu](#), Youcheng Zhang and Henning Sirringhaus; University of Cambridge, United Kingdom

Hybrid perovskites which are composed of both organic and inorganic components, have recently been found to possess excellent optical and electronic properties making them highly suitable for applications such as solar cells, light-emitting diodes, and thin film field-effect transistors (FETs) (1, 2). However, a deeper understanding of the complex charge transport in thin films of these hybrid materials is currently lacking. Here, we fabricated three-

dimensional perovskite FETs in the bottom-contact top-gate and the bottom-contact bottom-gate architectures using solution processing via the anti-solvent method (3) and identified unusual transfer characteristics that result in a lower than predicted field-effect mobility as well as unwanted hysteresis. To tackle these issues, we explore the effect of perovskite stoichiometry on the transfer characteristics of both methylammonium lead iodide and complex triple-cation perovskite FETs (3, 4). Those insights are correlated with the perovskite microstructure and local compositional information obtained using characterization techniques such as photoluminescence imaging, x-ray diffraction measurements and scanning electron microscopy, to unravel the central role of iodide ions in disrupting the expected FET transfer characteristics by partially screening the applied gate field. Furthermore, for each of the architectures, we present individual strategies in the perovskite processing methodologies and post-deposition cleaning protocols (5) that successfully suppress the unwanted ion migration. Our triple-cation-composition based FET device, optimized using Design of Experiments (DOE) principles, exhibits stable transfer characteristics with n-type behavior and remarkably low hysteresis even at room temperature. It also shows a good saturation electron field-effect mobility and an on/off ratio of $\sim 10^4$ at room temperature. Our work presents effective strategies to manage the ion migration and obtain improved device performance in organic-inorganic perovskite FETs, taking a step towards the realization of the predicted charge transport characteristics for these hybrid materials for use in different optoelectronic applications.

References

1. Green, M. A.; Ho-Baillie, A.; Snaith, H. J. The emergence of perovskite solar cells. *Nature Photonics* 2014, 8, 506-514.
2. J. Wang et al., Investigation of electrode electrochemical reactions in $\text{CH}_3\text{NH}_3\text{PbBr}_3$ perovskite single-crystal field-effect transistors. *Advanced Materials* 2019, 31, 1902618.
3. M. Saliba et al., Cesium-containing triple cation perovskite solar cells: improved stability, reproducibility and high efficiency. *Energy Environ. Sci.* 2016, 9, 1989-1997.
4. S. P. Senanayak et al., A general approach for hysteresis-free, operationally stable metal halide perovskite field-effect transistors. *Science Advances* 2020, 6, eaaz4948.
5. X.-J. She et al., A solvent-based surface cleaning and passivation technique for suppressing ionic defects in high-mobility perovskite field-effect transistors. *Nature Electronics* 2020, 3, 694-703.

12:15 PM EQ06.11.06

Electropatterned and Molecularly Imprinted Conjugated Polymers—Sensors and Nanostructured Devices Rigoberto C. Advincula^{1,2,3}; ¹Case Western Reserve University, United States; ²The University of Tennessee, Knoxville, United States; ³Oak Ridge National Laboratory, United States

Conjugated polymers and their use in organic electronics and have long been recognized and have made advances in display and electronic solid-state devices. The use of electropolymerization and electrodeposition have enabled the layering and formation of ultrathin functional polymer films useful for the transistor, display, and sensor devices. Utilizing control of the solution and electrochemical dielectric parameters, it is possible to tune and pattern surfaces where the polymer formed have controlled oxidation and reduction behavior which mediates the film workfunction and optical parameters. In this work, we report on the methods to prepare ultrathin dielectric and electronic materials of conjugated polymers primarily by electrochemical methods, highlighting the ability to pattern and control transport behavior up to the nanoscale. This will be demonstrated in the following: 1) electronanopatterning using SPM methods to prepare conjugated polymer network circuits, 2) electrodeposition in colloidal particle arrays and electropolymerization, and 3) electrochemically molecularly imprinted polymers. The results are devices that enable memory devices, mediated ion transport gates, and chemical and biological sensors respectively utilizing ultrathin film geometries, electrochemical control and surface characterization methods in devices.

SESSION EQ06.12: Novel Processing Methods

Session Chair: Oana Jurchescu

Monday Afternoon, December 6, 2021

EQ06-Virtual

1:00 PM *EQ06.12.01

Low Cost Manufacturing of μ LED Display by Fluidic Self-align Assembly (FSA) Technology Using Known-Good- μ LED Jong-Jan Lee; eLux, Inc., United States

Direct emission displays made with inorganic μ LEDs can potentially challenge LCD and OLED displays with better performance, efficiency and lifetime. Markets where microLED displays are likely to first appear are large information displays requiring high brightness, home theater applications benefitting from increased dynamic range and automotive displays in which high contrast and reliability are necessary. These displays are made possible by the integration of two mainstream technologies, namely GaN LED developed for general lighting and the large area active matrix backplanes developed for LCD displays.

The unique manufacturing challenge for μ LED displays is development of a technology to position and connect millions of small devices with zero defects and low cost. Conventional pick and place tools are capable of positioning μ LEDs, but the throughput of serial assembly is inadequate while mass-transfer methods have difficulty changing the pixel pitch. To address these challenges eLux has developed a massively parallel Fluidic Self-align Assembly (FSA) technology which positions each μ LED by capture of the device in a well structure that also contains the connecting electrodes.

FSA uses simple low-cost equipment to achieve assembly rates up to 50 million μ LEDs per hour and it is anticipated that production equipment could assemble an 8K display with 100 million LEDs in a few minutes. The technology is suitable for μ LEDs from 10 to 200 μm diameter offering flexibility to make a wide variety of displays with resolutions from 400 to 10 ppi or larger. Similarly, the microLED emitter area can be adjusted independently of the assembly technique to increase brightness and it is possible to produce displays over 5,000 cd/m^2 . Fluidic assembly applies relatively low force on the device so brittle materials such as red μ LEDs fabricated from AlGaInP can be assembled in the same way as blue and green emitting GaN μ LEDs.

A fully integrated manufacturing system for μ LED fluidic assembly will ensure that the assembled μ LEDs have acceptable performance with special emphasis on eliminating shorted or high resistance devices. Testing and binning used in the general lighting industry are not practical at the micron scale, so wafers are mapped by cathodoluminescence to identify defective μ LEDs. Based on the defect map, a selective harvest technique diverts bad μ LEDs from the suspension so only known good die are used for assembly. FSA relies on an excess of μ LEDs to ensure sufficient capture attempts for complete assembly, so it is also necessary to capture, filter and recycle unassembled μ LEDs.

With a suitable choice of complementary characteristic for the device and the trap site, it is possible to use fluidic assembly techniques to position nanowires or nanoparticles as well as μ LEDs. The presentation will give an overview of the integration issues with some suggestions for other possible applications and approaches.

1:30 PM *EQ06.12.02

Development of Ocean Chemical Sensors and Soft Actuators Through Printing Customizations Shuo Wu, Yichen Zhai and Tse Nga Ng; University of California, San Diego, United States

With our marine ecosystems under threat from climate change, there is an urgent need to continuously monitor marine conditions. One key indicator is the dissolved oxygen level, but existing sensors are limited by size and costs that preclude widespread non-intrusive monitoring. We present a new dual-gate design based on printed organic electrochemical transistors (OECTs) to track dissolved oxygen concentration in seawater, a highly challenging matrix owing to its high ionic strength and multitude of chemical interferents. The sensor achieved a detection limit of 0.3 ppm dissolved oxygen concentration in seawater. The device demonstrated reliable operation over five days and was capable of monitoring oxygenation changes arising from the photosynthesis cycles of saltwater macro-algae. In addition to oxygen, the dual-gate modulation principle is generalizable to other analytes with high redox potentials such as nitrates and dissolved carbon dioxide, and it offers a new design to realize compact, highly sensitive, economical in-situ sensors for harsh marine environments.

In addition to sensor fabrication, printing approaches can lead to devices that are readily customizable and economical for everyone to explore potential benefits and create new robotic applications. We demonstrated the printing integration of multi-material actuators, with an eye toward improving the fidelity and robustness of the printing process. We achieved compact soft actuators by using liquid-crystal elastomers (LCE) patterned by extrusion. An adjustable load was attached on the probe to control the pressure applied on the film. During the LCE alignment process, the probe velocity and load were tuned for gradient controls of alignment strength with various actuation strains based on different tool path strategies. The actuated samples were recorded with a 3D scanner to compare with the original 3D model. The quantitative results displayed a good index of 84.47% in structural similarity, successfully demonstrating the high fidelity of this approach.

2:00 PM EQ06.12.03

Increasing Photostability of Inverted Nonfullerene Organic Solar Cells by Using Fullerene Derivative Additives Marcella Günther¹, Dominic Blätte¹, Anna Lena Oechsle², Sergio Sánchez Rivas¹, Amir Abbas Yousefi Amin¹, Peter Müller-Buschbaum^{2,2}, Thomas Bein¹ and Tayebbeh Ameri^{3,1}; ¹Ludwig-Maximilians-Universität München, Germany; ²Technische Universität München, Germany; ³University of Edinburgh, United Kingdom

With efficiency now above 18%, organic solar cells are well on their way to commercial application. However, there are still major stability issues that drastically limit their lifetime. One problem that has recently become more apparent originates from the commonly used electron transport layer (ETL) zinc oxide. Although this material has very advantageous properties, such as low price, transparency and good conductivity, it has one major drawback, namely its photocatalytic activity, which degrades many good absorber materials. Typically, this problem is solved by adding a protective layer between the ETL and the absorber layer, however this results in a much more challenging manufacturing. A simpler approach would be to mix a protective compound directly into the absorbing layer. In this work we use a ternary approach by adding three different fullerene derivatives – PC₇₁BM, ICMA, and BisPCBM – to a PBDB-TF:IT-4F system in order to suppress the photocatalytic degradation of IT-4F on ZnO via the radical scavenging abilities of the fullerenes [1]. We show that already an addition of 5% fullerene can quintuple the lifetime of the solar cells under UV illumination. We attribute this improvement to a reduced photocatalytic decomposition of IT-4F in the ternary system, which results in a decreased recombination. We propose that the added fullerenes protect the IT-4F by acting as a sacrificial reagent, and thereby suppress the trap state formation. Furthermore, we show that the protective effect of the most promising fullerene ICMA is transferable to two other binary systems PBDB-TF:BTP-4F and PTB7-Th:IT-4F. Importantly, this effect can also increase the air stability of PBDB-TF:IT-4F. This work demonstrates that the addition of fullerene derivatives is a transferable and straightforward strategy to improve the stability of organic solar cells.

[1] ACS Appl. Mater. Interfaces 2021, 13, 16, 19072–19084

2:15 PM EQ06.12.04

Combining Screen and Aerosol Jet Printing Techniques for the Manufacturing of Organic Electrochemical Transistors (OECTs) for Utilization in Logic Circuits and Sensor Applications Anatolii Makhinia, Kathrin Hübscher, Jan Strandberg, Marie Nilsson, Valerio Beni and Peter Andersson Ersman; RISE Research Institutes of Sweden, Sweden

The reported study demonstrates a novel fabrication approach that combines the versatility of screen printing and the high resolution of aerosol jet printing to manufacture reliable and fast all-printed organic electrochemical transistors (OECTs) on PET substrates. For OECTs, both the area and physical thickness of the channels are of critical importance for rapid switching response. As a result, we take advantage of a robust screen printing process to fabricate all the layers, except for the channel that is deposited by aerosol jet printing technology. This fabrication strategy reduces the PEDOT:PSS-based channel volume by up to a factor of 15 compared to screen printed channels, giving rise to a faster switching response due to lowered device capacitance. The switching performance has been confirmed by dynamic and transfer sweep measurements for all-printed standalone OECTs, OECT-based inverters and 5-stage ring oscillator circuits. Remarkably fast switching response and propagation stage delays of just above 1 ms for all-printed OECT-based inverter and ring oscillators have been achieved, despite using a screen printed electrolyte layer solidified by UV curing. In contrast, previously reported fully screen printed OECT-based inverters and 5-stage ring oscillators exhibited propagation stage delays of ~50 ms and ~100 ms per stage, respectively [1]. Additionally, the all-printed OECT devices reveal a high ON/OFF ratio of 10³-10⁴, while keeping low switching voltages. This is evidenced by the fact that the input voltage window for the OECT-based inverter circuit was reduced to 1 V (square wave signal fluctuating between 0 V and 1 V), thereby prolonging the operational lifetime.

The results reported herein pave the way towards a cutting-edge fabrication approach that can tailor-made the device architecture to reveal the best possible match for various applications, depending on the requirements. The proposed approach was applied for the manufacturing of high-performance OECT-based devices, exemplified by OECT-based logic circuits with remarkable switching response as well as in sensor applications utilizing the high amplification in all-printed OECTs.

Acknowledgments: The research activities are funded within the BORGES project, under H2020-EU.1.3.1, grant agreement ID: 813863.

References:

[1] P. Andersson Ersman, et al. "All-printed large-scale integrated circuits based on organic electrochemical transistors." Nature Communications **10**, Article number: 5053 (2019).

2:30 PM EQ06.12.05

Transport Regimes, Material Utilization Efficiency and Film Production Rate in Low Pressure Organic Vapor Phase Deposition Ikenna H. Ozofor, Cecelia Kinane, Giselle Roca, Boning Qu, Stephen R. Forrest and Max Shtein; University of Michigan, United States

Organic vapor phase deposition (OVPD) is a technique for depositing active layers in organic optoelectronic devices, including OLEDs. In OVPD, organic material is evaporated into a stream of carrier gas, which transports it toward a cooled substrate, where organic vapor can be made to condense into a

smooth film. This approach decouples evaporation from transport and deposition, thereby offering increased stability of the deposition rate and doping ratio compared to the classical method of vacuum thermal evaporation (VTE). Thus, OVPD is a promising technique for low-cost volume production of multi-layer tandem OLEDs, where the number of active layers can exceed 25 in number. To advance deposition process and hardware design, we analyze transport mechanisms in OVPD, identifying key conditions and dominant factors. For a given hardware configuration, we show that diffusion dominates over convection in the upstream zone at carrier gas flow rates ≤ 50 SCCM and in the downstream zone when flow rate < 400 SCCM. These parameters can be scaled to hardware of different sizes. We also show how organic material flux, which determines film production throughput, can be extrapolated from convenient laboratory-scale experiments and computational fluid dynamics simulation. We further introduce a model that predicts material utilization efficiency, independent of organic vapor concentration. Results from this model compare well with experimental values, and they present pathways for process optimization and material waste minimization.

2:45 PM BREAK

SESSION EQ06.13: Processing and Applications II
Session Chair: Ioannis Kymissis
Monday Afternoon, December 6, 2021
EQ06-Virtual

4:00 PM EQ06.13.01

Emergent Opto-Electronic Properties in Molecular-Metal Polymer Nanocomposites Raphael Pfattner, Elena Laukhina, Marta Mas-Torrent, Elena Laukhina, Concepcio Rovira and Jaume Veciana; Institut de Ciencia de Materials de Barcelona (ICMAB-CSIC) and Networking Research Center on Bioengineering, Biomaterials and Nanomedicine (CIBER-BBN), Spain

Developing smart materials that can respond to an external stimulus is of major interest in artificial sensing devices able to read information about the physical, chemical and/or biological changes produced in our environment. Additionally, if these materials can be deposited or integrated on flexible, transparent substrates, their appeal is greatly increased.

The first [BEDT-TTF = bis(ethylenedithio)-tetrathiafulvalene based quasi-two-dimensional organic superconductor β -(BEDT-TTF) $_2$ I $_3$] was first reported back in 1984.^[1] Soon it became clear that ion radical salts (IRSs) derived from BEDT-TTF exhibit tuneable electronic band structures; therefore, such molecules are excellent building blocks for engineering a rich and diverse family of organic crystalline metals and semiconductors. Thanks to strong electron-electron and electron-phonon couplings, their anisotropic electronic structures exhibit many fascinating electronic and structural phase transitions, which can be controlled by external stimuli such as light, temperature, strain, pressure, and humidity, among others. Nevertheless, it is necessary to engineer these crystals into a proper material for sensing applications. This is done by forming polycrystalline layers of IRSs, derived from BEDT-TTF-based conductors, in nanocomposite bilayer (BL) films.

Such systems can be further tuned by choosing the nature of the IRSs enabling high sensitivity towards strain, pressure, temperature or even contactless radiation sensing *i.e.* bolometers.^[2,3] In another very recent example, bilayer films, composed of conducting polycrystalline layers of two dimensional BEDT-TTF-IRSs, hydroresistive sub-micron sized crystals on top of a polymeric host matrix permit to electrically monitor relative humidity in a stable and fully reversible fashion.^[4] At the percolation threshold, fascinating novel optoelectronic properties emerge (Insulator semiconductor-like metal transition).^[5] Mechanisms of responses are discussed and correlated with fundamental properties of charge transport in these systems. This sensor platform enables combining high electrical performance of single crystals with processing properties of polymers towards a simple, low-cost and highly sensitive platform for applications in robotics, biomedicine and human health care.

References:

- E. B. Yagubskii, I. F. Shchegolev, V. N. Laukhin, et al., JETP Lett., (1984), 39, 12.
- E. Laukhina, R. Pfattner, L. R. Ferreras, et al., Adv. Mater., (2009), 21, 1-5.
- R. Pfattner, V. Lebedev, E. Laukhina, et al., Adv. Electr. Mater., (2015), 1, 1500090.
- R. Pfattner, E. Laukhina, L. Ferlauto, et al., ACS Appl. Electr. Mater., (2019), 1, 1781.
- R. Pfattner, et al., (2021), submitted.

4:15 PM EQ06.13.02

Electron/Hole Transport Layer Work Function in Organic Devices Dalil Oussalah^{1,2}, Jérôme Vaillant¹, Benoît Racine¹, Jacques Baylet¹, Romain Paquet¹, Coralie Sésé¹, Christelle Laugier¹ and Raphael Clerc²; ¹Univ. Grenoble Alpes, CEA, Leti, France; ²Univ. Lyon, UJM-Saint-Etienne, CNRS, IOGS, Lab. Hubert Curien UMR5516, France

Introduction: Doped Hole (resp. Electron) Transport Layers HTL (resp. ETL) are commonly used in evaporated organic devices to achieve high work function hole contact (resp. low work function electron contact): in OLED to inject large current [1], in solar cell to increase the open circuit voltage Voc [2], and in photodetector to minimize the dark current [3]. However, the thickness of the HTL/ETL results from a delicate trade off. Indeed, on one hand, to minimize the detrimental impact of HTL/ETL on light absorption and series resistance effects, HTL/ETL must be kept as thin as possible. On the other hand, it is easier to reach an efficient work function by doping thicker layers. This later point is investigated more specifically in this work: an analytical model, numerical simulation and experiments are combined to identify this minimum acceptable thickness.

Simulation & Modeling: As it is surrounded by other materials with different work functions, the built in electric field within the HTL is never negligible, even in absence of applied voltage. In consequence, the Fermi level in ultra thin HTL layer, adjusted by doping, may differ from its (ideal) bulk value. A model has been derived to capture the impact of doping and thickness on the calculation of the HTL work function in two configurations: when the HTL is surrounded by two metals, when it is surrounded by a metal and an undoped organic semiconductor. Results, validated by numerical simulations, allows to determine the minimum acceptable thickness versus doping and electrostatic environment.

Experiments: Moreover, experiments were performed on a p-only structure (Ag/STTB:F4TCNQ (p-doped HTL)/ZnPc:C60 (active zone)/TiN) fabricated using common organic OPD/OLED materials. Samples feature different levels of doping and thickness. I-V curves has been fitted by a coherent set of physical parameters, confirming the capability of simulation of reproducing experiments. To extract the work function in situ, an innovative technic using I-Vs curves was implemented, following the work of X. Wei & al [4]. The results obtained clearly confirm the trend of the work function versus thickness curve predicted by theory. In high doped layers (10¹⁹ cm⁻³) a thickness of 10 nm is required to reach a suitable work function, while more than 20 nm is needed for lower doping (<10¹⁸ cm⁻³).

Conclusion: In summary, the impact of thickness and doping on the HTL work function in p-only template devices has been investigated in three complementary approaches: analytical modelling, numerical simulations and experiments. Results obtained proved that the obtaining of an efficient high work function HTL layer requires a minimum non negligible thickness, between 10 nm and 20 nm depending on doping level.

References: [1] C. Giebeler & al. J. Appl. Phys. 85, 608–615 (1999). [2] Y. Kinoshita & al., App Phys-92, 243309 (2008). [3] K. Kim & al., IEEE sensor, Vol 16, No 12, (2016). [4] X. Wei, M. Raikh, Z.V. Vardeny, Y. Yang, and D. Moses, Phys. Rev. B 49, 17480 (1994).

4:30 PM EQ06.13.03

Tunable and Narrowband Organic Photodetectors for Miniaturized Spectrometers on a Single Chip Shen Xing¹, Jonas Kublitski¹, Donato Spoltore¹, Koen Vandewal², Hans Kleemann¹, Johannes Benduhn¹ and Karl Leo¹; ¹IAPP, TU Dresden, Germany; ²Institute for Materials Research (IMO-IMOMECE), Belgium

Organic photodetectors (OPDs) are candidates for numerous novel applications including wearable electronics and biometric monitoring. Despite significant development, it is still challenging to simultaneously achieve tailorable optoelectronic properties and faint light sensitivity. Here, we propose a new concept by combining a transmission cavity structure with organic absorbers to achieve tunable and narrowband OPDs via a full-vacuum process. Benefiting from this strategy, remarkable performance such as narrowband photoresponse (full width at half maximum of around 40 nm), a large tunability from visible to near-infrared region, fast response speed, and ultrahigh specific detectivity ($> 10^{14}$ Jones) are simultaneously realized. To prove the potential application of this concept, multiple transmission cavity OPDs are integrated to be a miniaturized spectrometer whose performance is demonstrated. This novel concept extends the state-of-the-art OPDs, rivals silicon photodetectors, and will mature the spectroscopic photodetection for mobile applications.

4:45 PM EQ06.13.04

Innovative Fabrication and Processing Methods for Organic and Hybrid Electronics Christopher Landorf, Vijaya Kayastha, Rebekah Baggett, Anish Thukral and Marriana Nelson; Brewer Science, Inc., United States

Previously Brewer Science has reported on the solubilization of pristine carbon nanotubes in water, alcohols, and glycols through the use of super-acids and polyaromatic hydrocarbon derivatives. The goal of that research was to produce inks that allowed for rapid manufacturing of carbon-nanotube-based conductive thin films. These films do not require any post-processing steps, such as washing, to get rid of surfactants, and since the solubilizing functionality is non-covalently bonded to carbon nanotubes, the electronic structure of the carbon nanotube is preserved. In addition to enabling the production of films with excellent conductivity, these dispersions of carbon nanotubes also provide us with a unique environment to further explore reactivity for carbon nanotube functionalization. The lack of surfactants means that the surface of the tube is still accessible as a reactive surface, and since these carbon nanotubes are still highly conductive, further functionalization doesn't degrade the electrical properties. Carbon nanotubes have been exploited for their sensitivity to a variety of analytes, including gases; however, gas selectivity can be a challenge. In order to improve selectivity, carbon nanotubes can be functionalized through various means to target specific analytes. Using the unique reaction environment that Brewer Science has developed, we have successfully coated carbon nanotubes with a disordered tin oxide layer characterized as mixed oxides by Raman spectroscopy to target combustible analytes. Other metal oxides, including vanadium and titanium, have been reacted similarly. SEM images of films of the functionalized tube sets demonstrates that the metal oxide is deposited on the carbon nanotube surface, and minimal free metal oxide is observed. The resulting inks can be screen-printed between electrodes, allowing rapid manufacture of hundreds of devices. A thin layer of palladium is deposited as a catalyst, and with electronics developed by Brewer Science, the tin oxide-doped carbon nanotube films easily detect 100 ppm of carbon monoxide in our screening efforts. This same sensor, as printed, does not respond to other gases typical of tin oxide, such as methane. A sensor manufactured without either the tin oxide or the palladium does not respond to carbon monoxide.

5:00 PM EQ06.13.06

Enhanced Brightness Solution-Processed CsPbBr₃ Perovskite LEDs Using a Composite PEG-PVP Matrix Parvez Akhtar¹, Nidhi Dua¹, Raman Agrawal² and Madhusudan Singh¹; ¹Indian Institute of Technology Delhi, India; ²IIT Delhi, India

Imperfect surface coverage, pinholes and other defects in solution-processed perovskite (CsPbBr₃) thin films limit the radiative efficiency and stability of corresponding perovskite light-emitting diodes (LEDs). Significant effort on refinement of various deposition techniques, chemical compositions, functionalization and surface treatments have been reported in literature. In this work, we report on use of two inexpensive polymers - poly(ethylene) glycol (PEG) and polyvinylpyrrolidone (PVP) as a composite matrix for CsPbBr₃ to enhance surface coverage and uniformity of the deposited films in LEDs. A transparent perovskite precursor solution was prepared by mixing CsBr (99.999%, Sigma-Aldrich) and PbBr₂ (99.99%, Sigma-Aldrich) in DMSO with an optimized molar concentration ratio of 1.5:1 (0.2M) in a nitrogen glove box (Inert PureLab). After filtering, this solution was blended with separate PEG and PVP solutions (in dimethylsulfoxide (DMSO) and dimethylformamide (DMF), respectively, concentration > 5mg/ml) with a 6% net loading of the polymer solution to form the active ink. The ink was spin-coated on glass for film characterization. An orthorhombic phase (JCPDS(06-153-3063)) for CsPbBr₃ was confirmed using X-ray diffraction (Rigaku Miniflex, Cu-K α , 1.54Å), with the elemental composition confirmed using energy dispersive X-ray analysis (EDX). UV-Vis spectrometry (Perkin-Elmer) was used to infer a band gap of 2.38 \pm 0.015 eV. Photoluminescence spectra (Horiba Labram, with a 325 nm source) yield a single highly intense peak at 520 nm (FWHM: 20 nm). For polymer LED fabrication, indium tin oxide (ITO) coated glass substrates were cleaned in a standard multistep process prior to spincoating poly(3,4-ethylenedioxythiophene) polystyrene sulfonate (PEDOT:PSS, Baytron PVP), dehydration bake in air (120C), followed by spin-coating of perovskite ink under nitrogen, and an anneal at 75C. Samples were transferred under nitrogen for thermal evaporation at 2.3x10⁻⁶ Torr (Angstrom Engineering) of 2,2',2''-(1,3,5-Benzinetriyl)-tris(1-phenyl-1-H-benzimidazole) (TPBi, 300 Å), LiF (8Å) and Al (1000 Å) to complete the devices with a shadow-masked top contact of area 0.3 x 0.3 cm². Control devices (no polymer additive) were processed at the same time under identical conditions. Current-voltage (J-V) and light-intensity-voltage (L-V) characteristics were acquired using a Keithley 2450 SMU and a calibrated Si photodiode. The test (CsPbBr₃-PEG-PVP) perovskite device exhibited a lower turn-on voltage (4.1V vs 3.2V), higher luminance (392 cd/m² vs 1070 cd/m²), current efficiency (0.150 cd/A vs 0.254 cd/A), when compared to the control device. Electroluminescence spectroscopy measurements (Ocean Optics HR4000) reveal an emission at 518 nm (FWHM=17 nm) with Commission Internationale de l'éclairage (CIE1931) coordinates (0.13,0.75), in close agreement with measured PL. To study the likely source of these enhancements, we carried out comparative film analysis of test and control devices using field-emission scanning electron microscopy (FESEM, JEOL JSM-7800F Prime) and atomic force microscopy (AFM, Asylum Research MFP3D-SA). A reduced crystal grain size (204.1 nm to 101.1 nm) and nearly 100% surface coverage (compared to 81% found for control devices) found using FESEM suggests that the improved overall morphology and surface coverage plays a significant role in the improved performance. Further, a reduction in surface roughness (5.8 nm to 3.2 nm) and formation of a pinhole-free film is observed to increase yield by 20%. We are currently carrying out initial measurement of device lifetimes under accelerated test conditions under nitrogen and in air (after encapsulation) to further elucidate the relative prevalence of various device failure mechanisms in the test and control LEDs. We expect that these enhanced devices would find extensive applications in personal lighting, and transparent flexible display applications.

5:15 PM EQ06.13.07

Hybrid Organic-Inorganic Thin-Film Multispectral Photodetector Vladimir Pejovic^{1,2}, Epimitheas Georgitzikis¹, Itai Lieberman¹, Pawel Malinowski¹, Paul Heremans^{1,2} and David Cheyns¹; ¹imec, Belgium; ²KU Leuven, Belgium

Optoelectronic devices based on thin-film materials such as organic polymers and small molecules, colloidal quantum dots (CQDs), and perovskites have been demonstrated as a promising route to bring disruptions in various consumer and industrial domains. Thin-film photodetectors are emerging as new imaging technology, thanks to their versatile large-area and room-temperature fabrication. Highly sensitive organic photodetectors (OPDs) enable flexible image sensors and co-integration with OLED displays. However, no organic semiconductors have been synthesized so far that can offer competitive quantum efficiency in infrared beyond 1 μm wavelength – the same limitation associated with silicon photodiodes. On the other hand, the facile bandgap tunability of CQDs made them a promising alternative to conventional infrared image sensors based on compound semiconductors. Thanks to a possibility for monolithic integration with CMOS electronics, CQDs offer low-cost, high-throughput fabrication and unprecedented resolution in infrared, which is expected to enhance the development of industries such as autonomous driving, augmented/virtual reality, and others.

Here, we present our work in which we combine the two thin-film technologies in a single photodetector in order to leverage the best features of both, such as high visible sensitivity of OPDs and high infrared sensitivity of CQDs. The photodetector contains two stacked photodiodes connected in a back-to-back serial configuration. Each photodiode can be activated separately by selecting the bias voltage polarity, offering a multispectral capability. One photodiode is based on a solution-processed organic bulk heterojunction made of PTB7-Th and IECO-4F, and it exhibits sensitivity up to 1 μm wavelength, with high external quantum efficiency (EQE) of more than 60% at 700 nm and a low dark current density of 30 nA/cm² at 1 V reverse bias. The other photodiode is based on solution-processed PbS CQDs with their size tuned for absorption up to 1600 nm and it exhibits a dark current density of 800 nA/cm² at 1 V. We perform optical simulations based on a transfer matrix method and find that an intermediate thin silver layer can reduce the optical crosstalk between the two channels. Moreover, this thin film enables tuning of the CQD photodetector's response thanks to a strong optical cavity created with the back metal electrode, giving rise to a high EQE of more than 20% at different wavelengths in the 1-1.6 μm range. Transient measurements reveal a fast switching speed between the two photodiodes in the order of 10 μs .

By combining solution processing and physical vapor deposition, we developed a room-temperature, large-area compatible process that allows us to integrate polymers, CQDs, metal oxides, and metals in a single device. To ensure efficient charge carrier transport and low levels of dark current, we carefully engineered the device stack by controlling the surface passivation of CQDs and the energetic alignment at the interfaces. The presented photodetector is a two-terminal device that is compatible with the developed methods for integration of thin films with CMOS readout electronics, whereas its vertically stacked structure provides high spatial resolution for imaging. The presented photodetector has the potential to enable low-cost, high-resolution multispectral imaging and demonstrates how thin-film technologies can be exploited for new applications and functionalities.

5:45 PM BREAK

SESSION EQ06.14: Poster Session—Processing and Devices II

Session Chair: Paddy K. L. Chan

Monday Afternoon, December 6, 2021

EQ06-Virtual

6:30 PM EQ06.14.01

A Highly-Oriented Fibril-Like Rigid N-Type Polymer with High Electrical Performances Marc-Antoine Stoeckel¹, Han-Yan Wu¹, Chi-Yuan Yang¹, Ziang Wu², Yang Lu³, Jian Pei³, Han Young Woo², Magnus Berggren¹ and Simone Fabiano¹; ¹Linköping University, Sweden; ²Korea University, Korea (the Republic of); ³Peking University, China

Conjugated polymers are an enabling technology for numerous optoelectronic, bioelectronic, and energy harvesting/storage applications. The conductivity of several solution processable conjugated polymers, and therefore the performance of many of the corresponding devices, can be enhanced by molecular doping. For practical applications, both hole-transporting (p-type) and electron-transporting (n-type) conducting polymers are usually required. Unlike p-doped polymers that exhibit conductivities typically > 1000 S/cm, most n-doped polymers suffer from conductivity values < 1 S/cm. Various polymer design strategies, including planarization and stiffening of the polymer backbone, engineering of the donor-acceptor character, and control of the molecular dopant counterion-polymer side-chain miscibility are being explored. Despite great progress, n-doped conducting polymers do not yet meet the performance comparable to the best p-doped polymers. Here, we constructed highly ordered polymeric films, with thickness approaching unit cell dimension, and investigated their electrical properties. We used Langmuir-Schaeffer (LS) deposition technique to manufacture highly oriented polymeric monolayers with a low degree of defects. We used a combination of scanning probe microscopies, optical spectroscopy, GIWAXS, NEXAFS and electrical measurements to characterize the polymeric energetics, structural, and thermoelectric properties. We optimized the electrical performances of the ultra-thin films by n-doping them with strong reducing agents, reaching n-type conductivities of 4 S/cm, and a power factor of 1.5 $\mu\text{W/mK}^2$.

6:35 PM EQ06.14.02

Effect of Polymer Backbone on Optoelectronic Properties of Metallopolymers Nese Guven¹, Hajar Sultanova², Burak Ozer¹, Baris Yucel² and Pinar Camurlu¹; ¹Akdeniz University, Turkey; ²Istanbul Technical University, Turkey

Metallopolymers are a new generation of hybrid materials containing a transition metal complex and a π -conjugated backbone. Ruthenium complexes between transition metal complexes are extremely important with their stable redox transitions and electrochromic properties. Herein, monomers containing the redox active $[\text{Ru}(\text{bpy})_2\text{pytri}]^{2+}$ complex and various polymerizable thiophene derivatives such as SNS, EDOT and PProDOT were synthesized via click chemistry. As a result of electrochemical polymerization of monomers, new electrochromic metallopolymers based on polythiophene were obtained.

It was determined that polythiophene derivatives, which consist of the same complex unit and different polymerizable units, exhibit different band gaps and color properties depending on the backbone of the polymers. The band gaps of PSNS, PEDOT and PProDOT were calculated 2.44 eV, 1.84 eV and 1.94 eV, respectively. The neutral colors of the PSNS-Ru, PEDOT-Ru and PProDOT-Ru metallopolymers were determined yellow, green and orange, respectively. The switching times of PSNS-Ru, PEDOT-Ru and PProDOT-Ru were determined as 5.14 s, 2.52 s and 3.70 s, respectively.

All polymers showed their respective redox activities of both conjugated main backbone and metal complex indicating the effective manipulation of redox behavior of conducting polymers through engineering of the monomer structure.

***This work was financially supported by the National Science Foundation of Turkey (TUBITAK Project No: 215Z400) and Akdeniz University Research Funds (FDK-2019-4934).

6:40 PM EQ06.14.03

Late News: Effect of Water Treatment on Enhancing the Performance and Stability in Slot-Die Coated Organic Solar Cells [Nara Han](#)¹, Youn-Jung Heo², Yeonsu Choi¹ and Dong-Yu Kim¹; ¹Gwangju Institute of Science and Technology, Korea (the Republic of); ²Korea Institute of Industrial Technology, Korea (the Republic of)

In the field of organic electronic devices, it is generally unusual to use polar solvent in organic solvent-based active solution for improved efficiency and stability. Residual water in active solution has also been reported to adversely affect organic electronic devices. For blocking the contact of moisture, many researchers prepare and store organic electronic devices under nitrogen (N₂) atmosphere. However, we found that various hydrophilic solvents, such as water, methanol and isopropanol, as additives have an unexpectedly positive effect for enhanced efficiency and stability of solar cells. In this study, the D-A blend films (**ref-1**: PTB7-Th:PC₆₁BM, **ref-2**: PTB7-Th:EH-IDTBR and **ref-3**: PM6:Y6) with water treatment were slot-die coated and optimized for up-scaling production. Furthermore, we confirmed that the bulk heterojunction morphology and power conversion efficiency depend on the quantity (0~20 v/v%) of water introduced as a solvent additive. The effects of water addition were analyzed by using AFM, TEM, FT-IR and 2D GIWAXS measurements. As a result, enhanced efficiencies of 12% (ref-1/WT), 11% (ref-2/WT) and 12% (ref-3/WT) compared with efficiency of reference cells were achieved from the water addition. In addition, the improved stability (RH 60 % and room temperature in air) of the water additive incorporated devices was demonstrated as compared with reference cells, showing the excellent potential of eco-friendly and morphology-controllable additive for the printable organic solar cells.

6:45 PM EQ06.14.04

Improved Optical Confinement in Ambipolar Field-Effect Transistors via High Refractive Index Cladding Layers Towards Electrical Injection Organic Lasers [Yun Li](#)¹, Randy Sabatini², Shyamal Prasad³, Evan Hockings¹, Timothy Schmidt³ and Girish Lakhwani¹; ¹The University of Sydney, Australia; ²University of Toronto, Canada; ³University of New South Wales, Australia

Electrical injection organic solid-state lasers (OSL) promise easily processable devices for chemical sensing, point-of-care diagnostic and applications requiring wavelength tunable sources. While significant progress has been made with OSLs, persistent issues such as optical losses and short operational lifetimes in the devices prevent the realization of practical application. To circumvent these issues, novel injection architectures have been proposed. One such structure is the ambipolar field-effect transistor (FET).

In our work, mode-solver calculations demonstrate that improvements to optical confinement are possible in FET geometries, by using high refractive index cladding layers. Optical experiments show an increase in amplified spontaneous emission (ASE) efficiency and lowered ASE thresholds, which we attribute predominantly to the increased confinement. The results suggest that the structure can be potentially used to improve lasing characteristics for both optically pumped, and electrical injection organic lasers where thin, low refractive index active materials are required.

6:50 PM EQ06.14.05

The Shrink Film Scale Down Fabrication Method of the Low Voltage Operate Organic Field-Effect-Transistor [Shui Hong Siddhartha Dai](#)^{1,2}; ¹Hong Kong University, Hong Kong; ²Advanced Biomedical Instrumentation Centre, Hong Kong

Organic Field-Effect Transistors (OFETs) have been developed for different applications including bio-sensors, flexible memory, display drivers and etc. To enhance the functionality of OFET devices, downsizing the OFETs and increases their packing density are required. However, the traditional scaling-down fabrication method demands more involved fabrication processes such as photolithography, deep X-ray lithography, or e-beam lithography. To avoid these complicated processes, the current work presents an approach to downsize the OFETs by using the pre-stressed polystyrene (PS) shrink film substrates. It is a brand-new strategy for downsizing and improves the electrical performance of organic drivers. This method only needed common equipment (such as the oven or hot plate) and provided time effective downsizing fabrication process. After heating the film to 160 °C, over the glass transition temperature of PS, the shrink film will release its pre-loaded stress and the OFET devices will follow the shrink film substrates to shrink. The projective area of the device was reduced by 75%. The wrinkled structure can amplify the electrical field at the channel area and reduce the subthreshold voltage of the transistor. By using the AlO_x dielectric layer, the subthreshold voltage of the transistor is shifted from -1.44 V (before shrinking) to -0.18 V (after shrinking) with the subthreshold swing of 74 mV/dec and intrinsic gain of 4.151 x 10⁴. This study shows that fabricates OFET devices onto the shrink film substrate can provide a low cost and time-saving scale down method and the wrinkled structure would be one of the designs for the low voltage operated OFETs.

6:55 PM EQ06.14.06

Flexible High-Mobility, Bias-Stable Monolayer Organic Transistors Developed by Lamination Method [Zhenfei He](#) and Paddy K. L. Chan; The University of Hong Kong, Hong Kong

Solution processing is a facile fabrication method for large area, low-cost organic field-effect transistors (OFETs). Highly crystalline organic thin film by solution shearing offers a decent mobility, on/off ratio and subthreshold swing which are all important parameters to advance the OFET applications. To increase the device operation stability, self-assembled monolayers (SAMs) with low surface energy are usually used to eliminate the interface trap states locating at the semiconductor-dielectric interface. However, low surface energy which impedes solution wetting is a big challenge for the growth of highly crystalline thin film. To overcome the limitation, we replace the traditional fabrication method of in-situ growth of organic thin film by a transfer method. The high crystalline monolayer was grown on a high surface energy template substrate and transferred onto the low surface energy dielectric by using a temporary carrier. Both the morphology and the electrical property of organic monolayer remained undamaged during the transfer process and high mobility of 10 cm²V⁻¹s⁻¹ on SiO₂ was maintained. We further demonstrated a flexible, low-operation voltage OFET device with zero turn-on voltage, high on-off ratio 10⁷, and high mobility of 7 cm²V⁻¹s⁻¹, by transferring the high-quality active layer onto low surface-energy fluorinated-based SAM modified high-κ AlO_x dielectric and laminating source-drain electrodes. The transferred OFETs show a significant improvement against the bias stress effect. The device only showed 200mV threshold voltage shift after 10000s bias stress test. The fabrication method extended the application of highly crystalline organic active layer to flexible and conformal organic electronics.

7:00 PM EQ06.14.07

Feasibility of Fabricating High Mobility and Low Contact Resistance N-Type Polymer Field-Effect Transistors via Doping and Meniscus-Guided Coating Method. [Wanli Yang](#)¹, Paddy K. L. Chan¹ and Xugang Guo²; ¹The University of Hong Kong, Hong Kong; ²Southern University of Science and Technology, China

Despite the great progress have been made recent years in organic field-effect transistors (OFET), the n-type organic semiconductors with high mobility and reliability are still scarce. Doping of the meniscus-guided coated organic semiconductors (OSCs) is powerful technique for tuning the electrical properties of the active channel layer. Herein, towards the classic n-type polymer semiconductor P(NDI2DO-T2) (N2200), the better quality of the metal-organic interface between the N2200 and Au was achieved via employing cesium fluoride (CsF) doping and blade shearing method, respectively. Notably, when utilizing the CsF dopants at a low concentration (0.5wt%), the saturation mobility can be significantly

improved from 0.23 to 0.61 cm² V⁻¹ s⁻¹ as well as the threshold voltage from 29.7 to 10.1 V on glass substrate with CYTOP dielectric. In addition, a strong correlation between the contact resistance and the solution shearing speed is well observed with resistance decreasing from 7.9 kΩ cm for samples prepared under 0.005 mms⁻¹ to 3.1 kΩ cm for samples prepared by 5 mms⁻¹ shearing speed. Taking good advantages of these two techniques, a maximum electron mobility of 3 cm² V⁻¹ s⁻¹ and 1.23 cm² V⁻¹ s⁻¹ are achieved for the saturation and linear region operation, respectively. These results show the feasibility of alkali metal salt CsF as dopants and high-speed Meniscus-guided coating regulating the orientation of polymer fibers and demonstrate their promising applications in organic electronics.

7:05 PM EQ06.14.08

Ultra-Thin and Conformable Two-Dimensional Organic Thin-Film Transistor via Layer-by-Layer Transfer [Deng Zou](#)^{1,2} and Paddy K. L. Chan^{1,2}; ¹The University of Hong Kong, Hong Kong; ²Advanced Biomedical Instrumentation Centre, Hong Kong

Two-dimensional (2D) atomic crystals are extensively studied in recent years due to their exciting physics and device applications. However, there are still a number of technical challenges in achieving active layers with mono or bi-layer thicknesses while the electrical performance does not deteriorate. Here, we focus on organic field-effect transistors (OFETs) and fabricate them by a layer-by-layer transfer method with bottom-to-top 2D layers. The graphene bottom gate is atomically smooth and has few nanometers in thickness, which affords a pristine bottom interface for constructing upper 2D layers. High-quality C₁₀DNTT molecular crystal is deposited on fluorophlogopite mica by blade coating method, with precisely controlled thickness down to monolayer. Moreover, the van der Waal electrode is applied to ensure a clean and non-destructive interface for metal-semiconductor contact. As a result, the 2D OFET has a channel down to 1 μm length and the total thickness of the device is less than 200 nm. Simultaneously, the 2D OFET with ultra-thin fluorophlogopite mica dielectric shows high carrier mobility up to 12 cm²V⁻¹ s⁻¹, operating voltage within 1 V and decent subthreshold swing of 100 mV dec⁻¹. These electrical properties and the thickness allow them to conformally adhere onto non-planar surfaces for multifunctional applications, including electrophysiological signal detection on human. Our work unveils an exciting new class of two-dimensional OFETs for flexible electronic and photonic applications.

7:10 PM EQ06.14.09

Low Operating Voltage Organic Memory Transistor Based on Polymorphs of the Active Layer [Lizhi Yan](#) and Paddy K. L. Chan; The University of Hong Kong, Hong Kong

Organic memory transistor (OMT) is a promising candidate for the next generation memory devices towards human-machine interface applications. In this study, we developed nonvolatile optical memory transistor with [1]Benzothieno[3,2-b]benzothiophene (BTBT)-based p-type organic semiconductor as the active layer. We found that the polymorphs density of the active layer is corresponding directly to the OMT memory performance. The processing parameters, including deposition temperature (T), surface energy (γ), surface roughness (r) and film thickness (t), are pivotal to achieve fine control over the polymorphs of the deposited organic active layers and therefore, investigations of these parameters are highly desired. Here, we explore the effects of the processing factors mentioned above on the polymorphs morphology of the active layer under thermal evaporation and the memory performance of OMT. It is verified that T and γ are key parameters connected to the density of thin film polymorphs; r and t are also important in tuning the polymorphs density. Combining with the high-k dielectric material Al₂O₃, the memory transistor can operate at a low voltage during optical programming and electrical erasing process. Additionally, the transistor shows a field effect mobility up to 2.5 cm²V⁻¹s⁻¹ and excellent data retention for more than 12 hours with a current ratio higher than 10⁴ between the two binary states, which is a promising value for the OMT. Our findings provide valuable information in understanding the polymorphs morphology and the corresponding memory performance of BTBT-based organic semiconductor under thermal evaporation, which is believed to be with high potential in approaching next generation neuromorphic devices.

7:15 PM EQ06.14.10

A Dielectrophoresis-Chip with an OFET Array for Cell Trapping and Sensing [Piao Yingzhe](#)^{1,2}, Paddy K. L. Chan¹ and Xin Cheng²; ¹The University of Hong Kong, China; ²Southern University of Science and Technology, China

Microfluidics for cell trapping and pairing has become a very powerful platform for in vitro cell analysis. In many topics like the immune system and cancer biology, etc, using microfluidics chips to trapping cells and analyzing their behavior is very effective. Dielectrophoresis (DEP) with its compatibility with living cells is one of the mostly used method for cell manipulation. By integrating a FET sensor array into the DEP-chip, we can realize the combination of cell trapping and sensing. By using the organic field-effect transistors (OFETs) sensor array to measure the impedance of cells, we can monitor whether every trapping points which are designed and fabricated in the chip have successfully trapped a cell and the cell status (alive or dead). After identifying the successfully trapping, we can continue with subsequent manipulation like cell fusion, cell lysis, and DNA detection. It will be a very powerful platform for bio- and biomedical science.

7:20 PM EQ06.14.11

Solvent Toolkit for Electrochemical Characterization of Hybrid Perovskite Films Jason D. Slinker¹, [Sauraj Jha](#)¹ and Alexander Zakhidov²; ¹The University of Texas at Dallas, United States; ²Texas State University, United States

Organohalide lead (hybrid) perovskites have emerged as competitive semiconducting materials for photovoltaic devices due to their high performance and low cost. To further the understanding and optimization of these materials, solution-based methods for interrogating and modifying perovskite thin films are needed. In this work, we report a hydrofluoroether (HFE) solvent-based electrolyte for electrochemical processing and characterization of organic-inorganic trihalide lead perovskite thin films. Organic perovskite films are soluble in most of the polar organic solvents, and thus they were not considered suitable for electrochemical processing until now. We have enabled electrochemical characterization and demonstrated a processing toolset for these materials utilizing highly fluorinated electrolytes based on a HFE solvent. Our results show that chemically orthogonal electrolytes based on HFE solvents do not dissolve organic perovskite films and thus allow electrochemical characterization of the electronic structure, investigation of charge transport properties, and electrochemical doping of the films with in situ diagnostic capabilities.

7:25 PM EQ06.14.12

Electrochromic Properties of PEDOT Derivatives Containing Ru(II) Complex Nese Guven^{1,1}, Hajar Sultanova², Baris Yucel² and [Pinar Camurlu](#)^{1,1}; ¹Akdeniz University, Turkey; ²Istanbul Technical University, Turkey

In this study we display electrochromic properties of PEDOT derivatives containing Ru(II) complex which were synthesized through electrochemical homopolymerization of EDOT-Ru and copolymerization of EDOT-Ru with EDOT. All the metallopolymers revealed reversible electrochemical activity both in anodic and cathodic regions. Optoelectronic properties of metallopolymers were investigated by cyclic voltammetry, spectroelectrochemistry, kinetic and colorimetry measurements.

The band gap, optical contrast, switching time and coloration efficiency of the homopolymer (PEDOT-Ru) were determined as 1.77 eV, 33.72 %, 1.39 s

and 156.21 cm²/C, respectively. PEDOT-Ru exhibited multichromic behavior, displaying purple, green, yellow and transparent colors. The studies on copolymerization demonstrated that the electrochromic properties of the copolymers could be changed through comonomer feed ratio. All copolymers displayed multichromic behavior. The neutral state colors of P(EDOT-Ru-co-EDOT)₁, P(EDOT-Ru-co-EDOT)₂ and P(EDOT-Ru-co-EDOT)₃ copolymers were appeared as green, dark green and blue, respectively.

***This work was financially supported by the National Science Foundation of Turkey (TUBITAK Project No: 215Z400) and Akdeniz University Research Funds (FDK-2019-4934).

7:30 PM EQ06.14.13

Late News: Chalcogen Atom Substitution Effect in Novel Quinoidal Conjugated Polymers for Organic Field-Effect Transistors Yeonsu Choi¹, Yunseul Kim¹, Yina Moon¹, In-Bok Kim², Nara Han¹ and Dong-Yu Kim¹; ¹Gwangju Institute of Science and Technology, Korea (the Republic of); ²Research Institute of Solar and Sustainable Energies, Korea (the Republic of)

The field of semiconducting π -conjugated polymers (SCPs) have undergone fast development in recent decades due to their various applications in organic electronics, such as organic photovoltaics (OPVs), organic light emitting diodes (OLEDs), thermoelectrics and organic field-effect transistors (OFETs). In order to accomplish the high performance devices, a number of organic molecular building blocks based on aromatic rings have been designed and synthesized. Recently, the quinoid-type molecules have been considered as a promising candidate for active materials of organic electronics due to their superior electrical properties derived from more electron delocalized atmosphere facilitating efficient charge transport.

In this work, a novel quinoidal building block incorporating 3,4-ethylenedithiophene (EDTT) inducing intermolecular interaction *via* sulfur-sulfur interactions were designed and successfully synthesized. In addition to such intermolecular attraction, it has been reported that the conjugated molecules containing thioalkyl group show unique optoelectronic properties compared to molecules containing oxyalkyl group. Therefore, quinoidal polymeric semiconductors PmQEDTT-T2 and PmQEDOT-T2 that is 3,4-ethylenedioxythiophene (EDOT) incorporated structure instead of EDTT were copolymerized by Stille polymerization. The prepared quinoidal conjugated polymers exhibited significantly different properties such as electronic, optical properties and vibronic structures. Organic field-effect transistors were fabricated using PmQEDOT-T2 and PmQEDTT-T2 polymers as active layers, the highest hole carrier mobilities of 0.13 and 0.02 cm²/Vs were obtained, respectively. In this study, we will explain the substitution effect of atoms on quinoidal conjugated polymers in relation to microstructural analyses and molecular packing structures of thin films as well as thermal, optical, electrical and electrochemical properties.

7:35 PM EQ06.14.14

Late News: Flexible Glucose Biosensing via Carbon Nanotube-Based Electrodes on Elastomer Polymer Substrate Anthony Palumbo¹, Chenguang Zhao¹, Shichen Fu¹, Siwei Chen¹, Zheqi Li¹, Haoyu Wang¹, Kalle Levon² and Eui-Hyeok Yang¹; ¹Stevens Institute of Technology, United States; ²New York University, United States

Electrochemical wearable biosensors are suitable for diverse skin-attachable applications owing to their high performance, inherent miniaturization, and low cost [1], [2]. Incorporating flexible and stretchy materials enables electrochemical biosensors to impact a wide range of developing applications, including electronic skins [3], smart sensor bandages [4], and implantable medical devices [5]. Flexible/stretchable sensors need to be capable of accommodating various mechanical disturbances such as large bending, twisting and stretching, while retaining their performance for numerous cycles [6]. Though extensive efforts have been made, the performance of such flexible/stretchable electrodes under dynamic deformations issue need further studies, not only in scientific studies but also in any practical device applications.

Here, we study a flexible glucose sensor which can be subjected to various lateral strains via stretching, while providing reliable electrochemical sensing of biomarkers on a patient's skin, undeterred by daily activity and repetitive impacts. Vertically aligned carbon nanotubes (CNTs) grown via chemical vapor deposition (CVD) are embedded onto suspended polydimethylsiloxane (PDMS). The CNTs are coated with a conjugated polymer transducer layer via electropolymerization of polypyrrole (PPy), doped with glucose oxidase (GOx). The sensor is exposed to iterative concentrations of glucose, and GOx reacts in the presence of glucose, resulting in a concentration-dependent change of measurable current. For this sensor, we have developed CNT-based sensing electrodes on flexible substrates that exhibit reliable and stable performance under stretching up to 75%. Skin-attachable devices for continuous monitoring of patients will directly benefit the medical field, with potential applications towards smart sensor bandages, critical wound monitoring, and glucose detection for diabetes.

[1] A. J. Bandodkar and J. Wang, "Non-invasive wearable electrochemical sensors: A review," *Trends Biotechnol.*, vol. 32, no. 7, pp. 363–371, 2014.

[2] J. R. Windmiller and J. Wang, "Wearable Electrochemical Sensors and Biosensors: A Review," *Electroanalysis*, vol. 25, no. 1, pp. 29–46, 2013.

[3] D. Chen and Q. Pei, "Electronic muscles and skins: a review of soft sensors and actuators," *Chem. Rev.*, vol. 117, no. 17, pp. 11239–11268, 2017.

[4] H. Derakhshandeh, S. S. Kashaf, F. Aghabaglou, I. O. Ghanavati, and A. Tamayol, "Smart bandages: The future of wound care," *Trends Biotechnol.*, vol. 36, no. 12, pp. 1259–1274, 2018.

[5] G. A. Aitchison, D. W. L. Hukins, J. J. Parry, D. E. T. Shepherd, and S. G. Trotman, "A review of the design process for implantable orthopedic medical devices," *Open Biomed. Eng. J.*, vol. 3, p. 21, 2009.

[6] P. Lukowicz, T. Kirstein, and G. Tröster, "Wearable systems for health care applications," *Methods Inf. Med.*, vol. 43, no. 3, pp. 232–238, 2004.

7:40 PM EQ06.14.15

CNT-Based Flexible Electrodes Towards Sensors and Energy Storage Anthony Palumbo, Runzhi Zhang and Eui-Hyeok Yang; Stevens Institute of Technology, United States

Flexible electronics requires conformable substrates for a wide range of applications [1]. Conventional high-performance electronic materials such as silicon are not flexible, whereas many flexible materials, such as conducting polymers, are often characterized by poor electric properties [2]. Carbon nanotubes (CNTs) are promising owing to their excellent electronic properties and flexibility owing to their small diameter.

Here, we present stretchable electrodes composed of opposing layers of vertically aligned CNTs (VACNTs) partially embedded in a polydimethylsiloxane (PDMS) substrate; the tips of CNTs are partially embedded into PDMS. This unique synthesis permitted a rapid and facile integration of a flexible and stretchable platform for sensors and energy storage. VACNTs were grown using atmospheric-pressure chemical vapor deposition (APCVD) on a Si/SiO₂ substrate and transferred onto PDMS as a stretchable electrode. A liquid mixture of PDMS base and curing agent were mixed with a ratio of 10:1 and degassed under reduced pressure in a vacuum environment to remove gas bubbles. The liquid PDMS was heated on a hot plate at 65 °C for approximately 30 min to a state of partially cured PDMS. The CNT carpet was placed face-to-face onto the partially cured PDMS, and PDMS infiltrated between each individual carbon nanotube, owing to the capillary effect and the viscoelastic property of PDMS. As a result, tips of interwoven CNTs were embedded into PDMS. The CNT-PDMS sample was left in an ambient condition to fully cure PDMS. Two such CNT-PDMS electrodes were placed face-to-face and change of resistance occurs due to the external pressure applied orthogonal to the surface.

Here, we demonstrate a pressure sensor and a pseudocapacitor using VACNT/PDMS. To detect the pressure, two CNT-PDMS electrodes are arranged in a face-to-face configuration, so the increased pressure is directly proportional to a detectable change in resistance, enabled by increased contact between the opposing electrode surfaces. The measured resistance was maintained at stretching up to 180%, with a rapid response time during loading and unloading.

The sensor showed a stable performance for 10,000 loading/unloading cycles with the resistance retention of 82%. As a proof-of-concept, the sensor was successfully tested for measuring biological signals of a person, including pulse signature, muscle flexing, and step count/intensity. Towards an energy storage application, the CNT-PDMS electrode underwent electropolymerization of dodecylbenzene sulfonate polypyrrole (PPy(DBS)) to conformally coat individual CNTs, followed by deposition of a gel electrolyte, to create an all-solid state pseudocapacitor. In addition to high stretchability and stability, the pseudocapacitor exhibited a stable cyclic behavior up to 10,000 cycles of galvanostatic charge/discharge measurement. These novel CNT-based flexible electrodes demonstrated towards flexible sensor and energy storage devices. are very promising for wearable applications. This work will directly impact the development of biomedical and e-skin applications.

References

- [1] Wong, W. S. & Salleo, A. *Flexible electronics: materials and applications*. **11**, (Springer Science & Business Media, 2009).
- [2] Nyholm, L., Nyström, G., Mhryan, A. & Strømme, M. *Adv. Mater.* **23**, 3751–3769 (2011).

7:45 PM EQ06.14.16

ZIF—Silane Modified Electrochemical Lead Ion Sensor Jinu Joji and Praveen Ramamurthy; Indian Institute of Science Bangalore, India

The advancement in technology in the field of energy has contributed by different kinds of materials. Which includes polymer composites, metal derivatives, etc. There is a considerable increase in the usage of metal and its different structural derivatives. Heavy metals have been widely used for device applications. Hence contamination of natural resources by heavy metals is a major issue. Different sources like textile effluents, electronics industry, mining, industrial wastewater, are contributory. It causes adverse effects on health once it enters the food chain. So, great attention is required for the detection and removal of these metal ions.

Several methods have been explored for the removal and detection of heavy metals. Methods of removal include Adsorption, Ion exchange, Electrodialysis, Nanofiltration, etc. For the detection, electrochemical and spectroscopy methods, etc have been used. Materials like carbon nanostructures, polymer attached platforms, conjugated polymer, metal-organic frameworks (MOF's), covalent organic frameworks (COF's), etc. are act as receptors for metal ions. Further tunability of structure and functionalization could enhance the sensitivity. The current emerging materials of interest include framework structures like MOFs and COF's due to their ease of synthesis, scalability, stability, selectivity, and sensitivity. These porous architectures hold a high surface area. The change in electronic properties upon adsorption can be attributed to a sensing mechanism.

Zeolite imidazolium frameworks are a group of MOF's which are widely used for the adsorption of a wide range of analytes. Electrochemical device-based sensors based on MOF's are least explored. Modification of these frameworks has been done in numerous ways such as functionalization with various ligands, intercalation of ZIF in other MOF's, nanocomposite with graphene oxide, CNT, graphene, and other materials has shown improved sensing. In this study, ZIF-67 has been chosen as a sensing platform for lead ion detection. It is a cobalt metal-centered methyl imidazolium-based framework. Already it has shown good adsorption towards lead ions. Integrating it into a sensing platform is quite challenging. Cyclic voltammetric study in KCl/K₄Fe(CN)₆ exhibit ZIF-67 holds good catalytic behavior and sensitivity towards lead ions. Modification of ZIF-67 with 3-aminopropyl trimethoxysilane could increase sensitivity and selectivity due to the amine group's affinity towards lead ions. The sensitivity enhances with the incorporation of aminomethane siloxane compared to neat ZIF. The synthesized ZIF-67/3-aminopropyl trimethoxysilane was fabricated into a carbon paste electrode for further electrochemical sensing mechanism studies for lead ions detection.

7:50 PM EQ06.14.17

Flexible Multichannel Neural Probe Developed by Electropolymerization for Localized Stimulation and Sensing Na Xiao^{1,2,3}, Gary K.K. Chik^{1,2}, Jianni Deng^{1,2}, Chung Tin³ and Paddy K. L. Chan^{1,2}; ¹The University of Hong Kong, China; ²Advanced Biomedical Instrumentation Centre, China; ³City University of Hong Kong, China

Neural probe application has gotten more and more attention due to its advantages in microscale, material biocompatibility and flexible fabrication technology. Various kinds of biocompatible materials and electrochemical deposition methods were adopted to develop the neural probes so that it can minimize damage to the brain tissue and reduce the impedance for in-vivo applications. Here we designed a highly flexible gold electrode array, using SU8 and Parylene as supporting layer, coated with PEDOT:PSS to reduce the impedance and pHEMA to increase the bio-compatibility. We characterized the electrical performance of the probe for signal quality before in-vivo testing and then the probe was employed in the rat for signal acquisition and biocompatibility test. The length of the probe was tailor made for applying to different brain regions, including primary motor cortex, hippocampus, paraventricular thalamus and cerebellum, of the rat to record the single neuronal spike and local field potential. From both acute recording in anesthesia rats and 3 months long-term chronic recording in awake animals with implantation, our probes shown a good quality with the signal to noise ratio up to 20. The post-experiment dissection and immunohistochemistry staining illustrated a minor tissue damage and immune response comparing to the commercial metal electrode arrays. The proposed probe can be applied to variety of brain regions which provide a broad application in animal electrophysiological investigation and potential clinical usage.

7:55 PM EQ06.04.17

Late News: Novel and Exact Figure of Merit for Transparent Conductive Electrodes Aman Anand^{1,2}, MD Moidul Islam^{1,2}, Rico Meitzner^{1,2}, Ulrich S. Schubert^{1,2} and Harald Hoppe^{1,2}; ¹Laboratory of Organic and Macromolecular Chemistry (IOMC), Germany; ²Centre for Energy and Environmental Chemistry, Germany

Photovoltaic technologies depend largely on transparent conductive electrodes (TCEs). TCEs should, in theory, have the highest light transmission and conductivity. Both traits, however, must be balanced. The selection of the best TCE depends on the photovoltaic material system and is evaluated using so-called figures-of-merit (FOM). A novel and exact FOM is introduced here that explicitly analyzes the impact of TCEs on photovoltaic performance. This unique FOM has several important properties: normalization to the theoretically ultimately attainable photovoltaic performance, proportionality to the solar device's potential power output, and, thus, significant direction for the development of advanced TCEs. Here we evaluated TCE requirements for various photovoltaic material systems in relation to the spectral range in which they operate. Additionally, we also reassessed and compared a variety of realized state-of-the-art semitransparent electrodes.

8:00 PM BREAK

SYMPOSIUM EQ07

Defects and Strain Potential Enabled Emergent Behavior in Two-Dimensional Materials
November 29 - December 8, 2021

Symposium Organizers

Feng He, Harbin Institute of Technology
SungWoo Nam, University of California, Irvine
Michael Pettes, Los Alamos National Laboratory
Qing Tu, Texas A&M University

Symposium Support

Silver
National Science Foundation

* Invited Paper

SESSION Tutorial EQ07: Mechanics and Moirés in 2D Materials
Session Chairs: Feng He, Rui Huang, Allan MacDonald, SungWoo Nam and Qing Tu
Monday Afternoon, November 29, 2021
Virtual

1:30 PM

Mechanics of 2D Materials and Interfaces Rui Huang: The University of Texas at Austin, United States

Atomically thin materials such as graphene and other 2D materials are promising for a wide range of applications. Among many unique and attractive properties of 2D materials, mechanical properties play important roles in manufacturing, integration and performance for their potential applications. Mechanics is indispensable in the study of mechanical properties, both theoretically and experimentally. This tutorial aims to summarize the current understanding on the mechanics of 2D materials including linear and nonlinear elasticity, strength and toughness, as well as mechanical interactions such as adhesion and friction at the interfaces of 2D materials. Theoretical and computational models will be presented along with experimental methods for predicting and measuring the mechanical and interfacial properties of 2D materials.

Outline:

Linear and nonlinear elasticity
Strength and toughness
Adhesion and friction

3:00 PM BREAK

3:30 PM

Electronic Properties of Moiré Superlattices Allan H. MacDonald: The University of Texas at Austin, United States

When two or more van der Waals material layers are overlaid with small differences in lattice constant or overlaid with small relative twist angles they form two-dimensional moiré superlattices with unit cell areas that can be thousands of times larger than the unit cell areas of the underlying two-dimensional crystals. When the moiré superlattice materials are semiconductors or semimetals, low-energy electronic properties are accurately described by low-energy models that have the periodicity of the superlattice. These moiré materials act like crystals with artificial giant atoms. One of the most attractive properties of moiré materials is that the number of electrons per unit cell can be changed by more than one using electrical gates. I will survey the electronic properties of moiré materials, focusing on systems that have been achieved experimentally, including graphene bilayers and multilayers and systems based on traditional metal dichalcogenide layer building blocks.

SESSION EQ07.01: Strain Engineering of vdW Materials I

Session Chairs: Michael Pettes and Qing Tu
Tuesday Afternoon, November 30, 2021
Hynes, Level 2, Room 204

1:30 PM *EQ07.01.01

Strain and Defect Engineering of van der Waals Materials for Quantum Straintronics and Nano-Photonics Nai-Chang Yeh, Chen-Chih Hsu, Duxing Hao, Deepan K. Kumar, Stella Wang, Jiaqing Wang and Marcus L. Teague; California Institute of Technology, United States

Two-dimensional (2D) van der Waals materials exhibit a rich variety of properties that can be further tailored to achieve novel functionality by strain and

defect engineering. Here we describe a new paradigm of *quantum straintronics* based on strain engineering of monolayer (ML) graphene and 2H-phase transition metal dichalcogenides (TMDs), as well as novel photonic phenomena based on defect engineering of quasi-one dimensional (1D) graphene nanostripes (GNSPs).

Theory and experimental studies have found that non-trivial nanoscale strain in ML graphene can give rise to giant *pseudo-magnetic fields* (PMF) that dramatically modify the local electronic properties of graphene. Nonetheless, no realistic devices with spatially scaled-up PMF had been demonstrated until our recent work that achieved periodic graphene “wrinkles” by placing ML graphene on substrates with arrays of nanostructures and then by developing the strained graphene wrinkles into valley-Hall transistors *via e-beam lithography*. We found that the periodic graphene wrinkles formed a *valley splitter* that separated the K/K'-valley Dirac fermions and preserved the valley polarization. We further observed a wealth of novel quantum and topological phenomena, including flat bands of quantized Landau levels, spontaneous symmetry-breaking and spin polarization in the strong correlation limit, as well as quantum valley Hall and quantum anomalous Hall effects with different Chern numbers in the ballistic limit. Controllable electronic correlation could be further achieved by designing the magnitude and spatial distribution of strain and by varying the back-gate voltage. These findings suggest that nanoscale strain-engineering of ML graphene provides a new platform to control the topological electronic states and electronic correlation in 2D materials.

For ML semiconducting 2H-TMDs (*e.g.*, MoS₂ and WS₂) with strong spin-valley coupling, strain has been shown to induce variations in the optical bandgaps and exciton lifetimes. Our molecular dynamics simulations revealed additional symmetry breaking effects, suggesting that nanoscale strain engineering of ML TMDs may be employed to design the landscape of optical bandgaps and to lift the valley degeneracy to produce valley-polarized excitons for topological photonics and opto-valleytronic/spintronic device applications.

For quasi-1D GNSPs directly grown on silicon by PECVD, we found a number of novel photonic phenomena: [1] The GNSPs exhibited strong and wavelength independent optical absorption (absorption coefficient $\sim 10^6 \text{ cm}^{-1}$) from IR to visible light (Vis). [2] The photoluminescence (PL) spectra revealed an emission gap around the excitation frequency as well as both red- and blue-shifted broadband signals. [3] Unusually long carrier lifetimes (up to $\sim 12 \text{ ns}$) were found from the time-resolved PL studies with Vis lasers, and the lifetimes were nearly independent of temperature (from 15 K to 300 K). [4] The PL emissions were coherent, as manifested by the second-order temporal correlation function and the spatial interference patterns of the PL maps. [5] Under strong CW excitations, lasing phenomena with sharp peaks (FWHM linewidths $< 0.1 \text{ THz}$) at discrete frequencies from FIR to Vis were observed. We attribute these phenomena to the presence of topological defects that either naturally formed during the PECVD synthesis or engineered in the material by selective plasma radiation. These defects behaved like two-level color centers that coupled strongly to the high-mobility GNSPs, and the GNSPs provided significant confinement of photons due to strong subwavelength scattering and internal reflection. The GNSP matrix thus acted as an effective optical cavity for the color centers, and the observed photonic phenomena were consistent with cavity-QED. These findings suggest that defect engineering of quasi-1D GNSPs on silicon is a promising new approach for on-chip nano-photonics that are compatible with CMOS technologies.

2:00 PM *EQ07.01.02

Layered Quantum Materials—A New Platform for Quantum Technology [Andrea C. Ferrari](#); University of Cambridge, United Kingdom

Layered Materials (LMs) have potential for quantum technologies, as scalable sources of single photon emitters (SPEs)[1,2]. LM heterostructures can be built with tuneable properties depending on the constituent materials and their relative crystallographic orientation[3,4]. Quantum emitters in LMs hold potential in terms of scalability, miniaturization, integration. Generation of quantum emission from the recombination of indirect excitons in heterostructures made of different LMs is also promising. I will discuss how LM combinations can be used to generate SPEs and confinement of interlayer excitons[5].

- 1.C. Palacios-Berraquero et al., Nat. Commun. 8, 15093 (2017)
- 2.C. Palacios-Berraquero, et al., Nat. Commun. 7, 12978 (2016)
- 3.P. Rivera et al., Nat. Nanotech. 13,1004 (2018)
- 4.M. Barbone et al. Nat. Commun 9, 3721 (2018)
5. A. R. P. Montblanch et al. Commun Phys. 4, 119 (2021)

2:30 PM EQ07.01.03

Quasi-1D Exciton Channels in Strain-Engineered 2D Materials [Florian Dimberger](#)¹, Jonas D. Ziegler², Paulo E. Faria Junior², Rezlind Bushati^{1,3}, Takashi Taniguchi⁴, Kenji Watanabe⁵, Jaroslav Fabian², Dominique Bougeard², Alexey Chernikov^{2,6} and Vinod Menon^{1,3}; ¹The City College of New York, United States; ²Universität Regensburg, Germany; ³The Graduate Center, United States; ⁴International Center for Materials Nanoarchitectonics, Japan; ⁵Research Center for Functional Materials, Japan; ⁶Institute for Applied Physics, Germany

The gap between light-based communication technology and state-of-the-art electronic devices on the nanoscale constitutes a major obstacle towards integrated optoelectronic circuits. Two-dimensional transition metal dichalcogenides (2D TMDCs) harbour an enormous potential to bridge that gap by unifying strong light-matter interaction with exceptionally robust and simultaneously highly mobile exciton quasiparticles. However, steering these neutral quasiparticles along predesigned pathways has proven to be exceptionally challenging and only recently strain was identified as a key element in 2D TMDCs to gain real-space control over the exciton flow. Here, we demonstrate guiding of excitons along strain-engineered quasi-one-dimensional (1D) potential channels by combining mechanically flexible van der Waals heterostructures with single-crystal nanowires in hybrid 1D/2D systems. Using ultrafast, all-optical injection and time-resolved readout, we show near 100% anisotropy in the exciton propagation both at cryogenic and room temperatures. The vanishing diffusivity of excitons perpendicular to the channels highlights their efficient localization by the simultaneous action of confinement potentials and reduced scattering in strained regions. Such artificially induced anisotropy in a pristine, otherwise fully 2D semiconductor offers a highly promising, non-invasive platform to steer the flow of optical excitations and opens a path towards rich quasiparticle transport phenomena in 1D.

2:45 PM EQ07.01.04

Late News: Mechanical Tuning of the Electronic and Vibrational Properties of Epitaxial MoS₂ Through Ion Beam Modification [Shayani Parida](#)¹, Matt Chancey², Yongqiang Wang², Tanushree H. Choudhury³, Joan M. Redwing³, Avinash Dongare¹ and Michael Pettes²; ¹University of Connecticut, United States; ²Los Alamos National Laboratory, United States; ³The Pennsylvania State University, United States

Atomically thin transition metal dichalcogenides (TMDs), like MoS₂, with high carrier mobilities and tunable band gaps, are great candidates for next-generation optoelectronic devices. This study demonstrates the use of relatively low power (100 keV) ion beams to control the point defect levels in single and bilayer films of MoS₂. The use of ion irradiation towards controlling the localized strains and defect densities in TMDs is systematically probed to provide opportunities towards tuning the electronic and optical properties, like resistivity, and absorption and emission spectra. The use of relatively low power beams provides the scope to explore the novel phenomenon of ion implantation in 2D materials. Slight changes in the vibrational states and more significant changes in the photoluminescence (PL) of MoS₂ have been observed which might be explained by substrate straining as the ions penetrate the

2D materials before being trapped by the sapphire substrate. The effect of these strained microstructures on the vibrational states of the MoS₂ lattice is studied using PL and Raman spectroscopy. Recent unpublished alpha particle bombardment studies performed on WS₂ thin films also showed significant shifts in PL peaks (~5 nm). This novel capability provides insights into discerning the links between ion bombardment-induced mechanical straining of lattice and the emergent quantum properties. The study also combines experimental characterization with quantum mechanical simulations performed using density functional theory (DFT) framework to quantify the defect density and distributions; as well as further our understanding of the modifications observed in the optical and electronic band alignments with varying levels of atomistic defects.

3:00 PM EQ07.01.05

Emergent Axion Field Effects in Dynamically Deformed 2D Materials Ioannis Petrides and Prineha Narang; Harvard University, United States

In recent years, dynamical systems have proven to be a highly versatile platform for hosting exotic quantum phenomena. Specifically, high-dimensional topological physics, initially developed out of pure theoretical interest, has now been experimentally observed in physical systems, ranging from cold-atoms, to photonics, metamaterials and electrical circuits. At the heart of these experiments, the spatio-temporal evolution of the system's parameters induces a response proportional to a topological index defined in higher dimensions [1,2]. Drawing on this correspondence, we present a dynamical realization of an Axion field in a 2D material where strain is utilized towards engineering a controlled evolution. Such an approach extends the traditional description of 3D Axion insulators to lower-dimensional dynamical systems, in addition to predicting emergent responses in novel platforms.

Even though Axions are yet to be observed in particle physics and cosmology, they naturally arise in condensed matter systems. Specifically, recent research into the topological aspects of three-dimensional semiconductors and insulators has shown that electrons in certain materials are nontrivially coupled to an Axion field. Apart from the interesting responses to electromagnetic fields, e.g., fractional quantum Hall effect on the surface and magneto-electric polarizability, Axion field effects can be employed in numerous other fields, such as testing fundamental physics with dark matter detectors [3] or controlling electronic properties for technological applications [4]. Here, we present these effects in a completely different setting: in dynamical systems where physical observables are shown to depend stroboscopically on an Axion field defined over a higher-dimensional manifold – the phase-space of the system, i.e., the combined position, momentum and time coordinates.

Designing materials that can be easily controlled is of paramount importance when proposing realistic experiments. To this end, coupling electronic properties to strain offers a promising route towards tailoring dynamics. In particular, piezo-electromagnetic and deformation-induced symmetry breaking effects were shown to significantly change the electronic structure of materials. Here, we exploit such properties towards engineering systems that can be externally controlled via weak deformation fields.

References:

- [1] Petrides, I., Price, H.M. and Zilberberg, O., Six-dimensional quantum Hall effect and three-dimensional topological pumps. *Physical Review B*, 98(12), p.125431, 2018.
- [2] Petrides, I. and Zilberberg, O., Higher-order topological insulators, topological pumps and the quantum Hall effect in high dimensions. *Physical Review Research*, 2(2), p.022049, 2020.
- [3] D. J. Marsh, K. C. Fong, E. W. Lentz, L. Šmejkal, and M. N. Ali, "Proposal to detect dark matter using axionic topological antiferromagnets," *Physical review letters*, vol. 123, no. 12, p. 121601, 2019.
- [4] B. Zhao, C. Guo, C. A. Garcia, P. Narang, and S. Fan, "Axion-field-enabled nonreciprocal thermal radiation in weyl semimetals," *Nano Letters*, vol. 20, no. 3, pp. 1923–1927, 2020.

3:15 PM EQ07.01.06

Late News: Pressure Activated Diamond Phase in 2D Materials Martin Rejhon and Elisa Riedo; New York University Tandon School of Engineering, United States

Controlling phase transitions in 2D materials and switching between structures opens uncharted avenues in the use of 2D materials in mechanical, optical, electronics, and thermal applications. The first demonstration of a metastable phase transformation in bilayer graphene into an ultra-stiff single layer diamond phase has been recently achieved in ambient conditions and room temperature, with the sole application of a localized pressure [REF], this new phase was called diamane. This new single layer diamond phase is obtained in two-layer (one layer plus buffer layer) epitaxial graphene grown on SiC without chemical functionalization, and it is reversible to graphene upon release of pressure. Besides graphene, other 2D materials possess the structural characteristic necessary for sustaining a similar pressure-induced sp²-to-sp³ phase transition. In particular, two- and three-layer hexagonal boron nitride (h-BN) is shown to be convertible in a stable cubic phase (c-BN) under pressure. Furthermore, we conduct an electrical and mechanical investigation of 2D diamond phase formation as observed through pressure activation in hBN, single-layer epitaxial graphene, and quasi-free-standing H-intercalated two-layer graphene on SiC. In particular, we fabricate metal contacts on epitaxial graphene and hBN to study the change in electrical and optical properties before, during, and after the phase activation. This also allows to observe the time stability of the pressure-activated phase formation after the release of pressure.

3:30 PM BREAK

4:00 PM *EQ07.01.07

Designing the Bending Stiffness of 2D Heterostructures Edmund Han¹, Jaehyung Yu^{1,2}, Mohammad A. Hossain¹, Kenji Watanabe³, Takashi Taniguchi³, Elif Ertekin¹, Arend van der Zande¹ and Pinshane Y. Huang¹; ¹University of Illinois at Urbana-Champaign, United States; ²The University of Chicago, United States; ³National Institute for Materials Science, Japan

The bending stiffness of 2D materials and heterostructures governs their deformability, reconfigurability, and 3D structure. In particular, interlayer interactions play a major role in governing the bending of 2D materials, where they lead to an unusually low bending stiffness in few-layer graphene and a curvature-dependence of the bending stiffness [1]. The key role of interfaces in the bending of 2D multilayers also indicates potential methods to tune the deformability and 3D structures of 2D systems through interfacial engineering.

In this talk, we use aberration-corrected scanning transmission electron microscopy (STEM), density functional theory (DFT) simulations, and continuum mechanical models to examine the bending of 2D multilayers and heterostructures. We investigate the bending stiffness of graphene and MoS₂ multilayers, comparing the properties of stacks containing aligned, twisted, and heterointerfaces. We find that the bending properties of 2D materials and heterostructures is strongly tuned by the atomic arrangement of the interfaces present. For example, we find that the bending stiffness of 4-layer heterostructures containing two layers each of graphene and MoS₂ can be tuned from 20 eV to 80 eV by simply changing the order and interfacial atomic registry of the layers present. In addition, our measurements show that 2D heterostructures containing only misaligned interfaces exhibit ultra-low bending

stiffnesses that are the linear sum of the bending stiffness of each constituent monolayer, reaching the theoretical lower limit for stiffness in 2D materials. These properties arise from the low interlayer friction and sliding energy barrier of crystallographically misaligned interfaces, which DFT simulations indicate are two orders of magnitude lower in misaligned interfaces than in 2H-stacked MoS₂. Using these observations, we develop a model to predict and design the bending stiffness for arbitrary heterostructures as a function of thickness, system size, and the number and location of incommensurate interfaces [2]. Our techniques should enable the rational design of the out-of-plane structure of devices based on 2D materials, including illustrating how to incorporate slippable interfaces and create ultra-low bending stiffness structures for deformable, stress-resilient electronics.

- [1] E. Han et. al., *Nature Materials* **19**, 305-310 (2020).
[2] J. Yu et al., *Advanced Materials* **33**, 2007269 (2021).

4:30 PM *EQ07.01.08

Poking and Bulging of 2D Crystals Nanshu Lu; The University of Texas at Austin, United States

Recently, nano-tents and nano-bubbles formed by two-dimensional (2D) materials have seen a surge of interest because they are able to induce in-plane strain as well as strain gradient via out-of-plane deformation.[1] Our previous work has unveiled what sets the in-plane strains in terms of the shape characteristics of nano-tents and nano-bubbles.[2-4] Moreover, out-of-plane poking or bulging, also known as indentation or blister tests, are popular methods for the measurement of in-plane elasticity of thin sheets. For linear elastic sheets, a load-cubic deflection relation has been frequently assumed so that the stiffness of the sheet could be readily extracted. However, we find that recent results of indentation and bulge tests on 2D materials do not follow this relation, which can be attributed to the slippage of atomically smooth 2D materials against their supporting substrates.[5, 6] Besides, the interfacial slippage could cause instabilities in the sheet such as radial wrinkles in suspended region, with finite lengths.[4] To gain a quantitative understanding, we assume constant interfacial shear traction and study the wrinkling extent and the effective stiffness of thin sheets upon poking and bulging. We identify a single dimensionless parameter governing these mechanical responses—the sliding number—defined by comparing the sheet tension (that drives the slippage) with the interfacial traction (that resists the slippage).[7] We discuss several useful asymptotic behaviors emerging at small and large sliding numbers. These understandings are helpful for determining when the effect of the interfacial slippage (as well as other substrate-associated subtleties) can be neglected in these tests. At the end, we propose a simple poking/bulging methodology immune to the complexities caused by the slippage, pretension, Poisson's ratio, substrate roughness, etc., enabling a robust and accurate measure of 2D material stiffness.

- 1 Sanchez, D.A., Dai, Z., and Lu, N.: '2D Material Bubbles: Fabrication, Characterization, and Applications', *Trends in Chemistry*, 2021, 3, (3), pp. 204-217
2 Dai, Z., Hou, Y., Sanchez, D.A., Wang, G., Brennan, C.J., Zhang, Z., Liu, L., and Lu, N.: 'Interface-Governed Deformation of Nanobubbles and Nanotents Formed by Two-Dimensional Materials', *Physics Review Letters*, 2018, 121, (26), pp. 266101
3 Sanchez, D.A., Dai, Z., Wang, P., Cantu-Chavez, A., Brennan, C.J., Huang, R., and Lu, N.: 'Mechanics of spontaneously formed nanoblister trapped by transferred 2D crystals', *Proceedings of the National Academy of Sciences*, 2018, 115, (31), pp. 7884-7889
4 Dai, Z., Sanchez, D.A., Brennan, C.J., and Lu, N.: 'Radial Buckle Delamination around 2D Material Tents', *J Mech Phys Solids*, 2020, 137, pp. 103843
5 Akinwande, D., Brennan, C.J., Bunch, J.S., Egberts, P., Felts, J.R., Gao, H., Huang, R., Kim, J.-S., Li, T., Li, Y., Liechti, K.M., Lu, N., Park, H.S., Reed, E.J., Wang, P., Yakobson, B.I., Zhang, T., Zhang, Y.-W., Zhou, Y., and Zhu, Y.: 'A review on mechanics and mechanical properties of 2D materials—Graphene and beyond', *Extreme Mechanics Letters*, 2017, 13, pp. 42-77
6 Dai, Z., Lu, N., Liechti, K.M., and Huang, R.: 'Mechanics at the interfaces of 2D materials: Challenges and opportunities', *Current Opinion in Solid State and Materials Science*, 2020, 24, (4), pp. 100837
7 Dai, Z., and Lu, N.: 'Poking and bulging of suspended thin sheets: Slippage, instabilities, and metrology', *J Mech Phys Solids*, 2021, 149, pp. 104320

5:00 PM EQ07.01.10

In Situ Strain Engineering of Monolayer MoS₂ Photodetectors for High Photoresponse Ye Seul Jung and Yong S. Cho; Yonsei University, Korea (the Republic of)

Although strain engineering in 2D transition-metal dichalcogenides (TMDs) has been emerged as a critical way to control the electronic/optoelectronic properties, the presence of an in-situ compressive or tensile strain-applied in the flat state of 2D materials has never been reported in terms of photo-detecting capability. Herein, we propose a technical way of inducing intentional stress during the wet-transfer method of MoS₂ monolayer by using the pre-bent PET (polyethylene terephthalate) substrate for the photodetector of Au/MoS₂/Au structure, ultimately to investigate the strain-dependent photosensitivity modulations. As a highlight, the photocurrent reached a maximum value of 1.48 AW⁻¹ with an in-situ tensile strain of +1.08%, which corresponds to nearly 8 times increment compared to the reference sample. The enhancement originates from realigned energy bands at the MoS₂-Au interface through the strain-induced bandgap modulation. It is assumed that the in-situ tensile strain promotes the separation of photo-generated charge carriers and facilitates their transport. With extra strain imposed by post-bending of the in-situ strained sample, the photocurrent performance was further found to be improved to 1.77 AW⁻¹ due to the lowered Schottky barrier by the known piezophototronic effect.

SESSION EQ07.02: Poster Session
Tuesday Afternoon, November 30, 2021
8:00 PM - 10:00 PM
Hynes, Level 1, Hall B

EQ07.02.01

Direct Determination of the Linear Coefficient of Thermal Expansion of Low-Dimensional MoS₂ Kory Burns^{1,2}, Benjamin Bischoff³, Khalid Hattar² and Assel Aitkaliyeva¹; ¹University of Florida, United States; ²Sandia National Laboratories, United States; ³The University of Utah, United States

Low-dimensional Molybdenum Disulfide has shown remarkable potential for applications in flexible electronics and nanoscale photonics. However, a fundamental property that needs to be explored is the thermal expansion coefficient on free-standing MoS₂ because it is instrumental to the thermal management of nanomaterials. Currently, Raman spectroscopy methods and first-principles calculations provide order-of-magnitude differences, likely from the difficulty in obtaining accurate experimental measurements on 2D materials. In this contribution, we couple in-situ transmission electron microscopy (TEM) to supply uniform heating with selected area electron diffraction (SAED) patterns to analyze the defined regions upon heating. Next, we integrate advanced image analysis techniques to precisely align the diffraction pattern, outline Bragg peaks, and calculate the spacing of the d₁₀₀ and d₁₁₀ peaks. Through analysis of the uniaxial and biaxial changes of in-plane spacing, we show that properly indexing SAED peaks is a reliable tool to

investigate some thermal properties of MoS₂.

SESSION EQ07.03: Twisted vdW Heterostructures I
Session Chairs: Michael Pettes and Qing Tu
Wednesday Afternoon, December 1, 2021
Hynes, Level 2, Room 204

1:30 PM *EQ07.03.01

Ferroelectric Polar Domain Dynamics in Twisted Bilayer Transition Metal Dichalcogenides Philip Kim; Harvard University, United States

Controlling the interlayer twist angle in an artificial two-dimensional (2D) van der Waals (vdW) interface offers an experimental route to create a moire superlattice. One can create exotic electronic states by minimizing electronic bandwidth with a tunable moire length scale. However, in the small twist angle regime, vdW interlayer interaction can cause significant structural reconfiguration at the interface, creating the arrays of domain structures. Particularly, in the crystal symmetry engineered twisted bilayer polar crystals, unconventional ferroelectricity can arise to exhibit the ferroelectric switching mechanism. Here we performed an in-situ transmission electron microscopy (TEM) investigation on dual gated twisted bilayer transition metal dichalcogenides (TMD) devices that enable real-time observation of polar domain dynamics in a 2D system. In combination with the theoretical investigation, we find the polarizability of the twisted bilayer TMD sensitively depends on the moire length and the domain shapes. We also report on the angle-dependent development of ferroelectricity and unconventional domain antiferroelectricity in the twisted bilayer TMD that exhibits intriguing distinction from conventional ferroelectricity and antiferroelectricity.

2:00 PM DISCUSSION TIME

2:15 PM *EQ07.03.03

Nanometer-Scale Engineering and Analysis of Transition Metal Dichalcogenides with Atomic Force Microscopy Matthew R. Rosenberger; University of Notre Dame, United States

Two-dimensional materials (2DM) are atomically thin materials with extraordinary mechanical, electrical, and chemical properties that make them promising for next generation technologies in quantum communications, sensing, flexible and transparent electronics and optoelectronics, and energy conversion. The realization of new technologies based on 2DM requires both fundamental research on the materials science of 2DM and research that aims to bridge the gap between materials science and the engineering of real devices and systems. In this talk, I will describe our recent work on using atomic force microscopy (AFM) in conjunction with optical spectroscopy and transmission electron microscopy to understand the physics of strain and heterostructure interfaces in 2DM and leveraging that understanding to control material behavior. In the first part of this talk, I will discuss our work on using the AFM tip to write strain gradients into 2DM semiconductors with nanometer-scale precision. Briefly, we use the AFM tip to indent 2DM placed on top of a thin polymer layer, which results in strain texturing. We use this technique to deterministically place single photon emitters (SPEs) in WSe₂. [1] We find that electrical gating can lead to improved purity of SPEs created with this method. In the second part of the talk, I will discuss our investigations of the interfaces between 2DM layers, with a particular focus on the relative twist angle between layers. I will present experimental evidence of atomic reconstruction in WSe₂/MoSe₂ and WS₂/MoS₂ heterostructures. [2] We confirm the presence of atomic reconstruction through a combination of AFM and transmission electron microscopy. We find that the reconstructed domains have a pronounced dependence on the relative crystal orientation of the layers in the heterostructure. We also find intriguing electronic behavior of the domain boundaries between reconstructed domains. We use density functional theory modeling to understand the origin of the electronic behavior of the domain boundaries. These calculations suggest that flat bands in the conduction band may explain the observed electronic behavior.

[1] M. Rosenberger et al. *ACS Nano*, **2019**, 13 (1), 904-912 (DOI: 10.1021/acsnano.8b08730)

[2] M. Rosenberger et al. *ACS Nano*, **2020**, 14, (4), 4550-4558 (DOI: 10.1021/acsnano.0c00088)

2:45 PM EQ07.03.04

Strain Localization of MoSe₂/WSe₂ Interlayer Excitons Imaged by Scanning Tunneling and Nano-Photoluminescence Microscopies Thomas P. Darlington, Sara Shabani, Emanuil Yanev, Abhay Pasupathy and Peter Schuck; Columbia University, United States

Strain in the context of transition metal dichalcogenides (TMDs) has been shown to have a significant impact on the physics of both intralayer and interlayer excitons (ILE), e.g. in the former inhomogeneous strain can trap excitons in deep potential wells forming quantum-dot like localized states. For the monolayer TMDs these strain-induced electronic states have been investigated heavily with optical probes, revealing the emergence of single-quantum emitters at the inhomogeneous strain sites when cooled to cryogenic temperatures. However, to date strain induced localization of ILE's has predominately been investigated by broad far-field probes which obscure significant features of the strain field at the nanoscale. Because of the dramatic effect of strain on the opto-electronic properties of the ILE states, a detailed understand of the nanoscale variations present in heterolayers is crucial. In this presentation I will detail a combined nano-PL and STM study of nanobubbles in MoSe₂/WSe₂ heterostructures. Utilizing scanning tunneling and the nano-PL spectroscopies we find a consistent shifting of the indirect gap and ILE photoluminescence from the edge of the nanobubble to the center. Our hyperspectral STM imaging further shows the emergence of a strain-induced in-gap state at the nanobubble edge, that to our knowledge has not been observed in the literature. Our results demonstrate the dramatic effect of, and importance of, nanoscopic strain on the interlayer excitons in these state-of-the-art heterostructures.

3:00 PM EQ07.03.05

Late News: Nanoscale Probing Technique Based on Tip Induced Local Deformation of Moire Patterns on Graphite Surface by Scanning Tunneling Microscopy (STM) Nirjhar Sarkar, Prab Bandaru and Robert C. Dynes; University of California, San Diego, United States

A new nanoscale probing technique is employed using Scanning Tunneling Microscopy (STM) to study the local inter-layer potentials of different domains in moire landscapes on graphite surface. An anomalous tip-sample interaction based on local elastic deformation theory is exploited to deform the moire domains out of the plane on a scale of angstroms! This study of moire patterns under tip-induced strain not only reveals the VDW strength gradually varying on these patterns but also guides us in understanding the inter-layer bonding strength of other graphite features like step height and grain boundary.

3:15 PM EQ07.01.11

Inhibited Nonradiative Recombination at All Exciton Densities in Monolayer Semiconductors [Shiekh Zia Uddin](#)^{1,2} and Ali Javey^{1,2}; ¹University of California, Berkeley, United States; ²Lawrence Berkeley National Laboratory, United States

The upper limit of efficiency that any semiconductors can achieve in a light-emitting device is directly dictated by photoluminescence quantum yield (PL QY), which is a strong function of photocarrier density. Optoelectronic devices that are ubiquitously used for display or lighting applications such as light-emitting diodes (LEDs) often operate in a high photocarrier density regime, where all semiconductors experience elevated nonradiative carrier recombination, and thus diminished PL QY. Previously we have shown that, although 2D transition metal dichalcogenide (TMDC) monolayers exhibit near-unity PL QY at low carrier densities, their PL QY lowers significantly at high carrier densities like all other semiconductors. Despite extensive research to advance their material quality and device architecture, the inherent PL QY degradation in 2D TMDC monolayers at high exciton densities remains a major challenge for their utility towards high-performance optoelectronic devices. At low densities, neutral excitons in monolayer semiconductors recombine entirely radiatively even in the presence of a high native defect concentration. However, at high densities, recombination of neutral excitons is dominated by exciton–exciton annihilation (EEA), where an exciton nonradiatively recombines while colliding with another exciton. We show that EEA is resonantly amplified in TMDC monolayers by van Hove singularities (VHSs) present in their joint density of states. Logarithmically divergent VHSs are a topological hallmark of two-dimensional semiconductors, arising from saddle points in the energy dispersion. By applying small mechanical strain, we shift the EEA process away from the VHS resonance and circumvent the enhanced nonradiative EEA that plagues the PL QY at high exciton densities, leading to near-unity PL QY at all exciton densities in 2D TMDC monolayers (e.g. MoS₂, WS₂, WSe₂). This simple, scalable method suppresses all nonradiative recombination at all generation rates for both exfoliated and CVD-grown centimeter-scale TMDC monolayers, as long as they are direct, and their Fermi level is in the middle of the bandgap by electrostatic or chemical doping. Our results constitute the first critical step towards optoelectronic devices that retain their high efficiency at high carrier concentrations and put forth TMDC monolayers as a key material of choice for next-generation optoelectronic applications.

SESSION EQ07.04: Defect Engineering of vdW Materials I
Session Chairs: Michael Pettes and Qing Tu
Thursday Morning, December 2, 2021
Hynes, Level 2, Room 204

10:30 AM *EQ07.04.01

Deterministic Creation of Quantum Defects in van der Waal Materials [Han Htoon](#); Los Alamos National Laboratory, United States

Quantum defects of vdW materials have advanced to the forefront of quantum communication and transduction research due to their unique potential to access the valley pseudo-spin degree of freedom and facilitate integrate into quantum-photonics, electronic and sensing platforms via the layer-by-layer-assembly approach. Strain localized to a nm scale region of vdW has emerged as an effective means of creating quantum defects in vdW materials. This approach allows only a limited degree of control on placement, emission wavelength and quantum coherence properties of defects. Quantum defects realized to date emit at wavelengths shorter than 1 micron while the defects operating in telecommunication wavelength range are highly desirable. More importantly, how and why localized strain creates the quantum defects is poorly understood. Studies have suggested that strain simply activates the optical properties of naturally existing point defects.¹ Aiming to address these issues, Center for Integrated Nanotechnologies is developing novel strain engineering approaches in conjunction with ion beam implantation capabilities for deterministic creation of defects in vdW materials. Here in this talk I will provide an overview of these capabilities development efforts and recently discovered novel quantum defects: telecomm quantum emitters of MoTe₂² and quantum defects of TMD/2D magnet heterostructures realized via local strain engineering.

¹ Linhart, L., Paur, M., Smejkal, V., Burgdörfer, J., Mueller, T. & Libisch, F. *Phys. Rev. Lett.* **123**, 146401 (2019).

² Zhao, H., Pettes, M. T., Zheng, Y. & Htoon, H. *arXiv preprint arXiv:2105.00576* (2021)

11:00 AM EQ07.04.02

Defect Engineering of 2D van der Waals Materials for the Site-Selective Nucleation of Metal Nanoislands [Vera Zarubin](#)¹, Kate Reidy¹, Yang Yu², Ilya Charaev¹, Joachim D. Thomsen¹ and Frances M. Ross¹; ¹Massachusetts Institute of Technology, United States; ²Raith America, Inc., United States

The controlled formation of structural defects, ranging from single-atom vacancies to nanopores, has been broadly implemented as a method of modulating the properties of two-dimensional materials (2DMs). Moreover, theoretical studies predict that point defects in 2DMs provide nucleation sites for metal adatoms and clusters^{1,2} and that nanopores in graphene facilitate the growth of metal islands.³ These suggest that defect engineering may be extended to the site-selective growth of metals on 2DMs, enabling applications that require deterministic patterning of nanoscale features. Focused ion beams (FIBs) are well-suited for patterning 2DMs with nanometer precision and can be used to mill point defects⁴ and sub-10nm features⁵ in suspended 2DMs by tuning irradiation parameters that influence the ion dose and beam profile. To optimize the irradiation parameters for deterministic metal nucleation sites, an experimental investigation of defect creation mechanisms and metal-2DM interactions is required.

Here, we study the structural modifications that arise from FIB patterning of suspended 2DMs and the effects of patterning on subsequent metal nucleation and growth. Obtained by mechanical exfoliation of bulk crystals, layered 2DMs (graphene, MoS₂, WSe₂) are transferred to holey Si₃N₄ transmission electron microscope grids and annealed in ultra-high vacuum (UHV) to remove surface adsorbates, resulting in nearly pristine suspended membranes. Ions are delivered to the 2DM surface as arrays of spots and lines using He⁺ in the Zeiss ORION helium ion microscope and Si²⁺ and Au²⁺ in VELION FIB-SEM. Ion doses are calibrated and the resulting defects and nanopores are characterized with aberration-corrected scanning transmission electron microscopy. We evaporate metals (Au, Ti) onto the patterned 2DM surface in UHV and study, post-deposition, the extent to which the defects, ion species, dose rate, and 2DM thickness affect the metal nucleation and growth. We also heat the samples post-deposition to examine with *in situ* UHV transmission electron microscopy the effect of post-deposition annealing on island shape and size. The island geometry is well suited for automated image analysis to obtain statistics of the nucleation density and location. The materials preparation and analysis technique can be generalized to the site-selective growth of other materials, such as Si and Ge via chemical vapor deposition or metals via thermal and e-beam evaporation. This templating and nucleation control strategy opens routes towards the directed self-assembly of 3D nanoislands on 2DMs and other mixed-dimensional heterostructures.

¹ S. Malola, H. Häkkinen, and P. Koskinen, *Appl. Phys. Lett.* **94**, (2009).

² W. Ju, T. Li, X. Su, H. Li, X. Li, and D. Ma, *Phys. Chem. Chem. Phys.* (2017).

³ S. Antikainen and P. Koskinen, *Comput. Mater. Sci.* **131**, 120 (2017).

⁴ J.P. Thiruraman, P. Masih Das, and M. Drndić, *Adv. Funct. Mater.* **29**, 1904668 (2019).

11:15 AM EQ07.04.03

Atomically Resolved Imaging of Electronic Defects in a CVD Grown Transition Metal Carbide: α -Mo₂C [Saima A. Sumaiya](#)¹, [Omer Caylan](#)², [Goknur Buke](#)² and [Mehmet Baykara](#)¹; ¹University of California, Merced, United States; ²TOBB University of Economics and Technology, Turkey

There is a continuous pursuit for new materials to enable the development of small-scale, power-efficient electronics for next generation devices and applications. During the past decade and a half, two-dimensional (2D) materials have received particular attention in this regard with their extraordinary electronic characteristics. Defects in the form of vacancies, interstitials etc. have a profound influence on carrier transport and local conductance in these materials and as such, would constitute a key factor affecting device performance. Therefore, it is of critical importance to experimentally study defects in 2D materials, in terms of their atomic structure and influence on surface electronics. Motivated in this fashion, we present here an atomic-resolution study of native defects in thin crystals of α -Mo₂C, an emerging 2D transition metal carbide with attractive physical properties and potential to be employed in electronic applications. In particular, we perform conductive atomic force microscopy (C-AFM) experiments on α -Mo₂C crystals grown on copper foils via chemical vapor deposition, revealing the presence of two types of defects that either enhance or inhibit the local conductivity in their vicinity (referred to as “bright” and “dark” defects, respectively), over a lateral span of 2 to 10 nanometers. The simultaneous recording of topography maps together with atomic-resolution conduction maps allow us to make conclusions about the structure and location of defects in the crystals. Specifically, no features are detected in topography maps near both types of defects, suggesting that they are located below the top surface of the crystals. Additionally, while the influence of dark defects on the electronic landscape are diffuse such that the regular atomic structure of Mo₂C appears mainly undisturbed in conductivity maps, bright defects significantly distort the local conductivity, hinting at a stronger influence on local density of states. The findings presented here have the potential to provide critical fundamental information not only for electronic applications but also for other fields ranging from energy storage to catalysis where 2D transition metal carbides are envisioned to be used.

SESSION EQ07.05: Emerging Properties of vdW Materials I
Session Chairs: Michael Pettes and Qing Tu
Thursday Afternoon, December 2, 2021
Hynes, Level 2, Room 204

1:30 PM *EQ07.05.01

Layered Graphenic Structures for the Next Generation Lithium-Ion Batteries [Tereza M. Paronyan](#); HeXalayer LLC, United States

Rechargeable batteries are considered the key energy storage for portable electronics due to their ability to restore the charge and provide consistency in the voltage. Carbon-based materials remain the safest, cost-efficient, and environmentally stable anode material providing high-power density and energy compared to any other active materials.

I will discuss the advantageous layered graphenic structures versus commonly used graphitic negative electrodes in Lithium-ion batteries (LIB). The focus will be the study of interlayer structural features of multilayered graphene and its direct impact on Lithium intercalation. As-synthesized layered graphene with rotated layers is studied revealing that broken Van der Waals forces preceded intense Lithium diffusion and intercalation reaching up Li₂C₂ component formation. A large Li/electrolyte interface brings an enhanced charge-transfer kinetics resulting in effective charge/discharge cycling throughout hundreds of cycles with over 1800 mAh/g specific capacity.

This graphene anode's feasibility allows developing over 500 Wh/kg energy density in LIBs.

2:00 PM *EQ07.05.02

Direct Electron Imaging of Magnetic Topological Structures using 4D-STEM [Kayla Nguyen](#); University of Illinois at Urbana-Champaign, United States

Emerging 2-dimensional (2D) magnets provide opportunities for reducing magnetism to atomic length scales. For 2D magnets, investigations of their local magnetic structure will be important for future generations of magnetic memory storage, where current technologies utilizing ferromagnetic materials will soon reach fundamental scaling limits. In particular, 4-dimensional scanning transmission electron microscopy (4D-STEM) with the electron microscope pixel array detector (EMPAD) have provided ways to image magnetic domains, topological structures such as skyrmions and local chirality. In my talk, I will highlight new developments for imaging magnetic structures with 4D-STEM and how we can apply these new techniques to the investigation of magnetic properties in 2D materials.

2:30 PM EQ07.05.03

Magnetic Proximity Effect in TMD/2D-Magnet Heterostructures [Xiangzhi Li](#), Andrew C. Jones and Han Htoon; Los Alamos National Laboratory, United States

Van der Waals 2D magnets are recently discovered and have triggered significant research interests. These Magnetic 2D materials provide unique properties to study the magnetism response in the 2D limit, and thus an ideal platform for the integration with other atomic thin semiconductor heterostructures to explore the manipulate spin and photon degrees of freedom (DOF), facilitating control of spin degeneracy and light-matter interactions of well-defined quantum states. Magnetic proximity effect between monolayer transition metal dichalcogenides (TMDs) and 2D magnets have been proved in a few heterostructures (WSe₂/CrI₃ and MoSe₂/CrBr₃) based on manipulation of the PL intensity/linewidth and valley Zeeman splitting [1-3]. 0D strain-induced quantum emitters in WSe₂ are also employed to determine the proximity exchange interaction in WSe₂/CGT, WSe₂/FGT, and WSe₂/CrI₃ devices [4-6]. Band alignment and spin-dependent interlayer charge transfer are crucial for this effect which also strongly depends on the distance between layers due to the short range of the electronic wave function at the interface. However, most 2D magnets are sensitive to air which hinders the application of spintronic devices. In contrast with these extremely air unstable magnetic 2D materials, multiple 2D magnetic materials including the MPS₃ family (M = Mn, Ni, Cr, Co, Fe), CrPS₄, and CrSBr have emerged as environmentally stable materials providing a new opportunity for assembling air-stable devices. Moreover, the observation of magnetic exciton in CrPS₄, NiPS₃, and CrSBr with strong anisotropy also expands research possibilities of band alignment and many-body exciton interactions between them and TMDs. Here, we use monolayer WSe₂ as a probe to investigate the interplay between the magnetic proximity effect and valley pseudospin dynamics in air-stable 2D antiferromagnetic magnets (NiPS₃, CrPS₄, and CrSBr) heterostructures via polarization-resolved low-temperature PL, time-resolved PL, and magneto-optical spectroscopies. We will also report the interesting properties of strain-induced quantum defects created in TMD/2D magnet heterostructures.

References:

- [1] D. Zhong et. al Nature nanotechnology 2020, 15 (3), 187-191
- [2] T. P. Lyons et. al Nature communications 2020, 11 (1), 1-9
- [3] L. Ciorciar et. al Physical Review Letters 2020, 124 (19), 197401
- [4] K. Shanyan et. al Nano letters 2019, 10, 7301-7308
- [5] N. Liu et. al Nanoscale 2021, 13 (2), 832-841
- [6] A. Mukherjee et. al Nature communications 2020, 11 (1), 1-8

2:45 PM EQ07.05.06

Defect-Mediated Thermo-Mechanical Behavior of 2D Hybrid Organic-Inorganic Perovskites Doyun Kim¹, Eugenia S. Vasileiadou², Ioannis Spanopoulos², Mercouri G. Kanatzidis² and Qing Tu¹; ¹Texas A&M University, United States; ²Northwestern University, United States

2D hybrid organic-inorganic perovskites (HOIPs) are low-cost, high-performance semiconductor materials with great potential demonstrated in various fields, including photovoltaics, light-emitting diodes, lasers and field-effect transistors. During device fabrication and device operation, 2D HOIPs will go through various temperature statuses. Because of the hybrid organic and inorganic nature, the temperature fluctuation will cause significant influence on the mechanical behavior of 2D HOIPs, which is vital for material processing and device durability, but is largely unknown. We measured the in-plane elastic modulus E of a prototypical 2D HOIP, $(C_4H_7-NH_3)_2(CH_3NH_3)_4Pb_5I_{16}$ (abbreviated as C4n5) as a function of temperature across a range of technological interest (*i.e.*, -15 °C to 65 °C) by AFM stretching suspended 2D HOIP nanosheets. Unlike their 3D counterpart, $CH_3NH_3PbI_3$, which shows negligible temperature-dependent mechanical property, C4n5 exhibits a strong thermo-mechanical response in the tested temperature range. E is a non-monotonic function of temperature, which peaks slightly above room temperature, but are lower both at high and low temperature range. This trend clearly deviates from the general anharmonic expectation of the thermo-mechanical behavior for materials. Further structural analysis suggests that the observed thermo-mechanical behavior is due to the formation of gauche defects in the organic spacer molecules at the van der Waals interfaces, which mediates the mechanical coupling between the 2D layers. We further demonstrated that exposure to moisture results in defects in the 2D HOIP nanosheets and the defect density can strongly modulate the thermo-mechanical behavior of C4n5, probably due to a mix-phase of 2D and 3D HOIPs.

SESSION EQ07.06: Emerging Properties of vdW Materials II

Session Chairs: Feng He and SungWoo Nam

Tuesday Morning, December 7, 2021

EQ07-Virtual

8:00 AM *EQ07.06.01

2D Materials and Heterostructures—From Property Engineering to Emerging Memory and Neuromorphic Applications Feng Miao; Nanjing University, China

Two-dimensional (2D) materials and van der Waals (vdW) heterostructures have emerged as promising candidates for post-Moore electronics due to their unique electronic properties and atomically thin geometry. In this talk, I will start with an important type of in-memory computing device, robust memristors with excellent memory performance and thermal stability, which can be created from a vdW heterostructure composed of graphene/MoS₂-_xO_x/graphene.^[1] I will then discuss a prototype reconfigurable neural network vision sensor that operates via the gate-tunable positive and negative photoresponses of a WSe₂/BN heterostructure.^[2] A neuromorphic vision system with brain-inspired visual perception can be further realized by networking such retinomorph sensors with a memristive crossbar array.^[3] Our latest results on an electrically tunable homojunction for reconfigurable circuits,^[4] as well as a scalable massively parallel computing scheme in crossbar arrays^[5] will be presented in the last part of my talk.

References:

- 1) M. Wang, S. Cai, C. Pan, C. Wang, X. Lian, Y. Zhuo, K. Xu, T. Cao, X. Pan, B. Wang, S. Liang, J. Yang, P. Wang, F. Miao, **Nature Electronics** **1**, 130 (2018).
- 2) C. Wang, S. -J Liang, S. Wang, P. Wang, Z. Li, Z. Wang, A. Gao, C. Pan, C. Liu, J. Liu, H. Yang, X. Liu, W. Song, C. Wang, B. Cheng, X. Wang, K. Chen, Z. Wang, K. Watanabe, T. Taniguchi, J. Yang, F. Miao, **Science Advances** **6**, eaba6173 (2020).
- 3) S. Wang, C. Wang, P. Wang, C. Wang, Z. Li, C. Pan, Y. Dai, A. Gao, C. Liu, J. Liu, H. Yang, X. Liu, B. Cheng, K. Chen, Z. Wang, K. Watanabe, T. Taniguchi, S. -J Liang, F. Miao, **National Science Review** **8**, nwaal72 (2021).
- 4) C. Pan, C. Wang, S. -J Liang, Y. Wang, T. Cao, P. Wang, C. Wang, S. Wang, B. Cheng, A. Gao, E. Liu, K. Watanabe, T. Taniguchi, F. Miao, **Nature Electronics** **3**, 383 (2020).
- 5) C. Wang, S.-J Liang, C. Wang, Z. Yang, Y. Ge, C. Pan, X. Shen, W. Wei, Z. Zhang, B. Cheng, C. Zhang, F. Miao, **Nature Nanotechnology** (2021) (in press).

8:30 AM *EQ07.06.02

Graphene Interfaces for Electronics, Optoelectronics and Bio-Devices Vikas Berry; University of Illinois at Chicago, United States

The presentation will outline several chemical manipulation techniques developed in our laboratory to control the properties of graphene, including non-destructive functionalization, nanoparticle incorporation and biomolecular interfacing. The following topics will be discussed: (i) modification of phononic energy of antibody-coupled graphene when it interfaces with SARS-CoV-2 spike protein. (ii) phononic energy's modification with ionic flow over graphene, (iii) unique eta-6 organometallic approach to functionalize graphene in a vapor-phase process, while retaining its structural and electrical properties and offering chemical sites for nano-interfacing of plasmonic centers for enhanced photovoltaics; (iv) biointerfacing of graphene with electrogenic bacteria for microbial energy devices; and (vi) Photovoltaics via electronic coupling of graphene atop a bulk semiconductor to induce interfacial energy-band reorganization for light-sensitive junctions only one atom below the front surface.

9:00 AM EQ07.06.03

Late News: Long-Range Transport of 2D Excitons with Surface Acoustic Wave Ruoming Peng, Adina Ripin, Yusen Ye, Jiayi Zhu, Ting Cao, Xiaodong Xu and Mo Li; University of Washington, United States

Interlayer excitons in 2D semiconductors have emerged as a promising candidate for engineering excitonic devices, due to the strong coupling with light, large exciton binding energy, and gate tunability. However, the exciton is a charge-neutral particle that can not be controlled by the in-plane electric field

and thus inhibits the study of the exciton transport. Here, we demonstrate the directional transport of interlayer excitons in bilayer WSe₂ driven by the dynamic piezoelectric field induced by surface acoustic waves (SAW) on LiNbO₃. We show that at 100 K, the SAW-driven excitonic transport is activated above a threshold acoustic power and reaches a distance up to 20 μm which is far beyond the diffusion length, and only limited by the device size. Our work shows that acoustic waves are an effective contact-free approach to control exciton dynamics, which can provide a novel physical platform for the study of 2D excitons such as the exciton valley hall effect and also be promising for realizing 2D materials-based excitonic devices such as exciton transistors, switches, and transducers.

9:15 AM EQ07.06.04

Submicron Bi₂Se₃-WS₂ Pixels with Large (39.4%) Selectable Circular and Valley Polarization at Room Temperature [Zachariah Hennighausen](#)¹, Kathleen McCreary², Darshana Wickramaratne², Hsun-Jen Chuang², Bethany Hudak², Todd Brintlinger², Mehmet Noyan², Jisoo Moon², Berend Jonker², Rhonda Stroud² and Olaf van't Erve²; ¹National Research Council at Naval Research Laboratory, United States; ²U.S. Naval Research Laboratory, United States

Measuring and manipulating circular polarization is central to numerous existing and emerging technologies, including spintronics, bio-inspired navigation, valleytronics, quantum computing and communications, and spectroscopy. Here, we demonstrate a method to tune the photoluminescence (PL) intensity (factor of x161), peak position (38.4meV range), and degree of circular polarization (DoCP) (39.4% range) with extraordinary precision using a low-power laser in Bi₂Se₃-WS₂ 2D heterostructures. Few-layer, crystalline Bi₂Se₃ is grown on monolayer WS₂ using chemical vapor deposition (CVD). The Bi₂Se₃ grows at a ~0° twist angle, and density functional theory (DFT) calculations predict a coupling between the layers that possibly facilitates non-radiative recombination. The as-grown 2D heterostructure PL intensity is low; however, when exposed to a low-power laser (0.8mW) in ambient, the PL smoothly increases intensity, the peak position shifts, and the DoCP decreases. Atmospheric measurements suggest oxygen is absorbing into the 2D heterostructure. We use first-principles calculations to elucidate the role of oxygen incorporation on the electronic structure. We show that the intensity and peak position changes can be reversed by desorbing the oxygen using a laser in a nitrogen (N₂) environment, and that it can be reused. Our technology can be used to locally modify the valley polarization with submicron precision, a promising advancement for spintronics and valleytronics applications.

9:30 AM EQ07.06.05

Nano-Photoluminescence Mapping of Room-Temperature Strain-Localized Excitons in Array-Guided Nanowrinkles [Emanuil Yaney](#)¹, Thomas P. Darlington¹, Matthew Strasbourg², Nicholas Borys², James Hone¹ and Peter Schuck¹; ¹Columbia University, United States; ²Montana State University, United States

Quantum systems, and the field of quantum information science, are quickly becoming a hotbed for technological breakthroughs. At the heart of many of these technologies is the single-photon source (SPS). While a variety of systems are currently used for this purpose—from quantum dots to nitrogen-vacancy centers in diamond—they are not without their limitations. Often, cryogenic temperatures are required, tunability is lacking, or integration with other components is difficult. In an attempt to address some of these challenges, we examine a solid-state system with the potential of realizing tunable SPSs at room temperature by locally inducing large amounts of strain in a monolayer sheet of WSe₂. Due to the very low defect density and single crystal nature of the material, it is able to strongly conform to patterned substrate features. In so doing, nanoscale wrinkles are formed on, around, and in-between the structures, with orientations influenced by the patterned array. These highly strained regions can effectively localize excitons and produce room temperature low-energy emission, similar to that reported in our previous work on strained nanobubbles. When cooled to cryogenic temperatures, a rich milieu of sharp spectral features is revealed in these areas, which suggests that the emission seen at room temperature is quantum in nature and tunable with strain.

9:45 AM EQ07.06.06

On the Origin of Raman Peak Splitting in Monolayer 2D Materials—Metal Interfaces: MoS₂/Au [Mirjana Dimitrievska](#), Akshay Balgarkashi, Jin Jiang, Elias Stutz, Mitali Banerjee and Anna Fontcuberta i Morral; École Polytechnique Fédérale de Lausanne, Switzerland

Monolayer (ML) transition-metal dichalcogenides (TMDs) exhibit a direct bandgap and a relatively high carrier mobility. This makes them as excellent building blocks for applications in optoelectronics, photovoltaics and catalysis.

Electronic and optoelectronic applications with TMDs rely on the good functioning of the junction with metals. While the van der Waals nature of TMDs should in principle imply absence of states in the middle of the TMD bandgap, vacancies and point defects in the material may result in atom exchange and thus doping of the TMD by the metal. Chemical interaction at the interface, such as creation of metal-chalcogenide bonds, could lead to a configurational change in the TMD. In addition, ML TMDs can be easily perturbed by strain or charge transfer from the underlying layers due to their ultra-thin nature. Similar to classical low-dimensional structures, the physics of the metal- semiconductor junction shall dictate the behavior of the device. A fundamental understanding of the metal-TMD junction is thus extremely relevant for the reliability of TMD-based electronics and/or optoelectronics.

Raman spectroscopy is a versatile tool for characterization of 2D materials, especially in terms of quantifying the number of layers, and evaluating the effects of strain, doping and defects. In the case of monolayer TMDs, the most prominent features in the Raman spectra are in-plane (E_{2g}) and out-of-plane (A_{1g}) peaks. Among the recent Raman studies on TMD-metal interfaces, many have reported peak splitting of the A_{1g} and E_{2g} modes. A variety of attempts have been made to explain the peak splitting, usually in terms of strain and charge transfer effects. While these effects could cause splitting of individual peaks in some cases, they are insufficient to explain splitting in both A_{1g} and E_{2g} peaks simultaneously. To better understand the interaction at ML TMD-metal interfaces, which is extremely important for device performance, it is necessary to provide a full explanation of the mechanism causing the Raman peak splitting that occurs in this case.

In this work, we look into the origin of A_{1g} and E_{2g} peak splitting through a systematic measurement and simulation of Raman spectra, along with relevant literature review. We focus on MoS₂/Au as a representative system. We illustrate why strain and charge transfer cannot be the main contribution to the simultaneous splitting of both A_{1g} and E_{2g} Raman peaks. We propose a mechanism based on plasmon-phonon interaction and presence of extrinsic defects at the TMD-metal interface as the main driver leading to peak splitting. We attribute the new peaks to non-Γ phonon modes originating from in-plane (E_{2g}) and out-of-plane (A_{1g}) phonon branches at certain non-zero wave vector. We test the validity of our hypothesis by investigating samples with different interface configurations, including the exchange of Au with Al.

10:30 AM *EQ07.07.02

The Complex Role of Interfaces in Determining Phonon Transport in Two-Dimensional Materials Yan Wang; University of Nevada, Reno, United States

There has been a rising notion of the wave nature of phonons over the past decade. Notably, recent experiments and atomistic modeling have revealed ballistic transport of coherent phonons in superlattices containing dense interfaces. These coherent phonons allegedly arise from the interference of backscattered phonon waves at the densely packed interfaces, which should otherwise greatly hinder the transport of conventional, particle-like phonons. In this invited talk, we will discuss our recent findings of some exotic (and non-exotic) behaviors of coherent phonons in superlattices and phononic crystals, particularly in those made of two-dimensional materials. First, we will demonstrate that randomizing the layer thicknesses of a superlattice, which leads to localization of phonons, can reduce its thermal conductivity to even below the amorphous material limit, which can hardly be achieved by merely scattering phonons. Second, we will discuss the effect of reduced dimensionality on coherent phonon behaviors: can two-dimensional materials demonstrate more prominent coherent phonon transport than three-dimensional ones? what is the effect of anharmonic scattering on coherent phonons? can we find stronger phonon localization in two-dimensional systems than three-dimensional ones? We will explain these behaviors by decomposing thermal transport into coherent phonon and incoherent phonon contributions via the Landauer-Datta-Lundstrom approach. Detailed spectral phonon analysis will further reveal the interplay between coherent and incoherent phonons, as well as their respective effect on thermal transport.

11:00 AM *EQ07.07.03

Tunable Helical Edge States in van der Waals Materials Chun Ning (Jeanie) Lau; The Ohio State University, United States

Helical conductors, systems that have no bulk conduction but support dissipationless conducting states at their edges, may be engineered to realize Majorana statistics for quantum computation. Underlying these remarkable systems are the non-trivial topology of electronic structure in the bulk, arising from band inversion in the bulk and crossing of conduction and valence bands at the system boundary. In helical conductors, these counterpropagating states carry different spin quantum numbers, protecting the crossing and preventing a gap from opening in the spectrum of edge states. Traditional helical conductors, such as those achieved in topological insulator systems, are typically not tunable in situ, and helical conduction is only achieved over a narrow range of parameters.

Here we show that helical edge states are achievable and tunable in few-layer van der Waals materials. In Bernal-stacked trilayer and tetralayer graphene, we observe helical edge states at moderate and strong magnetic fields, respectively, arising from the competing effects of inter-layer coherence, electrostatic polarization and exchange interaction. As the interlayer potential and magnetic field varies, we observe a series of quantum transitions among the phases that host 2, 1 and 0 helical edge states on each edge. Our work highlights the complex competing symmetries in few-layer graphene and the rich quantum phases in this seemingly simple system [1, 2]. Lastly, in thin exfoliated Bi4I4 samples, which is a quasi-1D topological insulator and candidate for higher order topological states, we observe gate tunable magneto-transport and Josephson current. Our combined transport, photoemission, and theoretical results indicate that the gate-tunable channels consist of novel gapped side surface states, a 2D TI in the bottommost layer, and helical hinge states of the upper layers [3].

References

- [1] P. Stepanov, Y. Barlas, S. Che, K. Myhro, G. Voigt, Z. Pi, K. Watanabe, T. Taniguchi, D. Smirnov, F. Zhang, R. Lake, A. MacDonald, and C. N. Lau, Quantum parity Hall effect in Bernal-stacked trilayer graphene, Proc. Natl. Acad. Sci. 116, 10286 (2019).
- [2] S. Che, Y. Shi, J. Yang, H. Tian, R. Chen, T. Taniguchi, K. Watanabe, D. Smirnov, C. N. Lau, E. Shimshoni, G. Murthy, and H. A. Fertig, Helical Edge States and Quantum Phase Transitions in Tetralayer Graphene, Phys. Rev. Lett. 125, 036803 (2020).
- [3] Y. Liu, R. Chen, Z. Zhang, M. Bockrath, C. N. Lau, Y.-F. Zhou, C. Yoon, S. Li, X. Liu, N. Dhale, B. Lv, F. Zhang, K. Watanabe, T. Taniguchi, J. Huang, M. Yi, J. S. Oh, and R. J. Birgeneau, Gate-Tunable Transport and Unconventional Band Topology in Quasi-One-Dimensional a-Bi4I4 Field Effect Transistors, preprint, submitted (2021).

11:30 AM EQ07.07.04

Structural and Electronic Properties of a New 2D Material—Thiophene-Tetrathia-Annulenes (TTA-2D) Raphael M. Tromer¹, Levi C. Felix¹, Cristiano F. Woellner² and Douglas S. Galvao¹; ¹Universidade Estadual de Campinas - Unicamp, Brazil; ²Universidade Federal do Paraná, Brazil

Since the experimental realization of graphene [1], there is an increasing number of works for new two-dimensional materials (2D) [2]. In this work, we investigated using ab initio methods, the structural, electronic, and mechanical properties of a new 2D semiconductor material, named (TTA-2D) [3], which is topologically based on the molecular structure of Thiophene-Tetrathia-Annulene (TTA), which has been already synthesized. Our results showed TTA-2D has a small indirect bandgap semiconductor of about 0.6 eV with a semiconductor-metal transition when a uniaxial strain is applied. We also carried out molecular dynamics at high temperatures and observed that TTA-2D is thermally stable up to T = 1000 K. From optical analysis, our results also show that TTA-2D absorbs in a large energy range, from infrared to ultraviolet regions. The analysis of refractive and reflectivity index shows that TTA-2D reflects only 10% of the incident light within the visible region. Therefore, these results suggest that TTA-2D is a promising material for solar cell applications.

- [1] K. S. Novoselov, A. K. Geim, S. V. Morozov, D. Jiang, Y. Zhang, S. V. Dubonos, I. V. Grigorieva, and A. A. Firsov, Science, 306, 666 (2004).
- [2] R. M. Tromer, M. G. E. da Luz, M. S. Ferreira, L. F. C. Pereira, The Journal of Physical Chemistry C, 121, 3055 (2017).
- [3] R. M. Tromer, L. D. Machado, C. F. Woellner, and D. S. Galvao, Physica E 129, 114586 (2021).

11:35 AM EQ07.05.04

CO-Induced S Vacancy Formation for Phase Conversion of MoS₂ and WS₂—A DFT Study Deokgi Hong¹, Sungwoo Lee^{1,1}, Dae-Hyun Nam², Gun-Do Lee^{1,1} and Young-Chang Joo^{1,1,3}; ¹Seoul National University, Korea (the Republic of); ²Daegu Gyeongbuk Institute of Science & Technology, Korea (the Republic of); ³Advanced Institute of Convergence Technology, Korea (the Republic of)

Defect engineering in transition metal dichalcogenides (TMDs) is a key approach to controlling the properties of TMDs. Defects in TMDs like chalcogen vacancy can induce the phase conversion of TMDs. Because TMDs have different properties depending on the phase, controlling specific phase of TMDs through defect engineering is crucial to obtain specific properties.

For instance, group VI TMDs such as MoS₂ and WS₂ have thermodynamically stable H phase and unstable T phase. In application of these TMDs in hydrogen evolution reaction (HER), unstable T phase exhibits better performance. However, it is difficult to obtain and maintain the T phase, which causes stability problems. Many research groups have found the ways to tackle this issue. Formation of S vacancies (V_S) on TMD layer is one of the ways for the phase conversion of TMDs.

Recently, our colleagues proposed novel method of forming V_S for phase conversion of MoS₂ from stable H phase to unstable T phase. [1] In this method, S vacancy is formed on MoS₂ by the reaction between CO and S, and the phase conversion of MoS₂ occurs. This method was also applied to WS₂. It was

found that the phase conversion of WS₂ required higher annealing temperature and CO mole fraction than that of MoS₂. To reveal the mechanism of CO-induced phase conversion and elucidate the difference in the phase conversion conditions, we conducted DFT calculations. We calculated the reaction barriers of CO-mediated V_S formation and S diffusion to octahedral site of MoS₂ [2] and WS₂. V_S on the edge sites of MoS₂ and WS₂ were formed. Then, S atoms at the trigonal prismatic site diffused to the octahedral site. The reaction barrier for V_S formation on edge site and S diffusion to octahedral site of WS₂ was higher than that of MoS₂. By DFT calculation, we revealed the mechanism for CO-induced phase conversion of MoS₂ and WS₂. And we identified the cause of the difference in experimental conditions. Consequently, this work provides insights into the defect engineering for phase conversion of several TMD materials using gas-solid reactions.

References

Nam, D. H.; Kim, J. Y.; Kang, S.; Joo, W.; Lee, S. Y.; Seo, H.; Kim, H. G.; Ahn, I. K.; Lee, G. B.; Choi, M.; Cho, E.; Kim, M.; Nam, K. T.; Han, S.; Joo, Y. C. *Nano Lett.* 19, (12), 8644-8652 (2019).

Lee, S.; Hong, D.; Kim, J. Y.; Nam, D. H.; Kang, S.; Han, S.; Joo, Y. C.; Lee, G. D. *ACS Appl. Nano Mater.* 4, (5), 5496-5502 (2021).

SESSION EQ07.08: Defect Engineering of vdW Materials II

Session Chairs: Feng He and SungWoo Nam

Wednesday Morning, December 8, 2021

EQ07-Virtual

8:00 AM *EQ07.08.01

Creating Quantum Dot Arrays in Two-Dimensional Materials [Hui Deng](#); Univ of Michigan, United States

Large arrays of quantum dots at controlled positions could be pivotal for enabling practical applications of quantum dot systems. While single quantum dots have been widely studied in many material systems, creating a large array of quantum dots face different challenges. The engineering flexibility of atomically thin van der Waals crystals have brought about new possibilities to realize localized excitons. Here we explore two ways to create large arrays of quantum dots using transition metal dichalcogenides. First, we demonstrate rapid creation of large, rewritable arrays of localized emitters with high yield through strain engineering. Second, we show that uniform quantum dot arrays are naturally formed via moire potential confinement in twisted bilayers. Both types of quantum dot arrays are compatible with integration with other on-chip photonic structures and large scale fabrication.

8:30 AM EQ07.08.02

Modulating Water Slip Using Vacancy Defects—Towards Realistic Modeling of Hexagonal Boron Nitride Surfaces [Aniruddha Seal](#)^{1,2} and Ananth Govind Rajan²; ¹National Institute of Science Education and Research, India; ²Indian Institute of Science, India

Vacancy defects, despite being commonly present in nanomaterials, are inadequately understood in terms of their role in modulating interfacial fluid flow. In this work, we study the frictional properties of hexagonal boron nitride (hBN), an up-and-coming 2D material, by considering five different types of “realistic” vacancy defects present in it. In recent years, hBN has gained increasing attention for use in desalination membranes, oil-water separation devices, and osmotic energy harvesting, where hBN-water interfaces are ubiquitous. Thus, understanding solid-liquid friction on real hBN surfaces is important to design and develop such applications. Here, we present a combined quantum-classical approach to achieve this objective. To this end, we use quantum-mechanical density functional theory to obtain point charges to accurately represent the unique electric field produced by each of the five defects considered. Subsequently, using classical molecular dynamics simulations, we study the role of the vacancy composition and concentration in modulating the hBN-water friction coefficient, and the resultant slip length for water flow on hBN. Our findings demonstrate the use of vacancy defects to tune the water flow and slip on hBN, and indicate the promise of defective hBN as an alternative high-slip surface to graphene.

8:45 AM EQ07.08.03

Vacancy-Induced Emission in Proton Beam Irradiated Monolayer Semiconductors [Zhepeng Zhang](#), Haidong Liang, Leyi Loh, Yuan Chen, Yifeng Chen, Su Ying Quek, Bosman Michel, Andrew Bettiol and Goki Eda; National University of Singapore, Singapore

Defect engineering of atomically thin semiconductor crystals is an important approach to tailoring their optical properties for developing single-photon sources and valleytronic devices. Recently, He ion and electron beam irradiation of transition metal dichalcogenide (TMD) monolayers has been shown to induce single-photon emitting defects. Here, we report the generation of robust luminescent defects in chemical vapor deposition (CVD)-grown monolayer MoS₂ and WS₂ via proton beam irradiation with a wide range of ion beam fluences from 10¹¹ to 10¹⁴ cm⁻². These defects exhibit subgap photoluminescence peaks that are 100 to 200 meV below the neutral exciton peak. Remarkably, these emissions are robust even at room temperature, unlike the previously reported defect-induced emission. They exhibit sublinear power-dependent emission intensity and long emission lifetime (> 1ns), which are characteristics of localized emitters. Atomic resolution scanning transmission electron microscopy (STEM) images reveal that the areal density of sulfur vacancies is increased by ~10¹³ cm⁻² after ion beam irradiation, indicating that unpassivated sulfur vacancies are responsible for the observed localized emissions. We conduct DFT and GW-BSE calculations of TMDs with different defect configurations to further discuss the potential role of defect complexes.

9:00 AM EQ07.08.04

Optically Active Selenium Vacancies in MoSe₂ Induced by Proton Beam Irradiation [Yuan Chen](#), Haidong Liang, Leyi Loh, Bosman Michel, Andrew Anthony Bettiol and Goki Eda; National University of Singapore, Singapore

Deterministic creation of quantum emitters in transition metal dichalcogenides (TMD) has become a key challenge for their implementation into quantum technology. One of the promising routes to generating quantum emitters is controlled defect engineering by ion beam irradiation. In this study, we investigate the effect of high energy proton beam irradiation on deterministic creation of optically active defects in monolayer MoSe₂. We show that proton beam irradiation results in emergence of three narrow sub-gap emission peaks, which are stable up to 160 K. We probe the nature of the defects by studying their valley selectivity and the effect of electrostatic doping. Gate-dependent photoluminescence suggests that the sub-gap emission is suppressed when states near the conduction band edges are depopulated. Our observations are in good agreement with the recent theoretical predictions for selenium-vacancy-induced optical transitions in MoSe₂. Our scanning transmission electron microscopy (STEM) imaging reveals that proton beam irradiation results in increase in selenium vacancies but no changes in metal vacancy concentration, which further corroborates that these emissions are related to unpassivated selenium vacancies created by proton beam irradiation. Our work demonstrates that proton beam irradiation can serve as a simple approach to creating optically active defects in TMDs.

9:15 AM EQ07.08.06

Production of Defects in Suspended Graphene with High Density and Low Healing Energy Using Electron Irradiation [Ibikunle Ojo](#), Evan Hathaway, John Femi-Oyetero, Jingbiao Cui and Jose Perez; University of North Texas, United States

We report the production of defects in suspended graphene that have an extremely high defect density and low activation healing energy using electron irradiation at 20 keV from a scanning electron microscope (SEM). The graphene was suspended over microchambers etched in SiO₂, measuring 5 microns in diameter and 400nm in depth. The graphene completely seals the chamber with air at atmospheric pressure. The samples were then placed in an SEM system and irradiated to a dosage of about 1×10^{17} electrons/cm². The graphene effectively seals the microchamber so that the air pressure inside does not significantly decrease from atmospheric pressure during the irradiation. This produced an extremely high defect density with a sharp Raman D peak and Raman D peak height to G peak height ratio, I_D/I_G, of over 4.5. Thermal studies showed that the defects almost completely heal after annealing the sample at only 200 °C for 5 minutes. In contrast, microchambers in which the graphene does not completely seal the chamber show I_D/I_G ratios of 0.14. The high defect density achieved in the sealed microchambers is attributed to the atmospheric pressure inside and strain induced by the curvature. The low healing temperature rules out damage in the form of lattice defects such as vacancies. The method by which the defects were produced involving SEM, which is compatible with nanolithography, makes it useful for device applications.

9:30 AM EQ07.08.07

Engineering Defect-Related Color Centers in Hexagonal Boron Nitride Using Focused Ion Beams [Yue Xu](#)¹, Soumya Sarkar¹, Jing-Yang Chung^{1,1}, Manohar Lal¹, Sinu Mathew^{1,2}, T. Venky Venkatesan^{1,3} and Silvija Gradečak^{1,1}; ¹National University of Singapore, Singapore; ²Mahatma Gandhi University, India; ³The University of Oklahoma, United States

Hexagonal boron nitride (hBN), a van der Waals crystal with a honeycomb structure similar to graphene, has been widely investigated as a dielectric substrate for 2D-based devices. More recently, hBN has emerged as a prominent candidate for quantum nanophotonics due to the observation of a tunable single photon emission. These emitters have been associated with mid-gap states in ultra-wide bandgap hBN (~6eV) that originate from atomistic defects in the hBN lattice. Here, we report the observation of near-infrared (~ 800 nm) photoluminescence (PL) emission in hBN at room temperature caused by defects formed *via* focused He-ion beam irradiation. We tune PL intensity of the emitters by tailoring the defect generation in hBN as a function of the irradiation parameters. Raman spectroscopy and high-resolution scanning transmission electron microscopy imaging further confirm that the emerging PL response is correlated with point-defect states in hBN. We also demonstrate that similar results can be obtained by Ga-ion irradiation, confirming the PL emission to be related to intrinsic structural defects in hBN. Our work presents a platform to precisely create and control defect-related color centers in hBN that can serve as building blocks for next-generation nanophotonic and possible quantum devices.

9:35 AM EQ07.08.08

A Comprehensive Study of MoS₂ with Varying Layers Using Correlated Raman, PL, KPFM and TERS Imaging—Implications for Modulating Electronic Properties by Oxygen Plasma Induced Defects [Sanju Gupta](#); University of Central Florida, United States

Modulating physical (electrical, optical, and electrochemical) properties of transition metal dichalcogenides (TMDs) by oxygen plasma treatment has attracted a great deal of attention. However, the effect of exposure time on oxidation and etching process in oxygen plasma treatment and creating lattice defects still lacks systematic structural property investigations at the nanoscale. In this work, we have employed optical microscopy, scanning electron microscopy, micro- and nanoscale Raman (tip-enhanced, TERS) and photoluminescence (TEPL) spectroscopy, and scanning probe microscopy (atomic force and Kelvin Probe) to characterize changes in surface morphology, spectral signatures, electronic structure, oxidation, etching and/or clustering behaviors of atomically thin molybdenum disulfide (MoS₂) nanosheet layers, mechanically exfoliated on gold-coated substrates, treated by oxygen plasma with different times. For oxidation plasma (electron beam), the process is predominantly oxidation from 0 to 20s, while etching becomes the dominant behavior beyond 20s for monolayer (1L) to trilayer (3L) MoS₂ nanosheets under medium power oxygen plasma. By means of TERS, we uncover spectral heterogeneities, strain changes spatially localized to regions as small as 30 nm clustering domains due to sulfur vacancy followed by oxygenation and forming MoO₂/MoO₃, enhancement of certain Raman peaks due to strong electromagnetic confinement between the tip and MoS₂ and appearance of new peaks, often unobserved in confocal Raman spectroscopy. As for excitonic properties measured through photoluminescence spectroscopy, we observed evolution of trion peak and suppression or quenching of neutral exciton A peak with increased oxygen plasma exposure. We also estimated the concentration of sulfur vacancy via correlating the variation in characteristic E' and A' band position (~ 4 cm⁻¹) of MoS₂. We find that regions of maximum local strain correspond to the regions of topographic curvature extracted from AFM measurements. Likewise, we observed nanoscale variation in work function correlated with an alloy of MoS₂/MoO_{3-x}. The TERS study allowed us to determine various chemical compositional phases and built-in strain that arises when 2D materials interact with Au under oxygen plasma. This work is financially supported in parts by NSF and NSF-MRI Grants.

9:40 AM EQ07.08.09

Spatial Inhomogeneity in MoS₂ Monolayer Irradiated by Electron Beam for Different Times—Correlated Study by Raman, PL, AFM, KPFM and TERS Imaging [Sanju Gupta](#); University of Central Florida, United States

Modulating physical-chemical (electrical, optical, and electrochemical) properties of transition metal dichalcogenides (TMDs), particularly MoS₂, has attracted a great deal of attention for diverse technologies. In this work, we exposed exfoliated monolayer MoS₂ under electron beam irradiation with an energy of 15 keV for different times and investigated the possible effects of the structural defects intentionally created by electron-beam on electronic properties at the nanoscale. Among various ways in which an electron beam adversely affects the sample are: local heating, electrostatic charging, displacement damage, sputtering, and hydrocarbon contamination. However, the effects of exposure time on the oxidation and etching process in creating lattice defects by e-beam irradiation still lack systematic investigations. In this work, we have employed scanning electron microscopy, micro- and nanoscale Raman (tip-enhanced, TERS) and photoluminescence (TEPL) spectroscopy, atomic force, and Kelvin Probe microscopy to characterize changes in surface morphology, spectral signatures, oxidation, etching, and/or defect clustering, to obtain high-resolution images and quantitative measurements of the work function heterogeneities. We unravel the evolution of defects formed under electron beam irradiation and observe the formation of metastable defect domains with different work function values. The experiments show that material diffused outward forming ring-like morphologies which become prominent with increasing exposure time while sulfur vacancies formed after exposure to diffuse, coalesce, and migrate molybdenum atoms at the edge of the ring while leaving patches of MoS₂ in the center, suggested by work function variation bringing the system from a metastable to equilibrium ground state. In light of recent experimental evidence, the results provide the importance of defect control and determined that the amount of radiation damage is proportional to the electron dose; and the extent of the damage is proportional to the amount of energy deposited in the sample. The results of this study enhance understanding of the electrical properties of MoS₂ FET devices in terms of defect sites on the MoS₂ surface that work as trap sites, which can deteriorate the carrier mobility and carrier concentration similar to what occurs during oxygen plasma. This work is financially supported in parts by NSF and NSF-MRI Grants.

10:30 AM EQ07.09.01

Boosting Thermoelectric Performance of Ultrathin MoS₂ by Substrate-Induced Non-Uniform Strain Hong Kuan Ng^{1,2,1}, Kedar Hippalgaonkar^{2,3,1}, Goki Eda^{1,1,1} and Jing Wu^{2,1}; ¹National University of Singapore, Singapore; ²Institute of Materials Research and Engineering, Singapore; ³Nanyang Technological University, Singapore

Thermoelectric performance in 2D transition metal dichalcogenides (TMDs) are usually optimized through controlling carrier concentration, band engineering, and/or scattering mechanism. Applying uniform strain to TMDs has been demonstrated to increase electrical performance and carrier mobility owing to the alteration of electronic band structure and effective carrier mass. Here, we study the effects of non-uniform strain on the thermoelectric performance of MoS₂ using SiN_x substrates with a crested morphology. The non-uniform strain is demonstrated to suppress phonon-scattering which drastically enhances carrier mobility and thermoelectric power factor in crested MoS₂ by up to 2 orders of magnitude depending on carrier concentration as compared to conventional MoS₂ on flat SiO₂ surfaces. We investigate gate- and temperature-dependent carrier mobility and density to determine the mechanisms responsible for the drastic enhancement in thermoelectric performance. Distinctively, the ultra-high carrier mobility achieved at low carrier concentrations weakens the dependence of thermoelectric parameters on carrier concentration, therefore resulting in a substantial improvement in electrical conductivity without greatly compromising Seebeck coefficient. Our work provides a universal pathway towards engineering carrier mobility and superior thermoelectric performance for a wide range of room-temperature applications.

10:45 AM EQ07.09.02

Site-Controlled and Strain-Tunable Quantum Optical Emission in WSe₂ Monolayers Abel Martínez-Suárez^{1,2}, Matteo Savaresi³, Davide Tedeschi³, Victor M. G. Suarez¹, Johannes Aberl⁴, Moritz Brehm⁴, Aurelio Hierro-Rodriguez^{1,5}, Stephen McVitie⁵, Pablo Alonso-Gonzalez^{1,2}, Javier Martín-Sánchez^{1,2} and Rinaldo Trotta³; ¹University of Oviedo, Spain; ²Nanomaterials and Nanotechnology Research Center (CINN), Spain; ³Sapienza University of Rome, Italy; ⁴Johannes Kepler Universität Linz, Austria; ⁵University of Glasgow, United Kingdom

The development of novel ultra-compact two-dimensional (2D) photonic technologies for application in quantum information processing, relies on our ability to fabricate single photon sources (SPS) in 2D van der Waals materials where we are able to on-demand position them as well as tune their optical emission properties¹. However, the challenge still remains to fully understand their physical origin in order to be able to efficiently utilize them and how to actively tune their optical properties. One solution is to implement elastic strain engineering through the introduction of a novel class of piezoelectric actuators^{2,3}.

In this work, we demonstrate site-controlled SPSs with reversible tuning of their emission energy by placing WSe₂ monolayers on top of piezoelectric pillars capable of introducing in-plane isotropic strain fields⁴. Our findings prove that it is feasible to have a full control of the emission energy of these SPSs without affecting the single photon emission purity with relatively large energy shifts up to 18meV. The experimental results are further corroborated by finite element simulations along with analytical calculations showing that all SPSs can be energy blue-shifted. Interpretations on the origin of the SPSs will be discussed based on an exciton diffusion model accounting for the variations on the micro-photoluminescence spectra corresponding to individual quantum emitters. Our findings shed light on the understanding of the physical origin of SPSs in 2D monolayers and are of strong relevance for the practical implementation of single photon devices based on 2D materials for future applications in quantum information processing.

References:

- [1] A. Srivastava et al. Nat. Nanotechnol. 10 (2015) 491
- [2] J. Martín-Sánchez et al. Semicond. Sci. Technol. 33 (2018) 013001
- [3] R. Trotta, J. Martín-Sánchez et al. Nature Commun. 7 (2016) 10375
- [4] O. Iff, D. Tedeschi, J. Martín-Sánchez et al. Nano Lett. 19 (2019) 6931

11:00 AM EQ07.09.03

Effects of H₂O Interaction with Graphene Grain-Boundary Under Strain Julia T. Hatoum, Claire Andreasen and Zubaer M. Hossain; University of Delaware, United States

In recent years, graphene has captured wide attention among engineers and researchers for its unique electronic, thermal, chemical, and mechanical properties, which could revolutionize a number of application areas, including electronics, nanotechnology, drug delivery, sensors, and catalysis. Since discovery, extensive research has been conducted theoretically, experimentally, and computationally to investigate the behavior of pristine graphene under no strain conditions. With the goal of applications in mind, it is critical to develop a fundamental understanding of the properties of defective graphene under deformed or strained conditions. While grain boundary defects within the graphene lattice are known to degrade mechanical properties and decrease both electrical and thermal conductivity, they can serve as an important source for making the graphene layer function as a chemically reactive 2D material, which may be unattainable otherwise. Furthermore, assessing and analyzing defects in the lattice is essential for application because the prevalence of defects (especially grain boundaries) causes graphene's extrinsic effects to have greater influence on the material's behavior than its intrinsic properties. In this work, using density functional theory simulations, we investigated the energetics of an isolated H₂O molecule at a linear grain-boundary of pentagonal and heptagonal configurations formed between armchair and zigzag graphene sheets. Using SIESTA, we simulated a water molecule at an initial approach configuration parallel to the graphene lattice at different heights, and we analyzed the results of the relaxed configurations. Because we wanted to observe strain influence on the water molecule, we picked sites where the grain boundary induced tensions and compressions in the graphene lattice. Using these results, we investigated the total groundstate energies of the systems, the net force experienced by the carbon atoms, the orientations of the relaxed water molecules, and the electronic structure of the lattice. Our findings suggest that if the initial placement of the molecule is parallel to the lattice within the van der Waals interaction distance, the molecule undergoes a reorientation and the O atom faces the graphene lattice. On the other hand, if the initial position of the molecule is parallel but closer to the graphene lattice, the H atoms become more reactive and face toward the graphene lattice. We considered five different sites on the grain boundary defect and found similar behaviors throughout. An electronic structure analysis suggests that the electron redistribution at the grain boundary affects the behavior of the molecule; for electronic structure, we analyzed electronic charge and electron density to give us an indication of any polarization at the site and give insight into coulombic interactions at the defect. And through energy and force values that were calculated and plotted, we also found that chemical interactions between the water molecule and graphene lattice is negligible when the molecule is released more than 14.5Å above the sheet. Also, due to separation-distance dependent distinct chemical affinities between the C-O atom pairs vs. C-H atom pairs, the groundstate interaction is strongly affected by the initial position of the molecule. And finally, we looked at the possibilities of reorientation at relaxed states; we calculated the activation energies required to change the configurations of the relaxed water molecules and found that changes in such

configurations is unattainable at room temperature. The results are expected to have important implications to our understanding of strain-chemistry of defective graphene. This talk will present the analysis of these findings as well as their potential applications in catalysis and water purification.

11:15 AM EQ07.09.04

Late News: Probing Excitons in Curved MoTe₂ with Monochromated EELS and 4D-STEM [Yueming Guo](#)¹, Sergei V. Kalinin¹, Kai Xiao¹, Sergiy Krylyuk², Albert Davydov² and Andrew R. Lupini¹; ¹Oak Ridge National Lab, United States; ²National Institute of Standards and Technology, United States

Bound electron-hole pairs, known as excitons, are critical to the optical and electronic responses of semiconductors. Just as for traditional materials, this principle applies to the newly-emerged Van der Waals semiconductors such as 2H-MoTe₂. Distinct from conventional bulk semiconductors, the quasi 2D semiconductors are soft and can get buckled spontaneously at micro or nano scale. The mechanism of spontaneous breaking of periodicity in 2D crystals has been proven by David Mermin [1], which means that real 2D crystals either break or buckle [2]. The curvature effect on excitons has been theoretically investigated for various systems [3-5] but few experimental efforts for nanoscaled bucking effect on excitons have been dedicated to Van der Waals semiconductors.

Here, we explore the relationship between Gaussian curvature and the excitonic behaviors in multilayer 2H-MoTe₂ by acquiring electron energy loss spectroscopy (EELS) and 4D scanning transmission electron microscopy (4D STEM) over a curved area of a 2H-MoTe₂ flake. The same types of data have also been acquired from a flat area of the same sample with a similar thickness. We carried out these experiments on a NION monochromated, aberration-corrected STEM, which provides both good energy and spatial resolutions. An energy resolution of 30 meV (with 3meV/pix) and a spatial resolution of 1.5 Å is used here. Each diffraction pattern in the 4D STEM data shows the normal direction of the tangent plane at each spot on the curved surface, and therefore the Gaussian curvature can be computed. Exciton peaks are observed from monochromated EELS with a high exposure for each spot in the scan. Unlike tensile strain effects which show redshift of the exciton peaks [6], the A exciton peaks in the curved area show a blueshift of 20 meV on average. Further results are being analyzed and will be discussed.

References

- [1] N. D. Mermin, Phys Rev **176**, 250 (1968).
- [2] J. M. Carlsson, Nat Mater **6**, 801 (2007).
- [3] Y. Kayanuma and N. Saito, Solid State Commun **84**, 771 (1992).
- [4] T. G. Pedersen, Phys Rev B **67** (2003).
- [5] T. G. Pedersen, Phys Rev B **81** (2010).
- [6] O. B. Aslan *et al.*, Nano Lett **18**, 2485 (2018).

11:30 AM EQ07.09.05

Efficiency Roll-Off Free Electroluminescence in Monolayer Semiconductors by Strain Engineering [Naoki Higashitarumizu](#)^{1,2}, Shiekh Zia Uddin^{1,2}, Hyungjin Kim^{1,2} and Ali Javey^{1,2}; ¹University of California, United States; ²Lawrence Berkeley National Laboratory, United States

Two-dimensional transition-metal dichalcogenides (TMDCs) have attracted tremendous attention toward optoelectronic applications. Photoluminescence quantum yield (PL QY) in TMDC monolayer can approach unity at the low exciton generation rate, whereas the PL QY drastically droops at the high generation rate due to a nonradiative exciton-exciton annihilation (EEA), limiting their light-emitting device application. Here, we demonstrate a strain tunable transient-mode electroluminescence (EL) device composed of TMDC and gate oxide. WSe₂ and WS₂ monolayers exhibit near-unity PL QY even at the high exciton density by applying external tensile strain together with gate modulation due to the inhibition of van-Hove singularity resonance, which causes the EEA. With a small strain of 0.5%, notably, the WSe₂ monolayer shows EL enhancement by two order of magnitude and its internal quantum efficiency (QE) reaches 8% at maximum. Furthermore, this concept of EEA suppression by strain modulation is valid even in WSe₂ bilayer. Unstrained WSe₂ bilayer exhibits a low PL QY and EL QE at around 1% and 0.03%, respectively, because of its indirect bandgap nature. By strain modulation, however, we achieve ~50% PL QY and ~1.5% EL QE for a broad range of carrier densities. This improvement is attributed to the indirect-direct bandgap transition and EEA suppression, corroborated by density functional theory calculations. This approach will pave the way for practical optoelectronic device applications based on TMDC monolayer and even multilayers.

11:45 AM EQ07.01.09

Late News: Strain Determined Friction Properties Between MXenes and Other 2D Materials [Yanxiao Li](#); Missouri University of Science and Technology, United States

MXene, as a new type of 2-dimensional (2D) material, can be synthesized by removing A layers from MAX phases by HF etching. MAX phases are ternary carbides or nitrides with the general formula M_{n+1}AX_n, where M is an early transition metal, A is an A-group element (mostly group IIIA or IVA), X is either carbon or nitrogen with n value of 1, 2, or 3. During the selective etching process, the outer surfaces of the exfoliated MXene layers are always terminated with F, OH, and/or O groups. Thus, MXenes are referred to as M_{n+1}X_nT_x, where T represents the surface groups (F, OH, and/or O) and x is the number of terminations. Since now, about 20 different kinds of MXene have been prepared. More MXene materials are also expected to be exfoliated from more than 70 reported MAX phases in the future. To date, MXenes have shown attractive electronic, optical and magnetic properties, which have great potential in sensing, energy storage, and electromagnetic shielding applications. Their surface frictional properties are critically important to these applications involving layered structures and 2D interfaces. However, there has only been a few experiments conducted on MXenes. The interfacial frictional behaviors between MXenes and other 2D materials are still unknown.

Being a few atoms-thin, 2D materials have unique friction and wear properties that are different from those of their 3D counterparts. Lee et al. conducted the atomic force microscopy (AFM) friction experiments on interfaces between SiO₂ and a group of 2D materials (including graphene, MoS₂, NbSe₂ and h-BN). The results have shown that measured coefficient of frictions (COFs defined as the ratio between normal and tangential force) are dependent on both the surface conditions and the contact induced elastic deformations (which is a function of bending flexibility) of the 2D materials. Due to the rich surface chemistry of MXene based on various of possible terminating groups (F, OH, and/or O) and tunable monolayer thickness in terms of atomical structures (i.e., changing n in M_{n+1}X_nT_x), it was suspected that the friction between MXene and other 2D materials can be quite different from other 2D materials based on computational investigations. However, there have not been any experiments conducted on the frictional behaviors of MXenes with 2D materials. Most of the experiments conducted so far were limited to MXenes' frictional behaviors with 3D materials.

In this paper, we experimentally investigated the frictional behaviors of Ti₃C₂T_x and Ti₂CT_x MXenes against themselves as well as other 2D materials including graphene and MoSe₂. We measured the friction forces using both the bare SiO₂ spherical AFM probes as well as Ti₃C₂T_x and Ti₂CT_x MXenes coated probes on graphene, MoSe₂, Ti₃C₂T_x and Ti₂CT_x MXenes sheets with varying number of monolayers (1-25 monolayers), and normal forces (0-2 mN). We have found that the COFs for all the investigated 2D interfaces are below 0.01 indicating the super lubricant frictional behavior of MXenes on themselves and other 2D materials. A less significant number-of-monolayer effect on the friction was also observed for MXenes. The measured COFs were also found to be independent of the applied normal forces at contacts. These results indicate the great potential of MXenes as excellent lubricating materials for 2D homo-/heterostructured materials, also the mechanical vulnerability of 2D homo-/heterostructured materials containing MXenes under shear forces.

SESSION EQ07.10: Twisted vdW Heterostructures II
Session Chairs: Feng He and SungWoo Nam
Wednesday Afternoon, December 8, 2021
EQ07-Virtual

1:00 PM *EQ07.10.01

Intrinsic Strain Enables Lattice Reconstructions in Moiré Superlattices Jiamin Quan¹, Lukas Linhart², Miao-Ling Lin³, Daehun Lee¹, Chih-kang Shih¹, Keji Lai¹, Allan H. MacDonald¹, PingHeng Tan³, Florian Libisch² and [Xiaoqin E. Li](#)¹; ¹The University of Texas at Austin, United States; ²Vienna University of Technology, Austria; ³Institute of Semiconductors, China

In vertical van der Waals (vdW) homo- or heterobilayers, a finite twist angle between the two layers leads to a moiré superlattice that induces periodic modulations of atomic alignments and consequently, a periodic modulation of energy, ground-states, and excited states. While most prior experiments on moiré superlattices have been interpreted using a rigid lattice model in which the local atomic stacking is assumed to be determined by rotating pristine two-dimensional lattices, lattice reconstructions can occur in bilayers near a commensurate stacking style, driven by a competition between interlayer coupling and strain.

The lattice reconstructions have been visualized in various scanning probe experiments. Here, we report the signature of lattice reconstruction in phonon spectra in twisted MoS₂ bilayers measured by far-field Raman experiments. Over a range of small twist angles (0-6°), the phonon spectra evolve rapidly due to ultra-strong coupling between different phonon modes and atomic reconstructions of the moiré pattern. We further develop a new low-energy continuum model for phonons that overcomes the outstanding challenge of calculating properties of large moiré supercells and successfully captures essential experimental observations.

1:30 PM *EQ07.10.02

Moiré Metrology of Energy Landscapes in van der Waals Heterostructures [Dorri Halbertal](#); Columbia University, United States

The emerging field of twistronics has revolutionized quantum materials research. At the small twist limit, and particularly under strain, as atomic relaxation prevails, the emergent moiré superlattice encodes elusive insights into the local interlayer interaction. In this work we introduce moiré metrology as a combined experiment-theory framework to probe the stacking energy landscape of bilayer structures at the 0.1 meV/atomscale, outperforming the gold-standard of quantum chemistry. Through studying the shapes of moiré domains with numerous nano-imaging techniques, and correlating with multi-scale modelling, we assess and refine first-principle models for the interlayer interaction. We document the prowess of moiré metrology for three representative twisted systems: bilayer graphene, double bilayer graphene and H-stacked MoSe₂/WSe₂. Moiré metrology establishes sought after experimental benchmarks for interlayer interaction. Furthermore, in this talk we extend the previously reported framework of moiré metrology[1] to account for multi-layered structures, and demonstrate a few material systems where such a treatment is essential to describe experimental observations.

[1] Halbertal et al., Nat. Comm. 12, 242 (2021)

Dorri Halbertal¹, Nathan R. Finney², Sai S. Sunku¹, Alexander Kerelsky¹, Carmen Rubio-Verdú¹, Sara Shabani¹, Lede Xian^{3,4}, Stephen Carr^{5,6}, Shaowen Chen^{1,7}, Charles Zhang^{1,8}, Lei Wang^{1,9}, Derick Gonzalez-Acevedo^{1,7}, Alexander S. McLeod¹, Daniel Rhodes^{1,10}, Kenji Watanabe¹¹, Takashi Taniguchi¹¹, Efthimios Kaxiras¹², Cory R. Dean¹, James C. Hone², Abhay N. Pasupathy¹, Dante M. Kennes^{3,13}, Angel Rubio^{3,14}, D. N. Basov¹

¹Department of Physics, Columbia University, New York, NY, USA.

²Department of Mechanical Engineering, Columbia University, New York, NY, USA.

³Max Planck Institute for the Structure and Dynamics of Matter and Center Free-Electron Laser Science, Luruper Chaussee 149, 22761 Hamburg, Germany.

⁴Present address: Songshan Lake Materials Laboratory, Dongguan, Guangdong 523808, China.

⁵Department of Physics, Harvard University, Cambridge, Massachusetts 02138, USA.

⁶Present address: Brown University, Providence, RI 02912, USA.

⁷Present address: Department of Physics, Harvard University, Cambridge, MA 02138, USA.

⁸Present address: Department of Physics, University of California at Santa Barbara, Santa Barbara, CA 93106, USA.

⁹Present address: National Laboratory of Solid-State Microstructures, School of Physics and Collaborative Innovation Center of Advanced Microstructures, Nanjing University, Nanjing, China

¹⁰Present address: Department of Materials Science and Engineering, University of Wisconsin-Madison, WI 53706, USA.

¹¹National Institute for Material Science, Tsukuba, Japan

¹²John A. Paulson School of Engineering and Applied Sciences, Harvard University, Cambridge, Massachusetts 02138, USA.

¹³Institut für Theorie der Statistischen Physik, RWTH Aachen University, 52056 Aachen, Germany.

¹⁴Center for Computational Quantum Physics, Flatiron Institute, New York, NY 10010 USA.

2:00 PM EQ07.10.03

Topography Induced Plasmon Resonance in Graphene [Md Farhadul Haque](#)¹, Chullhee Cho¹ and SungWoo Nam^{1,2}; ¹University of Illinois at Urbana-Champaign, United States; ²University of California, Irvine, United States

Plasmons are collective oscillations of electrons. Plasmon resonance occurs when the collective oscillations of electrons are coupled efficiently with the incident photon through light-matter interactions. Graphene is uniquely advantageous for plasmon resonance when compared to conventional plasmonic materials due to extremely high quantum efficiency for light-matter interactions, low loss of the plasmon, and a wide range of tunability. Graphene plasmon resonance has been reported via nano-patterning, selective doping, or defect engineering. Our previous theoretical study has suggested that inducing surface inhomogeneity via wrinkling or crumpling of graphene thin films may offer increased plasmon resonance tunability over conventional electrical doping methods. Despite this significant potential, there has not yet been experimental evidence of topography-induced plasmon resonance on a semi-infinite atomically thin graphene layer. Here, we report experimental studies of plasmonic resonance tunability of a crumpled graphene using photo-induced force microscopy (PiFM). PiFM is an effective technique for probing light-matter interaction at a sub-20 nm spatial resolution, which is not possible with conventional optics-based technique due to the diffraction limit. By applying uniaxial compressive strain, we created crumpled structures of

graphene with controlled topography features (e.g., wavelength, aspect ratio) on a polymeric substrate. Using PiFM, we observed a wide tunability of plasmon resonance energy (1260-1732 cm^{-1}) which we attributed to both the variation in topography as well as efficient coupling with the incident photon. We further investigated the relationship between the plasmon resonance wavelengths and the topography features by spatially mapping the near-field optical responses. Our observed plasmon resonance followed a redshift trend with an increase in wavelength and aspect ratio of the crumples, which agrees well with our previously established theoretical model. Finally, we demonstrated enhanced chemical imaging of a polymethyl methacrylate (PMMA) film aided by the effective plasmon resonance of the underlying crumpled graphene structure. The coupling between PMMA phonon and graphene plasmon showed a two-fold increase in the obtained near-field optical response. Our results not only are the first experimental demonstration of the coupling between topography and plasmon resonance of semi-infinite atomically thin graphene layer but also suggest widely tunable, plasmonically-enhanced biosensing or spectroscopy in the infrared range.

2:15 PM *EQ07.10.04

Stacking Order Driven Optical and Vibrational Properties in ReS_2 Yongjian Zhou¹, Nikhilesh Maity², Abhishek K. Singh² and Yaguo Wang¹; ¹The University of Texas at Austin, United States; ²Indian Institute of Science, India

Two distinct stacking orders in ReS_2 are identified without ambiguity and their influence on vibrational, optical properties and carrier dynamics are investigated. With atomic resolution scanning transmission electron microscopy (STEM), two stacking orders are determined as AA stacking with negligible displacement across layers, and AB stacking with about a one-unit cell displacement along the a axis. First-principle calculations confirm that these two stacking orders correspond to two local energy minima. Raman spectra inform a consistent difference of modes I & III, about 13 cm^{-1} for AA stacking, and 20 cm^{-1} for AB stacking, making a simple tool for determining the stacking orders in ReS_2 . Polarized photoluminescence (PL) reveals that AB stacking possesses blue-shifted PL peak positions, and broader peak widths, compared with AA stacking, indicating stronger interlayer interaction. Transient transmission measured with femtosecond pump probe spectroscopy suggests exciton dynamics being more anisotropic in AB stacking, where excited state absorption related to Exc. III mode disappears when probe polarization aligns perpendicular to b axis. Our findings underscore the stacking-order driven optical properties and carrier dynamics of ReS_2 , mediate many seemingly contradictory results in literature, and open up an opportunity to engineer electronic devices with new functionalities by manipulating the stacking order.

2:45 PM EQ07.10.05

E-Beam Patterning of Dopants in Twisted Bilayer Graphene Ondrej Dyck¹, Andrew R. Lupini¹, Dale Hensley¹, Jacob L. Swett² and Stephen Jesse¹; ¹Oak Ridge National Laboratory, United States; ²University of Oxford, United Kingdom

E-beams have been suggested to be useful for fabrication on the atomic scale.¹ Here, we leverage techniques that have been developed recently for positioning dopants in single layer graphene²⁻⁵ to pattern arrays of dopants in twisted bilayer graphene (TBG) in a scanning transmission electron microscope. The process is governed by a feedback-controlled algorithm allowing patterning to proceed in an automated fashion. These techniques hold promise for the tailoring of TBG properties by the attachment of foreign atoms to defect sites.⁶

References

- (1) Dyck, O.; Ziatdinov, M.; Lingerfelt, D. B.; Unocic, R. R.; Hudak, B. M.; Lupini, A. R.; Jesse, S.; Kalinin, S. V. Atom-by-Atom Fabrication with Electron Beams. *Nat. Rev. Mater.* **2019**, *4* (7), 497–507. <https://doi.org/10.1038/s41578-019-0118-z>.
- (2) Dyck, O.; Zhang, C.; Rack, P. D.; Fowlkes, J. D.; Sumpter, B.; Lupini, A. R.; Kalinin, S. V.; Jesse, S. Electron-Beam Introduction of Heteroatomic Pt–Si Structures in Graphene. *Carbon* **2020**, *161*, 750–757. <https://doi.org/10.1016/j.carbon.2020.01.042>.
- (3) Dyck, O.; Zhang, L.; Yoon, M.; Swett, J. L.; Hensley, D.; Zhang, C.; Rack, P. D.; Fowlkes, J. D.; Lupini, A. R.; Jesse, S. Doping Transition-Metal Atoms in Graphene for Atomic-Scale Tailoring of Electronic, Magnetic, and Quantum Topological Properties. *Carbon* **2021**, *173*, 205–214. <https://doi.org/10.1016/j.carbon.2020.11.015>.
- (4) Dyck, O.; Kim, S.; Kalinin, S. V.; Jesse, S. Placing Single Atoms in Graphene with a Scanning Transmission Electron Microscope. *Appl. Phys. Lett.* **2017**, *111* (11), 113104. <https://doi.org/10.1063/1.4998599>.
- (5) Dyck, O.; Yoon, M.; Zhang, L.; Lupini, A. R.; Swett, J. L.; Jesse, S. Doping of Cr in Graphene Using Electron Beam Manipulation for Functional Defect Engineering. *ACS Appl. Nano Mater.* **2020**, *3* (11), 10855–10863. <https://doi.org/10.1021/acsanm.0c02118>.
- (6) This work was supported by the U.S. Department of Energy, Office of Science, Basic Energy Sciences, Materials Sciences and Engineering Division (A.R.L., S.J., O.D.) and by the Center for Nanophase Materials Sciences (CNMS), a U.S. Department of Energy, Office of Science User Facility (D.H.).

SYMPOSIUM EQ08

New Frontiers in the Design, Fabrication and Applications of Metamaterials and Metasurfaces
November 29 - December 8, 2021

Symposium Organizers

Wenshan Cai, Georgia Institute of Technology
Junsuk Rho, Pohang University of Science and Technology
Joel Yang, Singapore University of Technology and Design
Thomas Zentgraf, Universität Paderborn

Symposium Support

Silver

Nano Convergence (Korea Nanotechnology Research Society)

Bronze
Nanophotonics | De Gruyter

* Invited Paper

SESSION Tutorial EQ08: Artificial Intelligence in Nanophotonics, Metamaterials and Metasurfaces
Session Chairs: Patrice Genevet and Thomas Zentgraf
Monday Morning, November 29, 2021
Hynes, Level 2, Room 201

10:30 AM

An Overview of On-Demand Design of Metamaterials Enabled by Deep Learning [Yongmin Liu](#); Northeastern University, United States

Over the last years, deep learning has been used for on-demand design of metamaterials by representing and learning the mapping between the topology and composition of metamaterials and their associated optical properties. Prof. Liu will review the recent progress in on-demand design of metamaterials using deep learning, with an emphasis on various model architectures for specific photonic tasks. He will also provide the historical background, key algorithms, fundamentals and applications of deep learning used for design of metamaterials.

12:00 PM BREAK

12:30 PM

An Overview of Numerical Optimization Methods for Metasurfaces [Patrice Genevet](#); Centre de Recherche sur l'Hétéro-Epitaxie et ses Applications, France

Numerical optimizations search for local or global optimal solutions either by evolutionary or gradient-based approaches. The first method search solutions stochastically in an extensive parameter space allowing capture of global optima and the second strategy calculates the derivatives of the cost function and finds local optima. Prof. Genevet will review the recent advanced optimization method to further exploit metasurface capabilities. He will also discuss Bayesian-based optimization techniques which can reduce the computational cost substantially.

2:00 PM BREAK

3:30 PM

An Overview of Machine Learning-Assisted Global Optimization of Photonic Devices [Alexandra Boltasseva](#); Purdue University, United States

Machine learning has shown great promises for generating data by learning important features. By exploiting its versatility and efficiency, machine-learning assisted novel optimization methods have been reported coupled with conventional optimization framework including topology optimization and meta-heuristic optimization. In her tutorial, Prof. Boltasseva will present the recent progress in global optimization assisted by machine learning, with an emphasis on high efficiency and substantial improvement.

SESSION EQ08.02: Metasurfaces and Applications I
Session Chairs: Patrice Genevet and Thomas Zentgraf
Tuesday Morning, November 30, 2021
Hynes, Level 2, Room 201

11:00 AM *EQ08.02.01

Applications and Integration of "Regular" and "Topological" Metasurfaces [Patrice Genevet](#), Qinghua Song, Renato Martins and Samira Khadir; CRHEA, France

Metasurfaces offer complete control of optical wavefront, such as phase, amplitude and polarization at the subwavelength scale, enabling a new class of artificial two-dimensional optics. Metasurfaces hold great potential in on-chip optoelectronic integration applications, which will significantly promote the development of miniaturized optoelectronic systems. In this presentation, I will review our group results on Metasurfaces integration in VCSEL and new results on vectorial holography and LiDARs.

In this presentation, I will discuss basic design and fabrication methods of metasurfaces and summarize various applications for beam steering, polarization control^{1,4} and monolithic integration of metasurfaces in opto-electronic systems². As an alternative of conventional bulky, the development of this technology is expected to create a positive disruption in modern optical technologies, in particular in the fields of imaging, holography, 3D dynamic image rendering, AR/VR and LiDAR systems⁵, nonlinear optics⁶.

1. Q. Song, et al., *Science Advances* 7, no. 5, eabe1112 (2021)
2. Y. Xie, et al., *Nature nanotechnology* (2020), doi:10.1038/s41565-019-0611-y
3. M. Elsaywy, et al., *Laser & Photonics Review*, 1900445 (2020)
4. Q. Song, et al., *Nature Communications*, 11, 2651 (2020)
5. I. Kim, R.J. Martins et al., *Nature Nanotechnology* 16, (2021) doi: 10.1038/s41565-021-00895-3
6. T. Stolt, et al., *Physical Review Letters* 126, 033901, (2021)

We acknowledge funding from the European Research Council (ERC) under the European Union's Horizon 2020 research and innovation programme (Grant agreements no. 639109).

11:30 AM EQ08.02.02

Structural Colors with Silicon—Scalable and CMOS-Compatible Nanostructure Fabrication Using Metal Assisted Chemical Etch Akhila Mallavarapu^{1,2}, Brian Gawlik², Paras Ajay², Crystal Barrera², Mariana Castaneda² and S.V. Sreenivasan²; ¹University of Pennsylvania, United States; ²Univ of Texas-Austin, United States

Silicon nanostructures with precisely controlled geometries exhibit vivid structural colors, and enable high-performance optical devices such as metalenses and multispectral filters. The ability to reliably and repeatably control the nanostructure geometries (cross-section, sidewall profile and height) over large areas at low cost is essential for these applications.

High-throughput nanopatterning techniques, such as nanoimprint lithography, can precisely define the nanostructure cross-sections. However, control of sidewall profile and height is limited for traditional pattern transfer using plasma etch due to sidewall roughness, etch taper and loss of feature fidelity for high aspect ratio structures. Metal Assisted Chemical Etch (MACE or MacEtch) has superior etch anisotropy and sidewall profiles. It is an electroless catalyst-based wet etch, and is an inexpensive solution-based alternative to plasma etch. However, MacEtch has largely been demonstrated in literature over small areas, and lacks CMOS-compatibility due to the use of gold as a catalyst.

We present scalable solutions to address these MacEtch challenges, with a focus on adoption in high volume nanomanufacturing [1-3]. Wafer-scale reliable and repeatable fabrication of high aspect ratio silicon nanostructures using nanoimprint lithography and MacEtch is shown. A CMOS-compatible Ruthenium MacEtch process that is comparable in quality to the standard gold MacEtch is presented. Large-area characterization of the process with imaging spectroscopic scatterometry is used for full wafer data on critical dimension control, etch depth uniformity, and yield in silicon nanowire arrays. Varied geometries such as ultrahigh-aspect-ratio silicon nanowires, nanofins, and diamond-shaped cross-section nanopillars demonstrate the resolution and versatility of MacEtch.

The ability to make such large-area high aspect ratio nanostructure arrays with arbitrary geometries enables an extensive design space for optimization of silicon optical devices. Si nanostructure geometry can be tuned to provide a variety of structural colors, as shown by FDTD simulations and experimentally on 4-inch wafers. Thus, the results presented here remove a significant barrier to adoption of MacEtch as a next generation etch technology for scalable fabrication of silicon nanostructures for optical devices.

References:

- [1] Nano Lett. 2020, 20, 11, 7896–7905
- [2] ACS Appl. Mater. Interfaces 2021, 13, 1, 1169–1177
- [3] IEEE Trans. Nanotechnol. 2021, vol. 20, pp. 83-91

11:45 AM EQ08.02.03

Spin-Polarized Stimulated Raman Scattering in a High-Q Metasurface for Nanoscale Nonreciprocity Jefferson Dixon, Harsha Reddy, Sahil Dagli and Jennifer A. Dionne; Stanford University, United States

Nonreciprocal devices (i.e. optical isolators, circulators) allow light to pass in one-direction only, which is a critical component of photonic networks. Unfortunately, they remain large (>100um) and are a limiting step in the development of densely-integrated, ubiquitous photonic networks. Here, we fabricate and demonstrate high-Q metasurfaces for submicron nonreciprocal and self-isolated lasing.

Our metasurface is composed of disks 505nm in diameter and 230nm in height, which support ordinary electric (TE) and magnetic (TM) Mie modes. This highly symmetric metasurface geometry also supports antisymmetric counterparts to the ordinary, symmetric TE and TM modes, but these modes are not accessible from free-space radiation, leaving these modes in the dark (i.e. bound in the continuum of free-space radiation). By reducing the symmetry of the metasurface lattice through the introduction of biperiodic diameters (diameter_{diskA} = 495nm, diameter_{diskB} = 515nm), the anti-symmetric TE and TM modes become accessible to free-space radiation over a narrow spectral linewidth. As a result, the linewidth of the resonance (and hence its quality-factor) can be controlled by the degree of asymmetry, where smaller asymmetry results in larger quality-factors. Experimentally, we have achieved a quality factor exceeding 15,000, which enables us to observe Stimulated Raman Scattering at lower power thresholds and in this subwavelength formfactor.

In Stimulated Raman Scattering, photons at the pump frequency (ω_p) stimulate emission at the Stokes frequency (ω_s), which results in the amplification of a signal that is injected at the Stokes frequency. We facilitate amplification by aligning the pump and signal frequencies with the high-Q resonances of the metasurface, resulting in a doubly-resonant high-Q metasurface that more efficiently generates Raman amplification. If we consider this process in a spin-polarized basis, wherein the pump is circularly-polarized and the gain medium (i.e. the silicon metasurface) supports such circulating modes, spin-selection rules arise at the Stokes frequency that break Lorentz reciprocity. This nonlinear process enables nonreciprocal gain for a signal at the Stokes frequency and results in one-way, nonreciprocal Raman lasing in a subwavelength (230nm thick) device layer.

12:00 PM EQ08.02.04

Buckling Induced Phase Transition in Nanoelectromechanical Phononic Waveguides Paolo F. Ferrari, SunPhil Kim, Jonathan Bunyan, Ali Kanji, Alexander F. Vakakis, Sameh Tawfik and Arend van der Zande; University of Illinois at Urbana-Champaign, United States

Phononic crystals and metamaterials are an emerging class of engineered structures with applications ranging from vibrations control to heat transfer. Nanoelectromechanical phononic waveguides are 1D metamaterials that allow propagation of elastic waves by coupling several mechanical resonators together. Utilizing these waves as information carriers would allow on-chip mechanical logic and coupling between the optical, radio and mechanical domains. Achieving reconfigurability and tunability to condition and route these mechanical signals is of crucial importance. In this presentation, we will present a method to effectively switch on and off wave propagation in nanoelectromechanical waveguides. We fabricate phononic waveguides by suspending a 1D array of coupled drumhead resonators made from a silicon nitride film (~60 nm) in a Si/SiO₂ chip. Each resonator consists of a circular plate with a diameter of 10 μm , with a coupling length (overlap) of 1.35 μm . We actuate the waveguide electrostatically at one end, then characterize the band structure of the waveguides using dynamic Fabry-Perot laser interferometry. We relate the band structure to the shape of the corresponding Bloch modes, which are obtained by mapping the dynamic parameters of the waveguide by confocal laser mapping. The waveguides feature bands in the very high frequency range (10-50 MHz). By reducing the temperature from 300 to 80K, a thermally induced compressive stress buckles the waveguide, due to the mismatch in the coefficients of thermal expansion in the silicon nitride and the substrate. At higher temperatures, we observe strong tuning of the band frequencies. Then at a critical temperature corresponding with the buckling transition, transmission along the first pass band is interrupted, while higher bands continue to transmit. We employ finite element analysis to explain the observed behavior. We find that the

explanation of the band disappearance consists of two ingredients. First, through simulations with periodic boundary conditions, we find buckling affects the first pass band by continuously reducing the group velocity, until it reaches zero at the buckling transition, then inverts above the buckling transition. Second, by simulating the entire set of 60 unit cells forming a waveguide and comparing to spatial maps of transmission, we find the global buckling mode of the waveguide above the critical point adds disorder to the system by inducing non-uniform stresses in the unit cells. Because the buckling shape matches the modes of the first pass band, the disorder strongly affects the first pass band but only weakly affects the higher bands. In an analogy with condensed matter physics, this phenomenon resembles a phase transition, where the waveguide switches from a conducting to an insulating phase due to buckling. Our study shows for the first time the use of elastic instabilities to induce transitions in phononic metamaterials at the nanoscale, paving the way for more advanced forms of mechanically-induced reconfiguration in hybrid opto and electro-mechanical circuits.

SESSION EQ08.03: Novel Fabrication and Devices
Session Chairs: Patrice Genevet and Thomas Zentgraf
Tuesday Afternoon, November 30, 2021
Hynes, Level 2, Room 201

1:30 PM *EQ08.03.01

Designing Optical Metamaterials from Colloidal Nanocrystal Assemblies Cherie R. Kagan; University of Pennsylvania, United States

Colloidal plasmonic nanocrystals (NCs) are known for their size- and shape-dependent localized surface plasmon resonances and their solution-based printing and imprinting in device fabrication. We use NCs as building blocks of assemblies and exploit their chemical and physical (electrical, optical, mechanical, thermal) tailorability to design and fabricate optical metamaterials. Chemical exchange of the long ligands used in NC synthesis with more compact ligand chemistries brings neighboring NCs into proximity, increasing interparticle coupling and allowing us to tune through a dielectric-to-metal phase transition, seen by a 10^{10} range in DC conductivity and a dielectric permittivity ranging from everywhere positive to everywhere negative across the whole range of optical frequencies [1]. This ligand-controlled coupling is useful in the design of materials that are strong, ultrathin film optical absorbers [2] or strong optical scatterers [3]. Compact ligand exchange and thermal annealing of NC films also drives a large volume shrinkage in NC thin films, allowing a 10X tailorability in their Young's modulus [4-6]. By juxtaposing plasmonic NCs and bulk materials, we exploit their different chemical and mechanical properties to create misfit strain that drives the folding of NC/bulk bilayer heterostructures and the transformation of lithographically-defined two-dimensional structures into three-dimensional structures. We use the three-dimensional structures to demonstrate the scalable fabrication of large-area metamaterials with chiroptical responses of ~40% transmission difference between left-hand and right-hand circularly polarized light and that are suitable broadband circular polarizers [5,6].

(1) Fafarman, A. T.; Hong, S.-H.; Caglayan, H.; Ye, X.; Diroll, B. T.; Paik, T.; Engheta, N.; Murray, C. B.; Kagan, C. R. Chemically Tailored Dielectric-to-Metal Transition for the Design of Metamaterials from Nanoimprinted Colloidal Nanocrystals. *Nano Lett.* **2013**, *13* (2), 350–357. <https://doi.org/10.1021/nl303161d>.

(2) Chen, W.; Guo, J.; Zhao, Q.; Gopalan, P.; Fafarman, A. T.; Keller, A.; Zhang, M.; Wu, Y.; Murray, C. B.; Kagan, C. R. Designing Strong Optical Absorbers via Continuous Tuning of Interparticle Interaction in Colloidal Gold Nanocrystal Assemblies. *ACS Nano* **2019**, *13* (7), 7493–7501. <https://doi.org/10.1021/acsnano.9b02818>.

(3) Chen, W.; Tymchenko, M.; Gopalan, P.; Ye, X.; Wu, Y.; Zhang, M.; Murray, C. B.; Alu, A.; Kagan, C. R. Large-Area Nanoimprinted Colloidal Au Nanocrystal-Based Nanoantennas for Ultrathin Polarizing Plasmonic Metasurfaces. *Nano Lett.* **2015**, *15* (8), 5254–5260. <https://doi.org/10.1021/acs.nanolett.5b02647>.

(4) Zhang, M.; Guo, J.; Yu, Y.; Wu, Y.; Yun, H.; Jishkariani, D.; Chen, W.; Greybush, N. J.; Kübel, C.; Stein, A.; Murray, C. B.; Kagan, C. R.; Kubel, C.; Stein, A.; Murray, C. B.; Kagan, C. R. 3D Nanofabrication via Chemo-Mechanical Transformation of Nanocrystal/Bulk Heterostructures. *Adv. Mat.* **2018**, *30* (22), 1800233. <https://doi.org/10.1002/adma.201800233>.

(5) Guo, J.; Kim, J.-Y.; Zhang, M.; Wang, H.; Stein, A.; Murray, C. B.; Kotov, N. A.; Kagan, C. R. Chemo- and Thermomechanically Configurable 3D Optical Metamaterials Constructed from Colloidal Nanocrystal Assemblies. *ACS Nano* **2020**, *14* (2), 1427–1435. <https://doi.org/10.1021/acsnano.9b08452>.

(6) Guo, J.; Kim, J.-Y.; Yang, S.; Xu, J.; Choi, Y. C.; Stein, A.; Murray, C. B.; Kotov, N. A.; Kagan, C. R. Broadband Circular Polarizers via Coupling in 3D Plasmonic Meta-Atom Arrays. *ACS Photonics* **2021**, *8* (5), 1286–1292. <https://doi.org/10.1021/acsp Photonics.1c00310>.

2:00 PM *EQ08.03.02

Active Epsilon-Near-Zero Photonics Ho Wai (Howard) Lee¹, Aleksei Anopchenko¹, Sudip Gurung¹, Khant Minn² and Jingyi Yang¹; ¹University of California, Irvine, United States; ²Baylor University, United States

The optical response of epsilon-near-zero (ENZ) materials has been a topic of significant interest in the last few years as the electromagnetic field inside media with near-zero permittivity has been shown to exhibit unique optical properties, including strong electromagnetic wave confinement, non-reciprocal magneto-optical effects, and abnormal nonlinearity.

This talk will review our recent development on conducting oxide and metallic nitride epsilon-near-zero optics. I will present our recent advances on the study of enhanced ultrafast nonlinearity and broadband and field-effect tunable absorption in ultrathin transparent conducting oxide ENZ materials meta-film fabricated by atomic layer deposition technique. In addition, I will discuss the photoluminescence enhancement of 2D materials on epitaxial titanium nitride thin films grown by molecular-beam-epitaxy. These studies enrich the fundamental understanding of emission and nonlinear properties on ENZ thin films that could be important for the development of advanced nanoscale lasers/light sources, optical/bio-sensors, and nano-optoelectronic devices.

This work was supported in part by the National Science Foundation (grant number: 2113010) and Air Force Office of Scientific Research (AFOSR, Award number: FA2386-18-1-4099)

2:30 PM EQ08.03.03

Self-Assembly of Gold Nanoparticles Functionalized with Water-Soluble Synthetic Polymers into Two- and Three-Dimensional Superlattices Hyeon Jin Kim^{1,2}, Wenjie Wang², Honghu Zhang³, Guillaume Freychet³, Benjamin Ocko³, Alex Travesset^{1,2}, David Vaknin^{1,2} and Surya Mallapragada^{1,2}; ¹Iowa State University, United States; ²Ames Laboratory, United States; ³Brookhaven National Laboratory, United States

Here, we report on the self-assembly of gold nanoparticles functionalized with polyethylene glycol (PEG-AuNPs) into two- and three-dimensional superlattices at the liquid surface or in the bulk. Synchrotron-based small-angle X-ray scattering studies including X-ray reflectivity and grazing incidence

small-angle X-ray scattering showed that Gibbs monolayers of PEG-AuNPs were created at the liquid surface with a hexagonal structure by adding salt. Further increases in salt concentration and temperature led to the formation of 3D fcc-like structure in the bulk, which was confirmed by solution small-angle X-ray scattering. Interestingly, the interparticle distance (i.e., lattice constant) decreased with increasing temperature, showing negative thermal expansion. The strong dependence of interparticle distance on functionalized PEG chain lengths was also investigated by theoretical considerations.

2:45 PM EQ08.03.04

Nanocube Epitaxy for the Low-Cost Realisation of High-Quality Nanophotonic Gold Nanostructures [Anna Capitaine](#)^{1,2,3} and Beniamino Sciacca^{1,2,3}; ¹CINaM, France; ²Centre National de la Recherche Scientifique, France; ³Aix-Marseille Université, France

High-quality monocrystalline materials and nanostructures are key to high-efficiency optoelectronic devices (Polman et al., Science, 2016), plasmonic materials (Wu et al., Adv Mater, 2014) and metasurfaces (Koenderink et al., Science 2015). However, the techniques used to grow those materials are in most cases time consuming, expensive (high vacuum and temperature) and require lattice-matched substrate, whereas precise control over the nanoscale geometry can only be achieved after further nanofabrication steps, limiting nanostructured monocrystalline materials to niche applications.

It has been demonstrated that single-crystal silver nanocubes, grown in solution phase, could be used as building blocks for the fabrication of continuous monocrystalline 1D nano-structures through epitaxial welding of adjacent nanocubes (Sciacca et al, Adv Mater., 2017). We demonstrate here that this technique can be used as a general method to fabricate 1D and 2D monocrystalline gold (Au) nanopatterns and macroscopic thin films for the first time, and show that such nanostructures can then be transferred to virtually any kind of substrate, allowing for simple integration in optical and optoelectronic devices.

Monodisperse Au single-crystal nanocubes are first synthesized in solution at room temperature. Next, using capillary forces they are self-assembled in a polydimethylsiloxane (PDMS) mould containing pre-defined 1D and 2D nanoscale patterns, in a closely packed configuration, with individual nanocube subunits lying face-to-face. Then, spontaneous reduction of a gold salt (HAuCl₄) on nanocubes surface is performed in soft conditions (40°C, in aqueous environment), enabling for nanocube epitaxy and the formation of a continuous monocrystalline material in the time scale of a few minutes. We use high-resolution transmission electron microscopy, electron diffraction, and x-ray diffraction to provide evidence for epitaxy. The nanocube epitaxy process is thoroughly investigated and a mechanism is proposed, showing that by tuning few key parameters, we can also control the faceting of the resulting continuous monocrystalline nanostructures.

Finally, we show that such complex continuous Au nanostructures of arbitrary shapes can be transferred from PDMS to various substrate by contact printing. As a proof of concept, we show the realization of an optical device composed of monocrystalline Au patch-antenna arrays with tunable optical response, and compare the optical properties to FDTD simulations.

This low-cost solution proves a viable method for the fabrication of complex monocrystalline nanostructures and their use as a high-quality nanophotonic surface, paving the way for integration in more complex devices with unexplored geometries.

SESSION EQ08.04: Metasurfaces and Applications II

Session Chairs: Jason Valentine and Thomas Zentgraf

Tuesday Afternoon, November 30, 2021

Hynes, Level 2, Room 201

4:00 PM EQ08.04.01

Light-Induced Surface Structuring of Azopolymer Films [Stefano Luigi Oscurato](#)^{1,2}, [Pasqualino Maddalena](#)^{1,2} and [Antonio Ambrosio](#)²; ¹University of Naples, Italy; ²Istituto Italiano di Tecnologia, Italy

The light-induced structuration of amorphous azopolymer films is an emerging micro and nano-patterning method for the realization of diffractive optical elements. Sinusoidal surface reliefs, inscribed in a single lithographic step on azopolymer film surface through interference lithography, have been largely used as engineerable diffraction gratings for applications ranging from light couplers and optical filters to structural color and augmented reality devices. Advanced optical functionalities can arise from the additional structural control achievable on the surface geometry by moving beyond simple interference lithography.

The key feature that makes the azopolymers attractive over standard photoresist for photolithographic applications, not limited only to optics, lies in the direct, non-destructive, structuration of film surface, whose final geometry depends on the full electric field of the illuminating light, i.e. on its intensity pattern and its polarization distribution. This peculiar photo-response is the result of a reversible macroscopic material displacement, initiated by a multitude of microscopic light-fueled actuation of the azobenzene molecules under UV/visible illumination.

Controlling the spatio-temporal distribution of the illuminating electric field, together with the possibility of erasing previous surface patterns, allows the tailoring, even dynamically, of the surface topography and its optical functionality with higher degrees of freedom in respect to standard and more sophisticated photolithographic materials and techniques. Advanced structuration approaches range from very simple optical configurations, in which a single collimated light beam is used to generate ordered polarization-dependent microstructures over large scales, to holographic illumination schemes, where both the intensity and the polarization patterns can be engineered independently and used to inscribe high-quality surface reliefs of arbitrary complex geometries, including those of standard diffractive optical elements as gratings and lenses. Additional control on the surface geometry can be achieved with sequential exposures of a previously exposed or pre-patterned film, enabling even a three-dimensional manipulation of the topography in simple and cost-effective fabrication conditions.

Here, I will overview the recent advances in the design and realization of light-induced reliefs on the surface of the azopolymer films obtained in several illumination schemes, mainly focusing the attention on their potentialities in the realization of tunable and reconfigurable diffractive optical elements.

4:15 PM EQ08.04.02

Tuning Microwave Metadevices Using Organic Electrochemical Transistors [Giorgio Ernesto Bonacchini](#)^{1,2}, [Siew Ting Melissa Tan](#)¹, [Alexander Giovannitti](#)¹, [Tyler J. Quill](#)¹ and [Alberto Salleo](#)¹; ¹Stanford University, United States; ²Istituto Italiano di Tecnologia, Italy

In the past two decades, organic electronic materials have emerged as the key enablers of a large and diverse set of developing technologies. Traditional applications of organic semiconductors include energy harvesting devices, flexible and printed circuitry, optoelectronic and electro-mechanical actuators¹. New fields continue to bloom, as demonstrated by the recent rise of organic bioelectronics and organic neuromorphic devices^{2,3}. Interestingly, despite the extensive research conducted on this class of materials, their use in microwave applications has been comparatively modest, since organic electronics is

generally considered “slow” with respect to other semiconductor technologies – although focused efforts are being dedicated to challenge this view^{4,5}. In the past, this preconception has possibly led to underestimating the potential of organic transistors in microwave metadevices, whereas lately they have demonstrated great promise as tuning elements⁶.

In a recent work⁶, we introduced a new device configuration where organic electrochemical transistors – based on the conductive polymer PEDOT:PSS – actively tuned a set of sub-5GHz microwave metasurfaces and metamaterial-inspired resonant structures. The device structure consisted in individual (or multiple) microwave Split-Ring Resonators in which the split region is bridged by a thin-film conductive polymer, gated through an ionic medium by a lateral gate electrode. By applying a positive bias at the gate electrode, cations are injected within the bulk of the negatively biased organic semiconductor, decreasing the charge carrier density throughout the volume of the polymer⁷. This device configuration enables a fully reversible modulation mechanism that requires very low voltages (<1 V) thanks to the optimal mixed ion-electron transporting ability of PEDOT:PSS. We demonstrated this tuning strategy on a number of different resonant configurations, including magnetic and electric resonators, frequency-tuneable SRRs, dual-band devices, and in a reconfigurable metasurface. All materials were deposited by means of inkjet printing – a mass-scalable and cost-effective fabrication technique – onto plastic and flexible substrates.

The promising results achieved with PEDOT:PSS as the active material encourage a wider exploration of the continuously growing library of organic semiconductors. In this work, we demonstrate a set of tunable microwave devices using different p-type and n-type organic electrochemical transistors. By chemically engineering the organic semiconductors, we are able to operate our devices in selected voltage windows, with fine control over the voltage dependence of the metadevices’ scattering properties. As an example of a possible application, we exploit this strategy within a wireless biosensing platform operating in the 2-2.5 GHz range.

In conclusion, we believe that our tuning strategy based on organic electronic materials presents new exciting opportunities for the field of metadevices, possibly paving the way to a new generation of reconfigurable metasurfaces, fabricated on large-area flexible substrates via high-throughput deposition techniques. Moreover, this class of metadevices could potentially complement other emerging bioelectronic and neuromorphic technologies that are also based on organic electrochemical transistors, expanding the horizon of metamaterials research.

References:

1. Guo, X. & Facchetti, A. *Nat. Mater.* **19**, 922–928 (2020).
2. Ohayon, D. & Inal, S. *Adv. Mater.* 2001439 (2020). doi:10.1002/adma.202001439
3. Van De Burgt, Y., Melianas, A., Keene, S. T., Malliaras, G. & Salleo, A. *Nat. Electron.* **1**, 386–397 (2018).
4. Zschieschang, U. *et al. Adv. Funct. Mater.* **30**, 1903812 (2020).
5. Perinot, A., Passarella, B., Giorgio, M. & Caironi, M. *Adv. Funct. Mater.* **30**, 1907641 (2020).
6. Bonacchini, G. E. & Omenetto, F. G. *Nat. Electron.* (2021) – **In press**.
7. Rivnay, J. *et al. Nat. Rev. Mater.* **3**, 17086 (2018).

4:30 PM EQ08.04.03

Electrohydrodynamic Jet Printing of Near Infrared All-Dielectric Metasurfaces Brian Iezzi¹, Zahra Afkhami², Md Ferdous Alam³, David Hoelzle³, Kira Barton² and Max Shtein¹; ¹University of Michigan–Ann Arbor, United States; ²University of Michigan–Ann Arbor, United States; ³The Ohio State University, United States

Photonic metasurfaces structured using all-dielectric materials have gained increasing research interest due to low ohmic losses, compared to metals, and the tunability of refractive indices through oxide or semiconductor material selection. Metasurfaces are typically generated using photo- or electron beam-lithographic processes, affording high precision and repeatability, but at the expense of long prototyping cycles and high up-front cost. In this work, high-resolution electrohydrodynamic jet (e-jet) printing and various formulations of high refractive index silicon and germanium nanoparticle colloidal inks are combined to create all-dielectric metasurfaces with tunable response across the near-infrared spectrum (900-3000 nm). Finite-difference time-domain (FDTD) electromagnetic simulations are used to elucidate the relationship between the photonic response and meta-atom geometry and nanoparticle optical constants. These simulations are further guided by a predictive model of the printed spherical meta-atoms based on the ink formulation (e.g., nanoparticle loading percentage, ratio of solvents) and surface energetic properties of the substrate surface. Repeatable printing of metasurface structures with sub-micrometer radii and periodic spacing is demonstrated, and near infrared microspectroscopy measurements are compared to FDTD simulations predicting narrowband (sub-100 nm FWHM) resonant reflectors. The potential implementation of physics-guided reinforcement learning as a tool for optimizing printing parameters, in conjunction with *in-situ* metrology, is discussed as well. Beyond providing a rapid, cost-effective metasurface prototyping platform, e-jet printing enables the incorporation of multiple materials with differing refractive indices into the same structure as well as enabling beneficial, and custom-tuned, spherical meta-atom shapes that cannot be created easily *via* conventional lithographic techniques.

4:45 PM EQ08.04.04

Electro-Optic Modulation of Transmission in a Lithium Niobate Metasurface Helena Weigand, Viola Vogler-Neuling, Marc Reig Escalé, David Pohl, Felix U. Richter, Artemios Karvounis, Flavia Timpu and Rachel Grange; ETH Zurich, Switzerland

The field of active metasurfaces tremendously broadens the application range of planar free-space optics, as it overcomes the restriction of a design defining a fixed functionality. To achieve new flexibility, several approaches have been explored to alter the functionality after fabrication, e.g. changing the refractive index of the metasurface building material itself. This can be realized in a plethora of ways such as thermal tuning, phase change or electric tuning by e.g. free carrier injection. Although the advantage of electric tuning approaches is their fast speed, many of these come with an increased absorption of the material.¹ The electro-optic Pockels effect however, utilizes an electric field without introducing free carriers and is in theory able to tune the refractive index with PHz speed. The crucial parameter, the electro-optic coefficient, is exceptionally strong in lithium niobate (LN), which further combines a high damage threshold with a high refractive index and a low loss, transparent nature in the visible to near-infrared spectrum.

Here, we show transmission intensity modulation in a LN metasurface based on the Pockels effect, which is enhanced by 2 orders of magnitude compared to an unstructured LN film. The effect is observed for voltages as low as 1 V and a bandwidth of 2.5 MHz. We further report on the dispersive properties of this modulation amplitude linked to the metasurface transmission resonance.

We design and fabricate a metasurface from 500 nm LN thin-film on a SiO₂ buffer layer and 500 μm LN as substrate. The unit cells of the metasurface are pillars with a height of 200 nm and a radius of 135 nm, separated by a 500 nm period. The optical resonance of this geometry, dominated by an electrical dipole mode, is experimentally measured at a wavelength of 776.6 nm with a quality factor of 129.

To modulate the transmission, we access the r₃₃ electro-optic tensor component of LN using electrodes separated by 25 μm. We utilize the Pockels effect by applying a sinusoidal AC voltage to change the refractive index in the LN pillars and subsequently alter the resonance of the metasurface. A tunable laser probes the transmission between 765 and 780 nm to detect the change in transmitted intensity (modulation) with a photodiode.

We observe modulations already for voltages below 1 V, which allows driving our device with commercial microcontrollers. The modulation bandwidth ranges from 10 Hz to 2.5 MHz and is mainly limited by our electric setup. The modulation amplitude follows the derivative of the transmission, which is confirmed by simulations for our metasurface. As the geometry of the metasurface determines the transmission, we can engineer the electro-optic modulation by different metasurface unit cells and periods. The importance of nanostructuring further manifests in the experimentally observed enhancement by a factor of 80 when comparing the metasurface modulation to the spectrally flat modulation of an unstructured area.

To conclude, we investigate the modulation of transmission in a LN metasurface by the electro-optic Pockels effect. To the best of our knowledge, this is the first time an electro-optically induced transmission intensity modulation is observed in an all-dielectric metasurface. We show an enhancement of the modulation by two orders of magnitude as compared to an unstructured film, which stresses the impact of nanostructuring. Furthermore, we observe a dispersive behavior of the modulation amplitude, which is determined by the derivative of the transmission of the metasurface. Our device is so far the strongest and fastest electro-optic metasurface in LN. This is an important step towards potential future applications such as tunable metalenses, display applications or beam steering applications to further advance free-space data processing.

[1] Qiong He et al., *Research*, vol. 2019, 1849272, 2019.

5:00 PM EQ08.04.06

Late News: Active Angular Tuning and Switching of Brewster Quasi Bound States in the Continuum in Magneto-Optic Metasurfaces Diego R. Abujetas¹, Nuno de Sousa², Jose Manuel Llorens³, Jose A. Sanchez-Gil¹ and Antonio Garcia-Martin³; ¹Instituto de Estructura de la Materia (IEM-CSIC), Spain; ²Donostia International Physics Center (DIPC), Spain; ³Instituto de Micro y Nanotecnología, CSIC, Spain

Bound states in the continuum (BICs) emerge throughout Physics as leaky/resonant modes that remain, however, highly localized[1]. They have attracted much attention in Photonics, and especially in metasurfaces[2,3]. One of their most outstanding features is their divergent Q-factors, indeed arbitrarily large upon approaching the BIC condition (quasi-BICs) [4,5]. Here we investigate how to tune quasi-BICs in magneto-optic (MO) all-dielectric metasurfaces. The impact of the applied magnetic field in the BIC parameter space is revealed for a metasurface consisting of Si spheres with MO response. Through our coupled electric/magnetic dipole formulation, the MO activity is found to manifest itself through the interference of the (MO-induced) out-of-plane electric/magnetic dipole resonances with the in-plane magnetic/electric (directly induced) dipole, leading to a rich, magnetically-tuned quasi-BIC phenomenology, resembling the behavior of Brewster quasi-BICs for tilted vertical-dipole resonant metasurfaces. Such resemblance underlies our proposed design for a fast MO switch of a Brewster quasi-BIC by simply reversing the driving magnetic field. This MO-active BIC behavior is further confirmed in the optical regime for a realistic YIG nanodisk metasurface through numerical calculations. Our results present various mechanisms to magneto-optically manipulate BICs and quasi-BICs, which could be exploited throughout the electromagnetic spectrum with applications in lasing, filtering, and sensing [6].

References

- [1] Chia Wei Hsu, et al., *Nat. Rev. Mater.* **1**16048, (2016).
- [2] D.C. Marinica, et al., *Phys. Rev. Lett.*, **100**,183902 (2008).
- [3] Chia Wei Hsu, et al., *Nature* **499**, 188 (2013).
- [4] Kirill Koshelev, et al., *Phys. Rev. Lett.* **121**, 193903 (2018).
- [5] Diego R. Abujetas, et al., *Sci. Rep.* **9**, 16048 (2019)
- [6] Diego R. Abujetas, et al., *Nanophotonics* *submitted*(2021)

5:15 PM EQ08.04.08

Reconfigurable 2D Topological Mechanical Metamaterials with Dynamic Covalent Bonds Jason Christopher Jolly¹, Binjie Jin², YoungJoo Lee¹, Mohammad Charara³, Tao Xie², Stefano Gonella³, Xiaoming Mao⁴ and Shu Yang^{1,4}; ¹University of Pennsylvania, United States; ²Zhejiang University, China; ³University of Minnesota, United States; ⁴University of Michigan, United States

Topological mechanical metamaterials (TMMs) based on Maxwell lattices exhibit topologically protected states (both static and dynamic behavior), including polarized edge stiffnesses and directional acoustic wave transport, depending on their global conformation. Of particular interest is the 2D generalized kagome lattice (2D GKL) that offers a rich topological phase space and exhibits multiple auxetic, non-polarized and topologically polarized states, respectively. Prior work in TMMs have thus far either been theoretical investigations, toy-model demonstrations, or experimental studies on relatively large models with locked configurations. Here, we aim to explore the topological phase space upon reversible kinematic reconfiguration while being stable in each polarized or un-polarized configuration. To do so, we fabricate monolithic 2D GKL with ligament sizes on the order of 100 μ m from polycaprolactone diacrylate (PCLDA) and polycaprolactone divinyl (PCLDV) networks with dynamic covalent bonds. Dynamic bonds allow us to spatially program stress relaxation and intrinsic softening, respectively, via the breaking and re-forming of covalent bonds and a photo-catalytically modulated alteration of the network topology. Any elastic stress generated and stored in the hinges of a PCLDA 2D GKL following a soft-twisting kinematic topological reconfiguration can be 'annealed' to permanently lock a specific configuration of the lattice. The spatially programmable softening of the hinges in a PCLDV 2D GKL monolith on the other hand has the ability to drastically modulate the topologically protected static and dynamic mechanical behavior of the 2D GKL geometry without any topological alteration in a geometric sense. Our studies allow us to answer fundamental questions such as whether elastic strain energy stored during kinematic transformations affects topologically protected properties and is a big step forward in realizing active, device-like TMMs with potential applications as reconfigurable acoustic waveguides and energy absorbers with controllable depth of penetration.

SESSION EQ08.05: Soft Metamaterials and Bottom-up Approach
Session Chairs: Wenshan Cai and Thomas Zentgraf
Monday Morning, December 6, 2021
EQ08-Virtual

8:00 AM *EQ08.05.01

Chirality Control in Single Gold Nanoparticle Ki Tae Nam; Seoul National University, Korea (the Republic of)

Chiral structure controlled at nanoscale provides a new route to achieve intriguing optical properties such as polarization control and negative refractive index. However, asymmetric structure control with nanometer precision is difficult to accomplish due to limited resolution and complex processes of conventional methods. Here, we demonstrated novel chiral gold nanostructures exploiting chirality transfer between peptide and high-Miller-index gold surfaces. Enantioselective adsorption of peptides results in unequal development of nanoparticle surface and this asymmetric evolution leads to highly twisted chiral element in single nanoparticle making unprecedented 432 helicoid morphology. The synthesized helicoid nanoparticle showed strong optical activity which was substantiated by distinct transmittance color change of helicoid solution under polarized light.

8:30 AM *EQ08.05.02

Chiroptics with Reconfigurable Metamolecules and Metamaterials Yuebing Zheng; The University of Texas at Austin, United States

We apply directed assembly to realize reconfigurable chiral metamolecules and metamaterials consisted of nanoscale building blocks. New techniques such as opto-thermoelectric tweezers and optothermally gated photon nudging are developed for the reconfigurable directed assembly both in solutions and on solid-state substrates. We further demonstrate applications of the metamolecules and metamaterials in chiroptical spectroscopy for label-free enantiodiscrimination of drug molecules and abnormal metabolites in diabetes.

9:00 AM EQ08.05.04

Foot-Scale Acoustic Self-Limiting Assembly of Particles on Polymer [Liang Zhao](#)¹, Bchara Sidnawi¹, Jichao Fan², Thomas Scully¹, Weilu Gao², Qianhong Wu¹ and Bo Li¹; ¹Villanova University, United States; ²University of Utah, United States

Self-limiting assembly of particles, wherein assembly stops automatically once the limiting mechanism is turned on, represents state-of-the-art controllability. Here, we demonstrate a unique Acoustic Self-limiting Assembly of Particles (ASAP) to achieve foot-scale monolayer assembly of both inorganic and organic particles on flexible substrates in aqueous solutions. Unlike the dominating surface self-limiting mechanism, ASAP features a unique synergy of several designs. (1) Hard-to-wet surface energy design of hydrophobic particles and substrate in water ensures the energetic favorability of particle deposition on the substrate. (2) The acoustic field helps maintain the particles dispersion and energize them to collide with the substrate. (3) The viscoelastic behavior of polymer substrates helps absorb the kinetic energy of impacting particles to facilitate the assembly. (4) The assembled rigid particles convert the viscoelastic substrate into an elastic one, thereby preventing further formation of new layers. We have demonstrated the assembly of SiO₂ nanospheres (d = 500 nm-1000 nm, hydrophobic treated) and Poly(Methyl Methacrylate) microsphere (d = 1000-5000 nm) on various micro- and nanopatterned polydimethylsiloxane (PDMS) substrates. Such accurate assembly can be important for many applications. For example, as a proof-of-concept, we demonstrate that the produced films of mono- and bi-layer SiO₂ nanosphere show different colors due to Mie-resonance-induced optical coloration. It is important to note that the unique energy design of ASAP opens the gate toward many desirable but hard-to-assemble systems and thus enables unlimited functionalities. Moreover, ASAP is specially designed for viscoelastic polymer/bio substrates and may enable a wide range of applications in structural coloration, smart textile manufacturing, and drug delivery.

SESSION EQ08.06: Emerging Photonic Materials and Process

Session Chairs: Wenshan Cai and Junsuk Rho

Monday Afternoon, December 6, 2021

EQ08-Virtual

6:30 PM *EQ08.06.01

Nonlinear Metaphotonics and Metasurfaces [Yuri Kivshar](#); Australian National University, Australia

The field of nonlinear optics is a well-established discipline that relies on macroscopic media and employs propagation distances longer than a wavelength of light. Recent progress with electromagnetic metamaterials has allowed for the expansion of this field into new directions of new phenomena and novel functionalities. Nonlinear effects in thin, artificially structured materials such as metasurfaces do not rely on phase-matching conditions and symmetry-related selection rules of natural materials; they may be substantially enhanced by strong local and collective resonances of fields inside the metasurface nanostructures. Consequently, nonlinear processes may extend beyond simple harmonic generation and spectral broadening due to electronic nonlinearities.

For many years, plasmonics was considered as the only available platform for subwavelength optics, but the recently emerged field of Mie-resonant metaphotonics provides more practical alternatives for nanoscale optics by employing resonances in high-index dielectric nanoparticles and their structures such as metasurfaces. This talk aims to discuss recent advances and future emerging directions in the field of nonlinear metaphotonics and optical metasurfaces empowered by Mie resonances. We aim to discuss efficient spatial and temporal control of nonlinear light by employing multipolar Mie resonances and bound states in the continuum, with applications of these concepts to second-, third-, and high harmonic generation, self-action effects, upconversion, and lasing.

We will also discuss our recent results on asymmetric parametric generation of light in nonlinear metasurfaces with bianisotropic meta-atoms to generate images in the visible spectral range when illuminated by infrared radiation. By design, the metasurfaces produce different and completely independent images for the reversed directions of illumination, that is when the positions of the infrared transmitter and the visible light receiver are exchanged. Nonlinearity-enabled asymmetric control of light at a level of individual subwavelength resonators opens an untapped potential for developing novel nanophotonic components via dense integration of large quantities of nonlinear resonators into compact metasurfaces

7:00 PM *EQ08.06.02

The Ultra-Thin Nanophotonic Platform Using Transition Metal Dichalcogenides Layers [Su-Hyun Gong](#) and Junghyun Sung; Korea University, Korea (the Republic of)

The emergence of 2D materials stimulated intensive research on both electronic and photonic applications. Especially, transition metal dichalcogenides (TMDs) provided an excellent platform for photonic applications due to their strong light-exciton interaction. Various photonic devices such as a light-emitting device, laser, exciton-polariton device have been successfully demonstrated experimentally using TMD monolayers. However, multilayered TMDs has attracted far less attention than TMD monolayers because they become indirect bandgap materials. Here we show that multilayered TMD itself is a good platform for controlling light-matter interaction without integrating an external photonic structure. A TMD multilayer can be utilized for a passive optical structure because it possesses a high dielectric constant. For example, light guiding is possible along a multilayered TMD, which is very thin compared to the wavelength of the light. Because a high dielectric constant is owing to the exciton resonances, guided light along a TMD layer is referred to an exciton-polariton. The dispersion relation of the exciton-polariton in a TMD layer is very similar to that of surface plasmon polariton. Interestingly, we observed that the polarization of the exciton polaritons in a TMD layer is distinctive to surface plasmon polaritons because it inherits valley-dependent optical response from excitons in TMDs. We will also show that light can be further controlled using a patterned TMD multilayer. First of all, we designed an ultra-thin flat lens using a patterned TMD layer. We will show the optimized thickness and design of a TMD flat lens for efficient light focusing. Lastly, we will present the experimental observation on the lasing action in a bare TMD disk. A 50-nm thick TMD disk exhibits whispering gallery modes with a quality factor of ~400. The disk structure has a very high confinement factor for lasing action because the TMD disk offers both optical modes and optical gains. As a result, we observed the lasing operation under continuous-wave excitation at room temperature. We believe our results show a potential for the TMD-based nanophotonics offering a small mode volume but with a lower loss compared to the surface plasmon polaritons.

7:30 PM EQ08.06.03

Engineering Hyperuniform Phase Plates for Multispectral, Lensless Imaging Systems Yuyao Chen, Wesley Britton and Luca Dal Negro; Boston University, United States

Lensless imaging systems replace the lens of a traditional camera with engineered diffractive optical elements placed in close proximity (~2mm) to the image sensor plane, largely reducing the system volume and enabling on-chip imaging applications. In our recent work, we designed, fabricated, and characterized a novel multispectral lensless imaging system based on the design of hyperuniform phase plates (HPPs). In particular, we demonstrate the imaging capabilities and point-spread-function (PSF) engineering of HPPs based on from scalar random fields that are obtained by solving nonlinear reaction-diffusion equations. In particular, we focus on HPP structures and contour PSFs phase plates derived from the Gary-Scott (GS), Cahn-Hilliard (CH), and Swift-Hohenberg (SH) models that produce highly isotropic modulated transfer functions (MTFs) compared to state-of-the-art lensless imaging systems with contour PSFs based on the Perlin noise. Specifically, we demonstrate the importance of hyperuniform two-component isotropic random fields for the flexible design of novel diffractive phase plates and we introduce an efficient phase retrieval algorithm based on the Rayleigh-Sommerfeld diffraction theory that enables the fabrication of HPPs with desired PSFs. A device HPP structure within a four-level phase discretization approach is fabricated using scalable photolithography and its multispectral imaging behavior is demonstrated at different wavelengths using the high-fidelity (ADMM) optimization algorithm. The scalability of the proposed concepts to infrared spectral regions and their robustness against large photodetection noise will also be discussed.

7:45 PM EQ08.06.05

Focused Ion Beam (FIB) Induced Alignment-Controlled Herringbone Nanostructures on Germanium (100) Surface Bhaveshkumar B. Kamaliya^{1,2,3}, Mohammed Aslam¹, Jing Fu² and Rakesh G. Mote¹; ¹Indian Institute of Technology Bombay, India; ²Monash University, Australia; ³IITB-Monash Research Academy, India

To fabricate nanostructures, direct milling by the focused ion beam (FIB) is deemed as a mask-less and single-step fabrication technique; however, it is a time-consuming process due to pixel-by-pixel dwelling, and the effective beam size of FIB restricts minimum feature size. The self-organized nanostructures have an advantage over directly milled nanostructures owing to the low irradiation dose requirement. Also, self-organization does not possess any limitations on the minimum feature size. Thus, towards achieving miniaturization in the field of nanofabrication, FIB induced self-organization can be an easy and preferred approach. The formation of nanoripples on germanium, with enhanced wideband light absorption, has been reported by reorganization of the surface atoms due to FIB irradiation [1,2]. Systematic control on the topography progression of the germanium surface during FIB irradiation must be studied to attain complicated 3D geometries such as polygonal morphologies [3]. Such polygonal structures are essential as building blocks for photonic integrated circuits; however, superior complexities in morphologies such as corrugated [4] and herringbone patterns can be highly beneficial for hybrid microfluidic and optical sensing devices. The present work demonstrates controlled evolution and realization of complicated morphologies such as alignment-controlled herringbone nanostructures on the Ge surface by FIB induced self-organization. These periodic herringbone nanostructures were found to be evolved from the array of circular nanoholes and are jutting out of the surface, delivering the exclusive capability of FIB to create 3D nanostructures. As revealed by electron microscopy, Raman spectroscopy and molecular dynamics simulations, such complex morphologies were obtained by nanoscale control on the phase transformation of germanium surface during ion irradiation, leading to viscous-fingering process with site-specific self-organization. Moreover, the herringbone structures were manipulated with varying scanning strategies in order to modify their pitch and to orient the structures in a spiral manner. Germanium nanostructures exhibit improved THz emission; thus, such a possibility of easy direction and pitch control in Ge nanostructures can help to create scalable metasurfaces with superior light-matter interactions. The present study fosters the advancement in FIB processes towards manipulating the morphology of individual nanoholes (induced by each FIB-spots), offering a novel capability in the field of FIB-nanofabrication.

- [1] W. Zhou, A. Cuenat, and M. J. Aziz, Formation of Self-Organized Nanostructures on Ge during Focused Ion Beam Sputtering, in Conference Series-Institute of Physics, edited by A. G. Cullis and P. A. Midgley, Vol. 180 (Philadelphia; Institute of Physics; 1999, 2003), pp. 625–628.
- [2] B. Kamaliya, R. G. Mote, M. Aslam, and J. Fu, Enhanced Light Trapping by Focused Ion Beam (FIB) Induced Self-Organized Nanoripples on Germanium (100) Surface, *APL Mater.* 6, 036106 (2018).
- [3] B. Kamaliya, V. Garg, A. C. Y. Liu, Y. (Emily) Chen, M. Aslam, J. Fu, and R. G. Mote, Tailoring Surface Self-Organization for Nanoscale Polygonal Morphology on Germanium, *Advanced Materials* 33, 2008668 (2020).
- [4] B. Kamaliya, V. Garg, R. Mote, M. Aslam, and J. Fu, Controlled Self-Organization on Germanium Using Focused Ion Beam (FIB): From Quasi-Periodic Nanoripples to Well-Ordered Periodic Nanostructures, *Microscopy and Microanalysis* 26, 1684 (2020).

8:15 PM BREAK

SESSION EQ08.07: Tunable and Reconfigurable Metasurfaces
Session Chairs: Junsuk Rho and Joel Yang
Monday Afternoon, December 6, 2021
EQ08-Virtual

9:00 PM EQ08.07.03

Electrically Tunable Varifocal Metalens at Visible Wavelengths Trevon Badloe, Inki Kim, Yeseul Kim, Jooheon Kim and Junsuk Rho; Pohang University of Science and Technology, Korea (the Republic of)

Tunable optical devices powered by metasurfaces provide a new path for functional planar optics. In particular, lenses with tunable focal lengths could play a key role in various fields with applications in imaging, displays, and augmented and virtual reality devices. Here, we demonstrate an electrically controllable varifocal metalens at visible wavelengths by incorporating a metasurface designed to focus light at two different focal lengths, with liquid crystals to actively manipulate the focal length of the metalens through the application of an external bias. By utilizing hydrogenated amorphous silicon that is optimized to provide an extremely low extinction coefficient in the visible regime, the metalens is highly efficient with measured focusing efficiencies of around 44%. We numerically design and experimentally realize and characterize tunable focusing and demonstrate electrically tunable active imaging at visible wavelengths using the varifocal metalens combined with liquid crystals. Diffraction limited focusing and imaging is verified through the analysis of the measured optical intensities at the focal points, and the modulation transfer function. The varifocal metalens is used to demonstrate electrically modulated focus switching between the two designed focal planes, to display images of positive and negative target objects.

9:15 PM EQ08.07.04

All-Optical Reconfigurable Metamaterials Jingang Li and Yuebing Zheng; The University of Texas at Austin, United States

Colloidal metamaterials assembled from individual colloidal particles as building blocks exhibit unique collective behaviors beyond single components. Reconfigurable metamaterials with tunable optical properties are of significant interest in understanding the fundamental light-matter interactions at the nanoscale and developing active nanophotonic devices. Optical tweezers can precisely manipulate colloidal particles of variable sizes and materials. However, it has remained challenging for optical tweezers to assemble metamaterials due to the inability to control the interparticle and particle-substrate interactions.

To overcome these limitations, we have developed a series of optical techniques for all-optical reconfigurable metamaterials. Specifically, we invented opto-thermoelectric nanotweezers (*Nature Photonics* **2018**, *12*, 195-201) for versatile manipulation of nanoparticles with ultralow optical power and opto-thermoelectric assembly (*Science Advances* **2017**, *3*, e1700458) for reconfigurable construction of colloidal metamaterials with tunable bonding strength. To tackle the potential photothermal damages to nanoparticles, we further developed opto-refrigerative tweezers (*Science Advances* **2021**, *7*, eabh1101) as a noninvasive tool to trap and assemble metamaterials at the laser-cooling-generated low-temperature region.

In addition to the reconfigurable assembly of optical metamaterials in the liquid media, we developed optothermal nudging (*Nature Communications* **2019**, *10*, 5672) to directly manipulate colloids on a solid substrate. Reconfigurable construction of colloidal metamaterials is achieved with nanoscale accuracy, paving the way for the fabrication of active on-chip functional nanodevices. For instance, we demonstrate the all-solid-phase reconfigurable dielectric metamaterials with tunable optical chirality and their applications in enhanced chiral sensing (*Nano Letters* **2020**, *21*, 973-979; featured as a Front Cover article).

In summary, we have developed versatile optical approaches for bottom-up fabrication of reconfigurable metamaterials, which can operate both in the liquid media or on the solid substrate. Metamaterials with diverse configurations, sizes, and materials can be assembled at single-particle resolution. With highly enriched structures and tunable optical properties, the all-optical reconfigurable metamaterials provide a powerful platform to advance fundamental understandings in colloidal and materials sciences, investigate general design principles for functional metamaterials, and develop active devices for practical applications.

9:30 PM EQ08.07.05

On-Demand Mode Conversion and Wave-Front Shaping via On-Chip Metasurfaces Lin Deng and Yongmin Liu; Northeastern University, United States

To further reduce the overall size and increase the functionalities of integrated photonics, researchers have recently investigated the hybrid system by integrating metasurfaces with photonic waveguides. The wavevector of the guided mode can be modified or the mode coupling coefficient can be optimized with the aid of metasurfaces, ensuring the efficient conversion from the fundamental mode to higher-order modes^{1,2}. On the other hand, 2D phase shaping of the input planar waveguide mode was realized by deliberately controlling the local phase or reflective index with metasurfaces^{3,4}. However, to the best of our knowledge, a general approach for arbitrarily converting TM modes to TE modes or wave-front shaping for the cross-polarized waves is still lacking.

Here, we propose a new design strategy for mode converters and polarization rotators utilizing on-chip C-shaped plasmonic nanostructures, which support pronounced electric and magnetic resonances. Comparing to previous methods that convert the fundamental TE mode to other modes by modifying the wavenumber of guided waves^{1,2}, our design can directly generate the required wavefront of the desired TE modes from various TM modes even when the input mode and target mode have the same or very close wavenumbers. Also, the phase tuning range for the co-polarized light using the nano-bar structure in previous work can only cover 0 to π , which would potentially limit its applications. In contrast, the phase change of our C-shape nanoantenna can cover the 2π range, which could be more straightforward and flexible for higher-order cross-polarization modes conversion. In addition to the mode conversion, we demonstrate on-chip lenses that can shrink the spot size while rotating its polarization direction with a footprint of only 9.6 μm along the propagation direction. To the best of our knowledge, it is the first demonstration to achieve polarization rotation and wave-front shaping simultaneously inside the waveguide with the help of on-chip metasurfaces.

In summary, we propose and numerically demonstrate an innovative method for mode conversion and wave-front shaping, when the input guided mode is TM polarized. The rotation of the polarization and tuning of the local phase is achieved through the interaction of the on-chip metasurfaces and evanescent wave components of the waveguide. We envision that our concept may inspire novel applications such as mode division multiplexing, on-chip optical interconnection, optical router, and light detection and ranging.

1. Li, Z.; Kim, M.-H.; Wang, C.; Han, Z.; Shrestha, S.; Overvig, A. C.; Lu, M.; Stein, A.; Agarwal, A. M.; Lončar, M., Controlling propagation and coupling of waveguide modes using phase-gradient metasurfaces. *Nature nanotechnology* **2017**, *12* (7), 675.

2. Ohana, D.; Desiatov, B.; Mazurski, N.; Levy, U., Dielectric metasurface as a platform for spatial mode conversion in nanoscale waveguides. *Nano letters* **2016**, *16* (12), 7956-7961.

3. Wang, Z.; Li, T.; Soman, A.; Mao, D.; Kananen, T.; Gu, T., On-chip wavefront shaping with dielectric metasurface. *Nature communications* **2019**, *10* (1), 1-7.

4. Fan, Y.; Le Roux, X.; Korovin, A.; Lupu, A.; de Lustrac, A., Integrated 2D-graded index plasmonic lens on a silicon waveguide for operation in the near infrared domain. *ACS nano* **2017**, *11* (5), 4599-4605.

9:45 PM EQ08.07.07

Near-Infrared Reflection Modulation Through Electrical Tuning of Graphene Metasurfaces Ziqiang Cai and Yongmin Liu; Northeastern University, United States

Metasurfaces made of an array of rationally designed sub-wavelength structures have become one of the most promising frontiers in optics. By combining graphene with a metasurface, the functions of the metasurface can be electrically tuned with high tuning speed, high modulation efficiency, adaptability with silicon fabrication process as well as compactness. However, the tuning wavelengths of the demonstrated metasurfaces are mainly limited in the mid-infrared and terahertz spectra. There are some works that push the tuning wavelength of graphene metasurfaces close to the near-infrared region, but the experiment results either suffer from low tuning range (<5%) [1, 2] or require extremely high applied voltage (150V) to mechanically move graphene flakes [3, 4], imposing considerable limitations for practical applications.

In this presentation, we report a reflective-type tunable graphene metasurface operating in the near-infrared spectrum ($\leq 3.0\mu\text{m}$). The device combines metallic plasmonic structures with graphene to enhance graphene's interband transition, so that a decent tunability can be achieved. More specifically, the applied voltage can be rather small due to the 'step-like' change of graphene's conductivity. Moreover, since graphene's interband transition is less sensitive to its carrier mobility, our device can work well with wet-transferred Chemical Vapor Deposition (CVD) graphene that has low mobility. Thus, the device is robust and suitable for large-area fabrication. In addition, by carefully design the structure parameters, our tunable graphene metasurface can work in both near-infrared and mid-infrared spectra under different polarization of light.

Our design has been verified through both simulation and experiment, which agree well with each other. We achieved a reflection modulation ΔR of about 10% and a modulation depth $\Delta R/R_{\max}$ of 17% at $2.42\mu\text{m}$, with the applied voltage less than 15V. We have also fabricated another graphene metasurface that can work in both near-infrared and mid-infrared spectra at the same time. The corresponding reflection spectra have a modulation ΔR of about 9.5% and a modulation depth $\Delta R/R_{\max}$ of 18.2% at $2.30\mu\text{m}$, and a modulation ΔR of about 7.5% and a modulation depth $\Delta R/R_{\max}$ of 24.7% at $5.67\mu\text{m}$. We think that these results provide a new design strategy to advance electrically tunable metasurfaces.

1. Thareja, V., et al., Electrically tunable coherent optical absorption in graphene with ion gel. *Nano Lett*, 2015. 15(3): p. 1570-6.
2. Emani, N.K., et al., Electrical modulation of fano resonance in plasmonic nanostructures using graphene. *Nano Lett*, 2014. 14(1): p. 78-82.
3. Thackray, B.D., et al., Super-narrow, extremely high quality collective plasmon resonances at telecom wavelengths and their application in a hybrid graphene-plasmonic modulator. *Nano Lett*, 2015. 15(5): p. 3519-23.
4. Thomas, P.A., et al., Nanomechanical electro-optical modulator based on atomic heterostructures. *Nat Commun*, 2016. 7: p. 13590.

9:50 PM *EQ08.07.01

Active and Tunable Dielectric Nanoantennas and Metasurfaces Arseniy Kuznetsov; Institute of Materials Research and Engineering, Singapore

Nanoantennas and metasurfaces based on high-refractive index dielectric and semiconductor materials represent the new branch of resonant low-loss nanophotonics paving the way to real-life applications [1]. They can resonantly enhance light-matter interaction and control the phase and amplitude of scattered, transmitted or reflected light with nanoscale resolution. Recently, the toolkit of dielectric nanoantennas and metasurfaces has been strongly enriched by adding active and tunable functionalities. Active nanoantennas can enhance and emit light in preferred directions, becoming well-controlled nanoscale light sources. Tunable nanoantennas can dynamically switch the phase and amplitude of scattered light providing possibilities for nanoscale dynamic wavefront control. In this presentation, I will review our recent progress in the field of active and tunable dielectric nanoantennas and metasurfaces. I will show our demonstrations of nanoantenna lasers using the concept of bound states in the continuum (BIC) in dielectric nanoantenna structures interfaced with different active media [2-4]. This research paves the way to nanoscale laser devices with wavelengths ranging through the whole visible spectrum. Also, I will present our research on tunable nanoantennas and metasurfaces, demonstrating spatial light modulators with individually controlled micron-scale nanoantenna-based pixels [5]. These devices can provide novel solutions for 3D holographic displays [6] and compact solid-state Light Detection and Ranging (LiDAR) devices for autonomous vehicles.

References:

- 1) A. I. Kuznetsov et al., "Optically resonant dielectric nanostructures", *Science* 354, aag2472 (2016).
- 2) S. T. Ha et al., "Directional lasing in resonant semiconductor nanoantenna arrays", *Nature Nanotech.* 13, 1042 (2018).
- 3) V. Mylnikov et al., "Lasing Action in Single Subwavelength Particles Supporting Supercavity Modes", *ACS Nano* (2020), DOI: 10.1021/acsnano.0c02730
- 4) M. Wu et al., Room-temperature lasing in colloidal nanoplatelets via Mie-resonant bound states in the continuum. *Nano Letters* 20, 6005–6011 (2020).
- 5) S.-Q. Li et al., "Phase-only transmissive spatial light modulator based on tunable dielectric metasurface", *Science* 364, 1087 (2019).
- 6) W. Song et al., "Large-scale Huygens' metasurfaces for holographic 3D near-eye displays", arXiv:2010.04451.

10:50 PM BREAK

SESSION EQ08.08: Acoustic, Elastic and Mechanical Metamaterials
Session Chairs: Wenshan Cai and Thomas Zentgraf
Tuesday Morning, December 7, 2021
EQ08-Virtual

8:00 AM *EQ08.08.01

Topological Guiding of Stress Waves in Bolted Plate Structures Chun-Wei Chen¹, Rajesh Chaunsali², Johan Christensen³, Georgios Theocharis² and Jinkyu Yang¹; ¹University of Washington, United States; ²LAUM, France; ³Universidad Carlos III de Madrid, Spain

In the past decades, topological boundary states have been demonstrated in various fields, including photonics, electronics, and acoustics. However, their realization in mechanical systems, particularly in the setting of continuous plate structures, has been relatively unexplored. In this presentation, I will talk about how we can achieve topological guiding of stress waves in a ubiquitous platform of bolted plate structures. I will focus on the realization of three mechanical waveguiding phenomena: (1) 1D edge-state in a Z-shaped domain wall mimicking the quantum spin Hall effect; (2) asymmetric 0D corner localization in the same domain wall; and (3) another type of special non-propagating 0D localized state, so-called a mechanical analog of the Majorana bound states. The first two are realized in an ordered arrangement of embedded bolts in a hexagonal pattern, while the last is achieved using the non-periodic yet ordered mechanical system in the Kekulé distorted pattern. For experimental demonstrations, we adopt a laser Doppler vibrometer to scan the entire plate and create a 2D wavefield, which agrees well with numerical predictions. The topological waveguiding technique investigated in this study has a potential to enhance the degree of freedom in controlling stress waves in plate structures, which can be used for a variety of engineering applications, e.g., energy harvesting, vibration filtering, and structural health monitoring / nondestructive evaluations.

References

1. C. Chen, R. Chaunsali, J. Christensen, G. Theocharis, J. Yang, "Corner states in a second-order mechanical topological insulator," *Communications Materials* (in print, arXiv:2009.03525).
2. C. Chen, N. Lera, R. Chaunsali, D. Torrent, J. Vicente Alvarez, J. Yang, P. San-Jose, J. Christensen, "Mechanical analogue of a Majorana bound state," *Advanced Materials*, 1904386 (2019).
3. R. Chaunsali, C. Chen, J. Yang, "Experimental demonstration of topological waveguiding in elastic plates with local resonators," *New Journal of Physics*, 20: 113036, 2018.
4. R. Chaunsali, C. Chen, J. Yang, "Subwavelength and directional control of flexural waves in zone-folding induced topological plates," *Physical Review B*, 97: 054307, 2018.

8:30 AM EQ08.08.03

Interference, Scattering and Transmission of Acoustic Phonons in Si Phononic Crystals Yang Li¹, Adrian Diaz¹, Xiang Chen¹, David McDowell² and

Younging Chen¹; ¹University of Florida, United States; ²Georgia Institute of Technology, United States

In this talk, we report a multiscale study of the phonon transport processes in Si phononic crystals (periodic pore structures) using the concurrent atomistic-continuum method. The transient processes of phonon scattering and transmission in Si phononic crystals are visualized. The nature of phonon transport is demonstrated to be strongly dependent on the relation between the phonon wavelength and the period length, p , and the neck width, n , of the phononic crystal. Three distinct regimes have been observed: (1) phonons with wavelengths equal to $2.9p$ or larger propagate predominantly ballistically, which is accompanied by specular reflection of varying extents, depending on the wavelength of the phonons; the properties of these phonons are consistent with the phonon dispersion relations of a homogenous and harmonic system; (2) phonons with wavelengths $<n$ are partly reflected by the pore boundaries and partly propagate ballistically in the solid regions of the necks; two types of vibrational modes are identified: the single crystal Si phonon modes, and the vibrational modes resulting from internal surface scattering; (3) phonons with wavelength close to p are most strongly scattered, and the internal surface-related modes dominate the transport; these modes have the slowest group velocities and lowest energy transmission, and the transport is predominantly diffusive even for specimens originally at zero temperature. For phononic crystals that contain a single crystal heater at their center, the interface between the single crystal and the phononic structure provides a strong resistance to short wavelength phonons, leading to predominantly diffusive phonon transport and an average energy flux that is two orders of magnitude lower than a same-sized single crystal specimen.

8:45 AM EQ08.08.04

Late News: Exceptional Light Capturing Metamaterial for Solar Fuel Generation Joel Loh and mahdi Safari; University of Toronto, Canada

Abstract: Metamaterials are a new class of artificial materials that can achieve electromagnetic properties that do not occur naturally, hence they can also be a new class of photocatalytic structures. Harvesting primarily photonic energies to drive catalytic hydrogenation of carbon dioxide to methanol leads to highly sustainable fuel production in a solar refinery. Due to the limited selection of plasmonic metals in the visible, indirect catalysis is commonly performed with a plasmonic material attached to a catalytic material, via charge excitation and transfer. Photo-absorbing catalysts are sometimes achieved with stoichiometric bandgap modifications or with light trapping structural support that uses internal reflections, which can lead to catalytic trade-offs in the former and low internal light intensities in the latter. Here we show that metal catalysts can achieve photonic amplification and broadband absorption by decoupling optical properties from material composition as exemplified with a ZnO/Cu metamaterial surface comprising periodically arranged nanocubes. By refractive index engineering towards an index near that of vacuum, and via generalized sheet boundary conditions, it is possible to achieve a virtual perfectly absorbing copper film that absorb 98% of the visible without any modification of stoichiometric composition. The combination of plasmonics and broadband absorption doubles the electric field intensities across the absorption range and within the plasmonic band. This enhances catalytic rates by up to a factor of $\times 216$, in comparison to $\times 2$ to 4 enhancements of ZnO/Cu nanoparticles or films. The metamaterial catalyst shows consistent methanol production even at 50° incidence, which negates the need for solar tracking. These results show that metamaterials can act as a singular light harvesting device that collect and concentrate a broad band of the visible spectrum to substantially enhance photocatalysis of important reactions. We anticipate that achieving perfect absorption and confining electromagnetic fields within a nanoscale layer, through photonic designing of miniscule amounts of catalytic materials, which also circumvents low light penetration into bulk powders or pellets, can be a uniquely valuable and energy-efficient approach to photocatalyst engineering.

9:00 AM EQ08.08.05

Chiral Trabeated Elastic Meta-Beam with a Complete Bandgap Mechanism Jeonghoon Park, Dongwoo Lee, Yeongtae Jang and Junsuk Rho; Pohang University of Science and Technology, Korea (the Republic of)

Lots of research have been carried out to utilize elastic metamaterials for vibration reduction. Among them, flexural metamaterials have the advantage of being able to implement a bandgap in the low-frequency region but have a limitation in that it can reduce only the flexural waves. To break the limitation, we propose a novel complete bandgap mechanism created by overlapping a flexural and longitudinal bandgap to attenuate the propagation of all mechanical waves in the low-frequency region. To demonstrate the complete bandgap mechanism, a chiral trabeated elastic meta-beam has been proposed to realize a complete bandgap in periodically arranged beam-shape structures. By utilizing the longitudinal-torsional coupling characteristic of the chiral trabeated meta-beams, which are not found in achiral meta-beams, not only the flexural bandgap but also the longitudinal-torsional bandgap can be implemented in the same frequency region. We introduce an analytic model for the chiral trabeated meta-beam, and the dispersion curve is numerically calculated. We also calculate the dispersion curves from the finite element method, and it is confirmed that numerically and analytically calculated dispersion curves are in good agreement. It allows us to identify the complete bandgap region of the chiral meta-beam. We experimentally observe the complete bandgap in which all mechanical waves were inhibited. The chiral trabeated elastic meta-beam with the complete bandgap mechanism proposed in this study effectively reduces elastic waves and vibrations.

9:05 AM EQ08.08.06

Computational Design of Multifunctional Metamaterials for the Improved Combustion Performance Jose Ceja and Sungwook Hong; California State University, Bakersfield, United States

Aluminum nanoparticles (ANPs) are very promising additives in the combustion applications owing to their high energy density with an increased burning rate.¹ Unfortunately, the ANPs are easily aggregated, leading to an increase in their particle size, and thus lowering the combustion performance. This is primarily because the ANPs have a very high reactivity. As such, recent efforts have been made to synthesize novel metamaterials using ANPs and hydrocarbon precursors. For example, ANPs could be effectively coated by hydrocarbon precursors to lower their reactivity, thus preventing sintering effects of ANPs. However, an effect of precursor types of hydrocarbons on sintering behaviors of ANPs has yet to be understood at the molecular level. Here we perform reactive molecular dynamics (RMD) simulations using on ReaxFF² to investigate thermal behaviors of hydrocarbon coated ANPs. In particular, we employed different types of carbon precursors to evaluate the sintering behaviors of ANPs. Our RMD simulations suggest detailed reaction steps for the sintering process of the bare/hydrocarbon coated ANPs. Therefore, our RMD simulations will help provide a valuable input for experimental synthesis of a novel metamaterial for the improved combustion performance.

S.H. and R.E. acknowledge a start-up funding from School of Natural Science, Mathematics and Engineering at California State University, Bakersfield (CSUB).

References

- [1] Yetter, R. A.; Risha, G. A.; Son, S. F. Metal Particle Combustion and Nanotechnology. Proc. Combust. Inst. **2009**, 32, 1819–1838
- [2] Senftle, T. P.; Hong, S.; Islam, M. M.; Kylasa, S. B.; Zheng, Y.; Shin, Y. K.; Junkermeier, C.; Engel-Herbert, R.; Janik, M. J.; Aktulga, H. M. The ReaxFF Reactive Force-Field: Development, Applications and Future Directions. npj Comput. Mater. 2016, 2, 15011.

9:10 AM EQ08.08.07

Optical Response of Spherical Cavity with Temperature Effect in the Presence of Yukawa Potential Varsha Yadav¹, Mohamed Kria², L. M. Pérez³, V. Prasad¹, D. Laroze³, [Gen Long](#)⁴ and El Mustapha Feddi²; ¹University of Delhi, India; ²Mohammed V University in Rabat, Morocco; ³Universidad de Tarapacá, Chile; ⁴Saint John's University, United States

In the present study, we have investigated the effect of temperature and geometrical confinement on the behavior of spherical cavities with Yukawa potential presence inside the cavity within effective mass approximation. Using the Finite-element method, we have calculated the energy eigenvalue with the geometric and temperature effects into consideration. The optical transition from the ground to the excited state shows a blue shift in optical absorption coefficient and refractive index changes with an increase in temperature. The increase in the geometric size of the spherical cavity causes the redshift in the optical resonance peaks.

9:15 AM EQ08.03.05

Variable Stiffness Metamaterials to Tune Soft Robot Material Properties [Elze Porte](#), Sreekalyan Patiballa, Nidhi Pashine, Sophia Eristoff, Trevor Buckner and Rebecca Kramer-Bottiglio; Yale University, United States

Mechanical metamaterials can be used to alter the material behavior of soft robots, creating new possibilities to control deformations and enhance their performance. For example, auxetic structures have been embedded in elastomer capacitive sensors to increase the sensor sensitivity through a reduction in the Poisson's ratio. However, the stiffness of the embedded metamaterials needs to be much larger than the stiffness of the soft robots to retain the metamaterial properties. The larger stiffness often limits the range of motion and requires larger actuation forces. In this work, we present a variable stiffness metamaterial that can switch between exhibiting the properties of a metamaterial and soft elastomer. The variable stiffness is achieved by making auxetic structures from a Field's metal-silicone composite. The Field's metal is solid at room temperature and melts around 65°C, giving the composite a stiffness change around the melting temperature. The variable stiffness auxetic structure is embedded into a soft elastomer matrix representative of a soft robot. We investigate the mechanical behavior of auxetic structures with different architectures and Poisson's ratios embedded in different soft elastomers. We measure the Poisson's ratio and stiffness of the embedded structures during tensile tests. The results indicate that the material properties are dominated by the metamaterial in a stiff state (e.g., low Poisson's ratios) and by the elastomer in a soft state (e.g., enabling large strains, Poisson's ratio of 0.5). We show that the mechanical behavior of the embedded structure is both dependent on the rule of mixtures for composites and the architecture of the metamaterials. The Poisson's ratio of the embedded structure was lowest when the stiffness difference between the auxetic and elastomer matrix was highest, which was expected based on the rule of mixtures. We found that the Poisson's ratio of the auxetic structure was not a good indication of the Poisson's ratio when it is embedded into the elastomer. The auxetic structure with the lowest Poisson's ratio did not necessarily result in the lowest Poisson's ratio when embedded into the elastomer. Embedding the auxetic into an elastomer means that all voids in the structure are filled with elastomer, which changes the forces on the structure when strained. This means that for the design of embedded metamaterials both the stiffness of the components and the architecture of the metamaterials should be considered. We showcase the utility of the variable stiffness metamaterials by embedding them into soft capacitive sensors. The sensors show a high sensor sensitivity when measuring small strains (<5%) in the stiff state of the metamaterials (room temperature). When the auxetic structure is softened (>65°C) the sensors can be used to measure large strains (>10%) and require lower forces to be stretched. In conclusion, we developed a variable stiffness mechanical metamaterial that can be embedded in soft robotic structures to switch between favorable properties.

SESSION EQ08.09: Optical Metasurfaces
Session Chairs: Wenshan Cai and Junsuk Rho
Tuesday Afternoon, December 7, 2021
EQ08-Virtual

6:30 PM *EQ08.09.01

Nonlocal Metasurfaces [Andrea Alu](#); City University of New York, United States

In this talk, we discuss our recent theoretical and experimental progress in the area of metasurfaces, in particular on the role of engineered nonlocality to enable

a new degree of control over spectral and coherent features, in addition to wavefront manipulation.

We demonstrate frequency-selective and wavefront-selective responses based on these principles, of interest for augmented reality and secure communication applications.

We also discuss the impact of these concepts to manipulate thermal emission and photoluminescence and realize efficient, compact and highly flexible optical sources.

7:00 PM *EQ08.09.02

Optical Metasurfaces for Generating Customized Polarization Profiles [Xianzhong C. Chen](#) and Yuttana Intaravanne; Heriot-Watt University, United Kingdom

The polarization of light, as a fundamental degree of freedom, has been key to many applications ranging from quantum to classical optics. Light fields with spatially inhomogeneous polarization and intensity distributions play an increasingly important role in photonics due to their peculiar optical features and extra degrees of freedom for carrying information. Optical metasurfaces are ultrathin inhomogeneous media with planar structures of nanopatterns that can manipulate the optical properties of light at the subwavelength scale. The unprecedented capability of optical metasurfaces in the manipulation of the light's polarization at subwavelength resolution has provided an unusual approach for generating various polarization profiles. A compact metasurface platform has been demonstrated to arbitrarily engineer a polarization profile that is very difficult or impossible to realize with conventional optical elements. In this talk, we are going to report our recent progress on ultrathin metasurface devices for the realization of customized polarization profiles. The compact metasurface devices with customized polarization profile can greatly expand the range of applications of integrated optics in polarization topology, optical tweezers, nanolithography and photoalignment.

7:30 PM EQ08.09.04

Engineered Hydrogenated Amorphous Silicon for Functional Metasurfaces Working at the Visible Frequencies [Younghwan Yang](#)¹, Gwanho Yoon² and Junsuk Rho¹; ¹Pohang University of Science and Technology, Korea (the Republic of); ²Seoul National University of Science and Technology, Korea (the Republic of)

Dielectric metasurfaces which consist of periodic subwavelength structures have emerged as alternatives to conventional bulk refractive optical elements. Due to the requirement of miniaturization in commercial products such as smartphones, endoscopes, and LiDAR sensors, metasurfaces gain the attentions of industrial engineers. However, they suffer high production costs due to the high deposition cost of visibly transparent dielectrics including titanium dioxide, gallium nitride, and crystalline silicon. Here, we suggest engineered hydrogenated amorphous silicon, which is visibly transparent and exhibits a high-refractive index at the full-visible spectrum. It is deposited with plasma-enhanced chemical vapor deposition, which is commercially used for the deposition of large-area silicon-type films. We manipulate substrate temperature, chamber pressure, gas ratio and plasma power to obtain low-optical losses films at visible and we found that its optical losses are highly suppressed at the temperature of 200 degrees. Also, the chamber pressure is highly related to the complex refractive index and 45 mTorr of it makes the lowest extinction coefficient at the visible frequencies. We conducted X-ray diffraction and Raman spectroscopy and we found that lower extinction coefficient is suppressed as Si-H bonds increase. We also demonstrate beam-steering dielectric metasurfaces which steer the beam at a desired angle. We experimentally measured conversion efficiencies of 75%, 65%, and 42% at the wavelength of 635, 532, and 450 nm. Considering the high CMOS compatibility of hydrogenated amorphous silicon, it will be the dominant material for the commercialization of metasurfaces operating at the visible frequencies.

7:45 PM EQ08.09.05

Dynamically Tuneable Reflective Structural Colouration with Electroactive Conducting Polymer Nanocavities [Stefano Rossi](#) and Magnus P. Jonsson; Linköping University, Sweden

Displays form an integral part of modern society while they at the same time are responsible for a significant part of our energy consumption. The limited room for further improvement of emissive displays motivates the development of a complementary energy-effective reflective-based technology. However, it has been challenging to develop a high-performance e-paper in colour, since it is not only sufficient to optimize colour quality (chromaticity) but also to achieve high absolute reflection, having to rely only on ambient light. Recent research has explored various approaches to create highly reflective surfaces based on structural colouration of thin-film cavities, plasmonic or dielectric metasurfaces. These systems have further been combined with functional materials like liquid crystals, phase changing or electrochromic materials to switch such reflective surfaces on/off. However, most of those solutions suffer from low brightness or limited chromatic tunability. In addition, the traditional RGB subpixels division is not efficient for reflective displays, causing the loss of 2/3 of the light to reproduce a primary colour, which adds to the other losses of the optical system. To circumvent this issue, we need to develop reflective pixels with tuneable colours (monopixels) instead of relying on neighbouring subpixels with fixed colours. Recently, the use of materials with electrochromic properties to modulate nanooptical cavities and plasmonic devices has been proposed as a possible solution, but up to date no full tunability in the visible has been obtained yet.

We propose here a tuneable reflective nanooptical cavity that uses an electroactive conducting polymer (thieno[3,4-b]thiophene) as the actuating spacer layer, replacing the dielectric spacer in a conventional metal-insulator-metal (MIM) optical cavity. The cavity was fabricated with a thin semi-transparent layer of gold and chromium and bulk aluminium mirror, and it works combining both a broadband absorber and Fabry-Pérot effect to give a good overall reflectance, while also offering chemical stability. Integrating the nanocavity in an electrochemical cell, the doping and de-doping of the polymer spacer provided reversible tuning of the cavity's structural colour throughout the entire visible range and even beyond. The results indicated that the main working principle for the colour variation is the thickness change associated with the doping state of the polymeric spacer by counter-ions swelling, but a synergistic effect with refractive index change may also be possible. Furthermore, the cavity provided high peak reflectance (50-60%) with a difference within 10% between the reduced and oxidized states of the polymer. Both cyclic voltammetry and chronoamperometric techniques were investigated for the switching and we obtained a maximum wavelength change of 430nm for a nanohole-assisted optical cavity.

Our electroactive cavity concept may find particular use in reflective displays, by opening for tuneable monopixels that eliminate losses in brightness for traditional subpixel-based systems. Future work will preferably address remaining challenges such as long-term stability and improvement of uniformity, for example, by exploring alternative polymers, and strategies for improved polymer-metal adhesion. We believe that the presented concept to place functional polymers inside optical nanocavities may be used for other applications, like other types of tunable metasurfaces, as well as to study the polymers themselves, for example, using colour variations to extract information about spatial and temporal polymer thickness variations.

SESSION EQ08.10: Topological Metamaterials
Session Chairs: Junsuk Rho and Joel Yang
Tuesday Afternoon, December 7, 2021
EQ08-Virtual

9:00 PM *EQ08.10.01

High Dimensional Optical Meta-Devices—Classical to Quantum Mu Ku Chen, Xiaoyuan Liu, Jingcheng Zhang, Jiaqi Yuan and [Din-Ping Tsai](#); City University of Hong Kong, Hong Kong

Meta-surface can achieve light manipulation by the artificial nanoantenna array in a compact size. Various meta-devices have been demonstrated according to demands in Optics lately. For applications of full-color imaging and sensing, the correction of chromatic aberration is an important issue. Here, we developed the integrated-resonant unit to incorporate with the geometric phase method to realize achromatic meta-lens. The phase of different wavelengths can be compensated specifically. The full-color imaging is demonstrated by using GaN-based achromatic meta-lens. A 60 by 60 achromatic meta-lens array is used to implement the light field imaging system. The depth and moving speed of dynamic objects are achieved. A new type of high-dimensional quantum entanglement light source is demonstrated by using a meta-lens array which is composed of 10 by 10 meta-lens array. The multi-focusing spots can be delivered to the nonlinear crystal simultaneously and generate the multi entangled photon pairs. We demonstrated 2-, 3- and 4-dimensional two-photon path-entanglement with different phases coded by the meta-lenses. It is significant progress for the quantum light source and quantum applications such as optical quantum computation, quantum communication, and quantum cryptography. We have developed optical meta-devices for beam deflection and reflection, polarization control and analysis, holography, second-harmonic generation, laser, tunability, imaging, color display, focusing of light, multiplex color routing, light-field sensing, and high-dimensional optical quantum source. The meta-devices will come into our real-life very quickly because novel advantages of meta-devices are their novel properties, customizable, small size, lightweight, high efficiency, better performance, broadband operation, lower energy consumption, and Semiconductor process compatibility for mass production.

9:30 PM *EQ08.10.02

Metamaterial Systems Manifesting Non-Abelian Topology [Che-Ting Chan](#); Hong Kong Univ of S&T, Hong Kong

In recent years, topological phases protected by various symmetries have been extensively studied. Most topological systems that have been studied to date, including topological metamaterials, can be described using topological invariants that are integers. Very recently, the notion of non-Abelian topological

charges have been suggested to describe the properties of PT symmetric systems carrying three or more bands. Different from the Abelian topological viewpoint which is focused on a single band or band gap, these non-Abelian charges involve the simultaneous description of two more bulk bands and support non-trivial edge states that inherit the non-Abelian topological features. Furthermore, a system with an even or odd number of bands will exhibit noticeable differences in topological charge classifications. We designed parity and time-reversal (PT) symmetric models with 3 or 4 gapped bands as prototypical examples and we used transmission line networks to realize and characterize such systems experimentally. For the 3-band system, the non-Abelian topological charges belong to the quaternion group Q8 that describes the frame rotation of the eigenstate triad. We experimentally observed and characterized the eigenstate-frame rotation for various elements in the quaternion group. In addition, we proposed a non-Abelian quotient relation that predicts the distribution of edge/domain-wall states. For the 4-band system, the non-Abelian charges belong to the generalized quaternion group Q16, in which two new classes of topological charges emerge as well as edge states being special to the even-band systems. These non-Abelian charges are also experimentally observed through the 4D rotations of the eigenstate-frame. The corresponding edge/domain-wall states can also be described using the non-Abelian quotient relation. Being special to the even-band systems, we can obtain the domain-wall charge -1 without the assumption of the basepoint. Our prototypical systems offer a platform for the characterization and manipulation of non-Abelian topological charges, which may lead to interesting observables such as trajectory-dependent Dirac/Weyl node collisions in two-dimensional systems and various admissible nodal line configurations in three dimensions.

10:00 PM *EQ08.10.03

Manipulating Quantum Interference with Lossy Bianisotropic Metasurfaces Hong Liang¹, Tsz Kit Yung¹, Kai Ming Lau¹, Jiawei Xi¹, Wai Chun Wong¹, Shengwang Du², Wing Yim Tam¹ and Jensen Li¹; ¹Hong Kong University of Science and Technology, China; ²The University of Texas at Dallas, United States

Metasurfaces can lead to promising usage in quantum optics based on their freedom in wavefront control by engineering meta-atom's structures and resonances. Here, we numerically investigate how quantum interference can be controlled by using bianisotropic or inhomogeneous metasurfaces based on the Lindblad master equation formulation. By considering a bianisotropic metasurface with material loss from metal, we numerically demonstrate an asymmetric control of quantum interference with an origin from an exceptional point of the metasurface in the classical regime. We will also discuss possible experimental demonstration on measuring two photon coincidence by focusing the light using the same metasurface on a single photon avalanche diode (SPAD) camera.

10:30 PM EQ08.10.04

Novel Magnetic Nanostructures on Flexible Glass Guinevere Strack^{1,2}, Yassine AitElAoud³, Richard M. Osgood³ and Alkim Akyurtlu^{1,2}; ¹Printed Electronics Research Collaborative (PERC), United States; ²University of Massachusetts Lowell, United States; ³Optical and Electromagnetic Materials Team, US Army Combat Capabilities Development Command Soldier Center (DEVCOM Soldier Center), United States

Control over nanostructure fabrication on flexible substrates, in particular, 2D arrays and patterns, has been explored using traditional techniques such as e-beam lithography; however, the need for scalable fabrication strategies has resulted in a range of approaches, including nanoimprinting and nanosphere lithography. These techniques involve stamping a pattern into a polymer or assembling micro or nano polymer spheres to serve as a template or mask. In our previous work, we explored a range of approaches to fabricate ordered magnetic nanoparticle arrays on rigid or flexible substrates using nanosphere lithography.¹ One of the aforementioned fabrication methods relies on templating and thermal decomposition. The technique employs self-assembled polystyrene spheres, which serves as the template. A thin layer of metal is deposited onto the spheres and then the metal-coated polymeric pattern is subjected to temperatures high enough to degrade the polymer template and leave behind a metallic nanostructure. The resultant structure depends on several materials properties and process parameters, including the melting temperature and thickness of the metal, the substrate material, the size of the polymer template, and the heating parameters, such as the ramp time and the holding temperature. Using this method, we have fabricated Au, Au-Co, and Co metallic nanoparticle arrays on Si wafer and flexible glass substrates.² In addition, novel nanostructured films have been fabricated using thin layers of Ni and Co, including hollow hemispheres, and a structure with nanometric brain-type folding.

For the thermal degradation approach, we also applied intense pulsed light (IPL) to the metal-coated polymeric patterns to induce rapid heating on a millisecond time scale. The high energy density of the applied IPL causes the metal layer to heat enough to degrade or partially degrade the polymer template. The remaining structure is a pattern based on the original shape of the polymer template.³ The nanostructure shape and pattern depend on materials properties and process parameters, including the substrate material and the thickness and type of the metal film. Given that the application of IPL causes local heating, low temperature substrates—such as thermoplastics, textiles, and paper—can be used.

One of the substrates used in both fabrication approaches is flexible glass. This substrate is suitable for optical characterization using a Vis-NIR spectrometer with integrating sphere. Understanding the unique optical properties of each metasurface can enable novel applications, such as flexible plasmonic materials and reconfigurable magnetic materials.

1) *Fabrication Strategies for Large-Area, Flexible Magnetic Nanoparticle Arrays*. G. Strack, Y. AitElAoud, D. Slafer, R. M. Osgood III, and A. Akyurtlu, 2020 MRS Meeting, Boston, MA; virtual format; oral presentation F.FL03.03.09

2) *Fabrication of Ordered Au-Co Nanoparticle Arrays*. G. Strack and A. Akyurtlu, 2020 IEEE International Symposium on Antennas and Propagation and USNC-URSI Radio Science Meeting, Montreal, QB (virtual); 2-page paper <https://usnc-ursi-archive.org/aps-ursi/2020/pdfs/0000035.pdf>

3) *Large area nanoparticle arrays and method of making thereof*. G. Strack, Y. AitElAoud, R. M. Osgood III, and A. Akyurtlu; US Prov. Serial No. 63/04,0567 filed June 18th 2020

SESSION EQ08.11: Novel Design and Devices
Session Chairs: Wenshan Cai and Thomas Zentgraf
Wednesday Morning, December 8, 2021
EQ08-Virtual

8:00 AM *EQ08.11.01

Accelerating the Design of Photonic Metamaterials by Deep Learning Yongmin Liu; Northeastern University, United States

Over the past decades, we have witnessed tremendous progress and success of photonic metamaterials. By tailoring the geometry of the building blocks of metamaterials and engineering their spatial distribution, we can control the amplitude, polarization state, phase and trajectory of light in an almost arbitrary

manner. However, the conventional physics- or rule-based approaches are insufficient for designing multi-functional and multi-dimensional metamaterials, since the degrees of freedom in the design space become extremely large. Deep learning, a subset of machine learning that learns multilevel abstraction of data using hierarchically structured layers, could potentially accelerate the development of complex metamaterials and other photonic structures with high efficiency, accuracy and fidelity.

In this talk, I will present our recent works that employ advanced deep learning techniques to design and evaluate distinct photonic metamaterials, including 2D and 3D metamaterials that exhibit pronounced chiral or anisotropic responses [*ACS Nano* 12, 6326 (2018); *Advanced Materials* 31, 1901111 (2019)]. Our results show that deep learning, as a data-driven approach, can help to unveil the highly nonintuitive and nonlinear structure-property relationship in metamaterials. The developed deep learning models, after training, can evaluate the optical responses of metamaterials and inversely design them in less than seconds. Moreover, the model capacity can be substantially strengthened in use as we add more information into the database. This feature is fundamentally different from conventional approaches, in which almost every new design has a raw start, without contributions from prior experiences. Deep learning and other artificial intelligence techniques are currently transforming the areas of optical design, integration and measurement. More exciting advancements are anticipated as researchers with different background collectively contribute to this emerging field where photonics and artificial intelligence merge [*Nature Photonics* 15, 77 (2021)].

8:30 AM EQ08.11.02

Inverse Design of Spectrally Sensitive Multiband Absorbers Using Pruned Neural Networks [Sunae So](#) and Junsuk Rho; Pohang University of Science and Technology, Korea (the Republic of)

Recent advances in deep learning have enabled novel inverse design in the field of nanophotonics [1] by providing a new paradigm for discovering and extracting data representation. These design methods using deep learning have been proven to be particularly efficient in the task of designing multiple structures. Meanwhile, although large deep learning networks are generally known to perform better on a variety of tasks, practical applications require intensive networks that are small in size but perform well. Here, we report an inverse design of spectrally sensitive multiband absorbers using pruned neural networks (NNs) [2]. A five layered metal-insulator-metal structure with top grating structure is proposed and its structural parameters are designed by NNs. To achieve spectrally sensitive designs, additional spectral information of resonant wavelength is provided as well as reflection spectrum. The trained NNs have provided highly robust inverse design results, showing an average spectral error of 0.023. In particular, deep learning design results for several incrementally changing inputs not only demonstrate extremely high design efficiency but also show that deep learning has learned physics from the data. Finally, we discuss a network pruning method that reduces the size of the trained deep learning network with minimal performance degradation. The proposed pruning method leverages the observation of the trained network to guide its pruning, which is expected to significantly reduce the computational cost associated with network reduction.

[1] S. So*, T. Badloe*, J. Noh*, J. Bravo-Abad, and J. Rho. *Nanophotonics* 9(5), 1041-1057.

[2] S. So, Y. Yang, T. Lee, and J. Rho. *Photonics Research* 9(4), B153-B158.

8:45 AM EQ08.11.03

Embedding Statistical Machine Learning Model in End-to-End Design Loops for Multifunctional Metasurfaces [Yihao Xu](#)¹, Wei Ma², Bo Xiong³, Lin Deng¹, Ruwen Peng³ and Yongmin Liu¹; ¹Northeastern University, United States; ²Zhejiang University, China; ³Nanjing University, China

Supported by precisely designed nanostructures, metasurfaces provide an unprecedented means to control light on a completely planar platform. The advantage lies in their versatility and independent optical responses under varied illumination conditions. Conventional design methods for multifunctional metasurfaces usually follow a two-step, top-down process: First, the design goals are decoupled to obtain the phase requirements for each illumination condition. Then, the metasurfaces are assembled by multiplexing single-responsive meta-atoms or assembling multiple phase-tuning mechanisms such as geometric phase and resonant phase. This empirical intervention in the design process impedes the increase in functional complexity and becomes impractical as the number of design goals increases.

In this work, we propose to apply machine learning algorithms to capture the statistical features in the high-dimensional joint distribution of meta-atom design parameters and the corresponding optical responses, promoting a quantitative estimation of the strength of crosstalk between functions. With the help of the estimation, we improve the design capabilities under certain meta-atom design frameworks. Moreover, the developed machine learning model can be seamlessly embedded in the gradient-based and non-gradient optimization process to form an automatic end-to-end design loop of multifunctional metasurfaces. With the easy-to-manufacture single-layer structure, we have experimentally demonstrated metasurface focusing lenses and holograms working in eight controllable channels in the near-infrared region, where each channel is different combinations of incident frequency and polarization.

Our results show that the data-driven photonic design scheme has superior capabilities compared to traditional physical-guided methods, which will accelerate the development of unprecedented devices and systems for optical display, communication, and computing.

9:00 AM EQ08.11.04

Discovery and Insights into Organized Spontaneous Emulsification via Interfacial Self-Assembly of Amphiphilic Bottlebrush Block Copolymers [Xi Chen](#); Tianjin Key Laboratory of Composite and Functional Materials, China

Since the first discovery of spontaneous emulsification, the process has remained uncontrollable for centuries leading to unstable emulsion droplets with limited uses. Herein, it was found by in-situ observation that uniform water-in-oil (W/O) nano-emulsion droplets can be spontaneously formed and self-organized during solvent evaporation. Amphiphilic bottlebrush block copolymers are strongly adsorbed at the water/oil interface to stabilize the droplets, and their rod-like molecular conformation enables the well-control of droplet spherical curvature. After solvent removal, solidified thin films or microparticles with hexagonal closest packed nanopore arrays are produced in one-step templated by the ordered W/O emulsions. Pore diameter is precisely tunable in a wide range via changing spherical curvature of the water droplets dependent on degree of polymerization of the BBPC. The well-ordered porous structures give rise to full-spectrum structural colors. This work provides a general method for scalable production of well-ordered porous materials with greatly reduced energy consumption.

9:15 AM EQ08.11.05

Disordered Nanoparticle-Based Etalon for Fast Gas-Reactive Structural Colors and Sensor Application [Jaehyuck Jang](#), Junsuk Rho and Chunghwan Jung; Pohang University of Science and Technology, Korea (the Republic of)

Etalon, a cavity made from two parallel reflecting surfaces, allows light at resonant frequencies to pass through. The representative form of the etalon is the geometry of dielectric layers sandwiched by thin upper and lower metal slabs. However, the resonant frequency determined by effective optical path length between two reflecting surfaces is fixed once the device is fabricated. Accordingly, several attempts have been made to tune resonant features by replacing

the dielectric layer with phase change materials, phase transition metals (e.g. magnesium through hydrogenation), and gel-type polymer. Chitosan, one of the biopolymers derived from Chitin, has great capability to absorb water molecules from surroundings. Therefore, the metal-chitosan-metal etalon has shown a tunable resonant feature with respect to humidity environment, and proves the potential toward the humidity sensor [1]. However, the response time is rather slow (~ 1500 s) since the metal upper layer inevitably hinders the penetration of gas molecules into the chitosan polymer network. In this study, we would like to introduce disordered nanoparticle-based etalon structure for fast change of optical response (*i.e.* spectrum) and its application toward colorimetric sensors [2]. The gas-response time gets dramatically faster (~ 0.1s) because the disordered metal nanoparticles (MNP) forms membrane pores smaller than the mean free path of penetrating gas, known as Knudsen diffusion. The distance between adjacent MNPs acting as pores is an important factor to determine the response time of the device. Since the inter-distance is determined by the type of ligands attached to the MNP, we compare three types of samples in terms of temporal and spectral features: MNPs with Oleylamine ligand, MNPs with Thiocyanate ligand, and metallic film as the top layer on chitosan-(bottom reflector)-substrate. The entire geometry such as the radius of MNPs, type of ligand, and thickness of each layer is further optimized for the faster response time and sharper resonance features. This disordered nanoparticle-based etalon is next applied to reflective type tunable structural colors. In addition, we demonstrated an image sticker that changes the displayed image in response to external humidity, thus successfully showing the potential toward sensor and anti-counterfeiting application.

References

1. Jang, J. *et al.* Self-Powered Humidity Sensor Using Chitosan-Based Plasmonic Metal-Hydrogel-Metal Filters. *Adv. Opt. Mater.* **8**, 1901932 (2020).
2. Jang, J. *et al.* Disordered nanoparticle-based etalon for fast gas-reactive structural colors and sensor application. (In preparation).

9:30 AM EQ08.11.06

Late News: Bound State in the Continuum in Slab Waveguide Enables Low-Threshold Quantum-Dot Lasing [Mengfei Wu](#)^{1,2}, Lu Ding¹, Randy Sabatini², Laxmi Kishore Sagar², Golam Bappi², Ramon Paniagua Dominguez¹, Edward H. Sargent² and Arseniy Kuznetsov¹; ¹Institute of Materials Research and Engineering, A*STAR, Singapore; ²University of Toronto, Canada

Colloidal quantum dots (CQDs) are a promising gain material for solution-processed, wavelength-tunable lasers, with potential application in displays, communications, and biomedical devices. In this work, a ~ 300 nm-thick film of CQDs engineered for high optical gain is coated over an array of titanium dioxide (TiO₂) cylinders. The structure supports slab waveguide modes which, when coupled to the periodic array, give rise to symmetry-protected bound states in the continuum (BICs). The BICs have minimal radiation loss in the normal direction and thus possess extremely high quality factors. In particular, the BIC arising from a 2nd-order TE-polarized waveguide mode has a good spatial overlap with the gain medium, allowing us to achieve room-temperature CQD lasing with a low threshold of approximately 11 kW/cm² (peak intensity) under nanosecond optical pumping. Our work highlights that BICs are effective, surface-emitting lasing modes that allow versatile device structures to achieve low lasing thresholds.

SESSION EQ08.12: Metasurface and Plasmonic Devices

Session Chairs: Junsuk Rho and Joel Yang

Wednesday Afternoon, December 8, 2021

EQ08-Virtual

6:30 PM *EQ08.12.01

Ultrasensitive and Selective Gas Molecule Detection Using Vertically Oriented Metamaterial Absorber [Takuo Tanaka](#)^{1,1,2}; ¹RIKEN, Japan; ²Tokushima University, Japan

High-sensitive measuring or detecting techniques for biological and chemical components becomes imperative in our daily lives. Among the wide range of techniques, vibration spectroscopy, including infrared (IR) absorption spectroscopy and Raman scattering spectroscopy, is one of the most promising analysis methods due to its intrinsic label-free and noninvasive detection characteristics. But the weak signals caused by the inherently low absorption or scattering of the natural substance severely limits its practical applications. Recently, localized surface plasmon resonance in nanometer-scale metal structures has been shown to produce an enhanced electromagnetic field, and metamaterial-based plasmonic nanostructure using plasmonic-molecular coupling was proposed and high molecular sensitivity was realized [1-4]. However, this high sensitivity was realized only when analyte molecules are located in the vicinity of the localized plasmonic enhanced field (hot spot region); thus, introducing target molecules into the hot spot region to maximize plasmonic-molecular coupling is crucial to developing the sensing technology. To answer this requirement, we designed a metamaterial consisting of a vertically oriented metal-insulator-metal (MIM) structure with a 25 nm channel sandwiched between two metal films, which enables the delivery of molecules into the hot spot regions, offering an ultrasensitive platform for molecular sensing [5]. This metamaterial was applied to carbon dioxide and butane detection. We designed the structure to exhibit resonances at 4033 and 2945 cm⁻¹, which overlap with the C=O and -CH₂ vibration modes, respectively. The mutual coupling of these two resonant modes creates a Fano resonance, and their distinct peaks are clearly observed in the corresponding transmission dips. In addition, owing to its small footprint, such a vertically-oriented MIM structure enables us to increase the integration density and allows the detection of a 20 ppm concentration with suppressed background and high selectivity in the mid-infrared region.

[1] A. Ishikawa and T. Tanaka, *Scientific Reports* **5**, 12570 (2015).

[2] T. Le and T. Tanaka, *ACS Nano* **11**, 9780 (2017).

[3] T. Le, A. Morita, K. Mawatari, T. Kitamori, and T. Tanaka, *ACS Photonics* **5**, 3179 (2018).

[4] T. H. H. Le, A. Morita, and T. Tanaka, *Nanoscale Horiz.* **5**, 1016 (2020).

[5] D.-S. Su, D. P. Tsai, T.-J. Yen, and T. Tanaka, *ACS Sensors* **4**, 2900 (2019).

7:00 PM EQ08.12.02

Metamaterial Absorber for Intensifying Thermal Gradient Across Thermoelectric Device [Wakana Kubo](#); Tokyo University of Agriculture and Technology, Japan

Thermoelectric conversion is a technology based on direct conversion of heat energy into electricity; it is expected to be a promising tool for recovering waste heat for energy saving and more efficient fuel usage [1]. Since a thermal gradient across a thermoelectric device induces a potential difference between the hot and cold sides of the device, technology that increases the thermal gradients is the key for efficient power generation. Several attempts have been made to expand the thermal gradient across thermoelectric devices. Vertical geometric configuration of the thermoelectric bismuth telluride (Bi₂Te₃) device to the surface of a heater is a promising technology to enlarge the thermal gradient across the device. Nevertheless, power generation efficiencies of Bi₂Te₃ based thermoelectric devices remain at ~10%, indicating that further improvements in power generation efficiency are required. Hence, development of novel thermoelectric materials and concepts for improving the thermal gradient are necessary for extending the practical

applications of thermoelectric devices.

To increase the thermal gradient across a thermoelectric device, we utilized the localized surface plasmon resonance as the heat source [2, 3], and proposed the attachment of a metamaterial perfect absorber (MPA) on the surface of a Bi_2Te_3 thermoelectric device to realize a thermoelectric device than can generate electricity under homogeneous temperature environment [4].

In this report, we demonstrated a metamaterial- Bi_2Te_3 thermoelectric generation that can enlarge thermal gradient across a thermoelectric device. We observed an enhancement in output voltages triggered by MPA thermal radiation absorption.

References

- [1] R. Fitriani, B. D. Ovik, M. Long, et al., *Renew. Sust. Energ. Rev.* 64, 635 (2016).
- [2] W. Kubo, M. Kondo, and K. Miwa, *J. Phys. Chem. C* 123, 21670 (2019).
- [3] K. Miwa, H. Ebihara, X. Fang, and W. Kubo, *Appl. Sci.* 10, 2681 (2020).
- [4] S. Katsumata, T. Tanaka, and W. Kubo, *Opt. Express* 29, 16396 (2021).

7:15 PM EQ08.12.03

Directed Self-Assembly of Polymer Grafted Nanocrystal for Ordered 2D Superlattices Boyce Chang¹, Priscilla Pieters², Eric Dailing¹, A. Paul Alivisatos², Yi Liu¹ and Ricardo Ruiz¹; ¹Lawrence Berkeley National Lab, United States; ²University of California, Berkeley, United States

Nanocrystals have received tremendous attention arising from potential applications as metamaterials, plasmonics and semiconductor devices. A key factor in the development of nanocrystal-based devices is the ability to control assembly in a scalable manner. Despite impressive progress in this area, the majority of work have focused on kinetically driven processes such as solvent drying and liquid interfaces, which are undesirable for large scale fabrication. Replacing small molecule ligands with polymer grafts significantly improves processibility, creating particles that resemble star polymers. This allows access to thermodynamically stable structures and create a larger variety of design handles including molecular weight, chain architecture and grafting density. More importantly, the polymeric behavior opens the opportunity for techniques such as solvent vapor annealing and directed self-assembly to induce thermodynamically stable superlattice configurations of polymer grafted nanocrystals (PGNC), dramatically improving their development into potentially scalable devices. Herein, we explore methods to direct the assembly of PGNC 2D superlattices using pre-patterned substrates. A similar process flow utilized in directed self-assembly of block copolymers was implemented to generate lithographically defined patterns. We successfully demonstrate long-range orientational order of PGNCs using periodic stripes. The effects of surface topography, chemistry and PGNC architecture on the quality of the superlattice were investigated. This work serves as a guide to achieving 2D orientational order in PGNCs.

7:30 PM EQ08.04.05

VO_2 Based Dielectric Metasurfaces and Metamaterials for Reconfigurable Optical Systems Applications Jimmy John¹, Aditya Tripathi², Sergey Kruk³, Yael Gutierrez³, Helmut Karl⁴, Fernando Moreno⁵, Yuri Kivshar², Shriram Ramanathan⁶, Zhen Zhang⁶, Hai Son Nguyen¹, Lotfi Berguiga¹, Pedro Rojo-romeo¹, Régis Orobchouk¹ and Sébastien Cuffe¹; ¹Université de Lyon, France; ²The Australian National University, Australia; ³University Campus Ecotekne, Italy; ⁴Universität Augsburg, Germany; ⁵Universidad de Cantabria, Spain; ⁶Purdue University, United States

Metasurfaces and metamaterials have been at the forefront of optical progress in terms of applications over the past decades. With the growth of the telecommunications sector and quantum advances have propelled the requirement for compact, energy efficient and reconfigurable nanophotonic components in an optical system. All-dielectric meta-photonics research, in search for these ideal characteristics is reaching maturity, as optical devices based on dielectric metasurfaces are currently outperforming their conventional counterparts¹. However, the design and fabrication of efficient, switchable, and reconfigurable metamaterial-based components or meta-devices for practical applications² are still in their infancy and remain largely unexplored.

Since most metamaterial-based devices are functionally locked once fabricated, subsequent progress in the search for reconfigurable and switchable nanophotonic components has seen the increasing use of phase change materials, thanks to their stable switchable phases with different refractive indices. This makes them an attractive choice for various applications such as beam steering³, memory devices^{4,5}, electro-optical modulation⁶, neuromorphic computing⁷, metasurfaces and metamaterials^{8,9}.

Among all PCMs, vanadium dioxide (VO_2) is a prototypical example of functional materials exhibiting large changes in physical properties upon specific external excitation. Its easily controllable transition (optically, electrically or thermally at near-room temperatures) and the exceptionally large change in optical properties upon its insulator-to-metal transition (IMT) open interesting possibilities for dynamically tunable optical systems. Above all, change of its atomic structure during IMT is crystalline to crystalline in nature allowing the possibility of repeatability in the design of nanophotonic devices without the creation of defects.

Here, we demonstrate two different platforms and strategies to create highly tunable VO_2 -based building blocks for a multi-application metamaterial based optical system.

Our first strategy is based on VO_2 nanocrystals (NCs) embedded in SiO_2 , in which we show that the multipolar resonances supported by VO_2 NCs can be actively tuned through its insulator-to-metal transition (IMT) and tailored based on its size. By combining Mie theory and Maxwell-Garnett effective medium theory we retrieve the complex refractive index of the effective medium containing VO_2 NCs in SiO_2 . Through this, we show that the resulting NC metamaterial exhibits distinct tunability compared to the unstructured VO_2 thin film. In addition, we also show the possibility of designing these composite NCs in order to achieve refractive index variation with almost no variation in its extinction coefficient during its transition, in other words zero induced extinction value. This property is predominantly important for designing reconfigurable optical system with minimal losses.

Our second strategy is based on embedding a layer of VO_2 coupled to a dielectric metasurface consisting of silicon resonators. We demonstrate designing and fabrication strategy and characterize the resulting metasurface that is designed to support both electrical and magnetic Mie resonances. The interaction between these resonances and the incident light can be tuned depending upon the transition state of the VO_2 , and we show, first, 2 orders of magnitude modulation in metasurface transmission and second, a spectral modulation of near-perfect absorption. These spectral and magnitude modulations are accompanied by hysteresis-like behaviour that can be exploited for versatile memory effects and can find their application in optical communication, memory devices, detectors and sensors.

- 1: 10.1038/nphoton.2017.39.
- 2: 10.1038/nphoton.2017.126.
- 3: 10.1088/2040-8986/abbb5b
- 4: 10.1063/1.4758996
- 5: 10.1109/ACCESS.2020.3006899
- 6: 10.1364/FIO.2018.JW3A.96

SYMPOSIUM EQ09

Cutting-Edge Plasma Processes for Next-Generation Materials Science Applications
November 30 - December 6, 2021

Symposium Organizers

Rebecca Anthony, Michigan State University
Wei-Hung Chiang, National Taiwan University of Science and Technology
Davide Mariotti, Ulster University
Chi-Chin Wu, U.S. Army Research Laboratory

* Invited Paper

SESSION EQ09.01: Plasmas for Bio and Functional Materials
Session Chairs: Rebecca Anthony and Chris Hardacre
Tuesday Morning, November 30, 2021
Hynes, Level 1, Room 104

10:30 AM *EQ09.01.01

Surface Modification and Functionalization of Biomaterials by Plasma and Related Technology Paul K. Chu; City University of Hong Kong, Hong Kong

The interactions between biomaterials and biological tissues and body fluids depend on the surface properties of the biomaterials and biological interactions and response. However, many types of current biomaterials with favorable bulk characteristics cannot produce the desirable biological and biochemical effects and surface modification is one of the effective ways to alter selectively the surface properties of biomaterials and biomedical implants. By means of plasma surface modification, pre-designed surface properties such as biocompatibility and bacterial resistance can be endowed and at the same time, the inherent bulk properties such as mechanical strength can be maintained. Our research group has been conducting research on plasma immersion ion implantation and deposition (PIII&D) for more than 20 years. It is a non-line-of-sight technique and especially suitable for biomaterials and biomedical implants with a complex shape. Moreover, since the interface between biodegradable biomaterials and tissues and body fluids is dynamic, PIII&D offers the unique capability to optimize the interfacial physics and chemistry to achieve controlled and timely degradation and drug release. In this invited presentation, recent research activities in the Plasma Laboratory of City University of Hong Kong pertaining to surface treatment of biomaterials and biomedical devices, especially biodegradable and antibacterial materials, will be described.

Keywords: biomaterials, surface modification, plasma immersion ion implantation, antibacterial properties, osseointegration

11:00 AM EQ09.01.02

Surface Functionalization of Polymeric Surgical Meshes with Antibacterial Properties by Atmospheric Plasma Surface Modification and Silver Nanoparticles Immobilization Amin Zareei, Allison Thornton, Ulisses Heredia, Venkat Kasi and Rahim Rahimi; Purdue University, United States

Inguinal hernia occurs when an intestinal abdominal organ mostly part of small intestine protrudes into the inguinal canal through a weak spot in the abdominal muscles. Such weak spot results in the inner lining of the abdomen to push through the weakened area to form a balloon like sac. Up to date identified associated causes for inguinal hernia include increased pressure on the abdomen, pregnancy, obesity, heavy lifting and continuous coughing and sneezing. Recent data has shown that in the US, at least 10% of the population experiences some type of hernia that requires at least one million of abdominal hernia repair surgery each year. The hernia is repaired by an incision through the skin and then covered with a piece of surgical mesh. The most common material for such surgical meshes used in the US is polypropylene due to inert chemical property, light weight and mechanical strength that could withstand up to 170 mmHg of abdominal pressure. However, the main drawback with such polypropylene meshes (PoM) is bacteria growth induced infection after implanting the mesh in the body within the textile woven structure of the PoM. Such infection is mainly due to uneven topography of the mesh structure and is responsible for up to seven percent of post-operational complications that result in significant health risks and costs for prolonged patient treatment. Therefore, to address this issue, we have developed an innovative two-step process for fabrication of an antibacterial PoM via atmospheric plasma surface modification and functionalization and laser immobilization. First, the surface of the mesh was coated with 50 nm thick organosilicon by atmospheric plasma deposition system to enhance the hydrophilicity of the mesh surface and as a receptor layer for silver nanoparticles (AgNPs). Next, a thin layer of < 1 μ m AgNPs in the form of low viscosity ink was printed on the plasma deposited mesh via inkjet printing as an antibacterial agent. And then, non-destructive laser treatment technique was employed to selectively immobilize the deposited AgNPs onto the mesh. Such technique enables selective delivery of the laser thermal energy to the printed AgNP ink and fuse the particles together whereas the PoM is transparent to

the laser wavelength and would not get damaged under laser beam irradiation. In addition, such fusion enhances sustained antibacterial properties of the mesh by delaying the release of the AgNPs immobilized layer from the PoM when implanted. A systematic study was performed against *Staphylococcus aureus* and *Escherichia coli* to assess the antimicrobial properties of the AgNPs immobilized PoM. Moreover, thermal, optical and mechanical characterizations evidenced no significant effect of plasma surface modification and functionalization and laser AgNPs immobilization on microstructure of the PoM.

11:15 AM EQ09.01.03

Combat Corona Virus with Corona Discharge—Mask and Surface Disinfection Ying Zhong, Sriram Sundar Shankara Narayanan, Libin Ye and Zijian Weng; University of South Florida, United States

Because of the COVID-19 pandemic, there is need to urgently advance a safe, sustainable, and highly efficient disinfection technologies to treat face masks and various surfaces that are regularly exposed to public use. The demand of masks is challenging especially for the societies in less-developed areas across the world. Billions of used masks are threatening the environment as a new source of plastic pollution. Creating a safe and reliable method for mask reuse would help alleviate the situation. To this extent we developed a corona discharge (CD) based disinfection method to efficiently disinfect and recharge face masks simultaneously. Electric field, ions and reactive species generated by CD are the key components causing DNA damage and protein denaturation to effectively disinfect the 1.8 mm thick, dielectric, porous N95 masks. Up to 99.99% reduction in *E. coli* can be easily achieved under 10 mins, consuming only 1.25 W of power. This makes it ideal for affordable and portable disinfection and reuse applications. Further, up to 99.99999% reduction can be achieved after 3 cycles of treatment with optimized parameters. Most importantly, CD can simultaneously restore electrostatic charges on the mask surface to prevent filtration efficiency deterioration. It also provides an efficient disinfection solution for shared surfaces, confined spaces, and possibly open air reduce application of disinfectants and to mitigate the spread of COVID-19. We are also developing a corona discharge (CD) based disinfection robot with for the purpose of automatic and non-contact disinfection. The advance of CD disinfection will help us get better prepared for future pandemics.

SESSION EQ09.02: Plasmas for Catalysis and Energy
Session Chairs: Lorenzo Mangolini and Chi-Chin Wu
Tuesday Afternoon, November 30, 2021
Hynes, Level 1, Room 104

1:30 PM *EQ09.02.01

Non Thermal Plasma Catalysis for Emission Control and Clean Hydrogen Production Chris Hardacre; University of Manchester, United Kingdom

Hybrid non-thermal plasma catalysis has a significant potential to provide a low energy pathway to activate molecules and catalysts to enable processes to operate at lower temperatures than would occur if activated thermally. This talk will show how plasma activation can be utilised to promote the gas phase reactions for emission control and clean hydrogen production. The mechanism of the reactions determined by kinetic analysis and in-situ diffuse reflectance infra-red Fourier transform spectroscopy (DRIFTS) will be shown and how this differs from the thermally activated reactions. A new cell was developed to enable the DRIFTS measurements to be performed in the presence of the plasma. A range of catalysts have been examined including the use of metal organic frameworks which show high levels of stability under plasma activation which opens up the possibility of using them as heterogeneous catalysts in the gas phase which is challenging under normal operating conditions in many cases.

2:00 PM EQ09.02.02

Cold Atmospheric Plasma Deposition of Functional Conductive Polymers Ulisses Heredia, Venkat Kasi and Rahim Rahimi; Purdue University, United States

Conductive polymers such as polypyrrole (PPy), polyaniline (PANI) and poly(3,4-ethylenedioxythiophene) (PEDOT) are extensively used as sensing materials and conductive electrodes in printed and flexible sensors. As sensing materials, conductive polymers provide an electrical response to changes in temperature, gas concentration, humidity and/or radiation exposure that easily couple to simple electronics to achieve real-time detection and wireless readings. Typical synthetic methods for the fabrication of conductive polymer films are complex chemical processes that involve several steps of processing and the use of toxic solvents such as sulfuric acid, N-methylpyrrolidinone, and acetonitrile. Conductive polymers prepared via these methods are required to be in the form of suspended solutions which eventually need to be deposited onto desired substrates through either printing or additive manufacturing process. In addition, the films produced by these methods often exhibit inferior properties due to challenges associated with solvent-substrate incompatibility, poor film adhesion, remnant of toxic solvents in the films and long drying times. In order to address such drawbacks an effective approach is to deposit such functional conductive polymers directly onto the targeted substrates of interest.

Recently, cold atmospheric plasma chemical vapor deposition (CAP-CVD) has become an attractive approach to synthesize and deposit different organic and inorganic functional materials directly onto the desired substrate in atmospheric conditions. In CAP-CVD, conductive polymers are synthesized by plasma polymerization where the precursor of interest is introduced into the plasma stream and polymerized on the substrate by the action of the reactive species present in the plasma glow. Thus, post processing operations like solvent drying or sintering are eliminated. The resultant conductive polymer films can act as active layers to produce printed gas and radiation sensors with high quality, good adhesion, and intrinsic conductivity. Moreover, since this process deposits high quality films at high production rates, it is highly compatible with roll-to-roll manufacturing techniques to produce low cost printed sensors.

As proof of concept, a systematic study on different plasma processing conditions including power, an ionizing gas mix composed of oxygen and argon, and introduction of oxidants such as bromine was carried out on the CAP-CVD polymerization of PANI, PPy and PEDOT. In this work we present our investigation on the optimum processing conditions to deposit high quality conductive polymer films by CAP-CVD as well as the characterization of plasma conductive polymers by using Raman Spectroscopy, ATR-FTIR, TGA and SEM techniques.

2:15 PM EQ09.02.03

Pulsing as an Effective Strategy for the Reduction of the Energy Cost for the Non-Thermal Plasma Synthesis of Ammonia Minseok Kim, Giorgio Nava, Sharma S. Yamijala, Bryan Wong and Lorenzo Mangolini; University of California, Riverside, United States

Ammonia synthesis from N_2 and H_2 through non-thermal plasmas has recently attracted great attention as an alternative to standard ammonia production methods, such as the Haber-Bosch process (HB process). Production of ammonia through the HB process has made a significant positive contribution via

production of fertilizers directly linked to the high crop yields. However, the environmental problems associated with the HB process threatens the sustainable future of mankind with massive anthropogenic emissions, estimated at over 300 million metric tons of CO₂ annually [1]. Non-thermal plasmas could significantly reduce ammonia production associated greenhouse gas emissions as plasma-based reactors can be operated entirely by renewable energy resources. The synergistic effects between catalytic materials and plasmas in particular are being widely investigated to improve the yield and energy cost in plasma-driven ammonia production. One bottleneck in this effort is the lack of a microscopic-level understanding of the interaction between the low-temperature plasma and various materials. In this work, a non-thermal plasma was pulsed with different frequencies, respective to plasma residence time, in order to investigate effects on ammonia yield and related energy costs. The measurements were performed on an RF-driven plasma system including a quartz cylindrical plasma reactor whose diameter was 1", power supply, and matching network. The reaction products were sampled downstream of the reaction zone through a 50 μm orifice into a Residual Gas Analyzer (RGA). We observed a weak dependence of ammonia yield on various metallic catalysts [2]. This is consistent with a reaction mechanism that is initiated by the interaction between plasma-produced atomic nitrogen and the hydrogen terminated surface, via an abstraction mechanism. This pathway is consistent with the results from Born-Oppenheimer Molecular Dynamics (BOMD) simulation, which suggest that the direct surface abstraction pathway is fast and proceeds with near 100% probability. We have also investigated approaches to reduce the energy cost of this process and found that plasma pulsing is an effective strategy to achieve that. Measurements on energy cost was conducted at 60 W with various fraction of nitrogen flow rate per total flow rate (5%~90%). Based on the geometry of stainless-steel cone mesh utilized as a catalytic material, the residence time in the plasma reaction zone is around 40 msec. By decreasing the plasma on-time to 2 msec, it was possible to decrease the energy cost by roughly a factor of four, compared to the continuous plasma-on case. We interpret this measurement according to the following mechanism: plasma-produced atomic nitrogen diffuses to the catalyst surface on a time scale of one millisecond and it is quickly converted to ammonia, but the plasma is then rapidly extinguished to prevent it from dissociating the ammonia as it diffuses back into the reactor volume. In other words, pulsing utilized the electrical power input more efficiently as it is not used to re-dissociate the desired reaction product.

Reference:

- [1] Y. Tanabe et al., Developing More Sustainable Processes for Ammonia Synthesis. *Coordination Chemistry Reviews*, **257**, 2551–2564 (2013).
[2] S. S. R. K. C. Yamijala et al., Harnessing Plasma Environments for Ammonia Catalysis: Mechanistic Insights from Experiments and Large-Scale Ab Initio Molecular Dynamics, *The Journal of Physical Chemistry Letters*, **11**, 10469-10475 (2020).

2:30 PM *EQ09.02.04

Understanding the Cold Plasma Synthesis of Ammonia with Model Catalysts Sophia Gershman¹, Henry Fetsch¹, Fnu Gorky² and Maria Carreon³; ¹Princeton Plasma Physics Laboratory, United States; ²South Dakota School of Mines & Technology, United States; ³University of Massachusetts Lowell, United States

Ammonia is essential for food security due to its use in fertilizers. Currently, ammonia synthesis at industrial scale proceeds via Haber-Bosch (HB) process typically at ~500 C and 500 bar, which is the most energy-consuming process in the chemical industry. Global ammonia production (~249.4 million tons) consumes ~1-2% of the world's energy, 2-3% of the world's natural gas output, and emits over 300 million metric tons of CO₂. With such energy requirements, the HB process is only economically viable at large-scale plants running continuously. Consequently, ammonia synthesis is currently centralized, hampering the access to affordable fertilizers in remote areas. The development of simplified alternatives to HB at milder conditions and compatible with intermittent electric power (e.g. from renewable energy sources) is a critical step toward small-scale, decentralized ammonia production. During the past decade plasma catalytic ammonia synthesis has been driven by the cost-effective implementation of solar and wind sources, that would also reduce the carbon footprint of the process. The possible implementation of non-thermal plasma technology will be only feasible if there is an effective plasma catalytic system in terms of material selection and reactor design. However, to-date there is no fundamental basis for the rational selection of catalytic materials suitable for plasma systems. Selection of catalysts based on fundamental principles would help in developing new materials and further understanding the synergies in plasma catalytic processes.

One of our central hypotheses is that an optimal catalyst for plasma-assisted ammonia synthesis is one that delays the recombination of *adsorbed* hydrogen radicals (H*) into molecular hydrogen (H₂), allowing them to bind instead to the *adsorbed* nitrogen plasma activated species (N^{activated}) to form NH*. We postulated that a delay in recombination of hydrogen radicals can be achieved with catalysts that dissolve hydrogen more easily. Therefore, our interest in oxides stems from the possibility of facilitating hydrogen dissolution at mild reaction conditions. Moreover, oxides may promote NH* formation (an essential step in ammonia synthesis) by not binding strongly with nitrogen. An illustrative example is silica, where the N₂ adsorption obeys a peculiar mechanism governed by short-ranged forces.

Oxides, such as silica, are appealing materials for ammonia synthesis due to their: 1) lower electrical resistivity that can lead to more stable and uniform plasma discharges, a challenge in atmospheric plasmas; 2) readiness to dissolve hydrogen; 3) weakly bonding with nitrogen; 4) high chemical stability in the presence of water and some hydrocarbons, which are typical impurities in natural gas wells (hydrogen for ammonia production is typically obtained from steam reforming of methane), and 5) the presence of a porous structure with accessible pores for guest molecules diffusion. Herein we employ mesoporous silica SBA-15 with unimodal pore size of ~ 7 nm to assess the effect of ordered mesopores with and without being Ag impregnated. Interestingly, our data confirms the dominant presence of N₂ vibrational bands and a marginal benefit in the catalytic performance when using a metal i.e., Ag in this case. At specific discharge conditions SBA-15 performs better than the Ag impregnated mesoporous silica leading to the highest ammonia production of 11,000 ppm. Plasma on/off cycles demonstrate the desorption of ammonia when the plasma was turned off. Which can lead to future optimal reaction conditions for this reactor when adapted to intermittent renewable sources. We were able to measure a vibrational excitation temperature using the optical emission of the second positive N₂ vibrational band of 0.2±0.05 eV for SBA-15 and SBA-15-Ag.

SESSION EQ09.03: NP Synthesis and Processing I

Session Chairs: Paul Chu and Ming Xu
Tuesday Afternoon, November 30, 2021
Hynes, Level 1, Room 104

4:00 PM *EQ09.03.01

Plasma Synthesis of Nanoparticles for Applications in Plasmonics and Energetics Chris Rudnicki, Carla Berrospé Rodríguez, Giorgio Nava, Feiyu Xu, Michael R. Zachariah and Lorenzo Mangolini; University of California, Riverside, United States

The nucleation and growth of nanoparticles in low-temperature plasmas is recognized as a desirable powder synthesis technique. These systems impart a unipolar charge distribution onto particles dispersed within the ionized gas, slowing down growth via agglomeration and typically keeping the particle size well below 10 nm.[1] In addition, plasma-induced heating allows producing high quality single-crystal nanoparticles. While these properties are unique to these gas-phase processing technique, it can be argued that the full potential of low-temperature plasmas for nanoparticle synthesis and processing is still

severely underexplored. This talk will present two applications of low-temperature plasmas for nanoparticle growth that in our opinion suggest that there is significant room for growth in this field.

The first study involves the plasma synthesis of alternative plasmonic materials. Our group has recently shown that titanium and zirconium nitride nanoparticles can be obtained from low-temperature plasma reactors using the corresponding metal chlorides and ammonia as precursor couple.[2, 3] These ceramic materials have high free charge carrier density, showing plasmonic response in the visible part of the spectrum. Compared to standard plasmonic materials such as gold and silver, they are abundant, inexpensive and possess a high melting point, enabling application in high temperature environments. Example of the application of plasma-produce nitride particle for photochemistry and for wavelength-selective thermal emitters will be discussed in details.[4, 5]

The second case to be discussed is centered on the use of low-temperature plasma not to produce high-quality crystalline particles, but rather for the production of amorphous nanoparticles. Simple tuning of process parameters such as plasma power allows producing silicon particles with an amorphous structure. In addition, for the case of silicon particle produced using silane as precursor, we have found that these particle are rich in hydrogen. The hydrogenated amorphous silicon particles are highly desirable for application in nanoenergetics, where they show superior performance compared to their crystalline counterpart in terms of reaction kinetics because of the rapid release of hydrogen from the nanomaterial upon ignition.

1. Lopez, T. and L. Mangolini, *On the nucleation and crystallization of nanoparticles in continuous-flow nonthermal plasma reactors*. Journal of Vacuum Science & Technology B, 2014. **32**(6): p. 061802.
2. Alvarez Barragan, A., N.V. Ilawe, L. Zhong, B.M. Wong, and L. Mangolini, *A Non-Thermal Plasma Route to Plasmonic TiN Nanoparticles*. The Journal of Physical Chemistry C, 2017. **121**(4): p. 2316-2322.
3. Exarhos, S., A. Alvarez-Barragan, E. Aytan, A.A. Balandin, and L. Mangolini, *Plasmonic Core-Shell Zirconium Nitride-Silicon Oxynitride Nanoparticles*. ACS Energy Letters, 2018. **3**(10): p. 2349-2356.
4. Barragan, A.A., S. Hanukovich, K. Bozhilov, S.S.R.K.C. Yamijala, B.M. Wong, P. Christopher, and L. Mangolini, *Photochemistry of Plasmonic Titanium Nitride Nanocrystals*. The Journal of Physical Chemistry C, 2019. **123**(35): p. 21796-21804.
5. Berospé Rodriguez, C., A. Alvarez Barragan, G. Nava, S. Exarhos, and L. Mangolini, *Stabilizing the Plasmonic Response of Titanium Nitride Nanocrystals with a Silicon Oxynitride Shell: Implications for Refractory Optical Materials*. ACS Applied Nano Materials, 2020. **3**(5): p. 4504-4511.

4:30 PM EQ09.03.02

Nonthermal Plasma Synthesis of Indium Nitride Nanoparticles [Alexander Ho](#) and Rebecca J. Anthony; Michigan State University, United States

Indium nitride is a direct bandgap semiconductor with a small bandgap of 0.7 eV. Properties such as high electron mobility and low electron effective mass make this material suitable for a variety of optoelectronic and electronic devices. Indium nitride can also be alloyed with gallium nitride to form a ternary compound whose bandgap can take a value from 0.7 to 3.4 eV allowing for use in applications that span from the infrared to the ultraviolet range of the spectrum. Here we present on our work to synthesize indium nitride nanoparticles. A low-pressure plasma reactor made from a glass tube was supplied with precursor gases of trimethylindium and ammonia along with a background gas of argon. A 13.56 MHz RF power supply was used to generate a nonthermal plasma in the reactor between three external cylindrical electrodes. During synthesis conditions were controlled to obtain nanoparticles with specific characteristics and properties. From image analysis of TEM data, we have been able to obtain indium nitride nanoparticles with a diameter smaller than the Bohr-exciton radius of this material. Average nanoparticle size as small as 3.6 nm with a standard deviation of 0.5 nm have been synthesized. XRD was used to characterize the crystallinity of nanoparticles, by controlling the power delivery to the plasma particle crystallinity was controlled. Primarily crystalline nanoparticles were synthesized at 75 W of forward power with a diffraction pattern consistent with hexagonal indium nitride. Surface analysis of the particles was conducted using FTIR which showed characteristic absorptions from bonds containing indium, nitrogen, oxygen, carbon, and hydrogen. Optical properties of the nanoparticles were probed with photoluminescence measurements and absorption spectroscopy.

4:45 PM EQ09.03.03

Plasma-Enhanced Chemical Vapor Deposition to Produce Highly Energetic Core/Shell Nanostructures of Aluminum [Prawal P. Agarwal](#) and Themis Matsoukas; The Pennsylvania State University, United States

Aluminum (Al)-based nanoenergetic materials have emerged as promising propellants and fuel additives in civilian and defense-related applications due to their superior gravimetric energy density, green combustion, and abundance on the earth. The native oxide layer on the surface of Al particles provides stability during storage, but adds weight, contributes no energy, and acts as a barrier to oxidation under combustion. For particles in the nanometer range, these limitations are serious because the oxide represents a significant fraction of the total mass. Hence, there is a need to eliminate the adverse effects of oxide on the energetic performance of Al nanoparticles. In this work, we demonstrate a nonthermal plasma-enhanced chemical vapor deposition (PECVD) to prepare core/shell nanostructures of Al with significantly improved energy release. We deposit thin fluorocarbon films (CF_x) onto the surface of Al nanoparticles and study their energy release under thermochemical analysis. We suggest that the perfluoro-based plasma films can improve the overall energy released from Al nanoparticles by providing F for the reduction of Al₂O₃ via an exothermic reaction to produce AlF₃, thereby utilizing the oxide to produce energy. We accomplish this by coating Al nanoparticles with F containing film via plasma deposition of a perfluorocarbon precursor. By depositing the right amount of coating, we aim to reduce the oxide in situ. As a result of the removal of the oxide barrier, we can derive maximum chemical energy due to improved contact between oxygen and metallic Al. We prepare the Al/CF_x core/shell nanoparticles using perfluorodecalin (C₁₀F₁₈) as a coating precursor in PECVD for different periods ranging from 30-165 min, corresponding to film thickness from 5 to 22 nm, as measured using high-resolution transmission electron microscopy (HRTEM). The thickness of the deposited films shows a linear relationship with deposition time with a rate of 0.15 nm/min. This allows for nanometer-level control of the film thickness and precise control of the amount of F on the surface of Al. The coated samples and the uncoated control were studied by thermogravimetric analysis (TGA) and differential scanning calorimetry (DSC) to determine the effects of plasma films on their oxidation and energy release. All coated samples show increased weight gain, directly attributable to the conversion of Al into its oxide, and higher energy release relative to the uncoated control. In particular, at 55 min of plasma deposition, we obtain ~50% increase in the amount of energy released relative to the untreated sample. The composition of the plasma films was studied using high-angle annular dark-field (HAADF)-scanning transmission electron microscopy-(STEM)-energy dispersive spectroscopy (EDS), X-ray diffraction (XRD) analysis, and X-ray photoelectron spectroscopy (XPS). The results show the uniform distribution of F on Al nanoparticles and the presence of CF₃, CF₂, CF, and C-C bonds on the surface. The systematic increase of the energy released with deposition time is attributed to the increased amount of F in the coating. Optimum conditions are met when the amount of F matches the amount needed to react with the oxide on the particle surface. Above the optimum thickness, the gravimetric energy decreases because the coating adds more weight than the energy it extracts. In all cases, the energy of the treated particles is higher than that of the untreated control. This increase is further explained by the mechanism of interfacial reactions triggered due to the presence of perfluoro-based plasma films on the surface. XRD analysis along with SEM and TEM micrographs are used to support the claims in the explained mechanism. Thus, we conclude that the nonthermal plasma process has great potential in improving the performance of nanoenergetic materials by converting their native surface oxide into fuel.

5:00 PM EQ09.03.04

Surface Tailored Core-Shell Aluminum Nanoparticles via Two-Step Atmospheric Plasma Surface Modification and Coating [Chi-Chin Wu](#)¹, Scott D. Walck², Jianguo Wen³, Dinesh Thapa⁴ and Rose Pesce-Rodriguez¹; ¹U.S. Army Research Laboratory, United States; ²Service Engineering, United

States; ³Argonne National Laboratory, United States; ⁴Oak Ridge Associated Universities, United States

Core-shell metallic nanoparticles such as nano-aluminum (nAl) are sought-after potential energetic additives due to the high heat of combustion of Al and potentially faster burning rate enabled by the high surface area to volume ratio. This work describes a recent effort conducted at US Army Combat Capabilities Development Command-Army Research Laboratory to increase the reactivity of commercial nAl by a two-step atmospheric pressure plasma surface treatment and coating using custom-made dielectric barrier discharge plasma reactors. The commercial nAl particles of nominal 40-60 nm average size were first treated with a helium (He) plasma for 30 min, followed by a subsequent coating of carbonaceous materials by diluting carbon monoxide (CO) in the He plasma for different durations. The He-plasma treated nAl has thin roughened alumina shell with its thickness more than 40% less than the as-received nAl with an intact single crystalline Al core. High resolution transmission electron micrographs (HRTEM) revealed sporadic crystalline deposits on nAl surfaces and in gaps among particles and short-ordered structure in the amorphous alumina shell for all plasma-treated samples, confirmed to be γ -alumina via electron energy loss spectroscopy (EELS) at the scanning TEM (STEM) mode. All plasma-coated samples after the second step possessed dispersive thin layers of carbonaceous coating, as evident by nanoscale chemical analyses with elemental mapping and X-ray energy dispersive spectra (XEDS) at STEM mode. The coating was determined as aluminum carboxylate via Fourier transform IR spectroscopy, a product from chemical reactions of Al and carboxylic acid functional groups coated on the He-plasma modified alumina surface. This work demonstrates the preliminary success of exploiting a new approach for mitigating the inactive alumina shell and further tailoring the superficial morphology and chemical properties of core-shell commercial nAl via a two-step atmospheric pressure plasma process. The efforts also emphasize the significance of exploiting advanced materials characterization for a deeper understanding of the resultant nanoscale surface properties for ultimate optimization of plasma conditions.

5:15 PM EQ09.03.05

Plasma Assisted Growth of Hydrophobic Silicon Nanoparticles for Oil-Water Separation Sankhadeep Basu, Gabriel Ceriotti and Rebecca J. Anthony; Michigan State University, United States

Hydrophobic nanomaterials have drawn significant attention due to their applications in coatings, protein adsorption, nanomedicines, etc. For silicon nanomaterials, researchers have generally used external agents which react with the surface terminated Si-H bonds and render the surface hydrophobic. In the present work we investigate the hydrophobic nature of as-prepared silicon nanoparticles (SiNPs) produced in a nonthermal plasma reactor. SiNPs were synthesized in a flow-through reactor using silane with argon as the background gas. The total gas flowrate was 20 standard cubic centimeters per minute (scm) and with a reactor pressure of 1.4 Torr. The plasma as generated using radiofrequency (rf) power of 10W at 13.56MHz is delivered via ring electrodes encircling the reactor. SiNPs formed in the plasma were collected on a stainless-steel mesh filter at the reactor exhaust. Further examination under Scanning Electron Microscopy (SEM) revealed the formation of flow-through aggregated wires of around 12 microns in length and 7-8 microns in diameter, comprised of primary SiNPs. Transmission electron microscopy showed the primary particle size to be in range of 5-7 nm, but no electron diffraction rings were detected, indicating that the Si NPs were amorphous.

Contact angle measurements were performed to test the hydrophobicity of the as-prepared SiNPs. A water contact angle of 146° was observed demonstrating the near-superhydrophobic ($> 150^\circ$) nature of the aggregated SiNPs. The hydrophobic material was also successful in separating both vegetable cooking oil as well as heavy-duty pump oil from oil-water mixtures. Thermal experiments were also performed to illustrate the thermal stability of the hydrophobic nature. The nanomaterial was able to retain its hydrophobicity even at 450°C after 2h of heating showing robust stability. The material was also found to be stable under ambient air conditions as water contact angle did not change significantly even after a week of synthesis. These exciting properties signify the future prospects in coatings, biotechnology and more.

SESSION EQ09.04: Poster Session
Tuesday Afternoon, November 30, 2021
8:00 PM - 10:00 PM
Hynes, Level 1, Hall B

EQ09.04.01

Plasma Synthesis and Processing of Epitaxial β -FeSe/SrTiO₃ Heterostructures Kamron L. Kopecky¹, Adam D. Smith¹, Mphande N. Phiri², Sumner B. Harris¹ and Renato P. Camata¹; ¹The University of Alabama at Birmingham, United States; ²Alabama A&M University, United States

The combination of different materials in heterostructures often enables phenomena that are impossible to achieve in a single compound. A now-classic example is the interface-enhanced superconductivity of monolayer β -FeSe on (001)-oriented SrTiO₃ (STO). The observed superconducting gap in this system is substantially larger than in bulk β -FeSe due to a combination of electron doping and electron-phonon interactions at the FeSe/STO interface. Heterostructures derived from this FeSe/STO system are useful for the creation of layered quantum materials arrangements to study interface-enhanced processes, magnetic/superconducting proximity effects, and control of quantum properties via electrostatic gating. The plasma environment of pulsed laser deposition (PLD) is particularly suited for growing such heterostructures, either as stand-alone thin films on a variety of substrates or as designed multilayered and superlattice configurations. While characterizing the vacuum PLD environment in terms of the flux of depositing species, their kinetic energy, and the substrate temperature is generally considered sufficient for controlling film growth, in this work we explore how tuning more fundamental laser plasma parameters, such as the electron density and temperature, may alter the structure and interface of β -FeSe/STO heterostructures. We correlate measurements from Langmuir probe plasma diagnostics during FeSe growth with x-ray diffraction and x-ray reflectivity data from the epitaxial heterostructures obtained. Laser plasmas with electron density (n_e) below $\sim 5 \times 10^{19} \text{ m}^{-3}$ and electron temperatures (T_e) of 0.1-0.2 eV lead to epitaxial c -axis oriented β -FeSe/STO with clear thickness fringes in dynamical x-ray diffraction (Pendellösung oscillations), indicating high crystal quality and sharp interface. On the other hand, plasmas with $n_e \sim 10^{20} \text{ m}^{-3}$ and $T_e \approx 0.5$ -0.6 eV result in β -FeSe with a mixture of two epitaxial orientations, less defined interface, and a greater degree of mosaicity or defects. We will discuss how adjusting the laser plasma parameters may allow further control in plasma-mediated growth of β -FeSe/STO such as spatial modulation of nucleation sites, modification of island growth patterns, and activation of plasma-enhanced surface reactivity.

EQ09.04.02

The Angular Distribution of Species in Single- and Multi-Component Laser Plasmas for Materials Processing Audrey M. Collins¹, Jacob H. Paiste¹, Robert R. Arslanbekov² and Renato P. Camata¹; ¹The University of Alabama at Birmingham, United States; ²CFD Research Corporation, United States

The forward peaking of the angular distribution of plasma species is one of the most distinctive characteristics of plasmas produced by pulsed nanosecond UV laser ablation of solids. It is the result of gas dynamics effects and it depends strongly on the photo-physics of the laser-plasma interaction. In pulsed laser deposition, where the plasma may comprise a variety of chemical species and ionization states, chemical heterogeneity in the angular distribution may

affect the quality and properties of the resulting thin films. In processing applications, lack of control of the angular distribution may result in dissimilar effects in different locations of a single sample. In this work, we use a laser ablation/fluid plasma expansion model to simulate the angular distribution of single- and multi-species laser plasma expansions. We implement the model for plasmas produced by the ablation of elemental and compound metallic targets. The fluid simulation accounts for singly and doubly charged ions, as well as electrons and neutrals. The simulation is carried out over the centimeter distances required for proper evaluation of the angular distributions in a multidimensional setting using a state-of-the-art, open-source adaptive Cartesian mesh framework. The compressible solvers available in this framework (Riemann and all-Mach solvers) were adapted to include the equations of state of the plasma, which link local Saha equilibrium with augmented ideal gas expressions that include the internal degrees of freedom of the atomic species. Our implementation allows broad and detailed studies of the time-dependent angular behavior of all plasma constituents. This includes distributions of neutrals, ions, and electrons, as well as temperature and flow velocity profiles. As an example, the ablation of FeSe by the focused beam of a single KrF excimer laser pulse (248 nm, 25 ns, 10 mm² spot area), leads to a predicted angular distribution for peak number density of Fe⁰ with FWHM of ~80° at a fluence of 2.0 J/cm². The FWHM decreases to ~71° for 3.2 J/cm², in qualitative agreement with typical angular distributions observed in film growth. For the same conditions, the angular distribution for peak number density of Fe⁺ (i.e., singly charged ions) has FWHM of ~40° and ~22°, respectively. These results allow creation of spatially resolved maps of the degree of ionization during plasma irradiation of materials, enabling new types of gradients to induce materials transformations. We will discuss differences in elemental vs. compound metallic plumes and subtle variations in predicted angular distributions of different chemical species in compound plumes, which are critical for reproducible film synthesis and processing.

EQ09.04.03

Measurement and Simulation of the Plasma Parameters of a Bimetallic Laser-Produced Plasma [Mphande N. Phiri](#)¹, Braden L. Spiller², Adam D. Smith², Jacob H. Paiste², Robert R. Arslanbekov³ and Renato P. Camata²; ¹Alabama A&M University, United States; ²The University of Alabama at Birmingham, United States; ³CRD Research Corporation, United States

Pulsed laser deposition (PLD) is a versatile plasma-based technique for nonequilibrium growth of materials of complex stoichiometry. Kinetic manipulation of materials processing in PLD requires controlling the plasma parameters of its chemically intricate and transient plasma flows. In this research we compare trends in the plasma parameters measured for a laser plasma with predictions from a laser ablation/plasma fluid expansion simulation. Planar and cylindrical Langmuir probes were used to measure the ion and electron densities, as well as the electron temperature and Mach number of the plasma expansion. The laser plasma simulation couples laser-induced surface evaporation with fluid plasma expansion and is implemented in 2D-axisymmetric coordinates, effectively delivering predictions for the 3D temporal evolution of the corresponding plasma parameters. The simulation accounts for singly and doubly charged ions, as well as electrons and neutrals, and is performed in a multidimensional setting using a state-of-the-art, open-source adaptive Cartesian mesh (ACM) framework. The use of the dynamic ACM approach is essential for reliable evaluation of plasma parameters. This is because the initial ($t < 30$ ns) spatial resolution required near the target is tenths of microns, while the simulation domain is larger by multiple orders of magnitude. As the plasma plume expands ($t > 30$ -60 ns), the fine near-target resolution is no longer required for most of the simulation domain which allows the grid to be coarsened. However, proper resolution of the moving plasma front is still necessary throughout the entire plasma dynamics until the front reaches the anticipated substrate location. Only the very narrow plasma front region needs to be resolved for this purpose, while the remainder of the computational mesh can stay coarse. In this combined experimental and computational investigation, we analyzed a bimetallic plasma containing iron (Fe) and selenium (Se), obtained by ablating a solid pellet of FeSe with the 25 ns pulse of a KrF excimer laser (248 nm). For laser spot areas below 4.5 mm², the peak values of the experimental electron density, electron temperature, and Mach number of the expansion all increase gradually when laser fluence is in the 0.5-4.0 J/cm² range. The same trend is reproduced in the simulation. We will discuss how the measured time dependence of the plasma parameters can be used to constrain the simulation and test mechanisms of laser plasma formation that need to be invoked for accurate predictions of PLD plasmas containing multiple chemical species.

EQ09.04.04

Functionalization of Titanium by an Ionic Implantation Process by Plasma Oxygen Immersion [Michaël Redolfi](#)¹, [Brigitte Bacroix](#)¹, [Danièle Chaubet](#)¹ and [Laurent Berthe](#)²; ¹LSPM CNRS (UPR 3407), France; ²PIMM (UMR 8006), France

Titanium alloys are used in many industrial sectors including aeronautics and biomedical sectors, due to their low density combined with excellent mechanical properties (high strength and Young's modulus, corrosion resistance, etc.). Surface properties are also of paramount importance, for example to ensure good resistance to wear or to increase biocompatibility, main properties sought after in the biomedical field. Thus, many surface treatments are carried out, among which oxidation treatments, which in addition to the properties mentioned above, affect to varying degrees the fatigue resistance of the part treated depending on the degree of roughness, porosity and density adhesion of the formed layers. In the present work, we present an original oxidation treatment based on the coupled use of laser shock and microwave plasma oxygen implantation (MWPO) in order to improve in the first place the adhesion of the oxide layers, while inducing new functionalities. The process is versatile enough allowing (i) to obtain adherent oxide layers without adversely modifying the substrate, and (ii) to provide additional functions to the material treated, we propose here to explore a new combination of the two MWPO and ceramic conversion (CC) treatments, completed by preliminary mechanical hardening by laser shock. Here, the CC treatment consists of 2 successive stages of high temperature thermal treatment of oxidation then diffusion. The implementation of this process has been carried out initially on single-phase pure titanium. The treatment made up of 3 stages: (i) a preliminary surface treatment by laser shock, in order to create special grain boundaries on the surface making it possible to improve the diffusion of oxygen during the following two stages, (ii) an oxygen implantation step by MWPO process to produce more or less thick oxide layers, depending on the process parameters without modifying the substrate and (iii) a thermal step (of CC type) to allow more partial diffusion of oxygen and thus improve the adhesion of the layer. In order to keep the benefit of the previous steps and to simplify the process, this 3rd step has been carried in the plasma reactor at a lower temperature than the standard CC treatment. The characterization of the thickness and adhesion of the layers, the observation of the substrate microstructure by SEM/EBSD, the characterization of roughness and microhardness and the characterization of fatigue behavior have been performed.

SESSION EQ09.05: NP Synthesis and Processing II
Session Chairs: Ageeth Bol and Chi-Chin Wu
Wednesday Morning, December 1, 2021
Hynes, Level 1, Room 104

10:30 AM EQ09.05.01

Nanoparticle Growth Mechanics from Pulsed Plasma Exposure [Brandon A. Wagner](#), [Joseph Schwan](#), [Minseok Kim](#) and [Lorenzo Mangolini](#); University of California, Riverside, United States

Applications of pure nanoscale materials have rapidly expanded in recent years and with the development of non-thermal plasma as a synthesis method, these materials can be produced with high purity and narrow size distribution compared to standard thermal or wet production methods. Unfortunately, non-thermal plasma synthesis has been limited to structures below 10 nm in diameter due to unipolar charging effects inhibiting particle growth, thus restricting potential applications [1]. For instance, current efforts in lithium-ion battery development are focused on integrating nanoscale silicon into the anode with a theoretically optimal size near 100 nm in diameter [2]. The relaxation of particle net charge outside of a plasma and re-initiation of the plasma-instigated growth process merits investigation as the reduction of net charge may allow further particle growth through increased particle collision.

To perform this investigation, an RF capacitive plasma was simply pulsed at different frequencies with respect to a particle's residence time within the plasma reactor. Silicon particles were produced through the decomposition of silane gas in the plasma flowing through a cylindrical region top to bottom and collected onto a stainless steel mesh. Ex-situ characterization was performed via Transmission Electron Microscopy (TEM) and Scherrer's Analysis through X-Ray Diffraction (XRD). Effects of reactor pressure and length were tested and accounted for in the produced materials, showing generally understood trends. Additionally, pulsing frequency with respect to particle residence time, plasma exposure time (different pulsed frequencies with identical amounts of time in plasma), and duty cycle effects were tested. These pulsing trails enabled production of larger particle diameters in comparison to their non-pulsed counterparts. A constant plasma condition with a reactor pressure at 8 Torr produces nanopowder with average particle size of 8.0 nm; however, pulsing conditions were able to achieve an average particle size of 22.6 nm. Trends relating to crystallinity and new particle size limitations were also observed.

Materials produced at varying pulse rates were coated with graphitic carbon and tested in lithium-ion batteries to observe cycling stability and associated charge capacity. Finally, numerical simulations were performed to explain the altered charging and growth mechanics of particles repeatedly exposed to non-thermal plasma conditions.

[1] Lopez, T., Mangolini, L., On the nucleation and crystallization of nanoparticles in continuous-flow nonthermal plasma reactors. *J. Vac. Sci. Tech. B* 32(6), 061802 (2014)

[2] Zhu, G., Wang, Y., Yang, S., Qu, Q., Zheng, H., Correlation between the physical parameters and the electrochemical performance of a silicon anode in lithium-ion batteries. *J. Materiomics* 5(2), 163-175 (2019)

10:45 AM EQ09.05.02

Nonthermal Plasma Synthesis of Carbon Nanodots Sankhadeep Basu, [Cameron Papsen](#), Tanvi Nikhar, Sergey Baryshev and Rebecca J. Anthony; Michigan State University, United States

In recent years, carbon nanodots (CDs) have been of great interest for their applicability in areas such as solar energy harvesting, nano-sensing, photocatalysis, etc. Traditional routes for synthesis for CDs involve both top-down methods like laser ablation, electrochemical synthesis, and chemical oxidation, as well as bottom-up techniques like hydrothermal synthesis, microwave pyrolysis and others. In this work we report the synthesis of CDs in a nonthermal radiofrequency plasma reactor using methane as the carbon precursor. Nonthermal plasma synthesis offers several advantages over traditional routes in terms of simplicity, solvent free synthesis and near room temperature growth of nanoparticles. Radiofrequency power at 13.56 MHz was supplied through ring electrodes to a flow-through reactor. The methane precursor was diluted with argon and hydrogen (H_2), in varying concentrations, for a total flowrate of ~100 sccm. The reactor pressure was kept at 2.9 Torr. The CDs formed in the plasma were deposited onto arbitrary substrates via inertial impaction. The synthesized material was characterized using Transmission Electron Microscopy (TEM), Scanning Electron Microscopy (SEM), Raman spectroscopy, and UV-Vis optical absorption. Raman spectroscopy exhibited two significant features: the D band around 1330 cm^{-1} and the G band around 1590 cm^{-1} . While Raman spectroscopy did not reveal significant modifications in the bonding configuration upon changing synthesis parameters, by controlling the hydrogen content in the plasma via introduction of H_2 gas, there arose a dramatic shift in the visual appearance, nanostructure, and UV-Vis optical absorption. Under hydrogen-poor conditions, the CDs were black and accompanied by optical absorption across the visible range, while hydrogen-rich conditions led to white-appearing CD powders with an onset of optical absorption in the UV. TEM image analysis indicated that the average particle size was around 6nm under hydrogen-poor conditions, and much larger at >40nm for hydrogen-rich conditions. Additionally, the black CDs appeared to be in nano-onion-like morphologies, as evidenced with TEM imaging, while the white CDs appeared entirely amorphous with no layered structure within the primary particles, consistent with highly diversified sp^2 and sp^3 bonding within the CDs. Our future work will quantify the degree of sp^3 hybridization for CDs of both varieties, as well as measuring the effect of hydrogen during synthesis on the electrical conductivity of CD films created by inertial impaction directly from the reactor.

11:00 AM EQ09.05.03

Synthesis of 3D Films of Resonant Si Particle Absorbers by Filamentary Plasmas Mohammadali Eslamisaray¹, [Gunnar Nelson](#)¹, Parker Wray², Harry A. Atwater² and Uwe Kortshagen¹; ¹University of Minnesota, United States; ²California Institute of Technology, United States

Nonthermal plasmas have attracted increasing attention for the synthesis of groups IV and III-V semiconducting nanocrystals owing to their nonequilibrium environment which enables the nucleation, growth, and crystallization of materials with high melting point from gas phase precursors at room temperature. The resulting negatively charged nanocrystals with a narrow size distribution can be accelerated to a high velocity through a nozzle to form thin films via impaction onto a substrate. The scalability of this single step, ligand-free, amenable to doping, and high yield deposition technique has recently been demonstrated by depositing uniform nanoparticle films of tunable thickness and porosity on 125 mm-diameter silicon wafers. Despite impressive applications in electronic and light-emitting devices, plasma-synthesized thin films have come short in supporting optically-induced magnetic resonances (OMR) due to the small size of their constituent nanoparticles. This is mainly because of the short nanoparticle residence time in dusty plasma reactors with a uniform diffuse discharge resulting in particle sizes in the range of 2 to 10 nm. Synthesis attempts aimed for larger nanocrystals in diffuse discharges via changing the operating conditions, including the flow rates, operating pressure, tube size, and plasma power usually lead to either polycrystalline or amorphous nanoparticles, or nanocrystals with a wide size distribution. Here, we report the synthesis of monodisperse Si nanocrystals of over 80 nm with a standard deviation of 1.0 nm by intentionally operating the plasma in a regime where the discharge is constricted. In this regime, the plasma consists of two regions: a diffuse region that extends a few centimeters upstream of the RF electrode, and a striated high-luminosity plasma filament that rotates close to the wall of the tube between the RF electrode and the lower flange. Previous laser scattering studies have shown that the particle growth begins in the diffuse plasma and particles are trapped in a region upstream of the electrode. The filamentary plasma then most likely sinters the particles by annealing them to temperatures much higher than the gas temperature resulting in formation of single crystals. Using this method, we deposited a 550 nm thick fractal-like random film of resonant Si nanocrystals in an air host matrix with a 23% volume fill fraction on a glass substrate. Angle, polarization, and wavelength resolved reflection and transmission measurements of the film were performed. The film shows an absorption peak of close to an ideal blackbody at the particles' OMR with a broadened absorption tail emanating from the OMR and progressing out to longer wavelengths. Overall, the particle film is over 38% more absorbing compared to an antireflective-coated crystalline silicon slab of the same thickness using 77% less material. The particle film has antireflective properties regardless of the form of the incident excitation as evident by the fact that transmission \approx 1-absorption. Similar to a blackbody, there is a strong angle insensitivity of absorption up to angles of incidence as steep as 70 degrees at the OMR spectral

location. The film's optical response also shows significant polarization independence. This study paves the way for synthesis of resonant Si nanoparticles using nonthermal plasmas and displays the unique optical properties of 3D films fabricated by this single-step technique.

Acknowledgements: This work is supported by the Army Research Office under MURI project under W911NF-18-1-0240. Portions of this work were conducted in the Minnesota Nano Center, which is supported by the National Science Foundation through the National Nanotechnology Coordinated Infrastructure (NNCI) under Award Number ECCS-2025124.

SESSION EQ09.06: Synthesis and Processing I
Session Chairs: Rebecca Anthony and David Pai
Wednesday Afternoon, December 1, 2021
Hynes, Level 1, Room 104

1:30 PM *EQ09.06.01

Tailoring the Properties of 2D Transition Metal Chalcogenides Using Plasma-Enhanced Atomic Layer Deposition Ageeth A. Bol; Eindhoven University of Technology, Netherlands

2D materials have been the focus of intense research in the last decade due to their unique physical and chemical properties. This presentation will highlight our recent progress on the synthesis of two-dimensional transition metal di- and tri-chalcogenides (2DTMCs) for nanoelectronics and catalysis applications using atomic layer deposition (ALD). ALD-grown 2DTMC films typically exhibit a high density of out-of-plane 3D structures in addition to 2D horizontal layers. While the out-of-plane 3D structures are ideal for catalysis applications, the presence of such 3D structures can hinder charge transport, which hampers device applications. In this presentation I will show how we used mechanistic insight obtained by HRTEM and DFT simulations to tune the shape and density of the 3D structures during plasma-enhanced ALD. The obtained morphology control was further confirmed by electrocatalysis and electrical measurements.

In the second part of my talk I will demonstrate that we also can modulate the crystal phase of transition metal chalcogenides through plasma-enhanced ALD. Phase-control between the metallic TiS_2 and semiconducting TiS_3 phases was achieved by carefully tuning the co-reactant (H_2S gas vs plasma) and deposition temperature during ALD. These two material phases were differentiated using a variety of characterization techniques. This work sets the foundation for achieving electrical and catalytic property modulation through phase and morphology control in low-dimensional materials using plasma-enhanced ALD.

2:00 PM EQ09.06.02

Laser-Produced Plasmas in the Synthesis and Processing of 2D Materials Renato P. Camata; The University of Alabama at Birmingham, United States

Low-temperature plasmas (LTPs) have long been recognized as effective in enhancing physical and chemical processes during materials synthesis. The emergence of two-dimensional (2D) materials has renewed the interest in using LTPs for engineering these systems at the atomic scale. LTPs generated by laser ablation are of particular interest because of their rich chemistry and spatiotemporal phenomena. These plasmas can produce reactivity, temperature, and stress profiles to induce chemo-thermo-mechanical materials transformations that are not accessible by other approaches. The kinetic energy of ions can be tuned in the $\sim 1\text{-}400$ eV range and ion densities controlled between 10^9 and 10^{15} cm^{-3} . Compressive stress ranging from kPa to tens of GPa, due to energetic bombardment, and temperature pulses between hundreds and thousands of kelvin can be delivered by the leading edge of the plasma expansion. The sequence and timing of these conditions are adjustable, allowing new types of nonequilibrium processing. Despite their use in solid state physics for decades, there is a vast domain of unexplored plasma regimes with potential for breakthroughs in 2D materials research. In this talk, I will review the state of the art in plasma synthesis and processing of 2D materials, such as graphene, transition metal dichalcogenides, and atomic-monolayer epitaxial quantum materials. In particular, I will show how Langmuir probe, optical emission spectroscopy, gated-intensified CCD imaging, and laser-induced fluorescence spectroscopy diagnostics are being used in conjunction with particle-in-a-cell and fluid simulations to control plasma parameters and effect materials transformation in 2D and quantum materials.

2:15 PM EQ09.06.03

Non-Thermal Plasma Synthesis of Structural Materials Steven Herzberg, Lorenzo Mangolini and Suveen N. Mathaudhu; University of California, Riverside, United States

The low-temperature plasma synthesis of nanoparticles has many benefits over conventional powder production methods. Some of these include the ability to produce high purity semiconductor and ceramic nanoparticles with narrow size distributions[1]. By varying the ratio of precursors, the final composition of the materials can be finely controlled. In addition, the relatively low temperatures of non-thermal plasmas enable the production of amorphous nanoparticles, providing opportunities and potential applications that are still severely underexplored by the plasma community. This study focuses on the plasma processing of structural materials, with particular attention to amorphous ceramics. For this work, the silicon-carbo-nitride system (SiCN) was chosen because of its high temperature structural properties. SiCN has been shown to have good creep resistance and oxidation resistance[2] as well as high hardness[3] at temperatures past 1000°C . However, SiCN is primarily produced polymer pyrolysis and ceramisation of organosilicon precursors, which can make it difficult to control the final composition of the material and typically crystallizes during sintering. We have successfully produced bulk amorphous SiCN samples by sintering plasma-produced nanoparticles. The resulting hardness, fracture toughness, and microstructure of the samples will be discussed in detail.

[1] Mangolini, "Synthesis, Properties, and Applications of Silicon Nanocrystals."

[2] Raj et al., "Oxidation Kinetics of an Amorphous Silicon Carbonitride Ceramic."

[3] Herrmann et al., "Silicon Nitride/Silicon Carbide Nanocomposite Materials."

2:30 PM EQ09.06.04

Atmospheric Plasma Surface Modification to Enhance Performance of Printed All-Solid-State Ion Selective Electrode Sotoudeh Sedaghat, Venkat Kasi and Rahim Rahimi; Purdue University, United States

All-solid-state potentiometric sensors based on printed solid-contact ion-selective electrodes have shown great potential for point of care and portable diagnostic systems due to their simple integration, cost-effectiveness, and scalability. Despite the low cost such printed electrochemical sensors, they are often unsuitable for long-term monitoring application due to the sensor drift. One of the main causes of drift in printed ISEs is the water-layer-formation

between the ion selective membrane (ISM) and the electrode resulting in an interfacial potential change overtime. To date, significant efforts have been undertaken to improve the electrochemical performance and stability of the solid contact- ISM in order to modify the interfacial properties of ISM and electrode. However, their added fabrication steps, increased cost, and need of various chemical agents have restricted their wide application. In this study, we have attempted to address the current challenges by employing a simple, scalable, and novel atmospheric plasma surface treatment to modify the screen-printed carbon electrode surface and improve interfacial bonding between ISM and carbon electrode. As a proof of concept, the plasma surface modification effect was assessed with nitrate ISEs. Our results showed that plasma-treated electrodes had a significantly lower potential drift as compared to ISEs that were not surface treated with plasma. In addition, plasma treated ISEs demonstrated an improved reproducibility with less potential variation between fabricated sensors as compared to untreated electrodes. The enhanced electrochemical performance of plasma-treated ISE can be explained by the improved interfacial bonding and reduced water-layer, which was also confirmed by standard mechanical peel tests. Raman spectroscopy analysis of the carbon surfaces revealed a highly organized graphenic structure on the printed carbon surface originated by atmospheric plasma treatment. Effect of plasma treatment on reduced water uptake and generated graphene structure were further confirmed by electrochemical impedance spectroscopy with decreased charge transfer resistance for the plasma treated ISEs. Delamination of ISM for the untreated electrodes, as characterized by scanning electron microscopy (SEM), indicated the ingress of water at the interface for sensors with the untreated electrode while the plasma-treated electrodes showed a firmly packed configuration.

2:45 PM EQ09.06.05

Nonthermal Plasma Synthesis of Aluminum Nanoparticles from Aluminum Trichloride Uwe R. Kortshagen¹, Chad Beaudette¹, Himashi P. Andaraarachchi¹ and Chi-Chin Wu²; ¹University of Minnesota, United States; ²U.S. Army Combat Capabilities Development Command—Army Research Laboratory, United States

The synthesis of pure metal particles is of great interest for many applications including catalysis and metal additive manufacturing. For metal particle synthesis with nonthermal plasmas, metalorganic precursors with suitable vapor pressures are widely available. However, with many of these precursors it is difficult to avoid the incorporation of carbon contaminations into the metal particles. Metal chlorides are another group of attractive precursors. For many metals, chlorides are often produced as intermediates early in the extraction process or they are easily derived from other low-refined metal compounds. Most metal chlorides are liquid or solid at room temperature but many have attractive vapor pressures for low pressure synthesis. Here, we demonstrate the synthesis of aluminum (Al) nanoparticles from aluminum trichloride (AlCl₃). A vapor of AlCl₃ carried by an excess flow of argon is fed into a tubular low pressure nonthermal plasma reactor with one inch outer diameter operating at pressures around 5 Torr. Radiofrequency power between 80-200 W (nominal) is applied through inductive coupling. Hydrogen is added as a scavenger for chlorine. Aluminum nanoparticles with average diameters between 10-20 nm are produced with minimal chlorine contamination. While the nanoparticles oxidize rapidly when removed from the synthesis reactor, X-ray diffraction and transmission electron microscopy provide clear evidence for the presence of Al nanoparticles.

This work was primarily supported through the US Army Combat Capabilities Development Command—Army Research Laboratory under Cooperative Agreement W911NF-19-2-0283.

3:00 PM BREAK

SESSION EQ09.07: Diagnostics and Measurements
Session Chairs: Rebecca Anthony and Chi-Chin Wu
Wednesday Afternoon, December 1, 2021
Hynes, Level 1, Room 104

4:00 PM *EQ09.07.01

In Situ Optical Diagnostics of Plasma-Water Interfaces for Applications in Graphene Synthesis David Pai^{1,2}, Thomas Orriere², Francesca Caeilli², Karthik Thyagarajan², Darwin Kurniawan³, Yi-Chen Chang³, Jhih-Siang Yang³ and Wei-Hung Chiang³; ¹LPP CNRS Ecole Polytechnique, France; ²Institut Prisme CNRS Université de Poitiers ISAE-ENSMA, France; ³National Taiwan University of Science and Technology, Taiwan

Many approaches to graphene synthesis can require high temperature, strong/toxic reducing agents, or are expensive. The microplasma-electrochemical reactor (MEC), composed of an atmospheric-pressure microplasma with an aqueous solution as an electrode, may overcome these difficulties by providing physico-chemical conditions that are difficult to achieve otherwise. They can initiate non-equilibrium electrochemistry and nucleation in solution without additional heating or reducing agents, improving the efficiency of synthesis. In addition, the technological barrier to implementing MECs is low. MECs have successfully synthesized graphene quantum dot (GQD) synthesis in aqueous solution [1,2].

One of the main challenges going forward is to develop a detailed mechanism of GQD growth, which is a general difficulty in plasma-based nanomaterials synthesis due to the complexity of non-equilibrium plasma chemistry and interactions with surfaces. So far the relevant species and reactions have mainly been inferred from ex situ or macroscopic effects, with a limited degree of detail and certainty. The liquid-phase diagnostics of the plasma-water interfacial region can provide new insight into how the MEC transforms the precursor into GQDs. Current experimental techniques used for the analysis of liquid chemistry suffer from a lack of selectivity and/or degradation of dyes, chemical probes, or spin traps/probes introduced into the liquid. The spatial distribution of species is not often accessible. Most importantly, the majority of the diagnostics must be performed ex situ, removed from the plasma reactor and after treatment.

To address this challenge, we have developed an *in situ* multi-diagnostics approach to encompass a wide range of physical and chemical properties at the plasma-water interface. The centerpiece of this platform is *in situ* spontaneous Raman microspectroscopy, which offers several important advantages over the aforementioned diagnostic tools: non-intrusiveness, selectivity, versatility, and straightforward calibration. By developing a light-sheet technique, we have experimentally investigated the interfacial region with a spatial resolution as high as several tens of microns. To gain insight into the physical state of the solvent, we tracked the Raman spectrum of water. In particular, changes to the -OH stretch band shape indicate a weakening of the hydrogen bonding network of water with. These changes to the Raman spectra over the course of plasma treatment occur at both fast and slow time scales and become more pronounced as the detection volume approaches the interface. We also tracked the aqueous species H₂O₂ and NO₃⁻, whose concentrations both increase when approaching the interface to within several tens of μm [3]. An interfacial layer of excess NO₃⁻ concentration was found to extend 28 μm in depth. Similar interfacial layers have been modeled for transient species such as OH radicals but not for NO₃⁻, a stable product of plasma-activated water.

Raman spectroscopy of the liquid environment was complemented by *in situ* photoluminescence (PL) spectroscopy to track the appearance of GQDs in real

time. The PL spectrum evolves differently according to the depth of detection in the liquid, and so particle image velocimetry of the liquid flow field was performed to gain an understanding of possible transport mechanisms. These measurements of the liquid phase were complemented by optical emission spectroscopy of plasma properties such as the electron number density and presence of excited species as a function of the distance from the interface. Together, these experimental results represent the fullest description to date of the physico-chemical environment enabling GQD synthesis and mark an important step towards the discovery of the reaction mechanism.

4:30 PM EQ09.07.02

Time Resolved Ion and Electron Energy Distribution Functions During a HiPIMS Discharge David E. Barlaz¹, Zach Jeckell¹, Wolfgang Huber², Tom Houlahan², Ian Haehnlein², Brian Jurczyk² and David Ruzic¹; ¹Univ of Illinois, United States; ²Starfire Industries, United States

The expansion of HiPIMS as both a research and production technique has demonstrated the need to better understand transient events inherent to the discharge, specifically the Positive KickTM pulse, first commercialized by Starfire Industries, responsible for imparting ion energy to the workpiece at low gas temperatures. Previous research has shown that sputtered metal ions arrive at the workpiece with tunable ion energies depending on the conditions of the discharge, while limiting ion energies of working gases. Much remains to be understood about the nature of the plasma responsible for this.

In the current work, a Starfire Industries 2-2 Impulse[®] with Positive KickTM was utilized in conjunction with an Impedans Semion gridded energy analyzer to determine the transient nature of the ion energy distribution function (IEDF) during the positive kick pulse. Simultaneously, time resolved Langmuir probe data allowed for the plasma potential, electron energy-distribution function (EEDF), and normalized plasma density to all be resolved with μ s-resolution. An unbalanced magnetron was characterized for a variety of gas pressures, pulse lengths, kick pulse lengths and amplitudes.

Ion energies within 5% of the kick pulse bias voltage are consistently observed at the detector within several μ s of the beginning of the kick pulse indicating rapid transit times for the plasma across the chamber. Plasma transit times were mild functions of pressure, but not of pulse lengths or amplitudes, as measured both by the IEDF and plasma potential. Shifts in the IEDF early in the kick pulse suggest a transition between mechanisms for ion transport as the plasma sheath forms. Additionally, decay times for ion energy distributions occurred on similar time scales suggesting the plasma expansion enabled by the kick pulse is short lived. Ion energies above the kick pulse bias voltage are consistently absent over the conditions tested (Semion detection maximum for this configuration is 150 eV) indicating that the pulse conditions may be suitable for the minimization of instabilities that may be deleterious to both film quality and uniformity of deposition. These and other results will be discussed in conjunction with time resolved electron energy distribution measurements to provide an understanding of plasma dynamics and the effect of the magnetron's magnetic trap.

4:45 PM EQ09.07.03

Multidimensional Simulation of Laser-Generated Chalcogen Ion Plasmas in Length Scales Relevant for Materials Processing Jacob H. Paiste¹, Sumner B. Harris¹, Joseph Edoki², Robert R. Arslanbekov³ and Renato P. Camata¹; ¹The University of Alabama at Birmingham, United States; ²Alabama A&M University, United States; ³CFD Research Corporation, United States

Plasmas generated by laser ablation are of interest for materials processing because of their rich chemistry and spatiotemporal phenomena. The chemical diversity, variety of gas backgrounds, and shock wave characteristics of laser-produced plasmas are particularly conducive to kinetic control of materials synthesis. Measurements of laser plasma parameters using Langmuir probes, TOF mass spectroscopy, optical emission spectroscopy, laser-induced fluorescence, as well as photography and imaging techniques have established numerous correlations between plasma parameters and processing outcomes. These correlations represent a substantial body of knowledge, but do not provide an exhaustive picture of the laser plasma processing environment. This is due in part to the difficulty in gathering direct experimental information on the strongly time and space dependent plasma parameters at the plasma-surface boundary. Moreover, processing of 2D materials has raised new questions about the ion densities, kinetic energies, and plasma temperatures that are useful for manipulation of these atomically thin systems. In this context, laser plasma simulations may offer insights into the plasma characteristics in the vicinity of the processing area which, in conjunction with experiments, could reveal plasma conditions for controlling processes such as doping, defect annealing, and kinetically-driven phase transformations. The complexity and broad technical applications of laser-generated plasmas have for decades been motivators for their study via numerical simulations. Modern studies based on a variety of fluid, kinetic, and hybrid models are well described in the literature. The majority of investigations have focused on one-dimensional (1D) descriptions of single-element plumes, very close to the ablation target surface (<1 mm) and over short timescales (<1 μ s). Detailed analysis of this domain is valuable in applications dominated by near-target processes, such as micromachining, laser-induced breakdown spectroscopy, and laser sintering/additive manufacturing. Simulations up to several centimeters in length and times >10 μ s, have received much less attention but are needed to guide materials synthesis and modification approaches, where substrates are placed several centimeters away from ablation targets. Simulations over long distances are computationally costly and must include three-dimensional (3D) effects. They also need to account for the thermo-physical properties of specific chemical species. While embedding detailed mechanisms is desirable, simulations of practical utility need to be fast and meet predictive benchmarks. In this work we balance these demands using an effective model that incorporates standard features of UV nanosecond laser ablation plasmas: thermal evaporation, bremsstrahlung emission from plasma electrons, as well as photoionization and free-free laser absorption by the plasma. An additional effective plasma absorption coefficient is introduced as a stand-in term for other mechanisms that are impractical to account for directly—due to computational cost or unavailability of physical parameters. The effective model is constrained by Langmuir probe experimental data. The simulations are set up in a 2D-axisymmetric geometry using a solver with an adaptive Cartesian mesh. We simulate plasmas of selenium (Se) and tellurium (Te), which are of current interest in synthesis of transition metal chalcogenide materials. Predictions of Se and Te plasmas produced by 248-nm, pulsed nanosecond ablation of metal targets (4 J/cm² laser fluence and 1.8 mm² laser spot area) show chalcogen plumes with spatial gradients of plasma density that are steeper than those for more commonly studied copper (Cu) plumes by up to three orders of magnitude. Their spatial distributions have central bulges, in contrast to the edge-only ionization of Cu. The range of plasma temperatures for Se and Te is higher than for Cu by more than 0.5 eV.

5:00 PM EQ09.07.04

Plasma Enhanced Low Temperature Processing for Dopants Activation in CMOS Devices Yuanning Chen¹, Orlando Auciello² and Israel Mejia³; ¹MicorSol Technologies Inc., United States; ²The University of Texas at Dallas, United States; ³Center for Engineering and Industrial Development, Mexico

A novel plasma enhanced low temperature (around 400°C) process was developed for CMOS device dopant activation, post integrated circuits (ICs) fabrication processing, and for low temperature processing of organic and other materials needing low temperature conditioning. The main challenge for CMOS device processing is to maintain low thermal budget for source/drain's dopant activation while limiting dopant diffusion within the source/drain thickness layers, to produce optimal transistor performance. Low temperature processing of ICs is critical to eliminate undesirable materials alloying and structural changes in metals used in ICs' interconnect layers, and to limit diffusion-based doping profile changes in the CMOS source/drain regions, which degrade transistor performance and reliability.

Most frequently used annealing processes are furnace annealing, rapid thermal processing (RTP), arc flash annealing, laser annealing, and microwave

annealing (MWA). Recent publications show that MWA produce dopant activation at temperatures of 500-600°C, which are low compared to other processes, but still higher than the post IC processing target of 400°C.

An innovative plasma-based low temperature annealing process will be discussed, with plasma energy providing enhanced dopant activation at relatively low temperature with controlled nanoscale depth dopant diffusion. Preliminary experiments demonstrated good activation of phosphorus (P) dopant at 416 °C while maintaining a relatively uniform junction depth of ~ 20 nm.

Experiments involved using Si wafers implanted with 60 keV P ions with a dose of 5×10^{15} ions/cm². The Si surface temperature, read by a pyrometer, was around 416 °C during the annealing process. Four-point probe measurement revealed sheet resistance of the Si surface wafer before (77-163 KW/sq) and after (42-46 KW/sq) annealing, indicating very good activation of the P atoms at 416 °C.

Following annealing, the P-doped Si wafer was analyzed using X-ray photoelectron spectroscopy (XPS) depth profiling, to explore the distribution of P atoms from the surface into the bulk of the activated Si wafer. Prior to depth profiling, the sample was cleaned with low energy (1 kV) Ar ions bombardment for 2 minutes to remove adventitious carbon and oxygen atoms adsorbed on the surface of materials exposed to atmospheric conditions. The P-activated Si wafer surface cleaning was confirmed by the disappearance of the XPS C / O peaks. P atoms-depth profiling was performed by bombarding the Si surface with 5 keV Ar⁺ ions at 5 minutes interval plus XPS analysis, which revealed that the P 2p and Si 2p XPS peaks remain stable in intensity until full 40 minutes bombardment time. Measurement of the step between the original and etched Si surface, across the etched Si surface edge, revealed 20 nm depth. This value, together with the stable intensity of the XPS P 2p peak after etching indicates that the P dopant concentration is fairly uniform in the first 20 nm of the plasma-enhanced annealing activated Si wafer. Further longer time analysis will determine the P-atoms distribution throughout the entire junction depth.

The preliminary results reported here show that plasma enhanced low temperature processing can induce dopant activation at ~ 400 °C while maintaining shallow junction around 20 nm for fabrication of high-performance Si-based CMOS devices, as well as post IC processing. The process can also be used to condition organic and other materials requiring low temperature conditioning.

SESSION EQ09.08: Synthesis and Processing II
Session Chairs: Himashi Andaraarachchi and Attaul Haq
Monday Morning, December 6, 2021
EQ09-Virtual

8:00 AM *EQ09.08.01

Atmospheric Pressure Plasma Surface Modification of Materials for Environmental Protection and Remediation Antonella Uricchio¹, Teresa Lasalandra¹, Françoise Massines², Gael Plantard^{2,3} and Fiorenza Fanelli⁴; ¹University of Bari “Aldo Moro”, Italy; ²Laboratoire Procédés Matériaux et Energie Solaire, PROMES-CNRS, UPR 8521, France; ³University of Perpignan Via Domitia, France; ⁴National Research Council (CNR), Institute of Nanotechnology (NANOTEC), Italy

Atmospheric pressure non-equilibrium plasmas continue to attract considerable attention in surface engineering [1,2]. By providing unique reactive environments at moderate gas temperatures and atmospheric pressure, they have opened new opportunities to tailor the surface properties of materials as well as to prepare a variety of thin films with different chemical compositions, structures and morphologies. In this context, dielectric barrier discharges (DBDs) have played a major role due to their simple design and versatility. A plethora of DBD-based apparatuses and processes has been therefore devised to meet the ever-increasing demand for atmospheric pressure plasma technologies in various surface engineering applications. In this contribution we will present our recent advances in surface modification by DBDs with a special focus on the development of materials for environmental protection and remediation. The presented examples will include the design of surfaces for enhanced water condensation and recovery [3,4], the preparation of recyclable sorbents for the separation of hydrocarbon liquids from water [5], the deposition of photocatalytic thin films on macroporous supports for wastewater treatment [6], the plasma-assisted exsolution of nanoparticles on the surface of perovskite oxides as a promising approach towards the preparation of nanocatalysts for sustainable chemical production.

[1] F. Massines, C. Sarra-Bournet, F. Fanelli, N. Naudé, N. Gherardi *Plasma Processes and Polymers* 9 (2012) 1041.

[2] F. Fanelli, F. Fracassi, *Surface and Coatings Technology* 322 (2017) 174.

[3] F. Fanelli, A. M. Mastrangelo, F. Fracassi, *Langmuir* 30 (2014) 857.

[4] F. Fanelli, A. M. Mastrangelo, G. Caputo, F. Fracassi, *Surface and Coatings Technology* 358 (2019) 67

[5] F. Fanelli, F. Fracassi, *Plasma Processes and Polymers* 13 (2016) 470

[6] A. Uricchio, E. Nadal, B. Plujat, G. Plantard, F. Massines, F. Fanelli, *Applied Surface Science* 561 (2021) 150014.

8:30 AM EQ09.08.02

Toward a Single-Step Process to Produce a Zn-CNT Hybrid Material Ruairi McGlynn, Paul Brunet, Abhijit Ganguly, Hussein S. Moghaieb, Supriya Chakrabarti, Paul Maguire and Davide Mariotti; Ulster University, United Kingdom

New devices and applications are increasingly requiring tailored material properties which necessitates the development of advanced materials and novel nanocomposites to drive these new technologies. In addition to the material-specific properties there are two other key requirements to the success of new technologies, low-cost to performance ratio and a relative abundance of the materials. Two materials that can satisfy these requirements are carbon and zinc, with their derivative forms such as oxides or sulfides as well as micro- or nano-geometries widening the research impact to a myriad of applications. Blending these materials can lead to composite materials that greatly outperform each individual component material in energy storage applications. ZnO sites can act as pseudocapacitors to enhance the total capacitance, which when combined with a supportive carbon matrix leads to a highly reversible supercapacitor device.¹ Additionally, both ZnO and ZnS have high theoretical capacities in the application of lithium-ion battery anodes, and are relatively abundant, non-toxic, low-cost and environmentally friendly.^{2,3} Mechanical failure due to volume expansion and contraction during the charge and discharge can be alleviated by the usage of highly conductive, flexible and strong carbon-based supports can lead to a range of devices with enhanced performance.⁴

It is obvious that a wide range of applications and benefits are available from the combination of zinc oxides and sulfides with nanocarbons, though the question remains; how can this be achieved simply, at minimum cost and on a larger scale? Significant progress has been made in forming macroscopic

assemblies of CNTs by direct spinning CNT aerogels in a floating-catalyst chemical vapour deposition (FC-CVD) into a fibre or mat,^{5,6} which would represent a strong candidate for the supportive and conductive base. To create a composite material with the FC-CVD system as-is, these fibres and mats would have to be post-treated, diminishing the overall production rate. In this work, we detail the integration of an atmospheric-pressure plasma system with a FC-CVD system where we can successfully obtain a CNT-Zn composite material in a single step. XPS depth profiling measurements demonstrate that the zinc materials penetrate further into the composite when treated in-line compared with an off-line post-treatment. Application-related measurements are reported utilising the in-line produced composite material.

References

- (1) Sankapal, B. R.; Gajare, H. B.; Karade, S. S.; Salunkhe, R. R.; Dubal, D. P. Zinc Oxide Encapsulated Carbon Nanotube Thin Films for Energy Storage Applications. *Electrochim. Acta* **2016**, *192*, 377–384.
- (2) Zhang, Y.; Wei, Y.; Li, H.; Zhao, Y.; Yin, F.; Wang, X. Simple Fabrication of Free-Standing ZnO/Graphene/Carbon Nanotube Composite Anode for Lithium-Ion Batteries. *Mater. Lett.* **2016**, *184*, 235–238.
- (3) Zhang, W.; Huang, Z.; Zhou, H.; Li, S.; Wang, C.; Li, H.; Yan, Z.; Wang, F.; Kuang, Y. Facile Synthesis of ZnS Nanoparticles Decorated on Defective CNTs with Excellent Performances for Lithium-Ion Batteries Anode Material. *J. Alloys Compd.* **2020**, *816*, 152633.
- (4) Zhang, H.; Wang, Y.; Zhao, W.; Zou, M.; Chen, Y.; Yang, L.; Xu, L.; Wu, H.; Cao, A. MOF-Derived ZnO Nanoparticles Covered by N-Doped Carbon Layers and Hybridized on Carbon Nanotubes for Lithium-Ion Battery Anodes. *ACS Appl. Mater. Interfaces* **2017**, *9* (43), 37813–37822.
- (5) Li, Y. L.; Kinloch, I. A.; Windle, A. H. Direct Spinning of Carbon Nanotube Fibers from Chemical Vapor Deposition Synthesis. *Science* (80-.). **2004**, *304* (5668), 276–278.
- (6) Gspann, T. S.; Smail, F. R.; Windle, A. H. Spinning of Carbon Nanotube Fibres Using the Floating Catalyst High Temperature Route: Purity Issues and the Critical Role of Sulphur. *Faraday Discuss.* **2014**, *173*, 47–65.

8:45 AM *EQ09.10.05

On the Early Stages of Si Nanoparticles Growth in Non-Thermal Plasma Paolo Elvati, Xuetao Shi and [Angela Violi](#); Univ of Michigan, United States

The synthesis of nanoparticles (NPs) and films with non-thermal plasma assisted methods offers unique opportunities in the fields of bio-imaging, drug delivery, photovoltaics, microelectronics manufacturing, as well as in renewable energy efforts. The unique conditions of non-thermal plasma systems make them suitable for the synthesis of nanoparticles of materials with high melting points or with properties that are highly dependent on the NPs size distribution (luminescence, hardness). Plasmas also enable synthesis of compound nanoparticles such as group III-V semiconducting materials and metal oxides that require covalent bonding rather than the ionic bonding promoted by liquid phase synthesis.

Understanding the relationship between plasma operating parameters and particle growth, morphology, and composition can lead to the development of tailored nanomaterials and optimization of the conditions for the production of new and novel NPs. These relationships, however, are complicated by the variety of phenomena that occur in plasma and that dominate different stages of the particle growth. One of the key phenomena that controls the early stages of NP growth is the deposition of small species on the surface of incipient nanoparticles. This process is highly dependent on the shape and chemistry of both the small fragments and the surface of clusters, which makes its understanding and modelling still quite difficult.

In this work, we report on results from a computational investigation of silicon NPs with the goals of clarifying how operating conditions (temperature), size and surface of clusters influence the collision events and the dynamics of the surface growth mechanism. Specifically, we focus on the probability to form a bond between small silane fragments (SiH_x , $x = 1-4$) and large silanes Si_4 , Si_2H_6 , and $\text{Si}_2\text{H}_3\text{Si}$ molecules after a collision has taken place (sticking probability). To reduce the parameter space, we investigate the effect of temperature, size, and hydrogen surface coverage.

The results, obtained by using classical reactive molecular dynamics simulations, show that the sticking probability is the result of the interplay between two phenomena: physisorption and chemisorption. While some general trends are common to all types of collisions, like a decrease in the sticking probability with increasing temperature and hydrogen coverage, it is possible to observe a complicated dependence on the colliding species characteristics especially for temperatures below 400 K. This effect is the result of the different reaction pathways and the corresponding surface embedding that are possible for the small fragments, as well as the competing effect between desorption and physisorption to chemisorption conversion. Although the resulting sticking coefficients are not easily expressed in terms of the numerous factors that affect them, they constitute a good dataset for supervised learning models, which we used to quantify both the amount of potential computational effort that can be saved when analyzing similar systems, and to perform a regression of the sticking coefficients, when species that were not directly modelled are required.

9:15 AM EQ09.08.05

Surfactant-Free Copper Oxide Nanoparticles Synthesized by Plasma-Induced Non-Equilibrium Electrochemistry for Solar-Thermal Energy Conversion Hussein S. Moghaieb¹, Chiranjeevi Maddi¹, Praveen Kumar², Miryam Arredondo², Attaul Haq¹, Ruairi McGlynn¹, Harjit Singh³, Paul Maguire¹ and Davide Mariotti¹; ¹Ulster University, United Kingdom; ²Queen's University Belfast, United Kingdom; ³Brunel University, United Kingdom

Solar thermal collectors are one of the technologies used for harnessing and utilizing solar energy, in which the incident radiation is absorbed and converted into thermal energy for use in a wide variety of applications¹. However, conventional collectors, which rely on solid surface absorbers and use traditional heat transfer fluids, exhibit deficiencies due to large heat losses² and poor solar-thermal conversion (STC) performance.³ Direct absorption solar collectors (DASCs), therefore, were introduced to volumetrically absorb and convert solar radiation into heat,⁴ in which nanofluids (NFs) with their exceptional optical and thermal properties can significantly improve the STC efficiency.^{5,6}

In this work, copper oxides (CuO_x) were chosen due to their high thermal conductivity,⁷ broad absorption,⁸ high physical and thermal stability⁹, abundance at low cost and limited environmental impact with low toxicity.¹⁰ The synthesis of our surfactant-free CuO_x nanoparticles (sf- CuO_x NPs) was carried out with a custom-built system based on plasma-induced non-equilibrium electrochemistry (PiNE) which has recently demonstrated exceptional versatility for the production of a wide range of sf-NPs including oxides.¹¹ Furthermore, post-synthesis heat treatment was performed to determine the impacts on the size, morphology, surface structure, and chemical composition of the NPs.

Following, we re-dispersed sf- CuO_x NPs in ethylene glycol (EG) as a base fluid at different volume fractions up to 0.01%. After determining the solar absorption and scattering behaviours of the NFs using measurements from ultraviolet/visible/near-infrared spectroscopy over the wavelength range 280–2500 nm, the NFs were then exposed to simulated solar radiation of one sun ($\sim 1000 \text{ W/m}^2$) and the temperature change was recorded. Temperature measurements were then used to validate a 3-D numerical model employed in Ansys Fluent. The model results revealed that the STC efficiency reached a remarkable value of 81.92% at a volume fraction of as low as 0.01%, indicating that our sf- CuO_x NPs prepared by plasma-liquid interactions represent a promising candidate for NF-based DASCs.

References

1. Duffie, J. A. & Beckman, W. A. *Solar engineering of thermal processes*. (John Wiley & Sons, 2013).
2. Rasih, R. A., Sidik, N. A. C. & Samion, S. Numerical investigation of direct absorption solar collector using nanofluids: A review. in *IOP Conference Series: Materials Science and Engineering* vol. 469 12059 (IOP Publishing, 2019).
3. Chamsa-Ard, W., Brundavanam, S., Fung, C. C., Fawcett, D. & Poinern, G. %J N. Nanofluid types, their synthesis, properties and incorporation in direct solar thermal collectors: A review. **7**, 131 (2017).

4. Minardi, J. E. & Chuang, H. N. Performance of a "black" liquid flat-plate solar collector. *Sol. Energy* **17**, 179–183 (1975).
5. Otanicar, T. P., Phelan, P. E. & Golden, J. S. %J S. E. Optical properties of liquids for direct absorption solar thermal energy systems. **83**, 969–977 (2009).
6. Choi, S. U. S. & Eastman, J. A. *Enhancing thermal conductivity of fluids with nanoparticles*. (1995).
7. Ghosh, S. *et al.* Atmospheric-pressure dielectric barrier discharge with capillary injection for gas-phase nanoparticle synthesis. **48**, 314003 (2015).
8. Yang, Y., Xu, D., Wu, Q. & Diao, P. Cu 2 O/CuO bilayered composite as a high-efficiency photocathode for photoelectrochemical hydrogen evolution reaction. *Sci. Rep.* **6**, 35158 (2016).
9. Qiang, A., Zhao, L., Xu, C. & Zhou, M. Effect of Dispersant on the Colloidal Stability of Nanosized CuO Suspension. *J. Dispers. Sci. Technol.* **28**, 1004–1007 (2007).
10. Zhang, L. *et al.* In situ study of thermal stability of copper oxide nanowires at anaerobic environment. *J. Nanomater.* **2014**, (2014).
11. Saito, G. & Akiyama, T. Nanomaterial Synthesis Using Plasma Generation in Liquid. *J. Nanomater.* **2015**, 123696 (2015).

9:30 AM *EQ09.01.04

Plasma-Assisted Structural Design of Multifunctional Nanocarbon Materials for Extreme-Environmental Applications Ming Xu; Huazhong University of Science and Technology, China

Structural design has always been considered as one of the approaches to obtain and optimize material properties, realizing their value in applications. The same material will display different macro performances through the construction of different structures. One-dimensional and two-dimensional nanomaterials, such as carbon nanotubes, graphene, etc., have a series of excellent physical properties that other traditional materials cannot reach, and have become the preferred research materials in many application fields. Taking them as the "Building Blocks", the final performance of their assembly also depends on the structural design and construction. This time, we will show how to apply the concept of structural design to these nanostructured "building blocks" such as carbon nanotubes and graphene to achieve new breakthroughs in adhesion, sensing, energy storage in extreme environments [1-5].

References

- [1] M. Xu et al. *Science*, 330, 6009 (2010)
- [2] M. Xu et al. *Nat. Commun.*, 7, 13450 (2016)
- [3] X. Wan et al, *Nat. Catalysis*, 2, 259 (2019)
- [4] M. Zhang et al., *Adv. Func. Mat.*, 30, 2004564 (2020)
- [5] X. Gao et al., *Nat. Commun.*, 11, 6160 (2020)

SESSION EQ09.09: Synthesis and Processing III
 Session Chairs: Fiorenza Fanelli and Dilli Babu Padmanaban
 Monday Morning, December 6, 2021
 EQ09-Virtual

10:30 AM *EQ09.09.01

Bringing Plasmas to the Gas-Liquid Interface at the Surface of a Liquid Microdroplet Paul Maguire; Ulster University, Ireland

Microscopic liquid droplets are gaining attention as efficient microreactors for new chemical and nanomaterials processing techniques. Typically, aqueous droplets are introduced into a carrier fluid in a microfluidic channel. However, charged microdroplets, especially in the gas phase e.g. from electrospray, have exhibited interesting effects with regard to enhanced nanomaterials synthesis or accelerated reactions and, as yet, the mechanisms involved are unclear. When a low temperature plasma is added to the gas – liquid interface at a droplet surface, the plasma provides a much greater source of charge flux than other techniques. When the droplets travel through a low temperature plasma at atmospheric pressure a number of remarkable and unexpected effects have been observed. For flight times less than 1 millisecond, certain plasma-induced chemical reactions proceed significantly faster than in plasma – bulk liquid configurations and many orders of magnitude faster than in standard bulk chemistry. The plasma also delivers chemical radicals, photons and ions to the surface and the complex interplay between arriving flux, droplet surface charge, internal and external electric fields as well as the restricted volume and high surface to volume ratio, offers new avenues for microreactor development.

There is a large potential for new plasma-liquid processes in medical, chemical, biological, environmental and materials applications, and the plasma – microdroplet system has unique features that provide opportunities for exploitation, including a controlled gas environment, a large surface area to volume ratio for surface reactions, small volume for rapid mixing, and low droplet temperature which allows for a wide range of liquids, additives and precursors. Chemical synthesis and encapsulation in flight enables on-demand supply of materials and chemicals and also remote delivery, without intermediate filtration or purification stages. However synthesis rates need to be rapid i.e. closer to microseconds than minutes. Applications requiring instantaneous and remote chemical species and/or nanoparticles include, for example, plasma-medicine, agriculture and microreaction.

We have demonstrated the use of droplet streams where each individual droplet acts as a chemical microreactor to produce nanoparticles in flight, many orders of magnitude faster than reported by high energy radiolysis or chemical synthesis. The nature of the charge flux and the formation of a charged surface layer composed of solvated electrons is a critical aspect of this system but little explored or understood. Current theories of microparticle charging in a collisional plasma environment are very limited. While inflight charge measurements represent a significant challenge, in the high noise environment of a plasma, the relatively large size of the droplet (10 – 20 µm diameter) and the limited evaporation over the flight time, offer the prospect of using droplets as a spherical probe to develop enhanced collisional probe theories. We have measured the average charge of microdroplets of ~1E6 electrons, close to the Rayleigh limit and considerably higher than that obtained by other charging methods. Analytical – numerical and finite element simulations, in tandem with charge measurements, are being developed to better understand the droplet electrical environment and ultimately to link chemistry and charge in a consistent framework.

11:00 AM EQ09.09.02

Room Temperature and Time-Efficient Plasma-Induced Exsolution in Perovskites Oxides at Atmospheric Pressure Attaul Haq¹, Fiorenza Fanelli², Hesan Khalid¹, Bruno Alessi¹, Evangelos I. Papaioannou³, Kalliopi Kousi³, Ian S. Metcalfe³, Cristian Savaniu⁴, John T. Irvine⁴ and Davide Mariotti¹; ¹Ulster University, United Kingdom; ²National Research Council (CNR), Institute of Nanotechnology (NANOTEC), Italy; ³Newcastle University, United Kingdom; ⁴University of St Andrews, United Kingdom

Plasmas are widely used industrially for a wide range of processes including for surface cleaning, inducing functionality to the surfaces, chemical reduction of metal oxides and polymerization etc. Here we report the use of an atmospheric pressure plasma in a dielectric-barrier discharge (DBD) configuration for exsolving nanoparticles (NPs) from within the oxide matrix. Usually, the exsolution of NPs in perovskites oxides follows a thermal-reduction process in the presence of hydrogen at temperatures higher than 800 °C for more than 12 h. Surprisingly, DBD treatments of perovskites oxides ($\text{La}_{0.43}\text{Ca}_{0.37}\text{Ni}_{0.06}\text{Ti}_{0.94}\text{O}_{2.955}$, LCTN_{A-site deficient}) resulted in the exsolution of NPs within few minutes at ambient-temperature even without the need for hydrogen. The changes in the size and distribution of NPs in He-fed DBD at 1.2 kV and at 1 kV are compared. Furthermore, the role of hydrogen-containing DBD on the nature of exsolution has also been studied and compared with pure He DBD. The DBD not only induces oxygen vacancies but also provides free electrons that are sufficient for driving the exsolution of NPs from an estimated exsolution depth ranging from 15–45 nm. Such exsolved NPs are firmly socketed within the oxide surface and hence induced excellent catalytic activities as discussed in this contribution. The concept of exsolution on a variety of perovskites oxides can be demonstrated with our DBD system that can even directly be applied for an in-situ energy application [1-8].

References:

- [1] M. Emre Sener, Sanjayan Sathasivam, Robert Palgrave, Raul Quesada Cabrera and Daren J. Caruana, *Green Chem.*, 2020,22, 1406-1413 <https://doi.org/10.1039/D0GC00080A>
- [2] Ding-Xin Liu, Felipe Iza, Xiao-Hua Wang, Zhi-Zhen Ma, Ming-Zhe Rong, Michael G Kong, A theoretical insight into low-temperature atmospheric-pressure He+H₂ plasmas 2013 *Plasma Sources Sci. Technol.* 22 055016 <https://doi.org/10.1088/0963-0252/22/5/055016>
- [3] Islam, Q. A., Paydar, S., Akbar, N., Zhu, B., Wu, Y., Nanoparticle exsolution in perovskite oxide and its sustainable electrochemical energy systems, *Journal of Power Sources* 2021, 492, 229626, <https://doi.org/10.1016/j.jpowsour.2021.229626>.
- [4] Sun, X., Chen, H., Yin, Y., Cuman, M. T., Han, J. W., Chen, Y., Ma, Z., Progress of Exsolved Metal Nanoparticles on Oxides as High Performance (Electro)Catalysts for the Conversion of Small Molecules. *Small* 2021, 17, 2005383. <https://doi.org/10.1002/sml.202005383>
- [5] Kwon, O., Joo, S., Choi, S., Sengodan, S., and Kim, G., Review on exsolution and its driving forces in perovskites. *J. Phys. Energy* 2020, 2, 032001. <https://doi.org/10.1088/2515-7655/ab8c1f>
- [6] Zhu, T., Troiani, H., Moggi, L. V., Santaya, M., Han, M., Barnett, S.A., Exsolution and electrochemistry in perovskite solid oxide fuel cell anodes: Role of stoichiometry in Sr(Ti,Fe,Ni)O₃, *Journal of Power Sources* 2019, 439, 227077. <https://doi.org/10.1016/j.jpowsour.2019.227077>
- [7] V. Kyriakou, D. Neagu, E.I. Papaioannou, I.S. Metcalfe, M.C.M. van de Sanden, M.N. Tampakas, Co-electrolysis of H₂O and CO₂ on exsolved Ni nanoparticles for efficient syngas generation at controllable H₂/CO ratios, *Applied Catalysis B: Environmental* 2019, 258, 117950. <https://doi.org/10.1016/j.apcatb.2019.117950>
- [8] Myung, Jh., Neagu, D., Miller, D., Irvine, J. T. S. Switching on electrocatalytic activity in solid oxide cells, *Nature* 2016, 537, 528–531. <https://doi.org/10.1038/nature19090>

11:15 AM EQ09.09.03

Defluorination of the Fluoropolymer Surfaces for Composite Materials in the Industrial Market [Faegheh Fotouhi](#)^{1,2,3}, [Jacopo Profili](#)^{2,3}, [Morgane Laurent](#)⁴, [Sethumadhavan Ravichandran](#)⁴, [Gowri Dorairaju](#)⁴ and [Gaétan Laroche](#)^{1,2,3}; ¹Université Laval, Canada; ²Département de génie des mines, de la métallurgie et des matériaux, Centre de Recherche sur les Matériaux Avancés, Université Laval, Canada; ³Hôpital St. François d'Assise, Canada; ⁴Saint-Gobain Research North America, United States

Fluoropolymers are suitable for many applications, including textile, building, and biomedical materials. They are mainly used for their chemical inertness and low friction coefficient. However, for many applications, their low surface energy leads to poor adhesion during the assembly with other materials. Among the different techniques used to enhance the adhesion of polymers, atmospheric pressure discharges (APD) remain fast and cheap methods that are suitable for industrial applications. The highly energetic species present in the ionized gas allow the breaking of molecular bonds at the film surface and favor the recombination with polar free radicals from the discharge. Although this approach has been proven to be efficient, the understanding of the chemical and physical processes leading to these results remains not yet fully understood. In this study, we performed the modification of fluoropolymer surfaces at atmospheric pressure by using an inert plasma treatment equipped with a roll-to-roll system. The effect of the discharge on different fluoropolymers was studied through a detailed surface analysis before and after each treatment. The characterization of the extreme surface was carried out by X-ray photoelectron spectroscopy (XPS) in both survey and C1s high resolution. In addition, infrared spectroscopy in the attenuated total reflectance mode (IR-ATR) was used to evaluate the modifications observed on the first top micrometers of the samples. All results were correlated with the modification of the surface energy obtained from the static contact angle analysis measured using both water and diiodomethane. The dynamic contact angle was used to evaluate the affinity of the different functional groups deposited with water. The obtained results highlight the possibility to create new hydrophilic functionalities bonded on the fluoropolymer that is likely to improve the adhesion of these polymers in composite assemblies. These promising results constitute the first step toward a better understanding of the fundamental chemical modifications induced by using this relatively new approach. Keywords: Atmospheric pressure plasma, fluoropolymer, power, organic precursor, duty cycle.

11:30 AM *EQ09.09.04

Water-Soluble Luminescent Si Nanocrystals Through Colloidal PEGylation and Plasma Induced Acrylic acid Grafting [Himashi P. Andaraarachchi](#), [Zhaohan Li](#) and [Uwe R. Kortshagen](#); University of Minnesota Twin Cities, United States

Luminescent silicon (Si) nanocrystals are intriguing nanomaterials for biomedical application due to their unique optical properties and biocompatibility. Compared with cadmium containing fluorophores, Si nanocrystals are relatively non-toxic, abundant, and biocompatible. Synthesis of water-soluble Si nanocrystals is challenging as they are hydrophobic and mainly dispersible in non-polar organic solvents through hydrosilylation with non-polar alkyl ligands. A variety of approaches have been used to synthesize water-soluble Si nanocrystals through post synthetic surface modification with hydrophilic ligands including carboxylic acids, amines, hydroxyl groups, and hydrophilic polymers. Here, we demonstrate two approaches to synthesize water-soluble Si nanocrystals: A single ligand colloidal surface modification with polyethylene glycol (PEG) ligands and a two-step method of mixed-ligand surface modification through inflight surface functionalization with acrylic acid ligands coupled with colloidal PEGylation. Silicon nanocrystals were synthesized in a continuous-flow, low pressure capacitively coupled plasma reactor operating at pressure around 2 torr. In contrast to pristine hydrophobic Si particles, surface functionalized Si nanocrystals were dispersible in both water and biological buffer solutions and colloidal stable for about 24 h. Their surface properties were evaluated using X-ray photon spectroscopy and Fourier transform infrared spectroscopy. Transmission electron microscopy images provided evidence for both individual passivation and encapsulation of multiple nanoparticles together. The acrylic acid grafted-PEGylated Si nanocrystals were evaluated with MDA-MB-231 cell line and found that the cells are tolerant to these nanocrystals up to 30 µg/mL for 72 hours.

This work was primarily supported through the National Institute of Health under award R01DA045549.

12:00 PM EQ09.08.03

Microplasma-Based Synthesis of Metal-Oxide Transport Layers for Perovskite Solar Cell [Subha Sadhu](#), [Dilli Babu Padmanaban](#), [Chiranjeevi Maddi](#),

Slavia D. Dsouza, Paul Maguire and Davide Mariotti; Ulster University, United Kingdom

Perovskite solar cells are considered as “The Next Big Thing” in photovoltaics research as within only ten years the power conversion efficiency (PCE) has reached from 3.8% to 23%.^[1] Researchers worldwide are developing various procedures for mass scale fabrication of perovskite devices. The three main components of fabricating any types of solar cell devices are: absorbing layer to absorb photons followed by exciton formation, transport layers to conduct the charge carriers and metal contacts to transfer the carriers to the circuit. Transport layers are divided in two main categories electron transport layer (ETL) and hole transport layer (HTL) and metal oxides are largely favoured for both types of transport layers. Microplasma-based synthesis of metal-oxide transport layer is an emerging technology and a potential alternative to other chemical and physical synthesis methods.^[2] The one-step synthesis procedure is simple, less time consuming than other chemical method, can be performed in atmospheric condition and does not require any harsh or toxic chemicals. The transport layers can also be deposited easily with flexible substrates and do not need high temperature annealing which reduce the conductivity of the transparent conducting oxide substrates. In this contribution, we have synthesized HTL (NiO, CuO) and ETL (ZnO) through microplasma methods and directly deposited onto the device structure. From in-depth characterization techniques we observed that the as-synthesized metal-oxides are highly pure, stable and do not require any purification or annealing after the deposition. The absolute position of the band-edges can be tailored to match, for instance, with that of methyl ammonium lead iodide (MAPI) perovskite and the metal-oxides. The as-fabricated perovskite devices show promising photon to electron conversion efficiency.

12:15 PM BREAK

SESSION EQ09.10: General Session
Session Chair: Angela Violi
Monday Afternoon, December 6, 2021
EQ09-Virtual

4:00 PM *EQ09.10.01

Plasma-Driven Solution Electrochemistry—Synthesizing Materials at the Plasma-Liquid Interface [Peter Bruggeman](#); University of Minnesota, United States

Plasma-induced solution chemistry can be driven by electrons, ions, photons and radicals. In thermal catalytic, electrocatalytic, conventional electrolysis and plasmon-driven chemical transformations, metal surfaces play key roles. In contrast, in plasma-driven processes, electrons are produced in a gas phase plasma and injected into the interfacing liquid without the need for a solid electrode. The high-power density in plasmas enables exceptionally large yields of electrons, some having high energies up to 10 eV or more, leading to a high concentration of electrons in a near plasma-liquid interfacial region with a thickness up to a few tens of nm. These conditions enable unique chemical transformations including the synthesis of metallic nanomaterials enabled by the reduction of salt ion precursors. This presentation will provide an overview of our current understanding of the processes underpinning material synthesis at the plasma liquid interface and an outlook on opportunities to control such processes.

This work was supported by the Army Research Office under Grant Number W911NF-20-1-0105.

4:30 PM EQ09.10.02

Flexible Glass-Based pH Sensor Using Cold Atmospheric Plasma Deposition [Venkat Kasi](#), Ulisses Heredia, Sotoudeh Sedaghat and Rahim Rahimi; Purdue University, United States

pH is an essential parameter most commonly used to evaluate and control the conditions of various chemical and biological processes as well as to maintain the quality of products in many industries ranging from health care, food, environmental, chemical, and pharmaceutical industries. Different techniques including potentiometric, chemiresistive, capacitive, and optical methods have been developed for measuring pH. Among these methods, potentiometric sensing technique has gained considerable interest because of simple and low-cost fabrication process. Various functional materials including glass, metal oxides, and conductive polymers have been investigated for the fabrication of potentiometric based pH sensors. Generally, sensing performance of a pH sensor is evaluated in terms of its sensitivity, selectivity, working range, and repeatability. Most of the commercially available pH sensors consist of glass membrane as the sensing component because of several advantages of glass-based electrodes such as long service life, high accuracy, and excellent stability in various solutions. However, due to their bulkiness and poor mechanical properties, conventional glass-based sensors are not ideally suitable for wearable or flexible applications.

In recent years, cold atmospheric plasma (CAP) assisted deposition technique has gained much attention because of its feasibility in producing thin films with high quality and consistent properties in large scale onto desired substrates in atmospheric conditions. The CAP deposition technique eliminates the requirement of conventional slow vacuum deposition processes (e.g., CVD and PVD) while producing superior thin film deposition results compared to the conventional thermal spray coating technologies. In this work, we have demonstrated the use of CAP thin film glass deposition to fabricate flexible solid-state glass-based pH sensor using siloxane precursors in a simple and facile approach. Our sensitivity test results indicated that these sensors exhibit excellent sensitivity and selectivity over a wide physiologically relevant pH range. Additionally, in this study we investigated the morphology and chemical composition using SEM and FTIR and correlated with the sensing properties of the demonstrated all solid-state pH sensor.

4:45 PM EQ09.10.03

Plasma Induced Rapid Exsolution of Nanoparticles in Non-Stoichiometric Perovskite Oxides [Hessan Khalid](#)¹, Attaul Haq¹, Bruno Alessi¹, Evangelos I. Papaioannou², Kelly Kousi², Ian S. Metcalfe², Cristian Savaniu³, John T. Irvine³, Paul Maguire¹ and Davide Mariotti¹; ¹Ulster University, United Kingdom; ²Newcastle University, United Kingdom; ³University of St Andrews, United Kingdom

Exsolution of nanoparticles (NPs) for oxide support is considered as highly effective and efficient process for the synthesis of functional nanomaterial to be applied in catalysis and energy conversion applications. Unlike other nanoparticles decoration techniques (for instance deposition or impregnation), exsolution offers great control on the size and distribution of the particles and offers anchorage with the host matrix making them resilient to agglomeration. Conventionally, exsolution is performed in mild reducing atmosphere at elevated temperature, making them a relatively lengthy (10-30 hours) and energy demanding process. Herein a new dimension in exsolution is explored and NPs exsolution is demonstrated using low pressure plasmas, making exsolution to occur in minutes rather than hours. A non-stoichiometric (A-site deficient) perovskite oxide (POx) having a composition of $\text{La}_{0.43}\text{Ca}_{0.37}\text{Ti}_{0.94}\text{Ni}_{0.06}\text{O}_{2.955}$ (LCTN) treated in low pressure plasma in argon atmosphere results in the exsolution of nanoparticles. Particle size and density of the exsolved nanoparticles were optimized by tuning the treatment time and plasma power, which also helps in understanding the mechanism involved

in plasma enhanced exsolution. The average particle size does not change drastically and lies within the range of 19-22 nm for different plasma treatment times. However, the plasma density changes from 60 particles/ μm^2 to ~ 500 particles/ μm^2 when process time is increased from 10 minutes to 15 minutes. The creation of oxygen vacancies and a negative surface charge density are considered the main driving forces for plasma-induced exsolution. The effect of exsolved nanoparticles was analysed by employing CO catalytic testing to access CO_2 production rate. The catalytic reactivity of the plasma exsolved LCTN samples have been tested and present encouraging results. This makes plasma exsolution an interesting approach which will open new dimension in the field exsolution and provides future solutions in catalysis and energy conversion.

5:00 PM EQ09.10.04

Late News: Optical Emission Spectroscopy of an Atmospheric Pressure Dielectric Barrier Discharge for Surface Modification [Alex Destrieux](#)^{1,2,3}, Jacopo Profili^{2,3}, Morgane Laurent⁴ and Gaétan Laroche^{1,2,3}; ¹Université Laval, Canada; ²Département de génie des mines, des matériaux et de la métallurgie, Centre de Recherche sur les Matériaux Avancés, Université Laval, Canada; ³Hôpital Saint François d'Assise, Canada; ⁴Saint-Gobain, United States

Today, atmospheric pressure dielectric barrier discharges (DBD) have the potential to make the difference for the transition toward a cleaner and prosperous manufacturing processes. Compared to low pressure plasma, atmospheric pressure plasma does not require expensive pumping systems or closed reactors. For this reason, DBD processes are more suitable for industrial applications where large surfaces must be treated. Also, the possibility to operate surface modifications at room temperature makes DBDs particularly suitable for the modification of thermosensitive materials such as composite polymers.

In the last years, researchers have demonstrated that discharges at atmospheric pressure are very sensitive to the gas composition, the electrodes geometry, or the electrical excitation used. As an example, in nitrogen operating plasma, few tenth of ppm added can stabilize the discharge in a homogenous physical regime, while few hundreds of ppm can create a filamentary mode. These different physical regimes can differently affect the surface, provoke a change in the chemical reactions and finally lead to different surface properties. One can easily imagine that a small modification of the physical regime during an industrial process could provoke a strong modification of the performance of the final products.

Through this work, we aim to highlight the current understanding of the chemical reactions involved in a DBD process during the modification of a large polymer area. The remaining scientific challenges to control the physical regimes in an industrial reactor will also be presented. To gain insight into the physics of the discharge, optical emission spectroscopy (OES) and electrical characterization have been performed in real time. Measurements were performed at atmospheric pressure in flowing N_2 . N_2O was also admixed to understand the influence of impurities on the behavior and the species present in the discharge. Results show that in pure N_2 , the main feature of the spectra corresponds to transition of the N_2 second positive system (C-B). Several peaks of the NO (A-X) transition, as well as the CN (B-X) have been also observed. When a small amount of N_2O is added to the discharge, a complete disappearance of the CN and NO is denoted. The N_2 level and NO being excited mainly by direct electron impact, the absence of NO and the slight decrease of N_2 intensities have been related to the reduction of the electron temperature. In comparison, a decrease of CN emissions with the increase of N_2O has been related to lowered production of C or CN from the etching of fluoropolymer during the process. To confirm this, different electrical conditions have been compared. A modulated voltage has been created to control the ON time of the discharge. The results suggest that, by changing the duty cycle while maintaining the same mean power, optical emissions of the CN were less intense at lower voltage and higher duty cycle.

These results were correlated with XPS analysis of the surface. The analysis indicates that the lower the voltage, the higher the amount of CN present on the surface, which was correlated to the lesser CN concentration measured in the gas phase. This means that impurities and/or the electrical excitation of the discharge play an important role in the amount of CN on the surface, and hence on the adhesion improvements of the polymer. In conclusion, the real-time analysis of the CN emissions by OES seems a very promising method to control the process and ensure the good reproducibility of the surface properties.

5:05 PM EQ09.10.06

Atmospheric Pressure Plasma Synthesis of Bismuth Quantum Dots [Ankur U. Kambley](#), Bruno Alessi, Paul Maguire and Davide Mariotti; Ulster University, United Kingdom

Plasma processes operated at atmospheric pressure have been shown to be reliable and cost efficient methods¹ for material synthesis and surface engineering for micro/nanoscale fabrication. More specifically, atmospheric pressure microplasmas are of great interest for metal nanoparticle synthesis from bulk solid materials, by-passing conventional processes that require hazardous chemicals, numerous processing steps and/or expensive vacuum equipment.² Metal nanoparticles have shown interesting optical and electronic properties. At the nanoscale, metal nanoparticles exhibit a transition into a semiconductor behaviour and bandgap widening due to quantum confinement.^{3,4} Especially bismuth metal, owing to its large exciton Bohr's radius, starts exhibiting quantum confinement at diameter of $\sim 50\text{nm}$.⁴ This bismuth semimetal behaviour is highly desirable for optoelectronics, energy storage and thermoelectric applications.

Here we present work on the synthesis of bismuth quantum dots (Bi-QDs) by a one-step atmospheric pressure plasma process from a bismuth wire, either for direct deposition in the form of films or directly dispersed in liquid. Various plasma reactor architectures are examined to study the possible deposition conditions. The synthesised Bi-QDs are studied for their morphological, chemical, optical and electronic properties. The mean diameter of these QDs is in the range of 2-3 nm depending on the gas flow. XPS analysis shows the presence of oxidation peaks however XRD analysis show metallic peaks only which indicates the presence of surface oxidation which may have been caused by atmospheric interactions following the synthesis process.

Reference:

1. Velusamy, T. *et al.* Ultra-small CuO nanoparticles with tailored energy-band diagram synthesized by a hybrid plasma-liquid process. *Plasma Process. Polym.* **14**, 1–8 (2017).
2. Yao, D. *et al.* In Situ Fragmented Bismuth Nanoparticles for Electrocatalytic Nitrogen Reduction. *Adv. Energy Mater.* **10**, (2020).
3. El-Sayed, M. A. Some interesting properties of metals confined in time and nanometer space of different shapes. *Acc. Chem. Res.* **34**, 257–264 (2001).
4. Zhou, G., Li, L. & Li, G. H. Semimetal to semiconductor transition and thermoelectric properties of bismuth nanotubes. *J. Appl. Phys.* **109**, (2011).

5:20 PM EQ09.08.04

Rapid and One-Step Synthesis of Nickel Oxide Nanoparticle Thin Films Using Gas Phase Microplasma in Ambient Air [Dilli Babu Padmanaban](#), Slavia D. Dsouza, Paul Maguire and Davide Mariotti; Ulster University, United Kingdom

Microplasma techniques in recent times achieved attractive performance in nanomaterial processing. Microplasmas are special kind of sub-millimetre plasmas that are simple and easy to establish for different applications.^{1,2} With this technique several kinds of nanomaterials such as metal, transition metal oxides etc. were demonstrated with flexibility over the choice of precursors.³ Nickel oxide (NiO) is an excellent p-type semiconductor, which is widely employed as electrode material in many applications like supercapacitors, batteries, solar cells.^{4,5,6} NiO can be produced through chemical and physical deposition methods, however, most of current methods rely on toxic precursors and time consuming post-process steps.

In this work, we demonstrate the synthesis of nickel oxide nanoparticle thin film using a gas phase microplasma technique. The characteristics of the films

were studied for different oxygen precursor along with He carrier gas and film deposition conditions. It was observed that at a given He/O₂ gas mixture, the films appear with different macroscopic morphologies including columnar or planar features depending on the deposition condition. The nanoparticles deposited however exhibit diameters well below 10 nm. Surface chemical analysis and the investigation of the crystal structure show that the nanoparticle are composed of cubic NiO phase. We present the initial application of this process for transport layer in solar cell devices.

Reference:

- (1) Chiang, W.; Mariotti, D.; Sankaran, R. M.; Eden, J. G.; Ostrikov, K. (Ken). *Adv. Mater.* 2019, 32 (18), 1905508.
- (2) Mariotti, D.; Belmonte, T.; Benedikt, J.; Velusamy, T.; Jain, G.; Švrček, V. *Plasma Process. Polym.* 2016, 13 (1), 70–90.
- (3) Mariotti, D.; Sankaran, R. M. *J. Phys. D: Appl. Phys.* 2010, 43 (32), 323001.
- (4) Mamak, M.; Coombs, N.; Ozin, G. A. *Adv. Funct. Mater.* 2001, 11 (1), 59–63.
- (5) Jeng, J.-Y.; Chen, K.-C.; Chiang, T.-Y.; Lin, P.-Y.; Tsai, T.-D.; Chang, Y.-C.; Guo, T.-F.; Chen, P.; Wen, T.-C.; Hsu, Y.-J. *Adv. Mater.* 2014, 26 (24), 4107–4113.
- (6) Nelson, P. A.; Elliott, J. M.; Attard, G. S.; Owen, J. R. *Chem. Mater.* 2002, 14 (2), 524–529.

5:35 PM BREAK

SESSION EQ09.11: Synthesis and Processing IV
Session Chairs: Zheng Bo and I-Chun Cheng
Monday Afternoon, December 6, 2021
EQ09-Virtual

6:30 PM *EQ09.11.01

Plasma Materials Processing with Controlled Microdroplets—Printing and Particles Synthesis Tsuyohito Ito^{1,2}, Kaishu Nitta¹, Yoshiaki Shimizu² and Kazuo Terashima^{1,2}; ¹The University of Tokyo, Japan; ²National Institute of Advanced Industrial Science and Technology (AIST), Japan

With recent development of atmospheric-pressure technologies, various plasma applications with liquid/solution have been extensively studied. In this presentation, we are demonstrating pattern drawing as well as monodispersed spherical particle synthesis via atmospheric-pressure plasma using controlled microdroplets. Such microdroplets were ejected from an inkjet device with high reproducibility in place and size.

The first part of the presentation is about development of plasma-assisted inkjet printing, where inks during flight and after landing on a substrate are irradiated by atmospheric-pressure nonequilibrium plasma. Nanosecond pulsed discharge plasmas were applied here. When the ejected ink was exposed to plasma, reactive species from the plasma as well as rapid and local heating are expected to promote various reactions. Thus plasma-assisted inkjet printing could provide various advantages to inkjet printing, such as less pre- or post-treatments, low-temperature and rapid sintering/reduction, narrower pattern width, and/or on-site polymerization. Such advantages will be demonstrated with silver patterning using silver-nanoparticle-dispersed ink [1], poly(3,4-ethylenedioxythiophene) (PEDOT) pattern fabrication using 3,4-ethylenedioxythiophene (EDOT) monomer stock solution ink [2], and gold patterning using particle-free aqueous chloroauric acid solution ink [3].

The later part will be about monodispersed sub-micrometer spherical gold particles synthesis from chloroauric acid (HAuCl₄) solution [4]. While our previous study demonstrated that size-controlled particle synthesis with microdroplets generated by a mist atomizer, the particle sizes were distributed widely, originating from wide size distribution of the mist [5]. Here, by using an inkjet device, microdroplets were generated with high reproducibility. The plasma applied here was radio-frequency argon plasma. The synthesized sub-micrometer gold particles have a narrow size distribution (3%–9% standard deviation), and their diameters can be controlled at least in the 0.3–0.6 μm range by adjusting the concentration of the solution. Further details will be presented in the symposium.

- [1] M. Tsumaki, K. Nitta, S. Jeon, K. Terashima, T. Ito, *J. Phys. D: Appl. Phys.* 51, 30LT01 (2018).
- [2] K. Nitta, M. Tsumaki, T. Kawano, K. Terashima, T. Ito, *J. Phys. D: Appl. Phys.* 52, 315202 (2019).
- [3] K. Nitta, K. Ishizumi, Y. Shimizu, K. Terashima, T. Ito, *Materials Chemistry and Physics* 258, 123836 (2021).
- [4] K. Nitta, Y. Shimizu, K. Terashima, T. Ito, *J. Phys. D: Appl. Phys.* 54, 33LT01 (2021).
- [5] M. Tsumaki, Y. Shimizu, T. Ito, *Materials Letters* 166, 81 (2016).

7:00 PM *EQ09.11.02

Sputtering Deposition with Impurities—Another Key Parameter to Control Film Structures Naho Itagaki; Kyushu Univ, Japan

Structures of sputter-deposited films have been mostly determined in a way shown in the Thornton diagram, in which there are two key parameters: substrate temperature and sputtering pressure. Here we add another parameter, *impurity*, that adsorbs on, migrates on, and eventually desorb from the surfaces, and thus modify the film structures.

The first example is sputter deposition of single crystalline ZnO films on 18%-lattice mismatched sapphire substrates using N atoms as impurities. Generally, growth of single crystalline films on such large lattice mismatched substrates is impossible because the crystal growth ends up in the formation of relatively large three-dimensional (3D) islands (~100 nm in diameter) with large number of dislocations. Interestingly, however, we have observed that control of adsorption/desorption behavior of N atoms during deposition enables us to grow single crystalline ZnO films even on the sapphire substrates [1]. Here, buffer layers consisting of nano-sized 3D islands are initially grown by making N atoms adsorb on the surfaces. Next, ZnO films are fabricated on the 10-nm-thick buffer layers without N atoms. The crystal grains start to grow originating from the 3D islands, but in a short time, they coalesce to form two-dimensional (2D) layers. Eventually, the films grow in 2D mode having atomically flat surfaces. We consider that the desorption/adsorption behaviour of N atoms influences the surface energy and brings this interesting growth mode. During the buffer layer deposition, adsorbed N atoms lower the surface energy and lead to the formation of nano-sized grains. Such grains with high surface-to-volume ratio relieve the strain efficiently at the surface, resulting in the low dislocation density. On the other hand, N-atom desorption after the buffer layer deposition causes a drastic increase in the surface energy, which provides a driving force for coalescence of crystal grains and 2D-layer formation. In fact, we observed from vacuum ultraviolet absorption spectroscopy (VUVAS) and secondary ion mass spectroscopy that N solubility in ZnO is low of a few atomic ppm. This property makes N atoms segregate to the surface as well as to the grain boundaries, and thus reduces the surface free energy.

The next example is sputter deposition of amorphous In₂O₃:Sn (a-ITO) films on glass substrates. ITO films are essential for transparent electrodes, and a-ITO films have recently attracted attention due to the advantages such as surface smoothness, good short-range uniformity, low internal stress, and high etching rate. However, the mobility of conventional a-ITO films, fabricated below crystallization temperature, is quite low of 20–30 cm²/Vs. Furthermore, the amorphous phases are unstable and easily crystallized around 150°C, limiting the use of a-ITO films in practical devices. Here we show that impurities

can solve the problems again. We have succeeded in fabrication of a-ITO films at high temperature of 150°C using N atoms, where the films maintain the amorphous structures even after annealing at 300°C. Both VUVAS and x-ray fluorescence results indicate that the amorphization is caused not only by the incorporated N atoms into the films that disorder the bixbyite In_2O_3 structure, but by the adsorbed N atoms inhibiting the crystal nucleation, which are eventually desorbed from the surfaces. The most remarkable feature of the a-ITO films is the high carrier mobility over 50 cm^2/Vs , attributed to the high-temperature deposition leading both to increased film density and to enhanced short- and mid-range ordering in the amorphous structures.

We believe that sputtering deposition with “impurities” offer new opportunities for designing materials with unprecedented structures.

This work was supported by JSPS KAKENHI Grant Numbers JP21H01372, NTT collaborative research, and Toyota Riken Scholar.

[1] N. Itagaki, et al., *Sci. Rep.*, 10, 46691 (2020).

[2] T. Takasaki, et. al., *Proc. 9th ICRP*, 60, GT1.150 (2015).

7:30 PM EQ09.11.03

Boron Nitride Modified via Plasma Processing in Hydroquinone Solution for Preparation of Polyrotaxane Composite Kenichi Inoue^{1,2}, Taku Goto^{1,2}, Tsuyohito Ito^{1,2}, Yoshiki Shimizu², Yukiya Hakuta², Kohzo Ito¹ and Kazuo Terashima^{1,2}; ¹The University of Tokyo, Japan; ²National Institute of Advanced Industrial Science and Technology (AIST), Japan

Plasmas in solution provide attractive processing environments for surface modification of materials. The chemical species such as oxygen and hydroxyl radicals in plasma introduce functional groups on surface of materials [1,2], and such surface modifications on carbon nanotube or hexagonal boron nitride (hBN) were reported to help their dispersion in polymers for developments of composite materials [3,4]. Our group revealed that surface modification via plasmas in solution was effective to achieve tough composites with high filler contents [4]. However, the mechanism of dispersion via such plasma modification is not fully understood and the methods to evaluate the surface modification is still insufficient.

In this study, zeta potential was used as the indicator of surface modification of hBN particles for developing its composite elastomers with polyrotaxane.

Our previous study demonstrated that a plasma in solution with hydroquinone additive could produce water-dispersible hBN with higher zeta potential than hBN modified by a plasma in solution without additives [5]. Here, such water-dispersible hBN was dispersed into polyrotaxane as composite materials. Polyrotaxane is a unique polymer with movable crosslinking points allowing homogeneous deformation which agrees with ideal rubber elasticity [6]. The prepared hBN/polyrotaxane composites were observed with X-ray computed tomography (X-CT), and their tensile properties were measured.

In this experiment, plasmas were generated in flowing solution with cavitation bubbles dispersing hBN particles having a diameter of 0.2 μm by applying a bi-polar pulsed voltage [7]. Plasma processing in hydroquinone solution could produce water-dispersible hBN particles named as “HQpBN”, and hBN particles modified via plasma processing in pure water were named as “pBN”. The zeta potential measurement (ZetaView PMX 110, Particle-Metrix) confirmed that HQpBN had zeta potential of -43 mV at pH 7, slightly higher than -37 mV of pBN. Polyrotaxane composites with hBN concentration of 30 wt% were prepared with the pBN and HQpBN. X-CT (SkyScan1278, Bruker Inc.) observation revealed that pBN/polyrotaxane composite had pBN aggregate with size of 1–10 μm inside the composite, whereas HQpBN/polyrotaxane composite had no observable aggregates with a resolution of 0.5 $\mu\text{m}/\text{pixel}$. The pBN/polyrotaxane composite had tensile strength of 3.7 MPa and extension ratio at break of 1.6, whereas the HQpBN/polyrotaxane composite achieved tensile strength of 6.5 MPa and extension ratio at break of 2.0.

It was demonstrated that hBN with enlarged zeta potential showed uniform dispersion in composite and achieved high tensile properties of composite. These results suggest that the zeta potential can be an indicator of surface modification via plasma in solution with the purpose for preparing uniformly dispersed composites.

[1] J. P. Boudou, J. I. Paredes, A. Cuesta, A. Martínez-Alonso, and J. M. D. Tascón, *Carbon N. Y.* **41**, 41 (2003).

[2] N. Sakakibara, K. Inoue, S. Takahashi, T. Goto, T. Ito, K. Akada, J. Miyawaki, Y. Hakuta, K. Terashima, and Y. Harada, *Phys. Chem. Chem. Phys.* **23**, 10468 (2021).

[3] T. Shirafuji, Y. Noguchi, T. Yamamoto, J. Hieda, N. Saito, O. Takai, A. Tshchimoto, K. Nojima, and Y. Okabe, *Jpn. J. Appl. Phys.* **52**, 125101 (2013).

[4] T. Goto, M. Iida, H. Tan, C. Liu, K. Mayumi, R. Maeda, K. Kitahara, K. Hatakeyama, T. Ito, Y. Shimizu, H. Yokoyama, K. Kimura, K. Ito, Y. Hakuta, and K. Terashima, *Appl. Phys. Lett.* **112**, 101901 (2018).

[5] K. Inoue, T. Goto, M. Iida, T. Ito, Y. Shimizu, Y. Hakuta, and K. Terashima, *J. Phys. D: Appl. Phys.* **53**, 42LT01 (2020).

[6] K. Minato, K. Mayumi, R. Maeda, K. Kato, H. Yokoyama, and K. Ito, *Polymer*. **128**, 386 (2017).

[7] Y. Oka, K. Ohnishi, K. Asami, M. Suyama, Y. Nishimura, T. Hashimoto, K. Yonezawa, T. Nakamura, and M. Yatsuzuka, *Vacuum* **136**, 209 (2017).

7:45 PM EQ09.11.04

Three-Dimensional Porous Au/Ag Nanostructures Microplasma-Engineered Nanoassemblies on Cellulose for Surface Enhanced Raman Scattering Properties Jui-Yi Yeh; National Taiwan University, Taiwan

Assembly of functional nanostructures on substrates are useful for chemical and biomolecular sensing, optoelectronics, catalysis, and energy conversion and generation. However, conventional methods to produce assembly of nanostructures on substrates are usually time-consuming, complicated, and involving toxic and expensive chemicals. Here we report the fabrication method of microplasma-engineered nanoassembly (MEN) of plasmonic Au-Ag core-shell nanoparticle for ultrasensitive flexible surface-enhanced Raman scattering (SERS) substrates. Plasmonic Au-Ag core-shell NPs with tuned LSPR properties can be synthesized

and deposited on cellulose papers in one step with ambient condition using microplasmas[1]. The synthesized Au-Ag core-shell NPs are composed with crystalline-twinned Au cores coated by Ag shells via epitaxial growth under microplasmas, providing enhanced charge transportation during Raman scattering. 3D confocal microRaman scattering study shows that a large SERS volume was formed in the as-fabricated MEN substrates, leading significant SERS properties of 1 fM LoD and $\sim 10^{12}$ enhanced factor (EF) with the Rhodamine 6G (R6G) as the Raman probe. However, we also demonstrated the different kinds of Raman probe including Ketoprofen (KP), folic acid (FA), and Salicylic acid (SA). They are one of the important molecules of the human body. The limit of detection (LOD) of KP, FA and SA by Au@Ag SERS paper-based substrate can be low to 10^{-10}M , 10^{-12}M and 10^{-8}M . To sum up, Au@Ag material on paper-based substrate could provide SERS performance as sensitivities technique for the detection of human body molecular. In the future, our work demonstrates a scalable method to synthesize plasmonic nanoassemblies under ambient condition for emerging applications including nanocatalysis, sustainable energy, and biomedical imaging.

8:00 PM EQ09.11.05

Microplasma Nanoengineering of Emission-Tunable Colloidal Nitrogen-Doped Graphene Quantum Dots for Broad-Range Fluorescent pH Sensors Darwin Kurniawan¹, Kostya (. Ostrikov² and Wei-Hung Chiang¹; ¹National Taiwan University of Science and Technology, Taiwan; ²Queensland University of Technology, Australia

Graphene quantum dots (GQDs), one of the newest types of carbon nanoparticles (CNPs) with size <20 nm, have attracted many research attentions due to the highly tunable photoluminescence (PL) properties, biocompatibility, chemical and photo stability, and low toxicity. Doping GQDs with heteroatoms, such as nitrogen, can increase the PL quantum yield and has strong electron withdrawing ability. Therefore, nitrogen-doped GQDs as fluorescent pH monitor excels in sensitivity, selectivity, rapidity, and applicability comparing with the conventional electrochemical method, especially for bio-related and

medical applications. Good biocompatibility and low toxicity also make NGQDs more preferable to semiconductor quantum dots, organic fluorescent dyes, and noble-metal nanoparticles. As a matter of fact, pH value plays a very important and crucial role in all life forms. A small variation in pH not only endangers the lives of plants and animal but also human beings as it will mainly pollute our drinking water, which may cause some health issues, like physiological dysfunction or diseases. Moreover, with the fact the extracellular pH value of cancerous cell is lower than the intracellular pH value, early cancer diagnostic can be achieved.

Most of the approaches for synthesizing NGQDs are complex, time-consuming, in need of harsh reaction condition, and costly. Hereby, microplasma emerges as one of the most promising approaches for nanomaterials processing due to its facile, stable, efficient, and relatively low cost. The high electron density provided are very energetic (~10eV), which allows non-thermal dissociation of molecular gases to form high concentrations of reactive radical species, e.g. OH•, O•, O₂•, and NO•. These reactive radical species along with electrons are brought into the precursor solutions and will interact with the solution chemical species to form GQDs in a cascaded chemical reactions.

Here we report a novel and effective synthesis of the emission-tuneable NGQDs by nanoengineering the N dopant configuration and surface functionalities of GQD surfaces under ambient conditions using microplasmas. The emission-tuneable NGQDs was explored by precisely controlling the chemistry conditions of the reactions during the synthesis. This synthetic method leads to highly crystalline particles with easily tunable properties in high reproducibility from a simple chitosan biomass treated in different dilute acid solutions. Based on protonation and deprotonation of NGQDs surface functional groups, it is believed that the distinct proportions of surface functionalities can greatly influence the pH sensing performance. An optimum PL based pH probe with broad linear range of 1.78-13.56 and high accuracy can be obtained from acetic acid treated chitosan with high quantum yield up to ~30%. Moreover, the linear relationship between the UV absorption and the pH values are also obtained, covering from pH 1.25-10.17 and pH 10.17-13.24. The dual optical sensing characteristics allow for almost covering the entire pH range and better accuracy. Our work offers a promising strategy to engineer the functionalities of NGQDs applicable not only for optimal pH sensors but also for other applications with great potential.

8:15 PM BREAK

SESSION EQ09.12: Synthesis and Processing V
Session Chairs: Naho Itagaki and Tsuyohito Ito
Monday Afternoon, December 6, 2021
EQ09-Virtual

9:00 PM *EQ09.12.01

Applications of Atmospheric Pressure Plasmas in Interfacial Treatments for Perovskite Solar Cells I-Chun Cheng, Cheng-Che Hsu and Jian-Zhang Chen; National Taiwan University, Taiwan

Atmospheric pressure plasmas have drawn great attention in a wide variety of fields, such as surface engineering, material processing, biomedicine and agriculture. Possessing potential economic benefits in comparison with low-pressure plasmas, atmospheric pressure plasmas, without the requirement of vacuum technologies, are particularly attractive for processing large-area low-cost photovoltaic devices. Here we demonstrate examples of performance enhancement of n-i-p lead halide perovskite solar cells with the assistance of atmospheric pressure plasma treatments. In the first case, a nitrogen DC-pulse atmospheric-pressure plasma jet (APPJ) was applied to pre-treat the fluorine-doped tin oxide (FTO) glass substrates for perovskite solar cells. In comparison with a conventional 15-min UV-ozone treatment, a 10-s APPJ treatment can effectively decontaminate and enhance the wettability of FTO substrates and thus improve the cell efficiency by 27%. In the second case, a planar-type dielectric barrier discharge apparatus (DBD) was used to treat the absorber layers of perovskite solar cells. The perovskite absorber layer was formed by spin-coating a dimethylformamide solution containing CH₃NH₃I and PbI₂, followed by a soft-bake. Prior to the deposition of the spiro-OMeTAD hole transport layer, the DBD treatment was carried out in the nitrogen ambient. The result shows that a 20-s treatment can introduce the proper surface modification and grain growth of the perovskite absorber and thus improve the cell efficiency by 38%. In the third case, a low-temperature atmospheric-pressure dielectric-barrier-discharge-jet (DBDjet) was applied to post-treat the jet-sprayed silver nanowires (AgNWs) counter electrodes for fully solution-processed perovskite solar cells. The DBDjet treatment can remove the polyvinylpyrrolidone on the surface of AgNWs and thus improve the interfacial contacts among AgNWs and between the AgNWs layer and hole transport layer. A 33% enhancement in the cell efficiency was achieved when the AgNWs electrode was treated by the DBDjet for 10 times at a scan rate of 0.5 cm/s.

9:30 PM EQ09.12.02

Synthesis of Cuboid Cu(HBTC)(H₂O)₃ Using Plasma-in-Solution Treatment to Organic Ligands Moriyuki Kanno¹, Tsuyohito Ito¹, Yoshiki Shimizu² and Kazuo Terashima¹; ¹The University of Tokyo, Japan; ²National Institute of Advanced Industrial Science and Technology (AIST), Japan

Metal-organic frameworks (MOFs) or supramolecular coordination polymers are porous materials composed of metal ions and organic ligands. Due to their high surface area and designability, they are expected to be applied to catalyst, gas storage, and drug delivery. Moreover, they also serve as solid precursors for metals and metal oxide. Many porous transition metal oxides, such as CuO and Cu₂O, have been obtained by pyrolysis of MOFs under controlled atmospheres. Therefore, the control of the morphology of MOFs has recently attracted much attention in terms of both direct applications of MOFs and their application to intermediate materials for various metal or metal oxide materials synthesis. Here, we focused on Cu(HBTC)(H₂O), a MOF with Cu²⁺ ions and organic ligands, 1,3,5-tricarboxylbenzene (H₃BTC, trimesic acid), as raw materials. Cu(HBTC)(H₂O)₃ has been studied as an antibacterial material, a support agent for catalysts with metal nanoparticles, and intermediate material for Fe-BTC, which is a highly efficient nanozyme. Cu(HBTC)(H₂O)₃ is known as a one-dimensional material, but in recent years, the synthesis of two-dimensional nanosheets has been reported. In this study, using plasma-in-water treatment solution of H₃BTC, three-dimensional cuboid Cu(HBTC)(H₂O)₃ was synthesized [1]. It was also observed that the morphology changed with plasma treatment time. Plasma in liquid has been studied for applications in materials synthesis and surface modification, including the synthesis of MOFs [2]. However, the effect of plasma in liquid on organic ligands has not yet been clarified, and in this study, we observed the effect by treating only organic ligands with plasma in water. The plasma-treated solution of H₃BTC was also analyzed to study the effect of plasma-in-water treatment on the organic ligands by liquid chromatography, fluorescent emission spectra, and UV-Vis spectra. These results suggest that hydroxy groups are functionalized on the organic ligands by plasma-in-water treatment. Partial plasma treatment of raw materials, demonstrated here, could be useful in future studies on complex synthesis.

[1] M. Kanno, T. Ito, Y. Shimizu, and K. Terashima (submitted to *Plasma Processes and Polymers*)

[2] M. Kanno, T. Kitao, T. Ito, and K. Terashima, *RSC Advances* (in press)

9:45 PM EQ09.12.03

Microplasma-Reinforced Fabrication of Crosslinked Nitrogen-Doped Graphene Quantum Dot Sponges for Environmental Water Purification Applications Darwin Kurniawan¹, Kostya (. Ostrikov² and Wei-Hung Chiang¹; ¹National Taiwan University of Science and Technology, Taiwan; ²Queensland University of Technology, Australia

Quantum confinement of graphene quantum dots (GQDs) yields a unique photoluminescence (PL) properties which has been widely used for many applications including bioimaging, chemical and biological sensing, LED, optoelectronic devices, and energy related applications. This performance can be further enhanced by introducing heteroatom, such as nitrogen (N) into the sp² carbon core. The high electronegativity of N atom has been proven to provide better electron transfer for improving both sensing and catalytic performances. Despite the promising facts, the applicability of NGQDs have been hampered by their synthesis methods. Postgrowth N doping has been regarded as time consuming and requiring harsh reaction conditions, while the direct synthesis via top-down or bottom-up approach also suffers from uncontrolled NGQDs properties, long reaction time, laborious synthetic procedures, harsh reaction conditions, and scalability.

Moreover, the practicality of NGQDs can be further enhanced by incorporating the NGQDs in appropriate 3D matrices. Materials with 3D architectures like hydrogels and sponges have shown great potential in relevant applications due to their own merits. With regards to the presence of surface functional groups, the NGQDs not only able to act as stimuli response probe to the matrices, but also as nanoscale crosslinker via covalent or non-covalent interaction. As a result, the resulting composites exhibit better mechanical properties than the control groups. It is also envisaged that this nanoscale crosslinker is capable of replacing the conventional toxic crosslinker (*e.g.* EDC-NHS, glutaraldehyde, etc.), which further boosts the applicability either in biomedical or environmental field.

Water contamination has undoubtedly been one of the most concerning problem faced by many people. The contamination generally involves heavy metal ions (Hg²⁺, As³⁺, Cd²⁺, etc.), organic dyes (remazol brilliant blue R (RBBR), rhodamine B, congo red, etc.), and organic pollutants (nitroarenes family) which are highly toxic and dangerous to human being. Among other available methods, adsorption has been one of the most promising method to remove those contaminations from water owing to its effectiveness, efficiency, low cost, and simplicity.

Microplasma as gaseous discharge with one dimension geometrically confined to <1 mm emerges as an alternative way to promote crosslinking and polymerization process with the absence of toxic chemical crosslinker at ambient conditions. Besides, microplasma is also capable of cleaving polymeric chain to generate porous structures in the resulting 3D materials, resulting in enhanced pore size, surface area, hydrophilicity, and wettability. Herein, we utilized a microplasma system to synthesize NGQDs from chitosan at ambient conditions. The post-plasma solution was converted into NGQDs gel by neutralizing the unreacted chitosan with sodium hydroxide (NaOH) and subjected to another microplasma treatment for crosslinking process to generate NGQDs hydrogel. The fabricated NGQDs hydrogel can be further converted to NGQDs sponge by subsequent freeze-thawing method, showing remarkable water uptake and dye adsorption ability for RBBR. Our work provides an insight into the green and sustainable development of NGQDs sponge applicable for water environmental application.

10:00 PM EQ09.12.04

Microplasma-Assisted and One-Step Fabricated Silver/N-GQD Nanohybrids for Improve Raman Detection and PL Detection for Arsenic Species Jui-Yi Yeh¹ and Wei-Hung Chiang²; ¹National Taiwan University, Taiwan; ²National Taiwan University of Science and Technology, Taiwan

Recently experimental and theoretical works have reported that graphene quantum dots (GQDs), a unique form of zero dimensional nanostructure, and their exceptional properties make them promising in biosensing applications. Surface-enhanced Raman scattering (SERS) is an ultra-sensitive analytical technique for bio-molecules detection. While the potential of surface plasmon resonance (SPR) metals (*e.g.* Au and Ag) and graphene for SERS has been demonstrated, but the work of GQDs applied as SERS substrates is still lacking. Here we reported the rational design to develop GQD-based SERS active substrate.

Furthermore, modified GQD with metal nanostructures will lead to important advance for SERS-based detection. Here we demonstrate a facile synthesis of NGQD/AgNP nanohybrids by the atmospheric-pressure microplasma-assisted electrochemistry. Detailed nanomaterial characterizations including transmission electron microscopy, UV/Vis spectroscopy show that the microplasma-assisted electrochemical reaction can successfully grow Ag nanoparticles (AgNP) onto the NGQD surfaces to form the Ag@NGQD NP nanohybrids with heterodimeric nanostructures within minute scale. Besides, the photoluminescence (PL) optical study of NGQDs and AgNP@NGQD indicated that the non-radiative fluorescence resonance energy transfer (FRET) involved in the AgNP@NGQD nanohybrids. In the systematic Raman study, Rhodamine 6G (R6G) and B-carotene are selected as the Raman probe molecules. First we compare the SERS property of four kinds of Ag@NGQDs with different photoluminescence property (*e.g.* different emission wavelength), Raman results show that SERS performance of Ag@NGQD0.02 is highly influenced by overlap area in PL-UV image. The as-produced AgNP@NGQD nanohybrids shows superior SERS performance with high enhancement factor (EF) around 1x10⁸. We further studied the NGQD-AgNP nanohybrids with different FRET efficiency. The results revealed that FRET of the as-produced AgNP@NGQD nanohybrids is the dominant factor to SERS properties in our study.

On the other hand, the as-prepared Ag@NGQD exhibited excitation-independent behavior and high optical stability. Furthermore, based on the complexation between As³⁺ and Ag@NGQD, the fluorescence intensity of the Ag@NGQD could be greatly quenched by the addition of a small amount of As³⁺ ions. The linearity range is 0.1–1000 μM with a detection limit of 0.7 nM. For this reason, the proposed method was demonstrated to be selective and suitable for As³⁺ analysis in natural water samples. And, Ag@NGQD with the biosafety have the potentials for intracellular As³⁺ detection.

10:15 PM *EQ09.12.05

Plasma Fabrication of Graphene Nanostructures for Solar-Thermal Conversion Zheng Bo; Zhejiang University, China

Plasma technology plays a vital role in the manufacturing of materials for a wide range of industries. This talk presents a plasma-fabricated graphene nanostructure and its applications for solar-thermal conversion. In the plasma-enhanced chemical vapor deposition process, an electric field is produced by gas discharge and the graphene planes are grown along the electric field lines that converge normally onto the surface of substrates, forming vertically-arranged graphene nanosheets (VGs). With vertical orientation and open channels, VGs show the potential of constructing light traps that enable a high absorbance of 98% towards solar irradiation. Besides, plasma-enabled in-situ nitrogen doping during the graphene growth can mediate the surface wettability of the VGs from hydrophobic to hydrophilic. In particular, the hydrophilic N-doped VGs can serve as capillary pumps to provide sufficient water supply for solar-driven interfacial evaporation, and thus establish a high evaporation rate and high energy conversion efficiency in solar desalination applications.

Reference:

[1] Shenghao Wu, Guoping Xiong, Huachao Yang, Biyao Gong, Yikuan Tian, Chenxuan Xu, Yan Wang, Timothy Fisher, Jianhua Yan, Kefa Cen, Tengfei Luo, Xin Tu, **Zheng Bo***, Kostya (Ken) Ostrikov. Multifunctional solar waterways: plasma-enabled self-cleaning nanoarchitectures for energy-efficient

desalination. *Advanced Energy Materials*, 2019, 9, 1901286, <https://doi.org/10.1002/aenm.201901286>.

[2] Shenghao Wu, Guoping Xiong, Huachao Yang, Yikuan Tian, Biyao Gong, Huiwen Wan, Yan Wang, Timothy S. Fisher, Jianhua Yan, Kefa Cen, **Zheng Bo***, Kostya (Ken) Ostrikov. Scalable production of integrated graphene nanoarchitectures for ultrafast solar-thermal conversion and vapor generation. *Matter*, 2019, 1, 1017–1032, <https://doi.org/10.1016/j.matt.2019.06.010>.

[3] Biyao Gong, Huachao Yang, Shenghao Wu, Guoping Xiong, Jianhua Yan, Kefa Cen, **Zheng Bo***, Kostya (Ken) Ostrikov. Graphene array-based anti-fouling solar vapour gap membrane distillation with high energy efficiency. *Nano-Micro Letters*, 2019, 11:51, <https://doi.org/10.1007/s40820-019-0281-1>.

10:45 PM EQ09.12.06

Inverted Stranski-Krastanov Growth of Single-Crystalline Zn_{1-x}Mg_xO Films on Sapphire Substrates Using Magnetron Sputtering Daichi Takahashi, Daisuke Yamashita, Takamasa Okumura, Kunihiro Kamataki, Kazunori Koga, Masaharu Shiratani and Naho Itagaki; Kyushu University, Japan

Zn_{1-x}Mg_xO are promising materials for optoelectronic/excitonic devices because of the large exciton binding energy (60 meV) and the potentially tunable band gaps [1]. Ohtomo *et al.* have recently demonstrated the bandgap tuning of wurtzite Zn_{1-x}Mg_xO films in the range 3.4–4.15 eV [2], where the films have been grown by pulsed laser deposition (PLD). However, the large lattice mismatch between Zn_{1-x}Mg_xO films and commonly used substrates, such as sapphire, often results in poor crystal quality. Aiming to overcome this challenge, we here perform epitaxial growth of Zn_{1-x}Mg_xO films on sapphire substrates using *inverted* Stranski-Krastanov (*inverted* SK) mode [3]. In this mode, strain-relaxed nano-sized 3D islands (buffer layers) are initially grown by using impurities to control the surface energy. Then the islands coalesce to form 2D layer after the desorption of impurities, and eventually, films grow in 2D mode and form single crystals. This mode has enabled us to grow single crystalline films on large lattice mismatched substrates [3]. Here we demonstrate *inverted* SK growth of Zn_{1-x}Mg_xO films using N atoms as impurities, where sputtering method is employed for film deposition taking the advantages of the high dissociation degree of N₂.

All the films were fabricated by radio frequency magnetron sputtering. First, 10-nm thick buffer layers consisting of 3D islands were deposited on sapphire substrates at 780°C using N₂/Ar gas. Next, wurtzite Zn_{1-x}Mg_xO films were fabricated on the buffer layers at 800°C using O₂/Ar gas, and the films were post annealed in O₂ atmosphere at 880°C for 10 hours.

We have observed *inverted* SK growth and thus obtained high-quality single-crystalline Zn_{1-x}Mg_xO films of $x = 0.05$ – 0.33 . Atomic force microscopy measurement revealed that the films have atomically flat surfaces with root mean square roughness of 0.41–0.75 nm. The high crystal qualities of the films even with large Mg contents were also proved by x-ray diffraction analysis. The full widths at half maximum of the (0002) rocking curves are in the range between 0.05° ($x = 0.33$) and 0.07° ($x = 0.14$). These values are comparable to that of bulk single-crystal ZnO. Furthermore, we observed that the optical absorption edge shifts continuously toward the shorter wavelength with increasing x , and the band gap has been tuned in the range 3.37–4.03 eV. These results allow us to conclude that the combination of *inverted* SK growth and magnetron sputtering is a powerful method of growth of high-quality single-crystalline Zn_{1-x}Mg_xO films on lattice mismatched substrates.

This work was supported by JSPS KAKENHI Grant Numbers JP21H01372, NTT collaborative research, and Toyota Riken Scholar.

[1] K. Nakahara, *et al.*, *Appl. Phys. Lett.*, **97**, 013501 (2010)

[2] A. Ohtomo, *et al.*, *Appl. Phys. Lett.*, **72**, 2466 (1998).

[3] N. Itagaki, *et al.*, *Sci. Rep.*, **10**, 4669 (2020).

10:50 PM EQ09.12.07

Epitaxial Growth of (ZnO)_x(InN)_{1-x} Films on ZnO Substrate by Magnetron Sputtering—Impact of Substrate Surface Polarity Ryota Narishige, Daisuke Yamashita, Kunihiro Kamataki, Takamasa Okumura, Kazunori Koga, Masaharu Shiratani and Naho Itagaki; Kyushu University, Japan

We have developed novel semiconductors, (ZnO)_x(InN)_{1-x} (called “ZION” hereinafter), which are pseudo-binary alloys of ZnO and InN. ZION have tunable band gaps across the entire visible spectrum, high exciton binding energy of 30–60 meV, and high optical absorption coefficients of 10⁵ cm⁻¹, making ZION promising materials for optoelectronic and excitonic devices [1, 2]. Recently, we have succeeded in the heteroepitaxial growth of ZION films on sapphire, ZnO and GaN substrates by radio-frequency (rf) magnetron sputtering, where the temperature has been kept below 550°C so that the thermal dissociation of In–N bond is reduced. Furthermore, we found that under such conditions, “skewness”, the third moment of the surface height distribution of the substrates, is a key parameter for enhancement of adatom migration on the surface and thus for growth of high quality ZION films [3]. Beside the morphology, the surface polarity of the substrates might also play an important role in adatom migration since it affects the sticking coefficient of adatoms [4]. We here demonstrate epitaxial growth of ZION films on both O-polar and Zn-polar ZnO substrates and discuss the impacts on the migration as well as the crystal growth of ZION films.

ZION films were deposited on ZnO substrates by rf magnetron sputtering where the lattice mismatch between the film and the substrate is 1.6%. O₂, N₂ and Ar gases were used, and the gas flow rates were 1.8, 24.0, and 30.2 sccm, respectively. The total pressure was 0.50 Pa. ZnO and In targets with purity of 99.99% were used. The substrate temperature was 450°C. The deposition time was 220 seconds, and the film thickness on the O-polar and Zn-polar substrates were 25 and 35 nm, respectively. The chemical composition ratio was (ZnO)_{0.85}(InN)_{0.15}, confirmed by x-ray fluorescence spectrometry. The heteroepitaxial growth of ZION films on both surfaces were confirmed by high-resolution transmission electron microscopy (HRTEM), where all the films have atomically sharp interfaces with the substrates. Interestingly, however, the HRTEM images show a significant difference in the lattice relaxation process between the films. On Zn-polar ZnO surfaces, relaxation occurs at the beginning of the film growth, whereas on O-polar surfaces, ZION films are fully coherent with the 1.6%-lattice-mismatched ZnO substrates at least for 15 mono layers. We also found that the difference in the depth profile of the chemical composition. Rutherford back-scattering spectra show that on Zn-polar surfaces, there is no compositional change in the depth direction, indicating the particle flux toward the substrate mainly governs the film growth. While on O-polar surfaces, In and N contents decrease toward the surfaces, where adatoms tend to be incorporated into thermodynamically favored lattice positions. We consider that these differences are brought by the differences in the adatom migration, that is, O-polar surfaces provide smaller sticking coefficients and thus longer migration length of Zn/In atoms due to the smaller number of back bonds of Zn/In atoms on the surfaces [4]. This hypothesis is consistent with the facts that O-polar surfaces lead to lower deposition rate and to higher crystal quality of ZION films where the full-width at half maximum of (002) x-ray rocking curves is about 0.2°.

This work was supported by JSPS KAKENHI Grant Numbers JP21H01372, NTT collaborative research, Toyota Riken Scholar.

[1] N. Itagaki, *et al.*, *Mater. Res. Express*, **1**, 36405 (2014).

[2] K. Matsushima *et al.*, *Jpn. J. Appl. Phys.*, **52**, 11NM06 (2013).

[3] R. Narishige *et al.*, *Jpn. J. Appl. Phys.*, **60**, SAAB02 (2021).

[4] H. Kato, *et al.*, *J. Crystal Growth*, **265**, 375 (2004).

10:55 PM EQ09.12.08

High-Temperature Growth of Amorphous In₂O₃:Sn Films by Magnetron Sputtering Using Nitrogen Yuta Mido¹, Keigo Takeda², Daisuke Yamashita¹, Takamasa Okumura¹, Kunihiro Kamataki¹, Kazunori Koga¹, Masaharu Shiratani¹, Masaru Hori³ and Naho Itagaki¹; ¹Kyushu University, Japan; ²Meijo University, Japan; ³Nagoya University, Japan

In₂O₃:Sn (ITO) films are essential for transparent electrodes in flat panel displays, touch screens, and so on. Recently, amorphous ITO(a-ITO) has attracted

attention as an alternative to polycrystalline ITO due to the advantages such as surface smoothness, high etching rate and low internal stress. However, the mobility of conventional a-ITO films, deposited by sputtering below crystallization temperature of In₂O₃ (~150°C) is quite low of 20–30 cm²/Vs. Furthermore, the amorphous phases are unstable and they easily crystallize around 150°C, limiting the use of a-ITO films in practical devices. We have recently clarified that beside the substrate temperature, *impurity behavior* on the surfaces during the growth affects the film structures [1], and have succeeded in fabricating a-ITO films at 150°C using nitrogen as impurity, where the mobility is high of 50 cm²/Vs [2]. Here we demonstrate sputtering synthesis of a-ITO films at 350°C using nitrogen and see what happens if we increase the temperature far above the crystallization temperature of In₂O₃. ITO films were deposited by radio-frequency magnetron sputtering on quartz glass substrate at 350°C. Ar and N₂ gases were used and the total pressure was 0.9 Pa. The gas flow rate ratios of N₂ was 0–20%. In₂O₃:Sn (10wt.%) targets were used. The film thickness was 50 nm. N content in the films and the absolute N atom density in the plasma were measured by x-ray fluorescence (XRF) and vacuum ultraviolet absorption spectroscopy (VUVAS) [3], respectively.

X-ray diffraction (XRD) measurements revealed that a-ITO films are fabricated even at high temperature of 350°C using nitrogen. For the ITO films fabricated at N₂ flow rate ratios of 0–7%, diffraction peaks from In₂O₃ (222) plane are observed at 30.5°, while, no peaks are observed for the films fabricated at N₂ = 10–20%, indicating the films have amorphous structure. We found from VUVAS and XRF measurements that despite the high density of N atom in the plasma of 10¹¹ cm⁻³, being one order of magnitude higher than O atom density, N contents in the films are only a few at.%. These results suggest that the amorphization is caused not only by the N atoms incorporated into the films that disorder the bixbyite In₂O₃ structure, but by the adsorbed N atoms that inhibiting the crystal nucleation, which are eventually desorbed from the surfaces. Owing to the amorphous structure, the a-ITO films have smooth surface with the root mean square (RMS) roughness of 0.8 nm, which is half of that of films fabricated without N₂. The most remarkable feature of the a-ITO films is the high carrier mobility of 66 cm²/Vs. We consider that the high-temperature deposition leads both to increased film density and to enhanced short- and mid-range ordering in the amorphous structures, resulting in such high mobility.

This work was supported by JSPS KAKENHI Grant Number JP21H01372, NTT collaborative research, and Toyota Riken Scholar.

[1] N. Itagaki, et al., *Sci. Rep.*, **10**, 4669 (2020).

[2] T. Takasaki, et. al., *Proc. 9th ICRP*, **60**, GT1.150 (2015).

[3] S. Tada, et al., *J. Appl. Phys.* **88**, 1756 (2000).

SYMPOSIUM EQ10

Multiferroics and Magnetoelectrics
November 29 - December 8, 2021

Symposium Organizers

Jiamian Hu, University of Wisconsin-Madison
Tianxiang Nan, Tsinghua University
Eckhard Quandt, University of Kiel
Nian Sun, Northeastern University

* Invited Paper

SESSION Tutorial EQ10: Magnetoelectric Antennas—Materials, Design, Simulation, Fabrication, Test and Applications
Monday Morning, November 29, 2021
Hynes, Level 2, Room 206

8:30 AM

Magnetic, Piezoelectric and Magnetoelectric Materials for Magnetoelectric Antennas Nian Sun; Northeastern University, United States

- Introduction of magnetic materials, ferro/piezoelectric materials, and magnetoelectric materials.
- Characterization of magnetic materials, ferro/piezoelectric materials, and magnetoelectric materials.
- Magnetoelectric antennas from VLF to UHF and their applications

10:00 AM BREAK

10:30 AM

Magnetoelectric Antennas—Design, Simulation, Fabrication and Tests Hwaider Lin; Winchester Technologies, LLC, United States

- ME antenna: State of the art
- ME antenna: Design and fabrication
- ME antenna: Measurement and result
- ME antenna: Further works and discussion

12:00 PM BREAK

1:30 PM

Electrically Small Antennas and How Materials Can Help Ethan Wang; University of California, Los Angeles, United States

- Chu's theory in radiation of electrically small antennas
- Roles of mechanical, magnetic and magnetoelectric materials in electrically small antennas
- Full-wave modeling of piezoelectric and magnetoelectric effects in antennas
- Examples of electrically small antennas based on mechanical, magnetic and magnetoelectric effects

3:00 PM BREAK

3:30 PM

Phase-Field Simulation of ME Antennas Jiamian Hu; University of Wisconsin-Madison, United States

- Introduction to phase-field models for ferroic materials and devices
- Challenges for developing phase-field model for simulating ME antennas
- Results on phase-field simulations of ME antennas
- Related examples: Phase-field simulations of acoustically mediated spintronic emitters in millimeter-wave and terahertz range

SESSION EQ10.01 Multiferroics I
Session Chairs: Eckhard Quandt and Nian Sun
Tuesday Morning, November 30, 2021
Hynes, Level 2, Room 206

10:30 AM *EQ10.01.01

Broken Symmetries and Emergent Magnetoelectricity in Multiferroics Sang Wook Cheong; Rutgers, The State University of New Jersey, United States

We will first discuss the general connection between broken symmetries and emergent phenomena, especially magnetoelectricity in multiferroics in the framework of symmetry operational similarity (SOS). As a specific example of new phenomena associated with SOS, we will discuss toroidal magnetoelectricity in chiral and polar BaCoSiO₄.

11:00 AM *EQ10.01.02

Electric Field Control of Magnetism—What Does It Take to Get to 100 mV Switching? Ramamoorthy Ramesh; University of California, Berkeley, United States

Among the large number of correlated oxide materials, there exists a small set of materials which exhibit multiple order parameters; these are known as multiferroics, particularly, the coexistence of ferroelectricity and some form of ordered magnetism (typically antiferromagnetism). The scientific community has been able to demonstrate electric field control of both antiferromagnetism and ferromagnetism at room temperature. Current work is focused on ultralow energy (1 attoJoule/operation) electric field manipulation of magnetism as the backbone for the next generation of ultralow power electronics. We are exploring many pathways to get to this goal. In this talk, I will describe our progress to date on this exciting possibility. My specific focus will be on the materials physics behind getting to 100mV switching of magnetism (and ferroelectricity).

11:30 AM EQ10.01.03

Cryo-STEM Imaging of Charge Order Textures in a Manganite Ismail El Baggari^{1,2}, David Baek², Michael Zachman^{3,2}, Di Lu^{4,5}, Yasuyuki Hikita⁶, Harold Y. Hwang^{5,6}, Elizabeth Nowadnick⁷ and Lena Kourkoutis²; ¹The Rowland Institute at Harvard, United States; ²Cornell University, United States; ³Oak Ridge National Laboratory, United States; ⁴Northwestern University, United States; ⁵Stanford University, United States; ⁶SLAC National Accelerator Laboratory, United States; ⁷University of California, Merced, United States

In complex oxides, charge-ordered states involve a complex interplay between charge, spin, orbital and lattice degrees of freedom, and modulate important macroscopic phenomena such as magnetic order, metal-insulator transitions and colossal magnetoresistance. The intra-unit-cell arrangement within charge order superlattices can lead to even richer physics by breaking additional symmetries and allowing novel couplings. In half-doped manganites, for instance, charge order can reside on the sites (site-centered) or on the bonds (bond-centered), with each possibility leading to a distinct orbital and magnetic order arrangement. Previous theoretical work also predicts a third possibility: the formation of a mixed (or intermediate) state combining both site and bond orders [1]. This state leads to the formation of finite electrical dipoles within each supercell and is therefore predicted to be polar and possibly multiferroic. However, determining if such a state exists and distinguishing between various charge-ordered textures remain a challenge.

Here we demonstrate that atomic-resolution cryogenic scanning transmission electron microscopy (cryo-STEM) enables the visualization of charge-ordered states in manganites through the lens of the complex, picoscale lattice distortions that entwine with electronic transitions. In the model charge-ordered system Nd_{1/2}Sr_{1/2}MnO₃, we address the longstanding question of whether charge order resides on the sites or on the bonds. In addition to observing that the system hosts site-centered charge ordering, we discover the nanoscale coexistence of an intermediate state which mixes site and bond orders. In agreement with the theoretical proposals, we confirm that this intermediate state breaks inversion symmetry. Finally we show that nonlinear couplings of distinct lattice modes locally control the selection between these competing ground states [2].

[1] Efremov, D. V., Van Den Brink, J., & Khomskii, D. I. (2004). Bond-versus site-centred ordering and possible ferroelectricity in manganites. *Nature Materials*, 3(12), 853-856.

[2] El Baggari, I., Baek, D. J., et al. (2021). Charge order textures induced by non-linear couplings in a half-doped manganite. *Nature Communications*, 12(1), 1-7.

SESSION EQ10.02 Magnetolectrics I
Session Chairs: Eckhard Quandt and Nian Sun
Tuesday Afternoon, November 30, 2021
Hynes, Level 2, Room 206

1:30 PM *EQ10.02.01

Enabling Low-Voltage Multiferroics and Magnetolectrics Lane W. Martin; University of California, Berkeley, United States

Applications in advanced, beyond CMOS computing are driving researchers and industry alike to explore a broader set of materials than ever before. While industry has maintained, in some form, their ability to continually meet the demands of Moore's law by increasing the number of transistors on chip, largely in part from efforts in scaling and size reduction of the transistors themselves and the associated circuit area, the same cannot be said for energy scaling. In the last fifteen years, scaling has deviated from Dennard's trend which states that the power density of circuits stays roughly the same as transistors get smaller, assuming, concurrent voltage reductions are made. Herein lies the challenge – while we have reduced transistor and circuit size, voltages of operation have not been scaled at the same rate. As a result, power and energy dissipation now stands as one of the most pressing challenges for advanced nanoelectronics. This has motivated renewed attention to a wide variety of routes to reduce the voltage of operation of next-generation logic. Such approaches have thrust materials – including multiferroics and magnetolectrics – back into the mix as candidates for beyond CMOS computing.

Despite considerable research on multiferroic and magnetolectric materials in the last decade and advances in our ability to synthesize, control, characterize, and fabricate these materials, the requirements of beyond CMOS computing are already pushing these materials to their limits. Here, we will explore recent efforts to reduce the operating voltages of multiferroic and magnetolectric devices including exploring both new and old materials in ever decreasing sizes. We will focus on thin-film versions of magnetolectric composite structures based on piezoelectric/ferroelectric materials. For example, we will explore thin film ferromagnet/relaxor heterostructures and routes to quantify magnetolectric coupling in small scale devices. Specifically, in $\text{Fe}_{0.5}\text{Rh}_{0.5}/(0.68)\text{PbMg}_{1/3}\text{Nb}_{2/3}\text{O}_3-(0.32)\text{PbTiO}_3$ (PMN-PT) heterostructures, we will demonstrate routes towards 100 mV actuation and magnetolectric coefficients similar to those observed in other composite structures. In turn, we will discuss the implications of thin-film geometries for such applications and how substrate clamping impacts the response of materials. For example, we will explore how different types of relaxors (*e.g.*, PMN vs. $\text{BaZr}_{0.5}\text{Ti}_{0.5}\text{O}_3$) respond differently to substrate constraints and thus provide an impetus for the use of some relaxors over others in thin-film geometries. At the same time, we will explore how releasing such materials from the substrate – thereby producing free-standing versions of them – further changes their response to applied stimuli and could provide a pathway to the desired effects. Finally, we will explore the design of novel thin-film relaxor materials. We will look at how thin-film heterostructuring (namely as superlattices) could provide a novel route to improved relaxor behavior. To end, we will discuss where these ideas could lead us next and what metrics can be met using these materials and methods.

2:00 PM *EQ10.02.02

Room Temperature Multiferroicity in Orthoferrite Films and Nanocomposites Caroline Ross and Shuai Ning; Massachusetts Institute of Technology, United States

Multiferroic materials and nanocomposites offer the promise of electrically-controlled magnetism and a path towards magnetolectric memory and logic devices. Multiferroicity may be obtained in a single phase material or in a composite material consisting of a magnetic phase and a ferroelectric phase coupled by strain. Most research on single phase multiferroics has centered on BiFeO_3 , but we show here that room temperature multiferroicity can be produced in a single phase orthoferrite as a result of antisite defects. Ferroelectricity is obtained in thin films of Y-rich YFeO_3 , yttrium orthoferrite (YFO), a perovskite-structured canted antiferromagnet. The ferroelectricity is attributed to Y_{Fe} antisite defects which facilitate a non-centrosymmetric distortion. This mechanism is predicted to work analogously for other rare earth orthoferrites, with a dependence of the polarization on the radius of the rare earth cation. We then demonstrate the growth of two-phase epitaxial nanocomposites consisting of YFO and a magnetic spinel, CoFe_2O_4 (CFO). A nanocomposite consisting of pillars of CFO embedded epitaxially in a YFO matrix exhibits both robust ferroelectricity and ferrimagnetism at room temperature, as well as a strain-mediated magnetolectric coupling effect. This work expands the range of materials available for multiferroic and magnetolectric applications.

2:30 PM *EQ10.02.03

Magnetic Domain Wall Activity in High Sensitivity Magnetic Field Sensors—Magnetic Noise and Magnetic Domain Control Jeffrey McCord, Cai Müller, Phillip Durdaut, Elizaveta Golubeva, Viktor Schell, Anne Kittmann, Matic Jovičević Klug, Dennis Seidler, Lars Thormählen, Benjamin Spetzler, Dirk Meyners, Franz Faupel, Eckhard Quandt and Michael Höft; Kiel University, Germany

Magnetic domain formation reveals fascinating physics and is of great relevance for technological applications. Recent advances in thin film devices adopting magnetic films as sensing layers offer promising routes for sensing ultra-low magnetic signals, *e.g.* with magnetolectric (ME) cantilever sensors or surface acoustic wave (SAW) devices. As the sensors are operated by external stimuli of various frequencies, the complex physics of magnetic domain and domain wall activity at these modulation frequencies are one of the most important factors that determine the performance of the magnetic field sensors.

In-operando magnetic domain observation sheds light on the irreversible and hysteretic magnetization changes due to domain nucleation, domain wall resonances, domain wall flexure modes, precessional magnetization effects, and spin-wave like phenomena. Using time-resolved magneto-optical Kerr effect microscopy with time resolutions down to picoseconds, we show the effect of magnetic domains on the noise performance of ME, ΔE -effect, and SAW sensors. With the spatial and temporal domain analysis during sensor operation together with complementary electrical measurements, the micromagnetic origins are determined.

We identify specific magnetic domain wall processes as sensor-intrinsic noise sources. Magnetic noise originating from magnetic domain wall activity is the most relevant figure-of-merit for improving sensor performance. Even minimal magnetic domain activity restricts the achievable limit of detection. On various sensor specific examples, we demonstrate that understanding the magnetic domain physics and actively controlling magnetic domain behavior is key to improving sensor performance. The magnetic domain wall activity is directly related to magnetic losses. The presented data prove the significance of micromagnetic processes for real-world applications. Strategies for the elimination of domain wall activities and magnetic losses will be discussed. We acknowledge funding through DFG CRC 1261 “Magnetolectric Sensors: From Composite Materials to Biomagnetic Diagnostics”.

[1] P. Durdaut, E. Rubiola, J.M. Friedt, C. Müller, B. Spetzler, C. Kirchhof, D. Meyners, E. Quandt, F. Faupel, J. McCord, R. Knöchel, M. Höft, *Journal of Microelectromechanical Systems* **29**, 1347 (2020)

- [2] N.O. Urs, E. Golubeva, V. Rößisch, S. Toxværd, S. Deldar, R. Knöchel, M. Höft, E. Quandt, D. Meyners, J. McCord, *Physical Review Applied* **13**, 024018 (2020)
- [3] P. Hayes, M. Jovičević Klug, S. Toxværd, P. Durdaut, V. Schell, A. Teplyuk, D. Burdin, A. Winkler, R. Weser, Y. Fetisov, M. Höft, R. Knöchel, J. McCord, E. Quandt, *Scientific Reports* **9**, 16355 (2019)
- [4] M. Jovičević Klug, L. Thormählen, V. Rößisch, S. Salzer, M. Höft, E. Quandt, D. Meyners and J. McCord, *Applied Physics Letters* **114**, 192410 (2019)
- [5] A. Kittmann, P. Durdaut, S. Zabel, J. Reermann, J. Schmalz, B. Spetzler, D. Meyners, N.X. Sun, J. McCord, M. Gerken, G. Schmidt, M. Höft, R. Knöchel, F. Faupel and E. Quandt, *Scientific Reports* **8**, 278 (2018)
- [6] R.B. Holländer, C. Müller, M. Lohmann, B. Mozooni and J. McCord, *Journal of Magnetism and Magnetic Materials* **432**, 283–290 (2017)
- [7] J. McCord, *Journal of Physics D: Applied Physics* **48**, 333001 (2015) <div id="gtx-trans" style="position: absolute; left: 124px; top: 160px;">

3:00 PM EQ10.02.04

Control Of Unconventional Spin Torques in Epitaxial IrO₂ Thin Films Michael V. Patton¹, Tianxiang Nan², Lu Guo¹, Ding-Fu Shao³, Gahee Noh⁴, Saba Karimeddiny⁵, Phillip Ryan⁶, Evgeny Y. Tsybal³, Si-young Choi⁴, Dan Ralph⁵, Mark Ryzhowski⁷ and Chang-Beom Eom¹; ¹University of Wisconsin-Madison, United States; ²Tsinghua University, China; ³University of Nebraska–Lincoln, United States; ⁴Pohang University of Science and Technology, Korea (the Republic of); ⁵Cornell University, United States; ⁶Advanced Photon Source, Argonne National Laboratory, United States; ⁷University of Wisconsin–Madison, United States

Spin orbital torques (SOT) which are generated by a spin current are key to magnetic switching in spintronic applications. These SOTs can be generated by a spin source material via intrinsic mechanisms such as the spin Hall effect and can switch magnetizations without the need for external magnetic fields. Conventionally, the spin polarizations of these SOTs are limited due to the symmetry of the material allowing only for efficient in-plane magnetic switching. Unconventional SOTs arising from novel spin current polarizations however, have the potential to switch an arbitrary magnetization direction. Such SOTs have been reported in lower symmetry materials such as antiferromagnetic materials and transition metal dichalcogenides (TMDs) [1,2]. Here, we report the control of unconventional spin torques in epitaxial IrO₂ thin films. IrO₂ films with (001) and (111) orientation were grown by RF magnetron sputtering with a Py ferromagnetic overlayer and characterized using spin torque ferromagnetic resonance (ST-FMR). We find that the (001) orientation heterostructures have a conventional spin Hall conductivity (SHC) consistent with theoretical calculations and other experimental results [3]. The (111) orientation heterostructures show both conventional and unconventional spin torques consistent with trends predicted in our theoretical calculations. When charge current is applied along either of the crystallographic axes ([1-10] or [-1-12]), we see a noticeable unconventional contribution to the ST-FMR angular dependence from spins polarized along the charge current direction. We attribute these unconventional spin torques to the lower symmetry resulting from triclinic distortions in the (111) films. This work could provide further understanding of unconventional spin torques as well as controlling SOTs via epitaxial design.

[1] Nan, T., Quintela, C. X., Irwin, J., Gurung, G., Shao, D. F., Gibbons, J., Campbell, N., Song, K., Choi, S. Y., Guo, L., Johnson, R. D., Manuel, P., Chopdekar, R. V., Hallsteinsen, I., Tybell, T., Ryan, P. J., Kim, J. W., Choi, Y., Radaelli, P. G., Ralph, D.C., Tsybal, E. Y., Ryzhowski, M. S., & Eom, C. B. *Nature Communications*, 2020, 11(1)

[2] MacNeill, D., Stiehl, G. M., Guimaraes, M. H. D., Buhrman, R. A., Park, J., & Ralph, D. C. *Nature Physics*, 2017, 13(3), 300–305

[3] Bose, A., Nelson, J. N., Zhang, X. S., Jadaun, P., Jain, R., Schlom, D. G., Ralph, D. C., Muller, D. A., Shen, K. M., & Buhrman, R. A. *ACS Applied Materials and Interfaces*, 2020, 12(49), 55411–55416

This work was supported by a Vannevar Bush Faculty Fellowship (N00014-20-1-2844).

3:15 PM EQ10.02.05

Electrical Tuning of Spin to Charge Conversion Efficiency in Metal/SrTiO₃ Two-Dimensional Electron Gases for Future Spintronic Devices Srijani Mallik¹, Luis Moreno Vicente-Arche¹, Maxen Cosset-Cheneau², Paul Noel², Diogo Vaz¹, Felix Trier¹, Tanay Gosavi³, Chia-Ching Lin³, Dmitri Nikonov³, Ian Young³, Anke Sander¹, Agnès Barthelemy¹, Jean-Philippe Attané², Laurent Vila² and Manuel Bibes¹; ¹Unité Mixte de Physique CNRS/Thales, France; ²Université Grenoble Alpes, France; ³Components Research, Intel Corporation, United States

Recent studies on oxide spintronics rely exceedingly on the efficient spin-charge interconversion property of the two-dimensional electron gases (2DEGs) possessing a finite Rashba spin-orbit coupling. SrTiO₃-based 2DEGs are usually generated by the deposition of epitaxial oxides like LaAlO₃ or of reactive metals such as Al [1, 2]. Such 2DEGs are highly promising for the interconversion between charge and spin currents through the direct and inverse Edelstein and spin Hall effects. Here, we compare the formation and properties of 2DEGs generated in SrTiO₃ by the growth of Al, Ta, and Y ultrathin films by dc magnetron sputtering [3]. Both in-situ and ex-situ X-ray photoelectron spectroscopy studies revealed the quantification of reduced Ti states associated with 2DEG formation, their reoxidation by exposure to the air, and the transformation of the metal into its binary oxides. The carrier densities are extracted from magnetotransport measurements. Finally, we investigate the spin-charge conversion as a function of gate voltage by performing spin-pumping ferromagnetic resonance experiments on similar metal/SrTiO₃ samples with a capping of an extra NiFe layer. The trends for the spin to charge conversion efficiency for different metal/SrTiO₃ systems provide a systematic study as a function of the carrier density and the transparency of the metal oxide tunnel barrier [3]. Our results strongly influence the path to choose the correct metal/SrTiO₃ interface to achieve higher spin to charge conversion for future spin-based information readout e.g. Magneto Electric Spin-Orbit (MESO) logics proposed by Intel corporation.

[1] A. Ohtomo and H. Y. Hwang, *Nature (London)* **427**, 423 (2004).

[2] T. C. Rödel *et al.*, *Adv. Mater.* **28**, 1976 (2016).

[3] L. M. Vicente-Arche, S. Mallik, *et al.*, *Phys. Rev. Mater.* **5**, 064005 (2021).

Acknowledgments: The authors acknowledge support from the ERC Advanced Grant No. 833973 “FRESCO,” and Intel’s Science and Technology Center – Feinman.

3:30 PM BREAK

4:00 PM EQ10.02.06

Emergence of Ferroelectricity at the Morphotropic Phase Boundary of Ultrathin BiFeO₃ Johanna Nordlander^{1,2}, Bastien Grosso¹, Marta D. Rossell³, Aline Maillard¹, Elzbieta Gradauskaitė¹, Nicola Spaldin¹, Manfred Fiebig¹ and Morgan Trassin¹; ¹ETH Zürich, Switzerland; ²Harvard University, United States; ³Empa–Swiss Federal Laboratories for Materials Science and Technology, Switzerland

Multiferroic BiFeO₃ possesses a rich phase diagram of metastable phases that allows strain tuning of its room-temperature multiferroic properties in thin-film form. In particular, at large compressive strain a supertetragonal phase with giant polarization can be stabilized alongside the more common rhombohedral structure. Although BiFeO₃ in this mixed-phase regime is recognized as highly technologically relevant for multifunctional device integration, little is known about its ferroelectric state during the thin-film synthesis. Here, we demonstrate the robustness of polarization in ultrathin,

compressive-strained BiFeO₃ single layers and heterostructures during epitaxial thin-film growth. Using in-situ optical second harmonic generation (ISHG), we explore the emergence of ferroelectric phases at the strain-driven morphotropic phase boundary of BiFeO₃ in the ultrathin limit. Strikingly, we find that the epitaxial films grow in the ferroelectric tetragonal (T-) phase without exhibition of a critical thickness. The onset of monoclinic distortion of this T-phase and subsequent appearance of coexisting phases characteristic of the morphotropic phase boundary are confirmed only to develop post deposition and upon sample cooling. The robustness of polarization in the high-temperature T-phase against depolarizing-field effects is furthermore demonstrated during the growth of capacitor-like (metal/ferroelectric/metal) heterostructures. Our results show that strain-driven T-phase stabilization in multiferroic BiFeO₃ yields a prominent candidate material for realizing ultrathin ferroelectric devices with a well-defined polarization state.

4:15 PM EQ10.02.07

Novel Solid-Source Metal Organic MBE for Highly Perfect Metal and Metal Oxide Films Sreejith Nair, William Nunn, Hwanhui Yun, Anusha K. Manjeshwar, Anil Rajapitamahuni, Dooyong Lee, Andre Mkhoyan and Bharat Jalan; University of Minnesota, Twin Cities, United States

A fascinating consequence of electron correlation is the emergence of a wide range of quantum phases including superconductivity in perovskite oxides such as cuprates and ruthenates. In particular, ruthenates are difficult to grow in molecular beam epitaxy (MBE) due to the ultra-low vapor pressure of Ru. Additionally, Ru has high electronegativity which further makes it difficult for achieving complete oxidation, Ru → Ru⁴⁺ state under standard MBE conditions. The former issue has been dealt by supplying Ru using the electron-beam source whereas the oxidation issue is addressed by using highly reactive ozone. The use of electron-beam and ozone has adverse consequences on the stability of Ru beam-flux, which is critical for obtaining electronic-grade materials. Here, we show a novel solid-source metal-organic MBE approach that circumvents these issues by supplying a Ru containing metal-organic compound as a solid source of Ru for the growth of RuO₂.

Single crystalline, epitaxial RuO₂ films with scalable thicknesses were grown on a variety of substrates including r-Al₂O₃ and TiO₂ (110), (101), (100), and (001) as evident from high-resolution X-ray diffraction and scanning transmission electron microscopy (STEM). RuO₂ films with rocking curve full-width-half-maxima as low as 0.05° were obtained on TiO₂ (110) at substrate temperature of 300°C. Atomic force microscopy revealed atomically smooth film surfaces with a root mean square (rms) roughness value ~ 3 Å.

All films revealed metallic behavior down to 1.8 K with room temperature resistivities being comparable to bulk (35 μΩ-cm) for films as thin as 10 nm. The effect of film thickness, orientation, strain, and defects such as oxygen vacancies on the electrical properties will be discussed.

Finally, we also show the versatility of this novel MBE technique by demonstrating the growth of epitaxial and atomically smooth (001) platinum (Pt) films on SrTiO₃ (001). These films exhibited room-temperature resistivity of ~ 15 μΩ-cm, which is again comparable to that of the bulk single crystals. Importantly, these films showed a residual resistivity ratio (RRR) of 27, which is the highest reported value among Pt films grown to-date. We argue that the solid source MOMBE approach may potentially open up new physical vapor deposition (PVD) pathways (not just MBE) for “stubborn” materials such as delafossites, iridates, tungstates which contain elements that have low vapor pressures and are hard to oxidize in low pressure PVD approaches.

4:30 PM EQ10.02.08

Room-Temperature Ferroelectric Switching of Spin Hall Effect in GeTe Sara Varotto^{1,2}, Luca Nessi^{2,3}, Stefano Cecchi⁴, Jagoda Slawinska^{5,6}, Paul Noel⁷, Simone Petrò², Federico Fagiani², Alessandro Novati², Matteo Cantoni^{2,3}, Daniela Petti², Edoardo Albisetti², Marcio Costa⁸, Raffaella Calarco^{4,9}, Marco Buongiorno Nardelli⁵, Manuel Bibes¹, Silvia Picozzi⁹, Jean-Philippe Attané⁷, Laurent Vila⁷, Riccardo Bertacco² and Christian Rinaldi²; ¹CNRS/Thales, France; ²Politecnico di Milano, Italy; ³Istituto di Fotonica e Nanotecnologie IFN-CNR, Italy; ⁴Paul-Drude-Institut für Festkörperelektronik, Germany; ⁵University of North Texas, United States; ⁶University of Groningen, Netherlands; ⁷Université Grenoble Alpes, France; ⁸Fluminense Federal University, Brazil; ⁹Consiglio Nazionale delle Ricerche, Italy

Spin-to-charge conversion has been designated by Intel as a viable solution for beyond-CMOS computing elements [1], with very favourable scaling laws. In this context, ferroelectric Rashba semiconductors (FERSCs) provide a way for the non-volatile electric control of spin-to-charge conversion, of great importance for such computing elements.

The parent compound of FERSCs is germanium telluride (GeTe), a CMOS-compatible semiconductor characterized by a giant Rashba-type spin-orbit coupling at room temperature, arising from the symmetry breaking induced by ferroelectric displacement. Importantly, calculations revealed that the spin orientation of each Rashba sub-band is inverted upon ferroelectric polarization reversal [2]. Such prediction has been already demonstrated experimentally in epitaxial GeTe(111) thin films on silicon, by our spin and angle resolved photoemission measurements on two surfaces with inward or outward spontaneous polarization [2]. Thus, FERSCs allow for ferroelectric control of the spin-resolved band structure in semiconductors, with intriguing implications on the spin transport properties.

Here we demonstrate the non-volatile, ferroelectric control of spin-to-charge conversion at room temperature in GeTe epitaxial films [3]. First, we demonstrate the feasibility of the ferroelectric switching, despite the high density of free carriers. The switching is induced by voltage pulses applied to a gate electrode, while the readout of the written state is performed by electro-resistive measurements of the GeTe/metal junction. Using spin-pumping experiments, we measured a sizeable spin-to-charge conversion efficiency comparable to Pt. We show that the sign of the generated charge current is reversed for two opposite ferroelectric states controlled by a gate. Density functional theory calculations reveal the consistency of these observations with spin Hall effect in thin GeTe films.

Our results open a route towards devices combining spin-based logic and memory integrated into a silicon-compatible material, where ferroelectricity can be employed as a state variable to tune the spin-to-charge conversion.

C.R. acknowledges the project TWEET, grant no. 2017YCTB59 funded by MIUR. Work supported by the ERC Advanced Grant No. 833973 “FRESCO”

[1] S. Manipatruni *et al.*, Nature 565, 35–42 (2019)

[2] D. Di Sante *et al.*, Adv. Mater. 25, 509–513 (2013)

[3] C. Rinaldi *et al.*, Nano Letters, (2018); DOI: 10.1021/acs.nanolett.7b04829

[4] S. Varotto *et al.*, arXiv:2103.07646 (2021)

4:45 PM EQ10.02.09

Exchange Biased, Electrically Modulated Magnetoelectric Thin-Film Sensors Towards Biomagnetic Measurements Patrick Hayes, Eric Elzenheimer, Lars Thormählen, Elizaveta Golubeva, Jeffrey McCord, Gerhard Schmidt, Michael Höft, Dirk Meyners and Eckhard Quandt; CAU Kiel, Germany

Contact-less biomagnetic sensing constitutes the next frontier for advanced healthcare, creating novel diagnostic abilities using multichannel magnetocardiography (MCG) and magnetoencephalography (MEG) either as a single source of information for rapid patient screening or as fusion with

established methods such as electrocardiography and electroencephalography as a source for additional information. The main obstacle towards clinical biomagnetic diagnosis using magnetic imaging techniques is the lack of readily applicable sensor technology offering extremely low magnetic noise floors; realtime MCG measurements demand for a limit of detection (LOD) lower than 10 pT/ $\sqrt{\text{Hz}}$, reaching below 100 fT/ $\sqrt{\text{Hz}}$ enables even MEG signal acquisition. Such extremely minute amplitudes which are six to seven orders lower than earth's permanent magnetic field, demand lowest noise sensor technology as the low frequency signal regime below about 500 Hz is strongly affected by 1/f-noise.

In the presented work the piezoelectric (PE) phase of thin film magnetoelectric (ME) composites is actively excited, thus exploiting the converse ME effect [1], remedying shortcomings of the direct ME effect. The experimental work involves bulk micromachined thin film cantilever composites of mesoscopic scale (25mm x 2.5mm x 0.35 mm) of which high frequency mechanical resonances at about 500 kHz are studied. These resonances show high mechanical quality factors of about $Q \approx 1000$. This mechanical oscillation, being rigidly coupled into the magnetostrictive (MS) material phase leads to a voltage induced in a pickup coil surrounding the sensor composite. This converse ME voltage response with respect to small external fields shows high sensitivities in the order of kV/T and linearity up to a field magnitude of several μT , no external magnetic driving field is required.

The signal components of MCG lie in the range from 3 to about 150 Hz with vanishingly small amplitude $< \sim 100$ pT, this regime is targeted by this research. The entirely passive readout combined with low power requirements makes the presented ME sensor system suitable for integration into sensor arrays as anticipated for future biomagnetic imaging purposes. Using single layer MS FeCoSiB material, the measured noise floor in the low frequency regime shows an abrupt increase as soon as an excitation threshold of about 200 mV is reached. Intense magnetization activity in the MS phase poses the dominant source of noise, practically limiting the LOD at 10 Hz to about 70 pT/ $\sqrt{\text{Hz}}$ [1]. Using sophisticated magnetic layer systems such as exchange bias[2] enables to effectively lower the magnetically dominated noise, even at high drive levels, while maintaining high magnetic sensitivities.

In this contribution, we demonstrate the performance of electrically modulated thin film ME composites, using magnetron sputtered exchange biased, amorphous FeCoSiB films driven by aluminum nitride. This approach allows composite magnetoelectrics to detect low DC as well as AC magnetic fields of amplitudes down to ~ 10 pT/ $\sqrt{\text{Hz}}$ @ 10 Hz without the requirement of an external magnetic AC or DC bias field. In a human patient trial conducted in a magnetically shielded room, using averaging it was even possible to perform an MCG recording.

Funding via DFG, SFB1261 "Magnetoelectric Sensors: From Composite Materials to Biomagnetic Diagnostics" is gratefully acknowledged.

[1] P. Hayes, M. Jovičević Klug, S. Toxværd, P. Durdaut, V. Schell, A. Teplyuk, D. Burdin, A. Winkler, R. Weser, Y. K. Fetisov, M. Höft, R. Knöchel, J. McCord, E. Quandt, Converse Magnetoelectric Composite Resonator for Sensing Small Magnetic Fields. Scientific reports. 9, 16355 (2019)

[2] M. Jovičević Klug, L. Thormählen, V. Rößisch, S. D. Toxværd, M. Höft, R. Knöchel, E. Quandt, D. Meyners, J. McCord, Antiparallel exchange biased multilayers for low magnetic noise magnetic field sensors. Appl. Phys. Lett. 114, 192410 (2019)

5:00 PM EQ10.02.10

Polarization Switching Dynamics—A Molecular Dynamics Study Rajan Khadka and Pawel Koblinski; Rensselaer Polytechnic Institute, United States

In this work, we use molecular dynamics simulations to investigate the polarization switching dynamics in the single domain and 180° bidomain (i.e., including the preexisting domain wall) models in BaTiO₃ and KNbO₃. In a single domain study, for both materials, we observed that the hysteresis loop is essentially no-existent in the highest temperature non-cubic phase. We attribute this behavior to the observation of spontaneous local polarization fluctuations leading to the elimination of the nucleation barrier. Interestingly, in the case of the bidomain structure, while we observe domain migration driven by the electric field, at high fields new domain nucleation is severely suppressed by comparison with the single domain simulations. This behavior is explained by the suppression of simulation dimension fluctuations due to the presence of the two domains. We give further credence to this conjecture by demonstrating that artificial suppression of the simulation cell dimension fluctuations in the case of a single domain switching also suppresses new domain nucleation.

SESSION EQ10.03 Poster Session
Session Chairs: Tianxiang Nan and Nian Sun
Tuesday Afternoon, November 30, 2021
8:00 PM - 10:00 PM
Hynes, Level 1, Hall B

EQ10.03.04

High Data-rate Communication Enabled by Mechanical Non-Linear Response of Very Low Frequency (VLF) Magnetoelectric Antennas. Yifan He, Cunzheng Dong, Xianfeng Liang, Huaihao Chen and Nian Sun; Northeastern University, United States

The newly demonstrated very low frequency (VLF) magnetoelectric (ME) antennas [1] based on two-phase ME heterostructure have shown their capability and advantages in device miniaturization, ultra-sensitive magnetic field detection and communication in harsh environment. In this work, the authors utilized the non-linear electric field versus strain response of electrostrictive phase to achieve frequency mixing effect and intermodulation in the ME antenna. The proposed modulation scheme required simply an electrically applied superposition of carrier signal and baseband signal. To make the experimental demonstration, 5 layers of highly magnetostrictive Metglas foil were stacked and epoxy-bonded on both sides of a PMN-PT slab with a dimension of 50x5x0.2 mm, forming a two-phase ME heterostructure. The ME antenna had its maximum ME coefficient under 5.7 Oe DC magnetic field bias and the corresponding resonance frequency was 28.73 kHz. With a 30 Vpp carrier signal at 28.73 kHz and a baseband signal at 5 kHz with various amplitudes applied across the PMN-PT slab, two modulated frequency components at 23.73 kHz and 33.73 kHz were observed in picked-up near field signal. The analog modulation depth can be controlled by the amplitude of the baseband signal. The digital modulation test was also performed with a binary digit sequence of "0101..." at a data rate of 5 kbps as baseband signal, the picked-up modulated signal was successfully demodulated by an on-board demodulator, which indicated the potential application of high data rate communication using the proposed modulation scheme and PMN-PT material-based VLF ME antenna.

[1]. Dong, Cunzheng, Yifan He, Menghui Li, Cheng Tu, Zhaoqiang Chu, Xianfeng Liang, Huaihao Chen et al. "A portable very low frequency (VLF) communication system based on acoustically actuated magnetoelectric antennas." *IEEE Antennas and Wireless Propagation Letters* 19, no. 3 (2020): 398-402.

EQ10.03.05

Describing Hysteresis for Non-Switching Fields in Epitaxial Monoclinic PZT Films Using Polarization Rotation Model Philip Lucke¹, Muharrem Bayraktar¹, Andrey E. Yakshin¹, Guus Rijnders², Fred Bijkerk¹ and Evert P. Houwman²; ¹Industrial Focus Group XUV Optics, MESA+ Institute of Nanotechnology, University of Twente, Netherlands; ²Inorganic Material Science, MESA+ Institute of Nanotechnology, University of Twente, Netherlands

Hysteresis is a limiting factor for the actuation accuracy of $\text{PbZr}_{1-x}\text{Ti}_x\text{O}_3$ (PZT) ceramics and thin films. Explanation of hysteresis for these materials using phenomenological models such as Rayleigh model is a common practice. On the other hand, application of Rayleigh model and its variants results in significant discrepancies in explaining the hysteresis behavior in epitaxial thin films. Here, hysteresis in application-relevant, epitaxial, monoclinic $\text{PbZr}_{0.55}\text{Ti}_{0.45}\text{O}_3$ films were investigated for non-switching AC excitation fields at zero and 20 kVcm^{-1} DC bias cases. The hysteresis, loss and nonlinearity in the strain and polarization response of the films show unique features that is not expected from the Rayleigh model. The strain exhibits a hysteretic behavior and is linear with the excitation amplitude. However, the polarization is hysteretic and highly nonlinear over the investigated frequency range from 70 Hz to 5 kHz. The application of the bias shows almost no change for the strain response, whereas the loss tangent and nonlinearity of the polarization are significantly reduced.

The observations are explained by a new model, the so called polarization rotation model. This model describes the film properties as a result of the nonlinear rotation of the polarization vector within the monoclinic unit cell in response to the applied electric field, accompanied by a viscous interaction of the domains. The model can describe the scaling of the loss tangent and (non)linearity of the strain and polarization in an amplitude and frequency range that is far exceeding the applicable range of the Rayleigh model. It is shown that the nonlinear response and the hysteretic loss can be ascribed to two separate processes. The nonlinearity stems from the nonlinear nature of the rotation of the polarization vector. On the other hand, the hysteresis and ferroelectric loss stems from viscous interactions of domains during the rotation of the polarization vector.

[1] Lucke, P., Bayraktar, M., Birkhölzer, Y. A., Nematollahi, M., Yakshin, A., Rijnders, G., . . . Houwman, E. P. (2020). Hysteresis, Loss and Nonlinearity in Epitaxial $\text{PbZr}_{0.55}\text{Ti}_{0.45}\text{O}_3$ Films: A Polarization Rotation Model. *Advanced Functional Materials*, 30(52), 2005397. doi:https://doi.org/10.1002/adfm.202005397

[2] Lucke, P., Bayraktar, M., Schukink, N., Yakshin, A. E., Rijnders, G., Bijkerk, F., & Houwman, E. P. Influence of DC Bias on the Hysteresis, Loss, and Nonlinearity of Epitaxial $\text{PbZr}_{0.55}\text{Ti}_{0.45}\text{O}_3$ Films. *Advanced Electronic Materials*, 2100115. doi:https://doi.org/10.1002/aeml.202100115

EQ10.03.07

Observation of Topological Antiferromagnetic Phase at the Interface of Sputtered TI/FM Heterostructures Nirjhar Bhattacharjee¹, Adrian Fedorko¹, Valeria Lauter², Alexander Grutter³, Alexandria Will-Cole¹, Donald Heiman¹ and Nian Sun¹; ¹Northeastern University, United States; ²Oak Ridge National Laboratory, United States; ³National Institute of Standards and Technology, United States

Topological Insulators (TI) possess Dirac Surface Conducting States which are protected by Time Reversal Symmetry (TRS) [1]. However, a gap opening in the surface state bands through braking of TRS is needed for realization of Quantum Anomalous Hall Effect (QAH) which in turn can give rise to and Axion Insulator States and topological magnetoelectric effect [2-3]. Magnetic phase has been reported in TIs using doping [4-5] and proximity effect [6]. Recently, intrinsic magnetic TI (MTI) phase has been theoretically predicted in MBi_2Te_4 ($M = \text{Mn, Ni, Eu, V}$) family of compounds [7-8] and experimentally observed in MnBi_2Te_4 [9]. Here, we report growth of highly c-axis oriented TI, Bi_2Te_3 with nominal surface roughness ($\sim 1.3 \text{ nm}$) using sputtering and formation of a topological antiferromagnetic phase at the interface of $\text{Bi}_2\text{Te}_3/\text{Ni}_{80}\text{Fe}_{20}$ (Permalloy, Py) heterostructures. We grew samples of 40 nm c-axis oriented Bi_2Te_3 at 250 C followed by 20 nm of Py at room temperature. Since the growth of the FM on TI is carried out without breaking vacuum, the topologically nontrivial surface states are accessible to the FM species in their pristine condition. We observed large diffusion of Ni from Py and formation of distinct interfacial phase of $\text{Ni}_x\text{Bi}_y\text{Te}_z$. TSS catalyzed reaction [10] possibly leads to formation of a topologically non-trivial interfacial phase because of solid state reaction between Ni and Bi_2Te_3 and proximity effect. Zero Field Cooled (ZFC) magnetic hysteresis loop measurements at low temperatures showed a large spontaneous exchange bias which suggests presence of FM/AFM coupling in the samples. Further, Field Cooled (FC) measurements with field cooling at 1 T showed enhanced exchange bias field values of $\sim 160 \text{ Oe}$. We characterized the Neel Temperature of the AFM phase at $\sim 63 \text{ K}$. We further identified the antiferromagnetic phase at Ni intercalated Bi_2Te_3 interfacial layer using Polarized Neutron Reflectometry (PNR). The large exchange bias in the Ni intercalated Bi_2Te_3 interfacial layer clearly suggests a large exchange energy which is characteristic of super-exchange mediated VdW MTI compound [8]. The observation of magnetic phase at the interface layer further raises the possibility of QAH state and paves the way for further exploration of TI/FM based heterostructures and applications for energy efficient spintronic devices. Also, growth of high crystalline quality TI using sputtering opens up the path towards integration of crystalline TIs in industrial CMOS devices.

References:

1. Y. L. Chen, J. G. Anaytis and J.H. Chu et al., *Science* Vol. 325, p. 5937 (2009).
2. J. Wang, B. Liang and S.C. Zhang et al., *Phys. Rev. B* 92, 081107(R) (2015).
3. D. Xiao, J. Jiang and C. Z. Chang et al., *Phys. Rev. Lett.* 120, 056801 (2018).
4. C. Z. Chang, W. Zhao and J. S. Moodera et al., *Nat. Mat.* Vol. 14, p. 473–477 (2015).
5. C. Z. Chang, J. Zhang and Q. K. Xue et al., *Science* Vol. 340, Issue 6129, p. 167-170 (2013).
6. F. Katmis, V. Lauter and J. S. Moodera et al., *Nature*, Vol. 533, p. 513 (2016).
7. J. Li, Y. Li and Y. Xu et al., *Sci. Adv.* 5: eaaw5685 (2019).
8. Z. Li, J. Li and Y. Xu et al., *Phys Rev B*, 102, 081107(R) (2020).
9. Y. Deng, Y. Yu and Y. Zhang et al., *Science* Vol. 367, Issue 6480, pp. 895-900 (2020).
10. G. Li and C. Felser et al., *Appl. Phys. Lett.* 116, 070501 (2020).

EQ10.03.08

Low-Field Large Magnetocaloric Effect in Self-Assembled Iron Nanoparticles Embedded in Titanium Nitride Thin-Film Matrix Kaushik Sarkar, Surabhi Shaji, Manosi Roy and Dhananjay Kumar; North Carolina A&T State University, United States

A field-dependent transition from the superparamagnetic-to-superparamagnetic blocked state is realized during magnetization (M) versus temperature (T) measurements by controlling the size of the iron (Fe) particles in the confined layers of titanium nitride (TiN) thin-film matrix. The nanoscale Fe particles of uniform size and shape are embedded in a TiN/Fe/TiN multilayered pattern using a pulsed laser deposition (PLD) method. Crystallographic studies carried out using x-ray diffraction have indicated the epitaxial nature of TiN film. Applying the Maxwell relation to the M-T curves at various fields, $\delta M/\delta T$ vs. H plots are acquired, the integration of which provides quantitative information about the isothermal entropy change in the Fe nanoparticulate system. Our experimental data shows that a positive magnetocaloric effect (MCE) with a maximum entropy change of $\sim 2.27 \times 10^3 \text{ J/K m}^3$ can be achieved for the magnetic field in the range of 0.002 - 0.5 T for the TiN/Fe/TiN sample having Fe particles of the size $\sim 15 \text{ nm}$. All the change in entropy curves clearly shows a peak in the vicinity of blocking temperature. A broad isothermal entropy change over a wide range of temperature has been found for the same sample with a refrigeration capacity value of $8.9 \times 10^4 \text{ J/m}^3$.

EQ10.03.09

Electronic and Structural Characterization of Microstructured NdNiO₃ Thin Films [Patrick A. Singleton](#), Grace Pan, Dan Ferenc Segedin, Julia Mundy and Ismail El Baggari; Harvard University, United States

NdNiO₃ (NNO) is a member of the perovskite rare-earth nickelates whose phase diagrams host metal-insulator transitions and various magnetic orders [1]. These transitions can be tuned using a variety of knobs such as rare-earth substitution, epitaxial strain and dimensionality. Even more, reducing the dimensions of NNO devices can modulate the drops and jumps in resistivity across the metal-insulator transition [2]. Here we perform temperature-dependent electrical transport measurements to further examine the effect of the lateral dimensions of thin films of NNO on the metal-insulator transition. Focused ion beams microstructuring is used to reduce the dimensions of the device towards sizes comparable to the metallic and insulating domains near the transition temperature. In addition to measuring the temperature-dependent resistivity, we image the domain structure of NNO films at low temperatures using scanning transmission electron microscopy to investigate the relationship between the metal-insulator transition and the structural changes at the atomic level. These complementary measurements may reveal the interplay between atomic-scale changes, nanoscale domain arrangements, and the macroscopic properties of rare-earth nickelates and transition-metal oxides in general.

References

- [1] Mattoni, G., Zubko, P., Maccherozzi, F. et al. Striped nanoscale phase separation at the metal-insulator transition of heteroepitaxial nickelates. *Nat Commun* 7, 13141 (2016).
- [2] Hong Lee et al. Imaging and Harnessing Percolation at the Metal-Insulator Transition of NdNiO₃ Nanogaps. *Nano Letters* 19 (11), 7801-7805 (2019).

EQ10.03.11

Late News: Electric Field Control of Phonon Angular Momentum in BaTiO₃* [Kevin Moseni](#), Richard Wilson and Sinisa Coh; University of California, Riverside, United States

We studied the angular momentum of phonons in BaTiO₃ from first principles. We find that in the tetragonal phase of BaTiO₃ the average phonon angular momentum is significantly larger in directions perpendicular to polarization than parallel. Furthermore, there is additional anisotropy within the plane perpendicular to polarization. We analyze the interatomic force constants and build a simple effective model to reveal the origin of the anisotropies. Finally, we suggest experiments using BaTiO₃ as an electric field controllable phonon angular momentum reservoir.

*This work was supported by grant NSF DMR-1848074.

EQ10.03.12

Late News: Ab Initio Calculation of Magnetoelectric Tensors in Known Magnetoelectric Materials [Louis Alaerts](#) and Geoffroy Hautier; Dartmouth College, United States

Magnetoelectricity (ME) is the property of certain materials to exhibit a coupling between their electric and magnetic properties. This enables the control of magnetization with electrical fields, a process whose energy cost is order of magnitude lower than the direct control of magnetization with magnetic fields, paving the way towards low-power devices. Nowadays, ME has been reported in a large variety of materials but most of them are characterized by weak coupling constants. Furthermore, the effect only appears at low temperatures, putting heavy limitations for practical applications. One of the main challenges in this field is to develop materials with stronger coupling with higher operating temperatures.

The strength of the magnetoelectric coupling is given by the tensor α_{ij} which describes the magnitude of the polarization (magnetization) built by a magnetic (electric) field. The magnetoelectric coupling can be computed nowadays with ab initio techniques within the density functional theory (DFT) framework. Here, we present results on the ab initio computation of the ME tensor on a few known ME materials such as Fe₂Mo₃O₈, GaFeO₃ or Ni₃TeO₆. We compare the results to experimental data and discuss the importance of the electronic, ionic and strain components to the magnetoelectric tensor.

EQ10.03.13

A 3D-Printed Molecular Ferroelectric Metamaterial [Yong Hu](#) and Shenqiang Ren; University at Buffalo, The State University of New York, United States

Solution-processable molecular ferroelectrics, which show ferroelectric properties approaching inorganic perovskites, have amassed much recent attention due to their lightweight, tunable electro-optic and electromechanical coupling effects (1, 2). Spontaneous polarization and the ability to switch the electromechanical activity by an external electric or mechanical stimulus is of prime importance, establishing the basis for many metamaterial technologies (3, 4). Over the past decade, elastic metamaterials with resonant inclusions have gained significant traction owing to their unique response to incident dynamic loads, ranging from subwavelength band gaps, back-scattering immune wave guides, and topological pumps, to the design of logic gates, nonreciprocity, and diode-like formations. Despite their theoretical promise, such mechanical metamaterials remain hindered by the lack of adaptive stimuli-responsive materials which can be effectively tuned “on-demand” across the time and length scales dictated by such metamaterials. We present a continuous rapid printing strategy for the volumetric deposition of water-soluble molecular ferroelectric metamaterials with precise spatial control in virtually any three-dimensional geometry by means of an electric-field-assisted additive manufacturing (5). We demonstrate a scaffold-supported ferroelectric crystalline lattice that enables self-healing and a reprogrammable stiffness for dynamic tuning of mechanical metamaterials with a long lifetime and sustainability. A molecular ferroelectric architecture with resonant inclusions then exhibits adaptive mitigation of incident vibroacoustic dynamic loads via an electrically tunable subwavelength-frequency band gap. The findings shown here pave the way for the versatile additive manufacturing of molecular ferroelectric metamaterials.

Reference:

1. Z. Zhang *et al.*, Tunable electroresistance and electro-optic effects of transparent molecular ferroelectrics. *Sci. Adv.* **3**, e1701008 (2017).
2. D.-W. Fu *et al.*, Diisopropylammonium bromide is a high-temperature molecular ferroelectric crystal. *Science* **339**, 425-428 (2013).
3. W. Zhou, P. Chen, Q. Pan, X. Zhang, B. Chu, Lead-Free Metamaterials with Enormous Apparent Piezoelectric Response. *Adv. Mater.* **27**, 6349-6355 (2015).
4. L. Van Lich, T. Shimada, S. Sepideh, J. Wang, T. Kitamura, Multilevel hysteresis loop engineered with ferroelectric nano-metamaterials. *Acta Mater.* **125**, 202-209 (2017).
5. Y. Hu *et al.*, A 3D-printed molecular ferroelectric metamaterial. *Proc. Natl. Acad. Sci. U.S.A.* **117**, 27204-27210 (2020).

EQ10.03.14

Controlled Light Scattering on Domains Enabled by Ferroelectric Phase Transformations in PIN-PMN-PT Thomas R. Mion¹, Peter Finkel¹, Markys Cain², Margo Staruch¹, Jakub Kolacz¹, Alex Moser¹, Paul Thompson³, Gareth Nisbet⁴, John Daniels⁵ and Sam Lofland⁶; ¹U.S. Naval Research Laboratory, United States; ²Electrosiences Ltd., United Kingdom; ³European Synchrotron Radiation Facility, France; ⁴Diamond Light Source, United Kingdom; ⁵University of New South Wales, Australia; ⁶Rowan University, United States

It is generally accepted that most electro-optical materials are transparent and, often, piezoelectric by nature. Electrical switching of ferroelectric domains and consequent domain wall motion promotes a strong piezoelectric activity. However, light scatters strongly at refractive index discontinuities such as found at domain wall boundaries. Thus, simultaneously achieving high piezoelectric properties along with a high transparency remains elusive, until now. Here, we applied electrical and mechanical stresses to manipulate and reconfigure the domains in perovskite $\text{Pb}(\text{In}_{1/2}\text{Nb}_{1/2})\text{O}_3$ $\text{Pb}(\text{Mg}_{1/3}\text{Nb}_{2/3})\text{O}_3$ - PbTiO_3 domain-engineered single crystals. We demonstrated that, via the stress induced ferroelectric-ferroelectric phase switching, a highly transparent crystalline state develops as the polydomain structure reconfigures to a monodomain ferroelectric state. The unprecedented optical properties are achieved at very low electric fields (less than 1.5 kV/cm) with the piezo crystal retaining an excellent piezoelectric performance. We demonstrate a robust method to enhance or suppress light scattering at ferroelectric domain boundaries, manipulated by external electrical and mechanical stresses, realizing *on-demand* optical transmissivity and piezoelectricity outperforming state-of-the-art materials.

EQ10.03.15

Magnetic and Electrical Transport Properties of Ni/NiO Composite Thin Films Bishwajite Karmakar¹, Sajal Islam¹, Ariful Haque^{2,1} and Kartik Ghosh¹; ¹Missouri State University, United States; ²Texas State University, United States

In this paper, detailed magnetic and electrical transport properties of composite thin films consisting of antiferromagnetic (AFM) NiO and ferromagnetic (FM) Ni have been studied. Highly oriented NiO thin films were grown on sapphire (0001) substrate using pulsed laser deposition technique varying the growth parameters such as the oxygen pressure of the chamber and the substrate temperature. To obtain various percentage mixtures of Ni and NiO by means of introducing point defects (oxygen vacancies) into NiO crystal structure, the as-grown films were annealed in forming gas (Ar:96% and H₂:4%) varying the temperature from 3000 C to 5000 C with annealing time from 10 minutes to 100 minutes. The X-ray diffraction (XRD) data show that the as-grown NiO films have the rock salt structure and are preferentially grown on the sapphire substrate along the (111) planes. The phase mixture of Ni/NiO was obtained by annealing and was confirmed by XRD, Raman spectroscopy, and SEM-EDS. Additionally, the film transmittance degraded as a conspicuous amount of NiO crystal structure was converted into preferentially oriented pure Ni detected by XRD as well as Raman spectroscopy. The very sharp peak at 44.4° on XRD indicates the face-centered cubic crystal structure of Ni. Detailed magnetic properties were investigated using a superconducting quantum interference device (SQUID) magnetometer. The temperature and field-dependent magnetization $M(H, T)$ data show that pure NiO and Ni are antiferromagnetic and ferromagnetic, respectively. The Ni-rich samples show ferromagnetic behavior with lower saturation magnetization (1.2×10^{-3} emu) and higher coercivity of 150 Oe than pure Ni film. Ferromagnetism has also been observed in Ni-rich samples in the ferromagnetic resonance (FMR) experiment, and the FMR linewidth increases with decreasing Ni phase in the composite thin films. Pure NiO samples exhibit a very high resistivity of 812 Ohm-m, whereas, pure Ni just behaves like a normal metallic ferromagnet. However, the value of resistivity sharply decreases with increasing oxygen vacancies in NiO, and it behaves like a semiconductor. Finally, the behavior of the composite Ni/NiO thin films resemble a magnetic semiconductor leading to a promising application in the arena of spintronic devices.

EQ10.03.17

Nanoscale Multi-Modal Imaging of Multiferroics in Three Dimensions Luis Ortiz¹, Jingfeng Song¹, Bryan Huey¹, Dayne Sasaki², Yayoi Takamura² and Ramamoorthy Ramesh³; ¹University of Connecticut, United States; ²University of California, Davis, United States; ³University of California, Berkeley, United States

Ferromagnetic and multiferroic nanostructures are promising for next generation memory, logic, sensors, actuators, and nanoelectronics. In this work, we apply advanced scanning probe microscopy techniques including Magnetic Force Microscopy (MFM), Piezoresponse Force Microscopy (PFM), and Tomographic Atomic Force Microscopy (T-AFM) for nanoscale characterization of three multiferroic systems: homogeneous BiFeO₃ thin films, self-assembled BiFeO₃-CoFe₂O₄ (BFO-CFO) vertically aligned nanocomposites, and Lanthanum Strontium Manganite (LSMO) nanoarrays. Correlations between domain nanostructure and microstructural and engineered feature geometries are studied. Additionally, correlations between ferroelectric polarization and interfacial strain are directly investigated in 3 dimensions. Such correlated, multi-modal nanoscale imaging is promising for future optimization of multiferroic devices.

SESSION EQ10.04 Multiferroics II
Session Chairs: Eckhard Quandt and Nian Sun
Wednesday Morning, December 1, 2021
Hynes, Level 2, Room 206

10:30 AM *EQ10.04.01

Magnetolectric Correlations in Multiferroics at the Nanoscale Manfred Fiebig; ETH Zurich, Switzerland

Magnetolectric coupling phenomena in multiferroics were initially treated almost exclusively as bulk effects exhibited by homogeneous materials. In recent years, attention has moved to the nanoscale. On the one hand, magnetolectric phase control ultimately happens on the level of the mostly sub-micrometer-sized domains. On the other hand, domain walls, interfaces and thin films are nanoscale objects that have been proving to be the source of intriguing magnetolectric coupling effects. In my talk, I will therefore explore the fascinating world of magnetolectric correlations at the nanoscale in a number of examples, the diversity of which is intended to demonstrate the enormous potential of the nanoscale perspective on multiferroics.

[1] We show that in multiferroics with separately emerging magnetic and ferroelectric order (type I), the microscopic magnetolectric coupling can be intrinsically strong, even though the macroscopic leading-order magnetolectric effect is forbidden by symmetry. In hexagonal manganites like YMnO_3 an imbalance in the competing superexchange contributions couples the antiferromagnetic to the ferroelectric domains. The associated domain walls are a source of topological vortex-like magnetic singularities. --- Nat. Comms. 12, 3093 (2021).

[2] In certain multiferroics with jointly emerging magnetic and ferroelectric order (type II), like $(\text{Tb,Dy})\text{FeO}_3$, the multiferroic bulk state can be converted into multiferroic domain walls in a non-multiferroic environment. Electric or magnetic fields act on these confined multiferroic objects or return them to the bulk phase. --- Nat. Comms. 12, 2755 (2021).

[3] In epitaxial type-I multiferroic YMnO₃ thin films the coexistence of magnetic and ferroelectric order roots in the improper nature of the electrically polarized state. We find that its lattice-distortive origin permits to control the ferroelectric order via the mechanical clamping of the film to the substrate. This control is effective in the regime from a single monolayer to about 100 nm. Improper ferroelectrics hence offer additional degrees of freedom for tuning the magnetoelectric coupling in multiferroics. --- Nat. Comms. 10, 5591 (2019).

[4] As room-temperature multiferroic, BiFeO₃ is most promising for device applications. La alloying reduces the coercive field for magnetoelectric switching to the CMOS regime, but it also destroys the nano-domain patterning that is crucial for voltage-induced magnetization reversal. We show how the functionality of (La,Bi)FeO₃ films can be restored to the full potential of the BiFeO₃ parent compound by an electric-field training procedure. The training also initiates a giant net-polarization enhancement that survives in a device-like capacitor geometry. --- submitted.

11:00 AM EQ10.04.02

Training the Polarization in Integrated La_{0.15}Bi_{0.85}FeO₃-Based Devices Marvin J. Müller¹, Yen-Lin Huang^{2,3}, Saül Vélez¹, Ramamoorthy Ramesh^{2,3,2}, Manfred Fiebig¹ and Morgan Trassin¹; ¹ETH Zurich, Switzerland; ²University of California, Berkeley, United States; ³Lawrence Berkeley National Laboratory, United States

The integration of magnetoelectric multiferroics, hosting coexisting and coupled ferromagnetic and ferroelectric orders, into magnetoelectric spin-orbit logic devices holds promises for unprecedented performance and energy consumption reduction by several orders of magnitude.^[1,2] While static properties such as the coercive electric field are thoroughly studied and optimized, investigations on the evolution and coupling of the ferroic orders during electric-field cycling are sparse.^[3,4,5,6]

Here, we study the evolution of the ferroelectric order of the technologically most relevant magnetoelectric material, BiFeO₃, and its chemically engineered relative La_{0.15}Bi_{0.85}FeO₃. Using operando optical second-harmonic generation microscopy, we directly access the polarization of the films integrated in technologically relevant capacitor heterostructures during electric-field cycling. We demonstrate that electric-field training results in a spontaneous domain ordering and a giant enhancement of the net polarization in La_{0.15}Bi_{0.85}FeO₃. Furthermore, we track the evolution of this ordered domain configuration operando in the device architecture during repeated switching and find that it is stable for more than 10⁶ switching cycles. In conclusion, our operando investigations give unprecedented insights into the polarization evolution during real device conditions and, therefore, reveal hitherto hidden opportunities to probe the polarization dynamics and to optimize BiFeO₃-based integrated devices.

[1] S. Maniapatruni *et al.*, *Nature* **565**, 35 (2019).

[2] M. Trassin, *J. Phys. Condens.* **28**, 033001 (2016).

[3] J. Heron *et al.*, *Nature* **516**, 370 (2014).

[4] Y. Huang *et al.*, *Nat. Commun.* **11**, 2836 (2020).

[5] B. Prasad *et al.*, *Adv. Mater.* **32**, 2001943 (2020).

[6] E. Parsonnet *et al.*, *Phys. Rev. Lett.* **125**, 067601 (2020).

SESSION EQ10.05 Magnetoelectrics II
Session Chairs: Eckhard Quandt and Nian Sun
Wednesday Afternoon, December 1, 2021
Hynes, Level 2, Room 206

2:00 PM *EQ10.05.02

Sputter Deposited Magnetostrictive Multilayers for Advanced Magnetoelectric Sensors Dirk Meyners¹, Lars Thormählen¹, Dennis Seidler¹, Viktor Schell¹, Elizaveta Golubeva¹, Anne Kittmann¹, Frans Munnik², Jeffrey McCord¹ and Eckhard Quandt¹; ¹Kiel University, Germany; ²Helmholtz-Zentrum Dresden-Rossendorf, Germany

For different concepts of magnetoelectric sensors with sputter deposited magnetostrictive layers it could be shown that they can achieve low detection limits in the range of 100 pT/√Hz and below when used as magnetic field sensors in biomagnetically interesting frequency ranges [1-3]. To reach a further improved detection limit, during sensor operation a better control of the magnetization state of the magnetostrictive phase is required. This enables a reduction in magnetically induced noise contributions while maintaining the sensor sensitivity.

In the presented work, sensors are considered whose magnetostrictive phase is formed by (Fe₉₀Co₁₀)₇₈Si₁₂B₁₀ single or multilayers. Such magnetic layers show comparatively low magnetic anisotropy together with a significantly high magnetostriction. Process-related influences during sensor fabrication, layer stresses for example, can therefore affect the magnetic properties. In this context, we compare amorphous, magnetostrictive FeCoSiB films prepared by RF and DC sputter deposition. The chemical and magnetic properties determined by elastic recoil detection and magneto-optical magnetometry, respectively, are correlated with the resulting magnetoelectric sensor properties such as noise level and detection limit.

[1] S. Salzer, V. Röbisch, M. Klug, P. Durdaut, J. McCord, D. Meyners, J. Reermann, M. Höft, R. Knöchel, "Noise Limits in Thin-Film Magnetoelectric Sensors With Magnetic Frequency Conversion", in *IEEE Sensors Journal*, vol. **18**, no. 2, pp. 596-604, 2018.

[2] Zaeimbashi, M., Nasrollahpour, M., Khalifa, A. *et al.*, "Ultra-compact dual-band smart NEMS magnetoelectric antennas for simultaneous wireless energy harvesting and magnetic field sensing", *Nat. Commun.* **12**, 3141, 2021.

[3] V. Schell, C. Müller, P. Durdaut, A. Kittmann, L. Thormählen, F. Lofink, D. Meyners, M. Höft, J. McCord, E. Quandt, "Magnetic anisotropy controlled FeCoSiB thin films for surface acoustic wave magnetic field sensors", *Appl. Phys. Lett.* **116**, 073503, 2020.

This work was funded by the German Research Foundation (DFG) through the Collaborative Research Centre CRC 1261 "Magnetoelectric Sensors – From Composite Materials to Biomagnetic Diagnostics".

2:30 PM *EQ10.05.03

Low-Voltage Magnetoelectric Coupling in Membrane Heterostructures Shane Lindemann¹, Julian Irwin¹, Gi-Yeop Kim², Kitae Eom¹, Bo Wang³, Jianjun Wang³, Jiamian Hu¹, Long-Qing Chen³, Si-young Choi², Mark Rzchowski¹ and Chang-Beom Eom¹; ¹University of Wisconsin–Madison, United States; ²Pohang University of Science and Technology, Korea (the Republic of); ³The Pennsylvania State University, United States

Relaxor ferroelectrics, such as (1-x)Pb(Mg_{1/3}Nb_{2/3})O₃-(x)PbTiO₃ (PMN-xPT), exhibit giant piezoelectricity which arises from the presence of multiple symmetries near a Morphotropic Phase Boundary (MPB). The MPB in PMN-xPT lies around x = 35% and separates a Rhombohedral (R) phase, with

spontaneous polarization along the $\langle 111 \rangle$ crystallographic directions, from a Tetragonal (T) phase whose polarization lies along $\langle 100 \rangle$. [1] For compositions near the MPB, the presence of bridging Monoclinic (M) and Orthorhombic (O) phases help to facilitate large lattice distortions as the spontaneous polarization rotates between the competing symmetries in order to align with the applied field.

Bulk studies on (011) oriented PMN-PT single crystals have demonstrated non-volatile (i.e. permanent) 71/109 degree switching between in-plane and out-of-plane R polarization directions. [2] Such switching results in distinct strain states and forms the basis of low-power, ultrafast, memory storage devices when coupled with a ferromagnetic (FM) material. [3] Achieving low power, however, necessitates the use of thin films of PMN-PT. Additionally, the films must be removed from their substrates in order to prevent substrate clamping that eliminates their giant piezoelectricity. Here we demonstrate growth of epitaxial (011) PMN-PT thin films, followed by removal of the substrate via etching of a $\text{Sr}_3\text{Al}_2\text{O}_6$ (SAO) sacrificial layer. [4] By coupling with a FM Nickel overlayer, we demonstrate manipulation of in-plane magnetic anisotropy as seen by the Magneto-Optic Kerr Effect (MOKE). The coupling only requires 3V applied bias across the PMN-PT membrane, which is much lower than the $>100\text{V}$ needed using bulk PMN-PT. However, we do not see evidence of the 71/109 degree bi-stable switching as observed in the bulk studies. Instead we find that the piezo-driven coupling is dominated by polarization rotation from the nominally $\langle 111 \rangle$ oriented R states towards the [011] O state along the applied field direction. Our findings have significant implications on the design of strain-mediated devices based on relaxor-ferroelectrics such as PMN-PT.

[1] Noheda, B.; Cox, D. E.; Shirane, G.; Gao, J.; Ye, Z.-G. *Phys. Rev. B* 2002, 66 (5), 054104

[2] Wu, T.; Bur, A.; Zhao, P.; Mohanchandra, K. P.; Wong, K.; Wang, K. L.; Lynch, C. S.; Carman, G. P. *Appl. Phys. Lett.* 2011, 98 (1), 012504

[3] Hu, J.-M.; Li, Z.; Chen, L.-Q.; Nan, C.-W. *Nat. Commun.* 2011, 2, 553

[4] Lu, D.; Baek, D. J.; Hong, S. S.; Kourkoutis, L. F.; Hikita, Y.; Hwang, H. Y. *Nat. Mater.* 2016, 15 (12), 1255–1260

Acknowledgement: This work was supported by the Army Research Office through Grant W911NF-17-1-0462. MOKE measurement at the University of Wisconsin–Madison was supported by the US Department of Energy (DOE), Office of Science, Office of Basic Energy Sciences (BES), under award number DE-FG02-06ER46327.

3:00 PM BREAK

4:00 PM EQ10.05.04

Exchange Biased Multilayers for SAW Magnetic Field Sensors Viktor Schell, Elizaveta Golubeva, Lars Thormählen, Anne Kittmann, Jeffrey McCord, Dirk Meyners and Eckhard Quandt; Kiel University, Germany

Surface acoustic wave devices have found a wide field of applications since it was discovered that they can be excited by interdigital transducers on piezoelectric substrates in 1965. One of these applications gaining more interest in the recent years is the sensing of magnetic fields. Especially for the measurement of biomagnetic signals surface acoustic wave devices are promising candidates due to their ability to detect magnetic fields below $100 \text{ pT}/\text{Hz}^{1/2}$ over a large frequency range of 1 Hz to 100 kHz [1]. This large bandwidth in combination with a wide dynamic range make them also interesting for artificial current sensing.

For the sensing of magnetic fields Love waves give much higher sensitivities than Rayleigh wave based sensors, due to the strong confinement of the acoustic wave in the magnetostrictive film [2]. Love waves are horizontal shear waves which are guided to the surface by a layer of higher acoustic impedance than the substrate. Operating in a delay line configuration the magnetoelastically induced change of shear modulus of the magnetostrictive layer yields in a corresponding phase shift of the acoustic wave. The magnetically generated $1/f$ noise of this magnetostrictive film on top of the guiding layer turned out to be the limiting factor regarding the limit of detection of the sensors. One approach to reduce magnetic noise is to exchange bias the ferromagnetic phase by the coupling to an antiferromagnetic phase [3, 4]. With this, a single or nearly single domain state can be achieved and domain walls reduced or eliminated as they are the main source of phase noise in these devices.

In this work a layer system consisting of $(\text{Fe}_{90}\text{Co}_{10})_{78}\text{Si}_{12}\text{B}_{10} / \text{Ni}_{80}\text{Fe}_{20} / \text{Mn}_{70}\text{Ir}_{30}$ is used, where $(\text{Fe}_{90}\text{Co}_{10})_{78}\text{Si}_{12}\text{B}_{10}$ is the magnetostrictive layer and $\text{Ni}_{80}\text{Fe}_{20}$ is a seed layer for the antiferromagnetic $\text{Mn}_{70}\text{Ir}_{30}$ which induces the exchange bias. All films are deposited by means of magnetron sputtering on ST-cut Quartz substrates and ST-cut Quartz based SAW sensors while a magnetic field is applied during deposition to induce the exchange bias. Challenges concerning the deposition process on piezoelectric substrates, the magnetic behavior as well as the noise performance of the sensors will be discussed. The successful reduction of magnetically induced $1/f$ noise in the low frequency regime brings SAW magnetic field sensors closer towards biomagnetic applications.

[1] V. Schell, C. Müller, P. Durdaut, A. Kittmann, L. Thormählen, F. Lofink, D. Meyners, M. Höft, J. McCord, and E. Quandt, “Magnetic anisotropy controlled FeCoSiB thin films for surface acoustic wave magnetic field sensors,” *Applied Physics Letters*, 116, 2020.

[2] A. Kittmann, P. Durdaut, S. Zabel, J. Reermann, J. Schmalz, B. Spetzler, D. Meyners, N. X. Sun, J. McCord, M. Gerken, G. Schmidt, M. Höft, R. Knöchel, F. Faupel, and E. Quandt, “Wide Band Low Noise Love Wave Magnetic Field Sensor System,” *Scientific Reports*, vol. 8, no. 1, 278–287, 2018.

[3] E. Lage, C. Kirchner, V. Hrkac, L. Kienle, R. Jahns, R. Knöchel, E. Quandt & D. Meyners, “Exchange biasing of magnetoelectric composites”, *Nature materials*, 11, 523–529, 2012.

[4] M. Jovicevic Klug, L. Thormählen, V. Röbisch, S. D. Toxværd, M. Höft, R. Knöchel, E. Quandt, D. Meyners & J. McCord, “Antiparallel exchange biased multilayers for low magnetic noise magnetic field sensors”, *Applied Physics Letters*, 114, 2019.

This work was funded by the German Research Foundation (DFG) through the Collaborative Research Centre CRC 1261 “Magnetoelectric Sensors – From Composite Materials to Biomagnetic Diagnostics”.

4:15 PM EQ10.05.05

Control of Chirality in Magnetic Nanostructures via Nanosecond Electric Pulses Wael A. Aldulaimi¹, Baris Okatan², Kursat Sendur¹ and Ibrahim B. Misirlioglu¹; ¹Sabancı University, Turkey; ²Izmir Institute of Technology, Turkey

The stability of magnetism in reduced dimensions is a major scientific agenda in the pursuit of implementing magnetic nanostructures into spintronic devices. Methods to probe and control magnetization states of such structures in a deterministic manner include use of spin polarized currents, photon absorption and relatively recently, electric fields that tailor magnetoelectric coupling in multiferroic based structures. In theory, a short electric pulse is able to generate localized magnetic fields that can couple to the local magnetic dipoles electrostatically. Here, using the Landau-Lifshitz-Gilbert (LLG) formalism of magnetism dynamics combined with continuum Maxwell relations we study the response of a ferromagnetic permalloy nanodisc to nanosecond electric field pulses [1]. The dynamics of the magnetic order during this process are examined and discussed. Ferromagnet nanodiscs can relax to a vortex phase as the ground state due to the demagnetizing field. Our results demonstrate that the planar chirality of such a ferromagnet nanodisc can be switched via a time-wise asymmetric electric field pulse on the order of a few ns duration that generates radially varying tangential magnetic fields. These fields couple to the vortex state of the nanodisc ferromagnet electrostatically, revealing an effective and robust method to control chirality. The kinetics

of the chirality switching as a function of disc size is analyzed. We also go on to discuss the possibility to generate programmable metasurfaces based on the approach we develop where local magnetic states can be rapidly written onto thin magnetic films with ease and extraordinary precision.

[1] W. A. S. Aldulaimi, C. Akaoglu, M. B. Okatan, K. Sendur and I. B. Misirlioglu, "Chirality switching in ferromagnetic nanostructures via nanosecond electric pulses", under revision in *Annalen der Physik*, June 2021.

4:30 PM EQ10.05.06

Low Temperature Magnetic Transition and Spin-Lattice Coupling in epsilon-Fe₂O₃ Epitaxial Thin Films Zheng Ma¹, Nico Dix¹, Jesus López-Sánchez^{2,3,4}, Javier Herrero-Martín⁵, Victor G. Ivanov⁶, Vassil Skumryev^{7,8}, Florencio Sánchez¹, Pilar Marín^{2,3}, Jaume Gàzque¹, José Luis García-Muñoz¹ and Martí Gich¹; ¹Institut de Ciència de Materials de Barcelona (ICMAB-CSIC), Spain; ²Universidad Complutense de Madrid UCM, Spain; ³UCM ADIF, Spain; ⁴ESRF European Synchrotron, France; ⁵ALBA Synchrotron Light Source, Spain; ⁶University of Sofia, Bulgaria; ⁷Institució Catalana de Recerca i Estudis Avançats (ICREA), Spain; ⁸Universitat Autònoma de Barcelona, Spain

The intriguing low temperature softening of the high magnetic anisotropy epsilon Fe₂O₃ (eFO) nanoparticles [1] has been also observed in epitaxial stabilized eFO thin films on MgAl₂O₄(111) and flexible fluorophlogopyte mica (001) substrates. The selection of an adequate substrate and buffer layer leads to an excellent film quality with sharp (00L) eFO X-ray diffraction peaks and the formation of 3 in-plane twin domains compatible with the 3-fold symmetry of the substrate surface. At room temperature, the *M(H)* hysteresis loops show a strong magnetic anisotropy and absence of step-like magnetization drop due to soft components. A reduction of the magnetic anisotropy and coercive field occurs on cooling below 200 K, which is reminiscent of that found in randomly distributed nanoparticles. The *H_c* collapse is less pronounced in the epitaxial films (-40%) than in nanoparticles (-96%), but the (00L) out of plane-texture allows a better observation of temperature dependence of frequency shifts of Raman modes. The trends primarily agree with the anharmonic model at temperatures above ~ 200 K, whereas a marked phonon softening can be observed below this temperature for different modes. The transition has been also studied by X-ray absorption spectroscopy (XAS) measurements in total electron yield and fluorescence modes and by X-ray magnetic circular dichroism (XMCD) and transport measurements.

[1] M. Gich, C. Frontera, A. Roig, E. Taboada, E. Molins, H. R. Rechenberg, J. D. Ardisson, W. A. A. Macedo, C. Ritter, V. Hardy, J. Sort, V. Skumryev, and J. Nogués, *High- and Low-Temperature Crystal and Magnetic Structures of ε-Fe₂O₃ and Their Correlation to Its Magnetic Properties*, *Chem. Mater.* **18**, 3889 (2006).

SESSION EQ10.06 Multiferroics III
Session Chairs: Eckhard Quandt and Nian Sun
Thursday Morning, December 2, 2021
Hynes, Level 2, Room 206

10:30 AM *EQ10.06.01

Ferroelectric Control of Rashba States—Towards Non-Volatile Spintronics Driven by Ferroelectricity Manuel Bibes and Srijani Mallik; Unité Mixte de Physique CNRS/Thales, France

After 50 years of exponential increase in computing efficiency, the technology of today's electronics is approaching its physical limits, with feature sizes smaller than 10 nm. New schemes must be devised to contain the ever-increasing power consumption of information and communication systems, which requires the introduction of non-traditional materials and new state variables. As recently highlighted, the remanence associated with collective switching in ferroic systems is appealing to reduce power consumption¹. A particularly promising approach is spintronics, which relies on ferromagnets to provide non-volatility and to generate and detect spin currents. However, magnetization reversal by spin transfer torques is a power consuming process. This is driving research on multiferroics to achieve a low-power electric-field control of magnetization, but practical materials are scarce and magnetoelectric switching remains difficult to control. In this talk, we will propose an alternative strategy to achieve low-power spin detection and generation, in non-magnetic systems combining ferroelectricity and Rashba spin-orbit coupling². We will describe various materials strategies based on single materials, multilayers and two-dimensional electron gases. In particular we will show results on SrTiO₃-based electron gases in which a large electric field induces a ferroelectric-like state that enables a non-volatile control of its spin-orbit properties and spin-charge conversion capabilities³. These observations open the way to the electric-field control of spin currents and to ultralow-power spintronics, in which non-volatility would be provided by ferroelectricity rather than by ferromagnetism.

1. Manipatruni, S. Beyond CMOS computing with spin and polarization. *Nature Physics* **14**, 338 (2018).
2. Varignon, J., Vila, L., Barthélémy, A. & Bibes, M. A new spin for oxide interfaces. *Nature Phys* **14**, 322–325 (2018).
3. Noël, P. *et al.* Non-volatile electric control of spin–charge conversion in a SrTiO₃ Rashba system. *Nature* **580**, 483–486 (2020).

This work received support from the ERC Advanced grant n° 833973 "FRESCO".

11:00 AM *EQ10.06.02

An Antiferromagnetic Metal Phase from a Correlated Insulator Qi Song^{1,2}, Spencer Doyle¹, Grace Pan¹, Hanjong Paik², Colin Heikes³, Betül Pamuk², William Ratcliff³, Padraic Shafer⁴, John T. Heron⁵, Charles Brooks¹, Luca Moreschini⁴, Antia Botana⁶ and Julia Mundy¹; ¹Harvard University, United States; ²Cornell University, United States; ³National Institute of Standards and Technology, United States; ⁴Lawrence Berkeley National Laboratory, United States; ⁵University of Michigan–Ann Arbor, United States; ⁶Arizona State University, United States

Antiferromagnetic materials hold great promise for next-generation spintronics due to the combination of stability in external magnetic fields and the potential for ultrafast switching. Here, we explore a new antiferromagnetic metal for spintronic applications. We begin with a correlated insulator, NdNiO₃. NdNiO₃ has a metal-to-insulator transition that is concomitant with a paramagnetic to antiferromagnetic transition. We demonstrate that electron doping can induce a new antiferromagnetic metallic phase in NdNiO₃. We use a combination of neutron diffraction and resonant x-ray scattering to probe the magnetic order and angle resolved photoemission spectroscopy to demonstrate a new Fermi surface in the antiferromagnetic metal phase. Our materials show a large zero-field planar Hall effect and could find applications in heat-assisted magneto-recording.

11:30 AM DISCUSSION TIME

11:45 AM EQ10.06.04

Nonvolatile Electric Field Control of Inversion Symmetry Lucas M. Caretta¹, Yu-Tsun Shao², Antonio Mei², Bastien Grosso³, Pius Behera¹, Margaret McCarter¹, Eric Parsonnet¹, Edward Barnard⁴, Archana Raja⁴, Manfred Fiebig³, Nicola Spaldin³, David A. Muller², Darrell Schlom² and Ramamoorthy Ramesh¹; ¹University of California, Berkeley, United States; ²Cornell University, United States; ³ETH Zürich, Switzerland; ⁴Lawrence Berkeley National Laboratory, United States

Crystal symmetry in condensed-matter materials largely dictates their micro- and macroscopic properties, and new material functionalities can arise when inversion symmetry is broken and when symmetry changes. Thus, the ability to control crystal inversion symmetry on demand is of both fundamental and technological importance. Perhaps the most pervasive example of the manifestation of broken inversion symmetry is in ferroelectrics, where crystal structures that inherently break inversion symmetry directly lead to a switchable spontaneous electrical polarization. Recently, the ability to synthesize heteroepitaxial ferroelectric superlattice systems has enabled new methods to control ferroic order¹⁻⁴ and even crystal symmetry^{5,6}. Here, by using BiFeO₃/TbScO₃ superlattices as our model system, we take advantage of (i) the discontinuity of the spontaneous polarization; (ii) the lattice mismatch; and (iii) the octahedral tilt frustration between the two layers to engineer crystal inversion symmetry. We stabilize both a non-centrosymmetric polar and a centrosymmetric antipolar phase mediated by a first order phase transition at room temperature. Both phases are identified and characterized using a combination of high-resolution and four-dimensional (4D) scanning transmission electron microscopy (STEM), piezoforce microscopy (PFM), and confocal second harmonic generation (SHG) over atomic and mesoscopic length scales. Moreover, applying orthogonal in-plane electric fields to this mixed-phase system results in the deterministic, nonvolatile interconversion of the centrosymmetric and noncentrosymmetric phases, resulting in a three order of magnitude change in the non-linear optical (SHG) response of the system. Demonstration of such an optically addressable, multi-state memory device presents new avenues for cross-functional devices which take advantage of the interconversion between ferro- and anti-ferroelectric states.

1. Tang, Y. L. *et al.* Observation of a periodic array of flux-closure quadrants in strained ferroelectric PbTiO₃ films. *Science*. **348**, 547–551 (2015).
2. Yadav, A. K. *et al.* Observation of polar vortices in oxide superlattices. *Nature* **530**, 198–201 (2016).
3. Das, S. *et al.* Observation of room-temperature polar skyrmions. *Nature* **568**, 368–372 (2019).
4. Wang, Y. J. *et al.* Polar meron lattice in strained oxide ferroelectrics. *Nat. Mater.* **19**, 881–886 (2020).
5. Dong, W. *et al.* Emergent Antipolar Phase in BiFeO₃-La_{0.7}Sr_{0.3}MnO₃ Superlattice. *Nano Lett.* **18**, 15 (2020).
6. Mundy, J. A. *et al.* A high-energy density antiferroelectric made by interfacial electrostatic engineering. *arXiv:1812.09615* (2018).

SESSION EQ10.07 Magnetoelectrics III
Session Chairs: Eckhard Quandt and Nian Sun
Thursday Afternoon, December 2, 2021
Hynes, Level 2, Room 206

1:45 PM EQ10.07.02

Structural Tuning of Ferroelastic Domain Dynamics Induced by Thermal Stress Anisotropy John J. Scott¹, Blai Casals Montserrat², Ekhard K. Salje² and Miryam Arredondo¹; ¹Queen's University Belfast, United Kingdom; ²University of Cambridge, United Kingdom

Ferroics, namely ferroelastics, ferroelectrics, ferromagnets and multiferroics (more than one ferroic order), have been the subject of increasingly intense research over the best part of half a century; having applications as memory devices, mechanical switches and acousto-optic devices. All ferroics, when cooled below a critical temperature (T_c) between a high-symmetry paraphase and a low-symmetry ferrophase, develop energetically equivalent but differently orientated states (domains). Domains are separated by interfaces (domain walls), which exhibit properties unique to that of the bulk and often constitute the active component for novel devices.

Importantly, Ferroelastics play a vital role in the fundamental understanding of multiferroic switching, as a large majority of multiferroics exhibit a ferroelastic component which mediates many of the observed properties, such as (super-)conductivity¹ and magnetoelectricity².

Analogous to other ferroics, ferroelastics are defined by their hysteresis loop (strain vs stress). On a macroscopic scale the hysteresis can appear smooth, yet on a finer scale, is actually formed of small discrete jumps or 'jerks'.

Most driven systems exhibiting small discrete events, cover a broad range of sizes dubbed as 'crackling noise'³. Such distributions are examples of avalanches, where Mean-field theory allows for the statistical characterisation of domain wall movement by predicting the power law distribution of jerks as a scale-free process of the form $g(x)dx \sim x^{-\gamma}dx$, whereby $g(x)$ describes the probability (g) of a jump (x) and the critical exponent is characteristic of that system⁴. Such exponents can be implemented to describe the statistics of certain observables, such as the energy released (E) or area spanned (α) by events. These power-law critical exponents are scale invariant (no characteristic size/ time scale) and demonstrate a behaviour that is independent of the microscopic properties of that system. As such, systems that share the same critical exponent values are of the same 'universal class', where the statistical behaviour of one class can be utilised to garner insight into another system that macroscopically appears to be much different or more intractable, such as tectonic activity and the crackling of sweet wrappers⁵.

This study presents a new insight into the role that the aspect ratio (AR) has on ferroelastic domain dynamics, by probing two LaAlO₃ (LAO) samples with different AR (high vs low). In-situ heating polarised optical microscopy was used on LAO bulk where the samples were heated from room temperature (RT) to beyond its T_c (~545C°) and back.

It was observed that the AR influences i) the resultant domain pattern at RT, where a clear preference is given to the orientation parallel to the longer axis of the high AR (HAR) sample vs the low AR (LAR) sample, which exhibits a more even split and complex configuration of domain variants that meet at the centre and ii) each AR display some similarities in their dynamical behaviour at high temperatures while cooling down from T_c. At lower temperatures the AR induces distinct dynamic behaviour: the HAR samples display a propagating domain front that forms above RT and below T_c, leading to a global reconfiguration of the microstructure. This behaviour is explained in terms of thermal stress and the anisotropy present.

Moreover, statistical analysis shows that not only is there a difference in the overall criticality between the two samples, LAR:E=1.6 vs HAR:E=1.4, but that the HAR sample demonstrates a 'mixing' of the critical exponent before and after the global reconfiguration (E=1.66 to 1.33). This latter point is highlighted in the analysis of the maximum likelihood method statistics.

¹ T. Rojac, *et al.*, *Nat. Mater.* **16**(3), 322(2017).

² D. I. Khomskii, *J. Mag. & Mag. Mater.* **306**(1), 1(2006);

³ J. P. Sethna, *et al.*, *Nature* **410** (6825), 242(2001).

⁴ B. Casals, *et al.*, *Nat. Comms.* **12**(1)(2021).

⁵ F. Bohn, *et al.*, *Sci. Rep.* **8**(1)(2018).

2:00 PM EQ10.07.03

Ultra-High Room Temperature Carrier Mobility at Conducting Ferroelectric Domain Walls Measured by Corbino Disc Magnetoresistance [Conor J. McCluskey](#), Matthew Colbear, James McConville, Raymond McQuaid and Marty Gregg; Queen's University, Belfast, United Kingdom

Recently, an abundance of novel transport physics has been found at interfaces, much of which promises to be key in the development of future technologies. The unusual electronic and structural environment at the interface can lead to behaviours which deviate wildly from that in the individual bulk constituents, while remaining confined to the interface. Electrically conducting homointerfaces, such as the domain walls that separate different orientations of electrical polarisation within the same band-insulator [1,2], are of particular interest, as they boast the ability to be created, moved and erased on demand [3,4]. Thus, they offer an additional dynamic degree of freedom when compared to conducting heterointerfaces (between dissimilar band insulators, e.g. $\text{LaAlO}_3/\text{SrTiO}_3$ [5]), which are fixed in place. Despite this, understanding of charge transport and fundamental aspects of conduction at domain walls is lacking in comparison to the current state-of-the-art in heterointerfaces. Here, we try to address this disparity by reporting on a geometric magnetoresistance measurement of carrier mobility in approximately conical 180° domain walls, which occur in partially switched ferroelectric thin film single crystal lithium niobate. We show that the domain microstructure, which is usually a hurdle to overcome when performing transport measurements on domain walls, results in a domain wall geometry which is equivalent to that of the "Corbino disc"; a textbook sample arrangement for geometric magnetoresistance measurements. Analysis of our magnetoresistance data reveals that these domain walls exhibit an extremely high room temperature Hall mobility of $\sim 3,000\text{cm}^2\text{V}^{-1}\text{s}^{-1}$. This value much larger than that seen at bulk or interface oxides before. Finally, we discuss the insight this measurement gives us in terms of understanding the transport at lithium niobate conducting domain wall homointerfaces.

- [1] Seidel, J., Martin, L., He, Q. *et al.* Conduction at domain walls in oxide multiferroics. *Nature Mater* **8**, 229–234 (2009).
- [2] Schröder, M. *et al.* Conducting Domain Walls in Lithium Niobate Single Crystals. *Adv. Funct. Mater.* **22**, 3936–3944 (2012).
- [3] McQuaid, R., Campbell, M., Whatmore, R. *et al.* Injection and controlled motion of conducting domain walls in improper ferroelectric Cu-Ci boracite. *Nat Commun* **8**, 15105 (2017)
- [4] McGilly, L., Yudin, P., Feigl, L. *et al.* Controlling domain wall motion in ferroelectric thin films. *Nature Nanotech* **10**, 145–150 (2015).
- [5] Ohtomo, A., Hwang, H. A high-mobility electron gas at the $\text{LaAlO}_3/\text{SrTiO}_3$ heterointerface. *Nature* **427**, 423–426 (2004)

2:15 PM EQ10.07.04

Cross-Linking and Charging Molecular Magneto-electronics [Yulong Huang](#)¹, Yuxuan Chen², Yong Hu¹, Travis Mitchell¹, Lu An¹, Zheng Li¹, Jason Benedict¹, Huashan Li² and Shengqiang Ren¹; ¹The State University of New York at Buffalo, United States; ²Sun Yat-sen University, China

Magneto-electrics are witnessing an ever-growing success toward the voltage-controlled magnetism derived from inorganic materials. However, these inorganic materials have predominantly focused on the ferroelectromagnetism at solid-to-solid interfaces and suffered several drawbacks, including the interface-sensitive coupling mediators, high-power electric field, and limited chemical tunability. Here, we report a promising design strategy to shift the paradigm of next-generation molecular magneto-electrics, which relies on the integration between molecular magnetism and electric conductivity though an in situ cross-linking strategy. Following this approach, we demonstrate a versatile and efficient synthesis of flexible molecular-based magneto-electronics by cross-linking of magnetic coordination networks that incorporate conducting chain building blocks. The as-grown compounds feature an improved critical temperature up to 337 K and a room-temperature magnetism control of low-power electric field. It is envisaged that the cross-linking of molecular interfaces is a feasible method to couple and modulate magnetism and electron conducting systems.

2:30 PM EQ10.07.05

High-Throughput Computational Discovery of a New Magneto-electric Multiferroic—The Anti-Ruddlesden-Popper $\text{Eu}_4\text{Sb}_2\text{O}$ Maksim Markov¹, Louis Alaerts², Henriqu P. Miranda¹, Guido Petretto¹, Wei Chen¹, Janine George¹, Eric Bousquet³, Philippe Ghosez³, Gian-Marco Rignanese¹ and [Geoffroy Hautier](#)^{2,1}; ¹Institute of Condensed Matter and Nanosciences, Université Catholique de Louvain, Belgium; ²Thayer School of Engineering, Dartmouth College, United States; ³Université de Liège, Belgium

Magneto-electric multiferroic materials are greatly sought for their potential use in new devices. Combining ferroelectricity and magnetism in the same material has been a real challenge especially in perovskites. The search for new ferroelectric structural families beyond perovskites is one path towards the discovery of new multiferroic materials. Here, we report on our search for new ferroelectrics using high-throughput computing and a recently built database of more than 2,000 phonons[1]. Browsing the phonon database, we identify materials exhibiting dynamically unstable polar phonon modes, a signature of a potential ferroelectric. We identify one new family of ferroelectric materials: the anti-Ruddlesden-Popper phases of formula $\text{A}_4\text{X}_2\text{O}$ with A: a +2 alkali-earth or rare-earth element and X: a -3 anion Bi, Sb, As, and P [2]. We show that the unique geometrically-driven mechanism of ferroelectricity involves the movement of an anion in a cationic cage.

This new mechanism leads in the case of $\text{Eu}_4\text{Sb}_2\text{O}$ to a rare example of a material combining ferroelectricity and ferromagnetism.

- [1] Petretto, G., Dwaraknath, S., P.C. Miranda, H., Winston, D., Giantomassi, M., van Setten, M. J., Gonze, X., Persson, K. A., Hautier, G. & Rignanese, G.-M. (2018). *Sci. Data*, **5**, 180065.
- [2] Markov, M., Alaerts, L., Miranda, H. P. C., Petretto, G., Chen, W., George, J., Bousquet, E., Ghosez, P., Rignanese, G.-M. & Hautier, G. (2021). *Proc. Natl. Acad. Sci.* **118**, e2026020118.

2:45 PM EQ10.07.06

A Narrowband Spintronic Terahertz Emitter Based on Magnetoelastic Heterostructures [Shihao Zhuang](#) and Jiamian Hu; University of Wisconsin-Madison, United States

Narrowband terahertz (THz) radiation is crucial for high-resolution spectral identification, but a narrowband THz source driven by femtosecond (fs) laser has remained scarce. Here we computationally predict that a metal/dielectric/magnetoelastic heterostructure enables converting a fs laser pulse into a multi-cycle THz pulse with a narrow linewidth down to ~ 1.5 GHz, which is in contrast with the single-cycle, broadband THz pulse from the existing fs-laser-excited emitters. We show that such narrowband THz pulse originates from the excitation and long-distance transport of THz spin waves in the magnetoelastic film, which can be enabled by a short strain pulse obtained from fs laser irradiation of the metal film providing that the thicknesses of the metal and magnetoelastic films both fall into a specific range. Our results therefore reveal an approach to achieving optical generation of narrowband THz pulse based on heterostructure design, which also has implications in the design of THz magnonic devices.

3:00 PM *EQ10.07.07

Magneto-electric Antennas—A Novel Antenna Miniaturization Approach [Hwaider Lin](#)¹ and Nian Sun²; ¹Winchester Technologies, LLC, United States; ²Northeastern University, United States

Antenna miniaturization is one of the fundamental challenges for decades. Conventional small antennas use electric current for radiation which relies on

electromagnetic wave resonance that leads to antenna sizes comparable to the electromagnetic wavelength λ_0 . Here we demonstrated a new antenna miniaturization approach that acoustically actuated nanomechanical magnetolectric (ME) antennas with ferromagnetic/piezoelectric thin film resonators could successfully miniaturize the magnitude of 1 to 2 orders with one of the highest passive antenna gain within all nano to micro-scale antennas at a similar frequency. In this talk, we will present the ME antenna theory, calculations, comparison with conventional antennas, and a quick view of a biomedical application example. These micro-antennas with ultra-high sensitivity, high selectivity of the magnetic field, the integrated capability to CMOS technology, and ground plane immunity have great potential applications for bio-implantable antennas, biomedical applications, the internet of things, etc.

3:30 PM EQ10.07.08

Dehybridization of Surface States and Enhancement of Spin-Charge Conversion in Ultrathin Topological Insulator Bi_2Se_3 Films Hanbum Park¹, Kwangsik Jeong², Jonghoon Kim¹, Seok-Bo Hong¹, Chul Kang³ and Mann-ho Cho¹; ¹Yonsei University, Korea (the Republic of); ²Dongguk University, Korea (the Republic of); ³Gwangju Institute of Science and Technology, Korea (the Republic of)

A three-dimensional topological insulator (TI) has spin-momentum locked surface states, in which an interconversion between spin and charge currents occurs. This spin-charge conversion (SCC) enables various applications of TI films in the fields of spintronics. However, when the thickness of the TI film is reduced to a few nanometers, a finite energy gap appears at the Dirac point and the magnitude of spin-momentum locking decreases owing to hybridization between top and bottom surface states. As a result, the weak antilocalization and SCC phenomena, hallmarks of TI surface states, are suppressed.

In this study, we modulated the hybridization effect in ultrathin Bi_2Se_3 films via interface coupling with transition metal oxide HfO_{2-x} . The unbonded Hf *d*-orbital states accompanied by oxygen-vacancy defects enhanced spin-orbit coupling and induced asymmetric surface states in Bi_2Se_3 , which results in suppression of the hybridization effect. Accordingly, we observed a transition from weak localization to weak antilocalization due to the oxygen defects through magneto-transport measurements. In addition, we simulated the band structures of ultrathin Bi_2Se_3 as a function of the oxygen defects with density functional theory and observed reduced hybridization gap and enhanced spin-momentum locking. To investigate SCC phenomena, we introduced spintronic THz emission spectroscopy that is recently emerged as a unique technique for investigating ultrafast SCC in sub-picosecond timescales. Using the THz spectroscopy, we identified enhancement of SCC efficiency owing to the dehybridization of surface states. These results provide novel methods of controlling surface states of TI and developing TI-based electronic and spintronic devices.

SESSION EQ10.08 Multiferroics IV

Session Chair: Tianxiang Nan

Monday Morning, December 6, 2021

EQ10-Virtual

8:00 AM *EQ10.08.02

Coupling of Metal-Insulator and Magnetic Phases at Nickelate Interfaces Claribel Dominguez¹, Bernat Mundet^{1,2}, Jennifer Fowlie¹, Alexandru Georgescu³, Marta Gibert⁴, Yajun Zhang⁵, Alain Mercy⁵, Adrien Waelchli¹, Michel Viret⁶, Nicolas Jaouen⁷, Andreas Suter⁸, Philippe Ghosez⁵, Andy Millis³, Antoine Georges³ and **Jean-Marc Triscone**¹; ¹University of Geneva, Switzerland; ²EPFL, Switzerland; ³Flatiron Institute, United States; ⁴University of Zurich, Switzerland; ⁵University of Liege, Belgium; ⁶Université Paris-Saclay, France; ⁷Synchrotron SOLEIL, France; ⁸Paul Scherrer Institute, Switzerland

Perovskite nickelates (RENiO_3 , RE=Rare Earth, RE \neq La) are fascinating materials, well-known, for their metal to insulator transition (MIT) and unique antiferromagnetic ground state [1-3]. In this talk, I will discuss the phase diagram of the system and the physics of the MIT before focusing on $\text{NdNiO}_3/\text{SmNiO}_3$ superlattices that display, depending on the thickness of the individual layers, a single or double MIT and a single or double magnetic transition. The electronic state of the materials was revealed at the unit cell scale by STEM [4]. The critical wavelength Λ_{cMIT} below which a single MIT is observed is 16 unit cells – the corresponding critical wavelength for coupled magnetic transitions is $\Lambda_{\text{cAFM}} = 34$ unit cells. This model system allows the origin of the coupling at such oxide interfaces to be studied. The key finding is that the critical length scales are not set by the length scale of the propagation of structural motifs (for instance Ni-O-Ni bond angles) across the interface between the two materials, which ab-initio calculations and STEM analyses suggest is minimal, but rather by the balance between the energy cost of having metallic-insulating – magnetic-non-magnetic – phase boundaries and the energy gain of the bulk phases [5].

[1] M.L. Medarde, Journal of Physics Condensed Matter 9, 1679 (1997)

[2] G. Catalan, Phase Transitions 81, 729 (2008)

[3] S. Catalano et al., Reports on Progress in Physics 81, 046501 (2018)

[4] B. Mundet et al. Nano Letters 21, 6, 2436 (2021)

[5] C. Dominguez et al. Nature Materials, 19, 1182 (2020)

8:30 AM *EQ10.08.03

Voltage-Controlled Magnetolectric Spintronics and Devices Hao Wu, Bingqian Dai, Malcolm Jackson, Di Wu and **Kang L. Wang**; University of California, Los Angeles, United States

Spintronics is one of the most promising candidates for the next-generation memory and logic applications for integration with the complementary metal oxide semiconductor (CMOS) technology, such as the magneto-resistive random-access memory (MRAM). Compared to the electrical current-driven MRAM, [1,2] such as spin-transfer torque (STT) and spin-orbit torque (SOT), voltage-controlled magnetolectric random access memory (MeRAM) and alike have the advantages of low-power, high-speed and high-density.

Here, in the first part, we will discuss the fundamental physics of voltage-controlled magnetic anisotropy (VCMA) and the mechanism of VCMA-induced magnetization switching of the perpendicular magnetization; then we will show the progress of VCMA-based MeRAM, [3,4] and the comparison of MeRAM, STT-MRAM, SOT-MRAM. In the second part, we will present the interfacial Dzyaloshinskii-Moriya interaction (DMI) in heterostructures and the voltage-controlled DMI (VC-DMI) effect, and its role on the voltage control of the motion of domain walls and other spin textures such as skyrmions. Based on the VCMA and VC-DMI effects, we develop a method to resolve the need of precise timing of write pulses with the use of chiral symmetry breaking by DMI in the graded magnetic system [5] to achieve the deterministic VCMA switching. Finally, we will discuss the perspective of magnetolectric ferrimagnetic materials and structures for high-speed applications. The voltage-controlled spintronics has great potential for future low-power and high-density non-volatile memory and logic applications.

References:

- [1] K. L. Wang, J. G. Alzate, and P. Khalili Amiri, *Low-Power Non-Volatile Spintronic Memory: STT-RAM and Beyond*, J. Phys. D: Appl. Phys. **46**, (2013).
- [2] S. A. Wolf, D. D. Awschalom, R. A. Buhrman, J. M. Daughton, S. Von Molnár, M. L. Roukes, A. Y. Chtchelkanova, and D. M. Treger, *Spintronics: A Spin-Based Electronics Vision for the Future*, Science.
- [3] C. Grezes, F. Ebrahimi, J. G. Alzate, X. Cai, J. A. Katine, J. Langer, B. Ocker, P. Khalili Amiri, and K. L. Wang, *Ultra-Low Switching Energy and Scaling in Electric-Field-Controlled Nanoscale Magnetic Tunnel Junctions with High Resistance-Area Product*, Appl. Phys. Lett. **108**, (2016).
- [4] X. Li, T. Sasaki, C. Grezes, D. Wu, K. Wong, C. Bi, P. V. Ong, F. Ebrahimi, G. Yu, N. Kioussis, W. Wang, T. Ohkubo, P. Khalili Amiri, and K. L. Wang, *Predictive Materials Design of Magnetic Random-Access Memory Based on Nanoscale Atomic Structure and Element Distribution*, Nano Lett. **19**, 8621 (2019).
- [5] H. Wu, J. Nance, S. A. Razavi, D. Lujan, B. Dai, Y. Liu, H. He, B. Cui, D. Wu, K. Wong, K. Sobotkiewich, X. Li, G. P. Carman, and K. L. Wang, *Chiral Symmetry Breaking for Deterministic Switching of Perpendicular Magnetization by Spin-Orbit Torque*, Nano Lett. **21**, 515 (2021).

9:00 AM *EQ10.08.04

Probing Local Polarization, Electric Field and Charge Distribution in Ferroelectric Heterostructures and Polarization Vortices by Four-Dimensional Scanning Transmission Electron Microscopy [Xiaoqing Pan](#)^{1,2}; ¹University of California, Irvine, United States; ²University of California, United States

In ferroelectric/multiferroic heterostructures, intrinsic polarization and the resulting electric field generate a rich set of localized electrical properties that have recently begun to be studied by differential phase contrast imaging or four-dimensional scanning transmission electron microscopy (4D STEM). Due to the size of the probe in STEM, these emerging techniques are capable of imaging both the polarization and electric field over a wide range of length scales. But there is still much to be learned about how electron probe conditions affect the electric field measured with these techniques. Recently, we developed a real-space imaging technique that can directly map the local electric field and charge density of crystalline materials with sub-angstrom resolution, using scanning transmission electron microscopy (4D STEM) alongside an angle-resolved pixelated fast-electron detector. Using this technique, we image the interfacial charge distribution and ferroelectric polarization in a SrTiO₃/BiFeO₃ heterojunction in 4D, and reveal charge accumulation at the interface that is induced by the penetration of the polarization field of BiFeO₃. By performing Bader charge analysis on the acquired charge density maps, we demonstrate the existence of two-dimensional electron gas or hole gas (2DEG or 2DHG) at BiFeO₃/TbScO₃ interface, indicated by the fact that the charge state of each Fe/O column increases when the polarization points away from the interface and decreases when the polarization points toward the interface. Our charge-density imaging method advances electron microscopy from detecting atoms to imaging electron distributions, providing a new way of studying local bonding in crystalline solids.

By applying 4D STEM to image the electric field in (PbTiO₃)₁₆/(SrTiO₃)₁₆ superlattices, we demonstrate that measurements using electron probes of differing sizes reveal different electric field configurations. Using a picometer sized probe, we find the high-Z lead atomic columns exhibit a strong bias in the electric field correlated with the polarization direction. Using a nanometer sized probe, we find an electric field that is un-correlated with the polarization. Combining these results with phase-field simulations, we show that the dominant contribution of the electric field measured with 4D STEM changes from the dipole of individual unit cells, determined by the bonding structure of PTO, to the total electric field, determined by the strain and electrostatic boundary conditions, depending on the probe size. The separability of two different fields probed by 4D STEM offers possibility to reveal how each contributes to the electronic properties of the film.

SESSION EQ10.09 Magnetolectrics IV
Session Chairs: Jiamian Hu and Nian Sun
Monday Afternoon, December 6, 2021
EQ10-Virtual

1:00 PM *EQ10.09.01

Advanced X-Ray Characterization of Topological and Geometry-Induced 3D Spin Texture [Peter Fischer](#); Lawrence Berkeley National Lab, United States

Spin textures and their dynamics hold the key to understand and control the properties, behavior and functionalities of novel magnetic materials, which can impact the speed, size and energy efficiency of spin driven technologies. Topology, frustration, and bespoke geometries that impact spin textures have recently attracted significant scientific interest and led to intense research addressing a broad spectrum of challenging scientific and technological questions, including stability, dynamics, nucleation, and transport in novel spin textures, such as chiral bobsbers, magnetic hopfions and torons, skyrmion tubes, and curvilinear magnetism [1].

Advanced characterization tools that provide magnetic sensitivity to spin textures, disentangling the role of individual components in heterogeneous material at high spatial resolution, ultimately at buried interfaces and in all three dimensions [2], and at high temporal resolution to capture the spin dynamics across scales, are required to address those questions, and are therefore of large scientific interest.

Various magnetic soft X-ray spectro-microscopies [3] using polarized soft x-rays provide unique characterization opportunities to study the statics and dynamics of spin textures in magnetic materials combining X-ray magnetic circular dichroism (X-MCD) as element specific, quantifiable magnetic contrast mechanism with spatial and temporal resolutions down to fundamental magnetic length, time, and energy scales.

Current developments of x-ray sources aim to increase dramatically the coherence of x-rays opening the path to new techniques, such as ptychography [4] or x-ray photo-correlation spectroscopy (XPCS) [5] that allow unprecedented studies of nanoscale heterogeneity, complexity, and fluctuations.

I will review recent achievements and future opportunities with magnetic x-ray spectro-microscopies. Examples will address static properties and dynamic behavior of various magnetic skyrmion [6,7] and Hopfion [8] textures, including those on curved substrates [9] with potential application to novel magnetic logic and storage devices.

This work was supported by the U.S. Department of Energy, Office of Science, Office of Basic Energy Sciences, Materials Sciences and Engineering Division Contract No. DE-AC02-05-CH1123 in the Non-Equilibrium Magnetic Materials Program (MSMAG).

- [1] C.H. Back, et al, J Phys D: Appl Phys 53 (36), 363001 (2020)
[2] P. Fischer et al, APL Materials 8 010701 (2020)
[3] P. Fischer and H. Ohldag, Report on Progress in Physics 78 094501 (2015)
[4] X. Shi, et al, Appl Phys Letter 108, 094103 (2016)
[5] M. H. Seaberg, et al, Phys Rev Lett 119 067403 (2017)

- [6] S. Woo, et al., Nature Materials 15 501 (2016)
 [7] N. Kent et al, Appl Phys Lett 115 112404 (2019)
 [8] N. Kent et al, Nature Comm 12 1562 (2021)
 [9] R. Streubel et al, JAP 129 210902 (2021)

1:30 PM *EQ10.09.02

Magnetolectric Magnetic-Field Sensors—Simulation Models and Sensitivity Analysis Martina Gerken; Univ of Kiel, Germany

Magnetic-field sensors based on piezoelectric and magnetostrictive composite materials offer a low limit of detection and a high dynamic range. Here, a theoretical investigation of the sensitivity behavior of such composite magnetolectric sensors is presented. Our focus is on biomedical applications targeting magnetocardiography (MCG) and magnetomyography (MMG). For these applications, measurement frequencies on the order of 1 to 100 Hz and a limit of detection in the pT-range are relevant. The behavior of two types of composite sensors is investigated in simulations – resonant cantilever-type sensors and surface acoustic wave (SAW) sensors. By combination of the simulated sensitivity with a noise model the limit-of-detection is predicted. Theoretical predictions are compared to experimental results of fabricated sensors.

Analytic calculations are used to derive the scaling behavior of FeCoBSi-Si-AlN cantilever-type magnetolectric sensors. Sensitivity, noise, and resulting detection limits display different behavior with functional and substrate layer thicknesses [1]. For an improved limit of detection, a higher quality factor or thicker functional layers are necessary. For higher-mode operation, the finite-element method (FEM) is used to calculate the charge distribution along the cantilever. For higher modes, a change of sign in the charge distribution reduces the sensor sensitivity [2]. To prevent this and obtain maximum performance, sensors with segmented electrode are designed.

1D, 2D, 2.5D, and 3D FEM models for Love-wave propagation in magnetolectric SAW sensors were established [3]. Theoretical and experimental results show that SAW sensors with lower IDT pitches and thus higher frequencies have a higher sensitivity. With the higher frequency and staying at the same guiding layer thickness, there are higher order Love waves [4]. Their frequencies are even higher, but their sensitivity is lower compared to their fundamental mode. From simulations, it is observed that the wave energy is not as concentrated at the surface for the higher modes and thus has less overlap with the magnetostrictive layer.

Biomedical magnetic fields are typically not homogeneous. To analyze the effect of an inhomogeneous excitation, we conducted simulations of localized excitation by a small coil at different positions along the sensor axis [5]. The simulations predict a rich excitation-position-dependent and frequency-dependent response behavior.

In summary, geometry-dependent effects, higher-mode operation, and inhomogeneous excitation fields are evaluated for magnetolectric sensors. It is demonstrated that magnetic-field sensors suitable for magnetocardiography and magnetomyography with a limit of detection in the pT-range are achievable. In combination with the high linearity of the composite ME sensors unshielded and uncooled operation for wearable sensor systems is within reach.

This work is supported by the DFG Collaborative Research Center SFB1261.

- [1] Krantz, M. C.; Gerken, M. Limit of Thermal-Vibration Noise in Magnetic Field Detection with Magnetolectric-Composite Cantilevers. *Phys. Rev. Appl.* 2020, 13 (5), 054047.
 [2] Schmalz, J.; Krantz, M. C.; Knies, A.; Lüder, H.; Gerken, M. Signal-to-Noise Ratio Enhanced Electrode Configurations for Magnetolectric Cantilever Sensors. *AIP Adv.* 2020, 10 (7), 075314.
 [3] Schmalz, J.; Spetzler, B.; Faupel, F.; Gerken, M. Love Wave Magnetic Field Sensor Modeling — from 1D to 3D Model. In 2019 International Conference on Electromagnetics in Advanced Applications (ICEAA); IEEE, 2019; 0765–0769.
 [4] Schmalz, J.; Kittmann, A.; Durdaut, P.; Spetzler, B.; Faupel, F.; Höft, M.; Quandt, E.; Gerken, M. Multi-Mode Love-Wave SAW Magnetic-Field Sensors. *Sensors* 2020, 20 (12), 3421.
 [5] Özden, M.-Ö.; Teplyuk, A.; Gümüş, Ö.; Meyners, D.; Höft, M.; Gerken, M. Magnetolectric Cantilever Sensors under Inhomogeneous Magnetic Field Excitation. *AIP Adv.* 2020, 10 (2), 025132.

2:00 PM EQ10.09.03

Interfacial Mechanical Coupling in $\text{PbZr}_{0.2}\text{Ti}_{0.8}\text{O}_3/\text{LaNiO}_3/\text{SrTiO}_3$ Heterostructures Claudia Lau¹, Cristina Visani¹, Stephen Albright¹, Zhan Zhang², Myung Geun Han³, Yimei Zhu³, Sohrab Ismail-Beigi¹, Ankit Disa⁴, Divine Kumah⁵, Charles Ahn^{1,1} and Frederick Walker¹; ¹Yale University, United States; ²Argonne National Laboratory, United States; ³Brookhaven National Laboratory, United States; ⁴Max Planck Institute for the Structure and Dynamics of Matter, Germany; ⁵North Carolina State University, United States

Large conductivity modulation by the coupling of ferroelectric polarization to the strongly correlated oxide LaNiO_3 has been demonstrated at an epitaxial ferroelectric- LaNiO_3 interface. High quality PZT/LNO on STO heterostructures were grown by MBE and off-axis RF magnetron sputtering and fabricated into all-oxide field effect devices. Using operando synchrotron diffraction measurements, we correlate changes in the conductivity with structural changes in the ferroelectric and conducting oxide as the ferroelectric polarization is switched. Comparing crystal truncation rods with half-order LNO Bragg reflections, we determine that the LNO oxygen octahedra are compressed and elongated while inside a comparatively rigid cation sublattice as the PZT ferroelectric polarization is switched. This finding is supported by DFT calculations. The LNO tetragonality change is accompanied by rotations of the LNO oxygen octahedra, with the tilt angles increasing and decreasing to modify the channel conductivity in a manner consistent with theory and transport.

2:15 PM *EQ10.09.04

Magnetic Susceptibility Particle Mapping (MSPM) for Imaging SPIONs in Biomaterial Scaffolds Christine Selhuber-Unkel; Heidelberg University, Germany

3D scaffolds are essential in biomaterials science to resemble the natural 3D environment of living cells. However, many of these scaffolds are non-transparent or too thick for being imaged with conventional light microscopy. In such applications it would be very beneficial to achieve a magnetic detection of the cells after tagging them with magnetic superparamagnetic iron oxide nanoparticles (SPIONs) so that non-invasive imaging becomes possible. An interesting method in this context is Magnetic Susceptibility Particle Mapping (MSPM), which is able to detect magnetic nanoparticles in a

lab scale device. Our system is based on magnetoelectric (ME) sensors utilizing the Delta-E effect in combination with a permanent magnet, which generates a bias field for the sensor and at the same time magnetizes the SPIONs. The permanent magnet is placed above the sensor, and the sample is rotated through the gap in between at a defined frequency. The SPIONs in the sample are magnetized by the permanent magnet and generate an additional magnetic field, which is recorded by the ME sensor. The detection threshold of our MSPM system is about 20 μg SPIONs in a volume of 200 mm^3 , and the spatial resolution is in the range of a few mm. We have also equipped the MSPM system with a magnetorelaxometry extension by using a self-biased sensor, so that it is possible to distinguish between particles bound to a material and diffusing particles. To demonstrate the feasibility of the MSPM method, we will present data that show the distribution of cells in a hydrogel matrix and of magnetic particles in responsive hydrogels, which are interesting in the context of tissue engineering and soft actuators.

2:45 PM EQ10.09.05

Geometric Control of Domain Structure Stability in Ferroelectric Nanotubes Aiden Ross, Shihao Zhuang, Kwon Lee and Jiamian Hu; University of Wisconsin-Madison, United States

The field of nanoscale ferroelectrics has utilized geometric confinement in thin films, nanodots, nanoislands, and strained superlattices to stabilize flux closures, vortices, skyrmions, and other topologically non-trivial polar states. Ferroelectric nanotubes provide a unique geometry with a large surface-to-volume ratio and vertical to lateral aspect ratio, and from these unique geometric properties, new polarization domain structures can be stabilized. Using phase-field modeling, we simulated the equilibrium polarization domain structure in $\text{Pb}(\text{Zr}_{0.52}\text{Ti}_{0.48})\text{O}_3$ nanotubes under different height and wall thickness conditions, and three unique domain structures were found. Each domain structure comprises an array of periodic flux-closures and anti-flux-closures pairs formed to minimize elastic and electrostatic energy. These domain structures differ by the frequency of the flux-closure/anti-flux-closure pairs along the perimeter and height. We demonstrate that the thermodynamic stability of these domain structures can be tuned by changing the nanotube geometry with wall thickness and height.

2:50 PM EQ10.09.06

Hard Micromagnets for Microelectromechanical Systems Mani Teja Bodduluri, Thomas Lisee, Phillip Eckstein and Björn Gjodka; Fraunhofer Institute for Silicon Technology ISIT, Germany

Integration of high-performance and voluminous hard magnetic materials into microelectromechanical systems (MEMS) structures have prevalent potential applications in the areas of energy harvesting, loudspeaker, biomedical, and various other markets [1]. However, miniaturization of bulk hard magnets to hundreds of micrometers employing conventional top-down (micromachining, bonding, etc.) and bottom-up (sputtering, electro-deposition, etc.) approaches is challenging because of issues like high-temperature processes, patterning, the realization of complex structures, etc [2].

A novel technique based on the agglomeration of powder materials into rigid structures using atomic layer deposition (ALD), best adapted for MEMS fabrication processes, has been used to integrate high-performance and organic-free NdFeB micromagnets into MEMS structures [3,4]. 75nm of ALD deposited Al_2O_3 layer is ample to fully agglomerate the particles which are dry filled into the etched Si cavities (aspect ratios (t/l) of 0.25 to 5). Since the ALD process is a gas phase CVD technique it has the advantage to coat the particles detailedly with a homogeneous and conformal layer, as a result, the layer binds the particles together moreover protects them from corrosion.

In this study, we have investigated the salient factors and process parameters influencing the magnetic properties of the ALD agglomerated NdFeB micromagnets. A vibrating sample magnetometer was used to measure the magnetic properties. Low temperature (75°C) thermal ALD process of Al_2O_3 is developed to circumvent issues like oxidation during the deposition process and effects of thermal expansion mismatch. Besides fabricating micromagnets comprising of single hard magnetic material (NdFeB, SmCo) we fabricated hybrid micromagnets by mixing (in weight ratio) NdFeB, SmCo magnetic materials to improve the effective magnetic properties of the micromagnets. The hybrid micromagnets displayed better reversible temperature coefficients over a specified temperature range. We analyzed the susceptibility curves and recoil loops to understand the magnetic mechanism. Additionally, magnetic interactions in the agglomerated particles were interpreted from Henkel plots by measuring dc demagnetization remanence and isothermal remanence. The δM plot indicates negative values elucidating magnetostatic type of interactions.

1. Niarchos, D. "Magnetic MEMS: key issues and some applications." *Sensors and Actuators A: Physical* 109.1-2 (2003): 166-173.
2. Arnold, David P., and Naigang Wang. "Permanent magnets for MEMS." *Journal of microelectromechanical systems* 18.6 (2009): 1255-1266.
3. Lisee, T., et al. "A novel fabrication technique for MEMS based on agglomeration of powder by ALD." *Journal of Microelectromechanical Systems* 26.5 (2017): 1093-1098.
4. Bodduluri, Mani Teja, et al. "High-performance integrated hard magnets for MEMS applications." *MikroSystemTechnik 2019; Congress. VDE, 2019.*

2:55 PM EQ10.09.07

Effect of Bi-Axial Strain on Cation Rotations and Electronic Band Structure of the Antiperovskite Mn_3GaN Roman Malyshev¹, Ingeborg-Helene Svenum^{2,1}, Sverre M. Selbach¹ and Thomas Tybell¹; ¹NTNU – Norwegian University of Science and Technology, Norway; ²SINTEF Industry, Norway

Strain-engineering is a powerful technique to control the properties of perovskite oxides. The effect of bi-axial strain is effectively a rotation/tilt of the oxygen octahedra, altering bond angles and lengths. Antiperovskite materials, functional materials that can possess properties such as antiferromagnetism, superconductivity and topological effects, have a perovskite crystal structure. However, a cation is occupying the oxide anion position while the perovskite B-site is occupied by an anion. Recent progress in thin film deposition has advanced heterostructures of antiperovskites with oxide perovskites and other quantum materials. Here, a density functional theory (DFT) study of the effect of bi-axial strain on the cubic antiperovskite Mn_3GaN is presented. Mn_3GaN is antiferromagnetic with the Mn spins ordered in a Kagome $I^{2\bar{8}}$ structure. Contrary to perovskite oxides, the cation-octahedra of Mn_3GaN are resilient to strain and the system prefers to adjust into a centrosymmetric tetragonal structure. In order to understand this resilience, the implications of the intermetallic nature of antiperovskites are addressed, and a detailed mapping of how the chemical bonds are affected by strain in Mn_3GaN is compared to the effect of strain on the ionic bonds in the canonical cubic oxide perovskite SrTiO_3 . The stiffness of the Mn_3GaN phonon structure to strain will also be compared to phonon modes that cause octahedral rotations in perovskites. Lastly, the effect of biaxial strain of Mn_3GaN on electronic properties will be addressed via band structure investigations.

6:30 PM EQ10.10.01

Late News: Freestanding Ferroelectric Bubble Domains Saidur R. Bakaul¹, Sergei Prokhorenko², Qi Zhang³, Youstra Nahas², Amanda Petford-Long¹, Laurent Bellaiche² and Nagarajan Valanoor³; ¹Argonne National Laboratory, United States; ²University of Arkansas, Fayetteville, United States; ³University of New South Wales, Australia

Ferroelectric (FE) bubble-like domains contain specially ordered electric dipoles. These objects are considered as possible multifunctional topological defects^{[i],[ii]} that may find revolutionizing applications in the field of microelectronics, due to their exceptional electronic and mechanical behavior. These nanoscale objects arise only in ultrathin complex oxide ferroelectric-dielectric-ferroelectric heterostructures that are epitaxially clamped with flat substrates. The parameter space (epitaxial strain, screening, built-in field, etc.) that favors their formation is quite narrow, and epitaxial growth is necessary. Due to the need for stringent growth conditions, the formation of bubble domains is therefore only possible on select complex oxide platforms. As such, integration of these functional objects with mainstream microelectronics substrates such as silicon and germanium is beyond the current capability of direct synthesis technique. Recently discovered epitaxial layer transfer techniques^{[iii],[iv],[v]} can be a possible remedy in this regard. These techniques enable the epitaxially grown complex oxides to be freestanding by selectively detaching them from the host substrate. The freestanding complex oxides can be subsequently transferred to an arbitrary substrate.

In this work^[vi] we demonstrate that ferroelectric bubble domains can be stabilized in a freestanding epitaxial FE – DE – FE complex oxide heterostructure. We find that the FE bubbles are invariant to surface bending and mechanical perturbations up to a limit – suggesting the presence of an energy barrier to their breakdown. Local piezoresponse force mapping, together with field-dependent capacitance tuning and its agreement with calculations of capacitive response, confirm that the FE bubbles conserve their general electromechanical characteristics — this is in spite of a surface that is heavily rippled. We anticipate these results to be the starting point of a new paradigm for the exploration of electric skyrmions with arbitrary boundaries and physically flexible topological orders in ferroelectric curvilinear space.

[i] Y. Nahas, S. Prokhorenko, L. Louis, Z. Gui, I. Kornev, L. Bellaiche, *Nat Commun.* **2015**, *6*, 8542.

[ii] Q. Zhang, L. Xie, L. Guangqing, S. Prokhorenko, Y. Nahas, X. Pan, L. Bellaiche, A. Gruverman, N. Valanoor, *Adv. Mater.* **2017**, *29*, 1702375.

[iii] S. R. Bakaul, C. R. Serrao, M. Lee, C. W. Yeung, A. Sarker, S.-L. Hsu, A. K. Yadav, L. Dedon, L. You, A. I. Khan, J. D. Clarkson, C. Hu, R. Ramesh, S. Salahuddin *Nat. Commun.* **2016**, *7*, 10547.

[iv] S. R. Bakaul, C. R. Serrao, O. Lee, Z. Lu, A. Yadav, C. Carraro, R. Maboudian, R. Ramesh, S. Salahuddin *Adv. Mater.* **2017**, *29*, 1605699.

[v]. D. Lu, D. J. Baek, S. S. Hong, L. F. Kourkoutis, Y. Hikita, H. Y. Hwang, *Nat. Mater.* **2016**, *15*, 1255.

[vi] S. R. Bakaul, S. Prokhorenko, Q. Zhang, Y. Nahas, Y. Hu, A. Petford-Long, L. Bellaiche, N. Valanoor, *Adv. Mater.* (accepted, **2021**)

6:45 PM EQ10.10.02

Late News: Room temperature 0.55Pb(Zr0.52Ti0.48)O3-0.45Pb(Fe0.67W0.33)O3 Nanoscale Multiferroic Thin Films Prepared by Pulsed Laser Deposition Technique Karuna K. Mishra, Ivan Castillo and Ram Katiyar; University of Puerto Rico, United States

The discovery of single-phase magnetoelectric materials and studies of their coupling mechanisms between spin and polarization are important for next generation logic and memory devices. Highly (001) oriented 0.55Pb(Zr_{0.52}Ti_{0.48})O₃-0.45Pb(Fe_{0.67}W_{0.33})O₃ (0.55PZT-0.45PFW) multiferroic thin films were deposited on La_{0.67}Sr_{0.33}MnO₃ (LSMO) buffer layer coated on (LaAlO₃)_{0.3}(Sr₂AlTaO₆)_{0.7} (001) substrates by following two subsequent laser ablation processes in oxygen atmosphere employing pulse laser deposition technique. The 0.55PZT-0.45PFW films were found to grow in a tetragonal phase with orientation along (001) plane as inferred from x-ray diffractometry analysis. The temperature dependent dielectric measurements (80-730 K) on metal-ferroelectric-metal heterostructure capacitors in the frequency range of 10²-10⁶ Hz indicated broad and diffused dielectric peaks over a wide range of temperature 320-730 K and exhibits high dielectric constant ~2100 at 10 kHz at room temperature. The well saturated slim polarization hysteresis loop of the thin film capacitors suggests nano-scale ferroelectric ordering (relaxor type) in these films in accord with diffuse dielectric response results. An excellent high energy storage density with efficiency of ~62 % was estimated at an applied electric field of 1200 kV/cm. Magnetization studies involving Zero Field Cool and Field Cool magnetization curves on the thin films using PPMS down to 4 K indicated an irreversible magnetic ordering in the thin films. A saturated magnetization *M-H* loop with P_s value of 32 emu/cm² was observed at room temperature. The magneto-dielectric studies suggest robust direct evidence of magneto-electric coupling via strain at room temperature. These results suggest that our thin films are multiferroic (ferroelectric-ferromagnetic) at room temperature. These results will be presented in detail at the MRS Fall meetings.

7:00 PM *EQ10.10.03

Non-Trivial Orbital Torque in Ferromagnetic Metal/Cu/Al₂O₃ Junyeon Kim¹ and Yoshichika Otani^{2,1}; ¹RIKEN, Japan; ²University of Tokyo, Japan

So far, the orbital moment has not been seriously considered as an information carrier due to the orbital quenching in ordinary solid-state matters. However, as claimed in recent theoretical studies, we can expect nonzero orbital moment polarization against the orbital quenching whenever the orbital texture is formed in systems, e.g., surfaces or bulks [1,2]. Notably, the formation of orbital texture is irrelevant to the spin-orbit coupling strength (SOC). Thus we expect efficient orbital moment polarization even in a system composed of light elements. The magnetization of a magnetic layer feels a torque if the orbital polarization is transported to a magnetic layer. Hence, it is called orbital torque.

We systemically observe the orbital torque in ferromagnetic metal (FM)/Cu/Al₂O₃ trilayers [3]. Here we believe the Cu/Al₂O₃ interface is responsible for the orbital polarization. All samples in this study are prepared by the electron beam evaporation technique and photo-lithography. We utilized the ferromagnetic resonance technique to observe the torque efficiency. Interestingly, the orbital torque strongly depends on the FM materials. When the FM is CoFe or Fe, the torque efficiency reaches ~0.13, comparable to that for Ta or Pt. In contrast, the torque efficiency becomes almost zero when the FM is a Ni-based material.

Moreover, we find a significant annealing temperature dependence in the torque efficiency. After annealing at 400 C, the torque efficiency for the CoFe/Cu/Al₂O₃ trilayers becomes ~0.25, which is comparable to that for W. All these strong dependencies of torque efficiency on the FM materials and the annealing temperature reflect a characteristic transport of orbital moments. Commonly the change of the FM materials and the heat treatment modifies the interfacial/layer condition through the intermixing or separation. Since localized electrons transport information of the orbital moment, it is more sensitively affected by the material condition than spins.

Finally, we note that the spin Hall conductivity in the FM/Cu/Al₂O₃ trilayers is 3.4×10⁴ Ω⁻¹cm⁻¹, about 10-100 times larger than that for spin Hall materials

or topological insulators. Thus, we believe the FM/Cu/Al₂O₃ trilayers are superb for spin manipulation with low power consumption. We will give further discussions during the symposium.

[1] S. R. Park et al., Phys. Rev. Lett. **107**, 156803 (2011).

[2] D. Go et al., Phys. Rev. Lett. **121**, 086602 (2018).

[3] J. Kim et al., Phys. Rev. B **103**, L020407 (2021).

7:30 PM EQ10.10.04

Synthesis and Characterization of Bismuth Ferrite Using Conventional Ball-Milling, Nano-Agitator Milling and Calcination Methods Lyndon Smith¹, Jeffrey Shield², Rifat Mahbub², Vijaya K. Rangari¹ and Shaik Jeelani¹; ¹Tuskegee University, United States; ²University of Nebraska–Lincoln, United States

Bismuth ferrite is a well-known multiferroic ceramic. It shows ferroelectric and antiferromagnetic ordering at a Curie temperature of ~1100 K and a Néel temperature of ~653 K. Bismuth ferrite properties can be altered by varying shape and size of particles and also by doping other elements. In this study, bismuth ferrite was synthesized using three methods for comparison – a conventional high-energy shaker mill, a nano-agitator bead mill, and precipitation followed by calcination. Gadolinium (10%) and cobalt (10%) were used as dopants in the calcination method. The composition, morphology, and magnetic properties of the resulting particles were characterized with SEM, XRD, and VSM. The powders produced by both milling methods were weakly ferromagnetic. The particles produced from the nano-agitator mill process had a more uniform distribution of grain sizes than the conventional shaker mill process. The particles produced through calcination method were large polygons covered in smaller facets. This method is faster, but there are few options available for substitution of the B-site cation. The milling methods show fewer impurity phases than the calcination method.

7:45 PM EQ10.10.05

Study of the Magnetocaloric Behavior of La_{0.7}Ca_{0.3}MnO₃-xMO (M=Ni,Cu,Co) Nanocomposites Surendra Dhungana, Dipesh Neupane and Sanjay R Mishra; The University of Memphis, United States

Magnetic refrigeration has drawn the attention of many researchers due to its advantages over significant drawbacks of conventional cooling methods. The search is for a material with substantial relative cooling power (RCP), high magnetic entropy change (ΔS_m) and can operate at room temperature. La_{0.7}Ca_{0.3}MnO₃ exhibits high RCP of 243.1 J/Kg [1] and maximum ΔS_m of 6.99 J/Kg.K [1]. It has been pre-established that the composite formation undergoes multiple magnetic phase transition resulting in increase of RCP and ΔS_m [2]. For example, it is reported that ΔS_m and RCP is 2.32 J/Kg.K and 299 J/Kg for La_{0.45}Nd_{0.25}Sr_{0.3}MnO₃-2.5%NiO composite [2] and ΔS_m and RCP is 1.95 J/Kg.K and 298 J/Kg for La_{0.45}Nd_{0.25}Sr_{0.3}MnO₃-2.5%CoO composite [2]. All of these are improvement over ΔS_m and RCP value of 1.79 J/Kg.K and 296 J/Kg for pure La_{0.45}Nd_{0.25}Sr_{0.3}MnO₃ sample. In case of La_{0.45}Nd_{0.25}Sr_{0.3}MnO₃-2.5%CuO composite, significant increase in ΔS_m is reported to 3.95 J/Kg.K in compensation for decrease in RCP to 245 J/Kg which is attributed to the proximity between the critical temperature of La_{0.45}Nd_{0.25}Sr_{0.3}MnO₃, 240K and the Neel temperature of the CuO, 230K [2]. The MCE study on LCMO-MO (metal oxide) composites is not widely reported and with superior ΔS_m value of 6.99 J/Kg.K for La_{0.7}Ca_{0.3}MnO₃ [1] as compared to that of 1.79 J/Kg.K for La_{0.45}Nd_{0.25}Sr_{0.3}MnO₃ [2] better results are expected for LCMO-MO composite. Also, the recorded critical temperature of La_{0.7}Ca_{0.3}MnO₃ of 256K is significantly different from Neel temperature of used NiO, CuO and CoO which should yield higher ΔS_m and RCP. Other literatures have also recorded the performance improvement in manganite by composite formation with metal oxides [4]. This study presents the structural and magnetocaloric study of La_{0.7}Ca_{0.3}MnO₃ composite with metal oxides; NiO, CuO, CoO.

The (1-x)La_{0.7}Ca_{0.3}MnO₃-xMO (x=0, 0.25, 0.5 ; M=Ni, Cu, Co) nanocomposite samples were synthesized through autocombustion using nitrate salts followed by calcination. X-Ray Diffraction (XRD) and Scanning Electron Microscopy (SEM) were used to study structural characterize the samples. The XRD plots show no secondary phases and respective increase of the metal oxide phases with increase of their content. A grain refinement of LCMO phase was observed with the increased metal oxide phase in the composite. To study the magnetocaloric properties of the composites, magnetic isotherms were collected in the temperature range 100-300K and field up to 5T. The data is currently being analyzed to compare the magnetocaloric performance of the composites.

References

1. Wei Tang, Wenjian Lu, Xuan Luo, Bosen Wang, Xuebin Zhu, Wenhai Song, Zhaorong Yang, Yuping Sun, Particle size effects on La_{0.7}Ca_{0.3}MnO₃: size-induced changes of magnetic phase transition order and magnetocaloric study. Journal of Magnetism and Magnetic Materials. 322-16, 2360-2368 (2010)
2. D. Neupane, L. Hulsebosch, A. K. Pathak and S. R. Mishra, Magnetocaloric Study of La_{0.45}Nd_{0.25}Sr_{0.3}MnO₃/MO (MO=CuO, CoO, and NiO) Nanocomposites. IEEE Transactions on Magnetics. (2021)
3. Sheng-Bo Tian, Manh-Huong Phan, Seong-Cho Yu, Nam Hwi Hur, Magnetocaloric effect in a La_{0.7}Ca_{0.3}MnO₃ single crystal. Physica B: Condensed Matter. 327-2-4, 221-224 (2003)
4. M.S. Anwar, Faheem Ahmed, Rehan Danish, Bon Heun Koo, Impact of Co₃O₄ phase on the magnetocaloric effect and magnetoresistance in La_{0.7}Sr_{0.3}MnO₃/Co₃O₄ and La_{0.7}Ca_{0.3}MnO₃/Co₃O₄ ceramic composites. Ceramics International. (2014)

8:00 PM EQ10.10.06

Thermodynamic Stability of Polar Phases in Hf_{0.5}Zr_{0.5}O₂ Epitaxial Thin Films Bo Wang, Jianjun Wang and Long-Qing Chen; The Pennsylvania State University, United States

The discovery of robust ferroelectricity in ultrathin HfO₂-based materials has aroused surging interests in developing silicon-compatible ferroelectric nanoelectronics. To understand the fundamental origin of the ferroelectricity, epitaxial thin films of HfO₂-based oxides such as Hf_{0.5}Zr_{0.5}O₂ (HZO) have been successfully grown, wherein different polar phases have been detected, including the orthorhombic Pca2₁ phase and a newly discovered rhombohedral phase. However, it is not well understood how the misfit strains imparted by the substrate materials influence the stability of the polar phases. Here, we present a comprehensive thermodynamic model, developed based on our recently proposed strain phase separation theory, to predict and understand the stability and coexistence of polar and nonpolar phases in HZO epitaxial thin films. We demonstrate that the misfit strains imposed by substrates of different crystallographic structures (e.g., fluorite, perovskite, and hexagonal) can serve as a viable way to stabilize different polar phases. We establish film thickness – lattice constant phase diagrams for HZO thin films on different types of substrates, which can be utilized to understand the origin of ferroelectricity and guide the strain engineering of HfO₂-based ferroelectric thin films.

8:20 PM BREAK

SESSION EQ10.11: Magnetolectrics VI
Session Chairs: Jiamian Hu and Nian Sun
Monday Afternoon, December 6, 2021
EQ10-Virtual

9:00 PM EQ10.11.02

Acoustically Actuated Antennas Induced by Magnon-Phonon Coupling [Yahui Ji](#) and Tianxiang Nan; School of Integrated Circuits, Tsinghua University, China

Recently, acoustically actuated antennas based on the thin-film magnetolectric heterostructures have been demonstrated with 1-2 orders of magnitude miniaturization over the conventional counterparts. However, it remains challenging to improve their radiation efficiency and develop the high quality antenna modulation technique. Here, we computationally demonstrate a fully coupled model describing the radiation mechanism, including Newton, Maxwell and Landau-Lifshitz-Gilbert (LLG) equations, together with piezoelectric and magnetostrictive constitutive relations. We theoretically propose that magnons, the quanta of spin waves, can be utilized to strongly enhance the radiation efficiency of acoustically actuated antennas when magnon and phonon modes are coupled. In the strong coupling region, our model shows that the radiation efficiency can be 100-time enhanced, and antenna modulation can be substantially simplified. Additionally, a right-hand circular polarization (RHCP) radiation field can be observed.

9:15 PM EQ10.11.03

Late News: Boundary Conditions Manipulation of Polar Vortex Domains in BiFeO₃ Membranes via Phase-Field Simulations [Ren-Ci Peng](#)¹, Xiaoxing Cheng², Bin Peng¹, Ziyao Zhou¹, Long-Qing Chen² and Ming Liu¹; ¹Xi'an Jiaotong University, China; ²The Pennsylvania State University, United States

Polar vortex domains have recently become an emergent research field due to the abundant physical phenomena and potential applications in high-density memories. Here, we explore the mechanisms of creating polar vortex domains in the BiFeO₃ membranes subjected to different boundary conditions using phase-field simulations. A major difference is that the vortex in membrane can be stabilized even under short-circuit electrical boundary conditions compared to vortex in other systems, such as thin film or superlattice. We found that (i) the formation of polar vortex domains at the membrane interior under bending is mainly driven by the reduction of elastic energy under short-circuit boundary condition, and the vortex chirality (namely, clockwise and counterclockwise) could be identified by *n*-shape and *u*-shape bending; (ii) in the unbent open-circuit BiFeO₃ membrane case, exotic trapezoid-shaped vortex nanodomains form at the terminations of 109° domain walls (DWs) and partially charged 71° DWs, which is driven by the local depolarization field and the interplay among electrostatic, elastic, and gradient and Landau energies. We also examine Kittel's law by establishing the dependence of vortex periods on the membrane thickness. These results give further understanding of the effect of boundary conditions on the formation of polar vortex domains, guiding experimental designs of vortex-based high-density memories.

9:30 PM EQ10.11.04

Quantum Polar Skyrmions/Merons in Doped SrTiO₃ Heterostructures—A Topological Polaron [Takahiro Shimada](#)¹, Yuuki Ichiki¹, Tao Xu², Le Van Lich³, Jie Wang⁴ and Hiroyuki Hirakata¹; ¹Kyoto Univ, Japan; ²Chinese Academy of Sciences, China; ³Hanoi University of Science and Technology, Viet Nam; ⁴Zhejiang University, China

Realization of ultrasmall ferroics with nontrivial topological field textures such as vortices, skyrmions, and merons holds promise in novel technological paradigms. Such nontrivial ferroelectric orders and their functionalities, however, inevitably disappear below a critical size of several nanometers. In addition, very few topological structures can exist in ferroelectrics due to the lack of non-collinear interaction among electric dipoles, unlike the Dzyaloshinskii-Moriya (DM) interaction among spins in ferromagnetics. Here, we demonstrate from first-principles that "Polar Skyrmions and Merons" are formed in doped SrTiO₃ heterostructures. Doped (excess) electrons in SrTiO₃ are localized and form a polaronic state in the heterostructures (surfaces and grain boundaries), and give rise to skyrmionic and meronic dipole moments around the polaron formation sites due to the cooperative symmetry breaking of polarons and heterostructures. We further show that the topological number of polaronic state can be tailored by applied mechanical strain, i.e., strain engineering for polar topologies. Our discovery overcomes physical limitations of the critical size of 3-5nm where ferroelectricity disappears and the inability to form topological field (skyrmions, merons) of polarization due to absence of chiral interaction among electric dipoles, and realizes unique polar topological orders at ultimately electron(polaron)-scale. The clarified mechanism that local symmetry breaking via polaron formation coupled with heterostructures provides a novel approach to realize ultimate miniaturization of ferroic materials and opens up new fields to create the polar topological objects. Our result therefore adds a new class of functional polaron families as "Topological Polarons".

9:45 PM EQ10.11.05

Tuning Anharmonic Phonon Coupling Using Magnetism in Magnetolectric h-FeS [Dipanshu Bansal](#)^{1,2}, Jennier Niedziela³, Stuart Calder³, Tyson Lanigan-Atkins¹, Ayman Said⁴, Doug L. Abernathy³, Alexander Kolesnikov³, Haidong Zhou⁵ and Olivier Delaire¹; ¹Duke University, United States; ²Indian Institute of Technology Bombay, India; ³Oak Ridge National Laboratory, United States; ⁴Argonne National Laboratory, United States; ⁵The University of Tennessee, Knoxville, United States

Magnetolectric hexagonal iron sulfide (h-FeS) exhibits a fascinating coexistence of metal-insulator, structural and magnetic transitions, reflecting an intimate interplay of its spin, phonon, and charge degrees of freedom. Using comprehensive neutron and X-ray scattering measurements supported by first-principles electronic structure simulations, we show how a subtle competition of energetic and entropic free-energy components governs its thermodynamics and the sequence of phase transitions upon cooling.

We identify the critical role of the coupling between antiferromagnetic ordering and the instabilities of anharmonic phonons in the metallic phase in driving the metal-insulator transition. The antiferromagnetic ordering enables the emergence of two zone-boundary soft phonons, whose coupling to a zone-center mode drives the lattice distortion opening the electronic bandgap. Simultaneously, spin-lattice coupling opens a gap in the magnon spectrum that controls the entropy component of the metal-insulator transition-free energy. These results reveal the importance of spin-phonon coupling to tune anharmonic effects, thus opening new avenues to design novel technologically important materials harboring the metal-insulator transition and magnetolectric behaviors.

D. Bansal, J.L. Niedziela, S. Calder, T. Lanigan-Atkins, R. Rawl, A. Said, D.L. Abernathy, A.I. Kolesnikov, H. Zhou, and O. Delaire. "Magnetically

driven phonon instability enables the metal-insulator transition in h-FeS.” Nature Physics. Vol. 16, pg. 669-675, 2020

Funding: US Department of Energy, Office of Science, Basic Energy Sciences, Materials Sciences, and Engineering Division, under the Early Career award no. DE-SC0016166 (PI: O. Delaire).

10:00 PM EQ10.11.06

Investigation of Magnetic Ordering and Magneto-Caloric Effect in Pr₂MnNiO₆ [Rinku Kumar](#)¹, Ankita Singh², Mohd. Anas¹, Ramesh Chandra¹ and Vivek Malik¹; ¹Indian Institute of Technology Roorkee, India; ²Tata Institute of Fundamental Research, Mumbai, India

This work deals with the structural, magnetic and magneto-caloric properties of double perovskite Pr₂MnNiO₆ (PMNO) material. The bulk material was prepared in a single phase using the solid-state reaction method. The structural characterization showed monoclinic symmetry with the P21 / n space group. The temperature-dependent magnetic measurements were performed in presence of an applied magnetic field of 500 Oe, which showed a phase transition from paramagnetic to ferromagnetic at ~ 200K. The saturation (ZFC) magnetization shows the change in the slope below ~ 50 K, which may be attributed to the strong interaction between A-site (Pr) and B-site (Mn-Ni network) ions. We carried out the isothermal M vs H (hysteresis curve) measurements in the temperature range of 2K-190 K in the presence of a 0-10 T magnetic field to determine the change in magnetic entropy. The estimated value of magnetic entropy (-ΔS_M) is 1.6 J/Kg-K at 23 K under 10 T magnetic field. Interestingly, our report highlights the presence of low-temperature magneto-caloric effect in PMNO material.

10:35 PM BREAK

SESSION EQ10.12: Multiferroics V
Session Chairs: Jiamian Hu, Tianxiang Nan and Nian Sun
Wednesday Morning, December 8, 2021
EQ10-Virtual

10:30 AM *EQ10.12.01

Functionalizing the Néel vector in Collinear Antiferromagnets Ding-Fu Shao and [Evgeny Y. Tsymbal](#); University of Nebraska-Lincoln, United States

Antiferromagnetic (AFM) spintronics is an emerging field of research which exploits the antiferromagnetic order parameter, known as the Néel vector, to control spin- and orbital-dependent transport properties. This talk will address three novel approaches to functionalize the Néel vector in collinear compensated AFM metals via their response in transverse or longitudinal conductivity. The first approach utilizes room-temperature AFM metal MnPd₂ that allows the electrical control of the Dirac nodal line by the Néel spin-orbit torque [1]. The reorientation of the Néel vector leads to switching between the symmetry-protected degenerate state and the gapped state which modulates the spin Hall conductivity. The second approach involves the nonlinear anomalous Hall effect that can be used to detect the Néel vector in most compensated antiferromagnets supporting the antidamping spin-orbit torque [2]. The magnetic crystal group symmetry of these non-centrosymmetric antiferromagnets, such as CuMnSb, combined with spin-orbit coupling produce a sizable Berry curvature dipole and hence the nonlinear anomalous Hall effect. The third approach highlights antiferromagnets exhibiting a non-spin-degenerate Fermi surface and thus momentum-dependent spin polarization which can be functionalized in AFM tunnel junctions [3]. Using RuO₂ as a representative example of such antiferromagnets, a giant tunneling magnetoresistance effect is predicted for RuO₂-based AFM tunnel junctions. These results broaden the scope of materials and approaches, which can be exploited in AFM spintronics.

1. D.-F. Shao, G. Gurung, S.-H. Zhang, and E. Y. Tsymbal, “Dirac nodal line metal for topological antiferromagnetic spintronics,” *Physical Review Letters* 122, 077203 (2019).
2. D.-F. Shao, S.-H. Zhang, G. Gurung, W. Yang, and E. Y. Tsymbal, “Nonlinear anomalous Hall effect for Néel vector detection,” *Physical Review Letters* 124, 067203 (2020).
3. D.-F. Shao, S.-H. Zhang, M. Li, and E. Y. Tsymbal, “Spin-neutral currents for spintronics,” *arXiv*:2103.09219 (2021).

11:00 AM *EQ10.12.02

Giant Nonreciprocity in Magnetoacoustic Devices Piyush Shah¹, Derek Bas¹, Ivan Lisenkov², Alexei Matyushov³, Nian Sun³ and [Michael Page](#)¹; ¹Air Force Research Laboratory, United States; ²Independent Researcher, United States; ³Northeastern University, United States

Nonreciprocity, the property of merit for a variety of RF components such as isolators and circulators, is typically difficult to achieve with the magnitude required for applications. Many systems which demonstrate non-reciprocity are not suitable for scaling to the size, weight, and power required for applications, or do not exhibit a sufficient intensity of the effect for applications relevance. One such physical system which generally does not exhibit non-reciprocity is that of acoustic waves. Acoustic waves are an important medium for information transport, but they are inherently symmetric in time. By achieving non-reciprocity in an acoustic system, the decades of industrial research in this relatively mature field can be leveraged for new applications. The most promising route to accomplish this is by incorporating magnetic materials into surface acoustic wave (SAW) devices, as in the field of acoustically driven ferromagnetic resonance. While this field remained relatively small since the initial discovery, in the past year, many new reports investigating magnetic materials in SAW devices have been published. Motivated by this expanding field, I will discuss our recent work at the Air Force Research Laboratory on the discovery of giant nonreciprocity in the transmission of surface acoustic waves (SAWs) on a lithium niobate substrate coated with ferromagnet/insulator/ferromagnet (FeGaB/Al₂O₃/FeGaB) multilayer structure. I will discuss how this structure, with a unique asymmetric band diagram, can be exploited for very large non-reciprocal behavior. I will expand on magnetoelastic coupling theory to show how the magnetic bands couple with acoustic waves only in a single direction. In our devices, we measure 48.4 dB (ratio of 1:100,000) isolation which outperforms current state of the art microwave isolator devices in a novel acoustic wave system that facilitates unprecedented size, weight, and power reduction. Finally, I will discuss how these results offer a promising platform to study nonreciprocal SAW devices and other such magnetoacoustic devices.

11:30 AM EQ10.12.03

Influence of Boundaries and Geometrical Curvatures on Antiferromagnetic Textures [Oleksandr Pylypovskiy](#)^{1,2}, Artem V. Tomilo³, Yelyzaveta Borysenko³, Juergen Fassbender¹, Denis D. Sheka³ and Denys Makarov¹; ¹Helmholtz-Zentrum Dresden-Rossendorf e.V., Ukraine; ²Kyiv Academic University, Ukraine; ³Taras Shevchenko National University of Kyiv, Ukraine

A complex structure of magnetic subsystem in antiferromagnets (AFMs) determines challenges and technological perspectives for both, fundamental research and their applications for spintronic and spin-orbitronic devices [1]. In this respect, properties of the confined samples are of key interest because of the possibility to tune magnetic responses via effects of boundary and geometrical curvature [2]. Here, we consider textures in (i) AFM slabs with the Dzyaloshniskii-Morya interaction (DMI) of bulk symmetry [3] and (ii) the intrinsically achiral curvilinear spin chains arranged along space curves [4].

We derive a transition from spin lattice of G-type AFM to the sigma-model with the respective boundary conditions for the AFM order parameter [3]. The DMI influences a texture via boundary conditions modifying the ground state, domain wall shape and skyrmion profiles. Approaching the boundary in the slab with easy-axis anisotropy, the domain wall becomes broader and of mixed Bloch-Neel type near the top surface. Near the edges of the sample, the domain wall plane possesses and additional twist. Note, that the edge twists appear in achiral AFMs as well if the domain wall plane lies at an angle to the side faces [5]. Similarly, skyrmions of any radius become of the Bloch-Neel type approaching the top/bottom surfaces of the sample. The radius of narrow skyrmions changes up to 10% due to the boundary effects.

AFM spin chains arranged along space curves can model the simplest curvilinear nanoarchitectures. Their geometry is described by the curvature and torsion, determining local bends and twists of the curve. The geometry-driven anisotropy and inhomogeneous DMI render them as chiral helimagnets [6]. In addition, the exchange interaction generates the weakly ferromagnetic response, scaling linearly with curvature and torsion. The inter- and single-ion anisotropies in curvilinear AFM chains lead to the additional anisotropic contributions, scaling with curvature. The single-ion anisotropy leads to the homogeneous DMI mixing normal and tangential components of ferro- and antiferromagnetic vector order parameters. Both anisotropy models contribute to the additional easy axes, which determine the direction of the order parameters in spin-flop phase [4].

[1] V. Baltz et al, Rev. Mod. Phys. 90, 015005 (2018); A. Manchon et al, Rev. Mod. Phys. 91, 035004 (2019)

[2] P. Fischer et al, APL Mat. 8, 010701 (2020); R. Streubel et al, J. Appl. Phys. 129, 210902 (2021); D. D. Sheka, Appl. Phys. Lett. 118, 230502 (2021)

[3] O. V. Pylypovskiy et al, Phys. Rev. B 103, 134413 (2021)

[4] O. V. Pylypovskiy et al, Appl. Phys. Lett. 118, 182405 (2021)

[5] N. Hedrich et al, Nat. Phys. 17, 574 (2021)

[6] O. V. Pylypovskiy, D. Y. Kononenko et al, Nano Lett. 20, 8157 (2020)

11:45 AM EQ10.12.04

Resonant Elastic X-Ray Scattering of Sr₂CrReO₆ Epitaxial Films Guillaume Marcaud¹, Alex T. Lee¹, Sangjae Lee¹, Adam Hauser², Fengyuan Yang³, Zhan Zhang⁴, Hua Zhou⁴, Ignace Jarrige⁵, Sohrab Ismail-Beigi¹, Frederick Walker¹ and Charles Ahn¹; ¹Yale University, United States; ²The University of Alabama, United States; ³The Ohio State University, United States; ⁴Argonne National Laboratory, United States; ⁵Brookhaven National Laboratory, United States

Resonant Elastic X-Ray Scattering (REXS) is a powerful technique that combines X-Ray Diffraction (XRD) and X-Ray Absorption (XAS), which has elemental sensitivity to both the physical and electronic structure of materials. Due to the cross-section enhancement near an absorption edge, one can select for spin, charge, and orbital order. We apply this technique to rhenium-based double perovskite thin films, which are well known to possess an intricate interplay between structure and orbital electronic configuration. Especially, Sr₂CrReO₆ (SCRO) has been theoretically predicted to have order of the d_{xy} and d_{yz} orbitals on the rhenium sites. REXS has been performed on three SCRO thin films in different state of strain, compressive -1% on a (LaAlO₃)_{0.3}(Sr₂AlTaO₆)_{0.7} (LSAT) substrate, tensile +1% on a relaxed SrCr_{0.5}Nb_{0.5}O₃ buffer layer on LSAT and free of strain on SrTiO₃ (STO). We will discuss the presence and absence of orbital-order induced Bragg peaks in the three samples and compare Bragg peaks intensities as functions of the synchrotron energy through the L-II and L-III edges of Re in order to determine crystal site specific x-ray absorption spectra.

12:00 PM EQ10.12.06

Observing the Chiral Domain Boundaries in PbTiO₃/SrTiO₃ Superlattices Using Four Dimensional Scanning Transmission Electron Microscopy (4D-STEM) Sandhya Susarla¹, Pius Behera², Fernando Gómez-Ortiz³, Benjamin Savitzky¹, Colin Ophus¹, Peter Ercius¹, Ramamoorthy Ramesh^{2,1} and Javier Junquera³; ¹Lawrence Berkeley National Laboratory, United States; ²University of California, Berkeley, United States; ³Universidad de Cantabria, Spain

Polar vortices in PbTiO₃/SrTiO₃ superlattices are unique topological textures where local electric dipoles are arranged in a spiral fashion.¹ These structures are formed via careful control of strain, electrical, and electrostatic boundary conditions.¹ The unique arrangement of electric dipoles results in two major emergent properties: negative capacitance and chirality.^{2,3} While negative capacitance in this system is theoretically expected, the presence of the chirality is unexpected as these textures are formed from achiral objects. In this work, we have investigated the origins of chirality in this system by examining the three dimensional polarization network. To extract three dimensional information, conventional high-resolution scanning transmission electron microscopy (HR-STEM) can't be used directly since it is based on two dimensional projection. Recently, it has been shown that the depth dependence of four dimensional scanning transmission electron microscopy (4D-STEM) can be utilized to extract the underlying polarization.⁴ Utilizing 4D-STEM, we map out the three dimensional polarization network (lateral and axial polarization) in such textures. We found that the presence of the domain boundaries and dislocations influence the local handedness in these textures. The presence of the chirality is related to the local curvature of the domain boundary. We also find the ability to switch chirality is closely related to how the local polarization varies across the domain boundary. The emergence of chirality from the combination of non-chiral materials and ability to control the handedness has far-reaching implications for new electronics based on topological ferroelectric bits.

References:

1. Yadav, A. K. *et al.* Observation of polar vortices in oxide superlattices. *Nature* **530**, 198–201 (2016)

2. Yadav, A. K. *et al.* Spatially resolved steady-state negative capacitance. *Nature* **565**, 468–471 (2019)

3. Shafer, P. *et al.* Emergent chirality in the electric polarization texture of titanate superlattices. *Proc. Natl. Acad. Sci.* **115**, 915–920 (2018)

4. Nguyen, K. X. *et al.* Transferring Orbital Angular Momentum to an Electron Beam Reveals Toroidal and Chiral Order. *ArXiv201204134 Cond-Mat Physics*(2020).

12:15 PM BREAK

1:00 PM *EQ10.13.01

Induced Ferroelectricity in Epitaxial Nanocomposite SrTiO₃ Films E. Enriquez¹, A. P. Chen² and Quanxi Jia³; ¹The University of Texas Rio Grande Valley, United States; ²Los Alamos National Laboratory, United States; ³University at Buffalo—The State University of New York, United States

Over the past two decades, new discoveries and major advances have been made in the synthesis of oxide-based ferroic thin films and understanding their physical properties. Interface engineering, strain engineering, and defect engineering have been widely used to manipulate the physical properties of the ferroic films in classical lateral heterostructures. As a unique thin-film architecture, vertically aligned epitaxial nanocomposite films have also been widely studied in the past decade and great success has been achieved. However, strain-defect-microstructure-function correlation in such nanocomposite films has not been well-established yet. In this talk, we will overview our strategies in synthesis and characterization of vertically aligned epitaxial nanocomposite ferroic films. Using controlled synthesis, advanced probing, and theoretical modeling, we are able to understand the effect of interface strain on the induced ferroelectric properties in the vertically aligned epitaxial nanocomposite SrTiO₃ films.

1:30 PM EQ10.13.02

Combined Hydrogen- and Oxygen-Based Magneto-Ionic Control in Ni Films Maksim Kutuzau^{1,2}, Stefan Topolovec³, Markus Göbller³, Roland Würschum³, Sandra Schiemenz², Daniel Wolf², Jonas Zehner^{1,2}, Kornelius Nielsch^{2,4} and Karin Leistner^{1,2}; ¹Technische Universität Chemnitz, Germany; ²Leibniz IFW Dresden, Germany; ³Graz University of Technology, Austria; ⁴Technische Universität Dresden, Germany

Magneto-ionic control targets a change in the magnetic properties of materials by electrochemical reactions, which usually occur at low voltage and at room temperature (1). The most actively studied ions for magneto-ionic systems are oxygen (2,3) and hydrogen (4,5). In most cases, the effect of either oxygen or hydrogen is studied, despite the fact that a dual ion-switch, in which the hydrogen- and oxygen-based mechanisms are combined, may increase the versatility of magneto-ionics. A dual-ion switch has so far been studied only in oxide systems, and in this case major effects were restricted to low temperatures. A transfer to magneto-ionic metal systems with high Curie temperature would boost the perspectives for practical applications (6).

We report combined hydrogen- and oxygen-based magneto-ionic control of electrodeposited nanocrystalline nickel films in an aqueous alkaline electrolyte. To determine and analyze the magneto-ionic effect, *in situ* SQUID and *in situ* MOKE magnetometry measurements were used.

We demonstrate simultaneous voltage-control of magnetic moment and coercivity, caused by hydrogen- and oxygen-based mechanisms, respectively. The significant change in coercivity (up to 52 %) is associated with the removal of oxide pinning centers at the surface. It shows a training effect and becomes stronger with an increased number of cycles. The relatively small changes of magnetic moment (about 0.26%) are in a good agreement with the amount of hydrogen loaded into the Ni films in 1 M KOH (7). Both changes are reversible and repeatable at room temperature and require only a low voltage difference of about 1 V.

This combined ionic mechanism to tune magnetic metals may initiate a new direction in room-temperature magneto-ionics and expand the range of its practical applications.

1. Nichterwitz M, Honnali S, Kutuzau M, Guo S, Zehner J, Nielsch K, et al. Advances in magneto-ionic materials and perspectives for their application. APL Mater. 2021 Mar 1;9(3):030903.
2. Nichterwitz M, Honnali S, Zehner J, Schneider S, Pohl D, Schiemenz S, et al. Control of Positive and Negative Magnetoresistance in Iron Oxide-Iron Nanocomposite Thin Films for Tunable Magnetoelectric Nanodevices. ACS Appl Electron Mater. 2020 Aug 25;2(8):2543–9.
3. Zehner J, Soldatov I, Schneider S, Heller R, Khojasteh N, Schiemenz S, et al. Voltage-Controlled Deblocking of Magnetization Reversal in Thin Films by Tunable Domain Wall Interactions and Pinning Sites. Adv Electron Mater. 2020 Nov;6(11):2000406.
4. Tan A, Huang M, Avci C, Büttner F, Mann M, Hu W, et al. Magneto-ionic control of magnetism using a solid-state proton pump. Nat Mater. 2019 Jan;18(1):35–41.
5. Göbller M, Albu M, Klinser G, Steyskal E, Krenn H, Würschum R. Magneto-Ionic Switching of Superparamagnetism. Small. 2019 Nov;15(46):1904523.
6. Lu N, Zhang P, Zhang Q, Qiao R, He Q, Li H-B, et al. Electric-field control of tri-state phase transformation with a selective dual-ion switch. Nature. 2017 Jun;546(7656):124–8.
7. Proost J, Delvaux A. In-situ monitoring of hydrogen absorption into Ni thin film electrodes during alkaline water electrolysis. Electrochimica Acta. 2019 Nov;322:134752.

1:45 PM EQ10.13.03

Phase-Field Modeling of Charge Transport and Defect Properties in Ferroelectric Perovskite Oxides Rui Wang and Long-Qing Chen; The Pennsylvania State University, United States

The stability and evolution of mesoscale structures in solids often involve not only lattice structural and chemical inhomogeneities but also inhomogeneous distributions of electronic, atomic, and ionic defects. We present a general phase-field framework of coupled defect and microstructure evolution of perovskite ferroelectric oxides. In particular, starting from well-established classic thermodynamics, it offers an explicit formulation to obtain the electronic and lattice defect contributions to the thermodynamic properties using statistical/classical thermodynamics. In this model, we treat the ferroelectric perovskite oxide as a wide band-gap semiconductor and we derive all well-known thermodynamic relations related to defect reactions, equilibria including redox and electronic recombination/generation reactions. The model is applied to BiFeO₃ as a prototypical ferroelectric perovskite oxide system to study the interplay between mobile charges and stability of ferroelectric domains. It is demonstrated that the charged domain walls in BiFeO₃ are more likely to be stabilized with a larger amount of mobile charged defects, and the conductivity on domain walls can be tuned by the interactions and types of the charges within the ferroelectric system. It is also found that the mobile defect charges are responsible for the formation of local conductive paths and the bound charge separation at domain walls. The model would give insights to explore the electric properties and applications in ferroelectric perovskite oxides.

2:00 PM EQ10.13.04

Phase-Field Model of Light-Excited Carrier and Structural Dynamics of Ferroelectric Domain Structures Tiannan Yang and Long-Qing Chen; The Pennsylvania State University, United States

Charge carriers including electrons and holes as well as their dynamics play a significant role in determining material behaviors. Ferroelectric materials are quite commonly semiconductors, meaning that upon excitation by various stimuli such as light pulses, their carrier concentrations can be transiently raised by orders of magnitude from the equilibrium values, thus, giving rise to material properties and phenomena vastly different from those at equilibria. Here we develop a phase-field model for the dynamical phenomena of ferroelectric domain structures involving coupled charge carrier evolution and structural

responses under ultrafast external stimuli. As an example, we study the carrier and structural dynamics of various ferroelectric PbTiO₃ domain walls excited by a femtosecond above-band-gap light pulse. We find that the carrier concentration around charged domain walls relaxes with a two-component process at picosecond and nanosecond time scales for free carriers and carriers trapped at the domain walls, respectively. Meanwhile, a strong transient strain response is induced, which contains two fast oscillational components and a slower relaxational component, signifying rich dynamics involving domains, domain walls, and charges. The present work provides a general theoretical framework for studying carrier-mediated ultrafast processes in ferroelectric domain structures and thus for exploring dynamical functionalities of ferroelectric materials.

2:15 PM EQ10.13.05

Tunable Switching Behaviors and Topological Phase Transitions of a Ferroelectric Supercrystal Cheng Dai¹, Vladimir Stoica^{2,1}, Sujit Das³, Zijian Hong³, Lane W. Martin³, Ramamoorthy Ramesh³, John Freeland², Haidan Wen², Venkatraman Gopalan¹ and Long-Qing Chen¹; ¹The Pennsylvania State University, United States; ²Argonne National Laboratory, United States; ³University of California, Berkeley, United States; ⁴Zhejiang University, China

Understanding the phase transitions and switching behaviors of mesoscale topological structures in ferroic materials is critical to realize their potential applications in next-generation high-performance storage devices. In this work, we study the kinetic evolution of a mesoscale supercrystal with 3-D nanoscale periodicity in a PbTiO₃/SrTiO₃ superlattice under thermal and electrical stimuli using a combination of phase-field simulations and X-ray diffraction experiments. We construct a phase diagram of temperature versus polar state, showing the formation of the supercrystal from a mixed vortex and *a*-twin state and a temperature-dependent erasing process of a supercrystal returning to a classical *a*-twin structure. Under an electric field bias at room temperature, the vortex topology of the supercrystal irreversibly transforms to a new type of stripe-like supercrystal under an in-plane electric field. Under an out-of-plane electric field, the vortices inside the supercrystal undergo a topological phase transition to polar skyrmions. These results demonstrate the potential for the on-demand manipulation of polar topology and transformations in supercrystals using electric fields. The findings provide a theoretical understanding which may be utilized to guide the design and control of mesoscale polar structures and to explore novel polar structures in other systems and their topological nature.

2:30 PM EQ10.13.06

Structural Effects and the Formation of Small Polarons in of BiFeO₃ Iflah Larai^b and Anderson Janotti; University of Delaware, United States

The flexibility of manipulating the magnetic ordering and ferroelectric polarization at room temperature through the magnetoelectric effect in BiFeO₃ has attracted great attention to potential device applications. However, basic properties such as the electronic structure of BiFeO₃ is not yet well established. Reported band gap of multiferroic BiFeO₃ has been a subject of debate, with values reported in wide range of 2.5 - 3.1 eV. Presence of oxygen vacancy defects is a common occurrence in the synthesis of multiferroic BiFeO₃, which leads to room temperature conductivity that is often linked to polaron hopping. Using hybrid density functional theory calculations, we find a band gap of 3.4 eV for *R3c* BiFeO₃, which is slightly larger than a recent reported band gap of 3.1 eV for single crystals based on optical absorption and photoluminescence measurements. Our calculations reveals a strong dependence of the band gap and band edge positions on the antiferrodistortive rotations of the FeO₆ octahedra and ferroelectric displacement of Fe ions. The band gap decreases from 3.4 eV for the *R3c*, to 2.9 eV for the paraelectric *R3c*-, and to 1.6 eV for the cubic antiferromagnetic BiFeO₃, by significant lowering of the conduction band due to reduced O-2*p* Bi-6*p* coupling in the more symmetric structures, with simultaneous slight raising of the valence band that is dependent on Fe 3*d*-O 2*p* and Bi 6*s*-O 2*p* interactions. Lastly, we explored the formation of small hole and electron polarons in BiFeO₃ single crystals and propose a charge transport mechanism via polaron hopping, which can explain the observed room temperature conductivity in the material. Work supported by the NSF NSF Early Career Award grant no. DMR-1652994.

SESSION EQ10.14 Multiferroics VI
Session Chair: Jiamian Hu
Wednesday Afternoon, December 8, 2021
EQ10-Virtual

4:00 PM *EQ10.14.01

Voltage Controlled Néel Vector Rotation in Zero Magnetic Field Christian Binck^{1,2}, Ather Mahmood¹, Will Echtenkamp¹, Mike Street¹, Jun-Lei Wang¹, Shi Cao¹, Takashi Komesu¹, Peter Dowben^{1,2}, Pratyush Buragohain¹, Haidong Lu¹, Alexei Gruverman^{1,2}, Arun Parthasarathy³ and Shaloo Rakheja⁴; ¹University of Nebraska-Lincoln, United States; ²Nebraska Center for Materials and Nanoscience, United States; ³New York University, United States; ⁴University of Illinois at Urbana-Champaign, United States

Voltage-controlled switching of remnant magnetic states paves the way towards ultra-low power and non-volatile spintronics. In this presentation, I report on a journey, which took us from isothermal electric switching of exchange bias with the help of simultaneously applied electric and magnetic fields¹ to pure voltage-controlled antiferromagnetic spintronics in zero magnetic field and at CMOS compatible temperatures.² Nonvolatile Néel vector reorientation in the absence of an applied magnetic field, *H*, is demonstrated at CMOS compatible temperatures in prototype device structures which exploit the multi-functional properties of thin films of boron (B) doped Cr₂O₃. Boundary magnetization associated with the Néel vector orientation serves as state variable, which is read via magnetoresistive detection in a Pt Hall bar adjacent to the B: Cr₂O₃ film. Switching of the Hall voltage between zero and non-zero values implies Néel vector rotation by 90-degrees. Combined magnetometry, spin resolved inverse photoemission, electric transport and scanning probe microscopy measurements reveal B-dependent *T_N* and resistivity enhancement, spin-canting, anisotropy reduction, dynamic polarization hysteresis and gate voltage dependent orientation of boundary magnetization. The combined effect enables *H*=0, voltage controlled, nonvolatile Néel vector rotation at temperatures as high as 400 K. Theoretical modeling estimates switching speeds of about 100 ps making B: Cr₂O₃ a promising multifunctional single-phase material for energy efficient nonvolatile CMOS compatible memory applications.

REFERENCES

¹He, X., Wang, Y., Wu, N., Caruso, A. N., Vescovo, E., Belashchenko, K. D., Dowben, P. A. & Binck, C. Robust isothermal electric control of exchange bias at room temperature. *Nat Mater* **9**, 579-585, doi:10.1038/Nmat2785 (2010).

² Mahmood, A., Echtenkamp, W., Street, M., Wang, J.-L., Cao, S., Komesu, T., Dowben, P. A., Buragohain, P., Lu, H., Gruverman, A., Parthasarathy, A., Rakheja, S. & Binck, C. Voltage controlled Néel vector rotation in zero magnetic field. *Nature Communications* **12**, 1674, doi:10.1038/s41467-021-21872-3 (2021).

We acknowledge financial support by ARO through MURI W911NF-16-1-0472, the subsidiary of SRC nCORE through AMML and NSF through ECCS 1740136 and EPSCoR RII Track-1: Emergent Quantum Materials and Technologies (EQUATE), Award OIA-2044049, the Nebraska Nanoscale Facility: NNCL, and the Nebraska Center for Materials and Nanoscience.

4:30 PM *EQ10.14.02

Domain-Wall-Induced Electromagnons in Multiferroics Laurent Bellaiche; University of Arkansas, United States

The high demand for the development of multifunctional devices as well as the interesting mechanisms behind the coexistence of ferroic order parameters within the same phase in multiferroic materials has launched a new wave of research in recent years. The unique properties of some multiferroics such as magnetoelectric (ME) coupling, which allows the cross control of electrical dipole moments by applying magnetic fields (or conversely magnetic moments by electric field), open opportunities for designing novel sensors and memory devices with significantly lower power consumption and higher efficiency. Moreover, the existence of domains and excitations, such as electromagnons, awards multiferroic systems with richer multifunctionalities as well as the potential of enhancing ME responses and designing novel devices such as *electrically-driven* configurable magnonic circuits. Here we report the prediction of dynamical couplings between magnons and optical phonons in systems possessing ferroelectric domain walls that leads to the emergence of new hybrid quasi-particles, namely *domain-wall-induced* electromagnons. These quasi-particles induce THz resonances in magnetoelectric responses and preferentially localize either near the domain walls or near the middle of domains as a result of scatterings. Such features can be exploited to reach strikingly large ME conversion and designing more reliable and ultrafast ME devices with less energy consumption and using, e.g., local probes.

Acknowledgments. The authors are thankful to the Vannevar Bush Faculty Fellowship (VBFF) Grant No. N00014-20-1-2834 from the Department of Defense, DARPA Grant No. HR0011727183-D18AP00010 (under the TEE Program) and ONR Grants No. N00014-17-1-2818 and N00014-21-1-2086. B.X. further acknowledges the financial support from National Natural Science Foundation of China under Grant No. 12074277, the startup fund from Soochow University, and the support from Priority Academic Program Development (PAPD) of Jiangsu Higher Education Institutions.

5:00 PM EQ10.14.03

DFT-Based Resonant Inelastic Resonant Scattering Study of LaCoO₃, CoO and LaCoO₃/LaTiO₃ Superlattices Alex T. Lee, Sangjae Lee, Frederick Walker, Charles Ahn and Sohrab Ismail-Beigi; Yale University, United States

Cobalt cations in oxides can have multiple electronic configurations. While Co in CoO is in a 2+, high spin ($S=3/2$, $t_{2g}^5 e_g^2$) state, LaCoO₃ (LCO) has Co³⁺ that has multiple spin states depending on temperature: low-spin ($S=0$, $t_{2g}^6 e_g^0$), intermediate-spin ($S=1$, $t_{2g}^5 e_g^1$), and high-spin states ($S=2$, $t_{2g}^4 e_g^2$), which have nearly degenerate ground state energies. Recently, we have synthesized LaCoO₃/LaTiO₃ superlattices exhibiting strong orbital polarization [1]. Theoretical calculations show that Co is 2+ in these superlattices with two relevant low-energy spin states (low-spin $S=1/2$, $t_{2g}^6 e_g^1$ and high-spin, $S=3/2$, $t_{2g}^5 e_g^2$) [2,3].

Here, we combine Resonant Inelastic X-ray Scattering (RIXS), a powerful tool of local electronic states and low-energy excitations, with a DFT+U based theoretical approach to compute RIXS spectra. This approach is capable of describing both the broad, fluorescent features in RIXS (e.g., which are strong features for RIXS of LCO) as well as localized excitations (e.g., characteristic RIXS features of CoO). We find that this theoretical approach allows us to interpret the RIXS spectra for bulk materials and superlattices, and it also describes the changes of the experimental RIXS spectra as a function of the thickness of the cobaltate layers in the superlattices. We will briefly compare the DFT+U RIXS method to atomic and cluster calculations which do not describe the band-like features in condensed matter systems.

[1] S. J. Lee, A. T. Lee et al., Phys. Rev. Lett. 123, 117201 (2019)

[2] A. T. Lee and S. Ismail-Beigi, Phys. Rev. B 101, 144423 (2020)

[3] A. T. Lee, H. Park, and S. Ismail-Beigi, Phys. Rev. B 103, 125105 (2021)

5:15 PM EQ10.14.04

Vibrational Neutron Spectroscopy and Modelling using DFT of Organic Magneto-Ferroelectric TTF-BA Sanghamitra Mukhopadhyay; STFC Rutherford Appleton Laboratory, United Kingdom

Organic functional materials, particularly multiferroics, are very novel, because of their simultaneous magnetic and ferroelectric properties. These type of materials have many state of the art applications including flexible electronics, data and storage devices [1-4]. In these materials ferroelectricity can be tuned by applying magnetic fields. Since flexibility and multi-ferroicity rare combinations, organic multi-ferroics are candidates of intense research promising of designing new materials fit for the purpose. For these reasons these materials are in the focus of current research not only for fundamental scientific interests, but also of their potential use in new emerging technology, such as flexible electronics devices.

Generally, charge or proton transfer across chemically distinct donor-acceptor pairs, or movements of those protons in the centro symmetric to non-centrosymmetric positions are considered as the key mechanisms of the functionality of these materials [3]. In this context the dynamics of proton or the charge carriers are important to understand to do bespoke designing. Some of hydrogen bonded solids, namely croconic acid (C₅O₅H₂), 1-cyclobutene-1,2-dicarboxylic acid (CBDC, C₆H₈O₄) and 2-phenylmalondialdehyde (PhMDA, C₉H₈O₂) show high polarizability at room temperature [5]. As a continuation of our on-going effort in understanding dynamics of protons in ferroelectricity [6-10], in this work we investigate the dynamics of proton in tetrathiafulvalene-p-bromanil [(H₂C₂S₂C)₂ - C₆Br₄O₂] (TTF-BA). [2], which has shown its potential to be multiferroic at low temperatures. The motivation of this work to help not only to understand the finger print dynamics of ferroelectricity of these materials, but to design new organic ferroelectrics for technological use.

We have used inelastic neutron scattering (INS) to explore proton dynamics in TTF-BA. The INS experiment has been done at ISIS neutron and Muon Source. DFT based first-principles simulations have been done to model the INS spectrum to understand the mechanism of the multiferroic properties of this material. Both spin polarised and non-spin polarised calculations have been done using CASTEP code. PBE + GGA functionals have been used to determine the ground state structures. Quasi harmonic calculations have been performed to understand the mechanism of ferroelectricity. The responsible modes for ferroelectricity have been identified by normal mode and soft phonon analysis of these calculations.

The neutron spectroscopic experiment and DFT simulations indicate that C-H—Br bending modes carry the finger print signature of ferroelectricity of the molecule. In the talk the effect of spin polarisation on this mode will also be discussed.

References

[1] W. Qin et. al., Nanoscale, 7, 9122 (2015).

- [2] F. Kagawa et. al., Nat. Phys. **6**, 169 (2010).
 [3] S. Horiuchi et. al, Nat. Mat. **7**, 267 (2008),
 [4] S. Horiuchi et. al, Nature **463**, 789 (2010).
 [5] A. Stroppa et. al., Phys. Rev. B, **84**, 014101 (2011).
 [6] S. Mukhopadhyay et. al., Phys. Chem. Chem. Phys. **16**, 26234 (2014).
 [7] F. Fernandez-Alonso et. al, J. Phys. Soc. Japan, **82**, SA001, (2013).
 [8] S. Mukhopadhyay et. al., Chem Phys., **427**, 95 (2013).
 [9] S. Mukhopadhyay et. al., Phys. Chem. Chem. Phys. **19**, 32147 (2017).
 [10] S. Mukhopadhyay et al., J. Phys. Commun. **3**, 113001 (2019).

5:30 PM EQ10.14.05

Antiferromagnetic and Relaxor-Type Ferroelectric Behavior in Iron-Doped GdCrO₃ Jianhang Shi¹, Mohinder Seehra² and Menka Jain¹; ¹University of Connecticut, United States; ²West Virginia University, United States

Here we present a comparative study of the structural, magnetic, and dielectric properties of 960 nm thick film and bulk pellet of single-phase polycrystalline GdFe_{0.5}Cr_{0.5}O₃. The film was fabricated on a platinumized-silicon substrate by solution deposition and spin-coating methods. The bulk pellet was synthesized by the citrate solution route. Magnetic measurements show Néel temperature ~ 270 K for both the bulk and the film whereas dielectric measurements show ferroelectric to paraelectric transition with T_C ~ 525 K for bulk and 450 K for the film. The frequency dependent dielectric data of both samples is found to follow Vogel-Fulcher relation that implies relaxor-type diffusive ferroelectric behavior. Interfacial Maxwell–Wagner polarization was also observed at low frequencies. The electric polarization hysteresis loops, although leaky, are observed at room temperature revealing multiferroic nature. Details and discussions of these results will be presented.

5:45 PM EQ10.14.06

High-Tc Ferroelectricity in a New Molecular Magnetolectric Ytterbium (III) Complex Arseniy M. Buryakov¹, Maxim Ivanov^{1,2}, Artur Avdizhiyan¹, Ekaterina Mamontova³, Joulia Larionova³, Paula Maria Vilarinho², Elena Mishina¹ and Jerome Long³; ¹RTU MIREA, Russian Federation; ²University of Aveiro, Portugal; ³Université de Montpellier, France

Magnetolectric materials (ME) are multifunctional systems that combine magnetic and ferroelectric behaviors [1]. With the ability to switch ferroelectric (magnetic) domains by small external fields, ME create the basis for the development of low-consumption devices, including high-density data storage, spintronics, and optoelectronics [1]. For these applications, ME must have strong magnetolectric coupling at room temperature and above, which rarely observed for classical inorganic ME materials such as metal oxides [1, 2]. Synthesis of such inorganic ME at the atomic level is also a difficult task [1, 2]. However, there are several studies showing that molecular ME based on metal-organic complexes can be an alternative to the currently actively studied ME systems, in particular, transition metal oxides [3-5]. In addition, molecular ME have a wide functionality due to their flexibility, non-toxicity, and high manufacturability. Earlier, we showed the presence of a strong ME-coupling in a new molecular ZnYb complex, which combines ferroelectric and paramagnetic properties at room temperature [5]. This work represents further required fundamental study on the determination of ferroelectric Curie temperature (T_C) in the ZnYb compound and its distinct ferroelectricity type (uniaxial or multiaxial). Using nonlinear optical microscopy, we investigated anisotropic dependencies of the second harmonic generation (SHG) in the ZnYb single crystal. The ZnYb complex at room temperature is a monoclinic system described by the polar point group 2 [5]. In this case, the electric-dipole term is the main contribution to the SHG signal. Nonzero nonlinear susceptibility tensor components were defined for ZnYb complex. Temperature dependence of the SHG intensity in the range from 293 K to 493 K was obtained. To approximate this dependence, we used the classical Landau theory. Found values of T_C and critical exponent β are 473 K and 0.5, respectively. The nonzero SHG signal in the region above T_C is because chiral structures can crystallize only in noncentrosymmetric space groups. According to Aizu notation [3], the paraelectric phase in ZnYb belongs the species of orthorhombic noncentrosymmetric group 222 among the 88 ferroelectric species. The 222 → 2 phase transition characterizes the ZnYb compound as a uniaxial ferroelectric system. This results is also in good agreement with the Folk's theory, where the value of the critical exponent β = 0.5 corresponds strongly to ferroelectric system with uniaxial dipole interaction [6].

The reported study was supported by the Russian Science Foundation (project No. 20-79-10233). E.D. M. acknowledges the support of the Ministry of Education and Science of the Russian Federation (state task No. FSFZ-0706-2020-0022).

References

- [1] N.A. Spaldin, R. Ramesh, Nat. materials. **18**, 203 (2019).
 [2] M. Fiebig et al., Nat. Rev. Materials, **1**, 1 (2016).
 [3] T. Hang, et al., Chem. Soc. Rev. **40**, 3577 (2011).
 [4] W. Zhang, R. G. Xiong, Chem. Rev. **112**, 1163 (2012).
 [5] J. Long et al., Science. **367**, 671 (2020).
 [6] R. Folk, Phase Transitions, **67**, 645 (1999).

SESSION EQ10.15: On-Demand
 Sunday Morning, December 5, 2021
 On-Demand

8:00 AM EQ10.03.03

Multiferroic Bismuth Ferrite Nanoparticles via Pulsed Laser Ablation Astita Dubey, Maisarah Ismadi, Friedrich Waag, Stephan Barcikowski and Doru C. Lupascu; University of Duisburg Essen, Germany

Single phase multiferroic Bismuth Ferrite (BFO) Nanoparticles (NPs) are potential materials for spintronic devices, photovoltaics, photocatalysis, and memory storage due to their advantageous ferro-electromagnetic properties at room temperature and narrow band gap. We outline the synthesis of BFO utilising pulsed laser ablation technique in liquid (PLAL). Thorough characterization of the ablated NPs including powder X-ray diffraction (XRD), high-resolution transmission electron microscopy (HRTEM), high-angle annular dark-field imaging (HAADF), scanning transmission electron microscopy (STEM), and magnetometry have been performed. Laser ablated NPs have spherical morphology and consist of two kinds of NPs: primary and secondary. The sizes of primary particles are around 5 nm and of secondary particles are around 20 nm. After post-thermal treatment at 500 °C for 5 minutes, the NPs

are in the size range of 18 ± 5 nm. These NPs exhibit single phase, rhombohedral ($R3c$) crystal symmetry and are highly crystalline. The HAADF and STEM images unveil a homogeneous elemental distribution and a single ferroelectric domain, respectively for the ablated BFO NPs. Laser ablated BFO NPs show an increase in magnetic moment as compared to sol-gel synthesized BFO NPs (~50 nm) which may be due to the large number of uncompensated spins at the surface in smaller NPs. The laser ablation technique can tailor the NP sizes at low cost. It is quite reproducible approach.

8:05 AM EQ10.06.03

Towards the Electrical Control of Skyrmionic Spin Textures Combined with SrTiO₃ Two-Dimensional Electron Gases Luis Moreno Vicente-Arche^{1,2}, Srijani Mallik¹, Karim Bouzehouane¹, Sergio Valencia³, Nicolas Reyren¹, Agnès Barthelemy^{1,2} and Manuel Bibes¹; ¹CNRS/Thales, France; ²Université Paris-Saclay, France; ³Helmholtz-Zentrum Berlin für Materialien und Energie, Germany

SrTiO₃ (STO) two-dimensional electron gases (2DEGs) can be formed by depositing reactive metals such as Al onto STO single crystals: the metal oxidizes, forming oxygen vacancies in the STO and thus doping it in electrons^[1]. Such 2DEGs can then be used to interconvert spin and charge currents with great efficiency^[2]. In this presentation we will show that the metal oxide (e.g. AlOx) thus formed can be combined with ferromagnetic and heavy-metal-based ultrathin films to generate various types of magnetization configurations with in-plane or out-of-plane anisotropy, depending on their thicknesses. For specific compositions, these multilayers harbor magnetic bubbles, as imaged by magnetic force microscopy (MFM), X-ray photoemission electron microscopy (XPEEM), and NV-center microscopy, that likely have a skyrmionic character, due to the expected Dzyaloshinskii-Moriya interaction caused by the strong broken inversion symmetry. We will finally discuss how the Rashba spin-orbit coupling present in the 2DEG may be used to generate spin-orbit torques to manipulate spin textures.

[1] L. M. Vicente-Arche, S. Mallik, M. Cosset-Cheneau, P. Noël, D. C. Vaz, F. Trier, T. A. Gosavi, C.-C. Lin, D. E. Nikonov, I. A. Young, A. Sander, A. Barthélémy, J.-P. Attané, L. Vila, M. Bibes, *Phys. Rev. Materials* **2021**, 5, 064005.

[2] D. C. Vaz, P. Noël, A. Johansson, B. Göbel, F. Y. Bruno, G. Singh, S. McKeown-Walker, F. Trier, L. M. Vicente-Arche, A. Sander, S. Valencia, P. Bruneel, M. Vivek, M. Gabay, N. Bergeal, F. Baumberger, H. Okuno, A. Barthélémy, A. Fert, L. Vila, I. Mertig, J.-P. Attané, M. Bibes, *Nature Materials* **2019**, 18, 1187.

This project received funding from the ERC Advanced grant "FRESCO" n° 833973 and the ERA-NET QUANTERA European Union's Horizon H2020 project "QUANTOX" under Grant Agreement No. 731473.

SYMPOSIUM EQ11

Materials, Processes and Device Structures Enabling Next-Generation High-Frequency Flexible Electronics
November 30 - December 8, 2021

Symposium Organizers

Mario Caironi, Istituto Italiano di Tecnologia
Antonio Facchetti, Northwestern University/Flexterra Inc
Hans Kleemann, Technische Universität Dresden iAPP
Jun Takeya, The University of Tokyo

Symposium Support

Bronze
Novaled GmbH

* Invited Paper

SESSION EQ11.01: Materials and Deposition Techniques for High-Frequency Thin-Film Electronics I
Session Chairs: Mario Caironi and Hagen Klauk
Tuesday Morning, November 30, 2021
Hynes, Level 1, Room 111

10:30 AM *EQ11.01.01

Semiconducting Polymers for High Performance OFET and OECT Applications Iain McCulloch^{1,2}; ¹University of Oxford, United Kingdom; ²King Abdullah University of Science and Technology, Saudi Arabia

The evolution of organic electronics has now reached the commercial phase, with the recent market introduction of the first prototypes based on organic transistors and organic solar cell modules fabricated from solution. Understanding the impact of both the organic semiconductor design and processing conditions, on both molecular conformation and thin film microstructure has been demonstrated to be essential in achieving the required optical and electrical properties to enable these devices. Polymeric semiconductors offer an attractive combination in terms of appropriate solution rheology for printing processes, mechanical flexibility for rollable processing and applications, but their optical and electrical performance requires further improvement

in order to fulfil their potential. Synthesis of conjugated aromatic polymers typically involves carbon coupling polymerisations utilising transition metal catalysts and metal containing monomers. This polymerisation chemistry creates polymers where the aromatic repeat units are linked by single carbon-carbon bonds along the backbone. In order to reduce potential conformational, and subsequently energetic, disorder due to rotation around these single bonds, an aldol condensation reaction was explored, in which a bisatin monomer reacts with a bisoxindole monomer to create an isoindigo repeat unit that is fully fused along the polymer backbone. This aldol polymerization requires neither metal containing monomers or transition-metal catalysts, opening up new synthetic possibilities for conjugated aromatic polymer design, particularly where both monomers are electron deficient. Polymers with very large electron affinities can be synthesised by this method, resulting in air stable electron transport, demonstrated in solution processed organic thin film transistors. We present an electrical, optical and morphology characterisation of polymer thin films, illustrating structure-property relationships for this new class of polymers. Additionally, we will discuss the role of non-covalent short contacts on polymer backbone planarity, the subsequent minimisation of energetic disorder, and its effect on charge carrier mobility.

Organic electrochemical transistors (OECTs) have been shown to be promising devices for amplification of electrical signals and selective sensing of ions and biologically important molecules in an aqueous environment, and thus have potential to be utilised in bioelectronic applications. The sensitivity, selectivity and intensity of the response of this device is determined by the organic semiconducting polymer employed as the active layer. This work presents the design of new organic semiconducting materials which demonstrate significant improvements in OECT performance, through operation in accumulation mode, with high transconductance and low operating voltage.

11:00 AM *EQ11.01.02

Nanostructured Large-Area Electronics for High-Frequency Applications Thomas D. Anthopoulos; King Abdullah University of Science and Technology, Saudi Arabia

The relentless downscaling of the silicon transistor has fuelled the continuous innovations witnessed in the semiconductor industry over the past fifty years. Unfortunately, adopting a similar approach to emerging forms of electronics is not straightforward both in terms of technology and economics. In this talk I will first discuss the main challenges that emerging technologies - such as printed large-area electronics (LAEs) - face in combining scalable manufacturing with the required performance. I will then present recent work from our laboratory on new materials and processing paradigms that enable the development of LAEs with numerous functionalities and performance characteristics superior to the current state-of-the-art. Emphasis will be placed on showcasing the key role of innovating additive manufacturing as an enabling agent for next generation LAEs.

11:30 AM *EQ11.01.03

Customizing the Polarity of Single-Walled Carbon Nanotube Field Effect Transistors Using Solution-Based Additives Maria Antonietta Loi; University of Groningen, Netherlands

The polarity control in Semiconducting Single-Walled Carbon Nanotubes field effect transistors (s-SWNT FETs) is important to promote their application in logic devices. The methods to turn the intrinsically ambipolar s-SWNT FETs into unipolar devices that have been proposed until now, require extra fabrication steps that make their preparation longer and more complex. Here, we demonstrate that by starting from a highly purified ink of semiconducting single-walled carbon nanotubes sorted by a conjugated polymer, and mixing them with additives we are able to achieve unipolar charge transport. The three additives used are benzyl viologen (BV), 4-(2,3-Dihydro-1,3-dimethyl-1H-benzimidazol-2-yl)-N,N-dimethylbenzamine (N-DMBI), which give rise to n-type field effect transistors and 2,3,5,6-Tetrafluoro-7,7,8,8-tetracyanoquinodimethane (F₄-TCNQ), which gives rise to p-type transistors. BV and N-DMBI transform the s-SWNTs transistors from ambipolar with mobility of the order of 0.7 cm²/Vs to n-type with mobility up to 5 cm²/Vs. F₄-TCNQ transform the ambipolar transistors in p-type with mobility up 16 cm²/Vs.

SESSION EQ11.02: Materials and Deposition Techniques for High-Frequency Thin-Film Electronics II

Session Chairs: Hagen Klauk and Barbara Stadlober

Tuesday Afternoon, November 30, 2021

Hynes, Level 1, Room 111

1:30 PM EQ11.02.01

An Organic N-Type Conductive Ink for Thermoelectrics and Logic Applications Chi-Yuan Yang¹, Marc-Antoine Stoeckel¹, Tero-Petri Ruoko¹, Han-Yan Wu¹, Xianjie Liu¹, Nagesh B. Kolhe², Ziang Wu³, Yuttapoom Puttison¹, Chiara Musumeci¹, Matteo Massetti¹, Hengda Sun¹, Kai Xu¹, Deyu Tu¹, Weimin M. Chen¹, Han Young Woo³, Mats Fahlman¹, Samson A. Jenekhe², Magnus Berggren¹ and Simone Fabiano¹; ¹Linköping University, Sweden; ²University of Washington, United States; ³Korea University, Korea (the Republic of)

Conducting polymers are opening new possibilities that are impacting several technologies such as organic thermoelectrics but also opto- and bioelectronics applications.^[1] Among these polymers, PEDOT:PSS is the most successful one that can transport holes. With an electrical conductivity reaching thousands of S cm⁻¹ and an exceptional ambient stability, this ionic/electronic conductor has been integrated in multiple applications spanning from conducting layer in organic solar cells or light-emitting diodes to active material in sensors and actuators, supercapacitors or thermoelectrics.^[2] The versatility of the synthesis and processing of PEDOT:PSS is another reason of its success, being compatible with large scale deposition methods such as ink-jet printing or spray-coating, through an ink formulation that is water-based.

However, while PEDOT:PSS only transports holes (p-type), several opto- and bioelectronic applications include devices that require the integration of materials for transporting both charges; an n-type material able to transport electrons, combined with a p-type material that transport holes. To fill this gap, several n-type polymers were developed, without entirely reaching the performances of their p-type counterpart PEDOT:PSS. Most of these n-type conducting polymers, when properly doped, demonstrates electron conductivity of tens of S cm⁻¹. However, their use at the industrial scale is extremely limited due to their processing involving halogenated solvents that are harmful for the environment. Moreover, they usually lack of ambient and thermal stability, and can be hardly overprocessed due to a poor solvent stability, resulting in mediocre performances. Various approaches are explored in order to enhance the electrical performances of this class of n-type materials, from design rationalizations and adjustments of the chemical structure to the careful choice of dopants. For instance, polymeric backbone planarization and increased rigidity is a strategy towards superior properties for high-performing n-type conducting polymers.^[3,4]

Here we report on the use of the rigid ladder-type electron-conducting polymer poly(benzimidazobenzophenanthroline) (BBL) composing an n-type conductive ink for printed electronics.^[5] The ink is alcohol-based and composed of nanoparticles of BBL produced from a solvent exchange process. This system is doped by the amine-based polymer poly(ethyleneimine) (PEI) and is processable by spray-coating in air. A thermal activation allows the BBL:PEI thin-film to demonstrate an electrical conductivity up to 8 S cm⁻¹, with an excellent thermal stability. Interestingly, this film is stable even when

washed with common organic solvents typically used for microfabrication. Finally, we employed this material as active layer in thermoelectric generators demonstrating a power output of 56 nW for a ΔT of 50 K per p-n pair, and as ion-electron conductor in an organic electrochemical transistor (OECT) working in n-type depletion-mode regime. This device, coupled with a PEDOT:PSS-based OECT, was used for ternary logic application.

References

- [1] X. Guo, A. Facchetti, *Nature Materials* **2020**, *19*, 922.
- [2] H. Shi, C. Liu, Q. Jiang, J. Xu, *Advanced Electronic Materials* **2015**, *1*, 1500017.
- [3] S. A. Jenekhe, P. O. Johnson, A. K. Agrawal, *Macromolecules* **1989**, *22*, 3216.
- [4] Y. Lu, Z.-D. Yu, R.-Z. Zhang, Z.-F. Yao, H.-Y. You, L. Jiang, H.-I. Un, B.-W. Dong, M. Xiong, J.-Y. Wang, J. Pei, *Angewandte Chemie International Edition* **2019**, *58*, 11390.
- [5] C.-Y. Yang, M.-A. Stoeckel, T.-P. Ruoko, H.-Y. Wu, X. Liu, N. B. Kolhe, Z. Wu, Y. Puttisong, C. Musumeci, M. Massetti, H. Sun, K. Xu, D. Tu, W. M. Chen, H. Y. Woo, M. Fahlman, S. A. Jenekhe, M. Berggren, S. Fabiano, *Nat Commun* **2021**, *12*, 2354.

1:45 PM EQ11.02.02

Molecular Design of Stretchable/Elastic Polymer Semiconductors with High Electrical Performance [Yu Zheng](#) and Zhenan Bao; Stanford University, United States

Polymer semiconductors have recently gathered considerable interests for their potential to produce stretchable electronics for wearable and implantable device applications. The key target yet major challenge is to maintain high electrical performance under mechanical deformation. However, polymer semiconductors are typically π -conjugated systems with semi-crystalline thin film morphology, most of which experience device failure under low strain. In order to address this discrepancy, we iteratively developed three molecular design approaches.

We started with an in-depth investigation of structure-property relationships for a family of diketopyrrolopyrrole (DPP)-based conjugated polymers bearing hydrogen-bonding conjugation breakers (CBs) with different hydrogen-bonding strength and linker flexibilities. We concluded that CBs with a hydrogen-bonding self-association constant >0.7 and/or a denser packing tendency are able to induce higher polymer chain aggregation and crystallinity in thin films, resulting in a higher crack-on-set strain and a lower degradation in mobility during stretching. Detailed morphological characterizations suggested that crystallites alignment and hydrogen-bonding breakage are the main strain energy dissipation mechanisms. Such understanding well correlated molecular-level dynamic interactions with thin-film morphology and mechanical properties of polymer semiconductors, although this approach compromised the electrical performance.

To obtain highly stretchable polymer semiconductor without sacrifice in mobility, we investigated the potential of a high-performance conjugated polymer idacenedithiophene-co-benzothiadiazole (IDTBT) with originally low crystallinity. The polymer chains in amorphous region get involved in dissipating strain energy through conformation change. With this mechanism, IDTBT was found to be highly ductile and maintain sufficiently stable mobility of $\sim 0.6 \text{ cm}^2 \text{ V}^{-1} \text{ s}^{-1}$ at 100% strain without any crack formation. Despite its low crystallinity, the rigid and coplanar backbone configuration of IDTBT results in its efficient intrachain charge transport and thus high electrical performance. However, the plastic deformation of IDTBT leads to significant performance degradation after multiple stretching-releasing cycles due to wrinkle formation.

For realistic consumer electronics, robust elasticity is highly demanded. Therefore, we demonstrated a molecular design approach, covalently-embedded in-situ rubber matrix (iRUM) formation, which results in elastic semiconductors with high cyclic stability without comprising electrical performance. Additionally, iRUM approach can concurrently achieve solvent-resistance and photo-patternability, which are critical to realistic manufacturing. The rationally-designed good mixing of iRUM precursors with conjugated polymers significantly improves the crosslinking density of semiconductor films, serving as the key to achieve high elasticity. Besides, the charge transport is well maintained by leveraging reactivity difference between azide/C-H insertion and azide/C=C cycloaddition, leading to finely controlled competition between forming a rubber matrix and linking with conjugated polymer side chain. When applied in fully stretchable transistors, its mobility can be retained at 100% strain, and exhibits $0.93 \text{ cm}^2 \text{ V}^{-1} \text{ s}^{-1}$ record-high average mobility retention after 1000 stretching-releasing cycles at 50% strain. Unprecedented 5000 stable stretching-releasing cycles are achieved and such a cycle life is five times longer than any reported work. A fully patterned, elastic transistor array was fabricated via photo-patterning of iRUM-semiconductor, demonstrating its compatibility with solution-processed multilayer electronic device manufacturing. Our work represents a transition from soft/stretchable electronics to developing practical, long-cycling, and multifunctional electronics.

2:00 PM EQ11.02.03

Molecular Doping for High-Performance Organic Electronics [Alberto Scaccabarozzi](#)^{1,2}, Kalaivanan Loganathan², Thomas D. Anthopoulos² and Mario Caironi¹; ¹Italian Institute of Technology, Italy; ²King Abdullah University of Science and Technology, Saudi Arabia

The employment of organic semiconductors (OSCs) promises to widen the realm of electronics to countless new applications, thanks to the advantageous properties of soft matter. However, despite the plethora of fascinating opportunities, organic electronics has been progressing slower than expected due to difficulties in delivering high performance and reliability. In this framework, doping plays a fundamental role to overcome typical limitations. Indeed, even in the most successful organic-based technology -organic light-emitting diodes (OLEDs)- it was only when doped charge transport layers were introduced in standard device architectures, that the performance and the technological maturity required for industrialization of these devices were reached.

Interestingly, in recent years there has been a progressive transition from the simple employment of dopants in highly conducting layers, to their use into other fundamental parts of the devices. Active layers in organic thin-film transistors (OTFTs), for instance, have been almost entirely relying, until very recently, on pristine (*i.e.*, non-doped) organic semiconductors. Extensive efforts in optimizing structure-property relationships in these layers led to a level of device optimization that pushed this approach to its limits. In this context, the addition of dopants enabled the demonstration of OTFTs with unprecedented performance owing to an improved charge transport and reduced contact resistance.¹⁻³ Similarly, molecular dopants have been successfully employed in bulk heterojunctions to fabricate solar cells⁴ and photodetectors⁵ displaying enhanced properties.

In this work we cover different materials systems and show how doping can lead to increased charge carrier mobilities owing to synergistic effects both in terms of electronic and structural properties. Indeed, the addition of low concentrations of molecular dopants to the channel of OTFTs can be accompanied by changes in their charge transport mechanism, with the onset of a band-like transport, besides the achievement of extremely high mobilities. Furthermore, we show how the microstructure of the OSCs can be controlled upon blending them with dopants aiding the transport. The improvements of our blend systems are not limited to transistors, but are also valid also for photodetectors, solar cells and diodes. The latter are in particular very promising, since high frequency rectifiers are a central component that determine the frequency of operation and the power conversion efficiency in wireless energy harvesting (WEH) systems. Here we present a novel strategy in which an adhesion lithography fabrication route, yielding to electrodes separated by nanogaps $< 20 \text{ nm}$, is combined with doping to achieve co-planar nanogap Schottky diodes operating above 10 GHz.

Our results provide evidence that doping and innovative fabrication routes can pave the way towards future applications of GHz organic electronics.

References

1. Panidi, J. *et al.* Remarkable Enhancement of the Hole Mobility in Several Organic Small-Molecules, Polymers, and Small-Molecule:Polymer Blend Transistors by Simple Admixing of the Lewis Acid p-Dopant B(C₆F₅)₃. *Advanced Science* **5**, 1700290 (2018).
2. Scaccabarozzi, A. D. *et al.* Understanding Charge Transport in High-Mobility p-Doped Multicomponent Blend Organic Transistors. *Advanced Electronic Materials* **6**, 2000539 (2020).
3. Waldrip, M., Jurchescu, O. D., Gundlach, D. J. & Bittle, E. G. Contact Resistance in Organic Field-Effect Transistors: Conquering the Barrier. *Advanced Functional Materials* **30**, 1–31 (2020).
4. Lin, Y. *et al.* A Simple n-Dopant Derived from Diquat Boosts the Efficiency of Organic Solar Cells to 18.3%. *ACS Energy Letters* 3663–3671 (2020).
5. Wang, B. *et al.* Molecular Doping of Near-Infrared Organic Photodetectors for Photoplethysmogram Sensors. *J. Mater. Chem. C* (2021).

2:15 PM EQ11.02.04

Field Effect Transistors Based on Cumulenic sp-Carbon Atomic Wires—A New Paradigm for High Mobility Organic Semiconductors? Stefano Pecorario^{1,2}, Alberto Scaccabarozzi^{1,3}, Daniele Fazzi⁴, Carlo S. Casari² and Mario Caironi¹; ¹Istituto Italiano di Tecnologia, Italy; ²Politecnico di Milano, Italy; ³King Abdullah University of Science and Technology (KAUST), Saudi Arabia; ⁴Universität zu Köln, Germany

The achievement of high charge carrier mobility in solution processable organic semiconductors is a fundamental requirement for the development of organic field effect transistors operating at high frequency, therefore enabling middle-range wireless communication for the next generation of flexible electronic devices.

For this reason, in the last decades extensive efforts have been devoted to the chemical design of conjugated polymers and molecular semiconductors, reaching effective field effect mobilities $>10 \text{ cm}^2\text{V}^{-1}\text{s}^{-1}$, besides the employment of carbon nanostructures such as graphene and carbon nanotubes. Organic semiconductors consist in extended conjugated systems originating from overlapped π orbitals of adjacent sp²-hybridised carbon atoms. Herein, we report for the first time on the potential of sp-Carbon Atomic Wires as a new class of solution processable semiconductors for organic electronics. Carbon Atomic Wires are linear chains of sp-hybridized carbon atoms and represent the ultimate one-dimensional allotropic form of carbon.^[1] They exhibit two possible isomeric configurations: cumulenes (sequence of double bonds) and polyynes (sequence of single and triple alternated bonds). Theoretical studies have predicted outstanding mechanical, optical and electrical properties for these structures. However, only a few experimental studies have investigated their electronic properties in solid-state devices and, so far, they have focused mainly on molecular junctions or monolayers.^[2]

In this work we demonstrate the first example of organic field-effect-transistor (OFET) based on short cumulenic molecules, namely tetraphenylbutatriene [3]Ph.^[3] Furthermore, we discuss on our latest achievements in understanding and optimizing charge-transport properties in solution processed thin films of [3]Ph. In particular, we show how the control of large-area thin-films deposited via wire-bar coating, a scalable printing technique, allows achievement of field-effect-mobilities above $0.1 \text{ cm}^2\text{V}^{-1}\text{s}^{-1}$. Moreover, our [3]Ph-based transistors provide excellent operational stability in dark conditions, therefore addressing one of the major concerns for the application of Carbon Atomic Wires, and in general of organic semiconductors, in ambient conditions.

An in-depth characterisation of films obtained with different processing parameters allows to correlate microstructural and morphological features with the OFETs electrical performance. Our analysis highlights how these devices, based on the shortest of the cumulenes series, symbolize a promising starting point towards the exploration of sp-Carbon Atomic Wires with superior charge carrier mobility.

These results pave the way for the use of cumulenes as active material for organic electronics and open new possibilities for the chemical design of performant organic semiconductors based on sp-hybridised molecules.

[1] C. S. Casari, M. Tommasini, R. R. Tykwinski and A. Milani, *Nanoscale* 2016.

[2] M. R. Bryce, *J. Mater. Chem. C* 2021

[3] A. D. Scaccabarozzi, A. Milani, S. Peggiani, S. Pecorario, B. Sun, R. R. Tykwinski, M. Caironi, and C. S. Casari, *J. Phys. Chem. Lett.* 2020.

2:30 PM EQ11.02.05

Printing High-Performance 2D Oxide Transistors from Liquid Metals William J. Scheideler, Andrew B. Hamlin, Youxiong Ye, Julia Huddy and Md Saifur Rahman; Dartmouth College, United States

High-frequency flexible electronics demands high mobility channel materials suitable for low-temperature deposition. We present high-performance 2D In₂O₃ transistors printed from liquid Indium metal at temperatures compatible with low-cost polymer substrates. These ultrathin (2–4 nm) In₂O₃ channel materials demonstrate performance unseen in low-temperature sol-gel or nanoparticle systems, with low-field mobility greater than $40 \text{ cm}^2/\text{Vs}$ at 175 °C and $65 \text{ cm}^2/\text{Vs}$ at 250 °C processing compatible with PEN and Polyimide, respectively. We show through comparative XPS and XRD studies that a principal advantage of liquid-metal (LM) printed oxides relative to sol-gels is the ability to achieve crystalline and highly conducting films *as deposited*, avoiding hydroxide-dominated intermediate phases and eliminating the thermodynamic barrier posed by precursor decomposition.

Low-temperature Hall measurements reveal that, *as deposited*, these quantum-confined In₂O₃ channels exhibit Hall mobility of 12–20 cm²/Vs and electron concentrations of $\sim 1 \times 10^{19} \text{ cm}^{-3}$. Post-annealing in air further enhances electronic transport, allowing enhancement mode operation and tight control of the electronic density of states (eDOS) for monolayer and bilayer films, revealing the extremely steep band tail slope and lower deep state density of bilayer channels. Additionally, these devices exhibit ultra-low hysteresis and excellent current saturation, indicating the low defect density and stable back channel. This exceptional switching performance and the scalable simplicity of the LM printing method make these 2D oxide transistors promising devices for driving next-generation flexible electronic sensor and displays.

SESSION EQ11.03: Flexible Electronics—Fabrication

Session Chairs: Mario Caironi and Matteo Cucchi

Wednesday Afternoon, December 1, 2021

Hynes, Level 1, Room 111

1:45 PM *EQ11.03.01

Flexible Nanoscale Organic Transistors Hagen Klauk and Ute Zschieschang; Max Planck Institute for Solid State Research, Germany

Organic thin-film transistors (TFTs) can often be fabricated at temperatures around or below 100 degrees Celsius and thus on a wide range of unconventional substrates, including a variety of mechanically flexible and optically transparent polymers, such as polyethylene naphthalate (PEN). This makes organic TFTs a potential alternative to TFTs based on inorganic semiconductors, most notably low-temperature polycrystalline silicon (LTPS) and

indium gallium zinc oxide (IGZO), which typically require somewhat higher process temperatures that limit the choice of mechanically flexible substrate materials to ultrathin glass (which is prone to shattering) and polyimide (which has lower optical transmission compared with glass and PEN). For circuit and display applications, an important TFT parameter is the transit frequency, which is the highest frequency at which transistors are able to switch or amplify electrical signals. A field-effect transistor's transit frequency depends critically on the channel length and the parasitic gate-to-source and gate-to-drain overlaps. Most of the highest transit frequencies reported for organic TFTs to date have been achieved with channel lengths and gate-to-contact overlaps of around 1 μm . To explore the static and dynamic performance of flexible organic TFTs with nanoscale dimensions, we have used electron-beam lithography and fabricated low-voltage organic TFTs with channel lengths and gate-to-contact overlaps as small as 100 nm on flexible PEN substrates. These TFTs display useful static and dynamic characteristics, including on/off current ratios of nine orders of magnitude, subthreshold swings below 100 mV/decade, turn-on voltages of 0 V, negligibly small threshold-voltage roll-off, contact resistances below 1 k Ω -cm, and switching delays below 50 ns.

2:15 PM EQ11.03.03

Understanding the Effect of Processing on Structure Evolution and Dielectric Properties of Polymer Films Zeynep Mutlu, Mayank Jain, Venkat Kasi, Rahim Rahimi, Jiahao Mao and Mukerrem Cakmak; Purdue University, United States

Polymers have been used as flexible and easily processible dielectric materials for many years. Dielectric constant, dielectric loss and breakdown strength are critical for the successful application of a polymer dielectric. Numerous studies have been carried out to enhance the breakdown strength of polymers that have a reasonable dielectric constant. Taking advantage of their tailorability, this has been mainly achieved through the processing route where polymers are stretched to increase the orientation and superstructural organization, and hence the breakdown properties. This tends to lead to structural hierarchy forming tortuous path through thickness direction by the overlap of oriented crystalline and amorphous domains. However, it is challenging to understand the polymer responses under deformation. In this study we have investigated the effect of orientation on structural hierarchy (crystallinity, crystalline and amorphous chain orientation, superstructural organization) on the dielectric properties of Nylon 12. In addition to suppress the charge injection through the surfaces, SiO₂ coating was applied by using plasma enhanced chemical deposition.

2:30 PM EQ11.03.04

Modeling Rigidity in Conjugated Polymers Andrew T. Kleinschmidt, Tod Pascal and Darren J. Lipomi; University of California, San Diego, United States

Conjugated polymers are being asked to undergo more "polymer-like" behavior than ever before-- being strained, scratched, punctured, repeatedly elongated, and more. Computational modeling at the molecular dynamics level could speed up design of conjugated polymers considerably. However, these models must be able to consider "polymer-like" behavior as well. Accurate reflection of polymer nanostructure in molecular dynamics is key to determination of the polymer's mechanical properties. We find that the current state of modeling often neglects polymer rigidity. Forces meant to represent planarizing forces are often reduced or even eliminated by steric hindrance. We have thus developed a model that separates out steric forces from forces associated with electron delocalization and internal conjugation. We additionally find that there are two key types of torsion present even in a neat polymer film-- improper and dihedral. Both of these forces must be dealt with simultaneously to achieve accuracy. Finally, we compare homopolymers to donor-acceptor polymers and find the difference in rigidity is less than might be expected.

2:45 PM EQ11.03.05

Nanosoldering of Sensing Components on Conductive Textile Fibers Edward Fratto, Zhiyong Gu, Ramaswamy Nagarajan and Xuejun Lu; University of Massachusetts Lowell, United States

Ongoing research into the miniaturization and optimization of electronic device manufacture has driven component study to the nanoscale, sparking interest in device design on nontraditional substrates for highly specific, targeted applications. The emerging field of smart 'e-textiles' examines the translation of traditional device manufacturing strategies onto flexible textile substrates, driven by commercial and fundamental interest in textile-nanomaterial integration and conductive network wiring within woven architectures to imbue useful functionality to worn garments. In the interest of adapting thermally driven electronic interconnection strategies to temperature-sensitive materials, we provide an investigation into the modification of textile surfaces with nanosolder-inks, establishing conductive channels for signal communication and joining resistive sensing elements through soldered interconnection. Low melting temperature tin/indium nanosolder particles were synthesized via aqueous chemical reduction and formulated into conductive ethylene-glycol based inks at various loading concentrations. These nanoinks were applied to individual threads of various fabric blends by dip-dry coating, with degree of coverage evaluated in relation to number of coats and associated thermal/electrical processing to improve adhesion. Printed threads were exposed to infrared heating, allowing for targeted melting of solder particles without harming the woven fiber structure, confirmed visually and via monitoring change in electrical resistance. After melting, threads modified by nanoinks with incorporated graphene oxide platelets demonstrated sensing capability for temperature, humidity, liquid phase salinity, and chemical vapors. Signal generated by these sensing fibers was transmitted via thread-to-thread soldered interconnection, establishing the conductive wiring groundwork for a textile device platform. This realization of non-destructive robust solder joining on thermally delicate textile substrates represents a significant step towards full translation of electronic device manufacturing strategies onto a woven garment.

3:00 PM BREAK

4:00 PM EQ11.03.07

Long-Wavelength Instability-Coupled Alignment in a Semiconductor-Elastomer Blend for Stretchable Electronics Peter Dudenas¹, Eliot Gann¹, Guillaume Freychet², Lee Richter¹ and Dean DeLongchamp¹; ¹National Institute of Standards and Technology, United States; ²Brookhaven National Laboratory, United States

Flexible electronics are poised to significantly change device technologies, with applications across biological/medicinal, environmental, consumer, and industrial markets. Devices that are thin, conformable, and compliant open myriad design opportunities that are currently infeasible with today's rigid electronics. Some of the most promising material systems with these characteristics are semiconducting-polymer/elastomer (SPE) blends. The semiconducting polymer phase segregates into nanofibrils upon spin or blade coating and under certain conditions these fibrils can be aligned for directional charge transport. SPE blends have been shown to maintain excellent electronic properties under large strain, and have the advantage of being solution processable, enabling economical manufacturing scale-up.

In addition to the economic advantage solution-based processing confers, it also provides a large parameter space to optimize device fabrication. Solvent identity, polymer concentration, coating temperature, and coating speed are a few notable parameters available to tune. This allows for flexibility in the formulation process, but also creates a parameter space that can be difficult to optimize, and the optimum is often different with different coating methods. Of the many coating methods, meniscus-guided techniques are becoming more ubiquitous because of their ability to create aligned materials and are more directly translatable from lab to industrial scale manufacturing.

Here, we report on a long-wavelength instability in the blade coating process that leads to significant variation in the local semiconducting polymer fibril alignment for a DPP-TT:SEBS blend. Near-edge x-ray absorption fine structure (NEXAFS) is used to quantify the molecular alignment of DPP-TT in the fibrils and the surface composition of the films. The optical dichroic ratio from wide-field polarization imaging is directly correlated to fibril alignment as quantified by AFM, which provides a spatially resolved measurement of DPP-TT nanofibril alignment. These measurements are correlated to thin-film transistor data to characterize the impact on charge transport. Quantifying and potentially controlling coating instabilities are important for device optimization, especially in the scale-up process.

4:15 PM *EQ11.03.08

Doping Organic Semiconductors by Lewis Acids—A “Complex” Story [Thuc-Quyen Nguyen](#); University of California, Santa Barbara, United States

The ability to precisely control the equilibrium carrier concentration in organic semiconducting devices is of great interest. Solution processed doped layers are of extreme importance for high throughput production of organic electronic devices via roll-to-roll or ink-jet printing. In this talk, I will discuss tuning the conductivity of conjugated polymers containing Lewis basic sites by Lewis acids. Addition of the Lewis acid effectively p-dopes the hole transport in the parent polymer, leading to increases in the free hole density and conductivity. This methodology is advantageous since the polymer and Lewis acid have excellent solubility in organic solvents, negating the need for co-solvents that uses in molecular dopant such as F4TCNQ. We use a combination of techniques including electrical measurements, optical absorption, XPS, UPS, IPES, and electron paramagnetic resonance (EPR), electron-nuclear double resonance (ENDOR) and nuclear magnetic resonance (NMR) techniques in conjunction with density functional theory, to gain insight into the doping mechanism of 4,4-dihexadecyl-4H-cyclopenta[1,2-b:5,4-b']dithiophene (CPDT) and 2,1,3-benzothiadiazole (BT)-based (PCPDTBT) by Lewis acids, BCF. We suggest protonation of the CPDT moieties by the strong Brønsted acid BCF(H₂O), followed by electron transfer from a neutral polymer chain segment to a protonated chain forming a neutral, protonated radical species and a positively charged radical species (a positive polaron or a hole). Neher et al Neher and colleagues investigated doping of poly(3-hexylthiophene) (P3HT) by BCF and suggested that the overall reaction resulted in formation of H₂, rather than a radical species, as the final hydrogen-containing side product, with one possible route for H₂ formation being reaction of two radical species. DFT calculations predict that the protonation reaction and H₂ formation are highly endergonic. However, if we consider the formation of a larger anion, [BCF(OH)(OH₂)BCF]⁻, in which [BCF(OH)]⁻ is hydrogen bonded to another BCF(OH₂) complex, the protonation reaction and H₂ formation are exergonic.

SESSION EQ11.04: Designing UHF Printed Transistors
Session Chairs: Giuseppe Giccone and Jörn Vahland
Thursday Morning, December 2, 2021
Hynes, Level 1, Room 111

10:30 AM EQ11.04.01

Quasi-Self-Aligned Organic Thin-Film Transistors in Coplanar Top-Gate Configuration [Jörn Vahland](#), Karl Leo and Hans Kleemann; TU Dresden - Institut für angewandte Physik, Germany

Besides charge carrier mobility and contact resistance, the parasitic overlap capacitance is a key factor limiting the dynamic behavior of organic thin-film transistors. The most effective way to reduce parasitic overlap capacitances between source/drain and gate electrode is to employ self-aligned transistor architectures. However, so far self-alignment in organic transistors has only been achieved using non-scalable or complex fabrication processes. Here, we demonstrate quasi-self-aligned OTFTs in a coplanar top-gate architecture fabricated with reliable and scalable state-of-the-art fabrication techniques such as wet-chemical etching. Self-alignment is achieved by carrying out a wet-chemical etching process on top of the channel interface. We prove that for the right choice of etchant, the charge carrier transport properties of the channel interface are not deteriorated. The benefit of the self-aligned design lies in the reduction of the specific overlap capacitances which are two orders of magnitude (0.13 nF cm^{-2}) lower than for non-self-aligned devices (15 nF cm^{-2}). Furthermore, we highlight the potential of this approach for high-frequency operation of organic transistors and quantify the gain in cut-off frequency compared to non-self-aligned devices.

10:45 AM EQ11.04.02

Organic Mixed Ion-Electron Conductors in Microwave Metadevices [Giorgio Ernesto Bonacchini](#)^{1,2}, [Siew Ting Melissa Tan](#)¹, [Alexander Giovannitti](#)¹, [Tyler J. Quill](#)¹ and [Alberto Salleo](#)¹; ¹Stanford University, United States; ²Istituto Italiano di Tecnologia, Italy

The field of magnetic metamaterials has spurred increasing interest since the first experimental demonstrations of a negative refractive index metamaterial¹. The appeal of these photonic devices lies in the possibility to engineer media with tailored electromagnetic response, imparting them with unconventional wave propagation properties that cannot be achieved by ‘natural’ materials². Examples of metamaterials-enabled applications include artificial magnetism, arbitrary wave-front shaping, and cloaking. To overcome the practical limitations of static metamaterials, recent efforts have focused on the integration of passive microwave metamaterials with a number of active tuning mechanisms. These dynamic metadevices grant unprecedented control over the propagation of microwaves, enabling for example real-time modulation of light intensity and phase, as well as tunable spectral selectivity³.

A plethora of tuning strategies has been so far proposed for the realization of active metadevices. Among electrical strategies, established approaches such as the addition of lumped elements (e.g. varactor and pin diodes) to microwave resonators, or the use of materials such as graphene and III-V compound semiconductors, come with high fabrication complexity and cost compared to printed organic electronics⁴. Furthermore, these approaches cannot be easily translated into platforms where large-area formats and mechanical conformability are of essence.

A new device configuration has recently been proposed, where organic electrochemical transistors – based on the conductive polymer PEDOT:PSS – actively tune a set of sub-5GHz microwave metasurfaces and metamaterial-inspired structures⁵. These devices consist in individual (or multiple) microwave Split-Ring Resonators in which the split region is bridged by a transistor, gated through common electrolytes. This device configuration enables a fully reversible modulation mechanism, which requires very low voltages (<1 V) thanks to the mixed ion-electron transporting ability of PEDOT:PSS⁶. This tuning strategy can be readily implemented on different resonant configurations, including magnetic and electric resonators, frequency-tunable SRRs, dual-band devices, and in a reconfigurable metasurface.

The promising results achieved with PEDOT:PSS encourage a wider exploration of the continuously growing library of organic semiconductors. In this work, we demonstrate a set of tunable microwave devices using different p-type and n-type organic electrochemical transistors. By chemically engineering the organic semiconductors, we are able to operate our devices in selected voltage ranges, with fine control over the voltage dependence of the metadevices’ scattering properties. As an example of a possible application, we exploit this strategy within a wireless biosensing platform operating in the

2-2.5 GHz range.

In perspective, a metadvice tuning strategy based on organic electronic materials presents exciting opportunities for microwave technologies, possibly paving the way to a new generation of wireless interfaces for distributed sensing, fabricated on large-area flexible substrates via high-throughput techniques. Moreover, this class of metadvice could potentially complement other emerging neuromorphic technologies that are also based on organic electrochemical transistors, expanding the horizon of metamaterials research.

References:

1. Shelby, R. A., Smith, D. R. & Schultz, S. (80). **292**, 77–79 (2001).
2. Pendry, J. B., Schurig, D. & Smith, D. R. *Science* (80). **312**, 1780–1782 (2006).
3. Zhao, X., Duan, G., Li, A., Chen, C. & Zhang, X. *Microsyst. Nanoeng.* **5**, 1–17 (2019).
4. Caironi, M. & Noh, Y.-Y. *Large area and flexible electronics*. (Wiley-VCH, 2015).
5. Bonacchini, G. E. & Omenetto, F. G. *Nat. Electron.* (2021) - In press.
6. Rivnay, J. *et al. Nat. Rev. Mater.* **3**, 17086 (2018).

11:00 AM EQ11.04.03

Self-Aligned Amorphous Indium-Gallium-Zinc-Oxide TFTs Breaking the GHz Threshold [Christian Tückmantel](#), Utpal Kalita, Tobias Haeger, Manuel Theisen, Ullrich Pfeiffer and Thomas Riedl; University of Wuppertal, Germany

Thin-film transistors (TFTs) based on amorphous metal-oxide semiconductors have received enormous attention. While this technology has set new standards as backplane for flat-panel displays, there is a wide range of applications that only becomes accessible, if metal-oxide are capable of high-frequency operation. To this end, the transit frequency (f_T) and maximum oscillation frequency (f_{max}) become important figures of merit, which have not received adequate attention in metal-oxide based electronics, yet. These numbers are critically limited by parasitic elements in the device (such as capacitances). Compared to devices based on single crystalline silicon (c-Si) technology, the f_T of most metal-oxide TFTs in the literature is typically low. In fact, the best f_T of metal-oxide TFTs based on large area compatible and cost-effective standard lithography did not reach the GHz regime, as of yet. Here, we demonstrate the first a-IGZO based TFTs with a transit frequency $f_T > 1$ GHz. This is achieved by a rigorous reduction of parasitic elements ($L_{ov} = 300$ nm, $C_{GS} + C_{GD} = 800$ fF/mm) and a channel length L as low as $0.8 \mu\text{m}$, resulting from a substantially optimized self-alignment concept without sacrificing the typical advantages of optical lithography. At the same time, our TFTs set a new record in f_{max} of 3.1 GHz, which states a new high-frequency limit for power amplification in metal-oxide electronics.

We expect that our results will inspire metal-oxide based high-frequency circuit applications, such as communications systems, on large-area and even flexible substrates. As such, metal-oxide TFTs ultimately may become a meaningful platform for the realization of concepts discussed in the framework of the IoT.

11:15 AM EQ11.04.04

Conformable, Internal Ion-Gated Organic Electrochemical Transistor (IGT)-Based Multiplexer with Megahertz Operation [Claudia Cea](#), Zifang Zhao and Dion Khodagholy; Columbia University, United States

Organic transistor architectures that are able to interact with ions such as electrolyte-gated field effect transistors or electrochemical transistors are highly attractive devices for acquisition, transmission and processing of physiological signals. These devices are able to convert ions to electrons effectively and provide mechanical flexibility owing to their inherently soft channel materials. However, the temporal response of these devices, which directly translates into their operation speed, is defined by ion drift and mobility. As a result, they are limited to a few KHz speed regime. In addition, the lack of physically independent gate limits their ability to form integrated-circuits (ICs). Here we use internal ion-gated organic electrochemical transistors (IGTs) that are able to operate beyond the speeds dictated by ion mobility by creating local ion reservoirs inside the channel bulk. We demonstrate IGT-based amplifiers with uniform gain across their MHz range operation frequency. We characterize the electrical performance of these transistors with respect to various transistor sizes, contact area, and channel material composition, and determined the relationship between device geometry and gain, off current, leakage, and inter-transistor cross talk. Using these data and a high resolution vertical fabrication approach (capable of creating $<1 \mu\text{m}$ transistors), we then created high-density IGT-based conformable circuits that performed time-division multiplexing at speeds comparable to silicon based ICs for physiological signal acquisition and multiplexing. The unique features of IGT-based devices facilitate potential applicability to a broad range of flexible circuits that require safe, chronic implantation in humans, including brain-machine interfaces, wearable electronics, and therapeutic responsive stimulation devices.

SESSION EQ11.05: Flexible Electronics—Applications

Session Chairs: Matteo Cucchi and Jörn Vahland

Thursday Afternoon, December 2, 2021

Hynes, Level 1, Room 111

1:30 PM *EQ11.05.01

Tissue Equivalent, Conformal Medical Radiation Dosimeters Based on Organic Transistors [Oana D. Jurchescu](#); Wake Forest University, United States

Radiation therapy is one of the most effective medical procedures for cancer treatment: high-energy ionizing radiation is very effective in destroying cancer cells, but the risks of malignancies induced by peripheral radiation in healthy tissues surrounding the target volumes represents a serious concern for all patients and doctors alike. Positioning of the patient, inhomogeneities in the target (muscles/bones/adipose tissue), and even minor movements (e.g. breathing), can alter the received dose and targeted volume, and thus affect the outcome of the procedure. Therefore, being able to measure radiation doses with high accuracy is a critical aspect of diagnostics and treatment. In this presentation I will introduce a new type of radiation dosimeter, the RAD-OFET (RADiation Detector based on Organic Field-Effect Transistor), which can validate in real time the dose being delivered and ensure that for nearby regions an acceptable level of low dose is being received.¹ The RAD-OFETs exploit trap generation/annihilation in organic semiconductors,² are sensitive to doses relevant to many radiation treatment procedures and are robust when incorporated into conformal large-area electronic applications. Placement of the sensor directly onto the human body, coupled with the similarity in the Z-number between the electronically active layer and the human tissue, allows for direct measurement of the radiation dose, eliminating the need for extensive data processing faced by current technologies. The direct consequence is a greater precision and lower complexity in the medical equipment: their adoption in clinical settings will facilitate the application of therapeutic radiation with high precision, a process that will increase the effectiveness on treating cancerous tissue and minimize the impact on the surrounding healthy cells. These results uncover new opportunities for organic circuits that will improve the quality of healthcare through better, lower cost *in vivo* dose monitoring during radiation therapy.

- [1] A. M. Zeidell, T. Ren, D. S. Filston, H. F. Iqbal, E. Holland, J. D. Bourland, J. E. Anthony, O. D. Jurchescu, *Adv. Sci.* 7 (18), 2001522 (2020).
[2] H. F. Haneef, A. M. Zeidell, O. D. Jurchescu, *J. Mater. Chem C* 8, 759 (2020).

2:00 PM *EQ11.05.02

Imperceptible Energy Harvesting Device and Biomedical Sensor Based on Ultraflexible Ferroelectric Transducers and Ultraflexible High Frequency Organic Diodes [Barbara Stadlober](#)¹, Andreas Petritz^{1,2}, Esther Karner-Petritz^{1,2}, Philipp Schöffner¹, Takafumi Uemura^{2,3}, Teppei Araki^{2,3} and Tsuyoshi Sekitani^{2,3}; ¹Joanneum Research Forschungsgesellschaft mbH, Austria; ²Osaka University, Japan; ³AIST Advanced Photo-Bio Lab, Japan

Energy autonomy and conformability are essential elements in the next generation of wearable and flexible electronics for healthcare, robotics and cyber-physical systems. This study presents ferroelectric polymer transducers and organic diodes for imperceptible sensing and energy harvesting systems, which are integrated on ultrathin (1- μm) substrates, thus imparting them with excellent flexibility [1]. It was found that these ultraflexible ferroelectric polymer transducers (UFPTs) develop improved ferroelectric properties through thermal annealing resulting in an increased crystallinity. After poling the remnant polarization reaches values up to 70 mC/m² in close correlation with the crystallinity and the decrease of the dielectric constant. Simulations show that the sensitivity of ultraflexible ferroelectric polymer transducers can be strongly enhanced by the use of the ultrathin substrate. The ultrathin substrate furthermore allows the mounting of the transducers on 3D-shaped objects and the stacking in multiple layers. Indeed, UFPTs have improved sensitivity to strain and pressure as compared to devices on rigid thick substrates with values up to 15 nC/N; they have a fast response ($\ll 20$ ms/N) and an excellent mechanical stability with a bending radius down to 40 μm . Accordingly, they can be used as imperceptible wireless e-health patches for precise pulse and blood pressure monitoring.

For harvesting biomechanical energy, the transducers are combined with full wave organic rectifier circuits made of ultraflexible organic diodes. These diodes are based on organic thin film transistors with short-circuited drain and gate and are fabricated on the ultrathin substrate as well. The diodes have an excellent on/off ratio up to 10^7 and a transition voltage around 0V. Moreover they are exceptional in terms of operation frequency in the MHz regime. Transducers, diodes and ultrathin capacitors (needed as storage elements) were further combined to form an imperceptible, 2.5 μm thin, energy harvesting device with an excellent peak power density of 3 mW $\times\text{cm}^{-3}$. When placed on body joints like elbow or knee we estimate that over a day 100 -200 mJ can be generated by biomechanical motions like knee bending with such a system. This should be enough for vital parameter reading several times per day.

- [1] A. Petritz, E. Karner-Petritz, T. Uemura, P. Schöffner, T. Araki, B. Stadlober, T. Sekitani, *Nat. Comm.* (2021), 12:2399, <https://doi.org/10.1038/s41467-021-22663-6>

2:30 PM EQ11.05.03

Data Storage and Information Processing from Roll-to-Roll Printed Conjugated Polymeric Electrochemical Memristors [Benjamin T. Grant](#), Iurii Bandera and Stephen H. Foulger; Clemson University, United States

Conjugated polymeric electrochemical memristors (cPECMs) are a promising alternative towards next-gen bioinspired circuitry, such as memristive neuromorphic computers. Low gate switching voltages and low power consumption are easily achieved due to the wide range of redox potentials available. In the case of the p-type poly(3,4-ethylenedioxythiophene):poly(styrene sulfonate) (PEDOT:PSS), the conjugated PEDOT allows mobile holes to hop from one chain to another where, in the neutral form, holes are compensated by PSS anions. Major limitations of PEDOT:PSS devices are due to the inherent nature of the material to oxidize, which can impede the state retention and cycle stability of a device. In this effort, a water soluble, partially reduced self-doped PEDOT (S-PEDOT) that is synthesized and fabricated into an all-solid-state memristive device. This three-terminal device with a pre- and post-synaptic terminal is able to tune the device's conductance via electrochemical doping by means of voltage pulsing to the gate with a low power consumption for switching events (ca. 42 pJ/mm² for a 12 x 20 mm active area). S-PEDOT cPECMs are implemented to perform arithmetic and simple mathematics, execute information processing such as Boolean logic gates, display electrochromic behaviors, and can emulate essential artificial synaptic plasticities for learning and memory behaviors.

2:45 PM EQ11.05.04

Responsive Manipulation of Neural Circuit Pathology by Fully Implantable, Front-End Multiplexed Embedded Neuroelectronics [Zifang Zhao](#)¹, [Claudia Cea](#)¹, [Jennifer Gelinis](#)^{2,2} and [Dion Khodagholy](#)¹; ¹Columbia University, United States; ²Columbia University Medical Center, United States

Implantable bioelectronics are poised to unravel causal relationships between neural activity and brain function due to their ability to directly interact with neurons over extended periods of time. To facilitate advancements in both these basic science and translational research avenues, responsive implantable electronics are required to perform high performance data acquisition, stimulation and low-latency digital signal processing to enable real-time manipulation of neural networks and affect behavior. We introduce a multiplex-then-amplify (MTA) scheme that in contrast to current approaches (which necessitate an equal number of amplifiers as number of channels), only requires one amplifier per multiplexer, significantly reducing the number of components and size of electronics in multi-channel acquisition systems. It also enables simultaneous stimulation of arbitrary waveforms on multiple independent channels. We validated the function of MTA by developing a fully implantable, responsive embedded system that merges ability to acquire individual neural action potentials using conformable conducting polymer-based electrodes with real-time onboard processing, low-latency arbitrary waveform stimulation, and local data storage within a miniaturized physical footprint. We demonstrate all of these features in chronically implanted freely behaving rats, verifying high quality neurophysiological signal acquisition from the hippocampal-prefrontal cortex network over weeks. We implement an automated kindling procedure to generate epileptic neural networks as well as previously established responsive neurostimulation protocols known to affect memory.

The MTA design enables effective, self-contained, chronic neural network manipulation with translational relevance to treatment of neuropsychiatric disease.

3:00 PM EQ11.05.05

Late News: High-Frequency Rectifiers Based on Highly Flexible, Fully Printed Organic Diodes [Fabrizio A. Viola](#) and Mario Caironi; Italian Institute of Technology, Italy

The diffusion of portable and wearable technologies results in a growing interest in electronic devices having features such as flexibility, lightness-in-weight and wireless operation. Organic electronics was proposed decades ago as a potential candidate to fulfill such need, in particular targeting pervasive Radio-Frequency (RF) applications. Still, limitations in terms of device performances at RF, particularly severe when large-area and scalable fabrication techniques are employed. In this work we demonstrated that rectification of an electromagnetic wave at 13.56 MHz thanks to a fully inkjet printed polymer diode is possible. The rectifier, a key enabling component of future pervasive wireless systems, is fabricated through scalable large-area methods on plastic. Thanks to fine tuning of the barriers at the semiconductor-metal interfaces, the diode has a rectification ratio higher than 10^6 : at the best of our knowledge this is the first time that a fully inkjet printed diode with these performances has been obtained. When integrated in an organic rectifier, the excellent dynamic properties of the diode allow to rectify sinusoidal

signals above 20 MHz, well covering the near-field communication range. As demonstrated in this work, our fully printed polymer diode opens the possibility to couple power to a plastic foil, or in future other non-rigid substrates such as paper, by rectifying a 13.56 MHz AC electromagnetic wave, as requested in near-field RFID applications.

3:15 PM EQ11.05.06

Late News: ZnO TFTs for Giga-Hertz Wireless Systems Without Sub-Micron Lithography—Maximizing f_T , f_{MAX} , and $|Z_{OFF}/Z_{ON}|$ [Yue Ma](#), Can Wu, Yoni Mehlman, Sigurd Wagner, Naveen Verma and James C. Sturm; Princeton University, United States

We describe the key structure and material approaches towards recently demonstrated giga-Hertz large-area electronics (LAE) wireless systems using zinc-oxide (ZnO) thin-film transistors (TFTs) [1-4], and the resulting performance parameters. Today's LAE, such as flat-panel displays, operate at frequencies up to ~100 MHz. The next target is wireless applications [Internet of Things (IoT), 5/6G], where bringing LAE to the giga-Hertz regime opens new capabilities, enabling meter-scale radiative apertures for enhanced spatial resolution and power efficiency.

The two central performance goals that guide TFT design, fabrication, and in-circuit use, are: (1) for active device operation, achieving gain at high frequency, especially recognizing the potential for power gain (bound by f_{MAX}) rather than current gain (bound by f_T), and exploiting f_{MAX} -limited circuit operation to generate power at giga-Hertz frequencies; (2) for passive switch operation, achieving high off-to-on impedance ratio to reconfigure antenna elements. In terms of physical electronics, these goals are met in the following ways:

- f_T , the frequency up to which the TFT provides current gain, is determined by the electron transit time t between source and drain, and electron shunting by parasitic capacitances. t depends on electron mobility, channel length, and source/drain (S/D) contact resistance; while the shunting capacitances depend on the gate-source/drain (G-S/D) overlap regions. These are the knobs to turn for high f_T : the electron mobility is primarily set by the choice of semiconductor; minimal S/D contact resistance is achieved by selective etching; and channel length and G-S/D overlaps are minimized by self-aligning S/D to gate electrode. The f_T thus achieved is 0.4 GHz, for a typical ZnO TFT with channel length of 1 μm , biased at $V_{GS}=V_{DS}=6$ V with $V_T=2$ V.

- f_{MAX} , the frequency up to which the TFT provides power gain, depends on f_T , but can be made larger than f_T by reducing the sources of loss within the TFT. In practice, a factor that limits f_{MAX} is the power loss due to the gate resistance. This loss can be reduced by using a thick and highly conductive gate metal stack and multi-finger layout (putting fingers in parallel to reduce resistance along gate width). The f_{MAX} thus achieved is 2.0 GHz for the typical ZnO TFT and biasing.

- $|Z_{OFF}/Z_{ON}|$, the off-to-on impedance ratio of a TFT switch, depends on the conductance around an off channel, through G-S/D parasitic capacitances (which sets $|Z_{OFF}|$), as well as the t through the ZnO channel (which sets $|Z_{ON}|$). Conduction through the parasitic capacitances can be minimized via: (1) small G-S/D overlaps; and (2) the use of resonant inductors, which can be formed with high quality factor thanks to the sq. mm dimensions and low-loss substrates available in LAE. One important approach to reducing $|Z_{ON}|$ is to operate at high V_{GS} but low V_{DS} . This ensures high channel conductance while reducing TFT power dissipation to avoid thermal-induced breakdown [3]. The $|Z_{OFF}/Z_{ON}|$ thus achieved is ~48 at 2.4 GHz, with the half-bandwidth of ~350 MHz.

Based on these advanced ZnO TFTs, we demonstrated a cross-coupled LC oscillator operating at 1.25 GHz [1] and an LAE-based phased array system operating at 1 GHz with beamforming capability [2]. In a reconfigurable antenna with tunable directionality and operating frequency, ZnO TFT switches operate in the 2.4 GHz frequency band [3]. These giga-Hertz system performance results suggest that LAE is a promising candidate for wireless applications in IoT and 5/6G.

[1] Y. Mehlman et al., IEEE 2019 DRC pp. 63-64.

[2] C. Wu et al., Nat. Electron., in press.

[3] C. Wu et al., IEEE 2020 IEDM, paper 33-6.

[4] C. Wu et al., IEEE 2021 28th AM-FPD, pp. 51-54.

This work was supported by grants from Semiconductor Research Corporation (SRC), DARPA, and Princeton Program in Plasma Science and Technology (PPST). This work also utilized the Princeton PRISM cleanroom facilities.

3:30 PM BREAK

4:00 PM EQ11.05.07

Late News: Designing with Process Variability—Optimizing 5G (X-band) RF Antennas and Waveguides for Intrinsic Variability [Katherine Berry](#)¹, Eric Brown¹, Samuel Fedorka¹, Alkim Akyurtlu¹, Craig Armiento¹, Gary Walsh² and Corey Shemelya¹; ¹University of Massachusetts Lowell, United States; ²U.S. Department of the Army, United States

As advanced manufacturing techniques evolve, the mass production of lightweight, flexible electronics requires one to evaluate the levels of production variability that can be expected both in geometric dimensions and in the overall print fidelity of a direct-write (DW) printed design. These variations, introduced by inconsistent material effects in both the printing and curing stages of manufacture, generate behavior different from traditional rigid copper-milled designs. Even the smallest of these divergences in a critical dimension can significantly alter the high frequency response of the printed RF design. As such, this project evaluates the feature fidelity of micro-dispensed RF antennas and waveguides at 5G frequencies (X-band) on flexible 0.127mm-thick I-Tera MT40 dielectric substrate with silver nano-inks to determine repeatability, critical dimensions, and acceptable geometric tolerances in 8 GHz patch antennas and microstrip waveguides. All printed designs were characterized for surface roughness, print thickness, and feature fidelity. Two measures of geometric accuracy were also used across multiple critical features: variation in average feature size from design dimensions, and standard deviation of a feature's size from its average within a single print. The critical feature dimensions were determined to be waveguide width and impedance matching "inlets." S-Parameters were used as a measurement of RF performance, with the experimental range of each of the five measured features plotted separately against the respective antennas' responses to illuminate any outstanding trends between single feature variation and performance. These results were compared to simulation sets in order to determine whether trends were due to the feature alone, or to combinations of interdependent geometric variations. Based on these assessments, acceptable "as-printed" ranges of feature dimensions were developed to produce consistent, acceptable RF performance.

It was found that surface roughness and print thickness have no significant effect on performance, and that the level of variation in the microstrip width does not degrade port-to-patch transmission. However, variation in the dimensions of the impedance matching junction between the transmission line and patch plays a significant role in determining overall RF performance. In general, establishing the average standard deviation of printed traces in an RF antenna design determines the target transmission line width due to the non-linear effects of junction variability on impedance matching. By altering design parameters away from the traditional "ideal" dimensions and instead designing for a highly variable process, performance of up to -36dB was achieved in this study, with 70% of the dataset reaching -20dB or below. This is a significant improvement over traditional design dimensions which were predicted to range from -36dB to just -15dB. All printed results were compared to simulations and dual-clad copper laminate PCBs to verify process, design, and simulation accuracy.

Given the trends analyzed in this work, it is reasonable to expect that developing similar sets of feature dimensions can be applied to any DW printing process. Each DW process will introduce its own level of variability, but by designing the RF structures using the methods described here it becomes

possible to take full advantage of DW's compatibility with flexible substrates. The end result will be higher acceptable through-put while moving towards automated design and fabrication of flexible, on-demand, high-frequency systems.

4:15 PM EQ11.05.08

Late News: Multi-Material, Multi-Substrate, 5G RF Design for Flexible, Conformal and Non-Traditional Substrates [Samuel Fedorka](#), Bradley Pothier and Katherine Berry; UML, United States

Samuel Fedorka¹, Bradley Pothier¹, Katherine Berry¹, Gary F. Walsh², Corey Shemelya¹

1. University of Massachusetts Lowell, Printed Electronics Research Collaborative, 1 University Ave., Lowell, Massachusetts 01854

2. U.S. Army Combat Capabilities Development Command Soldier Center, 15 General Greene Ave., Natick, Massachusetts 01760

The past decade has seen a surge in additive manufacturing materials, devices, and applications bringing new form-factors to both new and existing technologies. Additionally, this unprecedented growth has led to a massive increase in the potential application space of printed electronics ranging from sensing to Radio Frequency (RF) antennas, systems, and components. As printed technologies advance, one must also examine the related RF designs, material systems, and fabrication techniques in order to adapt the technology to a variety of substrates and application environments. For example: a variety of new ink technologies and printable systems have been specifically designed to advance the field of AM, but there has been little research into designing fully integrated 5G RF systems with respect to these novel printing techniques. As such, these fully integrated solutions, i.e. materials, methods, design rules, and design constraints, required for the success printed RF systems/subsystems remains relatively unexplored in additive manufacturing (AM) research.

This work explores direct-write (DW) AM using silver nano-ink and RF-transparent spray coated THV Fluoropolymer on substrates ranging from "thick" laminated ultrahigh molecular weight polyethylene to standard "thin" flexible low-loss dielectric RF material. Using these techniques, an example RF circuit operating at 5G frequencies was designed and fabricated as a case study for DW RF sensing. This circuit consists of a 5G antenna, a Low Noise Amplifier, and an RF detector IC. All RF designs were simulated in ANSYS HFSS to ensure both printed and spray coated features produced the optimal RF response. Initial conducting elements were printed using a Nordson Pro4 direct-write, micro-pen dispensing system with final designs applicable to transition to an Optomec 5x as the processes/models are finalized for conformal geometries. The spray-coated fluoropolymer was shown to provide an RF transparent coating to improve component adhesion (i.e., capacitors, resistors, IC chips) and protect printed traces from external effects such as oxidation, without adversely affecting the RF performance. Also examined were additional 5G antenna designs on novel/alternative substrates (UHMWPE) where the spray coated polymeric layer was shown to be useful as a base layer in order to provide a smooth, "printable" surface (i.e., wettable surface) for printed RF antenna and waveguide systems. Additionally, the spray coated fluoropolymer was enabled full structural encapsulation through the deposition of subsequent layers.

This research is aimed to provide insight into how RF circuit design can be modified with new design constraints, substrates, and materials for a printed/flexible form factors while still maintaining high levels of performance. As such, we aim to present work that enables printed RF design/test to move from single component analysis to complete RF systems with integrated RF ICs, RF structures, DC components, DC ICs, novel substrates, and novel coatings in a variety of form factors.

4:30 PM EQ11.05.09

Optimization of Flexible Supercapacitors with Gel Polymer Electrolytes [Hamidreza Fallahtafti](#), Banafsheh Hekmatnia, Haleh Ardebili and Alamgir Karim; University of Houston, United States

Flexible energy storage devices such as supercapacitors (SCs) and lithium-ion batteries (LIBs) have attracted great attention for promising performances, such as high longevity and cycle life, fast charging-discharging rate, and high-power density. As a result, all-solid-state supercapacitors (ASSCs) are a great candidate for many applications, including wearable electronic devices, portable devices, and electric vehicles (EVs).

In this study, a high-performance flexible supercapacitor with gel polymer electrolyte was developed with optimal design, fabrication, mechanical, safety and electrochemical performance. The optimum ratio of materials was determined for durable, long cycle life, high performance, flexible, and environmentally friendly supercapacitors (SCs). A flexible thin film of electrolyte was fabricated with a thickness of 475 μm . Since the electrodes were composed of nanocarbon with a high specific area, the fabricated supercapacitor was lightweight, flexible, and low cost with high electrochemical performances.

Moreover, comprehensive mechanical testing of the electrolyte, such as stretchability, flexibility, yield stress, and ultimate tensile strength (UTS), was conducted by the MARK-10 apparatus. As a result, the elongation of the gel polymer electrolyte (GPE) was 355%. Besides flexibility, different design strategies were adopted to provide additional stretchability in the supercapacitors.

Furthermore, electrochemical tests, including cyclic voltammetry (CV) and galvanostatic charge and discharge (GCD), has been conducted to evaluate the performance of the fabricated supercapacitors. In addition, SEM, FTIR, and AFM were used to characterize the change in the performance while in different bending angles.

SESSION EQ11.06: Materials and Deposition Techniques for High-Frequency Thin-Film Electronics III

Session Chairs: Hans Kleemann and Shu-Jen Wang

Monday Morning, December 6, 2021

EQ11-Virtual

8:00 AM *EQ11.06.01

Solution-Processed Semiconducting Carbon Nanotubes for Transistors and Complementary Circuits [Jana Zaumseil](#); Heidelberg University, Germany

Large volumes of highly purified dispersions of semiconducting single-walled carbon nanotubes have become readily available through polymer-wrapping and shear-force mixing. Such nanotube inks can be further stabilized by small molecule additives and thus enable the reproducible deposition (e.g., by aerosol jet printing, spincoating or zone-casting) of semiconducting nanotube layers of variable thickness from sparse to dense. These networks are employed in thin film transistors with high hole and electron mobilities ($5\text{-}50\text{ cm}^2\text{V}^{-1}\text{s}^{-1}$). Through intentional doping it is possible to create purely n-type or p-type transistors with on/off current ratios exceeding 10^7 , which are suitable for complementary and high-frequency circuits. Here, we will discuss the basic charge transport properties and limitations of nanotube networks, novel n-dopants as well as routes toward low-voltage circuits on flexible substrates.

8:30 AM *EQ11.06.02

Factors Limiting Charge Transport in Highly Doped Conducting Polymers [Henning Siringhaus](#); Cambridge University, United Kingdom

Doping of semiconducting polymers has seen a surge in research interest driven by emerging applications in sensing, bioelectronics and thermoelectrics. A recent breakthrough was a doping technique based on ion-exchange, which separates the redox and charge compensation steps of the doping process. The improved microstructural control this process allows enables us for the first time to systematically address a longstanding but still poorly understood question: what limits the electrical conductivity at high doping levels? Is it the formation of charge carrier traps in the Coulomb potentials of the counterions, or is it the structural disorder in the polymer lattice? Here, we apply ion-exchange doping to several classes of high mobility conjugated polymers and identify experimental conditions that achieve near 100% doping efficiency under degenerate conditions with nearly 1 charge per monomer. We demonstrate very high conductivities up to 1200 S/cm in semicrystalline polymer systems, and show that in this regime conductivity is poorly correlated with ionic size, but strongly correlated with paracrystalline disorder. This observation, backed by a detailed electronic structure model that incorporates ion-hole and hole-hole interactions and a carefully parameterized model of disorder, indicates that trapping by dopant ions is negligible, and that maximizing crystalline order is critical to improving conductivity.

9:00 AM *EQ11.06.03

Development of High Performance Metal Halide and Perovskite Transistors Yong-Young Noh; Pohang University of Science and Technology, Korea (the Republic of)

Achieving high-performance and reliable transistors based on metal halide perovskites has been pursued for decades yet remains challenging because of the absence of highly qualified perovskite channels. Herein, we report inorganic perovskite thin-film transistors with exceptional performance using high-crystallinity and uniform cesium-tin-triiodide-based semiconducting layers with moderate hole concentrations and superior Hall mobilities, which are enabled by the judicious engineering of film composition and crystallization. The optimized devices exhibit high field-effect hole mobilities of over 50 square centimeters per voltage-second and large current modulation greater than 10^8 as well as high operational stability and reproducibility. Our results represent a key step towards employing printable perovskite semiconductors in cost effective transistors and circuits.

9:30 AM EQ11.06.04

Stable Twisting of Carbon Nanotubes into Semiconducting Chiralities by Low-Work-Function Contact Jiangtao Wang¹, Gregory Pitner², Xiang Ji¹, Jiadi Zhu¹, Jinchi Han¹, Han Wang², Lain-Jong Li² and Jing Kong¹; ¹Massachusetts Institute of Technology, United States; ²TSMC Corporate Research, United States

To realize the projected speed, efficiency, and scalability of carbon nanotube (CNT) based electronics, the key fundamental challenge is the growth of horizontally-aligned arrays of defect-free CNT with a semiconducting purity >99.99%. Until recently, selective CNT synthesis methods utilized either the native free energy or native stability difference between the growth of semiconducting CNTs (s-CNTs) and metallic CNTs (m-CNTs). However, such native energy separation is too small to sufficiently suppress the random thermal fluctuation at the 800-900°C growth temperature and fails to delivery semiconducting carbon nanotubes with required >99.99% s-CNT purity. Here we report an approach to open a larger gap in the free energy between m-CNT and s-CNT during both epitaxial growth and chirality change by contacting growing CNTs with low work-function electrodes such as Hafnium Carbide or Titanium Carbide. First, the remarkable difference of quantum capacitance between m-CNT and s-CNT separates the CNT free energy plot of CNTs into two branches. Second, when in contact with low work-function electrodes CNTs and tipped catalysts will be negatively charged (n-doped) due to the electrode work-function, which causes an increase in free energy gap between m-CNTs and s-CNT and a reduction of the twisting barrier from m-CNT to s-CNT. Third, the large aspect ratio of CNTs enables a strong local electric field generated by the charge stored at the CNT tip to contribute a prominent electrostatic effect that greatly affects the total free energy change. As a result, stable twisting of horizontally aligned CNTs from initially mixed m-CNT and s-CNT chiralities to s-CNT chiralities is achieved by applying a weak perturbation (10V/mm-alternating electric field). These results validate that a lower work-function contact does result in a higher selectivity towards s-CNTs at a reduced applied electric field. Our observations also open a possibility to select the catalytic pathway through the contact engineering and will pave the way for practical applications of CNT electronics.

9:45 AM EQ11.06.05

Large Area Doped Rubrene Thin-Film Electronics Ilia Lashkov, Shu-Jen Wang, Hans Kleemann and Karl Leo; Technische Universität Dresden, Germany

Organic and molecular electronics is a promising field for many applications, particularly flexible electronics [1] [2], since it allows the processing of electronic circuits at low temperatures on a variety of substrates, including flexible sheets [3]. Despite continuous improvements in the charge carrier mobility of both n- and p-type thin-film transistors, the performance of these devices is not yet attractive enough for commercial applications. A substantial hurdle to the realization of effective organic-based analog and digital circuits is the lack of scalable high-charge-carrier-mobility organic semiconductors with low contact resistances in transistors [4]. Devices based on organic single-crystalline rubrene with superior mobility of over $10 \text{ cm}^2 \text{V}^{-1} \text{s}^{-1}$ have been previously shown [5]. However, such single crystals are difficult to grow and handle and are less suited for integrated electronics, which limits the commercial attractiveness of this material. Here, we demonstrate vacuum-processed and, subsequently, thermally annealed highly crystalline rubrene thin films which enable the realization of large-area high-frequency circuits. We fabricate organic thin-film transistors (OTFTs) based on highly ordered rubrene films with different underlayers and reach charge carrier mobilities over $5 \text{ cm}^2 \text{V}^{-1} \text{s}^{-1}$ (for a channel length of $L = 100 \text{ }\mu\text{m}$ and width of $W = 1000 \text{ }\mu\text{m}$). Moreover, we significantly reduce the contact resistance of the transistors down to $1 \text{ k}\Omega \text{ cm}$ by utilizing contact doping [6]. We analyze the uniformity of the crystals and show that such rubrene thin-film transistors are well suited for large-area electronics.

[1] H. Sirringhaus, *Adv. Mater.* **2014**, 26, 1319.

[2] B. Lussem, C-M. Keum, D. Kasemann, B. Naab, Z. Bao, K. Leo, *Chem. Rev.* **2016**, 116, 22, 13714.

[3] B. Lim, H. Sun, J. Lee, Y-Y Noh, *Sci Rep.* **2017**, 7, 164.

[4] J-W. Borchert, B. Peng, F. Letzkus, J-N. Burghartz, P. Chan, K. Zojer, S. Ludwigs, H. Klauk, *Nat Commun.* **2019**, 10, 1119.

[5] J. Takeya, M. Yamagishi, Y. Tominari, R. Hirahara, Y. Nakazawa, *Appl. Phys. Lett.* **2007**, 90, 102120.

[6] S-J. Wang, M. Sawatzki, H. Kleemann, I. Lashkov, D. Wolf, A. Lubk, F. Talnack, S. Mannsfeld, Y. Krupskaya, B. Büchner, K. Leo, *Mat. Today Phys.* **2021**, 17, 100352.

8:00 AM EQ11.07.01

High-Speed Solution-Processed Organic Single-Crystal Transistors for Active-Matrix Flexible Mini-LED Displays Jun Takeya^{1,2,3} and Tatsuyuki Makita^{1,3}; ¹The University of Tokyo, Japan; ²Organo-Circuit Inc., Japan; ³Pi-Crystal Inc., Japan

Images such as large mammals have impacted psychology of human species since the beginning of their history. Indeed, demand for technologies of meter-size large-area digital advertisement has been essentially very large, though the current devices are not well-prevalued because of high cost, large weight, and high power consumption. We developed a method to produce LED pixels on printed backplanes of active matrices based on high-mobility organic semiconductors. Due to the light-weight film-based materials of low-cost printed organic active matrices, which is also very effective in reducing power consumption, the present technology meets the requirement for the large-area digital signage. The present devices are formed on a sheet of PEN film with the thickness of 0.1 mm, so that the large-area movies can be shown hung on the ceilings of buildings or under mobile drones.

High-performance solution-processed transistors are employed with recently developed technologies of ultrathin organic semiconductor single crystalline films suitable for large-area production with low energy consumption. The films are easily formed to large area from solution at relatively low temperature at 80 degrees centigrade [1]. Extremely thin crystal films are controllably grown to a few molecular layers with the thickness of only 10 nm, so that material cost can be only 0.01 USD per cm². Such prospect bears increasing reality because of recent research innovations in the field of material chemistry, charge transport physics, and solution processes of printable organic semiconductors. Particularly important are new processing technologies for continuous growth of the organic single-crystalline semiconductor "wafers" from solution and for lithographical patterning of semiconductors and metal electrodes. The active-matrix transistors are successfully formed with 60-Hz frame rate and more than 1-mA on current to illuminate the LEDs, thanks to the high carrier mobility as high as 10 cm²/Vs in the single-crystal organic semiconductors.

[1] A. Yamamura, J. Takeya et al., *Adv. Electron. Mater.* 3, 1600456 (2017); S. Watanabe, J. Takeya et al., *Communications Physics* 1, 37 (2018); A. Yamamura, S. Watanabe, J. Takeya et al., *Sci. Adv.* 4, eaao5758 (2018); T. Makita, S. Kumagai, A. Kumamoto, M. Mitani, J. Tsurumi, R. Hakamatani, M. Sasaki, T. Okamoto, Y. Ikuhara, S. Watanabe, and J. Takeya, *PNAS* (2019), DOI.org/10.1073/pnas.1909932116; T. Sawada, A. Yamamura, M. Sasaki, K. Takahira, T. Okamoto, S. Watanabe and J. Takeya, *Nat. Commun.* volume 11, Article number: 4839 (2020) DOI.org/10.1038/s41467-020-18616-0

8:15 AM *EQ11.07.02

Establishing a Process Design Kit for Low Contact Resistance OTFT with MHz Switching Frequencies Simon Ogier, Dan Sharkey and Alejandro Carreras; SmartKem, United Kingdom

Organic thin-film transistor (OTFT) devices have been fabricated using a maximum processing temperature of 80 degrees Celsius, rendering them compatible with a range of low-cost, transparent and flexible substrates. Charge mobility at a transistor channel length (L) of 5 μm is 3cm²/Vs. Such performance is compatible with a wide range of voltage or current driven display device applications fabricated on plastic or glass. A small variation of mobility with channel length suggests a very low contact resistance (~100 Ohms), enabling good use of channel length scaling to increase operating frequencies in digital circuits. Current driven applications, such as local dimming mini-LED backlights, AMOLED or voltage driven displays and sensor arrays have been demonstrated using SmartKem's OTFT materials. These are fabricated using process techniques common to flat panel display backplanes (sputtering, photolithography, dry/wet etching), providing a low cost of manufacture per unit area substrate.

The design of digital circuitry using transistor devices is aided by electronic design automation (EDA) tools which enable the accurate layout of a circuit using a process technology helping to deliver a consistent device performance. This presentation describes work to establish a process/technology design kit (PDK/TDK) for devices using the SmartKem OSC material stack. The PDK contains the device dimensions, overlaps, etc relating to the OTFT device and these are coded in software into parameterizable cells (p-cells). Device modelling and circuit simulations are used to predict electrical performance of the designs prior to tape out of the mask set for fabrication. PDK roadmaps are presented relating to improvements in device operating voltage and fabrication techniques, showing the potential for achieving circuits with higher operating frequency at a lower voltage in subsequent batch runs.

8:45 AM *EQ11.07.03

Flexible Sub-Micron Thin-Film Transistors Based on Oxide Semiconductors Niko Münzenrieder, Giuseppe Cantarella and Luisa Petti; Free University of Bozen-Bolzano, Italy

Wearable devices seamlessly integrated into everyday objects and able to conform to the movement of soft artificial and natural surfaces are considered one of the next major steps in the development of electronics for consumer products and industrial applications. The main application scenarios of such imperceptible electronics include the collection of data from the environment or the interaction with humans, to enable e.g. smart personalized healthcare devices or efficient Industry 4.0 processes. This requires the wireless transmission of data and the conditioning of a variety of analogue sensor signals using flexible, cheap, and environmentally-friendly components.

Thin-film transistors (TFTs), based on oxide semiconductors, most prominently amorphous Indium-Gallium-Zinc-Oxide (IGZO), and fabricated on large-area polymer substrates, are a suitable approach to fabricate active electronics if high bendability and electrical performance are required simultaneously. Such devices are investigated since more than a decade, hence their DC performance is well understood and reliable fabrication processes for systems, such as display backplanes, are established. However, the realization of highly scaled sub-micron devices on thermally and mechanically instable plastic substrates, together with the optimization of their analogue and high-speed performance, is less investigated. Here, various fabrication techniques and device structures, as well as theoretical models to predict the AC performance, resulting in flexible IGZO TFTs with channel length as short as 160 nm, are presented. Their AC performance is analysed, and it is discussed how analogue integrated circuits, such as amplifiers, buffers, or multiplexers made from these TFTs, can be used to realize front-end conditioning circuits for wearable sensors.

The IGZO TFTs presented here are manufactured on free standing polyimide foils. These TFTs are fabricated using high-k atomic layer deposition (ALD) grown Al₂O₃ insulating and passivation layers, metallic contacts, and RF sputtered IGZO with a stoichiometric composition of In:Ga:Zn:O = 1:1:1:4. The maximum process temperature used is 150°C. They exhibit state of the art DC performance including field effect mobilities up to ≈15 cm²/Vs, on-off current ratios >10⁸, subthreshold swings of ≈125 mV/dec., and threshold voltages allowing the operation of devices and circuits at voltages <5 V. The TFTs also stay fully functional when exposed to tensile or compressive strain induced by bending radii as small as 50 μm.

Here, the AC performance of these TFTs will be shown. All devices are designed with ground-signal-ground contact pads to enable their reliable AC characterization using a two-port network analyser. To minimize the channel length and hence to maximize the operation frequency of flexible IGZO TFTs, different fabrication methods are evaluated. These include conventional bottom gate TFTs, transistors structured by self-alignment, focused ion beam milling, or direct laser writing, as well as vertical TFTs and double gate TFT geometries.

The characterisation of all these devices showed that conventional bottom gate TFTs, with a channel length of 1 μm, and gate overlaps of 5 μm can exhibit a transit frequency up to 47 MHz. This value is in agreement with corresponding transconductance and gate capacitance measurements. At the same time, the AC performance is limited by the lateral dimensions of the TFTs. It was found that although traditionally smaller feature structures are beneficial, in the case of short and flexible IGZO TFTs, a careful optimisation of the capacitances and contact resistances is required. Consequently, the shortest transistors

do not exhibit the highest frequencies, but a transit frequency of 135 MHz is demonstrated for 500 nm long self-aligned transistors even while exposed to 0.5% tensile strain. These in turn, enable the fabrication of fully flexible circuits able to operate in the megahertz regime.

9:15 AM *EQ11.07.04

Organic Thin-Film Transistors for High Performance Logic Circuits—Realization of Short Channel, High Mobility, Low Contact Resistance and Threshold Voltage Control Masatoshi Kitamura and Yoshiaki Hattori; Kobe University, Japan

The organic thin-film transistor (TFT) is a key device for flexible electronics. The field-effect mobility for p-channel TFTs has reached up to $10 \text{ cm}^2 \text{ V}^{-1} \text{ s}^{-1}$, which is close to those of InGaZnO TFTs used in flat panel displays. We have been trying to realize short channel, high mobility organic TFTs for high frequency operation, and control the threshold voltage for actual applications.

A key issue for realization of short channel, high mobility organic TFTs is reducing contact resistance between organic channel materials and contact electrodes. We have used contact electrodes modified with benzenethiol derivative to realize low contact resistance. The modification demonstrated wide work function tuning for contact electrodes. The measured work function of modified Au electrodes was in a relatively wide range between 4.24–6.02 eV. We have applied modified electrodes to bottom-contact organic TFTs. The organic TFT having C10 DNNT as a channel material exhibited very high channel conductance. This is due to the low contact resistance, which is about $20 \Omega \text{ cm}$ under a gate voltage of -10 V .

We have used modified electrodes for high frequency operation in organic TFTs. The current-gain cutoff frequency was measured for evaluation of operational frequency in organic TFTs. The cutoff frequency was estimated by direct measurement of the gate and drain modulation currents. The measured cutoff frequencies for both C60 and pentacene TFTs increase consistently with reducing channel length. Cutoff frequencies of about 28 and 11 MHz were obtained from C60 and pentacene TFTs with a channel length of $2 \mu\text{m}$, respectively.

The threshold voltage control is an important issue for actual application. We have reported the threshold voltage control in organic TFTs realized by oxygen plasma treatment. Exposing a SiO₂ gate dielectric surface in organic TFTs to oxygen plasma shifted the threshold voltage to positive gate voltage. The threshold voltage shift depended on plasma treatment time, AC power for plasma generation, and gate dielectric thickness. The threshold voltage change was explained by negative charges induced on and/or near the surface of the gate dielectric. The threshold voltage change on the order of 1 V was roughly proportional to plasma treatment time. The predictable change enables the control of threshold voltage in this range. In actual, we used organic TFTs with controlled threshold voltages for application to logic circuits. Operation of logic inverters consisting of organic TFTs with different threshold voltages was demonstrated as an application of TFTs with controlled threshold voltage. Furthermore, a ring oscillators consisting of organic inverters operated at supply voltages in the range of 15–25 V. Combination of techniques about short channel, high mobility, low contact resistance, and threshold voltage control will realize high performance circuit consisting of organic TFTs.

SESSION EQ11.08: Flexible Electronics – Fabrication and Applications
Session Chairs: Henning Sirringhaus and Shu-Jen Wang
Wednesday Morning, December 8, 2021
EQ11-Virtual

8:00 AM *EQ11.08.01

Circuit Design Approaches for Different Thin-Film Technologies Kris Myny¹, Hikmet Çeliker¹ and Wim Dehaene²; ¹imec, Belgium; ²KU Leuven, Belgium

The necessity of higher operation speed in electronic circuits is inevitable as there is a big amount of data being produced and transferred in our daily lives through different ways of digital communication. This argument is valid for silicon based integrated circuits as well as for thin-film-transistor based integrated circuits. Improvements in device processes have equal importance as circuit design techniques in order to achieve high frequency operation within the field of thin film transistors (TFT). In this invited presentation, we will provide an overview of different circuit design approaches specifically focusing on fast operating thin-film circuits combined with two main technology aspects: scaling and higher mobility materials.

Transistor downscaling has been proven to be key for Si CMOS electronics to obtain better figures of merit and consequently improve the operating speed of the integrated circuits. A analogy can be made for TFT-based circuits, whereby the minimum achievable channel length of TFTs on flexible substrates is mainly depending on photolithography accuracy, limiting it in many cases to μm -ranges. A self-aligned amorphous Indium-Gallium-Zinc-Oxide (a-IGZO) TFT technology allows n-type only TFTs to have a channel length down to $1.5 \mu\text{m}$. Thanks to the self-aligned structure, overlap the capacitance between source/drain and gate of a TFT are mostly eliminated. These have been instrumental in demonstrating an ISO14443-A compatible flexible NFC barcode tag operating at 13.56 MHz [1].

Besides scaling of the transistor footprint, upscaling of the number of routing metals also helps increasing the operation speed and reducing footprint of thin-film ICs. Combining the design strategies already available for unipolar technologies with these process developments, performance and robustness of digital thin-film ICs have been increased continuously. One example is a Two-Stage Resistor-Load Logic standard cell library for digital applications [2]. We have demonstrated that this logic topology shows better speed performance than the conventional one-stage resistor-load topology. It is also more robust against the impact of global variability. To demonstrate this, a 4-bit digital multiplier using the new topology with $0.8 \mu\text{m}$ channel length TFTs is fabricated. It shows a speed performance up to 1 MHz.

The second important technology factor in the performance of thin-film ICs is the semiconductor material. For instance, Low-temperature polysilicon (LTPS) is attractive because of its higher mobility and the availability of complementary transistors. Because of its polycrystalline structure, minimum channel length of LTPS TFTs is larger than a-IGZO devices. In the presentation, we will show a performance comparison between logic gates realized with a-IGZO and LTPS technologies. Having complementary transistors enables circuit designers to use similar techniques as used in silicon CMOS designs. To demonstrate the capabilities of LTPS, we will also compare the measurement results of two different flip-flop architectures in terms of speed performance and power consumption.

References:

[1] Myny, Kris, et al. "15.2 A flexible ISO14443-A compliant 7.5 mW 128b metal-oxide NFC barcode tag with direct clock division circuit from 13.56 MHz carrier." 2017 IEEE International Solid-State Circuits Conference (ISSCC). IEEE, 2017.

[2] Celiker, Hikmet, et al. "Two-Stage Resistor-Load Logic for Digital Applications on Flexible Substrates" 2021 IEEE International Conference on Flexible and Printable Sensors and Systems (FLEPS). IEEE, 2021. (to be published)

Acknowledgement - This work has received funding from the European Research Council (ERC) under the European Union's Horizon 2020 research and innovation programme under grant agreement No 716426 (FLICs project).

8:30 AM EQ11.08.02

Organic-Inorganic Nanomaterials Based Piezoelectric Nanogenerator for Self-Powered Structural Health Monitoring Md. Masud Rana^{1,2}, Asif

Abdullah Khan^{1,2}, Guangguang Huang¹, Nanqin Mei¹, Resul Saritas^{1,2}, Boyu Wen^{1,2}, Steven Zhang¹, Weiguang Zhu¹, Peter Voss³, Eihab-Abdel Rahman^{1,2}, Zoya Leonenko¹, Shariful Islam³ and Dayan Ban^{1,2}; ¹University of Waterloo, Canada; ²Waterloo Institute for Nanotechnology, Canada; ³Shimco North America Inc, Canada

Recently Structural Health Monitoring (SHM) is being widely assessed by the aerospace industry to enhance the safety and consistency of aircraft structures. The use of built-in sensor networks coupled with continuous structural integrity monitoring on an aircraft can provide vital real-time information concerning the condition, damage state, and/or service environment of the structure, which could significantly reduce the cost compared to scheduled manual inspection. Sustainable and durable piezoelectric nanogenerators (PENGs) with good flexibility, high performance, and superior reliability under inconsistent environments are a promising candidate for modern Wireless Sensor Network (WSN)-based SHM application. Numerous materials have been used to fabricate PENGs such as lead zirconate titanate (PZT), barium titanate (BaTiO₃), ZnO, Na/KNbO₃ and ZnSnO₃ nanoparticles have great piezoelectric coefficients and superior energy conversion efficiencies. However, research progress is often impeded due to fragility, heavyweight, low durability, complex synthesis and fabrication process, and high toxicity of many of these materials. This research demonstrates the prospect of comprehending a self-powered wireless sensing system based on a piezoelectric nanogenerator (PENG) which is prominently anticipated to address the aforementioned issues. Here we present a flexible self-powered PENG sensor for the quantitative measurement of abnormal vibration based on WSN with the distinctive mesoporous structure via a drop-cast technique, and successfully demonstrated proof-of-the-concept applications. The well-dispersed and controllable size of ZnO nanoparticles (NPs) endows the composite film with the advantages of ZnO NPs and the virtues of the poly(vinylidene fluoride) (PVDF) matrix. A high voltage electrical poling of the porous PVDF film was performed with an electric field of 70-120 V/μm-1 for 5-6 hours with a DC voltage of 0-6 kV. No short circuit or noticeable voltage fluctuation was detected up to the maximum voltage of 6 kV. The poled porous PVDF composite films were sandwiched between electrodes. For the characterization purpose, the electrical connections were made from both of the top and bottom electrodes by very thin and flexible copper conductors. The self-powered wireless structural health monitoring system is a combination of an energy generation part, a part of sensing, and an integrated circuit (IC) part. A custom-made IC is placed on top of the PENG device, which is driven by the PENG device, monitors the surrounding environment automatically and transfers the signal to a receiver wirelessly. The performance of PENG based on the porous PVDF is systematically studied. The open-circuit voltage of the PENG device of 50wt.% ZnO was measured within a frequency range from 10Hz to 50Hz (varied frequency by Vibration Research's VR9500 Revolution unit) to examine the feasibility which is close to oscillation frequencies under a practical environment. The peak-to-peak output open-circuit voltage of the PENG was measured to be 84.5V at 30 Hz frequency. The peak output power ($P=I^2R$) 78μW and the corresponding peak power density of 12μW/cm² were achieved at a load resistance of 7MΩ, which is sufficient for driving the entire system. Such a PENG device produces electrical energy from the shaker vibration, and charge an input capacitor (1 μF) through a rectifier circuit. When the charging voltage of the input capacitor reaches ~ 5V, which was regulated by a zener diode, it discharges energy through a buck converter module to an output storage capacitor (220 μF). The charging and discharging cycle of the input capacitor continues until the output capacitor is charged up to ~ 3.1V, and by then, it empowers the whole system and sends the signal to a remote receiver. These results demonstrate the great potential of porous PVDF based film for the simple and cost-effective fabrication of high-performance piezoelectric energy harvesting devices.

8:45 AM EQ11.08.03

Thermal Management of Flexible Electronics Enabled by Programmable Liquid Metal Microstructures A B M Tahidul Haque, Ravi Tutika and Michael D. Bartlett; Virginia Polytechnic Institute and State University, United States

Emerging flexible electronics technologies including wearable biodevices, soft robotics, and stretchable sensors demand efficient thermal management to dissipate and distribute heat. One significant challenge in these systems is that the low thermal conductivity of flexible substrates limits device functionality by accumulating heat which leads to deteriorated charge transport and unstable electro-mechanical performance. To overcome these challenges, liquid metal (LM) dispersed elastomers have shown unique combinations of soft mechanical response with exceptional electrical and thermal functionalities. However, approaches to control LM microstructure in composites are needed to further enhance properties to enable heat dissipation and improved interfacial compatibility in flexible electronic systems. Here, we present an innovative approach to control LM microstructure in soft composites to enhance heat distribution while maintaining the soft, mechanical characteristics needed for flexible electronics. Through a mechanical reconfiguration and thermal relaxation process, we orient and elongate LM droplets in elastomers at high concentration (up to 70% by volume). Through this microstructural control in soft composites, we demonstrate a material which simultaneously achieves a high thermal conductivity of 13 W/mK ($> 70 \times$ increase over polymer matrix) and low modulus (< 1.0 MPa) in stress-free conditions. As a lightweight, conductive, and transferrable medium for flexible substrates, we also extend the LM morphology programming concept for micron sized thin films. The thickness tunable (30-70 μm) thin films are composed of disk-shaped LM droplets which can be electrically activated for circuit integration. This enables high stretchability (strain limit $> 700\%$) and metallic electrical conductivity (sheet resistance $< 0.1 \Omega/\text{sq}$) in soft films. We demonstrate these materials for rapid heat dissipation of high-power devices on flexible substrate, wearable robotics, and electronics integrated flexible circuits. We envision that the material, process, and device development strategy using the LM programmed composites will enable next-generation high-frequency flexible transistors, stretchable electronics, and soft robotics.

9:00 AM EQ11.08.04

Flexible Triboelectric Laminate for Mechanical Energy Harvesting as an Energy Source for Electronics Kaspars Malnieks, Andris Sutka, Artis Linarts and Linards Lapčinskis; Riga Technical University, Latvia

Triboelectric generator (TEG) devices have attracted considerable interest in the field of mechanical energy harvesting due to their low weight and mechanical softness. The charge transfer in TEG devices has been attributed to electron transfer, ion transfer, and material transfer [1] with the discussions still ongoing. There are many innovative TEG devices from low-cost materials presented in the literature for mechanical energy harvesting from human motion, vibrations, wind, water flow, and waves.[2-4] However, all TEG devices as a rule contain movable parts to magnify the dipole moment between triboelectric charges obtained from contact-separation. This specific requirement complicates the integration of TEG devices into energy harvesting systems. Alternative soft materials that exhibit bulk electromechanical response are piezoelectric polymers and their nanocomposites. For example, fluoropolymers such as poly(vinylidene fluoride) (PVDF) and PVDF co-polymers exhibit the piezoelectric d_{33} coefficient as high as 20–28 pC N⁻¹ due to large dipole polarization between hydrogen and fluorine atoms.[5] However, to obtain high electromechanical response, the poling procedure at high electric fields (10–30 kV cm⁻¹) for prolonged periods (24 h or more) has to be applied. The necessity to apply high electric field limits moreover, the alignment of dipoles in the polymer is not stable and depolarization of PVDF is often observed over the course of days even at room temperature. Herein we are presenting the triboelectric laminates where the polymer bilayers with different triboelectric properties are stacked to form laminates, together with the separator mesh between each bilayer and for an electrodes we use flexible polyisoprene conductive carbon black composite. The proposed design ensures the formation of aligned macroscopic dipoles across the volume of triboelectric laminate and provides the desired electromechanical response. When the force is applied, the triboelectric charges on opposite surfaces of bilayers are formed due to triboelectrification. The mesh provides the macroscopic dipole formation between the distinct triboelectric layers. Different triboelectric surface properties of polymer bilayers result in dipole alignment. Triboelectric laminate generates the open-circuit voltage (V_{OC}) of 29 V and short-circuit current (I_{SC}) of 15 nA. Volumetric energy density of 21.13 μJ cm⁻³ and a peak average power density of 46.19 μW cm⁻³ are observed. Triboelectric laminate shows an effective piezoelectric constant d_{33} of 9.83 pC N⁻¹, higher than reported for piezoelectric polymer like nylon-11 and there is no need to apply an external electric field to polarize the material and to observe the piezoelectric response. In addition, the electromechanical response of the triboelectric laminate does not disappear over

time. The triboelectric laminate is produced from cheap, mechanically flexible materials that can be produced in large quantities.

This work has been supported by the European Regional Development Fund within the Activity 1.1.1.2 “Post-doctoral Research Aid” of the Specific Aid Objective 1.1.1 “To increase the research and innovative capacity of scientific institutions of Latvia and the ability to attract external financing, investing in human resources and infrastructure” of the Operational Programme “Growth and Employment” (No.1.1.1.2/VIAA/3/19/404)

- [1] S. Lin, L. Xu, C. Xu, X. Chen, A. C. Wang, B. Zhang, P. Lin, Y. Yang, H. Zhao, Z. L. Wang, *Adv. Mater.* 2019, 31, 1808197.
- [2] Z. Tian, J. He, X. Chen, T. Wen, C. Zhai, Z. Zhang, J. Cho, X. Choua, C. Xue, *RSC Adv.* 2018, 8, 2950.
- [3] L. Zhao, L. Liu, X. Yang, H. Hong, Q. Yang, J. Wang, Q. Tang, *J. Mater. Chem. A* 2020, 8, 7880.
- [4] C. Rodrigues, D. Nunes, D. Clemente, N. Mathias, J. M. Correia, P. Rosa-Santos, F. Taveira-Pinto, T. Morais, A. Pereira, J. Ventura, *Energy Environ. Sci.* 2020, 13, 2657.
- [5] K. S. Ramadan, D. Sameoto, S. Evoy, *Smart Mater. Struct.* 2014, 23, 033001.

9:05 AM EQ11.08.05

Low Temperature Crystallization of Ge Thin Films for Channel Layers of Thin-Film Transistors by Gold-Induced Layer Exchange [Narin Sunthornpan](#), Kenjiro Kimura and Kentaro Kyuno; Shibaura Institute of Technology, Japan

Fabricating high quality semiconductor thin films on plastic substrates is becoming increasingly important which is crucial in realizing high-speed electronic devices on plastic substrates. Germanium (Ge) thin film is one of the promising candidates among semiconductors which can be fabricated on flexible substrates at low temperature. Ge has many excellent properties such as higher electron and hole mobilities and smaller energy bandgap compared to silicon (Si), which is advantageous in applications such as thin-film transistor, solar cell, and next generation MOSFET. Metal-induced crystallization (MIC) technique by gold (Au) catalyst is one of the promising candidates to crystallize Ge films because of its low crystallization temperature. Nevertheless, further knowledge about the crystallization process is needed to improve the quality of the film. In this work, the Au layer thickness dependence of the crystallization process has been investigated in detail. It is found that the grain size, crystal orientation and crystallization temperature are sensitive to the Au layer thickness. Ge films crystallized with thinner Au films show lower crystallization temperature and higher (111) crystal orientation. A hole mobility as high as 50 cm²/Vs is achieved by annealing a Ge(30nm)/Au(9nm) bilayer at 220 °C, which is low enough to fabricate electronic devices on plastic substrates such as polyimide.

The Au and Ge films were fabricated by RF magnetron sputtering process on Si wafer with 100 nm thermally grown oxide (SiO₂) layer. Au films ranging from 9 to 34 nm were deposited on the wafer and subsequently Ge films (27 and 55 nm) were deposited on the Au layer. Au/Ge bilayers were crystallized by using MIC technique at 220 °C under N₂ ambient. Structural properties were examined by X-ray diffraction (XRD), scanning electron microscope (SEM) and electron backscattered diffraction (EBSD). Ge films crystallized with thinner Au film showed higher Ge (111) orientation, which was confirmed by XRD and EBSD observation. From the Hall effect measurement, p-type behavior and hole mobility as high as 50 cm²/Vs was achieved for the Ge film crystallized by annealing a Ge(30nm)/Au(9nm) bilayer film. Transistor action was also demonstrated successfully by using these films as channel layers. These findings will open up the possibility to apply MIC technique to crystallize Ge thin film at temperatures as low as 220 °C, which is low enough to fabricate thin-film semiconductor on various inexpensive plastic substrates.

9:10 AM *EQ11.08.06

Scalable Growth of Doped Organic Thin-Film Crystals for High Frequency Applications [Shu-Jen Wang](#), Michael Sawatzki, Hans Kleemann and Karl Leo; TU Dresden, Germany

The current generation of organic electronic devices such as the established OLED technology are based on amorphous thin-films with low carrier mobility due to their disordered molecular orientation. For high frequency device operation, higher carrier mobility is generally required. Here, we present the growth of highly crystalline organic thin-film crystals using vacuum deposition technique where the thickness of the films can be precisely tuned using epitaxy [1, 2]. In addition, organic dopants can be incorporated into the thin-film crystals during the deposition process that allow us to tune the properties of the individual layers. Finally, we integrate these doped highly crystalline thin films into devices to enable novel applications.

- [1] S. Wang, M. Sawatzki, H. Kleemann, I. Lashkov, D. Wolf, A. Lubk, F. Talnack, S.11 Mannsfeld, Y. Krupskaya, B. Büchner, K. Leo, *Mater. Today Phys.* **2021**, 17, 100352.
- [2] M. Sawatzki, H. Kleemann, B. Boroujeni, S. Wang, J. Vahland, F. Ellinger, K. Leo, *Adv. Sci.* **2021**, 8, 2003519.

SESSION EQ11.09: Design of UHF Printed, Flexible Transistors, Circuits and Characterization II
Session Chairs: Hans Kleemann and Jörn Vahland
Wednesday Morning, December 8, 2021
EQ11-Virtual

10:30 AM *EQ11.09.01

Toward Accurate Prediction of Transit Frequency in Organic Transistors [Chang-Hyun Kim](#); Gachon University, Korea (the Republic of)

In this presentation, an analytical theoretical description of the ac transit frequency of organic field-effect transistors is proposed. The model is built upon an advanced physical description of the contact resistance as a key mathematical component. Such a treatment self-consistently and predictively correlates the transit frequency to a number of materials, geometrical, and operational parameters. By navigating a broad parametric space, it is found that the ambitious gigahertz operation is observable only in highly downscaled devices, and the intrinsic carrier mobilities and charge-injection barriers required to reach that regime are specified.

11:00 AM *EQ11.09.02

Polymeric Devices for Infrared Upconversion Imagers and Energy Storage Ning Li, Lulu Yao and [Tse Nga Ng](#); University of California, San Diego, United States

The shortwave infrared spectral region is particularly powerful for a variety of applications including environmental monitoring and medical diagnosis,

enabling greater penetration depth and improved resolution in comparison to visible light. Upconversion imagers that combine photosensing and display in a compact structure are attractive since they avoid the costly and complex process of pixilation. Here, we have implemented polymeric upconversion imagers that combined photo-sensing and display in a compact structure, to extend the capability of human and machine vision to 1400 nm. The photoresponse exhibited a high external quantum efficiency of 35% at a low bias of ≤ 3 V with -3 dB bandwidth of 10 kHz. The large active area of 2 cm² enabled demonstrations such as object inspection, imaging through smog, and concurrent recording of blood vessel location and blood flow pulses. In addition to visualisation of infrared radiation, this class of narrow bandgap polymers showed highly delocalized redox states and operated as stable n-type anodes in energy storage devices. The redox polymer was used in supercapacitors and achieved a high areal power density of 227 mW/cm², allowing rapid charging and relevant to ac line filtering applications. The capacitance retention was 84% after 11,000 full redox cycles, offering the critical benefit of long cycle life. This work demonstrated the application of a new class of stable redox-active materials suitable to meet the energy storage needs for short-range wireless electronics.

11:30 AM *EQ11.09.03

Engineering OFETs Architecture Towards High Frequency [Annalisa Bonfiglio](#), Piero Cosseddu and Andrea Spanu; University of Cagliari, Italy

Despite the impressive advances that organic electronics has faced in the past 30 years, which led to the introduction of a variety of devices for a great number of different applications (such as, for example, the mobile phone industry and the biomedical field), organic field effect transistors still suffer from undeniable limitations, and present clearly subpar performances, especially with respect to standard silicon-based devices. In particular, despite the many advantages that organic transistor have in terms of low fabrication costs, easy processing techniques (often from solution), flexibility, and large area deposition, their actual employment for high-performance applications is still slowed down by several issues, such as the low mobility of organic semiconductors, the not-so-easy miniaturization, and poor long term stability of organic molecules, which generally lead to not always trivial encapsulation steps in order to avoid early aging due to the extreme sensitivity of such molecules to oxygen and moisture. These limitations have repercussions in the use of OFET-based devices in applications where high operation frequencies are needed, such as IoT, where smart devices are thought to intercommunicate and exchange continuous information in real time, and front-end circuits developing. An obvious approach to somehow dodge this limitation, which is in fact due to the intrinsic nature of the employed materials, and thus obtaining transistors with a suitable switching rate, is related to finding new ways to shorten the transistor channel length. However, a further challenge is doing so without excessively complicating the fabrication process. In fact, a lot of effort has been put in the past 20 years towards the reduction of devices dimensions, which is generally obtained using rather complicated approaches.

In order to meet the aforementioned goals, an accurate design is mandatory in order to minimize all the side effects that could limit the operational frequency of these devices. In this work we will report the approach that we have developed along the years in order to improve OFET performances. First of all, cut off frequency is strongly limited by all the device parasitic capacitances, therefore, thanks to the transparency of the employed substrates we have developed a self-alignment process that allowed us to achieve operational frequencies, very close to the MHz even with relatively low mobility semiconductors. More recently, in order to further close the gap with standard semiconductor-based devices, we have developed and optimized an easy and upscalable procedure for routinely fabricating submicrometer size OFETs with limited parasitic capacitances. These two factors turned out to be crucial to achieve cut off frequencies well above the MHz even with the employment of low mobility semiconductors, and without the need of employing expensive high resolution techniques. The proposed approach, thanks to its versatility and impressive performance can open up interesting new paths in the field of organic electronics for logic and front-end circuits developing and IoT applications.

12:00 PM EQ11.09.04

Integrated Complementary Organic Circuits and Ring Oscillators for Ultra-High-Frequency Logic Circuits [Erjuan Guo](#) and Hans Kleemann; Technische Universität Dresden, Germany

Relatively long channel lengths of lateral-channel dual-gate organic thin-film transistors typically leads to slow inverter operation. Vertical channel dualgate organic thin-film transistors are a promising alternative due to their short channel lengths, however, the lack of appropriate p- and n-type devices has limited the development of complementary inverter circuits. Here we show that organic vertical n-channel permeable single- and dualbase transistors and vertical p-channel permeable base transistors can be used to create integrated complementary inverters and ring oscillators. With operating voltages < 2.0 V, the threshold voltages of the n-type OPDBTs are changed across a wide range from 0.12 to 0.82 V by varying the voltage of the additional base. Thus, the vertical dual-base transistors enable a widerange of switching voltage controllability of complementary inverters. In addition, the inverters exhibit small switching time constants at 10 MHz, and the 7-stage complementary organic ring oscillators exhibit short signal propagation delays of 11 ns per stage at a supply voltage of 4 V. This underlines the potential of vertical organic transistors for high-frequency logic circuit applications

SYMPOSIUM EQ12

Optical Probes of Nanostructured, Organic and Hybrid Materials
November 30 - December 8, 2021

Symposium Organizers

Natalie Banerji, University of Bern
Ilaria Bargigia, Wake Forest University
Carlos Silva, Georgia Institute of Technology
Mark Wilson, University of Toronto

* Invited Paper

SESSION EQ12.01: Excitonic Processes in Organic Materials I
Session Chairs: Rishi Shivare and Carlos Silva
Tuesday Morning, November 30, 2021
Hynes, Level 2, Room 207

11:00 AM EQ12.01.03

The Role of Polarization-Induced Exciton-Polaron Quenching in Limiting OLED Efficiency Evgeny Pakhomenko and Russell J. Holmes; University of Minnesota, United States

Many common electron transport layer (ETL) materials employed in organic light-emitting devices (OLEDs) show a preferred orientation of molecular permanent dipole moments. This phenomenon is known as spontaneous orientation polarization (SOP), and leads to the formation of bound polarization charge, with polarons (typically holes) accumulating at the ETL/emissive layer interface to balance this charge. Previous study of phosphorescent OLEDs constructed using a polarized electron transport layer of tris-(1-phenyl-1H-benzimidazole) (TPBi) found that SOP-induced hole accumulation led to substantial exciton-polaron quenching *prior* to device turn-on. This quenching was found to reduce peak device external quantum efficiency by ~ 20%. This is in contrast with the prevailing understanding of exciton kinetics in OLEDs, where it is generally assumed that exciton-polaron quenching is only significant under high injection. This work examines the generality of this result by systematically probing polaron accumulation and quenching in phosphorescent OLEDs constructed using archetypical ETLs with varying degrees of SOP. Exciton quenching is quantified by the lock-in measurement of emitter photoluminescence during device operation. The use of a lock-in method allows emitter photoluminescence to be probed *in situ* even after turn-on by rejecting device electroluminescence. In comparison to device-efficiency based analyses of quenching, this technique decouples luminescence loss due to exciton-polaron quenching from inefficiencies in exciton formation. We find SOP-induced luminescence quenching to be a general phenomenon, here observed for devices based on several polar ETL materials. The onset-voltages for exciton-polaron photoluminescence quenching are in good agreement with conventional displacement current measurements, suggesting that this optical technique can be generally used to assess the magnitude of SOP. It is found that exciton quenching is a major limiting factor for determining peak internal quantum efficiency. These findings contrast the common practice of attributing lower-than-expected peak efficiency to charge balance losses and highlight the impact of SOP on OLED device efficiency, and the need to consider SOP-induced quenching in device design and analysis.

11:15 AM EQ12.01.04

Singlet Heterofission in Tetracene-Pentacene Thin-Film Blends Luca Moretti¹, Clemens Zeiser², Daniel Lepple², Margherita Maiuri¹, Giulio Cerullo¹ and Katharina Broch²; ¹Politecnico di Milano, Italy; ²University of Tubingen, Germany

Singlet fission (SF) is the photophysical process where an excited singlet state is converted into two triplets on the ultrafast timescales [1]. SF gained increasing attention in recent years due to the capability to overcome the Shockley-Queisser limit of single junction solar cells [2]. Different approaches to control the key parameters of SF (molecular arrangement, electronic coupling or energy balance) are often based on covalently bound dimers of SF chromophores. Another promising way to control the energy balance of SF and the optical bandgap is to combine two different chromophores. Here we focus on two prototypical SF chromophores pentacene (PEN, exothermic SF) and tetracene (TET, endothermic SF), and we exploit the advantage of intermolecular heterofission where two triplets are formed on different chromophores. In this work we investigate thin film blends with 5%, 25%, 50% and 75% of PEN with ultrafast transient absorption (TA) spectroscopy to study the impact of neighbouring TET molecules on the photophysics of crystalline PEN. We consider the TA of the neat compounds excited resonantly as references for understanding the interaction in the blends.

The results for PEN:TET blends performed with PEN excitation (to rule out energy transfer from TET to PEN) show a change in the relative position and intensity of the Davydov-components of the PEN photobleaching (PB) until the energetically higher one dominates at 5% PEN blend. The presence of excited state absorption (ESA) of triplets in all blends indicates that they are still being formed via SF despite the presence of TET. The 5% PEN blend shows a build-up of a negative signal around TET PB, as well as a disappearing SE at long delays. Global Analysis (GA) performed on the TA data, assuming SF to be the dominating channel, showed two different processes for the 5% PEN blend. The first one, occurring with 165 fs time constant was attributed to homofission of PEN, while a second 26 ps process was attributed to heterofission of PEN isolated among TET neighbours. The low heterofission rate can be explained by the endothermicity of the process. For PEN concentrations exceeding 5% there is no evidence of this process, since homofission outcompetes heterofission thanks to its exothermicity. Time constants from GA of the other blends confirm the robustness of PEN homofission [3] against the incorporation of weakly interacting compounds due the fact that SF in PEN proceeds via a coherent pathway where the triplet pair state directly mixes into the photoexcited bright state.

The study is completed with TA measurements exciting the TET, where the interpretation of TA and GA becomes complex as TET homofission and Förster resonance energy transfer (FRET) from TET to PEN additionally can occur. For high PEN concentration, FRET followed by PEN homofission outcompete TET homofission and heterofission [4]. The TA data for the 5% PEN blend present complex multi-exponential dynamics that reflect the relaxation of excited PEN and TET molecules via a multitude of channels. The persistence of the TET GSB at long delays is again evidence for TET triplets, which can be populated either via heterofission or TET homofission.

In conclusion we observe heterofission of a singlet from PEN to two triplets on one PEN and one TET, after direct excitation of PEN chromophores, showing that heterofission is observable in weakly interacting systems bridging the gap between studies of doped single crystals [5] and strongly coupled systems such as heterodimers [6]. Our approach allows continuous tuning of the optical bandgap along with the singlet and triplet energies by varying the mixing ratio without significant impact on PEN homofission time constants.

[1] J. Phys. Chem. C 123, 3923–3934 (2019)

[2] J. Appl. Phys. 32, 510–519 (1961)

[3] Nat. Commun. 9, 954 (2018)

[4] Angew. Chem. Int. Ed. 59, 19966–19973 (2020)

[5] Phys. Status Solidi B 83, 249–256 (1977)

[6] J. Am. Chem. Soc. 141, 17558–17570 (2019)

11:30 AM EQ12.01.05

Transient Strain Induced Electronic Structure Modulation in a Conducting Polymer Imaged by Scanning Ultrafast Electron Microscopy Taeyong Kim, Saejin Oh, Usama Choudhry, Carl Meinhart, Michael L. Chabinc and Bolin Liao; University of California, Santa Barbara, United States

Understanding the opto-electronic properties of conducting polymers under external strain are essential for their applications in flexible opto-electronic and photovoltaic devices. While prior studies have highlighted the impact of static strain applied on a macroscopic length scale, accessing structural relaxation under the local transient deformation was challenging due to the lack of spatiotemporal resolution using conventional methods. Here, we employ the newly developed scanning ultrafast electron microscopy (SUEM) to image the dynamical effect of the photo-excited transient strain in poly(3-hexylthiophene) (P3HT) facilitated by high space-time resolutions. We observe that the photo-induced SUEM contrast, corresponding to the local change of secondary electron emission, exhibits a ring-shaped spatial profile with a rise time of around 500 ps, beyond which the profile persists near the absence of spatial diffusion. We attribute the observation primarily to the electronic structure modulation induced by a local strain field owing to high elastic modulus, as supported by a finite-element numerical analysis. Our work provides insights into tailoring opto-electronic properties using transient mechanical deformation in conducting polymers, and demonstrates the versatility of SUEM to study photo-physical processes in various materials. This work is based on research supported by the Army Research Office under the award number W911NF-19-1-0060.

SESSION EQ12.02: Light-Induced Phenomena in Hybrid Perovskites I
Session Chair: Steven Cundiff
Tuesday Afternoon, November 30, 2021
Hynes, Level 2, Room 207

2:00 PM *EQ12.02.04

Energy Transport Processes in Hybrid Perovskite Nanomaterials William Tisdale; Massachusetts Institute of Technology, United States

Hybrid organic-inorganic halide perovskites are a newly rediscovered class of solution-processable semiconductor materials with surprisingly promising optoelectronic performance. When fabricated in a nanostructured form – either as layered 2D quantum wells or colloidal nanocrystals – hybrid perovskite nanomaterials exhibit a combination of interesting properties revealing both quantum mechanical and classical composite effects. In this talk, I will discuss the thermal, electronic, and excitonic properties of hybrid perovskite nanomaterials as a function of composition, structure, and temperature – and what these experimental observations tell us about the interactions between the organic and inorganic subphases of this interesting class of materials.

2:30 PM EQ12.02.05

Defects in Tin Halide Perovskites Antonella Treglia^{1,2}, Isabella Poli¹, Samuele Martani^{1,2}, Giulia Folpini¹, Alex Barker¹ and Annamaria Petrozza¹; ¹Istituto Italiano di Tecnologia (IIT), Italy; ²Politecnico di Milano, Italy

Tin halide perovskites (THPs) have emerged as a promising alternative to Lead Halide Perovskites (LHPs). The interest has grown not only because of the reduced environmental toxicity, but also due to the narrow bandgap (between 1.3 and 1.4 eV). We have recently reported that the optoelectronic quality of Sn-based perovskites is inherently comparable to LHP.¹ Despite this, device efficiency and stability are still limited.² Sn-based perovskites show a very interesting interplay of shallow and deep defects that can be either stable in the bulk or at the surface of the material. The dominant effect of one or the other can be tuned by differentiating the fabrication process. Even though there is general agreement on the beneficial effect of additives (mostly SnF₂)^{3,4} the mechanisms at the basis of the observed improvement in optoelectronic properties are yet not understood.

We have unraveled the optoelectronic properties of FA_{0.85}CS_{0.15}SnI₃ thin films providing a comprehensive picture of the competing radiative and non-radiative recombination processes with a combination of steady-state, time-resolved, and pump-probe spectroscopic techniques. We also discuss the origin of these competing processes in relation to the presence of additives. The interpretation of experimental results is supported by simulations describing free and trapped-carrier dynamics in a simplified system.

We show that the content of Sn⁴⁺ in the precursors' solution has a critical effect on optoelectronic properties drastically reducing the radiative efficiency. We suggest that surface Sn(IV), incorporated in the film from solution, might act as an electron trap enhancing non-radiative recombination that results dominant over doping-induced monomolecular radiative recombination.⁵ A moderated improvement of optoelectronic properties upon SnF₂ addition could still not match the performances of the pristine sample. This suggests that the introduction of the additive on one side might reduce the doping but conversely introduces additional non-radiative decay channels that fundamentally limit the radiative efficiency. The optimal percentage is not generally fixed but depends on the initial oxidation state of the precursors. We eventually show that an excess of the additive creates a Sn-rich growth condition that might result in the formation of deep defects⁶, with an overall detrimental effect on optoelectronic performances.

(1) Poli, I.; Kim, G.; Wong, E. L.; Treglia, A.; Folpini, G.; Petrozza, A. High External Photoluminescence Quantum Yield in Tin Halide Perovskite Thin Films. *ACS Energy Letters* 2021, 6, 609–611. <https://doi.org/10.1021/acsenerylett.0c02612>.

(2) Milot, R. L.; Klug, M. T.; Davies, C. L.; Wang, Z.; Kraus, H.; Snaith, H. J.; Johnston, M. B.; Herz, L. M. The Effects of Doping Density and Temperature on the Optoelectronic Properties of Formamidinium Tin Triiodide Thin Films. *Advanced Materials* 2018, 30 (44). <https://doi.org/10.1002/adma.201804506>.

(3) Gupta, S.; Cahen, D.; Hodes, G. How SnF₂ Impacts the Material Properties of Lead-Free Tin Perovskites. *Journal of Physical Chemistry C* 2018, 122 (25), 13926–13936. <https://doi.org/10.1021/acs.jpcc.8b01045>.

(4) Savill, K. J.; Ulatowski, A. M.; Farrar, M. D.; Johnston, M. B.; Snaith, H. J.; Herz, L. M. Impact of Tin Fluoride Additive on the Properties of Mixed Tin-Lead Iodide Perovskite Semiconductors. *Advanced Functional Materials* 2020, 2005594, 1–13. <https://doi.org/10.1002/adfm.202005594>.

(5) Ricciarelli, D.; Meggiolaro, D.; Ambrosio, F.; De Angelis, F. Instability of Tin Iodide Perovskites: Bulk p-Doping versus Surface Tin Oxidation. *ACS Energy Letters* 2020, 5 (9), 2787–2795. <https://doi.org/10.1021/acsenerylett.0c01174>.

(6) Meggiolaro, D.; Ricciarelli, D.; Alasmari, A. A.; Alasmay, F. A. S.; Angelis, F. De. Tin vs. Lead Redox Chemistry Modulates Charge Trapping and Self Doping in Tin/Lead-Iodide Perovskites. *J. Phys. Chem Lett.* 2020, 11, 3546–3556. <https://doi.org/10.1021/acs.jpclett.0c00725>.

2:45 PM *EQ12.02.06

Hot Exciton Dynamics in Two-Dimensional Organic-Inorganic Hybrid Perovskites Daniel Straus^{1,2}, Sebastian Hurtado Parra¹, Natasha Iotov¹, Qinghua Zhao¹, Michael Gau¹, Patrick Carroll¹, James Kikkawa¹ and Cherie R. Kagan¹; ¹University of Pennsylvania, United States; ²Princeton University, United States

Two-dimensional, organic-inorganic hybrid perovskites (2DHPs) are stoichiometric compounds composed of alternating sheets of corner-sharing, metal-halide octahedra and organoammonium cationic layers. We study 2DHPs containing single lead iodide layers separated by intervening substituted,

phenethylammonium (PEA) cations with the chemical structure $(x\text{-PEA})_2\text{PbI}_4$, where $x = \text{F, Cl, Br, or CH}_3$. These 2DHPs form type-I heterojunctions in which excitons and carriers are strongly confined to the lead halide layers with exciton binding energies > 150 meV. We use x-ray diffraction and variable-temperature steady-state and time-resolved absorption and photoluminescence (PL) measurements to uncover the correlation between their structure and photophysical properties. $(\text{PEA})_2\text{PbI}_4$ excitonic absorption and PL spectra at 15 K show splittings into regularly spaced resonances every 40–46 meV [1]. Anti-Stokes hot exciton PL is observed at the same energy as the optical absorption resonances. Replacing a single atom in the *para* position of the PEA-cation phenyl group increases its length and therefore the interlayer spacing, but leaves the cross-sectional area unchanged and results in structurally similar metal halide frameworks [2]. As the cation length increases, the absorption spectra broaden and blueshift, but the PL spectra remain invariant. Substitution in the *ortho* position with progressively larger cations increasingly distorts and strains the inorganic framework [3]. Ortho substitutions change the number of and spacing between the discrete excitonic resonances and increase the hot exciton PL by $> 10\times$. By correlating the atomic substitutions on the cation with changes in the excitonic structure, we show that the origin of the discrete excitonic resonances is consistent with a vibronic progression caused by strong exciton-phonon coupling to a phonon on the organic cation. The properties of 2DHPs can be tailored by the selection of the cation without directly modifying the inorganic framework.

(1) Straus, D. B.; Hurtado Parra, S.; Iotov, N.; Gebhardt, J.; Rappe, A. M.; Subotnik, J. E.; Kikkawa, J. M.; Kagan, C. R. Direct Observation of Electron-Phonon Coupling and Slow Vibrational Relaxation in Organic-Inorganic Hybrid Perovskites. *J. Am. Chem. Soc.* **2016**, *138* (42). <https://doi.org/10.1021/jacs.6b08175>.

(2) Straus, D. B.; Iotov, N.; Gau, M. R.; Zhao, Q.; Carroll, P. J.; Kagan, C. R. Longer Cations Increase Energetic Disorder in Excitonic 2D Hybrid Perovskites. *J. Phys. Chem. Lett.* **2019**, *10* (6), 1198–1205. <https://doi.org/10.1021/acs.jpcclett.9b00247>.

(3) Straus, D. B.; Hurtado Parra, S.; Iotov, N.; Zhao, Q.; Gau, M. R.; Carroll, P. J.; Kikkawa, J. M.; Kagan, C. R. Tailoring Hot Exciton Dynamics in 2D Hybrid Perovskites through Cation Modification. *ACS Nano* **2020**, *14* (3), 3621–3629. <https://doi.org/10.1021/acsnano.0c00037>.

SESSION EQ12.03: Light-Induced Phenomena in Hybrid Perovskites II

Session Chairs: Matthew Beard and Steven Cundiff

Tuesday Afternoon, November 30, 2021

Hynes, Level 2, Room 207

4:00 PM *EQ12.03.01

Multidimensional Coherent Spectroscopy of Perovskite Nanocrystals Steven Cundiff¹, Albert Liu¹, Gabriel Nagamine², Diogo Almeida² and Lazaro Padilha²; ¹University of Michigan, United States; ²Universidade Estadual de Campinas, Brazil

Perovskite nanocrystals have attracted much attention recently because of their high luminescence quantum efficiency compared to traditional nanocrystals. We have used multidimensional coherent spectroscopy to study excitonic states in perovskite nanocubes and nanoplatelets at low temperature.

The studies reveal coherences involving triplet states of a CsPbI_3 nanocube ensemble [1]. Picosecond time scale dephasing times are measured for both triplet and inter-triplet coherences, from which we infer a unique exciton fine structure level ordering composed of a dark state energetically positioned within the bright triplet manifold.

In an ensemble of colloidal CsPbI_3 perovskite nanoplatelets, we determine the homogeneous line broadening [2]. We demonstrate a dependence of not only their intrinsic line widths but also of various broadening mechanisms on platelet geometry. We find that decreasing nanoplatelet thickness by a single monolayer results in a 2-fold reduction of the inhomogeneous line width and a 3-fold reduction of the intrinsic homogeneous line width to the sub-millielectronvolts regime. In addition, our measurements suggest homogeneously broadened exciton resonances in two-layer (but not necessarily three-layer) nanoplatelets at room-temperature.

These results provide new insight into the coherent dynamics of excitonic states in perovskite nanocrystals as well as information about the underlying electronic states.

[1] A. Liu, D. B. Almeida, L. G. Bonato, G. Nagamine, L. F. Zagonel, A. F. Nogueira, L. A. Padilha, and S. T. Cundiff, "Multidimensional coherent spectroscopy reveals triplet state coherences in cesium lead-halide perovskite nanocrystals," *Science Advances* **7**, eabb3594 (2021).

[2] A. Liu, G. Nagamine, L. G. Bonato, D. B. Almeida, L. F. Zagonel, A. F. Nogueira, L. A. Padilha, and S. T. Cundiff, "Toward Engineering Intrinsic Line Widths and Line Broadening in Perovskite Nanoplatelets," *ACS Nano* **15**, 6499–6506 (2021).

4:30 PM EQ12.03.02

Nanoscale Chemical Heterogeneity Dominates the Optoelectronic Response over Local Electronic Disorder and Strain in Alloyed Perovskite Solar Cells Kyle Frohna¹, Miguel Anaya¹, Stuart Macpherson¹, Jooyoung Sung¹, Tiarnan A. Doherty¹, Yu-Hsien Chiang¹, Andrew Winchester², Keshav M. Dani², Akshay Rao¹ and Samuel D. Stranks^{1,1}; ¹University of Cambridge, United Kingdom; ²Okinawa Institute of Science and Technology, Japan

Halide perovskites perform remarkably in optoelectronic devices including tandem photovoltaics^{1,2}. However, this exceptional performance is striking given that perovskites exhibit deep charge carrier traps and spatial compositional and structural heterogeneity³⁻⁵, all of which should be detrimental to performance. In this presentation, I will discuss how we resolve this long-standing paradox by providing a global visualisation of the nanoscale chemical, structural and optoelectronic landscape in halide perovskite devices⁶. This was made possible through the development of a new suite of correlative, multimodal microscopy measurements combining quantitative optical spectroscopic techniques and synchrotron nanoprobe measurements. We show that compositional disorder dominates the optoelectronic response, while nanoscale strain variations, even of large magnitude ($\sim 1\%$), have only a weak influence. Nanoscale compositional gradients drive carrier funneling onto local regions associated with low electronic disorder, drawing carrier recombination away from trap clusters associated with electronic disorder and leading to high local photoluminescence quantum efficiency. These measurements reveal a global picture of the competitive nanoscale landscape, which endows enhanced defect tolerance in devices through spatial chemical disorder that outcompetes both electronic and structural disorder.

1 Al-Ashouri, A. *et al.* Monolithic perovskite/silicon tandem solar cell with $>29\%$ efficiency by enhanced hole extraction. *Science* **370**, 1300, doi:10.1126/science.abd4016 (2020).

2 Xu, J. *et al.* Triple-halide wide-band gap perovskites with suppressed phase segregation for efficient tandems. *Science* **367**, 1097,

doi:10.1126/science.aaz5074 (2020).

3 Doherty, T. A. S. *et al.* Performance-limiting nanoscale trap clusters at grain junctions in halide perovskites. *Nature* **580**, 360-366, doi:10.1038/s41586-020-2184-1 (2020).

4 Correa-Baena, J.-P. *et al.* Homogenized halides and alkali cation segregation in alloyed organic-inorganic perovskites. *Science* **363**, 627, doi:10.1126/science.aah5065 (2019).

5 Feldmann, S. *et al.* Photodoping through local charge carrier accumulation in alloyed hybrid perovskites for highly efficient luminescence. *Nat. Photonics* **14**, 123-128, doi:10.1038/s41566-019-0546-8 (2020).

6 Frohna, K. *et al.* Nanoscale Chemical Heterogeneity Dominates the Optoelectronic Response over Local Electronic Disorder and Strain in Alloyed Perovskite Solar Cells. *arXiv e-prints*, arXiv:2106.04942 (2021).

4:45 PM EQ12.03.03

Understanding the Mechanistic Role of Atomic Doping in Perovskite Nanocrystals to Enhance Their Luminescent Properties Sascha Feldmann; University of Cambridge, United Kingdom

Nanocrystals based on halide perovskites offer a promising material platform for highly efficient lighting and as quantum emitters. Using transient optical spectroscopies supported by ab initio calculations, we study excitation recombination dynamics in atomically doped lead halide perovskite nanocrystals which exhibit dramatically improved luminescent properties.

Unexpectedly, we find an increase in the intrinsic excitonic radiative recombination rate upon doping, which is typically a challenging material property to tailor. We can attribute the enhanced emission rates to increased exciton localization through lattice periodicity breaking from dopants, which increases exciton effective masses and overlap of electron and hole wavefunctions and thus the oscillator strength.

The important interplay between electronic and structural effects involving dopant and halide ions will be elucidated. Our report of a generalizable strategy for improving luminescence efficiencies in perovskite nanocrystals will be valuable for maximizing the performance of light-emitting applications.

5:00 PM EQ12.03.04

Observation of the Chiral Phonon Activated Spin Seebeck Effect Kyunghoon Kim¹, Eric Vetter¹, Liang Yan², Yu Yang³, Xiao Li³, Lifa Zhang³, Jun Zhou³, Wei You², Dali Sun¹ and Jun Liu¹; ¹North Carolina State University, United States; ²University of North Carolina at Chapel Hill, United States; ³Nanjing Normal University, China

Utilization of the interaction between spin and heat currents is the central focus of the field of spin caloritronics. The recent emergence of chiral phonons possessing angular momentum arising from the broken symmetry of the lattice creates the potential for generating spin currents at room temperature in a non-magnetic material in response to a thermal gradient, precluding the need for an applied magnetic field or polarized ferromagnetic contacts. In this talk, we will show the observation of spin currents generated by chiral phonons in a two-dimensional layered hybrid organic-inorganic perovskite semiconductor implanted with chiral cations when subjected to a thermal gradient. Identified by transient magneto-optical Kerr effect measurements, the spin polarization direction shows a strong dependence on the chirality of the semiconductors. Our findings indicate the potential of chiral phonons for spin caloritronic applications and offer a new route toward spin generation in the absence of magnetic materials.

SESSION EQ12.04: Excited States in Nanostructures I
Session Chairs: Stephane Kena-Cohen and Carlos Silva
Wednesday Morning, December 1, 2021
Hynes, Level 2, Room 207

10:30 AM EQ12.04.01

Probing Carrier Dynamics in Liquid Phase Exfoliated Graphene via Terahertz Spectroscopy Harrison Loh, Alan D. Bristow and Kostas Sierros; West Virginia University, United States

Liquid phase exfoliation (LPE) of graphene nanosheets from bulk graphite powders is of interest in materials science for graphene production because of the potential for environmentally benign production using green and non-toxic solvents in addition to well defined and controllable chemistry. Graphene flakes are suitable for many solution processing and fabrication methods such as direct ink writing for applications ranging from printable electronics and energy storage to optoelectronics and sensing. Because many of the desired applications for graphene are centered around its electrical conductivity and hence carrier transport, it is important to measure carrier conductivity and mobility, and correlate the finds with the LPE procedures for optimizing and tailoring the synthesis. To this end, terahertz time-domain spectroscopy is employed as a non-contact method of probing the carrier transport for a variety of graphene layers and graphite powders. Fitting the data to transport models, such as variants of the Drude model, provide conductivity and mobility characteristics that can be linked to microscopic scattering mechanism that are related to the LPE process. This characterization is expected to inform the preparation of exfoliated flake materials for more desirable properties for electronic and optoelectronic applications.

10:45 AM EQ12.04.02

Composite Fast Scintillators Based on Fluorescent Metal–Organic Framework Nanocrystals Angelo Monguzzi; Università degli Studi di Milano-Bicocca, Italy

Scintillators are materials that produce light pulses upon interaction with ionizing radiation, therefore they are widely employed in radiation detectors. In advanced medical-imaging technologies, fast scintillators enabling a time resolution of tens of picoseconds are required to achieve low-noise and fast imaging at the millimeter length scale. [1] Because, commonly used bulk and nanostructured materials, both organic and inorganic, does not offer the synthetic versatility required to have full control over the properties affecting the time resolution, composite systems are currently intensively investigated with the aim to overcome the performance traditional scintillators. [2]

We demonstrate that composite materials based on fluorescent metal–organic framework (MOF) nanocrystals can work as fast scintillators. We present a prototype scintillator fabricated by embedding MOF nanocrystals in a polymer. The MOF comprises zirconium oxo-hydroxy clusters, high-Z linking nodes interacting with the ionizing radiation, arranged in an orderly fashion at a nanometric distance from 9,10-diphenylanthracene ligand emitters. Their incorporation in the framework enables fast sensitization of the ligand fluorescence, thus avoiding issues typically arising from the intimate mixing of complementary elements. This proof-of-concept prototype device shows an ultrafast scintillation rise time of ~50 ps, thus supporting the development of new scintillators based on engineered fluorescent MOF nanocrystals. We further developed the scintillating MOF concept by realizing hetero-ligand

fluorescent nanocrystals with large Stokes shift of 750 meV showing a fluorescence quantum efficiency as large as 70%. The Stokes shifted emission is successfully activated by diffusion-mediated non-radiative energy transfer within the crystalline framework between the co-ligands, thus obtaining a fast scintillator with zero re-absorption effects that it strictly required for high-resolution medical imaging and other applications involving the detection of high energy radiation and particles.

REFERENCES

- [1] Conti, M. & Bendriem, B. *Clin. Transl. Imaging* **7**, 139–147 (2019).
- [2] Hajagos, T. J., et al. *Adv. Mater.* **30**, 1706956 (2018).
- [3] J. Perego, I. Villa, et al. *Nature Photonics* **15**, 393–400 (2021).

11:00 AM EQ12.04.03

Resolve Temporal Changes in the Excited State Lifetimes of Single Quantum Dots by Statistical Methods Yonglei Sun and Jing Zhao; University of Connecticut, United States

A mechanistic understanding of the photo-excited states in colloidal quantum dots (QDs) is the essential step toward unleashing their full potential in various optoelectronic applications. Fluorescence spectroscopy at the single-particle level is a powerful tool to study the excited states in QDs and has revealed a number of phenomena such as photoluminescence (PL) intensity blinking and lifetime blinking in recent decades. However, interpreting fluorescence data of single QDs is still challenging to date. For one thing, excited state lifetimes and PL intensities of single QDs are correlated, but unfortunately the fluctuation of PL intensity in single QDs is non-ergodic. Moreover, the PL signal from single QDs is often weak and noisy because the single QD emission is intrinsically weak, and current detection efficiency of single-photon detectors is far from perfect. These effects become even more pronounced when studying excited state lifetimes of single QDs, for the accuracy and reliability of derived lifetimes depend upon the purity and size of the data. So far, most studies analyzed excited state lifetimes of single QDs without preselecting the data or preselected the data by setting subjective bins and/or thresholds. As a result, the excited state lifetimes were actually derived from mixed states and lack reproducibility, from where the true photophysics may be blurred. To overcome these difficulties, we utilize statistical methods to derive well-defined excited state lifetimes of single QDs. We employ change-point analysis to break down the arrival time series of compact CdSe/CdS core/shell QDs so that the consecutive bins that belong to the same state could be analyzed altogether. We then perform multi-exponential fitting and tests of significance to verify that in the single QD PL decay curves there is an additional lifetime component whose value is roughly half of that of the single exciton lifetime. The additional lifetime component in this type of QDs is assigned to lifetime blinking that happens too fast to be detected by traditional binning analysis methods. We propose that lifetime blinking happens when a negative trion forms in the core of a QD after photoexcitation while non-radiative processes are not activated. However, the easy accessibility to efficient non-radiative processes results in the short durations of lifetime blinking events in this type of QDs.

11:15 AM EQ12.04.04

Ultrafast Pump-Probe Microscopy Investigation of the Carrier Dynamics in Anisotropic Rhenium Disulfide (ReS₂) Nanoflakes Sarah Sutton, Jason Malizia, Alexis Glaudin, Cullen Walsh and John Papanikolas; University of North Carolina at Chapel Hill, United States

We have studied the anisotropic optical and electronic properties of ReS₂ flakes using ultrafast pump-probe microscopy. In contrast to other highly symmetric TMDCs like MoS₂ and WS₂, ReS₂ remains a direct bandgap semiconductor regardless of the number of layers due to its low-symmetry distorted 1T crystal structure. This low symmetry also gives rise to anisotropic optical and electronic properties. We have used polarization-resolved pump-probe microscopy to investigate the anisotropic carrier dynamics in ReS₂ nanoflakes. In these experiments, a localized region on a single nanoflake is excited with a linearly polarized 440 nm femtosecond laser pulse focused through a microscope objective. A second 880 nm laser pulse with variable arrival time and polarization probes how the excitation evolves in time. Carrier recombination dynamics were studied by measuring the difference in the transmission of the 880 nm probe as its time delay increases with respect to the initial 440 nm pump. At fixed time delays, changes due to polarization were resolved by rotating the probe polarization. The resulting polar plots illustrate how changes in excited carrier population influence the anisotropic optical properties in ReS₂ nanoflakes.

11:30 AM EQ12.04.05

Late News: Spin-Orbit Driven Terahertz Optical Response in Ferromagnetic Fe-Co-Al Alloys Ming Lei and Sinisa Coh; University of California, Riverside, United States

We study the optical conductivity response of simple ferromagnetic alloys driven by spin-orbit coupling. The spin-orbit coupling leads to a band splitting near the Fermi surface in the range of 10-100 THz. This band-splitting energy range provides an opportunity to study the optical conductivity in the THz regime. The optical conductivity response is sensitive to the details of the structure and chemical composition. For simple alloys, like Fe-Co alloys, we find that there is not much dependence of optical conductivity response in the THz range. However, we find the optical conductivity response changes sign from positive in Fe to negative in Fe-Al alloys. Furthermore, those features are washed away at 10 THz but remain only at 100 THz because of the short electron lifetime.

11:45 AM EQ12.04.06

Probing Structural and Compositional Parameters on Hafnia Nanoparticles with Up-Conversion Xavier H. Guichard and Alessandro Lauria; ETH Zurich, Switzerland

NIR-Vis up-conversion (UC) plays a key role in many emerging applications such as theranostics, solar energy harvesting, sensing and others.^[1] While rare earth (RE) up-conversion luminescence in fluoride nanoparticles is extensively studied,^[2] fewer reports are available on RE-doped metal oxide UC nanoparticles, despite their high chemical stability. In particular, HfO₂ nanocrystals seem to be a promising alternative because of their high inertness and biocompatibility.^[3] Nevertheless, the polymorphism observed in hafnia when high RE doping levels are used, prevents a clear understanding of the parameters relevant for controlled and improved UC. Therefore, a finer control over doping levels and crystal structure is necessary to optimize the optical performance.

In this work, we studied the influence of structural and compositional modifications on the up-conversion luminescence (UCL) recorded in Er/Yb co-doped hafnia nanocrystals obtained by a colloidal solvothermal synthesis. The up-conversion characteristics of the materials were monitored in dependence of structural parameters such as crystal size and lattice symmetry, determined by means of X-ray diffraction and transmission electron microscopy (TEM), and originating from the multifunctional doping.^[4] We report that the cubic polymorph of hafnia expresses much higher up-conversion efficiency with respect to monoclinic nanoparticles. On the other hand, the elemental analysis carried out by TEM energy dispersive X-ray spectroscopy (EDS) allowed us

to correlate the composition of Er/Yb/Lu:HfO₂ with the main UC features like efficiency and the ratio between green and red emission deriving from radiative recombination on Er³⁺ centres. These results give useful insights about the phenomena responsible for UCL features in hafnia nanocrystals, enabling their employment in various fields, thanks to improved UC intensities and control over the emission profile. Moreover, the experimental platform described here permitted to possibly explain the inhomogeneity of doping in mixed polymorphs by analysing UCL profiles as probes of the local rare earth environment.

[1] B. Zhou, B. Shi, D. Jin, X. Liu, *Nat. Nanotechnol.* **2015**, *10*, 924.

[2] S. Wilhelm, *ACS Nano* **2017**, *11*, 10644.

[3] I. Villa, C. Villa, A. Monguzzi, V. Babin, E. Tervoort, M. Nikl, M. Niederberger, Y. Torrente, A. Vedda, A. Lauria, *Nanoscale* **2018**, *10*, 7933.

[4] A. Lauria, I. Villa, M. Fasoli, M. Niederberger, A. Vedda, *ACS Nano* **2013**, *7*, 7041.

SESSION EQ12.05: Strong Light-Matter Interactions and Quantum Phenomena I

Session Chair: Carlos Silva

Wednesday Afternoon, December 1, 2021

Hynes, Level 2, Room 207

1:30 PM *EQ12.05.01

Nanostructured Materials for Infrared Light-Emission Stephane Kena-Cohen; Polytechnique Montreal, Canada

In this talk we will describe recent advances in our group towards developing efficient infrared emissive devices using nanostructured materials. First, we will discuss the realizing of ultrastrong light-matter coupling in microcavities containing dense films of single chirality semiconducting nanotubes. We will show that this allows for hybridization with the K-momentum dark exciton and the bright direct exciton mediated by the optical field. As a result, new opportunities arise for enhancing the luminescence efficiency by bypassing losses associated to the optically forbidden dark exciton transition.

We will then describe our work on the spectroscopy and realization of LEDs using the two-dimensional (2D) semiconductor black phosphorus (BP). Black phosphorus is unique amongst 2D materials in that it possesses a direct bandgap, which is highly tunable from 0.3 eV in the bulk, to ~2 eV at the monolayer level. In addition, it possesses significant in-plane anisotropy, with the transition dipole moment strongly oriented along the armchair direction. We will describe the first realization of LEDs based on BP, which rely on the use of BP/Molybdenum disulfide heterojunctions. These emit at 3.8 μm with an internal quantum efficiency of ~1%. Then, we will discuss strategies for increasing the scalability of black phosphorus devices through the use of solution-processing technique and the realization of cm x cm-scale homogeneous thin films of BP-fullerene via the Langmuir-Blodgett technique. This will highlight an outstanding problem in the community in understanding the strong discrepancy between the optical response of nanosheets as compared to bulk crystals. We will postulate on the likely origin of this discrepancy.

2:00 PM EQ12.05.02

Charge Accumulation Driven by Fluid-Like Flow of Quasiparticles in a Semimetal WTe₂ at Room Temperature Young-Gwan Choi¹, Manh-Ha Doan¹, Maxim N. Chernodub^{2,3} and Gyung-Min Choi^{1,4}; ¹Sungkyunkwan University (SKKU), Korea (the Republic of); ²Université Tours, France; ³Far Eastern Federal University, Russian Federation; ⁴Institute for Basic Science, Korea (the Republic of)

Recently, the fluid-like behavior of charge carriers in condensed matter systems has attracted much interest. For example, the ultraclean graphene can host a hydrodynamic charge flow at low temperatures, when momentum conserving carrier-carrier scattering is much faster than momentum relaxing scattering. In analogy with whirlpools in flowing water, the viscous electronic flow generates vortices in the electronic fluid in graphene. The vortices drive electric current against an applied field, resulting in a negative nonlocal voltage near current sources and drains. The alternating, sign-flipping pattern in the *voltage* close to the contacts is an experimentally detectable signature of the electronic viscous behavior.

We observe visually similar *charge*-alternating accumulation patterns in tungsten ditelluride in the semimetallic phase at room temperature by using a polarization-sensitive laser microscopy technique with an electrical bias. To observe charge distribution, we utilize an electro-optical effect, which is a polarization variation resulting from optical refractive index change due to the local carrier density variation. The spatial charge distribution shows exceptionally long relaxation profiles, ~1.4 μm, which are much more extended than a charge screening length in conventional semimetals (usually a few nanometers). We analyze that the nonlocal negative charge current and the sizeable spatial size of the charge domains are supported by the long recombination time of electron-hole pairs in this nearly-compensated two-component Weyl semimetal.

We show theoretically that these peculiar charge accumulation patterns appear due to the unbalanced diffusive behavior of electrons and holes. Our analytical calculations in a two-component model indicate that the Ohmic electric current can produce hydrodynamic-like whirlpool structures in the neutral electron-hole current close to the injection contacts. The whirlpools in the neutral current spatially correlate with the charge accumulation regions. We argue that it is the backflow of a neutral current which leads to the experimentally observed exotic alternating charge distribution near the contacts. Moreover, the fluid-like behavior of the neutral quasiparticle current can be described in terms of a modified Navier-Stokes equation equipped with higher-derivative terms.

We find that the extremely long relaxation length and alternating distribution of charge in semimetal WTe₂ can be described by the pseudo-hydrodynamic flow of neutral quasiparticle. We expect that the unconventional flow of neutral quasiparticle in WTe₂ is responsible for many interesting physical effects at room temperature.

2:15 PM EQ12.05.03

Molecular Polaritons Generated from Strong Coupling between CdSe Nanoplatelets and a Dielectric Optical Cavity Liangyu Qiu, Arkajit Mandal, Ovishek Morshed, Mahilet Meidenbauer, William Girten, Pengfei Huo, Nick Vamivakas and Todd Krauss; University of Rochester, United States

Coupling electronic states of molecules or nanoparticles to the quantized radiation field inside an optical cavity creates a set of new photon-matter hybrid excitations, called polaritons. As opposed to atoms, the vibrational modes of molecules provide new degrees of freedom to mediate the quantum transduction between electronic and photonic states, offering new paradigms for quantum materials and chemical science. We will discuss the formation of CdSe nanoplatelet (NPL) exciton-polaritons in a distributed Bragg reflector (DBR) cavity [1]. The molecule-cavity hybrid system is in the strong coupling regime with an 83 meV Rabi splitting, characterized from angle resolved reflectance and photoluminescence measurements. Mixed quantum-classical dynamics simulations are used to investigate the polariton photophysics of the hybrid system by treating the electronic and photonic degrees of freedom (DOF) quantum mechanically and the nuclear phononic DOF classically. Our numerical simulations of the angle-resolved photoluminescence (PL) agree extremely well with the experimental data, providing a fundamental explanation of the widely-observed asymmetric intensity distribution of the upper and

lower polariton branches. Our results also provide mechanistic insights into the importance of phonon-assisted nonadiabatic transitions among polariton states, which are reflected in the various features of the PL spectra. This work provides a facile and direct path for the coupling of nanoparticle electronic states with the photon states of a dielectric cavity to form a hybrid system, and provides a new platform for investigating cavity-mediated physical and chemical processes, providing the emerging quantum information science field the knowledge for preparing next generation quantum systems.

(1) L. Qiu, A. Mandal, O. Morshed, M. T. Meidenbauer, W. Girten, P. Huo, A. N. Vamivakas, and T.D. Krauss *J. Phys. Chem. Lett.* **12**, 5030–5038 (2021).

2:30 PM EQ12.05.04

Elucidation of Ultrafast Photophysics in Carbon Nanotube Exciton-Polaritons Using 2D White-Light Spectroscopy Minjung Son, Ryan Allen, Abitha Dhavamani, Michael Arnold and Martin Zanni; University of Wisconsin–Madison, United States

Semiconducting carbon nanotubes (CNTs) are promising candidates for next-generation optoelectronic and photovoltaic devices due to their strong absorptivity and easily tunable photophysical properties. However, device performance is typically limited by sub-10 nm exciton diffusion lengths as well as energy loss via trap states and non-radiative pathways. An emerging approach that has the potential to overcome these limitations is to utilize hybrid light-matter states known as exciton-polaritons, where the strong coupling between photons and excitons leads to energy delocalization over the length of the entire cavity, which is typically hundreds of nanometers. We demonstrate the fabrication of a donor-acceptor polaritonic system bearing semiconducting single-walled CNTs with two different band gap energies, and characterization of the energy flow therein using transient reflection and two-dimensional white-light (2DWL) spectroscopies. The CNT layers are spatially separated by a 150-nm thick insulating polymer layer, ruling out the possibility of energy transfer due to direct donor-acceptor contact. The transient and 2DWL spectra reveal a 300-fs growth of the lower-polariton excited-state population upon photoexcitation into the higher-lying upper-polariton state, indicative of a polariton-assisted long-range energy transport process over a ~300-nm distance. These results highlight the potential of polaritonic microcavities as a tool for tailoring and optimizing material properties toward desired device performance.

2:45 PM EQ12.05.05

Modification of High-Harmonic Generation in Non-Relativistic Quantum Electrodynamics Davis Dave Welakuh Mbangheku and Prineha Narang; Harvard University, United States

Experiments at the intersection of condensed matter physics and chemical dynamics are now able to control and alter the properties of quantum matter on demand in regimes of strong-coupling. In such experiments, strongly coupling the complex matter system to a mode of an optical high-Q cavity leads to the emergence of hybrid light-matter states that influence the physical, chemical and spectroscopic properties of the matter system. An example of a physical process that can be modified is second-harmonic generation (SHG) where the efficiency of the process can be increased by strongly coupling to photons [1, 2]. To date, an *ab initio* approach to this process has not been investigated in the context of strong light-matter coupling. In this context, we present an *ab initio* strong light-matter description of SHG from a molecular system within the framework of quantum-electrodynamical density functional theory (QEDFT) [3, 4]. We investigate the efficiency of the process for a single molecular system coupled to a cavity mode as well as for the case of collectively coupled molecules. From these first principles calculations, we deduce how collective strong coupling influences non-linear properties of the matter system. Also, we show the spectrum of the photon field of the corresponding SHG in this talk.

[1] J. Schmutzler, et al., *Phys. Rev. B* **90**, 075103 (2014),

[2] T. Chervy, et al., *Nano Lett.* **16**, 12, 7352-7356 (2016),

[3] M. Ruggenthaler et al., *Phys. Rev. A* **90**, 012508 (2014),

[4] J. Flick and P. Narang, *Phys. Rev. Lett.* **121**, 113002 (2018).

SESSION EQ12.06: Spectroscopic Insights into Bioelectronics

Session Chair: Carlos Silva

Wednesday Afternoon, December 1, 2021

Hynes, Level 2, Room 207

4:00 PM *EQ12.06.01

First *In Situ* THz Measurements on Organic Electrochemical Transistors—Accessing Intrinsic Conductivity of Bipolarons and Polarons Gonzague Rebetz, Dimitra Tsokkou, Olivier Bardagot, Julien Réhault and Natalie Banerji; University Bern, Switzerland

Organic electrochemical transistors (OECTs) are highly sensitive sensors used in increasingly challenging biologic applications such as wearable textiles with integrated biosensors and *in vivo* recording of brain activity.[1,2] They can be described as an ionic circuit embedded with an electronic circuit. When gating the OECT with a voltage bias, ions penetrate and modify the doping level of the organic channel thereby changing its conductivity at both macro- and microscopic scales.

One of today's challenges to further develop this promising technology lies in the fundamental understanding of the interplay between doping level and conductivity. [3] Previous investigations have addressed this question via macroscopic approaches which are inherently sensitive to the device geometry and morphology.[3-4] In this work, we propose an innovative *in situ* bottom-up approach that allows the determination of the intrinsic conductivity of bipolarons and polarons.

We use UV-VIS-NIR absorption spectroelectrochemistry combined with a multivariate curve resolution (MCR) analysis [4] to extract the neutral, polaron and bipolaron populations at different voltages. The microscopic conductivity is then probed via *in situ* THz spectroscopy [5], which represents the first measurement of this kind on OECTs. For archetypal PEDOT:PSS-based OECTs, we find that bipolarons are slightly more localized than the polarons and thus demonstrate a lower microscale mobility. However, the higher density of charges in bipolarons counterbalances their lower mobility and explains why bipolarons largely contribute to the total microscale conductivity.

Finally, we will present the two main perspectives of this new THz measurement technique in the field of OECTs:

1. Combined with macroscopic conductivity measurements, microscopic conductivity offers the prospect to disentangle underlying mechanisms limiting long-range charge transport such as device geometry and/or morphological features.

2. Determining the fundamental conductivity properties of doped species like bipolarons and polarons represents a necessary step to push microscale modelling of devices by linking the doping level and conductivity at the smallest possible level.

- [1] Gualandi I., Marzocchi M., Achilli A. *et al.*, *Sci Rep*, 2016, 6, 33637.
- [2] Khodagholy D., Doublet T., Quilichini P. *et al.* *Nat Commun*, 2013, 4, 1575.
- [3] Colucci R., de Paula Barbosa, H. F., Günther, F., Cavassin, P., & Faria, G. C. (2020). Recent advances in modeling organic electrochemical transistors. *Flexible and Printed Electronics*, 5(1), 013001.
- [4] Rivnay J., Inal S., Salleo A. *et al.*, *Nat Rev Mater*, 2018, 3, 17086
- [5] De Juan A., Jaumot J., Tauler R. Multivariate Curve Resolution (MCR). Solving the mixture analysis problem. *Anal. Methodes* 6, 4964-4976 (2014)
- [6] Unuma T., Yamada N., Nakamura A. *et al.* Direct observation of carrier delocalization in highly conducting polyaniline. *Appl Phys Lett* 103, 053303 (2013)

4:30 PM *EQ12.06.02

Spectrally Resolved Ion Dynamics in Mixed Ionic-Electronic Conducting Polymers with High Spatial and Temporal Resolution Scott T. Keene¹, Raj Pandya¹, Juliana P. Maria², Maximilian Moser², Christopher Schnedermann¹, Iain McCulloch^{2,3}, Akshay Rao¹ and George G. Malliaras¹; ¹University of Cambridge, United Kingdom; ²University of Oxford, United Kingdom; ³King Abdullah University of Science and Technology, Saudi Arabia

Mixed ionic-electronic conducting polymers have recently emerged as a promising material choice for bioelectronic devices due to their low impedance, soft mechanical properties, and ability to transduce ionic signals to electronic currents.¹ The unique behaviour of mixed conducting polymers arises from ion intercalation through the bulk of the material which can modify the oxidation state, and therefore charge carrier concentration, of the semiconducting polymer backbone. However, the physics of ion-doping in polymers is still unclear² with increasingly complex experiments and models being developed to capture the internal electric fields,³ ionic distributions,⁴ and structure-property relationships.⁵ Here, we utilize the electrochromic response of mixed conducting polymers to monitor ion motion optically at the length scales (from 1 μm to 500 μm) and timescales (from 1 ms to 10 s) relevant to device operation. We fabricate devices with polymer/electrolyte interface orthogonal to the substrate to limit ionic penetration to single plane, similar to previously investigated "ionic moving front" geometries.⁶ Using spectrally- and time-resolved transmission microscopy, we monitor the change in visible light absorption of mixed conducting polymer backbone as it is doped/de-doped when ions flow out of/into the bulk. Contrary to previous work at much larger distances (several mm) and longer times (from 5 s to 1 min),^{6,7} we observe a linear relationship between time and the distance of the doping front from the polymer/electrolyte interface. Furthermore, the results reveal unintuitive relationship between the phase-front velocity and the applied electrochemical potential, with larger de-doping potentials resulting in slower electrochromic transitions. We explore a range of organic mixed conducting materials, both p-type and n-type, with varying degrees of swelling during bulk doping to identify the structure-property relationships for ion dynamics in mixed conducting polymers. Finally, using finite element analysis, we reconstruct the internal electric field evolution near the polymer/electrolyte interface based on the experimental results. This work helps resolve the fundamental physics of electrochemical doping in mixed conducting polymers and provides guidance for optimizing the polymer microstructure and chemical functionality for improved bioelectronic devices.

- [1] J. Rivnay *et al.* *Nat. Rev. Mater.* 3, 17086 (2018)
- [2] B.D. Paulsen *et al.* *Nat. Mater.* 19, 13-26 (2020)
- [3] K. Tybrandt *et al.* *Sci. Adv.* 3, eaao3659 (2017)
- [4] V. Kaphle, *et al.* *Nat. Comm.* 11 (2020)
- [5] I. Bargigia *et al.* *J. Am. Chem. Soc.* 143, 294-308 (2021).
- [6] E. Stavrinidou *et al.* *Adv. Mater.* 25, 4488-4493 (2013)
- [7] J. Rivnay *et al.* *Nat Comm.* 7, 11287 (2016)

5:00 PM *EQ12.06.03

Resolving Mixed Electronic-Ionic Transport at Nanometer Length Scales in Polymer Electrochemical Cells Using Color Impedance Spectroscopy Zhiting Chen¹ and Erin L. Ratcliff²; ¹The University of Arizona, United States; ²University of Arizona, United States

Conductive polymers exhibit hybrid electronic-ionic transport properties that are critical to understanding functionality in electrochemical devices for energy conversion and storage and biosensing. Electrochemical impedance spectroscopy enables the resolution of charge transport in both the frequency and energy domains, but often is complicated by complex circuit analysis necessary to estimate non-Faradaic (double layer) and Faradaic (charge transfer) contributions, often where these two events are coupled together. Optical spectroscopies offer specificity but often lack the sensitivity of electrochemical techniques. Ultimately, neither EIS nor spectroscopic methods alone afford the sensitivity and specificity to confidently isolate charge transfer and transport processes in conductive polymer/electrolyte systems.

Herein we demonstrate the use of color impedance spectroscopy (CIS) to resolve electrolyte effects on electrical charge transport in a prototypical material: poly(3-hexylthiophene) (P3HT). In CIS, the modulated transmittance tracks the motion of Faradaic charges in the films via the optical signatures attributed to P3HT polarons with resolution in both energy and frequency. This approach allows for characterization of the dynamics of charge transport in the context of Coulombic binding effect between counterions and polarons. Using CIS, we observe that at low doping potentials, only a small fraction of polarons are actually mobile and respond to electric field modulation at moderate frequencies. We attribute this to the localization of the polarons via long-range Coulombic interactions with counterions; i.e. Coulombic trapping. Increasing the electrochemical doping increases the steady-state carrier density and increases the fraction of mobile carriers. This is consistent with a more homogenous energetic environment, i.e. the reduction in quantity and/or trap energy. The chemical information gained and the CIS method development described here should be instructive for future efforts to quantify charge transfer/transport structure-property relationships, with applications to energy conversion and storage and biosensing.

SESSION EQ12.07: Poster Session I
Session Chairs: Christian Oelsner and Carlos Silva
Wednesday Afternoon, December 1, 2021
8:00 PM - 10:00 PM
Hynes, Level 1, Hall B

EQ12.07.01

Study of Structural, Electrical and Optical Properties of Copper Oxide Phase Mixture Thin Films Grown by Pulsed Laser Deposition Rifat Ara A.

Shams¹, Jacob Berry¹, Ariful Haque² and Kartik Ghosh¹; ¹Missouri State University, United States; ²Texas State University, United States

CuO and Cu₂O, both being small and direct bandgap materials, have been studied and implemented individually as an active layer of solar cell from early age of manufacturing. A mixture of these two-phase contents at different ratios can bring variance in absorbance and electrical conductivity which can present new and diverse aspect in solar cell fabrication with added efficiency. Previous works was successful to vary the phase mixture and the nanoparticle (NP) structure provided very high absorption co-efficient but poor electrical conductivity. By controlling the PLD parameters and subsequent processing steps we figured out a way to vary the phase mixture of copper oxide thin films to maximize the electrical conductivity and absorption in the solar spectrum. Phase mixture with different CuO/Cu₂O ratios was obtained using pulsed laser deposition through varying growth parameters such as oxygen pressure in the chamber and temperature of the substrate. i. To obtain the structure-property correlation we have performed the X-ray diffraction, Raman spectroscopy, scanning electron microscopy, electrical measurements and optical transmittance measurements by UV-VIS spectroscopy on the samples. The TOPAS analysis of the XRD data from all the samples has shown various percentage of CuO and Cu₂O and one of the samples also had metallic Cu phase. Owing to the change in the phase content in the copper oxide thin films we have observed some consistent variations in the electrical and optical properties. And so far, a thin film copper oxide phase mixture (CuO 61.60%-Cu₂O 38.15%) with a thickness of 200 nm yielded an absorption co-efficient of 7.02E+6 cm⁻¹ which is greater than that of commercially available pure CuO (1.19E+5 cm⁻¹). The measured resistivity of this sample was obtained to be 0.034 Ω-m indicating a doped semiconducting composite. This phase mixture, with the maximum absorption coefficient and suitable electrical property, can be implemented as the absorption layer of a solar cell which would help attaining maximum efficiency in the copper oxide based low-cost heterojunction solar cell. Moreover, the presence of Cu in one of the sample hints the possibility of NP incorporation with more controlled and reduced amount of copper in the film.

EQ12.07.03

Synthetic Advancements to Control Size, Morphology and Optical and Electrical Properties of Blue-Luminescent Two-Dimensional Silver Phenylselenolate Watcharaphol Paritmongkol, Woo Seok Lee, Tomoaki Sakurada, Wenbi Shcherbakov-Wu, Seung Kyun Ha and William Tisdale; Massachusetts Institute of Technology, United States

Silver phenylselenide (AgSePh) is a blue-emitting two-dimensional (2D) semiconductor with in-plane anisotropy, large exciton binding energy, non-toxic and earth-abundant elemental composition, and a scalable synthetic method that is compatible with modern microelectronics. Unlike transition metal dichalcogenides and 2D layered perovskites, AgSePh features covalent bonding between its organic and inorganic components, becoming a *truly hybrid organic-inorganic* semiconductor with chemical stability and a unique bandgap tunability through organic modification. Although AgSePh contains multiple desirable characteristics for modern electronics, its performance is still limited by the crystal size and quality produced by conventional synthetic methods. In this presentation, we will show two synthetic advancements to produce AgSePh thin films with controllable grain size from <200 nm to >5 μm and AgSePh microcrystals with improved crystal size from ~2 μm to >1mm. Systematic optical and electrical characterizations to confirm higher crystalline quality with lower defect densities in these samples will be presented. Furthermore, mechanistic insight into the improved syntheses will be elucidated, and an application of this knowledge to grow single crystals will be shown. We expect these improved synthetic methods to facilitate the studies on the fundamentals and applications of this exciting new material.

EQ12.07.04

Late News: Photodegradation of Organic Dyes in Single and Multi-Component in the Presence of Titanium Dioxide Nanoparticles Alondra A. Lugo Ruiz, María J. Paz Ruiz and Sonia J. Bailón- Ruíz; University of Puerto Rico at Ponce, United States

Over 17% of water contamination in the world is due to the discharge of wastewater from textile and dyeing industries. These industries use a large portion of organic dyes, which are found to be toxic, carcinogenic, and can be difficult to remove. Conventional treatments have been studied and found to be ineffective for the removal of the dyes. However, one effective way to remove them from our water sources is by a photocatalytic degradation process using semiconductor nanoparticles. Titanium dioxide (TiO₂) is a semiconductor material with intrinsic optical and electronic properties and is one of the most used photocatalyst for the degradation of these organic contaminants. The photocatalytic capacity of TiO₂ nanostructures is based on the generation of electron-hole pairs due to the Ultraviolet (UV) excitation of TiO₂. The objective of this investigation is to assess the organic dyes individually and combined, in the presence of Titanium Dioxide nanoparticles. Photodegradation studies were evaluated in the presence of dyes like Malachite Green Chloride (MG) and Methyl Violet (MV) at different concentrations of TiO₂ nanoparticles (10, 15, 25, and 50 ppm). Following the UV irradiation of the dyes at certain time intervals, it was found that 15 ppm TiO₂ degraded MG and MV more swiftly than the other concentrations, with a result of ~90% and ~98%, respectively. Our future studies include evaluating the photocatalysis of the mixture of both dyes (multi-component) in the presence of TiO₂.

EQ12.07.05

Late News: Electrical Conductivity and Optical Properties of ITO Powder Surface-Modified with Nano-Ni Particles Jeong Hye Jo, Su Hyeong Kim and Young Soo Yoon; Gachon University, Korea (the Republic of)

Generally, ITO thin film is deposited by sputtering which is required a high-vacuum and high-temperature process, resulting in high manufacturing costs. On the other hand, spin coating method has advantages such as efficient cost, simplicity, fast and mass production. So, it can be another method for manufacturing ITO thin films. However, Since the ITO thin films deposited by spin coating method has a porous surface, electrical conductivity is lower than that of ITO thin films deposited by sputtering.

The electronic conductivity of nickel-plated ceramic is improved by electroless Nickel plating, and it is verified that nickel increase conductivity. [1]. In this study, We confirmed with 4-point probe that spin-coating Nickel plated ITO (ITO@Ni) increase electrical conductivity. [2-4] The composition and morphological of nickel deposited on ITO were characterized by transmission electron microscope (TEM) and SEM-EDX analysis. ITO@Ni powder becomes the source of ITO@Ni colloid ink to be used in spin coating. Particle size and ink dispersion were measured by electrophoresis light scattering (ELS). ITO@Ni was deposited by spin coater. Transmittance and conductivity was respectively measured with UV-Visible Spectrophotometer and 4-point probe. When pure ITO and ITO containing 10wt% of nickel were deposited as one layer, the transmittance was lowered from about 97% to 90%. Sheet resistance of ITO@Ni multilayer appears less than 30ohm/square.

As a result, Transmittance and conductivity had a trade-off relationship according to nickel ratio. It is expected that spin-coating ITO@Ni can be used as a transparent electrode without high vacuum and high temperature process.

[1] Pratihari, S. K., Sharma, A. D., & Maiti, H. S., Materials Chemistry and Physics, (2006), 96(2-3), 388-395.

[2] Alavi, B., Aghajani, H., & Rasooli, A., Thin Solid Films, (2019), 669, 514-519.

[3] Uysal, M., Karşioğlu, R., Alp, A., & Akbulut, H., Ceramics International, (2013), 39(5), 5485-5493.

[4] Kumar, D. S., Suman, K. N. S., & Kumar, P. R., International Journal of Advanced Science and Technology, (2016), 97, 59-68.

EQ12.07.06

Late News: Production of Tin Dioxide Nanoparticles in Aqueous Phase Fabio Santiago, Alondra A. Lugo Ruiz and Sonia J. Bailón- Ruíz; UPR Ponce,

Puerto Rico

When mentioning emerging fields, nanoparticle research is at the forefront due to their unique physical and chemical properties. Tin dioxide (SnO_2) is a n-type semiconductor with potential photocatalytic properties, based on the fact that they exhibit a large surface area. Additionally, tin is a nontoxic material and a safe alternative in the cleaning of bodies of water. Considering these facts, this research aims at the production of SnO_2 nanoparticles in aqueous phase to study their spectroscopic properties using characterization techniques, specifically UV-vis and spectrofluorometer analysis.

Tin dioxide synthesis was made in the presence of tin chloride (SnCl_2), cetyltrimethylammonium bromide (CTAB), ammonium hydroxide and deionized water. The reaction time was optimized to 6-hours and the fluorescence was studied by using a spectrophotometer evidencing a peak at 403nm when excited at a wavelength of 280nm. While, UV-vis analysis denoted a peak at 303nm.

Taking into consideration SnO_2 spectroscopic properties and expected photocatalytic tendencies, future studies will be focused on the degradation of organic dyes.

EQ12.07.07

Late News: Effect of Various ZnO Interfacial Layer on the Nanostructured Photovoltaic Properties Based on Organic Materials [JunYoung Kim](#), JaeMin Jeon and DongYeol Shin; Gyeongsang National University, Korea (the Republic of)

Recently, research on nanostructured photovoltaic cells based on organic materials has been actively conducted to improve power conversion efficiency through the development of new device structures, synthesis of new organic materials and applied to charge extraction layer. This study applies various ZnO thin films (sol-gel process based on high and low temperature and nanoparticle process) as electron extraction layer in nanostructured photovoltaic cells based on PBDB-T:ITIC, and the correlation between ZnO and photovoltaic cells performance was analyzed. When the ZnO thin film was formed by the high temperature (450°C) sol-gel process, the sheet resistance of ITO electrode was increased up to 5 times. As a result, the power conversion efficiency was low at 4.12%. In the nanoparticle process, butanol-based ZnO has better dispersion and surface properties than IPA-based ZnO, resulting in improved polymer solar cell performance (PCE of 6.35% and 4.58% with butanol and IPA-based ZnO respectively). In addition, ZnO precursor solution with a low-temperature (150°C) sol-gel process was developed, and as a result of applying it as an electron extraction layer of a nanostructured photovoltaic cells, the device performance was greatly improved (PCE of 8.89%). The main reason for the improvement of the device performance is that the ripple-shaped surface is formed, which facilitates extraction of electrons and has excellent surface roughness.

EQ12.07.08

Dichalcogenide Monolayer-Plasmonic Heterostructures [Haydee Pacheco](#) and Deirdre O'Carroll; Rutgers, The State University of New Jersey, United States

Investigating the optical properties of transition metal dichalcogenide (TMDs) monolayers has recently become a promising research direction towards direct bandgap two-dimensional (2D) semiconductor applications. Monolayer 2D-TMDs emit light efficiently in the form of two distinct excitonic emission features, referred to as the A-peak (ground state) and B-peak (higher spin-orbit split state). These emission peaks can be tuned to promote a higher intensity ratios and therefore, to reduce the opportunity for undesirable intervalley scattering. Our work provides insight into the degree of valley polarization in MoS₂ monolayers and of MoS₂/plasmonic/heterostructures that can help maximize the optically-induced valley polarization by inducing a population imbalance between the two inequivalent valleys. Our monolayers are produced by lithium intercalation as well as by epitaxial growth on sapphire, while the heterostructures are fabricated using plasmonic nanostructures such as Ag nanoparticles. We observe that high quality samples produce enhanced emission from the B-exciton relative to the A-exciton, which corresponds to an increased degree of valley polarization. As it turns out, the relative optical orientation of these peaks, occurring at 612 nm and 675nm in MoS₂ monolayers, remains efficient even at room temperature. We take advantage of this fact and make use of a modified circular polarization luminescence (CPL) emission spectroscopy system. More specifically, our system consists of a static achromatic quarter wave plate (QWP) that converts L-CPL and R-CPL light to orthogonal linearly polarized light; later both L-CPL and R-CPL states are analyzed by automated rotation of a linear polarizer prior to whole-spectra detection with a CCD spectrometer. We present the analysis of the A- and B-exciton photoluminescence intensity ratio of both intrinsic and induced circular polarization emission in these structures.

EQ12.07.09

Structuring Exciton Transfer Pathways via Angular Control in Metal-Organic Frameworks [Ruomeng Wan](#), Dong-Gwang Ha, Jinhu Dou, William Tisdale and Mircea Dinca; Massachusetts Institute of Technology, United States

Metal-organic frameworks (MOFs) are crystalline materials consisting of organic building blocks and metal clusters. Traditionally known as a versatile system for manipulating chemical processes, MOFs' potential has recently been extended beyond controlling the movement of molecules to structuring the flow of energy. The promise of MOF as a platform for photophysical studies lies in its ability to lock chromophores into a variety of packing distances and geometries. Since photophysical processes are highly sensitive to the communication among neighboring molecules, MOFs provide a synthetic handle for structuring exciton dynamics. Taking advantage of this unique opportunity, herein we present a strategy that allows inhibition of singlet exciton transfer in a spin-selective fashion. The angular arrangement of chromophores inside the donor-acceptor MOF is visualized with high resolution transmission electron microscopy, and the exciton dynamics are probed by time-resolved spectroscopy. Connecting the structural and photophysical properties demonstrates that spin-selective control over exciton transfer can be synthesized with long-range structural order. We envision that this strategy can be applied to increasing the efficiency of photophysical processes that involve interplay between transfer of excitons of different spin states, such as solid-state triplet-triplet annihilation upconversion.

EQ12.07.10

Non-Perturbative Nonlinear Optical Properties of Single Chirality Carbon Nanotube Thin Films Near the Exciton Resonance [Pierre-Luc Thériault](#)¹, Abitha Dhavamani², Louis Haeblerle¹, Michael Arnold² and Stephane Kena-Cohen¹; ¹Polytechnique Montréal, Canada; ²University of Wisconsin Madison, United States

The lack of materials with large ultrafast nonlinearities currently limits the rise of optical information processing as a solution to efficiently process the ever-growing amount of data collected for big data and artificial intelligence applications. Optical processing schemes still need to interface with electronics for key functions which require nonlinear functions such as switching. Due to the weak nonlinear response of bulk materials, current optical switching technologies function at high threshold power which makes them unpractical. The development of efficient switching would be greatly helped by materials showing a fast and strong nonlinear optical response. Low-dimensional nanostructured materials like carbon nanotubes are predicted to have large and fast nonlinearities. Several groups have attempted to measure optical nonlinearities in single-walled carbon nanotube (CNT) thin films using the Z-scan technique. However, the use of a mixture of chiralities masked the resonant excitonic behavior and the analysis didn't account for the limited validity of common approximations when z-scan is used to study strongly nonlinear or absorbing films. In fact, the common approximations used in Z-scan fail drastically near electronic resonances.

In this work, we study the nonlinear optical properties of single chirality carbon nanotubes thin films using the Z-scan technique at wavelengths ranging from 917 nm to 1550 nm covering the near, on, and off-resonant excitation regime. Our investigation reveals a large enhancement of the nonlinear response near the excitonic resonance (1003 nm) of the film. In this regime, we observe a 15-fold enhancement of the nonlinear parameters. A nonlinear refractive index (n_2) as large as $3.4 \pm 0.2 \text{ cm}^2/\text{GW}$ and $-0.50 \pm 0.06 \text{ cm}^2/\text{GW}$ are measured on the blue and red sides of the resonance respectively. Large changes in the imaginary refractive index attributable to saturable 1-photon absorption are also observed for the near and on-resonance regimes together. The changes are well into the non-perturbative regime, where variations of the real and imaginary refractive index are on the order of the linear index, for intensities of less than $5 \text{ GW}/\text{cm}^2$. To account for the non-perturbative nature of the response, we developed a numerical beam propagation code that extracts the nonlinear properties of the thin film from the transmittance measurement, for an arbitrary nonlinear refractive index model, free of approximations. The strength of the nonlinearities in high-density single chirality CNT thin films, together with their compatibility with the silicon photonics fabrication processes, makes them a promising material for the development of nonlinear devices for optical signal processing.

EQ12.07.11

Late News: Ultrafast Dynamics of Photoexcited Carriers in Two-Dimensional Transition Metal Oxides and Carbo-Oxides Erika Colin-Ulloa¹, Ryan Hanna¹, Michelle H. Frasch¹, Hussein Badr², Kiana Montazeri², Michel Barsoum², Ronald L. Grimm¹ and Lyubov Titova¹; ¹Worcester Polytechnic Institute, United States; ²Drexel University, United States

Enhanced light-matter interactions and high surface to volume ratio in two-dimensional (2D) materials makes them promising candidates for application in solar energy conversion and optoelectronics. Recently, we have reported on a scalable, near ambient bottom-up synthesis of 2D transition metal oxides and carbo-oxides from non-layered precursors. Here we investigate the nature and dynamics of photoexcitations in 2D $\text{TiC}_{1-x}\text{O}_{1+x}$ and 2D Mn_xO_y using a combination of time-resolved photoluminescence spectroscopy and pump-probe spectroscopy. Both classes of materials are indirect gap semiconductors with the gap as high as 4.1 eV for Ti-based films and as low as 2.37 eV for Mn-based films. However, even high band gap films have considerable optical absorption across the visible range due to pronounced band tail states. Some of the films also exhibit efficient optical emission. Tuning optical excitation from the ultraviolet to the infrared range, we study the transient changes in optical properties and the lifetime of photoexcitations to uncover the nature and origin of the optically active states that play critical roles in solar energy conversion processes.

EQ12.07.13

Sensitive Time-resolved Luminescence Spectroscopy of CIGS Solar Cells Combined with Spatial Resolution Christian Oelsner, Eugeny Ermilov, Volker Buschmann, Frank Birke, Matthias Patting and Rainer Erdmann; PicoQuant, Germany

Over the years, luminescence spectroscopy has established itself as one of the fundamental methods for analyzing the photophysical properties of a variety of samples, ranging from simple organic molecules to semiconductor materials and photovoltaic (PV) devices. Combining spectral and lifetime information of a sample's luminescence signals provide a deeper insight into its photophysical processes. This can be further enhanced by including spatial information. Acquiring steady-state and time-resolved spectroscopic data at multiple, well defined points of interest (POI) of the sample can help in inferring structural-to-photophysical relationships in PV materials. Gathering such information is an important step toward the optimization of structure as well as preparation process of such materials in order to increase the performance of PV devices.

Here we will demonstrate the performance of a spectrometer-microscope assembly based on the FluoTime300 spectrometer and FluoMic add-on for investigating a Copper Indium Gallium Selenide (CIGS) based solar cell in terms of steady-state and time-resolved luminescence spectroscopy at different micrometer sized POIs. We will show that acquiring data at well defined excitation / detection areas can provide deeper insights into relationships between structure and photophysical behavior of CIGS solar cells. This additional information are not readily available when investigating such a sample with a conventional spectrometer as the luminescence signal is averaged over a much larger area (typically 1 mm^2 or more).

SESSION EQ12.08: Excitonic Processes in Organic Materials II

Session Chairs: Gonzague Rebetz and Carlos Silva

Thursday Morning, December 2, 2021

Hynes, Level 2, Room 207

10:30 AM EQ12.08.01

PBI-Based Biomimetic Complex for Efficient Light-Conversion Unveiled via Ultrafast Spectroscopy Vasilis Petropoulos¹, Mattia Russo¹, Francesco Rigodanza², Luca Moretti¹, Andrea Sartorel², Maurizio Prato³, Giulio Cerullo¹, Marcella Bonchio² and Margherita Maiuri¹; ¹Politecnico di Milano, Italy; ²University of Padova, Italy; ³University of Trieste, Italy

Converting solar energy into chemical energy is a promising strategy towards the production of solar electricity and stored fuels. Until now, most of the supramolecular complexes that undergo symmetry breaking charge separation (SB-CS) process, mimicking the photosynthetic special pair, reveal strong competing pathways of long-lived excitons and/or excimeric traps. Recently, a new supramolecular framework was developed taking inspiration from the minimal component in the photosynthetic organisms, defined as "Quantasome" (QS) [1]. The artificial QS is composed of a self-assembled perylene bisimide (PBI) and a polyoxometalate (POM) catalyst as a guest, building highly ordered three-dimensional (3D) noncovalent assemblies in water. We study a series of QS assemblies, with a redox-inactive and a redox-active POM catalyst as guest, Q-1 and Q-2 complexes respectively. Structural information extracted from Powder X-Ray Diffraction (PXRD) proves that the QS structures are mimicking the organization of the thylakoids in the granum domain of the chloroplasts.

We perform Ultrafast Transient Absorption (TA) spectroscopy to unveil the photo-physical pathways after photo-excitation. The samples are pumped with a sub-100 fs laser pulse peaked at 520 nm, while the probe pulse covers a broad spectral window spanning from 560 nm to 1000 nm. Q-1 and Q-2 complexes exhibit excited state absorption (ESA) bands originating exclusively from the superposition of PBI radical anion and cation. Our TA data show ultrafast ($< 150 \text{ fs}$) and quantitative formation of symmetry-broken charge transfer (SB-CT) excitonic states, delocalized over a number of PBI units. After excitation, there is an evident sharpening of the line-widths accompanied by partial peak-shifts over 0.8 ps timescale, suggesting electronic relaxation towards a more localized lower-energy Charge Separated (CS) state. After the localization of the charges into CS states, the Q-1 and Q-2 complexes follow different excited-state pathways. The Q-1 undergoes bi-exponential recombination, involving photo-generated PBI⁺ and PBI⁻, with 80 ps and 1 ns lifetime components. In Q-1, the quantitative SB-CS is followed by long-lived charges with an unprecedented k_{CS}/k_{CR} ratio with respect to geminate perylene-based systems in literature [2]. On the contrary, the Q-2 undergoes 8 ps hole transfer from PBI⁺ to POM which is followed by bi-exponential recombination, involving photo-generated POM⁺ and PBI⁻, with 60 ps and $> 1 \text{ ns}$ lifetime components. In this case, the presence of long-lived charges in the catalytic sites can lead to efficient water splitting.

To investigate the mechanism in QS structures leading to long-lived charges, we performed TA Anisotropy measurements. Anisotropy is sensitive to the relative polarization displacement of the photo-generated charges. We track the anion motion due to the anisotropy of the signal detected at the anion ESA peak (820 nm). The prominent depolarization for Q-1 and Q-2 complexes, suggests that the charges are not localized in the space they were created after photoexcitation, and instead they rapidly move in the 3D space [3]. The overall high anisotropic depolarization denotes that charge pairs in QS undergo an efficient dissociation and have a high mobility, consistent with the observation of long-lived CS states.

Hence, the ability to control the outcome application of the long-lived charges can be obtained through the suitable choice of the guest catalyst in the Quantasome-like self-assembly organization.

References

- [1] Bonchio, M. *et al. Nat. Chem.* **11**, 146–153 (2019).
- [2] Spenst, P., Young, R. M., Wasielewski, M. R. & Würthner, F. *Chem. Sci.* **7**, 5428–5434 (2016).
- [3] Moia, D. *et al. J. Am. Chem. Soc.* **138**, 13197–13206 (2016).

10:45 AM EQ12.08.02

Short Excited State Lifetimes Mediate Charge Recombination Losses in Organic Solar Cell Blends with Low Charge Transfer Driving Force [Rishi R. Shrivhare](#)¹, Gareth J. Moore¹, Andreas Hofacker², Sebastian Hutsch², Stefan Mannsfeld², Frank Ortman³ and Natalie Banerji¹; ¹Department of Chemistry and Biochemistry (DCB), University of Bern, Switzerland; ²Technische Universität Dresden, Germany; ³Technische Universität München, Germany

The field of organic photovoltaics (OPV) has undergone a resurgence in recent years owing to the swift increase in efficiency values of the solar cells. Highly efficient OPV systems demand a concomitant increase in the short-circuit current density (j_{SC}) and the open-circuit voltage (V_{OC}). In order to optimize the V_{OC} losses, majority of the high-efficiency OPV systems employ donor:acceptor combinations with near-zero energetic offset for the interfacial charge transfer reaction. In our study, we have investigated a blend of a low optical-gap diketopyrrolopyrrole (DPP) polymer and a fullerene derivative: PC[70]BM, with a near-zero driving force of ~ 50 meV for the interfacial electron transfer. In order to probe a sequence of events that ultimately lead to the formation of free charges, we employ a series of complementary spectroscopic and theoretical tools. Using femtosecond transient absorption (TA) and electroabsorption (EA) spectroscopy, we quantify the charge transfer (CT) and recombination dynamics and as well as the charge transport at early timescales. Firstly, we observe unusually short S_1 and CT state lifetimes in the investigated system (~ 13 -14 ps) and significant geminate charge recombination (gCR). Secondly, electron transfer is found to be ultrafast with a time constant of ~ 240 fs. The finding of ultrafast electron transfer was found to be consistent with a semiclassical Marcus-Levich-Jortner (MLJ) description at low driving force and low reorganization energy (λ_{reorg}). At low S_1 -CT offset, a short-excited state lifetime mediates charge recombination because i) back-transfer from the CT to the S_1 state followed by S_1 recombination can occur and ii) additional S_1 -CT hybridization can decrease the CT lifetime as a result of intensity borrowing effects. Both effects were confirmed by density functional theory (DFT) calculations. In addition, we employed time-resolved electromodulated differential absorption (EDA) spectroscopy to probe the transport of charge carriers on a sub-nanosecond time scale. We observed relatively slow dissociation of charges (tens of picoseconds) from the interfacial CT state, in contrast to polymer:fullerene blends with high CT driving force. We identify low local charge carrier mobility as a primary reason for the slow rise of the free charge population. Lastly, we performed simulations using a four-state kinetic model using Gaussian manifold of states and thus entailing the effects of energetic disorder (σ). These simulations enabled us to discern the role of interfacial CT state disorder (σ_{CT}) and the energetic disorder in the bulk of the film (σ_{bulk}). Firstly, the simulations reveal that the free charge yield could be increased from the observed 12% to 60% by increasing the S_1 and CT lifetimes to ~ 150 ps. Alternatively, by decreasing the interfacial CT state disorder (σ_{CT}) and increasing the bulk disorder (σ_{bulk}) the yield of free charge generation can be enhanced to 65% despite short excited state lifetimes.

11:00 AM EQ12.08.03

Amplification of Optoelectronic Properties through Homoconjugation in Three-Dimensional Molecular Structures [Iain A. Wright](#); Loughborough University, United Kingdom

The development of new molecular and macromolecular materials for organic light emitting devices (OLEDs) and organic solar cells (OSCs) is constantly evolving thanks to new insights into the interactions between light and matter. There is a great deal of work currently underway towards harnessing useful excited state properties of organic molecules and polymers such as room temperature phosphorescence,[1] thermally activated delayed fluorescence,[2] and singlet fission [3], making use of intermolecular interactions between individual donor and acceptor molecules which can yield efficient luminescence and simple devices.

The influence of three-dimensional molecular topology on the photophysical and electrochemical behaviour of organic semiconducting materials can be truly defining in how well such a molecule performs in any given application. Small changes in, for example, the dihedral angle between two rings in a molecule can make the difference between efficient or poor luminescence, charge transport, processability etc.[4-5]

Structure property relationships which take consideration of molecular geometry in three dimensions are required.

Here, the results of studies on new organic molecules which have been designed to make use of twisted, contorted or otherwise three-dimensionally defined structures will be presented. Using such 3D structures allows us to exploit or enhance photophysical processes towards obtaining higher efficiencies in organic electronic applications.

Particular focus will be given to the exploitation of homoconjugation – the through-space overlap of molecular orbitals – on the enhancement of defining photophysical parameters of new donor-acceptor compounds for use in OLEDs and OSCs. [6]

References:

- [1] B. Xu, H. Wu, J. Chen, Z. Yang, Z. Yang, Y.-C. Wu, Y. Zhang, C. Jin, P.-Y. Lu, Z. Chi, S. Liu, J. Xu and M. P. Aldred, *Chem. Sci.*, 2017 **8**, 1909
- [2] M. Zhang, C. J. Zheng, H. Lin and S.L. Tao, *Mater. Horiz.*, 2021, **8**, 401
- [3] T. Ullrich, D. Munz, D. M. Guldi; *Chem. Soc. Rev.*, 2021, **50**, 3845
- [4] R. Huang, J. S. Ward, N. A. Kukhta, J. Avó, J. Gibson, T. Penfold, J. C. Lima, A. S. Batsanov, M. N. Berberan-Santos, M. R. Bryce and F. B. Dias, *J. Mater. Chem. C*, 2018, **6**, 9238
- [5] I. A. Wright, A. Danos, S. Montanaro, A. S. Batsanov, A. P. Monkman, M. R. Bryce, *Chem. Eur. J.*, 2021, **27**, 6545
- [6] S. Montanaro, D. G. Congrave, M. K. Etherington, I. A. Wright, *J. Mater. Chem. C*, 2019, **7**, 12886

11:15 AM EQ12.08.05

Energy and Carrier Dynamics in Radical Organic Semiconductors [Sebastian Gorgon](#)¹, Qinying Gu¹, Alexander Romanov², Feng Li³, Emrys Evans⁴ and Richard H. Friend¹; ¹University of Cambridge, United Kingdom; ²University of Manchester, United Kingdom; ³Jilin University, China; ⁴Swansea University, United Kingdom

Radical organic semiconductors have unpaired electrons, leading to unusual physics that can be utilised in next-generation optoelectronics. High stability and luminescence can be achieved by molecular design, thus taming the typical reactivity of radical systems. In particular, emitters based on the tris(2,4,6-

trichlorophenyl)-methyl (TTM) radical moiety have recently been shown to fluoresce within the spin-doublet manifold with near-unity internal quantum efficiency. The ground state open-shell electronic structure, in combination with strong light absorption and emission, makes these materials promising for organic light-emitting diodes and photovoltaics with eliminated triplet losses. The integration of radicals into devices requires a detailed understanding of their fundamental energy and electron transfer mechanisms.

Here, a model system of closed-shell energy donor and open-shell acceptor is used to study energy transfer into radical materials via time-resolved optical spectroscopy, and signatures of direct triplet to doublet energy transfer are observed. In combination with temperature-dependent time-resolved photoluminescence measurements and modelling, these results allow us to propose the mechanism and yield for this process. Additionally, we present new insights into the photophysics of TTM derivatives on picosecond timescales. This work demonstrates a new method of harvesting dark triplet states, enabling lowering efficiency losses in optoelectronic devices.

SESSION EQ12.09: Excited States in Nanostructures II

Session Chair: Jiri Vanicek

Thursday Afternoon, December 2, 2021

Hynes, Level 2, Room 207

1:45 PM EQ12.09.01

Non-Destructive Photoluminescence Investigation of PV Devices with High Spatial Resolution Microscope Techniques [Christian Oelsner](#), Volker Buschmann, Felix Koberling, Matthias Patting and Rainer Erdmann; PicoQuant, Germany

Investigations of photovoltaic devices and semiconductors are essential to enhance the efficiency of preparation methods as well as their electronic and optical properties. Different parameters define these properties, e.g., number of defects and trap states, interface interactions, energy and electron transfer behavior and, of course, absorption properties and response to photon stimulation.

Surface characterization of such materials is usually done with scanning electron, scanning tunnel and atomic-force microscopes, which can gather information about homogeneity, conductivity, carrier mobility and defect center of films, semiconductors or within devices. But there still is a lack of information about important parameters that are necessary for understanding and optimizing the preparation and efficiencies of these materials.

We present here how combining time-resolved laser scanning microscopy – offering a broad range of techniques – with a spectrometer results in a valuable and powerful toolbox. This combination of microscopic (e.g., FLIM, PLIM, fast switch between widefield and confocal resolution, or carrier diffusion measurements) and spectroscopic methods (such as time-resolved photoluminescence or wavelength dependent emission scanning) allows investigating the photophysical properties of semiconductors, nanoparticles, QDs, polymers, solid-states as well as nanostructures on a whole new level. This additional information enables gaining a deeper understanding of both photophysical processes as well as structure-property relationships, which will help for the optimization of properties and efficiencies in practical applications.

2:00 PM EQ12.09.02

Plasma-Induced Heating—Interaction Between a Low-Temperature Plasma and Graphene [Carla Berrospe Rodríguez](#), Joseph Schwan and Lorenzo Mangolini; University of California, Riverside, United States

The energetic interaction between low-temperature plasma and the surface of materials produces a phenomenon commonly refer as plasma heating. This phenomenon, which plays a critical part in many plasma-driven processes [1], is very difficult to characterize and therefore poorly understood. Low-temperature plasma is used to activate several important surface reactions, since it can accelerate the surface kinetics, leading to processes such as reactive ion-etching, atomic layer deposition and heterogeneous chemistry, among others. One interesting example is the heat induction due to the recombination of atomic hydrogen at the surface nanoparticles in dusty plasmas to synthesized refractory materials [2]. However, the low rate of heat dissipation from the particles to the background gas, leads to a significant temperature increment and therefore, leaving unknown the real contribution of plasma heating into the temperature profile.

In this work, we present a Raman spectroscopic approach to quantify plasma-induced heating on a two-dimensional material as a surface-sensitive temperature probe. We use graphene because it is atomically thin, and it has a well characterized Raman signature. In addition, it is well known that graphene has been implemented into a variety of fields such as sensing, graphene-based catalysis or electrochemical energy conversion and others [3]. The temperature of the plasma-exposed graphene surface is obtained by Raman thermometry characterization [4]. We simultaneously measure the signal intensity of the Stokes and anti-Stokes G Raman band, while plasma impinging in the surface. The measurements are calibrated bringing the graphene temperature up to 200 °C, by means of a vacuum chamber-heater, to increase the thermal population of the vibrational modes and therefore enhance the anti-Stokes signal, which is significantly low compared to the Stokes signal at room temperature. When graphene is exposed to a radiofrequency (RF) argon plasma, its temperature raises to approximately 350 °C and its linearly dependent on the plasma input power. We strengthen our experimental results using a heat transfer model in COMSOL, where we discard the possibility of temperature increment due to gas heating by the plasma. In addition, we find a heating dependence on the plasma composition, where hydrogen-diluted argon decreases the surface temperature as hydrogen concentration increases in exponential-like behavior. Finally, we show evidence of anisotropic etching by hydrogenation, increasing disorder in the material structure and reducing the size of graphene domains. This study highlights the potential of two-dimensional materials, particularly graphene, to understand better plasma related phenomena.

[1] G. S. Oehrlein and Y. H. Lee, Reactive ion etching related Si surface residues and subsurface damage: Their relationship to fundamental etching mechanisms. *J. Vac. Sci. Technol.*, A5, 1585 (1987).

[2] L. Mangolini and U. Kortshagen, Selective nanoparticle heating: Another form of nonequilibrium in dusty plasmas, *Phys.Rev.* E79, 026405 (2009).

[3] K. M. F. Shahil and A. A. Balandin, Thermal properties of graphene and multilayer graphene: Applications in thermal interface materials. *Solid State Commun.* 152, 1331(2012)

[4] A. G. Souza Filho, A. Jorio, J. H. Hafner, C. M. Lieber, R. Saito, M. A. Pimenta, G. Dresselhaus, and M. S. Dresselhaus, Electronic transition energy E_{ii} for anisolated (n,m) single-wall carbon nanotube obtained by antiStokes/Stokes resonant Raman intensity ratio, *Phys.Rev.* B63, 241404 (2001).

2:15 PM EQ12.09.03

Origin of Photoluminescence from Carbon Dots [Nasir Javed](#), Zhongkai Cheng and Deirdre O'Carroll; Rutgers, The State University of New Jersey, United States

Carbon-based luminescent nanoparticles, which are usually referred to as carbon dots (CDs), are becoming increasingly popular for light-emitting applications due to their attractive optical properties and low-cost synthesis. CDs exhibit strong excitation-wavelength-dependent and -independent photoluminescence (PL) emission that can be tuned throughout the visible spectrum. However, their structure and the origin of their PL emission is still debated. In this study, CDs are synthesized by a solvothermal method using citric acid and 1,5-diaminonaphthlene, and X-ray photoelectron spectroscopy (XPS), UV-visible absorption, PL emission, Fourier transform infrared (FTIR), and Raman spectroscopies are used to investigate their structure and the origin of PL emission. The average size of the purified CDs is 19.5 nm with the majority of particles in the size range of 10 nm to 25 nm. XPS shows that the CDs also contain oxygen (31%) and nitrogen (9%) in addition to carbon (60%). FTIR and nuclear magnetic resonance (NMR) spectroscopy analysis show that the CDs are composed of aromatic as well as aliphatic carbon.

To investigate the photonic properties of the CDs, PL emission from the CDs is studied using different excitation wavelengths in different water-miscible solvents. Two distinct excitation-wavelength-independent PL emission bands are observed from the CDs: one deep violet emission band at 400 nm and another green emission band at ~520 nm. The PL quantum yield (QY) varies from 3.5% to 9.4 % with polarity of the solvents. Time-resolved PL (TRPL) emission measurements reveal that the CDs have short PL lifetime (≤ 8 ns) with a double exponential decay. The excitation-wavelength-independent PL emission, and the short PL lifetime imply that the CDs are likely to be composed of molecular clusters instead of graphitic crystals. Double exponential decay suggests that the CDs may be composed of two different types of fluorophores. The structure and optical properties of individual fluorophores are studied for the first time by dissolving the CDs in low-polarity, water-immiscible solvents, and separating the green-emitting molecules by solvent extraction. The PL QY of the green-emitting molecules after separation increases to 53.6%, and TRPL emission of these molecules decays with a single exponential with a lifetime of 5.8 ns. The structure of the green-emitting molecules is determined by using 1D (^1H and ^{13}C) and 2D (^1H - ^{13}C correlation spectroscopy, ^1H - ^{13}C heteronuclear multiple quantum coherence and ^1H - ^{13}C heteronuclear multiple bond correlation) NMR spectroscopies, which reveal that the molecules mainly have aromatic structure with pyridinic nitrogen doping. Finally, time-dependent density functional theory (TD-DFT) calculations are carried out to further study the excited states in the green-emitting molecules and to confirm that the green emission arises from the same molecules. From this study, it is concluded that the CDs are mainly composed of molecular fluorophores and that PL arises from individual molecules within the CD clusters.

2:30 PM EQ12.09.04

Dynamics of Photoexcited Carriers in Single-Crystal BiOI(001)—Interplay Between Charge Carriers, Interfaces and Environment [Amy M. Welch](#), Julia Martin, Erika Colin-Ulloa, Kateryna Kushnir, Leonardo N. Coelho, Katarina M. Himmelberger, Ronald L. Grimm and Lyubov Titova; Worcester Polytechnic Institute, United States

With a 1.8 eV band gap in the red region of the visible spectrum, bismuth oxyiodide (BiOI) may be viable as a top absorber in tandem-junction photovoltaics or a non-toxic photocatalyst for degradation of environmental pollutants. Viability requires understanding the interplay between interfacial chemical states, ambient atmosphere, and the resulting dynamics of photoexcited carriers in this 2D layered material. We synthesized single-crystal BiOI(001) via vapor transport and explored the behavior of optically excited carriers using time-resolved THz spectroscopy (TRTS) and time-resolved photoluminescence spectroscopy (TRPL). Under inert environments or chemical passivation, above-band-gap excitation with UV or blue light yields free carriers with mobilities that rival crystalline silicon, and hundreds-of-picosecond lifetimes that recombine with both band-edge and defect-related emission. In contrast to in vacuo behavior, PL intensities show a rapid and irreversible attenuation with increasing exposure to the 485 nm excitation light. We discuss the results in the context of BiOI for energy harvesting and sensing applications, and highlight pathways for chemical passivation for stable, efficient operation under illumination in air.

2:45 PM EQ12.09.05

Near-Field Optical Microscopy of Silicon Arrays Composed of Subwavelength Light Funnel Arrays [Ankit Chauhan](#)¹ and Gil Shalev^{2,1}; ¹Ben-Gurion University of the Negev, Israel; ²Ben-Gurion University of Negev, Israel

Light trapping in arrays composed of subwavelength light funnel arrays (LF arrays) is a promising approach towards efficient broadband absorption of the solar radiation and surface arrays of subwavelength structures has an additional advancement towards ultra-thin photovoltaic (PV) cells. In the following we examine the origin of light trapping enhancement in LF arrays as compared to nanopillar (NP) arrays and we show that light trapping enhancement is due to favorable strong optical coupling between adjacent light funnels which is not realized in NP. We suggest that the enhanced light trapping and absorption in dense LF arrays is governed by strong modal excitation coupled with high filling ratio, unlike the absorption in dense optimized nanopillar arrays which is governed by weak modal excitation and high filling ratio. Finally, we make the distinction between two types of optical overlap: weak overlap in which the coupling between the sparse array modes and the impinging illumination increases with array densification, and strong overlap where the array densification introduces new highly absorbing modes. Finally, the study of the resonant behaviour of silicon non-imaging light concentrators (NLCs) provide a new route for achieving efficient control of both electric and magnetic components of light. We use near-field scanning optical microscopy (NSOM) to measure the near-field light intensity as function of array geometry.

3:00 PM EQ12.09.06

Surface-Mediated Ensemble Energy Transfer in Core-Only CdSe NCs [Minhal Hasham](#) and Mark W. Wilson; University of Toronto, Canada

Semiconductor nanocrystals (NCs) exhibit bright, narrow, and size-tunable emission across the visible and infrared spectrum with large absorption cross-sections and high quantum yields. A recent use for NCs gaining interest is triplet fusion based incoherent photon upconversion (TUC), which is a rising strategy to generate emissive spin-singlet states from two spin-triplet excitons. While TUC motifs have found success in biomedical imaging applications and have recently been employed to initiate photochemical transformations, an understanding of sensitization mechanisms is required.

Here NCs are promising sensitizers due to their small exchange splitting and facile surface functionalization routes. These factors allow for minimal energy loss and direct injection of triplets to surface bound transmitters, along with the ability to load >1 transmitter per NC. In the archetypal core-only CdSe/9-anthracenecarboxylic acid (9-ACA), the role of the commonly observed trap during triplet sensitization remains unclear, as do the energetics of this surface-oriented trap state.

Here, we use time-resolved photoluminescence to probe energy transfer in hybrid CdSe/10-(4-methoxyphenyl)anthracene-9-carboxylic acid (MeOPh-ACA) systems. We observe rapid transfer from both band-edge and trap states and show that transfer occurs from states which would appear to be thermodynamically uphill if their photon energy was a faithful proxy of chemical potential. Notably, we observe comparable quenching from band-edge and trap states, with similarly rapid kinetics. Further, we synthesize MeOPh-ACA, a 9-ACA derivative with stabilized frontier orbitals with respect to bare 9-ACA. When paired with a sufficiently small (<2 nm) CdSe NC sensitizer, both Dexter-like correlated energy transfer and sequential charge transfer are thermodynamically favourable mechanisms to sensitize the spin-triplet state on the organic ligand. Even with this new available pathway, we observe no change in the rate of energy transfer, while continuing to observe comparable quenching from band-edge and trap states. Finally, we find that these trap states are not pathological for TUC, and observe upconverted photon emission when our system is paired with free-floating annihilator.

Our results suggest that the deeply Stokes-shifted photoluminescence from these nanocrystals arises from energetically shallow surface-oriented states which localize the exciton shortly after irradiation, but that selection rules for exchange-mediated transfer qualitatively differ. Our observation of commensurate quenching from band-edge and trap states suggests that the band-edge and trap band are in rapid thermal equilibrium and supports the hypothesis that traps in CdSe NCs are 'shallow' i.e., of comparable energy to the band-edge. Taken together, these observations have the practical implication that the trap band can be used as a surrogate to monitor the population of band-edge excitations. These findings indicate that surface traps in core-only CdSe NCs may not hinder energy transfer during triplet sensitization and that the trap photon energy is not an honest representation of its free energy.

SESSION EQ12.10: Theoretical Frameworks for Excited States Dynamics
Session Chairs: Ferdinand Grozema and Carlos Silva
Thursday Afternoon, December 2, 2021
Hynes, Level 2, Room 207

4:00 PM *EQ12.10.02

Finite-Temperature, Anharmonicity and Duschinsky Effects on the Two-Dimensional Electronic Spectra from *Ab Initio* Thermo-Field Gaussian Wavepacket Dynamics [Jiri Vanicek](#) and Tomislav Begušić; Ecole Polytechnique Fédérale de Lausanne, Switzerland

Accurate description of finite-temperature vibrational dynamics is indispensable in the computation of two-dimensional electronic spectra. Such simulations are often based on the density matrix evolution, statistical averaging of initial vibrational states, or approximate classical or semiclassical limits. While many practical approaches exist, they are often of limited accuracy and difficult to interpret. Here, we use the concept of thermo-field dynamics to derive an exact finite-temperature expression that lends itself to an intuitive wavepacket-based interpretation. Furthermore, an efficient method for computing finite-temperature two-dimensional spectra is obtained by combining the exact thermo-field dynamics approach with the thawed Gaussian approximation for the wavepacket dynamics, which is exact for any displaced, distorted, and Duschinsky-rotated harmonic potential but also accounts partially for anharmonicity effects in general potentials. Using this new method, we directly relate a symmetry breaking of the two-dimensional signal to the deviation from the conventional Brownian oscillator picture.

[1] T. Begušić and J. Vanicek, *J. Phys. Chem. Lett.*, **12**, 2997 (2021).

[2] T. Begušić and J. Vanicek, *J. Chem. Phys.* **153**, 184110 (2020).

[3] T. Begušić and J. Vanicek, *J. Chem. Phys.* **153**, 024105 (2020).

4:30 PM EQ12.10.03

Monte Carlo Simulation of Secondary Electron Emission under Photoexcitation [Wenkai Ouyang](#), Xiangying Zuo and Bolin Liao; University of California, Santa Barbara, United States

Understanding the photogenerated charge carrier transport in semiconductors is crucial, particularly for applications toward high-efficiency photovoltaic cells and photosensors. Scanning ultrafast electron microscopy (SUEM) is an emerging technique that can visualize photocarrier transport by measuring the spatial-temporal change of secondary electron emission as a result of photoexcitation. Despite the increasing demonstrations of SUEM capability, the physical picture of the image contrast mechanisms of SUEM remains incomplete. In this work, we implement Monte Carlo simulation based on the Mott elastic scattering cross section and Landau's theory of statistically distributed energy loss for inelastic collision; we simulate the secondary electron yield (SEY) of doped silicon under photoexcitation. Photoexcitation will induce both photocarriers in the bulk and the surface photovoltaic voltage (SPV) effect that modifies the surface band bending. Photoexcited carriers result in the change of the inelastic scattering cross section which is determined by the electron energy loss functions (ELF). Time-dependent density functional theory (TDDFT) is applied to evaluate the ELF for both n-type and p-type Si with different doping concentrations and transient electronic temperatures, but only marginal changes of SEY are observed. In contrast, SPV effect changed the surface transmission probability for secondary electrons, and SEY of n-type Si had a 3% ~5% increase while p-type Si had a 3%~5% decrease. This study provides a detailed understanding of SUEM image contrasts and lays the foundation for precise interpretation of ultrafast electron microscope images.

This work is based on research supported by the Army Research Office Young Investigator Program under the award number W911NF-19-1-0060.

SESSION EQ12.11: Poster Session II
Session Chair: Carlos Silva
Thursday Afternoon, December 2, 2021
8:00 PM - 10:00 PM
Hynes, Level 1, Hall B

EQ12.11.01

Late News: Structural, Electrical and Optical Properties of Electroless Silver Plated $\text{La}_x\text{Ba}_{1-x}\text{SnO}_3$ for Transparent Electrode Using Non-Vacuum Process [Su Hyeong Kim](#)¹, Jeong Hye Jo¹ and Sun Hee Kim²; ¹Gachon university, Korea (the Republic of); ²Incheon National University, Korea (the Republic of)

Transparent electrodes for electronic devices have to unique properties such as transmittance of more than 80% in visible light and sheet resistance of less than $10^3\Omega$. ITO (Indium Tin Oxide) is the TCO (Transparent Conductive Oxide) used in almost transparent electrodes. ITO uses indium, which is a rare earth, and has the drawbacks of high cost and low mobility.[1] Consequently, the many research of TCO like ZnO, STO (SrTiO_3), BSO (BaSnO_3) to replace ITO were being studied. LBSO ($\text{La}_x\text{Ba}_{1-x}\text{SnO}_3$) is a transparent conductive oxide candidate to replace ITO due to its wide bandgap of 4.05 eV, high transmittance in visible light, mobility, and carrier density. [2], [3] For high crystallinity, these properties of LBSO required a vacuum process that had drawbacks such as high cost, low deposition rate, shadow effect, etc. Thus, a thin film deposition method using a non-vacuum process has been studied, but there are problems in depositing several layers and having lower performance compared to vacuum processes [4] High resistance of thin film using non-vacuum process can be improved by electroless silver plating, and it is confirmed that silver nano particle increase conductivity. [5] In this research, using

non-vacuum process improve of low deposition rate and high equipment cost in vacuum process, and overcome low thin film quality and high sheet resistance in non-vacuum process deposition method through electroless silver plating. It has been verified that LBSO thin films deposited using non-vacuum process have a sheet resistance of less than $10^3 \Omega$, a work function of more than 5 eV, and a transmittance of more than 80% in visible light. The above-mentioned LBSO can also open new ways toward intrinsically next-generation transparent electrodes to replace ITO.

[1] Terzini, E., P. Thilakan, and C. Minarini. *Materials Science and Engineering: B* 77.1 (2000): 110-114.

[2] Luo, X., et al. *Applied Physics Letters* 100.17 (2012): 172112.

[3] Sanchela, Anup V., et al. *Journal of materials chemistry C* 7.19 (2019): 5797-5802.

[4] Wang, Zhaokui, et al. *ACS applied materials & interfaces* 3.7 (2011): 2496-2503.

[5] Babaahmadi, Vahid, Majid Montazer, and Wei Gao. *Carbon* 118 (2017): 443-451.

This research was funded and conducted under the Competency Development Program for Industry Specialists of the Korean Ministry of Trade, Industry and Energy (MOTIE), operated by Korea Institute for Advancement of Technology (KIAT). (No. P0012453, Next-generation Display Expert Training Project for Innovation Process and Equipment, Materials Engineers)

EQ12.11.02

Asymmetric-Donor (D₂D₂')-Acceptor (A) Conjugates for Simultaneously Accessing Intrinsic Blue-RTP and Blue-TADF Harsh Bhatia^{1,2} and Debdas Ray²; ¹University College London, United Kingdom; ²Shiv Nadar University, India

The development of new photoluminescent (PL) materials with simultaneous room-temperature phosphorescence (RTP) and thermally activated delayed fluorescence (TADF) features is highly desirable for bio-imaging, security applications and sensors due to the involvement of both singlet and longer lived triplet states.¹ In this work we have systematically designed two multiple donors and single acceptor based molecular systems which can simultaneously harness the triplet state via two different channels. We designed the molecules by taking cue from the idea that the free lone pair of electron containing phenoxy donors when linked to the phthalonitrile (PN) acceptor gives rise to RTP emission. When carbazole connects angularly with PN acceptor, it give rise to TADF emission. In this work we have connected both the donors to the single acceptor PN. Here we discuss the photophysical studies of two carbazolyl-phenoxy-phthalonitrile conjugates (CPPN, CPPNF).² The detailed spectroscopic studies of CPPN and CPPNF along with two daughter compounds of phenoxy-phthalonitrile (PPN, PPNF) in polar and non-polar hosts confirmed efficient blue-RTP from the higher-energy locally excited (LE) triplet state (T_{PPN}) due to the phenoxy-phthalonitrile (PPN) part. While the blue-TADF was observed via the reverse intersystem crossing from the low-lying charge transfer triplet state (T_{CzPN}) of the carbazolyl-phthalonitrile (CzPN) part to the singlet (S_1) charge transfer state of the same CzPN part. Moreover, it was observed that the higher lying LE triplet state (T_{PPN}) acts as an intermediate for spin-vibronic coupling^{3,4} to cause the reverse intersystem crossing. Such PL characteristics are observed due to the energetic proximity of $^3LE_{PPN}$, $^1CT_{CzPN}$ and $^3CT_{CzPN}$.⁵ In the hydrogen-bonded matrix and crystals, we found faint persistent green-RTP characteristics of the PPNF due to supramolecular interactions and aggregation of the molecule. This study paves the way to understand the involvement of different excited states associated with TADF and RTP processes of asymmetric-donor-acceptor systems.

References:

1. Data, P.; Takeda, Y.; *Chem. Asian J.* **2019**, *14*, 1613-1636.

2. Bhatia, H.; Ray, D.; *Mater. Adv.* **2020**, *1*, 1858-1865.

3. Chen, X., -K.; Kim, D.; Bredas, J. -L. *Acc. Chem. Res.* **2018**, *51*, 2215-2224.

4. Etherington, M. K.; Gibson, J.; Higginbotham, H. F.; Penfold, T. J.; Monkman, A. P. *Nat. Commun.* **2016**, *7*, 13680.

5. Samanta, P. K.; Kim, D.; Coropceanu, V.; Bredas, J. -L. *J. Am. Chem. Soc.* **2017**, *139*, 4042-4051.

EQ12.11.07

Reverse Intersystem Crossing Enhancement in Organic Devices via Heavy-Atom Effect in Host Molecules Alexandre Malinge¹, Shiv Kumar², William Skene³, Eli Zysman² and Stephane Kena-Cohen¹; ¹Polytechnique Montréal, Canada; ²University of St Andrews, United Kingdom; ³Université de Montréal, Canada

The performance of Organic Light-Emitting Diode (OLEDs) has considerably improved with the discovery of Thermally-Activated Delayed Fluorescence (TADF) materials that can harvest dark triplet excitons. In TADF molecules, the triplet excitons are transferred to emissive singlet excitons by a process called reverse intersystem crossing (rISC). However, the collection of triplet excitons remains a challenge for OLEDs that suffer from a poor efficiency at high current (roll-off). Indeed, the drop of the performance is mainly due to polaron-exciton deactivation and exciton-exciton annihilation coming from the high density of triplet excitons and their relatively long lifetime. In order to overcome that problem, the rISC process can be faster in order to decrease the density of triplet excitons to limit their interactions. It is shown that this process can be enhanced by a stronger spin-orbit coupling, generated by a heavy-atom effect in the host molecules.

Derivatives of 1,3-Bis(N-carbazolyl)benzene (mCP) were synthesized by adding bromine or iodine atoms in order to increase the heavy-atom effect in the mCP host. It results in a greater phosphorescence of the host due to a better transfer between singlet and triplet states. Then, photophysical studies were carried out on different TADF guest molecules. The lifetime of the excitons has been reduced while keeping a high photoluminescent quantum yield when using halogenated molecules as host and the rate of rISC has been multiplied by a factor of 10. The use of spin-orbit coupling through the heavy-atom effect in the host molecule could be a solution to the strong roll-off and degradation observed in OLED devices.

EQ12.11.08

Tunable Electronic Properties of Two-Dimensional Hybrid Organic-Inorganic AgSe_nTe_{1-n}Ph by Composition Control Woo Seok Lee, Watcharaphol Paritmongkol, Tomoaki Sakurada and William Tisdale; Massachusetts Institute of Technology, United States

Silver phenylselenolate (AgSePh) is an emerging hybrid organic-inorganic two-dimensional (2D) semiconductor due to its unique properties such as narrow blue emission, in-plane anisotropy and high exciton binding energy. To expand an application of this novel 2D semiconductor, a systematic method for precisely controlling its band gap, which determines electronic and optical properties, is required. One of the simplest and the most effective way to tune the band gap is making an alloy and controlling its composition. Herein, we show that the chemical transformation reaction between silver film and the mixture of diphenyl diselenide (Ph₂Se₂) and diphenyl ditelluride (Ph₂Te₂) vapors produces 2D silver phenylchalcogenolate alloy (AgSe_nTe_{1-n}Ph) thin films with controllable Se to Te ratio depending on partial pressure of Ph₂Se₂ and Ph₂Te₂ vapors during reaction. Systematic structural and optical characterization to confirm tunable structural and optical properties as well as homogeneity of alloys will be presented. Furthermore, the emission mechanisms of AgSe_nTe_{1-n}Ph alloy films depending on chalcogen ratio will be discussed. This work provides an insight to design novel 2D hybrid organic-inorganic semiconductors with desirable optical properties.

EQ12.11.09

Real-Time and In Situ Viscosity Monitoring in Industrial Adhesives Using Luminescent Cu(I) Phenanthroline Molecular Sensors Ankit Dara¹, Derek Mast¹, Anton Razgoniaev², Felix Castellano³ and Alexis D. Ostrowski¹; ¹Bowling Green State University, United States; ²Duke University, United States

States; ³North Carolina State University, United States

Monitoring the viscosity of polymers in real-time remains a challenge, especially in confined environments where traditional rheological measurements are hard to apply. In this study, we have utilized $[\text{Cu}(\text{diptmp})_2]^+$ (diptmp = 2,9-diisopropyl-2,4,7,8-tetramethyl-1,10-phenanthroline) as an optical probe for real time sensing of viscosity in various adhesives during the curing process (viscosity increases) via changes in luminescence. The emission lifetime of the triplet metal to ligand charge transfer (³MLCT) state of $[\text{Cu}(\text{diptmp})_2]^+$ in epoxy adhesive increased exponentially similar to viscosity values obtained from oscillatory rheology. The longer lifetime in higher viscosity materials was attributed to changes in the excited state deactivation processes from a known Jahn-Teller distortion in the Cu(I) geometry from tetrahedral in the ground state to square planar in the excited state. The real-time viscosity was also monitored reversibly by emission lifetime during polymer swelling (viscosity and lifetime decrease) and unswelling (viscosity and lifetime increase). Monitoring emission lifetime, unlike absorption lifetime in our previous study, allowed us to measure viscosity in opaque samples which scatter light. The optical probe $[\text{Cu}(\text{diptmp})_2]^+$ in Gorilla Glue™ adhesive, showed a clear correlation of emission intensity or lifetime to viscosity during the curing process. We have also compared these lifetime changes using $[\text{Ru}(\text{bpy})_3]^{2+}$ (bpy = bipyridine) as a control. $[\text{Cu}(\text{diptmp})_2]^+$ showed not only higher emission lifetime but also more ubiquity as a real-time viscosity sensor.

EQ12.11.10

Robust Estimation of Charge Carrier Diffusivity Using Transient Photoluminescence Microscopy [Narumi Wong](#), Seung Kyun Ha, Kristopher Williams, Marc A. Baldo, James W. Swan and William Tisdale; Massachusetts Institute of Technology, United States

Studying charge transport in emergent semiconducting materials is particularly challenging as structural inhomogeneities in the material can play an influential role, leading to dynamics that require resolution of sub-diffraction limited length-scales and femtosecond time-scales. Transient photoluminescence (PL) microscopy can provide the spatial and temporal resolution required to image diffusion of excitons and free charge carriers in optoelectronic materials. In excitonic materials, extraction of key material parameters such as diffusion coefficients can be simplified as the bound electron and hole move together. However, in materials where transport is dominated by free charge carriers, extracting diffusivities accurately from this multi-dimensional data requires good physical models coupled with statistically robust fitting algorithms. In this work, I present a detailed numerical framework for modeling the free charge carriers in transient PL microscopy experiments, and provide model and parameter analyses using a Markov Chain Monte Carlo sampler as part of the fitting algorithm. This approach is applied to lead-halide perovskites and transition metal dichalcogenides to obtain statistically confident estimates of ambipolar charge carrier diffusivities for these materials.

EQ12.11.20

Time-Dependent Photoluminescence of Titanium Carbo-Oxide Nanostructures [Ryan Hanna](#)¹, Erika Colin-Ulloa¹, Michelle H. Frasch¹, Kateryna Kushnir¹, Hussein Badr², Michel Barsoum², Ronald L. Grimm¹ and Lyubov Titova¹; ¹Worcester Polytechnic Institute, United States; ²Drexel University, United States

Nanostructured metal oxides such as TiO₂ or ZnO represent state-of-the-art photocatalysts for water splitting and waste treatment. While highly efficient, they are limited by the need for ultraviolet illumination. Recently, we have developed a simple one pot approach for fabrication of nanostructured titanium carbo-oxide TiC_{1-x}O_{1+x} (x=0.25-0.5) which is photocatalytically active under visible excitation. Here we investigate the photophysical properties of TiC_{1-x}O_{1+x} films using time-resolved photoluminescence spectroscopy. UV-VIS spectroscopy shows an indirect band gap at ~ 4.1 eV, higher than that of TiO₂, and sub-gap states that absorb in the visible range. Excitation with below band gap, 485 nm light results in a broadband optical emission centered around ~ 2.1 eV. Its decay is bi-exponential, with the ~ 1ns fast component in all studied films, and the slower component that varies in 5-12 ns range depending on synthesis duration. We hypothesize that radiative recombination at the nanostructure surfaces is responsible for the slower process, with longer processing yielding smaller nanostructures and higher surface recombination rates. Lifetime of optically excited carriers has major implications for photocatalysis and other applications, and we demonstrate here that it can be tuned it during one-pot titanium carbo-oxide nanostructure synthesis.

SESSION EQ12.12: Spatio-Temporally Resolved Optical Probes of Materials

Session Chairs: Natalie Banerji and Rishi Shivare

Monday Afternoon, December 6, 2021

EQ12-Virtual

1:00 PM *EQ12.12.01

Nanoscale Stroboscopic Tracking Microscopy of Electronic and Thermal Energy Through Optical Elastic Scattering [Naomi S. Ginsberg](#)¹, Hannah Weaver¹, James Utterback¹, Milan Delor², Cora Wentz³, Joelson Wong³, Harry A. Atwater³, Dipti Jasarasaria¹, Eran Rabani¹, Aditya Sood⁴, Burak Guzelturk⁴ and Aaron Lindenberg⁴; ¹University of California, Berkeley, United States; ²Columbia University, United States; ³California Institute of Technology, United States; ⁴Stanford University, United States

I will describe our transient optical approaches to directly image the nanoscale transport dynamics of various types of quasiparticles in a wide range of hierarchical semiconducting and conducting materials. For example, by characterizing the mean squared expansion of initially localized charge carriers, bound electron-hole pairs, heat, and sound, we elucidate the impact of various material heterogeneities on electronic and thermal transport and also the interplay between heat and charge distributions.

1:30 PM *EQ12.12.02

Spatial and Temporal Imaging of Exciton Transport in Two-Dimensional Heterostructures [Libai Huang](#); Purdue University, United States

Charge-transfer (CT) excitons at hetero-interfaces play a critical role in light to electricity conversion using nanostructured materials. However, how CT excitons migrate at these interfaces is poorly understood. Atomically thin and two-dimensional (2D) nanostructures provide a new platform to create architectures with sharp interfaces for directing interfacial charge transport. Here we investigate the formation and transport of interlayer CT excitons in van der Waals (vdW) heterostructures based on semiconducting transition metal dichalcogenides (TMDCs) employing transient absorption microscopy (TAM) with a temporal resolution of 200 fs and spatial precision of 50 nm.

We have investigated interlayer exciton dynamics and transport modulated by the moiré potentials in WS₂-WSe₂ heterobilayers in time, space, and momentum domains using transient absorption microscopy combined with first-principles calculations. Experimental results verified the theoretical prediction of energetically favorable K-Q interlayer excitons and unraveled exciton-population dynamics that was controlled by the twist-angle-dependent energy difference between the K-Q and K-K excitons. Spatially- and temporally-resolved exciton-population imaging directly visualizes exciton

localization by twist-angle-dependent moiré potentials of ~100 meV. Exciton transport deviates significantly from normal diffusion due to the interplay between the moiré potentials and strong many-body interactions, leading to exciton-density- and twist-angle-dependent diffusion length. These results have important implications for designing vdW heterostructures for exciton and spin transport as well as for quantum communication applications. We have also imaged the transport of interlayer CT excitons in 2D organic-inorganic vdW heterostructures constructed from WS₂ layers and tetracene thin films. Photoluminescence (PL) measurements confirm the formation of interlayer excitons with a binding energy of ~ 0.3 eV. Electron and hole transfer processes at the interface between monolayer WS₂ and tetracene thin film are very rapid, with time constant of ~ 2 ps and ~ 3 ps, respectively. TAM measurements of exciton transport at these 2D interfaces reveal mobile CT excitons, with diffusion constant of ~ 1 cm²s⁻¹. The high mobility of the delocalized CT excitons could be the key factor to overcome large CT exciton binding energy in achieving efficient charge separation.

2:00 PM BREAK

SESSION EQ12.13: Excited States in Nanostructures III
Session Chairs: Libai Huang and Mark Wilson
Monday Afternoon, December 6, 2021
EQ12-Virtual

4:00 PM *EQ12.13.01

Tuning Exciton Extraction Dynamics by Twisting and Stacking van der Waals Materials [Matt W. Graham](#); Oregon State University, United States

Using time-space resolved ultrafast microscopy on 2D materials or single-crystal singlet-fission crystals, we show how long-range interlayer electronic coupling can be selectively enhanced either by applying an *E*-field or by twisting the layer stacking orientation. In both cases, transient interlayer exciton states form and drive the optoelectronic material response. Considering first twisted bilayer graphene (*t*BLG), we discovered how stacking-angle tunable absorption resonances form a strongly-bound exciton state owing to the symmetrized rehybridization of the interlayer *2p* orbitals. Using two-photon photoluminescence and intraband-transient absorption microscopies, we have recently imaged the photoemission and exciton dynamics from single-grains of *t*BLG. After resonant excitation, our results suggest the formation of strongly bound (up to 690 meV), metastable interlayer exciton states. Our observation of resonant PL emission from twisted bilayer graphene materials is best explained by the theoretically predicted coexistence of strongly bound interlayer excitons and metallic graphene continuum states. We show how stacking angle-tunable interlayer excitons states may permit new photocurrent extraction routes from quasi-stable interlayer excitons.

Unlike stacked graphene, semiconducting 2D transition metal dichalcogenides (TMDCs) have diffuse interlayer *d*-orbital overlap. To enhance interlayer electronic coupling in TMDCs, we apply an interlayer-directed *E*-field, inducing electron-hole dissociation. Time-resolved photocurrents show that stacked WSe₂ devices can have both IQE >50% and fast (<60 ps) picosecond electron escape times. Our ultrafast photocurrent rates kinetics give the same *E*-field-dependent electronic escape and dissociation rates seen from optical ultrafast microscopy. To rationalize these fast electronic escape rates, we show the ratio of the electronic rates accurately predicts the actual WSe₂ device photocurrent generation efficiency. Collectively, we show how optical and photocurrent-based ultrafast microscopies together provide an analytical extraction of the photocurrent-generating ultrafast dynamics in van der Waals stacked materials and organic singlet fission materials.

References

- [1] H. Patel, L. Huang, C.J. Kim, J. Park, M. W. Graham, Stacking Angle-Tunable Photoluminescence from Interlayer Exciton States in Twisted Bilayer Graphene, *Nature Comm*, 10, 1445 (2019).
- [2] K. T. Vogt, S.-F. Shi, F. Wang, M. W. Graham, Ultrafast photocurrent and absorption microscopy of few-layer TMD devices isolate rate-limiting dynamics driving fast and efficient photoresponse, *J Phys Chem C*, 124, 28, 15195–15204 (2020)

4:30 PM EQ12.13.02

Composition, Crystalline Phase Transformation and Emission of Si-Rich-HfO₂:Pr Films Prepared by Magnetron Sputtering Tetyana V. Torchynska¹, Leonardo Gabriel Vega-Macotela², José Oliveros-García³, Manuel Alejandro Garcia Andrade⁴, Larysa Khomenkova^{5,6} and Fabrice Gourbilleau⁷; ¹Instituto Politecnico Nacional, ESFM, Mexico; ²Instituto Politecnico Nacional, ESIME Zac, Mexico; ³Instituto Politecnico Nacional, UPIITA, Mexico; ⁴Instituto Politecnico Nacional, ESIME Cul, Mexico; ⁵V. Lashkaryov Institute of Semiconductor Physics at NASU, Ukraine; ⁶National University "Kyiv-Mohyla Academy, Ukraine; ⁷CIMAP, UMR CNRS/CEA/ENSICAEN/UNICAEN, France

The impact of annealing at different temperatures and times on the morphology, composition, the transformation of crystal phases, and emission of Si-rich-HfO₂ films prepared by radio-frequency magnetron sputtering and doped with the rare-earth Pr element has been investigated. The follows methods: scanning electronic microscopy (SEM), energy dispersive X-ray spectroscopy (EDS), X-ray diffraction (XRD), Raman scattering and photoluminescence (PL) have been used. Thermal annealing was carried out at 800, 900, 1000 and 1100C for 30 min or for times 5, 15, 20 and 60 min at 1000°C in nitrogen atmosphere.

The films are characterized by the fine grain structures with the maximum grain size of 40nm. The composition of the films varied significantly at annealing with the oxidation increasing at high annealing temperatures. The annealing causes the transformation and separation of the crystal phases from the hafnia silicates at low annealing temperatures to the tetragonal HfO₂ and SiO₂ phases detected after high temperature (1000 or 1100°C) treatments. The great variety of the visible and infrared PL bands related to the optical transitions in the 4f inner shells of the Pr³⁺ ions and via native host matrix defects were detected in the PL spectra. Their contribution depends on the annealing temperature and governs the shape of total PL spectra. The impact of crystalline phase transformation at annealing on the peculiarities of the PL excitation and emission spectra of rare-earth Pr³⁺ ions are analyzed and discussed.

4:35 PM EQ12.13.03

Phase Change Vanadium Dioxide Microstructures—Size Dependence and Photodetection [Sumaiya Kabir](#)¹, [Shruti Nirantar](#)¹, [Cuong Ton-That](#)², [Sharath Sriram](#)¹, [Sumeet Walia](#)¹ and [Madhu Bhaskaran](#)¹; ¹RMIT University, Australia; ²University of Technology Sydney, Australia

The conventional high-speed semiconductor-based photodetectors involve limited wavelengths of operation and usually incorporate complex and expensive fabrication. Vanadium dioxide is a phase change material that undergoes an insulator to metal transition near room temperature. This material has drawn attention to broadband optoelectronic applications due to its unique band structure and versatile electronic and optical properties. However, vanadium dioxide-based photodetectors reported so far involve complex structures that lack scalability and constrained wavelength response similar to commercial photodetectors. Herein, two-terminal planar devices based on vanadium dioxide thin film are presented where devices were fabricated by using

standard micro-/nano-fabrication. To enhance the photoresponse of our photodetector devices, we use two novel techniques. Firstly, we explore the effect of the size of photodetector devices in photoresponse at broadband wavelengths ranges from ultra-violet to near-infrared. With the miniaturization of device size, the photoresponsivity increases. Finally, we investigated photoresponse in the insulator-to-metal transition slope (50-60 °C) and beyond insulator-to-metal transition slope (65 °C) regions. The co-existence of the insulator and metallic domains in these regions significantly enhances the photoresponse. The ability to manipulate the phase transition and the photoresponse with device size opens opportunities for designing and controlling functional domains of vanadium dioxide for scalable micro- and nano-scale devices and sensor applications. This work enables a technology where phase change oxides can contribute to ultra-fast and compact optoelectronic applications.

4:50 PM *EQ12.13.04

WITHDRAWN 12/6/2021 EQ12.13.04 Triplet Energy Transfer from Semiconductor Nanocrystals to Organic Molecules: Fundamentals and Applications Kaifeng Wu; Chinese Academy of Sciences, China

In recent years, sensitization of molecular triplets using inorganic semiconductor nanocrystals *via* triplet energy transfer (TET) has emerged as a new area with potential applications ranging from photochemical photon upconversion to organic synthesis. We investigated the fundamental mechanisms of the inorganic/organic TET by building well-defined model systems and applying state-of-the-art time-resolved spectroscopy tools. In doing so, we uncovered the essential role of quantum confinement of nanocrystals in facilitating electronic coupling required for triplet energy transfer. We also established a unified picture of charge-transfer-mediated triplet energy transfer mechanisms, which greatly expanded the scope of molecular triplet sensitization using nanocrystals. Additionally, we demonstrated that nontoxic nanocrystals such as CuInS₂ and InP were also capable of sensitizing molecular triplets for efficient photon upconversion. These contributions will serve as a roadmap for the design of nanocrystal-molecule triplet sensitization systems for photon upconversion as well as many other photochemical applications.

5:20 PM EQ12.13.05

Late News: Enhancement of Photoelectron Emission Efficiency from Quantum Dot Solids, Through Electrical Field Biasing of Interfaces Kasra D. Eshraghi and Prab Bandaru; University of California, San Diego, United States

It is shown through comparison with experimental results that the efficiency of quantum dot (QD) film-based photoemission would be impacted by an inadequate supply of electrons from an electron source. An explanation for the related photocurrent *droop*, as arising from restricted electron transmission at the substrate-QD interface as well as between the QDs, is proposed. It is suggested that interfacial potential based biasing schemes could considerably enhance electronic coupling for improved transmission and quantum efficiency. Modeling of the system through application of a 1-dimensional transfer matrix algorithm (TMA) to smoothly varying potential profiles indicates that electric fields of ~450 MV/m would be necessary for ensuring electron transmission coefficients close to unity.

5:25 PM *EQ12.01.02

Optimizing the Efficiency of Solid-State Photochemical Upconversion Systems—Effects of Temperature and Morphology Ferdinand C. Grozema; Delft University of Technology, Netherlands

Triplet-triplet annihilation upconversion is a promising approach for application in solar cell devices since it allows the conversion of sub-bandgap infrared photons into visible photons that can be absorbed by the underlying cell. Most examples of photochemical upconversion are either in solution or glassy polymer matrices, which is undesirable from a technological point of view. In this contribution we demonstrate a solid state approach in which absorption of near infrared light is followed by direct electron injection into an inorganic substrate. We use time-resolved microwave photoconductivity experiments to study the injection of electrons into the electron-accepting substrate (TiO₂) in a trilayer device consisting of a triplet sensitizer (fluorinated zinc phthalocyanine), triplet acceptor (methyl substituted peryleneimide) and smooth polycrystalline TiO₂. Absorption of light at 700 nm leads to the almost quantitative generation of triplet excited states by intersystem crossing. This is followed by Dexter energy transfer to the triplet acceptor layer where triplet annihilation occurs and concludes by injection of an electron into TiO₂ from the upconverted singlet excited state.

The effect of temperature on the triplet upconversion process in the solid is largely unexplored. We have investigated the effect of temperature on exciton diffusion and overall charge injection efficiency into metal oxide TiO₂ resulting from upconversion in a triple-layer system composed of TiO₂, methyl substituted perylene diimide (PDI-CH₃) and hexadecafluorinated zinc phthalocyanine (F₁₆ZnPc). We used the time resolved microwave photoconductivity technique to probe free mobile charge carriers that are generated at a planar heterojunction interface from upconverted singlet excitons. The charge yield is found to be thermally activated, which is attributed to thermally activated exciton diffusion, in combination with a phase change in the PDI-CH₃ crystalline material at higher temperature. These results show that crystal engineering can be a valuable approach to optimization of solid state upconversion.

[1] Felter, K. M.; Fravventura, M. C.; Koster, E.; Abellon, R. D.; Savenije, T. J.; Grozema, F. C., Solid-State Infrared Upconversion in Perylene Diimides Followed by Direct Electron Injection. *ACS energy letters* **2019**, 5(1), 124-129.

[2] Kevin M. Felter, Jetsabel M. Figueroa-Tapia, John W.A. Suijkerbuijk and Ferdinand C. Grozema, Optimizing the efficiency of solid state trilayer upconversion systems: Effects of temperature and morphology. *Submitted for publication*, **2021**.

5:55 PM BREAK

SESSION EQ12.14: Insights from Advanced Spectroscopy Tools

Session Chairs: Natalie Banerji and Sophia Hayes

Tuesday Morning, December 7, 2021

EQ12-Virtual

8:00 AM *EQ12.14.01

2D Electronic Spectroscopies Towards Quantum Technology Applications—The Example of Semiconductor Quantum Dots and Metal-Organic Hybrid Systems Elisabetta Collini^{1,2}; ¹University of Padova, Italy; ²Padua Quantum Technologies Research Center, Italy

Multidimensional coherent techniques in the visible range, 2D electronic spectroscopy (2DES) in particular, have been developed starting from the beginning of 2000, and historically they have been mainly exploited for the investigation of subtle dynamic mechanisms of energy and charge transport in biological complexes. Only later, these techniques have been recognized to be particularly valuable also for the study of transport processes in artificial

nanomaterials and nanodevices.

Recent results obtained applying ZDES (including 'action-based techniques') to the study of nanomaterials will be overviewed, focusing the attention on semiconductor nanocrystals ('quantum dots') in solid-state devices and metal-organic hybrid systems.

In particular, the characterization of coherent mechanisms active in the transport of excitation energy in these materials will be presented. This is particularly meaningful towards the possible application of these nanomaterials for quantum technology.

8:30 AM EQ12.14.02

Tip-Enhanced Second Harmonic Generation Microscopy for *In Situ* Nanoscale Corrosion Imaging Yoonsoo Rho¹, SeokJae Yoo¹, Dan Durham¹, Andrew M. Minor^{1,2}, Hee K. Park³ and Costas Grigoropoulos¹; ¹University of California, Berkeley, United States; ²Lawrence Berkeley National Laboratory, United States; ³Laser Prismatic LLC, United States

Second harmonic generation (SHG), a nonlinear optical process where two photons of the same energy generate a single photon of twice the energy, is an optical fingerprint to probe an inversion symmetry of crystal structure of nonlinear materials. This symmetry-dependent characteristics of SHG are particularly important in the study of chemical properties in functional nanostructures whose crystal structure can be altered by chemical reactions facilitated by their high surface-to-volume ratio. SHG also provides a simple, non-invasive, and vacuum-free optical method, which can be easily integrated with various gas flow and temperature control systems for in-operando study. However, the fundamental limitations such as the intrinsically low SHG efficiency and the limited spatial resolution have rendered the nanoscale nonlinear optics studies for the functional nanostructures challenging. Here, we developed a tip-enhanced *in-situ* nano-imaging of second harmonic generation (SHG) for nanoscale corrosion process studies based on the scanning near-field optical microscopy (SNOM) platform. We proposed that strong nonlinear responses of Au tips can be used as an optical probe for SHG signals of a nonlinear sample. This possibly originates from a resonant energy transfer between the Au tip and the sample in nonlinear process, while neither the Purcell effect nor the plasmonic field enhancement can explain the SHG enhancement in our tip-enhanced microscopy. Integrated with environmental control system, we probed *in-situ* nanoscale corrosion process occurred at the surface of zinc oxide (ZnO) nanowires, which was supplemented by correlative tunnelling electron microscopy (TEM) studies. Further, our tip-enhanced SHG nano-mapping can visualize multipolar SHG by Mie-resonance in dielectric silicon nanowires, manifested by the characteristic fringe patterns apparent in nanoscale SHG images. Thus, we believe that the presented tip-enhanced SHG microscopy for in-operando test can provide powerful means for nanoscale probing of optical and chemical properties of nanostructures.

8:45 AM EQ12.14.03

Excitonic and Spin Dynamics of the Antiferromagnetic 2D Semiconductor NiPS₃ Andrii Shcherbakov¹, Stanislav Bodnar¹, Kevin Synnatschke^{2,3}, Claudia Backes² and Felix Deschler¹; ¹Walter Schottky Institute Technical University of Munich, Germany; ²Universität Heidelberg, Germany; ³Trinity College Dublin, The University of Dublin, Ireland

Antiferromagnets (AFMs) are promising materials for spintronic and opto-electronic applications due to natural spin dynamics in the THz range and, at the same time, no net magnetization. This leads to the absence of stray fields which is a key property for data storage applications. A promising approach here is to combine the unique magnetic properties of AFMs with the strong coupling of optical and magnetic properties of semiconductors. Recently, semiconducting AFMs attract a lot of attention with several studies focusing on van der Waals layered AFMs from metal phosphotrichalcogenides such as NiPS₃, FePS₃, and MnPS₃. For our studies, we have chosen NiPS₃ because of its non-trivial exciton behavior of singlet and triplet states. To investigate light-induced dynamics in the excited, state spin, and electronic populations in semiconducting NiPS₃, we use time-resolved transient absorption (TA). This technique provides access to spectral information about changes in absorption induced by excitation of non-equilibrium carrier populations and the dynamics of the carrier and exciton recombination. We will further report our results on time and spectrally resolved optical detection of the Neel vector at cryogenic temperatures through complex Zhang-Rice excitonic states of NiPS₃ antiferromagnet by using Faraday rotation experiments. We also demonstrate the manipulation of the spin structure via application of the external magnetic field in the range of 1 T. Application of the external magnetic field leads to changes in polarization properties of PL. Finally, we provide a comparison of such dynamics for chemically exfoliated NiPS₃ from scalable solution-based fabrication, by varying the size of flakes and their thickness from monolayers, up to bulk materials.

SESSION EQ12.15: Light-Induced Phenomena in Hybrid Perovskites III

Session Chairs: Natalie Banerji and Elisabetta Collini

Tuesday Morning, December 7, 2021

EQ12-Virtual

10:30 AM *EQ12.15.01

Spectroscopic Signatures of Magnetic Ordering and Coupling to Excitons in 2D Xiaoyang Zhu; Columbia University, United States

We have developed spectroscopic techniques to probe unprecedented properties of a 2D layered semiconductor, CrSBr. Using second harmonic generation (SHG), we find that monolayers are ferromagnetically (FM) ordered below a Curie temperature $T_C = 146$ K, an observation enabled by the discovery of a large magnetic dipole SHG effect in the centrosymmetric structure. In multilayers, the ferromagnetic monolayers are coupled antiferromagnetically (AFM) with a Néel temperature of $T_N = 148 - 132$ K (decreasing with increasing thickness). Symmetry analysis establishes magnetic dipole and magnetic toroidal moments as order parameters of FM monolayer and AFM bilayer, respectively. The embodiment of both magnetic and semiconducting properties in this material allows the magnetic control of interlayer electronic coupling, as manifested in tunable excitonic transitions. Excitonic transitions in bilayer CrSBr and above can be drastically changed when the magnetic order is changed from paramagnetic to AFM as T is lowered below T_N or as it is switched from layered AFM to the field-induced FM state. The magnetic-excitonic coupling is attributed to the spin-allowed interlayer hybridization of electron and hole orbitals in the FM, but not AFM state. Our work uncovers a magnetic approach to engineer electronic and excitonic effects in layered magnetic semiconductors.

11:00 AM *EQ12.15.02

Electron-Phonon Coupling and Carrier Transport in Halide Perovskites from First Principles Feliciano Giustino; The University of Texas at Austin, United States

During the past decade halide perovskites have risen to prominence as a novel class of energy and optoelectronic materials. A fundamental question in the materials science of halide perovskites is how lattice vibrations influence their electronic and transport properties. In this talk I will describe first-principles investigations of electron-phonon couplings in hybrid organic-inorganic lead halide perovskites [1,2] and all-inorganic lead-free halide double perovskites

[3], and I will analyze the atomic-scale mechanisms underpinning charge transport in these systems. I will show how the lower mobilities of halide perovskites, as compared to standard inorganic semiconductors, are linked with the heavy atomic masses and the resulting low vibrational frequencies. Furthermore, I will show that lead-free halide double perovskites exhibit lower carrier mobilities than their lead-halide counterparts because they possess much heavier band effective masses. For both lead-based and lead-free perovskites, carrier scattering by longitudinal optical polar phonons is found to be the main source of mobility degradation. Building on this understanding, I will discuss a universal scaling law for the carrier mobility in these compounds, and illustrate possible avenues to design new halide perovskites with improved carrier transport properties.

[1] M Schlipf, S Poncé, F Giustino, Phys. Rev. Lett. 121, 086402 (2018).

[2] S. Poncé, M. Schlipf, F. Giustino, ACS Energy Lett. 4, 456 (2019).

[3] J. Leveillee, G. Volonakis, F. Giustino, J. Phys. Chem. Lett. 12, 4474 (2021).

11:30 AM EQ12.15.03

Amplified Spontaneous Emission in Quasi-2D and 3D Perovskite Gain Materials—Influences of Excitonic Versus Free Carrier Emission Yang Li^{1,2}, Isabel Allegro², Milian Kaiser¹, Aditya J. Malla², Bryce Richards^{1,2}, Ulrich Lemmer^{1,2}, Ulrich W. Paetzold^{1,2} and Ian Howard^{1,2}; ¹Institute of Microstructure Technology, Karlsruhe Institute of Technology, Germany; ²Light Technology Institute, Karlsruhe Institute of Technology, Germany

Quasi-two-dimensional (2D) perovskites are promising optoelectronic materials for lighting due to their excellent luminescent properties and color tunability. The recent demonstration of optically pumped continuous-wave (CW) lasing at room temperature stipulated the promise that these materials are also candidates for realizing electrically driven lasers from solution-processed materials. Excitonic emission from the quantum wells (QWs) of quasi-2D perovskite accounts for their superior light emission at low excitation fluences and can enhance LED performance. However, at high excited-state densities (necessary for lasing) the emission efficiency of 3D samples overtakes that of quasi-2D samples whose excited-state population is dominated by excitons. In this contribution, it is explained by the 2nd order rate of bimolecular radiative recombination increasing with fluence in the 3D sample (whose excited-state population is dominated by free charge carriers) making the emission more efficient and the radiative rate faster with increasing excitation density. Before the lasing threshold, the bimolecular radiative rate in the 3D materials apparently exceeds the radiative rate in the excitonic materials. The efficiency of the excitonic emission is also reduced by exciton-exciton annihilation, leading the 3D samples to become brighter at high fluences. In terms of amplified spontaneous emission (ASE) threshold, these effects mean that the ASE threshold is higher for the quasi-2D samples (~600 $\mu\text{J cm}^{-2}$) whose excited-state population is dominated by excitons than for the 3D samples (~130 $\mu\text{J cm}^{-2}$).

Furthermore, we then demonstrate that the ASE threshold in quasi-2D samples is significantly affected by the type and concentration of the 2D spacer used. The 2D spacer content affects the ASE threshold by two mechanisms. Firstly, the spacer content has a large influence on the surface roughness. The smoother the film, the longer the photon lifetime within the film, and therefore the higher the photon density within the film. As the ASE threshold is related to the product of the photon and excited-state density in the film, these higher photon densities work to reduce the ASE threshold. Secondly, the spacer nature and content influence the excited states that are present in the quasi-2D films. Moving from butylamine to naphthylmethylammonium (NMA) 2D spacers and decreasing the spacer concentration in the film shifts the emission mechanism towards free carrier radiative recombination and away from excitonic emission. This shift towards free carrier recombination based emission is associated with a reduction in the ASE threshold (from > 600 $\mu\text{J cm}^{-2}$ to ~200 $\mu\text{J cm}^{-2}$) of the quasi-2D materials. The best ASE thresholds in quasi-2D materials that we achieved used low concentrations of 40% NMA spacer, and thermal imprinting to reduce the roughness. In this case, we achieved a threshold of 200 $\mu\text{J cm}^{-2}$ similar to those in the 3D material. Our findings are closely relevant to many of the widely concerned 2D/3D perovskite materials these days.

In terms of optimizing quasi-2D materials for gain applications, our results suggest that careful consideration of the excited-state population and emission mechanism should be made. We propose that an excited-state population in the quasi-2D material dominated by free charge carriers may be the most favorable for their gain performance, and should be the focus of further material engineering efforts. Irrespective, a close examination of the excited states present in the quasi-2D materials and their influence on the optical gain in these materials will be of continued relevance to their development.

11:45 AM EQ12.15.04

Mobility, Quantum Efficiency and Defect Density from High Throughput Spectroscopy of CsPbBr₃ Nanowires Stephen Church¹, Hoyeon Choi¹, Nawal Al-Amairi¹, Ella Sanders², Eitan Oksenberg³, Ernesto Joselevich² and Patrick Parkinson¹; ¹University of Manchester, United Kingdom; ²Weizmann Institute of Science, Israel; ³AMOLF, Netherlands

Structural and material inhomogeneities in microstructures can have large effects on the optical properties and functional performance [1]. In this study, we demonstrate a novel way to harness this variation to probe the optoelectronic properties of the material. This is achieved using high-throughput spectroscopy to gather statistically significant, large experimental datasets of microstructures [2]. The methodology was applied to in-plane CsPbBr₃ nanowires (NWs), which are promising for nano-photonics applications, showing good waveguiding [4] and luminescence properties [3] as well as demonstrating lasing at elevated carrier densities [5].

Optical microscopy with a machine vision camera was used to identify and measure the width and length of >10,000 NWs. The optoelectronic properties of each nanowire were characterised using room temperature photoluminescence (PL) spectroscopy and time correlated single photon counting techniques. The measurements were repeated when exciting carriers at the air/NW interface and the substrate/NW interface to probe the inhomogeneity in each NW. Differences in the bandgap were observed due to tensile effects at the NW/substrate interface [6]. Two carrier lifetimes were observed: a fast lifetime (~2ns) associated with carriers at the air/NW interface and a slow lifetime (~8ns) associated with carriers in the bulk. A single recombination model was developed to explain correlations between the NW geometry and the results. This model, when applied to the large volume of experimental data, is unique in that it provides a large breadth of information about the growth, and can simultaneously determine values for the diffusion length, carrier mobility, trap densities and internal quantum efficiency (IQE). These values are compatible with those from small-scale studies in the literature, and the IQE was verified independently using temperature dependent PL. Importantly, the model requires minimal a-priori knowledge and can therefore be applied to other material ensembles in a statistically rigorous way, including those which have not been previously studied.

[1] Al-Abri, R. et al. (2021). Photonics 3(2), 22004.

[2] Parkinson, P. et al. (2020) Proc. SPIE 112910K.

[3] Oksenberg, E. et al. (2021) Adv. Funct. Mater. 31, 2010704.

[4] Shoaib, M. et al. (2017) J. Am. Chem. Soc. 139, 15592–15595.

[5] Schlaus, A. P. et al. (2019) Nat. Commun. 10, 265.

[6] Oksenberg, E. et al (2018). Nano Letters 18(1), 424.

12:00 PM EQ12.15.05

Photoexcited Charge Carrier and Spin Dynamics in Methylammonium Lead Bromide Doped by Magnetic Transition Metals Stanislav Bodnar¹,

Jonathan Zerhoch¹, Timo Neumann^{1,2}, Lissa Eyre¹, Barbara Sergl¹ and Felix Deschler¹; ¹Walter Schottky Institute of Munich Technical University (Walter Schottky Institut Technische Universität München), Germany; ²University of Cambridge, United Kingdom

One of the most challenging tasks for LED applications is emitting 100% polarized light from the device. Typically, this is achieved by introducing an additional layer of polarization filter which leads to losing half of the light intensity. To overcome this issue, one has to find a system with a high degree of photoluminescence (PL) polarization. A promising approach here is using magnetic metal doping in combination with a highly efficient semiconductor. Metal-halide perovskites have attracted the attention of many scientific groups around the world as one of the most promising candidates for solar cell applications and light-emitting diode (LED) technology. In our work, we will present how doping of methylammonium lead bromide ($\text{CH}_3\text{NH}_3\text{PbBr}_3$) with the transition metals Ni, Co, and Mn induces dramatic changes in the magneto-optical properties and carrier dynamics due to interactions between the magnetic moments of the dopants and Coulomb interactions of the excitons.

We have chosen to use transient absorption (TA) spectroscopy at cryogenic temperatures with applied magnetic fields of up to 1 T to investigate changes in the optical properties induced by magnetic metal doping in $\text{CH}_3\text{NH}_3\text{PbBr}_3$, since it gives spectral information about the energies of electronic states and dynamic properties of the photoexcited carriers. We find a change in the main ground state bleach (GSB) peak position in doped $\text{CH}_3\text{NH}_3\text{PbBr}_3$, which depends on the transition metal used. The main GSB peak of pure $\text{CH}_3\text{NH}_3\text{PbBr}_3$ at 4 K is at 2.32 eV. Doping $\text{CH}_3\text{NH}_3\text{PbBr}_3$ with Mn and Ni leads to a shift of the main peak to lower energies by 0.04 eV and 0.08 eV, respectively, while doping with Co leads to a shift to higher energies by 0.02 eV. The modifications of the TA spectra are associated with changes of the bandgap energy, which is the result of doping-induced lattice expansion or compression. For all investigated samples, we observed energy splitting of the TA spectra for two different circular polarizations of the pump pulse. We interpret this splitting as the result of a light-induced Zeeman effect which arises from the spin-polarized photoexcited charge carriers due to angular momentum selection rules of the optical transitions. For the pure $\text{CH}_3\text{NH}_3\text{PbBr}_3$ case, we observed splitting in the range of the 8 meV, while for the Ni-doped material, this splitting is around 17 meV. We attributed this significant enhancement in the splitting energy to the exchange coupling of the photoexcited charge carrier spins with the Ni ion spins. The presence of the Ni spins in the crystal lattice also affects the lifetime of the photo-induced Zeeman splitting. Undoped $\text{CH}_3\text{NH}_3\text{PbBr}_3$ shows a lifetime of the Zeeman splitting in the range of 30 ps, while for the Ni-doped samples this lifetime is exceeding 1300 ps which is an indication of one order of magnitude longer spin lifetime in the Ni-doped sample, compared to undoped $\text{CH}_3\text{NH}_3\text{PbBr}_3$. The reason for this significantly different behavior could be a long-range order of the Ni spins, potentially indicating magnetic spin order, which we are currently exploring. The long lifetime of the Zeeman splitting could also indicate a long lifetime of circularly polarized PL.

SESSION EQ12.16: Excitonic Processes in Organic Materials III

Session Chairs: Felipe Herrera and Mark Wilson

Tuesday Afternoon, December 7, 2021

EQ12-Virtual

1:00 PM *EQ12.16.01

Excited State Dynamics of a Conjugated Polyelectrolyte Self-Assembled with ss-DNA *Sophia C. Hayes*¹, Eliana Nicolaidou¹, Anthony Parker² and Michael Towrie²; ¹University of Cyprus, Cyprus; ²Central Laser Facility, Science & Technology Facilities Council, Rutherford Appleton Laboratory, United Kingdom

Control over the conformation of conjugated polymers using nucleic acids (NAs) as templates can be very advantageous in inducing unique and readily controllable properties. Complexation of NAs with conjugated polyelectrolytes (CPEs) such as cationic polythiophenes (CPT) is facilitated by the presence of charged side groups on the backbone.¹ Previous studies on the biosensing ability of a certain CPT has revealed a tremendous impact of the ssDNA sequence on the conformational and optical response of the polymer.^{2,3} The complex formed of CPT and oligocytosine (dC_{20}) strands is especially noteworthy due to the formation of highly ordered and extended chains due to π -stacking between the cytosine bases and thiophene rings, further stabilized by π -stacking with the imidazole side chain.^{4,5} This stands in contrast to the complex with oligoadenosine (dA_{20}), where π -stacking between the bases limits any stacking interactions with the polymer resulting in a flexible and torsionally disordered conformation. Interestingly, though, our previous ultrafast transient absorption (TA) work showed that both complexes showed only excitonic behavior, with similar and much faster decay dynamics compared to the polymer alone, which forms interchain aggregates.⁵

Therefore, we used TRIR to directly probe the role of NA templating in the excited state species formed in the two complexes, which is responsible for the faster dynamics observed with vis-NIR probes, as well as compare the photophysics of loosely bound complexes with the more rigid and ordered systems. We find that with excitation of the polymer in the visible (532 nm) both complexes form the P_0 intrachain polaron evidenced by a broad absorption background that decays faster than the delocalized polaron DP_1 formed in the case of CPT alone. The lower intensity of the P_0 absorption in the CPT/ dA_{20} case is consistent with increased intrachain disorder, while higher interchain long range order leads to the higher DP_1 absorption.⁶ The rigid complex formed in the case of CPT/ dC_{20} limits the geometric relaxation observed in the C=C stretch Fano antiresonance, in agreement with the reduced reorganization energy calculated from resonance Raman intensity analysis and the limited evolution of the stimulated emission in the TA data.⁵ Excitation in the UV (266 nm) shows that a charge transfer complex is formed between CPT and dC_{20} with the observation of the cytosine anion and a broad absorption background, in contrast to CPT/ dA_{20} case, where the TRIR spectra solely reflect the excited state behavior of the oligoadenosine. These results show that non-covalent interactions between NAs and CPTs can determine the excited state species formed, which has implications to the applicability of these complexes in molecular electronics.

Rubio-Magnieto, J. et al, *Soft Matter* **2015**, *11*, 6460–6471.

Liu, Y. et al, *J. Photochem. Photobiol. C Photochem. Rev.* **2009**, *10*, 173–190.

Duan, X. R. et al, *Acc. Chem. Res.* **2010**, *43*, 260–270.

Charlebois, I. et al, *Macromol. Biosci.* **2013**, *13*, 717–722.

Peterhans, L. et al, *Chem. Mater.* **2020**, *32*, 7347–7362.

Pochas, C. M.; Spano, F. C. *J. Chem. Phys.* **2014**, *140*, 244902.

1:30 PM *EQ12.16.04

Control of Exciton Dynamics for Efficient Photon Upconversion in Solid Materials *Nobuhiro Yanai*; Kyushu University, Japan

Controlling the behavior of molecular excitons in solids is crucial for the expression of optical functions. We have been interested in the triplet diffusion and upconversion of triplet into singlet in solid materials, especially in densely packed dyes in solid environments where molecular diffusion is limited. As an example, we present a system of emitter dyes densely integrated in epoxy resins. Epoxy resins have a high oxygen barrier property, which is used as

an encapsulant for OLEDs. We have succeeded in dispersing the dye in epoxy resins with a high concentration of more than 1 M by appropriate molecular design, and achieved a high upconversion efficiency in air. We will show how the emitter density plays an important role not only in the triplet diffusion between emitters, but also in the circumvention of back energy transfer from emitter to sensitizer.

The introduction of singlet energy collectors to more actively prevent back energy transfer will also be presented. We show that the singlet energy collectors play an important role in effectively suppressing the back energy transfer from emitter to sensitizer, and can also compete with the free triplet generation by the singlet fission.

2:00 PM EQ12.16.03

Exploring the Multiple Resonance Thermally Activated Delayed Fluorescence Mechanism and Its Contribution to the State of the Art

3rd Generation OLEDs Kleitos Stavrou¹, Andrew Danos¹, Toshiki Hama², Takuji Hatakeyama² and Andrew Monkman¹; ¹Durham University, United Kingdom; ²Kwansei Gakuin University, Japan

Organic light emitting diodes (OLEDs) are considered the most recent commercially available lighting and display technology. Until now, only the first two generations of OLEDs were used in the market but not until recently the 3rd generation made huge steps towards real life applications. Using a thermally activated delayed fluorescence (TADF) sensitizer and a multiple resonance (MR) TADF emitter in a host matrix, hyper-fluorescence (HF) OLEDs already achieved higher efficiencies and comparable lifetimes with the ones already in the market. In this work, we focus on understanding the mechanism of the MR-TADF emitters using steady-state and time-resolved spectroscopic methods. Evidence of hot transitions from vibrational excited states is shown experimentally along with a temperature dependant singlet-triplet state energy gap (ΔE_{ST}). Combining the two, a reverse intersystem crossing (rISC) mechanism that involves thermally activated reverse internal conversion (rIC) from the T_1 to the T_n ($n \geq 2$) state followed by rapid (r)ISC to the S_1 state, is deduced. The existence of an intermolecular specie, due to the planarity/rigidity of the molecule, is assigned to an excimer which affects the optical performance even at concentrations below those used in devices. HF-OLEDs, using v-DABNA as the emitter, exhibit an increase of maximum external quantum efficiency (EQE), compared to a control device. Forster resonance energy transfer (FRET) studies show that although FRET efficiency decreases with decreasing emitter concentration, the overall device efficiency is higher, indicating that excimer quenching affects the OLED's performance.

2:15 PM EQ12.16.05

Entropy, Delocalization, and Marcus-Theory Explain Ultrafast Free-Charge Generation in Excitonic Semiconductors Joshua Carr^{1,2}, Taylor Allen², Bryon Larson², Obadiah Reid^{1,2} and Garry Rumbles^{1,2}; ¹University of Colorado Boulder, United States; ²National Renewable Energy Laboratory, United States

Understanding how Frenkel excitons efficiently split to form free-charges in low-dielectric constant organic semiconductors has proven extremely difficult, with many different models proposed in recent years to explain this exceptional phenomenon. Here, we present evidence that a simple model invoking a modest amount of charge delocalization, a sum over the available microstates, and the Marcus rate constant for electron transfer can explain many seemingly contradictory phenomena reported in the literature. We use an electron-accepting fullerene host matrix diluted sensitized with a series of electron donor molecules to test this hypothesis. The donor series enables us to tune the driving force for photoinduced electron transfer over a range of 600 meV, mapping out normal, optimal, and inverted regimes for free-charge generation efficiency, as measured by time-resolved microwave conductivity. However, the photoluminescence of the donor is found to be rapidly quenched as the driving force increases, with no evidence of inverted behavior, or the linear relationship between photoluminescence quenching and charge generation efficiency one would expect. This behavior is self-consistently explained by competitive formation of bound charge-transfer states and long-range or delocalized free-charge states, where both rate constants are described by the Marcus rate equation. Moreover, the model predicts a suppression of the inverted regime for high-concentration blends and efficient ultrafast free-charge generation, providing a mechanistic explanation for why Marcus inverted-behavior is rarely observed in device studies.

2:30 PM EQ12.16.06

Photophysical Approach to Study Matrix Effects on TADF Materials Larissa G. Franca, Kleitos Stavrou and Andrew Monkman; Durham University, United Kingdom

Thermally activated delayed fluorescence (TADF) emitters are considered a novel class of molecules for applications in organic light-emitting diodes (OLEDs). Due to the small energy gap between triplet and singlet state, reverse intersystem crossing (rISC) is allowed. This efficient mechanism has the ability to convert triplet states into an emissive singlet state, which enhances the internal quantum efficiency (IQE) towards 100%. In the context of an OLED, the TADF emitters are mainly incorporated in a matrix of host molecules. Apart from a better control of the electrical transport properties in the emission layer, the host molecules also prevent emitter self-quenching, a great source of non-radiative losses. The aim of this work is the use of DMAC-TRZ as a TADF emitter 'probe' to differentiate the environmental effects of a range of solid state host materials in guest-host systems. A variety of typical TADF OLED hosts with different characteristics was studied. This provides a clearer understanding of guest-host interactions and what effects emitter performance in solid state. Using time-resolved photoluminescence (PL) measurements, the CT state energy distribution was obtained from the full width at half maximum (FWHM) of the emission band. By correlating FWHM with other photophysical properties such as the apparent dynamic redshift of CT emission onset, we obtain the disorder-induced heterogeneity of D-A dihedral angles. Concentration dependence studies show that aggregation contributes to reducing photoluminescence efficiency. In our study, we explore the hosting potential of two host materials of similar chemical structure: mCPCN and mCBPCN, demonstrating the divergent photophysical behavior of DMAC-TRZ as a guest molecule.

References:

Stavrou, K.; Franca, L. G.; Monkman, A. P. Photophysics of TADF Guest-Host Systems: Introducing the Idea of Hosting Potential. *ACS Appl. Electron. Mater.* **2020**, *2* (9), 2868–2881.

2:45 PM BREAK

SESSION EQ12.17: Strong Light-Matter Interactions and Quantum Phenomena II

Session Chair: Mark Wilson

Tuesday Afternoon, December 7, 2021

EQ12-Virtual

4:00 PM *EQ12.17.01

Controlling Light-Matter Interaction with Molecular Vibrations in Mid-Infrared Resonators Felipe Herrera^{1,2}; ¹Universidad de Santiago de Chile,

Chile; ²ANID - Millennium Institute for Research in Optics, Chile

Nanoscale infrared (IR) resonators with sub-diffraction limited mode volumes and open geometries have emerged as new platforms for implementing cavity quantum electrodynamics (QED) at room temperature [1,2]. The use of infrared (IR) nano-antennas and tip nanoprobes to study strong light-matter coupling of molecular vibrations with the vacuum field can be exploited for IR quantum control with nanometer and femtosecond resolution. In order to accelerate the development of molecule-based quantum nano-photonics devices in the mid-IR, we developed a generally applicable semi-empirical quantum optics approach to describe light-matter interaction in systems driven by mid-IR femtosecond laser pulses.

The theory is shown to reproduce recent experiments on the acceleration of the vibrational relaxation rate in infrared nanostructures [3], and also provide physical insights for the implementation of coherent phase rotations of the near-field using broadband nanotips [4]. We then apply the quantum framework to develop general tip-design rules for the experimental manipulation of vibrational strong coupling and Fano interference effects in open infrared resonators. We finally propose the possibility of transferring the natural anharmonicity of molecular vibrational levels to the resonator near-field in the weak coupling regime, to implement intensity-dependent phase shifts of the coupled system response with strong pulses. Our semi-empirical quantum theory is equivalent to first-principles techniques based on Maxwell's equations, but its lower computational cost suggests its use as a rapid design tool for the development of strongly-coupled infrared nanophotonic hardware for applications ranging from quantum control of materials to quantum information processing.

[1] T. W. Ebbesen. *Acc. Chem. Res.* 49, 2403, 2016.

[2] F. Herrera and J. Owrutsky. *J. Chem. Phys.* 152, 100902, 2020.

[3] B. Metzger et al. *Phys. Rev. Lett.* 123, 153001, 2019.

[4] E. A. Muller et al. *ACS Photonics*, 5, 3594, 2018.

4:30 PM *EQ12.17.02

Molecular Polaritons—Photophysics and Photochemistry Joel Yuen Zhou; University of California San Diego, United States

Strong light-matter coupling reveals itself in dramatic changes in linear and nonlinear response spectroscopy. In particular, the emergence of so-called polariton (hybrid light-matter) modes that are well-separated in energy from bare material transitions indicates the onset of strong coupling. However, a more subtle question arises as to the extent to which polariton modes can alter photochemical and photophysical processes of interest. An important aspect that is not highlighted enough in molecular polaritonics studies is that whether the strong coupling happens with one or a few molecules (as in plasmonic nanocavities) or with a thermodynamic ensemble (of $>10^6$ molecules/photon mode) dramatically affects the outcome of the molecular process of interest. Here I will discuss effective strategies to take advantage of the various flavors of strong coupling phenomena to control photochemistry and photophysics.

5:00 PM EQ12.17.03

Phase-Field Model of Coupled Electron and Lattice Dynamics in Correlated Material Systems Tiannan Yang¹, Yihuang Xiong¹, Yin Shi¹, Yakun Yuan², Yi Wang¹, Venkatraman Gopalan¹, Ismaila Dabo¹ and Long-Qing Chen¹; ¹The Pennsylvania State University, United States; ²University of California, Los Angeles, United States

We establish a phase-field model for coupled electron and lattice dynamics in correlated material systems under ultrafast excitation. The model integrates a phase-field description of phase transitions with other notable mechanisms at picosecond-to-nanosecond timescales to deliver a comprehensive spatiotemporal profile of excitation and relaxation transients of the system. Combined with first-principles calculation of electronic and phonon properties, we theoretically examine the light-excited electron and lattice dynamics in strongly correlated material $\text{Ca}_3\text{Ru}_2\text{O}_7$ involving a coupled electronic and magnetic phase transition. We demonstrate that the excited-state dynamics contains a three-component relaxation process of carrier concentration across picosecond-to-nanosecond timescales, which is supported by evidence from previous experimental works. A strong temperature dependence of all relaxation components within a wide range across the phase transition temperature is revealed. This model provides in-depth theoretical insights of the dynamical properties of complex electronic systems and ultrafast phenomena that lies within them. It can be applied to various material systems for predicting the electronic and lattice dynamics under different ultrafast external stimuli, including light pulses, electric fields, and currents, etc.

5:15 PM *EQ12.15.02

Electron-Phonon Coupling and Carrier Transport in Halide Perovskites from First Principles Feliciano Giustino; The University of Texas at Austin, United States

During the past decade halide perovskites have risen to prominence as a novel class of energy and optoelectronic materials. A fundamental question in the materials science of halide perovskites is how lattice vibrations influence their electronic and transport properties. In this talk I will describe first-principles investigations of electron-phonon couplings in hybrid organic-inorganic lead halide perovskites [1,2] and all-inorganic lead-free halide double perovskites [3], and I will analyze the atomic-scale mechanisms underpinning charge transport in these systems. I will show how the lower mobilities of halide perovskites, as compared to standard inorganic semiconductors, are linked with the heavy atomic masses and the resulting low vibrational frequencies. Furthermore, I will show that lead-free halide double perovskites exhibit lower carrier mobilities than their lead-halide counterparts because they possess much heavier band effective masses. For both lead-based and lead-free perovskites, carrier scattering by longitudinal optical polar phonons is found to be the main source of mobility degradation. Building on this understanding, I will discuss a universal scaling law for the carrier mobility in these compounds, and illustrate possible avenues to design new halide perovskites with improved carrier transport properties.

[1] M Schlipf, S Poncé, F Giustino, *Phys. Rev. Lett.* 121, 086402 (2018).

[2] S. Poncé, M. Schlipf, F. Giustino, *ACS Energy Lett.* 4, 456 (2019).

[3] J. Leveillee, G. Volonakis, F. Giustino, *J. Phys. Chem. Lett.* 12, 4474 (2021).

5:45 PM BREAK

10:30 AM *EQ12.18.01

Optical Probes of Exciton / CT Mixing in Long-Lived Donor/Acceptor Complexes David S. Ginger¹, Yun Liu¹, Zilong Zheng^{2,3}, Veaceslav Coropceanu^{4,2} and Jean-Luc Brédas^{4,2}; ¹University of Washington, United States; ²Georgia Institute of Technology, United States; ³Beijing University of Technology, China; ⁴The University of Arizona, United States

We seek to understand the lower limits of non-radiative recombination losses from charge transfer states in organic donor/acceptor systems. These factors underpin applications ranging from organic photovoltaics to organic LEDs and lasers. As an extreme case, we study a model thermally activated delayed fluorescence (TADF) system that exhibits both a high photoluminescence quantum efficiency (PLQY = ~22%) and comparatively long PL lifetime, while simultaneously yielding appreciable amounts of free charge generation (photocurrent external quantum efficiency EQE of 24%). In solar cells, this blend exhibits non-radiative voltage losses of only ~0.1 V, among the lowest reported for an organic system. Notably, we find that the non-radiative decay rate, k_{nr} , is on the order of $1E-5$ /s, roughly 4-5 orders of magnitude slower than typical OPV CT states. Surprisingly however, this rate is still orders of magnitude too *fast* compared to predictions by Marcus-Levich-Jortner two-state theory. By comparing experimental PL and electroabsorption spectroscopy with theory, we conclude that CT-local exciton (LE) hybridization is present and that this mixing greatly increases the non-radiative recombination rate of the CT state. We discuss implications of this finding for different optoelectronic devices.

11:00 AM *EQ12.18.03

In Situ Transient Absorption Spectroscopy of Evolving Molecular Aggregates Cathy Y. Wong; University of Oregon, United States

The electronic structure and exciton dynamics of the molecules and polymers that form the active layer in organic electronic devices can change dramatically during solution deposition and thermal annealing. As solvent vaporizes, molecules aggregate and become electronically coupled, sometimes dramatically changing the exciton dynamics and thus the suitability of the material for electronic devices. Similar changes occur during thermal annealing, as the relative orientation of molecules change. The exciton dynamics of molecules in solution and in films of aggregates can be measured using transient absorption spectroscopy. However, the progression of exciton dynamics during film formation and thermal annealing is unknown, as measurements typically cannot be performed quickly enough to collect accurate transient absorption spectra of the evolving molecular aggregates. The exciton dynamics of evolving material systems can be measured by increasing the speed of data collection. Single-shot transient absorption spectroscopy using tilted pulses can measure transient spectra with up to a 60 ps pump-probe time delay in 8 ms, with an adequate signal-to-noise ratio achieved in just a few seconds. The exciton dynamics of intermediate aggregation states are revealed during the formation of an organic film and during thermal annealing. This type of measurement provides insight into the complex process of organic film formation and how the excitonic properties of a film emerge.

11:30 AM EQ12.18.04

Activated Carbon Aging Processes Characterization by Raman Spectroscopy Sari Katz¹, Alexander Pevzner², Vladislav Shepelev², Sharon Marx², Hadar Rotter², Tal Amitay Rosen² and Ido Nir²; ¹On Sabbatical leave from Soreq NRC, Israel; ²Israel Institute for Biological Research, Israel

Activated carbon is used as an adsorbent material for various hazardous materials. Typically, active carbon is impregnated with metal oxides in order to improve its adsorbing capabilities towards inorganic low molecular weight gases, and high vapor pressure compounds by chemisorption mechanism. Exposure of activated carbon to humid air leads to water adsorption. As a result, the carbon surface and the impregnants are changing over time. The impregnants are dissolve and migrate to the external surface of the carbon following gradual recrystallization. The aging process may reduce the chemisorption capacity of the activated carbon.

In this study, the effect of aging on activated carbon from coconut husks source, impregnated with zinc oxide and the organic additive triethylenediamine, was studied by non-destructive Raman spectroscopy as well as energy dispersive spectroscopy. Raman spectroscopy enables the chemical characterization of a packed activated carbon samples. Energy dispersive spectroscopy was used to characterize the surface elements of the native and aged activated carbon. Accelerated aging was achieved by water adsorption on the carbon, followed by storage at 50°C in a closed container. The study shows that the aging process increased the oxygen content on the carbon surface, both by introducing carboxyl and epoxides groups on the carbon surface, as well as migration of the metal oxide impregnants to the carbon granules' external surface. The aging process was studied by two laser excitation wavelengths (532 nm and 785 nm) Raman spectroscopy. Raman spectroscopy is commonly used to study carbonaceous materials molecular structure. It allows to characterize the graphitic sp^2 versus disordered sp^2 carbon, amorphous carbon sp^3 degree, and their stress state. In general, the G-band at ~1582 cm^{-1} , is of E_{2g} mode symmetry, which is common to all sp^2 carbon systems, and results from the in-plane bond stretching of the C-C bond in graphitic materials. The full-width at half-maximum of the G band increases monotonically with the degree of disorder in the graphitic lattice. The D-band at ~1350 cm^{-1} , is an A_{1g} breathing mode symmetry, it is associated with carbon atoms having disordered sp^3 carbon atoms. The intensity ratio ($R = I_D/I_G$) of D and G bands, is used to assess the sp^3/sp^2 carbon ratio, which represents the degree of disordered carbon atoms. An increase in this ratio results from a reduction in the crystalline size. The Raman D and G band shifts were followed by double Lorentzian model fitting. The aging outcome indicated by a D band position upshift from 1337 cm^{-1} to 1340 cm^{-1} and 1342 cm^{-1} , that can be explained by the compression of the activated carbon structure. The aging process leads to I_D/I_G increase indicating a reduction in the size of the crystal. In addition, the low frequency Raman bands were used to study the aging process of the carbon. Higher oxygen content on the carbon external surface was presented by elevated Raman intensities of the epoxide's groups at 643 cm^{-1} . This finding indicates oxidation of the carbon surface during the aging. Furthermore, higher content of the $sp-sp^2$ amorphous carbon at 405 cm^{-1} and 418 cm^{-1} was found in aged carbon, indicating carbon structure configuration changes with aging. The increased content of zinc on the carbon granules external surface, due to its migration during the aging, was portrayed by the creation of new vibration bands at 333 cm^{-1} and 991 cm^{-1} with aging. In addition, the higher content of oxygen on the carbon surface with aging, and the higher content of the impregnated metal was demonstrated by energy dispersive spectroscopy characterization.

Raman spectroscopy was found to be a powerful non-destructive method for analyzing the aging process of impregnated activated carbon.

11:35 AM EQ12.18.05

Influence of Surface Modification of BaTiO₃ Nanoparticles by Hydrolyzed Chitosan on the Optical Response Intensity of the Second Harmonic Luis M. Angelats Silva¹, Fredy R. Perez-Azahuanche¹, Jose A. Roldan-Lopez^{1,2}, Nikita A. Emelianov³, Rudy B. Céspedes-Vasquez¹ and Miguel A. Valverde-Alva²; ¹Universidad Privada Antenor Orrego, Peru; ²Universidad Nacional de Trujillo, Peru; ³Kursk State University, Russian Federation

Spherical titanium barium nanoparticles with an average size about 100 nm in the tetragonal crystal phase were obtained by peroxide synthesis and then with formation of OH groups on its surface by hydrogen peroxide. To reduce the toxic effect, the surface of nanoparticles was chemically modified with hydrolyzed chitosan obtained from shrimp exoskeleton (*Penaeus vannamei*). The chitosan obtained and the modified surface were analyzed by X-ray diffraction, Raman spectroscopy and Infrared. Influence of surface modification on the optical response intensity of the second harmonic was investigated using a Nd:YAG laser 1064 nm (2.8, 4.5 and 8.1 mJ/pulse).

11:40 AM *EQ12.02.03

Carrier, Exciton and Spin Dynamics in Perovskite 2D Layered Systems [Matthew C. Beard](#); National Renewable Energy Lab, United States

Controlling charge and energy flow in functional systems can be beneficial for solar energy conversion and utilization. The marriage of colloidal semiconductor nanocrystals and functional organic molecules has brought unique opportunities in emerging photonic and optoelectronic applications. In this presentation I will discuss our studies of controlling the charge carrier dynamics, light/matter interactions, and spin populations in these novel hybrid systems. In one effort we are exploring the use of novel organic hybrid systems at and near interfaces to control the carrier dynamics and reduce surface recombination but also to protect grain boundary surfaces from degradation. With respect to controlling spins we have recently studied and developed a novel class of chiral hybrid semiconductors based upon layered metal-halide perovskite 2D Ruddlesden-Popper type structures. These systems exhibit chiral induced spin selectivity whereby only one spin sense can transport across the film and the other spin sense is blocked. From these systems we can achieve a high degree of spin current polarization and injection when used as a contact layer. We have developed novel spin-based LEDs using mixed NCs as the light emitting layer that promotes light emission at a highly spin-polarized interface. The LED spin-polarization is limited by spin-depolarization within the MHP NCs. Thus understanding and controlling the spin-depolarization is an important goal. Here we discuss the charge carrier recombination rate and spin-coherence lifetimes in single crystals of 2D Ruddlesden-Popper perovskites. Layer thickness dependent charge carrier recombination rates are observed with the fastest rates for $n = 1$ due to the large exciton binding energy and the slowest rates for $n = 2$. Room temperature spin-coherence times also show a nonmonotonic layer thickness dependence with an increasing spin-coherence lifetime with increasing layer thickness from $n = 1$ to $n = 4$, followed by a decrease in lifetime from $n = 4$ to bulk. The longest coherence lifetime of ~ 7 ps is observed in the $n = 4$ sample. We also studied the spin-coherence lifetimes as a function of exciton binding energy and find that the spin-lifetime increases with decreasing exciton binding energy.

SYMPOSIUM EQ13

Nitride Materials—Synthesis, Characterization and Modeling
November 30 - December 8, 2021

Symposium Organizers

Bjorn Alling, Linkoping University
Rachel Oliver, University of Cambridge
Minghui Yang, Chinese Academy of Sciences
Andriy Zakutayev, National Renewable Energy Laboratory

Symposium Support

Silver

Taiyo Nippon Sanso

* Invited Paper

SESSION EQ13.01: Transition Metal Nitrides
Session Chairs: Eva Monroy and Andriy Zakutayev
Tuesday Morning, November 30, 2021
Hynes, Level 2, Room 202

10:30 AM *EQ13.01.01

Transition Metal Nitride Semiconductors [Daniel Gall](#); Rensselaer Polytechnic Institute, United States

We explore new transition metal nitride compounds using a combination of epitaxial layer growth, first-principles calculations, and measurements of electronic and optical properties as a function of composition and structure. (1) Rock salt structure: ScN has a $E_g = 0.92$ eV indirect bandgap and a carrier concentration that is controlled by F doping. CrN forms a charge-transfer insulator with $E_g = 0.2 \pm 0.4$ eV, but oxygen exposure results in a two-dimensional metallic CrN_xO_y surface layer. The addition of Al to form $\text{Sc}_{1-x}\text{Al}_x\text{N}$ and $\text{Cr}_{1-x}\text{Al}_x\text{N}$ compounds increases the bandgap with $dE_g/dx = 2.75$ and 2.81 eV, respectively. $\text{Ti}_{0.5}\text{Mg}_{0.5}\text{N}$ has a 0.7-1.7 eV bandgap. However, a high density of N vacancies act as n-type dopants resulting in a highly degenerate semiconductor. The vacancy formation is suppressed when alloying with Al, yielding $(\text{Ti}_{0.5}\text{Mg}_{0.5})_{1-x}\text{Al}_x\text{N}$ alloys with E_g increasing with x . (2) Wurtzite structure: Alloying AlN with Sc causes a drop in the direct bandgap for $\text{Al}_{1-x}\text{Sc}_x\text{N}$ with $dE_g/dx = -9.23$ eV and a structural instability with a non-linear composition dependence in bond angle and length that causes the reported piezoelectric enhancement. $(\text{Ti}_{1-x}\text{Mg}_x)_{0.25}\text{Al}_{0.75}\text{N}$ exhibits a stability peak at $x = 0.5$ with a minimum in the lattice constant ratio c/a that is caused by a Fermi-level shift into the bandgap and a trend toward nondirectional ionic bonding, leading to a maximum in the expected piezoelectric stress constant.

11:00 AM EQ13.01.03

Analysis of Niobium Nitride Films for Saturated Micrometer Wide Superconducting Single-Photon Detectors [Owen Medeiros](#), Marco Colangelo, Akshay Agarwal, Ilya Charaev, Brenden Butters and Karl Berggren; Massachusetts Institute of Technology, United States

Superconducting single-photon detectors used for quantum optics, LIDAR, and astronomy, have traditionally been fabricated in a meander with strip widths around 100 nm. The narrow width was designed to be similar to the diameter of a hot spot formed by an incident photon. However, recent work has shown strips as wide as 3 μm were able to detect single photons by fine tuning the film's sputtering conditions¹⁻³. Wider detectors show improved signal-to-noise ratio, and higher fabrication yield when compared to traditional detectors of the same active area. The increased performance of these detectors obtained by material deposition optimization suggests that by porting this process to traditional-width detectors may increase their sensitivity at mid-infrared wavelengths. This has prompted the recent work towards wide detectors in nitrogen rich niobium nitride (NbN)^{4,5}, however this work has ignored any characterization of the atomic structure of the material, instead focusing on electrical characterization of the thin film only. Here we study thin film NbN using sputtering conditions similar to previous work and fabricate single photon detectors between 0.5 and 3 μm wide. We observe saturated photon counts at 1550-nm wavelength in a 2.5 μm wide strip with a large inductor patterned in series to prevent latching. We characterize the film's atomic structure by performing x-ray diffraction (XRD) and transmission electron microscopy (TEM) and compare the results with RF-bias sputtered NbN⁶. We observe an increase in the 111-phase of NbN for the nitrogen rich films used to fabricate wide wire single photon detectors. These results suggest that the continued development of the NbN phase shown here would improve the detector performance. This optimization would allow for the detection of low energy photons in the mid-infrared⁷ and lead to the development of large area single-photon detectors for dark matter detection⁸, high energy physics⁹, or biomedical imaging¹⁰.

1. Korneeva, Y. P. et al. Optical Single-Photon Detection in Micrometer-Scale NbN Bridges. *Phys. Rev. Applied* 9, 064037 (2018).
2. Charaev, I. et al. Large-area microwire MoSi single-photon detectors at 1550 nm wavelength. *Appl. Phys. Lett.* 116, 242603 (2020).
3. Chiles, J. et al. Superconducting microwire detectors based on WSi with single-photon sensitivity in the near-infrared. *Appl. Phys. Lett.* 116, 242602 (2020).
4. Zolotov, P. I. et al. Dependence of Photon Detection Efficiency on Normal-State Sheet Resistance in Marginally Superconducting Films of NbN. *IEEE Trans. Appl. Supercond.* 31, 1–5 (2021).
5. Vodolazov, D. Y., Manova, N. N., Korneeva, Y. P. & Korneev, A. A. Timing Jitter in NbN Superconducting Microstrip Single-Photon Detector. *Phys. Rev. Applied* 14, 044041 (2020).
6. Dane, A. E., McCaughan, A. N., Zhu, D. & Zhao, Q. Bias sputtered NbN and superconducting nanowire devices. *J. Phys. D Appl. Phys.* (2017).
7. Verma, V. B. et al. Single-photon detection in the mid-infrared up to 10 μm wavelength using tungsten silicide superconducting nanowire detectors. *APL Photonics* vol. 6 056101 (2021).
8. Hochberg, Y. et al. Detecting Sub-GeV Dark Matter with Superconducting Nanowires. *Phys. Rev. Lett.* 123, 151802 (2019).
9. Polakovic, T., Armstrong, W., Karapetrov, G., Meziani, Z.-E. & Novosad, V. Unconventional Applications of Superconducting Nanowire Single Photon Detectors. *Nanomaterials* (Basel) 10, (2020).
10. Schaart, D. R., Ziegler, S. & Zaidi, H. Achieving 10 ps coincidence time resolution in TOF-PET is an impossible dream. *Medical Physics* vol. 47 2721–2724 (2020).

SESSION EQ13.02/CH02.03: Joint Session: Solid State Chemistry of Nitride Materials

Session Chairs: Brent Melot and Andriy Zakutayev

Tuesday Afternoon, November 30, 2021

Hynes, Level 2, Room 202

1:30 PM *EQ13.02/CH02.03.01

Advances and Challenges in Mapping the Stability Landscape of Novel Nitride Materials [Wenhao Sun](#); University of Michigan, United States

Despite the great promise of nitrides as functional materials, exploration of the nitrides chemical space has been relatively limited compared to oxides and other chalcogenides/pnictides. Recently, we used a suite of computational materials discovery and informatics methods to construct a large stability map of the inorganic ternary metal nitrides [W. Sun. *et al.*, *Nature Materials*, 2019], revealing exciting opportunities for the discovery of novel nitride materials. Here, I will briefly review the computational methods we used to construct this stability map and will describe a new class of II_x-TM-N ternary nitride semiconductors experimentally realized from our 2019 search. However, since our 2019 search efforts, we have encountered new challenges to more comprehensively survey and design nitride materials. In this talk, I will examine these challenges and discuss our strategies for their solution: in particular, 1) search strategies for Zintl-based metal-rich nitrides which are relevant as permanent magnets, ammonia synthesis catalysts and superhard materials; 2) strategies for the facile synthesis of metastable nitrides based on computationally-guided ammonolysis and metathesis reactions, and 3) the $p\text{O}_2$ and $p\text{N}_2$ chemical potential boundaries between nitrides, oxynitrides and oxides.

SESSION EQ13.03: New Nitride Semiconductors

Session Chairs: Daniel Gall and Stefan Nikodemski

Tuesday Afternoon, November 30, 2021

Hynes, Level 2, Room 202

4:00 PM EQ13.03.01

Electrical Control in ZnSnN₂ by Tailoring Intrinsic and Extrinsic Defects [Vegard S. Olesen](#), Simon Cooil, Vetle Øversjøen, Lasse Vines and Andrej Yu Kuznetsov; University of Oslo, Norway

Ternary nitrides are a novel and emerging class of semiconductors with potential impact within a wide range of applications, including solar cells, power electronics, and overall water-splitting [1]. Zn-IV-N₂, with IV = Sn, Ge or Si, represents an earth-abundant alternative to conventional III-nitrides, currently dominating the optoelectronic market and playing a vital role in a quest for record-high efficiency solar cells, specifically in multi-junction architectures. Zn-IV-N₂ semiconductors exhibit close similarities to the III-nitrides in terms of the functional properties, e.g., optical band gap tunability [2-4]. Such close similarities invite for both the knowledge transfer and combinational utilization of the III-nitride and Zn-IV-nitride systems. The main challenge for Zn-IV-N₂ in general, and for ZnSnN₂ in particular, is in controlling intrinsic and extrinsic defects, governing the carrier concentration (n). Typically, for as-grown stoichiometric ZnSnN₂, n remains in the range of 5×10^{19} - 5×10^{20} cm⁻³, where possible defects causing the degeneracy have been identified by first-principles calculations; the tin-zinc antisite (Sn_{Zn}), the nitrogen vacancy (V_N), and the zinc interstitial (Zn_i), are all defects probable to occur and form shallow donors [5,6]. Furthermore, common impurities such as oxygen substituting for nitrogen (O_N), hydrogen interstitials (H_i) and

substitutional hydrogen (H_N), also form donor states in $ZnSnN_2$ [5,6]. The prevailing route for controlling n is the fabrication of Zn-rich $ZnSnN_2$, effectively reducing and enhancing the formation probability of Sn_{Zn} donors and Zn_{Sn} acceptor [7], but the carrier mobility (μ) remains unacceptably low ($< 10 \text{ cm}^2 \text{ V}^{-1} \text{ s}^{-1}$). Possible p -type dopants in $ZnSnN_2$ have also been identified by first-principles calculations, where Na_{Zn} and K_{Zn} are predicted to exhibit deep acceptor levels, while Li_{Zn} is predicted to be a shallow acceptor [8]. However, the corresponding experimental explorations are rare or missing. Here, we report on $ZnSnN_2$ thin films grown by high-power impulse magnetron sputtering (HiPIMS), with carrier concentration reducing strategies, such as shallow acceptor doping with Li and off-stoichiometric growth. We thus extend our work on epitaxial $ZnSnN_2$ growth exhibiting a dislocation density of 1×10^{10} – $5 \times 10^{10} \text{ cm}^{-2}$, i.e., comparable to III-nitrides grown without dislocation-reducing strategies [9], in order to obtain electrical control. Our preliminary results confirm that the Sn_{Zn} antisite is the dominant intrinsic defect, as n is reduced, and hence also the optical band gap (from $\sim 1.78 \text{ eV}$ to $\sim 1.28 \text{ eV}$) due to reduced Burstein-Moss shift, when moving towards more Zn-rich conditions. Moreover, we confirm that Li acts as an acceptor in $ZnSnN_2$, reducing n in the stoichiometric film by an order of magnitude, while keeping μ at a reasonable high value, $\mu \sim 60 \text{ cm}^2 \text{ V}^{-1} \text{ s}^{-1}$. As predicted by Wang *et al.* [8], Li_{Zn} is a shallow acceptor in $ZnSnN_2$; however, in the interstitial configuration (Li_i), Li may act as a donor too. Nevertheless, even though both Li_{Zn} and Li_i are possible to occur in our samples, the significant reduction in n for the stoichiometric film suggests that the majority of the incorporated Li is in the form of Li_{Zn} acceptors. Thus, controlling the interplay between intrinsic and extrinsic defects may lead to a breakthrough in the development of $ZnSnN_2$.

- [1] Schepf, R. R. *et al.*, ACS Energy Letters, **5**, 2027-2041, 2020
- [2] Lahourcade, L. *et al.*, Advanced Materials, **25**, 2562-2566, 2013
- [3] Kikkawa, S. *et al.*, Solid State Communications, **112**, 513-515, 1999
- [4] Osinsky, A. *et al.*, Proceedings 2000 IEEE/Cornell Conf. on High Perform. Devices, 2000
- [5] Tsunoda, N. *et al.*, Physical Review Applied, **10**, 011001, 2018
- [6] Chen, S. *et al.*, Advanced Materials, **26**, 311-315, 2013
- [7] Fioretti, A. *et al.*, Journal of Materials Chemistry C, **3**, 11017, 2015
- [8] Wang, T. *et al.*, Physical Review B, **95**, 205205, 2017
- [9] Olsen, V. S. *et al.*, Advanced Optical Materials, 21000015, 2021

4:15 PM EQ13.03.03

Accelerated Simulation of Elastic and Thermodynamic Properties of Materials at High Temperature Ferenc Tasnádi¹, Florian Bock¹, Qurat Ul-Ain¹, Alexander Shapeev², Magnus Odén¹ and Igor A. Abrikosov¹; ¹IFM Linköping University, Sweden; ²Skolkovo Institute of Science and Technology, Russian Federation

Refractory nitrides (TiN, ZrN, Hf, etc.) and nitride alloys ($Ti_{1-x}Al_xN$, etc.) form a class of materials with high industrial relevance for hard coatings of cutting tools [1] or for plasmonic-based devices [2]. For these applications the major objectives are the material's high-temperature thermal and elastic properties. A recently developed combination of quantum mechanical calculations with machine-learning interatomic potentials [3], is utilized to calculate materials elastic constants with high accuracy. On-the-fly training of these potentials allows us to perform the calculations with more than two orders less computational effort than using state-of-the-art ab initio molecular dynamics simulations. The derived elastic constants are used to calculate surface acoustic waves and Brillouin light scattering (BLS) spectra. The results are compared with experiments. Furthermore, we investigate high-temperature bcc phase of titanium and predict very weak temperature dependence of its elastic moduli [4], called Elinvar effect, similar to the behavior observed for so-called GUM alloys. However, the effect in bcc-Ti is intrinsic and therefore unique.

- [1] See, for example, F. Tasnádi *et al.*, Phys. Rev. B **85**, 144112 (2012); F. Tasnádi *et al.*, Appl. Phys. Lett. **97**, 231902 (2010); D. Holec *et al.* Phys. Rev. B **90**, 184106 (2014); F. Tasnádi *et al.*, Mater. Des. **114**, 484 (2017).
- [2] U. Guler *et al.*, Mater. Today **18**, 227 (2015), Catellani *et al.*, Phys. Rev. B **95**, 15145 (2017); M. Kumar *et al.*, ACS Photonics **3**, 43 (2016); U. Guler *et al.*, Faraday Discuss. **178**, 71 (2015).
- [3] I. S. Novikov *et al.*, Mach. Learn.: Sci. Technol. **2** 025002 (2021).
- [4] A. Shapeev *et al.*, New. J. Phys. **22**, 113005 (2020).

SESSION EQ13.04: Poster Session I: Ceramic, Nanoparticle and Transition Metal Nitride
 Session Chairs: Wenhao Sun and Andriy Zakutayev
 Tuesday Afternoon, November 30, 2021
 8:00 PM - 10:00 PM
 Hynes, Level 1, Hall B

EQ13.04.01

Atomistic Modeling of Hot-Press Sintering of AlN Ceramics Aoyan Liang, Chang Liu and Paulo Branicio; University of Southern California, United States

The sintering of AlN ceramics has been intensely investigated and it is reasonably understood. The increasing possibilities offered by the outstanding properties of nanostructured ceramics underline the necessity to also understand the sintering process of AlN ceramic nanoscale powder. Here, we use atomistic molecular dynamics simulations to study the hot-press sintering of AlN nanoceramics. We employ nanopowder samples composed of nanoparticles with 8, 12, and 16 nm: namely, samples AlN-8, AlN-12, and AlN-16. Densification simulations are run for 6 ns under a hydrostatic pressure of 1 GPa and sintering temperature of 1,900 K. An extra simulation is performed for an 8 nm sized nanoparticle system at a lower pressure of 0.1 GPa (sample AlN-8-0.1). Results show that the sample AlN-8 reaches 99% densification, the highest of all systems. 96.2%, 95.6%, and 93.2% densifications are achieved for the samples AlN-8-0.1, AlN-12, AlN-16, respectively. Grain size distribution statistics shows that the AlN-8 system experience significant microstructural evolution from 3 to 6 ns of the sintering process developing a wide distribution of grain sizes from 4 to 15 nm with a large average grain size of $\sim 11 \text{ nm}$. These results reveal a two-stage sintering process: (1) Initial swift densification that is rooted at the high diffusivity of surface atoms. (2) Intense grain growth driven by grain boundary migration. Moreover, a wurtzite-to-rocksalt structural phase transformation occurs at the nanoparticles contact points in the AlN-16 sample during the sintering. These exciting results offer nanoscale insights into the intriguing hot-press sintering of nanoscale ceramics and shed light on the densification and microstructural evolution processes.

EQ13.04.02

Molecular-Level Sintering Additives for Densification of SiAlON Ceramics Kade McGarrity and Holly Shulman; Alfred University, United States

SiAlON ceramics are solid solutions of Al and O in the Si_3N_4 lattice. They are used as wear parts and gas turbine engine blades, and more recently have shown promise for application as biomedical implants. The densification of SiAlONs is generally achieved using sintering additives and/or pressure-assisted sintering techniques. Traditionally, additives such as alumina and yttria powders are utilized. In this work, we investigate the use of organic precursors rather than powders in order to incorporate sintering additives at the atomic or molecular level. This presentation will highlight the densification, strength, elastic modulus, hardness, microstructure, and phase assemblage of SiAlONs fabricated via atomic-scale as well as conventional additives. It was found that the use of molecular precursors may enhance densification by providing a very fine scale distribution of solute atoms which are more readily available to the Si_3N_4 starting powder than atoms confined to powder particles.

EQ13.04.04

Synthesis of Silicon Nitride Nanoparticle Films from Silane-Nitrogen Non-Thermal Radio-Frequency Plasma [Gunnar Nelson](#), Himashi P. Andaraarachchi, Ognjen Ilic and Uwe R. Kortshagen; University of Minnesota Twin Cities, United States

Silicon nitride (SiN_x) is ubiquitous in photovoltaic technology as a dual-purpose passivation layer and antireflection-coating. It also is used as a durable coating/material in industrial settings as it is a high-strength ceramic. Recent work has explored nanoscale silicon nitride morphologies such as nanowires, nanopores, nanocomposites, and others. Specifically, nanoparticle (NP) SiN_x is a promising nano-scale form as it has applications in battery technology, passive radiative cooling films, and as passivation layer on silicon nanoparticles for improving photo-luminescence. Also hot-pressed and sintered SiN_x from a powder is an attractive route to high mechanical strength materials. These studies outline the need for SiN_x NP with a narrow size distribution, minimal aggregation, high purity, and high throughput. However, producing SiN_x nanoparticles with current top-down techniques does not meet the high yield and narrow size distribution requirements. Bottom-up techniques such as gas phase synthesis typically require very high temperatures and use ammonia as the nitrogen precursor as it has lower bonding energy than diatomic nitrogen. Ammonia, however, is caustic and requires several safety precautions. Nonthermal plasma NP synthesis has been shown to be a promising technique which meets these production requirements and can deposit uniform films over a wide area with tunable thickness and porosity. Here, we report SiN_x NP synthesis with this technique using a silane-nitrogen plasma. After synthesis, the particles are accelerated through a nozzle to sonic speeds to deposit ballistically onto a rastered substrate. Resulting SiN_x NP films show low visible absorption suggesting stoichiometric silicon nitride. This study shows that silicon nitride nanoparticles can be produced in this high-yield, scalable, and tunable synthesis process.

Acknowledgement: This work is supported by the Army Research Office under MURI project under W911NF-18-1-0240.

SESSION EQ13.05: AlScN Ferroelectric Nitrides
Wednesday Morning, December 1, 2021
Hynes, Level 2, Room 202

11:45 AM *EQ13.05.01

Switching Dynamics in Ferroelectric AlN-Based Films Keisuke Yazawa^{1,2}, Daniel Drury^{1,2}, Andriy Zakutayev^{2,1} and [Geoff L. Brennecke](#)¹; ¹Colorado School of Mines, United States; ²National Renewable Energy Laboratory, United States

The 2019 report from Fichtner, et al.[1] of ferroelectric switching in $\text{Al}_{1-x}\text{Sc}_x\text{N}$ thin films further increased interest in this materials system that was already the darling of the piezoelectric thin film community. This system now promises both resonator-quality piezoelectric properties and the potential to enable a class of next-generation compute-in-memory hybrids if switching voltages can be sufficiently scaled. Hayden, et al.[2] recently expanded the family of AlN-based ferroelectrics to include $\text{Al}_{1-x}\text{B}_x\text{N}$ and even unmodified AlN, adding to the excitement over potential for integrated functionality. The large switchable spontaneous polarization values, enormous coercive fields, and remarkably square hysteresis loops of AlN-based ferroelectrics draw sharp contrast to HfO_2 -based ferroelectrics and highlight the need for better understanding the switching behaviors in these novel ferroelectrics to effectively leverage this switchable polarization.

Using a custom-built high power measurement capability in addition to commercial test equipment, we have studied the polarization reversal behavior of AlN-based ferroelectric thin films across more than 9 orders of magnitude in time. This talk summarizes our findings on the effects of chemistry (intentional alloying elements such as scandium and boron as well as unintentional contaminants such as oxygen), measurement temperature, film structure and stress state, and electrodes on switching dynamics. Combined with complementary measurements of Rayleigh behavior and polarization retention, these studies provide strong hints at the underlying mechanisms controlling ferroelectricity in these new AlN-based ferroelectrics.

[1] S. Fichtner, N. Wolff, F. Lofink, L. Kienle, and B. Wagner, "AlScN: A III-V semiconductor based ferroelectric," J. Appl. Phys., 125, 114103 (2019). doi: 10.1063/1.5084945

[2] J. Hayden, M.D. Hossain, Y. Xiong, K. Ferri, W. Zhu, M.V. Imperatore, N. Giebink, S. Trolier-McKinstry, I. Dabo, and J.-P. Maria, "Ferroelectricity in boron-substituted aluminum nitride thin films," Phys. Rev. Mater., 5, 044412 (2021). doi: 10.1103/PhysRevMaterials.5.044412

12:15 PM EQ13.05.04

Characterization of the Structure, Composition and Strain in Ultrathin Ferroelectric Aluminum Scandium Nitride Films [Pariasadat Musavigharavi](#), Andrew C. Meng, Dixiong Wang, Jeffrey Zheng, Alexandre Foucher, Roy H. Olsson and Eric A. Stach; University of Pennsylvania, United States

We present characterizations of the local atomic structure and nanoscale chemistry of ferroelectric aluminum scandium nitride thin films ($\text{Al}_{1-x}\text{Sc}_x\text{N}$) using advanced transmission electron microscopy (TEM) techniques. An $\text{Al}_{1-x}\text{Sc}_x\text{N}$ ($x = 0.36$) film of ~ 20 nm thickness was grown on a Pt(111)/Ti/SiO₂/Si(100) substrate via pulsed DC co-sputtering. The homogeneous distribution of scandium and the formation of defects in the epitaxial growth of 2.1% lattice-mismatched AlScN on Pt are reported. We also examined the strain distribution across the AlScN/Pt interface. The "four-dimensional scanning TEM" (4D-STEM) technique was employed to systematically investigate the nanoscale order by measuring the average spacing between atoms within certain regions in the film and determining the strain. It was conclusively shown that AlScN crystallites preserve the piezoelectric wurtzite-type structure in the (001) preferential orientation normal to the substrate. The strain map confirms a significant increase in the out-of-plane component of the lattice parameter ($\sim 9\%$) at the AlScN/Pt interface. The lattice parameter in the Pt template decreases as a function of distance from the Pt/Si interface. The study of the atomic crystal structure and the chemical composition of the AlScN thin film provides useful information that will aid future applications of this material in ferroelectric memories and microelectromechanical systems.

SESSION EQ13.06: III-N Semiconductors for Optoelectronics
Session Chairs: Ana Cros and William Doolittle
Wednesday Afternoon, December 1, 2021
Hynes, Level 2, Room 202

2:00 PM *EQ13.06.02

Distribution of Ge Dopants in AlGa_xN—A Chemical and Structural Investigation Down to the Nanoscale Catherine Bougerol¹, Eric Robin², Enrico Di Russo³, Edith Bellet-Amalric², Vincent Grenier², Akhil Ajay², Lorenzo Rigutti³ and Eva Monroy²; ¹Institut Néel - CNRS, France; ²CEA-IRIG, France; ³UNIROUEN-CNRS, France

The potential of Ge as n-type dopant for AlGa_xN materials is currently under consideration. Ge is known to generate significantly less local tensile strain than silicon, whatever the Al mole fraction of the alloy. However, at high doping concentrations, the issue of the effective dopant incorporation and its spatial distribution is relevant. Formation of precipitates or diffusion of dopants along structural defects may occur [1]. Recently, we have demonstrated plasma-assisted molecular-beam epitaxy growth of Al_xGa_{1-x}N planar layers with Ge nominal concentrations up to 10²¹ cm⁻³ [2]. Here, we present a structural analysis of Al_xGa_{1-x}N:Ge samples with x covering the full compositional range (0 ≤ x ≤ 1), together with the measurement of Ge concentration and its spatial distribution from the μm range down to the nm scale [3]. Our study is based on a combination of X-ray diffraction (XRD) and quantitative energy dispersive X-ray spectrometry (EDX) coupled to high-resolution scanning transmission electron microscopy (HR-STEM) and atom probe tomography (APT).

In Al_xGa_{1-x}N:Ge samples with x > 0.4, top-view SEM observations reveal the presence of μm-size crystallites at the surface. The nature of such crystallites is pure Ge, as verified by EDX. Inside those layers, we have also identified Ge-rich inclusions with a size of tens of nanometers, generally associated with Ga-rich regions around structural defects. With these local exceptions, the Al_xGa_{1-x}N:Ge matrix presents homogenous Ge composition. The Ge concentration in the matrix, i.e. away from the precipitates, was obtained from the ratio of the EDX signal between doped and undoped samples. The Ge content in the binary AlN matrix is extremely low, and it increases linearly with the Ga mole fraction in ternary Al_xGa_{1-x}N, which suggests that the Ge incorporation takes place by substitution of Ga atoms. The maximum percentage of Ga sites occupied by Ge saturates around 1%. These solubility issues and the Ge segregation phenomena should play a role in the efficiency of Ge as n-type dopant, even at Al concentrations where Ge DX centers are not expected to manifest. In view of these results, the extracted solubility limit of Ge in Al_xGa_{1-x}N can have direct impact on the performance of Al_xGa_{1-x}N-based UV light emitting diodes. In principle, the Ge content should be kept below these limits to prevent a degradation of carrier transport due to scattering at structural defects. Co-doping or the use of surfactant species should be explored to attain Ge concentrations beyond the solubility limit.

References

- [1] L. Amichi, *et al.*, *Nanotechnol.* **31**, 045702 (2020).
- [2] R. Blasco, *et al.*, *J. Phys. D.: Appl. Phys.* **52**, 125101 (2019).
- [3] C. Bougerol, *et al.*, *ACS Applied Materials & Interfaces* **13**, 4165 (2021).

2:30 PM DISCUSSION TIME

2:30 PM EQ13.06.04

Has the InGa_xN Nanowires Surface an Influence on Luminescence Efficiency? Alexandre Concorde¹, Joël Bleuse and Bruno Daudin; CEA Grenoble, France

The remarkable properties of InGa_xN/GaN nanowires (NWs) heterostructures emitting at 480 nm and grown by PA-MBE, namely a large amount of free surface favouring strain relaxation and the expected absence of extended defects make them attractive for the development of a new generation of highly efficient light emitting diodes (LEDs). However, as a counterpart of these potential advantages, the surface itself may act as a non-radiative recombination centre. To clarify this issue, the effect of surface passivation by deposition of an aluminium oxide material, using the Atomic Layer Deposition technique was investigated by time resolved photoluminescence experiments. It appears that the photoluminescence decay - which follows a power law - before passivation is markedly shorter than following passivation, emphasizing the role of the NW surface as a non-radiative recombination channel in the case of InGa_xN/GaN NWs heterostructures. Furthermore, Micro-photoluminescence spectroscopy experiments performed on InGa_xN/GaN NWs for laser excitation power density ranging from 10⁻⁴ W.cm⁻² to 10⁶ W.cm⁻², exhibit a bell shape curve, typical of a defect saturation regime. As the power law dependence of the photoluminescence prevents from determining a single lifetime, the standard phenomenological ABC model cannot be used to describe it. Hence, we developed a theoretical model that accounts for the carrier generation, the radiative recombination, the capture of carriers by non-radiative defect states — leading to their saturation, as well as the Auger losses. The internal quantum efficiency and the nature of carrier recombination (monomolecular or bimolecular) are quantitatively assessed by this model, as a function of the excitation power.

SESSION EQ13.07: III-N Epitaxy and Nanowires
Session Chairs: Geoff Brenneka and Jon-Paul Maria
Wednesday Afternoon, December 1, 2021
Hynes, Level 2, Room 202

4:00 PM *EQ13.07.01

Exploring the Properties of GaN Epilayers on van der Waals Substrates—The Case of Graphene and Muscovite Mica Ana Cros¹, Saül Garcia-Orrit¹, Núria Garro¹, Oleksii Klymov¹, María José Recio-Carretero¹, Marion Gruart², Remy Vermeersch², Fabrice Donatini², Catherine Bougerol², Bruno Gayral², Stéphanie Pouget², Edith Bellet-Amalric², Nicolas Mollard², Hanako Okuno², Jean-Luc Rouvière², Nathaniel Feldberg² and Bruno Daudin²; ¹Univ de Valencia, Spain; ²Univ. Grenoble-Alpes, France

The quality of III-nitride epilayers depends strongly on the characteristics of the substrate. The reduction of the number of extended defects in lattice mismatched epitaxial GaN layers grown on the most used substrates, namely sapphire and silicon, requires complex growth strategies that, despite the continuous advances, result in higher costs of the final device. The mismatch in thermal expansion coefficients of III-nitride layers and, for instance, Si substrate, is an additional source of extended defects associated with a strong substrate/layer chemical bonding. This motivates the exploration of alternative substrates, including the renewed interest in van der Waals epitaxy, where epitaxial growth is achieved through weak dipolar interactions. Materials such as graphite, mica, MoS₂ or GaSe, have layered structures bonded via weak van der Waals interaction and can be easily cleaved, presenting very flat surfaces and the absence of dangling bonds. When GaN is grown on them, these substrates allow a significant relaxation of the epilayer strain and facilitate, at the same time, layer detachment [1].

We study the case of GaN grown by molecular beam epitaxy on graphene and muscovite mica as possible van der Waals substrates, addressing epilayer morphology, crystallographic phase and orientation, surface potential and strain. We also study the changes experienced by the graphene substrate during growth: doping, strain and, under certain conditions, the intercalation of a self-limited bilayer of metal atoms below graphene [2, 3]. In the case of mica, we observe that part of the strain accumulated in the GaN layer during growth relaxes by the formation of three-dimensional structures in the shape of telephone cord buckles, straight blisters or by more complex arrangements. The characteristics of these structures are analyzed in relation to the compressive strain of the surrounding material, the achieved relaxation and layer adhesion [4].

[1] Kim, J., Bayram, C., Park, H., Cheng, C. W., Dimitrakopoulos, C., Ott, J. A., Reuter, K. B., Bedell, S. W., & Sadana, D. K. (2014). Principle of direct van der Waals epitaxy of single-crystalline films on epitaxial graphene. *Nature Communications*, 5, 1–7. <https://doi.org/10.1038/ncomms5836>

[2] Gruart, M., Feldberg, N., Gayral, B., Bougerol, C., Pouget, S., Bellet-Amalric, E., Garro, N., Cros, A., Okuno, H., & Daudin, B. (2020). Impact of kinetics on the growth of GaN on graphene by plasma-assisted molecular beam epitaxy. *Nanotechnology*, 31(11), 115602. <https://doi.org/10.1088/1361-6528/ab5c15>

[3] Feldberg, N., Klymov, O., Garro, N., Cros, A., Mollard, N., Okuno, H., Gruart, M., & Daudin, B. (2019). Spontaneous intercalation of Ga and In bilayers during plasma-assisted molecular beam epitaxy growth of GaN on graphene on SiC. *Nanotechnology*, 30(37), 375602. <https://doi.org/10.1088/1361-6528/ab261f>

[4] Daudin, B., Donatini, F., Bougerol, C., Gayral, B., Bellet-Amalric, E., Vermeersch, R., Feldberg, N., Rouvière, J.-L., Recio Carretero, M. J., Garro, N., Garcia-Orrit, S., & Cros, A. (2021). Growth of zinc-blende GaN on muscovite mica by molecular beam epitaxy. *Nanotechnology*, 32(2). <https://doi.org/10.1088/1361-6528/abb6a5>

4:30 PM *EQ13.07.02

Chemical and Kinetic Mechanisms to Overcome Perceived Limitations in III-Nitride Epitaxy William A. Doolittle, Zachary Engel, Habib Ahmad, Christopher Matthews and Keisuke Motoki; Georgia Institute of Technology, United States

III-Nitride epitaxy is fraught with many challenges ranging from phase separation to high defect densities to doping limitations. Traditional epitaxy has suggested that high temperatures are required to maintain long surface diffusion lengths and thus, high material quality. Unfortunately, high temperature environments also introduce significant complications and limitations in practically achievable compositions and doping ranges. Furthermore, huge variations in the effective metal-fluxes from one growth system to another at traditional epitaxy growth temperatures makes it difficult to achieve commercial scalability. By deviating from the normal high temperature epitaxy via the control of surface chemistry and adding intentional kinetic limitations on adatom diffusion, we can achieve significant improvements in the material quality of traditionally difficult materials to grow such as AlInN and InGaN. Non-phase separated InGaN has been grown throughout the miscibility gap and record Indium-content solar cells produced via a low temperature variant of molecular beam epitaxy called metal modulated epitaxy (MME). MME offers the ability to control major factors in phase separation: growth at low temperature avoids InGaN decomposition and indium desorption; high growth rates limit the lateral separation of surface adatoms; and fine-control of excess-metal dose per shutter cycle prevents extreme build-up of a metal adlayers and allows control over vertical segregation of indium and gallium. Likewise, highly luminescent AlInN has been produced that has x-ray diffraction (XRD) figures of merit 11 times better than previous literature. Furthermore, MME has been expanded to grow high crystal quality AlInN over the entire composition range. Additionally, low temperature MME AlInN growth near the composition that would be lattice matched to GaN (~18% In) shows XRD figures of merit rivaling the best in the literature. By modeling and controlling surface chemistry, especially vertical phase segregation, remarkably coherent superlattices can be obtained in AlGaIn and InGaIn ternary systems and can be maintained coherent for many microns thicknesses. MME achieves excellent uniformity and thickness control suitable for commercial use primarily because of low temperature growth while simultaneously achieving high quality films via enhanced adatom diffusion through its additional growth control parameter of excess-metal dose per shutter cycle. Additionally, by using substantially lower growth temperatures than other methods, MME can enhance the doping concentration of traditionally difficult dopants such as magnesium and beryllium exceeding prior doping limits by more than 40 times and for more traditional dopants like Si and Ge by factors of 2 to 4. This has led to a new understanding of the acceptor energy wherein a wide acceptor energy band forms because of the Pauli Exclusion principle compared to a single isolated energy in traditionally doped cases. Using these highly advanced low temperature doping methods, tunnel junctions with record conductance and strong negative differential resistance have been demonstrated and used in GaN and AlGaIn homojunction devices even up to 58% Al. These advances have enabled the first tunnel junction contacted III-Nitride solar cell with much higher uniformity and improved the 270 nm DUV optical output of LEDs by as much as 110%. Finally, we will demonstrate that by a combination of low temperature growth and control of surface chemistry, for the first time we have been able to demonstrate p-type aluminum nitride with hole concentrations exceeding $1 \times 10^{18} \text{ cm}^{-3}$ and showed a first time heterojunction p-AlN/n-GaN diode with modest rectification showing future potential for future deep ultraviolet, high-power and high-frequency devices capable of operation in extreme radiation and heat environments.

5:00 PM EQ13.07.03

Towards a Better Understanding of Electronic Transport in Si Doped AlN Nanowires Remy Vermeersch^{1,2}, Eric Robin¹, Ana Cros³, Gwénoél Jacopin², Bruno Daudin¹ and Julien Pernot²; ¹CEA Grenoble, France; ²CNRS Neel Institute, France; ³University of Valencia, Spain

Thanks to its ultra-wide band gap, AlGaIn and AlN nanowires (NWs) are attractive candidates for deep UV light emitting diodes (LED). The absence of extended defects, such as dislocations, as well as the morphology of nitride NWs, are favorable to improve the dopants incorporation, the internal quantum efficiency and light extraction. In this context, some of us recently reported axial pn junction realization with Mg acceptors in the p-region and Si donors in the n-region [1]. Thus, it becomes crucial to understand and describe in detail the transport mechanisms at the origin of the current flow inside the individual nanodevices. The n-type doping of AlN nanowires remains a blind spot in recent research and is as important as its p-type counterpart in order to achieve the best performances for nanowire-based DUV LEDs.

In this work, we investigate the electrical properties of n-type AlN NWs grown by molecular beam epitaxy using several silicon fluxes. The current voltage measurements show that all the samples exhibit an Ohmic regime at low bias (< 0.2 V) and a space charge limited current regime assisted by traps for higher voltage (> 0.2 V). This regime occurs in semiconductor with moderate carrier density either because of a near-surface depletion or because of a weak ionization of relatively deep dopants. The conductivity reaches a maximum of 6.10^{-6} S/cm for intermediate Si flux before dropping down to 4.10^{-6}

9 S/cm at larger flux, in good agreement with high compensation effects observed in bulk AlN [2]. Temperature dependent measurements from 180 K to 600 K revealed that NW conductivity is a combination of the two identified silicon levels at 75meV and 270meV [3]. Due to a high surface level pinning energy of 2.1eV [4], the NW diameter is shown to be a key parameter of particular importance in order to not reach its full depletion, decreasing the free electrons concentration at thermal equilibrium and leading to poor conductivity. The full model and analysis will be presented and discussed in this presentation. Those results point towards the need for larger nanowires and/or surface passivation to ensure better electron injection, enabling the realization of efficient UV LEDs.

- [1] A.-M. Siladie et al, *Nano Lett.* 19, 8357-8364 (2019)
- [2] J. S. Harris et al, *Appl. Phys. Lett.* 112, 152101 (2018)
- [3] M.H. Brenckenridge et al, *Appl. Phys. Lett.* 118, 112104 (2021)
- [4] P. Reddy et al, *J. Appl. Phys.* 116, 123701 (2014)

5:15 PM EQ13.07.04

Inhomogeneous Si and Mg Dopant Distribution in GaN Nanowires Ece Aybeke^{1,2}, Alexandra-Madalina Siladie^{3,4}, Remy Vermeersch^{3,4}, Eric Robin^{3,4}, Oleksandr Synhavskiy^{1,2}, Bruno Gayral^{3,4}, Julien Pernot⁴, Georges E. Bremond^{1,2} and Bruno Daudin^{3,4}; ¹Institut des nanosciences de Lyon, France; ²Institut National des Sciences Appliquées, France; ³CEA Grenoble, France; ⁴Université Grenoble Alpes, France

Introduction of electrical dopant species in semiconductors generally results in increasing built-up strain for increasing dopant densities, till reaching the solubility limit and/or a strain relaxation stage associated with extended defect formation. By contrast doping in nanowires (NWs) obeys a specific regime, associated with their unique morphology. In the case of GaN NWs grown on Si (111) by molecular beam epitaxy, the eased strain relaxation due to the large amount of free surface favors the incorporation of Si dopant at concentrations higher than in layers [1]. Also, specific adatom surface diffusion and reconstruction-stabilized sidewall stoichiometry are affecting dopant incorporation. Hence, atom probe tomography [2] and energy-dispersive X-rays spectroscopy (EDX) [3] experiments at the nanoscale demonstrate that preferential Mg incorporation through the m-plane side walls of GaN NWs leads to a higher Mg density in the NW periphery, about ten times larger than in the NW core. Scanning spreading resistance microscopy (SSRM) experiments were performed to investigate the effect of inhomogeneous dopant distribution on the electrical transport properties of n-type and p-type GaN NWs at the nanoscale. In Si-doped GaN NWs a conductive core surrounded by a more resistive shell was put in evidence, which is assigned to the depletion resulting from Fermi level pinning on m-plane surface states. By contrast, in the case of Mg-doped GaN NWs, the SSRM is one order of magnitude smaller at the periphery than at the centre of the Mg-doped GaN. This experimentally demonstrates that peripheral Mg incorporation in GaN NWs indeed counterbalances the depletion resulting from Fermi level pinning on m-plane surface states, which results in preferential current flow in the highly doped shell. For the same samples as measured by SSRM, EDX reveals a Mg concentration of about $2-4 \times 10^{20}/\text{cm}^3$ in periphery, higher by more than one order of magnitude compared to the NW centre where the Mg content is below the experimental detection limit of $10^{19}/\text{cm}^3$. The coexistence of these different electrical conduction channels, specific to NWs, opens new prospects on the full understanding of the opto-electrical properties of NW-based devices such as visible or UV light emitting diodes.

- [1] Z. Fang et al, *Nano Lett.* 15, 6794 (2015)
- [2] A.M. Siladie et al, *Nanotechnology*, 29, 255706 (2018)
- [3] E. Aybeke et al, submitted

SESSION EQ13.08: Computational Prediction and Bulk Synthesis of New Nitride Materials
Session Chairs: John Attfield and Minghui Yang
Monday Morning, December 6, 2021
EQ13-Virtual

8:00 AM *EQ13.08.01

Computational Design and Exploration of Ternary Zinc Nitride Semiconductors [Fumiyasu Oba](#); Tokyo Institute of Technology, Japan

The search for novel semiconductors is increasingly important as the applications of semiconductors become more prevalent in modern society. This situation stimulates not only experimental but also computational explorations of as-yet-unreported semiconductors, typically using first-principles calculations. In such computational searches, reliable design principles, as well as accurate and efficient computational schemes, are key requirements for the successful identification of target materials and functionalities. In this talk, I will discuss the design and exploration of nitride semiconductors using first-principles calculations, with a focus on ternary zinc nitrides. Topics to be covered include the theoretical prediction and experimental verification of new nitride semiconductors such as CaZn_2N_2 , SrZn_2N_2 , and related alloys with direct band gaps covering most of the visible light range [1-3]. Computational methods for predicting fundamental and defect properties of semiconductors and their applications to nitride semiconductors will also be discussed [4].

- [1] Y. Hinuma, T. Hatakeyama, Y. Kumagai, L. A. Burton, H. Sato, Y. Muraba, S. Iimura, H. Hiramatsu, I. Tanaka, H. Hosono, and F. Oba, *Nat. Commun.* 7, 11962 (2016).
- [2] R. Kikuchi, K. Ueno, T. Nakamura, T. Kurabuchi, Y. Kaneko, Y. Kumagai, and F. Oba, *Chem. Mater.* 33, 2864 (2021).
- [3] M. Tsuji, H. Hiramatsu, and H. Hosono, *Inorg. Chem.* 58, 12311 (2019).
- [4] F. Oba and Y. Kumagai, *Appl. Phys. Express* 11, 060101 (2018).

8:30 AM *EQ13.08.02

Exploring Polymorphism and Cation Disorder in Mg-IV-N₂ Semiconductors [Ann L. Greenaway](#)¹, Rekha Schnepf^{1,2}, Amanda Loutris¹, Karen Heinselman¹, Rachel Woods-Robinson^{1,3}, Celeste Melamed^{1,2}, Jesse Adamczyk², Brooks Tellekamp¹, Sage Bauers¹, Andriy Zakutayev¹, Steven Christensen¹, Stephan Lany¹ and Adele Tamboli¹; ¹National Renewable Energy Laboratory, United States; ²Colorado School of Mines, United States; ³University of California, Berkeley, United States

While the III-N compounds revolutionized solid-state lighting, there is ongoing work to identify nitrides which enable technologies currently inaccessible with III-Ns, such as bridging the “green gap”. This has led to the investigation of increasingly complex materials which potentially have increased property tunability over the III-Ns, such as II-IV-N₂ compounds ZnGeN_2 and ZnSnN_2 . Interest in these materials is driven by their cation site disorder, which may be harnessed to tune bandgap without a corresponding change in lattice parameter [1]. At the same time, it is increasingly clear that metastable nitrides are highly synthesizable compared to other compounds [2], increasing the diversity of nitride materials which can be utilized in emerging technologies.

While interest in the Zn-based II-IV-N₂ compounds has been high, Mg-IV-N₂ compounds (IV = Si, Ge, Sn) are substantially underexplored in comparison. However, these materials not only display the potential for bandgap tunability *via* cation disorder of II-IV-N₂ compounds, but also multiple low-energy metastable polymorphs, as exemplified by MgSnN₂ [3]. The wurtzite-type, ground-state polymorph of MgSnN₂ has a ~2.4 eV bandgap, but it can also form as a >2.9 eV, high dielectric constant rocksalt-type metastable phase. Here, we present ongoing work on the synthesis of the Mg-IV-N₂ family of compounds, seeking to understand and control polymorph formation to enable property tuning across the group.

First, we discuss our combinatorial approach to the synthesis of the Mg-IV-N₂ compounds, beginning with MgSnN₂ [3]. The metastable rocksalt-type polymorph of MgSnN₂ was found to form as a secondary phase to the wurtzite-type polymorph at substrate temperatures below 200 °C and at high Mg content on Si substrates, but also as part of a mixed wurtzite/rocksalt phase on GaN substrates at high temperatures. The close effective lattice match between GaN (001) and rocksalt MgSnN₂ (111) surfaces promotes the formation of the rocksalt at those high temperatures, an effect that we seek to leverage in ongoing work exploring control of polymorph formation *via* epitaxial strain energy of different substrates. We will discuss related phenomena in MgSiN₂ and MgGeN₂, and present trends across this family of materials, with broad lessons for development of emerging nitride semiconductors.

This material is based on work funded by a Director's Postdoctoral Research Fellowship (LDRD) at the National Renewable Energy Laboratory and by the Office of Science, Basic Energy Sciences, Material Sciences and Engineering Division.

- [1] Schnepf et al, *ACS Energy Letters* (2020).
- [2] Greenaway et al, *Annual Review of Materials Research* (2021).
- [3] Greenaway et al, *Journal of the American Chemical Society* (2020).

9:00 AM *EQ13.08.03

Strain-Induced Creation and Switching of Anion Vacancy Layers in Perovskite Oxynitrides SrV(O,N)₃, Hiroshi Kageyama; Kyoto University, Japan

In oxides, the oxygen-vacancy ordering often occurs, leading to the emergence of novel functional properties, as exemplified by YBCO. On the other hand, oxynitrides are expected to have functions beyond oxides due to the difference in nitrogen and oxygen (e.g., valence and polarizability), but there are no reports on anion-vacancy ordering. In my talk, a successful example of anion-vacancy order is shown by SrVO_{2.2}N_{0.6}, where anion-vacant layers appear periodically along the 111 direction when perovskite oxide SrV(IV)O₃ powder is treated with NH₃ at about 600°C. We suggest that the anion-deficient ordering is originated from the oxidation of V⁴⁺ to V⁵⁺ by N₃/O²⁻ exchange and the preference of pentavalent V for tetrahedral coordination. More surprisingly, when the same treatment was applied to a single-crystal SrVO₃ thin film, the direction of the vacancy planes (111, 112) and the periodicity (5-fold, 6-fold) changed depending on the substrate used. The biaxial strain effect was verified by first-principles calculations. Like oxide heterostructures, the oxynitride has a superlattice of insulating and metallic blocks. Given the abundance of perovskite families, this study provides new opportunities to design superlattices by chemically modifying simple perovskite oxides with tunable anion-vacancy patterns through epitaxial lattice strain.

T. Yamamoto et al., *Nat. Commun.* 11, 5923 (2020).

H. Kageyama et al., *Nat. Commun.* 9, 772 (2018).

9:30 AM *EQ13.08.04

New Polar Oxynitride Perovskites Amparo Fuertes; ICMAB-CSIC, Spain

Perovskite oxynitrides ABO₂N or ABON₂ (A=rare earth or alkaline earth metal; B=transition metal) are important heteroanionic materials that show high permittivities, photocatalytic activity under visible light and colossal magnetoresistance among other relevant properties. (1) Pseudocubic oxynitride perovskites derived from the Pm-3m aristotype are centrosymmetric and show symmetry lowering for tolerance factors (t) below 1. All anion sites show similar coordination environments with cations, which favours the partial or total disorder of nitrogen and oxygen. The observed high relative permittivities and ferroelectricity in compounds such as SrTaO₂N and BaTaO₂N have been ascribed to local electrical dipoles (2) from cis order of nitrides, induced by covalency. (3)

Hexagonal perovskites formed by sequences of cubic and hexagonal close packed AX₃ layers are stabilized for tolerance factors greater than 1 and show two well differentiated environments for anions, in sharing vertex and sharing faces of the BX₆ octahedra, providing the possibility of selective occupation by nitride and oxide. This talk will present results on the new polar compound BaWON₂ that is the first example of a hexagonal perovskite oxynitride. (4) It shows the 6H polytype and crystallizes in the non-centrosymmetric space group P6₃mc, with cell parameters a=5.85073(2) and c=14.53220(9) Å. The two anions N³⁻ and O²⁻ are completely ordered in the vertex shared and face shared positions of the WX₆ octahedra respectively. The preferred occupation of the more electronegative O atom at face-shared sites is a consequence of the weaker bonding for these positions, with W-X-W angles ≈90°, compared with corner-shared sites, with W-X-W angles ≈180°. Total anion order, together with the large electrostatic repulsion between W⁶⁺ cations in the face shared octahedra, and second order Jahn-Teller effect induce highly distorted environments in three inequivalent WX₆ octahedra stabilizing the non-centrosymmetric structure. The spontaneous polarization, calculated from the crystal coordinates and formal electrical charges of all atoms, is ≈17.7 μC/cm², parallel to the c axis. BaWON₂ is a semiconductor with a band gap of 1.1 eV and a relative permittivity of 200-230 in the 10-100 K temperature range, and shows a second harmonic generation (SHG) signal under excitation with a Ti:sapphire laser. The observed remarkably large permittivity is consistent with anisotropic, multi-anionic bond network in the structure, which in turn shall promote anharmonicity of the bond dynamics and subsequently the observed non-linear optical response. This achievement contrasts with earlier results on ABO₂N perovskites with pseudocubic centrosymmetric structures that lead to large dielectric permittivity and piezoresponse under electric field bias, ascribed to field-response of nanopolar regions, but without long range polar order.

References

1. A.Fuertes, *APL Mater.* 2020, 8, 020903.
2. A.Hosono, Y.Masubuchi, S. Yasui, M. Takesada, T. Endo, M. Higuchi, M. Itoh and S. Kikkawa, *Inorg. Chem.* 2019, 58, 16752.
3. M. Yang, J.Oró-Solé, J.A. Rodgers, A. B. Jorge, A.Fuertes and J. P.Attfield, *Nat. Chem.*, 2011, 3, 47.
4. J. Oró-Solé, I.Fina, C.Frontera, J.Gázquez, C.Ritter, M.Cunquero, P. Loza-Alvarez, S.Conejeros, P.Aleman, E.Canadell, J.Fontcuberta and A.Fuertes, *Angew. Chem. Int. Ed.* 2020, 59, 18395.

10:30 AM *EQ13.09.01

Zn-IV-N² Semiconductors, Homovalent Alloys and ZnGeN₂-GaN Alloys Grown by MOCVD for Optoelectronic Applications [Kathleen Kash](#); Case Western Reserve University, United States

The prospect of combining members of the large family of heterovalent ternary nitride semiconductors with each other and with the III-nitrides opens up new avenues for band structure engineering, lattice matching with different substrates, and new applications. There is interest in ZnSnN₂, with a band gap in the range of 1-2 eV that tunes with the degree of disorder on the cation sublattice, for its application to single junction solar cells [1]. Alloys of ZnGeN₂ and GaN are of interest for photocatalytic applications such as water splitting [2].

A major aim of our work on developing the growth of these materials by MOCVD is to improve the efficiency of nitride LEDs at green and longer wavelengths by taking advantage of the large predicted type II band offsets of the Zn-IV-nitrides with the III-nitrides. Band offsets at the ZnGeN₂-GaN interface greater than 1 eV in both the conduction and valence bands have recently been confirmed experimentally [3]. Appropriate insertion of a few-unit-cell-wide Zn-IV-nitride layer into a conventional InGaN quantum well is predicted to improve the electron-hole wave function overlap substantially, thus increasing the emission efficiency while also providing the benefit of reducing the In content in the InGaN quantum well for emission at a given wavelength, compared to the conventional InGaN structure [4].

In order to realize these proposed LED structures, the growth temperature for the Zn-IV-nitride or alloy insertion layer should be matched to that for the InGaN quantum well. However, the temperatures for the growth of high quality InGaN [5]. On the other hand, the case is reversed for ZnSnN₂, and the growth temperature for producing high quality ZnSnN₂ layers is too low. ZnSn_xGe_(1-x)N₂ presents a solution to matching the optimal growth temperature of the insertion layer to InGaN; the growth window of the homovalent alloy is fortuitously broadened over that for pure ZnSnN₂.

Growth of thick layers of ZnSnN₂, as are necessary for other applications such as photovoltaics, is problematic by MOCVD. We find that if the precursors (in this work, DEZn, TMSn and NH₃) are flowed continuously with a DEZn-to-TMSn ratio that produces stoichiometric ZnSnN₂ for thin layers, for thicker layers Sn droplets accumulate on the growth surface and cause decomposition of the underlying ZnSnN₂, in a reversal of the process that produces vapor-liquid-solid growth of ZnSnN₂ [6]. Pulsing the Sn precursor is an effective route to preventing the accumulation of Sn droplets.

The temperature window for MOCVD growth of the heterovalent ZnGeN₂-GaN alloy is also broadened over that for pure ZnGeN₂. The incorporation rate of Zn into the film is enhanced by the addition of Ga, and, correspondingly, the incorporation of Ge is depressed.

This work was supported by funding from the U.S. Department of Energy (DE-EE0008718) and from the National Science Foundation (DMREF-SusChEM-1533957).

[1] R. A. Makin, K. York, S. M. Durbin, N. Senabulya, J. Mathis, R. Clarke, N. Feldberg, P. Miska, C. M. Jones, Z. Deng, L. Williams, E. Kiyoupakis, and R. J. Reeves, *Phys. Rev. Lett.* **122**, 256403 (2019).

[2] T. Suehiro, M. Tansho, and T. Shimizu, *J. Phys. Chem. C* **121**, 27590 (2017).

[3] M. R. Karim, B. A. Noesges, B. H. D. Jayatunga, M. Zhu, J. Hwang, W. R. L. Lambrecht, L. J. Brillson, K. Kash, and H. Zhao, *J. Phys. D: Appl. Phys.* **54**, 245102 (2021).

[4] L. Han, K. Kash, and H. Zhao, *J. Appl. Phys.* **120**, 103102 (2016), and subsequent work.

[5] M. R. Karim, B. H. D. Jayatunga, M. Zhu, R. A. Lalk, O. Licata, B. Mazumder, J. Hwang, K. Kash, and H. Zhao, *AIP Advances* **10**, 065302 (2020).

[6] P. C. Quayle, G. T. Junno, K. He, E. W. Blanton, J. Shan, and K. Kash, *Phys. Status Solidi B* **254**, 1600178 (2017).

11:00 AM EQ13.09.02

Synthesis and Characterization of Sputter-Deposited Zn₂VN₃ Thin Films—A Combined Theoretical and Experimental Study [Siarhei Zhuk](#) and Sebastian Siol; Empa, Switzerland

Nitrides are promising functional materials for a variety of applications. Despite their technological importance many promising theoretically predicted metal nitrides are yet to be discovered.[1] This is partly rooted in their challenging synthesis as compared to oxides. Non-equilibrium PVD in ultra-high vacuum conditions, such as reactive RF-magnetron sputtering, provides ideal prerequisites for the formation of novel metastable nitride thin films.[2] Furthermore, combinatorial sputtering approaches are extremely effective for a rapid screening of the associated complex synthesis phase-spaces.[3]

In this study, an epsilon-support vector regression machine learning (ML) algorithm was used in combination with density functional theory (DFT) calculations using Heyd-Scuseria-Ernzerhof (HSE) functionals to identify interesting candidates from computational materials databases for a combinatorial PVD screening.[4,5] Zn-V-N was selected as a promising material system for a comprehensive experimental phase screening mainly due to the presence of a potentially stable Zn₂VN₃ semiconducting phase with properties suitable for optoelectronic applications.[4,5]. We carried out a combinatorial PVD screening of the entire Zn-V-N phase space. RF co-sputtering of Zn and V targets was carried out in mixed plasma of Ar and N₂ to grow combinatorial libraries on plain glass substrates. N₂ was supplied directly to the sputter plasma to increase the N₂ dissociation rate and consequently increase the N chemical potential. Automated mapping characterization of the sample libraries was performed using X-ray diffraction (XRD), X-ray fluorescence (XRF), X-ray photoelectron spectroscopy (XPS) and four-point probe techniques. In addition, selected samples were studied using hard X-ray photoelectron spectroscopy (HAXPES), Rutherford backscattering spectrometry (RBS), elastic recoil detection analysis (ERDA), photoluminescence (PL) and optical spectrophotometry.

XRD analysis revealed the presence of an orthorhombic Zn_{1-x}V_xN phase over a large compositional range from Zn₂VN₃ to ZnVN₂, with a narrow process window for single-phase Zn₂VN₃. The measured XRD patterns are consistent with the corresponding calculated patterns.[4] Following the combinatorial screening, we were able to improve the crystallinity and isolate the Zn₂VN₃ phase on larger substrates (51 x 51) mm². A combined RBS/ERDA analysis on these samples demonstrates that the material is stoichiometric with only trace amounts of O, well below 1 at. %. Further, XPS/HAXPES analysis confirms this result with Zn and V being present in oxidation states of +2 and +5, respectively, as expected for Zn₂VN₃. The Fermi level is located ~ 1 eV above valence band maximum indicating a weak p-type doping. Zn₂VN₃ thin films exhibit a resistivity of 0.42 Ωcm. Moreover, PL spectra measured at room temperature exhibits three distinctive peaks at 2.65 eV, 2.85 eV and 3.05 eV with a tail towards 2 eV. The latter is consistent with a significant amount of sub-band gap absorption measured using optical spectrophotometry. This could be due to the presence of anti-site defects and as well as scattering on amorphous phase impurities.

In conclusion, we performed an experimental screening of the Zn-V-N phase space and isolated the novel semiconducting Zn₂VN₃ phase. The experimental

results are consistent with DFT calculations, which predict direct band gap of 2.35 eV and p-type conductivity for Zn_2VN_3 . However, further studies are required to improve optoelectronic properties of the compound.

References:

- [1] W. Sun *et al.* Nat. Mater. 18 (2019) 732–739.
- [2] A. Zakutayev, J. Mater. Chem. A 4 (2016) 6742–6754.
- [3] K. Alberi *et al.* J. Phys. D: Appl. Phys. 52 (2019) 013001.
- [4] A. Jain *et al.* APL Mater. 1 (2013) 011002.
- [5] S. Lany, Phys. Rev. B 87 (2013) 085112.

11:15 AM EQ13.09.03

The Impact of Oxygen on the Degeneracy of Zinc Nitride Layers Elise I. Sirotti, Stefan Böhm and Ian Sharp; Technische Universität München, Walter Schottky Institut, Germany

Zinc nitride (Zn_3N_2) has a small direct bandgap, is composed of only earth-abundant elements, and possesses characteristics such as a high mobility that make it a promising semiconductor material for optoelectronic applications. However, non-degenerate Zn_3N_2 is rare and the cause of the high charge carrier concentration remains unknown. Prior density functional theory calculations have predicted oxygen and hydrogen as being responsible for the strong n-type doping but this has not been conclusively verified experimentally. In this work, we studied the role of oxygen on the structural, electrical, and optical properties of Zn_3N_2 grown by plasma-assisted molecular beam epitaxy. The crystalline quality is optimized by tuning both flux and growth temperature, resulting in single phase (222) oriented Zn_3N_2 with a rocking curve full width at half maximum of 0.031° . In addition, we have developed an amorphous GaN capping layer that can be directly deposited onto air-sensitive Zn_3N_2 , which shows excellent promise for protecting the material without adversely impacting its electronic properties. To analyze the influence of oxygen on the material properties, the amount of incorporated oxygen in the layer was tuned by changing the elemental base pressure in the growth chamber. Hall and temperature-dependent conductivity measurements reveal high mobilities ranging from 100 to $210 \text{ cm}^2\text{V}^{-1}\text{s}^{-1}$, as well as a clear correlation between the oxygen concentration in the sample and the bulk charge carrier concentration. In particular, the carrier concentration of nominally oxygen-free Zn_3N_2 can be decreased from 10^{20} cm^{-3} to 10^{17} cm^{-3} via controlled oxygen incorporation, without significantly impacting the high mobility of the material. Photothermal deflection spectroscopy shows a concurrent decrease in the bandgap with increasing oxygen concentration (decreasing free electron concentration), consistent with a reduced Burstein-Moss shift.

11:30 AM EQ13.09.04

Deposition and Characterization of Copper Nitride and Tantalum Nitride Thin Films for Electronic Applications Md Maidul Islam and Daniel Georgiev; The University of Toledo, United States

Copper nitride (Cu-N) and tantalum nitride (Ta-N) films have potential applications in photovoltaic solar cell technology and electronic devices, in general. These thin film materials are non-toxic and can be obtained from readily available low-cost precursors. Cu-N can be used in absorber layers of solar cells because of its high optical absorption coefficient and energy band gap that are almost ideal for efficient absorption of light in the solar spectrum. Cu-N films can be doped both p-type and n-type, they are defect tolerant, and their surfaces can be passivated by a native oxide. On the other hand, Ta-N films are chemically inert and corrosion resistant, which makes them very attractive for various functions in integrated circuits, including thin film resistors and diffusion barrier layers. Furthermore, carrier-selective contact materials, rectifying contacts, and Schottky diodes have been developed based on Ta-N. Recently, there has been interest in the Cu-Ta-N ternary semiconductor alloy system for electronic device applications, which has been the motivation for our work and interest in the binaries that comprise this ternary system. Our intention is to work on the fabrication and study applications of films from the ternary system after gaining a good understanding of the sputtering deposition of the related binaries as well as their properties. In this work, Cu-N and Ta-N films were deposited on glass or Si substrates by reactive RF magnetron sputtering of Cu or Ta in a nitrogen-containing atmosphere. Films with thicknesses of several hundred nanometers were obtained by systematically varying the substrate temperature at a fixed N:Ar sputtering gas ratio or by varying the N:Ar gas ratio at a fixed substrate temperature. The film morphology was examined by both top-view and cross-sectional-view scanning electron microscopy, and the films' chemical composition was established by energy-dispersive X-ray spectroscopy. Four-probe resistivity measurements and optical spectrophotometry were performed, and the optical band gaps were calculated by a standard Tauc's plot technique. The crystallinity of the film's material was studied by X-ray diffraction in a small-angle X-ray scattering geometry. The film properties are influenced by the RF power used during the deposition, the substrate temperature, the overall deposition pressure, and the N:Ar gas ratio. The color of the Cu-N films that were obtained was reddish-brown with slight variation among the different types of samples, while the Ta-N films had a metallic luster for lower nitrogen gas fractions and were more brownish-transparent for higher nitrogen gas fractions. Both types of film surfaces were relatively smooth and uniform, with a granular structure, which contained dense pyramid-like grain shapes for Cu-N and irregular cauliflower-like shapes for Ta-N. The optical band gap of Cu-N films ranges from 1.3 to 1.4 eV and decreases with increasing the substrate temperature. For Ta-N, the band gap varies from 1.62 to 1.77 eV and shows an increasing trend with increasing the nitrogen concentration in the sputtering gas mixture. This work is in progress and some of the results obtained so far appear to match published reports, while in other cases there are differences, or there is no published work that could be used for reference. All indications are that reactive RF sputtering can be used as an efficient, low-cost, and flexible method to fabricate Cu-N and Ta-N films and stacks of such films for device applications. We will report on these and any new results that are becoming available as well as on their analysis, and we expect that this work will be of significant interest to applications and the understanding of metal nitrides, in general.

11:45 AM EQ13.09.05

Site Disorder and Its Impact on Simulated Band Gap in ZnGeN_2 Jacob Cordell^{1,2}, Jie Pan², Linda Pucurimay^{2,3}, Celeste Melamed^{1,2}, Garritt Tucker¹, Adele Tamboli² and Stephan Lany²; ¹Colorado School of Mines, United States; ²National Renewable Energy Laboratory, United States; ³Princeton University, United States

The ability to tune electronic structure through cation ordering while maintaining lattice constants closely matched to III-Vs makes II-IV-N₂ materials promising for tuning band gaps for use in energy-relevant devices such as LEDs and PV. However, characterizing the degree of ordering in synthesized materials presents challenges due to the large number of variables besides ordering which also influence diffraction and spectroscopy techniques. Through simulations, we develop a picture of site disorder in ZnGeN_2 at short- and long-range, isolated from other structural effects as the state of the system relates to the energetics under nonequilibrium conditions. In ZnGeN_2 , the non-isovalent character of the disordered species (Zn^{2+} and Ge^{4+}) subjects the cation ordering to strong short-range order effects which influence band structure by decreasing the band gap relative to ordered ZnGeN_2 from 3.5 eV to 2.0 eV with small but non-dilute fractions of cations present as anti-site pairs. ZnGeN_2 exhibits pronounced discontinuities in enthalpy and order parameters, which correspond to a first-order phase transition and narrowed forbidden gap in the density of states as well as an onset in localized states in disordered material. We use Monte Carlo simulations to model cation disorder, which in turn use a cluster expansion to approximate the formation enthalpy of a cation configuration. Converged configurations are relaxed in volume and lattice parameters through Density Functional Theory as 1,024 atom supercells. We calculate nitrogen coordination as a short-range order parameter and the Bragg-Williams and stretching parameters as long-range order parameters. We then relate these order parameters with the mixing entropy, free energy of the system and electronic properties to draw relations between order and

electronic structure.

12:00 PM EQ13.09.06

Late News: Characterization of ZnGeN₂ Thin Films on Heteroepitaxial Mismatched AlN Substrates Brooks Tellekamp¹, [Moira Miller](#)^{2,1}, Anthony Rice¹ and Adele Tamboli¹; ¹National Renewable Energy Laboratory, United States; ²Colorado School of Mines, United States

The GaN ternary analog ZnGeN₂ is proposed as a green-to-amber emitter able to be integrated easily into current GaN light emitting diode (LED) heterostructures. However, growing ZnGeN₂ on GaN makes accurate material characterization difficult due to their similar optical and structural properties. This ambiguity motivates this work where we present ZnGeN₂ grown on lattice mismatched AlN templates and regrown AlN buffer layers by molecular beam epitaxy. We present highly accurate lattice parameters using multiple reflections and a least squares regression ($a = 3.1962 \text{ \AA} \pm 0.0032 \text{ \AA}$ and $c = 5.2162 \text{ \AA} \pm 0.0015 \text{ \AA}$ [c/a ratio = 1.632]) enabled by the full relaxation of ZnGeN₂ and get a lattice-mismatch of 0.22%. We find the preferred growth temperature for ZnGeN₂ on AlN is 450 C by reflection high-energy electron diffraction, X-ray diffraction, and atomic force microscopy characterization. We also present photoluminescence attributed to ZnGeN₂ with a broad recombination band centered around 2.96 eV. Theory suggests that disordered material will emit light as a broad peak in the 2.5-3 eV region, suggesting that we have disordered material. Here we provide insight into the properties of ZnGeN₂ and provide direction for further studies modeling and characterizing GaN/ZnGeN₂ heterostructures.

12:05 PM EQ13.09.07

Chemical State Analysis of Ternary Zinc Nitride by Photoelectron Spectroscopy—Applications in Materials Discovery and Design [Sebastian Siol](#), Siarhei Zhuk and Jyotish Patidar; Empa-Swiss Federal Institute of Materials Science and Technology, Switzerland

Photoelectron spectroscopy (PES) has long been considered a standard characterization technique in the development of new semiconducting materials. Despite its mainstream use for the analysis of surface chemistry and electronic structure of new materials, conducting meaningful PES on nitrides is challenging. Handling nitride samples in air usually results in surface oxidation as well as the formation of adsorbate layers, which complicates and quite often prevents meaningful PES measurements.[1] Unfortunately, few labs possess the experimental infrastructure to perform clean (i.e. UHV) transfers from synthesis to characterization environments and sputter cleaning the samples often results in sputter damage or a reduction of the surface.

In this study, we show how a combination of X-ray photoelectron spectroscopy (XPS) and laboratory based hard X-ray photoelectron spectroscopy (HAXPES) was successfully used on ex-situ treated ternary zinc nitrides to complement accelerated phase discovery in Zn-V-N thin films deposited by combinatorial reactive co-sputtering.

The presented concepts can be applied to many different material systems. In particular, we discuss how to gain valuable insights for the design and discovery of new nitrides using chemical state analysis based on the Auger parameter (AP) concept.[2] The core level emission lines of many oxides and nitrides show considerable overlap, which makes analysis of nitride samples exhibiting surface oxides challenging. Auger lines are more sensitive to changes in the local chemical environment, which can make it easier to distinguish oxide and nitride phases. In addition, the AP can show considerable shifts upon the formation of new phases or changes in the microstructure, providing valuable, complimentary insights to conventional structural analysis (e.g. X-ray diffraction or Raman spectroscopy).[3]

For the Zn-V-N material system, a new potentially stable phase was discovered by XPS mapping characterization via analysis of the modified AP for Zn. The latter was calculated using the kinetic energy of the Zn LMM Auger line as well as the binding energy of the Zn 2p_{3/2} core level emission. The Zn AP showed a distinct shift for some samples (>0.3 eV), which directly correlated with the occurrence of a new phase, as confirmed by XRD and RBS. In addition, we used a laboratory-based HAXPES system equipped with monochromatic Cr-K α X-ray source (5414.7 eV) to perform measurements with an information depth of over 20 nm. In a contrast, an XPS measurement using monochromatic Al-K α excitation (1486.7 eV) can probe only up to 10 nm deep.[3] Consequently, the results of the HAXPES analysis are much less affected by the presence of surface oxides or adsorbates, which allowed us to not only to probe the chemical composition of the material, but more importantly investigate the Zn and V oxidation states as well as the doping of the material without the need of any sputter cleaning.

These results highlight how novel photoelectron spectroscopy techniques can produce important insights for the discovery and design of new nitride materials, even when the samples exhibit surface oxides or adsorbates. Specifically, measurements of the AP can be used to identify new phases and changes of the microstructure in previously underexplored material systems.

References

- [1] G. Greczynski *et al.* Progress in Materials Science. (2020) 100591.
- [2] C. D. Wagner, Faraday Discuss. Chem. Soc. 60, (1975) 291.
- [3] S. Siol *et al.* Surf. Interface Anal. 52 (2020) 802–810.

12:10 PM EQ13.09.08

Structural and Electronic Effects of Cation Radius Mismatch in II-IV-N₂ Semiconductors [Malhar Kute](#), Zihao Deng, Sieun Chae and Emmanouil Kioupakis; University of Michigan, United States

The II-IV-N₂ class of heterovalent ternary nitrides have gained significant interest as alternatives to the III-nitrides for electronic and optoelectronic applications. In this study, we apply first-principles calculations based on density functional theory to systematically investigate the effects of structural distortions due to cation size mismatch on the cation sublattice disorder and the valence band structure in this class of materials. We find that larger size mismatch between the group-II and the group-IV cations results in stronger lattice distortions from the ideal hexagonal ratio, which in turn inhibits the propensity of these materials towards octet-rule violating cation disorder. We also demonstrate that the formation energy of a single cation antisite pair, which is fast and simple to calculate, is a strong indicator of a material's propensity towards disorder. Furthermore, the breaking of in-plane symmetry leads to a splitting of the top three valence bands at Γ , which is also directly related to the magnitude of structural distortions. Our work demonstrates that the structural and functional properties of the II-IV-N₂ materials can be finely tuned through controllable structural distortions that stem from the choice of cations.

12:15 PM EQ13.09.09

A Two-Dimensional Layered Semiconductor, Alkaline Earth Transition Metal Nitrides; High-Purity Bulk Synthesis and Electronic Properties Characterization [Shigeru Kimura](#), Akihiro Shiraishi, Xinyi He, Takayoshi Katase, Keisuke Ide, Hidenori Hiramatsu, Hideo Hosono and Toshio Kamiya; Tokyo Institute of Technology, Japan

Ternary transition metal nitrides, $AETMN_2$ ($AE = \text{Sr, Ba}$; $TM = \text{Ti, Zr, Hf}$), are expected to exhibit unique electro-magnetic properties since they possess two-dimensional (2D) electron transport layers in their natural layered crystal structures, and their conduction band minimums are formed mainly of $TM d_{xy}$ orbitals like SrTiO₃-based 2D electron gas system [1,2]. However, high purity bulk samples of $AETMN_2$ have not yet been synthesized,

hindering their intrinsic physical properties. To overcome the problem, we herein propose a 2-step process for the synthesis of high purity $AETMN_2$. We realized high-purity polycrystalline bulks and investigated the electronic structure and electronic properties of $AETMN_2$.

Polycrystalline bulks of $AETMN_2$ were synthesized by the high-temperature solid-state reactions of $2AENH + 2TMN \rightarrow 2AETMN_2 + H_2$. Since the complete nitridation of Sr and Ba metals, i.e. SrN_3 and BaN_3 phases, by direct annealing under N_2 gas is difficult, we made $AENH$ powders through the nitridation of AEH_2 hydrides as the starting precursors. Then, to achieve a high nitrogen chemical potential during the solid state reactions of $AENH + TMN$, the NaN_3 powder is used as N-source.

By optimizing the annealing temperature and stoichiometric ratio, high purity $AETMN_2$ bulks with phase purity more than 90 mol% were obtained. From diffuse reflectance spectra, the optical bandgap was estimated to be 1.7 eV ($SrTiN_2$), 2.0 eV ($BaZrN_2$), and 2.2 eV ($BaHfN_2$). The ρ - T of all $AETMN_2$ exhibit semiconducting behavior. Arrhenius plot of $\ln \sigma (1/\rho)$ versus $1000/T$ is nearly linear over the temperature range 100-300 K, and an activation energy (E_A) increased from 2.9 meV ($SrTiN_2$) to 116 meV ($BaHfN_2$). Seebeck coefficient of all $AETMN_2$ were negative and increased from -26 $\mu V/K$ ($SrTiN_2$) to -117 $\mu V/K$ ($BaHfN_2$), indicating that $AETMN_2$ are n-type semiconductor and the unintentional impurity doping is suppressed in $BaHfN_2$. We will discuss the difference of impurity incorporation in $AETMN_2$ by calculating the defect formation enthalpies of intrinsic defects and oxygen/hydrogen impurities in $AETMN_2$ at the conference.

[1] D. H. Gregory et al., *Inorg. Chem.* 37, 3775 (1998), [2] I. Ohkubo et al., *Chem. Mater.* 26, 2532 (2014).

12:20 PM EQ13.09.10

Characteristics of Hf(M)SiBCN ($M = Y, Ho, Ta, Mo$) Materials—Role of the M Choice [Martin Matas](#), Michal Prochazka, Jaroslav Vlcek and Jiri Houska; University of West Bohemia, Czechia

Nitride-, carbide- and boride-based alloys of light main-group elements are attractive due to unique combinations of properties ranging from optical transparency through high hardness to high-temperature stability and oxidation resistance. The properties, in the first place electrical conductivity, can be further modulated by addition of early transition metals. In this contribution, amorphous nitrogen-rich Hf(M)SiBCN thin films are investigated by combining magnetron sputtering of composite B_4C -Si-Hf-M targets in Ar + N_2 reactive atmosphere with *ab-initio* calculations [1]. First, we study the effect of the M choice and fraction on calculated mechanical properties and formation energy of crystalline MN and $Hf_xM_{1-x}N$ nitrides. We discuss the dependence of formation energy on the crystal structure and on the distribution of Hf and M in the metal sublattice. The calculated mechanical properties of MN correlate with those measured on HfMSiBCN. The driving force towards N incorporation, monotonically decreasing with increasing periodic-table group number of M according to the calculated formation energy of MN , very well correlates with measured electrical conductivity and extinction coefficient of HfMSiBCN. Second, we use *ab-initio* molecular dynamics to model the amorphous HfMSiBCN materials themselves. The calculated band gap, localisation of states around the Fermi level and bonding preferences of M atoms (in particular their tendency to bind with N) also correlate with the measured metallicity and confirm the possibility of predicting the trends in characteristics of HfMSiBCN using those of MN . Third, we identify an optimum target composition leading to hard (>20 GPa) HfMSiBCN materials with a relatively high conductivity at a given extinction coefficient. The results are important for the design of transparent and/or conductive hard high-temperature coatings.

[1] M. Matas, M. Prochazka, J. Vlcek, J. Houska, *Acta Mater.* 206 (2021) 116628

12:25 PM BREAK

SESSION EQ13.10: Nitrides for Quantum and Other Applications
Session Chairs: Rachel Oliver and Sebastian Siol
Monday Afternoon, December 6, 2021
EQ13-Virtual

1:00 PM *EQ13.10.02

Novel Nitride Thin-Film Materials for Thermoelectrics Studied by Experiments and Theory [Per Eklund](#); Linköping Univ, Sweden

Thermoelectric devices have the potential to contribute to energy harvesting in society by directly converting heat into electricity or vice versa. However, the conversion efficiency of thermoelectric devices of today is limited. The critical material-dependent parameter is the figure of merit ($ZT = S^2T/rk$, where r is the electrical resistivity, S is the Seebeck coefficient and k is the total thermal conductivity). In this lecture, I present an overview of our experimental and theoretical investigations of CrN-, ScN-, and $Ca_3Co_4O_9$ -based thin films. ScN thin films exhibit an anomalously high power factor (S^2/r) for transition metal nitrides of 2.5 - 3.3×10^{-3} W/mK² at 800 K. We have explained this result, from first-principles calculations, by nitrogen vacancies generating an asymmetric sharp feature in the density of states which allows low electrical resistivity with relatively large S . However, ScN has high thermal conductivity, thus its ZT is low (~0.2). To reduce lattice thermal conductivity, potential strategies are nanostructuring, alloying or nanoinclusion formation. We have modeled the thermal conductivity in pure ScN as a function of grain size using time-dependent effective potentials (TDEP), correlating the ideal thermal conductivity of an infinite ideal crystal with the thermal conductivity reduction of grain-size effects, and alloying trends in mixing thermodynamics of ScN-based solid solutions. Pure CrN exhibits n-type conduction with a high power-factor enabled by a high electron concentration thermally activated from N vacancies, and alloys can be made of rocksalt-Cr_{1-x}Sc_xN. We have demonstrated that it can be rendered p-type by Al alloying in combination with N superstoichiometry.

References

- 1) P Eklund, S Kerdsonpanya, B Alling (*invited review*) *J. Mater. Chem. C* 4, 3905 (2016)
- 2) Y Du, J Xu, B Paul, P Eklund (*invited review*) *Appl. Mater Today* 12, 366 (2018)
- 3) A le Febvrier, N Van Nong, G Abadias, P Eklund *Appl. Phys. Expr.* 11, 051003 (2018)
- 4) S Kerdsonpanya, O Hellman, ..., B. Alling, P Eklund *Phys Rev B* 96, 195417 (2017)
- 5) M. A. Gharavi, ..., B. Alling P. Eklund, *Materials Today Communications*, 28 102493 (2021)

1:30 PM *EQ13.10.03

Extending the Nitride Material Platform for Classical and Quantum Information Systems [Debddeep Jena](#); Cornell University, United States

The nitride semiconductor materials GaN, AlN and InN revolutionized solid state lighting in the last two decades and are currently doing the same for high-speed and high-voltage electronics, and deep-ultraviolet photonics. As the semiconducting properties, it is becoming increasingly clear that this material

family has far more to offer ranging from communication at high frequencies, to harsh environment and high voltage digital electronics, to quantum communications and computation. In this talk, I will present recent developments in the synthesis and integration of nitride semiconductors, magnets, ferroelectrics, and superconductors towards an exciting new platform that feeds off the many past successes of photonics and electronics with GaN.

A missing piece in the classical computation paradigm for nitride semiconductors was the p-channel transistors with high hole mobilities. This problem has found an exciting solution in the discovery of undoped polarization-induced 2-dimensional hole gases in epitaxially grown GaN quantum wells on AlN substrates. This new material-driven discovery is a key enabler for digital CMOS with wide-bandgap nitride semiconductor that can operate in harsh environments.

Substitution of Al or Ga of AlN or GaN with other group-III metals such as the transition metals Sc and Y, or the metal B is bringing in new physical properties into the nitride family. In particular, I will talk about a) the growth and properties of ScN, a narrow-bandgap semiconductor, and b) the impact of substitution of Al by Sc, Y, and B on the structural and electro-mechanical properties of AlN. These materials boost the piezoelectric properties of AlN so much so that for certain compositions ferroelectricity is observable in both sputtered and MBE grown layers.

The epitaxial growth of metallic and superconducting NbN and TiN, and its heterostructures with AlN and GaN polar semiconductors will be discussed. Epitaxial metal/AlN heterostructures are enabling new forms of integrated epitaxial bulk acoustic wave (epiBAW) filters with the potential to scale to far thinner structures and extend the speed of such devices. It is allowing the direct integration of such filters with AlN/GaN/AlN quantum well high-electron mobility transistors (HEMTs) for highly integrated RF systems. These epitaxial heterostructures are also finding use in superconducting single-photon detectors (SNSPDs) and in new forms of microwave qubits.

2:00 PM *EQ13.10.04

Novel Rocksalt Nitride Semiconductors—From Prediction, to Realization, to Integration [Sage Bauers](#)¹, Anuj Goyal¹, Sarah Jones², Brian Gorman², Serena Eley², Stephan Lany¹ and Andriy Zakutayev¹; ¹National Renewable Energy Laboratory, United States; ²Colorado School of Mines, United States

Integrated discovery workflows are effective tools for identifying candidate functional materials in underexplored chemistries. Nitrides represent one such chemical space: the number of known nitrides is an order of magnitude less than known oxides. At the same time, many of the known inorganic nitrides—and (Al, Ga, In)-N semiconductors in particular—are useful in thin-film technological applications. Thus, our team has developed a workflow for discovering new inorganic nitrides based on data-mining the materials project, performing structure prediction calculations, experimentally screening materials using combinatorial exploration, and performing targeted, epitaxial growth of compelling candidate compositions.

One family of new compounds, described as either $MgTMN_2$ (TM =group 4 transition metal) or Mg_2TMN_3 (TM =group 5 transition metal), were identified using such a discovery pipeline. These materials represent a class of medium-gap ($E_G=0.9-2.4$) semiconducting nitrides which adopt a rocksalt-derived crystal structure. This is a departure from normal structure/property relationships in functional inorganic nitrides, where compounds tend to belong to one of two primary families—hexagonal main-group metal nitride semiconductors or cubic transition-metal nitride superconductors. Furthermore, the material properties can be controlled with the metal composition in these ternary composition spaces. For example, electronic transport properties can be tuned using the cation $Mg:TM$ ratio from metallic (TM -rich) to non-degenerately doped (Mg -rich).

We found that the lattice parameters of some of these materials are compatible with the two primary families of technologically important nitrides, suggesting the possibility for epitaxial integration of these materials into functional devices. For example, we have observed epitaxial alignment when $MgZrN_2$ and Mg_2NbN_3 are grown via sputter-deposition onto MgO , GaN, and Al_2O_3 substrates, as well as underlying superconducting ZrN and NbN epilayers. Inspired by these results, we are now evaluating Mg_2NbN_3 as a barrier layer in tunnel junctions with NbN superconducting layers. The combination of elemental abundance, compelling properties, and structural compatibility highlights the potential of these new $Mg-TM-N$ materials for integration with known nitrides.

2:30 PM EQ13.01.02

NbN/III-N Heterostructures Grown by MBE for Superconducting Electronic Devices [John G. Wright](#)¹, Maxwell Drimmer², Yiwen Chu², Huili G. Xing¹ and Debdeep Jena¹; ¹Cornell University, United States; ²ETH Zürich, Switzerland

The development of single crystal III-N semiconductor heterostructures has been central to the success of III-N materials in wide range of electronic and optoelectronic applications. With this fact in mind, we have pursued the ability to integrate materials with previously inaccessible properties, such as metals, superconductors, and piezoelectrics, into single crystal III-N heterostructures. New and improved III-N devices become possible with access to the larger design space offered by these new materials and properties.

We present our development of novel III-N heterostructure containing NbN grown by molecular beam epitaxy (MBE). NbN, a metal and superconductor with critical temperature around 15 K, has been shown to possess structural and chemical compatibility sufficient to enable epitaxial integration of NbN into III-N heterostructures. We have investigated the growth of both GaN and AlN on NbN thin films by MBE. Our systematic study of the nucleation and growth of AlN on NbN demonstrate that lattice and symmetry matching between AlN and NbN enables the growth of high crystal-quality AlN on NbN. Atomically smooth ultra-thin AlN films can be nucleated directly on NbN, and thicker AlN films grown on NbN exhibit [0 0 2] rocking curve FWHM values as low as 250 arcsecond, which we believe to be the lowest value reported for AlN grown on a metal.

The crystal quality of our AlN films significantly surpasses that of AlN films deposited on non-epitaxial metallic electrodes, which are commonly utilized to produce piezoelectric acoustic resonators. We utilize our AlN/NbN heterostructure to produce high-overtone bulk acoustic resonators (HBARs), and are investigating the coupling of NbN/AlN HBARs to qubits to create hybrid quantum systems.

In addition, we have developed epitaxial NbN/AlN Josephson junctions grown on low dielectric loss sapphire substrates. We are exploring the properties of these materials and devices, and the suitability of these structures for quantum computing applications. MBE grown single crystal AlN/NbN heterostructures are a promising platform for the development of high coherence time Josephson junctions for quantum computing due to the chemical purity and lack of structural defects at the MBE grown NbN/AlN interface. This is especially promising in light of the limit on qubit coherence time set by two-level systems in the amorphous barriers of Nb/Al/AlO_x/Nb Josephson junctions.

8:00 AM *EQ13.11.01

Control of Ferroelectric Property in $(Al_{1-x}Sc_x)N$ Films Prepared by Sputtering Method Hiroshi Funakubo¹, Shinnosuke Yasuoka¹, Ryoich Mizutani¹, Takahisa Shiraishi¹, Akinori Tateyama¹, Takao Shimizu^{1,2}, Masato Uehara³, Hiroshi Yamada³, Morito Akiyama³, Yoshiomi Hiranaga⁴ and Yasuo Cho⁴; ¹Tokyo Institute of Technology, Japan; ²National Institute for Materials Science, Japan; ³National Institute of Advanced Industrial Science and Technology, Japan; ⁴Tohoku University, Japan

Experimental evidence of ferroelectricity of $(Al_{1-x}Sc_x)N$ films by Fichtner *et al* in 2019 open the novel applications of nitride films using ferroelectric properties [1]. It includes low power nonvolatile ferroelectric memories (FeRAMs) as well as resistance-type memories using ferroelectric tunnel junction (FTJ). The most important feature of the ferroelectricity of these nitrides is their large remanent polarization (P_r) after releasing an applied voltage that is more than 5 times larger than that of present-fashioned HfO₂-based ferroelectric films and more than 3 times larger than that of Pb(Zr,Ti)O₃ films presently used in FeRAMs. This large P_r has a potential to realize high density FeRAMs. High Curie temperature beyond 1000 °C is another feature of the ferroelectricity of nitrides that makes it possible to use at high temperatures.

In my presentation, we introduce our results of ferroelectricity of $(Al_{1-x}Sc_x)N$ films prepared by sputtering method. Obtained results are listed as follows [2,3].

- 1) P_r and coercive field (E_c) values can be controlled by the crystal anisotropy of $(Al_{1-x}Sc_x)N$ films
- 2) Ferroelectricity was observed down to 9 nm in thickness. This means a fundamentally small decrease of P_r with decreasing film thickness.
- 3) Ferroelectricity was observed for the films deposited at low temperature including room temperature.

These results show that ferroelectric nitrides are novel and one of the most promising candidates for memory applications using their ferroelectricity.

[1] Fichtner, *et al.*, J. Appl. Phys., **125**, 114103 (2019).

[2] Yasuoka *et al.*, J. Appl. Phys., **128**, 114103 (2020).

[3] Yasuoka *et al.*, Phys. Status Solidi (A), *accepted*.

8:30 AM EQ13.11.02

Inverting the Polarity of Scandium Aluminum Nitride (ScAlN) Piezoelectric Thin Films by Using Si Addition Sri Ayu Anggraini, Masato Uehara, Kenji Hirata, Hiroshi Yamada and Morito Akiyama; National Institute of Advanced Industrial Science and Technology, Japan

Among nitride semiconductor materials, wurtzite phase scandium aluminum nitride (ScAlN) has the highest piezoelectric coefficient which is why it has been touted as a future material for many promising electronic applications including the radio frequency (RF) resonators [1-2]. A highly *c*-oriented ScAlN piezoelectric thin film could exhibit either aluminum/scandium (Al/Sc) or nitrogen (N) polarity. The use of thin films with Al/Sc-polarity or N-polarity could lead to different electronic property which potentially affect the performance of the developed devices. For example, integrating both N-polar and Al-polar layers in a solidly mounted resonator BAW (SMR-BAW) was found to enhance the ability of the device to work at higher frequency when compared with that using a single layer Al-polar thin film [3]. Since ScAlN has been widely used as filter material for wireless telecommunication devices, controlling the polarity of ScAlN-based thin films is expected to promote the development of broadband filter that can function at higher frequency range in 5G communication technology. As a method to control the polarity, addition of silicon (Si) into AlN has been reported to inverse the polarization direction of non-doped aluminum nitride (AlN) from Al-polar to N-polar [4]. Therefore, in this study, we propose the use of Si as dopant to control the polarity of ScAlN piezoelectric thin film.

All thin films were fabricated by using radio frequency (RF) magnetron sputtering system. The concentration of Sc and Si was controlled by adjusting the power of cathodes for each corresponding target during deposition process. Positive d_{33} value indicates that the thin film has Al/Sc-polarity while negative d_{33} value indicates that the thin film has N-polarity. All $Sc_xAl_{1-x}N$ thin films exhibited positive d_{33} values which indicate that the thin films have Al-polarity. However co-addition of Sc and Si into AlN was found to result in thin films with inverted polarity. For example, co-addition of 30 at.% Sc and Si with concentration in the range of 8-20 at.% (Sc/Si < 4) was found to result in thin films that exhibited N-polarity. While co-addition of 10 at.% Si and Sc with concentration higher than 40 at.% (Sc/Si > 4) yielded in thin film that showed Al-polarity. It is evident that the polarity inversion of $(ScSi)_xAl_{1-x}N$ was found to be largely relies on the concentration of Sc, Si and their ratio. These results indicate that Si addition can also be used not only to inverse the polarity of AlN but also to control the polarization direction of ScAlN, particularly for Sc concentration that is less than 40 at.%. Other than changes in polarization direction, effect of co-addition of Sc and Si into AlN on changes in crystal structure, lattice parameters and surface state have been studied and will be discussed.

References:

[1] M. Akiyama, T. Kamohara, K. Kano, A. Teshigashara, Y. Takeuchi, N. Kawahara, *Adv. Mater.* (2009) 21, 593.

[2] M. Moreira, T. Torndahl, I. Katardjiev, T. Kubart, *J. Vac. Sci. Technol. A* 33 (2015) 021518.

[3] Mizuno, T. *et al.* In *2017 19th International Conference on Solid-State Sensors, Actuators and Microsystems (TRANSDUCERS)*. 1891.

[4] S. A. Anggraini, M. Uehara, K. Hirata, H. Yamada, M. Akiyama, *Scientific Reports* (2020) 10, 4369.

8:45 AM EQ13.11.03

Pyroelectric Tomography of AlScN with Sub-Micron Resolution Stefan Tappertzhofen; TU Dortmund University, Germany

Novel lead-free ferroelectric and pyroelectric materials such Aluminum Scandium Nitride (AlScN) show great potential for development of CMOS-compatible temperature and motion sensors. A key challenge is the understanding of the origin of pyroelectricity and the profile of the spontaneous polarization in AlScN, that could be, for example, related to thermal deformation and corresponding piezoelectric mechanical clamping. A powerful tool to analyze the spontaneous polarization in three dimensions with sub-micron resolution is the Laser Intensity Modulation Method (LIMM). In this study, we report on the LIMM tomography of ferro-/pyroelectric AlScN thin-films using Fabry-Perot quantum-cascade mid-infrared, and near-infrared lasers. We discuss the influence of Scandium on the thermal and pyroelectric properties of AlScN based on our LIMM measurements. In particular, we report on thermal conductivity levels of AlScN two to three orders of magnitude lower than for conventional AlN films, which we contribute to phonon/alloy scattering mechanisms. We also characterized the profile of the spontaneous polarization as a function of the sample temperature, ambient conditions, and bias-voltage. Our tomography results are complemented by thermal simulations, and advanced microscopic and spectroscopic techniques. Our findings gain insight into important material properties of AlScN and provide guidelines for engineering of novel lead-free pyroelectric devices.

9:00 AM EQ13.11.04

Combinatorial Synthesis of Ferroelectric $Al_{1-x}Sc_xN$ Films Keisuke Yazawa^{1,2}, Daniel Drury^{2,1}, Geoff L. Brennecke² and Andriy Zakutayev¹; ¹National Renewable Energy Laboratory, United States; ²Colorado School of Mines, United States

Wurtzite ferroelectrics such as $Al_{1-x}Sc_xN$ are promising nitride materials for piezoelectric and ferroelectric applications in 5G communication and non-

volatile memories. Finding the upper Sc concentration limit and the lower thickness limit, both of which reduce the coercive voltage of the materials system, is important for the applications due to the large coercive electric field of the $\text{Al}_{1-x}\text{Sc}_x\text{N}$ nitride alloys. However, rocksalt phase transition in Sc rich side and ferroelectric hysteresis degradation in thinner films hinder the efforts in decreasing coercive voltage. Combinatorial approaches have emerged in the past decade as important tools for rapidly screening new compositions and thicknesses, in the search for new and improved structures and properties of the materials. One of the common concerns voiced about combinatorial approaches is that a focus on chemistry and thickness de-emphasizes effects of microstructure, which is very important in piezoelectric and ferroelectric applications. This common concern implies that the properties of combinatorial libraries are often not representative of the structures and properties of traditionally-fabricated homogeneous samples.

In this study, we demonstrate $\text{Al}_{1-x}\text{Sc}_x\text{N}$ films deposited by combinatorial co-sputtering with ferroelectric response across the sample library rivaling that of single-composition samples [1]. The composition and thickness gradients in the combinatorial $\text{Al}_{1-x}\text{Sc}_x\text{N}$ library co-sputtered from Al and Sc metal targets range from $x = 0.25$ to 0.5 and 250 to 150 nm. XRD $q-2q$ patterns show the wurtzite – rocksalt phase transition across the composition gradient. Even in this inhomogeneous library, the Al rich region ($x = 0.25$) exhibits a well saturated ferroelectric hysteresis loop and larger breakdown field. As expected, the Sc rich region ($x = 0.5$) side does not show fully opened hysteresis loop due to the larger leakage contribution and lower breakdown electric field. As for the thickness gradient, thinner region (150 nm) possesses large leakage current contribution to the hysteresis loop compared to the thicker side (250 nm) at the same composition. As a result of this study, the systematic comparison map among composition, thickness, crystal structure, microstructure, and electric characterization gives us insights of physics and chemistry behind the ferroelectricity in $\text{Al}_{1-x}\text{Sc}_x\text{N}$ nitride alloys with wurtzite structure.

[1] K. Yazawa et al, Appl. Phys. Lett., 118, 162903 (2021)

9:15 AM *EQ13.11.05

Nitrides at Multimegabar Compressions—From Fundamental Discoveries to practical applications Igor A. Abrikosov¹, Ferenc Tasnadi¹, Alena V. Ponomareva², Maxim Bykov³, Elena Bykova³, Ekaterina A. Smirnova², Maxim Belov², Natalia Dubrovinskaia^{4,1} and Leonid Dubrovinsky⁴; ¹Linköping University, Sweden; ²NUST "MISIS", Russian Federation; ³Howard University, United States; ⁴University of Bayreuth, Germany

Behavior of matter at extreme conditions challenge accepted concepts within materials science [1]. Nitrides have been found to have the largest fraction of metastable phases, and very high accessible thermodynamic range of metastability [2]. Combining theoretical simulations with experiment and broadly varying external parameters, pressure, temperature and composition we report on several novel nitrides with fascinating crystallochemistry [3] and properties attractive for applications [4,5]. First, we explore the Re-N system at high pressure up to 1 TPa and compare thermodynamics of experimentally synthesized phases with those obtained in theoretical structure predictions and reported in the literature. We point out a remarkable observation: tough most of the synthesized Re nitrides are stable at the synthesis pressure, and their energies are below the convex hull formed by the predicted structures, they have not been identified by the state-of-the-art structure prediction algorithms.

Next, we pay attention to a serious drawback of the high-pressure synthesis: the discovered materials cannot be always recovered at ambient conditions and the quantity of the produced material does not allow to carry out a characterization of their physical and mechanic properties. We argue that theoretical simulations have important role in identifying materials of interest for various applications, and in guiding their quenching to ambient pressure. We report the synthesis of metallic, ultracompressible and very hard rhenium nitride pernitride $\text{Re}_2(\text{N}_2)(\text{N})_2$. Unlike known transition metals pernitrides, it contains both pernitride $(\text{N}_2)^{4-}$ and discrete N^{3-} anions, which explains its exceptional properties. Importantly, $\text{Re}_2(\text{N}_2)(\text{N})_2$, which was discovered via a reaction between rhenium and nitrogen in a diamond anvil cell at pressures from 40 to 90 GPa has been recovered at ambient conditions, and a route to scale up its synthesis has been developed [4].

Finally, we demonstrate that the diamond anvil cell technique can be used for synthesis of layered materials, precursors of novel 2D-materials. We illustrate this considering a triclinic phase of beryllium tetranitride tr-BeN_4 which upon decompression from the synthesis pressure of ~ 85 GPa to ambient conditions, transforms into a compound with atomic-thick BeN_4 layers interconnected via weak van der Waals bonds. Theoretical calculations for a single BeN_4 layer show that its electronic lattice is described by a slightly distorted honeycomb structure reminiscent of the graphene lattice and the presence of Dirac points in the electronic band structure at the Fermi level. The BeN_4 layer, i.e., beryllonitrene, represents a qualitatively new class of 2D materials that can be built of a metal atom and polymeric nitrogen chains and host anisotropic Dirac fermions [5].

In summary, the fundamental understanding of the physical principles behind the formation of high-pressure materials generated in our studies is essential for the accelerated knowledge-based design of novel materials.

[1] E. Bykova, *et al.*, Nature Commun. **9**, 4789 (2018).

[2] W. Sun *et al.*, Sci. Adv. **2**, e1600225 (2016).

[3] M. Bykov, *et al.*, Angew. Chem. Int. Ed. **59**, 10321 (2020).

[4] M. Bykov, *et al.*, Nature Commun. **10**, 2994 (2019).

[5] M. Bykov, *et al.*, Phys. Rev. Lett. **126**, 175501 (2021).

SESSION EQ13.12: Transition Metal Nitrides and Related Materials

Session Chairs: Bjorn Alling and Rebecca Smaha

Tuesday Morning, December 7, 2021

EQ13-Virtual

10:30 AM *EQ13.12.01

New Transition Metal Nitrides John P. Attfield; University of Edinburgh, United Kingdom

Transition metal nitrides are typically based on metals in low oxidation states and have many useful properties, for example, ZrN was recently discovered to be an outstanding ORR (Oxygen Reduction Reaction) catalyst for electrochemical applications [1]. However, stabilisation of solid nitrides of transition metals in high oxidation states, comparable to those in oxides and fluorides, has proved difficult due to the well-known inertness of nitrogen and the tendency to evolve dinitrogen gas. A high pressure method using sodium azide has recently been demonstrated to overcome these issues leading to the synthesis of a highly oxidised iron(IV) nitride, Ca_4FeN_4 [2].

[1] Y. Yuan et al, Nature Mat. 19, 282–286 (2020). <https://doi.org/10.1038/s41563-019-0535-9>

[2] S. D. Kloss et al, Nature Comm. 12, 571 (2021). <https://doi.org/10.1038/s41467-020-20881-y>

11:00 AM *EQ13.12.02

High Throughput Fabrication of Plasmonic Nitride Nanostructures Panos A. Patsalas¹, Spyridon Kassavetis¹, Stavros Panos¹, Afroditis Koutsogianni¹, Christos Kapnopoulos¹, Gregory Abadias², Sophie Camelio², David Babonneau², Ilias Fekas¹, Spiliotis Dellis¹ and Nikolaos Kalfagiannis³; ¹Aristotle University, Greece; ²University of Poitiers, France; ³Nottingham Trent University, United Kingdom

Conductive transition metal nitrides (TMN) have been considered for applications in micro- and opto-electronics such as diffusion barriers and ohmic contacts to III-nitrides; recently, they are revisited as alternative plasmonic materials, which are refractory, spectrally tunable, CMOS-compatible, and durable in high electric fields. The most prominent examples of TMNs are TiN and ZrN. The refractory character of TMN and their growth predominantly by reactive sputtering are simultaneously blessings and curses, as they limit the fabrication of nitride plasmonic nanostructures to top-down processes, so far. Despite of the spatial accuracy of top-down processing, such fabrication is time consuming, costly, and of limited scalability. In this work, alternative routes of fabrication of TMN nanostructures are critically reviewed and presented. In particular, we focus on the fabrication of nano-islands and dichroic nanowires supported on silicon wafers and silica, and colloidal nanoparticles. We emphasize on emerging techniques that may be applied on meso- or macro-scopic scales, such as nanosphere lithography (NSL) combined with ionized reactive magnetron sputtering, glancing angle deposition (GLAD), and laser ablation in liquids (LAL). We critically evaluate the assets and drawbacks of each individual fabrication technique, and we evaluate the optical and plasmonic performance of the produced nanostructures using finite difference time domain (FDTD) calculations. There is, unfortunately, a feature that is present in all the presented manufacturing schemes: TMN typically contain a considerable amount of point defects that are known to affect the properties of the host crystal. We provide thorough experimental evidence that in TMN nanostructures the point defects tend to be outdiffused to the surface, thus limiting the deterioration of their performance, at least from the optical and plasmonic point of view; in fact, we show that for many TMN and under certain conditions the polycrystalline samples may be equivalent, if not superior, to epitaxial samples. This feature adds to the feasibility of NSL, GLAD and LAL to produce efficient TMN nanostructures on large areas and/or in large volumes.

11:30 AM *EQ13.12.03

MXenes - 2D Nitrides and Carbonitrides for Future Technologies Christopher E. Shuck, Grayson Deysler, Patrick Urbankowski, Kanit Hantanasirisakul and Yury Gogotsi; Drexel University, United States

2D carbides and nitrides, known as MXenes, are among the most recent, but quickly expanding material families. The field is experiencing rapid growth with more than 1000 papers published on MXenes each year. Major breakthroughs have been achieved in the past 3-4 years, including the discovery of 2D M₅C₄ carbides with the twinned layers and CVD synthesis of MoSi₂N₄, representing a new family of 2D nitrides. Synthesis of dozens of predicted MXenes, demonstration of superconductivity in MXenes with specific surface terminations, stronger interactions with electromagnetic waves compared to metals, metallic conductivity combined with hydrophilicity and redox activity, have led to numerous applications. The outstanding mechanical properties of Ti₃C₂, combined with its conductivity and strong interfaces, have been used in polymer, ceramic, and metal matrix composites. The reversible redox activity of transition metal atoms in the outer layers of MXene flakes combined with high electronic conductivity have led to applications in a variety of batteries and electrochemical capacitors. MXenes are promising candidates for energy storage and related electrochemical applications, but applications in optoelectronics, plasmonics, electromagnetic interference shielding, electrocatalysis, medicine, sensors, or water purification are equally exciting. At the same time, the majority of studies were conducted using carbide MXenes. Relatively few nitrides (Ti₂N and Ti₄N₃) and carbonitrides (Ti₃CN and Ti₂C_{0.5}N_{0.5}) have been produced by etching MAX phases. A few more were synthesized by replacing carbon by nitrogen in 2D carbides using high-temperature retreatments. While synthesis of nitrides is more challenging compared to carbides, theoretical predictions of attractive optoelectronic and magnetic properties of 2D nitrides fuel further efforts.

12:00 PM EQ13.12.05

Metal Nitrides—From Structure Design to Applications Yao Yuan, Fengdong Qu, Siqi Liu, Hangjia Shen, Haichuan Guo and Minghui Yang; Chinese Academy of Sciences, China

Transition metal nitrides (TMNs) as a class of metallic interstitial compounds, by tuning chemical composition through suitable selection of parent metals and introducing different amounts of nitrogen atoms into the lattice of parent metals could allow TMNs to be either semiconducting or metallic. In the last 5 years, our team using different synthetic methods have successfully prepared TMNs which show great practical value to catalysis and sensors. The observations have been theoretically rationalized. Using both experimental and theoretical results, we have been analyzing the relationship of crystal and surface structure and have correlated it to the activity for the related applications. In particular, major breakthroughs from our lab involved the discovery that ZrN shows better catalytic property than Pt/C for oxygen reduction reaction¹, Surface oxide-rich activation layer (SOAL) on Ni₂Mo₃N for rapid and durable oxygen evolution reaction² and ternary metal nitride based fuel cell type methanol sensor³.

References

- Y. Yuan, J. Wang, S. Adimi, H. Shen, T. Thomas, R. Ma, J. P. Attfield, M. Yang, Zirconium nitride catalysts surpass platinum for oxygen reduction, *Nature Materials* **19**, 282 (2020).
 Y. Yuan, S. Adimi, X. Guo, T. Thomas, Y. Zhu, H. Guo, G. S. Priyanga, P. Yoo, J. Wang, J. Chen, P. Liao, J. P. Attfield, M. Yang, Surface oxide-rich activation layer (SOAL) on Ni₂Mo₃N for rapid and durable oxygen evolution reaction, *Angewandte Chemie International Edition* **59**, 41, 18036 (2020).
 C. Huang, S. Adimi, D. Liu, H. Guo, T. Thomas, J. P. Attfield, S. Ruan, F. Qu, M. Yang, Pt/WN based fuel cell type methanol sensor, *Journal of Materials Chemistry A*, 2021. DOI: 10.1039/D1TA02433G.

SESSION EQ13.13: Rare Earth Nitrides and Related Materials

Session Chairs: Sage Bauers and Panos Patsalas

Tuesday Afternoon, December 7, 2021

EQ13-Virtual

1:00 PM *EQ13.13.01

The Outrageous Ferromagnetism of Rare-Earth Nitride Semiconductors Joe Trodahl; Victoria University, New Zealand

Most of the 14 rare-earth nitrides (REN) are *intrinsic* ferromagnetic semiconductors. Their magnetism resides in the 4f shell with a strong spin-orbit interaction that locks the spin and orbital magnetic moments together, a contrast to the quenched orbital magnetic moments in the d shell of transition-metal ferromagnets. The contribution of both spin *and* orbital magnetic moments delivers outrageous magnetisations across the series: coercive fields from 0.01T to 10 T, zero magnetic moment in otherwise conventional ferromagnetic SmN, composition tuning of magnetic moment, coercive field and the net angular

momentum in (Gd,Sm)N and (Gd,Nd)N alloys. All of these promise enhanced efficacy in various device structures, for which the doping control of electronic conduction further broadens their technical potential.

The REN are a favourite playing field of theorists, but experimentalists are deterred by the reputation of nitride film growth as problematic. We began growing them in 2006, motivated by a prediction that some are half metals, to find that they are semiconductors. They are readily grown in a N_2 atmosphere of 10^{-5} mbar; there is no need for activated nitrogen. Surprisingly a freshly deposited rare-earth film spontaneously breaks the enormously strong triple bond of N_2 , a reaction which is itself of substantial chemical interest. We have developed growth of polycrystalline and epitaxial films, mixed rare-earth nitride alloys and superlattices, both stoichiometric and n-doped by nitrogen vacancies when grown at a reduced N_2 pressure.

Following a brief description the thin-film growth that is at the core of our programme, I will describe the highlights from our 15 years exploring these materials: their huge range of magnetic states, their coupled electronic-magnetic responses, a surprising incidence of heavy-fermion superconductivity and hints of a Kondo lattice state. The study is supported by DFT computations, a variety of laboratory-based transport and magnetisation measurements and X-ray spectroscopic investigations at various synchrotrons.

1:30 PM EQ13.13.02

Rare-Earth Nitride Alloys Jackson Miller^{1,2}, Joe Trodahl¹ and Ben Ruck^{1,2}; ¹Victoria University of Wellington, New Zealand; ²MacDiarmid Institute, New Zealand

The rare-earth nitrides are associated with many remarkable magnetic behaviours. These range from the near-zero moment of ferromagnetically aligned samarium nitride (SmN), through the $J = 0$ ground state of europium nitride (EuN) to the more conventional magnetism of gadolinium nitride (GdN). In all cases, the electrical transport of these materials can be controlled over multiple orders of magnitude through n-type nitrogen vacancy doping. Thus they may be classed as intrinsic ferromagnetic semiconductors.

The coupling of gadolinium and samarium in a ternary alloy ($Gd_xSm_{1-x}N$) allows the independent tuning of the magnetic properties, as well as the electrical conduction. The magnetism comes from the localised 4f moments of the rare-earths and interpolates the magnetic behaviours of the two endpoints GdN and SmN, whose disparate behaviours offer a deal of scope in tuning the alloy magnetism. Moreover, the orbital dominated nature of the magnetic moment of SmN ensures that these alloys host magnetic moment (net $m = 0$) and angular momentum (net $J = 0$) compensation points. These features, added to the exhibition of perpendicular magnetic anisotropy offer significant benefits for magnetic recording applications. We will describe the features of these materials with reference to studies of their magnetization, XMCD (X-ray Magnetic Circular Dichroism) and electron transport, which establish their suitability for future device development.

1:45 PM EQ13.13.03

Cryogenic Magnetic Memory Element Using Rare Earth Nitrides Catherine Pot^{1,2}, William F. Holmes-Hewett^{1,2}, Jackson Miller^{1,2}, Sam Devese^{1,2}, Joe Trodahl¹ and Ben Ruck^{1,2}; ¹Victoria University of Wellington, New Zealand; ²MacDiarmid Institute, New Zealand

The rare-earth nitrides are mostly intrinsic ferromagnetic semiconductors at cryogenic temperatures and have vast potential applications in magnetic memory (MRAM) structures. The 15 members of the series offer the selection of both saturation magnetisation and coercive field required for these devices. We will report layered MRAM structures with two compositions of $Gd_xSm_{1-x}N$, separated by an exchange-blocking layer, and describe their performance under (i) current applied through an insulating exchange-blocking layer (tunnelling MRAM geometry) and (ii) in-plane current in a metallic exchange-blocking layer (GMR geometry). Both the high-impedance tunneling and the low-impedance GMR devices show binary data storage action.

2:00 PM EQ13.13.04

Defect Hopping to Ballistic Band Transport—Investigating the Insulator to Metal Transition in Vacancy Doped SmN William F. Holmes-Hewett, Bob Buckley, Ben Ruck and Joe Trodahl; Victoria University of Wellington, New Zealand

The magnetic properties of the rare-earth nitride series are determined largely by the occupation of the 4f electron shell. In a select few members of the series this shell also directly influences electrical transport. Here we discuss a combined experimental and computational study of nitrogen-vacancy doped SmN. We show that the material crosses an insulator-to-metal transition as samples are increasingly doped with nitrogen vacancies. At low doping levels, the transport can be understood as variable range hopping between defect states, while at high doping levels extended state metallic transport is seen. In the intermediary 'anomalous metallic' region where transport is in a mixed 4f-5d band, there are indications of more exotic ground states, such as unconventional superconductivity and a Kondo lattice. These may coexist with ferromagnetic order.

2:15 PM EQ13.13.05

Synthesis and Characterization of the First Nitride Perovskite, $LaWN_3$ Rebecca Smaha¹, Kevin Talley¹, Sage Bauers¹, Rachel Sherbondy^{2,1}, Craig L. Perkins¹, David Diercks², Geoff L. Brennecka² and Andriy Zakutayev¹; ¹National Renewable Energy Lab, United States; ²Colorado School of Mines, United States

While the impressive flexibility and tunability of the perovskite crystal structure ABX_3 has allowed materials in this family to exhibit a very wide range of properties, nearly all reported perovskites have oxygen or halides as the anion. Nitride perovskites have long presented a synthetic challenge due to the difficulty of completely excluding oxygen during synthesis and the high oxidation states required for the A and/or B site cations. This phase space is nearly unexplored, and the greater covalency of nitrogen makes nitrides attractive for semiconducting and other functional applications in renewable energy. Recently, we reported on the experimental realization of the first oxygen-free nitride perovskite— $LaWN_3$ —as a thin film, crystallizing in polar space group $R3c$. [1] The oxygen-free character of $LaWN_3$ is determined by Auger Electron Spectroscopy, and the structure is determined by synchrotron based X-ray diffraction. $LaWN_3$ exhibits a large piezoelectric response and signs of ferroelectricity, making it the first stable nitride ferroelectric compound. This opens a host of possible avenues to target novel compounds for functionalization, including as potential multiferroics for spintronic applications.

Here we report on the synthesis and detailed investigation of the structure and electronic properties of thin film $LaWN_3$ and analogous novel nitride perovskites. The films were grown through using combinatorial radiofrequency plasma sputtering and characterized via spatially-resolved structural, electronic, and optical measurements, allowing correlation to the films' composition. The combinatorial synthesis methods and high-throughput characterization used in this study allows rapid exploration of the phase space, accelerating the discovery of novel materials and pinpointing which have promising properties for functional applications.

[1] Talley, K.; Perkins, C.; Diercks, D.; Brennecka, G.; Zakutayev, A. arXiv:2001.00633, 2020.

2:30 PM EQ13.13.06

Growth of New Cerium-Containing Nitride Perovskites Rachel Sherbondy¹, Rebecca Smaha², Allison Mis¹, Megan Holtz¹, Kevin Talley², Andriy Zakutayev² and Geoff L. Brennecka¹; ¹Colorado School of Mines, United States; ²National Renewable Energy Laboratory, United States

Perovskite materials, those with a crystal structure related to the mineral perovskite and typically with the formula ABX_3 , are well known across a number of fields, such as ultrasonics and photovoltaics. These fields use perovskites that have oxygen or halides on the X (anion) site of the perovskite structure, but there are relatively few perovskites that have nitrogen as the anion. In this work, new nitride perovskites of composition $CeMoN_3$ and $CeWN_3$ were grown as thin films using a high-throughput approach. These films were grown using reactive sputtering with a chemical gradient in cation stoichiometry. After growth, films were annealed under flowing nitrogen to explore the phases present at a number of different conditions. The crystallization path revealed a competing defect phase within the fluorite family of crystal structures, which is reported here for the first time and is similar to the fluorite family phase that is observed in the $Pb(Zr,Ti)O_3$ (PZT) system. For $CeMoN_3$, the perovskite phase was grown using post growth annealing of thin films in a flowing nitrogen atmosphere at a temperature of 900°C for 10 minutes. For the $CeWN_3$ system, growing a perovskite phase was best accomplished during growth conditions that emphasized nitrogen reactivity. The fluorite-family phase was present for both compositions at high Ce content (well above the 1:1 perovskite stoichiometry) and when either temperature or nitrogen reactivity were low. A nitrogen plasma source offered a way to increase nitrogen reactivity at the surface of the film growth to induce growth, especially in $CeWN_3$. For both of these composition families, the high-throughput technique offered insight into the defects that form in off-stoichiometry regions of the film, which serve as a comparison to tell a more complete story of the crystallization of the perovskite phase. For both films, a crystallization path to the perovskite phase is presented and verified by x-ray diffraction. Preliminary property information was also gathered to demonstrate the changes after crystallization of the perovskite phase from the fluorite phase.

SESSION EQ13.14: GaN and Related Nitride Materials
Session Chairs: Huili Xing and Minghui Yang
Wednesday Morning, December 8, 2021
EQ13-Virtual

8:00 AM *EQ13.14.01

Chemistry of Ammonothermal Nitride Semiconductor Synthesis Rainer Niewa; Univ of Stuttgart, Germany

The ammonothermal process is a promising route for the synthesis and crystal growth of various nitride-based semiconductor materials with potential for technological applications. This method typically employs ammonobasic or ammonoacidic mineralizers in supercritical ammonia and was proven to be capable of growing a broad variety of nitrides like InN crystals and freestanding GaN wafers as well as a broad variety of further interesting nitride-based materials. Such chemical transport reactions for crystal growth require use of high-pressure autoclaves, typically operated at process parameters of up to 3 MPa and 600 °C and protection against corrosion provoked by the aggressive medium.

For a successful synthesis and crystal growth, not only a good knowledge of the process parameters and technological challenges is necessary, but also a profound understanding of the chemical processes that govern the feedstock dissolution, the material transport and the deposition in the crystallization zone. In order to obtain deeper insights, we have studied the chemistry of the ammonothermal crystal growth utilizing various mineralizers. Soluble intermediates and their influence on the crystal growth in supercritical ammonia depending on the chemical nature of the mineralizer as well as the pressure and temperature conditions will be discussed with emphasis on crystal growth of AlN, GaN, InN and the feasible synthesis of Zn_3N_2 .

8:30 AM *EQ13.14.02

Laser-Assisted MOCVD GaN Epitaxy and Developments of Ternary Nitrides, Heterostructures and Quantum Wells Hongping Zhao; The Ohio State University, United States

Wide bandgap GaN ($E_g \sim 3.4$ eV) with the intrinsic breakdown field $E_{br} \sim 3.5$ MV/cm and high electron mobilities $\mu_n \sim 1000$ cm²/Vs possesses the Baliga figure-of-merit (FOM) at least 5X better than SiC and almost 1000X better than Si for power devices. Vertical GaN devices have been demonstrated with true avalanche breakdown [1]. The current key challenge to achieve high power operation for GaN vertical device with high breakdown voltage (V_{br}) and low on resistance (R_{on}) is on the development of thick GaN drift layer with low controllable doping (N_d-N_a). Key impurities in MOCVD GaN serving as charge compensation centers were systematically investigated. For example, mechanisms of Fe incorporation in MOCVD GaN were identified and addressed [2]. Laser-assisted MOCVD (LA-MOCVD) growth technique was used to enable fast GaN epitaxy while suppressing C impurity incorporation [3]. The effects of LA-MOCVD GaN growth parameters on GaN growth rate, impurity incorporation and charge transport properties will be discussed. GaN PN diodes with breakdown voltage ~ 3 kV are demonstrated.

Expanded from III-nitrides, ternary II-IV-N₂ material system possesses unique properties beyond well-developed III-nitrides. Particularly, II-IV-N₂/III-N heterostructures with close lattice matching and large band offsets can potentially address existing challenges facing in pure III-nitride based devices. Closely lattice-matching ZnGeN₂/(In)GaN heterostructures have been demonstrated with large band offsets of >1 eV [4, 5]. In this talk, MOCVD developments of ZnGeN₂, ZnGeN₂/GaN heterostructures and InGaN/ZnGeN₂ quantum well structures will be discussed.

Acknowledgement:

The authors acknowledge the funding support from Advanced Research Projects Agency-Energy (ARPA-E) DE-AR0001036, U.S. Department of Energy's Office of Energy Efficiency and Renewable Energy (EERE) under the Advanced Manufacturing Office, FY18/FY19 Lab Call. The authors also acknowledge the funding support from the U.S. Department of Energy (DE-EE0008718) and the National Science Foundation (DMREF-SusChEM-1533957).

[1] I. C. Kizilyalli, A. P. Edwards, H. Nie, D. Disney, D. Bour, IEEE Tran. on Elec. Dev., 60, 3067, 2013.

[2] Y. Zhang, Z. Chen, W. Li, H.-S. Lee, M. R. Karim, A. R. Arehart, S. A. Ringel, S. Rajan, H. Zhao, J. Appl. Phys., 127, 215707, 2020.

[3] Y. Zhang, Z. Chen, K. Zhang, Z. Feng, H. Zhao, Physica Status Solidi (RRL), 2100202 (2021). doi.org/10.1002/pssr.202100202

[4] M. R. Karim, B. H. D. Jayatunga, M. Zhu, R. A. Lalk, O. Licata, B. Mazumder, J. Hwang, K. Kash, and H. Zhao, AIP Advances 10, 065302, 2020.

[5] M. R. Karim, B. A. Noesges, B. H. D. Jayatunga, M. Zhu, J. Hwang, W. R. L. Lambrecht, L. J. Brillson, K. Kash, and H. Zhao, J. Phys. D: Appl. Phys., 54, 245102 (2021).

9:00 AM DISCUSSION TIME

9:15 AM EQ13.14.05

Late News: Multi-Carbon Complexes in Highly C-Doped GaN John L. Lyons¹, Evan R. Glaser¹, Mary Ellen Zvanut², Subash Paudel², Malgorzata Iwinska³, Tomasz Sochacki³ and Michal Bockowski³; ¹Naval Research Laboratory, United States; ²The University of Alabama at Birmingham, United

States; ³Polish Academy of Sciences, Poland

Due to its deep acceptor level, carbon doping can lead to highly resistive gallium nitride. But recent experiments indicate that other configurations of carbon become important in heavily C-doped GaN. Here we investigate the properties of heavily C-doped GaN grown by hydride vapor phase epitaxy using optical experiments and hybrid density functional theory (DFT) calculations. Prior work established that carbon acceptors (C_N) give rise to a yellow luminescence (YL) band near 2.2 eV, along with a blue luminescence band (BL) near 2.9 eV. Photoluminescence measurements show the YL band shifting as a function of carbon concentration, suggesting a change in the behavior of carbon species as carbon content increases. With hybrid DFT we calculate the electrical and optical behavior of multi-carbon complexes which may arise in heavily doped material. We compare the behavior of these complexes to the isolated centers, and find that the dicarbon donor-acceptor ($C_{Ga}-C_N$) complex is a candidate to explain the shift in the YL peak. Tricarbon complexes have modest binding energies but high formation energies, and also give rise to optical transitions inconsistent with the observed spectra. The split dicarbon interstitial on the gallium site is identified as a low-energy species with a large binding energy, that may act to compensate carbon acceptors. Local vibrational modes are calculated for carbon impurity centers and compared to recent experiments. Dicarbon and tricarbon complexes involving C_{Ga} and C_N exhibit modes only slightly higher than the isolated species, while carbon interstitials and related complexes give rise to vibrational modes significantly higher than C_{Ga} and C_N .

[1] *Phys. Rev. B* **104**, 075201 (2021).

This work was supported by the ONR/NRL 6.1 Basic Research Program.

9:20 AM EQ13.14.06

Thermodynamics and Growth of V-pit Defects on Wurtzite GaN Polar Surfaces Su-Hyun Yoo, Liverios Lymperekis and Jorg U. Neugebauer; Max-Planck-Institut für Eisenforschung, Germany

Controlling surface defects is a key to reduce efficiency losses in wurtzite (WZ) GaN-based optoelectronic and power electronic devices. Inverted pyramids or V-pits are a prominent and often observed extended defect in heteroepitaxially grown GaN surfaces. They are widely accepted to be detrimental for optoelectronic devices. Recently, there is an increasing interest in the effect of V-pits on the efficiency of power electronic devices. V-pits are commonly associated with threading dislocations, can reach lateral sizes as large as a few hundred nms, and are buried inside the buffer layer of the heteroepitaxial structures [1]. The buried nature of this defect makes experimental investigations challenging. Therefore, despite their importance, an in-depth understanding of their origin, size, and shape is still lacking.

In the present work, we combine first-principles calculations with elasticity theory and investigate thermodynamic stability and growth of V-pits at GaN (0001) surfaces. The nucleation and properties (e.g., size and shape) of these defects are governed by the complex interplay between dislocation's strain and core energies, surface energies, and oversaturation. A prerequisite to accurately describe these defects is the identification of their absolute surface energies that constitute the inverted pyramid, i.e., polar, semipolar, and/or non-polar planes. Therefore, in the first step, we calculate roughly 300 different GaN surfaces having low index (0001), (10-1n), and (11-2n) orientations, where $n=0, \dots, 3$. Although absolute polar and semipolar WZ surface energies are ill-defined, the energies of the semipolar planes can be aligned with respect to those of polar ones. Furthermore, we exploit geometric similarities between {0001} WZ surfaces with higher symmetry {111} zincblende surfaces to calculate "absolute" polar surface energies. For these calculations, we employ our recently developed methodologies, which address the spontaneous polarization fields and allow us to identify accurate surface energetics and electronic structures of WZ surfaces [2, 3]. Based on these calculations we construct a 'V-pit' phase diagram, which describes the equilibrium size and shape of V-pits as a function of the ambient growth conditions, i.e., the Ga and H chemical potentials reflecting oversaturation. This diagram reveals that under typical MOCVD growth conditions, the GaN polar planes are intrinsically unstable against the formation of V-pits at sites where screw threading dislocations reach the surface. The defect formation is driven by the preferential decoration of the surfaces by hydrogen, which reduces the surface energies. The remaining surface energy is compensated by releasing the energy stored in the dislocation core and strain field. Our calculations predict equilibrium lateral sizes up to a few tenths of a nm. Although this is smaller than the experimentally observed maximum size, the size of the energetically favorable V-pit nucleus may be enhanced by surface kinetics, i.e., the presence of Ehrlich-Schwoebel barriers. On the other hand, under typical MBE growth conditions and the lack of hydrogen, V-pits are energetically unfavorable. Based on these results we will further discuss the electronic properties of the V-pit side facets and how they influence critical device parameters such as work functions and ionization energies.

This project has received funding from the ECSEL Joint Undertaking (JU) project UltimateGaN under grant agreement No 826392. The JU receives support from the European Union's Horizon 2020 research and innovation program and Austria, Belgium, Germany, Italy, Slovakia, Spain, Sweden, Norway, Switzerland.

[1] S. Besendörfer *et al.*, *J. Appl. Phys.* **127**, 015701 (2020)

[2] S.-H. Yoo, *et al.*, *npj Comput. Mater.* **7**, 58 (2021)

[3] S.-H. Yoo, *et al.*, *Phys. Rev. Mater.* **5**, 044605 (2021)

9:25 AM EQ13.14.07

Investigation of Self-Assembled GaN Nanowire Growth Mechanism Nian Jiang, Hannah J. Joyce, Saptarsi Ghosh, Simon M. Fairclough, Rachel Oliver and Carmen M. Fernandez-Posada; University of Cambridge, United Kingdom

One of the major challenges faced by the III-Nitride materials is caused by the absence of a suitable substrate, which results in high dislocation densities in epitaxially grown planar structures. Nanowire geometries are drawing the attention of the III-nitride community for their narrow diameter and small footprint, enabling efficient strain relaxation, thus dislocation free III-nitride nanowires. Yet, a solid understanding of the growth mechanisms for self-assembled III-Nitride nanowires is to be developed, despite many successfully demonstrated devices based on the III-nitride nanowires.

The self-assembled GaN nanowires/nanorods can be achieved via two major growth methods: one with a dielectric mask and one without a pre-deposited dielectric mask. Typically, the GaN nanowires grown with dielectric masks have metal (e.g. Ga) polarity, and have a growth rate comparable to their planar counterparts, while the ones grown directly on a sapphire substrate has a growth rate that is of orders of magnitude higher, and they are mostly with N-polarity.

In this study, we conducted a systematic study of self-assembled GaN nanowires on c-Sapphire substrates grown by metalorganic chemical vapor deposition (MOCVD) through X-ray photoelectron spectroscopy (XPS), atomic force microscope (AFM), scanning electron microscopy and transmission electron microscope. Self-assembled GaN nanowires were grown on c-sapphire substrates in a Veeco Propell Power GaN MOCVD, using ammonia (NH_3), trimethylgallium (TMGa) and silane (SiH_4) as precursors. The substrates were kept in H_2 flow at 1060°C for 5 min to decontaminate the surface followed by a 10 min nitridation step at 1080°C. The temperature was then dropped to (1035 – 1050)°C for GaN nanowire growth. Growth was initiated with a

nucleation step followed by a 15s growth interruption before 10 min nanowire growth with $[\text{NH}_3]/[\text{TMGa}] = 6 - 24$ and $[\text{SiH}_4] = 0.8 - 1.6 \mu\text{mol}/\text{min}$. The substrate surfaces after the decontamination, nitridation and nucleation steps were studied by XPS and AFM to understand the initiation of nanowire growth. The polarities of as-grown structures were studied by SEM after 30 min etching by KOH solution at room temperature.

We confirmed that the nitridation treatment of the c-Sapphire substrate forms a thin layer of AlN that leads to the N-polarity of the subsequently grown GaN nanowires. The reported $\text{Al}(\text{NO})_x$ complex associated with the metal-polar III-nitride growth¹, is not observed in the samples after nitridation step, and is consistent with the observation of predominate N-polar GaN nanowires. The nucleation step is essential for GaN nanowire growth, yet this step does not control the nanowire diameters as reported². We found that the broad distribution of nanowire lengths is caused by the different growth mechanisms. Typically, N-polar GaN nanowires' growth rate is 15 – 23 atomic bilayers/sec compared to 2 – 4 atomic bilayers/sec of the Ga-polar nanowires. The N-polar GaN nanowires were found with two distinctive growth rate region – one with (15 ± 2) atomic bilayers/sec and one with (23 ± 2) atomic layers/sec. TEM results suggest screw dislocations may be one of the causes of the growth rate differences.

Understanding the underlying growth mechanisms of N-polarity GaN nanowire growth and their fast growth rate will provide insides to the III-Nitride materials growth community and shine lights to explore the full potential of III-nitride nanowires.

References:

¹ S. Mohn, N. Stolyarchuk, T. Markurt, R. Kirste, M.P. Hoffmann, R. Collazo, A. Courville, R. Di Felice, Z. Sitar, P. Vennéguès, and M. Albrecht, *Phys. Rev. Appl.* **5**, 1 (2016).

² R. Koester, J.S. Hwang, C. Durand, D. Le Si Dang, and J. Eymery, *Nanotechnology* **21**, (2010).

9:30 AM EQ13.14.08

Amorphous Boron Nitride—Ab Initio Study of Its Vibrational Properties David Hinojosa¹, Isafas Rodríguez¹, Alexander Valladares², Renela M. Valladares² and Ariel Valladares¹; ¹Universidad Nacional Autónoma de México - Instituto de Investigaciones en Materiales, Mexico; ²Universidad Nacional Autónoma de México - Facultad de Ciencias, Mexico

Boron nitride (BN) is a structurally versatile insulator since it can be found in several crystalline structures with outstanding mechanical and electrical properties, making this material to be attractive for technological applications. Seeking to improve its features, first principles studies for the amorphous phase (a-BN) have been carried out by several groups, focusing on the electrical [1] and structural [2] properties, pressure-induced phase transformations [1], and hydrogenated a-BN [3]. In this work we shall contribute to the understanding of the a-BN by generating an amorphous structure by means of *ab initio* Molecular Dynamics on a 216-atom supercell, following the *undermelt-quench* approach which has proven to give good structures for structurally disordered materials [4, 5] and studying the vibrational density of states for the samples obtained.

[1] M. Durandurdu. Amorphous boron nitride at high pressure. *Philosophical Magazine* **96** (2016), pp. 1950–1964, DOI:10.1080/14786435.2016.1183830.

[2] D.G. McCulloch, D.R. McKenzie, C.M. Goringe. Ab initio study of structure in boron nitride, aluminum nitride and mixed aluminum boron nitride amorphous alloys, *Journal of Applied Physics* **88** (2000), pp. 5028–5032. DOI:10.1063/1.1316790.

[3] T.A. Üçhöyük, M. Durandurdu. Hydrogenated amorphous boron nitride: A first principles study, *Journal of Non-Crystalline Solids* **502** (2018), pp. 159–163 DOI:10.1016/j.jnoncrysol.2018.08.021.

[4] Z. Mata-Pinzón, A.A. Valladares, R.M. Valladares, A. Valladares. Superconductivity in Bismuth. A New Look at an Old Problem. *PLoS ONE* **11** (2016), e0147645. DOI:10.1371/journal.pone.0147645.

[5] D. Hinojosa-Romero, I. Rodríguez, A. Valladares, R.M. Valladares, A.A. Valladares. Ab initio Study of the Amorphous Cu-Bi System. *MRS Advances* **4** (2019), pp. 81–86. DOI:10.1557/adv.2019.83.

9:35 AM EQ13.14.09

Late News: UV Photodetector Based on Wide Bandgap Gap p-type MnO Quantum Dots /n-type GaN Structures via pn Junction Hadeel Alamoudi, Bin Xin, Mohamed Nejib Hedhili, Somak Mitra and Iman S. Roqan; King Abdullah University of Science and Technology, Saudi Arabia

Developing p-type wide-bandgap semiconductors with bandgap energy corresponding to UV-C spectral region (> 280 nm) is still challenging. This issue motivated us to explore wide-bandgap p-type MnO quantum dots (QDs) with the bandgap of > 4 eV synthesized by femtosecond laser ablation in liquid (FLAL), which is a cost-effective technique. In this study, we demonstrate for the first time a pn-junction photodetector based on p-MnO QDs/n-GaN. As a part of this work, MnO target in ethanol was ablated by ultrafast Ti:Sapphire laser (at 800 nm and 75 MHz) to synthesize the wide-bandgap p-MnO QDs under ambient conditions. We subsequently demonstrate the p-type conductivity of the QDs using Kelvin probe (KP), as well as via field-effect transistor (FET) measurements. X-ray diffraction (XRD), transmission electron microscopy and Raman spectroscopy were also performed to ascertain the p-type MnO composition. Absorption spectroscopy findings indicated that the bandgap was in the 4–5 eV range. The solution-processed MnO QDs were simply spray-coated on Si-doped GaN to fabricate MnO/GaN-based solar-blind DUV photodetector. X-ray Photoelectron Spectroscopy (XPS) analysis reveals the heterojunction band alignment of p-MnO QDs/n-GaN and the band offset at the heterojunction interface, demonstrating a good band alignment between GaN and MnO QDs with type II. Electrical characterizations show a good photocurrent response, as well as self-powered characteristics. This study provides new insights into the use of p-type MnO QDs for III-nitride devices.

9:40 AM EQ13.14.10

Late News: Optical Characterization of Carrier Recombination Process in GaPN Alloys: Excitation Source and Nitrogen Concentration Dependence Hiroki Iwai, Sanjida Ferdous, Norihiko Kamata, Shuhei Yagi and Hiroyuki Yaguchi; Graduate School of Science and Engineering, Saitama University, Japan

III-V-N alloys have been receiving much attention for optoelectronic device applications because of their attractive features, for example, large gap bowing and splitting of conduction band. In particular, GaPN alloys are candidate materials for intermediate band solar cells (IBSCs). Since some defects due to nitrogen atoms in III-V-N alloys are found to act as nonradiative recombination (NRR) centers, however, it is crucial to study non-radiative recombination processes in GaPN alloys for improving the efficiency of solar cells. In this study, therefore, we evaluate the carrier recombination process in GaPN alloys with various nitrogen concentrations by using an optical technique, two-wavelength excited photoluminescence (TWEPL).

The samples used in this work were grown by metalorganic chemical vapor deposition. A 300 nm-thick GaP buffer layer and a 500 nm-thick $\text{GaP}_{1-x}\text{N}_x$ ($x = 0.105\%$, 0.56% , 0.75% , 1.4% and 3.2%) were grown in sequence on 400 μm -thick GaP substrates with an orientation of (100). Trimethylgallium, phosphine, and dimethylhydrazine were used as Ga, P, and N sources, respectively.

The TWEPL measurements were carried out using above-gap excitation (AGE) and below-gap excitation (BGE) light. While the sample was excited by AGE light, BGE light was irradiated at the same point of AGE spot. We measured PL intensities with BGE ($I_{\text{AGE+BGE}}$) and without BGE (I_{AGE}), and derived the normalized PL intensity ($I_{\text{N}} = I_{\text{AGE+BGE}}/I_{\text{AGE}}$). We used two light sources for AGE; $\lambda = 374 \text{ nm}$, 3.32 eV and $\lambda = 532 \text{ nm}$, 2.33 eV for conduction band (CB) excitation and intermediate band (IB) excitation, respectively. For BGE, we used 0.81 eV (1532 nm), 0.93 eV (1340 nm), 1.17 eV (1064 nm), 1.27 eV (980

nm), and 1.46 eV (850 nm). The sample was immersed in liquid nitrogen (77 K) to prevent temperature rise effect due the excitation light sources. First, we studied the nitrogen dependence of the integrated PL intensity by AGE and found that the PL intensity of 3.2% sample was the lowest in all the samples, indicating that 3.2% sample is the most significantly affected by NRR centers. The PL intensity of 1.4% sample was the highest and the samples with nitrogen concentration of 0.105%, 0.56% and 0.75% showed the PL intensity between 3.2% and 1.4%; however, the PL intensity of 0.105% sample was a little lower than 0.56% and 0.75% because isolated N-N pairs emissions are dominant for 0.105%. Second, we investigated the BGE power dependence of normalized PL intensity (I_N) based on TWEPL method. For IB excitation, I_N value increased and became saturate for all the BGE sources, showing that some electrons are excited from valence band (VB) to NRR centers or from NRR centers to IB. The I_N value of 3.2% was higher than that of 1.4% sample. This is consistent with the integrated PL intensity result that 3.2% sample is significantly affected by NRR centers. For CB excitation, in contrast, I_N value was almost constant for 1.4% and 3.2% samples, which is clear evidence that the carrier relaxation and subsequent recombination processes are much different for CB and IB excitation. Therefore, we found that the reduction of NRR centers located between VB and IB is important for reducing the relaxation from CB to NRR centers, and thus improving the efficiency of CB excitation. We will clarify the carrier recombination process in GaPN alloys with different nitrogen concentrations by combining the experimental results of time-resolved photoluminescence measurements.

SESSION EQ13.15: AlGa_N and Related Nitride Materials
Session Chairs: Bjorn Alling and Tongtong Zhu
Wednesday Morning, December 8, 2021
EQ13-Virtual

10:30 AM *EQ13.15.01

Why Should We Invest in Ultrawide Bandgap Nitride Semiconductors? Huili G. Xing; Cornell University, United States

To fully unleash the potential of a semiconductor, it is critical to 1) control its defect levels below the limits that the targeted applications can tolerate, 2) control its doping in both n-type and p-type, and 3) engineer the most effective carrier injection into the conduction and valence bands, i.e. excellent ohmic contacts. A DUV emitter is an epitome of devices where these requirements need to be met. Even for an application that can be successful in engineering only one band of the semiconductor, availability of adequate control of the other band expands the design and operation space of the device tremendously. I will discuss advances in fundamental science and technology development that promise solutions for DUV devices, power and RF electronics.

11:00 AM EQ13.15.02

Novel Approach for Growth of High-Quality Aluminum Indium Nitride Covering the Entire Composition Range Zachary Engel, Habib Ahmad and William A. Doolittle; Georgia Institute of Technology, United States

Aluminum Indium Nitride (AlInN) has shown great potential in the fields of optoelectronics, photovoltaics, and electronics. It has shown potential as an electron blocking layer and quantum well material in light emitting diodes (LEDs), as an absorbing material in solar cells, and as a barrier layer in high electron mobility transistors (HEMTs). Additionally, AlInN has a wide range of useful properties, including a tunable bandgap from 0.65 to 6.1 eV, a high absorption coefficient, high polarization coefficients to allow for high density 2D hole and electron gasses, and the ability to be grown lattice matched to GaN at a composition of about 18% indium. However, despite the proven useful applications and properties of the alloy, crystal quality issues have plagued this material. Due to the large mismatches between the two binary alloys, AlN and InN, a large miscibility gap exists for the ternary material. Additionally, the growth temperatures required to achieve state-of-the-art quality InN and AlN differ in extremes of ≥ 500 °C. At the preferred temperature required for superb AlN, it is difficult to incorporate indium into a film. Conversely, at growth temperatures that allow for high or complete indium incorporation, aluminum adatom mobility is traditionally extremely low. Thus, a nontraditional method must be employed to grow this challenging material.

For these reasons, Aluminum Indium Nitride was grown over the entire composition range from InN to AlN using a non-traditional method, Metal Modulated Epitaxy (MME). MME is an extremely low temperature modification of molecular beam epitaxy (MBE) performed at temperatures where desorption and thermal decomposition are negligible, utilizing cyclic, high metallic doses to establish a low bond strength surface layer resulting in higher adatom mobility. MME has shown great potential in the past for the growth of AlInN, demonstrating the ability to grow high indium content AlInN with state-of-the-art crystal quality and sub-nm RMS roughness. By utilizing pulsed cation fluxes with high metal fluxes, short metal doses, and a metal rich III/V ratio at substrate temperatures low enough to prevent In-N decomposition and In desorption, adatom kinetics have been improved, improving film structural and optical properties. Using this approach, MME has produced Al_{0.3}In_{0.7}N with X-ray rocking curves 11 times better than prior literature. This non-traditional approach was expanded to look at 9 compositions from 10% to 90% Al, each at multiple substrate temperatures. Because the optimal substrate temperature varies with composition, 27 samples ranging from: 10-40% Al were grown at 300, 350, and 400 °C; 50-70% Al were grown at 350, 400, and 450 °C; and 80-90% Al were grown at 400, 450, and 500 °C. High structural quality was observed over the entire composition range but varied with growth temperature for different compositions, with (0002) X-ray diffraction (XRD) rocking curve full-width at half-maximum (FWHM) values as low as 163 arc-sec even near the center of the composition range where phase separation is predicted to be problematic. Atomic force microscopy (AFM) measurements showed smooth surfaces throughout the composition range with RMS roughness' ranging between 0.16 to 3 nm. Photoluminescence measurements of high indium content AlInN show promising luminescence at wavelengths traditionally difficult for efficient InGa_N emission while the luminescence efficiency varies with composition and growth conditions.

11:15 AM EQ13.15.03

Enhanced Performance of Al_{0.4}Ga_{0.6}N Solar-Blind Photodetectors by Localized Surface Plasmon Resonance in Pd Nanoparticles Shuchi Kaushik¹, Prashant Bisht¹, Che-Hao Liao², Xiaohang Li², Bodh Raj Mehta¹ and Rajendra Singh¹; ¹Indian Institute of Technology Delhi, India; ²King Abdullah University of Science and Technology, Saudi Arabia

The ever-increasing demand for “solar-blind” (insensitive to photons with wavelengths longer than ~285 nm) photodetectors (PDs) in healthcare, space science, and technology, and the military requires focusing on state-of-the-art PDs. Owing to its appealing properties of tunable wide bandgap (3.4 to 6.2 eV), high-temperature robustness, chemical and radiation hardness, Al_xGa_{1-x}N has emerged as the most suitable candidate for fabricating solar-blind PDs [1]. However, the “5S” requirements of high spectral selectivity, sensitivity, speed, signal-to-noise ratio, and stability for a commercial PD emphasize novel strategies to improve the performance parameters of AlGa_N-based solar-blind PDs. In the last two decades, the localized surface plasmon resonance (LSPR) in metal nanoparticles (NPs) has proved to be a promising strategy to enhance the performance of semiconductor PDs [2]. The role of Al NPs has been investigated to improve the performance of AlGa_N solar-blind PDs. However, the reported responsivity values were only 0.288 AW⁻¹ at 5 V [3] and 2.34 AW⁻¹ at 20 V [4]. Therefore, there is a need to explore other metal NPs that may prove better than Al NPs for AlGa_N solar-blind PDs.

In this work, we report a significant enhancement in the performance parameters of $\text{Al}_{0.4}\text{Ga}_{0.6}\text{N}$ solar-blind PDs mediated by LSPR in Pd NPs. The interdigitated electrode (IDE) geometry (width and inter-electrode spacing $20\ \mu\text{m}$) of metal-semiconductor-metal (MSM) PDs was fabricated on MOCVD grown $\text{Al}_{0.4}\text{Ga}_{0.6}\text{N}$ epilayers. Pd NPs were deposited on one of the PDs using an integrated gas-phase setup and then annealed at $500\ ^\circ\text{C}$ to obtain AlGaN PD with Pd NPs. On decorating the $\text{Al}_{0.4}\text{Ga}_{0.6}\text{N}$ film by Pd NPs, a significant enhancement in the current at $500\ \text{nm}$ (visible) and $280\ \text{nm}$ (solar-blind) was observed. At $-5\ \text{V}$, the photo-to-dark current ratio (PDCR) was found to increase by 99.7% and 71.7% at 500 and $280\ \text{nm}$, respectively. Similarly, at $-10\ \text{V}$, the enhancement was 99.6% and 85.0% at the two wavelengths. The observed results are attributed to the increased absorption and hot-carrier generation by LSPR in the Pd NPs. As a result, the performance parameters of the PD, such as responsivity and specific detectivity, were found to improve significantly. At $-10\ \text{V}$, the peak responsivity was found to increase by 75% , reaching a maximum value of $2.2\ \text{AW}^{-1}$ at $220\ \text{nm}$ with an incident optical power of only $1.7\ \mu\text{W}$, indicating the ability to detect even weak signals. It was observed that the responsivity increased with the increasing bias, and an enhancement by 71% was observed in the responsivity at $280\ \text{nm}$ for the PD with NPs. To compare the sensitivity of the PDs, the specific detectivity was calculated, and its variation with the incident wavelength was analyzed. At $-10\ \text{V}$, the maximum value of specific detectivity was found to increase by 82% , and a peak value of $3.4 \times 10^{13}\ \text{Jones}$ was calculated. In conclusion, a significant increase in the PDCR, peak responsivity, and specific detectivity by 85% , 75% , and 82% , respectively, was observed for $\text{Al}_{0.4}\text{Ga}_{0.6}\text{N}$ solar-blind PD on decorating with Pd NPs.

References

- [1] D. Li *et al.*, *Adv. Opt. Photonics*, vol. 10, no. 1, p. 43, (2018).
- [2] X. Chang *et al.*, *Appl. Surf. Sci.*, vol. 464, p. 455–457, (2012).
- [3] G. Bao *et al.*, *Opt. Express*, vol. 22, no. 20, p. 24286, (2014).
- [4] W. Zhang *et al.*, *Appl. Phys. Lett.*, vol. 106, no. 2, p. 021112, (2015).

11:30 AM EQ13.06.03

Understanding Dislocation Induced Formation of Nanopipes in III-Nitrides from First Principles Liverios Lymperakis, Su-Hyun Yoo and Jorg U. Neugebauer; Max-Planck-Institut für Eisenforschung GmbH, Germany

Threading dislocations constitute a long standing and highly debated issue in the field of III-nitride materials. Typical dislocation densities in nitride based devices can be as high as of 10^8 to $10^{10}\ \text{cm}^{-2}$. These defects have recently attracted considerable interest due to their detrimental role in power electronics. *c*-type screw dislocations are considered to be one of the major limiting factors in achieving the full potential of nitride based power electronic devices. Specifically, screw dislocations as well as the associated V-pits have been proposed to be the root cause of device leakage and breakdown [1,2]. An intriguing feature of these defects is that experimental evidences suggest that they are associated with open core structures, thus forming nanopipes with diameters of a few nm [3]. On the other hand, early as well as recent first principles calculations indicate that the formation of nanopipes is energetically unfavorable under typical growth conditions [4,5]. However, these calculations do not explicitly consider the effect of core and/or do not consider the effect of impurities such as hydrogen that is abundant in MOCVD growth or dopand species such as C and Mg.

In order to resolve the aforementioned discrepancies and provide an understanding on the formation and the properties of dislocation induced nanopipes in III-nitrides we combine first principles with large scale empirical potential calculations within the Implicit Boundaries Multiscale Scheme [6]. Using this approach we investigate the energetics, atomic structure and electronic properties of *c*-type screw dislocations in GaN and AlN. Based on these calculations we construct a screw dislocations' phase diagram which describes the energetically most favorable core structures as function of the species' chemical potentials. We explicitly consider the effect of H, C, and Mg as well as the formation of superscrew dislocations, i.e., dislocations with Burgers vector multiple lattice constants. Although nanopipes exhibit large free surface areas which increase the energy, they can be energetically favorable if the surface energy is compensated by the core and strain energy of the material removed to create the open core screw dislocation. Our calculations indicate that under MBE growth this requirement is not met and the formation of nanopipes is energetically highly unfavorable. However, a general trend that emerges from the aforementioned phase diagram is that nanopipes become energetically favorable at higher H chemical potentials. Indeed, under typical MOCVD or MOVPE growth conditions the cation and anion dangling bonds at the open core inner surfaces are passivated by NH_x molecules and H atoms, respectively. This reduces considerably the surface energy and the formation of nanopipes with hexagonal cross section and equilibrium diameters ranging from approx. 1 to 2 nm are energetically favorable. Based on these results we will discuss the electronic properties of the nanopipes, the diffusion and incorporation of C and Mg dopands at the open core structure as well as implications these defects may have on the efficiency of the electronic devices.

This project has received funding from the ECSEL Joint Undertaking (JU) project UltimateGaN under grant agreement No 826392. The JU receives support from the European Union's Horizon 2020 research and innovation program and Austria, Belgium, Germany, Italy, Slovakia, Spain, Sweden, Norway, Switzerland.

- [1] K. Nomoto *et al.*, *IEEE Electron Device Lett.* **37**, 161 (2016).
- [2] S. Besendörfer *et al.*, *J. Appl. Phys.* **127**, 015701 (2020)
- [3] S. Usami *et al.*, *Appl. Phys. Lett.* **112**, 182106 (2018).
- [4] J. E. Northrup, *Appl. Phys. Lett.* **78**, 2288 (2001).
- [5] L. Pizzagalli *et al.*, *Phys. Rev. Materials* **2**, 064607 (2018).
- [6] L. Lymperakis *et al.*, *Phys. Rev. Lett.* **93**, 196401-1 (2004).

11:45 AM EQ13.15.04

Growth and Optical Characteristics of High-AlN Content AlGa_xN on AlN Templates by RF-MBE Under Metal-Rich Conditions Mahiro Hayasaki and Takeyoshi Onuma; Kogakuin University, Japan

Recently, UV-C lights are getting explosive attention for UV sterilization. $\text{Al}_x\text{Ga}_{1-x}\text{N}$ is a direct bandgap material covering from 3.4–6.0 eV. It is one of the most promising one to realize semiconductor-based UV-C emitter. However, metal-rich growth of high-AlN content AlGa_xN by RF-MBE has known to be suffered from drawback due mainly to the difference in the bonding energy of Ga-N and Al-N [1,2]. In this study, high-AlN content $\text{Al}_x\text{Ga}_{1-x}\text{N}$ films were grown by RF-MBE. Impact of change in group-III to nitrogen supply ratio on their crystallinity and optical property are studied to phenomenologically understand the growth kinetics.

$\text{Al}_x\text{Ga}_{1-x}\text{N}$ films were grown on 425-nm-thick *c*-plane AlN on Al_2O_3 templates [3] at substrate temperature of $775\ ^\circ\text{C}$. Beam equivalent pressures of Al and Ga sources were fixed at 2.0×10^{-7} and 3.0×10^{-7} Torr, respectively. N_2 gas flow rate was varied in between 0.3–2.0 sccm by fixing RF input power of 150 W. Growth time was controlled by the group-III source supply for 1 hour with maintaining the reactive nitrogen source supply during the heating and cooling processes above $300\ ^\circ\text{C}$. Photoluminescence (PL) spectra were measured at room temperature (RT) using a frequency-quintupled (213 nm) Q-switched YAG:Nd laser. Reflectance spectra were measured at RT using a 25 W Deuterium and a 20 W Tungsten Halogen lamps.

XRD 2 θ - ω pattern for the film with $\text{N}_2=0.3\text{--}0.5\ \text{sccm}$ only shows a (0002) diffraction peak of AlN. Diffraction peaks of GaN and AlGa_xN additionally appeared for the films with 0.7–2.0 sccm. Furthermore, the AlGa_xN peaks for 0.7–2.0 sccm exhibited a shoulder at higher and lower diffraction angle side, respectively. Al mole fraction *x* was measured by X-ray reciprocal space mapping to be 0.67–0.88, confirming the growth of high-AlN content AlGa_xN.

Film thicknesses were assessed by the spectroscopic ellipsometry measurements to be 387~416 nm for AlN overlayers at $N_2=0.3\text{--}0.5$ sccm, 420~653 nm for AlGaIn at $N_2=0.7\text{--}2.0$ sccm, and 4~73 nm for GaN grown on top of the AlGaIn layer. PL spectra exhibited near-band-edge emission peaks for GaN at around 3.3~3.4 eV and for AlGaIn at around 4.3~4.8 eV. Furthermore, the AlGaIn peak for 1.0 and 2.0 sccm clearly shows double peaks. The reflectance spectra show the multiple interference fringes in which three periodic oscillations are overlapped, and the averaged effective bandgap energies of AlGaIn layers were estimated to 5.09~5.43 eV.

The overall results can be understood by the growth model [1], in which the Al-N bond is favorably formed under the metal rich condition. The additional lower-Al-content AlGaIn and GaN overlayers were found to be grown during the cooling process by nitriding the excess Al and Ga metals.

This work was supported in part by Takahashi Industrial and Economic Research Foundation. The authors grateful to Prof. A. Yoshikawa of Chiba University for his continuous encouragements.

[1] E. Iliopoulos and T. D. Moustakas, *Appl. Phys. Lett.* **81**, 295 (2002). [2] M. Shirazi-HD *et al.*, *J. Appl. Phys.* **123**, 161581 (2018). [3] H. Fujikura *et al.*, *Appl. Phys. Express.* **13**, 025506 (2020)

11:50 AM EQ13.15.05

Defect Detection in AlGaIn Barrier of AlGaIn/GaN Schottky Diodes Philippe Ferrandis^{1,2,3}, Matthew Charles^{2,4}, Marc Veillerot^{2,4} and Charlotte Gillot^{2,4}; ¹Université de Toulon, France; ²Univ. Grenoble Alpes, France; ³Institut Néel, France; ⁴CEA, LETI, France

The AlGaIn/GaN heterostructure has been demonstrated to be a promising candidate for high power amplifiers in the microwave communication system and high-voltage power switches [1]. The combination of GaN device performance with the low cost of silicon substrates enhances the interest of this technology. Despite numerous improvements of GaN power components during the last decades, charge trapping effects at deep levels still lead to dynamic on-resistance and switching losses [2]. To detect these deep traps and determine in which part of the device structure they are located, capacitance deep level transient spectroscopy (DLTS) has been applied to GaN Schottky barrier diodes (SBDs) [3].

However, hole-like traps are frequently observed in DLTS spectra of devices with n-type AlGaIn/GaN heterojunctions without any minority carriers. Many works refer to previous studies carried out in AlGaAs/GaAs systems to explain the nature of these DLTS signals. Hence, hole-like traps are often associated with surface states at the ungated SiN/AlGaIn interface [4]. They are sometimes related to bulk traps in the AlGaIn layer [5] or to the transfer of electrons by tunneling effect from the traps in the lower half of the AlGaIn bandgap into the states in the GaN buffer [6].

To our knowledge, no deep investigation exists to clearly identify the origin of hole-like traps in AlGaIn/GaN heterojunctions. A detailed understanding of the trapping mechanism involved in this anomalous DLTS signal is of fundamental importance to learn which defects affect device performance such as the gate-lag, for instance [5].

This work introduces a deep study on a hole-like signal which appears in DLTS spectra of AlGaIn/GaN SBDs. A correlation between the amplitude of the peak and the reverse leakage current of the diode has been demonstrated and a mechanism is proposed to explain the formation of the hole-like signal. During the pulse voltage, electrons move by tunneling conduction from the two-dimensional electron gas (2DEG) towards the AlGaIn layer where they are captured on deep donor states. When the temperature is increased and the reverse voltage is applied on the anode, the thermal energy removes electrons from the traps and the 2DEG is refilled by the reverse leakage current of the diode. The hole-like signal results from the return of electrons into the 2DEG.

The simulation of the DLTS peak using a model involving a transient time constant, which takes into account the thermal activation energy of the reverse leakage current of the diode, leads to the extraction of two deep levels in AlGaIn. The concentration of the dominant trap depends on the ammonia partial pressure used to perform the AlGaIn layer and was calculated at $4.1 \times 10^{13} \text{ cm}^{-3}$ and $5.3 \times 10^{13} \text{ cm}^{-3}$ for the two tested SBDs. With the help of secondary ion mass spectrometry studies, this trap was assigned to nitrogen antisite defects. The second trap was tentatively associated with Ga vacancy related defects.

The proposed model allows an explanation of the origin of traps reported in the literature. In addition, this work demonstrates that information can be extracted from a hole-like signal in AlGaIn/GaN heterojunctions to access features of traps in AlGaIn. We also demonstrated that the amplitude of the hole-like signal is an indication of the quantity of electrons which leave the 2DEG. Since the reduction of electrons in the 2DEG directly results in a decrease of device performance, the appearance of a hole-like signal in DLTS spectra of AlGaIn/GaN heterojunctions should be thoroughly investigated.

[1] E. A. Jones *et al.*, *IEEE J. Emerg. Sel. Topics Power Electron* **4**, 707 (2016)

[2] M. Meneghini *et al.*, *IEEE Trans. Electron Devices* **58**, 2996 (2011)

[3] P. Hacke *et al.*, *J. Appl. Phys.* **76**, 304 (1994)

[4] T. Okino *et al.*, *IEEE Electron Device Lett.* **25**, 523 (2004)

[5] A. Y. Polyakov *et al.*, *ECS J. Solid State Sci. Technol.* **6**, S3034 (2017)

[6] K. L. Enisherlova *et al.*, *Russ. Microelectron.* **48**, 28 (2019)

11:55 AM EQ13.15.06

Defect Analysis of a Thin Channel AlGaIn/GaN Transistor Julien Bassaler¹, Farid Medjdoub², Yvon Cordier³ and Philippe Ferrandis⁴; ¹Univ. Grenoble Alpes, CNRS, Grenoble INP, Institut Néel, France; ²CNRS-IEMN, Institute of Electronics, Microelectronics and Nanotechnology, France; ³Université Côte d'Azur, CNRS, CRHEA, France; ⁴Université de Toulon, Univ. Grenoble Alpes, CNRS, Institut Néel, France

AlGaIn/GaN high electron mobility transistor (HEMT) are known to be promising devices for high voltage applications. But the voltage range of the commercially available devices is not exceeding 650 V. To achieve operating voltages above kV, several solutions have been tested. One of them is the use of a thinner GaN channel combined with an ultra-wide bandgap material as a buffer in order to reduce its impact on the overall breakdown voltage.

The device studied in this work is an AlN-based HEMT [1] grown by molecular beam epitaxy. It is composed of a 6 μm thick commercial AlN-on-sapphire template, a 190 nm AlN buffer, a 8 nm GaN channel, a 10 nm AlGaIn barrier layer with 90% aluminum molar fraction to ensure a high sheet carrier density and a 5 nm in-situ grown SiN_x cap layer. Ti/Al/Ni/Au ohmic contacts are deposited on top of the barrier layer and Ni/Au is used to form the gate metal. Characterization by capacitance deep-level transient spectroscopy (DLTS) has been performed between 77 K and 500 K. A reverse voltage V_R from -1 V to -7 V has been applied between the gate and the ohmic contact. The filling pulse voltage V_P was fixed at -0.5 V.

For a reverse voltage $V_R > -5$ V, the depleted layer is under the gate. A DLTS peak can be observed at $T_{\text{max}} = 123$ K for a period width of $T_W = 10$ ms. The Arrhenius plot gives an activation energy of $E_a = 0.18$ eV and a capture cross-section of $\sigma_n = 1.2 \times 10^{-15} \text{ cm}^2$. The amplitude of the peak is saturating for a filling pulse time of $t_p = 10$ ms, indicating this is a point defect. It could be related to a N-vacancy defect [2][3]. For a reverse voltage $V_R < -5$ V, the depleted area extends under the SiN_x cap layer. At least five new peaks appear on the DLTS spectra at $T_{\text{max}} = 158, 190, 294, 375, 443$ K for the same period width of 10 ms. Their activation energies are consequently higher than the first identified defect. When the negative voltage is applied on the gate contact, the negative charges in the SiN_x are pushed back towards the ohmic contact and let positive charges on the gate side. The electrons of the channel are attracted by these positive charges and are captured by the defects in the AlGaIn layer. This leakage mechanism has already been proposed for another

AlGaIn/GaN HEMT [4]. The peaks resulting from this phenomenon are not visible on the DLTS spectra for $V_R > -5$ V because the probed area is not under the SiN_x cap layer. It is expected that the large lattice mismatch between AlGaIn and GaN layers, resulting from the high aluminum concentration of AlGaIn, leads to the formation of defects. Additional levels which appear in DLTS spectra for $V_R < -5$ V could then be related to interface states or border traps in AlGaIn.

The DLTS results enabled to highlight defects in the high aluminum concentration barrier layer and the leakage mechanisms occurring between the channel and the barrier. These results will help to improve critical properties of the AlN-based HEMT with a thin channel.

References:

- [1] I. Abid et al., *Micromachines* 10, 690 (2019)
- [2] L. Polenta et al., *Appl. Phys. Lett.* 76, 2086 (2000)
- [3] Z-Q. Fang et al., *Proc. 11th International Conference on Semiconducting and Insulating Materials*, 35 (2000)
- [4] P. Ferrandis et al., *J. Phys. D: Appl. Phys.* 53 185105 (2020)

12:00 PM EQ13.15.08

Late News: Revealing Sub-Quantum-Well Effect on Carrier Dynamics in High Efficiency DUV AlGaIn/AlGaIn-Based Multiple-Quantum- Wells Iman S. Roqan¹, Idris Ajia¹, Sergei Lopatin¹, Dhaifallah Almalawi¹ and Zhiqiang Liu²; ¹King Abdullah University of Science and Technology, Saudi Arabia; ²Institute of Semiconductors, Chinese Academy of Science, China

We reveal the role of the sub-well centers and related carrier dynamics mechanisms in enhancing the DUV emission of AlGaIn/AlGaIn multiple quantum wells (MQWs) when AlN substrate is grown homoepitaxially using MOCVD, thus eliminating the dislocation effect. As a part of this work, a 400 nm thick AlN layer was initially regrown on a thick (0001) AlN substrate at 1250 °C, followed by a 20×Al_{0.6}Ga_{0.4}N/AlN superlattice (SL) layer. Subsequently, a 1 μm thick n-AlGaIn layer was grown, followed by a nominal 5-period Al_{0.4}Ga_{0.6}N/Al_{0.5}Ga_{0.5}N (3 nm/12 nm) MQW active layer capped by a 30 nm p-Al_{0.65}Ga_{0.35}N electron blocking layer (EBL). Both plan-view and cross-sectional images obtained via scanning transmission electron microscopy (STEM) reveal dislocation defect-free epitaxial layers of very high crystalline quality, as well as ultra-thin Al-rich sub-quantum barrier layers. Energy dispersive x-ray (EDX) compositional analysis of the STEM cross-sections indicates that the formation of these layers can be ascribed to the diffusion of Al adatoms towards the top of the barriers, creating shallow sub-wells within the barrier regions. Advanced carrier dynamic analyses via photoluminescence (PL), power-dependent time-resolved PL (TRPL) spectroscopy and PL excitation measurements show that these sub-wells/sub-barriers resulted in additional carrier confinement and exciton localization centers. As a result, internal quantum efficiency is enhanced via staggered carrier repopulation into the MQWs to reach its maximum (~ 85%) and remains high (> 60%) after a slight droop at high carrier densities. We show that this slight efficiency droop is due to Auger recombination counteracted by a simultaneous increase in radiative recombination processes at high power density, demonstrating the role of sub-wells/barriers in efficiency enhancement.

12:05 PM EQ13.15.09

Al Flux Control in Growth of AlN on AlN Templates by RF-MBE Tomoya Yamaguchi and Takeyoshi Onuma; Kogakuin University, Japan

The use of deep ultraviolet (DUV) light for sterilization is attracting much attention behind recent global situation regarding COVID-19. AlGaIn is the most promising candidate material [1,2]. Recent developments of high quality AlN template [3] as well as AlN bulk substrate [4] accelerate improvements of performance of DUV emitters. Nevertheless the developments of the template and substrate, precise control of conditions is still necessary for growth of Al_xGa_{1-x}N by RF-MBE. In general, metal-rich condition is preferred to maintain high crystallinity and flat surface. Meanwhile, Al atoms tend to be stronger bonded to the surface, and Ga and N atoms are hardly incorporated into the alloy lattice even if Ga and N are sufficiently supplied [5]. Therefore, control of Al flux is crucial to eliminate Al precipitation and to suppress composition fluctuation in Al_xGa_{1-x}N alloy. In this study, AlN thin films were grown on AlN templates as functions of Al flux and growth temperature. Effects of the parameters on crystallinity and surface flatness are discussed. AlN templates were 431-nm-thick c-plane AlN prepared on Al₂O₃ by halide vapor phase epitaxy (HVPE) [3]. 181 to 432-nm-thick AlN films were grown for 1 hour with N₂ gas flow rate of 0.3 and RF input power of 150 W. Substrate temperature was varied as $T_s=775, 800, \text{ and } 850$ °C, and Al equilibrium vapor pressure was varied as $\Phi_{Al}=1.0 \times 10^{-7}$ Torr and 2.0×10^{-7} Torr. The samples were evaluated by atomic force microscopy (AFM), laser microscopy, X-ray diffraction (XRD), and spectroscopic ellipsometry.

All the XRD $2\theta-\omega$ patterns predominantly show a (0002) diffraction peak of AlN. The patterns for $\Phi_{Al}=2.0 \times 10^{-7}$ Torr additionally show a (111) diffraction peak of Al metal. The peak appeared regardless of T_s , and the intensity decreased with increasing T_s . It was also confirmed by the laser microscope images that the amount of Al precipitates decreased with increasing T_s . On the contrary, the films grown with $\Phi_{Al}=1.0 \times 10^{-7}$ Torr showed no tendency of Al precipitation at all T_s . The results imply that the growths with $\Phi_{Al}=2.0 \times 10^{-7}$ Torr were Al-rich conditions, and growths with $\Phi_{Al}=1.0 \times 10^{-7}$ Torr were stoichiometric or slightly N-rich conditions. Furthermore, the growth rate decreased for $\Phi_{Al}=2.0 \times 10^{-7}$ Torr at the lowest T_s of 775°C. It was suggested that excess Al supply induced a formation of Al layer, which are no longer contribute to the growth, and resulted in a decrease in film thickness [6]. Root mean square roughness obtained from the surface AFM images was improved from 3.7 nm at $(\Phi_{Al}, T_s)=(2.0 \times 10^{-7}$ Torr, 800°C) to 1.4 nm at $(\Phi_{Al}, T_s)=(1.0 \times 10^{-7}$ Torr, 800°C). The results indicate that the Al precipitation degrade the surface flatness, and it must be eliminated to obtain crystallinity as is the same with the AlN template.

This work was supported in part by Takahashi Industrial and Economic Research Foundation. The authors grateful to Prof. A. Yoshikawa of Chiba University for his continuous encouragements.

- [1] H. Hirayama, *J. Appl. Phys.* 97, 091101 (2005).
- [2] M. Kneissl and J. Rass, III-Nitride Ultraviolet Emitters (Springer International Publishing, Cham, 2016).
- [3] H. Fujikura *et al.*, *Appl. Phys. Express* 13, 025506 (2020).
- [4] Y. Kumagai *et al.*, *Appl. Phys. Express* 5, 055504 (2012).
- [5] M. Shirazi-HD *et al.*, *J. Appl. Phys.* 123, 161581 (2018).
- [6] V. N. Jmerik *et al.*, *J. Cryst. Growth* 354, 188 (2012).

SESSION EQ13.16: InGaIn and Related Nitride Materials

Session Chairs: Kathleen Kash and Rachel Oliver

Wednesday Afternoon, December 8, 2021

EQ13-Virtual

1:00 PM *EQ13.06.01

Ab Initio Insights into Fundamental Intrinsic Growth and Materials Limitations in Group-III-Nitrides Su-Hyun Yoo, Liverios Lymperakis and Jorg U. Neugebauer; Max-Planck-Institut für Eisenforschung, Germany

Their large direct bandgap, high thermal stability and surprisingly large insensitivity against even large defect concentrations have made group-III-nitrides the alloy system of choice in manufacturing light emitting devices and make them highly attractive for high-power applications. Despite the amazing progress that has been achieved in understanding, controlling and processing these materials fundamental issues remain unresolved that severely limit device performance. Infamous examples are the efficiency droop in the green region of the optical spectrum, the spontaneous formation of extended defects during epitaxial growth such as V-pits, or the formation of long-range electrostatic fields due to spontaneous polarization.

Understanding the origin of the underlying fundamental mechanisms requires an in-situ observation of atomic-scale phenomena during epitaxial growth, which makes it hard and often even impossible to explore them by experimental techniques. Recent developments and progress in first principles calculations provide now a powerful tool to unravel the mechanisms that are the fundamental cause for limitations in these materials [1,2]. In the presentation a brief overview about key concepts of the novel approaches will be given. It will be further demonstrated how they help to uncover hitherto unknown surface phenomena such as frustrated hybridization [3] that explain the origin of droop as a phenomenon originating at the surface rather than in bulk.

[1] S.-H. Yoo, M. Todorova, D. Wickramaratne, L. Weston, C.G. Van de Walle, and J. Neugebauer, *Finite-size correction for slab supercell calculations of materials with spontaneous polarization*, npj Comput. Mater. **7**, 58 (2021).

[2] S.-H. Yoo, L. Lymparakis, and J. Neugebauer, *Efficient electronic passivation scheme for computing low symmetry compound semiconductor surfaces in density-functional theory slab calculations*, Phys. Rev. Mater. **5**, 044605 (2021).

[3] L. Lymparakis, T. Schulz, C. Freysoldt, M. Anikeeva, Z. Chen, X. Zheng, B. Shen, C. Chèze, M. Siekacz, X. Q. Wang, M. Albrecht, and J. Neugebauer, *Elastically frustrated rehybridization: Origin of chemical order and compositional limits in InGaN quantum wells*, Phys. Rev. Mater. **2**, 011601(R) (2018).

1:30 PM EQ13.16.02

Growth of High-Quality InGaN on N-Polar GaN Substrates by Plasma-Assisted Molecular Beam Epitaxy at High Temperatures Ruby Wellen, Kamruzzaman Khan and Elaheh Ahmadi; University of Michigan–Ann Arbor, United States

In recent years, nitrogen-polar based devices have emerged as a potential source for novel and innovative developments in the field of GaN technology. With a different polarity, surface reactivity, and growth dynamic, N-polar GaN demonstrates notable advantages over Ga-polar GaN. The benefits of N-polar also span the typical compounds grown on Ga-polar GaN substrate. $\text{In}_x\text{Ga}_{1-x}\text{N}$ is especially interesting to investigate due to its attractive applications in optoelectronic devices. However, InGaN growth on GaN is challenging for several reasons, one of which concerns the conflicting values for the optimum growth temperatures of GaN and InGaN. To better examine such obstacles, this study explores InGaN growth on N-polar GaN by plasma assisted Molecular Beam Epitaxy (MBE) with high temperature. Samples were grown within a range of temperatures from 600° to 670°C, although typically InGaN films on Ga-polar GaN are grown around 100° less. The resulting N-polar InGaN samples achieved higher indium incorporation compared to Ga-polar growths. With further experimentation, the desirable growth conditions can be established and applied for development of higher performance InGaN devices.

1:45 PM EQ13.16.03

Atomic-Scale Localization Centers in Strain-Compensated In-rich InGaN Architectures for Red Emission Jing-Yang Chung^{1,2}, Zackaria Mahfoud³, Govindo Syaranamual¹, Li Zhang¹, Stephen Pennycook^{1,2}, Silvija Gradečak^{1,2} and Bosman Michel^{2,3}; ¹Singapore-MIT Alliance for Research and Technology, Singapore; ²National University of Singapore, Singapore; ³A*STAR (Agency for Science, Technology and Research), Singapore

A remarkable increase in the quantum efficiency of long-wavelength III-nitride light emitters has been demonstrated by AlN or AlGaIn strain-compensating interlayers that cap In-rich InGaN quantum wells (QWs). However, the structural non-uniformity within these strain-compensated heterostructures, and its effect on the local and overall optical properties, has not yet been satisfactorily addressed.

In this work, we use aberration-corrected scanning transmission electron microscopy (STEM) combined with cathodoluminescence (CL) in the STEM to study optical inhomogeneities resulting from various atomic-scale localization centers in red-emitting AlN capped InGaN/GaN QW devices. By probing the spectral response of individual InGaN QWs with nanometer spatial precision, we show that a secondary blueshifted emission originates within the QW near to the AlN interlayer. On the other hand, the presence of criss-crossing inversion domains intrinsically linked to the strain fields surrounding V-pits result in further distinct blueshifts. Finally, high intensity luminescence can be directly correlated to In-rich quantum dots spontaneously nucleated at intersecting V-pit regions. This study highlights the importance of controlling thickness modulation of interlayers and threading dislocation densities to ensure compositional and optical homogeneity in strain-compensated In-rich optoelectronic devices targeted for practical applications. Our results also suggest the nanoscopic origins for the significant emission wavelength shift with injection-current observed in red-emitting devices.

2:00 PM EQ13.16.04

Detection and Suppression of Compositional Fluctuations in InGaN Light Emitting Diodes Tara P. Mishra^{1,2}, Jing-Yang Chung^{1,2}, Zeyu Deng¹, Silvija Gradečak^{1,2,3}, Stephen Pennycook^{1,2} and Pieremanuele Canepa^{1,2}; ¹National University of Singapore, Singapore; ²Singapore-MIT Alliance for Research and Technology, Singapore; ³Massachusetts Institute of Technology, United States

$\text{In}_x\text{Ga}_{1-x}\text{N}$ light-emitting diodes (LEDs) with higher In content have reduced efficiency compared to their lower In counterparts. The origin of this reduction in efficiency is still not fully understood, although compositional fluctuations in $\text{In}_x\text{Ga}_{1-x}\text{N}$ quantum wells have been linked with the efficiency of LEDs. We combined atomic-resolved electron energy loss spectroscopy (EELS) imaging with first-principles multiscale computational models to obtain a statistical distribution of the compositional fluctuations in $\text{In}_x\text{Ga}_{1-x}\text{N}$ LEDs at different indium concentrations. By analyzing a large dataset of EELS data, we obtain the statistical distribution of the compositional fluctuations as a function of the $\text{In}_x\text{Ga}_{1-x}\text{N}$ composition. We show that although lower In content $\text{In}_x\text{Ga}_{1-x}\text{N}$ with $x \sim 18\%$ LEDs mostly show compositional fluctuations in the limit of a random alloy, the distribution of compositional fluctuation drastically changes in $\text{In}_x\text{Ga}_{1-x}\text{N}$ LEDs with higher In content ($\geq 24\%$) [1]. Therefore, a distinctly different mechanism for carrier localization can be expected for $\text{In}_x\text{Ga}_{1-x}\text{N}$ LEDs of different In content, which would ultimately affect the performance of the LEDs [2]. Our theoretical approach directly incorporates strain effects in the $\text{In}_x\text{Ga}_{1-x}\text{N}$ quantum wells, resulting from the epitaxial growth. Based on our theoretical model, we will showcase a new method to prevent compositional fluctuations in higher In content $\text{In}_x\text{Ga}_{1-x}\text{N}$ LEDs.

References:

1. Tara P. Mishra *et al.*, Physical Review Materials **5**, 024605 (2021).
2. C. M. Jones *et al.*, Appl. Phys. Lett **111**, 113501 (2017).

2:15 PM EQ13.16.05

Identification of Extended Defects in Long Wavelength InGaN Light Emitters Jing-Yang Chung^{1,2}, Tara P. Mishra^{1,2}, Govindo Syaranamual¹, Li Zhang¹, Bosman Michel^{2,3}, Stephen Pennycook^{1,2} and Silvija Gradečak^{1,2}; ¹Singapore-MIT Alliance for Research and Technology, Singapore; ²National

University of Singapore, Singapore; ³A*STAR (Agency for Science, Technology and Research), Singapore

Extended defects in In-rich quantum wells (QWs) hamper the fabrication of efficient long-wavelength III-nitride light emitting diodes (LEDs). A detailed understanding on their nature, formation mechanism, and the resulting properties is crucial for the design of more efficient optoelectronic devices. With the advent of 5th order aberration correctors in scanning transmission electron microscopes (STEMs), the direct imaging of atom displacements becomes possible, allowing an unambiguous interpretation of the atomic structure of defects. However, at the moment there is no broad reference for STEM-based atomic-resolution defect classification such as those which exists for conventional TEM.

We demonstrate high-angle annular dark-field (HAADF) depth-sectioning as a convenient tool to distinguish between various defect types in In-rich QWs. We show that different planar defects – the dominant defect type emerging from the QWs – are identifiable by their unique atomic column overlap configurations. Through this method, we reveal that defects commonly identified as edge type dislocations in conventional QWs are instead isolated sub-5-nm type I₂ basal stacking faults (BSFs). Electron energy loss spectroscopy mapping of the QWs suggests the origins of these small diameter BSFs to be local compositional fluctuations, which have theoretically been predicted to increase in QWs with higher strain. Through the engineering of a strain relaxed architecture, we show that a pathway for defect-free long wavelength InGaN LEDs can be achieved.

2:20 PM EQ13.16.07

Bandgap Energies of Cubic Al_xIn_{1-x}N_ySb_{1-y} Calculated by the Dielectric Method Hiroyuki Naoi, Shion Iwai and Rinko Ohara; National Institute of Technology, Wakayama College, Japan

Group III–V quaternary alloy semiconductors are attractive materials due to their capability of covering a relatively wide wavelength range at least between those values of their constituent binary compounds. These alloy systems are also attractive due to their capability of changing their bandgap energies even under a fixed lattice constant [1]. The latter nature furthermore opens a possibility of fabricating high-quality layers of these alloys lattice-matched to an underlying layer or a substrate with a low density of crystal defects.

Among a number of group III–V quaternary alloys, this study is focused on cubic Al_xIn_{1-x}N_ySb_{1-y} in terms of not only a wide range of its usable light wavelengths spanning from the ultraviolet to infrared regions but also its lattice matching ability to Si, GaAs, and GaN substrates. Furthermore, this alloy system can potentially be grown in the cubic phase over the entire composition range, since each of the four constituent binary compounds of this alloy system can be grown in the cubic phase [2, 3]. The large difference in the atomic radius between N and Sb should cause large energy gap bowing. This may lower the minimum bandgap energy value of this alloy system to below that of InSb, which has the lowest bandgap energy value among the four constituent binary compounds.

It should be noted that Sakai et al. calculated bandgap energies of a number of group III–V quaternary alloy semiconductors incorporating Nitrogen as group V element [4] by means of the dielectric method [5–8] using band parameters of the constituent binary compounds. Al_xIn_{1-x}N_ySb_{1-y} was also included in this pioneering and comprehensive work [4]. The band parameters for cubic group–III nitrides were scant at that time and more substantial data has become available in recent years including drastically revised parameters of InN. Furthermore, bandgap energies of cubic Al_xIn_{1-x}N_ySb_{1-y} have not been calculated by other methods to the best of authors' knowledge.

In this study, direct and indirect bandgap energies of cubic Al_xIn_{1-x}N_ySb_{1-y} were calculated by means of the dielectric method [5–8]. We referred to a review article for the lattice constant and the direct and indirect bandgap values of the constituent cubic group–III nitrides, AlN and InN [3]. In contrast with Sakai et al.'s work [4], we show all energy set of interest: Γ -valley direct (E_T), X - Γ indirect (E_X), and L - Γ indirect (E_L) bandgap energies of this alloy system as contour maps. The transition types of this alloy system were also distinguished on the alloy composition space by simply comparing the calculated E_T , E_X , and E_L values.

The calculation results showed that cubic Al_xIn_{1-x}N_ySb_{1-y} converted its band structure from direct to indirect transition types by variation of x and y values. The bandgap range covered in the direct transition regime was between – 5.38 [eV] and 4.60 [eV], indicating that cubic Al_xIn_{1-x}N_ySb_{1-y} can be applicable for optical devices over a wide wavelength range longer than 270 [nm]. Al_xIn_{1-x}N_ySb_{1-y} lattice-matched to either Si or GaAs resulted in having only negative bandgap energies at all possible compositions. On the other hand, Al_xIn_{1-x}N_ySb_{1-y} lattice-matched to GaN was of direct transition type at all possible compositions, with bandgap energies ranging between 2.02 [eV] and 3.81 [eV].

1. Sadao Adachi, *Properties of Semiconductor Alloys: Group-IV, III-V, and II-VI Semiconductors* (WILEY, West Sussex, 2009).
2. I. Vurgaftman, J. R. Meyer, and L. R. Ram-Mohan, *J. Appl. Phys.* **89** 5815 (2001) and references therein.
3. I. Vurgaftman and J. R. Meyer, *J. Appl. Phys.* **94** 3675 (2003) and references therein.
4. S. Sakai, Y. Ueta, and Y. Terauchi, *Jpn. J. Appl. Phys.* **32** 4413 (1993).
5. J. A. Van Vechten, *Phys. Rev.* **182** 891 (1969).
6. J. A. Van Vechten, *Phys. Rev.* **187** 1007 (1969).
7. J. A. Van Vechten, *Phys. Rev.* **B1** 3351 (1970).
8. Y. Ueta, Doctoral Dissertation (The University of Tokushima, March 1995).

SESSION EQ13.17: On-Demand
Sunday Morning, December 5, 2021
On-Demand

8:00 AM EQ13.04.07

Epitaxial Growth and Materials Characterization of Single Crystalline Boron Rich B(Al)N Ternary Alloys Phuong Vuong¹, Adama Mballo¹, Suresh Sundaram², Gilles Patriarche³, Yacine Halfaya⁴, Tarik Moudakir⁴, Simon Gautier⁴, Paul Voss², Jean-Paul Salvestrini^{1,2} and Abdallah Ougazzaden^{2,1}; ¹CNRS, IRL 2958 Georgia Tech, France; ²Georgia Institute of Technology, France; ³CNRS, Centre de Nanosciences et de Nanotechnologies, France; ⁴Institut Lafayette, France

Hexagonal boron nitride (h-BN) is a unique 2D III nitride material. It is interesting for applications in electronics and opto-electronics because of its properties such as high thermal conductivity and a wide bandgap (~ 6eV), and its graphite-like 2-D structure makes it interesting for convenient lift-off of devices. AlN, on the other hand, is the most studied material for applications in the deep UV regime, but its high crystalline quality and p-type doping are challenging. To date there have been few reports of boron-rich BAlN alloys. These alloys may enable choice of the bandgap and facilitate lattice/strain engineering for applications. They would enhance emission efficiency in the deep UV for UV LEDs and allow for the achievement of an electron blocking layer.

In this work, we report the growth of boron rich BAlN alloys with Al content up to 17% on 2-inch sapphire substrates by Metal-Organic Vapor Phase

Epitaxy (MOVPE). Characterization of the surface morphology of BAIN alloys shows a transition stage from a completely 2D to a 3D granular surface when the Al content is increased. A shift in the position of the 002 plane reflection peak to higher diffraction angles in the 2 theta-omega scan along with a decrease in intensity was observed, evidence of the formation of layered BAIN alloys. Cross sectional transmission electron microscopy (TEM) studies demonstrate the formation of a single BAIN hexagonal phase with the presence of wurtzite Al rich BAIN phases in a matrix of layered hexagonal B rich BAIN. A band-to-band transition around 5.86 eV has been observed, which shifted slightly to lower energy with increasing Al incorporation. The bowing parameter in boron rich BAIN alloy systems was evaluated to be around 0.65 ± 0.05 eV. This is encouraging evidence of boron rich BAIN alloy formation, motivating further exploration of growth conditions and the study of fundamental BAIN properties for applications in deep UV optoelectronics.

8:15 AM EQ13.14.03

Matryoshka Phonon Twinning in α -GaN Bin Wei^{1,2,3}, Qingan Cai³, Jiawang Hong¹ and Chen Li³; ¹Beijing Institute of Technology, China; ²Henan Polytechnic University, China; ³University of California, Riverside, United States

Understanding lattice dynamics is crucial for effective thermal management in high-power electronic devices because phonons dominate thermal transport in most semiconductors. This study utilizes complementary inelastic X-ray and neutron scattering techniques and reports the temperature-dependent phonon dynamics of α -GaN, one of the most important third-generation power semiconductors. A prominent Matryoshka phonon dispersion is discovered with the scattering tools and confirmed by the first-principles calculations. Such Matryoshka twinning throughout the three-dimension reciprocal space is demonstrated to amplify the anharmonicity of the related phonon modes through creating abundant three-phonon scattering channels and cutting the phonon lifetime of affected modes by more than 50%. Such phonon topology effectively contributes to the reduction of the in-plane thermal transport, thus the anisotropic thermal conductivity of α -GaN. The results not only have significant implications for engineering the thermal performance and other phonon-related properties of α -GaN, but also offer valuable insights on the role of anomalous phonon topology in thermal transport of other technically important semiconductors.

SYMPOSIUM EQ14

Materials and Devices for Controlling Quantum-Coherent Spin Dynamics
December 1 - December 6, 2021

Symposium Organizers

Lee Bassett, University of Pennsylvania
Marcus Doherty, Australian National University
Danna Freedman, Northwestern University
Bernhard Urbaszek, Institut National des Sciences Appliquées de Toulouse

* Invited Paper

SESSION EQ14.01: Magnonic Materials and Dynamics
Session Chair: Michael Flatté
Wednesday Afternoon, December 1, 2021
Hynes, Level 2, Room 201

1:45 PM *EQ14.01.01

Spin-Magnon Coupling in Ultra-Low Loss Magnetic Resonators Ezekiel Johnston-Halperin; The Ohio State University, United States

The emergence of coherent magnons as a potential transduction channel for coupling remote spin qubits has generated intense interest in both the theoretical limits for these strategies and the practical barriers to their implementation. Here, we present recent progress on both fronts enabled by the emergence of the molecule-based coordination compound vanadium tetracyanoethylene (V[TCNE]_x), an ultra-low loss ferrimagnet with magnetic excitations whose quality factor, Q , exceeds 8,000 (corresponding to a linewidth of 0.51 Oe at 9.86 GHz) and whose Gilbert damping ($\alpha = 4 \times 10^{-5}$) is competitive with highly polished spheres of yttrium iron garnet (YIG). In contrast to other molecule-based materials V[TCNE]_x exhibits a Curie temperature of over 600 K with robust room temperature hysteresis with sharp switching to full saturation. Further, since V[TCNE]_x is grown via chemical vapor deposition (CVD) at 50 C it can be conformally deposited as a thin film on a wide variety of substrates and patterned using electron-beam lithography without introducing additional loss [1]. We will discuss how this combination of properties, coupled with an extremely low saturation magnetization ($M_s = 100$ Oe), allows access to a regime of magnetization dynamics that is theoretically predicted to yield cooperativities in excess of 10 for spin-magnon coupling in realistic device geometries (e.g., micron-scale magnon resonators) [2]. Further, we will present studies of the temperature dependent linewidth that show a modest peak at a temperature of 10 K and a recovery of room-temperature values at 5 K [3]. This behavior is consistent with models of coherent scattering from two level fluctuators (TLF) developed in YIG, but with a sensitivity to TLFs that is roughly 6 times lower. These results indicate the potential for the lowest damping measured in a magnetic system when temperatures are further reduced into the milliKelvin regime. Finally, we will present the results of combined theory-experiment study of the electronic structure of V[TCNE]_x that provides quantitative agreement between density functional theory (DFT) calculations and electron energy loss spectroscopy (EELS) at both the band edge and for core-level atomic

transitions. This study reveals a distinction between apical and planar TCNE for octahedrally coordinated V^{2+} , and provide insight into the aging mechanisms of this material. Taken together, these results demonstrate the unique application potential of $V[TCNE]_x$ for quantum information technologies and provide clear directions for further development and study.

- [1] “Low-damping ferromagnetic resonance in electron-beam patterned, high-Q vanadium tetracyanoethylene magnon cavities” A. Franson, N. Zhu, S. Kurfman, M. Chilcote, D. R. Candido, K. S. Buchanan, M. E. Flatté, H. X. Tang, and E. Johnston-Halperin, *APL Mater.* 7, 121113 (2019).
- [2] “Predicted strong coupling of solid-state spins via a single magnon mode” D. Candido, G. Fuchs, E. Johnston-Halperin, and M.E. Flatté, *Materials for Quantum Technology* 1(1), 011001 (2020).
- [3] “Exploring a quantum-information-relevant magnonic material: Ultralow damping at low temperature in the organic ferrimagnet $V[TCNE]_x$ ” H. Yusufi, M. Chilcote, D. R. Candido, S. Kurfman, D. S. Cormode, Y. Lu, M. E. Flatté, and E. Johnston-Halperin, *AVS Quantum Sci.* 3, 026801 (2021).

2:15 PM EQ14.01.02

Noble Metal Underlayer Influence on the Temperature-Dependent Gilbert Damping in $L1_0$ FePd Films with Large Perpendicular Magnetic Anisotropy Dingbin Huang¹, Delin Zhang², Jian-Ping Wang², Daniel B. Gopman³ and Xiaojia Wang²; ¹University of Minnesota Twin Cities, United States; ²University of Minnesota, United States; ³National Institute of Standards and Technology, United States

The moderate bulk perpendicular magnetic anisotropy (PMA, $K_u \approx 1$ MJ/m³) and low Gilbert damping ($\alpha < 0.01$) make $L1_0$ -FePd a strong candidate for energy-efficient, dense spintronic devices with non-volatility down to 10 nm pitch or even lower. Existing applications subject spintronic devices to a wide temperature operating range from -55°C to 150°C . In order to better address the technological viability of FePd based devices, it is of utmost importance to evaluate the anisotropy strength and Gilbert damping of $L1_0$ -FePd at elevated temperatures. In this work, we examine the impacts of buffer layers (e.g., Cr/Pt, Cr/Ru, and Cr/Rh) on the Gilbert damping and PMA of FePd at elevated temperatures (up to 150°C) using the ultrafast, laser-based time-resolved magneto-optical Kerr effect (TR-MOKE) metrology. Our initial data suggest Cr/Ru has a weaker spin-pumping contribution to α of the FePd layer at RT compared with Cr/Pt and Cr/Rh. However, the Gilbert damping of Cr/Ru/FePd increases faster with temperature compared with that of Cr/Pt/FePd and Cr/Rh/FePd. The buffer/seed layers also affect the reduction of effective anisotropy field ($H_{k,eff}$) at elevated temperatures, which is presumably correlated with the $L1_0$ ordering of the FePd layers.

2:30 PM EQ14.01.03

Raman Spectroscopy, Aging and Laser Patterning of the Low-Loss Ferrimagnet Vanadium Tetracyanoethylene Hil Fung Harry Cheung¹, Michael Chilcote¹, Huma Yusuf², Donley S. Cormode², Yueguang Shi³, Seth Kurfman², Andrew Franson², Michael E. Flatté^{3,4}, Ezekiel Johnston-Halperin² and Gregory Fuchs^{1,5}; ¹Cornell University, United States; ²The Ohio State University, United States; ³The University of Iowa, United States; ⁴Eindhoven University of Technology, Netherlands; ⁵Kavli Institute at Cornell for Nanoscale Science, United States

Vanadium tetracyanoethylene ($V[TCNE]_x$; $x \approx 2$) is an organic-based ferrimagnet with low magnetic damping and compatible with a wide variety of substrates. These properties make it an attractive candidate in the field of coherent magnonics. However, similar to many organic-based materials, $V[TCNE]_x$ is air sensitive. While encapsulation extends its lifetime in ambient conditions from hours to weeks, its aging mechanism is not well understood. Here we use confocal microscopy, microfocused Raman spectroscopy, ferromagnetic resonance, and magnetometry to study $V[TCNE]_x$. We identify key Raman peaks in $V[TCNE]_x$ with C=C, C≡N vibrational modes, which are consistent with *ab initio* theory. We correlate changes in magnetic properties with changes in Raman intensity and in photoluminescence. These results enable optical characterization of local $V[TCNE]_x$ film quality, which is invaluable when local magnetic characterization is not possible. We also find similar changes can be induced by high intensity laser illumination. We utilize this method for laser patterning $V[TCNE]_x$ by selectively removing magnetism and study the damping, anisotropy, and spin wave modes of patterned structures.

2:45 PM EQ14.01.04

First Principles Calculation of the Electronic Structure of $V(TCNE)_2$ Yueguang Shi and Michael E. Flatté; The University of Iowa, United States

Over the past two decades there has been growing interest in organic magnetic materials, due to their potential applications in the field of magnonics and spintronics.[1,2,3,4] Vanadium tetracyanoethylene, $V(TCNE)_2$, is a room temperature ferrimagnetic semiconductor with a $T_c \sim 600$ K [5], which has very low loss ferromagnetic resonance and spin-wave propagation [1,2]. Previous first principles calculations of the electronic structure have indicated an indirect band gap substantially larger (0.8 eV) than experimentally inferred (0.5 eV) [6,7]. The study of Ref. 6 used a local-orbital basis with B3LYP hybrid functional. Here we explore the electronic structure using a plane-wave code VASP [8,9,10] with Perdew-Burke-Ernzerhof (PBE) functionals with Hubbard model corrections, and hybrid functional Heyd-Scuseria-Ernzerhof (HSE06). We confirm that the structure of $VTCNE$ has a triclinic unit cell with each V atom surrounded by 6 organic ligands, as found in Ref. 6. However, in contrast to the previous study we found a direct band gap of 0.4 eV located at a different k-point. This band gap better agrees with the experimental inference from the conductivity activation energy [7]. We also studied magnetic anisotropy, optical properties, elastic properties of $V(TCNE)_2$ and other metal TCNE materials with other metal substitutes. Further studies also involve magnetic dynamics, magnetoelastic properties, and oxidized or doped $V(TCNE)_2$ systems.

We acknowledge funding from NSF Grant No. DMR-1808742.

- [1] H. Yu, M. Harberts, R. Adur, Y. Lu, P. C. Hammel, E. Johnston-Halperin, and A. J. Epstein, *Appl. Phys. Lett.* 105, 012407 (2014).
- [2] N. Zhu, X. Zhang, I. H. Froning, M. E. Flatté, E. Johnston-Halperin, and H. X. Tang, *Appl. Phys. Lett.* 109, 082402 (2016).
- [3] H. Liu, C. Zhang, H. Malissa, M. Groesbeck, M. Kavand, R. McLaughlin, S. Jamali, J. Hao, D. Sun, R. A. Davidson, L. Wojcik, J. S. Miller, C. Boehme, and X. V. Vardeny, *Nat. Mater.* 17, 308–312 (2018).
- [4] A. Franson, N. Zhu, S. Kurfman, M. Chilcote, D. R. Candido, K. S. Buchanan, M. E. Flatte, H. X. Tang, and E. Johnston-Halperin, *APL Materials* 7, 121113 (2019).
- [5] J. M. Manriquez, G. T. Yee, R. S. McLean, A. J. Epstein, and J. S. Miller, *Science* 252, 1415 (1991).
- [6] G. C. De Fusco, L. Pisani, B. Montanari, and N. M. Harrison, *Phys. Rev. B* 79, 085201 (2009).
- [7] V. N. Prigodin, P. R. Nandyala, K. I. Pokhodnya, J. S. Miller, and A. J. Epstein, *Adv. Mater.* 14, 1230 (2002).
- [8] G. Kresse and J. Hafner, *Phys. Rev. B* 47, 558 (1993); *ibid.* 49, 14 251 (1994).
- [9] G. Kresse and J. Furthmüller, *Comput. Mat. Sci.* 6, 15 (1996).
- [10] G. Kresse and J. Furthmüller, *Phys. Rev. B* 54, 11 169 (1996).

3:00 PM BREAK

4:00 PM EQ14.01.05

Corner Spin-Wave Modes of a Tapered $V[TCNE]$ Bar Kwangyul Hu¹, Denis R. Candido¹ and Michael E. Flatté^{1,2}; ¹University of Iowa, United States

States; ²Eindhoven University of Technology, Netherlands

Spin-wave excitations may become highly localized near the edges or surfaces of a magnetic material. Confinement to a small mode volume enhances the magnetic oscillations associated with a single magnon, and thus the local fringe fields that can couple to, e.g., localized spin qubits. This enhancement is critical for achieving high cooperativity spin-magnon transduction and high gate to decoherence ratio spin-spin coupling[1,2]. Localized modes at the edges of a finite magnetic structure originate from internal inhomogeneous demagnetization field at the boundaries[3-6]. For this reason, the edge modes are dependent on the shape of the surfaces and it is possible for the edge modes in non-trivial structures to have unusual properties. Furthermore the nature of these modes may depend strongly on the magnetization of the bar, and low-moment materials have not been extensively explored.

Here we present the spin wave edge modes in a micron-scale magnetic bar of a low-moment material that has tapered edges, with magnetic field in-plane, perpendicular to the bar axis. We used the micromagnetic modeling program MUMAX3[7] to simulate the spin wave excitations. The magnetic material was a low loss semiconducting organic ferrimagnet, V[TCNE] that has a saturation magnetization $M_s=7560$ A/m, an exchange stiffness constant $A_{ex}=2.2\times 10^{-15}$ J/m, a Gilbert damping constant $\alpha=4\times 10^{-5}$ and a gyromagnetic ratio $\gamma=2.7\times 10^{10}$ Hz/T [8]. The results show that it is possible to excite highly-localized corner modes with resonance frequencies above the uniform mode, in contrast to the well-known edge modes of perpendicular-wall bars which have frequencies below the uniform mode. We also performed analytic calculations and obtained similar results based on a formalism for inhomogeneous systems[9]. Our work extends the understanding of spin wave edge dynamics in non-trivial structures and suggests potential applications of these new corner modes with very small mode volume to quantum information science.

*We acknowledge funding from NSF Grant No. DMR-1808742.

- [1] D. R. Candido, G. D. Fuchs, E. Johnston-Halperin and M. E. Flatté, *Mater. Quantum Technol.* **1**, 011001 (2020).
- [2] M. Fukami, D. R. Candido, D. D. Awschalom and M. E. Flatté, arXiv:2101.09220v [quant-ph], (2021).
- [3] J. Jorzick et al., *Phys. Rev. Lett.* **88**, 047240 (2002).
- [4] B. B. Maranville, et al., *J. Appl. Phys.* **99**, 08C703 (2006).
- [5] R. C. McMichael and B. B. Maranville, *Phys. Rev. B.* **74**, 024424 (2006).
- [6] J. Jersch et al., *Appl. Phys. Lett.* **97**, 152502 (2010).
- [7] Vansteenkiste et al., *AIP Adv.* **4**, 107133 (2014).
- [8] A. Franson, et al., *AIP Adv.* **7**, 121113 (2019).
- [9] B. A. Kalinikos and A. N. Slavin, *J. Phys. C: Solid State Phys.* **19**, 7013 (1986).

4:15 PM EQ14.01.06

Time-Resolved Optical Detection of Magnetization Vectors Driven by Pulsed Spin-Orbit Torque Young-Gwan Choi¹ and Gyung-Min Choi^{1,2}; ¹Sungkyunkwan University (SKKU), Korea (the Republic of); ²Institute for Basic Science, Korea (the Republic of)

Spin Hall effect (SHE) driven spin-transfer torque facilitates an efficient manipulation of magnetization with flowing charge current. In aspect of experimental technique, electronic measurement methodologies have widely been used for SHE-driven spin-transfer torque analysis, e.g. Hall measurements, spin transfer ferromagnetic resonance, and so on. However, electronics methods usually detect final static states of the magnetization vector of the ferromagnetic layer, and it is difficult to observe detailed dynamic motion during ultrafast precessional process. Here, we demonstrate a time-resolved technique for pulsed electric current and following pulsed spin torque. We investigate the magnetization precession dynamics, driven by pulsed spin current, by using time-resolved magneto-optical Kerr effect with femtosecond laser. A low-temperature-grown GaAs-based photo-switch can convert an optical pulse to charge current pulse that results in pulsed spin-orbit torque (SOT). We argue that this technique is useful for investigating the current-driven SOT effect in ultrafast time-domain regime.

SESSION EQ14.02: Solid-State Spin Qubits I
Session Chair: Mikey Wojnar
Thursday Morning, December 2, 2021
Hynes, Level 2, Room 201

10:45 AM EQ14.02.02

Suppression of the Optical Linewidth and Spin Decoherence of a Quantum Spin Center in a p-n Diode Denis R. Candido^{1,2} and Michael E. Flatté^{1,2}; ¹The University of Iowa, United States; ²The University of Chicago, United States

We present [1] a quantitative theory of the suppression of the optical linewidth due to charge fluctuation noise in a p-n diode, recently observed in Ref. 2. We connect the local electric field with the voltage across the diode, allowing for the identification of the defect depth from the experimental threshold voltage. Furthermore, we show that an accurate description of the decoherence of such spin centers requires a complete spin-1 formalism that yields a bi-exponential decoherence process, and predict how reduced charge fluctuation noise suppresses the spin center's decoherence rate.

The material is based on work supported by the U.S. Department of Energy, Office of Basic Energy Sciences, under Award Number DE-SC0019250.

- [1] Denis R. Candido and Michael E. Flatté, arXiv:2008.13289
- [2] C. P. Anderson, A. Bourassa et al., *Science* **366**, 1225 (2019).

11:00 AM EQ14.02.03

Single-Shot Readout and Coherence Protection of Novel Qubit States in Hexagonal Boron Nitride Rohit Babar¹, Gergely Barcza², Anton Pershin², Oscar Bulancea Lindvall¹, Örs Legeza², Igor A. Abrikosov¹, Adam Gali² and Viktor Ivady^{1,2,3}; ¹Linköping University, Sweden; ²Wigner Research Centre for Physics, Hungary; ³Max Planck Institute for Physics of Complex Systems, Germany

Point defect qubit sensors in semiconductors have demonstrated their outstanding potential for new discoveries in material science and medicine. The

sensitivity and the spatial resolution of these sensors are currently limited by the distance between the qubit and the target, the spin coherence, and the readout characteristics of the qubit. Here, we report on the peculiar magneto-optical properties and on demand creation of a novel point defect qubit on the surface of hexagonal boron nitride (hBN). The electronic structure of the studied point defect enables optical initialization and single-shot readout of the spin states, while the reported large transverse zero-field splitting gives rise to robust clock transitions between the spin states and elongated coherence time at zero magnetic field. The stress absorption capabilities of the microscopic structure enable further tailoring of the properties of the qubit. Our results thus provide an alternative for advancing nano-scale sensing and magnetic resonance imaging utilizing few layer hBN platforms.

11:15 AM *EQ14.02.04

Probing Spin Dynamics on Diamond Surfaces Using a Single Quantum Sensor [Nathalie P. de Leon](#); Princeton University, United States

Understanding the dynamics of a quantum bit's environment is essential for the realization of practical systems for quantum information processing and metrology. We use single nitrogen-vacancy (NV) centers in diamond to study the dynamics of a disordered spin ensemble at the diamond surface. Specifically, we tune the density of "dark" surface spins to interrogate their contribution to the decoherence of shallow NV center spin qubits. When the average surface spin spacing exceeds the NV center depth, we find that the surface spin contribution to the NV center free induction decay can be described by a stretched exponential with variable power n . We show that these observations are consistent with a model in which the spatial positions of the surface spins are fixed for each measurement, but some of them reconfigure between measurements. In particular, we observe a depth-dependent critical time associated with a dynamical transition from Gaussian ($n=2$) decay to $n=2/3$, and show that this transition arises from the competition between the small decay contributions of many distant spins and strong coupling to a few proximal spins at the surface. These observations demonstrate the potential of a local sensor for understanding complex systems and elucidate pathways for improving and controlling spin qubits at the surface.

SESSION EQ14.03: Spin-Based Quantum Memories

Session Chair: Daniel Laorenza

Thursday Afternoon, December 2, 2021

Hynes, Level 2, Room 201

1:30 PM *EQ14.03.01

Nuclear Spin Quantum Memories in Silicon and SiC [Guido Burkard](#); University of Konstanz, Germany

Nuclear spins in solids show long coherence times and could therefore be employed as quantum memories in quantum processors or quantum networks. However, their good isolation from the environment also makes it challenging to prepare and measure (i.e., write and read) nuclear spins, or to coherently transfer information to and from electronic or photonic qubits. We have developed and modelled a method for the readout of a phosphorous donor nuclear spin by probing the transmission of a microwave resonator coupled to a silicon quantum dot-donor system subjected to a transverse magnetic field gradient. We have identified optimal readout points with strong signal contrast to facilitate the implementation of nuclear spin readout. Furthermore, we investigate the potential for achieving coherent excitation exchange between a nuclear spin qubit and microwave cavity photons. A different approach is possible for transition metal (TM) defects in silicon carbide (SiC) that represent another promising platform in quantum technology, especially because some TM defects emit in the optical spectrum into one of the telecom bands. We present a theory for the interaction of an active electron in the D-shell of a TM defect in SiC with the TM nuclear spin and derive the effective hyperfine tensor within the Kramers doublets formed by the spin-orbit coupling [2]. Based on our theory we discuss the possibility to exchange the nuclear and electron states with potential applications for nuclear spin manipulation and long-lived nuclear-spin based quantum memories.

[1] J. Mielke, J. R. Petta, and G. Burkard, accepted for publication in PRX Quantum [arxiv:2012.01322]

[2] B. Tissot and G. Burkard, arXiv: 2104.12351

2:00 PM EQ14.03.02

Numerical Modeling of Multi-Qubit Spin Dynamics in a Hyperfine Field [Christopher Ciccarino](#) and [Prineha Narang](#); Harvard University, United States

Spins in solid state defects represent promising building blocks for quantum information applications. For these purposes, maintaining the desired quantum state of these spins is crucial, however it is generally not straightforward, as spins can interact with various degrees-of-freedom of the solid state host. In many cases, hyperfine interactions between the electronic spin of the defect and the nuclear spins of the host lattice dominate decoherence. In these scenarios, the cluster-correlation expansion (CCE) method [1,2] has proven to be a useful numerical tool in qualitatively and quantitatively capturing the effective spin coherence of the combined spin-bath system, and more recent generalizations have included population dynamics as well [3]. In this work, we discuss extending this generalized CCE method to capture the spin dynamics of two qubit spins coupled with a common bath of nuclear spins [4]. Using this framework, we evaluate the spin dynamics in a variety of defect qubit candidate systems, where we also consider different defect pair separations, magnetic field strengths, and pulse sequence schemes. We study the interplay of the two qubits and the role of the hyperfine spin bath and highlight particularly important quantum-dynamical processes involved in these various regimes.

1. Yang and Liu, PRB, 78, 085315 (2008)

2. Yang and Liu, PRB, 79, 115320 (2009)

3. Yang et al, Annals of Physics, 413, 168063 (2020)

4. Ciccarino and Narang, in preparation.

SESSION EQ14.04: Quantum Point Defects I

Session Chair: Bernhard Urbaszek

Monday Morning, December 6, 2021

EQ14-Virtual

8:00 AM *EQ14.04.01

Scaling of Quantum Coherence in Solid-State Spin Defects Shun Kanai^{1,1,1}, F. Joseph P. Heremans^{2,3}, Hosung Seo⁴, Gary Wolfowicz^{2,3}, Christopher P. Anderson^{3,3}, Sean Sullivan², Mykyta Onizhuk³, Giulia Galli^{2,3,3}, David Awschalom^{2,3,4} and Hideo Ohno^{1,1,1}; ¹Tohoku University, Japan; ²Argonne National Laboratory, United States; ³University of Chicago, United States; ⁴Ajou University, Korea (the Republic of)

Solid-state defect centers have achieved various quantum functionalities, and further development of their functionalities as well as the expansion of viable qubit material options are critical issues in quantum information science [1-5]. The electron spin coherence time T_2 , is one of the most critical material parameters for defect center qubits. Recently, cluster correlation expansion (CCE) calculations have emerged as a promising tool to simulate the T_2 of materials with dilute spinful nuclei *e.g.*, diamond and SiC [6-10]. Here we show a surprising scaling relationship of T_2 on g -factor, spin quantum number, and the densities of electron and nuclear spins based on the CCE calculations, constituting a simple new tool for the exploration of qubit materials [11]. We calculate T_2 of the well-known qubit materials (*e.g.*, diamond, SiC, and Si) with second-order CCE calculations which include pairwise transitions of the nuclear spins, and show the CCE result agrees well with the experimentally observed T_2 . Especially, the nuclear spin baths are shown to decouple under external magnetic fields typically encountered in experiments (> 30 mT). For a dilute ($< 10^{22}$ cm⁻³) spinful nuclear bath with a single nuclear species, T_2 is proportional to the nuclear spin density $n^{-1.0}$, which reproduces the previous experimental reports. Furthermore, based on the CCE calculations, we calculate the coefficients of $n^{-1.0}$ for all stable nuclear spin species, and find that T_2 of electron spin with spin $S = 1/2$ and electron g -factor $g_e = 1/2$ is expressed by $T_2 = 1.5 \times 10^{18} \times |g|^{-1.6} T^{-1.1} n^{-1.0}$ (seconds), where g is the nuclear spin g -factor and I the nuclear spin quantum number, which we further generalize to the case for the electron spin with $S \neq 1/2$ or $g_e \neq 1/2$, and show that CCE reproduces the experimentally reported T_2 on the known materials. This quantitative and algebraic expression for T_2 offers qubit materials exploration without extensive computations; for example, we obtain the predicted T_2 of over 12,000 qubit host candidates with bandgap > 1 eV, and show that there are more than 700 materials with $T_2 > 1$ ms. Among these, SiC stands out as the only non-chalcogenide [11]. This study will provide a guideline for material exploration and will be an important resource for understanding nuclear spin bath decoherence in lesser-known compounds.

We thank He Ma, Jaewook Lee, and Huijin Park for their help in cross-checking the CCE predictions. This work was supported in part by JSPS Kakenhi Nos. 19KK0130 and 20H02178, the cooperative research of RIEC, the EFRC Center for Novel Pathways to Quantum Coherence in Materials (NPQC) supported by DOE/BES, National Research Foundation of Korea (NRF) grant funded by the Korea government (MSIT) Nos. 2018R1C1B6008980, 2018R1A4A1024157, and 2019M3E4A1078666, AFOSR FA9550-19-1-0358, the Center for Novel Pathways to Quantum Coherence in Materials, and an Energy Frontier Research Center funded by the U.S. Department of Energy, Office of Science, Basic Energy Sciences in collaboration with the U.S. Department of Energy, Office of Science, National Quantum Information Science Research Centers.

References

- [1] J.R. Weber, W.F. Koehl, J.B. Varley *et al.*, Proc. Natl. Acad. Sci. U.S.A. **107**, 8513-8518 (2010).
- [2] J. Wrachtrup, Proc. Natl. Acad. Sci. U.S.A. **107**, 9479-9480 (2010).
- [3] M. Atature *et al.*, Nat. Rev. Mater. **3**, 38-51 (2018).
- [4] A. Alkauskas *et al.*, Nanophotonics **8**, 1863-1865 (2019).
- [5] G. Wolfowicz, F.J. Heremans, C.P. Anderson *et al.*, Nat. Rev. Mater., 1-20 (2021). doi:10.1038/s41578-021-00306-y
- [6] W. Yang and R.B. Liu, Phys. Rev. B **78**, 085315 (2008).
- [7] S.J. Balian *et al.*, Phys. Rev. B **89**, 045403 (2014).
- [8] L. Hall *et al.*, Phys. Rev. B **90**, 075201 (2014).
- [9] H. Seo *et al.*, Nat. Commun. **7**, 12935 (2017).
- [10] M. Onizhuk *et al.*, PRX Quantum **2**, 010311 (2021).
- [11] S. Kanai *et al.*, arXiv 2102.02986 (2021).

8:30 AM EQ14.04.02

Stacking Fault-Qubit Complexes in SiC for Quantum Technology Applications Rohit Babar¹, Viktor Ivády^{1,2,3} and Igor A. Abrikosov¹; ¹Linköping University, Sweden; ²Wigner Research Centre for Physics, Hungary; ³Max Planck Institute for the Physics of Complex Systems, Germany

Spin defect qubits in SiC are strong candidates for scalable quantum communication technology. It is possible to encode and manipulate quantum information in a qubit under optical excitation. However, the qubit properties are often compromised by charge-state instabilities and phonon coupling, which result in diminished spin-initialization fidelity and limited room-temperature operation. Engineering of stacking faults in SiC offers a material-based solution towards stabilizing the qubit charge state at room temperature [1]. In this talk, we theoretically investigate stacking fault-qubit complexes in SiC and demonstrate that the local environment within a stacking fault gives rise to distinct qubit configurations. We report zero-field splitting values above 60 MHz for these complexes, that can further improve the coherence protection scheme achieved for basally oriented qubits in SiC [2]. Further, the calculated magneto-optical and hyperfine parameters can assist in identification of previously unassigned PL signals. Our results demonstrate the quantum-well feature of stacking faults can be exploited to develop robust spin qubits in SiC.

- [1] V. Ivády, J. Davidsson, A. L. Falk, P. V. Klimov, N. T. Son, D. D. Awschalom, I. A. Abrikosov, and A. Galí, Nature Commun. **10**, 5607 (2019)
- [2] K. C. Miao, J. P. Blanton, C. P. Anderson, A. Bourassa, A. L. Crook, G. Wolfowicz, H. Abe, T. Ohshima, D. D. Awschalom, Science **369**, 1493 (2020)

8:45 AM *EQ14.04.03

Spin Coherence and Optical Properties of the Silicon Vacancy in 4H-SiC Samuel G. Carter¹, Hunter B. Banks², Ignas Lekavicius², Oney O. Soykal², Shojan P. Pavunny³, Daniel J. Pennachio², Jenifer R. Hajzus³, Matthew T. Dejarld³, Andrew L. Yeats¹, Peter G. Brereton⁴, Evan R. Glaser¹, Andrew Purdy¹, Edward Bielejec⁵, Rachael Myers-Ward¹, D K. Gaskill^{1,6} and Thomas L. Reinecke¹; ¹U.S. Naval Research Laboratory, United States; ²NRC Research Associate at the U.S. Naval Research Laboratory, United States; ³ASEE Research Associate at the U.S. Naval Research Laboratory, United States; ⁴U.S. Naval Academy, United States; ⁵Sandia National Laboratories, United States; ⁶University of Maryland, United States

Defects in SiC are of significant interest for quantum information and sensing, due to the combination of long spin coherence times, optical spin polarization, and industrial maturity of the material system. The ideal defect system should have long spin coherence times, homogeneous spin and optical transitions, bright emission, and efficient optical initialization and readout. We have characterized many of these spin and optical properties of the V₂ silicon vacancy in 4H-SiC for both single defects and ensembles, showing quite promising results as well as some non-ideal behavior. This defect is notable as it is one of the few that shows spin coherence at room temperature and also has an S=3/2 spin system. For single Si vacancies, we have performed low temperature photoluminescence excitation spectroscopy of the spin-dependent optical transitions, showing two sharp lines with linewidths near the radiative lifetime limit, corresponding to the m_s=±1/2 and m_s=±3/2 spin states. Time resolved measurements show significant differences between these two transitions that we understand and theoretically model in terms of the intersystem crossing, which occurs at different rates for the two spin states and has implications for spin initialization and readout. Spin coherence in this system is strongly influenced by the presence of nuclear spins, despite the low natural abundance of isotopes with nonzero spin. The nuclear spin environment gives rise to inhomogeneous dephasing and strong effects on spin echo measurements, particularly at low magnetic fields. We have grown isotopically purified SiC with a very low abundance of ²⁹Si and ¹³C to strongly suppress

the influence of nuclear spins. Our room temperature spin coherence measurements show large improvements in the coherence times, with particular improvement in the inhomogeneous dephasing time T_2^* , reaching 20 μs in the $m_s = \pm 1/2$ basis. We consider the prospects of this system for quantum sensing and for an efficient spin-photon interface.

This work was supported by the U.S. Office of Naval Research, the OSD Quantum Sciences and Engineering Program, the Defense Threat Reduction Agency, and the Center for Integrated Nanotechnologies, an Office of Science User Facility operated for the U.S. Department of Energy (DOE) Office of Science. Sandia National Laboratories is a multi-mission laboratory managed and operated by National Technology and Engineering Solutions of Sandia, LLC., a wholly owned subsidiary of Honeywell International, Inc., for the U.S. Department of Energy's National Nuclear Security Administration under contract DE-NA-0003525.

9:15 AM *EQ14.04.04

Random-Access Microwave Quantum Memories Joseph Alexander¹, Oscar Kennedy¹, James O'Sullivan¹, Mantas Šimėnas¹, Ana Villanueva Ruiz De Temino¹, Christoph Zollitsch¹, Kamanasish Debnath², Akel Hashim³, Christopher Thomas⁴, Irfan Siddiqi³, Stafford Withington⁴, Klaus Mølmer², Philippe Goldner⁵ and John Morton¹; ¹University College London, United Kingdom; ²Aarhus University, Denmark; ³University of California, Berkeley, United States; ⁴University of Cambridge, United Kingdom; ⁵Chimie Paris Tech–École Nationale Supérieure de Chimie de Paris, France

Quantum memories capable of faithfully storing and recalling quantum states on-demand are powerful ingredients in building quantum networks and quantum information processors. As in conventional computing, key attributes of such memories are high storage density, long storage lifetimes and random access, or the ability to read from or write to an arbitrarily chosen register. However, achieving such random access with quantum memories in a dense, hardware-efficient manner remains a challenge, for example requiring dedicated cavities per qubit or pulsed field gradients.

In this talk I will introduce a variety of spin systems in different host materials that are particularly promising for the realisation of microwave quantum memories, including various donors in silicon and optical defects in YSO. I will present recent progress in extending the spin coherence lifetimes in such systems, which impacts the timescale over which the microwave quantum memory is able to faithfully store coherent states. I will also present a protocol that uses chirped pulses to encode qubits within the spin ensemble, offering both random access and naturally supporting dynamical decoupling to further enhance the memory lifetime. Finally, I will discuss recent progress on the implementation of this protocol using different spin systems.

9:45 AM EQ14.04.05

Development of a Scalable Quantum Memory Platform—Er Doped TiO₂ Thin Films on Silicon Manish Kumar K. Singh¹, Gary Wolfowicz², Jianguo Wen², Abhinav Prakash², Sean Sullivan², Alan Dibos², F. Joseph P. Heremans^{2,1}, David Awschalom^{1,2} and Supratik Guha^{1,2}; ¹University of Chicago, United States; ²Argonne National Laboratory, United States

Recent work exploring rare earth ions as qubits has demonstrated key milestones – such as high cyclicity and high Purcell factor in nanophotonic devices (Raha et al, Nature Comm., 2020) – needed for controlling qubits based on rare earth atoms in a solid-state host. However, the material platform (Er-doped bulk crystals) used in these key studies is difficult to scale and integrate with other semiconductor technology. This capability is necessary for the high qubit densities needed in some advanced quantum applications and thin film host materials that enable scalable deployment is a topic of active research. Here we report on our progress in this direction.

Using the synthesis technique of metal-organic molecular beam epitaxy (MOMBE), we report the growth and characterization of Er-doped TiO₂ thin films – both in single crystal TiO₂ (on r-sapphire and strontium titanate), as well as in polycrystalline films (on silicon). Using XRD and TEM we confirm the dependence of the TiO₂ phase (anatase or rutile) on growth substrate and temperature. The lifetime of the first optical excitation (of Er³⁺) in our films varies with film structure and thickness, ranging from 1 to 1.85 ns in our films. Through low temperature photoluminescence characterization, we obtained an inhomogeneous linewidth of 5.2 GHz (T=3.4 K), which is about an order of magnitude larger than the value of 460 MHz reported on bulk Er-doped TiO₂ crystals (Phenicie et al., ACS Nano, 2019). This linewidth is thermally broadened and should reduce further at lower temperatures. In addition, we find that the linewidth depends on the thickness, and presence of buffer or capping layers, which we describe by an empirical model. Further, measurement of spectral diffusion, which sets the upper limit on the value of T_2^* , is shown to reduce with Er concentration. Altogether, our study explores and presents data that highlight the potential to engineer a solid-state qubit platform using thin film hosts.

SESSION EQ14.05: Quantum Metrology and Simulation

Session Chairs: Lee Bassett and Bernhard Urbaszek

Monday Morning, December 6, 2021

EQ14-Virtual

10:30 AM *EQ14.05.01

Quantum Metrology Using Spins in Diamond Nanostructures and Nanoparticles Helena S. Knowles; University of Cambridge, United Kingdom

Nanoscale quantum probes are a versatile platform for studying solid state and living systems in a non-invasive way. They can be embedded in a sample of interest and can thus provide in situ, nanoscale information, for example from inside thick biological structures such as cells. In this talk, I will present results on using Nitrogen-Vacancy centres (NVs) in diamond nanocrystals and ensembles of NVs in diamond nanobeams for local sensing of magnetic fields and temperature.

First, I will discuss the detection of NMR signals from multiple nuclear species in a (19 nm)³ volume using a versatile NV-NMR device inside a diamond nanocrystal of ~25 nm diameter. Within this volume, we are able to sense ~1000 molecules[1]. These promising devices are robust to photobleaching and environmental changes, have low toxicity, and an ability to measure multiple spin species with high specificity. While the spin concentration extracted from the measured NMR signal amplitude is subject to errors due to the geometric variability of nanodiamonds devices, this error can be corrected for using an in-situ calibration scheme based on exploiting the signal from a thin layer of reference nuclei on the diamond surface. We are also able to perform nanoscale measurements of temperature inside living cells, a key tool for investigating thermogenesis on a sub-cellular level.

Second, I will present a quantum sensor composed of a dense spin ensemble in a diamond nanobeam that operates as a collection of independent, unperturbed sensors working in parallel[2]. We experimentally demonstrate fault-tolerant decoupling of spin-spin interactions, achieving a five-fold enhancement of spin coherence time. This is made possible by a novel dynamical decoupling sequence that simultaneously suppresses disorder,

interactions, and imperfections in control operations[3]. We utilize the extended coherence time to demonstrate an increase in magnetic field sensitivity of over 40% compared to conventional sensing protocols such as the XY8 sequence. These results demonstrate a significant enhancement by breaking the natural interaction limit of dense ensembles, and reveal the potential of tailored control in complex, interacting ensembles.

[1] Holzgrafe et al., *Phys. Rev. Appl.* **13**, 044004 (2020)

[2] Zhou et al., *Phys. Rev. X* **10** 031003 (2020)

[3] Choi et al., *Phys. Rev. X* **10** 031002 (2020)

11:00 AM *EQ14.05.02

Nanoscale Vector AC Magnetometry with a Single Nitrogen-Vacancy Center in Diamond [Paola Cappellaro](#), Guoqing Wang, Yi-Xiang Liu and Yuan Zhu; Massachusetts Institute of Technology, United States

Detection of AC magnetic fields at the nanoscale is critical in applications ranging from fundamental physics to materials science. Isolated nitrogen-vacancy centers in diamond can achieve the desired spatial resolution with high sensitivity. Still, vector AC magnetometry currently relies on using different orientations of an ensemble of sensors, with degraded spatial resolution. Here I will present a novel protocol that exploits a single NV to reconstruct the vectorial components of an AC magnetic field, by tuning a continuous driving to distinct resonance conditions. As an experimental proof-of-principle, I'll show how to map the spatial distribution of an AC field generated by a copper wire on the surface of the diamond. The proposed protocol combines high sensitivity, broad dynamic range, and sensitivity to both coherent and stochastic signals, with broad applications in condensed matter physics.

11:30 AM *EQ14.05.03

A Programmable Quantum Simulator Based on Spins in Diamond [Tim Hugo Taminiau](#); Delft University of Technology, Netherlands

Spins associated to optically active defects in diamond provide a versatile platform for quantum science and technology. In this talk, I will discuss our recent advances in realizing programmable quantum simulators based on individually controllable carbon-13 nuclear spins in diamond. I will present how one can use a single nitrogen-vacancy (NV) centre to detect, characterize and control a large number of nuclear spins in its environment [1,2]. By controlling the interactions between the spins it becomes possible to create a variety of many-body Hamiltonians with tuneable parameters. As an example, I will discuss our investigation of a discrete-time crystal stabilized by many-body localization, a new out-of-equilibrium phase of matter [3].

[1] M. H. Abobeih et al., *Nature* **576**, 411 (2019)

[2] C. E. Bradley et al., *Phys. Rev. X* **9**, 031045 (2019)

[3] J. Randall et al., arXiv:2107.00736 (2021)

SESSION EQ14.06: Quantum Point Defects II

Session Chairs: Lee Bassett and Marcus Doherty

Monday Afternoon, December 6, 2021

EQ14-Virtual

4:00 PM *EQ14.06.01

Coherent Control of Spin Defects in Hexagonal Boron Nitride [Vladimir Dyakonov](#); University of Wuerzburg, Germany

Optically active defects in solids with accessible spin states are promising candidates for quantum applications. While several candidates in 3D crystals including diamond and silicon carbide have been extensively studied, the coherent control of color centers in 2D materials is still an open issue. We recently investigated a bright 850nm fluorescence in irradiated hexagonal boron nitride (hBN) and found it spin-dependent. Using magnetic resonance techniques such as optically detected magnetic resonance (ODMR), we identify this fluorescence associated with a particular defect, a negatively charged boron vacancy V_B^- , possessing a spin triplet ($S=1$) ground state and a zero-field splitting D/h of 3.48 GHz. Moreover, we realized a coherent control of these defects by applying pulsed ODMR protocols. In particular, we measured spin-lattice relaxation time T_1 of 18 μ s and spin coherence time T_2 of 2 μ s at room temperature. T_1 increases by three orders of magnitude at cryogenic temperature following a $T^{-5/2}$ power law, while T_2 remains almost unaffected. Employing electron spin-echo envelope modulation (ESEEM) we were able to separate the quadrupole and hyperfine interactions with the surrounding nuclei. Finally, by applying a two-frequency "hole-burning" technique, we partially decoupled the electronic spin state from its inhomogeneous nuclear environment, which prolonged the spin coherence time by a factor of three. Our results can be important for employment of spin-decorated hBN layers as local probes in hybrid quantum systems, however, requires careful defect and heterostructure engineering.

4:30 PM *EQ14.06.02

Quantum Control of Color Center Spins [Sophia Economou](#); Virginia Tech, United States

Color centers such as the NV, SiV and SnV centers in diamond and vacancy centers in silicon carbide are leading qubits for quantum repeater networks. These systems have a spinful ground state, which is used as a qubit to encode information, optical transitions for spin-photon entanglement and long-range quantum communication, and are coupled to nuclear spin qubits which, given their long coherence times, can be used as an additional memory register. This talk will present high-fidelity designs for entangling gates between the defect and nuclear spin qubits which selectively couple one nuclear spin while decoupling the rest. Optical control protocols tailored to SiV and SnV centers in diamond that overcome cross talk and leakage errors will also be discussed.

5:00 PM EQ14.06.03

Theory and All-Electrical Detection of Spin-Coherent Trap State Dynamics at the Si/SiO₂ Interface [Nicholas Harmon](#)¹, James Ashton², Patrick Lenahan² and Michael E. Flatte³; ¹Coastal Carolina University, United States; ²The Pennsylvania State University, United States; ³University of Iowa, United States

Interfacial trap states have been a subject of study due to the detrimental effect they have on conventional electronic devices (e.g. source of leakage currents). The same states also deleteriously impact quantum coherent devices through spin-spin interactions (when the trap state is paramagnetic) or charge fluctuations. Recently, an upside for interfacial trap states has been discovered [1]: interfacial spins may serve as quantum sensors due to how transport or

recombination through the sensors intimately depends on the local field environment.

In this work, we present theoretical and experimental results determining the role that spin-dependent processes at deep levels plays in governing recombination through interfacial traps. For paramagnetic trap states, capture of electrons or holes is limited by spin statistics. For instance, a neutral trap with $S = 1/2$ only captures spins with opposite orientation (assuming a negatively charged ground state of $S = 0$). These spin-dependent processes are incorporated into a generalized Shockley-Read-Hall model. Magnetic interactions (e.g. hyperfine) at each of the combining spins modify capture efficiency; the probability of capture is determined by solving the stochastic Liouville equation for the spin density matrix. Using this formalism, we calculate magnetoresistance for dangling bond defects at the Si/SiO₂ interface. The results from the model agree well with our experiments measuring recombination current in a Si/SiO₂ MOSFET. Chief among our conclusions is that a large number of nuclei interact with the trap spin which necessitates a semiclassical approximation for the hyperfine interaction. Lastly, we examine how the quantitative theory can be utilized in the service of all-electrical quantum magnetometry using interfacial trap states.

[1] C. J. Cochrane, J. Blackberg, M. A. Anders, P. M. Lenahan, *Phys. Rev. X* **5**, 041023 (2015)

[2] N. J. Harmon, J. P. Ashton, P. M. Lenahan, M. E. Flatté, arXiv:2008.08121v1

The project or effort depicted was or is sponsored by the Department of the Defense, Defense Threat Reduction Agency under Grant HDTRA 1-18-1-0012 and Grant 1-16-0008. The content of the information does not necessarily reflect the position or the policy of the federal government, and no official endorsement should be inferred.

5:45 PM BREAK

SESSION EQ14.07: Coherent Magnonics
Session Chair: Marcus Doherty
Monday Afternoon, December 6, 2021
EQ14-Virtual

6:30 PM *EQ14.07.01

Magneto-Rotation Devices and Spin Current Generation in the Presence of Acoustic Cavities Jorge Puebla¹ and Yoshichika Otani^{1,2}; ¹RIKEN, Japan; ²University of Tokyo, Japan

In this contribution, I present our most recent research on magnon-phonon coupling. A fundamental form of magnon-phonon interaction is an intrinsic property of magnetic materials, the “magnetoelastic coupling.” This form of interaction has been the basis for describing magnetostrictive materials and their applications, where strain induces changes in internal magnetic fields. Unlike magnetoelastic coupling, more than 40 years ago, it was proposed that surface acoustic waves may cause surface magnons via a rotational motion of the lattice in anisotropic magnets [1]. However, a signature of this magnon-phonon coupling mechanism, termed magneto-rotation coupling, has been elusive. We recently demonstrated a nonreciprocal acoustic wave attenuation with an unprecedented ratio of up to 100% rectification, which is understood as a consequence of the magneto-rotation coupling [2]. Considering the broad application of the general acoustic device in sensing, filtering, and information transportation, the intriguing nonreciprocal features of our magneto-rotation devices suggest an extraordinary versatility of acousto-magnetic applications.

As well-known, the coupling of surface acoustic waves with ferromagnetic layers also induces acoustic ferromagnetic resonance, consequently acting as a method of spin current generation [3, 4]. An intriguing scenario is to explore the spin current generation when the strength of magnon-phonon coupling is improved. We have carefully engineered an acoustic wave device in the presence of an acoustic cavity consisting of two acoustic reflectors separated by a distance equal to a multiple of the acoustic wavelength of our device. In our acoustic cavity device, we observed enhancements of up to two times in acoustic ferromagnetic resonance and up to three times more spin current generation than a non-cavity reference device [5]. The apparent discrepancy between the enhancements of energy absorption in acoustic ferromagnetic resonance (two times) and the enhancements of the spin current generation (three times) is an open question. Beyond the enhancement of spin current generation, improvements of magnon-phonon coupling towards the strong coupling regime can have significant consequences such as early on-sets of nonlinear effects, enhancement of magnon propagation length, condensation, and transfer of coherent phase information.

[1] Maekawa and M. Tachiki, Surface acoustic attenuation due to surface spin-wave in ferro- and antiferromagnets AIP Conference Proceedings **29**, 542 (1976)

[2] M. Xu, K. Yamamoto, J. Puebla, K. Baumgaertl, B. Rana, K. Miura, H. Takahashi, D. Grundler, S. Maekawa, Y. Otani, Nonreciprocal surface acoustic wave propagation via magneto-rotation coupling. *Sci. Adv.* **6**, eabb1724 (2020)

[3] M. Xu, J. Puebla, F. Auvray, B. Rana, K. Kondou, and Y. Otani, *Phys. Rev. B* **97**, 180301(R) (2018)

[4] J. Puebla, M. Xu, B. Rana, K. Yamamoto, S. Maekawa, and Y. Otani, *J. Phys. D* **53**, 264002 (2020)

[5] Y. Hwang, J. Puebla, M. Xu, A. Lagarrigue, K. Kondou, and Y. Otani, Enhancement of acoustic spin pumping by acoustic distributed Bragg reflector cavity *Appl. Phys. Lett.* **116**, 252404 (2020)

7:00 PM EQ14.07.02

Phase-Field Simulations on Temperature-Related Behaviors of Skyrmions Yu Wang¹, Takahiro Shimada¹, Shizhe Wu², Yuelin Zhang², Jinxing Zhang², Jie Wang³ and Hiroyuki Hirakata¹; ¹Kyoto University, Japan; ²Beijing Normal University, China; ³Zhejiang University, China

Controlling static and dynamic behaviors of the bubble-like magnetic skyrmion exhibits great potential in the application of spintronics. Especially, as a natural property, temperature plays an important role in the control of skyrmion behaviors. For example, statically, the temperature can lead to the phase transition of the topological magnetic structures (such as skyrmions) by affecting their stability; dynamically, fluctuated or inhomogeneous temperature fields can drive the skyrmion motion. However, due to the limitation of existing hypothesis-based simulation methods, the study of temperature-related behaviors of skyrmions from the perspective of thermodynamic free energy is rare. Here, we developed a temperature-related phase field simulation to predict and explain the skyrmion behaviors in temperature fields. Statically, we demonstrate the skyrmion lattice of a room-temperature ferromagnetic thin film lose the thermal stability near the 340 K, and obtain the temperature-magnetic field-strain phase diagrams of topological structures in MnSi thin film, which consists with the experimental results very well. Dynamically, we study the rectilinear motion of the individual asymmetrical skyrmion driven by temperature gradients, and propose a kinematic equation to describe it. Therefore, these works demonstrate the temperature-related phase field simulation is a reliable method to simulate the skyrmion behaviors in temperature fields, and propose the thermodynamics explanation on both static and dynamic

features of skyrmions, which is anticipated to be the theoretical support for further research about temperature-related behaviors of skyrmions and their potential applications in functional devices.

7:15 PM EQ14.07.03

Direct Neutron Scattering Observation of Spin-Phonon Coupling in Nickel Oxide [Chen Li](#)^{1,1}, Qiyang Sun¹, Lin Jiao² and Doug L. Abernathy²; ¹University of California, Riverside, United States; ²Oak Ridge National Laboratory, United States

Antiferromagnetic (AFM) materials have great potentials for spintronics applications due to their robustness against disturbance. The physics of mutual interactions between lattice and spin degrees of freedom in AFMs, leading to unusual transport phenomena of spin and heat, has been a subject of continuing interest. In the current work, temperature and field dependent inelastic neutron scattering measurement were performed to investigate the magnon-phonon interactions in AFM nickel (II) oxide. Giant phonon anomalies are observed by inelastic neutron scattering in the first Brillouin zone, showing magnon-like behaviors. Atomistic simulation and scattering simulation attribute such anomalies to strong spin-phonon coupling and the broken symmetry of related phonon modes. Such couplings have important implications on the properties of both phonon and spin dynamics. Additionally, the discovery provides a direct approach to quantify such spin-lattice interactions via a revised inelastic neutron scattering formalism.

7:30 PM EQ14.07.04

THz Dynamics of Emerging Low-Dimensional Antiferromagnets [Jun Xiao](#)^{1,2,3}, Chenyi Xia¹, Jake Wisser¹, Yuri Suzuki^{1,2} and Aaron Lindenberg^{1,2}; ¹Stanford University, United States; ²SLAC National Accelerator Laboratory, United States; ³University of Wisconsin–Madison, United States

Antiferromagnets are a type of quantum material where electron exchange interactions result in antiparallel or non-collinear microscopic spin correlations with negligible macroscopic magnetization. Given their low-loss THz magnetic resonance and insensitivity to stray fields, antiferromagnetic spintronics holds great potential in realizing high-speed communications and robust in-memory computing¹. Emerging low-dimensional antiferromagnets such as nanoscale oxide thin films and van der Waals layered materials^{2,3}, are expected to further pave the way for ultimate antiferromagnetic device miniaturization. Here we investigate the THz magnetic dynamics of such novel material systems. Using cryogenic THz emission spectroscopy as a direct probe of the time-dependent magnetization, we observed nontrivial THz signals generated by ultrafast optical pumping of NiO thin films and NiPS₃ crystals. Their unique THz emission dependence as a function of optical fluence, THz polarization, and temperature, shows direct sensitivity to the magnetic ordering symmetry and picosecond spin dynamics. Our findings will advance the understanding of the underlying physics that governs the dissipation and electrodynamics of low-dimensional antiferromagnetic materials with large tunability for ultrafast and compact spintronic devices.

1. Jungwirth, T., Sinova, J., Manchon, A., Martí, X., Wunderlich, J. & Felser, C. The multiple directions of antiferromagnetic spintronics. *Nature Physics* **14**, 200–203, doi:10.1038/s41567-018-0063-6 (2018).

2. Lee, J.-U., Lee, S., Ryoo, J. H., Kang, S., Kim, T. Y., Kim, P., Park, C.-H., Park, J.-G. & Cheong, H. Ising-Type Magnetic Ordering in Atomically Thin FePS₃. *Nano Letters* **16**, 7433–7438, doi:10.1021/acs.nanolett.6b03052 (2016).

3. Kang, S., Kim, K., Kim, B. H., Kim, J., Sim, K. I., Lee, J.-U., Lee, S., Park, K., Yun, S., Kim, T., Nag, A., Walters, A., Garcia-Fernandez, M., Li, J., Chapon, L., Zhou, K.-J., Son, Y.-W., Kim, J. H., Cheong, H. & Park, J.-G. Coherent many-body exciton in van der Waals antiferromagnet NiPS₃. *Nature* **583**, 785–789, doi:10.1038/s41586-020-2520-5 (2020).

7:45 PM EQ14.07.06

Revealing the Origin of the Feature-Rich MEL Response of OLEDs Based on Ordered Singlet-Fission/Triplet-Fusion Materials [Sebastian Engmann](#)^{1,2}, Emily G. Bittle¹, Lee Richter¹, Rawad Hallani^{3,4}, John Anthony⁴ and David Gundlach¹; ¹National Institute of Standards and Technology, United States; ²Theiss Research, United States; ³King Abdullah University of Science and Technology, Saudi Arabia; ⁴University of Kentucky, United States

Magneto-electroluminescence (MEL) is a powerful tool to study singlet fission and triplet fusion dynamics in organic light emitters as the functional form of the MEL response can be qualitatively attributed to the dominant processes within the device. In this study, we will present a quantitative model for the MEL response, valid over a wide current range, and apply it to devices based on Rubrene, and three solution processable anthradithiophene emitters. By varying the chemical motif, we are able to systematically vary the film structure between highly textured, poly-crystalline to amorphous. We find significant diversity in the MEL, with the textured films showing feature-rich MEL responses. We will show that features in the MEL response coincide with field direction dependent crossings of the projections of the coherent triplet pair state onto the singlet state of the spin-Hamiltonian. Furthermore, we will discuss the effect of the film structure on the observable MEL response.

8:00 PM EQ14.07.07

Effectiveness of Different Heat Treatments in Attaining Very Low Gilbert Constant in Sputtered Co₂FeAl Thin Film on Si (100) [Soumyarup Hait](#)¹, Sajid Husain², Vineet Barwal¹, Nanhe K. Gupta¹, Lalit Pandey¹, Peter Svedlindh³ and Sujeet Chaudhary¹; ¹Indian Institute of Technology Delhi, India; ²Mixed Unit Of Physics CNRS, Thales, France; ³Uppsala University, Sweden

The current-driven switching of the magnetization of a ferromagnetic (FM) layer in a multilayer stack continues to be one of the intensively investigated topics of research interest both from the fundamental as well as technological points of view. To achieve the switching with lower (critical) current, it is highly desirable that the FM layer must possess a high value of spin-polarization (such as in Heusler alloys), sufficiently low Gilbert damping α_{int} and preferably low values of both saturation magnetization M_S and anisotropy energies.

In this work, the effectiveness of two different approaches used in growing sputtered FM films suitable for such current induced switching applications is investigated in detail. In particular, the effectiveness of maintaining high substrate temperature (T_S) during deposition versus *in situ* annealing of the films at high temperature (T_A) after sputtering at room temperature is compared with an objective to obtain thin films of Heusler alloy Co₂FeAl (CFA) having optimally low α_{int} and 12–17% smaller M_S by employing ion beam sputtering technique and Si(100) as substrates. In each of the two series of CFA films, appropriately suitable choices of T_S and T_A (lying in 300–773K range) were explored for optimally tailoring their structural, static and dynamic magnetization properties.

Structural studies revealed that although all the CFA films of the two series were polycrystalline but the post-deposition annealed films were structurally optimal with higher density (6.36 ± 0.09 g/cm³) and lower interface roughness (0.48 ± 0.03 nm) compared to the CFA films grown at high T_S (6.23 ± 0.06 g/cm³, 0.61 ± 0.01 nm). While the higher density for the post annealed films is accredited to the removal of the voids at higher T_A , the higher interface roughness of the films grown at higher T_S is attributed to the non-uniform growth of films at higher T_S .

In-plane field-angle dependent longitudinal magneto optical Kerr effect (L-MOKE) study on these CFA films revealed the existence of a coupling between the uniaxial and biaxial magnetic anisotropies, whose origin is attributed to the employed deposition geometry. Contribution of both the anisotropies are separated and the calculations suggest that the uniaxial anisotropy is *dominant* over biaxial anisotropy in all the CFA films.

Ferromagnetic resonance (FMR) spectroscopy measurements, performed in both the field configuration, viz. in-plane as well as out-of-plane, revealed a

lowest value of $1.19 (\pm 0.08) \times 10^{-3}$ of α_{int} in the film post-annealed at 773K. In addition, the observed non-linear relation between the α_{int} and the dynamical 'g'-factor suggests that the contribution of spin-orbit interaction to the damping is far less compared to the damping contribution from the DOS present near the Fermi level. It is remarkable to note that the *as-grown* CFA films sputtered at room temperature exhibited a record lowest value of $1.73 (\pm 0.09) \times 10^{-3}$ of α_{int} . Attainment of such a small value of Gilbert damping and having moderate magnetization in high spin polarized Co_2FeAl Heusler films sputtered on the Si (100) substrate opens up their great application potential in future spintronics devices.

8:15 PM BREAK

SYMPOSIUM EQ15

Soft Matter Materials and Mechanics for Haptic Interfaces
November 30 - December 8, 2021

Symposium Organizers

Bianchi Bianchi, University of Pisa
Charles Dhong, University of Delaware
Marcia O'Malley, William Marsh Rice University
Tristan Trutna, Facebook Reality Labs

Symposium Support

Gold
Reality Labs Research

* Invited Paper

SESSION EQ15.01: Materials for Haptic Interfaces I

Session Chair: Charles Dhong

Tuesday Morning, November 30, 2021

Hynes, Level 1, Room 110

10:30 AM *EQ15.01.02

Robotic Fabrics and Liquid Metal-Based Stretchable Circuits—Two Wearable Technologies for Haptic Interfaces Trevor Buckner, Shanliangzi Liu and [Rebecca Kramer-Bottiglio](#); Yale University, United States

Robotic fabrics and stretchable electronics are broad-category technologies that may play a role in next-generation haptic interfaces. In this talk, we will present two recent works and speculate on their applications to wearables.

First, we will present an implementation of robotic fabrics by integrating functional fibers into conventional fabrics using typical textile manufacturing techniques. We will introduce a set of actuating and variable-stiffness fibers, as well as printable in-fabric sensors, which allow for robotic closed-loop control of everyday fabrics while remaining lightweight and maintaining breathability. By designing actuators, sensors, and structural components that conform to a fiber-based geometry, our methodology shows that simple fabrics can be functionalized to create self-deploying structures, morphing airfoils, and damage-responsive tourniquets, among other wearable and haptic devices.

Second, we will present biphasic Ga-In (bGaIn): a printable, solid-liquid biphasic material that maintains a near-constant resistance under extreme strains; maintains direct, consistent, and stretchable electrical connections with conventional electronic components; and is mechanically stable when applied onto numerous soft materials. bGaIn is produced by thermally treating eutectic GaIn nanoparticles to create a mixture of liquid and crystalline solids. It shows a high initial conductivity of 2.06×10^6 S/m and near-constant resistance at strains over 1,000%. We have employed bGaIn as a stretchable interconnect to interface with commercial electronic components—including resistors, capacitors, light-emitting diodes (LEDs), operational amplifiers, and microcontrollers—by simply pressing the electronics into the bGaIn trace. Using bGaIn vertical interconnect accesses (VIAs) to connect traces on the top and bottom layers, we have converted conventional multilayer PCB designs into stretchable circuit board assemblies (SCBAs) that maintain performance while experiencing large strains. Finally, the applicability of bGaIn stretchable circuits to wearables will be shown with a stretchable signal conditioning circuit integrated into a smart sensing garment.

11:00 AM EQ15.01.03

Measurement of Lateral Force and Slipping Based on Optical Fiber Mechanism [Michael Han](#) and Cindy Harrett; University of Louisville, United States

Humans excel at controlling their gripping force during manipulation tasks so that objects don't slip, while avoiding too-strong pressures that damage soft objects. In this presentation, we develop a soft optical sensor for slipping measurement in gripping applications. The principle is micro-bending of a soft optical fiber by lateral forces and its effect on optical transmission from emitter to receiver. The optical fiber deformation is intensified by a stress-concentrating structure. Based on the data, we describe the empirical relationship between intensity and lateral force with a function.

When it comes to robotic grasping, measuring tactile information is critical for human-like performance. In the case of the human grasping process, cutaneous sensory input determines how grasping forces are modulated. Lateral-force tactile sensors for robotic hands, and sensors that can measure lateral forces experienced in human test cases, will help robots emulate human dexterity in manipulation tasks.

Considering the human case, we need to detect both slipping (lateral forces) and grasping forces (normal forces) in real-time, thereby holding objects with optimum forces—not crushing, but also not dropping the object. In that case, lateral forces and the relative slipping amount provide direct and indirect information for determining slippage and grasping normal force respectively. Therefore, it is natural to identify contact mechanisms, which can provide friction force and normal force information. Furthermore, based on the contact mechanism it can make tactile sensors be designed and analyzed in accordance with the situation.

Because our optic fibers are fabricable and elastic, we can make them available to analyze the contact mechanism assuming under Hooke's laws. In particular, we measured lateral force by using an elastomeric optical fiber through the stress concentrating structure that deforms the fiber in response to the shear forces of the surface. In other words, we investigate the relationship between light power intensity variations and lateral forces and figure out its viability to grasping applications. Moreover, based on the stress concentrating structure, we investigate how variables related to surface contact dynamics depend on applied forces. In this study, the regions of lateral force sensing are in the 1 – 5 cm² range and the detected displacements are on the 1 – 5 mm scale. Although it could be changed by the stress concentrating structure due to its material and configuration, the lateral forces are low under 20N for this displacement range.

11:15 AM *EQ15.01.04

A General Strategy to Impart Electronic Conductivity to Hydrogels Laure V. Kayser; University of Delaware, United States

Human-machine interfaces are increasingly prevalent in society to enhance productivity and performance (e.g., automated driving), aid people with sensory and motor deficiencies (e.g., tactile displays, assistive exoskeletons), and allow remote tasks (e.g., surgery, bomb deactivation). This field, and particularly haptics and robotics, is gradually switching from hard and bulky materials to softer, lightweight, and conformable ones. As such, new electronic materials are needed to enable finer tasks and sensations, more realistic human-machine interactions, and less intrusive assistive devices. Additionally, ionic and electronic conductivity are both required to transduce biological to electronic signals and vice versa. For this purpose, we have developed a general approach to synthesize electronically and ionically conductive hydrogels with tunable mechanical properties. Instead of using rigid metal nanoparticles or stiff conductive polymers, we use a water-soluble derivative of 3,4-ethylene dithiophene (EDOT) functionalized with oligo-ethylene oxide side chains (EDOT-DEG) directly polymerized in a range of hydrogels commonly used for biological interfaces. The resulting conductive hydrogels have low impedance and resistance, and similar mechanical properties as the initial—non-electronically conductive—hydrogels. Importantly, the shape and size of the hydrogel is retained after the polymerization of the conductive PEDOT-DEG polymer. In this presentation, I will share our synthetic approach towards these materials, their characterization, and a vision of how they could address challenges in interfacing electronics with the human body.

SESSION EQ15.02: Materials for Haptic Interfaces II

Session Chair: Tristan Trutna

Tuesday Afternoon, November 30, 2021

Hynes, Level 1, Room 110

1:30 PM EQ15.02.01

Textile-Based Wearable Haptic Devices Barclay J. Umetsu, Jeffrey Berning, Nicolas Escobar, Mark Schara, Zane A. Zook, Marcia K. O'Malley and Daniel J. Preston; Rice University, United States

Wearable haptic devices use intuitive tactile signals to enable alternative pathways for communication in “noisy” environments and immersive virtual reality experiences. These wearable devices often employ rigid electromechanical components, including onboard motors that require gearboxes for appropriate torques in squeeze cues and rotating eccentric masses for vibration cues [1]; incorporation of these rigid components hinders the construction of unobtrusive, comfortable, and lightweight wearables.

Soft haptic devices overcome this limitation by leveraging intrinsic compliances to apply haptic cues while maintaining flexibility and light weight, with most approaches utilizing either (i) compliant pneumatic systems composed of inflatable bladders or (ii) flexible electronic systems. Focusing on the former, typical pneumatic systems are composed of molded elastomers or bonded thermoplastic sheets which create chambers that can apply kinesthetic or tactile feedback when inflated [2]. However, these materials introduce challenges for seamless and discreet integration into everyday wearable devices, clothing, and other attire.

Here, we present a new approach for soft haptics based on textiles bonded with an adhesive thermoplastic. The adhesive thermoplastic allows tunable actuator geometries and strong bonds between textiles. Textiles are low-profile, ubiquitous, and most importantly, comfortable and conformal to the human body [3], and this approach enables easy and inconspicuous integration into clothing because textiles can be sewn into or bonded onto existing garments.

We selectively bond textiles to each other through heat and pressure to define internal bladders and pathways for flow of pressurized air, driving actuation of the haptic devices. The geometry of the customizable bladders facilitates squeeze, stretch, and vibration cues, while the channels route the pressurized air to the actuators through tailored pathways. The addition of a patterned intermediate layer between textiles permits the formation of these features by preventing adhesion in defined locations. Moreover, fluidic and systematic instabilities can be designed and exploited to provide simpler control [4] than existing pneumatic counterparts that rely on bulky electromechanical regulators for actuation [5].

Soft haptic devices based on textiles and fluidic actuation allow facile fabrication and operation, and the ease of integration into everyday garments and wide array of design possibilities highlight a promising strategy for integration in wearable devices. Our textile-based approach to wearable haptics can supplement the more traditional, yet often saturated, modes of communication (visual, aural, etc.) while delivering salient information to a user in an inconspicuous, lightweight, and comfortable manner.

[1] C. Pacchierotti, S. Sinclair, M. Solazzi, A. Frisoli, V. Hayward, and D. Prattichizzo, “Wearable Haptic Systems for the Fingertip and the Hand: Taxonomy, Review, and Perspectives,” *IEEE Transactions on Haptics*, vol. 10, no. 4, pp. 580–600, Oct. 2017, doi: 10.1109/TOH.2017.2689006.

[2] R. Niiyama, D. Rus, and S. Kim, “Pouch Motors: Printable/inflatable soft actuators for robotics,” in *2014 IEEE International Conference on Robotics and Automation (ICRA)*, May 2014, pp. 6332–6337, doi: 10.1109/ICRA.2014.6907793.

[3] V. Sanchez, C. J. Walsh, and R. J. Wood, “Textile Technology for Soft Robotic and Autonomous Garments,” *Advanced Functional Materials*, vol. 31,

no. 6, p. 2008278, 2021, doi: 10.1002/adfm.202008278.

[4] A. Rajappan, B. Jumeat, and D. J. Preston, "Pneumatic soft robots take a step toward autonomy," *Science Robotics*, vol. 6, no. 51, Feb. 2021, doi: 10.1126/scirobotics.abg6994.

[5] E. M. Young, A. H. Memar, P. Agarwal, and N. Colonnese, "Bellowband: A Pneumatic Wristband for Delivering Local Pressure and Vibration," in *2019 IEEE World Haptics Conference (WHC)*, Jul. 2019, pp. 55–60. doi: 10.1109/WHC.2019.8816075.

1:45 PM *EQ15.02.02

Materials for Epidermal Haptic Interfaces [John A. Rogers](#); Northwestern University, United States

Immersive systems for virtual and augmented reality (VR/AR) will transform the way that we interact with computer-generated environments and, by extension, with one another. Interfaces that add spatio-temporally controlled physical sensations to well-developed audio and video components of VR/AR systems will qualitatively enhance the user experience. These technologies have myriad potential uses in remote health care, in prosthetic control, in physical rehabilitation, in social media, in entertainment and in training. This talk summarizes our most recent work in this area, with a focus on concepts in materials science and electrical engineering for thin, soft, lightweight sheets that embed wirelessly powered and addressed arrays of high-speed, millimeter-scale mechanical actuators, capable of gently laminating onto the skin. We highlight the capabilities through several example application areas, and we outline frontier opportunities for continued research.

2:15 PM EQ15.02.03

Smart Knit Textiles for Soft Robotic Garments [Vanessa Sanchez](#), Kausalya Mahadevan, Katia Bertoldi and Robert J. Wood; Harvard University, United States

Soft robotic garments represent a promising approach to provide a wearer with mobile assistance for haptic communication, grasping and reaching, and dynamic thermoregulation [1]. For these devices to be as wearable as everyday clothing, it is necessary for them to be created from compliant, lightweight, breathable, and stretchable materials, and textiles satisfy all of these needs. Textile-based soft robotic components, including sensors, actuators, and integration components (which connect to power and control elements) are gaining traction to enable these properties; however, they are traditionally developed separately using different manufacturing processes due to their diverse requirements in terms of mechanical and electrical properties. In order to build a full robotic garment with distributed sensing and actuation, subcomponents must be manufactured discretely and subsequently connected together using cut-and-sew processing. Such manufacturing strategies increase complexity and also reduce durability by adding potential failure points.

To overcome these challenges, we leverage weft knitting as a strategy to create integrated robotic textile materials. Weft knitting is a single additive manufacturing process that can form monolithic 3D shell shapes out of multiple materials [2,3]. Simultaneously, the ability to vary the knit stitch pattern (including changing stitch symmetry and geometry) and material choice enables mechanical diversity, which is necessary to optimize for separate component needs [4,5]. Here, we investigate the ability of weft knitting to create integrated textile actuators and sensors, and we show how the knit architecture, dictated by stitch pattern, leads to tailorable properties required for these components. Specifically, we explore how the stitch pattern changes knit mechanical properties, including stress-strain behavior and Poisson's ratio, for use in fluidic actuators. We also study how varied knit architectures change the sensitivity, linearity, and range of knit strain sensors. We demonstrate fully integrated robotic textile components (sensors, actuators, and conductive signal lines) based on these strategies.

[1] Sanchez, V., Walsh, C. J., & Wood, R. J. *Advanced Functional Materials*, 31(6), 2021.

[2] Underwood, J. "The Design of 3D Shape Knitted Preforms." RMIT University, 2009.

[3] Hodgins, J., McCann, J., Grow, A., Albaugh, L., Mankoff, J., Matusik, W., & Narayanan, V. *ACM Transactions on Graphics*, 35(4), 2016.

[4] Poincloux, S., Adda-Bedia, M., & Lechenault, F. *Physical Review X*, 8(2), 2018.

[5] Bueno, M. A., & Camillieri, B. Structure and mechanics of knitted fabrics. In *Structure and Mechanics of Textile Fibre Assemblies* (2nd ed.). Elsevier Ltd. 2019

2:30 PM EQ15.02.04

Materials Control of Tactile Sensations for Haptics and Touch Psychophysics [Charles Dhong](#); University of Delaware, United States

For the sense of sight, we can purchase HD screens to recreate nearly any image or movie. For touch, we are not yet able to recreate the variety of sensations from our everyday experiences. However, an accurate and rich recreation of tactile sensations could have broad implications in human machine interfaces, soft robotics, and disability rehabilitation. While most haptic devices rely on reconfigurable bumps or electrical stimulation, one possible avenue we explore for is creating tactile sensations through materials chemistry.

A challenge behind controlling touch is that touch is a complex mechanical event between the finger—a heterogenous and deformable interface—and an object. During touch, friction generated between the finger and object produces a variety of mechanical vibrations, which ultimately forms a tactile perception. In this talk, we describe our efforts to use materials coating to both control touch and to study touch. In the first part, we will discuss our efforts in using silane-derived monolayers and our findings that humans can perceive single atom substitutions within silane-coated silicon wafers, thus opening the possibility for molecular-scale control over touch. In the second part, we use tools from materials chemistry to enable psychophysical investigations on the perception of softness. By creating samples which react to touch in a known manner, we can perform our investigations with high "ecological validity", i.e., perform studies in a manner similar to everyday human exploration. We will discuss our key findings that the perception of softness is universal between subjects, and thus is a repeatable and controllable tactile percept.

2:45 PM *EQ15.02.05

Intrinsically Soft Actuators and a Route to High Density Arrays in Small Form Factors [Robert Shepherd](#); Cornell University, United States

Since the modern concepts for virtual reality and augmented reality were first introduced in the second half of the twentieth century, the field has strived to develop technologies that could create realistic experience for the user to immerse themselves in a fully or partially virtual environment. While there has been great progress in visual and auditory technologies, haptics has seen much slower technological advances. The challenge is because skin has densely packed mechanoreceptors distributed over a very large area with complex topography; devising something as targeted as an audio speaker or television where sensory input is made into something as specific as an ear canal or iris seems to be a more difficult task. To compound the difficulty of a somewhat universal haptic solution, the soft and sensitive nature of the organ makes it difficult to apply solid state electronic solutions that cannot address large areas without causing discomfort. The emerging field of soft robotics, where many actuators and sensors are built from materials science innovations, offers potential solutions towards this challenge. In this article, we first provide an overview of haptic output and input technologies to identify opportunities for soft robotics to provide solutions for haptics. We then introduce mechanisms of intrinsically soft actuators and sensors and discuss soft haptic output and input devices categorized by device form of wearable, graspable, or touchable interfaces. We also review the definition and history of virtual and

augmented reality and show examples of soft haptic devices demonstrated in VR/AR environments. Finally, we will introduce an innovative solution to the multiplexing vs. sensory density problem facing haptics.

3:15 PM EQ15.02.06

Multistable Self-Folding Knit Textiles for Deployable Structures [Kausalya Mahadevan](#), Vanessa Sanchez and Katia Bertoldi; Harvard University, United States

The existing familiarity of textiles makes them ideal for lightweight, breathable, wearable soft robots and shape changing deployable garments. These garments are often manufactured by weft-knitting. The weft-knitting process allows us to alter the topology of a manufactured textile through an infinite number of stitch patterns, which allows for precise control of both the tactile and mechanical properties. We harness the existing symmetry in a knit stitch to manipulate the natural curvature of the material into a self-folding pattern. While traditional knit textiles are monostable and return to a single rest state when a load is removed, we leverage this folding to design a textile with multiple stable configurations. This multistable textile is evaluated by mechanical testing and predicted by a finite element model. We investigate how the distribution of stitches affects both the mechanical properties and the energy landscape of the knit. Understanding the relationship between the stitch pattern and the mechanical properties allows us to tune the behavior of these structures; we can select the switching load and design the shape of the structure in each stable state. By fine tuning the geometric parameters in the structure, we exploit the bistability to realize shape changing garments and deployable structures.

3:30 PM EQ15.02.07

Mixed-Conducting Particulate Composites for High Resolution Human-Machine Interfaces [Han Yu](#), Richard Yao, Claudia Cea and Dion Khodagholy; Columbia University, United States

The ability to decode hand gestures is critical for natural human-machine interaction, immersive virtual reality, and creation of effective prosthetics. Although technologies such as video tracking have been applied for hand gesture recognition, they restrict the user's mobility as they need to capture images of the body with several optical devices surrounding the user, and the cameras must maintain clear line-of-sight with all movements. Therefore, bioelectronics that are able to directly acquire and communicate the electrical activity of the human peripheral nervous system to machines have the potential to overcome these limitations. However, it is challenging to non-invasively acquire high-resolution electrophysiology signals that allow representation of ongoing muscle activity in the body. Effective contact and adhesion between conformable high-density electrodes and human skin are essential for the success of this kind of interface. Here we present a novel device that combines conformable electronics and organic mixed-conducting particulate composites (MCPs) to acquire reliable and high-spatiotemporal resolution muscle activity at the level of individual motor neuron action potentials. We demonstrated that MCP can establish anisotropic conduction with the tissue allowing the creation of high-density conformable electronics for the peripheral nervous system. We developed a 10x12 high density conformable array of electrodes combined with mixed conducting particulate composites with similar particle size as skin roughness to cover approximately 500 mm² of muscle area. We performed electrophysiological recordings in humans and non-human primates while subjects performed predefined tasks and movements. We are able to cluster the acquired action potentials into a large number of putative single motor units (MUs) using a template matching-based clustering algorithm. The action potential firing pattern was then correlated with the corresponding movement to establish a decoding model to allow construction of gestures. As such, our approach facilitates investigation into the neural mechanics of our sensorimotor system and enables creation of effective bioelectronic interfaces.

SESSION EQ15.03: Materials for Haptic Interfaces III

Session Chair: Charles Dhong

Wednesday Morning, December 1, 2021

Hynes, Level 1, Room 110

10:30 AM EQ15.03.01

Hybrid Response Pressure Sensors Nanshu Lu and [Kyoungho Ha](#); The University of Texas at Austin, United States

Soft pressure sensors with high sensitivity over a wide pressure range are required for various applications such as electronic skins for human-mimetic robotics and electronic tattoos for mechanophysiology measurement. In the last decade, most research aiming at increasing the sensitivity of capacitive pressure sensors focused on developing dielectric materials with added air gaps and/or higher dielectric constants. After extensive research, sensitivity has been significantly improved at low pressure range, e.g. 1 kPa, but still decays drastically as the pressure increases. To overcome this challenge, we engineered a soft capacitive pressure sensor based on an electrically conductive porous nanocomposite. The porous nanocomposite was fabricated by molding the mixture of functionalized carbon nanotubes (f-CNT) and Ecoflex out of a nickel (Ni) foam. The nanocomposite was 600- μ m thick and 86% porous with open cells and tubular ligaments. With enough f-CNT doping (e.g. 0.25 wt%), the nanocomposite became electrically conductive with both piezoresistive and piezocapacitive characteristics. An ultrathin dielectric layer was added between the conductive nanocomposite and the electrode to ensure the whole device was still capacitive. This hybrid response pressure sensor (HRPS) was measured to have a sensitivity of 3.13 /kPa within 0-1 kPa, 1.65 /kPa within 1-5 kPa, 1.16 /kPa within 5-10 kPa, 0.68 /kPa within 10-30 kPa, and 0.43 /kPa within 30-50 kPa of pressure ranges. The hybrid response was fully understood through a simplified circuit model, which has been validated by experimental measurements and could be used to determine the optimal f-CNT loading. We have successfully applied this sensor to measure very subtle surface pulse waves of the radial artery, the common carotid artery, and the temporal artery, even under large preloads such as a VR (virtual reality) headset.

10:45 AM EQ15.03.02

Late News: Macro-Assembly of Carbon Nanotube Wrapped Textile Yarn for Multifunctional Wearable Electronic Applications [Md. Milon Hossain](#) and Philip Bradford; North Carolina State University, United States

Carbon nanotube (CNT) is a promising material for multifunctional wearable electronic applications due to their excellent electrical conductivity, low density, and superior strength. However, the shorter length of CNTs and nanoscale dimension restricts them for macro assembly and bulk scale processing. Therefore, different synthesis methods emerged for the macro-assembly of the CNTs. Here we report a solid-state and straightforward process of producing CNT-wrapped textile yarns for multifunctional wearable electronic applications. Highly aligned and millimeter-tall CNTs were synthesized on a quartz substrate by chemical vapor deposition. Two CNTs arrays were placed on a custom-made spinning device, and the textile yarn was inserted as a core. Both the arrays were wrapped over the textile yarns for producing highly conductive and strong yarn.

The produced yarn has a diameter similar to the conventional textile yarns essential for the bulk production of electrodes. Scanning electron microscope (SEM) showed successful wrapping of CNTs over different textile yarns. The CNT-wrapped yarns are suitable for textile processing such as weaving and

knitting, sewing, and embroidering into apparel and have excellent electrical conductivity. Both the strength and conductivity of the CNT-wrapped yarn can be customized for various applications. A 1% thermoplastic polyurethane nanocoating increased packing density by aligning the fibers along the yarn axis and increasing the strength two folds. We have demonstrated the use of the yarns in different multifunctional applications such as motion sensors, powering LEDs and heating garments. The yarn was seamlessly integrated into 3D knitted gloves and used for finger movement detection. The yarn exhibited a large resistance change when the finger was bent and returned to the initial position in relaxing conditions. When the yarn is connected to a power source, the yarn can transfer the power lighting 12V LED. A knitted wrist band was produced for wearable thermotherapy, and when connected to 3V, it can generate heat higher than skin temperature and reach about 46 degrees Celcius. The yarn can also be used as a flexible electrode for different physiological health monitoring such as electrocardiography and electromyography.

SESSION EQ15.04: Materials for Haptic Interfaces IV
Wednesday Afternoon, December 1, 2021
Hynes, Level 1, Room 110

1:30 PM EQ15.04.01

Liquid Crystal Elastomers with Enhanced Directional Actuation to Electric Field Hayden E. Fowler¹, Philipp Rothmund^{2,1}, Christoph Keplinger^{2,1,1} and Timothy White^{1,1}; ¹University of Colorado Boulder, United States; ²Max Planck Institute for Intelligent Systems, Germany

Liquid crystal elastomers (LCEs) are stimuli-responsive materials. Programming the local orientation within LCEs is a promising route to realize 3-D deformations. Recent demonstrations have shown these materials can exhibit exceptional work capacity of upwards of 40 J/kg. However, the inefficient and slow responses of LCEs to heat and light limit the functional integration of these materials in many applications. Electrical control of LCEs continues to be a preferred stimuli for use in actuation. Recently, electromechanical actuation of LCEs at ambient conditions was realized by exploiting the unique mechanical anisotropy (e.g., association of modulus with orientation) of aligned LCEs. By coating both sides of an aligned LCE with compliant electrodes and applying voltage, the LCE film is compressed in its thickness, leading to deformation in the planar area. However, due to the mechanical anisotropy, the LCE deforms preferentially in the lower modulus direction, leading to directional mechanical response in these actuating elements. Here, we are concerned with understanding the role of materials properties on the electromechanical response of LCEs. Using a newly developed materials chemistry and employing established processing methods, reliable electromechanical actuation is realized in LCEs with high mechanical anisotropy and uniaxial actuation strains up to 17.5%. The uniaxial actuation behavior is closely predicted using previously developed theory and the physical materials properties of the LCEs. Response times of 1 Hz are demonstrated. Furthermore, 3-D deformations from flat sheets to cones are demonstrated.

1:45 PM *EQ15.04.02

Organic Haptics—Soft Materials for Artificial Touch Darren J. Lipomi; University of California, San Diego, United States

Human culture is replete with artifacts that interact with the senses of sight, hearing, taste, and smell. Material objects whose purpose is to produce a thoughtful or emotional response through the sense of touch, however, are rare. In this talk, I present my group's recent work on the intersection between the science of soft materials and the science of touch. This field, which we have named "organic haptics," combines active polymers, contact mechanics, and psychophysics. We are beginning to understand the ways in which stick slip friction, adhesion, and capillary forces between planar surfaces and human skin affect the ways materials produce tactile objects in consciousness as mediated by the sense of touch. This work, which combines human subject experiments, laboratory mockups of human skin, and analytical models accounting for friction, has led to several important observations. In particular, we have elucidated the mechanism by which humans can differentiate hydrophilic from hydrophobic surfaces when bulk parameters such as hardness, roughness, and thermal conductivity are held constant. We examined the role of relief structures in the skin—i.e., fingerprints—in determining the human ability to differentiate between surfaces. We have taken the insights from these psychophysical experiments to design new electroactive and ionically conductive materials to produce "actuator skins" whose goal is to produce realistic sensations for applications in tactile therapy, instrumented prostheses, education and training, and virtual and augmented reality.

2:15 PM EQ15.04.03

Microstructured Materials for Controlling the Pressure Response of Soft Optical Skins Michael Portaro, Rio Brittany and Cindy K. Harnett; University of Louisville, United States

Soft optical pressure-mapping elastomeric skins are an intrinsically stretchable and deformable platform for human-like tactile sensing. In this work, we investigate how the microstructure of an elastomer layer controls its light transmission as a function of pressure. Under pressure, voids in a soft, optically-transmissive material will preferentially compress, making the microstructured material densify. Not only do the voids control the tactile feel of the layer, but shrinking surface voids can increase the solid contact area that the elastomer makes with an underlying waveguide core, causing more light to exit the waveguide at the pressure location. Whether the voids are randomly distributed or deterministically placed by molding, the surface takes on new optical and mechanical properties thanks to its microstructure. Developments in this area will lead to all-polymer surfaces that measure and map deformation on a force scale controlled by the material's design.

Optical waveguiding in a core-clad structure requires a cladding that has a lower index of refraction than the core. The refractive index (RI) describes the speed of light in the material, with higher RI materials having higher optical density, shorter wavelengths for a given frequency, and slower light velocity than in a low RI material. The ideal high-index core, low-index cladding structure enables rays with a sufficiently shallow incidence angle to achieve total internal reflection (TIR) at the core-cladding interface, the principle behind long-distance optical fiber communication. Normally the cladding is a solid material. Here, the cladding is an elastomer with RI between 1.4 and 1.6, containing voids: air pockets with RI close to 1. Voids are created using two methods: molding liquid-cure elastomers on micromachined substrates, and incorporating porogens into liquid-cure elastomers.

Two principles apply to these porous materials at different size scales: 1) for large features (> 0.1 micron relative to the 940 nm sensor wavelength in this research), more of the light escapes the core where the cladding is solid compared to where the cladding has a void. Therefore the light loss increases as pressure increases the solid fraction of the total contact area. Scattering and interference also occur at the interfaces between air and solid. 2) For sub-wavelength features (< 0.1 micron), scattering and interference become less of an issue, and the material behaves as a composite with a refractive index somewhere between solid and air, proportional to the solid volume fraction.

To characterize the optical pressure response of these structured materials, we developed an instrument to measure transmission vs. incidence angle as a function of pressure for soft films having thicknesses between 0.5 and 3 millimeters. Applied pressures were in the 0-0.1 MPa (0-15 PSI) range that

humans typically use to manipulate objects. Optical microscopy of molded surfaces, for example a hexagonal array of 180-micron diameter silicone hemispheres (RI=1.41), showed that the solid contact area with a glass slide (RI=1.55) did increase under pressure. We found that increasing pressure on the sample increased the amount of light escaping the glass at incidence angles below the TIR angle for the glass-to-solid elastomer interface.

Changing the designs of the micromachined features might allow one to further tune the pressure response, for example buckling at a threshold pressure or responding to shear forces. The work here was performed on liquid-cure elastomers, but porogens incorporated into 3D printable filaments such as thermoplastic urethane could enable additive manufacturing of microstructured soft optical surfaces without high-resolution printing.

SESSION EQ15.05: Poster Session
Session Chair: Charles Dhong
Wednesday Afternoon, December 1, 2021
8:00 PM - 10:00 PM
Hynes, Level 1, Hall B

EQ15.05.01

Late News: Multilayered Joints with Adjustable Linear and Rotational Stiffnesses via Electro-Stiction Phenomenon Yuri Cho, Hyun-Ki LEE, Mijin KIM and Seung Tae CHOI; Chung-Ang University, Korea (the Republic of)

The electro-stiction phenomenon provides the frictional force between two contacting electrodes covered with high dielectric media, of which an applied electric field produces the Maxwell force to attract the two electrodes. Such an electro-stiction force is mechanically and electrically simple and has a fast response speed. But it requires a relatively high driving voltage. In this study, we developed robotic joints having adjustable linear and rotational stiffnesses by stacking many electro-stiction layers, composed of dielectric film/electrode/frame/electrode/dielectric film. Polyoxymethylene copolymer (POM-C) is used for the frame of thickness 1 mm, and Au is sputtered onto the POM-C frame as the electrode of thickness 24 nm. A relaxor ferroelectric polymer, poly(vinylidene fluoride-trifluoroethylene-chlorotrifluoroethylene (P(VDF-TrFE-CTFE))), is used as the dielectric film material since the electro-stiction force is proportional to the relative permittivity of the dielectric material. The P(VDF-TrFE-CTFE) film is first dip-coated on the Au electrode and frame, followed by lamination of the 5 μm thick P(VDF-TrFE-CTFE) film, which is fabricated by the adhesion-mediated film transfer technique (AMFTT). The multilayered structure is an effective way to produce high electro-stiction force with low driving voltage, but all layers must be kept at a constant distance to attract neighboring layers with the same force. In this study, by extending the edge of the structure, drilling a hole, and aligning many frames through an elastic string, the multilayered frames can be simultaneously controlled with the same applied voltage. Therefore, two bundles of frames can freely slide each other without applied voltage, while they can experience different linear and rotational stiffnesses when the applied voltage is changed.

EQ15.05.02

Transparent Omni-Directional Stretchable Circuit Lines Made by Junction-Free Grid of Expandable Au Lines Minsik Kong and Unyong Jeong; Pohang University of Science and Technology, Korea (the Republic of)

Although various stretchable optoelectronic devices have been reported, omni-directionally stretchable transparent circuit lines have been a great challenge. We engineer the cracks and fabricate highly conductive patterned metal circuit lines in which Au grids are embedded. Au is deposited selectively in the cracks to form a grid without any junction between the grid lines. Since each grid line is expandable under stretching, the circuit lines are stretchable in all the directions. This study shows that a thin coating of Al on the oxide surface enables precise control of the cracks (crack density, crack depth) in the oxide layer. High optical transparency and high stretchability can be achieved simultaneously by controlling the grid density in the circuit line. We integrate light-emitting diodes (LEDs) directly on the circuit lines and demonstrate stable operation under 100% stretching.

EQ15.05.03

Electroluminescent Liquid Dielectric Actuators Using Silica-Coated ZnS:Cu Jae Rim Lee and Byung Yang Lee; Korea University, Korea (the Republic of)

Multifunctional soft actuators can impart soft robots with diverse properties in a limited space, enabling the integration of several functionalities in a single device. Recently, soft electroluminescent actuators have been reported, where a dielectric elastomer is combined with electroluminescent particles under combined AC and DC driving signals. Here, we present an electroluminescent soft actuator that utilizes a liquid dielectric as the active material with EL phosphor particles dispersed in it. By coating the surface of the ZnS with silica, we solved the problem of agglomeration of the ZnS particles in the dielectric liquid, resulting in uniform luminescence throughout the device active region. The soft actuators showed strain values of 34% and maximum EL values of 25 cd/m^2 for a single actuator and over 34 cd/m^2 for five stacked actuators. The strain values are comparable to previous works. We expect our EL actuator devices will be used as new smart components for soft robotics and interactive sensors where external stimulus can be displayed as color signals.

EQ15.05.04

Semi-Crystalline Polymer Films to Probe the Effects of Crystallinity on Tactile Discrimination Abigail Nolin and Charles Dhong; University of Delaware, United States

Human touch is critical to the human experience, especially those with low vision and sensory impaired disorders. The field of haptics aims to design materials that recreate tactile sensation. Sensations in fine touch derive from the dynamic frictional forces that arise at the interface between human skin and the surface of a material, and these forces depend on both pressure and sliding velocity. Current approaches rely on physical controls such as mechanical vibrations, bumps, or pins, but the mechanical forces in fine touch arise from not only physical surface features, but the chemical properties of the material itself. Crystallinity is a classic material structure property used to control the mechanical forces of a material and has wide applicability in many material systems. Semi-crystalline polymers can have both amorphous and crystalline regions, and the degree of crystallinity can be controlled through many processes including annealing the polymer at an ideal crystallization temperature. Crystallinity has well-defined effects on mechanical forces, most notably an increase in modulus, but also has effects on frictional forces. Increasing crystallinity correlates with higher molecular order and higher shear strengths, resulting in lower coefficients of friction and less sensitivity to contact pressure. To connect tactile perception with degree of crystallinity, chemically similar atactic and isotactic polystyrene films were prepared and then annealed to induce crystallization. Films were compared for tactile distinguishability with an in-house mechanical testing set-up and human testing. We demonstrated that humans could distinguish films which differed by only degree of crystallinity as predicted by frictional force curves and characterized through microscopy and GIWAXS. Connecting tactile

discriminability with degree of crystallinity has immediate use in developing switchable haptics devices with materials such as liquid crystal elastomers or conjugated polymers.

EQ15.05.05

Electrochemiluminescence Skin with Piezo-Ionic Effect and Mass Transport Phenomenon [Jong Ik Lee](#)^{1,2}, Hanbin Choi³, Ik-Soo Shin^{4,2}, Do Hwan Kim³ and Moon Sung Kang¹; ¹Sogang University, Korea (the Republic of); ²Graphenide Technology, Korea (the Republic of); ³Hanyang University, Korea (the Republic of); ⁴Soongsil University, Korea (the Republic of)

Electrochemiluminescence (ECL) has been recently exploited to form alternative light-emitting devices, referred to as phenomenon electrochemiluminescence device (ECLD). Unlike conventional light-emitting devices, an ECLD requires mass transfer of oxidants/reductants as well as charge transfer reactions in an electrolytic environment. In this talk, we propose the electronic skin (e-skin) device exploiting the characteristic mass transfer phenomenon within ECLD, as an alternative strategy capable of transducing mechanical stimuli into visual readout rely on ECL. First, we investigate the influence of the mass transfer and electron transfer kinetics on emission of ECLDs. Then, we fabricated an e-skin based on ECL layer employing thermoplastic polyurethane as a matrix polymer. The proposed material platform shows the visco-poroelastic response to mechanical stress, which induces a change in the distribution of the ionic luminophore in the film referred to as the piezo-ionic effect. This piezo-ionic effect is exploited to develop a simple device containing the composite layer sandwiched between two electrodes, which is termed ECL skin. Emission from the ECL skin is examined, which increases with the applied normal-/tensile- stress. Additionally, locally applied stress to the ECL skin is spatially resolved and visualized without the use of spatially distributed arrays of pressure sensors. The simple fabrication and unique operation of the demonstrated ECL skin are expected to provide new insights into the design of materials for human-machine interactive electronic skins.

References

- [1] Electrogenerated Chemiluminescence, Ed: Bard, A. J. Marcel Dekker, New York, 2004.
- [2] Kang, M. S. et al. ACS Appl. Mater. Interfaces 2018, 10, 48, 41562–41569
- [3] Kim, D. H. et al. Nat. Commun. 2019, 10, 1, 1-13
- [4] Kang, M. S. et al. ACS Photonics 2018, 5, 2, 267–277

Keywords: electrochemiluminescence; light-emitting device; light-emitting electrochemical cells; ionic liquid

SESSION EQ15.06: Soft Matter Materials and Mechanics in Haptic Interfaces I

Session Chair: Charles Dhong

Monday Afternoon, December 6, 2021

EQ15-Virtual

4:00 PM EQ15.06.02

Reconfigurable 3D Structures of Spatially Programmed Liquid Crystal Elastomers and Their Ferromagnetic Composites Yi Li and [Xueju Wang](#); University of Connecticut, United States

Reversible programming of 3D soft mesostructures is desired for many applications including soft robotics and biomedical devices. The large, reversible shape changes of liquid crystal elastomers (LCEs), which result from the coupling between the alignment of liquid crystal (LC) molecules and the macroscopic deformation of polymer networks, have attracted much attention for such applications. In this talk, I will discuss our recent effort in developing a facile and versatile strategy to create reconfigurable, freestanding 3D mesostructures of LCEs and magnetic LCE composites that are inaccessible with existing techniques via spatially programming LC molecules. Experimental and theoretical results of more than 20 reconfigurable 3D LCE mesostructures of diverse configurations and their large, reversible shape-switching behaviors over multiple cycles will be demonstrated. In addition, an LCE gripper and a robot of ferromagnetic LCE composites that simultaneously responds to magnetic and thermal stimuli for diverse biomimetic behaviors, especially crawling underneath a narrow crack, will be used to illustrate the integration of other functional materials to LCEs for multifunctional systems.

4:15 PM *EQ15.06.03

Tactile Sensing and Perception for Human–Robot Systems [Veronica Santos](#); University of California, Los Angeles, United States

The sense of touch is vital for any system in which humans use machines to physically interact with the world. An artificial sense of touch is especially useful when complementary sensory modalities, such as vision, are limited or unavailable. I will highlight past and present work to enhance the functionality of artificial hands in human-robot systems. I will describe our efforts to develop multimodal tactile sensor skins and our experiences with a variety of deformable, low-cost and commercially available tactile sensor designs. I will discuss the use of machine learning to perceive tactile directionality and salient geometric features, along with a tactile perception pipeline for haptically locating objects buried in granular media. Finally, I will present work in which reinforcement learning is used for the tactile-driven manipulation of deformable objects, such as sheets of paper, ziplock bags, and computer cables. Real-time tactile perception and decision-making capabilities could be used to advance semi-autonomous robot systems and reduce the cognitive burden on human teleoperators for applications that include assistive technology, manufacturing, the handling of dangerous materials, and remote healthcare and work in space.

4:45 PM EQ15.06.04

Increasing Performance of Soft Dielectric Elastomer Artificial Muscles via Nanomaterial Composite Electrical Insulators Max Herzog, [Maduran Palaniswamy](#), Chuck Rutledge, Shardul S. Panwar, Michael Jones and Michael P. Rowe; Toyota Research Institute of North America, United States

The fields of soft robotics and human-machine interfaces are rapidly evolving but are still limited by the commercial viability of soft actuator technologies. When compared against other soft actuators (e.g. shape-memory alloys, pneumatics/hydraulics), dielectric elastomers provide a superior balance between performance metrics like actuation frequency, stroke length, and implementation hardware but fall short when comparing force output. Additional benefits of dielectric elastomers are that they are compliant, low profile, lightweight, and scalable, making them ideal in wearable, e-textile, and haptic interface platforms. The force output of dielectric elastomer artificial muscles depends on a few key parameters (e.g. electrode area, dielectric fluid volume, applied voltage, geometry of thin-films); it is well known that increasing the dielectric constant of the electrically insulating materials within the actuator has a nominally linear relationship to force output, but it is challenging to access high-dielectric polymers that can be used in artificial muscle fabrication.

Diverging away from homo- and co-polymers, high dielectric constants can be alternatively accessed through nanomaterial composite films. This methodology allows for the use of high-dielectric inorganic materials (which are typically very rigid) in soft robotic applications. Inorganic nanomaterial composites using titanium dioxide, Fe_3O_4 , and barium titanate were formed in a sandwich structure with polymer layers of biaxially-oriented polypropylene and poly(ethylacrylate acrylamide). Composites consisting of conductive, organic nanomaterials (e.g. graphene, carbon nanotubes) and their combinations with inorganic materials were also fabricated. The microstructure, composition, and electrical properties of these nanomaterial composite films were analyzed using scanning electron microscopy (SEM), Raman and FT-IR spectroscopy, and capacitance measurements. Changes in the dielectric constant were measured indirectly through material property analysis and mechanical studies of the artificial muscle actuator performance. These modifications showed artificial muscle maximum force output improvements greater than 2.5x compared to control muscles without nanomaterial incorporation. Actuator performance gains were in spite of any added thickness to the electrical insulators from the addition of nanomaterial. Efforts to decrease dielectric relaxation time and increase the actuator duty cycle by using a graphene-doped titanium dioxide nanomaterial composite found that conductive carbon can have a dramatic impact on performance. These nanomaterial composite advancements are particularly attractive because their drop-in quality allows for application in artificial muscle technologies without impacting existing actuator design. Such fundamental material insights push the field of soft robotics towards improving real-world human-machine interactions.

5:00 PM EQ15.06.05

Effect of the Magnetic Field-Assisted Synthesis of PVB/ Fe_2O_3 Magnetic Polymers Films on the Magnetic Properties for Haptic Actuators [Sara Gomez](#), Beatriz C. Lopez-Walle and Edgar Reyes-Melo; Universidad Autonoma de Nuevo Leon, Mexico

Haptic actuator research presents a challenge correlating fundamental knowledge between the properties of the materials and their behaviour on haptic systems. Specifically, the analysis of the magnetic properties of magnetic polymers produced by assisting the synthesis process with a magnetic field is still promising. In this work, magnetic polymer films (thickness: ~ 0.020 mm) were made by the *in situ* synthesis of iron oxide nanoparticles (Fe_2O_3) in a polymeric matrix of polyvinyl butyral (PVB). This synthesis is performed by applying a constant magnetic field during the nucleation and growth of the Fe_2O_3 nanoparticles. Consequently, an increase in the reaction time was also necessary during this process. Therefore, a change in the magnetic properties (and the magnetic response) of the resulting magnetic polymer films was obtained. The magnetic characterization of the resulting PVB/ Fe_2O_3 magnetic polymer films was performed using a vibrating sample magnetometer (VSM). The magnetization curves showed that in samples produced without the magnetic field, the maximum magnetic magnetization is similar (about 0.89 emu/g) and, in samples obtained with the magnetic field, the maximum magnetic magnetization is different (from 0.32 emu/g to 0.66 emu/g). Thereby, the orientation of the magnetic field could have affected the maximum magnetic magnetization. These results will improve the use of magnetic actuators in haptic systems like soft robots for manipulating actuators, aquatic actuators, or mimic animals.

5:15 PM EQ15.04.04

Failure Mechanisms of Embedded Flexible Strain Sensors for Soft Robotics [Akshay Kakar](#), Derrick Banerjee, Edward M. Sabolsky and Kostas Sierros; West Virginia University, United States

Flexible sensors are being used in a variety of applications such as biomedical, textile robotics, and wearable devices. The ability of the sensors to function while deformed proves their adaptability for being implemented into various soft robotic structures, which makes them more desirable than conventional rigid sensors. Therefore, it is important to study the mechanisms through which the sensors reach their functional limits and begin to fail. In this study, we used PDMS as the matrix and silver-based ink for printing linear strain sensors. The sensors with varying vol.% of binder, dispersant, and solvent were embedded using two methods: lay-up and direct-writing. The failure mechanisms of these sensors were then studied based on the electro-mechanical performances, deformation tolerance, and durability while under varying levels of tension and compression using a universal testing machine. The desirable ink composition and fabrication method were evaluated based on the sensor's conductivity, stretchability, bendability, and longevity.

5:30 PM EQ15.08.04

A Soft Neuromorphic Mechanosensor Using Ferromagnets [Si Li](#), Hian Hian See, Aeree Kim, Jingyi Yang, Kelu Yu and Benjamin C. Tee; National University of Singapore, Singapore

Mechanosensors in biological somatosensory system encode mechanical stimuli into electrical pulse (i.e. action potential) for tactile perception and learning. Inspired by the nature of biological action potentials, we present a soft neuromorphic mechanosensor that enable robust tactile application even in aquatic environments. The soft ferromagnetic material in the mechanosensors generates electrical pulses under external stimuli. The decoded responses from the specific pulse sequences exhibit a highly linear function with the mechanical stimuli. Assisted with machine learning algorithms, we achieved high accuracy multi-pixel differentiation and underwater object recognition in robotic and flexible human-machine interface applications. We anticipate that this new soft neuromorphic mechanosensor will potentially enable new forms of robots and human-machine interfaces.

SESSION EQ15.07: Soft Matter Materials and Mechanics in Haptic Interfaces II

Session Chair: Charles Dhong
Tuesday Morning, December 7, 2021
EQ15-Virtual

10:30 AM *EQ15.07.01

Deciphering Physical Cues and Dimensions that Underlie Our Sense of Compliance [Gregory J. Gerling](#); University of Virginia, United States

Mobile phones, tablets, and watches have become a normal part of everyday life. The next generation of devices will enable touch feedback, become flexible, and extend increasingly rich and immersive interactions into virtual reality. Remote touch interactions will convey an object's compliance, or softness, as with fruits such as plums and tissues such as skin. In addition to applications in entertainment and personal productivity, such interactions will enable surgeons to distinguish gallbladder and prostate tissue and ducts from fat and bone, small children to feel a parent's hand, and consumers to inspect and compare products, clothing, and work pieces. While promising new possibilities, the displays under development do not yet feel natural. They also face severe limitations in terms of weight, power, and actuation range. To inform devices to replicate naturalistic interactions of this sort, we have been working to define how the finger pad must deform in space and time to adequately convey a natural sense of compliance.

Object softness, of which compliance is one major dimension, is thought to be encoded by relationships of force, displacement, and contact area at the finger pad. This talk will describe work to understand how time-dependent cues, or information in the rate of change of skin over a spatial field, govern the

encoding of compliance. To do so, we have first developed experimental devices to control the force, indentation, and or their rates in passive touch. We concurrently developed an ink-based method to measure biomechanical contact of the finger pad. Human-subjects studies show that temporal, force-rate cues are more efficient in discriminating compliances, by reducing the amount of deformation of the finger pad and stimulus, which aligns with ongoing skin remodeling. To further study force-rate cues, but under an active touch paradigm, we developed a compliance illusion by introducing spheres of various elasticities and curvatures, derived from finite element simulations of the finger pad. The illusion is that participants cannot discriminate, in passive touch, spheres that are small and compliant versus large and stiff, which generate equivalent contact areas. In active touch, however, participants easily discriminate these spheres, and may utilize cues tied to proprioceptive joint angle, the rate of change of contact area, or surface penetration depth. This special case tells us that our perception of softness is a product of both sensation and volition, and depends upon both afferents in skin and proprioception. To further evaluate these cues, we developed a stereo imaging technique to capture skin deformation while interacting with objects of varied elasticity. We have also standardized a way to characterize the elasticity of test stimuli used by others in similar studies and begun to study ecological interactions with naturalistic fruits in order to reproduce observed skin deformation with dynamic displays.

11:00 AM *EQ15.07.04

OPEN DISCUSSION: Organic Haptics—Soft Materials for Artificial Touch [Darren J. Lipomi](#); University of California, San Diego, United States

Open Discussion

11:30 AM EQ15.07.02

Tactile perception of micro-structured materials [Roland Bennewitz](#); INM - Leibniz Inst for New Materials, Germany

Roughness at the micrometer scale has been identified as a key tactile dimension in the haptic perception of materials. There is a longstanding tradition to create well-defined surface structures with the goal to elucidate mechanisms underlying roughness perception. We will discuss results of two tactile perception studies with micro-structured stimuli.

Randomly rough surfaces were created by 3D printing with independently varied topography and spectral distribution of roughness. We found that the tactile perception of similarity follows the amplitude of roughness at smaller length scale rather than the topographic resemblance. The interaction between surface asperities and fingertip skin led to higher friction for higher microscale roughness. Individual friction data allowed us to construct a psychometric curve which relates similarity decisions to differences in friction [1].

We also produced fibrillar samples from materials with varying elastic modulus. The perception of similarity between samples with different fibril length and different elastic modulus followed the bending of the sub-millimeter scale fibrils, which were arranged in regular arrays on the surface.

[1] R. Sahli, A. Prot, A. Wang, M.H. Müser, M. Piovarči, P. Didyk, R. Bennewitz, Tactile perception of randomly rough surfaces, Scientific Reports, 10 (2020) 15800.

11:45 AM *EQ15.07.03

Self-Healable Soft Materials for Sensing and Actuation [Benjamin C. Tee](#); National University of Singapore, Singapore

Haptic devices can elicit sensations remotely or in virtual environments. Sensing and actuation are required in order to digitize real world interactions and transmit it to an actuation device or system. In this talk, I will discuss strategies to enable soft electromagnetic materials to sense the environment and simultaneously actuate. Such materials can potentially be made self-healable, and allow for mechanical recovery in performance despite mechanical damage. Repair can be effected simply by mechanical contact of the damage areas. It is envisioned that such materials can be useful in the growing field of haptic devices and systems.

12:15 PM EQ15.08.05

Soft Rubbery Electronics and Sensors for Robotics [Cunjiang Yu](#); University of Houston, United States

Soft sensory devices that mimic the human skin with multiple sensors spatially distributed to extract information in a temporal manner are technically challenging yet promising for many emerging applications from haptic interfaces, to medical robotics and to skin prosthesis among others. Although drastic advances already been made in developing various soft devices with various functions, one of the long-lasting challenges is to have biology-similar materials and structures to physically mimic the human skin. This presentation will introduce rubbery electronics, which is a new type of electronics with skin/tissue-like softness and mechanical stretchability, constructed all based on elastic rubbery electronic materials. The innovations in rubbery electronic materials and devices set the foundation for rubbery electronics, integrated system and their broad usages, such as active matrix based tactile sensory skins, soft neurobotics, etc. This presentation will introduce fully rubbery based active matrix tactile sensory skin that is able to sense the touch spatiotemporally that could be equipped for various robotics and robotic interfaces. This presentation will also demonstrate a soft neurobotics which is constructed with neurologic function integrated skin on soft robotics to decode the external interactions into neurological signals for decision making.

SESSION EQ15.08: Soft Matter Materials and Mechanics in Haptic Interfaces III

Session Chair: Tristan Trutna

Tuesday Afternoon, December 7, 2021

EQ15-Virtual

1:00 PM EQ15.08.01

Increased Performance by Matching Electric Fields from Triboelectric and Ferroelectric Charges in Nanogenerators [Linards Lapčinskis](#)¹, Kaspars Malnieks¹, Artis Linarts¹, Kaspars Pudzs² and Andris Sutka¹; ¹Riga Technical University, Latvia; ²Institute of Solid State Physics, Latvia

The field related to triboelectric nanogenerator (TENG) devices is emerging rapidly by continuously presenting new original and creative TENG concepts for conversion of mechanical energy into electricity.¹ The working principle of TENG is straightforward - upon contact-separation or sliding of two triboelectric material (often polymer) coated electrodes surface charges are formed on the triboelectric materials, which induce an electrostatic charge on the conductive electrodes. As electrodes move, a potential difference is created causing a current flow in the external electric circuit. Evidently, TENG devices can be used as excellent self-powered force sensors and haptic sensor arrays.^{2,3} Up to now devices have been integrated into a range of objects - fabrics,⁴ wearables,⁵ interior objects,⁶ and even implantable devices.⁷

Additionally embedding ferroelectric dipoles in contacting polymer layers is known to effectively enhance the performance of TENG. However, dipoles can form also between the opposite triboelectric surface charges on the contacting ferroelectric films. Up to now this similarity has been neglected in the

relevant studies. Our research demonstrates that proper attention to the alignment of the distinct dipoles present between two contacting surfaces and in composite polymer/BaTiO₃ ferroelectric films can lead to up to four times higher energy and power density output compared with cases when dipole arrangement is mismatched. For example, TENG device based on PVAc/BaTiO₃ shows energy density increase from 32.4 μJ m⁻² to 132.9 μJ m⁻² when comparing devices with matched and mismatched triboelectric and ferroelectric dipoles. The presented strategy and understanding of resulting stronger electrostatic induction in the contacting layers enable the development of TENG devices with greatly enhanced properties. Greater generated energy allows easier integration with MEMS and since the output signal is stronger - more precise electromechanical response and sensing.

References:

1. *Sci. Technol. Adv. Mater.* 2019; 20: 758-773
2. *Nano Energy* 2021; 79: 105431
3. *Nano Energy* 2020; 78: 105266
4. *ACS Appl. Mater. Interfaces.* 2014; 6: 14695-14701
5. *Adv. Mater.* 2015; 27: 2367-2376
6. *Sci. Rep.* 2016; 6: 22253
7. *Nat. Commun.* 2018; 9: 5349

1:05 PM EQ15.08.02

Multi-Stimuli Responsive Reduced Graphene Oxide Patterned Azo-Liquid Crystalline Polymer Networks for Stretchable Electronics with Tailored Morphologies Woongbi Cho¹, Jisoo Jeon¹, Wonsik Eom², Tae Hee Han² and Jeong Jae Wie¹; ¹Inha University, Korea (the Republic of); ²Hanyang University, Korea (the Republic of)

The concept of 'kirigami' has been of interest in the field of stretchable electronics because the kirigami patterned structure can increase the degree of freedom for deformation beyond the intrinsic limits of the original material. Furthermore, shape-reconfiguration of tunable electronics can be achieved by the introduction of kirigami-engineered design for programmable materials such as azo-benzene functionalized liquid crystalline polymer networks (azo-LCN). In this presentation, we introduce a facile coating process for patterned reduced graphene oxide (rGO) as well as integration of the patterned rGO along with shape-reconfigurable azo-LCN. The rGO patterned azo-LCN (azo-LCN/rGO) demonstrates about 500 % higher storage modulus of 6.4 GPa than neat azo-LCN (1.3 GPa) and an electrical conductivity of 380 S cm⁻¹ at 4 times the number of rGO coating cycles. In addition, multi-stimuli (i.e. UV, NIR, focused solar ray, and direct heat) responsive actuation of azo-LCN/rGO is achieved by photochemical isomerization of azobenzene moiety in conjunction with the coefficient of thermal expansion (CTE) mismatch via photothermal effects. In particular, the convolution of photochemical and photothermal effects provides enhanced actuation performance of the azo-LCN/rGO bilayer from the neat azo-LCN monoliths. Finally, the kirigami pattern allows the azo-LCN/rGO to endure a higher strain beyond the strain capacity of azo-LCN/rGO without permanent damages to its own body or deterioration of electrical performance. The kirigami-engineered azo-LCN/rGO demonstrates passive, active and hybrid types of shape-morphing under mechanical tension, UV, and simultaneous stimuli of UV and tension, respectively. Toward shape-reconfigurable and stretchable electronics, we demonstrate UV-induced shape-morphing of the kirigami-engineered azo-LCN followed by 60 % of mechanical strain by tension without increase in electrical resistance.

1:10 PM EQ15.08.03

Wearable Haptic Feedback Based on Electrohydraulic Actuators Yitian Shao; Max Planck Institute for Intelligent Systems, Germany

Current virtual reality (VR) techniques can provide synthesized graphics and sounds that allow the user to explore the virtual world but permit comparatively limited haptic feedback. One challenge frequently encountered by wearable haptics designers is the dilemma between the need for generating sufficiently large haptic signals and the desire for keeping the device small and lightweight for better wearability. Indeed, a bulky and heavy haptic device may constrain the movement of the user and cause fatigue. Actuators made from smart materials can have high power-to-weight ratio and therefore can provide sufficient haptic feedback with limited size and weight.

Here, we present our recent design of a wearable haptic device made from electrohydraulic actuators [1]. The device consists of a flat dielectric pouch filled with liquid dielectric. Six pairs of hydrogel electrodes are attached to opposite sides of the pouch and enclosed by insulating rubber. Made from soft and compliant materials, the device can be attached to the skin as a body-worn haptic interface. Voltage applied to any pair of hydrogel electrodes generates electrostatic force, which closes the gap and displaces the liquid dielectric between them. Activation of multiple pairs of electrodes can produce both static and dynamic spatial patterns to provide feedback to a large area of the skin. The device is thin (< 3.5 mm), lightweight (< 35 grams), and capable of producing substantial displacement (> 2 mm) and forces (> 0.8 N) for haptic feedback. The wearability of the device allows long-term usage in VR systems. Since the feedback provides a softness feeling, potential applications of the device include wearable interfaces for social haptics and medical training simulators in VR. Currently, in our unpublished work, we further improved the design to enable more complex haptic feedback patterns, larger displacement and force output, and full portability of the whole system.

[1] Yitian Shao, Siyuan Ma, Sang Ho Yoon, Yon Visell, and James Holbery, "Surfaceflow: Large area haptic display via compliant liquid dielectric actuators". In 2020 IEEE Haptics Symposium (HAPTICS), pp. 815-820.

1:15 PM *EQ15.08.06

Haptics—Emerging Material Technologies and Touch Interaction Yon Visell; University of California, Santa Barbara, United States

Haptics refers to our capacities for touch perception and physical interaction with our surroundings. Haptic technologies hold the potential to transform how we interact within environments that are increasingly interwoven with digital information. However, technologies for furnishing tactile information to the skin, our largest sensory organ, are rudimentary when compared with biological capabilities. I will describe the challenges involved in characterizing and engineering for the human sense of touch. I will discuss recent research in my lab that aims to meet these challenges through research on haptics and emerging material technologies, including several projects that elucidate key synergies between materials, mechanics, and capabilities of biological and engineered systems, and how this research is yielding new technologies for haptics and robotics.

1:45 PM BREAK

1:50 PM EQ15.08.08

Spatial Independent Zone for Body-Motion Unaffected Haptic Sensors Chanho Jeong and Tae-il Kim; Sungkyunkwan University, Korea (the Republic of)

Haptic sensors are devices for measuring any physical quantities that can be received from a tactile sense. They measure from temperature, pressure to their advanced concepts such as roughness, vibration, pain, etc. Most haptic sensors are designed to be placed close to the skin for the purpose of haptic. This

can be attributed to the tremendous development of 2D flexible devices. Despite such advanced haptic sensors, haptic sensors always suffer from motion noise. Even though the sensor reads the necessary data, it is mixed with noise and cannot transmit meaningful information. Accordingly, many researchers tried to solve the problem with various ideas such as strain/bending insensitive pressure sensors, uni-directional sensors, decoupled strain-temperature sensors, etc., and published quite meaningful research results. However, another difficulty arises when the different sensors studied in their own methods need to be combined once more to be used in the complex sensing system of the haptic.

Unlike previous studies, we did not focus on the sensor itself, but rather focused on the surrounding environment where the haptic sensors are located. Haptic sensors are mostly in the form of a flexible film in order to be close to the skin, and are affected by the relaxation, contraction, and bending of the skin. Here, we have focused on stress-transformation in this skin. In an environment where only one-way normal force of contraction and relaxation is applied, such as skin, stress transformation shows that there is a region where stress in a specific direction does not exist. At this time, it is necessary to focus on the fact that most flexible sensors are in the form of a 2D film and have little reactivity to normal stress acting perpendicular to the 2D film unless they have a bi-layer structure. From the perspective of research up to now, it was taken for granted that the flexible sensor was located on the same surface as the skin surface due to the morphological factor of the 2D film. This is the most vulnerable positioning method to the force transmitted by contraction and relaxation. However, even though it is a 2D film, it is a different story if it maintains a different angle from the skin surface. The force transmitted from the skin can be made to act in a direction in which the sensor does not respond. Taking advantage of this, we found a specific area that stress from the dynamic motion does not affect the device. In this area, the strain sensor is insensitive to contraction, tension, and bending, but reacts sensitively to the external pressure that must be read as a real tactile sense. Furthermore, since this study is not limited to sensors, it can be applied to universal 2d flexible sensors. Therefore, we performed a measurement experiment with a 2d temperature sensor in the corresponding area. It was possible to measure the desired temperature without being affected by motion noise.

Our research was more about the environment surrounds the strain sensor rather than the sensor itself. It means it is applicable to many other already-made sensors without an additional device.

1:55 PM EQ15.08.09

Chemical Heterogeneity in Grafted Particle Nanocomposites Measured in Rheology Di Wu and Pinar Akcora; Stevens Institute of Technology, United States

Structural and chemical heterogeneity around nanoparticles have strong influences on mechanical properties of nanocomposites. The phase stability of polymer grafted nanoparticles in polymer melt is governed by the mixing of chemically different polymers in the particle-polymer interfacial regions. In this work, poly(methyl methacrylate) (PMMA)-grafted Fe_3O_4 nanoparticles with the same grafting density but with two different chain lengths are synthesized and dispersed in poly(methyl acrylate) (PMA) at different molecular weights. The mechanical responses of the composites are measured in rheometer. The grafted particle composites exhibit the higher rubber plateau modulus than adsorbed samples. This is attributed to the higher number of segments interacting with the matrix chains, and this conformational factor on interfacial layers on nanoparticles tune thermal-stiffening and reinforcement of composites. It was found that intermediate molecular weight of grafted chains reinforces the composite better at high temperatures. For both long and short grafted particles, rubber plateau modulus and entanglement density decreased due to phase separation of grafted particles. Moreover, the interface entanglements recover and re-entangle more with the large deformation experiments with the short graft and matrix chains.

2:00 PM *EQ15.08.10

Open Discussion—Materials Control of Tactile Sensations for Haptics and Touch Charles Dhong; University of Delaware, United States

Open Discussion

2:30 PM *EQ15.04.05

Soft Robotics for Haptics—Industrial Perspective on Challenges and Philosophy Yigit Menguc^{1,2}; ¹Facebook, United States; ²Oregon State University, United States

Our coordination and convergence challenges in industrial soft robotics are defined by task uniqueness (no one has ever tried to do what we do) and expansive multidisciplinary (...→chemistry→materials→mechanics→design→...). Such an environment makes it hard to scope and align research for the individual scientists, engineers, and designers, and makes prioritizing the work ambiguous for the academic and industrial organization.

The history of scientific discovery highlights certain research teams (Bell Labs, PARC, Rad Lab) that implemented strategic organizational and tactical behavioral innovations that lead to a culture of convergence. All research may be considered on a two dimensional space defined by the axes of Fundamental↔Applied and Curiosity-Driven↔Use-Inspired. Industrial soft roboticists are working in the quadrant of Fundamental, Use-Inspired research — called Pasteur's Quadrant — that is neither pure basic nor pure applied research.

Much like academia, industrial research into soft robotics is based on the fundamental questions that push each subsystem forward. The anatomy of soft robots spans actuators, sensors, control, power, and the mechanical structural (skin, bone, etc). The divergence between academia and industry is in terms of value assigned to system integration and to reliability/replicability. System integration is often considered technical and without intellectual merit, yet the gaps in human knowledge around holistic system design is vast -- especially in soft robotics. Risk assessment, balancing, and mitigation drive much of the industrial research portfolio management -- and a major attribute of this process is assessing the reliability and replicability of novel technology. The current academic incentive for novelty and first-to-press discounts the value of replicability/reliability that drives industrial research. Strengthening the alignment and bridging the divergence between academy-industry must be our goal in soft robotics research if it is to broadly translate its impact to society.

SESSION EQ15.09: Soft Matter Materials and Mechanics in Haptic Interfaces IV

Session Chair: Charles Dhong

Wednesday Morning, December 8, 2021

EQ15-Virtual

10:30 AM EQ15.09.01

3D and 4D Printing of Stimuli-Responsive Materials and Actuation Devices Rigoberto C. Advincula^{1,2,3}; ¹Case Western Reserve University, United States; ²The University of Tennessee, Knoxville, United States; ³Oak Ridge National Laboratory, United States

The use of 3D printing for rapid prototyping of functional and biocompatible polymeric materials enables new functionality of polymeric materials for

devices useful in flexible and wearable electronics. The use of thermoplastics, thermosets, and elastomers based on their outstanding thermo-mechanical properties have to be married with their 3D printability. In addition, for actual biomedical device applications, their in-vivo or in-vitro functions have to be considered. A number of 3D printing methodologies (FDM, SLA, SLS, VSP) can make use of new blended or formulated compositions that incorporated stimuli-responsiveness. Herein, we demonstrate the ability to deploy 3D and 4D printing methods of designed (materials and geometry) polymer materials. This will be demonstrated in the following: 1) biomedical grade thermoplastic polyurethanes (TPU) with compatibility to mammalian NIH 3T3 cells and elastomeric response. 2) Shape-memory polybenzoxazine-epoxy polymers that enable T and P response, and 3) Actuator devices to measure mechanical response in motion detection. The 4D printing allows the design of new materials and applications based on integrating the chemistry of conversion with the printing mode. For example, these materials have been printed via viscous extrusion printing (VEP) or VSP and then converted to an elastomeric actuating material with very high cyclic compressibility. Other work based on the use of SLA, SLS, FDM, towards high strength nanocomposite and biomaterials will also be discussed.

10:45 AM *EQ15.09.02

Active Haptics in Clothing—Approaches and Obstacles for Designing Soft Wearable Systems Lucy Dunne; University of Minnesota, United States

Textile- and clothing-based haptic systems remain a persistent challenge for research and industry. Integrating mechanical actuation into structures with variable and unpredictable geometry and mechanics is a new level of complexity for system design. The field of flexible electronics has afforded a degree of conformability to electronic devices, but does not yet meet the 3D drapability or comfort requirements expected of clothing-like wearability, particularly for systems that require simultaneous access to many parts of the body. Developing effective wearable haptic systems requires accommodating many facets of user and system needs, which are often in conflict. This talk will explore challenges and current approaches related to: haptic modalities in clothing; fabrication and manufacture of soft actuation devices; understanding and affording perceptibility of actuators in clothing systems; sizing and fit across a user population; and balancing the comfort/functionality tradeoffs in system design.

11:15 AM EQ15.09.03

Stretchable Printed Giant Magnetoresistive Sensors for On-Skin Interactive Electronics Eduardo Sergio Oliveros Mata¹, Minjeong Ha², Gilbert Santiago Cañón Bermúdez¹, Yevhen Zabala^{1,3}, Juergen Fassbender¹ and Denys Makarov¹; ¹Helmholtz-Zentrum Dresden-Rossendorf, Germany; ²Electronics and Telecommunications Research Institute, Korea (the Republic of); ³Polish Academy of Sciences, Poland

Printed electronics are expected to be implemented as a set of industrial technologies that will facilitate the on-demand fabrication of imperceptible^[1] and shapeable^[2] devices. Conductive pastes are typically composed of polymeric matrices with embedded conductive fillers. The properties of the fillers can be exploited to deliver functional devices as printed transistors^[3], displays^[4], and sensors^[5]. The smart integration of such elements will allow task-specific integration in consumer electronics and even personalized wearable devices.

Aiming to develop on-skin printed interfaces, it is necessary to ponder mechanical, performance, and health safety considerations. Integrating magnetic sensors on interactive platforms is attractive due to their touchless, action-at-distance nature, which increases the reliability of the devices^[6]. In the past, solution processable magnetic field sensors have been fabricated from composite pastes embedding magnetic particles. Among the previous reports on printable magnetic sensors^[7], there are not examples of devices able to maintain high performance sensing during usual skin deformations. Concomitantly, there is a lack of research on skin-compliant printed magnetic sensors able to perform below the 40 mT safety continuous exposure threshold established by the World Health Organization^[8].

Here, we will present the fabrication and implementation of stretchable printed magnetic field sensors. They are based on composite pastes with embedded flakes of [Py/Cu]₃₀ Giant Magnetoresistance (GMR) thin-film stacks. We demonstrated printed GMR sensors on ultrathin (3- μ m-thick Mylar) foils which are skin compliant, and with maximum sensitivity at 0.88 mT. The stretchable sensors maintained stable sensing performance at 16 μ m bending radius and 100 % strain which corresponds to two orders of magnitude increase with respect to previous reports. We demonstrate the implementation of the technology on interactive applications after laminating the printed sensors on the user's skin to navigate through digital maps and scroll through text documents. The ability of the sensor to comply with the skin creases and deformations, and to detect field changes in the safe threshold limit, place this technology as a prospective method for fabricating on-demand printed human-machine interfaces^[9].

[1] M. Melzer et al., *Nat. Commun.* **6**, 6080 (2015)

[2] D. Makarov et al., *Appl. Phys. Rev.* **3**, 011101 (2016)

[3] J.A. Lim et al., *Adv. Func. Mater.* **20**, 3292 (2010)

[4] S. Cho et al. *ACS Appl. Mater. Interfaces* **9**, 44096 (2017)

[5] X. Wang et al. *ACS Appl. Mater. Interfaces* **10**, 7371 (2018)

[6] P. Makushsko et al., *Adv. Func. Mater.*, 2101089 (2021)

[7] E.S. Oliveros Mata, et al. *Appl. Phys. A* **127**, 280 (2021)

[8] Static Fields. *World Health Organization*. (2006)

[9] M. Ha, E.S. Oliveros Mata, et al. *Adv. Mater.* **33**, 2005521 (2021)

11:30 AM *EQ15.09.04

Haptic Illusions from Soft Wearable Haptic Devices Allison Okamura; Stanford University, United States

Haptic devices allow touch-based information transfer between humans and intelligent systems, enabling communication in a salient but private manner that frees other sensory channels. For such devices to become ubiquitous, they must be intuitive and unobtrusive – properties that can be achieved using soft materials that interface comfortably with the body. The amount of information that can be transmitted through touch is limited in large part by the location, distribution, and sensitivity of human mechanoreceptors. Not surprisingly, many haptic devices are designed to be held or worn at the highly sensitive fingertips, yet stimulation using a device attached to the fingertips precludes natural use of the hands. In this talk, we will explore the design of haptic feedback mechanisms that can be worn on the body, which achieve compelling haptic stimulation using a combination of soft robotics approaches and an understanding of human haptic illusions.

In creating wearable soft haptic devices, one can consider an approach that transmits information through many contacts, taking advantage of “unused real estate” on the surface of the skin to deliver haptic cues over a large area. One example uses a sequence of discrete contacts delivered to the forearm by pneumatic pouches attached to a growing haptic device constructed from flexible low-density polyethylene, called HapWRAP. Controlled air flow through tubes and pouches allows HapWRAP to grow out of a compact housing unit and provide a combination of directional and force feedback to a user. When activated, HapWRAP grows up and around the forearm; its loops form a temporary sleeve. After growth, pneumatic actuators inflate and deflate to stimulate mechanoreceptors in the skin at distinguishable locations, or in sequence to allow the haptic illusion of a traveling contact on the skin.

Alternatively, a wearable haptic device can use a single contact, but apply multi-modal feedback and/or multiple degrees of freedom of simulation to transmit information to the user. We created a multi-modal haptic device with a rigid rotational housing and three soft fiber-constrained linear pneumatic actuators. Soft pneumatic actuators were used because of their compliance, light weight, and simplicity, while rigid components provided robust and precise control. The soft pneumatic actuators provide linear horizontal and vertical movements, and the rigid housing, affixed to a motor, provides rotational movement of the tacter. The device can produce normal, shear, vibration, and torsion skin deformation cues by combining the movement of the soft pneumatic actuators with the rotational housing. The device generates haptic illusions in that the skin deformation, which is inherently tactile in nature, can generate the sensation of a world-grounded force applied to the arm.

12:00 PM *EQ15.03.03

Actuation Requirements for Maximizing Information Transmission Through the Skin Hong Z. Tan; Purdue University, United States

This talk will present an information-theoretical approach to maximizing information transmission through haptic displays. While the talk will not focus on soft materials per se, it will provide the engineering specifications for actuation materials and mechanisms based on psychophysical data. Our past research over several decades have provided empirical evidence that the human skin is capable of receiving complex information at a rate of at least 12 bits/s, a rate that is significantly above the demonstrated performance of most haptic displays. A major challenge is the lack of suitable actuation mechanisms for wearable haptic displays.

I will cover the following topics in this talk:

- 1) The need for an information-theoretical approach to haptic interface research;
- 2) The derivation of 12 bits/s from natural tactile speech communication methods;
- 3) Guidelines for maximizing information transmission based on empirical evidence;
- 4) Recent success in transmitting English words via a tactile sleeve with an embedded array of broadband actuators.

I will conclude the talk with a set of engineering specifications for soft materials and mechanisms capable of delivering broadband actuation on the skin surface to achieve high information transmission rates.

SYMPOSIUM EQ16

Infrared and Thermal Photonic Materials and Their Applications
November 30 - December 8, 2021

Symposium Organizers

Svetlana Boriskina, Massachusetts Institute of Technology
Artur Davoyan, University of California, Los Angeles
Zhe Fei, Iowa State University of Science and Technology
Georgia Papadakis, ICFO – Institute of Photonic Sciences

* Invited Paper

SESSION EQ16.01: Near Field Heat Transfer
Session Chairs: Svetlana Boriskina and Artur Davoyan
Tuesday Morning, November 30, 2021
Hynes, Level 1, Room 102

10:30 AM *EQ16.01.01

Near-Field Heat Transfer in Non-Hermitian Many-Body Systems Philippe Ben-Abdallah; Université Paris-Saclay, France

In this talk I will discuss some thermomagnetic effects for radiative heat exchanges in non-Hermitian many-body systems [1]. Contrary to Hermitian systems, the non-Hermitian systems are optically non-reciprocal. This breaking of symmetry gives rise to some singular radiative behaviors that we detail in this talk.

The first effect is a thermal analog of Hall effect [2] which exists in magneto-optical networks in presence of an external magnetic field. This effect consists in the appearance of a temperature gradient and therefore a heat flux transversally to the direction of a primary temperature gradient.

The second effect is a giant thermal magneto-resistance [3] within these systems. Similarly to the famous magnetoresistance [4] reported in ferromagnetic/normal metal multilayers, variations of thermal resistance of about 50% has been highlighted in nanoparticle networks with magnetic fields of magnitude of 500mT opening so the way to an ultrafast tunability of heat transfers mediated by an external field.

Next we analyze the radiative heat transfers in Weyl semimetals networks. Contrary to magneto-optical systems these Weyl networks are intrinsically non-reciprocal even without applied magnetic field. Hence an anomalous Hall effect [5] can exist in these media.

To finish we discuss some potential applications for these effects to control heat flux at nanoscale and to cool down solids using an external magnetic field.

References :

- [1] S.-A. Biehs, R. Messina, P. S. Venkataram, A. W. Rodriguez, J. C. Cuevas and P. Ben-Abdallah, *Rev. Mod. Phys.*, **93**, 025009 (2021).
- [2] P. Ben-Abdallah, *Phys. Rev. Lett.* **116**, 084301 (2016).
- [3] I. Latella and P. Ben-Abdallah, *Phys. Rev. Lett.* **118**, 173902 (2017).
- [4] M. N. Baibich, J. M. Broto, A. Fert, F. Nguyen Van Dau, F. Petroff, P. Etienne, G. Creuzet, A. Friederich, and J. Chazelas, *Phys. Rev. Lett.* **61**, 2472 (1988).
- [5] A. Ott, S.-A. Biehs and P. Ben-Abdallah, Anomalous photon thermal Hall effect, *Phys. Rev. B* **101**, 241411 (2020).

11:00 AM EQ16.01.02

Tuning the Spectrum of Near-Field Thermal Radiation Using Quantum Dots [Saman Zare](#) and Sheila Edalatpour; University of Maine, United States

Thermal emission observed at sub-wavelength distances from the emitting medium is referred to as the near-field thermal radiation. Thermal radiation in the near-field regime can exceed the far-field blackbody limit by orders of magnitude and be quasi-monochromatic. These unique properties of near-field thermal radiation have attracted significant attention for many potential applications such as waste heat recovery using thermophotovoltaic devices, near-field photonic cooling, and thermal rectification. Most of near-field applications require tuning the spectrum of near-field thermal radiation. So far, the near-field spectra are tuned by engineering materials at the sub-wavelength scale. These sub-wavelength-engineered materials are referred to as metamaterial. Thermal emission by metamaterials, which is significantly different from that of the corresponding bulk materials, can be tuned by modifying the geometry and size of the sub-wavelength features in the material. In this study, we propose tuning the spectrum of near-field thermal radiation by engineering the materials at the quantum scale. We show that modulating the electronic structure of materials by capitalizing on the quantum confinement effect provides a powerful mechanism for tuning the peak location of near-field thermal radiation.

For this purpose, we calculate the local density of states (LDOS) thermally emitted by lead chalcogenide quantum dots (QDs) of various diameters ranging from 3.3 nm to 6.8 nm at a near-field distance from the QDs. To find the thermal LDOS, the size-dependent dielectric function of the QDs is extracted from their measured absorbance spectra using the Maxwell-Garnett effective medium theory, the Kramers-Kronig relation and an optimization technique. The thermal discrete dipole approximation is used for finding the LDOS based on the framework of fluctuational electrodynamics and using the extracted dielectric function data. The thermal LDOS emitted by periodic and random arrays of QDs shows a peak around the bandgap energy of the QDs. The bandgap energy, which is affected by the quantum confinement in the QDs, can be tuned by changing the size and thus the level of quantum confinement of the QDs. The wavenumber of the peak LDOS emitted by PbS QDs can be shifted by up to 4490 cm^{-1} by changing the diameter of the QDs from 3.7 nm to 6.8 nm. It is also demonstrated that the peak location of the near-field radiative heat transfer between two arrays of QDs shows the same level of tuning as the thermally emitted LDOS.

Acknowledgment:

This work is supported by the National Science Foundation under Grant No. CBET-1804360.

11:15 AM EQ16.01.03

Exploring Near-Field Enhanced Electrical Power Output in an Efficient Thermophotovoltaic Energy Conversion System [Rohith Mittapally](#), Byungjun Lee, Linxiao Zhu, Ju Won Lim, Dejiu Fan, Stephen R. Forrest, Pramod Sangi Reddy and Edgar Meyhofer; University of Michigan, United States

Thermal radiation from a hot body is well described by Planck's law. However, Planck's law is not applicable when the gap size or the characteristic dimensions of the involved objects are much smaller than the thermal wavelength. Specifically, when a hot and a cold object are placed at nanoscale gaps, orders of magnitude enhancement in the radiative energy transfer is expected due to contributions from the evanescent waves. This can dramatically enhance the performance of thermophotovoltaic (TPV) energy conversion, which involves a hot emitter radiating photons that excite electron hole pairs in a photovoltaic (PV) cell. The performance of a TPV system can be characterized by the electrical power density and the efficiency of the radiative energy conversion. Recent TPV studies in the far-field demonstrated impressively high efficiencies (~30%) but at low power densities due to operation in the far-field. Several theoretical proposals have shown that dramatic enhancement in power density can be achieved by reducing the gap to tens of nanometers. However, such demonstrations have been challenging due to difficulties in maintaining nano-gap separations between a hot emitter (>1000 K) and a cold cell (~300 K). In this talk, we will first describe the development of micro-fabricated doped silicon emitters that can be resistively heated to temperatures as high as 1270 K. Next, we will describe how high power (~5000 W/m²) and high efficiency (~7%) TPV energy conversion can be achieved when the hot emitter is placed at nanometric separations (<100 nm) from a custom fabricated thin-film InGaAs-based PV cell designed for high internal quantum efficiency and for minimized sub-bandgap absorption. Finally, we will present strategies for achieving even larger energy conversion efficiencies.

11:30 AM EQ16.01.04

Near-Field Radiative Heat Transfer Between Time Reversal Symmetry-Breaking Weyl Semimetals with Fermi Arc Surface States [Simo Pajovic](#), Yoichiro Tsurimaki, Xin Qian, Svetlana V. Boriskina and Gang Chen; Massachusetts Institute of Technology, United States

Recently, time reversal symmetry-breaking Weyl semimetals have attracted great attention in the field of thermal radiation because of their strong, intrinsic electromagnetic nonreciprocity in the mid-IR. Previous models have emphasized their potential to realize the breakdown of Kirchhoff's law of radiation (i.e., the inequality of spectral directional emissivity and absorptivity) and highly directional emitters and absorbers. Their far-field nonreciprocity is linked to nonreciprocal surface plasmon polaritons, which suggests even stronger nonreciprocity is possible in the near-field, where surface modes dominate the radiative heat transfer. The effects of Fermi arc surface states (a defining characteristic of Weyl semimetals) on surface modes and near-field radiative heat transfer remain largely unexplored. Here, we model the near-field radiative heat transfer between two planar time reversal symmetry-breaking Weyl semimetals, explicitly including the effects of Fermi arc surface states in Maxwell's equations. We show that the inclusion of Fermi arc surface states creates new surface modes that exhibit strong nonreciprocity and exotic behavior. These modes, which can exist at relatively large wavevectors, contribute non-negligibly to the heat transfer, contrasting our previous studies in which Fermi arc surface states did not significantly affect far-field radiative heat transfer. Our work further points to the applicability of Weyl semimetals in nonreciprocal, tunable radiative heat transfer systems and highlights the importance of Fermi arc surface states beyond as a hallmark of Weyl semimetals. This work is supported by ARO MURI (Grant No. W911NF-19-1-0279) via the University of Michigan.

11:45 AM EQ16.01.05

Near-Field Thermal Radiation from Room to High Temperature—Calibration and Temperature Dependence Christophe Lucchesi¹, Maud Piqueras¹, Ali Alkurdi¹, Jean-Marie Bluet², Rodolphe Vaillon³ and [Pierre-Olivier Chapuis](#)¹; ¹CNRS - INSA Lyon, France; ²INSA Lyon, France; ³IES, France

Near-field radiative effects can be observed through two different manifestations. First, the distance dependence of the flux exchanged between two bodies

at different temperatures is different from the prediction from the macroscopic theory. This is now well established for large bodies, such as parallel-surfaces and sphere-plane configurations [1]. Second, the temperature dependence of the flux exchanged is also expected to be different in the near field [2,3], as sizes and temperatures are tightly connected [4]. Only moderate temperature differences (up to 400 K) between emitter and receiver were probed so far, and only few materials were tested. We therefore focus on near-field radiative heat transfer measurements between microspheres and planar substrates [5] for record temperature differences larger than 900 K, with the emitter being heated up to 1200 K [6]. This allows observing the temperature dependence of near-field radiative heat transfer for various materials (SiO₂, graphite and InSb). It is shown that the temperature exponent n of the near-field radiative power, ranging between 2 and 3 in various cases, is lower than that in the far field, which itself can deviate from $n = 4$ well-known in the Stefan-Boltzmann law. These results are obtained thanks to a careful calibration of thermal cantilevers by combined means of Raman thermometry and FEM simulations. They indicate that power increase due to decreasing distance and rising emitter temperature do not act with equal footing, which has key implications for energy harvesting such as thermophotovoltaics.

References:

[1] C. Lucchesi *et al.*, *Nanoscale Horizons* 6, 201 (2021) [2] T. Kralik *et al.*, *Phys. Rev. Lett.* 109,224302 (2012) [3] Y. Tsurimaki *et al.*, *J. Quant. Spectrosc. Radiat. Transfer* 187, 310–321 (2017) [4] K.L. Nguyen *et al.*, *Appl. Phys. Lett.* **112**, 111906 (2018) [5] C. Lucchesi *et al.*, *Nano Lett.* 21, 4524 (2021) [6] C. Lucchesi *et al.*, *to be published*.

Acknowledgments: Financial support by the French National Research Agency (ANR) grant ANR-6-CE05-0013 (Demo-NFR-TPV), by EU EIC Pathfinder FETPROACT-EIC-05-2019 grant 951976 (TPX-Power) and partial funding by the French "Investment for the Future" program (IDEXLYON ANR-16-IDEX-0005) are acknowledged.

SESSION EQ16.02: Active and Tunable Infrared Metaplatforms

Session Chairs: Artur Davoyan and Bo Zhao

Tuesday Afternoon, November 30, 2021

Hynes, Level 1, Room 102

1:30 PM *EQ16.02.01

Controlling the Optical Properties of Conducting Oxides for Time-Varying Metasurface Applications [Alexandra Boltasseva](#)¹, Vladimir Shalaev¹, Soham Saha¹, Marcello Ferrara², Vincenzo Bruno², Michael Wood³, Richard Schaller⁴ and Benjamin Diroll⁴; ¹Purdue University, United States; ²Heriot-Watt University, United Kingdom; ³Sandia National Laboratories, United States; ⁴Argonne National Laboratory, United States

The fast and large optical response changes in transparent conducting oxides (TCOs), namely, ITO and AZO, under external optical excitation have recently led to the demonstration of nonlinearity enhancements and all-optical addition of signal. In this talk, techniques to control the optical responses of TCOs will be discussed as well as nonlinear optical effects enabled by the so-called epsilon-near-zero (ENZ) region of the TCOs. Recent results on extending the ENZ regime from the visible to the mid-infrared wavelength region by utilizing metal- and optical doping will be reported. Specifically, we tailored the ENZ points of cadmium oxide from 11 μm to 5 μm by yttrium doping, to develop fast all-optical switches in the mid-IR regime. Secondly, utilizing undoped zinc oxide, we showed real-time control over the permittivity by interband pumping, achieving unity order refractive index change, and picosecond-speed reflectance modulation in the telecom regime. In addition, by employing titanium nitride with a nanosecond response, and aluminum-doped zinc oxide with a picosecond response, we tuned the switching speed of a metasurface from the nanosecond to the picosecond scale. This results could pave the way to designing novel nonlinear optical devices spanning the telecom to the mid-infrared regime.

2:00 PM EQ16.02.02

Electrolyte-Gated La_{1-x}Sr_xCoO_{3- δ} (LSCO) for Tunable Infrared Nanophotonics—Fundamental Optical Properties and Applications in Active Metasurfaces [Rohan D. Chakraborty](#), Vipul Chaturvedi, Chris Leighton and Vivian E. Ferry; University of Minnesota Twin Cities, United States

Material systems with tunable optical properties are in high demand for mid- and far-infrared applications, including infrared sensing, thermal imaging, and radiative cooling. Such materials can also enable active metasurfaces, which can serve different optical functions simply by tuning the refractive index of a material layer. Here, we present the perovskite cobaltite La_{1-x}Sr_xCoO_{3- δ} (LSCO) as a new material candidate for tunable nanophotonics that demonstrates increased light modulation depth and convenient electrical control for infrared applications.

We focus on electrolyte-gated transistors featuring perovskite LSCO at $x = 0.5$ (LSCO50), which is a metallic ferromagnet with a low formation enthalpy and high diffusivity of oxygen vacancies. Using electrolyte gating with ionic liquids/gels, it has been shown that positive gate voltage and resulting oxygen vacancy formation in ~ 10 -nm-thick LSCO50 drives a topotactic transformation from the metallic perovskite phase to an insulating oxygen-vacancy-ordered brownmillerite phase, La_{1-x}Sr_xCoO_{2.5}, and thus a metal-insulator transition (MIT).

Here, we show via *ex situ* spectroscopic ellipsometry and Kramers-Kronig consistent dispersion models that this electrochemically-induced MIT produces significant, nonvolatile refractive index changes between the perovskite and brownmillerite phases of LSCO50, both of which are air-stable. In particular, the insulating brownmillerite phase is a high-index, low-loss dielectric ($n > 3$, $k < 0.4$) in the mid-infrared, while the metallic perovskite phase remains highly lossy.

We then implement electrochemically-gated LSCO50 as the active layer in a reconfigurable, mid-infrared plasmonic absorber designed with finite-difference time-domain (FDTD) electromagnetic simulations. In the ungated state, strong optical losses in metallic-phase LSCO50 hinder surface plasmon resonance and yield a spectrum of higher reflectance, but the insulating phase accessed by electrochemical gating allows incident radiation to couple into highly-absorbing resonant modes, significantly lowering the reflectance of the metasurface. Such a device could enable many infrared applications including dynamic thermal imaging and infrared camouflage, and cements electrolyte-gated LSCO50 as a promising vehicle for tunable nanophotonics.

2:15 PM EQ16.02.03

Electrochemically Tunable Mid-IR Metasurface by Conducting Polymers [Po-Chun Hsu](#); Duke University, United States

Metasurface design is a powerful approach to create exotic and desirable properties that do not appear in nature. The quasi-2D and deep-subwavelength structure suggests the device can be made ultrathin, lightweight, and flexible. By coupling the metasurface with mid-IR light, one can enhance performance or create new functionality in the frequency regime of phonons, which has wide applications in molecular vibrational spectroscopy, imaging, and thermal management. In particular, by employing index-tunable materials in metasurfaces, one can modulate the thermal radiation to stabilize the heat balance,

which can be a game-changer for future energy-efficient wearable/portable thermoregulation. This dynamic mid-IR metasurface device is orders of magnitude more efficient than traditional thermoregulation such as thermoelectric devices or resistive heaters because it controls the heat transfer coefficient rather than directly pumping heat. Although there are various ways to achieve tunable mid-IR metasurface, special considerations are needed to optimize the thermoregulation performance in tuning range and switching time. In this talk, I will introduce our recent research progress in using conducting polymers for mid-IR emissivity tuning and comparative study for ordinary versus metasurface design. Conducting polymers are widely known for their electrochemically tunable optoelectronic properties, and they have the suitable plasmon frequency to work as a mid-IR plasmonic material. The change of carrier density is driven by electrochemical reaction, which implies large contrast. The switching speed is not as fast as electrostatic gating but nevertheless more than enough for wearable technology and room temperature thermoregulation. Despite the potential impacts on applications for personal health and space heating/cooling energy efficiency, mid-IR electrochromic properties of conducting polymers have not been thoroughly studied, limiting their utility for tunable metamaterials. I will share our study on conductive polymer charge transport and optoelectronic properties, hoping to enrich the material palette for tunable mid-IR materials.

2:30 PM *EQ16.02.04

Atomic Layer Deposited VO₂ Thin Films for Modulated Optoelectronic Devices Virginia Wheeler¹, Chase Ellis¹, Marc Currie¹, Jason Avila¹, Joshua Caldwell², Joseph Tischler³, Austin Howes⁴, Zhihua Zhu², David Curie², Richard Haglund², Ahmed Morsy⁵, Romil Audhkhasi⁵, Michelle Povinelli⁵ and Jason G. Valentine²; ¹U.S. Naval Research Laboratory, United States; ²Vanderbilt University, United States; ³The University of Oklahoma, United States; ⁴Northrop Grumman Corporation, United States; ⁵University of Southern California, United States

VO₂ is a phase change material that undergoes a first order crystalline phase transition at a critical temperature ($T_c = 68^\circ\text{C}$), resulting in significant changes in intrinsic electrical and optical properties, especially in the infrared. Optical changes with this phase transition are of particular interest as passive and active components of optoelectronic devices, specifically for thermal regulation and modulated signaling. Realizing this type of device often requires the integration of thin, conformal VO₂ films with complex, non-planar structures (like metamaterials). Thus, atomic layer deposition (ALD) is an ideal deposition method in these cases. In this work, we will discuss the ALD process optimization and characterization of thin VO₂ films itself and subsequent integration into different optoelectronic structures for active modulation. In particular, we will present a few examples based on nanopillar arrays.

Traditional metal-based plasmonic materials suffer from high optical losses, which has promoted research towards alternative low-loss materials that can support plasmonic-like effects. One such approach employs phonon-mediated collective-charge oscillations (surface phonon polaritons, SPhPs) that are supported by nanostructured polar dielectric materials (SiC, AlN, etc), which inherently are low-loss. Geometric design of the nanostructures enables spectral tuning of resonant features between the longitudinal and transverse optical phonons of the polar material, typically in the infrared regions. However, the spectral position and amplitude of these resonances remain fixed after fabrication. Integrating phase change materials with these structures provides a way to achieve active modulation of resonances.

As an example, nanopillar arrays were etched into SiC and AlN to create narrowband resonances in the long-wave infrared region. These structures were subsequently coated with ALD VO₂ films with different thicknesses (8-75nm). As-deposited VO₂ films are highly conformal and amorphous, and cause the resonances to shift and broaden due to the different dielectric environment. However, after annealing the films at 525°C in 6x10⁻⁵ Torr, the VO₂ films crystallize resulting in sharper resonances and spectral locations close to the initial uncoated structures. Temperature-dependence reflectance and emission measurements show that by heating through the VO₂ transition temperature, the amplitude of the resonances can be modulated. Full signal modulation (ie. on/off) requires at least a 16nm VO₂ film.

ALD VO₂ films can be applied to other optoelectronic pillar arrays derived from different, non-polar semiconductors, such as Si, to enable active focusing/defocusing or optical limiting [1] using metasurface concepts. Additionally, we have demonstrated the ability to use these in planar stacks for thermal homeostasis [2]. We will briefly go over several of these concepts the advantages and disadvantages of ALD VO₂ films in each.

[1] Howes et al, *Nano Lett.* 20(6), 4638-4644 (2020).

[2] Morsy et al, *Scientific Reports* 10, 13964 (2020).

3:00 PM *EQ16.02.05

Dynamic Infrared Metasurfaces Based on Phase Change Media Jason G. Valentine; Vanderbilt University, United States

The use of nano and microstructured metasurfaces provides new freedom in infrared optic design as it allows precise control over the phase, amplitude, and polarization at a surface. Realizing dynamic tuning of these properties is a critical step towards achieving more advanced functionality and improved operational bandwidth. In this talk, I outline several approaches towards achieving dynamic tuning by incorporating metasurfaces with phase change media. I will explore both thermal and electrical activation of these metasurfaces for achieving dynamic tunability in both the infrared regime. The metasurface can be used for a variety of purposes including spectral signature control, thermal management, and adaptive systems.

3:30 PM BREAK

SESSION EQ16.03: Emergent Infrared Materials and Phenomena

Session Chairs: Artur Davoyan and Virginia Wheeler

Tuesday Afternoon, November 30, 2021

Hynes, Level 1, Room 102

4:00 PM *EQ16.03.01

Full Control of Far-Field Thermal Radiative Properties with Nonreciprocal Materials and Nanophotonic Designs Bo Zhao^{1,2}; ¹Stanford University, United States; ²University of Houston, United States

Objects around us constantly emit and absorb thermal radiation. The basic properties that characterize these two processes are emissivity and absorptivity, respectively. For reciprocal systems, the emissivity and absorptivity for a given direction, polarization, and frequency are tightly restricted to be equal by Kirchhoff's law of thermal radiation [1]. This restriction limits the control of thermal radiation and contributes to an intrinsic loss mechanism in photonic energy harvesting systems.

Existing approaches to violate Kirchhoff's law typically utilize conventional magneto-optical effects in the presence of an external magnetic field. However, these approaches require either a strong magnetic field (~3T) [2] or narrow-band resonances under a moderate magnetic field (~0.3T) [3], because the nonreciprocal effect in conventional magneto-optical materials is usually weak in the thermal wavelength range. The nonreciprocal effect is also only confined in a relatively narrow angular range. Meanwhile, in these designs, the angular distribution of emissivity and absorptivity is symmetric with respect to the normal direction, meaning that the emissivity in the θ direction is always equal to the absorptivity in the $-\theta$ direction. This equality significantly restricts the ability to separately control the emissivity and absorptivity in the angular degree of freedom.

In this talk, I will show that the axion electrodynamics in magnetic Weyl semimetals can be used to construct strongly nonreciprocal thermal emitters [4,5]. Such a thermal emitter can near completely violate Kirchhoff's law over broad angular and frequency ranges, without requiring any external magnetic field. Meanwhile, I will introduce a general coupled-mode theory framework for nonreciprocal thermal emitters. I will discuss the necessary conditions for the nanophotonics design to decouple the link between emissivity in the θ direction and the absorptivity in the $-\theta$ direction so that one can achieve complete control of emissivity and absorptivity in the angular degree of freedom. Finally, I will present a case study using nanophotonic design and magnetic Weyl semimetal to achieve nonreciprocal thermal emission in semitransparent emitters [6].

Reference

- [1] G. Kirchhoff, *Annalen Der Physik* 185, 275 (1860).
- [2] L. Zhu and S. Fan, *Phys. Rev. B* 90, 220301 (2014).
- [3] B. Zhao, Y. Shi, J. Wang, Z. Zhao, N. Zhao, and S. Fan, *Opt. Lett.* 44, 17(2019).
- [4] B. Zhao*, C. Guo*, C. A. C. Garcia, P. Narang, and S. Fan, *Nano Lett.* 20, 1923 (2020).
- [5] Y. Tsurimaki, X. Qian, S. Pajovic, F. Han, M. Li, and G. Chen, *Phys. Rev. B* 101, 165426 (2020).
- [6] Y. Park, V. Asadchy, B. Zhao, C. Guo, J. Wang, and S. Fan, arXiv:2105.08954.

4:30 PM EQ16.03.02

Thermochromic Coatings for Energy-Efficient Smart Windows Resulting from Phase Separation of VO₂ in SiO₂ on SiO₂-Coated Float

Glass Cindy Yeung^{1,2}, Roberto Habets^{1,2}, Luc Leufkens^{1,2}, Fallon Colberts³, Kathleen Stout³, Marcel A. Verheijen^{4,5}, Zeger Vroon^{3,1,2}, Daniel Mann^{1,2} and Pascal Buskens^{1,2,6}; ¹TNO, Netherlands; ²Brightlands Materials Center, Netherlands; ³Zuyd University of Applied Sciences, Netherlands; ⁴Eurofins Material Science Netherlands BV, Netherlands; ⁵Eindhoven University, Netherlands; ⁶Hasselt University, Belgium

Vanadium dioxide displays thermochromic properties based on a reversible metal-insulator transition which is caused by the structural phase transition from monoclinic VO₂ (M) to rutile VO₂ (R) and *vice versa*. We developed a single layer coating comprising VO₂ (M) and SiO₂ starting from a mixture of pre-oligomerized tetraethoxysilane and vanadium(IV) oxalate dissolved in an alcohol-water mixture [1,2]. After dip coating and subsequent solvent evaporation under ambient conditions, we obtained a homogeneous mixture of both components as xerocoat on silica-coated float glass. During the thermal anneal at 450°C in inert gas atmosphere phase separation occurred. This yielded coatings comprising V-rich and Si-rich nanodomains, the size and shape of which depended on the V/Si ratio in the starting mixture. Size and shape of the nanodomains were determined by performing scanning transmission electron microscopy – energy dispersive X-ray studies on scraped off coating material. The thermochromic coatings resulting from these experiments combine high visible light transmission $T_{vis} > 60\%$ with a large solar modulation $\Delta T_{sol} \geq 10\%$, as demonstrated via UV-vis-NIR spectrophotometric analyses performed below and above the switching temperature. In addition to T_{vis} and ΔT_{sol} , the switching hysteresis width studied. The relationship between the coating size, shape and concentration of VO₂ domains and the optical properties of the coating was studied in detail. Additionally scraped off coating material has been isolated and measured with differential scanning calorimetry to determine the switching enthalpy and relate that to the amount of VO₂ (M) in the obtained mixture of vanadium oxides. When applied in insulating glass units, the coating has a positive impact on energy savings for heating and cooling of buildings in intermediate climates, which is demonstrated through energy performance simulations. For a typical house in the Netherlands, energy savings up to 24% were forecasted [3]. In addition, we demonstrate a coating life time of > 10 years in insulating glass units through accelerated life time tests, including switching fatigue studies.

4:45 PM EQ16.03.04

Optical Properties of Oxides at High Temperatures Jonathan Kaufman and Keivan Esfarjani; University of Virginia, United States

We present the results of our density functional theory simulations of the optical properties of some oxides at high temperature. To validate, we simulate the band structure and dielectric constant of one of the archetypal oxides for which many experimental data is available i.e. MgO. To overcome the gap underestimation, we use the GGA+U approximation. At high temperatures, defects affect the optical properties, and therefore we simulate the dielectric constant of this system with O and Mg vacancies as the dominant defects. They induce respectively donor and acceptor levels in the gap and cause interband transitions of lower energies. The change of the dielectric constant as a function of defect concentration will be discussed in this work.

5:00 PM EQ16.03.05

Giant Optical Anisotropy in Quasi-1D Hexagonal Perovskite-Derived Chalcogenide A_{1+x}TiS₃ (A=Sr, Ba) Boyang Zhao¹, Jad Salman², Guodong Ren³, Hongyan Mei², Shantanu Singh¹, Shanyuan Niu¹, Arashdeep Thind³, Huandong Chen¹, Rohan Mishra³, Mikhail A. Kats² and Jayakanth Ravichandran^{1,1}; ¹University of Southern California, United States; ²University of Wisconsin–Madison, United States; ³Washington University in St. Louis, United States

Birefringent and dichroic crystals are critical building blocks for devices such as polarizers, filters, and phase matching elements in optical systems. However, in the mid-wave (MWIR) and long-wave (LWIR) infrared spectral ranges, there is still a shortage of optically anisotropic materials. In this work, we show perovskite-derived chalcogenides—A_{1+x}TiS₃ (A=Sr, Ba)—are a platform for achieving giant optical anisotropy across the MWIR and LWIR and can play a key role in next-generation infrared optics. We grew high-quality A_{1+x}TiS₃ crystals of various shape and orientation by chemical vapor transport. Electron microscopy studies revealed 1D chains of face-sharing TiS₆ octahedra with a highly anisotropic electronic structure, which infers a large optical anisotropy. We used polarized infrared spectroscopy combined with spectroscopic ellipsometry to extract the optical properties of these materials and discovered refractive-index differences between the ordinary and extraordinary axes of up to two across the MWIR and LWIR, as well as large dichroism. We applied Density Function Theory (DFT) on A_{1+x}TiS₃ structure and discovered that such optical anisotropy originates from the structural modulation of TiS₆ octahedral. We anticipate A_{1+x}TiS₃ (A=Sr, Ba) and other quasi-1D materials will be useful for next-generation imaging and sensing applications, especially for miniaturized photonic devices. This study also lays ground for material designs towards highly electronic and optic anisotropic materials.

SESSION EQ16.04: Phonon Polariton Excitations—2D and Beyond
Session Chairs: Svetlana Boriskina and Zhe Fei
Wednesday Morning, December 1, 2021
Hynes, Level 1, Room 102

10:30 AM *EQ16.04.01

Programable Hyperbolic Polaritons in van der Waals Semiconductors [Aaron Sternbach](#)¹, Sanghoon Chae¹, Simone Latini², Andrey Rikhter³, Yinming Shao¹, Baichang Li¹, Daniel Rhodes⁴, Brian Kim¹, Peter Schuck¹, Xiaodong Xu⁵, Xiaoyang Zhu¹, Richard Averitt³, James Hone¹, Michael Fogler³, Angel Rubio^{2,6} and Dmitri Basov¹; ¹Columbia University, United States; ²Max Planck Institute for the Structure and Dynamics of Matter, Germany; ³University of California, San Diego, United States; ⁴University of Wisconsin–Madison, United States; ⁵University of Washington, United States; ⁶Center for Computational Quantum Physics (CCQ), Flatiron Institute, United States

Programming materials with light and interrogating their properties within the resultant transient states is an important goal of modern condensed matter physics. Polaritons - where strong dipole active resonances hybridize with photons - are central to transient nano-optical exploration. Infrared nano-imaging can be used to detect these polaritonic waves, yielding detailed information on the properties of host materials that support these polaritons. The naturally layered class of van der Waals (vdW) materials are particularly intriguing in this regard due, in-part, to their often strongly anisotropic behavior. In materials hosting both strong anisotropy and strong dipole active resonances sub-diffractive polaritonic wave packets, that travel as conical rays with hyperbolic dispersion throughout the materials' bulk, can emerge. We utilized femtosecond photoexcitation to agitate crystals of the vdW semiconductor WSe₂ and interrogated these crystals in the transient state with near-field optical microscopy [1]. Our time-resolved nano-imaging data reveals key signatures of optical hyperbolicity, appearing on the sub-picosecond timescale.

[1] AJS et al., Science 371, 617–620 (2021)

SESSION EQ16.05: Emergent Infrared Materials and Excited States
Session Chairs: Artur Davoyan and Zhe Fei
Wednesday Afternoon, December 1, 2021
Hynes, Level 1, Room 102

1:30 PM *EQ16.05.01

Thermal and Electrical Properties of Some of the Narrow Gap Semiconductors and Topological Conductors [Mona Zebarjadi](#); University of Virginia, United States

Narrow gap semiconductors and topological semimetals/metals are important in infrared applications and can be used for harvesting radiative thermal energy. The band structure of these materials can change with temperature when the material goes through a phase change and it affects the material's thermal, electrical, and magnetic properties. In this talk, I will discuss several materials, their band structure in different phases, and how the band structure and the electron-phonon scattering affect the electrical, and thermomagnetic properties. I will discuss our results on NbSe₂ sample, a topological metal/semimetal, that goes through charge density wave (CDW) transition, and superconducting phase at lower temperatures. The band structure of both 1T and 2H phase appears semimetallic in the normal phase while a gap opens up in the CDW phase. I will also discuss the Mo_{1-x}W_xTe₂ single crystal samples, another topological semimetal, which are going through 2H-1T phase change, and show how the Seebeck and the Nernst coefficients are affected. Finally, I will discuss the case of FeSb₂, a highly correlated narrow-gap semiconductor with debates on the effect of phonon-drag as opposed to correlation on its transport properties and specifically on the Seebeck coefficient.

2:00 PM *EQ16.05.02

Metastructure Design for Actively Tailoring Thermal and Nonthermal Radiation [Harry A. Atwater](#); California Institute of Technology, United States

Photonic designs with active elements have the potential to exquisitely tailor the properties of thermal radiation, including modulation of the intensity, phase, linewidth, wavevector and scattered wavefront. We describe the coupling of tunable permittivity graphene elements to resonant nanophotonic structures for i) modulation of emissivity between 10% and 97% by Fermi level modulation, ii) active steering and focusing of thermal radiation, iii) dramatic emission line narrowing of thermal emitters from linewidths characteristic of blackbody emitters to those more closely resembling light-emitting diodes.

Pulsed laser excitation of graphene is shown to exhibit ultrabright non-thermal emission, arising from spontaneous emission of plasmons generated by cooling of the nonequilibrium carrier distribution. Our observation of the non-thermal contribution of Fermi-level-dependent radiation constitutes the first experimental demonstration of hot plasmon emission arising from a photo-inverted carrier distribution in graphene. This previously unobserved mechanism generates bright nonthermal radiation in the far field, as the generated plasmons are outcoupled from the excited graphene by gold nanoantennas, with implications for design of future ultrafast and ultrabright mid-infrared emission processes and light sources.

For the vast majority of materials, Kirchoff's Law dictates that absorptivity and emissivity are equal for any particular wavelength or angle, a property that has fundamental implications for infrared photonics. While previous theoretical work has suggested that Kirchoff's Law could be violated using magneto-optical materials, the required magnetic field strengths were impractically large. We demonstrate in the present work the first definitive experimental observation of Kirchoff Law violated in magnetoelectric heterostructures. We find that the required magnetic field for reciprocity breaking can be reduced by over an order of magnitude, bringing it within the range of practical experiments with simple permanent magnets. By combining the magneto-optical character of doped InAs crystals in the epsilon-near-zero wavelength regime with guided mode resonance waveguides, we have observed violations of Kirchoff's Law as large as 50% in experiment. These results open up new opportunities for the manipulation of thermal radiation in the long wavelength infrared regime.

2:30 PM EQ16.05.03

Ultrafast Polariton Dynamics Following Remote Heating via Mid-Infrared Pump-Probe Spectroscopy John A. Tomko¹, [William D. Hutchins](#)¹, Daniel M. Hirt¹, Joseph Matson², Katja Diaz-Granados², Joshua Caldwell² and Patrick E. Hopkins¹; ¹University of Virginia, United States; ²Vanderbilt University, United States

The reduced dimensions of electronic devices lends itself toward rapid bottlenecks in thermal dissipation; heat conduction becomes limited due to interface scattering of thermal carriers when material geometries approach the nanoscale. Thus, additional thermal transport pathways are necessary in further developing next-generation RF and power electronics. In this work, we consider two potential means of doing so: i) enhancing interfacial heat transport rates through non-equilibrium processes and ii) accessing polariton-mediated transport mechanisms.

In the first case, we elucidate a novel energy transduction pathway that can efficiently transfer heat across metal-semiconductor interfaces, where traditional thermal boundary resistances greatly mitigate heat flow. This energy transfer mechanism, termed Ballistic Thermal Injection, is demonstrated in gold/cadmium oxide (CdO) heterostructures. We find that under non-equilibrium conditions, photo-excited metals can undergo an electron-mediated ballistic energy transfer process that can remotely modulate the electronic environment of an underlying degenerate semiconductor; namely the plasmonic resonance of this semiconductor. We term this effect 'ballistic thermal injection' (BTI) to distinguish it from the well-studied charge injection effects caused by hot electrons traversing an energy barrier. Our results are explained through transient reflectivity (TDTR) measurements to understand the fundamental carrier dynamics at the Au/CdO interface. Additionally, we perform mid-infrared, ultra-fast pump-probe experiments to obtain spectral, temporal, and ultimately spatial resolution of the electronic environment within the CdO layer following excitation of the Au film. Ultimately, the carrier dynamics derived from the transient spectra fully agree with our TDTR results, and can only be accurately modeled by the BTI process rather than by charge injection.

With regards to polariton-mediated heat transfer pathways, from an experimental perspective, many of the recent advances have been investigated from the perspective of thermoreflectance measurements, such as TDTR or FDTR, where the role of these potential thermal carriers is inferred by trends in thermal conductivity measurements. While certainly of merit, these methods provide an experimental measure of the average temperature of a system rather than a direct probe of the vibrational carrier of interest. In this work, we further employ our tunable-wavelength, mid-infrared ultrafast pump-probe spectroscopy system to perform such a measurement. In particular, we investigate the phonon dynamics of both h-BN and SiC following pulsed excitation of a metal contact, providing a direct measure of the temporal dynamics of the optical phonon mode, the highly-reflective Reststrahlen band, and phonon-polaritons in these material systems during heating. These results demonstrate a unique regime of polariton-mediated heat transfer: the generation of a thermal radiation-induced phonon polariton. In other words, we demonstrate the ability to stimulate phonon polaritons in h-BN via remote heating of a metal contact, thus allowing for enhanced radiative heat transfer in device heterostructures.

2:45 PM EQ16.05.04

Hyperbolic Shear Polaritons in Low-Symmetry Crystals Nikolai Passler¹, Xiang Ni², Guangwei Hu³, Joseph Matson⁴, Martin Wolf¹, Matthias Schubert⁵, Andrea Alu², Joshua Caldwell⁴, Thomas G. Folland⁶ and Alexander Paarmann¹; ¹Fritz Haber Institute, Germany; ²The City College of New York, United States; ³National University of Singapore, Singapore; ⁴Vanderbilt University, United States; ⁵University of Nebraska–Lincoln, United States; ⁶University of Iowa, United States

The lattice symmetry of a crystal is one of the most important factors in determining its physical properties. Low-symmetry crystals offer powerful opportunities to control light propagation, polarization, and phase. When such materials featuring extreme optical anisotropy, they can support a hyperbolic response, enabling coupled light-matter interactions, also known as polaritons, with highly directional propagation and compression of light to deeply sub-wavelength scales. In this talk we show how low-symmetry crystals can support hyperbolic shear polaritons, a new polariton class arising in the mid- to far-infrared due to shear dissipation in the dielectric response. This feature can emerge in materials where the dielectric tensor cannot be diagonalized, that is, in low-symmetry monoclinic and triclinic crystals where multiple damped oscillators with non-orthogonal relative orientations contribute to the optical response. This results in a non-zero complex off-diagonal terms in the dielectric tensor which cannot be removed by coordinate rotation. Hyperbolic shear polaritons complement previous observations of hyperbolic phonon polaritons in orthorhombic and hexagonal crystal systems, unveiling new features, such as the continuous evolution of their propagation direction with frequency, tilted wavefronts, and asymmetric responses.

As an exemplar case, we will describe the hyperbolic shear polaritons supported by the polar optical phonons of the monoclinic semiconductor β -Ga₂O₃. We will describe an approximate framework for how to classify polaritons in low-symmetry materials with non-orthogonal oscillators, and how this predicts a continuous rotation of the polariton direction frequency. We will then go on to experimentally demonstrate how hyperbolic shear polaritons can be measured using orientation sensitive prism type coupling experiments. Finally, we will show the specific role of the off-diagonal terms play in creating new types of light propagation, and how this influences our treatment of the polaritons. This interplay between diagonal loss and off-diagonal shear dissipation in the dielectric response of these materials has implications for new forms of non-Hermitian and topological photonic states. We anticipate that our results will motivate new directions for polariton physics in low-symmetry materials, which include geological minerals, many common oxides, and organic crystals, significantly expanding the material base and extending design opportunities for compact photonic devices.

3:00 PM BREAK

SESSION EQ16.06: Radiative Heat Transfer—Breakthrough Phenomena
Session Chairs: Artur Davoyan and Zhe Fei
Wednesday Afternoon, December 1, 2021
Hynes, Level 1, Room 102

4:00 PM EQ16.06.01 INVITED PRESENTATION BY PILON LAURENT WILL BE PRESENTED VIRTUALLY NEXT WEEK IN EQ16.14

4:30 PM *EQ16.06.02

Coherent Thermal Emission by Metasurfaces Zongfu Yu; University of Wisconsin--Madison, United States

Engineering the coherent properties of thermal emission plays an important role in many applications, such as energy harvesting, light sources, imaging and remote temperature sensing. Whereas thermal emission from bulk materials is generally incoherent, it has been shown that structured material, which have at least one of its structure parameters comparable with the thermal wavelengths, can greatly modify the coherence of thermal emission due to excitation of optical modes in the photonic structures. Most of existing works so far can only realize simple function such as spectral and directional selectivity. More complex control such as focusing and holography, remains difficult to achieve. The limited control of thermal emission is a result of the simple structures used in most previous works, which are either periodic structures or small structures whose sizes are around the wavelength of thermal photons. They do not offer enough degrees of freedom to accomplish complex control. To overcome this limit, we use large-area emitters with inhomogeneous structures that offer a large design space. Fine tuning the structural features allows us to exploit collective wave effects of thermal photons and to realize sophisticated control of thermal emission such as focused thermal emission and thermal holography.

5:00 PM EQ16.06.03

Beyond Traditional Polyethylene Fibers for Passively Cooling Monomaterial Textiles Volodymyr Korolovych¹ and Svetlana V. Boriskina^{1,2}; ¹Institute for Soldier Nanotechnologies, Massachusetts Institute of Technology, United States; ²Massachusetts Institute of Technology, United States

Considering the adoption of the sustainable circular bioeconomy, polyethylene (PE) fibers produced from green, renewable raw material are becoming more and more critical for everyday clothes, bedding textile and wearables due to their low environmental footprint and combination of material low-cost, durability with lightweight, high UV resistance and infrared (IR) transparency. [1-4] It is not surprising that the unique properties of green PE can be exploited to engineer high-performance sustainable fibers with mechanical properties tunable by design. Here, we explore the role of polyethylene molecular architecture in engineering mechanical properties and surface morphology of fibers based on the traditional fossil sourced raw PE and sugarcane-derived, renewable raw PE material. A range of fibers with different material parameters have been fabricated by a low-cost melt-extrusion method, mechanically and optically characterized, and classified according to their crystallographic structure as well as elongation, strength, recovery properties, and surface morphology. Differential scanning calorimetry and X-ray scattering techniques confirmed that by combining precise engineering of molecular structure we can adjust structural disorder in PE fibers, which results in crystallinity of fibers ranging from ~8% to ~60% and different crystallite orientation along the fiber axis. This tunability of the fiber molecular structure translates into a wide range of elongation at break, specific stiffness and specific strength values as well as tunable infrared transparency and thermal conductivity values. These results demonstrate feasibility of low-cost, large-scale fabrication of green PE fibers with a wide range of mechanical performance, smooth fiber surfaces, and variable cross-sectional shapes, paving the road to engineering mono-material high-performance sustainable textiles. These mono-material textiles can find applications in passive cooling technologies and are 100% recyclable at the end of their lifecycle.

This work was supported by the DEVCOM Soldier Center through the US Army Research Office (W911NF-13-D-0001), the Advanced Functional Fabrics of America (AFFOA) Institute (W15QKN-16-3-0001), the MIT Deshpande Center, and the US Department of Energy (DE-FG02-02ER45977). We thank B. A. Welsh (DEVCOM SC) for help with PE fiber fabrication and Braskem and Dow Chemical Company for providing raw olefin polymers.

[1] Alberghini, M.; Hong, S.; Lozano, L.M.; Korolovych, V.; Huang, Y.; Signorato, F.; Zandavi, S.H.; Fucetola, C.; Uluturk, I.; Tolstorukov, M.Y.; Chen, G.; Asinari, P.; M. Osgood III, R.; Fasano, M.; Boriskina, S.V. Sustainable polyethylene fabrics with engineered moisture transport for passive cooling. *Nature Sustainability* **2021**, 1-10.

[2] Boriskina, S. V. An ode to polyethylene, *MRS Energy Sustain.* **2019**, 6, E14.

[3] Lozano, L. M.; Hong, S.; Huang, Y.; Zandavi, H.; El Aoud, Y. A.; Tsurimaki, Y.; Zhou, J.; Xu, Y.; Osgood, R. M.; Chen, G.; Boriskina, S. V. Optical engineering of polymer materials and composites for simultaneous color and thermal management. *Opt. Mater. Express* **2019**, 9, 5.

[4] Tong, J.K.; Huang, X.; Boriskina, S.V.; Loomis, J.; Xu, Y.; Chen, G. Infrared-transparent visible-opaque fabrics for wearable personal thermal management. *ACS Photonics* **2015**, 2, 769-778.

5:15 PM EQ16.06.04

Enhancing Passive Radiative Cooling in Solar Modules Using Microstructures with Mie-Like Resonances Evelijn Akerboom¹, Tom Veeken¹, Chris Hecker² and Albert Polman¹; ¹AMOLF, Netherlands; ²University of Twente, Netherlands

Photovoltaic systems show a strong reduction in conversion efficiency when their temperature rises due to hot carrier cooling and non-radiative recombination in the solar cells. One key factor that determines the steady-state cell temperature is the radiative cooling rate: every solar cell shows spontaneous emission of infrared light. The spontaneous emission is determined by the emissivity, which is linked to the absorptivity by Kirchhoff's law ($\epsilon = A = 1 - R - T$). To achieve the maximal radiative cooling rate for a silicon solar cell, and given the absorption spectrum of the earth's atmosphere, the emissivity should be minimal in the spectral range from the Si bandgap at 1.1 to 4 micron and be maximal beyond that range.

Here, we propose two designs based on resonant microstructures; one for bare silicon solar cell and a second for a silica-based solar module glass. Both designs enhance the emissivity, and hence the radiative cooling rate, by reducing the reflection and transmission in a well-defined spectral range beyond 4 micron. They effectively enhance the absorption of infrared light. The design is based on Mie-like resonances in spherical or cylindrical structures that show strong forward scattering of light and thereby decrease the reflectivity. Finite-difference-time-domain (FDTD) simulations are used to optimize the geometry of the radiative cooling microstructures, by minimizing the reflectance in the infrared.

For the bare silicon solar cell, we find an optimized design composed of a close-packed hexagonal array of glass microspheres (diameter 20 micron) that is fabricated by drop casting from an aqueous suspension on silicon. The hemispherical reflectivity of the stack is measured using Fourier Transform Infrared Spectroscopy (FTIR) with an external integrating sphere. The measured reflectivity of bare silicon is reduced from 80 to 10 percent by adding the close-packed monolayer of glass spheres, for wavelengths larger than 7 micron.

To determine the radiative cooling power we measure, using a thermocouple, the temperature of different designs under direct sunlight on a sunny summer day in Amsterdam. The preliminary results of the silicon covered with glass spheres, show a clear decrease in temperature of approximately 5 degrees with respect to the bare silicon reference under solar illumination. Reference reflectivity measurements at wavelength below the Si bandgap show the effect is not due to reduced incoupling of below-gap sunlight into the cell, hence demonstrating a significant radiative cooling effect.

For the silica-based solar module glass, we use a periodic hexagonal array of quartz cylinders (diameter 3.5 micron, height 2.25 micron, pitch 6.13 micron). The cylinders are fabricated into a thin quartz plate with UV lithography and reactive ion etching using C_4F_8/Ar . The micropatterned plate is then placed on top of a silicon sample. The unpatterned stack shows a strong reflection peak at 9 micron, due to a stretching vibration in the quartz crystal. This peak is reduced from 75 to 30 percent, due to the forward scattering of the induced electric dipole in the microcylinders.

The new radiative cooling microstructure design concept can be applied to every kind of solar cell, with or without module glass. The resonant radiative cooling concept can be applied to all devices operating in outside ambient that benefit from a low operation temperature.

EQ16.07.01

Near-Field Thermophotonic Devices with AlGaAs Emitters and Cells [Julien Legendre](#) and P.-Olivier Chapuis; CNRS-CETHIL, France

Thermophotonics (TPX) is a technology close to thermophotovoltaics (TPV), where a heated light-emitting diode (LED) is used as the active emitter of the system [1]. By doing so, the emission profile can be tuned: initially in the infrared range, it can be shifted by means of electroluminescence to a spectral range matching better the gap of a photovoltaic cell. With the development of LEDs and the increase of their achievable quantum efficiency, TPX has come out as an attractive concept for both energy harvesting and refrigeration [2]. The many studies on near-field (NF) thermal radiation and their application into efficient NF-TPV devices [3] highlight the possibility to extend the concept to near-field thermophotonics (NF-TPX) [4], where enhanced energy conversion is due to both electric control and wave tunneling.

This contribution analyzes numerically the capabilities of NF-TPX systems. Several methods modelling the charge carriers behaviour for NF-TPV systems [5-6] are compared for NF-TPX in terms of precision and computation time. For both the LED and the PV cell, the capabilities of PN and PIN AlGaAs junctions are analyzed. The results include detailed IV characteristics around the maximum power point, highlighting in particular the advantages in comparison to far-field TPX and NF-TPV. The impact of the doping levels and the thickness of each element are amongst the studied parameters. The capabilities of NF-TPX to harvest energy are assessed for thermal sources of few hundreds of degrees Celsius [7].

[1] N.P. Harder and M.A. Green, *Semicond. Sci. Technol.* 18,S270,2003 [2] T. Sadi et al., *Nat. Phot.*14, 205, 2020 [3] C. Lucchesi et al., *Nano Lett.*21, 4524, 2021 [4] B. Zhao et al., *Nano Lett.*18, 5224, 2018 [5] E. Blandre et al., *Sci. Rep.*7, 15860, 2017 [6] W.A. Callahan et al., *Phys. Rev. Appl.*15, 54035, 2021 [7] J. Legendre and P.O. Chapuis, submitted.

We acknowledge the funding of EU H2020 FET Proactive (EIC) programme through project TPX-Power (GA 951976).

EQ16.07.02

Photonic Multilayer Structure for Near-Infrared Blocking as Energy-Saving Window [Jiwon Kim](#)¹, Sangwon Baek¹, Jae Yong Park¹, Kwang ho Kim² and Jong-Lam Lee¹; ¹POSTECH, Korea (the Republic of); ²Pusan National University, Korea (the Republic of)

Blocking near-infrared (NIR) is indispensable for saving energy consumed to maintain an interior temperature in buildings. However, it is hard to achieve both high visible transmittance and high NIR reflectance for energy-saving windows. Here, we demonstrate a TiO₂/Ag/TiO₂/SiO₂/TiO₂ multilayer film on a glass substrate to block the entire NIR (800 ≤ λ ≤ 2500 nm) while maintaining high visible transmittance. We first design and optimize the thickness of a TiO₂/Ag/TiO₂ structure; the metal layer exceeds NIR and the dielectric layers increase visible transmittance with zero reflection condition. To further enhance NIR-blocking efficiency, we implement a TiO₂ back reflector with a SiO₂ spacer to TiO₂/Ag/TiO₂ structure. TiO₂ layer with high refractive index sandwiched between glass substrate and SiO₂ with low refractive indices can induce additional Fresnel reflection without sacrificing transmittance in visible light. The optimal photonic multilayer film shows solar energy rejection 89.2% (reflection 86.5%, absorption 2.7%) in NIR, visible transmittance 69.9%. Furthermore, the blocking capability in NIR of the designed multilayer film is maintained over a wide range of incident angles of light.

EQ16.07.03

Ultrafast Phonon Polariton Dynamics Resolved via Femtosecond Mid-Infrared Spectroscopy [William D. Hutchins](#)¹, Daniel M. Hirt¹, John A. Tomko¹, Patrick E. Hopkins¹, Joshua Caldwell², Joseph Matson² and Katja Diaz-Granados²; ¹University of Virginia, United States; ²Vanderbilt University, United States

As electronic devices continue to reduce towards nanoscale dimensions, understanding heat transport mechanisms at these scales becomes vital. In most non-metallic materials heat dissipates according to the movements of phonons or phonon-like waves. The efficiency of this phonon-mediated heat transport is dictated by various characteristics of these modes including their lifetime, scattering rate, and velocity. Thus, characterization of these properties is crucial to making more effective devices. From an experimental perspective, the majority of recent advances in such characteristics stems from ultrafast thermoreflectance measurements, namely TDTR and FDTR, where phonon transport is inferred from trends in thermal conductivity of materials. In other words, these methods measure the average temperature of a material following pulsed excitation rather than directly monitoring the individual mode of interest. In this work, we develop a novel ultrafast pump-probe technique that allows us to directly couple to vibrational modes of interest with sub-picosecond time resolution, thus characterizing the aforementioned phonon dynamics.

Our technique relies on a wavelength tunable mid-infrared probe pulse, allowing us to directly resonate with vibrational heat carriers, thus providing a direct measure of phonon dynamics in nanoscale material systems. In particular, we investigate the phonon dynamics in hexagonal boron nitride (h-BN) and silicon carbide; the high frequency optical modes in these materials lends itself to the potential for manipulation of thermal radiation in near room temperature conditions. Thus we investigate the ultrafast temporal dynamics of the transverse optical (TO) modes, the high reflectivity Reststrahlen band, and a unique regime of polaritonic heat transfer: the generation of a thermal radiation-induced phonon polariton. For the first time, we experimentally demonstrate the ability to stimulate phonon polaritons in h-BN through remote heating of a metal contact. Our results open the door for future experiments to manipulate and guide phonons via heterostructures, which could increase thermal efficiency of microelectronics.

EQ16.07.05

Late News: Conduction-radiation Coupling and Slowing-down of Thermal Relaxation Between Two Closely Separated Solids [Riccardo Messina](#), Marta Reina and Philippe Ben-Abdallah; Université Paris-Saclay, France

Two bodies at different temperatures experience a photon-mediated heat exchange, even when separated by vacuum. This radiative heat flux is limited by Stefan-Boltzmann's law in the far field, i.e. when the separation distance between the bodies is large compared to the thermal wavelength. The pioneering works of Rytov, Polder and van Hove and the development of the theoretical formalism of fluctuational electrodynamics allowed to show that in the near-field regime the heat flux can instead exceed this limit even by orders of magnitude for shorter distances. Surprisingly, the huge majority of works exploiting fluctuational electrodynamics neglect the possible existence of a temperature gradient due to the coupling between radiative heat transfer between the bodies and conduction within each body, and assume a perfectly uniform temperature inside each of them. We have recently developed a theory to describe the conduction-radiation coupling between solids of arbitrary size separated by a subwavelength gap [1]. The essence of this approach is based on the combination of Boltzmann's equation to deal with the transport of heat carriers inside the solids (valid for any heat-transport regime) and fluctuational electrodynamics to calculate the radiative power locally dissipated in each body. By means of this approach we show that the interplay between conduction and radiation can indeed result in an observable temperature profile within each solid. Moreover, we show that, as a result of this temperature profile, the radiative heat flux exchanged between two parallel slabs at nanometric distances can be orders of magnitude smaller than the one predicted by the conventional theory. These results could have important implications in the fields of

nanoscale thermal management, near-field solid-state cooling, and nanoscale energy conversion. By exploiting our formalism, we have also highlighted a significant slowing-down of the thermal relaxation process [2] in the extreme near-field regime at distances where the heat flux exchanged between the two solids is comparable or even dominates over the flux carried by conduction inside each solid. This mechanism, leading to a strong effective increase of the system thermal inertia, should play an important role in the temporal evolution of thermal state of interacting solids systems at nanometric and subnanometric scales.

References

- [1] M. Reina, R. Messina, and P. Ben-Abdallah, Phys. Rev. Lett. 125, 224302 (2020)
- [2] M. Reina, R. Messina, and P. Ben-Abdallah, arXiv:2106.15471 (2021, accepted on Phys. Rev. B)

EQ16.07.06

Enhancing Light-Matter Interaction Using Ultrafast Q-Switching Pavel Shafirin; University of California, Los Angeles, United States

Using resonant structures for enhancing light-matter interactions is a popular topic of research. The field localisation that they provide allows to amplify all kinds of processes, such as absorption and nonlinear effects. One limiting factor of resonant structures is their limited bandwidth, especially for the high-Q resonances the bandwidth is too small to effectively interact with short laserpulses. In this work we present a method, that allows to resolve this issue by dynamically switching the Q-factor of the resonance and allowing short pulses to effectively couple to the resonant mode. We demonstrate the effect using a simple theoretical model based on coupled mode theory and then show a potential implementation of the technique using a dielectric metasurface that we model using FDTD. In both models we consider the using our approach to increase the efficiency of third harmonic generation and show a significant increase in the generated harmonic.

SESSION EQ16.08: Radiative Heat Transfer—New Insights
Session Chairs: Svetlana Boriskina and Zhe Fei
Thursday Morning, December 2, 2021
Hynes, Level 1, Room 102

10:30 AM *EQ16.08.01

Shaping Asymmetric Responses for Infrared Light with Meta-Gratings Stavroula Foteinopoulou; University of New Mexico, United States

Photonic structures with asymmetric responses to impinging light are highly desirable across the EM spectrum, even more so for infrared (IR) light, as they introduce new capabilities for integrated beam manipulation as well as thermal management applications. Here we discuss the key principles leading to extreme asymmetry in reflection or in both reflection and transmission in metagratings comprising building-blocks that lack inversion symmetry along the propagation direction. Although counterintuitive, we explain how such extremely asymmetric responses in these passive systems are entirely consistent with the reciprocity principle. We further showcase examples relevant to highly efficient uni-directional thermal IR sources and directional higher-harmonic generation.

11:00 AM EQ16.08.03

Late News: Configure Phonon Polaritons in van der Waals Materials Siyuan Dai; Auburn University, United States

The manipulation of light at small scales is one of the ultimate goals for nanophotonics. For this purpose, polaritons – hybrid light-matter waves that propagate in a confined length scale – are typically involved. Recent results of polaritons in van der Waals materials reveal a series of advances, including atomic scale localization, dynamic tunability, relative low-loss and topologically protected states. These advances are attributed to the unique physical properties in reduced dimensions and the configurability through van der Waals structuring and stacking. In this talk, I will show new merits of phonon polaritons that can be obtained through van der Waals configuration. I will talk about the tunability implemented into phonon polaritons by van der Waals heterostructuring hexagonal boron nitride with graphene and vanadium dioxide, where the polaritons can be tuned dynamically and reversibly via electrostatic gating and temperature control. I will also talk about the geometry and topology configuration of phonon polariton wavefront by twisting stacked slabs of molybdenum trioxide.

11:15 AM EQ16.08.04

Current Flux Imaging of a Micromagnetic Electrofoil David Mayes¹, Maxwell Grossnickle¹, Farima Farahmand¹, Mark Lohmann¹, Mohammed Aldosary¹, Junxue Li¹, Vivek Aji¹, Jing Shi¹, Justin C.W. Song² and Nathaniel Gabor¹; ¹University of California, Riverside, United States; ²Nanyang Technological University, Singapore

Individual electrons in conductors are transported via diffusion, yet current-voltage characteristics in a device are governed by the collective flow of current along streamlines. Despite being at the core of our understanding of electronic and optoelectronic charge transport, the intrinsic global pattern of current streamlines - described by the Shockley-Ramo theorem - has never been imaged. Here, we unveil a microscopy method to image the streamlines along which current naturally flows through ultrathin photodetector devices. Combining scanning photovoltage microscopy with a highly uniform, rotating magnetic field, we probe the photoresponse of atomically pristine thermospintronic heterostructures composed of platinum on yttrium iron garnet (YIG). Under focused laser excitation, a local out-of-plane temperature gradient produces a corresponding out-of-plane spin current in the YIG layer by the Spin Seebeck Effect, which, according to the Inverse Spin Hall Effect, scatters electrons in the platinum layer away from an external, saturating magnetic field. Much like tracers in a wind tunnel map the flow of air around an aerodynamic airfoil, we use a scanning laser beam as a source of directional charge current to map the flow around precisely engineered wing shaped devices, or electrofoils. Photocurrent streamlines can be contorted, compressed or expanded by changing the shape and angle of attack of the electrofoil devices. By imaging and manipulating photocurrent streamlines, we demonstrate an intensive imaging technique to visualize and characterize charge flow in quantum materials.

SESSION EQ16.09: Infrared 2D Materials
Session Chairs: Artur Davoyan and Zhe Fei
Monday Morning, December 6, 2021
EQ16-Virtual

10:30 AM *EQ16.09.01

Infrared s-SNOM Imaging and Spectroscopy of Polaritons at STO-Based Surfaces and Interfaces Yixi Zhou, Weiwei Luo, Margherita Boselli, Adrien Bercher, Adrien Waelchli, Willem Rischau, Stefano Gariglio, Jean-Marc Triscone and [Alexey Kuzmenko](#); University of Geneva, Switzerland

Infrared spectroscopy probes charge, spin and lattice dynamics and therefore is a useful tool to elucidate the physical origin of ordered phases in quantum oxides and interfaces. However, conventional infrared measurements are diffraction limited and do not provide nanoscale resolution. The technique of scattering-type scanning near-field optical microscopy (s-SNOM) based on the near-field interaction between an atomic-force microscope (AFM) tip and the sample, overcomes the diffraction limit, while keeping all the advantages of conventional spectroscopy. We present variable temperature s-SNOM mapping and infrared near-field spectra of surface phonon polaritons in SrTiO₃ and coupled phonon-plasmon polariton modes in (nano-)structures realized at LaAlO₃/SrTiO₃ interfaces [1,2]. We report a long phonon-polariton propagation length exceeding 100 microns, which shows a significant temperature dependence. Our results suggest that strontium titanate and related oxide interfaces are potentially promising for (far-)infrared plasmonic applications.

[1] W. Luo, M. Boselli, J.-M. Pouchard, I. Arzuffi, J. Teyssier, D. van der Marel, S. Gariglio, J.-M. Triscone and A.B. Kuzmenko, *Nature Communications* **10**, 2774 (2019).

[2] M. Boselli, G. Scheerer, M. Filippone, W. Luo, A. Waelchli, A.B. Kuzmenko, S. Gariglio, T. Giamarchi, and J.-M. Triscone, *Phys. Rev. B*, **103**, 075431 (2021).

11:00 AM *EQ16.09.02

Multipole-Engineered van der Waals and High-Refractive-Index Nanostructures [Viktoriia Babicheva](#); University of New Mexico, United States

Transition metal dichalcogenides belong to the family of van der Waals materials and exhibit unique optical and electronic properties, including high tunability, strong nonlinearity, and anisotropy stemming from the van der Waals layers of the material [1]. Most importantly, these materials have a high refractive index and small non-radiative losses in the infrared spectral range. One can operate in the regime when the period of the nanoantenna array is comparable to the wavelength of multipole resonance of a single nanoantenna, which results in optical coupling between nanoantenna and the excitation of lattice resonances [2].

We consider various multipole excitations in such van der Waals and high-index nanostructures, and we design metasurfaces with the properties of directional scattering based on the excited multipoles. We take advantage of both the same-multipole couple and cross-multipole coupling of nanoscatterers in the lattice. We show the nanostructure Mie resonances and coupling between nanoantennas and substrate in the van der Waals nanoantenna array. Such nanoantenna arrays with collective excitation and Mie resonances have a high potential to be utilized in infrared metasurfaces and photonic elements.

The computational efforts are supported by UNM Research Allocations Committee, award RAC2022.

References

[1] V. E. Babicheva and J. Moloney, "Lattice Zenneck modes on subwavelength antennas," *Laser & Photonics Reviews* **13**, 1800267 (2019).

[2] V. E. Babicheva and A. Evlyukhin, "Multipole lattice effects in high refractive index metasurfaces," *Journal of Applied Physics* **129**, 040902 (2021).

11:30 AM EQ16.09.03

Dynamic Spectrum Optoelectronics with Black Phosphorus [Hyunjin Kim](#)^{1,2} and Ali Javey^{1,2}; ¹University of California, Berkeley, United States; ²Lawrence Berkeley National Laboratory, United States

Optoelectronics devices operating at different wavelength ranges require materials with different bandgaps. Although varying chemical compositions or integrating materials with different bandgaps could tailor the operating wavelength range depending on their target applications, increased complexity of their fabrication and necessity for precise control of thickness and/or compositions of materials have made it impractical for realization of actively tunable optoelectronics. Strain is an effective method to modulate the electronic and optical properties of semiconductors by mechanically altering their structure. Reversible and controllable tuning of bandgap in semiconductors can be achieved even within a single device *via* application of elastic strain. While bulk crystalline materials possess a limited maximum amount of strain, two-dimensional (2D) layered materials, such as graphene and transition metal dichalcogenides (TMDCs), can sustain much larger elastic strain, thus allowing for wide tuning of their optical bandgap using strain.

Black phosphorus (bP) has shown unique response upon strain, including anomalous strain dependence of bandgap, tunable van der Waals interactions, and piezoelectricity. These unprecedented strain-dependent characteristics are attributed to a puckered lattice structure of bP, of which bandgap has extraordinary sensitivity to strain. To fabricate devices where reversible strain application is viable, semiconductor materials are required to be in a form of thin membrane. As opposed to bulk crystalline semiconductors, this is readily achievable in bP due to its thin-membrane nature and by mechanical exfoliation to obtain the desired thickness of the bP membrane. Especially, bP with thickness greater than 6 layers has its bandgap spanning over near-infrared (NIR), short-wavelength infrared (SWIR), and mid-wavelength infrared (MWIR) ranges where there is a rapidly increasing demand for optical communications, thermal imaging, health monitoring, spectroscopy, and gas sensing. Strain-induced bandgap modification in bP has recently been studied by several studies and they have shown potentials of bP as tunable optical materials. However, despite the considerable interest in IR regime for optoelectronic applications, such as light-emitting diodes and photodetectors, a device-compatible approach towards tunable optoelectronics with high performance at room temperature is yet to be demonstrated.

Here, we present bP with strain-tunable bandgap and its applications for room-temperature infrared optoelectronic devices with actively variable operating wavelength ranges. Covering from 2.3 μm to 5.5 μm , we demonstrate wide-range tuning of bP bandgap with a combination of compressive and tensile strain. Repeatable and continuous tuning of electrically-pumped MWIR light emission is achieved by utilizing a strained bP-MoS₂ heterostructure on a flexible substrate. Moreover, the low Auger recombination velocity of bP offers much higher theoretical limit of the quantum efficiency in our tunable bP-LED, compared to other materials with similar bandgaps (e.g. InAs and PbSe). We further exploit strain-tunable bandgap of bP to develop a spectrally variable photodetector with high responsivity that can extend its cutoff wavelength by applied strain. Finally, by leveraging the tunable light emission properties of strained bP, we demonstrate multiplexed non-dispersive infrared (NDIR) gas sensing, where multiple gases (e.g. CO₂, CH₄, and H₂O) are detected using a single light source. Our approach bridges the existing technological gap in optoelectronics at infrared wavelength regimes, where III-V and II-VI materials have limited their widespread utilization due to their high cost and stringent requirement for fabrication process by epitaxial growth. Also, our solution decouples the complexity in the device structure and tuning capability in the operating wavelength range without the necessity for sacrificing its performance.

11:35 AM EQ16.09.05

Mid-Infrared Polarization Manipulation via Natural In-Plane Hyperbolic van der Waals Crystals [Nihar R. Sahoo](#), Saurabh Dixit, Anuj K. Singh and Anshuman Kumar; Indian Institute of Technology Bombay, India

Mid-infrared (IR) spectral range has significant potential application in thermal imaging, free-space communication, molecule sensing and others. Thus mid-IR sources, detectors and other opto-electronic components have a vast demand in this era. Furthermore, polarized IR light is a valuable addition in IR imaging techniques as it can distinguish various features of an object. However, conventional wire grid mid-IR polarizers are bulky, designed using complex lithography techniques and exhibit form birefringence. Hence, the integration of conventional mid-IR polarizers with chip-scale devices is challenging. Recently, van der Waals (vdW) materials exhibiting natural in-plane hyperbolicity in the mid-IR spectral region, like α -MoO₃, have garnered research attention. These vdW single crystals demonstrate several benefits over conventional devices, e.g., non-lithographic fabrication approach, facile integration with nano-scale platforms and room temperature operation. In this work, we investigate the infrared optical response of α -MoO₃ thin film for the application of a reflecting type polarizer.

We fabricate the α -MoO₃ using the thermal physical evaporation technique and transfer the as grown α -MoO₃ flakes to a silicon substrate using the mechanical exfoliation method. XRD, HRTEM and SEED confirm the orthorhombic nature of MoO₃ flake. Further, polarization-dependent Raman studies reveal the in-plane anisotropic nature of α -MoO₃. Moreover, the optical response of α -MoO₃ thin film in the mid-IR spectral region displays anisotropic reflectance for p- and s- polarized incident light, which can be exploited as a reflecting type mid-IR polarizer. We explain our results as a manifestation of strong in-plane hyperbolic anisotropy of α -MoO₃ single crystals in the mid-IR spectral region. We verify these experimental results using full-wave numerical simulations and using semi-analytical model based on the transfer matrix method. We perform extensive device optimization and the optimized thickness of α -MoO₃ thin film lies between 1500 nm to 2500 nm where it shows an extinction ratio of more than 5 dB over a bandwidth more than (200 cm⁻¹) with reflectance above 60%. We further experimentally evaluate the temperature resilience of our device and discuss our findings in the context of polarizer performance metrics. This work opens up new avenues for naturally hyperbolic vdW thin-films to be utilized to realize sub-wavelength optical devices with ease of fabrication and chip-scale integration.

11:50 AM EQ16.09.06

A Photothermal Generator via Solar Harvesting Through Spectral Selective Multilayer Transparent Thin Films Mengyao Lyu¹, Jou Lin¹, John Krupczak² and Donglu Shi¹; ¹University of Cincinnati, United States; ²Hope College, United States

To address the critical energy issues, the utilization of solar energy has been one of the main approaches to produce clean energy for many technical, environmental, and ecological advantages. Conventional solar harvesting has been limited to 2D surfaces such as photovoltaic (PV) solar cells. We report solar harvesting via multiple layers of thin films which are spectral-selectively rendered transparent. In this fashion, solar harvesting is transformed from 2D to 3D with much greater energy density. The key requirements are that these films must not only exhibit strong UV and NIR absorptions for harvesting sufficient solar photon energies, but also high average visible transmittance (AVT) for permitting light passing through many layers. We have designed and synthesized photothermal materials from two families of materials: iron oxide (Fe₃O₄@Cu_{2-x}S) and porphyrin compounds (chlorophyllin), both are optically characterized with significant UV and NIR absorptions and high AVTs. Analogous to multilayer capacitors, we have constructed a photothermal generator (PTG) with parallel multilayers of transparent thin films of Fe₃O₄@Cu_{2-x}S and chlorophyllin sealed in a cuboid. As simulated solar light passing through these transparent films, they are photonically activated to generate sufficient heat on each layer, raising the maximum temperature to 76.1 °C. The thermal energy generated has increased from 5074.3 J (one layer) to 55,465.8 J (ten layers) for the Fe₃O₄@Cu_{2-x}S system, and increased from 3826.3 J (one layer) to 56,143.9 J (ten layers) for the chlorophyllin system, both have more than tenfold of increase. The solar photothermal conversion efficiencies of the PTG have reached greater than 60% for both systems. Also discussed is the mechanism underlying the structural effects on optical absorption and photothermal heating.

12:25 PM BREAK

SESSION EQ16.10: Infrared Metasurfaces and Emergent Materials

Session Chairs: Artur Davoyan and Georgia Papadakis

Monday Afternoon, December 6, 2021

EQ16-Virtual

1:00 PM *EQ16.10.01

Use of Time-Dependent Refractive Index Modulation to Achieve Strong Violation of Kirchhoff's Law Alok Ghanekar¹, Jiahui Wang², Shanhui Fan² and Michelle Povinelli¹; ¹University of Southern California, Los Angeles, United States; ²Stanford University, United States

Many naturally occurring materials obey Kirchhoff's Law, the statement that the absorptivity and emissivity of a material are equal for any given wavelength and solid angle. This fundamental property both underlies and limits a variety of applications, from energy harvesting to remote sensing. In the last several years, there has been growing interest in strategies for breaking Kirchhoff's Law, with effort focused on strategies using magneto-optical materials. However, these strategies require use of an external magnet for implementation. Here, we consider an alternate method, which instead uses time-dependent modulation of the material refractive index. This approach would eliminate the need for an external magnet, potentially allowing the violation of Kirchhoff's Law in electronically modulated, semiconductor systems. In this work, we use numerical simulations to design a nonreciprocal infrared thermal emitter with strong Kirchhoff violation.

We start with a dielectric grating that supports guided-mode resonances and impose a spatially- and time-varying index modulation. We calculate the conversion of incoming light to sideband frequencies using a coupled finite-element method (FEM) simulation formalism. For the lossless system, as in previous work, we find that modulation gives rise to nonreciprocal reflection effects. In the forward direction, mode conversion due to index modulation significantly reduces the reflection. In the reverse direction, the absence of mode conversion results in much higher reflection. We thus observe a strong direction-dependence to the reflected signal.

We then introduce loss into the system to create a material capable of thermal emission. We observe continued direction-dependence in the reflectivity, along with the emergence of a resonant reflection dip in the reverse direction. We then use a generalized coupled-mode formalism valid for time-modulated systems to relate the absorptivity and emissivity at a given angle and frequency to the scattering matrix of the modulated material. In the weak-modulation limit, we choose the modulation to correspond to the maximum conversion rate of the lossless system. In this case, we predict a large contrast between absorptivity and emissivity at wavelengths in the mid-infrared, using realistic modulation frequencies of 10's of GHz. In the strong-modulation limit, we further increase the modulation strength to observe directional Rabi splitting. In this case, we observe even higher contrast between emissivity and

absorptivity.

Our results thus suggest the feasibility of achieving violations of Kirchoff's Law without the use of magneto-optics, providing a route to the use of nonreciprocal emissive effects in a variety of novel energy conversion and sensing applications.

1:30 PM EQ16.10.02

Room-Temperature GeSn Nanowires SWIR and MWIR Photodetectors Lu Luo, Simone Assali, Mahmoud R. Atalla, Sebastian Koelling and Oussama Moutanabbir; Polytechnique Montréal, Canada

Abstract: During the last decade, the opto-electronic properties of direct bandgap and metastable GeSn semiconductors have been intensively investigated from short-wave IR (SWIR: 1.5-3 μm) to mid-wave IR (MWIR: 3-8 μm) wavelengths.[1] By engineering materials properties a plethora of infrared photonic devices have been developed, such as lasers, LEDs, and photodetectors[2,3,4,5] However, GeSn thin films are typically under compressive strain due to the large lattice mismatch with Ge interlayer used in the growth on Si substrate. And plastic relaxation during lattice-mismatched growth results in the formation of defects and dislocations, thereby reducing device performance. By exploiting nanowire (NW) morphology, elastic strain can be relaxed due to the compliant nature of the nanoscale core, thus avoiding the formation of structural defects and resulting in a higher crystalline quality compared to thin film materials, without compromising optoelectronic properties.[6]

With this perspective, we discuss in this work discuss the opto-electronic devices made of Ge/GeSn core/shell NWs and operating at room-temperature across SWIR-MWIR wavelengths. NWs with a tunable Sn content ranging from 8 at.% to >20 at.% were grown in a CVD reactor using either a Si or Ge (111) substrate and their structural properties will be discussed down to the atomic level by combining Transmission Electron Microscopy (TEM) and Atom Probe Tomography (APT). Single Ge/Ge_{0.92}Sn_{0.08} NW SWIR photodetectors that were fabricated on a SiO₂/Si substrate exhibit excellent light detection performance at room temperature, with a responsivity of 2.7 A/W under 1550 nm illumination at 1 V and an extended cutoff wavelength of 2.1 μm compared to the 1.6 μm typical to Ge. Moreover, the single NW photodetector shows a degree of polarization with the polarization ratio up to 32%. The back-gated single NW FET geometry allows to estimate the mobility in the Ge/Ge_{0.92}Sn_{0.08} core/shell NW at 50 K, which is two times higher than that in Ge NWs. The tunability of the cutoff wavelength of the NW photodetector from 2.1 μm to higher wavelengths up to 6 μm will be demonstrated using NWs at Sn content of 20 at.% and higher and their performance will be discussed by combining temperature-dependent responsivity measurements. The broadband tunability of GeSn NWs across the infrared range has a tremendous potential for the development of on chip data communication and sensing devices using scalable, Si-compatible fabrication processes.

[1] O. Moutanabbir, et al. Appl. Phys. Lett. 118, 110502 (2021)

[2] S. Wirths, et al. Nat. Photonics 9.2, 88-92 (2015)

[3] S. Assali, et al. Appl. Phys. Lett. 112.25, 251903 (2018)

[4] M.R.M. Atalla, et al. Adv. Funct. Mater. 31.3, 2006329 (2021)

[5] H. Tran, et al. J. Appl. Phys. 124, 013101 (2018)

[6] S. Assali, et al., Nano Lett 17, 1538–1544 (2017)

1:45 PM EQ16.10.03

Extended X-Ray Absorption Fine Structure Spectroscopy (EXAFS) Studies of Sn-Vacancy Defect Complexes in Optoelectronic Ge/Ge-Sn Core/Shell Nanowires John Lentz¹, Michael Braun¹, Apurva Mehta², Ryan Davis² and Paul McIntyre^{1,2}; ¹Stanford University, United States; ²SLAC National Accelerator Laboratory, United States

Germanium-tin alloys may provide a path toward efficient mid-infrared (IR) wavelength optoelectronics in a materials system that is all group IV, and therefore chemically compatible with silicon-based complementary metal oxide semiconductor (CMOS) technologies. They, therefore, hold promise as a potential IR source for on-chip optical interconnects, and for monolithic integration of IR detectors with silicon circuitry. A direct bandgap can be achieved in Ge by incorporating a metastably high Sn composition of about 8–10 at%. However, the optoelectronic properties of these materials have been limited to date, which is thought to be caused largely by a high concentration of grown-in vacancies and vacancy-containing defect clusters. Isolated vacancies act as acceptor-type defects and are present due to the low-temperature at which these alloys are grown¹. Moreover, complexing of Sn atoms and vacancies is theoretically predicted and can create trap levels near mid gap², thus promoting non-radiative carrier recombination. In order to measure the presence and behavior of these complexes in largely strain-free³ single crystal Ge-Sn shells grown by reduced pressure chemical vapor deposition around Ge nanowires, we have used extended x-ray absorption fine structure spectroscopy (EXAFS). EXAFS is one of the few techniques able to probe the detailed local structure of point defect complexes. We report measurements sensitive to the presence and concentration of Sn-vacancy complexes in Ge/Ge-Sn core/shell nanowires, to provide clearer understanding of how these defects affect the material's optoelectronic properties.

1. Nakatsuka *et al.* Mobility behavior of Ge_{1-x}Sn_x layers grown on silicon-on-insulator substrates. *Jpn. J. Appl. Phys.* **49**, (2010).

2. Tahini *et al.* Diffusion of tin in germanium: A GGA+U approach. *Appl. Phys. Lett.* **99**, 1–4 (2011).

3. Meng *et al.* Coupling of coherent misfit strain and composition distributions in core-shell Ge/Ge_{1-x}Sn_x nanowire light emitters. *Mater. Today Nano* **5**, 100026 (2019).

2:00 PM EQ16.10.04

The Origin of Intraband Optical Transitions in Ag₂Se Colloidal Quantum Dots and Their Utilization for Infrared Detectors Ayaskanta Sahu; New York University, United States

In the past 30 years, material scientists have largely capitalized on the grand appeal of utilizing quantum confinement to obtain size-tunable inter-band optical transitions and implement colloidal quantum dots (CQDs) in optoelectronic applications throughout the electromagnetic spectrum. The infrared region is particularly exciting with applications in telecommunications, night-time surveillance, and satellite imaging for agricultural water conservation. While most progress with CQDs in the infrared (IR) has been achieved using inter-band transitions in Pb- and Hg-based heavy metal compounds, intra-band optical transitions originating from external- or self- dopants can potentially expand the library of materials to generate IR-optoelectronic devices with non-toxic materials. In this talk, I will focus on my group's work on recently discovered silver chalcogenide (Ag₂Se) quantum dots that exhibit distinct optical absorption in the mid wave-IR wavelength spectrum. These CQDs demonstrate a narrow bandgap metastable tetragonal phase, not available in bulk, and contain excess electrons in the lowest level of the conduction band. This allows for intra-band optical transitions between the first and the second conduction energy level which can significantly decrease Auger recombination rates and avoid the need for cryogenic cooling. I will present a detailed study of the size-dependent inter-band to intra-band optical transition and compare the competing effects of quantum confinement, environmental Fermi level and particle stoichiometry to provide guidelines for stable electron occupation of the 1S_c state and obtaining tunable mid wave IR absorption.

2:15 PM *EQ16.10.05

Far-Infrared (THz) Applications of Ultrafast Semiconductor Metasurfaces Igal Brener; Sandia National Laboratories and Center for Integrated Technologies, United States

Semiconductor metasurfaces have become attractive for applications in nonlinear optics, control of light emission and switching. In particular, metasurfaces made from direct bandgap semiconductors with low carrier lifetime combined with design concepts that include topology and symmetry can lead to new ways to emit and detect far-infrared radiation.

Ultrafast photodetection with semiconductor devices typically requires structures with fast photoresponse with minimal volume of the photodetection active area. In particular, photoconductive (PC) detectors for far-infrared (THz) pulses rely on devices made from semiconductors exhibiting sub-picosecond lifetime, high absorption of a short gating pulse and high on-off photoconductive contrast. These simultaneous requirements have been extremely difficult to meet using standard and uniform photoconducting semiconductors. However, perfect absorption in semiconductor metasurfaces has created a new path to a new family of photoconductive detectors with unmatched performance. Perfect absorption in dielectric metasurfaces require overlapping two resonances of opposite symmetry in the meta-atoms, critically coupled to the intrinsic absorption of the semiconductor. Moreover, in order to collect the photocurrent, the metasurfaces should provide a continuous current path to the collecting electrodes. Using these concepts, we show a new family of THz photoconductive detectors that can operate with ultralow gating powers (tens of μW) and exceed most other performance parameters of conventional PC detectors. These highly efficient PC detectors are applicable to a wide range of THz spectroscopy and imaging systems, particularly those where low power operation is required such as detector arrays and cryogenic environments.

Finally, I will also present our latest results on THz emission from these ultrafast semiconductor metasurfaces.

2:45 PM EQ16.10.06

A Comparative Study on the Switching Kinetics of W/VO₂ Micron-Sized Powders and Nanoparticles Lavinia Calvi^{1,2}, Luc Leufkens^{3,4}, Cindy Yeung^{3,4}, Roberto Habets^{3,4}, Romy van Geijn^{3,4}, Janique Hupperetz^{3,4}, Daniel Mann^{3,4}, Ken Elen^{1,2}, An Hardy^{1,2}, Marlies Van Bael^{1,2} and Pascal Buskens^{1,3,4}; ¹Hasselt University, Institute for Materials Research (IMO), DESINE Group, Belgium; ²IMEC Vzw, IMOMEC Associated Laboratory, Belgium; ³The Netherlands Organisation for Applied Scientific Research (TNO), Netherlands; ⁴Brightlands Materials Center, Netherlands

Monoclinic vanadium dioxide VO₂ (M) is a thermochromic material based on its reversible metal-insulator transition (MIT). The MIT results from the underlying structural phase transition (SPT) from monoclinic VO₂ (M) below to rutile VO₂ (R) above the transition temperature (T_0) and *vice versa*. The SPT and associated MIT are of great interest for the implementation in energy efficient glazing as VO₂ (M) exhibits a high transmission for solar infrared (IR) radiation below T_0 while above T_0 IR light is blocked. This can lead to significant reduction in energy consumption for heating and cooling of buildings in intermediate climates.

In order to apply VO₂ (M) in thermochromic energy efficient glazing, dopants are required to lower T_0 from 68°C to 20-30°C. Another challenge is the preparation of high quality doped VO₂ nanoparticles for use in coatings and polymer films. To obtain such nanoparticles, we prepared W-doped VO₂ powders and subsequently subjected them to bead milling. We investigated the switching kinetics of undoped and W-doped VO₂ (M) micron-sized powders [1] and nanoparticles. These studies were carried out using data obtained from differential scanning calorimetry, and isoconversional methods were applied for the kinetic analysis. Undoped and W-doped VO₂ (M) powders were prepared via solution-phase reduction of V₂O₅ with oxalic acid followed by solvent removal and thermal annealing. Nanoparticles were obtained through wet bead milling of the powders dispersed in 2-propanol. The results show that the activation energy of the SPT is temperature dependent and decreases when the difference between the material temperature and T_0 increases. Additionally, the activation barrier for both VO₂ (M) to VO₂ (R) and *vice versa* is similar for undoped and W-doped VO₂ (M) powders, and ranges between 138-563 kJ mol⁻¹. This indicates that similar defects are involved in the SPT of VO₂ (M) to VO₂ (R) and *vice versa* [1]. Wet bead milling effectively decreased the VO₂ particle size from 10-50 μm in powders to 50-500 nm for nanoparticles dispersed in 2-propanol. This leads to a decrease in switching enthalpy from 47 to 28 J g⁻¹, amongst others caused by partial loss of crystallinity during bead milling. The activation energy decreases with decreasing particle size. Simultaneously an asymmetry in the switching kinetics occurs and increases with progressive milling. This suggests that the defects introduced into the crystal structure by bead milling affect the transitions VO₂ (M) to VO₂ (R) and *vice versa* differently. In conclusion, W-doping of the VO₂ was successful in tailoring the transition temperature and from the kinetic studies we find that the switching temperature selected should be 2-3°C below the desired in order to facilitate a rapid SPT and MIT. Additionally, wet bead milling was successfully applied to achieve VO₂ nanoparticles. Milling induces asymmetry in the switching kinetics. The produced particles can be further used for the implementation in coatings and films for studying the relationship between the particle size and switching enthalpy and the optical properties of the resulting coatings and films for smart window applications.

References

1. Calvi L, Leufkens L, Yeung CPK, et al. A comparative study on the switching kinetics of W/VO₂ powders and VO₂ coatings and their implications for thermochromic glazing. *Sol Energy Mater Sol Cells*. 2021;224(2021):110977. doi:10.1016/j.solmat.2021.110977

SESSION EQ16.11: Emergent Infrared Systems
Session Chairs: Siyuan Dai and Zhe Fei
Monday Afternoon, December 6, 2021
EQ16-Virtual

9:00 PM EQ16.11.02

Late News: Two-Dimensional Ti₃C₂T_x with Low Infrared Emissivity for Thermal Management and Energy Harvesting Yang Li and Baoling Huang; Hong Kong University of Science and Technology, Hong Kong

In nature, the infrared emissivity of most materials and surfaces are quite large (>0.8), such as woods, glasses, stones, human body surfaces, many plastics, and so on. Apart from polished metals, low-emissivity materials and surfaces (<0.2) are relatively scarce, especially among those dark color materials with high visible absorption. However, those materials and surfaces with low infrared emissivity but high visible absorption are highly demanded for many specific applications, such as visible and IR camouflage, solar thermal harvesting, and thermal management. For instance, even with higher surface temperatures, the low emissivity endows those materials/surfaces with the counter-intuitive ability to conceal themselves from IR detection due to the limited thermal radiation, showing great potential in IR camouflage. Moreover, owing to their dark color, they can easily blend themselves with the environment at night or under weak light. In other words, these visible black but infrared white materials are attractive in multispectral (visible-IR) camouflage. In addition, in solar thermal areas, such low-emissivity black materials can achieve high solar-thermal conversion efficiency due to the

suppression of radiative heat losses. However, the lack of such ideal intrinsic materials has been a long-standing challenge for decades. For this reason, great efforts have been made in developing subwavelength photonic crystals and metamaterials/metasurfaces using complicated and costly nanofabrication methods. It is preferable if there was a flexible intrinsic material with strong, broadband solar absorption but low mid-IR emissivity. In this study, for the first time, we discovered that the black 2D $\text{Ti}_3\text{C}_2\text{T}_x$ MXene film shows strong reflection up to 90% for the mid-IR wavelengths, resulting in a quite low emissivity of ~ 0.1 . Associated with its high solar absorption (90%), it achieves a record-high spectral selectivity (8.2) among reported black materials to the best of our knowledge. Excellent intrinsic spectral selectivity is offered by the $\text{Ti}_3\text{C}_2\text{T}_x$ MXene in a free-standing form as well as coatings on versatile substrates, even on porous, rough surfaces, showing much wider applications than metamaterials. The great potential of 2D $\text{Ti}_3\text{C}_2\text{T}_x$ in visible-IR camouflage was demonstrated. Further studies also reveal that some other commercially available MXenes are also potential IR white materials.

9:15 PM EQ16.11.03

Human Hand as a Powerless Infrared Light Source for Multilevel Information Encryption [Shun An](#), Wen Shang and Tao Deng; Shanghai Jiao Tong University, China

The utilization of man-made, electricity-powered light sources as external stimuli for anti-counterfeiting and other applications is limited by the cost, energy consumption, and lack of human-compatibility. In this work we explore the use of human hand as a natural and powerless infrared (IR) light source and demonstrated the integration of human hand into the anti-counterfeiting systems to enhance the human-compatibility of the system. This hand-based IR anti-counterfeiting approach enables both multilevel information encryption and unclonable coding. We also demonstrate the simultaneous decoding of both the visible code and the IR code overlaid on a flexible label without interference, which makes it promising for high level dual- or multiple-mode anti-counterfeiting. A smartphone-based IR camera is also integrated into this anti-counterfeiting system, which offers the possibility of instantly uploading the coding data to the database to further enhance the effectiveness of the anti-counterfeiting process. Compared to traditional passive light sources and other external stimuli, using human hand as active stimuli enhances the security level of the system, as well as the portability and accessibility of the anti-counterfeiting system, which will help further open up the possibility of integrating not only human hand, but also potentially other human components into the functional systems and processes.

9:20 PM EQ16.11.04

Infrared Emissivity of Polyurethane/Al Composite Coating with Different Floating Position of Al-Particles [Juyeong Nam](#), Injoong Chang, Junesoo Lim and Hyung Hee Cho; Yonsei University, Korea (the Republic of)

During the decades, the infrared survivability of aircraft has been an important issue for ally's air force enhancement in the modern battlefield. In the development of IR sensors, the signature from airframes in the long-wave infrared (LWIR, 8-12 μm) band could be used for target aircraft tracking. Infrared seekers detect aircraft using the contrast radiant intensity between target aircraft and background. For this reason, we thought that we could reduce contrast signature intensity for infrared camouflage. When the background is the sky, because the infrared signature of the sky is low, many studies have been conducted to lower the surface emissivity of the target in the detection wave band. However, when the background is ground, soil, or forest such as look-down situation, we confirmed that there is an optimal emissivity to minimize the contrast signature. Because the polyurethane (PU) based paint is applied to aircraft, in general, through spray coating, we developed PU/Al composite coating that can be applied to aircraft with the same coating method. Polyurethane (PU)/Al composite coating with low infrared emissivity was prepared via spray coating method using PU paint, Al-particles, and ethanol as adhesive, functional pigment, and agent for spraying, respectively. The effect of floating position and amount of Al-particles on infrared emissivity has been discussed. In order to uniformly spray Al-particles, we mixed particles with ethanol at a weight percent of 0.5% and sprayed them using an air-spray gun. The vertical position of Al-particles in a thin PU paint layer was controlled by varying the drying time of PU paint, which takes 48 hours to completely dry. Also, the amount of Al-particles on the coating surface was controlled by varying the number of spraying. To analyze optical properties, we measured the optical emittance and reflectance using FT-IR, and also the apparent temperature using IR camera in infrared band. The results show that the reflectivity increases, therefore, the surface emissivity decreases in the LWIR band, as the vertical floating position is closer to the top surface. Also, the surface emissivity decreases when there are more particles in the coating, and especially, this effect is greater when the floating position of the particle is on the top surface.

9:25 PM EQ16.11.05

Tunable Multiband Coloration Metamaterial for Visible to Infrared Optical Confusing Applications [Injoong Chang](#)¹, Taehwan Kim², Namkyu Lee³, Junesoo Lim¹, Juyeong Nam¹, Maroosol Yun¹ and Hyung Hee Cho¹; ¹Yonsei University, Korea (the Republic of); ²Samsung Electronics, Korea (the Republic of); ³Forschungszentrum Juelich GmbH, Germany

Optical confusion refers to a creature's camouflage technique by which it assimilates itself with the surroundings through manipulation of its colors and patterns. Inspired by these coloration and patterning strategies, artificial tunable materials to control their visible colors or infrared signatures have researched in display, energy, and military application fields. With the development of multiband imagery sensors, optical confusing camouflage must not only be able to control the signature intensity but also be able to mimic patterns of surroundings. Moreover, it must have multiband characteristics. Conventional visible camouflage mimics the colors and patterns of the surroundings and, therefore, creates pixelated digital camouflage patterns. However, conventional infrared camouflage has been focused on reducing signature of target by assuming averaged background signature. Therefore, optical confusion by patterning the colors and signatures in the visible and infrared ranges simultaneously is the most appropriate approach to developing advanced multispectral camouflage.

Herein, we propose a tunable multiband coloration metamaterial (TMCM) devised by arranging pixelated silicon nanowire fractal structures (SiNW-FSs). In this study, we fabricated SiNW-FSs by using one of the wet etching methods, which is metal-assisted chemical etching (MaCE). We calculated the fractal properties of the SiNW-FSs to verify their fractality. As a result, we found that the SiNW-FSs exhibited constant fractal dimension values and a 39% increase in lacunarity, which quantified their morphological heterogeneity with etching time increase. Moreover, we measured their multispectral optical properties, namely, reflectivity and emissivity in the visible and infrared ranges, respectively. We concluded that we could tune the reflectivity and emissivity in each waveband. Finally, through imagery measurements, we confirmed the superior multiband optical confusing effect of the TMCM against a modeled background, which imitates the real environment, compared with that of conventional single-spectral camouflage surfaces. The TMCM is expected to help improve the understanding of the multispectral characteristics of randomly distributed nanostructures and aid the development of state-of-the-art stealth technology.

9:30 PM EQ16.11.06

GeSn/Ge Core-Shell Nanowire Photonic Crystals for Resonant Infrared Photonics [Siyang Peng](#)^{1,2}, Michael Braun¹, John Lentz¹, Andrew C. Meng¹, Zhengrong Shang¹, Alberto Salleo¹ and Paul McIntyre¹; ¹Stanford University, United States; ²Westlake University, China

Mid-infrared light sources are key components for future chemical sensing, on-chip optical interconnect and LIDAR technologies. GeSn alloys can be synthesized under silicon CMOS compatible conditions. Therefore, GeSn can open pathways for miniaturization of mid-infrared devices such as on-chip

molecular sensors, optical interconnects and thermal cloaking devices. Most importantly, direct band gap GeSn is a promising material for on chip integration of light emitters. Previous research on GeSn films has shown mid-infrared lasing at increasing temperatures, initially (in 2015) at less than 90K and, in more recent reports, at or near room temperature. It has also been shown that GeSn nanowires with high-Sn content exhibit strong direct-gap photoluminescence at room temperature. Compared to GeSn thin films, GeSn nanowires are less constrained to lattice match with misfitting (e.g. Ge, Si) substrates and therefore may achieve higher Sn contents without strain and defects that promote non-radiative recombination. Additionally, unlike in a planar GeSn film where the emission angle is limited to $< 13^\circ$ by its high refractive index ($n > 4$), GeSn nanowires provide a platform to design the optical density of states for highly efficient light extraction directly from the light emitting material. GeSn nanowires may also constitute a superior medium for absorption and generation of photocarriers.

We demonstrate room temperature mid-infrared photodetection using resonantly absorbing GeSn/Ge core-shell nanowire photonic crystals. We have synthesized GeSn/Ge core-shell single crystal nanowires with up to 6% Sn that exhibit strong direct-bandgap photoluminescence at room temperature, with a fixed periodic, varying radius and Sn compositions. To synthesize the nanowire device, gold catalysts were patterned on Ge [111] substrate and then two step VLS growth was performed to synthesize Ge core and GeSn shell. The vertical nanowire photodetection device consists of arrays of nanowires in-filled with PMMA insulating layer, an ITO top contact (electron selective) and an aluminum bottom contact (hole selective). We performed selective area FTIR reflectance characterization, which indicates the reflectance maximum changes predictably as the radius and composition of the photonic crystal arrays varies. Reflectance data are in agreement with FDTD full wave simulation of resonant wavelengths and band structures of photonic crystal arrays. We performed photocurrent characterization with an FTIR spectrometer at room temperature. The photocurrent spectrum of Ge/GeSn nanowire photonic crystals have absorption edges up to 2.4 μm , a many-fold enhancement due to resonant absorption, and a photocurrent spectrum that is tunable by varying the photonic crystal geometry.

9:45 PM EQ16.11.07

Thermal Hysteresis Loop in IR Reflectivity of Nanostructured Phase-Change-Material VO₂ Kazutaka Nishikawa, Masamichi Yoshimura and Yoshihide Watanabe; Toyota Technological Institute, Japan

Vanadium dioxide (VO₂) shows a metal-insulator phase transition around 70 °C (T_c), and is drawing attention due to the anomalous physical properties. The optical property in infrared (IR) light region is drastically changed with the transition due to increased free carrier by 4 digits. The VO₂ at metal state (over T_c) has high reflectivity in IR region, and low reflectivity at insulating state (below T_c). Also, it is well known that the transition temperature is modified by the additional elemental doping such as W and Mg.

VO₂ is a promising material to realize future devices such as “smart glass” and “thermal memory” due to temperature-switchable IR properties. Typically, VO₂ shows a temperature hysteresis during heating and cooling processes. The “smart glass” requires narrow temperature-hysteresis-width. In contrast, the “thermal memory”, which can record and read information with temperature states, requires broad temperature-hysteresis-width to store thermal information. Thus, it is essential for realizing such future devices to control the hysteresis width in optical properties of VO₂. In this study, we have fabricated nanostructured VO₂ with different morphologies and measured the temperature width of the hysteresis by IR reflectivity measurements. We found that the hysteresis width is highly dependent on the VO₂ nanostructures [1].

We fabricated VO₂ nanostructures by sputtering deposition and subsequent lamp annealing. For the sputtering deposition, we used a V metal disc as a sputtering target, and deposited V thin films on Si substrates at 350 °C. For the lamp annealing, the samples were annealed at 600 °C by changing the annealing times (1-90 min) and O₂ pressures (2-15 Pa). We observed the morphology of VO₂ by SEM, and recorded IR reflectivity changing the sample temperature in both heating and cooling processes. We found that the fabricated samples were formed by VO₂ nanoparticles on the Si substrates, and that the aggregation of VO₂ nanoparticles was changed by controlling the annealing times and the O₂ pressure during annealing. The isolation of VO₂ nanoparticles progressed with annealing time, and the long-time annealing (90 min) induced highly isolated VO₂ nanoparticles. From the temperature-dependent IR reflectivity measurements, we estimated the hysteresis width (ΔT) at the wavelength of 2.5 μm . For the highly aggregated VO₂ nanoparticles, which were fabricated by short-time annealing (1 min) and low O₂ pressure (2 Pa), the values of ΔT were small. The value of ΔT increased with the decrease of aggregation of VO₂ nanoparticles. We have fabricated VO₂ nanostructures with the different ΔT of 17 °C and 61 °C by changing the annealing conditions. Also, in cooling process, two-step decreases in reflectivity were observed for the slightly aggregated VO₂ nanoparticles. Such two-step decreases in IR reflectivity were not observed for highly aggregated or highly isolated VO₂ nanoparticles.

[1] K. Nishikawa, M. Yoshimura, and Y. Watanabe “Growth of nanostructured VO₂ via controlling oxidation of V thin films: Morphology and phase transition properties” *Journal of Applied Physics* **129**, 185303 (2021).

10:00 PM EQ16.11.09

Three-Dimensional Construction from Two-Dimensional Glassy Polymers via Photothermal Effects Jae Gyeong Lee, Sukyoung Won, Jeong Eun Park and Jeong Jae Wie; Inha University, Korea (the Republic of)

Photothermal heating method has been emerged as a contactless shape manipulating system in materials community. Although numerous methods are documented to achieve 2D to 3D construction, photothermal method has an advantage of using inexpensive near infrared (NIR) light and uniform stimulus with contactless system. The common photothermal method uses black ink patterned hinges on shape memory polymers (SMP) with local light absorption. However, remaining hinges could induce further undesirable actuation after 3D construction. In this study, we employed adhesive tape patterns instead of black ink patterns to achieve transparent 3D structures. The black adhesive tape patterns were irradiated with NIR light to induce local light absorption. When the temperature of the black adhesive patterned area exceeds the polymer's glass transition temperature, biaxially-stretched polymeric chains recover its conformation to random coils, resulting in contraction. We present the 3D complex structures from radial and chiral 2D tape patterns to control the curvature. We also demonstrate sequential folding by distinct light absorption time. Furthermore, we will discuss shape-morphing with multi-material including papers and conductive paste to reconfigure the 3D structures and conductivity.

10:05 PM EQ16.11.10

Development of a Drift-Free Transmission Infrared Spectroscopy System for Long-Term Stable Measurement of Reactions in Aqueous Solutions Yuta Kurokawa, Takumi Goto, Takuji Ube and Takashi Ishiguro; Tokyo University of Science, Japan

Transmission infrared (IR) spectroscopy is one of the best methods for quantitative detection of chemical species with high accuracy. However, the evaluation of chemical reactions in aqueous solutions is usually difficult due to the strong IR absorption of water itself. We avoided this difficulty by fabricating an optical cell with an optical path length of about a few micrometers: the thickness of water through which IR rays can penetrate^{1,2}. To evaluate the absorbance: A using a single optical cell, we measure the transmitted light I₀ and I_s for the empty cell and the cell filled with a specimen, respectively, and calculate $A = -\log(I_s/I_0)$. However, since the measurement times of I₀ and I_s are different, stable quantitative measurement is difficult due to instrument drift (e.g., temperature change of the interferometer or detector) or accidental fluctuations. In this study, we fabricated a microfluidic cell with two adjacent channels and developed a transmission IR spectroscopy system that can simultaneously measure I₀ and I_s using a linear array detector. A two-channel microcell was fabricated by photolithography technique on a CaF₂ substrate and sealed with a CaF₂ window plate. This was mounted on a transmission IR spectroscope (IRT7000, Jasco Inc.) equipped with a linear array (16 parallel detectors). The linear array detectors were cooled by a 5L

liquid nitrogen tank, allowing continuous measurements for about a week. One channel was filled with dry nitrogen gas, while the other channel was filled with ethanol solution (20 mass%) for simultaneous measurement of I_0 and I_s . Simultaneous measurements were made 512 times during 100 seconds, and data was transferred in 20 seconds, which was repeated as one cycle.

When the measurements were made at the same time: t , the time variation, or drift, of $I_0(t)$ and $I_s(t)$ was fluctuated synchronously. In order to evaluate the stability of this IR measurement system, we calculated the time variation of the ratio of $\text{Int}(I_s(t))/\text{Int}(I_0(t))$. Here, $\text{Int}(I_0(t))$ and $\text{Int}(I_s(t))$ were calculated by integrating the respective spectra of $I_0(t)$ and $I_s(t)$ in the range of 2000 to 2250 cm^{-1} after sensitivity correction. For example, in the case of simultaneous measurements, $\text{Int}(I_s(t))/\text{Int}(I_0(t))=0.98733\pm 0.00012$. In a normal measurement, i.e. using one cell, it takes about one hour to change the cell contents. Therefore, the time difference of $\text{Int}(I_s(t+\tau))/\text{Int}(I_0(t))$ was evaluated as $\tau=1$ hour. The error in this case was ± 0.00150 . In other words, the stability of the measurement was improved by a factor of 12.5.

The system was found to be capable of stable quantitative absorbance measurements over a long period of time, even in the presence of external disturbances. As a result, this system can be applied to the measurement of slow chemical reactions in aqueous solution, such as photosynthesis, photocatalysis, and cellular metabolism.

References

1. T.Ube, T.Harumoto, and T.Ishiguro, In situ transmission infrared spectroscopy of hydroxylation of aluminum thin film and subsequent dehydration processes, *J. Appl. Phys.*, 53(2014), 066701-1 - 066701-4,
2. T.Ube, Y. Yoneyama, and T.Ishiguro, In situ Measurement of the pH-dependent Transmission Infrared Spectra of Aqueous Lactic Acid Solutions, *Anal. Sci.*, 33(2017)1395-1400

10:25 PM BREAK

SESSION EQ16.13: Metasurfaces and Metaplatforms for Infrared
Session Chairs: Sheila Edalatpour and Georgia Papadakis
Wednesday Afternoon, December 8, 2021
EQ16-Virtual

1:00 PM *EQ16.13.01

Mid-Infrared Metasurfaces for Biosensing and Tunable Optical Control Hatice Altug; École Polytechnique Fédérale de Lausanne, Switzerland

Metasurfaces have recently emerged as a breakthrough platform for manipulating light at the nanoscale with the use of engineered dielectric and plasmonic nanostructures. They can be tailored to operate over a broad spectrum ranging from terahertz to middle-infrared (Mid-IR) and ultraviolet. Mid-IR metasurfaces are particularly important for the wavelengths between 3 to 20 μm because this range includes two atmospheric windows and fundamental absorption bands of chemicals and biomolecules. Infrared absorption spectroscopy taps into these absorption bands, so called “fingerprints”, for label-free and chemical-specific biosensing. Nevertheless, conventional infrared absorption suffers from several limitations such as low signal levels, difficulty to operate in aqueous environment and bulky and expensive instrumentation. In this talk I will present our recent work with plasmonic and dielectric Mid-IR metasurfaces for realizing novel Mid-IR biosensors through surface enhanced infrared absorption spectroscopy (SEIRA) and incorporation of dielectric metasurfaces with phase change materials for programmable phase control [1-4]. I will also present a versatile nanofabrication process enabling wafer-scale and CMOS-compatible manufacturing of efficient dielectric and plasmonic mid-infrared metasurfaces [5].

With metallic nanoantennas our lab has been developing ultrasensitive SEIRA based biosensors. Most recently, we introduced a deep learning-augmented Mid-IR nanoplasmonic metasurface, which provides a universal platform to study dynamic biological processes involving analytes from all four major biomolecular classes [1]. The optofluidic device incorporating multiresonant plasmonic metasurface and microfluidics enabled to collect a vast amount of spectrotemporal data, which is then used to construct a deep neural network for accurate analyte discrimination. The capabilities of the new method are demonstrated by dynamically monitoring a multistep bioassay containing sucrose- and nucleotides-loaded liposomes interacting with a small, lipid membrane-perforating peptide.

In low-loss dielectric metasurfaces, we harness their high-Q resonances to implement compact Mid-IR biosensors. One of our devices utilizes large-area imaging with a 2D pixelated metasurface to detect Mid-IR molecular fingerprints without the need for spectrometry and frequency scanning [2]. The metasurface is designed to provide strong near-field enhancement, where the resonance positions of individual metapixels are varied over a target Mid-IR range. With this one-to-one mapping between spectral and spatial information, enhanced absorption signatures of analytes are sampled at multiple spectral points and translated into a 2D barcode-like spatial absorption map for imaging-based detection. In another device, we expanded the operational spectral range of dielectric metasurfaces for spectroscopy by using angle scanning and polarization aspect together. The system provided an impressively wide spectral coverage from 1100 cm^{-1} to 1800 cm^{-1} at 1.4 cm^{-1} resolution [3].

Current metasurfaces are often locked to a fixed functionality due to their static constituent materials. Extending into tunable metasurfaces can enable active optical elements such as tunable lenses, dynamic holograms and spatial light modulators for key application areas including adaptive spectroscopy. Recently, we introduced a tunable all-dielectric Mid-IR Huygens' metasurface consisting of multi-layer Ge meta-units with strategically incorporated phase change material [4]. Through hyperspectral imaging measurements we showed optical programming of a light phase profile into the metasurface with single meta-unit precision and a maximum light phase tunability of 81% of full 2π phase shift.

References:

- [1] John-Herpin et al. *Advanced Materials* (2021)
- [2] Tittl et al. *Science* (2018)
- [3] Leitis et al. *Science Advances* (2019)
- [4] Leitis et al. *Advanced Functional Materials* (2020)
- [5] Leitis et al. Under Review (2021)

1:30 PM *EQ16.13.02

Light-Absorption in Nano-Antennas—From Self-Heating to Reconfigurable Metasurfaces Giulia Tagliabue; École Polytechnique Fédérale de Lausanne, Switzerland

By engineering light absorption in dielectric nanoantennas, we explore new opportunities for the manipulation of temperatures at the nanoscale as well as

the design of reconfigurable metasurfaces.

In the last decade, optical nanoantennas have revolutionized light manipulation and control at the nanoscale. Light absorption was initially considered a purely detrimental process, reducing the efficiency of optoelectronic devices. Recently, however, it has attracted growing interest, enabling novel light-energy conversion pathways and offering intriguing opportunities for reconfigurable systems. In particular, going beyond metallic nanostructures, I will introduce the opportunities offered by dielectric nanoantennas for thermophotonics and, more specifically, for thermo-optical reconfigurable devices. In the first part of the talk, I will discuss self-induced optical heating effects in highly absorbing Silicon (Si) and Germanium (Ge) nanoresonators. In particular, I will show recent calculations demonstrating that, due to thermo-optical effects, self-heating can give rise to a complex, non-linear relationship between illumination intensity and temperature, even for moderate illumination intensities relevant for applications such as Raman scattering [1]. Subsequently, I will discuss how self-induced optical heating could be employed in optical devices and metasurfaces. In particular, I will present our recent efforts in the design of thermally reconfigurable metalenses [2].

[1] T.V. Tsoulos, G. Tagliabue – Self-induced thermo-optical effects in silicon and germanium dielectric nanoresonators - *Nanophotonics* 9 (12), 3849-3861

[2] A. Archetti, R.J. Lin, F. Kiani, N. Restori, TV Tsoulos, G. Tagliabue – Thermally Reconfigurable Metalens - in preparation.

2:00 PM *EQ16.13.03

Near-Field Infrared Optical Characterization Techniques of Twisted and Indirectly Nanostructured 2D Material Heterostructures [Frank Koppens](#); ICFO - The Institute of Photonics Sciences, Spain

Two-dimensional (2D) materials offer extraordinary potential for control of light and light-matter interactions at the atomic scale. In particular, twisted 2D materials has recently attracted a lot of interest due to the capability to induce moiré superlattices and discovery of electronic correlated phases [1,2]. In this talk, we present nanoscale optical techniques such as near-field optical microscopy and photocurrent nanoscopy, and reveal with nanometer spatial resolution unique observations of the infrared and photothermal properties of twisted 2D materials.

We report on the photo-thermoelectric nano-imaging within the Moire unit cell of small-angle twisted graphene [4] and interband collective modes in charge neutral twisted-bilayer graphene near the magic angle [3]. The freedom to engineer these so-called optical and electronic quantum metamaterials [1] is expected to expose a myriad of unexpected phenomena. As an example for indirectly patterned polaritons, we introduce and demonstrate a novel multimodal reflection mechanism of the ray-like optical excitations in hyperbolic materials, such as hBN.

References

[1] Song, Gabor et. al., *Nature Nanotechnology* (2019)

[2] Cao et al., *Nature* (2018)

[3] Hesp et al., *Nature Physics* (2021). Arxiv 1910.07893.

[4] Hesp et al., *Nature Communications* (2020)

[5] Epstein et al., *Science* (2020)

[6] Herzig Sheinfux et al., (2021)

2:30 PM *EQ16.13.04

Towards Complete Optical Coupling to Localized Optical Modes [Javier Garcia de Abajo](#)^{1,2}; ¹ICFO, Spain; ²ICREA, Spain

The large mismatch between the free-space light wavelength and the spatial extension of localized optical modes, particularly at infrared frequencies, results in a poor light-mode coupling, which poses a serious problem in the design of practical structures for light and thermal radiation management. As a possible way to address this issue, we propose the use of perfect scatterers, which enable complete coupling between free space radiation and arbitrarily small localized modes when they are placed at suitable positions and the external light is also optimally structured in the far field. We discuss quantum perfect scatterers consisting of two-level atomic/molecular systems, as well as classical perfect scatterers provided by Mie-mode-supporting dielectric cavities. Our results open a practical route to circumvent the long-standing photon-polariton wavelength mismatch problem in nanophotonics.

SESSION EQ16.14: Infrared 2D Materials—Continued

Session Chairs: Artur Davoyan and Zhe Fei

Wednesday Afternoon, December 8, 2021

EQ16-Virtual

4:00 PM *EQ16.14.01

Nanophotonics with Phonon Polaritons in 2D Materials [Rainer Hillenbrand](#); CIC nanoGUNE BRTA, Spain

Phonon polaritons - light coupled to optical lattice vibrations - in 2D materials exhibit ultra-short wavelengths, long lifetimes and strong field confinement, which allow for manipulating infrared light at the nanometer scale. Here, we discuss real-space nanoimaging studies of ultra-confined infrared phonon polaritons, essentially in thin hexagonal boron nitride layers and nanostructures, using scattering-type scanning near-field optical microscopy (s-SNOM) and nanoscale infrared Fourier transform (nano-FTIR) spectroscopy. We visualize and analyze phonon polaritons in nanoscale waveguides and resonators. Particularly, we will demonstrate that phonon polaritons can be utilized to achieve vibrational strong coupling with nanoscale amounts of organic molecules.

4:30 PM *EQ16.08.02

Highly Broadband Spectral Control of Thermal Radiation by Exploiting Air as a Functional Element [Andrej Lenert](#), Tobias Burger, Deju Fan, Zachary J. Berquist, Andrew J. Gayle, Neil P. Dasgupta and Stephen R. Forrest; University of Michigan, United States

Air can play a key role within photovoltaic and photothermal materials, owing to its non-absorbing, low-index, low-thermal-conductivity properties. However, exploiting these unique properties is challenging because it requires an approach that accommodates the undesirable properties of air, namely the lack of structural support. Here, I discuss our recent progress in realizing thermophotovoltaic (TPV) cells¹ and refractory solar thermal absorbers^{2,3} that incorporate air in a way that does not compromise their functional stability. In doing so, we overcome key limitations in TPV and solar thermal conversion, namely a lack of broadband spectral control, and realize record-high efficiencies. With such high-efficiency approaches, TPV-based thermal batteries can serve as a solution to the long-duration electricity storage problem, while concentrated solar thermal can access a high-temperature regime and, in turn,

provide efficient, on-demand power generation and industrial process heat.

1. Fan, D., Burger, T., McSherry, S., Lee, B., Lenert, A. & Forrest, S. R., "Near-perfect photon utilization in an air-bridge thermophotovoltaic cell," *Nature* **586**, 237–241 (2020). DOI: 10.1038/s41586-020-2717-7
2. Berquist, Z. J., Turaczy, K. K. & Lenert, A., "Plasmon-Enhanced Greenhouse Selectivity for High-Temperature Solar Thermal Energy Conversion," *ACS Nano* (2020). DOI: 10.1021/acsnano.0c04982
3. Gayle, A. J., Berquist, Z. J., Chen, Y., Hill, A. J., Hoffman, J. Y., Bielinski, A. R., Lenert, A. & Dasgupta, N. P., "Tunable Atomic Layer Deposition into Ultra-High-Aspect-Ratio (>60000:1) Aerogel Monoliths Enabled by Transport Modeling," *Chem. Mater.* **33**, 5572–5583 (2021). DOI: 10.1021/ACS.CHEMMATER.1C00770

5:00 PM *EQ16.06.01

Radiative Properties of Optically Clear Mesoporous Silica Films and Monoliths [Laurent Pilon](#) and Refet Yalcin; University of California, Los Angeles, United States

This talk presents new synthesis methods and characterization of optically transparent mesoporous silica thin films and monoliths with tunable infrared properties. The material featured porosity that can be adjusted from 50 to 90% with narrow pore size distribution varying between 5 and 20 nm and silica building blocks between 2 and 10 nm. As a result, the materials are transparent in the visible while their infrared properties can be tuned to achieve very high and/or spectrally selective thermal emission at room temperature. The material optical behavior observed across the spectrum is interpreted thanks to numerical simulations of electromagnetic wave transport through realistic computer-generated mesoporous materials. Particular attention is paid to the effects of dependent scattering, absorption, and fractal architecture of the mesoporous structure. The novel materials investigated could be used for passive thermoregulation of buildings.

SESSION EQ16.15: On-Demand
Sunday Morning, December 5, 2021
On-Demand

8:00 AM EQ16.03.03

High-Temperature Photonics with Refractory Metals [Margaret A. Duncan](#)¹, Mariama Rebello Sousa Dias² and Marina Leite¹; ¹University of California, Davis, United States; ²University of Richmond, United States

The continuous growth of the field of photonics over the last several decades has led to a myriad of groundbreaking applications, from ultrafast quantum computation to long-distance data transmission to energy conversion. However, most of the current research in photonics is performed at room temperature in an ambient environment. Determining the optical behavior of materials in different environments and at higher temperatures is crucial to understanding their properties and thus the performance of devices in the real world. Similarly, certain materials with advantageous mechanical and thermal properties such as refractory metals remain minimally explored in the optical regime. Because of this, refractory metals have for the most part been overlooked for photonic applications, even though their refractive indices may prove highly useful to many situations, e.g. thermophotovoltaics (TPV). We resolve the effects of environment (air, N₂, and Ar) and temperature (25 – 600°C) on the complex refractive index of seven refractory metals (Cr, Hf, Mo, Ru, Ta, Ti, and W) as well as TiN by performing *in situ* ellipsometry, where all thin films are fabricated via sputtering. Our *in situ* ellipsometry experiments suggest a reaction at high temperatures between certain refractory metals and an N₂-rich environment. For example, we show a maximum change of 38% for the refractive index and 24% for the extinction coefficient in Mo, and a maximum change of 23% for the refractive index and 47% for the extinction coefficient in W. This change remains even after the temperature is lowered. We note that TiN has the added benefit of including nitrogen, making it less likely to react when placed in an N₂-rich environment at high temperatures. When exposed to an inert Ar environment, many of the refractory metals showed similarly substantial changes in refractive index beginning around 500°C. We complement the optical measurements with morphological and chemical analyses of the films' surface by combining atomic force microscopy, transmission electron microscopy, and X-ray photoelectron spectroscopy of the substrates before and after being held at high temperatures, to analyze the possible physical and surface changes that have occurred. With these experimentally obtained temperature-dependent refractive indices, we provide an example application, quantifying the performance of these refractory metals in an example TPV absorber/emitter. Here, we find a 3-fold increase in efficiency by using refractory metals when compared to other current state-of-the-art absorber/emitters, proving their value for modern photonic applications.

SESSION EQ16.12: Near Field Radiation Control
Session Chairs: Georgia Papadakis and Giulia Tagliabue
Wednesday Morning, December 8, 2021
EQ16-Virtual

10:30 AM *EQ16.12.01

Incandescent Metasurface Modulated Beyond 10 MHz Leo Wojszwyk, Anne Nguyen, Cheng Zhang, Anne-Lise Coutrot, Benjamin Vest and [Jean-Jacques Greffet](#); Institut d'Optique, France

Incandescent sources such as hot membranes and globars are widely used for mid infrared spectroscopic applications. The emission properties of these sources can be tailored by means of resonant metasurfaces: control of the spectrum, polarization and directivity has been reported. For detection or communication applications, fast temperature modulation is desirable but is still a challenge due to thermal inertia. Reducing thermal inertia can be achieved using nanoscale structures at the expense of a low absorption and emission cross section. Here, we introduce a metasurface that combines nanoscale heaters to ensure fast thermal response and nanophotonic resonances to provide large monochromatic and polarized emissivity. The metasurface is based on platinum and silicon nitride and can sustain high temperatures. We report a peak emissivity of 0.8 and an operation up to 20 MHz, six orders of magnitude faster than commercially available hot membranes.

11:00 AM *EQ16.12.02

Near-Field Heat Transfer and Energy Conversion in Nanoscale Gaps Pramod Sangi Reddy; University of Michigan, United States

Understanding radiative heat transfer in nanoscale gaps and devices is of considerable interest for creating novel energy conversion devices. In this talk, I will first describe ongoing efforts in our group to experimentally elucidate nanoscale radiative heat transfer. Specifically, I will present our recent experimental work where we have addressed the following questions: Can existing theories accurately describe radiative heat transfer in single nanometer sized gaps? Can radiative thermal conductances that are orders of magnitude larger than those between blackbodies be achieved? In order to address these questions we have developed a variety of instrumentation including novel nanopositioning platforms and microdevices, which will also be described. Further, I will discuss possible applications of near-field thermal radiation for energy conversion and photonic cooling. Finally, I will briefly outline how these technical advances can be leveraged for future investigations of nanoscale heat transport and near-field thermophotovoltaic energy conversion.

11:30 AM EQ16.12.03

Exploring Phonon Polariton Heat Transfer Channels Across Nanoscale Gaps Using an Electron Beam Isobel C. Bicket^{1,1}, Connor Wong¹, Yao-wen Yeh², Joshua Tefal¹, Nabil Bassim^{1,1} and Maureen Joel Lagos^{1,1}; ¹McMaster University, Canada; ²Rutgers, The State University of New Jersey, United States

Understanding near-field radiative heat transfer (NFRHT) underpins the management of thermal energy for the development of novel heat-control technologies. Evanescent near-fields couple across nanoscale gaps, making these platforms a classic case study for NFRHT phenomena. Most studies on NFRHT in gaps provide limited spectral information, with the exception of scanning probe microscopies [1], in which the spatial resolution is limited to tens of nm. Spectral information can also be obtained using far-field IR probes, in which case much of the spatial sensitivity is lost and optically dark modes are unreachable. Challenges remain in understanding the spectral and spatial properties of NFRHT channels provided by bright and dark surface phonon polaritons (SPhP) in dielectric-based nanogaps. Detecting all of the available SPhP modes present in a gap and their spatial distribution; understanding the role of gap size and shape in tuning the spectral response; and nanoscale imaging of the local temperature profile across the gap is needed to further our understanding of NFRHT limits and nanoscale thermal emission.

We study the near-field spectral response of SiC nanogaps as small as 5 nm, with different temperature gradients across the gap. We use an atom-sized electron beam in a monochromated transmission electron microscope to conduct electron energy loss spectroscopy (EELS) measurements of the IR response [2]. We image the spatial distribution of both bright and dark SPhP modes, providing rich spectral information with nm spatial resolution [3]. For temperature measurements, we use a recently-developed method to locally measure thermal profiles across the gap using phonon EELS signal [4]. We fabricate SiC nanogaps between two rods using a focused ion beam, producing gaps ranging from 40-280 nm. Under heating, the gaps may shrink, down to 5 nm. Our EELS data reveals a broad spectral peak: the amalgamation of a rich spectrum of SPhP modes. We notice that the shape, intensity, and maximum of the EELS peak depends on the gap size and shape, and on the probe location in the gap. For example, the high energy modes within the peak are stronger in the centre of the gap than near the open sides, indicating strong high energy near-fields at the gap centre due to the formation of highly localized modes in these narrow gaps (<50 nm). Our results suggest that spectral tunability can be obtained even with small gaps, potentially affecting spectral heat flux and thermal emission. To gain further insight into the variety of SPhP in the gap, we conduct boundary element simulations of coupled nanorods with varying cross-sectional geometries. We find that a large variety of coupled modes exist, including new face-type modes with extremely localized near-fields, dependent on the cross-sectional shape. Our results provide relevant information on channels for NFRHT beyond the traditional coupled dipolar modes.

Our fabricated gaps are designed to exhibit different temperature profiles; some gaps have the same temperature on either side while other gaps have hot and cold sides, according to our local temperature measurements. In thermally symmetric gaps, the near-field intensity drops towards the centre, but is symmetrically distributed on either side and increases under heating. In thermally asymmetrical gaps, the near-fields near the hotter rod are stronger, due to an increase in thermal phonon population [4]. Our work studying the spatial distribution and temperature gradients present in coupled SPhP represents progress towards understanding the available channels for NFRHT and thermal emission in nanogaps.

Acknowledgements

MJL and NDB acknowledge NSERC of Canada for financial support. We thank P. Batson for access to the Rutgers University Nion microscope.

References

- [1] Cuevas & García-Vidal, *ACS Photonics*, **5**, 10, 2018.
- [2] Krivanek *et al.*, *Nature*, **514**, 7521, 2014.
- [3] Lagos *et al.*, *Nature*, **543**, 7646, 2017.
- [4] Lagos & Batson, *Nano Lett.*, **18**, 7, 2018.

11:45 AM EQ16.12.04

Analysis of Nano-Resistor Light Emission Areas in Solid State Incandescent Light Emitting Devices Yue Kuo and Jia Quan Su; Texas A&M Univ, United States

The Solid State Incandescent Light Emitting Device (SSI-LED) was reported recently (1,2,3). It emits the warm white light from visible to near IR wavelength range, which is similar to that emitted from a conventional incandescent lamp or that of the sunlight in the same wavelength range. The principle of the light emission of this kind device is the thermal excitation of nano-resistors formed from the breakdown of a MOS capacitor with a metal oxide high-k gate dielectric. It can be operated continuously for more than 20,000 hours in air without failure. The electrical, optical, and material properties of the SSI-LED have been investigated. In general, the intensity and spectrum of the emitted light is related to the material and structure of the nano-resistor, i.e., the original gate dielectric properties, and the applied voltage. In this paper, authors investigated the relationship between the (light emission area/whole gate area) ratio and the operation condition as well as the gate dielectric material using the J Mapping method. The cause of the high light emission density on the edge of the device will also be discussed.

1. Y. Kuo and C.-C. Lin, *Appl. Phys. Letts.*, **102**(3), 031117 (2013).
2. Y. Kuo, *IEEE Trans. Elec. Dev.*, **62**(11), 3536-3540 (2015).
3. A. Shukla and Y. Kuo, *ECS J. Solid State Sci. Technol.*, **9**, 065017 (2020).

12:00 PM *EQ16.12.05

Engineering the Spectrum of Near-Field Thermal Radiation Using Thermal Metamaterials Sheila Edalatpour; University of Maine, United States

The near-field effects of radiative heat transfer arise when at least one of the characteristic lengths of the system, i.e., the size of the objects and their separation distance, is smaller than the dominant thermal wavelength (approximately 10 μm at room temperature). Radiative heat transfer in the near field can be quasi-monochromatic, polarized, coherent, and it can exceed the far-field blackbody limit by several orders of magnitude. These unique properties are highly promising for many advanced and state-of-the-art technologies in waste heat recovery, nanoscale-resolution imaging, photonic cooling, thermal management of electronic devices, and thermal rectification through a vacuum gap. The quasi-monochromatic nature of near-field radiative heat transfer

plays a central role in these technologies. For example, quasi-monochromatic thermal emission has been reported to improve the performance of nano-gap thermophotovoltaic devices which are proposed for waste heat recovery. Another example is a thermal diode, which allow heat to flow only in a preferred direction. In this case, thermal rectification is achieved by capitalizing on temperature dependence of the resonance frequency of thermal emission. Development of the near-field applications requires materials with designer near-field thermal spectra. Materials with designer near-field spectra are rarely found in nature. As such, metamaterials that are engineered at the sub-wavelength scale have been proposed for controlling the spectral distribution of near-field thermal radiation.

Achieving customized near-field spectra using metamaterials requires reliable and computationally efficient theoretical models for designing the material as well as robust experimental techniques for characterization of the designed materials. This talk starts with an overview of near-field thermal radiation, its significance and applications, and it continues with a discussion of various metamaterials, including nanopillars, gratings, and Mie-resonance based metamaterials, proposed for tuning the spectrum of near-field thermal radiation. Next, the numerical and approximate models used for designing metamaterials is reviewed, and an experimental technique for characterizing the spectrum of near-field thermal radiation is presented. Finally, the measured near-field and far-field thermal radiation spectra for metamaterials made of silicon carbide nanopillars are presented and discussed.

SYMPOSIUM EQ17

Emerging Materials for Contacts and Interfaces in Optoelectronics
November 30 - December 8, 2021

Symposium Organizers

Stefaan De Wolf, King Abdullah University of Science and Technology
Alex Martinson, Argonne National Laboratory
Monica Morales-Masis, University of Twente
Philip Schulz, Centre National de la Recherche Scientifique

* Invited Paper

SESSION EQ17.01: Printable Electronic Materials and Organic Semiconductors
Session Chair: Thomas Riedl
Tuesday Morning, November 30, 2021
Hynes, Level 2, Room 203

10:30 AM *EQ17.01.01

Interfacial Electronic Properties in Organic Solar Cell, a Two Study Case—Fullerene vs Non Fullerene Acceptor at TiO₂ Surface and 4P-NPD as Exciton Blocking Layer in Inverted Solar Cell Architecture Nadine Witkowski¹, Dylan Amelot¹, Hervé Cruguel¹, Mariam Ahmad², Mehrad Ahmadpour² and Morten Madsen²; ¹Sorbonne University, France; ²University of Southern Denmark, Denmark

Solar energy is by far the most abundant and widespread renewable energy resource, which is maintenance-free and envisioned to play a key role in the energy transition needed for the next decades. Organic photovoltaics (OPVs) technology, offering now power conversion efficiency of over 18%, is expected to provide alternative implementation technologies such as large area flexible panels for urban compatible exploitation with cost-effective printing techniques.

Organic solar cells architectures have become increasingly complex with stacking of both organic and inorganic materials optimized to provide largest efficiency in the final device. The rational design of electronic levels at the organic/organic interfaces or at the organic/inorganic interfaces is of fundamental importance in the transport of charges for improved efficiency. The use of electron spectroscopies carried out using synchrotron radiation allows an in-depth investigation of the electronic interplay at the interface evidencing charge transfer, band bending or chemical bonding together with a detailed picture of the band alignment.

In this context, we have used electron spectroscopies to investigate metal oxide interfacial layers acting as electron-transport layer (ETL) in organic solar cells, namely TiO₂, in connection with acceptor molecules. During past twenty years, fullerenes have been dominant as electron accepting materials for designing high performance organic solar cells, however their drawbacks mainly in terms narrow absorption spectra have motivated their replacements by non-fullerene electron acceptor molecules. The comparison between C₇₀ and non-fullerene acceptor, namely ITIC molecule, at the interface with low temperature sputtered TiO₂ ETL will be presented. It will be shown that resonant photoemission is a powerful technique capable in revealing the role of defects states present at the TiO₂ interface.

In the second example presented, we will focus our interest on organic/organic interfaces. It has been evidenced that the efficiency of organic solar cell suffers from the recombination of photo-induced electron-hole pair or excitonic state at the interface between the electron donor and the hole transport layer (HTL) or electrode. One of the strategies to limit this recombination consists in introducing an exciton blocking layer (EBL) at the interface between the electron donor and the HTL. Such strategy has been recently used successfully in an inverted solar cell design, in which a molecule commonly used in OLED, 4P-NPD has demonstrated its abilities as EBL in a planar heterojunction of 4P-NPD/DBP. Surprisingly, the optimal thickness of the EBL giving higher power conversion was found to be less than one nm. Our investigation of interfacial electronic properties in 4P-NPD/DBP heterojunction reveals the

strong influence of DBP in term of band alignment on ultra-thin layer of 4P-NDP favoring the charge transport across the device.

The presented work is a joint study by Sorbonne Université and University of Southern Denmark and supported by Danmarks Frie Forskningsfond, DFF FTP project 'React-PV', Danish Ministry of Higher Education and Science project 'SMART', Horizon2020 project CALIPSOplus.

11:00 AM EQ17.01.03

Novel Solution-Combustion Technique for the Synthesis of Impurity-Free BaSnO₃ Nanoparticles at 130 °C Sushobhita Chawla¹, Garima Aggarwal¹, Akash Kumar² and Balasubramaniam Kavaipatti¹; ¹Indian Institute of Technology Bombay, India; ²Gachon University, Korea (the Republic of)

Conventionally, thin-film synthesis of the high mobility, high figure of merit BaSnO₃ is achieved *via* cost-intensive, high temperature, high vacuum methods. *Chimie-douce* techniques for nanoparticle synthesis of this material are often accompanied by impurity phases such as BaCO₃, SnO₂ and Ba₂SnO₄, necessitating high annealing temperatures, consecutively rendering it impractical for numerous applications. Lowering the synthesis temperature to obtain phase pure BaSnO₃ can expand the horizons for its optoelectronic applications, with an obvious reduction in the thermal budget.

In this work, we have developed a novel solution combustion technique for the synthesis of BaSnO₃ nanoparticles. A peroxy/superoxy precursor to the nanoparticles is first synthesized by co-precipitation of the tin and barium salts *via* the H₂O₂ assisted route. We find that the crystallization temperature of BaSnO₃ is significantly reduced by adding an organic solvent to the precursor; temperatures as low as 130 °C lead to phase pure BaSnO₃ nanoparticles. The role of the organic solvent is established as the component responsible for an exothermic reaction occurring around 130 °C, that leads to crystalline BaSnO₃ formation. Importantly, this method allows for facile incorporation of dopants. Such low synthesis temperatures enable BaSnO₃ to be used in devices having temperature limitations during device processing, such as perovskite-based solar cells in an *n-i-p* architecture or heterojunction Si solar cells.

11:15 AM DISCUSSION TIME

11:30 AM EQ17.01.05

Late News: Transferrable Ag Nanogrid Electrodes by Unidirectional Electrospinning for Semitransparent Perovskite Solar Cells Jieun Lee, Beomjune Shin, Seongheon Kim, Seong Ho Cho, Yonghoon Jung, Ki-Tae Park, Changgyun Son, Young Ho Chu, Da Gil Ryu, Sunggun Yoon, Munkyeong Choi, Ho-Young Kim and Yun Seog Lee; Seoul National University, Korea (the Republic of)

Semitransparent solar cells are used in diverse energy-related applications, such as Building Integrated Photovoltaics (BIPV), automobile windows, and wearable electronic devices. Perovskite is fairly attractive as an active layer in semitransparent solar cells. When this material is used, the thickness of the light absorption layer can be easily controlled based on a solution-based process. On the contrary, the fabrication of a transparent electrode layer in film solar cells with great performance remains a challenge so far. Since the layers of perovskite solar cells are substantially thin, the transparent electrode should be manufactured with the low surface roughness to prevent a detour current path between the different layers. In addition, the transparent electrode should be fabricated in low-temperature, moreover, the use of polar solvents is not beneficial because the active layer of solar cells can be damaged. In this contribution, the Ag nanogrid electrode is fabricated by using directional electrospun polyethylene oxide (PEO) nanofibers as an etching mask in the wet etching process. Because polar solvents are not used, and high temperature is not required in this process, electrodes can be fabricated on Polydimethylsiloxane (PDMS) substrate; hence, electrodes can be transferable to various surfaces or shapes. In addition, when this method is applied, the high scalability can be achieved, such as for the roll-to-roll process for large-area substrates. The fabricated transferrable Ag nanogrid transparent electrodes has the transmittance of 92.7% (at 550 nm) and the sheet resistance of 18.0 Ω/sq. Furthermore, the MAPbI_{2.5}Br_{0.5} based perovskite semitransparent solar cell with Ag nanogrid electrode attached as the top electrode was manufactured. And the performances, such as J-V characteristics, quantum efficiency, and transmittance, were investigated. Consequently, we report a semitransparent solar cell with an average visible wavelength transmittance (AVT) of 25.2%, and a power conversion efficiency (PCE) of 12.7%. Therefore, the light utilization efficiency rates (LUE) of 3.21%, which is the highest value in the conventional perovskite semitransparent solar cells, can be identified.

SESSION EQ17.02: Perovskite and Organic Solar Cells

Session Chair: Nadine Witkowski

Tuesday Afternoon, November 30, 2021

Hynes, Level 2, Room 203

1:30 PM EQ17.02.01

Think Small—Hole-Selective Monolayers for Solar Cells Artiom Magomedov¹, Ernestas Kasparavicius¹, Amran Al-Ashouri², Eike Köhnen², Yuanbao Lin³, Yuliar Firdaus³, Bor Li², Thomas D. Anthopoulos³, Tadas Malinauskas¹, Steve Albrecht² and Vytautas Getautis¹; ¹Kaunas University of Technology, Lithuania; ²Helmholtz-Zentrum Berlin für Materialien und Energie, Germany; ³King Abdullah University of Science and Technology, Saudi Arabia

Several emerging technologies from the field of organic electronics have a great promise to disrupt our everyday lives. To achieve this goal, new materials need to be developed, that would meet the high expectations of the market.

Traditionally, self-assembled monolayers (SAMs) were widely used in material sciences for the modification of the interfaces of various semiconducting oxides. However, there were not many examples, where the SAMs would have an individual role, rather than that of the “assisting” or “improving”. The most significant demonstration of the power of the SAMs is dye-sensitized solar cells. There, in a combination with the mesoporous scaffold, a single layer of the dye molecules was sufficient to ensure efficient absorption of the light. Nevertheless, there were still only several examples of the other types of semiconducting SAMs demonstrated over the years.

Recently in our work, we have introduced carbazole-based phosphonic acids into the p-i-n perovskite solar cell architecture. It was used instead of the traditional hole-transporting materials, formed by a spin-coating method. Instead, the layers were formed on top of the indium tin oxide electrode by a simple dipping procedure.

Initially, phosphonic acid with dimethoxydiphenylamine-substituted carbazole chromophore was used for the construction of the proof-of-concept devices, showing a promising efficiency of over 17%. Eventually, the structure was simplified, and the devices with the [2-(9H-carbazol-9-yl)ethyl]phosphonic acid (**2PACz**) have demonstrated over 20% efficiencies, outperforming polytriarylamine (PTAA) standard. In further work **2PACz** was used as a starting compound for the structural modifications, leading to some exceptional results.

The first example is a material called **Me-4PACz** ([4-(3,6-dimethyl-9H-carbazol-9-yl)butyl]phosphonic acid), which was used to fabricate record-breaking silicon/perovskite tandem solar cell, with 29.2% efficiency [1]. Another example is **Br-2PACz** ([2-(3,6-dibromo-9H-carbazol-9-yl)ethyl]phosphonic acid),

which was used in bulk-heterojunction solar cells, to give 18.4% efficiency, which is one of the highest reported values in the literature [2]. The incorporation of the monolayers into devices as a functional layer is leading to a breakthrough in several aspects. First, due to the ultimately low thickness of the layer, the amount of the required material is significantly reduced. Next, the defined orientation of the molecule (“anchor” attached to the surface, while “head” staying on the surface), gives a promise for the more rational design of the materials. Finally, conventional synthetical procedures are allowing the creation of large libraries of the materials, making it possible to fine-tune the properties of the layer.

1. A. Al-Ashouri et al. *Science*, **370**(6522) p. 1300-1309 (2020)
2. Y. Lin et al. *ChemSusChem*, Early View (2021)

1:45 PM EQ17.02.02

Indium Oxide Grown by Atomic Layer Deposition as Impermeable Top Electrode in Semi-Transparent Perovskite Solar Cells Florian Zimmermann, Tobias Gahlmann, Manuel Theisen, Kai O. Brinkmann, Cedric Kreusel and Thomas Riedl; Bergische Universität Wuppertal, Germany

The efficiency of perovskite solar cells (PSCs) almost reached that of silicon photovoltaics. Owing to the facile band-gap tunability of halide perovskites, partially see-through, i.e. semi-transparent, solar cell architectures with appealing colour impression become attractive. This opens up innovative areas of application, such as window integration, house facades, and in vehicles. Another essential challenge for PSCs is the susceptibility of the perovskite material to the effects of outside gases, such as moisture and oxygen.

A key element of semi-transparent cells is the semi-transparent top electrode. Previously, we have shown that networks of silver nanowires^[1] or thin metal layers, such as Ag^[2], can be used to realize such electrodes. Both concepts are based on metals that are easily corroded by halide containing species potentially leaking from the perovskite (e.g. at elevated temperature). To mitigate this issue, an impermeable ALD grown SnO_x electron transport layer is typically inserted to prevent halide migration and to protect the perovskite against subsequent deposition processes.

While the SnO_x is highly transparent and an excellent permeation barrier, it lacks the intrinsic electrical conductivity ($5 \times 10^{-3} \text{ S cm}^{-1}$) to qualify as a stand-alone semi-transparent top electrode without the requirement of additional metals.

In this work we propose ALD grown In₂O₃ from Cyclopentadienylindium(I) (CpIn) as semi-transparent top electrode with a high electrical conductivity of $2 \times 10^3 \text{ S cm}^{-1}$, which is six orders of magnitude higher than that of SnO_x and on par with that of sputtered indium tin oxide (ITO). Even at growth temperatures as low as 80°C and without any post deposition annealing, our In₂O₃ layers provide a high charge carrier density in the order of 10^{21} cm^{-3} and an electron mobility up to 23 cm²/Vs. In stark contrast to sputter deposited ITO the ALD grown In₂O₃ provides outstanding properties as diffusion barrier, exemplified by a low water vapor transmission rate (WVTR) of $4.8 \times 10^{-4} \text{ g (m}^2\text{d}^{-1})$ at 70°C/70%rH, which is orders of magnitude lower than number typically quoted for sputtered ITO^[3].

Finally, a high optical transmittance of over 80% in the wavelength range from 400-1000 nm for layers with a thickness of 100 nm and a sheet resistance of 45 W/sq, qualifies the In₂O₃ as an excellent semi-transparent electrode to realize semi-transparent PSCs. Details of the growth conditions using oxygen and water as co-reactants in the ALD process as well as the requirement of a proper seed layer for the In₂O₃ on top of the perovskite will be discussed. In first experiments, we applied our In₂O₃ as semi-transparent top electrode in semi-transparent PSCs, which afford notable efficiencies up to 16.5%.

- [1] Gahlmann et al., *Adv. Energy Mater.* **2020**, 10, 1903897
- [2] Zhao et al., *Adv. Energy Mater.* **2017**, 7, 1602599
- [3] Behrendt et al., *Adv. Mater.* **2015**, 27, 5961-5967

2:00 PM *EQ17.02.03

Engineering the Interfaces of Highly Efficient Perovskite/Organic Multi-Junction Solar Cells Thomas Riedl; Wuppertal University, Germany

Hybrid halide perovskites have overwhelmed the field of photovoltaics with unprecedented progress and skyrocketing efficiencies. Their facile bandgap tunability renders perovskite solar cells excellent building-blocks for multi-junction architectures, that provide the prospect to overcome fundamental efficiency limits of single-junctions. While perovskite/silicon or all-perovskite tandem cells have shown some remarkable progress, as of yet, perovskite/organic tandem cells show subpar efficiencies of ~20 per cent, limited by the low open circuit voltage of wide-gap perovskite cells, and serious optical/electrical losses introduced by the interconnect between the sub-cells.

Organic and perovskite semiconductors share similar processing technologies, which makes them attractive partners in multi-junction architectures. More importantly, the introduction of non-fullerene acceptors has boosted the efficiency of organic solar cells to levels beyond 18 per cent.

Here, we demonstrate perovskite/organic tandem cells with an efficiency up to 24 per cent, setting a new milestone for perovskite/organic tandem devices, which now for the first time outperform the most efficient single junction perovskite cells in *p-i-n* architecture. In an optimistic scenario, we envision that perovskite/organic tandem architectures bear a realistic prospect to reach efficiencies above 31 per cent.

This progress is not least based on significant improvements on the most critical interfaces in such a device:

Firstly, we managed to overcome interfacial losses, that are the predominant reasons limiting the performance of wide-gap perovskite cells. This allows us to access previously unreached territory of combined high open circuit voltage and fill factor. At the same time, our findings evidence that the proper choice of charge extraction layers allows to mitigate the detrimental halide segregation typically encountered in mixed-halide perovskites.

Secondly, we introduce a novel recombination interconnect for the two sub-cells, that is based on an ultra-thin (~1.5 nanometers) metal-like indium oxide layer. This interconnect offers unprecedented low optical and electrical losses, which unlocks the exploitation of the full potential of the two sub-cells without any discount. It can be foreseen that the applicability of this novel interconnect is not limited to perovskite/organic tandem cells but we expect that it will likewise revolutionize other tandem architectures.

SESSION EQ17.03: Metal Halide Perovskite Materials and Stability
Session Chairs: Philip Schulz and Nadine Witkowski
Tuesday Afternoon, November 30, 2021
Hynes, Level 2, Room 203

2:30 PM *EQ17.03.01

Defect Characterization and Passivation in Printable Electronic Materials—An Electrochemical and Spectroscopic Perspective Linze Du, Michel

De Keersmaecker, Joshua Hill, Neal R. Armstrong and [Erin L. Ratcliff](#); University of Arizona, United States

This talk will focus on the combined use of photoelectron spectroscopy and electrochemical methods as a unique feedback loop to i) characterize the origin of defects in printable electronic materials; ii) quantify the energetics and effective density of states within the gap under applied voltage conditions; and iii) assess the validity of different passivation strategies using ionic liquid (IL) layers.

Defects and near-surface mid-gap states are a fundamental challenge in semiconductor materials. For example, in photovoltaic devices, controlling defects of charge selective layers and photoactive layers is critical to energy level alignment, functionality, and overall performance. For printable semiconductor materials and devices, a number of factors can increase the concentration of mid-gap defects, which can be coupled to complex Lewis and/or Bronsted acid/base chemistries, and redox reactions. We have recently shown that we can electrochemically quantify defect density and energetics in thin film optoelectronic materials using solid electrolytes, where the electrolytes act as transparent top contact in the dark and under illumination. Operando diffraction and spectroscopic tools can then be used under device-relevant conditions to probe changes in lattice spacing and band energetics.

Herein we expand on this to consider layer-by-layer vacuum deposition of IL films on prototype optoelectronic materials. Interfaces are characterized using photoemission spectroscopies (XPS/UPS) primarily to elucidate changes in band edge energetics at the electronic material/IL heterojunction. Striking differences are seen in the energetics and composition of these heterojunctions depending on the type of semiconductor substrate and type of IL deposited, which enhances our understanding of the electrostatic interactions between ILs and printed semiconductor materials which impact on both defect characterization and defect mitigation.

3:00 PM *EQ17.03.02

Metal Halide Perovskite Interface Reactivity—Towards Understanding Doping and Degradation [Barry P. Rand](#); Princeton University, United States

Metal halide perovskite semiconductors have captured significant interest in the thin film optoelectronics community. As one example, certified photovoltaic efficiencies of metal halide perovskite solar cells currently exceed 25%, making them competitive in the laboratory with well-established technologies like multicrystalline-Si, CdTe, and CIGS. Also recently, gains have been made in perovskite-based light emitting devices (LEDs), with external quantum efficiency (EQE) of approximately 20% realized for bromide (green) and iodide (red/near-infrared) based perovskite emission layers. But in order to better understand the physics of device operation as well as degradation, we need to understand what can occur at interfaces of halide perovskites with other materials. For example, we have determined that metal halide perovskites not only feature mixed ionic-electronic motion but are also considerably chemically reactive, for example via redox or acid-base reactions. In addition, it may be possible to exploit this reactivity to allow for charge transfer doping, as we have shown perovskite systems with the ability to illustrate charge transfer states as well as doping with important implications on perovskite optoelectronic devices.

SESSION EQ17.04: Nanowire and Semiconductor Coatings

Session Chair: Elvira Fortunato

Wednesday Morning, December 1, 2021

Hynes, Level 2, Room 203

10:30 AM EQ17.06.04

Spotlight Talk—Transparent Amphiphobic Surfaces from Metal-Organic Frameworks [Vikramjeet Singh](#) and Manish K. Tiwari; University College London, United Kingdom

Transparent amphiphobic surfaces (repelling water and other low surface tension liquids) are of great interest in applications such as self-cleaning, anti-icing, anti-fouling, condensation and water harvesting etc. Current state-of-the-art in highly liquid repellent surfaces highlights several limitations on their use in practical applications. For example, superhydrophobic surface (SHS) suffer from instabilities/collapse of air pockets/cushion responsible for high liquid contact angles. Similarly, the retention of slippery behaviour in lubricant infused surfaces (SLIPS) and other smooth surfaces (SS) are restricted by eventual lubricant depletion and mechanical susceptibility of short molecular chains, respectively. Herein, we present a way to overcome these challenges by combining a robust nanohierarchical morphology with long flexible alkyl chains and achieve high drop mobility (~10 times than SLIPS) and amphiphobicity (Singh et al., Nano Lett. 2021, 21, 8, 3480–3486). High drop mobility comparable to superhydrophobic surfaces is achieved due to nanohierarchy i.e. reduced solid fraction (= 0.4). Precisely controlled nanohierarchy is obtained from surface grown metal-organic frameworks (MOFs) via layer-by-layer method. Covalently attached zirconium-based MOFs (OH-UIO-66) on glass substrate are used for demonstration due to their highly stable framework structure and easy synthesis. We observed a free sliding of vegetable oil, alcohols or other polar liquids at <15°. In addition to the excellent optical transparency and robustness, our surface enables a unique combination of additional desirable properties, e.g., resistance to high-speed liquid impact due to high capillary pressure generated from MOF nanopores ($V = 35$ m/s, $We_t = 42,500$), thermal stability up to 200 °C, and mechanical stability of scratch resistance. Moreover, benefiting from inherent porous structure of MOFs, our surface is able to absorb carcinogenic pollutants such as dyes and volatile organic compounds (VOCs) from water. These features endow the usage of the presented nanohierarchical MOF coating in applications such as windows, hand-held displays, goggles, wind screens, optoelectronics and so on.

10:35 AM EQ17.06.13

Spotlight Talk—3D Printing of Transparent Polysiloxanes Using Direct Ink Writing [Michael Ford](#), Colin Loeb, Lemuel Pérez Pérez, Stuart Gammon, Steven Guzorek, Hawi Gameda, A. Golobic, August Honnell, Justin Erspamer, Eric Duoss, Thomas Wilson and Jeremy Lenhardt; Lawrence Livermore National Laboratory, United States

Mixtures of silica and polysiloxane form thixotropic inks useful for 3D printing. However, 3D printed structures of these inks have typically been opaque due to the refractive index mismatch between the base polysiloxane and silica. By tuning the composition of the base polysiloxane, we matched the refractive index to formulate transparent inks. The transparent inks transmit up to ca. 90% of 700 nm light through 1 cm and remain transparent when solidified. We observed and characterized a thermochromic effect, where the inks change in opacity depending on refractive index mismatch and temperature. We also observed that the rheological properties of the ink depend on the distribution of silica particles, which is dictated by silica functionality, weight content, and processing. We demonstrate utility of these inks by printing encapsulants for LEDs, scintillators, and microfluidic mixing devices.

10:40 AM EQ17.06.15

Spotlight Talk—Late News: Large Area, Multi-Pulse Laser Lifetime of Purified Nematic Liquid Crystals at Near Infrared Wavelengths Selim Elhadi¹, Andy Bayramian¹, Stavros Demos² and Kenneth Marshall²; ¹Seurat Technologies, Inc., United States; ²University of Rochester - LLE, United States

Nematic liquid crystals (LC's), ubiquitous in high information density displays, are typically composed of rod-shaped molecules that can exhibit large dielectric anisotropy, high birefringence and excellent transparency. These properties make them well suited for use in many optical components in high power laser systems, including polarization controllers and optoelectronic devices for beam shaping in 3D metal printing [*"A new era In metal part production"*, available at www.seuratech.com]. Recently, the single shot laser damage threshold of both saturated and un-saturated nematic LC's revealed an intrinsic relationship between the degree of chemical bond saturation within LC molecules and laser damage [Kosc *et al*, *Scientific Reports* 2019, 9 (1), 16435]. Extrinsic factors such as alignment layer material selection and preparation, particulate contamination and LC chemical purification can also play an important role in determining the optical response and durability of the liquid crystals. In this study we investigate the efficacy of several absorption-based purification methods and their impact on the laser damage behavior of nematic LC'S. We focus on the lifetime of purified and as-prepared LC'S when exposed to multiple laser pulses at kW's average power, over cm² areas, at near infrared wavelength and 20 to 40 Hz rep rates. Numerical simulations are used to estimate the degree of heat accumulation during exposure to rationalize the LC lifetime results.

10:45 AM EQ17.04.07

Interfacing Silicon with Doped Coatings for Band Modulation and Improved Light Emission Sufian Abedrabbo¹, El Mostafa Benchafia¹, Ahmad Al-Qawasmeh¹, Anthony T. T. Fiory² and Nuggehalli M. Ravindra³; ¹Khalifa University of Science and Technology, United Arab Emirates; ²Integron Solutions, United States; ³New Jersey Institute of Technology, United States

The recent report of a breakthrough in light emission in silicon-germanium alloys has renewed interest in light emission in silicon related materials and structures. The ability to tailor solid-solid interfaces, for a desired functionality, is of enormous interest in a vast variety of applications in materials science and engineering. In this work, engineered doped coatings catalyzed by several acids are deposited on silicon to introduce random interfacial stresses that can modulate the silicon bandgap. This modulation has been demonstrated to be beneficial by adding two functionalities to ordinary Czochralski-Si. It has appreciably improved bandgap radiative recombination of carriers by over two folds which leads to the possibility of engineering silicon-enabled absorber by circumventing Auger recombination processes, i.e. better light emitter and photovoltaic candidate at the same time. This talk will brief properties of the films that lead to light emission enhancement and will present the room-temperature photoluminescence results as well as the nature of the interfacial strains and will quantify bandgap modulations. Theoretical interpretation of these interesting results will be presented along with some comparative studies of stressed and alloyed silicon.

11:00 AM EQ17.04.06

De-Densifying Metallic Nanowire Networks Using Betweenness Centrality Adam Trebach¹, Evan Toth², Woo Hyun Chae¹, Jatin Patil¹, Ki-Jana Carter¹, Thomas Sannicola¹ and Jeffrey C. Grossman^{1,1}; ¹Massachusetts Institute of Technology, United States; ²Northeastern University, United States

Silver nanowire networks show great promise as transparent conductors, but many nanowires in these materials participate only meagerly in conduction. Using graph theoretic measures to rank the importance of different nanowires, we show that simulated networks can be strategically de-densified to below the percolation threshold while maintaining low resistance. We achieve performance reaching 63% of the theoretical maximum, a roughly 91% gain over the performance predicted by percolation theory. Furthermore, the mathematical methods applied here are sufficiently general to apply to any networked material in which there is a non-monotonic relationship between density and performance.

11:15 AM EQ17.04.05

Encapsulation of Silver Nanowires via Metal-Oxynitride Reactive Sputtering for Highly Stable Transparent Electrodes Jatin Patil, Maya Reese, Eric Lee and Jeffrey C. Grossman; Massachusetts Institute of Technology, United States

Silver nanowire networks (AgNWs) are a promising candidate for transparent electrodes due to their high transparency, low sheet resistance, flexibility, and potential for low-cost implementation, owing to their high DC-to-optical conductivity ratio and low metal loading. These properties make it suitable for applications such as transparent heaters and solar cell electrodes. Unfortunately, AgNWs are susceptible to electrical, thermal and chemical degradation, which have largely stifled their implementation; effective encapsulation strategies are needed. To ensure the encapsulation approaches are scalable, industrial scale, high throughput deposition methods should be targeted. Moreover, encapsulation methods should use low cost, high-abundance elements with low-temperature processing. A variety of encapsulation approaches have been considered in the past, but physical vapor deposition approaches are the most promising for these criteria.

In this work, reactive pulsed DC and RF magnetron sputtering at room temperature are demonstrated as a promising approach to encapsulate AgNWs with thin films. Since using O₂ as a reactive gas can significantly oxidize and damage the AgNWs and active layer surfaces, N₂ is used as a reactive gas under moderate base chamber pressures (0.5×10⁻⁴ Torr). Low- to moderate- cost metal sputtering targets (Al, Ti, Zr) are then used to deposit as little as 20 nm of oxynitrides using mixed Ar and N₂ gas flow with high deposition rates. Oxynitride-encapsulated AgNW films show exceptional electrothermal stability, surviving at temperatures of 100°C more than unencapsulated AgNWs (>250°C). They also show exceptional chemical stability, where the electrical properties of Al oxynitride encapsulated wires stay nearly unchanged after >7 days under modified Damp Heat testing conditions (80°C, 80%RH). This work demonstrates a versatile approach to encapsulating AgNWs with sputtering, which can be extended to encapsulate lithographically patterned electrodes and other solar cell device architectures.

SESSION EQ17.05: Oxide Electronics and Transparent Conductive Oxides

Session Chair: Anna Regoutz

Wednesday Afternoon, December 1, 2021

Hynes, Level 2, Room 203

1:30 PM *EQ17.05.01

The Past, Present and Future of Oxide Electronics Elvira Fortunato, Emanuel Carlos, Rita Branquinho, Pedro Barquinha and Rodrigo Martins; NOVA University Lisbon, Portugal

Oxide electronic materials is one of the most promising technologies for electronic devices, as distinct from the traditional silicon technology. The fact that

circuits based on conventional semiconductors such as silicon and conductors such as copper can be made transparent by using different materials, the so-called transparent semiconducting and conducting oxides (TSOs and TCOs, respectively), is of great importance and allows for the definition of innovative fields of application with high added value.

Oxide electronic materials are becoming increasingly important in a wide range of applications including transparent electronics, optoelectronics, magnetoelectronics, photonics, spintronics, thermoelectrics, piezoelectrics, power harvesting, hydrogen storage and environmental waste management. Synthesis and fabrication of these materials, as well as processing into particular device structures to suit a specific application is still a challenge. Further, characterization of these materials to understand the tunability of their properties and the novel properties that evolve due to their nanostructured nature is another facet of the challenge.

In this paper we will present the most important landmarks achieved by these stimulating scientific area as well as some insights to emerging applications.

2:00 PM EQ17.05.02

Enhancement in Photo-Absorbing Performance of Hafnium–Indium–Gallium–Zinc Oxide Based Optoelectronic Devices by Reduction Treatment with Sodium Dithionite [Min Seong Kim](#)¹, Joohye Jung^{1,2}, Hyung Tae Kim¹, Dong Hyun Choi¹, Sujin Jung¹ and Hyun Jae Kim¹; ¹Yonsei University, Korea (the Republic of); ²Samsung Display, Korea (the Republic of)

During the last decade, the constant growth of interest in the field of optoelectronic devices has been observed in almost every commercial electronic device. Advances in interdisciplinary researches and industrial approaches have practically improved the optical characteristics of optoelectronic devices comparable with conventional silicon-based photodiodes. Among these extensive ranges of studies, transparent metal oxide semiconductors such as indium–gallium–zinc oxide or indium-zinc oxide have emerged as an important candidate owing to the wide variety of their electronic and optical properties, for instance, high field-effect mobility, low off-state current, optical transparency, high uniformity in large area deposition and processing versatility. However, the wide bandgap above 3 eV of metal oxide layer fundamentally restricts its light absorption range under about 420 nm which is the spectrum of ultraviolet and blue light. In this regard, more detailed researches about metal oxide semiconductors-based optoelectronic devices are required, which focus on how to engineer them for excellent responsivity upon the visible light and stability concurrently. Studies focusing on expanding the absorption range of metal oxide semiconductors-based phototransistors have been conducted by inserting a visible light absorption layer such as nanomaterials, quantum dots, perovskite, or two-dimensional materials. Although these results manifested the feasibility of metal oxide semiconductors-based optoelectronic devices, they still have some inherent barriers for practical large-scale devices due to the high cost and complicate fabrication process. In this work, we introduce a facile method to control the photoresponse characteristic of oxide semiconductor under visible light using a reducing agent, sodium dithionite ($\text{Na}_2\text{S}_2\text{O}_4$), that is able to compensate for the aforementioned limitations. $\text{Na}_2\text{S}_2\text{O}_4$ exhibits strong reducing properties due to its weak S-S bond. Photoresponse characteristic of hafnium–indium–gallium–zinc oxide (HIGZO) thin-film was enlarged to absorb visible light by modulating sub-gap states and oxygen vacancy of HIGZO through reduction treatment, immersing in $\text{Na}_2\text{S}_2\text{O}_4$ solution. Moreover, we revealed that photoresponsivity of HIGZO thin-film is easy to control substantially depending upon the molarity of $\text{Na}_2\text{S}_2\text{O}_4$. This controllability plays a key role in widening its potential applications and fine adjustment of performance from phototransistor to photo memory such as neuromorphic devices using persistent photoconductivity (PPC). Specifically, we achieved HIGZO phototransistors with photoresponsivity of 626.32 A/W, photosensitivity of 3.32×10^7 , and detectivity of 7.18×10^{11} Jones under 10 mW/mm² of red light using 0.1 M of $\text{Na}_2\text{S}_2\text{O}_4$. In addition, HIGZO photomemory-based neuromorphic devices with a paired-pulse facilitation index of 142.6% under the input pulse of red light with 1 mW/mm² intensity were fabricated by increasing the molarity of $\text{Na}_2\text{S}_2\text{O}_4$ to 0.5 M. As a result, we successfully demonstrated the facile method for improving the performance of HIGZO optoelectronic devices by controlling the photoresponse characteristic which makes it possible to be applied in various optoelectronic applications.

2:15 PM EQ17.05.03

Unravelling the Chemical Conversion of Sub-10 nm Metal Oxide Thin-Film Precursors—An IRSE Study [Christina Koutsiki](#), Demosthenes Koutsogeorgis and Nikolaos Kalfagiannis; Nottingham Trent University, United Kingdom

The last decade has witnessed a remarkable development in thin film technologies, the application of which has marked a new era in electronics research and industry. To this end, thin film-based optoelectronic devices have created the foundation of outstanding technology applications, from flexible displays to smart window coatings, to name a few. Whilst the demand for improvement in device performance is increasing, Metal Oxides (MOs) have lately emerged as a prominent class of optoelectronic materials, whilst gathering a plethora of unique features such as increased carrier mobility, high optical transparency and mechanical stability. Besides their advantages, MOs present an excellent compatibility with solution processes, thus providing the opportunity of a novel, high-throughput manufacturing scheme of MO-based high-performance optoelectronic devices.

“Sol-gel” is established as one of the currently favourable solution processes, as it uniquely links MOs to solution processing. This deposition of organometallic precursors *via* wet techniques, followed by a subsequent thermal treatment, enables the formation of high-quality MOs, while accommodating essential advantages such as ambient processing conditions and composition tuning. The growing implementation of sol-gel ultra-thin MO layers (<10 nm) in optoelectronic devices renders the assessment and control of their optoelectronic properties essential. However, the cost and time-consuming features of current characterization techniques such as XPS and TEM hinders their implementation in a high-throughput production line. In addition, their “destructive” character (Pt deposition in TEM, Argon etching in depth-profile XPS) allows only for final product analysis, thus restricting the possibility of *in situ* monitoring during fabrication. Therefore, the presence of non-invasive, highly-sensitive characterization techniques could introduce a remarkable upgrade of MO thin film manufacturing.

To address this challenge, we propose Infra-Red Spectroscopic Ellipsometry (IRSE) as an alternative and novel approach towards the clarification of the sol gel precursor conversion stages, the control of which leads to high quality MO ultra-thin films. Particular focus is being paid in the role of substrates, as their optoelectronic properties may tune the presence of spectral features, thus allowing the detection of vibrational modes in ultra-thin films (~ 1 nm). In this study, $\text{In}(\text{NO}_3)_3$ dissolved in 2-Methoxyethanol ($\text{C}_3\text{H}_8\text{O}_2$) is converted into an ultra-thin In_2O_3 film (<10 nm), a popular MO semiconductor, widely used as a Transparent Conductive Oxide (TCO) host. The individual stages are captured by IRSE, aiming to shed light into the sol gel reaction conversion. For this, various substrates are being utilized (Al, TiN, Au and Si (including highly doped)), aiming to enhance the IRSE sensitivity, thus provide a clear monitoring of the conversion process through vibrational mode detection. We thus identify the intermediate products during transition towards In_2O_3 . This introduces IRSE as a new route towards the detection of sol-gel stages in ultra-thin films, with its implementation in solution processing technologies being potentially essential. The suggested methodology can also be employed in the non-destructive characterization of an expanded material palette, such as 2-D materials. This approach could constitute a novel tool in thin film industry, thus boosting the new generation of optoelectronic devices.

2:30 PM EQ17.05.04

Solid Phase Epitaxial Growth of the Transparent Conducting Oxide SrVO_3 [Samuel Marks](#), Lin Lin, Peng Zuo, Patrick Strohbeen, Ryan Jacobs, Dongxue Du, Jason Waldvogel, Rui Liu, Donald Savage, John Booske, Jason K. Kawasaki, Susan Babcock, Dane Morgan and Paul Evans; University of Wisconsin–Madison, United States

SrVO_3 thin films with a high figure of merit for applications as transparent conductors were crystallized from amorphous layers using solid phase epitaxy (SPE). Epitaxial metal oxides incorporating multivalent ions can be formed with thermodynamics and kinetics derived from crystallization processes that are initiated at buried amorphous/crystalline interfaces. We report crystallization methods allowing control of the ionic valence during crystallization and

the synthesis of epitaxial SrVO₃ on SrTiO₃. The SrVO₃ layers exhibited room temperature resistivity as low as $2.5 \times 10^{-5} \Omega \text{ cm}$ and visible light transmission ranging from 0.89 to 0.52 for thicknesses from 16 to 60 nm. Amorphous SrVO₃ was deposited at room temperature using radio-frequency sputtering and crystallized by heating in a gas environment with selected oxygen activity. The lattice parameters and mosaic angular width of x-ray reflections from the crystallized films are consistent with partial relaxation of the strain resulting from the epitaxial mismatch between SrVO₃ and SrTiO₃ in the 60 nm layer while the 16 nm layers were found to be fully strained. A reflection high-energy electron diffraction study of the kinetics of SPE indicates that crystallization occurs via the thermally activated propagation of the crystalline/amorphous interface, similar to SPE in other perovskite oxides. Thermodynamic calculations based on density functional theory predict the temperature and oxygen partial pressure conditions required to produce the SrVO₃ phase and are consistent with the experiments. The separation of deposition and crystallization processes used in this work are scalable to large areas and can form the basis of technologies incorporating complex oxide electronic materials in emerging devices.

2:45 PM EQ17.05.05

CaCuP—A Degenerate Wide Band Gap Phosphide for Transparent Conducting Applications Joe Willis^{1,2}, Andrea Crovetto³ and David O. Scanlon^{1,2}; ¹University College London, United Kingdom; ²Diamond Light Source, United Kingdom; ³Helmholtz-Zentrum Berlin, Germany

In modern day life, transparent conducting materials (TCMs) are ubiquitous, playing an integral role in touch and display screens, solar cells and smart windows. P-type TCMs have often been overshadowed by n-type TCMs, due to the increased difficulty in synthesis, poorer stability and inferior optoelectronic properties. With technologies such as pop up windshield displays and fully transparent touch-display screens on the horizon, there is an impending need for the development of a high performance p-type TCM, in turn allowing the fabrication of a transparent p-n junction.

In 2017, CaCuP (and MCuP where M = Mg, Sr, Ba) was identified as a potential p-type TCM by Williamson et al, owing to its large valence band dispersion and optical absorption onset at around 2.7 eV.[1] Powders were synthesised and pressed into pellets, which were shown to be phase pure from XRD analysis, to possess a strong absorption onset of around 2.7 eV, and to display p-type conductivity of around $2 \times 10^{-3} \text{ S cm}^{-1}$, with the origin of this conductivity suggested to be Cu vacancies. For a nominally undoped pressed powder sample, this was an impressive level of conductivity, and served as the motivation for this work.

Formation energies for the intrinsic defects in CaCuP have been calculated using hybrid density functional theory within VASP. The Cu vacancy possesses extremely low formation energies under cation poor growth conditions, and is stable into the valence band giving rise to degenerate semiconducting behaviour. The resulting hole charge density is delocalised through the Cu-P layers of the material, indicating high charge carrier mobility and conductivity.

Phase pure thin films have been successfully grown across a Cu gradient via the pulsed laser deposition technique. The measured room temperature conductivity is 1040 S cm^{-1} , a vast improvement over the pressed powder samples. Hall measurements indicate a mobility of $36 \text{ cm}^2 \text{ V}^{-1} \text{ s}^{-1}$ and a carrier concentration of around $1.8 \times 10^{20} \text{ cm}^{-3}$, supporting the defect calculation results and indicative of a degenerate semiconductor. Temperature dependent charge transport calculations are being performed using the AMSET code[2] to assess if this is the intrinsic material limit, or if improved electronic properties could be achieved with a better optimised deposition process. The optical behaviour of these films is not straightforward, with a larger absorption coefficient than expected seen at the indirect band gap value of around 1.2 eV – optical defect transition calculations are being performed in order to understand this further.

[1] B. A. D. Williamson et al, *Chem. Mater.*, **29**, 2402-2413 (2017).

[2] A. M. Ganose et al, *Nat. Comm.*, **12**, 2222 (2021).

SESSION EQ17.06: Poster Session
Session Chair: Davide Ceratti
Wednesday Afternoon, December 1, 2021
8:00 PM - 10:00 PM
Hynes, Level 1, Hall B

EQ17.06.01

Late News: Solution-Processed Cathode Interfacial Layers for Efficient Energy Level Alignment in Organic Photovoltaics Jisu Hong^{1,2}, Zhang Dongbo¹, Hyeok-jin Kwon², Chan Eon Park², Soon-Ki Kwon¹ and Yun-Hi Kim¹; ¹Gyeongsang National University, Korea (the Republic of); ²Pohang University of Science and Technology, Korea (the Republic of)

Organic Photovoltaics (OPVs) have now attained high power conversion efficiencies (PCEs) over 15%, and research on OPV fabrication via solution processes on flexible substrates, and replacement of toxic halogenated solvents by environmentally benign solvents, is underway, as are extensive efforts to improve the PCEs. In this work, we synthesized solution processable cathode interfacial materials and used in OPVs. Two small-molecule interfacial materials with phosphine oxide and benzimidazole groups were designed to induce strong interface dipoles and chelate with the metal electrodes. We used isopropanol, an environmentally benign solvent, to dissolve the small-molecule materials and spin-coated solutions onto photoactive layers. The interfacial materials formed ohmic contacts between the electron acceptor materials and the OPV cathodes due to the strong interface dipoles. As the highest occupied molecular orbital (HOMO) energy level of the interfacial materials is -7.05 eV, hole carriers cannot travel toward the cathode. The appropriate energy levels of the interfacial materials and the efficient energy level alignment facilitated charge extraction at the cathodes and increased the PCEs of OPVs. Of the two, BIPO (with two benzimidazole groups) more efficiently formed smooth interfacial layers on active layers that allowed of better energy level alignment between the electron acceptor materials and the cathodes.

EQ17.06.02

Helical Self-Assemblies of Pt(II) Complexes Exhibit Strong Circularly Polarized Luminescence Emission Dong Yeun Jeong¹, Seung Yeon Yu², Jong Jin Park³, Jong Hyun Kim³ and Youngmin You¹; ¹Ewha Womans university, Korea (the Republic of); ²Ewha Womans University, Korea (the Republic of); ³Ajou University, Korea (the Republic of)

Circularly polarized luminescence (CPL) refers to the differential photoemission between left- and right-handedly polarized lights. The polarity of CPL provides a unique principle for photonic applications, including three-dimensional displays and quantum encryption. However, previous CPL-active materials have suffered from a trade-off between a photoluminescence quantum yield (PLQY) and a luminescence dissymmetry factor (g_{lum}). We recently

discovered that helical co-assemblies of square-planar cycloplatinated complexes could overcome the intrinsic limitation. This strategy exploited an asymmetric exciton coupling and the magnetically allowed metal-metal-to-ligand charge-transfer (MMLCT) transition within the Pt(II) complex co-assemblies. However, utility of this strategy is limited because it inevitably requires chiral guest molecules to form helical co-assemblies.

In this research, we have developed a combined top-down and bottom-up strategy which enables strong CPL emissions without chiral guest molecules. Our strategy takes advantage of the chiral induction effect exerted by counter anions of charge-cationic Pt(II) complexes. The Pt(II) complexes stack in a face-to-face fashion to form helical self-assemblies, where the helical sense is dictated by the point chirality of counter anions. We tailored the chemical structures of the counter anions, including (*R*)-/(*S*)-tetrahydrofuran-2-carboxylates ((*R*)-/(*S*)-TC), *L*-/*D*-dipivaloyl tartarate (*L*-/*D*-PT), and *L*-/*D*-dibenzoyl tartarate (*L*-/*D*-BT).

The Pt(II) complex self-assemblies could be grown by in-situ anion metathesis between [(2-phenylpyridinato)(4,4'-bis(nonyl)-2,2'-bipyridine)platinum]ClO₄ ([PtN]ClO₄) and tetrabutylammonium (TBA) salts of the chiral anions in 1,2-dichloroethane (1,2-DCE):CH₃CN (8:2, wt/wt). The formation of PtN self-assemblies were supported by an emergence of the MMLCT absorption at 500 nm and the strong MMLCT phosphorescence at 613 nm (PLQY = 0.19 for the [PtN]₂BT self-assemblies). The MMLCT transitions of the self-assemblies were chiroptical, as seen from strong couplets at 500 nm in electric circular dichroism. Among the tested anions, BT having the -2 charge and the elongated π -conjugation structure resulted in the most tight and helical stacking of PtN. As expected, helical supramolecular structures were absent for the self-assemblies of [PtN]ClO₄.

To further enhance the CPL activities, we allowed the self-assembly formation within microchannels with a 28 μ m width which were formed by a conformal contact between a glass substrate and a poly(dimethylsiloxane) mold. The self-assemblies of [PtN]₂BT formed within the microchannels exhibited a two-fold improvement in PLQY (0.32) over that (0.19) of the self-assemblies formed onto the planar glass substrate. In addition, an order of magnitude enhancement in $|g_{lum}|$ was also found; g_{lum} (572 nm) were -0.12 and 0.13 for the self-assemblies of [PtN]₂L-BT and [PtN]₂D-BT, respectively, grown within the microchannels, whereas g_{lum} (572 nm) were -0.027 and 0.037 for the dropcasted self-assemblies of [PtN]₂L-BT and [PtN]₂D-BT, respectively. The notable improvement in $|g_{lum}|$ was attributed to the tight and ordered supramolecular packing structures. Our approach is valuable as it does not rely on chiral guest molecules. The successful combination with soft-lithographic techniques will stimulate the future research to construct CPL-active materials.

EQ17.06.03

High-Efficiency Thermally Activated Delayed Fluorescence Emitters with High Horizontal Orientation and Narrow Deep-Blue Emission Youngnam Lee and Jong-In Hong; Seoul National University, Korea (the Republic of)

Highly efficient 10-(5,9-dioxa-13b-boranaphtho[3,2,1-de]anthracen-7-yl)-10*H*-dispiro[acridine-9,9'-anthracene-10',9''-fluorene] (OBOTsAc) and 10-(2,12-di-*tert*-butyl-5,9-dioxa-13b-boranaphtho[3,2,1-de]anthracen-7-yl)-10*H*-dispiro[acridine-9,9'-anthracene-10',9''-fluorene] (tBuOBOTsAc) emitters, comprising almost perpendicularly linked rigid 5,9-dioxa-13b-boranaphtho[3,2,1-de]anthracene (OBO) electron acceptors and a rigid and linear tri-spiral acridine electron donor, are reported here. OBOTsAc and tBuOBOTsAc show deep-blue emission (λ_{max} = 452 and 446 nm) with narrow full width at half maximum (FWHM) values of 50 and 48 nm, respectively. Due to the rigid and twisted structures, and the appropriate singlet and triplet energy levels of both emitters, 10 wt% doped films of OBOTsAc and tBuOBOTsAc in a bis[2-(diphenylphosphino)phenyl]ether oxide (DPEPO) host show efficient thermally activated delayed fluorescence (TADF) emission and photoluminescence quantum yields (PLQYs) of 97% and 90%, respectively. Moreover, linear-shaped OBOTsAc and tBuOBOTsAc lead to excellent horizontal emitting dipole orientations (88% and 90%, respectively). Consequently, organic light-emitting diode (OLED) devices using OBOTsAc and tBuOBOTsAc exhibit maximum external quantum efficiencies (EQEs) of 31.2% and 28.2%, respectively, and Commission Internationale de l'Éclairage (CIE) coordinates of (0.147, 0.092) and (0.149, 0.061), respectively.

EQ17.06.04

Spotlight Talk—Transparent Amphiphobic Surfaces from Metal-Organic Frameworks Vikaramjeet Singh and Manish K. Tiwari; University College London, United Kingdom

Transparent amphiphobic surfaces (repelling water and other low surface tension liquids) are of great interest in applications such as self-cleaning, anti-icing, anti-fouling, condensation and water harvesting etc. Current state-of-the-art in highly liquid repellent surfaces highlights several limitations on their use in practical applications. For example, superhydrophobic surface (SHS) suffer from instabilities/collapse of air pockets/cushion responsible for high liquid contact angles. Similarly, the retention of slippery behaviour in lubricant infused surfaces (SLIPS) and other smooth surfaces (SS) are restricted by eventual lubricant depletion and mechanical susceptibility of short molecular chains, respectively. Herein, we present a way to overcome these challenges by combining a robust nanohierarchical morphology with long flexible alkyl chains and achieve high drop mobility (~10 times than SLIPS) and amphiphobicity (Singh et al., Nano Lett. 2021, 21, 8, 3480–3486). High drop mobility comparable to superhydrophobic surfaces is achieved due to nanohierarchy i.e. reduced solid fraction (= 0.4). Precisely controlled nanohierarchy is obtained from surface grown metal-organic frameworks (MOFs) via layer-by-layer method. Covalently attached zirconium-based MOFs (OH-UIO-66) on glass substrate are used for demonstration due to their highly stable framework structure and easy synthesis. We observed a free sliding of vegetable oil, alcohols or other polar liquids at <15°. In addition to the excellent optical transparency and robustness, our surface enables a unique combination of additional desirable properties, e.g., resistance to high-speed liquid impact due to high capillary pressure generated from MOF nanopores ($V = 35$ m/s, $We_l = 42,500$), thermal stability up to 200 °C, and mechanical stability of scratch resistance. Moreover, benefiting from inherent porous structure of MOFs, our surface is able to absorb carcinogenic pollutants such as dyes and volatile organic compounds (VOCs) from water. These features endow the usage of the presented nanohierarchical MOF coating in applications such as windows, hand-held displays, goggles, wind screens, optoelectronics and so on.

EQ17.06.05

Improved Charge Injection in Metal-Polymer Interfaces of Inverted Organic Electronic Devices Using Dithiolane-Based Self-Assembled Monolayers Sneha Sreekumar, Marzieh Hydari, Zhongkai Cheng, Hemanth Maddali, Elena Galoppini and Deirdre O'Carroll; Rutgers, The State University of New Jersey, United States

The fabrication of polymer-based organic light-emitting diodes (OLEDs) using the inverted method, where the device is built on top of a metal back electrode has advantages over more conventional OLED fabrication methods. For example, the inverted method provides a way to control the structure and morphology of the metal electrode. This, in turn, enables improved light management by control of the photonic and plasmonic behavior within the OLED devices. Ag is a good option as a back metal electrode in OLEDs because of its low optical loss, high reflectivity and high conductivity. However, Ag has a work function (~4.4 eV) which is not compatible with the band gap of many polymeric organic semiconductors.

Poly(9,9-dioctylfluorene-*alt*-benzothiadiazole) (F8BT) is a conjugated polymer commonly used in OLED prototypes that has high electron affinity (~3.3 eV), large ionization potential (~5.9 eV), and high fluorescence quantum yield. Combining F8BT with an Ag back electrode results in a high barrier height for charge injection, which results in poor device performance and a high turn on voltage. A method to overcome this, as some studies on organic field-effect transistors (OFETs) have, used self-assembled monolayers (SAMs) of sulphur compounds like thiols to reduce the work function of Ag and the barrier height for charge injection into the polymer.

Here, we have extended this methodology in using the more commercially available lipoic acid (LA) and its derivatives to form SAMs in between Ag back electrodes and F8BT thin films. By selecting LA, we can tailor the functional groups at one end of the compound by converting the acid to an ester,

allowing the influence of difference alkyl chains as well as chain lengths to be investigated. We have studied how having two sulphur linkages instead of one in the case of conventional thiols like 1-decanethiol(1-DT), as well the dipole orientation of the molecules can change the work function of Ag and improve the contact at the metal-polymer interface. X-ray photoelectron spectroscopy and Raman spectra reveal the binding properties of the SAMs, while current density-voltage and ultraviolet photoelectron spectroscopy measurements show that (\pm)- α -lipoic acid and (\pm)-4-phenylbutyl 5-(1,2-dithiolan-3-yl)pentanoate improve the charge injection greatly by changing the work function of the Ag and by altering the morphology of the semiconducting polymer. The results obtained gave us valuable insight into the effect of chain length and functional groups of the SAMs in engineering morphological and electronic properties of the metal-polymer interface.

EQ17.06.07

Facile and Rapid Fabrication of p-type Copper Iodide Nanowire Networks and Utilization in UV Photodetectors Muhammed A. Calasin¹, Serkan Koylan¹, Loay Madbouly¹, Sensu Tunca¹, Yusuf Tutel¹, Sahin Coskun² and Husnu E. Unalan^{1,1}; ¹Middle East Technical University, Turkey; ²Osmangazi University, Turkey

Semiconductors industry necessitate p-type materials in a wide range of applications like photovoltaics, light-emitting diodes, detectors, transistors and thermoelectrics. Copper iodide (CuI) has received significant interest as an alternative beyond silicon. Intriguing optoelectronic properties of CuI include but not limited to, direct and wide bandgap (3.1 eV measured as thin film), high hole mobility (in excess of 40 cm²/V.s) and large exciton binding energy (62 meV). Direct iodination of copper thin films allows production of CuI films even at room temperature, which makes CuI a suitable candidate for flexible and transparent electronics. In this study, γ -CuI nanowire networks were fabricated through direct vapor iodination of copper nanowire (Cu NW) networks. Cu NWs were synthesized and purified by solution means and deposited onto glass substrates by spray coating [1,2]. A house-made setup was used for the vapor iodination of Cu NW networks. The transformation of Cu to γ -CuI was monitored through investigating morphological, structural, chemical and optoelectronic properties of the fabricated γ -CuI NW networks. Upon 120 seconds exposure to iodine vapor, initially smooth Cu NW surface became rough, indicating transformation to γ -CuI with a zinc-blende structure. γ -CuI NWs were found to consist of only Cu⁺ and I⁻. Hall-effect measurements revealed a mobility and resistivity of 12 cm²/V.s and 19.9 ohm-cm, respectively. Optical transmittance of γ -CuI NW networks was over 68% in the wavelength range of 300-1200 nm, while that of Cu NWs was 85%. The direct optical band gap value was determined as 3.2 eV with the help of Tauc's plot. Following materials characterization, UV-photodetectors in metal-semiconductor-metal structure were fabricated using γ -CuI NW networks. A three times increase in current was registered in response to UV light illumination (with a wavelength 365 nm) under 5 V.

References

- [1] Tigan, D., Genlik, S. P., Imer, B., & Unalan, H. E. Transparent Thin Film Heaters Based on Copper Nanowire Networks
- [2] Sevim Polat Genlik, Dogancan Tigan, Yusuf Kocak, Kerem Emre Ercan, Melih Ogeday Cicek, Sensu Tunca, Serkan Koylan, Sahin Coskun, Emrah Ozensoy, and Husnu Emrah Unalan
ACS Applied Materials & Interfaces 2020 12 (40), 45136-45144

EQ17.06.08

Polyimide Doped Indium-Gallium-Zinc Oxide Based Transparent and Flexible Phototransistor for Visible Light Detection Kiseok Kim^{1,2}, Min Seong Kim¹, Jusung Chung¹, Dongwoo Kim¹, I Sak Lee¹ and Hyun Jae Kim¹; ¹Yonsei University, Korea (the Republic of); ²LG Display Co., Ltd., Korea (the Republic of)

Nowadays, displays are evolving as a way of interacting with users rather than simply conveying information. Interactive display is one of the new high-value-added display technologies and means a display that enables interaction between users and display devices through interface technology with transparent display panels that incorporate various sensors. These interactive displays can perform various roles, such as providing new experiences to users through interaction with users and responding to emergency situations through real-time environment awareness. For the implementation of these interactive displays, research on transparent and flexible phototransistors for embedding in transparent display panels is essential. The phototransistor is an essential element to perform various functions such as user's touch, motion, and gaze recognition. To apply it to transparent displays, it is also essential to ensure transparency, to facilitate processing for large-area substrates, and to have low off current for high photosensitivity. Therefore, oxide semiconductors with high transparency, large area processability, and reasonable mobility (~ 10 cm²/Vs) are suitable candidates for the channel layer of phototransistors. However, oxide semiconductors cannot absorb visible light with large bandgap energy of ~ 3.0 eV. For fabricate an oxide semiconductor-based phototransistor that can absorb the full range of visible light, one of the most widely used methods is to add absorption layer such as chalcogenides, organics, perovskites, and nanodots. However, in the case of the materials that can absorb visible light, it is not transparent due to a small bandgap. Thus, it is difficult to fabrication transparent phototransistors.

In this work, we propose a method for fabricating polyimide (PI) doped single layer (PSL) phototransistor that is transparent and can absorb visible light. Amorphous indium-gallium-zinc oxide (IGZO) and PI can be deposited using co-sputtering process for the channel layer itself to absorb visible light. The PI is well known in the display industry as a flexible substrate and can be made into a sputter target, so it can be used in sputter equipment. We used a SiO₂/p⁺-Si substrate in which SiO₂ is thermally oxidized on a p⁺-Si wafer; the p⁺-Si and SiO₂ were used as gate and gate insulator, respectively. On the SiO₂/p⁺-Si substrate, the PSL phototransistor was deposited as a channel layer using a co-sputtering process; a shadow mask was used for patterning. The powers of IGZO and PI were set to 150 W and 0 to 30 W, respectively. After that, thermal annealing was performed at 300 °C for 1 hr. Finally, aluminum was deposited as a source/drain using a shadow mask for patterning. When fabricating the PSL phototransistor, it was optimized by controlling the sputter power of the PI target. We confirmed that the PSL phototransistor fabricated with sputter power of PI 10 W featured excellent optoelectronic characteristics compared with other PSL phototransistors. In addition, when compared with the IGZO phototransistor, the optoelectronic characteristics of the PSL phototransistor also improved in red lights at 1mW/mm² intensity. Specifically, photoresponsivity improved from 14.43 to 623.79 A/W, photosensitivity improved from 2.30 $\times 10^9$ to 9.89 $\times 10^6$, and detectivity improved from 8.92 $\times 10^6$ to 5.83 $\times 10^{11}$ Jones. Furthermore, as the bending test was conducted 10,000 times, the flexible PSL phototransistor exhibited stable optoelectronic characteristics.

As the phototransistors can be fabricated with an organic material, this manufacturing method shows mechanical flexibility and reliability, which enables its usage in the display industry in the future.

EQ17.06.09

Silver Nanoparticles-Decorated Titanium Oxynitride Nanotube Arrays for Enhanced Solar-Assisted Hydrogen Generation Nageh K. Allam; American University in Cairo, Egypt

We demonstrate, for the first time, the synthesis of highly ordered titanium oxynitride nanotube arrays sensitized with Ag nanoparticles (Ag/TiON) as an attractive class of materials for visible-light-driven water splitting. The nanostructure topology of TiO₂, TiON and Ag/TiON was investigated using FESEM and TEM. The X-ray photoelectron spectroscopy (XPS) and the energy dispersive X-ray spectroscopy (EDS) analyses confirm the formation of the oxynitride structure. Upon their use to split water photoelectrochemically under AM 1.5 G illumination (100mW/cm², 0.1M KOH), the titanium oxynitride nanotube array films showed significant increase in the photocurrent (6mA/cm²) compared to the TiO₂ nanotubes counterpart (0.15mA/cm²). Moreover, decorating the TiON nanotubes with Ag nanoparticles (13 \pm 2nm in size) resulted in exceptionally high photocurrent reaching 14mA/cm² at

1.0V/SCE. This enhancement in the photocurrent is related to the synergistic effects of Ag decoration, nitrogen doping, and the unique structural properties of the fabricated nanotube arrays.

EQ17.06.10

Experiments and DFT Calculations of DTO Crystal [Iskander G. Batyrev](#) and Rosario C. Sausa; DEVCOM U.S. Army Research Laboratory, United States

X-ray diffraction (XRD) and Raman spectroscopy measurements of relatively new energetic crystal DTO [N-(1,7-dinitro-1,2,6,7-tetrahydro-[1,3,5]triazino[1,2-c][1,3,5]oxadiazin-8(4H)-ylidene)nitramide] are accompanied by DFT calculations. Calculated XRD and Raman spectra are in reasonable agreement with experiments. Calculated vibrational spectra identified in terms of atomic movements help us determine the 'weakest link' in the molecular crystal, whereas DFT partial charge density calculations related with N, C, and O atoms are used to find most chemically active atoms in crystal decomposition. In addition, the calculations show that the cage-containing N atoms provide the main contribution near the bottom of the DTO valence band. The DTO band gap calculated with hybrid function is compared to the band gap of several other energetic materials with regards to impact sensitivity.

EQ17.06.11

Investigation of the Electronic Structure and Triplet Emission Energy of Ir(azp)₂(acac)—an Organometallic Infrared Emitter [Nasir Javed](#), Jinyu Chong and Deirdre O'Carroll; Rutgers, The State University of New Jersey, United States

Infrared (IR) emitting phosphorescent materials have unique photophysical properties which make them useful for applications in optoelectronic devices. Ir(azp)₂(acac) (Bis(1-monoazaperylene)iridium(acetylacetonate)) is a promising phosphor for IR emitting applications; however, little information is available about the frontier orbitals and triplet states of this molecule. Here, density-functional theory (DFT) is used to calculate the singlet and triplet electronic structure of Ir(azp)₂(acac), and the triplet emission energy. Typically, DFT calculation results of organometallic phosphors, especially of iridium-based emitters, are reported with varying accuracy compared to experimental results. Therefore, first a calculation method is established by carrying out DFT calculations of two well-known organometallic phosphorescent materials: Flrpic (Bis[2-(4,6-difluorophenyl)pyridinato-C²,N](picolinato)iridium) and Ir(ppy)₃ (tris(2-phenylpyridine)iridium). A set of different hybrid functionals that are a mixture of Hartree-Fock exchange with DFT exchange-correlation (e.g., B3LYP, M05, M06), or a long-range correlation functional (e.g., CAM-B3LYP), are used with different basis sets including double-zeta (such as LANL2DZ) and polarized triple-zeta basis sets (such as DEF2TZVP) to optimize the ground state and triplet state geometries of the molecules in solvents (using polarizable continuum model) and in the gas phase. It is determined that the B3LYP functional performs better as compared to other functionals in terms of performance as well as accuracy; most likely because it uses non-local correlation, which works better with large molecules. From the DFT calculations of Flrpic and Ir(ppy)₃, and comparing the calculation results with relevant literature, it is determined that the LANL2D basis set gives results within less than 0.2 eV of error. The DEF2TZVP, being a bigger basis set used with the B3LYP functional, gives the most accurate energy levels; however, it requires much longer computational time. Later, the B3LYP functional and DEF2TZVP basis set are used to carry out geometry optimization of Ir(azp)₂(acac) in the ground state and in the first triplet state in dichloromethane and in the gas phase. Energy levels of the highest occupied molecular orbital (HOMO), lowest unoccupied molecular orbital and first triplet level (T₁) are determined from the optimized geometry. Finally, the triplet emission energy is calculated from the difference in energy level of T₁ and HOMO. This study not only provides useful information about the frontier orbitals and triplet states of Ir(azp)₂(acac) but also will help researchers working in the field in selecting appropriate functionals and basis sets for DFT calculations of the similar molecules.

EQ17.06.12

Optimization of Indium Oxide Thin Films by Molecular Beam Epitaxy [Erika V. Ortega Ortiz](#), Johanna Nordlander, Margaret Anderson, Charles Brooks and Julia Mundy; Harvard University, United States

Transparent conducting oxide (TCO) thin films play an important role in the development of optoelectronic devices. To fulfill their function as contacts and interfaces in optoelectronics, these materials need to perform well in terms of electronic conductivity, while at the same time maintaining their optical transparency. The most widely-used TCO is indium tin oxide. However, a remaining long-standing challenge in the synthesis of such indium-oxide-based thin films is achieving a sufficiently high crystalline quality and smooth surface morphology, which has complicated their integration into next-generation nanoscale devices. Here, we use oxide molecular beam epitaxy to explore the optimal growth parameters for both undoped and doped indium oxide on various technologically relevant substrates. By combining in-situ electron diffraction during thin-film growth with post-deposition X-ray diffraction and atomic-force microscopy, we achieve improved epitaxy and smoothness of our films as an important step to facilitate their integration in nanoscale optoelectronic devices.

EQ17.06.13

Spotlight Talk—3D Printing of Transparent Polysiloxanes Using Direct Ink Writing [Michael Ford](#), Colin Loeb, Lemuel Pérez Pérez, Stuart Gammon, Steven Guzorek, Hawi Gameda, A. Golobic, August Honnell, Justin Erspamer, Eric Duoss, Thomas Wilson and Jeremy Lenhardt; Lawrence Livermore National Laboratory, United States

Mixtures of silica and polysiloxane form thixotropic inks useful for 3D printing. However, 3D printed structures of these inks have typically been opaque due to the refractive index mismatch between the base polysiloxane and silica. By tuning the composition of the base polysiloxane, we matched the refractive index to formulate transparent inks. The transparent inks transmit up to ca. 90% of 700 nm light through 1 cm and remain transparent when solidified. We observed and characterized a thermochromic effect, where the inks change in opacity depending on refractive index mismatch and temperature. We also observed that the rheological properties of the ink depend on the distribution of silica particles, which is dictated by silica functionality, weight content, and processing. We demonstrate utility of these inks by printing encapsulants for LEDs, scintillators, and microfluidic mixing devices.

EQ17.06.14

AZO/TiO₂ Core-Shell Heterojunction Nanorods for Dye-Sensitized Solar Cells Hiroto Ando, Mahito Yamamoto and [Mitsuru Inada](#); Kansai University, Japan

It is well known that increasing the surface area and reducing the electrical resistance of the photoanode electrode are important factors for realizing a highly efficient dye-sensitized solar cell. Long and dense nanorods are a suitable structure for obtaining a large surface area. However, in long nanorods, the photoexcited carriers tend to recombine before reaching the electrode, which causes a decrease in photoelectric conversion efficiency. Therefore, a low resistivity material is desired as the nanorod material. ZnO possess higher electron transport properties than traditional anode material, TiO₂, and thus improve the conversion efficiency of the solar cell. However, bare ZnO nanorods are prone to chemical etching. In this point, the ZnO/TiO₂ core-shell heterojunction is candidate for the nanodot, because TiO₂ shell can prevent both the chemical etching and material corrosion caused by the external

environment such as acid and/or alkali solutions. Nevertheless, the conversion efficiency of present ZnO/TiO₂ nanorod dye-sensitized solar cells is not sufficiently high. In this study, we adopted Al-doped ZnO (AZO) as the core nanorod material. This is because the resistivity of AZO is lower than that of ZnO, so higher conversion efficiency can be expected.

AZO/TiO₂ core-shell heterojunction nanorods are prepared by a combination of hydrothermal method and successive ionic layer absorption and reaction (SILAR) method. Fluorine-doped tin oxide (FTO) sheet glass was used as substrate. AZO seed layer was deposited on the FTO glass substrate by sputtering. AZO nanorods were prepared by immersing the substrate in a mixture solution of zinc nitrate hexahydrate, aluminum nitrate hexahydrate, hexamethylenetetramine and polyethyleneimine at 90°C for 3 hours. TiO₂ shell layer was then prepared by SILAR method, repeatedly dipping three kinds of solution, "titanium tetraisopropoxide + diethanolamine + IPA", "IPA" and "deionized water", in this order. From SEM observations, the typical length and diameter of the nanorods were 1.6 μm and 60 nm, respectively.

Comparing the performance of our dye-sensitized solar cells using AZO nanorods and that of ZnO nanorods, the short-circuit current increased by 12% and the photoelectric conversion efficiency improved by 43% by using AZO nanorods.

EQ17.06.15

Spotlight Talk—Late News: Large Area, Multi-Pulse Laser Lifetime of Purified Nematic Liquid Crystals at Near Infrared Wavelengths [Selim Elhadji](#)¹, Andy Bayramian¹, Stavros Demos² and Kenneth Marshall²; ¹Seurat Technologies, Inc., United States; ²University of Rochester - LLE, United States

Nematic liquid crystals (LC's), ubiquitous in high information density displays, are typically composed of rod-shaped molecules that can exhibit large dielectric anisotropy, high birefringence and excellent transparency. These properties make them well suited for use in many optical components in high power laser systems, including polarization controllers and optoelectronic devices for beam shaping in 3D metal printing [*"A new era in metal part production"*, available at www.seuratech.com]. Recently, the single shot laser damage threshold of both saturated and un-saturated nematic LC's revealed an intrinsic relationship between the degree of chemical bond saturation within LC molecules and laser damage [Kosc *et al*, *Scientific Reports* 2019, 9 (1), 16435]. Extrinsic factors such as alignment layer material selection and preparation, particulate contamination and LC chemical purification can also play an important role in determining the optical response and durability of the liquid crystals. In this study we investigate the efficacy of several absorption-based purification methods and their impact on the laser damage behavior of nematic LC'S. We focus on the lifetime of purified and as-prepared LC'S when exposed to multiple laser pulses at kW's average power, over cm² areas, at near infrared wavelength and 20 to 40 Hz rep rates. Numerical simulations are used to estimate the degree of heat accumulation during exposure to rationalize the LC lifetime results.

SESSION EQ17.07: Advanced Characterization and Theory
Session Chairs: Artiom Magomedov and Philip Schulz
Thursday Morning, December 2, 2021
Hynes, Level 2, Room 203

10:30 AM *EQ17.07.01

Probing Buried Interfaces in Device Heterostructures Using Soft and Hard X-Ray Photoelectron Spectroscopy [Anna Regoutz](#); University College London, United Kingdom

Interfaces govern the behaviour of all electronic devices. Herbert Kroemer coined the famous phrase "the interface is the device" in his 2000 Nobel Prize lecture, and we are still applying tremendous effort to understand interfaces in new material generations, with transparent and wide band gap materials being no exception. Understanding gained for the bulk behaviour of materials can often not be extended to their behaviour in structured film stacks, where interfaces play a vital role.

This talk will give an overview of analytical strategies to probe buried interfaces between metallisation, dielectrics and semiconductors using both soft and hard X-ray photoelectron spectroscopy (XPS and HAXPES). It will contrast opportunities and limitations of these techniques to qualitatively and quantitatively explore heterostructures both in the laboratory and at synchrotron sources. It will explore how the different types of spectral features, such as shallow and deep core levels, Auger lines, and valence spectra, can be used to understand aspects of device critical interfaces such as elemental distributions, local chemical environments, intermixing and interdiffusion, and interface defects.

To illustrate the capabilities of PES techniques to address device interfaces and their structure and electronic structure, application examples including bulk Ga₂O₃, transparent conducting oxide (TCO) based transistors and diodes and copper-based industrial metallisation schemes will be used.

11:00 AM EQ17.07.02

Understanding the Surface Chemistry of Tin Dioxide Gas Sensors [Luisa Herring Rodriguez](#)¹, Chris Blackman¹ and David O. Scanlon^{1,2,3}; ¹University College London, United Kingdom; ²Diamond Light Source, United Kingdom; ³Thomas Young Centre, United Kingdom

Tin dioxide (SnO₂) is one of the most studied and used metal oxide semiconductors and is often used in gas sensors. Despite the extensive research into SnO₂ and its wide range of uses, its surface chemistry is still not fully understood. A detailed literature search of previously proposed surface structures and gas adsorption mechanisms for SnO₂ reveals many conflicting models with zero consensus. This disparity between different mechanistic theories demonstrates the need for a more thorough investigation into SnO₂ if we are to design new gas sensing materials in a methodical way in the future.

In this work, we use levels of accuracy within a Density Functional Theory (DFT) framework which have hitherto been inaccessible due to their computational expense. We initially calculate the optoelectronic properties of bulk SnO₂ and systematically investigate the effect of slab and vacuum thickness on surface model validity. We go on to calculate the energetics and electronic structures for a range of proposed surface defects, as well as for various proposed gas adsorption sites.

Our initial results show that larger slab models than those previously used are required to accurately represent the SnO₂ crystal structure. Overall, this work highlights how modern first-principles methods can elucidate surface phenomena in well-studied materials and paves the way for the rational design of new inorganic compounds for gas sensing applications.

11:15 AM EQ17.07.03

Rapid Recombination by Cadmium Vacancies in CdTe [Seán R. Kavanagh](#)¹, Aron Walsh² and David O. Scanlon³; ¹University College London & Imperial College London, United Kingdom; ²Imperial College London, United Kingdom; ³University College London, United Kingdom

The ability to accurately model, understand and predict the behaviour of crystalline defects would constitute a significant step towards improving photovoltaic device efficiencies and semiconductor doping control, accelerating materials discovery and design.¹ In this work, we apply hybrid Density Functional Theory (DFT) including spin-orbit coupling to accurately model the atomistic behaviour of the cadmium vacancy (V_{Cd}) in cadmium telluride (CdTe).¹ In doing so, we resolve several longstanding discrepancies in the extensive literature on this species.

CdTe is a champion thin-film absorber for which defects, through facilitation of non-radiative recombination, significantly impact photovoltaic (PV) performance, contributing to a reduction in efficiency from an ideal detailed-balance limit of 32% to a current record of 22.1%. Despite over 70 years of experimental and theoretical research, many of the relevant defects in CdTe are still not well understood, with the definitive identification of the atomistic origins of experimentally observed defect levels remaining elusive.²⁻⁴

In this work, through identification of a tellurium dimer ground-state structure for the neutral Cd vacancy, we obtain a single negative-U defect level for V_{Cd} at 0.35 eV above the VBM, finally reconciling theoretical predictions with experimental observations. Moreover, we reproduce the polaronic, optical and magnetic behaviour of V_{Cd} ¹ in excellent agreement with previous Electron Paramagnetic Resonance (EPR) characterisation.^{5,6} We find the cadmium vacancy facilitates rapid charge-carrier recombination, reducing maximum power-conversion efficiency by over 5% for *untreated* CdTe—a consequence of tellurium dimerisation, metastable structural arrangements, and anharmonic potential energy surfaces for carrier capture.

The origins of previous discrepancies between theory and experiment, namely incomplete mapping of the defect potential energy surface (PES) and approximation models, are highlighted and discussed. Importantly, these results demonstrate the necessity to include the effects of both metastability and anharmonicity for the accurate calculation of both charge-carrier recombination rates in emerging photovoltaic materials and the efficiency limits imposed by both native and extrinsic defect species.

¹ Y.-T. Huang, S. R. Kavanagh, D. O. Scanlon, A. Walsh and R. L. Z. Hoyer, *Nanotechnology*, 2021, **32**, 132004.

² S. R. Kavanagh, A. Walsh and D. O. Scanlon, *ACS Energy Lett.*, 2021, **6**, 1392–1398.

³ A. Lindström, S. Mirbt, B. Sanyal and M. Klintonberg, *J. Phys. D: Appl. Phys.*, 2015, **49**, 035101.

⁴ J.-H. Yang, W.-J. Yin, J.-S. Park, J. Ma and S.-H. Wei, *Semicond. Sci. Technol.*, 2016, **31**, 083002.

⁵ A. Shepidchenko, B. Sanyal, M. Klintonberg and S. Mirbt, *Scientific Reports*, 2015, **5**, 1–6.

⁶ P. Emanuelsson, P. Omling, B. K. Meyer, M. Wienecke and M. Schenk, *Phys. Rev. B*, 1993, **47**, 15578–15580.

SESSION EQ17.10: Advanced Characterization, New Materials and Concepts I

Session Chairs: Alex Martinson and Nathanaelle Schneider

Monday Afternoon, December 6, 2021

EQ17-Virtual

1:00 PM *EQ17.10.01

Thin-Film Solar Cell Structures as Revealed by Electron and X-Ray Spectroscopies [Marcus Baer](#)^{1,2,3}; ¹Helmholtz-Zentrum Berlin für Materialien und Energie GmbH, Germany; ²Helmholtz-Institute Erlangen-Nürnberg for Renewable Energy, Germany; ³Friedrich-Alexander-Universität Erlangen-Nürnberg, Germany

The multitude of layers, interfaces, elements, impurities, defects, etc. contributing to the structure, function, and performance of optoelectronic devices means that characterization and fundamental understanding of the chemical and electronic structures of each component, as well as their interactions at interfaces, are crucial to support technical progress. The deliberate combination of complementary electron and x-ray spectroscopies can reveal crucial information that open routes to insight-driven strategies to improve device performance.

To showcase the power of this approach, several examples from the field of photovoltaics will be presented. In particular, the chemical and electronic structures (including energy level alignment) of the emitter/absorber and absorber/back contact interfaces for Cu(In,Ga)Se₂ (CIGSe) thin-film solar cell absorbers and how they are modified by different alkali post-deposition treatments will be presented and discussed against the background of the respective device performances.

1:30 PM EQ17.10.02

Strong Fermi-Level Pinning at Metal Contacts to Halide Perovskites [Kootak Hong](#)^{1,2}, Ki Chang Kwon², Kyoung Soon Choi³, Carolin M. Sutter-Fella¹ and Ho Won Jang²; ¹Lawrence Berkeley National Laboratory, United States; ²Seoul National University, Korea (the Republic of); ³Korea Basic Science Institute, Korea (the Republic of)

The performance of halide perovskite-based electronic and optoelectronic devices is often related to interfacial charge transport. To shed light on the underlying physical and chemical properties of CH₃NH₃PbI₃ (MAPbI₃) in direct contact with common electrodes Al, Ti, Cr, Ag, and Au, the evolution of interfacial properties and Fermi level pinning is systematically studied. Given a unique experimental facility, pristine interfaces without any exposure to ambient air were prepared. We observe aggregation of substantial amounts of metallic lead (Pb⁰) at the metal/MAPbI₃ interface, resulting from the interfacial reaction between the deposited metal and iodine ions from MAPbI₃. It is found that the Schottky barrier height at the metal/MAPbI₃ interface is independent of the metal work function due to strong Fermi level pinning, possibly due to the metallic Pb⁰ aggregates, which act as interfacial trap sites. The charge neutrality level of MAPbI₃ is consistent with the energy level of Pb⁰-related defects, indicating that Pb⁰ interfacial trap states can be nonradiative recombination sites. This work underlines that control of chemical bonding at interfaces is a key factor for designing future halide perovskite-based devices.

1:45 PM *EQ17.10.03

Making Contact with Emerging Photovoltaic Materials [Aron Walsh](#); Imperial College London, United Kingdom

Device architectures for high-performance solar cells have evolved over decades to maximise current collection and to minimise voltage losses. The two main challenges caused by moving to new systems is the change in crystal structure and the variation in electron energies (ionisation potential and electron

affinity). These issues are magnified for non-cubic crystals where anisotropic materials properties can result in a mismatch between the ideal orientations for absorption and transport versus the preferred orientation for crystal growth. I will discuss our development and application of computational tools to accelerate the design process including the electron-lattice-strain (ELS) descriptor[1] and its extension to systems including Sb₂Se₃, SnS, and CuBiS₂ [2,3].

1. Screening procedure for structurally and electronically matched contact layers for high-performance solar cells: hybrid perovskites, *J. Mater. Chem A* 4, 1149 (2016); <https://doi.org/10.1039/c5tc04091d>

2. Finding a junction partner for candidate solar cell absorbers enargite and bournonite from electronic band and lattice matching, *J. App. Phys.* 125, 055703 (2019); <https://doi.org/10.1063/1.5079485>

3. Upper limit to the photovoltaic efficiency of imperfect crystals from first principles, *Energy Environ. Sci.* 13, 1481 (2020); <https://doi.org/10.1039/D0EE00291G>

2:15 PM EQ17.10.04

Optical Properties of OLED Materials by TDDFT Nobuhiko Akino; Hosei University, Japan

Organic light emitting diodes (OLEDs) have been of great interest for display and lighting applications during decades and they have recently been utilized in smartphones and flat-panel displays. After the development of fluorescent materials, the phosphorescent materials have been introduced and have achieved high efficiency. However, phosphorescent materials require expensive heavy metal such as Ir and Pt. Recently, thermally activated delayed fluorescence (TADF) materials have been developed as a new class of light emitting material where triplet excitons are converted into singlet excitons without heavy metals in phosphorescent materials.[1] Theoretically, an internal quantum efficiency of 100%, the same as for phosphorescent materials, can be expected.

In order to study the optical properties of materials, we have employed the time dependent density functional theory (TDDFT), which is one of the most prominent and widely used methods for calculating excited states of various molecules, and it is recognized as a powerful tool for studying their electronic transition. In our calculations, the real-time and real-space (RSRT) techniques are employed in solving time dependent Kohn-Sham equation by the finite difference approach [2,3] without using explicit bases such as plane waves and Gaussian basis. Within the frame work of this approach, we can solve for the wave functions on the grid with a fixed domain, which encompasses the physical system of interests.[4]

In this study, we have focused on the spectrum of OLED materials. For material design, it is highly desirable to simulate the spectral profile, not only the peak wavelength of absorption and/or emission, but also its spectrum shape. RSRT-TDDFT is applied to analyze some typical organic materials to study their spectrum profiles. In addition to the conventional fluorescent materials, phosphorescent and TADF materials are studied. Although the research is in an early stage, current results show that this approach may be able to simulate the spectrum profile reasonably well and to apply the material design.

REFERENCES

[1] K. Goushi, K. Yoshida, K. Sato, C. Adachi, *Nat. Photonics*, **6**(2012), 253

[2] E. Runge, E. K. U. Gross, *Phys. Rev. Lett.* **52**, 997(1984)

[3] K. Yabana and G.F. Bertsch, *Phys. Rev.* **B54**, 4484(1996)

[4] N. Akino and Y. Zempo, *MRS Advances*, **1**(2016), 1773

2:30 PM EQ17.10.05

Experimental Realization of P-Type Transparent Conductive Phosphides Andrea Crovetto^{1,2}, Thomas Unold¹ and Andriy Zakutayev²; ¹Helmholtz-Zentrum Berlin, Germany; ²National Renewable Energy Laboratory, United States

Despite long-standing research efforts to develop p-type transparent conductive materials (TCMs), the current generation of optoelectronic devices still relies exclusively on n-type TCM contacts due to their much better trade-off between conductivity and transparency. An important issue in oxide-based p-type TCMs is the deep energy and localized nature of the 2p oxygen states in the valence band, which has negative consequences on both hole dopability and hole mobility in most oxides.

Recent computational work [1,2] has identified several earth-abundant phosphides (particularly BP and CaCuP) that could potentially outperform the existing p-type TCMs. These phosphides have shallow, disperse valence bands that are ideal for high hole dopability and mobility. Although their indirect band gaps are rather low (around 2 eV), their direct band gaps are much wider and could ensure transparency in thin film samples. However, thin films of CaCuP have not been made yet, and previously reported BP thin films have not been thoroughly evaluated as transparent contacts [3].

Using a unique combinatorial sputter chamber with reactive PH₃ gas, we have synthesized BP and CaCuP films as a function of various process parameters. Last year we gave a preliminary report of their properties at this conference. This year, we will discuss their suitability as p-type TCMs in much greater detail.

In particular, we have found that the electrical conductivity of CaCuP under optimized growth conditions is almost on par with the conductivity of state-of-the-art n-type TCMs such as ITO and FTO, even in the absence of any extrinsic dopant. However, CaCuP films are only moderately transparent in the visible region due to unexpectedly high absorption strength above the indirect band gap.

We have also found that BP can be doped p-type up to remarkably high hole concentrations by using extrinsic dopants combined with off-stoichiometry. However, it is challenging to obtain BP films of high crystal quality by sputter deposition. This issue has so far prevented us from reaching high hole mobilities.

Despite the experimental challenges, we confirm that both CaCuP and BP could be outstanding transparent conductors if their growth processes could be further improved. More generally, the field of metal phosphides appears to be a fertile search space for potential p-type transparent conductors.

[1] B. Williamson et al., *Chem. Mater.*, **29**, 2402–2413 (2017).

[2] J. Varley et al., *Chem. Mater.*, **29**, 2568–2573 (2017).

[3] A. Fioretti, M. Morales-Masis, *J. Photonics Energy*, **10**, 042002 (2020)

2:45 PM EQ17.10.06

Ultrafast, Low-Noise Solution-Processed Quantum Dot Photodetectors with Amorphous Selenium Transport Layer Haripriya Kannan¹, Atreyo

Mukherjee², Triet Ho², Jann Stavro³, Adrian Howansky³, Neha Nooman², Dragica Vasileska⁴, Wei Zhao³, Amirhossein Goldan³ and Ayaskanta Sahu¹; ¹New York University, United States; ²Stony Brook University, College of Engineering and Applied Sciences, United States; ³Stony Brook University, United States; ⁴Arizona State University, School of Electrical, Computer and Energy Engineering, United States

Effective sensing of optical signals by a solid-state detector that convert photons to electricity are widely used in digital imaging, optical communications, remote-sensing, spectroscopy, and astronomy. These photodetectors should possess high sensitivity, i.e., the ability to differentiate signal from noise, especially at low light intensities down to single-photon level. In recent years, colloidal quantum dots (CQDs) have gained significant attention in optoelectronics due to their wide spectral tunability, high absorption coefficients, and large oscillator strengths. Colloidal quantum dots also allow facile solution-processing that enables an easy room-temperature integration onto variety of substrates, rigid or flexible, including read-out integrated circuits with near-unity fill factor. In semiconductor optoelectronics, fast and sensitive photodetection is achieved when photocarrier recombination is limited by physically separating holes and electrons through electron/hole-transport layer. In our work, we developed vertical-stack photodetectors, which uses a solution-processed nanocrystal photoconversion layer coupled to an amorphous selenium wide-bandgap avalanche charge transport layer, in the desired p-i-n fabrication sequence that enables compatibility with active-matrix readout circuitry. Amorphous-selenium detectors have gained significant attention due to their single-carrier hole impact ionization phenomenon achieving high gains (~1000) with a very low excess noise factor and are suitable for a large-area deposition at room-temperature without damaging the underlying read-out circuits. Here, in our recent work on colloidal quantum dot/glass avalanche transport layer heterostructures, optical absorption and electrical transport are physically separated which enables increased flexibility for spectral tuning and increased charge extraction reaching high specific detectivity (5×10^{12} Jones), fast photoresponse with megahertz 3-dB electrical bandwidth (~ 25 Mhz), ultra-low dark current density (~ 10 pA/cm²), low noise current (~ 20 fW/Hz^{1/2}), and high linear dynamic range (~ 150 dB).

SESSION EQ17.11: Advanced Characterization, New Materials and Concepts II
Session Chairs: Fan Fu and Philip Schulz
Monday Afternoon, December 6, 2021
EQ17-Virtual

4:00 PM *EQ17.11.01

Space-Resolved Photoelectron Spectroscopy to Probe Heterostructures Dipankar Das Sarma; Indian Inst of Science, India

X-ray photoelectron spectroscopy has played an enormous role in developing our understanding of a range of interesting materials over the last five decades, primarily arising from its ability to energy-resolve electrons ejected from any sample due to its interaction with sufficiently high energy photons, thereby defining one of the most powerful spectroscopic techniques. However, when combined with space-resolution to achieve a microscopy based on this spectroscopy, it can provide us with unique information, not available otherwise. In my presentation, I shall describe two qualitatively different ways^{1,2} to achieve such a space-resolution to provide complementary insights into diverse systems.

In the first part of the presentation, I shall focus on an elusive metastable phase, existing only as small patches in chemically exfoliated few-layer, thermodynamically stable 2H phase of MoS₂ that is believed to critically influence properties of MoS₂ based devices. Its electronic structure is little understood in absence of any direct experimental data and conflicting claims from theoretical investigations. I shall present data^{3,4} to conclusively resolve this issue based on probing the electronic structure of chemically exfoliated few layer systems using lateral-space-resolution in photoemission spectroscopy.

In the second approach, I shall explore the rapidly expanding field that deal with emergent properties at a variety of interfaces formed in heterostructured materials, including optically active nanomaterials. It is in general difficult to probe directly the nature of such interface states since these are typically buried under a depth and represent a very small volume fraction of the entire sample. We have shown over the years^{2,5-10} that x-ray photoelectron spectroscopy with a widely tunable photon energy from synchrotron sources can be used very effectively to obtain vertical-space resolution leading to layer-resolved electronic structure information; This makes this technique an ideal probe to investigate interface properties in diverse heterostructured systems. I shall illustrate this by discussing electronic properties of a few interesting systems, such as LaAlO₃-SrTiO₃, magnetic tunnel junctions with CoFeB and MgO, and optical properties of highly luminescent semiconductor nanoparticles with integrated internal interfaces.

References:

1. D. D. Sarma *et al.*, Phys. Rev. Lett. **93**, 097202 (2004).
2. D. D. Sarma *et al.*, Chem. Mater. **25**, 1222 (2013).
3. Banabir Pal *et al.*, Phys. Rev. B **96**, 195426 (2017).
4. Debasmita Pariari *et al.*, Applied Materials Today **19**, 100544 (2020); and APL Mater. **8**, 040909 (2020).
5. S. Sapra *et al.*, J. Phys. Chem. B **110**, 15244 (2006).
6. Pralay K. Santra *et al.*, J. Am. Chem. Soc. **131**, 470 (2009).
7. D. D. Sarma *et al.*, J. Phys. Chem. Lett. **1**, 2149 (2010).
8. Banabir Pal *et al.*, J. Electron Spectrosc. Relat. Phenom. **200**, 332 (2015).
9. Sumanta Mukherjee *et al.*, Phys. Rev. B **91**, 085311 (2015).
10. Sumanta Mukherjee *et al.*, EPL (Europhys. Lett.) **123**, 47003 (2018).

4:30 PM EQ17.11.02

Organic Electronics with Solution-Processed Electron Transport Layers Based on ZnO and MgO Ioannis Ierides^{1,2}, Kunping Guo^{1,2}, Isaac Squires³, Giulia Lucarelli⁴, Thomas M. Brown⁴ and Franco Cacialli^{1,2}; ¹University College London, United Kingdom; ²London Centre for Nanotechnology, United Kingdom; ³Imperial College London, United Kingdom; ⁴Università degli Studi di Roma Tor Vergata, Italy

Electron transport layers (ETLs) have been instrumental in breaking the efficiency boundaries of optoelectronic devices. A key ETL for organic electronics is ZnO, however, depending on its preparation it can be a sub-optimal ETL suffering from surface defects. The application of a thin interlayer between ZnO and the active layer of optoelectronic devices has proven to be a successful method to achieve performance enhancements. Ultrathin MgO in combination with metal oxides such as SnO₂ and TiO₂ to form effective ETLs has afforded tremendous success in various solution-processed systems, such as perovskite photovoltaics. However, its application to improve ZnO based ETLs for organic electronics is limited.¹

In our work, we investigate MgO as a modifying interlayer on top of a ZnO ETL formed by simple solution-processing and low temperature annealing and

apply it to organic photovoltaics (OPVs). We show that the modified ETL enhances the performance of OPV devices with respect to a single ZnO ETL without significantly affecting the photon capture rate and blend morphology. The ZnO/MgO ETL is shown to have a more uniform top surface with a root mean square roughness decreasing from 4.5 ± 0.2 nm to 3.2 ± 0.4 nm and a lower work function (by 0.11 ± 0.05 eV) compared to the single ZnO ETL, which is expected to be beneficial to electron extraction. We demonstrate that insertion of the thin MgO interlayer in devices leads to a reduced leakage current and an increase in the shunt resistance. The power conversion efficiency of OPVs employing the ZnO/MgO ETL is enhanced by $\approx 10\%$ (relative increase) as a result of a boosted short circuit current density and fill factor.²

1. J. Dagar et al., "Highly efficient perovskite solar cells for light harvesting under indoor illumination via solution processed SnO₂/MgO composite electron transport layers", *Nano Energy*, 49, (2018) 290–299.

2. I. Ierides et al., "Inverted organic photovoltaics with a solution-processed ZnO/MgO electron transport bilayer", *J. Mater. Chem. C*, 9, (2021) 3901–3910

4:45 PM EQ17.11.03

Late News: Transfer of Oxide Electrode Sheet with Wide Bandgap of 4.6 eV Lizhikun Gong, Mian Wei, Hiromichi Ohta and Tsukasa Katayama; Hokkaido University, Japan

Transparent conductive oxides (TCOs) are essential for optoelectronic devices. Among TCOs, ITO is widely utilized due to its high electrical conductivity (~ 10000 S cm⁻¹) and easy synthesis. However, the bandgap of ITO (~ 3.5 eV) is insufficient compared to the requirements of electrodes for deep-ultraviolet light-emitting diodes (DUV-LEDs) ($h\nu > 4.1$ eV). As the electrode, La-doped SrSnO₃ (LSSO) is promising due to its both wide bandgap (~ 4.6 eV) and high electrical conductivity (~ 3000 S cm⁻¹). Nevertheless, there is a problem that single-crystal LSSO epitaxial film requires high deposition temperature, which is beyond the heat resistant temperature of the DUV-LEDs. In order to solve this problem, we proposed a lift-off and transfer method, which enables preparation of LSSO sheet on many kinds of substrates at room temperature.

The LSSO thin films were heteroepitaxially grown on the water-soluble Sr₃Al₂O₆ (SAO)^[3,4]-buffered SrTiO₃ (STO) substrate by pulsed laser deposition method. Then, we removed the SAO layer with water. The LSSO sheet was further transferred on glass or PET substrates.

The out-of-plane X-ray diffraction (XRD) patterns of the LSSO/SAO bilayer film and transferred LSSO sheet clearly exhibited the LSSO peaks without any impurity peaks. In addition, the sheet exhibited coexistence of high electrical conductivity (~ 1600 S cm⁻¹) and wide bandgap (~ 4.6 eV) at room temperature. The single-crystal LSSO sheet with lateral size of 5 mm \times 5 mm was successfully obtained.

[1] H. Ohta et al., *Appl. Phys. Lett.* **76**, 2740 (2000).

[2] M. Wei et al., *Appl. Phys. Lett.* **116**, 022103 (2020).

[3] D. Lu et al., *Nat. Mater.* **15**, 1255 (2016).

[4] P. Singh et al., *ACS Appl. Electron. Mater.* **1**, 1269 (2019)

4:50 PM EQ17.11.04

Carbon Based Materials for Hole- Extraction in Perovskite Solar Cells G.R.A. Kumara¹, D.G.B.C. Karunaratne¹, A.D.T. Medagedara¹, R.M.G. Rajapakse², Dhayalan Velauthapillai³, Punniamoorthy Ravirajan⁴, A. G. U. Perera⁵, Ajith DeSilva⁶ and K. Tennakone^{1,5}; ¹National Institute of Fundamental Studies, Sri Lanka; ²University of Peradeniya, Sri Lanka; ³Western Norway University of Applied Sciences, Norway; ⁴University of Jaffna, Sri Lanka; ⁵Georgia State University, United States; ⁶University of West Georgia, United States

Performance of perovskite solar cells (PSCs) are largely determined by the nature of the hole -collector material and its interface with the perovskite. The molecular solid Spiro-OMeTAD; inorganic p - type semiconductors such as CuSCN, CuI and NiO; conducting polymers; metals and forms of carbon have been used as the hole -collector materials. PSCs based on metals and carbon are often referred to as hole- collector free perovskite solar cells. A misleading statement, because it is not clear how the hole extraction property has arisen, as the of nature of the true interface remain uncertain. Metals are often coated with oxide layers and in many instances different forms of carbon had been blended other substances and reported as carbon electrodes without empathizing role of the binder.

Compared to metals, carbon and its blends turn out be more suitable to understand mechanism by which the holes photo-generated in perovskite are transferred to the cathode of the solar cell. Carbon when perfectly purified contains no solid surface layers; but liable to be populated with surface groups. Therefore in the case of carbon; the grain structure, grain size and surface groups are the main relevant parameters, characterizing the material. An extensively studied carbon material which can be easily purified is coconut shell charcoal. In the present work; the rectification properties of the perovskite/carbon interface and IV characteristic of cells are examined in detail by pressing coconut shell derived carbon powder on the perovskite surface deposited on TiO₂ by the usual procedure. Results indicate that the grain electrical conductivity, grain size and pressure applied are the crucial factors determining the cell efficiency. Experimental details and possible electron-hole separation mechanisms at the perovskite/carbon will be discussed.

4:55 PM EQ17.11.05

Strategies to Enhance the Capability of Carrier Injection to the Effective Channel for Bottom-Gated Amorphous Oxide Thin-Film Transistors Mingyuan Liu¹, Hyeonhun Kim¹, Han Wook Song² and Sunghwan Lee¹; ¹Purdue University, United States; ²Korea Research Institute of Standard and Science (KRISS), Korea (the Republic of)

Over the two decades, amorphous oxide semiconductors (AOSs) and their thin film transistor (TFT) channel application have been intensely explored to realize high performance, transparent and flexible displays due to their high field effect mobility ($\mu_{FE} = 5\text{-}20$ cm²/Vs), visible range optical transparency, and low temperature processability (25-300 °C).[1-2] The metastable amorphous phase is to be maintained during operation by the addition of Zn and additional third cation species (e.g., Ga, Hf, or Al) as an amorphous phase stabilizer.[3-5] To limit TFT off-state currents, a thin channel layer (10-20 nm) was employed for InZnO (IZO)-based TFTs, or third cations were added to suppress carrier generations in the TFT channel. To resolve bias stress-induced instabilities in TFT performance, approaches to employ defect passivation layers or enhance channel/dielectric interfacial compatibility were demonstrated.[6-7]

Metallization contact is also a dominating factor that determines the performance of TFTs. Particularly, it has been reported that high electrical contact resistance significantly sacrifices drain bias applied to the channel, which leads to undesirable power loss during TFT operation and issues for the measurement of TFT field effect mobilities. [2, 8] However, only a few reports that suggest strategies to enhance contact behaviors are available in the literature. Furthermore, the previous approaches (1) require an additional fabrication complexity due to the use of additional treatments at relatively harsh conditions such as UV, plasma, or high temperatures, and (2) may lead to adverse effects on the channel material attributed to the chemical incompatibility between dissimilar materials, and exposures to harsh environments. Therefore, a simple and easy but effective buffer strategy, which does not require any additional process complexities and not sacrifice chemical compatibility, needs to be established to mitigate the contact issues and therefore achieve high performance and low power consumption AOS TFTs.

The present study aims to demonstrate an approach utilizing an interfacial buffer layer, which is compositionally homogeneous to the channel to better align work functions between channel and metallization without a significant fabrication complexity and harsh treatment conditions. Photoelectron spectroscopic measurements reveal that the conducting IZO buffer, of which the work function (Φ) is 4.37 eV, relaxes a relatively large Φ difference between channel IZO ($\Phi=4.81$ eV) and Ti ($\Phi=4.2-4.3$ eV) metallization. The buffer is found to lower the energy barrier for charge carriers at the source to reach the effective channel region near the dielectric. In addition, the higher carrier density of the buffer and favorable chemical compatibility with the channel (compositionally the same) further contribute to a significant reduction in specific contact resistance as much as more than 2.5 orders of magnitude. The improved contact and carrier supply performance from the source to the channel lead to an enhanced field effect mobility of up to 56.49 cm²/Vs and a threshold voltage of 1.18 V, compared to 13.41 cm²/Vs and 7.44 V of IZO TFTs without a buffer. The present work is unique in that an approach to lower the potential barrier between the source and the effective channel region (located near the channel/dielectric interface, behaving similar to a buried-channel MOSFET [9]) by introducing a contact buffer layer that enhances the field effect mobility and facilitates carrier supply from the source to the effective channel region.

This work is partially supported by the U.S. National Science Foundation (NSF) Award No. ECCS-1931088 and the KRISS Improvement of Measurement Standards and Technology for Mechanical Metrology, Award No. 20011028.

This presentation is based on our recent publication, M. Liu et al. *ACS Applied Electronic Materials*, 2021 (In press) (DOI: 10.1021/acsaem.1c00284).

5:00 PM EQ17.11.06

Improvement of Light-Harvesting in Perovskite Solar Cells by Post-Modification with a Fluorescent Layer Timur Atabaev; Nazarbayev University, Kazakhstan

Perovskite solar cells (PSCs) with a standard sandwich structure suffer from optical transmission losses due to the substrate and its active layers. Developing strategies for compensating for the losses in light-harvesting is of significant importance to achieving a further enhancement in device efficiencies. In this work, the down-conversion effect of carbon quantum dots (CQDs) was employed to convert the UV fraction of the incident light into visible light. For this, thin films of poly(methyl methacrylate) with embedded carbon quantum dots (CQD@PMMA) were deposited on the illumination side of PSCs. Analysis of the device performances before and after application of CQD@PMMA photoactive functional film on PSCs revealed that the devices with the coating showed an improved photocurrent and fill factor, resulting in higher device efficiency.

5:05 PM EQ17.11.07

Fabrication and Characterization of Wrinkle Free Nanometer Rigid Thin Film on Soft Substrate Maryam Jalali-Mousavi¹ and Jian Sheng^{1,2}; ¹Texas A&M University, United States; ²Johns Hopkins University, United States

Flexible electronics and electro-optics have drawn a significant attention in recent years. Successful fabrication of flexible mirrors or transparent electronics will require deposition of relatively rigid thin films on soft compliant substrates. However, direct deposition of a rigid film on soft substrates often suffers from wrinkling or buckling due to the interfacial instability arising from the substrate compression beyond a critical strain. Wrinkled surfaces cause severe reduction in reflectivity and low transmittance. In this work, we report a novel technique to fabricate wrinkle free deposited rigid thin films on soft substrate by suppressing the instability with a nm-layer of jamming nanoparticles. The thickness of the jammer can tailor the wrinkle periodicity and the roughness of the surface. The technique is robust and readily applicable to wide variety of materials. For demonstration system, we selected Poly(dimethylsiloxane) (PDMS), poly(monochloro-p-xylylene) (parylene C) as jammer and various metals (*e.g.*, Cu, Al, Ti). Different jammer layers varying from 40nm to 2um are deposited on 1mm PDMS substrate followed by sputter deposition of 50nm thin metal film. The surface morphology of the samples was analyzed by atomic force microscopy (AFM). The results showed that as the jammer thickness increases, the wrinkle wavelength increases accordingly and when the thickness exceeds a threshold (*e.g.*, ~150nm), wrinkles are suppressed. Nanoindentation measurements also show the interfacial stiffness increases by two orders of magnitude as the jammer thickness increases. When the layer reaches 150nm, the metal-jammer-PDMS composite becomes increasingly elastic and deviates substantially from viscoelastic behavior. A dual power law emerges in Young's relaxation modulus.

5:10 PM EQ17.11.09

Computational Fermi Level Engineering and Doping-Type Conversion of Mg:Ga₂O₃ via Three-Step Processing Anuj Goyal¹, Andriy Zakutayev¹, Vladan Stevanovic^{2,1} and Stephan Lany¹; ¹National Renewable Energy Laboratory, United States; ²Colorado School of Mines, United States

Ga₂O₃ is being actively explored for optoelectronic (phosphorus, and electroluminescent devices, solar-blind photodetectors) application due to its ultra-wide bandgap and low projected fabrication cost of large-size and high-quality crystals. Efficient *n*-type doping of Ga₂O₃ has been achieved, but *p*-type doping faces fundamental obstacles due to compensation, deep acceptor levels, and the polaron transport mechanism of free holes. However, aside from achieving *p*-type conductivity, plenty of opportunities exists to engineer the position of the Fermi level for improved design of Ga₂O₃ based devices. We use first principles defect theory and defect equilibrium calculations to stimulate a 3-step growth-annealing-quench synthesis protocol for hydrogen assisted Mg doping in beta Ga₂O₃, considering the gas phase equilibrium between H₂, O₂, and H₂O, which determines the H chemical potential. We predict Ga₂O₃ doping-type conversion to a net *p*-type regime after growth under reducing conditions in the presence of H₂ followed by O-rich annealing, which is similar process to the Mg acceptor activation by H removal in GaN. We show there is an optimal temperature that maximizes the Ga₂O₃ net acceptor density for given Mg doping level. After quenching to operating temperatures, the Ga₂O₃ Fermi level drops below mid-gap down to +1.5 eV above the valence band maximum, creating significant number of uncompensated neutral Mg_{Ca}⁰ acceptors. The resulting free hole concentration in Ga₂O₃ is very low due to deep energy level of these Mg acceptors, and hole conductivity is further impeded by the polaron hopping mechanism. However, the Fermi level reduction down to +1.5 eV and suppression of free electron density in this doping type converted Ga₂O₃ material is of significance and impact for the design of Ga₂O₃ based optoelectronic devices.

5:15 PM EQ17.11.10

Solar-Blind Photodetectors Based on Gallium Oxide and Their Performance Analysis Against Swift Heavy Ions Damanpreet Kaur and Mukesh Kumar; Indian Institute of Technology Ropar, India

The UV-C (< 280 nm of wavelength) part of the solar spectrum is highly dangerous to living organisms, with exposure often causing changes in their genetic make-up. Thankfully, the ozone layer in the atmosphere absorbs almost all of this radiation, thereby providing us with natural protection. The complete absorption leads to a very low background signal of UV-C on earth. This unique characteristic can be exploited in the fabrication of highly sensitive photodetectors which are responsive to UV-C only from other sources on earth, leading to the development of the so-called solar-blind photodetectors (SBPD). Solar-blind photodetectors are deep-UV photodetectors that show sensitivity to only UV-C radiation. They show no response when placed in natural sunlight and thus have applications ranging from ozone-hole monitoring, missile tracking, flame detection, space exploration, UV sterilization systems, non-line-of-sight communications, etc. Traditionally, SBPDs were fabricated using mature technologies such as silicon. However, a

band gap of 1.1 eV renders the devices to have a broadband photoresponse, thus necessitating the use of costly optical filters. Wide band gap semiconductors offer a solution to this problem by removing the need for any filters due to their suitable band gap. Gallium oxide is a new, ultra-WBG material with properties that are promising for its use as a functional material in the fabrication of SBPDs. It has an apt band gap of 4.6-5.3 eV (depending on the polymorph) making it intrinsically solar-blind. Moreover, it is highly chemically and thermally stable (M.P. ~ 1730°C), has a high breakdown voltage and is extremely radiation hardened and hence it can be employed for use in extreme environment applications (high temperature and high radiation conditions). Some of these applications include employment in nuclear, geothermal or space exploration, which require the material to be immune (at least partially) to all sorts of radiation. This requires extensive studies to investigate the effect that each type of radiation might have on the material as well as on the performance of its devices.

We have undertaken such a study on the radiation hardness and device performance of amorphous and polycrystalline gallium oxide thin film against heavy ion (Ag^{7+}) irradiation with a high energy of 100 MeV. We found that the amorphous thin film shows better resilience to the radiation as compared to the polycrystalline film. Changes in the morphology and crystal structure of the material were thereby investigated. There occurs recrystallization and formation of nano-pores in the amorphous film while the polycrystalline film shows destruction of the larger crystallites. The photodetectors fabricated on the irradiated films exhibit good device integrity albeit with a decrease in performance. The change in performance is linked to the change in the material's defect density which is confirmed by photoluminescence study. The optical defects, which are responsible for the high photoconductive gain in gallium oxide, undergo ionization-induced defect annealing and thus lead to an overall decrease in performance. The radiation-damaged performance of the photodetectors is recovered by annealing at moderate temperatures in air ambient, so much so that the amorphous based photodetector not only recovers but shows a two order of magnitude increase in its responsivity. This study not only shows the high radiation hardness of gallium oxide against Swift Heavy Ions but may also serve as a stepping stone for the use of high energy irradiation as a tool for defect engineering in gallium oxide based devices.

5:20 PM EQ17.11.11

Theoretical Investigation of Electronic Structure Properties of $\text{ZnO}_{1-x}\text{Se}_x$ for Photoanode Applications Arini Kar, Gurudayal Behera, Balasubramaniam Kavaipatti and Dayadeep S. Monder; Indian Institute of Technology Bombay, India

Despite high chemical stability in an aqueous environment, application of ZnO as a visible light photoanode in photoelectrochemical cells (PECs) is limited due to its large bandgap. Alloying ZnO with ZnSe reduces the electronic bandgap of ZnO, as observed experimentally at low alloy compositions. In this work, we have performed density of states and electronic band structure calculations using DFT to determine the band gap of wurtzite solid state solutions of $\text{ZnO}_{1-x}\text{Se}_x$ over the entire composition range to develop deeper insight into the system. The band gap calculated using the delta-sol method shows a bowing behaviour, with a minimum bandgap at $x=0.5$, as predicted by the band anticrossing (BAC) model. Difference in the electronegativities of O and Se atoms in the lattice leads to hybridization of O-2p and Se-4p electronic states which can be clearly observed from the projected density of states and band structure plots. Interaction between these electronic states also leads to a split in the valence band edge at O-rich end and a split in the conduction band edge at the Se-rich end. These are observed as dips in the density of states plot at the respective band edges. In addition, the curvature of the valence band maxima and conduction band minima reduce at the O-rich end and Se-rich end, respectively. This implies an increased effective mass of the charge carriers and hence a decreased mobility. These fundamental insights will help in employing suitable alloy compositions in PECs for optimal photocurrent density.

5:25 PM EQ17.11.12

Excimer Laser Crystallization and Doping of Epitaxial Ga_2O_3 Thin Films for Ultraviolet Optoelectronics Devices Kazuki Watanabe¹, Ryoya Kai¹, Naho Kaneko¹, Shohei Hisatomi¹, Tomoaki Oga¹, Satoru Kaneko^{2,1}, Akifumi Matsuda¹ and Mamoru Yoshimoto¹; ¹Tokyo Institute of Technology, Japan; ²Kanagawa Institute of Industrial Science and Technology, Japan

Ultraviolet optoelectronics devices have attracted much interest for a variety of applications to use photolithography, biochemical and so on. Among the wide-bandgap semiconductors, Ga_2O_3 with the bandgap of about 5 eV is considered as one of the eco-friendly candidates used for ultraviolet optoelectronics devices. The development of the Ga_2O_3 -based devices relies on the feasibility of growing impurity-doped p-type conductive Ga_2O_3 thin films.^[1] It has been reported that n-type Ga_2O_3 semiconductors have been prepared via impurity doping of 4+ cations like Si^{4+} .^[2] On the other hand, to fabricate p-type Ga_2O_3 semiconductors, potential dopants like Mg^{2+} and Zn^{2+} are presented.^[3] However, as far as we know, there is no report on fabrication of impurity-doped p-type Ga_2O_3 thin films.

So far, we have investigated the pulsed excimer laser-induced room-temperature epitaxial crystallization of $\beta\text{-Ga}_2\text{O}_3$ thin films on the NiO-buffered sapphire substrates.^[4,5] Different from the conventional high-temperature growth of $\beta\text{-Ga}_2\text{O}_3$ thin films, crystallization of amorphous Ga_2O_3 thin films via excimer laser annealing at room-temperature is expected to suppress phase separation and precipitation, and also to induce unusual impurity doping. In this study, for the purpose of controlling the electrical properties such as p- or n-type of $\beta\text{-Ga}_2\text{O}_3$ thin films by laser-induced impurity doping, we evaluated the effects of laser irradiation conditions and/or thin film compositions on the crystal growth and conductivity of the impurity-doped amorphous Ga_2O_3 thin films.

In the experiment, Li element was used as one of impurity dopants because Li is expected as monovalent p-type dopant.^[6] The amorphous 5 at% Li-doped Ga_2O_3 thin film (50-80 nm-thick) was grown on the atomically stepped $\alpha\text{-Al}_2\text{O}_3$ (0001) substrates with about 2 nm thick MgO (111) buffer layer by pulsed laser deposition (PLD) equipped with pulsed KrF excimer laser ($\lambda=248$ nm, $d=20$ ns, and $E\sim 1.2$ J/cm²) at room-temperature in ultra-high vacuum ($\sim 10^{-6}$ Pa) using a sintered 5 at% Li-doped $\beta\text{-Ga}_2\text{O}_3$ target. The obtained amorphous Ga_2O_3 thin film were subsequently crystallized in the solid-phase by excimer laser annealing (ELA), in which KrF excimer laser beam (not focused, $E\sim 175$ mJ/cm²) was irradiated from the substrate side at room-temperature in air. As a result, it was verified from the XRD and RHEED analyses that 5 at% Li-doped $\beta\text{-Ga}_2\text{O}_3$ (-201) epitaxial film was obtained on the MgO (111) (2 nm thick) buffered $\alpha\text{-Al}_2\text{O}_3$ (0001) substrate. Li inclusion in the $\beta\text{-Ga}_2\text{O}_3$ thin film after ELA was confirmed from TOF-SIMS measurements (operated by the Open Facility Center of Tokyo Inst. Tech.). These results indicate that ELA process induces solid-phase epitaxy at room-temperature and suppress re-evaporation of Li in Ga_2O_3 crystallization. In addition, TOF-SIMS measurements also indicate the possible diffusion of Al^+ and Mg^+ elements into the thin film. The optical property of the epitaxial 5 at% Li-doped $\beta\text{-Ga}_2\text{O}_3$ thin films were evaluated by UV-vis measurements, which revealed a transmission over 90% of light in the visible region (360-830 nm) and rapid absorption in the UV region (~ 360 nm). In addition, the optical bandgap of the 5 at% Li-doped $\beta\text{-Ga}_2\text{O}_3$ thin film was estimated about 4.81 eV, being about 0.1 eV smaller than that of the non-doped $\beta\text{-Ga}_2\text{O}_3$ thin film (4.9 eV). It is suggested that the impurity Li atoms have been largely activated as acceptors in the $\beta\text{-Ga}_2\text{O}_3$ film to modify the energy level of the valence band top. The electrical properties are also reported in the presentation on the day.

[1] F. Alema et al., Phys. Status Solidi. 214, 1600688 (2017).

[2] F. B. Zhang et al., J. Mater. Sci.: Mater. Electron 26, 9624 (2015).

[3] Y. Su et al., J. Alloys Compd. 782, 299 (2019).

[4] D. Shiojiri et al., J. Cryst. Growth 424, 38 (2015).

[5] H. Morita et al., J. Vac. Sci. Technol. A 39, 043414 (2021).

[6] A. Kyrtos et al., Appl. Phys. Lett. 112, 032108 (2018).

5:30 PM EQ17.11.13

Vacuum-Ultraviolet Excimer Light Derived Conductivity and Structural Modification of Pure NiO Epitaxial Thin Films Kenta Kaneko¹, Tomoaki

Oga¹, Hiroki Shoji¹, Shohei Hisatomi¹, Satoru Kaneko^{2,1}, Mamoru Yoshimoto¹ and Akifumi Matsuda¹; ¹Tokyo Institute of Technology, Japan; ²Kanagawa Institute of Industrial Science and Technology, Japan

Recently, perovskite solar cells have attracted interests, and are of significance in photovoltaic energy conversion. Nickel oxide (NiO) with wide-bandgap of $E_g \sim 3.4$ eV is one of the p-type semiconductors utilized as hole transport layers in the devices [1]. Aliovalent doping of such as Li⁺ have commonly applied to enhance its p-type conduction according to improved carrier concentration. Meanwhile, there are some researches of uv-ozone treatment of polycrystalline NiO films using mercury lamps, that altered resistance and electronic states was reported [2,3]. Modification of p-type conduction without impurity doping would advance development and properties of multilayered optoelectronic devices; although it still requires further research on the influence of film structure as well as illuminance and ambience of the irradiation. Application of vacuum-ultraviolet (VUV) light with larger photon energy and efficient production of active oxygen species would contribute to further modification of properties. In this study, noticeable conductivity improvement of epitaxial NiO thin films by excimer VUV-light irradiation was verified, and the effect of the treatment on structure and morphology of the films was investigated.

The epitaxial NiO (111) thin films were grown on atomically stepped α -Al₂O₃ (0001) single crystal substrates by pulsed laser deposition (PLD) technique using a KrF excimer laser ($\lambda=248$ nm, $E \sim 1.2$ J/cm²) and a pure NiO sintered target. The thin film growth took place at room-temperature (not-heated intentionally) in 1×10^{-3} Pa O₂ (base pressure $\sim 3 \times 10^{-6}$ Pa). The NiO thin films were subsequently introduced to VUV-light treatment procedure using a Xe₂ excimer lamp ($\lambda=172$ nm, $E \sim 65$ mW/cm² at lamp surface). The VUV-light was irradiated to thin film surfaces in air, vacuum, or inert gas at the distance of 0.5–2.0 mm. The electric property of NiO (111) thin films was measured by four-probe DC method. The resistivity of the PLD-grown 40 nm-thick epitaxial NiO (111) thin film was $\sim 7 \times 10^3$ Ω cm, although VUV-light irradiation in air at 0.5 mm drastically reduced the value by three-digits, that $\sim 4 \times 10^0$ Ω cm and $\sim 2 \times 10^0$ Ω cm were obtained after the treatment for 60 and 120 minutes, respectively. The epitaxial structure was retained even after VUV-light irradiation of 120 min according to the XRD and RHEED results, while observed slight reduction of the (111) plane spacing suggested redox reaction of the film. Thus, the demonstrated conductivity improvement of NiO (111) thin films due to VUV-light irradiation would advance optoelectronic application of the material. In addition, influence of conditions of thin film preparation and VUV-light treatment on the structures and properties would also be presented.

[1] S. E. Habas et al., *Chem. Rev.* 110 (2010) 6571–6594.

[2] G. H. Aydogdu et al., *J. Appl. Phys.* 108 (2010) 113702.

[3] R. Islam et al., *ACS APPL. Mater. Interfaces* 9 (2017) 17201–17207.

5:35 PM BREAK

SESSION EQ17.13: Transparent Conductive Oxides and Solar Cell Applications
Session Chairs: Marcus Baer and Alex Martinson
Tuesday Morning, December 7, 2021
EQ17-Virtual

10:30 AM EQ17.13.01

Unusual Epitaxy of Nd:ZnO Thin Films on c-Cut Sapphire Under Oblique Incidence Magdalena Nistor¹, Eric Millon², Christophe Cachoncinlle², Corneliu Ghica³, Christian Hebert⁴ and Jacques Perrière⁴; ¹NILPRP, Romania; ²Université d'Orléans, France; ³NIMP, Romania; ⁴Sorbonne Universités & CNRS, France

ZnO thin films typically grow with the c-axis normal to the substrate leading to a columnar microstructure with the (002) ZnO planes parallel to the substrate surface. Tuning the incident angle of the species reaching the substrate changes the morphology and microstructure of the film. In this work Nd-doped ZnO thin films were grown by pulsed-electron beam deposition (PED) on c-cut sapphire substrates under oblique angle incidence, at 10^{-2} mbar oxygen pressure and for a substrate temperature of 500°C. Transmission electron microscopy, X-ray diffraction and pole figures analyses were performed to obtain the film microstructure together with their electrical and optical properties. The Nd-doped ZnO thin films were smooth, compact and constituted with columnar grains inclined at about $17^\circ \pm 4^\circ$ from the normal to the substrate surface. From X-ray diffraction and transmission electron microscopy experiments, the wurtzite phase of Nd-doped ZnO thin films was observed with the c-axis inclined around 35° with respect to the normal axis of the substrate, with a three-fold azimuthal symmetry. Epitaxial relationships between Nd-doped ZnO films and sapphire substrate were determined from the pole figures and compared with those obtained for the films grown under non-oblique angle incidence. Classical in-plane epitaxy with a 30° rotation between the two hexagonal unit cells of ZnO and c-cut sapphire was observed under non-oblique incidence [1, 2]. For the films grown under oblique incidence, the 35° angle tilt of the ZnO c-axis from the normal to the substrate is explained by the epitaxy of the (229) ZnO plane on the (002) sapphire plane. This particular orientation, which has never been reported previously, is obtained from the rotation of the [001] ZnO direction around the [1-10] ZnO one, which allows the (229) ZnO plane to be parallel to the (002) sapphire substrate one [2]. A new well-defined epitaxial relationship was observed between the (229) ZnO on (002) Al₂O₃ plane although the large lattice mismatch and symmetry mismatch. This unusual epitaxy will be discussed, as well as the effect of tilted growth on the electrical and optical properties of Nd-doped ZnO films. These epitaxial c-axis tilted Nd-doped ZnO thin films are also interesting for sensitive and disposable biosensors working as film bulk acoustic resonators in the shear acoustic mode for biological and medical applications. [1] M. Nistor, L. Mihut, E. Millon, C. Cachoncinlle, C. Hebert, J. Perrière, *RSC Adv.* 6, 41465 (2016); [2] M. Nistor, E. Millon, C. Cachoncinlle, C. Ghica, C. Hebert, J. Perrière, *Appl. Surf. Sci.* 563, 150287 (2021)

10:45 AM *EQ17.13.02

Rapid Vapor-Phase Deposition of Oxide Overlayers on Thermally-Sensitive Device Stacks for Optoelectronics Rob Jagt¹, Virgil Andrei¹, Solène Béchu^{2,3}, Motiar Rahaman¹, Leonardo Lari⁴, Ravi D. Raninga¹, Tahmida N. Huq¹, Weiwei Li¹, Mark Nikolka¹, Muriel Bouttemy^{2,3}, Mathieu Fregnaux^{2,3}, Vlado Lazarov⁴, Philip Schulz^{2,5}, Erwin Reisner¹, Judith L. MacManus-Driscoll¹ and Robert Hoye⁶; ¹University of Cambridge, United Kingdom; ²Institute Photovoltaïque d'Île de France, France; ³Institut Lavoisier de Versailles (ILV), France; ⁴University of York, United Kingdom; ⁵CNRS, France; ⁶Imperial College London, United Kingdom

Oxides play a critical role in a wide range of optoelectronic devices as the charge-selective layer. Whilst the electronic properties of oxides generally improve with increasing growth temperature, the processing window is limited when depositing over device stacks, owing to the thermal sensitivity of the active layer. A prominent example of a thermally-sensitive active layer is methylammonium lead iodide (MAPbI₃) perovskite.^[1] This talk explores the use of atmospheric pressure chemical vapor deposition (AP-CVD) as a means to broaden the processing window of oxide overlayers on optoelectronic device stacks. AP-CVD produces oxide films with similar uniformity, density and conformality as films grown by atomic layer deposition (ALD), but with orders of magnitude higher growth rates, and without the need for a vacuum chamber. We investigate the growth of TiO₂ over MAPbI₃ films. We show that

growth rates of $1.19 \pm 0.04 \text{ nm s}^{-1}$ are achievable, which allows 7 nm TiO_2 films to be grown in 6 s (compared to >30 min for ALD). The rapid processing allows us to deposit TiO_2 directly onto MAPbI_3 films at 150°C without any structural, chemical or electronic damage, as found from X-ray diffraction, X-ray photoemission spectroscopy and time-resolved photoluminescence measurements. In MAPbI_3 photovoltaic devices, we show that TiO_2 growth temperatures can exceed 180°C without any drop in efficiency. This is $>70^\circ\text{C}$ larger than achievable with ALD or solution-based methods for growing oxide overlayers, resulting in more conductive TiO_2 films which lead to increases in device performance. We show that these results can be generalised to triple-cation perovskites, as well as to AP-CVD SnO_2 overlayers. In particular, we show that the high density of the oxide overlayers improves fill factors by reducing dark currents, reaching up to 84% (with 19.4% steady-state power conversion efficiency) for triple-cation perovskite devices covered with 60 nm SnO_2 .^[1]

More broadly, we demonstrate the wider applicability of AP-CVD to grow oxide electron transport layers on the perovskite-inspired material bismuth oxyiodide (BiOI). We show through transmission electron microscopy that AP-CVD ZnO films are highly conformal to the textured BiOI surface, resulting in photovoltaic devices with external quantum efficiencies reaching 80% at 450 nm wavelength.^[2] We demonstrate the benefits of this oxide-based device structure for achieving improved performance and stability across multiple light-harvesting applications.

References:

- [1] Raninga, Jagt, ..., Hoye, *Nano Energy*, **2020**, *75*, 104946
[2] Hoye, *et al.*, *Adv. Mater.*, **2017**, *29*, 1702176

11:15 AM EQ17.13.03

Towards Lead-Free Perovskite Device Architectures—Interface Simulations of Tin-Based Heterostructures Pedesseau Laurent¹, Pingping Jiang¹, Boubacar Traore², Mikael Kepenekian², George Volonakis², Claudine Katan² and Jacky Even¹; ¹FOTON Institute - INSA Rennes, France; ²ISCR CNRS, France

Following the emergence of lead halide perovskites as record-breaking materials for emerging photovoltaic applications, lead-free perovskites are gaining interest as novel materials which are compatible with inkjet-printing based technologies^{1,2,3}. Bulk properties are of the prime importance, but charge transport can be rapidly altered across the interface of perovskite/ (hole or electron) transport layer (HTL or ETL). Yet, due to the size and complexity of the interface systems, a thorough ab initio modeling of the interfaces remains elusive to-date. Within this work, to explore the atomic-scale details of the structural and electronic properties of these materials, we employ state-of-the-art density functional theory (DFT) based calculations of model tin-based heterostructures. We investigate in particular three-dimensional corner-sharing Sn-based perovskites, their surface and interface properties and calculate the interaction of the materials with charge transport layers (CTLs). Our approach reveals the electronic band alignments and dielectric mismatches between perovskite layers and the most important hole and electron transport layers that have been used in prototype thin film device architectures^{4,5}. In an effort to understand the fundamental physico-chemical mechanisms that govern the interactions between the photo-active absorber material and CTLs, we also probe the influence of surface termination on structural and electronic properties at $\text{FASnI}_3/\text{C}_{60}$ (as ETL) interfaces and $\text{FASnI}_3/\text{NiO}_x$ (as ETL) interfaces. Our findings give a detailed insight into the interface engineering necessary for optimizing the next generation of environmental-friendly high-performing opto-electronic devices.

This DROP-IT project¹ has received funding from the European Union's Horizon 2020 research and innovation Program under the grant agreement No 862656. The information and views set out in the abstracts and presentations are those of the authors and do not necessarily reflect the official opinion of the European Union. Neither the European Union institutions and bodies nor any person acting on their behalf may be held responsible for the use which may be made of the information contained herein.

References:

- (1) DROPIT <https://www.uv.es/dropit/> (accessed June 22, 2021).
(2) Volonakis, G.; Filip, M. R.; Haghighirad, A. A.; Sakai, N.; Wenger, B.; Snaith, H. J.; Giustino, F. Lead-Free Halide Double Perovskites via Heterovalent Substitution of Noble Metals. *J. Phys. Chem. Lett.* 2016, *7* (7), 1254–1259. <https://doi.org/10.1021/acs.jpclett.6b00376>.
(3) Volonakis, G.; Haghighirad, A. A.; Milot, R. L.; Sio, W. H.; Filip, M. R.; Wenger, B.; Johnston, M. B.; Herz, L. M.; Snaith, H. J.; Giustino, F. $\text{Cs}_2\text{InAgCl}_6$: A New Lead-Free Halide Double Perovskite with Direct Band Gap. *J. Phys. Chem. Lett.* 2017, *8* (4), 772–778. <https://doi.org/10.1021/acs.jpclett.6b02682>.
(4) Traore, B.; Pedesseau, L.; Blancon, J.-C.; Tretiak, S.; Mohite, A. D.; Even, J.; Katan, C.; Kepenekian, M. Importance of Vacancies and Doping in Hole Transporting Nickel Oxide Interface with Halide Perovskites. *ACS Appl. Mater. Interfaces* 2020. <https://doi.org/10.1021/acsami.9b19457>.
(5) Canicoba, N. D.; Zagni, N.; Liu, F.; McCuistian, G.; Fernando, K.; Bellezza, H.; Traoré, B.; Rogel, R.; Tsai, H.; Le Brizoual, L.; et al. Halide Perovskite High-k Field Effect Transistors with Dynamically Reconfigurable Ambipolarity. *ACS Materials Lett.* 2019, *1* (6), 633–640. <https://doi.org/10.1021/acsmaterialslett.9b00357>.

11:30 AM EQ17.13.04

Indirect Excitation and Luminescence Activation of Tb Doped Indium Tin Oxide and Its Impact on the Host's Optical and Electrical Properties Paul Llontop, Miguel Piñeiro, Carlos Torres, Erik Perez and Jorge A. Guerra; Pontificia Universidad Católica del Perú, Perú

The effect of terbium doping on the electrical, optical and light emission properties of sputtered indium tin oxide thin films was investigated. The films were prepared by radio frequency dual magnetron sputtering maintaining a high optical transmittance in the ultraviolet and visible spectral regions and an electrical resistivity ranging from $5\text{E}-3$ to $0.3 \Omega\text{cm}$. Terbium-related luminescence is achieved after thermal treatments at 470°C in air at atmospheric pressure. Electrical resistivity and optical transmittance were registered after each annealing step to evaluate the compromise between the achieved light emission intensity, electrical and optical properties. Additionally, Tb-related luminescence thermal quenching is assessed by temperature-dependent photoluminescence measurements, from -190°C to 300°C , under non-resonant excitation. Thermal quenching activation energies suggest an effective energy transfer mechanism from the ITO host to the rare-earth ions. This indirect excitation mechanism is tentatively modeled using a spherical potential well, as well as a tight-binding one-band approximation, approach for a short-range charge trapping process and subsequent formation of bound excitons to rare-earth ion clusters.

11:45 AM *EQ17.13.06

ALD-Oxide Materials and Surface Modification for Next-Generation PV Devices Nathanaelle Schneider^{1,2}; ¹CNRS, UMR-IPVF 9006, France; ²Institut Photovoltaïque d'Ile de France (IPVF), France

Zinc oxide is an extensively studied n-type semiconductor for various applications such as light emitting devices, detection of chemicals or solar cells,¹ which often needs to be doped, modified or protected.

Doped-ZnO films can replace conventional transparent conductive oxides (TCO), especially in high aspect ratio structures. For example, radial junction silicon nanowire (Si NW) based solar cells, which allow to decouple light absorption and charge carrier collection, are highly interesting but challenging to top contact.² Use of ALD-Ti:ZnO (TZO) as the top electrode has proven the applicability of ALD-TZO as TCO and the unique capabilities of ALD, showing superior optoelectrical properties, conformally covering the Si NWs, and yielding a PV diode behavior with external quantum efficiency response surpassing the conventional ITO top electrode.³

In other cases, it is beneficial to modify the properties of the ZnO surface, for instance by the grafting of organic molecules.⁴ ALD-ZnO surfaces were modified by phosphonic acid derivatives with different spacer and functionalizing groups (2-aminoethylphosphonic acid, 2-AEPA; 4-aminobenzylphosphonic acid, 4-ABzPA; and 4-fluorobenzylphosphonic acid, 4-FBzPA). The resulting ZnO surfaces were characterized, used as a mean to passivate the reactive interface between ALD-ZnO and a hybrid organic inorganic metal halide perovskite, and complete solar cell devices were prepared.⁵ Finally, ZnO-based films often need to be protected to prevent their degradation. Al:ZnO (AZO) window layer is reported as the primary component responsible for the degradation of CIGS solar cells. The feasibility to prevent AZO degradation and encapsulate module-level (10×10 cm²) CIGS solar devices by a 10 nm ALD-Al₂O₃ barrier layer was demonstrated.⁶ However, solar panels in field operation are also exposed to various chemical air pollutants such as in (NH₄)₂SO₄ in rural, and NaCl in marine environments. Their effects were studied by placing AZO w/ and w/o encapsulation in specific climatic test conditions. This demonstrated the necessity to consider atmospheric chemistry when evaluating barrier protection capacities of encapsulants and assessing the durability of PV materials and devices.⁷

References

¹ Z.L. Wang, *J. Phys. Condens. Matter* **16**, R829 (2004).

² S. Misra, L. Yu, M. Foldyna, and P. Roca i Cabarrocas, *IEEE J. Photovolt.* **5**, 40 (2015).

³ D. Coutancier, S.-T. Zhang, S. Bernardini, O. Fournier, T. Mathieu-Pennober, F. Donsanti, M. Tchernycheva, M. Foldyna, and N. Schneider, *ACS Appl. Mater. Interfaces* (2020).

⁴ I. Lange, S. Reiter, M. Pätzelt, A. Zykov, A. Nefedov, J. Hildebrandt, S. Hecht, S. Kowarik, C. Wöll, and G. Heimel, *Adv. Funct. Mater.* **24**, 7014 (2014).

⁵ O. Fournier, C.D. Bapaume, D. Messou, M. Bouttemy, P. Schulz, F. Ozanam, L. Lombez, N. Schneider, and J. Rousset, *ACS Appl. Energy Mater.* **4**, 5787 (2021).

⁶ S.-T. Zhang, M. Guc, O. Salomon, R. Wuerz, V. Izquierdo-Roca, A. Pérez-Rodríguez, F. Kessler, W. Hempel, T. Hildebrandt, and N. Schneider, *Sol. Energy Mater. Sol. Cells* **222**, 110914 (2021).

⁷ S.-T. Zhang, A. Maltseva, G. Herting, J.-F. Guillemoles, N. Schneider, I. Odnevall Wallinder, and P. Volovitch, (submitted).

SESSION EQ17.14: Photoelectrochemistry, Catalysis and III/V Materials
Session Chairs: Erkan Aydin and Philip Schulz
Tuesday Afternoon, December 7, 2021
EQ17-Virtual

1:00 PM *EQ17.14.01

Charge-Selective Contacts in Energy Conversion Photoelectrochemistry Joel W. Ager^{1,2} and Rajiv R. Prabhakar²; ¹University of California, Berkeley, United States; ²Lawrence Berkeley National Laboratory, United States

Solar photovoltaic (PV) and photoelectrochemical (PEC) energy conversion share the same fundamental requirements of photon absorption, charge separation, and selective carrier collection [1]. In addition, in order to produce storable chemical energy, PEC systems must drive multi-electron transfer reactions, i.e. water oxidation (OER, a 4 electron process) for a photoanode and hydrogen evolution (HER) or carbon dioxide reduction (CO₂R) for a photocathode (2-18 electron processes) [2]. In a small number of cases it has been possible to have a single material perform all of the requisite steps and remain stable under operation: water oxidation photoanodes composed of TiO₂ or Fe₂O₃ are examples. However, in the vast majority of cases, it has been beneficial to construct multi-material PEC systems, with different components chosen for optimal light absorption, selective carrier collection/passivation, and catalysis.

In this context, the choice of electron transfer layers (ETLs) for PEC CO₂R reduction will be discussed. While it is attractive to design semiconductor absorbers based on the position of their conduction band relative to the standard state redox potentials of a given CO₂ reaction, e.g. CO₂/CO, CO₂/HCOOH, CO₂/CH₄, etc., this analysis neglects the fact that these multi-electron reactions occur via a series of elementary proton coupled electron transfers, with each step having its own redox potential [3]. For this reason, either solid state or molecular CO₂R co-catalysts are usually integrated with the absorber in PEC CO₂R studies [4,5].

These concepts will be illustrated through the design and operation of Si-based CO₂R photocathodes. Adroit use of charge selective contacts allows for considerable flexibility in design. For example, in contrast to conventional photocathode designs which employ p-type absorbers, we used a back illumination geometry with an n-type Si absorber to permit the use of absorbing metallic catalysts which would otherwise block the light. Hole collection was enabled by p⁺ implant on the illumination side while TiO₂ as applied as an ETL on the catalyst side. Selectivity to C-C coupled products was achieved by using hierarchical Au-Ag-Cu nanostructures as electrocatalysts. The photovoltage, 550-600 mV under simulated 1-sun illumination, and photocurrents exceeding 30 mA cm⁻² confirm the carrier selectivity and passivation of the front and back interfaces. Under simulated diurnal illumination conditions, over 60% faradaic efficiency to C₂₊ hydrocarbon and oxygenate products (mainly ethylene, ethanol, propanol) is maintained for several days [6].

As further examples of the PEC design space for CO₂R, use of other oxides as ETLs (e.g. Al₂O₃ and TaO_x) and the prospects of achieving cascade CO₂R [7] on the PEC surface will be discussed.

This material is based on work performed by the Liquid Sunlight Alliance, which is supported by the U.S. Department of Energy, Office of Science, Office of Basic Energy Sciences, Fuels from Sunlight Hub under Award Number DE-SC0021266.

Wurfel, U.; Cuevas, A.; Wurfel, P. Charge Carrier Separation in Solar Cells. *IEEE J. Photovoltaics* **2015**, *5*, 461–469.

Osterloh, F. E. *ACS Energy Lett.* **2017**, *2*, 445–453.

Peterson, A. A.; Abild-Pedersen, F.; Studt, F.; Rossmeisl, J.; Nørskov, J. K. *Energy Environ. Sci.* **2010**, *3*, 1311

Arai, T.; Tajima, S.; Sato, S.; Uemura, K.; Morikawa, T.; Kajino, T. *Chem. Commun.* **2011**, *47*, 12664.

Qiu, J.; Zeng, G.; Ha, M.-A.; Ge, M.; Lin, Y.; Hettick, M.; Hou, B.; Alexandrova, A. N.; Javey, A.; Cronin, S. B. *Nano Lett.* **2015**, *15*, 6177–6181.

Gurudayal; Beeman, J. W.; Bullock, J.; Wang, H.; Eichhorn, J.; Towle, C.; Javey, A.; Toma, F. M.; Mathews, N.; Ager, J. W. *Energy Environ.*

Sci. **2019**, *12*, 1068–1077.

Lum, Y.; Ager, J. W. *Energy Environ. Sci.* **2018**, *11*, 2935–2944.

1:30 PM *EQ17.14.02

Cascade Photoelectrochemical CO₂ Reduction Using Spatially Patterned Tandem Photovoltaics Adele Tamboli¹, Ann L. Greenaway¹, Calton J. Kong², Fry Intia¹, Myles A. Steiner¹, Grace A. Rome¹, Talysa R. Klein¹, Rajiv R. Prabhakar², Emily Warren¹ and Joel W. Ager²; ¹National Renewable Energy Laboratory, United States; ²Lawrence Berkeley National Laboratory, United States

One of the primary challenges facing solar conversion of CO₂ to fuel is the selectivity of the CO₂ reduction reaction to a single, ideally liquid, product. One method for improving selectivity is to use a cascade approach, where sequential steps of the multi-step reduction reaction are driven in series using different catalysts and adjacent microenvironments[1]. Each of these catalysts should be supplied with the ideal photocurrent and photovoltage to drive its respective reaction step. As a model system, we are considering the conversion of CO₂ to ethylene using a patterned, multi-terminal photovoltaic device as a photocathode. This two-step reaction (CO₂ to CO, then CO to C₂H₄) can be driven by two terminals of a three-terminal tandem (3TT) photovoltaic cell, where the third terminal drives the oxidation reaction. We have previously demonstrated 3TTs for photovoltaic applications[2], and will present the operational principles of these devices as well as experimental results using III-V semiconductors as a model system. We show that we can achieve the necessary photovoltages and photocurrents from the rear “R” and middle “Z” contact of these devices to drive the two CO₂ reduction reactions, using the top “T” contact to drive oxidation[3]. Then, we will present a model for how this device is expected to operate in an integrated photoelectrochemical cell[4]. Finally, we will discuss surface protection schemes using a transparent, conductive encapsulant[5] with embedded catalysts to protect the semiconductor from degradation, while providing the required electrical conduction and catalyst integration.

This material is based on work performed by the Liquid Sunlight Alliance, which is supported by the U.S. Department of Energy, Office of Science, Office of Basic Energy Sciences, Fuels from Sunlight Hub under Award Number DE-SC0021266.

[1] Y. Lum and J.W. Ager, *Energy Environ. Sci.* 2018

[2] J.F. Geisz et al., *submitted*

[3] E.L. Warren et al., *ACS Energy Letters* 2020

[4] C.J. Kong et al., *in prep*

[5] T.R. Klein et al., *J. Phys. D.* 2021

2:00 PM EQ17.14.03

Achieving High Product Selectivity in Silicon Photocathodes by Cascade Catalysis for CO₂ Reduction Rajiv Ramanujam Prabhakar and Joel W. Ager; Lawrence Berkeley National Laboratory, United States

In this work, a sequential catalysis approach by light was employed to achieve high product selectivity for CO₂ reduction. By employing light, regions with high photovoltage and low photovoltages was achieved by using photo-absorbers with different opto-electronic properties. In the low photovoltage region, CO₂ would be reduced to CO and at the high photovoltage region, CO would be reduced to useful products such as ethylene and ethanol with high selectivity. Different photovoltage regions was achieved on Silicon photocathodes by tuning the band edge of Silicon using surface dipoles. The surface dipoles were fabricated on Silicon photocathodes using a solution processed technique like spin coating. The regions of different photovoltages were investigated using surface photovoltage (SPV) and kelvin probe force microscopy (KPFM). SPV shows the increase in the photovoltage of Silicon photocathode upon deposition of the surface dipole. KPFM measurements also reveal an increase in the surface potential with the dipole on Silicon. By accomplishing voltage tunability using this strategy, high product selectivity could be achieved by sequential catalysis using light. The results and outcome of this work would bring a paradigm shift in the methodology of obtaining high product selectivity in CO₂ reduction research.

2:15 PM EQ17.14.04

Investigation of Ni/Au/Ni Ohmic Contact and Dry Etch Mask to p-type GaN for Vertical Top-Down Nanowire Optoelectronics Matthew Seitz, Bryan Melanson, Matthew Hartensveld and Jing Zhang; Rochester Institute of Technology, United States

Vertical GaN nanowires have emerged over the past decade as promising candidates for next-generation optoelectronics, which are of great importance for applications such as novel display systems, micro-LEDs, and nanowire LEDs. The small footprint of these nanowire devices allows for increased device scaling and three-dimensional (3D) integration. Typically, GaN nanowires can be formed through either bottom-up or top-down fabrication processes. Metal organic chemical vapor deposition (MOCVD) or molecular beam epitaxy (MBE) are often used to grow nanowires in the bottom-up approach, however these techniques have many drawbacks, including complex growth conditions and non-uniformities in nanowire diameter, height, and spacing, which can only be partially corrected using expensive selective area epitaxy. Top-down fabrication on the other hand, makes use of the well-developed processes to form nanowires from a monolithic, planar epitaxial stack. Our previous works have explored top-down fabrication approaches for GaN nanowires extensively, for device applications such as vertical nanowire LEDs and vertical transistors. Our top-down fabrication approach consists of patterning a 200 nm thick Ni hardmask on top of a 300 nm thick layer of SiO₂ which has been deposited on the GaN epitaxial stack. The Ni layer is then used to mask Cl-based dry etches of the underlying SiO₂ and GaN to form approximately 3 μm tall nanowires with diameters of approximately 1 μm down to 20 nm. Following and hydroxyl-based wet etch and deposition of the n-metal contact at the base of the nanowires, an HF-based wet etch is used to remove the Ni etch mask from the tops of the nanowires by etching the SiO₂ to allow for formation of a Ni/Au p-contact. Ni/Au is typically preferred as a p-contact as it exhibits superior contact resistance to Ni, due to the high work function of Au (5.1 eV). While this process has proved successful, the use of a SiO₂ liftoff layer adds complexity to the fabrication process in the form of additional deposition, dry etch, and wet etch steps. It is therefore desirable to develop a method of embedding an ohmic contact beneath the Ni dry etch mask so that it does not require a lift-off process. This can be achieved through exploration of a novel metal stack which acts as both an ohmic contact to p-GaN as well as an effective etch mask for dry etching of higher aspect ratio GaN nanowire structures.

In this work, we have developed a process to embed the low-resistance ohmic contact with the dry etch hard mask, which leads to the realization of vertical GaN nanowire transistors with promising current injection. This novel structure is composed of a 20 nm Ni layer deposited via electron beam evaporation, a 20 nm Au layer directionally deposited via thermal evaporation. This metal stack was then annealed at 500°C for 10 minutes under oxygen. After this anneal, the bottom Ni/Au layers form a low resistance ohmic contact with the p-GaN through diffusion and the formation of NiO. Following the anneal step, a final and conformal 200 nm Ni capping layer deposited via electron beam evaporation. Electrical performance of this full contact stack was measured via the transmission line model (TLM) using 10 μm x 30 μm contact pads at separation distances ranging from 25 μm to 75 μm. Our measurements indicate that the inclusion of this additional capping layer still provides a good ohmic contact with GaN, showing a specific contact resistance as low as 0.14 Ω/cm². By including an additional capping layer in our electrical contacts, the metal stack can serve both as a low resistance ohmic contact and additionally as a hard mask for Cl-based inductively coupled plasma (ICP) etching. These promising results suggest that our proposed process could be used for the successful fabrication of high aspect ratio vertical GaN nanowire optoelectronic devices.

2:30 PM *EQ17.14.05

III-V Semiconductor Solid-State Design and Interface Engineering for High-Efficiency Photoelectrolysis [Todd G. Deutsch](#), Myles A. Steiner and James L. Young; National Renewable Energy Laboratory, United States

Photoelectrochemical (PEC) water splitting, which is the direct electrolysis of water with one of the half-reactions occurring on an immersed semiconductor electrode, has made good progress in solar-to-hydrogen (STH) efficiency in the last several years. III-V semiconductor materials have demonstrated the highest STH efficiencies mostly due to their excellent optoelectronic properties, bandgap tunability, and ease of monolithic multijunction fabrication. Many unique semiconductor layers must work in harmony to achieve a device that can spontaneously split water upon illumination. The layers that constitute the solid-state device establish the current and voltage generated under illumination while the strata closer to the electrolyte greatly influence the electrochemical performance.

During this talk we will describe the process of designing and testing a multijunction semiconductor structure optimized for maximum STH efficiency. We grew III-V semiconductors with metalorganic vapor phase epitaxy using the inverted metamorphic approach to obtain non-lattice-matched absorber junctions. We used over a dozen distinct III-V layers to achieve a tandem absorber with a 1.8 eV band gap top junction and 1.2 eV bottom junction. While the photovoltaic performance of these devices was exceptional, they were unable to perform photoelectrolysis without a bias due to an unoptimized interface with the electrolyte. We grew a highly doped emitter layer on the wide band gap material to create a buried junction which improved the open-circuit voltage of the PEC structures by > 500 mV. This configuration achieved 14% STH efficiency, which was short of our target efficiency (15%), so we grew a solid-state, surface-passivating "window layer" that is lattice-matched to the wide band gap material. While this device structure had improved voltage and current, the window layer is chemically unstable in our acidic electrolyte. We grew a thin, highly-doped, lattice-matched capping layer to protect the underlying window layer. Finally, we sputtered PtRu nanoparticulate cocatalysts on the photoelectrode surface to lower the kinetic overpotential of the hydrogen evolution reaction. We rigorously benchmarked the STH efficiency of the resulting device and observed greater than 16% conversion of sunlight into hydrogen fuel [1]. Still more work remains to be done to engineer the semiconductor/electrolyte interface to address insufficient stability.

[1] *NATURE ENERGY* 2, 17028 (2017).

SESSION EQ17.15: Organic, Hybrid and Metal Halide Perovskite Electronics

Session Chairs: Giulia Grancini and Robert Hoyer

Wednesday Morning, December 8, 2021

EQ17-Virtual

8:00 AM *EQ17.15.01

Dopant-Free Hybrid Silicon Heterocontacts—Interface Energetics and Solar Cell Performance [Steffen Duhm](#); Soochow University, China

Dopant-free heterocontacts are frequently utilized as charge-carrier selective contacts of hybrid silicon solar cells with high power conversion efficiencies. Although these interfaces are well characterized from a device perspective, the physics and chemistry of contact formation mechanisms are still not well understood. We use X-ray photoelectron spectroscopy (XPS) to track core-level shifts upon contact formation and accessing the built-in potential. Furthermore, vacuum-level shifts are measured by ultraviolet photoelectron spectroscopy (UPS). By spin-coating ultrathin layers of the conducting polymer PEDOT:PSS on hydrogen-terminated n-Si we can track the Si core-levels upon contact formation and get direct evidence for inversion layer formation. In addition, our XPS and UPS data allows us to speculate that PEDOT passivates Si surface states. Furthermore, we demonstrate that the built-in potential measured with XPS correlates well with the open-circuit voltage of model solar cells. The same holds for devices with dopant-free MoO₃/n-Si or LiF/p-Si heterocontacts as main building blocks. Strikingly, the insulator LiF forms a Schottky contact with p-Si and facilitates an ohmic contact in n-Si.

8:30 AM EQ17.15.02

Efficient Electron Injection into Various Organic Semiconductors Utilizing Superbase [Tsubasa Sasaki](#)¹, [Munehiro Hasegawa](#)², [Kaito Inagaki](#)³, [Taku Oono](#)¹, [Katsuyuki Morii](#)^{2,4}, [Takahisa Shimizu](#)¹ and [Hirohiko Fukagawa](#)¹; ¹NHK Science & Technology Research Laboratories, Japan; ²Nippon Shokubai Co., Ltd., Japan; ³Tokyo University of Science, Japan; ⁴Nippon Shokubai Research Alliance Laboratories, Osaka Univ., Japan

Tuning the carrier injection barrier between organic semiconductors and electrodes in organic optoelectronic devices is of pivotal importance for their future development. The electron affinity (EA) of materials used in organic light-emitting diodes (OLEDs) is smaller than that of materials used in other organic devices. Therefore, chemically reactive alkaline elements such as Li/Cs have been essential for fabricating the electron injection layer (EIL) near the cathode. Because such alkali elements are highly chemically reactive and easily oxidize in the presence of ambient oxygen and moisture, there is a strong desire to eliminate reactive materials from devices, especially flexible optoelectronic devices.

The method of fabricating a low-work-function (WF) electrode that eliminates reactive alkali elements, which are widely used for electron injection, from organic devices has been the subject of intense study in recent years. Zhou et al. reported electrodes with a WF of about 3 eV by utilizing polyethyleneimine, and some organic devices without reactive alkali elements have been demonstrated [1]. Very recently, an electrode with a WF of 2.4 eV has been reported by Tang et al. [2]. However, alkali elements are still essential in most OLEDs to achieve a barrier-free contact between the cathode and the organic layer, since the EA of materials used in OLEDs is about 2.0 eV.

Here, we succeeded in injecting electrons into various organic materials owing to the discovery of an EIL that can significantly reduce the WF around the cathode [3]. The novel electron injection material found in this study is the superbase 2,6-bis(1,3,4,6,7,8-tetrahydro-2H-pyrimido[1,2-a]pyrimidin-1-yl)pyridine (Py-hppz), which can reduce the WF near an Al cathode from 4.3 to 2.0 eV by utilizing both a coordination reaction [4] and the formation of hydrogen bonds [5]. To investigate the correlation between the EA of the electron transport materials and the electron injection properties, OLEDs were fabricated using 17 different materials for the electron transport layer (ETL). The actual EA of these materials was measured by low-energy inverse photoemission spectroscopy (LEIPS). We found that the operating voltage was low when the actual EA was above 2.0 eV, even if the molecular structures were different, such as a compound with nitrogen-containing heterocycles and aromatic hydrocarbons. A compound with nitrogen-containing heterocycles has conventionally been considered to be essential for delivering electrons from the cathode to the light-emitting layer in OLEDs. However, by tuning the WF near the cathode to about 2.0 eV using a superbase, it is possible to deliver electrons from the cathode to the light-emitting layer independent of the molecular structure. On the basis of these results, we fabricated a simple-structure blue OLED with 9-(naphthalen-1-yl)-10-(naphthalen-2-yl)anthracene (1-2ADN) as the emitting host material, and we also used it as the ETL. Then, an OLED with low operating voltage, high efficiency and high operational stability was realized in spite of the simple device structure. This liberation of the materials used in OLEDs by utilizing superbases can enable the realization of device structures that was previously impossible.

Our breakthrough discovery represents a departure from the conventional wisdom and is expected to contribute to significant progress in the development of various devices such as OLEDs, perovskite LEDs, organic/perovskite solar cells, organic semiconductor laser diodes, and organic transistors.

- [1] Y. Zhou et al., *Science* vol.336, p.327 (2012).
 [2] C. G. Tang et al., *Nature* vol.573, p.519 (2019)
 [3] T. Sasaki et al., *Nat. Commun.* vol.12, p.2706 (2021).
 [4] H. Fukagawa et al., *Nat. Commun.* vol.11, p.3700 (2020).
 [5] H. Fukagawa et al., *Adv. Mater.* vol.31, e1904201 (2019).

8:45 AM EQ17.15.03

Perylene Diimides (PDI)s as Cathode Interlayer in Organic Solar Cells Julien Leoni¹, Alison Campbell¹, Tom Raeber², Mei Gao², Anthony Chesman² and Girish Lakhwani¹; ¹University of Sydney, Australia; ²CSIRO Manufacturing, Australia

Owing to their good photophysical properties, perylene diimides have shown great potential in many fields, such as photo-redox catalysis, bio-imaging and optoelectronic devices. In fact, imine functionalized PDI derivatives have recently been used as cathode interlayers in organic solar cells (OSCs) significantly improving their efficiency. To create the most suitable interface between the bulk heterojunction (BHJ) and the electrode, these materials are processed with an alcohol-based solvent. This combination enables multiple properties that were examined to understand the full extent of how this cathode enhances charge carrier dynamics as well as the exciton dissociation in the OSC's active layer.

A PTQ10:IDIC conventional organic solar cell was reproduced and used as a reference for this project. Several OSCs were fabricated under different conditions and studied through a series of standard PV and spectroscopic characterizations. Indeed, pristine BHJ, alcohol treated BHJ and the addition of a PDI based interlayer were compared. However, one of the key characterization methods used was light intensity variation measurements that were conducted to enlighten us on the types of recombination. This method enables the extraction of the ideality factor through various approaches and can greatly expand our knowledge of the OSC's inner workings.

9:00 AM EQ17.15.04

A Metal-Free Synthetic Protocol for Blue POSS(R)₈ Materials for OLED Applications Rina Mahato, Parvez Akhtar, Madhusudan Singh and Chinmoy K. Hazra; Indian Institute of Technology Delhi, India

Polyhedral oligomeric silsesquioxane (POSS)[1] based organic light-emitting devices (OLEDs) have significant potential applications in displays and solid-state lighting[2], based on favorable charge transport, light absorption, and emission, resulting high efficiency OLEDs[3]. The conventional method of attaching the emitters with the POSS core is metal-assisted hydrosilylation, which often involves the use of expensive metals, such as Pt. Since metal incorporation in POSS(R)₈ affects the cost of the device, and also increases the environmental footprint of the synthetic process, a metal-free synthetic strategy is highly desirable. In this work, we propose a highly efficient, easily accessible, metal-free Lewis acid-catalyzed hydrosilylation process for the synthesis of POSS(R)₈ under very mild conditions, and report on initial results for a blue emitter. A Lewis acid, B(C₆F₅)₃ [tris(pentafluorophenyl)borane], is used to activate the Si-H bond group as a constituent of frustrated Lewis pairs (FLP). For the blue emitter[2,4], we have modified the traditional diphenyl group with a more conjugated pyrene moiety. The characteristic peaks of alkenes at δ 5.74 (ddt, J = 17.1, 9.6, 6.8 Hz, 1H), 4.96 – 4.84 (m, 2H), 2.19 – 2.09 (m, 2H), the methyl group at δ 1.36 – 1.24 (m, 3H) ppm from ¹H-NMR and the quaternary carbon peak at δ 40.56 ppm from ¹³C-NMR confirms the successful synthesis of the emitter. Currently, we are optimizing the reaction conditions for the synthesis of different types of POSS(R)₈ starting from different emitters where B(C₆F₅)₃ can be used as a metal-free catalyst. This reaction will be monitored by using thin-layer chromatography (TLC) and FT-IR spectroscopy. The synthesized products will be characterized by ¹H-NMR, ¹³C-NMR, ²⁹Si-NMR, high-resolution mass spectrometry (HRMS), FT-IR, and

thermogravimetric techniques. The newly developed protocol would provide a more industrially relevant and more environmentally benign process, and contribute significantly to commodity chemical production of [POSS(R)₈] due to their significant applications in OLEDs. Characterization data of blue emitter (B2): Yellow fluorescent solid (125 mg, 89% yield). ¹H-NMR (500 MHz, CDCl₃) δ 8.38 – 8.23 (m, 4H), 8.23 – 7.96 (m, 14H), 7.73 – 7.66 (m, 3H), 5.74 (ddt, J = 17.1, 9.6, 6.8 Hz, 1H), 4.96 – 4.84 (m, 2H), 2.19 – 2.09 (m, 2H), 1.97 (q, J = 7.4 Hz, 2H), 1.53 (s, 2H), 1.36 – 1.24 (m, 3H) ppm; ¹³C-NMR (101 MHz, CDCl₃) δ 152.62, 140.25, 139.08, 138.87, 138.25, 131.57, 131.04, 130.60, 129.67, 128.65, 127.74, 127.49, 127.42, 126.05, 125.39, 125.25, 125.14, 125.00, 124.83, 124.70, 119.93, 40.56, 33.47, 30.92, 29.31, 26.86 ppm.

- [1] (a) Wu, J.; Mather, P. T. *J. Macromol. Sci., Polym. Rev.* **2009**, *49*, 25–63; (b) Kuo, S. W.; Chang, F. C. *Prog. Polym. Sci.* **2011**, *36*, 1649–1696.
 [2] Froehlich, J. D.; Young, R.; Nakamura, T.; Ohmori, Y.; Li, S.; Mochizuki, A. *Chem. Mater.* **2007**, *19*, 4991–4997.
 [3] (a) Yang, X.; Froehlich, J. D.; Chae, H. S.; Harding, B. T.; Li, S.; Mochizuki, A.; Jabbour, G. E. *Chem. Mater.* **2010**, *22*, 4776–4782; (b) Carmoa, D. R.; Filhob, N. L. D.; Stradiottoa, N. R. *Material Research* **2004**, *7*, 499–504.
 [4] Hazra, C. K.; Gandhamsetty, N.; Park, S.; Chang, S. *Nat. Commun.* **2016**, *7*, 13431–13440.

9:15 AM EQ17.15.05

Morphology- and Surface Chemistry-Controlled NaTaO₃ as Highly Efficient Electron Extraction Layer for Halide Perovskite Solar Cells Kootak Hong, Finn Babbe, Guosong Zeng, Francesca M. Toma and Carolin M. Sutter-Fella; Lawrence Berkeley National Laboratory, United States

Lack of stability is one of the major limitations towards halide perovskite solar cell (HPSC) commercialization. As charge transport layers are critical for device performance and stability, the development of charge transport layers with excellent chemical stability and good energy level alignment for efficient charge transfer is of high research interest. TiO₂ and SnO₂ are widely employed as electron transport layers. However, HPSCs with TiO₂ layer suffer from poor stability due to ultraviolet (UV) light-induced O² desorption leading to degradation of halide perovskites. SnO₂ shows temperature-induced degradation and exhibits a lower conduction band compared to halide perovskites resulting in a voltage loss. To achieve better stability and efficiency of HPSCs, it is essential to identify alternative wide band gap materials that are UV-stable and show favorable energy level alignment.

Here, we report on the flux-mediated synthesis of morphology- and surface chemistry-controlled NaTaO₃ thin films and their application as an electron transport layer for HPSCs. The synthesized NaTaO₃ films have a band gap of ~ 4 eV, which makes them more chemically robust under UV illumination and slows down the degradation of halide perovskites, leading to enhanced stability of HPSCs. By varying the precursor chemistry, the resulting microstructure of NaTaO₃ films can be varied from smooth thin films to nanocubes. The latter is possibly useful to increase photon recycling. More efficient photoluminescence quenching of the halide perovskite emission, as a measure for charge extraction efficiency, is observed with the NaTaO₃ in comparison to the SnO₂ layer. In addition, the precursor chemistry can be used to tune the charge extraction ability of NaTaO₃ thin films via surface chemistry modifications.

9:30 AM *EQ17.15.06

Interfacial Engineering Enables Efficient and Stable All-Perovskite Flexible Tandem Solar Cells Fan Fu, Yannick Zwirner, Huagui Lai and Ayodhya Tiwari; Empa-Swiss Federal Laboratories for Materials Science and Technology, Switzerland

Single-junction perovskite solar cells (~ 1.5 eV) have reached certified efficiency of 25.5%, on par with c-Si technology. Due to the broad bandgap

tunability of perovskites, all-perovskite tandem solar cell (TSC), which consists of a wide-bandgap (WBG, 1.75-1.85 eV) perovskite top subcell and a narrow-bandgap (NBG, 1.2-1.3 eV) perovskite bottom subcell, hold great promise to break the Shockley-Queisser limit of single-junction solar cells via reduced thermalization loss. With only a few years' developments, efficiencies over 25% have been demonstrated in both 4-terminal and 2-terminal all-perovskite TSCs. Despite the promising progress, all-perovskite tandems are still far from reaching their practical efficiency potential (>30%), and the long-term (>1000 hours) stability under operational conditions remains a major concern.

All-perovskite TSCs are complex multilayer devices featuring over 10 thin film layers. Each of these layers has its own functionality, such as charge extraction and transport, defect passivation, broadband transparent conducting electrode, etc., and are equally important to achieve high efficiency and stability. In this contribution, we present comprehensive studies on factors limiting the efficiency and stability of WBG and NBG perovskite subcells. We use advanced materials and device characterizations, including scanning transmission electron microscopy, time-of-flight secondary ion mass spectrometry, time-resolved photoluminescence (TRPL), (hard) X-ray photoelectron spectroscopy, thermal admittance spectroscopy, etc., to gain insights on optical, compositional, structural, and electronic properties in WBG and NBG perovskite absorbers and at interfaces to adjacent layers. We will present interfacial engineering (such as tuning band alignment and implementing surface passivation strategies) tailored for WBG and NBG perovskite layers and associated interfaces to mitigate the photovoltaic performance and stability loss mechanisms. With this approach, we demonstrate over 22% all-perovskite TSCs on flexible polymer foils with promising operational stability. In the end, we will discuss the opportunities and challenges towards 25% flexible all-perovskite TSCs on both 4-terminal and 2-terminal architecture.

SESSION EQ17.16: On-Demand
Sunday Morning, December 5, 2021
On-Demand

8:00 AM EQ17.08/EN04.02.02

Photo-Engineered Optoelectronic Properties of Transparent Conductive Oxides *via* Reactive Laser Annealing (ReLA)—The Consequence of Defects [James Hillier](#), Demosthenes Koutsogeorgis and Nikolaos Kalfagiannis; Nottingham Trent University, United Kingdom

Transparent conductive oxides (TCOs) are appealing materials for electronic and photonic applications as, amongst other advantages, their properties can be modulated by engineering their defects. Optimisation of this adjustment is, however, a complex design problem. In this work we address this problem following two ways: (i) establishing new high-throughput methods to selectively tune these properties towards the requirements of the application and (ii) developing better insights into the optoelectronic properties of TCOs. Specifically, we investigated the selective modification of the optoelectronic properties of sputtered tin-doped indium oxide (ITO), aluminium-doped zinc oxide (AZO) and gallium doped zinc oxide (GZO) thin films *via* laser annealing (LA) within an environmental cell containing a wide set of reducing and oxidising reactive gas mixtures.

In order to elucidate the precise mechanisms behind the ReLA process, the optical properties modifications were related to the structural, compositional, and electronic properties. In one case, where the sputtering conditions were optimised to produce an ITO thin film with low resistivity ($4 \times 10^{-4} \Omega\text{cm}$), infrared-visible (0.034-3.4 eV) spectroscopic ellipsometry and Hall Effect measurements revealed a modulation of the optoelectronic properties that is dependant upon the ambient gas mixture. Explicitly, reducing environments (5% H_2 in N_2) promoted a greater enhancement of the carrier concentration. Examination of the X-ray diffractograms and cross-sectional Transmission Electron Microscopy images did not reveal any ReLA-induced structural modifications. However, X-ray photoelectron spectroscopy and energy-dispersive X-ray concluded that the modification of the optoelectronic properties of the ITO films arose from purely compositional changes (creation/filling of oxygen vacancies and activation of substitutional Sn dopants). The precise ReLA induced modifications were not identical for all TCO thin films. In the case of ITO thin films grown with "un-optimised" sputtering conditions (with a higher resistivity of $7 \times 10^{-3} \Omega\text{cm}$), the alteration of the optoelectronic properties was more significant and did not arise from changes to the composition alone. Instead, the depth-dependence of the laser annealing process was uncovered *via* a combination of advanced ellipsometric modelling and cross-sectional transmission electron microscopy. For the AZO and GZO films that form distinct grains even for room-temperature sputter depositions, the role of the grain boundary scattering on the optoelectronic properties is more significant. Therefore, we focussed our attention on the crystal structure in this case. By carefully considering the interplay between the compositional alterations and crystal structure changes for a wide range of TCO films, we revealed the influence of both the intra-grain and inter-grain carrier transport properties for doped ZnO and ITO thin films.

Altogether, we demonstrate that ReLA can be utilised to target specific defects within the TCO films and engineer them to achieve specific alterations to the optical and electronic properties. Hereby, ReLA is established as a novel and versatile tool to tailor the properties of TCO films towards the requirements of potential electronic and photonic applications.

SYMPOSIUM EQ18

Emerging Materials for Quantum Information
November 30 - December 8, 2021

Symposium Organizers

Susan Coppersmith, University of New South Wales
Vincenzo Lordi, Lawrence Livermore National Laboratory
Shashank Misra, Sandia National Laboratories
Giordano Scappucci, TU Delft University of Technology

Symposium Support

Silver

Lawrence Livermore National Laboratory (Lawrence Livermore National Security, LLC)

* Invited Paper

SESSION EQ18.01: Semiconductor Qubits I
Session Chairs: Kyungjean Min and Rick Silver
Tuesday Afternoon, November 30, 2021
Hynes, Level 1, Room 109

1:30 PM *EQ18.01.01

Solid-State Atom-Based Devices for Analog Quantum Simulation Rick Silver^{1,2}, Xiqiao Wang², Jonathan Wyrick¹, Fan Fei², Ranjit Kashid¹, Pradeep Namboodiri¹, Ehsan Khatami³, Albert Rigosi¹ and Garnett Bryant¹; ¹National Institute of Standards and Technology, United States; ²University of Maryland, United States; ³San Jose State University, United States

NIST is using atomically precise fabrication to develop devices for use in quantum information processing. We are using hydrogen-based scanning probe lithography for deterministic placement of individual dopant atoms with atomically aligned gates to fabricate single/few atom transistors, few-donor/quantum dot devices for spin manipulation, and arrayed few-donor devices for analog quantum simulation.

In this talk I will discuss the analog quantum simulation of an extended Hubbard model using arrays of few atom structures in silicon. These atomic clusters form the sites of a Hubbard model array in the strong interaction regime, where we vary the tunnel coupling with atomic precision between nearby dots from a weakly to strongly tunnel coupled regime.

Using an extended Hubbard model we explore the impact of site-by-site disorder on charge occupation and the Hubbard band structure. Numerical simulations of the model reveal the nature of charge distributions and magnetic correlations for different parameter sets. We quantify the electron addition energy spectrum through Coulomb blockade and charge stability analysis and demonstrate tuning of the array's energy spectrum using gates. We map the Hamiltonian parameters to the physical system to tune the charge occupation, the spatial distribution of the eigenstates, localization/delocalization transition, and Hubbard band structure. We identify resonant and inelastic conductance paths and extract coherent tunnel coupling strength.

Details of the STM-fabrication will be described as well as quantum transport measurements from several arrays of few atom clusters ranging from 1x2 double dots to a multi-gate 3x3 dot array to explore the rich Hubbard physics of quantum dot-arrays.

2:00 PM EQ18.01.02

Sequential Atomic-Scale Placement and Alignment of P and B for Bipolar APAM Devices James H. Owen, Robin Santini, Ehud Fuchs and John Randall; Zyvex Labs LLC, United States

The ability to place both *n*-type and *p*-type dopants relative to each other with atomic precision is crucial to the application of Atomically Precise Advanced Manufacturing (APAM) beyond quantum computing. While PH₃ and AsH₃ are highly selective precursors for donor dopants [1-3], the direct equivalents for B and Al are unstable. However, diborane has been used to create a p-n junction[4], and halide precursors, BCl₃ and AlCl₃ are proving promising for acceptor dopants[5].

In this work, we have developed an APAM process for the sequential placement of P and B using PH₃ and BCl₃. First, Hydrogen Depassivation Lithography is used to create patterns on a H:Si(001) substrate. PH₃ is dosed onto the sample and adsorbs selectively into these patterns. An incorporation anneal then drives the adsorbed P into the top layer of the substrate. The sample is repassivated with atomic H before returning to the STM for the second dopant step. A similar process of patterning, dosing with BCl₃ and incorporation completes the bipolar device. The P regions are patterned, dosed and incorporated first, as the incorporation anneal temperature for PH₃ is higher than for BCl₃.

Alignment marks on the sample allow rapid relocation of the device area, and we have developed a high-speed dI/dV imaging method[6] to locate surface or buried dopants. The dI/dV imaging provides much higher contrast of the dopants than the topographic image, so that dopant patches can be relocated quickly in the STM using low-resolution, large-area scans. It also allows for precise alignment of new patterns to existing dopant patches. After both dopants have been incorporated, the surface is repassivated, and the presence of both dopants is confirmed in the STM. The dopant device can then be buried in epitaxial silicon. After burial, dI/dV imaging is then used to confirm the location of the bipolar device for electrode deposition.

1: Fuchsle, M. *et al.* A Single-Atom Transistor. *Nat Nano* **2012**, *7*, 242–246.

2: Wang, X. *et al.* Atomic-Scale Control of Tunneling in Donor-Based Devices. *Commun. Phys.* **2020**, *3*, 82.

3: Stock, T. J. Z.; Warschkow, O.; Constantinou, P. C.; Li, J.; Fearn, S.; Crane, E.; Hofmann, E. V. S.; Kölker, A.; McKenzie, D. R.; Schofield, S. R.; *et al.* Atomic-Scale Patterning of Arsenic in Silicon by Scanning Tunneling Microscopy. *ACS Nano* **2020**, *14*, 3316–3327.

4: Škeren, T. *et al.* Bipolar Device Fabrication Using a Scanning Tunneling Microscope. *Nat. Electron.* **2020**, *3*, 524–530.

5: Dwyer, K. J. *et al.* Area-selective deposition and B delta-doping of Si(100) with BCl₃; Radue, M. S. *et al.* AlCl₃-Dosed Si(100)-2x1: Adsorbates, Chlorinated Al Chains, and Incorporated Al. arxiv (2021)

6: Alemansour, H. *et al.* High Signal-to-Noise Ratio Differential Conductance Spectroscopy. *J. Vac. Sci. Technol. B* **2021**, *39*, 010601.

2:15 PM EQ18.01.03

Experimental Measurements of Atomic Scale Decoherence Mechanisms in Planar Germanium Quantum Wells Brian Gorman¹, Megan Holtz¹, Edwin Supple¹, Chomani Gaspe² and Christopher Richardson²; ¹Colorado School of Mines, United States; ²Laboratory for Physical Sciences, United States

Holes in compressively strained germanium quantum wells is an emerging spin qubit system to overcome the challenges associated with valley degeneracy in silicon. The local electrostatic potential is critical to control the qubit state, and through the deformation potential there is a need to understand the local strain environment. Nanometer-scale experimental assessment of the strain in the quantum well is lacking due to the high spatial resolution and nearly single atom detectability required. Using combined Transmission Electron Microscopy and Atom Probe Tomography, strain variations are herein shown to be experimentally accessible in Ge quantum wells grown via MBE on SiGe buffer layers. Using 4-D STEM, anisotropic strain in the Ge layer was mapped in real space to better than 1 nm and lattice parameters measured to better than 0.1 Å in multiple crystallographic directions. The Ge quantum well was found to be tetragonally strained in defect-free regions and partially relaxed near threading dislocations. Combining TEM with APT, the SiGe/Ge internal

interface structure was mapped in 3-D and shown to have sub-nm interfacial roughness. Individual ^{73}Ge atoms with non-zero nuclear spins are uniquely identified within the Ge quantum well in order to provide another metric that quantum wells can be characterized in order to explore potential interactions between nuclear and hole spins.

2:30 PM *EQ18.01.04

Modeling SiGe Heterostructures and Devices for Si-Based Qubits Mark Gyure; University of California, Los Angeles, United States

A current bottleneck for the development of semiconductor-based qubits is the need for high fidelity simulations that can assist in the device design process and minimize expensive and labor-intensive fabrication cycles. This need is largely unmet – there are very few publicly or commercially available simulation tools that are well suited for this task and, as devices get more complex and time consuming to fabricate, the need only continues to grow.

UCLA has developed simulation capabilities over the last several years to meet this need. We have developed and implemented grid-based software components that can be combined to create very accurate simulations of localized quantum mechanical systems. These software components support the construction of simulations that can be used to model everything from the properties of semiconductor heterostructures to the behavior of multiple interacting electrons.

This talk will describe how our simulation tools, which model realistic device features including gate geometries and dielectric layers, can be used to design SiGe heterostructures and devices for Si-based qubits. We will show that full configuration interaction (FCI) methods can be used to generate highly accurate energy spectra for multi-electron and coupled few-electron quantum dots including important quantities like the exchange interaction between electrons in nearest neighbor dots including the effects of magnetic fields and valley physics. The exchange interaction is the foundation of most two qubit gates in semiconductor dots and being able to predict its behavior as a function of gate geometry and bias is critically important to optimizing the design of qubit devices.

3:00 PM EQ18.01.05

Impact of Ti/Pd Gates on the Stability of Si/SiO₂ Quantum Dots Kyungjean Min^{1,2} and M. D. Stewart, Jr.²; ¹University of Maryland, College Park, United States; ²National Institute of Standards and Technology, United States

Gate-defined Si/SiO₂ based single electron devices (SEDs) are a promising platform to implement spin qubits and a quantum standard of the Ampere. Noise can limit the performance and integrability of devices for each of these applications. One of the measures of low-frequency charge noise control is known as charge offset drift. The device stability at low frequencies is usually attributed to the presence of defects which are influenced by materials choices, fabrication processes and device design. Poly-Si gated silicon SEDs are known to have smaller charge offset drift (0.01e) than the metallic gates SEDs as observed in the charge offset drift measurement of Al gates SEDs (0.15e). The reactivity of the Al can produce defective AlO_x formation as the inter-gate dielectric as well as underneath the gate, increasing charge offset drift and degrading device performance. However, Pd gates which are much less reactive than Al, may induce fewer defects while preserving the benefits of metal-gated devices such as simplified fabrication, reduced parasitic resistances, and reduced grain size. To assess the impact on stability of Pd gates, we fabricate and measure SEDs with a combination of Ti/Pd and poly-Si gates with thermally grown SiO₂ as the inter-gate dielectric. This choice preserves a high level of tunability and functionality in the devices provided by overlapping gate design, while also avoiding defects associated with a deposited inter-gate dielectric. Our latest measurement results and the implications for device performance will be discussed.

3:15 PM EQ18.01.06

Antisite Defect Qubits in Monolayer Transition Metal Dichalcogenides Jeng-Yuan Tsai¹, Jinbo Pan¹, Hsin Lin², Arun Bansil³ and Qimin Yan¹; ¹Temple University, United States; ²Academia Sinica, Taiwan; ³Northeastern University, United States

Like the classical bit that launched the modern electronic age, the quantum bit or qubit lies at the heart of the ongoing quantum information revolution that is expected to transform science and society in previously unimaginable ways. Although solid-state defects such as the diamond-NV centers in three-dimensional hosts have been demonstrated as promising qubits, atomically-thin two-dimensional (2D) materials offer an exciting new paradigm for qubit fabrication and operation at room temperature. Using data-driven approaches and a symmetry-based hypothesis for qubit discovery, we show that neutral anion-antisite defects in six transition metal dichalcogenide (TMD) monolayers as viable spin qubits. We show how the optical transitions and triplet-singlet intersystem crossing paths in the qubit provide a complete cycle for initialization, manipulation, and readout of the qubit. The operational principles of the qubit are illustrated through an in-depth discussion of the antisite qubit in WS₂. Our study opens a new pathway for creating spin-qubits and multi-qubit platforms for quantum information technologies based on defects in 2D solid-state systems.

SESSION EQ18.02: Superconducting Qubits I
Session Chair: William Strickland
Wednesday Afternoon, December 1, 2021
Hynes, Level 1, Room 109

1:30 PM EQ18.02.01

Long-Lived Transmons with Different Electrode Layouts Kungang Li, Sudeep Dutta, Zachary Steffen, Dylan Poppert, Shahriar Keshvari, Jeffery Bowser, Ben Palmer, Christopher Lobb and Frederick Wellstood; University of Maryland, United States

The relaxation time T_1 of superconducting qubits has increased by orders of magnitude over the last two decades. To test whether quasiparticles are a significant contributor to the loss, we have repeatedly measured T_1 in Al/AIO_x/Al transmons with electrodes with different superconducting gaps. In one device, the first layer electrode was formed by deposition of nominally pure aluminum, while the counter-electrode was formed by deposition of oxygen-doped aluminum. The superconducting energy gap of the electrode depends on the grain size, which depends on the oxygen doping as well as the layer thickness. The device showed relatively large fluctuations in T_1 , varying from about 100 μs to just over 300 μs at 20 mK. In other transmons, we formed the first layer electrode by deposition of oxygen-doped aluminum, while the counter-electrode was formed by deposition of nominally pure aluminum. These devices showed a similar range of large fluctuating T_1 values, as well as a maximum T_1 over 300 μs . Measurements of the T_1 of these transmons as a function of temperature shows similar temperature dependence, with the relaxation time at high temperature dropping due to the thermally-generated quasiparticles.

1:45 PM EQ18.02.02

Structural Characterization of Nitride Josephson Junctions Grown via Molecular Beam Epitaxy Using Scanning Transmission Electron Microscopy and Atom Probe Tomography [Edwin Supple](#)¹, Megan Holtz¹, Christopher Richardson^{2,3} and Brian Gorman¹; ¹Colorado School of Mines, United States; ²University of Maryland, United States; ³Laboratory for Physical Sciences, United States

Current implementations of superconducting qubits have short decoherence times attributed, in part, to losses to two level systems. These two level systems reside in dielectric materials and at interfaces in the device. Josephson junctions made of (Nb,Ti)N superconductors and AlN junction barrier grown via molecular beam epitaxy on sapphire have the potential to eliminate the amorphous material hosting two level systems and thus potentially improve qubit coherence times. Here, we utilize 4-D scanning transmission electron microscopy (STEM) to determine nanometer-scale changes in crystallographic structure, cation ordering, and orientation of the superconductors in a NbTiN / 2 nm AlN / NbTiN device stack grown on c-sapphire. We find that the NbTiN is rock salt structured and highly oriented towards $\langle 111 \rangle$ but with rotations about that axis corresponding to step edges in the c-sapphire. The AlN structure, orientation, roughness and thickness were investigated using correlative 4-D STEM and Atom Probe Tomography (APT). Under these growth conditions, the AlN can exhibit island growth on the lower NbTiN, leading to nm scale changes in thickness and shorts across the barrier junction. As a result, the top NbTiN has randomly oriented crystallographic structure. APT was also utilized to determine local changes in point defect chemistry at the internal interfaces. Changes in the nitrogen stoichiometry are observed near the AlN barrier, leading to negatively charged vacancies that may be a source of decoherence.

2:00 PM EQ18.02.03

Transparent Superconductor Candidates—Intercalated ITO [Emma K. Batson](#)¹, Marco Colangelo¹, John Simonaitis¹, Mayuran Saravanapavanantham¹, Madison King², Johanna Nordlander³, Margaret Anderson³, Erika V. Ortega Ortiz³, Vladimir Bulović¹, Stephanie K. Hurst², Julia Mundy³, Phillip D. Keathley¹ and Karl Berggren¹; ¹Massachusetts Institute of Technology, United States; ²Northern Arizona University, United States; ³Harvard University, United States

There are an increasing number of circuit architectures that put optical modes on-chip with superconducting microwave electronics, such as microwave-to-optical transducers which could help link quantum networks.[1, 2] However, such devices are frequently limited by absorption of the optical field in the superconducting electronics. This loss leads to a reduction in the quality factor of the optics, and may also induce quasi-particle generation which reduces the performance of the superconducting material. Although fine-tuning the geometry of the circuit can decrease optical absorption in the superconductor, the absorption could be further reduced if the electronics were made of a superconductor which was transparent to visible light.

In this work, we study sodium-doped ITO as a potential transparent superconductor. ITO, which has previously been studied as a transparent conductor with a low carrier concentration and a high mobility, has recently been shown to superconduct when electrochemically doped via intercalation of sodium ions.[3] However, the doping is also associated with a visible change in the optical properties of the material that has not previously been quantitatively measured. We develop an electrochemical cell for doping ITO and study how the process affects its electrical and optical properties. We use ITO on different substrates, including glass and silicon, with different doping levels set by intercalation time. We measure how doping changes the optical properties of the ITO using ellipsometry and spectrophotometry across the visible spectrum and near infrared. We also measure the room temperature resistivity and superconducting transition temperature, and their relationship to the optical properties. Based on these measurements, we evaluate the suitability of sodium-doped ITO as a transparent superconductor.

[1] Optica 7.12 (2020), pp. 1714–1720

[2] Optica 7.12 (2020), pp. 1737-1745

[3] Appl. Phys. Lett. 101, 252603 (2012)

2:15 PM EQ18.02.04

Late News: Microwave Absorption of Near-Surface InAs Quantum Wells on Pseudomorphic III-V Buffer Layers [William M. Strickland](#), Joseph O'Connell Yuan, Aminatou Dabokemp, Mehdi Hatefipour, Dylan Langone and Javad Shabani; New York University, United States

Qubits on solid state devices could potentially provide the rapid control necessary for developing scalable quantum information processors. Materials innovation and design breakthroughs have increased the functionality and coherence of qubits substantially over the past two decades. Here we show by improving the interface between InAs and Al, one can reliably fabricate voltage-controlled Josephson junction field effect transistors (JJ-FET) to be used in tunable qubits, resonators, and couplers. We find that band gap engineering is crucial in realizing a two-dimensional electron gas near the surface. In addition, we show that coupling between the semiconductor layer and the superconducting contacts can affect qubit properties.

We analyze materials systems with varied growth conditions on the pseudomorphic buffer layer and quantum well active region for the purposes of making JJ-FET devices. In samples with a high indium content graded buffer layer, we find that surface roughnesses decrease drastically with the graded buffer layer growth temperature. We also find that samples with isotropic roughnesses along the $\langle 110 \rangle$ and $\langle 1-10 \rangle$ directions show a higher mobility than those with anisotropic roughnesses. We study the effects of the quantum well growth temperature over a range of 445°C to 465°C on 2DEG mobility. We grow a thin 1-6 nm $\text{In}_{0.81}\text{Al}_{0.19}\text{As}$ capping layer in order to discern the effects of surface scattering on the quantum well and measure density and mobility as a function of the $\text{In}_{0.81}\text{Al}_{0.19}\text{As}$ layer thickness. We compare the measured densities to those calculated by solving the Schrödinger and Poisson equations self-consistently, where the presence of a thin $\text{In}_{0.81}\text{Al}_{0.19}\text{As}$ top layer causes the density and mobility increase, due to the decreasing conduction band energy of InAs and to separation from surface scattering sites.

We test these structures in coplanar waveguide (CPW) resonator devices using microwave transmission measurements, we study the quality factor on each device at high and low power and extract TLS losses in each materials combination. We also present anharmonicity and coupling strengths measured from one and two-photon absorption in a quantum two-level system engineered in a fabricated JJ-FET.

2:30 PM EQ18.02.05

Ultra-High Vacuum Electron-Beam Evaporated Niobium for Low-Loss Superconducting Coplanar Waveguide Resonators [Daria Kowsari](#)¹, Kaiwen Zheng¹, Jonathan Monroe¹, Nathan Thobaben², Xinyi Du¹, Patrick Harrington^{1,3}, Erik Henriksen^{1,1}, David Wisbey² and Kater Murch¹; ¹Washington University in St. Louis, United States; ²Saint Louis University, United States; ³Massachusetts Institute of Technology, United States

Material losses limit the performance of superconducting qubit processors. Recent advances in the fabrication techniques and materials science have reduced the majority of decoherence sources such as quasiparticles, magnetic vortices, and radiation, leaving two-level system (TLS) defects as the most prominent source of loss. Due to its high transition temperature and critical field, niobium is one of the common materials used to achieve highly coherent devices. Conventional niobium deposition methods, such as DC magnetron sputtering can result in a damaged substrate-metal interface during the deposition due to the presence of high energy argon ions. To eliminate this source of damage, here we report on a refined growth technique for extremely low-loss niobium thin films using an electron-beam evaporator. The films are deposited in an ultra-high vacuum pressure environment (< 5 nTorr) with deposition rates as low as 1.2 nm/min. The resulted films exhibit a superconducting transition temperature of 9.2 K and residual-resistivity ratio as high of 5.1 for a film with a thickness of 200 nm, proving the absence of any trace of impurities, despite the low deposition rate. To further study the sources of

loss in our films, we fabricated the films into coplanar waveguide (CPW) resonators to extract the TLS loss tangent of the niobium using microwave measurements. Notably, we utilized a CPW gap of 2 μm to maximize coupling to the TLSs at the interfaces, and thereby gain a more reliable estimate of the defects in the films. Our results show that after passivating the niobium surface using a buffered oxide etch, we achieve TLS loss tangents as low as 1×10^{-7} , well below the previous limits.

2:45 PM EQ18.02.06

Niobium Coplanar Waveguide Microwave Resonators with Nitrogen Plasma Passivated Surface Kaiwen Zheng¹, Daria Kowsari¹, David Wisbey² and Kater Murch¹; ¹Washington University in St. Louis, United States; ²Saint Louis University, United States

The quality factor of superconducting coplanar waveguide resonators correlates strongly with the coherence properties of planar superconducting qubits. Recent works have shown that the microwave loss of niobium microwave resonators is dominated by an oxide layer of approximately 5 nm thick at the metal-air interface. Although the microwave loss can be reduced by removing the oxide layer using buffered oxide etch, the oxide regrows in a time frame of several hours. Our work demonstrates a novel method of preventing the regrowth of surface oxide by passivating the metal surface using nitrogen plasma. We will present data of surface and microwave characterizations of resonators passivated using this method.

SESSION EQ18.03: Topological Qubits I
Session Chairs: Chunyi Huang and Javad Shabani
Thursday Morning, December 2, 2021
Hynes, Level 1, Room 109

10:30 AM *EQ18.03.01

Progress in Realizing Topological Superconductivity in Planar Josephson Junctions Javad Shabani; New York University, United States

Recently the drive to understand and control the order parameter characterizing the collective state of electrons in quantum heterostructures has attracted great interest. New physical behavior can emerge that is absent in the isolated constituent materials. With regards to superconductivity this has opened a whole new area of investigation in the form of topological superconductivity. Topological superconductivity are expected to host exotic quasi-particle excitations including Majorana bound states which hold promise for fault-tolerant quantum computing. Recent theory predicts in superconductor-semiconductor devices, Majorana bound states can emerge and are accompanied by a topological phase transition. We study epitaxial Al/InAs Josephson junctions in presence of Zeeman field where we find a transition between trivial and topological superconductivity. We observe a minimum of the critical current at the topological transition, indicating a closing and reopening of the superconducting gap induced in InAs, with increasing magnetic field. By embedding the Josephson junction in a phase-sensitive loop geometry, we measure a π -jump in the superconducting phase across the junction when the system is driven through the topological transition. These findings reveal a versatile two-dimensional platform based on epitaxial superconductors and semiconductors.

11:00 AM EQ18.03.02

InAs Nanowires on Nanomembranes—Growth and Device Aspects Didem Dede¹, Kristopher Cervený², Chunyi Huang³, Valerio Piazza¹, Nicholas P. Morgan¹, Martin Friedl¹, Lucas Güniat¹, Jean-Baptiste Leran¹, Jaime Segura Ruiz⁴, Valentina Bonino⁴, Lincoln Lathon³, Dominik Zumbuhl² and Anna Fontcuberta i Morral¹; ¹Ecole Polytechnique Federale de Lausanne, Switzerland; ²Universität Basel, Switzerland; ³Northwestern University, United States; ⁴European Synchrotron Radiation Facility, France

Even though many advances have been made in the field of quantum computing, Majorana fermions, the exotic mystery of topological qubits, have yet to be conclusively identified and are thus still waiting to be explored.^[1] Materials science is still the bottleneck of this progress; high-quality semiconductor nanowires (NWs) in a precise configuration are required, as well as a deeper understanding of their structural, electrical, and transport properties. Previously, selective area growth of horizontal In-based NW networks by molecular beam epitaxy has been proposed for these systems due to the scalability of the process, inherent properties of the material, and the cleaner environment of the machine.^[2,3] Growing NWs on defect-free GaAs templates or nanomembranes (NMs) results in high crystal quality, eliminating undesired impurity incorporation coming from the substrate. As a result, these NWs show field-effect gating, quantum coherence, and induced superconductivity.^[3,4] Moreover, the carrier concentration of the In(Ga)As NW branches can be enhanced by quasi-remotely doping the (111)B GaAs NMs. This results in the observation of weak anti-localization, an indication of strong spin-orbit interaction (SOI), and enhanced coherence length and mean free path.^[5] However, the maximum achievable In concentration on these NMs is 50%, and Si dopants accumulate at the NW/NM interface contributing to the donor interface scattering. Thus, advancements are still necessary to achieve the optimal material design for efficient quantum transport.

In this study, we address several challenges related to the design, growth, and exploitation of horizontal NWs grown epitaxially on NMs. First, we explore the crystal orientation of the GaAs substrate as a design parameter for changing the morphology of the In(Ga)As NWs. Since growths on (111)B, (100), and (110) are all governed by both thermodynamics and kinetics, the GaAs NMs have different morphologies and facets depending on the surface energy. Consequently, the NW geometry and the amount of In incorporation in the wire change depending on the substrate orientation. We demonstrate that growth on (100) substrates results in NWs that grow conformally around a low-aspect-ratio NM. These nanowires can be nearly pure InAs and exhibit only a narrow-intermixed region. For growth on (110) substrates, the NWs have a trapezoidal cross-section with a moderate In concentration. Subsequently, we explore the possibility to modify the morphology of the NMs by adding a small amount of Sb during the epitaxial growth (less than 5 at%). Sb acts as a “morphactant” in the system, favoring the formation of a flat top facet. This provides a smoother growth surface for the InAs NW, helping to decrease the scattering at the NM-NW interface. We also investigate new routes to suppress Si dopant diffusion in remotely-doped structures by two different approaches: (i) suppressing dopant mobility during the growth by decreasing the temperature and (ii) introducing a few-nm thick trapping layer after the doped layer growth. Dopant displacement was characterized by atom probe tomography. Finally, we investigate the magnetotransport properties of some of the quasi-remotely doped NWs. By fabricating a dual gated architecture at each side of the NW, we aim to keep carrier density constant while changing the electric field across two gates. This novel device design would make it possible to tune the SOI present in these NWs.

References

- [1] P. Yu *et al.*, *Nat. Phys.* **2021**, *17*, 482.
- [2] M. Friedl *et al.*, *Nano Lett.* **2018**, *18*, 2666.
- [3] F. Krizek *et al.*, *Phys. Rev. Mater.* **2018**, *2*, 093401.
- [4] S. Vaitiekėnas *et al.*, *Phys. Rev. Lett.* **2018**, *121*
- [5] M. Friedl *et al.*, *Nano Lett.* **2020**, *20*, 3577.

Acknowledgments: Funding from Swiss National Science Foundation, NCCR QSIT

11:15 AM EQ18.03.03

Breakdown of Induced p±ip Pairing in a Superconductor-Semiconductor Hybrid Duc Phan¹, Jordan Senior¹, Areg Ghazaryan¹, Mehdi Hatefipour², William M. Strickland², Javad Shabani², Maksym Serbyn¹ and Andrew P. Higginbotham¹; ¹IST Austria, Austria; ²New York University, United States

Superconductor-semiconductor hybrids are platforms for exploring the rich phenomena that can emerge from effective p-wave superconductivity. Spin-orbit coupling, combined with the proximity effect, causes the two-dimensional semiconductor to inherit p±ip intraband pairing, and application of magnetic field can then result in transitions to the normal state, partial Bogoliubov Fermi surfaces, or topological phases with Majorana modes. Experimentally probing the hybrid superconductor-semiconductor interface, however, is challenging due to the shunting effect of the conventional superconductor. Consequently, the nature of induced pairing remains an open question.

I will discuss the use of planar superconducting resonators to probe induced superconductivity in a two dimensional Al-InAs hybrid system. We have observed a strong, anisotropic suppression of superfluid density and enhanced dissipation driven by magnetic field, which cannot be accounted for by the depairing theory of an s-wave superconductor. These observations are explained by a picture of independent intraband p±ip superconductors giving way to partial Bogoliubov Fermi surfaces. Within this picture, we provide the first characterization of key properties of the hybrid superconducting system, with implications for routes to Majorana physics. In addition, this work raises questions surrounding the stability of Bogoliubov Fermi surfaces.

11:30 AM EQ18.03.04

Remote Doping in Nanowires for Quantum Computing Chunyi Huang¹, Didem Dede², Martin Friedl², Valerio Piazza², Anna Fontcuberta i Morral^{2,2} and Lincoln Lauhon¹; ¹Northwestern University, United States; ²EPFL, Switzerland

The manipulation of Majorana zero modes in networks of semiconductor nanowires is a promising route to quantum computing. A central challenge to this approach is to achieve control of both nanowire morphology and network topology. We have previously demonstrated wafer-scale growth of high mobility branched InAs nanowires (NWs) supported on GaAs nanomembranes (NMs) by molecular beam epitaxy (MBE).^[1] Here we address the challenge of controlling the NW morphology and dopant incorporation simultaneously. Modulation of growth temperature and III-As ratios can be used to determine the nanowire morphology by controlling anisotropic growth in these non-planar heterostructures. However, the incorporation kinetics of the dopants are generally facet-dependent, such that the ideal growth conditions for self-assembled NWs may not match the conditions needed to achieve the ideal doping profile. We have used atom probe tomography (APT)^[1] to make 3D compositional measurements at the atomic scale to understand the relationship between nanowire faceting and dopant incorporation under a range of growth conditions.

In our initial work, atom probe tomography analysis found that Si dopants accumulate at the top of the (111) facet of InGaAs nanowires,^[3] which will produce scattering from the ionized donors. Follow-up work was successful in introducing Si below the NW/NM interface, but with strong facet dependent doping and with incomplete control of morphology. The talk will describe strategies to mitigate facet dependent doping while maintaining precise dopant positioning beneath a well-defined channel. We visualized buried growth interfaces by introducing dilute Al marker layers during growth, providing new insights into how faceting varies with temperature and III-As ratios in a continuous manner. Si diffusion can be suppressed by doping at reduced temperatures, leading to dopant profiles that are less diffuse both along the growth axis and along the growth interface. However, the growth interface shape changes as the temperature is increased for the definition of the InAs nanowire grown. The precise determination of the nanowire morphology and dopant distribution by atom probe tomography lays an essential foundation to understanding the origin of transport properties, and provides new strategies to mitigate Si segregation and facet-dependent doping.

References:

- [1] Friedl, M., Cerveny, K., *et al.* Remote doping of scalable nanowire branches. *Nano Letters* **2020**, *20*, 3577.
- [2] Chang, A. and Lauhon, L., Atom probe tomography of nanoscale architectures in functional materials for electronic and photonic applications. *Current Opinion in Solid State and Materials Science* **2018**, *22*, 171.
- [3] Friedl, M., *et al.* Template-assisted scalable nanowire networks. *Nano Letters* **2018**, *18*, 2666.

11:45 AM EQ18.03.05

Reversed Phase Transformation of β→α-Sn at Elevated Temperatures Towards Quantum Material Integration on Silicon Shang Liu, Alejandra V. Covian, Xiaoxin Wang and Jifeng Liu; Dartmouth College, United States

α-Sn and SnGe alloys have recently attracted much attention as a new family of topological quantum materials [1,2]. Depending on strain, they can be topological insulators or topological Dirac semimetals (TDS), the latter being a 3D counterpart of graphene with the Dirac cone protected by crystal symmetry and spin-orbit coupling. Recently, theoretical predictions have also shown that SnGe alloys with >40% Sn composition can be a TDS under compressive strain [2]. If verified experimentally, the wide range of SnGe alloys could greatly enrich the family of 3D TDS since only a few of them have been discovered so far [1,3,4]. They are also naturally compatible with Si-based integrated circuits as alloys based on Group IV elements. However, bulk α-Sn is stable only at <13°C. High Sn composition SnGe alloys have been rarely studied experimentally since they are well beyond the equilibrium solubility limit [5]. Moreover, the integration of α-Sn on silicon has also been hindered by a large lattice mismatch, and epitaxial α-Sn is limited to InSb substrates so far. To address these challenges, we demonstrate that ~4 at.% Ge-doped α-Sn microdots can be grown on native oxide on Si substrate via a *reversed* phase transformation from β to α-Sn at 300-500°C, seeded by Ge-rich GeSn nanoclusters in the as-deposited materials instead of heteroepitaxy from the Si substrate. This result is exactly opposite to the bulk phase diagram that says α-Sn cannot be formed at >13°C. It also shows that Ge-doped α-Sn can be stabilized at elevated temperatures without the help of coherent epitaxial interface as in the common case of α-Sn growth on InSb substrates. The size of α-Sn dots reaches up to 280 nm in diameter and 150 nm in thickness, ~10x larger than the upper size limit for α-Sn formation reported before. Raman spectroscopy, X-ray diffraction (XRD), Energy-dispersive X-ray spectroscopy (EDS), and high-resolution transmission electron microscopy (HRTEM) have been used to confirm the formation and determined the Ge composition in α-Sn. A compressive strain of ~-0.6% is introduced to Ge-doped α-Sn, which makes it one of the few candidates for 3D TDS according to theoretical predictions. This work presents the first instance of α-Sn grown at relatively high temperature on Si without epitaxy, breaking through the long-existing constraints in substrate selection, size/thickness limit, and thermal stability of α-Sn growth towards topological quantum material integration on Si. These TDS microdots could be coupled through graphene towards quantum device applications [6]. Furthermore, since we found that Ge-rich GeSn nanoclusters can effectively seed the growth of Sn-rich α-SnGe in this study, this process could potentially be scaled up using selective epitaxial growth on GeSn virtual substrates on Si for high-quality quantum device integration.

Reference

- [1] Xu, *et al.* Phys. Rev. Lett. **118**, 146402 (2017).
- [2] Lan, *et al.* Phys. Rev. B **95**, 20, 201201 (2017).

- [3] Wang, et al. Nature materials 15, 38–42 (2016).
[4] Liu, et al. Science 343, 864–867 (2014).
[5] Predel, B. Ge-Sn (Germanium-Tin) Landolt-Börnstein - Group IV Physical Chemistry 5F(Ga-Gd – Hf-Zr) (1996)
https://materials.springer.com/lb/docs/sm_lbs_978-3-540-44996-6_1506
[6] Wu, et al. Advanced Materials 32.2, 1905632 (2020).

SESSION EQ18.04: Semiconductor Qubits II
Session Chairs: Vincenzo Lordi and John Nichol
Monday Morning, December 6, 2021
EQ18-Virtual

10:30 AM *EQ18.04.01

Atomic-Scale Material Insights for Silicon Based Qubits Sven Rogge; Univ of New South Wales, Australia

Spins bound to electronic dopant atoms in silicon are promising qubits since they interact weakly with their environment, resulting in exceptional coherence times of the order of seconds. Characterising and controlling their properties and interactions is essential to fulfil the prerequisite for accurate quantum state manipulation needed to build scalable quantum computers. An extra challenge in silicon originates from the indirect bandgap that leads to a spatial modulation of the qubit's wavefunction at the atomic scale that is incommensurate with the host lattice. This presentation will cover innovative methods to probe the quantum states encoded of individual and interacting atom qubits in silicon, including single electron-tunnelling in nanoscale transistors, scanning tunnelling microscopy to directly image the wave-function at the atomic scale and radio frequency reflectometry. Together with the development of atomistic simulations of realistic devices, these methods bring new insights to the understanding of the impact of the valley degree of freedom in silicon to accelerate the engineering of atom-based quantum processors.

11:00 AM *EQ18.04.02

Bridging the Classical-Quantum Divide with Implanted Ions—Engineered Donors in Enriched Silicon David N. Jamieson^{1,2}; ¹University of Melbourne, Australia; ²Centre for Quantum Computation and Communication Technology, Australia

We have developed a strategy to implant near-surface donor atoms into silicon that form the components of quantum computer devices employing the donor nuclear and electron spins. Our devices address the challenge of bridging the internal donor quantum states to read-out circuitry and hence the classical observer. One and two atom devices can be engineered by implanting a small number of ions, subject to Poisson statistical distributions, then finding optimally located donors by sweeping surface control gates to induce electron exchange with an adjacent single electron transistor. Enriched 28-Si substrates, depleted in the nuclear spin 1/2 29-Si isotope, give long donor nuclear and electron spin coherence times. For large scale devices we have developed a strategy integrating a plasma ion source, which produces donor ions with random arrival times, together with an active substrate that signals the implantation of each ion. The ion implantation site is defined by a nanostencil incorporated in an AFM cantilever that also allows for non-destructive, in-situ imaging of location markers to align the implanted donors to sub-100 nm precision. The signals are generated from the e-h pairs induced in the substrate using high sensitivity readout electronics which has also provided insights into the physics of the ion stopping process for near-surface doping. We have developed the capability to implant molecules of 31-PFx (x=1,2,3,4), Sb isotopes and 209-Bi all within a mean 20 nm of the silicon surface. In the case of PFx molecules, the F bystander ions generate e-h pairs, then diffuse away during post-implantation annealing for donor activation. Signals from the ion-induced electron hole pairs also show that discrete ion impacts suffer much lower levels of charge recombination in the substrate compared to continuous ion irradiation. In parallel we have demonstrated a method to locally deplete the non-zero nuclear spin isotope 29-Si to 250 ppm using high fluence ion implantation. Electron Spin Resonance measurements of near-surface 31-P donors material with 29-Si depleted to 3000 ppm with this method produced a T2-Hahn electron coherence time of 285 μs which is commensurate with previous work on enriched silicon. Also, the signal amplitude as a function of time showed a single component exponential decay without the need for a third order term imposed by residual 29-Si. For a large-scale device, this would potentially allow both 29-Si depletion and donor array construction in the same ion implantation system.

Acknowledgements: This work is supported by the Australian Research Council Centre of Excellence for Quantum Computation and Communication Technology (CQC2T, CE170100012) and the US Army Research Office (Contract no. W911NF-17-1-0200). We acknowledge the AFAiIR node of the NCRIS Heavy Ion Capability for access to ion-implantation facilities at EME, ANU, Silicon Quantum Computing for access to the electron spin resonance infrastructure, the Surface Analysis Laboratory, SSEAU, MWAC, UNSW for SIMS, and the contribution of collaborators in CQC2T including A.M. Jakob, D. Holmes, B.C. Johnson, J.C McCallum, A. Morello, S. Rogge.

11:30 AM *EQ18.04.03

Charge Noise in Semiconductor Quantum Dot Spin Qubits John Nichol; University of Rochester, United States

Electron spins in semiconductor quantum dots are a leading platform for quantum computing because they have extremely long coherence times and are compatible with advanced semiconductor manufacturing techniques. However, most two-qubit gates between spins rely on electric fields to manipulate the wavefunctions of the electrons. Spurious electric-field noise, or charge noise, can cause decoherence of multi-spin systems and is a significant obstacle to large-scale quantum computing with electron spins. I will describe what we know about charge noise in semiconductor quantum dots and potential strategies to mitigate its effects.

12:00 PM *EQ18.04.04

Qubits Made by Advanced Semiconductor Manufacturing Anne-Marije Zwerfer¹, Tobias Krähenmann¹, Thomas Watson², Lester Lampert², Hubert George², Ravi Pillarisetty², Stephanie Bojarski², Payam Amin², Sergei Amitonov¹, Jelmer Boter¹, Roman Caudillo², Diego Corras-Serrano², Juan Pablo Dehoillain¹, Gabriel Droulers¹, Eric Henry², Roza Kotlyar², Mario Lodari¹, Florian Lüthi², David Micalak², Brennen Mueller², Samuel Neyens², Jeanette Roberts², Nodar Samkharadze¹, Gouji Zheng², Otto Zietz², Giordano Scappucci¹, Menno Veldhorst¹, Lieven Vandersypen¹ and James Clarke²; ¹QuTech and Delft University of Technology, Netherlands; ²Intel Components Research, Intel Corporation, United States

Spin qubits that are hosted in electrically-controlled, silicon quantum dots are promising candidates for implementing quantum technology. Due to their small size, relatively long coherence times and their compatibility with the semiconductor industry they offer great promises, both for qubit performance and for scaling. To pave the road towards large-scale quantum computing, making use of common CMOS fabrication techniques, like optical lithography and chemical-mechanical polishing is key. Spin qubit devices to date, however, still rely on the flexibility of e-beam lithography and mostly lift-off

techniques.

Here, we present the first qubits in isotopically enriched 28 Si-MOS fabricated entirely with optical lithography in an industrial 300 mm process line. These devices are fully fabricated with optical lithography and chemical-mechanical polishing techniques for patterning, compatible with state-of-the-art fabrication. This leads to an extremely high nanofabrication yield across the full wafer. Furthermore, due to the large number of devices characterized, we can study correlations between room-temperature and low-temperature device behavior. In these devices, we demonstrate well-controlled single and double quantum dots in the multi-electron regime, which is also reproducible across the wafer for several wafers. Moreover, we demonstrate charge sensing with a signal-to-noise ratio high enough for single shot readout. With this, we form high-quality qubits in the single-electron regime, comparable to qubits in academic devices, but with much better prospects for scaling.

SESSION EQ18.05: Superconducting Qubits II
Session Chair: Vincenzo Lordi
Tuesday Morning, December 7, 2021
EQ18-Virtual

10:30 AM EQ18.05.01

Steps Towards Homogenous Transition Metal Nitride Thin Film Growth for Josephson Junctions Using PAMBE Austin Thomas, Nicholas Grabon, Alan Kramer and Christopher Richardson; University of Maryland, United States

Nitride superconductors are attractive materials for superconducting quantum circuits. This work investigates methods of growing an isolated phase of NbN_x to create a materials platform that can be used for an epitaxial Josephson junction (JJ) that may perform better than existing platforms by eliminating interface defects. NbN_x has been used for JJ fabrication due to its high critical temperature, along with its mechanical and chemical stability when compared to pure Nb JJ layers. However, our work has shown that when growing NbN_x with Plasma Assisted Molecular Beam Epitaxy (PAMBE), several distinct crystallographic phases of the nitride are present, and isolation of an individual phase for JJ fabrication proved to be difficult.

Isolation of the rock salt δ - NbN phase is necessary for growing $\text{Nb}_x\text{Ti}_{1-x}\text{N}$ films where the (111) plane has the same atomic spacing as the (0001) plane of AlN. These lattice-matched, abrupt interfaces may reduce defects at the insulating barrier, reducing energy loss in Josephson junction devices. The composition of $\text{Nb}_x\text{Ti}_{1-x}\text{N}$ can be adjusted to the correct lattice constant for lattice matched growth. These transition metal nitrides are mechanically and chemically stable, with high critical temperatures, making them ideal for superconducting devices.

PAMBE grown NbN_x and $\text{Nb}_x\text{Ti}_{1-x}\text{N}$ films on Al_2O_3 (0001) are investigated regarding phase stabilization with varying substrate temperature, buffer layers, and alloyed composition. The rock salt phase of NbN_x is desired for heterostructure growth, and this phase is verified using high-resolution x-ray diffraction (HRXRD) and electron backscatter diffraction (EBSD). Atomic force microscopy (AFM) and electrical characterization of the normal and superconducting states are used to determine suitability for $\text{Nb}_x\text{Ti}_{1-x}\text{N}(111)|\text{AlN}(0001)|\text{Nb}_x\text{Ti}_{1-x}\text{N}(111)$ and $\text{NbN}_x(111)|\text{AlN}(0001)|\text{NbN}_x(111)$ Josephson junction heterostructures.

Samples were grown using a custom DCA M600 MBE system with a base pressure better than $1\text{e-}10$ Torr. Samples were grown on $2''$ C-plane sapphire wafers, which were degreased and thermally cleaned before growth. A RF plasma generator is used for nitrogen incorporation, while Nb is deposited using an electron beam evaporator. Ti is deposited using a high-temp effusion cell. Nitrogen flux was set at 0.6 sccm at 500W, and Nb flux was kept between $0.5\text{E}17$ and $3.5\text{E}17$ m^2s^{-1} . Substrate temps during growth were set at between 800°C and 1000°C by thermocouple.

δ - NbN grows predominantly at 1000°C with our growth technique, though phases γ - Nb_4N_3 and ϵ - NbN are still present in our films. To isolate the rock salt phase further, we investigate the effects of TiN buffer layers, along with alloying NbN_x with Ti. We have also observed that Ti incorporation in NbN_x films at lower temperatures increases the rock salt phase stability. For δ - NbN , XRD and EBSD results show uniform, single phase growth, while AFM results show a smooth, striated surface with a roughness of $< 1\text{nm}$, ideal for JJ fabrication. Internal quality factors of these thin films are investigated by way of superconducting coplanar microwave resonator measurements.

10:45 AM EQ18.05.02

Suppression of Nb Suboxides via Oxygen Scavenging by TiN Deposition Mahmut Sami Kavrik¹, Shaul Aloni¹, Frank Ogletree¹, Irfan Siddiqi^{1,2} and Adam Schwartzberg¹; ¹Lawrence Berkeley National Laboratory, United States; ²University of California, Berkeley, United States

Quantum computers are an inevitable need for energy efficiency in large scale computation and absolute information security demanded in both military and civil applications. Among the proposed platforms, superconducting qubit-based processors are leading candidates because of its scalability, gate speed, and microwave control. However, the realization of feasible quantum processors is inhibited prominently by the decoherence processes emerging from materials-inherent defects such as suboxides on Nb based superconducting qubits. In recent work, microwave losses scaling inversely with NbO_x thickness in Nb resonator devices has been demonstrated indicating the impact of the suboxides on coherence time. DFT calculations by Griffin et. al., shown that sub-stoichiometric Nb_2O_5 has paramagnetic phase that can be a source of the decoherence. In this work we investigated impact of Nb_2O_5 on coherence time by selectively eliminating Nb_2O_5 via oxygen scavenging by TiN deposited on resonators by atomic layer deposition. In comparison to Nb resonators with native oxide, TiN passivated resonators shows traces of Nb_2O_5 while NbO and NbO_2 persist on the Nb according to photoemission spectroscopy. Controlled selective reduction of Nb_2O_5 to NbO on Nb resonators hence mitigation of the associated defects with TiN passivation suggest a viable step towards development of the large-scale fault tolerant quantum processor.

11:00 AM EQ18.05.03

Using Superconductive Resonators to Characterize Charge Noise in Oxides Sueli Skinner Ramos, Rupert Lewis, William Kindel, Tzu-Ming Lu and Tom Harris; Sandia National Laboratories, United States

Solid state quantum information technologies are highly sensitive to material defects. In particular, charge centers at oxide interfaces have been shown to cause charge noise in electron-spin quantum dot qubits and negatively impact device yield, long-term stability, qubit coherence, and measurement fidelity. Semiconductor spin qubits are typically fabricated using standard metal-oxide-semiconductor gates to accumulate or deplete the two-dimensional electrons regions and localize single electrons in a quantum dot. These gates require an oxide layer, giving rise to two material-oxide interfaces that may contain charge defects that adversely affect the qubit performance. As such, thorough characterization of defects in an oxide layer interface is crucial for optimizing the behavior of quantum information devices. Several measurement techniques using operational qubits have already been established, however these techniques are limited in bandwidth and require long measurement times to fully characterize the charge noise spectrum of a single device. In this work we develop superconductive coplanar waveguide (CPW) resonators as a potentially much faster, scalable, and less expensive alternative charge-noise characterization technique to quantify the quality of oxides. To calibrate our technique, we present measurements of two different oxides, a high-quality

gate oxide and an oxide with intentional defects.

Funding Acknowledgment: SNL is managed and operated by NTESS under DOE NNSA contract DENA0003525

11:15 AM EQ18.05.04

Lessons Learned While Seeking Superconducting Al Doped Silicon [Joshua Pomeroy](#), Ke Tang, Karen A. DeRocher and Frederick Meisenkothen; National Institute of Standards and Technology, United States

Single crystal silicon, super-saturation doped with aluminum, has the promise of realizing superconductivity within a semiconductor with a transition temperature above 4 K, a substantial increase over similar demonstrations with boron and gallium, but is yet to be realized. In this talk, the process of saturation doping a clean silicon surface, overgrowing it with an encapsulating silicon layer and electrically activating the dopants is presented. Emphasis will be put on the determination of the surface-saturation doping density, found to be 3.4×10^{14} atoms/cm², which involves comparative measurements from scanning tunneling microscopy (STM), secondary ion mass spectroscopy (SIMS) and atom probe tomography (APT). Additional discussion on the electrical activation efficiency, low temperature transport modelling and prospects for increase the stable dopant atom density will be presented.

11:30 AM EQ18.05.05

Probing Sources of Decoherence at Interfaces in Superconducting Qubit Systems [Akshay A. Murthy](#), Mattia Checchin, Alexander Romanenko and Anna Grassellino; Fermi National Accelerator Laboratory, United States

Superconducting qubits have emerged as a potentially foundational platform technology for addressing complex computational problems deemed intractable with classical computing. Despite recent advances enabling multiqubit designs that exhibit coherence lifetimes on the order of hundreds of μ s, material quality and interfacial structures continue to curb device performance. When niobium is deployed as the superconducting material, two-level system defects in the thin film and adjacent dielectric regions introduce stochastic noise and dissipate electromagnetic energy at the cryogenic operating temperatures. In this study, through a combination of correlative electron microscopy imaging and diffraction methods and secondary ion mass spectrometry, we conduct a detailed investigation to disentangle the role specific fabrication procedures play in introducing such dissipation mechanisms in these complex systems. From these measurements, we find that during film deposition, oxide and silicide layers form at metal/substrate and metal/air interfaces and can reduce coherence times. Additionally, we observe that impurity species such as resistive niobium hydrides and carbides are incorporated within the niobium layer through the subsequent lithographic patterning steps, which impact the superconducting properties of the thin film. Armed with these findings, we seek to intelligently fabricate superconducting qubits and extend coherence times.

11:45 AM EQ18.05.06

Evolution of Tunneling Density of States in Nb/Al Based N/I/S Junctions with Al Thickness [Zachary Barcikowski](#)^{1,2} and [Joshua Pomeroy](#)²; ¹University of Maryland, United States; ²National Institute of Standards and Technology, United States

Nb/Al bilayers are of great interest for applications such as X-ray detectors or Josephson junctions where Al enables high-quality tunnel barrier fabrication and can be used to modify the Nb superconducting state. To investigate the evolution of the superconducting bilayer states with Al thickness, we fabricated a series of Nb/Al/AlOx/normal metal tunnel junctions with different Al thicknesses and measured the tunnel junction properties. Tunneling density of states spectra are presented in the regime of $T_{c, Nb} > T > T_{c, Al}$ and reveal larger zero-bias conductance than can be explained by a change in superconducting transition temperature with Al thickness alone. We model the data using the Blonder-Tinkham-Klapwijk (BTK) theory and discuss trends in BTK barrier strength, superconducting energy gap, and Dynes broadening as a function of Al film thickness and temperature.

12:00 PM *EQ18.05.07

Reproducible Materials Measurements for Superconducting Qubits and Resonators [Corey Rae H. McRae](#)^{1,2}; ¹University of Colorado Boulder, United States; ²National Institute of Standards and Technology, United States

Superconducting quantum circuits are a promising hardware implementation for large-scale quantum computing, but materials losses continue to significantly limit scalability and single-qubit performance. These cryogenic microwave materials losses can thus be characterized by coherence measurements of qubits and resonators. However, experimental factors such as thermalization, packaging, and microwave electronics have significant effects on these coherence measurements as well. In this talk, I outline a roadmap towards reproducible measurements of qubits and resonators and their further application to the investigation and characterization of materials losses.

SESSION EQ18.06: Ion Trap and Novel Qubits
Session Chairs: Susan Coppersmith and Shashank Misra
Tuesday Afternoon, December 7, 2021
EQ18-Virtual

1:00 PM *EQ18.06.01

The Influence of Material Choices on Trapped Ion Performance [Todd Barrick](#), B. K. McFarland, M. C. Revelle and D. L. Stick; Sandia National Laboratories, United States

Surface electrode ion traps permit the individual storage, manipulation, and optical addressing of atomic ions for applications such as highly sensitive sensors, atomic clocks, and quantum computing, to name a few. For these applications to be successful, one must have precise control over the quantum state of the ion, which includes its motional state during entangling operations. Therefore, the ion must be isolated from environmental perturbations like electric field noise which uncontrollably excite the motion of ions. Here, we study the influence of materials used in the fabrication of surface electrode ion traps and how they contribute to electric field noise that resonantly couples to the motional (secular) frequency of a trapped ion. In addition, we will also show experimental data that compares motional heating at different frequencies and with different capacitive grounding methods.

1:30 PM EQ18.06.03

First-Principles Study of sp³-doped (6,5) Single-Walled Carbon Nanotubes as a Potential Optically Interfaced Solid-State Spin Qubit [Kasidet Jing](#) [Trerayapiwat](#)¹, [Xuedan Ma](#)^{2,3} and [Sahar Sharifzadeh](#)^{1,1}; ¹Boston University, United States; ²Argonne National Laboratory, United States; ³The University of Chicago, United States

Single-walled carbon nanotubes (SWCNTs) doped with sp³ defects are a promising class of optoelectronic materials with bright tunable photoluminescence and demonstrated single-photon emission capability. Recently, we have shown that doping of (6,5) SWCNT via diazonium reaction results in an isolated electron spin with bright photoemission in the near-infrared range. In order to understand the spin-orbit coupling (SOC) and the spin decoherence mechanism in this material, we apply density functional theory (DFT) simulations, complemented by experiment, on a variety of sp³ defects attached to (6,5) SWCNT. We determine that doping the SWCNT with a heavy atom does not necessarily result in spin-orbit splitting in the near-gap states (a measure of SOC in the excited state) if there is no overlap between the unpaired spin and the metal's atomic orbitals; this overlap can be enforced by choosing a defect with a direct sp³ carbon-metal bond. Furthermore, the strength of spin-orbit splitting increases with reduction of the metal-tube separation or larger intrinsic SOC on the heavy atom. Additionally, we simulate dephasing by considering spin-bath interactions as the source of decoherence. We apply the cluster correlation expansion method with a pure-dephasing spin Hamiltonian to doped SWCNT in presence of water molecules at near 0 K and estimate the magnitude of T₂.

1:45 PM EQ18.06.04

Late News: Tailoring Quantum Oscillations of Excitonic Schrodinger's Cats as Qubits Amit Bhunia¹, Mohit Kumar Singh¹, Maryam Al Huwayz^{2,3}, Mohamed Henini² and Shouvik Datta¹; ¹IISER-Pune, India; ²The University of Nottingham, United Kingdom; ³Princess Nourah Bint Abdulrahman University, Saudi Arabia

We report [<https://arxiv.org/abs/2107.13518>] experimental detection and control of Schrodinger's Cat like macroscopically large, quantum coherent state of a two-component Bose-Einstein condensate of spatially indirect electron-hole pairs or excitons using a resonant tunneling diode of III-V Semiconductors. This provides access to millions of excitons as qubits to allow efficient, fault-tolerant quantum computation. In this work, we measure phase coherent periodic oscillations in photo-generated capacitance as a function of applied voltage bias and light intensity over a macroscopically large area. Periodic presence and absence of splitting of excitonic peaks in the optical spectra measured by photocapacitance point towards tunneling induced variations in capacitive coupling between the quantum well and quantum dots. Observation of negative 'quantum capacitance' due to screening of charge carriers by the quantum well indicate Coulomb correlations of interacting excitons in the plane of the sample. We also establish that coherent resonant tunneling in this well-dot heterostructure restricts the available momentum space of the charge carriers within this quantum well. Consequently, the electric polarization vector of the associated indirect excitons collectively orients along the direction of applied bias and these excitons undergo Bose-Einstein condensation below ~100 K. Generation of interference beats in photocapacitance oscillation even with incoherent white light further confirm the presence of stable, long range spatial correlation among these indirect excitons. We finally demonstrate collective Rabi oscillations of these macroscopically large, 'multiparticle', two-level, coupled and uncoupled quantum states of excitonic condensate as qubits. Therefore, our study not only brings the physics and technology of Bose-Einstein condensation within the reaches of semiconductor chips, but also opens up experimental investigations of the fundamentals of quantum physics using similar techniques.

Operational temperatures of such two-component excitonic BEC can be raised further with more densely packed, ordered array of QDs and/or using materials having larger excitonic binding energies. However, fabrications of single crystals of 0D-2D heterostructures using 2D materials (e.g. transition metal di-chalcogenides, oxides, perovskites etc.) having higher excitonic binding energies are still an open challenge for semiconductor optoelectronics. As of now, these 0D-2D heterostructures can already be scaled up for mass production of miniaturized, portable quantum optoelectronics devices using the existing III-V and/or Nitride based semiconductor fabrication technologies.

SESSION EQ18.07: Semiconductor Qubits III
Session Chairs: Nico Hendrickx and Vincenzo Lordi
Wednesday Morning, December 8, 2021
EQ18-Virtual

8:00 AM *EQ18.07.01

Quantum Computing with Spins in Germanium Nico Hendrickx; QuTech and Kavli Institute of Nanoscience, Delft University of Technology, Netherlands

The prospect of building quantum circuits using advanced semiconductor manufacturing techniques position quantum dots as an attractive platform for quantum information processing. Initial demonstrations of one and two-qubit logic have been performed in gallium arsenide and later silicon. However, until recently, interconnecting larger spin qubit systems has remained a challenge.

Over the past years, hole states in strained germanium quantum wells have emerged as a host for spin qubits. These states have favourable properties for defining extended spin qubit arrays. The small effective mass relaxes constraints on lithography, the low degree of disorder enables reproducible quantum dots, the lack of a valley degeneracy ensures a well-defined qubit state and the strong spin-orbit coupling allows for local and electrical qubit control.

Within four years time, this platform [1] has rapidly evolved from materials growth to supporting multi-qubit logic [2]. In this talk, I will discuss our group's efforts on the development of this system, starting from material growth and characterization [3] to our recent results on operating a highly-connected two-dimensional qubit array [4]. We implement qubit logic all electrically and the exchange interaction can be pulsed independently to freely program one, two, three, or four qubit gates. Furthermore, we show that we can extend the quantum coherence by several orders of magnitude by implementing dynamical decoupling. All these techniques are combined to perform a quantum circuit that generates a four-qubit Greenberger-Horne-Zeilinger state, showcasing coherent operation of all four qubits together. This positions strained germanium as a unique material for quantum applications. I will furthermore discuss strategies, challenges, and opportunities in scaling these systems up as a step towards the realization of scalable qubit tiles for fault-tolerant quantum processors.

[1] Scappucci, G. et al. *The germanium quantum information route*. Nature Reviews Materials (2020);

[2] Hendrickx N.W. et al. *Fast two-qubit logic with holes in germanium*. Nature **577** 487-491 (2020);

[3] Sammak, A. et al. *Shallow and Undoped Germanium Quantum Wells: A Playground for Spin and Hybrid Quantum Technology*. Advanced Functional Materials **29** 14 (2019);

[4] Hendrickx N.W. et al. *A four-qubit germanium quantum processor*. Nature **591** 580-585 (2021).

8:30 AM *EQ18.07.02

Manipulation of Three-Spin States in a Si/SiGe Triple Quantum Dot Kenta Takeda; RIKEN, Japan

Semiconductor quantum dots are one of the most promising platforms for quantum computing due to their nanofabrication capability for scaling-up. Recent technical advances have enabled high-fidelity one- [1,2] and two-qubit [3] gates for spins in quantum dots. The next crucial step toward scaling up is the demonstration of genuinely multipartite entanglement, an essential resource for quantum error correction. This requires at least three qubits with the full capabilities of control and measurement, a lot further than individual qubit manipulation. In this talk, we first show individual initialization, measurement, and universal manipulation of three electron spins in our Si/SiGe triple quantum dot device. Second, we show generation and characterization of a three-qubit Greenberger–Horne–Zeilinger state, a type of maximally entangled state that is usable to implement a bit-flip or phase-flip quantum error correcting code. We obtain a state fidelity of 88.0 % by quantum state tomography, which witnesses a genuine three-qubit entanglement. We anticipate that our results will enable exploration of multi-spin correlations and demonstration of multi-qubit algorithms in scalable silicon-based quantum computing devices.

[1] J. Yoneda et al., Nat. Nanotechnol. 13, 102–106 (2018).

[2] C. H. Yang et al., Nat. Electron. 2, 151–158 (2019).

[3] W. Huang et al., Nature 569, 532–536 (2019).

9:00 AM EQ18.07.03

Can Plasma Oxidized AlO_x SETs Detect Charge Motion on Silicon MOS Quantum Dots? Yanxue Hong^{1,2}, Kyungjean Min², M. D. Stewart, Jr.² and Joshua Pomeroy²; ¹University of Maryland, United States; ²National Institute of Standards and Technology, United States

The design and development of charge stable, plasma oxidized Al/AIO_x/Al single-electron transistors (SETs) for use as charge sensors in single metal layer gated silicon MOS quantum dots will be presented, extending an integrated architecture that enables fabricating both devices simultaneously. In previous work, we achieved long-term charge offset stability (best $\Delta Q_0 = 0.13 e \pm 0.01 e$ over 7.6 days) by using plasma oxidized AlO_x as tunnel barriers in Al/AIO_x/Al SETs [1], and persistent charge sensing (SNR > 5) of controllable quantum dots on single metal gate layer silicon MOS quantum dot devices [2]. By calculation, the required minimum coupling capacitance between these two devices is approximately 2.8 aF for the AlO_x SET to detect the charge motion on the MOS quantum dot. Here we will present the design of streamlined fabrication process of fabricating Al/AIO_x/Al SETs and MOS quantum dots simultaneously, preliminary modeling and calculations for charge sensing feasibility of vertically and laterally aligned configurations. This integrated architecture is expected to be useful as a diagnostic qubit platform for simplifying the process flow, testing gate materials and tunnel barrier materials, and detecting oxide interface defects, etc.

References:

[1] Hong, Yanxue, et al. "Reduction of charge offset drift using plasma oxidized aluminum in SETs." *Scientific reports* 10.1 (2020): 1-9.

[2] Hong, Yanxue, et al. "Developing single-layer metal-oxide-semiconductor quantum dots for diagnostic qubits." *Journal of Vacuum Science & Technology B, Nanotechnology and Microelectronics: Materials, Processing, Measurement, and Phenomena* 39.1 (2021): 012204.

9:15 AM EQ18.07.04

Defect Detection in Silicon-on-Insulator Transistors for Quantum Information Systems Philippe Ferrandis^{1,2,3}, Thomas Bédécarrats^{4,2} and Mikael Cassé^{4,2}; ¹Université de Toulon, France; ²Univ.Grenoble Alpes, France; ³Institut Néel, France; ⁴CEA, France

Among promising materials for the realization of future quantum processors, silicon has several assets. A silicon quantum bit (qubit) device can be performed with an industry-standard fabrication process and allows a co-integration with classical control hardware [1]. However, an excellent control of carrier transfer in the channel of the transistor is required, ruling out any electrical active defects, which could act as recombination centers. Such an optimization of the device necessitates a fine characterization of the channel to evaluate the purity of the material.

In this work, we investigate the presence of defects in the channel of a fully depleted silicon-on-insulator (FDSOI) transistor designed for qubit applications. A buried oxide of 145 nm formed on a silicon substrate is covered by an 11 nm thick unintentionally doped silicon channel. A SiO₂/HfSiON bilayer and a TiN metallic electrode compose the gate. P-doped source and drain contact regions were realized by implantation. A Si₃N₄ layer is used to passivate uncovered silicon areas. To enlarge the capacitance of the gate and allow measurements, 111 cells were connected in parallel.

The ON state of the transistor is achieved by applying a negative voltage to the gate. Source and drain electrodes were connected together and voltage pulses were applied to the gate contact to perform capacitance deep level transient spectroscopy (DLTS) measurements between 77 K and 350 K. A depleted section of the channel extends beneath the gate and towards the source and drain regions when applying a positive voltage to the gate contact. By tuning a positive reverse bias and negative voltage pulses, we were able to probe the channel and localize the electrical active defects responsible for the DLTS signal.

Three hole traps, labelled H1, H2 and H3, were detected by DLTS at respectively 0.54 eV, 0.57 eV and 0.65 eV above the valence band edge. The apparent capture cross sections of these levels are respectively $7.9 \times 10^{-16} \text{ cm}^2$, $2.4 \times 10^{-14} \text{ cm}^2$ and $3.3 \times 10^{-12} \text{ cm}^2$. H1 and H2 are donor-like states whereas H3 is an acceptor-like state.

Electrical simulations using Synopsys demonstrated that the DLTS probed zone is nearby gate edges and extends towards the source and drain contacts when the gate voltage changes from 0 V to 1 V. According to this feature, all traps have been localized very close to the source and drain implanted zones. The origin of these traps is likely related to damages produced during the formation of the p-doped regions and are assigned to bulk [2] and Si/SiO₂ interface defects [3].

In the temperature range 77 K – 350 K, no traps have been detected in the active region, i.e. below the gate contact. Finally, this investigation highlights the good quality of the channel material and the ability of the studied FDSOI transistor to work as a qubit device.

[1] R. Maurand et al., Nat. Commun. 7, 13575 (2016)

[2] E. Fretwurst et al., Nucl. Instr. and Meth. in Phys. Res. A 388, 356 (1997)

[3] E. Simoen et al., Phys. Status Solidi C 13, 718 (2016)

9:30 AM EQ18.07.05

Atomic-Level Origin of Valley Splitting Variations in Silicon Quantum Dots Brian Paquelet Wuetz¹, Merritt Losert², Sebastian Koelling³, Lucas Stehouwer¹, Anne-Marije Zwerver¹, Stephan Philips¹, Mateusz Madzik¹, Nodar Samkharadze⁴, Xiao Xue¹, Gouji Zheng¹, Sergey Amitonov¹, Mario Lodari¹, Amir Sammak⁴, Lieven Vandersypen¹, Susan Coppersmith⁵, Oussama Moutanabbir³, Mark Friesen² and Giordano Scappucci¹; ¹TU Delft, Netherlands; ²University of Wisconsin–Madison, United States; ³Polytechnique Montréal, Canada; ⁴TNO, Netherlands; ⁵University of New South Wales, Australia

²⁸Si/SiGe heterostructures provide a compelling host material for a scalable quantum computer, due to the long coherence times of electron spin qubits and compatibility with industry. Here we study ²⁸Si/SiGe heterostructures characterized by different roughness of the critical Si/SiGe quantum well interface to understand the energy splitting of the lowest lying conduction valleys (valley splitting). To improve control of valley splitting in ²⁸Si/SiGe, we implement a feedback loop for materials stack engineering which includes several elements. We use atom probe tomography to provide atomic 3D reconstruction of the material stack and statistical understanding of compositional variations at the Si/SiGe interface over nanoscale dimensions relevant for qubits in quantum

dots. We feed the resulting data into a tight binding model to compute the valley splitting in real quantum wells and dots with varying quantum well thickness, Si/SiGe interface width, and interface chemical roughness. We complete the feedback loop by comparing the obtained simulation results with the valley splitting measured in heterostructure field effect transistors and quantum dots, making use of cryomultiplexer technology for achieving statistical significant metrics with high-throughput. We envision that such a feedback cycle - consisting of atomic understanding of the critical material stack interfaces fed into device modelling and high-throughput cryogenic measurements- may help to engineer optimal stacks for large and controlled values of valley splitting in Si/SiGe.

SESSION EQ18.08: Topological Qubits II
Session Chair: Shashank Misra
Wednesday Morning, December 8, 2021
EQ18-Virtual

10:30 AM EQ18.08.01

High-Throughput Search for Magnetic Topological Materials Using Spin-Orbit Spillage, Machine Learning and Experiments [Kamal Choudhary](#); National Institute of Standards and Technology, United States

Magnetic topological insulators and semimetals have a variety of properties that make them attractive for applications, including spintronics and quantum computation, but very few high-quality candidate materials are known. In this paper, we use systematic high-throughput density functional theory calculations to identify magnetic topological materials from the 40000 three-dimensional materials in the JARVIS-DFT database. First, we screen materials with net magnetic moment $>0.5\mu_B$ and spin-orbit spillage (SOS) >0.25 , resulting in 25 insulating and 564 metallic candidates. The SOS acts as a signature of spin-orbit-induced band-inversion. Then we carry out calculations of Wannier charge centers, Chern numbers, anomalous Hall conductivities, surface band structures, and Fermi surfaces to determine interesting topological characteristics of the screened compounds. We also train machine learning models for predicting the spillages, band gaps, and magnetic moments of new compounds, to further accelerate the screening process. We experimentally synthesize and characterize a few candidate materials to support our theoretical predictions.

10:45 AM EQ18.08.02

Unconventional Magnetism and Spin Dynamics in the Frustrated Triangular Lattice Antiferromagnet Ba_2MnTeO_6 [Joydev Khataua](#)^{1,2,3}, T. Arh^{4,5}, Shashi B Mishra¹, H. Luetkens⁶, A Zorko^{4,5}, B. Sana¹, M. S. Ramachandra Rao^{7,2}, B. R. K. Nanda^{1,1,3} and P Khuntia^{1,2,3}; ¹Indian Institute of Technology Madras, India; ²Quantum Centre for Diamond and Emergent Materials, Indian Institute of Technology Madras, India; ³Functional Oxide Research Group, Indian Institute of Technology Madras, India; ⁴Jozef Stefan Institute, India; ⁵University of Ljubljana, Slovenia; ⁶Paul Scherrer Institute, Switzerland; ⁷Nano Functional Materials Technology Centre and Materials Science Research Centre, Indian Institute of Technology Madras, India

Frustrated magnets wherein complex interplay between emergent degrees of freedom, macroscopic ground state degeneracy and competing magnetic interactions can lead to correlated quantum phenomena with exotic excitations highly relevant for potential technological applications. We present thermodynamic, and muon spin relaxation (μ SR) measurements accompanied by density functional theory (DFT) results on the double-perovskite Ba_2MnTeO_6 in which Mn ions constitute a perfect triangular lattice. Magnetic susceptibility and specific heat data show the presence of a phase transition at $T_N = 21$ K. The magnetic specific heat result infers the presence of antiferromagnetic magnon excitations with a gap of 1.4 K below T_N . μ SR reveals the presence of static internal magnetic field below T_N and short-range spin correlations high above T_N . Furthermore, critical slowing-down of spin dynamics at T_N and the persistence of spin dynamics even in the magnetically ordered state have been detected by μ SR. Three-dimensional magnetic ordering in this frustrated magnet is attributed to the presence of a weak ferromagnetic inter-layer interaction.

11:00 AM EQ18.08.03

Quantum Anomalous Hall Insulators for Topological Quantum Computing [Igor Altfeder](#)¹, Robert Walko¹, Albert Davydov², Seng Huat Lee³, Zhiqiang Mao³ and Alexander Balatsky²; ¹The Ohio State University, United States; ²National Institute of Standards and Technology, United States; ³The Pennsylvania State University, United States; ⁴University of Connecticut, United States

Bound states of electric charge and magnetic monopole are anticipated to behave as anyons, i.e. 2D quantum states obeying fractional statistics. Image magnetic monopoles can be induced in topological systems with broken time-reversal symmetry, such as quantum Hall (QH) and quantum anomalous Hall (QAH) insulators, using a point charge located above the surface. In our experiments with the QAH insulator, charge-monopole composite is produced by the electric field of scanning tunneling microscope (STM) tip, which confines the current vortex of monopole inside ~ 1 nm radius quantum dot. Our studies are performed using magnetic topological insulator $MnBi_2Te_4$ whose surface is modified by STM-lithography to prepare room temperature QAH state displaying unusually high Chern number. We found a rich spectrum of many-body effects and nonlinear behavior manifested in the trapping of tunneling electrons by the current vortex and interaction of monopole with the Mn spin subsystem. High-Chern-number charge-monopole composites are anticipated to be non-Abelian anyons with potential applications in fault-tolerant topological quantum computing.

11:15 AM EQ18.08.04

Performing Sensitive Broadband Microwave Spectroscopy on μ m-scale Materials [Antonio L. Levy](#), Zachary S. Barcikowski, Joshua Pomeroy, Pradeep Nambodiri, Rick Silver and Neil M. Zimmerman; National Institute of Standards and Technology, United States

We have developed a new simple broadband microwave spectroscopy technique for μ m-scale flakes in which, unlike existing techniques, μ m-scale flakes effect orders-of-magnitude (>30 dB) changes in the transmissivity without requiring sophisticated sample preparation or measurement techniques. Broadband microwave spectroscopy is a sensitive probe of the physics of material systems which has been used to study novel physics of mm-scale thin film material systems, such as ordered electron phases, superconductors, and metal-insulator transitions. In recent years, interesting materials have emerged which are only available as μ m-scale flakes, and whose novel physics might be better understood through broadband microwave spectroscopy; examples include twisted bilayer graphene [4], 2D materials in which many-body phases are observed [5], and artificial lattices for analog quantum simulations [6]. With most current GHz broadband spectroscopy techniques, the signal for smaller (μ m-scale) flakes is too weak to be useful [1, 2, 3].

In the new technique, a CPW containing a series gap in the signal line over the flake is fabricated on the chip, and the transmission spectrum is measured. The spectra are then normalized, we can immediately see spectral features, and we can also extract the complex conductivity. We present results from proof-of-principle experiments conducted for μ m-scale P^+ monolayer regions encapsulated in Si, whose conductivity spectrum is expected to be constant in frequency for microwave frequencies. These results show a broadband change in the transmissivity of more than 40 dB, indicating the ability to perform

sensitive contact-free conductivity spectroscopy on μm -scale flakes. We then show through theory and simulations that one will be able to qualitatively measure spectral features of interest, and quantitatively deduce the frequency-dependent complex conductivity. These experimental and theoretical results show that this technique could make profound contributions to the characterization of 2D materials in the coming years.

References

- [1] L. W. Engel, *et al.* Solid State Comms. 104 167 (1997)
- [2] Y. Oamura *et al.* Phys. Rev. Lett. 122 057202 (2019)
- [3] K. Steinberg *et al.* Phys. Rev. B 77 214517 (2008)
- [4] Y. Cao, *et al.* Nature 556 43 (2018)
- [5] S. Chen *et al.* Phys. Rev. Lett. 122. 026802 (2019)
- [6] J. Salfi *et al.* Nat. Comms. 7 1 (2016)

11:30 AM EQ18.08.05

Quantum Simulations with P-Doped Silicon Nanostructures Maicol A. Ochoa^{1,2}, Keyi Liu^{1,2}, Emily Townsend^{1,2}, Michal Gawelczyk³, Michal Zielinski³ and Garnett Bryant^{1,2}; ¹National Institute of Standards and Technology, United States; ²University of Maryland, United States; ³Nicolaus Copernicus University, Poland

Atomically precise phosphorus-doped silicon nanostructures that incorporate few-atom arrays are attractive architectures for the solid-state implementation of quantum computing technologies and quantum simulations. These devices readily integrate with traditional electronic devices and can be fabricated to control critical properties, such as tunnel couplings and on-site charging energies. Furthermore, single-electron transport and quantum control of the electronic state is possible using atomically aligned gates, source, and drain contacts. Significantly, few-atom devices arranged in any number of different geometries are ideal for exploring a variety of many-body physics effects. This talk presents atomistic calculations and a detailed analysis of the many-electron states and transport properties of devices with two and four P atoms. In particular, we investigate mappings of these systems into the extended range Fermi-Hubbard model and study how the model parameters vary with the array's geometry and electron number. Our approach consists of self-consistent solutions to the Schrodinger-Poisson equations and incorporates the effect of the silicon matrix, electron-electron interactions, and corrections due to exchange and correlation. We also carry out transport calculations beyond the mean-field treatment by using the non-equilibrium Green functions based on the extended Fermi-Hubbard many-electron eigenstates to calculate Coulomb blockade diagrams. By comparing the predictions made with the Fermi-Hubbard model with the results of our detailed atomistic calculations for different dopant geometries, we show when exchange and correlation effects and coupling to higher energy orbitals missing in the Fermi-Hubbard model become important in predicting the stability diagrams of these devices.

11:45 AM EQ18.08.06

Disorder Induced Phase Transitions in Magnetic Topological Insulators Swarnava Ghosh and Markus Eisenbach; Oak Ridge National Laboratory, United States

Topological insulators are a class of quantum materials that have gaps in the bulk but metallic edge or surface states, which are protected by time reversal symmetry. Long-range magnetic order in a topological insulator can break the time reversal symmetry, open an exchange gap in the surface states, thereby leading to exotic topological quantum phenomena. Just like ordinary materials, defects are also omnipresent in topological insulators. The concentration of defects are low; few parts per million for vacancies to few percent for dopants. This makes first principles simulations of defects at realistic concentrations extremely challenging due to the large cell sizes required. We use the Locally Self Consistent Multiple Scattering (LSMS) code to solve the Kohn-Sham equations at realistic concentrations of disorder in the intrinsic magnetic topological insulator MnSb_2Te_4 . We present the role of disorder such as doping and site-mixing on the magnetic ground state of the intrinsic magnetic topological insulator MnSb_2Te_4 . Our results show magnetism can be tuned by carefully controlling the concentration of defects in MnSb_2Te_4 .

Acknowledgements:

This research was funded in part by the U. S. Department of Energy, Office of Science, Basic Energy Sciences, Materials Sciences and Engineering Division and it used resources of the Oak Ridge Leadership Computing Facility, which is supported by the Office of Science of the U.S. Department of Energy under Contract No. DE-AC05-00OR22725.

SESSION EQ18.09: Topological Qubits III
Session Chairs: Pengzi Liu and Shashank Misra
Wednesday Afternoon, December 8, 2021
EQ18-Virtual

1:00 PM EQ18.09.01

Synthesis of Narrow SnTe Nanowires Using Alloy Nanoparticles Pengzi Liu^{1,2}, Hyeuk Jin Han^{1,2}, Julia Wei¹, David Hynek^{1,2}, James L. Hart^{1,2}, Myung Geun Han³, Christie J. Trimble^{4,4}, James Williams^{4,4,4}, Yimei Zhu³ and Judy Cha^{1,2,5}; ¹Yale University, United States; ²Yale West Campus, United States; ³Brookhaven National Laboratory, United States; ⁴University of Maryland, United States; ⁵Canadian Institute for Advanced Research Azrieli Global Scholar, Canada

The last decade has witnessed substantial progress in probing topological states of matter whose wavefunctions possess a distinct topological invariant signature barring adiabatic deformation from a trivial phase to a non-trivial phase [1]. The search for topological materials is of profound scientific significance and will have applications for spintronics, low-dissipation electronics and quantum computing. Particularly, one dimensional (1D) topological superconductor systems, which are predicted to host localized Majorana bound states (MBSs), can be leveraged for fault-tolerant and scalable topological quantum computing. However, realizing 1D topological superconductors is challenging in synthesis of topological nanowires with sufficiently good sample quality, which can reveal and control the topological properties. Careful studies on precise control of the morphology and dimensions of topological nanowires along the axial and radial directions remain sparse.

In this work, we developed a reliable vapor-liquid-solid (VLS) route to synthesize narrow SnTe nanowires with diameters under 100 nm using Au-Sn-Te alloy nanoparticles as growth catalysts with high yield [2]. Experimentally, this was achieved by performing CVD growths twice. In the first growth, gold nanoparticles react with SnTe vapor to form alloy nanoparticles. In the second growth, the alloy nanoparticles catalyze the growth of narrow SnTe nanowires. The average diameter of the SnTe nanowires grown using alloy nanoparticles is 85 nm, in contrast to the 240 nm obtained using gold

nanoparticles. Transport measurements showed a diameter-dependent residual resistance ratio and magnetoresistance.

We also observed that the ferroelectric transition temperature of SnTe nanowires is diameter-dependent, whose trend suggests that the carrier density decreases for narrower nanowires, likely due to the removal of bulk electron carriers. *In situ* cryogenic transmission electron microscopy (cryo-TEM) experiments down to 25 K confirmed the expected structural transition from the room-temperature cubic phase to the low-temperature rhombohedral phase for these SnTe nanowires. Electron diffraction data and TEM images at 25 K show there are two crystallographic orientations for the low-temperature rhombohedral domains in these SnTe nanowires. Simulation results suggest that both 109 and 71° domain walls are possible to explain our observations. The narrow SnTe nanowires are important to study the nature of the superconductivity induced in these nanowires, which was recently suggested to have a pairing symmetry of $s \pm is$ via Josephson junction measurements [3]. They also serve as a model system for the investigation of possible multiband superconductivity, Majorana bound states, and the interplay between ferroelectricity and topological orders.

1. Qi, X.-L. and S.-C. Zhang, *Topological insulators and superconductors*. Reviews of Modern Physics, 2011. **83**(4): p. 1057-1110.
2. Liu, P., et al., *Synthesis of narrow SnTe nanowires using alloy nanoparticles*. ACS Applied Electronic Materials, 2021. **3**(1): p. 184-191.
3. Trimble, C.J., et al., *Josephson detection of time-reversal symmetry broken superconductivity in SnTe nanowires*. npj Quantum Materials, 2021. **6**(1): p. 61.

1:15 PM EQ18.09.02

Coexistence of Superconductivity, Fluctuations and Spin-Orbit Splitting in $\text{Sn}_{1-x}\text{In}_x\text{Te}$ Thin Film [Jiashu Wang](#), William Powers, Seul-Ki Bac, Logan Riney, Maksym Zhukovskiy, Tatjana Orlova, Xinyu Liu and Badih Assaf; University of Notre Dame, United States

SnTe is identified to be a topological crystalline insulator, whose surface states are protected by crystal mirror symmetry. It has been recently found that by In doping, $\text{Sn}_{1-x}\text{In}_x\text{Te}$ (SIT) can be superconducting and also maintains its topological surface states. However, the non-trivial character of superconductivity in SIT remains debated. Most previous research of SIT was focused on single crystals. The growth and analysis of SIT thin films are necessary to search for boundary Majorana states. Here, we investigated the MBE growth of $\text{Sn}_{1-x}\text{In}_x\text{Te}$ ($x=0.05-0.3$) thin films (~100nm) on BaF_2 (111), and characterized them by X-ray diffraction, Transmission electron microscopy and magneto-transport measurement. A superconducting transition is consistently observed in films, and the critical temperature T_c increases as we increase the In concentration up to 3.5K. Hall measurements show that In is more likely to act as an electron donor instead of an acceptor as reported in earlier works on single crystal. The normal state is shown to host coexisting weak localization (WL) and weak antilocalization (WAL), analyzed using a 2D Hikami Larkin Nagaoka model. The WL only occurs in superconducting samples, indicating that electrons from trivial spin-orbit split states may play a dominant role in the superconducting state. Close to but above T_c , a signature of Maki-Thompson superconducting fluctuations is also observed. Overall, our findings motivate further experiments to find the origin of a possible spin-orbit splitting and study its impact on the pairing symmetry of $\text{Sn}_{1-x}\text{In}_x\text{Te}$. Work supported by NSF-DMR-1905277.

1:30 PM *EQ18.09.03

Mobility and Spin Orbit in InAs Heterostructures [Maja Cassidy](#); Microsoft Quantum, Australia

Semiconductor heterostructures based on III-V materials such as InAs are candidate systems for realizing a topological quantum computer based on Majorana zero modes due to their high mobility, strong spin-orbit interaction, and ability to be proximitized by a nearby superconductor. While each of these components can be realized alone, combining them into a single device exhibiting all effects simultaneously and reproducibly remains a significant engineering challenge. In this talk, I will discuss materials processing that limits mobility in InAs 2DEG quantum wells during device fabrication, and discuss strategies for increasing this mobility by repairing the semiconductor-dielectric interface. I will also discuss the effect that these fabrication processes have on the spin orbit coupling within these heterostructures, and pathways to maximizing both mobility and spin orbit in a device.

2:00 PM EQ18.09.04

Heteroepitaxy of Dirac Semimetal Cd_3As_2 by Metal-Organic Chemical-Vapor Deposition [Anthony Rice](#), Christopher R. Tait, Steven Lee, Julia Deitz, Mark Rodriguez, Wei Pan, Taisuke Ohta, Darrell Alliman, Gregory Peake, Annette Sandoval, Nichole Valdez and Paul Sharps; Sandia National Laboratories, United States

We present progress on the synthesis of semimetal Cd_3As_2 by metal-organic chemical-vapor deposition (MOCVD). Specifically, we have optimized the growth conditions needed to obtain technologically useful growth rates and acceptable thin-film microstructures, with our studies evaluating the effects of varying the temperature, pressure, carrier-gas type, and group-V:II molar flow ratio for MOCVD of Cd_3As_2 when performed using dimethylcadmium and tertiarybutylarsine precursors. In the course of the optimization studies, exploratory Cd_3As_2 growths have been carried out on GaSb substrates, InAs substrates, strain-relaxed InAs buffer layers grown on GaSb substrates, and near-lattice-matched AlGaAsSb-alloy buffer layers grown on GaSb substrates. Notably, the InAs-terminated substrate surfaces yield desirable, nearly epitaxial results, while the pure GaSb surfaces instead yield laterally nonuniform, poor-quality, polycrystalline results. For the films presenting epitaxially on InAs, two different growth regimes are seen that depend strongly on the V:II ratio. For Cd_3As_2 thin films grown at a lower V:II ratio near 1.7, extensive microstructural studies have been performed by using multiple advanced imaging microscopies and x-ray diffraction (XRD) modalities. The as-grown films are 5-75 nm in thickness and consist of highly oriented, coalesced polycrystals with lateral domain widths of 30-80 nm. The most optimized films are smooth and specular, exhibiting a surface roughness as low as 1.0 nm rms. Under cross-sectional imaging, the Cd_3As_2 -InAs heterointerface appears smooth and abrupt at a lower film thickness, ~30 nm, but becomes quite irregular as the average thickness increases to ~55 nm. The films are strain-relaxed with a residual biaxial tensile strain ($\epsilon_{xx} = +0.0010$) that opposes the initially compressive lattice-mismatch strain of Cd_3As_2 coherent on InAs ($\epsilon_{xx} = -0.042$). For more recent Cd_3As_2 thin-film growths done at a higher V:II ratio near 8.0, there appears to be a substantially improved thin-film microstructure, with thickness fringes emerging in both XRD 2theta-omega scans and x-ray reflectivity scans, which are absent for the growths at lower V:II ratio. Further microstructural characterization of the higher-V:II-ratio films remains as work in progress. Importantly, phase-identification studies find a thin-film crystal structure consistent with the $P4_2/nbc$ space group for growth at the lower V:II ratio; in contrast, the space group appears to change to either $I4_1cd$ or $I4_1acd$ for growth at the higher V:II ratio. These observed space groups place MOCVD-grown Cd_3As_2 among the Dirac semimetals of substantial interest for topological quantum materials studies. Our presentation will highlight selected results from the above-described research to grow Cd_3As_2 thin films by MOCVD, with a focus on growth-parameter trends, microstructural characterization, and electronic properties.

Supported by the Laboratory Directed Research and Development program at Sandia National Laboratories, a multimission laboratory managed and operated by National Technology and Engineering Solutions of Sandia, LLC., a wholly owned subsidiary of Honeywell International, Inc., for the U.S. Department of Energy's National Nuclear Security Administration under contract DE-NA-0003525.

2:15 PM EQ18.09.05

Collective Mode Spectroscopy of Unconventional Superconductors [Nicholas Poniatowski](#), Jonathan Curtis, Amir Yacoby and Prineha Narang; Harvard University, United States

The study of unconventional superconducting states remains at the forefront of condensed matter physics research, driven in large part by the desire to understand the superconducting ground states of novel quantum materials. One of the defining features of any superconducting state is its collective mode spectrum, which encodes the dynamics of the order parameter. We will discuss how one can leverage the collective mode spectrum of unconventional superconducting states to gain new insights into their order parameter symmetry, making use of existing experimental probes [1,2]. In particular, we will discuss the existence and possible detection of a unique class of collective modes which can be used to identify and characterize time-reversal symmetry breaking superconductors [3].

References

- [1] R Shimano & N Tsuji, *Annu. Rev. Condens. Matter Phys.* 11, 103 (2020)
- [2] L Schwarz, et al., *Nat. Comm.* 11 287 (2020)
- [3] N Poniatowski, et al., arXiv:2103.05641

2:30 PM EQ18.09.06

Characterization of In_{1-x}Mn_xAs/GaSb Quantum Wells by Shubnikov de Haas Oscillations and Cyclotron Resonance Logan Riney¹, Xinyu Liu¹, Joaquin B. Ortiz², Roland Winkler^{3,4}, Jiashu Wang¹, Seul-Ki Bac¹, Louis-Anne DeVaulchier², Yves Guldner², Tatyana Orlova¹, Maksym Zhukovskiy¹, Margaret Dobrowolska¹, Jacek K. Furdyna¹ and Badih Assaf¹; ¹University of Notre Dame, United States; ²École Normale Supérieure, France; ³Northern Illinois University, United States; ⁴Argonne National Laboratory, United States

At the interface of InAs/GaSb, the broken gap alignment leads to an anti-crossing between the InAs s-like conduction levels and the GaSb p-like valence levels. The hybridization of these levels cause a topological gap to open. The observation of the quantum anomalous Hall effect (QAHE) is expected to occur if the s-p ordering is inverted (non-trivial) for one spin species and trivial for the other, which can be achieved through the introduction of magnetism into system. In this work, we characterize a series of Mn doped InAs/GaSb type-II quantum wells. We show the successful growth of 15nm InAs/ 10nm GaSb quantum wells using transition electron microscopy (TEM). Using SQUID magnetometry, we find the samples host a paramagnetic order. Robust SdH oscillations and Hall quantization between 1.5K and 50K are observed in magneto-transport. We perform magneto-optics up to 15T to measure the cyclotron mass. We report a discrepancy between the carrier mass calculated from SdH oscillations and cyclotron resonance. The manifestation of paramagnetism in this system makes it an ideal platform for measuring the magnetic exchange interaction.

SYMPOSIUM EQ19

Diamond and Diamond Heterojunctions—From Growth to Applications
November 30 - December 7, 2021

Symposium Organizers

Anke Krueger, Julius-Maximilians-Universität Würzburg
Emmanuel Scorsone, Commissariat à l'énergie atomique et aux énergies alternatives
Mariko Suzuki, University of Cádiz
Oliver Williams, Cardiff University School of Physics and Astronomy

* Invited Paper

SESSION EQ19.01: Surfaces and Characterization
Session Chair: Emmanuel Scorsone
Tuesday Morning, November 30, 2021
Hynes, Level 1, Room 101

10:30 AM *EQ19.01.01

Diamond Interfaces by TEM Castro P. Villar¹, Beatriz Soto¹, Gonzalo Alba¹, Jesus Canas², José C. Piñero¹, Javier Navas¹, Marina Guitiérrez¹, Josep Montserrat³, Philippe Godignon³ and Daniel Araujo¹; ¹Universidad de Cádiz, Spain; ²Institute Néel-CNRS, France; ³Centro Nacional de Microelectrónica - CSIC, Spain

Despite the superior Baliga's figure of merit of diamond with respect to other wide band gap materials [1], it is still not extensively used for electronic devices, in general, or power electronic devices, in particular. Aspects such as size of diamond substrates, extreme mechanical hardness, capability of getting high quality n-type doped layers or reproducibility of high quality growings are some of the reasons that make difficult to implement diamond in power electronics market and constitute a set of challenges to overcome in the manufacture of devices. But not only this, manufacture also involves deposition of other materials on diamond grown layers, as oxides gates for MOS transistors, metals for ohmic or Schottky contacts, which not always are well controlled. In addition, diamond surface termination is also determinant in how all these materials are finally bounded to diamond. Indeed, electrical characteristics depend directly on the latter. Therefore, electrical performances directly result from the structural way in which other materials, as metals or

oxides, are bound to diamond.

Transmission electron microscopy (TEM) is one of the most powerful tools to directly analyze interfaces. Information about roughness of the interface, atomic arrangement, chemical environment, crystalline nature of the oxide onto diamond, orientation relations between diamond and crystals forming the deposited layer, energy gap of the oxide, chemical composition variations or formation of interface specimens can be obtained through TEM related techniques as HREM, HR-STEM, EDX and (V)EELS. XPS or DFT-periodic calculations are complementary to understand the TEM related results and can give relationships to electrical characteristics.

This contribution will present an overview about diamond interfaces characterization carried out at the University of Cádiz on different electronic devices studied by TEM related techniques. In particular, several interfaces as metal/diamond, oxides/diamond and carbides/diamond by means of their atomic interface configuration, i.e., atomic bondings and grain configuration, are investigated and related to their electrical characteristics. In addition, TEM spectroscopies complemented by XPS measurements are shown to be of first importance to understand band setting at such interfaces. Role of interface states and their relation with crystallinity of oxide in MOS stacks will be discussed for Al₂O₃ and ZrO₂ MOSCAPs and MOSFETs. Al₂O₃ is the most common oxide for these purposes and it is well characterized [2], although ZrO₂ is also a promising candidate due to its high dielectric constant [3], large band gap and high breakdown field. Performance of diamond based-Schottky diodes is also greatly dependent on diamond surface terminations [4] and, in the case of tungsten carbide contacts, some results on the WC/O-diamond are presented identifying crystallinity and stoichiometry of WC phases. Oxygen termination has also an important role in Zr/diamond Schottky interfaces.

[1] B.J. Baliga. *IEEE Electron Devices Lett.* 10 (1989) 455-457

[2] J. Cañas *et al. Appl. Surf. Sci.* 461 (2018) 93-97

[3] D. Vanderbilt *et al. Thin Solid Films* 486 (2005) 125-128

[4] N. Donato *et al. J. Phys. D: Appl. Phys.* 53 (2020) 093001

11:00 AM EQ19.01.02

Interface States and Charges Induced by ZrO₂ Deposited by Different Methods on O-Terminated Diamond Capacitors Beatriz Soto¹, Castro P. Villar¹, Daniel Araujo¹ and Julien Pernot²; ¹University of Cádiz, Spain; ²University of Grenoble Alpes, France

One of the bottlenecks in the fabrication of diamond-based electronic devices is related to the diamond interface state passivation. The surface termination quality and the fact of not having a native oxide hinders high performance and reliability of the device. The improvement of the oxide/diamond interface quality leads to a minimization of the interface states density in the diamond gap which strongly modify the electrical response. The starting point of this study is the interesting characteristics of the ZrO₂ such as the high dielectric constant (of the order of 19.7), the high band gap (6eV characterized by Electron energy loss spectroscopy), its band setting providing a barrier for holes (of the order of 2eV) or the high breakdown field (of the order of 2MVcm⁻¹). In the present contribution, different zirconia layers have been deposited by two methods: Atomic layer deposition and radio frequency Sputtering. The crystallinity of the layers has been studied by High resolution electron microscopy and its related Fast Fourier transform and by X-ray diffraction. The band alignment will be established by X-ray photoelectron spectroscopy. Also, by Energy dispersive X-ray spectroscopy is possible to analyse the stoichiometry throughout the dielectric comparing the oxygen content, and thus the possibility of finding electron-trapping mechanisms, from the two methods of deposition. Finally, the analysis of the electrical characteristics (I-V, C-V, C-f) for zirconia deposited under several conditions allows an understanding of how microstructure influences electrical performance.

11:15 AM EQ19.01.04

Mapping Boron Distribution by Cathodoluminescence in P-Type Monocrystalline Diamond Nicolas Tappy¹, Christian Monachon² and Anna Fontcuberta i Morral¹; ¹Ecole Polytechnique Fédérale de Lausanne, Switzerland; ²Attolight SA, Switzerland

The spatially resolved and non-destructive measurement of impurities and defects in diamond is key for the deployment of diamond in electronics. Techniques used so far such as the X-ray Topography using synchrotron radiation for monitoring defects in substrates exhibits a low scalability. In the large-scale production picture, the lack of high throughput characterization technique could rapidly become a bottleneck. We propose that Cathodoluminescence Spectroscopy (CL) is a useful alternative, because of its sensitivity to defects. In addition to this, the excitonic spectrum of diamond has been useful to measure dopant concentrations in diamond for many years, but relies on prior knowledge of the setup performances, i.e. a diamond standard of known doping level for the calibration of the setup.

Going beyond this state-of-the-art, we study dopants in diamond using Time-Resolved CL (TR-CL) with a picosecond time resolution, and CL spectral imaging. TR-CL evidences that the excitation dynamics of a CL experiment are significantly different from their PL counterparts, because many excitons are generated in a very small interaction volume even if few electrons impact the sample. This novelty provides direct, quantitative access to the electrically active Boron concentration in a sample, regardless of compensation or non-incorporated impurities, with sub-micron spatial resolution and attractive measurement throughput. We demonstrate how this can be applied to map doping variations in a Boron-doped High-Pressure-High-Temperature diamond substrate across growth sectors, which shows doping concentration varying over 1 order of magnitude, in the 1.5e16 – 4.0e17 [cm⁻³] range. The measurements are performed at a spatial scale sufficient to resolve crystalline defects, and study their impact on the spectral signal and Boron incorporation.

11:30 AM EQ19.01.05

Investigating Novel Electrochemiluminescence Reactions Utilising Boron Doped Diamond Electrodes in Aqueous Solutions Samuel Stewart, Emmanuel Scorsone and Matthieu Hamel; CEA-LIST, France

Electrochemiluminescence (ECL) is a technique where chemical species generated at the surface of an electrode interact; producing an excited state, which then emits photons. The intensity of the emitted light is proportional to the concentration of the target molecule and so is quantifiable. Exploiting features of both electrochemical analysis and chemiluminescence, the use of ECL has become very popular in many areas due to the wide range of advantages it displays over more conventional fluorescence techniques: the ability to control the exact time and position of the photon emission, the absence of background optical signal (high signal/noise ratio) and good selectivity.

ECL generally occurs where the oxidized and reduced forms of the target analyte are produced by sweeping from cathodic to anodic potential, or vice versa. The recombination of these two species is what produces the excited state. However, in aqueous solutions this becomes difficult as the relatively high and low potentials needed can cause the electrolysis of water, disrupting the ECL process. This is usually overcome with the use of a co-reacting species, where the luminescent species are oxidized at the electrode together with the co-reactant, giving a strong reducing agent. However, these additional compounds can often be expensive and significantly reduce the selectivity of the technique.

Boron Doped Diamond electrodes have several advantages over other electrode materials. The most important for ECL assays is that it possesses a wide potential window in water, meaning we have the ability to mitigate the splitting of water without the need for the addition of co-reacting species. Another is BDD ability to withstand very high and low potentials (over 1.5V and under -1.5V), this has already been implemented for the in-situ electrochemical cleaning of the electrode for both electrochemical and ECL analysis. It also means that we have the ability to apply these very high potentials for the rapid production radicals (hydroxyl and super oxide) at the surface of the electrode. Many ECL assays depend on the interaction of the target analytes with these

radicals, like in the case of indolic compounds, to produce the excited state that give the ECL signal – but are often performed in organic solvents or with co-reactants. The robustness of diamond gives the opportunity to create ECL reactions and analyses of these compounds in aqueous solution. Here, we investigate the potential of using the unique properties of diamond electrodes to produce novel ECL assays.

SESSION EQ19.02: Devices
Session Chair: Bohuslav Rezek
Tuesday Afternoon, November 30, 2021
Hynes, Level 1, Room 101

1:30 PM *EQ19.02.01

Non Volatile Photo-Switch Using a Diamond pn Junction Julien Pernot^{1,2}, Cédric Masante¹, Martin KAH¹, Gwérolé Jacopin², Clément Hébert³ and Nicolas Rouger²; ¹Univ. Grenoble Alpes, France; ²Centre National de la Recherche Scientifique, France; ³Institut national de la Santé et de la Recherche Médicale, France

Ultrawide bandgap semiconductor technologies offer potentially revolutionary advances in the rapidly developing areas of quantum communication, short wavelength optics, smart energy conversion and biomedical interfaces. These strongly demanding technologies can be partly constructed using conventional devices but new hybrid architectures are needed to overpass current performances and add functionalities. Here, we propose a new concept based on the specific properties of a diamond pn junction combined with both an electric and optical control of the depletion region. Using this junction as a gate in a junction field effect transistor, we report a proof of concept of a non volatile diamond photo-switch. A diamond pn junction made with nitrogen deep donors in the n-side is demonstrated to be optically activated thanks to visible light. The n-type diamond gate is almost devoid of free carriers in the dark and thus insulating. Illuminating the device renders the standard electrical gate control of the transistor efficient. Without illumination, the device is frozen, keeping a permanent memory of the current state. This new way of operating the device opens numerous possibilities to store and transfer information or energy with applications in the field of electrical aircraft or aerospace electronics, power electronics, bio-electronics and quantum communication.

2:00 PM EQ19.02.02

High Voltage (-580 V) Vertical- Diamond MOSFET by 2DHG Channel and Implementing p-Drift Layer Kosuke Ota¹, Jun Nishimura¹, Naoya Niikura¹, Aoi Morishita¹, Atsushi Hiraiwa¹ and Hiroshi Kawarada^{1,2}; ¹Waseda Univ., Japan; ²Kagami Memorial Research Institute for Materials Science and Technology, Japan

Diamond has excellent physical properties as a semiconductor material, such as a high breakdown electric field (~10 MV/cm), the highest thermal conductivity among solid materials (~22 Wcm⁻¹K⁻¹), and a low dielectric constant (~5.7), and is expected to be applied to high-power, high-frequency p-FETs. To realize high-power and high-speed switching complementary inverters, there is an urgent need to develop vertical p-channel power FETs comparable with n-type FETs and suitable for integration. We have reported vertical-type diamond MOSFET using two-dimensional hole gas (2DHG) which is induced at any C-H diamond surface independent from crystal orientation covered by high temperature ALD-Al₂O₃[1][2][3]. However, the drift layer by lightly B doped layer (p- layer) has not been implemented because the controllability of lightly doping of boron into diamond is very difficult. In this work, we fabricated (001) vertical-type 2DHG diamond MOSFET with a p-drift layer and achieved a breakdown voltage of V_B: -580 V, which is the highest among the vertical diamond MOSFETs currently reported.

Fabrication process was as follows. First, a p-drift layer ([N]: 1.0 × 10¹⁶ cm⁻³, [B]: 8.0 × 10¹⁷ cm⁻³) of 4 μm was deposited on a p⁺-type diamond substrate using the microwave plasma chemical vapor deposition (MPCVD) method and nitrogen-doped layer of 2 μm were deposited as a vertical current blocking layer on a p-drift layer by the MPCVD method. Second, trench with a depth (D_T) of 3 μm, a width (W_T) of 6 μm are formed by inductively coupled plasma reactive ion etching using O₂ plasma. After trench formation, a 300 nm regrown undoped layer was deposited by the MPCVD method to induce the 2DHG and secure the drift layer on the trench sidewall. Third, source electrodes (Ti/Pt/Au) were formed and the 200-nm-thick Al₂O₃ was deposited as the gate insulator through the high-temperature atomic layer deposition (ALD) method. Finally, drain electrodes (Ti/Au) was formed on the back surface of the substrate and gate electrode (Al) was formed to complete the vertical-type device. The source-gate length (L_{SG}), gate-trench (L_{GT}), gate-drain (L_{GD}), source-drain (L_{SD}) and gate length (L_G) for this device are 3 μm, 4 μm, 10 μm, 17 μm, 4 μm, respectively. The area size of an active region for this device (L_{SS} × W_G = 7.5 × 10⁻⁶ cm²) is defined by multiplying the distance between the trench-side edges of two sources (L_{SS}: 30 μm) and the gate width (W_G: 25 μm).

From the I_D-V_{DS} characteristics, the maximum drain current density (I_{D,max}) normalized by the gate width is 210 mA/mm at V_{DS}: -50 V and V_{GS}: -20 V. In the active region, the I_{D,max} is 1400 A/cm² and the on-resistance (R_{on}) is 23 mΩcm². The drain current density obtained in this study is comparable to that of a vertical device of the same device size without a p-drift layer [1]. No gate leakage current is observed at room temperature (300 K) and on/off ratio is about 6 orders of magnitude. A high breakdown voltage of -580 V is achieved, this value is more than 60 % (200 V) higher than the breakdown voltage (V_B: -359 V) [1] of a device of the same size without a p-drift layer, and is the highest value reported for vertical diamond FETs. From the above, it can be confirmed that the p-drift layer does not significantly reduce the current value and increase the breakdown voltage. In the near future, a p-type power trench diamond MOSFET with high voltage and low ON-resistance will be realized by increasing the thickness of the p-drift layer (currently 4 μm) to about 10 μm, implementing a trench gate structure [3] and a high-density boron-doped layer [4] under the source electrode in this device structure.

[1] N. Oi, H Kawarada et al., *Sci. Rep.*, vol. 8, Art. No. 10660, (2018).

[2] J. Tsunoda, H. Kawarada et al., *Carbon*, **176**, 349-357, (2021).

[3] J. Tsunoda, H. Kawarada et al., *IEEE TED*, accepted, (2021).

[4] S. Imanishi, H. Kawarada, et al., *IEEE EDL*, **42**, 2, 204-207, (2021).

2:15 PM EQ19.02.03

Late News: 1kV Normally-off Lateral Diamond Reverse Blocking MESFET Jesus Canas^{1,2}, Alex Pakpour-Tabrizi³, Richard Jackman³ and Etienne Gheeraert¹; ¹Institute NEEL-CNRS, France; ²universidad de cadiz, Spain; ³University College London, United Kingdom

Diamond transistors are promising for high temperature, power and frequency applications in harsh environments, including those with high radiation levels. This is due to the unique properties of diamond as a wide band-gap (5.5eV) semiconductor. The majority of Diamond field-effect transistors (FETs) fabricated to-date use a 2D hole gas that emerges when an H-terminated diamond surface comes into contact with a range of adsorbates and/or selected metal oxides. However, this unconventional manner of creating a p-type region in a semiconductor suffers from instability and reproducibility problems and low operational mobility issues.

Several lateral O-terminated diamond FET concepts and architectures have been recently fabricated while for vertical FETs, traditionally favored for high

power devices, fabrication is still challenging despite the recent efforts of the diamond device community. The reported lateral devices display 'normally-on' characteristics, which are not ideal for high power applications. Further, reported breakdown voltages are typically poor in comparison to diamond's full potential mainly due to limitations in substrate and epilayer quality alongside existing processing capabilities. In this work, these problems are addressed. A novel and a *normally-off* lateral Schottky-drain reverse blocking (RB) MESFET based on molybdenum Schottky contacts on O-terminated boron doped diamond has been fabricated. The device display a current level of 70 μ A/mm and a transconductance of 147 μ S mm⁻¹ at 425 K. Importantly, the blocking voltage capabilities of the devices at this temperature are >1 kV with no leakage current and reproducible characteristics after the high voltage stress test.

2:30 PM EQ19.02.04

C-Si Bonded 2DHG Diamond MOSFETs—Improvement of Interface Characteristics by Thin Gate Insulating Film Yuta Nameki, Te Bi, Wenxi Fei, Jun Nishimura, Naoya Niikura, Atsushi Hiraiwa and Hiroshi Kawarada; Waseda University, Japan

Diamond is the next generation wide bandgap semiconductor material, which can realize high performance power devices. The H-terminated (C-H) diamond has low activation energy, high carrier mobility¹ and high hole density. We have ever developed C-H diamond MOSFETs reported high drain current density² and high breakdown voltage³. However, C-H diamond has a weak oxidation resistance, there is a problem that it is difficult to apply it to commercialization. Therefore, we proposed C-Si bonded (C-Si) diamond structure using SiO₂ to achieve further diamond device development. The SiO₂ is advantageous for power devices in terms of chemical stability and wide bandgap, so it can be used as the gate insulator in the diamond power device applications. In previous study, we fabricated C-Si diamond MOSFETs with the boron-doped diamond selective growth by using the SiO₂ as the mask for the formation of source-drain electrode and the gate insulator^{4,5}. The C-Si diamond device had C-Si bonds as the p-channel. We consider C-O-Si on the diamond-SiO₂ interface can reduce the interface state and improve the field-effect mobility. In addition, the C-Si diamond MOSFET achieved normally-off operation⁴ and wide temperature stability (~673 K)⁵. In this study, we have further improved the characteristics by thinning the SiO₂ gate insulating film. The fabrication process is as follows. The 2 mm undoped layer was grown on nitrogen-doped (001) diamond substrate by microwave plasma chemical vapor deposition (MPCVD). The 100 nm SiO₂ layer was formed on the substrate by utilizing tetra ethoxy silane chemical vapor deposition (TEOS-CVD). The source-drain patterns were formed by the inductive coupled plasma reactive ion etching. Then, boron-doped diamond ([B]:~10²¹ cm⁻³) was selectively grown by MPCVD on the selectively etched undoped diamond layer by 50 nm with the SiO₂ mask patterns with. The growth temperature and microwave output power of MPCVD were 1200 K and 360 W, respectively. The C-Si diamond interface has been formed between the undoped diamond and the SiO₂ mask during selective growth of boron-doped diamond layer. Source-drain electrode were deposited on the surface of the selected boron-doped diamond. Ohmic contacts were formed by annealing (773 K). The SiO₂ film was removed by ICP-RIE, apart from the channel region. The 100 nm Al₂O₃ was deposited as a gate insulating on the diamond substrate using the high temperature ALD method (723 K). Finally, gate electrode (Al) was deposited so as to overlap the source-drain electrode by 2 mm. The gate width, gate length and channel length were 25, 14-22 and 4-12 mm, respectively. The maximum drain current density of the C-Si diamond MOSFET normalized by gate width is 108 mA/mm at V_{DS} of -30 V and V_{GS} -40 V, and the maximum transconductance is 3.1 S/mm at the V_{DS} of -30 V. The field effect mobility (m_{EF}) is 122 cm²V⁻¹s⁻¹. This value is comparable or better than that of C-H diamond MOSFETs. In addition, the C-Si diamond MOSFET have the normally-off operation with threshold voltage V_{th} of -0.2 V. This result exhibits that the C-Si bond contributes to normally-off operation of diamond MOSFET indicating a new V_{th} control mechanism. Furthermore, this device has a thin gate insulating film, which results in low subthreshold characteristics and a steep on /off ratio. In addition, the maximum drain current density increases due to the increased capacity of the oxide film. The drain current on/off ratio is about 7 orders of magnitude at 300 K. In future, C-Si diamond MOSFET be expected to vertical-type diamond devices, and it will contribute significantly to the diamond p-FET for CMOS circuits combined with GaN or SiC n-FETs.

¹Y. Sasama, T. Yamaguchi, et al., APL Mater. 6(2018)

²K. Hiram, M. Kasu, et al., Jpn. J. Appl. Phys. 51, no.9.(2012)

³Y. Kitabayashi, H. Kawarada, et al. IEEE Electron Device Lett. 38(2017)363.

⁴W. Fei, H. Kawarada et al., Appl. Phys. Lett. 116, 212103(2020)

⁵T. Bi, H. Kawarada et al., Carbon, 175, 525-533(2021)

2:45 PM EQ19.02.05

Propagation Characteristics for Seawater Wireless Communication up to 25 m of Transmission Distance by Utilizing Diamond Solution Gate FET Hirotsuka Sato, Teruaki Takarada, Shuto Kawaguchi, Yu H. Chang and Hiroshi Kawarada; Waseda University, Japan

We have investigated the characteristics of electric signal propagation in seawater by utilizing diamond solution gate FET (SGFET) [1]. The channel surface of a SGFET and a gate electrode are directly immersed in solutions and the drain current (I_{DS}) can be remotely modulated by electric signals (V_{GS}) applied on the gate electrode via solution. Due to these properties, we proposed a new electric seawater communication method utilizing the gate electrode as a transmitter, seawater as propagation medium and SGFET as a receiver [2].

Seawater wireless communication has been required in a wide range of fields such as environmental research, scuba diving, and autonomous underwater vehicle. In seawater, radio waves have short transmission distances, due to the high electric conductivity of seawater. Present seawater wireless communication mainly employs the use of acoustic waves. Recently optical waves are considered or. Optical waves face some drawbacks due to turbidity absorbing scattering centers such as sands, planktons in seawater. While acoustics waves exhibit relatively low absorption, they have low frequency band (~kHz) [3].

To address these issues, we have proposed a new seawater wireless communication method utilizing a diamond SGFET that can operate in electrolyte solutions as the receiver. Diamond SGFET can respond to AC electric signals applied on the electrically independent gate electrode, which indicates successful wireless communications. SGFET output signals were observed as differential pulses responding to the input square potential change. In addition, we have reported that increasing the ion concentration in the electrolyte solution favors signal propagation [2]. The result suggests that the signals are not propagated by radio waves, but that sodium and chloride ions in the solution play an important role in propagation. However, the mechanism for signal propagation has not been clarified yet. In this work, we evaluate the amplitude (V_{peak}) of the differential pulses and investigate the effect of the transmission distance (gate-SGFET channel distance) up to 25 m on the output characteristics in order to consider the mechanism of signal propagation. This communication system composes of three components: a gate electrode as the transmitter, an SGFET as the receiver, and an electrolyte solution as the propagation medium. 3.5 % NaCl solution was filled into PVC tubes with a length of 1 to 25 m (diameter = 2.5 cm). The transmission distance was changed by inserting the gate electrode and SGFET at both ends of each tube. The gate electrode was applied up to 10 MHz and 1 V amplitude square waves electric signal (v_G). The drain electrode of SGFET was connected to a load resistance (R_L) and was applied with a supply voltage (V_{DD}). Then, drain-source voltage (v_{DS}) and load resistance voltage (v_{RL}) were measured as outputs.

The output characteristics show that SGFET respond to v_G at least 200 kHz frequency at the distance of 25 m. The amplitude (V_{peak}) at 50 kHz drastically decreases from 1 m ($V_{peak} > 80$ mV) to 10 m ($V_{peak} < 10$ mV). On the other hand, V_{peak} at 50 kHz gradually decreases from 10 m to 25 m, and we observe that V_{peak} is about 5 mV at 25 m. However, the response above 500 kHz is not observed at 25 m even though diamond SGFET can respond at 10 MHz input voltage v_G at 1 m. This is because the propagation of differential pulses caused by the derivative of input voltage v_G is delayed and the upper limit of frequency response becomes lower as the distance increases.

We explain these results by introducing two types of propagation models; ion conduction current due to solution resistance R_s , and ion plasma wave model

that is propagation as longitudinal waves of sodium and chloride ions.

- [1] H. Kawarada, et al, Phys. Stat. Sol. (a) 185 (2001) 79.
- [2] K. Tadenuma, H. Kawarada et al., MRS Fall 2019.
- [3] H. Kaushal and G. Kaddoum, IEEE access 4 (2016) 1518.

3:00 PM EQ19.02.06

Lowest Contact Resistance for High Drain Current Density >1A/mm at Diamond MOSFETs with Heavily Boron-Doped Source and Drain Fuga Asai¹, Ken Kudara¹, Masakazu Arai¹, Atsushi Hiraiwa¹ and Hiroshi Kawarada^{1,2}; ¹Waseda Univ, Japan; ²Kagami Memorial Research Institute, Japan

Diamond has a wide band gap (5.5 eV), high thermal conductivity (22 W/cm K), and high breakdown field. Therefore, Diamond is expected to apply RF amplifier. We fabricated high-voltage Diamond MOSFETs with Al₂O₃ (200 nm) as gate insulator formed by high temperature ALD process. We achieved the highest output power density $P_{out} = 3.8$ W/mm [1] in p-type FETs. The high output has been obtained by reducing on-resistance, increasing operating voltage $V_{DS,Q}$ and current density $I_{D,Q}$, and increasing actual current by extending the gate width W_G . The device with extended W_G may reduce current density because of self-heating, and influence characteristics of devices caused by increase of gate resistance.

In this work, we fabricated ALD-Al₂O₃ MOSFETs with a boron-doped layer on a pure (111) diamond and evaluated DC and RF performance as well as contact resistance in detail. Devices were fabricated on a pure (111) diamond. We etched selectively by ICP-RIE through the evaporated metal mask to form space for heavily boron-doped epitaxial layer (150 nm of p⁺⁺ layer) for source and drain. Source and Drain electrodes are deposited Ti/Pt/Au (20 nm/30 nm/90 nm). The thickness of Al₂O₃ gate insulator is 200 nm. And we adopted double gate finger structure for the reduction of gate resistance. From I_{DS} - V_{DS} characteristics, the maximum drain current density $I_{D,max}$ of 1.03 A/mm, R_{on} of 23 Ω mm was obtained at $V_{GS} = -28$ V and $V_{DS} = -40$ V. To obtain even higher current density, it is valid to shorten the distance between the source and drain, for example. It is expected that the drain current density achieves 1.5 A/mm when L_{SD} is designated 0.5 μ m. This small L_{SD} device has been manufactured by using electron beam lithography when we coat resist of metal mask for p⁺⁺ layer. We measured TLM pattern on the substrate which are (a) 2DHG and p⁺⁺ layer and (b) only 2DHG without p⁺⁺ layer. As for (a), contact resistance $R_{contact}$ was 1.77 Ω mm and sheet resistance R_{sheet} was 6.7 k Ω /sq. As for (b), $R_{contact}$ was 27.5 Ω mm and R_{sheet} was 16.8 k Ω /sq. These results suggest that p⁺⁺ layer under the source and drain area reduce both contact resistance and sheet resistance. (c) In order to evaluate the contact resistance between boron-doped layer and 2DHG, we measured contact resistance to p⁺⁺ layer and sheet resistance R_{sheet} of p⁺⁺ layer to be 0.49 Ω and 64 Ω /sq, respectively. From these results, each element of resistance can be calculated. $R_{TIC-Boron}$ was 0.49 Ω mm, R_{Boron} was 0.32 Ω mm, $R_{Boron-2DHG}$ was 0.96 Ω mm. This result suggests that the barrier between boron-doped layer and 2DHG is not a serious problem because the contact resistance (=0.96 Ω mm) is very small. And the large signal performance of a device was evaluated by using a load pull system at 1 GHz. As for the power output density measured by the load pull system, 3.6 W/mm was obtained on the device of $W_G = 200$ μ m. This value is almost equal to the maximum value of Diamond MOSFETs (= 3.8 W/mm), which was obtained at $W_G = 100$ μ m; that is, actual power in this new device is almost twice as that of former maximum value.

In summary, we fabricated boron-doped MOSFETs on a pure (111) diamond substrate and evaluated DC and RF performance as well as contact resistance between boron-doped layer and 2DHG. As a result, over 1 A/mm of drain current density was obtained. To obtain even higher current density, it is valid to shorten the L_{SD} . As for the TLM measurement, boron-doped layer reduced both contact resistance and sheet resistance. Then we found that the barrier between the boron-doped layer and 2DHG is not a serious problem. As for the large signal performance, power output density 3.6 W/mm was obtained. This is to be equal to the maximum value of Diamond MOSFETs, but actual output power is twice than that of maximum value.

This work is supported in part by MEXT Project on Design & Engineering by Joint Inverse Innovation for Materials Architecture.

- [1] S. Imanishi, H. Kawarada et al: IEEE EDL.40 (2019) 279

SESSION EQ19.03: Nanodiamond I
Session Chair: Philippe Bergonzo
Tuesday Afternoon, November 30, 2021
Hynes, Level 1, Room 101

4:00 PM *EQ19.03.01

Nanodiamonds Under Control—Size and Synthesis Dependent Properties, Composites, Interfaces and Application Examples from Health to Sensors, Photocatalysis and Energy Bohuslav Rezek¹ and Stepan Stehlik²; ¹Czech Technical University, Czechia; ²The Czech Academy of Sciences, Czechia

Nanodiamonds science and technology has been extensively explored in the past decade with prospects and examples of applications from biomedicine to quantum technologies. Ample reviews and seminal articles are available [Mochalin, Nature Nanotechn. 7 (2012) 11; Arnault (Ed.), Nanodiamonds, Elsevier, 2017]. Yet many scientific and application related problems remain to be addressed. Driving motivation is to better understand, control, and make use of nanodiamonds unique properties for photocatalysis, energy harvesting, sensing, health and safety. In this contribution, we review our recent progress in technology to better control nanodiamond properties and we analyze interactions (structural, chemical, electronic, optical) of nanodiamonds with molecules and inorganic materials by correlating microscopic, spectroscopic, and computational methods. We focus on two representative types of nanodiamonds (NDs) produced by HPHT or detonation synthesis that in some aspects exhibit distinctively different features.

We present a technology of controllable and high-yield purification and size reduction of both types of NDs down to 2 nm (mode size) by using annealing in air at optimized temperatures of 450-520 °C for 10-50 min. The effect differs on HPHT and detonation NDs. Size and nitrogen inhomogeneity in the primary DND particles is revealed via salt-assisted deaggregation. We characterize the effect of size on multiple methods, from DLS and AFM to SAXS and Raman. We observe distinct size-related effects on surface chemistry and Raman spectral features (incl. breathing modes) in sub-5nm range on HPHT and detonation NDs. We show that even at the molecular size the nanodiamond surfaces can be reversibly modified from oxidized to hydrogenated by thermal processes.

We demonstrate use of such controlled nanodiamonds on various examples. For instance, 2 nm H-DNDs enable formation of extremely dense (10^{13} cm⁻²), thin (2 nm), and smooth (RMS < 0.8 nm) nucleation layers and then highly uniform sub-6 nm CVD diamond films. Photoluminescence of SiV centers in the films < 10 nm is fully switched between on and off states by O/H surface terminations. Nanodiamonds themselves inherently assume electrical charge on substrates (up to 0.4 V) that affects both electron emission and photoluminescence. Surface potential of nanodiamonds is affected also by adsorbed water that forms a thicker layer on hydrogenated and binds more tightly on oxidized NDs as shown by TGA and FTIR. Specific interaction with biological solutions leads to formation of different protein corona on 2 nm O/H DNDs and thereby to different interaction with cell membrane and cytotoxicity. On bacteria, the most pronounced long-term inhibition of E. coli growth (45%) is provided by hydrogenated NDs, via oxidative stress predominantly. We show that composites of nanodiamonds with other materials represent a promising future direction. TiO₂/nanodiamond composites exhibit more efficient photocatalytic degradation of soman via enhanced hole transfer. Ag/nanodiamond composites exhibit better stability and photoactive effects than

Ag nanoparticles alone. Based on AFM and FTIR analysis, hydrogenated or oxidized DNDs in composites with Au nanoparticles provide control of drug molecule adhesion and assembly (upright or layered) both on nanodiamond and Au and thereby control also impedance biosensor response. Nanodiamond surface chemistry controls also assembly of polypyrrole-DND complexes and thereby generation of photovoltage. Based on the experiments and theoretical DTF computing, polyfunctional DNDs with both oxygen and hydrogen surface groups may be the best nanodiamonds for PV, serving as effective inorganic electron acceptor. We demonstrate prototype spin-coated DND-PPy solar cell incl. cross-sectional SEM analysis.

We gratefully acknowledged the long-term support from the Czech Science Foundation, Ministry of Education Youth and Sport, and the project CZ.02.1.01/0.0/0.0/15_003/0000464 (CAP).

4:30 PM EQ19.03.02

Valence Band Electron Energy Loss Spectroscopy Study of Boron-Doped Nanodiamonds Souvik Bhattacharya¹, Jonathan Boyd², Amir H. Talebi³, Sven Reichardt³, Olga A. Shenderova⁴, Nicolò Maccaferri³, Ludger Wirtz³, Giuseppe Strangi² and R. Mohan Sankaran¹; ¹University of Illinois at Urbana-Champaign, United States; ²Case Western Reserve University, United States; ³University of Luxembourg, Luxembourg; ⁴Adamas Nanotechnologies, United States

Doped semiconductors exhibit interesting optical and optoelectronic properties such as localized surface plasmon resonances^{1,2} and carrier-phonon coupling³. Boron-doped diamond is a wide band-gap, p-type semiconductor which has been previously found to produce interesting phenomena such as electron-phonon coupling that leads to Fano resonances⁴ and superconductivity⁵. Here, we characterize boron-doped nanodiamond powders by electron-energy loss spectroscopy (EELS) using a scanning transmission electron microscope to reveal potentially new optical transitions. The nanodiamond samples were synthesized commercially by high-pressure-high-temperature methods and obtained from Adamas Nanotechnologies. The particles were imaged using high-resolution transmission electron microscopy to confirm the crystalline structure and measure their size which was on the order of 0.5-1 microns. The boron concentration was estimated to be ca. 800 ppm by comparing the Fano line shape of the main peak in the Raman spectrum to results in the literature⁴. For EELS, we focused on the valence-band where a clear shoulder was observed on the zero-loss peak (ZLP). Through data processing, the ZLP was either deconvoluted or subtracted from the inelastic scattering spectra using the reflected-tail method and fitted using Voigt peaks to identify multiple peaks in the range of 0.1-0.2 eV. We note that the feature was completely absent in a control undoped nanodiamond sample synthesized under the same conditions. We present theoretical simulations to explain the origin of this signal, which suggest that the new resonances are driven by low-lying electronic excitations in the valence band. We also investigate the role of resonant electron-phonon coupling, which was previously shown to lead to observable changes in the electronic and vibrational properties in boron-doped diamond⁶.

References:

1. J. A. Faucheaux, A. L. D. Stanton, and P. K. Jain. *The Journal of Physical Chemistry Letters* **5** (6), 976-985 (2014).
2. Z. Liu, Y. Zhong, I. Shafei, R. Borman, S. Jeong, J. Chen, Y. Losovyj, X. Gao, N. Li, Y. Du, E. Samello, T. Li, D. Su, W. Ma, and X. Ye. *Nature Communications* **10** (1), 1394 (2019).
3. N. H. Protik and D. A. Broido. *Physical Review B* **101** (7), 075202 (2020).
4. V. Mortet, I. Gregora, A. Taylor, N. Lambert, P. Ashcheulov, Z. Gedeonova, and P. Hubik. *Carbon* **168**, 319-327 (2020).
5. T. Yokoya, T. Nakamura, T. Matsushita, T. Muro, Y. Takano, M. Nagao, T. Takenouchi, H. Kawarada, and T. Oguchi. *Nature* **438** (7068), 647-650 (2005).
6. F. Caruso, M. Hoesch, P. Achatz, J. Serrano, M. Krisch, E. Bustarret, and F. Giustino. *Physical Review Letters* **119** (1), 017001 (2017).

4:45 PM EQ19.03.03

Formation of Water-Soluble Onion-Like Carbon by Laser Irradiation of Colloidal Detonation Nanodiamonds Irena Bydžovská^{1,2}, Ekaterina Shagieva¹, Ivan Gordeev¹, Oleksandr Romanyuk¹, Zuzana Nemecková³, Jiri Henych^{3,4}, Lukas Ondic¹, Alexander Kromka¹ and Stepan Stehlik¹; ¹Institute of Physics, AS CR, Czechia; ²Czech Technical University in Prague, Czechia; ³Institute of Inorganic Chemistry of the Czech Academy of Sciences, Czechia; ⁴J.E. Purkyně University in Ústí nad Labem, Czechia

Industrial-scale production and narrow size distribution make detonation nanodiamonds (DNDs) a convenient precursor for onion-like carbon (OLC) formation. Apart from frequently used high-temperature annealing of DNDs in an inert environment, their laser irradiation in liquid can be effectively used for the OLC formation. Due to processing in chemically reactive environment, the produced OLCs can carry specific surface functional groups that mediate their solubility in various solvents¹. Moreover, the transformation was shown as a reversible process, i.e. nanodiamonds (NDs) were back-transformed after the OLC laser irradiation².

In this work, we focused on this process more in detail by monitoring the surface chemistry, zeta potential, and structure of DNDs as a function of laser irradiation duration. Firstly, we used fully deaggregated hydrogenated DNDs (H-DNDs) dispersed in ethanol which were irradiated by a 532 nm NdYAG laser with energy 150 mJ in a pulse (5 J/cm²) at 10 ns pulse duration and 10 Hz repetition rate. The irradiation lasted for 1, 2, 3, 4, 5, 10, 20, 40, and 60 minutes giving a rise to nine samples. With increasing irradiation time, the brown colloid of the pristine H-DND gradually changed to black and finally turned to a transparent yellow colloid. FTIR measurements revealed a monotonical decrease in the C-H₂ bands intensities and an increase of the C-O and C=O features. This was accompanied by a zeta potential decrease from 54 mV for the pristine sample down to 34 mV for the 10 min sample. The 20 and 40 min samples were already colloiddally unstable. Gradual photo-oxidation of the H-DNDs was confirmed by XPS which revealed an increase of the oxygen content with increasing laser irradiation time. The formation of OLC-like structure was proven by transmission electron microscopy (TEM). In addition, TEM also showed a gradual loss of nanoparticle character with increasing the irradiation time. The 40 min sample no longer consisted of ~5 nm particles but an interconnected chain-like mesostructure. Two fundamental aspects were investigated by Raman spectroscopy. First, we focused on the time-dependent H-DND transformation into OLC structures. In agreement with XPS and TEM, Raman measurements confirmed the gradual increase of the sp² C with increasing laser irradiation time. However, no OLC-to-ND back transformation was detected. Second, we investigated the laser-treated samples after their purification from sp² carbon by air annealing treatment. Surprisingly, for all samples irradiated up to 40 min, the typical and unchanged DND Raman spectrum was successfully recovered after the annealing in air at 450°C for 300 min. This finding indicates the inhomogeneous sp³ to sp² transformation during the laser irradiation process as well as the insensitivity of the DND Raman spectra to the surface chemistry, size, and transient structural changes. Our results demonstrate the potential and limits of the laser irradiation technique as an effective tool for the controllable formation of water-soluble OLCs and bring deeper understanding to relations between sp³ and sp² nanocarbons.

(1) Jang, D. M.; Im, H. S.; Back, S. H.; Park, K.; Lim, Y. R.; Jung, C. S.; Park, J.; Lee, M. Laser-Induced Graphitization of Colloidal Nanodiamonds for Excellent Oxygen Reduction Reaction. *Phys Chem Chem Phys* **2014**, *16* (6), 2411–2416. <https://doi.org/10.1039/C3CP54039A>.

(2) Xiao, J.; Ouyang, G.; Liu, P.; Wang, C. X.; Yang, G. W. Reversible Nanodiamond-Carbon Onion Phase Transformations. *Nano Lett.* **2014**, *14* (6), 3645–3652. <https://doi.org/10.1021/nl5014234>.

SESSION EQ19.04: Poster Session I
Session Chairs: Emmanuel Scorsone and Mariko Suzuki
Tuesday Afternoon, November 30, 2021
8:00 PM - 10:00 PM
Hynes, Level 1, Hall B

EQ19.04.01

Dislocations as Topological Wires and Magnets Sevim Polat Genlik and Maryam Ghazisaeidi; The Ohio State University, United States

Dislocations—one dimensional topological defects—in electronic materials, are considered to have a negative influence on electronic properties; their presence is thought to cause non-radiative recombination of charge carriers which lead to overheating of the crystal and malfunction of the device. Therefore, great effort has been made to produce dislocation-free crystals. However, recent studies show that dislocations can also be turned into useful functional features. For instance, it is reported that magnetic properties of dislocations differ from the lattice due to broken symmetry of the magnetic order and local non-stoichiometry of the dislocation core [1][2]. In another study, it is shown that inherent screw dislocations in certain elemental and compound semiconductors generate coherent spin currents through spin orbit coupling effect [3]. Thus, dislocations, with unique and localized magnetic and electronic properties, as well as their interactions in attracting point defects could be engineered to designing next generation technological devices and there is need for a thorough theoretical understanding of their influence on electronic and magnetic properties by means of atomic scale modelling which provide a predictive way to model strongly distorted dislocation core region.

We present a systematic study of the core structure and electronic and magnetic properties of various dislocations in diamond using density functional theory (DFT). DFT calculations are performed with the Vienna ab initio Simulation Package (VASP), using norm-conserving pseudopotentials. Exchange and correlation contributions are treated within both the generalized gradient approximation and hybrid HSE06 (Heyd-Scuseria-Ernzerhof) functionals. To be able to satisfy periodic boundary conditions and to minimize long range elastic field interactions, supercells with two dislocations having opposite sign Burgers vectors (i.e. dislocation dipole) are used, which result in an infinite quadrupolar array of dislocations. The analysis of the electronic band structure along the dislocation line together with band decomposed charge density distributions reveal mid-gap energy states induced by broken atomic bonds in the dislocation core. Deep levels associated with dislocations are found to be donor type (n-type) charged dislocations. In addition, we compute the interaction of dislocations with nitrogen-vacancy centers. These results have a strong potential for tailoring the functionality of dislocations in various elemental and compound semiconductors for future electronic devices.

[1] Shimada, T., Xu, T., Araki, Y., Wang, J., & Kitamura, T. (2017). Multiferroic dislocations in ferroelectric PbTiO₃. *Nano letters*, 17(4), 2674-2680.

[2] Sugiyama, I., Shibata, N., Wang, Z., Kobayashi, S., Yamamoto, T., & Ikuhara, Y. (2013). Ferromagnetic dislocations in antiferromagnetic NiO. *Nature nanotechnology*, 8(4), 266.

[3] L. Hu, H. Huang, Z. Wang, W. Jiang, X. Ni, Y. Zhou, V. Zielasek, M. G. Lagally, B. Huang, F. Liu, "Ubiquitous Spin-Orbit Coupling in a Screw Dislocation with High Spin Coherency" *Phys. Rev. Lett.* 121, 066401 (2018).

EQ19.04.02

Generation of Anti-Reflective Diamond Surfaces Based on Artificial Moth-Eye Nanostructures Louise Kaeswurm and Joachim Spatz; Max Planck Institute for Medical Research, Germany

Reflectivity has always been a problem for a variety of processes involving interfaces and electromagnetic waves. For most substrates, the reflectivity can be reduced by introducing thin anti-reflective (AR) coatings. However, the conventional coating technology reaches its limit when dealing with diamond: due to the high refractive index of diamond it is nearly impossible to find suitable coating materials.

The bioinspired approach to achieve anti-reflective surfaces leads to so called moth-eye nanostructures, pillar-like structures with sizes in the nano- and micrometer-regime on the surface of the substrate. In nature, the structures have proven to effectively reduce the reflectivity. Copying these structures has shown that artificial moth-eye structures are also capable of reducing the reflectivity to a minimum. Here, the AR effect is not based on destructive interference created by defined layers of an AR coating and therefore does not depend on the fulfillment of interference conditions. In the case of moth-eye nanostructures, a density effect leads to continuous refractive index matching. Due to this, the AR properties are not limited to certain wavelengths or angles of incidence but are achieved for a broad band of incoming wavelengths and angles of incidence. This already poses a great advantage compared to the limited possibilities of conventional coating methods. Additionally, the size and shape of the pillar like structures have an impact on the enhanced optical properties, making it possible to tailor the structures to achieve the desired optical performance. Furthermore, by changing the optical properties in a surface-based and intrinsic process, the challenge of finding suitable coating materials can be neglected and the unique thermal, mechanical and electronic properties of diamond are not falsified by a comparably fragile coating.

So far, conventional lithographic methods have been used to generate such structures. These methods are comparably laborious, especially for large areas. We propose a new method to produce artificial moth-eye structures in polycrystalline diamond: using the self-assembly based block copolymer micellar lithography (BCML) and reactive ion etching (RIE), we found a possibility to implement moth-eye nanostructures in different materials. Originally developed for glassy silicon dioxide (SiO₂), the process has been refined for a variety of different substrates, ranging from simple glasses like SiO₂ to semiconductors like silicon up to high-performance materials like sapphire and diamond. In comparison to the conventional lithographic methods widely used to produce these moth-eye structures, the self-assembly based BCML method is comparably fast but still as reliable as conventional methods. For diamond, the structuring process has increased the maximum transmission over 15 % compared to the untreated substrate, also reducing the reflectance severely. These advantages show the significance of the presented method, especially for high performance materials with atypical properties such as diamond.

SESSION EQ19.05/EQ03.01: Joint Session: Quantum Applications of Diamond I
Session Chair: Julien Pernot
Wednesday Morning, December 1, 2021
Hynes, Level 1, Room 101

10:30 AM *EQ19.05/EQ03.01.01

Challenges of CVD Single Crystal Diamond Engineering for Quantum Applications Jocelyn Achard¹, Alexandre Tallaire^{2,1}, Ovidiu Brinza¹, Midrel Ngandeu¹, Chaimaa Mahi¹, Audrey Valentin¹, Riadh Issaoui¹, Vianney Mille¹ and Fabien Benedic¹; ¹LSPM-CNRS, France; ²IRCP-CNRS, France

The development of applications in quantum sensing require dedicated solid-state material platforms with unprecedented control over quality, purity and

doping. Indeed, Quantum Technologies (QT) explore our ability to coherently control the peculiar properties of nanoscale quantum systems and harness their potential in a wide range of fields including health, communications, security and environment. In particular, sensors and devices having a disrupting performance as compared to classical systems are foreseen in a relatively short-term [1].

Atomic-scale defects in solid-state materials are among the most promising candidates and several platforms are being considered such as donors in silicon, color centers in semiconductors (NVs in diamond and SiC), rare-earth ions in oxides, quantum dots etc. One of the inherent drawbacks of the extreme sensitivity of such spin systems to the field they are supposed to measure, is the necessity to carefully control their close crystalline environment in order to maximize coherence properties. This pushes the fabrication technologies to their limits and requires that tailored materials are produced on purpose. In this presentation, we will review the main challenges in the synthesis of suitable “quantum-grade” materials with a special emphasis to color centers in diamond and more specifically NV centers. Issues related to controlling their density and maximizing their coherence properties through precise engineering will be discussed. (i) Atomic scale defects need to be selectively doped on demand within the matrix. High amounts are usually preferred in most sensing schemes but limits exist in the ability to control growth at high doping levels as well as to avoid interaction between nearby spins. (ii) Nuclear spins within the matrix itself might cause unwanted decoherence and growth of isotopically enriched materials allows considerably extending T_2 times or investigating specific coupling schemes with nearby spins. This has serious implications on the precursors used for material synthesis. (iii) In the same vein, magnetic sensitivity of a sensor based on NV ensembles can be considerably increased by producing diamond with NV centers having preferential orientation which can be obtained by using diamond substrates with specific crystallographic orientation such as (111) or (113) (iv) Controlling the spatial localization of color centers is crucial to the sensing device since their interaction strongly depends on the distance to the field that is to be sensed. Positioning them close to the surface with ion implantation is an efficient and widely followed approach but which comes along with the generation of residual defects that can seriously impact the spin properties.

[1] Degen, C. et al. *Reviews of Modern Physics* **2017**, 89 (3), 035002.

11:00 AM *EQ19.05/EQ03.01.02

Engineering New Solid State Quantum Defects for Quantum Networks [Nathalie P. de Leon](#); Princeton University, United States

Engineering coherent systems is a central goal of quantum science and quantum information processing. Point defects in diamond known as color centers are a promising physical platform. As atom-like systems, they can exhibit excellent spin coherence and can be manipulated with light. As solid-state defects, they can be produced at high densities and incorporated into scalable devices. Diamond is a uniquely excellent host: it has a large band gap, can be synthesized with sub-ppb impurity concentrations, and can be isotopically purified to eliminate magnetic noise from nuclear spins. Currently-known color centers in diamond either exhibit long spin coherence times or efficient, coherent optical transitions, but not both. We have developed new methods to control the diamond Fermi level in order to stabilize a new color center, the neutral charge state of the silicon vacancy (SiV) center. This center exhibits both the excellent optical properties of the negatively charged SiV center and the long spin coherence times of the NV center, making it a promising candidate for applications as a single atom quantum memory for long distance quantum communication. We have recently discovered bound exciton transitions associated with SiV0, which enable efficient optical spin polarization and optically detected magnetic resonance. Finally, I will describe our efforts to integrate SiV0 centers in nanophotonic devices, specifically in heterogeneously integrated III-V/diamond nanophotonic platforms designed to enhance the atom-photon interaction and achieve quantum frequency conversion to the telecom band.

11:30 AM *EQ19.05/EQ03.01.03

Enhanced Quantum Sensitivity for Diamond Spins via Real-Time Control [Lee Bassett](#); University of Pennsylvania, United States

Despite the technological maturity of nitrogen-vacancy (NV) centers in diamond as a platform for quantum technology, their performance in most applications is hindered by imperfect state initialization and readout [1]. This is especially true for quantum sensing, where the NV center’s charge and spin stability are typically degraded by proximity to surfaces and impurities. This talk will present a framework for optimizing the performance of NV-center quantum sensors using all-optical techniques that improve the signal-to-noise ratio through spin-to-charge conversion [2] and deterministic charge initialization [3]. I will also discuss recent efforts to create nanodiamond assemblies and to characterize their material and quantum properties, towards the realization of new sensing modalities.

D. A. Hopper, H. J. Shulevitz, and L. C. Bassett, *Micromachines* **9**, 437 (2018)

D. A. Hopper et al., *ACS Nano* **12**, 4678 (2018).

D. A. Hopper et al., *Phys. Rev. Applied*, **13**, 024016 (2020).

This work was supported by the NSF through a CAREER award (ECCS-1553511) and the University of Pennsylvania Materials Research Science and Engineering Center (MRSEC) (DMR-1720530).

SESSION EQ19.06/EQ03.02: Joint Session: Quantum Applications of Diamond II

Session Chair: Nathalie de Leon

Wednesday Afternoon, December 1, 2021

Hynes, Level 1, Room 101

1:30 PM *EQ19.06/EQ03.02.01

Inversion Symmetric Color Centers in Diamond for Quantum Technology Gergo Thiering¹, Anton Pershin¹ and [Adam Gali](#)^{1,2}; ¹Wigner Research Centre for Physics, Hungary; ²Budapest University of Technology and Economics, Hungary

Inversion symmetry makes the color centers insensitive to stray electric fields in diamond which enables to create indistinguishable solid state single photon sources. The most studied and employed representative is the negatively charged silicon-vacancy defect [SiV(-)] in diamond. However, the fine electronic structure of SiV(-) limits the coherence times of the electron spin, thus it is not practical. One possible route is to use isovalent tin or lead which are predicted to possess longer coherence times [1]. Alternatively, SiV(0) and their akin isovalent variants [2] may be used where the ground state spin has a long coherence time [3]. We show that the excited state of SiV(0) is highly complex in which the Rydberg excited states can be used to optically readout the spin state which is a crucial step towards coherent manipulation of single SiV(0) centers. We identify further inversion symmetric color centers in diamond such as the negatively charged magnesium-vacancy [MgV(-)] defect. We find that the electronic structure of MgV(-) permits the coexistence of two loosely separated spin-states, where both can emerge as a ground state and be interconverted depending on the temperature and external strain. These results demonstrate a route to control the magneto-optical response of a qubit by modulating the operational conditions [4]. We also identified the negatively charged nickel-vacancy center in diamond which has favorable spin coherence time at cryogenic temperature which can be coherently controlled

by all-optical means. This work was supported by the Ministry of Innovation and Technology and the National Research, Development and Innovation Office of Hungary (NKFIH) within the Quantum Information National Laboratory of Hungary, the National Quantum Technology Program (NKFIH Grant no. 2017-1.2.1-NKP-2017-00001). A.G. acknowledges the National Excellence Program (NKFIH Grant no. KKP129866), the EU QuantERA project “Q_magine” (NKFIH Grant no. 127889) as well as the support of the European Commission within the Quantum Technology Flagship Project ASTERIQS (Grant no. 820394).

[1] G. Thiering and A. Gali, *Phys. Rev. X* **8**, 021063 (2018)

[2] G. Thiering and A. Gali, *npj Comp. Mat.* **5**, 18 (2019)

[3] Zi-Huai Zhang, Paul Stevenson, Gergo Thiering, Brendon C. Rose, Ding Huang, Andrew M. Edmonds, Matthew L. Markham, Stephen A. Lyon, Adam Gali, and Nathalie P. de Leon, *Phys. Rev. Lett.* **125**, 237402 (2020)

[4] Anton Pershin, Gergely Barcza, Örs Legeza, and Adam Gali, *npj Quantum Information* **7**, 99 (2021)

2:00 PM EQ03.03.02

Multi-Frequency Spin Dependent Transient Spectroscopy [Kenneth Myers](#) and Patrick Lenahan; The Pennsylvania State University, United States

Long ago, Chen and Lang¹ demonstrated spin dependent deep level transient spectroscopy in metal-oxide-semiconductor (MOS) capacitors, combining the advantages of both electron paramagnetic resonance (EPR) and deep level transient spectroscopy (DLTS). EPR and the closely related electrically detected magnetic resonance (EDMR)² techniques are able to identify the chemical and physical nature of paramagnetic point defects while DLTS has the capability to determine point defect energy levels. We report on a simplification of the Chen and Lang method which we term spin dependent transient spectroscopy (SDTS) and demonstrate the magnetic field and frequency independence of this technique. Additionally, we show that it can be extended to utilize near zero field magnetoresistance (NZFMR)³ spectroscopy. Our SDTS measurements were performed on negative-bias-temperature-stressed⁴ Ti-Al/SiO₂/p-Si capacitors.

In our SDTS measurements we somewhat modified the spin dependent DLTS technique of Chen and Lang, utilizing a single boxcar averager for time-resolved data acquisition. In addition, we show that this modified technique has essentially the same sensitivity at X-band (≈ 9.4 GHz) and quite low RF (≈ 500 MHz) frequencies. The physics of this method is quite simple. Applying a voltage pulse to the metal gate brings the interface Fermi level from near the valence band to near the conduction band. This creates a current transient due in part to charge carriers filling defect levels at the insulator-semiconductor interface. Since the capture process can be spin dependent, the recombination component of the transient can be affected by magnetic resonance. These observed spin dependent events allow for the identification of the involved interface states.

We have made these measurements as functions of the pulse voltage (V_{min}), sustained base voltage (V_{max}), pulse time, and acquisition window. Each of these parameters has an effect on the amplitude of the spin dependent response. We focus on the pulse and base voltages of our waveform in order to determine energy levels in the bandgap. Additionally, we show that we can perform SDTS at high and low fields/frequencies as well as in the NZFMR regime. In conclusion, we show that SDTS is a potentially powerful new tool with comparable sensitivity to other EDMR techniques with the advantage of observing interface states in simple metal-insulator-semiconductor structures.

¹ M.C. Chen and D. V. Lang, *Phys. Rev. Lett.* **51**, 427 (1983).

² D. Kaplan, I. Solomon, and N.F. Mott, *J. Phys. Lettres* **39**, 51 (1978).

³ N.J. Harmon, S.R. McMillan, J.P. Ashton, P.M. Lenahan, and M.E. Flatte, *IEEE Trans. Nucl. Sci.* **67**, 1669 (2020).

⁴ D.K. Schroder and J.A. Babcock, *J. Appl. Phys.* **94**, 1 (2003).

2:15 PM EQ03.04.01

Sensing Nuclear Spins of Adsorbed Molecules on a Diamond Surface with Shallow NV Centers [Konstantin Herb](#), John Abendroth, Tianqi Zhu, Erika Janitz and Christian Degen; ETH Zurich, Switzerland

The structure elucidation of macromolecules and molecular complexes is an important topic in molecular biology and biochemistry. The nitrogen vacancy center (NV center) is seen as a promising platform for scaling nuclear magnetic resonance down to the single-molecule level. However, the sensing capability of near-surface NVs – a necessary prerequisite for single-molecule NMR – is severely limited by charge state instabilities and decoherence due to surface traps and electronic and magnetic surface noise, respectively. Here, we report on strategies to improve the stability of NV centers and their coherence properties by controlled termination of the diamond surface, and to functionalize the diamond surface to bind molecules of interest.

In this talk, we discuss the creation of 3 to 7 nm deep NVs in nano-structured diamond surfaces that show T_2 coherence times of 50 to 300 μ s. The creation of photonic structures boosts the collection efficiency and allow us to follow single NV centers as the diamond undergoes surface termination and functionalization steps. We investigate the effects of oxygen- and nitrogen-termination, and find that the former improves the electron spin coherence properties if annealing is performed below the graphitization-threshold. Further, we chemically functionalize the diamond surface with fluorinated silanes and show that, after silanization, a ¹⁹F NMR signal can be detected. The successful functionalization is further confirmed by complementary X-ray Photoelectron Spectroscopy (XPS) and fluorescence measurements. We give an outlook on the steps needed to perform nuclear magnetic resonance (NMR) measurements on the single-molecule level.

SESSION EQ19.07: Hybrid Structures
Session Chair: Jocelyn Achard
Wednesday Afternoon, December 1, 2021
Hynes, Level 1, Room 101

4:00 PM EQ19.07.01

Diamond CVD Deposition on CF for Aerospace Applications [Josué Millán Barba](#)^{1,2}, Hicham Bakkali¹, Marina Guitierrez¹, Fernando Lloret¹, Roberto Guzmán de Villoria³, Manuel Dominguez¹, Ken Haenen⁴ and Daniel Araujo¹; ¹University of Cádiz, Spain; ²Foundation for the research development and application of composite materials (FIDAMC), Spain; ³University of Salamanca, Spain; ⁴University of Hasselt, Belgium

Carbon fibers reinforce polymers (CFRP) is the principal structural material used in the aerospace industry due to its high strength-low weight ratio as well as its high stiffness. In contrast, CFRP is a bad electrical and heat conductor. This limits heat dissipation which causes high damages when lightning impacts occur. In addition, the aircraft structure should act as a Faraday cage to protect electronic devices which is not possible with standard CFRP. In this work it is evidenced that the use carbon fiber coating made of highly doped boron polycrystalline diamond (HDBPD), increases the electrical conductivity

of carbon fiber (CF) for the manufacture of aeronautical structures.

HDBPD was deposited by microwave plasma enhanced chemical vapor deposition (MW PE CVD) on one commercial carbon fiber used in the aerospace industry, specifically HexTow AS7 from Hexcel, using a clamshell ASTeX 6500 series reactor. The growth conditions chosen to avoid fiber damage due to plasma were: low temperature (700 °C) and pressure (35 Torr), 1% methane and 40 Sccm of trimethylborane (TMB). Once the polycrystalline diamond was deposited on a commercial tow, different individual fibers were taken to prepare samples for transmission electron microscopy (TEM) and atomic force microscopy (AFM). Both the traditional polishing as Focus Ion Beam (FIB) methods were used to check to check the suitability of both methods in this type of CF/diamond material to avoid sample preparation artifacts.

Electron beam techniques such as high-resolution electron microscopy (HREM), electron energy loss spectroscopy (EELS) and scanning electron microscopy (SEM), were used to determine their CF/interface/diamond nanostructure. HREM showed that an intermediate layer grows on the fiber surface first, on which the polycrystalline diamond is subsequently formed. The analysis of this layer by EELS revealed its strong sp^2 character which is in accordance with the bibliography where this layer is described as Carbon nanowalls. The subsequent polycrystalline diamond layer was ~1 micrometer thick and contained spherical grains averaging 70 nanometers.

The electrical properties of the HDBPD-carbon fiber were measured using conductive and scanning microwave impedance microscopy atomic force microscopy (C-AFM and sMIM-AFM) and Kelvin method. The improvement of the electrical conductivity of the CF is evidenced after HDBPD deposition.

4:15 PM EQ19.07.02

TCAD Simulation of High Power β -Ga₂O₃/Diamond Heterojunction PIN Diodes Cristian J. Herrera-Rodriguez¹ and Timothy Grotjohn^{1,2}; ¹Michigan State University, United States; ²Fraunhofer USA, United States

CVD Diamond is one of the most promising semiconductor materials for high power applications, because of its exceptional mechanical, electronic and thermal properties, such as wide band-gap, high breakdown electric field, high mobility and high thermal conductivity. Diamond bipolar devices are promising for ultra-high voltage applications (>10kV), but diamond PN junctions provides limitations due to (1) a high turn-on voltage (~5V) giving a significant on-state voltage drop and (2) n-type diamond having higher resistivity and poor ohmic contacts. In order to address this problem, the implementation of an alternative n-type UWBG semiconductors with shallow donor dopants should be considered. Beta-Gallium Oxide (β -Ga₂O₃) is a semiconductor that has gained significant attention due to its attractive properties like its wide bandgap (4.85eV) and high breakdown field in the range of 8 MV/cm. Also, commercially available larger area high quality β -Ga₂O₃ wafers will lead to potentially more affordable high performance power devices. Diamond's outstanding thermal properties can serve as a heat dissipater at high power operations, compensating the poor thermal conductivity of β -Ga₂O₃. As an experimental demonstration of a diamond/ Ga₂O₃ pn junction device structure a photodiode [1] has been demonstrated in the literature using a nanomembrane of Ga₂O₃ on diamond.

In this study we report the device modeling using TCAD Sentaurus and analysis of n-type β -Ga₂O₃/p-type diamond heterojunction PIN diodes for future applications in power electronic devices. Material parameters input entered into the TCAD model will be presented. The heterojunction modeled had a band discontinuity of $\Delta E_c=2.7\text{eV}$ at the conduction band and $\Delta E_v=2.1\text{eV}$ at the valence band. It was observed that at voltages >5V, the on-state shows conductivity modulation in the drift region in the forward regime. The current density, carrier concentration and carrier recombination spatial distribution for the diamond intrinsic region with a thickness of 1 μm as a function of temperature and carrier lifetime will be examined.

[1] H. Kim *et al.*, "Ultrawide-Bandgap p-n Heterojunction of Diamond/ β -Ga₂O₃ for a Solar-Blind Photodiode," *ECS J. Solid State Sci. Technol.*, vol. 9, no. 4, p. 045004, Apr. 2020, doi: 10.1149/2162-8777/ab89b8.

4:30 PM EQ19.07.03

A Scanning Nonlinear Dielectric Microscopic Investigation of Al₂O₃/Diamond MOS Interfaces Yu Ogata¹, Kohei Yamasue¹, Xufang Zhang², Tsubasa Matsumoto², Norio Tokuda² and Yasuo Cho¹; ¹Tohoku University, Japan; ²Kanazawa University, Japan

Recently, inversion type p-channel diamond MOSFETs with normally off characteristics have been demonstrated for the first time [1]. However, the improvement of the channel mobility is one of the major issues towards the practical application of the diamond based power devices [2]. The previous studies have suggested that high interface defect density (D_{it}) at the Al₂O₃/diamond interface significantly reduce the channel mobility [2].

Although such macroscopic evaluation method employed in the previous studies is capable of quantitatively evaluating D_{it} with good energy depth resolution, the lateral resolution is quite limited. On the other hand, recently there have been reports suggesting that interface traps have an inhomogeneous spatial distribution, which makes characterizing interface traps with high lateral resolution quite interesting and important [3].

In the present study, in order to give microscopic insights on the physical origin of the high D_{it} , we investigate the Al₂O₃/diamond interfaces using scanning nonlinear dielectric microscopy (SNDM) [4, 5].

SNDM permits nanoscale evaluation of local MOS capacitance [5] which can perform local differential capacitance (dC/dV) imaging, local CV profiling [6], and local deep level transient spectroscopy (DLTS) using a time-resolved SNDM (tr-SNDM) setup [7].

The samples were fabricated from highly B-doped p⁺- diamond layer grown on the back side of a high-pressure and high-temperature p-type (111) substrate for ohmic contact formation and had a 50 nm thickness atomic layer deposited Al₂O₃ top layer [1, 2]. We measured three different samples, whose diamond surfaces were terminated by H, O, and OH-groups, respectively.

At first, local CV profiles were here obtained. The H-terminated sample exhibited strongly negative shift reflecting the formation of surface accumulation layer, while the O- and OH-terminated samples showed depletion at 0 V. The three profiles also showed different behaviors in the transition from depletion to accumulation, suggesting D_{it} is highest in the O-terminated samples followed in order by the OH- and H-terminated samples. We could find that these local CV profiles also showed microscopic spatial fluctuations, which might be correlated with D_{it} [8].

Second, we measured dC/dV images of two different areas with atomic flatness and high roughness in the OH-terminated sample. In both images, there are non-uniformly distributed dark, or low dC/dV, spots indicating the low slope of local CV profiles. Since dC/dV becomes lower due to higher D_{it} broadening the local CV profile, the observed images possibly visualize the high D_{it} spots non-uniform distributing at the Al₂O₃/OH-terminated diamond interface and the difference of the interface by the flatness of the diamond surfaces.

Finally, we also performed local DLTS on the same sample. We found the non-uniform D_{it} distribution, again. In addition, the line-shaped features

of D_{it} distribution could be observed especially in the atomic flat area. The line-shaped features might be related to the variation of D_{it} at the atomic steps in the buried interface. In fact, the previous study by conductive atomic force microscopy and Kelvin probe force microscopy also showed the steps seem to generate D_{it} [8].

- [1] T. Matsumoto et al., *Sci. Rep.* 6, 31585 (2016).
- [2] T. Matsumoto et al., *Appl. Phys. Lett.*, 114, 242101 (2019).
- [3] N. Chinone, A. Nayak, R. Kosugi, Y. Tanaka, S. Harada, H. Okumura, and Y. Cho, *Appl. Phys. Lett.*, 111, 061602 (2017).
- [4] Y. Cho, A. Kirihara, and T. Saeki, *Rev. Sci. Instrum.*, 67, 2297 (1996).
- [5] Y. Cho, "Scanning Nonlinear Dielectric Microscopy: Investigation of Ferroelectric, Dielectric, and Semiconductor Materials and Devices", Elsevier, ISBN 9780128172469 (2020).
- [6] K. Suzuki et al., in 2019 IEEE International Integrated Reliability Workshop (IIRW) (2019).
- [7] Y. Yamagishi and Y. Cho, *Appl. Phys. Lett.* 111, 163103 (2017).
- [8] E. H. Nicollian and A. Goetzberger, *Bell Labs Tech. J.* 46, 1055 (1967).

4:45 PM CLOSING COMMENTS

SESSION EQ19.08/EQ03.05: Joint Session: Quantum Applications of Diamond III
Session Chairs: Peter Knittel and Anke Krueger
Monday Morning, December 6, 2021
EQ19-Virtual

8:00 AM *EQ19.08/EQ03.05.01

Diamond Quantum Sensors—From Growth to Applications Mutsuko Hatano; Tokyo Institute of Technology, Japan

Diamond is an excellent host for spin-based qubits, and the spin in diamond has excellent properties. Nitrogen-vacancy (NV) center in diamond is one of the most promising candidates for quantum sensing. The energy levels of NV centers are sensitive to magnetic fields, electric fields, strain, and temperature, enabling scalable applications from the atomic to the macroscopic range [1].

Core technologies on material, sensor systems, and applications for energy electronics and life science are introduced.

Materials

Selectively aligned NV ensemble formed by distinctive CVD-growth for scalable applications.

The heteroepitaxial growth of NV-contained diamond on Si substrate for large area and on-chip integration.

Multi-scale and multi-modal sensor systems

- Direct sensing of nano-scale internal electric-field in the power device [2]
- EV battery monitoring [3]
- Magnetocardiography (MCG) of mammalian animals [4]

This work was supported by MEXT QLEAP Grant Number JPMXS0118067395.

The author would like to thank Lab and Q-LEAP members for their contributions and helpful discussion.

- [1] L. Doherty et al., *Phys. Rep.* 528, 1 (2013).
- [2] Bang Yanget et al., *Physical Review Applied* 14, 044049 (2020).
- [3] Y. Hatano et al., *APL* 118, 034001 (2021).
- [4] K. Arai et al., *arXiv*2105.11676 (2021).

8:30 AM *EQ19.08/EQ03.05.02

Plasma CVD Synthesis of Nitrogen-Vacancy Centers in (111)-Oriented Diamond Hiromitsu Kato, Moriyoshi Haruyama, Yukako Kato, Masahiko Ogura and Toshiharu Makino; AIST, Japan

Nitrogen vacancy (NV) center in diamond has much attention as a quantum material that can realize spin-based sensing due to its excellent characteristics such as long coherence time, fast manipulation rates, optical initialization and readout, etc. Precise control of material-related parameters including NV concentrations, axis alignment, volume, charge-state, are essential for higher sensitivity and are important to bring the NV centers closer to quantum application in practical use. Plasma-enhanced chemical vapor deposition (CVD) with microwave is one of the major approaches to introduce well-defined NV centers in diamond, as well as electron beam irradiation and ion implantation techniques. So far, we have already proposed following ideas based on semiconductor engineering; the charge-state stabilization by n-type Fermi control [1,2], longer coherent time by phosphorus and carbon isotopic control [3], perfect alignment of NV axis [4], device applications with PIN junction [5-7]. All these achievements are based on our comprehensive progresses of CVD diamond growth, impurity doping, junction management, and device fabrication processes. Details will be discussed focusing on technical aspects peculiar to plasma CVD engineering of diamond NV centers.

Acknowledgments

This work was partially supported by MEXT Q-LEAP (JPMXS0118067395), JST CREST (JPMJCR1773), MIC R&D (JPMI00316), and JST Moonshot R&D (JPMJMS2062).

References

- [1] H. Kato, M. Ogura, T. Makino, D. Takeuchi, and S. Yamasaki, *Appl. Phys. Lett.* 109, 142102 (2016).
- [2] Y. Doi, T. Fukui, H. Kato, T. Makino, S. Yamasaki, T. Tashima, H. Morishita, S. Miwa, F. Jelezko, Y. Suzuki, and N. Mizuochi, *Phys. Rev. B* 93, 081203(R) (2016).
- [3] T. Murai, T. Makino, H. Kato, M. Shimizu, T. Murooka, E. D. Herbschleb, Y. Doi, H. Morishita, M. Fujiwara, M. Hatano, S. Yamasaki, and N. Mizuochi, *Appl. Phys. Lett.* 112, 111903 (2018).
- [4] E. D. Herbschleb, H. Kato, Y. Maruyama, T. Danjo, T. Makino, S. Yamasaki, I. Ohki, K. Hayashi, H. Morishita, M. Fujiwara and N. Mizuochi, *Nat. Commun.* 10, 3766 (2019).
- [5] H. Kato, M. Wolfer, C. Schreyvogel, M. Kunzer, W. Muller-Sebert, H. Obloh, S. Yamasaki, and C. Nebel, *Appl. Phys. Lett.* 102, 151101 (2013).
- [6] T. Iwasaki, W. Naruki, K. Tahara, T. Makino, H. Kato, M. Ogura, D. Takeuchi, S. Yamasaki, and M. Hatano, *ACS Nano* 11, 1238 (2017).

[7] N. Mizuochi, T. Makino, H. Kato, D. Takeuchi, M. Ogura, H. Okushi, M. Nothaft, P. Neumann, A. Gali, F. Jelezko, J. Wrachtrup and S. Yamasaki, *Nat. Photonics* 6, 299 (2012).

9:00 AM EQ19.08/EQ03.05.03

Fabrication of High-Density NV Ensemble Using Vacancies Created by Transmission Electron Microscope Kyosuke Hayasaka¹, Kyotaro Kanehisa¹, Tetsuya Tatsuishi¹, Yuta Saito¹, Yuki Ueda¹, Kazuki Otani¹, Takashi Tani¹, Shinobu Onoda², Junichi Isoya³, Shinpei Enomoto⁴, Shozo Kono⁴ and Hiroshi Kawarada^{1,4}; ¹Waseda University, Japan; ²QST, Japan; ³University of Tsukuba, Japan; ⁴ZAIKEN, Japan

Negatively charged nitrogen vacancy (NV) center is expected to be a platform for magnetic sensors and quantum communications because of its optically detectable spin properties and long coherence time [1]. One of the most leading application of NV center is magnetic sensor with high sensitivity even at room temperature. Especially, the sensitivity of a magnetic sensing scales with the square root of its quantum coherence time and the total number of NV centers [1]. Thus, enhanced NV concentration while maintaining long coherence times is desired to improve magnetic sensitivity. Ion implantation is frequently used to increase NV concentration [2]. However, this method results in unwanted paramagnetic defects or charge traps due to knock-on-atoms [3]. Delta-doping with CVD diamond growth is also used to create high density NV ensemble [4]. Yet, this technology has the problem of low N-to-NV conversion efficiency. Therefore, it is an effective approach to maximize N-to-NV conversion efficiency while suppressing damage to the substrate by electron irradiation.

Single-ended accelerator [5] or TEM [6] is used to create vacancies on the substrate with electron irradiation. TEM can adjust the electron irradiation amount per unit time by narrowing the beam diameter. As a result, it is possible to irradiate a high dose of electrons that cannot be achieved by the accelerator. TEM also has the advantage of being easily accessible compared to the accelerator. In fact, several groups have reported using a 200-keV TEM for (100) diamonds, while none have reported for (111) diamonds. Since (111) diamond can incorporate more dense nitrogen atoms than (100) diamond [7], electron irradiation of (111) diamond is promising for the realization of high density NV ensemble. Hence, by irradiating (111) diamond with electrons, we investigated the change in NV density and spin properties in the irradiated region and estimated the magnetic sensitivity.

We irradiated nitrogen-rich ($[N]=4\times 10^{19}$ [cm⁻³]) HPHT (111) diamond with electrons using 300-keV TEM (JEOL JEM-3010) because the minimum energy of electrons required to form a defect in (111) diamond is 220-keV [8]. Next, a custom-built laser scanning confocal fluorescence microscope (CFM) was used to estimate the concentration of NV center. We also measured the coherence time of the NV ensemble. We then implemented photoluminescence measurements (RENISHAW inVia Basis) to confirm the presence of vacancy as GR1 center in PL spectrum.

As a result, the PL spectra in the electron-irradiated region showed that the peak intensity at 638 nm, which is the ZPL of , intensified with increasing electron dose. The volume density of the NV center in the NV ensemble increased with increasing electron fluence from 10^{16} to 10^{22} [cm⁻²]. The NV volume density was calculated by comparing the luminescence intensity of the CFM image in the NV ensemble with that of the Single NV center. At a dose of 1.0×10^{22} [cm⁻²], the NV volume density reached to 8×10^{18} [cm⁻³], which is one of the highest NV density. The coherence time remained on the order of even when the electron fluence was increased, which is expected to improve the magnetic sensitivity.

This work was supported by This work was supported by MEXT Quantum Leap Flagship Program (MEXT Q-LEAP) Grant Number JPMXS0118067395.

- [1] V. M. Acosta, D. Budker *et al.*, *Phys. Rev. B* 80, 115202 (2009).
- [2] E. E. Kreinsasser, Kai-Mei C. Fu *et al.*, *Appl. Phys. Lett.* 108, 202401 (2016).
- [3] G. Davies, T. Anthony *et al.*, *Phys. Status Solidi A* 186(2), 187 (2001).
- [4] M. Chandran, A. Hoffman, *et al.*, *Appl. Phys. Lett.* 109, 221602 (2016).
- [5] C. Zhang, J. C. Fang *et al.*, *J. Phys. D: Appl. Phys.* 50 505104 (2017).
- [6] D. Farfurnik, N. Bar-Gill *et al.*, *Appl. Phys. Lett.* 111, 123101 (2017).
- [7] R. C. Burns, C. M. Welbourn *et al.*, *J. Cryst. Growth* 104 257-79 (1990).
- [8] J. Koike, D. M. Parkin, and T. E. Mitchell, *Appl. Phys. Lett.* 60, 1450 (1992).

9:15 AM EQ19.08/EQ03.05.04

Study of Electronic and Optical Properties of NV Centers in Diamond for Sensing Applications—First Principles Density Functional Theory and Experimental Approach Hari P. Paudel¹, Scott Crawford², Benjamin Chorpeng² and Yuhua Duan²; ¹Leidos Inc/NETL DOE, United States; ²U.S. Department of Energy National Energy Technology Laboratory, United States

The nitrogen-vacancy (NV) center in a nanodiamond (ND) crystal is one of the best candidate materials for quantum sensing and metrology at elevated environmental conditions. The NV center can be used to achieve an unprecedented level of sensitivity for sensing applications at high temperatures and pressures. In addition, the NV center is proven to be useful for magnetic field sensing. This opens avenues for applications in the sensing of valuable minerals such as rare earth elements (REEs) in crude and waste subsurface materials which carry free electronic spins locally. In this work, we present our computational and experimental studies on electronic and optical properties of bulk diamond with N impurity and N with a carbon (C) vacancy defect. Experimentally, we encapsulate NDs in MOF/polymer materials. We measure the transverse spin relaxation time of NV center in bare and encapsulated NDs. In order to study the surfaces with shallow NV center that are useful for the quantum sensing applications, we will introduce different doping elements on the surfaces and present surface electronic properties.

9:30 AM *EQ03.03.01

Nanoscale Probing of 2D Magnetic Order Joerg Wrachtrup; University of Stuttgart, Germany

The investigation of magnetic order in 2D materials requires dedicated probes. While conventional probes of magnetism with nanoscale resolution, like Lorenz microscopy or MFM fail for few layer- or monolayer samples, STM requires dedicated sample preparation. NV-based magnetic probes on the other hand are very well suited to provide quantitative data with a few ten nm spatial resolution and sufficient sensitivity, even for monolayer samples. In the talk I will describe experiments on CrBr₃ which show the domain structure of the material [1]. Upon imaging material with different number of layers we gained insight into interlayer coupling and its impact on magnetic order. We also measure magnetic order over a wide range of temperatures and derive information on the physics of the phase transition of CrBr₃. We also measured CrI₃ samples of different thickness and relative order and find signatures of periodic magnetic order in twisted multilayers. [1] Qi-Chao Sun *et al.* *Magnetic domains and domain wall pinning in atomically thin CrBr₃ revealed by nanoscale imaging*, *Nature Comm.* 12, 1989 (2021)

10:30 AM *EQ19.09/EQ03.06.01

Single Crystal Diamond Growth by Chemical Vapor Deposition for High-End Applications—Recent Trends and State of the Art Matthias Schreck and Theodor Grünwald; University of Augsburg, Germany

In order to profit from diamond's unique material properties for demanding device applications, high quality single crystals are needed. For their synthesis by chemical vapor deposition (CVD) two alternative strategies are currently being explored with great effort. The first is based on homoepitaxy using low-dislocation-density crystals from the high pressure high temperature (HPHT) method as growth seeds. While the obtained crystals excel in terms of highest structural quality, the concept still suffers from limitations in size. In the alternative heteroepitaxy concept, diamond is nucleated and grown on a single crystal surface of a foreign material. Among all potential crystalline materials, iridium has been identified as unique. A major advantage of heteroepitaxy consists in its better scalability which has been demonstrated in 2017 by the realization of a diamond/Ir/YSZ/Si(001) wafer with a diameter of 92 mm [1]. However, the minimum values in dislocation density ($7 \times 10^6 \text{ cm}^{-2}$) and mosaic spread (FWHM: polar 0.03° and azimuthal 0.05°) [2], are still significantly higher than for homoepitaxially grown crystals.

After reviewing the current state of the art, recent and new attempts to reduce the dislocation densities are described. These comprise different variants of epitaxial lateral overgrowth (ELO) and metal assisted termination (MAT).

Next, the properties of threading dislocations in heteroepitaxial diamond as traps for holes and electrons have been investigated. The experimentally derived lifetime values facilitate estimations of the corresponding capture cross sections and extrapolations on critical defect densities for potential applications [2].

Progress in dislocation density reduction and increase in lateral dimensions call for efficient techniques to duplicate the wafers so that the excellent structural properties once achieved on large area substrates can be transferred to new samples. In this context, a new smart-cut process with easy scalability has been developed [3].

In the final part, gain formation as an old and fundamental problem in the application of diamond as solid state ionization chamber for dosimetry of high energy radiation is discussed. A model is presented that can quantitatively explain the formation of gain and its huge variation ranging from less than 1 to more than 10^6 [4].

[1] M. Schreck, S. Gsell, R. Brescia, M. Fischer: Ion bombardment induced buried lateral growth: the key mechanism for the synthesis of single crystal diamond wafers, *Sci. Rep.* **7**, 44462 (2017).

[2] M. Schreck, P. Ščajev, M. Träger, M. Mayr, T. Grünwald, M. Fischer, S. Gsell: Charge carrier trapping by dislocations in single crystal diamond. *J. Appl. Phys.* **127**, 125102 (2020).

[3] M. Schreck, M. Mayr, M. Weini, M. Fischer, S. Gsell: Liftoff of single crystal diamond by epitaxial lateral overgrowth using SiO_2 masks, *Diamond Relat. Mater.* **101**, 107606 (2020).

[4] T. Grünwald and M. Schreck: Photoconductive gain in single crystal diamond detectors, *J. Appl. Phys.* **129**, 124502 (2021).

11:00 AM *EQ19.09/EQ03.06.02

Development and Optimization of CVD Diamond Growth Processes for Magnetic-Field Sensing Applications Andrew M. Edmonds, Matthew Markham, Pierre-Olivier Colard and Daniel Twitchen; Element Six, United Kingdom

Quantum technologies is attracting significant investment due to the range of potential applications, but behind any new technology are enabling materials. Diamond is one such material and ensembles of negatively-charged nitrogen-vacancy (NV^-) centers constitutes a promising platform for sensing applications utilizing the quantum properties of this defect. However, the sensitivity of present NV^- ensemble devices and the need for diamond material with reproducible properties has the potential to hinder progress toward many envisioned commercial-scale applications.

The work covered in this presentation will address the material-related aspects of these challenges by discussing the progress towards the development of chemical vapor deposition (CVD) growth processes incorporating high substitutional-nitrogen (N_S) concentrations (> 8 parts-per-million carbon atoms), specifically targeted for magnetic-field sensing. Through this optimisation process the effects of N-doping during CVD growth have also been investigated by characterization of the as-grown sample properties, including concentrations of $[\text{N}_\text{S}^0]$ and $[\text{N}_\text{S}^+]$, as well as color.

Through detailed study of varying CVD processes for high- $[\text{N}_\text{S}]$ diamond it is shown that increased nitrogen incorporation does not necessarily result in increased densities of unwanted vacancy-related defects which act as a source of broadband absorption in as-grown CVD diamond (commonly resulting in a brown coloration). Previously suggested correlations between $[\text{N}_\text{S}^+]$ and the level of broadband absorption, as well as the bands at 360 nm and 520 nm are also investigated and strong links have been established in this study. Measurements of the NV^- concentration, charge ratio and contrast suggest that these grown-in defects have a detrimental impact on the NV^- ensemble properties observed after irradiation and annealing.

This work also investigated the potential to produce material with reproducible as-grown $[\text{N}_\text{S}]$ at a level of ~ 16 ppm, to demonstrate increased scale production of plates with improved NV^- ensemble properties. NV^- concentration, NV^- charge ratio, strain homogeneity, and T_2^* after irradiation and annealing were investigated in such material by characterizing a batch of samples treated to create 3.8 ppm of NV^- centers. The measured NV^- and NV^0 concentrations in these samples varied by less than 7% (1 standard deviation) and exhibited well-controlled strain inhomogeneity, as characterized by NV^- -strain mapping and (as a proxy) birefringence. The resulting $T_2^* = 1 \mu\text{s}$ in material enriched with $>99.99\%$ ^{12}C was as expected for the concentration of N, establishing that other sources of decoherence have been controlled. The resulting samples also have a high measured fraction of $[\text{NV}^-]/[\text{NV}]$ in UV-Vis, which ensures a high optically-detected-magnetic-resonance (ODMR) contrast ($>10\%$), which results in enhanced device sensitivity.

The material reported in this work enables immediate sensitivity improvements for present quantum-sensing devices utilizing bulk samples. Additionally, the progress towards μm -scale thickness layers of equivalent material grown on high-purity substrates for magnetic-field imaging applications will be presented.

11:30 AM EQ19.09/EQ03.06.03

Investigation of Germanium-Vacancy Colour Centre Formation in Nanocrystalline CVD Diamond Rani Mary Joy¹, Paulius Pobedinskas¹, Celine Noel², Daen Jannis³, Nicolas Gauquelin³, Johan Verbeeck³, Laurent Houssiau² and Ken Haenen¹; ¹U Hasselt / IMO-IMOMEC / IMEC, Belgium; ²University of Namur, Belgium; ³University of Antwerp, Belgium

Nitrogen-vacancy (NV^-) centres in single crystal diamond (SCD) have been extensively investigated as promising platforms for photonics, sensing, imaging, and other applications¹. However, the constraints with such systems include inferior optical properties of NV^- centres and limitations in the SCD upscaling process. A promising alternative to the NV^- centre are the Group IV element (Si, Ge, Sn, Pb) defects in diamond². As nanocrystalline diamond (NCD) has wafer scalability, it is interesting to investigate the colour centre formation in NCD layers. In addition, recent studies have demonstrated GeV as a potential temperature sensor³.

This study reports *in-situ* germanium-vacancy (GeV) fabrication in NCD on Ge substrates using the microwave plasma-enhanced chemical vapour deposition technique. Detonation nanodiamond seeded Ge substrates are exposed to 1% CH₄ in H₂ plasma at 3000 W and 45 Torr process conditions. We discuss the challenges in such an approach, such as the proximity of deposition temperature to Ge's melting point (937°C) and the absence of a carbide phase at the NCD / substrate interface, potentially limiting adhesion. Nevertheless, the gas-phase plasma etching of the substrate, followed by Ge-vacancy formation in diamond, ensures that the Ge substrate can act as a solid dopant source.

Electron energy loss spectroscopy analysis confirms that carbide phases are absent; instead, an amorphous carbon layer of 2 nm forms at the diamond/substrate interface. Hence, growing thicker NCD films (~9 µm) self-separating freestanding GeV incorporated diamond films with dimensions up to 1 × 1 cm² can be fabricated. Room temperature photoluminescence (PL) measurements reveal a ~602 nm peak characteristic of GeV formation in diamond^{4,5}. We also present time-of-flight secondary ion mass spectroscopy (ToF-SIMS) results that confirm Ge incorporation in NCD and discuss the non-uniformities in Ge incorporation in the film with PL mapping supported by the high-resolution ToF-SIMS elemental imaging technique. In addition, we also present studies to achieve uniformly distributed GeV in nanodiamonds via spontaneous nucleation as well as overgrowth GeV formation studies in polycrystalline diamond substrates.

References

1. Aharonovich, I., Greentree, A. D. & Prawer, S. Diamond photonics. *Nat. Photonics* **5**, 397–405 (2011).
2. Bradac, C., Gao, W., Forneris, J., Trusheim, M. E. & Aharonovich, I. Quantum nanophotonics with group IV defects in diamond. *Nat. Commun.* **10**, 1–13 (2019).
3. J. W. Fan. *et al.*, Germanium-Vacancy Color Center in Diamond as a Temperature Sensor, *ACS Photonics*, **5**, 765–770 (2018)
4. Iwasaki, T. *et al.* Germanium-Vacancy Single Color Centers in Diamond. *Sci. Rep.* **5**, 1–7 (2015).
5. Ralchenko, V. G. *et al.* Observation of the Ge-Vacancy Color Center in Microcrystalline Diamond Films. *Bull. Lebedev Phys. Inst.* **42**, 157–164 (2015).

11:45 AM BREAK

SESSION EQ19.10: Poster Session II

Session Chairs: Anke Krueger, Emmanuel Scorsone, Mariko Suzuki and Oliver Williams
Monday Afternoon, December 6, 2021
EQ19-Virtual

1:00 PM EQ19.10.01

p-Type Diamond/n-Type β-Ga₂O₃ Heterojunctions Fabricated Using Direct-Bonding Technique Phongsaphak Sittimart^{1,2}, Shinya Ohmagari^{1,1}, Takashi Matsumae¹, Hitoshi Umezawa¹ and Tsuyoshi Yoshitake²; ¹National Institute of Advanced Industrial Science and Technology (AIST), Japan; ²Kyushu University, Japan

Heterojunctions comprising of p-type diamond substrates and thin exfoliated n-type β-Ga₂O₃ layer were fabricated using direct-bonding technique at a low temperature. Due to using low temperature for the fabrication, formation of p-type diamond/n-type β-Ga₂O₃ heterostructure was, therefore, possible. In this work, p⁺-diamond/n-Ga₂O₃ and p⁻-diamond/n-Ga₂O₃ heterostructures were fabricated using direct-bonding technique. From electrical investigations, p⁺-diamond/n-Ga₂O₃ heterostructure exhibited ohmic behavior, resulting from p⁺-diamond substrate behaving as a metallic layer. In the case of p⁻-diamond/n-Ga₂O₃ heterostructure, it showed a rectifying action as a conventional *pn* heterojunctions with turn-on voltage ~4.5 V, rectifying ratio >10⁹ at ±10 V and leakage current < 10⁻¹² A. Ideality factor and barrier height of p⁻-diamond/n-Ga₂O₃ heterojunctions were 2.7 and 1.51 eV, respectively. Electrical comparison between p⁻-diamond/n-Ga₂O₃ heterojunctions and β-Ga₂O₃ Schottky junctions confirmed that p-type diamond/n-type β-Ga₂O₃ heterojunctions were truly formed using direct-bonding technique. This confirmation is suggesting that lightly doped diamond and β-Ga₂O₃ are preferable to realize the formation of diamond/β-Ga₂O₃ heterojunctions. Energy band diagram of the fabricated *pn* heterojunctions was provided. This work can serve as an important reference for fabrication of diamond/β-Ga₂O₃ heterojunctions for application in future electronic devices operating under extreme conditions such as high-power, high temperature and strong radiation.

1:05 PM EQ19.10.02

Controllable Crystal Plane Curvature of CVD Single Crystal Diamond and Its Boundary Between Single-Crystalline and the Polycrystalline within Adjusted Constrained System Shengyuan Bai, Ramón D. Díaz, Aj Bensman and Elias Garratt; Michigan State University, United States

Great details remain unclear to overcome the challenges in diamond growth using Microwave Plasma Assisted Chemical Vapor Deposition (MPACVD). This research will report the single crystal diamond (SCD) grown in several angled holders designed to achieve better epitaxial lateral outgrowth (ELO) and to maintain an optimized lateral growth rate. Multiple depositions are carried out using angled holders from larger angled pockets to smaller angled pockets. These results in larger size ELO with possible PCD growth, intermediate smooth ELO growth, and inward lateral growth.

All as-grown samples are measured with the X-ray rocking curve (XRC) mapping technique to reveal the crystallographic structural properties, and compared to that of the original substrates. Diamond 400 crystal plane curvature/flatness and morphology, XRC FWHM of 400/113/111 diamond peaks are plotted using self-made analytical software to compare the quality revolution before and after the growth. Quantitative birefringence maps are also taken to present the internal crystal structural defects within the CVD diamond. Other than these, the growth behavior within such kinds of adjusted constrained systems will be analyzed to reveal the preference of atomic level diamond growth.

Mapping results show that CVD SCD grown using wider angled pocket, though with PCD rims, has better flatness (small curvature) and higher average structural quality (small FWHM); Diamond grown with intermediate pocket, with pure SCD growth, also has not only a good lateral growth behavior, but also intermediate crystal morphology and intermediate structural quality; Those are using smaller pocket results area shrink, but with larger crystal plane curvature, indicating the CVD SCD is compressed due to the smaller size of the pocket.

Cross polarized birefringence and quantitative birefringence images of all samples care taken to understand the internal structure of the CVD SCDs.

Thus, an intermediate choice would be the best way for iterative SCD growth to maintain the lateral growth rate and the crystal quality at the same time.

1:10 PM EQ19.10.03

Introducing a Unique Technique for Measuring Electrical Conductivity of Heteroepitaxial Diamond at High Temperatures and Determining the

Activation Energy Maddy Behravan; Converse College, United States

Diamond is an attractive material for high power electronic devices because of its unique properties such as wide band-gap and high thermal conductivity. Heteroepitaxial growth of diamond offers the possibility of making devices over a large surface area. In order to characterize electrical properties of heteroepitaxial diamond and address its suitability for electronic application, a diamond device is fabricated from a nominally undoped heteroepitaxial diamond film. The diamond film was grown using plasma enhanced chemical vapor deposition (PECVD). Here the temperature-dependent DC electrical conductivity $\sigma(T)$ of heteroepitaxial diamond is reported. Owing to its extremely low conductivity at room temperature, measurements of current-voltage characteristics were made between 300 °C and 550 °C.

A particular technique was used to measure electrical conductivity of heteroepitaxial diamond at high temperature, which provided for a precise measurement circuits enabling thermal control with sufficient stability for electrical measurements of very small currents ($<10^{-13}$ A). Ohmic contacts with diamond and procedures for preparing diamond surface will be addressed. In this study, a single activation energy of 1.40 eV is found for the diamond device. The heteroepitaxial diamond conductivity profile closely matches that of previously studied natural Type IIa diamond. A thermally activated electrical conductivity $\sigma(T)$, with single activation energy 1.40 eV, does not match natural diamond, but does match previously studied homoepitaxial diamond, suggesting the presence of electronic states comparable with synthetic diamond.

1:15 PM EQ19.10.05

Porous Boron-Doped Ultrananocrystalline Diamond Grown on Anodized 3D Titanium Grid Laís G. Vernasqui¹, Neidenêi G. Vernasqui¹ and Manuel Rodrigo²; ¹National Institute for Space Research (inpe.br), Brazil; ²Universidad de Castilla-La Mancha, Spain

Porous DDB morphology for the electrochemical oxidation process has been a focus of researches in recent years due to the unique DDB properties as well as the possibility to allow contact between the electrolyte and the material, raising the electrochemical area and enhancing the electrode efficiency. In this context, the film porosity may be controlled from nano to macroporous according to the substrate porosity or using some specific diamond surface post-growth treatment. Regardless of the material porous size or its applicability, it is normal to use a seeding pre-treatment with diamond powder to enhance the diamond growth by chemical vapor deposition (CVD) process. Nonetheless, we are presenting diamond films got without substrate seeding. This approach was obtained with success using titanium dioxide nanotube substrate (DTNT) produced on a titanium grid. This process allowed greater surface control and homogeneity. DTNT is a singular substrate because the formed hydrocarbon radicals originated from the methane/hydrogen mixture are used to grow diamond. From this system, the TiO₂-TiC conversion enables and enhances diamond nucleation, which is also increased by the substrate porosity. Besides, carbide formation avoids the usual hydrogen attack observed on titanium substrate also preventing the titanium hydride evolutions. In this context, this work aiming at the ultrananocrystalline boron-doped diamond film growth without seeding on DTNT electrochemically anodized on 3D Ti grid (B-UNCD_{WS}/DTNT/Ti_{GRID}). The samples were analyzed physically and morphologically by scanning electron microscopy (SEM), micro-Raman scattering spectroscopy, and X-ray diffraction. Electrochemical characterizations were performed regarding the B acceptor concentration evaluations from Mott-Shottky curves while from cyclic voltammetry the reversibility study in redox pair was performed. The Ti grid (25x25x1 mm) was cleaned in acetone and polished in acid solution. Subsequently, the sample was anodized in a 40°C glycerol solution containing fluoride for 3h under 60 V. The counter electrode was a Pt network as an open cylinder that was able to evolve the Ti grid for both sides assuring their simultaneous anodization. After anodization, the sample was put in a hot filament CVD reactor to grow B-UNCD without the diamond powder seeding process. Diamond growth was also provided on the sample backside following a similar procedure. SEM images confirmed a continuous and uniform 3D film following the substrate morphology for both sample sides. The pore bottoms and walls were covered by ultrananocrystalline diamond in addition to the CVD balls diamond clusters with their density increase with increasing the film growth time. Also, Raman spectra, as well as XRD diffractograms, confirmed the B-UNCD_{WS}/DTNT/Ti_{GRID} quality and crystallinity. Their good electrochemical response with doping level from 10¹⁸ to 10²⁰ B.cm⁻³ and satisfactory reversibility in a redox pair confirmed them as promising new electrode material, mainly for anodes in the electrooxidation process.

1:20 PM EQ19.10.07

Synthesis of Nanodiamond Film by UV Laser Annealing of PTFE Pratik Joshi, Siddharth Gupta, Roger Narayan and Jagdish Narayan; North Carolina State University, United States

Nanodiamond (ND) synthesis by nanosecond laser irradiation has sparked a tremendous scientific and technological interest. Herein we have demonstrated the conversion of PTFE (low thermal conductivity polymer) into NDs by the melting route. Notably, UV laser irradiation of PTFE at low energy densities (0.6-0.8 Jcm⁻²) was effective for amorphization and subsequent melting of amorphous PTFE to obtain NDs. High energy densities (>1 Jcm⁻²) generated ablation with minimal control over amorphization and melting. COMSOL simulations yielded a melt regrowth velocity of 5.6 m/s. We also noted that the graphitic content in these NDs may be controlled by altering the number of shots. Finally, this ND film was utilized as a seed layer to selectively generate adherent and dense CVD microdiamond film.

1:25 PM EQ19.10.11

Late News: Scalable Fabrication of Clean Nanodiamonds via Salt-Assisted Air Oxidation—Implications for Sensing and Imaging Tongtong Zhang and Zhiqin Chu; The University of Hong Kong, Hong Kong

Nanoscale diamond particles, generally known as nanodiamonds (NDs), have several outstanding material qualities, offering a wide range of potential for basic science and industrial applications. In particular, a number of optically addressable impurity defects, such as nitrogen-vacancy (NV) centers residing in the diamond lattice, have been deployed for next-generation quantum technologies due to their unique spin properties. Currently, there are mainly two methods for the large-scale fabrication of NDs: “bottom-up” detonation NDs and “top-down” milling of bulk high-pressure high-temperature (HPHT) diamond. It is well known that the raw ND powders (i.e., detonation or HPHT) contain a considerable amount of unwanted impurities [e.g., ultra-small (<10 nm) sized NDs, disordered carbons, metal, and metal oxides], which are naturally introduced during synthesis and processing. And previous reports demonstrated that the non-diamond phases present at the surface of NDs are detrimental to the properties of embedded quantum defects (e.g., NV centers). Therefore, the removal of those impurities becomes a critical step before the ultimate applications of the NDs. Several purification methods, like the air oxidation (at 400 - 600 °C) and wet chemical (e.g., HNO₃/H₂SO₄/HClO₄, molten KNO₃) treatments, have been adopted to remove the adsorbed impurities on NDs. Despite the considerable effort devoted to overcoming these challenges, it is still difficult to obtain NDs with a well-defined surface, especially when examined at the individual particle level.

Here, we developed a simple, reliable and reproducible purification method, namely the salt-assisted air oxidation (SAAO) treatment, requiring only one additional pre-step, i.e., mixing NDs with a proper amount of salt crystals (e.g., sodium chloride) prior to conventional air oxidation method. Our inspiration for this method came from the cooking procedure used in the preparation of a well-loved Chinese snack, fried chestnuts with stones. The role of the salt crystals added in NDs powder is closely analogous to that of the stones added in the Chinese snack, and ensures that the NDs (the “chestnuts”) are evenly and thoroughly etched by SAAO. This method rounds the original shard-like shape of the NDs with clean surface, and can be scaled up to permit their manufacture in large quantities. We also investigated the underlying mechanism of the SAAO process, i.e., the “salt-assisted etching atmosphere” would easily etch away non-diamond impurities and significantly accelerate the oxidation of NDs as well. These findings will significantly enhance the scope of these little gemstones in diverse scientific and industrial fields, particularly in demanding areas such as biomedical and quantum sensing requiring

stable and sound surface functionalities.

SESSION EQ19.11: Sensing
Session Chair: Matthias Schreck
Tuesday Morning, December 7, 2021
EQ19-Virtual

8:00 AM *EQ19.11.01

Diamond Quantum Sensing of Cell Mechanics Quan Li; Chinese Univ of Hong Kong, Hong Kong

The long spin coherence time of NV center electrons make it particularly attractive for bio-sensing applications. The NV centers are particularly sensitive to the magnetic field projected along the NV axis, so that orientation change of a diamond sample (containing NVs) would cause detectable modulation in its optically detected magnetic resonance spectrum, a method known as the vector magnetometry. This method has excellent spatial resolution and measurement sensitivity on the orientation change of NVs in the diamond sample. In the present work, we will discuss a newly developed scheme to investigate the mechanical properties of soft materials using diamond nanoparticles as the quantum sensors. The feasibility of the method is firstly demonstrated using polydimethylsiloxane (PDMS) film and gelatin microparticle. The excellent sensitivity and spatial resolution associated with such a technique enable the disclosure of heterostructured nature of the former, and effect of surface tension in the latter. We then study the mechanical properties of fixed HeLa cells using the nanodiamond-sensing-enabled non-local deformation measurement, enabling observation of the competition between elasticity and capillarity upon indentations on cells. The works are carried out in collaboration with Renbao Liu, Yue Cui, Wenghang Leong, Kangwei Xia, and Chufeng Liu. We acknowledge funding from GRF of RGC (Project No. 14300720), CRF of RGC (Project No. C4007-19G); and ANR/RGC (project No. A-CUHK404/18).

8:30 AM *EQ19.11.02

Towards Next Generation Diamond-Based Sensor Devices Oliver Roman Opaluch, Lahcene Mehmel, Nimba Oshnik and Elke Neu-Ruffing; Technische Universität Kaiserslautern, Germany

Individual, luminescent point defects in diamond termed color centers are stable, atomically small quantum systems. Such individual quantum systems are extremely sensitive sensors, e.g., for magnetic fields. Their strength is to harness quantum mechanics for ultimate sensitivity and versatility while simultaneously boosting spatial resolution in imaging.

To fully exploit the potential of this novel class of sensors, dedicated diamond materials as well as nanostructures are needed. We here present our work on using large area, heteroepitaxial diamond for sensing applications. We also discuss recent results on integrating diamond with two-dimensional, luminescent transition metal dichalcogenides to establish a hybrid sensor material. The talk will furthermore summarize recent advances in fabricating diamond nanostructures for sensing. In addition to material and process optimization, we employ optimal control algorithms to shape the laser pulses as well as microwave pulses that address the color center spins.

9:00 AM *EQ19.11.03

Diamond Sensing of Magnetic Transitions and Fluctuations of Nanoparticles Renbao Liu^{1,2,2}; ¹The Chinese University of Hong Kong, Hong Kong; ²THE CHINESE UNIVERSITY OF HONG KONG, Hong Kong

Nitrogen-vacancy (NV) center spins in diamond are good quantum sensors for their long quantum coherence times. In particular, quantum coherence of NV centers can be manipulated even at high temperature. Therefore, we can use NV centers to detect magnetic transitions and fluctuations of nanoparticles for a broad range of materials. Here we will present examples of controlling quantum coherence of NV centers at high temperature, detection of magnetic transitions of single nanoparticles, measurement of magnetic fluctuations near Currier temperatures of magnetic nanoparticles, and methods for improving magnetometry sensitivity near zero magnetic fields (which is important for non-invasive study of magnetic properties of materials).

This work was supported by Hong Kong RGC Collaborative Research Fund Project C4006-17G and was done in collaboration with Q. Li, G.-Q. Liu, C. F. Liu, N. Wang, K. Xia, W.-H. Leong, T. Zhang, X. Feng, M. H. Kwok, H. Zeng, S. H. Li, F. Dolde, A. Finkler, A. Denisenko, S. Yang, J. Wrachtrup, X. D. Cui, and H. Fedder.

References:

1. C. F. Liu *et al*, National Science Review **8**, nwa194 (2021).
2. G. Q. Liu *et al*, Nature Communications **10**, 1344 (2019).
3. T. Zhang *et al*, Nature Communications **9**, 3188 (2018).
4. N. Wang *et al*, Physical Review X **8**, 011042 (2018).

SESSION EQ19.12: Growth, Doping, Processing and Characterization
Session Chair: Ken Haenen
Tuesday Morning, December 7, 2021
EQ19-Virtual

10:30 AM *EQ19.12.01

Diamond Etching Based on Carbon Solid Solution into Nickel for Wafer and Device Fabrication Processes Norio Tokuda¹, Xufang Zhang¹, Tsubasa Matsumoto¹, Takao Inokuma¹, Christoph E. Nebel^{2,1} and Satoshi Yamasaki¹; ¹Kanazawa Univ, Japan; ²Diamond and Carbon Applications, Germany

Diamond is expected to be the semiconductor material of the next-generation high-power and high-frequency devices as well as quantum technologies because of its superior physical and electronic properties. Etching is one of the most important techniques for semiconductor wafer and device fabrication processes. The etching techniques for SiC and GaN as next generation power semiconductor materials have been already established. However, the

diamond etching technique has not yet reached the required quality for semiconductor wafer and device processing because of the inherent difficulties arising by its extremely high physical hardness and chemical stability. Recently, we have reported a novel diamond etching process based on the carbon (C) solid solution into Ni [1-5]. The etching is a solid-solid reaction, which occurs at Ni/diamond interfaces. Therefore, the process can selectively etch diamond surfaces in contact with Ni. We also demonstrated diamond imprint lithography with Ni mold [2] and surface planarization with flat Ni plates [3] based on this novel diamond etching process. Additionally, the diamond etching shows a high etching rate (~10 $\mu\text{m}/\text{min}$) and strong anisotropy [4,5], which is similar to the anisotropic Si etching using KOH solution for device fabrication. This novel diamond etching processes will be introduced in detail.

Acknowledgements

This work was partially supported by Adaptable and Seamless Technology transfer Program through Target-driven R&D (A-STEP) from Japan Science and Technology Agency (JST), Kanazawa University SAKIGAKE Project 2020 and JSPS KAKENHI Grant Number JP18KK0383.

References

- [1] K. Nakanishi, N. Tokuda et al., *Dia. Relat. Mater.* 68 (2016) 127.
- [2] T. Tabakoya, N. Tokuda, *Dia. Relat. Mater.* 114 (2012) 108294.
- [3] K. Sakauchi, N. Tokuda et al., *Dia. Relat. Mater.* 116 (2021) 108390.
- [4] M. Nagai, N. Tokuda et al., *Sci. Rep.* 8 (2018) 6687.
- [5] M. Nagai, N. Tokuda et al., *Dia. Relat. Mater.* 103 (2020) 107713.

11:00 AM EQ19.12.02

On the Observation of Mott-Gurney Behavior in Diamond Schottky and PIN Diodes Kelly Woo¹, Mohamadali Malakoutian¹, Manpuneet Benipal², Franz A. Koeck³, Robert Nemanich³ and Srabanti Chowdhury¹; ¹Stanford University, United States; ²Advent Diamond Inc., United States; ³Arizona State University, United States

Diamond is perhaps the most attractive candidate for ultra-high voltage (multi-kV) power electronics due to its large bandgap (5.47 eV), high breakdown electric field (10 MV/cm), high carrier mobility, high thermal conductivity (10-20 W/cm.K), and low coefficient of thermal expansion (~1.1 $\mu\text{m}/\text{mK}$) [1]. Thus, the development of diamond Schottky barrier diodes and PIN diodes may lead to much more efficient power electronics. The diamond diodes fabricated in this work have shown superlinear current-voltage curves in the forward bias region following the Mott-Gurney law, allowing for higher on-current densities at lower voltages.

In this work, intrinsic layers of varying thicknesses (~0.5-7 μm) and n-type top layers of 100nm with up to $5 \times 10^{19} / \text{cm}^3$ phosphorous doping were grown on (111) and (100)-oriented diamond p+ (type IIb diamond) substrates by Microwave Plasma Enhanced Chemical Vapor Deposition. To fabricate the diode, Ti/Pt/Au was evaporated on the backside of the p+ diamond plate to form an ohmic contact, and depending on the crystal orientation, the circular contacts made to the n-layer on top were either ohmic or Schottky. Because phosphorous incorporation is significantly improved on (111) oriented surfaces as opposed to (100) substrates, the diodes on the (111) substrate have shown PIN diode behavior, whereas the diodes based on the (100) substrates exhibit Schottky diode behavior [3].

In our Schottky devices, we have observed that the turn on characteristics can be analyzed through the thermionic emission equation $J_F = A^* T^2 \exp(-q\Phi_B / (kT)) [\exp(-qV_F / (nkT) - 1)]$, where A^* is the Richardson constant, Φ_B is the Schottky barrier height, and n is the ideality factor [2][3]. However, at higher voltages after turn-on, the current exhibits Mott-Gurney behavior or space charge limited current. Because of the low doping densities in the intrinsic layers of the devices, the total on current at higher bias regions are instead dominated by charge carriers injected from the highly doped adjacent regions as opposed to the intrinsic carriers present in the drift region. As a result, the current can be described by the equation $J_{MG} = (9/8) \epsilon_0 \epsilon_r \mu V^2 / d^3$, where ϵ_r is the relative permittivity of diamond, μ is the carrier mobility, V is the bias voltage, and d is the drift region thickness [2]. This behavior, a characteristic notable in vacuum diodes, allows for greater current densities at lower forward biases in comparison to traditional diode behavior which typically exhibits linear behavior based in Ohm's law. Diode current increasing as the square of the voltage applied across it should be viewed favorably in power electronics as it may allow for lower voltage operation at equivalent current output, thus leading to lower power consumption and reduction of thermal runaway effects. This observation of Mott-Gurney's law is an indication of highly developed diamond growth techniques producing high quality material, as well as optimized diode fabrication. Additionally, it was observed that as the intrinsic layer thicknesses were increased, the turn on voltage and onset of Mott-Gurney effect was shifted to higher voltages. Also, by elevating the temperature (up to 400°C) the current was increased due to increased ionized carriers and a lower turn-on voltage was observed. As a result, the onset of Mott-Gurney effect was shifted to lower voltages as well.

This work was supported by ULTRA, an Energy Frontier Research Center funded by the U.S. Department of Energy (DOE).

- [1] Tsao, J. Y., et al., *Adv. Electron. Mater.*, 4, 1600501 (2018).
- [2] Brezeanu, M, et al., *Diamond and Related Materials*, Volume 17, Issues 4–5, 2008, 736-740.
- [3] Dutta, M, et al., *IEEE Electron Device Letters*, Vol. 35, Num. 5, 2017

11:15 AM EQ19.12.05

Phosphorus Doping Considerations for Controlled Diamond Interfaces Franz A. Koeck and Robert Nemanich; Arizona State University, United States

Diamond based electronics could exploit the unique materials properties (carrier mobilities, breakdown voltage, thermal characteristics) that would enable superior devices in particular for high-power, high frequency applications. Practical solid state devices necessitate n-type and p-type material with controlled properties specifically the doping concentration and its profile, both, in the bulk and at interfaces. Interface or near surface doping properties will also be important for heterostructures. While abrupt doping profiles should provide preferred performance, these abrupt interfaces are not always observed and cannot always be reliably prepared. As a result, graded junctions would then define device characteristics like current flow, switching speed and breakdown voltage. We present results for phosphorus doped homoepitaxial diamond on (111) substrates. The epitaxial layers were prepared by microwave-plasma assisted chemical vapor deposition utilizing a 200ppm trimethylphosphine (TMP) in hydrogen mixture as dopant source in addition to hydrogen and methane to achieve a phosphorus concentration $> 1 \times 10^{19} \text{ cm}^{-3}$. With a dual-wavelength pyrometer and optical emission spectroscopy, the in-situ growth characterization was related to results from secondary ion-mass spectroscopy (SIMS), which was utilized to determine the doping profile of the epitaxial diamond layer. Phosphorus doped homoepitaxial diamond layers were grown on intrinsic CVD substrates in various plasma focusing geometries and a relation to the doping profile was established. With enhanced plasma focusing a shift toward a more abrupt doping profile was observed. Optical emission spectroscopy of the phosphorus related signal (930nm) during growth indicated a relation to the doping profile. With dual-wavelength pyrometer temperature measurements a small change (5°C or about 0.5%) in the growth temperature resulted in a change of about 7% in the doping concentration. These observations indicated the sensitivity of the phosphorus incorporation on the growth temperature and availability of donor species in the reactor. We will further elaborate on the effects of the substrate surface (miscut angle, polishing) on the phosphorus incorporation.

This work was supported as part of ULTRA, an Energy Frontier Research Center funded by the U.S. Department of Energy, Office of Science, Basic

11:30 AM EQ19.12.06

Analytical Expression of the Fermi Level for Doped and Compensated Diamond—A Tool for the Diamond Electronics Analysis Gonzalo Alba¹, Beatriz Soto¹, Jesus Canas^{1,2}, Castro P. Villar¹, Rodrigo Alcántara¹ and Daniel Araujo¹; ¹University of Cádiz, Spain; ²Institut Néel, France

Diamond outstanding properties make it a promising candidate for its application on high-power rectifying electronic devices. The intrinsic nature of diamond is related to the diamond electronic devices strong dependence on doping, and surface/interface phenomena. The understanding and control of such phenomena is key for the development of reliable electronic devices that can compete with current silicon-based solutions.

The position of the Fermi level is a fundamental parameter that has served for the prediction of the ideal band diagram of electronic devices and is also required for the extraction of some of its fundamental operational parameters. Among others, the Schottky barrier height of metal-diamond junctions can be estimated based on Capacitance-Voltage (C-V) measurements by which the resulting built-in potential is added to the Fermi level to diamond valence band energy distance. For Metal-oxide-diamond structures the ideal flat band voltage is obtained as the metal-diamond Fermi level distance, which allows to identify and estimate the oxide charge net density by comparison to the experimental C-V value. Other techniques such as Kelvin Probe Atomic Force Microscopy or X-ray photoelectron spectroscopy also allows the determination of the Fermi level position and requires theoretical values for the characterization of the diamond electronic phenomena.

Besides its wide application, the calculation for the diamond Fermi level position is commonly made based on numerical calculations. In the present contribution, an analytical expression for the Fermi level on diamond is deduced in order to simplify diamond-based electronic device design and analysis procedures. The limits of this expression, i.e. the validity of the Boltzmann approximation, are discussed and its application to some real cases shown.

11:45 AM EQ19.12.07

Diamond Field-Effect Transistors with Modulation Doping Makoto Kasu¹, Niloy Chandra Saha¹, Seong-Woo Kim² and Toshiyuki Oishi¹; ¹Saga University, Japan; ²Adamant Namiki Precision Jewel, Japan

Diamond semiconductor can be used to develop high-power devices owing to its wide bandgap of 5.47 eV and superior properties compared to SiC and GaN. Till date, we have demonstrated field-effect transistors (FETs) with NO₂ p-type doping on hydrogen-terminated diamond (H-diamond) with an output power density of 345 MW/cm² [1]. However, conventionally doped diamond FET structures have several problems, such as lower hole mobility (μ) (~100 cm²/V s) in the channel than in the bulk (>1200 cm²/V s) and degradation of hole channel during lengthy operations. To overcome these limitations, we propose modulation or selective doping in diamond. We separated the NO₂ acceptor impurities from the hole channel on H-diamond using an Al₂O₃ gate insulator layer in the FET structure.

First, we investigated the modulation-doping effect by employing Hall effect measurements of a modulation-doped sample with the structure Al₂O₃/NO₂/Al₂O₃ spacer layer/H-diamond by changing the thickness of Al₂O₃ spacer layer. KENZAN Diamonds[®], high-quality (001) heteroepitaxial diamonds [2]. The results revealed that the sample with an Al₂O₃ spacer layer thickness of 8 nm exhibited maximum mobility by maintaining high hole sheet concentration. Thus, we observed the effects of modulation doping unambiguously.

Second, we performed temperature-variable Hall effect measurements of the modulation-doped sample and observed that the high mobility and hole sheet concentration were retained until at least 500 K. Thus, the thermal stability was improved. The low temperature dependence of mobility exhibited the characteristics of modulation doping.

Next, we fabricated modulation-doped diamond FETs. The NO₂ p-type doping was performed on the H-diamond surface to form the access channels and on the 8-nm-thick first Al₂O₃ gate insulator layer. The diamond FETs exhibited a maximum drain current density of -627 mA/mm and maximum transconductance of 131 mS/mm. The effective mobility increased to 2465 cm²/V s near the gate threshold voltage, which was a factor of 3.7 greater than that of the conventionally doped FETs, and was near the highest reported value (3800 cm²/V s) in the purest form of diamond. The off-drain voltage was -703 V and the on-state resistance was 37.55 Ω mm. Consequently, Baliga's figure-of-merit, an available output power density of the modulation-doped FET, was obtained experimentally as 179 MW/cm².

[1] N. C. Saha *et al.*, IEEE Electron Device Lett., 41, 1066 (2020).

[2] S.-W. Kim *et al.*, Appl. Phys. Lett., 117, 202102 (2020).

12:00 PM EQ19.12.08

Homoepitaxial Growth Mechanism of Heavily Nitrogen Doped Diamond (111) Films Yuta Nakano¹, Shu Inagaki¹, Kazuki Kobayashi¹, Xufang Zhang^{1,2}, Tsubasa Matsumoto^{1,2}, Takao Inokuma¹, Satoshi Yamasaki², Christoph E. Nebel^{2,3} and Norio Tokuda^{1,2}; ¹Graduate School of Natural Science and Technology, Kanazawa Univ., Japan; ²Nanomaterials Research Institute, Kanazawa Univ., Japan; ³Diamond and Carbon Applications, Germany

High-quality nitrogen-doped diamond is expected to be applied for power devices and high-sensitive quantum sensors at room temperature [1,2]. For example, for n-channel MOSFETs, to reduce the contact resistance, it is important to use diamond films with high nitrogen concentration ([N]). In addition, for high-sensitive quantum sensors, to improve the sensor sensitivity, it is important to increase [N] involving high [NV⁻] with high film quality. However, previous studies have reported that high [N] doping causes nucleation and deterioration of film quality, but the details about nucleation mechanism are not yet known [3,4]. Thus, in this study, we investigated the effect of N-doped growth on nucleation and used lateral growth modes to eliminate nucleation factors other than N-doping [5,6]. Furthermore, we analyzed the nucleation mechanism using first-principles calculations. As a result, it was found that the carbon atoms in the plasma are more easily adsorbed by the nitrogen atoms than the carbon atoms on the substrate. Moreover, by optimizing the N-doped lateral growth conditions, we succeeded in developing a growth technique that suppresses 2D nucleation as much as possible.

Atomically flat diamond surfaces were grown by homoepitaxial lateral growth on HPHT Ib type diamond (111) mesas in order to prevent 2D nucleation and hillocks due to dislocations in the diamond substrate; then homoepitaxial N-doped growth was carried out under N₂/CH₄ = 0 ~ 2000 % for 10 min. The surface morphology was evaluated with a laser microscope and an atomic force microscope. The nucleation mechanism was examined by the potential energy surface (PES) calculation using Octopus as a simulator.

Acknowledgements: This work supported by Kanazawa University SAKIGAKE Project 2020 and Q-LEAP.

[1] T. Matsumoto *et al.*, Sci. Rep. **6**, 31585 (2016).

[3] H. Ozawa *et al.*, Phys. Status Solidi A **215**, 1800342 (2018).

[4] E. Boettger *et al.*, J. Appl. Phys. **77**, 6332 (1995).

[5] A. T. Sowers *et al.*, J. Appl. Phys. **86**, 3973 (1999)

[6] N. Tokuda *et al.*, Jpn. J. Appl. Phys. **51**, 9R (2012).

[7] H. Ozawa *et al.*, Appl. Phys. Express **10**, 045501 (2017).

1:00 PM *EQ19.13.01

Inverse Design of Multi-Functional Diamond Nanoparticles Using Machine Learning [Amanda Barnard](#) and Sichao Li; Australian National University, Australia

Inverse design, which predicts the required structure based on a desired property, is a necessary part of industrial design. Property/structure relationships of materials are far more difficult than the forward structure/property relationships, however, since there could be numerous combinations of materials characteristics that present the same properties and conventional predictions do not distinguish between them. They are even more challenging in nanomaterial design, where the design space is even greater, and materials are prized for their multi-functionality. Optimization based on hypothetical databases predicted using machine learning has shown promise in recent years, but suffers from a high computational cost, lack of specificity, and no guarantee that the optimal nanomaterial has been found. There are simply too many unknown variables (structural characteristics) and not enough known variables (properties) for optimization to be reliable. In this presentation we will describe an alternative approach to inverse design that overcomes each of these limitations. By drawing on the multi-functionality of nanomaterials and using multi-target machine learning methods, we develop a workflow that is fast, easy to use, and predicts the characteristics of a single nanoparticle that simultaneously meets a set of performance criteria, with a fault tolerance. The method focuses the outcome on the most important characteristics in an entirely data-driven way, and with comparable accuracy and generalizability as traditional forward structure/property machine learning predictions. We have demonstrated the new inverse design workflow on diamond nanoparticles, an important platform with significant potential for a range of industrial applications.

1:30 PM EQ19.13.02

Density Functional Theory Study of the Adsorption of Nitric Oxide and Nitrous Oxide on Hydrogen-Terminated Diamond (100) Surfaces [Jenille Cruz](#)¹, Michael Groves¹ and Mahesh Neupane²; ¹California State University, Fullerton, United States; ²CCDC US Army Research Laboratory, United States

Diamond's unique geometric and electronic properties have gathered interest, for it can undergo a surface transfer doping mechanism which can then be used to build high-field, high-frequency device applications [1]. Recent experimental evidence suggests that adsorbing NxOy functional groups on hydrogen-terminated diamond surfaces could play an important role in improving device parameters such as current density and threshold voltage [2, 3]. In this research, we performed a computational study on the adsorption of the NxOy functional groups on diamond (100) surfaces using Density Functional Theory (DFT). The adsorption energies were calculated to predict the most favorable structure. Band structures and density of states will be reported to explain the electronic properties of the most favorable system for device design. Nudged Elastic Band calculations will also be reported for the adsorption pathways to form these most stable adsorbate configurations. This research will present several models of NxOy functional groups on diamond (100) surfaces and will provide critical insight into surface electronic properties of the diamond surfaces for surface doped diamond devices.

Acknowledgement: ORAU-Journeyman Fellowship sponsored by CCDC US Army Research Laboratory, Adelphi, MD

1. K. G. Crawford et al., IEEE Transactions on Electron Devices, 67, 6 (2020).
2. M. Kasu, Jpn. J. Appl. Phys. 56, 01AA01 (2017).
3. N. C. Saha et al., IEEE Electron Device Letters, 42 (6), 903-906 (2021).

1:45 PM *EQ19.13.03

Development of Electrochemical Application on Boron-Doped Diamond Electrodes [Yasuaki Einaga](#); Keio University, Japan

Boron-doped diamond (BDD) electrodes are very attractive material, because of their wide potential window, low background current, chemical inertness, and mechanical durability.[1] In these years, we have reported several examples for electrochemical sensor applications.[2] Here, novel microsensing systems for *in vivo* real time detection of local drug kinetics are reported. Furthermore, applications for electrochemical organic synthesis[3] including CO₂ reduction[4], and electrochemiluminescence (ECL) systems[5] are also reported.

Microsensing system for *in vivo* real time detection of local drug kinetics[2b]

We have developed a microsensing system for *in vivo* real time detection of local drug kinetics and its physiological relevance. The system consists of two different sensors of both a micro-sensor composed of BDD microelectrodes with tip diameter ~40 μm and a glass microelectrode. By using the system, we have first tested bumetanide, a diuretic that is ototoxic but applicable to epilepsy treatment.

CO₂ reduction[4]

We investigated the electrochemical reduction of CO₂ to HCOOH in a flow cell using BDD electrodes. The faradaic efficiency (FE) for the production of HCOOH was as high as 94.7%. The selectivity for the production of HCOOH was more than 99%. Furthermore, recently, by optimizing certain parameters and conditions used in the electrochemical process with BDD electrodes, such as the electrolyte, the boron concentration of the BDD electrode, and the applied potential, we were able to control the selectivity and efficiency with which carbon monoxide is produced.[4c] Recently, an intermittent flow cell system was presented. A stop-start motion of the flow conditions in the intermittent cell was created using a piston pump, and this considerably increases the rate of electrochemical conversion of CO₂ to HCOOH compared to a continuous flow system.[4d]

Electrochemiluminescence (ECL)[5]

A novel coreactant-free electrogenerated chemiluminescence (ECL) system is developed where Ru(bpy)₃²⁺ emission was obtained on BDD electrodes. The method exploits the unique ability of BDD to operate at very high oxidation potential in aqueous solutions and to promote the conversion of inert SO₄²⁻ into the reactive coreactant S₂O₈²⁻. This novel procedure was rather straightforward, not requiring any particular electrode geometry, and, since the coreactant was only generated *in situ* the interference with biological samples was minimized. The underlying mechanism was similar to that of the Ru(bpy)₃²⁺/S₂O₈²⁻ system. Furthermore, recently, another ECL system was presented. The system took advantage of the unique properties of BDD to promote oxidation of carbonate (CO₃²⁻) into peroxydicarbonate (C₂O₆²⁻), which further reacted with water to form hydrogen peroxide (H₂O₂), which acted as a coreactant for Ru(bpy)₃²⁺ ECL.

References

- Bull. Chem. Soc. Jpn.*, **91**, 1752 (2018)., *Chem. Soc. Rev.*, **48**, 157 (2018).
(a) *Proc. Natl. Acad. Sci.*, **113**, 8981 (2016). (b) *Nat. Biomed. Eng.*, **1**, 654 (2017). (c) *Science*, **359**, 1287 (2018). (d) *Anal. Chem.*, **92**, 13742 (2020).
Angew. Chem. Int. Ed., **51**, 5443 (2012).
Angew. Chem. Int. Ed., **53**, 871 (2014). (b) *Angew. Chem. Int. Ed.*, **57**, 2639 (2018). (c) *J. Am. Chem. Soc.*, **141**, 7414 (2019). (d) *ACS Sustainable Chem.*

Eng., 9, 5298 (2021).

(a) *J. Am. Chem. Soc.*, **138**, 15639 (2016). (b) *J. Am. Chem. Soc.*, **142**, 1518 (2020).

2:15 PM EQ19.13.04

Fabrication and Characterization of the Boron Nitride/Boron Doped Diamond Heterostructure Avani Patel, Jesse Brown, Kari Slotten, David Smith and Robert Nemanich; Arizona State University, United States

Boron Nitride is an ultra-wide bandgap material with significant potential as an active or dielectric layer in high-power switches, high-frequency transistors, diodes, detectors, and other applications. The cubic phase (c-BN) is a semiconductor with a 6.4 eV bandgap and a near lattice match to diamond. The layered hexagonal phase (h-BN) may perform as a dielectric in hydrogen terminated-diamond field effect transistors. High-quality BN / diamond heterostructures (whether as heteroepitaxial semiconductor or as a gate dielectric) requires a smooth interface. At Arizona State University, we have grown BN thin films on B-doped, p-type diamond substrates using electron cyclotron resonance microwave plasma chemical vapor deposition (ECR MPCVD). By varying the growth conditions, the BN layer can have predominant c-BN or h-BN structure. Results show that a smooth, flat interface can be achieved for layers that are predominantly h-BN, while some c-BN layers show island growth and relatively rough interface structures. The morphology of the interface and growth surface is characterized with optical phase contrast microscopy and cross section TEM. The electrical properties of the mixed phase c/h-BN are electrically characterized using lithographically patterned contacts. Results correlate the growth parameters with the morphology and electrical properties of the c/h-BN – diamond heterostructure.

This work was supported as part of ULTRA, an Energy Frontier Research Center funded by the U.S. Department of Energy, Office of Science, Basic Energy Sciences under award DE-SC0021230.

2:30 PM EQ19.01.03

Phosphorus Incorporation and Its Effects on Residual Stress in Linear Antenna CVD Nanocrystalline Diamond Films Rani Mary Joy^{1,2}, Paulius Pobedinskas^{1,2}, Daen Jannis^{3,5}, Nicolas Gauquelin^{3,5}, Kamatchi J. Sankaran⁴, Fernando Lloret⁵, Derese Desta¹, Hans-Gerd Boyen^{1,2}, Jan D'Haen^{1,2}, Johan Verbeeck^{3,5} and Ken Haenen^{1,2}; ¹Hasselt University, Belgium; ²IMEC vzw, Belgium; ³University of Antwerp, Belgium; ⁴CSIR, India; ⁵Universidad de Cádiz, Spain

Owing to its superior mechanical and tribological properties, diamond is an attractive candidate used in various applications, including micro / nanoelectromechanical systems (MEMS / NEMS) [1]. Although single crystal diamond (SCD) has been successfully integrated and used for such MEMS / NEMS based devices, high fabrication costs and limited upscaling hinders its wide industrial usage. Such bottlenecks can be mitigated using nanocrystalline diamond (NCD) and (U)NCD as an alternative. Furthermore, with the availability of large-area diamond deposition systems, such as the linear antenna microwave CVD (LA MW CVD), such (U)NCD based devices can potentially be fabricated on an industrial scale [2]. However, very few studies have reported stress studies, an essential parameter for device integration, in NCD films grown in such systems [3].

In this work, we present residual stress studies in NCD films (~250 nm thick) deposited on silicon substrates in the LA MW CVD system. We compare intrinsic and doped films grown in a H₂/CH₄/CO₂ plasma and with varying phosphine (PH₃) gas concentrations up to a maximum [P]/[C] ratio of 8090 ppm and substrate temperatures between 400°C and 900°C while maintaining working pressure at 0.23 mbar and MW power at 2800 W process conditions.

Scanning electron microscopy results reveal that under increasing [P]/[C] ratios, the film morphology transitions from NCD with randomly faceted grains to ultra-NCD-like with dendrite features. Similar morphology changes also occur at higher substrate temperatures above 800°C. Raman analysis verifies diamond formation, and the corresponding sp³/sp² bonded carbon ratios correlate well with the associated changes in film morphology. Substrate curvature measurements reveal compressive stress in all the samples in this study, with residual stress decreasing under increasing [P]/[C] concentrations in the plasma and higher substrate temperatures. The lowest value of -0.25 GPa is observed for the NCD films grown with a [P]/[C] ratio of 8090 ppm and 900°C substrate temperature. Furthermore, transmission electron microscopy results indicate that additional impurities, such as silicon and oxygen, are present in the deposited films.

Based on the above results, a qualitative relationship between the sp³ content and projected mean grain size is proposed and the origin and the role of impurities in residual stress evolution in LA MW CVD diamond films is discussed. Finally, X-ray photoelectron spectroscopy results that indicate successful phosphorus incorporation into the carbon matrix for the layers deposited at 900°C are presented.

References

- [1] O. Auciello and D. M. Aslam, *Journal of Materials Science* **56**, 7171-7230 (2021).
- [2] S. Drijckoningen *et al.*, *Scientific Reports* **6**, 35667 (2016).
- [3] A. Taylor *et al.*, *Diamond & Related Materials* **69**, 13-18 (2016).

SESSION EQ19.14: Nanodiamond II
Session Chair: Emmanuel Scorsone
Tuesday Afternoon, December 7, 2021
EQ19-Virtual

4:00 PM *EQ19.14.01

Multicolor Fluorescent Diamond Particles for Multiplexed Imaging and Sensing Olga A. Shenderova¹, Nicholas Nunn², Marco Torelli¹, Alexander Zaitsev³, Alexander I. Shames⁴, Alexander Smirnov², Carlos Meriles⁵ and Ashok Ajay⁶; ¹Adamas Nanotechnologies, United States; ²North Carolina State University, United States; ³College of Staten Island, CUNY, United States; ⁴Ben-Gurion University of the Negev, Israel; ⁵City University of New York-City College of New York, United States; ⁶University of California, Berkeley, United States

Nitrogen is the most common impurity in diamond and forms different types of color centers, particularly via combination of one or more N atoms with vacancies. Traditional production of fluorescent diamond particles focuses primarily on the introduction vacancies via irradiation with high energy electrons and subsequent thermal annealing to promote vacancy diffusion and formation of stable optical centers with N. The N content and state are inherited from diamond synthesis and N rearrangement via diffusion is typically not considered for modifications during traditional post-synthesis processing. As a result, the fluorescent color palette is typically restricted to particles emitting only in red or green, either from NV centers produced in type Ib synthetic diamond containing single N atoms, or NVN centers produced in type Ia natural diamond containing N pairs, respectively. Recently, we

demonstrated that ultra-high temperature annealing (>1500 °C) facilitating N diffusion in the lattice, generates conditions for the controlled formation of one-, two- and three-atom nitrogen complexes with vacancies in electron irradiated type Ib synthetic diamond, providing vibrant luminescence in the red (NV), green (NVN) and blue (N3 centers) spectral ranges [1]. Remarkably, this treatment also enhanced the optically induced ¹³C hyperpolarization [2], which promotes a new paradigm in dual-mode fluorescence/magnetic resonance imaging enabled by multicolor fluorescent nanodiamonds [3]. Ultra-high temperature annealing also significantly impacts the quantum properties of NV centers, leading to increased spin-lattice (T1) and spin-spin (T2, T2*) coherence times, increased ODMR contrast, and magnetically induced fluorescence contrast. This opens routes for multiplexed labeling in combination with sensing when NV centers coexist with NVN or N3 centers within individual particles. We discuss opportunities for nano- and microparticulate diamond in a number of imaging and sensing applications in biological and industrial fields based on controlled and reproducible formation of specific color centers previously not possible in type Ib synthetic diamond.

[1] L. Dei Cas, S. Zeldin, N. Nunn, et al., From Fancy Blue to Red: Controlled Production of a Vibrant Color Spectrum of Fluorescent Diamond Particles, *Advanced Functional Materials* 2019, 1808362.

[2] M. Gierth, V. Krespach, Al. I. Shames, et al., Enhanced Optical ¹³C Hyperpolarization in Diamond Treated by High-Temperature Rapid Thermal Annealing, *Adv. Quantum Technol.*, 2000050 (2020).

[3] X. Lv, J. Walton, E. Druga, et al., Background-free dual-mode optical and ¹³C magnetic resonance imaging in diamond particles, *PNAS*, 2021 118 (21) e2023579118.

4:30 PM EQ19.14.02

Surface Functionalized Nanodiamond with Protein Repulsion and Targeting Capabilities Viktor Merz and Anke Krueger; Julius-Maximilians-Universität Würzburg, Germany

The chemical, physical and biological properties of a material are strongly related to its surface. For nanodiamond (ND), this holds true as well. And its surface can be modified easily using its broad variety of surface groups.[1] Thus, ND is attractive for applications in biological environments as it also possesses high biocompatibility and low toxicity. Further, it is available in large quantities and additional characteristics, such as luminescence from lattice defects make them candidates for applications such as imaging, drug delivery etc.

However, when nanoparticles are dispersed in typical cell culture media or body fluids, proteins from these media are adsorbed and a so-called “protein corona” forms around the particles. This corona can mask the actual functional moieties of the surface and is rather strongly attached by non-covalent interactions. Both, the colloidal stability and the physiological properties are not controllable anymore.[2]

Here, we report nanodiamond functionalized with a multifunctional surface termination,[3] consisting of zwitterionic moieties as headgroups in combination with oligoethylene glycol chains attached to hydrophobic chains to improve the colloidal dispersion in buffered cell culture media and the prevention of protein corona formation. Further, the attachment and effect of other charged surface groups such as small peptides will be discussed.

This project has received funding from the Volkswagenstiftung under Grant Agreement no. 88393

[1] A. Krueger, D. Lang, *Adv. Funct. Mater.* 22 (2012), 890.

[2] W. C. W. Chan, C. D. Walkey, *J. Am. Chem. Soc.* 134 (2012), 2139.

[3] V. Merz, J. Lenhart, Y. Vonhausen, M. E. Ortiz Soto, J. Seibel, A. Krueger, *Small* (2019) 1901551.

4:45 PM *EQ19.14.03

Direct and Quantitative Characterization of Detonation Nanodiamond Dispersion in Biomedical Relevant Media Using Cryo-TEM Shery L. Chang, Inga Kuschnerus and Haotian Wen; University of New South Wales, Australia

Detonation nanodiamonds (DNDs) are diamond nanoparticles synthesized through detonation process with a size-range of 3-5nm. Their small size, non-toxicity and biocompatibility has drawn huge interests, particularly in the biomedical field. To capitalize the large total surface area and flexible surface chemistry afforded by the unique particle size and surface structure, understanding the DND dispersion behaviour has been one of the endeavours to improve their application potential in the biomedical field.

We have recently shown that purified DNDs dispersed in water, without any additional surface modification, exhibit a striking lacey network-like morphology, formed dynamically by self-assembled chain-like structures. This discovery was carried out using direct cryo-TEM imaging of the DND dispersions. Moreover, using cryo-TEM electron tomography, we found that there is a preferential orientation of the DND aggregates that results in a 2-D planar superstructure. These new findings have significant impact on the performance of DNDs, particularly for biomedical applications. For example, in drug delivery applications, the monodispersed DNDs offer higher surface area that can promote drug loading whereas the formation of aggregate can slow down the release.

In light of the importance of the DND dispersion and their aggregate morphology distributions to the biomedical applications, we have conducted a systematic study of purified and surface functionalized DNDs dispersed in biomedically relevant media with varying pH and saline content. The large datasets generated in our studies using cryo-TEM was analyzed using our recently developed machine learning (ML) based approach. The ML analysis from cryo-TEM datasets on DND assembly will offer direct and quantitative information regarding the aggregation behavior as well as its size and morphology distribution in biomedical relevant media which is a crucial step towards a better design of DNDs for biomedical and further applications.

5:15 PM EQ19.14.04

Enhancement of Thermal and Structural Properties of Diamond Nucleation on GaN HEMTs Mohamadali Malakoutian¹, Kelly Woo¹, Shubhra Pasayat² and Srabanti Chowdhury¹; ¹Stanford University, United States; ²University of California, Santa Barbara, United States

The significantly high thermal conductivity of diamond up to 2200 W/m.K makes it an ideal choice for heat spreading applications by integration to high-frequency high-power devices such as GaN high-electron-mobility-transistors (HEMTs). One of the approaches for diamond integration to GaN HEMTs is chemical vapor deposition (CVD) of polycrystalline (PC) diamond on top of the device [1]. PC diamond has a lower thermal conductivity (100-1000 W/m.K) compared with single crystal diamond depending on its average grain size [2]. However, this lower thermal conductivity is still higher than any other competing materials such as Si₃N₄, GaN, AlGaN, and SiC. Besides thermal conductivity, the thermal boundary resistance (TBR) between the diamond heat spreading layer and GaN device is a key property which determines diamond cooling capabilities, as it can change the whole GaN channel thermal resistance. The smoothness/abruptness of the interface between diamond and GaN along with the nature of diamond nucleation during the CVD growth defines the TBR value.

Due to the presence of high temperature H₂-plasma in the CVD chamber during diamond growth, it is challenging to grow diamond without any protection layer on top of the GaN. This protection layer (MOCVD-grown Si₃N₄) not only protects the GaN channel from exposure to H₂-plasma and decomposition but also enhances diamond adhesion to the substrate by promoting covalent bonding. Carbon diffusion inside the Si₃N₄ replaces some of the nitrogen atoms (2N + 3H₂ ↔ 2NH₃) and transforms a portion of this layer to SiC which forms covalent bonds with diamond [3]. However, it is essential to identify which carbon state is nucleating on SiC in the first 1-2 nm of the diamond nucleation layer. It can be amorphous carbon (sp² a-C) or sp³ diamond depending on the nucleation recipe before the main growth. The ideal case is to nucleate sp³ carbon states on SiC as it yields a lower thermal resistance at the interface. In this work, we identify the local carbon state by using scanning tunneling electron microscopy (STEM) to perform electron energy loss spectroscopy

(EELS), a technique which studies the excitations from the 1s orbital of carbon to the states above the Fermi level (K-edge) [4]. This study showed that by using a low-density CH₄/H₂-plasma and high temperature (> 700 °C) for diamond nucleation, a monolayer of sp² a-C is first formed on the surface and then the carbon state gradually transforms to sp³ diamond. With this nucleation method, carbon only diffused ~1 nm inside the Si₃N₄ protection layer. On the other hand, when using a high density CH₄/H₂-plasma at lower temperatures (~ 600 °C) no a-C peak was observed on the K-edge intensity mapping spectra and sp³ carbon immediately nucleated on SiC layer. In this sample carbon diffused into the Si₃N₄ layer ~ 5 nm due to the highly energized CH₃⁺ radicals in the chamber. According to the Si₃N₄ thickness before the diamond growth and the target use of the remaining portion of the Si₃N₄ we can select accurate plasma parameters (microwave power, chamber pressure, CH₄ concentration, and sample surface temperature) for the nucleation stage of the diamond growth. Our nucleation recipe achieved both strong adhesion of the diamond to the substrate and low thermal resistance interface formation enabling high efficiency channel cooling capabilities at higher power levels.

This work was partially supported by the Semiconductor Research Corporation (SRC) and DARPA under the JUMP program.

[1] M. Malakoutian et al., Crystals, vol. 9, num. 10, p. 498, 2019.

[2] J. Anaya et al., Acta Materialia, vol. 103, pp. 141–152, 2016.

[3] M. Malakoutian et al., Cryst. Growth Des., vol. 21, num. 5, pp. 2624–2632, 2021.

[4] D. Muller et al., Nature, vol. 366, pp. 725–727, 1993.

5:30 PM CLOSING REMARKS

SYMPOSIUM EQ20

Beyond Graphene 2D Materials—Synthesis, Properties and Device Applications
November 29 - December 8, 2021

Symposium Organizers

Zakaria Al Balushi, University of California, Berkeley
Cinzia Casiraghi, University of Manchester
Joshua Robinson, The Pennsylvania State University
Hyeon Jin Shin, Samsung Advanced Institute of Technology

Symposium Support

Silver
Penn State 2DCC-MIP

* Invited Paper

SESSION EQ20.01: Advanced Manufacturing of 2D Materials
Session Chairs: Zakaria Al Balushi and Joshua Young
Monday Afternoon, November 29, 2021
Hynes, Level 2, Room 207

1:30 PM EQ20.01.01

Synthesis and Processing of Chemically Stable V₂CT_x MXene with Improved Properties [Kyle Matthews](#), Teng Zhang, Christopher E. Shuck, Armin VahidMohammadi and Yury Gogotsi; Drexel University, United States

Two-dimensional (2D) transition metal carbide and nitrides, MXenes, exhibit promising properties in different applications such as energy storage, sensing, and optoelectronics, to name a few. (1) These materials have a general formula of M_{n+1}X_nT_x where M is a transition metal, X is carbon and/or nitrogen, and T_x represents surface functional groups on the outer layers. Since the discovery of MXenes in 2011, research has mainly focused on Ti₃C₂T_x because of its established synthesis protocols and high chemical stability, while investigation of other experimentally made, stoichiometric MXenes has been trailing behind. Among other MXenes, M₂XT_x MXenes such as Vanadium carbide (V₂CT_x) promise exceptional theoretical properties due to the increased active surface area in M₂XT_x MXenes and the multiple available oxidation states in Vanadium systems. Despite its attractive properties, however, research related to V₂CT_x has mostly been limited to its multilayered state due to rapid oxidation after delamination. Herein, we have developed improved etching and delamination protocols through formulating new etchants and intercalants to increase the yield of synthesis and prepare high-quality and less defective V₂CT_x flakes. Furthermore, we show that through post-processing protocols the shelf life of delaminated V₂CT_x dispersions can be extended from only a few hours to multiple months with almost no degradation. Various characterization techniques such as X-ray diffraction (XRD), scanning electron microscopy (SEM), UV-Vis, and thermogravimetric analysis were used to investigate the synthesized materials. The combined synthesis and post-processing protocols presented here result in high quality and chemically stable V₂CT_x that shows improved electronic properties.

1. A. VahidMohammadi, J. Rosen, Y. Gogotsi, The world of two-dimensional carbides and nitrides (MXenes). *Science* (80-.). **372**, eabf1581 (2021).

1:45 PM EQ20.01.02

Selective-Area van der Waals Epitaxy of h-BN/Graphene Heterostructures via Defect-Engineering Using Focused He Ion Beam Joao Marcelo Lopes¹, Martin Heilmann^{1,2}, Victor Deinhardt^{3,4}, Abbas Tahraoui¹ and Katja Höflich^{3,4}; ¹Paul-Drude-institut für Festkörperelektronik, Leibniz-Institut im Forschungsverbund Berlin e.V., Germany; ²IMEC, Belgium; ³Ferdinand-Braun Institut gGmbH, Leibniz-Institut für Höchstfrequenztechnik, Germany; ⁴Helmholtz-Zentrum Berlin für Materialien und Energie GmbH, Germany

Van der Waals (vdW) heterostructures combining dissimilar 2D materials offer a great prospect for the realization of atomically thin devices with tailored properties [1]. To achieve a high density, bottom-up integration, the synthesis of such heterostructures via vdW epitaxy is a promising alternative to mechanical transfer, which is problematic in terms of scaling and reproducibility. Nevertheless, due to the weak bonding between 2D crystals, vdW epitaxy is sensitive to various surface defects, usually leading to uncontrolled nucleation and thus non-uniform growth of polycrystalline material [2]. Hence, the control over nucleation location is considered to be one of the key challenges to achieve scalable and high-quality fabrication of 2D heterostructures [3]. In this contribution, we report on the use of focused ion beam (FIB) within a He ion microscope [4] as a novel tool to deliberately create atomic scale defects in graphene on SiC(0001), which act as nucleation sites for atomically h-BN grown via molecular beam epitaxy. Thereby, we demonstrate a mask-less, selective-area growth of h-BN/graphene heterostacks, in which nucleation yield and crystal quality of h-BN is controlled by the ion beam parameters used for the defect formation. The epitaxially grown h-BN exhibits electron tunneling characteristics comparable to those of h-BN flakes exfoliated from high-quality bulk crystals [5]. Our results open a new pathway for the scalable fabrication of not only h-BN/graphene systems, but also of other vdW heterostructures composed of 2D materials that can be synthesized via vdW epitaxy, such as layered semiconductors [3] and ferromagnets [6].

References

- [1] Yankowitz et al., Nat. Rev. Phys. 1, 112 (2019).
- [2] Heilmann et al., 2D Mater. 5, 025004 (2018).
- [3] Robinson, ACS Nano 10, 42 (2016).
- [4] Deinhardt et al., Beilstein J. Nanotech. 12, 304 (2021).
- [5] Britnell et al., Nano Lett. 12, 1707 (2012).
- [6] Lopes et al., arXiv:2104.09184 (2021).

2:00 PM EQ20.01.03

Design and Fabrication of Boron-Rich 2D MXene Flakes for High Efficiency Neutron Absorption Shi-Hyun Seok, Ju-Hyoung Han, Young Ho Jin, Jaewon Wang, Jaeun Park and Soon-Yong Kwon; Ulsan National Institute of Science and Technology, Korea (the Republic of)

Neutron radiation is extremely hazardous because it can induce radioactivity in most irradiated substances, including body tissues. Therefore, construction of effective nuclear reactors and repositories with appropriate neutron shielding or absorption measures to prevent exceeding nuclear criticality is necessary. B₄C is widely used as a neutron-shielding material for reactor systems because of its high neutron-absorption efficiency (i.e., neutron-absorbing cross section for ¹⁰B). Several composites such as borated stainless steel, B₄C-reinforced Al, and B₄C-reinforced polymers have been developed. However, the practical application of these composites in the fabrication of containers or casks is limited because of their low B content and insufficient workability. In addition, their relatively thick thickness (> 1 cm) required for sufficient neutron shielding severely hinder the light-weight application. Two-dimensional (2D) transition metal carbides, namely MXenes, have recently attracted considerable attention for several applications because of their large surface area, good mechanical properties, and the presence of numerous chemically active sites. The layered structure and surface functional groups of MXenes facilitate the formation of large interlayer spaces and confer high interfacial strength, respectively. In our work, 2D Ti₃C₂T_x (T refers to surface termination group) MXene flakes were chosen to cooperate with B₄C neutron absorbing powder to fabricate hierarchically layered composite films by vacuum filtration. Through the control of particle sizes and resultant electrostatic repulsion, a homogeneous dispersion of MXene flakes and B₄C powder, both with negative surface charges, was obtained. By the self-intercalation of the submicron B₄C powder between the vacuum-filtrated 2D MXene flakes with sufficiently large lateral sizes up to several micrometers, a hybrid film was successfully developed. Notably, the film showed a wide range of boron capacity (20–60 wt%) and the B₄C reinforcements were uniformly dispersed in the MXene flakes, forming multi-interfacial layers: this was facilitated by the van der Waals interactions and the hydrogen bonds formed upon the addition of a small amount of an organic binder. The free-standing hybrid film exhibited excellent neutron absorption ability (with an absorption capacity of ≈39.8 %) at an ultralow thickness (< 40 μm), leading to a macroscopic cross-section of ≈127.6 cm⁻¹, which is the highest value among the previous reports on boron-based neutron shielding materials to date (typically, 1–34 cm⁻¹). Moreover, the mechanical flexibility of 2D films and simple processing showed the possibility for shielding surfaces of any shape with reduced net weight and volume. Thus, the as-prepared film can be used as an efficient neutron-absorbing coating material not only in nuclear repositories, but also in other fields requiring accurate shielding such as spacesuit, radiation medical, and neutron transmutation doping.

2:15 PM EQ20.01.04

Engineering High-Mobility 2D In₂O₃ Semiconductors Printed From Liquid Metals Andrew B. Hamlin, Youxiong Ye, Julia Huddy, Md Saifur Rahman and William J. Scheideler; Dartmouth College, United States

2D conducting metal oxides offer outstanding optoelectronic properties for applications in sensing, microelectronics, and flexible electronics. Here, we unlock the ultra-high electron mobility of 2D oxides formed by a rapid, liquid-metal (LM) printing process that transfers ultrathin (~ 2 nm), crystalline monolayers and bilayers of In₂O₃ at low temperatures just above the melting point of indium (156 °C). We demonstrate the use of quantum confinement and low-temperature post-annealing to control the electronic density of states (DOS) of the 2D In₂O₃, fabricating thin-film transistors with ultrahigh mobility (μ₀ > 65 cm²/Vs) at linear printing speeds from 0.6 to 36 meters/min.

LM-printed monolayer and bilayer InO_x were characterized by XRD and TEM to understand their thickness-dependent crystallinity. The films exhibit a mixture of large crystalline domains (20–40 nm, laterally) of cubic In₂O₃ and amorphous regions as deposited. Post-annealing at temperatures from 150 to 250 °C further enhances the crystallinity and grain size, as observed via the (222) cubic peak as well as through TEM imaging and diffraction patterns. UV-Vis measurements indicate that this post-annealing regulates the Burstein-Moss shift in the optical bandgap, lowering the free carrier concentration and leading to positive threshold voltages in high-performance 2D transistors. To our knowledge, this is the first report of such scalable (30 cm²) device integration of these atomic-scale 2D oxides at deposition temperatures broadly suitable for high-performance flexible electronics.

2:30 PM EQ20.01.05

Preparation and Patterning of 2D MoS₂ from Solution-Processed Precursors Using EHD Jet Printer Thi Thu Thuy Can and Woon-Seop Choi; Hoseo University, Korea (the Republic of)

Recently, transition-metal dichalcogenides (TMDs) have attracted much attention as new materials for electronics devices, electrocatalysts, photocatalysts, sensors, batteries, and bio-applications. Most TMDs are two-dimensional (2D) materials with a single layer. Bonds between each layer are made up of Van der Waals bonds, while intra-layer atoms bind together as covalent bonds.

Chemical vapor deposition (CVD) with sulfur gas is the most popular method for synthesizing large-scale 2D materials with high quality. Various MoS₂ can be obtained from this method using various precursors with different properties, process temperatures, and substrate materials. Solution process methods show advantages for preparing films with large size, high throughput, low cost, thickness control, and an environmentally friendly process. Even though there is sulfur in the precursors of the solution-process synthesis methods, supplementing the sulfur that is lost in the high-temperature CVD process is unavoidable.

We developed a unique solution process to obtain large-size and uniform MoS₂ atomic layers without CVD (CVD-free). MoS₂ atomic layers could be fabricated using the S-rich precursor solution and one-step annealing. The sulfurization process is omitted to simplify the entire process, and wafer-scale and larger-scale synthesis of MoS₂ can be achieved by simple thermal treatment. The atomic layers of the synthesized MoS₂ were identified as 2 layers for 0.0070 M, 3 layers for 0.0125 M, and 5 layers for 0.0250 M of MoS₂ solution by STEM-FIB. MoS₂ patterns were made at a resolution of around 150 μm with highly uniform coverage using electrohydrodynamic (EHD)-jet printing for the first time. The EHD jet-printed MoS₂ TFTs show good electrical properties of 19.4 cm² V⁻¹ s⁻¹.

2:45 PM *EQ20.01.06

Going Where Silicon Cannot Reach—Print-in-Place and Recyclable Electronics from Low-Dimensional Nanomaterials Aaron D. Franklin; Duke University, United States

For decades we've been hearing about the promise of printing electronics directly onto any surface. However, despite significant progress in the development of inks and printing processes, reports on fully, direct-write printed electronics continue to rely on excessive thermal treatments and/or fabrication processes that are external from the printer. In this talk, recent progress towards print-in-place electronics will be discussed; print-in-place involves loading a substrate into a printer, printing all needed layers, then removing the substrate with electronic devices immediately ready to test. A key component of these print-in-place transistors is the use of inks from various nanomaterials, including: 2D graphene and hexagonal boron nitride, 1D carbon nanotubes, and quasi-1D silver nanowires. Using an aerosol jet printer, these mixed-dimensional inks are printed into functional 1D-2D thin-film transistors (TFTs) without ever removing the substrate from the printer and using a maximum process temperature of 80 °C with most processing occurring at room temperature. To achieve this, significant advancements were made to minimize the intermixing of printed layers, drive down sintering temperature, and achieve sufficient thin-film electrical properties. Devices are demonstrated on various substrates, including paper, and evidence of the potential for printing directly onto biological surfaces will be shown. What's more, recent progress towards a completely recyclable printed transistor will be discussed, fabricated entirely using nanoscale carbon-based inks. These demonstrations give evidence for an electronic future involving devices with fabrication and/or function that goes beyond what is possible with silicon-based technologies.

SESSION EQ20.02: Physical Properties in 2D Materials I—Ferroelectricity, Magnetism and Beyond

Session Chair: Zakaria Al Balushi
Monday Afternoon, November 29, 2021
Hynes, Level 2, Room 207

4:00 PM EQ20.02.02

Study of Novel Mixed Metallic Chalcophosphates van der Waals System—Fe_{2-x}Co_xP₂S₆ Matthew Cheng¹, Yea-Shine Lee¹, Daniel Chica¹, Eric Qian¹, Abishek Iyer¹, M. Arslan Shehzad^{1,2}, Roberto dos Reis^{1,2}, Mercouri G. Kanatzidis¹ and Vinayak Dravid^{1,2,3}; ¹Northwestern University, United States; ²Northwestern University Atomic and Nanoscale Characterization Experimental (NUANCE) Center, Northwestern University, United States; ³International Institute for Nanotechnology (IIN), Northwestern University, United States

The metal chalcophosphates (MPX₃) are layered van der Waals materials that have recently gained attention due to their intrinsic magnetic properties. These systems are composed of [P₂X₆]⁴⁻ bipyramid anion units, where each P is tetrahedrally bonded to three chalcogen atoms. These anion units are surrounded in a honeycomb arrangement by metal cations, where each metal cation site is octahedrally coordinated to chalcogen atoms. By incorporating different metal cation species into the available octahedral sites different magnetic phases can be induced. Among the metal chalcophosphates, Fe₂P₂S₆ and Co₂P₂S₆ are known for their interesting magnetic properties. Fe₂P₂S₆ is unique as it exhibits out-of-plane orientation magnetic moments when cooled under its Neels temperature. In contrast, Co₂P₂S₆ exhibits in-plane alignment of magnetic moments. However, mixing these metallic cations Fe_{2-x}Co_xP₂S₆ has not been studied yet. This mixed metallic system can be used as a platform to study new form of magnetic states through magnetic frustration.

Here, we present a thorough investigation of the mixed Fe_{2-x}Co_xP₂S₆ system and study the structure, chemical states, and magnetic behavior as the Fe:Co is varied. A novel flux method is used which enables us to synthesize a series of Fe_{2-x}Co_xP₂S₆ with different Fe:Co (1:0, 7:1, 1:1, 1:7, and 0:1). Elemental studies have confirmed the single crystals stoichiometry of these mixed cation systems. This was further supported by structural analysis which confirms a linear expansion of the lattice from Co to Fe. All of the mixed metal cation systems exhibits a transition from a paramagnetic to antiferromagnetic state when cooled beneath each system's Neels temperature. Interestingly, we found a dependence of the transition temperature to the ratio of Fe:Co. Furthermore, this dependence is confirmed by the electronic structural behavior which showed two distinct work functions in the Fe_{2-x}Co_xP₂S₆ system. This strong correlation is likely linked to a distinct ordering that is apparent from high resolution electron energy loss spectroscopy. This work provides an in-depth road map for the investigation of mixed metallic cation chalcophosphates and can be utilized as a resource for future studies on low dimensional materials in next generation electronic devices.

Acknowledgements

This work was supported by the Army Research Office (Grant W911NF1910335) and NSF Division of Material Research (NSF Grant DMR-1929356). This work made use of the EPIC facility of Northwestern University's NUANCE Center, which has received support from the SHyNE Resource [National Science Center the Keck Foundation, and the State of Illinois through IIN]. M.C. acknowledges support from the NSF Graduate Research Fellowship under Grant DGE-1842165.

4:15 PM EQ20.02.03

Computational Discovery and Investigation of Two Dimensional Ferroelectric Materials Mo Li, Olamide Omisakin, Hao Mei and Joshua Young; New Jersey Institute of Technology, United States

Two dimensional materials with ferroelectricity (i.e., having a switchable spontaneous electric polarization) have recently been proposed as components for ultrathin electronic devices. However, such materials with large out-of-plane polarizations, ideal for such applications, are challenging to find. Recently, Chandrasekaran et al. proposed that the functionalized MXene Sc₂CO₂ has a metastable state with an out-of-plane electric polarization larger than other common 2D ferroelectrics. [1] In this work, we used density functional theory (DFT) calculations to investigate additional M₂CX₂ materials (M = Sc, Y, La

and $X = O, F$). We found that (1) chemical substitution of Sc with Y and/or O with F can preferentially stabilize the ferroelectric phase as the ground state (with the dynamic stability verified with phonon calculations); (2) such substitution can also be used to systematically tune the polarization and band gap; and (3) these monolayers display large piezoelectric coefficients. We then demonstrate how these properties can be continuously tuned by the application of external strain or by alloying to create $Sc_2Y_{2(1-x)}CO_2$ monolayers. These findings demonstrate that, as with traditional bulk ferroelectrics, chemical substitution and external stimuli are powerful ways to stabilize and control the properties of low dimensional ferroelectric materials. Finally, we extend this to new families by using a high throughput DFT approach to scan through a database of 2D materials and compute their polarization to find and verify new 2D ferroelectric materials with out-of-plane polarizations.

[1] A. Chandrasekaran, A. Mishra, A. K. Singh, *Nano Letters* 17 3290 (2017)

4:30 PM EQ20.02.04

Intrinsic Stacking Disorder in Exfoliated $MoTe_2$ Due to Dimensional Confinement James L. Hart^{1,1}, Myung Geun Han², David Hynek^{1,1}, Elisabeth Bianco³, John A. Schneeloch⁴, Yu Tao⁴, Despina Louca⁴, Lena Kourkoutis³, Yimei Zhu² and Judy Cha^{1,1}; ¹Yale University, United States; ²Brookhaven National Laboratory, United States; ³Cornell University, United States; ⁴University of Virginia, United States

T-type $MoTe_2$ has drawn increasing attention due to properties such as extreme magnetoresistance, exotic superconductivity, and non-trivial band topology. In bulk, $MoTe_2$ undergoes a layer stacking transition from the $1T'$ to the T_d phase at $T_c \sim 250$ K, which alters the topology (higher-order topological insulator to Weyl semimetal) and induces ferroelectricity. Determining the layer stacking in thin film $MoTe_2$ is essential for device applications, but to date, the stacking remains poorly understood in nanoscale $MoTe_2$ samples. Here, we present *in situ* cryogenic transmission electron microscopy (cryo-TEM) measurements of exfoliated $MoTe_2$ flakes from 17 to 700 K, complemented by quantitative multi-slice simulations, electrical transport measurements, and Raman spectroscopy. Across the studied temperature range of 17 – 700 K, we find that the layer stacking in exfoliated $MoTe_2$ flakes is highly disordered, with nanoscale $1T'$ and T_d domains, as well as regions with seemingly random stacking. With cooling to 17 K (230 K below the bulk T_c), there is a modest increase in T_d -type stacking, but the stacking remains mainly disordered. Through comparison with measurements of exfoliated WTe_2 flakes – which retain the same T_d stacking found in bulk WTe_2 – we argue that the observed disorder in $MoTe_2$ is not due to mechanical exfoliation. Instead, we argue that the observed disorder is an intrinsic effect of dimensional confinement. The observation of highly disordered stacking in exfoliated $MoTe_2$ has significant implications for the interpretation of superconductivity, giant nonlinear hall effect, and other exotic properties measured in thin $MoTe_2$ flakes.

4:45 PM EQ20.02.05

Electrically Detected Phase Transition of Two-Dimensional Ferromagnetic Insulator by Proximity Effect with Graphene Tuan K. Chau¹, Sung J. Hong² and Dongseok Suh¹; ¹Sungkyunkwan University, Korea (the Republic of); ²Kangwon National University, Korea (the Republic of)

Since monolayer graphene was discovered and its electrical transport properties were well studied [1-3]. The graphene field effect transistor (FET) was used for probing the oxygen vacancies of $SrTiO_3$ substrate, studying the interface with a ferroelectric substrate, or detecting the hidden localized states at the interface with h-BN [4-6]. Recently, various 2D magnetic materials ($Cr_2Ge_2Te_6$, CrI_3 , Fe_3GeTe_2 , etc.) were reported [7-9]. With van der Waals type of the material, its heterostructures have been extensively investigated, demonstrating their fundamental properties and prototypical devices [10,11]. In this study, we have investigated proximity-coupling between 2D magnet ($Cr_2Ge_2Te_6$, CGT) and graphene. The transport parameters such as hysteresis in back-gate voltage sweep, carrier density, and mobility were abruptly changed at a temperature around ~ 60 K corresponding to Curie temperature (T_C) where CGT transfer from paramagnetic to ferromagnetic phase. In addition, the quantum Hall state of graphene with filling factor $n = 6$ similarly shows critical occurrence near T_C , which can be attributed to the additional contribution of magnetization. These results imply that graphene can be utilized to monitor the magnetic phase transition of the adjacent CGT layer. Therefore, graphene-based vdW heterostructures is expected to become a novel electrical platform for exploring various phases in 2D magnetic insulators.

References

1. K. S. Novoselov *et al.*, *Science* 306, 666 (2004).
2. V. P. Gusynin. *et al.*, *Phys. Rev. Lett.* 95 (2005).
3. Y. Zhang. *et al.*, *Nature*, 438 (2005)
4. K.T. Kang. *et al.*, *Adv. Mater.* 29 (2017), Article 1700071
5. N. Park. *et al.*, *ACS Nano* 9, 10729 (2015)
6. T. K. Chau. *et al.*, *Curr. Appl. Physics.* 23, (2021)
7. Gong, C. *et al.*, *Nature* 546, 265 (2017).
8. Huang, B. *et al.*, *Nature* 546, 270 (2017).
9. Deng, Y. *et al.* *Nature* 563, 94-99 (2018).
10. Gong, C. & Zhang. *Science* 363, eaav4450 (2019).
11. Gibertini, M. *et al.*, *Nat. Nanotechnol.* 14, 408-419 (2019).

5:00 PM EQ20.02.06

Atomistic Spin Textures On-Demand in the van der Waals Layered Magnet $CrSBr$ Julian Klein¹, Thang Pham¹, Joachim D. Thomsen¹, Jonathan Curtis², Michael Lorke³, Matthias Florian³, Alexander Steinhoff³, Ren Wiscons⁴, Jan Luxa⁵, Zdenek Sofer⁵, Frank Jahnke³, Prineha Narang² and Frances M. Ross¹; ¹Massachusetts Institute of Technology, United States; ²Harvard University, United States; ³Institut für Theoretische Physik, Germany; ⁴Columbia University, United States; ⁵University of Chemistry and Technology Prague, Czechia

The observation of long-range magnetic order in van der Waals layered materials down to the monolayer limit has sparked great interest for the study of low-dimensional magnetism. [1] However, the air-sensitivity of conventional magnetic layered materials like CrI_3 has hindered further nanoscale investigation. Recently, $CrSBr$ [2] has been rediscovered: it is a layered magnet that shows air stability and therefore presents exciting opportunities for atomistic measurements and manipulation. $CrSBr$ is a semiconductor with a bandgap of approximately 1.6 eV. It has a high Néel temperature of 145 K and shows strong light-matter interaction, which makes this material interesting for the study of magneto-transport and magneto-optical excitations. [3, 4] Here, we establish $CrSBr$ as a material platform that allows unprecedented nanoscale control over structural and therefore magnetic properties. Layered materials in general offer a myriad of degrees of freedom to tailor the crystal structure down to the single atom scale. In the case of $CrSBr$, we find that controlled irradiation with electrons in a scanning transmission electron microscope induces a local phase transformation. [5] The transformed material is also a 2D layered structure, but its layers are perpendicular to those in the original material. We investigate the mechanism of the phase transformation by tracking individual atom column intensities as well as local strain, column by column. We find that the phase transformation occurs through Cr atom migration into the van der Waals gap and we show examples of twin boundaries and grain boundaries, controlled knock-out of rows of Cr atoms, and moiré twisted $CrSBr$. Ab-initio and spin-wave theory suggest that the individual layers in the new phase are magnetic, and the material has an energy gap and a fully spin-polarized band structure. We therefore anticipate that directing this phase transformation at the atomic scale can create spin textures with specific properties that could be tailored towards applications. Overall, we propose that $CrSBr$ and other air-stable magnets with similar crystal structure will become unique platforms for the design, measurement, and application of nanoscale magnetic textures.

- [1] Huang, B. et al. *Nature* **546**, 270–273 (2017)
 [2] Göser, O. et al. *J. Magn. Magn. Mater.* **92**, 129 (1990)
 [3] Telford, E. J. et al. *Adv. Mater.* **32**, 1 (2020)
 [4] Lee, K. et al. *Nano Lett.* **21**, 3511 (2021)
 [5] Klein, J. et al. to be submitted (2021)

5:15 PM EQ20.02.07

Ferromagnetic Quasi-One Dimensional van der Waals Lattices—A New Platform Towards Freestanding Magnetic Nanowires Yi Qu¹, Maxx Arguilla¹, Qiang Zhang² and Mircea Dinca¹; ¹Massachusetts Institute of Technology, United States; ²Oak Ridge National Laboratory, United States

The demand towards accessing one-dimensional (1D) magnetic nanostructures has grown tremendously—as driven by numerous discoveries of novel physical properties in these systems as well as their integration into next-generation data storage devices and bioengineered artificial organelles. However, with current bottom-up synthetic pathways, achieving precise control over crystallinity, long-range morphology, and surface termination in magnetic nanowires, especially as they approach the Angstrom size regime, remains challenging. In this talk, we will describe our recent efforts in developing a new material platform to access freestanding ferromagnetic nanowires from top-down routes. We realize this by exfoliating a unique class of bulk magnetic crystals comprised of quasi-1D inorganic chains that are predominantly held together by van der Waals (vdW) forces. Based on these quasi-1D vdW crystals, we establish the intrinsic magnetic anisotropy in the bulk structure *via* powder neutron diffraction and demonstrate that these bulk 1D vdW crystals can be readily exfoliated into 10 ± 2.8 nm thick nanowires using solution-phase exfoliation. As expected from exfoliating a vdW lattice, the resulting nanowires possess cylindrical cross-sections with negligible anisotropy and surfaces that are resistant towards oxidation in ambient conditions. We find that the reduction in size of the bulk crystal, upon exfoliation into long and thin nanowires, directly decreases the magnetic ordering temperature of these phases and results to a significant increase in both the coercive field and remanence, both of which are the hallmarks of a hard ferromagnet. Overall, these findings collectively demonstrate the adaptability of well-established exfoliation methods into new classes of functional vdW lattices, which we envision would enable unique opportunities in the creation of 1D magnetic nanostructures and the realization of new magnetic properties and applications at or near the limit of 1D confinement.

5:30 PM EQ20.02.08

Cavity-Enhanced Linear Dichroism in a van der Waals Antiferromagnet Huiqin Zhang¹, Zhuoliang Ni¹, Aofeng Bai², Jason Lynch¹, Deep M. Jariwala¹, Frank Peiris² and Liang Wu¹; ¹University of Pennsylvania, United States; ²Kenyon College, United States

The coupling of electronic states with crystal lattice underlies a wealth of condensed matter phenomena. Coupling of electronic charge with lattice vibrations or distortions underlies superconductivity, charge density wave and metal-insulator transitions. In contrast, coupling between electronic charge and spins has been scarcely investigated, particularly in the optical domain. The recent discovery of anti-ferromagnetic (AFM) insulators of the form MPX_3 ($M = \text{Fe, Mn, Ni}$; $X = \text{S, Se}$) has opened new avenues in studying spin-charge correlations via optical means. Here we report such an interaction in AFM FePS₃ crystals which induces strong in-plane anisotropy, resulting in linear dichroism (LD). We identify that this LD is characteristic of the AFM spin ordering in the crystal coincident with the Neel transition temperature (~ 118 K). Further, we show that the LD is tunable both spectrally and in magnitude up to near-unity ($\sim 98.4\%$) levels when coupled to an optical cavity. Finally, through transfer-matrix simulations, we also demonstrate the dispersion of the LD in the visible-near infrared range as a function of the cavity length and the FePS₃ thickness. We observe a close agreement between experiments and simulations and prove that the LD can be enhanced from 5% (in bulk) to 98.4% (in ~ 200 nm thick samples) by virtue of cavity coupling and engineering the dielectric stack. Our findings open a new route to probing spin-charge coupling in magnetic materials and have implications in the design of novel birefringent nanophotonic elements.

5:45 PM EQ20.02.09

Monolayer Half van der Waals Heavy Metals via Confinement Heteroepitaxy Alexander Vera, Wilson Yanev, Cequn Li, Kaijie Yang, Boyang Zheng, Timothy Bowen, Siavash Rajabpour, Yuanxi Wang, Vincent Crespi, Chaoxing Liu, Jun Zhu, Nitin Samarth and Joshua A. Robinson; The Pennsylvania State University, United States

Atomically thin heavy metals (Pb, Bi) are expected to exhibit strong spin orbit coupling and broken spin degeneracy, making them viable candidates for next-generation quantum applications in both spin-dependent devices (i.e. spintronics) and spin-dependent phenomena (ex. quantum spin Hall effects). However, most ultrathin, mono-elemental metals are extremely sensitive to oxidation and degradation in ambient conditions. To answer this, our group has developed a synthesis route known as confinement heteroepitaxy (CHet), through which we have created large-area, atomically thin 2D-Pb, 2D-Bi, and 2D-PbGa capped by a quasi-freestanding epitaxial graphene which provides air-stability. Through our *ex-situ* characterization work, we have demonstrated strong spin splitting (~ 500 meV) and a unique out-of-plane spin polarization for 2D-Pb, superconductivity up to 3K in 2D-PbGa, and strong photoluminescence in 2D-Bi, implying their potential as precursors for next-generation, quantum spin technologies.

SESSION EQ20.03: Large Scale Electronic Grade Synthesis of 2D Materials I

Session Chairs: Zakaria Al Balushi and Deep Jariwala

Tuesday Morning, November 30, 2021

Hynes, Level 1, Room 103

10:30 AM *EQ20.03.01

Epitaxy of TMDs on Sapphire—Progress Toward Wafer-Scale Single Crystal Monolayers Haoyue Zhu, Tanushree H. Choudhury, Nicholas Trainor, Benjamin Huet, Thomas McKnight, Anushka Bansal and Joan M. Redwing; The Pennsylvania State University, United States

Wafer-scale synthesis of semiconducting transition metal dichalcogenide (TMDs) monolayers such as MoS₂, WS₂ and WSe₂ is of significant interest for device applications to circumvent size limitations associated with the use of exfoliated flakes. Epitaxy is required to achieve single crystal monolayers over large areas via coalescence of TMD domains with the same crystallographic direction. Sapphire has emerged as a promising substrate for wafer-scale epitaxy due to its commensurability with the hexagonal lattice of TMDs and its good thermal and chemical stability. However, the three-fold symmetry of TMDs typically results in inversion domains, also referred to as 60° twins, on substrates such as c-plane sapphire forming twin boundaries upon coalescence that are generally undesired.

In this study, we demonstrate the epitaxial growth of TMD monolayers on 2" diameter c-plane sapphire substrates with a significantly reduced density of inversion domains. Steps on the sapphire are shown to break the surface symmetry giving rise to a preferred domain orientation. Metalorganic chemical vapor deposition (MOCVD) was used for the epitaxial growth of WSe₂ and WS₂ monolayers on c-plane sapphire in a cold-wall horizontal quartz-tube reactor. A three-step nucleation-ripening-lateral growth process, carried out at temperatures ranging from 850°C to 1000°C, was used to achieve epitaxial films using W(CO)₆, H₂Se and H₂S as precursors in a H₂ carrier gas. Nucleation was observed to occur at the terrace edge and the growing domains align epitaxially with the underlying (0001) sapphire lattice. As a result of the nucleation process, the domains grow with a zig-zag edge facing the terrace edge which imparts a preferential direction to the domains. The percentage of domains with a preferred direction ranges from 75%-86% depending on MOCVD growth conditions. Continued lateral growth for times ranging from 10-30 minutes results in fully coalesced TMD monolayers that are epitaxially oriented on the sapphire, as assessed by in-plane x-ray diffraction, with a reduced density of inversion domain boundaries and good circular helicity. The results demonstrate the important role of surface structure in nucleation and epitaxial growth of TMD monolayers.

11:00 AM EQ20.03.02

CMOS Compatible Substitutionally Doped N- and P-type 2D WSe₂ Azimkhan Kozhakhmetov¹, Samuel Stolz², Anne Marie Tan^{3,4}, Rahul Pendurthi¹, Saiphaneendra Bachu¹, Furkan Turker¹, Nasim Alem^{1,5,6}, Jessica Kachian⁷, Saptarshi Das^{1,1,5}, Richard Hennig⁴, Oliver Gröning², Bruno Schuler² and Joshua A. Robinson^{1,6}; ¹The Pennsylvania State University, United States; ²Empa-Swiss Federal Laboratories for Materials Science and Technology, Switzerland; ³Nanyang Technological University, Singapore; ⁴University of Florida, United States; ⁵Materials Research Institute, The Pennsylvania State University, United States; ⁶Two-Dimensional Crystal Consortium, The Pennsylvania State University, United States; ⁷Intel Corporation, United States

Doping is the cornerstone of modern semiconductor technology where extrinsic semiconductors are the fundamental building blocks of everyday electronic devices. Recently emerged two-dimensional (2D) transition metal dichalcogenides (TMDs) are actively considered as one of the potential materials system for next-generation electronics, where significant progress has been made in the wafer-scale synthesis of pristine TMDs as large as 300 mm. Even though electronic-grade, industrial-scale intrinsic materials exist, to date, similar success does not hold for scalable doping of TMDs, which remains at the proof-of-concept stage.

In this study, we present scalable rhenium (n-type) and vanadium doping (p-type) of 2D WSe₂ films at front-end-of-line (FEOL) and back-end-of-line (BEOL) compatible temperatures via gas source chemical vapor deposition (CVD). Detailed experimental and theoretical studies demonstrate that Re and V substitutionally replace W atoms in the WSe₂ lattice and introduce discrete energy states that lie close to the conduction band and valance band, respectively. The concentration of the dopants can be precisely controlled down to <0.0001 at % and confirmed with a combination of x-ray photoelectron spectroscopy (XPS) and time-of-flight secondary ion mass spectroscopy (ToF-SIMS). Incorporated Re and V atoms break the translational symmetry of the host lattice resulting in increased density of defect-activated Raman modes. Moreover, the density of positive and negative trions is increased as a function of V and Re atom concentration leading to the complete quench of the photoluminescence spectra due to the non-radiative recombination nature of the trions. Transport measurements verify the n- and p-type nature of the rhenium and vanadium dopants, respectively. Moreover, we demonstrate that the dopants are not efficiently ionized in monolayer WSe₂ due to ineffective Coulomb screening and a strong dependence of dopant ionization energy on the thickness of the 2D films. Our findings are the first demonstration of extrinsic 2D semiconductors that are fully compatible with state-of-the-art Si processing which will be indispensable in constructing a heterogeneous platform for "Beyond Moore" technology.

11:15 AM EQ20.03.03

BEOL Compatible MOCVD-Grown Re-Doped MoS₂ for Next Generation Cu/TMD Hybrid Interconnects Riccardo Torsi, Yu-Chuan Lin and Joshua A. Robinson; The Pennsylvania State University, United States

The International Roadmap for Semiconductors expressed the urgent need for ultrathin (~1nm) diffusion barrier materials for copper interconnects. Recently, 2D transition metal dichalcogenides (TMD) such as MoS₂ have been proposed as a possible solution to this technological need as they can offer excellent diffusion blocking capabilities even at low thickness unlike conventional barrier materials. The challenge with 2D TMD integration as barrier materials is that synthesis of high-quality layers is typically achieved via vapor-phase techniques like chemical vapor deposition (CVD) at temperatures much higher than the back-end-of-line (BEOL) limit (<500C). In this study we demonstrate the growth of nanometer thick Re-doped MoS₂ via metal organic chemical vapor deposition (MOCVD) at BEOL-compatible temperatures with excellent Cu diffusion barrier performance. Employing Re₂(CO)₁₀ as a gas-source dopant precursor within the MOCVD process, we exhibit unprecedented control over Mo-substitutional doping concentration even up to degenerate levels confirmed by a combination of X-ray photoelectron spectroscopy (XPS) and Time-of-Flight Secondary Ion Mass Spectrometry (ToF-SIMS) measurements. With this precise regulation of dopant source flux and resulting Re concentration, we show how both diffusion blocking capabilities and carrier mobility of the grown MoS₂ films change as a function of dopant concentration. Time dependent dielectric breakdown (TDDB) tests are employed to measure the breakdown time and benchmark the Re-doped MoS₂ films against industry standard barrier materials (Ta/TaN) as well as other 2D nanosheet-based diffusion barriers. Carrier mobility on the other hand is extracted by fabricating back-gated and electrolyte double layer gated field-effect transistors (FETs). These results show that degenerately doped MoS₂ films are a promising candidate for ultrathin next-generation Cu/TMD hybrid interconnects.

11:30 AM EQ20.03.04

Polycrystalline MoS₂ Thin Films at 100 °C by Plasma-Enhanced Atomic Layer Deposition Miika Mattinen¹, Farzan Gity², Emma Coleman², Ray Duffy², Erwin Kessels¹ and Ageeth A. Bol¹; ¹Eindhoven University of Technology, Netherlands; ²Tyndall National Institute, Ireland

Semiconducting transition metal dichalcogenides (TMDCs), such as MoS₂, exhibit vast potential in a variety of applications due to their unique and favorable electronic, optical, and mechanical properties. However, the commonly used gas-phase TMDC deposition methods require high temperatures that are incompatible with many applications and substrates, in particular the emerging field of flexible electronics.¹

In this contribution, we demonstrate wafer-scale deposition of polycrystalline MoS₂ thin films at very low temperatures down to 100 °C using plasma-enhanced (PE) atomic layer deposition (ALD). ALD is a scalable, semiconductor industry compatible gas-phase method producing uniform, high-quality thin films with accurately controlled thickness. These attributes have led to rapidly growing interest in ALD for preparing TMDCs.^{2,3}

Our PEALD process is based on self-limiting, alternating surface reactions of a metalorganic molybdenum precursor Mo(NⁱBu)₂(NMe₂)₂ and mixed H₂S/H₂/Ar plasma.⁴ We have identified the critical role of hydrogen during the plasma step in controlling the composition and properties of molybdenum sulfide films. By increasing the H₂/H₂S ratio, we are able to deposit polycrystalline MoS₂ films at temperatures as low as 100 °C. To the best of our knowledge, this represents the lowest temperature for crystalline MoS₂ films prepared by any chemical gas-phase method.

Based on thorough film characterization, we find that adding hydrogen in the plasma helps avoid excess sulfur incorporation at low temperatures. The correct stoichiometry, in turn, enables crystallization of MoS₂. Furthermore, the H₂/H₂S ratio is found to control growth rate, film morphology, and electrical properties. For example, electrical conductivity can be increased by at least four orders of magnitude by increasing the H₂/H₂S ratio. Thus, the PEALD process enables tailoring molybdenum sulfide films to meet the requirements of different applications. We are currently investigating the

electronic transport properties of our MoS₂ films prepared at conditions that are compatible with flexible electronics as well as other applications and substrates with a low thermal budget.

1 Yao and Gang, *J. Appl. Phys.* **2020**, 127, 030902

2 Mattinen et al., *Adv. Mater. Interfaces* **2021**, 8, 2001677

3 Kim et al., *Adv. Mater.*, **2021**, 2005907

4 Sharma et al., *Nanoscale*, **2018**, 10, 8615

11:45 AM EQ20.03.05

Highly Controlled Alloying of 2D MoS₂, WS₂ and NbS₂ by Atomic Layer Deposition Jeff J. Schulpen¹, Cindy Lam¹, Marcel A. Verheijen^{1,2}, Erwin Kessels¹, Vincent Vandalon¹ and Ageeth A. Bol¹; ¹Technische Universiteit Eindhoven, Netherlands; ²Eurofins, Netherlands

Semiconducting 2D transition metal dichalcogenides (TMDs) such as MoS₂ and WS₂ have many unique properties such as stable excitons at room temperature and direct-gap luminescence at monolayer thickness, making them promising materials for various applications such as photovoltaics, optical sensing and catalysis. In particular, alloys of 2D TMDs hold great potential due to their composition-controlled properties, making them more versatile than pure TMDs. Hence, there is a clear need for a synthesis method of 2D TMD alloys that can exert excellent control over the alloy composition. While TMD alloys have been synthesized by chemical vapor deposition (CVD), the control of this method is limited, which is exemplified by the lack of control over *atomic ordering* (i.e. mixing or clustering of the alloy's constituents).

In this work we employ plasma-enhanced atomic layer deposition (ALD) to synthesize the 2D TMD alloys Mo_xW_{1-x}S₂ and Nb_xW_{1-x}S₂. As MoS₂ and WS₂ are both semiconductors, Mo_xW_{1-x}S₂ is a good case study for a tunable-bandgap semiconductor. The growth of the nanocrystalline Mo_xW_{1-x}S₂ alloys is shown to be exceptionally well-behaved, as their composition follows the ideal rule of mixtures. Beyond resulting in excellent control over fundamental properties such as the bandgap (evidenced by optical absorption spectroscopy), this ideal alloying behavior enables us to control the *atomic ordering* (i.e. mixing or clustering) of the alloys in the deposition process. Specifically, it is shown by atomic resolution HAADF-STEM that the atomic ordering can be tuned from a randomly mixed Mo_xW_{1-x}S₂ alloy to an alloy that exhibits clusters of MoS₂ and WS₂. When a sub-monolayer film with clustered atomic ordering is grown, the resulting film effectively consists of 2D core-shell nanoparticles (MoS₂ islands epitaxially bordered by WS₂) which are expected to have fascinating novel properties.

On the other hand, Nb is a group-VB transition metal whereas W is a group-VIB transition metal, making Nb_xW_{1-x}S₂ a relevant case study for electronic applications where well-controlled doping is desired. For the NbS₂ – WS₂ alloy system, we observe similarly well-behaved rule-of-mixtures growth. The electronic properties of the Nb_xW_{1-x}S₂ alloy are studied based on Hall measurements and their suitability for transistors is evaluated. Furthermore, the atomic arrangement of the alloy is studied using HAADF-STEM to gain fundamental insight into the alloying behavior of the NbS₂ – WS₂ system.

Our results demonstrate excellent control over the composition and *atomic ordering* of 2D TMD alloys by ALD, thus enabling fine tuning of the material properties as well as the emergence of novel properties, thereby opening up many possibilities for next-generation devices based on 2D materials.

SESSION EQ20.04: Advances in Memory and Logic Enabled by 2D Materials

Session Chairs: Zakaria Al Balushi and Aaron Franklin

Tuesday Afternoon, November 30, 2021

Hynes, Level 1, Room 103

1:30 PM *EQ20.04.01

2D Atomic Memory and Computing/Communication Applications Deji Akinwande; The University of Texas at Austin, United States

This talk will present our latest research adventures on 2D atomic nanomaterials towards greater scientific understanding and applications. In particular, the talk will highlight our work on non-volatile memory (atomristors) that can be employed in various applications including information storage, brain-inspired computing, and zero-power RF/THz switches. Non-volatile memory device based on atomically-thin materials is an application of defects, and is a rapidly advancing field with rich physics that can be attributed to metal ion binding to native defects. The promising 2D materials for neuromorphic computing include a library of TMDs (e.g. MoS₂), and hBN. In particular, hBN memory devices feature very low switching energy, a relatively wide range of stable programmable resistance states, and good endurance and retention. Recent progress has also demonstrated wafer-scale integration of 2D memory devices with a prospect to leverage silicon electronics for fully integrated systems.

2:00 PM *EQ20.04.02

2D/3D Heterostructures for Advanced Logic and Memory Devices Deep M. Jariwala; University of Pennsylvania, United States

The isolation of a growing number of two-dimensional (2D) materials has inspired worldwide efforts to integrate distinct 2D materials into van der Waals (vdW) heterostructures. While a tremendous amount of research activity has occurred in assembling disparate 2D materials into “all-2D” van der Waals heterostructures and making outstanding progress on fundamental studies, practical applications of 2D materials will require a broader integration strategy. I will present our ongoing and recent work on integration of 2D materials with 3D electronic materials to realize logic switches and memory devices with novel functionality that can potentially augment the performance and functionality of Silicon technology. First, I will present our recent work on gate-tunable diode¹ as well as tunnel junction devices based on integration of 2D chalcogenides with Si and GaN. I will show that combining 2D semiconductors with 3D semiconductors allows highly-tunable diode devices with applications in logic. Following this I will present our recent work on non-volatile memories based on Ferroelectric Field Effect Transistors (FE-FETs) made using a heterostructure of MoS₂/AlScN² and I also will present our work on Ferroelectric Diode devices based on thin AlScN and ultrafast switching in them.^{3,4} Finally, I will also present our recent and ongoing work on probing buried 2D semiconductor/3D metal interfaces⁵ and their impact on contact polarity and resistance engineering in electronic and opto-electronic devices.

I will end by giving a broad perspective on future opportunities of 2D semiconductors in basic science and applied microelectronics technology.

References:

1. Miao, J.; Liu, X.; Jo, K.; He, K.; Saxena, R.; Song, B.; Zhang, H.; He, J.; Han, M.-G.; Hu, W.; Jariwala, D. *Nano Letters* **2020**, 20, (4), 2907-2915.

2. Liu, X.; Wang, D.; Kim, K.-H.; Katti, K.; Zheng, J.; Musavigharavi, P.; Miao, J.; Stach, E. A.; Olsson, R. H.; Jariwala, D. *Nano Letters* **2021**, 21, (9),

3753-3761.

3. Liu, X.; Zheng, J.; Wang, D.; Musavigharavi, P.; Stach, E. A.; Olsson III, R.; Jariwala, D. *Applied Physics Letters* **2021**, 118, (20), 202901.

4. Wang, D.; Musavigharavi, P.; Zheng, J.; Esteves, G.; Liu, X.; Fiagbenu, M. M. A.; Stach, E. A.; Jariwala, D.; Olsson III, R. H. *physica status solidi (RRL)–Rapid Research Letters* **2021**, 10.1002/pssr.202000575.

5. Jo, K.; Kumar, P.; Orr, J.; Anantharaman, S. B.; Miao, J.; Motala, M. J.; Bandyopadhyay, A.; Kisslinger, K.; Muratore, C.; Shenoy, V. B.; Stach, E. A.; Glavin, N. R.; Jariwala, D. *ACS Nano* **2021**, 15, (3), 5618-5630.

2:30 PM EQ20.04.04

Field-Effect Conductivity Scaling for Two-Dimensional Materials with Tunable Impurity Potentials Chulin Wang, Lintao Peng, Spencer Wells, Jeffrey Cain, Yi-Kai Huang, Vinayak Dravid, Mark C. Hersam and Matthew Grayson; Northwestern University, United States

In this work, a scaling law is demonstrated in the conductivity of gated two-dimensional (2D) materials with tunable concentration of impurity scatterers, such as from shallow capacitively charged traps or adsorbed gas molecules. For the same device at different concentration of scatterers, a single scaled conductivity curve is observed upon rescaling the non-linear gate-dependent conductivity by a mobility scaling factor r to represent different strength of impurity-induced scattering potential while simultaneously shifting the gate voltage by an amount ΔV_g to represent different concentrations of impurity-induced doping. The scaling effect is demonstrated first by cooling an encapsulated black phosphorus (BP) 2D multilayer at $T_L = 100$ K with charge trap scatterers that are populated by cooling down from room temperature under a gate bias. A second case of mobility scaling is observed in a Bi_2Se_3 2D monolayer at room temperature exposed to gas adsorbate scatterers. The 2D nature of these samples weakly screens the charge of the adjustable density of point-like scatterers. The observed scaling in the conductance curve can be explained with a simple mobility model whereby the screened potential of individual scatterers determines the scaled conductivity versus density curve.

In the case of BP multilayers, the sample is tested under a series of bias cooling process which appears to remotely charge a trap layer with a tunable concentration of impurity scatterers. A gate bias is first applied on the back gate at room temperature. Then, the sample is cooled down to $T_L = 100$ K under the same gate voltage, namely the bias cooling voltage V_{BC} . Once the sample reaches T_L , the gate bias is then swept. For each V_{BC} , a distinct field-effect conductivity curve is obtained at T_L . The lineshapes of these curves have little in common. Remarkably, however, these curves can be empirically aligned onto a single curve if one artificially scales the conductivity by a factor r and shifts the gate voltage by ΔV_g , where a distinct pair of parameters r and ΔV_g is associated with each V_{BC} . The model is validated by taking Hall measurements for each bias cooling voltage V_{BC} , whereby the carrier densities are also observed to collapse onto a single curve upon shifting the gate voltage by ΔV_g .

These observations are interpreted with a charge-trap model. It is commonly known that the BP is susceptible to surface oxidization. The oxidization sites host charge traps that can be capacitively loaded. During the bias cooling process, the charge traps that have deep energy barriers are effectively frozen out, thereby determining the strength of the scattering potential and the concentration of doping in the device at T_L . Further, our analysis suggests that the mobility-limiting factors are charged impurity scattering and surface roughness scattering in the positive and negative limits of gate bias, respectively. The shallow charge trap model described here shows how naively estimated field-effect mobilities may be commonly over-estimated in 2D FET devices.

The Bi_2Se_3 monolayer device is studied under a gaseous environment from vacuum to forming gas to air. Various field-effect conductivity curves are obtained in each environment. Following the conductivity scaling analysis, the parameters indicate that the impurities are positively charged and scattering strength increases irrespective to the type of gas molecules present.

The scaled 2D conductivity analysis introduced in this work can serve as a fingerprint for a given material over an extended gate voltage range, allowing one to determine the characteristic field-effect conductivity with any impurity density and gate voltage for a given type of impurity. From the slope of the mobility scaling factor r plotted versus gate shift ΔV_g , one can further determine whether the impurities are acceptor-like or donor-like.

SESSION EQ20.05/SB06.03: Joint Session: Fabrication and Characterization of 2D Materials for Bioelectronics and Healthcare

Session Chairs: Zakaria Al Balushi and Dmitry Kireev

Tuesday Afternoon, November 30, 2021

Hynes, Level 1, Room 103

4:00 PM *EQ20.05/SB06.03.01

Novel van der Waals Materials and Their Potential for Biosensing Shengxi Huang; The Pennsylvania State University, United States

Emerging 2D and topological quantum materials have gained increasing attention due to their unique electronic and optical properties, and have shown promise in sensing applications. The realization of sensing devices using these materials still faces several challenges. For example, it is critical to gain clear understandings of (1) the fundamental light-matter interactions and their relations to the atomic structures, which govern many key material properties and device performances; and (2) the coupling with other nanostructures and molecules, which is a required structure for sensing devices and systems. This talk introduces new discoveries and pioneering works on these critical challenges, and novel applications of these materials in biochemical sensing. The first part of this talk presents light-matter interactions and techniques to augment material performance, including 3D Weyl semimetals, 2D Janus transition metal dichalcogenides, and 1D nanoscrolls. The characterization techniques employed, including low-frequency Raman spectroscopy, polarization- and time-resolved spectroscopy, and ultrafast electron diffraction, can be widely used in other material systems. The second part of this talk focuses on the interaction of 2D materials with organic molecules and related sensing applications. In particular, a novel enhancement effect of molecular Raman signals on 2D surface was discovered, which offers a new paradigm of biochemical sensing with high specificity, high multiplexity, and low noise. The selection rule for the 2D material substrates has been revealed, which is critical for device design. Two sensing applications for Alzheimer's disease and respiratory viruses will also be discussed. Overall, the works presented in this talk are significant in fundamental quantum science, and offer important guidelines for practical applications in sensing and quantum technologies. The methodologies used here also provide a framework for the future study of many emerging materials and sensing scenarios.

4:30 PM *EQ20.05/SB06.03.02

Novel 2D Material Based Devices for Biosensing Deblina Sarkar; Massachusetts Institute of Technology, United States

Sensors are ubiquitous in today's world starting from healthcare to security and forensic industries. Especially, 2D materials are highly promising for sensing applications because of their large surface to volume ratio, possibility to obtain pristine interfaces and opportunities for unique device design leveraging the ability from Van der Waal's heterostructures. Here, we will discuss the advantages of 2D material based Field effect Transistors (FETs) for highly sensitive and label-free electrical detection of biomolecules. Going beyond conventional FETs, we will discuss how novel quantum mechanical transistors can overcome the fundamental limitations in sensitivity of conventional electrical biosensors. We will also present how 2D materials can particularly enable the development of such novel quantum mechanical devices, which can open up new avenues in point-of-care applications.

5:00 PM *EQ20.05/SB06.03.03**Realizing Biomimetic Neuromorphic Functionality with 2D Material Electronic Devices** Mark C. Hersam; Northwestern University, United States

The exponentially improving performance of conventional digital computers has slowed in recent years due to the speed and power consumption issues that are largely attributable to the von Neumann bottleneck (i.e., the need to transfer data between spatially separate processor and memory blocks). In contrast, neuromorphic (i.e., brain-like) computing aims to circumvent the limitations of von Neumann architectures by spatially co-locating processor and memory blocks or even combining logic and data storage functions within the same device. In addition to reducing power consumption in conventional computing, neuromorphic devices also provide efficient architectures for emerging applications such as image recognition, machine learning, and artificial intelligence [1]. With this motivation in mind, this talk will explore how the reduced dielectric screening in 2D nanoelectronic materials enables opportunities for novel gate-tunable neuromorphic devices [2]. For example, by utilizing self-aligned, atomically thin p-n heterojunctions, dual-gated Gaussian heterojunction transistors have been realized, which show fully tunable anti-ambipolar transfer characteristics that are suitable for artificial neurons, competitive learning, and spiking circuits [3]. In addition, by exploiting field-driven defect motion in monolayer transition metal dichalcogenides, gate-tunable memristive phenomena have been achieved, which serve as the basis of hybrid memristor/transistor devices (i.e., 'memtransistors') that concurrently provide logic and data storage functions [4]. The planar geometry of memtransistors further allows multiple contacts to the channel region and dual gating that mimic the behavior of biological systems such as heterosynaptic responses [5]. Overall, this work introduces new foundational circuit elements for neuromorphic computing in addition to providing alternative pathways for studying and utilizing the unique quantum characteristics of 2D nanoelectronic materials [6].

[1] V. K. Sangwan, *et al.*, *Nature Nanotechnology*, **15**, 517 (2020).[2] M. E. Beck, *et al.*, *ACS Nano*, **14**, 6498 (2020).[3] M. E. Beck, *et al.*, *Nature Communications*, **11**, 1565 (2020).[4] V. K. Sangwan, *et al.*, *Nature*, **554**, 500 (2018).[5] H.-S. Lee, *et al.*, *Advanced Functional Materials*, **30**, 2003683 (2020).[6] X. Liu *et al.*, *Nature Reviews Materials*, **4**, 669 (2019).

SESSION EQ20.06: Poster Session I

Session Chairs: Zakaria Al Balushi and Joan Redwing

Tuesday Afternoon, November 30, 2021

8:00 PM - 10:00 PM

Hynes, Level 1, Hall B

EQ20.06.01**Structure and Properties of a Novel Heptacoordinated Complex Based on Sr²⁺ and 1,2,4,5-tetrakis(4-carboxyphenyl)benzene** Muhammad Usman^{1,2}, Lydia Ogebulu¹, Evgenii Oskolkov^{3,1}, Raúl Castañeda¹ and Tatiana Timofeeva¹; ¹New Mexico Highlands University, United States; ²Academia Sinica, Taiwan; ³University at Buffalo, The State University of New York, United States

Metal-organic frameworks (MOFs) have emerged as a class of structurally diverse materials with immense potential for many applications. Their often fascinating properties, apart from composition, depend strongly on the structure. An important subclass – MOFs based on naturally abundant and generally non-toxic alkaline metals – have recently offered a sustainable alternative to conventional rare-earth and transition metal complexes. Among the elements of the alkaline metals group, strontium (Sr) currently remains the most exotic and least studied in context of metal-organic complexes. However, few recent reports have suggested Sr-based complexes' suitability as semiconducting materials, which is rare for the class of MOFs. In this work two structurally different Sr²⁺ MOFs of the same composition were prepared by introducing slight changes into the synthesis conditions. Single crystal diffraction data was obtained and used to determine the structures of both complexes. The discovered structural differences have shown that control of crystalline structure and topology by small changes in preparation method is possible for similar alkaline metal complexes. High stability to temperatures up to 250 C° was confirmed by thermogravimetric analysis. Optical properties were studied and bandgap values determined. With facile synthesis method, synthetic tunability and remarkable properties both complexes exhibit high promise in semiconducting technology.

EQ20.06.02**Pseudo-Polymorphism in Layered Tetragonal FeS Intercalates** Kirill Kovnir^{1,2}; ¹Iowa State University, United States; ²US DOE Ames Laboratory, United States

Tetragonal iron sulfide and selenide, FeQ (Q = S, Se), adopt the simplest crystal structures of the iron-based superconductors. Their layered structures are suitable for development of the hybrid magnetic and superconducting materials by the intercalation of the host species in the interlayer space. Low-temperature solution-assisted intercalations provides an access to rich phase space of intercalates based on C,N,O,H-containing molecular species. A complete description of the Fe-Q layer as well as the intercalate is required to accurately link these structural aspects to a material's bulk properties. While interplanar van der Waals stacking is ideal for diverse intercalation it can limit crystal quality and in turn complicate the structure-properties analysis. To determine exact composition and challenging complex crystal structures of two pseudo-polymorphic Fe-S-en (en = ethylenediamine) layered hybrid phases we applied a synergistic combination of elemental composition, decomposition behavior, high-resolution synchrotron X-ray diffraction and total scattering, ⁵⁷Fe Mössbauer spectroscopy, and electron diffraction methods. The intricate interplay between Fe vacancies, puckering of the Fe-s layers, number and charge of the intercalated species, structural distortion, and magnetic properties will be discussed. Our work shows an importance of detailed characterization of the crystal structure of intercalated compounds to understand the origin of the observed properties and develop proper structure-properties relationships.

EQ20.06.03**Quasi-One-Dimensional Transition-Metal Trichalcogenide for Low-Dimensional Electronic Device Applications** Archit Dhingra, Alexey Lipatov, Alexander Sinitkii and Peter Dowben; University of Nebraska-Lincoln, United States

Transition metal trichalcogenides (TMTs) are quasi-one-dimensional semiconductors with modest band gaps that offer an opportunity to fabricate transistors with widths less than 10 nm, as they lack undesirable edge effects that plague other well-studied two-dimensional materials (namely: graphene-based materials and transition metal dichalcogenides). Among the family of TMTs, TiS₃, ZrS₃, and In₄Se₃ are n-type semiconductors, while HfS₃ is a p-type semiconducting trichalcogenide with high spin-orbit coupling. Besides, in addition to their electronic properties and adequate band gaps, their opto-

electronic properties project them as promising candidates for photodetector applications. That is to say, potential of TiS_3 , ZrS_3 and In_4Se_3 for photodetector applications is now known owing to successful experimental demonstrations of working light polarization-dependent phototransistors made from these TMTs; and this is consistent with appreciable photo-response of HfS_3 reported elsewhere.¹ Furthermore, temperature-dependent X-ray photoemission spectroscopy (XPS) and Raman spectroscopy have been employed to investigate and quantify the extent of electron-phonon scattering in these transition metal trichalcogenides. The Debye–Waller factor plots (based on the temperature-dependent XPS) for S 2p and Hf 4f core-levels of HfS_3 suggest that there exists a phase transition between 225 K and 240 K; however, no such phenomenon is seen for TiS_3 , ZrS_3 , and In_4Se_3 . Thus, HfS_3 exhibits higher electron-phonon scattering at temperatures above 240 K than at temperatures below 225 K. Generally, it is clear that phonon scattering affects carrier mobilities of transition metal trichalcogenides. Nonetheless, the interaction between the Au metal contacts and the various transition metal trichalcogenides, which differs substantially, also affects the measured carrier mobilities. The Au thickness-dependent XPS measurements confirm Schottky-barrier formation at the Au/ HfS_3 and Au/ In_4Se_3 interfaces, which is different from what is seen at the Au/ TiS_3 and Au/ ZrS_3 interfaces. This, in turn, implies that the work function of Au is less than that of HfS_3 because the formation of a Schottky-barrier at the metal/p-type semiconductor interface is only possible if the work function of the p-type semiconductor is higher than that of the metal. Nevertheless, noteworthy in this regard is that for other Au/TMT interfaces, some complex interfacial chemistry also plays a big role. Yet, there are good reasons to believe that the fabrication of transition metal trichalcogenides-based Schottky transistors, Schottky diodes, and phototransistors are all possible. These results are important as they open new pathways for efficient integration of logic and sensing, which is key to robotics applications.

1. W. -W. Xiong, J. -Q. Chen, X. -C. Wu, J. -J. Zhu, *J. Mater. Chem. C* **2**, 7392 (2014). DOI:10.1039/C4TC01039F

EQ20.06.04

Graphene Growth on Non-Metallic Substrates by Chemical Vapor Deposition Sandra Rodriguez Villanueva^{1,2}, Frank Mendoza³, Alvaro Instan¹, Brad Weiner⁴, Ram Katiyar¹ and Gerardo Morell^{1,2}; ¹University of Puerto-Rio Piedras, United States; ²Molecular Sciences Research Center, United States; ³University of Puerto Rico at Mayagüez, United States; ⁴University of Puerto Rico at Río Piedras, United States

For optoelectronic applications, graphene is usually grown on metallic substrates then transferred into a dielectric. This process leaves large amounts of residual chemicals and a high risk of wrinkling or breakage of the film. A solution is to grow graphene directly on the dielectric, but this still is very challenging.

In this work, we show the direct synthesis of graphene on SiO_2/Si and SiC by hot-filament chemical vapor deposition. The graphene deposition was conducted at low pressures (35 Torr) with a mixture of methane in hydrogen and a substrate temperature $\sim 900^\circ\text{C}$ followed by abrupt cooling to room temperature. A thin strip of copper layer was sputtered in the middle of the SiO_2/Si substrates as a catalytic material. The structural properties of the graphene films were analyzed using Raman Spectroscopy, Atomic Force Microscopy (AFM), and X-ray photoelectron spectroscopy (XPS). Raman mapping and AFM measurements indicate the growth of few-layer graphene films in all cases. X-ray photoelectron spectroscopy confirmed the presence of graphene deposition on SiO_2/Si and SiC substrates. The results show that the effect of the surface catalytic of copper allows the graphene growth beyond the copper strip and all over the SiO_2/Si substrates.

EQ20.06.05

Polarity Switch of WS_2 Transistors Through *In Situ* Ion Beam-Modified Contacts Alexander T. Mangus, Hattan Abuzaid and Aaron D. Franklin; Duke University, United States

As modern transistor technologies reach their physical limits, new materials are being actively explored for device scaling strategies, novel device structures, or integration strategies. Two-dimensional (2D) transition metal dichalcogenides (TMDs) show promise because their atomic thickness enables aggressive channel length scaling and they are compatible with low thermal budget fabrication into transistors. For TMDs to be practical for logic transistors, complementary (both n- and p-type) devices need to be realized. Typically, semiconductors tend to show either p- or n-type behavior in transistors, depending on how their energy bands align with the Fermi level of the source/drain contact metals. Theoretically, metals can be carefully chosen by considering their work functions to give n- or p-type devices based on preferential carrier injection to the conduction or valence band, respectively. However, in real devices, Fermi-level pinning and related effects limit the effectiveness of this approach. In previous works, modification of the metal-TMD interface with an Ar^+ ion beam has been shown to enhance device performance in MoS_2 transistors, with increased on-current and on/off-current ratio [1-2]. In this study, we demonstrate the effect of this *in-situ* Ar^+ ion beam modification of the metal-TMD contact interface for Pd-contacted WS_2 transistors. The ion beam was used to modify the inert surface of the TMD (selectively in the contact regions) to generate dangling bonds for promoting improved carrier injection with the Pd. Having the ion beam in the same high vacuum chamber as the electron beam evaporator for metal deposition enabled a fully *in-situ* process, which reduced contamination from ambient exposure before contact deposition. To eliminate flake-to-flake variation, multiple modified and unmodified devices were fabricated on each flake of the mechanically exfoliated WS_2 . Raman spectroscopy was used to study the impact of the ion beam modification on the WS_2 surface. An unanticipated polarity switch in these WS_2 transistors was driven by the ion beam modification, which enhanced the p-branch current, causing a polarity switch compared to the devices with unmodified Pd- WS_2 contacts. The p-branch on-current in the modified devices showed an enhancement of two to three times, on average, over the n-branch on-current of the unmodified devices. This discovery presents a unique path towards complementary WS_2 devices to be easily fabricated with the addition of an ion beam modification step to the fabrication process. Based on these findings, ion beam effects should be studied more extensively on other TMDs using a multitude of different metals to thoroughly characterize the enhancement and polarity switching effects that may occur.

EQ20.06.06

2D Nanocoating for High-Voltage Discharge Resistant Dielectrics Antigoni Konstantinou, Hiep Nguyen, Yifei Wang and Yang Cao; University of Connecticut, United States

There are serious safety concerns with materials that are used in high-voltage applications because electric arc represents one of the most severe thermal plasma energy discharges involving extremely high temperature ($>25\text{kK}$). Therefore, the need for electrical discharge resistant dielectrics is imperative for safe high voltage design. A milestone of the 2D materials that are still using in this kind of applications is mica, of which the best properties are retained in the form as tape insulation. On the other hand, modern applications require conformal coating or injection molded insulation with superior discharge resistance and mica does not fulfill this requirement. Also, high layer thickness of mica insulation system behaves as a barrier for heat conduction dissipation. Therefore, the development of a novel polymer-based coating with self-assembling, inorganic 2D nanofiller montmorillonite (MMT) appears to be a promising way to overcome these problems. In this study, spray coating is applied to Kapton substrates to significantly increase discharge resistance. The electric performance of 2D nanoclay coated dielectrics is extensively characterized via voltage endurance and breakdown strength testing. The samples are further characterized using microscopy, x-ray diffraction, and broadband dielectric spectroscopy.

References

1. Xia, J.; Li, Z.; Nasreen, S.; Ronzello, J.; Teng, H.; Jacobs, L.; Cao, Y., Discharge Resistant Nano-Coatings. In *2018 IEEE Conference on Electrical Insulation and Dielectric Phenomena (CEIDP)*, 2018; pp 183-186.

EQ20.06.07

Preparation of Ge(111) Substrates for Bismuthene and Stanene [Jessica Dong](#), Kaylyn Holmes, Ruizhe Kang, Jennifer Hoffman, Charles Brooks and Julia Mundy; Harvard, United States

Monolayers of bismuth and tin arranged in a honeycomb lattice hold great promise for next-generation electronics. These materials, so-called “bismuthene” and “stanene”, could host a quantum spin Hall effect near room-temperature. Unlike graphene, however, these materials cannot be readily exfoliated from a bulk crystal and must be stabilized in the thin film form. Here we use molecular-beam epitaxy to construct these metastable structures. We discuss the preparation of the Ge(111) surface as a platform for our epitaxial deposition.

EQ20.06.08

Interface Chemistry, Band Alignment and Thermal Stability of Metal Contacts on MoS₂ [Xinglu Wang](#), Seong Yeoul Kim, Yi Shen and Robert Wallace; The University of Texas at Dallas, United States

The high contact resistance of transition-metal dichalcogenide (TMD)-based devices is one of the bottlenecks that limit the application of TMDs in various domains. The contact resistance of TMD-based devices is strongly related to the interface chemistry and band alignment at the contact metal/TMD interfaces. To understand the metal/MoS₂ interface chemistry and band alignment, Ni and Ag metal contacts are deposited on MoS₂ bulk and chemical vapor deposition bilayer MoS₂ (2L-MoS₂) film samples under ultrahigh vacuum (UHV, $\sim 3 \times 10^{-11}$ mbar) and high vacuum ($\sim 3 \times 10^{-6}$ mbar) conditions. X-ray photoelectron spectroscopy (XPS) is used to characterize the interface chemistry and band alignment of the metal/MoS₂ stacks. Ni forms covalent contact on MoS₂ bulk and 2L-MoS₂ film by reducing MoS₂ to form interfacial metal sulfides. In contrast, van der Waals gaps form at the Ag/MoS₂ bulk and Ag/2L-MoS₂ film interfaces, proved by the absence of an additional metal sulfide chemical state and the detection of Ag islands on the surface. Different from other metal/MoS₂ systems studied in this work, Ag shows potential to form an Ohmic contact on MoS₂ bulk regardless of the deposition ambient. Fermi levels (E_F 's) are pinned near the intrinsic E_F of the 2L-MoS₂ film with high defect density regardless of the work function of the metal, which highlights the impact of substrate defect density on the E_F pinning effect and contact resistance.

To achieve reliable MoS₂ based devices with a higher thermal budget, it is imperative in understanding the impact of thermal treatment on the interface chemistry of the Ni/MoS₂ interface. 1 nm Ni films were deposited on CVD 1L-MoS₂/SiO₂/Si and 2L-MoS₂/SiO₂/Si wafers, and exfoliated MoS₂ bulk crystal in UHV. *In-situ* XPS was employed to study the interface chemistry and band alignment after Ni deposition and subsequent stepwise UHV annealing up to 400 °C. Ni in-diffusion is detected for all the Ni/MoS₂ systems after annealing at 300 °C in UHV. The defects generated by Ni reduction of MoS₂ and Ni in-diffusion cause the interfacial reaction at the MoS₂/SiO₂ interface after annealing at 400 °C for the CVD MoS₂ film systems. This work highlights the influence of the processing condition on the interface chemistry and band alignment of metal contacts/TMD/oxide stacks and their implications on the device performance. The interface reaction between CVD few-layer MoS₂ film and SiO₂/Si wafer necessitates the careful processing of the transferred or deposited TMD thin films on oxide substrates.

This work was supported in part by NEWLIMITS, a center in nCORE, a Semiconductor Research Corporation (SRC) program sponsored by NIST through award number 70NANB17H041.

EQ20.06.09

How Surface Tension Matters in Polymer-Free Graphene Transfer [Aisha A. Okmi](#)^{1,2}, Ninxin Li¹, Guanhui Gao³, Yelyzaveta Rublova⁴, Tara Jabegu¹, Diren Maraba¹, Rui He⁵, Yue Zhang⁶, Xuemei Xiao⁶, Pei Dong⁵, Boxing Xu⁶ and Sidong Lei^{1,7}; ¹Georgia State University, United States; ²Jazan University, Saudi Arabia; ³Rice University, United States; ⁴Institute of Chemical Physics, University of Latvia, Latvia; ⁵George Mason University, United States; ⁶University of Virginia, United States; ⁷Center of Nano-Optics, Georgia State University, Atlanta, United States

Although chemical vapor deposition (CVD) enables large graphene sheets, the polymer-free transfer techniques of this type of graphene are still challenging. The main reason that complicates graphene's current direct transfer techniques is the non-understood effect of high surface tension (ST) of water on graphene during this type of transfer. For instance, it is widely accepted that ST of water (72 dyne/cm) would break graphene sheets during metal etching or solution replacement. In this work, we have achieved several experiments and calculations to unveil the actual effect of high ST on graphene and to provide a simple, effective, and clean method to achieve graphene transfer. We designed a specific way that allows tuning surface tension of liquids underneath graphene. We successfully transferred graphene at ST lower than the initial ST (ST of the water) and provided a wide range of liquids that can be used to replace water underneath graphene. Leveraging the high ST of water, a graphene water membrane (GWM) would be formed, providing a new understanding of the graphene-water molecules dynamics. GWM was functioned successfully to deliver graphene to varied substrates. Our work removes the long believed idea that high ST has a damaging effect on graphene. Additionally, it expands the graphene applications in several fields, such as sensors and actuators.

EQ20.06.14

Dominating Interlayer Resonant Energy Transfer in Type-II 2D Heterostructures [Arka Karmakar](#)¹, Abdullah Al-Mahboob¹, Christopher E. Petoukhoff¹, Oksana Kravchyna¹, Nicholas S. Chan¹, Takashi Taniguchi², Kenji Watanabe² and Keshav M. Dani¹; ¹Okinawa Institute of Science and Technology Graduate University, Japan; ²National Institute for Materials Science, Japan

Type-II heterostructures (HSs) are building blocks of next generation electronic and optoelectronic devices. Till date, studies have shown that the interlayer charge transfer (CT) mechanism is the dominating carrier relaxation pathway in type-II transition metal dichalcogenide (TMD) HSs. This work shows in a type-II HS formed between monolayers of group-6 and group-7 TMD materials, nonradiative energy transfer (ET) dominates over the traditional CT process even *without* a charge-blocking interlayer. Without charge-blocking interlayer, the measured ET efficiency is 70%, which leads to 3.6 times photoluminescence (PL) enhancement from the acceptor material in HS area. By completely blocking the interlayer CT process we achieved more than one order magnitude higher PL emission from the acceptor material in the HS area. The PL enhancement factor (I/I_0) shows a distance (d) dependency of $1/d^2$, revealing the interaction between the TMD layers via 2D-to-2D dipole coupling. This study not only provides significant insight into the competing interlayer processes, but also shows an innovative way to increase the PL quantum yield of the desired TMD material using ET process.

EQ20.06.18

Late News: Degradation of 2D Materials Formed by Crosslinking of Hydrophilic Macromolecules [Rainhard Machatschek](#)^{1,2}, Shivam Saretia^{1,2} and Andreas Lendlein^{1,2}; ¹Helmholtz Zentrum Hereon, Germany; ²University of Potsdam, Germany

In 2D materials, each constituent is permanently in contact with the environment. While this is beneficial for applications such as catalysis or sensors, such exposure to its surrounding makes 2D materials susceptible to mechanical stress, chemical modification and degradation. Clearly, the prospective application of 2D materials determines whether degradation or long-term stability is required. Yet, the degradation behavior of 2D materials under different environmental conditions remains largely unexplored.

Here, we use the Langmuir monolayer technique to study the preparation and degradation of 2D materials, formed in situ by the reaction of monolayers of

hydrophilic polymers with suitable cross-linkers. In particular, we are interested in the influence of acidic, alkaline and oxidative environments on the mass loss and the mechanical properties of the 2D sheets. We show how functional groups that are particularly susceptible to distinct environmental factors enable a rapid loss of mass and mechanical strength. The experimental results are compared to existing theoretical models for the degradation of 2D polymer networks, as a first step towards a prediction of the environmental fate of these fascinating materials.

[1] S. Saretia, R. Machatschek, B. Schulz, B., A. Lendlein, Reversible 2D networks of oligo (ϵ -caprolactone) at the air–water interface. *Biomedical Materials*, 14(3), 034103 (2019).

[2] S. Saretia, R. Machatschek, T. Bhuvanesh, A. Lendlein. Effect of Water on Crystallization and Melting of Telechelic Oligo (ϵ -caprolactone) s in Ultrathin Films. *Advanced Materials Interfaces*, 8(7), 2001940 (2021).

SESSION EQ20.07: Physical Properties in 2D Materials II—Transport

Session Chair: Zakaria Al Balushi

Wednesday Morning, December 1, 2021

Hynes, Level 1, Room 103

10:30 AM EQ20.07.01

Origins of Fermi Level Pinning for Ni and Ag Contacts on Transition Metal (Mo and W) Dichalcogenides—Interface Chemistry and Band Alignment Xinglu Wang, Seong Yeoul Kim, Yi Shen and Robert Wallace; The University of Texas at Dallas, United States

Transition metal dichalcogenides (TMDs) are intriguing due to their unique properties and potentials for applications in next-generation electronic devices. However, strong Fermi level (E_F) pinning manifests at the metal/TMD interfaces, which could tremendously restrain the carrier injection into the channel. In this work, we illustrate the interface chemistry and band alignment of Ni and Ag on the Molybdenum and Tungsten based (Mo, W-based) TMDs. Ni reduction of all the TMD substrates and the formation of intermetallic products are detected by X-ray photoelectron spectroscopy (XPS) after *in-situ* ultra-high vacuum (UHV, $\sim 3 \times 10^{-11}$ mbar) and *ex-situ* high vacuum (HV, $\sim 3 \times 10^{-6}$ mbar) metal depositions. E_F 's are pinned close to the middle of the bandgap for Ni contacts with MoSe₂ and MoTe₂. In contrast, Ni tends to form n-type and p-type Schottky contacts with WS₂ and WSe₂, respectively. Van der Waals interfaces form between Ag and TMDs with E_F 's pinned close to the intrinsic E_F 's of the TMDs, indicating the impact of the natural defects of the TMD substrates. The oxidation of metal contacts and the metal/TMD interfaces are observed for most of the *ex-situ* HV samples. The metal deposition mechanism is characterized by atomic force microscopy and the surface morphology is correlated to the interface chemistry. The implications of interface chemistry on the *true* band alignment of Ni and Ag contacts on Mo and W-based TMDs will be discussed. This work improves the understanding of the possible E_F pinning origins at the metal/TMD interfaces.

This work was supported in part by NEWLIMITS, a center in nCORE, a Semiconductor Research Corporation (SRC) program sponsored by NIST through award number 70NANB17H041.

10:45 AM EQ20.07.02

Metal Particle-Enabled Width-Controlled Growth of Atomically-Thin Molybdenum Disulfide Nanoribbons with Width-Dependent Quantum Transport Behavior Xufan Li¹, Baichang Li², Jincheng Lei³, Ksenia V. Bets², Xiahan Sang⁴, Yang Liu², Raymond R. Unocic⁴, Boris I. Yakobson³, James Hone² and Avetik R. Harutyunyan¹; ¹Honda Research Institute USA Inc., United States; ²Columbia University, United States; ³Rice University, United States; ⁴Oak Ridge National Laboratory, United States

Transition metal dichalcogenides (TMDs) exhibit a variety of electronic behaviors depending on the number of layers and width. Therefore, developing facile methods for their controllable synthesis is of central importance. We present a way to control the width by employing metal nanoparticles and the number of layers by substrates. We found that on some types of substrates metal nanoparticle promotes both heterogenous nucleation of the first layer of TMDs (e.g., MoS₂) and simultaneously homoepitaxial tip growth of a second layer via vapor-liquid-solid (VLS) mechanism, resulting in bilayer nanoribbons with the width down to sub-10 nm as controlled by the nanoparticle diameter; while on some other types of substrates single layer of MoS₂ nanoribbons are directly grown via the VLS mechanism through the metal nanoparticle. Simulations further confirm the VLS growth mechanism towards nanoribbons and its orders of magnitude faster growth speed compared to the conventional non-catalytic growth of flakes. Width-dependent photoluminescence and Coulomb-blockade oscillation observed in the transfer characteristics of the nanoribbons at temperatures up to 60 K demonstrate the width evinces the value of this proposed synthesis strategy for future nanoelectronics.

11:00 AM EQ20.07.03

Phonon-Mediated Hydrodynamic Transport in Layered Quantum Materials Yaxian Wang, George Varnavides and Prineha Narang; Harvard University, United States

Hydrodynamic electron flow in condensed matters has been one of the most active research areas recently. While progress from both theory and experimental techniques are made, open questions regarding the underlying mechanisms in layered quantum materials still remain. We utilize *ab initio* techniques to treat the electron scattering events explicitly, and show in combination with the Boltzmann transport equation a generic metric of hydrodynamic transport taking into account temperature, channel width, and impurity length, which can be directly verified by various experimental techniques.

We start by investigating different electron scattering mean free paths in WTe₂, and show that that phonon mediated electron-electron interaction could lead to much shorter momentum conserving mean free path (l_{mc}) than momentum relaxing l_{mr} , facilitating hydrodynamic behavior in systems where the direct Coulomb interaction is largely screened [Vool 2021].

We then present the transport regime limits in PdCoO₂, and identify the finite size effects in both the quasi-hydrodynamic and quasi-ballistic transport regimes, which leads to the in-plane conductivity anisotropy observed recently [Maja 2019, Maja 2021]. We further discuss the dynamics of phonons through the lifetime hierarchy from interactions with electrons and the lattice, and confirm that phonons do play an important role in the electronic transport phenomena [Varnavides, Wang 2021].

Finally, we predict prominent hydrodynamic effects in other layered semimetals ZrSiS and TaAs₂, and propose a few key ingredients including high carrier mobility, large electron-phonon matrix elements, and slow phonon-phonon scattering. The plethora of low symmetry crystals whose Fermi surfaces are composed of d orbitals from the transition metal and p orbitals from the metalloids provides a much larger pool for further study. This work provides *ab initio* signatures of material-specifics to explore hydrodynamic electron flow in a much larger family of condensed matter systems, and thus offers insights into further study of electron interactions through transport phenomena.

11:15 AM *EQ20.07.04

Light Matter Interaction and Quantum Confinement in 2D Polar Metals Margaux Lassaunière¹, Jakob Henz¹, Wen He², Siavash Rajabpour³, Alexander Vera³, Katharina Nisi¹, Shruti Subramanian³, Su Ying Quek², Joshua A. Robinson³ and Ursula Wurstbauer¹; ¹University of Münster, Germany; ²National University of Singapore, Singapore; ³The Pennsylvania State University, United States

Important for all (quantum) optical technologies is the manipulation of the light-matter interaction to achieve a high level of control, particularly in technologically relevant solid-state nanomaterials. Atomically thin two-dimensional layered materials receive great interest because of their unique properties. A novel class of atomically thin materials such as 2D polar metals such as 2D gallium or 2D indium and their ternary alloys that exhibit fascinating properties like superconductivity [1,2] strong nonlinear optical properties emerging by giant second harmonic generation [3] and epsilon near zero behavior in the visible and NIR range [4]. The layer dependence of the energies of localized plasmons due to interband transition strongly suggest quantum confined 2D metal films. In contrast, monolayers and hetero-bilayers of semiconducting transition metal dichalcogenides (SC-TMDCs) excel due to their strong exciton dominated light matter interaction with the possibility to study and manipulate dense and correlated exciton ensemble [5-7] and to realize quantum light sources [8].

In this talk, we will introduce the rather new class of 2D materials, 2D polar metals and focus on their linear optical response measured by imaging spectroscopic ellipsometry in dependence of the temperature covering room temperature to 800mK. At low temperatures emergent behavior such as superconductivity occurs such that we are able to monitor the dielectric functions across the phase transitions.

We acknowledge funding by the Deutsche Forschungsgemeinschaft (DFG, German Research Foundation) under Germany's Excellence Strategy – EXC 2089/1 – 390776260 and projects Wu 637/4- 1, 4 – 2, 7-1 and SPP 2244.

References

- [1] N. Briggs et al. Nature Materials 19 (6), 637-643 (2020).
- [2] S. Rajabpour et al. arXiv:2106.00117 (2021).
- [2] M. A. Steves et al. Nano Letters 20, 11, 8312–8318 (2020).
- [3] K. Nisi et al. Advanced Functional Materials 2005977, 1-11 (2020)
- [4] B. Miller, et al., Nano Lett. 17(9), 5229–5237 (2017).
- [5] J. Kiemle et al. Phys. Rev. B 101, 121404(R) (2020).
- [6] L. Sigl et al. Physical Review Research 2, 042044(R) (2020)
- [7] J. Klein et al. ACS Photonics 8, 2, 669–677 (2021).

11:45 AM EQ20.08.02

Intercalation-Induced Phase Transition in Ta-WTe₂ Mengjing Wang, Aakash Kumar, Hao Dong, John Woods, Joshua Pondick, Alyssa Shiyu Xu, Peijun Guo, Diana Qiu and Judy Cha; Yale University, United States

Intercalation of lithium into van der Waals gaps of two-dimensional (2D) materials has been exploited to induce useful electronic and structural phase transitions enabled by its high electron doping power on the order of 10^{14} e/cm². For example, semiconducting 2H-MoS₂ can be transformed into metallic 1T'-MoS₂ with lithium intercalation. Despite the extensive studies of lithium intercalation in MoS₂ and WS₂, the effects of lithium intercalation in other 2D transition metal dichalcogenides have rarely been explored. Herein, we report a reversible structural phase transition in 2D semi-metallic Td-WTe₂ by electrochemical lithium intercalation. The phase transition dynamics were systematically investigated with a combination of *in situ* characterization tools to monitor the changes in the optical, structural, and electrical properties of WTe₂ as a function of intercalation driving voltage in real-time. The intercalation-induced new phase was probed structurally by *in situ* polarization angle-dependent Raman spectroscopy, which revealed new Raman peaks as well as a distinct symmetry for the high-frequency intralayer and low-frequency interlayer vibration modes at the phase transition point. Surprisingly, the new phase shows an increase of longitudinal resistance by two orders of magnitude and a significant reduction of carrier density at the phase transition point, probed by *in situ* Hall measurements as a function of intercalation. The *in situ* transport data suggests that the new phase has a distinct electronic band structure from the T_d phase. Based on our observations and *ab initio* calculations, we suggest possible crystal structures and corresponding electronic band structures for the intercalation-induced phase in WTe₂.

12:00 PM EQ20.08.05

Two-Dimensional Charge Order Stabilized in Clean Polytype Heterostructures Suk Hyun Sung¹, Noah Schnitzer², Steve Novakov¹, Ismail El Baggari³, Xiangpeng Luo¹, Jiseok Gim¹, Nguyen Vu¹, Zidong Li¹, Todd Brintlinger⁴, Yu Liu⁵, Wenjian Lu⁵, Yuping Sun⁵, Parag Deotare¹, Kai Sun¹, Liuyan Zhao¹, Lena Kourkoutis², John T. Heron¹ and Robert Hovden¹; ¹University of Michigan, United States; ²Cornell University, United States; ³The Rowland Institute at Harvard, United States; ⁴U.S. Naval Research Laboratory, United States; ⁵Institute of Solid State Physics, Chinese Academy of Sciences, China

Strong evidence suggests that transformative correlated electron behavior may exist only in unrealized clean 2D materials such as 1T-TaS₂ [1]. Unfortunately, experiment [2, 3] and theory [4] suggest that extrinsic disorder in free standing 2D layers impedes correlation-driven quantum behavior. Here we demonstrate a new route to realizing fragile 2D quantum states through epitaxial polytype engineering of van der Waals materials [5]. The isolation of truly 2D charge density waves (CDWs) between metallic layers stabilizes commensurate long-range order and lifts the coupling between neighboring CDW layers to restore mirror symmetries via interlayer CDW twinning. The twinned-commensurate (tC-) CDW reported herein has a single metal-insulator phase transition at ~350 K as measured structurally and electronically. Fast in-situ transmission electron microscopy and scanned nanobeam diffraction map the formation of tC-CDWs. This work introduces epitaxial polytype engineering of van der Waals materials to access latent 2D ground states distinct from conventional 2D fabrication.

CDWs are an emergent periodic modulation of the electron density that permeates a crystal with strong electron-lattice coupling [6, 7]. TaS₂ and TaS_xSe_{2-x} host several CDWs that spontaneously break crystal symmetries, mediate metal-insulator transitions [6, 8], and compete with superconductivity [9–11]. These quantum states are promising candidates for novel devices [12–15], efficient ultrafast non-volatile switching [16, 17], and suggest elusive chiral superconductivity [18, 19]. Unfortunately, extrinsic and thermal disorder in free standing 2D layers degrades correlation-driven quantum behavior and clean 2D CDWs or superconductivity are near absent. Room temperature access to spatially coherent CDWs and clean 2D confinement could enable a paradigm shift toward device logic and quantum computing.

Here we show the critical temperature for spatially-coherent, commensurate (C-) CDW in 1T-TaS₂ can be raised to well above room temperature (~150 K above the expected transition) by synthesizing clean interleaved 2D polytypic heterostructures [5]. This stabilizes a collective insulating ground state (i.e. C-CDW) not expected to exist at room temperature. We show the formation of these spatially coherent states occurs when 2D CDWs are confined between metallic prismatic polytypes. Metallic layers screen impurity potentials to suppress the disordered nearly-commensurate (NC-CDW) phase. At the same time, interleaving disables interlayer coupling between CDWs. This raises the critical temperature of the C-CDW and forms out-of-plane twinned commensurate (tC) CDWs as revealed by scanned nanobeam electron diffraction. These results demonstrate polytype engineering as a route to isolating 2D

collective quantum states in a well-defined extrinsic environment with identical chemistry but distinct band structure.

- [1] K. Law and P. Lee, *Proc. Natl. Acad. Sci.*, **114**: 6996–7000 (2017).
- [2] Y. Yu et al., *Nat. Nanotechnol.*, **10**: 270–276 (2015).
- [3] A. Tsen et al., *Proc. Natl. Acad. Sci.*, **112**: 15054–15059 (2015).
- [4] L. Nie et al., *Proc. Natl. Acad. Sci.*, **111**: 7980–7985 (2014).
- [5] S. H. Sung et al., *Arxiv*, 2102.09079 (2021).
- [6] J. A. Wilson et al., *Adv. Phys.* **24**: 117–201 (1975)
- [7] S.-K. Chan et al., *J. Phys. F: Met. Phys.* **3**, 795 (1973)
- [8] S. Hellmann et al., *Nat. Commun.* **3**, 1069 (2012)
- [9] E. Navarro-Moratalla et al., *Nat. Commun.* **7**, 11043 (2016)
- [10] R. Ang et al., *Nat. Commun.* **6**, 6091 (2015)
- [11] L. Li et al., *npj Quantum Mater.* **2**, 11 (2017)
- [12] D. N. Basov et al., *Nat. Mater.* **16**, 1077–1088 (2017)
- [13] Y. Tokura et al., *Nat. Phys.* **13**, 1056–1068 (2017)
- [14] M. J. Hollander et al., *Nano Lett.* **15**, 1861–1866 (2015)
- [15] G. Liu et al., *Nat. Nanotechnol.* **11**, 845–850 (2016)
- [16] I. Vaskivskiy et al., *Nat. Commun.* **7**, 114422 (2016)
- [17] A. W. Tsen et al., *Proc. Natl. Acad. Sci.* **112**, 15054–15059 (2015)
- [18] A. Ribak et al., *Sci. Adv.* **6**, eaax9480 (2020)
- [19] R. Ganesh et al., *Phys. Rev. Lett.* **113**, 177001 (2014)

SESSION EQ20.09: Inorganic-Organic and Hybrid 2D Materials
Session Chairs: Zakaria Al Balushi and Azimkhan Kozhakhmetov
Wednesday Afternoon, December 1, 2021
Hynes, Level 1, Room 103

4:00 PM EQ20.09.01

Stages in the Structural and Chemical Modification of Zeolitic Imidazole Frameworks (ZIFs) Under Electron-Beam Irradiation [Supriya Ghosh](#) and Andre Mkhoyan; University of Minnesota, Twin Cities, United States

Zeolitic imidazole frameworks (ZIFs) are a type of metal organic framework (MOF), where Zn metal atoms are tetrahedrally coordinated to imidazole linkers.¹ ZIFs are widely studied as potential materials of interest in electronic devices and sensor applications due to their low-dielectric constants. For device applications, high precision patterning of the ZIFs is essential, which has been demonstrated by using an electron and X-ray beam. To optimize these patterning techniques, it is necessary to understand the structural and chemical changes happening in the MOF framework upon electron-beam irradiation. This has been widely studied in other inorganic crystalline materials like zeolites, but is limited for MOFs.² Here, we study the transition of a ZIF-L MOF from an ordered crystalline state to a disordered amorphous state using dose-controlled transmission electron microscopy (TEM) coupled with electron energy-loss spectroscopy (EELS) to simultaneously monitor chemical changes during the transition.

First, structural changes in ZIF-L were monitored using dose-dependent electron diffraction. It was observed that at an accumulated dose of $\sim 100 \text{ e}/\text{\AA}^2$, there is a complete loss in diffraction intensity along with the appearance of broad amorphous like peaks indicating the formation of an amorphous ZIF-L phase. Further, shifts in diffraction peaks with dose indicates a decrease in the lattice parameters, which is also observed as particle shrinkage in the high-angle annular dark-field scanning TEM (HAADF-STEM) images. Thus, in the initial stages of beam exposure, it can be concluded that there is a collapse of the porous framework resulting in the formation of a “disordered” amorphous ZIF-L phase, retaining the short-range order of the parent framework. To study the chemical changes in ZIF-L during this transformation, core-level EELS spectra were obtained from C, N and Zn as a function of dose to monitor changes in the fine-structure which are sensitive to the local chemical environment. At doses $< 100 \text{ e}/\text{\AA}^2$, changes in the fine-structure were minor indicating no changes in the local bonding of the amorphous ZIF-L. At higher doses $> 500 \text{ e}/\text{\AA}^2$, considerable changes were observed in the core-level EELS fine-structure, resulting from the radiolytic modification of the imidazole linkers by the loss of methyl groups and ring opening reactions, degrading the linker in the second stage of the structural modification. These results point to a completely radiolytic behavior of the electron-beam-ZIF interaction. Further, these structural modifications impact the dielectric properties of the material by shifting the energy for the optical transitions, which are important for device applications.³

References:

1. Park K.S., Ni Z., Cote A. P., Choi J. Y., Huang R., Uribe-Romo F.J., Chae H. K., O’Keeffe M., Yaghi O. M., PNAS July 2006, 103(27) 10186-10191.
2. Kumar P., Kim D. W., Rangnekar N., Xu H., Fetisov E. O., Ghosh S., Zhang H., Xia Q., Shete M., Siepmann J. I., Dumitrica T., McCool B., Tsapatsis M., Mkhoyan K. A., Nat. Mater. 2020, 19, 443-449.
3. Ghosh S., Yun H., Kumar P., Conrad S., Tsapatsis M., Mkhoyan K. A., Chem, Mater., 33, 2021.

4:15 PM EQ20.09.02

Designer Quantum States in van der Waals Heterostructures and Metal-Organic Frameworks [Orlando J. Silveira](#)¹, Peter Liljeroth¹, Teemu Ojanen² and Adam Foster¹; ¹Aalto University, Finland; ²Tampere University, Finland

In general, the progress in the field of condensed matter comes from the discovery of new materials with novel properties. For instance, the discovery of two dimensional (2D) materials such as graphene in 2004 and transition metal dichalcogenides (TMDs) in 2005 had great impact on the scientific community, giving rise to tremendous and ongoing activity in both theoretical and experimental fields. Following that, van der Waals (vdW) heterostructures have gained attention, where two or more atomically thin layers interact with each other through weak vdW forces, and induced effects due to the proximity of the layers lead to intriguing properties that can be engineered for several practical applications. Recently, with the advance on experimental techniques to fabricate and isolate new materials, as well as to probe their features, other novel properties have also been reported intrinsically in 2D materials: spontaneous magnetization, quantum Hall effect and superconductivity. Nonetheless, the rational design of new heterostructures combining these materials, and thus their properties, allows the development of new quantum phases of matter that have not been observed in stand-alone materials, such as the topological superconductivity, which has aroused great interest in recent years due to the potential applications in topological quantum computers. Here we present results obtained for the 2D magnetic CrBr₃ monolayer deposited on top of the layered superconductor NbSe₂, as well as the metal-organic framework M-DCA (with M=Cu, Co and Ni) deposited either on graphene or NbSe₂, focusing mainly on their electronic and structural

properties obtained through density functional theory (DFT) and tight-binding (TB) calculations. We compare these directly to state-of-the-art Scanning Tunneling Microscopy experiments and develop a framework for the systematic design of quantum materials.

4:30 PM EQ20.09.03

1D van der Waals Molecular Wires—Exfoliation Energies, Electronic Properties and How to Find Them in the Lab Yanbing Zhu¹, Daniel Rehn², Evan Antoniuk¹, Gowoon Cheon¹, Rodrigo Freitas³, Aditi Krishnapriyan⁴ and Evan Reed¹; ¹Stanford University, United States; ²Los Alamos National Laboratory, United States; ³Massachusetts Institute of Technology, United States; ⁴Lawrence Berkeley National Laboratory, United States

Two-dimensional (2D) materials derived from van der Waals (vdW)-bonded layered crystals have been the subject of considerable research focus, but analogous one-dimensional (1D) materials have received less attention while potentially also exfoliable and useful for optical or electronic applications. These bulk crystals consist of covalently bonded multi-atom atomic chains with weak van der Waals bonds between adjacent chains. Using density-functional-theory-based methods, we find the binding energies of several 1D families of materials to be within typical exfoliation ranges possible for 2D materials. In addition, we compute the electronic properties of a variety of insulating, semiconducting, and metallic individual wires and find differences that could enable the identification of and distinction between 1D, 2D, and 3D forms during mechanical exfoliation onto a substrate. We find 1D wires from chemical families of the forms PdBr₂, SbSeI, and GePdS₃ are likely to be distinguishable from bulk materials via photoluminescence. Like 2D vdW materials, we find some of these 1D vdW materials have the potential to retain their bulk properties down to nearly atomic film thicknesses, including the structural families of HfI₃ and PNF₂, a useful property for some applications including electronic interconnects.

Machine learning methods are also used to predict previously undiscovered low-dimensional van der Waals materials, targeting compositions with conductive and potentially magnetic properties. We find different models trained on different subsets of the data recover similar predicted unsynthesized 1D materials, illustrating model robustness. A particular composition, MoI₃, which is predicted by the model to be 1D, is indeed confirmed to exist with wire-like subcomponents. We train on classes of materials tailored for potential experimental synthesizability, specifically for chalcogen, halogen, and pnictogen-containing compounds due to their ease of synthesis using chemical vapour deposition (CVD) and chemical vapour transport (CVT).

SESSION EQ20.10: Poster Session II
Session Chairs: Zakaria Al Balushi and Azimkhan Kozhakhmetov
Wednesday Afternoon, December 1, 2021
8:00 PM - 10:00 PM
Hynes, Level 1, Hall B

EQ20.10.08

Inhomogeneity in Large Area Exfoliated Transition Metal Dichalcogenide Monolayers Mohammad A. Hossain, Yue Zhang and Arend van der Zande; University of Illinois at Urbana-Champaign, United States

In nanomaterial synthesis, there is a tradeoff between scalability, material quality and uniformity. The tradeoff is especially evident in the case of two dimensional (2D) materials, which are layered materials with single or few atoms thick layers that are held together by weak van der Waals forces. Semiconducting transition metal dichalcogenides (TMDC) from the family of 2D materials offer opportunities including exploring strongly bound excitons and engineering highly deformable, high mobility electronics. However, progress in translating these materials from scientific curiosities to applications is largely limited by the availability of synthesis techniques that are both scalable and yet lead to high quality materials. A new approach gaining momentum is to use large area exfoliation through selective adhesion of bulk 2D materials to metal adlayers to get monolayers with the quality and lateral sizes similar to the starting bulk crystal. These techniques rely on the stronger adhesion of gold to the TMDC layers compared to the interlayer van der Waals adhesion in the bulk crystal[1-6].

In this work, we demonstrate a modified gold mediated technique for large area exfoliation of high quality TMDC monolayers over millimeter scales which leads to much higher yield and uniformity compared with previous approaches. With the higher uniformity from the exfoliation, we discover a surprising inhomogeneity in the quality of the starting bulk crystal at ~ 100 um length scales which was not evident through traditional exfoliation techniques.

Our technique adds an additional step by relaxing the gold adhesion layer when laminating onto the 2D bulk surface, leading to better conformation at the Au-TMDC interface. As a result, we were able to exfoliate monolayers with lateral sizes up to 5 mm, limited only by the size of the starting bulk crystal. To make direct quantitative comparison, we exfoliated large monolayers of WSe₂ from the same bulk crystal using multiple large area exfoliation techniques. On average, the yield was 75% using our approach compared with 45% for other similar approaches. In addition, our approach leads to fewer cracks, higher reproducibility, and higher optical uniformity from other approaches.

Intriguingly, by comparing optical maps of sequential transfers from the same bulk crystal, we observe inhomogeneities in the optical response on the scale of 100 μm that are in the same relative positions on each monolayer. By comparing the photoluminescence peak positions and intensities, we relate these variations to discrete changes in the defect density or material doping present in the bulk crystals.

These results show that the uniformity of exfoliation is now limited not by the uniformity of transfer, but the quality of the starting material. The variations even within bulk crystals show that care must be taken when comparing properties based on defect density – highly pertinent to many device applications relevant to properties including doping, contact engineering, excitonic states, and mobility.

References:

- [1] Liu, F., et al. Disassembling 2D van der Waals crystals into macroscopic monolayers and reassembling into artificial lattices. *Science* 2020, 367, 903–906
- [2] Moon, J.Y., et al. Layer-engineered large-area exfoliation of graphene. *Science Advances* 2020, 6(44), eabc6601
- [3] Desai, S.B., et al. Gold-mediated exfoliation of ultralarge optoelectronically-perfect monolayers. *Advanced Materials* 2016, 28(21), 4053–4058
- [4] Huang, Y., et al. Universal mechanical exfoliation of large-area 2D crystals. *Nature Communications* 2020, 11(1), 1–9
- [5] Velicky, M., et al. Mechanism of gold-assisted exfoliation of centimeter-sized transition-metal dichalcogenide monolayers. *ACS Nano* 2018, 12(10), 10463–10472
- [6] Magda, G.Z., et al., Exfoliation of large-area transition metal chalcogenide single layers. *Scientific Reports* 2015, 5(1), 1–5

EQ20.10.10

Finite-Size Effects of Electron Transport in Anisotropic Quasi-Two Dimensional Metals [George Varnavides](#)^{1,2}, Yaxian Wang¹, Philip J. Moll³, Polina Anikeeva² and Prineha Narang¹; ¹Harvard University, United States; ²Massachusetts Institute of Technology, United States; ³École Polytechnique Fédérale de Lausanne, Switzerland

Non-magnetic delafossite metals, such as PdCoO₂ and PtCoO₂, exhibit single-band, quasi-two dimensional Fermi surfaces (FS) which can host extremely long carrier mean free paths, despite their high carrier-density^{1,2}. This provides opportunities to investigate unconventional carrier transport where the intrinsic scattering mechanisms additionally compete with the micro-scale device's length-scale, resulting in finite-size effects such as the recently observed crystal symmetry-forbidden directional "quasi-ballistic" transport^{3,4}. Interestingly, the hexagonal FS of these delafossite metals deviates strongly from a circular FS - with pronounced facets, leading to an anisotropic Fermi velocity distribution^{3,4}.

Here, we parametrize the electronic 2D Boltzmann transport equation (BTE) to account for the in-plane FS anisotropy and include both momentum-relaxing and momentum-conserving interactions⁵. This allows us to investigate unconventional electronic transport in these systems by numerically solving the anisotropic BTE, across a range of momentum-relaxing and momentum-conserving interaction lengthscales, to create transport regime plots for each FS orientation. Using first principles calculations of the (momentum-relaxing) electron-phonon and (momentum-conserving) phonon-mediated electron-electron interactions, we populate the resulting transport regime plots and classify electronic transport in PdCoO₂ between the "quasi-diffusive", "quasi-ballistic", and "quasi-hydrodynamic" transport limits as a function of temperature.

Consistent with experimental observations we find the directional dependence of electron flow, which gives rise to crystal symmetry-forbidden in-plane resistivity anisotropy, is strongest at low temperature in the "quasi-ballistic" regime, i.e. in the absence of momentum-conserving interactions⁵. As momentum-conserving interactions increase, leading to collective flow which acts to homogenize the current distribution, the effect gets weaker in the "quasi-hydrodynamic" regime identified between 10-25 K, albeit still expected to be measurable⁵. This work provides insights into understanding electron transport from microscopic scattering mechanisms and Fermi surface geometries, paving the way for designing finite-size devices from high carrier-density quasi two-dimensional metals.

¹ C.W. Hicks, A.S. Gibbs, A.P. Mackenzie, *et al.*, Phys. Rev. Lett. 109, 116401 (2012)

² R. Daou, R. Fresard, V. Eyert and A. Maignan, Science and Technology of Advanced Materials 18, 919 (2017)

³ M.D. Bachmann, A.L. Sharpe, A.W. Barnard, *et al.*, Nature Communications 10, 1 (2019)

⁴ M.D. Bachmann, A.L. Sharpe, A.W. Barnard, *et al.*, arXiv:2103.01332 (2021)

⁵ G. Varnavides, Y. Wang, P.J.W. Moll, P. Anikeeva, and P. Narang, arXiv:2106.00697 (2021)

EQ20.10.11

Mechanical Properties and Thermal Stability of a Free-Standing Monolayer Amorphous Carbon [Levi C. Felix](#)¹, Raphael M. Tromer¹, Pedro Autreto², Luiz A. Ribeiro³ and Douglas S. Galvao¹; ¹State University of Campinas, Brazil; ²Universidade Federal do ABC, Brazil; ³Universidade de Brasil, Brazil

Recently, the first synthesis of a free-standing monolayer amorphous carbon (MAC) was reported [1]. MAC is a pure carbon structure composed of randomly distributed five, six, seven, and eight atom rings and has many structural differences from a random network. Its electronic properties are similar to boron nitride. Also, several nanostructures, such as nanotubes and nanoscrolls, build from MACs were found to be stable [2]. In this work, we have investigated, through fully atomistic reactive molecular dynamics simulations the structural and thermal MAC properties. Our results [3] show that MAC and graphene (G) sheets of similar dimensions have quite distinct mechanical behavior. In general, G exhibits one stage of the elastic regime, followed by abrupt fracture (brittle), while MAC exhibits several structural stages where the stress values drop, but with no abrupt fractures (ductile). These stages present structural reconstructions followed by the appearance of linear atomic chains (LAC) in the final fracture stages. LAC are commonly observed in fractured carbon-based nanostructures [4]. These extensive MAC reconstructions are possible due to the large distribution of bond lengths and bond angle values, and the presence of different types of rings, which creates multiple stress release channels. The G and MAC fracture dynamics are also different, while PG presents abrupt fractures and fast crack propagation, MAC exhibits more localized fractures that prevent fast crack propagation and works as efficient stress release mechanisms. MAC is softer than G, their corresponding Young's modulus values are 881 and 587 GPa, respectively. MAC also exhibits remarkable thermal stability with a melting point (5368K) very close to that of G (5643K).

[1] C. -T. Toh, H. Zhang, J. Lin, A. S. Mayorov, Y. -P. Wang, C. M. Orofeo, D. B. Ferry, H. Andersen, N. Kakenov, Z. Guo, I. H. Abidi, H. Sims, K. Suenaga, S. T. Pantelides and B. Özyilmaz, Nature **2020**, 577, 199-203.

[2] R.M. Tromer, L.C. Felix, L.A. Ribeiro, D.S. Galvao, Physica E **2020**, 130, 114683.

[3] L. C. Felix, R. M. Tromer, P. A. S. Autreto, L. A. Ribeiro Junior and D. S. Galvao, J. Phys. Chem. C **2020**, 124 (27), 14855-14860.

[4] F. R. Eder, J. Kotakoski, U. Kaiser, J. C. Meyer, Sci. Rep. **2014**, 4, 4060.

EQ20.10.15

Layered CuIn₇Se₁₁ for Near-Infrared and Polarization-Sensitive Photodetector [Ningxin Li](#); Georgia State University, United States

Ternary copper indium selenide (CIS), as a novel two-dimensional (2D) material, has a high external quantum efficiency and a sufficiently narrow bandgap (1.1 eV), making it a promising candidate for the development of ultra-thin and flexible current photodetectors. Since CIS can exhibit a variety of structures depending on the ratio between Cu and In, here, we investigate the optoelectronic response characteristics of the new 2D atomically layered ternary compound that was synthesized with the ratio between Cu and In was 1:7 (CuIn₇Se₁₁), consistent with the range where the layered phase forms. We discovered that, unlike conventional 2D materials which have the blue-shifted phenomena in photoconductivity spectra as the thickness decreases, the CuIn₇Se₁₁ shows an opposite trend of red-shift. This unique feature makes it an ideal candidate for a red light or near-infrared photodetector material. Additionally, we unveil a strong linear polarization dependence in its photoconductivity response, which also exhibits an intriguing relationship with the sample thickness and working temperature. This may indicate a phase transition occurs at low temperature and induced the variation in dipolar transition law. Our study will provide an alternative material system for the fabrication of highly-effective polarization-sensitive visible and near-infrared photodetector.

EQ20.10.16

Late News: Chemical Design of Molecular Frameworks as Stimuli Responsive Phase Change Materials [Dara E. Weiss](#); Johns Hopkins University, United States

While the permanent porosity and crystalline structure of metal-organic frameworks (MOFs) has been exploited for gas sequestration and catalysis, recent attention has focused on the potential for MOFs to enable a new generation of sensors, actuators, and low-power consumption electronics. To do so,

chemical design of MOFs and other molecular frameworks that exhibit stimuli-responsive properties is necessary. Previous work from the Kempa group demonstrated the gas-phase assembly of 2D MOFs comprised of redox-active, stimuli-responsive $\text{Mo}_2(\text{isonicotinate})_4$ paddlewheels. Here we present and investigate the tunable properties of MOFs assembled from derivatives of this di-Mo paddlewheel. A notable example is comprised of $\text{Mo}_2(\text{isonicotinamide})_4$ clusters, which we show can be assembled using solution- and gas-phase methods into MOFs with 2D and quasi-1D topologies. X-Ray diffraction (XRD) data collected on $\text{Mo}_2(\text{isonicotinate})_4$ and on $\text{Mo}_2(\text{isonicotinamide})_4$ MOFs at various partial pressures of CO_2 reveal the structural origins of interlayer gas uptake anomalies. These data suggest that the commensurately stacked 2D monolayers can dynamically and reversibly re-order to assume new phases in response to external stimuli. Device transport measurements can reveal not only the significant modulation of framework conductivity corresponding to the induced phase changes, but also the role of the metal-ligand coordination environment. These efforts lay the groundwork for implementation of these designer molecular frameworks as switches and dynamically tunable membranes.

EQ20.10.17

Late News: Photo-Transistor Based on 2D Materials Heterojunction with Periodically Arrayed Nanopore Structures for Enhancing Performance [Min-Hye Jeong](#), Sang-Hyun Lee, Hyun-Soo Ra and Jong-Soo Lee; Daegu Gyeongbuk Institute of Science and Technology, Korea (the Republic of)

Two dimensional materials are promising building blocks for various optoelectronic application such as ultra-high-mobility transistors, tunable p-n junction diodes, solar cells, light-emitting diodes and their unique properties have attracted attention. However, in the case of monolayer materials, strongly bound excitons generated by Coulomb interaction inhibit the formation of free carriers due to the absence of internal potential. Here, we demonstrate p-n junction phototransistor, which has a novel hybrid photonic crystal structure for improve the optical properties of the photo transistor in active area. To understand enhanced optical properties and optoelectronic interaction with our novel hybrid structure, we have performed density functional theory calculations as well as Raman spectroscopy, Photoluminescence (PL), Time-Resolved Photoluminescence (TR-PL) and measurement of electrical and optical transport properties for device characteristics. The characteristics of the heterojunction devices with PANS reveal enhanced photodetector figures-of-merit compared with pristine heterojunction devices. The phototransistor with novel hybrid photonic crystal structure shows dramatically enhanced photo current (A), responsivity (A/W) and detectivity (Jones). Therefore, it is important advantage in using our novel hybrid nanopores structure in optoelectronic application.

EQ20.10.18

Late News: Reversible and Controllable Threshold Voltage Modulation for n-channel MoS₂ and p-channel MoTe₂ Field-Effect Transistors via Multiple Counter Doping with ODTs/Poly-L-lysine Charge Enhancers [Seung G. Seo](#) and Sung Hun Jin; Incheon University, Korea (the Republic of)

Confronted by the inherent physical limitations in scaling down Si technology, transition metal dichalcogenides (TMDCs) as alternatives are being tremendously researched and paid attention to. However, mature counter doping technology for TMDCs is still elusive, and thus, a controllable and reversible charge enhancer is adopted for acceptor (or donor)-like doping via octadecyltrichlorosilane (ODTS) (or poly-L-lysine (PLL)) treatment. Furthermore, multiple counter doping for TMDC field-effect transistors (FETs), combined with a threshold voltage (V_{th}) freezing scheme, renders the V_{th} modulation controllable, with negligible degradation and decent sustainability of FETs even after each treatment of a representative charge enhancer. In parallel, the counter doping mechanism is systematically investigated via photoluminescence spectroscopy, X-ray photoelectron spectroscopy, atomic force microscopy (AFM), surface energy characterization, and measurement of optoelectronic properties under illumination with light of various wavelength. More impressively, complementary inverters, composed of type-converted molybdenum ditelluride (MoTe_2) FETs and hetero-TMDC FETs in enhancement mode, are demonstrated via respective ODTs/PLL treatment. Herein, driving backplane application for micro-light-emitting diode (μ -LED) displays and physical validation of a corresponding counter doping scheme even for flexible polyethylene terephthalate (PET) substrates could be leveraged to relieve daunting challenges in the application of nanoscale Si-based 3D stacked systems, with potential adoption of ultralow power and monolithic optical interconnection technology.

EQ20.10.19

Late News: Type-Controllable MoTe₂ Thin-Film Transistors Driven Quantum Dot Light-Emitting Diodes with Ligand Modification [Geunwoo Baek](#)¹, [Seung G. Seo](#)², [Donghyo Hahn](#)³, [Wan Ki Bae](#)³, [Jeonghun Kwak](#)¹ and [Sung Hun Jin](#)²; ¹Seoul National University, Korea (the Republic of); ²Incheon National University, Korea (the Republic of); ³Sungkyunkwan University, Korea (the Republic of)

Recently, transition metal dichalcogenide (TMDC) has gained tremendous interests in electronic/optoelectronic applications because it has prominent optical/electrical properties, a controllable bandgap, superior electrostatic gate coupling, and immunity to a short channel effect. Despite these outstanding merits, the study of emerging devices incorporated with TMDC thin film transistors (TFTs) and quantum dot light-emitting diodes (QLEDs) has been rarely reported. In this sense, TMDCs have one of the excellent candidates to realize the switching device for QLED displays in lieu of conventional Si technology. So, we adopted a molybdenum ditelluride (MoTe_2) as a switching component exhibiting a negligible Fermi-level pinning phenomenon, light insensitive properties, and the availability of type conversion. In this study, molecular doping by Poly-L-lysine (PLL) is adopted for a type conversion of MoTe_2 TFTs and surface ligand modification is utilized for the improvement of QLED performance. Based on these methodologies, we firstly demonstrate active-matrixed light-emitting devices, composed of ultra-thin MoTe_2 TFTs and highly efficient QLEDs. As a result, the driving capability of MoTe_2 TFTs for the operation of QLEDs display provides the successful and advanced applications as next generation display backplane transistors of QLEDs.

EQ20.10.22

Low-Temperature and Magnetoresistance Behavior of Ti₃C₂-MXene for Sensing Applications [Krzysztof Grabowski](#), [Kamil Goc](#), [Tomasz Straczek](#), [Shreyas Srivatsa](#), [Tadeusz Uhl](#) and [Czeslaw Kapusta](#); AGH University of Science and Technology, Poland

MXenes are a family of two-dimensional (2D) nanomaterial. Titanium Carbide MXene (Ti_3C_2 -MXene) is the first inorganic compound discovered among the MXene family in 2011. Ti_3C_2 -MXenes have been studied extensively for their physical properties and chemical stability. There have also been many applications of these MXenes for sensing applications. In this present work, we discuss the response of Ti_3C_2 -MXene nanomaterials to low-temperature. The Ti_3C_2 -MXene samples are tested for their change in electrical resistivity for a wide range of temperatures (3K – 300 K). The unique behaviors observed in Ti_3C_2 -MXene as well as their precursor MAX (Ti_3AlC_2 -MAX) phase material are presented. Then the magnetoresistance behavior of Ti_3C_2 -MXene and Ti_3C_2 -MAX phase materials are studied at various temperatures leading to their analysis and reporting. These unique behaviors of Ti_3C_2 -MXenes have the capability for sensor development and thus extensive repeatability tests are conducted. The sensing applications of Ti_3C_2 -MXene at low temperatures with their magnetoresistance behavior opens avenues for the application of these sensors for space technology and explorations. Finally, the possibilities of various sensors using the magnetoresistance behavior are envisaged.

EQ20.20.21

Graphene Confined in Layered Silicate [Barbara Pacakova](#)¹, [Marian Matejdes](#)², [Paulo H. Michels Brito](#)¹, [Leander Michels](#)¹, [Josef Breu](#)² and [Jon O. Fossum](#)¹; ¹Norwegian University of Science and Technology, Norway; ²Bayerisches Polymer Institut und Lehrstuhl für Anorganische Chemie 1, Universität Bayreuth, Germany

The real use of graphene in electronic devices, such as field-effect transistors (FET), meets several principal complications. Opening of graphene band gap usually leads to significant drop of electron mobility; limitation of Klein tunneling paradox can prevent graphene-based devices from switching into the OFF state. Some of the complications can be overcome by combining graphene with insulating layers in two-dimensional heterostructures that allow for fabrication of a graphene-based FET with a high ON and OFF switching ratio¹, and precise control over graphene doping. However, fabrication of such heterostructures is not trivial. The best performing heterostructures are made by manual assembly, which is not very efficient method for their mass production.

We have prepared two-dimensional heterostructures more efficiently, by growing graphene from a nitrogen-carbon precursor inside the confined space of a layered silicate. This approach promises simultaneous band-gap opening in graphene and formation of final heterostructures in one step. The resulting structure has the form of a multi-layered sandwich composed of nitrogen-doped (N-doped) graphene-like layers and the single layer sheets of synthetic layered silicate, sodium fluorohectorite.

Can such a large-scale production method generate well-defined and homogeneous clean system useable for FET or other electronic applications of graphene? To answer this question, we need to examine the layered heterostructure itself, to reveal the nature of the N-doped graphene-like layers. As the initial point, it is of high benefit to know how are the nitrogen atoms distributed within the graphene lattice. Electronic transport properties of sandwich multi-layers, which are important parameters for device performance, can be then explained in the context of geometry of individual layers.

Nitrogen doping of graphene is the efficient way of band-gap modification, as it allows band-gap opening and its transformation to an *n* or a *p*-type semiconductor². Nitrogen can be incorporated into the graphene lattice in three different configurations^{2,3}, with planar *sp*² (pyridinic and pyrrolic) and tetrahedral *sp*³ (quaternary N) hybridizations. Depending on the level of the *sp*²-N doping and the geometry of the N-doped graphene lattice, band gap can vary from 0.14 eV up to 0.7 eV⁴. Characteristic C-C, N-C and N-N bond lengths depend on the lattice configuration and differ from the un-doped graphene^{2,4}.

Growth of the N-doped graphene in confined space³ is a promising method superior to the other preparation strategies, as it provides selective formation of pyridinic and pyrrolic groups in the graphene lattice and suppress formation of quaternary N. Carbon lattice doped with planar N-sites can serve as useful building block for use in the supercapacitors, batteries, transistors, fuel cells and other semiconductor applications², and also possess high activity in the oxidation reduction reactions³ in contrast to the lattice containing quaternary N. In all cases, types of nitrogen doping, lattice geometry and defects together with the lattice distortions significantly alter both properties, performance and the suitable application potential of the N-doped graphene². Its combination with layered silicate is a promising step towards the real applications.

References.

1. Britnell, L., Gorbachev, R. V. Jalil, R. *Science* **286**, 947–951 (2012). 2. Wang, H., Maiyalagan, T. & Wang, X. *ACS Catal.* **2**, 781–794 (2012). 3. Ding, W. *et al. Angew. Chemie - Int. Ed.* **52**, 11755–11759 (2013). 4. Rani, P. & Jindal, V. K. *RSC Adv.* **3**, 802–812 (2013). 5. Breu, J., Seidl, W., Stoll, A. J., Lange, K. G. & Probst, T. U. *Chem. Mater.* **13**, 4213–4220 (2001). 6. Rojas, W. Y. *et al. Langmuir* **34**, 1783–94 (2017). 7. Chuang, C.-H. *et al. Sci. Rep.* **7**, 42235 (2017). 8. Ehlert, C. *et al. Phys. Chem. Chem. Phys.* **16**, 14083–95 (2014).

SESSION EQ20.11: Optics Enabled by 2D Materials
Session Chairs: Daniel Bediako and Joan Redwing
Thursday Morning, December 2, 2021
Hynes, Level 1, Room 103

10:30 AM *EQ20.11.01

Atomically Thin Canvas for Quantum Optoelectronics Hongkun Park; Harvard Univ, United States

Transition metal dichalcogenide monolayers are atomically thin semiconductors that can host tightly bound excitons. Recent advances in materials growth and fabrication have enabled the preparation of high-quality van der Waals heterostructures incorporating these two-dimensional materials. In this presentation, I will describe our efforts to use these heterostructures as a “canvas” to realize new quantum optoelectronic devices for excitons and electrons. I will discuss how we improve the spectral/spatial uniformity and coherence of excitons and realize atomically thin mirrors and active metasurfaces. I will also describe our recent observation of long-sought electron Wigner crystal phases in these heterostructures without a magnetic field or moiré potential. Our studies illustrate that the heterostructures made of atomically thin semiconductors are an attractive solid-state platform for exploring novel excitonic and correlate-electron phenomena.

11:00 AM EQ20.11.02

Rydberg Exciton Emission Dynamics in Monolayer MoTe₂ Souvik Biswas¹, Joeson Wong¹, Eoin Caffrey¹, Sergiy Krylyuk², Hamidreza Akbari¹, Kenji Watanabe³, Takashi Taniguchi³, Albert Davydov², Zakaria Al Balushi^{1,4} and Harry A. Atwater¹; ¹California Institute of Technology, United States; ²National Institute of Standards and Technology, United States; ³National Institute for Materials Science, Japan; ⁴University of California, Berkeley, United States

Low dimensional systems, such as monolayer TMDCs, host strong non-hydrogenic Rydberg-series excitonic resonances that dominate the optical spectrum. Here, we investigated the dynamical radiative properties of the excitonic Rydberg series-driven photoluminescence in monolayer MoTe₂. High quality hBN-encapsulated MoTe₂ monolayer heterostructures with electrical contacts and back gate, which enabled modulation of the doping density in MoTe₂, were fabricated to perform low temperature (~4.5K) photoluminescence measurements. We observed bright, narrow emission from the first three states of the excitonic Rydberg series, namely A1s, 2s and 3s with record linewidths of ~3, 6 and 10 meV, respectively. All these states exhibit linear scaling with incident excitation pump fluence. Upon injecting excess free charges on either electron or hole side in MoTe₂, dipole oscillator strengths were rapidly transferred from the excitonic to the corresponding trionic (charged exciton/attractive polaron) states. Energy shifts between the neutral and dressed excitonic states were observed as a function of gate voltage, which strongly depend on the Rydberg state of the exciton – indicating strong excitonic wavefunction dependent screening properties and electron-exciton interaction. Our findings provide a route to realize exotic excitonic phases in monolayer or twisted bilayer MoTe₂.

11:15 AM EQ20.11.03

Temperature and Gate Dependent Refractive Index Modulation and Epsilon-Near-Zero Response in Monolayer Molybdenum Diselenide Melissa Li, Souvik Biswas, Claudio U. Hail and Harry A. Atwater; California Institute of Technology, United States

Dynamic control of the optical scattering properties in resonant nanostructures is central to the realization of active nanophotonics, but concepts thus far

have primarily used dielectric or plasmonic Mie resonances which have limited electrical tunability. Here, we report over 200% modulation in both the real and imaginary part of the complex refractive index in hBN-encapsulated monolayer molybdenum diselenide (MoSe_2) by tuning the exciton resonances. Gate modulated control of the Fermi level allows us to explore the doping dependence of the A and B exciton resonances for temperatures between 4 K to 150 K. We observe both a temperature and carrier density dependent variation in the permittivity and transition from metallic to dielectric response in the epsilon-near-zero wavelength range. We attribute the change in the refractive index to the interplay between radiative and nonradiative channels that are dependent on carrier density and temperature. Our findings of large electrical tunability of the complex refractive index is accompanied by large changes in reflectance amplitude and phase, suggesting the potential of monolayer MoSe_2 as an active material for emerging photonics applications.

11:30 AM EQ20.11.04

Deeply Subwavelength Light Confinement and Guiding with Bulk Transition Metal Dichalcogenides Haonan Ling and Artur Davoyan; University of California, Los Angeles, United States

In this work we investigate theoretically and experimentally light guiding in nanometer-scale waveguides made of transition metal dichalcogenides (TMDCs). We explore the limits of light guiding and show that in certain configurations owing to unique material properties light can be squeezed and guided in nanometer thick channels. In our experimental effort we discuss the fabrication approach and the preliminary measurements examining performance of such waveguides.

TMDCs are an emerging type of layered van der Waals semiconductors possessing unique electronic and optical properties [1,2], which make them promising candidates for photonic applications. Specifically, bulk TMDCs are of great interest for a range of optical applications, including metasurfaces [3], gratings [4], and nano-resonators [5,]. Recently promise of bulk TMDCs for integrated nanophotonics [6] was also explored. Here we show that owing to their unique optical properties, including high refractive index, room temperature excitonic resonance and strong anisotropy, bulk TMDCs are capable of guiding light in a deeply subwavelength regime.

We begin our analysis with a study of dispersion relations and influence of materials anisotropy on optical field confinements in slab waveguides. We show that owing to high refractive index light can be efficiently guided in 120 nm thick TMDC flakes. We then examine the limits of light guidance in structures made of bulk TMDCs, especially in nanometer-size void waveguides, which are formed within a bulk of MoS_2 material. In such systems we find that the light can be efficiently confined in very narrow air channels, down to even sub-nanometer scale. We show that by selecting appropriate waveguide dimensions over 75% of the power can be squeezed into a waveguide with less than 35 nm air gap across a broad spectral range (visible to near infrared). We then study how material anisotropy influences the light confinement and guidance and show that interlayer voids provide a simpler approach to device fabrication and experimental study of the phenomenon. Finally we discuss the influence of losses and show that such waveguides can be low loss in the sub-band gap regime. Our theoretical findings are of direct interest to highly confined optical interconnects and to light materials coupling in atomic size channels of 2D materials.

Lastly, we discuss pathways for experimental demonstration of light guiding in such nanometer scale devices. We discuss our approach to fabricating such nanoscale waveguides, in which we have optimized processes to obtaining structures made of ~ 100 nm MoS_2 . Next we discuss design and fabrication of grating coupler excitation of bulk MoS_2 waveguides. We then perform far-field measurements in 800 nm-1100 nm band that indicate that light can be efficiently guided in such subwavelength structures.

In conclusion, our work paves the way to a new type of highly confined low loss optical waveguides, which will find use in a broad range of applications including among others integrated photonics, quantum optics and sensing.

References

1. Wang, Qing Hua, et al. "Electronics and optoelectronics of two-dimensional transition metal dichalcogenides." *Nature nanotechnology* 7.11 (2012): 699-712.
2. Mak, Kin Fai, and Jie Shan. "Photonics and optoelectronics of 2D semiconductor transition metal dichalcogenides." *Nature Photonics* 10.4 (2016): 216-226.
3. Liu, Chang-Hua, et al. "Ultrathin van der Waals metalenses." *Nano letters* 18.11 (2018): 6961-6966.
4. Zhang, Huiqin, et al. "Hybrid exciton-plasmon-polaritons in van der Waals semiconductor gratings." *Nature communications* 11.1 (2020): 1-9.
5. Verre, Ruggero, et al. "Transition metal dichalcogenide nanodisks as high-index dielectric Mie nanoresonators." *Nature nanotechnology* 14.7 (2019): 679-683.
6. Ling, Haonan, Renjie Li, and Artur R. Davoyan. "All van der Waals Integrated Nanophotonics with Bulk Transition Metal Dichalcogenides." *ACS Photonics* 8.3 (2021): 721-730.

11:45 AM *EQ20.11.05

High Quality Factor Polariton Nanoresonators and Planar Programmable Optics with van der Waals Materials Michele Tamagnone¹, Xinghui Yin², Antonio Ambrosio¹ and Federico Capasso²; ¹Istituto Italiano di Tecnologia, Italy; ²Harvard University, United States

Nanophotonics is expected to play a key role in the next decades. The miniaturization and integration of these components has, however, an additional challenge with respect to nanoelectronics devices, namely the diffraction limit. If dielectric materials are used, light cannot be confined and guided if the size of the waveguides and components is below a critical size which is determined by the wavelength and the refractive index of the used dielectric material.

However, this limit can be circumvented if materials supporting polaritons are used instead of dielectrics. Polaritons consist in a strong interaction between light and a dipole-carrying excitation (e.g. plasmons, phonons and excitons).

Phonon polaritons in van der Waals (vdW) materials such as hexagonal boron nitride (h-BN) and molybdenum trioxide (MoO_3) have been extensively studied with techniques including near-field scanning optical microscopy (NSOM) and are considered as particularly good candidates for miniaturized photonics in the mid-infrared [1-6].

In this contribution we will first present some recent results from our group. We first demonstrate high quality factor phonon polaritons resonators (with Q reaching almost 500) based on isotopically pure h-BN and MoO_3 [6]. Compared to previous devices based on non-isotopically-pure hBN [3], these resonators can achieve a Q factor up to 3 times larger due to the intrinsic higher quality of the phonon in the material [4]. The resonators (arrays of disks with thickness of tens of nanometers and diameters of hundreds of nanometers) have been fabricated with electron beam lithography followed by reactive ion etching of the vdW materials. Using FTIR spectroscopy and NSOM we observed and studied the resonance in both the reststrahlen bands for hBN and in all 3 reststrahlen bands in MoO_3 , finding high quality factors in all hBN bands and in the third band of MoO_3 . Strikingly, the resonance is maintained even if the volume of the resonator is 10^6 times smaller than the cube of the wavelength in free space, and thanks to the hyperbolic properties of hBN and MoO_3 it can be pushed further down.

We then determined a theoretical upper bound on the quality factor of the resonators working for polaritonic resonators in the sub-wavelength limit. Through rigorous manipulation of Maxwell's equations, we found that the linewidth of the resonator can never be smaller than the intrinsic linewidth of the polaritonic resonance.

Second, we will show flat reconfigurable photonic devices based on a heterostructure of isotopically pure hBN deposited on a thin layer of the phase-change material GeSbTe [5]. With a laser diode we can induce crystallization of GST ("write" process) and we can restore the amorphous state ("erase"

process). Because the crystalline form has much larger refractive index, we can induce waveguides for hBN phonon polaritons via substrate effects. We demonstrated fully programmable and reprogrammable lenses, metalenses and prisms for bidimensional polaritons. We also created guided wave resonators with periodic substrate patterning, which are akin to photonic crystals but with phonon polaritons. Finally, we will discuss applications of these devices for bio-chemical sensing and photodetectors.

- [1] D. N. Basov et al. "Polaritons in van der Waals materials." *Science* 354.6309 (2016).
- [2] T. Low, et al. "Polaritons in layered two-dimensional materials." *Nature materials* 16.2, 182-194 (2017).
- [3] M. Tamagnone, et al. "Ultra-confined mid-infrared resonant phonon polaritons in van der Waals nanostructures." *Science advances* 4.6, eaat7189 (2018).
- [4] A. J. Giles et al. "Ultralow-loss polaritons in isotopically pure boron nitride." *Nature Materials* 17.2, 134-139 (2018).
- [5] K. Chaudhary et al. "Polariton nanophotonics using phase-change materials." *Nature Communications* 10.1, 4487 (2019).
- [6] M. Tamagnone et al. "High quality factor polariton resonators using van der Waals materials." *arXiv preprint* 1905.02177 (2019).

SESSION EQ20.12: Advanced Characterization of 2D Materials I/Twisted 2D Layers
Session Chairs: Zakaria Al Balushi and Souvik Biswas
Thursday Afternoon, December 2, 2021
Hynes, Level 1, Room 103

1:30 PM EQ20.12.01

Microscopic Carrier Distribution Imaging of Atomically-Thin van der Waals Semiconductors by Scanning Nonlinear Dielectric Microscopy Kohei Yamasue and Yasuo Cho; Tohoku University, Japan

Atomically-thin van der Waals semiconductor materials have attracted much attention because of their superior and unique material properties. However, the precise control of carrier doping levels is still a challenge due to their intrinsic high surface-to-volume ratio [1]. In fact, MoS₂ can be p-doped in bulk by Nb doping but show p- to n-type transition as the number of layers decreases [2]. In addition, the performance of the devices using these materials is often affected by a semiconductor-substrate interface and the doping levels may also be changed through various treatments in device process.

Imaging microscopic carrier distributions will help the understanding the mechanism of the doping level changes. As a key imaging technology, here we demonstrate that scanning nonlinear dielectric microscopy (SNDM) permits the imaging of dominant carrier distribution of atomically-thin layers [3]. SNDM normally measures the voltage derivative of local capacitance (dC/dV) below the tip. SNDM imaging is useful because dC/dV images reflect the dominant carrier distributions. The polarity of dC/dV is inverted depending on the polarity of dominant carriers and its magnitude varies with dominant carrier concentration. It is also notable that, because of capacitance sensing using near-field microwave electric fields, this microscopy can image atomically-thin materials on a substrate without preparing contact electrodes to the sample or fabricating test device structures.

Here we report the details of dominant carrier distributions in Nb-doped MoS₂ layers mechanically exfoliated on a SiO₂/Si substrate [4]. The sample had a bulk p-doping level of $5 \times 10^{19} / \text{cm}^3$. By dC/dV imaging of a sample with various thickness, we visualized p- to n-type transition of Nb-doped MoS₂. As expected, thick layers were actually p-doped but we found that, as the layer number (L) decreased, hole concentration became lower. In more detail, for layers with $L > 6$, dC/dV signals did not depend on L significantly, while for $L \leq 6$, they significantly varied with the decrease of L. The signals became zero at $L = 3$ once, the polarity was finally inverted for $L = 2, 1$. This implies that a counter n-doping effect called surface electron accumulation [5] manifested for $L \leq 6$ and dominated the doping levels for $L = 1$ and 2. We could estimate surface level to be $1 \times 10^{13} / \text{cm}^2$. In addition, from our analysis, we suggest that a large part of p-type carriers supplied from Nb accepters were trapped at the interface states. The density of trapped carriers were estimated to be on the order of $10^{12} / \text{cm}^2$. These results are actually consistent with the previous literatures [1, 2]. Furthermore, we also examined the impact of ultraviolet-ozone (UV/O₃) treatment on p-doping level. UV/O₃ treatment can be used prior to the growth of gate dielectric films to make a nucleation layer on the dangling bond-free materials [5]. We performed UV/O₃ treatment of the sample in air ($\sim 10 \text{ mW/cm}^2$, 185 nm and 254 nm). We found that the signal polarity was inverted even on the thicker layers after the treatment. This shows that UV/O₃ treatment has n-type doping effect, which is strong enough to cause p- to n-type transition even on the thicker layers. The results here demonstrate that SNDM provides microscopic key information for understanding and controlling the doping levels in atomically-thin van der Waals semiconductors.

References:

- [1] M. D. Siao et al., *Nature Commun.* 9, 1442 (2018).
- [2] N. Fang et al., *Adv. Funct. Mater.* 29, 1904465 (2019).
- [3] Y. Cho, *Scanning Nonlinear Dielectric Microscopy: Investigation of Ferroelectric, Dielectric, and Semiconductor Materials and Devices*. Elsevier, 2020, ISBN 9780128172469
- [4] K. Yamasue and Y. Cho, *J. Appl. Phys.* 128, 074301 (2020).
- [5] Azcatl et al., *Appl. Phys. Lett.* 104, 111601 (2014).

1:45 PM DISCUSSION TIME

2:00 PM *EQ20.12.03

Strategies for Local Control of the Structure and Properties of the 2D Layered Magnet CrSBr Frances M. Ross; Massachusetts Institute of Technology, United States

Two dimensional (2D) materials with magnetic properties open exciting new design opportunities for nanoscale magneto-electric devices. The layered magnet CrSBr is particularly interesting because of its stability in air, giving this material a key advantage for device integration compared to other 2D magnets such as CrI₃. Since practical devices based on 2D materials often involve contacting, patterning or modifying the layers, it is important to develop methods for controlling the structure and properties of CrSBr at the local, nanoscale level. Here we discuss strategies for achieving this goal, making use of approaches that have proved promising for other 2D materials. We first discuss local control of structure. We find that electron beam irradiation in a scanning transmission electron microscope induces a surprising structural change, where certain atoms migrate into the van der Waals gap to create a new phase with layer direction (and, in theory, magnetization) perpendicular to the initial layers. The ability to modulate the magnetization direction deterministically is of great interest for device applications. We also study local chemical modulation in solid-solution alloys such as CrSCl_xBr_{1-x}. In these materials we investigate the distribution of the alloying elements, aiming to understand magnetism and phase transformations in such tailored 2D magnets. We finally discuss strategies for contacts, focusing on the opportunities for epitaxial growth of metals and other 3D crystals onto the CrSBr surface. We have developed an approach to grow single crystal or heterostructured metals on graphene, hBN and transition metal dichalcogenides; the 2D/3D contact resistance is known to improve for larger crystals with fewer grain boundaries. We will explore how nucleation and epitaxy phenomena play out for

pristine and patterned CrSBr with its distinctive crystal symmetry. We believe that atomistic level structural and chemical modification and control are crucial for understanding properties and designing novel low-dimensional magnetic devices that use these fascinating materials.

2:30 PM EQ20.12.04

The Structural and Vibrational Properties of Intrinsic and Extrinsic Defects in the 2D Layered van der Waals Magnet CrSBr Kierstin P. Torres¹, Julian Klein¹, Thang Pham¹, Joachim D. Thomsen¹, Kate Reidy¹, Agnieszka Kuc^{2,3}, Michael Lorke⁴, Jan Luxa⁵, Zdenek Sofer⁵ and Frances M. Ross¹; ¹Massachusetts Institute of Technology, United States; ²Helmholtz-Zentrum Dresden-Rossendorf, Institut Forschungsstelle Leipzig, Germany; ³Jacobs University Bremen, Germany; ⁴Universität Bremen, Germany; ⁵University of Chemistry and Technology Prague, Czechia

Layered two-dimensional (2D) magnetic materials have intriguing low-dimensional magnetic physics and promising applications in spintronic and magneto-electronic devices. CrI₃ has emerged as a well-studied 2D magnet. [1] However, its poor stability in ambient conditions has been a significant hindrance towards its integration in devices, heterostructures, and further experiments. In contrast, the layered van der Waals antiferromagnet CrSBr [2] is suggested to be air-stable in the mono- and few-layer limit, making it a promising alternative for magneto-transport and magneto-optical studies and device applications. [3, 4] In addition, CrSBr is a semiconductor with a bandgap of ~1.6 eV, a Néel temperature of 145 K, and a strong light-matter interaction. In this work, we investigate the crystal stability and impact of defects on mono-, bi- and few-layer CrSBr using a combination of Raman spectroscopy, scanning transmission electron microscopy (STEM) and helium ion irradiation in a helium ion microscope (HIM). We study two types of samples: (i) CrSBr exfoliated via the scotch tape method and stored at ambient conditions over intervals up to months, and (ii) CrSBr exfoliated and irradiated with helium ions. We find that in pristine, mono-, and few-layer CrSBr, Raman peak shifts are a direct fingerprint of the layer number. By varying the excitation laser energy, we additionally observe resonant Raman modes due to enhanced electron-phonon coupling. Studying Raman line shapes of mono-, bi-, and few-layer CrSBr over long time periods, we find that this material is stable under ambient conditions, with only slight changes in peak shape over time. We also compare CrSBr flakes before and after annealing. At the monolayer level, changes between the annealed and unannealed spectra are most pronounced. This agrees with STEM images of annealed monolayers that display significant degradation and defect formation, whereas bilayers appear to be stable. To better understand the influence of defects on the vibrational properties, we intentionally introduce defects through controlled helium ion irradiation. With increasing helium ion dose, Raman peaks shift and broaden significantly, suggesting increased defect concentration and phonon confinement, as further manifested by our STEM studies. We further corroborate our results by ab-initio calculations of the phonon dispersion. Overall, we demonstrate how Raman spectroscopy is useful towards assessing the stability of CrSBr and its suitability in device applications.

2:45 PM *EQ20.13.01

Physical and Chemical Impacts of Atomic Reconstruction in Twistrionic 2D Layers Daniel K. Bediako; University of California, Berkeley, United States

Atomically thin or two-dimensional (2D) materials can be assembled into bespoke heterostructures to produce some extraordinary physical phenomena. Likewise, these highly manipulatable materials are useful platforms for exploring fundamental questions of interfacial chemical/electrochemical reactivity. In this talk, I will discuss how spontaneous mechanical deformations (atomic reconstruction) and resultant intralayer strain fields at twisted bilayer graphene have been quantitatively imaged using Bragg interferometry, based on four-dimensional scanning transmission electron microscopy, and the impact of these mechanical deformations to the electronic band structure of these moiré superlattices. The talk will then explore how various degrees of freedom that are unique to 2D materials may be used to tailor interfacial charge transfer at well defined mesoscopic electrodes and the outlook for new paradigms of functional materials for energy conversion and low-power electronic devices.

SESSION EQ20.25: On-Demand
Sunday Morning, December 5, 2021
On-Demand

8:00 AM EQ20.10.23

Load-Dependent Friction Hysteresis on Graphitic Surfaces in *n*-alkanes Behnoosh Sattari Baboukani¹, Zhijiang Ye² and Prathima Nalam³; ¹University at Buffalo, United States; ²Miami University, United States; ³University at Buffalo, The State University of New York, United States

Recent advances in two-dimensional (2D) materials such as graphene, molybdenum disulfide (MoS₂), boron nitride (BN), *etc.*, have opened a new path in utilizing the atomically thin layers as oil-based additives due to their ultra-low shear strength, weak interlayer interactions, and the surface chemical stability. It is crucial to develop a fundamental understanding of the dissipation mechanisms for 2D materials in the presence of hydrocarbons to control friction using 2D materials as additives in oil-based lubrication. This work presents the load-dependent atomic force microscope (AFM) friction measurements in *n*-hexadecane solutions on two graphitic surfaces, i.e., highly oriented pyrolytic graphite (HOPG) and exfoliated few-layer graphene (FLG). A sublinear increase in the friction forces with load was measured on both graphitic surfaces, with FLG measuring 30% higher friction force than HOPG (at 60 nN). Further, the nanoscale friction forces exhibit hysteresis between the loading (increasing) and unloading (decreasing) normal forces. Below a specific transition load, higher friction forces were measured during unloading than the loading for a given load, while above the transition load, the friction hysteresis becomes insignificant. The origins for friction force and load-dependent friction hysteresis were explored by measuring the adhesion and roughness of the graphitic surfaces and the solvation layering behavior. Similar RMS roughness values and insignificant adhesion forces were obtained among the graphitic surface; however, higher forces were required to squeeze the solvation layers out of contact for FLG compared to HOPG surfaces. Molecular dynamics (MD) simulations assisted in understanding the impact of solvation layers of *n*-hexadecane on the load-bearing capacity and the friction forces of the graphitic interfaces. The load-dependent friction hysteresis originates from the irreversible reorganization of *n*-hexadecane solvation layers on the graphitic surfaces during the loading and unloading phenomena.

8:05 AM EQ20.08.04

Complex Hysteresis and Memory Effects Observed in the Charge-Density-Wave Phases of the Transition Metal Dichalcogenide TaS_{1.2}Se_{0.8} Benjamin Smith¹, Aimee Nevill¹, Liam Farrar², Charles Sayers³, Sara Dale¹, Simon Bending¹, Daniel Wolverson¹ and Enrico da Como¹; ¹University of Bath, United Kingdom; ²University of St Andrews, United Kingdom; ³Politecnico di Milano, Italy

The tantalum dichalcogenides (TaS₂, TaSe₂ and their intermediate alloys) are members of the layered transition metal dichalcogenide (TMD) family of materials. The tantalum dichalcogenides present a variety of different phases at different temperatures and pressures including metallic [1], Mott insulating [2], charge density wave (CDW) [3] and superconducting [4]. Of particular interest are the low-temperature CDW phases, which display further phase transitions between different CDWs (e.g., commensurate CDW, incommensurate CDW and quasi-commensurate CDW). An understanding of the interplay

of these different phases would provide a valuable insight into the nature of the electron-electron and electron-phonon interactions in these materials. Further, such properties of the tantalum dichalcogenides support their use in a variety of applications where different resistive states can be easily switched using temperature or pressure - for example, for data storage or other memory applications [5] [6].

Here, we shall present our studies on the intermediate alloy $\text{TaS}_{1.2}\text{Se}_{0.8}$. Large-area crystals have been grown in-house, using a chemical vapour transport method. We have characterised the material using a variety of experimental techniques, including temperature-dependent electrical transport, Raman spectroscopy and X-ray diffraction. These measurements have revealed the hysteretic properties of this alloy over a single cooling-heating cycle (320 – 4 K for the transport measurements). Furthermore, we have observed a fascinating ‘memory effect’ in this material, in which a second cooling-heating cycle yields a completely different hysteresis loop. This ‘memory effect’ has been observed in multiple crystals from several different growth batches and has been observed in both our transport and Raman measurements. The effect appears to be closely linked to the doping concentration we have used ($S = 1.2$, $\text{Se} = 0.8$), as we have not observed any such memory effect in crystals grown with slightly different stoichiometries (e.g., $S = 1.3$, $\text{Se} = 0.7$). We have further examined this effect by using a range of cooling/heating rates. These measurements have displayed a clear dependence on cooling/heating rate, which provide us with crucial insights into the mechanisms of the CDW phase transitions, in particular the nearly-commensurate to commensurate transition, in which domains of commensurability increase in size and eventually merge to form a fully-commensurate system. Meanwhile, our Raman measurements are vital in helping us to understand the CDW mechanism in this material, and the contributions of electron-electron and electron-phonon interactions in the formation and transitions of the CDWs.

- [1] A. K. Geremew et al., ACS Nano 13, 6, 7231–7240 (2019)
- [2] Y. D. Wang et al., Nat Commun 11, 4215 (2020)
- [3] F. J. Di Salvo et al., Phys. Rev. B 12, 2220 (1975)
- [4] Y. Liu et al., Appl. Phys. Lett. 102, 192602 (2013)
- [5] M. Yoshida et al., Sci. Adv. 1, e1500606 (2015)
- [6] I. Vaskivskiy et al., Nat. Commun. 7:11442 doi: 10.1038/ncomms11442 (2016)

8:20 AM EQ20.12.02

Correlative and Cryogenic Imaging of TMDs Thomas Dieing¹, Ute Schmidt¹, Patrick Altmann², Mirko Bacani² and Olaf Hollricher¹; ¹WITec GmbH, Germany; ²attocube systems AG, Germany

WSe_2 and MoS_2 , as transition metal dichalcogenides (TMDs), belong to a new class of nanomaterials with great potential for optoelectronic device applications. Thickness, changes in crystal symmetry, and growth defects are a few fundamental parameters that define the electronic, optical and thermal properties of two-dimensional (2D) crystals and for which different characterization techniques are required. In addition, the dependency of material characteristics on temperature and/or external magnetic fields is receiving increasing attention. Here we present the correlative analysis of these TMDs using Atomic Force Microscopy (AFM), Photoluminescence (PL) Imaging, Second Harmonic Generation (SHG) imaging and confocal Raman imaging under ambient and cryogenic conditions. The combination of the insights obtained by AFM, PL, SHG and Raman on WSe_2 measured under ambient conditions allow an interpretation of the cause of PL wavelength emission shifts, strain states and contaminations during the growth process. The strongly localized peak shift variations around the rim of the WSe_2 flake and their possible explanations based on the correlative results are particularly interesting. The addition of temperature-dependent PL imaging using a cryostat capable of cooling the sample down to 2K also allows the determination of the peak shift, both on the rim as well as in the center of such a flake, as a function of temperature. The newly established CryoRaman system, a combination of a WITec confocal Raman microscope and an attocube attoDry2100 closed-cycle cryostat, uses a high NA low temperature objective that allows for optical resolution close to that which is available under ambient conditions. Using this system, it was possible to discern low frequency Raman bands of WSe_2 for layering identification and observe them under varying polarization directions of the incoming laser light at cryogenic temperatures. The ability to apply high magnetic fields (up to 12T) additionally enables observation of the effect of the magnetic field on the recorded Raman spectra and reveals further properties of the TMDs.

SESSION EQ20.14: Large Scale Electronic Grade Synthesis of 2D Materials II
Session Chairs: Jieun Lee and Hyeon Jin Shin
Monday Morning, December 6, 2021
EQ20-Virtual

8:00 AM EQ20.14.01

A New Computational Framework for Structural Characterization and Edge-Growth Kinetics of Transition Metal Dichalcogenides—ReaxFF Reactive Force Field Nadire Nayir^{1,2,3,4}, Yuanxi Wang^{1,1}, Danielle Hickey^{1,1}, Yanzhou Ji¹, Tanushree H. Choudhury¹, Long-Qing Chen^{1,1}, Nasim Alem^{1,1}, Joan M. Redwing^{1,1}, Vincent Crespi^{1,2} and Adri van Duin^{1,1}; ¹The Pennsylvania State University, United States; ²Karamanoglu Mehmetbey University, Turkey

Presented by Nadire Nayir
Mechanical Engineering, The Pennsylvania State University, State College, PA, United States.
2D Crystal Consortium, The Pennsylvania State University, State college, PA, United States.
Physics, Karamanoglu Mehmetbey University, Karaman, Turkey.

We introduce new reactive potentials (ReaxFF)^{1,2,3,4} for large-scale molecular dynamics simulations of the synthesis, processing, and characterization of two-dimensional transition metal dichalcogenides (MoS_2 , WSe_2 , MoSe_2 , and WS_2), guided by an extensive quantum mechanical dataset on both periodic and non-periodic systems and validated against HAADF/STEM experiments. These new potentials are designed to capture the most essential features of TMD thin films and elucidate the structural transition from metallic to semiconducting phases, the energetics of various defects, and the Se-vacancy migration barrier. The new ReaxFF descriptions provide valuable insights into nucleation of the 1T-phase on the 2H basal plane or edges, rotational and translational grain boundaries, and the coupled effect of chemical potential and edge stability on the formation of S- and W-oriented grain boundaries. Since controllable edge-mediated growth kinetics of 2D- MoSe_2 are of great interest to the 2D community, these potentials are trained further against the edge formation energies of MoSe_2 nanoribbons with different Se coverages, we believe they will be a powerful complementary tool to experimental studies by simulating the edge-growth kinetics of 2D- MoSe_2 at high speed and low cost.

- [1] Ostadhosseine, A.; Rahnamoun, A.; Wang, Y.; Zhao, P.; Zhang, S.; Crespi, V. H.; van Duin, A. C. T. ReaxFF Reactive Force-Field Study of Molybdenum Disulfide (MoS_2). J. Phys. Chem. Lett. 2017, 8 (3), 631–640. <https://doi.org/10.1021/acs.jpcclett.6b02902>.

[2] N. Nayir, Y. Wang, S. Shabnam, D.R. Hickey, L. Miao, X. Zhang, S. Bachu, N. Alem, J. Redwing, V.H. Crespi, A.C. T. van Duin, Modeling for structural engineering and synthesis of two-dimensional WSe₂ using a newly developed ReaxFF reactive force field, *J. Phys. Chem. C* 124 (51) (2020) 28285–28297, <https://doi.org/10.1021/acs.jpcc.0c09155>.

[3] N. Nayir; Y. Wang; Y. Ji; T. H. Choudhury; J. M. Redwing; L.-Q. Chen; V. H. Crespi; A. C. T. van Duin. Theoretical Modeling of Edge-Controlled Growth Kinetics and Structural Engineering of 2D-MoSe₂. *MatSciEng B* Vol. 271, Sep. 2021, 115263, DOI:10.1016/j.mseb.2021.115263

[4] N. Nayir; Y. Shin; Y. Wang; M. Sengul; D. R. Hickey; M. Chubarow; T. Choudhury; N. Alem; J. Redwing; V. Crespi; A. C. T. van Duin, Development of a ReaxFF Force Field for 2D-WS₂ and Its Interaction with Sapphire (under review at JPCC).

8:15 AM EQ20.14.02

Effects of Growth Substrate on the Nucleation of Monolayer MoTe₂ David Hynek¹, Raivat Singhania², James L. Hart¹, Benjamin Davis², Mengjing Wang¹, Nick Strandwitz² and Judy Cha¹; ¹Yale University, United States; ²Lehigh University, United States

MoTe₂ is a 2D transition metal dichalcogenide with small energy differences between its polymorphs, allowing access to a wide range of electronic states including the room-temperature semiconducting 2H state and semimetallic 1T' state, and low-temperature topological T_d state. Due to this, MoTe₂ is a model material for studying phase transformations and structure-property relationships and has potential applications in low-power, non-volatile phase change memory.

These phase changes can be induced through application of strain and charge doping, and are affected greatly by the choice of substrate. Thus, understanding the interfacial effects between MoTe₂ films and substrate is important for selective synthesis and control over different crystalline phases of MoTe₂. Further, while there are many growth studies to investigate the effects of substrate for 2D sulfides and selenides, there is a lack of fundamental understanding of the growth mechanisms for the tellurides.

Here, we examined the effect of the substrate on the morphology and crystalline phase of MoTe₂ by tracking the nucleation and growth of MoTe₂ on different substrates (*CrystEngComm* **2021**, doi:10.1039/d1ce00275a). We grew monolayer MoTe₂ by converting MoO_x thin films deposited on three different substrates: sapphire Al₂O₃ (0001), amorphous SiO₂, and amorphous AlO_x, following the synthesis method we developed for large-area MoTe₂ thin films (*ACS Nano* **2021**, 15, 1, 410–418). We systematically examined the early stages of the conversion reaction occurring on the three substrates to elucidate the substrate effects on the nucleation of MoTe₂. We observe that the chemical composition of the substrate is more important than the surface topography and crystallinity of the substrate, with high quality monolayer 2H MoTe₂ formed on both Al₂O₃ (0001) and AlO_x in contrast to mixed phase 2H/1T' MoTe₂ formed on SiO₂, as determined by Raman spectroscopy, x-ray photoelectron spectroscopy, cross-sectional transmission electron microscopy, and atomic force microscopy. We attribute these results to increased wetting between Te or Mo atoms on AlO_x vs. SiO₂, which allows for improved lateral mobility and reconfiguration. Our work highlights the role of chemistry regarding substrate interactions during the synthesis of 2D materials and particularly the diffusion of metal species on different oxide films.

8:30 AM EQ20.14.03

Wafer-Scale Epitaxial TMD Monolayers—Comparison of MOCVD Growth and Properties with Different Metals and Chalcogens Nicholas Trainor¹, Tanushree Choudhury^{1,2}, Mikhail Chubarov¹, Kasra Momeni³, James Spencer Lundh¹, Danielle Hickey¹, Tianyi Zhang¹, Amritanand Sebastian¹, Haoyue Zhu¹, Baokun Song⁴, Yueli Chen⁴, Benjamin Huet¹, Anushka Bansal¹, Sukwon Choi¹, Nasim Alem¹, Mauricio Terrones¹, Deep M. Jariwala⁴, Saptarshi Das¹ and Joan M. Redwing¹; ¹The Pennsylvania State University, United States; ²Indian Institute of Technology Bombay, India; ³The University of Alabama, United States; ⁴University of Pennsylvania, United States

Monolayers of transition metal dichalcogenides (TMDs) are promising materials for electronic, optoelectronic, spintronic and valleytronic devices. Furthermore, wafer-scale epitaxial growth of TMD monolayers has been demonstrated^{1,2}; however, fundamental understanding of these processes is limited. In this work, we demonstrate and compare the epitaxial growth of MoS₂, WS₂ and WSe₂ on 2" c-plane sapphire wafers using metal-organic chemical vapor deposition (MOCVD). Heat and mass transport within the reactor was modelled with computational fluid dynamics (CFD) to help predict and understand the effect of process parameters such as substrate rotation on the growth rate and uniformity of the TMD films. The films displayed uniform thickness and topography across the wafer, as measured via atomic force microscopy. X-ray diffraction measurements confirmed the films were epitaxial with respect to the sapphire substrate, while dark field transmission electron microscopy was used to image microstructural features such as translational and anti-phase grain boundaries in the coalesced monolayers. Different excitonic species such as trions and defect-bound excitons were observed with variable-temperature photoluminescence (PL) spectroscopy, while optical properties measured by spectroscopic ellipsometry closely matched predictions from theoretical models. The electronic properties of the films were measured using FETs, with the sulfide and selenide films having carrier mobilities of ~20 cm²/Vs and ~2.5 cm²/Vs, respectively. The lower carrier mobility in the WSe₂ films correlates with defect-related exciton emission which was observed in the PL spectrum.

We also systematically studied how the transition metal and chalcogen species affected the growth of the monolayers. For example, under similar growth conditions, WSe₂ exhibited larger domains and lower nucleation densities compared to WS₂ films, which suggests that surface diffusivity is higher on sapphire under a selenium ambient compared to sulfur. For W-containing TMDs, a three-step nucleation-ripening-lateral growth process was more effective in achieving uniform domain size compared to a single-step growth process. In contrast, no such difference was observed for MoS₂; several possible causes are currently under investigation. Understanding these trends will prove useful in the rational selection of growth parameters for TMD films.

(1) Zhang, X.; Choudhury, T. H.; Chubarov, M.; Xiang, Y.; Jariwala, B.; Zhang, F.; Alem, N.; Wang, G.-C.; Robinson, J. A.; Redwing, J. M. Diffusion-Controlled Epitaxy of Large Area Coalesced WSe₂ Monolayers on Sapphire. *Nano Lett.* **2018**, 18 (2), 1049–1056.

(2) Chubarov, M.; Choudhury, T. H.; Hickey, D. R.; Bachu, S.; Zhang, T.; Sebastian, A.; Bansal, A.; Zhu, H.; Trainor, N.; Das, S. Wafer-Scale Epitaxial Growth of Unidirectional WS₂ Monolayers on Sapphire. *ACS Nano* **2021**, 15 (2), 2532–2541.

8:45 AM EQ20.14.04

Synthesis and Phase Tuning of MoTe₂ Nanosheets by Chemical Vapor Deposition Pinaka Pani Tummala^{1,2,3}, Christian Martella¹, Sara Ghomi⁴, Samarsadat Mirenayat⁵, Alessio Quadrelli⁶, Mario Alia¹, Matteo Cocuzza⁴, Cristina Lenardi⁶, Luca Nobili⁵, Roberto Mantovan¹, Alessio Lamperti¹ and Alessandro Molle¹; ¹CNR-IMM, Italy; ²KU Leuven, Belgium; ³Università Cattolica del Sacro Cuore, Italy; ⁴Politecnico di Torino, Italy; ⁵Politecnico di Milano, Italy; ⁶Università degli Studi di Milano, Italy

Among transition metal dichalcogenides (TMDs), molybdenum ditelluride (MoTe₂) shows significant attention due to its polymorphic nature from semiconductor to topological insulator and Weyl-semimetal. To date, considerable efforts have been devoted for synthesizing large area MoTe₂ suitable for the fabrication of devices to be integrated in different applications. As compared to other synthesis methods, chemical vapor deposition (CVD) is a facile and promising way for synthesizing large scale MoTe₂ nanosheets.

Here we report the CVD growth and controlled phase tuning strategies for obtaining 1T' (metallic) and 2H (semiconducting) molybdenum ditelluride (MoTe₂) nanosheets via two ways: 1) co-deposition of tellurium and MoO₃ powder precursors and 2) tellurization of pre-deposited Mo thin film. In first

case, we employed CVD through powder precursors targeting large area growth of thin MoTe₂ nanosheets with controlled allotropic 1T' and 2H phases. We investigated how the local tellurium vapor concentrations determines the MoTe₂ phase (2H and 1T') depending on the flow rate of the Ar carrier gas and with the insertion of a physical barrier in the reaction chamber. The effect of the physical barrier is also reflected in the shape of the crystallite population and in their log-normal areal distribution pointing out to a homogeneous nucleation mode of the MoTe₂ crystals [1]. On the other hand, in tellurization we show a detailed study of the heterogeneous vapor-solid reaction between an e-beam pre-deposited molybdenum film and tellurium vapor, thus yielding a large area growth of MoTe₂ onto SiO₂/Si substrate [2]. MoTe₂ growth is mainly influenced by involved kinetics, tellurium concentration and geometry configurations inside the CVD furnace. As grown MoTe₂ nanosheets were characterized by several techniques such as Raman spectroscopy, scanning electron microscopy (SEM), atomic force microscopy (AFM) and X-ray photoelectron spectroscopy (XPS). This study is a crucial step for enabling 1T' and 2H-MoTe₂ integration in numerous potential applications in novel micro- and nano-electronics, quantum technologies, integrated photonics, and thermoelectric devices.

References:

C. Martella, Alessio Quadrelli, Pinaka Pani Tummala, Cristina Lenardi, Roberto Mantovan, Alessio Lamperti, Alessandro Molle, *Cryst. Growth Des.* **2021**, *21*, 5, 2970–2976.

Jin Cheol Park, Seok Joon Yun, Hyun Kim, Ji-Hoon Park, Sang Hoon Chae, Sung-Jin An, Jeong-Gyun Kim, Soo Min Kim, Ki Kang Kim, Young Hee Lee, *ACS Nano* **2015**, *9*, 6, 6548–6554

9:00 AM EQ20.14.05

Oxide Scale Sublimation Chemical Vapor Deposition: Controllable Growth of Monolayer MoS₂ Crystals on Catalytic Glass Xu Yang, Shisheng Li, Naoki Ikeda and Yoshiki Sakuma; National Institute for Materials Science, Japan

Abstract

In this study, a newly-proposed oxide scale sublimation chemical vapor deposition (OSSCVD) technique is demonstrated for the controlled growth of two-dimensional (2D) monolayer MoS₂ crystals. With the new reactor configuration, MoO₃, which is generated in situ by flowing O₂ over Mo metal surface, can be sublimated by heating and supplied separately from the H₂S source in a controlled manner through mass flow controllers and pneumatic switching valves. A series of proof-of-concept growth experiments with varied gas flow rate and growth time was carried out using high-temperature resistant alkali-aluminosilicate glass, Dragontrail (DT-glass), as catalytic substrate. We confirmed that OSSCVD enables the growth of MoS₂ with significantly improved flexibility, controllability, and reproducibility that are absent in the conventional powder-source CVD. As a result, single-crystalline MoS₂ triangular domains as large as 25 μm was observed reproducibly, followed by the fully-covered continuous MoS₂ layer within 25 minutes. Photoluminescence and Raman spectroscopies revealed that both the achieved domains and the continuous film possess monolayer MoS₂ features and good optical quality. Meanwhile, the characteristics of fabricated field effect transistors showed maximum electron mobility of 13 cm²/Vs, indicating a good electrical property as well. Utilizing DT-glass as substrate, the MoS₂ growth process is strongly affected by suppressed nucleation density and enhanced lateral growth, probably due to the catalytic effect of sodium and/or potassium in the glass. Particularly, we found that before growth in situ DT-glass substrate treatment by H₂S enables a remarkably enlarged domain size with reduced domain density. Intriguingly, these growth improvements might be primarily related to the alkali metal elements extracted from DT-glass to the reactor inner walls rather than the modification on the glass surface during the H₂S pretreatment process. The results achieved in this work open new avenues for growing high-quality MoS₂ and other 2D transition metal dichalcogenides using the simple OSSCVD and the cost-effective catalytic glass substrate. More details will be presented at the conference.

Acknowledgments

This work was partly supported by Innovative Science and Technology Initiative for Security Grant Number JPJ004596, ATLA, Japan, and JSPS KAKENHI (No. JP17H03241)

9:15 AM EQ20.14.08

Tuning Electronic Structure in Wafer-Scale Continuous Monolayer MoS₂ by Chemical Vapor Deposition Shu-Ju Tsai¹, Yi-Cheng Lin¹, Sumayah Shakil Wani², Yu-Lun Chueh² and H. Hoe Tan³; ¹Taiwan Instrument Research Institute, National Applied Research Laboratories, Taiwan; ²National Tsing Hua University, Taiwan; ³The Australian National University, Australia

Monolayer molybdenum disulfide (ML-MoS₂) with excellent exotic electronic and optical properties has shown great potential for applications in transistors, sensors, energy harvesting, light-emitting diodes, catalysis, flexible devices, etc. However, it is a great challenge to achieve wafer-scale growth of continuous monolayer for MoS₂ and to control the doping because of its intrinsic *n*-type conductivity. Substitution doping (such as Nb, Mn, N atoms) has been proved to be an effective approach to tune their native properties toward *p*-type and enhance device performance. Herein, we report the growth of sulfur-rich large-area monolayer MoS₂ by a one-step chemical vapor deposition method. Much attention will be paid to the electric properties and the atomic structures of the sulfur-rich MoS₂ using Kelvin Probe Force Microscopy (KPFM, Bruker ICON) and X-ray photoelectron spectroscopy (XPS), respectively. Further studies of electrical measurements indicate that the *p*-type transport behavior can be observed in sulfur-rich MoS₂ field-effect transistor (FET) devices. The results of these studies will have a considerable impact on the tuning the electronic structure of two-dimensional TMDs, and create new direction for fundamental study and their novel device applications.

9:20 AM EQ20.14.10

Wafer-Scale Epitaxial MoSe₂ on Epitaxial hBN—A Combination of MBE and MOVPE Katarzyna Ludwiczak, Aleksandra K. Dabrowska, Johannes Binder, Mateusz Tokarczyk, Jakub Iwanski, Grzegorz Kowalski, Rafal Bozek, Roman Stepniewski, Wojciech Pacuski and Andrzej Wyszomlek; University of Warsaw, Poland

Ultrathin transition metal dichalcogenides (TMD) are two-dimensional semiconductors exhibiting exceptional optical, mechanical and chemical properties. Hence, they can complement other layered materials like graphene in various next-generation nanodevices.

High-quality TMD monolayers can be obtained by mechanical exfoliation - a process that is extremely time-consuming, non-deterministic and provides flakes of only a few-micrometers in size. Here, we present a heteroepitaxial method to grow single layer MoSe₂ directly on hBN, allowing to overcome the before mentioned problems.

In our approach, we use Metalorganic Vapour Phase Epitaxy (MOVPE) to grow few-nanometres thick layers of hexagonal boron nitride (h-BN) on two-inch sapphire substrates [1,2]. We present thorough optical and structural studies, demonstrating a high structural quality of the samples. h-BN possesses a wide bandgap (~6 eV) that makes it a perfect insulating barrier in heterostructures and is also known to improve optical properties of other layered materials due to the lack of dangling bonds on its surface [3]. Therefore, we use the epitaxial h-BN as a substrate for a subsequent growth of a monolayer of molybdenum diselenide (MoSe₂) using Molecular Beam Epitaxy (MBE) [4].

We studied the optical quality of the obtained TMD layers as a function of h-BN substrate thickness by performing Raman scattering and photoluminescence measurements. For the samples from well-optimized processes, we observe excitonic lines that can be resolved into two peaks corresponding to the neutral exciton A and trion at low temperatures (4 K), indicating that the material is of excellent optical quality.

Further characterization includes optical mapping of the whole two-inch samples, which proves a high homogeneity of the material. Such measurements additionally demonstrate the formation of a single atomic layer of MoSe₂. Our results constitute a large step towards the wafer-scale growth of van der Waals heterostructures, which is of crucial importance for future applications. Our work also demonstrates for the first time, that using epitaxial h-BN, MoSe₂ of excellent optical quality can be scaled up to the size of 2 inch wafers. Moreover, the presented method can be easily applied to grow other TMD which can be used to construct optoelectronic devices such as photodetectors, LEDs and phototransistors.

[1] K. Pakula, A. Dabrowska, M. Tokarczyk, R. Bozek, J. Binder, G. Kowalski, A. Wyszomolek, R. Stepniewski "Fundamental mechanisms of hBN growth by MOVPE" arXiv: **1906.05319 (2019)**

[2] A.K. Dabrowska, M. Tokarczyk, G. Kowalski, J. Binder, R. Bozek, J. Borysiuk, R. Stepniewski, A. Wyszomolek, "Two stage epitaxial growth of wafer-size multilayer h-BN by metal-organic vapor phase epitaxy – a homoepitaxial approach", 2D Mater., **8, 015017 (2021)**

[3] F. Cadiz, E. Courtade, C. Robert, G. Wang, Y. Shen, H. Cai, T. Taniguchi, K. Watanabe, H. Carrere, D. Lagarde, M. Manca, T. Amand, P. Renucci, S. Tongay, X. Marie, and B. Urbaszek, "Excitonic Linewidth Approaching the Homogeneous Limit in MoS₂-Based van der Waals Heterostructures" Phys. Rev. X **7, 021026**

[4] W. Pacuski, M. Grzeszczyk, K. Nogajewski, A. Bogucki, K. Oreszczuk, J. Kucharek, K. E. Polczynska, B. Seredynski, A. Rodek, R. Bozek, T. Taniguchi, K. Watanabe, S. Kret, J. Sadowski, T. Kazimierczuk, M. Potemski, and P. Kossacki, "Narrow Excitonic Lines and Large-Scale Homogeneity of Transition-Metal Dichalcogenide Monolayers Grown by Molecular Beam Epitaxy on Hexagonal Boron Nitride", Nano Lett. **20, 3058–3066 (2020)**

9:25 AM EQ20.14.11

MBE Growth of VS₂ Layer and Its Electronic Structure [Hyuk Jin Kim](#)¹, Byoung Ki Choi¹, In Hak Lee², Min Jay Kim¹, Tae Gyu Rhee¹ and Young Jun Chang¹; ¹University of Seoul, Korea (the Republic of); ²Korea Institute of Science and Technology, Korea (the Republic of)

Vanadium disulfide (VS₂) has recently attracted much attention due to their intriguing properties, such as charge density wave (CDW), ferromagnetism, and surface catalytic behavior. However, VS₂ has received relatively little experimental research compared to other vanadium chalcogenides (VSe₂, VTe₂), so physical properties of VS₂ such as an origin of CDW, and ferromagnetism are experimentally unsettled. Here, we report MBE growth of VS₂ with different thicknesses. We investigated temperature dependent electronic structure studies by using angle-resolved photoemission spectroscopy (ARPES) measurements and show the signature of CDW transition above 300 K. Furthermore, we investigated enhanced water-dissociation properties of few layer VS₂ layers by using ambient pressure X-ray photoemission spectroscopy (APXPS) measurements. These results suggest promising properties of VS₂ and related metallic sulfides.

9:30 AM EQ20.14.12

Growth of InSe on Si(111) 7x7 Surface By Molecular Beam Epitaxy [Derrick Shao Heng Liu](#), Maria Hilse and Roman Engel-Herbert; The Pennsylvania State University, United States

InSe was recently reported as another candidate in the family of layered semiconductor material with tremendous application potential because of its high charge carrier mobility of above 1000 cm²/Vs at room temperature, a high photoresponsivity and sizeable principal optical bandgap of 1.2 eV in the bulk that can be tuned by the number of InSe layers up to 1.9 eV in a bilayer structure, a natural ultra-thin body form factor suitable to ensure excellent electrostatic control over the channel and synthesis parameters compatible with the stringent back-end-of-line requirements. In this talk the results of InSe thin films grown by molecular beam epitaxy (MBE) on Si(111) will be presented. By taking advantage of excellent in-situ control and monitoring capability of MBE, specifically a precise temperature control using IR cameras as well as employing the approach of controlled flux gradients across the wafer, we have identified suitable growth conditions to synthesize single phase InSe, thus demonstrating the capability of large scale high-quality InSe film on 3 inch Si(111) wafers despite the very narrow growth parameter window. We will discuss how different growth parameters affect the phase formation and surface morphology of the films. We have mapped out the growth parameter space for which single phase InSe can be grown in the temperature range between 350°C to 500°C. The single phased InSe films are confirmed by reflection high energy electron diffraction (RHEED) and X-ray diffraction. The films surface morphology is found to be affected by the chemistry composition of the growth front and growth temperature. In-rich growth fronts at lower temperatures promote the formation of pyramid-like triangles, while lower growth rates and higher temperature suppressed the pyramid formation, giving rise to smooth film surfaces with atomic terraces. Raman and photoluminescence (PL) measurements as well as X-ray photoelectron spectroscopy results will be correlated with the growth conditions and transport measurements to provide a comprehensive understanding towards wafer scale high quality growth of this promising semiconductor.

SESSION EQ20.15: Optical Properties of 2D Materials
Session Chairs: Azimkhan Kozhakhmetov and Riccardo Torsi
Monday Afternoon, December 6, 2021
EQ20-Virtual

1:00 PM *EQ20.15.02

Exciton-Polaritons in van der Waals Materials Explored by Electron Beams [Nahid Talebi](#); Christian Albrechts Universität zu Kiel, Germany

Semiconducting van der Waals materials, including transition metal dichalcogenides (TMDCs) and tetradymites are fascinating platforms for strong light-matter interactions. Thanks to their weak anisotropic dielectric screening, their excitonic landscape include bright and dark-exciton with large binding energies. Therefore, excitons can be excited, for example by optical means, at the room temperature. Normally, exciton-photon interactions are in the form of weak interactions, as revealed from luminescence spectroscopy. Strong exciton-photon couplings though could lead to the emergence of exciton polaritons allowing for coherent transfer of the electromagnetic energy with applications in optoelectronic devices. Strategies for enhancing the coupling between excitons and photons include the exploitation of photonic resonators or plasmonic effects. Such strong-coupling effects thus normally incorporate optical means for excitations and detections. Here, we use cathodoluminescence spectroscopy technique that is based on the spontaneous interaction of electron beams with the optical modes, hence could be a signature of the spontaneous coherence caused by collective polaritonic polarizations in the material [1, 2]. Our talk thus constitute three explorations: First, we investigate exciton-photon couplings in thin WSe₂ films [3]. Thanks to the Fabry-Perot-like resonances in thin films, the guided photonic modes pursue a longer interaction time with exciton A in the material and hence undergo a strong interaction with exciton A. We will show that the strong-coupling effect could be traced out by observing the splitting in the eigen energies and be detected spectroscopically, whereas the near-field interference effects demonstrate the excitation of exciton polaritons with their dispersions perfectly matching our theoretical results. Second, the interaction between exciton polaritons and the optical modes of a plasmonic lattice

is investigated. We will show that depending on the thickness of the WSe₂ film, the excitons luminescence response is either quenched or enhanced, signifying the interplay between the strong-coupling and screening effects. Third, we investigate exciton polaritons in Bi₂Se₃ thin films [4]. Thanks to the hyperbolic response of the material, hyperbolic exciton polaritons are excited that in contrast with the excitons polaritons in WSe₂ – that are bulk polaritons – are bound to the surfaces and edges of the materials. We particularly show that hyperbolic edge exciton-polariton sustain a long propagation length with promising applications in optics-electronics interconnects.

References:

- [1] N. van Nielsen, M. Hentschel, N. Schilder, H. Giessen, A. Polman, N. Talebi, “Electrons generate self-complementary broadband vortex light beams using chiral photon sieves,” *Nano Letters* **20** (8), 5975-5981 (2020)
- [2] N Talebi, S Meuret, S Guo, M Hentschel, A Polman, H Giessen, P. A. van Aken, “Merging transformation optics with electron-driven photon sources,” *Nature communications* **10** (1), 1-8 (2019)
- [3] M. Taleb, F. Davoodi, F. Diekmann, K. Rossnagel, N. Talebi, “Charting the Exciton-Polariton Landscape in WSe Thin Flakes by Cathodoluminescence Spectroscopy,” arXiv preprint arXiv:2101.01465 (2021)
- [4] R. Lingstädt, N. Talebi, M. Hentschel, S. Mashhadi, B Gompf, M Burghard, “Interaction of edge exciton polaritons with engineered defects in the hyperbolic material Bi₂Se₃,” *Communications Materials* **2** (1), 1-11 (2021)

1:30 PM *EQ20.15.01

Probing Excitons in 2D Semiconductors and Heterostructures in Momentum Space [Tony F. Heinz](#)^{1,2}; ¹Stanford University, United States; ²SLAC National Accelerator Laboratory, United States

One of the characteristic features of 2D semiconductors is the strong role of many-body electronic effects that result from the reduced dimensionality and reduced dielectric screening in these systems. In particular, the optically excited states of 2D materials and heterostructures are dominated by exciton transitions, giving rise to many distinctive properties, such as sharp, strong features and the ability to tune transition energies by external dielectric screening.

Despite our deepening understanding of excitons in 2D semiconductors and their heterostructures through advances in optical spectroscopy, some fundamental aspects of the properties of excitons in 2D semiconductors have been difficult to address directly by experiment. These include a determination of the location in momentum space of the electron and hole forming an exciton and a determination of the actual excitonic wavefunction. In this talk, we will describe recent advances in the application of time-resolved ARPES (angularly resolved photoemission spectroscopy) based on femtosecond laser sources [1,2]. This technique allows one to investigate the nature of excited states of 2D materials directly in momentum space.

We will present results demonstrating how the method allows us to identify the valley characteristics of both the electron and hole forming excitons in both 2D semiconductors and 2D heterostructures in the transition metal dichalcogenide family. The dynamics of exciton relaxation and scattering can also be captured in ultrafast pump-probe measurements. Further, the measured dispersion characteristics of the electrons photoemitted from an exciton, as opposed to a photoemission of excited free carriers, show a distinctive dispersion relation reflecting the characteristics of the remaining hole. A particularly important possibility of this approach is the direct imaging of the excitonic wavefunction through its mapping into the momentum distribution of the photoemitted electrons. We will demonstrate how this can be applied not only to isolated monolayers, but also to interlayer excitons in semiconductor heterostructures.

This work was performed in collaboration with the group of Keshav Dani at OIST, Japan, with theoretical contributions for Ting Cao at the University of Washington and Felipe da Jornada at Stanford University.

- [1] J. Madéo et al., *Science* **370**, 1199-1204 (2020).
- [2] M. K. L. Man et al., *Science Adv.* **7**, eabg0192 (2021).

2:00 PM EQ20.15.03

Interlayer Exciton Mediated Second Harmonic Generation Control in Transition Metal Dichalcogenides Shivangi Shree^{1,2}, Delphine Lagarde², Laurent Lombez², Cedric Robert², Andrea Balocchi², Kenji Watanabe³, Takaaki Taniguchi³, Xavier Marie², Iann C. Gerber², Mikhail Glazov⁴, Leonid Golub⁴, Ioannis Paradisanos² and Bernhard Urbaszek²; ¹University of Washington, United States; ²Institut National des Sciences Appliquées de Toulouse, France; ³National Institute for Materials Science, Japan; ⁴Ioffe Institute, Russian Federation

Non-linear optical spectroscopy of atomically thin crystals gives crucial insights into their physical properties and investigates potential applications. Second harmonic generation (SHG) is a non-linear optical process, where two photons coherently combine into one photon of twice their energy. SHG is vital both as a spectroscopic tool and also for applications of a large class of materials such as II-VI and III-V semiconductors, nanotubes, magnetic- and non-magnetic layered materials, perovskites and antiferromagnetic oxides.

Efficient SHG occurs for crystals with broken inversion symmetry, such as transition metal dichalcogenide monolayers. Here we show tuning of non-linear optical processes in an inversion symmetric crystal. This tunability is based on the unique properties of bilayer MoS₂, that shows strong optical oscillator strength for the intra- but also interlayer exciton resonances. As we tune the SHG signal onto these resonances by varying the laser energy, the SHG amplitude is enhanced by several orders of magnitude. In the resonant case the bilayer SHG signal reaches amplitudes comparable to the off-resonant signal from a monolayer. In applied electric fields the interlayer exciton energies can be tuned due to their in-built electric dipole via the Stark effect. As a result the interlayer exciton degeneracy is lifted and the bilayer SHG response is further enhanced by an additional two orders of magnitude, well reproduced by our model calculations [1]. Since interlayer exciton transitions are highly tunable also by choosing twist angle and material combination in heterostructures our results open up new approaches for designing the SHG response of layered materials.

- [1] Shivangi Shree et al, arXiv 2104.01225

2:15 PM EQ20.15.04

Improving Exciton Valley Polarization by Scattering [Jun Yan](#)¹, Yueh-Chun Wu¹, Takashi Taniguchi² and Kenji Watanabe²; ¹University of Massachusetts Amherst, United States; ²National Institute for Materials Science, Japan

Scattering in a device often causes performance degradation. Here we experimentally demonstrate a counter-intuitive enhancement of device performance induced by scattering. In monolayer MoS₂, we show that scattering can markedly improve its excitonic valley polarization. We report seven- and twelve-

folds of valley polarization enhancement due to thermally activated and charge doping induced scattering respectively. This interesting effect is attributed to the disruption of valley pseudospin precession arising from rapid modulation of exciton momentum and concomitant exchange interaction field, which is analogous to motional narrowing in nuclear magnetic resonance spectroscopy. Our work advances understanding of valley depolarization mechanisms in transition metal dichalcogenide atomic layers and illustrates a novel approach for controlling and improving valleytronic devices.

2:30 PM EQ20.15.05

Factors Influencing Valley Splitting in 2D Heterointerfaces Steven T. Hartman and Ghanshyam Pilania; Los Alamos National Laboratory, United States

With the recent advances in synthesis and characterization of two-dimensional materials, there is great interest in exploiting their favorable electronic properties to create compact devices. In particular, materials which lack inversion symmetry can break degeneracy between otherwise equivalent crystal momentum valleys if the time-reversal symmetry is also removed. This allows the generation of valley-polarized carrier populations, because each valley preferentially absorbs a certain polarization of light and the lack of degeneracy changes the absorption frequency for each valley. Traditionally, the symmetry has been broken with an external magnetic field, but the proximity effect of a magnetic substrate layer can potentially induce stronger Zeeman splitting of the valleys without the need for a bulky magnet. A number of computational studies have identified valleytronic/substrate material pairs which break the degeneracy between valleys, and a few have been experimentally verified. However, a systematic understanding is absent because most studies only test one or two interfaces, and differing methods make it hard to compare results.

For this reason, we have done a larger computational search of eight different materials pairs in three possible stackings, with the goal of identifying the design principles which generate much greater valley splitting in certain interfaces than in others. The valleytronic layers are transition metal dichalcogenides (Mo,W)(S,Se)₂, while we use two antiferromagnetic (Mn, Ni)PSe₃ substrates or the ferromagnets CrBr₃ and CrGeTe₃ to generate the proximity effect; we choose the specific pairs according to their predicted strain and band alignment, as well as their experimental relevance. While there are several common definitions of valley splitting, we select the difference between same-spin excitation energies at K vs. K'. Our first-principles calculations find a wide range of valley splittings from -26.7 to 9.8 meV, with strong dependence on both chemistry and stacking pattern. The largest valley splitting is obtained in a ferromagnetic interface which has unusually strong band hybridization between the two layers, and we analyze the possible effects of this hybridization. We identify several factors which can influence the sign and magnitude of the valley splitting.

"Strong Zeeman Splitting in Orbital-Hybridized Valleytronic Interfaces," Steven T. Hartman and Ghanshyam Pilania (in preparation).

2:45 PM EQ20.15.06

Organic-Polymer Coated Superacid-Treated Tungsten Disulfide with Air-Stable Strong Photoluminescence Intensity Takahiro Nakahara, Takeshi Yoshimura, Norifumi Fujimura and Daisuke Kiriya; Osaka Prefecture University, Japan

Monolayer transition metal dichalcogenides (TMDCs) have attracted attention as direct band-gap semiconductor materials consisting of three atomic thin-layer (0.7 nm thick). A near-unity photoluminescence (PL) quantum yield of a monolayer MoS₂ was demonstrated via treatment with a superacid molecular (bis(trifluoromethane)sulfonimide (TFSI)) under excitation laser intensity of 10⁻⁴~10⁻² W cm⁻² [1]. Recently, the superacid treatment followed by UV irradiation leads to strong photoluminescence with high yield [2]. In this study, we examined the same treatment on tungsten disulfide (WS₂), which has sulfur in its structure similar to MoS₂ and investigated the relationship between the superacid molecular treatment and UV light irradiation, as well as the dependence on the solvent to prepare the superacid solution. Furthermore, we achieved the air-stability of the superacid-treated WS₂ by coating with an organic polymer for more than 30 days.

A mechanically exfoliated monolayer WS₂ was immersed in 1 mg/mL superacid solution followed by UV light irradiation. PL measurements were performed for the samples as-exfoliated, TFSI-treated, and UV light irradiated after the TFSI-treatment. The as-exfoliated WS₂ shows strong PL intensity compared to MoS₂ cases, and the magnitude of the intensity is more than 300 times. The PL intensities of a monolayer WS₂ after the TFSI-treatment and the following UV light-irradiation were 7 times and 11 times enhancement, respectively, from the as-exfoliated sample. The magnitude of the enhancement was not as large compared to the previous MoS₂ cases [2], however, the PL intensity of the monolayer WS₂ of the treatment showed about 10 times stronger than that of MoS₂.

To further investigate the modulation of PL intensity of the monolayer WS₂, the solvent dependency of TFSI solution was investigated by comparing the hydrophobic 1,2-dichloroethane (DCE) and the hydrophilic acetonitrile. As a result, it was confirmed that the PL intensity of the hydrophilic acetonitrile was almost twice that of the hydrophobic DCE on average. This behavior would be due to the wettability of the acetonitrile solution of TFSI on WS₂.

We further achieved the stabilization of the strong photoluminescence of the superacid-treated WS₂ for more than 30 days in the air by coating with organic polymers. This behavior would be due to the physical separation of the TFSI molecules from the adsorption of H₂O molecules.

According to the above results, the combination of TFSI treatment and UV light irradiation results in strong photoluminescence enhancement in WS₂. In addition, the TFSI solution was prepared using hydrophilic acetonitrile as a solvent, which enabled us to investigate the optimal method for increasing the PL intensity in this system. We developed the stabilization of the strong photoluminescence of the superacid-treated WS₂ by coating with an organic polymer for more than 30 days in the air. In the presentation, we will discuss the detailed mechanism of air stability as well.

[Reference]

[1] M. Amani, D. H. Lien, D. Kiriya, et al., Science, 350, 1065, 2015.

[2] Y. Yamada, K. Shinokita, Y. Okajima, et al., ACS Appl. Mater. Interfaces, 2020, 12, 36496-36504.

SESSION EQ20.16: Twisted Layers and Moiré Superlattice

Session Chairs: Maria Hilde and Joshua Robinson

Monday Afternoon, December 6, 2021

EQ20-Virtual

4:00 PM *EQ20.16.01

The Magic of Moiré Materials Allan H. MacDonald; The University of Texas at Austin, United States

Two-dimensional crystals that are overlaid with a difference in lattice constant or a relative twist form a moiré pattern. In semiconductors and semimetals, the low-energy electronic properties of these systems are described by Hamiltonians with the periodicity of the moiré pattern, opening up a strategy to make artificial two-dimensional crystals with lattice constants on the ten nm scale. I refer to these artificial crystals as moiré materials. Because of their large lattice constants, the band filling factors of moiré materials can be electrically tuned over large ranges without introducing chemical dopants. Moiré materials, can be used to flexibly simulate the physics of real atomic scale crystals, and to create new states of matter. I will overview progress that has been made in understanding the low-temperature properties of twisted graphene and transition-metal dichalcogenide multilayers, the first moiré materials,

and provide a perspective on prospects for future room-temperature applications. My talk will emphasize the physics of broken spin/valley flavor symmetries including the frequent emergence of Chern insulator states, and moiré material ferromagnetism and superconductivity.

4:30 PM *EQ20.16.02

Direct Imaging of Wigner Crystal States in a WSe₂/WS₂ Moiré Superlattice Michael Crommie^{1,2,3}, Hongyuan Li¹, Shaowei Li^{1,3,4}, Mit H. Naik¹, Takashi Taniguchi⁵, Kenji Watanabe⁵, Sefaattin Tongay⁶, Alex Zettl^{1,2,3}, Steven Louie^{1,2} and Feng Wang^{1,2,3}; ¹University of California, Berkeley, United States; ²Lawrence Berkeley National Laboratory, United States; ³Kavli Energy NanoScience Institute, United States; ⁴University of California, San Diego, United States; ⁵International Center for Materials Nanoarchitectonics, Japan; ⁶Arizona State University, United States

Moiré superlattices in transition metal dichalcogenide (TMD) heterostructures host novel correlated quantum phenomena due to the interplay of narrow moiré flat bands and strong, long-range Coulomb interactions. One such phenomenon is the Wigner crystal, a 2D crystallization of electrons. Recent optical spectroscopy has provided evidence of generalized Wigner crystal states in TMD moiré superlattices (a generalized Wigner crystal is one in which the electrons can fractionally fill a lattice). Direct observation of 2D Wigner crystals in real space, however, has remained an outstanding challenge. Scanning tunneling microscopy (STM) in principle has sufficient spatial resolution to image a Wigner crystal, but conventional STM measurements perturb fragile Wigner crystal states in the process of measurement. Here I will discuss recent work where we have performed real-space imaging of 2D Wigner crystals in a WSe₂/WS₂ moiré heterostructure using a new non-invasive STM spectroscopy technique. This involves the use of a graphene sensing layer placed in close proximity to an occupied WSe₂/WS₂ moiré superlattice. The STM tunnel current into the graphene sensing layer is modified by the underlying electron lattice of the Wigner crystal in the WSe₂/WS₂ heterostructure. Our measurement directly visualizes different lattice configurations associated with Wigner crystal states at fractional electron fillings of $n = 1/3, 1/2$, and $2/3$, where n is the electron number per site (n is controlled by voltages that can be separately applied to both a top and a bottom gate). The $n=1/3$ and $n=2/3$ Wigner crystal states are observed to exhibit triangular and a honeycomb lattices, respectively, in order to minimize nearest-neighbor Coulomb interactions. The $n = 1/2$ state, on the other hand, spontaneously breaks the original C3 symmetry and forms a stripe structure in real space.

5:00 PM EQ20.16.03

Quantum Anomalous Hall Effect in Magic-Angle van der Waals Materials—Enabler of Cryogenic Memory Systems Shamiul Alam¹, Md Shafayat Hossain² and Ahmedullah Aziz¹; ¹University of Tennessee, Knoxville, United States; ²Princeton University, United States

The quantum anomalous Hall effect (QAHE) stems from the interplay between magnetism and the energy band structure of topological materials. The hallmark of QAHE is the precise quantization of Hall resistance at $\pm h/e^2$ ($h = \text{Planck's constant}$, $e = \text{charge of an electron}$) without an external magnetic field. Notably, QAHE features topologically protected, dissipation-less current channels along the edge of the sample, and thus can be of great interest for emerging electronic devices. However, there is no clear pathway to utilize QAHE at the device/circuit/system level. Recently, intrinsic QAHE has been observed in twisted bilayer graphene (tBLG) moiré heterostructure¹ and tri-layer graphene², where the well-defined QAH states can be tuned by applying a bias current. Leveraging this aspect, we propose and construct a cryogenic non-volatile memory system using tBLG moiré heterostructure³. We define the memory states ('1' and '0') with the two Hall resistance states ($\pm h/e^2$). We utilize the hysteretic dependence of Hall resistance on the bias current to write into the accessed cell. During a read operation, the Hall voltage of the accessed cell shows different polarities depending on the stored memory state. Finally, the polarity of the Hall voltage is sensed using a voltage comparator to decide the memory state stored in the accessed cell. The designed memory system can operate with ultra-low power because of the nano-ampere level of bias current requirement for switching between two Hall resistance states. To scale up, we design a memory array (similar to a 3D Cross-point array) with novel peripherals (accessing and sensing mechanism) to ensure the highest scalability, minimum leakage power, and to avoid accidental data manipulation. Thanks to its small cell size and simple peripherals, the designed QAHE based memory array promises to solve the scalability issue faced by the state-of-the-art superconducting memories. We believe, this work will provide a framework for realizing memory systems based on the emerging magic-angle Van der Waals materials for cryogenic applications.

References:

1. Serlin, M. *et al.* Intrinsic quantized anomalous Hall effect in a moiré heterostructure. *Science* **367**, 900–903. doi:10.1126/science.aay5533 (2020).
2. Chen, S. *et al.* Electrically tunable correlated and topological states in twisted monolayer–bilayer graphene. *Nat. Phys.* doi:10.1038/s41567-020-01062-6 (2020).
3. Alam, S. *et al.* A non-volatile cryogenic random-access memory based on the quantum anomalous Hall effect. *Sci. Rep.* doi:10.1038/s41598-021-87056-7 (2021).

5:15 PM EQ20.16.04

Orientation-Dependent Linear and Nonlinear Optical Properties in Layered 2D Materials Manpreet Boora, Geeta Sachdeva, Jae Yong Suh and Ravindra Pandey; Michigan Technological University, United States

Transition metal dichalcogenides (TMDs) of semiconductor band structures have recently emerged as a new family of two-dimensional (2D) materials. TMDs can have a tunable bandgap in the range of 1 – 3 eV, which enables their application in ultrathin field-effect transistors, sensors, and optoelectronic devices. Tungsten-based TMDCs such as WS₂ and WSe₂ have electronic states that support a strong interlayer coupling, and they exhibit an indirect-to-direct band gap transition when the number of layers decreases. After the discovery of magic angles in twisted graphene, it was found that electronic flat bands appeared for relatively small angles close to 0° and 60° in twisted bilayers of TMDs. We propose to explore the linear and nonlinear optical properties at these relatively small twist angles so that we could understand the optical physics behind the singularities appearing at these twist angles. At small relative twist angles, the stacking can generate the so-called Moiré excitons with Moiré patterns. The transitions of the Moiré excitons can be measured by photoluminescence spectroscopy, which enables the study of interlayer coupling effects. The electrical and optical properties of these stacks are significantly influenced by the twist angle, reflecting the modulated electronic band structure due to angle-dependent interlayer coupling. In our work, we use density functional theory (DFT) calculations on the electronic and optical properties of multilayer WS₂ and WSe₂. Calculations of the band structures, frequency-dependent dielectric function, and optical absorbance for mono, bi, and trilayers of WS₂ and WSe₂ shows that the optical properties strongly depend on the twist angles between two or more stacked layers. Also, many possible combinations of the crystal axes in bilayer TMDs, which cause a change in the symmetry, enable us to control the nonlinear properties. Based on DFT calculations, we propose to study the nonlinear optical properties of TMDs, such as second and third harmonic generations as a function of the number of layers and stacking orientation.

5:30 PM EQ20.16.05

Tuning Interlayer Coupling in Twisted Janus MoSSe/MoS₂ Heterostructures Kunyan Zhang¹, Yunfan Guo², Daniel Larson³, Ziyang Zhu³, Shiang Fang⁴, Efthimios Kaxiras³, Jing Kong² and Shengxi Huang¹; ¹The Pennsylvania State University, United States; ²Massachusetts Institute of Technology, United States; ³Harvard University, United States; ⁴Rutgers, The State University of New Jersey, United States

Interlayer coupling in van der Waals heterostacks governs a variety of optical and electronic properties. Janus transition metal dichalcogenides (TMDs), a newly emerged TMD with out-of-plane asymmetry, offers a simple and versatile approach to tune the interlayer coupling. Our previous work has

demonstrated that Janus MoSSe can enhance the interlayer coupling with MoS₂ by up to 13% compared to the corresponding TMD bilayers. Here, we employed Janus MoSSe to tune the interlayer phononic and intralayer excitonic properties of Janus MoSSe/MoS₂ by forming heterostructures with S/S and Se/S interfaces, in which the sulfur or selenium side of MoSSe is in contact with bottom MoS₂, and with twist angles between the in-plane crystalline axes. The S/S heterobilayer exhibited a stronger interlayer coupling than the Se/S heterobilayer as shown by low-frequency Raman modes. The stronger interlayer coupling was in agreement with the density-functional theory calculations and was explained by a smaller interlayer distance in S/S heterostructures. Besides, the intrinsic dipole at S/S and Se/S interfaces led to enhanced and reduced charge transfer and thus different intralayer exciton relaxation, respectively. Our work opens the avenue to manipulate the asymmetry of Janus TMD to tailor the van der Waals interfacial interactions.

5:45 PM EQ20.16.06

Late News: First-Principles Calculations of Minimally Twisted MoSe₂/WSe₂ Bilayers [Madeleine Phillips](#) and C. S. Hellberg; Naval Research Laboratory, United States

We present density functional theory (DFT) calculations of MoSe₂/WSe₂ bilayers twisted a small angle (~ 3°-5°) away from the commensurate 2H stacking. As the twist angle decreases, our calculations show the emergence of flat bands in both conduction and valence bands. The degeneracies of the flat bands suggest their origins in features of the 2H band structure. We also analyze the atomic relaxation of the twisted MoSe₂/WSe₂ bilayer away from the rigid moiré structure. While full reconstruction is not achieved at the angles we study, we begin to see the increase in area of regions of low energy stacking. We show that the states associated with the conduction and valence band flat bands are localized in different regions of local stacking. The localization of states is pronounced even though reconstruction is incomplete.

SESSION EQ20.17: Phase Modulation in Synthetic 2D Materials II

Session Chairs: Zakaria Al Balushi and Christopher Smyth

Monday Afternoon, December 6, 2021

EQ20-Virtual

6:30 PM EQ20.17.01

Gallium Sulfide as a Novel 2D Phase Change Semiconductor [Stefano Dicorato](#)^{1,2}; ¹Institute of Nanotechnology, CNR-NANOTEC, Italy; ²University of Bari "Aldo Moro", Italy

In recent years, phase-change materials (PCMs) have received increasing attention because of their unique properties, exploited in data storage/processing applications. PCMs require pronounced contrast in optical and/or electrical properties between two different structural state. Alternative PCMs to conventional chalcogenide alloys, containing Ge, Sb, and Te, (GST) are being extensively studied.

In the rising family of two-dimensional, 2D, materials, group (III) chalcogenides such as, GaS, Ga₂S₃, GaSe, GaTe, gallium sulfide, GaS is interesting as phase-change material in the optical range due to its wide bandgap of approximately 2.4 eV in the bulk form. GaS is a layered van der Waals semiconductor consisting in the stacking of covalently bond S-Ga-Ga-S atomic planes, where the successive tetralayers are held together via van der Waals forces. Few layers of GaS have successfully been produced by mechanical exfoliation, liquid exfoliation⁴, chemical vapor deposition (CVD), Atomic Layer Deposition (ALD), and used in field effect transistors (FET), near-blue light emitting devices, photodetectors², energy storage, gas sensing³, and in hydrogen evolution catalysis.

Here we present characteristics of few layers GaS grown by CVD. We establish the interplay between number of layers, from monolayers up to 10 layers, of GaS and its structural, optical and electrical properties. Those characteristics have been determined through an extensive characterization by Raman spectroscopy, run as a function of laser wavelength and number of GaS layers, scanning electron microscopy (SEM) used to image the morphology of the layers and count the number of layers, X-ray photoelectron spectroscopy to determine the chemical Ga:S ratio and hence, stoichiometry of the layers, spectroscopic ellipsometry used to determine the dielectric function and optical gap as a function of number of layers, as well as photoconductivity measurements also depending on number of layers.

The effect of thermal processing on those structural, compositional, opto-electronic properties is also thoroughly discussed for the first time to the best of our knowledge.

We also present results on 2D heterojunctions of GaS/graphene for blue-light photodetector, exploring different configurations of GaS/Graphene coupling. We also discuss the role of graphene electron transfer on the phase change dynamics of GaS. This study represents a step forward 2D phase change heterostructures.

Acknowledgement: This work has been supported by the European Union's Horizon 2020 research and innovation program under grant agreement no. 899598 – PHEMTRONICS.

6:45 PM EQ20.17.02

Tailoring the Optical and Electrical Properties of MoTe₂ via Electrochemical Intercalation of Lithium [Alyssa Shiyu Xu](#), Joshua Pondick, Mengjing Wang and Judy Cha; Yale University, United States

Intercalation of lithium ions is one of the most effective methods to realize structural transformation and to tune the optical and electrical properties of two-dimensional transition metal dichalcogenides (2D TMDs). Numerous studies have focused on the phase transition from semiconducting 2H phase to metallic 1T (or 1T') phase in MoS₂ and WS₂ induced by the intercalation of lithium ions. However, few reports explore the effects of lithium intercalation in other TMDs, such as Mo- or W- ditellurides. In particular, novel electronic and energy devices can be achieved using the lithium-intercalated MoTe₂ with its intriguing electrical, topological and catalytic properties. Density-functional theory (DFT) calculations suggest that lithium-adsorbed T'-MoTe₂ is thermodynamically more stable than H-MoTe₂ at the same electron-doped level and the energy barrier to trigger the H to T' phase transition for monolayer MoTe₂ should be less than that for monolayer MoS₂ or MoSe₂ by lithium intercalation. [1]

Here, we report electrochemical lithium intercalation into 2H- and 1T'-MoTe₂ flakes. We observe that intercalated lithium dopes electrons to 2H-MoTe₂, as evidenced by the downshift of the peak position and broadening of the full-width at half maximum (FWHM) of A_{1g} peak in Raman spectroscopy.

Further, the n-type doping of intercalated lithium to 2H-MoTe₂ is confirmed by the increase in conductivity of 2H-MoTe₂ with lithium intercalation. However, *in situ* Raman spectroscopy shows that 2H-MoTe₂ does not convert to 1T' phase by the intercalation of lithium ions, but directly breaks down to Mo metal clusters and lithium tellurides at an applied electrochemical voltage of 0.7 – 0.8 V. For 1T'-MoTe₂, the 1T' phase is stable down to 1.2 V of the applied electrochemical voltage, and a new phase is observed with no prominent Raman peaks between 0.8 – 1.1 V before becoming amorphous at 0.7 V. Our study thus suggests that, while calculations indicate that lithium-intercalated 1T'-MoTe₂ might be thermodynamically more stable than 2H phase, experimentally this is not realized. We hypothesize that this discrepancy is due to a high nucleation barrier of the 1T' phase, where the nucleation barrier

cannot be overcome by the applied electrochemical voltage at room temperature. Our results thus highlight the importance of phase transition pathways, in addition to the final phases at thermodynamic equilibrium, in intercalation-induced phase transitions in 2D TMDs.

[1] *Journal of Materials Chemistry C* **8**, 4432-4440

7:00 PM EQ20.17.03

Li-Intercalation-Induced Phase Transition in As_2P_3 Dinushika C. Vithanage, Manthila Rajapakse, Bhupendra Karki, Kazi Jannatul Tasnim, Ali Ibrahim Alzahrani, Usman Abu, Gamini Sumanasekera, Jacek Jasinski and Ming Yu; University of Louisville, United States

Layered As_2P_3 compounds were synthesized from red phosphorus and gray arsenic by chemical vapor transport growth method. A systematic study on electrochemical intercalation in As_2P_3 was carried out by both *in-situ* Raman scattering and *ex-situ* X-ray diffraction (XRD). A dedicated electrochemical cell under Galvanostatic discharge for *in-situ* Raman spectroscopy studies was used to study time evolution of vibrational modes under lithiation. During Lithium intercalation in As_2P_3 , an abrupt shift in characteristic Raman peak positions of As_2P_3 after $x = 0.06$ (in $\text{Li}_x(\text{As}_2\text{P}_3)_{1-x}$) was observed. At this degree of lithiation (x), an emergence of new peaks $\sim 200 \text{ cm}^{-1}$ and $\sim 406 \text{ cm}^{-1}$ were also observed. It is believed that an intercalation induced phase transition taking place at this specific intercalation level. *Ex-situ* XRD spectra also show evidence for different structural phases in the pristine alloy (before intercalation) and after intercalation beyond $x=0.06$. Raman shifts indicate competing effects of strain and charge transfer at the initial intercalation levels followed by structural reorganization before the phase transition. In the final stages of the intercalation, the entire process is governed by charge transfer.

7:15 PM EQ20.17.04

Heterointerface Control over Lithium-Induced Phase Transitions in MoS_2 Heterostructures Joshua Pondick, Aakash Kumar, Mengjing Wang, Sajad Yazdani, John Woods, Diana Qiu and Judy Cha; Yale University, United States

Phase transitions of two-dimensional (2D) materials and their heterostructures enable many applications including electrochemical energy storage, catalysis, and memory. These phase transitions are initiated by nucleation, and the transition pathways between phases are complex and heavily influenced by factors such as nanoscale confinement and interfaces. To effectively exploit these phase transitions for device applications, understanding the thermodynamics and kinetics of the nucleation pathways is essential; however, nucleation pathways remain virtually unexplored for many 2D transition metal dichalcogenides (TMDs) that have been demonstrated to undergo phase transitions.

Here we demonstrate that the lithium intercalation-induced 2H-1T' phase transition in the TMD MoS_2 proceeds via nucleation of the 1T' phase at a heterointerface by monitoring the phase transition of MoS_2 /graphene and MoS_2 /hexagonal boron nitride (*h*BN) heterostructures during intercalation with Raman spectroscopy *in situ*. We observe that graphene- MoS_2 heterointerfaces require an increase of 0.8 V in applied electrochemical potential to nucleate the 1T' phase in MoS_2 , while *h*BN- MoS_2 heterointerfaces do not. The increased nucleation barrier at graphene- MoS_2 heterointerfaces is due to the reduced doping power of lithium to MoS_2 at the heterointerface as lithium also dopes graphene based on *ab initio* calculations. Further, we show that the growth of the 1T' domain propagates along the heterointerface, rather than through the interior of MoS_2 . Our results provide the first experimental observations of the heterogeneous nucleation and growth of intercalation-induced phase transitions in two-dimensional materials and heterointerface effects on the phase transition.

7:30 PM EQ20.17.05

Energetics of Black $\text{As}_x\text{P}_{1-x}$ Alloy and the Effect of Li Intercalation Kazi Jannatul Tasnim, Md Rajib Khan Musa, Manthila Rajapakse, Dinushika C. Vithanage, Gamini Sumanasekera, Jacek Jasinski and Ming Yu; University of Louisville, United States

A methodical density functional theory calculation has been performed to understand the effect of alloying in stabilizing black $\text{As}_x\text{P}_{1-x}$ system and the role of Li intercalation on black $\text{As}_x\text{P}_{1-x}$ alloy. The structures of black $\text{As}_x\text{P}_{1-x}$ alloy were constructed by randomly substituting phosphorus (P) atoms with arsenic (As) atoms in the framework of the black phosphorus. Various distributions of As atoms for a given As concentration were considered and the constructed alloy systems were optimized within a full relaxation process which allows all the atoms fully relaxed with no restriction on the lattice symmetry and volume. It was found that in the energetically most stable black $\text{As}_x\text{P}_{1-x}$ alloys, both As and P atoms prefer to forming armchair As-As and P-P bonds, aligning along zigzag direction. Due to the larger atomic size of As, a local distortion was found after the release of the local strain. The in-plane lattice constants (a and c) and the volume approximately follow the Vegard's law, but the vertical lattice constant (b) shows a fluctuation as the function of As concentration. The Li interaction has been performed on $\text{Li}_x(\text{As}_{0.375}\text{P}_{0.625})$ system. Our results show that a structural transformation occurs under the Li intercalation. With increasing Li concentration, the AB stacking of black $\text{As}_{0.375}\text{P}_{0.625}$ flipped from symmetric to antisymmetric ordering, then the lattice transferred from orthorhombic to rhombohedral, and a bond-breaking happened with an assembly of buckled rhombohedral nanoribbons and zigzag chains. This study pointed out that Li atoms intercalated in black $\text{As}_{0.375}\text{P}_{0.625}$ could act as 'catalyst' in a local structural transformation, indicating a possible pass way for structural phase transition and even a discovery of novel materials.

7:45 PM EQ20.17.06

Competing Forces Behind Charge Density Wave in Transition Metal Dichalcogenides Mohammad Saeed Bahramy; University of Manchester, United Kingdom

Charge density wave (CDW) is one of the most common, yet least understood, quantum phenomena in condensed matter physics. Occurring in metallic systems, it forms a new ordered state with a distorted lattice structure and modulated charge density distribution. Astonishingly, these modulations emerge in various patterns with disparate dimensional characteristics, even within the same family of materials. In this talk, I propose a general framework [1], that helps us to unify distinct trends of CDW instability. To show this, I focus on an isoelectronic group of transition metal dichalcogenide, $2H\text{-MX}_2$ ($M=\text{Nb}$, Ta and $X=\text{S}$, Se) which are best known for their puzzling CDW orderings. For example, while NbSe_2 exhibits a strongly enhanced CDW order in two dimensions, TaSe_2 and TaS_2 behave oppositely, with CDW being absent in NbS_2 entirely. Combining Raman scattering spectroscopy with first-principles calculations, I show that such a disparity arises from a competition of ionic charge transfer, electron-phonon coupling, and electron correlation. Despite its simplicity, the approach presented here, in principle, explain dimensional dependence of CDW in any material, thereby shedding new light on this intriguing quantum phenomenon and its underlying mechanisms.

[1] D. Lin, S. Li, J. Wen, H. Berger, L. Forró, H. Zhou, S. Jia, T. Taniguchi, K. Watanabe, X. Xi, M. S. Bahramy, *Nature Communications* **11**, 2406 (2020).

8:00 PM EQ20.17.07

Highly Anisotropic Properties of $(\text{PbSe})_{1+\delta}(\text{VSe}_2)_{1,2}$ 2D Layered Rotationally Disordered Charge Density Wave Heterostructures Yu Wang¹, Danielle Hamann², Dmitri Cordova², Marisa Choffel², Zhi Cai¹, Evguenia Karapetrova³, Li Shi⁴, David Johnson² and Stephen Cronin¹; ¹University of Southern California, United States; ²University of Oregon, United States; ³Argonne National Laboratory, United States; ⁴The University of Texas at Austin, United States

We explore the effect of charge density wave (CDW) phase transition on the in-plane and cross-plane properties of $(\text{PbSe})_{1+\delta}(\text{VSe}_2)_1$ and $(\text{PbSe})_{1+\delta}(\text{VSe}_2)_2$ heterostructures. For in-plane transport measurements of $(\text{PbSe})_{1+\delta}(\text{VSe}_2)_1$, we observe an abrupt 86% increase in the Seebeck coefficient, 245% increase in the power factor, and a slight decrease in resistivity before and after the CDW transition. This phenomenon is not observed in $(\text{PbSe})_{1+\delta}(\text{VSe}_2)_2$ and is highly unusual compared to the general trend observed in other materials. The abrupt transition shows a deviation from the Mott relationship through electron-electron and electron-phonon interactions. Raman spectra analysis of the $(\text{PbSe})_{1+\delta}(\text{VSe}_2)_1$ material shows the emergence of additional peaks associated with CDW transition in VSe_2 material. Temperature-dependent in-plane X-ray diffraction (XRD) spectra show a change in the in-plane thermal expansion coefficient of VSe_2 layers in $(\text{PbSe})_{1+\delta}(\text{VSe}_2)_1$ due to lattice distortion. The increase in the power factor and a slight decrease in the resistivity due to CDW suggest a potential mechanism for enhancing the thermoelectric performance at the low temperature region. Anisotropic transport measurements of $(\text{PbSe})_{1+\delta}(\text{VSe}_2)_1$ show 4 orders of magnitude differences between cross-plane and in-plane resistivities over the entire measured temperature range (77 - 300 K). There is a 30% change for cross-plane resistivity of $(\text{PbSe})_{1+\delta}(\text{VSe}_2)_1$ during the measured temperature range, while the change of in-plane resistivity is only less than 8%. The designed measurement platform can be generalized to explore anisotropic properties of various 2D layered heterostructures.

8:05 PM EQ20.17.08

Vapor Phase Intercalation of Cesium into Black Phosphorous Usman Abu, Md Rajib Khan Musa, Manthila Rajapakse, Bhupendra Karki, Dinushika Chathurani Vithanage, Yu Ming, Gamini Sumanasekara and Jacek Jasinski; University of Louisville, United States

Among the bulk of post-graphene 2D layered materials, black phosphorous (BP) has attracted much attention since the isolation of its layers in 2014 because of its exotic properties which include: high carrier mobility, in-plane anisotropy, and thickness-dependent bandgap. Intercalation has been used to expand the versatility of BP by tuning its properties and inducing structural phase transitions for diverse applications. This happens by introducing foreign atoms (intercalants) into the van der Waals (vdW) gaps of BP. There have been past attempts to understand the underlying mechanism of intercalation in BP using different intercalants and intercalation strategies. Herein, we carry out an ex-situ study of the structural evolution and an in-situ study of the electrical transport properties of BP as it is intercalated with cesium (Cs) in the vapor phase. The Raman studies of Cs-intercalated and pristine BP indicates a redshift of its characteristic vibrational modes (A^1_g, B_{2g} and A^2_g) relative to the pristine ones where B_{2g} and A^2_g modes shifted 1.3 times faster than A^1_g mode; reinforcing the established preference of alkali ions to intercalate in the in-plane direction (arm-chair and zig-zag) of BP rather than the out-of-plane direction while the x-ray diffraction (XRD) patterns of Cs-intercalated BP suggest weakening vdW interactions between BP layers. Scanning electron microscopy (SEM) was done to quantify the amount of Cs intercalated into BP while x-ray photoelectron spectroscopy (XPS) was used to analyze the chemistry of these samples. Density functional theory (DFT) calculations were also carried out to help explain experimental findings.

8:10 PM EQ20.17.09

Origins of Charge Density Wave Sliding-Based Switching in Layered 1T-TaS₂ Materials from First Principles Vishal Ravi¹, Sophie Weber², Jonah B. Haber^{2,1}, Eran Maniv^{2,1}, Shannon Haley^{2,1}, James G. Analytis^{2,1} and Jeffrey Neaton^{2,1,3}; ¹University of California, Berkeley, United States; ²Lawrence Berkeley National Laboratory, United States; ³Kavli Energy NanoScience Institute at Berkeley, United States

Layered van der Waals materials, in particular transition metal dichalcogenides (TMDs) exhibit a wide variety of exotic electronic and photophysical phenomena, such as non-trivial topology and valleytronics [1]. These desirable properties, combined with their quasi-two-dimensional nature, make TMDs particularly attractive as candidate materials for nanoscale non-volatile logic and memory devices. The TMD 1T-TaS₂ is particularly promising for device applications due to its rich phase diagram, including multiple distinct charge density wave (CDW) phases, all of which can be manipulated by electromagnetic perturbations. Specifically, 1T-TaS₂ exhibits multiple distinct charge density wave (CDW) phases. We focus on the low-temperature, commensurate CDW phase which manifests as an in-plane Star of David-type deformation of the tantalum sublattice. An additional degree of freedom arises from numerous metastable stacking configurations of the adjacent CDW layers. The onset of the Star of David CDW transforms the material's electronic structure at low temperatures [2] in a way that enables a metal-insulator transition upon cooling through a critical temperature. Within this low-temperature, insulating CDW phase, recent experiments have demonstrated that 1T-TaS₂ can be switched between states of high and low resistance by application of orthogonal current pulses. While anisotropic switching has been observed in thin-film flakes in the insulating state at low temperatures [3], this behavior arises even in the 3D limit, although the role played by the interlayer stacking on the nature of the CDW phase and switching is unknown. Motivated by previous calculations demonstrating the dramatic effect of CDW stacking on the electronic structure of 1T-TaS₂, we investigate the hypothesis that the resistivity switching may be caused by a current-induced change in the CDW stacking sequence using first-principles density functional theory calculations. For a number of stacking sequences, we examine the computed band structure's anisotropy in connection with the possible dynamics and mechanisms of CDW movement, and we propose a model for the nature of 2D CDW sliding, identifying low-energy pathways for CDW motion. Using this detailed information, we construct a quantitative hypothesis to explain the switching behavior observed experimentally [4]. Our work leads to new understanding of CDWs in layered van der Waals materials and their dynamics, and could reveal novel energy-efficient routes for the electric field control of logic and memory for the next generation of switching devices. [1] Manzeli, S., Ovchinnikov, D., Pasquier, D. et al. 2D transition metal dichalcogenides. *Nat Rev Mater* 2, 17033 (2017). <https://doi.org/10.1038/natrevmats.2017.33> [2] Ritschel, T., Trinckauf, J., Koepf, K. et al. Orbital textures and charge density waves in transition metal dichalcogenides. *Nature Phys* 11, 328–331 (2015). <https://doi.org/10.1038/nphys3267> [3] Svetin, D., Vaskivskiy, I., Brazovskii, S. et al. Three-dimensional resistivity and switching between correlated electronic states in 1T-TaS₂. *Sci Rep* 7, 46048 (2017). <https://doi.org/10.1038/srep46048> [4] Maniv, E., Haley, S., Analytis, J. G., Metastable Slidetric Switching in Bulk 1T-TaS₂, unpublished work.

8:25 PM BREAK

SESSION EQ20.18: Ferroelectricity and Magnetism in 2D Materials

Session Chairs: Li Lain-Jong and Hyeon Jin Shin

Monday Afternoon, December 6, 2021

EQ20-Virtual

9:00 PM *EQ20.18.01

Layer Dependent and Air Stable Ferromagnetism in Atomically Thin van der Waals CrPS₄ Jieun Lee; Seoul National University, Korea (the Republic of)

Ferromagnetism in two-dimensional materials presents a promising platform for the development of novel ultrathin spintronic devices with new functionalities. Recently discovered ferromagnetic van der Waals crystals such as CrI₃, readily isolated two-dimensional crystals, are highly tunable

through external fields or structural modifications. However, there remains a challenge because of material instability under air exposure. In this talk, we report the observation of a new air stable and layer dependent ferromagnetic (FM) van der Waals crystal, CrPS₄, using magneto-optic Kerr effect microscopy. In contrast to the antiferromagnetic (AFM) bulk, the FM out-of-plane spin orientation is found in the monolayer crystal. Furthermore, alternating AFM and FM properties observed in even and odd layers suggest robust antiferromagnetic exchange interactions between layers. The observed ferromagnetism in these crystals remains resilient even after the air exposure of about half a day, opening a door to the practical applications of van der Waals spintronics.

9:30 PM EQ20.18.02

Late News: Thickness and Spin Dependence of Raman Modes in 2D Magnetic Fe₃GeTe₂—A First-Principles Study [Liangbo Liang](#), Xiangru Kong and Tom Berlijn; Oak Ridge National Lab, United States

Two-dimensional (2D) layered magnetic materials have attracted increasing attention after the 2D ferromagnetic order was first discovered in chromium compounds such as CrI₃ and Cr₂Ge₂Te₆. The family of 2D magnets continues to grow larger and larger: in addition to insulating CrI₃ and Cr₂Ge₂Te₆, Fe₃GeTe₂ as a 2D magnetic metal has also joined the family. The outstanding physical properties in Fe₃GeTe₂ demonstrate its potential values in fundamental research and future applications. Before any practical applications of 2D magnets, the lattice vibrations (i.e., phonons), the magnetic orders (i.e., spins), and their coupling need to be understood first. Raman spectroscopy is among the most fast and reliable experimental techniques that can probe both phonons and spins in 2D magnetic materials. To explain and guide experimental Raman measurements, first-principles modeling of Raman scattering based on density functional theory (DFT) is often required. Here, I will highlight a recent Raman modeling-driven project on Fe₃GeTe₂ [1]. Its phonon vibrations and Raman intensities were calculated from the bulk to the monolayer. The spin-phonon coupling effect was investigated by considering different interlayer magnetic orders: ferromagnetic and antiferromagnetic. The frequencies of Raman modes in Fe₃GeTe₂ were found to exhibit considerable dependence on both the layer number and spin order. The results not only reveal the notable spin-phonon interactions in Fe₃GeTe₂, but also demonstrate that Raman modes can be utilized for characterizing the sample thickness and interlayer magnetic order in Fe₃GeTe₂.

References

[1] X. Kong, T. Berlijn, **L. Liang***, “Thickness and spin dependence of Raman modes in magnetic layered Fe₃GeTe₂”, *Advanced Electronic Materials*, 2001159 (2021).

9:45 PM EQ20.18.04

Origin and Stabilization of Ferrielectricity in Layered Thiophosphates—A First-Principles Case Study of CuInP₂Se₆ [Nikhil Sivadas](#), Peter Doak and Panchapakesan Ganesh; Oak Ridge National Laboratory, United States

Recently, ferroelectricity in layered materials “*beyond graphene*” has attracted a lot of attention because of its applications in high-density nonvolatile memory devices. However, very few layered materials demonstrate switchable out-of-plane polarization. Of them, the transition metal thiophosphates are a promising family of *beyond graphene* materials that host out-of-plane ferrielectricity (FiE) with large values of polarization [1-2]. Further, research efforts in these materials have reported a plethora of properties including negative piezoelectricity, negative electrostriction, large dielectric tunability, and unconventional field-induced switching behavior, all of which depend strongly on the polarization [3-5]. Despite the growing interest, a clear understanding of the origin and stabilization of the polar phase is still lacking in transition metal thiophosphate.

Using first-principles calculations and group-theoretical methods, we study the origin and stabilization of FiE in CuInP₂Se₆ [6]. We find that the polar distortions of metal atoms create most of the polarization in the FiE phase. Surprisingly, the stabilization of the FiE phase comes from an anharmonic coupling between the polar mode and a fully symmetric Raman-active mode comprising primarily of the Se atoms. This coupling is large, with the degree of anharmonicity is comparable to improper ferroelectrics. Thus, the origin of polarization is different from the factors that stabilizes the FiE phase in CuInP₂Se₆, unlike conventional ferroelectrics. Our results open possibilities for dynamical control of the single-step ferroelectric switching barrier by directly tuning the Raman-active mode. These finding has important implications not only for designing next-generation microelectronic devices that can overcome the voltage-time dilemma [7] but also in understanding the emergent responses in these materials.

[1] V. Misonneuve et al., *Phys. Rev. B* **56**, 10860 (1997).

[2] F. Liu et al., *Nat. Comm.* **7**, 12357 (2016).

[3] A. Dziazgys et al., “Piezoelectric domain walls in van der Waals antiferroelectric CuInP₂Se₆”, *Nat. Comm.* **11**, 3623 (2020).

[4] J. A. Brehm et al., “Tunable quadruple-well ferroelectric van der Waals crystals”, *Nat. Mat.* **19**, 43 (2020)

[5] Y. Qi and A. M. Rappe, *Phys. Rev. Lett.* **126**, 217601 (2021).

[6] N. Sivadas et al., “Origin and stabilization of ferrielectricity in CuInP₂Se₆”, arXiv:2106.08783

[7] T. Schenk et al., *Reports on Progress in Phys.* **83**, 086501 (2020).

10:00 PM EQ20.18.05

MnPS₃—A Different Twist on 2D Materials [Kevin Roccapriore](#)¹, Nan Huang², Vinit Sharma^{1,2}, David G. Mandrus^{1,2} and Sergei V. Kalinin¹; ¹Oak Ridge National Laboratory, United States; ²The University of Tennessee, Knoxville, United States

Owing to dimensionality constraints, two-dimensional materials are of great interest for a number of different applications ranging from nanophotonics and plasmonics to mechanics and nanoelectronics.^{1,2} Much focus has been on the ubiquitous graphene, as well as transition metal dichalcogenides,³ where several applications and unique physics have been uncovered.⁴ Recently, the emergent field of twistrionics has enabled tremendous functionality based on twist angle between two single atomic layers.^{5,6} Consequently, a great number of alternative materials have been overlooked and is arguably a source of many missed opportunities.

Here we explore the electronic and structural properties of MnPS₃ using scanning transmission electron microscopy (STEM) and monochromated electron energy loss spectroscopy (EELS). Previous work on MnPS₃ has largely considered it as a candidate for an antiferromagnetic 2D magnet by studying its magnetic ordering.^{7,8} Through electron microscopy, we find that compared to other layered materials, MnPS₃ is a host for several unique characteristics. We focus on two of these phenomena that we have recently discovered by STEM-EELS in which both great utility and distinct physics reside.

One of the most striking behaviors of MnPS₃ is its sensitivity to electron beam irradiation. The effect this has on the crystal structure of MnPS₃, however, is remarkable, and to our knowledge, is the first time such an effect has been observed. By electron beam irradiation, we observe the spontaneous formation of Moiré patterns with varying length scales. In effect, the electron beam in the STEM provides a modification tool that selectively induces the formation of Moiré patterns. Moreover, several degrees of freedom are present in this capability and consequently several Moiré wavelengths can be produced by the electron beam. We consider different mechanisms of Moiré pattern formation, explore the electronic property changes of the modified material as measured by STEM-EELS, as well as discuss possible applications this holds.

A second property of MnPS₃ of potential great interest to the nanophotonics community lies in its support of localized plasmon resonances. Particularly, we find through hyperspectral STEM-EELS analysis that an edge plasmon near 5 eV is supported in varying number of layers. Crucially, the localization length of the edge plasmon is on the order of two-unit cells – i.e., it is extremely confined, and at the same time is relatively strong. Moreover, due to the

electron beam sensitivity of MnPS₃, edges can be engineered at will by controlling the position and dose of the electron beam, paving the way toward quantum nanophotonic and plasmonic applications. We discuss the plasmonic behavior of the system and suggest its candidacy as a nanophotonic waveguide and emitter.

1. A.N. Grigorenko *et al. Nature Photon* **2012** 6, 749–758.
2. D. Akinwande, *et al. Extreme Mechanics Letters* **2017** 13, 42–77.
3. Y.P.V. Subbaiah *et al. Adv. Funct. Mater.* **2016** 26, 2046–2069.
4. A. Splendiani *et al. Nano Lett.* **2010** 10, 1271–1275.
5. S. Carr *et al. Phys. Rev. B* **2017** 95, 075420.
6. Y. Cao *et al. Nature* **2020** 583, 215–220.
7. Y.-J. Sun *et al. J. Phys. Chem. Lett.* **2019** 10, 3087–3093.
8. G. Long *et al. Nano Lett.* **2020** 20, 2452–2459.

This effort is based upon work supported by the U.S. Department of Energy (DOE), Office of Science, Basic Energy Sciences (BES), Materials Sciences and Engineering Division.

10:15 PM *EQ20.13.02

Twistronics with Real Time Control [Cory Dean](#); Columbia University, United States

The ability to isolate atomically thin crystals, such as graphene, boron nitride, and the transition metal dichalcogenides, and then mechanically layer them to form new heterostructures has driven a recent revolution in materials design. These layered structures are held together by weak van der Waals forces, rather than chemical bonding making it possible to readily mix and match 2D materials spanning a wide range of properties, virtually at will. More recently it has been demonstrated that the weak interlayer coupling also makes it possible to arbitrarily tune the rotation angle between adjacent layers and that varying this twist angle can lead to dramatic transformations in electronic, optical and magnetic of the combined heterostructure. Exploiting this new degree of freedom, which has been termed twistronics, has already revealed remarkable new opportunities with twisted layered structures demonstrating the ability to tune through metallic, insulating, semiconducting, semimetal, magnetic, superconducting, and topological behaviour by simply varying the twist angle. So far the vast majority of studies have reported static devices, where the twist angle is established during the fabrication process such that each device represents a single twist angle. However the weak interlayer bonding means that it is possible to realize devices where the twist angle can be dynamically varied post-fabrication. Here I will discuss our ongoing efforts to develop improved in-situ control with the goal towards realizing fully tunable devices structures consisting of just two atomic layers. I will discuss recent progress in terms of mechanical rotation of individual monolayers, improved understanding of interfacial dissipation mechanisms, implementation of in-situ feedback of twist angle and new approaches towards developing non-mechanical control of the heterostructure geometry at the nanoscale. Prospects for realizing functional twistronic devices with real-time in-situ control will be discussed.

10:45 PM BREAK

SESSION EQ20.19: Device Transport in 2D Materials
Session Chairs: Nadire Nayir and Hyeon Jin Shin
Tuesday Morning, December 7, 2021
EQ20-Virtual

8:00 AM *EQ20.19.01

Pinning-Free Metal Contacts to MoS₂ Monolayers for FET Applications [Li Lain-Jong](#); University of Hong Kong, Hong Kong

Two dimensional materials (2D) have desirable properties such as high mobility at an atomic thickness, superior electrostatic control, and potential for low-power electronics. Forming a low resistance contacts to 2D such as MoS₂ is one key challenge for realizing 2D electronics. The presence of Schottky barrier height (SBH), associated with the metal-induced gap states (MIGS), limits the contact performance. In a top contact geometry, we find that the semimetallic bismuth contacted to MoS₂ monolayers lead to a pinning-free Ohmic contact. A record-low contact resistance (RC) of 123 Ω μm is achieved. For the edge contact geometry, Fermi-level pinning-free Ni-MoS₂ edge contact transistor devices are obtained using in-situ etching and metal deposition. We conclude that the edge contact fabrication processes strongly affect the electrical characteristics such as Schottky barrier height where the in-situ process gives the best performance and pinning-free characteristics.

8:30 AM *EQ20.19.02

Drawing Devices on Paper with van der Waals Materials [Andres Castellanos-Gomez](#); Spanish National Research Council, Spain

A big chunk of the price tag of electronic components is due to the cost of silicon wafer substrates. Although silicon is a highly abundant and cheap element, the transformation and processing from the raw material into high quality silicon wafers results very costly. In fact, the cost of silicon substrates constitutes ~1/3rd of the total cost of a memory chip and about ~1/10th of the cost of a high-end state of the art micro-processor. The societal, industrial and technological demands of ultra-low-cost electronic components has spurred the quests towards lower cost substrates. This has motivated a surge of works on paper-based electronics in the last years. In fact, paper substrates cost (~0.1 €/m²) is orders of magnitude lower than that of polymer substrates (PET ~2 €/m² and PI ~30 €/m²) and crystalline silicon (~1000 €/m²).

Despite the promises of paper-based electronics, there are several challenges to be solved. One of the major challenges is that the rough, fiber-based structure of paper makes it impossible to fabricate devices using conventional lithographic techniques. In this talk I will discuss our last works to integrate different van der Waals materials onto standard paper substrates [1-4].

- [1] J Azpeitia *et al. Materials Advances* (2021)
- [2] W Zhang *et al. Applied Materials Today* (2021) 23, 101012
- [3] M Lee *et al. Nanoscale* (2020) 12 (43), 22091-22096
- [4] A Mazaheri *et al. Nanoscale* (2020) 12 (37), 19068-19074

9:00 AM EQ20.19.03

Unlocking the Potentials of Emerging Two-Dimensional Materials for Electronic and Optoelectronic Devices Mohammed Amer; University of California, Los Angeles, United States

Devices based on 2-Dimensional materials have been extensively investigated in recent years. Reasons such as superior electrical, optical, thermal, and mechanical properties have made these materials attractive for the next generation of devices. Yet, the realization of these 2D devices is still hindered by many challenges including a comprehensive understanding of the electrical and optical characteristics of 2D materials. In this talk, I will discuss our recent work carried out on different 2-D devices. First, I will discuss our recent development of our new pulsed thermal annealing technique to produce a controlled and tunable light emission from black phosphorus nanosheet. This tunable light emission exhibits a wide bandwidth reaching up to 110nm. This wide bandwidth has been found to be caused by the formation of black phosphorus oxide, which exhibit a direct bandgap that can cause radiative processes at room temperature.

Second, I will demonstrate our recent work on Hafnium Diselenide (HfSe₂), an emerging 2D material that exhibit a bandgap of ~1.1eV which is analogous to silicon. I will show how HfSe₂ can exhibit conductivity switch using deterministic laser induced methods. This conductivity switch has been observed in both phases of HfSe₂ (1T and 2H). This conductivity switch has been attributed to an increase in the Schottky barrier height at the contacts, which pushes the Fermi level closer to the valance band, causing the observation of this conductivity switch.

Moreover, I will discuss our recent results obtained on Germanium Sulfide devices. Due to its similar structure to black phosphorus, GeS can be a promising material for device applications. Yet, GeS based devices are facing a major challenge due to the high contact resistance obtained. I will demonstrate our new method of 2D doping of GeS that exhibit an intentional conductivity switch from *p*-type to *n*-type with a conductivity enhancement reaching more than 10 folds. Our technique relies on deterministic deposition of degradable black phosphorus nanosheets which chemically interacts with GeS channel. We also observe a striking Negative Differential Resistance (NDR) accompanied during the transient doping of GeS devices. We characterize these devices and show that this NDR behavior is caused by partial doping in the transient state, which creates resonant tunneling paths causing the observation of this remarkable NDR behavior.

Finally, I will discuss our recent fabrication work on exfoliated Tellurene nanosheets for device applications. This material which exhibits superior thermoelectric and optoelectronic properties, is facing a major exfoliation challenge. Previous work has demonstrated solution processing technique to obtain few layers Te nanosheets. Yet, additive chemicals during liquid exfoliation may impose a potential risk in altering the pristine nature of Tellurene. I will demonstrate Tellurene thinning using specific oxygen annealing technique. Morphology measurements show a favorable thinning direction which is attributed to the anisotropy of the material. This thinning method can be a stepping milestone towards pristine few layers Tellurene devices. Our results demonstrate promising future for 2D materials to be used in device applications.

9:15 AM EQ20.19.04

Unraveling the Effect of Defects, Domain Size and Chemical Doping on Photophysics and Charge Transport in Covalent Organic Frameworks Raja Ghosh; University of California, San Diego, United States

Understanding the underlying physical mechanisms that govern charge transport in two-dimensional (2D) covalent organic frameworks (COFs) will facilitate the development of novel COF-based devices for optoelectronic and thermoelectric applications. In this context, the low energy mid-infrared absorption contains valuable information about the structure-property relationships and the extent of intra- and inter-framework "hole" polaron delocalization in doped and undoped COF structures. A theory describing the spatial coherence length of polarons in disordered COFs is presented, revealing a simple relationship between the oscillator strength of the mid infrared absorption band and the polaron coherence function. Emphasis is placed on the fundamental nature and origin of the components polarized along the intra- and inter-framework directions and their dependence on the spatial distribution of disorder as well as the position of the dopant counter-anion relative to the framework. The Hamiltonian, represented in a multiarticle basis set,¹ has been successful in quantitatively reproducing recently measured spectra recorded in doped COF films and our analysis provides conclusive evidence of why iodine doped COFs have so far shown lower bulk conductivity compared to doped polythiophenes.² Finally, we propose new research directions to address existing limitations and improve charge transport in COFs for applications in functional molecular electronic devices.

1. Raja Ghosh and Frank C. Spano, "Excitons and Polarons in Organic Materials", *Acc. Chem. Res.* 2020, 53, 10, 2201–2211

2. Raja Ghosh and Francesco Paesani, "Unraveling the Effect of Defects, Domain Size, and Chemical Doping on Photophysics and Charge Transport in Covalent Organic Frameworks", *Chem. Sci.* 2021, 10.1039/d1sc01262b

9:30 AM EQ20.19.05

Effect of Surface Functional Groups on MXene Conductivity Rabi Khanal and Stephan Irlle; Oak Ridge National Laboratory, United States

MXenes are a rapidly developing class of two-dimensional materials with suitable properties for use in emerging electrochemical energy storage devices, including batteries and supercapacitors. The chemical synthesis of MXene leads to the surfaces being functionalized with different functional groups (O, OH, and F). Since MXene layers are only atomically thin, such surface functionalities can play an essential role in the electrical conductivity of MXene. Conductivity is a key for both the transport and storage of ions in MXene during their energy applications. While there are some experimental studies on the electrical conductivity of MXene, theoretical conductivity studies are rare. Investigations of charge carrier transport in MXene nanowires necessarily involves calculations with hundreds of atoms at the quantum level, which typically requires extraordinary computational resources. Complications due to the surface structure variability increases with model system size and increasing numbers of functional groups. The density-functional tight-binding (DFTB) approach enables the treatment of complex systems with several hundred to thousands of atoms at the quantum level at reduced computational cost with good accuracy compared to DFT. In this study, we use DFTB calculations with the nonequilibrium Green's functions (NEGF) technique to calculate in-plane transport in the MXenes (i.e., within the MXene layers) as a function of composition. All MXene compositions were found to show a linear relationship between current and voltage at lower potentials, indicating their metallic character. However, their I-V curves, i.e., conductivity, show different trends among different compositions. MXenes without any surface terminations (Ti₃C₂) show higher conductivity compared to MXenes with surface functionalization (Ti₃C₂O₂ and Ti₃C₂(OH)₂). Among the MXenes with O and OH termination, MXenes with O surface termination have lower conductivity than OH surface termination. Conductivity changes with the ratio of O and OH on the MXene surface. I-V curves and their conductivities correlate with transmission functions and the electronic density of states (DOS) around the Fermi level. The surface composition-dependent conductivity of the MXenes provides a path to tune their conductivity for enhanced pseudocapacitive performance.

Acknowledgment: This material is based upon work supported by the Fluid Interface Reactions, Structures and Transport (FIRST) Center, an Energy Frontier Research Center funded by the U.S. DOE Office of Science. The research used resources of the National Energy Research Scientific Computing Center (NERSC), a U.S. Department of Energy Office of Science User Facility operated under Contract No. DE-AC02-05CH11231.

9:45 AM EQ20.19.06

Layer-Number Dependence of Metallic Transport Behavior in MoS₂ by Molecular Charge Transfer Doping [Keigo Matsuyama](#), Takeshi Yoshimura, Norifumi Fujimura and Daisuke Kiriya; Osaka Prefecture University, Japan

Transition metal chalcogenides (TMDCs) are two-dimensional semiconductor materials with a thickness of ~0.7 nm at the monolayer limit. A carrier modulation method of TMDCs is surface charge transfer doping by a junction with other materials such as potassium, Cs₂CO₃, and polyvinyl alcohol, etc. [1] One of the strongest modulating agents is the molecular benzyl viologen (BV) [1,2]. In previous work, BV-molecular treated MoS₂ showed degenerate semiconducting behavior without electrostatic gate-dependence in the metal-oxide-semiconductor field-effect-transistors (MOSFETs). However, the device characteristics of the organic BV-doped TMDC MOSFET have not been characterized sufficiently, and the metallic behavior by the molecular-doped has not been examined yet. The metallic behavior should be analyzed from the temperature-dependent transport behavior. In this study, we demonstrate the temperature and magnetic-field dependence of the monolayer and multilayer MoS₂ MOSFETs and characterize the behavior of the organic BV-treated MoS₂ as the metallic state and discuss the conduction mechanism of the device.

We fabricated back-gated MOSFET using monolayer and multilayer (~10 nm thick) MoS₂ flakes on Si/SiO₂ substrate and carefully measured the transport properties in the temperature range from cryogenic (~2K) to room temperature. The conductance of the device increased with decreasing the temperature in both monolayer and multilayer devices without applying gate-voltage. Therefore, the BV-doped MoS₂ obviously transformed from a semiconductor to a metallic situation.

As expected from the temperature-dependency of the BV-doped MoS₂ MOSFET, the transfer characteristic curves of BV-treated devices showed a gate-independent behavior with an ON/OFF ratio of ~10¹ in both monolayer and multilayer devices at room temperature. We further analyzed the gate- and temperature-dependency of the MOSFETs of monolayer and multilayer MoS₂ MOSFETs. In the case of monolayer MoS₂ MOSFET, the conductance just increases with decreasing the temperature even applying negative gate-voltage. On the other hand, the conductivity in the multilayer sample decreases under the negative gate-voltage with decreasing the temperature, therefore, the transport mechanism would be different in the monolayer and multilayer samples. To discuss further the details of the transport behavior, we focused on the contact resistance of the BV-doped devices. Monolayer MoS₂ MOSFET shows small gate-dependency of the contact resistance, therefore, the direct current path between the electrode and MoS₂ channel would be constructed. On the other hand, the multilayer MoS₂ device showed a large dependence of the gate voltage, this may be attributed to the additional carrier conduction under the multilayer MoS₂. In the presentation, we will discuss the details of the transport behaviors.

[Reference]

- [1] P. Luo *et al.* Nanoscale Horiz., 4, 26-51 (2019).
- [2] D. Kiriya *et al.* J. Am. Chem. Soc. 136, 7853-7856 (2014).
- [3] K. Matsuyama *et al.* ChemistryOpen, 8, 908-914 (2019).

9:50 AM EQ20.19.07

Brain-Mimic Optoelectronic Memory Functions of Vertically Aligned Graphene/Diamond Heterojunctions Yuga Ito, Yuki Mizuno and [Kenji Ueda](#); Nagoya University, Japan

Graphene/diamond (carbon sp²-sp³) interfaces have attracted much attention because the interfaces become sources of various interesting electronic phenomena. Recently, we found that vertically-aligned graphene (VG)/diamond heterojunctions (C sp²-sp³ interfaces) became photo-controllable memristors [1], which are optically controllable memory-resistors with nonvolatile memory and switching functions. One of the most important application of the photo-controllable memristors is thought to be optoelectronic memory, which possess both photo-sensing and data storage function. In this study, we demonstrate that VG/diamond heterojunctions can be used as special types of optoelectronic memory, that is, brain mimic optoelectronic memory, that exhibit some of the basic functions of the human brain, such as an excitatory postsynaptic current (EPSC) and transition from short (STM) to long-term memory (LTM) states.

VG/diamond bilayers were grown *in situ* by using microwave plasma CVD, and VG/diamond junctions with diameters of 80-160 μm were fabricated using the bilayers [1, 2]. The *I-V* characteristics of these junctions in response to photoirradiation were measured using blue light emitting diodes (LEDs) or a fluorescent lamp in air at room temperature.

Raman, SEM and TEM results suggest that VG/diamond heterostructures with sharp interfaces were successfully formed. The VG/diamond junctions exhibited hysteretic *I-V* characteristics. The resistance of the junctions was changed to low or high resistance states by the light irradiation with bias voltage application and the resistance states was maintained in nonvolatile manner. The resistance difference ratio between the HRS and LRS (= R_{HRS}/R_{LRS}) was approximately 10² and was maintained for 2 days.

The VG/diamond junctions also exhibited clear responses to optical pulses and brain-like optoelectronic memory properties were observed. The junctions' current, which depended on the conductivity of the junctions, increased stepwise in response to each optical pulse, and a value of approximately 11 nA was obtained after applying 10 optical pulses. The current was subsequently maintained without significant deterioration. This generation of a current after frequent stimulation (via optical pulses) is analogous to the generation of the EPSC at biological synapses. Thus, the present VG/diamond junctions can be said to have produced an EPSC in response to optical stimulation. The magnitude of the EPSC generated by the junctions could be tuned by varying the intensity, width, frequency and numbers of the optical pulses, suggesting good controllability of the EPSC based on applying optical spikes. The energy consumption per event under these conditions was estimated to be approximately 440 pJ. This energy value is quite low and suggests the possibility of fabricating devices that mimic brain functions with very low energy consumption.

The memory retention time of the junctions was changed from shorter to longer by increasing the irradiated numbers of optical pulses. The behaviors of conductance decay can be described well by using the following decay function, $G(t)/G_0 = \exp[-(t/\tau)^{\beta}]$, which was often used for analysis of forgetting characters of the human brain. The relaxation time τ for above 7 pulses became ~2 orders higher than those for below 4 pulses. The memory character of the junctions was changed by optical pulses, and transition from STM to LTM states was caused by stronger optical stimulation. These kind of STM-LTM transition was also caused by controlling frequency of optical pulses. These results indicate that the VG/diamond junctions can be used as novel brain mimic optoelectronic memory devices, where weakly stimulated information was lost immediately and only strongly stimulated information was kept for a long time.

Ref.: [1] K. Ueda *et al.*, J. Mater. Res. 34 (2019) 626, [2] K. Ueda *et al.*, Appl. Phys. Lett. 117 (2020) 092103.

9:55 AM EQ20.19.08

2D Heterostructures with Fe:MoS₂ Toward Magnetic Tunneling Junction [Siwei Chen](#), Zitao Tang, Mengqi Fang, Shichen Fu, Kyungham Kang and Eui-Hyeok Yang; Stevens Institute of Technology, United States

The emergence of two-dimensional (2D) magnets offers exciting opportunities to discover new physical phenomena. Theoretical studies predicted that substitutional doping of magnetic atoms in transition metal dichalcogenide (TMD) monolayers would enable 2D ferromagnets at room temperature, which is a critical requirement for practical applications [1]. Experimental observations of magnetism have been made in bulk TMDs or transition metal-doped few-layer TMDs, using dopants, including V, Mn, Co, Ni, Cu, Nb and Re [2, 3]. Recently, the RT ferromagnetism was successfully demonstrated in *in-situ* Fe-doped MoS₂ (Fe:MoS₂) and V-doped WSe₂ (V:WSe₂) *via* chemical vapor deposition (CVD) [4, 5]. These 2D magnets can be used as electrodes or

barriers in vdW magnetic tunnel junctions (MTJs). Previous reports include an MTJ using MoS₂, CrI₃, or graphene as a tunneling barrier and using Fe₃GeTe₂ or Cr₂Ge₂Te₆ as magnetic electrodes [6–8]. The magnetic switching in the MTJ can be achieved using spin-transfer torque (STT), where the orientation of the Fe layer can be flipped using a spin-polarized current. A fast current-induced magnetization switching (CIMS) is important for high-speed and low power next-generation spintronics devices [9], which we expect to achieve using 2D magnets. Here, we present the layer-transfer of graphene and Fe-doped MoS₂ (Fe:MoS₂) monolayers on hBN toward fabricating an MTJ consisting of a Fe/hBN/Fe:MoS₂ heterostructure. This Fe:MoS₂ monolayers were synthesized *via* low-pressure chemical vapor deposition to induce magnetic properties at a room temperature. Here, hBN is used as the tunneling barrier, Fe:MoS₂ as the free layer, and Fe thin film as the fixed layer. As a next step, we will characterize the junction magnetoresistance inside an ultra-low vibration cryogen-free cooling closed-cycle cryostat with a temperature range from 4 K to 300 K. We will measure the CIMS by applying short current pulses over the junction. This work is expected to pave the way to developing van der Waals spintronics based on various magnetic transitional metal dichalcogenides.

References:

- [1] Y. Wang, S. Li, and J. Yi, *Scientific Reports*, **6** (1), 24153, (2016).
- [2] Y.-C. Lin, *Advanced Science*, **8** (9), 2004249, (2021).
- [3] T. Zhang, *ACS nano*, **14** (4), 4326–4335, (2020).
- [4] F. Zhang, *Advanced Science*, **7** (24), 2001174, (2020).
- [5] S. Fu, *Nature Communications*, **11** (1), 2034, (2020).
- [6] Z. Fei, B. Huang, *Nature Materials*, **17** (9), 778–782, (2018).
- [7] K. Shayan, *Nano Letters*, **19** (10), 7301–7308, (2019).
- [8] S. Jiang, *Nature Materials*, **17** (5), 406–410, (2018).
- [9] S. Ikeda, *Nature Materials*, **9** (9), 721–724, (2010).

SESSION EQ20.20: Poster Session III: Processing of Carbon Based and Beyond 2D Materials
 Session Chairs: Cinzia Casiraghi and Andres Castellanos-Gomez
 Tuesday Morning, December 7, 2021
 EQ20-Virtual

10:30 AM EQ20.20.01

Laser-Induced Graphene with Controlled Heteroatom-Doping Based on Molecularly Engineered Polyimides Ki-Ho Nam, Moataz Abdulhafez, Golnaz Najaf Tomarac and Mostafa Bedewy; University of Pittsburgh, United States

Localized graphitization of aromatic polyimides (PIs) can be achieved by laser direct write process owing to the high absorptance in the infrared wavelength range of commercial CO₂ laser cutting/scribing machines. This one-step photothermal process allows the formation of unique hierarchical nano-/micro-structured graphene patterns on the surface of polyimide film. Nevertheless, controlling chemical doping in this laser-induced graphene, has been limited thus far. Herein, we present a facile approach for manufacturing patternable, heteroatom-doped, hierarchically porous graphene from molecularly engineered PI films using a continuous-wave 10.6 μm laser in ambient air. Conventional two-step polymerization of PIs was carried out from 4,4'-oxydianiline and three different commercially available tetracarboxylic dianhydrides with different internal linkages such as phenylene, trifluoromethyl or sulfone groups. We show that the chemical structure of PIs and laser fluence of the incident radiation affect the gas evolution, inducing different structure rearrangements, as interesting heteroatom self-doping (N-doping, F-doping, S-doping) and consequently different electrical and electrochemical properties. Impressively, the electrical resistivity of F-doped laser-induced graphene can be precisely tuned to lower than ~13 Ω sq⁻¹. Moreover, these fabricated graphene electrodes are capable of detecting nanomolar concentrations of neurotransmitter, which is promising for implantable neural probes. Hence, the proposed laser one-step synthesis of graphitic structures can be readily extended for the fabrication of various advanced materials including early diagnosis of neurological disorders.

10:35 AM EQ20.20.02

Synthesis of Two-Dimensional Plasmonic Molybdenum Oxide Nanomaterials by Femtosecond Laser Irradiation Fan Ye^{1,2}, Darren Chang^{1,2}, Ahsan Ayub¹, Khaled Ibrahim^{1,2}, Ahmed Shahin^{1,2}, Reza Karimi¹, Shawn Wettig¹, Joseph Sanderson¹ and Kevin Musselman^{1,2}; ¹University of Waterloo, Canada; ²Waterloo Institute for Nanotechnology, Canada

A novel process to synthesize plasmonic MoO_{3-x} nanosheets is demonstrated, in which MoS₂ powders suspended in ethanol/water are irradiated with pulses from a femtosecond laser, resulting in simultaneous Coulomb explosion, photoexfoliation, and oxidation. The oxidation process is found to start with the formation of hydrogen-bonded molybdenum oxide (H_xMoO₃), followed by the release of -OH₂ groups to create oxygen vacancies, and finally the MoO_{3-x} is oxidized to MoO₃ after extended irradiation. The formation of H_xMoO₃ is the critical step to create enough oxygen vacancies for localized surface plasmon resonance (LSPR), and this step is attributed to H₃⁺ dissociated from ethanol under femtosecond laser irradiation. It is found that 80-90% ethanol is the optimal concentration to synthesize plasmonic MoO_{3-x}, where the balance of water facilitates the release of the -OH₂ groups to create the required vacancies. It is shown that different organic solvents like methanol, 1-propanol and isopropyl alcohol that were reported to generate large amounts of H₃⁺ under femtosecond laser irradiation can also oxidize MoS₂ into plasmonic MoO_{3-x}. The LSPR properties of the synthesized MoO_{3-x} are evaluated by UV-vis spectroscopy and photothermal conversion measurements.

10:40 AM EQ20.20.03

Low Temperature Direct Growth of Multilayer Graphene on SiN_x/Si Through Ni Catalyzed Solid Phase Reaction for EUV Pellicle Hyeoung Kim^{1,2}, Junhyeok Jeon^{1,2}, Sangmin Lee¹, Seul-Gi Kim¹, Ki-Bum Kim³, Hyeongkeun Kim¹, Hyun-Mi Kim¹ and Ji-Beom Yoo²; ¹Korea Electronics Technology Institute, Korea (the Republic of); ²Sungkyunkwan University, Korea (the Republic of); ³Seoul National University, Korea (the Republic of)

Graphene has a transmittance higher than 85% for extreme ultraviolet (EUV) light (13.5 nm) and high in-plane Young's modulus. Graphene can satisfy all characteristic indicators as a material of EUV pellicles. Among the many techniques developed for synthesizing high-quality graphene, metal induced crystallization (MIC) of amorphous carbon is a unique technique for fabricating uniform multilayer graphene (MLG) that has an advantage in pellicle application due to no additional transfer process. In this study, we investigated Ni catalyzed crystallization of amorphous carbon on SiN_x/Si substrate, and further on diffusion mechanism between amorphous carbon and Ni. We found the optimal conditions to form a highly uniform MLG as a material for EUV pellicle. We observed the effect of carbon density and thickness ratio of Ni and carbon layer (t_c/t_{Ni}) on the MIC and succeeded in forming uniform graphene on 8 inch wafer with short annealing of 1 h at 500°C. The density of amorphous carbon was tuned by changing sputtering conditions such as power and gas flow rate. The formation of MLG on SiN_x/Si was confirmed by Raman spectroscopy, atomic force microscopy, cross-section transmission

electron microscopy. The kinetic model between amorphous carbon and nickel was substantiated by experimental findings based on amorphous carbon/Ni stacked structures of various thicknesses and densities with different heat treatment conditions.

10:45 AM EQ20.20.05

Synthesis of Graphene Nanoribbons and Nanosheets Formed in Metals by an Electrocharging Assisted Process, Their Properties and

Applications Lourdes G. Salamanca-Riba¹, Oded Rabin^{1,1}, Manfred Wuttig¹ and Shenjia Zhang²; ¹University of Maryland, United States; ²General Cable, United States

Carbon nanostructures, such as graphene and carbon nanotubes incorporated in metals have recently gained great interest for the possibility of enhancing the electrical and thermal conductivities as well as mechanical strength of the metal. This is possible because of the combination of excellent charge carrier mobility, thermal conductivity and mechanical strength of the carbon nanostructures and the high density of electrons in the metal. The improved properties make these nanocarbon metal composites unique candidates in applications such as high power transmission lines, interconnects, heat exchangers, motors, photovoltaic cells and transparent electrodes, among others. We developed a process to synthesize graphitic nanostructures in metals by the application of a high electrical current to liquid metal containing particles of activated carbon. The process called electrocharging assisted process transforms the activated carbon particles from amorphous to crystalline graphitic nanoribbons in the liquid metal. Upon solidification of the metal the nanoribbons self-assemble with an epitaxial relation with the metal. We have used Al 1350 and activated carbon particles of ~100 nm and obtained samples with global electrical conductivities more than 5% higher than the parent alloy as well as enhanced local stiffness, measured by nanoindentation. The conductivity enhancement is correlated with increasing crystallite size and concentration of the produced graphitic nanostructures. We have investigated different parameters in the process such as applied current, duration of the current, stirring speed of the liquid metal (with and without Argon bubbler) to optimize the process. The approach is scalable to large scale manufacturing.

Supported by DOE EERE Award EE0008313.

10:50 AM EQ20.20.07

Sonication-Based Selective Removal of Mechanically-Exfoliated Bulk MX₂ Flakes on the Substrate Tatsuya Nakamoto, Takeshi Yoshimura, Norifumi Fujimura and Daisuke Kiriya; Osaka Pref. Univ, Japan

Two-dimensional (2D) materials gather attention because of their large carrier mobility, transparency, and high-optoelectronic characters in a thin-confined structure. Transition metal chalcogenides (TMDCs) with the formula of MX₂ (M = transition metals, X = chalcogen atoms) are a family of 2D materials; MoS₂ is a representative material of TMDCs, which shows direct bandgap in a single layer. The single-layer MoS₂ further shows distinctive physical properties such as piezoelectric effect and second harmonic generation due to its symmetry-breaking structure.

It would be important to obtain thin layers selectively on the substrate to study 2D materials effectively. Usually, samples are prepared via a mechanical exfoliation method because the method is simple, and the exfoliated crystals usually show good crystallinity. Although the exfoliation method can transfer monolayers on the substrate, a large number of bulk flakes are simultaneously obtained. The bulk flakes cause trouble to make devices because the electric lines sometimes may disconnect by overwrapping the thick flakes. Once transfer the flakes, it is very hard to remove the bulk flakes selectively. In this study, we show our method of selective removal of bulk flakes from the substrate and maintain thin layers including monolayers by applying sonication in organic solvents.

MoS₂ flakes are transferred on a Si/SiO₂ substrate using a general mechanical exfoliation method with scotch tape. Various thick flakes cover the substrate. Then, the substrate is sonicated under an organic solvent for 5 minutes at most. After the sonication, the bulk flakes are selectively removed, and the thin layers, including monolayers, remain on the substrate.

In the process of flake-removal process, the solvent is critical. In some solvents, the selectivity is very low, and a lot of bulk flakes remained on the surface. This removal process is highly solution-dependent. The relationship between the solvent and residual rate is analyzed in terms of polar dispersion factors of the solvents. In the presentation, we will show the details of the mechanism of the selective removal of the sonication method.

10:55 AM EQ20.20.08

High Performance Self-Powered MoS₂/ReS₂ Broadband Photodetector Riya Wadhwa and Mukesh Kumar; Indian Institute of Technology Ropar, India

Two dimensional (2D) layered materials emerged enormously in the past decade, largely being investigated fundamentally and practically. The unique layered structure and atomic-scale thickness make them attractive to have exclusive electrical and optical properties than their bulk counterparts. 2D layered materials easily integrated and formed heterostructure due to the dangling bond free surfaces. Heterostructure can access more functioning ability beyond its individual constituent. However, for novel electronic/optoelectronic device applications, it is very critical to understand the charge carrier dynamics at the interface of heterostructures. Here, we report a highly sensitive self-powered MoS₂/ReS₂ broadband photodetector, covering visible (400 nm) to NIR (1100 nm) regime with a high value of responsivity 42.61 A/W at 1V under the illumination of 800 nm, which is approximately 16 times of the reference pristine MoS₂ photodetector. The favourable energy band alignment of n-n hetero-junction is responsible for enhanced photo-responsivity and self-driven feature of the detector. Moreover, fast rise/decay transient photoresponse (20/19 ms) strongly advocate the spatial separation of charge carrier across the interface. This work facilitates the understanding of fundamental interfacial study of a new growing van der waals heterostructures for the development of novel device applications.

11:00 AM EQ20.20.09

Harnessing the Bendability of Atomically Thin MoS₂ Layers Grown by Perylene Assisted Chemical Vapour Deposition Christian Martella¹, Erika Kozma², Pinaka Pani Tummala¹, Paolo Targa³, Davide Codegoni³, Alessio Lamperti¹ and Alessandro Molle¹; ¹CNR Institute for Microelectronics and Microsystems, Italy; ²Consiglio Nazionale delle Ricerche, Italy; ³ST Microelectronics, Italy

Two-dimensional (2D) layered materials exhibit an intrinsic attitude to sustain high curvature angle without rupture.^[1] Therefore, shaping 2D layers into complex curved geometries is emerging as an exciting way to access unprecedented physical properties driven by two different responses to the strain-induced morphological modifications. On one hand, deformations of the atomic lattice positions lead to energetic bandstructure modifications with dramatic impacts on the opto-electronic properties of the 2D materials.^[2] On the other hand, accommodation of strain through slip-and-shear mechanisms of the layers leads to superlubricity.^[3]

Here we show that shape transformations in atomically thin MoS₂ layers can be controlled in the first stage of their formation by means of chemical vapor deposition on pre-patterned substrates by design. Aiming at harnessing the local curvature of mono- and few-layers MoS₂, we functionalize the pre-patterned substrates via aromatic perylene molecules serving as nucleation seeding promoters.^[4] Based on the analysis of atomically resolved transmission electron microscope images, we demonstrated that the so-grown MoS₂ layers bend conformally without rupture and detachment from the substrate even at the extreme geometric features (asperities, edges, etc..) only when the seeding promoter is used. Moreover, theoretical energetic arguments allow us to quantitative derive the role of the perylene molecules to increase the interfacial adhesion energy between MoS₂ and SiO₂ substrate by balancing the strain and bending energy contributions.

References

- [1] C. Martella, C. Mennucci, E. Cinquanta, A. Lamperti, E. Cappelluti, F. Buatier de Mongeot, A. Molle, *Adv. Mater.* **2017**, *29*, 1605785.
 [2] A. Castellanos-Gomez, R. Roldán, E. Cappelluti, M. Buscema, F. Guinea, H. S. J. van der Zant, G. A. Steele, *Nano Lett.* **2013**, *13*, 5361.
 [3] J. Yu, E. Han, M. A. Hossain, K. Watanabe, T. Taniguchi, E. Ertekin, A. M. Zande, P. Y. Huang, *Adv. Mater.* **2021**, *33*, 2007269.
 [4] C. Martella, E. Kozma, P. P. Tummala, S. Ricci, K. A. Patel, A. Andicsová Eckstein, F. Bertini, G. Scavia, R. Sordan, L. G. Nobili, M. Bollani, U. Giovannella, A. Lamperti, A. Molle, *Adv. Mater. Interfaces* **2020**, *7*, 2000791.

11:05 AM EQ20.20.10

High-Performance NO₂ Sensor Based on an Atomically Ordered TMD Alloy Mehmet Dogan^{1,2}, Amin Azizi^{1,3}, Hu Long^{1,2,3}, Jeffrey Cain^{1,2,3}, Kyunghoon Lee^{1,2,3}, Rahmatollah Eskandari¹, Alessandro Varieschi¹, Emily C. Glazer¹, Alex Zettl^{1,2,3} and Marvin L. Cohen^{1,2}; ¹University of California, Berkeley, United States; ²Lawrence Berkeley National Laboratory, United States; ³Kavli Energy NanoScience Institute, United States

Developing sensors that can be operated at room-temperature and ambient conditions has been an important goal for a wide range of applications. Coupled with this goal is the desire to have sensors that are small, low-power, fast and able to detect small concentrations of a molecular species. Here, we demonstrate a room-temperature, highly sensitive, selective, stable, and reversible chemical sensor based on single layer and few layers of the transition-metal dichalcogenide alloy Re_{0.5}Nb_{0.5}S₂. This alloy exhibits short-range ordering of atomic species due to the geometric frustration in the triangular sublattice that corresponds to the transition metal atoms. The resulting sensing device exhibits a thickness-dependent carrier type due to the band alignment changing with thickness. Upon exposure to NO₂ molecules, its electrical resistance considerably increases or decreases depending on thickness. The sensor is highly selective to NO₂ with only minimal response to other gases such as NH₃, CH₂O, and CO₂. Surprisingly, in the presence of humidity, the sensor shows complete reversibility with fast recovery at room temperature, in contrast with other similar sensors whose performance is lowered with humidity. In this presentation, we focus on the theoretical analysis of the sensing platform and identify the atomically sensitive transduction mechanism. We also explain the structural properties of the Re_{0.5}Nb_{0.5}S₂ and its electronic properties.

Acknowledgments: This work was primarily supported by the U.S. Department of Energy, Office of Science, Office of Basic Energy Sciences, Materials Sciences and Engineering Division under contract no. DE-AC02-05-CH11231, within the sp²-bonded Materials Program (KC2207), which provided for materials synthesis, chemical sensitivity tests, and atomic structure calculations. Additional support was provided by the National Science Foundation under grant no. DMR-1807233, which provided for STEM measurements, and under grant no. DMR-1926004, which provided for calculations of precise electronic structures. Computational resources were provided by the DOE at Lawrence Berkeley National Laboratory's NERSC facility and the NSF through XSEDE resources at NICS.

11:10 AM EQ20.20.11

Heteroepitaxy and Property of Triple-Layered Ruddlesden-Popper Phase La_{n+1}Ni_nO_{3n+1} with Tetravalent-Dopants Akifumi Matsuda¹, Shohei Hisatomi¹, Yuki Goto¹, Satoru Kaneko^{2,1} and Mamoru Yoshimoto¹; ¹Tokyo Institute of Technology, Japan; ²Kanagawa Institute of Industrial Science and Technology, Japan

Lanthanum nickelates (La_{n+1}Ni_nO_{3n+1}) with two-dimensional perovskite structure, so called Ruddlesden-Popper phases, have attracted interests for their electronic properties derived from their layered structure and mixed valence Ni-ions^[1]. These two-dimensional perovskite layers are also expected as precursors to develop infinite-layer nickelate such as Sr-doped NdNiO₃ for which superconducting behavior was reported recently^[2]. Epitaxy of multilayered La_{n+1}Ni_nO_{3n+1} thin films and characterizing their structure, electronic state, and properties according to interfacial strain and aliovalent doping would contribute to further comprehension of their solid-state physics. There are also reports of La_{n+1}Ni_nO_{3n+1} for its metal-insulator-transition according to oxygen deficiency, and applicability to SOFC cathodes and gas sensors^[1,3]. However, aliovalent doping in La₄Ni₃O₁₀ epitaxial thin films similar to La₂NiO₄ and La₃Ni₂O₇ still requires further researches to understand its effect on structure and properties^[5,6]. In this study, epitaxial growth of triple-layered La₄Ni₃O₁₀ thin films and the effect of tetravalent dopants substituting La³⁺ on the growth, structure, and electric properties was investigated. The lanthanum nickelate thin films were grown on single crystal substrates such as SrTiO₃, NdGaO₃, and LaAlO₃ by pulsed laser deposition technique equipped with a KrF excimer laser (λ=248 nm, d~20 ns, and E~1.0 J/cm²). The films were deposited at substrate temperature range from room-temperature (not heated intentionally) to 750°C in ~10 Pa O₂-flowed ambience (base pressure ~3×10⁻⁶ Pa) using sintered targets of pure and (Hf⁴⁺, Sn⁴⁺) co-doped La₄Ni₃O₁₀. The thin films were subsequently post-annealed in high-purity O₂ atmosphere (1 atm, 200 sccm) at temperature up to 1100°C to improve crystallinity as well as to modify the crystal phases and the valence of Ni-ions. The epitaxy of La₄Ni₃O₁₀ (001) thin films after annealing in O₂ was verified by {001} diffraction and four-fold planar symmetry detected in XRD 2θ/ω and φ scans, while epitaxial growth of La₂NiO₄ (100) was observed for the as-grown films. The Hf and Sn-doped La₄Ni₃O₁₀ (001) thin films with thickness of ~100 nm demonstrated low resistivity of ~5×10⁻³ Ωcm at room-temperature. The obtained epitaxial thin films would allow us further formation and analyses of aliovalent doped and multi-layered infinite layer nickelates reduced from the Ruddlesden-Popper phase. Additional detailed structural analyses of the doped La₄Ni₃O₁₀ thin films, and the effect of the tetravalent doping on the electronic property would also be discussed.

- [1] K.-T. Wu et al., *J. Mater. Chem. A*, *5* (2017) 9003–9013.
 [2] D. Li et al., *Nature*, *572* (2019) 624–627.
 [3] V. Pardo et al., *Phys. Rev. B*, *83* (2011) 245128.
 [4] S. Yoo et al., *RSC Advances*, *2* (2012) 4648–4655.
 [5] R. J. CaVa et al., *Phys. Rev. B*, *43* (1991) 1229–1232.
 [6] S. A. Nedilko et al., *J. Alloys Compd.*, *367* (2004) 251–254.

11:15 AM EQ20.20.12

Late News: Synthetic Control Over Edge Structure in WSe₂ Crystals Reynolds Dziobek-Garrett, Shreya Sriramineni, Ona Ambrozaite and Thomas Kempa; Johns Hopkins University, United States

Recent developments have shown that chemical synthesis is a powerful tool for controlling the size, shape, and composition of two-dimensional (2D) crystals with broad implications for their implementation in optoelectronic and quantum devices. However, the gas-phase reactions carried out by most researchers are not conducive to precise manipulation of the 2D crystal edge structure. Here we demonstrate a salt-assisted low-pressure chemical vapor deposition method, which enables growth of 2D WSe₂ monolayers whose edge morphology can be tuned from straight, to sawtooth, to fractal-like by adjusting the ratio of WO₃ to NaCl. We discuss the volatility of the metal precursor and its role in dictating not only the edge structure, but also the defect density within the as-grown crystals. These studies provide important insight into new 2D crystal growth modes and synthetic strategies for producing crystals with unique structures and optoelectronic properties.

11:20 AM EQ20.20.13

Enhancing Low-Frequency Raman Scattering in Exfoliated CVD-Grown 2D Nanosheets of Transition Metal Dichalcogenides Using Metal/Dielectric Substrates Bharathi Rajeswaran, Rajashree Konar, Eti Teblum, Hagit Aviv, Gilbert D. Nessim and Yaakov Tischler; Bar-Ilan University, Israel

Layered 2D sheets of Transition Metal Dichalcogenides (TMDCs) exhibit interesting optical and electronic properties such as indirect to direct bandgap transition and valley-spin coupling when scaling from bulk to a few layers. TMDCs are also flexible and versatile for constructing a wide range of heterostructures with atomic-level control over their layer thickness, devoid of issues pertaining to lattice mismatch. Hence layered TMDCs have the potential for realizing novel high-performance optoelectronic devices over a broad operating spectral range. Therefore, a detailed structural study on these materials is important to develop novel electronic and optoelectronic devices. Low-Frequency Raman (LFR) Spectroscopy is an ideal tool to investigate the signature structural information and the layer-to-layer dependency of TMDCs. LFR is a highly efficient technique for material analysis and layer identification with significant advantages over other vibrational or fluorescence spectroscopy methods. This technique remains to date one of the most popular characterization tools because of its non-invasive nature and ultra-fast detection limits. With LFR measurements, crucial information such as the tilt and number of layers can be determined. For instance, enhancement in optical properties can be understood by monitoring the evolution of the in-plane (shear- E'/E_g) and the out-of-plane ((A'/A_{1g})) vibration modes with the number of layers. In this work, we explore a combination of metal/dielectric substrates to enhance the LFR scattering of different 2H-TMDC layers of WSe₂, WS₂, MoSe₂, and thereby to understand the structure of these nanoscale films. Phase-pure 2H-TMDCs were grown via an in-built two furnace ambient pressure CVD and the layers of exfoliated flakes were studied. Layer thickness and number of layers of 2H-MoSe₂, WSe₂, and WS₂ were varied. We used different substrates such as coatings of Al₂O₃ with different thickness on top of Al mirror layer, Al coated glass and Raman-grade CaF₂ among other substrates, to study bi-layers and a few layers of the above-mentioned TMDCs. We observe an enhancement of 30 times in LFR signal corresponding to WSe₂ and WS₂ on an Al₂O₃ coated Al substrate with oxide thickness of 80 nm and Al thickness of 200 nm.

References:

1. X. Yu and K. Sivula, *ACS Energy Lett.*, 2016, **1**, 315–322.
2. B. Chen, X. Zhang, K. Wu, H. Wang, J. Wang and J. Chen, *Opt. Express*, 2015, **23**, 26723.
3. F. Chen, L. Wang, T. Wang and X. Ji, *Opt. Mater. Express*, 2017, **7**, 1365.
4. Z. Jia, J. Xiang, F. Wen, R. Yang, C. Hao, and Z. Liu, *ACS Appl. Mater. Interfaces*, 2016, **8**, 4781–4788.
5. Rajashree Konar, Bharathi Rajeswaran, Hagit Aviv, Eti Teblum, Ilya Grinberg, Yaakov Raphael Tischler, Gilbert Daniel Nessim (JMC C, submitted)

11:25 AM EQ20.20.14

Late News: Method for Enrichment with Semiconducting Single-Walled Carbon Nanotubes by Aerosol N₂O Etching Alena A. Alekseeva¹, Dmitry Krasnikov¹, Grigory Livshitz¹, Stepan Romanov¹, Pavel Sorokin², Andrey Klimovich³ and Albert Nasibulin¹; ¹Skolkovo Institute of Science and Technology, Russian Federation; ²University of Science and Technology MISIS, Russian Federation; ³A.M. Prokhorov General Physics Institute, Russian Federation

Nowadays, flexible electronics demands new materials for integrated circuits of high flexibility and stretchability [1]. Single-walled carbon nanotubes (SWCNTs) are one of the most promising materials for utilization in the flexible integrated circuits owing to the outstanding electrical and mechanical properties [2]. However, the electronic and optoelectronic applications demand an advanced control of the nanotubes properties such as: length distribution, defectiveness, and most importantly ratio of semiconducting/metallic SWCNTs [3].

Most synthesis methods yield in 1/3 of metallic SWCNTs, thus, obtaining purely semiconducting species is a complex multistep procedure. Common strategies include either precise chirality distribution tuning during SWCNTs synthesis, post-synthesis etching of SWCNTs powders and films by oxidizing agents, or chirality separation. However, despite being well-established, these methods are suffering from multistage treatments, induced damage of SWCNTs [4], and irreversible attachment of surfactants that diminish performance of semiconducting devices [5].

Herein we report a simple one-step method for selective etching of metallic SWCNTs with nitrous oxide in aerosol phase. Our approach bases on faster oxidation rate of metallic SWCNTs compared to semiconducting ones, with advantage of aerosol chemical vapor deposition method, providing flow of individual SWCNTs in gas phase. We show a scalable method for obtaining semiconducting enriched SWCNT films with selectivity of 97% by treatment of pristine SWCNT aerosols for 6 sec at 600°C in the atmosphere of 30% N₂O. We assess structural changes in the nanotubes structure using comprehensive set of methods: UV-vis-NIR and Raman spectroscopies, differential mobility of aerosol particles, X-ray photoelectron spectroscopy, scanning and transmission electron microscopies and investigate the mechanism employing the DFT studies. We verify optimal etching conditions by equivalent sheet resistance, and temperature dependence of resistance dependencies, and the performance of SWCNT thin films as a channel material for thin film field-effect transistors, which showed an average improvement of on/off current ratio from 10⁰-10¹ to 10³-10⁴ and open state resistance from 10² to 10⁹ Ω/μm for statistics over 9000 devices.

[1] Q. Huang and Y. Zhu, "Printing Conductive Nanomaterials for Flexible and Stretchable Electronics: A Review of Materials, Processes, and Applications," *Adv. Mater. Technol.*, vol. 4, no. 5, pp. 1–41, 2019, doi: 10.1002/admt.201800546.

[2] Jariwala, D., Sangwan, V. K., Lauhon, L. J., Marks, T. J., & Hersam, M. C. (2013). Carbon nanomaterials for electronics, optoelectronics, photovoltaics, and sensing. *Chemical Society Reviews*, 42, 2824–2860. <https://doi.org/10.1039/c2cs35335k>

[3] Rao, R., Pint, C. L., Islam, A. E., Weatherup, R. S., Hofmann, S., Meshot, E. R., Hart, A. J. (2018). Carbon Nanotubes and Related Nanomaterials: Critical Advances and Challenges for Synthesis toward Mainstream Commercial Applications. *ACS Nano*, 12(12), 11756–11784. <https://doi.org/10.1021/acsnano.8b06511>

[4] Hu, H., Zhao, B., Itkis, M. E., & Haddon, R. C. (2003). Nitric Acid Purification of Single-Walled Carbon Nanotubes. *Journal of Physical Chemistry B*, 107(50), 13838–13842. <https://doi.org/10.1021/jp035719i>

[5] Wei, N., Laiho, P., Khan, A. T., Hussain, A., Lyuleeva, A., Ahmed, S., Kauppinen, E. I. (2020). Fast and Ultraclean Approach for Measuring the Transport Properties of Carbon Nanotubes. *Advanced Functional Materials*, 30(5), 1–9. <https://doi.org/10.1002/adfm.201907150>

Financed by: Russian Science Foundation № 17-19-01787

11:30 AM EQ20.20.15

Drain-Gate Connected Graphene/TMD Diode with Near Unity Ideality Factor Mihyang Park and Woojong Yu; Sungkyunkwan University, Korea (the Republic of)

Two-dimensional materials such as graphene, transition metal dichalcogenide(TMD), h-BN have been studied in various fields and their stacking

heterostructures have also received great attention. However, devices fabricated by stacking two-dimensional materials have an issue about ideality factor that cannot reach unity compared to the PN junction diode.

To solve this problem, we fabricated a two-terminal diode without forming the heterojunction or doping, just simply connecting the gate and drain. We used graphene as a bottom gate and TMD such as MoS₂ and WSe₂ as a conducting channel. Our gate-drain connected diode obtained ideality factor near unity. When drain-gate voltage is negative, which is reverse bias, Schottky barrier height is high so that current flow can be suppressed. In contrast, when drain-gate voltage is positive, which is forward bias, Schottky barrier height is low so that current can flow easily. This is further confirmed by Schottky barrier height modulation with varying drain-gate voltage by low-temperature measurement. The Schottky barrier height difference of 0.2eV was observed between the reverse bias and forward bias. The important role of the drain-connected bottom gate was also confirmed with varying carrier density with different drain-gate voltage, by hall-bar measurement. Due to the drain-gate connected structure, when a reverse bias is applied to the drain, the bottom gate is also negatively charged and a negative field is applied to the channel, thereby lowering the carrier concentration. Similarly, when it is forward bias, the carrier concentration in the channel increases due to the positively charged bottom gate.

11:35 AM EQ20.20.16

Investigations of MoS₂ on Carrier Selective Contacts for Photovoltaic Applications Colleen Lattvak¹, Martin Vehse¹, Marco A. Gonzalez² and Carsten Agert¹; ¹DLR Institute of Networked Energy Systems, Germany; ²Carl von Ossietzky University of Oldenburg, Germany

Molybdenum disulfide (MoS₂) is a transition metal dichalcogenide known for its exceptional optoelectronic properties in its few- and monolayer form. It has a band gap in the range of 1.2 to 1.9 eV, depending on the layer thickness. This, along with other optoelectronic properties such as high absorptivity, makes MoS₂ a promising absorber layer in photovoltaic (PV) applications, like PV windows. Through optical simulation and Raman and photoluminescence (PL) spectroscopy we investigate the potential of MoS₂ in combination with the transparent carrier selective contacts molybdenum oxide and titanium oxide. The optical simulations show that this combination of layers has the potential to be semi-transparent and color neutral with possible current densities of 1 to 5 mA/cm² and average visible transmittance of 42% and 32% for device stacks with monolayer and few layer (< 5nm) MoS₂, respectively. Results from Raman and PL spectroscopy indicate that molybdenum oxide and titanium oxide influence the contribution of excitonic charge carriers in the MoS₂ absorber. This is observed in the form of spectral shifts in both Raman and PL. This can be explained by doping and screening effects induced by the metal-oxide layers. Both metal oxides can induce charge carrier extraction from the MoS₂, observed as quenching of the PL spectra. We compare these effects in exfoliated single crystalline MoS₂ flakes and transferred centimeter scale atomic layer deposition grown MoS₂ films and find that they are the same. This indicates that the knowledge gained from studying single crystalline flakes can be transferred to large area MoS₂ films which are a possible route to realize larger scale applications. The results from our optical simulation and optical spectroscopy, we will show the potential of this layer stack for applications such as transparent photovoltaic windows.

11:40 AM EQ20.20.17

Position-Controlled Fabrication of Vertically-Aligned Mo/MoS₂ Core-Shell Nanopillar Arrays Louis Maduro, Marc Noordam, Maarten Bolhuis, Laurens Kuipers and Sonia Conesa-Boj; Delft University of Technology, Netherlands

The fabrication of two-dimensional (2D) materials, such as transition metal dichalcogenides (TMDs), in geometries beyond the standard platelet-like configuration exhibits significant challenges which severely limit the range of available morphologies. These challenges arise due to the anisotropic character of their bonding, van der Waals out-of-plane while covalent in-plane. Furthermore, industrial applications based on TMDs nanostructures with non-standard morphologies require full control on the size-, morphology- and position in the wafer scale. Such a precise control remains an open problem whose solution would lead to the opening of novel directions in terms of electronic and optoelectronic applications. Here, we report on a novel strategy to fabricate vertical position-controlled Mo/MoS₂ core-shell nanopillars (NPs). Metal-molybdenum (Mo) NPs are first patterned in a silicon wafer using lithography and cryo-etching. These Mo NPs are then used as scaffolds for the synthesis of Mo/MoS₂ core/shell NPs by exposing them in a rich sulfur environment. Cross-sectional transmission electron microscopy (TEM) analysis reveals the well-defined morphologies and the Mo/MoS₂ core/shell nature of the NPs. We demonstrate that individual Mo/MoS₂ core/shell NPs exhibit enhanced second order nonlinear optical processes, with an intensity increase up to a factor 40 as compared with regular MoS₂ flakes. Our results, and specifically the high degree of morphology- and position-control achieved on the core/shell NPs, represent an important step towards realising one-dimensional TMD-based nanostructures as building blocks of a new generation of sensors, nanophotonic devices, and hydrogen evolution reactions.

11:45 AM EQ20.20.18

Centimetre Scale Synthesis of Monolayer WS₂ Using Single Zone APCVD—Study of Growth Mechanism and Photodetector Properties Pallavi Aggarwal, Shuchi Kaushik, Prashant Bisht, Madan Sharma, Aditya Singh, Bodh Raj Mehta and Rajendra Singh; Indian Institute of Technology Delhi, India

Importance of two-dimensional transition metal dichalcogenide (2D TMDC) has been well known due to their novel optical and electrical properties but their growth mechanism has still been unclear. In this study, we have accomplished 1×1 cm² monolayer WS₂ film on sapphire substrate using single zone atmospheric pressure chemical vapor deposition (APCVD) method. The work is centered upon the detailed explanation on the growth of large area film by employing the importance of alkali halides and other growth parameters like gas flow rate, growth time, quantity of sulfur powder with respect to WO₃ powder, and substrate temperature. Structural and optical characterization were done using optical microscopy, Raman spectroscopy, Raman mapping, photoluminescence, UV-Visible spectroscopy, atomic force microscopy (AFM), and high-resolution transmission electron microscopy (HRTEM). Herein, optical microscopic images represent different stages of the growth of thin film, UV-Visible absorption spectra show the presence of A, B, and C excitons indicating its broad range absorption capability, Raman and PL spectra show peaks characteristic to the monolayer WS₂, and the thickness is 1 nm as measured from the height profile image which further confirms it to be monolayer. Moreover, single crystal nature of the as-grown film is deduced from the HRTEM images and SAED pattern which depict only single set of diffraction planes. Chemical composition of the film is confirmed from XPS spectra which exhibit peak characteristic to W⁺⁴ and S²⁻ ions in bulk WS₂ revealing its complete sulfurization. Following the high quality of the as-grown films as deduced from the afore mentioned characterizations, photodetector was fabricated by using standard e-beam lithography technique to study its photo response over a wide range of wavelengths from 380 nm to 660 nm. Responsivity and detectivity spectra indicate broad range photo-response from UV to visible region with highest value of 847 mA/W and 6.27× 10¹² Jones at 380 nm, respectively.

11:50 AM EQ20.20.19

Water-Soluble Layer Assisted Transfer of Large-Area MoS₂ for Application in Photodetectors Madan Sharma, Aditya Singh and Rajendra Singh; Indian Institute of Technology Delhi, India

Molybdenum disulfide (MoS₂), having excellent optical and electrical properties and tunable bandgap, offers new opportunities for next-generation electronic devices. It is difficult to grow MoS₂ onto most substrates (specially on flexible substrates) due to growth limitations such as temperature, growth promoters, precursors, etc. In the present work, we have first grown large-area (centimeter-scale) trilayer MoS₂/SiO₂ via CVD and then transferred onto various substrates (sapphire, SiO₂, flexible substrates) without degradation of film quality. To transfer the MoS₂, a water-soluble layer (Na₂S/Na₂SO₄) was

grown on the growth substrate during the growth of MoS₂ film, such that the MoS₂ lies on top of the water-soluble layer. Upon treating with DI water, the water-soluble film dissolves, causing the MoS₂ film to lift off and float to the surface. The film is then cleaned and transferred onto the desired substrate. Optical, morphological, and XPS results show that transferred film is highly clean and damage-free. A broadband (NIR-Vis-UV) photodetector was also fabricated onto transferred 3L MoS₂/sapphire to show the compatibility of the transfer process with the nanodevice fabrication. The photocurrent was enhanced 100 times and 10 times to dark current in UV and visible region, respectively. The maximum responsivity was found to be 8.6 mA/W. The proposed work offers enormous potential for the industrial implementation of 2D material technology platforms. Also, this process may be used to transfer other 2D materials like WS₂, MoSe₂, etc.

11:55 AM EQ20.20.20

Synthesis of Orientation Controlled WS₂ Thin Films for Enhanced Gas Sensing Performance Prashant Bisht¹, Arvind Kumar¹, Branson Belle² and Bodh Raj Mehta¹; ¹Indian Institute of Technology Delhi, India; ²SINTEF Industry, Norway

In this study, in-plane, and out-of-plane growth of WS₂ on SiO₂/Si substrate has been achieved using pulsed laser deposition technique. We have systematically studied the effect on the growth of the thin films at different sets of pressure (30 mTorr, 50 mTorr, and 70 mTorr) and temperature (400 °C, 500 °C, and 600 °C). Samples grown at the combination of low temperature and low vacuum showed a vertical flake-like growth, whereas at high temperature and high vacuum horizontal growth was achieved. XRD and Raman spectra show the formation of the 2H-WS₂ phase with (002) dominant plane which reflects the layered growth. FESEM, AFM, and HRTEM depict the growth evolution at different deposition parameters and thickness of the thin film. XPS compares the chemical state and composition of the as-grown films. Deposition pressure and substrate temperature were found crucial for controlling the stoichiometry and texture of WS₂ thin film. Furthermore, the gas sensing performance of the as-grown horizontal and vertical film has been compared. Later showed an enhanced response and selectivity towards NO₂ gas with a LOD of 100ppb at room temperature. The reason might be ascribed to the presence of a comparatively large number of active edge sites which are more reactive as compared to the flat basal planes present in the horizontal film.

12:00 PM EQ20.10.13

Phase Engineering of Group VIB Transition Metal Dichalcogenides via a Thermodynamically Designed Gas-Solid Reaction Geosan Kang¹, Dae-Hyun Nam², Gun-Do Lee¹ and Young-Chang Joo¹; ¹Seoul National University, Korea (the Republic of); ²Daegu Gyeongbuk Institute of Science & Technology, Korea (the Republic of)

2D transition metal dichalcogenides (TMDs) have been increasingly studied due to their wide range of optical, mechanical, chemical, and electric properties, from metal to insulator. 2D TMDs has graphene-like layered structure but with a controllable wide-bandgap by their atomic arrangement. Structural phase control in TMDs provides a variety of material phenomena that can be applied to tune the intrinsic properties. In general, group VIB TMDs can have thermodynamically stable semiconducting 2H phases and metastable metallic 1T phases. Recently, S vacancy-driven atomic diffusion has been studied to be an efficient approach for polymorphic transition from 2H-MoS₂ to 1T-MoS₂ by using carbon monoxide (CO)-mediated gas-solid reaction. Gas-solid reaction behaviors in nanomaterials can be predicted by their thermodynamic Gibbs free energy. The processing parameters of gas-solid reactions, such as the temperature and pressure, can be predicted using thermodynamic calculations that can be applied to drive targeted reactions. By using thermodynamic predictions and the properties of gas-solid reactions, the targeted reaction can be selectively induced among various competing reactions in multicomponent systems.

In this study, phase engineering of group VIB TMDs: WS₂ and MoS₂ was performed via CO-based gas-solid reactions with thermodynamic prediction. We predicted the thermal stability of chemical compounds corresponding to the process conditions and designed a process window map with the temperature and CO ratio. Each predicted phases appeared as oxides, sulfides, carbides and metals. In the synthesis of TMDs with precursors in a CO-mediated reaction environment, the metallic species exhibited a variety of phases within the quaternary-element system with Sulfur, Oxygen and Carbon. The trend of experimental fabrication was consistent with the prediction by the thermodynamic model. Synthesized TMDs exhibited 2H- to 1T-phase transition. 1T transition ratios was compared in two different TMDs according to the process parameters. The reaction between CO and S atoms became more active with increasing temperature, CO ratio, and calcination time that promote considerable S vacancy formation and cause phase transition. This revealed that gas-solid reactions-induced S vacancy formation triggered T-phase formation in not only MoS₂ but also WS₂.

This work presents the possibility of phase engineering TMDs through thermodynamic prediction, thereby helping to improve the synthesis efficiency of targeted materials and promoting expanded phase engineering of a variety of 2D nanomaterials as well.

12:05 PM EQ20.10.20

Late News: A Facile Strategy for the Synthesis of Tungsten Disulfide Monolayers from Solid Oxide Precursor Grown by Pulsed Laser Deposition Denys Miakota¹, Ganesh Ghimire¹, Raymond R. Unocic², Rajesh Ulaganathan¹, Fabian Bertoldo¹, Sara L. Engberg¹, Kristian S. Thygesen¹, David Geohegan² and Stela Canulescu¹; ¹Technical University of Denmark, Denmark; ²Oak Ridge National Laboratory, United States

Two-dimensional (2D) WS₂ is among the most intriguing representatives of the semiconducting transition metal dichalcogenide (TMD) family with a direct bandgap ~2 eV. WS₂ material shows extraordinary properties at the monolayer limit, such as strong light absorption, one of the lowest electron effective masses, high (>6.4%) photoluminescence yield (which can be further enhanced via doping), excellent thermal stability, mechanical flexibility and access to valley degree of freedom. Strong light absorption and emission at visible wavelengths opens great opportunities for its integration in ultrathin optoelectronic devices, such as light-emitting diodes, photodetectors, photovoltaic cells, and microcavity lasers.

However, for any practical application of WS₂, it is required to find a method to grow uniform and highly oriented WS₂ monolayers with a precise control over the layers number on a large scale. Tremendous efforts were devoted to study 2D TMD growth and examine their electronic and structural properties. Recently, several approaches were suggested to obtain a wafer-scale production of TMD monolayers. These methods include chemical vapor deposition (CVD), metal-organic chemical vapor deposition (MOCVD)¹, magnetron sputtering, and molecular beam epitaxy (MBE), etc. Pulsed laser deposition (PLD) is one of the prominent ways to synthesize TMD monolayers, which has demonstrated its potential for 2D materials synthesis both via direct growth² and two-step process³.

In this paper, we report on two-step synthesis of WS₂ mono- and multilayers by high-temperature sulfurization of oxygen-deficient tungsten oxide films obtained by PLD on sapphire. PLD is an established method to grow high-quality oxides with sharp interfaces, and it offers great opportunities to control crystalline quality of the material and its composition. This is achieved by deposition of precursors at different substrate temperatures and background gases (oxygen and argon). The X-ray photoelectron spectroscopy (XPS) results reveal that by changing the growth conditions in the PLD process, the properties of WO_x precursors can be significantly varied.

Next, we unravel how the presence of intrinsic oxygen vacancies in the tungsten suboxide (WO_x) precursor leads to a more facile conversion from WO_x to WS₂ films in a CVD process. Our study suggests that native oxygen vacancies in the PLD-grown precursors can serve as niches through which sulfur atoms enters the lattice and facilitates the growth of WS₂ crystals with high photoluminescence (PL) emission and large domain size. Indeed, the overall PL emission increases ~40 fold while the full width of half maximum (FWHM) of the PL peak decreases significantly for WS₂ crystals synthesized from precursors with a high content of oxygen vacancies as compared to that obtained from nearly stoichiometric counterpart. Based on atomic resolution images we will discuss intrinsic, grain boundaries, bilayer WS₂ crystal orientation evolve from nearly stoichiometric oxides to highly reduced oxide

precursors.

Our studies reveals how the epitaxial WO_x precursors with tunable properties grown by PLD can be used to independently control the nucleation, lateral growth and ultimately the WS_2 domain size.

1. Cun, H. *et al.* Wafer-scale MOCVD growth of monolayer MoS_2 on sapphire and SiO_2 . *Nano Res* 12, 2646–2652 (2019).
2. Bertoldo, F. *et al.* Intrinsic Defects in MoS_2 Grown by Pulsed Laser Deposition: From Monolayers to Bilayers. *ACS Nano* 15, 2858–2868 (2021).
3. Xu, X., Wang, Z., Lopatin, S., Quevedo-Lopez, M. A. & Alshareef, H. N. Wafer scale quasi single crystalline MoS_2 realized by epitaxial phase conversion. *2D Mater* 6, (2019).

SESSION EQ20.21: Advanced Characterization of 2D Materials II
Session Chairs: Cinzia Casiraghi and Nahid Talebi
Tuesday Afternoon, December 7, 2021
EQ20-Virtual

1:00 PM *EQ20.21.01

Challenges and Opportunities with 2D- Nanoporous Membranes [Aleksandra Radenovic](#); Ecole Polytechnique Federale Lausanne, Switzerland

Atomically thin (2D) nanoporous membranes are an excellent platform for a broad scope of academic research. Their thickness and intrinsic ion selectivity (demonstrated for example, in molybdenum disulfide MoS_2) make them particularly attractive for single molecule biosensing experiments and osmotic energy harvesting membranes. Currently, one of the significant challenges associated with the research progress and industrial development of 2D nanopore membrane devices is small scale thin film growth and small area transfer methods. This challenge has been recently tackled. Beyond large area growth and integration into devices, several other essential aspects such as mechanical stability and pore geometry, pore shape stability and its chemical termination require close attention from the community working with the 2D nanoporous membrane.

1:30 PM EQ20.21.02

Fingerprinting the Impact of p- and n-type Dopants on the Structural and Local Electrical Properties of Indium Selenide by Means of State-of-the-Art Transmission Electron Microscopy [Abel Brokkelkamp](#)¹, Sergiy Krylyuk², Laurien Roest¹, Isabel Postmes¹, Jaco ter Hoeve^{3,4}, Juan Rojo^{3,4}, Albert Davydov² and Sonia Conesa-Boj¹; ¹TU Delft, Netherlands; ²National Institute of Standards and Technology, United States; ³Vrije Universiteit Amsterdam, Netherlands; ⁴Nikhef, Netherlands

Indium Selenide (InSe) is a remarkable two-dimensional quantum material whose characteristic properties include a bandgap that increases with fewer layers and a high controllability of p- and n-type doping. Furthermore, its bandgap can lie in the near infrared region, depending on the specific crystalline phase adopted. Indium Selenide is known to crystallize in either the $\beta(2\text{H})$ -, $\gamma(3\text{R})$ - or the $\epsilon(2\text{H})$ -phase. Of these three crystalline phases, only the $\beta(2\text{H})$ and $\gamma(3\text{R})$ ones exhibit a direct bandgap, which makes them particularly suitable for optoelectronic applications. However, while the $\beta(2\text{H})$ -phase can be easily disentangled from the other, the $\gamma(3\text{R})$ - and $\epsilon(2\text{H})$ -phases are indistinguishable from the in-plane point of view and appear also very similar from the out-of-plane one. An attractive possibility to tailor the optoelectronic properties of InSe is based on the introduction of dopants, which leads to structural defects and can modify the crystalline structure and symmetry properties of the material. In this work, we investigate p- and n-doped (as well as undoped) Indium Selenide by means of Transmission Electron Microscopy and related techniques. We determine the crystalline phase present in these Indium Selenide specimens with High Resolution TEM by means of a systematic investigation of both in- and out-of-plane cross-sections, and compare the structural differences arising from different types and amounts of doping. We further assess the impact of dopants on the local electronic properties using Electron Energy-Loss Spectroscopy (EELS) by comparing how relevant features in the spectra (including surface- and edge-related properties) depend on the doping. Finally, we deploy Machine Learning techniques for a model-independent subtraction of the Zero Loss Peak, which makes possible identifying in an unbiased manner the impact of dopants in InSe in the ultra-low-loss region of the EELS spectra.

1:45 PM EQ20.21.03

In Situ Environmental Scanning Electron Microscopy of Aging Dynamics in 2D Materials [Ye Fan](#)¹, Ryo Mizuta¹, Peter Voorhees² and Stephan Hofmann¹; ¹University of Cambridge, United Kingdom; ²Northwestern University, United States

2D materials have been under the spotlight for over a decade. Given the multitude of promising properties demonstrated at lab-scale, a host of disruptive technologies with exponentially improved performances were expected to revolutionise markets ranging from integrated electronics to catalysis. In reality, however, the emergence of such game-changers has been significantly delayed. One major reason is the aging and failure of 2D materials in real working environments [1,2], the dynamics of which remain poorly characterised.

Here, we present an *in situ* study of the thermal oxidation of transition metal dichalcogenide monolayers to foster a fundamental understanding of the corrosion and aging dynamics in 2D materials. The full corrosion process is monitored in real-time, from the nanometre to sub-millimetre scale, utilising a custom *in situ* environmental SEM (ESEM), permitting conventional theories of materials corrosion to be tested in the 2D limit. We focus on the emergence of corrosion pits in WS_2 monolayers during oxidation, leveraging the ESEM's large field of view to simultaneously track up to 10^3 to 10^4 pits. The corrosion kinetics are quantified by analysing the growth kinetics of individual pits, based on which the corrosion kinetics are found to transition from a reaction-limited to a diffusion-limited regime as a function of oxidation temperature. Moreover, an acceleration of corrosion is found to occur when adjacent corrosion pits coalesce with each other. All results are compared with phase field modelling, which provide a predictable model for the 2D thermal oxidation process. Our study demonstrate the power of the *in situ* ESEM in elucidating material aging mechanisms 2D materials at the nanoscale.

References:

- [1] Gao et al., *ACS Nano*, 2016, 10(2), 2628
- [2] Li et al., *J. Mater. Chem. A*, 2019, 7(9), 4291

2:00 PM EQ20.21.04

Late News: 2D MXenes—Visible Black But Infrared White Materials [Yang Li](#), Xiong Cheng, He Huang, Tianshou Zhao and Baoling Huang; Hong Kong University of Science and Technology, Hong Kong

In nature, most of the visible black materials have high absorption/emission in the mid-IR region (2.5-20 μm). Visible black materials with low infrared absorption/emission (or IR white) are rare but highly desired in numerous areas, such as solar energy harvesting, multispectral camouflage, thermal

insulation, and information security management. Due to the lack of wavelength selectivity in intrinsic materials, such counter-intuitive properties are generally realized by constructing complicated subwavelength metamaterials such as plasmonic nanostructures and photonic crystals with costly nanofabrication techniques. Here, for the first time, the intrinsically low mid-IR emissivity (down to 10%) of the black 2D $\text{Ti}_3\text{C}_2\text{T}_x$ MXene is reported. Associated with a high absorbance of 90% in average over the solar spectrum, it embraces the best wavelength selectivity among the reported intrinsic black solar absorbing materials. Its appealing potentials in multispectral camouflage, smart textiles, and anti-counterfeiting applications are experimentally demonstrated. First-principles calculations reveal that the IR emissivity of MXene relies on both the nanoflake orientations and terminal groups, indicating great tunability. The calculations also suggest more potential low-emissivity MXenes including Ti_2CT_x , Nb_2CT_x , and V_2CT_x . This work opens the avenue to further exploration of a family of intrinsically low-emissivity materials with over 70 members.

2:15 PM EQ20.21.05

Detecting Charge Dissipation and Conductance Switching in Graphene Nanodevices in a STEM Ondrej Dyck¹, Jacob L. Swett², Andrew R. Lupini¹, Jan Mol² and Stephen Jesse¹; ¹Oak Ridge National Laboratory, United States; ²University of Oxford, United Kingdom

Feedback-controlled electroburning of graphene nanoribbons has been shown to be effective at creating nanogaps within the ribbon.¹⁻³ Molecules introduced into these nanogaps form tunnel junctions which can form the basis for molecular rectifiers, switches, transistors, or sensors.³ Secondary electron e-beam induced current (SEEBIC) is a technique that can be used to reveal sample conductivity and connectivity with high spatial resolution in a scanning transmission electron microscope (STEM).^{4,5} Here, we use feedback-controlled electroburning *in situ* to observe the evolution of the sample while it is being burned. We leverage the SEEBIC technique to image conductive, connected regions of the sample and diagnose device failures. When a nanogap is formed, producing a non-ohmic device response, the SEEBIC signal is observed to display dynamic contrast variation. A significant component of this contrast variation can be attributed to conductance switching in the high resistance region of the graphene nanodevice as the beam differentially charges the substrate. These results suggest that the SEEBIC imaging technique can be leveraged to provide information about charge flow and dynamic variations in conductance at the nanometer scale.⁶

References

- (1) Sarwat, S. G.; Gehring, P.; Rodriguez Hernandez, G.; Warner, J. H.; Briggs, G. A. D.; Mol, J. A.; Bhaskaran, H. Scaling Limits of Graphene Nanoelectrodes. *Nano Lett.* **2017**, *17* (6), 3688–3693. <https://doi.org/10.1021/acs.nanolett.7b00909>.
- (2) S. Lau, C.; A. Mol, J.; H. Warner, J.; D. Briggs, G. A. Nanoscale Control of Graphene Electrodes. *Phys. Chem. Chem. Phys.* **2014**, *16* (38), 20398–20401. <https://doi.org/10.1039/C4CP03257H>.
- (3) Prins, F.; Barreiro, A.; Ruitenber, J. W.; Seldenthuis, J. S.; Aliaga-Alcalde, N.; Vandersypen, L. M. K.; van der Zant, H. S. J. Room-Temperature Gating of Molecular Junctions Using Few-Layer Graphene Nanogap Electrodes. *Nano Lett.* **2011**, *11* (11), 4607–4611. <https://doi.org/10.1021/nl202065x>.
- (4) Hubbard, W. A.; Mecklenburg, M.; Chan, H. L.; Regan, B. C. STEM Imaging with Beam-Induced Hole and Secondary Electron Currents. *Phys. Rev. Appl.* **2018**, *10* (4), 044066. <https://doi.org/10.1103/PhysRevApplied.10.044066>.
- (5) Dyck, O.; Swett, J. L.; Lupini, A. R.; Mol, J. A.; Jesse, S. Imaging Secondary Electron Emission from a Single Atomic Layer. *Small Methods* **2021**, *5* (4), 2000950. <https://doi.org/10.1002/smt.202000950>.
- (6) This work was supported by the U.S. Department of Energy, Office of Science, Basic Energy Sciences, Materials Sciences and Engineering Division (A.R.L., S.J., O.D.). The authors acknowledge use of characterization facilities within the David Cockayne Centre for Electron Microscopy, Department of Materials, University of Oxford, alongside financial support provided by the Henry Royce Institute (Grant ref EP/R010145/1).

2:20 PM EQ20.21.06

Infrared and Magnetic Study of the van der Waals Semiconductor $\text{Co}_2\text{P}_2\text{S}_6$ Ben Mallett^{1,2}, Kiri Van Koughnet¹, Shen V. Chong^{1,2}, Bob Buckley^{1,2}, Benjamin Conner³ and Michael Susner³; ¹Robinson Research Institute - Victoria University of Wellington, New Zealand; ²The MacDiarmid Institute for Advanced Materials and Nanotechnology, New Zealand; ³Air Force Research Laboratory, United States

We report the results of a study of the temperature-dependent infrared spectroscopy and magnetism of single crystals of the antiferromagnetic semiconductor, $\text{Co}_2\text{P}_2\text{S}_6$. For comparison, we also report results on a second crystal substituted with 20% non-magnetic, closed-shell Zn. Concurrent with other, recent reports we observe a transition from a paramagnetic to antiferromagnetic state with a Neel temperature at $T_N \sim 120$ K. The magnetic transition is strongly reflected in differences between the infrared spectra taken above and below T_N . At 300 K we identify 4 relatively narrow phonon modes and a very broad mid-IR absorption while below T_N we observe that several new phonons appear, and a number alter their oscillator strength. The lowest energy mode exhibits significant asymmetry. With Zn doping significant changes occur at low energies where the motion is dominated by the transition metal atoms while the high energy modes, where motion is largely restricted to the sulphur atoms, are less affected.

2:25 PM EQ20.21.07

A Clean TEM Sample Preparation Technique for CVD-Grown TMD Monolayers Shichen Fu, Mengqi Fang, Zitao Tang, Siwei Chen, Kyungnam Kang and Eui-Hyeok Yang; Stevens Institute of Technology, United States

Transmission electron microscopy (TEM) and scanning transmission electron microscopy (STEM) are extensively used to characterize chemical vapor deposition (CVD)-grown transition metal dichalcogenides (TMDs). To prepare the specimens for such an imaging, a polymethyl methacrylate (PMMA) assists wet-etching transfer technique is often used^[1]. Here, PMMA residues can affect the TEM image quality, especially under high-magnifications. While thermal annealing under vacuum is typically performed to reduce the residue problem, the process can still damage TMD monolayers due to their poor in-air stability^[2]. Here, we present an enhanced sample preparation technique for the TEM imaging of CVD-grown TMD monolayers, and the sample attachment onto a TEM grid, reducing TMD oxidation of monolayers. The new steps incorporated in this process include a thorough PMMA removal using acetone at 60 C followed by annealing at 350 C in 0.01 mTorr for 4 hours, which was corroborated by measuring Energy-dispersive X-ray spectroscopy (EDS). In addition, we dropped PMMA in a liquid form onto the TEM grid to fully cover the sample with the grid, ensuring a firm attachment of TMDs onto the grid during acetone washing. The sample was checked by scanning electron microscope (SEM), which confirmed that the TMD monolayers were successfully transferred onto TEM grids. Further, combining the EDS and EELS measurements, a significantly reduced carbon signal was observed. The high-resolution TEM (HRTEM) showed no polymer residues over the imaged regions, while the atomic structures were clearly seen. Several STEM images were also collected, and no e-beam radiation damage was observed.

Reference

- [1] L. Zhang, *Nanoscale* **2017**, *9*, 19124.
- [2] K. Kang, *Adv. Mater.* **2017**, *29*, 1603898.
- [3] J. Lin, *APL Mater.* **2016**, *4*, 116108.

2:30 PM EQ20.21.08

In Situ Spectroscopic Ellipsometry for Monitoring Bi_2Se_3 Growth in Molecular Beam Epitaxy Maria Hilsel¹, Xiaoyu Wang², Phoebe Killea², Frank Peiris² and Roman Engel-Herbert¹; ¹The Pennsylvania State University, United States; ²Kenyon College, United States

Two-dimensional materials cover a large range of high-interest properties such as high mobility, piezo- and ferroelectricity, scalable band gap, and topological non-trivial band structures to name a few. The key to access and study those properties lies in high-quality materials synthesis, which in turn requires precise control over relevant growth parameters. The complex interplay of rate and relative flux ratio of the supplied constituents as well as substrate temperature at the growth front determines film growth rate, and stoichiometry. However, to date, there is no unifying method to measure these parameters in real time. Commonly used methods to monitor flux rates or film thickness and temperature differ in accuracy and applicability. Consequently, rather large unintentional deviations exist in reported values which presents a sizeable problem in the reproducibility of growth conditions, in particular for the growth temperature.

With our work, we propose in-situ spectroscopic ellipsometry (SE) as an alternative method that offers the potential for absolute temperature measurements and simultaneous determination of physical film thicknesses in-operando and non-destructively which furthermore can be used by any deposition technique. Using in-situ SE during molecular beam epitaxy (MBE) growth, we have developed a precise model for the dielectric function of Bi_2Se_3 thin films grown on Al_2O_3 substrates that allows to extract and thus monitor film thickness and growth temperature simultaneously. Throughout our work, we used an infrared (IR) camera system and X-ray reflectivity (XRR) to calibrate our SE measurements against absolute temperature in-situ and against physical film thickness ex-situ for which we capped Bi_2Se_3 films with an amorphous Se layer to protect them against oxidation under ambient pressure conditions.

In the first part we demonstrate the dielectric model for the Al_2O_3 substrate and the thickness dependence for the Bi_2Se_3 thin film model at the fixed growth temperature of 225 °C for 5 samples. The dielectric model obtained by in-situ SE proofed to be very sensitive to film thickness changes with a precision of about 1 %.

In the second part we show in-situ SE measurements performed on the same samples at different temperatures to demonstrate temperature dependent changes in the dielectric function of Bi_2Se_3 for fixed film thickness. Having thus decoupled thickness and temperature related changes in the dielectric function, we included temperature effects in our model, which allowed us to monitor the film temperature with a precision of about 10 K.

Based on the presented data, in-situ SE bears the potential to serve as an ultimate baseline for thickness and temperature calibration for two-dimensional materials, thus enhancing reproducibility and advancing material quality.

SESSION EQ20.22: Poster Session IV: Physical Properties of 2D Materials
Session Chairs: Joshua Robinson and Andrey Voevodin
Tuesday Afternoon, December 7, 2021
EQ20-Virtual

4:00 PM EQ20.22.01

Unique 2D Metal Chalcogenide Material Synthesis by Molecular Building Blocks Veronika Brune, Fabian Hartl, René Weißing, Michael Wilhelm and Sanjay Mathur; University of Cologne, Germany

The lacking control of large scale and homogeneous preparation of well-known 2D van der Waals materials MS_2 ($\text{M} = \text{Mo}^{\text{IV}}, \text{W}^{\text{IV}}, \text{Ti}^{\text{IV}}, \text{Sn}^{\text{IV}}$), MS ($\text{M} = \text{Sn}^{\text{II}}, \text{Ge}^{\text{II}}$) for commercial application, motivated us to develop a unique synthetic approach to molecular precursors for layered 2D van der Waals materials. A uniform synthesis route of molecular building blocks for controlled formation of stable precursor class $[\text{M}(\text{SEtN}(\text{Me})\text{EtS})_x]$ ($\text{M} = \text{Mo}^{\text{IV}}, \text{W}^{\text{IV}}, \text{Ti}^{\text{IV}}, \text{x} = 2$; $\text{M} = \text{Ge}^{\text{II}}, \text{Sn}^{\text{II}}, \text{x} = 1$) was observed by using chelating SNS ligand systems and suitable metal precursors, which have been fully characterized by NMR, TG-DSC, mass spectroscopic and single crystal analysis. Following the simple synthetic protocol of new metal chalcogenide complexes isolation of (air)stable molecular precursors have been performed. These complexes enabled the targeted preparation of homogeneous crystalline 2D MoS_2 , WS_2 , TiS_2 , SnS_2 and SnS by varying thermal based decomposition experiments as well as using wet chemical decomposition routes, resulting in SnS and SnS_2 particles. The as prepared 2D materials have been identified by XRD, XPS, SEM and TEM analysis.

The presented molecular building blocks provide an extraordinary synthetic approach to a unique molecular precursor class for 2D material preparation.

4:05 PM EQ20.22.02

Band Engineering and Quantum Well Formation in Semiconducting Defective Graphene Multilayers—A First-Principles Study Yuta Taguchi, Masayuki Toyoda and Susumu Saito; Department of Physics, Tokyo Institute of Technology, Japan

Two dimensional van der Waals "heterostructures", which consist of two dimensional materials such as pristine graphene, hexagonal boron nitride and transition-metal dichalcogenides, have attracted much attention because they have various interesting electronic properties. The heterostructures are expected to be promising device materials in the next generation. Up to now, two dimensional materials without intentional defects have been used. However, periodically modified graphene with various types of defects, "graphene antidot lattices", are also expected to be the components of the heterostructures in the near future. Graphene antidot lattices have been studied theoretically for the last two decades and it is known that they can be semiconductors with the band gap values of 0 to 2 eV. We have studied the electronic properties of the graphene antidot lattices with the triangular defects in the super honeycomb arrangement. It is found that the band gap value can be tuned between 0.1 and 1.3 eV and the eigenvalue at the conduction band edge is nearly independent of the size of the defects while the eigenvalue at the valence band edge is strongly dependent on the size of the defects with the super-honeycomb-lattice-constant fixed. We should design both Type1 and Type2 quantum well structures by stacking the graphene antidot lattices with the triangular defects in the super honeycomb arrangement. From this background, we investigate the electronic properties of the trilayer systems consisting of the graphene antidot lattices with the triangular defects in the super honeycomb arrangement by performing first-principles electronic structure calculations within the framework of the density-functional theory. We study the stabilities, the electronic structures and the electronic states of the valence and conduction band edges. A graphene sheet with smaller band gap is sandwiched between two sheets with larger band gaps. It is found that electronic structures near the valence edge are independent of the stacking sequence while the electronic structures near the conduction band edge strongly depend on the stacking sequence. Interestingly, it is also found that both electrons and holes are expected to be confined in the middle layer for some cases. In other words, these types of trilayer graphene systems have Type1 quantum well structure. This result opens a new way of realizing a very thin quantum well laser of graphene antidot lattices. We will also report on the effect of the chemical doping and the electronic field.

4:10 PM EQ20.22.05

$\text{N,N}'$ -Dimethylformamide Sensor in a Contaminated Solution Based on the Specific Interaction on Molybdenum Disulfide Akito Fukui¹, Hiroaki Onoe², Shun Itai², Keiko Ishikura², Hidekazu Ikeno¹, Yuh Hijikata³, Jenny Pirillo³, Takeshi Yoshimura¹, Norifumi Fujimura¹ and Daisuke Kiriya¹; ¹Osaka Prefecture University, Japan; ²Keio University, Japan; ³Hokkaido University, Japan

$\text{N,N}'$ -dimethylformamide (DMF) is one of the industrially important solvents. DMF is easily absorbed into the human body by inhalation or skin

absorption. DMF is metabolized to generate N-methylformamide (NMF), which is highly toxic for the human body^[1]. In addition, DMF molecule shows cytotoxicity, and 50% inhibitive concentration is about 1 v/v% in a culture fluid^[2]. Therefore, it is important to monitor DMF concentration at a scale of 0.1 % in a situation of contaminated solution. However, it is so far not easy to monitor DMF in solutions because of the low reactivity of DMF molecules, and the coexistence of polar molecules such as water prohibits the detection of DMF molecules. In this study, we examine the interaction between DMF molecules and transition metal dichalcogenides and found a specific interaction with DMF molecules on the surface. This specific interaction enables to generate DMF sensor to monitor the concentration even in a contaminated solution such as a cell culture fluid.

A metal-oxide-semiconductor field-effect transistor (MOSFET) was fabricated by a standard lithography process. The channel material is MoS₂ in this study. Transfer characteristic curves of MoS₂ MOSFET show usual n-type behavior with an average ON/OFF ratio of 10⁵. By treating DMF solution, the drain current dramatically increases, and the MOSFET shows small electrostatic modulation by applying gate voltage. From the MOSFET characteristics, DMF molecules show n-type donor property to MoS₂ with achieving degenerate doping level. By using the strong donor ability of DMF molecules for MoS₂, we examined the DMF sensor in contaminated solutions. A microfluidic chamber was fabricated over the MoS₂-MOSFET device, and DMF-mixed solution in 0.15 M NaCl_{aq} was introduced in the microchannel. MOSFET monitors the MoS₂ surface state and we found that the drain current can successfully distinguish the DMF concentration in NaCl solution at the concentration level of 0.1 v/v%.

To further investigate the mechanism of DMF-MoS₂ interaction, we calculated the frontier orbitals of DMF and band alignment with MoS₂ by DFT (B3LYP) method. From the calculation, we found that the location of the HOMO energy level of DMF molecule is under the conduction band of MoS₂, therefore, the n-type behavior would not be a usual electron transfer process. By further DFT calculation with the structural optimization of the interaction between DMF and MoS₂ and we found that the DMF molecules would be specifically oriented on the oxygen adatoms on MoS₂.

[1] N. Sun et al., *Sensors & Actuators: B. Chemical*, 261, 153-160 (2018)

[2] Jamalzadeh. L et al., *Avicenna J Med Biochem.*, 4(1):e33453. (2016)

4:15 PM EQ20.22.06

Novel Bipolar Exfoliated Graphene-Based Electrochemical Aptasensors for Sensitive Label-Free Detection of Cancer Biomarkers Shahrzad Forouzanfar, Iman Khakpour, Nezhdeh Pala, Chunlei Wang and [Borzooye Jafarizadeh](#); Florida International University, United States

Early detection of cancer can noticeably increase the survival chance of many cancer patients. Quantifying cancer biomarkers detectable from blood is an efficient way for the early detection of cancer diseases. In recent years, the application of synthetic DNA or RNA-based bio-recognizers (i.e., aptamers) in cancer biomarker sensor development has been vastly investigated. Electrochemical label-free aptamer-based biosensors (also known as aptasensors) are highly suitable for point-of-care applications. In this study, the application of bipolar exfoliated (BPE) graphene for developing cancer biomarker label-free aptasensors is explored. Graphene as a single, two-dimensional layer of carbon atoms has very remarkable features suitable for biosensor applications. The common graphene synthesis methods require complicated and costly processes and excessive use of harsh chemicals, as well as complex subsequent deposition procedures. In this study, a single setup has been used for exfoliation, reduction, and deposition of graphene nanosheets on a conductive electrode based on the principle of bipolar electrochemistry of graphite in deionized water. We investigated the properties of aptasensors based on graphene oxide (GO) deposited on a positive electrode feeding electrode and reduced-GO (rGO) deposited on a negative electrode feeding electrode. The PDGF-BB affinity aptamers were covalently immobilized by binding amino-tag terminated aptamers and carboxyl groups of GO and rGO surfaces. In this study, Fourier-transform infrared spectroscopy (FTIR) was used to study the surface characteristics of synthesized graphene and developed aptasensors. The scanning electron microscopy (SEM) was used to study the morphology of the bipolar exfoliated GO and rGO. The SEM study demonstrated that the rGO has a porous vertically aligned structure with pore sizes of around 100 nm, while GO has bulky flattened plates with random cracks. Cyclic voltammetry (CV) and differential pulse voltammetry (DPV) were used for characterizing the BPE graphene-based aptasensors in different stages of development and their sensing performances. The turn-off sensing strategy was implemented by measuring the peak-currents from DPV plots. The optimized aptasensor based on rGO showed a wide linear range of 0.75 pM-10 nM, high sensitivity of 7.83 A Logc⁻¹ (unit of c, pM), and a low detection limit of 0.53 pM. However, the optimized aptasensor based on GO reached its saturation point around 150 pM. This study demonstrated that bipolar electrochemistry is a simple yet efficient technique that could provide high-quality graphene for biosensing applications. Considering the BPE technique's simplicity and efficiency, this technique is highly promising for developing feasible and affordable lab-on-chip and point-of-care cancer diagnosis technologies. <!--[endif]-->

4:20 PM EQ20.22.08

Tailoring Laser Induced Graphene Porosity for Pressure Sensing [Tessa Van Volkenburg](#)^{1,2}, Nick Kantack¹, Spencer Langevin¹ and Zhiyong Xia¹; ¹Johns Hopkins University Applied Physics Laboratory, United States; ²Johns Hopkins University, United States

Laser induced graphene (LIG) is a rapid fabrication technique for producing passive sensors that are lightweight, flexible, and tailored for applications ranging from biometric analysis to chemical detection. Through laser irradiation of a substrate surface, typically polyimide, a porous graphene can be formed whose electrical properties depend on the laser fluence, substrate composition, and atmosphere used. Though less conductive than traditional printed electronics, the porous nature has previously been leveraged to create piezoresistive sensors that change their conductivity in response to temperature, strain, or pressure. Additionally, the inherent robustness of polyimide substrates allows for application to extreme environments including space and ocean exploration. In this work, we expand on previous efforts to create LIG sensors for pressure measurement by correlating laser fluence and resultant graphene porosity to sensor hydrostatic response. The impact of laser fluence is investigated through changing speeds, powers, and density (pulses per inch) of the laser beam, and characterizing the porous structures formed with scanning electron microscopy. Hydrostatic testing at pressures up to 2,000 psi was also performed with supporting electronics to determine sensor response and validate the repeatability of the fabrication method. Through this work, we aim to demonstrate that by controlling the porosity of the graphene formed, and characterizing its piezoresistive response with respect to pressure, on demand passive pressure sensors can be fabricated for targeted pressure ranges and applications.

4:25 PM EQ20.22.09

Late News: Unusual-High Ion Conductivity in Large-Scale Patternable Two-Dimensional MoS₂ Wonbong Choi¹, [Sanket D. Bhoyate](#)¹ and Juhong Park^{1,2}; ¹University of North Texas, United States; ²Ark Power Technology, United States

The advancement of ion transport applications will require the development of new materials with a high ionic conductivity that is stable, scalable, and micro-patternable. We report unusually high ionic conductivity of Li⁺, Na⁺, and K⁺ in 2D MoS₂ nanofilm exceeding 1 S/cm, which is more than two orders of magnitude when compared to that of conventional solid ionic materials. The high ion conductivity of different cations can be explained by the mitigated activation energy *via* percolative ion channels in 2H-MoS₂ including the 1D ion channel at the grain boundary, as confirmed by modeling and analysis. We obtain field-effect modulation of ion transport with a high on/off ratio. The ion channel is large-scale patternable by conventional lithography, and the thickness can be tuned down to a single atomic layer. The findings yield insight into the ion transport mechanism of van der Waals solid materials and guide the development of future ionic devices owing to the facile and scalable device fabrication with superionic conductivity.

4:30 PM EQ20.22.10

Investigating Effects of Graphene Layers on Photonics Properties in MoS₂/Graphene Heterostructure Ensemble Prepared by Dry Transfer Method for Optoelectronic Applications [Sanju Gupta](#); University of Central Florida, United States

Two-dimensional layered materials that harvest or transduce light energy are of paramount interest. In this context, two-dimensional transition metal dichalcogenides such as molybdenum disulfide (MoS₂) are attractive for harnessing optoelectronics. In this work, we report the integration of MoS₂ with a strong electron accepting graphene yielding novel MoS₂ (1-2L)/graphene (1-2L) heterostructure ensemble by facile and efficient dry transfer method. We also found additional hetero-interfaces due to folded flakes such as MoS₂/MoS₂/graphene and MoS₂/MoS₂/Au hetero-interfaces. We characterized the heterointerfaces using correlated micro-Raman spectroscopy, photoluminescence (PL) spectroscopy, atomic force microscopy, Kelvin probe microscopy and conducting AFM, tip-enhanced Raman spectroscopy (TERS), and tip-enhanced photoluminescence (TEPL) techniques to gain insights into the structural quality, hetero-interfaces, and excitonic effects to elucidate the role of a number of graphene layers which are crucial in modulating the light emission. We studied the charge transfer in these vertical heterostructures unraveling the interlayer electronic coupling. We demonstrate strong evidence that the excitonic properties of MoS₂ are most effective for two layers of graphene layers underneath leading to a significant enhancement of the PL response as compared to MoS₂ supported on one-layer graphene and directly on the gold-coated substrate. We observed a marginal increase in work function with increasing MoS₂ layer as anticipated and for heterointerfaces which are indicative of electron injection. We measured C-AFM without light (dark) and with light in view of photoconducting properties of heterointerfaces and found a rectifying behavior with an apparent increase in current by almost twice for MoS₂/graphene heterostructures in contrast to MoS₂/Au which shows ohmic behavior. Our findings signify the importance of substrate engineering when constructing 2D multilayered architectures for harvesting or storing light energy. This work is financially supported in parts by NSF and NSF-MRI Grants.

4:35 PM EQ20.22.11

Late News: Dielectric and Substrate Engineered Tuning of Photoluminescence in Monolayer WS₂ [Tamaghna Chowdhury](#), Diptabrata Paul and Atikur Rahman; IISER Pune, India

The dielectric environment strongly influences the photoluminescence (PL) of transition metal dichalcogenide (TMD) monolayers. The PL spectra are usually modified by the defect states present in the monolayer and substrate interface. To study the effect of substrate defects on PL, we have gradually increased the separation between substrate and WS₂ by placing hBN of various thicknesses in between. Further dielectric engineering was done by patterning the substrate with holes and pillars. In this way, we were able to tune the contribution of trion and exciton in the PL of WS₂. An excitation power-dependent study was also done to understand the tuning mechanism of PL in various kinds of engineered substrates. The charge of the substrate defects is also important in determining the nature of the PL spectra in monolayer WS₂. This effect was also studied by treating the substrate with APTES which changes the nature of the charge carried by a SiO₂/Si substrate. This study will be important for the fabrication of valleytronic and excitonic interconnects.

SESSION EQ20.23: Physical Properties and Transport of 2D Materials
Session Chairs: Zakaria Al Balushi and Nicholas Trainor
Tuesday Afternoon, December 7, 2021
EQ20-Virtual

6:30 PM EQ20.23.01

Heavy Ion and Laser Irradiation Effects on MoS₂ Memtransistors [Christopher M. Smyth](#)¹, John M. Cain¹, Eric J. Lang¹, Khalid Hattar¹, Xiaodong Yan², Jiangtan Yuan², Matthew Bland², Taisuke Ohta¹, Stanley Chou¹, Vinod K. Sangwan², Mark C. Hersam^{2,2} and Tzu-Ming Lu¹; ¹Sandia National Laboratories, United States; ²Northwestern University, United States

Recently, a diverse range of memristive phenomena have been demonstrated in 2D transition metal dichalcogenides (TMD) in vertical and lateral device architectures. TMD-based memristors can exhibit unipolar and bipolar resistive switching, tunable set voltage, a resistance ratio as high as 10⁵, endurance up to 10⁷, thus, presenting a new opportunity for ultra-scaled memory cells [1-3]. The lateral architecture is implemented as a gate tunable memristor and relies on bias-induced Schottky barrier modulation, which either originates from defect migration or charge trapping/detrapping processes [4]. High performance is achieved in the lateral memristor architecture across an unusually wide defect density range up to ~50% [3]. Therefore, due to its inherent defect tolerance and ultrathin body [5], the TMD memristor may provide superior durability of in-memory computation in harsh radiation environments.

In this presentation, I will discuss the effects of 48 keV Au⁺ irradiation and 532 nm laser irradiation on the physical and electrical properties of the MoS₂ memristor as a function of photon exposure or 48 keV Au⁺ fluence. We employ X-ray photoelectron spectroscopy, Atomic Force Microscopy, Raman spectroscopy, and transmission electron microscopy to elucidate the structural and chemical effects of the radiation species and dose on polycrystalline MoS₂ grown by chemical vapor deposition. The V_G-dependent I_D-V_D response and gate-contact capacitance are measured ex-situ as a function of radiation dose to evaluate the radiation tolerance of the memristor and deconvolute the radiation effects in the gate oxide, respectively.

The S:Mo ratio of the MoS₂ decreases from 1.9 to 0.3 and the relative concentration of MoO_x increases from 0.1 to 0.5 after an ion fluence of 9E15 cm⁻². The E_{2g} mode exhibits a ~6 cm⁻¹ red shift and the intensities of the LO(M) and TO(M) defect modes increase after an ion fluence of 1E14 cm⁻², which corroborates the significant increase in defect concentration in the MoS₂ with increasing ion fluence. The ON/OFF ratio of the memristor devices is reduced from ~10 to ~0 after serial exposure to an ion fluence of 1E13 cm⁻² and a 532 nm laser. Interestingly, some memristor devices that are only ion irradiated retain initial electrical performance despite a significant increase in gate-contact capacitance. Our preliminary results suggest the MoS₂ memristor exhibits impressive tolerance to ionizing radiation.

This work was supported by a Laboratory Directed Research & Development program at Sandia National Laboratories. Sandia National Laboratories is a multimission laboratory managed and operated by National Technology & Engineering Solutions of Sandia, LLC, a wholly owned subsidiary of Honeywell International, Inc., for the U.S. DOE's National Nuclear Security Administration under contract DE-NA-0003525. The views expressed in the article do not necessarily represent the views of the U.S. DOE or the United States Government. This work was performed, in part, at the Center for Integrated Nanotechnologies, an Office of Science User Facility operated for the U.S. Department of Energy (DOE) Office of Science.

References:

[1] V. K. Sangwan et al. *Nature Nanotechnol.* 2015, 10, 403-406

- [2] R. Ge et al. *Nano Lett.* 2018, 18, 434-441
 [3] M. Wang et al. *Nature Electronics* 2018, 1, 130-136
 [4] V. K. Sangwan et al. *Nature* 2018, 554, 500-504
 [5] A. J. Arnold et al. *ACS Appl. Mater. Interfaces* 2019, 11, 8391-8399

6:45 PM EQ20.23.02

Xene Routes Towards Device Integration Christian Martella¹, Daya Sagar Dhungana¹, Chiara Massetti^{1,2}, Emiliano Bonera², Carlo Grazianetti¹ and Alessandro Molle¹; ¹CNR Institute for Microelectronics and Microsystems, Italy; ²Università degli Studi di Milano-Bicocca, Italy

Xenes, the two-dimensional (2D) monoelemental graphene-like materials, promise to open new research frontiers in the technological exploitation of atomically thin materials because of their scalability and of their rich physics varying from one member to another.^{1,2} However, significant challenges are at stake when considering the Xenes synthesis, stabilization and manipulation. Because of their artificial nature, Xene deposition usually requires an extreme control of the experimental conditions including growth temperature and substrate choice, in particular when an epitaxial matching is necessary. Moreover, strategies for overcoming the stabilization issues related to their manipulation in ambient condition are to be implemented. Taking the silicene case, namely the 2D buckled form of silicon, as paradigmatic of the Xenes family, here we show that meeting these requirements is often a matter of adopting smart experimental solutions. For example, the use of single crystal metal films grown on cleavable mica substrates allows for the development of manipulation schemes enabling portability and transfer of the Xene layers by means of mechanical and chemical delamination.³ In addition, the in-situ encapsulation of the silicene enables us to preserve the structural integrity against aging and degradation.⁴ Here we demonstrate that, when disassembled from the substrate, silicene of different forms, i.e. single layer, multilayer or heterostructured layers,⁵ can be bent by reshaping or rolling it around any macroscopic surface or object showing the emergence of a strain feature in its Raman response. Bendable silicene and Xenes may thus hold high potential for strain sensor devices. The work is within the ERC-COG 2017 Grant N0. 772261 "XFab".

- [1] A. Molle, J. Goldberger, M. Houssa, Y. Xu, S.-C. Zhang, D. Akinwande, *Nat. Mater.* **2017**, 16, 163.
 [2] C. Grazianetti, C. Martella, A. Molle, *Phys. status solidi – Rapid Res. Lett.* **2020**, 14, 1900439.
 [3] C. Martella, G. Faraone, M. H. Alam, D. Taneja, L. Tao, G. Scavia, E. Bonera, C. Grazianetti, D. Akinwande, A. Molle, *Adv. Funct. Mater.* **2020**, 30, 2004546.
 [4] A. Molle, G. Faraone, A. Lamperti, D. Chiappe, E. Cinquanta, C. Martella, E. Bonera, E. Scalise, C. Grazianetti, *Faraday Discuss.* **2020**, DOI 10.1039/c9fd00121b.
 [5] D. S. Dhungana, C. Grazianetti, C. Martella, S. Achilli, G. Fratesi, A. Molle, *Adv. Funct. Mater.* **2021**, 2102797.

7:00 PM EQ20.23.03

Achieving Open-Circuit Voltages Greater Than 500 mV by Applying Perovskite-Like Carrier-Selective Contacts to Transition Metal Dichalcogenide Solar Cells Cora Went¹, Joeson Wong¹, Phil Jahelka¹, Morgaine Mandigo-Stoba² and Harry A. Atwater¹; ¹California Institute of Technology, United States; ²University of California, Los Angeles, United States

Two-dimensional transition metal dichalcogenides (TMDCs) are promising candidates for ultrathin photovoltaics due to their high absorption coefficients and intrinsically passivated surfaces.¹ However, careful selection of carrier-selective contacts for efficient TMDC solar cells has never been seriously considered. Here, we demonstrate that open-circuit voltages greater than 500 mV are achievable in ultrathin (total cell thickness less than 150 nm) TMDC solar cells modeled on inverted perovskite device architectures. Currently, the highest efficiency inverted (p-i-n) perovskite solar cells employ the polymer hole-transporting layer PTAA as a bottom contact and the organic electron-transporting layer C60 as a top contact.^{2,3} Following this inverted perovskite geometry, we fabricate carrier-selective contact TMDC solar cells. We start with a template-stripped gold substrate, spin coat 10 nm of PTAA, exfoliate 15 nm of tungsten disulfide, thermally evaporate 10 nm of C60, and finally thermally evaporate 20 nm of silver with a bathocuproine interlayer. These devices achieve open-circuit voltages greater than 500 mV even with nonideal optical design. Using transfer matrix calculations, we demonstrate that short-circuit current greater than 20 mA/cm² is possible in a similar electronic architecture illuminated from the bottom through an ITO-coated glass substrate, with a 100-nm silver top contact as a back-reflector. We fabricate these devices and characterize them for their optoelectronic properties using one-sun illumination in a solar simulator, absorption and quantum efficiency measurements, photocurrent mapping, and power-dependent current-voltage sweeps. Finally, we discuss pathways to greater than 10% one-sun power conversion efficiencies. Our work demonstrates the transferability of perovskite carrier-selective contacts to TMDC solar cells, opening up the possibility for TMDCs to become a new low-cost, high-efficiency photovoltaic technology.

References:

1. D. Jariwala, A. R. Davoyan, J. Wong, H. A. Atwater, Van der Waals Materials for Atomically-Thin Photovoltaics: Promise and Outlook. *ACS Photonics* **4**, 2962–2970 (2017).
2. X. Zheng et al., Managing grains and interfaces via ligand anchoring enables 22.3%-efficiency inverted perovskite solar cells. *Nat. Energy* **5**, 131–140 (2020)
3. F. Li, et al., Regulating Surface Termination for Efficient Inverted Perovskite Solar Cells with Greater Than 23% Efficiency. *J. Am. Chem. Soc.* **142**, 20134–20142 (2020).

7:15 PM EQ20.23.04

Engineering the Electronic Structure of Two-Dimensional Materials with Near-Field Electrostatic Effects of Self-Assembled Organic Layers Qunfei Zhou¹, Bukuru Anaclat², Trevor Steiner³, Michele Kotiuga⁴ and Pierre Darancet⁵; ¹Northwestern University, United States; ²Pomona College, United States; ³University of Minnesota, United States; ⁴Ecole Polytechnique Federale de Lausanne, Switzerland; ⁵Argonne National Laboratory, United States

Engineering the electronic and physical properties, such as work function, band gaps and transport properties for two-dimensional (2D) materials is essential for their promising applications in advanced electronic and optoelectronic devices. In this work, we study the effect of experimentally self-assembled organic monolayers on the electronic properties of 2D materials using first-principles density functional theory calculations. Unlike surfaces of bulk materials, we find that 2D materials are strongly impacted by near-field electrostatic effects resulting from high multipoles of the organic layer electronic density. We show this effect can lead to significant (~0.5V) modulation of the in-plane potential experienced by the electrons within 4 Å of the molecular layer, with a transition between near- and far-field. We develop an electrostatic theory of this effect, showing that the effect of the molecular layer is akin to the one of a discretized planar charge density, which can be derived from the multipole moments of the molecules. Solving this model computationally and analytically, we propose implementations of this effect to generate novel electronic properties for electrons in 2D materials. As a proof of principle, we show that the near-field potential of phthalocyanine molecular monolayers deposited on graphene leads to bandgap opening.

7:30 PM EQ20.23.05

Effects of Molecular Structure and Chemistry on Molecular Doping to MoS₂ Serrae Reed¹, Milad Yarahi¹, Yifeng Chen², Yiren Zhong¹, David

Charboneau¹, Julia Curley¹, Fabian Menges¹, Nilay Hazari¹, Hailiang Wang¹, Su Ying Quek² and Judy Cha¹; ¹Yale University, United States; ²National University of Singapore, Singapore

Surface functionalization of 2D materials with organic electron donors (OEDs) is a powerful pathway to modulate the electronic properties of 2D materials. However, understanding of the doping mechanism is largely limited to categorization of molecular dopants as n- or p-type based on the relative position of the molecule's redox potential to the Fermi level of 2D host. Systematic studies to examine factors beyond redox potential for molecular doping are critically lacking. In our previous work, we showed that an organic dopant based on 4,4 bipyridine (DMAP-OED) has a doping power of 0.63-1.26 electrons per molecule to MoS₂ at maximum functionalization conditions.^[1] We calculated the molecular doping by measuring the carrier density of functionalized MoS₂ field effect transistors and estimating the molecular surface coverage of DMAP-OED by atomic force microscopy. We also observed that the molecular arrangement and surface coverage greatly affects the doping power of the molecule.

In this study, we use monolayer MoS₂ as a model 2D system and two molecular dopants, Me- and ^tBu-OED, which have the same redox potential but different ligand groups to probe the effects of molecular size and ligand chemistry on the molecular surface coverage and doping power to MoS₂. We show that, for the same functionalization conditions, the doping powers of Me- and ^tBu-OED are 0.22-0.44 and 0.11 electrons per molecule, respectively, demonstrating that the molecular size and ligand chemistry critically affect molecular doping. Using the stronger dopant, Me-OED, a carrier density of $1.10 \times 10^{14} \text{ cm}^{-2}$ is achieved in MoS₂, the highest doping level to date in MoS₂ by surface functionalization. We thus show that proper tuning of the molecular ligand chemistry and size is essential in the rational design of powerful molecular dopants.

[1] M. Yarali, Y. Zhong, S. N. Reed, J. Wang, K. A. Ulman, D. J. Charboneau, J. B. Curley, D. J. Hynek, J. V. Pondick, S. Yazdani, N. Hazari, S. Y. Quek, H. Wang, J. J. Cha, *Advanced Electronic Materials* 2020, n/a, 2000873.

7:45 PM EQ20.23.06

In Situ Collecting Ultrafast Hot Carrier as Photocurrent in Monolayer WS₂ Pan P. Adhikari¹, Peijiang Wang², Chendi Xie¹, Hao Zeng², Victor Klimov³ and Jianbo Gao¹; ¹Clemson University, United States; ²University at Buffalo, SUNY, United States; ³Los Alamos National Laboratory, United States

Extracting hot carriers as a photocurrent remains a challenge in materials science and quantum devices because the hot carrier lifetime is within the range of ultrafast picosecond. A more profound challenge is to understand the hot carrier drift dynamics. Here, we collect hot carriers as a photocurrent *in-situ* 2D WS₂ single layer photoconductor, characterized by the ultrafast photocurrent spectroscopy (UPCS). The hot carrier is induced by the rich exciton species interaction, attributed to the trion Auger recombination under low exciton density and biexciton Auger recombination at high exciton density, respectively. We further identify the hot carrier transport properties, manifested by the minimum mobility of $\sim 10 \text{ cm}^2/\text{Vs}$ and drift length of $\sim 8 \text{ nm}$.

8:00 PM EQ20.23.07

Ultra-Thin Amorphous Boron Oxynitride Dielectric Produced by RF Magnetron Sputtering Corey Arnold¹, Chukwudi E. Iheomamere¹, Spencer Gellerup¹, Nicholas Glavin², Christopher Muratore³, Nigel D. Shepherd¹ and Andrey A. Voevodin¹; ¹University of North Texas, United States; ²Air Force Research Laboratory, United States; ³University of Dayton, United States

Advancement in flexible microelectronics based on 2D materials urgently needs reliable, high dielectric strength and chemically inert dielectric materials, which can be economically produced using large area and low-temperature synthesis techniques. Among possible candidate dielectric materials, ultra-thin amorphous boron oxynitride recently emerged as an attractive material, which can be synthesized at low temperatures using physical vapor deposition methods. In this study, amorphous boron oxynitride films were deposited at room temperature on rigid and flexible substrates using radio frequency magnetron sputtering of a hexagonal boron nitride target in various argon-nitrogen background gas ratios. The effect of nitrogen content in the sputtering gas, changes in target-to-substrate distance, and magnetron power density to the target on the film composition were investigated with X-ray photoelectron spectroscopy and correlated to the dielectric breakdown strength and bandgap obtained from current-voltage measurements and Tauc plots, respectively. Films grown in pure Ar atmosphere at a large target-to-substrate distance displayed compositions containing metallic boron, which led to a decrease in the dielectric breakdown strength. The use of Ar:N₂ mixtures and pure N₂ eliminated metallic boron bonding. Decreasing the target-to-substrate distance and target power density during reactive sputtering resulted in B:N stoichiometry ratio closer to one and about 25 – 30 at.% oxygen. Amorphous boron oxynitride films grown in pure N₂ at a small target-to-substrate distance exhibited dielectric breakdown strength of 2.1 – 2.4 MV cm⁻¹, smooth surface topography, and a bandgap of 5.4 eV. Charge transport was field-dependent, with field-enhanced Schottky emission, Frenkel-Poole emission, and space-charge-limited conduction being observed in various field ranges. Test MIS structures comprised of $\sim 30 \text{ nm}$ thick boron oxynitride insulator and transparent ZnO semiconductor also grown at room temperature revealed a low interface trap concentration N_{it} of $7.3 \times 10^{10} \text{ cm}^{-2}$, and interface state density N_{ss} of $7.5 \times 10^{12} \text{ eV}^{-1} \text{ cm}^{-2}$. The results demonstrate the suitability of amorphous boron oxynitride for applications as an insulator or gate dielectric in flexible or transparent thin-film transistors and other electronics when a low processing temperature is required.

8:15 PM EQ20.23.08

Rapid Growth of Monolayer 2D Transition Metal Dichalcogenide Films for Large-Area Electronics Mengqiang Zhao¹, Danzhen Zhang², Chengyu Wen³ and A T Charlie Johnson³; ¹New Jersey Institute of Technology, United States; ²Drexel University, United States; ³University of Pennsylvania, United States

The large-scale growth of semiconducting thin films on insulating substrates enables batch fabrication of atomically-thin electronic and optoelectronic devices and circuits without film transfer. Here we report an efficient method to achieve rapid growth of large-area monolayer MoSe₂ films based on spin coating of Mo precursor and assisted by NaCl. Uniform monolayer MoSe₂ films up to a few inches in size were obtained within a short growth time of 5 min. The as-grown monolayer MoSe₂ films were of high quality with large grain size (up to 120 μm). Arrays of field-effect transistors were fabricated from the MoSe₂ films through a photolithographic process; the devices exhibited high carrier mobility of $\sim 27.6 \text{ cm}^2 \text{V}^{-1} \text{s}^{-1}$ and on/off ratios of $\sim 10^5$. The growth method was also applicable to other 2D transition metal dichalcogenides (TMDs), and rapid growth of large-area monolayer MoS₂, WS₂, and WSe₂ films were all successfully achieved. Our findings provide insight into the batch production of uniform thin TMD films and promote their large-scale applications.

10:30 AM EQ20.24.02

Hexagonal Metal Oxide Monolayers Derived from the Metal-Gas Interface Bao Yue Zhang and Jian Zhen Ou; RMIT University, Australia

Metal oxides, which is one of the most abundant substances in nature, are rarely found to be layered crystal. This hinders their potential to form into two-dimension (2D) since the cleavage of weak, interlayer van der Waals bonds in layered bulk crystal serves as the benchmark to obtain the atomically thin high-quality 2D layers such as ZnO¹. 2D-like non-layered metal oxides are usually created *via* a space-confined-growth^{2,4} or soft-chemically exfoliation of unilamellar bulk crystal⁵, in which external ionic groups may be induced to stabilize the crystals. In this talk, I will discuss our recent discovery of a series of the layered planar hexagonal phase of oxide from elements across the transition metals, post-transition metals, lanthanides and metalloids⁶. These oxides can be naturally formed from metallic surfaces under a controlled oxidation environment without involving sophisticated equipment or other chemicals. Subsequently, the hexagonal 2D metal oxide monolayers can be readily exfoliated on a substrate in a mechanical manner, similar to the way of obtaining graphene and other layered metal chalcogenides. We have selected the hexagonal TiO₂ as a representative to reveal the distinct properties of such hexagon crystal coordinated oxides apart from their bulk counterparts. The monolayered and few-layered hexagonal TiO₂ shows p-typed semiconductor behavior with the hole mobility up to 950 cm²V⁻¹s⁻¹ at room temperature. This research topic can possibly expand the exploration of metal oxides in the 2D quantum regime and initiate numerous applications in the future.

Reference

- 1 Tusche, C., Meyerheim, H. & Kirschner, J. Observation of depolarized ZnO (0001) monolayers: formation of unreconstructed planar sheets. *Physical review letters* **99**, 026102 (2007).
- 2 Xiao, X. *et al.* Scalable salt-templated synthesis of two-dimensional transition metal oxides. *Nature communications* **7**, 1-8 (2016).
- 3 Yang, J. *et al.* Formation of two-dimensional transition metal oxide nanosheets with nanoparticles as intermediates. *Nature materials* **18**, 970-976 (2019).
- 4 Son, J. *et al.* Epitaxial SrTiO₃ films with electron mobilities exceeding 30,000 cm² V⁻¹s⁻¹. *Nature materials* **9**, 482-484 (2010).
- 5 Ma, R. & Sasaki, T. Nanosheets of oxides and hydroxides: ultimate 2D charge bearing functional crystallites. *Advanced materials* **22**, 5082-5104 (2010).
- 6 Zhang, B. Y. *et al.* Hexagonal metal oxide monolayers derived from the metal-gas interface. *Nature Materials*, doi:10.1038/s41563-020-00899-9 (2021).

10:45 AM EQ20.24.03

Universal Synthesis of Layered Materials by Microwave-Induced-Plasma Assisted Method Apoorva Chaturvedi and Edwin H. Teo; Nanyang Technological University, Singapore

Layered van der Waals (vdW) materials, consisting of atomically thin layers, are of paramount importance in physics, chemistry, and materials science owing to their unique properties and various promising applications. However, their fast and large-scale growth via a general approach is still a big challenge, severely limiting their practical implementations. Here, we report a universal method for rapid (~60 min) and large-scale (gram scale) growth of phase-pure, high-crystalline layered vdW materials from their elementary powders via microwave plasma heating in sealed ampoules. This method can be used for growth of 30 compounds with different components (binary, ternary, and quaternary) and properties. The ferroelectric and transport properties of mechanically exfoliated flakes validate the high crystal quality of the grown materials. Our study provides a general strategy for the fast and large-scale growth of layered vdW materials with appealing physicochemical properties, which could be used for various promising applications.

11:00 AM EQ20.24.04

Two-Dimensional Janus Nanomaterials for Controllable Delivery and Imaging Application Wei Wang and Sehoon Chang; Aramco Services Company, United States

Anisotropic nanomaterials composed of two halves with different structure, chemistry, or polarity, known as Janus nanomaterials, have distinct properties when compared to symmetrically functionalized analogues. These materials have recently gained significant attention in many applications such as electronic thin films, drug delivery, sensors, optics, oil/water separation membranes, photoactivated micromotors, photocatalysts, and interfacial modification. Two dimensional (2D) Janus nanosheets are especially intriguing considering their interfacial properties as well as their ability to assemble into higher order and hybrid structures. In this research, we describe an approach to mass synthesis of Janus nanosheets consist of graphene, metal and ceramic materials in highly controllable ways via a novel "Interfacial Nanoreactor" system. We have characterized and proven the asymmetric structures of the synthesized Janus graphene nanosheets by Langmuir-Blodgett (LB) surface pressure-area (π -A) curves, fluorescence spectroscopy, contact angle measurement and scanning electron microscope (SEM) characterizations. As an example of applications in oil and gas industry, we have demonstrated that the Janus nanosheets with proper hydrophilic/hydrophobic functionalization can be directed onto interface of aqueous-organic bi-phase system and significantly lower the interfacial tension (IFT) between aqueous and organic phases, which promotes the oil recovery process in oil reservoir. With loading of proper imaging contrast agents (dyes or quantum dots) on one side and controlled hydrophilicity or hydrophobicity on the other side, the Janus nanosheets can be directed to confined microporous area, which enables to probe structural microheterogeneity of geological samples such as shale rocks by optical or microscopic imaging techniques.

11:15 AM EQ20.24.05

Late News: New Routes to Assessing and Enhancing the Yield of Hexagonal Boron Nitride Using Sustainable Liquid Phase Exfoliation Techniques Kai Ling Ng¹, Barbara M. Maciejewska¹, Zhicheng Xu¹, Dillon McGurty¹ and Nicole Grobert^{1,2}; ¹University of Oxford, United Kingdom; ²Williams Advanced Engineering, United Kingdom

The suitability of solvents for the efficient liquid phase exfoliation (LPE) to produce 2D materials such as hexagonal Boron Nitride (hBN) from their bulk starting materials is typically assessed by UV-Vis concentration measurements. However, UV-Vis concentration characterisation of liquid phase exfoliated 2D materials relies on good materials dispersibility within a given solvent for the data to reflect the actual solvent exfoliation efficiency.

'Green' solvents possess low boiling points and toxicity, which are the attractive solvent choice for LPE of 2D materials but the yield is low due to the limited materials dispersibility in these solvents. Therefore, the efficient liquid phase exfoliation to produce 2D materials is still largely relying on e.g., 1-Methyl-2-pyrrolidinone (NMP) which unfortunately is harmful to the environment and therefore hinders the large scale production. Here, to assess the exfoliation efficiency of 2D materials in 'green' solvents independently of their dispersibility, we performed dedicated exfoliation efficiency studies to enhance the yield of liquid phase exfoliated hBN and compared yields to the most studied 2D materials system to date, e.g. graphene.

We found that isopropanol (IPA) has the highest exfoliation efficiency (comparable to that of NMP), despite the poor dispersibility of graphene in IPA. We could also show that the dispersibility and concentration of layered materials in IPA is higher after a brief post-exfoliation sonication treatment without damaging the exfoliated 2D materials.

By studying shear-mixing processes and understanding the actual exfoliation efficiency of the solvents in detail, it is possible to double the hBN yield (and increase the graphene yield 10-fold) using IPA as the exfoliation medium. Our studies prove that the yield of hBN (and graphene) in green solvents is not limited by the exfoliation efficiency but it is due to its poor dispersibility in green solvents. Our findings pave the way for other post-exfoliation methods to optimise the yield through sustainable solvents exfoliation for industrial-scale, especially for hBN production.

11:30 AM EQ20.24.06

Late News: Synthesis of Two-Dimensional Silicon Carbide—Bridging Theory and Experiment [Sakineh Chabi](#); University of New Mexico, United States

In the past decade, research in the field of two-dimensional materials has exponentially transitioned from fundamental studies to the development of complex 2D devices. While an increasing number of 2D materials, including graphene, and hexagonal-boron nitride, have been synthesized successfully in the lab, others have only been theoretically predicted. One very important example is two-dimensional silicon carbide (2D SiC). Theoretical studies have predicted that monolayer SiC has a stable planar graphene-like structure, a direct bandgap of about 2.58 eV, strong excitonic effects, and highly tunable electronic, optical, and magnetic properties. These characteristics are of great importance for many applications and make 2D SiC a potential game-changer for future energy-related technologies. Experimentally, however, the growth of 2D SiC has challenged scientists for decades, mainly because unlike graphite or other layered materials, bulk SiC is not a van der Waals layered structure. Bulk SiC is a covalently bonded material, and it is one of the strongest materials. Further still, bulk SiC exists in more than 250 polytypes, further complicating the synthesis efforts. Importantly though, our group has made groundbreaking progress on the synthesis of 2D SiC. We successfully grow the first monolayer SiC by adopting a unique wet exfoliation method, in which 6H-SiC was used as a precursor. The exfoliated 2D SiC nanosheets, are 100% stable in air and show visible light emission at around 480 nm (2.58 eV), which is in good agreement with theoretical predications.

As a stable atomic thick semiconducting material, 2D SiC has the potential to bring revolutionary advances across various technological fields ranging from power electronics, and optoelectronics to quantum information processing and beyond. 2D SiC can address countless drawbacks associated with the gapless nature of graphene, silicon semiconductors (narrow band gap and low voltage breakdown), environmental instability of silicene and few-layer black phosphorous and the indirect bandgap of bulk SiC.

11:45 AM EQ20.24.07

Patterning Laser Induced Graphene on Flexible Substrates with Spatial Control of Morphology Moataz Abdulhafez, Ki-Ho Nam, Golnaz Najaf Tomaraei and [Mostafa Bedewy](#); University of Pittsburgh, United States

Laser induced graphene (LIG) is an emerging technique that enables directly patterning conductive carbon electrodes for a plethora of flexible devices, including supercapacitors and sensors. While the morphology and chemistry of the porous three-dimensional graphene produced by this method were previously shown to be tunable, the ability to create functional gradation wherein different parts of the patterned graphene exhibit different morphology and/or chemistry on the same flexible substrate has not been previously achieved. Here, we present a new methods for creating functionally graded LIG based on utilizing controlled gradients of optical energy flux to create spatial gradients of LIG morphologies having different electrical conductivities. Importantly, we demonstrate the seamless transition between neighboring regions having different porosity and conductivity. To demonstrate the morphology transitions in the LIG, we developed a method to continuously sweep laser fluence values by controlling the defocus level of the sample surface. This sweep enabled identifying the precise fluence thresholds that correspond to morphological transitions: first, from isotropic porous morphology to anisotropic networks at 12 J/cm²; second, from anisotropic networks to aligned nanofibers at 17 J/cm². Hence, our results provide new insights into the fluence-dependence of the physicochemical processes underlying LIG formation. Moreover, our approach enables generating a morphology diagram for LIG, which facilitates precise tunability of both the morphology, electrical and electrochemical properties of LIG patterns, based on easy-to-control processing parameters, such as laser power and degree of beam defocusing. In addition, this unprecedented ability to create spatially varying morphologies opens the door for one-step fabrication process of complex flexible devices with high surface area electrodes that are integrated with relatively denser and more electrically conducting traces.

Here, we present two methods for creating functionally graded laser induced graphene materials: The first method utilizes controlled gradients of optical energy flux to create spatial gradients of LIG morphologies having different electrical conductivities. The second approach creates spatially controlled surface functionalization through releasing the LIG in vacuum, nitrogen or oxygen environment in a controlled chamber. Through the second laser, patterned LIG surfaces can be created, leading to patterned surface properties and electrochemical properties.

SYMPOSIUM SB01

Engineered Functional Multicellular Circuits, Devices and Systems
November 30 - December 8, 2021

Symposium Organizers

Kate Adamala, University of Minnesota
Seokheun Choi, Binghamton University, The State University of New York
Liang Guo, The Ohio State University
Pinar Zorlutuna, University of Notre Dame

Symposium Support

Silver
Science Robotics | AAAS

* Invited Paper

SESSION SB01.01: Cellular Interface Engineering
Session Chairs: Kiara Cui and Cecilia Leal
Tuesday Afternoon, November 30, 2021
Sheraton, 3rd Floor, Dalton

1:30 PM *SB01.01.01

Forming Input/Output (I/O) Interfaces with Excitable Cells and Tissue Using Nanocarbons Tzahi Cohen-Karni; Carnegie Mellon University, United States

We focus on developing a new class of nanoscale materials and novel strategies for the investigation of biological entities at multiple length scales, from the molecular level to complex cellular networks. Our highly flexible bottom-up nanomaterials synthesis capabilities allow us to form unique hybrid-nanomaterials that can be used in various input/output bioelectrical interfaces, i.e., bioelectrical platforms for chemical and physical sensing and actuation. We developed a breakthrough bioelectrical interface, a 3D self-rolled biosensor arrays (3D-SR-BAs) of either active field effect transistors or passive microelectrodes to measure both cardiac and neural spheroids electrophysiology in 3D. This approach enables electrophysiological investigation and monitoring of the complex signal transduction in 3D cellular assemblies toward an organ-on-an-electronic-chip (organ-on-e-chip) platform for tissue maturation investigations and development of drugs for disease treatment. Utilizing graphene, a two-dimensional (2D) atomically thin carbon allotrope, we demonstrated a new technique to simultaneously record the intracellular electrical activity of multiple excitable cells with ultra-microelectrodes that can be as small as the size of an axon ca. 2 μ m in size. The outstanding electrochemical properties of our hybrid-nanomaterials allowed us to develop electrical sensors and actuators, e.g., sensors to explore the brain chemistry and sensors/actuators that are deployed in a large volumetric muscle loss animal model. Finally, using the unique optical properties of nanocarbons, e.g., graphene-based hybrid-nanomaterials and 2D nanocarbons, we have formed remote, non-genetic bioelectrical interfaces with excitable cells and modulated cellular and network activity with high precision and low needed energy. In summary, the exceptional synthetic control and flexible assembly of nanomaterials provide powerful tools for fundamental studies and applications in life science and potentially seamlessly merge nanomaterials-based platforms with cells, fusing nonliving and living systems together.

2:00 PM *SB01.01.02

Computer Designed Organisms Built from Embryonic Amphibian Cells Douglas Blackiston^{1,2}, Sam Kriegman³, Josh Bongard³ and Michael Levin^{1,2}; ¹Tufts University, United States; ²Wyss Institute, United States; ³The University of Vermont, United States

The fields of biology and robotics have seen an emergence of interdisciplinary work aimed at building machines that contain biological components, designed to solve a wide variety of problems that challenge traditional robots including: robustness to damage, increased biocompatibility, and a programmable internal biochemistry. These efforts have largely coalesced around biohybrid designs, combining synthetic scaffolds or components alongside living cells and tissues. In complement to this approach, we have developed methods for constructing fully biological machines from embryonic amphibian cells, engineered to exhibit a specific behavior. As part of these studies, we demonstrate a scalable pipeline for creating functional computer designed organisms: AI methods automatically design diverse candidate lifeforms in silico to perform some desired function, and transferable designs are then created using a cell-based construction toolkit to realize living systems with the predicted behaviors. Although some steps in this pipeline still require manual intervention, complete automation in future would pave the way to designing and deploying unique, bespoke living systems for a wide range of functions.

2:30 PM SB01.01.03

Stress-Induced Electrical Signaling in Microalgae Cohorts Paulo R. Rocha¹, Lode Vandamme² and Ricardo Leite³; ¹University of Coimbra, Portugal; ²Eindhoven University of Technology, Netherlands; ³Instituto Gulbenkian de Ciéncia, Portugal

Diatoms are early Jurassic microalgae, a photosynthetic group with a major environmental role on the planet due to the biogeochemical cycling of silica and global fixation of carbon. However, they can evolve into harmful blooms through a resourceful communication mechanism, not yet fully understood. Harmful algae blooms in water supply reservoirs must be eradicated due to unwanted toxin production and filter blocking at water treatment works. Until now there has been no efficient consensus that harmful microorganisms such as diatoms communicate with each other and no accurate and self-sustained tool to monitor such communication.

Here, we demonstrate the ability to electrically monitor a diatom cohort. The breakthrough is realized by means of a unique measurement setup based on low impedance electrodes that exploit the large Helmholtz-Gouy-Chapman double-layer capacitance. The sensing system comprises a transducer based on a metal/Si/SiO₂/Au electrode. Small extracellular voltages of diatoms adhered to the electrode induce a displacement current that is enhanced by a gain factor proportional to the double-layer capacitance.

The origin is paracrine signalling, which is a feedback, or survival, mechanism that counteracts changes in the physicochemical environment. The intracellular messenger could be related to Ca²⁺ ions since spatiotemporal changes in their concentration match the characteristics of the intercellular waves. Our conclusion is supported by using a Ca²⁺ channel inhibitor. The transport of Ca²⁺ ions through the membrane to the extracellular medium is blocked and the intercellular waves disappear. The translation of microalgae cooperative signalling paves the way for early detection and prevention of harmful blooms and an extensive range of stress-induced alterations in the aquatic ecosystem

2:45 PM *SB01.01.04

Synapse- and Neuron-Inspired Biomolecular Materials and Devices Joseph S. Najem; The Pennsylvania State University, United States

The rise of Artificial Intelligence and the Internet of Things applications in biological domains poses questions about the best way to build computing devices that are biocompatible, low-power, and adaptable. We believe an approach that takes inspiration from the brain could grant an answer. For instance, biological neurons process signals and compute by integrating incoming stimuli and initiating action potentials to convey information within the nervous system without loss. The process from generation to propagation is regulated by membrane potential and voltage-activated sodium and potassium channels. Moreover, synaptic plasticity is responsible for learning, processing, and information retention. These key features inspire and guide the design of neuron- and synapse-like materials for applications in signal processing, computing, and lossless propagation of information. To this end, we have recently

demonstrated that lipid bilayer membranes formed between two lipid-encased water droplets in oil (i.e., droplet interface bilayers or DIBs) can exhibit memcapacitive and memristive properties, suitable for emulating synapse and neuron functions. Here, we describe a dynamic neuristor consisting of two biomolecular memristors in parallel, while operating according to the same principles as the Hodgkin-Huxley model. The biomolecular memristors consist of insulating biomembrane doped with voltage-driven, pore-forming alamethicin peptides. To capture the switching dynamics of the sodium and potassium channels, we used DPhPC- and BTLE-based memristors, which can offer fast and slow switching dynamics, respectively. The neuristor exhibits a firing behavior similar to a biological neuron and a power efficiency that far exceeds metal oxide-based memristors. This novel neuristor can be implemented in applications ranging from adaptive nonlinear control to signal processing. Additionally, we will discuss our approach to scaling up networks of biomolecular synapses and neurons using microfluidic crossbar array devices. We describe how these devices can be implemented in online learning and reservoir computing applications. These results serve as a foundation for a new class of low-cost, low-power biomolecular materials to support neuromorphic computing applications in biological environments.

3:15 PM SB01.01.05

A Microfluidics-Based *In Vitro* Model of Anterior-Posterior Gut Patterning [Kiara W. Cui](#), Leeya Engel, Kevin J. Liu, Kyle M. Loh, Lay Teng Ang and Alexander Dunn; Stanford University, United States

In this work, we demonstrate, for the first time, spatially controlled differentiation of human pluripotent stem cells (hPSCs) into the anterior foregut (AFG) and mid/hindgut (MHG) cell types within a single cell monolayer using chemical gradient-generating microfluidics. This result represents an advance in the ongoing efforts to harness the processes by which complex tissues arise during embryonic development *in vitro*—a long-standing goal of tissue engineering and regenerative medicine. In embryos, uniform populations of stem cells are exposed to spatial gradients of diffusible extracellular signaling proteins, known as morphogens. Varying levels of these signaling proteins induce stem cells to differentiate into distinct cell types at different positions along the gradient, thus creating spatially patterned tissues.

To accomplish this spatially controlled differentiation, or patterning, we combined principles of engineering and biology to develop a novel, reproducible, and easily accessible method for the anterior-posterior patterning of hPSCs. We performed a 6-day, on-chip differentiation protocol within a commercially available microfluidic chip. We used finite element analysis to model the distribution of morphogens within the microfluidic device and determined that the chip can generate two stable and opposing linear morphogen gradients. Quantitative analysis of immunofluorescence data showed that expression of AFG and MHG markers is localized to their respective morphogen sources and that both display a decreasing linear profile with increasing distance from their sources. This platform thus allows us to explore fundamental questions about how a single population of stem cells differentiate into multiple cell types along a body axis in response to exposure to morphogen gradients, such as whether the response in marker expression is graded or discretized as well as the influence of neighboring cells on cell fate decisions. Our *in vitro* model contributes to the stem cell and developmental biology toolkit and may eventually pave the way to create increasingly spatially patterned tissue-like constructs *in vitro*.

3:30 PM *SB01.01.06

Remodeling of Biological Membranes Adsorbed to Crumpling 2D Materials Devices [Cecilia Leal](#), Marilyn Porras-Gomez, Hyunchul Kim, Nurila Kamar, Mohan Teja Dronadula, Narayana Aluru and Arend van der Zande; University of Illinois at Urbana-Champaign, United States

We study the structural evolution of biologically relevant phospholipid membranes adsorbed onto deformable 2D substrates. We introduce a novel way to remodel lipid bilayers using polydimethylsiloxane substrates or graphene, which can be uniaxially stretched and wrinkled on demand. X-ray, microscopy and simulation data revealed that phospholipid membranes undergo restructuring at the nano and molecular scale. These observations have repercussions on membrane order, permeation, and directing the insertion of proteins for applications in biotechnological applications such as biosensing.

SESSION SB01.02: Multicellular Circuits and Devices I

Session Chairs: Kate Adamala and Seokheun Choi

Wednesday Morning, December 8, 2021

SB01-Virtual

8:00 AM *SB01.02.01

***In Vitro* Neuronal Network-on-a-Chip Technology—From Millimeter to Centimeter-Scale Networks** [Yoonkey Nam](#); Korea Advanced Institute of Science and Technology, Korea (the Republic of)

In vitro neural cultures have been used as an experimental model system to study basic neuroscience, design advanced cell-based biosensing platform, and utilize as testbeds for novel neurotechnology. Many types of primary cultured neurons (e.g. rat/mouse cortical or hippocampal neurons) go through developmental processes (neurite outgrowth, axon/dendrite formation), and form a matured neuronal network with functional synapses during the extended cultivation period. To investigate the functional developments during the network formation, neurons are cultivated on a planar-type microelectrode array (MEA) chip, and electrophysiological activity is measured from multiple sites in the network. Conventional MEA chips provide a few millimeter-sized recording area with sparse or dense microelectrodes, which limits the physical size of the cultured neuronal networks under the investigation. Large-scale neuronal networks on the order of a few centimeters are rarely investigated by the limited availability of the MEA chips that provide recording electrodes distributed over a large area. This talk introduces a scaling up the network size to centimeter scale on a microslide-sized MEA chip. The chip is equipped with 256 channels which are subdivided into 16 millimeter-sized recording areas with 16 channels. The large-scale MEA chips were fabricated by conventional microfabrication processes, and recording sites were made of low-impedance electropolymerized conductive polymers (PEDOT:PSS). On this large-scale MEA chip with clustered recording areas, we designed an ultra-large-scale, modular neuronal network connected by biological connections (e.g. axons). Neuronal network modules, composed of primary cultured neurons, were patterned on the MEA chip using soft-lithography, and each module was connected later by removing alginate hydrogel mask. The alginate hydrogel was used as a removable cell-repulsive surface to temporarily limit the cell adhesion and neurite outgrowth. Using this method, the development of network activity could be more precisely measured and analyzed. The emergence of synchronized, propagating network bursts were readily measured, and their time course could be analyzed. We found network-size dependent signal propagation properties in the cultured neuronal networks.

8:30 AM *SB01.02.02

Emerging Technology for Biohybrid Systems [Shoji Takeuchi](#)^{1,2}; ¹The University of Tokyo, Japan; ²Kanagawa Institute of Industrial Science and Technology, Japan

While manufacturing is evolving and new devices are coming out one after another, it is still difficult to artificially create functions such as molecular recognition, material production, and self-organization that are found in living organisms. We have developed a biohybrid device that combines living organisms and machines. The biohybrid devices can be categorized into 4 groups: (i) biohybrid-sensors that can detect target molecules at highly selective and sensitive manner, (ii) biohybrid-reactors that mimic biological reaction in our body, and thus are useful for drug testing or tissue transplant for cell therapy, (iii) biohybrid-actuators that shows highly energy efficient motion and (iv) biohybrid-processors that achieve low-energy and highly parallel computing like our brain. Here, I would like to talk about a couple of our recent results regarding biohybrid sensors and actuators.

9:00 AM SB01.02.03

Rapid and Simple Antibiotic Susceptibility Testing by Monitoring Bacterial Extracellular Electron Transfer [Zahra Rafiee](#) and Seokheun Choi; Binghamton University, The State University of New York, United States

A rapid and simple antibiotic susceptibility testing (AST) is critical to provide valuable information on the antibiotic efficacy and their right doses for treatment against bacterial infections. Although emerging genotypic ASTs are very useful and fast, it is difficult to characterize unknown bacteria. Even "gold standard" phenotypic ASTs require a relatively long time for culturing and monitoring. This work creates a powerful yet simple method to assess antibiotic effectiveness against electrogenic bacteria, which enables rapid, high-throughput, and real-time monitoring. The proposed AST approach continuously monitors extracellular electron transfer by bacterial cells, parallelly and controllably formed on a paper-based sensing array. The transferred electrons are based on microbial metabolic activities and are inversely proportional to the concentration of potential antibiotics, leading to the early detection of antimicrobial drug resistance in bacteria.

Extracellular electron transfer (EET) is a remarkable bioelectrochemical process used by certain microorganisms for growth, overall cell maintenance, and information exchange with surrounding microorganisms or environments. Almost all environments, even those involving harsh conditions, host microorganisms performing EET. Recent studies have demonstrated electrogenicity by even Gram-positive microorganisms, which have thick cell walls that limit effective electron transfer. Other microorganisms have demonstrated weak electrogenic capacity in microbial consortia, involving direct interspecies electron transfer (DIET) and EET-involved cell-to-cell communications. Even many microbial pathogens such as *Pseudomonas aeruginosa* use quorum sensing inter-cellular communication by producing diffusible signaling molecules (e.g., autoinducers) and redox active compounds to control virulence during infections and defend their immediate niche against competing microorganisms and environmental stresses. The redox-active compounds can also serve as extracellular soluble mediators for microbial EET. Therefore, the electrical outputs from the bacterial EET can be used as a measurement to evaluate the antibiotic efficacy. When the antibiotics are effective against those pathogenic exoelectrogens, their metabolic activities can be inhibited, thus decreasing their electron transfer reactions. The changes in electrical outputs can be measured to assess the antibiotic effectiveness against the pathogen.

In this work, a paper-based 8-well sensing array offers a rapid and simple approach to characterize bacterial electrical response in the different concentrations of antibiotics. A common Gram-negative pathogenic bacterium *Pseudomonas aeruginosa* wild-type PAO1 and first-line antibiotic gentamicin (GEN) are used in our experiments. Eight different concentrations of antibiotics (1, 2, 4, 8, 16, 32, 64, and 128 ug/ml) are pre-loaded and dried on the sensing units. When bacterial samples are loaded into the array, antibiotic exposures allow sufficient inhibition to the bacterial metabolisms, and the readout becomes sensitive enough to show small variations in electric output caused by changes in antibiotic effectiveness. The result generates quantitative, actionable minimum inhibitory concentration (MIC) values within an hour by measuring electricity produced by bacterial metabolism instead of the days needed for growth-observation methods. This work will explore the viability of this system as a practical and reliable AST tool. The project outcomes will address grand challenges in microbial infections critical to U.S. healthcare and the economy, through enabling sensors that will augment human health, safety, and well-being by providing information to effectively treat the infections and better control the spread of the antibiotic resistance.

9:15 AM SB01.02.04

Late News: Cardiac Muscle-Cell-Based Coupled Oscillator Network for Vertex Coloring Problems [Jiaying Ji](#)¹, Xiang Ren¹, Jorge Gómez¹, Mohammad K. Bashar², Shukla Nikhil², Suman Datta¹ and Pinar Zorlutuna¹; ¹University of Notre Dame, United States; ²University of Virginia, United States

Inspired by the natural biological system's efficiency and complexity, biocomputing that utilizes or mimics natural information processing inherent in living organisms provides a new computational approach that performs computing in a massively parallel way with energy efficiency. Here, we present a new biocomputing platform, a cardiac muscle-cell-based bio-oscillator network, for solving computationally hard problems such as vertex coloring problems, which entail computing the minimum number of colors required to assign colors to all vertices in a graph such that every adjacent vertex have a different color. The computing components of the network are composed of bio-oscillators, cardiomyocytes (CMs), and coupling elements, cardiac fibroblasts (CFs). We aim to harness the unique phase ordering produced by the coupled bio-oscillators to approximate the optimal solution to the vertex coloring problem. We first studied the synchronization behavior of a pair of coupled bio-oscillators that exhibited stable phase delays caused by the time lag in transporting electrical signals through the coupling elements. Such delays can be exploited to build up the phase ordering in multi-node oscillators. Then, we aimed to use the bio-oscillator network to solve multi-node vertex coloring problems (9 nodes and 64 nodes) through mapping the vertices and edges onto the CMs and CFs. The micropatterning method based on topographic features and mobile blockers was implemented for creating the controlled cell distribution. On the theoretical front, we developed a polynomial-time post-processing scheme that uses the bio-oscillator solution as a starting point to improve the solution to be comparable to the heuristic algorithm. Moreover, the bio-oscillator-based computational model can have a performance advantage at large nodes compared to the heuristic algorithm. We also benchmarked the energy and latency for graph coloring using coupled bio-oscillators and conventional CMOS oscillators. The energy consumption of the cardiac-cell and CMOS oscillators for networks of different sizes indicated that cardiac cells consume lesser energy in computing the graph coloring solution which can lead to significant energy savings in larger networks.

SESSION SB01.03: Multicellular Circuits and Devices II
Session Chairs: Seokheun Choi and Pinar Zorlutuna
Wednesday Morning, December 8, 2021
SB01-Virtual

10:30 AM SB01.03.01

Paper-supported 3-D Cell Culturing, Sensing and Biofabrication for Exploring Research Frontiers in Electromicrobiology [Anwar Elhadad](#) and Seokheun Choi; Binghamton University, The State University of New York, United States

Electromicrobiology is a discipline emerging from studies of microbial electron exchange with external electrodes and of novel electrochemical properties of microorganisms. Intensive study in electromicrobiological engineering has created a plethora of new concepts and potential applications, offering

sustainable environmental solutions for the production of energy as well as valuable products. However, the microbial electrochemical technique has not yet been leveraged for practical applications. Several significant research gaps must be addressed before electromicrobiology is viable and scalable, and the need to address these gaps is growing more urgent with the increasing concerns over the energy-climate crisis and environment pollution. For example, researchers do not yet fully understand the interplay between electrodes and active microbes, and factors controlling the rate and extent of the exchange process are still ill-defined. Additionally, more research is needed to ascertain which microbial species or consortia of species are best suited for efficient electron transfer.

The overarching purpose of this work is to pursue advanced, innovative approaches that elucidate/maximize microbial electron exchange with electrodes, and translate basic findings within the field of electromicrobiology into practical, real-world applications that support environmental sustainability. In this work, a range of innovative approaches are investigated with the major goals of investigating fundamental factors responsible for determining efficient electron exchange with external devices, and exploring three-dimensional biofabrication and engineering of synthetic polymicrobial biofilms. This research provides a foundation for enhanced performance in electromicrobiology. The project uses the new field of 3D, paper-based cell culturing, sensing and biofabrication platforms that mimic microbe-electrode interactions in biofilms. In particular, stacks of patterned papers provide creative and unique solutions for 3D bacterial cultures of controlled biofilm geometry, high-throughput monitoring of microbial electrical properties and layer-by-layer construction of an artificial biofilm. This research addresses key issues in electromicrobiology: (i) promote/accelerate the discovery and characterization of customized and novel exoelectrogens, (ii) establish fundamental knowledge to determine critical factors in electron transfer at the microbial/anode interface, and (iii) optimize bacterial synergistic interactions in synthetic bacterial communities.

Multiple layers of paper containing bacterial cells can be stacked to form a layered 3D model of the overall biofilm construct and mass transport of nutrients/oxygen into this 3D system can be regulated to explore the microbial energy production within controlled biofilms. Different stack configurations allow us to generate many different experimental setups to better understand key mechanisms underlying electron harvesting from microorganisms and other fundamental factors determining their electron-generating capabilities. De-stacking the multi-layered biofilm construct also allow layer-by-layer analysis for pH distribution and cellular viability. In this 3D model system, *Synechocystis* sp. PCC 6803 on the top layer exploits photosynthesis to produce carbohydrates, which are used as a carbon source by other microbial communities. Then, the facultative aerobic *Bacillus subtilis* are inserted into the middle layer of the co-culture to produce riboflavin as an electron shuttle, which significantly improves power generation of exoelectrogens, *Shewanella oneidensis*, on the bottom layer. Furthermore, *Bacillus subtilis* can remove oxygen and thus maintain an anaerobic condition for the optimized electrogenic process of *Shewanella* sp. This 3D system demonstrates a significantly increased power output.

10:45 AM SB01.03.02

A Three-Dimensional Blood-Brain Barrier Model Using *Ex Vivo* Brain Tissue Brian O'Grady¹, Alexis Yates¹, Michael Geuy¹, Hyosung Kim¹, John Wiksw¹, Matthew Schrag^{1,2} and Ethan Lippmann¹; ¹Vanderbilt University, United States; ²Vanderbilt University Medical Center, United States

Introduction: Dysfunction of the blood-brain barrier (BBB) is implicated in several neurological disorders. As such, it is highly desirable to develop new models to study BBB pathology. However, these studies are hampered by the complex multi-cellular hierarchy and cellular interactions that are required to create a physiologically relevant model that accurately depicts the structure and function of the BBB. To address these limitations, we have been developing a vascularized, anatomically-representative three-dimensional (3D) model of the BBB in a perfusable, 3D printed microfluidic chip using *ex vivo* mouse and human tissue embedded in a biomimetic hydrogel. Overall, our 3D BBB model provides a unique system that allows for dynamic interrogation of the BBB in healthy and diseased tissue.

Methods and Materials: Microfluidic devices were fabricated using a stereolithographic 3D printed mold. This mold was vapor deposited with Parylene C to provide a physical barrier to prevent cytotoxic leaching into the casted polydimethylsiloxane and hydrogel. Fresh mouse and/or human brain tissue were collected and minced in a 1mL conical tube filled with 500 μ L of Hank's Balanced Salt solution for 5 minutes. The vial was then centrifuged at 2500 rpm. After centrifugation, the vial was tilted and the liquid top layer was aspirated. Then, 100 μ L of minced tissue was transferred to 1mL of 10% gelatin conjugated with an N-cadherin biomimetic peptide and thoroughly mixed. Subsequently, microbial transglutaminase was added to the hydrogel for crosslinking (2% final solution), mixed and poured into the microfluidic device. The hydrogel was cured for 30 minutes at 37°C, followed by immediate perfusion of the peripheral channels. Vascular growth in the hydrogels was imaged with confocal immunofluorescence 7 days following tissue embedding.

Results and Discussion: We established a neurovascular *ex vivo* model using mouse and human brain tissue embedded in a hydrogel containing a peptide from the extracellular epitope of N-cadherin. This tissue spontaneously sprouts vasculature in our microfluidic platform to form a perfusable vascular network. The two flanking perfusion channels are independently perfusable with media and growth factors to direct vascularization to the channels, while the middle channel was designed for 3D hydrogels impregnated with tissue. Neovascularization could be observed in real-time from the embedded tissue, and immunostaining revealed vessels that were several millimeters in length and consisted of anatomically correct positioning of endothelial cells and pericytes separated by a collagen IV basement membrane. Excitingly, human brain tissue from a patient with CAA, a disease characterized by the accumulation of amyloid- β deposition in the vascular walls, could grow vasculature that exhibited hallmarks of the disease including amyloid accumulation and arterioles devoid of smooth muscle cells.

Conclusions: We have shown that human and mouse brain tissue in our hydrogel exhibits continuous vascular growth with anatomically correct hierarchy and expression of characteristic markers of vascular cell phenotypes. This new platform also supports the use of diseased primary human tissue to produce brain vasculature with alterations characteristic of the underlying cerebral vascular architecture pathology. Thus, we believe this new tool will be a powerful platform for building more complex brain models with proper organization and assessing therapeutic efficacy of drugs for a broad range of neurological disorders.

11:00 AM SB01.03.03

On-Demand Paper Bio-batteries Activated by Human Body Fluids Mya Landers and Seokheun Choi; Binghamton University, The State University of New York, United States

With the growing demand for point-of-care (POC) and in-field diagnostic testing, paper attracts significant attention as a substrate for simple, low-cost, and disposable analytical devices. A porous, hydrophilic network of intertwined cellulose fibers promotes excellent mechanical, dielectrical and fluidic properties in paper. These properties mean microfluidic assays and electronic/mechanical components can be built into paper, offering the transformative potential of generating important function for POC diagnostic devices. Recent advances in paperfluidic and papertronic technologies offer more decentralized diagnostic analyses with portability, automation, and the capacity to produce test results in shorter times at a reduced cost. However, there has been a significant challenge in realizing a truly stand-alone and self-sustainable diagnostic platform that does not rely on a competent laboratory service or smartphone's built-in functions. The key challenge is to develop a miniaturized on-chip power source for those paper-based POC devices in a more effective and efficient way. Power autonomy is one of the most critical requirements for the devices so they can work independently and self-sustainably in limited-resource and remote regions, where a stable electrical supply is not available. Even standard batteries are not suitable in those areas because of their cost, incompatibility with paper, and potential danger to the environment. Smartphone built-in batteries are not always available. Also, conventional energy harvesting technologies (e.g. solar, thermal, mechanical, chemical energy) are too overqualified and expensive as a power source for single-use, disposable POC tests, which require relatively small power consumption for only a couple of minutes. What is needed is a low-cost, disposable, and eco-friendly micro-power source that can be easily integrated with paper-based devices and be readily activated even in those challenging field conditions.

Here we provide a realistic and accessible solution as a novel power source that can enable a self-powered paper-based diagnostic test for anyone,

anywhere, and anytime. The work creates a paper-based microbial fuel cell (MFC) device that is pre-inoculated with *Bacillus subtilis* endospores and can be activated with a drop of human body fluids, such as sweat or saliva. *B. subtilis* endospores are a resilient, desiccation-resistant state of the bacteria that can develop in a nutrient-deficient environment. These endospores are pre-loaded into the anode of the device and begin germination and electricity generation once nutrients become available. Dropping bodily fluids onto the device's inlet introduces these nutrients to the endospores and activates the biobattery. The design consists of several individual MFC units that can be easily connected through a simple folding mechanism to achieve a higher output power.

Since they are low-cost, fast-acting, and disposable, paper-based MFCs have shown potential for applications in powering a variety of low-power, POC diagnostic tools, especially in resource-limited environments that lack dependable access to other forms of power. Conventional MFC operation often requires exoelectrogen-containing or nutrient-rich water from the environment to be applied to the MFC for activation, but access to such a water source may not always be available. Using bodily fluids to activate the device allows for it to be readily used even in dry climates without access to nutrient-rich environmental water. Since local bacteria may also be incapable of generating electricity, some previous MFC devices have included pre-inoculated, lyophilized exoelectrogens, but lyophilized bacteria have been shown to suffer from significant performance decline over time during storage. Using dehydrated *B. subtilis* endospores instead extends the durability and shelf-life of the MFC, while still allowing for rapid, on-demand electricity generation once activated.

11:15 AM *SB01.03.04

Soft Reconfigurable Electronics Through Tunable Percolation Networks [Carmel Majidi](#); Carnegie Mellon University, United States

Nervous tissue has the extraordinary ability to reconfigure the synaptic connections between its neurons and form new neural pathways. This mechanism of neuroplasticity allows for dynamic adaptations in response to learning or to repair tissue damaged by injury. Achieving this reconfigurability in engineered systems could allow future machines and electronics to be more adaptive, sustainable, and robust to damage. Such capabilities will be especially critical in emerging fields like soft robotics and stretchable electronics, which are designed to match the versatility and rich multifunctionality of soft natural organisms and tissue. In this talk, I will highlight progress in creating bioinspired circuits that are soft, stretchable, and electrically reconfigurable. This includes recent work on electrically conductive hydrogel composites in which a soft hydrogel is embedded with percolating networks of silver flakes that reversibly reconfigure under hydration, heat, and electrical stimulation. I will also present our ongoing work on creating self-reconfigurable soft circuits using liquid metal (LM). Eutectic gallium indium (EGaIn) is selected as the LM alloy due to its enabling combination of high electrical conductivity and fluidic deformability. When embedded in soft elastomer, microscale droplets of EGaIn can be selectively connected to form electrically conductive pathways that reconfigure in response to mechanical loading and damage. To demonstrate their potential role in future soft material technologies, I will present examples of how these Ag-hydrogel and LM-elastomer composites can be used for sensing, power transmission, and actuation in soft robotics and stretchable electronics applications.

SYMPOSIUM SB02

From Hydrogel Fundamentals to Novel Applications via Additive Manufacturing
November 30 - December 8, 2021

Symposium Organizers

Ferenc Horkay, National Institutes of Health
Marc In het Panhuis, University of Wollongong
David Londono, DuPont

Evgenia Vaganova, The Hebrew University of Jerusalem

* Invited Paper

SESSION SB02.01: Structure Property Relationships in Gels I
Session Chair: Elizabeth Cosgriff-Hernandez
Tuesday Morning, November 30, 2021
Sheraton, 2nd Floor, Republic A

10:30 AM *SB02.01 .01

Tough Hydrogel Coatings via Diffusion-Mediated Redox Polymerization [Elizabeth Cosgriff-Hernandez](#) and Megan Wancura; The University of Texas at Austin, United States

Our lab has developed hydrogel coatings for electrospun vascular grafts that resist platelet adhesion and promote endothelial cell adhesion for acute and sustained thromboresistance.¹ To improve homogeneity of the coating, we developed a diffusion-mediated redox polymerization method to generate conformal hydrogel coatings with improved thickness control.² Reduced thickness of the hydrogel coating resulted in reduced damage due to forceps gripping; however, these coatings still displayed damage due to twisting and torqueing associated with implantation that exposed the underlying thrombogenic substrate.³ In this study, we developed a new hydrogel chemistry based on interpenetrating networks of polyether urethane diacrylamide

(PEUDAm) and poly(*N*-acryloyl glycinamide) (pNAGA) with improved damage resistance. Investigation of the redox hydrogel coating methodology was then used to identify parameters that enabled fabrication of hydrogel-mesh vascular grafts with requisite laminate strength.

First, the reducing agent, iron gluconate (IG), was adsorbed onto the electrospun mesh substrate, then the coated substrate was immersed in an aqueous macromer solution with the initiator, ammonium persulfate (APS). IG diffusion from the mesh substrate into the APS solution results in the formation of persulfate radicals and crosslinking of the PEUDAm hydrogel. The hydrogel coating thickness was controlled with incubation time. The effect of solution viscosity and rate of crosslinking on hydrogel coating laminate strength was studied by systematically tuning molecular weight and APS concentration to identify parameters for suitable coating application. A second network was introduced by swelling in NAGA and photopolymerization with the total hydrogel coating thickness set by the first PEUDAm hydrogel coating.

Our studies identified key parameters necessary to apply these coatings using redox diffusion-mediated crosslinking with improved control of hydrogel thickness. Reducing initiator concentration was necessary to slow cure rate to promote better penetration of higher molecular weight macromers and prevent swelling-mediated delamination; however, reduction of initiator concentration also required additional consideration of gelation time to achieve sufficient crosslink density. The resulting hydrogel coatings were resistant to damage from suturing and torquing of coatings under 180° twisting with hemostat gripping. We hypothesized that the increased molecular weight between crosslinking points facilitated greater elongations and the additional hydrogen bonding motifs dissipated fracture energy to increase the resistance to hydrogel coating damage with handling. These results demonstrate the improved damage resistance of PEUDAm-NAGA hydrogels and the potential of this hydrogel design for coating vascular grafts.

References:(1) Browning, M. B., et al. *Acta Biomaterialia* **2012**, 8 (3), 1010-21; (2) Wancura, M., et al. *J. Mater. Chem. B* **2020**, 8 (19), 4289-4298. (3) Post, A., et al. *Acta Biomaterialia* **2018**, 69, 313-322;

11:00 AM *SB02.01 .02

Establishing Rules for How N- and O- Glycans Modify Interfacial Phenomena at Biological Surfaces Anjolaoluwa L. Bamtefa, Elbethel L. Dantae and Preethi Chandran; Howard University, United States

The surfaces of host cells and pathogens are covered with short polymers of sugars known as glycans attached to the proteins and lipids in the biological membranes. There are two predominant types of glycans - N and O glycans. N-glycans have a highly conserved structure, constitute greater than 50% of the glycosylation type in secreted proteins. O-glycans have a more varied structure and are present in the mucins of host cells. Among the five sugars typically present in N- and O- glycans, four are common to both. The goal is to determine if there are clear rules for how the interfacial phenomena on biotic and abiotic surface varies with the sugar composition of the glycans present, particularly their terminal sugar profile. Terminal sugars on N- and O-glycans were systematically removed and the changes in aggregation and adhesion patterns were monitored. Rules of adhesion and aggregation between different combinations of terminal glycan sugars were verified in multiple systems. Mannose sugars consistently showed short-range 'Velcro-like' adhesions with other mannose sugars, whereas SA residues showed long-range 'slime-like' adhesions with other terminal SA sugars in the presence of salt. The adhesion patterns were not sensitive to the structure of sugar presentation - they existed irrespective of whether the sugars were present in abiotic monolayers or in N-glycans or in O-glycans. In addition to these sugar-sugar self-adhesions, cross-adhesions were observed only between specific pairs of sugars. N-glycans abound on the surfaces of viruses such as HIV, Ebola, Dengue, SARs, and Influenza. O- glycans abound on mucins present in the mucus gel within respiratory, gastric, and vaginal cavities. Rules for which sugars on these glycans will self- and cross-adhere would enable predicting when pathogens will self-aggregate, when mucins will adhere to pathogens, how glycosylated abiotic surfaces will behave in host environment, and how changes in glycosylation that occur with age, race, and chronic conditions will alter the interfacial phenomena on biotic and abiotic surfaces.

11:30 AM SB02.01 .03

Polyanion Induced Phase Separation of Resilin-Based Intrinsically Disordered Proteins—Applications in Microstructured Hydrogels Cristobal Garcia and Kristi Kiick; University of Delaware, United States

Resilin-like polypeptides (RLPs) are intrinsically disordered proteins (IDPs) that may undergo liquid-liquid phase separation (LLPS). This IDP property is involved in the control of the formation and dissolution of membraneless organelles inside cells through interactions between the IDP amino acids or interactions with polyanions such as RNA. Polyphosphate is a polyanion that is capable of promoting the LLPS of resilin-based IDPs, emulating the behavior observed between other IDPs and RNA in living cells. By regulating the concentration and localization of polyphosphate deposited over acrylamide functional RLP solutions, transition temperature gradients are generated, allowing the creation of different types and sizes of microstructures upon crosslinking of the resulting emulsions. These studies help us to take advantage of a phenomenon naturally occurring in cells and utilize it for making RLP-based hydrogels with controlled microstructures with potential applications in fields such as tissue engineering and drug delivery.

11:45 AM SB02.01 .04

Additive Manufacturing of Shape-Changing Engineered Living Materials Laura K. Rivera Tarazona¹, Tarjani Shukla², Kanwar A. Singh¹, Akhilesh Gaharwar¹, Zachary T. Campbell² and Taylor H. Ware^{1,1}; ¹Texas A&M University, United States; ²The University of Texas at Dallas, United States

Shape transformation in response to changes in environmental conditions is a prevalent function observed in living systems, from the blooming of flowers to muscle actuation. Current shape-changing synthetic materials that mimic this behavior typically respond to non-specific stimuli such as pH, light, or temperature. Nevertheless, these stimuli are not specific to the material and may affect various components of the surrounding environment. New materials are needed that respond mechanically in a programmed manner by detecting specific biochemical cues. In this work, we develop 3D-printable engineered living materials (ELMs) capable of responding to very specific and pre-determined biochemical stimuli. We synthesize shape-changing ELMs from living probiotics embedded in cellulose nanocrystal (CNC)/polyacrylamide hydrogels. The effects of CNC at concentrations between 5-14 wt% and 11-22 wt% were studied to evaluate ELM volume expansion in active (with yeast) and passive (cell-free) composites respectively. Using direct ink write printing, we spatially patterned cellular proliferation within a monolith to induce complex shape transformations. By encapsulating genetically engineered probiotics (*Saccharomyces boulardii*) that proliferate only in the presence of specific biochemical cues, ELM capsules were designed that deliver a model drug. To create these drug delivery devices, structures composed of cell-free and yeast-embedding materials were printed to obtain hollow capsules containing a hydrophobic model drug. In this device, the ELM portion, containing an engineered *S. boulardii* strain, only changes in volume in the presence of a particular amino acid, which leads to expansion of one portion of the capsule. This expansion ruptures the device and releases 11 % ± 3 % of the total model drug to the surrounding environment within 48 h of growth. The use of genetically modified probiotics enables devices that respond to subtle biological cues found in the surrounding environment. Our study may enable new opportunities to develop drug-delivery devices for the diagnosis and treatment of gastrointestinal disorders.

1:30 PM *SB02.02.01

Design of 3D Printable Homocomposite Hydrogels with Synergistically Reinforced Molecular-Colloidal Networks Orlin D. Velev; North Carolina State University, United States

We report the design and properties of a new class of self-reinforced homocomposite hydrogels (HHGs) comprised of interpenetrating networks of multiscale hierarchy. They are made possible by the introduction of novel soft matter called soft dendritic colloids (“dendricolloids”). The dendricolloids are fabricated by a process of the eddy-guided polymer precipitation in turbulently sheared liquid medium. They have hierarchical morphology similar to molecular-scale polymer dendrimers, but two orders of magnitude larger in scale [Nature Mater. 18:1315, 2019]. The branched dendricolloids have very large excluded volume, and are surrounded by a corona of polymer nanofibers, which are highly adhesive due to van der Waals forces. Dendricolloids made of alginate can serve as reinforcement networks of molecular alginate, forming jointly homocomposite hydrogels [Nature Comm. 12:2834, 2021]. The reinforcement of the molecular gel with the nanofibrillar colloidal network of the same biopolymer results in a remarkable increase in the mechanical properties of the homocomposite hydrogels. The HHG’s show $>3\times$ larger storage modulus and $>4\times$ larger Young’s modulus than either constitutive network at the same concentration. The synergistically reinforced colloidal-molecular HHGs open numerous opportunities for formulation of biocompatible gels with robust structure-property relationships. They can be used in 3D printing with Homocomposite Thixotropic Paste (HTP), a method that was originally developed in our group for 3D printing with ultrasoft silicone HTP [Adv. Mater. 29:1701554, 2017]. The homocomposite hydrogels enable the making of thixotropic pastes for precise and efficient 3D printing via extrusion. We will demonstrate how the ratio of the HHG precursors facilitates precise control of the yield stress and timed rate of self-reinforcement. The resulting hydrogel architectures have excellent mechanical properties and potential for broad range of biomedical and soft robotics applications.

2:00 PM SB02.02.03

Design Polyrotaxane-Based 3D Printing Hydrogels for Direct Ink Writing Chenfeng Ke; Dartmouth College, United States

Natural materials are programmed hierarchically to form homo- and heterogeneous three-dimensional (3D) architectures, yielding intelligent systems that can complete complex tasks. Designing artificial materials that mimic and even improve upon natural systems requires the precise spatiotemporal control of molecular entities’ chemical structures, assemblies, homo- and heterogeneous placements, and macroscale 3D architectures. My research aims to develop next-generation responsive polymers by integrating cyclodextrin (CD)-based polypseudorotaxanes with the direct ink writing technique. The understanding and control of the molecular-to-macroscale hierarchical assembly within in a pre-designed 3D geometry enables the fabrication of responsive polyrotaxanes to complete complex tasks.

In this presentation, I will introduce our development of a CD-based sidechain polypseudorotaxane system and the synthesis of 3D-printable hydrogels with spatiotemporally programmable shape morphing and dynamic mechanical properties. We demonstrated a *de novo* molecular design to synthesize sidechain polypseudorotaxanes with tunable nano-to-macroscale properties for multi-material 3D printing. These sidechain polypseudorotaxanes were formed by copolymers with PEG sidechains and α -CDs. When α -CDs fully covered the PEG sidechains, the rod-like polypseudorotaxane sidechains acted like rigid collagen helices at the nanoscale to aggregate in water, forming crystalline bundles at the mesoscale. We revealed that longer copolymer chains formed disordered polypseudorotaxane crystalline aggregates through systematic variations of the copolymer chain lengths, which exhibited physically crosslinked 3D networks with good 3D printability. Shorter copolymer chains favored ordered lamella crystalline aggregates. Upon α -CD threading and dethreading, copolymers with varied PEG grafting densities showed different stiffness. When these sidechain polypseudorotaxane networks were covalently crosslinked, they were transformed into α -CD-responsive mechanically adaptive hydrogels, featuring more than 100 times elastic moduli change and multi-stage shape persistence. By incorporating a slide-ring crosslinker in the hydrogel, we achieved large tensile strain and significant elastic-to-plastic property variation upon α -CD (de)threading. These discoveries enabled us to integrate two α -CD-responsive hydrogels through multi-material 3D printing and fabricate a sea cucumber mimic possessing multi-stage stiffness change and shape morphing. Our demonstration of designing a macroscale multi-responsive system directly from simple molecular entities showcased an integrated nano-to-macroscale design.

References

- [1] Q. Lin, X. Hou, and C. Ke, Angew. Chem. Int. Ed. 2017, 56, 4452-4457.
- [2] Q. Lin, L. Li, M. Tang, X. Hou, and C. Ke, J. Mater. Chem. C, 2018, 6, 11956-11960.
- [3] L. Li, Q. Lin, M. Tang, E. Tsai, and C. Ke, Angew. Chem. Int. Ed. 2021, 60, 10186-10193.

2:15 PM SB02.02.04

Late News: 3D Printing of Living Microbial Fuel Cell Anode Megan Freyman, Tianyi Kou, Shanwen Wang and Yat Li; University of California, Santa Cruz, United States

3D printing helps to provide further control on electrode design. By using 3D printing to tune the geometry, porosity and dimensions of the structure mass transport to functional microbes or sites in the structure can be improved. By embedding living microbes directly into the ink, we can create 3D printed structures to help harness the activity of microbes and use them in functional devices. Here we demonstrate the incorporation of the living bacteria *Shewanella Oneidensis* MR-1 (*S. Oneidensis* MR-1) directly into an ink used for creating 3D printed structures. *S. Oneidensis* MR-1 has been commonly used in microbial fuel cells (MFC). By incorporating *S. Oneidensis* MR-1 into a sodium alginate-cellulose ink we showed that *S. Oneidensis* MR-1 survives the 3D printing process through the prominent degradation of methyl orange azo dye from the surrounding solution in the presence of the living 3D printed structure. The viability was further confirmed using confocal microscopy. By incorporating carbon black into this ink we further demonstrate the direct printing of a living MFC anode. Electrochemical measurements showed there was good charge transfer between the *S. Oneidensis* MR-1 and the electrode surface. To our knowledge, this is the first report on implementing 3D printed bacteria structure as a living electrode for an MFC system. The capability of printing living and functional 3D bacterial structure could open up new possibilities in design and fabrication of microbial devices as well as fundamental research on the interaction between different bacterial strains, electrode materials, and surrounding environments.

2:30 PM SB02.02.05

Microgel Building Blocks Control Granular Hydrogel Mechanics Börte Emiroglu, Andrew J. deMello and Mark W. Tibbitt; ETH Zurich, Switzerland

Traditional polymeric hydrogels are often static in nature with nanoscale pores, which can limit cell infiltration, spreading, and extracellular matrix deposition. Granular hydrogels overcome these limitations, due to their macroporous structure [1]. Composed of micro-scale building blocks (microgels), granular hydrogels can undergo a glass transition into a jammed state, giving rise to macroscale elasticity. The resulting voids between microgels form a

three-dimensional interconnected network of pores. Recent studies have exploited granular hydrogels to meet the complex demands of cell culture [2] and regenerative medicine [3,4]. Despite the wide interest in granular hydrogels, the mechanism by which the properties of the building blocks control the rheological behavior of these systems remains largely unexplored and is essential to ensure robust translation.

In this work, we relate the emergence of granular hydrogel mechanics to building block properties and provide in depth understanding of the dynamic rheology of soft and jammed granular systems. Thiol-ene based microgels were formed leveraging microfluidic templating for precise synthesis of the building blocks. The microgels were then jammed to produce macroscopic materials that behave like an elastic solid at low strain, but also exhibit shear-thinning and self-healing properties. Oscillatory shear rheometry showed that the mechanical properties of granular hydrogels can be tuned over several orders of magnitude through the control of microgel stiffness and size. To unveil the emergence of the macroscale behavior of granular hydrogels, we computationally generated jammed hard sphere packings and simulated the three-dimensional soft microgel scaffolds. We leveraged contact mechanics principles to establish predictive descriptions of the mechanical response. The model revealed that the extent of contact deformation is proportional to the size and inversely proportional to the stiffness of the microgels, which dictates the linear viscoelastic plateau moduli and zero shear viscosity [5]. With our predictions of the contact landscape of the building blocks, we further explained the differences in the non-linear rheology of granular hydrogels. The results expand our ability to tailor the material properties of granular hydrogels toward a range of biomedical applications and enable advanced engineering of granular hydrogels of complex architecture.

We are translating our study on the relationship between building block properties and the macroscopic response into rational design of granular hydrogels for the development of in vitro models and the engineering of regenerative biomaterials. We present additional results on the effects of controlled microgel environments that enable cell spreading, proliferation, and differentiation.

[1] Bhattacharjee, T., et al. *ACS Biomater. Sci. Eng.* **2016**, 2, 10, 1787-1795.

[2] Caldwell A.S., et al. *Biomaterials*. **2020**, 232, 119725.

[3] Shin, M., et al. *Adv. Sci.* **2019**, 1901229.

[4] Griffin, D., et al. *Nature Mater.* **2015**, 14, 737-744.

[5] Emiroglu, D.B., et al. *in preparation*.

2:45 PM SB02.02.06

Multiphysics Modeling of Ionically Conductive Hydrogels Nikola Bosnjak, Max Tapermeister, Hongyi Cai and Meredith N. Silberstein; Cornell University, United States

Recently there has been an increase in demand for soft and biocompatible electronic devices capable of withstanding large stretch. Conductive hydrogels present a promising class of soft materials for the emerging applications due to their ability to realize charge transport across wet and swollen polymer networks, while preserving the desired mechanical and chemical features. As opposed to electron transfer in traditional electrical conductors, the charge transport across a polymer swollen with an electrolyte solution is achieved through ion migration – such materials are therefore known as ionotronic. The applications of ionically conductive hydrogels are vast, from healthcare and soft robotics to sensors. Moreover, the ability to successfully predict ion migration in soft and wet materials opens the door for implementation of biocompatible hydrogels as an interface between living tissue and external devices.

Hydration level and water diffusion through the polymer network have a significant impact on both the conductive and mechanical behavior of hydrogels. In addition to water molecules and mobile ionic species, fixed charge groups might be tethered onto the polymeric backbone. As a consequence of variation in pH, the ions might interact with the fixed groups through association/dissociation chemical reactions, thus changing the overall electrolyte strength. This significant environmental responsiveness of hydrogels identifies them as active materials with highly tunable properties, and therefore front-runners for implementation in soft electric circuits and devices.

Ionotronic materials and systems are characterized primarily through DC measurements, electrochemical impedance spectroscopy (EIS), and thermo-mechanical testing. EIS consists of applying a time-varying voltage across the material while measuring the corresponding current, and provides insights into the underlying electrochemical mechanisms driving the ion transport. Despite the rapid increase in the number of potential applications and experimental procedures, there is a lack of overarching design tools, hindering the further advance of ionotronic technology. The main challenge in developing reliable simulation capabilities is the complex and coupled electro-chemo-mechanical behavior of ionically conductive hydrogels.

In this work, we propose a multiphysics framework involving the coupled effects of ion transport, electric fields, network hydration, and large deformation. In addition, the developed constitutive model takes into account the difference in conductivity at various hydration levels, along with association/dissociation chemical reactions triggered by pH variations. The model also provides capabilities for computing current generated by the time-varying voltage, and prediction of EIS results based on material microstructure and environmental conditions. We numerically solve this multiphysics system by employing the finite element method. Such an approach will enable quantitative evaluation of material design and ionotronic devices. The accuracy of the developed model and numerical method is ensured through validation against the EIS data. The usefulness of the developed multiphysics model is showcased by simulating the representative ion transport problems and the operation of a soft ionotronic device.

3:00 PM SB02.02.07

Gel Spiderweb Robots [Younghoon Lee](#), Won Jun Song and Jeong-Yun Sun; Seoul National University, Korea (the Republic of)

Spiders possess fascinating multi-feats with spiderweb for maximizing adhesion force. Here, we explore an approach to behavioral characteristics of *cyclosa japonicas* inspired ionic spider webs (ISWs), which is capturable, self-powered sensible and vibrationally dust-cleanable, all of which the principles are solely based on electrostaticity in a single platform [1]. It was made with ionically conducting organogels encapsulated with dielectric elastomers as a strand shape. Its thinness and transmittance led ISWs could be camouflageable. Plasma etching and (heptadecafluoro-1,1,2,2-tetrahydrodecyl)trichlorosilane treatment on dielectric elastomer readily boosted cleanability and it even prevented the evaporation of organogel, which led increase of durability of ionic spider web. Its high stretchability and translucency led it endure applied strain upto 50 % to capture targets larger than ISWs, which cannot be realized by rigid one, and realized it can be camouflageable, respectively. The ISW robustly captured a wide range of materials including a leaf, acryl, glass, and aluminum of which weight is 50 times heavier than its own weight. The capturability was ensured with its additional feats including electrostatic sensing ability and resonance cleanability.

References

[1] Lee, Y., Song, W. J., Jung, Y., Yoo, H., Kim, M. Y., Kim, H. Y., & Sun, J. Y. (2020). Ionic spiderwebs. *Science Robotics*, 5(44).

3:15 PM BREAK

4:00 PM SB02.02.08**Micellar Hybrid Nitric Oxide-Scavenging and Sequential Drug-Releasing Hydrogel for Combinatorial Treatment of Rheumatoid Arthritis** Taejeong Kim and Won Jong Kim; Pohang University of Science and Technology, Korea (the Republic of)

Selective depletion of overproduced nitric oxide (NO) with nanoscavengers is a promising approach for treating rheumatoid arthritis (RA), preventing both oxidative/nitrosative stress and the upregulation of immune cells. However, its practical applications are limited owing to the minimum time interval between intra-articular injections and unwanted off-target NO depletion. At an appropriate level, NO plays a crucial role in modulating various biological functions. To address this issue, we herein report the rational design of an injectable in situ micellar hybrid NO-scavenging and sequential drug-releasing (M-NO) gel platform for the combinatorial treatment of RA by incorporating a “clickable” NO-cleavable cross-linker (DA-NOCCL). This network is held together with micellar structures to achieve a self-healing capability for visco-supplementation and on-demand dual drug (both hydrophilic and hydrophobic)-releasing properties, depending on the NO concentration. Moreover, consecutive NO-scavenging action reduces pro-inflammatory cytokine levels in LPS-stimulated macrophage cell lines in vitro. Finally, the intra-articularly injected M-NO gel with anti-inflammatory dexamethasone significantly alleviated the symptoms of RA, with negligible toxicity, in animal models.

This proposed concept and the platform with favorable results showed promising application potential for the combinatorial treatment of various NO-related diseases, delivering various hydrophobic and hydrophilic drugs in a single platform with a consecutive NO-scavenging action.

4:15 PM SB02.02.09**Late News: Enhanced Strength and Shape Memory in Microgel Filled Biopolymer Networks** Vignesh Subramaniam and Thomas E. Angelini; University of Florida, United States

Biopolymer networks comprise an essential and substantial proportion of 3D bioprinting materials because of their abundance and role in living tissues. While biopolymers serve to strengthen tissues in vivo, biopolymer networks in vitro are notoriously soft and weak; bioprinted structures made from biopolymer networks exhibit the same limitations. To stiffen and strengthen printable in vitro biopolymer networks, we developed a biomaterial made from collagen-1 in which the polymer mesh-space is filled with micron-scale microgel particles made from polyethylene glycol (PEG). We find that this combination of material components synergistically enhances the system material properties. For example, by filling in the mesh space of the polymer networks with low volume fraction microgels, the elastic modulus can increase by more than an order of magnitude. By packing the microgels into the polymer network at volume fractions approaching jamming, the material takes on a shape-memory property, where the material will spontaneously lock-in deformations at intermediate strain levels; reversal of these strains requires a stress-reversal and results in the material returning to its original deformation state. This new class of materials opens up wide possibilities in its capacity as a 3D bioprinting material and has potential applications in fabrication of model tissues.

4:30 PM SB02.02.10**Stretchable Anti-Fogging Tapes for Diverse Transparent Materials** Shaoting Lin, Yueying Yang, Jiahua Ni, Xuanhe Zhao and Gang Chen; Massachusetts Institute of Technology, United States

Surface wetting prevents surface fogging on transparent materials by facilitating filmwise condensation with specific chemistry but suffers from material and geometry selectivity. Extreme environments associated with high humidity and mechanical loading further limit their anti-fogging persistence. Here, we report a stretchable anti-fogging tape (SAT) that can be applied to diverse transparent materials with varied curvatures for persistent fogging prevention. The SAT consists of three synergistically combined transparent layers: i) a stretchable and tough layer with large elastic recovery, ii) an enduring anti-fogging layer insensitive to ambient humidity, and iii) a robustly and reversibly adhesive layer. The SAT maintains high total transmittance (>90%) and low diffuse transmittance (<5%) in high-humidity environments, under various modes of mechanical deformations, and over a prolonged lifetime (193 days tested so far). Two applications are demonstrated, including the SAT-adhered eyeglasses and goggles for clear fog-free vision, and the SAT-adhered condensation cover for efficient solar-powered freshwater production.

4:45 PM SB02.02.11**Fracture and Fatigue of Ideal Polymer Networks** Shaoting Lin, Jiahua Ni, Dongchang Zheng and Xuanhe Zhao; Massachusetts Institute of Technology, United States

Soft materials have enabled diverse modern technologies, but their practical deployment is usually limited by their mechanical failures. Fracture and fatigue of polymer networks are two important causes of mechanical failures of soft materials. A soft material fails by fracture when a monotonic load reaches its *fracture toughness* or fails by fatigue when a cyclic load reaches its *fatigue threshold*. Fracture toughness is usually much larger than fatigue threshold for randomly crosslinked polymer networks (e.g., elastomers and gels). This work systematically studies the fracture and fatigue of ideal polymer networks with controlled densities of dangling-chain defects. We show that the fracture toughness and fatigue threshold of an ideal polymer network almost without defects are the same. After introducing a low density of dangling-chain defects into the ideal polymer network, its fracture toughness and fatigue threshold still maintain approximately the same. The fracture toughness of the ideal polymer network is also independent of the loading rate. We further use the recently developed defect network model to explain the fatigue threshold (*i.e.*, intrinsic fracture energy) of ideal polymer networks with controlled densities of dangling-chain defects.

SESSION SB02.03: Poster Session I: From Hydrogel Fundamentals to Novel Applications via Additive Manufacturing

Session Chairs: Preethi Chandran and Orlin Velev

Tuesday Afternoon, November 30, 2021

8:00 PM - 10:00 PM

Hynes, Level 1, Hall B

SB02.03.01**Thermosensitive Hydrogel-Based Desalination System Driven by Diurnal Temperature Variation** Hoyeon Kim and Jonghwi Lee; Chung-Ang University, Korea (the Republic of)

Solar desalination system has been considered as an effective method to address the global water scarcity, which thanks to its eco-friendliness and sustainability. However, the heat loss of evaporation surface to water reservoir, fouling due to the formation of salt crystals on evaporation surfaces and

water channels, and the difficulty of continuous brine supply without external power are the major obstacles in the practical use of the solar desalination. Herein, through the separation of water pumping and evaporation part, a novel solar desalination system showed no heat loss during evaporation and had an antifouling property. Moreover, using thermosensitive hydrogel composites, a solar desalination system could work by diurnal temperature variation. An irreversible water flow was achieved by using composites of thermosensitive poly(N-isopropylacrylamide) (PNIPAm) hydrogel and hydrophobic polydimethylsiloxane (PDMS), which have fast deswelling kinetics responsive to temperature above 32 °C (LCST). The composites were made by directional melt crystallization (DMC) of solvent. By the DMC method, a porous PNIPAm having aligned and continuous three-dimensional pores was prepared. The structure enables a combination of two different materials. It can be achieved by the infiltration of PDMS to the aligned pores of PNIPAm. Anisotropic composites have PNIPAm/PDMS phase at the bottom of the composites, which has a faster deswelling rate than pure PNIPAm phase. As temperature rises above the LCST of PNIPAm, water can be released from the top surface of the PNIPAm, and this water pumping could be repeated by the diurnal temperature variance. Average pump efficiency of our composites is 88%. Between the pumping composite and the water reservoir, porous polyethylene glycol (PEG) was placed for the water channel. PEG can absorb brine from the water reservoir and diffuse brine into the entire phases of PNIPAm/PDMS composite. Water from the pumped brine evaporates on the surface of reduced graphene oxide (rGO) coated cellulose paper, which showed broad range of light wavelength. When brine is released, the rGO coated cellulose paper float, and salt accumulation is formed at the bottom of the paper. This crystallized salt is dissolved in the next pumped water. Our three-dimensional solar desalination system was operated stably in several cyclic tests in one-sun condition. Diurnal operating strategy makes the solar evaporator eco-friendly, and the antifouling properties increase the sustainability of solar desalination.

SB02.03.02

Injectable and Conductive Alginate and Poly (3,4-Ethylenedioxythiophene) (PEDOT) Based Soft Electrodes for Neural Regenerative Applications Ivana Perkucin, Tianhao Chen, Kylie Lau, Cindi M. Morshead and Hani E. Naguib; University of Toronto, Canada

Electroconductive biocompatible polymers have been of interest for use in a wide range of biomedical applications such as biosensors, regenerative therapeutics and prostheses. This surge of curiosity has sparked the development of soft functional materials to meet these demands. In the field of neural regenerative medicine, we have demonstrated that resident brain neural precursor cells are electrosensitive cells that respond to electric field application by proliferating, differentiating and migrating in a rapid and directed fashion. Harnessing these properties can potentially be used to facilitate neural regeneration following injury or disease. The design of current electrodes, typically made of conductive metals, are stiff and result in additional tissue injury as a result of implantation. The mechanical mismatch of these materials to the soft and wet physiological conditions that they would be subjected to in their use in the brain, presents significant limitations of this technology as a potential therapeutic. Recently, there has been interest in using biologically derived polymers for their relative abundance and consequently, economic feasibility. Sodium alginate is an attractive example of such and can be used to form hydrogels whose soft and flexible nature as well as functionality in aqueous environments presents a potential solution to this issue of mechanical mismatch. We have fabricated a novel conductive and biocompatible hydrogel that more closely mimics the modulus of the brain as a solution to this problem. By designing a hydrogel based system comprised of alginate and conductive polymer, poly(3,4-ethylenedioxythiophene) (PEDOT), we propose an innovative new material for use in the development of novel neural regenerative therapeutics. These alginate/PEDOT blends exhibit shear thinning behaviour at both ambient and body temperatures as well as exhibit satisfactory conductivity for their intended therapeutic application.

SB02.03.04

Heterotypic Supramolecular Hydrogels Formed by Noncovalent Interactions in Inflammasomes Adrianna Shy, Huaimin Wang, Zhaoqianqi Feng and Bing Xu; Brandeis University, United States

Inspired by the work of Stupp and colleagues on the supramolecular exchange of oppositely charged molecules, we used two complementary peptides derived from ASCPYD inflammasomes. The addition of the positive and negatively charged complements in water produced heterotypic hydrogels dependent on ratio and the use of N-terminal acetyl or naphthalene capping groups. We found that mixing one naphthalene capped positively charged peptide at 0.5wt% with an acetyl capped negatively charged complement created hydrogels across all ratios of 0.5, 1, 2, 3, and 4 times the amount of positively charged peptide. The addition of the peptides of the oppositely charged peptides in solution produces heterotypic hydrogels. Rheology measurement shows that ratios of the complementary peptides affect the viscoelasticity of the resulted hydrogel. Circular dichroism indicates that the addition of the complementary peptides results in electrostatic interactions that modulate self-assembly. Lastly, transmission electron microscopy reveals that the ratio of the complementary peptides controls the morphology of the heterotypic peptide assemblies. This work illustrates a rational, biomimetic approach that uses the structural information from the protein data base (PDB) for developing heterotypic peptide materials via self-assembly.

SB02.03.05

Leveraging LCST Behavior in Thermoresponsive Polymers to Enable Reliable Cooling-Triggered Reactions Romario Lobban and Leon Bellan; Vanderbilt University, United States

Much work has been done on the use of heating to trigger reactions via the temperature-dependent removal of a barrier or constraint separating reagents. An example of this method is the use of wax microbeads to encapsulate reagents which are only liberated to react with each other when the wax is melted by heating. Far less work, however, has been done on the use of cooling to achieve a similar goal. Numerous applications, such as those involving components or materials susceptible to persistent low temperatures and cases in which energy for heating is not available would benefit from this inverse approach. Hence, in this study we explore whether LCST polymers can be reliably used as thermoresponsive constraints that allow reagents to react only upon cooling. We aim to achieve this by loading reagents into separate adjacent blocks of thermoresponsive polymer gels- in this case, 400 cP methylcellulose- and showing that said reagents can only react with each other after the temperature of the polymer falls below its LCST. Additionally, to demonstrate generalizability and the innate robustness of the concept, we explore situations involving radically different reaction types: one reaction based on a colorimetric enzyme assay (using a colorless HRP solution to oxidize a colorless TMB substrate, resulting in a soluble blue reaction product), and another based on a change in pH (using basic colorless NaOH solution to change colorless slightly acidic phenolphthalein solution from colorless to pink). Finally, to explore the tunability of the process, we alter the LCST of the polymer and observe the resulting change in the extent of cooling necessary to allow a chemical reaction to occur. This change in LCST is achieved by adding different quantities of NaCl to methylcellulose and is corroborated by rheology.

At elevated temperatures (above the LCST), the reagents remain sequestered in separate gels and no reaction occurs. We have demonstrated that this "OFF" state is stable for extended periods of time. When the system is allowed to cool, the gels liquify and flow into each other, allowing mixing of the embedded reagents ("ON" state). By quantitatively assessing the progress of the stated color change reactions over time, we determine that these reactions are triggered reproducibly at different temperatures based on the polymer's tuned LCST (determined by the NaCl content of the methylcellulose), as well as the proximity of the reagent-laden gels and viscosity of the liquified materials after cooling. With no NaCl present, reactions are triggered 18 minutes (the time required for the gels to liquify and flow into each other) after cooling below 50 degrees Celsius. With 1.5% and 2% NaCl, reactions are triggered 18 minutes after cooling below 36 and 30 degrees Celsius, respectively. In all three cases, the same geometry is used (to maintain the same gel proximity) and the viscosity of liquified materials is similar. We therefore conclude that thermoresponsive polymers can, in fact, act as reliable temperature-sensitive

constraints that allow reagents to react only upon cooling. We successfully demonstrate that this method can be applied to a variety of reactions and that the temperature required for triggering a reaction can be predictably and reproducibly tuned.

SB02.03.06

High Elastic Modulus, Ion-Responsive Hydrogel with Controlled Response [Abhishek Pachauri](#) and Jeffrey Bates; University of Utah, United States

Hydrogels possess outstanding biocompatibility and swelling properties and thus find extensive applications in fields such as biomedical devices and soft robotics. Here, a high elastic modulus hydrogel with improved strength and toughness is synthesized. The hydrogel can be stretched many times its initial dimensions, where the material returns to its original shape in a reversible manner. Glucose solution is used as the chemical stimulus and the hydrogel swells several times its initial size when immersed in glucose solution and shrinks when it is removed from the solution. This swelling and deswelling behavior of the hydrogel can be used to perform useful work. The swelling behavior of the hydrogel as a function of the amount of glucose in the solution is studied. Rheology of hydrogel material is investigated so that the material has desired properties for 3D printing. Mechanical and viscoelastic properties of hydrogel before and after swelling are tested. The swelling kinetics are analyzed, so that swelling and deswelling behavior can be precisely controlled.

SESSION SB02.05: Biological Gels
Session Chairs: Alan Grodzinsky and Nir Kampf
Wednesday Morning, December 1, 2021
Sheraton, 2nd Floor, Republic A

10:30 AM *SB02.05.01

Hydration Lubrication by Polymer Assemblies and Hydrogel Composites [Nir Kampf](#)¹, Weifeng Lin¹, Monika Kluzek¹, Somasundaram A. Angayarkanni², Noa Iuster¹, Eyal Shimoni¹, Ronit Goldberg³ and Jacob Klein¹; ¹Weizmann Institute of Science, Israel; ²SRM Institute of Science and Technology, India; ³Liposphere Ltd., Israel

About 20% of the world's total energy consumption is spent to overcome friction. Friction is also present in biological systems such as in hips and joints, and correlated with joint diseases such as osteoarthritis. Due to the molecular complexity of the biological systems, the mechanism of lubrication is still not clear. Apart from our efforts to find the major components responsible for the low friction in biological systems, we also try to exploit nature's solution for lubricating interfaces such as cartilage by mimicking nature's strategies of boundary lubrication, which lead to an extreme reduction of friction in aqueous environments. In my talk, I will present several examples of bio-inspired lubrication by polymers and in polymer networks. We carried out systematic investigations from the molecular to the macroscopic level, demonstrating excellent lubrication by polymer assemblies (1) and hydrogel composites (2), attributed to the hydration lubrication mechanism acting at highly-hydrated boundary layers.

- 1) Angayarkanni et al., (2019) *Langmuir*. 35, 48, p. 15469-15480.
- 2) Lin et al., (2020) *Science*. 370, 6514, p. 335-338.

11:00 AM *SB02.05.02

A Human Microphysiological System to Model Breakdown of Hydrogel-Like Cartilage Caused by Osteoarthritis [Alan Grodzinsky](#); Massachusetts Institute of Technology, United States

Traumatic joint injuries can initiate early cartilage degeneration in the presence of elevated levels of inflammatory cytokines, leading to post-traumatic osteoarthritis (PTOA). There are currently no disease-modifying drugs for osteoarthritis, and a major challenge is the ability to achieve sustained levels of potential therapeutics *inside* a target tissue, with no side effects, after intra-articular delivery. We have developed a human *in vitro* microphysiological system (MPS) for studies of drug discovery for OA/PTOA as well as drug delivery into cartilage. Human knee osteochondral plugs subjected to a single impact mechanical injury are co-cultured with joint capsule synovium. Cytokines secreted mainly from the synovium emulate the inflammatory component of the response to joint injury. Combination therapeutics (e.g., glucocorticoids, growth factors) are tested which can inhibit matrix degradation and cell death in cartilage. Experiments involving this human knee MPS were recently launched on SpaceX-21 to the International Space Station to study the effects of microgravity and radiation on disease-like progression and the effects of selected therapeutics. Parallel *in vitro* and animal studies are aimed at approaches to targeted tissue drug delivery. For these studies, electrostatic interactions involving cationic nanoparticles to which drugs are functionalized are found to augment transport into and through the cartilage tissue. Thus, the transport properties of the negatively charged gel-like extracellular matrix of cartilage, even during initial degradative stages of the disease model, can provide benefit to enhance drug delivery.

11:30 AM SB02.05.03

Towards Hydrogel-Capped Titanium Implants for Cartilage Repair [Jiacheng Zhao](#), Feichen Yang, William Koshut, Alina Kirillova, Cambre Kelly and Heng Xu; Duke University, United States

There are approximately 900,000 people in the US suffering from damage to the articular cartilage, with the knee being most commonly affected. Articular cartilage lacks a vasculature and has a limited ability to heal. A variety of surgical treatments have been developed to repair cartilage lesions. Current strategies for cartilage repair include microfracture, autologous chondrocyte implantation (ACI) and osteochondral allograft transfer (OAT). These strategies suffer from high failure rates (25-50% at 10 years), long rehabilitation times (more than 12 months) and decreasing efficacy in patients older than 40-50 years. Focal joint resurfacing with traditional orthopedic materials is being explored as an alternative strategy, but due to their high stiffness and coefficient of friction relative to cartilage, these implants may ultimately contribute to joint degeneration through abnormal stress and wear. A focal joint resurfacing method that is widely available, allows immediate weight bearing, has short recovery times and has low long-term failure rates remains an unmet need.

Our strategy to address this need is to (1) develop a material that mimics the properties of cartilage and (2) attach this material to a titanium base to enable integration with bone. We developed the first hydrogel to achieve the strength and modulus of cartilage in both tension and compression. This hydrogel also exhibits cartilage-equivalent tensile fatigue at 100,000 cycles. The hydrogel was created by infiltrating a PVA-PAMPS double-network hydrogel into a bacterial cellulose (BC) nanofiber network. The BC provides tensile strength in a manner analogous to collagen in cartilage. The PAMPS provides a fixed negative charge and osmotic restoring force similar to the role of aggrecan in cartilage. The hydrogel is not toxic, has the same aggregate modulus and permeability as cartilage, has a coefficient of friction 45% lower than cartilage, and is 4.4 times more wear-resistant than a PVA hydrogel. These properties make the BC-PVA-PAMPS hydrogel an excellent candidate material for the replacement of damaged cartilage. Current strategies for adhering hydrogel to a surface are 10 times weaker than the shear strength with which cartilage is attached to the bone. The

osteocondral junction is characterized by collagen nanofibers anchoring cartilage to bone. We sought to mimic this strategy by bonding freeze-dried BC to porous titanium with a hydroxyapatite-forming cement. The cement penetrates about 10 microns into the bacterial cellulose, forming a nanofiber-reinforced zone of adhesion. The PVA-PAMPS hydrogel is then infiltrated into the bonded bacterial cellulose. This strategy achieved a shear strength of attachment three times greater than the state of the art. Such improved strategies for attaching hydrogels to a titanium surface with sufficient strength to allow for weight-bearing can enable the creation of hydrogel-capped titanium implants for cartilage repair.

11:45 AM SB02.05.04

Chemistry of Metal-Organic Frameworks as Hydrogels and Silicone Patches in Wound Healing [UnJin Ryu](#) and Kyung Min Choi; Sookmyung Women's University, Korea (the Republic of)

Metal-organic frameworks, called MOFs, are crystalline porous materials constructed by repeating metal clusters and organic linkers thus having permanent porosity. The structure and characters of MOF libraries have been widely reported and some MOFs have been applied to the wound healing process by using the porosity to release drugs, gases, and metal ions promoting the wound healing process. However, our research focused on removing substances from living organisms, and these studies have not been reported before.

In the wound healing process, the important mediators that lead to inflammation and scar formation are nitric oxide, cytokines, and reactive oxygen species (ROS). However, the overproduction of these inflammatory agents causes abnormal inflammation and excessive scarring, so it is challenging to control adequate amounts of mediators to complete wound healing with barely scarred.

In this study, MOF was introduced to suppress the excess nitric oxide, cytokines, and ROS, that based on their MOF's own structure such as micropores, surface, and catalytic activities. we systemically devised and applied a MOF hybrid hydrogel (and silicone patch) that optimizes the wound healing performance by removing excess immune mediators with MOF as well as simultaneously supplying moisture and uniformly applying MOF by hydrogel matrix. After the removal of excess mediators was experimentally analyzed based on MOF chemistry, the wound healing process of MOF was analyzed through cell-derived substances, and finally applied the MOF to animal testing for a real actual wounded environment. It was confirmed that the wound recovered rapidly within 14 days after the introduction of MOF-hydrogel, which showed that the system incorporating MOF is effective in wound healing.

SESSION SB02.06: Gels and Applications

Session Chair: Catalin Picu

Wednesday Afternoon, December 1, 2021

Sheraton, 2nd Floor, Republic A

1:30 PM SB02.06.01

Strength and Toughness of Stochastic Networks: Dependence on Structural Parameters and Network Architecture [Catalin R. Picu](#), Sai Deogekar and Shengguang Jin; Rensselaer Polytechnic Institute, United States

Network materials are encountered broadly in the engineering and natural worlds and gels are an important subset of this broad class. These materials have a molecular or fiber network as their main structural component and perform various functions of which the most prevalent is structural. The integrity of network materials is critical in many applications. Therefore, it is of interest to determine ways to control their strength and toughness. This work focuses on the relation between structural parameters of the network, the network architecture and its strength and toughness. We report the dependence of the strength on network density, crosslink density and strength, and fiber properties. We also investigate the toughness of networks without pre-existing defects and report its dependence on the same set of structural parameters. We observe and characterize the intermittent dynamics of rupture in networks and relate it to similar processes in other materials with stochastic structure. Network design rules emerge from these results. Numerical results are compared with equivalent experimental data.

1:45 PM SB02.06.02

Anomalous Collagen Fiber Reorientation in the Facet Capsule Ligament: Mechanism and Implications [Jacob Merson](#), [Mark Shephard](#) and [Catalin R. Picu](#); Rensselaer Polytechnic Institute, United States

Multiscale models are employed to study how the microscopic and tissue scale properties of the facet capsule ligament of the spine combine to cause anomalous collagen fiber realignment (AR). The facet capsule ligament, located between the spinal processes, is primarily made up from type I collagen. Fiber reorientation in the FCL has been linked to neck and back pain and it is therefore a critical phenomenon to understand. Anomalous realignment is experimentally observed in the FCL using quantitative polarized light imaging (QPLI). However, no experimental techniques are currently available to probe the root causes of anomalous realignment. This talk will discuss how the interplay of tissue scale collagen orientation, fiber scale instabilities, and fiber failure can cause anomalous realignment in the facet capsule ligament.

2:00 PM SB02.06.03

Developing a Platform to Evaluate Photoswitches and Their Mechanical Work [Friedrich Stricker](#), [Jesus G. Campos](#), [Minwook Park](#), [Kyle Clark](#) and [Javier Read de Alaniz](#); University of California, Santa Barbara, United States

Materials adapting their shape reversibly to external stimuli have gathered increasing attention for a range of applications in medicine and robotics. In particular, photoresponsive systems have shown promise through the facile and benign nature of the trigger. However, most photoresponsive molecules, which can be used to convert light into mechanical work, are susceptible to decomposition upon conditions commonly used in preparation of polymeric systems. In this work we present new light-responsive liquid crystalline network (LCN) systems using benign Diels-Alder chemistry and employ this novel platform to compare a range of different photoswitches from the well-established azobenzene scaffold to the novel Donor-Acceptor Stenhouse adducts.

2:15 PM SB02.06.06

Thermal Stabilisation of Biologics Using Reversible Dynamic Covalent Hydrogels [Bruno Marco Dufort](#) and [Mark W. Tibbitt](#); ETH Zurich, Switzerland

Biologics—including peptides, therapeutic proteins, enzymes, monoclonal antibodies, vaccines, and viral vectors—comprise the majority of new drugs entering the market. However, biologics are highly susceptible to thermal fluctuations during storage and transport, as aggregation, denaturation, and oxidative degradation render them ineffective. In order to guarantee their quality and safety, biologics must be maintained within a tight temperature window (2–8 °C) from manufacture to point of use. This global 'cold chain' infrastructure cost over 17 billion USD in 2020 and poses significant health

risks as failures in the cold chain can lead to community health outbreaks, as in the case of ineffective vaccines. An emerging strategy to impart thermal stabilisation is to immobilize biologics directly within a protective matrix that can hold the molecules in place to resist conformational changes and prevent translation. One of the major challenges for these matrix-based approaches, however, is to achieve on-demand release of the biologics from the protective matrix.

To meet these challenges, we designed a safe and easy-to-use synthetic reversible hydrogel for the encapsulation and stabilisation of a broad range of biologics against thermal stress [1]. Our approach is based on the use of dynamic covalent boronic ester cross-links that enable on-demand recovery through network dissolution upon addition of sugars [2, 3]. Using these reversible hydrogels, we thermally stabilised a wide range of biologics, starting with model enzymes (β -galactosidase, leucine aminopeptidase, and alkaline phosphatase). We attributed protection to the formation of polymer networks around the biologics, which restricted their mobility and physically restrained them from interacting with each other, reducing aggregation and activity loss after exposure to heat. In addition, we showed that the gels could be used to protect extremely heat sensitive therapeutic enzymes, such as *E. coli* DNA gyrase and human topoisomerase I. Both enzymes could be stored within the gels for months at room temperature without significant activity loss, vastly outperforming the unencapsulated (free) enzymes.

Finally, we present our results on the thermal stabilisation of vaccines. We stabilised a protein-based vaccine, recombinant influenza A H5N1 hemagglutinin, and a live virus, adenovirus Type 5 (Ad5). Viral vectors, such as Ad5, are central to gene therapy and genome editing techniques (i.e., CRISPR-Cas9), and are becoming increasingly important for use in vaccine development (i.e., COVID-19 vaccines). Live viruses such as Ad5 present a particular challenge for thermal stabilisation because both protein conformation and nucleic acid integrity must be preserved to retain viral infectivity and immunogenicity; even simple drying of live viruses is often challenging. Gel-encapsulated Ad5 outperformed free Ad5 at all tested temperatures (4 °C to 65 °C) and retained close to 100 % activity after 4 weeks at 27 °C, while the infectivity of free Ad5 decreased by 3 logs. In total, our work demonstrates that reversible hydrogels are suitable for the thermal stabilisation of multiple classes of biologics, with little formulation work required to stabilise each type of biologic. The ability to protect biologics from thermal stress with a simple material solution offers a useful approach to mitigate the costs and risks associated with reliance on a continuous cold chain for biologic transport and storage.

[1] Marco-Dufort et al., *in preparation*.

[2] Marco-Dufort et al., *J. Am. Chem. Soc.* **2020**, *142*, 15371.

[3] Marco-Dufort et al., *Biomacromolecules* **2021**, *22*, 146.

3:30 PM SB02.06.07

Digitally Programmable Living Materials from Biowaste Suitu Wang, Laura K. Rivera Tarazona, Mustafa K. Abdelrahman and Taylor H. Ware; Texas A&M University, United States

Materials manufacturing strategies that use little energy, valorize waste, and result in degradable products are urgently needed. Strategies that transform abundant biomass into functional materials form one approach to new manufacturing, but the resulting products of the biomass are often dictated by the organisms. From a biology standpoint, morphogenesis of biological tissues is a “manufacturing” mode without energy-intensive processes, large carbon footprints, and toxic wastes. However, most living organisms cannot form materials that are suitable for engineering applications. Inspired by biological morphogenesis, we have proposed a manufacturing strategy by embedding living *Saccharomyces cerevisiae* (baker’s yeast) within a synthetic acrylic, such as poly(2-hydroxyethyl acrylate), hydrogel matrix. The resulting living composites derive functionality from both the biological activity and material properties. By culturing the living composites in media derived from bread waste, encapsulated yeast cells can proliferate resulting in a dramatic dry mass and volume increase of the whole living composite. After growth, the final composite is up to 96 wt% biomass and 590% larger in volume than the initial object. By spatial-patterning the cell viability through UV irradiation or photodynamic therapy, the living composites can also form complex user-defined relief surfaces or 3D objects during growth. The resulting living composites also have tunable mechanical properties by controlling the extent of the cell growth or the selection of polymer matrix. After growth and drying, the modulus of the composites can be tuned from 290 MPa to 856 MPa. Ultimately, the grown structures can be degraded into water-soluble polymers and yeast. The accelerated degradation of the living composites can be tuned by changing the molecular weight of polyester crosslinkers from 4 to 8 days. The proposed living composite strategy cultured from biowaste may pave the way for future ecologically friendly manufacturing of materials.

2:45 PM BREAK

3:45 PM SB02.06.08

Design and Use of a Thermogelling Methylcellulose Nanoemulsion to Formulate Nanocrystalline Oral Dosage Forms Liang-Hsun Chen and Patrick Doyle; Massachusetts Institute of Technology, United States

Oral drug products have become indispensable in modern medicine because of their exceptional patient compliance. However, poor bioavailability of ubiquitous low-water-soluble active pharmaceutical ingredients (APIs) and lack of efficient oral drug formulations remain as significant challenges. Nanocrystalline formulations are an attractive route to increase API solubility, but typically require abrasive mechanical milling and several processing steps to create an oral dosage form. Using the dual amphiphilic and thermoresponsive properties of methylcellulose (MC), a new thermogelling nanoemulsion and a facile thermal dripping method are developed for efficient formulation of composite particles with the MC matrix embedded with precisely controlled API nanocrystals. Moreover, a fast and tunable release performance is achieved with the combination of a fast-eroding MC matrix and fast-dissolving API nanocrystals. Using the versatile thermal processing approach, the thermogelling nanoemulsion is easily formulated into a wide variety of dosage forms (nanoparticle suspension, drug tablet, and oral thin film) in a manner that avoids nanomilling. Overall, the proposed thermogelling nanoemulsion platform not only broadens the applications of thermoresponsive nanoemulsions but also shows great promise for more efficient formulation of oral drug products with high quality and tunable fast release.

4:00 PM SB02.06.09

Late News: Digital Lensless Holographic Traction Force Microscopy in Alginate Hydrogels Optimized for Additive Manufacturing Sebastian Ocampo Gutierrez, Brayan Patiño-Jurado, Carlos Paucar and Claudia Garcia; Universidad Nacional de Colombia, Colombia

The general knowledge of many cell-based processes comes from experimentation on flat surfaces, mainly in culture wells made of either a polymer or glass. These are 2D, stiff and non-physiological environments, which are simple for experimentation, yet do not replicate all the conditions a cell experiences in vivo.

In this work a methodology to develop an alginate hydrogel based material with calcium phosphate particles suspensions is presented. This material has the potential to act as a scaffold with a complex architecture processed via additive manufacturing, and is shown in the shape of a triply periodic minimal surface. Being a known biocompatible material, and formed in a shape suitable for cell culturing, a method to capture information from this scaffold is presented.

The formed hydrogel shows elastic properties suitable to implement traction force microscopy (TFM), a computational technique to compute force fields exerted on the substrate. This is achieved using digital lensless holographic microscopy, a holographic technique that vastly reduces costs, experimental setup and permits the analysis of transparent objects with sizes in the range of a few micrometers. The calcium phosphate particles in the hydrogel are used as fiducial markers to calculate displacement in TFM. This way, a complex, more physiological environment can be achieved, and the means to recover information such as traction forces are shown to work, facilitating acquisition to offer biological insight.

SESSION SB02.07: Hydrogel Characterization and Application
Session Chairs: Emiliós Dimitriadis and Gaio Paradossi
Tuesday Morning, December 7, 2021
SB02-Virtual

10:30 AM *SB02.07.01

Surface Morphology Changes and Micromechanics in PNIPAAm Based Micro- and Nanogels Particles Fabio Domenici¹, Elisabetta Tortorella¹, Barbara Ceroni¹, Yosra Toumia¹, Letizia Oddo¹, Sharad Pasale¹, Ester Chiessi¹, Mark Telling², Sarah Rogers² and Gaio Paradossi¹; ¹Università degli Studi di Roma Tor Vergata, Italy; ²STFC ISIS Facility, United Kingdom

Gels thermal responsivity is usually associated to a Volume Phase Transition, VPT. However, different and equally relevant for biomedical applications, responsive behaviors to temperature can be found in micro- and nanogel particles.

In this contribution we report on the morphological changes around physiological temperature of hybrid nanogel particles made by crosslinking via click chemistry an azido-derivative of hyaluronic acid, HA, and a derivative of poly(N-isopropyl acrylamide), PNIPAm, having propargyl functions at both ends, with interesting fallouts concerning targeting and drug delivery. In *in vitro* tests, doxorubicin loaded nanoparticles with a PNIPAAm/HA ratio of 33 % (w/w) increased its cytotoxicity on HT-29 tumor cells over the NIH 3T3 healthy fibroblasts, by a factor of two.

In this HA/PNiPAAm nanogel, the hydrophobic – hydrophilic interplay of the two crosslinked polymer components gives rise to a reshuffling of the surface composition passing a quite narrow threshold around 33 °C, taken as the VPT temperature, VPTT, of the system. In this process, the room temperature surface structure is a collection of PNIPAAm and hyaluronate patches. Approaching the VPTT, the PNIPAAm hydrophobicity promotes the interparticle aggregation. Above the VPTT, the NiPAAm residues self-segregate in the particle core, leaving the charged HA moiety on the surface. This moieties redistribution, and not the size reduction, within the microgel particle, assessed by an atomic force microscopy, AFM, study of the surface, dynamic light scattering, DLS, zeta potential analysis and small angle neutron scattering, SANS, is at the base of the recognition of tumor cells via the interaction HA/receptors of overexpressed CD44 transmembrane proteins and of the specific drug delivery mechanism.

In PNIPAAm hydrogels, drug release has been often coupled with the temperature response of the matrix. However, besides the temperature, responsiveness to other state variables, such as pressure, or to the combination of both temperature and pressure can be considered. Two microgels having PNIPAAm as the only polymer component but different architectures, obtained by precipitation polymerization, were investigated: a morphology with (i) an un-crosslinked core and a crosslinked shell of PNIPAM chains and a softer one, (ii), having crosslinked PNIPAM chains as particle core with a shell of tethered un-crosslinked PNIPAM chains to the core. Confocal microscopy was a useful tool to validate the different morphologies. Differential scanning calorimetry, DSC, and DLS were used to follow the microgels as a function of temperature, pressure and both, pressure being osmotically controlled with a high molecular weight non-interacting polymer. Under osmotic stress, soft microgels can be compressed above the VPTT, reaching extremely low hydration degrees. The microgel volume behavior as a function of pressure and temperature allowed to estimate the isothermal compressibility and thermal expansion coefficients for the different morphologies. The VPT enthalpy is scarcely affected by the network architecture, whereas the work on osmotically stressed PNIPAAm is strongly influenced by the morphology. As biological counterpart, a very low cytotoxicity was highlighted by MTT tests of all morphologies on HaCAT cell line, while it is noteworthy that the softer morphology (ii) of microgels enhances the phagocytosis by RAW 264 macrophages.

11:00 AM *SB02.07.02

Biopolymer-Particle Composites Designed to Match the Mechanical Properties of Soft Biological Tissues Paul A. Janmey; University of Pennsylvania, United States

Fibrous networks are ubiquitous in biology. The mechanical properties of the biopolymer fibers, the way in which the fibers are linked into networks, and the types of cells or particles within the network mesh all affect the macroscopic mechanical response of the material. Filamentous polymer networks containing volume-conserving particles are found in the cytoskeleton and extracellular matrix of animal cells and tissues, bacterial biofilms, fungal mycelia, and other structures spanning multiple biological kingdoms. The responses of biomaterials to uniaxial and shear deformations depends critically on the volume fraction of particles within networks and on the binding of particles to the network, but current data suggest that the mechanical properties of the particles themselves have only minor effects on the response of the composite material. Controlling biopolymer network connections and incorporation of appropriately sized particles within them can lead to viscoelastic properties that mimic those of biological tissues more closely than polymer networks alone.

11:30 AM *SB02.07.03

Mapping the Mechanics of Cartilage Matrix, Nature's Almost Perfect Hydrogel Emiliós K. Dimitriadis¹, Preethi Chandran², Edward Mertz¹, Ferenc Horkay¹ and Peter Basser¹; ¹National Institutes of Health, United States; ²Howard University, United States

Cartilage matrix is composed of a dense collagen mesh within which the highly charged glycoprotein, aggrecan, is produced by chondrocytes and remains entangled in high concentrations. The inclusion and entanglement of large complexes of aggrecan molecules attached to long hyaluronic acid chains is responsible for matrix osmotic swelling that profoundly affects the behavior of the composite tissue. The equilibrium between the swelling and the mechanical constraints imposed by the collagen matrix is what provides cushioning of bones at load bearing joints. The relationship between osmotic and mechanical properties on one hand, and matrix composition and architecture on the other, is poorly understood. The composition of the tissue changes through tissue depth. Moreover, in growing cartilage, the relative composition and organization of the different components changes with time and along the bone axis and in the vicinity of chondrocytes, the pericellular matrix (PCM). Axial mapping of the mechanics is further complicated due to the need to physically section the tissue to gain access.

Here we study mouse cartilage. Even though mice are extensively used as model systems for a wide range of pathologies including arthritis, there are limited studies mapping matrix mechanics across different regions. Newborn mouse cartilage adds the complication that the tissue is densely populated with chondrocytes creating a complex 3-D composite that is continuously varying both in space and time. Nanomechanical studies, typically performed by

indenting tissue sections, are subject to errors due to matrix collapse, surface roughness and loss of aggrecan from the section surface by diffusion and degradation. Furthermore, data interpretation often poses its own challenges not least because of the natural inhomogeneity of the tissue.

Here, we performed high-resolution (1 μ m) elasticity mapping of the knee cartilage matrix of newborn mice. The indentations were performed on thin (~12 μ m) cartilage sections that were cut parallel to the bone longitudinal axis and mildly fixed to minimize loss of aggrecan. We chose the diameter of the microspheres used as indentation probes and we applied indentations that were large enough as to minimize the effects of surface roughness and geometric inhomogeneities. To consistently analyze the data, we developed a novel method for obtaining an effective contact point on the tissue surface. Our model fitting protocol ensures that we are probing bulk matrix properties and minimizes the effects of surface damage, tissue inhomogeneity and finite sample thickness. Matrix regions were extracted by correlation with optical images. Our results show interesting variation of properties between different regions and large variations in the vicinity of chondrocytes. The latter presented an additional challenge because the septa between chondrocytes are often very narrow adding to the difficulty of interpretation. Further modeling and analysis points to continuously and strongly varying properties of the PCM. The variability of matrix elasticity across the growing cartilage will be described and possible correlations with composition will be discussed.

12:00 PM *SB02.07.04

Bio-Inspired Hydrogels as Superglue in Seawater [Hailong Fan](#) and Jian Ping Gong; Hokkaido University, Japan

Many efforts have been made on developing adhesives for the marine environment that are inspired by organisms that fix themselves to underwater surfaces, like mussels. These catechol-based glues are easily oxidized and so eventually lose their adhesiveness, making them less than satisfactory for their intended purpose. Recently, we explored the possibility of developing adhesives that utilize electrostatic interaction to stick to negatively charged surfaces such as rocks, glass, and metals under the sea [1]. We built polymer chains made from two types of monomers as building blocks. One contains a positively charged "cationic" residue and the other contains an "aromatic" ring. In biosystems, adjacent cationic-aromatic amino acid sequences in proteins are known to facilitate electrostatic interactions in saline water. It has been challenging, however, to introduce such sequences in synthetic polymers due to difficulties in controlling monomer sequences. We discovered that the synthetic polymers with adjacent cationic-aromatic sequences could easily be manufactured using a highly scalable, cost-effective method through cation- π complex-aided free-radical polymerization. We found that the two residue types in polymers bonded together to form a hydrogel that stuck well to negatively charged solid surfaces in saltwater. Hydrogels composed of a variety of cationic-aromatic monomer combinations exhibited fast, strong, but reversible adhesion to the surfaces. Adhesion was largely thanks to the electrostatic interaction between the positively charged residues on the polymers and the negatively charged surfaces. But, interestingly, polymers made from these cationic - aromatic monomers without adjacent sequences weren't nearly as adherent, indicating that adjacent aromatic residue enhances electrostatic interaction in high ionic strength environments. Based on the above result, we also developed hydrogel adhesives working in pure water [2].

References

- 1) Hailong Fan, Jiahui Wang, Zhen Tao, Junchao Huang, Ping Rao, Takayuki Kurokawa, Jian Ping Gong, "Adjacent Cationic-Aromatic Sequences Yield Strong Electrostatic Adhesion of Hydrogels in Seawater", *Nature Communications*, 10, 5127 (2019).
- 2) Hailong Fan, Jiahui Wang, Jian Ping Gong, "Barnacle Cement Protein-Inspired Tough Hydrogels with Robust, Long-Lasting, and Repeatable Underwater Adhesion", *Advanced Functional Materials*, 31(11), 2009334 (8 pages) (2021) (Web 2020)

SESSION SB02.08: 3D Printing
Session Chairs: Preethi Chandran and Orlin Velez
Tuesday Afternoon, December 7, 2021
SB02-Virtual

1:00 PM *SB02.08.01

3D Printable Hybrid Hydrogels with Hierarchical Structure Pramod Dorishetty, Rajkamal Balu, Naba Dutta and [Namita Choudhury](#); RMIT University, Australia

The development of protein-based 3D printable hydrogels with required physicochemical and structural tunability is a critical challenge. One of our major focus is to design and develop novel 3D printable hydrogels that must possess both appropriate mechanics to be printable, are both shear-thinning and self-healing, and possess appropriate biocompatibility to support cellular interaction. Many widely used bioinks do not currently allow for this flexibility. By expanding the number and tunability of materials that are available for 3D printing, we aim to fabricate complex, multi-material constructs [1-7] and use of customizable, engineered scaffolds to support cell or microbiota growth with controlled porosity, elasticity, water absorption characteristics and mechanical properties. This presentation will highlight the effects of different types of nanocellulose on the hierarchical structure (nano-micro), mechanical properties (compression and shear), cellular response, and the printability of the fabricated protein/polysaccharide biomimetic hydrogels. The incorporation of fibrous polysaccharide significantly increased the toughness of the hydrogel without compromising cellular activities. The extrusion-based 3D printing of protein based hydrogels photochemically co-crosslinked between globular protein and fibrous protein has also been investigated in this work. The hierarchical structure of hybrid inks and their organizational transition during printing condition (shear) was investigated using small-/ultra-small-angle neutron scattering combined with rheology (Rheo-SANS/USANS). The properties of fabricated hydrogels was investigated using photorheology and atomic force microscopy; where, the hybrid hydrogels exhibited tuneable storage and Young's modulus. The 3D printed hybrid hydrogels showed micropore size significantly higher than their solution casted counterparts. Moreover, the fabricated hybrid hydrogels show good mouse fibroblast cell attachment, viability and proliferation demonstrating their potential for tissue engineering applications.

References

- (1) Dorishetty, P.; Balu, R.; Sreekumar, A.; de Campo, L.; Mata, J. P.; Choudhury, N. R.; Dutta, N. K. *ACS Sustainable Chem. Eng.* **2019**, 7 (10), 9257-9271.
- (2) Kundu, B.; Kurland, N. E.; Bano, S.; Patra, C.; Engel, F. B.; Yadavalli, V. K.; Kundu, S. C. *Prog. Polym. Sci.* **2014**, 39 (2), 251-267.
- (3) Whittaker, J. L.; Choudhury, N. R.; Dutta, N. K.; Zannettino, *J. Mater. Chem. B* **2014**, 2 (37), 6259-6270.
- (4) Whittaker, J. L.; Dutta, N. K.; Elvin, C. M.; Choudhury, N. R. *J. Mater. Chem. B* **2015**, 3 (32), 6576-6579.
- (5) Whittaker, J. L.; Dutta, N. K.; Zannettino, A.; Choudhury, N. R. *J. Mater. Chem. B* **2016**, 4 (33), 5519-5533.
- (6) Balu, R.; Reeder, S.; Knott, R.; Mata, J.; de Campo, L.; Dutta, N. K.; Choudhury, N. R. *Langmuir* **2018**, 34 (31), 9238-9251.
- (7) Dorishetty, P.; Balu, R.; Athukoralalage, S. S.; Greaves, T. L.; Mata, J.; de Campo, L.; Saha, N.; Zannettino, A. C. W.; Dutta, N. K.; Choudhury, N. R. *ACS Sustainable Chem. Eng.* **2020**, 8 (6), 2375-2389.

1:30 PM *SB02.08.02

Desolvation Induced Shape Change for 4D Printing Hang (Jerry) Qi; Georgia Inst of Technology, United States

3D printing of structures and devices with shape or property change, or 4D printing, are highly desirable in many applications such as mechanical actuators, soft robotics, and artificial muscles. Early work in 4D printing used shape memory polymers (SMPs) as the shape change mechanism, but SMPs require complicated thermo-mechanical loading and most SMPs do not have reversible shape change capability. It is still a challenge to develop simple methods to freestanding, reversible, shape changing structures and devices. Desolvation is a novel method for shape changing devices where polymers with different crosslinking densities can absorb different amount of water or solvent to create different deformation. In recent years, our group has explored using the desolvation concept as a means for 4D printing. We first found that the light intensity gradient along the thickness direction created by photoabsorbers can be used to generate bending deformation. The level of the bending deformation depends on the light irradiation dose, which can be further controlled by light intensity. Therefore, by controlling light intensity pattern, we could create different bending distributions, or origami. This concept was further used to create reversible origami-based shape transformations. We then further developed such method to print 3D structures with rapid shape transformation by carefully managing the light penetration among different layers. Finally, we applied this method to extrusion based DIW printing of inks with high short fiber glass content to create shape-changing stiff structures. The design of all these desolvation-based 4D printing methods were guided by the theoretical modeling to achieve more accurate control of shape transformation.

2:00 PM SB02.08.03

3D Printing MRI Phantoms for Microscopic Anisotropy Velencia Witherspoon¹, Nikolay V. Lavrik², Michal Komlos¹ and Peter Basser¹; ¹National Institutes of Health, United States; ²Oak Ridge National Laboratory, United States

One major challenge facing the advancement of diffusion-weighted imaging (DWI) methods is phantom development and fabrication. Isotropic diffusion phantoms are not sufficient to validate and calibrate more advanced DWI sequences that aim to distinguish between isotropic hindered diffusion and anisotropic randomly oriented restricted diffusion. Enhancing the contrast between these descriptions of diffusion regimes is the goal of most diffusion MRI method development teams. In reality, the size of the microstructural features that exhibit this behavior in biological tissue is on the order of 1-10 μm , while the features of the most commonly used phantoms are on the order of 20-100 μm . We plan on addressing the technical challenge of fabricating a 3D phantom that contains both randomly oriented highly anisotropic and isotropic structural features. We hope to reach high aspect ratios for these features to better resemble the target brain tissue. We tested this 3D Printed MRI phantom using DWI that reproduced the size and orientation distribution of the 3D printed pores. A portion of this research was conducted at the Center for Nanophase Materials Sciences, which is a DOE Office of Science User Facility.

2:15 PM SB02.08.04

3D Bioprinted Inflammation Modulating Polymer Scaffold for Chronic Wound Healing Aparna Adumbumkulath¹, Crystal S. Shin², Richard Lee², Adam Nelson¹, Ghanashyam Acharya² and Pulickel Ajayan¹; ¹Rice University, United States; ²Baylor College of Medicine, United States

Wound healing is a complex, highly organized biological and physiological process comprising of four overlapping phases: hemostasis, inflammation, re-epithelialization, and remodeling. A standard wound healing process is dependent on leukocyte recruitment and a cascade of pro- and anti-inflammatory cytokine responses. Over expression of the inflammatory cytokines such as interleukins (IL-1, IL-6) and tumor necrosis factor (TNF- α) as well as excessive recruitment of neutrophils and macrophages arrests the healing process in the chronic inflammatory phase. Once the wound is stalled in this phase, it becomes chronic or non-healing and is prone to infections. Chronic foot ulcers are one of the most common chronic wound condition arising from complication of diabetes, suffered by ~25% of diabetic patients. These confer a high-risk prognosis for lower extremity amputation to prevent the spread of infection. Current standard of care for chronic foot ulcer includes wound debridement, wound dressings for moisture balance, revascularization procedures to treat ischemia and improve blood flow, and hyperbaric oxygen therapy. Pharmacological treatments include using biological actives like topical formulations of growth factors or anti-inflammatory cytokines. The efficacy of topical formulations is hindered by their proteolytic breakdown in the hostile environment that results in therapeutically ineffective concentration and prevents their diffusion into deeper wound layers. Moreover, these approaches are labor intensive, expensive and focus on treating the symptoms of inflammation rather than the inflammation itself. Thus, it is important to develop de novo multivalent materials that can unlock the local inflammatory phase by extracting the molecular drivers of inflammation in a highly selective and concerted fashion and aid in the reparative phase. In this work, we developed a novel non-pharmacological approach to modulate chronic inflammation. A 3D-bioprinted polymer scaffold was fabricated by in-situ phosphate crosslinking of a poly (vinyl alcohol) polymer, that when applied on the wound, can modulate local inflammation by sequestering pro-inflammatory cytokines from the wound site via physicochemical and electrostatic interactions. Moreover, this polymer scaffold also contributes to the rapid wound healing by disrupting the constant recruitment of leukocytes to the wound site. We demonstrated the therapeutic efficacy of the polymer scaffold in a skin excision mouse model by applying the gel directly on the wound. The ability of the scaffold to capture the positively charged pro-inflammatory cytokines were evaluated by Luminex assay on the scaffold removed from the mice. Compared to the controls (PVA crosslinked with glycidyl methacrylate), the polymer scaffold was more effective in capturing the pro-inflammatory cytokines (IL-1 α , IL-6 and TNF- α). Furthermore, flow cytometry studies showed that leukocytes were captured by the scaffold. These studies support that the polymer scaffold enhanced wound healing by trapping the excess pro-inflammatory cytokines and leukocytes in a tightly controlled manner and disrupting the chronic inflammatory cycle in wounds.

2:30 PM *SB02.08.05

3D Bioprinting—What Cells Find Attractive in a Gel Gordon Wallace; University of Wollongong, Australia

3D Bioprinting enables the fabrication of structures with living cells, biomaterials and other active ingredients (e.g. drugs and/or growth factors) strategically arranged in three dimensions. The biomaterials used are traditionally hydrogels since these provide adequate mechanical support to ensure structure integrity along with a cytocompatible environment.

The engagement of cells with the biomaterial (gel or the precursors) during and after printing determines the success or otherwise of any 3D Bioprinting strategy.

The interaction of gel or the precursors and cells determines the ability to retain viable suspensions in bioink reservoirs.

The rheological properties of the gels used determines how they behave and how they might protect cells during printing.

The modulus and porosity of gels determines the capacity of cells to interact with each other and the immediate environment.

Using several 3D bioprinting case studies aimed at meeting clinical challenges we will explore the critical properties of gels for such applications.

The clinical challenges include:

- cartilage regeneration in the knee (1,2)

- islet cell transplant ion to treat diabetes (3,4)
- skin regeneration (5,6)

With a view to developing protocols that are implementable in the clinic we will also review some of the additional requirements such gels must meet. These include the availability of a reliable and reproducible source material and compatibility with sterilisation methods traditionally used.

The cell - gel engagement is short lived and the temporal dimension is critical to a successful relationship. The role of the gel as a function of cell and tissue development time will be discussed.

References

- (1) Duchi, S., Francis, S., O'Connell, C.D., Aguilar, L.M.C., Doyle, S., Yue, Z., Wallace, G.G., Choong, P.F., Di Bella, C. FLASH: Fluorescently Labeled Sensitive Hydrogel to monitor bioscaffolds degradation during neocartilage generation, *Biomaterials* 2021, 264, 120383.
- (2) O'Connell, C.D., Di Bella, C., Thompson, F., Augustine, C., Beirne, S., Cornock, R., Richards, C.J., Chung, J., Gambhir, S., Yue, Z., Bourke, J., Zhang, B., Taylor, A., Quigley, A., Kapsa, R., Choong, P., Wallace, G.G. Development of the Biopen: A handheld device for surgical printing of adipose stem cells at a chondral wound site, *Biofabrication* 2016 8, 015019.
- (3) Kim, J., Hope, C.M., Gantumur, N., Perkins, G.B., Stead, S.O., Yue, Z., Liu, X., Asua, A.U., Kette, F.D., Penko, D., Drogemuller, C.J., Carroll, R.P., Barry, S.C., Wallace, G.G., Coates, P.T. Encapsulation of Human Natural and Induced Regulatory T-Cells in IL-2 and CCL1 Supplemented Alginate-GelMA Hydrogel for 3D Bioprinting, *Advanced Functional Materials* 2020, 30 (15), 2000544.
- (4) Liu, X., Carter, S.-S.D., Renes, M.J., Kim, J., Rojas-Canales, D.M., Penko, D., Angus, C., Beirne, S., Drogemuller, C.J., Yue, Z., Coates, P.T., Wallace, G.G. Development of a co-axial 3D printing platform for biofabrication of implantable islet-containing constructs, *Advanced Healthcare Materials* 2019, 8 (7), 1801181.
- (5) Zhou, Y., Kang, L., Yue, Z., Liu, X., Wallace, G.G. Composite Tissue Adhesive Containing Catechol-Modified Hyaluronic Acid and Poly-L-lysine, *ACS Applied Bio Materials* 2020, 3 (1), 628-638.
- (6) Daikuara, L.Y., Yue, Z., Skropeta, D., Wallace, G.G. In vitro characterisation of 3D printed platelet lysate-based bioink for potential application in skin tissue engineering, *Acta Biomaterialia* 2021, 123, 286-297.

SESSION SB02.09: Poster Session II: From Hydrogel Fundamentals to Novel Applications via Additive Manufacturing
 Session Chairs: Ferenc Horkay and Marc In het Panhuis
 Tuesday Afternoon, December 7, 2021
 SB02-Virtual

9:00 PM SB02.09.01

Biocompatible Fluidic Device Formed Through the Buckle-Delamination of Hydrogel Films [Riku Takahashi](#)¹, Hiroki Miyazako², Aya Tanaka¹ and Masumi Yamaguchi¹; ¹NTT Basic Research Laboratories and Bio-Medical Informatics Research Center, NTT Corporation, Japan; ²NTT Basic Research Laboratories, NTT Corporation, Japan

Biocompatible fluidic systems play a vital role in a wide range of biological applications, such as tissue engineering, biochemical sensing, cell-to-cell interaction studies, microfluidic bioreactors and so on. Hydrogels are one of the best candidates to use as a base material when fabricating the above systems due to their characteristic properties, including compliance similar to biological tissues, permeability to small molecules, biocompatibility with most cells and optical clarity under visible light. On the other hand, the swelling properties (volume change) of hydrogels is considered to be a negative factor in flow channel design, and therefore non/less-swelling hydrogels tend to be used to fabricate hydrogel-based fluidic systems. By leveraging the swelling properties of hydrogels, we can turn this disadvantage into a unique, new method to create fluidic devices from various functional hydrogels. In this study, we demonstrate the use of swelling-driven buckle-delamination, a physical phenomenon observed in hydrogel/solid substrate bilayer composites, for fabricating fluidic channels.^[1] By spatially controlling the interfacial bonding between a thin polyacrylamide (PAAm) gel film and a glass substrate, swelling-driven compressive stress induces the formation of channel architectures through a buckle-delamination process. Connecting flow tubes to the channels with a 3D printed connector results in a fluidic device, enabling pressure-driven flow without leakage or rupture. Furthermore, by stacking less-swelling bulk gels on the device, we obtained a tough, permeable, and biocompatible fluidic device, which successfully demonstrates the use of both swelling and less-swelling hydrogels as base materials for developing fluidic systems. Finally, we performed cell cultures with the device and applied chemical stimulation to cells through diffusion of molecules from the fluidic channels.^[2] This work should shed light on the design of diverse hydrogel-based fluidic systems and may be useful for applications in the fields of bioanalysis, tissue-engineering and cell biology.

[1] R. Takahashi, *et al. ACS Appl. Mater. Interfaces*, 2019, **11**, 28267-28277.

[2] R. Takahashi, *et al. Lab Chip*, 2021, **21**, 1307-1317.

9:05 PM SB02.09.02

Late News: Capsule-Shaped Self-Oscillating Gel with Cell-like Surface Fluctuation [Won Seok Lee](#), Takafumi Enomoto, Aya M. Akimoto and Ryo Yoshida; The University of Tokyo, Japan

[Introduction]

The fluctuation of biological membranes has fascinated scientists and engineers with various backgrounds. The membrane fluctuation induces essential features for life, such as cell compartmentalization, cell motility, cell division, and vesicle trafficking. The membrane fluctuation is derived from the following parameters: the thermal fluctuation of phospholipids in the membrane layer, ATP-dependent conformational changes of transmembrane proteins. Mimicking the membrane fluctuation using artificial active matters is important to understand the origin of the dynamic behavior of life. In this context, our group has developed self-oscillating gels with living organism-like functions. The self-oscillating gel shows dynamic behavior by chemo-mechanical motion, driven by a Belousov-Zhabotinsky (BZ) reaction. The self-oscillating gel is fabricated by introducing a tris(2,2'-bipyridine)

ruthenium ($\text{Ru}(\text{bpy})_3^{2+}$), a metal catalyst for the BZ reaction, into a thermoresponsive hydrogel network. Cyclic redox changes of $\text{Ru}(\text{bpy})_3$ ($\text{Ru}(\text{bpy})_3^{2+} \leftrightarrow \text{Ru}(\text{bpy})_3^{3+}$) during the BZ reaction lead the gel to present periodic and autonomous swelling-deswelling oscillation without any external stimuli.¹ Here we present a self-oscillating capsule-shaped gel that shows the cell-like membrane fluctuation. Self-oscillating gels are one of the promising materials for mimicking the membrane fluctuation because the gels show the regional deformation randomly and spontaneously in various regions. We fabricated a capsule-shaped hollow structure using the self-oscillating gel, which provides a structural resemblance compared with biological cells. The capsule-shaped gel exhibits the surface fluctuation by the propagation of the BZ reaction wave similar to the shape fluctuation of the living cells.

[Materials and Method]

The capsule-shaped hollow self-oscillating gel was fabricated by four processes described below: (1) An alginate/calcium (Alg/Ca) spherical bead, which is a template of the capsule-shaped gel, was fabricated by adding sodium alginate solution to CaCl_2 solution. (2) Poly((*N*-isopropylacrylamide)-*co*-(*N*-(3-aminopropyl)methacrylamide)) (poly(NIPAAm-*co*-NAPMAm) layer was synthesized by immersing the Alg/Ca gel into ammonium persulfate (APS) solution and monomer solution, in a sequence. (3) The Alg/Ca template was dissolved by putting the gel into a sodium citrate solution. (4) $\text{Ru}(\text{bpy})_3$ -NHS was conjugated to capsule-shaped hollow gel. The gel surface fluctuations by volumetric oscillation during the BZ reaction were evaluated.

[Result and Discussion]

The cross-sectional images of the gels in each fabricating process show that the capsule-shaped hollow structure was successfully formed. On a millimeter scale, the volumetric oscillation of the self-oscillating gel appears with a spreading chemical signal by the BZ reaction.² Therefore, in this study, the chemical signals of the BZ reaction run along to the surface of the entire gel, causing the surface fluctuating phenomenon like a living red blood cell. Moreover, it becomes clear that the amplitude of fluctuation increases as layer thickness grows. The thickened self-oscillating gel layer leads to improved local deformation, which brings about the more intense surface fluctuation phenomenon. The thickness deformation-induced surface fluctuation could correspond to the effect of the ATP-driven conformational change of protein, which induces the shape fluctuation in the living cells. We expect that this study can be utilized to realize the artificial cell which shows various cell-like functions.

[Reference]

1. Yoshida, R. Self-oscillating polymer gels as biomimetic and smart softmaterials. *Adv. Mater. Lett.* **9**, 836–842 (2018).
2. Kim, Y. S., Tamate, R., Akimoto, A. M. & Yoshida, R. Recent developments in self-oscillating polymeric systems as smart materials: From polymers to bulk hydrogels. *Mater. Horizons* **4**, 38–54 (2017).

9:10 PM SB02.09.03

Fabrication of Porous PDMS Sponges Using Spontaneously Self-Removing Sacrificial Templates Alex Keller, Khalid Zainulabdeen, Holly Warren and [Marc In het Panhuis](#); University of Wollongong, Australia

Poly(dimethylsiloxane) (PDMS) sponges are an emergent technology, garnering much attention in recent years due to their unique mechanical properties, high surface area and hydrophobicity/oleophilicity. In this work, a hydroscopic calcium chloride hard template is used to prepare a PDMS sponge in 6 hours, faster than previously reported template removal methods. Furthermore, the unique deliquescent properties of the calcium chloride are harnessed to provide a spontaneously self-removing sacrificial template within 4 days. The resultant PDMS sponges displayed excellent mechanical robustness, exhibiting maximum tensile and compressive stress values of 110 ± 20 kPa and 2.8 ± 0.1 MPa, respectively. The PDMS sponges displayed far greater preferential absorption of toxic solvents over simulated gastric fluid.

9:15 PM SB02.09.04

Living Hydrogels as Toxicity Indicators Kharina Fenton and [Marc In het Panhuis](#); University of Wollongong, Australia

Living hydrogels were made by embedding microalgae of the species *Chlorella vulgaris* in alginate-based hydrogels. It was shown through detection of chlorophyll-a content that these algal cells were able to grow as expected within the hydrogel matrix. This system was formed the basis for a *Chlorella vulgaris* algal (hydrogel) sensing system for the detection of the exposure to toxic compounds. For example, exposure to dichloroethane resulted in a 43% decrease in *Chlorella vulgaris* growth. This work demonstrates that living hydrogel materials containing *Chlorella vulgaris* cells can successfully act as toxicity indicators. This could suggest their suitability in applications of living hydrogels in water quality assessment.

9:20 PM SB02.09.05

Synthesis and Characterisation of a 3D-Printable Gelatin—Epoxy Amine Double Network Hydrogel Anne Kelly and [Marc In het Panhuis](#); University of Wollongong, Australia

There is a current need for the development of robust smart materials for a variety of medical, consumer, and manufacturing applications. In addition, these materials require the ability to act as 3D printable inks to undergo rapid prototyping. A UV curable gelatin-epoxy amine double network hydrogel with water content of 80% can be simply produced by a one-pot synthesis. This synthesis method can be performed by methacrylating the individual networks by either a one-step process (simultaneously) or a two-step process (independently). It was found that the two-step process is more effective in producing a mechanically robust material, capable of exhibiting a compressive stress at failure of 2.5 ± 0.2 MPa. Significantly, a new 3D printing method has been developed to allow the material to be cured post printing resulting in no significant loss in mechanical strength compared to gels prepared by casting. This method uses the entanglement of gelatin (below 37°C) to give support to the individual printed layers of the structure eliminating the need for UV curing after each layer is printed. Post printing, the structure can be UV cured to increase the mechanical strength of the material to that of the hydrogels prepared by casting. It is envisaged that this new printing method in conjunction with new hydrogel chemistries can be utilised to fabricate new materials for applications ranging from biomedical devices to soft robotics.

9:25 PM SB02.09.06

3D Printed Living Hydrogels Mohammed Al-Mossawi, Paul Molino, Holly Warren and [Marc In het Panhuis](#); University of Wollongong, Australia

In this presentation the 3D printing of living hydrogels based on alginate-gelatin gels embedded green algae *Chlorella Vulgaris* is presented. It is shown that alginate-gelatin gels crosslinked with 0.05M CaCl_2 displayed excellent mechanical properties whilst still allowing for suitable algal cell growth. The latter was determined using dissolved oxygen ratio.

The rheological flow behaviour of these hydrogels systems was investigated to assess their potential for extrusion printing. Our results indicated that a combination involving 4% (w/w) alginate and 4% (w/w) gelatin resulted in a mechanically robust 3D structure that maintained algal cell viability. 3D printed living hydrogel with excellent mechanical stability offer new possibilities to connect the inorganic and biological worlds.

9:30 PM SB02.09.07

3D Printing of Surgical Staples Osama Al Takhayneh, Holly Warren and Marc In het Panhuis; University of Wollongong, Australia

There are several techniques used in the manufacturing of bone implants such as 3D printing. Rapid prototyping/3D printing is an important process in the development of implants used in bone fixation surgeries, its importance lies within the ability to customize and create patient specific systems to increase the efficiency of bone fixation surgeries. The main aim of this study was to develop and test new (and softer) materials for the purpose of surgical staples using 3D printing. Our results indicate that the mechanical characteristics of staples is suitable to enable their use in low impact locations within the body (such as upper extremities). This study demonstrated that biocompatible polymers are a viable alternative for metal alloys in the use of surgical staples.

9:35 PM SB02.09.08

Cartilage Hierarchy and Function Ferenc Horkay¹, Peter Bassler¹ and Erik Geissler²; ¹National Institutes of Health, United States; ²Universite Grenoble Alpes, France

The biochemistry of cartilage has been extensively studied in the last couple of decades. The major proteoglycan component of cartilage extracellular matrix is the high molecular weight ($1 \times 10^6 < M < 3 \times 10^6$) bottlebrush shaped aggrecan. In the presence of hyaluronic acid (HA) and link protein, aggrecan self-assembles into a supramolecular structure with as many as 100 aggrecan molecules attached as side chains on a filament of HA. This supramolecular array yields a hydrated, viscous gel that provides the osmotic properties necessary for the cartilage to resist deswelling under compressive load. In cartilage these complexes are interspersed in the collagen matrix.

Imaging techniques (electron microscopy, atomic force microscopy, etc) have revealed the size and structural pattern of large distinct aggrecan-HA acid complexes. Such methods yield detailed information on the morphology within a selected area of the sample. However, the interactions that govern the morphology and dynamics of aggrecan-HA assemblies in solution remained poorly understood. Owing to the complexity of the aggrecan-HA system the determination of the relationship between its structure and function requires a range of experimental approaches combining both physical and biochemical techniques.

We investigate the spatial organization both in solutions of aggrecan and aggrecan-HA complexes over a length scale range between 1 and 500 nm. The static properties are studied by small angle neutron scattering (SANS) and static light scattering (SLS), while the dynamics are probed by dynamic light scattering (DLS). The length scale range probed by scattering methods detects changes in the architecture on the supramolecular scale. Changes at the molecular level are detected by virtue of the average effect that they exert on the larger scale structures. Better understanding of the organization of aggrecan assemblies and their effect on cartilage mechanical properties is essential to advance our knowledge of arthritis and develop treatment strategies.

9:40 PM SB02.09.09

Structural Change of Colloidal Silica Solution Under Shear Stress Keishi Akada¹, Soichiro Okubo², Kazuya Tokuda², Koji Yamaguchi², Takamasa Onoki², Tatsuya Yamada³, Ryota Jono³, Hiroshi Ushiyama³, Syogo Tejima³ and Jun-ichi Fujita¹; ¹University of Tsukuba, Japan; ²Sumitomo Electric Industries, Ltd., Japan; ³Research Organization for Information Science & Technology, Japan

Background:

In some colloidal suspensions, viscosity increases (shear thickening) or decreases (shear thinning) when shear stress is applied. The shear thickening material is a candidate for wide range applications such as damper systems in machinery, and such phenomena can cause a flow to be obstructed. However, these viscosity changes occur in a dynamic process in which shear is applied, and the viscosity returns to its original state when the shear stress is removed. Therefore, it has been difficult to measure the dynamic microstructural changes that lead to the shear thickening phenomena. In this study, we performed simultaneous measurements of solution viscosity and small-angle X-ray scattering (SAXS) using an X-ray transmission solution cell. By observing the structural changes of colloidal particle clusters under shear stress in real time, we investigated the aggregation process of colloidal particles responsible for the phenomenon.

Experiment:

The silica colloid sample was prepared by dispersing a silica sol (Snowtex ST-S, Nissan Chemical) with a particle size of 8 nm in a 0.8 wt% PEG solution [1]. The viscosity and SAXS were measured simultaneously using a rheometer (ONRH-1, Ohna Tech Inc.) in combination with a polycarbonate X-ray transmission Couette cell. The obtained spectra were divided into perpendicular and parallel components with respect to the direction of the cylinder rotation, and it was plotted against the scattering vector Q . The experiments were performed at the Sumitomo Electric Beamline BL16 at the Kyushu Synchrotron Light Source Center and Spring-8 BL40XU.

Results:

The viscosity measurement results of the silica colloidal solution showing shear thickening properties. This property was observed at a shear rate of 10 [1/s], where the viscosity increased rapidly. SAXS spectra were acquired while rotating at a constant speed at the shear rate before and after the viscosity change, and the spectra in direction of perpendicular and parallel to the rotation were compared. In both directions, a characteristic peak at about 3.4 [1/nm] was observed, which is attributed to a particle cluster spacing and reflects an isotropic cluster dispersion. The anisotropic shift of the peaks were observed after viscosity increase. The spacing of the parallel to the shear direction decreased, while that of perpendicular increased, suggesting that a compressive force was applied to the cluster in the direction of rotation. These results suggest that the application of shear stress caused an aggregating cluster and an increasing viscosity [2]. These results demonstrated an effectiveness of the viscosity-SAXS measurement method.

Acknowledgments:

This work was supported by Innovative Science and Technology Initiative for Security Grant Number JPJ004596,ATLA, Japan.

[1] Kamibayashi, M., Ogura, H. & Otsubo, Y. *J. Colloid Interface Sci.* **321**, 294–301 (2008).

[2] Cheng, X., McCoy, J. H., Israelachvili, J. N. & Cohen, I. *Science* **333**, 1276–9 (2011).

9:45 PM SB02.09.10

3D Printing of Tough and Stretchable Hydrogels Kusuma Betha Cahaya Imani and Jinhwan Yoon; Pusan National University, Korea (the Republic of)

Tough and stretchable hydrogels are highly studied in recent years, due to its promising potential applications in various field such as for actuators, wearable electronic devices, and soft robotics. To have a hydrogel with improved mechanical property, its viscoelastic dissipation needs to be enhanced, which is difficult to be obtained in a hydrogel containing of covalent bonds only. To overcome this problem, in this study, physical interaction in form of ionic bond and micelles incorporations are used. For the micelles, Pluronic F-127 micelles was chosen, other than for mechanical enhancement, it also has the capability to have a quick viscosity shift depending on temperature. This capability is generated owing to its structure, a triblock copolymer which consists of hydrophobic poly (propylene oxide) (PPO) core block and hydrophilic poly (ethylene oxide) (PEO) side blocks. At elevated temperature, the hydrophobic core block dehydrates, which leads to micelles formation and increasing its viscosity. The controllable viscosity is highly useful for 3D

printing, as it is important to prevent the spread of the ink upon deposition to a substrate. The Pluronic F-127 was also synthesized to have methacrylate group to allow photo-polymerization after printing, to have immediate permanent shape. With this method, hydrogels with complex shapes in various toughness and stretchability could be achieved, and it opens the possibility for further applications.

9:50 PM SB02.09.11

Reversible Clustering Dynamics of Thermo-Responsive Hydrogel Micropillar Arrays by Capillary Force and Temperature [Jiseong Choi](#), Suim Lim and Seongmin Kang; Chungnam National University, Korea (the Republic of)

High aspect ratio pillar structure was suitable for implementing various functional surfaces due to the easy shape transform. The high aspect ratio pillars composed of elastomers or rigid polymers were unstable and easily clustered by external forces such as capillary forces. This clustering property was used in various field. However, easy clustering property of the high aspect ratio pillars posed an obstacle to apply functional surfaces because special treatment was essential for high aspect ratio pillars to return to their original state from clustering state. Therefore, we reported reasonable criteria to control the clustering phenomena in high aspect ratio pillar arrays. We adjusted two main factors that were the crosslinker density of thermal-responsive hydrogels and the temperature of the surrounding environment to control the elastic modulus, which was the most important characteristic for clustering property of high aspect ratio pillars. Experimentally, the clustering behavior of the high aspect ratio pillars was respectively analyzed by changing the mechanical property according to the water content and temperature. In addition, theoretical analysis supported the criteria for controlling condition with clustering and de-clustering phenomena of the high aspect ratio pillars.

9:55 PM SB02.09.12

Late News: Modeling the Behavior of Hydrogel Modified Pore Fluids for Geotechnical Applications [Varun Nimmagadda](#)¹, Albert Tam^{2,3}, Shoumik Saha² and Dilip Gersappe²; ¹University of Michigan–Ann Arbor, United States; ²SUNY-Stony Brook, United States; ³Lynbrook High School, United States

Recent advances in bioremediation techniques in geotechnical engineering has pioneered the replacement of pore water in soil by biopolymers to improve the physical and hydraulic properties of soils. In determining the type of biopolymer additive that will not reduce the soil strength, several factors need to be considered. Ideally, the biopolymer-based pore fluid needs to be self-assembling and can recover after deformation. Recent advances in geotechnical engineering have shown hydrogels as a soil additive to improve soil stability. Hydrogels, particularly with clay additives, can help mitigate soil erosion, reduce soil swelling, and optimize soil near building foundations. While experiments have successfully demonstrated the effect of hydrogels on soil strength, these studies depend on trial and error to identify the suitable biopolymer and type and concentration of clay fillers.

This study analyzes hydrogel systems consisting of two types of polymer chains and clay nanoplatelets dispersed in an explicit solvent and assesses the effect of clay filler structure, filler amount, and polymer-polymer attraction on the mechanical and structural properties of the hydrogel. To simulate the formation and behavior of the hydrogel, the systems were studied using coarse-grained molecular dynamics. A series of simulations were run using various combinations and concentrations of clays and the different polymers. We analyzed the effect of including interactions between the clay and the polymers and polymer – polymer interactions. Mechanical properties were measured via viscosity and stress autocorrelation (SAC) calculations, while the radial distribution function (RDF), was used to measure degree of phase separation or random mixing of polymers.

Our results show that by changing the polymer-polymer interaction we observed morphologies ranging interpenetrating networks to single polymer networks. Higher percentage of clay fillers and larger values of attraction between the polymers allows us to tailor the viscosity of the hydrogel pore fluid. High shear rates lowered viscosity values, leading to the pore fluids being shear thinning in nature. Overall, our results show that by choosing the hydrogel components and the nanofiller, the properties of the pore fluid can be controlled. These results will allow better design and selection of the biopolymer-based pore fluids for various biogeotechnology applications.

10:00 PM SB02.09.13

Dynamically Changing the Transmission Property of Hydrogel using Metal Microstructures Fabricated by Multi-Photon Photoreduction [Hirofumi Tomikawa](#), Kaneto Tsunemitsu, Yo Nagano and Mitsuhiro Terakawa; Keio University, Japan

All-optical switching, or dynamically changing optical properties by light stimulation, has received much attention because of its capability of non-contact controlling. Volume phase transition of temperature-responsive hydrogel causes change of optical transmittance, and metal nanoparticles embedded in the hydrogel can enhance the transmittance change by light stimulation, owing to photo-thermal conversion via the localized surface plasmon resonance (LSPR). In this study, we propose a method to control spatially-localized optical transmittance of temperature-responsive hydrogel by external light stimulation, by the use of the metal microstructures fabricated with multi-photon photoreduction (MPR) method. MPR is the reduction of metal ions induced by ultrashort laser pulses which enables direct writing of metal microstructures composed of the nanoparticles. Grating microstructures with different line spacing were fabricated inside poly(N-isopropylacrylamide) (PNIPAm) hydrogel containing gold ions by computer-aided femtosecond-laser scanning. Since the gold microstructures formed in the hydrogel showed an absorbance peak around 520 nm, 520 nm laser diode (maximum laser power: 50 mW) was used as the light source of stimulation. As a result, decrease in the transmittance (more than 66 %) was observed at laser powers higher than 7 mW for the light stimulation, when hydrogel with line spacing of 5 μm was used. The threshold of the laser power that required to decrease the transmittance became higher as hydrogel with wider line spacing was used, demonstrating transmission property can be easily changed with the same materials and the fabrication method. Our results indicate the potential to fabricate all-optical switching devices with hydrogel.

10:05 PM SB02.03.03

Functionalized Conductive Hydrogels Applied to the Discriminative Detection of Heavy Metals [João P. Braga](#)¹, [Guilherme R. De Lima](#)¹, [Giovani Gozzi](#)² and [Lucas Fugikawa-Santos](#)²; ¹São Paulo State University – UNESP, Brazil; ²São Paulo State University – UNESP, Brazil

Ionic conductive hydrogels can be used in many sensing and actuators applications, including chemical detection, artificial skin, and biosensors. We report herein the development of a discriminative sensor array used to detect heavy metals commonly found dissolved in waters in aquatic ecosystems. Each sensing unit is comprised by 4 interdigitated electrodes on which poly(ethylene glycol):poly(ethylene glycol) diacrylate (PEG:PEG-DA) films were formed by UVA (370 nm) curing. After crosslinking, the hydrogels were washed and functionalized by drop casting solutions of 3 different organic semiconductors: poly(3-hexathiophene) (P3HT), poly(o-methoxy aniline) (POMA) and a poly(vinyl carbazole):2-(4-biphenyl)-5-(4-tert-butylphenyl)-1,3,4-oxadiazole (PVK:PBD) blend. The resulting sensor array was formed by 3 electrodes with organic semiconductor functionalized hydrogels, in addition to a “blank” hydrogel film, used as reference. Water solutions of iron (Fe), manganese (Mn) and molybdenum (Mo), at concentrations varying from 20 ppm up to 200 ppm were used to demonstrate the discriminative capability for heavy metal detection by using the global electrode response extracted from electrical impedance/capacitance measurements. The frequency-dependent response of the electrodes was analyzed by considering a generalized Warburg impedance model to extract the electrical response parameters. The electrical characteristics of the functionalized hydrogels were compared to the changes in the morphological, thermal and physio-chemical properties of the films, analyzed via scanning electron microscopy,

thermogravimetry analysis, FTIR and Raman spectroscopy.

SESSION SB02.10: Hydrogel Applications
Session Chairs: Jack Douglas and Richard Leapman
Wednesday Morning, December 8, 2021
SB02-Virtual

10:30 AM OPEN SLOT

10:30 AM *SB02.10.01

Evidence of Many-Body Interactions in the Virial Coefficients of Polyelectrolyte Gels Jack F. Douglas¹ and Ferenc Horkay²; ¹National Institute of Standards and Technology, United States; ²National Institutes of Health, United States

The phase behavior of materials ranging from gases to polymer solutions can often be understood semi-quantitatively in terms of their first few virial coefficients that quantify intermolecular interactions in the limit of low molecular concentration. The second (A_2) and third (A_3) virial coefficients, or their equivalent *chi*-interaction parameters in a polymer solution context, have correspondingly been adopted as fundamental measures of intermolecular interaction having fundamental significance for materials classification, design and characterization. It is often implicit in this type of description of phase behavior that the interactions between the molecules can be described by *pairwise decomposable interactions* and it is not clear if patterns of phase behavior applies to complex liquids, such as ionic and polyelectrolyte solutions, polyelectrolyte gels, etc. in which many-body interactions associated with polymer and ion solvation, and hydrogen bonding interactions of the water molecules, and the associated “hydrophobic effect” governing solvation of charged molecules or uncharged moieties in water, might lead to entirely different patterns of phase behavior. Along these lines, simulations of simple hydrophobic solutes (modeled as Lennard-Jones molecules or simple molecules such as methane or noble gases) in water at ambient temperatures have indicated that while the interaction of two particles may be predominantly repulsive, corresponding to a positive second virial, the interactions between many particles can become attractive, corresponding to higher virials being negative, and this can lead to phase separation. This pattern of phase behavior is exhibited experimentally by all the polyelectrolyte gels that we study. We thus observe clear evidence of many-body interactions on the solution properties of polyelectrolyte gels.

11:00 AM *SB02.10.02

Imaging Cells and Tissues in 3D at the Nanoscale with Electron Probes Richard D. Leapman and Maria A. Aronova; National Institutes of Health, United States

Microscopies based on focused electron probes allow the cell biologist to image the 3D ultrastructure of eukaryotic cells and tissues extending over large volumes, thus providing new insight into the quantitative relationship between cellular architecture and function of organelles. Here we compare three such techniques: (i) electron tomography in conjunction with axial bright-field scanning transmission electron microscopy (BF-STEM), (ii) serial block face scanning electron microscopy (SB-SEM), and (iii) focused ion beam scanning electron microscopy (FIB-SEM). The advantages and limitations of each approach are illustrated by their application to determining the 3D ultrastructure of human blood platelets, and insulin-secreting beta cells of mouse pancreatic islets of Langerhans. In comparing the three methods, we consider specimen geometry, specimen preparation of stained polymer embedded cells and tissues, beam damage and automated segmentation methods. Many features of the organelles contained in blood platelets can be visualized using all three approaches, but STEM tomography offers an almost isotropic resolution of ~ 3 nm, compared with ~5 nm in FIB-SEM, and an anisotropic resolution of ~5 nm in the block-face plane and ~30 nm perpendicular to the block-face in SB-SEM. In this regard, we demonstrate that STEM tomography is advantageous for visualizing the platelet canalicular system consisting of interconnected membranous cisternae. In contrast, SB-SEM enables visualization of large numbers of complete platelets, each of which extends ~2 μ m in minimum dimension, whereas an electron tomogram acquired in the BF-STEM can typically only visualize about half of a platelet volume due to a rapid non-linear loss of signal in specimens of thickness greater than ~1.5 μ m. Although cellular and tissue volumes acquired by FIB-SEM are typically smaller than those acquired by SB-SEM, the improved spatial resolution perpendicular to the block-face in FIB-SEM facilitates more accurate 3D segmentation of the ultrastructure.

11:30 AM *SB02.10.03

Photo-Crosslinkable Polymer Platform—From Bioinks to Shape Memory Polymers Sandra Van Vlierbergh^{1,2}; ¹Ghent University, Belgium; ²Vrije Universiteit Brussel, Belgium

Biofabrication is a specific area within the field of tissue engineering which takes advantage of rapid manufacturing (RM) techniques to generate 3D structures which mimic the natural extracellular matrix (ECM). A popular material in this respect is gelatin, as it is a cost-effective collagen derivative, which is the major constituent of the natural ECM. The material is characterized by an upper critical solution temperature making the material soluble at physiological conditions. To tackle this problem, the present work focusses on different gelatin functionalization strategies which enable covalent stabilization of 3D gelatin structures [1, 2].

In a second part, synthetic acrylate-encapped, urethane-based precursors (AUP) based on polyethers and polyesters, will be discussed with exceptional crosslinking behaviour and CAD-CAM mimicry compared to conventional materials [3]. Within this synthetic material class, also insight will be provided on the shape memory properties of polyester-based AUPs (two filed patents). Both chain growth and step growth polymerization mechanisms (see figure) along with their mechanical properties and processability potential will also be addressed.

Several polymer processing techniques will be covered including conventional 3D printing using the Bioscaffolder 3.1 and two-photon polymerization [4, 5]. A number of biomedical applications will be tackled including adipose tissue engineering [6, 7], vascularization [8], ocular applications [9], etc. In a final part, attention will be paid to the valorization of our biomaterial platform technology through the launch of our spin-off company Xpect-INX. The results show that chemistry is a valuable tool to tailor the properties of (bio)polymers towards processing while preserving the material biocompatibility.

1. J. Van Hoorick et al., *Macromolecular Rapid Communications*, 2018, 39, 1800181.
2. J. Van Hoorick et al., *Biomacromolecules* 2017, 18, 3260-3272.
3. A. Houben et al., WO 2017/005613.
4. J. Van Hoorick et al., *Biofabrication*, 2020, accepted.
5. A. Arslan et al., *Materials Today*, 2020, accepted.
6. L. Tytgat et al., *Acta Biomaterialia*, 2019, accepted.
7. L. Van Damme et al., *Biomaterials Science*, 2020, submitted.

8. L. Tytgat et al., *Macromolecular Bioscience* 2020 accepted.
9. J. Van Hoorick et al., *Advanced Healthcare Materials* 2020 accepted.

SESSION SB02.11: Biopolymers and Tissue Science
Session Chairs: Peter Basser and Christopher Bettinger
Wednesday Afternoon, December 8, 2021
SB02-Virtual

1:00 PM *SB02.11.01

Osmotic and Load-Bearing Properties of Cartilage Peter Basser; National Institutes of Health, United States

Cartilage is a load-bearing tissue that derives its stiffness from a fibrous network, mainly consisting of collagen type II, which is pre-stressed by the osmotic swelling pressure of negatively charged proteoglycan assemblies imbedded in the collagen matrix¹. Changes in the relative amounts of the main constituents will affect the macroscopic properties of cartilage. A decrease in tissue water content that might occur in some disease states could alter these properties and lead to impaired joint function. For example, previous findings indicate that osteoarthritic cartilage contains more water than healthy cartilage and exhibits poorer load-bearing properties.¹

We intend to determine how the interactions of the major biochemical constituents of articular cartilage influence its osmotic and mechanical behavior. One of the basic challenges of existing biomimetic cartilage models and modeling is that the pre-stress is largely ignored. However, in cartilage pre-stress exists even in the absence of external loading and plays an important role in defining the load-bearing properties of this tissue¹. Recently, we developed a pre-stressed biomimetic composite gel system consisting of a relatively stiff poly(vinyl alcohol) (PVA) matrix which encloses weakly cross-linked poly(acrylic acid) microgel particles. This model allows us to explore how changes in composition affect the swelling and mechanical behavior. There are three major determinants of the biomechanical behavior of articular cartilage. The first is the osmotic swelling pressure that reflects the interactions between the polymeric components of the tissue and the ions. The second is the elastic resistance of the cartilage matrix itself, and the third is the fluid-solid interaction that can affect hydration. It is demonstrated that our model satisfactorily describes the osmotic and swelling properties of healthy and osteoarthritic cartilage.²

1. Basser, P. J., Schneiderman, R., Bank, A., Wachtel, E. & Maroudas, A. Mechanical properties of the collagen network in human articular cartilage as measured by osmotic stress technique. *Archives of Biochemistry and Biophysics* **351**, 207–219 (1998).
2. Horkay, F., Basser, P.J. Composite Hydrogel Model of Cartilage Predicts Its Load-Bearing Ability. *Scientific Reports* **10**, 8103 (2020).

1:30 PM *SB02.11.02

Multifunctional Hydrogels from Mechanistic Design to Practical Applications Jie Zheng; University of Akron, United States

Nature designs a vast library of soft materials in living bodies to fulfil many unique and specific functions, including strong mechanics, high actuation and sensitivity, better biocompatibility, and fast self-healing property. Sure nature soft materials offer a rich reservoir for rational design and engineering of synthetic soft materials (polymers and hydrogels). Herein, we uniquely integrate theoretical models, molecular simulations, and biophysical experiments to conduct fundamental and applied research at the interface of computational structural biology, biophysics, biomaterials, and nanotechnology, with the goals of better understanding of biophysicochemical interactions at the biological interfaces and rationally engineering biomolecules for practical applications in biomaterials and medicine. In this talk, I will show different general strategy to design soft living materials with extraordinary properties. Guided by our computational theory, I will demonstrate the design of synthetic polymers and peptides for antifouling coatings, smart hydrogels, and amyloid inhibitors. The interplays between theory, experiments and design will be emphasized throughout the talk.

2:00 PM *SB02.11.03

Genipin Crosslinked Networks—From Bioplastics and Biogels to Next-Generation Embolization Coils Emily Augustine, Spencer Matonis, Gaurav Balakrishnan, Durva Naik and Christopher J. Bettinger; Carnegie Mellon University, United States

Genipin is a naturally occurring small molecule that has been used extensively as a protein crosslinker for engineering application-specific biomedical materials. Genipin crosslinked proteins have been used for applications ranging from tissue engineering scaffolds to drug delivery matrices. Here, we will discuss the use of genipin as an enabling additive to improve the mechanical properties and processability of both collagen-based networks for medical devices and fibrin-based networks for use as a strategy for reinforcement after embolization. In the first part of the talk, we will describe structure-processing-property relationships in genipin/collagen hybrids. The composition and processing history of these precursor materials can be controlled to produce materials ranging from rigid bioplastics to compliant hydrogel-based networks. Applications as structural materials in biomedical devices and bioelectronics will be discussed. In the second part of the talk, we will describe the use of genipin as a crosslinker to improve the robustness of fibrin networks in the context of embolization devices. Specifically, we will describe genipin-eluting polymer fibers as an approach to improve the efficacy of embolizing intracranial aneurysms. Diffusion-reaction kinetics of genipin released from polymeric fibers within fibrin hydrogels using an in vitro aneurysm flow model will be described. Taken together, this talk will elaborate on the use of genipin as an enabling component of protein-based hydrogels as biomedical materials.

2:30 PM SB02.11.04

Synthesis of Polymer Nanoparticles and Their Assemblies Nikunj Kumar Visaveliya; The City College of New York, United States

When two or more nanoscale components assemble, they create new, advanced, and multifunctional composite systems. The assembly systems reveal advanced property/function that is not possible to achieve by individual types of nanoparticles alone. A wide range of various assemblies can be prepared such as self-assembly, templated assembly, directed assembly, etc. Considering the chemical nature of polymeric materials which are soft and flexible, it is more challenging and interesting to create the engineering architectures of nanoscale assemblies in hierarchical order. In general, the engineering of polymer nanoparticles with controlled properties is very promising for various applications. Polymer nanoparticles' interior is mainly made up of the cross linked network. On the other side, the surface of polymer nanoparticles can be tailored with soft, flexible, and responsive molecules and macromolecules as potential support for the controlled particulate assemblies. Molecular surfactants and polyelectrolytes as interfacial agents improve the stability of the nanoparticles whereas a swellable and soft shell like cross linked polymeric layer at the interface can significantly enhance the uptake of guest nano constituents during their interactions to form the assembly architectures. Moreover, layer by layer surface functionalization holds the ability to provide a high variability in assembly architectures of different interfacial properties. Based on these aspects, various assembly architectures of polymer

nanoparticles of tunable size, shapes, morphology, and tailored interfaces together with controllable interfacial interactions are presented here. The microfluidic supported platform has been used for the synthesis of constituent polymer nanoparticles of various structural and interfacial properties, and their assemblies are prepared in batch or flow conditions.

2:45 PM SB02.11.05

Messy to Ordered—Fiber Diameter Controls the Shape-Morphing Behavior of 2D Networks of Mesoscale Responsive Fibers Shiran Ziv Sharabani and Amit Sitt; Tel Aviv University, Israel

In recent years, there has been a continuous endeavor to develop synthetic shape-morphing materials of different architectures and scales and to decipher the underlying principles that govern their behavior and functionality. Here, we present 2D highly ordered shape-morphing networks of interconnected mesoscale fibers, constructed of a thermoresponsive copolymer. The networks are fabricated using the jet writing approach, which enables a high spatial precision over fiber deposition, a well-defined long-range order, and high control over the fiber diameter.

When immersed in a hot aqueous environment, the networks maintain their ordered as-spun morphology. However, upon cooling below, the fibers swell and the networks shape-morph, exhibiting two distinct morphing behaviors that are determined by the diameter of the diameter and the mesh density. In the case of thick fibers or dense networks, the networks swell while preserving their original ordered morphology and expands homogeneously. In the case of thin fibers and sparse networks, upon swelling the fibers exhibit significant in-plane buckling, and the network loses its ordered morphology. However, regardless of the morphing mode, the networks exhibit memory and return to their originally ordered, as spun, configuration upon heating. Simulations of the morphing of the network using a mesh-of-springs model indicated that for mesoscale hydrogel fibers, the change in the mechanical properties during the swelling process can induce a transition between the two morphing modes as a function of the fiber diameter.

The morphing behavior exhibited for networks of mesoscale morphing fibers differs significantly from bulk systems and macroscale networks of similar compositions, and hence demonstrates a novel structure-and-function relationship, which was not exhibited in other 2D morphing systems. Such meshes may be used in novel applications, ranging from artificial micro-muscles to shape-morphing optical devices, and may provide insights into the morphing mechanisms of complex biological filament networks such as actin-myosin and microtubules networks.

SESSION SB02.12: Structure Property Relationships in Gels II

Session Chairs: Ferenc Horkay and Jie Zheng

Wednesday Afternoon, December 8, 2021

SB02-Virtual

4:00 PM SB02.12.01

Pushing the Boundary of Thermally Responsive Hydrogel in Osmotic Processes via Materials Designs Nupur Gupta, Yen Nan Liang and Xiao Hu; Nanyang Technological University, Singapore, Singapore

Stimuli-responsive hydrogels forms an interesting class of crosslinked hydrophilic polymeric materials, capable of absorbing large amount of water without dissolving. Their physical properties can be easily tuned to different external stimulus such as heat, light, pressure, pH, ionic strength, etc., by careful selection of functional groups and proper molecular design. This has in turn rendered their tremendous potential use for a wide array of applications such as biosensing, actuation, smart electronics, sensing and as osmotic agents.

Our research group has demonstrated previously use of thermally responsive hydrogels as smart regenerable draw agents for quasi-continuous forward osmosis (FO) where the swelling pressure of hydrogel drives the water permeation across the semi-permeable membrane [1, 2]. Hence, it can easily overcome reverse solute diffusion, one of the major drawbacks using conventional draw solutes and provide direct water recovery by heating the hydrogel above its volume phase transition temperature. High water recovery using N-isopropylacrylamide based hydrogels has gained special attention as its hydrophilicity can be tuned at physiological temperature i.e., 32 °C. On heating above this temperature, the change in the polymer solvent interaction results in conformational change of the polymer resulting in water release. However, its slow response and low absorption capacity has left them obscure to be used as draw agents.

To overcome the low absorption capacity and enhance the water release kinetics semi-IPN architecture of the hydrogel was previously proposed by our research group. By dispersing a hydrophilic polyelectrolyte, like poly sodium acrylate (PSA), within the PNIPAM network not only the water absorption capacity of the hydrogel can be improved but also fast water release was also observed. Yet only low water flux was achievable using the above system when used for FO. Although semi-IPN hydrogel is widely studied, yet there is no systematic study done regarding retention of polyelectrolyte within the gel network. Based on our recent work we have found that a number of factors play a critical role in defining the morphology of the semi-IPN hydrogel and also for enhanced retention of PSA in PNIPAM network[3]. Using a series of model PNIPAM/PSA semi-IPN hydrogel we not only determined the optimum synthesis conditions for higher retention of PSA within the PNIPAM network but also decoupled the swelling/deswelling kinetics from the measured swelling ratio. Using a lower polymerization temperature, more dense and homogenous structure is formed resulting in faster water uptake whereas higher polymerization temperature results in more porous fibrillar like structure with faster water release kinetics. By optimizing the polymerization temperature, PSA concentration and Mw we were able to synthesize PNIPAM/PSA semi-IPN hydrogel with swelling ratio as high as 260 g/g with fast swelling kinetics. The ongoing work in this direction entails on tailoring compositional and morphological properties for enhancing interaction between hydrogel and membrane surface to improve the water flux and permeation.

References:

1. Cai, Y., et al., *Exploration of using thermally responsive polyionic liquid hydrogels as draw agents in forward osmosis*. RSC Advances, 2015. 5(118): p. 97143-97150.
2. Cai, Y., et al., *Towards temperature driven forward osmosis desalination using Semi-IPN hydrogels as reversible draw agents*. Water Research, 2013. 47(11): p. 3773-3781.
3. Gupta, N., et al., *Design Rationale for Stimuli-Responsive, Semi-interpenetrating Polymer Network Hydrogels—A Quantitative Approach*. Macromolecular Rapid Communications, 2020. n/a(n/a): p. 2000199.

4:15 PM SB02.12.02

Negatively Charged Hydrogel Microfibers for Three-Dimensional Cell Culture Scaffolds Sungrok Wang, Jongwon Lee, Sangwoo Lee and Myung-Han Yoon; Gwangju Institute of Science and Technology, Korea (the Republic of)

Polymeric microfibers have been utilized as porous scaffolds for various types of three-dimensional (3-D) cell cultures but there still exist practical issues

such as limited bioactivity, unfavorable mechanical stiffness, poor dimension controllability, etc. In this research, we developed water-soluble polymer (e.g., polyvinyl alcohol, hyaluronic acid and gelatin)-based negatively-charged hydrogel microfibers with enhanced bioactivity and adjustable mechanical properties. In order to increase dimensional controllability of hydrogel microfibers, we homogenized these microfibers and precipitated them by adding cationic polyelectrolyte, leading to the entangled hydrogel microfibrillar network with microscale porosity. Furthermore, because those fibers were made by combination with natural polymers, the hydrogel microfibrillar network was degradable by enzyme treatment (>95% by hydrolase such as collagenase or hyaluronidase). Also following the degree of crosslinking, the degradability and size of entangled hydrogel microfibrillar network were well modulated by controlling their composition and fiber diameters. Finally, we demonstrated that these colloidal hydrogel microfibers mixed with cells could be patterned by using a conventional 3D printer, suggesting that resultant hydrogel microfiber scaffolds are suitable for various types of 3-D cell cultures.

4:30 PM SB02.12.03

Late News: Ultra-Tough and Stiff Ionogels by *In Situ* Phase Separation [Meixiang Wang](#) and Michael Dickey; North Carolina State University, United States

Ionogels are compelling materials for energy storage devices, ionotronics, and actuators due to their excellent ionic conductivity, thermal and electrochemical stability and nonvolatility. However, most existing ionogels suffer from low strength and toughness. Here, we report a simple one-step method to achieve ultra-tough and stretchable ionogels by randomly copolymerizing two common monomers in ionic liquid. Copolymerization leads to a single covalent network with controllable polymer- and solvent-rich phases that form *in situ* due to the phase behavior of the polymer in ionic liquid. The polymer-rich phase forms hydrogen bonds that dissipate energy and thereby toughen the ionogel during extension, while the solvent-rich phase remains elastic to enable large strain. The copolymer ionogels composed of acrylamide and acrylic acid exhibit extraordinary mechanical properties, including fracture strength (12.6 MPa), fracture energy (~24 kJ m⁻²), and Young's modulus (46.5 MPa), setting new records among reported ionogels. The tough ionogels are highly stretchable (~600% strain) and possess good self-recovery, as well as excellent self-healing and shape-memory properties. This concept extends to other monomers and ionic liquids, which offers a promising and general way to tune microstructure *in situ* during one-step polymerization that solves the longstanding mechanical challenges in ionogels.

SYMPOSIUM SB03

Transformative Nanostructures with Therapeutic and Diagnostic Modalities
November 30 - December 7, 2021

Symposium Organizers

Jennifer Dionne, Stanford University
Isabel Gessner, Harvard Medical School-Massachusetts General Hospital
Gerardo Goya, University of Zaragoza
Sanjay Mathur, University of Cologne

* Invited Paper

SESSION SB03.01: Transformative Nanostructures with Therapeutic and Diagnostic Modalities I
Session Chair: Polina Anikeeva
Tuesday Morning, November 30, 2021
Sheraton, 2nd Floor, Independence East

10:30 AM *SB03.01.01

Controlled Delivery Technologies for Modulating the Immune System to Engineer Potent and Durable Vaccines [Eric A. Appel](#); Stanford University, United States

Vaccines can take one of several forms, but those based on subunit antigens (representative subunits of the pathogen for which immunity is desired) offer the greatest safety profile and scalability, but generally elicit weaker and less durable immune responses. Failure to elicit a sufficiently strong response likely arises from inappropriate temporal control over antigen/adjuvant presentation and immune cell activation. Either short-term presentation of these signals, or misalignment of their presentation along different timelines, results in poor affinity maturation of antibodies and poor immune memory responses. When considering the iterative selection process occurring during somatic hypermutation and antibody affinity maturation in B lymphocytes, it is intuitive that prolonged lymphocyte activation and antigen exposure would lead to the generation of higher-affinity antibodies. Moreover, the immune system is highly spatially organized and so spatiotemporal control over vaccine exposure is crucial to potent and safe responses. In this work we will discuss novel technologies for improving the spatiotemporal presentation of vaccine components to the immune system. In particular we will describe an injectable hydrogel platform providing unique drug delivery capabilities for the long-term co-delivery of antigen and adjuvant in subunit vaccines and discuss the impact of prolonged vaccine delivery on humoral immune responses. We demonstrate that prolonged hydrogel-based immunizations greatly enhance the magnitude and duration of antibody responses, enhance and prolong germinal responses, and lead to 1000-fold enhancement in antibody affinity maturation when compared to the same vaccine delivered in bolus. These advanced materials technologies, therefore, have the potential to provide

vastly superior vaccine performance through the precise and sustained delivery of subunit vaccines that take advantage of natural immune mechanisms for building long-lasting and potent immunity.

11:00 AM SB03.01.02

Delivering an Antibody Against SARS-CoV-2 from a Subcutaneous Supramolecular Hydrogel Depot Catherine Meis and Eric A. Appel; Stanford University, United States

Supramolecular hydrogels are promising materials to address challenges associated with the formulation of biotherapeutic drugs, such as antibodies, which often suffer from a lack of stability in formulation and poor pharmacokinetics. To address these challenges, we have developed an injectable polymeric materials platform to encapsulate and deliver macromolecular drug cargo. Our modular, tunable supramolecular hydrogel system is comprised of a polymer matrix that is physically cross-linked by polymeric nanoparticles, resulting in a material which exhibits shear-thinning and self-healing properties, both desirable characteristics for an injectable drug delivery vehicle. In vitro drug release assays and diffusion measurements indicate that our materials dramatically prolong the release of antibodies and improve formulation stability under severe stressed aging conditions. To investigate the performance of these materials in vivo, antibodies against SARS-CoV-2 were delivered in mice to assess the pharmacokinetics of an antibody delivered in our hydrogel compared to standard routes of administration. In addition, a model was implemented to further understand how the materials design impacts the ability of the hydrogel to modulate pharmacokinetics in vivo, enabling customization of the hydrogel properties to achieve the target pharmacokinetic profile based on properties of both the hydrogel formulation and the specific antibody drug. The model will help inform future materials design efforts to generate long-acting antibody-based drug products for a variety of important therapeutic applications.

11:15 AM SB03.01.03

Therapeutic Targeting of lncRNAs for Cancer Therapy Jan M. Hoelzl^{1,2} and Ralph Weissleder^{1,3}; ¹Massachusetts General Hospital Research Institute, United States; ²Heidelberg University Medical Center, Germany; ³Harvard Medical School, United States

Long non-coding RNAs (lncRNAs) are emerging as a new player in the field of cancer research. They show tissue -and sometimes even cell-specific expression and have potential in therapeutic and diagnostic settings. Whilst research in this area is still in its early stages, promising lncRNA candidates have been identified. Therapeutically, the most widely used approach is to silence cancer-associated lncRNAs with RNase H competent antisense oligonucleotides (ASOs). While this approach is promising, in vivo ASO delivery to tumors remains a hurdle. Different advances in nano compositions of lipid nanoparticles (LNPs), lipoplexes and exosomes offer some possibilities to maximize tumoral and minimize hepatic delivery. Here, I will present on the role that these nanotechnologies, specifically LNPs, could play in the development of novel ASO-based cancer therapeutics and will also discuss remaining problems with this approach and next steps that have to be taken in order to move such novel drugs towards the clinic. I will also explore possibly targetable lncRNAs associated with different cancers. It is expected that collaborative efforts in nanotechnology and cancer biology may lead to therapeutic platforms that could usher in a new era of therapeutics.

11:30 AM SB03.01.04

Late News: Development of a Polymer-Lipid Core-Shell Nanoparticle for Improved Drug Loading and Layer-by-Layer Functionalization Emily Han¹, Joelle L. Straehla^{1,2} and Paula Hammond^{1,1}; ¹Massachusetts Institute of Technology, United States; ²Dana-Farber/Boston Children's Cancer and Blood Disorders Center, United States

Introduction: Efficient encapsulation of therapeutic agents is a key factor when designing a nanoparticle (NP) drug delivery platform. For some hydrophobic small molecules, encapsulation within polymer-lipid core-shell NPs is more efficient than polymer- or lipid-based NPs. Most well-studied core-shell formulations incorporate poly(ethylene glycol) (PEG) as a stealth molecule to extend circulation time, but there are disadvantages to PEG as well, including limited uptake into cancer cells and the potential for allergic reactions. In addition, surface PEG limits the ability to perform layer-by-layer (LbL) functionalization.

Objectives: We sought to develop a stable core-shell NP without PEG that can efficiently load hydrophobic drugs and serve as a biocompatible anionic substrate for layer-by-layer (LbL) functionalization. LbL assembly involves the iterative adsorption of oppositely charged polyelectrolytes onto charged NP cores in a simple and scalable water-based system. LbL NPs have key advantages including preserving the biological activity of therapeutic agents, controlling drug release behavior, and adding functional targeting groups to the surface. Here we report a new polymer-lipid core-shell NP formulation with a poly(lactic-co-glycolic acid) (PLGA) core and a lipid shell, with the eventual goal of loading a class of poorly soluble small molecule inhibitors for a targeted cancer application.

Methods: We first tested a suite of lipids with anionic head groups for solubility in water-miscible organic solvents to maintain compatibility with the nanoprecipitation method. Next, lead lipid candidates were combined with soy lecithin in the aqueous phase, and a panel of core-shell NPs were formed via nanoprecipitation with 50:50 esterified PLGA in the organic phase (protocol adapted from Chan et al. *Biomaterials*, 30, (2009), 1627). NPs were characterized for dynamic light scattering size, polydispersity, and zeta potential. Transmission electron microscope (TEM) imaging was used to investigate NP morphology. Finally, lead formulations were used as core templates for layering, with cationic poly-L-arginine (PLR) as the first layer and anionic poly-L-aspartic acid (PLD) as the terminal layer.

Results: We identified two lipids with anionic head groups that were soluble in ethanol, 1,2-dipalmitoyl-sn-glycero-3-phospho-(1'-rac-glycerol) (16:0 PG) and 1-palmitoyl-2-oleoyl-sn-glycero-3-phospho-(1'-rac-glycerol) (16:0-18:1 PG), making them ideal for the nanoprecipitation method. They had higher solubility than analogously structured phosphoethanolamine (PE)-based lipids, likely due to the PG head group bearing more negative charge. Incorporating 16:0 PG and 16:0-18:1 PG with soy lecithin at a molar ratio of 3:7, we were able to form NPs with favorable properties for drug delivery. The z-averaged diameter, number mean diameter, and zeta potential of the formulations are as follows: 186 nm, 130 nm, -53 mV (16:0 PG formulation); 175 nm, 117 nm, -61 mV (16:0-18:1 PG formulation); 157 nm, 89 nm, -52 mV (1,2-Distearoyl-sn-glycero-3-phosphoethanolamine-Poly(ethylene glycol) (DSPE-PEG) control). 16:0-18:1 PG was chosen as the lead candidate after dry-state TEM imaging confirmed the core-shell structure. This formulation also formed stable LbL NPs, with surface charge reversal after layering with PLR (63 mV) and PLD (-56 mV).

Discussion: Our data suggests that polymer-lipid core-shell nanoparticles without PEG are a promising formulation to improve hydrophobic drug loading, avoid clinical disadvantages of PEG, and take advantage of the layering capabilities of LbL technology. Ongoing work with this formulation includes drug loading, release characterization, and the generation of an expanded LbL NP library with functionalization for specific cancer applications.

11:45 AM SB03.01.05

Multimodal Nanotracking for Exosome-Based Therapy in DMD Valeria Secchi¹, Chiara Villa², Yvan Torrente² and Angelo Monguzzi¹; ¹University of Milano-Bicocca, Italy; ²Fondazione IRCCS Ca' Granda Ospedale Maggiore Policlinico, Italy

Duchenne Muscular Dystrophy (DMD) is one of the most common forms of muscular dystrophy caused by mutations in the dystrophin gene that result in absent or insufficient functional dystrophin, a cytoskeletal protein that enables the strength, stability, and functionality of myofibres. Progressive muscular damage and degeneration occurs in people with DMD, resulting in muscular weakness, associated motor delays, loss of ambulation, respiratory impairment, and cardiomyopathy. Up to now there is no cure for DMD.

Recently, promising outcomes are revealed from the therapeutic use of exosomes: small extracellular vesicles secreted by cells and found in body fluids. Exosomes can be seen as exciting biological carriers, thanks to their ability to traverse biological barriers, to transport functional RNAs between cells and to be better tolerated by the immune system. They can be considered as surrogate for cell-based therapy with a stronger safety, for their well-documented active therapeutic role.

In this context, our aim is the development of a stable, therapeutic, tissue-specific exosome-based approach in the field of DMD, supported by the use of advanced multimodal probes, in order to track and specifically direct the exosomes to dystrophic muscles. For this reason, we combined fluorescent, labeling and ferromagnetic functionalities on single nano-object through self-assembly interactions to obtain a multimodal probe for high contrast non-invasive in vitro imaging and efficient in vivo tracking of exosomes in dystrophic mice. The multimodal probe is made of inert and biocompatible chrysotile nanotubes (NTs). The positive surface potential of NTs could be exploited for anchoring anionic species, exosomes included, in aqueous environment, following an ionic self-assembly scheme. A magnetic functionality is introduced through the interaction of NTs with anionic functional groups of the TAU capping ligand of ferrite magnetic nanoparticles (MAG NPs). Moreover, the fluorescent functionality is introduced by a red emitting chromophore. Side-by-side fluorescence imaging and magnetic resonance (MRI) experiments have confirmed the effectiveness of ferromagnetic Nanotubes as multimodal contrast agents.

In particular, the strong ferromagnetic properties of these probes will enable the driving of regenerative exosomes under high magnetic field by a clinically applicable permanent magnet, for a specific targeted in vivo delivery towards interested tissue. The possibility to specifically direct exosomes to dystrophic muscle will allow the development of a controlled release of sufficient exosome amount at disease target site for a clinical outlook of personalized highly efficient and safe nanomedicine.

¹ C. Villa, M. Campione, B. Santiago-González, F. Alessandrini, S. Erratico, I. Zucca, M. G. Bruzzone, L. Forzenigo, P. Malatesta, M. Mauri, E. Trombetta, S. Brovelli, Y. Torrente, F. Meinardi, and A. Monguzzi Self-Assembled pH-Sensitive Fluoromagnetic Nanotubes as Archetype System for Multimodal Imaging of Brain Cancer *Adv. Funct. Mater.* 2018, 1707582

SESSION SB03.02: Transformative Nanostructures with Therapeutic and Diagnostic Modalities II

Session Chair: Emmanuel Flahaut
Tuesday Afternoon, November 30, 2021
Sheraton, 2nd Floor, Independence East

1:30 PM *SB03.02.01

Coupling Pro-Apoptotic TRAIL Factor to Superparamagnetic Iron Oxide Nanoparticles to Build Efficient Nanohybrid Drugs for Cancer Therapy Hanene Belkahl^{1,2,2}, Andrei Alexandru Constantinescu², Tijani Gharbi², Florent Barbaut¹, Miryana Hemadi¹ and Souad Ammar¹; ¹Universite de Paris, France; ²Université Bourgogne Franche-Comté, France

TRAIL (Tumor Necrosis Factor-related apoptosis-inducing ligand), a cytokine belonging to the TNF superfamily, attracted major interest in oncology owing to its selective antitumor properties [1]. Therapeutic clinical trials using soluble TRAIL or antibodies targeting the two main agonist receptors (TRAIL-R1 and TRAIL-R2) have, however, failed to demonstrate their efficacy [2]. Attempts to increase its antitumor activity include, amongst others, its functionalization by nanoparticles [3], particularly magnetic nanoparticles (MNPs). Such carriers allow concentrating TRAIL [4] which can be driven to a defined target site by local application of an external DC-magnetic field. They also offer the possibility of monitoring TRAIL delivery by magnetic resonance imaging (MRI) and the possibility to increase antitumor TRAIL functionality by magnetic hyperthermia [5]. Magnetic iron oxide MNPs, magnetite and maghemite, have the right magnetic properties [6] and exhibit relatively low toxicity [7]. For this reason, they were specifically produced with different average sizes, i.e. 10 and 100 nm (magnetic single core versus magnetic multicore) [4], and were attached to TRAIL through peptide coupling, engaging respectively carboxylic or amino protein group to evaluate both the effect of their size and their chemical bounding on TRAIL antitumoral activity on malignant mammal cells. They were also subsequently submitted to an external AC-magnetic field to confirm their capability to eradicate residual TRAIL resistant tumoral cells through local heating [5]. Clearly, the properties of TRAIL and the multimodal characteristics of MNPs hold great promise for the treatment of cancer and pave the way for the generation of new and efficient drugs.

[1] A. Ashkenazi, R. C. Pai, S. Fong, et al., *J. Clin. Invest.*, 1999, 104, 155–162.

[2] O. Micheau, S. Shirley, F. Dufour, *Br. J. Pharmacol.*, 2013, 169, 1723–1744

[3] H. Belkahl, G. Herlem, F. Picaud et al., *Nanoscale*, 2017, 9, 5755–5768.

[4] H. Belkahl, A. Haque, A. Revzin et al., *J. Interdiscip. Nanomed.*, 2019, 4, 34–50.

[5] H. Belkahl, E. Mazarío, J. S. Lomas et al., *Theranostics*, 2019, 9, 5924–5936.

[6] S. Laurent, S. Dutz, U. O. Hafeli et al., *Adv. Colloid Interface*, 2011, 166, 8–23.

[7] A. Hanini, A. Schmitt, K. Kacem et al., *Int. J. Nanomedicine*, 2011, 6, 787–794.

2:00 PM SB03.02.02

Design of Luminescence and Surface Chemistry of Hafnia Nanoparticles for Biological Applications Xavier H. Guichard and Alessandro Lauria; ETH Zurich, Switzerland

Luminescent materials are used in a variety of applications, from lighting and display technologies to scintillators for high-energy radiation detection. ^[1] A particular interest has grown towards nanoscale phosphors, proposed also for innovative bio-imaging excited by infrared radiation or photosensitizers for cancer self-lighting photodynamic therapy. ^[2]

The employment of nanoparticles in these applications relies on the ability to tailor their photo-physics, which is based on the control over structural features like their size, composition and crystal symmetry able to impact their optical properties. Moreover, to be suitable for specific applications, the surface chemistry of these materials must be adapted to provide homogeneous stable dispersions/inks and thus facilitate handling and deposition, as well as efficient cellular uptake.

Colloidal nanocrystals of HfO₂ can be synthesized from molecular precursors by a solvothermal route, where both fluorescence and structural control can be achieved thanks to the multifunctional role of rare earth (RE) doping. ^[3] While RE dopant ions activate the visible luminescence of nanocrystals, at the same time, their incorporation can also stabilise the cubic polymorph of HfO₂ at room temperature. Such a structural change can significantly affect the optical quality of sintered polycrystalline scintillator ceramics as well as the performance of RE-based upconversion. In addition, the native surface chemistry of such nanoparticles allows their further adaptation to either organic solvents or, alternatively, to aqueous biological environments, enabling cellular uptake and making them suitable as non-toxic probes for optical imaging, and possibly therapy. ^[4]

In this talk the control over the structure/function relationship in HfO₂ doped nanoparticles is discussed, together with its implications towards and

functional inks for innovative deposition/assembly of nanoparticle based optical materials as well as for advanced bio-imaging.

- [1] S. V. Eliseeva, et. al., *New J. Chem.* 35, 1165 (2011).
- [2] B. del Rosal, et. al., *Adv. Funct. Mater.* 28, 1803733 (2018).
- [3] A. Lauria, et. al., *ACS Nano* 7, 7041 (2013).
- [4] I. Villa, et. al., *Nanoscale* 10, 7933 (2018).

2:15 PM *SB03.02.05

Modulating Neuronal Signaling with Magnetic Nanotransducers Polina Anikeeva; Massachusetts Institute of Technology, United States

The mammalian nervous system spans spatial scales from centimeters to nanometers, and functions at time scales from microseconds to decades. To access this spatiotemporal complexity, we envision tools capable of modulating individual receptors at the nanoscale in behaving organisms at the macroscale. Weak magnetic fields offer unprecedented access to the arbitrary locations within the body due to the low conductivity and negligible magnetic permeability of biological matter. To convert weak magnetic fields into biological signals, we design and synthesize a range of nanotransducers. Based on their composition and geometry, these nanotransducers can be tailored to dissipate heat or apply force or torque. We leverage magnetothermal and magnetomechanical transduction mechanisms to enable wireless remote control of a variety of receptors in neurons and thus modulate animal behavior and physiology.

2:45 PM SB03.02.06

Development of Colloidal Magnetic Nanoparticles with Strong Liquid-Phase AC Field Response for Remote Thermometry and Sensing

Applications Adam Bicchì, Thanh Bui, Eduardo Correa, Cindi Dennis, Solomon Woods and Angela Hight Walker; National Institute of Standards and Technology, United States

Colloidal magnetic nanoparticles (MNPs) are an important class of nanomaterials being investigated for use in a host of therapeutic and diagnostic modalities such as medical imaging, remote sensing, drug delivery, and hyperthermia. These applications exploit the very soft magnetic behavior found in certain materials, often ferrites, when they are confined in size to tens of nanometers in diameter or less. Such nanoscale magnets produce a strong collective response to applied alternating (AC) magnetic fields, while simultaneously remaining dispersed in heterophasic liquid media. Further, the synthesis of these magnetic colloids employs inexpensive, scalable, highly tailorable solution chemistry routes that both allow fine control of their properties and afford a practical route to commercialization.

Recently, we have been developing remote magnetic thermal imaging as a potential diagnostic application of colloidal MNPs. This measurement will employ dispersed particles to construct a 3D visual representation of temperature throughout a volume. The technique is based on the temperature-dependent collective response of MNPs to applied AC magnetic fields coupled with simultaneously applied DC fields to afford spatial control over the region in which the measurement is conducted. However, significant challenges remain in the development of this metrology, including a need to increase both the MNPs' magnetic thermosensitivity and magnitude of AC field response.

Here, we report on our development of MNPs with a robust liquid-phase response to applied AC magnetic fields, specifically for solution-phase remote thermometry and other sensing applications. First, a series of colloidal nanocrystals based on ferrites were synthesized *via* solution routes in a variety of sizes and compositions. These MNPs were then systematically investigated using liquid-phase AC and DC field magnetometry measurements. An arbitrary-wave magnetic particle spectrometer was employed to measure magnetic AC susceptibility, allowing for a rigorous analysis of the temperature- and frequency-dependent AC response from 1 Hz to 30 MHz. These results were cross-correlated with detailed structural characterization, including electron microscopy, optical spectroscopy, and X-ray/electron diffraction, which underpins the inherent magnetic properties of the particles.

We find the relaxation dynamics in solution are strongly dictated by the structural and compositional properties of the MNPs. Specifically, particle size and compositional doping act as levers to optimize the liquid-phase AC response through the manipulation of interparticle and intraparticle magnetic spin interactions. Using these guidelines, we find the set of structural parameters that produce the most robust thermosensitive magnetic response. Collectively, these studies illuminate the complex behavior of MNPs under AC driving fields, reveal extensive correlations between nanoscale atomic structure and their liquid-phase magnetic response, and provide guidelines for the design of MNPs used in magnetic thermal imaging and other remote sensing applications.

3:00 PM SB03.02.07

Magnetic Silica-Coated Particles with Enhanced Brightness (MagSiGlow) Isabel Gessner^{1,2}, Elias A. Halabi Rosillo^{1,2,3}, Katherine S. Yang^{1,2} and Ralph Weissleder^{1,2}; ¹Massachusetts General Hospital, United States; ²Harvard Medical School, United States; ³Swiss National Science Foundation, Switzerland

Magnetic nanoparticles are extremely useful tools for purifying biological targets in complex mixtures. Magnetofluorescent nanoparticles have additional benefits allowing for sensing and multiplexing. Although the chemical coupling of conventional organic dyes to silicon dioxide shells is straightforward, densely packing can lead to quenching and non-radiative decay pathways. These unwanted side effects, significantly reduce the overall brightness of a given particle. To circumvent this issue, we implement a new method to sparsely distribute dye labeling on multiple coating layers, yielding distinctively bright magnetic silica-coated fluorescent particles, which we termed MagSiGlow. In this study, we describe the design and synthesis of MagSiGlow particles using novel and commercially available fluorophores detectable in different color channels. Additionally, we discuss experiments where implementing MagSiGlow particles facilitates detection of extracellular vesicles and visualization of living cells using flow cytometer and confocal microscopy.

3:45 PM SB03.02.08

Opto-Thermo-Electrohydrodynamic Tweezers (OTET) for On-Chip Trapping and Analysis of Single Extracellular Vesicles Justus C. Ndukaife, Chuchuan Hong and Sen Yang; Vanderbilt University, United States

The year 2018 Nobel Prize in Physics was awarded for Optical Tweezers and their application in biological systems. Optical tweezers have emerged as a powerful tool for the non-invasive trapping and manipulation of colloidal particles and biological cells. However, the stable trapping of nanometer-scale biological objects such as proteins, small extracellular vesicles, and virions has been met with challenges due to the diffraction limit of light. Significantly increasing the laser power can provide sufficient trapping potential depth to trap nanoscale objects. Unfortunately, the significant optical intensity required predisposes the trapped biological specimens to photo-toxicity and thermal stress. I will discuss a new paradigm for optically controlled nanotweezers termed Opto-Thermo-Electrohydrodynamic Tweezers (OTET) that enables the stable trapping and dynamic manipulation of nanoscale biological objects such as EVs with negligible photothermal heating and light intensity. The OTET platform employs a finite array of plasmonic nanoholes illuminated with light in conjunction with an applied a.c. electric field to create the spatially varying electrohydrodynamic potential that can rapidly trap single nanoscale

EVs on-demand. I will also discuss potential translational biomedical applications of this new technology for early cancer detection via EV-based liquid biopsy. This novel non-invasive optical nanotweezer is expected to open new horizons in life science and medicine by offering an unprecedented level of control of tiny nano-sized biological objects in solution without photo-induced damage.

3:30 PM BREAK

SESSION SB03.03: Transformative Nanostructures with Therapeutic and Diagnostic Modalities III
Session Chairs: Souad Ammar and Eric Appel
Wednesday Morning, December 1, 2021
Sheraton, 2nd Floor, Independence East

10:30 AM *SB03.03.01

Carbon Nanotubes Based Hydrogels for Transdermal Drug Delivery Juliette Simon^{1,2,3}, Georgios Kougkoulos^{1,2,4}, Bastien Jouanmiquet³, Muriel Golzio³, Emmanuel Flahaut^{2,1} and Zarel Valdez-Nava^{4,1}; ¹University of Paul Sabatier, France; ²CNRS / CIRIMAT, France; ³CNRS / IPBS, France; ⁴CNRS / LAPLACE, France

Large molecules such as insulin are too big to be able to cross the skin and reach the blood flow through passive diffusion, unlike smaller molecules such as nicotine for example. Needles are thus usually required to cross this natural barrier. In order to improve the life quality of patients using regular hypodermal injections, alternative delivery methods are needed. Carbon-based nanoparticles, free or associated with a polymer matrix, are increasingly used in innovative biomedical applications [1]. We are developing a non-invasive transdermal delivery route, using a two-in-one nanocomposite device and the reversible permeabilisation of the skin, thanks to electroporation. The device is a nanocomposite with a biocompatible hydrogel matrix containing carbon nanotubes (CNTs), which combines both purposes of assisting the permeabilisation and storing the molecule to be delivered. The inclusion of CNTs in the hydrogel matrix is also intended to prevent their release during operation of the device, with a safe(r) by design strategy in mind. Previous work from our group described an enhanced drug delivery of dextran FITC through permeabilised skin for devices containing CNTs [2]. Later, the electrical characterisation of those devices was performed [3]. However, although the proof of concept was validated, such devices are still far from practical applications and the optimisation of electroporation parameters, depending on the intended use, is still in progress. We will describe and discuss our most recent advances.

References:

[1] Simon, J.; Flahaut, E.; Golzio, M. Overview of Carbon Nanotubes for Biomedical Applications. *Materials* 2019, 12(4), 624. <https://doi.org/10.3390/ma12040624>

[2] Guillet, J.-F.; Flahaut, E.; Golzio, M. A Hydrogel/Carbon-Nanotube Needle-Free Device for Electrostimulated Skin Drug Delivery. *ChemPhysChem* 2017, 18 (19), 2715–2723. <https://doi.org/10.1002/cphc.201700517>

11:00 AM SB03.03.02

Injectable Nanoparticle-Based Hydrogels Improve the Safety and Efficacy of Potent Immunostimulatory CD40 Agonist Antibodies Santiago Correa, Juliana Idoyaga and Eric A. Appel; Stanford University, United States

When properly deployed, the immune system can render deadly pathogens harmless, eradicate even metastatic cancers, and provide long-lasting protection from diverse diseases. However, realizing these remarkable capabilities is inherently risky, as disruption to immune homeostasis can lead to dangerous complications and autoimmune disorders. While current research is continuously expanding the arsenal of potent immunotherapeutics, there is a technological gap when it comes to controlling when, where, and how long these drugs act on the body. We previously described a polymer-nanoparticle (PNP) based hydrogel that is biocompatible, long lasting, and injectable^{1,2}, traits that we hypothesized would improve controlled local delivery of immunotherapy.

To test this hypothesis, we explored PNP hydrogel-mediated delivery of CD40 agonist antibody (aCD40), a potent immunostimulant that has been shown to improve outcomes in combination immunotherapy, but poses considerable dose-limiting toxicity.³ PNP hydrogels were formed by mixing CD40 agonist antibody (CD40a), dodecyl-modified hydroxymethylcellulose (HPMC-C₁₂), and poly(ethylene glycol)-b-poly(lactic acid) nanoparticles (PEG-PLA NPs) to generate gels with 2 wt% HPMC-C₁₂, 10 wt% PEG-PLA NPs, and the desired dose of CD40a (ranging from 10-100 mg). HPMC-C₁₂ and PEG-PLA NPs were prepared as described previously¹.

Using positron emission tomography (PET) imaging, we quantitatively tracked how delivery strategy (e.g., hydrogel vs. local bolus) shaped aCD40 pharmacokinetics over the course of 12 days. PET studies demonstrated that hydrogels substantively altered antibody pharmacokinetics to favor drug exposure in target tissues. Our data indicate that hydrogels increased exposure at the injection site by $96 \pm 13\%$ ($q = 4 \times 10^{-6}$) and at the tumor draining lymph node by $35 \pm 19\%$ ($q = 5 \times 10^{-3}$) over the course of the 12-day study. Locoregional hydrogel delivery also circumvented dose-limiting toxicity commonly associated with aCD40 therapy (e.g., acute weight loss and hepatotoxicity). Using Luminex multiplexed cytokine assays, we also evaluated how delivery strategy shaped the induction of effector cytokines in systemic circulation and in tumor draining lymph nodes. We found that hydrogels substantively attenuated the induction of systemic cytokines, particularly across a number of pro-inflammatory cytokines (IFN γ , TNF α , IL6, and IL1b) commonly associated with cytokine storm syndrome, another common side effect of aCD40 therapy. Despite reducing cytokine levels systemically, hydrogel delivery generated a more potent immune response, as measured by effector cytokine (IFN γ , CXCL10) levels within tumor-draining lymph nodes (TdLN). Correspondingly, hydrogel-mediated locoregional aCD40 therapy was more tolerable and effective than even locoregional bolus injections, and synergized with PD-L1 blockade (40% survivors in combo-therapy arms vs. 0% survivors in monotherapy arms, n=10, $p_{\text{adj}} < 0.03$).

Overall, this study provides compelling evidence that PNP hydrogels can improve aCD40 pharmacokinetics and pharmacodynamics, leading to greater tolerability and therapeutic efficacy in the B16F10 model of melanoma. Notably, PNP hydrogels mediated these effects without the need to modify their cargo in any way. Therefore, we anticipate that this approach may also improve the safety of other potent immunostimulants, and is thus a highly translatable solution to the problem of immune-related adverse effects.

References:

1. Appel, E.A. et al. Nat Commun 6, 6295 (2015).
2. Stapleton, L.M. et al. Nat Biomed Eng 3, 611-620 (2019).
3. O'Hara, M.H. et al. The Lancet Oncology 22, 118-131 (2021).

11:15 AM SB03.03.04

Enzyme-Triggered Depolymerization of Polymeric Micelles for Targeted Anticancer Therapy Jaehyun Park, Seokhee Jo, Junseok Lee and Won Jong Kim; Pohang University of Science and Technology, Korea (the Republic of)

The high activity of specific enzymes in cancer has been utilized as tumor-specific trigger for anticancer drug delivery. NAD(P)H:quinone oxidoreductase-1 (NQO1), an overexpressed enzyme in certain tumor types, maintains homeostasis and inhibits oxidative stress caused by elevated reactive oxygen species (ROS) in tumor cells. The activity of NQO1 in certain types of cancer cells is increased compared to that in normal cells. Interestingly, NQO1 catalyze the reaction of trimethyl-locked quinone propionic acid (QPA) to a lactone-based group via intramolecular cyclization. Toward this objective, we synthesized amphiphilic block copolymer (QPA-P) composed of QPA-locked polycaprolactone (PCL) as a hydrophobic block and poly(ethylene glycol) (PEG) as a hydrophilic block. This polymer formed a self-assembled micelle via hydrophobic interaction. QPA-locked PCL block was depolymerized by NQO1 via a cascade two-step cyclization process, which eventually mediated the disassembly of micelle and released anticancer drugs at the target cancer cells. The micelles showed NQO1-responsive intracellular drug release and enhanced anticancer effects in vivo. These results indicate that enzyme-responsive depolymerization process could be a promising strategy for improving therapeutic efficacy of polymer-based anticancer drug delivery carrier.

SESSION SB03.04: Transformative Nanostructures with Therapeutic and Diagnostic Modalities IV
 Session Chairs: Souad Ammar and Eric Appel
 Wednesday Afternoon, December 1, 2021
 Sheraton, 2nd Floor, Independence East

1:30 PM SB03.04.02

H₂O₂ Detection with Silver-Platinum Core-Shell Nanowires Serkan Koylan¹, Sensu Tunca¹, Gokhan Polat², Mete Batuhan Durukan^{1,1}, Dongkwan Kim³, Yunus E. Kalay¹, Seung H. Ko³ and Husnu E. Unalan^{1,1,1}; ¹Middle East Technical University, Turkey; ²Necmettin Erbakan University, Turkey; ³Seoul National University, Korea (the Republic of)

Detection of hydrogen peroxide (H₂O₂) possess an essential role in both analysis and applications (chemical synthesis, cosmetics, biology, medicine, food, paper and textile industries) in bioelectronics. Electrochemical detection of H₂O₂ seems to be the highly promising due to its simplicity, fast response and low cost. Enzyme-free electrochemical sensors were demonstrated utilizing metal nanostructures, particularly silver (Ag) based nanostructures, for the detection of H₂O₂. Oxidation tendency of Ag together with its degradation in the presence of H₂O₂ necessitates use of a protective coating for Ag based amperometric sensors. In this work, a platinum (Pt) shell layer was deposited onto Ag NWs to improve the oxidation stability so then they can be used for the detection of H₂O₂. Ag-Pt core-shell NW electrodes were used for the detection of H₂O₂ with different concentrations (10, 50, 100 mM) at an applied potential of +0.8 V (vs. Ag/AgCl). The fabricated Ag-Pt core-shell NWs electrode showed a high sensitivity of 0.04 μA/μM over a wide linear range of concentrations (16.6 - 990.1 μM) with a low detection limit (10.95 μM), the regression equation was determined as $I(\mu A) = 1.61 + 0.04 \times [H_2O_2]/\mu M$ with a correlation coefficient R² of 0.9947. Using the 90% initial step change in the current, the response time of the sensor was 4.74 seconds. Fabricated sensors gave response only to H₂O₂ which proved interference selectivity. A simple and highly reproducible method for the fabrication of H₂O₂ sensors with highly repeatable response was demonstrated, which can be further expanded to other bioelectronics applications requiring electrochemical stability.

This work was supported by the Scientific and Technological Research Council of Turkey (TUBITAK) under grant no 117E539.

1:45 PM SB03.04.03

Probing Peptide Conformation on Carbon Nanotube for Volatile Organic Compound Sensors Daniel Sim^{1,2}, Zhifeng Kuang¹, Nicholas Bedford³, Jorge L. Chávez¹, Jennifer A. Martin¹, Ahmad Islam¹, Benji Maruyama¹, Rajesh Naik¹ and Steve S. Kim¹; ¹Air Force Research Laboratory, United States; ²UES, Inc., United States; ³University of New South Wales, Australia

Ubiquitous, autonomous, and real-time chemical sensing can provide abundant information related to the warfighter health and performance status. For example, volatile organic compounds (VOCs) found in exhaled breath are critical biomarkers for assessing human health and physiological status. Biorecognition elements (BREs) are biological materials exhibiting specific affinity to the target molecules. Short peptides (generally composed of 5-15 amino acid residuals) are promising BREs for selective VOC detection. They provide chemical stability and design flexibility to sensing the targeted biomarker. Peptide BRE-coated CNT chemiresistor has emerged as a miniaturized sensor platform for wearable applications. Previous peptide-functionalized CNT gas sensors have shown detecting explosives and bacterial food contamination byproducts. However, the peptide sensing mechanism of a peptide-CNT pair is yet unclear. We presumed that the conformation of the peptide on the CNT surface affects the molecular accessibility to the BRE-CNT interface. Here, we present a peptide conformation model to investigate peptides' affinity towards VOC on a CNT chemiresistor platform. This model predicts the conformation of the peptide on the CNT surface using peptide-CNT interaction energy obtained from a molecular dynamics simulation. A near-edge X-ray absorption fine structure (NEXAFS) spectroscopy experimentally validates the peptide conformation model by observing the peptide alignment to the CNT. Then, a peptide-functionalized CNT chemiresistor was tested to various gases to investigate how the conformation affects VOC sensing. The result shows that the vertically oriented peptide on the CNT surface hinders VOC access to the peptide-CNT interface, resulting in a significantly low sensor signal than the CNT chemiresistor with the horizontally oriented peptide. Our results strongly indicate that molecular accessibility is a key factor detrimental to the VOC sensing from peptide-CNT devices. This finding is crucial for designing the peptide sequence specific to target VOC, and ultimately, developing sensitive CNT-based VOC sensors.

2:00 PM SB03.04.04

Late News: Biomimetically Self-Assembled DNA—Inorganic Hybrid Nanoarchitectures for Quantitative Intracellular Aptasensing Nayoung Kim, Eunjung Kim, Hyemin Kim, Michael R. Thomas, Adrian Najer and Molly Stevens; Imperial College London, United Kingdom

Aptamers, nucleic acid analogs of antibodies, have shown promise in molecular diagnostics capitalizing on their programmable nature and high affinity/selectivity towards cognate ligands. Despite the breadth of biomolecular targets ranging from biofluid biomarkers to cellular analytes, a biologically deliverable aptasensor that enables to accurately monitor endogenous biomolecular abundance still remains elusive. DNA nanoassembly

aptasensors built from short staple DNA stands have shown particular success based on their precise Förster resonance energy transfer (FRET)-based operations; nonetheless, challenges are often associated with relatively low structural stability, its labor-/time-intensive fabrication, and the complex sensor operations that limit the design generalizability and necessitate computational modeling. Here, we present high-throughput biomimetic crystallization-driven DNA self-assembly as a route to tackle the challenges and produce a highly programmable and agile intracellular ratiometric aptasensor.[1] The probes are formulated by rolling circle amplification (RCA), whereby multifunctional elements-encoded polymeric DNA strands are enzymatically produced and self-compacted into DNA–inorganic hybrid nanoarchitectures. Harnessing the programmability of RCA template, the obtained DNA nanoparticles are intrinsically encoded with three functional features: 1) Tumor targetability using cell-targeting aptamer, 2) Ratiometric aptasensing of cellular analytes empowered by a tripartite duplexed aptasensor and 3) Synergistic assistance of cellular internalization by cholesterol decoration. The resultant probes possess biocompatibility, structural integrity and sequence-driven multifunctionalities which can be readily customized using the template without the need of computational modeling or any modification of fabrication procedures. Taking LNCaP human prostate adenocarcinoma cells and intracellular adenosine triphosphate as an exemplar target system, we illustrate the targeted delivery of our probe and subsequent ratiometric signaling triggered by intracellular target analyte recognition events. The limitations often associated with intensimetric-signaling intracellular probes are elegantly leveraged by our approach, where the quantitative detection is demonstrated with drug-treated cells and corresponding ratiometric FRET signal changes from internalized aptasensors. To the best of our knowledge, this represents the first demonstration of harnessing biomimetic crystallization to construct a DNA nanosensor that is capable of target-responsive biomolecular detection within intracellular environments. We envision that the proposed probe has substantial promise as a biologically deliverable probe that can be readily tailored across wide-ranging target systems, being capable of the quantitative monitoring of biomolecular profiles.

[1] **N. Kim**, E. Kim, H. Kim, M. R. Thomas, A. Najer, M. M. Stevens, Tumor-Targeting Cholesterol-Decorated DNA Nanoflowers for Intracellular Ratiometric Aptasensing, *Advanced Materials*, **2021**, 33, 2007738.

2:15 PM SB03.04.06

PDMS Composites with Photostable NIR Dyes for Multi-Modal Ultrasound Imaging and Optical Ablation India Lewis-Thompson, Shaoyan Zhang and Richard J. Colchester; University College London, United Kingdom

All-optical ultrasound imaging has emerged as an imaging paradigm well-suited for minimally invasive surgical procedures. With this modality, ultrasound is generated when pulsed or modulated light is absorbed within a coating material. The ensuing heat rise causes a corresponding pressure rise which propagates as ultrasound. Using optic fibres to deliver light for ultrasound generation and reception allows complementary therapeutic and imaging modalities to be integrated to create highly miniaturised devices. One area of interest for these devices is combined imaging and optical ablation, to provide real-time monitoring of ablation lesion depth. However, combining modalities requires carefully engineered composite materials with wavelength-selective absorption. Previous research has demonstrated the use of gold nanoparticles and crystal violet dye for co-registered ultrasound and photoacoustic imaging [1]. However, these materials were limited by material degradation with prolonged exposure and limited ultrasound pressures and bandwidths.

We present the optimisation of a nanocomposite material that comprises a near infrared absorbing dye in a polydimethylsiloxane (PDMS) host on the distal tip of optical fibres. The optical absorption of this composite has a pronounced peak at 1064 nm, allowing the absorption of laser light for ultrasound generation. Optical transmission through the composite was low for wavelengths below 900 nm allowing for the transmission of laser light at 808 nm for tissue ablation. Crucially, the composite demonstrates a high photostability to laser exposure, allowing continuous ultrasound imaging for larger periods of time (several hours). Varying the dye concentration allows for strong optical absorption for ultrasound generation, whilst maintaining higher transmission at shorter wavelengths for complementary modalities.

Our studies demonstrate that ultrasound pressures in excess of 1 MPa can be generated, sufficient for M-mode imaging at centimetre scale depths and consistent with other ultrasound generating materials [1,2]. Further, the corresponding ultrasound bandwidths (25 MHz), will enable high resolution imaging. We have used this composite to provide ultrasound imaging for the monitoring laser ablation of tissue in real-time, allowing the tracking of lesion depth. By optimising the optical absorption of the composite, light delivery for laser ablation is possible through the same optical fibre used for ultrasound generation. This would allow for device miniaturisation and coaxially aligned imaging and tissue ablation.

[1] S. Noimark *et al.*, "Polydimethylsiloxane Composites for Optical Ultrasound Generation and Multimodality Imaging," *Adv. Funct. Mater.*, vol. 28, no. 9, p. 1704919, Feb. 2018, doi: 10.1002/adfm.201704919.

[2] S. Noimark *et al.*, "Carbon-Nanotube-PDMS Composite Coatings on Optical Fibers for All-Optical Ultrasound Imaging," *Adv. Funct. Mater.*, vol. 26, no. 46, pp. 8390–8396, Dec. 2016, doi: 10.1002/adfm.201601337.

3:00 PM BREAK

SESSION SB03.05: Poster Session I: Transformative Nanostructures with Therapeutics and Diagnostic Modalities

Session Chair: Sanjay Mathur

Wednesday Afternoon, December 1, 2021

8:00 PM - 10:00 PM

Hynes, Level 1, Hall B

SB03.05.03

Late News: Glutathione-Depleting Nanocomposites for Amplification of Oxidative Stress in Sonodynamic Therapy Wooram Um, Yeari Song and Jae Hyung Park; Sungkyunkwan University, Korea (the Republic of)

The upregulation of glutathione (GSH) in cancer contributes to the resistance of cancer cells against oxidative stress and apoptosis. Thus, it is considered a crucial barrier that inhibits the therapeutic efficacy of reactive oxygen species-mediated cancer therapy. Herein, we develop glutathione-depleting nanocomposites (dGSH-NC) for amplifying the oxidative stress in sonodynamic therapy of cancer. dGSH-NC is composed of titanium dioxide nanoparticles and manganese dioxide surface for providing ultrasound-responsive ROS generation and GSH depletion. Further, GSH reduces manganese dioxide to manganese(II) ion that induces additional intracellular ROS generation. In SCC7 cells, dGSH-NC remarkably inhibits GSH in SCC7 cells and produces reactive oxygen species to amplify the cellular oxidative stress. In the presence of ultrasound, dGSH-NC exhibited an improved cytotoxic effect than that of bare titanium dioxide nanoparticles, and exposed cells presented necrotic cell death features.

SB03.05.04

Late News: Impact of Surface Properties on Nanoprobe-Analyte Interaction Kaleigh M. Ryan, Ajita Nair, Zelin Wang, Yuxuan Wu, Lu Wang and Laura Fabris; Rutgers University, United States

Surface enhanced Raman spectroscopy (SERS) is gaining popularity as a diagnostic technique, due to its ability for multiplexed detection and ultra-high sensitivity. So far, in the majority of its clinical applications, it has relied on the use of nanoprobe for indirect detection. In general, the nanoprobe brightness decreases exponentially as the Raman reporter molecule moves away from the nanoparticle surface, and local enhancement factors can vary dramatically on specific locations of the nanoparticle due to the presence of "hot spots". In order to develop a SERS based diagnostic platform with maximum sensitivity and reliability, it is imperative to understand the orientation and binding behavior of the Raman reporter on the nanoparticle surface, as well as under what conditions its orientation may change. Herein, we investigate analyte orientation and interaction on the nanoparticle surface using two different nanostar morphologies, surfactant-free nanostars and 6-branched nanostars, and three different analytes, thiophenol, 4-aminothiophenol, and crystal violet. Nanoprobe-analyte interactions are characterized by Raman spectroscopy and nanostar morphologies by transmission electron microscopy (TEM). Molecular dynamics simulations were conducted to verify the changes in analyte-nanoprobe interaction. It was found that signal amplification provided by surfactant-free nanostars and 6-branched nanostars can follow dramatically different trends depending on the analyte molecular structure. Molecular orientation on the nanoprobe surface was demonstrated to vary with changing analyte concentration.

SB03.05.05

Drug Delivery via Surface Modified Scintillating Nanoparticles Jeremy M. Quintana^{1,2}, David Arboleda¹, Isabel Gessner^{1,2}, Miles Miller^{1,2} and Ralph Weisleder^{1,2}; ¹Massachusetts General Hospital, United States; ²Harvard Medical School, United States

Antibody and nanoparticle mediated drug delivery to solid tumors can improve pharmacokinetics and dynamics of local payloads and decrease systemic toxicity. Despite these obvious advantages, there remains considerable room for improvement. We have previously shown that localized bursts of radiation can enhance local myeloid cell delivery and result in improved anti-tumor effects. To further enhance target specificity, we hypothesized that radiation induced drug release could represent a powerful complementary approach. Here, we developed scintillating yttrium oxide nanoparticle that emit UV light upon excitation with external X-ray irradiation, resulting in the release of attached UV-activatable prodrugs. Using Fourier-transform infrared spectroscopy, zeta potential and dynamic light scattering measurements, we have demonstrated and optimized the covalent modification of the nanoparticle surface with a prodrug. The release kinetics and total drug release were then observed by X-ray irradiation, followed by drug quantification using liquid chromatography. Likewise, the *in vitro* activation of the prodrugs has been demonstrated in culture, following X-ray irradiation. We show that these X-ray activatable nanoparticles efficiently release active cytotoxic agent with precise control due to the external radiation beam.

SB03.05.06

Anatase TiO₂-Coated Gold Nanobipyramids for Combinational Photothermal and Photodynamic Therapy Dohyub Jang^{1,2}, Subin Yu³, Dong June Ahn², Sehoon Kim¹ and Dong Ha Kim³; ¹Korea Institute of Science and Technology, Korea (the Republic of); ²Korea University, Korea (the Republic of); ³Ewha Womans University, Korea (the Republic of)

Photodynamic therapy is increasingly being recognized as a non-invasive feature and local treatment. Especially, inorganic photocatalysts, such as titanium dioxide (TiO₂), are regarded alternative materials for organic photosensitizer due to their high photo-stability, biocompatibility and significant photocatalytic ability. However, inorganic photocatalysts have critical threshold in the absorption of low energy photons to introduce in cancer therapy owing to their large band gap.

Meanwhile, plasmonic noble metal-based nanomaterials has drawn important attraction in recent years due to their broadly tunable localized surface plasmon resonance properties derived from the collective oscillation of surface free electrons under incident light. According to recent studies, anisotropic gold nanomaterials with tunable aspect ratio can generate strong electric fields at their tips. Particularly, gold nanobipyramids possessing sharp-tip morphology induce much stronger electric fields against gold nanorods commonly used in photothermal therapy. With suitable biocompatibility, plasmonic gold nanomaterials were investigated for cancer treatment and became a promising candidate to redeem the limitations of TiO₂ in biomedical applications. Upon strategic coupling with TiO₂, LSPR-induced hot carriers of plasmonic Au nanomaterials are injected into the conduction band of TiO₂ over the Schottky barrier, which can be consumed for the reduction of oxygen.

Despite of these advantages, Au NBP is hard to utilized due to their low thermal stability. To date, the synthesis of Au/TiO₂ heterostructures with crystalline TiO₂ requiring annealing steps at high temperature after amorphous TiO₂ coating. In order to convert the amorphous phase of TiO₂ to anatase phase, high temperature treatment is necessary. However, sharp tip gold nanomaterials such as Au NBP lose their tip during annealing process. Therefore, undesirable morphological disruption is occurred during annealing step, leading to LSPR peak changes. Moreover, TiO₂ shell agglomeration could not be avoided. These leads to low photocatalytic effects during NIR laser irradiation.

Herein, we newly developed anatase TiO₂-decorated Au NBP (Au NBP/a-TiO₂) as a novel metal/semiconductor core/shell colloidal heterostructure for NIR-responsive phototherapy. This is the first time that introducing low temperature hydrothermal method to crystalline anatase TiO₂ onto Au NBP surface, while preserving a well-defined Au NBP/a-TiO₂ morphology with sharp-metal tips without any aggregation. Strategically, the highly energetic LSPR-derived hot electrons generated by incident NIR light were injected directly into the conduction band of the anatase TiO₂ nanoclusters, inducing the reduction of oxygen to superoxide and finally producing hydroxyl radical species. Simultaneously, the LSPR-induced photothermal effect was investigated for combinational photothermal and photodynamic cancer therapy. Our work emphasizes the facile and mild fabrication of anatase TiO₂ decorated anisotropic plasmonic nanostructures, while expanding the promise of novel NIR-responsive nanostructures with remarkably superior efficiency for synergistic photo-induced cancer treatments.

SB03.05.07

Plasmon-Triggered Upconversion Luminescence and Hot Carrier Injection in Novel Au NR@TiO₂@UCNP Nanostructures—Mechanism and Application in Photothermal and Photodynamic Cancer Therapy Subin Yu¹, Dohyub Jang², Hong Yuan³, Wen-Tse Huang³, Minju Kim¹, Filipe Marques Mota¹, Ru Shi Liu³, Hyukjin Lee¹, Sehoon Kim² and Dong Ha Kim¹; ¹Ewha Woman's University, Korea (the Republic of); ²Korea Institute of Science and Technology, Korea (the Republic of); ³National Taiwan University, Taiwan

Lanthanide-doped upconversion nanoparticles (UCNP) have been attracted great attention with the unique ability to convert low-energy NIR radiation to high-energy UV-vis light in biomedical applications. UCNP additionally possesses unique properties, including good photostability with biological transparent excitation wavelength, tunable emission band, and low cytotoxicity. However, the UCNP showcases the intrinsic low quantum efficiency for practical applications as a result of insufficient absorption cross-section area and surface defects. To overcome this limitation, the incorporation of localized surface plasmon resonance (LSPR) has been suggested as a promising way. In this work, anatase titania-coated gold nanorods (Au NR@aTiO₂) were decorated with UCNP. aTiO₂ was integrated as a spacer between plasmonic Au NR and UCNP to avoid the quenching of UCL. Au NR and UCNP components showed characteristic absorbance in the NIR region, detailed characterization of the resulting core@shell nanostructures revealed enhanced UCNP-derived UV-vis emission due to the plasmonic properties of Au NR.¹ In presence of UCNP, the emitted UV light was proposed to excite the aTiO₂ semiconductor and play a key role in the generation of reactive oxygen species (ROS). In addition, emitted visible light from UCNP was re-absorbed

by Au NR which was well matched with the transverse absorption peak of Au NR to further generate the hot carriers. The resultant hot carriers could inject into the conduction band of aTiO_2 to further generate the ROS. LSPR-induced photo-thermal effect was also investigated by temperature-rise profile. *In vitro* and *in vivo* phototherapy effect was induced on U87MG (Glioblastoma astrocytoma). Interestingly, the overall therapeutic effects of our hybrid nanostructures were enhanced under laser irradiation, confirming the combinational photothermal and photodynamic effects. Thus, serving as a multifunctional phototherapy agent, the hybrid nanostructures herein introduced are suggested to be a valuable addition in deep-range noninvasive cancer phototherapy studies.

SB03.05.08

A Feasible Phenylboronic Acid-Based Delivery Platform of Anti-PD-L1 Antibody for Effective Cancer Immunotherapy [Junha Lim](#), Junseok Lee, Sungjin Jung and Won Jong Kim; Pohang University of Science and Technology (POSTECH), Korea (the Republic of)

The immune checkpoint blockade (ICB) for tumor therapy is promising in the clinic. Among some ICB drug, Anti-PD-L1 antibody (aPD-L1 antibody) blocks the overexpressed PD-L1 of the tumor cell membrane and enhance the antitumor effect of cytotoxic T cell. However, these antibody therapies still have several challenges of poor delivery efficiency and immune-related adverse events. Herein, we designed the delivery platform for systemic controlled release of aPD-L1 antibody. Through the formation of pH-responsive phenylboronic ester between PBA group on polymeric phenylboronic acid (pPBA) and diol on inherent glycosylation site of the antibody, a polymeric phenylboronic acid-antibody (pPBA-Ab) nanocomplex was prepared by simply mixing pPBA and antibody. As the basic key point of effective delivery, we focused on the property of antibody nanocomplex, which are protection from external attack and release at tumor lesion. In various *in vitro* assays, Our antibody nanocomplex protected antibody by shielding effect of polymer shell and released antibody from acidic pH which are known as hallmarks of tumor. Furthermore, antibody complex exhibited longer circulation and enhanced tumor accumulation *in vivo*, which led to a significant antitumor effect when compared to free antibody. Overall, we propose the potential of our antibody nanocomplex platform as a successful delivery system for a therapeutic application that improved antitumor immunity.

SB03.05.09

Novel CuInS₂ Quantum Dot-PDMS Nanocomposites for All-Optical Multimodality Imaging Semyon Bodian¹, Richard Colchester¹, Thomas J. Macdonald², Sunish J. Mathews¹, Edward Z. Zhang¹, Paul C. Beard¹, Ivan P. Parkin¹, Adrien Desjardins¹ and [Sacha Noimark](#)¹; ¹University College London, United Kingdom; ²Imperial College London, United Kingdom

Highly optically absorbing nanocomposites have broad versatility with applications ranging from solar cell technology to biomedical imaging. One area in which these nanocomposites have shown particular promise, is optical ultrasound generation. We report the development of CuInS₂ quantum dot (CIS QD)-polydimethylsiloxane (PDMS) nanocomposites with wavelength-selective optical absorption properties for all-optical multimodality imaging. Using bottom-up fabrication methods, micron-scale thickness CIS QD-PDMS nanocomposites were created on highly miniature optical fibre substrates. These nanocomposites were engineered to exhibit high optical absorption (> 90%) at 532 nm for optical ultrasound generation and high optical transmission (> 95%) at wavelengths greater than 700 nm, enabling other modalities such as photoacoustic imaging and spectroscopy.

Pulsed laser excitation light at 532 nm transmitted by the optical fibre was absorbed by the coating and ultrasound generation was achieved *via* the photoacoustic effect. These CIS QD-PDMS nanocomposites generated high ultrasound pressures of up to 3.7 MPa (laser fluence: 153.4 mJ/cm², distance: 1.5 mm) with corresponding -6 dB ultrasound bandwidths of 18 MHz. Using 532 nm and 1064 nm laser excitation sources for ultrasound and photoacoustic imaging respectively, a co-registered image of a carbon black ink-filled tube gel wax phantom was obtained with good correspondence between the ultrasound image and photoacoustic signals. Due to their wavelength-selective optical absorption properties, these high-performance fibre-based ultrasound transmitters show promise for diagnostic and therapeutic clinical applications such as the imaging of atherosclerotic plaques in coronary arteries, or use in photodynamic therapy for cancer treatment.

SESSION SB03.06: Transformative Nanostructures with Therapeutic and Diagnostic Modalities V

Session Chairs: Isabel Gessner and Sanjay Mathur

Monday Morning, December 6, 2021

SB03-Virtual

8:00 AM *SB03.06.01

Nanostructure of NIR-Excited Photo Dynamic Therapy for Killing Three Birds with One Stone Kohei Soga¹, Masakazu Umezawa¹, Kyohei Okubo¹, Masao Kamimura¹ and Hsin-Cheng Chiu²; ¹Tokyo University of Science, Japan; ²National Tsing Hua University, Taiwan

Photo dynamic therapy (PDT) is one of the important therapeutic methods for cancer treat especially for skin cancer. Currently, a sort of dye, such as chlorin e6, are used for generating singlet oxygen for killing cancer by irradiating visible light. However, the penetration depth of the visible excitation light is only limited to be less than a millimeter. We proposed to use near infrared (NIR) light for the excitation to penetrate into tissues with centimeter order depth. Upconversion (UC) luminescence is a specific phenomenon observable for the rare-earth ions in ceramic hosts to emit green and red visible light under NIR excitation. We had reported a nano-structure by combining the UC ceramic nano phosphors with red emission (660 nm) to generate singlet oxygen by exciting the chlorin e6 on the surface. Simultaneous emission of NIR luminescence (1550 nm) can be used for NIR fluorescence imaging for diagnosis. The structure can kill two birds with one stone [M. Kamimura et al., Chem. Lett. 2017, 46, 1076–1078(doi: 10.1246/cl.170322)]. Rose Bengal (RB) is another known dye for the PDT to be excited with green light. The UC nano phosphor can also be designed to emit 550-nm green light efficiently. Here, we designed a new nanostructure for using the RB for the NIR-excited PDT agent. Basically the position of the RB is important. The RB is known to have toxicity. If the RB is exposed to the surface of the structure, the toxicity cannot be avoided. We designed to form a nano micelle structure with hydrophobic core with PLGA and PEGylated hydrophilic shell. The RB was installed to the border position of the border of the PLGA core and PEG shell. For installing the RB at a proper position, C₁₈RB was used for sticking the C18 part to the hydrophobic core to locate the RB on the border. Singlet oxygen generation effectively killed cancer cells with 980-nm NIR excitation. As well, NIR imaging was successfully performed by observing 1550-nm luminescence. Also, the toxicity of the RB was effectively suppressed. Therapy, diagnosis and toxicity suppression are the three birds. One stone killed three birds [K. Tezuka et al., ACS Appl. Bio Matter, 2021, 4 4462-4469 (doi: 10.1021/acsbm.1c00213)]! The nanostructure for utilizing the merits of transparency of the NIR photonics [K. Soga et al. ed., "Transparency in Biology," Springer, 2021(doi: 10.1007/978-981-15-9627-8)] will be furthermore discussed.

8:30 AM *SB03.06.02

Multimodalities of Diamond Nanoparticles for Imaging and Drug Delivery in 3D Cellular Models Elena Perevedentseva^{1,2}, Y.-C. Lin¹, Z.-R. Lin¹, C.-

C Chang¹ and Chia-Liang Cheng¹; ¹National Dong Hwa University, Taiwan; ²Russian Academy of Sciences, Russian Federation

Nanoparticles (NP) exhibit some interesting bio-medical applications and the development are in high degree determined by new facilities opened by the NP's multifunctionalities. Among all developed nanoparticles, nanodiamond (ND) and ND-based hybrid complexes are promising due to their biocompatibility, variable sizes, structure, surface chemistry, and physical properties. Recent works have demonstrated exciting advantages of ND for theranostic applications, including bio imaging and drug delivery. ND's surface chemistry allows advanced methods of functionalization with the molecules of interest extending the applications, for example, ND enhanced drug delivery and efficiency has been observed, including effects on chemoresistant tumors and direct delivery across blood-brain barrier.

In this presentation, nanodiamond-gold core-shell (ND@Au) hybrid nanoparticles are synthesized combining properties and advantages of Si-doped nanodiamond and nanogold. It is shown that the ND@Au nanoparticles are biocompatible. NDs are demonstrated as imaging agent for Raman mapping, one-photon Fluorescence imaging, two-photon Fluorescence Lifetime Imaging, and high-resolution X-ray microscopy utilizing absorption properties of Au in the nanoshell. This demonstrated the synergistical effects of combining gold and nanodiamond render then useful markers in bio tracing and imaging. When drug molecules are conjugated onto ND, the composed ND-X complexes are demonstrated in a 3D cellular model (multicellular tumor spheroid, MCTS), consisted of large collection of cells in a three dimensional format extend about 0.7 mm in diameter; resemble the configuration of a tumor, ideal for evaluating the cytotoxicity and cytotoxicity mechanism of ND-drug complex and their efficacy. The drug molecules can be released in a pH dependent manner and enhanced drug efficacy can be achieved. Although this work presents only few examples, they demonstrate wide perspectives of development of NP with new synergy properties and of their use.

9:00 AM *SB03.06.04

Tailoring the Bioactivity of Inorganic Nanomaterials Inge K. Herrmann^{1,2}; ¹ETH Zurich, Switzerland; ²Empa-Swiss Federal Laboratories for Materials Science and Technology, Switzerland

The well-controlled synthesis of nanoscale materials is arguably one of the most important achievements of material science in the past decades. With the push to simplify biomedical material designs, inorganic nanomaterials have regained interest. Especially metal and metal oxide nanomaterials have attracted significant attention due to the scalability and robustness of their synthesis and their tailorable composition and architecture. While fascinating results have been achieved by loading inorganic nanoparticles with organic molecules, my presentation will focus on purely inorganic systems. In the first part, I will present an approach to unite tissue adhesion, based on nano-bridging, with bioactivity for wound healing applications. Uniting these properties requires control over nanoparticle architecture and freedom of choice in materials. Liquid-feed flame spray pyrolysis (LF-FSP) fulfills these requirements, while offering scalable and sterile synthesis. By utilizing the versatility of LF-FSP, we have united the wound closure properties of bioglass with the anti-inflammatory properties of ceria in one nanoparticle hybrid system. Careful selection of the bioglass composition and the hybrid architecture gives access to hard and soft tissue healing properties. In addition, by adjusting LF-FSP process parameters, we are able to control the oxidation state of the ceria, which governs anti-oxidative and anti-microbial properties of the hybrid. By tailoring the architecture of the hybrid nanoparticles, temporal control of the material bioactivities can be achieved in order to optimally address the different phases of the wound healing cascade. In the second part, I will show how LF-FSP gives access to ultra-small, near-monodisperse hafnium dioxide nanoparticles with excellent radio-enhancement properties. Such radio-enhancers can be employed to increase the x-ray absorption cross-section of tumor compared to healthy tissues. Direct benchmarking of the LF-FSP-made hafnia against gold nanoparticles, the current gold standard in the field, rationalizes their use based on their superior radio-enhancement performance. The competitive radio-enhancement properties for near-monodisperse nanoparticles produced by scalable and sterile flame spray synthesis offer a route to overcoming key roadblocks in the translation of nanoparticle-based radio-enhancers.

9:30 AM SB03.06.05

Polymeric Matrices for High-Resolution Dual-Mode MALDI MS and MS Imaging of Low Molecular Weight Compounds Franziska Lissel^{1,2}; ¹Leibniz Institute of Polymer Research, Germany; ²Dresden University of Technology, Germany

Matrices for matrix assisted laser desorption/ionization mass spectrometry (MALDI MS) is a standard tool to investigate high molecular weight (HMW) compounds, e.g. proteins and polymers. Small organic matrices (SOMs) generally consist of an aromatic ring to absorb the laser energy and transfer it to the HMW analyte, and an ionizing functional group to transfer charge. Now the MALDI analysis of low molecular weight (LMW) compounds is coming into focus [1], to use this fast and reliable method to e.g. trace metabolomic changes in tumor development. Here, SOMs are problematic as they give rise to noise in the LMW part of the spectrum (are not "MALDI-silent"), are generally not "dual mode" (i.e. supporting measurements in both ion modes) and in MALDI MS imaging (MSI), their uneven surface coverage limits spatial resolution.

We develop polymeric matrices to enable MALDI analytics of LMW compounds, thereby turning the initial MALDI MS concept of "small matrices – big analytes" on its head.

For conjugated polymers (CPs), the conjugated backbone translates into a strong optical absorption, alkyl side chains make the CPs solution-processable and allows to coat uniform thin films. We tested several CPs as matrices and found that they are MALDI silent in the full measurement range (>m/z= 150k) except at high laser intensities, when fragmentation of the solubilizing sidechains starts [2]. Most importantly, the CPs allow the analysis of noise-free analysis of LMW analytes. Also, the CPs are dual-mode matrices, and the analyte ionization ability is competitive to standard SOMs in both positive and negative mode. MALDI MSI experiments were carried out visualize morphologies of rat brain sections, and the uniform thin films allowed a spatial resolution of 10 nm, which is high for MSI and was limited by the resolution of the instrument. SEM analyses of the films indicates that using more advanced instruments, even higher resolutions are possible using CPs.

It is a general assumption that high crystallinity is a crucial prerequisite for MALDI matrices. Yet polymers are only capable of adopting a semi-crystalline morphology, i.e., forming crystalline and amorphous domains. The analytes are therefore expected to be incorporated in the crystalline domains, and efficiency is expected to depend on the polymer's degree of crystallinity. To explore this, we synthesized two fully amorphous NDI(T2) and fluorene copolymers carrying long and branches sidechains on both monomers [3]. Both turned out to be excellent MALDI silent dual-mode matrices, suggesting that in CP matrices analyte incorporation takes place in the amorphous phase.

Finally, the polymerization of high-performing SOMs can retain the advantageous properties of the SOM while increasing their vacuum stability and making them MALDI silent in the LMW area. The polymerized SOMs were used in MALDI MSI measurements of breast cancer xenografts, and showed excellent ion extraction abilities [4].

References:

- [1a] Calvano, Monopoli, Cataldi, Palmisano: *Anal. Bioanal. Chem.* **2018**, 410, 4015; [1b] Qiao, Lissel: *Chem. Asian J.* **2021**, doi:10.1002/asia.202100044.
- [2] Horatz, Giampa, Karpov, Sahre, Bednarz, Kiri, Voit, Niehaus, Hadjichristidis, Michels, Lissel: *J. Am. Chem. Soc.* **2018**, 140 (36), 11416.
- [3] Horatz, Ditte, Prenveille, Zhang, Jehnichen, Kiri, Voit, Lissel: *ChemPlusChem* **2019**, 84 (9), 1338.

SESSION SB03.07: Transformative Nanostructures with Therapeutic and Diagnostic Modalities VI
Session Chairs: Gerardo Goya and Inge Herrmann
Monday Morning, December 6, 2021
SB03-Virtual

10:30 AM *SB03.07.01

Multistage Signal-interactive Nanoparticles Improve Tumor Targeting Through Efficient Nanoparticle-Cell Communications [Hélder A. Santos](#)^{1,2}; ¹The University Medical Center Groningen, Netherlands; ²University of Helsinki, Finland

Communication between biological components is critical for homeostasis maintenance among the convergence of complicated bio-signals. For therapeutic nanoparticles (NPs), the general lack of effective communication mechanisms with the external cellular environment causes loss of homeostasis, resulting in deprived autonomy, severe macrophage-mediated clearance, and limited tumor accumulation. Here, we develop a multistage signal-interactive system on porous silicon particles through integrating the Self-peptide and Tyr-Ile-Gly-Ser-Arg (YIGSR) peptide into a hierarchical chimeric signaling interface with “don’t eat me” and “eat me” signals. This biochemical transceiver can act as both the signal receiver for amantadine to achieve NP transformation and signal conversion as well as the signal source to present different signals sequentially by reversible self-mimicking. Compared with the non-interactive controls, these signal-interactive NPs loaded with AS1411 and tanespimycin (17-AAG) as anticancer drugs improve tumor targeting 2.8-fold and tumor suppression 6.5-fold and showed only 51% accumulation in the liver with restricted hepatic injury. Here, we demonstrate that constructing a signal-interactive NP system improves NP-cell communication efficiency. Moreover, we show that the functional chimeric peptide design enables orderly integrating of multiple signal modules and the signal-interactive NPs reduce liver accumulation and promote tumor targeting in an animal cancer model.

11:00 AM SB03.07.02

Mesoporous NiO Electrodes for Enzymatic Electrochemical Sensing of Xanthine [Anuja Tripathi](#)^{1,2}, Natasha Singer², Anastasia L. Elias¹, Abebaw B. Jemere² and Kenneth D. Harris^{2,1}; ¹University of Alberta, Canada; ²National Research Council Canada, Nanotechnology Research Centre, Canada

The freshness of fish meat is the most important criterion in the pre-consumption quality control process. Complex microbiological processes lead to the loss of freshness and subsequent spoilage. Six hours after death, autolytic decomposition of adenosine triphosphate (ATP, the energy-storing molecule found in cells) leads to xanthine (XA) production. XA concentration increases with storage time, and thus it can be used as an indicator of fish freshness. Current analytical methods of XA determination that are based on chromatography, colorimetry, spectrophotometry or mass spectrometry are time consuming, expensive and require experienced operators. Electrochemical sensor platforms on the other hand are attractive due to their simple operation, low cost, low sample volume requirements, and speed of analysis. In recent years, enzyme-based electrochemical biosensors, employing xanthine oxidase (XO) for selective recognition and catalysis of XA, have become promising for XA determination in fish and meat samples because of their low detection limits, high selectivity and sensitivity.

The working electrode material is a key factor affecting the analytical performance of electrochemical biosensors, and integration of nanomaterials in the working electrode has previously improved sensor performance. Though carbon based nanomaterials, metal and metal oxide nanostructures that have favorable electrical properties and biocompatibility have been reported for enzymatic biosensor fabrication, mesoporous NiO electrodes are rarely used for electrochemical enzymatic detection of XA. Mesoporous NiO electrodes are ideal for electrochemical biosensor fabrication owing to their large surface area for enzyme immobilization, high isoelectric point, biocompatibility, chemical stability and fast electron transfer features. Moreover, NiO has a redox couple of its own (Ni³⁺/Ni²⁺), paving the way for reagentless biosensing. In this work, we fabricate mesoporous NiO electrodes to immobilize XO, and we demonstrate sensitive and selective amperometric determination of XA. Electrodes were formed using the glancing angle deposition (GLAD) technique, and the large surface area and internal porosity of the GLAD films should allow immobilization of large quantities of the XO enzyme, which combined with the excellent electrical properties of the GLAD electrode allowed amperometric detection of XA at +0.5 V vs Ag/AgCl with excellent sensitivity, detection limit and response time. The sensor was also used to measure XA in a fish sample.

Sensor fabrication and performance

Nanocolumnar and mesoporous NiO films (thickness ~500 nm) were deposited on ITO using GLAD. XO was physisorbed into the pores of activated GLAD NiO electrode by incubating in XO-loaded PBS buffer, pH 7.4. In brief, the NiO electrode was first electrochemically activated using 0.1 N NaOH for 25 cycles at 10 mV/s. 20 µl 0.18 U/mg XO was then immobilized in the activated NiO electrode for 4 hours at room temperature. The modification of the NiO GLAD film with XO was characterized by electrochemistry and FTIR techniques. XO catalyzes the oxidation of XA to uric acid and hydrogen peroxide (H₂O₂), and therefore, using an optimized measurement condition, current was monitored by applying +0.5 V vs Ag/AgCl to the electrode. This current was proportional to the concentration of XA. The amperometric sensor rendered a dynamic range of 60 nM to 3.5 µM, with a limit of detection of 2 nM, limit of quantitation of 6 nM and a sensitivity of 0.01 µA/nM. The sensor showed little interference from common fish sample matrices (such as glucose, uric acid, hypoxanthine) and the common fish preservative (sodium benzoate). The sensor could also be stored in buffer at 4°C for over a week without losing its performance.

11:15 AM *SB03.07.03

Carbon Dots—Multifunctional Nanomaterials for Bioimaging and Biosensing Applications [Rafik Naccache](#); Concordia University, Canada

In recent years, nanomaterials (defined as materials < 100 nm in a single dimension) have garnered significant interest for the development of novel applications in the physical and life sciences. This is especially true for luminescent nanoparticles, which have been investigated for the development of sensors, imaging and diagnostic probes. Recently, a relatively new class of luminescent nanomaterials, namely carbon dots, has come to light. Carbon dots, sometimes known as carbonogenic dots, are carbon, oxygen, nitrogen and hydrogen containing materials that are typically water dispersible and can be prepared from an abundant number of inexpensive sources including small molecules such as citric acid, amino acids and sugars. Of particular interest are their optical properties, which can be tailored via careful selection of the starting precursors and the desired synthesis route resulting in the ability to generate fluorescence from the blue to the near infrared regions of the spectrum. In addition to their versatile optical properties, these carbon dots are generally known to have low cytotoxicity and good biocompatibility. Combined with their small size and versatile optical properties, developing carbon dots as a nanoplatform can be achieved as these nanodots lend themselves for integration in a myriad of applications most notably in bio-imaging, sensing and drug delivery, among others. Our work focuses on achieving a fundamental understanding of the synthesis of these carbon dots in order to control their size and achieve homogenous surface chemistry and optical properties. We can also endow them with chirality during synthesis opening up novel avenues for chiral sensing applications. As they are fluorescent, we have investigated their development as bimodal imaging probes for optical and magnetic

resonance imaging applications. We have also exploited their temperature and pH dependent optical properties in order develop novel tools that can be used for intracellular sensing applications.

11:45 AM *SB03.07.04

Dual Action Chemo-Radio Labeled Targeted Nanocarriers with High Efficacy Against Triple Negative Breast Cancer Shaista Ilyas¹, Annika Szymura¹, Sabri Sahnoun², Pardes Habib³, Felix Mottaghy² and Sanjay Mathur¹; ¹Institute of Inorganic and Materials Chemistry, University of Cologne, Germany; ²Department of Nuclear Medicine, University Hospital RWTH Aachen, Germany; ³Department of Neurology, RWTH Aachen University, Germany

The therapeutic index of established nuclear medicine procedures for an aggressive type of cancer such as triple negative breast cancer, (TNBC, lacking estrogen, progesterone receptors, and excess HER2 protein) is typically low due to the lack of targeted therapies and limited stability of radiolabeled carrier molecules in physiological environment. In this study, we developed a potential dual-purpose therapeutic nanocarrier (mesoporous silica particles) by integrating complementary functionalities (folate ligand, DOTA chelator) and payloads (doxorubicine, radionuclides ⁶⁸Ga/¹⁷⁷Lu) into one nanocarrier through covalent conjugation strategies. The nanocarriers, [⁶⁸Ga]Ga-DOTA-FA and [¹⁷⁷Lu]Lu-DOTA-FA demonstrated an outstanding radiochemical yield of > 98 % showing successful incorporation of radionuclides to DOTA cavity. Moreover, radiolabeled nanocarrier exhibited excellent stability in PBS and human serum during 3 h (⁶⁸Ga) and 120 h (¹⁷⁷Lu). In addition, the labeled FA-DOTA@mSiO₂ exhibited a favorable partition coefficient (log P) of -3.29 ± 0.08, suggesting highly hydrophilic carriers. *In vitro* studies using 3 different TNBC cell lines with FA-DOTA@mSiO₂ carriers demonstrated a significant cell internalization suggesting specific targeting of folate receptor in TNBC cells. Interestingly, FA-capped nanocarrier revealed a significant time dependent cell uptake after labeling with ¹⁷⁷Lu in SUM149PT (33 %) MDA-MB-231 (9%), BT20 (28%) compared to nanocarrier without FA. In Annexin-V based apoptosis studies, combined delivery of ¹⁷⁷Lu radiations and DOX induced significant cell death to TNBC cells earlier at different time points. *In ovo* studies using fertilized chicken eggs, exhibited higher uptake of dual-purposed nanocarriers (PET imaging). Our data suggests that dual functions nanocarriers has great potential in delivering radiation and drug doses for TNBC tumor treatment and highlight further studies to evaluate its preclinical therapeutic efficacy.

SESSION SB03.08: Transformative Nanostructures with Therapeutic and Diagnostic Modalities VII

Session Chair: Hélder Santos

Monday Afternoon, December 6, 2021

SB03-Virtual

1:00 PM SB03.08.02

Formation and Stability of Dendronized Vesicles Akash Banerjee¹, Acacia Tam² and Meenakshi Dutt¹; ¹Rutgers, The State University of New Jersey, United States; ²Cornell University, United States

Nanoparticles that block fundamental bacterial functions like quorum sensing could potentially replace conventional antibiotic therapies. Vesicles that bind interfacially to charged biomolecules could be used to block these quorum sensing pathways. Towards this goal, dendronized vesicles (DVs) consisting of polyamidoamine dendron-grafted amphiphiles (PDAs) and dipalmitoyl-sn-glycero-3-phosphocholine lipids are investigated. The molecular dynamics simulation technique in conjunction with an explicit solvent coarse-grained force field is employed. The key physical factors responsible for the stability of DVs as a function of the dendron generation and relative concentration are identified. The threshold concentration of each dendron generation that yields stable DVs is determined. Lower dendron generations rupture the DVs at high relative concentrations due to the electrostatic repulsions between the terminally protonated amines. Whereas, intermediate dendron generations demonstrate a mushroom-to-brush transition. Such conformational changes in the dendrons expand the outer DV surface, resulting in instability in the DV bilayer. DVs encompassing dendrons with higher generations incur stresses on the bilayer due to their high charge density and spontaneous curvature. Minimization of asymmetric stresses across the bilayer are understood by studying the self-organization of PDAs on the DV surface. A conducive set of conditions is determined for the formation of a single cluster of PDAs that decorates the DV surface like a mesh. Results from this study can potentially guide the design and synthesis of nanoparticles which target quorum sensing pathways in bacteria. Beyond applications in prevention of bacterial infections, these nanoparticles can be used in diverse applications, e.g. biomedicine, energy or bioelectronics, that require synthetic dendronized cells or the adsorption and transport of charged species.

1:15 PM *SB03.08.03

Combinatorial Immunotherapies and Treatment Response to Immunotherapies with Nanoscale Probes Rizia Bardhan^{1,2}; ¹Iowa State University, United States; ²Nanovaccine Institute, United States

Immunotherapies have driven a paradigm shift in the landscape of cancer treatment and currently many immune active drugs are in FDA trial for cancer therapies. Yet, the distribution of many of these drugs remains low in the tumor due to rapid *in vivo* degradation or low accumulation. Further, which patients are good candidates for immunotherapies remains a challenge incurring high costs of unsuccessful therapies and unnecessary side effects. In this talk I will show the utility of inorganic nanoprobess (gold nanostars) designed in my lab for rapid and noninvasive detection of multiple immunomarkers of cancer to enable patient selection for immunotherapies, as well as response to treatment after immunotherapy. We combined a clinical and pre-clinical imaging technique, positron emission tomography with surface-enhanced Raman spectroscopy (ImmunoPET-SERS) *in vivo* by labeling gold nanostars with radiolabels, Raman reporter molecules, and targeting antibodies. Multimodal ImmunoPET-SERS seamlessly integrates depth-resolved whole-body imaging and high sensitivity of PET with high spatiotemporal resolution and multiplexing of SERS providing dynamic immunomarkers profiling *in vivo*. ImmunoPET-SERS was used to determine the immunomarker status of mice treated with combinatorial immunotherapy; we demonstrated real-time feedback of CD8+ infiltration and PD-L1 status in tumors which was confirmed with IHC *ex vivo*. We are also tracking both CD8+ T cells and Natural Killer (NK) cells *in vivo* to examine response to immunotherapies. I will also show the utility of organic nanoprobess (liposomes) for highly effective combinatorial immunotherapies integrating mild hyperthermia and hypoxic drugs with immune checkpoint blockade for enhanced treatment outcome in aggressive breast tumors. In summary, my talk will show nanoscale probes can be engineered to have multifunctional properties from therapeutic response to monitoring treatment efficacy *in vivo*.

1:45 PM SB03.08.04

Domain Aggregation and Associated Pore Growth in Lipid Membranes Yue Liu^{1,2}, Guijin Zou³ and Huajian Gao^{1,3,4}; ¹Brown University, United States; ²University of Michigan, United States; ³Institute of High Performance Computing, Singapore; ⁴Nanyang Technological University, Singapore

Recent experiments have shown that certain molecular nano-agents can selectively penetrate and aggregate in bacterial lipid membranes, leading to their

permeability and rupture, and as such can effectively address the looming crisis on antimicrobial resistance by killing bacteria even in their dormant state - the so-called “persisters”. So far, the discovery of these agents is still mainly restricted to empirical screening with limited physical understanding. To help reveal and understand the underlying mechanisms, here we establish a theory to show that the deformation energy of the membrane tends to limit the growth of molecular domains on a lipid membrane, resulting in a characteristic domain size, and that the domain aggregation significantly reduces the energy barrier to pore growth. Coarse-grained molecular dynamics simulations are performed to validate such domain aggregation and associated pore formation. This study sheds light on how lipid membranes can be damaged through molecular domain aggregation and contributes to establish a theoretical foundation for the next-generation membrane-targeting nanomedicine to effectively target bacteria with high antimicrobial resistance against conventional antibiotics.

SESSION SB03.09: Transformative Nanostructures with Therapeutic Diagnostic Modalities VIII
Session Chair: Eva Hemmer
Monday Afternoon, December 6, 2021
SB03-Virtual

4:00 PM *SB03.09.01

Beyond Cryo-Microscopy—Current-Controlled Transmission Electron Microscopy for Beam-Sensitive Material Imaging [Petra D. Specht](#)¹ and [Christian Kisielowski](#)²; ¹University of California, Berkeley, United States; ²Lawrence Berkeley National Laboratory, United States

Since the DoE funded TEAM project ended in the United States with the development of spherical and chromatic aberration correction in 2009 single atom sensitivity is established for transmission electron microscopy (TEM) imaging. Theoretically, every material could be imaged in full atomic resolution, and every atom could be resolved within all material structures. In an experimental setup, however, electron beam sensitivity of a given material determines which original structures can be resolved in reality. Therefore, our focus in the last decade has been on minimizing electron beam induced material damage, and to find alternative ways to image beam sensitive materials without altering its original structure. At least, if a material is altered under the electron beam the dynamics of this behavior should be recorded, too. Such dynamic considerations led to the development of current-controlled TEM.

Low dose rate and pulsed electron beams were applied to image pristine properties of MgCl₂, a Ziegler-Natta catalyst which is both air and electron beam sensitive. The particular choice of pulse and delay times allowed to mitigate damage caused by phonon accumulation. The total electron dose can be extended more than ten times before material alterations set in. Changing electron currents while imaging polymers or various catalytic nano-crystals by varying dose rates and / or the irradiated areas had similar effects. Using direct electron detectors facilitated those experiments, and allowed for the use of ultra-low currents where single electrons are delivered to interact with the material under investigation. We find that the beam current limits material alterations in the ultra-low current regime rather than the deposition of electron charge.

With the application of current-controlled TEM the onset of material changes is found to be generally delayed. The experimental setup may be used in combination with cryo-microscopy, and could further postpone material alterations, even in soft materials.

Work at the Molecular Foundry was supported by the Office of Science, Office of Basic Energy Sciences, of the U.S. Department of Energy under Contract No. DE-AC02-05CH11231.

4:30 PM *SB03.09.02

Plasmon-Mediated Optical Biosensing and Photodynamic Therapy [Nianqiang Wu](#); University of Massachusetts Amherst, United States

Surface plasmon resonance (SPR) is characteristic of strong light harvesting, enhanced localized electromagnetic field and tunable energy donation. As a result, SPR has a great potential in biosensing, drug delivery and theranostics. In this work, SPR has been used to develop new fluorescence and surface-enhanced Raman scattering (SERS) sensors. In particular, SPR enables sensitive detection of analytes in human fluidic samples in the biological transparency window in the near-infrared spectral range. In addition, SPR can be incorporated with inorganic semiconductors to create new stable agents for photodynamic therapy.

5:00 PM SB03.09.03

Intracellular Trafficking Study and Rapid Purification of Lysosomes Using Magnetic Plasmonic Nanoparticles [The Son Le](#)¹, [Mari Takahashi](#)¹, [Yuichi Hiratsuka](#)¹, [Kazuaki Matsumura](#)¹, [Tomohiko Taguchi](#)² and [Shinya Maenosono](#)¹; ¹Japan Advanced Institute of Science and Technology, Japan; ²Tohoku University, Japan

The rapid and efficient purification of lysosomes is the key to uncover the mechanistic insights of lysosomal activity using proteomics analysis. The traditional method for isolating lysosomes such as the density-gradient ultracentrifugation technique often takes a long time and the intact structure of lysosomes is not preserved.^[1] Therefore, it may lead to a change of protein composition in labile lysosomes as well as detach and/or denature of membrane proteins on it. Recently, the nanoparticle-based fractionation method which uses superparamagnetic iron oxide nanoparticles (SPIONs) for targeting lysosomes through the endocytosis pathway has been used for the isolation of lysosomes to identify disease-related alternation in protein composition.^[2] The versatility of SPIONs together with the quick and gentle nature of magnetic isolation are advantages of this technique. However, to obtain a highly-purified lysosomal fraction with high yield, it is important to determine the appropriate timing for performing magnetic separation, since the time-dependent localization of SPIONs in different organelles (*i.e.* early endosome, late endosome, and lysosome) depends on cell type, loading condition, incubation time, *etc.* To screen localization of SPIONs in a large number of cells, they are often labeled with the fluorescent dye to be monitored by fluorescent microscopy. However, besides the photobleaching problem, dye labeling of nanoparticles could have dye-leaking or influence on nanoparticle uptakes.^[3] Therefore, to further sophisticate the SPIONs-based isolation technique, it has been demanded to develop a new type of magnetic probes with intrinsic imaging capability to both precisely visualize the intracellular transport and quickly obtain high purified isolation fraction. Herein, to satisfy those requirements, we have developed magnetic-plasmonic Ag/FeCo/Ag core/shell/shell nanoparticles (MPNPs) for lysosome isolation. Since dextran has been well-known as a fluid phase cargo, which is internalized *via* pinocytosis rather than receptor-mediated endocytosis and eventually delivered to lysosomes. In this study, the MPNPs were encapsulated in phospholipid micelles followed by conjugation with amino dextran (aDxt). The hydrodynamic size of aDxt-conjugated MPNPs (aDxt-MPNPs) was ~50 nm at pH in the range of 4-10, which is suitable for efficient cellular uptake through various pathways. Owing to plasmonic property, the intracellular trafficking of aDxt-MPNPs could be simply visualized by confocal laser scanning microscopy (CLSM). After determining the intracellular fate of aDxt-MPNPs, lysosomes were quickly isolated using a MACS separator (Miltenyi Biotec). The purity and the intactness of the lysosome fraction were confirmed by western blot and CLSM images. Furthermore, we will discuss

the influence of the elapsed time from homogenization to the magnetic separation on the protein composition in lysosomes.

References:

- B. D. Beaumelle *et al.*, *J. Cell. Biol.* **111**, 1811-1823 (1990).
A. K. Tharkeshwar *et al.*, *Sci. Rep.* **7**, 41408 (2017).
S. Snipstad *et al.*, *Cytometry A* **91**, 760-766 (2017).

5:15 PM SB03.09.04

Nano-Analytical Characterization of Metal-Organic-Framework Biotransformation [Anna Neuer](#)^{1,2}, Alexander Gogos², Alexandre Anthis^{1,2} and Inge K. Herrmann^{1,2}; ¹ETH Zurich, Switzerland; ²Empa-Swiss Federal Laboratories for Materials Science and Technology, Switzerland

In biomedical research, metal-organic-frameworks (MOF) have attracted increasing interest over the past decade. MOFs hold promises as drug delivery agents, radioenhancers and application in theranostic and personalized medicine. Zeolite-imidazole-framework-8 nanoparticles (ZIF-8) are amongst the most extensively studied MOFs featuring anti-inflammatory and anti-microbial properties when doped with ceria.^{1,2} Alternatively, hafnium-based MOFs have been shown to enhance radiation therapy damage in tumor cells via reactive oxygen species creation.³ However, clinical translation for such novel materials remains challenging and tight control over nanomaterial chemistry during nanomedical life-cycle is needed. While stability and dissolution have been studied in the past for several MOFs, a detailed understanding of the intracellular behaviour and potential phase-transformation and/or generation of secondary nanomaterials is missing. Compared to their metal oxide counterparts, MOFs typically exhibit higher instability, making them prone to degradation/biotransformation. For biomedical applications, the fate of these new materials is, next to efficacy and toxicity, a major determinant of clinical success.

To overcome the gap between material engineering and medical application, and enable more rationalized safe-by-design material development, we investigated the environment-dependent biochemical-transformation of different nano-particulate MOFs containing essential (Zn, Fe) and non-essential (Hf, Ce) metal ions in physiologically relevant liquids and *in-vitro* systems. We present biotransformation kinetics of a biomedically relevant set of MOFs, including findings of particle transformation with changes in elemental distribution and morphological appearance with potential formation of nanomaterial from degradation products. Taken together, our nano-analytical characterization approach offers a route to follow the biological fate of MOF-based nanomedicines.

References

- [1] Feng S, Zhang X, Shi D, Wang Z. *Front Chem Sci Eng.* 15 (2020) 221; [2] Li X, Qi M, Li C, et al. *J Mater Chem B.* 44 (2019) 6955; [3] Ni K, Lan G, Chan C, et al. *Nat Commun.* 1 (2018) 2351

5:30 PM SB03.09.05

An Interdisciplinary Approach to Biosensors to Meet the Market Need for Faster Diagnosis in Health Care [Laure Abensur Vuillaume](#)¹, Thierry Leichle^{1,2}, Mathieu Grajoszex³, Marie-Pia d'Ortho³, Paul Voss^{1,4}, Jean-Paul Salvestrini^{1,5} and Abdallah Ougazzaden^{1,4}; ¹IRL 2958 GeorgiaTech CNRS, France; ²LAAS-CNRS, Université de Toulouse, France; ³DMH – APHP and Université de Paris, France; ⁴Georgia Institute of Technology, School of Electrical and Computer Engineering, United States; ⁵Georgia Tech Lorraine, France

To improve the efficiency of current medical practices, more significant data from technology is needed. One lever to optimize medical decision time is to shorten the delay from biological test to results. In the field of fast biological tests, biosensors have received increasing attention over the last decades and several technologies have been developed to deliver portable, cheap and sensitive analytical systems. Nevertheless, two main obstacles prevent the marketing of these biosensors: 1) an accurate analysis of the market in terms of real needs for medical practices and 2) perfect matching with current medical recommendations. We identify several obstacles that prevent the marketing of biosensors today: 1/ prior precise study of the market (needs for medical practices that fit perfectly into the current recommendations); 2/ technological realization that can meet this need; 3/ Knowledge of standards and validation and calibration procedures. Our study is divided into 5 phases: 1/ Determination of the use case(s) and the biomarkers of interest with an international opinion survey of physicians from all specialties; 2/ Design of a laboratory prototype; 3/ Manufacturing of a more advanced prototype suitable for the first steps of clinical validation phase; 4/ Interconnection with artificial intelligence and biological gold standard; 5/ Multicentric study for validation as a medical device. For this purpose, we have assembled an interdisciplinary team with medical doctors, engineers, and experts on market validation with the goal of identifying the most promising use cases in human medicine and creation of the most suitable biosensors anchored in medical practices. In this work, we first determine the use case(s) and the biomarkers of interest through an international opinion survey conducted among physicians from a broad range of specialties. We distributed a questionnaire via our networks and professional social networks for a voluntary survey of physicians about existing needs for rapid biological diagnosis and what this might change in their daily practice. More than 200 physicians from 10 different countries and 19 different medical specialty responded to our survey. 48,5% of participants think that it would save medical time (fluidity in the hospital environment, saving time in ambulatory care), 55,5% think it could improve their medical practice (guide a course of action, help a therapeutic decision, avoid unnecessary treatment) and 31,5% think that this could lead to faster and easier patient referrals.

As a result, the main biomarkers of interest identified by our panel are troponin (50%), PCR (30,5%), d-dimères (26,5%), BNP or NT-proBNP (12,5%), and respiratory viruses (9,5%).

Our study is based on the creation of biosensors, in a trans and interdisciplinary manner, so that they can be perfectly integrated into daily medical practice and respect all the issues at stake, in terms of diagnostic sensitivity, cost/efficiency and service to the patient. The biosensors are based on AlGaIn/GaN High Electron Mobility Transistors (HEMTs). GaN-based HEMTs have demonstrated high sensitivity as detectors, sensors and biosensors and have the advantage of extreme chemical stability and are biocompatible. Furthermore, the basic technology is widely commercialized and mature, making for rapid industrial upscaling.

In this presentation, we will describe the interest of the various biomarkers that were identified in our study and we will compare medical practices, literature, recommendations of good practices and technological possibilities, in order to define the best use case for biosensors.

This study is of importance in terms of future public health, making it possible to provide the medical community and the patient with one or more relevant tools for the fluidity of care.

6:30 PM SB03.10.01

Engineering Nano-Architected Surfaces to Steer Soft and Hard Tissue Interactions on Tissue Level Dental Implants [Judith Ng](#)^{1,2}, Martin Tobias Matter¹, Kerda Keevend¹, Stefanie Guimond², Markus Rottmar² and Inge K. Herrmann^{1,2}; ¹ETH Zurich, Switzerland; ²Empa–Swiss Federal Laboratories for Materials Science and Technology, Switzerland

Dental implant failures arise from poor integration of the implant with surrounding soft and hard tissues. Osseointegration and periosteal integration are crucial to their prevention. A persistent challenge is the inconsistency between tissue surrounding an implant and natural periodontal tissue around natural teeth. This increases vulnerability to peri-implant diseases, affecting soft and hard tissue integration and highlighting the need for implants with improved osseointegration and periosteal integration potential. Implant surface nanostructures promote osseointegration; however, designs which improve the soft tissue response have yet to be identified. We present novel nanoparticle coatings applied to surfaces in a single step technique driven by liquid-feed flame spray pyrolysis, which uniquely permits the construction of bespoke nanoparticle architectures from a breadth of inorganic precursors. This highly scalable technique has the potential to create multi-layer nanostructures of differing thicknesses, diverse patterns, and pore sizes – qualities as diverse as the inorganic building blocks of which these nanoparticle layers are composed. Novel nanoparticle-based coatings with bioactive inorganic architectures can enhance osseointegration, reduce the inflammatory response, and possess exemplary process versatility and stability, permitting precise control over the synthesis process, and so too, evaluation of the concomitant soft tissue bioresponse.

6:35 PM SB03.10.02

Late News: Facile Fabrication of Silk Protein for a Versatile Drug Carrier [Anh T. Dao](#), Farsai Taemaitree, Motohumi Nakamura, Ryuju Suzuki, Yoshitaka Koseki and Hitoshi Kasai; Tohoku University, Japan

Drug delivery technologies have been quickly innovated in the last few decades, especially in aspect of combination with nanotechnology to advance into multifunctional drug carriers, which can accomplish targeting a tumor, delivering therapeutic molecules, imaging and monitoring drug response. Many models were built and tested; still the challenge is at the choice of the appropriate materials and the facilitation of carrier preparation to achieve both safety and efficacy. Reflecting such needs, silk protein was chosen to provide a biodegradable and biocompatible matrix for carrying drug molecules. Such system with controllable structures and compositions can be an advanced type of drug carriers and further contribute to the improvement of cancer therapy. Silk protein originated from *Bombyx mori* silkworm was dissolved in various types of aqueous solution, including LiBr [1], CaCl₂/Ethanol [2], and formic acid solutions. In this research, the fabrication of silk NPs from the obtained silk protein solution was carefully monitored to achieve various morphologies and structures, through the reprecipitation method. Silk NPs were obtained in narrow size distribution, with the average diameter can be tuned from 10 to 100 nm. The surface charges of as-synthesized silk nanoparticles can be either negative or positive, depending on preparation conditions, brings out the possibility of loading different types of drugs. The obtained silk NPs showed good drug uptakes, adequate stability in aqueous and almost no toxicity at cellular level. The research also provides a NP library with diverse structures and properties, which can be used to manipulate the drug delivery performance. The results are discussed in terms of UV-Vis, DLS, XRD, TEM, XPS, and CLSM.

[Acknowledgement] This work was supported by JSPS KAKENHI for Early-Career Scientists Grant Number JP19K15388.

[References] [1] A. Matsumoto J. Phys. Chem. B **110** (2006) 21630; [2] Anh T.N. Dao et al. Polym. Degrad. Stab. **153** (2018) 37.

6:40 PM SB03.10.03

Study of the Interaction of Human Serum Albumin with β -Cyclodextrin Modified Gallium Oxide Nanoparticles Using Fluorescence Spectroscopy [Nitza Falc3n-Cruz](#) and Rolando Oyola-Mart3nez; University of Puerto Rico-Humacao, United States

Gallium oxide nanoparticles (GaO-(OH)) have been proposed for biomedical applications such as diagnostics and therapeutic approaches, like cancer treatments. Understanding its interaction with biological components, like proteins, is an important factor for the development of new nanomaterials. Gallium oxide nanoparticles conjugated with β -cyclodextrin (GaO-CD) were synthesized using a wet-chemical route, characterized by molecular spectroscopic and imaging techniques, and further used to probe equilibrium interactions with human serum albumin (HSA). In this work, we have used the sensitivity of the single tryptophan (Trp) fluorescence of HSA to monitor the interaction between GaO-CD and the protein at different temperatures. The binding and quenching constants were determined using Stern-Volmer analysis. Also, the thermal stability of the complex was followed by fluorescence spectroscopy using a simple two-state model. A weak interaction of HSA with GaO-CD, relative to other nanomaterials, like gold nanoparticles, was observed. In addition, results show no change in temperature of unfolding (T_m) of the protein, implying that GaO-CD does not affect HSA tertiary structure.

SESSION SB03.11: Transformative Nanostructures with Therapeutic and Diagnostic Modalities IX

Session Chairs: Jennifer Dionne and Rafik Naccache

Tuesday Afternoon, December 7, 2021

SB03-Virtual

1:00 PM *SB03.11.01

Rare-Earth-Based Nanoparticles—From Microwave-Assisted Synthesis to Multimodal Bioprobes [Eva Hemmer](#); University of Ottawa, Canada

The remarkable optomagnetic properties of the rare-earths (RE) make RE-based materials ideal for biomedical applications, including diagnostic (e.g., imaging, nanothermometry) and therapeutic (e.g., drug delivery, photodynamic therapy) approaches. This is due the unique electronic properties of the f-elements allowing for upconversion and near-infrared emission under near-infrared excitation as well as high magnetic moments. Yet, challenges remain; low emission intensity and efficiency of small nanoparticles (NPs), and reliable, fast synthesis routes. As material chemists, we tackle these challenges with new designs of RE-NPs by chemically controlled synthesis, application-oriented surface chemistry, and understanding of structure-property-relationships. Sodium rare-earth fluorides (NaREF₄) are our favorite materials, and we developed a fast and reliable microwave-assisted synthesis approach allowing crystalline phase and size control in the sub 15nm realm. Such control is crucial for the understanding of fundamental structure-property relationships and to optimize their optical and magnetic properties, when aiming for the design of next-generation optical probes or contrast agents for magnetic resonance imaging. For instance, NaGdF₄ NPs are gaining interest as alternative MRI contrast agent, while co-doping with RE³⁺ ions renders them excellent candidates for photoluminescent optical probes. The hexagonal crystalline phase of NaGdF₄ is known as the more efficient host material for upconversion emission, yet interestingly, it was found that its cubic counterpart shows superior performance as MRI contrast agent. Having a fast and reliable synthesis route towards NaREF₄ NPs on hand, we now explore various nanoparticle architectures and compositions with

the goal to optimize their optomagnetic properties, ultimately resulting in the design of biocompatible multimodal bioprobes.

This presentation will shed light on recent results and remaining challenges in the field of RE-based nanostructures with respect to their microwave-assisted synthesis as well as structural and optomagnetic properties, seeking biomedical application, while also touching on hyperspectral imaging as an emerging analytical tool offering spatio-spectral information about RE-based materials.

1:30 PM SB03.11.02

Tuning the In-Plane Anisotropy of CoFeB Films for Disk-Shaped Nanoparticles for Biomedical Applications Subas Scheibler^{1,2}, Oguz Yildirim², Mihai Gabureac², Inge K. Herrmann¹ and Hans J. Hug²; ¹ETH Zürich, Switzerland; ²Empa-Swiss Federal Laboratories for Materials Science and Technology, Switzerland

Magnetic separation offers an elegant and efficient route to selectively capture and remove specific compounds from blood (or other body fluids), which are inaccessible to current blood cleansing technologies, such as dialysis and hemosorption [1]. However, currently available superparamagnetic iron oxide nanoparticles (SPIONs) impose significant performance limits arising from their physical properties. Their low saturation magnetization coming from their oxidic nature results in a poor magnetic response, which severely limits performance.

The development of disk-shaped nanoparticles fabricated by lithographic methods and thin film deposition enables a precise control of size, geometry, material composition and magnetic properties such as interlayer exchange coupling and magnetic anisotropies.

In this work, we develop magnetic thin film systems for synthetic antiferromagnetic (SAF) coupled disk shaped particles with tunable in-plane anisotropies. The antiferromagnetic coupling is obtained by the stray field interaction of the two ferromagnetic layers. These SAF particles are designed to show zero net-magnetization in absence of a magnetic field – hence allowing perfect colloidal stability. Upon application of a magnetic field overcoming the antiferromagnetic coupling, a high net-magnetization can then be obtained, which translates into a large magnetic moment and magnetic force, acting on the particles in a gradient field allowing efficient capturing.

In order to synthesize such synthetic antiferromagnets, we evaluated strategies to obtain the required magnetic anisotropies. We report results obtained by deposition of soft magnetic CoFeB layers on Ta seed layers grown by oblique sputtering and compare the resulting anisotropies to those obtained by deposition of the magnetic layer in an applied field. Moreover, for the CoFeB layers on the oblique-sputtered seeds we compare the anisotropies obtained for different CoFeB-thicknesses to distinguish between a surface or interface induced anisotropy or a bulk anisotropy term. While with oblique sputtering, a wide range of in-plane anisotropies can be achieved (2kJ/m³ – 25kJ/m³), the anisotropy remains much smaller when CoFeB films are deposited in field (1.35kJ/m³).

Our work shows that in-plane anisotropies in magnetically soft systems can be tuned over a wide range by oblique seed-layer depositions or in-field depositions. These thin film systems open up the path for a new kind of magnetic disk shaped nanoparticles for prospective use in magnetic blood purification.

[1] Anthis AHC, Matter MT, Keevend K, Gerken LRH, Scheiber S, Doswald S, Gogos A, Herrmann IK, Tailoring the Colloidal Stability, Magnetic Separability, and Cytocompatibility of High-Capacity Magnetic Anion Exchangers, ACS Applied Materials and Interfaces, 2019.

1:45 PM SB03.11.03

Self-Organization of Iron Sulfide Nanoparticles into Multi-Compartment Supraparticles as Artificial Viruses for DNA Delivery Emine S. Turali-Emre, Ahmet Emre, Kadiyala Usha, Scott J. VanEpps and Nicholas Kotov; University of Michigan, United States

Gene and gene editing therapies have been widely investigated for the treatment of inherited or acquired genetic diseases. Efficient delivery of therapeutic agents has become a significant barrier in clinical applications due to the toxicity and instability of the vectors in the complex intracellular environment. Among non-viral vectors, individual inorganic nanoparticles (NPs) have become a popular strategy for nucleic acid delivery. However, the nanoshell geometry of viruses that creates a compartment to protect the cargo from its environment is still advantageous. Recreation of these compartments' formation has both technological and fundamental importance. In this study, we show that L-cysteine stabilized iron sulfide NPs can self-assemble into multi-compartment supraparticles (SPs) with nanoshell geometry. The transmission electron microscopy results showed that constituent NPs initially form ~55nm cup-like structures and then mature into positively charged ~75nm SPs with ca. 190 interconnected compartments. The results of selected area electron diffraction and energy dispersive X-ray spectroscopy confirm SPs are formed from FeS₂ and Fe₂O₃ NPs. Elemental mapping showed that Fe₂O₃ NPs are located on the surface of the SP and protecting FeS₂ and compartments from the surroundings. DNA was loaded in the compartments during the formation of supraparticles. We tested these complexes in circular dichroism, UV-Vis spectroscopy, electrophoretic mobility shift, and protection assays. Our results show successful DNA encapsulation in compartments. These pDNA-SP complex protect DNA against degradation, penetrate through cellular membranes and facilitate endolysosomal escape. Therefore, the development of these particles can be used as an effective cargo delivery tool for gene and gene-editing therapies.

2:00 PM SB03.11.04

Mixed-Halide Nanocrystals—From NIR-to-Vis Upconverters to Luminescent Thermometers Federico A. Rabuffetti; Wayne State University, United States

Bulk mixed halides constitute an important class of optical materials used as detection and storage phosphors in medicine. However, the potential of their nanocrystalline counterparts in biophotonic applications such as imaging and sensing is largely unexplored. In this talk I will highlight the potential of mixed-halide nanocrystals as luminescent thermometers capable of operating in a broad temperature range, from cryogenic to physiological temperatures. First, I will describe the chemistry that enables the synthesis of size- and shape-controlled mixed-halide nanocrystals with sizes ranging from 20 to 100 nm. Then, I will show how controlled amounts of rare-earth ions may be incorporated into these nanocrystals to generate a family of color-tunable NIR-to-visible upconverters. Finally, I will demonstrate that rare-earth-doped mixed halide nanocrystals serve as optical temperature sensors in the 100–400 K range. These luminescent thermometers can be excited within the first biological window.

SESSION SB03.12: On-Demand
Sunday Morning, December 5, 2021
On-Demand

8:00 AM SB03.02.03

Late News: Design of Theranostic Nanocomplex for Drug Delivery and Photodynamic Therapy Against HER2+ Breast Cancer Elder De la Rosa¹, Gonzalo Ramirez², Sandeep Panikar³, Tanya Camacho⁴ and Pedro Salas²; ¹Universidad De La Salle Bajio, Mexico; ²CFATA-UNAM, Mexico; ³UNAM,

Mexico; ⁴CIATEJ, Mexico

Design of theranostic nanocomplex has gained a lot of attention because its capability for simultaneous imaging, detection and therapy. In particular, high selectivity nanocomplex for photodynamic therapy and drug delivery are important tools to fight the cancer problem. Here, we report recent results on the design of theranostic complex based on the use of upconversion nanoparticles (UCNP) which convert near infrared (NIR) excitation at 970 nm into blue, green, red and NIR emission tuned with the lanthanide doping ion. Such nanoparticles are ideal for overpassing the limited penetration depth of conventional photodynamic therapy (PDT), also useful for imaging and detection. Green and red emissions were obtained with the introduction of Er³⁺ ion. The green and red emission is used as an excitation source for zinc phthalocyanine (ZnPc), a photosensitizer (PS) bounded to the surface of UCNP. PS transfers energy to molecular oxygen in the surroundings to produce reactive oxygen species (ROS) able to induce death of breast cancer cells (BCC). Selectivity was obtained by the conjugation with Trastuzumab (Tras), a specific monoclonal antibody for selective detection and treatment of HER2-overexpressing malignant BCC. With the use of nanocomplex UCNP-ZnPc-Tras, was observed selective tracking of SKBR-3 HER2+ BCC by using a confocal microscope and reducing cells viability to 80% upon 200mg/ml load and 5 minutes of irradiation. Furthermore, PS was replaced for a photocatalytic TiO₂/ZrO₂ shell which is excited with blue light coming from Tm³⁺ ions enhancing the ROS production and then killing cancer cells up to 88%. In this case, emission band at 801 nm was used for tracking cells at deep tissue. Indeed, we report the fabrication of immunoliposomes nanocomplex loaded with UCNP, PS for PDT and drugs for chemotherapy. Results shows a combined chemo-photodynamic synergistic effect killing cells up to 80% after 10mM load and 5 minutes of irradiation. The specificity of our nanocomplex was achieved by conjugating a newly discovered anti-HER2 peptide screened from a phage display peptide library. The high selectivity of the peptide-conjugated was confirmed by confocal imaging of SKBR-3 (HER2-positive) and MCF-7 (HER2-negative) breast cancer cell lines, illustrating its target-specific nature. Results suggest great potential for multifunctional theranostic nanocomplex for detection, imaging and therapy of cancer.

We acknowledge financial support from UDLNB and CONACYT through grant 259192.

8:15 AM SB03.05.10

Stimuli-Responsive Mesoporous Silica Nanoparticles for Applications in Cancer Theranostics [Nikola Knezevic](#), Minja Mladenovic, Mirjana Mundzic and Aleksandra Pavlovic; University of Novi Sad, Serbia

Mesoporous silica nanoparticles (MSN) exhibit highly beneficial features for devising nanosystems applicable in cancer therapy, imaging, or diagnostics. The high surface area of MSN, which can be easily postsynthetically functionalized with different organosilanes, in addition to their structured porosity available for loading cargo molecules, allows plethora of opportunities for devising multifunctional and multipurpose nanostructures. In this context, our research focuses on devising MSN-based cancer theranostics, containing different modalities for targeting specific cancer microenvironment, and the capabilities for delivering cargo therapeutic molecules upon exposure to the specific conditions of this environment, such as tissue acidosis or elevated concentration of glutathione and other cancer-related biomolecules. Thus, specific surface modification and controlling the release process of therapeutic molecules enables utilization of MSNs as unique facilitators toward enhancing the efficacy and precision of cancer treatment, imaging and sensing.

SYMPOSIUM SB04

Materials and Algorithms for Neuromorphic Computing and Adaptive Bio-Interfacing, Sensing and Actuation
November 30 - December 7, 2021

Symposium Organizers

Paschalis Gkoupidenis, Max Planck Institute
Priyadarshini Panda, Yale University
Francesca Santoro, Istituto Italiano di Tecnologia
Yoeri van de Burgt, Technische Universiteit Eindhoven

Symposium Support

Bronze
Neuromorphic Computing and Engineering (NCE) | IOP Publishing

* Invited Paper

SESSION SB04.01: Materials and Devices for Neuromorphic Computing
Session Chair: Paschalis Gkoupidenis
Tuesday Morning, November 30, 2021
Sheraton, 2nd Floor, Liberty B

10:30 AM *SB04.01.01

Using New Materials for Brain-Like Computing—From Fundamental Mechanisms to High-Performance Devices [Alberto Salleo](#); Stanford

University, United States

The brain can perform massively parallel information processing while consuming only ~1- 100 fJ per synaptic event. I will describe an electrochemical neuromorphic device that switches at low energy (~80 fJ), and displays a large number of distinct, non-volatile conductance states within a ~1 V operating range. The tunable resistance behaves very linearly, allowing blind updates in a neural network when operated with the proper access device. These devices also display outstanding endurance achieving over 10^9 switching events with very little degradation. I will describe our recent efforts at scaling and materials selection, allowing us to reach 20 ns write pulses and operation at high temperature (up to 120°C). In particular, we developed a fully lithographic process that allowed us to demonstrate sub- μm channel devices, opening the door to integration with Si driving circuitry. By carefully deuterating the electrolytes, we provide strong evidence that the secret to the high speed and low energy switching properties of these artificial synapses is the combination of electronic and protonic transport. Finally, we demonstrate that the working mechanism is quite general by fabricating and operating high-performance synapses based on MXenes. This generality is promising in terms of monolithic integration as MXenes can be chosen to be BEOL compatible with Si.

11:00 AM *SB04.01.02

Large-Scale Crossbar Arrays of Analog Memristors for In-Memory Computing [Qiangfei Xia](#); University of Massachusetts, United States

It becomes increasingly difficult to improve the speed-energy efficiency of traditional digital processors because of limitations in transistor scaling and the von Neumann architecture. Computing systems augmented with emerging devices such as memristors offer an attractive solution. A memristor, also known as a resistance switch, is an electronic device whose internal resistance state is dependent on the history of the current or voltage it has experienced. Because of its small size and fast switching speed, a memristor consumes a small amount of energy to update the internal state (training). Within large-scale crossbar arrays, memristors perform in-memory computing by utilizing physical laws, such as Ohm's law for multiplication and Kirchhoff's current law for accumulation. The current readout (inference) at all columns is finished simultaneously regardless of the array size, offering massive parallelism in vector-matrix multiplication and accelerating neural computing. This talk will first introduce an analog memristor that meets most requirements for in-memory computing in artificial neural networks. We will then showcase the integration of large-scale crossbar arrays of these memristors and the implementation of multilayer neural networks for several machine learning applications.

11:30 AM SB04.01.03

Oxygen Vacancy Based Electrochemical Memory Yields Deterministic Analogue Switching and Nonvolatile State Retention [Yiyang Li](#); University of Michigan, United States

In-memory computing with combined logic and memory functionality is a promising energy-efficient solution for data-intensive processes like machine learning. A crucial component towards in-memory computing is the analogue nonvolatile resistive memory element. Two-terminal filamentary valence-change memory (VCM) based on metal oxides are extremely difficult to control due to the formation of a nanosized filament. On the other hand, more predictable and deterministic solutions like electrochemical random-access memory (ECRAM) based on the intercalation of lithium and proton ions have poor state retention when scaled to nanosized dimensions, and often utilize materials that are difficult to integrate into CMOS processes. A memory solution possessing all of these requirements have been elusive.

In this work, we combine the VCM and ECRAM concepts by replacing the highly mobile lithium and proton ions in ECRAM with less mobile oxygen vacancies. As a three-terminal ECRAM cell with a solid electrolyte, it possesses highly desirable linear and deterministic analogue switching at moderately elevated temperatures (~100-150C). On the other hand, the low mobility of oxygen vacancies at room temperatures provide nonvolatile state retention for days and weeks at scale without a selector, while also enabling the use of CMOS-compatible transition metal oxides. We further show how the switching and retention time are related to fundamental material properties like ionic resistance and chemical capacitance, and how changes in material processing conditions can be used to control the switching and retention properties.

11:45 AM SB04.01.04

Reliability of ZrO₂-ReRAM Based Memristive Crossbars in Inference Dominated Applications [Johannes Mohr](#)¹, [Christopher Bengel](#)¹, [Stefan Wiefels](#)², [Rainer Waser](#)^{1,2}, [Stephan Menzel](#)² and [Dirk J. Wouters](#)¹; ¹RWTH Aachen University, Germany; ²Forschungszentrum Jülich GmbH, Germany

In recent years, many novel computing paradigms have emerged that promise to complement the classic von-Neumann architecture, such as artificial neural networks and computation-in-memory. It is expected that these will enhance the functionality of everyday devices, such as in edge-AI and the internet of things as well as in datacenters for green-IT.

Analog accelerators based on crossbar arrays of non-volatile memristive devices (such as resistive switching ReRAM) are believed to be well suited for many of these applications, as they offer efficient (i.e., fast parallel and low power) operation and high integration densities. However, because of their high write energy and limited write count, applications of interest are limited to read-dominated ones, such as ANN inference or database queries. Yet, the effect of ReRAM device reliability issues as variability and drift on the crossbar operation needs to be explored.

To characterize the reliability of the crossbar, a representative computation is needed. The vector dot-product was chosen here because it can serve as a computational primitive for constructing more complicated operations such as matrix or tensor multiplications, which are among the most utilized operations in neural networks. Therefore, it can reveal the key behaviors, while still being sufficiently simple to allow for easy interpretation of the results. We fabricated crossbar structures based on a ZrO₂/Ta ReRAM device stack. These feature a number of cells connected with one electrode to a common bitline, and can be viewed as a column of a passive memory array. The measurements presented were performed on 8-bit words stored in these. To perform a computation, an input voltage vector is applied to the block, the sum of the currents through all memristive devices is then the calculated dot-product. Using this configuration, we experimentally demonstrated the feasibility of the operation. From these experiments, a number of important conclusions could be drawn regarding the memristive device characteristics. For example, it was found (using binary weights) that the spread in current levels depends strongly both on the accuracy of the programmed low resistance state value and on the resistance level of the high resistance state.

Furthermore, we identified typical failure mechanisms, such as read disturb, which is a change or drift in the device resistance caused by repeated reading of the cells or random bit-flips. We show how these are influenced by the magnitude of the applied voltages, and compare the behavior to that expected from the characterization of single cells. We demonstrate how they can be understood based on the material properties, such as the non-linear device kinetics being a key driver of low resistance state degradation. This allows us to identify the best operating conditions.

In a real world application the crossbar does not operate as a standalone device, but in conjunction with CMOS periphery. This periphery is needed to convert between the analog domain of the crossbar and the digital domain of the rest of the system. The impact of the measured device level failures on this interfacing between the analog and digital world is investigated through simulation. For these, we fitted our physics based compact model JART VCM v1b to measured data from the cells, which is able to describe the device-to-device and cycle-to-cycle variability, as well as mechanisms such as read disturb and random telegraph noise.

SESSION SB04.02: Biointerfacing and Biosensing
Session Chair: Yoeri van de Burgt
Tuesday Afternoon, November 30, 2021
Sheraton, 2nd Floor, Liberty B

1:30 PM *SB04.02.01

Translational Neuroelectronics Dion Khodagholy; Columbia University, United States

As our understanding of the brain's physiology and pathology progresses, increasingly sophisticated technologies are required to advance discoveries in neuroscience and develop more effective approaches to treating neuropsychiatric disease. To facilitate clinical translation of advanced materials, devices, and technologies, all components of bioelectronic devices have to be considered. Organic electronics offer a unique approach to device design, due to their mixed ionic/electronic conduction, mechanical flexibility, enhanced biocompatibility, and capability for drug delivery. We design, develop, and characterize conformable organic electronic devices based on conducting polymer-based electrodes, particulate electronic composites, high-performance transistors, conformable integrated circuits, and ion-based data communication. These devices facilitate large-scale neurophysiology experiments and have led to discovery of a novel cortical oscillation involved in memory consolidation as well as elucidated patterns of neural network maturation in the developing brain. The biocompatibility of the devices also allowed intra-operative recording from patients undergoing epilepsy and deep brain stimulation surgeries, highlighting the translational capacity of this class of neural interface devices. In parallel, we are developing the high-speed conformable implantable integrated circuits and embedded acquisition and storage systems required to make high channel count, chronic neurophysiological recording from animals and human subjects possible. This multidisciplinary approach will enable the development of new devices based on organic electronics, with broad applicability to the understanding of physiologic and pathologic network activity, control of brain-machine interfaces, and therapeutic closed-loop devices.

2:00 PM *SB04.02.02

Stable Self-Healing Neural Circuits in Millimeter-Sized Animal Jacob T. Robinson; Rice University, United States

By understanding the self-healing properties of biological systems it may be possible to build robust artificial systems with similar stable operation. Here we discuss how the nervous system of the Hydra - a millimeter-sized aquatic cnidarian - can reorganize itself in a matter of hours to regain function after half the neurons are lost. By studying how this simple nervous system confined to two layers of cells achieves this robust control of the body we hope to reveal ways we may be able to design and build robust, soft, biological neural control systems.

2:30 PM SB04.02.03

Polymeric Thin-Film Memristor Integration with Sensors onto Reconfigurable Structures for *In Situ* Processing of Tactile Inputs Subhadeep Koner¹, Yongchao Yu¹, Katherine Riley², Juan C. Osorio², Carlos Montenegro², Janav Udani², Harith Morgan², Andres F. Arrieta² and Stephen Sarles¹; ¹University of Tennessee, United States; ²Purdue University, United States

In animals, and especially humans, trained neural networks form associative learning patterns that allow rapid classification and decision making (e.g. object identification via touch sensing). In contrast, current engineered systems are unable to sense and classify information without significant instrumentation and software. But this might be possible in hardware alone if a system were constructed in a way that combines materials for distributed sensing, intrinsic computing (for classification), and memory (for learning). Only a handful of research works by Bao et.al, Lee et.al, Zhu et.al have tried to explore the artificial sensory nervous system, mostly using transistors, with just one work by Zhang et.al used threshold dependent switching devices for data processing.

Recently, Arrieta, et al demonstrated thin, flexible dimpled sheets, comprised of planar arrays of bi-stable domes, which reconfigure their global shapes in emergent forms when specific domes are inverted. The global shape of the sheet is dictated by both the local pattern and sequence of dome inversions. We propose to leverage the complex mechanics of these dimpled sheets combined with polymeric thin film non-volatile memristors to provide a novel foundation for combining autonomous reconfiguration with distributed sensing and embedded memory—akin to a peripheral nervous system—for onboard classification in engineered structures.

In this study, we demonstrate that dome inversion events can be sensed and remembered by integrating resistive strain sensors connected electrically to memory storage elements. The former is achieved by printing conductive traces into the dimpled sheets at positions near the individual domes, while the latter consists of polymeric thin-films that function as memory resistors. When the two are connected in series and biased with voltage, a transient change in sensor resistance caused by deformation of the dome encodes a permanent change in the resistance of the memristor. Through fabrication and experiments, we study the design and integration of both the sensor and memory storage elements for effective operation. An amplification circuit is used to magnify the changes in sensor resistance occurring during dome deformation, which allows the memristor voltage to eclipse the switching threshold. Using 1 sensor:1 memristor pairs, we demonstrate spatially distributed transduction and memory of dome inversions, and by applying a pulsatile voltage, we demonstrate incremental changes in the state of the memristor, which allows for temporal encoding of dome inversion events. These capabilities set the stage for an era of smart sensing and memory (via memristors) applications with emerging systems (reconfigurable sheet) that interact with the world for autonomous classification of tactile information.

2:45 PM SB04.02.04

Organic Electrochemical Networks for Brain-Inspired Computation and Classification Tasks of Biosignals and Biofluids Matteo Cucchi, Hans Kleemann and Karl Leo; TU Dresden, Germany

Early detection of malign patterns in patients' biological signals can save millions of lives. In this regard, artificial intelligence and machine learning can be used to detect patterns with super-human abilities. However, the practical clinical application of these methods is mostly constrained to an offline evaluation of the patients' data. In-vivo and real-time use of machine learning is so far only a vision, hampered by the difficult integration of traditional electronics and dedicated hardware into the human body.

Previous studies have identified organic electrochemical transistors (OECTs) as ideal candidates in bioelectronics for biosignal monitoring and sensing. However, using them for pattern recognition in real-time has so far not been achieved. Likewise, OECT-based artificial synapses have been proposed, but never integrated into networks.

In the present study, we produce and characterize brain-inspired random networks composed of OECTs and employ them for time-series predictions and classification tasks using the machine learning framework known as reservoir computing.

Due to their biocompatibility and low energy consumption, these networks could serve in implantable devices to carry out real-time on-chip computation.

We successfully pattern these networks on flexible and biocompatible substrates and we apply them to learning tasks with classical databases (classification of flowers and time-series predictions).

Furthermore, we show the potential use of the networks for biofluid monitoring and biosignal analysis. For this purpose, we classify 4 classes of arrhythmic

heartbeats with an accuracy of 88%. Each measurement is performed in PBS solution, in order to mimic the interface between the polymer and the biological cellular environment.

The results of this study introduce a novel paradigm for biocompatible computational platforms and may enable the development of ultra-low power consumption hardware-based artificial neural networks capable of interacting with body fluids, sensing chemicals, and monitoring biological tissues.

3:00 PM SB04.02.05

An Organic Artificial Synapse Coupling Optical and Electronical Readouts to Replicate Multiple-Neurotransmitters-Based Learning and Forgetting Patterns Giovanni Maria Matrone^{1,2}, Csaba Forro^{1,3}, Claudia Lubrano¹, Ugo Bruno¹, Bas de Jong⁴, Stefano Cinti⁵, Yoeri van de Burgt² and Francesca Santoro¹; ¹Istituto Italiano di Tecnologia IIT, Italy; ²Technische Universiteit Eindhoven, Netherlands; ³Stanford University, United States; ⁴Cicci Research, Italy; ⁵University of Naples Federico II, Italy

In biological neural networks communication relies on electric signals in the form of action potentials (APs) that trigger the release of neurotransmitters at the synapses, thus influencing the mechanisms of synaptic plasticity that regulates over time the transmission efficiency across the synaptic cleft.

Neuromorphic computing and its progress intrinsically depend on faithfully replicating the communication mechanisms of biological neural networks. As such, electrical to chemical signal transduction is essential to fully mimic brain functions and establish in future an active interaction with biological tissues¹. The potential transition from fully artificial to bio-hybrid, integrated synapses is only enabled by neuromorphic systems that display synaptic conditioning based on biochemical signalling activity which typically involves more than one neuromodulator.

The conductive polymer mixture PEDOT:PSS can be exploited for the electrochemical detection of electroactive neurotransmitters² (i.e. dopamine, serotonin, ascorbic acid) through redox reactions while providing a suitable biocompatible interface with cells and neurons³.

Here, we report the first demonstration of a neuromorphic platform recapitulating the synergetic concourse of multiple neurotransmitters (NTs) that control synaptic weight modulation. This novel symmetric electrochemical neuromorphic organic device (SENODE) is capable of identifying three neurotransmitters that are simultaneously present and through modular microfluidic channels to mimic the recycling machinery of the synaptic cleft and control the output to replicate exocytosis-driven synaptic potentiation and depression⁴. Hence, the platform allows to transduce the neurotransmitters-mediated chemical signal, eliciting an output that is stored and read as a change in the polymer's conductance, a reversible neuromorphic phenomenon that replicates neuronal's short-term and long-term plasticity⁵. Moreover, by exploiting PEDOT:PSS electrochromism, the system's readout is alternatively monitored as a variation of the polymer's transmittance. The combination of the two readout mechanisms allows to emulate high order biological processes such as intrinsic forgetting, memory consolidation and NTs co-modulation, while also classic conditioning processes are replicated. Hence, the possibility to combine different NTs and input stimuli enable to program the synapse weights opens the way to the integration of array of devices which recreate complex, more refined brain's learning processes.

1. Markram, H. A history of spike-timing-dependent plasticity. *Front. Synaptic Neurosci.* **3**, (2011).
2. Gualandi, I. *et al.* Textile Organic Electrochemical Transistors as a Platform for Wearable Biosensors. *Sci. Rep.* **6**, 33637 (2016).
3. Asplund, M. *et al.* Toxicity evaluation of PEDOT/biomolecular composites intended for neural communication electrodes. *Biomed. Mater.* **4**, 045009 (2009).
4. Gu, C., Larsson, A. & Ewing, A. G. Plasticity in exocytosis revealed through the effects of repetitive stimuli affect the content of nanometer vesicles and the fraction of transmitter released. *Proc. Natl. Acad. Sci.* **116**, 21409–21415 (2019).
5. Abbott, L. F. & Regehr, W. G. Synaptic computation. *Nature* **431**, 796–803 (2004).

3:15 PM BREAK

SESSION SB04.03: Materials and Concepts for Neuromorphic Electronics

Session Chair: Robert Nawrocki

Tuesday Afternoon, November 30, 2021

Sheraton, 2nd Floor, Liberty B

4:00 PM *SB04.03.01

Evolvable Organic Electronics Based on *In Situ* Polymerization Magnus Berggren; Linkoping University, Sweden

Neuromorphic electronics is a promising approach to enable dedicated computing at the site of sensing and actuation at the same time it offers new strategies to perform signal processing. Neuromorphic devices and systems combine signal processing and memory functionality in a manner to enable “training” and “evolution” of hardware to improve its performance for identification, perception and/or quantifying data and information. Our approach takes use of operating organic electrochemical devices and systems in electrolyte media containing electroactive monomers. This approach allows us to evolve the actual physical dimensions of devices while operating and performing signal processing. Organic electronic materials are unique in the sense that they can operate and be manufactured at the same conditions, which here allow us to make novel neuromorphic technology that relies on evolving critical device parameters of organic electrochemical transistors. We will report on device architectures, manufacturing approaches, materials and system design for organic evolvable electronics.

4:30 PM SB04.03.02

Particulate Composite Anisotropic Ion Conductor Richard Yao and Dion Khodagholy; Columbia University, United States

Ions are the primary charge carrier in physiological environments. Conventional inorganic electronic materials used in bioelectronic devices rely on surface capacitance for conversion of ionic potentials to electrons at the tissue interface for electrophysiological sensing and stimulation. In contrast, conducting polymers have mixed ion and electron conductivity that enables ion-based modulation of electronic charge carriers. However, it is not possible to individually control the properties of these polymers' ion and electron conducting domains. Mixed-conducting particulate composites are an emerging material that allows precise tuning of ionic and electronic conduction states by varying particle size and density in a scaffolding matrix. We hypothesized that a similar strategy could be used to create an anisotropic ion conductor by controlling the particle path (ionic mean free path) length to allow ion conductivity only within the lateral plane. To test our hypothesis, we synthesized anisotropic ion conducting films composed of biocompatible ion conducting particles and organic dielectric materials. Electrochemical impedance spectroscopy and scanning electron microscopy measurements were performed to characterize the degree of anisotropy and mean free path of particles. We showed that such composites have uniformly distributed particles, hydration stability over weeks, scalable thickness, tunable out-of-plane conductivity, and consistent anisotropy for various particle and scaffold materials. Additionally, an anisotropic ion conductor can be designed as a soft, stretchable, and conformable transducer that directly interfaces with the skin for neural

interface applications. We demonstrated the application of this material by acquiring biological signals via electrocardiography. Furthermore, we applied this ion membrane in organic electrochemical transistors (OECTs) to eliminate crosstalk between transistors, which is conventionally caused by the use of a shared electrolyte. This enables the fabrication of high-density transistor arrays, opening the avenue for organic integrated circuits and OECT-based neuromorphic computing devices. The development of this novel anisotropic ion conducting film has a wide range of implications and potential applications, ranging from anisotropic interfaces with biological tissue for high-resolution electrophysiology recordings and large-scale integration of ionic circuits, to directional control and programming of synaptic weights for artificial neural network and neuromorphic devices.

4:45 PM SB04.03.03

Biomembrane-Based Reservoir Computing for Image Classification [Joshua Maraj](#), Jessie Ringley and Stephen Sarles; The University of Tennessee, Knoxville, United States

Biomembrane-based devices exhibit unique capabilities in the realm of neuromorphic applications. Doping model lipid membranes with voltage-active species transforms them into low voltage volatile memristors that dynamically process incoming signals in a manner consistent with sensory synapses in the retina and olfactory systems. Unlike the brain however, volatile memristor networks do not have a built-in method to interpret processed signals. Reservoir computing (RC) may be one such way to interpret the nonlinear, history-dependent outputs from such networks. In the simplest terms, a reservoir is a network of nodes with inputs and outputs whose connection topology and weights do not change. Classification can be performed on reservoir outputs using supervised learning techniques to train a “readout layer” of artificial neurons, independent of the internal connectivity that defines the reservoir itself. Recently, volatile, solid-state memristors have been successfully used to create a reservoir for enabling image classification and chaotic temporal forecasting tasks. Low voltage, organic, and biocompatible materials, including those that more faithfully emulate the short-term plasticity of biological synapses, however, have not yet reported these capabilities but have the necessary properties to show similar success.

Herein, we propose the use of monazomycin-doped droplet interface bilayers (MzDIB) as candidates for reservoir computing nodes. We hypothesize that this material composition has unique properties that can reduce the overall size of the reservoir which will reduce footprint and energy expenditure. Using physical modeling, numerical simulation, and image classification tasks, we show that MzDIBs can accurately classify handwritten numbers digitized as small (5x5) or large (20x22) pixel representations of digits with appropriately sized reservoirs. A custom 5x5 pixel digit dataset consisting of ten distinct representations of each integer 0-9 is tested as proof of concept, with the larger 20x22 images consisting of the MNIST handwritten digit dataset with black borders removed. To process images using voltage-activated MzDIBs, pixel rows of image are converted into time varying voltage inputs fed at different rates into the reservoir. The voltages cause bi-directional, time-varying changes in membrane conductance due to Mz channel formation, such that the simulated final conductance states are then used as inputs to a 196x10 readout layer for image classification. We show that classification using a MzDIB reservoir network is feasible. Fully realized arrays with more complex connectivity have the potential to be hardware based reservoir computers due to their low operation voltage, biocompatibility, and ease of assembly.

5:00 PM SB04.03.04

Independent Impact of the Electrode Thermal Environment on the Analog Response of HfO_x-Based Filamentary Neuromorphic Devices [Matthew P. West](#)¹, Robert H. Montgomery¹, Georges Pavlidis², Riley Hanus¹, Fabia Farlin Athena¹, Andrea Centrone², Samuel Graham¹ and Eric M. Vogel¹; ¹Georgia Institute of Technology, United States; ²National Institute of Standards and Technology, United States

Filamentary adaptive oxides operate on nanosecond time scales, with local temperatures as high as 1000 K, yet the impact of the thermal environment on their analog operation is often ignored. These devices are a promising new technology for neuromorphic and biomimetic computing applications, which require linear, analog resistance changes. Filamentary oxides can be set to a continuum of resistance states based on the amount of oxygen ions within a nanosized area, called a filament. If the maximum current is well controlled, the oxygen deficient region can be partially re-oxidized by reversing the bias, thus increasing the resistance of the device. The resistance is modulated by applying voltage pulses for times varying many orders of magnitude, from seconds to nanoseconds. The ability to realize these devices in neuromorphic computing models such as spike timing dependent plasticity or pattern recognition relies on achieving a repeatable, linear resistance change. Understanding the role that the thermal environment has on the distribution of oxygen ions will inform material choices for the electrodes, substrates, and packaging of neural network chips.

The main mechanisms that drive the oxygen ions in and out of the filament are drift, diffusion, and thermophoresis [1]; all of which are heavily influenced by the temperature. Temperature gradients are the driving force for thermophoresis, which is very strong in these devices due to a localized high temperature region where all the current passes. Previous work showed changing the thermal conductivity of the substrate by an order of magnitude, from 138 W/m-K to 1.2 W/m-K, increased the percent change in the resistance of a single pulse from 150% to 450% [2]. It was determined that when the substrate thermal conductivity was low, the electrode acted as a heat sink. To influence the thermal environment of the switching oxide more directly, this work focuses on changing the thermal properties of the electrodes while maintaining the same chemical environment near the filament. Previous studies have explored the impact of the electrodes in direct contact with the filament [3], however, this layer also alters the bonding and release of oxygen ions, and thus these experiments did not independently change the thermal environment. In this study, the thermal environment imposed by the electrodes will be independently changed by surrounding the filamentary HfO_x active layer with thin, 5 nm gold layers. The bulk of the electrodes will then be varied between silver, platinum, and TiN having thermal conductivities of ~429, 72, and 25 W/m-K. Initial finite element modeling suggests that increasing the thermal conductivity of the electrodes reduces the initial resistance change to the first pulse. This is important because these devices typically have a large initial resistance change that quickly levels off, instead of the desired linear change with the number of pulses. The digital, analog, and operation temperature of these devices are compared and supported by modelling work. By tailoring the thermal environment of the device, the temperature gradient is manipulated thus altering relative magnitudes of three main thermal driving forces, drift, diffusion, and thermophoresis. Fundamentally understanding how the electrode materials influence the local temperature distribution will lead to more reliable and repeatable filamentary devices for neuromorphic applications.

This work was supported by the AFOSR MURI under Award No. FA9550-18-1-0024. In part at the Georgia Tech Institute for Electronics and Nanotechnology, a member of the NNCI, which is supported by the NSF (ECCS-2025462). This material is based upon the work supported by the NSF GRFP under Grant No. DGE-1650044.

[1] D. G. Pahinkar, *et al. AIP Advances* 10, 035127 (2020)

[2] M. P. West, *et al. Applied Physics Letters* 116, 063504 (2020)

[3] W. Wu, *et al. IEEE Electron Device Letters* 38, 1019-1022 (2017)

SESSION SB04.04: Poster Session I: Materials and Algorithms for Neuromorphic Computing and Adaptive Bio-Interfacing, Sensing and Actuation
Tuesday Afternoon, November 30, 2021
8:00 PM - 10:00 PM
Hynes, Level 1, Hall B

SB04.04.01

Impact of Oxygen Concentration at the HfO_x/Ti Interface on the Behavior of HfO_x Filamentary Memristors [Jinho Hah](#), Matthew P. West, Fabia Farlin Athena, Riley Hanus, Eric M. Vogel and Samuel Graham; Georgia Institute of Technology, United States

Towards future computing and nonvolatile memory (NVM), memristors have gained wide attention for their in-memory computing and neuromorphic computing applications [1, 2]. The resistive switching (RS) dynamics in memristors rely critically on oxygen ions and their recombination with oxygen vacancies to partially rupture and form the conductive filament (CF) [3] for modulating the device between the low resistance state (LRS) and high resistance state (HRS).

In this study, we investigated the effect of oxygen ion concentration at the HfO_x/Ti interface on set and reset operation, LRS, and HRS characteristics in HfO_x-based filamentary memristors. Devices with higher oxygen ion concentrations at the interface were fabricated by performing oxygen plasma treatment at varying times on the as-grown ~5 nm HfO_x active layer via atomic layer deposition (ALD). Detailed x-ray photoelectron spectroscopy (XPS) analysis and its depth profile results verify the excess oxygen ion present at the HfO_x/Ti interface, and thin TiO_x layer has been formed between the HfO_x and Ti layers, resulting in a HfO_x/TiO_x/Ti structure. This change in interface chemistry at the active layer and capping layer near the top electrode have impacted the set transition behavior more gradual, favorable for analog logic computation. This work demonstrates the importance of oxygen ion concentration and motion in controlled growth of CF during memristor set operation.

- [1] J. J. Yang et al., *Nature Nanotechnology*, **3**(7), 429–433 (2008).
- [2] J. J. Yang et al., *Nature Nanotechnology*, **8**(1), 13–24 (2013).
- [3] Y. Li et al., *J. of Physics D: Applied Physics*, **51**, 503002 (2018).

SB04.04.02

Artificial Synapse with Neurotransmitter and Spike-Timing Dependent Plasticity (STDP) Modulation for Neuronal Micro-Circuitry [Charles-Théophile Coen](#), Setareh Kazemzadeh, Aref Saberi and Yoeri van de Burgt; Technische Universiteit Eindhoven, Netherlands

For more than a decade, a shift of paradigm has taken place within neural implant engineering with the idea of implementing active components and bringing out modalities capable of modulating the biological surroundings. Examples span from integration of micro-LED for photostimulation of cells, to microfluidic systems for local drug delivery.

This shift has been a cornerstone in neuroengineering that allowed to move from a passive monitoring to a dynamic modulation of the nervous system. Nonetheless, one of the missing parts is the ability to emulate certain functions of the neural system, such as neuronal connectivity, network plasticity or local computing. Indeed, to achieve a biologically relevant modulation, it is crucial to mimic as closely as possible neuronal processes happening in the body. The next generation of devices needs thus to focus on implementing biomimetic aspects to not only interface with the nervous system, but recreate these biological functions to locally sense, process and modulate it.

The central nervous system is at the essence of our ability to learn, memorize and compute information and at the core of this intricate and complicated network lays the synapse and its capacity of passing information from one neuron to another. The first building blocks to recreate the functions of this key element have already been developed with a non-volatile electrochemical neuromorphic organic device (ENODE)¹ which showed short- and long-term plasticity, laying down the foundation of neuromorphic devices for bio applications. Another important milestone has been the modulation of a biohybrid synapse through the inhibitory neurotransmitter dopamine released by neuron-like cells².

In this work, we propose to further develop these technologies and to create an artificial synapse capable of creating neuronal micro-circuits. In its nature, the synapse can strengthen or weaken over time and different mechanisms cooperate to achieve this plasticity, such as the release of neurotransmitters by the presynaptic neuron or the time difference of firing between the pre- and postsynaptic neurons. We are therefore investigating the modulation of an artificial synapse through the presynaptic release of inhibitory or excitatory neurotransmitters and through a spike-time dependent plasticity (STDP) phenomenon. An unconnected pair of neurons is coupled together thanks to this artificial synapse showing a plasticity at the chemical level, with the neurotransmitters, and in the time domain, with the STDP, allowing a more truthful modulation.

This work thus aims at creating an artificial synapse that emulates as closely as possible its biological counterpart and presents a platform capable of creating a closed-loop neuronal micro-circuit based on neuromorphic devices.

1. Van De Burgt, Y. *et al.* A non-volatile organic electrochemical device as a low-voltage artificial synapse for neuromorphic computing. *Nature Materials* vol. 16 414–418 (2017).
2. Keene, S. T. *et al.* A biohybrid synapse with neurotransmitter-mediated plasticity. *Nat. Mater.* **19**, 969–973 (2020).

SESSION SB04.05: Materials and Devices for Neuromorphic Computing and Learning
Session Chair: Robert Nawrocki
Wednesday Morning, December 1, 2021
Sheraton, 2nd Floor, Liberty B

10:30 AM *SB04.05.01

Novel Organic Materials and Architectures for Neuromorphic Computing [George G. Malliaras](#); University of Cambridge, United Kingdom

The realization of bioinspired circuits that mimic the signal processing capabilities of the brain demands the reproduction of both short- and long-term aspects of synaptic plasticity on a single device level. The emergence of organic electronics has made available a host of new materials and devices with properties that are well-suited to address this challenge. We show how mixed conductivity in organic semiconductors can be leveraged to control neuromorphic functions similar to the basic short-term and long-term synaptic plasticity. Namely, we demonstrate that the timescales for functions such as depression, adaptation and dynamic filtering can be controlled by tuning the ratio of electronic/ionic mobility. We further show that 3D printing can be leveraged to develop new architectures for neuromorphic computing.

11:00 AM *SB04.05.02

Control of Ion Trapping for Non-Volatile Electrochemical Transistors Jonathan Rivnay; Northwestern University, United States

Materials processing and synthetic design serve as ideal avenues to control the transport properties of polymer-based mixed ionic/electronic conductors. Small changes in chemistry can affect the materials electronic mobility, swelling, ion uptake and stability. Devices based on these materials have thus opened up new opportunities in bioelectronics, energy, and neuromorphic computing. Associative learning, a critical learning principle to improve an individual's adaptability, has been emulated by few organic electrochemical devices. However, complicated bias schemes, high write voltages, as well as process irreversibility hinder the further development of associative learning circuits. Here, we present a non-volatile organic electrochemical transistor (OECT) based on a poly(3,4-ethylenedioxythiophene):tosylate (PEDOT:Tos)/ Polytetrahydrofuran (PTHF) composite. This device can continuously and reversibly change its conductance state at a write bias less than 0.8 V and the state retention time can be longer than 200 min without decoupling the write and read operation. By incorporating a pressure sensor and a photoresistor into the gate terminal of volatile and non-volatile OECTs, a neuromorphic circuit is demonstrated with the ability to associate two physical inputs (light and pressure), which may have implications for biomimetic devices like electronics-skin and neuroprosthetics. To unravel the non-volatility of this material, UV-Vis-NIR spectroscopy, X-ray photoelectron spectroscopy (XPS) and grazing-incidence wide-angle X-ray scattering (GIWAXS) are used to characterize the oxidation level variation, compositional change and the structural modulation of the PEDOT:Tos/PTHF films in various conductance states. These studies support the finding that non-crystalline PTHF retains injected cations, and thus allowing for the non-volatile memory behavior of the composite OECT devices. The implementation of the associative learning circuit as well as the understanding of the non-volatile material represent critical advances for organic electrochemical devices in neuromorphic applications.

11:30 AM SB04.05.03

Organic Neuromorphic Electronics for Local Control and Learning—Path Planning Robot in a Maze Imke Krauhausen^{1,2}, Dimitrios Koutsouras¹, Armantas Melianas³, Scott T. Keene⁴, Katharina Lieberth¹, Hadrien Ledanseau¹, Rajendar Sheelamanthula⁵, Alexander Giovannitti³, Fabrizio Torricelli⁶, Iain McCulloch^{5,7}, Paul Blom¹, Alberto Salleo³, Yoeri van de Burgt² and Paschalis Gkoupidenis¹; ¹Max Planck Institute for Polymer Research, Germany; ²Technische Universiteit Eindhoven, Netherlands; ³Stanford University, United States Minor Outlying Islands; ⁴University of Cambridge, United Kingdom; ⁵King Abdullah University of Science and Technology, Saudi Arabia; ⁶University of Brescia, Italy; ⁷University of Oxford, United Kingdom

Artificial intelligence applications have demonstrated their enormous potential for complex processing over the last decade. However, they are mainly based on digital operating principles while being part of an analogue world. Moreover, they still lack the efficiency and computing capacity of biological systems. Neuromorphic electronics emulate the analogue information processing of biological nervous systems.¹ Organic artificial synapses exhibit volatile as well as tunable/non-volatile conductance states that replicate the behavior of their biological counterparts.²⁻⁶ In this work we present a path planning robot that uses a small-scale, locally-trained organic neuromorphic circuit to navigate through a maze. The neuromorphic circuit responds and adapts to environmental stimuli directly, as it is integrated with the robot sensors. The on-chip integration of sensor signals together with low-power organic neuromorphic electronics paves the way toward stand-alone, brain-inspired computing circuitry in autonomous and intelligent robotics.⁷

References

- C. Mead, Neuromorphic electronic systems. *Proc. IEEE* 78, 1629-1636 (1990).
- P. Gkoupidenis et al. Synaptic plasticity functions in an organic electrochemical transistor. *Appl. Phys. Lett.* 107 (26), 263302 (2015).
- P. Gkoupidenis et al. Neuromorphic functions in PEDOT:PSS organic electrochemical transistors, *Adv. Mater.* 27 (44), 7176 (2015).
- Y. van de Burgt et al. A non-volatile organic electrochemical device as a low-voltage artificial synapse for neuromorphic computing. *Nat. Mater.* 16, 414 (2017).
- E. J. Fuller et al. Parallel programming of an ionic floating-gate memory array for scalable neuromorphic computing, *Science* 364 (6440), 570 (2019).
- A. Melianas et al. Temperature-resilient solid-state organic artificial synapses for neuromorphic computing, *Sci. Adv.* 6, (27) eabb2958 (2020).
- C. Wan et al. Artificial Sensory Memory. *Adv. Mater.* 1902434, 1–22 (2019).

11:45 AM SB04.05.04

Smart and Adaptable Biosensor Based on Organic Neuromorphic Circuit Eveline van Doremale^{1,2} and Yoeri van de Burgt^{1,2}; ¹Eindhoven University of Technology, Netherlands; ²Institute for Complex Molecular Systems, Netherlands

Traditional computing systems are unable to capture the capability of the brain in real world information processing as evidenced by the anticipated end to Moore's law. Neuromorphic computing aims to mimic the efficiency of the brain in complex classification tasks by applying learning directly in hardware and is promising for local edge computing applications such as smart point-of-care devices (1). However, straightforward tuneability, low power consumption and high accuracy are necessary for successful implementation of such applications (2). Recently, organic materials have emerged as building blocks for neuromorphic systems due to their low operation voltage, biocompatibility and excellent tunability properties (3). Nevertheless, fully autonomous bioelectronic applications demand not only the acquisition of biological signals, but also local data processing, storage and the extraction of specific features of merit (4). Here we show a smart biosensor based on organic neuromorphic devices that can be fully trained in hardware to classify a model disease (e.g. cystic fibrosis). We use ion selective electrodes that are able to detect physiological levels of potassium and chloride and serve as the input to the hardware-implemented neural network. We demonstrate the flexibility and versatility of the neuromorphic system by on-chip retraining with different input signals as well as by classification of logic gates. These results pave the way for adaptive biosensors, smart point-of-care devices and personalized healthcare.

1. Fuller et al., *Science*, 2019
2. Van de Burgt et al., *Nature Materials*, 2017
3. Van de Burgt et al., *Nature Electronics*, 2018
4. Van Doremale et al., *J. Mater. Chem. C*, 2019

Wednesday Afternoon, December 1, 2021
Sheraton, 2nd Floor, Liberty B

1:30 PM *SB04.06.01

High-Aspect-Ratio Nanoelectrodes for the Recordings of Neuronal Signals with Sub-Threshold Signal Resolution [Andreas Offenhaeuser](#)¹, Pegah Shokohimehr¹, Bogdana Cepkenovic^{1,2} and Vanessa Maybeck¹; ¹Forschungszentrum Julich, Germany; ²RWTH Aachen University, Germany

Silicon-based microstructures are gaining importance in fundamental neuroscience and biomedical research. Precise and long-lasting neuro-electronic hybrid systems are at the center of research and development in this field. Nowadays, the best approach to study the electrophysiological activity of neurons in vitro and in vivo is based on planar microelectrode arrays (MEA) or field-effect transistors (FET) which can be integrated with microfluidic devices. However, the weak coupling between cell membrane and electrode surface is one of the major limiting factors and technology of 3D nanostructures for cell-chip coupling is currently a vivid field of investigation. Our present study focuses on the investigation of cell-chip interfaces with 3D nanoelectrodes for extracellular recordings. In particular 3D nanostructures with a high aspect ratio have become a suitable interface between neurons and electronic devices, since the excellent mechanical coupling to the neuronal cell membrane allows very high signal-to-noise ratios. In the light of an increasing demand for a stable, non-invasive and long-term recording at subthreshold resolution, we present a combination of vertical nanostraws with nanocavities. These structures provide a tight coupling with rat cortical neurons, resulting in high amplitude sensitivity and post-synaptic resolution capability, as directly confirmed by combined patch-clamp and MEA measurements.

2:00 PM SB04.06.02

Sensing, Thresholding and Associative Memory in Multistable Metasheets Juan C. Osorio¹, Carlos Montenegro¹, Katherine Riley¹, Harith Morgan¹, Subhadeep Koner², Yongchao Yu², Stephen Sarles² and [Andres F. Arrieta](#)¹; ¹Purdue University, United States; ²The University of Tennessee, Knoxville, United States

Organisms display a remarkable ability to perform complex functions in unstructured settings thanks to their co-evolved neuromechanical systems. Filtering, thresholding, and nonlinear amplification are common features found in organisms' mechanosensing. In contrast to engineering systems that rely on electrical filtering, organisms often employ distributed mechanical filters intimately integrated within their material architecture to extract only the necessary information from the environment. Filtering and signal thresholding are often achieved by careful positioning of geometrical features in the form of hairs or cilia spiders' legs, bats' wings, and fish's skins to sense the surrounding conditions mechanically.

An equally important aspect in neuromechanical systems is the capacity to form and retain memory that classifies different external stimuli. A crucial such mechanism is the ability to recall events from partial information, often described as associative memory. Integrating mechanosensing and memory formation as intrinsic properties in soft systems constitutes a new frontier in the development of engineered materials with potential applications in robotics, morphing structures, and wearables.

We report on multistable metamaterial architectures exhibiting hybrid units that enable filtering, thresholding, transduction, and associative memory formation, providing a route to synthetic neuromechanical systems. Our hybrid constitutive units collocate a geometrically bistable structure, a piezoresistive sensor, and a polymeric memristor. Specifically, we leverage the local bistability of constitutive units to filter external inputs, which are only transduced once the specific force threshold required to induce unit inversion (snap-through) is reached. The resulting unit inversion causes a nonlinear strain field that amplifies the external input, subsequently inducing transduction into an electrical signal leveraging collocated piezoresistive strips. The transduced signals trigger memristance changes which allow for memory retention. Notably, successive transduced signals accumulate changes of memristance, thereby enabling the formation of associative memories following a Hebbian rule within the paradigm of Hopfield networks. We demonstrate that the final accumulated signal on our memristors can be used to recall several spatiotemporal forcing patterns acting on metasheet featuring N hybrid units. Our metamaterials offer the rudiments of neuromechanical systems while requiring minimal external power and digital electronics, opening a route to engineered structures with organism-inspired functionality.

2:15 PM BREAK

SESSION SB04.07: Neuronal and Synaptic Electronics
Session Chair: Paschalis Gkoupidenis
Wednesday Afternoon, December 1, 2021
Sheraton, 2nd Floor, Liberty B

4:00 PM *SB04.07.01

Spiking Organic Electronics Synaptic Circuits Mohammad Javad Mirshojaeian Hosseini¹, Elisa Donati^{2,3,4}, Giacomo Indiveri^{2,3,4} and [Robert A. Nawrocki](#)¹; ¹Purdue University, United States; ²Institute of Neuroinformatics, Switzerland; ³University of Zurich, Switzerland; ⁴ETH Zurich, Switzerland

Spiking Neural Networks (SNN), provide distributed computational capability and emulate the brain processing principles. Compared to conventional Artificial Neural Networks (ANN) that encode the information in the magnitude of the signal, SNN function based on modulation of spike frequency and pulse width [1]. Due to intrinsic compatibility with brain signaling, one of the target applications of SNN hardware implementation, known as neuromorphic systems [2], are Brain-Computer Interfaces (BCI) [3]. With a handful of exceptions [4], such implementations are typically implemented using silicon technology, which is physically hard and rigid, and non-biocompatible, resulting in a permanent damage to the brain's soft tissue. Organic electronics are physically soft and flexible, biocompatible, and offer low-cost, large-area fabrication, for direct interface with biological tissues [5].

Synapses play a crucial role in neural networks by interfacing between adjacent neurons [1]. They are responsible for tuning the neural signals and, as such, are critical in memory, learning, and cognition.

We report on the fabrication of a physically flexible organic electronics, spiking synaptic circuits. Organic Field-Effect Transistors (OFETs) were fabricated on rigid glass and physically flexible 50 μm thin Polyimide substrates. OFETs' architecture was bottom-gate top-contact, and fabricated through thermal deposition of Cr (3 nm)/Au (50 nm) as the gate electrode, 400 nm of Parylene diX-SR as the dielectric, 30 nm of dinaphtho[2,3b:2',3'-f]thieno[3,2-b]thiophene (DNTT) as the p-type and N,N'-bis(n-octyl)-x:y,dicyanoperylene3,4,9,10-bis(dicarboximide) (PDI8-CN2, also referred to as N1200) as the n-type organic semiconductors. A 50 nm layer of Au served as the source and the drain electrodes. A layer of Parylene encapsulated the structure. Non-fabrication-integrated commercial capacitors were used to accelerate the fabrication and the characterization process. Future work will include all

integrated, all-organic circuits.

The results demonstrate that the fabricated log-domain integrator synapse [6], a variant of the linear charge-and-discharge synapse, can implement a true linear integrator circuit. The circuit exploits the logarithmic relationship between subthreshold OFET gate-to-source voltages and their channel currents. It provides proportional output current based on continuously tunable synaptic weights. We also demonstrate the effects of synaptic weighting voltage, synaptic capacitance, and disparity in pre-synaptic signals on circuit time constant.

Crucially, we show that our organic synaptic circuits can provide time constants that are more than 200 times longer compared to silicon-based synaptic circuits, recorded in excess of 6 seconds. Also, theoretical calculations are commensurate with empirically recorded time constants.

We believe that this work is the first demonstration of a spiking organic electronic synaptic circuit. Time constants in the range of seconds are considered critical for future integration of synaptic neuromorphic circuits with biological neurons, for future implantable BMIs. Furthermore, with our previously demonstrated spiking organic electronic Axon-Hillock somatic circuits [7], it paves the way for future all-organic, flexible and biocompatible neuromorphic computing.

- [1] F. Rieke and D. Warland, *MIT Press*, 1999.
- [2] R.A. Nawrocki, et al., *IEEE Trans. Ele. Dev.*, 63 (10), 2016.
- [3] F. Boi, et al., *Front. Neuro.*, 10 (563), 2016.
- [4] R.A. Nawrocki, et al., *IEEE Trans. Ele. Dev.*, 61 (10), 2014.
- [5] G. Schwartz, et al., *Nat. Comm.*, 4 (1), 2013.
- [6] P. Merolla and K. Boahen, *MIT Press*, 2004.
- [7] Hosseini, MJM, et al., *J.Phys.D: Appl.Phys.*, 54, 104004, 2021.

4:30 PM SB04.07.02

Solid-state Organic Electrochemical Transistor with Adjustable Biomimetic Properties for Spiking Neurons Hsin Tseng¹, Anton Weissbach¹, Lukas M. Bongartz¹, Laurie E. Calvet², Karl Leo¹ and Hans Kleemann¹; ¹Technische Universität Dresden, Germany; ²C2N, Université Paris-Saclay-CNRS, France

Neuromorphic devices and circuits offer huge potential for hardware-based neuromorphic computing and next-generation, power-efficient artificial intelligence (AI). Organic electrochemical transistors (OECTs) and related devices emerged as an interesting class of devices for neuromorphic computing as the interplay between ions and electrons in OECTs can be considered biomimetic. The research on OECTs mainly focuses on developing powerful and versatile artificial synapses for conventional AI paradigms, e.g., feed-forward neural networks. However, because of their biomimetic operation, OECTs might also be used to build bio-inspired spiking neurons for next-generation power-efficient computing. Here, we show an OECT with photo-patternable solid electrolyte advancing towards the integration of bio-inspired neurons. We discuss how the neuromorphic properties of OECTs, i.e. the time constants of the ionic and electronic subcircuit of the device, can be controlled by process and device parameters. We also demonstrate the first step towards the integration of Morris-Lecar inspired neurons, which offer type-I and type-II excitability in their spiking behavior. In particular, we discuss how the specific properties of the solid-state electrolyte OECTs, such as threshold voltage, subthreshold slope, hysteresis, and off-current leakage, influence the function of the subcircuit of our biomimetic neuron. The solid-state electrolyte OECT paves the foundation towards the integration of neuromorphic devices beyond artificial synapses, and the small-scale integration of OECTs exhibit potential for building blocks of next-generation spiking neuron circuits.

4:45 PM SB04.07.03

Neuromorphic Memory with Hydrogen Doped Rare-Earth Perovskite Nickelates Tae Joon Park, Hai-Tian Zhang and Shriram Ramanathan; Purdue University, United States

Strongly correlated perovskite nickelates (RNiO₃) have attracted great interest in condensed matter sciences due to its unique electrical properties such as metal-to-insulator transition. Hydrogenation induced electron doping leads to a phase transition in this material system independent of temperature. The electrical conductivity of RNiO₃ is extremely sensitive to the electron occupancy of Ni 3d orbitals. The electron from hydrogen occupies Ni eg orbital and results in remarkable resistance change by several orders of magnitude. The proton resides on interstitial sites of NiO₆ octahedra and can be mobile under electric fields. In this work, we applied high-speed voltage pulses and measured the resistance changes of hydrogen doped NdNiO₃ devices fabricated with conducting oxide (FTO) electrodes. We will discuss the effect of voltage pulses on proton migration in the nickelate device, which enables thousands of analog states with highly tunable electronic structures. Interestingly, non-volatile memory trees can be demonstrated in perovskite nickelate device at room temperature by applying consecutive positive or negative voltage pulses emulating synaptic weight branching noted in animal brains. This behavior is akin to magnetic frustration in spin-glasses at low temperatures. The complex synaptic behavior in perovskite nickelate devices can open up new avenues for design of memories for neuromorphic computing.

5:00 PM SB04.07.04

Stochastically Switching HfO₂/TiO_x ReRAM Devices for Spiking Neural Network Synapses Felix J. Cüppers¹, Christopher Bengel², Melika Payvand³, Rainer Waser^{1,2}, Stephan Menzel¹ and Susanne Hoffmann-Eifert¹; ¹Forschungszentrum Jülich GmbH, Germany; ²RWTH Aachen University, Germany; ³ETH Zürich, Switzerland

In today's computing architectures, fundamental physical limits are increasingly prohibiting performance improvements. At the same time, the amount of data, recorded by an ever rising number of sensors in various applications, is growing rapidly. In order for computers to keep up with this contradiction, new computing paradigms are required. Neuromorphic technologies are seen as key solutions as they can be employed at the edge of the sensors, rendering the need for storing the data or sending them to remote clouds. Augmenting these devices with emerging memory technologies empowers them with non-volatile and adaptive properties, which are desirable for low power and online learning requirements at the edge, independently from remote cloud computers. However, an energy- and area-efficient realization of such systems requires disruptive hardware and algorithm changes. Solutions based on memristive devices are in the focus of research and industry due to their low-power and high-density online learning potential. Specifically, the filamentary-type valence change mechanism (VCM) memories have shown to be promising candidates. Because of CMOS compatibility, HfO₂-based cells are among the most researched devices and are nearing industrial maturity. In consequence, physical models capturing a broad spectrum of experimentally observed features such as the pronounced cycle-to-cycle and device-to-device variability are required for accurate evaluation of the proposed concepts. In this study, we present an in-depth experimental analysis of device-to-device and cycle-to-cycle variability of filamentary-type bipolar switching HfO₂/TiO_x nano-sized crossbar devices. A match of the experimentally obtained statistics and variabilities to our physically motivated, variability-aware JART VCM compact model [1] is established. The high degree of agreement between model and experiment allows us to evaluate the concept of parallel memristive devices forming a single synapse. Both experimental and theoretical results are presented and conditions for favorable properties of such synapses are defined. The interplay of cycle-to-cycle and device-to-device variability is analyzed in detail and descriptive figures of merit are defined, since the proposed concept should retain its functionality in case of devices with lower variability.

These parallel compound synapses form a synaptic array which is at the core of many neuromorphic chips. We exploit the cycle-to-cycle variability of the single devices for stochastic online learning which has shown to increase the effective bit precision of the synapses [2]. Finally, we demonstrate the stochastic switching operation as synapse update method in a Spiking Neural Network which classifies two patterns. In this small scale demonstrator, perfect accuracy is achieved, proving the feasibility of this alternative synapse concept. [3]

- [1] C. Bengel, A. Siemon, F. Cüppers, S. Hoffmann-Eifert, A. Hardtdegen, M. von Witzleben, L. Hellmich, R. Waser and S. Menzel, Variability-Aware Modeling of Filamentary Oxide based Bipolar Resistive Switching Cells Using SPICE Level Compact Models, *TCAS I* **67**, 4618–4630 (2020)
[2] S. Gupta, A. Agrawal, K. Gopalakrishnan and P. Narayanan, Deep Learning with Limited Numerical Precision, 1737–1746 (2015)
[3] C. Bengel, F. Cüppers, M. Payvand, R. Dittmann, R. Waser, S. Hoffmann-Eifert and S. Menzel, Utilizing the Switching Stochasticity of HfO₂/TiO_x-Based ReRAM Devices and the Concept of Multiple Devices for the Classification of Overlapping and Noisy Patterns, *Frontiers in Neuroscience* **15**, 621 (2021)

SESSION SB04.08: Materials for Neuromorphic Devices
Session Chair: Yoeri van de Burgt
Monday Morning, December 6, 2021
SB04-Virtual

10:30 AM *SB04.08.01

“Lithionics”—On the Design of Lithium Oxides for Novel Neuromorphic Computing Functions Jennifer L. Rupp; Massachusetts Institute of Technology, United States

Next generation of energy storage may largely benefit from fast Li⁺ ceramic electrolyte conductors to allow for safe and efficient batteries. With recent discoveries in thin film processing solid-state lithium ion conductors, such as Li-garnets and LIPON or LiSICON-based solids, have been recently considered as candidate materials not only for next-generation solid-state batteries but also for neuromorphic computing via memristors owing to the fast ionic transport in the solid-state electrolyte.

In the first part of this talk, we review current needs and challenges in the field of solid state batteries. We underline the advantages of various Li solid-state conductor materials and reflect on opportunities of thin film processing, being a requirement to define precisely the Lithium stoichiometries and related electronic state changes for transition metal ions, miniaturize the device, and reach high energy/information densities for energy storage, computation, and sensing.

In the second part, we focus on Li-film processing and controlling Lithium stoichiometries to reach fast conductive phases for Li garnets and Li titanates as solid state battery components, and memristive neuromorphic computing units. Insights on structure-phase-transport interaction and implications on performances will be exemplified for energy storage aiming high energy densities, and modulations of synaptic artificial weights through lithium induced metal-to-insulator transitions in lithium titanate memristors.

11:00 AM SB04.08.02

Ruthenium Prussian Blue Analogue for Electrochemically Programmed Artificial Synapses Donald A. Robinson, Austin Bhandarkar, Elliot J. Fuller, Vitalie Stavila, David Ashby, Catalin Spataru, Christopher Bennett, Matthew Marinella, Mark D. Allendorf and A. A. Talin; Sandia National Laboratories, United States

Artificial neural networks based on electrochemical random-access memory (EC-RAM) represent an emerging strategy for low power analog computing. EC-RAM synapses operate by virtue of linear/symmetric resistance tuning through electrochemically gated control of the charge state of a resistive channel. The exploration of promising active materials for EC-RAM functionality was previously limited to semiconducting organic polymers and metal oxides. Here we demonstrate a Ru-based Prussian Blue Analogue (RuPBA), an electroactive mixed valence semiconductor with a cyanide-bridged framework structure, as a new candidate material for EC-RAM devices. Our fabrication method employs inkjet printing to prepare both the RuPBA and ionogel electrolyte films. The RuPBA channel resistance depends on the electrochemically tunable ratio of Ru^{II} to Ru^{III} and the degree of cation intercalation in the micropores of the material. The relationship between charge state, resistance, and electronic structure is elucidated using *in-operando* Raman and UV/Vis/NIR spectroscopy. The RuPBA devices exhibit excellent linearity, symmetry, and consistency during pulsed voltage programming, as well as long term retention of conductance state.

11:15 AM SB04.08.03

Modeling and Measurement of Non-Linear Electrical Properties of Self-Assembled Ag₂S Nanowire Resistive Switching Networks for Neuromorphic Applications Mahshid Hosseini, Nikolay Frick, Damien Guilbaud, Ming Gao and Thomas LaBean; North Carolina State University, United States

Among the outstanding capabilities of biological brains is their ability to visualize, memorize, and recognize objects in erratic and unstable environments. The strength, versatility, and fault-tolerance of brains result from the sheer number of synaptic connections between neurons that is estimated to be ~10¹⁴-10¹⁵ in a human brain. Reactivation of specific groups of neurons and the strength of connections between them play important roles in memorization and information processing. In the age of new information and communications technologies, these traits, among others, serve as motivation for design choices in development of bio-inspired computing technologies. Neuromorphic computing and artificial neural networks today represent an example of the most successful bio-inspired technologies that excel in a broad range of classification and regression tasks.

A large portion of current efforts to reach the goal of neuromorphic systems focuses on the use of ordered nanodevice structures, most notably the memristor crossbar array. Lithographic fabrication of such ordered structures inherently limits neuromorphic systems' complexity and scale and cannot mimic the sheer scale of complex interconnections of biological neural networks. In this study, two-dimensional, stochastic, self-assembled, bio-inspired, highly interconnected silver sulfide (Ag₂S) nanowire networks are studied experimentally and through simulation to investigate their usefulness for neuromorphic hardware applications, potentially for use in Reservoir computers. Resistive switching behaviors resulting from the electromigration interaction between memristive nanowires are explored. Single memristive Ag₂S nanowire, as well as small, randomly assembled networks of NWs with countable numbers of components, are also studied. We further compare experimental measurements with predictions from a novel simulation model, the "stochastic drift R_{ON} memristor model". This computational model suggests that R_{ON}, the resistance observed in the memristors' ON state, is not a constant but rather a function of the volume fraction of reduced silver ions in the Ag₂S matrix. In the experimental memristive systems described, several crucial synaptic functions are demonstrated, such as learning, forgetting, paired-pulse facilitation, and short-term plasticity. Some aspects of the physical mechanisms of the devices are also inferred from the observed behaviors. The self-assembled nanodevices and device networks described in this research

are first steps toward three-dimensional randomly self-assembled nanocomposite memristor networks for neuromorphic computing applications. Such materials represent promising candidates for next-generation biomimetic hardware. A critical issue yet to be resolved involves interfacing such memristive device networks with multi-electrode arrays such that finer-grained substates of the networks' electrical behaviors can be simultaneously and continuously read and routed for biologic-like computational tasks. This work aims to provide a convenient, low cost and low-power physical implementation for Reservoir Computing research with potential applications in communications, signal processing, and control.

11:30 AM SB04.08.04

Closed-Loop Biomimetic Synapse for Neuromorphic Network Design Ugo Bruno, Daniela Rana and Francesca Santoro; Italian Institute of Technology, Italy

As conventional silicon based computing techniques are reaching their limits in terms of energy consumption and density[1], neuromorphic platforms are emerging as new computational paradigm[2], with the ultimate goal of replicating the efficiency of the brain in terms of parallel computation. Among the plethora of the available materials and structures, organic electrochemical transistors (OECTs) have emerged for their natural ionic-to-electronic signal transduction, biocompatibility and possibility of operating in aqueous environment[3]. In particular, PEDOT:PSS based OECTs have been exploited to recapitulate neurotransmitter-mediated synaptic plasticity[4], in which the oxidation of a neurotransmitter modulates the doping state of the transistor, resulting in a change in device conductivity, de facto emulating the synaptic conditioning naturally occurring in biological synapses.

While successfully recapitulating spike-dependent plasticity, this approach still lacks the self-regulation mechanisms naturally found in neuronal networks: when the post-synaptic neuron is engaged in the neurotransmitter-mediated communication, receptor recycling occurs[5], while astrocytes provide a feedback onto the presynaptic terminal, to reduce or increase the release of such neurotransmitter[6]. Moreover, the PEDOT:PSS-based neuromorphic transistor, if used as a building block of an artificial network, would lead to a continuous de-doping of the devices, ultimately leading to the exhaustion of the network dynamics, because of the unidirectional modulation of the synaptic weight.

Taking inspiration from the nigrostriatal DA pathway, in which the endogenously generated H₂O₂ activates K⁺ channels, inhibiting DA neuron firing[7], a closed-loop synapse is proposed, in which the bidirectional modulation of the synaptic weight is shown. In particular, the output current of the device closes a feedback loop, allowing for a controller to drive a microfluidic system. As a result, an influx of dopamine (DA), and its subsequent oxidation, is used to cause the de-doping of both OECT gate and channel, while the inverse reaction can be induced by the introduction of hydrogen peroxide (H₂O₂). The presence of the control system proposed here introduces the astrocytes-like effect of presynaptic input regulation, naturally found in neural networks. This enables for synaptic weight control while avoiding the uncontrolled doping/de-doping of the PEDOT:PSS.

Ultimately, this platform paves the way for the creation of biomimetic complex systems. A network of artificial neurons can be designed in which the output depends on the presence of a neurotransmitter while each node can still be individually controlled, to induce and study topology-dependent dynamics propagation across the network.

1. Hassan, S., Humaira & Asghar, M. Limitation of Silicon Based Computation and Future Prospects. in 2010 Second Int. Conf. Commun. Softw. Netw. 559–561 (2010). doi:10.1109/ICCSN.2010.81
2. van de Burgt, Y., Melianas, A., Keene, S. T., Malliaras, G. & Salleo, A. Organic electronics for neuromorphic computing. Nat. Electron. 1, 386–397 (2018).
3. Friedlein, J. T., McLeod, R. R. & Rivnay, J. Device physics of organic electrochemical transistors. Org. Electron. 63, 398–414 (2018).
4. Keene, S. T., Lubrano, C., Kazemzadeh, S., Melianas, A., Tuchman, Y., Polino, G., Scognamiglio, P., Cinà, L., Salleo, A., van de Burgt, Y. & Santoro, F. A biohybrid synapse with neurotransmitter-mediated plasticity. Nat. Mater. 19, 969–973 (2020).
5. Jung, N. & Haucke, V. Clathrin-Mediated Endocytosis at Synapses. Traffic 8, 1129–1136 (2007).
6. Newman, E. A. New roles for astrocytes: Regulation of synaptic transmission. Trends Neurosci. 26, 536–542 (2003).
7. Rice, M. E. H₂O₂: A Dynamic Neuromodulator. The Neuroscientist 17, 389–406 (2011).

11:45 AM SB04.08.05

Oxygen Composition Dependence of Forming Characteristics in Analog Resistive Switching Cells with Pt/TaO_x/Ta₂O₅/Pt Stack Structure Toshiki Miyatani¹, Tsunenobu Kimoto¹ and Yusuke Nishi^{1,2}; ¹Kyoto University, Japan; ²NIT Maizuru College, Japan

Resistive switching (RS) cells are promising as synaptic devices owing to analog controllability of the cell resistance. However, most transition metal oxide-based RS cells often show an abrupt decrease in the cell resistance (set process), resulting in the difficulty of the analog control of the cell resistance by the applied voltage [1]. Moreover, although some studies have reported gradual set processes, the mechanism of the gradual set processes is not clear [2]. Therefore, no design rules exist to improve the analog RS characteristics. In our previous study, we reported that analog RS characteristics can be obtained by adjusting the applied voltage after the unique forming process (semi-forming) in Pt/TaO_x/Ta₂O₅/Pt cells [3]. In this study, we mainly investigated the impacts of oxygen composition of the TaO_x layer on the semi-forming characteristics for the purpose of clarifying the mechanism of the semi-forming and subsequent analog RS phenomena.

We fabricated platinum (Pt)/tantalum sub-oxide (TaO_x)/tantalum oxide (Ta₂O₅)/Pt stack cells on a SiO₂/Si substrate. A 60-nm-thick Pt bottom electrode (BE) was deposited by DC sputtering. Then, a 10-nm-thick Ta₂O₅ and a 20-nm-thick TaO_x layer were deposited by reactive RF sputtering with different oxygen gas flow rates. The oxygen composition of the TaO_x layer was controlled by appropriately adjusting the oxygen gas flow rate between 0.8 sccm and 1.2 sccm. Finally, 25-nm-thick Pt top electrodes (TE) with various diameters (100–300 μm) were formed by electron beam evaporation. We evaluated forming characteristics by performing a current sweep on the Pt/TaO_x/Ta₂O₅/Pt cells with the BE grounded at room temperature.

Two types of initial transition processes occur in the Pt/TaO_x/Ta₂O₅/Pt cells. One is the transition process to a low resistance state (LRS) less than 100 Ω, which is conventionally called a forming phenomenon. The other is the transition process to a higher resistance state than the LRS, which is defined as a semi-forming phenomenon. Next, we examined dependences of the oxygen composition (*x*), initial resistance (*R*_{ini}), and occurrence frequency of the semi-forming phenomenon (*F*_{semi}) on the oxygen flow rate during deposition of a TaO_x layer (*f*_{O_x}). First, *x* is proportional to *f*_{O_x}, and the *f*_{O_x} range of 0.8–1.2 sccm corresponds to the *x* range of 1.3–2.0. Second, as *x* linearly increases, *R*_{ini} exponentially increases and *F*_{semi} tends to decrease. Here, we have reported that *R*_{ini} is mainly dominated by the hopping conduction through oxygen vacancies (V_OS) in the Ta₂O₅ layer [4]. The density of localized states corresponding to the V_O density was estimated from the temperature dependence of *R*_{ini} in each Pt/TaO_x/Ta₂O₅/Pt cell, resulting in that the density of localized states exponentially decreased from roughly 10²² cm⁻³eV⁻¹ to 10¹⁹ cm⁻³eV⁻¹ as *x* linearly increased from 1.3 to 1.7. In other words, the density of V_OS supplied from the TaO_x layer to the Ta₂O₅ layer decreases with increasing *x*.

From the above results, although the semi-forming phenomenon is more likely to occur as more V_OS are supplied to the Ta₂O₅ layer, the more supplied V_O causes the decrease in *R*_{ini}, bringing about a decrease in the resistance range of RS operation. To obtain the semi-forming and subsequent analog RS characteristics in the high-resistance range for reduction of power consumption, it is necessary to appropriately control the oxygen composition of the TaO_x layer.

[1] D. Ielmini, *Microelectronic Engineering*, **190**, 44 (2018).

[2] R. Waser *et al.*, *Faraday Discuss.* **213**, 11 (2019).

[3] T. Miyatani *et al.*, 2020 virtual MRS spring/fall meeting, F. NM07. 06. 06.

[4] T. Miyatani *et al.* *Jpn. J. Appl. Phys.* **58**, 090914 (2019).

12:00 PM SB04.08.06

Optimization of Projected Phase Change Memory for Application in Analog Neuromorphic Computing Ning Li¹, Kevin Brew², Timothy Philip², Charles Mackin³, Juntao Li², Andrew Simon², Ching-Tzu Chen¹, Syed Ghazi Sarwat⁴, Seong Soon Jo², Injo Ok², Praneet Adusumilli², Malte Rasch¹, Matthew BrightSky¹, Geoffrey W. Burr³, Abu Sebastian⁴, Nicole Saulnier² and Vijay Narayanan¹; ¹IBM T.J. Watson Research Center, United States; ²IBM Research - Albany NanoTech, United States; ³IBM Almaden Research Center, United States; ⁴IBM Research-Zurich, Switzerland

Phase change memory (PCM) is a promising candidate for non-von Neumann based analog in-memory computing – particularly for inference of previously-trained Deep Neural Networks [1,2], as well as Neuromorphic computing [3,4]. Many factors including resistance values, memory window, resistance drift, read noise, and programming accuracy impact the performance of PCM in analog neuromorphic computing applications. We previously showed that resistance drift and noise of a mushroom-type PCM device can be reduced by introducing an additional projection liner [5]. The projection liner comprised of a non-phase change material could decouple the read operation from the write operation and help mitigate the non-ideal attributes such as drift and noise.

Here, we perform a systematic study of the electrical properties of these PCM devices—including resistance values, drift, noise, and endurance—and discuss the implications for in-memory computing. We optimize the PCM and projection liner materials to have effective drift mitigation while retaining a large enough memory window. We also examine how endurance cycling affects the phase change materials and the electrical characteristics of the devices. The results show that the liner is helping to maintain a rather constant reset resistance throughout the endurance cycles. With a widened memory window, no degradation in the drift mitigation through the cycling, and reduced read noise, these cycled PCM devices are shown to deliver excellent balance of performance for analog AI applications. Finally, the performance of these PCM devices for neural network inference is analyzed for state-of-the-art image processing and natural language processing tasks.

[1] P. Narayanan, et al., Fully On-Chip MAC at 14nm Enabled by Accurate Row-Wise Programming of PCM-Based Weights and Parallel Vector-Transport in Duration-Format, Proc. VLSI Tech. Symposium, 2021

[2] R. Khaddam-Aljameh, et al., HERMES Core – A 14nm CMOS and PCM-based In-Memory Compute Core using an array of 300ps/LSB Linearized CCO-based ADCs and local digital processing, Proc. VLSI Circuits Symposium, 2021

[3] I. Boybat, et al., Neuromorphic Computing with Multi-Memristive Synapses, Nature Communications 9, 2514, 2018

[4] G. W. Burr, et al., Neuromorphic computing using non-volatile memory, Advances in Physics: X, 2:1, 89, 2017

[5] R. Bruce, et al., Mushroom-type phase change memory with projection liner: an array-level demonstration of conductance drift and noise mitigation, Proc. IRPS, 2021

SESSION SB04.09: Materials and Devices for Neuromorphic Computing I

Session Chair: Priyadarshini Panda

Monday Afternoon, December 6, 2021

SB04-Virtual

1:00 PM *SB04.09.01

Artificial Intelligence with Radio-Frequency Spintronic Synapses Nathan Leoux¹, Alice Mizrahi¹, Danijela Marković¹, Dédalo Sanz-Hernández¹, Juan Trastoy¹, Paolo Bortolotti¹, Leandro Martins², Alex Jenkins², Ricardo Ferreira² and Julie Grollier¹; ¹Université Paris-Saclay, France; ²International Iberian Nanotechnology (INL), Portugal

For numerous Radio-Frequency applications such as medicine, RF fingerprinting or radar classification, it is important to be able to apply Artificial Neural Network on RF signals. In this work we show that it is possible to apply directly Multiply-And-Accumulate operations on RF signals without digitalization, thanks to Magnetic Tunnel Junctions (MTJs). These devices are similar to the magnetic memories already industrialized and compatible with CMOS. These devices are promising RF emitters. Like biological neurons, MTJs are non-linear oscillators, and it was already proven that they can efficiently emulate neurons in the framework of reservoir computing. These junctions can also be used as detectors and rectify RF signals.

We show experimentally that a chain of these MTJs between 250 and 400 nm of diameters can rectify simultaneously different RF signals, and that the synaptic weight encoded by each junction can be tune with their resonance frequency. Our architecture benefits both from frequency-multiplexing of the RF inputs and from the frequency selectivity of MTJs to route the information with a compact architecture.

Through simulations we train a layer of these junctions to solve the dataset “digits” with an accuracy as good as software neural networks (99.96 %). Finally, we show that our system can scale to multi-layer neural networks using MTJs to emulate neurons. In the future these MTJs could be scaled down to 10 nm.

Our proposition is a parallel and compact system that allows to receive and process RF signals in situ and at the nanoscale.

This work was supported by the European Research Council ERC under Grant bioSPINspired 682955, the French ANR project SPIN-IA (ANR-18-ASTR-0015) and the French Ministry of Defense (DGA).

1:30 PM *SB04.09.02

Memristor-Based Neuromorphic Design for Temporal Pattern Processing and Learning Hai Li, Ziru Li and Brady Taylor; Duke University, United States

Memristor technology provides a more efficient solution to emulating the behaviors of synapses and neurons in neuromorphic systems compared to conventional CMOS technology. Memristive resistances can store synaptic weights, while memristive nonlinearity can be exploited for neuron circuits. Achieving the advanced learning capabilities and adaptability of the brain requires further circuitry to leverage the characteristics of these memristive devices. Basic spike-based learning algorithms such as spike-timing-dependent plasticity (STDP) have previously been demonstrated. In addition, circuits for exploiting novel device dynamics for flexible and powerful training rules will promote computationally efficient intelligence that approaches that of the human brain.

Spike-based encoding methods enable more efficient data processing when applied to memristor-based hardware for artificial deep (DNNs) and spiking neural networks (SNNs). In these designs, the memristor-based synapses take in binary spike trains rather than analog voltages, avoiding power-hungry analog-to-digital conversions and thus elevating energy efficiency. Encoding data as a binary spike train has historically involved generating proportional

spike rates. However, an increase in data value corresponds to an increase in the number of spikes. Temporal coding encodes data as discrete timings of voltage spikes for a much more efficient and precise method of representing data. For example, time-to-first-spike (TTFS) encodes data as the arrival time of the first spike during a predefined time period [1]. It minimizes spike numbers by using only one spike to carry data.

In realizing such neuromorphic systems, new ideas and approaches must be advocated. Architectures consisting of simple crossbar synapses and integrate-and-fire neurons should be adapted in favor of more biologically derived but often oversimplified models. Each component of a neural system incorporates its own unique dynamics and offers opportunities for a behaviorally parallel circuit to be developed and incorporated into a sophisticated neuromorphic design. Furthermore, the fast-shrinking factor size of novel devices promotes the potential for computationally dense neuromorphic building blocks. Following these methodologies, we proposed a memristor-based single-spiking processing engine with a set of circuitry designs for supporting DNN inference with the TTFS scheme, leading to faster computations and lower energy consumption [2]. Compared to conventional memristor-based dot product engines that encode data as the amplitude of voltages or currents, this design leverages the advanced spike-based encoding to shorten the computational period and pursue high efficiency. Furthermore, we demonstrated in-situ learning in a memristor crossbar using a methodology for single-spike-encoded STDP that could be incorporated into a TTFS system [3].

In our future exploration, we will investigate techniques for building large-scale memristor-based neuromorphic systems with online learning capabilities. The targeted system should support both the inference of input data and the update of neural network parameters. Circuit/architecture-level designs are required to implement either supervised or unsupervised learning rules with memristors while ensuring the forward and backward data paths do not interfere with each other.

References:

- [1] S. Thorpe, A. Delorme, and R. Van Rullen, "Spike-based strategies for rapid processing," *Neural Networks*, vol. 14, no. 6-7, pp. 715-725, 2001.
- [2] Z. Li, B. Yan, and H. Li "ReSiPE: ReRAM-based Single-Spiking Processing-In-Memory Engine," in 2020 57th ACM/IEEE Design Automation Conference (DAC), pp. 1-6, 2020.
- [3] B. Taylor, A. Shrestha, Q. Qiu, and H. Li. "IS1R-Based Stable Learning Through Single-Spike-Encoded Spike-Timing-Dependent Plasticity." 2021 IEEE International Symposium on Circuits and Systems (ISCAS), pp. 1-5, 2021.

2:00 PM *SB04.09.03

Robust RRAM-Based In-Memory Computing in Light of Model Stability Gokul Krishnan¹, Li Yang¹, Jingbo Sun¹, Jubin Hazra², Xiacong Du¹, Maximilian Liehr², Karsten Bechmann², Rajiv Joshi³, Nathaniel C. Cady², Deliang Fan¹ and Yu Cao¹; ¹Arizona State University, United States; ²SUNY Polytechnic Institute, United States; ³IBM T.J. Watson Research Center, United States

Artificial intelligence (AI) today outperforms humans for a variety of applications, such as computer vision and natural language processing. Higher accuracy comes at the cost of increased computational complexity and model size, stressing already limited memory access.

RRAM-based in-memory computing (IMC) provides a dense and parallel structure to achieve high performance and energy efficiency in AI computing. The increased energy-efficiency is attributed to a full-custom design following the assumption that all weights are stored on-chip. However, such an assumption results in a significant area overhead, especially when the AI model size is rapidly increasing. Hence, model compression (e.g. pruning and quantization) is necessary for RRAM-based in-memory acceleration.

When an AI model is mapped to realistic RRAM devices, it will suffer from various non-idealities, such as statistical variations, quantization error, stuck-at-faults, and limited resistance ratio. These issues pose a significant challenge to designing robust RRAM-based IMC architectures. For instance, statistical variations in RRAM cause deviations in the programmed resistance, leading to a significant loss in post-mapping accuracy (i.e., accuracy in the presence of RRAM variations) for AI models. To mitigate the post-mapping accuracy loss, variation-aware training (VAT) is employed. VAT exploits the inherent redundancy in the AI model by embedding the device variations, based on a log-normal or normal distribution model, into the training process to achieve a variation-tolerant model, with no need of re-training for each individual RRAM chip.

Under model pruning and quantization, the efficacy of conventional VAT methods is reduced due to increased model sensitivity to variations, although a lower precision may help improve the tolerance. These algorithmic and device issues interact with each, affecting the optimal design choice of RRAM-based IMC. Hence, there is a need for a more systematic solution for robust RRAM-based in-memory computing with sparse and quantized AI models. In this work, we propose a model stability-based VAT approach to recover the post-mapping accuracy with model compression. The proposed method utilizes VAT to train the compressed model with different scales of device variations and search for the most stable model to improve post-mapping accuracy. For a given model, higher model stability implies better tolerance of variations and thus, higher post-mapping accuracy. The model stability is visualized by the loss landscape and evaluated by the roughness score. A lower roughness score indicates a smoother loss landscape and a more stable model. We utilize a structured pruning method and model quantization to compress the AI model. The pruning method considers the mapping of the model on to the RRAM crossbar for best IMC performance. We illustrate that pruning results in a less stable model, while quantization improves the model stability.

For accurate modeling, we measured statistical variations from a 65nm CMOS/RRAM 1T1R chip and developed a cross-layer benchmarking tool. This tool incorporates RRAM device models, IMC architecture, pruning and quantization, and evaluation of model stability and outputs post-mapping accuracy, hardware performance, and model stability.

The major contributions of this work are as follows: (1) Based on the roughness score and loss landscape, we present that quantization (low-precision) improves the model stability, but pruning reduces the stability; (2) We propose a model stability-based VAT method, which searches the most stable model under variations to achieve the best post-mapping accuracy, without knowing the exact amount of RRAM testing variations upfront; and (3) We demonstrate that the proposed method achieves up to 19%, 21%, and 11% improvement in post-mapping accuracy on CIFAR-10, CIFAR-100, and SVHN datasets, respectively.

2:30 PM SB04.09.04

Electric Mott Transition and Neuromorphic Applications of Mott Insulators Laurent Cario, Julien Tranchant, Marie-Paule Besland, Benoit Corraze and Etienne Janod; CNRS-Université de Nantes, France

A great challenge in the field of neurocomputing is to mimic the brain behaviour by implementing artificial synapses and neurons directly in hardware. So far, many works were devoted to the realisation of artificial synapses but the realisation of artificial neurons in hardware is still scarce. This work shows that Mott insulators are interesting inorganic materials to consider in order to achieve this goal.

Mott Insulators experience resistive switching above a threshold electric field [1-4]. This resistive switching is related to the creation of hot carriers leading to an electronic avalanche breakdown and a burst of current in the electronic circuit (Firing event) [2]. Moreover, under a train of electric field pulses, narrow gap Mott insulators behave as a leaky integrators of hot carriers and this phenomenon could be modelled assuming the creation of a metallic phase at the local scale [3,4]. Narrow-gap Mott insulators subjected to electric pulsing can therefore implement the three basic functions Leaky Integrate and Fire (LIF) of artificial neurons [5]. A simple two terminal device made of Mott insulator thin film can therefore be considered as a promising LIF artificial neuron. This work shows the realisation and tests of such downscalable artificial neurons made with Mott insulators. [6]

References:

- [1] E. Janod, *et al.*, *Adv. Funct. Mater.* 2015, 25, 6287.
- [2] V. Guiot, *et al.* *Nat Commun* 2013, 4, 1722; P. Diener, *et al.*, *Phys. Rev. Lett.* 2018, 121, 016601; D. Babich, *et al.*, *Physics and Simulation of*

Optoelectronic Devices XXVIII; 2020, 112740B..

[3] P. Stoliar *et al.*, Adv. Mater. 2013, 25, 3222.

[4] P. Stoliar *et al* Phys. Rev. B 2014, 90, 045146.

[5] P. Stoliar *et al.*, Adv. Funct. Mater. 2017, 27, 1604740; F. Tesler, *et al.*, Phys. Rev. Appl. 2018, 10 (5), 054001; C. Adda *et al.* J. Appl. Phys. 2018, 124 (15), 152124.

[6] C. Adda *et al.*, MRS Com. 2018, 8, 835–841.

2:45 PM SB04.09.05

Beyond-CMOS Vanadium Dioxide Devices and Oscillators for Brain-Like Information Processing Stefania Carapezzi¹, Gabriele Boschetto¹, Siegfried Karg² and Aida Todri-Sanial¹; ¹LIRMM, University of Montpellier, CNRS, France; ²IBM Research Europe - Zurich, Switzerland

In recent years, the improvement of traditional computing machines has been assisted by the Moore's law. However, nowadays, further shrinking of device dimensions is currently impeded by the reaching of physical limits. Additionally, the separation between storage and processing of data in von Neumann classical machines is power consuming, in contrast with the trend of reduction of energy intake for greener electronics. The human brain is an example of how sophisticated tasks may be accomplished by a computing engine with reduced power consumption. Then, neuromorphic computing can provide new precious insights, ready for being hardware-translated. In this respect, oscillatory neural networks (ONNs) are appealing ultra-low-power neuromorphic architectures able to perform intelligent tasks, such as pattern recognition [A]. In the present contribution, we propose the innovative concept of implementing ONN by Beyond Complementary-Metal-Oxide-Semiconductor (CMOS) devices. In particular, we show experimental and simulation results of oscillators based on vanadium dioxide (VO₂). VO₂ is a transition metal oxide (TMO) that undergoes a phase transition from a high-resistive monoclinic (M1) crystal structure to a low-resistive tetragonal rutile-like (R) one. This phase transition takes the name of insulator-to-metal transition (IMT) and it is triggered by temperature. The IMT brings a resistive switching in VO₂, where the resistivity change may be up to several orders of magnitude. It has been observed that the switch in resistance occurs as well in VO₂ two-terminal devices, where self-heating is thought to play the main role. This occurrence is a key factor in implementing highly compact and scalable oscillators. We will investigate devices fabricated on Si-compatible technology on SiO₂ substrate [B]. The lattice mismatch between the VO₂ layer and the SiO₂ substrate gives rise to a typical granular texture. We will use dedicated technology computer-aided design (TCAD) 3D electrothermal simulations of VO₂ devices [C] and of the associated VO₂ oscillators to assess the impact of this grainy structure over the device performances with a multi-scale approach that considers material properties and device architectures. Our findings will help shed light on the entangled thermal and electrical behavior of VO₂ oscillators and can help provide guidelines for the successful implementation of ONN technology.

[A] A. Todri-Sanial, S. Carapezzi, C. Delacour, M. Abernot, T. Gil, E. Corti, et al., "How Frequency Injection Locking Can Train Oscillatory Neural Networks to Compute in Phase," preprint, hal-lirmm.ccsd.cnrs.fr/lirmm-03164135, 2021.

[B] E. Corti, J. A. Comejo Jimenez, K. M. Niang, J. Robertson, K. E. Moselund, B. Gotsmann, et al., "Coupled VO₂ Oscillators Circuit as Analog First Layer Filter in Convolutional Neural Networks," Front. Neurosci., vol. 15, 2021

[C] S. Carapezzi, C. Delacour, G. Boschetto, E. Corti, M. Abernot, A. Nejim, et al., "Multi-Scale Modeling and Simulation Flow for Oscillatory Neural Networks for Edge Computing," 19th IEEE Interregional NEWCAS Conference, 2021.

SESSION SB04.10: Biointerfacing and Artificial Sensorimotor Systems II

Session Chair: Yoeri van de Burgt

Monday Afternoon, December 6, 2021

SB04-Virtual

4:00 PM *SB04.10.01

Organic Nervetronics for Artificial Afferent/Efferent Nerves Yeongjun Lee¹, Jin Young Oh², Yeongin Kim³, Alex Chortos⁴, Wentao Xu⁵, Dae-Gyo Seo⁶, Gyeong-Tak Go⁶, Zhenan Bao⁷ and Tae-Woo Lee⁶; ¹Samsung Advanced Institute of Technology, Korea (the Republic of); ²Kyung Hee University, Korea (the Republic of); ³Massachusetts Institute of Technology, United States; ⁴Purdue University, United States; ⁵Nankai University, China; ⁶Seoul National University, Korea (the Republic of); ⁷Stanford University, United States

Biological nerves can efficiently process complex information in real-time. To implement biological event-driven and parallel operation artificially, organic nervetronics have been upsurged. The artificial synapses can be combined with sensors and actuators to emulate the functions of biological sensory and motor neurons with a simple circuit structure. Furthermore, compared to CMOS-based von Neumann computing systems, they consume 10⁻⁶ times less energy to operate. This organic nervetronics can be a new strategy for soft robotics and neuroprosthetics by emulating biological neuroplasticity events that have not been existed nerve before.

Here, we developed an artificial nerve that emulates biological afferent and efferent nerve. The flexible artificial afferent nerve consists of a resistive pressure sensor, organic ring oscillator, and artificial synapse. Sensory signals are converted into spike signals and processed in the artificial synapse, thus movement, simultaneous pressure, and braille characters can be detected through an artificial afferent nerve. The connection of biological organs and artificial afferent nerves shows a hybrid reflex arc that shows future applicability for neural prostheses. The movement of the detached cockroach leg can be controlled by external sensory information. Also, an artificial auditory system was developed by integrating a triboelectric nanogenerator an artificial synapse. The optoelectronic artificial efferent nerve can be constructed by integration of a photodetector, stretchable artificial synapse, and a polymer actuator (role of an artificial muscle). This optoelectronic artificial sensorimotor nerve emulates optogenetically engineered neurons and synapses. The contraction of artificial muscles well imitates biological muscle contraction. Furthermore, the system can distinguish alphabet Morse code for optical wireless communication method. Our flexible organic artificial nervous systems suggest a promising strategy for bioinspired electronics, soft robotics, and neuroprosthetics. Neuroplasticity-based artificial nerves can be used for restoring the biological afferent and efferent nerve response which can pave a new way to technology without using bulky electronic devices.

4:30 PM SB04.10.03

Stress-Based Control of Ferroelectric Memristors Youri Popoff^{1,2}, Laura Bégon-Lours¹, Mattia Halter^{1,2}, Heinz Siegwart¹ and Bert Offrein¹; ¹IBM Research GmbH - Zurich Research Laboratory, Switzerland; ²ETH Zürich, Switzerland

The impact of stress on the properties of thin film materials plays a crucial role in the performance of integrated devices. Indeed, in the last decades, stress engineering has been purposefully used to enhance the conduction of CMOS transistors thanks to increased carrier mobility under stress [1, 2]. Drawing inspiration from this successful use of stress in integrated devices, we turn our focus to integrated analog synapses used in Artificial Neural Networks which are key to bridging the computing bottleneck in Von-Neumann architectures [3]. In particular, the stress-based control of memristors is of interest.

Not only is static stress targeted, but an external pressure source e.g. from an actuator or from a sound wave can be used as an additional input to the individual synapses in the learning process [4].

In this work we investigate the change in electrical conductivity caused by varying the pressure applied to integrated Ferroelectric Memristor devices. In these devices fabricated on Si with a CMOS compatible process, the switching of the polarization of the 3.5 nm $\text{Hf}_x\text{Zr}_{1-x}\text{O}_2$ ferroelectric thin film layer in the stack has an influence on the electrical conduction. The state of the memristor is written by applying an electric field and it is read out with the measured current [5].

For this study, we show the development of a custom indenter setup which uses a flat sapphire tip 100 μm in diameter to apply pressure (forces potentially up to 20 N). A calibrated load cell and motorized stage allow for a PID-controlled tuning of the applied force and thus exerted pressure on the device under test.

Increase of the Low Resistive State (2 M Ω LRS) up to 10% per 0.7 N applied force (0.56 GPa) on devices of 40 μm diameter can be shown. On the other hand, the High Resistive State (HRS) is much less impacted by the pressure. By releasing the pressure and electrically cycling the device, the change in resistive state is reversible and the device operation is preserved after the pressure cycling. Changes up to 60% can be measured, however at the cost of a non-reversible state behavior or loss of the device after too much cycling. Variation in device dimensions and application of stress is used to investigate the physical mechanism behind the change in resistance.

Moreover, we propose a novel device concept where integrated piezoelectric actuators at the low micrometer and nanometer scale can be used to apply stress on the Ferroelectric Memristors [6]. When used as a synapse, the 2-port device gains through the actuator an additional input to control its state, thus mimicking the control of biological synapses by neuromodulators.

This study validates the use of stress as a new way of controlling analog memristors and this stress-based approach opens up a multitude of new opportunities for the operation of synaptic networks.

1 K. Rim, J. L. Hoyt, and J. F. Gibbons, International Electron Devices Meeting, 1998

2 J. L. Hoyt et al., International Electron Devices Meeting, 2002

3 H. Jeong, and L. Shi, J. Phys. D: Appl. Phys., 2019

4 J. Fompeyrine, Y. Popoff, S. Abel, US20210034320A1, 2021

5 L. Bégon-Lours, M. Halter, Y. Popoff, Z. Yu, D. F. Falcone, and B. J. Offrein, ESSDERC, 2021

6 J. Fompeyrine, Y. Popoff, S. Abel, US2020235294A1, 2020

4:45 PM SB04.10.04

Supported Lipid Bilayers as Biomimetic Approach to Tune Neuromorphic Plasticity Claudia Lubrano, Chiara Ausilio, Ugo Bruno and Francesca Santoro; Istituto Italiano di Tecnologia, Italy

Neurodegenerative diseases and brain damage require the constant development of new technologies able to replicate synaptic functionalities and replace damaged connections. As widely reported in literature, synaptic communication is based on electrochemical mechanisms: certain stimuli might induce the release of neurotransmitters from the pre-synaptic site and the consequent recognition of these molecules at the post-synaptic receptors, thus causing the propagation of an action potential from one cell to another.¹ In this scenario, neuromorphic devices represent a powerful platform to recreate artificial neural networks, which will offer the chance to improve implantable devices towards the replacement and repair of injured brain areas. In particular, organic neuromorphic devices, such as PEDOT:PSS organic electrochemical transistor (OECT), offer a unique approach: in addition to the well-known biocompatibility of PEDOT:PSS, owing to its ionic-to-electronic current transduction, the conductance of these devices can be modulated through external stimuli (*i.e.* ionic flow) and the altered conductance state is retained over long time, replicating to some extent the physiological synaptic plasticity.² Recently we have successfully established a direct coupling between PC12 neuron-like cells, able to secrete dopamine (DA)³, and an organic neuromorphic device, thereby recreating an *in vitro* model of the synaptic system which simulate both long and short-term plasticity through the oxidation of DA.⁴

Here, we aim to recapitulate not only the same functionalities of neurons (*i.e.* synaptic plasticity) using an organic neuromorphic device, but also to have a biomimetic platform replicating the physiological neuronal membrane by means of supported lipid bilayers (SLBs), simplified in-vitro models of cell membranes with potential bio-technological applications⁵. We evaluated the role of SLB composition on the OECT plasticity, analyzing how the bilayer fluidity affects the ions flow towards the neuromorphic channel, thus modulating the de-doping level of the PEDOT:PSS. Furthermore, we explored SLBs with neuronal composition in order to resemble the functioning of biological synapses. We expect that such platform thanks to its learning capabilities and biomimetic properties, could really interact with biological neurons, monitoring their activities and providing feedback accordingly, thus creating an artificial biohybrid functional network. This biohybrid platform might be further exploited to engineer future implantable devices able to replace damaged connections either in pathological networks in neurodegenerative diseases, or in case of amputations to create adaptive prosthetics able to reduce the mismatch between these artificial parts and the human body.

References.

1. Burns, M. E. & Augustine, G. J. Synaptic structure and function: Dynamic organization yields architectural precision. *Cell* **83**, 187–194 (1995).

2. Gkoupidenis, P., Schaefer, N., Garlan, B. & Malliaras, G. G. Neuromorphic Functions in PEDOT:PSS Organic Electrochemical Transistors. *Adv. Mater.* **27**, 7176–7180 (2015).

3. Westerink, R. H. S. & Ewing, A. G. The PC12 cell as model for neurosecretion. *Acta Physiol.* **192**, 273–285 (2008).

4. Keene, S. T., Lubrano, C., Kazemzadeh, S., Melianas, A., Tuchman, Y., Polino, G., Scognamiglio, P., Cinà, L., Salleo, A., van de Burgt, Y., Santoro, F. A biohybrid synapse with neurotransmitter-mediated plasticity. *Nat. Mater.* (2020).

5. Richter, R. P., Bérat, R. & Brisson, A. R. Formation of Solid Supported Lipid Bilayers an Integrated View. *Langmuir* **22**, 3497–3505 (2006).

5:00 PM SB04.06.04

A Novel Approach for the Analysis of Multivariate Impedance Data—Making Possible the Development of Calibrated Sensor Arrays Lucas Fugikawa-Santos¹, João P. Braga², Vinicius M. Oliveira³ and Vitor B. Leite²; ¹São Paulo State University - UNESP, Brazil; ²University of São Paulo State—UNESP, Brazil; ³University of Maryland, United States

Functionalized sensor arrays are commonly used in the detection and sensing of chemical compounds in electronic tongue/nose systems. The analysis of the multivariate complex impedance data from sensor arrays is based on the global selectivity principle, which allows the qualitative discrimination of substances and their corresponding concentrations. However, frequently used analytic methods such as principal component analysis (PCA) and interactive document map (IDMAP) are non-quantitative methods and do not allow the development of calibratable devices. We propose a novel approach for the analysis of multivariate impedance data from sensor arrays used as electronic tongue devices. The method allows the representation of the data in a quantitative 2-D space where devices produced using similar fabrication parameters yields similar values when exposed to the same compound, at the same concentration. To prove the concept of the method, an extensive set of experiments was carried out, comprising the impedance (capacitance) vs. frequency spectra from 8 different types of electrodes (functionalized with organic semiconducting films), and 5 types of analytes, at different concentrations.

Triplicated devices were also tested to confirm the reproducibility of the electrical impedance response. The result was a large, multivariate dataset, which required innovative computational aid to be analyzed. Although unspecific electrodes for the detection of substances were used in the experiments, several combinations of electrode arrays were possible to discriminate the analytes, with good reproducibility of the response. The concentration dependence of the electrode array response also permitted the determination of the detection limit for each compound, as well as each detection calibration curve. The method can be easily extended to smart sensing applications, including biosensors, which demand reliable and quantitative analysis.

SESSION SB04.11: Poster Session II: Materials and Algorithms for Neuromorphic Computing and Adaptive Bio-Interfacing, Sensing and Actuation
Session Chair: Paschalis Gkoupidenis
Monday Afternoon, December 6, 2021
SB04-Virtual

9:00 PM SB04.11.01

Neuromorphic Device Based on Non-Volatile Organic Electrochemical Transistors Yuyang Yin, Shaocong Wang, Zhongrui Wang and Paddy K. L. Chan; The University of Hong Kong, China

Neuromorphic computing systems mimicking biological neural network show significant advantages in the efficiency for processing complex data. As a major building block of the new-generation computing hardware, artificial synapses such as those based on novel memory devices are capable to store and process information on the same device, mitigating the von Neuman bottleneck of digital systems featuring physical separation of memory and processing units and thus large time and energy overheads in running AI tasks. To harvest the advantage of in-memory computing, synapses are required to update their weights in a linear and repeatable way, and the operation is supposed to be fast and low power-consumption for in situ training, which remains one of the biggest challenges to various in-memory computing based neuromorphic systems. Besides, the long-term non-volatile memory property of the artificial synapse for retaining the weight value is critical to the learning performance. Here, we demonstrate a neuromorphic device by employing non-volatile organic electrochemical transistors (OECTs) as artificial synapses, which can provide analog weight updates with decent linearity while costing low power supply. The non-volatility of the synapse endows the possibility to emulate long-term synaptic plasticity, augmented by linear and repeatable weight modulation, provides a promising scheme to physically implement mainstream machine learning techniques such as gradient descent. This would significantly benefit the neuromorphic hardware in terms of power consumption, speed, form factors and cost. To verify this, we performed ANN simulations based on the weight update data of the transistors for the learning and recognition of the MNIST handwritten digits dataset. The results indicate the potential of this non-volatile OECT device for further moving towards smart and efficient edge neuromorphic computing hardware.

9:03 PM Q&A

9:05 PM SB04.11.02

Electrode Material Dependence of Electrical Characteristics in Double Ta₂O₅-Based Resistive Switching Cells Tomoaki Ohno and Yusuke Nishi; National Institute of Technology Maizuru College, Japan

Resistive switching cells as one of the next-generation nonvolatile memories to replace the Flash have been extensively studied because of their potential use for neuromorphic devices. However, the mechanism of resistive switching and the origin of conductive filaments in resistance change materials remain controversial. At present, many combinations of electrode metals and resistance change materials have been reported. In particular, conductive filaments in conductive-bridge random access memories are formed by electrode metal such as silver (Ag) extending from the counter electrode instead of oxygen vacancies, and in several cases quantization phenomenon appears upon a voltage pulse application to the cell [1]. In this study, we focus on the effect of electrode materials on the forming and resistive switching characteristics in double tantalum oxide (Ta₂O₅)-based resistive switching cells to clarify the origin of the conductive filament created by the forming.

The resistive switching cells were fabricated as described below. A platinum (Pt) bottom electrode was prepared by dc sputtering. A 10-nm-thick Ta₂O₅ resistance change layer and a subsequent 10-nm-thick TaO_x (x=1.6) oxygen-vacancy reservoir layer were deposited by reactive rf sputtering with different oxygen gas flow rates [2]. Next, top electrodes (TEs), such as Pt, Ag, and gold (Au), were deposited through a metal mask by resistive heating (Ag and Au) or electron beam (Pt) evaporation. We examined the differences in initial resistance, forming voltage, and resistive switching characteristics of three types of cells, Ag, Au, and Pt-TE cells. The bottom electrode was grounded, and voltages were applied to the top electrodes with a diameter of 100 μm using a semiconductor parameter analyzer Keithley 2450. Current or voltage sweeps were applied to the top electrodes to investigate electrode material dependence of initial resistance and forming characteristics, or resistive switching characteristics, respectively.

The results of initial resistance were 5 k~300 kΩ for the Ag-TE cells, 10 k~200 kΩ for the Au-TE cells, and 2 k~3 kΩ for the Pt-TE cells. Besides, the variations of forming voltage at which a cell resistance reaches sub-kΩ were 6~8 V, 7~10 V, and 5 V for the Ag, Au, and Pt-TE cells, respectively, indicating that the Pt-TE cells were more stable with less variation. These results remain unchanged even after a few months except for Ag-TE cells, which show a clear reduction in the forming voltage and the initial resistance. Although the reason for the reduction is unclear at present, Ag ions may be gradually dissolved from the Ag-TE layer to the Ta₂O₅ layer over time, owing not to the oxidation of metal-TE leading to an increase in the cell resistance. Note that the three types of cells after the specific forming show analog resistive switching characteristics upon bipolar voltage sweeps irrespective of the reduction above. These results reveal that an initial state in every cell does not involve the analog resistive switching.

Moreover, Ag and Au-TE cells exhibit discrete conductance fluctuation before the forming, while Pt-TE cells show continuous conductance increase [3]. The appearance frequency of the cell conductance based on quantized conductance is apparently high in Ag-TE cells. From viewpoint of the large variation of initial conductance and forming voltage, Ag ions can pass through the TaO_x layer with random ion collisions and form conductive filaments composed of Ag atoms during the conductance fluctuation and the forming, instead of oxygen vacancy rows supplied from the reservoir layer. Furthermore, in contrast, Pt-TE cells show possibly gradual diffusion of oxygen vacancies from the reservoir layer at the forming.

[1] T. Tsuruoka et al., *Nanotechnology*, 23, 435705 (2012).

[2] T. Miyatani et al., *MRS Advances*, 4, 2601 (2019).

[3] Y. Nishi et al., *Journal of Applied Physics*, 124, 152134 (2018).

9:08 PM Q&A

1:00 PM *SB04.12/SB08.16.01

Keynote: Designing New Materials for Neural Interfacing Molly Stevens; Imperial College London, United Kingdom

This talk will provide an overview of our recent developments in polymer materials with unique electrochemical properties for use in neural bio-interfacing. We design, synthesise and fabricate conjugated polymer-based scaffolds presenting complex electrical and topographical cues that support neural stem cell adhesion, growth and differentiation [1]. I will discuss the applications of our facile strategy for controlled functionalisation and post-polymerisation of the aromatic backbone of conjugated polymers for selective cell stimulation [2]. Our recent developments in the context of bioelectronic nanostructured surfaces for biosensing and interfacing will be discussed [3,4].

[1] K. Ritzau-Reid... M. M. Stevens. "An electroactive oligo-EDOT platform for neural tissue engineering." *Advanced Functional Materials*. 2020. DOI: 10.1002/adfm.202003710.

[2] A. Creamer... M. M. Stevens, M. Heeney. "Quantitative post-polymerisation functionalisation of conjugated polymer backbones and its application in multi-functionalised semiconducting polymer nanoparticles." *Nature Communications*. 2018. 9: 3237.

[3] S. Higgins... M. M. Stevens. "High-aspect-ratio nanostructured surfaces as biological metamaterials." *Advanced Materials*. 2019. DOI: 10.1002/adma.201903862.

[4] C. Chiappini... M. M. Stevens, E. Tasciotti. "Biodegradable silicon nanoneedles delivering nucleic acids intracellularly induce localized *in vivo* neovascularization." *Nature Materials*. 2015. 14: 532-539.

1:30 PM *SB04.12/SB08.16.03

Enhanced Bio-Interfacing and Sensing Based on Spatiotemporal Dynamics and Ionic-Electronic Signal Amplification Fabrizio Torricelli; University of Brescia, Italy

The seamless integration of biology with electronics demands for new bio-inspired approaches able to detect, process and amplify both ionic and electronic information. Ions are the ubiquitous biological and physiological regulators, being involved in most of the fundamental processes of every living organism. Ions enable the communication between cells and the metabolic and bioenergetic processes, playing a key role in hydration, pH regulation, and osmotic balance across cell membranes. Biological systems, including animals and plants, communicate and process information using as carriers ions, small molecules, and electronic charges. In the nervous system, stimuli are collected from distributed sensory receptors, computation then takes place locally or centrally, and when necessary, feedback signals drive sensorimotor processes. The technological potential of co-integration between electronics and biology stems from the ability of electronics to bi-directionally interact with biological systems, and even more importantly to emulate biological functions.^[1,2]

Using state of art organic electrochemical materials and devices, we show the design and validation of unconventional iontronic circuit and system approaches for (i) integrated ion-sensing amplifier and (ii) spatiotemporal dynamic multiplexing of ionic signals in a shared liquid medium of communication. The ion-sensing amplifier integrates both selective ion-to-electron transduction and local signal amplification demonstrating a sensitivity larger than $2300 \text{ mV V}^{-1} \text{ dec}^{-1}$, which overcomes the fundamental limit.^[3] It provides both ion detection over a range of five orders of magnitude and real-time monitoring of variations two orders of magnitude lower than the detected concentration, viz. multiscale ion detection. The iontronic multiplexing system discriminates locally random-access events with no need of peripheral circuitry or address assignment, thus decreasing significantly the integration complexity.^[4] The form factors allow for intimate bio-interfacing communication in shared medium. The ion-sensing amplifier and the spatiotemporal dynamic iontronic multiplexer are fundamental building blocks for multifunctional bio-interfacing and sensing in the emerging fields of bioelectronics, wearables, and neuromorphic computing or sensing.

[1] S. Vassanelli, M. Mahmud, *Front. Neurosci.* 2016, 10, 438.

[2] C. Lubrano, G. M. Matrone, C. Forro, Z. Jahed, A. Offenhaeusser, A. Salleo, B. Cui, F. Santoro, *MRS Commun.* 2020, 10, 398.

[3] P. Romele, P. Gkoupidenis, D. A. Koutsouras, K. Lieberth, Zs. M. Kovacs-Vajna, P. W. M. Blom, F. Torricelli, *Nat. Commun.* 2020, 11, 3743.

[4] D. A. Koutsouras, M. Hassanpour Amiri, P. W. M. Blom, F. Torricelli, K. Asadi, P. Gkoupidenis *Adv. Funct. Mater.* 2021, 31, 2011013.

2:00 PM SB04.12/SB08.16.05

Capacitive Coupling Phenomenon in Multi-Conductive Layer Bioelectronic Devices Remy Cornuejols^{1,2}, Sofia Drakopoulou², Gerwin Dijk², Rodney O'Connor², Christophe Bernard¹ and Shahab Rezaei-Mazinani²; ¹Aix-Marseille Université, France; ²École des Mines de Saint-Étienne, France

Increasing number of electrodes in neural recording and stimulation devices is a key aspect to improve the spatial resolution. To keep appropriate dimensions for clinical applications, utilization of multiple layers of superimposed conductive leads helps to maximize the number of electrodes in a limited available space. However, close conductive lines with different electrical charges can lead to a crosstalk effect between channels due to capacitive coupling. To understand and quantify this phenomenon on devices made of gold leads with Parylene C encapsulation, we present a study on the influence of the thickness of inter-conductive insulation layer on capacitive coupling and Parylene C permeability. Subsequently, *in vitro* experiments were conducted on a multielectrode array, consisting of spatially distributed multi conductive-layer electrode clusters. This helped to quantify capacitive coupling. Furthermore, *in vivo* experiments were carried out to measure crosstalk in multi conductive layer electrocorticography probes, interfacing the brain. Finally, by shedding light on the optimal insulation-layer thickness between conductive layers, this study will help to optimize organic-bioelectronic sensor's structure, to increase number of electrodes, thus spatial resolution of devices. Therefore, this will lead to an efficient detection of biological events and facilitate interfacing of these devices with small anatomical structures.

4:00 PM *SB04.13.01

Employing the Non-Linear Response of Synaptic Polymer Networks for Reservoir Computing Hans Kleemann, Matteo Cucchi, Lautaro N. Petruskas and Karl Leo; Technische Universität Dresden iAPP, Germany

The emerging field of organic electrochemical neuromorphic devices is gaining enormous interest as such devices show distinct synaptic properties, operate at a low voltage, and enable biocompatible, intelligent sensor units which might be used, e.g., for real-time classification of bio-signals. So far the focus of research is mainly on the synaptic properties of single organic electrochemical transistors and related devices with the emphasis to control the strength and time constants of synaptic plasticity. However, to do computation, e.g., in a feedforward neural network, a very large number of identical synaptic devices is required with very strict definitions in terms of their synaptic properties to enable efficient learning. Due to these challenges, organic electrochemical synaptic networks have not been used for complex classification tasks.

In this contribution, I discuss how networks of synaptic organic electrochemical devices can be employed to solve complex classification tasks by utilizing a brain-inspired approach of computation denoted as echo-state or reservoir computing. Reservoir computing, a kind of recurrent neural network, is an approach where a low-dimensional input signal is mapped onto a high-dimensional output through a non-linear transformation which exponentially increases the probability to classify the input data according to the features being selected. The reservoir itself does not require training which makes this technique very fast and power-efficient compared to other machine learning approaches.

We create such a reservoir by growing dendritic networks of the benchmark material PEDOT:PF6 in an array of electrodes using field-directed electropolymerization. This method enables us to grow random networks of conductive polymer fibers with a diameter down to 1 μm . As these fibers, each operating as an organic electrochemical transistor, are connected through the liquid electrolyte, a situation of complex resistive and capacitive coupling is created in the network. Hence, if an input signal is applied to the reservoir, the signal is distorted in a highly non-linear and transmitted to the output. The degree of non-linearity of the polymer reservoir depends on the balance between inhibitory and excitatory fibers and the strength of capacitive coupling. Implementing a delayed feedback loop connecting input and output of the reservoir (so-called single-node reservoir), the complexity of the system at hand is proven by chaotic oscillations. Ultimately, the single-node reservoir is utilized to demonstrate standardized classification tasks such as heartbeat classification, classification of flowers, time-series prediction, and others.

4:30 PM SB04.13.02

Enhanced Performance of Ag/HfO₂/Pt-Based Diffusive Threshold Switches for Energy-Efficient Neuromorphic Computing Solomon Amsalu Chekol¹, Rainer Waser^{1,2} and Susanne Hoffmann-Eifert¹; ¹Forschungszentrum Jülich GmbH, Germany; ²RWTH Aachen University, Germany

Brain-inspired neural networks are emerging as potential alternatives to the traditional von-Neumann architectures, mainly due to their unique structure of combining the memory and processor, giving them the ability to learn more efficiently^[1]. Such neural architectures are composed of computing and memory elements, representing the neuron and synapse functions, respectively. Neurons are used to execute current summation, integration, and firing. As frequent integrating and firing events are involved, the power consumption needs to be low enough to ensure an energy-efficient computing element. Currently, neuronal functionality is often performed using a conventional CMOS-based neuron. However, a CMOS neuron, made of several transistors and a capacitor, is area- and energy-inefficient^[2]. Hence, there has been a great interest in searching for an alternative neuron device by deploying new concepts, designs, and materials. Recently, a compact neuron design has been exploited utilizing two-terminal threshold switching (TS)-based elements, owing unique features such as thresholding and self-relaxation behaviors.

In our previous work, we developed Ag/HfO₂/Pt-based volatile electrochemical metallization (v-ECM) devices^[3]. The stack was built from atomic layer deposited (ALD) 3 nm HfO₂ sandwiched between an Ag top electrode and a Pt bottom electrode. The thin HfO₂ layer serves as electrolyte matrix for the formation/rupture of an Ag filament. The fabricated device exhibits an extremely low-leakage current (I_{off}) of < 100 fA and ultra-low threshold voltage (V_{th}) of < 0.2 V, guaranteeing a low power consumption. In most threshold switching devices such as ovonic threshold switches (OTS) and insulator-to-metal transition (IMT) devices, the I_{off} and V_{th} show a tradeoff, meaning that the improvement in leakage current comes with increased V_{th} and vice versa. In this regard, v-ECMs have a unique advantage of providing low I_{off} and low V_{th} values simultaneously.

Some of the main concerns in such devices are the volatility range (stuck-at-ON) and the switching variability. The morphology of the conductive filament ultimately defines how fast the device relaxes back to the initial state. Excessive Ag in the filament could lead to a non-volatile state. Often, this happens during the initial forming stage, since a relatively higher voltage is required to initiate the switching. Therefore, controlling the amount of Ag constituting the filament is important. The formation/rupture of conductive filaments in v-ECM is closely related to the electrochemical dynamics of the active metal, such as Ag, which could determine the switching speed and the morphology of the filament. In addition to the material's property, the electrochemical dynamics can be modulated by external factors like the electric field, bias duration, and temperature.

In this presentation, we will discuss the advantages of Ag/HfO₂/Pt based TS for artificial neuron applications, and potential improvements to enhance performance such as variability, volatility, and switching speed. For this purpose, different approaches to control the Ag concentration in the matrix - such as hot forming and annealing - will be discussed. Finally, a proof of concept artificial spiking neuron functionality of our device will be shown.

B. Chen, et. al., "Efficient in-memory computing architecture based on crossbar arrays," *2015 IEEE International Electron Devices Meeting (IEDM)*, 2015, pp.

G. Indiveri, et. al., "Neuromorphic Silicon Neuron Circuits," *Frontiers in Neuroscience*, vol. 5, pp. 73, 2011.

S. A. Chekol, et. al., "An Ag/HfO₂/Pt Threshold Switching Device with an Ultra-Low Leakage (< 10 fA), High On/Off Ratio (> 10¹¹), and Low Threshold Voltage (< 0.2 V) for Energy-Efficient Neuromorphic Computing," *2021 IEEE International Memory Workshop (IMW)*, 2021, pp. 1-4.

4:45 PM SB04.13.03

Neuromorphic Learning with NiO Sandip Mondal, Zhen Zhang and Shriram Ramanathan; Purdue University, United States

Non-associative learning represents fundamental mechanisms by which organisms interact with their environment. Early studies in neuroscience using sea slugs as model systems demonstrated the synaptic origins of habituation and sensitization. In this presentation, we will discuss non-associative learning mechanisms in NiO, a canonical Mott insulator. By varying the Ni:O stoichiometry, it is possible to obtain a range of transport gaps as well as p-type conduction. Using different stimuli such as oxygen chemical potential and UV light, we have been able to obtain current-voltage characteristics (resistance evolution) that emulate cellular learning in two-terminal NiO devices. Spectroscopic evidence on representative samples indicates that modulation of oxygen vacancy concentration through the film thickness is responsible for such non-associative learning. A set of samples carefully prepared under different oxygen partial pressures (by varying Ar-O₂ ratio) have been studied for resistive switching and learning under electric field pulsing. We find that samples with near-stoichiometric composition do not show switching behavior. However, interestingly, we are able to control the memory formation dynamics in oxygen-deficient samples by training under similar electric field strengths. We have studied such samples in-depth using X-ray scattering techniques and performed drift-diffusion modeling of current-voltage curves to understand the mechanisms behind learning and glass-like relaxation; and will be discussed in this presentation. Mott materials with carefully chosen defect structures possess highly tunable electronic structures and appear to be promising candidates for neuromorphic computation.

8:00 AM SB04.06.03

Flexible Neuromorphic-Neurotransmitter Biohybrid Interface Setareh Kazemzadeh and Yoeri van de Burgt; Eindhoven University of Technology, Netherlands

Neuromorphic devices represent a powerful platform to create artificial neural networks, which will offer the chance to improve implantable devices towards the replacement of brain injuries. As widely reported in literature, the dominant synaptic communication is based on electrochemical mechanisms by releasing neurotransmitters [1]. However most of the existing implantable prosthetics are designed to operate mainly through intrinsic potentials of the brain, overlooking the chemical aspect. In this scenario, neuromorphic devices offer a unique new perspective: these devices can “learn” by receiving stimuli, changing their plasticity similar to physiological synaptic plasticity [2]. Recently we demonstrated a biohybrid synapse that formed a bidirectional coupling between PC12 neuron-like cells and an organic neuromorphic device. Applying a positive bias at the gate leads to oxidation of dopamine secreted from cells and the release positive ions in the electrolyte solution as well as electrons donated to the PEDOT:PSS channel. These processes de-dope the material resulting in a permanent change of resistance of the channel. Additionally, this device shows a high state retention after the pulses are stopped resembling long-term plasticity [3]. This work opens the pathway towards combining artificial neuromorphic systems with biological neural networks for future brain implants. Here we show a further expansion of these biohybrid synapses towards highly reliable prosthetics. Oxidized dopamine gradually forms a layer of polydopamine on the interface of cells and the device, which may result in blockage and limit the device sensitivity. Moreover, in case of prosthetic implants the device must be highly biocompatible and flexible. To tackle these challenges, we introduce a new technique of fabricating flexible organic electrochemical devices on highly biocompatible flexible substrates. These devices use polydopamine as a solid state electrolyte and simultaneously act as a de-doping agent for the PEDOT:PSS layer to increase the resistance of the channel for neuromorphic memory. A more resistive channel avoids excessive current through the device which decreases the energy consumption. The presence of amine in the PEDOT:PSS channel also reduces the diffusion of amines into the electrolyte leading to more stability and higher state retention. Furthermore, using polydopamine as the solid electrolyte significantly increases the energy barrier for ion/proton diffusion which eliminates the need for an access device or resistor. This will significantly increase the ease of design, fabrication and integration of these neuromorphic devices in biological environments. Polydopamine as a biomaterial melanin is inherently biocompatible, which is essential for viable bioelectronic material [4]. We expect these new flexible biocompatible ENODes can be used to bridge hybrid synaptic connections and could further be utilized in an array fashion for integration of future brain-machine interfaces.

References

- [1] M. E. Burns and G. J. Augustine, “Synaptic structure and function: Dynamic organization yields architectural precision,” *Cell*, vol. 83, no. 2, pp. 187–194, Oct. 1995.
- [2] J. J. Jun et al., “Fully integrated silicon probes for high-density recording of neural activity,” *Nature*, vol. 551, no. 7679, pp. 232–236, 08 2017.
- [3] S. T. Keene, C. Lubrano, S. Kazemzadeh, A. Melianas, Y. Tuchman, G. Polino, P. Scognamiglio, L. Cinà, A. Salleo, Y. van de Burgt and Francesca Santoro. “A biohybrid synapse with neurotransmitter-mediated plasticity”, *Nature Materials*, VOL 19, 2020, 969–973.
- [4]. Lee, H., M.Dellatore, S., M.Miller, W. & B.Messersmith, P. Mussel-Inspired Surface Chemistry for Multifunctional Coatings. *J. Chem. Inf. Model.* 318, 1689–1699 (2007).

SYMPOSIUM SB05

Antimicrobial Materials Against Coronaviruses and Other Nosocomial Pathogens
November 30 - December 8, 2021

Symposium Organizers

Reza Ghiladi, North Carolina State University
Vijay Mhetar, Kraton Corporation
Frank Scholle, PhotoCide Protection, Inc.
Qingqing Wang, Jiangnan University

SESSION SB05.01: Antimicrobial Materials I
Tuesday Morning, November 30, 2021
Sheraton, 2nd Floor, Liberty C

10:30 AM OPENING COMMENTS

10:35 AM *SB05.01.01

Continuously Self-Disinfecting and Broad-Spectrum Polymers—Next Steps Toward Preventing the Spread of Highly Contagious Microbes Reza Ghiladi, Frank Scholle and [Richard Spontak](#); North Carolina State University, United States

Some of the pathogenic challenges currently facing the global community are becoming increasingly life-threatening. For instance, infectious microbes such as SARS-CoV-2 and MRSA constitute major healthcare concerns as invisible predators primarily, but not restricted to, stalking the elderly and immune-compromised. In response, various materials-related methods involving nanoparticles or surface functionalization have been proposed to combat this menace, but many are either limited to specific microbes or promote environmental contamination. In this work, we introduce two promising antimicrobial strategies in which several polymer films and coatings serve as exemplars to demonstrate their potential. The first focuses on embedding photosensitive dye molecules capable of generating singlet oxygen, a strong oxidizing agent, into polymer matrices as films, as well as coatings on polymer fibers and other substrates. In the presence of molecular oxygen and incoherent visible light, this system inactivates at least 99.9999% of two Gram-positive bacterial strains, as well as at least 99.9% of three Gram-negative bacterial strains (belonging to the ESKAPE family of bacteria primarily responsible for nosocomial infections) and three virus strains, in *ca.* 1 h under the conditions employed. Moreover, these materials retain their antimicrobial efficacy even after a month of exposure to light. Alternatively, a vastly different method employs anionic polymer surfaces that are inherently capable of promoting a dramatic pH reduction, resulting in a hostile acidic environment that rapidly kills at least 99.99% of the pathogens tested (including 3 drug-resistant bacteria such as MRSA, as well as *C. difficile* and the SARS-CoV-2 and HCoV229E viral strains) in less than 5 min. These materials afford highly effective and largely unexplored pathways to rapid, scalable and broad-spectrum microbial inactivation.

11:05 AM SB05.01.02

Superhydrophobic and Self-Sterilizing Surgical Mask with Spray-Coated Carbon Nanotubes [Ritesh Soni](#), Shalikh Ram Joshi, Mamata Karmacharya, Hyegi Min, Shin Kwan Kim, Sumit Kumar, Gun H. Kim, Yoon K. Cho and Chang Y. Lee; Ulsan National Institute of Science and Technology, Korea (the Republic of)

Coronavirus has affected the entire global community owing to its transmission through respiratory droplets. This has led to the mandatory usage of surgical masks for protection against this lethal virus in many countries. However, the currently available disposable surgical masks have limitations in terms of their hydrophobicity and reusability. Here, we report a single-step spray-coating technique for the formation of a superhydrophobic layer of single-walled carbon nanotubes (SWCNTs) on melt-blown polypropylene (PP) surgical mask. The sprayed SWCNTs form nanospine-like architecture on the PP surface, increasing the static contact angle for water from $113.6^\circ \pm 3.0^\circ$ to $156.2^\circ \pm 1.8^\circ$ and showing superhydrophobicity for various body fluids such as urine, tear, blood, sweat, and saliva. The CNT-coated surgical masks also display an outstanding photothermal response with an increase in their surface temperature to more than 90°C within 30 s of 1 sun solar illumination, confirming its self-sterilization ability. Owing to the cumulative effect of the superhydrophobicity and photothermal performance of the SWCNTs, the CNT-coated masks show 99.99% higher bactericidal performance towards *Escherichia coli* than pristine masks. Further, the virucidal ability of the SWCNT-coated mask, tested by using virus-like particles, was found to be almost 99% under solar illumination. As the spray-coating method is easily scalable, the nanotube-coated mask provides cost-effective personal protection against respiratory diseases.

11:35 AM CLOSING COMMENTS

SESSION SB05.02: Antimicrobial Materials II
Session Chair: Reza Ghiladi
Tuesday Afternoon, November 30, 2021
Sheraton, 2nd Floor, Liberty C

1:30 PM OPENING COMMENTS

1:35 PM *SB05.02.01

Understanding and Tuning the Visible-Light Induced Photodynamic Properties of TiO₂ [Elizabeth C. Dickey](#); Carnegie Mellon University, United States

In recent years, the rise in antibiotic-resistant bacteria and other nosocomial pathogens has highlighted the need for passive, self-cleaning surfaces and personal protective equipment. The motivation to develop such materials has been emphasized in the past year with the outbreak of the coronavirus pandemic. Numerous classes of materials have been explored for such applications, including metal oxides, organic photosensitizers, and other compounds. Our interdisciplinary team is currently working with titania (TiO₂), a common photocatalytic agent known for its production of reactive oxygen species (ROS), in an attempt to lower the band-gap and increase light absorption in the visible region (>400 nm) and test for antimicrobial ability. We reduce the bandgap into the visible spectrum via the introduction of mid-gap states using various doping techniques. In particular, we pursue cationic and self-doping methods with readily available components and develop a facile synthesis method. The procedure rapidly reaches completion under mild reaction conditions (ambient temperature, 1 atm) to produce visible-light absorbing TiO₂. Multiple characterization techniques are utilized to investigate the properties of the formed particles and determine the effect of the doping on the band-gap and the subsequent pathogen inactivation. Crystallographic structure, UV-Vis absorption properties, particle morphology, the cationic valence state and other properties are investigated to assess the materials' viability for self-cleaning surfaces.

Materials are exposed to a variety of pathogens: methicillin resistant *Staphylococcus aureus* (MRSA), multi-drug resistant *Acinetobacter baumannii* (MDRAB), and human coronavirus 229E (HCoV-229E) to determine their overall antimicrobial efficacy through antimicrobial photodynamic inactivation (aPDI). Various concentrations of particles (5 and 10 mg/mL), light intensities (65 ± 5 and 85 ± 5 mW/cm²), and illumination times (30, 60, and 90 minutes) are tested. The particles exhibit promising antimicrobial properties with inactivation up to the limit of detection (6 log units, 99.9999%). Further investigations utilizing ROS scavengers and probes are performed to determine the primary mechanism of inactivation. Long term viability and

photobleaching studies are also explored, demonstrating the particles' ability to be exposed to intense illumination for extended periods with no effect on overall antimicrobial properties. Inductively coupled plasma optical emission spectroscopy is utilized to confirm dopants were not leaching from particles and acting as cytotoxic agents.

Several coating methods (slot-die and spray coating) are employed to test particle compatibility with surface application and reuse. This is done by slot-die and spray coating a UV-curable polymer matrix, containing photoactive TiO₂ particles onto glass slides and woven materials. Slot-die coating is chosen because it gives a uniform film across a variety of length scales and translates well to industrial surface coating applications. Similarly, spray coating can aid in applying these particles to personal protective equipment such as N-95 masks as well as other woven materials like curtains and upholstery commonly found in hospitals and other public areas. Further aPDI tests are being performed on coated materials to ascertain how well antimicrobial behavior can be transferred and utilized in the public sector.

2:05 PM SB05.02.02

Grain Size Effects and Mechanisms for Increased Antimicrobial Efficiency in Ultrafine-Grained Bulk Copper Evander Ramos¹, Isabella Bagdasarian¹, Yaqiong Li¹, Masuda Takahiro², Y. Takizawa², Justin Chartron¹, Alex Greaney¹, Zenji Horita², Joshua Morgan¹ and Suveen N. Mathaudhu¹; ¹University of California, Riverside, United States; ²Kyushu University, Japan

Copper and its alloys have long been known for their antiviral and antibacterial properties, and in the course of the global pandemic, research on ways to accelerate their effectiveness have come to the forefront. Recent studies have reported that when the crystal size of bulk copper reduces towards the nanoscale, the anti-viral and anti-microbial efficiency increases non-linearly. The mechanisms for this are diverse, and include the increase in volume fraction of ionic pathways to the surface, oxidation-reduction, topological features and others. In this study, we investigate the antibacterial characteristics of nanocrystalline pure copper produced by severe plastic deformation (SPD), and based on a literature review and our own emerging data, attempt to unravel the mechanisms that promote bacteria or cell destruction as a function of grain size. The versatility of SPD methods allows for the fabrication of bulk components that, unlike thin-film coating approaches, may enable scalability of medical applications.

2:20 PM *SB05.02.03

Laser-Induced Surface Modification to Improve Antimicrobial Properties of Metal Surfaces Rahim Rahimi; Purdue University, United States

Currently, over a million people die each year due to some form of antibiotic-resistant infection. At the same time, the fast mutation of other pathogenic organisms – fungi, viruses and parasites – are also developing resistance to the drugs that are used to tackle them almost as quickly as new ones can be made. A devastating example is the recent outbreak of SARS-CoV-2 virus that began in December 2019 in China, and by March 15, 2021, the global case rate reached 120 million and 2.65 million people died around the world. This pandemic can be explained by the fact that today's world is a global village, with many shared areas and surfaces (e.g., door handles, airplanes, and hospitals) that can serve as routes by which infectious diseases can easily spread around the world within hours. For instance, the SARS-CoV-2 virus has been shown to remain active for up to three days on plastic and stainless-steel door handles and up to 24 hours on cardboard. Some bacteria – including E. Coli and MRSA – can survive for several months on inanimate surfaces. Consequently, special attention has been devoted to the development of new material and surfaces with antimicrobial and antiviral properties that are less susceptible to resistance and can minimize the spread of pathogens at bay. Among different materials, copper (Cu) and silver (Ag) have been recognized as most widely used and well-documented materials that can effectively inactivate different microbes upon direct contact. However, these metals require a few hours of direct contact with the bacteria or virus that lands on its surface to completely inactivate them. Furthermore, it is impractical to make all high-risk surfaces in public places (e.g., buttons and door handles) and medical instruments out of Ag or Cu due to several limiting factors such as cost, weight and mechanical properties.

In this presentation, we will discuss two novel use of laser surface nano texturing and immobilization technologies to enhance the bacterial rate of killing of such metal surfaces (Cu and Ag) as well as effectively immobilize them onto other biologically inert metallic surface. This presentation is divided into two main sections, each showcasing one of these technologies and their applications. In the first section, we will describe a one-step laser nanotexturing process to enhance the bactericidal properties of Cu surfaces via concurrent selective modification of surface topography and chemistry of laser nanotextured copper. This process provides a unique and facile approach for creating robust Hierarchical Micro/Mesoporous structures directly onto metal surfaces in ambient conditions, eliminating complexities of chemical etching as well as metal nanoparticles synthesis and coating processes. In this section we will look at the surface chemistry and morphology that changes with the laser processing conditions and how these surface properties enhance the overall antibacterial properties of the Cu surface against a range of gram positive and negative antibiotic resistant bacteria.

In the second part of this talk, we will showcase the use of a combination of laser nanotexturing and laser immobilization to selectively reduce Ag ionic compounds directly onto the surface of biologically inert titanium metal implants. We will discuss the systematic experimental studies (e.g., elemental and surface morphology analysis) that were conducted with different laser processing condition and silver coating compositions which resulted in both improved cellular integration and antibacterial properties while having minimal change in the bulk mechanical properties of the titanium substrate. We will conclude this presentation by briefly commenting on our efforts to translate some of these technologies into clinical practice and the future directions.

2:50 PM CLOSING COMMENTS

SESSION SB05.03: Poster Session: Antimicrobial Materials

Session Chair: Reza Ghiladi

Tuesday Afternoon, November 30, 2021

8:00 PM - 10:00 PM

Hynes, Level 1, Hall B

SB05.03.01

Dual-Dyed Photodynamic Antimicrobial Polyethylene Terephthalate/Cotton Blended Fabrics with Variable Color Expression Chenyu Jiang¹, Wangbingfei Chen², Reza Ghiladi¹, Qingqing Wang² and Qufu Wei²; ¹North Carolina State University, United States; ²Jiangnan University, China

Aiming to develop scalable, potent, color variable, and comfortable antimicrobial textiles that can help reducing infection transmission in healthcare facilities, we explored photodynamic antimicrobial polyethylene terephthalate (PET)/cotton blended fabric (TC) comprising of photosensitizer-conjugated cotton fibers and disperse dye dyed PET fibers. A small library of TC blended fabrics was constructed wherein the PET fibers dyed with different traditional disperse dyes dominated the color of the fabrics and thereby enables variable color expression, while cotton fibers were covalently coupled with thionine acetate as photosensitizer generating photobiocidal under illumination. Physical (SEM, CLSM, TGA and mechanical strength), colorimetric (K/S and *CIE*Lab values) characterizations were employed to investigate the resultant fabrics and the photooxidation studies with DPBF demonstrated the ability

of these materials to generate reactive oxygen species (i.e., singlet oxygen) upon visible light illumination. The best results of these materials demonstrated the 99.985% (~3.82 log unit reduction, $P = 0.00208$) photodynamic inactivation of Gram-positive *S. Aureus*, and achieved detection limit 99.99% inactivation (4 log unit reduction, $P \leq 0.0001$) against Gram-negative *E. coli* upon illumination with visible light (60 min; ~300 mW/cm²; $\lambda \geq 420$ nm). Different disperse dyes on the fabric were observed no photophysical competition relation, leading to lower aPDI efficiency, with photosensitizer and furthermore, playing a 'protection' role for photosensitizer during the photobleaching process which ends up improving the photostability of these materials. Taken together, these results suggested the feasibility of low cost, scalable and color variable thionine conjugated TC blended fabrics as potent self-disinfecting textiles.

SB05.03.02

Safety and Effectiveness Assessments of Gold Nanorods Coated Titanium Surfaces for Near-Infrared Photothermal Treatment Against Biofilms Kanny R. Chang¹, Thilak Mudalige², Jiwen Zheng², Matthew Silverman¹, Patrick Regan¹ and Jayaleka Amarasinghe¹; ¹U.S. Food & Drug Administration, Office of Regulatory Affairs, United States; ²U.S. Food & Drug Administration, United States

Bacterial biofilms are communities of microbes encased within a self-produced slimy extracellular polymeric substance (EPS) attached to a surface. Biofilms can enable bacteria to survive in hostile environments and release fresh bacteria into the environment. Compared to their planktonic counterparts, biofilm bacteria embedded in layers of EPS are highly resistant to antibiotics and conventional disinfection strategies as compared to their planktonic counterparts. Particularly, medical implant-associated biofilms accounts for significant increase in chronic diseases and mortality worldwide.

To eliminate biofilm colonization on medical implants, various strategies including antibiotics, disinfectants, cationic materials, and anti-biofilm coatings have been attempted so far with some success. Surfaces coated with gold nanorods (GNRs) have been demonstrated to be promising as they are capable of eradicating bacterial biofilm upon exposure to near-infrared (NIR) radiation. When exposed to NIR, GNRs can generate plasmonic photothermal heat that can inhibit microbial biofilms and thereby, reduce implant failures and the need for revision surgeries. However, the performances of these surfaces may differ as the fabrication methods vary. In addition, the biocompatibility and anti-biofilm performances of such functionalized surfaces prepared by various methods are not yet fully investigated.

This study addresses the regulatory knowledge gap in evaluating safety and effectiveness of GNR-coated titanium surfaces with antibiofilm activity. Herein, we have used medical grade titanium as a model material and coated GNRs by different techniques via thiol- or amine-terminated silane.

Successful deposition of GNRs was confirmed and quantified by scanning electron microscope and X-Ray spectroscopies. The results showed that the more polar amine-terminated silane achieved a higher amount of deposited nanorods on titanium. Biocompatibility testing was conducted in vitro on human osteoblast, macrophages, and fibroblast cells by following ISO-10993 Part 5: Tests for *in vitro* cytotoxicity. Titanium coated with GNRs solutions up to 200 µg/mL did not show significant cytotoxicity and were favorable to cell attachment and proliferation. In addition, toxicological assessments, such as cytotoxicity and measurement of inflammatory cytokine levels, are conducted on fabricated surfaces exposed to NIR. Anti-biofilm performance of the GNR-coated surfaces in the presence or absence of NIR will be tested against *Staphylococcus aureus* and *Nontuberculous mycobacterial* biofilms. The results of this research will help the FDA assess medical device submissions that use similar nanomaterial-based anti-biofilm technology.

SB05.03.03

Characterizing Hydrodynamic Wear of Superhydrophobic Materials Daniel Braconnier; Northeastern University, United States

Hydrophobic coatings rely on chemical apolarity and hierarchical roughness to achieve high contact angles and low roll-off angles that lead to self-cleaning and antibacterial properties. Current hydrophobic coatings tend to be delicate and lose their properties easily when subjected to water spray. Many of these coatings become impaled (pinned) with water droplets immediately after incremental hydrodynamic wear from water spray. This hydrodynamic wear differs from seemingly more aggressive mechanical wear including scratching with sandpaper - a common approach used to claim both self-similarity of a material and extreme robustness against wear. However, the hydrodynamic wear of these self-similar materials can quickly erode the hydrophobic constituents, exposing more hydrophilic materials that lead to quick wetting out despite the self-similarity of the greater material. In this work, we systematically study several approaches that have claimed robustness against wear and find that most approaches fall short of application requirements for withstanding a simple onslaught of water spray. Through quantifying hydrodynamic wear, we have also been able to demonstrate an advancement on the leading systems through developing a novel superhydrophobic material. We compare a popular off-the-shelf industry solution to these recent academic works, as well as offer an analytical model that nicely predicts the hydrodynamic wear of these systems.

SB05.03.04

Late News: (Garcia High School Student) Repurposing Waste Fabric by Synthesizing Silver Nanoparticles on Deweaved Cotton Fibers Elizabeth Zhang¹, Ivan J. Yuan², Jacob T. Zerykier³, Ayush Agrawal⁴, Tianyu Dong⁵, Guanchen Zhu⁶, Haojun Xu⁷, Michael Cuiffo⁸, Stephen Walker⁸ and Miriam Rafailovich⁸; ¹Phillips Academy, United States; ²Shanghai High School International Division, China; ³Rambam Mesivta-Maimonides High School, United States; ⁴Canyon Crest Academy, United States; ⁵Northview High School, United States; ⁶Experimental High School Attached to Beijing Normal University, China; ⁷The Madeira School, United States; ⁸Stony Brook University, The State University of New York, United States

Silver nanoparticles (Ag NPs) have well-studied antimicrobial properties effective against many types of bacteria and fungi. Fine Ag NPs have also demonstrated antiviral activity against H1N1 (influenza), SARS-CoV-2, and other viruses.^[1,2] The antimicrobial properties of Ag NPs are due to the release of silver ions that inhibit respiratory enzymes of bacteria and fungi. In its main antiviral mechanism, Ag NPs bind to and inactivate membrane proteins, thereby preventing the virus from entering the host cell.^[1] Applications of Ag NPs in textiles have gained worldwide attention due to the importance of antimicrobial textiles for wound dressings, medical equipment and staff uniforms, bedsheets, and others. Because textiles serve as a medium for microbe growth and cross-contamination, there is a growing demand for antimicrobial textiles. To reduce waste, especially since the textile industry produces over 10 million tons of waste cotton cloth globally each year, this study seeks to synthesize Ag NPs on discarded cotton muslin tailoring cloth.^[3] Cotton fabric can be deweaved into cellulose fibers, which act as a stabilizing agent on which silver nanoparticles can be synthesized through the reduction of silver nitrate with trace amounts of sodium borohydride.

Fabric was deweaved by stirring in a 3:1 by volume ratio solution of 0.5 M citric acid and 0.5 M sodium nitrate at 50 °C and 600 rpm for 15 minutes. After drying, the fibers were used for the synthesis of silver nanoparticles in two ways. Both samples were treated with a solution of 20 mL silver nitrate (0.01 M) and 2-5 drops of sodium borohydride (0.01 M) until a color change was observed. The first sample was placed for 20 minutes at room temperature, while the second sample was ultrasonicated for 20 minutes at 40 °C. Both samples were then air-dried. The solution used in the synthesis process, which contained silver nitrate, sodium borohydride, and silver nanoparticles, was then analyzed using UV-Vis spectrometry. Results showed a peak at 325 nm, which is characteristic of silver nanoparticles.^[4] The samples were then observed with SEM to visualize the size and features of the nanoparticles, and EDX was simultaneously performed to verify the existence of silver. The fibers heated in the ultrasonicator showed a higher silver signal in EDX than the non-heated samples, and the silver coating was present on more parts of the fibers in the ultrasonicated sample. The size of the nanoparticles was below the resolution of the SEM. X-ray photoelectron spectroscopy showed that the silver in the nanoparticles existed in both elemental and oxidized forms, both of which are antimicrobial.^[5]

We then performed an antibacterial test using *S. aureus* and *E. coli*. Deweaved fibers without Ag NPs did not exhibit any antibacterial properties, while both species of bacteria showed zones of exclusion when the Ag NP-containing fibers were used. The zone of exclusion was larger in the culture of *S. aureus*, suggesting that silver nanoparticles may be more effective against Gram-positive bacteria. Experiments are underway in order to determine the antiviral properties of the silver coating against H1N1 influenza. Hence, this technique has the potential to produce antiviral and antibacterial fibers that can be incorporated into textiles.

- [1] Mori, Y., et. al, *Nanoscale Res. Lett.*, **2013**, 8, 93
- [2] Jeremiah, S., et. al, *Biochem. Biophys. Res. Commun.*, **2020**, 533, 195
- [3] Mohamed S., et. al, *Polymers*, **2021**, 13, 626
- [4] Santos, K. de O., et. al, *J. Phys. Chem. C.*, **2012**, 116, 4594
- [5] Dharmaraj, D., et. al, *J. Drug Deliv. Sci. Technol.*, **2021**, 61, 102111

SESSION SB05.04: Antimicrobial Materials III
Session Chair: Reza Ghiladi
Wednesday Morning, December 1, 2021
Sheraton, 2nd Floor, Liberty C

10:30 AM OPENING COMMENTS

10:35 AM SB05.04.01

Photodynamic and "pH-drop" Antimicrobial Materials for Infection Prevention in Hospital Environments Reza Ghiladi; North Carolina State University, United States

Efforts to control hospital acquired infections (HAIs) have been hampered by the emergence of drug-resistant pathogens, necessitating the pursuit of advanced functional materials that are capable of the self-disinfection of such microbes in hospital environments. To that end, we have explored the feasibility of antimicrobial photodynamic inactivation (aPDI) of bacteria and viruses using photodynamic materials, as well as pathogen inactivation using "pH-drop" based materials. *In vitro* aPDI studies were performed against bacteria and viruses employing photosensitizer-embedded or conjugated nanofibrillated cellulose, polyacrylonitrile or nylon nanofibers, dual-dyed wool/acrylic blended fibers, olefinic block copolymers, and spray coatings. Pathogens were cultured, deposited onto the materials, and subsequently illuminated with visible light (400–700 nm, 65–80 mW/cm², 5–60 min), and their survivability was determined via colony counting or plaque assay methods. For natural polymer scaffolds, cellulose-porphyrin conjugates (either as nanocrystals, nanofibers, or paper sheets) were found to be highly effective against a broad spectrum of pathogens: our best results demonstrated that *S. aureus*, *A. baumannii*, *P. aeruginosa* and *K. pneumoniae* all exhibited photodynamic inactivation by 99.99+%, as well as inactivation of dengue-1 virus (>99.995%), influenza A (~99.5%), and human adenovirus-5 (~99%). As an alternative strategy, non-covalent approaches to photodynamic materials using artificial polymers were also explored: i) using electrospinning, cationic porphyrin and BODIPY photosensitizers were embedded into polyacrylonitrile and nylon nanofibers, and the resultant nonwoven materials possessed both antibacterial and antiviral activities; ii) using melt-pressing, we developed a photosensitizer-embedded olefinic block copolymer that exhibited excellent antimicrobial properties against a range of microbes, including Gram-positive and Gram-negative drug-resistant bacteria, as well as against enveloped and non-enveloped viruses. More recently, we have explored photodynamic coatings on polymer microfibers for pathogen inactivation, and have demonstrated population reductions of >99.9999 and 99.6% for *S. aureus* and antibiotic-resistant *E. coli*, respectively, after exposure to visible light for 1 h. In response to the current COVID-19 pandemic, we also confirmed that these coated fibers can inactivate a human common cold coronavirus serving as a surrogate for the SARS-CoV-2 virus. In a non-photodynamic approach, excellent antimicrobial properties were achieved through the use of charged multiblock polymers wherein the midblock was selectively sulfonated: the resultant hydrophilic and water-swellaible polymers led to self-sterilizing surfaces that rapidly act (killing more than 99.9999% in just 5 min) against a wide range of Gram-positive and -negative bacteria, as well as enveloped and non-enveloped viruses. Together, these results demonstrate that such materials may have widespread applicability for non-specific pathogen disinfection, and further research may lead to their application in hospitals and healthcare-related industries where novel materials with the capability of reducing the rates of transmission of a wide range of bacteria, viruses, and fungi, particularly of antibiotic resistant strains, are desired.

10:50 AM SB05.04.02

Laser Functionalized Carbon Membranes with Exceptional Antimicrobial Properties Sina Nejadi¹, Seyed Ahmad Mirbagheri², Jose F. Waimin¹, Marisa Grubb¹, Samuel Peana¹, David M. Warsinger¹ and Rahim Rahimi¹; ¹Purdue University, United States; ²K. N. Toosi University of Technology, Iran (the Islamic Republic of)

Biofilms and microbial colonies are ubiquitous on nearly any substrate exposed to water and can easily spread microorganisms causing severe conditions in water filtration systems. To defeat the formation of biofilm, deposition of silver nanoparticles (AgNPs) on water treatment membranes has been widely exploited through various techniques including physical vapor deposition and chemical vapor deposition, however, the deposited AgNPs are not effectively anchored to the surface. In this study, we functionalized the surface of a carbon membrane via a CO₂ laser in order to generate oxygen containing species to aid perfect attachment of AgNPs on the membrane surface while providing a superhydrophilic surface. Various characterizations including SEM, XRD, and EDX displayed the nanotextures, enhanced surface roughness, and significant alteration of surface chemistry caused by laser processing. To validate the strong AgNPs attachment to the surface, vigorous mechanical agitation as well as probe sonication were performed. Finally, direct contact killing along with antibiofouling properties of laser functionalized carbon membrane with immobilized AgNPs was performed and compared to the pristine membrane. The results demonstrated an exceptional antibacterial of the laser functionalized membrane to fully eradicate the pathogenic bacterial strains of *Escherichia coli* and *Pseudomonas aeruginosa*. It is believed that the developed technology opens new opportunities towards a rapid, scalable, and cost-effective preparation technique for fabrication of carbon membranes with outstanding antimicrobial activities suitable for water purification applications.

11:05 AM SB05.04.03

Anti-Biofilm Activity of Chiral Graphene Quantum Dots and Their Effects on Functional Bacterial Amyloid Proteins Misché Hubbard, Christopher Altheim, Scott J. VanEpps and Nicholas Kotov; University of Michigan, United States

The ability of bacteria to form complex structures called biofilms create numerous human health and industrial problems. These 3D architectures are defined by the extracellular polymer substance (EPS) that consists of a protective assembly of biomolecules surrounding encased planktonic bacterial cells. The current strategies for targeting biofilms weaken the EPS layer but are typically organic in nature and are subject to enzymatic degradation.

Nanoparticles are a promising new class of anti-biofilm agents for their highly tunable physical and chemical properties, stability, and ability to interact with biological molecules, namely proteins. Here, we report the anti-biofilm activity of L-cysteine or D-cysteine derived chiral graphene quantum dots (L/D-GQDs) against amyloid rich *Staphylococcus aureus* (*S. aureus*) biofilms. Both enantiomers are capable of biofilm disruption. Notably, D-GQDs displayed higher affinity for amyloid fibers causing increased biofilm dispersal compared to L-GQDs. Chiral GQDs mimic peptide binding proteins, interfering with the self-assembly phenol soluble modulins (PSMs), the monomeric form of amyloid fibers responsible for biofilm structuring and multiple other virulence factors. The effect of chiral GQDs on key PSM functions including cytolysis, neutrophil production, and anti-biofilm properties were also explored. The chiral interactions between GQDs and biofilm components give rise to a highly tunable antibiofilm NP platform.

11:20 AM SB05.04.04

The Effect of Pillar Stiffness on Mechanical Bactericidal Efficacy of UV Nanoimprint Lithography Patterned Polymeric Surfaces [Sophie Lohmann](#), Abinash Tripathy, A. Milionis, Anja Keller, Martin Loessner and Dimos Poulikakos; ETH Zürich, Switzerland

The world is facing a growing challenge of antibiotic resistance, making diseases assumed benign with antibiotic treatment once again a looming threat to all members of society. Surfaces play an important role in the transmission of bacterial pathogens. Not only can bacteria survive on surfaces, but in aqueous surroundings, surfaces allow the formation of biofilms, stable bacterial ecosystems that make it extremely difficult to remove bacterial contamination. Preventing bacterial transmission on surfaces is relevant in a variety of settings such as public transport, sanitary facilities, electronic devices, food production and in particular, health care. Hospitals are fertile breeding grounds for antibiotic resistance, as patients gather there, bringing many different types of pathogens. Compromised immune systems combined with the widespread use of antibiotic agents promote the development of antibiotic resistance.

Therefore, there is a growing push to develop antibacterial and bactericidal surfaces to reduce the transmission of bacterial pathogens. Common approaches towards designing antibacterial surface employ the release of biocidal agents. Though effective in some applications, biocide releasing systems can contribute to antibiotic resistance, as release rates decrease with time. Furthermore, biocide release can result in undesired pollution of its environment. Especially nanoparticles, commonly used as biocide agents, have toxic effects on other organisms even at low concentration.

To kill bacteria while avoiding the use of biocidal agents, nanotopographies can be designed to mechanically kill adhered bacteria by rupturing the cell membrane during the adhesion process. This form of bactericidal action was initially discovered on cicada and dragonfly wings, which inspired the production of nanostructures on black silicon. Further studies have been conducted on graphene, titanium and gold, as well as stiff polymers such as PMMA and polystyrene. However, the mechanism leading to bacteria death is not yet fully understood. Recent literature points to differences in bactericidal effects of extremely sharp nanostructures such as vertical graphene and carbon nanotubes that could cut the bacterial membrane versus wider nanopillars or nanocones. It is speculated that the latter functions by exerting lateral force on the membrane that leads to membrane rupture.

In order to make use of bactericidal properties of nanotopographies in a wide range of applications, it is necessary to fabricate such surfaces on a large variety of materials. Polymers are widely used in food, sanitation and health settings and often times soft or flexible surfaces are required. It is therefore necessary to understand the interplay between pillar geometry and elastic modulus on the bactericidal mechanism. Furthermore, fabrication methods need to permit low-cost upscaling to large surface areas of varying geometries.

We have developed a nanoimprint lithography process for rapid, simple and scalable fabrication of nanopillar arrays using UV-curable polymeric resins, therefore permitting the use of a wide range of polymers with varying material properties. In addition, surface material properties can differ from the bulk material by combining polymer foil as a carrier with UV-curable resin for the surface topography.

Using this process, we have fabricated nanopillar arrays of different pillar diameters, spacings and materials in order to investigate the effect of pillar geometry and elastic modulus on bactericidal efficacy. After incubation of samples in bacteria-PBS suspension, the number of live and dead cells on each array are quantified via fluorescent live/dead staining. High-resolution SEM imaging shows the change in bacterial morphology and degree of pillar-bending.

Our results help to shed light on bactericidal mechanisms of nanopillars and determine pillar diameter, periodicity and stiffness in order to optimize bactericidal action.

11:35 AM SB05.04.05

Fluorous-Cured Protein Films as Anti-Fouling and Drug-Eluting Antimicrobial Coatings for Medical Implants [Sanjana Gopalakrishnan](#), Li-Sheng Wang, Yi-Wei Lee, Jiaxin Zhu, Stephen Nonnenmann and Vincent M. Rotello; University of Massachusetts Amherst, United States

Nosocomial bacterial infections are a major health crisis, often occurring due to bacterial contamination of medical devices or implants. Antimicrobial coatings are promising materials for preventing bacterial contamination of medical devices. Protein-based materials offer a sustainable and biocompatible strategy for combatting bacterial infections, either by harnessing antimicrobial properties of native proteins or through the fabrication of antimicrobial-loaded protein scaffolds. However, the high aqueous solubility of proteins often results in materials with poor aqueous stability and mechanical properties. Therefore, current strategies rely on physical or chemical treatments to enhance the stability of protein-based materials and prevent rapid degradation in biological milieus. Thermal treatment is an additive-free approach for stabilizing protein films, but proteins are prone to denaturation at high temperatures leading to loss of function.

We employed a thermal treatment approach in fluoros media (hereafter referred to as fluoros-cured or FC) to enhance aqueous stability of protein films while minimizing protein denaturation. We hypothesized that the fluoros environment prevents rearrangement of proteins at the interface during heat treatment thereby minimizing denaturation. Through this strategy, we developed anti-fouling protein coatings for medical implants, by harnessing the native properties of BSA (Bovine serum albumin). FC-BSA films retained most of the secondary structure of the native protein but remained stable in aqueous media. FC-BSA films were hydrophilic and had an overall negative charge, similar to native BSA. The negative charge of the film prevents bacterial contamination through electrostatic repulsion. Conformal BSA coatings were generated on dental implants (screws) by dip-coating in BSA solution followed fluoros-curing. FC-BSA coated dental implants successfully resisted contamination from *E. coli*.

Anti-fouling FC-BSA films provided passive protection against bacterial contamination by preventing bacterial adhesion on the surface. However, they cannot actively eliminate bacteria as BSA is not an inherently biocidal protein. We hypothesized that electrostatic interactions may be utilized to load antibiotics into FC-BSA films to impart antibacterial activity. FC-BSA films were loaded with a cationic antibiotic colistin sulfate by incubating the films in antibiotic solution overnight. Release of colistin was modulated by ionic strength of supernatant – high ionic strength results in slow release of colistin while low ionic strength results in a rapid burst-release. The colistin-loaded FC-BSA not only retained their anti-fouling behavior while also eliminated bacteria in the vicinity of the dental implant.

Colistin-loaded FC-BSA films are biocompatible antibacterial coatings for medical implants, offering passive protection in the form of anti-fouling behavior as well as active antimicrobial activity through release of antibacterial agents. Thermal treatment in fluorinated media offers an additive-free, sustainable, and biodegradable approach for fabricating protein-based materials while retaining the native properties of protein precursors.

11:50 AM CLOSING COMMENTS

SESSION SB05.05: Antimicrobial Materials IV
Session Chair: Reza Ghiladi
Tuesday Afternoon, December 7, 2021
SB05-Virtual

1:00 PM OPENING COMMENTS

1:05 PM *SB05.05.01

Metal Oxide Nanostructures as Antimicrobial Agents Mohammed Kuku^{1,2}, Ahmad Fallatah^{1,3} and Sonal Padalkar¹; ¹Iowa State University of Science and Technology, United States; ²1. Department of Mechanical Engineering, Jazan University, Jazan, Saudi Arabia, Saudi Arabia; ³2. Space and Aeronautics Research Institute, King Abdulaziz City for Science and Technology, Saudi Arabia

The field of nanotechnology has grown immensely in the last couple of decades owing to the unique properties exhibited by nanomaterials. One such class of nanomaterials are the metal oxide nanoparticles or nanostructures ranging in size from 1 to 100 nm and available in several different shapes. These metal oxide nanostructures find applications in many fields including catalysis, drug delivery, sensing, semiconductors etc. Along with these aforementioned applications, metal oxide nanostructures are favorable candidates as antimicrobial agents.

In the present seminar, the synthesis, characterization and testing of metal oxide nanostructures as antimicrobial agents will be discussed. The influence of nanostructure size and shape on their antimicrobial performance will be evaluated. Additionally, the influence of underlying substrates of the nanostructures on antimicrobial performance will also be addressed. Finally, a tentative guideline will be provided to obtain the best performing antimicrobial nanostructures through the above-mentioned investigation.

1:35 PM SB05.05.02

Carbon Nanomaterials for Antimicrobial Surfaces Laure Giraud^{1,2}, Celine Cougoule³, Audrey Tourrette^{1,2}, Etienne Meunier³ and Emmanuel Flahaut^{2,1}; ¹University of Paul Sabatier, France; ²CNRS / CIRIMAT, France; ³CNRS / IPBS, France

Carbon Nanomaterials such as carbon nanotubes as well as graphene and related materials, present many exceptional properties, including antimicrobial ones. The transfer of the latter through their incorporation into materials has generated a growing interest especially the last ten years [1]. However, due to their intrinsic toxicity not only for microbes but also potentially for humans and the environment, their potential release in use conditions is a central issue in terms of practical applications.

Our work stands at the interface between materials science / chemistry and biology, thanks to the fruitful collaboration between our two laboratories. It focuses on the comparison of different carbon nanomaterials against 2 kinds of pathogens: bacteria and viruses. After deposition of carbon nanomaterials onto a surface, we measure the antibacterial activity against both gram + (*S. aureus*) and gram - (*P. aeruginosa*) bacteria. In the current context of the COVID-19 pandemic, we also investigate the antiviral activity of the same carbon nanomaterials against SARS-CoV-2. This work is especially important in the current context of the worldwide withdrawal from the market of face masks containing "graphene" for safety reasons, while the literature about the actual antiviral activity of such nanomaterials is clearly deficient.

Our most recent results will be presented and discussed considering the many technical challenges associated to such research.

Reference:

L. Giraud, A. Tourrette, E. Flahaut
Carbon, 182, (2021), 463-483

"Carbon nanomaterials-based polymer-matrix nanocomposites for antimicrobial applications: a review"

1:50 PM SB05.05.03

Covalently Attached Liquid-Like Solid Surfaces Prevent Biofilm Formation Yufeng Zhu¹, Glen McHale², Jack Dawson¹, Steven Armstrong², Gary Wells², Hongzhong Liu³, Waldemar Vollmer¹, Paul Stoodley⁴, Nick Jakubovics¹ and Jinju Chen¹; ¹Newcastle University, United Kingdom; ²University of Edinburgh, United Kingdom; ³Xi'an Jiaotong University, China; ⁴The Ohio State University, United States

Biofilms are a major issue for industries from global shipping to health underpinning significant markets for antifouling paints and coatings, and antimicrobial surfaces. To combat biofilm growth porous/textured solid surfaces with a lubricant locked-in to the structure by capillary forces have been used to create a stable hemi-solid/hemi-liquid surface or a continuous liquid lubricant coating – a so-called Slippery Liquid Infused Porous Surface (SLIPS). However, performance under flow conditions where there is shear stress at the surface, such as in catheters, remains a concern due to flow-induced depletion of the lubricant. Here, we report an anti-biofilm surface strategy using liquid-like solid surfaces where the risk of lubricant loss is completely removed. Our coating is a Slippery Omniphobic Covalently Attached Liquid-like (SOCAL) surface, developed as an ultra-slippery non-pinning surface for sessile droplets. This surface displays similar wetting properties to SLIPS through its grafted PDMS coating that behaves as a liquid phase approximately 150°C above its glass transition temperature. However, since it does not flow and is optically transparent, mechanically durable and thermally stable, it offers significant potential for stable anti-biofilm coatings. In this study, SOCAL surface reduced biofilm formation of *Staphylococcus epidermidis* and *Pseudomonas aeruginosa*, two key biofilm forming bacterial pathogens, by 3 to 4 orders of magnitude compared to polydimethylsiloxane (PDMS) in both static and dynamic culture conditions. This liquid-like solid surface approach offers a new strategy for biofilm resistant surfaces under flow conditions and may find application in medical devices, biosensors and many other areas where biofilms are problematic.

2:05 PM SB05.05.04

Understanding the Zwitterionic Hydration from *Ab Initio* Simulations Pranab Sarker, Md Symon Jahan Sajib and Tao Wei; Howard University, United States

Biofouling is a global problem that stemmed from the gradual accumulation of biomolecules and microorganisms, such as barnacles and algae, on a

submerged surface. It causes pitting and crevice corrosion of vessels' metal surfaces and increases the drag on vessels while sailing. An affordable solution in this regard requires developing a non-toxic, eco-friendly, and sustainable-in-all-marine-environments anti-biofouling coating. Trimethylamine-N-oxide (TMAO), a naturally occurring zwitterionic biopolymer found in the deepwater sea fish, is a promising candidate to this end. Its two oppositely charged moieties are directly connected, possessing zero zwitterionic separation. Experimentally, the antibiofouling property of zwitterions increases as the zwitterionic separation decreases. Employing *ab initio* molecular dynamics, we thus investigate hydration of TMAO and another zwitterion with a larger separation, carboxybetaine (CBAA1). Our simulations show an inhomogeneous water distribution for both TMAO and CBAA1. Due to the strong hydrogen bonding, a condensed layer of water surrounds the negative moieties. In contrast, the positive moieties have less hydration due to the shielding of three methyl groups.

While comparing the hydrogen bond strength between the zwitterionic oxygens and water molecules, TMAO has far stronger bonding than CBAA1, as validated and quantified by the geometric and quantum theory of atoms in molecules analyses, respectively. Moreover, we utilize the symmetry-adapted perturbation theory (SAPT) to investigate the zwitterion-water interactions. Our SAPT analysis demonstrates that the electrostatic interaction is the dominant attractive term in zwitterions' interactions with hydrogen-bonded-water molecules. The charge transfer between zwitterionic oxygen and water hydrogen plays a critical role in hydrogen bonding, although it is not the dominant term. In the case of TMAO, it is larger, indicating the more rigidity of hydrogen bonding in TMAO than in CBAA1. Our analysis elucidates the origin of the solid antibiofouling behavior of TMAO.

2:20 PM SB05.05.05

Highly Durable and Functionalized Polyurethane Coatings for Protection of Infectious Aerosols and Elimination of Bacteria Moonhyun Choi and Jinkee Hong; Yonsei University, Korea (the Republic of)

Severe acute respiratory syndrome coronavirus 2 (SARS-CoV-2) or Coronavirus Disease 2019 (COVID-19), characterized as a pandemic at 2020 march, is affecting 216 countries and territories around the world. The issues of hygiene to defend against germs and viruses have risen significantly. For antiviral and antibacterial, it is important to prevent anti-microbial and anti-fouling on the surface because of transmission of pathogens droplets and surface contact. We thus developed multi-functionalized polyurethane coating materials and techniques to satisfy both strategies. PU has been widely used commercially and can be controlled with a variety of mechanical properties, such as hardness, toughness, elasticity and so on due to chemical bonding and physical interaction.

Firstly, we synthesized perfluoro tert butanol-hexamethylene diisocyanate (PFtB-HDI) containing of an umbrella-like structure for anti-fouling of airborne infectious particles (< 5 μm in diameter). The fluorine-containing PU coatings have highly hydrophobic properties, scratch resistance and durability after laundry with commercial detergent, which means the coating has a potential of reusability and decreasing waste plastic. The PFtB-HDI-PU-coated fabric had an improved aerosol protection performance without changing its air and moisture permeability.

Secondly, we prepared a quaternary ammonium alkyl chain-isocyanate (QAC-NCO) for coating with curing and bactericidal effect. The coatings were prepared with reacting polyol (pHEMA or PEG) and QAC-NCO. This coating contains QCA as a killer of bacteria and urethane bond for durability on the outside and inside. After QAC-NCO coating, percent (%) of bacteria killed for *Staphylococcus aureus* (*S. aureus*) and *Pseudomonas aeruginosa* (*P. aeruginosa*) were decreased up to 99.8% and 98.4%, respectively. Our coating systems is based on a polyurethane coating. Therefore, it has a high potential of realizing good performance by applying it to many fields where urethane coating is used.

2:35 PM CLOSING COMMENTS

SESSION SB05.06: Antimicrobial Materials V
Wednesday Morning, December 8, 2021
SB05-Virtual

8:00 AM OPENING COMMENTS

8:05 AM *SB05.06.01

Potential Strategies for Photosensitizer Embedded Anti-Microbial Materials Qingqing Wang¹, Huiyiing Shen¹, Reza Ghiladi², Qufu Wei¹ and Chenyu Jiang²; ¹Jiangnan University, China; ²North Carolina State University, United States

Photosensitizers immobilized onto various matrixes as self-disinfecting materials has been widely reported in the last few decades. However, the antimicrobial photodynamic inactivation (aPDI) efficiency of those materials was restricted by different factors including the photosensitizer itself, immobilization strategy, light availability, illumination conditions, etc. In view of this, we have focused on the potentiation of photoactive materials in which different photosensitizers have been embedded to either electrospun nanofibers (*Mater. Sci. Eng. C*, **2021**, 111502), bacterial cellulose (BC) (*Cellulose* **2020**, 27, 991-1007), or traditional textile fabrics (*ACS Appl. Mater. Interfaces* **2019**, 11, 29557–29568). The photodynamic antimicrobial membrane comprised of electrospun cellulose acetate (CA) microfibers into which the photosensitizer protoporphyrin IX (PpIX) was *in situ* embedded (abbr. PpIX/CA) achieved a 99.8% reduction in Gram-positive *S. aureus* after illumination (Xe lamp, 500 W, $\lambda \geq 420$ nm; 30 min), with a lower level of reduction (86.6%) for Gram-negative *E. coli*. Potentiation with potassium iodide was found to be an effective way to further enhance the antimicrobial efficacy of the PpIX/CA microfibrillar membrane, achieving 99.9999% (6 log units) inactivation of both *S. aureus* and *E. coli* in the presence of 25 and 100 mM KI, respectively. As an alternative strategy, we have embedded another promising photosensitizer molybdenum disulfide (MoS₂) into BC membrane by a facile *in-situ* growth followed by a dip-coating process to coat a chitosan layer on its surface (abbr. BC/MoS₂-CS). When compared with BC/MoS₂ membrane, which showed a 95% reduction of *S. aureus* and 99.9% inactivation of *E. coli*, the addition of chitosan led to a satisfying synergistic effect between chitosan and MoS₂, showing a 99.998% reduction of *S. aureus* and 99.988% inactivation of *E. coli*. More recently, we have developed photosensitizer-luminous powder dual-coated fabrics using silk-screen printing, and demonstrated that this strategy is able to produce antimicrobial materials working not only in light-available area but also in the dark. Our conclusion is that those photosensitizer-embedded materials, that are not so desirable in anti-microbial efficacy, may still have widespread applicability when appropriate potentiation method was employed.

– References –

1. T. Wang, H. Ke, S. Chen, J. Wang, W. Yang, X. Cao, J. Liu, Q. Wei, R. A. Ghiladi and Q. Wang "Porous Protoporphyrin IX-Embedded Cellulose Diacetate Electrospun Microfibers in Antimicrobial Photodynamic Inactivation" *Mater. Sci. Eng. C*, 2021, 111502.
2. T. Wang, L. Xu, H. Shen, X. Cao, Q. Wei, R. A. Ghiladi, and Q. Wang "Photoinactivation of Bacteria by Hypocrellin-Grafted Bacterial Cellulose" *Cellulose* 2020, 27, 991-1007
3. W. Chen, J. Chen, L. Li, X. Wang, Q. Wei, R. A. Ghiladi, and Q. Wang "Wool/Acrylic Blended Fabrics as Next Generation Photodynamic Antimicrobial Materials" *ACS Appl. Mater. Interfaces* 2019, 11, 29557–29568.

8:35 AM SB05.06.02

Photoactive Carbon Dots as a New Class of Broad Spectrum Antibacterial and Antiviral Agents [Liju Yang](#)¹ and Ya-Ping Sun²; ¹North Carolina Central University, United States; ²Clemson University, United States

Infectious diseases caused by pathogenic bacteria and viruses represent a huge global challenge in public health and have prompted the in-demand search for novel and effective alternative antimicrobial agents. We have recently developed carbon dots (CDots) as a new class of effective and efficient visible/natural light-activated antimicrobial agents, with demonstrated ability against a wide range of bacteria and viruses. CDots are surface-functionalized small carbon nanoparticles (CNPs), represent the nanoscale carbon allotrope at zero-dimension. Attributed to the π -plasmon-associated electronic transitions, CDots have remarkable broad optical absorptions in the entire visible spectrum, extending into both near-UV and near-IR, making them excellent visible light-excitabile agents. Mechanistically, upon photoexcitation on CDots, there are rapid charge transfers and separation to form electrons and holes redox pairs, followed up the radiative recombinations of the separated redox pairs resulting in emissive excited states, which are responsible for photodynamic production of classical reactive oxygen species (ROS). The combined action of the initially separated redox pairs and the generated classical ROS are responsible for the observed uniquely effective photoinduced antimicrobial function of CDots.

We have demonstrated the highly effective photoactive antimicrobial activities of CDots against various bacteria and viruses, ranging from laboratory model bacteria (*E. coli*, *Bacillus Subtilis*), pathogenic foodborne bacteria (*Listeria*, *Salmonella*), to multi-drug resistant (MDR) nosocomial pathogens (*Enterococcus*), as well as various viruses (model MS2 virus, vesicular stomatitis virus (VSV), and marine norovirus (MNV)). For the bacterial species tested, the treatments with 0.1 mg/mL CDots under 1 h household light illumination achieved up to more than 7 log viable cell reductions, demonstrating the high efficiency of photoinactivation by CDots. For viruses tested, the treatment with 5 mg/mL to viral samples containing 10⁶ PFU/mL under 1 h household light illumination inactivated all the viruses, diminishing viral infectivity to their host cells. Bacterial damages by CDots treatments, including elevated levels of lipid peroxidation, increased membrane permeability, and cytoplasmic structural disruptions, are evident. Degradation in viral proteins and genomic RNAs are also observed.

Along with these demonstrated highly effective antimicrobial activities, our studies on property-function correlations have revealed that the optical properties, the surface functional groups and charges, and the passivation layers of CDots are highly correlated with their antimicrobial activities, which make CDots tunable and expandable material platforms for further improvement. With their tunable structures and uniquely advantageous properties together with their non-toxic nature, CDots present new opportunities for effective control and prevention of infectious diseases.

Acknowledgement: The research was supported by NSF grants #1855905, #2102021, #2102056, and USDA grant #2019-67018-29689.

8:50 AM SB05.06.03

Superhemophobic and Antivirofouling Coating for Mechanically Durable and Wash-Stable Medical Textiles [Anthony Galante](#), Sajad Haghani, Eric G. Romanowski, Robert M. Shanks and Paul W. Leu; University of Pittsburgh, United States

Medical textiles have a need for repellency to body fluids such as blood, urine, or sweat that may contain infectious vectors that contaminate surfaces and spread to other individuals. Similarly, viral repellency has yet to be demonstrated and long-term mechanical durability is a major challenge. In this work, we demonstrate a simple, durable, and scalable coating on nonwoven polypropylene textile that is both superhemophobic and antivirofouling. The treatment consists of polytetrafluoroethylene (PTFE) nanoparticles in a solvent thermally sintered to polypropylene (PP) microfibers, which creates a robust, low-surface-energy, multilayer, and multilength scale rough surface. The treated textiles demonstrate a static contact angle of $158.3 \pm 2.6^\circ$ and hysteresis of $4.7 \pm 1.7^\circ$ for fetal bovine serum and reduce serum protein adhesion by $89.7 \pm 7.3\%$ (0.99 log). The coated textiles reduce the attachment of adenovirus type 4 and 7a virions by $99.2 \pm 0.2\%$ and $97.6 \pm 0.1\%$ (2.10 and 1.62 log), respectively, compared to noncoated controls. The treated textiles provide these repellencies by maintaining a Cassie-Baxter state of wetting where the surface area in contact with liquids is reduced by an estimated 350 times (2.54 log) compared to control textiles. Moreover, the treated textiles exhibit unprecedented mechanical durability, maintaining their liquid, protein, and viral repellency after extensive and harsh abrasion and washing. The multilayer, multilength scale roughness provides for mechanical durability through self-similarity, and the samples have high-pressure stability with a breakthrough pressure of about 255 kPa. These properties highlight the potential of durable, repellent coatings for medical gowning, scrubs, or other hygiene textile applications.

9:05 AM SB05.06.05

Polyethylenimine-Functionalized Silver Nanoparticles as Potential Antiviral and Antibacterial Disinfectant [Atul K. Tiwari](#) and Prem C. Pandey; Indian Institute of Technology Banaras Hindu University, India

Polyethylenimine in the presence of organic reducing agent allow the formation of functionalized Silver nanoparticles of controlled particle size distribution. The nanoparticles exhibited potent antimicrobial activity against drug resistant bacterial and also to viruses. as a function of size of silver nanoparticles. Fluorescence imaging of Ag-NPs revealed selective transfection of Ag-NPs across the cell membrane as a function of the polymeric MW; differential interaction of the cytoplasmic proteins during antimicrobial activity was observed and will be discussed during presentation.

9:20 AM SB05.06.06

Late News: (Garcia High School Student) Fogging H1N1 Virus to Quantify the Survival Rate on Various Surfaces Timothy J. Reinholdt, Kuan-Che Feng, [Francis H. White](#), Qianhui Hong and Miriam Rafailovich; Stony Brook University, The State University of New York, United States

The COVID-19 pandemic has made the general public more aware of the threat of viruses. With that comes interest in how long pathogens are able to survive on surfaces, to help minimize potential exposures. Hypochlorous Acid, or HOCl is an endogenous substance found in mammals, and effective against a wide range of microorganisms¹. This research will determine the efficacy of Hypochlorous Acid for eliminating the H1N1 Virus, which is responsible for a highly contagious respiratory disease², and identify the survival rate on various surfaces.

To identify the reduction rate of H1N1, a plaque assay was executed to calculate the PFU of H1N1 plated on PLA (Polylactic Acid), Polystyrene (280K), and Aluminum at different timeframes. The samples were allocated into vials with 0.2% BSA in MEM (minimum essential media) and vortexed to promote uniformity. Subsequently, the new virus solution underwent a ten-fold serial dilution to perform a plaque assay. The virus was then replaced by the gum medium (0.2% BSA, 0.5% TrypLE Select, 1% PenStrep and 25% Tragacanth gum). Lastly, the plates were placed in the incubator for 3 days and later stained with 1% crystal violet, with 4% formaldehyde and 50% methanol dye. The PFU of each well was counted and documented.

In relation to time (in hours), drying in a room temperature environment was significantly more susceptible to viruses surviving than at 4°C and -20°C, despite the variance in surfaces. In a 4°C refrigerator, the penny, an impure copper surface, had the lowest H1N1 survival surface rate (blank) in coin currencies. For the 24 hour series, PLA—at room temperature—achieved the most resistance to the H1N1 virus with a 2-log reduction. Most notably, an Aluminum surface drying for 48 hours produced a 3-log reduction, which resulted in a 99.9% H1N1 elimination.

At room temperature, all tested surfaces reached antiviral capabilities (at least 4-log reduction or 99.99% elimination) between 24 and 50 hours; however, this span significantly increases the likelihood of pathogens to spread via surfaces. Therefore, the addition of Hypochlorous Acid, a common disinfectant, was deemed necessary to increase the log reduction of H1N1 in a shorter time frame.

To observe the disinfecting effect of Hypochlorous Acid, 350 and 510 ppm (low and high) concentrations were used. Firstly, the H1N1 virus was deposited on three different surfaces: Polystyrene (280K), Aluminum, and PLA. The plated virus samples were then fogged with HOCl at 2.5 minutes, 5 minutes, 7.5

minutes, and 10 minutes with a 5 minute interval of rest for the different concentrations. For H1N1 deposited on all surfaces, there was an increasing correlation between log reduction and time (in minutes) for both chlorine concentrations, denoting that longer fogging cycles eliminates more virus particles. Specifically, Aluminum and Polystyrene infected surfaces exposed to high chloride concentration were considered antiviral between 5 and 7.5 minutes. For low chloride concentration, surfaces plated with H1N1 produced a 4-log reduction between 7.5 and 10 minutes. Therefore, these results provide promising evidence that makes hypochlorous acid fogging, a cheap and readily available substance, a potential method of disinfecting with high efficacy.

1Block, Michael S, and Brian G Rowan. "Hypochlorous Acid: A Review." *Journal of oral and maxillofacial surgery : official journal of the American Association of Oral and Maxillofacial Surgeons* vol. 78,9 (2020): 1461-1466. doi:10.1016/j.joms.2020.06.029 2Lee, Spike W., et al. "Risk Overgeneralization in Times of a Contagious Disease Threat." *Frontiers in Psychology*, vol. 11, 2020, doi:10.3389/fpsyg.2020.01392.

9:25 AM SB05.06.07

Evaluation of Antifungal Activity of Ca₂Fe₂O₅ against *Candida utilis* with Changing Susceptibility upon Cultivation Svetlana Vihodceva¹, Olga Muter² and Andris Sutka¹; ¹Riga Technical University, Latvia; ²University of Latvia, Latvia

Candida species are the most common fungi isolated from nosocomial infections (e.g., hospital-acquired infections), and biofilms formed by these organisms are associated with drastically enhanced resistance against most antimicrobial agents. Nowadays, also rare fungal species of low pathogenic potential, or even species never described before as a cause of disease, are being more commonly detected in health-care settings. Thus, an intensive search and development of the novel anti-fungal agents is of current interest. This study reports the impact of Ca₂Fe₂O₅ nanoporous powder on yeast *Candida utilis* – as a fungal model – at different phases of growth, i.e., early exponential, mid-log and stationary phases. After 120 min incubation, the fungicidal activity of nanoporous powder was observed, i.e., log reduction of 2.81 and 2.58 for mid-log and stationary culture, respectively, reaching the maximum of 4 log reduction after 7 days. The early exponential culture of *C. utilis* showed an enhanced resistance to Ca₂Fe₂O₅ with a log reduction 4.04 during the 7 days exposure. Our results not only showed that Ca₂Fe₂O₅ have the potential to effectively decrease the *C. utilis* cell growth, but also indicated the importance of the physiological state of the test culture. Obtained results may contribute to better understanding of the difference in fungicidal efficacy of antimicrobial materials.

Acknowledgments: This work has been supported by the European Regional Development Fund within the Activity 1.1.1.2 "Post-doctoral Research Aid" of the Specific Aid Objective 1.1.1 "To increase the research and innovative capacity of scientific institutions of Latvia and the ability to attract external financing, investing in human resources and infrastructure" of the Operational Programme "Growth and Employment" (No. 1.1.1.2/VIAA/2/18/331).

9:30 AM SB05.06.08

Capture-and-Release Filtration of Aerosolized Bacteria Using Liquid Nets Daniel Regan, Chun Ki Fong, Justin Hardcastle and Caitlin Howell; University of Maine, United States

Materials and methods of collecting bioaerosol for performing analysis on potential biological threats is at an all-time high after over a year of battling COVID-19. Currently, filter-based air samplers capture the highest yield and ratio, while liquid impingers offer the best chance to maintain pathogen viability. In this body of work, we present a novel approach to filter-based filtration by fabricating liquid nets. Infusing polytetrafluoroethylene filters with a perfluoropolyether oil resulted in improved rate of release of captured *Escherichia coli* aerosols onto culture plates. Furthermore, wetting meltblown polypropylene filters with the same perfluoropolyether oil improved the rate of release, as well as the overall colonies transferred and cultured. The efficiency of bioaerosol transfer demonstrated by the liquid-infused filters could provide a better representation of the airborne pathogens within an environment, enabling informed actions by infectious disease experts and medical professionals.

9:35 AM CLOSING COMMENTS

SYMPOSIUM SB06

Graphene and Related 2D Materials for Bioelectronics and Healthcare
November 30 - December 8, 2021

Symposium Organizers

Deji Akinwande, The University of Texas at Austin
Matthew Cole, University of Bath
Andreas Offenhaeusser, Forschungszentrum Julich
Litao Sun, Southeast University

* Invited Paper

SESSION SB06.01: Fabrication and Characterization of 2D Materials for Bioelectronics and Healthcare I
Session Chair: Dmitry Kireev

Tuesday Morning, November 30, 2021
Sheraton, 2nd Floor, Constitution A

10:30 AM *SB06.01.01

Graphene-Based Electrode for Cortical Maps and Epilepsy Treatment [Jong-Hyun Ahn](#); Yonsei University, Korea (the Republic of)

Cortical maps, which are indicative of cognitive status, are shaped by experience. Previous mapping tools, such as penetrating electrodes and imaging techniques, are limited in assessing high-resolution brain maps largely owing to their invasiveness and poor spatiotemporal resolution, respectively. In this talk, we developed a flexible graphene-based multichannel electrode array for electrocorticography (ECoG) recording, which enables us to assess cortical maps in a time- and labor-efficient manner. The flexible electrode array, formed by chemical vapor deposition (CVD)-grown graphene, provides low impedance and electrical noise because of the creation of a good interface between the graphene and brain tissue, which improves the detectability of neural signals. In addition, we present the results of simultaneous recordings of multiple cortical sites and responsive neurostimulations for epilepsy treatment carried out in free-moving rats. Flexible graphene-based electrode array which stably wraps onto the cortex surface of a living rat's brain, exhibiting a superior signal-to-noise ratio. The graphene multichannel electrode successfully detected brain signals with high-throughput spatiotemporal resolution and substantially suppressed pilocarpine-induced epileptic discharges and behavior. The simultaneous recording and neurostimulation in awake animals can lead to a fundamental change in the approaches used for the treatment of medically intractable epilepsy.

11:00 AM SB06.01.02

Graphene Quantum Dots Synthesized from Reduced Graphene Oxide for Near-Infrared *In Vitro/In Vivo/Ex Vivo* Bioimaging Applications Md Tanvir Hasan^{1,2}, [Bong Han Lee](#)³, Ching-Wei Lin^{3,4}, Ainsley McDonald-Boyer^{5,2}, Roberto Gonzalez-Rodriguez^{6,2}, Satvik Vasireddy², Uyanga Tsedev^{4,4}, Jeffery Coffey², Angela Belcher^{4,4,4} and Anton V. Naumov²; ¹National Institute of Standards and Technology, United States; ²Texas Christian University, United States; ³Academia Sinica, Taiwan; ⁴Massachusetts Institute of Technology, United States; ⁵Rice University, United States; ⁶University of North Texas, United States

Near-infrared (NIR) emissive nanomaterials are desired for bioimaging and drug delivery applications due to the high tissue penetration depth of NIR light, enabling *in vitro/ex vivo/in vivo* fluorescence tracking. Considering the scarcity of NIR-fluorescing biocompatible nanostructures, we have for the first-time synthesized nanometer-sized reduced graphene oxide-derived graphene quantum dots (RGQDs) with NIR (950 nm) emission highly biocompatible *in vitro* with no preliminary toxic response *in vivo*. RGQDs are obtained in a high-yield (~90%) top-down sodium hypochlorite/UV-driven synthetic process from non-emissive micron-sized reduced graphene oxide (RGO) flakes. This oxidation of RGO yields quantum dots with an average size of 3.54 ± 0.05 nm and a highly crystalline graphitic lattice structure with distinguishable lattice fringes. RGQDs exhibit excitation-independent emission in the visible and NIR-I region with a maximum NIR quantum yield of ~7%, where *in situ* fluorescence measurements of the synthesis also showed an interdependence of evolution for the visible and NIR-I emissions. Unlike their parent material, RGQDs show substantial biocompatibility with ~75-80% cell viability up to high (1 mg/mL) concentrations verified via both MTT and luminescence-based cytotoxicity assays. Tracked *in vitro* via their NIR fluorescence, RGQDs exhibit efficient internalization in HeLa cells maximized at 12 h with further anticipated excretion. *In vivo*, RGQDs introduced intravenously to NCr nude mice allow for fluorescence imaging in live sedated animals without the need in sacrificing those at imaging time points. Their distribution in spleen, kidneys, liver, and intestine assessed from NIR fluorescence in live mice, is further confirmed by excised organ analysis and microscopy of organ tissue slices. This outlines the potential of novel RGQDs as NIR imaging probes suitable for tracking therapeutic delivery in live animal models. A combination of smaller size, water-solubility, bright NIR emission, simple/scalable synthesis, and high biocompatibility gives RGQDs a critical advantage over a number of existing nanomaterials-based imaging platforms.

11:15 AM SB06.01.03

Exfoliated and Stabilized Biological Carbon Nanotube (CNT) Dispersions, Conductive Films, and Biocatalysts for the Bioengineering Applications [Ankarao Kalluri](#)¹ and Challa V. Kumar^{1,2,2}; ¹University Of Connecticut, United States; ²University of Connecticut, United States

As carbon nanotubes (CNT) emerging in the healthcare and bioengineering field, it is essential to produce toxic-free, biofriendly, biocompatible, water-soluble, fewer defects, highly concentrated, and stable biological CNT solutions. We report stable and high-quality multi-walled carbon nanotube (MWCNT) dispersions using proteins as a dispersing agent by a simple stirring on the benchtop. Bovine serum albumin (BSA), anionic or cationic BSA, ovalbumin, lysozyme, and hemoglobin are used to disperse MWCNT, and the dispersions and exfoliation efficiency depended on the charge, size, and nature of the protein. We achieved a minimum dispersion limit ~5 mg/ml and a maximum up to ~12 mg/ml and the undispersed CNT is easily removed by centrifugation and washing or precipitation. The BSA-coated CNT showed controllable surface charge, stable dispersions at pH 7 to 14 and stability over a wide temperature (2–50 °C) up to 6 months. Furthermore, the CNT dispersions loaded on the cellulose filter paper to fabricate the metal-free and conductive bio-CNT films. The bio-CNT films showed a resistance of <30 Ω/sq and conductivity >10000 S/m, greater than the electrical conductivity reported for CNT-polymer composites. This general, powerful approach is used to produce environmentally benign, biocompatible CNT dispersions by a simple method that can be adapted under resource-limited conditions.

Keywords: Carbon nanotubes, protein, bio-conductivity films, biocatalysts

11:30 AM SB06.01.04

Biocompatibility of Large Area Electronic-Grade 2D Materials with Stem Cells and Motor Neurons [RT Jayanth](#)¹, Nicholas White², Dmitry Kireev^{1,2}, Martha Serna^{1,2}, Emmanuel Okogbue^{3,3}, Yeonwoong Jung^{3,3,3}, Shelly Sakiyama-Elbert² and Deji Akinwande^{1,2,2}; ¹University of Texas at Austin, United States; ²The University of Texas at Austin, United States; ³University of Central Florida, United States

Two-dimensional (2D) materials have the potential to become the functional elements of future bioelectronic interfaces. So far, studies directed towards understanding their biocompatibility have mostly utilized exfoliated flakes and suspensions resulting in large uncertainty and discrepancies in their cytotoxicity measures. In this work, as a first step before incorporating them in bioelectronic interfaces, we have performed a comprehensive experimental study of *in vitro* cell-viability of large-scale sheets of electronics grade 2D materials that include platinum diselenide (PtSe₂), platinum ditelluride (PtTe₂), molybdenum disulfide (MoS₂), and graphene. These materials were selected because of their superior electronic and mechanical properties, and their atomically thin layered structure which facilitates efficient surface chemical functionalization. We cultured embryonic stem cells (ESCs) and ESC-derived motor neurons (MNs) on the surface of these large-area 2D sheets and quantified cell-viability using the 3-(4,5-dimethylthiazol-2-yl)-2,5-diphenyltetrazolium bromide (MTT) assay and the Lactate Dehydrogenase (LDH) assay. Live-dead fluorescence imaging was performed to qualitatively understand the trends in cellular growth and proliferation. The results suggest that PtSe₂ displays cell-viability values on par with those of the controls, graphene, and MoS₂. Contrarily, PtTe₂ displays the lowest cell-viability value amongst all the 2D materials when observed through the lens of the MTT assay but displays cell-viability similar to that of the controls when observed through the lens of the LDH assay. We provide experimental validations to explain for this discrepancy with PtTe₂'s cell-viability and present an overall view on how our study can be further developed to incorporate other 2D materials and cell-viability measurement assays. We believe these results from the *in vitro* biocompatibility experiments can help large-area 2D materials

become an alternative for both future cell-culture scaffolds and bioelectronic implants.

SESSION SB06.02: Fabrication and Characterization of 2D Materials for Bioelectronics and Healthcare II

Session Chair: Dmitry Kireev

Tuesday Afternoon, November 30, 2021

Sheraton, 2nd Floor, Constitution A

1:30 PM SB06.02.01

Graphene Obtained from Renewable Materials—From Biosensors to Supercapacitors [Elvira Fortunato](#), Tomas Pinheiro, Sara Silvestre, Ana Carolina Marques and Rodrigo Martins; NOVA University Lisbon, Portugal

Graphene has emerged as a novel material with enhanced electrical and structural properties that can be used for a multitude of applications from supercapacitors to biosensors.

The use of laser irradiation to induce networks of graphene-based structures towards cost effective, flexible device fabrication has been a highly pursued area, with application of laser engraving in various polymeric substrates.

In this work, we report the application of this approach towards commonly available, eco-friendly and low-cost substrates, namely office paper and cork to be used as a standard glucose biosensor and supercapacitor.

As proof-of-concept amperometric, enzymatic biosensors were developed, exhibiting a good analytical performance in physiologically relevant glucose levels in blood, with linear sensitivity range between 0.5 and 15 mM, with a limit of detection of 130 μ M and a sensitivity as high as 27.23 μ A/mM.

Furthermore, flexible microcapacitor has been also developed on cork exhibiting an outstanding performance with an areal capacitance of 1.39 mF cm⁻² (107.26 mF cm⁻³) at 0.005 mA cm⁻².

It was proved that is possible to join sustainable materials and low-cost techniques for laser induced graphene electrodes production, representing a mandatory step for a clean and green future in wearable and self-sustainable electronics.

1:45 PM SB06.02.03

Tuning the Properties of Printed Graphene to Create Electrochemical Sensors and Integrated Open Microfluidics for In-field Environmental and Health Monitoring Systems Zachary Johnson, Nate Garland, Kelli Williams, Bolin Chen, Carmen L. Gomes and [Jonathan Claussen](#); Iowa State University, United States

Printed graphene (PG) has recently shown promise in the fabrication of low-cost, flexible electrical circuits. However, biosensing applications involving PG have been constrained due in part to low resolution printing, destructive post-print annealing steps, low electrochemical reactivity, and/or relatively smooth, planar non-electroactive surfaces.

In this presentation, we demonstrate how low-cost printed and flexible PG circuits can be fabricated and functionalized fluid transport and electrochemical sensing. First, we demonstrate how the utility of PG is expanded through high-resolution patterning, post-print laser annealing, and biorecognition agent functionalization techniques. A new graphene patterning technique [i.e., inkjet maskless lithography (IML)] is used to form high resolution, flexible graphene films (line widths down to 20 μ m) that significantly exceeds current graphene inkjet printing resolution (line widths \sim 60 μ m). We build upon this technique and add salt porogens into the graphene inks [i.e., salt impregnated inkjet maskless lithography (SIIML)] to increase the micro/nano surface area of the printed graphene to further improve biosensor performance. Next, a rapid pulse laser annealing technique with a continuous CO₂ laser is used to tune the electrical conductivity, surface wettability, surface roughness, and electrochemical reactivity of the IML PG. Finally, we demonstrate how a newer variant of nano/microstructured PG called laser induced graphene (LIG) can be fabricated. This graphene fabrication technique utilizes a scalable direct-write laser fabrication process that converts polyimide into LIG which eliminates the need for chemical synthesis of graphene, ink formulation, masks, stencils, pattern rolls, and post-print annealing commonly associated with other PG sensors.

Finally, we demonstrate how these graphene-based circuits can be biofunctionalized with enzymes [phosphotriesterase (PTE) and acetylcholinesterase (AChE)] for organophosphate sensing or ion selective membranes for ammonium, nitrate, and potassium sensing in river water soil slurry, or urine samples. The PTE and AChE enzymes offer distinct sensing paradigms where PTE is activated by organophosphates and AChE is inhibited. The detection limits of the biosensors so far have achieved approximately 0.6 nM for organophosphate pesticides which well below the concentration limits we would expect for drinking water or soil samples. We also demonstrate how LIG electrodes were capable of monitoring four major neonicotinoids (CLO, IMD, TMX, and DNT) with low detection limits (CLO - 823 nM; IMD - 384 nM; TMX - 338 nM; and DNT - 682 nM) and a rapid response time (\sim 10s) using square wave voltammetry without chemical/biological functionalization. Finally, we demonstrate how the surface wettability of the LIG can be tuned in order to create narrowing, wedge-shaped hydrophilic tracks surrounded by superhydrophobic walls that permit movement of fluid along the tracks by net Laplace pressure (i.e., open microfluidics). Such definitive control over material properties enables the creation of LIG-based integrated open microfluidics and electrochemical sensors that are capable of splitting a single water sample along four multifurcating paths to three ion selective electrodes (ISEs) for potassium (K⁺), nitrate (NO₃⁻), and ammonium (NH₄⁺) monitoring and to an enzymatic pesticide sensor for organophosphate pesticide (parathion) monitoring. The ISEs displayed near-Nernstian sensitivities and low limits of detection (LODs) (10^{-5.01} M, 10^{-5.07} M, and 10^{-4.89} M for the K⁺, NO₃⁻, and NH₄⁺ ISEs, respectively) while the pesticide sensor exhibited the lowest LOD (15.4 pM) for an electrochemical parathion sensor to date. Hence, this unique and tunable fabrication approach to PG is expected to enable a wide range of real-time, point-of-use health and environmental sensors.

2:00 PM SB06.02.04

In Situ Graphene Liquid Cell Scanning Transmission Electron Microscopy Studies Investigating Antibacterial Mechanisms of Multimetallic Nanoparticles [Abhijit H. Phakatkar](#), Tolou Shokuhfar and Reza Shahbazian-Yassar; University of Illinois at Chicago, United States

Continuously emerging antimicrobial resistance (AMR) in bacteria is a global challenge. Herein, we propose the strategy to utilize bactericidal multimetallic ternary (Fe/Ni/Cu) nanoparticles (NPs) to address the rising AMR challenge. The ternary NPs were synthesized by using aerosol mediated nebulized spray pyrolysis method. The pure metallic FCC crystal structure of NPs was confirmed by using atomic resolution high angle annular dark field (HAADF) scanning transmission electron microscopy (STEM) analysis. Further energy dispersive X-ray spectroscopy (STEM-EDS) technique was used to confirm the elemental composition of synthesized NPs. In-situ graphene liquid cell (GLC) STEM novel approach was utilized to investigate the antibacterial mechanisms of action of these ternary NPs against *Escherichia Coli* (*E. Coli*) bacteria. Cryo-electron microscopy and conventional transmission electron microscopy (TEM) coupled with ultramicrotomy are well-studied and widely utilized approaches to investigate the antibacterial mechanisms of actions of bactericidal nanomaterials. Although these approaches have shown potential to evaluate the nanoscale antibacterial mechanisms,

there exists challenges with lower spatial resolution and the tedious steps involved for the sample preparation. In-situ GLC STEM approach allows faster sample preparation with minimal efforts and can provide insights of dynamic nanoscale events of antibacterial mechanisms of action. Moreover, GLC has unique advantages with higher spatial resolution and capability to reduce the electron beam damage, especially for the soft matter. In the present study, graphene coated TEM gold grids were prepared by transferring chemical vapor deposition (CVD) grown graphene upon etching of the copper substrate. To prepare GLC pockets, 0.3 μ L of reaction solution was encapsulated between two graphene coated TEM grids. *E. Coli* bacteria were cultured prior to the experiments in the LB broth culture media for 4 hours under 37°C incubation. For in-situ GLC experiments, the final concentration of cultured *E. Coli* bacteria was as low as 20 CFU/ml. To acquire better contrast during STEM study and to reduce the organic content in the cell media, cultured bacteria were transferred into the ultrapure water for GLC studies. For investigating the antibacterial mechanisms of ternary NPs, NPs with 25 μ g/ml concentration were mixed with cultured *E. Coli* bacteria in water medium. Upon 10 minutes of interaction, the NPs treated bacteria were immediately encapsulated between TEM grids for GLC studies. STEM-imaging and STEM-EDS mapping acquired in GLC clearly indicate the presence of nitrogen (N), oxygen (O), carbon (C), chlorine (Cl) and phosphorus (P) diagnostic ions, mapping the bacterium morphology and cellular integrity. Cl is responsible for the osmotic balance in the bacterium, while N is associated with amino acids. P is present in the phosphorylated proteins and deoxyribonucleic acid, while O and C are present in almost all cellular components. The cellular integrity of control bacterium was disrupted upon treating with ternary NPs for 10 minutes. Fe, Ni, and Cu metal ions were observed inside the bacterium cytoplasm and along the cell wall, confirming the synergistic release of metal ions. Results also confirm that the ions release rate from the ternary NPs follows a trend, as Cu ions > Ni ions > Fe ions. Further organic corona formed around the NPs was investigated to be the bacterium cytoplasmic and cell membrane components. Synergistic and varying rate of (Fe/Ni/Cu) ions release from the ternary NPs can inactivate the bacteria without allowing to develop AMR and can provide prolonged bactericidal efficiency. The present work investigates the real time nanoscale mechanisms of antibacterial activity of multimetallic NPs, encouraging the developments of novel drug delivery strategies.

2:15 PM SB06.02.05

Towards 2D Heterostructure Nanopore for DNA Characterization and Sequencing Sihan Chen¹, Siyuan Huang¹, Jangyup Son¹, Kenji Watanabe², Takashi Taniguchi², Arend van der Zande¹ and Rashid Bashir¹; ¹University of Illinois at Urbana-Champaign, United States; ²National Institute for Materials Science, Japan

Sequencing the human genome has helped to improve our understanding of disease, inheritance and individuality. Solid-state nanopores could potentially meet the demand for even cheaper and faster genome sequencing, owing to their superior mechanical, chemical and thermal robustness and durability, and potential for integration into high-density electronic arrays.¹ Despite the promise, solid state nanopores have yet to demonstrate DNA sequencing. Two key challenges remain, i.e., achieving few-base spatial resolution and slowing the translocation of the DNA molecule. 2D materials such as graphene² and MoS₂³ have emerged as attractive possibilities, since the thickness of these films is in the range of a few nucleotides. However, atomic membranes alone are not robust in fluid under an electric field.⁴ 2D materials sandwiched within dielectrics could provide a stable platform,⁵ but the resulting stack thickness limits the spatial resolution. Resolving these challenges requires new sensing mechanisms beyond ionic currents and translocation control. This work reports a novel solid state nanopore sensor that has the desired spatial resolution of sub nanometer, integrated electrical sensing, and can potentially control the translocation of the DNA molecule. In this architecture, the nanopore is drilled through a vertical 2D heterostructure consisting of n-type MoS₂ and p-type WSe₂. The heterostructure forms an atomically thin out-of-plane p-n diode. The diode is passivated by atomic layer deposition (ALD) of HfO₂ for electrical insulation. We validated the robustness of the 2D heterostructure nanopore architecture with ionic sensing, by acquiring thousands of DNA translocation events under three different ionic biases. Then we demonstrated modulation of ionic current by 2D diode interlayer potential. Ionic current modulation is more effective with smaller pores and lower salt concentrations, and thus is not caused by leakage or edge electrochemistry. Modulation of ionic transport is also more effective under forward bias than under reverse bias, as a larger fraction of in-plane bias drops across the vertical p-n junction under forward bias.⁶ Finally, we obtained signatures of DNA translocation in ionic and diode channels simultaneously. DNA translocation in 10 mM KCl resulted in current increase in ionic channel, as well as current increase in diode channel. The diode channel had better signal-to-noise ratio than the ionic channel. To our knowledge, these proof-of-principle experiments are first-of-its-kind demonstration of 1) simultaneous detection of DNA translocation in a 2D diode nanopore device in both ionic and electrical channels, and 2) modulation of ionic current by the interlayer potential of 2D diode.

References:

- (1) Lindsay, S. The Promises and Challenges of Solid-State Sequencing. *Nat. Nanotechnol.* **2016**, *11* (2), 109–111.
- (2) Garaj, S.; Hubbard, W.; Reina, A.; Kong, J.; Branton, D.; Golovchenko, J. A. Graphene as a Subnanometre Trans-Electrode Membrane. *Nature* **2010**, *467* (7312), 190–193.
- (3) Feng, J.; Liu, K.; Bulushev, R. D.; Khlybov, S.; Dumcenco, D.; Kis, A.; Radenovic, A. Identification of Single Nucleotides in MoS₂ Nanopores. *Nat. Nanotechnol.* **2015**, *10* (12), 1070–1076.
- (4) Graf, M.; Lihter, M.; Thakur, M.; Georgiou, V.; Topolancik, J.; Ilic, B. R.; Liu, K.; Feng, J.; Astier, Y.; Radenovic, A. Fabrication and Practical Applications of Molybdenum Disulfide Nanopores. *Nat. Protoc.* **2019**, *14* (4), 1130–1168.
- (5) Venkatesan, B. M.; Estrada, D.; Banerjee, S.; Jin, X.; Dorgan, V. E.; Bae, M. H.; Aluru, N. R.; Pop, E.; Bashir, R. Stacked Graphene-Al₂O₃ Nanopore Sensors for Sensitive Detection of DNA and DNA-Protein Complexes. *ACS Nano* **2012**, *6* (1), 441–450.
- (6) Lee, C. H.; Lee, G. H.; Van Der Zande, A. M.; Chen, W.; Li, Y.; Han, M.; Cui, X.; Arefe, G.; Nuckolls, C.; Heinz, T. F.; et al. Atomically Thin P-n Junctions with van Der Waals Heterointerfaces. *Nat. Nanotechnol.* **2014**, *9* (9), 676–681.

SESSION SB06.04: 2D Bioelectronic Sensing I

Session Chair: Dmitry Kireev

Wednesday Morning, December 1, 2021

Sheraton, 2nd Floor, Constitution A

10:30 AM *SB06.04.01

Graphene-Based Sensors for Real-Time Monitoring of Physiological Parameters Mantian Xue¹, Anthony Taylor², Wei-Hung Weng¹, Jiadi Zhu¹, Yiyue Luo¹, Ang-Yu Lu¹, Elaine McVay¹, Jing Kong¹ and Tomas Palacios¹; ¹Massachusetts Institute of Technology, United States; ²Edwards Vacuum, United States

This paper describes the use of graphene-based sensors for the real-time detection of physiologically-relevant ions and volatile organic compounds (VOCs). Specifically, we have developed a robust sensing platform with more than 200 sensing units on a transparent glass substrate connected to a custom hand-held readout circuit. This system is then combined with a novel calibration algorithm and machine learning software to provide excellent reproducibility and accuracy over a wide range of physiologically-relevant analytes. For example, using this system, potassium, sodium and calcium ions

have been detected and their relative concentrations have been identified in complex multi-ion electrolytes. An analytical study of the impact of sensor redundancy on the sensitivity and reproducibility of the sensing platform will be presented. The impact of device calibration and machine learning data analysis on system performance will also be discussed. Finally, the use of the graphene sensing platform for the detection of VOC's in both breath and skin will be described, as well as the potential of this technology for diagnosis of different disease.

11:00 AM SB06.04.02

Graphene and hBN/Graphene Heterostructure Channels for Ultra-Sensitive Field-Effect Transistor Biosensing of SARS-CoV-2 Spike Protein S1 Subunit Nicholas E. Fuhr, Mohamed Azize and David Bishop; Boston University, United States

Stemming the exponential growth of emergent infectious disease (e.g., COVID-19) requires prompt detection of infection followed by isolation and treatment of the afflicted. If unchecked, infectious evolutionary events can upend the fundamental institutions constituting *Homo sapiens'* society and economy. Here, a biosensing platform is realized via surface functionalization of a two-dimensional channel comprised of graphene/hexagonal boron nitride (hBN) heterostructure field-effect transistor with monoclonal immunoglobulin G specific for SARS-CoV-2 antigen protein. Several surface functionalization schemes with real-time monitoring of surface modification and sensation on both G- and hBN/G-FETs have been performed. These low-cost devices have been observed to be ultra-sensitive to ≥ 200 ag/mL SARS-CoV-2 spike protein S1 subunit in 1X phosphate buffered saline. This is ~ 1 -3 orders of magnitude lower than contemporary molecular diagnostics (i.e., RT-PCR and ELISA, respectively). Graphene and hBN/graphene materials and fabrication process are characterized with Raman spectroscopy, X-ray reflectometry, atomic force microscopy, and biosensor performance evaluated with two- and three-terminal electrical measurements. The G- and hBN/G-FET devices used in this study contribute to the growing body of knowledge regarding graphene applications in biosensing by including a passivating hexagonal boron nitride layer and help pave the path toward lab-on-chip platforms for point-of-care applications.

11:15 AM *SB06.04.04

Graphene-Based Materials for Biosensing Platforms Arben Merkoçi^{1,2}; ¹Catalan Institute of Nanoscience and Nanotechnology and The Barcelona Institute of Science and Technology, Spain; ²ICREA - Institutio Catalana de Recerca i Estudis Avançats, Spain

Graphene-related materials (GRM) such as graphene oxide (GO) and graphene quantum dots (GQDs) display advantageous characteristics with interest for building innovative biosensing platforms and even smart devices such as nano/micromotors for a myriad of uses including sensing. Quenching of the fluorescence induced by GO or photoluminescence of GQDs can easily operate in synergy with various other nanomaterials and platforms opening the way to several unprecedented biosensing strategies and unique nanomotor technologies. Taking advantage of GRMs we are developing simple, sensitive, selective and rapid biosensing platforms that include: a) GO – based microarray & laterals flow technologies taking advantages of high quenching efficiency of GO. A “turn ON by a pathogen” device will be shown as a highly sensitive detection system using plastics or paper/nanopaper substrates; b) GQDs–based sensors for contaminants detection based on the use of multifunctional composite materials that enable rapid, simple and sensitive platforms in connection to smartphone; c) electroluminescent-based approaches d) A water activated GO transfer technology using wax printed membranes for fast patterning of a touch sensitive device with interest for electronic devices including sensing as well as for a cost-efficient nanomotor building technology for several applications. This work is supported by EU (Graphene Flagship), CERCA Programme / Generalitat de Catalunya.

SESSION SB06.05: Wearable Bioelectronics with 2D Materials I

Session Chair: Dmitry Kireev

Wednesday Afternoon, December 1, 2021

Sheraton, 2nd Floor, Constitution A

1:30 PM *SB06.05.01

Wireless Graphene E-Tattoos for Long-Term Mental Stress Monitoring Nanshu Lu; The University of Texas at Austin, United States

Mental stress negatively impacts more than 77% population in our modern societies. Electrodermal activity (EDA), a.k.a. galvanic skin response (GSR), is an emotion-induced skin conductance change due to sweat gland activity, which has been widely used as a quantitative index of mental stress levels for decades. Palm has the highest density of eccrine sweat glands which are filled up under psychological stimuli, such as mental stress, primarily. However, state-of-the-art EDA monitors suffer from limitations such as obstructiveness, short-term wearability, motion artifacts, etc. My group has previously engineered mechanically and optically imperceptible wearable sensors named graphene e-tattoos (GET).[1-3] Herein, we introduce a wireless, long-term wearable (e.g. 24 hours), high-fidelity palm EDA sensor based on 150-nm-thick GET. The ultrathin GET can fully conform to the finest texture of human skin, resulting in an interface impedance even lower than that of the wet Ag/AgCl gel electrodes. GET is laminated on the palm and needs to extend to the wrist to connect to a wristwatch which provides data acquisition, storage, and wireless transmission. The orders-of-magnitude mismatch of stiffness and thickness between the GET and the wristwatch poses a significant challenge for the electrical connection in between. We propose a simple yet effective solution named “heterogenous serpentine ribbon (HSR).” Compared with contacts between straight GET and metal ribbons, HSR offers a ten-fold strain reduction. We have successfully applied such GET-watch-based wearable EDA sensor for long-term, continuous, and ambulatory EDA sensing during our daily activities as well as during sleep. The HSR could be a generic solution to robustly connect any ultrathin and ultrasoft e-tattoos to smartwatches or rigid PCBs, which could significantly expand the sensing modalities of future smartwatches and other wearable devices.

1 Ameri, S.K., Ho, R., Jang, H.W., Tao, L., Wang, Y.H., Wang, L., Schnyer, D.M., Akinwande, D., and Lu, N.: ‘Graphene Electronic Tattoo Sensors’, *Acs Nano*, 2017, 11, (8), pp. 7634-7641

2 Ameri, S.K., Kim, M., Kuang, I.A., Perera, W.K., Alshiekh, M., Jeong, H., Topcu, U., Akinwande, D., and Lu, N.: ‘Imperceptible Electrooculography Graphene Sensor System for Human-Robot Interface’, *npj 2D Materials and Applications*, 2018, 2, pp. 19

3 Kireev, D., Ameri, S.K., Nederveld, A., Kampfe, J., Jang, H., Lu, N., and Akinwande, D.: ‘Fabrication, characterization and applications of graphene electronic tattoos’, *Nature Protocols*, 2021, 16, (5), pp. 2395-2417

2:00 PM SB06.05.03

Van der Waals Semiconductor Enabled Miniaturized Color Sensing Ningxin Li, Aisha A. Okmi, Tara Jabegu, Udagamage K. Wijewardena, Diren Maraba and Sidong Lei; Georgia State University, United States

The miniaturized image sensor has received great attention recently, due to their significances in micro-robotics. Current research mainly focuses on developing curved image sensors to correct the field curvature induced by the small lens. However, the innovations in color image sensors are so far very

rare, because of the two major challenges. First, conventional image sensors typically adopt a Bayer filter to endow the laterally arranged pixel with the function of color sensing, rendering a large device profile. Second, aggravated optical chromatic aberrations due to lens system simplification is another difficulty. In this study, we developed a novel vertical color recognition structure (CRS) by stacking multiple layers of van der Waals semiconductors (vdW-S) including $\text{CuIn}_7\text{Se}_{11}$, InSe , and GaS as the sensing layers which are sensitive to red, green, and blue light from bottom to top, and the neighboring sensing layers are separated with flexible and transparent insulating materials, such as mica or hexagonal boron nitride to prevent short circuits. Meanwhile, adjusting the thickness of these insulating layers makes it feasible to align each of the sensing layers to their respective focal plan to compensate the chromatic aberration. Experimentally, upon the successful fabrication of the CRS, by carefully selecting the vdW-S and control their thicknesses, each sensing layer obtained the desired spectral responses, as well as excellent photoresponsivity linearly depending on incident light power. In addition, depending on the structural superiority of the vertical stacking design, the simulation of chromatic aberration correction based on this CRS is also achieved. The as-developed CRS can serve as individual pixels and implement miniaturized full color image sensor through a scalable fabrication and integration of them, with incomparable advantages in a compact size, aberration correction function for the utilization in medical care, environmental surveillance, and many other areas.

SESSION SB06.06: Poster Session: 2D Materials for Bioelectronics

Session Chair: Dmitry Kireev

Wednesday Afternoon, December 1, 2021

8:00 PM - 10:00 PM

Hynes, Level 1, Hall B

SB06.06.02

Energetically Preferred Bilayered Coacervation of Oppositely Charged Inorganic Nanoplatelets Minchul Sung^{1,2}, Jaemin Hwang¹, Bokgi Seo¹, Daeyeon Lee² and Jin Woong Kim¹, ¹Sungkyunkwan University, Korea (the Republic of); ²University of Pennsylvania, United States

Colloidal particles with 2-dimensional geometry exhibit high adhesion energy at the interface so there have been studied to synthesized new types of particles with a tailored platelet structure. Compared to typical spherical particles, high aspect ratio of 2D nanoparticles not only stabilize interface more effective but also enhance the interaction between particles due to their large lateral surface area. A platform is introduced for bilayered coacervation of oppositely charged nanoplatelets (NPLs) at the oil-water interface. To this end, we synthesized two types of zirconium hydrogen phosphate (ZrHP) NPLs, cationically charged NPLs (CNPLs), and anionically charged NPLs (ANPLs) by conducting surface-initiated atom transfer radical polymerization. Taking advantages of the platelet geometry and controlled wettability, we demonstrated that ANPLs and CNPLs coacervate themselves to form a bilayered NPL membrane at the interface, which was directly confirmed by confocal laser scanning microscopy. Via theoretical consideration using the hit-and miss Monte Carlo method, we determined that electrostatic attraction-driven coacervation of ANPLs and CNPLs at the interface shows a minimum attachment energy of $\sim 10^6 k_B T$, which is comparable to the cases where NPLs charged with the same type of ions are attached. This unique and novel interfacial coacervation behavior allowed use to develop a pH-responsive smart Pickering emulsion system. All of these results highlight that platelet-type colloids are indeed effective in inducing controllable interfacial adsorption and desorption at interfaces, as well as interactions between them, and also pave ways to develop various interfacial engineering technologies.

SB06.06.03

Interface of Electrogenic Bacteria and Reduced Grapheneoxide: Energetics and Electron Transport Sheldon Cotts, Bijentimala Keisham, Jay Rawal, Vikas Berry and Roshan Nemade; University of Chicago, United States

A synergistic, nanoscale electrical interface with the membranes of exoelectrogenic microbes will have a transformative impact on biological cell-based electronic devices. Here, we report that a conformal graphenic interface on biocatalytic *Geobacter sulfurreducens* membrane results in quantum-capacitance induced n-doping in reduced graphene oxide (rGO) that further enhances electron shuttling from the membrane to improve electron harvesting from the electrogenic organism. The quantum coupling of rGO with the connected protein-membrane channels leads to an additional electron density of $3.91 \times 10^{12} \text{cm}^{-2}$ and an increase in the in-plane phonon vibration energies (G) of rGO by $\sim 5 \text{cm}^{-1}$. This n-doping enhances the electron transfer rate from the cell membrane into the rGO via a net driving potential of 158 meV with a 3-fold increase in the power density. The synergistic electron-harvesting and conformal membrane-interfacing of flexible 2D nanomaterials can lead to an evolution in the design of microbe-circuitry to power stand-alone nanodevices.

SB06.06.04

Fabrication Constraints of Flexographic Printed Graphene Electrodes for Chemical Sensing Rebecca R. Tafoya¹, Bryan Kaehr¹, Michael Gallegos¹ and Ethan B. Secor²; ¹Sandia National Laboratories, United States; ²Iowa State University of Science and Technology, United States

To leverage recent advances in the production of printed graphene electrodes, there exists a need to develop a graphene ink suitable for high-throughput fabrication processes. Herein, we fine-tune previously developed graphene ink, formulated with exfoliated graphene and an ethyl cellulose stabilizing polymer, to be suitable for flexographic printing. Further, the impact of process parameters and ink formulation are investigated by analyzing print quality and electrical properties. Characterization reveals anisotropic electrical properties due to striations caused by viscous fingering. Ambient environmental responses are characterized, which inform the scope of graphene electrode applications and need for functionalization of graphene in complex environments. Overall, this work informs the viability of graphene as an environmental and biological sensor and outlines fabrication constraints of production scale printed graphene electrodes.

SB06.06.05

Dual COVID-19 and Influenza Virus Detection via Antibody-Functionalized Graphene Field-Effect Transistors Neelotpala Kumar, Dalton Towers, Dmitry Kireev, Andy Ellington and Deji Akinwande; University of Texas at Austin, United States

The advent of pandemic caused by SARS-CoV-2 (COVID-19) has highlighted the requirement of devices capable of carrying out rapid differential diagnosis of various viruses that may manifest similar physiological symptoms but demand tailored treatment plan. Annually, the world undergoes multiple cycles of seasonal Flu infection which now poses a bigger challenge, exacerbated by the pandemic. In this work, we demonstrate liquid-gated graphene field effect transistor (GFET) based rapid biosensing device capable of making differential diagnosis between Influenza (H3N2) and COVID-19 viruses. The device consists of four onboard GFETs arranged in a quadruple architecture, where each quarter is functionalized with specific antibody to utilize the antibody-antigen reaction on graphene's surface to indicate the presence of either Influenza (H3N2) or COVID-19. The antigen-antibody interaction is

dependent on uniform diffusion of virus delivered in low ionic strength phosphate buffered saline, entailing a facile operating procedure, where the user is only required to pipette in a drop of the viral solution onto the device.

Our devices were successfully tested against a range of concentrations of both the viruses (COVID-19 and Influenza), indicating extremely high sensitivity. Unlike the standard polymerase chain reaction-based testing kits which have a turn-around time of at least three hours, our device has a lower response time of a few milliseconds; hence enabling rapid diagnosis. Furthermore, the device is highly specific as confirmed by cross-reactivity tests: the COVID-19 functionalized channels are not reactive to the Influenza virus, and the Influenza-functionalized channels are not reactive to the COVID-19 spike protein. In addition, both the channels are not reactive to the introduction of bovine serum albumin, confirming excellent specificity of the multi-targeted biosensor.

SESSION SB06.07: 2D Neurotechnologies
Session Chair: Dmitry Kireev
Tuesday Afternoon, December 7, 2021
SB06-Virtual

4:00 PM *SB06.07.01

Graphene Transistors for Biosensing Applications Amaia Zurutuza; Graphenea, Spain

Over the past two decades, graphene has attracted a great deal of attention due to its extraordinary properties. When these properties are translated into applications graphene could have a large impact in various industries and markets such as telecommunications, healthcare, automotive, etc. However, for this to occur there are many milestones that have to be achieved such as graphene manufacturing (growth and transfer) and device fabrication at relevant wafer scales, before moving to component fabrication and system integration into the final product.

Graphene's electronic and mechanical properties make it an ideal candidate to be applied in various types of sensors. The sensors' market is extremely large since we are dealing with the automotive, electronics and healthcare industries among others. Therefore, it is an excellent starting platform for graphene applications. For example, the current COVID-19 pandemic has demonstrated the urgent need for fast diagnostics in order to minimise and control its effects, here, biosensors based on graphene field effect transistors (GFETs) have shown great potential as a platform for future diagnostics.

During this talk, I will cover the fabrication of graphene at wafer scale and the use of graphene in various types of sensors including MEMS [1,2], ion sensors (ISFETs) [3-5], gas sensors [6] and biosensors. Depending on the type of sensor, the graphene requirements including the transfer and characterisation vary considerably.

REFERENCES

- S. Wagner, T. Dieing, S. Kataria, A. Centeno, A. Zurutuza, A. Smith, M. Ostling, and M. Lemme, *Nano Lett.*, 17 (2017) 1504.
- C. Berger, R. Philips, A. Centeno, A. Zurutuza and A. Vijayaraghavan, *Nanoscale*, 9 (2017) 17439.
- N. Tran, I. Fakhri, O. Durnan, A. Hu, A. Aygar, I. Napal, A. Centeno, A. Zurutuza, B. Reulet, and T. Szkopek, *Nanotechnology*, 32 (2021) 045502.
- I. Fakhri, O. Durnan, F. Mahvash, I. Napal, A. Centeno, A. Zurutuza, V. Yargeau, and T. Szkopek, *Nature Commun.*, 11 (2020) 3226.
- I. Fakhri, A. Centeno, A. Zurutuza, B. Ghaddab, M. Sijaj, and T. Szkopek, *Sens. Actuators B Chem.*, 291 (2019) 89.
- C. Mackin, V. Schroeder, A. Zurutuza, C. Su, J. Kong, T.M. Swager and T. Palacios, *ACS Appl. Mater. Inter.*, 10 (2018) 16169.

4:30 PM *SB06.07.02

Graphene-Based Active Neural Sensors for Brain Monitoring and Mapping Jose A. Garrido; Catalan Institute of Nanoscience and Nanotechnology - ICN2, Spain

Large effort is being dedicated to the integration of novel materials into neural interface devices capable of providing an efficient and consistent activity for the duration of their functional lifetime. Recording capabilities need to be such that they allow the detection of brain activity over large areas and with a high spatial resolution. For stimulation applications, a suitable charge injection capacity is required in order to elicit a response from the tissue being targeted without causing damage. Additionally, these devices must be biocompatible and mechanically compliant with neural tissue. Because its two-dimensional nature, graphene exhibits a rather unique combination of physicochemical properties which make it an attractive platform for neural technologies.

This contribution will focus on the recording capabilities of active sensor technology based on single-layer graphene, highlighting its potential for the development of the next-generation neural prostheses and brain-computer interfaces. Recently, solution-gated field-effect transistors (SGFET) based on graphene are being explored with increasing interest as novel transducers for neural signals. The electrochemical stability of graphene and its facile integration with flexible substrates were among the initial triggers that attracted the interest of the community to develop flexible neural probes for brain interfacing. In addition, other properties such as the high carrier mobility and the field effect associated to single-layer graphene allows for the implementation of an active sensor configuration that will be shown in this contribution to offer significant advantages with respect to the classical passive metallic electrodes. Further, this presentation will discuss how SGFET-type sensors allow us the implementation of multiplexing strategies, time-domain and frequency-domain multiplexing, that reduce the footprint of connectivity, permitting an aggressive scaling up in the number of recording sites. Very interestingly, we will demonstrate that SGFETs also have a distinctive capability to expand the temporal resolution of classical electrocorticography technologies, allowing the recording of the relatively unexplored infra-slow brain activity and, thus, potentially enabling the study of novel biomarkers for monitoring neurological disorders.

Acknowledgements. This work has been partially funded by the EU Horizon 2020 programme under Grant Agreement no. 881603 (GrapheneCore3) and no. 732032 (BrainCom)

5:00 PM *SB06.07.03

Graphene-Based Neural Interfaces for Multimodal Probing Brain Activity Duygu Kuzum; University of California, San Diego, United States

The complexity of neural activities has challenged both neuroscience research and clinical practice for decades. Understanding neuronal dynamics and information processing performed by neural populations requires advanced technologies with high-resolution sensing and stimulation capability. Clinical neuromodulation therapies widely used for neurological disorders also depend on the ability to manipulate the dynamics of neural circuits. Conventional

neural interfaces offering electrical, optical, or chemical signals have greatly advanced our understanding of neural functions, however, most of these technologies are based on a single functionality. Combining multiple functionalities in a single system has recently been pursued as an integrative approach in new neurotechnology development. Graphene has recently emerged as a neural interface material offering several outstanding properties, such as optical transparency, flexibility, high conductivity, functionalization and biocompatibility. The unique combination of these properties in a single material system makes graphene an attractive choice for multi-modal probing of neural activity. In this talk, I will present our recent work on graphene-based neural interfaces, highlight key applications, and finally discuss future directions and potential advances for graphene-based neurotechnologies in both basic neuroscience research and medical applications.

5:30 PM SB06.07.04

Hexagonal Boron Nitride Heat Dissipation Neural Opto-Probe for *In Vivo* Applications-- [JuSeung Lee](#) and Tae-il Kim; Sungkyunkwan University, Korea (the Republic of)

Due to the development of various advanced new materials and process technologies, electronic devices are being reduced in size to a microscale and are being integrated with high density in a limited area. Through this, energy is saved and performance and efficiency are greatly improved, but heat generated from components of device concentrated in a narrow area is a new problem that cannot be found in previous conventional devices. In particular, in the case of the micro light emitting diodes (LEDs), the heat problem more stands out as it is used as densely integrated injectable or wearable devices for photodynamic therapy, optogenetics, and various sensors. The heat generated by the LED causes problems such as deterioration of light emitting performance, change of emission wavelength property, and reduction of lifespan, which can be a fatal disadvantage to the device.

Although in order to solve this problem, recent research tried to control the LEDs temperature through various methods such as size reduction, pulsed operation, and high thermal conductivity substrate, these are acceptable in limited applications, and it is difficult to apply on the bio-injectable devices. Here, we present an injectable neural opto-probe using the Boron Nitride (BN) as a heat dissipation layer. BN is a 2D inorganic material with excellent thermal stability, electrical insulation property, and high thermal conductivity. Recently, various research using it as a heat dissipation material have been published. We applied the BN to neural opto-probe device as a heat dissipation layer to effectively disperse the heat generated during operation. The temperature of the device is verified through finite element method simulation and actual IR temperature measurement to ensure heat dissipation performance of up to 40°C or higher. This heat dissipation performance increased the thermal stability of the device, thereby increase the emitting efficiency of the LEDs and preventing the red shift of the wavelength of the LEDs by spreading the heat from the heat source. The heat dissipation neural opto-probe has superior emitting performance than general devices, and the penetration depth of light *in vivo*, especially in the brain, has been greatly increased. Through this, it was possible to develop a device that can effectively deliver light to a wider range in applications such as PDT and optogenetics.

5:45 PM SB06.07.05

Diagnosis and Treatment of Epilepsy Using Hybrid Structured Graphene-Based Multielectrode Array [Jejung Kim](#)¹, Jeongsik Lim¹, Sangwon Lee², Sunggu Yang² and Jong-Hyun Ahn¹; ¹Yonsei University, Korea (the Republic of); ²Incheon National University, Korea (the Republic of)

In decades, neural interfacing devices have attracted huge attention because they can provide not only diagnosis of neurodegenerative diseases but also treatment for a patient suffering from them. Recent researches on surface neural electrodes on the cortical surface have suggested that recording ECoG can diagnose neurodegenerative diseases and also treat them with electrical stimulation. In order to achieve the chemically stable, biocompatible, and electrochemically conductive neural interface, various materials have been investigated such as noble metals, conductive polymers, and nanomaterials. However, each of them has still several defects such as non-transparency, instability in long-term implantation, their mechanically stiff nature, which impede the chronic biomedical use of implantable devices. Graphene is one of the nanoscale forms of carbon materials, which consists of a single-atomic hexagonal lattice of sp² hybridized carbon atoms. It is an attractive candidate for implantable biomedical devices due to its excellent electrochemical property, biocompatibility, chemically inert nature, and mechanically flexibility.

Herein, we suggest graphene-based neural electrode arrays for the treatment of epilepsy. We investigated various graphene-based electrodes for improving the neural interface. First is 4-layer doped graphene. The second one is graphene/Au/graphene sandwich structure. The sandwich structure was synthesized with the followed process: (1) conventional CVD growth process of graphene on copper foil (2) deposition of nanoscale thick gold layer on it (3) wet transfer of monolayer graphene coated with PMMA on it. The sandwich structure takes both advantages of electrical conductivity of gold and electrochemical property and a good interface with neural cells of graphene. We electrochemically characterized these graphene-based electrode arrays and long-term stability and biocompatibility after *in-vivo* implantation. Finally, we successfully demonstrated detection of epileptic form neural activity and treatment of epilepsy using electrical stimulation *in-vivo* rat experiments. These graphene-based electrodes showed very high signal-noise-ratio compared with other neural electrodes and the capability to treat brain diseases. We expect that our graphene-based electrode arrays can demonstrate a breakthrough toward the non-invasive medical application of neural devices.

SESSION SB06.08: Wearable Bioelectronics with 2D Materials II

Session Chair: Dmitry Kireev

Wednesday Morning, December 8, 2021

SB06-Virtual

8:00 AM *SB06.08.01

Wellness and Eye Tracking with Graphene-Based Flexible Photodetectors [Frank Koppens](#); ICFO, Spain

Sensors for ubiquitous sensing purposes should be low-cost, invisible and seamlessly integrable with many different surfaces such as bendable plastic, textiles and glass. Graphene based light sensors [1,2] are inherently flexible and transparent and can be integrated with low-cost CMOS technology [3], hence providing a disruptive platform for future wearables and vision devices.

We will show a prototype non-invasive wellness monitor based on hybrid nanoparticle-2D material systems. We leveraged graphene's flexible and transparent properties to create a wearable device that is conformal to the human body so that it can reliably extract vital signs such as heart rate, breathing rate and oxygen saturation [4]. Furthermore, we present a graphene-based UV-sensing patch. It records harmful UV-exposure on the skin. The patch does not need a battery as a smartphone provides energy via wireless power transfer.

Moreover, we present the first transparent camera based on an array of graphene photodetectors. These transparent image sensors can have a far-reaching impact on human-computer interfaces, smart displays, and eye-tracking for augmented and virtual reality. The operation of these devices presents a fundamental shift in how we think about image sensor, as these devices can be hidden in plain sight.

References

- [1] G. Konstantatos, et al., Nature Nanotechnol., 7 (2012)
- [2] Nikitskiy et al., Nat. Commun., 7 (2016)
- [3] Goossens et al., Nat. Phot. 11 (2017)
- [4] Polat et al., Science Advances (2019)

8:30 AM *SB06.08.02

Integration of Graphene Materials with Textiles Fibers and Fabrics for Applications in Wearable Bio-Electronics [Monica Craciun](#), University of Exeter, United Kingdom

Graphene materials are emerging systems for wearable electronics and smart textiles applications due to their exceptional properties such as electrical conductivity, optical transparency and mechanical flexibility. These properties offer opportunities for the seamless incorporation of electronic devices in textiles, unlocking a future where interacting with bio-electronic devices will be as simple as getting dressed. In this invited talk, I will give an overview of our developments in the integration of graphene materials with flexible substrates, including textile fibers and fabrics for various wearable applications. In our earlier studies [Sci. Rep. 5, 9866 (2015) and Sci. Rep. 7, 4250 (2017)] we demonstrated a versatile method to coat a wide range of common insulating textile fibres with monolayer and few layer graphene grown by Chemical Vapor Deposition. Fibre materials such as polypropylene, polylactic acid, polyethylene and nylon, of tape and cylindrical shapes, display sheet resistance values as low as 600 Ohm/sq, demonstrating that the high conductivity of graphene is not lost when transferred to textile fibres. These graphene-based conductive fibres were used as a platform to build integrated electronic devices directly in textiles. For example, we demonstrated graphene electronic textile fibers that function as touch-sensors and light-emitting devices [npj Flexible Electronics 2, 25 (2018)]. We also demonstrated the weaving of such graphene electronic fibres in a fabric which enabled the realization of pixels for displays and position sensitive functions. Finally, we recently demonstrated the use of graphene-coated polypropylene (PP) textile fibers as temperature sensors within a low-operating voltage carbon-graphene e-textile system [ACS Appl. Mater. Interfaces 12, 26, 29861 (2020)]. For the development of fabric-based wearable devices, one of the critical challenges is the seamless incorporation of electronics in textiles that will preserve their softness and comfort. A key feature is the realisation of electrically conductive coatings on textile that conform to the irregular and coarse structures of the textile fabrics. Therefore, a different approach compared to fibers is needed for creating conductive textile fabrics without compromising the properties of the fabric. We recently demonstrated a simple, low-cost, efficient, and highly scalable method of ultrasonic spray coating for coating three types of textile fabrics, meta-aramid, polyester and nylon, with a water based graphene nanoplatelets suspension [J. Phys. Mater. 4 014004 (2021)]. These conductive textile fabric electrodes show a sheet resistance as low as 4.5 kOhm/sq without any intentional doping or required additives for improved adhesion. Such fabric electrodes have applications in sensors or energy-harvesting wearable technologies.

One of the main advantages of 2D materials for various applications is that they can be prepared in form of water-based solutions. The high yield and cost-effectiveness of this method make them of great interest for printed electronics, composites, and bio- and healthcare technologies. In the final part of my talk I will discuss our developments in this area. I will present the integration of high quality graphene films obtained from scalable water processing approaches in emerging energy harvesting devices [Adv. Mater. 30, 1802953 (2018)], opening new possibilities for self-powered electronic skin, flexible and wearable electronics. Building on this work, we developed a method for the fabrication of micrometer-sized well-defined patterns in water-based 2D materials [Adv. Sci. 6, 1802318 (2019)]. This method was used to create humidity sensors with performance comparable to that of commercial ones. These sensor devices are fabricated onto a 4 inch polyethylene terephthalate (PET) wafers to create all-graphene humidity sensors that are flexible, transparent, and compatible with current roll-to-roll workflow.

9:00 AM SB06.08.03

Direct Writing of Highly Crystalline Laser-Induced Graphene on Polydimethylsiloxane for Wearable Devices [Shuichiro Hayashi](#), Fumiya Morosawa, Rikuto Miyakoshi and Mitsuhiro Terakawa; Keio University, Japan

Laser-based modification of polymers has been emerging as a versatile method to simultaneously synthesize and pattern electrically conductive structures on polymer substrates for flexible device applications. By simply irradiating and scanning the polymer substrate with a laser beam, optical and thermal effects are induced near the focal spot, and electrically conductive graphitic carbon (ie., laser-induced graphene, LIG) can be directly patterned onto the substrate. Although laser modification is promising for the fabrication of flexible devices, polymer precursors used in previous studies are limited to inelastic materials, such as polyimide (PI) and biomasses (ie., cellulose). We have been studying the femtosecond laser-induced graphitization of a well-known elastomer, polydimethylsiloxane (PDMS). PDMS-based LIG generally shows comparably lower conductivity than those of structures fabricated from PI, possibly due to the aliphatic structure of PDMS, hindering graphitization. However, fabrication of highly conductive structures, composed of highly-crystalline graphene, was achieved by irradiating femtosecond laser pulses at a high repetition rate onto the surface of native PDMS. The structures fabricated by using our method exhibited an electrical conductivity as high as $\sim 51.6 \text{ S m}^{-1}$, which is, to the best of our knowledge, the highest value achieved (ie., $\sim 300\%$ of highest value previously reported) using the laser modification of PDMS. Raman analyses of the fabricated structures indicated the formation of highly crystalline and few-layered graphene by laser irradiation, which is considered to contribute to the high conductivity of the fabricated structures. Furthermore, when the fabricated structures were excited using UV light (365 nm), photoluminescence was observed for the fabricated structures. The emission spectra obtained from the structures indicated two peaks centered at 400 nm and 720 nm, suggesting the formation of nano-sized carbonaceous (ie., carbon quantum dots, graphene quantum dots) and siliconaceous (ie., silicon carbide, porous silicon) structures, respectively. The structures fabricated with the proposed method exhibited piezoresistive behavior, and by exploiting the elasticity of PDMS, in combination with the high conductivity of the fabricated structures, a soft, small, and sensitive (ie., $\sim 2.2 \text{ kPa}^{-1}$) piezoresistive sensor that could detect pressures as low as approximately 0.1 Pa was realized. When compression cycle tests were performed on the sensors, the relative changes in resistance to applied pressure at the end of compression cycles were comparable to those at the beginning, indicating high stability and repeatability. The high sensitivity indicated by the sensor, regardless of the small size, is attributable to the elasticity of the PDMS substrate. Furthermore, a PDMS-based ring-shaped heart rate (HR) monitor capable of obtaining the pulse wave-form, and resultantly the HR, of the human subject from just the index finger was demonstrated; indicating the potential of the structures fabricated with the proposed method for health monitoring applications.

SESSION SB06.09: 2D Bioelectronic Sensing II
Session Chair: Dmitry Kireev
Wednesday Morning, December 8, 2021
SB06-Virtual

10:30 AM SB06.09.01

Detection of SARS-CoV-2 Receptor-Binding Domain Using Surface-Enhanced Raman Scattering and Machine Learning Kunyan Zhang¹, Ziyang Wang¹, He Liu¹, Néstor Perea-López¹, Allen M. Minns¹, Randall M. Rossi¹, Scott E. Lindner¹, Xiaolei Huang¹, Mauricio Terrones^{1,2} and Shengxi Huang¹; ¹The Pennsylvania State University, United States; ²Shinshu University, Japan

COVID-19 was one of the leading causes of death in the United States in 2020 and early 2021 and it continues to threaten public health. Thus, it is imperative to understand and identify SARS-CoV-2 including different mutant lineages. Surface-enhanced Raman spectroscopy (SERS) can provide characteristic fingerprints of biomolecules, and with the assistance of machine learning, can become a powerful tool to rapidly identify and understand complicated biosamples. In this work, we developed a platform combining SERS and machine learning to detect the receptor-binding domain (RBD) of SARS-CoV-2 spike protein, a key component related to the infection and transmission. The Raman modes of SARS-CoV-2 RBD were enhanced by gold nanoparticles under a 785 nm laser. To understand the origin of the Raman modes, we analyzed the correlation between the Raman spectra of SARS-CoV-2 RBD and compositing amino acids using our *Frequency Matching* algorithm and achieved high consistency with the genome sequence. In addition, we can classify RBDs of SARS-CoV-2 and MERS-CoV with accuracy, precision, and recall all over 97% using machine learning classifiers. Our SERS-machine learning integrated platform holds promise for rapid detection of SARS-CoV-2 mutants that hinder the immunity efficacy.

10:45 AM SB06.09.02

Transparent, graphene-based Organic Charge-Modulated Field-Effect Transistor for chemical sensing Stefano Lai¹, Ylea Vlamidis², Neeraj Mishra², Vaidotas Miseikis², Pier Carlo Ricci¹, Camilla Coletti², Piero Cosseddu¹ and Annalisa Bonfiglio¹; ¹University of Cagliari, Italy; ²Istituto Italiano di Tecnologia, Italy

In recent years, graphene and its derivatives have been demonstrated as valuable materials for the development of several kind of biochemical sensors. In particular, its integration in Field-Effect Transistor (FET) structures as active layer has been thoroughly explored in literature. Nonetheless, graphene-based FETs are typically characterized by poor switching properties, which severely limit their actual exploitation in electronic circuits. Moreover, proposed devices typically need a reference electrode in the measurement environment, which is another important limitation for their actual exploitation in a real application scenario.

Here, we report an innovative approach, using graphene as conductive element in a peculiar device structure named Organic Charge-Modulated FET (OCMFET). The OCMFET is a floating gate Organic FET, where a part of the floating gate, namely the sensing area, is exposed to the measurement environment. Through a modification of the sensing area with a proper biochemical receptor, the floating gate can act as a probe for the investigated analytes, which is recognized by means charge variations/modulations induced in the measurement environment and then transduced in a variation of the threshold voltage of the transistor. By decoupling the sensing element by the active layer of the transistor, it is possible to exploit at their best the peculiar properties of graphene as sensing element, while the transistor structure can be optimized to reach electronic performances suitable for the future integration into electronic systems. Moreover, the OCMFET operates in a electrically-floating environment, i.e. the need for a reference electrode in solution is avoided.

It is noteworthy that, although the OCMFET working principle has been already successfully exploited in several kinds of biochemical sensors, conventional materials and fabrication processes have been always employed, as well as chemical functionalization processes of the sensing area. In this new version of the OCMFET, graphene is used for defining the floating gate and the sensing area of the OCMFET, while the other elements in the transistor structure are defined by means of large area, industrial-like techniques such as Chemical Vapor Deposition and inkjet printing. Moreover, we report a straightforward, non-covalent modification of graphene by means of molecules hosting a pyrene moiety, which ensures an highly stable functionalization without affecting the optical and electrical properties of graphene.

As a result, the fabrication process here proposed is suitable for future scale-up to an industrial scale. Taking advantage of the peculiar optical properties of graphene and of the organic materials employed for the fabrication of the transistor structure, highly transparent devices have been fabricated, showing a transmittance higher than 90%.

The actual functionality of this new OCMFET implementation as biochemical sensor has been demonstrated considering pH sensing as a benchmark. Graphene has been non-covalently functionalized with pyrene peptides hosting chemical groups that can change their charge state with pH. A complete characterization in a wide pH range (3-12) has been carried out using peptides with different net charge profiles. This study paves the way to the development of novel, high-performing sensors integrating graphene and organic semiconductor-based devices.

11:00 AM SB06.09.03

Improving Biosensors Through Understanding the Bonding of Amine Groups on CVD Graphene Elizabeth J. Legge^{1,2}, Muhammad M. Ali³, Hina Y. Abbasi³, Benjamin Reed¹, Barry Brennan¹, Zari Tehrani³, Vlad Stolojan², S Ravi P. Silva², Owen J. Guy^{3,3} and Andrew J. Pollard¹; ¹National Physical Laboratory, United Kingdom; ²University of Surrey, United Kingdom; ³Swansea University, United Kingdom

Graphene biosensors are a rapidly growing area of research, due to graphene's desirable properties, such as the ease of chemical functionalisation, high electrical conductivity, and high surface area. To achieve the required selectivity for this application area, graphene must be functionalised with an appropriate molecule, which can vary depending on the analyte under investigation. For some sensors, amine groups are required to bind to antibodies then used for the detection of biomarkers. However, there are a range of possible methods to functionalise graphene with amine, and the optimal method is still unclear.

Typically, covalent functionalisation is more durable, due to the greater bond strength, but this can disrupt the sp^2 carbon structure and thus degrade the electrical conductivity. Non-covalent functionalisation is expected to be less durable but maintains the sp^2 lattice and electrical conductivity. In our work we have investigated the differences between a covalent functionalisation, using 4-nitrobenzene diazonium tetrafluoroborate (4-NBD) to bind nitro-phenyl groups and subsequently phenyl amine groups to graphene, and a non-covalent functionalisation, using 1,5-Diaminonaphthalene (DAN) to form poly(1,5-diaminonaphthalene) (pDAN) layers on graphene.

The I_D/I_G ratio from the Raman spectra of graphene can be used as an indication of the level of disorder, and therefore can approximate the level of sp^3 defects due to molecules bound to the graphene. Consequentially, it is typically used to confirm the success of a functionalisation process. However, Bissett, M. A *et al.* and Knirsch, K. C. *et al.* both previously reported unexpected changes in the I_D/I_G , where the I_D/I_G increased with functionalisation, but decreased again after an external force, due to strain and a chemical process respectively. Greenwood, J. *et al.* also reported changes in the Raman spectra after scanning tunnelling microscopy (STM) on functionalised highly oriented pyrolytic graphite (HOPG).

The work presented here on amine functionalised chemical vapor deposition (CVD) graphene shows that while covalent functionalisation is usually the method of choice, it is not necessarily preferable over non-covalent alternatives. Removal of functional groups from CVD graphene with contact-mode

atomic force microscopy (AFM) explains unexpected changes in the Raman spectra, and suggests the durability of covalent functionalisation can be similar or worse than non-covalent functionalisation.

By using a combination of imaging techniques, we demonstrate some imaging challenges that can occur and the importance of using different analytical techniques to investigate the physicochemical properties of biosensors. Our characterisation combines the use of contact-mode AFM, tapping-mode AFM, Raman spectroscopy and time-of-flight secondary ion mass spectrometry (ToF-SIMS). We have also shown how different functionalisation processes affect the operation of a pH sensor, showing a higher sensitivity for the non-covalent process compared to the covalent process.

11:15 AM *SB06.09.04

Ultrasensitive Detection of Crumpled Graphene Biosensors for DNA and Proteins Michael T. Hwang^{1,2}, Insu Park², Mohammad Heiranian², Amir Taqieddin², Seungyong You², Yerim Kim², Juyoung Leem², Yuhang Jing^{2,3}, Vahid Faramarzi², Angela A. Pak², SungWoo Nam^{2,2,2}, Arend van der Zande^{2,2}, Narayana Aluru^{2,2} and Rashid Bashir^{2,2,2}; ¹Gachon University, Korea (the Republic of); ²University of Illinois at Urbana-Champaign, United States; ³Harbin Institute of Technology, China

Electrical field effect sensors are an important class of devices that can enable point-of-care sensing by probing the intrinsic charge in the biological entity to be sensed. Use of graphene and especially curved or crumpled graphene for this application is especially promising. We have recently reported the lowest limit of detection (LoD) on electrical label-free field effect-based sensors using single or double stranded DNA molecules on the crumpled graphene FET platform. These devices with even millimeter scale channels show an ultra-high sensitivity detection in buffer and human serum sample down to 600 zM and 20 aM, respectively. Computational simulations reveal that the nanoscale deformations can form 'electrical hot spots' in the sensing channel which reduce the charge screening at the concave regions. We have also used the crumpled graphene field effect transistor-based biosensing of important biomarkers including small molecules and proteins. We show that dopamine can be captured by an aptamer and the conformation change of the probe molecule induced electrical signal changes in the sensor. Three different kinds of proteins were captured with specific antibodies including interleukin-6 (IL-6) and two viral proteins. All tested biomarkers were detectable with the highest sensitivity reported on a label-free electrical platform. Significantly, two COVID-19 related proteins, nucleocapsid (N-) and spike (S-) proteins antigens were successfully detected in PBS with extremely low LoDs. This label-free electrical tests can contribute to the challenge of rapid, point of care diagnostics for infectious disease and other important clinical conditions.

11:45 AM SB06.09.06

Highly Sensitive One-Dimensional Material-Based Biosensor for Residual Cancer Cell Detection Sophia Chan¹, Denise Lee¹, Maria P. Meivita¹, Lunna Li¹, Yaw Sing Tan², Christine Cheung³, Natasa Bajalovic¹ and Desmond K. Loke^{1,4}; ¹Singapore University of Technology and Design, Singapore; ²Agency for Science, Technology and Research, Singapore; ³Nanyang Technological University, Singapore; ⁴Changi General Hospital, Singapore

Nanoscale materials present excellent electrical and optical characteristics that can be harnessed for biosensing applications. Moreover, these materials are biocompatible and can be employed for cancer cell-specific detection, making them ideal candidates for bioelectrical sensing. Here, we developed an electrical-based biosensor based on one-dimensional (1D) materials with specific biosensing activity towards breast cancer cells. High sensitivity of the cancer cells were achieved within a heterogeneous population. Atomistic simulations and experimental studies indicate a 1D material-facilitated change in electrical conductivity. Our results provide a promising method of harnessing 1D materials for cell-specific bioelectrical sensing, and has the potential to recognize residual cancer cells within a clinical setting.

SESSION SB06.10: Fabrication and Characterization of 2D Materials for Bioelectronics and Healthcare III

Session Chair: Dmitry Kireev

Wednesday Afternoon, December 8, 2021

SB06-Virtual

1:00 PM *SB06.10.01

Water-Based and Biocompatible 2D Material Inks for Bioelectronics and Healthcare Cinzia Casiraghi; University of Manchester, United Kingdom

Liquid-phase exfoliation (LPE) [1] allows mass-scalable, cost-effective and versatile production of graphene and other 2-dimensional (2D) material formulations suitable for a wide range of applications. This approach can be also applied to biomedical applications, as LPE can be easily performed in water via non-covalent functionalisation with stabilisers. In particular, pyrene derivatives have shown to be more effective exfoliating agents than traditional surfactants and polymers [2], while providing defect-free 2D materials in water [3-4].

In this talk I will show that non-covalent functionalization with pyrene derivatives is a simple one-pot approach that allows to make 2D material formulations with strong potential for biomedical applications. In particular, anionic, cationic and amphoteric graphene inks can be easily made by tuning the pyrene derivative used as stabilizer [5-7]. Cationic graphene dispersions show exceptional biocompatibility, intracellular uptake profile and stability in the biological medium, even with protein serum, making them a very attractive material for nanomedicine applications [7]. Finally, I will show that our graphene formulations can be used in combination with other materials to make a viscoelastic surface microelectrode array, which plastically deforms to allow conformation to the complex geometry of soft tissues such as brain [8].

[1] Hernandez, Y. et al. Nat. Nanotechnol. 3, 563 (2008)

[2] Parviz, D. et al. ACS Nano 6, 8857 (2012)

[3] Yang, H. et al. Carbon. 53, 357 (2013)

[4] Yang, H. et al, 2D Materials 1, 011012 (2014)

[5] Shin et al, Mol. Syst. Des. Eng., 2019, DOI:10.1039/C9ME00024K

[6] Shin et al, Faraday Discussion, <https://doi.org/10.1039/C9FD00114J>

[7] Shin et al, Nanoscale, 2020, DOI: 10.1039/D0NR02689A

[8] Tringides et al, just accepted

1:30 PM SB06.10.02

Development of Non-Bonded Interaction Parameters between Molybdenum Disulfide and Water Abhishek T. Sose¹, Esmat Mohammadi¹, Preeya F. Achari¹, Samrendra Singh² and Sanket Deshmukh¹; ¹Virginia Tech, United States; ²CNH Industrial, United States

Molybdenum Disulfide (MoS₂) has shown potential for applications in the field of electronic devices that can be used in the fields of bioelectronics to healthcare. In almost every application MoS₂ is exposed to water or humidity, making it important to study the interactions between MoS₂ and water. Here to explore the structure of water at the MoS₂ surface, we have developed the non-bonded force-field (FF) parameters between the MoS₂ surface and three different water models. A single-layered MoS₂ surface was represented with Stillinger-Weber (SW) potential and SPC, SPC/E and SPC/Fw water models were used. In order to develop the non-bonded FF parameters, we have employed all-atom (AA) molecular dynamics (MD) simulations integrated with particle swarm optimization (PSO). The new parameters were optimized to reproduce the experimental contact angle of the water droplet on the MoS₂ surface as well as the binding energy of a water molecule in four different orientations placed above the MoS₂ surface. Using the newly developed parameters, we showed that the binding energies between water molecules and the MoS₂ surface is equal to ~ -6.5 kJ/mol, which is in good agreement with the previously reported values in the literature. We have also analyzed the structural properties of water molecules in a droplet on a MoS₂ sheet to validate the precision of the developed parameters. The analysis includes z-density profile of oxygen atoms, average hydrogen bond distribution per water molecule, and the angle made by the O-H vector with the normal to the MoS₂ sheet.

1:45 PM SB06.10.03

Direct Conversion of PTFE into Reduced Graphene Oxide by Ultraviolet Laser Writing Method Parand R. Riley, Roger Narayan and Jagdish Narayan; North Carolina State University, United States

Reduced graphene oxide has caused a flurry of excitement between researchers for its numerous applications including flexible electronics, biosensing, batteries, supercapacitors, photovoltaics, and optical devices. We report a simple and cost-effective method for the direct writing of reduced graphene oxide (rGO) from polytetrafluoroethylene (PTFE). The ArF excimer laser with a wavelength of 193 nm was utilized for the fast and non-equilibrium transition of PTFE into rGO in ambient conditions with no additional steps for the reduction of graphite. We show that this method has the capability of writing rGO from PTFE on different substrates. The Raman, SEM, and TEM studies indicated that an energy density window of 0.8-1.1 J.cm⁻² was necessary for providing the appropriate undercooling to form rGO structure. The studies suggested the mechanism of the transformation from PTFE into rGO is the photothermal process in which the chains of PTFE experience unzipping, melting, degassing of volatile components, and restructuring under the ablation threshold.

2:00 PM SB06.10.04

Late News: Next-Generation PPE: Synergistic Antimicrobial Activity and Low-Cytotoxicity of Graphene-Derivative and Nanoparticles on Cotton/Silk Fabrics Shovon Bhattacharjee¹, Rakesh Joshi², Muhammad Yasir², Anurag Adhikari¹, Abrar Ahmad Chughtai², David Heslop², Rowena Bull¹, Mark Willcox² and C Raina MacIntyre¹; ¹The Kirby Institute, UNSW Sydney, Australia; ²UNSW Sydney, Australia

During epidemics or pandemics of emerging infections, personal protective equipment (PPE) is a critical non-pharmaceutical intervention that significantly reduces the spread of pathogens, especially when drugs and vaccines are unavailable. Due to many shortcomings of conventional PPE, there is a need for sustainable, re-usable high-performance PPE with antimicrobial properties. Herein, we report antimicrobial, biocompatible, and multifunctional cotton/silk fabrics coated with reduced graphene oxide (RGO) and silver (Ag)/copper (Cu) nanoparticles (NPs) by using a silane coupling agent followed by chemical reduction and vacuum heat treatment. Results reveal that due to the synergistic impact of NPs and RGO, incorporating a tiny amount of Cu and Ag NPs on top of the RGO boosts the bactericidal activity. All RGO-Ag/Cu NPs coated cotton/silk fabrics showed ~99% inhibition of *Escherichia coli* and *Pseudomonas aeruginosa* (Gram-negative bacterium). RGO-Ag NPs coated cotton/silk fabrics showed inhibition of 78–99% *Staphylococcus aureus* (Gram-positive bacterium). All the developed samples sustained their remarkable antimicrobial activity even after ten times washing. The RGO-Cu NPs cotton/silk demonstrated better inhibition of *Candida albicans* (Fungi), than all other samples. Additionally, developed fabrics exhibited lower cytotoxicity (<30%) than the pure, untreated fabrics, suggest good biocompatibility. These findings indicate that RGO– Cu/Ag NPs coated cotton/silk fabrics have excellent potential to be used in PPE development, such as protective clothing and face masks.

2:15 PM SB06.10.05

Study of Interaction of Polycaprolactone/Graphene Scaffold Using CompuCell3D Kartik S. Menon¹, Aparna K. Menon¹, Praseetha P. Nair¹, Bhushan V. Dharmadhikari² and Prabir Patra³; ¹Government Engineering College, India; ²Minnesota State University, United States; ³University of Bridgeport, United States

Introduction: Polycaprolactone (PCL)/Graphene nanocomposites emerge as promising scaffolds in biomedical applications owing to their unique properties. Understanding molecular level interactions of PCL/Graphene is inevitable to explore its potentials. Here we attempt a computational approach to study the interaction of PCL scaffold and Graphene nanoparticles using the software package, CompuCell3D (CC3D). CC3D is a flexible, scriptable modeling environment, which allows the rapid construction of sharable virtual tissue in-silico simulations of a wide variety of multi-scale, multicellular problems.

Materials and Methods: The computational package, CC3D, used in this work is based on the Cellular Potts Model (CPM). CPM is a spatial lattice-based formalism that is extensively applied to understand complex multicellular behaviors in tissue morphogenesis. The technique is based on the free energy minimization using a dynamic Monte Carlo simulation algorithm where the cell behavior depends on a balance of forces described by the Hamiltonian function.

Results and Discussion: The biocompatibility of the PCL scaffold can be improved in the presence of graphene quantum dots due to their high electron mobility and conductivity. Attractive interaction between graphene and PCL is observed in the simulated results, which is primarily due to the natural hydrophobicity of graphene and PCL nanofibers. Van der Waal's interaction also contributes to the same. As the concentration of GQDs increases, the hydrophilicity of the scaffold increases, changing the trend in their interaction. Basic properties of the solvent like viscosity and chain length play an essential role in the scaffold's stability.

Conclusions: Simulation studies for PCL/Graphene interaction using CC3D were conducted. The results obtained indicate improved interaction of PCL and graphene. Reduced cytotoxicity of graphene GQDs is expected as PCL molecules surround it. Moreover, improvement in the diffusional properties of the system is anticipated. The simulation results are to be validated with experimental studies. Further simulation studies are to be conducted using CC3D to find out and optimize the parameters that influence the system and the system's permeability to check the efficiency of the same as a permeable membrane.

SYMPOSIUM SB07

Soft, Healable Materials and Devices for Biological Interfaces and Wearables
November 30 - December 8, 2021

Symposium Organizers

Derya Baran, King Abdullah University of Science and Technology
Fabio Cicoira, Ecole Polytechnique de Montreal
Wei Lin Leong, Nanyang Technological University
Shiming Zhang, The University of Hong Kong

* Invited Paper

SESSION SB07.01: Soft, Healable Materials and Devices for Biological Interfaces and Wearables I

Session Chairs: Fabio Cicoira, Wei Lin Leong and Cunjiang Yu

Tuesday Morning, November 30, 2021

Sheraton, 2nd Floor, Back Bay B

10:30 AM *SB07.01.01

Designing a Universal OECT Platform for Sensing at Biological Interfaces and in Wearables Jonathan Harris, Songyan Yu and [Erin L. Ratcliff](#); University of Arizona, United States

This talk will focus on device physics, interface characterizations, and viability of organic electrochemical transistors (OECTs) for chemical sensors. OECTs are printable, biocompatible and exhibit a hybrid electrical-ionic conduction mechanism which gives rise to high levels of gate electrode amplification at low operating voltages.

To develop a “universal” platform that can detect a range of biomarkers, ranging from redox active to not, we take inspiration from a number of different approaches to chemical sensing, including the ultra-high sensitivity of electrochemical-based approaches and the biomarker selectivity of biorecognition elements. Through a number of strategic interface modifications, we show high levels of transconductance at low operating voltages and low detection limits for biomarkers of interest, where the only difference between platforms is the bio-recognition element used for capture. The final architecture is a floating gate OECT. Briefly, an organic semiconductor is used as the channel element and is interfaced with a printable solid state electrolyte. Channel modulation is driven by voltage drops at faradiac floating gate electrodes, one of which is interfaced with complex fluids, such as human sweat, as a demonstration for wearables. A second application considers yeast sensing, with applications to food and beverage industries to biofuels.

Funding acknowledgement: This material is based on research sponsored by the Nano-Bio Materials Consortium (NBMC) in a partnership between the Air Force Research Laboratory (AFRL) and SEMI under agreement number [FA8650-18-2-5402]. The U.S. Government is authorized to reproduce and distribute reprints for Government purposes notwithstanding any copyright notation thereon. The views and conclusions contained herein are those of the authors and should not be interpreted as necessarily representing the official policies or endorsements, either expressed or implied, of Air Force Research Laboratory, the U.S. Government, or SEMI-FlexTech.

11:00 AM SB07.01.02

Strain-Insensitive Intrinsically Stretchable Transistors and Circuits [Weichen Wang](#); Stanford University, United States

Intrinsically stretchable electronics can form intimate interfaces with the human body, creating devices that could be used to monitor physiological signals without constraining movement due to its tissue-like mechanical properties. The seamless integration between intrinsically stretchable devices and human body will benefit both signal qualities and wearing comfort, which are essential for the future wearable electronics.

However, mechanical strain invariably leads to the degradation of the electronic properties of the devices, which severely limits the applications of quantitative processing of physiological signals. Here we show that strain-insensitive intrinsically stretchable transistor arrays can be created using an all-elastomer strain engineering approach, in which the patterned elastomer layers with tunable stiffnesses are incorporated into the transistor structure. By varying the cross-linking density of the elastomers, areas of increased local stiffness are introduced, reducing strain on the active regions of the devices.

This approach can be readily incorporated into existing fabrication processes, and we use it to create arrays with a device density of 340 transistors cm^{-2} and a strain insensitivity of less than 5% performance variation when stretched to 100% strain. We also show that it can be used to fabricate strain-insensitive circuit elements, including NOR gates, ring oscillators and high-gain amplifiers for the stable monitoring of electrophysiological signals.

11:15 AM SB07.01.03

A Stretchable and Strain-Unperturbed Pressure Sensor for Motion-Interference-Free Tactile Monitoring on Skins Qi Su^{1,2}, Qiang Zou², [Yang Li](#)¹, Yuzhen Chen³, Lihua Jin³ and Sihong Wang¹; ¹The University of Chicago, United States; ²Tianjin University, China; ³University of California, Los Angeles, United States

A stretchable pressure sensor is a necessary tool for perceiving and recording physical interactions that take place on soft/deformable skins present in human bodies. However, all existing types of stretchable pressure sensors have an inherent limitation, that is the interference of stretching with pressure

sensing accuracy. This has been a roadblock in providing quantitative pressure sensing under motion-induced stretching, preventing the deployment of pressure sensors in a number of human-integrated applications. Here, we report the design of a novel stretchable pressure sensor that achieves intrinsically strain-unperturbed performance while providing a high pressure sensitivity of 2.2 kPa^{-1} . This is realized through the synergistic creations of electrical double-layer based interfacial-capacitive sensing mechanism and the pyramid microstructure with designed stiffness hierarchy. Specifically, the use of an ionic elastomer for the micro-pyramids renders the sensor's overall capacitance dominated by the electrical double-layer formed at the interface between the tip of the pyramid and the top electrode, which remains almost unchanged under in-plane stretching. This is enabled by the patterned stiffening micro-electrodes underneath each of the pyramids, together with the assist from a pair of soft spacers that keep the two ends of the sensor with the same separation distance between the top and bottom layers. Under different strain states, the sensor can maintain not only a highly stable capacitance value when there is no pressure, but also the same capacitance changing behaviors to normal pressures, exhibiting 98% strain-insensitivity up to 50% strain. Besides the strain-unperturbed performance, our design also provides a low detection limit (0.2 Pa) and a high response speed to pressures ($\sim 50 \text{ ms}$), as well as repeatable and robust sensing performance. The stretchability and low modulus of our sensor allows it to be attached to the human body with soft embodiments and great conformability. Being the first sensor that can provide all the desired characteristics for quantitative pressure sensing on a deformable surface, it has been demonstrated to realize the accurate sensation of touching information on human skin even in the presence of stretching deformation (under revision).

11:30 AM SB07.01.04

Soft Multimodal Sensor for Sensing and Distinguishing of Pressure, Strain and Temperature Li-Wei Lo, Haochuan Wan, Junyi Zhao and Chuan Wang; Washington University in St. Louis, United States

Soft wearable sensors are essential components for applications such as motion tracking, human-machine interface and soft robots. However, most of the reported sensor are either specifically designed to target an individual stimulus or capable of responding to multiple stimuli (e.g. pressure and strain) but without the ability to distinguish them. Here we report an elastomeric foam-based three-dimensional sensor that can not only respond to but also distinguish three different kinds of stimuli (pressure, strain and temperature). The sensor utilizes a porous poly(dimethylsiloxane) (PDMS) template coated with a poly(3,4-ethylenedioxythiophene) polystyrene sulfonate (PEDOT:PSS) conductive polymer through a low-cost dip-coating process. Responses to different types of stimuli can be differentiated by simultaneously recording resistance and capacitance changes. When pressure is applied normal to the top surface of the sensor, the conductive network of PEDOT:PSS and the air-gap inside the pores are both being compressed, resulting in a decrease in electrical resistance and increase in capacitance. In contrast, when the sensor is being stretched, the PEDOT:PSS network exhibits an increase in electrical resistance and a decrease in capacitance due to the elongation in distance between the two electrodes. Moreover, the sensor can also respond to change in temperature due to the enhancement of charge transport within PEDOT under elevated temperatures. As the temperature increases from $20 \text{ }^\circ\text{C}$ to $80 \text{ }^\circ\text{C}$, the sensor exhibits a decrease in resistance but no noticeable change in capacitance. We have also systematically studied the effect of the pore size on the sensor sensitivity to different stimuli and have found that smaller pore size generally leads to better sensor performance. With its high sensitivity to pressure, strain and temperature stimuli, we have demonstrated the use of the 3D porous sensor on an artificial hand for object detection, gesture recognition and temperature sensing applications.

11:45 AM SB07.01.05

Sono Healing of Conductive Nanomaterial Network on Polymer Substrate for Reusable Flexible Electronics Bo Li and Thomas Scully; Villanova University, United States

Advanced manufacturing technology to repair and regenerate nanomaterial-on-polymer flexible electronics (NPFes) will be crucial for their sustainable and affordable applications. Unlike healing strategies for bulk systems, here, we demonstrated an ultra-fast and eco-friendly sono healing method that selectively repairs the ultra-thin nanomaterial network assembled on polymer for NPFes. The sono healing method highlights a unique energy design of hydrophobic nanomaterial and hydrophobic polymer substrates in water solution such that the nanomaterial will reorganize the network at substrate-water interface energized by sono field (40 kHz and 0.3 W/cm^2). The graphene ultrathin film assembled on polydimethylsiloxane (PDMS) was used as the demonstration system. To mimic the complex deformation in the practical applications of an NPF device, we used a combined stretch-twist method to initiate the network damage, and the healing process was performed by putting the damaged graphene/PDMS devices back to pure DI water with sonication for 1 min. The damage degree can be defined as R_d/R_0 , where R_d is the sample resistance after the damage and R_0 is the initial resistance, while a healing degree is defined as R_r/R_0 where R_r is the regenerated resistance after sono healing. Healing coefficient $R_r/R_0 = 1$ means full regeneration. We have demonstrated that for damage degree less than 10, full regeneration or even enhanced conductive network ($R_r/R_0 < 1$) can be realized. For more severe damage (e.g., $R_d/R_0 = 26.6$), the healing process can recover the resistance close to its original resistance ($R_r/R_0 = 3.2$). The morphology observation suggests that sonication can help rearrange the disturbed graphene network, merging the cracks and reattaching the delaminated graphene flakes, even without a new supply of nanomaterial in the solution. As a proof-of-concept, we have first demonstrated the regeneration of a flexible resistor in a circuit with a lighting diode. The recovered light intensity is the direct evidence of functional recovery. We have also demonstrated the regeneration of a strain sensor where, the gauge factor, the factor describing the strain sensitivity, can be recovered. We have further explored the influence of nanomaterial shape on reparability by studying two other carbon allotropes: 0D carbon black and 1D carbon nanotube and find that 2D graphene presents the best recovery capability. In summary, the selective, ultra-fast, and clean sono healing method will be extremely valuable for eco-repairing flexible devices for biological interfaces and wearables.

SESSION SB07.02: Soft, Healable Materials and Devices for Biological Interfaces and Wearables II

Session Chair: Fabio Cicoira

Tuesday Afternoon, November 30, 2021

Sheraton, 2nd Floor, Back Bay B

1:30 PM *SB07.02.01

Stretchable, Degradable and Healable Conducting and Semiconducting Polymers Darren J. Lipomi; University of California, San Diego, United States

Mechanical deformability underpins many of the advantages of organic semiconductors in applications from flexible solar cells to wearable devices for healthcare and virtual touch. The mechanical properties of these materials are, however, diverse, and the molecular characteristics that permit charge transport can render the materials stiff and brittle. In this talk, I describe the ways in which molecular structure and solid-state packing structure govern the mechanical properties of organic semiconductors, especially of π -conjugated polymers. In particular, I describe how low modulus, good adhesion, and absolute extensibility prior to fracture enable robust performance, along with mechanical "imperceptibility" if worn on the skin. The discussion focuses on

the mechanisms by which mechanical energy is either stored (i.e., elastically) or dissipated (i.e., by plastic deformation or fracture). Mechanical energy is mediated at the level of both the molecular structure (determined by synthesis) and solid-state packing structure (determined by processing techniques). Development of metrological methods are critical for the accurate determination of the mechanical properties of thin films of materials for which only small quantities are available from laboratory-scale synthesis. We often find that the interplay between the semiconducting polymer and the substrate influence the mechanical properties and the fracture behavior. Computational molecular dynamics simulations have been particularly helpful in predicting the molecular mechanisms responsible for deformation. The talk concludes with applications of organic semiconductor devices in which every component is intrinsically stretchable or highly flexible.

2:00 PM SB07.02.02

Ionic Polydimethylsiloxane-Silica Nanocomposites—From Synthesis and Characterization to Self-Healing Property Clément Mugemana¹, Ahmad Moghimikheirabadi², Daniel F. Schmidt¹, Martin Kröger² and Argyrios Karatrantos¹; ¹Luxembourg Institute of Science and Technology, Luxembourg; ²ETH Zurich, Switzerland

Polydimethylsiloxane (PDMS) is the most widely explored and utilized polysiloxane, possessing an extremely low glass transition temperature, excellent thermal stability, high permeability and good biocompatibility.¹ As a liquid at room temperature, most applications require PDMS to be chemically crosslinked and / or combined with nanofillers to realize the requisite mechanical properties. Cross-linking PDMS via reversible dynamic bonds such as hydrogen bonds,² ionic interactions,³ or metal complexes⁴ has led to smart self-healable materials. While mechanical reinforcement of PDMS by nanofillers is well-known, the realization of consistently high levels of dispersion of nanofillers in a PDMS matrix remains a challenge. One strategy to control nanoparticle dispersion involves grafting ionic functional groups to the nanoparticle surface (thus creating so-called nanoparticle ionic materials, or NIMs⁵) and combining these charged nanoparticles with a polymer matrix containing functional groups with the opposite charge. Following such an approach, we describe ionic PDMS-silica nanocomposites from (cationic) ammonium-functionalized PDMS and (anionic) sulfonate-functionalized silica nanoparticles, formulated with the aim of influencing the distribution and dispersion of the nanoparticles. The impact of the PDMS molecular weight, charge density and charge location on the distribution, dispersion of ionic silica nanoparticles and on the mechanical reinforcement of the resultant nanocomposites is explored. The potential for self-healing arising from reversible ionic interactions located at the interface between polymer matrix and highly dispersed silica nanoparticles is investigated by studying the impact of ionic nanoparticles loading and the PDMS molecular weight under different healing conditions, i.e. temperature and humidity. Finally, coarse-grained molecular dynamics simulations are carried out to calculate the lifetimes of temporary ionic crosslinks between the nanoparticles and the polymer matrix comprising these nanocomposites⁶.

References

1. Wolf, M. P.; Salieb-Beugelaar, G. B.; Hunziker, P., PDMS with designer functionalities Properties, modifications strategies, and applications. *Progress in Polymer Science* **2018**, *83*, 97-134.
2. Ge, S.; Samanta, S.; Tress, M.; Li, B.; Xing, K.; Dieudonné-George, P.; Genix, A.-C.; Cao, P.-F.; Dadmun, M.; Sokolov, A. P., Critical Role of the Interfacial Layer in Associating Polymers with Microphase Separation. *Macromolecules* **2021**, *54* (9), 4246-4256.
3. Lai, J.-C.; Li, L.; Wang, D.-P.; Zhang, M.-H.; Mo, S.-R.; Wang, X.; Zeng, K.-Y.; Li, C.-H.; Jiang, Q.; You, X.-Z.; Zuo, J.-L., A rigid and healable polymer cross-linked by weak but abundant Zn(II)-carboxylate interactions. *Nature Communications* **2018**, *9* (1), 2725.
4. Li, C.-H.; Wang, C.; Keplinger, C.; Zuo, J.-L.; Jin, L.; Sun, Y.; Zheng, P.; Cao, Y.; Lissel, F.; Linder, C.; You, X.-Z.; Bao, Z., A highly stretchable autonomous self-healing elastomer. *Nature Chemistry* **2016**, *8* (6), 618-624
5. Rodriguez, R.; Herrera, R.; Archer, L. A.; Giannelis, E. P., Nanoscale Ionic Materials. *Advanced Materials* **2008**, *20* (22), 4353-4358.
6. Moghimikheirabadi, A.; Mugemana, C.; Kröger, M.; Karatrantos, A. V., Polymer Conformations, Entanglements and Dynamics in Ionic Nanocomposites: A Molecular Dynamics Study. *Polymers* **2020**, *12* (11), 2591.

2:15 PM SB07.02.03

Dynamic Metal-Ligand Coordinated PDMS with Tunable Surface Hydrophilicity Xinyue Zhang and Meredith N. Silberstein; Cornell University, United States

Polydimethylsiloxane (PDMS) has been widely used in biomedical, soft lithography, marine antifouling, flexible electronics, and other fields due to its appealing physical and chemical properties. However, the surface energy of PDMS is low and it is highly hydrophobic, which not only yields poor adhesion to substrates but also facilitates undesired adsorption of substances such as protein, biofouler, etc. These drawbacks limit the lifetime and application of PDMS. Moreover, traditional surface modification techniques do not work well on the PDMS surface, because its low glass transition temperature allows the chain to move easily and cover up the modified surface. To overcome this challenge, we investigated a series of dynamically crosslinked PDMS containing metal-ligand coordination, which show tunable surface wettability. The intrinsic hydrophilic functionality is introduced by the metal-ligand coordination, and therefore hydrophilicity of the bulk PDMS can be tailored by the choice of metal cations, counterions, and coordination density in the polymer matrix. The possible mechanisms in the context of metal-ligand bond dynamics are discussed. We show that a properly designed PDMS system with metal-ligand coordination can improve PDMS hydrophilicity as well as control the surface reconstruction speed.

2:30 PM SB07.02.05

Vitrimers and Vitriemer Nanocomposites—Thermomechanical and Self-Healing Properties Amber M. Hubbard¹, Yixin Ren¹, Peter Papaioannou¹, Dominik Konkolewicz², Alireza Sarvestani³, Catalin R. Picu⁴, Gary Kedziora¹, Ajit Roy¹, Vikas Varshney¹ and Dhriti Nepal¹; ¹Air Force Research Laboratory, United States; ²Miami University, United States; ³Mercer University, United States; ⁴Rensselaer Polytechnic Institute, United States

With sustainability at the forefront of materials research, recyclable polymers, such as vitrimers, have garnered increasing attention since their introduction in 2011. In addition to a traditional glass transition temperature (T_g), vitrimers have a second topology freezing temperature (T_v) above which dynamic covalent bonds allow for rapid stress relaxation, self-healing, and shape reprogramming. Herein, we demonstrate the self-healing, shape memory, and shape reconfigurability properties of this unique material with an aim towards recyclability and increased part lifetime. In addition, a variety of nanofillers (e.g., graphene, clay) are introduced to make vitriemer nanocomposites. We demonstrate an increase in the T_v as a function of nanofiller concentration, while nanofiller composition produces a negligible change in T_v . Furthermore, we establish the addition of nanofillers into the vitriemer matrix increases the mechanical properties but does not hinder the recyclability of these composites as explored via thermomechanical testing. These photothermally activated composites allow for shape memory and shape reconfigurable applications such as actuators and self-healing components.

2:45 PM SB07.02.06

The Mechanical Study of Polyelectrolyte Complexes with Copolymers Hongyi Cai, Yuval Vidavsky and Meredith N. Silberstein; Cornell University, United States

Oppositely charged polyelectrolytes in solution can associate and form polyelectrolyte complexes (PECs), which are widely used in hydrogels, self-

assembly and drug/nucleic acid deliveries. They are versatile materials with morphologies ranging from solid precipitates to liquid-like coacervates to micelles and nanoparticles. People can regulate PECs with both internal factors, like the charged species, and external stimuli, like the environmental ionic strength. Ionic bonds within the materials can break and reform, acting as dynamic crosslinkers to enable self-healing and easy reprocessing while maintaining mechanical strength. One unexplored strategy to modify the mechanical properties of PECs is using copolymers. In this work, we incorporate monomers with different degrees of hydrophilicity into the PEC system. Unlike traditional PECs that are brittle when dried, the resulting materials show elastomeric behavior with high stretchability and self-healing. Further, mechanical strength can still be maintained after equilibration in water. We will present both chemical and mechanical characterization, and demonstrate how the comonomer type and ionic component ratio affects bulk PEC behavior. This can be an inspiration for future development of soft iontronics used in biological wearable devices.

3:00 PM *SB07.02.07

Organic Mixed Conductors for Bioelectronics—Understanding the Fundamentals and Putting Them to Good Use [Alberto Salleo](#); Stanford University, United States

Conjugated mixed conductors have attracted much attention lately as soft materials with applications in bioelectronics, energy storage and brain-like computing. In addition to the well-known PEDOT:PSS blend, new families of polymers with glycolated side-chains have been recently developed with promising performance. Interestingly, details of how charge transport occurs and how it's related to ionic transport are still not well understood in both PEDOT:PSS blends and newer materials. This lack of understanding hinders the rational design of the next generation of high-performance materials. In this talk I will show the result of experiments that suggest that while its role in ion transport is well understood, the insulating PSS phase also plays an unexpected role in electronic transport in PEDOT:PSS blends, suggesting new design rules to control electronic transport in these materials. Furthermore, I will show how the microstructure of glycolated polymers must exhibit a balance between aggregates and disordered regions in order to ensure optimal electrochemical performance such as low turn-on voltage and lack of hysteresis. Hence, these important operational parameters do not depend only on energy levels but also on microstructure, making materials more challenging and introducing the importance of processing. Finally, I will show how understanding these materials properties is useful towards using them in high-performance devices such as biosensors.

3:30 PM BREAK

4:00 PM SB07.02.08

Fully Organic Compliant Dry Electrodes Selfadhesive to Skin for Long-Term Motion-Robust Epidermal Biopotential Monitoring [Jianyong Ouyang](#); National University of Singapore, Singapore

Biopotential signals such as ECG, EMG and EEG are vital for diagnosis and rehabilitation. Long-term biopotential monitoring is important. However, the conventional Ag/AgCl gel electrodes are not suitable for long-term biopotential monitoring because of the vaporation of the liquid phase and poor contact to skin during body movement. Thus, wearable dry electrodes are needed for long-term biopotential recordings but are limited due to the problems related to their contact with the skin, especially during body movements and sweat secretions, leading to high skin/electrode impedance and motion artifacts. Here, I will present our recent an intrinsically conductive polymer dry electrodes with excellent self-adhesiveness, stretchability, and conductivity. The electrodes shows much lower skin-contact impedance and noise in static and dynamic measurement than the current dry electrodes and standard gel electrodes, and they can give rise to high-quality biopotential signals including ECG, EMG and EEG in various conditions such as dry and wet skin and during body movement. Therefore, these dry electrodes can be used for long-term healthcare monitoring in complex daily conditions.

4:15 PM SB07.02.09

Fatigue-Resistant Hydrogel Optical Fibers for Long-Term Light Delivery In Dynamic Organs [Xinyue Liu](#), [Siyuan Rao](#) and [Xuanhe Zhao](#); Massachusetts Institute of Technology, United States

Biophotonics offers promise for disease detection and treatment through the light transmission between the optical devices and tissues. However, integration of optical devices (optical fibers included) with dynamic tissues remains challenging, as those devices with limited deformability constrain the natural movement of the tissues or even body. Here, we report a fatigue-resistant hydrogel-based optically stimulating technology that utilizes nanocrystalline hydrogels as optical fibers for optogenetic control of the peripheral nervous system. The hydrogel optical fibers are soft and stretchable to conform to the flexible substrates, and meanwhile the formation of polymeric nanocrystalline domains in hydrogels confers fatigue-resistance to these hydrogel materials against repeated deformation (fatigue strength 1.4 MPa). In addition, hydrogels with polymeric nanocrystals exhibit high transparency that reduces light absorption or scattering and a relatively high refractive index that minimizes interfacial light leakage, which synergistically contributing to efficient light transmission. Light transmission ability, mechanical and optical stability, and stimulation functionalities are demonstrated in vitro, ex vivo and in vivo. The light pulses delivered from the light source through the long hydrogel implant were able to activate the mouse sciatic nerve for four weeks, during which the mouse experienced extra exercise and the hydrogel fiber underwent repeated deformation (> 30,000 cycles) in the mouse.

4:30 PM SB07.02.10

Fluorinated Elastomers as Soft and Long-Lived Dielectrics for Scalable Brain-Machine Interfaces [Paul Le Floch](#)¹, [Siyuan Zhao](#)¹, [Nicola Molinari](#)¹, [Junsoo Kim](#)¹, [Ren Liu](#)¹, [Hao Sheng](#)¹, [Chanan Sessler](#)^{2,3}, [Guogao Zhang](#)¹, [Zhigang Suo](#)¹, [Boris Kozinsky](#)¹, [Xiao Wang](#)^{2,3} and [Jia Liu](#)¹; ¹Harvard University, United States; ²Broad Institute of MIT and Harvard, United States; ³Massachusetts Institute of Technology, United States

This presentation will discuss the development of bioelectronics for brain-wide neural activity mapping at single-cell resolution, in a chronically stable manner, a tool that will greatly advance our understanding of brain, help to build advanced neuroprosthetics, and enable new forms of communication between brain and machines. High spatiotemporal resolution and large bandwidth brain mapping requires implantation of thousands to millions of nanoelectronic probes into the brain. While multiplexed microscale brain probes are realized by nanofabrication techniques for microelectronics, the large mechanical mismatch reduces their scalability and long-term biocompatibility in the brain. Therefore, development of scalable, soft, and stretchable nanoelectronics mimicking the mechanical and physiochemical properties of the neural tissues is crucial to further increase the bandwidth of communication between brain and electronics without any adverse effects over the years. In this lecture, I introduce soft nanoelectronics for scalable brain-machine interfaces by using fluorinated elastomers as ultra-soft dielectric insulation and biofluid barriers. I will first discuss the choice of fluorinated elastomers, incentivized by molecular dynamics simulations, which reveal that this class of elastomers displays an outstandingly low ionic diffusivity at body temperature and could lead to an ultra-low ionic conductivity. Then, I will show how this result is confirmed by two experiments to quantify the ionic conductivity in dielectric polymers exposed to biofluids, namely Electrochemical Impedance Spectroscopy (EIS) and a novel technique that we name External Electrolyte Conductimetry (EEC). The observed ultra-low ionic conductivity in fluorinated elastomers provides the long-term electrical insulation required for brain implants. Finally, I will present a novel nanofabrication process using a perfluoropolyether elastomer allows the fabrication of ultra-soft, scalable brain probes, which can record individual neuron's activity over the course of multiple months, with a vanishing immune response over time. This technology will provide stable and long-term brain-machine interfaces as an electrophysiological tool for neuroscience and biomedicine. Furthermore, the

material and fabrication procedures developed in this work will not only impact brain implantation, but also offer high-performances soft materials for soft robotics, epidermal electronics, regenerative medicine, and biomedical devices.

SESSION SB07.03/SB02.04: Keynote: Hydrogel Bioelectronics

Session Chair: Fabio Cicoira

Tuesday Afternoon, November 30, 2021

Sheraton, 2nd Floor, Back Bay B

5:00 PM *SB07.03/SB02.04.01

Keynote: Hydrogel Bioelectronics Xuanhe Zhao; Massachusetts Institute of Technology, United States

Whereas human tissues and organs are mostly soft, wet and bioactive; machines are commonly hard, dry and biologically inert. Merging humans, machines and their intelligence is of imminent importance in addressing grand societal challenges in health, sustainability, security, education and joy of living. However, interfacing humans and machines is extremely challenging due to their fundamentally contradictory properties. At MIT Zhao Lab, we exploit *soft materials technology* to form long-term, high-efficacy, multi-modal interfaces and convergence between humans and machines. In particular, hydrogels with similar mechanical and physiological properties as various biological tissues have been explored as an ideal material candidate for such human-machine interfaces and convergence. This talk will focus on *Hydrogel Bioelectronics*. I will first discuss the general principles to design hydrogels to be extremely tough, adhesive, strong, fatigue-resistant, and electrically conductive. I will then introduce a 3D printing method for the fabrication of various hydrogel bioelectronic devices, including wearable, ingestible and implanted devices. Thereafter, I will discuss in vivo tests on the long-term biocompatibility and efficacy of the hydrogel bioelectronics in rat and pig models. I will conclude the talk with a perspective on future human-machine convergence enabled by soft materials technology.

SESSION SB07.04: Poster Session I: Soft, Healable Materials and Devices for Biological Interfaces and Wearables

Session Chair: Fabio Cicoira

Tuesday Afternoon, November 30, 2021

8:00 PM - 10:00 PM

Hynes, Level 1, Hall B

SB07.04.01

Transparent, Conductive and Skin-Adhesive PVA Organohydrogels for Strain Sensing and Wearable Technology Applications Jennie Paik, Boonjae Jang, Sunghyun Nam, Jiajie Li and L.Jay Guo; University of Michigan–Ann Arbor, United States

Conductive polymer gels can enable innovative wearable technologies due to their mechanical robustness and flexibility. However, biocompatibility and processability remain obstacles in realizing these materials' commercialization, while devices made from these materials must maintain sustained adhesion and electrical connectivity under duress so that sensing performance is not negatively impacted. Herein, we have addressed these challenges by developing a multifunctional PVA-based organohydrogel material for use as a transparent, skin-adhesive strain sensor for motion monitoring. While ice templated PVA hydrogels are biocompatible, they are neither transparent nor conductive, and their flexibility degrades due to water loss over time. The introduction of Zn^{2+} ions into the hydrogel imparts ion conductivity, while plasticization by Zn^{2+} -water complexes yields a fourfold increase in rupture strain. Partial solvent exchange with the high-dielectric-constant solvent glycerol improves skin adhesion twofold, reduces water loss up to 20%, and reduces electrical resistance from the megaohm (M Ω) to the kilohm (k Ω) regime, resulting in a transparent, skin-adhesive, elastomeric, conductive organohydrogel. The material shows high gauge factor (1.69 at 21.5% strain), making it a potential low-cost candidate for a stretchable electronic material. Subsequent work will characterize the relationship between the electrical performance and gel microstructure using electrical, spectroscopic, and microscopic methods, which is believed to play a role in the transport of ionic species through the material. Due to the availability and biocompatibility of the component materials, we believe that our multifunctional organohydrogel is a promising development in making wearable technology more accessible to society at large.

SB07.04.02

Wearable Triboelectric Nanogenerators with Thermoplastic Polyurethane/Silver Nanowire Textiles for Human Machine Interface Doga Doganay¹, Melih O. Cicek¹, Mete Batuhan Durukan¹, Burak Altuntas¹, Erdem Agbahca², Sahin Coskun³ and Husnu E. Unalan¹; ¹Middle East Technical University, Turkey; ²Tubitak Ulakbim, Turkey; ³Eskisehir Osmangazi University, Turkey

Electronic textiles received considerable attention both in scientific field and in the market since early 2010s. Fabrication of electronic textiles over large areas is problematic and require urgent solutions. Functional materials should be homogeneously decorated via low cost and scalable methods. These functional textiles must retain their functions after certain number of washing cycles. More importantly, these wearable electronics consume high power and necessitate large and bulky batteries that significantly reduce user comforts. Herein this study proposes a combined, facile, scalable and low cost solution for the aforementioned problems. Silver nanowires (Ag NW) were decorated onto conventional cotton textiles via dip and dry method. Thermoplastic polyurethane (TPU) films were then hot pressed onto these textiles and functioned as both the protection and electrification layer for machine washable wearable TENGs. TPU/Ag NW fabric TENG electrodes produced a maximum power output of 1.25 W/m² when polylactic acid/aluminum (PLA/Al) foil TENG electrodes were used as the top electrode. Electrical resistance, joule heating performance and voltage output of TPU/Ag NW fabric TENGs were monitored to investigate their washing stability. It was observed that the electrodes performed stably up to 15 washing cycles. Finally, a self-powered e-wristband was developed and used as a human machine interface, which showed the true potential of the TPU/Ag NW fabric TENGs.

SB07.04.04

Late News: An Electrically Recoverable, Sintering-Free Conductor for Intrinsically Stretchable Electronics Sun Hong Kim¹, Geunwoo Baek¹, Donghee Son² and Jeonghun Kwak¹; ¹Seoul National University, Korea (the Republic of); ²Sungkyunkwan University, Korea (the Republic of)

There are have been many progresses of stretchable electronics for epidermal and wearable devices, soft robotics and implantable devices. Despite

remarkable progresses in conventional electronics, soft materials for skin electronics have been required due to its nature of skin-like properties enabling reduction of modulus mismatch. However, it is still challenging to achieve high conductivity and high stretchability of soft materials simultaneously. Herein, we present an electrically recoverable, sintering-free conductor for durable electronic skin devices. As fabricated conductor shows electrical recovery under strains and high conductivity without any post treatments. With printing technology, we realized the system that features a rigid-island structure interconnected with our conductor, which is optimized by controlling the evaporation rate of solvent (~160% stretchability and ~18,550 S/cm conductivity). Devised design has potential to enhance both areal density and structural reliability while avoiding the thermal degradation of heat-sensitive stretchable electronic components. To show the feasible application, stretchable sensory-neuromorphic system, comprising a stretchable capacitive pressure sensor, a resistive random-access memory, and a quantum dot light-emitting diode, respectively. Even in the skin deformation range, each device operated well, accurately recognizing various patterned stimuli via an artificial neural network with training/inferencing functions. In the future, our work is expected to be an important step toward robust electronic skin system.

SESSION SB07.05: Soft, Healable Materials and Devices for Biological Interfaces and Wearables III

Session Chair: Fabio Cicoira

Wednesday Morning, December 1, 2021

Sheraton, 2nd Floor, Back Bay B

10:30 AM *SB07.05.01

Liquid Metal Enabled Soft, Healable and Stretchable Electronics Michael Dickey; North Carolina State University, United States

Gallium-based liquid metals have remarkable properties: melting points below room temperature, water-like viscosity, low-toxicity (unlike Hg), and effectively zero vapor pressure (they don't evaporate). They also have, by far, the largest interfacial tension of any liquid at room temperature. Yet, these liquid metals can be patterned into non-spherical shapes (cones, wires, etc) due to a thin, oxide skin that forms rapidly on its surface. This talk will describe recent efforts in our research group to harness this oxide to pattern and manipulate metal into shapes—such as wires and particles—that are useful for applications that call for soft and deformable metallic features, such as wearables. It is possible to pattern the metal in a number of ways, including injection into microchannels or by direct-write 3D printing at room temperature, to form ultra-stretchable wires, deformable antennas, and microelectrodes. Liquid metal conductors can be rendered into self-healing circuits by either (1) encasing liquid metal wires in a self-healing polymer, (2) using dielectrophoresis to assemble microdroplets of liquid metal into conductive paths that span damaged portions of circuits, or (3) harnessing shear from cutting to create autonomously healing circuits. Liquid metal circuits can also be designed to respond to touch in unique and useful ways. I will show how this principle can be utilized to create soft circuit elements that can perform simple logic in response to touch, which is interesting because such circuits can carry out logic operations without the use of conventional transistors. Taken in sum, this work has implications for soft and stretchable electronics; that is, devices with desirable mechanical properties for human-machine interfacing, soft robotics, and wearable electronics.

11:00 AM SB07.05.02

Dissolving Microneedles Delivering Cancer Cell Membrane Coated Nanoparticles for Cancer Immunotherapy Wonchan Park and Sei Kwang Hahn; POSTECH, Korea (the Republic of)

Recently, a variety of tumor vaccines and immune system stimulators such as toll-like receptors (TLRs) agonists have been widely investigated for cancer immunotherapy via transdermal delivery. Despite these great research efforts, low efficiency and discomfort remain a huge technical hurdle for the development of immunotherapeutics. Here, we design a facile method to deliver drugs to the skin through microneedles (MNs) to stimulate the immune system in two ways. As one of the tumor vaccines, cancer cell membrane proteins can act as tumor-specific antigens that are presented to antigen presenting cells (APCs) to activate the immune system. In addition, a toll-like receptor 7 (TLR7) agonist of imiquimod (R837) can suppress cancer cell growth by inhibiting angiogenesis. Using poloxamer 407 (F127) as a nanocarrier, F127 nanoparticles (F127 NPs) are loaded with R837 and then coated with cancer cell membranes (M). These F127-R837@M NPs are loaded in rapidly dissolving MNs and delivered through the skin. MNs loaded with F127-R837@M NPs show significant inhibition of cancer cell growth in both prophylactic vaccination and antitumor immunotherapy in vivo. The dual immune system stimulating F127-R837@M NPs would be effectively used for cancer immunotherapy.

11:15 AM SB07.05.03

Photo-Patternable, Large-Area Particle-Packed-State Liquid Metal Film Coated via Solution Shearing for Soft Electronics Gun-Hee Lee; Korea Advanced Institute of Science and Technology, Korea (the Republic of)

Liquid metal (LM) is considered one of the most promising conducting materials for soft electronics due to its unique combination of metal-level high conductivity with exceptional deformability and stretchability. However, their practical applicability has thus far been limited due to the challenges of generating chemically and mechanically stable film over a large-area and the need for non-standard fabrication approaches. Here, we report materials and manufacturing methods that enable multiscale patterning (from microns to centimeters) and multilayer integration of 'solid-state liquid metal (SSLM)' with the conventional cleanroom process. In this work, solution shearing of a polyelectrolyte-attached LM particle ink is used to generate SSLM films. The stabilized LM particles were observed to form a close-packed thin-film without particle rupture when coated under an evaporative regime. This is essential in enabling a subsequent photolithographic lift-off process at wafer-scale to produce high-resolution features (~10 μm) of varying thicknesses on various substrates. Demonstrations of wearable multilayer tactile sensing systems and stretchable skin-interfaced electronics validate the simplicity, versatility, and reliability of this manufacturing strategy, suggesting broad utility in the development of advanced soft electronics.

11:30 AM SB07.05.04

Late News: Partially Graphitized Synthetic Polyphenols Enables Wear-Resistant Antimicrobial Coating Kyueui Lee^{1,2}, Minok Park², Katerina Malollari², Jisoo Shin², Sally M. Winkler², Yuting Zheng², Jung Hwan Park³, Costas Grigoropoulos² and Phillip Messersmith²; ¹Kyungpook National University, Korea (the Republic of); ²University of California, Berkeley, United States; ³Kumoh National Institute of Technology, Korea (the Republic of)

Grafting antimicrobial polymers on public surfaces may minimize the spread of diseases. For this, surface functionalization is essential. However, conventional approaches such as hydroxylation are limited to specific substances. Surface-independent multifunctional coating including polydopamine (PDA) can be a promising alternative, however, its inherently weak wear resistance prevents practical applications. To overcome this problem, we developed the laser annealing process that can partially graphitize PDA to induce mechanical enhancement while its inherent catechol functionality can be preserved. The post-treated functional coating showed significantly increased mechanical resistance compared to the original PDA, which was confirmed by scratch testing using a nanoindenter. Surprisingly, the laser-annealed coating showed even better wear resistance compared to strong inorganic materials

(e.g., quartz and TiO₂). To further introduce antimicrobial ability, thiolated polyethylene glycol (PEG) was grafted on the coating. Due to the presence of catechol functional groups on the surface, the PEG-SH was easily grafted through Michael-type addition. The bacterial attachment was significantly reduced (5-fold) on the PEGylated laser-annealed PDA compared to PEGylated PDA. This was found to be due to the delamination of the PDA layers under ambient conditions. We believe that our work can provide an insight into designing antimicrobial surfaces that can slow down pandemics including COVID-19.

11:45 AM SB07.05.05

Fully Bioresorbable, Leadless, Battery-Free Cardiac Pacemaker Yeonsik Choi¹, Rose T. Yin², Igor Efimov² and John A. Rogers¹; ¹Northwestern University, United States; ²George Washington University, United States

Temporary cardiac pacemakers provide critical functions in pacing through periods of need during post-surgical recovery. The percutaneous leads and externalized hardware associated with these systems present, however, risks of infection and constraints on patient mobility. Furthermore, the pacing leads can become enveloped in fibrotic tissue at the electrode-myocardium interface, which thereby increases the potential for myocardial damage and perforation during lead removal. Here, we report a bioresorbable, leadless, and fully implantable cardiac pacemaker for post-operative control of cardiac rate and rhythm during a stable operating timeframe that subsequently undergoes complete dissolution and clearance via natural biological processes. A combined set of *in vitro*, *ex vivo*, and *in vivo* studies across mouse, rat, rabbit, canine, and human cardiac models demonstrates that these devices provide an effective, battery-free means for pacing hearts of various sizes with tailored geometries and timescales for operation and bioresorption. These features enable programmable cardiac pacing in a manner that overcomes all of the key disadvantages of traditional temporary pacing devices. As such, this novel cardiac pacemaker may serve as the basis for the next generation of post-operative temporary pacing technology.

SESSION SB07.06: Soft, Healable Materials and Devices for Biological Interfaces and Wearables IV

Session Chair: Fabio Cicoira

Wednesday Afternoon, December 1, 2021

Sheraton, 2nd Floor, Back Bay B

1:30 PM SB07.06.01

Late News: Smart Materials for Flexible, Self-Healing and Conductive Interfaces Antonio Riul Jr^{1,2}, Gabriel Gaal¹, Anerise Barros^{1,2}, Maria Braunger¹, Mawin M. Jimenez¹, Carlos A. Avendano², Monica Jung de Andrade², Manuel Quevedo-Lopez², Fernando Alvarez¹ and Ray Baughman²; ¹University of Campinas, Brazil; ²The University of Texas at Dallas, United States

Self-healing materials inspire the next generation of multifunctional wearables and IoT appliances. Nonetheless, it is crucial to fabricate thin films enabling seamless and conformational coverage irrespective of the complexity of shape and geometry of the surface for electronic skins, smart textiles monitoring body signals, soft robotics, wearables and storing energy devices. Within this context, the layer-by-layer (LbL) technique is a versatile approach for homogeneously dispersing materials into various matrices. Moreover, it provides molecular level thickness control and conformational configuration on virtually any surface. Poly(ethyleneimine) (PEI) and poly(acrylic acid) (PAA) are materials primarily employed in LbL structures due to their intrinsic ability to form self-healing coatings at room temperature. However, it is still challenging to achieve thin composite films having high conductivity, good healing strength, and controlled mechanical properties at ambient conditions. Here, PEI and PAA were mixed with conductive materials such as gold nanorods, poly(3,4-ethylene dioxathiophene) polystyrene sulfonate (PEDOT:PSS), reduced graphene oxide and multi-walled carbon nanotubes in distinct LbL film architectures. Electrical (AC and DC), optical (Raman spectroscopy), and mechanical (nano-indentation) measurements were performed to evaluate the impact of the different fillers in the electrical and mechanical properties of the multilayered structures. As a proof-of-concept a self-healing electronic-tongue was assembled using different geometries. We were able to distinguish basic tastes at low molar concentration, below the human threshold. We also tested the self-healing e-tongue setup as a glucose sensor, distinguishing different concentrations of glucose in artificial sweat, a first step towards a long-term wearable biosensor. The results are promising for the manufacture of self-healing conductors by design, as the mechanical properties were balanced with the healing and electrical efficiencies. The formed nanostructures have the potential for creating smart surface layers having unique features that solve technological challenges.

1:45 PM SB07.06.02

Self-Limiting Electrospray Deposition of Composite Gelled Electrospray Liquids (GELs) Michael Grzenda, Zhiyi Chen and Jonathan Singer; Rutgers, The State University of New Jersey, United States

In electrospray deposition (ESD), strong electric fields are applied to solutions exiting narrow capillaries in order to produce monodisperse droplets that are attracted to grounded substrates. Self-limiting electrospray deposition (SLED) is a recently discovered phenomena where insulating polymers below their glass transition temperature are deposited onto conductive surfaces. The growing film eventually cannot dissipate charge effectively which leads new material to be repulsed by the film, causing the incoming droplet to target uncoated conducting regions of the substrate. This targeting effect occurs on complex 3D objects, even on surfaces not facing the needle, as well as on small 2D and 3D features less than the characteristic size of the spray. The resulting polymer films demonstrate a wide range of complex morphologies, including nanowires forests and hollow shells. When nanoparticles are added to these morphologies, the self-assembly acts to separate the particles within the polymer network, allowing, for example, a conformal 3D composite foam of methylcellulose nanowires to display the single particle plasmon of embedded gold nanoparticles even at high loadings. In this work, we explore the use of SLED solutions as a carrier for unmodified functional nanoparticles with the goal of providing new functionalities to the target spray substrates. This is accomplished using a shear-thinning gelling agent in combination with a SLED-compatible polymer to form a gelled electrospray liquid (GEL). GELs can easily suspend nanoparticles, regardless of their composition for prolonged periods at particle loadings of up to 70 volume %, while the shear thinning capability maintains spray stability. This targeted nanoparticle delivery is envisioned as an advanced manufacturing technique ideal for upgrading and functionalizing conductive traces in flexible electronics with high efficiency or adding surface modification to soft robotic structures. The current work explores films created using GELs composed of several different nanoparticles, including silver electronic particles and mica pigments, and demonstrates corresponding changes in surface properties.

2:00 PM SB07.06.03

Sintering Liquid Metal Nanoparticles by a CO₂-Laser Cutter Soouk Im, Jan Genzer and Michael Dickey; North Carolina State University, United States

Liquid metals are intrinsically soft. They have been studied intensively as conductive materials in soft and wearable electronics. Among liquid metals,

eutectic gallium indium (EGaIn) is an alloy with 75 wt% gallium and 25 wt% indium, which has a low melting point (15.7 °C) low-toxicity, and near-zero vapor pressure at room temperature. EGaIn spontaneously reacts with oxygen in ambient conditions to form a few-nanometer thick gallium oxide layer at the surface. This oxide layer can even form in water with a low oxygen concentration (~ppm). When bulk liquid metal (~mm diameter) is sonicated, it breaks into nanoparticles (~100 nm) composed of a liquid core and an oxide shell. Films of these particles have poor electrical conductivity due to the oxide layer. Still, particles can merge to form conductive paths if the applied stress is enough to break the oxide [1]. A focused laser beam has also been used to sinter liquid metal particles. Kramer et al. proposed the laser beam provides a localized heat source to break the oxide layer and coalesce the particles [2]. They used a ytterbium pulsed fiber laser with a different sintering mechanism from a conventional laser cutter operated by a CO₂ laser. Here, we investigate CO₂ laser-sintered liquid metal nanoparticles to understand better how laser sintering works. Liquid metal particles were prepared by sonication with isopropanol. Particle films were obtained by casting the solution on glass slides and subsequently evaporating the solvent. After sintering with a CO₂ laser, the EGaIn particle film had low resistance (~1 Ω), but the particle morphology only changed slightly, unlike reported previously [2]. We also found changes in rheological properties after sintering, indicating that the CO₂ laser beam broke the oxide of the particles. Lastly, since the particle film remained conductive on a latex glove after bending and stretching, particle films sintered using lasers have potential applications in soft wearable devices.

References

- [1] Y. Lin, J. Genzer, M. D. Dickey, *Adv. Sci.* 2020, 7, 2000192.
- [2] S. Liu, M. C. Yuen, E. L. White, J. W. Boley, B. Deng, G. J. Cheng, R. Kramer-Bottiglio, *ACS Appl. Mater. Interfaces* 2018, 10, 28232.

SESSION SB07.07: Soft, Healable Materials and Devices for Biological Interfaces and Wearables V
Session Chairs: Wei Lin Leong and Shiming Zhang
Monday Morning, December 6, 2021
SB07-Virtual

8:00 AM *SB07.07.01

Nanomesh Pressure Sensor Without Sensory Interference [Takao Someya](#), Sunghoon Lee and Tomoyuki Yokota; The University of Tokyo, Japan

Precise measurement of finger manipulation is critical to understand and reproduce the sense of natural touch. Huge advances have been made in developments in soft and flexible sensors for finger motions monitoring helping to decrease physical interferences due to the sensor attachment. For example, a use of stretchable substrates and/or a reduction in sensor thickness have substantially improved the conformability of sensors to the skin enabling more accurate monitoring of finger touch. Recently, ultra-thin (a few μm) sensors have been also demonstrated, which significantly reduce the loss in sensation. However, there is still challenge to monitor finger touch while maintaining the natural touch feeling. Covering the skin with any object, even a super thin layer significantly affects sensory information which results in a distortion of the inherent control. Here, we succeeded in monitoring finger pressure with an undetectable effect on human sensation using sensors directly attached to the highly sensitive fingertip. To minimize sensory interference, we developed ultra-thin nanomesh sensors composed of compliant nanoporous structures. To objectively and quantitatively evaluate the effect of the nanomesh material on human sensation, we investigated the grip force during object grasp. The sensor-applied finger exhibits comparable grip forces with those of the bare finger, even though the attachment of a 2-μm-thick polymeric film results in a 14% increase in the grip force. Furthermore, this nanomesh structure allows the simultaneous achievement of high mechanical durability against shearing and friction over hundreds of kilopascals while the ultra-thin compliant structure preserves the human sensitivity. Our new methodology, which removes the effect caused by the electronics, offers the possibility to accurately monitor biological information in a natural state to a variety of fields such as biomedical, sports, and entertainment applications.

8:30 AM *SB07.07.02

Wearable Electronics Using a Textile-Centric Design Approach Yunyun Wu, Sara Mechael, Yiting Chen and [Tricia B. Carmichael](#); Univ of Windsor, Canada

Clothing is ubiquitous in daily life, making textiles an ideal platform for the next generation of wearable electronics. New electronic textiles (e-textiles) will incorporate sensors to detect biometric data, light-emitting devices to display data, and integrated wiring and power sources. The fabrication of these e-textiles requires the integration of functional materials into the textile, while maintaining wearability, softness, and stretchability. The challenge with this integration is that the porous, 3D structures of textiles are obviously different from the flat and rigid surfaces conventionally used for device fabrication. Textiles present a non-planar surface for fabrication and readily absorb and wick solutions of functional inks, which can stiffen the textile and compromise wearability. In this presentation, we discuss the use of solution-based electroless metallization to fabricate conductive textiles. A key advantage of this approach is the ability of the aqueous plating solution to permeate into the textile structures to deposit conformal, uniform gold coatings on the surfaces of individual fibers that comprise the yarns, leaving the void structure of the textile intact. We also discuss how the ready availability of the considerable variety of textiles offers a great opportunity to advance the e-textile field by incorporating textile structures into the device design. In this textile-centric design paradigm, textiles play an integral role in the operation of e-textile devices rather than acting merely as passive device carriers. We discuss how the open structure of a low-denier nylon and spandex ultrasheer fabric can be used as a framework for highly stretchable transparent electrodes in wearable and stretchable light-emitting devices, and how the tufted structure of a velour fabric can form the basis for an architectural engineering approach to protect brittle electroactive materials from strain for the fabrication of stretchable textile-based lithium-ion batteries.

9:00 AM *SB07.07.03

Intrinsically Stretchable Healable Semiconductors for Skin-Inspired Electronics [Jin Young Oh](#); Kyung Hee University, Korea (the Republic of)

In this talk, I will address molecular designs and material processing of intrinsically stretchable healable semiconductors for skin-inspired electronics.

- 1) Incorporation of dynamic intermolecular interaction unit into semiconducting polymers.
- 2) Blending of intrinsically stretchable semiconducting polymer and self-healable elastomer.
- 3) Applications for skin-inspired electronics.

9:30 AM SB07.07.04

Late News: A Highly Stretchable and Transparent Conducting Polymer and the High-Resolution Patterning for Large-Area Capacitive Sensors [Tokihiko Shimura](#)¹, Shun Sato¹, Kaoru Yamashita¹, Shuma Abe¹, Taizo Tominaga¹, Minoru Ashizawa², Hiroki Ishikuro¹ and Naoji Matsuhsa^{1,3}; ¹Keio University, Japan; ²Tokyo Institute of Technology, Japan; ³JST PRESTO, Japan

Stretchable and transparent conducting polymers have been demonstrated in various applications, such as wearable/implantable devices and robotic skins, which enables biosensing for healthcare and facilitates human-machine interaction. Several approaches to achieve high-resolution patterning have been reported, including inkjet printing and photolithography.[1,2] However, it is difficult to simultaneously improve conductivity and stretchability due to the materials limitation in each patterning process. Therefore, a method of achieving precise patterning without compromising the electrical and mechanical characteristics has been desirable.

Here we have realized a highly conductive and stretchable polymer conductors, and the patterning in high-resolutions (tens of micrometers). The material consists of PEDOT:PSS and Lithium Bis(pentafluoroethanesulfonyl)imide (LiBETI), which improves its conductivity and stretchability, spin-coated on a thermoplastic polyurethane (TPU) substrate. Our conducting polymer doped with LiBETI showed a high conductivity of 328 S/cm at 0% strain, and 196 S/cm at 100% strain although that with Lithium Bis(trifluoromethanesulfonyl)imide (LiTFSI) showed 272 S/cm at 0% strain and 98 S/cm at 100% strain.[3] Moreover, our material showed a very high crack-on-set strain of 160%, which is the highest value among the previously reported stretchable conducting polymers to the best of our knowledge. It also showed high transparency of 86% (at a wavelength of 550 nm, including a TPU substrate). Furthermore, the high-resolution patterning (smaller than 20 μm) was achieved by UV-laser ablation which can be carried out over large areas at a high throughput.

The utility of our material was demonstrated by two types of sensors. One is a stretchable and transparent capacitive strain sensor. Our strain sensor showed high stretchability of 100%, and high linearity, which enabled radial artery pulse monitoring. Another is a stretchable, transparent, and large-area capacitive touch sensor matrix. Our 7×7 matrix sensor was able to detect single-point and multi-point touches even while sensor was stretched at 30% strain. Our transparent, thin-film sensors are expected to be used in next-generation human-computer interfaces which can be attached on the surfaces of humans and robots.

This work was supported by JST, PRESTO Grant Number JPMJPR20B7, Japan. Part of this work is supported by The Amada Foundation, JGC-S scholarship foundation, The Mazda Foundation, and The Kao Foundation for Arts and Sciences.

[1] Y. Q. Zheng, *et al.* "Monolithic optical microlithography of high-density elastic circuits." *Science* **373**, 88-94 (2021).

[2] U. Kraft, *et al.* "Ink Development and Printing of Conducting Polymers for Intrinsically Stretchable Interconnects and Circuits." *Advanced Electronic Materials* **6**, 1900681 (2020).

[3] Y. Wang, *et al.* "A highly stretchable, transparent, and conductive polymer." *Science Advances* **3**, e1602076 (2017).

9:45 AM SB07.07.05

Printable Elastomeric Electrodes with Sweat-Enhanced Conductivity for Wearables Jian Lv, Gurunathan Thangavel and Pooi See Lee; Nanyang Technological University, Singapore

Human sweat has always been considered a negative factor for electrode conductivity because of the enhanced corrosion behavior of bulk metals in the presence of saline solution. Here, we designed printable, photocurable, and textile-based silver flakes-poly(urethane-acrylate) (Ag-HPUA) electrodes of which the resistance can be reduced by human sweat in both original and stretched states. The electrodes are composed of Ag flakes and HPUA binder with hydrophilic, photocurable, and high stretchable properties. The specially designed HPUA binder contains hard segments made up of carbamate groups (-NH-C=O-O-) and soft segments made up of aliphatic polyether (-O-) or polyester (-CO-O-) backbone that was capped with acrylate (C=C) functionality at each end. When the Ag-HPUA encounters the sweat, the lactic acid, and Cl⁻ work synergistically to enhance the conductivity rapidly and permanently by removing the surfactant on the Ag flakes surfaces and sintering the exposed Ag flakes. The key factors (pH, Cl⁻, and gradual sweating) and the mechanism of the reaction between the Ag-HPUA electrode and sweat have been elaborated. Sweat can also significantly improve the electrode's durability to stretching deformation. The on-body test has shown that the resistance of the electrode can be reduced from 3.02 Ω to 0.6 Ω after the subject started to secrete sweat. As an example, a type of stretchable sweat-based Zn-Ag₂O battery using Ag-HPUA as the current collector was directly printed on textile to supply energy for a wearable wireless temperature sensor. Apart from acting as the electrolyte, human sweat also enables the battery to operate under stretching. Our approach uses sweat that is harmless to human skin as the sintering agent that reduces the resistance of printed stretchable electrodes during wearing, providing a new route in the design of printed stretchable devices.

SESSION SB07.08: Soft, Healable Materials and Devices for Biological Interfaces and Wearables VI
Session Chair: Shiming Zhang
Monday Morning, December 6, 2021
SB07-Virtual

10:30 AM SB07.08.01

Bioinspired Flexible Microneedle Patches for Improved Transdermal Drug Delivery Jie Hao Tay¹, Yu Han Lim¹, Mengjia Zheng¹, Wen See Tan¹, Qian Shi¹, Chenjie Xu² and Juha Song¹; ¹Nanyang Technological University, Singapore; ²City University of Hong Kong, Hong Kong

Microneedle (MN) technology is well-known, extensively researched and has been growing in market size. However, designs to enhance the functionality of MN patches are still lacking. Most MN patches are fabricated as a stiff, single arrays. This is problematic as the human skin is intrinsically curved, and hyperelastic. Applying a stiff entity to dynamic surfaces of the skin results in geometric incompatibility and induces pre-stress conditions at the interface. After removal of the application force, the hyperelastic skin returns to its pre-stretched state, where the adhesive strength between skin and MN patch is lower than the recovery stress of skin, causing interfacial delamination. Particularly, anatomical regions with large surface area and complex surface topography are prone to causing interfacial problems, and exhibit low contact stability. Hence, there is a mismatch in current MN patch functionality and application requirements onto human skin, where patch delamination and partial MN penetration result in inconsistent and poor drug delivery efficiency. In this study, we propose a novel MN patch design – bioinspired by the multi-scale principle of naturally segmented fish armour systems – by translating stiff individual MN tips onto a macro-scale flexible assembly substrate, for an adaptive and highly flexible MN patch with enhanced drug delivery capabilities. Through this approach, microneedle patches showed significantly improved penetration efficiency, even under dynamic cyclic loading conditions. We confirmed improved contact stability, penetration efficiency and large surface coverage of those bioinspired microneedle patches, varying microneedle materials from fast dissolvable to slowly degradable polymers, through both *in vitro* and *in vivo* tests. We envisage that this bioinspired flexible microneedle platform can be used for various functional transdermal drug delivery platforms or long-term epidermal biosensors.

10:45 AM SB07.08.02

Late News: Soft, Miniaturized and Self-Adhesive Interface in Wearable Sensor Network for Systematic and Quantified Assessment of Full-Body Kinematics Young Joong Lee, Hyoyoung Jeong, Jae-Young Yoo and John A. Rogers; Northwestern University, United States

Early detection of atypical movement due to neuromotor pathology can expedite timely therapeutic intervention that promotes recovery. Continuous monitoring of body kinematics near surgical sites can provide safe recovery and rehabilitation process. A particular challenge in identifying and monitoring such neuromotor or psychiatric assessment is in qualitative and subjective assessment. Advanced kinematic assessment and treatment rely on medical records, clinical exams, and imaging methods that require expert evaluations or expensive medical facilities and raise privacy issues. These requirements prevent broad access to the assessment due to cost and geographic proximity.

Here, we introduce a soft, flexible, and miniaturized skin-interfaced sensor network as an alternative solution, which are placed at strategic locations across the body to capture full-body kinematics of subjects as well as vital signs quantitatively and continuously. Biocompatible, thin, and self-adhesive encapsulation ($< 180 \mu\text{m}$ thickness) with a fiberglass fabric ($< 20 \mu\text{m}$ thickness) embedded facilitates soft, intimate contact to the skin without irritation and disrupting signal sensitivity of the mechanoacoustic sensor which enables capturing of gross and subtle movements. The resulting quantitative measurements from time-synchronized wireless sensors integrated with 3-axis accelerometer and 3-axis gyroscope can be analyzed across the full range of spatio-temporal scales to identify body balance and motor behaviors of each body part such as the torso, arms, legs, and head. These quantitative measurements can serve as basis for 3D motion reconstruction in avatar form, enabling remote assessments by experts with de-identified means. The sensor network system presented here has potential applications in long-term tracking of atypical motor development in infants with elevated risks of neuromotor pathology, real-time tracking and feedback based on neck activity level in patients recovering from thoracic surgery to enhance personal awareness of health status, and guidance for posture correction in athletes' performances.

11:00 AM SB07.08.03

An Electroactive Filter with Tunable Porosity Vasileios Oikonomou¹, Johannes Gladisch¹, Maximilian Moser², Iain McCulloch^{2,3}, Magnus Berggren¹ and Eleni Stavrinidou¹; ¹Linköping University, Sweden; ²University of Oxford, United Kingdom; ³King Abdullah University of Science and Technology, Saudi Arabia

Advanced materials with stimuli responsive volume change are of interest for a wide range of applications, from actuators, microfluidics and drug delivery. Conjugated polymers change their volume when electrochemically doped/dedoped via the exchange of ions and solvent with an electrolyte. Here, we demonstrate an electroactive filter with tunable porosity, composed of a metallic mesh coated with the conjugated polymer pg3T2. Pg3T2 is a polythiophene polymer with ethylene glycol side chains that reversibly expands by 300% upon addressing, relative to its previous contracted state, outperforming any other conjugated polymers. By optimizing the polymer coating on the metallic mesh, we achieved highly controllable porosity during electrochemical addressing. The pores reversibly opened and closed, and their diameter could be defined by the applied potential within a dynamic range of $40 \mu\text{m}$. Among hundreds of pores from different samples 90 % of them could be completely closed while only less than 1 % were inactive. Finally, we demonstrate control of dye flow through the electroactive filter, highlighting the potential for controlled large molecule delivery applications

11:15 AM SB07.02.04

Nanophase Separation in Triblock Copolymers—A Strategy to Achieve Low Modulus, Elastic Deformation and Good Mobility in Polymer Semiconductors Franziska Lissel^{1,2}; ¹Leibniz Institute of Polymer Research, Germany; ²Dresden University of Technology, Germany

The elastic modulus of polymer semiconductors (PSCs) (0.1 - 1 GPa for typical PSCs) is still orders of magnitudes away from human skin (0.1 - 10 MPa). Also, PSCs are brittle and structurally fragile, prohibiting their application in mechanically strenuous environments, or leading to the break-down of electric functionality.

Different pathways were explored to lower the modulus of PSCs, e.g. non conjugated spacers [1], changing the regioregularity of the backbone [2], or modifying the sidechains [3], to name a few. Lowering the modulus is generally associated with a decrease in mobility, and balancing the requirements of high mobility and low modulus when designing a PSC is challenging.

Here, we draw on an old concept in polymer engineering to approach the problem: Covalently linking two polymer chains into a block copolymer leads to separation on the nanoscale due to the thermodynamic incompatibility of the chains. The phases retain their respective properties (T_g, etc). A similar approach was used before to realize elongability (plastic deformation) in PSCs [4].

Combining PSCs with biocompatible elastomers in block copolymers gives materials that have a low modulus, can be deformed elastically and retain good mobility [5]. We synthesized triblock co-polymers (TBCs) by covalently end-capping poly-diketopyrrolopyrrole-thienothiophene (PDPP-TT), a high-performance D-A PSC, with two elastomeric polydimethylsiloxanes (PDMS) blocks to combine favorable electrical and mechanical properties in one system. The resulting nanophase segregation of both components, preserves the features of both moieties (PDPP-TT and PDMS) in their respective domains. The TBCs are soft and durable: the TBC with the highest PDMS content has a low modulus (6 MPa) in the range of mammalian skin and shows no crack formation up to 85% strain. The TBC achieves a mobility of $0.1 \text{ cm}^2\text{V}^{-1}\text{s}^{-1}$, in the range of the fully conjugated reference polymer ($0.7 \text{ cm}^2\text{V}^{-1}\text{s}^{-1}$). In a doped state, the block copolymer maintains electronic functionality over more than 1500 cycles at 50% strain. Also, the TBC can be shear-coated at high speeds (up to 10 s cm^{-1}) and still reliably give smooth films [6]. While the high speeds result in increased film thickness (up to 600 nm), no degradation of the electrical performance was observed, as was frequently reported for polymer-based OFETs.

Finally, using physisorption, organic field-effect transistor (OFET)-based biosensors can be fabricated which detect both SARS-CoV-2 antigens as well as anti-SARS-CoV-2 antibodies in less than 20 minutes. The biosensor was produced by functionalizing an intrinsically stretchable and semiconducting triblock copolymer (TBC) film either with the anti-S1 protein antibodies (S1 Abs) or receptor-binding domain (RBD) of the S1 protein, targeting CoV-2-specific RBDs and anti S1 Abs, respectively. The device demonstrates a high sensitivity of about 19%/dec and limit of detection (LOD) 0.36 fg/mL for anti-SARS-Cov-2 antibodies, and at the same time, a sensitivity of 32%/dec and LOD of 76.61 pg/mL for the virus antigen detection [7].

References:

- [1] Mun, Wang, Oh, Katsumata, Lee, Kang, Wu, Lissel, Rondeau-Gagné, Tok, Bao: *Adv. Funct. Mater.* **2018**, 28, 1804222.
- [2] Kim, Kim, Lee, Yu, Kim, Song, Shin, Oh, Jeon, Kim, Kim: *Macromolecules* **2015**, 48, 13, 4339.
- [3] Savagatrup, Makaram, Burke, Lipomi: *Adv Funct Mater* **2014**, 24, 1169.
- [4] Müller, Goffri, Breiby, Andreasen, Chanzy, Janssen, Nielsen, Radano, Siringhaus, Smith, Stingelin-Stutzmann: *Adv. Funct. Mater.* **2007**, 17, 2674.
- [5] Ditte, Perez, Chae, Hamsch, Al-Hussein, Komber, Formanek, Mannsfeld, Fery, Kiri, Lissel: *Adv. Mat.* **2021**, 2005416
- [6] Ditte, Perez, Hamsch, Kiri, Mannsfeld, Voit, Krukskaya, Lissel: *Polymers* **2021**, 13 (9), 1435
- [7] Ditte, Nguyen Le, Ditzer, Sandoval Bojorquez, Chae, Bachmann, Baraban, Lissel: *under review 2021*

1:00 PM SB07.09.02

Late News: (Garcia High School Student) Web Interface for the Operation of a Robotic Arm Audrey Wong¹, David Tarrab², Lauren Yu³, Dyllan Hofflich⁴, Matthew Garcia⁵, Shubham Agrawal⁶, Dasharadhan Mahalingam⁶ and Nilanjan Chakraborty⁶; ¹Beckman High School, United States; ²Ramaz Upper School, United States; ³Brea Olinda High School, United States; ⁴Pelham Memorial High School, United States; ⁵Plainedge High School, United States; ⁶Stony Brook University, The State University of New York, United States

Ailments like Parkinson's disease, carpal tunnel syndrome, arthritis, and cerebral palsy can leave individuals severely limited in mobility and unable to perform essential tasks. The diseases and impairments listed above all damage functionality in the upper arms. The use of a robotic arm to perform activities of daily living (ADL's) may be able to address these limitations.

The goal of this study is to control a robotic arm with eye-gaze technology or a Tongue Touch Keypad (TTK) through the shared context of a web interface. Created with HTML, CSS, and JavaScript, the interface was designed to facilitate clear communication between the user and robot arm. To allow the robotic arm to complete a task with missing information, the interface included a query-based system that would allow the user to supply additional information to aid the robot in performing a task. Important design decisions included the size and placement of buttons as well as the display of information on the interface to address the heightened error that follows eye-tracking.

This web interface will ultimately be built into the robot arm system to allow for its full testing and use by individuals. Two different pipelines will be present, the first using a wheelchair-mounted camera to acquire the coordinates of objects. The second will act upon the user's interactions with the interface as an object with a corresponding movement is selected; this information is then sent to the robot arm for the requested action to be executed. This backend development will be completed using ROS (Robot Operating System) and further project development will include optimizing communication between nodes, which include the web interface, camera, and various modalities of user interaction.

1:15 PM SB07.09.03

Late News: An Organic Electrochemical Transistor-Assisted Integrated Photodetector for Photoplethysmogram Signal Acquisition Yizhou Zhong, Diego Rosas Villalva, Luis H. Hernandez, Derya Baran and Sahika Inal; King Abdullah University of Science and Technology, Saudi Arabia

The unique characteristics of an organic electrochemical transistor (OECT) distinguish it from other transistors and make it a promising electrophysiological interface for a living system. In this work, we report a photodetector integrating an organic photodiode (OPD) and an OECT for physiological signal acquisition. The OPD module exhibits strong absorption in the visible and NIR wavelengths while the OECT is a p-type enhancement mode device. The high gain of the OECTs endows the integrated photodetector with a ca. 200 times increase in the photocurrent generated and at least a 100 times improvement in both the response and the external quantum efficiency compared to the OPD alone. We evaluated the performance of the integrated photodetector as a reliable transducer for photoplethysmogram (PPG) signal acquisition and suggest its high potential as a wearable biosensor.

1:30 PM SB07.09.04

Lightweight and Flexible Conducting Polymer Sponges and Hydrogels for Excellent EMI Shielding Applications Biporjoy Sarkar and Fabio Cicoira; Polytechnique Montreal Canada, Canada

Conducting polymers have extensively been used in the soft wearable electronic devices, and, successfully replaced the conventional metals in electromagnetic interference (EMI) shielding applications. In the present work, three dimensional (3D) foams and hydrogels derived from the most popular conducting polymer poly(3,4-ethylene dioxithiophene) polystyrene sulfonate (PEDOT:PSS) have been used to study EMI properties in the frequency range between 8 to 12.4 GHz. The 3D PEDOT:PSS foams endowed a unique complex porous micro-features that offer excellent electrical response under compressive forces, due to the coalescence of micro-features in the foam structure. Interestingly, the compressive strain enhanced the shielding effectiveness (SE) value of PEDOT:PSS foam by 60% of the pristine value. For the first time, highly conducting PEDOT:PSS hydrogel films were developed to show the highest SE value of about 105 dB. Both reflection and absorption attributed to the total shielding effectiveness. These results would open a new horizon for the development of a new class of EMI shielding materials.

SESSION SB07.10: Soft, Healable Materials and Devices for Biological Interfaces and Wearable VIII
Session Chairs: Fabio Cicoira and Shiming Zhang
Monday Afternoon, December 6, 2021
SB07-Virtual

4:00 PM SB07.10.01

Supervised Folding of Origami Soft Actuators Enabled by Magnetic e-Skins Eduardo Sergio Oliveros Mata¹, Minjeong Ha², Gilbert Santiago Cañón Bermúdez¹, Jessica Liu³, Benjamin A. Evans⁴, Joseph B. Tracy³ and Denys Makarov¹; ¹Helmholtz-Zentrum Dresden-Rossendorf, Germany; ²Electronics and Telecommunications Research Institute, Korea (the Republic of); ³North Carolina State University, United States; ⁴Elon University, United States

Reconfigurable^[1], soft^[2], and lightweight^[3] actuators are expected to be implemented in robotic systems biomimicking the multifunctional and adaptive capabilities of living organisms. The integration of sensing elements in soft actuators enables smart motion events increasing reliability, efficiency, and safe integration in diverse environments^[4]. Specifically, for origami-based systems^[5], the tracking of the orientation and the readiness of the folding is important to achieve reliable assembly of the structures.

Integration of sensing elements with soft actuators is typically addressed with stimuli-responsive materials^[6] and commercial sensors^[7] that lack feedback capabilities and high compliancy, respectively. Recent approaches measuring strain^[8], curvature^[9], and optical^[10] signals have been demonstrated for localized single folding in soft actuators. Until recently, there were no reports of an onboard sensing platform that enables the folding of multiple flaps as needed for origami.

Here, we will show the integration of flexible e-skins on magnetic actuators for supervision of the sequence and folding assembly of hinges defined on the fly. Highly compliant magnetic sensors (GMR and Hall effect) were laminated on ultrathin magnetic origami actuators enabling the detection of the readiness for actuation, the orientation, and the hinge folding process. The actuator, a magnetic composite based on a shape memory polymer with embedded NdFeB microparticles, actuates during a light softening and magnetic stimuli sequence^[11]. We optimized the thickness (60 μm) and composition (NdFeB - 40 wt%) of the composite to achieve the 180 deg basic fold for origami structures. The capabilities of the system with laminated sensing e-skin

were demonstrated after self-guided assembly of the origami platform with multiple hinges into box- and boat-like layouts^[12]. We envision that further development of alike self-supervised systems will bring closer the realization of adaptive mechatronic soft systems for different environments and even remote applications.

- [1] H. Song et al., *Nano Lett.* **20**, 5185 (2020)
- [2] Y.F. Zhang et al., *Adv. Func. Mater.* **29**, 1806698 (2019)
- [3] C. Lu et al., *Materials* **13**, 656 (2020)
- [4] S. Cheng et al., *Adv. Mater. Interfaces* **6**, 1900985 (2019)
- [5] M. Taghavi et al., *Sci. Robot.* **3**, (2018)
- [6] L. Hines et al., *Adv. Mater.* **29**, 1603483 (2017)
- [7] M. Salerno et al., *Sens. Actuators, A* **265**, 70 (2017)
- [8] S. Mousavi et al., *ACS App. Mater. Interfaces* **12**, 15631 (2020)
- [9] A. Koivikko et al., *IEEE Sens. J.* **18**, 223 (2018)
- [10] C. Wang et al., *Adv. Mater.* **30**, 1706695 (2018)
- [11] J. A.-C. Liu et al., *Sci. Adv.* **5**, eaaw2897 (2019)
- [12] M. Ha, E.S. Oliveros Mata et al., *Adv. Mater.* 2008751 (2021)

4:15 PM SB07.10.02

Mechanically Tough Ionogels for Stretchable Electroluminescent Devices Jinhwan Yoon; Pusan National University, Korea (the Republic of)

Double network (DN) ionogels comprising soft and brittle polymer networks were prepared to fabricate high-performance stretchable electronics such as electroluminescent (EL) devices. As a highly stretchable electrode, conducting ionogels of a double network structure which are further reinforced by the ionic and covalent crosslinking of the network were prepared. Based on their excellent mechanical properties and high conductivity, the developed ionogels are envisioned as stretchable ionic conductors for extremely stretchable EL devices. The EL device fabricated with the developed ionogel exhibits stable working operation under an ultrahigh elongation of over 1200% as well as severe mechanical deformations such as bending, rolling, and twisting. Furthermore, the developed ACEL devices also display stable luminescence over 1000 stretch/release cycles or at temperatures as harsh as 200 °C.

4:30 PM SB07.10.03

Flexible Magnetoreceptor with Tunable Intrinsic Logic for On-Skin Touchless Human-Machine Interfaces Pavlo Makushko^{1,2}, Eduardo Sergio Oliveros Mata¹, Gilbert Santiago Cañón Bermúdez¹, Mariam Hassan^{3,4}, Sara Laureti³, Christian Rinaldi³, Federico Fagiani⁵, Gianni Barucca⁴, Nataliia Schmidt⁶, Yevhen Zabala^{1,7}, Tobias Kosub¹, Rico Illing¹, Oleksii Volkov¹, Igor Vladymyrskyi², Juergen Fassbender¹, Manfred Albrecht⁶, Gaspare Varvaro³ and Denys Makarov¹; ¹Helmholtz-Zentrum Dresden-Rossendorf, Germany; ²National Technical University of Ukraine "Igor Sikorsky Kyiv Polytechnic Institute", Ukraine; ³Consiglio Nazionale delle Ricerche, Istituto di Struttura della Materia, Italy; ⁴Università Politecnica delle Marche, Italy; ⁵Politecnico di Milano, Italy; ⁶Institute of Physics, University of Augsburg, Germany; ⁷The H. Niewodniczanski Institute of Nuclear Physics, Polish Academy of Sciences, Poland

Flexible magnetoreceptive electronic skins are game changer for prospective personal appliances, human-machine interactions and augmented reality applications^[1]. Mechanically compliant magnetoresistive sensors have been introduced as touchless human-machine interfaces enabling the interaction with magnetic objects by means of proximity sensing, motion, and orientation tracking features^[2,3]. Although basic interactive functionality has been demonstrated, the current on-skin magnetoreceptors are not yet employed as advanced spintronics-enabled switches and logic elements for skin compliant electronics. The major limitation remains primarily due to the use of magnetic layer stacks, which are in-plane magnetized and, hence, are mainly sensitive to magnetic fields oriented within the sensor plane.

Introducing flexible Hall effect sensors^[4,5] could provide a solution to this conundrum, however, they cannot be intrinsically tuned to be bistable as needed for switches, and thus require additional flexible electronic modules. Considering the lower performance of flexible electronics compared to their rigid counterparts in terms of integration density and speed^[6], full-fledged interactive systems should be built based on smart sensors with intrinsic logic functionality, which can be tailored by the material properties rather than by the circuit design.

Here, we present the first mechanically flexible spin valve switch sensitive to the out-of-plane magnetic fields^[7]. The spin valve device is realized on a flexible polyethylene naphthalate (PEN) foil relying on Co/Pd multilayers with perpendicular magnetic anisotropy and synthetic antiferromagnet as a reference layer. By tuning the strength of magnetic coupling between free and reference layers we can tailor the functionality of the flexible device to act as a momentary or permanent (latching) switch. We show mechanical stability of the devices as they retain performance upon bending up to 3.5 mm bending radius and withstand more than 600 bending cycles without sacrificing their functionality. Due to the intrinsic memory function, the magnetic latching switches can reliably operate in an environment with strong magnetic disturbances.

Unambiguous interpretation of the out-of-plane magnetic fields provides intuitive understanding of the input stimuli and prevents from false triggering. We demonstrate the performance of our device as a touchless interactive interface for augmented reality system as well as its tolerance to the magnetic field disturbances. We showcase the great potential of this new kind of flexible magnetoreceptive functional elements for realization as on-skin human-machine interfaces for virtual- and augmented reality applications.

- [1] D. Makarov, M. Melzer, D. Karnaushenko, and O. G. Schmidt, *Applied Physics Reviews* **3**, 011101 (2016).
- [2] M. Melzer, M. Kaltenbrunner, D. Makarov, D. Karnaushenko, D. Karnaushenko, T. Sekitani, T. Someya, and O. G. Schmidt, *Nature Communications* **6**, 6080 (2015).
- [3] G. S. C. Bermúdez, H. Fuchs, L. Bischoff, J. Fassbender, and D. Makarov, *Nature Electronics* **1**, 589 (2018).
- [4] Z. Wang, M. Shaygan, M. Otto, D. Schall, and D. Neumaier, *Nanoscale* **8**, 7683 (2016).
- [5] H. Heidari, E. Bonizzoni, U. Gatti, F. Maloberti, and R. Dahiya, *IEEE Sensors Journal* **16**, 8736 (2016).
- [6] G. A. Salvatore, N. Münzenrieder, T. Kinkeldei, L. Petti, C. Zysset, I. Strebel, L. Büthe, and G. Tröster, *Nature Communications* **5**, 2982 (2014).
- [7] P. Makushko, E. S. O. Mata, G. S. C. Bermúdez, M. Hassan, S. Laureti, C. Rinaldi, F. Fagiani, G. Barucca, N. Schmidt, Y. Zabala, T. Kosub, R. Illing, O. Volkov, I. Vladymyrskyi, J. Fassbender, M. Albrecht, G. Varvaro, and D. Makarov, *Advanced Functional Materials* 2101089 (2021).

4:45 PM *SB07.12.05

Novel Electroactive Interfaces for Biomedical Applications Jadranka Travas-Sejdic; The University of Auckland, New Zealand

Conducting polymers (CPs) are emerging as one of the most promising functional materials for bioelectronics and biointerfaces due to their high biocompatibility, intrinsic electrical and ionic conductivity, tunable mechanical properties and the capability of being functionalized through chemical modification.

In this presentation, I will discuss novel bioelectronic materials and devices, based on conducting polymers, as well as a direct printing technique, useful in making both 2D and 3D polymer electronics. The examples will include: (i) electrochemically switchable, flexible, electrospun, microporous substrates for

selective captures and releases of intact extracellular vesicles[1] and (ii) 3D printed polymer microelectrode arrays for 3D electrical stimulation of neural stem cells[2].

References:

- [1] Akbarinejad A; Hisey, C.; Brewster, Diane ; Ashraf, J.; Chang, V.; Sabet, S.; Nursalim, Y.; Lucarelli, V.; Blenkiron, C.; Chamley, L.; Barker, D.; Williams, D.; Evans, C.; Travas-Sejdic, J., Novel Electrochemically Switchable, Flexible, Microporous Cloth that Selectively Captures, Releases and Concentrates Intact Extracellular Vesicles, ACS Applied Materials and Interfaces, 2020,12, 35, 39005–39013
- [2] E. Tomaskovic-Crook, P. Zhang, A. Ahtiainen, H. Kaisvuo, C.-Y. Lee, S. Beirne, Z. Agrawe, D. Svirskis, J. Hyttinen, G. G Wallace, J. Travas-Sejdic (co-corresponding author), J. M Crook, Human Neural Tissues from Neural Stem Cells Using Conductive Biogel and Printed Polymer Microelectrode Arrays for 3D Electrical Stimulation, Advanced Healthcare Materials, 2019, 8, 1900425

5:15 PM BREAK

SESSION SB07.11: Poster Session II: Soft, Healable Materials and Devices for Biological Interfaces and Wearables
Session Chairs: Fabio Cicoira and Shiming Zhang
Monday Afternoon, December 6, 2021
SB07-Virtual

9:00 PM SB07.11.02

Highly Conductive, Self-Healable and Stretchable Solid-State Ionic Conductors Minsu Kim, Dae Hyun Cho, Kyunggook Cho and Keun Hyung Lee; Inha University, Korea (the Republic of)

Solid-state nonvolatile ionic conductors, known as ionogels, consisting of polymer network and ionic liquid have attracted significant attention as promising solid electrolytes for electrical and electrochemical devices because of their outstanding physicochemical properties including low vapor pressure, high ionic conductivity, and superior mechanical property including stretchability and elasticity. For the long-term operation of deformable devices, the active layers can properly function without performance degradation from the external mechanical stress including large and/or successive strain. The introduction of self-healing functionality in ionogels prevents physical and functional degradation from the mechanical breakdown and thus significantly improves their tolerance to the external stress. In this work, we developed highly conductive and self-healable solid electrolytes with outstanding stretchability (fracture strains more than 600%). The effect component ions on the mechanical and electrical properties were systemically investigated. In addition, these ion gels were successfully employed in stretchable strain sensors and the healed devices displayed nearly identical electrical signals compared to undamaged sensors.

9:05 PM SB07.11.03

A Textile-Based Stretchable Supercapacitor with Wide Temperature Tolerance for Wearable Application Hanchan Lee and Jeong Sook Ha; Korea University, Korea (the Republic of)

Along with the extensive development of wearable electronics for integration into the body or clothes, textile-based devices have attracted great attention. At the same time, the necessity for wearable energy storage devices stable under harsh environmental conditions of temperature and humidity as well as deformations of bending and stretching has been also increased, for a reliable application to daily lives. In this work, a textile-based stretchable supercapacitor with a tolerance over a wide temperature range between -30 and 80 °C is reported. The textile-based stretchable supercapacitor with MWCNT/RGO nanocomposite electrodes and ionic liquid-based gel-type electrolyte exhibits high electrochemical performance, temperature tolerance, and mechanical stability: High areal capacitances of 28.0, 30.4, and 30.6 mF/cm² are obtained at -30 , 25, and 80 °C temperatures, respectively, while the capacitance remains stable over three repeated cycles of cooling and heating between -30 and 80 °C. The fabricated supercapacitor is stable under stretching up to 50% and 1000 repetitive cycles of stretching by 30%. With the supercapacitors, a temperature sensor and a liquid crystal display is simultaneously operated in the temperature range between -20 and 80 °C. The supercapacitors woven into a nylon glove drive a micro-LED under the bending of the index finger and retain the capacitance after being immersed in water for a few days. This work demonstrates the high potential application of our textile supercapacitor as a wearable energy storage device under severe conditions of high/low temperatures, high humidity, and movements of the body.

9:10 PM SB07.11.04

Stretchable QD-LED Array for Bio-Signal Monitoring Yonghui Lee and Jeong Sook Ha; Korea University, Korea (the Republic of)

Display device that can visually present various bio-signals is one of the future core technologies required for skin attachable wearable electronics. Quantum dot light emitting diode (QD-LED), which can be used for high performance display devices, exhibits many advantages such as a narrow bandwidth, a high color purity, a high environmental stability, easy and fast processing, and a high brightness at low voltages. In this study, we report on the fabrication of a stretchable QD-LED array for the visual display of the skin-attached sensor signals of the body movements and skin temperatures. On a stretchable elastomer substrate of Ecoflex/PDMS, an array of a rigid NOA63 islands is formed. Then, the array of CdSe/ZnS QD-LEDs are fabricated on top of the islands array and electrically connected by using liquid metal Galinstan interconnections. Of particular importance, a flexible and high-performance Au grid/Ethylene glycol doped PEDOT:PSS transparent electrode was used as a replacement of conventionally used ITO for stable performance of the QD-LEDs under deformations. Such a design architecture can minimize the strain applied to the QD-LEDs via concentrating the strain onto the soft elastomer film substrate and the Galinstan interconnections. As a result, the fabricated QD-LED array exhibits a stable operation under both 50% uniaxial and 30% biaxial strains. After attachment of the stretchable QD-LED array, the extent of knee bending, and the change of skin temperature are displayed as a change in the pattern of the QD-LED array. This work demonstrates the potential application of our stretchable array of QD-LEDs to facile and daily monitoring of health conditions in the form of visual display.

9:15 PM SB07.11.05

Self-Healable Organic Electrochemical Transistors Xihu Wu and Wei Lin Leong; NTU, Singapore

The use of conjugated polymers for bioelectronics applications is especially attractive due to their favorable properties, namely, chemical stability, facile processability, biocompatibility as well as enabling an amiable interface with living cells and tissues. One new class of devices that leverage these many attributes of conjugated polymers is organic electrochemical transistors (OECTs). Owing to their high transconductance and thus capable of amplifying

small biologic or ionic signals into electronic output. OECTs are especially promising for diverse biomedical applications such as the detection of ions, metabolites, alcohol, DNA, and cells. Poly(3,4-ethylenedioxythiophene):poly(styrenesulfonate) (PEDOT:PSS) has been extensively used as self-healable OECT channel layer and demonstrated outstanding transconductance values.^[1] The OECT performances are influenced by the combination of ionic-electronic conduction properties of the active material. Although there are not many reports on self-healable PEDOT:PSS, there have been efforts to improve the mechanical properties of PEDOT:PSS. One of the challenges in developing self-healable conjugated polymers for organic electrochemical transistors (OECTs) lie in maintaining good both ionic and electronic properties. Incorporation of stretchable polymer matrix, such as polyurethane, polyacrylic acid, polyethylene glycol, natural rubber, have been done to boost the self-healability and mechanical properties of PEDOT:PSS films, however, these composites struggle with either poor ionic conductivity or poor electrical conductivity even with relatively high PEDOT:PSS content. In this text, we demonstrate a solid state OECT that is self-healable and possess good electrical performance, by utilizing a matrix of PEDOT:PSS and non-ionic surfactant, Triton X-100 as channel, and ion conducting poly(vinyl alcohol) hydrogel as a quasi-solid-state polymer electrolyte. Details of the self-healing mechanism, device performance including the transconductance, response time and electrochemical doping/de-doping stability before and after healing were presented. These findings will contribute to the development of high performing and robust OECTs for wearable bioelectronic devices.

9:20 PM SB07.11.06

Breathable and Waterproof Fibrous Organic Electrochemical Transistors for On-Skin Electronics [Shuai Chen](#) and Wei Lin Leong; Nanyang technological university, Singapore

Recently emerged on-skin electronics with applications in human-machine interfaces and on-body healthy monitoring call for the development of high-performance skin-like electrodes and semiconducting polymers. The development of waterproof and breathable membranes that can provide a high level of protection for human skins and a comfortable contact between electronics and human skin are the pressing demands for on-skin electronics. However, major challenges still remain such as the limited durability and permeability of gas and liquid, which hindering the long-term stability and reusability. Therefore, it is highly desirable to develop a type of. Herein, we reported a fibrous electrolyte membrane containing polymer matrix and ionic liquid by electrospinning method, which is highly robust, breathable, waterproof, and conformal with human skin, after bonding a parylene layer with fibers. In addition, the parylene layer can also improve the connection of junctions between fibers, which showed improved conductivity of electrodes and organic semiconducting layer. Serving as fibrous substrate and electrolyte of organic electrochemical transistors (OECTs), the ions can freely transport along the fibers and across the bridged fibers and the gate bias can control the ionic injection from the fibrous electrolyte to channel to modulate the conductivity of organic semiconductor. The waterproof and breathable capabilities of fibrous OECTs enable comfortable contact after attaching to human skin, which can also reduce the interfacial impedance to achieve local amplification of the high-quality electrocardiography signals. These results indicated that our fibrous OECTs have huge potential for on-skin electronics such as non-invasive medical monitoring, sophisticated electronics, and electronics textiles.

9:25 PM SB07.11.07

Interactive Electrochromic Display of Bio-Signals [Dong Sik Kim](#) and Jeong Sook Ha; Korea University, Korea (the Republic of)

We report on the fabrication of an interactive display system consisting of a stretchable array of electrochromic devices and temperature and strain sensors for visual display of a skin temperature and bending of wrist. The electrochromic device is prepared by coating poly(3-hexylthiophene) and tungsten trioxide as electrochromic materials on a flexible and transparent electrode of indium tin oxide coated polyethylene terephthalate, and subsequent assembly of thus prepared electrodes using a gel-type electrolyte of Li-doped 1-butyl-3-methylimidazolium bis(trifluoromethylsulfonyl)imide/poly(methyl methacrylate). The fabricated ECD exhibits three different colors due to the redox reaction of the electrochromic materials at the corresponding potential: magenta, violet, and blue at -1.5 V, 0.5 V, and 1.5 V, respectively. By using the patterned liquid metal Galinstan interconnections, a stretchable array of the ECDs is fabricated based on a strain relieving mechanism with an island-bridge design resulting in a mechanical stability under repetitive stretching up-to 30%.

A high performance strain sensor is fabricated by embedding fragmentized graphene foam (GF) inside poly(dimethylsiloxane) thin film. Also, a temperature sensor is prepared by embedding multi-walled carbon nanotubes/polyaniline composite into poly(vinyl alcohol) film. With the integrated system, strains due to wrist bending and the skin temperatures measured by the sensors are displayed as the changes in the color pattern of the ECD array via an aid of an Arduino circuit. This work demonstrates a high potential application of our system to wearable healthcare devices with instant recognition of various bio-signals.

9:30 PM SB07.11.08

Room-Temperature Growth of Ultra-Flat Transparent Conducting ZnO Thin Films on the Morphologically and Chemically Surface-Modified Polymer Substrates for Flexible Optoelectronics Devices [Tomoaki Oga](#)¹, [Naho Kaneko](#)¹, [Kenta Kaneko](#)¹, [Satoru Kaneko](#)^{2,1}, [Akifumi Matsuda](#)¹ and [Mamoru Yoshimoto](#)¹; ¹Tokyo Institute of Technology, Japan; ²Kanagawa Institute of Industrial Science and Technology, Japan

The combination of flexible transparent polymer substrates and wide band-gap oxide semiconductors with superior electrical and/or magnetic properties is highly expected to be applied to the wearable optoelectronics devices. Most of the optoelectronics devices using the highly crystal orientated oxide semiconductors such as ZnO thin films are fabricated on the glasses or single crystal substrates at high temperatures. On the other hand, thermoplastic cyclic olefin polymers (COPs) used in this study have extremely low hygroscopicity, high transparency and relatively high heatproof temperatures (about 150°C), so they are the possible flexible substrates applied to the wearable optoelectronics and bioelectronics devices. For growth of the highly crystalline oxide thin films on the polymer substrates with irregularly roughened surfaces, we had better employ the thin film techniques to control the nucleation and growth direction of oxides at low temperatures as well as polymer surface modification.

So far, we reported the nanoscale smoothening and patterning on the polyimide or PMMA acrylic polymer substrates, which had the surfaces with 0.3 nm-high atomic steps and about 500 nm-wide ultra-flat terraces by applying thermal nanoimprinting using atomically stepped sapphire molds.[1] As a result, the crystallinity and surface roughness of oxide thin films deposited on the surface-controlled polymer substrates were greatly improved.[2] In this study, we investigated the effects of oxide buffer-layer insertion as well as nanoimprinted surface modification of the COP polymer substrates on the crystal growth manner and electronic properties of ZnO thin films deposited on the substrates at room-temperature. Development of the advanced low-temperature growth techniques of high-quality functional oxide thin films on the flexible polymers will open the new field in the application of oxide-polymer hybrid flexible and wearable devices.

In the experiment, thermoplastic COP (ZF16-188, ZEON; $T_g \sim 163^\circ\text{C}$, $t \sim 188 \mu\text{m}$) sheets were used as polymer substrates. Two kinds of surface modifications of COP substrates were carried out successively as follows; (1) thermal nanoimprinting of 0.3 nm-height atomic-step array and terrace pattern using $\alpha\text{-Al}_2\text{O}_3$ single crystal molds (2 MPa, 180°C , 5 min, in 10^3 Pa-Ar gas), and then (2) buffer layer insertion on the substrate by pulsed laser deposition (PLD) of an amorphous oxide thin film such as aluminum oxide or gallium oxide. Then, ZnO semiconductor thin films ($t \sim 40 \text{ nm}$) were grown at room-temperature on the surface-modified, and as-received COP substrates by PLD using a sintered ZnO target and a KrF excimer laser ($\lambda = 248 \text{ nm}$, $d \sim 20 \text{ ns}$) under O_2 gas of 10^{-3} Pa .

As a result, the ZnO thin film grown on the nanoimprinted and Ga_2O_3 buffered COP substrate exhibited an ultra-flat surface with 0.3 nm-high atomic step-and-terrace pattern and RMS roughness of about 0.15 nm. From XRD and RHEED measurements, it was found that the present ZnO thin film had a drastic improvement in c-axis oriented growth and crystallinity compared to that grown on the untreated COP substrate. Furthermore, the electric conductivity of

the ZnO thin films on the surface-modified COP substrate was increased by one-order of magnitude to $4 \times 10^{-2} \Omega \text{cm}$ than that on the untreated substrate. Thus, the present physical and chemical surface modification of the polymer substrate was considered to enhance the homogeneous nucleation and crystal orientation at the initial stage of oxide thin film growth, resulting in the development of the ultra-flat surface and c-axis oriented crystal growth of the ZnO thin film on the COP substrate.

[1] G. Tan et al., *Nanotech.*, **27**, 295603 (2016), [2] T. Oga et al., *Jpn. J. Appl. Phys.*, **59**, 128001 (2020).

9:35 PM SB07.11.09

Nano-Scale Growth Study of Calcium Phosphate Thin Films on the Nanopatterned and Chemically-Modified Polymer Sheets for Flexible Apatite-Based Biodevices Naho Kaneko¹, Yuto Maeda¹, Tomoaki Oga¹, Kazuki Watanabe¹, Kenta Kaneko¹, Tomohiro Hayashi¹, Evan Angelo Q. Mondarte¹, Satoru Kaneko^{2,1}, Akifumi Matsuda¹ and Mamoru Yoshimoto¹; ¹Tokyo Institute of Technology, Japan; ²Kanagawa Institute of Industrial Science and Technology, Japan

Biocompatibility of the devices is an important factor for application in the biomedical field. Calcium phosphate (Ca-P), particularly hydroxyapatite (HAp), is well known as bioceramics with high biocompatibility and Ca-P materials are used in biosensors due to unique protein adsorption [1]. Since flexibility and stretchability are essential factors for future wearable electronics, electronic skin, implantable biomedical devices, and soft robotics [2], combination of flexible polymer substrates and Ca-P thin film would contribute to development of new biodevices. On the other hand, the nanoscale size and shape of Ca-P crystals and aggregates are considered to play critical roles in their applications [3]. Deposition and growth characterization of Ca-P thin films on the nanopatterned polymer substrates is expected to lead to nanoscale control of Ca-P thin film growth.

So far, we have reported atomic-scale nanopatterning of polymer sheets such as polyimide (PI) and acrylic resin (PMMA) by applying originally developed thermal nanoimprint technique, in which we could fabricate the 0.3 nm-high atomically stepped patterns on the PI and PMMA sheets [4]. The nanoscale-aligned surface morphology on the polymer substrates was found to control the crystal nucleation and growth direction of functional inorganic thin films on their surfaces [5]. In this study, we investigated the nanoscale growth manner of calcium phosphate thin films on the nanopatterned and chemically-modified polymer sheets using the ex-situ and liquid-environment in-situ AFM for development of the flexible apatite-based biodevices.

In the experiment, the Ca-P thin films were grown on the polyethylene terephthalate (PET) sheets with atomically stepped patterns, which pattern was transcribed on a PET surface by nanoimprinting (pressure of 0.2 MPa for 5 min at 85°C in air) using a replica PI (Mitsui Chemicals Co., ECRIO® VICT-Bnp, $T_g=265^\circ\text{C}$). The nanopattern replica mold was fabricated by transcription of 1 nm-high bunching stepped sapphire mold [4]. Before thin film growth, the transcribed atomically stepped PET substrates were “modified” by treatment in NaOH aq. (0.1 M) at 60°C for 10 min to form carboxylate groups on the surface. The atomically stepped patterns were kept on the PET substrate even after the alkali-treatment. For Ca-P thin film growth, the surface-modified PET substrate was immersed in Hanks' Balanced Salt Solution (HBSS(+); Fuji-Film Wako Pure Chemical Co., No. 082-08961) at 37°C for 1 h. After deposition, the samples were picked up, cleaned with ultrapure water, and dried using nitrogen blower.

From ex-situ AFM observations, precipitation of nanoparticles was observed on the entire substrate. For the analysis of the particle, watershed algorithm was used. The particle distribution result indicated that the statistical mode radius and height of the nanoparticles were about 25 nm and about 3 nm, respectively. The size of the grown nanoparticles was similar to that of the aggregates of prenucleation clusters, that is, the basic unit of the final Ca-P crystals reported previously [6]. These AFM observations would be expected to advance understanding of the initial growth of Ca-P materials on the polymer substrates, leading to the nanoscale design of flexible apatite-based biodevices.

[1] H. Zhang et al., *J. Electroanal. Chem.*, **624** (2008) 79.

[2] R. Dong et al., *Adv. Mater.*, **31** (2019) 1805033.

[3] K. Lin et al., *Acta Biomater.*, **10** (2014) 4071.

[4] G. Tan et al., *Nanotech.*, **27** (2016) 295603.

[5] T. Oga et al., *Jpn. J. Appl. Phys.*, **59** (2020) 128001.

[6] A. Det et al., *Nat. Mater.*, **9** (2010) 1010.

9:40 PM SB07.11.11

Soft, Self-Healing and Highly Adhesive Hydrogels for Human Healthcare Xin Zhou and Fabio Cicoira; Polytechnique Montréal, Canada

Soft, healable, and adhesive conductive materials with Young's modulus matching biological tissues are highly desired for bioelectronics. Here, we report soft, self-healing, stretchable, highly adhesive and conductive hydrogels obtained by mixing polyvinyl alcohol, sodium tetraborate, and a commercial screen printing paste containing Poly (3,4-ethylenedioxythiophene) doped with polystyrene sulfonate (PEDOT:PSS) and diol additives. The as-prepared hydrogels exhibited high plastic stretchability (>1000%), high adhesion on pig skin (1.96 N/cm^2), a moderate conductivity, a low compressive modulus (0.3 - 3.7 KPa), and remarkable self-healing properties. Epidermal electrodes prepared using the hydrogel demonstrated high-quality recording of electrocardiography (ECG) and electromyography (EMG) signals compared to commercial Ag/AgCl gel electrodes.

9:45 PM SB07.11.12

Epidermal Graphene Sensors and Machine Learning for Estimating Swallowed Volume Beril Polat; University of California, San Diego, United States

Assessment of liquid intake is necessary to obtain a complete picture of an individual's hydration status. Measurements using state-of-the-art wearable devices have been demonstrated, but none of these devices have combined high sensitivity, unobtrusiveness, and automated estimation of volume, i.e., using machine learning. Such a capability would have immense value in a variety of medical contexts, such as monitoring patients with dysphagia or the performance of athletes. Here, an epidermal sensor platform is combined with machine learning to measure swallowed liquid volume based on signals obtained from the surface of the skin. The key component of the device is a composite piezoresistive sensor consisting of single-layer graphene decorated with metallic nanoislands and coated with a highly plasticized form of the conductive polymer poly(3,4-ethylenedioxythiophene):poly(styrenesulfonate) (PEDOT:PSS). Surface electromyography (sEMG) signals obtained with conventional electrodes are used in concert with the strain measurements. The use of strain and sEMG measurements together both (1) improve the accuracy of estimated volumes and (2) permit the differentiation of swallowing from motion artifacts. In a cohort consisting of 11 participants, the combined measurements of strain and sEMG—processed by the machine learning algorithm—were able to estimate unknown swallowed volumes cumulatively between 5 to 30 mL of water with greater than 92% accuracy. Ultimately, this system holds promise for numerous applications in sports medicine, rehabilitation, and the detection of nascent dysfunction in swallowing.

9:50 PM SB07.11.13

Electrochemical and Operational Stability of Ion-Gel Gated Organic Transistors Mona Azimi and Fabio Cicoira; Polytechnique Montreal, Canada

Electrolyte gated transistors (EGTs) benefits from low operating voltage and high charge carrier mobility. However, concerns about the confinement of liquid electrolytes and inhibition of leakage of liquid are of utmost importance in the fabrication of EGTs. Ion gels are a suitable solution for solving the aforementioned problems. In this work, we fabricated a low voltage ion-gel gated organic transistors based on donor-acceptor copolymer, poly(N-alkyldiketopyrrolo-pyrrole-dithienylthieno[3,2-b]thiophene) (DPP-DTT). We studied the transistor characterization of ion-gel gated transistors using ionic

liquid-based gel and hydrogel. Gels based on ionic liquid composed of (1-ethyl-3-methylimidazolium bis(trifluoromethylsulfonyl)imide ([EMIM][TFSI]) and poly(vinylidene fluoride-co-hexafluoropropylene) (P(VDF-HFP)). Electrochemical and operational stability of ionic liquid-based gel gated devices in ambient condition were conducted, and the results revealed significant stability, most likely due to the well-ordered compact lamellar structure of the organic semiconductor. In addition, hydrogel-based on polyvinyl alcohol (PVA) and sodium chloride (NaCl) was used as gating medium. The operational stability of the hydrogel gated transistor is also studied in ambient and different relative humidity conditions. Totally, this study will contribute to development of highly stable organic transistors using ionic liquid-based gels and hydrogels as gating media.

SESSION SB07.12: Soft, Healable Materials and Devices for Biological Interfaces and Wearables IX
Session Chairs: Fabio Cicoira, Wei Lin Leong and Shiming Zhang
Tuesday Morning, December 7, 2021
SB07-Virtual

8:00 AM *SB07.12.01

Organic Electrochemical Transistors for Protein Detection Sahika Inal; King Abdullah University of Science and Technology, Saudi Arabia

Conjugated polymers provide a unique toolbox for establishing electrical communication with biological systems. In this talk, I will show how these materials are used in organic electrochemical transistors (OECTs) to detect biological species in physiological media. I will introduce two types of OECT based sensors; one that detects Alzheimer's disease biomarkers with performance exceeding the state-of-the-art,^{1,2} and the other that detects coronavirus spike proteins at the physical limit.³ Having challenged these sensors with patient samples, I will discuss areas where proof-of-concept organic biosensor platforms may fail. By tackling each of these problems, we improve device performance to a level that marks a considerable step toward biochemical sensing of infectious and noninfectious disease biomarkers. I will highlight that the advances in biosensor device design stem from in-depth investigations of the active materials' transport properties, device operation principles and carefully designed biorecognition units.

S. Wustoni et al *Biosensors and Bioelectronics*, 2019, 143, 111561.

A. Koklu et al *ACS Nano* 2021,15, 8130.

K. Guo et al, *Nat. Biomed. Eng.* 2021 <https://doi.org/10.1038/s41551-021-00734-9>

8:30 AM SB07.12.02

Development of Biomimetic Hydrogel Skin Interfaces for Sweat Extraction and Analysis in Wearable Devices Tamoghna Saha, Tate Knisely, Jennifer Fang, Sneha Mukherjee, Michael Dickey and Orlin D. Velev; North Carolina State University, United States

Sweat is an essential biofluid for monitoring individuals' health as it contains several key biomarkers. However, sampling sweat for analysis is still challenging as most of the commercially available sweat sensing devices are either invasive in nature or work only during active perspiration. We demonstrate a new principle for the design of flexible and wearable patches, based on biomimetic hydrogel interface. These devices are capable of extracting sweat under both resting and actively perspiring conditions using osmotic pressure difference for pumping, and evaporation for liquid disposal.¹ The patch is composed of silicone that hosts a polyacrylamide hydrogel disk and a paper channel with an evaporation pad at the end. The hydrogel, which contacts the skin, is pre-equilibrated with glycerin, glucose, or NaCl solution to build up the desired osmotic strength to extract sweat from the skin, which is then sampled on a paper channel.² We investigate the performance of the patch using a model biomarker (dye) solution. *In-vitro* testing with a gelatin-based model skin platform revealed that both glucose and glycerin-infused gels facilitate high analyte accumulation on the evaporation pad, with glucose hydrogels having the highest driving pressure. The cumulative dye collection also depends on the dimensions of the paper channel, hydrogel area and paper pore size. Human trials show the potential to extract sweat and analyze it for lactate under both resting and non-resting conditions within a period of two hours. We used lactate as a concept demonstrator, as sweat appears to be more informative medium for lactate quantification than blood. The ability to measure lactate enables monitoring metabolism and oxidative stress levels in athletes and military personnel. Our group is currently investigating how this hydrogel enabled sweat sampling concept can be integrated in continuously operating wearable devices using enzymatic electrochemical sensors³, and with microneedle patches for long-term interstitial fluid (ISF) sampling.

1. Shay, T., Saha, T., Dickey, M.D., and Velev, O.D. (2020) *Biomicrofluidics*, **14**, 034112.

2. Saha, T., Fang, J., Mukherjee, S., Dickey, M.D., and Velev, O.D. (2021) *ACS Appl. Mater. Interfaces*, **13**, 8071.

3. Yokus, M.A., Saha, T., Fang, J., Dickey, M.D., Velev, O.D., and Daniele, M.A. (2019) *IEEE SENSORS*, 2019-October, 1-4.

8:45 AM SB07.12.03

Thermoplastic poly(2-methoxyethyl acrylate)-based Polyurethane and Its Antithrombogenicity Shunsuke Tazawa¹, Tomoki Maeda^{1,2}, Masamitsu Nakayama^{1,3} and Atsushi Hotta¹; ¹Keio University, Japan; ²Ibaraki University, Japan; ³Tokai University Graduate School of Medicine, Japan

In this study, thermoplastic poly(2-methoxyethyl acrylate)-based polyurethane (PMEA-based PU) with reversible crosslinkings constructed through hydrogen bonds, was synthesized by reversible-addition fragmentation transfer (RAFT) polymerization and polyaddition using diisocyanate. The newly synthesized thermoplastic PMEA-based PU possessed excellent antithrombogenicity.

Poly(2-methoxyethyl acrylate) (PMEA) is known as an excellent biocompatible liquid for its antithrombogenicity [1,2]. However, major applications of PMEA are always limited to antithrombogenic coating because the glass transition temperature of PMEA is around -30°C, meaning that PMEA is viscous liquid at room temperature. Therefore, by solidifying PMEA, the usage of PMEA will become significantly broadened as a bulk material. To obtain PMEA-based PU, hydroxyl-terminated PMEA (HO-PMEA-OH) was first synthesized by RAFT polymerization with a RAFT agent consisting of hydroxyl groups at both ends. Then, HO-PMEA-OH was reacted with diisocyanate to form urethane bonds for the introduction of hydrogen bonding. The synthesized HO-PMEA-OH by RAFT polymerization (the prepolymer of PMEA-based PU) was a viscous liquid. After the polyaddition reaction with diisocyanate, a solid standing film of PMEA-based PU could be obtained. The existence of the urethane bonds in PMEA-based PU was confirmed by NMR and FTIR. The existence of the hydrogen bonding in PMEA-based PU was also confirmed by FTIR.

Thermoplastic and mechanical properties of PMEA-based PU were analyzed by dynamic mechanical analysis (DMA). The storage modulus of PMEA-based PU was 2.3×10^5 Pa, while that of HO-PMEA-OH was 2.5×10^3 Pa. As for the thermoplastic property, the melting point of PMEA-based PU was 73°C, while HO-PMEA-OH was in the liquid state from 0°C to 100°C. All these results indicated that, by introducing reversible crosslinkings by hydrogen bonds, PMEA-based PU successfully became solid and thermoplastic.

Antithrombogenicity of PMEA-based PU was also evaluated through platelet-adhesion testing. The number of platelets on PMEA-based PU was 17 cells per $22,570 \mu\text{m}^2$. In fact, the numbers of platelets on fluorinated diamond-like carbon (F-DLC), a well-known highly antithrombogenic material [3], and on polycarbonate, a commercially used material in the medical field (e.g., the blood circuit) were 73 cells and 295 cells, respectively. The results of the

platelet adhesion test confirmed that PMEA-based PU possessed excellent antithrombogenicity compared to the conventional antithrombogenic materials.

References

- [1] C. Sato, M. Aoki and M. Tanaka, *Colloids Surf., B*, 2016, 145, 586–596.
- [2] K. Akamatsu, T. Furue, F. Han and S. Nakao, *Sep. Purif. Technol.*, 2013, 102, 157–162.
- [3] T. Hasebe, S. Nagashima, A. Kamijo, M. W. Moon, Y. Kashiwagi, A. Hotta, K. R. Lee, K. Takahashi, T. Yamagami, T. Suzuki, *Diamond Relat. Mater.* 2013, 38, 14-18.

9:00 AM SB07.12.04

Dynamic Defects, Bacterial Biofilms and Medical Device Infections Dalal Asker, Tarek Awad, Desmond van den Berg and Benjamin Hatton; University of Toronto, Canada

Indwelling medical devices such as catheters, prosthetic heart valves and reconstructive implants are susceptible to microbial biofilm colony formation and serious infection. Does mechanical deformation of elastomer biomaterials (such as PDMS silicone) affect microbial surface colonization? Recently we found that bacteria prefer the tensile (convex) side of deformed silicone tubing, by about a factor of 3-4 times, over the compressive (concave) side. Why should this be? In general, there is not a very good understanding of microbial-surface interactions at early stages of growth. But we do know they're very sensitive to surface defects and roughness (scratches, grooves, etc). We have recently shown that elastomers such as silicone (polydimethylsiloxane, PDMS) or polyurethane form surface microcracks much more readily than has been previously recognized, and these surface defects become primary sites for initial microbial attachment. We show that even mild mechanical contact or deformation of PDMS materials, such as by surface wiping, is enough to generate these microcracks. The deformation of silicone tubing then appears to open up these microcracks, as dynamic defects that become sites for initial attachment of *Pseudomonas aeruginosa*. That a typical, mild deformation of elastomer medical devices can make them significantly more susceptible to infection appears to be a previously unrecognized mechanism for medical device-associated infections. We speculate that a wide range of elastomeric medical devices and components, from silicone breast implants to prosthetic heart valves and vascular grafts may be susceptible, and we present simulation data about localized strains in some typical devices that may be problematic.

SESSION SB07.13: Soft, Healable Materials and Devices for Biological Interfaces and Wearables X
Session Chairs: Fabio Cicoira and Shiming Zhang
Tuesday Afternoon, December 7, 2021
SB07-Virtual

1:30 PM *SB07.13.01

Hybrid Approaches to Soft Electronics Benjamin C. Tee; National University of Singapore, Singapore

Wearable electronics closely contacts the skin interface to collect health parameters and understand the environment¹. For devices that contact soft tissues such as skin, appropriate mechanical moduli is required to integrate more seamlessly into human activities. Simultaneously, exciting research in materials science and engineering of soft materials can enable self-healing functions in artificial materials that repair autonomously like biological skin^{2,3}. In this talk, I will discuss our work in using a hybrid soft-hard approach to create soft devices that can bend and stretch. Such approaches can also lower the viscoelastic properties of soft materials for sensing applications⁴. These devices can be used in wearable or human-machine interface technologies for healthcare applications⁵.

References

1. Zhao, Y. et al. (2019). Design and applications of stretchable and self-healable conductors for soft electronics. *Nano Convergence*.
2. Guo, H. et al. (2020). Artificially innervated self-healing foams as synthetic piezo-impedance sensor skins. *Nature Communications*.
3. Cao, Y., et al. (2019). Self-healing electronic skins for aquatic environments. *Nature Electronics*.
4. Yao, H. et al. (2020). Near-hysteresis-free soft tactile electronic skins for wearables and reliable machine learning. *Proceedings of the National Academy of Sciences*.
5. Yao, H. et al. (2021). Augmented Reality Interfaces Using Virtual Customization of Microstructured Electronic Skin Sensor Sensitivity Performances. *Advanced Functional Materials*.

2:00 PM SB07.13.02

Pushing OECTs Toward Wearables—The Development of a Miniaturized Device Characterization System Xinyu Tian¹ and Shiming Zhang^{1,2}; ¹The University of Hong Kong, China; ²Terasaki Institute, United States

Portable and wearable devices are highly demanded to achieve the goal of decentralized and personalized healthcare. Organic electrochemical transistors (OECTs), which combine advantages of both an electrochemical cell and a microelectronic transistor, have high signal amplification ability and are energy efficient. OECTs have been widely explored for application in emerging research areas including health monitoring, bioelectronic interfacing, and neuromorphic computing. However, despite these advances, a miniaturized OECT characterization system is still missing, which is an indispensable building block to realize the feat of fully integrated OECTs for portable and wearable applications. The development of a miniaturized OECT characterization system is challenging because it requires transdisciplinary efforts among device engineering, microelectronics, embedded systems, wireless communication, and software engineering.

In this work, we report our recent breakthrough on the development of the world's first miniaturized system, namely "personalized electronic reader for electrochemical transistors" (PERfECT), for portable OECT characterizations. Our PERfECT is a coin-sized flexible module that measures an OECT wirelessly and is controllable with a personalized APP on a mobile. Experimental validation demonstrates that PERfECT can measure various kinds of electrolyte-gated transistors including ECTs and FETs, with a low current detection limit of 1 nA, a high sampling rate of 200K per second, a gate pulse as short as 20 μ s. The figure of merits of PERfECT is comparable to that of lab-used bulky equipment. Moreover, PERfECT is equipped with all functions of an electrochemical workstation such as cyclic voltammetry (CV), amperometry, potentiometry, and electrochemical impedance spectroscopy (EIS). These merits, altogether, make PERfECT a highly pursued system for commercial uses.

PERfECT contributes to the OECT community by bridging the last-mile gap between OECTs and a fully integrated miniaturized system for portable and

wearable applications.

2:15 PM SB07.13.04

Localized Heating of Lab-on-Chip Devices by Flexible Transparent Electrodes Based on Silver Nanowire Networks Dorina T. Papanastasiou¹, Abderrahime Sekkat¹, Viet Huong Nguyen², Magali Le Goff³, Carmen Jimenez¹, David Munoz-Rojas¹, Franz Bruckert¹ and Daniel Bellet¹; ¹LMGP-Grenoble INP-CNRS-UGA, France; ²Phenikaa University, Viet Nam; ³Université Grenoble Alpes, France

In situ biological observations present challenges related to the accurate temperature control of the biological medium. Several heating elements have been coupled with microfluidic systems during fluorescence monitoring under a microscope. However, they are either complicated or costly to be mounted, or they are not transparent enough to facilitate the observations. Very few examples have reported the use of transparent heater (TH) devices for *in situ* experiments. Among them, traditional technologies, like the indium tin oxide (ITO), suffer from serious drawbacks like the scarcity of raw material and the brittleness of the film. Silver nanowire (AgNW) networks are one of the most promising alternative transparent electrodes (TE) since: i/ they exhibit excellent optical and electrical properties, ii/ they are very flexible, and iii/ they can be fabricated by low-cost, solution-based techniques suitable for large scale production.

In the present work we propose a transparent, flexible, light-weight transparent heater integrated to a lab-on-chip set-up. Using a low power-supply, we are able to accurately control the thermal cycles inside the microfluidic channels and reach efficient heating-cooling rates comparable to other laboratory and/or commercial instruments. In addition, localized heating with micrometric resolution can be achieved by using a single TH elements and applying the same voltage. To do so, we have used a simple approach of putting 3D-printed masks during the spray deposition of the AgNW networks. These patterned regions have different density, resulting to different local electrical resistance. This can be exploited for example for heating selectively different microfluidic channels at different temperatures. Physical modelling can be supplementary used to predict and design such transparent heaters. Meanwhile, in order to ensure a stable and reproducible performance, we have encapsulated the AgNW network with a thin, protective zinc oxide (ZnO) film. As already demonstrated in our previous studies, such AgNW/ZnO nanocomposites retains the high transparency and flexibility of bare networks. Developed by atmospheric-pressure atomic layer deposition (AP-SALD), it can be done in the open-air (i.e. without the need of a deposition chamber) and rather low temperatures, which makes it compatible with up-scalable processes and very promising for industrial implementation.

2:30 PM *SB07.13.05

Soft Rubbery Bioelectronics Cunjiang Yu; University of Houston, United States

Seamlessly merging electronics with biology is of imminent importance in addressing grand societal challenges in health and joy of living. However, the main challenge lies in the huge mechanical mismatch between the current form of rigid electronics and the soft nature of biology. Our approach is to create rubbery electronics to solve the challenge. Rubbery electronics is a new type of electronics, with tissue-like softness and mechanical stretchability, which is constructed all based on elastic rubbery electronic materials. Rubbery electronics allows seamless integration with soft deformable tissues and organs. The innovations in rubbery electronic materials and devices set the foundation for rubbery electronics, integrated system and their broad usages, such as wearables and implantables. The presentation will firstly briefly present our recent results on the development of materials, manufacturing and devices, including rubbery semiconductors, fully rubbery transistors, logic gates, integrated electronics, and sensors. It will then demonstrate rubbery implantable and wearable electronics to showcase their vast implications in biomedical area with their clear merits of being able to harmonically interface with soft human tissues and organs for sensing, diagnosis, preventing and therapy purposes. In particular, a rubbery bioelectronic epicardial patch and a drawn-on-skin (DoS) motion-artifact free wearable bioelectronics will be demonstrated.

SESSION SB07.14: Soft, Healable Materials and Devices for Biological Interfaces and Wearables XI

Session Chair: Fabio Cicoira

Tuesday Afternoon, December 7, 2021

SB07-Virtual

4:00 PM SB07.14.02

Self-Healing Liquid Metal Composite for Reconfigurable and Recyclable Soft Electronics Ravi Tutika, A B M Tahidul Haque and Michael D. Bartlett; Virginia Tech, United States

Soft electronics and robotics are in increasing demand for diverse applications. However, in contrast to rigid electronics, which are protected with stiff external supports and enclosures when deployed, soft electronics must maintain extreme compliance and cannot use these traditional means of protection, which can render them vulnerable and lead to premature disposal. This creates a need for soft and stretchable functional materials with resilient and regenerative properties to survive in unstructured environments. Here we show a liquid metal-elastomer-plasticizer composite for soft electronics with robust circuitry that is self-healing, reconfigurable, and ultimately recyclable. This is achieved through an embossing technique for on-demand formation of conductive liquid metal networks which can be reprocessed to rewire or completely recycle the soft electronic composite. Through this approach we achieve a combination of high electrical conductivity, high stretchability, and robust tolerance to damage. The embossing approach further enables soft, stretchable wiring to be created with resistance tunability over two orders of magnitude, while achieving conductivities as high as 45,400 S/cm at large strains. These skin-like electronics stretch to 1200% strain with minimal change in electrical resistance, sustain numerous damage events under load without losing electrical conductivity, and are recycled to generate new devices at the end of life. These soft composites with adaptive liquid metal microstructures can find broad use for soft electronics and robotics with improved lifetime and recyclability.

4:15 PM SB07.14.03

Carbon Nanotube-Conducting Polymer Core-Shell Microfibers for Bioelectrical Energy Storage Devices Myung-Han Yoon; Gwangju Institute of Science and Technology, Korea (the Republic of)

Carbon nanotubes (CNTs) are one of the most commonly used electrodes for fiber-type energy storage devices as they exhibit mechanical flexibility/durability, light weight, excellent electrical conductivity, and thermal/chemical stability. Nonetheless, the relatively low electrical double capacitance have limited their practical applications to fiber- and/or textile-type supercapacitors. In this research, we developed the CNT-PEDOT:PSS (poly(3,4 ethylenedioxythiophene):poly(styrene sulfonate)) core-shell microfibers via yarning and self-fusion. The core-shell microfibers were fabricated by yarning multi-strands of PEDOT:PSS microfibers (shell) onto the CNT microfiber with enhanced wettability (core), followed by the self-fusion of PEDOT:PSS microfibers. The resultant core-shell microfibers showed high electrical conductivity (~6,000 S/cm), large capacitance (~0.2 F/cm), and stable charging/discharging behaviors with minimal voltage drop and capacitance degradation. We expect that these fibers can be beneficial for flexible power

sources in wearable and textile electronics and stimulation electrodes in implantable bioelectronics.

4:30 PM SB07.14.04

Spider's Pad Inspired Dynamic Noise-Free Bioelectronics [Byeonghak Park](#) and Tae-il Kim; Sungkyunkwan University, Korea (the Republic of)

Soft materials such as elastomers and gels provide the potential for applications in bioelectronics that can be used in biophysiological monitoring. However, these applications are limited by the presence of dynamic mechanical noise artifacts in monitored signals under 30 Hz, for example due to walking and respiration. Although signal processing techniques such as bandpass filtering can be used to selectively remove such artifacts, this can compromise the distorted target signals after signal processing. Here, we present the "Selective frequency fading Hydrogel for a viscoElastic Dampening (SHIELD)", composed of a mixture of chitosan and gelatin. This material was inspired by the viscoelastic cuticular pad in a spider, used to separate target biophysiological signals while minimizing mechanical noise. The SHIELD exhibits viscoelastic properties with a frequency-dependent phase transition that results in a rubbery state that damps low-frequency noise, and a glassy state that transmits the desired high-frequency signals. The relaxation time as a proxy of the transition frequency varies with temperature and molecular weight, enabling to modulate transition frequency and resulting in selective damping capabilities. Instead of the additional signal processing after detecting from conventional sensor and electrodes or damping materials, we show that the SHIELD can be integrated with mechanosensors for the detection of biophysiological signals, or can be used as an electrode for sensing electrophysiological signals under the noisy mechanical conditions that arise in real-world applications involving medical patients. The SHIELD offers the possibility of proceeding to the practical real-time interactions between humans and devices and expanding the potential of advanced biomedical applications.

4:45 PM SB07.14.05

Late News: Highly Compliant, Flexible, Transparent, sub 150 Nanometers Thick, Fully Solution Processed All-Organic Transistor [Fabrizio A. Viola](#) and Mario Caironi; Italian Institute of Technology, Italy

The advancements in the field of electronics have paved the way to the development of new applications, such as wearable or tattoo electronics, where the employment of ultra-conformable devices is required. One of the main strategies to improve the device mechanical conformability is the reduction of its total thickness, of which the substrate usually represents the biggest contribution. To this end, organic materials can be considered enablers, owing to their advantageous mechanical characteristics, not achievable with inorganic counterparts, and to the possibility to obtain films with thicknesses at the nanometric scale. To date most of the reported approach for ultra-thin organic devices are based on physical deposition techniques that are not cost-effective. In this work we have successfully fabricated ultra-flexible, 143 nm-thick all-organic field-effect transistors, based on an ultra-thin solution processable dielectric, adopting only solution based techniques, such as spin-coating and inkjet printing. The devices can operate at low voltages and, thanks to their very low thickness, can conform to human skin in an imperceptible way and sustain bending radii as low as 0.7 mm, thus setting a new limit in thickness and flexibility. Moreover, this is the first demonstration of ultra-thin fully solution processable transistors, including the substrate. The electrical characterization showed a very good reproducibility, and the stability test in air make the devices in principle compatible with single-day, disposable usage. Moreover, the employed materials and their very low thickness guarantee a high transparency of the device. Besides providing an alternative and valid technological solution for the cost-effective fabrication of ultra-thin devices, the proposed approach can be a candidate for a plethora of possible use ranging from wearable to tattoo/epidermal electronics where conformability, ultra-flexibility and transparency are necessary.

5:00 PM SB07.14.06

Leak-Tight Anastomosis Hydrogel Sealants Using Mutually Interpenetrating Networks [Alexandre Anthis](#)^{1,2}, Xueqian Hu², Martin Tobias Matter^{1,2}, Anna Neuer^{1,2}, Kongchang Wei³, Andrea A. Schlegel⁴, Fabian H.L. Starsich^{2,1} and Inge K. Herrmann^{1,2}; ¹ETH Zürich, Switzerland; ²Empa-Swiss Federal Laboratories for Materials Science and Technology, Switzerland; ³Empa-Swiss Federal Laboratories for Materials Science and Technology, Switzerland; ⁴University Hospital Birmingham, United Kingdom

Intestinal anastomotic leaking involving the release of chemically aggressive, microbially active fluids into the abdomen through defective suture or staple sites, remains one of the most dreaded postoperative complications of abdominal surgery. Depending on the site and the patient condition, incidence rates of up to 21% and mortality as high as 27% are reported. Currently available surgical sealants only poorly address the issue, with most commonly used fibrin-based glues failing due to insufficient adhesion and chemical instability.

In this study, a leak-tight, chemically highly resistive and mucoadhesive hydrogel sealant, which is grafted on the surface of the intestinal wall via the use of a mutually interpenetrating network, is presented. This latter traverses both hydrogel and tissue yielding tissue compatible, deep anchorage. In contrast to clinically used, fibrin-based sealants (such as Tachosil), the developed poly(acrylamide-methyl acrylate-acrylic acid) (P(AAm-MA-AA)) adhesive patch does not degrade and exhibits high performance tissue adhesion under the harshest digestive conditions present in the abdominal cavity. The biocompatible hydrogel patch effectively seals anastomotic leaks in human relevant, *ex vivo* intestinal models, greatly surpassing commercial sealants (time to patch-failure >24 hours compared to 5 minutes for commonly used Tachosil). Importantly, the developed adhesive patch paves the way for the application of both mechanically and chemically robust sealants suitable for the treatment and prevention of intestinal anastomosis leaks.

5:15 PM SB07.14.07

Predicting Temporal Evolution of Self-Healing and Mechanical Properties of Intrinsic Self-Healing Polymers Through Deep Learning [Hashina Parveen Anwar Ali](#)¹, Zichen Zhao¹, Yu Jun Tan¹, Yao Wei¹, Qianxiao Li^{1,2} and Benjamin C. Tee¹; ¹National University of Singapore, Singapore; ²Agency for Science, Technology and Research, Singapore

The temporal evolution of self-healing intrinsic polymers is generally characterized through destructive testing of many samples as computational modeling and simulations cannot capture this phenomenon. We propose a new machine learning model called Self-healing Property Evolution using the Energy-functional Dynamical (SPEED) model to identify polymers' self-healing dynamics quickly. By training on a small set of experimental measurements, this model can predict the material property and understand the self-healing mechanics of polymers by using images of cuts dynamically healing over time. The potential and interface energies showing the effective physics behind the self-healing polymer are revealed by the SPEED model too. We validate this approach on toughness measurements of an intrinsic self-healing conductive polymer by capturing over 100,000 image frames of cuts to build the ML model. The close accuracy of our SPEED model predictions of toughness with experimental data over time shows that the SPEED model can be applied to predict the temporal evolution of macroscopic properties using few measurements as training data.

5:30 PM SB07.14.08

Intrinsically Stretchable Phosphorescence Organic Light Emitting Materials for Next Generation Stretchable Displays [Je-Heon Oh](#) and Jin-Woo Park; Yonsei University, Korea (the Republic of)

Stretchable electronics, especially stretchable organic light-emitting diodes (OLED), are one of the promising technologies in display industries. The stretchable OLEDs can be used in various applications such as stretchable smartphones, 3-dimensional tactile displays, and various bioelectronics devices

including optogenetics. Until now, stretchable light-emitting panels have been developed using stretchable interconnects and rigid OLEDs. However, this approach has critical limitations such as low diode density per unit area and complexity in the device fabrication process. Hence, stretchable light-emitting diodes consisting of intrinsically deformable materials should be developed for realizing the stretchable displays. Recently, we successfully fabricated an intrinsically stretchable fluorescent OLED. A commercial fluorescent polymer was blended with a non-ionic surfactant to significantly improve the mechanical properties without degrading the electrical properties of the OLED emission layer (EML). However, fluorescence emitting materials, in general, have the disadvantage of low internal quantum efficiency (IQE) of 25% at maximum in comparison to the phosphorescent emitting materials with IQE reaching up to 100%. In this work, we designed a solution-processable and intrinsically stretchable phosphorescent EML (*isp*-EML) by blending a small molecule emitting dopant together with the mixture of a polymer host, small molecule host and a plasticizer. The microstructure-modifying plasticizer enhanced the mechanical properties of the polymer but did not have any degenerating effect on the electrical and luminescent properties of the *isp*-EML. The crack onset strain of *isp*-EML was significantly improved from 5% to 100% and Young's modulus of *isp*-EML was reduced from 2,870 MPa to 267 MPa as the weight % of the plasticizer increases. The morphology change of the polymer host according to the ratio of the plasticizer and small molecules was analyzed through transmission electron microscopy (TEM) and atomic force microscopy (AFM), and it was predicted that the change in the conformation of the polymer host improved the mechanical properties. Furthermore, in the light emission characteristics of *isp*-EML, the luminance and efficiency of the PHOLED with *isp*-EML showed higher performance (3,500 cd/m², 9.4 cd/A) than PHOLED without plasticizer at EML (2,452 cd/m², 7.0 cd/A). This was because of the change in solubility of the small molecule dopant in the host solution according to the presence of the plasticizer and the change in morphology inside the *isp*-EML.

SESSION SB07.15: Soft, Healable Materials and Devices for Biological Interfaces and Wearable XII
Session Chair: Fabio Cicoira
Wednesday Morning, December 8, 2021
SB07-Virtual

10:30 AM *SB07.15.01

Self-Healable Elastomers and Gel-Based Materials for Wearables Pooi See Lee; Nanyang Technological University, Singapore

Elastomers and gel-based materials are attractive for epidermal hybrid electronics due to their tunable mechanical compliances and versatile properties. Many stimuli receptive interface for bidirectional human-machine interactions require tactile sensors that are intrinsically soft, skin conformable and dynamically deformable. While addressable touch input can be realized using capacitive, resistive, piezoelectric or triboelectric signals, the output signals often require integrated transduction mechanism or signal feedback channels on a compliant interface. In addressing these needs, we investigate the use of elastomers and ionic gel-based materials that provide the advantages of skin compliant, ease of processibility and added functionality such as self-healability.

Strategy to design self-healable and tough elastomer is pursued through the realization of dynamic hierarchical hydrogen bonds in the network of functionalized polyurethane. A high tensile strength with elongation break and high toughness elastomer is attained, and the self-healing efficiency can be enhanced by incorporation of plasticizers, making it attractive for rugged wearables. On the other hand, conductive hydrogel composites have been designed for the preparation of strain sensors. The use of hydrogel ionic conductor was shown to be effective current collector by harnessing the electrical double layer for triboelectric nanogenerators, allowing them to be mounted onto skin or curvilinear surfaces. Printable ionic gels with controllable rheological characteristics can be inkjet patterned into transparent deformable touch panels. The transparent touch interface is capable of remarkable signal fidelity under dynamic interactive conditions. We have also prepared thermally stable gels with self-healing ability and found applications in soft dielectric actuators for haptics and wearables.

11:00 AM SB07.15.02

Performance Comparison and Optimization of Stretchable Organic Electrochemical Transistors on Soft Substrates Dingyao Liu¹ and Shiming Zhang^{1,2}; ¹The University of Hong Kong, China; ²Terasaki Institute, United States

Organic electrochemical transistors (OECTs) based on poly(3,4-ethylene dioxythiophene) doped with polystyrene sulfonate (PEDOT: PSS) have attracted tremendous attention in the past decade due to their applications in bioelectronic interfaces, biomedical sensing, and neuromorphic computing. Moving forward, stretchable OECTs are demanded to promote their applications at soft biological interfaces to minimize their mechanical mismatch with the environments. However, despite recent advances, stretchable OECTs are suffering from lower performance than those fabricated on glass, attributable to the irregular and the impurified surface of the soft substrates.

In this work, we systematically benchmarked and compared the performance of stretchable OECTs on different soft substrates, including the commonly used polydimethylsiloxane (PDMS), styrene-ethylene-butylene-styrene (SEBS), polyolefin elastomer (POE), and thermoplastic polyurethane (TPU). We concluded that TPU, a widely used substrate in the soft electronics industry, is the best substrate to elevate the overall performance of stretchable OECTs. For example, the ON/OFF ratio of OECT on TPU is significantly higher than devices on other reference substrates and is comparable to the device performance on the glass. The fabrication process of stretchable OECTs on TPU was strategically simplified and standardized to ease its future integration with TPU-based soft electronics in the industry.

This work contributes to the OECT community by presenting a stretchable OECT unit with the highest performance so far. It serves as an indispensable building block to fill the gap between OECTs and soft electronics. This work motivates us to further develop fully integrated soft OECT arrays towards soft biosensing, bioelectronic interfacing, and neuromorphic computing applications.

11:15 AM SB07.15.03

Photothermal Enhanced Self-healing Liquid Metal Dielectric Elastomer Actuators Matthew Tan, Hyunwoo Bark, Gurunathan Thangavel and Pooi See Lee; Nanyang Technological University, Singapore

Infrared (IR) light has been used to stimulate a series of physiological reactions in the body for its recovery. Inspired by this approach, we utilize photothermal effects induced by IR light to restore the properties of dielectric elastomer actuators (DEAs) after damage by accelerating re-formation of hydrogen bonds through enhanced chain mobility. These actuators, often coined as artificial muscles are composed of carboxyl functionalised polyurethane films that display high fracture and mechanical toughness. With liquid metal (LM) nanoparticles inclusions, photothermal and dielectric properties of these composites can be drastically enhanced for accelerated self-healing and actuation respectively. Concurrently, a higher thermal conductivity (up to 800% increase) of LM composites imparts efficient heat dissipation with lower thermal drift under cyclic heating. Photothermal effects lead to on-demand

thermal softening behaviours that reduce electric field requirements (up to 40%) to achieve 50% area strains. By modulating the power of IR light from 200 to 800 mW cm⁻², these actuators can achieve a variety of stiffness that leads to greater control over actuation performances. Therefore, by applying photothermal effects on LM DEAs, not only can self-healing efficiencies and actuation performances be improved; but offers an alternative control strategy to tune the stiffness of DEAs on-demand to augment actuation.

11:30 AM SB07.15.04

Self-Adhesive, Stretchable and Non-Volatile Ionic Conductors Based on Associating Polymer Networks for Accurate Motion

Monitoring Kyunggook Cho, Sol An, Jeong Hui Kim, Jieun Nam, Myungwoong Kim and Keun Hyung Lee; Inha University, Korea (the Republic of)

Interest in wearable and stretchable skin-type sensors has grown rapidly and its application scope has been expanded in many areas. However, insufficient contact between the sensors and the target object causes low-quality signals which is a major hurdle for precise monitoring of complex movement of the human body. Here in, self-adhesive, stretchable, and non-volatile ionic conductors, known as ionogels, composed of an associating polymer network and ionic liquid were demonstrated. The new networks were designed by noncovalent association of two diblock copolymers, where phase-separated micellar clusters are interconnected via hydrogen bonds between corona blocks. The optimized ionogels exhibit outstanding self-adhesive characteristics (lift-off force \approx 93.3 N/m), stretchability (strain at break \approx 720%), and thermal stability (\approx 150 °C) without solvent evaporation. These ionic conductors were successfully applied to stretchable on-skin strain sensors, generating accurate electrical signals in accordance with the active motions of body parts including wrist, finger, ankle, and neck while maintaining full contact with the skin.

11:45 AM SB07.15.05

Recovery of Macro Properties of Damaged Polymer Films Through Self-Healing Under Supercritical CO₂ Levent Sendogdular, Selda Topcu Sendogdular, Bilge Bozdogan and Berna Aktas; Erciyes University, Turkey

Most of the thermoplastic polymer thin films are known to perform linear dilation anomalies normal to the substrate (lamellar direction) under supercritical CO₂ (scCO₂), which fluctuates in correlation with glass transition temperature. In this study, polymer swelling was found to be taking place in three dimensional space (expansion) instead of just normal direction to the substrate. And this phenomena enables the self-healing of damaged polymer thin films under scCO₂ as plasticization process. Here, CO₂ has been chosen as *an universal and environmentally friendly post-processing method* that is free of the polymer's nature and chemical structure.

Polymers' self-healing can be considered in different levels regarding polymer chain interactions where physical properties like electrical conductivity is known to be affected by intermolecular structure. Charge transfer is directly controlled with polymer chain order, crystallinity; therefore, recovery process has to take place on micrometer and even on nanometer scale.

Conjugated polymer thin films like P3HT films on substrate have two different chain orientations: lamellar (normal to the substrate) and π - π orientations (parallel to the substrate). And π - π chain stacking and order is more affective on polymer electrical conductivity than lamellar stacking; hence, in-situ x-ray and neutron studies showed that scCO₂ annealing promotes chains' swelling along with increased crystallinity on x-ray synchrotron studies.

SEM and optical microscope results proved 100% recovery especially for the films of which thicknesses are coherent with the width of the discontinuity in the film. To further investigate the self-healing in nano-scale, electrical conductivity experiments were performed on damaged regioregular poly(3-hexylthiophene-2,5-diyl) (P3HT) films exposed to scCO₂. In conclusion, before and after scCO₂ conductivity tests supported microscope results showing full recovery of polymer film.

12:00 PM SB07.15.06

Flexible Multifunctional Sensorics for Strain and Magnetic Field Measurements Yevhen Zabala^{1,2}, Alexey Maximenko^{2,3}, Michal Krupinski², Arkadiusz Zarzycki², Marcin Perzanowski², Piotr Horeglad², Marta Marszalek² and Denys Makarov¹; ¹Helmholtz-Zentrum Dresden-Rossendorf, Germany; ²The Henryk Niewodniczanski Institute of Nuclear Physics Polish Academy of Sciences, Poland; ³Jagiellonian University, Poland

As an alternative for conventional rigid electronics, there is tremendous progress in the area of mechanically soft electronics [1,2], where functional elements are fabricated on flexible and even elastic membranes that can be bent, folded, or twisted. This technology enables an appealing possibility to adjust the shape of the devices at will after their fabrication and paves the way to their use for smart skin, smart textile applications, where the functional elements should conform to a dynamically varying and curved surface of an object. Examples of soft functional elements include organic photovoltaics [3], light-emitting diodes [4], thin-film transistors [5], batteries [6], sensors and actuators [7] to name just a few.

Flexible magnetic field sensors [8,9] are crucial components of flexible interactive on-skin and wearable electronics as they allow to monitor of any type of motion. Typically, magnetic thin films are used for flexible magnetoelectronics to detect in-plane magnetic fields [10-14]. To acquire the sensitivity to out-of-plane magnetic fields, Bi-based Hall effect sensors have proven their efficiency for smart wearables and electromobility applications [15,16].

Semi-metallic Bi thin films reveal extremely high magnetoresistance (MR) and a strong Hall effect even at room temperature when patterned to a small lateral size. This is possible due to a much lower electron effective mass in bismuth in comparison to other metals. This results in the electron mean free path of the order of micrometres, which is lower only than the mean free path of graphene.

Here, we explore the extreme strain sensitivity of Bi thin films to realise a multifunctional flexible device, which can measure strain and magnetic fields simultaneously. The sensors are fabricated on 12-um-thick polyimide foils capped with Bi thin films of different thickness from 20 to 100 nm. The sensors are mechanically stable and withstand severe mechanical bending down to the radii of about 1 mm for 10.000 bending cycles. The fabrication method allows realising ultrathin and flexible Bi-based Hall effect sensors with the sensitivity of 5 Ohm/T, which is a record high for this type of sensors. We propose and validate the measurement sequence relying on the spinning current approach to decouple the signals measured by a single sensor element in transversal and longitudinal resistance channels. Furthermore, we developed a method to analyse the measured transversal and longitudinal resistances to assess the out-of-plane component of the magnetic field (Hall effect) and vector components of the in-plane strain (tenselectric effect). We apply these sensors as a component of smart skin for soft robotics and human-machine interfaces.

In this presentation, we will demonstrate the key aspects linking the fundamental properties of Bi thin films with their practical implementation in flexible sensor devices for simultaneous strain and magnetic field sensing.

This work was supported by the National Centre for Research and Development within LIDER V program, Poland (project Nr.: LIDER/008/177/L-5/13/NCBR/2014).

- [1] S. Bauer et al., Adv. Mater. 26, 149 (2014).
- [2] T. Someya et al., MRS Bulletin 42, 124 (2017).
- [3] M. Kaltenbrunner, Nat. Commun. 3, 770 (2012).
- [4] T.-H. Han, Nat. Photon. 6, 105 (2012).
- [5] L. Petti et al., Appl. Phys. Rev. 3, 021303 (2016).
- [6] L. Hu, ACS Nano 4, 5843 (2010).
- [7] J.C. Yeo, Adv. Mater. Technol. 1, 1600018 (2016).

- [8] D. Makarov, Appl. Phys. Rev. 3, 011101 (2016).
[9] G.S. Canon Bermudez et al., Adv. Funct. Mater. (2021). DOI: 10.1002/adfm.202007788
[10] M. Ha et al., Adv. Mater. 33, 2005521 (2021).
[11] E.S. Oliveros Mata et al., Applied Physics A 127, 280 (2021).
[12] J. Ge et al., Nat. Commun. 10, 4405 (2019).
[13] G.S. Canon Bermudez et al., Nat. Electron 1, 589 (2018).
[14] G.S. Canon Bermudez et al., Science Adv. 4, eaao2623 (2018).
[15] M. Melzer et al., Adv. Mater. 27, 1274 (2015).
[16] I. Mönch et al., IEEE Trans. Magn. 51, 4004004 (2015).

SESSION SB07.16: On-Demand
Sunday Morning, December 5, 2021
On-Demand

8:00 AM SB07.16.01

Wearable Multi-Functional Sensor Sheet with Feedback Alarm System [Kuni Takei](#)¹, Kaichen Xu², Yusuke Fujita¹, Satoko Honda¹, Yuyao Lu¹, Takayuki Arie¹ and Seiji Akita¹; ¹Osaka Prefecture University, Japan; ²Zhejiang University, China

Daily continuous health condition monitoring is now of great interests using multi-functional flexible sensors. In particular, vital signals from skin are most likely most convenient way to measure continuously data collections. For this purpose, flexible sensor sheets allow it to detect multiple information from skin precisely due to conformable covering over skin surface. To realize this platform, multiple developments including flexible sensors, wireless system, and potential application are required. In this study, we develop three sensors integrated with wireless and signal processing circuit system. The system makes a feedback alarm if abnormal human condition signals are detected. As a proof-of-concept, 10 directional tilt sensors, respiration sensor, and wet sensor attached onto a diaper are developed.

First, tilt sensor is discussed. To make simple tilt detections, conduction between two electrodes via a liquid metal of GaInSn (galinstan) is used.

Depending on the tilt direction, galinstan encapsulated in a chamber formed by PDMS can be moved and makes the connection between the electrodes. By reading on and off state of the electrodes, tilt direction can be extracted. However, galinstan surface is often oxidized readily in air due to Ga-based metal, resulting in residue of galinstan on the surface. This residue sometimes causes the shortage between the electrodes. To prevent the malfunction of tilt sensor, laser-induced graphene (LIG) in PDMS was used. In addition, to make almost non-wettability between the LIG/PDMS and galinstan, laser treatment over the LIG/PDMS was applied. This treatment realizes the long stability for more than several months with high contact angle (>155 degree) and low sliding angle (<5 degree). After charactering fundamental properties, 10 directional tilt sensor was successfully fabricated.

Next, respiration and wet sensors are explained briefly. For the respiration sensor, LIG transferred into PDMS was used to monitor the resistance change under strain. Because the sensor sheet is attached on a rubber belt region of a diaper, strain caused by inflation and deflation of abdominal can be detected. The gauge factor was calculated to be 9, and hysteresis was confirmed to be almost negligible. For the wet sensor, stacked ZnIn₂S₄ (ZIS) nanosheets were used. Due to proton hopping on the surface of ZIS, conductivity is changed depending on the number of water vapor corresponding to humidity level. Resistance change ratio between RH 30 % and 70 % shows about 30 %. Importantly, this humidity sensor is stable for a long-time cycle test more than several days.

Finally, all sensors were integrated on a film and connected to a wireless circuit system. Output signal was transmitted to a smartphone via low-energy Bluetooth. The program was designed to make feedback alarm functions if the conditions are abnormal. When a baby sleeps in the prone position, alarm is initiated to notify a carer. In addition, when respiration stops more than 10 s or diaper is a wetting condition, each alarm is also started.

In conclusion, this study demonstrated a wireless body condition sensor sheet with feedback alarm function. Long-time stable tilt, respiration, and wet sensors are realized to be used for wearable device applications. Furthermore, wireless feedback alarm function is integrated with the flexible sensor sheets, which show the great advance for the flexible electronics.

SYMPOSIUM SB08

Bioelectronics—Materials and Interfaces
November 29 - December 8, 2021

Symposium Organizers

Tzahi Cohen-Karni, Carnegie Mellon University
Sahika Inal, King Abdullah University of Science and Technology
Jonathan Rivnay, Northwestern University
Flavia Vitale, University of Pennsylvania

* Invited Paper

SESSION SB08.01: Materials and Devices I

Session Chairs: Tzahi Cohen-Karni, Nicolette Driscoll, Raghav Garg, Sahika Inal, Jonathan Rivnay, Daniel San Roman, Flavia Vitale and Yingqiao Wang
Monday Morning, November 29, 2021
Hynes, Level 3, Room 304

9:45 AM *SB08.01.01

Bacterial Photoenzymes Entrapped in Polydopamine Thin Films for Photoconversion [Gianluca M. Farinola](#)¹, Danilo Vona¹, Rossella Labarile¹, Gabriella Buscemi^{1,2}, Roberta Ragni¹, Francesco Milano³ and Massimo Trotta²; ¹University degli Studi-Bari Aldo Moro, Italy; ²Institute for Physical-Chemical Processes (IPCF), CNR, Italy; ³CNR-ISPA, Institute of Sciences of Food Production, Italy

Reaction Centers (RCs) are specific transmembrane proteins of photosynthetic microorganisms that convert photons into charge separated states, with extremely high photoconversion efficiency. Our research group has demonstrated that bioconjugation of tailored molecular organic antennas represents an efficient strategy to enhance the light harvesting capability of RC extracted from *Rhodobacter sphaeroides* R26 photosynthetic bacterium [1-3]. Moreover, RC based photoelectrochemical cells [4,5], photosensors [6] and photoactive transistors [7] have been developed. RCs have been also integrated in semiconducting thin films deposited onto metal electrodes [8], and stabilized in soft structures like vesicles and polymersomes [9] before integration in electronic systems. Recently, we have developed chemical methods to optimize the interface of *Rhodobacter sphaeroides* RCs with electrodes, avoiding protein denaturation. To this aim, an adhesive biocompatible polymer, polydopamine (PDA), has been used. PDA can be easily produced by oxidative polymerization of dopamine in mild aqueous aerated conditions. It acts as an efficient coating layer for RC photoenzymes, improving the electrode/protein interface without altering the enzyme photoactivity [10]. PDA can be further functionalized to improve its light transmittance, allowing an increase of photocurrent generation of PDA coated RCs [11]. Hence, this polymer can be envisaged as a promising biocompatible adhesive material to efficiently interface photoenzymes with electrodes in bioelectronic devices for solar energy conversion.

[1] F. Milano, R.R. Tangorra, O. Hassan Omar, R. Ragni, A. Operamolla, A. Agostiano, G.M. Farinola, M. Trotta, *Angew. Chem. Int. Ed.*, **51**(44), 11019-11023 (2012).

[2] O. Hassan Omar, S. La Gatta, R.R. Tangorra, F. Milano, R. Ragni, A. Operamolla, R. Argazzi, C. Chiorboli, A. Agostiano, M. Trotta, G. M. Farinola, *Bioconjugate Chem.* **27**, 1614-1623 (2016).

[3] S. la Gatta, F. Milano, G. M. Farinola, A. Agostiano, M. Di Donato, A. Lapini, P. Foggi, M. Trotta, R. Ragni, *Biochimica et Biophysica Acta-Bioenergetics*, **1860** (4), 350-359 (2019).

[4] F. Milano, F. Ciriaco, M. Trotta, D. Chirizzi, V. De Leo, A. Agostiano, L. Valli, L. Giotta, M.R. Guascito, *Electrochim. Acta*, **293**, 105-115 (2019).

[5] F. Milano, A. Punzi, R. Ragni, M. Trotta, G. M. Farinola, *Adv. Funct. Mater.*, **29** (21), 1805521, (2019).

[6] M. Chatzipetrou, F. Milano, L. Giotta, D. Chirizzi, M. Trotta, M. Massauti, M.R. Guascito, I. Zergioti, *Electrochemistry Communications*, **64**, 46-50 (2016).

[7] M. Di Lauro, S. la Gatta, C.A. Bortolotti, V. Beni, V. Parkula, S. Drakopoulou, M. Giordani, M. Berto, F. Milano, T. Cramer, M. Murgia, A. Agostiano, G.M. Farinola, M. Trotta, F. Biscarini, *Adv. Electronic Mater.* **6** (1), 1900888 (2020).

[8] E. D. Glowacki, R. R. Tangorra, H. Coskun, D. Farka, A. Operamolla, Y. Kanbur, F. Milano, L. Giotta and N. S. Sariciftci, *J. Mater. Chem. C*, **3** (25), 6554-6564 (2015).

[9] R. R. Tangorra, A. Operamolla, F. Milano, O. Hassan Omar, J. Henrard, R. Comparelli, F. Italiano, A. Agostiano, V. De Leo, R. Marotta, A. Falqui, G.M. Farinola, Trotta M., *Photochem Photobiol Sci.*, **14**(10), 1844-1852 (2015).

[10] M. Lo Presti, M. M. Giangregorio, R. Ragni, L. Giotta, M. R. Guascito, R. Comparelli, E. Fanizza, R. R. Tangorra, A. Agostiano, M. Losurdo, G. M. Farinola, F. Milano, M. Trotta *Adv. Electron. Mater.* **2000140**, (2020).

[11] G. Buscemi, D. Vona, R. Ragni, R. Comparelli, M. Trotta, F. Milano, G. M. Farinola, *Adv. Sustain. Syst.*, doi.org/10.1002/adsu.202000303 (2021).

10:15 AM *SB08.01.02

Integrating Organic Bioelectronic Materials into Biological and Neuronal Systems [Magnus Berggren](#); Linköping University, Sweden

Applying organic electronics technology to biological systems, such as cells and neuronal tissue, is a promising strategy to answer many of the long-standing questions of biology and neuro-signaling. Further, such approach may also provide new solutions for therapy and prosthesis applications, especially to combat neurodegenerative disorders or diseases. The fidelity of such methodology depends heavily on the quality of interfacing foreign device technology with soft and complex biological systems. Several approaches have been conducted in the past to improve the matching between organic electronics and biology with respect to mechanical, chemical, electrical and signaling characteristics. Here, a novel approach is reported where organic electronic materials is applied to the biological system in the form as monomers, followed by bio-interfacing and in-situ polymerization. The resulting system is a self-organized electrode and device technology that integrates and interfaces with cells and tissues in a highly conformable and tight manner. The chemical approach, electrical characteristics as well as the performance when operating such in vivo-manufactured organic bioelectronics will be reported.

10:45 AM SB08.01.03

Granules-Enabled Tissue-Like Systems for Bioelectronics [Jiuyun Shi](#), Yin Fang, Yiliang Lin, Aleksander Prominski and Bozhi Tian; The University of Chicago, United States

Biological tissues are multiscale, cooperative across different components, dynamically responsive, and in many cases strain-stiffening. One key challenge in creating bioelectronic devices with tissue-like features is to recapitulate the multiscale tissue architectures and the unique dynamic mechanical responsiveness. If these could be achieved, the bioelectronic devices would allow for seamless biointerfaces and the sensing or modulating of the biological signals with high efficiency. In this work, we designed a granules-enabled hydrogel composite, with multiple naturally occurring biopolymers and synthetic hydrogels as the key components. Mechanical and in-situ x-ray characterizations reveal that the strong inter-molecular and inter-granular interactions between the components give rise to the exceptional tissue-like strain-stiffening behaviors. Due to mechanical match with the real tissues, our tissue-like materials have enabled the pneumatically actuated bioelectronic devices for applications such as the recording of the heart electrocardiogram (ECG) signal ex-vivo.

11:00 AM SB08.01.04

A Universal and Facile Approach for Building Multifunctional Conjugated Polymers for Human-Integrated Electronics [Nan Li](#), Yahao Dai, Yang Li and Sihong Wang; The University of Chicago, United States

Functional polymer semiconductors based on π -conjugated structures have shown distinct promise for the development of human-integrated electronics, owing to their solution processability for large-area fabrication, mechanical softness and even stretchability, as well as low cost. However, among the wide range of functional properties required for this application domain, which include, but not limited to, biochemical sensing, chemotherapeutic property, bio/immune-compatibility, micro-patternability, tissue/skin adhesion, stimuli-responsiveness, numerous of them face synthetic challenges to be imparted onto conjugated polymers and thus combined with efficient charge-transport property. Currently, the absence of these functional properties poses the major obstacle for taking advantage of the unique properties of conjugated polymers to benefit the development of human-integrated electronics. Here, we establish a “click-to-polymer” (CLIP) synthesis strategy for conjugated polymers, which enables the use of a click reaction for the facile and versatile attachment of diverse types of functional units to a pre-synthesized conjugated-polymer precursor. This can be utilized to realize both bulk and surface functionalization in/on the deposited thin films. Through demonstrating the applicability on four types of functional groups that each carry distinct emerging properties, for instance, ion conduction and immune-modulation, we show that functionalized polymers from this CLIP method can still retain good charge-carrier mobility above 0.1 square centimeters per volt per second. The obtained electrical performance is much higher compared to that from conventional synthesis approach for the incorporation of long polar groups. On the other hand, the surface functionalization does not cause any influence on the mobility while bringing in new surface properties. To demonstrate the usefulness of this CLIP strategy, we realized two highly desired functions on conjugated polymers: the direct photo-patterning with sub-10 μm resolution enabled by the incorporation of benzophenone groups; and the amplified biomolecular sensing enabled by the incorporation of *N*-hydroxysuccinimide (NHS) ester that can conjugate with enzymatic bioreceptors. Both the performances advance the state of the art of realizing these two types of functions on conjugated polymers. We expect the expanded use of this synthesis approach will largely enrich the functional properties from conjugated polymers and facilitate the electronic-biological interfacing in the future. (Under revision)

11:15 AM SB08.01.05

Hybrid Pneumatic–Magnetic Soft Actuator with Novel Channel Integration for Multiple Axis Actuation [Ji Eun Lee](#), Yu-Chen Sun and Hani E. Naguib; University of Toronto, Canada

Soft actuators are garnering considerable attention, due to their ability to perform tasks that are difficult or impossible for traditional electromechanical robotic technologies. The flexibility and control exerted by soft actuators is ideal for biomimicking of the complex and delicate movements emerging from soft muscles. These soft actuators are often fabricated from smart materials, being able to respond and actuate when exposed to a specific external stimulus. With such advantages as flexibility, lightweight, and deliverance of a wide range of movement, smart materials based soft actuators can be utilized in applications from satellite mirror control to miniaturized medical devices and biomimetic robotic grippers.

This study reports a novel soft actuator that combines the advantages of pneumatic and magnetic responsive systems for achieving a multi-directional actuation behaviour. The fabricated Fe_3O_4 /silicone hybrid actuator balances the two distinct pneumatic and magnetic stimuli responses by allowing each stimuli to overcome each other's disadvantages and optimizing these components. The micro soft pneumatic actuator is fabricated utilizing 3D printed wires to create unique singular motions, forming unique “S”, “L”, or a hook shape. The magnetic actuation is integrated into the silicone soft body through Fe_3O_4 nanoparticles and complements this pneumatic movement. It was reported that the Fe_3O_4 had a significant impact on the mechanical property of the silicone matrix, the incorporation reducing the elastic modulus of the silicone elastomers. This was favorable overall, allowing the pneumatic actuation to occur under a lower pressure requirement while producing a high blocking force. Additionally, it was observed that the magnetic nanoparticles alignment within the samples enhanced the magnetic deflection and susceptibility at a lower magnetic field. The demonstrated hybrid soft actuators could lift objects 3.4 times its own weight. Furthermore, a gripper system was designed with two operational soft actuators in parallel configuration. It could grab objects larger than the gripper width due to a secondary magnetic actuation. Using the advantage of the multi-directional pneumatic/magnetic actuation, such hybrid soft actuator has the capability to be utilized in biomimicking or biomedical applications where unique maneuverability and force control is required.

11:30 AM SB08.01.06

Gating Dual Channel Ionic Transport in Conducting Polymers via Hydrophobicity [Tamanna T. Khan](#)¹, Terry McAfee², Thomas Ferron³ and Brian Collins¹; ¹Washington State University, United States; ²Lawrence Berkeley National Laboratory, United States; ³National Institute of Standards and Technology, United States

Mixed electron/ion transport in organic materials is enticing due to the potential applications in electrochemical transistors, bioelectronics, printed electronics, and sensors. PEDOT:PSS is a model mixed conductor with a morphology consisting of PEDOT:PSS-rich gel particles embedded within a PSS matrix. Our previous study reported heterogeneous ion mobility. However, the origins behind this heterogeneity were not explored in detail. We present the existence of two separate ion channels in PEDOT:PSS originating from a bilayer morphology that naturally forms from the differing surface energies of the two components during solution casting. A higher ion mobility occurs in a PSS-rich ~10 nm top channel versus a slower PEDOT-rich bulk. We demonstrate the ability to gate ion flow by using different ion barrier materials of increasing hydrophobicity that drives ions out of the top channel. By increasingly removing the PSS top channel, the ion mobility approaches that of the bulk. These results reveal that the measured ion mobility can be skewed without taking surface layers into effect. Finally, we demonstrate sensing of UV exposure over time through switching a hydrophobic barrier layer to hydrophilic, an effect that attracts ions into the fast channel and increases ion transport. Understanding how polymer nanostructure and hydrophobicity can control ion mobility and potentially transduction to electron transport will enable these devices to be used in wide-ranging sensing applications.

NSF, Electronic and Photonic: Grant#1905790

SESSION SB08.02: Materials and Devices II

Session Chairs: Tzahi Cohen-Karni, Nicolette Driscoll, Raghav Garg, Sahika Inal, Jonathan Rivnay, Daniel San Roman, Flavia Vitale and Yingqiao Wang
Monday Afternoon, November 29, 2021
Hynes, Level 3, Room 304

1:30 PM SB08.02.01

Shape-Morphing Materials for Deployable Intracortical Probes [Mahjabeen Javed](#)¹, Rashed T. Rihani², Joseph Pancrazio² and Taylor H. Ware¹; ¹Texas A&M University, United States; ²The University of Texas at Dallas, United States

Intracortical microelectrode arrays (MEAs) used for diagnostic and treatment purposes, such as prosthetic devices, are currently limited in their chronic reliability. Several biotic and abiotic factors have been identified that lead to device failure *in vivo*. Abiotic causes of failure include delamination, metal corrosion, and insulation damage. At the biotic level, failure occurs as a result of initial tissue damage caused by insertion and the immune response elicited by the chronic persistence of a foreign object, which leads to glial scarring and neuronal death. This foreign body response of the tissue leads to disruptions in the functionality of the implanted devices, interfering with their ability to stimulate or record. We are developing shape-changing, liquid crystal polymer (LCP) based ultramicroelectrode arrays where probes of minimal cross-sectional area deploy to predetermined locations, away from the site of implantation and the associated foreign body response. We hypothesize that the deployment of these flexible probes with subcellular dimensions will mitigate the foreign body response, allowing for a more successful long-term implantation. We have shown that liquid crystal polymers are highly resistant to degradation when exposed to accelerated aging conditions. Prior work demonstrated liquid crystal polymer-based electrodes deploying distances of hundreds of micrometers away from the site of implantation in agar brain phantom and rodent brain tissue. However, one limitation of this work was that due to the low elastic modulus of the liquid crystal polymer, the devices were of mm-scale (0.07 mm²). Here, we aim to describe a novel approach to synthesize a semicrystalline liquid crystal polymer with increased elastic modulus, that may allow for the deployment of electrodes of much smaller size in a volume of cortical tissue. We employ a thiol-ene approach to synthesize liquid crystal polymer networks that crystallize after polymerization. Directed self-assembly can be used to pattern the molecular orientation of the liquid crystal monomer mixture prior to crosslinking. This alignment of molecular order enables controlled deployment of the device after insertion. Liquid crystal polymer substrates are synthesized where the crosslinker content is varied from 0% to 40% to optimize the mechanical properties. At 40% crosslinker content, Young's modulus of the liquid crystal polymer is 400 MPa, with an actuation strain of up to 130%. Electrode arrays can be fabricated on these crystalline liquid crystal polymer substrates using photolithography. We envision, that this approach to develop deployable neural interfaces will overcome some critical challenges that currently hinder the chronic functionality and longevity of intracortical devices.

1:45 PM SB08.02.02

Dual-Color Organic LEDs for Co-Located Optogenetic Activation and Inhibition of Cellular Activity Giuseppe Ciccone¹, Ilenia Meloni², Rodrigo F. Lahore³, Hans Kleemann¹, Peter Hegemann³, Karl Leo¹ and Caroline Murawski²; ¹Dresden Integrated Center for Applied Physics and Photonic Materials (IAPP) and Institute for Applied Physics, Technische Universität Dresden, Germany; ²Kurt-Schwabe-Institut für Mess- und Sensortechnik Meinsberg e.V., Germany; ³Institute for Biology, Experimental Biophysics, Humboldt-Universität zu Berlin, Germany

Photo-stimulation of neurons allows optogenetics to evoke and probe cellular activity with high spatial and temporal resolution. Light-responsive proteins are genetically expressed across the plasma membrane to control fluxes of ions in response to light with specific wavelength and intensity. Recently, light-sensitive proteins that combine two separate photosensitive cores into a single domain have been developed by covalent linking of a cation-conducting and an anion-conducting channel, to provoke neuronal excitation and inhibition with a single optogenetic tool¹. Traditionally, light sources such as lasers or LEDs are used for addressing biological targets. Although these devices are adequate for *in vitro* studies, their bulkiness, low biocompatibility, and poor mechanical matching with biological systems make them less appealing for *in vivo* applications. Organic LEDs (OLEDs) may overcome these limitations, since they offer mechanical flexibility, excellent optical tunability, and can be patterned on the micron scale. Thus, OLEDs have the potential to increase the precision of optogenetic targeting while providing also a softer interface between light source and tissue². Here, we present two stacked OLED architectures that can emit light with two different emission colors from the same pixel³, addressing the single domains of bidirectional ion channels expressed in *Drosophila melanogaster* larvae and ND7/23 cells. Tuning of the OLED layers' thicknesses allowed us to well match the OLED emission spectra to the activation spectra of the tandem photo-sensitive proteins *GtACR2-Chrimson* and *GtACR2-ChRmine*. Our work shows that OLEDs can provide narrowband light emission with minimal crosstalk between sub-pixels, enabling us to switch between optogenetic activation and inhibition of *Drosophila* larvae and ND7/23 cells.

1. Vierock, J. *et al.* BiPOLES: a tool for bidirectional dual-color optogenetic control of neurons. *bioRxiv* 2020.07.15.204347 (2020) doi:10.1101/2020.07.15.204347.

2. Kim, D. *et al.* Ultraflexible organic light-emitting diodes for optogenetic nerve stimulation. *Proceedings of the National Academy of Sciences of the United States of America* **117**, 21138–21146 (2020).

3. Fröbel, M. *et al.* Get it white: Color-tunable AC/DC OLEDs. *Light: Science and Applications* **4**, 247 (2015).

2:00 PM SB08.02.03

Porosity-Based Silicon Heterostructures for Modulation of Hearts and Nerves Aleksander Prominski^{1,2,2}, Menahem Y. Rotenberg³ and Bozhi Tian^{1,2,2}; ¹University of Chicago, United States; ²The University of Chicago, United States; ³Technion–Israel Institute of Technology, Israel

Biocompatible and leadless stimulation is the ongoing goal of bioelectronics research with a broad potential for clinical translation. New soft, thin, and efficient materials must be developed to achieve biological modulation suitable for medical treatments. Photosensitive semiconductor nanowires and patterned membranes were found to be suitable materials for wireless optical modulation. However, the preparation of p-i-n junctions is time-consuming, requires dedicated instrumentation, and may need additional metal modifications to achieve sufficient photoelectrochemical activity in saline. To this end, we sought a new approach for the generation of highly photoelectrochemically active materials fabricated directly from a thin crystalline silicon substrate. In this presentation, I will discuss our recent advances in the synthesis of nanoporous/non-porous silicon membranes and their application for remote non-genetic biological modulation with light. Specifically, we have developed a simple, wet-processing technique to generate nanoporous silicon-based photoelectrochemical devices. We have shown how nanostructuring of the material surfaces can improve the modulation efficiency and biocompatibility at the device and tissue interfaces. We have successfully applied silicon devices to stimulate hearts and nerves in a rat model using light pulses. We have achieved highly efficient modulation in which the radiant exposure necessary for the modulation is on the same scale as in the approaches based on optogenetics. We hope that our materials designs and synthetic methods enable new tools for bioelectronic research and future clinical therapies.

2:15 PM SB08.02.04

Shape-Actuated Bioelectronics Christopher M. Proctor; University of Cambridge, United Kingdom

Significant advances have been made in the last two decades in interfacing electronic devices with the nervous system. Organic electronic materials in particular have emerged as ideal materials for interfacing with the neural tissues due to their flexibility, biocompatibility and moreover their electronic and ionic conductivity. To that end, significant research efforts are being pursued to develop minimally invasive, implantable organic electronic devices integrating recording, stimulating, and drug delivery features. Here we report recent developments towards such dynamic devices for neural interfacing that take full advantage of the favorable properties offered by conducting polymers and polymer substrates. It is shown that thin, flexible devices can incorporate microfluidic channels to enable actuated shape control. Furthermore, we show such features open the door to novel implantation strategies that can reduce the surgical footprint required for implantation of large bioelectronic devices. We anticipate this work will accelerate the development of a new generation of minimally invasive implants for neural interfacing.

2:30 PM SB08.02.05

Material and Device Designs in Biomimetic Polymer Electronics Sihong Wang; The University of Chicago, United States

The vast amount of biological mysteries and biomedical challenges faced by human provide a prominent drive for seamlessly merging electronics with biological living systems (e.g. human bodies) to achieve long-term stable functions. Towards this trend, one of the key requirements for electronics is to possess biomimetic form-factors in various aspects for achieving the long-term biocompatibility. To enable such paradigm-shifting requirements, polymer-based electronics are uniquely promising for combining advanced electronic functionalities with biomimetic properties. In this talk, I will introduce our new molecular-design, chemical-synthesis and physical-processing concepts for polymer semiconductors, which enabled the incorporation of multiple biomimetic properties with advanced electronic functionalities. Fundamental understandings that have been obtained about the structure property relationship on these unprecedented material designs are serving as the foundation for opening up this new research direction for polymer semiconductors. Furthermore, enabled by these new materials, we have also created new device designs and fabrication processes for building unprecedented functional devices (i.e., sensors and circuits) that are intrinsically stretchable with unperturbed performance when operating conformably on human bodies. Collectively, our research is opening up a new generation of electronics that fundamentally change the way that the humans interact with electronics.

SESSION SB08.03: Neurotech I

Session Chairs: Tzahi Cohen-Karni, Nicolette Driscoll, Raghav Garg, Sahika Inal, Jonathan Rivnay, Daniel San Roman, Flavia Vitale and Yingqiao Wang
Tuesday Morning, November 30, 2021
Sheraton, 2nd Floor, Independence West

10:30 AM *SB08.03.01

Accessing Neurobiological Complexity with Multifunctional Fibers Polina Anikeeva; Massachusetts Institute of Technology, United States

The past decade has delivered unprecedented speed of development of neurotechnologies. Modern complimentary metal-oxide-semiconductor (CMOS) fabrication has yielded high-resolution electrophysiology and robust back-end interfaces for probes implanted in the brains of rodents and even non-human primates. Combining electrophysiology with modern opto- and chemogenetic approaches, as well as with the emergence of photopharmacological tools remains a challenge. Furthermore, multifunctional neural interfaces with organs other than the brain present additional challenges associated with dimensions, reduced redundancy, vascularization, and susceptibility to the immune response. In this talk, I will discuss our recent efforts in multi-material fiber design that address some of the challenges of the neurobiological complexity and create stable multifunctional interfaces to the central and peripheral nervous systems.

11:00 AM *SB08.03.02

Peripheral Nerve Interfaces—Optimizing Wireless Optoelectronic Stimulation Mary J. Donahue; Linköping University, France

The informational density and relative accessibility of the peripheral nervous system make it an attractive site for therapeutic intervention. Although electrode-based electrophysiological interfaces for peripheral nerves have been under development for over half a century, achieving spatial specificity and minimally invasive devices remains challenging. The value in tackling this challenge lies in the possibility to treat disorders such as, for example, chronic pain, overactive bladder, depression, and epilepsy. We aim to improve peripheral nerve interfaces through the use of wired flexible electrode arrays to intelligently design wireless organic electrolytic photocapacitor (OEPC) stimulation devices. Through the use of OEPCs we achieve capacitive stimulation pulses delivered by non-toxic materials as tissue-penetrating deep-red light is transduced into electrical signals. We therefore avoid faradaic reactions and the products thereof, and accomplish safe, non-invasive neuromodulation.

11:30 AM SB08.03.03

Conductive Polymer Coating on 3D Nanoprobes for High-Performance Neural Recording and Stimulation Ines Muguet^{1,2}, Ali Maziz¹, Laurent Mazon¹, Fabrice Mathieu¹ and Guilhem Larrieu¹; ¹LAAS-CNRS, France; ²Université Paul Sabatier, France

Understanding the functioning of the brain and the mechanisms involved in neuronal networks is one of the biggest scientific challenges yet to overcome. Within this field, remarkable advances were made, thanks to the development of a new generation of *in-vitro* micro-electrode arrays, in which the sensing elements are miniaturized and 3D-structured. Such devices, called Nanostructured Electrode Arrays (NEAs), offer real benefits, as they possess a high spatial resolution and an important surface-to-volume ratio leading to a higher affinity with cells. This technology enables to stimulate and record the neuronal activity at the single-cell level. However, reducing the size of the electrodes diminishes their effective area, which increases their impedance, leading to a loss in signal resolution. It also negatively affects the charge injection properties, a key parameter for stimulation processes.

Here, we demonstrate for the first time the ability to selectively deposit a nanolayer of poly(3,4-ethylenedioxythiophene)-poly(styrenesulfonate) (PEDOT:PSS), a conductive polymer, on metal 3D nanoprobes through electrochemical deposition. These polymer-coated nanoelectrodes have been fully characterized, both electrochemically and morphologically, to establish a direct relationship between the synthesis conditions, the final morphology, and the conductive features

First, nanowires-based NEAs were fabricated at wafer scale using a cost-effective top-down approach, combining conventional lithography tools, plasma etching, sacrificial oxidation, metal deposition, and chemical etching steps. All sensing electrodes are formed by 7 connected vertical platinum-silicide nanowires. Each nanowire is 4µm high and has a diameter of 400nm. All the conductive access lines are insulated from the liquid media and only the nanowires are in contact with the solution. The nanoprobes were coated with PEDOT:PSS via electrochemical deposition. Different polymerization routes have been investigated, from galvanostatic to potentiodynamic, showing a large range of layer morphology. After optimizing the coating conditions, conformal and homogenous PEDOT:PSS layers were successfully deposited, down to 75nm thin. Indeed, Scanning Electron Microscopy demonstrated that the nanowires were wrapped tightly by the polymer coating, keeping the high aspect ratio of the nanoprobes.

The recording properties of the probes were evaluated, by performing Electrochemical Impedance Spectroscopy measurements in saline media. The impedance values (at 1kHz) of the coated nanoprobes decreased by 2 orders of magnitude compared to bare nano-electrodes. Cyclic voltammetry and voltage transients experiments have also been conducted, to estimate the charge injection capabilities of the polymer-coated NEAs. Results indicated an enhancement in delivering a higher charge at the 3D electrode-electrolyte interface. In fact, the charge storage capacity increased up to 10 times and the charge injection limit doubled compared to bare electrodes.

Thanks to their improved performances, PEDOT-coated 3D-nanostructured devices open new perspectives to stimulate and record the *in-vitro* neuronal

activity with higher spatial and signal resolution.

SESSION SB08.04: Neurotech II

Session Chairs: Tzahi Cohen-Karni, Nicolette Driscoll, Raghav Garg, Sahika Inal, Jonathan Rivnay, Daniel San Roman, Flavia Vitale and Yingqiao Wang
Tuesday Afternoon, November 30, 2021
Sheraton, 2nd Floor, Independence West

1:30 PM *SB08.04.01

Manipulation and Integration of Sub-10kPa Materials for Neural Interfaces Michael Shur, Noaf Alwahaab, Jennifer Macron and Stephanie P. Lacour; Ecole Polytechnique Federale de Lausanne, Switzerland

Neural tissues are non-linearly elastic materials that display viscoelasticity and plasticity. They are extremely soft with elastic modulus in the 100 Pa to several kPa. Hydrogels are a unique class of materials that may be tuned to mimic the mechanical properties of neural tissues. Their high-water content and porous micro-structure greatly resemble the natural structure of the extracellular matrix. On the other end, the very same features impose many challenges e.g. swelling, electrical insulation or mechanical robustness for their integration into microfabricated devices. This talk will report on our efforts to integrate hydrogels as coating or structural materials to design, manufacture and test biomimetic neural interfaces.

In air, hydrogels dry progressively, leading to massive shrinkage of the organic network. Kept in water, they can swell up to more than ten times their initial volume. When used as a coating, re-swelling of the hydrogel film results in important shear stress at the interface with the encapsulated device. When used as the bulk carrier, the soft material *in vivo* may display stiffer properties than those *in vitro*. In both cases, this significant volume change is not compatible with the cohesion of a multilayer system and has irreversible impact on the structural and functional properties of the soft neural interface.

We are engineering and manipulating several hydrogels ranging from low swelling poly(2-hydroxyethyl methacrylate) [PHEMA] to anti-fouling zwitterionic hydrogels via ultra-soft polyacrylamide (PAAm) gels. Our observations are that hydrogels improve the biomimetic design of neural interfaces but their integration triggers additional challenges related to process compatibility and stability and *in vivo* use that call for further optimization.

2:00 PM SB08.04.02

Late News: Selective Targeting and Electrophysiological Recording of Distinct Neural Cell Types with Mesh Electronics Theodore J. ZWang^{1,2}, Anqi Zhang³ and Charles M. Lieber⁴; ¹Massachusetts General Hospital, United States; ²Harvard Medical School, United States; ³Stanford University, United States; ⁴Harvard University, United States

Selective targeting and modulation of functionally distinct cell types and neuron subtypes is central to the bottom-up understanding of the complex neural circuitry. While the optogenetically engineered cells can express light-sensitive channelrhodopsins in a cell type-specific manner and enable targeted optical stimulation, such cell type specificity has not been demonstrated with implantable electronic probes. We address this challenge by modifying the surface of mesh electronics, an implantable neural probe that does not elicit chronic inflammatory immune response and allows for recording of neurons in deep brain structures for over one year. The device surface was functionalized with antibodies or aptamers capable of recognizing and targeting specific cell surface receptors for neurons, astrocytes, microglia, or dopaminergic neuron subtypes and was implanted in the hippocampus of mice. Time-dependent histology studies revealed the intimate association of the targeted cell types with the electronics, without affecting the distribution of other cell types. *In vivo* chronic electrophysiology showed that the identity of cells associated with the electronics had a significant influence on the properties of recordings. Recordings from electronics with modifications targeting dopaminergic neuron subtypes showed selective modulation under the influence of known dopamine receptor agonists and antagonists. These surface modifications may be extended to other neurotechnologies and could benefit the study of neural cells in model systems where genetic modifications are difficult or not possible.

2:15 PM SB08.04.03

Ti₃C₂MXene Microelectrode Arrays with Tunable Optical and Electrochemical Properties Sneha Shankar¹, Brendan Murphy¹, Yuzhang Chen¹, Quincy Hendricks¹, Nicolette Driscoll¹, Tyler Mathis², Natalia Noriega², Hajime Takano¹, Yury Gogotsi² and Flavia Vitale¹; ¹University of Pennsylvania, United States; ²Drexel University, United States

Microelectrode arrays are widely adopted tools to investigate neuron-level and microscale circuit dynamics underlying brain function and disease. While standard microelectrodes enable detecting electrophysiological signaling, developing devices with optical stimulation, and recording capabilities, allows mapping neural dynamics at higher spatial and temporal resolution, and across multiple scales. Thus, there is a need of novel materials and processes to realize microelectrode arrays with tunable optical and impedance properties, while minimizing interference from photoelectric artifacts. Here we demonstrate novel processing and fabrication approaches to develop low-impedance microelectrode arrays with tunable optical properties based on Ti₃C₂MXene. Specifically, we explored several processing parameters and conditions, such as the concentration of the precursor solution as well as film thickness, to optimize sheet resistance, transparency, and electrochemical interface impedance of the Ti₃C₂MXene films. The resulting films are ~20nm thick, have a 550 nm transmittance of 60% and sheet resistance of 60 Ω/□. The corresponding figure of merit is 14, which is comparable to or higher than other optoelectronic transparent films used for neural interfacing. Then we fabricated parylene C-based 4 x 4 micro electrocorticography (μECOG) arrays using microfabrication techniques and solution processing of MXene. The arrays have 50 μm x 50 μm recording sites spaced 500 μm apart and an overall footprint of 2.75 mm x 2.75 mm. Electrochemical impedance spectroscopy measurements at 1kHz show a predominantly capacitive response and an average impedance modulus ranging from 143 kΩ ± 157 to 555 kΩ ± 103 (5 devices, 68 channels) which is 2 to 5 times lower than previously developed transparent graphene interfaces. To evaluate the feasibility of acquiring multimodal signals *in vivo* in a relevant disease model, signal recording ability and quality, we tested the devices *in vivo* in an epilepsy mouse model. We were able to successfully record epileptiform activity and simultaneous monitor calcium fluorescence fluctuations. Continued work with electrodes will involve dissecting recorded data and probing neural dynamics through concurrent optogenetic stimulation of neuronal activity to understand disordered mechanisms.

2:30 PM SB08.04.04

Multi-Dimensional Fuzzy Graphene Based I/O Bioelectronics for Tissue Innervation Raghav Garg¹, Mehrdad Javidi¹, Daniel J. San Roman¹, Yingqiao Wang¹, Samuel Gershanok¹, Stephen Badylak², Douglas Weber¹ and Tzahi Cohen-Karni¹; ¹Carnegie Mellon University, United States; ²University of Pittsburgh, United States

Complete recovery from volumetric muscle loss injuries requires adequate structural regeneration of the lost tissues with proper innervation. Although

various tissue engineering strategies have been developed to facilitate regeneration, restoring adequate innervation remains an open challenge. Electrical stimulation has emerged as a promising intervention to enhance tissue innervation after trauma and restore motor control. This has been achieved via input/output (I/O) bioelectronics that interface engineered materials with biological entities. Recently, graphene and its composites have gained interest as building-blocks for bioelectronics due to their advantageous electrochemical properties and biocompatibility. However, graphene-based bioelectronics exhibit a two-dimensional (2D) topology resulting in limited electrochemical performance. Ideal bioelectronics need to leverage on three-dimensional (3D) topologies to maximize the exposed surface-area and enhance interaction with interfaced biological entities.

Here we report a breakthrough hybrid-nanomaterial based on nanowire-templated 3D fuzzy graphene (NT-3DFG) and poly(3,4-ethylenedioxythiophene)-polystyrene sulfonate (PEDOT:PSS), for functional I/O bioelectronics. The hybrid-nanomaterial leverages on high surface-area of free-standing graphene flakes of NT-3DFG and the high charge storage capacity of PEDOT:PSS. The resultant hybrid-nanomaterial exhibits lower electrode impedance, cathodic charge storage capacity (CSC_C) up to 24.87 ± 5.40 mC/cm², and charge injection capacity (CIC) up to 13.21 ± 3.6 mC/cm² with footprint as small as 20 μm. We interface the developed hybrid-nanomaterial with *in-vivo* systems to effect cellular- and tissue-scale electrophysiology via electrical stimulation; and record the resultant electrical activity as electromyograms (EMG). Through our platform, we demonstrate the importance of extending the topology of nanomaterials to 3D to develop the next generation of functional I/O bioelectronics.

2:45 PM SB08.04.05

Viscoelastic Surface Electrode Arrays to Interface with Viscoelastic Tissues [Christina M. Tringides](#)^{1,2}, Nicolas Vachicouras³, Irene de Lazaro¹, Alix Trouillet³, Stephanie P. Lacour³ and David Mooney¹; ¹Harvard University, United States; ²Massachusetts Institute of Technology, United States; ³EPFL, Switzerland

Living tissues are non-linearly elastic materials that exhibit viscoelasticity and plasticity. Man-made, implantable bioelectronic arrays mainly rely on rigid or elastic encapsulation materials and stiff films of ductile metals that can be manipulated with microscopic precision to offer reliable electrical properties. Here, we engineer a surface microelectrode array that replaces both the traditional encapsulation and conductive components with viscoelastic materials. Our entirely viscoelastic array overcomes previous limitations in matching the stiffness and relaxation behavior of soft biological tissues by using hydrogels as the outer layers. We introduce a novel hydrogel-based conductor made from an ionically conductive alginate matrix enhanced with carbon nanomaterials (e.g. graphene, carbon nanotubes). These high aspect ratio additives provide electrical percolation even at low loading fractions, and we fabricate ultra-soft viscoelastic conductive electrodes and electrical tracks that intimately conform to the convoluted surface of the heart or the brain cortex. Our combination of conducting and insulating viscoelastic materials, with top-down manufacturing, allows for the versatile fabrication of electrode arrays compatible with *in vivo* recording and stimulation.

3:00 PM *SB08.04.06

Millimeter-Sized Wireless Bioelectronics [Jacob T. Robinson](#); Rice University, United States

Millimeter-sized bioelectronic implants can provide advanced therapies with minimal invasiveness providing a potential alternative to traditional pharmaceuticals. To create devices with millimeter-sized form factors we must overcome the challenges of sending data and power to miniature battery-free devices. This is particularly challenging for devices implanted deep within tissue because the body absorbs electromagnetic radiation at frequencies typically used for wireless data and power transmission. Here, we describe how magnetic materials like magnetoelectrics and superparamagnetic nanoparticles can enable precise control of neural circuits and millimeter-sized bioelectronic devices. Specifically, we show that these materials can improve the speed, reliability, and power densities possible with miniature bioelectronics

3:30 PM BREAK

4:00 PM SB08.04.08

Ti₃C₂ MXene Flakes for Optical Control of Neuronal Electrical Activity [Yingqiao Wang](#)¹, Raghav Garg¹, Jane E. Hartung², Adam Gold³, Dipna A. Patel³, Flavia Vitale⁴, Michael S. Gold², Yury Gogotsi³ and Tzahi Cohen-Karni¹; ¹Carnegie Mellon University, United States; ²University of Pittsburgh, United States; ³Drexel University, United States; ⁴University of Pennsylvania, United States

Understanding cellular electrical communications in both health and disease necessitates precise subcellular electrophysiological modulation. Nanomaterial-assisted photothermal stimulation was demonstrated to modulate cellular activity with high spatiotemporal resolution. Ideal candidates for such an application are expected to have high absorbance at the near-infrared (NIR) window, high photothermal conversion efficiency, and straightforward scale-up of production to allow future translation. Here, we demonstrate two-dimensional (2D) Ti₃C₂ (MXene) as an outstanding candidate for remote, nongenetic, optical modulation of neuronal electrical activity with high spatiotemporal resolution. Ti₃C₂ photothermal response measured for the first time at a single-flake level resulted in local temperature rises of 2.31 ± 0.03 K and 3.30 ± 0.02 K for 625 nm and 808 nm laser pulses (1 ms, 10 mW), respectively. Dorsal root ganglia (DRG) neurons incubated with MXene film (25 μg/cm²) or MXene flakes dispersion (100 μg/mL) for 24 h did not show a significant effect on cellular viability, indicating that MXene is non-cytotoxic. DRG neurons were photothermally stimulated using MXene films and flakes with as low as tens of micro-joule per pulse incident energy (635 nm, 2 μJ for film, 18 μJ for flake) with sub-cellular resolution. MXene's straightforward and large-scale synthesis will allow translation of the reported photothermal stimulation approach in multiple scales, thus presenting a powerful tool for modulating electrophysiology from single cell to three-dimensional (3D) engineered tissues.

SESSION SB08.05/SB11.03: Keynote Session: Biostimulation and Bioelectronics

Session Chairs: Herdeline Ardoña, Tzahi Cohen-Karni, Nicolette Driscoll, Raghav Garg, Sahika Inal, Jonathan Rivnay, Daniel San Roman, Flavia Vitale and Yingqiao Wang

Tuesday Afternoon, November 30, 2021
Sheraton, 2nd Floor, Independence West

5:00 PM *SB08.05/SB11.03.01

Keynote: Material Building Blocks for Bioelectronics—Micelles, Pores and Granules [Bozhi Tian](#); University of Chicago, United States

Bioelectronics devices have the potential for realizing personalized medicine and brain-machine interfaces. While significant progress has been made in this area, there is still room for improving the material designs to achieve better functionalities at the interfaces with cells and tissues. In particular, applying biomimetic design principles enables the development of new devices with improved properties in terms of their signal transduction efficiency and biocompatibility. In this talk, I will present a few latest processes in our lab, where new material building blocks have been identified for building

bioelectronics systems. I will discuss a micelle-enabled self-assembly process to prepare a binder-free (i.e., monolithic), carbon-based, and flexible micro-supercapacitor-like system for various types of bioelectronic interfaces. The devices can operate under either micro-supercapacitor-like or a traditional monopolar electrode configuration under physiological conditions, yielding modulation of cardiomyocytes *in vitro*, excitation of isolated heart and retinal tissues *ex vivo*, stimulation of sciatic nerves *in vivo*, as well as bioelectronic cardiac recording. I will also present a newly developed nanoporous/non-porous heterojunction for improved biointerfaces. Without any interconnects or metal modifications, the heterojunction enables efficient non-genetic pulse stimulation of isolated rat hearts *ex vivo* and sciatic nerves *in vivo* with radiant exposure similar to that used in optogenetics. Finally, I will showcase a class of granules-enabled hydrogel composites, with multiple naturally occurring biopolymers and synthetic hydrogels as the key components. The composites have many tissue-like properties, such as strain-stiffening behaviors. The granules-enabled tissue-like materials have enabled the pneumatically actuated bioelectronic devices for applications such as recording the heart electrocardiogram signal *ex vivo*. At the end of my talk, I will present future material development in our lab.

SESSION SB08.06: Tissue Engineering

Session Chairs: Tzahi Cohen-Karni, Nicolette Driscoll, Raghav Garg, Sahika Inal, Jonathan Rivnay, Daniel San Roman, Flavia Vitale and Yingqiao Wang
Wednesday Morning, December 1, 2021
Sheraton, 2nd Floor, Independence West

10:30 AM *SB08.06.01

3D Conducting Polymer Scaffold Devices for Organ-on-Chip Applications Roisin Owens; University of Cambridge, United Kingdom

In vitro models of biological systems are essential for our understanding of biological systems. In many cases where animal models have failed to translate to useful data for human diseases, physiologically relevant *in vitro* models can bridge the gap. Many difficulties exist in interfacing complex, 3D cell biology models with technology adapted for monitoring function. Polymeric electroactive materials and devices can bridge the gap between hard inflexible materials used for physical transducers and soft, compliant biological tissues. An additional advantage of these electronic materials is their flexibility for processing and fabrication in a wide range of formats. In this presentation, I will discuss our recent progress in pushing conducting polymer devices, to 3D, to simultaneously host and monitor complex multi-cellular models of tissues and organs. Building on our previous work that showcased a bioelectronic model of the human intestine, we are now incorporating elements of the microbiome and the immune system as well as the enteric nervous system. Coupling this model with our model of the neuro-vascular unit (including blood brain barrier) currently in progress, will bring us to our goal of a physiologically representative *in vitro* model of the gut-brain-microbiome axis.

11:00 AM SB08.06.02

3D Conducting Polymer/ECM Scaffolds for the Maintenance and Differentiation of Human Neuronal Cells *In Vitro* Chiara Barberio and Janire Saez; University of Cambridge, United Kingdom

Advances in three-dimensional (3D) cell culture modeling have extensively contributed to generate new sophisticated cell culture configurations broadening our understanding of cellular physiology and pathology for a wide range of biomedical applications (e.g., drug discovery, tissue engineering and regenerative medicine). Compared to two-dimensional (2D) cell culture, which is overall too simplistic and lacking most of the cell-cell and cell-environment interaction occurring in the *in vivo* milieu, such 3D formats are capable of resembling the tissue microenvironment in a more biomimetic manner¹. Scaffold-based systems integrating natural and/or synthetic materials are extensively exploited in tissue engineering to develop tissue-specific microenvironments for better supporting cell survival and outgrowth, by providing the chemical and physical cues of the natural extracellular matrix (ECM)². Using a freeze-drying technique, we engineered porous 3D composite scaffolds consisting of poly(3,4-ethylene-dioxythiophene) doped with polystyrene sulfonate (PEDOT:PSS), containing ECM-derived proteins (i.e., Collagen, Hyaluronic Acid and Laminin) for hosting neural 3D cell culture. The highly porous microstructure of these scaffolds was characterised optically by scanning electron microscopy (SEM) along with confocal microscopy, and their conducting properties via electrochemical impedance spectroscopy (EIS). The resulting scaffolds exhibited remarkable mechanical stability and water uptake capacity, directly proportional to the increasing collagen/HA content. We further tested the cytocompatibility profile of these scaffolds and ultimately, their suitability for supporting neural differentiation of neuroblastoma-derived SH-SY5Y cells. We observed that the presence of ECM proteins within the scaffold backbone improves cell survival and proliferation rate compared to the pristine substrate, thus promoting cell propensity to differentiate into mature neurons and generate 3D neural networks. In conclusion, these conducting platforms used here for neuronal cell culture could be potentially amenable for regulating neuronal cell behaviour in a 3D configuration and customised for a variety of tissue engineering applications. Ultimately, to gain more insight into the effects of conducting polymers on neural firing, recording of electrophysiological activity of neurons cultured in 3D will be attempted via simultaneous EIS and MEA (microelectrode array).

References:

1. Moysidou CM, Barberio C, Owens RM. Advances in Engineering Human Tissue Models. *Front Bioeng Biotechnol.* 2021;8:620962. doi:10.3389/fbioe.2020.620962
2. Ullah S, Chen X. Fabrication, applications and challenges of natural biomaterials in tissue engineering. *Appl Mater Today.* 2020;20. doi:10.1016/j.apmt.2020.100656

11:15 AM SB08.06.03

Electrochemical Impedance Spectroscopy as a Tool for Monitoring Cell Differentiation from Floor Plate Progenitors to Midbrain Neurons in Real Time Aya Elghajji¹, Bastian Hengerer², David Tosh¹ and Paulo R. Rocha³; ¹University of Bath, United Kingdom; ²Boehringer Ingelheim Pharma GmbH & Co. KG, Germany; ³University of Coimbra, Portugal

Spinal cord injuries constitute an important clinical target. Emerging therapies to treat central nervous system (CNS) injuries seek to implant neural progenitor cells (NPCs) to promote repair of the neural network subsequent to neural injury. A debilitating aspect of this approach is the inability to non-invasively monitor NPCs during migration and differentiation at injured spots, which critically affects the therapeutic efficacy of neural repair.

Here we show that electrical impedance spectroscopy (EIS) can be used as a non-invasive and real time tool to probe cell adhesion and differentiation from midbrain floor plate progenitors into midbrain neurons, on Au electrodes coated with human laminin. The electrical data and equivalent circuit modelling are consistent with standard microscopy analysis and reveals that within the first 6 hours progenitor cells sediment, and attach to the electrode within 40 hours. Between 40 and 120 hours midbrain progenitor cells differentiate into midbrain neurons, followed by an electrochemically stable maturation phase. The ability to sense and characterize non-invasively and in real time cell differentiation opens up unprecedented avenues for implantable therapies and differentiation strategies.

11:30 AM *SB08.06.04**Bioelectronics for Hybrid Tissues and Disease Modeling** Brian Timko; Tufts University, United States

Hybrid bioelectronic systems offer a unique route toward achieving two-way electronic communication with living cells and tissues. In this talk, we will discuss recent advances in both devices and biomaterials that achieved stable and seamless interfaces with surrounding cells and tissues. We will first present an overview of our recent heart-on-a-chip platform which integrated both extra- and intracellular devices for monitoring cardiac electrophysiology during episodes of acute hypoxia. This system allowed us to monitor not only cell-cell communication (e.g., wavefront propagation) but also action potentials at several spatially-distinct regions simultaneously. Our platform provided a unique route toward undertraining the role of hypoxia on ion channel dynamics. For example, we found that APs shortened during hypoxia, consistent with proposed mechanisms by which oxygen deficits activate ATP-dependent K^+ channels that promote membrane repolarization. We will next discuss routes toward extending our bioelectronic platform to 3D, enabling new classes of hybrid, devices-embedded tissues. We developed a Photo-crosslinkable Silk Fibroin (PSF) derivative that was compatible with conventional photolithography processes and enabled flexible scaffolds with well-defined geometries and cm-scale uniformity. Our freestanding PSF-based scaffolds supported bioelectronic devices, provided excellent electrical passivation, and adhered both cardiac and neuron model cells, opening new avenues toward engineered brain hybrids. Finally, we will present a new class of electromagnetic stimulation elements which achieved highly-localized cellular activation. Taken together, these research directions open new avenues for engineered, bioelectronics-innervated cardiac and brain systems.

SESSION SB08.07: Bioelectronic Devices

Session Chairs: Tzahi Cohen-Karni, Nicolette Driscoll, Raghav Garg, Sahika Inal, Jonathan Rivnay, Daniel San Roman, Flavia Vitale and Yingqiao Wang
 Wednesday Afternoon, December 1, 2021
 Sheraton, 2nd Floor, Independence West

1:30 PM *SB08.07.01**Materials for Bioelectronic Medicines—From Neuroregeneration and Drug Delivery to Cardiac Pacing** John A. Rogers; Northwestern University, United States

Bioresorbable electronic materials form the basis for broad classes of temporary implants with unique capabilities that address unmet clinical needs. Such types of devices can provide therapeutic functionality during the time course of a natural biological process such as healing, and then harmlessly disappear into the body, without a trace. Here, bioresorption eliminates unnecessary device load on the body in a way that bypasses the need for secondary surgical extraction. This talk describes the latest advances in the active and passive materials components of these systems, with examples in devices for (1) neural stimulation, (2) cardiac pacing and (3) programmable drug release.

2:00 PM SB08.07.03**Ti₃C₂ MXene Enables High-Resolution, Gel-Free Electroencephalography** Nicolette Driscoll¹, Brian Erickson², Meikang Han², Georgios Mentzelopoulos¹, Yury Gogotsi², John Medaglia² and Flavia Vitale¹; ¹University of Pennsylvania, United States; ²Drexel University, United States

Electroencephalography (EEG) is a widely used technique for clinical diagnostics and monitoring, for neuroscience research, as well as for non-invasive brain-computer interface (BCI) applications. Despite over 100 years of EEG research, the technology has benefitted from relatively few fundamental innovations in materials that enhance its resolution and form factor while maintaining high-quality signals. Today's EEG technologies have limited spatial resolution because the sensors are relatively large (~1 cm diameter) and they typically require the use of conductive gels or pastes to achieve sufficiently low electrode-skin interface impedance. Such gelled or "wet" electrodes are prone to shorting *via* gel-bridging when they are placed close together for dense spatial sampling, which has made it challenging to push the spatial resolution limits of EEG technology. Gel-free or "dry" EEG electrode technologies offer an alternative solution to the limitations of wet EEG sensors. Existing dry EEG technologies, however, rely on large-area electrodes with poor spatial resolution in order to reduce contact impedance, and rigid, uncomfortable pillar structures to contact the scalp. Here, we present a novel gel-free EEG electrode technology based on the 2D nanomaterial Ti₃C₂ MXene which is capable of recording high-fidelity EEG signals from dry electrodes with high spatial resolution. The electrodes comprise a MXene composite aerogel which is compliant to enhance subject comfort, and can be molded into 3D "mini-pillar" geometries for contacting the scalp through hair. The high conductivity of Ti₃C₂ MXene, along with the porous structure of the composite foam, gives the electrodes low skin contact impedance, allowing high-fidelity EEG recording from mm-scale electrodes with signal quality comparable to standard gelled electrodes. To demonstrate the ability to map scalp EEG at high density, we fabricated 16-channel high-density EEG grids with 3 mm-diameter MXene contacts and 3 mm spacing, which offers higher spatial sampling than the densest EEG systems available today. We used these grids to record EEG signals on human subjects in frontal regions while they completed a battery of attention and working memory tasks shown to have frontal EEG signatures related to task performance. In these experiments, the MXene electrode grids were centered over F3 and F4 EEG coordinates (10-5 system) such that we obtained a total of 32 channels of high-density EEG signal across two frontal regions. Using this paradigm, we explore whether current source density transforms of the ultra high-density enabled by MXene reveal more detailed and localized correlates of frontal attentional function than previously observed. Furthermore, we demonstrate that the MXene electrodes are compatible with magnetic resonance imaging (MRI) and transcranial magnetic stimulation (TMS) due to the low magnetic susceptibility of Ti₃C₂ MXene. The magnetic compatibility of Ti₃C₂ MXene opens up the possibility of concurrent structural or functional MRI, TMS, and EEG recording.

2:15 PM SB08.07.04**Rational Spatial Design of a Bioelectronic Interface** Vedran Derek¹, Nikola Habek¹, Aleksandar Opančar¹, Marta Nikić¹, Anja Mioković¹, Malin Silvera Ejneby² and Eric Glowacki^{3,2}; ¹University of Zagreb, Croatia; ²Linköping University, Sweden; ³Brno University of Technology, Czechia

Essential properties of the bioelectronic materials and interfaces, such as their abilities to exert effective stimulation or enable recording of biological signals, their interface electrochemistry and physiological stability, are widely studied and optimized from the individual perspective of the studied property. Lately, attention was focused on volume electrodes¹ and 3D structuring of bioelectronic devices² on all scales. We will demonstrate how optimizing the two-dimensional and three-dimensional structuring of the bioelectronic interfaces of a model device can amplify, suspend or channel the desired effects in comparison to trivial structures such as highly symmetric planar or rod-like electrodes. As a model device, we have used the organic electrolytic photocapacitor (OEPc), an organic semiconductor-based optoelectronic device capable of capacitive coupling with the excitable tissues. OEPcs have been shown to effectively modulate single cell membrane potentials³, to elicit action potentials in explanted retinal tissue⁴, and to chronically stimulate a peripheral nerve in a rodent model⁵.

We will discuss the basic principles guiding the active and return electrode spatial design for enhanced stimulation intensity and improved and controlled

stimulation localization, demonstrated by the results of FEM numerical modelling, measurements of 3D transductive electric potential field maps in extracellular phantom, and in-vitro stimulation experiments. Multifold enhancement of the performance of the 3D micro-pyramid structured OEPC in comparison to the planar OEPC was observed, with the enhancement strongly depending on the micro-pyramid size and their density, while rationally designed 2D electrode shapes enabled localized and effective tissue stimulation, which would not be possible with the previously used simple designs. We will show how our optimization toolset can be extrapolated and applied to a more general class of bioelectronic interfaces.

- [1] Pitsalidis, C. et al, Transistor in a tube: A route to three-dimensional bioelectronics, *Science Advances*, 4(10), p. eaat4253. doi: 10.1126/sciadv.aat4253 (2018)
- [2] Pennacchio, F. A. et al. 'Bioelectronics goes 3D: new trends in cell–chip interface engineering', *Journal of Materials Chemistry B*, 6(44), pp. 7096–7101 (2018)
- [3] M. Jakesova et al, Optoelectronic control of single cells using organic photocapacitors, *Science advances*, 5 (2019) eaav5265
- [4] D. Rand et al, Direct Electrical Neurostimulation with Organic Pigment Photocapacitors, *Adv. Mater.* 30 (2018), 1707292
- [5] M. Silvera-Ejney et al, A chronic photocapacitor implant for noninvasive neurostimulation with deep red light, *bioRxiv* (DOI: 10.1101/2020.07.01.182113), accepted for publication (*Nature Biomedical Engineering*, June 2021)

2:30 PM SB08.07.05

High-Sensitivity and Real-Time Monitoring of Cell Layers with Dynamic-Mode Current-Driven OEECT Katharina Lieberth¹, Daria Harig¹, Paschalis Gkoupidenis¹, Paul Blom¹ and Fabrizio Torricelli²; ¹Max-Planck-Institute for Polymer Research, Germany; ²University of Brescia, Italy

To use the organic electrochemical transistor (OEECT) as a biosensor is of great importance, as it is a state-of-the-art technique in the field of drug delivery.^[1] Allowing ion-to-electron conversion and having a high amplification of gating due to volumetric capacitance, enables the OEECT to operate with aqueous electrolytes at low voltages.^[2] When utilizing the OEECT as an inverter in a current-driven configuration, a constant current is applied at the channel by an external power supply. It was found that the OEECT offers an enhanced sensitivity compared to standard transfer characteristics of an OEECT.^[3] Even small variations in the ionic current can be detected with the OEECT, which is required to study changes in the cell layer morphology, such as tight junction modulation.^[4] Tight junction barriers of epithelial cell layers impede the transcellular pathway of nutrients and drugs from organs into the blood.^[5,6] Hence, monitoring tight junction modulations is crucial for drug delivery.^[7] As a well-established model for oral drug delivery, the epithelial colon carcinoma (Caco-2) cell line,^[8] found in the small intestine, was used to evaluate reversible modulation of tight junctions over time. Recently, we showed the suitability of OEECTs to *in-situ* monitor temporal barrier modulation and recovery, which can offer valuable information for drug delivery applications.^[9] Here, the origin of the enhanced sensitivity of OEECTs with integrated barrier tissue in current-driven configuration is demonstrated. As next step, we have addressed both experimentally and theoretically the dynamics of OEECTs operation. Understanding of the dynamics is a prerequisite to tune the sensitivity of the OEECT in accordance with the resistance of the barrier under investigation. The quantitative agreement between experiment and modelling of the transient OEECT characteristics allows us to directly translate the current-driven OEECT characteristics into a resistance of the barrier tissue under investigation.^[10]

- [1] N. Y. Shim, D. A. Bernards, D. J. Macaya, J. A. DeFranco, M. Nikolou, R. M. Owens, G. G. Malliaras, *Sensors* **2009**, 9896.
- [2] J. Rivnay, P. Leleux, M. Sessolo, D. Khodagholy, T. Hervé, M. Flocchi, G. G. Malliaras, *Adv. Mater.* **2013**, 25, 7010.
- [3] M. Ghittorelli, L. Lingstedt, P. Romele, N. I. Craciun, Z.M. Kovács-Vajna, P.W.M. Blom, F. Torricelli, *Nat. Commun.* **2018**, 1441;
- [4] L. V. Lingstedt, M. Ghittorelli, M. Brückner, J. Reinholz, N. I. Craciun, F. Torricelli, V. Mailänder, P. Gkoupidenis, P. W. M. Blom, *Adv. Healthcare Mater.* **2019**, 8, e1900128.
- [5] M. Ramuz, A. Hama, M. Huerta, J. Rivnay, P. Leleux, R. M. Owens, *Adv. Mater.* **2014**, 7083.
- [6] L. H. Jimison, S. A. Tria, D. Khodagholy, Gurfinkel M., E. Lanzarini, A. Hama, G. G. Malliaras, R. M. Owens, *Adv. Mater.* **2012**, 5919.
- [7] G.T.A. McEwan, M. A. Jepson, B. H. Hirst, N. L. Simmons, *Biochem. et Biophys. Acta* **1993**, 1148, 51.
- [8] M. S. Balda, K. Matter, *Seminars in cell & developmental biology* **2000**, 11, 281.
- [9] K. Lieberth, M. Brückner, F. Torricelli, V. Mailänder, P. Gkoupidenis, P.W.M. Blom, *Adv. Mater. Tech.* **2021** 6, 2000940
- [10] K. Lieberth, D. Harig, P. Gkoupidenis, P.W.M. Blom, F. Torricelli (in progress)

3:45 PM *SB08.07.06

Transformable Cuff Electrodes for Closed-Loop Stimulation of Small Peripheral Nerves Lukas Hiendlmeier^{1,2}, Francisco Zurita^{1,2}, Tetsuhiko Teshima^{2,1}, Fulvia Del Duca^{1,2} and Bernhard Wolfrum^{1,2}; ¹Technical University of Munich, Germany; ²NTT- Research, United States

Peripheral nerve interfaces are important for implementing neuromodulation strategies. For example, feedback loops can be employed to control the behavior of tissue by modulating the activity of the innervating input as a response to a biomarker. Cuff electrodes represent an important class of such nerve interfaces that are often used for applications in bioelectronic medicine. Large nerves, with diameters in the range of one mm or above, can be easily stimulated with appropriate cuff electrodes. However, the stimulation strategies often lack specificity as several fibers are typically addressed simultaneously. Stimulating small nerves, below 100 μm , can generate more specific responses but poses additional challenges for device development as well as handling during an operation. Here, we present a type of self-foldable cuff electrodes that can be readily applied *in vivo* for addressing small peripheral nerves. The devices are fabricated combining 3D printing and lithographic approaches employing strongly swelling materials. We demonstrate the usability of the nerve cuff electrodes after implantation on the extensor motor nerves by implementing a simple closed-loop strategy to control the angles of a locust's legs in real time. Extensor motor nerves are stimulated using trains of stimulation pulses with a gradual response of the leg position determined by the applied stimulation frequencies. We monitor the leg's angles using a flexible sensor and implement the feedback loop with a simple control algorithm on a microcontroller. The design of the cuff electrodes allows straightforward implantation and removal without impairment of the nerve functionality.

3:00 PM BREAK

4:15 PM SB08.07.07

Fully Implantable, Ion-Gated, Organic Integrated-Circuits for Chronic, Closed-Loop Epileptic Interventions Claudia Cea, Zifang Zhao, Jennifer Gelinas and Dion Khodagholy; Columbia University, United States

Bioelectronic devices are increasingly required to not only acquire biologic signals, but also to process them in real-time. For a subset of patients with epilepsy, responsive neurostimulation in the form of implanted devices are promising form of treatment. However, the only components capable of performing these functions at present are silicon-based, non-biocompatible, bulky, and need rigid encapsulation in physiologic environments. Here, we demonstrate a fully implantable, soft, biocompatible, neural acquisition and processing device based on complementary internal ion-gated organic electrochemical transistors (IGTs). A key function of these responsive neurostimulation devices is accurate detection of epileptic discharges. This detection can be challenging due to the variable amplitude of the neural potentials based on the location of the recording electrode with respect to local dipoles and

the reference electrode. We combined a depletion and enhancement mode IGTs to create a non-linear rectification circuit that can be chronically implanted to recorded and detect epileptiform inter-ictal discharges (IEDs). This device was used to process signals acquired from the hippocampus of a freely moving epileptic rat. The IGT-based non-linear rectification circuit accurately detected epileptic discharges, with receiver operating characteristics that surpassed traditional filter thresholding methods. Therefore, IGTs and their ability to efficiently integrate enhancement and depletion mode devices within individual circuits can improve real-time processing of disease-relevant neurophysiological signals and have the potential to form fully implantable, conformable acquisition and processing units for bioelectronic devices. Overall, we have shown that e-IGTs can serve as reliable components for bioelectronic devices, with the potential to improve our ability to transduce and modulate physiologic signals. E-IGTs are also suitable for translation to use in humans, offering a safe, reliable, and high-performance building block for chronically implanted bioelectronics.

4:30 PM SB08.07.08

Ions-Based High-Bandwidth Communication for Bioelectronics Zifang Zhao¹, Claudia Cea¹, Georgios Spyropoulos², Jennifer Gelinas^{3,3} and Dion Khodagholi¹; ¹Columbia University, United States; ²Ghent University, Belgium; ³Columbia University Medical Center, United States

High-density neural interfaces are continuously progressing towards seamless integration of brain and electronics. As more effort has been dedicated to implantable devices, effective and non-invasive data communication between the implant and outside electronics becomes a critical unresolved issue, because biologic tissue absorbs most of the electromagnetic waves. Here we introduce the ionic communication (IC) that utilizes ions and water polarization for high-speed data communication. We describe the working principles of IC, and investigated the effect of material and geometrical properties such as area, material composition, ion type/concentration, and operating frequency and on the performance of the IC in the form of gain and spatial propagation. Based on these measurements, we developed a model to accurately estimate IC-based communication's propagation depth in the body and established a multi-line implantable IC with several hundred MHz bandwidth. We chronically implanted conformable IC devices with no extruding elements and were able to acquire and transmit high-quality electrophysiological data at the level of signal neurons' action potentials from freely moving rats. The IC and the resulting devices set the foundation for non-invasive, fully-implantable communication strategy for biomedical implantable systems, such as brain-computer interfaces, responsive neurostimulation devices, deep-brain-stimulators and cochlear implants that require a low consumption, high bandwidth wireless communication system.

4:45 PM SB08.07.09

High Energy Return on Investment—Efficient Natural Perspiration Based Biofuel Cells for Bioenergy Harvesting Lu Yin, Jong-min Moon, Juliane Sempionatto, Sheng Xu and Joseph Wang; University of California, San Diego, United States

Self-powered wearable systems relying on bioenergy harvesters commonly require excessive energy inputs from the human body and are highly inefficient when accounting for the overall energy expenses. A harvester independent from the external environment for sedentary states has yet to be developed. Herein, we present a touch-based lactate biofuel cell that leverages the high passive perspiration rate of fingertips for bioenergy harvesting. Powered by finger contact, such bioenergy harvesting process can continuously collect hundreds of mJ of energy during sleep without movements, representing the most efficient approach compared to any reported on-body harvesters. To maximize the energy harvesting, complementary piezoelectric generators were integrated under the biofuel cell to further scavenge mechanical energy from the finger presses. The harvesters can rapidly and efficiently power sensors and electrochromic displays to enable independent self-powered sensing. The passive perspiration-based harvester establishes a practical example of remarkably high energy return-on-investment for future self-sustainable electronic systems.

5:00 PM SB08.07.10

An Implantable and Flexible Multi-Electrode Neural Probe using Active Matrix Design of IGZO Thin-Film Transistors Array Jiwon Chae, Gooun Pyo, Sujin Heo, Kwonsik Shin, Sohee Kim and JaeEun Jang; Daegu Gyeongbuk Institute of Science and Technology (DGIST), Korea (the Republic of)

An implantable probe with an electrode array can precisely record brain signals from different groups of neurons simultaneously, yet maintaining high spatial resolution is still challenging. Each electrode of a dot matrix type needs an individual wire, and then, it is appropriate only for a few electrodes. A passive matrix design is better, since the total number of wires needed is $C+R$, where C is the number of columns and R is the number of rows in the passive array, respectively. However, the passive matrix design showed a cross talk issue among neighboring cells. In contrast, an active matrix design also needs $C+R$ number of wires to fabricate $C \times R$ number of electrodes, but it can induce a good electrical isolation among cells. CMOS technology has been studied for high density electrodes. However, stiff silicon-based probes induce inflammation in the tissue. Therefore, flexible polymer-based probes can handle this problem by reducing mechanical mismatch between a probe and neural tissue and growth of the glial sheath. Here, we fabricated polyimide-based flexible neural probes with a 4×8 array of electrodes based on the active matrix design of a-IGZO thin-film transistors (TFTs) for neural signals recording. We measured electrical properties and conducted electrical signal recording tests. Our neural probe design has advantages in high spatial resolution, flexibility due to polyimide (PI) probe pattern, and high mobility of IGZO TFTs. We easily fabricated probes using photoresist PI (jsr-wpr 1201) by photolithography on a sacrificial layer. Then, back gate IGZO TFT was fabricated on the PI probe, followed by PI encapsulation layer photolithography. The sacrificial layer was wet etched, while the probe has $50\mu\text{m}$ spacing and $20\mu\text{m}$ diameter holes for large area undercut. Our $25\mu\text{m}$ thickness PI probe is flexible and can endure a-IGZO TFT annealing temperature. The cell size is $86\mu\text{m} \times 200\mu\text{m}$ and the electrode size is $40\mu\text{m} \times 80\mu\text{m}$. To obtain a high signal-to-noise ratio (SNR), a high-performance transistor is studied. The width-length of the transistors is designed to $50\mu\text{m}/10\mu\text{m}$, and the field-effect mobility is $20\text{ cm}^2/\text{Vs}$ and on current is $7 \times 10^{-5}\text{A}$ under a low driving voltage, 5V. The on-off ratio is 1.1×10^7 and the threshold voltage (V_{th}) is 2.7V. The passive matrix design consists of one transistor in a cell. A gate line turns on the TFT applying 5V which is higher than the V_{th} , and a drain line senses the signal. For amplifying signals, the active matrix design consisting of two transistors in a cell is also fabricated. By applying 5V, the switching TFT is turned on, and the sensed signal can be measured on the drain line. One transistor works as a switch and another works as an amplifier. The shank, a sensing area of the probe, was placed in the PBS solution, and we recorded electrical signals using a function generator, an oscilloscope, and a power supply. Signals were recorded and compared to the dot matrix design. Our active matrix design probes successfully amplified the amplitude value of electrical signals. Therefore, our active matrix design TFT electrode array probe can be used for accurate neural recordings with high SNR and would open a new generation of flexible neural probes with high spatial resolution.

SESSION SB08.08: Poster Session I: Bioelectronics—Materials and Interfaces

Session Chairs: Tzahi Cohen-Karni, Raghav Garg, Jonathan Rivnay, Daniel San Roman, Flavia Vitale and Yingqiao Wang

Wednesday Afternoon, December 1, 2021

8:00 PM - 10:00 PM

Hynes, Level 1, Hall B

SB08.08.01

A Comprehensive 3D FEM Model of Excitable Tissue and Capacitive Electrode Interface [Aleksandar Opančar](#), Anja Mioković, Nikola Habek and Vedran Derek; Department of Physics, Faculty of Science, University of Zagreb, Croatia

The interface of excitable cells and stimulation or recording electrodes is essential for bioelectronic applications. Parameters such as the electrode impedance and capacitance, interface electrochemistry, surface structuring and long term in vivo stability have been thoroughly studied. However, in many applications, especially clinical ones, only trivial electrode geometries are used, resulting in increased charge density thresholds. Using optimized electrode geometries and stimulation protocols may overall be more effective, especially in the case of implanted bioelectronic devices with limited current generation capabilities.

For highly localized target specific electrostimulation, electrode design and stimulation protocol are crucial parameters to consider. We consider multiple planar and 3D electrode configurations for stimulating excitable cells and tissues, and different stimulation protocols using pulsed and modulated current. A comprehensive finite element method (FEM) model encompassing realistic capacitive photo-electrode (organic electrolytic photocapacitor – OEPC) and tissue model is made in COMSOL Multiphysics® software. Electrodes are characterized by their contact electrical properties, contact capacitance and contact resistance, while the OEPC is characterized by its equivalent circuit model. Realistic cell membranes and action potential propagation are implemented using the Hodgkin–Huxley model which can be tailored to a specific cell type.

We show that using the optimized electrode configuration enables multifold current density enhancement at the targeted stimulation area which enables effective cell and tissue excitation while minimising the residual effect on the surrounding tissue. Our numerical findings are validated in vitro using cortical neuron cell cultures and mouse brain slices.

SB08.08.02

Passivation Strategies for Enhanced BioFET Performance and Stability in Ionic Solutions [Faris M. Albarghouthi](#), Nicholas Williams, Joseph Andrews, Shiheng Lu, Jay Doherty, Steven Noyce and Aaron D. Franklin; Duke University, United States

Increasing demand for personalized medicine has led to a surge of research into electronic biosensing approaches, particularly those involving the use of a field-effect transistor (FET) as the transduction element in ion-sensitive FET-like structures. While electrical biosensors adhere to many of the tenets of the so-called “ideal biosensor,” one limitation that could hinder their success in a solution-gated setup is gate leakage. As electrical devices become immersed in solution (such as physiological liquid), improper passivation of the components results in electrical current leaking between the BioFET and the solution, thus compromising the transduction signal and preventing sensitive biological detection. Focus in the field has been on singular demonstration of BioFET applications, yet there is no consensus on device design and passivation strategy, which leads to difficulty comparing results between reports that ostensibly investigate similar phenomena, particularly with regards to gate leakage.

In this work, we investigate various passivation strategies for printed, solution-gated carbon nanotube (CNT) BioFETs. Contact-only photoresist passivation is investigated alongside whole-device dielectric passivation, particularly in the context of gate leakage reduction, long-term device stability, and wafer-scale device yield. We find that while optimized photoresist-only and dielectric-only passivation both result in high-quality BioFETs, the combination of the two – coating the contacts with a photoresist then the entire device with a dielectric – results in highly consistent performance, with more than 90% of tested devices displaying nA-level gate leakage with on/off-current ratios greater than 10^3 in solution. The photoresist+dielectric strategy also results in the best stability over 500 testing cycles, demonstrating robust performance on a timescale exceeding that required for most biomolecular binding reactions to occur. Finally, we show that the addition of a polyethylene glycol (PEG) polymer layer, which reduces non-specific protein adsorption and increases Debye length, has no significant impact on device performance both in initial device metrics and after long-term cycling when polymerized on these passivation structures. Ultimately, these results help pave the path toward the development of a truly high-yield, sensitive, stable, and robust electrical biosensing platform.

SB08.08.03

Electrical Transduction of Prothrombin Time Using Printed Nanoparticle-Based Sensors [Brittani L. Carroll](#), Nicholas X. Williams, Jay Doherty, Steven Noyce and Aaron D. Franklin; Duke University, United States

Heart failure affects over 6.4 million people in the United States alone, with over 550,000 new cases emerging annually. Ventricular assist devices (VADs) have become a popular means of long-term care; yet, due to their thrombogenic nature, patients are frequently prescribed anticoagulation medication (e.g., warfarin). To ensure dosages remain in the therapeutic window for this strong anticoagulation drug, periodic blood-based testing (every 1-4 weeks) is required to measure patients' prothrombin time/international normalized ratio (PT/INR), which reflect the clotting tendency of blood and hence the extent of anticoagulation. This frequent, clinic-based monitoring of PT/INR is cumbersome and costly; thus, an at-home monitoring system to ensure adequate coagulation times would be transformative for those on warfarin therapy.

Although point-of-care (POC) coagulometers are commercially available and have been demonstrated to reduce the burden on both patients and the healthcare system, only a small percentage of VAD patients perform POC self-testing. Current POC coagulometers and reagent cartridges are high cost, which limits insurance coverage, and are inconsistent in device performance. Therefore, there is a need for an alternative device that offers an at-home and portable measurement of PT/INR that is low-cost, accurate, and user friendly. In this work, a fully printed POC PT/INR test using electrical transduction is demonstrated. In order to create a low-cost device, an inexpensive testing platform was designed, which consists of aerosol jet printed silver nanoparticle electrodes. The functionality of the device was demonstrated in whole blood derived from both animal and human subjects. Given the necessity of a robust sensor, identical clotting times were measured on both a ridged and a flexible substrate tested under bending strain. In addition, a handheld sensor with low-cost electronics was designed and shown to have a measurement accurate to within a standard deviation of the costly, stationary, computer-based testing system. Finally, to improve upon the accuracy of developed handheld devices, multiple sensing modalities were combined to incorporate on-chip calibration for the impedimetric coagulometer. Taken together, these results lay the groundwork for fully printed impedimetric sensors, which address the unmet need for a low-cost, robust, POC device, potentially improving outcomes for VAD patients by early detection of aberrations in PT/INR.

SB08.08.04

Detecting Cancer Biomarkers Electrically Using Single-Molecule Techniques for Future Liquid Biopsy Applications—Understanding Bioelectronics Fingerprints at the Nucleic Acid Bioelectronic Interface [Keshani G. Pattiya Arachchilage](#), Subrata Chandra, Jordan Ventura, Sarah Currier, Steven Ayoub and Juan Artes Vivancos; University of Massachusetts Lowell, United States

Cancer is one of the most frequent causes of death globally and kills more than 8 million people per year.¹ Early diagnosed cancers are relatively easier to treat and cure. Cancer biomarkers, such as circulating free tumor nucleic acids (ctNA), are promising for detecting cancers early.^{2,3} There are various techniques to screen cancers and liquid biopsy is one of them.² This is a promising approach since it is used to diagnose tumor-specific biomarkers non-invasively.² Detecting ctNA in body fluids is challenging, because of the low ctNA concentration and the low frequency of mutations compared to wild-type sequences.² Nanotechnology bioelectronics methods can help to address this challenge. In particular, the Scanning Tunneling Microscopic (STM)-assisted break junctions method (STM-BJ)⁴ has recently allowed the first demonstration of detection and identification of RNA from E.Coli via single-molecule conductance.⁵ This is an ideal new method for liquid biopsy bioelectronics since it is non-invasive, highly sensitive, and specific.

This work focuses on characterizing ctNAs and investigating an effective method for their ultra-sensitive detection in complex samples using STM-BJ. The study's main hypothesis is that the sequences of ctNAs can be used to detect cancers electrically, by finding their unique electronic fingerprints. We focus the study on KRAS, BRAF, and Nras as effective cancer biomarkers, in agreement with data from the Pan-Cancer Analysis of Whole Genomes (PCAWG) Consortium of the International Cancer Genome Consortium (ICGC) and The Cancer Genome Atlas (TCGA).^{6,7} We already have obtained some preliminary data for RNA sequences for KRAS biomarker and we expect to understand the bioelectronics interface between genetic material(ctNA) and nanostructured electrodes. Our initial analysis and the results pave the way for the early detection of bioelectronic fingerprints from biomarkers, such as ctDNA and ctRNA, through liquid biopsy using nanotechnology. This new bioelectronics method may allow beginning treatments early, potentially saving many lives from cancer patients in the future.

References

1. Campbell PJ, Getz G, Korbel JO, et al. Pan-cancer analysis of whole genomes. *Nature*. 2020;578(7793):82-93. doi:10.1038/s41586-020-1969-6
2. Das J, Kelley SO. High-Performance Nucleic Acid Sensors for Liquid Biopsy Applications. *Angew Chemie - Int Ed*. 2019. doi:10.1002/anie.201905005
3. Henry NL, Hayes DF. Cancer biomarkers. *Mol Oncol*. 2012;6(2):140-146. doi:10.1016/j.molonc.2012.01.010
4. Xu B, Tao NJ. Measurement of single-molecule resistance by repeated formation of molecular junctions. *Science (80-)*. 2003;301(5637):1221-1223. doi:10.1126/science.1087481
5. Li Y, Artés JM, Demir B, et al. Detection and identification of genetic material via single-molecule conductance. *Nat Nanotechnol*. 2018;13(12):1167-1173. doi:10.1038/s41586-018-0285-x
6. Rheinbay E, Nielsen MM, Abascal F, et al. Analyses of non-coding somatic drivers in 2,658 cancer whole genomes. *Nature*. 2020;578(7793):102-111. doi:10.1038/s41586-020-1965-x
7. Detection of BRAF mutation in thyroid papillary carcinomas by mutant allele-specific PCR amplification (MASA) in: *European Journal of Endocrinology* Volume 154 Issue 2 (2006). <https://eje.bioscientifica.com/view/journals/eje/154/2/1540341.xml>. Accessed June 8, 2020.

SB08.08.06

Degradation Mechanisms in Organic Electrochemical Transistors Emily Schafer, Ruiheng Wu, Dilara Meli, Bryan D. Paulsen and Jonathan Rivnay; Northwestern University, United States

Organic electrochemical transistors (OECTs) leverage the volumetric capacitance of mixed conducting conjugated polymers to enable efficient signal transduction and amplification at the biotic/abiotic interface, which is advantageous for applications such as electrophysiology and biosensing. The specific properties of conducting polymer OECT channel materials can be synthetically tailored to meet a variety of application and device requirements, such as biocompatibility, high degree of amplification, fast switching times, processability, and more. However, issues of OECT stability must be addressed in order to realize long-term biological interfacing. First and foremost, the mechanisms of OECT degradation have yet to be directly assessed. Further, a common standard for quantifying OECT stability has yet to be adopted across the field, limiting the general utility of published OECT stability results. Without addressing the fundamental issues of OECT stability and degradation, the translational potential of OECTs is unlikely to be realized.

We therefore have quantified OECT degradation during cycling with a suite of electrical, electrochemical, and *in situ* spectroscopic measurements which enable the separate investigation of OECT channel degradation near the source and drain electrodes, and allow the deconvolution of bias and current stress effects. Employing a prototypical P-Type polythiophene based polymer with oligoethylene glycol side chains, we find OECT degradation to be a complex phenomenon, exacerbated by the coexistence of oxidating and reducing potential environments arising near the source and drain electrodes during device operation. These environments depend on both the mass transport of electrochemically produced reactive species and the residence time of electronic charge carriers in the channel. Interestingly, device implementations that avoid the coexistence of oxidating and reducing potential environments drastically improve device stability. To test the universality of these results we have extended our studies to N-type and other P-type conjugated polymers.

Our results identify clear material properties targets (highest occupied and lowest unoccupied molecular orbital level positions) for directing the rational design of next generation OECT channel materials to maximize device stability. Further, we elucidate the most stable OECT biasing schemes and circuit implementations to maximize device stability, particularly for long-term biological sensing. Finally, we present suggestions for straightforward and rigorous OECT stability evaluation and discuss key caveats to consider when interpreting OECT stability results in the literature.

SB08.08.08

Late News: Modeling Quantum Transport in Bacterial Nanowires for Nanoelectronics William Livernois and M.P. Anantram; University of Washington, United States

Heme-based nanowires found in the pili of *Geobacter sulfurreducens* bacteria show great promise as a biomaterial for sensors and nanodevices. These nanowires, which consist of stacked cytochromes in a protein scaffold, have been shown to have high metallic-like conductivity. The structure was only recently determined using cryo-EM techniques, showing alternating perpendicular and parallel coordinated heme porphyrins with a repeating six heme subunit that forms a helical wire. Previous studies have modeled charge transport in cytochromes using Marcus theory, which combines modeling methods with a semi-classical electron hopping model that uses transition states to determine rate kinetics. While this has yielded models that match some cytochrome systems, the electronic behavior of the pili nanowires indicates that coherent and decoherent transport contribute significantly to overall conductivity.

The electronic properties of these nanowires were investigated using density functional theory (DFT) with a localized atomic orbital basis in Gaussian 16. Terminated sub-units of the nanowire structure were investigated, looking at the dependency of quantum transmission on spin states and iron oxidation states. The generated Hamiltonian was used with the non-equilibrium Green's function method to calculate quantum transmission and determine the single molecule conductance. The results show that the Fe (II) neutral structure has a moderate band gap (2.3-2.7eV) that drops significantly with a single oxidized heme site, and further oxidation restoring the original band gap. The quantum transmission was similarly affected, with resulting conductances matching experimental results. This demonstrates the nanowire sensitivity to oxidation state, which can be modulated chemically to change conductivity.

SB08.08.09

Late News: Biosynthetic Electronics with Encoded Functionalities Yixin Zhang; Tufts University, United States

Living electronics that converge the unique functioning modality of biological and electrical circuits has the potential to transform both fundamental biophysical/biochemical inquiries and translational biomedical/engineering applications. The intrinsic mismatches in physiochemical properties and signaling modality at biotic/abiotic interfaces, however, have made the seamless integration challenging. Here we demonstrate the effective hybridization of living and artificial components through a bottom-up approach, where electrochemically active bacteria (such as *Shewanella*) initiate the interaction and drive the assembly of electronic building blocks to design and formulate new functions across multiple length scales. In particular, by exploiting graphene

oxide (GO) as the solid-state electron acceptors, the bacterial metabolism leads to the construction of fully integrated 3-D living hydrogel material with significantly reduced interfacial charge transfer barrier. Combining desirable material and signaling attributes from both biotic and abiotic components, as assembled biohybrids feature mechanical integrity, optimal mass/charge transport, and bioactive performance. In particular, the electrical conductivity and morphology/shape of the living hydrogel can be simply tuned by changing ratios of two precursor solutions: bacteria and GO and using culture reactors with different shapes, respectively. With minimized charge transfer barrier between biological and electrical centers in our living system, it also enables us to quantitatively “read” intrinsic biological functions/activities based on detected electrical signals. Here we proved this possibility by translating bacteria’s metabolism towards heavy metal ions into the measurable electrical signals with both shape and magnitude being linked to specific bio activities. Lastly, we also proved that our hydrogel system is compatible to be interfaced with other biological machineries and therefore, could introduce more advanced functions to our system, such as photosynthetic function. In summary, these works describe by forging the structural and functional synergy between biological and electrical circuits, the as-formed “living electronics” is expected to open-up new opportunities for many cross-disciplinary applications in biosynthesis, sensing, energy transduction, and hybrid information processing.

SB08.08.10

The Influence of Regiochemistry on the Performance of Organic Mixed Ionic and Electronic Conductors Roman Halaksa¹, Ji Hwan Kim², Peter A. Finn¹, Hyungju Ahn³, Myung-Han Yoon² and Christian Nielsen¹; ¹Queen Mary University of London, United Kingdom; ²Gwangju Institute of Science and Technology, Korea (the Republic of); ³Pohang Accelerator Laboratory, Korea (the Republic of)

The field of organic bioelectronics has experienced a dramatic development in recent years and during its existence has shown a number of applications such as metabolite sensing, drug delivery, fabrication of neuromorphic devices, and many more.

The organic electrochemical transistor (OECT), which combines both a sensor and a signal amplifier in its structure, is an ideal tool for the interface between biological and artificial systems. Currently, the OECT research is dominated by commercial PEDOT:PSS, which, however, has a number of disadvantages, such as operation in depletion mode, the difficulty of its chemical modification, and very high acidity. Therefore, it is necessary to focus development on other materials as well to remedy these unwanted properties. Both ionic and electrical conductivity are required for OECTs to function properly. It is therefore beneficial to functionalize the OECT active materials with hydrophilic moieties (such as glycol chains), but also to pay attention to their position so that the resulting material can remain structurally organized in order to preserve its electrical conductivity.

In this study, a series of four p-type polymer materials with a high density of glycol side chains were designed, synthesized, and subsequently fully characterized. By choosing different comonomer units, both straight and bent polymer geometries were achieved, with each polymer having been synthesized in two regioisomeric variants depending on the exact positioning of the glycol side chains. All polymers were found to operate efficiently in OECT accumulation mode. Subsequent detailed research revealed that even a small positioning change of side chains can have a major effect on molecular packing and electrochemical properties and can lead to nearly 6-fold increase of the OECT figure of merit.

SB08.08.12

The Pyroelectricity of M13 Virus Han Kim^{1,2}; ¹University of California, Berkeley, United States; ²Lawrence Berkeley National Laboratory, United States

Pyroelectricity is a physical phenomenon of polarization change under temperature fluctuation in the environment. Biological building blocks, such as amino acids, nucleic acids (DNA and RNA), proteins, and biomaterials such as soft and hard tissues with hierarchical structures are composed of polar molecules and are also known to induce pyroelectric properties. However, the understanding of the biological pyroelectric effect is still lacking due to the configurational complexity and few model system. Here, we present the M13 virus as a novel model system to demonstrate the structure-and-function relationship of biological pyroelectricity at the molecular level. M13 virus is a benign and non-harmful virus to infect only bacterial host cells. It has a filamentous shape with 880 nm in length and 6.6 nm in diameter. The M13 virus is assembled with 2700 copies of major pVIII coat protein hierarchically with spontaneous polarization. We observe that the pyroelectricity of the M13 is induced by the non-centrosymmetric structure and spontaneous polarization of the major coat protein (pVIII). With molecular dynamics simulations and circular dichroism spectroscopy, we demonstrate that the alpha-helical structure of pVIII changes to a random coil upon heating, resulting in the change in polar characteristics of M13. By fabricating unidirectionally polarized M13 film, we characterize the macroscopic pyroelectric potential of the M13 surface under various temperature fluctuations using Kelvin probe force microscopy. Further, we measure the pyroelectric voltage and current generated by pulse-modulated near-infrared laser under various frequencies and intensities. Our bioengineering approach shows how the hierarchical assembled polar molecules contribute to the pyroelectricity in a biological system and how we can develop novel virus-based self-powered systems and biomedical applications in the future.

SB08.08.13

Effects of the Doping Elements (Co, Mn, Mg) on Ultrasonic Spray Deposited NiO Thin Films and Their H₂O₂/Glucose Sensing Behavior Yusuf Tutel, Serkan Koylan, Sensu Tunca and Husnu E. Unalan; Middle East Technical University (METU), Turkey

Due to their low cost, wide band gap semiconducting nature, high chemical stability and admirable durability, nickel oxide (NiO) thin films were frequently utilized in electrochromic smart windows, p-type transparent conducting electrodes, photovoltaics (PVs), organic light-emitting diodes (OLEDs), gas sensors and functional layers for chemical sensors [1]. Chemical sensors used in healthcare have utmost importance, hydrogen peroxide (H₂O₂) and glucose being the two typical analytes. Excess H₂O₂ in the environment may lead to serious health problems as diabetes, cardiovascular disorders, cancer, and concerning neurodegenerative diseases so that an accurate, rapid and reliable method to detect H₂O₂ is of great importance [2]. Likewise, measurement of glucose concentration is also highly critical for clinical diagnosis of diabetes, fermentation and food quality control [3]. To date, many methods for determining H₂O₂ and glucose have been developed, but these methods are often time-consuming and expensive. On the other hand, electrochemical detection of H₂O₂ and glucose can be performed in a cost-effective manner, on-site with high sensitivity, using simple instrumentation. Electrochemical detection with enzyme-free electrodes has superior pH and temperature stability performance compared to that of enzyme-based sensors. Transition metals, metal oxides and their alloys are suitable candidates for the determination of H₂O₂ and glucose sensors owing to their electrocatalytic properties. And the sensor characteristics can simply be tuned by doping the electrochemically active thin films. In this work, NiO and doped NiO (cobalt, manganese and magnesium) thin films were deposited via ultrasonic spray deposition (USD) method. Then, deposited thin films were annealed to crystallize. The addition of different dopant atoms on the morphological, optical and electrochemical sensing properties of NiO thin films have been systematically investigated. Significant decrease in the crystallite sizes was observed upon doping NiO thin films. Likewise, the bandgap of doped NiO thin films decreased drastically compared to undoped NiO thin films (3.74 eV). Detection of H₂O₂ and glucose was performed using a 3-electrode setup where 0.1 M sodium hydroxide was used as an electrolyte, the fabricated thin film electrodes acted as working electrodes and Ag/AgCl and Pt wire were used as a reference and counter electrodes, respectively. The addition of interferences with different concentrations was monitored through the change in the current response at an applied potential of +0.65V (vs. Ag/AgCl). The NiO thin film H₂O₂ sensor showed a sensitivity of 1.5 μA/μM with a limit of detection of 3.8 μA. The response time was calculated as 5 seconds using 90% of initial step change in the current. These results showed the promise of ultrasonic spray deposited NiO thin films for amperometric detection of H₂O₂ and glucose.

SESSION SB08.09: Biosensors I

Session Chairs: Tzahi Cohen-Karni, Nicolette Driscoll, Raghav Garg, Sahika Inal, Jonathan Rivnay, Daniel San Roman, Flavia Vitale and Yingqiao Wang
Thursday Morning, December 2, 2021
Sheraton, 2nd Floor, Independence West

10:30 AM SB08.09.01

Three-Dimensional Graphene Microelectrode Arrays for Detection of Wound Healing Biomarkers Daniel J. San Roman¹, Yingqiao Wang¹, Raghav Garg¹, Mangesh Kulkarni², Bryan Brown², Stephen Badylak² and Tzahi Cohen-Karni¹; ¹Carnegie Mellon University, United States; ²University of Pittsburgh, United States

Volumetric muscle loss (VML) injuries that result in fibrotic tissue formation and degradation of skeletomuscular function represent a significant hurdle for affected patients and clinicians. Upon wound formation, macrophages and neutrophils are recruited to the site to release cytokines and growth factors for proliferation and innervation. To understand the state of the wound and thus plot an optimal trajectory for rapid regeneration, one must track the wound healing process by spatially mapping key regulatory wound biomarkers, such as nitric oxide (NO). While single-point NO probes for acute measurements have been demonstrated, improvements in device stability and the number of sensing nodes are needed to achieve smart biointerfaces for in vivo applications. Here we leverage novel nanomaterials and their exceptional electrochemical properties to construct three-dimensional fuzzy graphene (3DFG) microelectrode arrays (MEAs) for the multiplexed electrochemical sensing of NO. We report in vitro results for 3DFG MEAs capable of detecting NO at physiological concentrations in the nanomolar regime. We investigate the effects of sensor size and semipermeable selective coatings to optimize the performance of our sensor arrays and benchmark performance against conventional Pt-based sensor arrays. Finally, we demonstrate our devices on a flexible platform for in vivo NO detection (rodent model) to aid in monitoring inflammatory wound states.

10:45 AM SB08.09.02

All-Printed Organic Electrochemical Transistors for Detecting Macronutrients in Raw Plant Sap Elliot Strand¹, Eloise Bihar¹, Sangil Han², Sean Gleason³, Megan Renny¹, George G. Malliaras², Robert McLeod¹ and Gregory L. Whiting¹; ¹University of Colorado, United States; ²University of Cambridge, United Kingdom; ³United States Department of Agriculture, United States

Conscious cultivation of plants has sustained human civilization for millennia. Maintaining optimal levels of macronutrients like potassium (K⁺) and calcium (Ca²⁺) is critical for promoting healthy plant growth and development. However, there remains no technical solution for monitoring these vital nutrients in plants in real-time. Existing nutrient detection methods typically require the excavation and transportation of plant samples to off-site laboratories for characterization, which is labor intensive and time consuming. Organic electrochemical transistors (OECTs) are devices that can monitor plant chemical levels in real-time due to their high sensitivity, low voltage and power requirements, and compatibility with living tissue. Additionally, OECTs can be fabricated using readily scalable additive manufacturing techniques (e.g., inkjet and screen printing) making them suitable for applications where many sensors are required under capital constraints.

This presentation will describe the development of fully printed, mechanically flexible, and ion selective OECTs that can accurately detect macronutrient concentrations in raw whole plant sap in real-time. The performance of these devices is drastically improved by doping PEDOT:PSS with common sugar alcohols to generate “internal ion reservoirs” within the OECT channel. The all-printed OECTs show maximum transconductances over 5 mS, which, as far as we are aware, is the highest reported for a fully printed OECT. By utilizing ion selective membranes (ISMs), OECT-based ion sensors are fabricated that show super-Nernstian sensitivity, selectivity to the target ion against similar ions over five orders of magnitude in concentration, and a limit of detection (LOD) as low as 10 μM. This work provides a potential path to high-throughput, low-cost, high spatiotemporal assessment of plant nutrition, enabling correlation of sap chemical composition to overall plant and soil health, and the potential for massive efficiency gains in agriculture.

SESSION SB08.10: Biosensors/Wearables

Session Chairs: Tzahi Cohen-Karni, Nicolette Driscoll, Raghav Garg, Sahika Inal, Jonathan Rivnay, Daniel San Roman, Flavia Vitale and Yingqiao Wang
Thursday Afternoon, December 2, 2021
Sheraton, 2nd Floor, Independence West

1:30 PM *SB08.10.01

Novel Materials and Devices for Bioelectronic Medicine George G. Malliaras; University of Cambridge, United Kingdom

As the discovery of new drugs becomes slower and more expensive with time, there is an urgent need for a new approach to treating disease. Bioelectronic medicine, which uses electrical stimulation to influence neural behaviour, has emerged as a powerful technology to that end: Deep brain stimulation, for example, has shown exceptional promise in the treatment of neurological and neuropsychiatric disorders, while stimulation of peripheral nerves is being explored to treat autoimmune disorders. To bring these technologies to patients at scale, however, significant challenges remain to be addressed. Key among these is our ability to establish stable and efficient interfaces between electronics and the human body. I will show examples of how this can be achieved using new electronic materials and devices engineered to communicate with the body and evolve with it.

2:00 PM SB08.10.02

On-Body Seismology for Continuous Monitoring of Tissue Mechanics Changsheng Wu¹, Chenhang Li², Heling Wang¹, Mengdi Han¹, Ziwu Song³, Zihao Zhao³, Jiahong Li¹, Lin Shu¹, Haixu Shen⁴, Tzu-Li Liu¹, Wenbo Ding³, Yonggang Huang¹, John A. Rogers¹ and Xiaoyue Ni²; ¹Northwestern University, United States; ²Duke University, United States; ³Tsinghua University, China; ⁴California Institute of Technology, United States

Recent progress in wearable devices provides new opportunities for precise, non-invasive, long-term recording of body mechanics. The soft device incorporating a single MEMS accelerometer captures subtle vibration of the skin with a resolution of 1×10^{-4} g/sqrt(Hz) in frequency range 0 to 800 Hz. In this study, we introduce an on-body mechano-acoustic sensing technology based on a skin-mounted accelerometer array to assess the mechanical profiles of subdermal tissues in-vivo, similar to seismology. A system-level wearable device construction, optimized for a comfortable skin interface and high precision, incorporates a broadband dual-accelerometer sensor, an audio actuator, and a Bluetooth System-on-Chip and enables a wireless, automated operation. An automated algorithm, leveraging the spectral analysis of surface waves (SASW) methods, computes the depth-sensitive, elastic modulus information of the propagation media from the mechanical dispersion relationship. Comprehensive theoretical and experimental investigation verifies that the device, together with the automated data-processing platform, provides a precise, robust, and non-invasive evaluation of the elasticity with a resolution

of ~5 kPa and depth information in the range of ~1-140 mm of various phantom materials (Young's modulus $E = 10-1500$ kPa). The device also identifies the softening of pork tissues with increasing injected water content and the changes of modulus of brachioradialis muscle under different levels of tension. The results are in agreement with the in-parallel Ultrasound Elastography measurements. A quantitative assessment of the stiffness profile of the rectus femoris muscle during leg-press exercise demonstrates the continuous monitoring capability in the ambulant environment that can support long-term clinical assessment of different tissues and disease states in a large population.

2:15 PM SB08.10.03

Topological Supramolecular Network Enabled Highly Conductive and Stretchable Organic Bioelectronics Yuanwen Jiang and Zhenan Bao; Stanford University, United States

Intrinsically stretchable bioelectronic devices based on soft and conducting organic materials have been regarded as the ideal interface for seamless and biocompatible integration with the human body. However, the grand challenge remains for the conducting polymer to possess both high mechanical ductility and good electrical conduction at cellular level feature sizes. This longstanding material limitation in organic bioelectronics has impeded the full exploitation of its unique benefits.

Here, we introduce a new molecular engineering strategy based on rationally designed topological supramolecular networks, which allows effective decoupling of competing effects from multiple molecular building blocks to meet complex requirements. We achieve two orders of magnitude improvement in the conductivity under 100% strain in physiological environment, along with the capability for direct photopatterning down to 2 μm .

These unprecedented capabilities allow us to realize previously inaccessible bioelectronic applications including high-resolution monitoring of 'soft and malleable' creatures, e.g., octopus, and localized neuromodulation down to single nucleus precision for controlling organ-specific activities through delicate tissues, e.g., brainstem.

2:30 PM SB08.10.04

Bimetallic Nanocatalysts Immobilized in Nanoporous Hydrogels for Long-Term Robust Continuous Glucose Monitoring of Smart Contact Lens Su-Kyoung Kim and Sei Kwang Hahn; POSTECH, Korea (the Republic of)

Smart contact lenses for continuous glucose monitoring (CGM) have great potential for huge clinical impact. To date, their development has been limited by challenges in rapid detection of glucose without hysteresis for tear glucose monitoring to track the blood glucose levels. Here, we demonstrate that bimetallic nanocatalysts immobilized in nanoporous hydrogels in smart contact lenses enable reliable CGM in diabetic rabbits. After redox reaction of glucose oxidase, the nanocatalysts facilitate rapid decomposition of hydrogen peroxide and nanoparticle-mediated charge transfer with drastically improved diffusion via rapid swelling of nanoporous hydrogels. The ocular glucose sensors result in high sensitivity, fast response time, low detection limit, low hysteresis, and rapid sensor warming-up time. In diabetic rabbits, smart contact lens can detect tear glucose levels consistent with blood glucose levels measured by a glucometer and a CGM device, reflecting rapid concentration changes without hysteresis. The CGM in a human demonstrates the feasibility of smart contact lenses for further clinical applications.

3:00 PM BREAK

SESSION SB08.11: Materials/Chem

Session Chairs: Tzahi Cohen-Karni, Nicolette Driscoll, Raghav Garg, Sahika Inal, Jonathan Rivnay, Daniel San Roman, Flavia Vitale and Yingqiao Wang
Thursday Afternoon, December 2, 2021
Sheraton, 2nd Floor, Independence West

4:00 PM *SB08.11.01

Tuning the Functionality of Mixed Ionic-Electronic Conductors Using Block Copolymers Laure V. Kayser; University of Delaware, United States

The development of bioelectronic devices for sensing or actuation requires materials that have properties similar to that of biological entities. In particular, a strong emphasis has recently been placed on minimizing the mechanical mismatch between 'hard' electronics and 'soft' biological tissues to reduce tissue scarring and increase device longevity. This mismatch can be partially addressed by using conductive polymers instead of inorganic materials. Not only do polymers have a lower Young's modulus, but they can also behave as mixed ionic-electronic conductors. This mixed conduction is essential to transduce electronic to biological (ionic) signals (e.g., in neurological electrodes) and vice versa (e.g., in organic electrochemical transistors). Amongst organic mixed conductors, the polyelectrolyte complex poly(3,4-ethylenedioxythiophene):poly(styrene sulfonate) (PEDOT:PSS) is probably the most commonly used. While some properties of PEDOT:PSS are highly desirable for bioelectronics such as its high conductivity and biocompatibility, it remains difficult to access new functionality without using a composite approach. A major challenge stems from the lack of control over the molecular structure of PEDOT:PSS, which leads to a highly disordered morphology in the solid state. Instead of taking a blending approach toward functionalizing PEDOT:PSS, we have developed a method to direct its solid-state assembly using block copolymers. Our approach uses block copolymers of PSS with neutral polymers to drive the self-assembly of PEDOT particles in solution while imparting additional functionality. In this presentation, I will share some of our results showing the importance of controlling the molecular structure of PEDOT:PSS to access properties relevant to bioelectronics, such as volumetric capacitance and reversible self-assembly.

4:30 PM SB08.11.02

Ambipolar Organic Electrochemical Transistors Based on the Bulk Heterojunction Morphology Eyal Stein¹, Oded Nahor¹, Iuliana P. Maria², Jonathan Rivnay³, Iain McCulloch^{4,2} and Gitti L. Frey¹; ¹Technion--Israel Institute of Technology, Israel; ²University of Oxford, United Kingdom; ³Northwestern University, United States; ⁴KAUST, Saudi Arabia

Organic Electrochemical Transistors (OECTs) offer transduction and high amplification of biological signals. Both p-type and n-type mixed ionic and electronic conductors and their corresponding OECT devices are gaining significant interest. Ambipolar OECTs, however, offer additional advantages including simplifying the design and fabrication of OECT-based complementary circuits, detecting biological multifunctional analytes, enabling versatile device architectures such as vertical OECTs, reducing device footprint and increasing the density of elements, etc. Still, ambipolar OECTs are scarce because it is difficult to balance the performance and stability of the device when operating under the negative and the positive conditions. Here we show that the bulk-heterojunction approach, borrowed from organic solar cells, can be harnessed to achieve ambipolarity in an OECT device. More specifically,

a semiconducting polymer and small molecule are judiciously selected, blended at suitable ratios and annealed to yield the morphology optimal for mixed conductivity and ionic-electronic coupling. We demonstrate the approach using a common OECT p-type polymer and an n-type fullerene derivative and show, for the first time, a truly balanced ambipolar OECT device. Electrical and electrochemical techniques are used to follow the physical processes under bias, while the morphology is studied using Xray techniques and VPI. Device stability as a function of time and temperature are also investigated. Changes in the morphology induced by time and temperature are associated with device performance to realize structure-property relationships in bulk-heterojunction-based OECTs.

4:45 PM SB08.11.03

Role of Molecular Mass and Processing on the Performance of an Oligoethylene Glycol-Substituted Polythiophene Based Organic Electrochemical Transistor Lucas Flagg¹, Ulyana S. Cubeta¹, Jonathan W. Onorato², Christine Luscombe², Chad R. Snyder¹ and Lee Richter¹; ¹National Institute of Standards and Technology, United States; ²University of Washington, United States

Organic electrochemical transistors (OECTs) are a novel device architecture, emerging as a potential platform for biosensors and neuromorphic computing. In an OECT, volumetric doping (gating) of the active semiconductor is achieved through ingress of electrolyte ions, under potential control. This opens unique transduction modalities, due to the mixed (ionic and electronic) modes of conduction. This also challenges established paradigms for the operation of traditional, organic field-effect transistors as operation involves the dynamic swelling of the active layer by both solvent and ion. Poly(3-(methoxyethoxyethyl)thiophene) (P3MEEMT) has emerged as an interesting, prototypical OECT material, differing from the classic OFET material, regioregular poly(3-hexyl)thiophene (P3HT), by the replacement of the non-polar alkyl side chains with oligoethylene glycol (OEG). In an early study of P3MEEMT,[1] it was observed to exhibit the counter-intuitive behavior of degraded charge transport upon thermal processing. We have conducted a detailed study of the variation of the structure and OECT performance of P3MEEMT with thermal processing. In the study we compare polymers with number average molecular mass, M_n , varying from (13 to 87) kg/mol. Using GIWAXS to characterize the degree of crystallinity and crystal orientation distribution, we find the OEG side chains introduce rich thermal processing behavior. All polymers exhibit only moderate and nearly isotropic order when coated from chlorobenzene. Low M_n material adopts an edge-on structure, with monotonically increasing degree of crystallinity with increasing anneal temperature. In contrast, high M_n material first adopts a face-on orientation when annealed at (115 to 125) °C, and then a nearly isotropic crystal distribution when annealed above the last crystal melt transition near 145 °C. Remarkably, the OECT device behavior (C^*m) is nominally independent of the severe differences in orientation distribution across M_n at anneal temperatures below 120 °C. Consistent with the earlier report,[1] 13 kg/mol M_n material exhibits a degradation in C^*m when melt-annealed (at $T \geq 145$ °C), in striking contrast to the higher M_n (≥ 23 kg/mol) material that exhibits anneal T independent performance. In accord with recent studies for the M_n dependence of transport in P3HT[2] we attribute the drop in performance of annealed, low M_n P3MEEMT to the phenomena of tie-chain-pullout and ripening of the crystalline domains.

[1] L.Q. Flagg, et al. J Am Chem Soc 2019, doi: 10.1021/jacs.8b12640

[2] K. Gu, et al. ACS Macro Lett 2018 doi: 10.1021/acsmacrolett.8b00626

5:00 PM SB08.11.04

Controlling Morphology, Adhesion and Electrochromic Behaviour of PEDOT Films Through Molecular Design and Processing Christina J. Kousseff, Fani E. Taifakou, William G. Neal, Matteo Palma and Christian Nielsen; Queen Mary University of London, United Kingdom

The structure-based tuneability of the electronic and optical properties of conjugated polymers has enabled their application across a range of fields, including energy harvesting and optoelectronics. However, in the context of biological sensing, the use of conjugated polymers has thus far incorporated little specificity in terms of covalent modification.

Developing robust, highly selective, biologically compatible sensing platforms is of critical importance because the measurement of analyte concentrations in biological samples is crucial for the management or detection of many diseases. Currently, many devices which function for this purpose are complex, multi-component systems. However, directed synthetic strategy with conjugated polymers enables the fine-tuning of analyte specificity, electroactive or optical functionality, and physical and morphological properties, within a single multi-purpose material. In addition, these entirely organic systems offer affordability, biocompatibility, and simple design and fabrication.

I will present my work on a novel covalently-modified PEDOT polymer featuring a 15-crown-5 moiety. The introduction of such a group is shown to enhance a diverse range of characteristics in comparison to regular PEDOT, including: adhesion to ITO substrates, physical and electrochemical integrity, film uniformity, and spectroelectrochemical properties. Furthermore, we find that the long-term electrochromic behaviour of PEDOT-Crown is altered in the presence of its chelating ion, sodium, compared to unmodified and analyte-free controls, which may open the door to its application as a sensor material. The adaptable nature of the synthetic pathway also unlocks access to range of potential sensor materials, featuring differently modified PEDOTs specific to other biomarkers, a space we have begun to explore.

5:15 PM SB08.11.05

Role of Side Chain Redistribution on the Morphology of Hydrated Organic Mixed Ionic-Electronic Conductors Lucas Flagg¹, Maximilian Moser², Iain McCulloch^{2,3}, Dean DeLongchamp¹ and Lee Richter¹; ¹National Institute of Standards and Technology, United States; ²University of Oxford, United Kingdom; ³KAUST Solar Center (KSC), Saudi Arabia

Organic mixed ionic-electronic conductors (OMIECs) are a class of materials that have recently drawn interest as materials for next generation biosensors. For these applications, cycling stability is an important parameter that is not yet well understood. Recent work has shown that redistributing the ethylene glycol side chain units along the backbone, while maintaining a constant number of ethylene glycol units, can be used to optimize the cyclability of polythiophenes. In this system the polymers with unevenly distributed sidechains showed a greatly suppressed active (in response to bias) swelling as measured by quartz crystal gravimetry. This reduced swelling in response to electrochemical bias correlated with increased cycling stability.¹ Here we investigate this side chain redistribution series using grazing incidence x-ray scattering (GIWAXS) with *in-situ* potential control to examine the passive and active swelling of the polymer crystallites in addition to the bulk film. We find that when the side chain is evenly distributed, the polymer crystallites swell minimally upon contact with electrolyte, implying that most of the swelling occurs in the amorphous regions of the film. However, in polymers with highly uneven side chain distribution, contact with electrolyte causes the formation of a hydrated crystal lattice that is ~ 50 percent expanded relative to the dry lattice. We hypothesize that this hydrated crystal lattice minimizes mechanical strain caused by cycling and helps explain the greater cycling stability of these polymers. Additionally, we examine the role of different anions in swelling both the hydrated state and the dry state of the polymer films to further understand electrochemically induced swelling of these films. Overall, this work provides insights into the synthetic design of highly cyclable OMIEC materials.

References

(1) Moser, M.; Hidalgo, T. C.; Surgailis, J.; Gladisch, J.; Ghosh, S.; Sheelamanthula, R.; Thiburce, Q.; Giovannitti, A.; Salleo, A.; Gasparini, N.; Wadsworth, A.; Zozoulenko, I.; Berggren, M.; Stavrinidou, E.; Inal, S.; McCulloch, I. Side Chain Redistribution as a Strategy to Boost Organic

SESSION SB08.12: Biosensors II

Session Chairs: Tzahi Cohen-Karni, Victor Druet, Sahika Inal, David Ohayon, Jonathan Rivnay, Sneha Shankar and Flavia Vitale
Monday Morning, December 6, 2021
SB08-Virtual

8:00 AM SB08.12.01

Electrical Characteristics of Solution-Gated Ultrathin Channel ITO-Based Transistor Fabricated by One-Step Procedure and Biomolecular Recognition Based on Its Chemical Modification [Xianqi Dong](#), Akiko Saito and Toshiya Sakata; The University of Tokyo, Japan

We previously proposed a one-step procedure for fabricating a solution-gated ultrathin channel indium tin oxide (ITO)-based field-effect transistor (FET) biosensor.¹ A thin-film sheet was placed on both ends of a metal shadow mask, which were contacted with a glass substrate. The bottom of the metal shadow mask corresponding to the channel was slightly raised from the substrate, resulting in the creeping of some particles into the gap during sputtering. Owing to this modified metal shadow mask, a thin ITO channel (< 30–40 nm) and thick ITO source/drain electrodes (ca. 100 nm) were simultaneously fabricated during the one-step sputtering. The thickness of ITO films was critical for them to be semiconductive, depending on the maximum depletion width, similarly to 2D materials. The ultrathin ITO channel worked as an ion-sensitive membrane as well, owing to the intrinsic oxidated surface directly contacting with an electrolyte solution. The solution-gated 20-nm-thick channel ITO-based FET, with a steep subthreshold slope (SS) of 55 mV per decade (pH 7.41) attributable to the electric double-layer capacitance at the electrolyte solution/channel interface and the absence of interfacial traps among electrodes formed in one step, demonstrated an ideal pH responsivity (~56 mV/pH). Therefore, the chemical modification of the ITO channel surface is expected to contribute to biomolecular recognition with ultrahigh sensitivity owing to the remarkably steep SS. In this study, we fabricate the solution-gated ultrathin channel ITO-based FET on glass substrate by one-step sputtering, then modify it with an aptamer, which binds to a specific target biomolecule (e.g., dopamine). Moreover, the fundamental electrical properties of the solution-gated ultrathin channel ITO-based FET with and without aptamer are investigated.

The ITO device was prepared on a glass substrate by sputtering. The ITO channel was immersed in 0.2% 3-aminopropyltrimethoxysilane (APTMS) solutions for 30 min. After the surface was washed by deionized (DI) water, the ITO transistor was heated for 10 min at 120°C. Then, the ITO channel was immersed in the mixed solution of 10% dimethyl sulfoxide (DMSO) and 90% phosphate buffered salts (PBS), containing 1 mM *N*-succinimidyl 3-maleimidobenzoate (MBS) for 1 h, and then the surface was washed with DI water. Finally, 5 mM dopamine aptamer solution (pH 7.4) was dropped on the ITO channel surface overnight. Using the prepared device, the fundamental electrical properties such as transfer characteristics (I_D - V_G), output characteristics (I_D - V_D), and real-time monitoring (I/V - t) were collected.

The solution-gated ultrathin channel ITO-based FET showed a good sensitivity near the Nernstian response to pH. Besides, by setting a gate potential in the subthreshold regime, the ITO device, which is modified by aptamer, should be capable of detecting dopamine with high sensitivity.

Reference

1. T. Sakata et al., *ACS Appl. Mater. Interfaces*, under revision (2021).

8:15 AM *SB08.12.02

Bioelectronic Single-Molecule Label-Free Sensing with Large-Area Transducing Interfaces [Luisa Torsi](#); University of Bari A. Moro, Italy

Nanosized bioelectronic detecting interfaces seem the privileged pathway to single-molecule detections. However, while giving access to rarer events, this *near-field* approach is unsuited to detect at concentrations lower than nanomolar because of the diffusion-barrier issue. *Large-area* (μm^2 - mm^2 wide) bioelectronic transistors are perceived as unsuited due to the irrelevant footprint of a single molecule on a much larger detecting interface. *Indeed, detecting such an event would be like spotting the wave generated by a single droplet of water falling on a one-kilometer-wide pond.* However, many field-effect large-area biosensors have been shown to detect at limit-of-detection below femtomolar, being also naturally suited for point-of-care applications. Here the field is reviewed, illustrating device architectures, materials used, and target analytes that can be selectively detected. The sensing mechanisms and the amplification effects enabling the large-area bioelectronic sensor to detect at the physical limit are also detailed

8:45 AM SB08.12.04

A Wearable Microneedle-based Potentiometric Sensing System for Continuous Monitoring of Multiple Electrolytes in Skin Interstitial Fluid [Huijie Li](#) and [Yi Zhang](#); University of Connecticut, United States

Electrolytes play a pivotal role in regulating cardiovascular functions, hydration, and muscle activation. The current standards for monitoring electrolytes involve periodic sampling of blood and measurements using laboratory techniques, which are often uncomfortable/inconvenient to the subjects and add considerable expense to the management of their conditions. The wide range of electrolytes in skin interstitial fluids (ISF) and their correlations with plasma create exciting opportunities for applications such as electrolyte and circadian metabolism monitoring. However, it has been challenging to monitor these electrolytes in the skin ISF. In this study, we report a minimally invasive microneedle-based potentiometric sensing system for multiplexed and continuous monitoring of Na^+ and K^+ in the skin ISF. The potentiometric sensing system consists of a miniaturized stainless-steel hollow-microneedle to prevent the sensor delamination and a set of modified microneedle electrodes for multiplex monitoring. We demonstrate the measurement of Na^+ and K^+ in artificial ISF with a fast response time, excellent reversibility and repeatability, adequate selectivity and negligible potential interferences upon the addition of physiologically relevant concentration of metabolites, dietary biomarker and nutrients. In addition, the sensor maintains the sensitivity after multiple insertions into the chicken skin model. Furthermore, the measurements in artificial ISF using calibrated sensors confirms the accurate measurements of physiological electrolytes in artificial ISF. Finally, the agarose gel model and chicken skin model experiments demonstrate sensor's potential for minimally invasive monitoring of electrolytes in skin ISF. The developed sensor platform can be adapted for a wide range of other applications, including real-time monitoring of nutrients, metabolites and proteins.

9:00 AM SB08.12.05

Late News: The Role of Oxygen in the Operation of Organic Enzymatic Metabolite Sensors [Victor Druet](#)¹, [Anil Koklu](#)¹, [David Ohayon](#)¹, [Prem Nayak](#)¹, [Xingxing Chen](#)¹, [Iain McCulloch](#)^{1,2} and [Sahika Inal](#)¹; ¹KAUST, Saudi Arabia; ²University of Oxford, United Kingdom

When combined with oxidase enzymes, the NDI-T2 based electron transporting polymer led to high performance metabolite sensors, yet their working mechanism has been poorly understood.^{1,2} Here using in-situ oxygen, hydrogen peroxide, and pH analysis during device operation, we shed light into the biocatalysis at the semiconducting polymer interface. We demonstrate the significant role that oxygen plays during the operation of glucose sensors made

of n-type organic electrochemical transistors (OECTs). We show that the oxygen reduction capability of our polymer is mainly responsible for the observed sensing performance, where a strong correlation has been seen in the amount of solution oxygen and the charge carrier density of the n-type film in the OECT channel. Our results show the importance of in operando analysis for understanding polymer-catalytic enzyme activity, as well as the importance of ambient oxygen in the operation of n-type devices.

1: Pappa, A. M.; Ohayon, D.; Giovannitti, A.; Maria, I. P.; Savva, A.; Uguz, I.; Rivnay, J.; McCulloch, I.; Owens, R. M.; Inal, S., Direct metabolite detection with an n-type accumulation mode organic electrochemical transistor. *Science advances* 2018, 4 (6), eaat0911.

2: Ohayon, D.; Nikiforidis, G.; Savva, A.; Giugni, A.; Wustoni, S.; Palanisamy, T.; Chen, X.; Maria, I. P.; Di Fabrizio, E.; Costa, P. M., Biofuel powered glucose detection in bodily fluids with an n-type conjugated polymer. *Nature materials* 2020, 19 (4), 456-463.

SESSION SB08.13: Wearables/Biosensors

Session Chairs: Tzahi Cohen-Karni, Victor Druet, David Ohayon, Jonathan Rivnay, Sneha Shankar and Flavia Vitale

Monday Afternoon, December 6, 2021

SB08-Virtual

6:30 PM *SB08.13.01

Self-Powered, Ultraflexible Photonic Skin for Continuous Bio-Signal Detection Takao Someya¹, Tomoyuki Yokota¹, Hiroaki Jinno¹ and Kenjiro Fukuda²; ¹The University of Tokyo, Japan; ²RIKEN, Japan

Organic semiconductor devices are actively being applied to the next generation of wearable electronics, taking advantage of their lightweight, thinness, and flexibility. Flexible displays based on organic light-emitting diodes (LEDs) are being used in smartwatches and wristband applications to help reduce power consumption. Pulse oximetry has also been realized by combining organic LEDs with organic photodetectors. By making these organic optical sensors flexible, they can be attached directly to a human's skin with little discomfort and enable long-term health monitoring. However, it is still difficult to integrate such thin organic optical sensors with power sources at the system level. In addition, ultra-thin organic LEDs are not stable enough to operate in air, which hinders long-term monitoring of biological signals.

Here, we present an ultra-thin, self-powered organic optical system for monitoring photoplethysmogram (PPG). The system consists of three ultra-thin electronic devices: a polymer LED (PLED), an organic solar cell, and an organic photodetector. By adopting an inverted structure and a polyethyleneimine ethoxylate (PEIE) layer doped with 8-quinolinolathritium (Liq) as the electron transport layer (ETL), organic light-emitting diodes exhibit improved operation stability under ambient air conditions. Because of the intrinsic air operational stability of inverted PLED with PEIE:Liq electron injection layers, the ultra-flexible OLED fabricated without passivation shows 70% of the initial brightness lifetime of 11.3 hours in air, which is more than three times the lifetime of conventional ultra-flexible OLEDs. In addition, the built-in light sensor showed high linearity with respect to the output of 0.98 of the PLED light sources. Such a self-powered ultra-flexible PPG sensor can stably monitor the blood flow pulse signal of human hands.

7:00 PM SB08.13.02

Wireless Human-AI Collaborative System for Enhancing Machine Decision-Making Using Tattoo-Like Electronics Joohwan Shin; Sungkyunkwan University, Korea (the Republic of)

"A.I. Artificial Intelligence" (2001), Steven Spielberg's film, features a robot that tries to understand human emotions via communication. However, human sentiments, which are nonverbal communication tools, are very ambiguous in terms of interpretation and are difficult for machines or artificial intelligence (AI) to translate technically. If AI understands a user's mental state, AI will learn the right decisions from humans in unclear situations that have been difficult to judge. Here, we introduce a wirelessly operative, neuroadaptable (adaptable in relation to his/her mindset), communicable "Human-AI Collaborative System" (HACS) based on the earbud-like wireless EEG device (e-EEGd) composed of tattoo-like electrodes, connectors, and a wireless EEG earbud. The HACS can make up for AI-based machines' incorrect decisions to revise and reinforce its decision accuracies according to P300 event-related potential (ERP) in volunteers' brain signals. It is based on the P300 EEG signal, one of ERP components, positive rises around 300 msec after an unexpected external stimulus is applied due to the human decision-making process³⁷. In the case of the HACS, an unexpected behavior of the AI-based machine causes the P300. Since the intensity of P300 is small and the frequency range overlaps with the range of motion artifact, it is vital to measure high-quality EEG and accurately classify only P300 among various noises and components. We proposed an integration strategy based on gradually increasing thickness from ultra-thin electrodes (900 nm) to rigid earbud measurement system that enables lower motion artifacts. The e-EEGd conformally adheres to the skin on the head, minimizes volunteer motion artifacts, and continuously records EEG even while the volunteer is walking, driving, etc, which expands the variety of situations in which this technology can be used. The device weighs only 8.24 g, which is several times lighter than other available EEG devices, and generates 8.5-times less artifactual noise. The e-EEGd enables the achievement of high signal-to-noise ratio (SNR) EEG signals and transmits EEG signals wirelessly with minimal delay (up to 15 ms). We measured the P300 component with 12 subjects using e-EEGd by sensory stimulation and controlling the unexpected behavior of the autonomous machines. In addition, based on the measured P300, we conducted a signal processing and classifier optimizing study for efficient and fast real-time classification to be performed on an AI-based machine. The HACS can immediately correct unexpected working of AI-based machines or reinforce the system choices based on the presence/absence of the P300 in the user's EEG. We demonstrated potential applications of the HACS and the e-EEGd with embedded real-time classification on AI-based machines, including virtual assistants, maze solvers, and autonomous remote-controlled (RC) cars.

7:15 PM SB08.13.03

Patch Type Glucose Sensor for Prediabetes Based on Microneedle and Self-Powered Supercapacitor Hyejun Kil and Jin-Woo Park; Yonsei University, Korea (the Republic of)

Pre-diabetic patients with glucose levels between diabetes and normal can recover to normal levels without medication if their blood glucose management is well done. However, unlike diabetics who keep blood glucose levels with medication prescribed by doctors, pre-diabetes patients should make significant efforts to control blood glucose through diet and regular exercise. The basis of blood glucose management is blood glucose measurement. A commonly used blood glucometer is a one-time measurement through blood collection by a sharp needle, which is an invasive method. Hence, patients feel pain at each measurement. Recently, continuous blood glucometers using microneedles have been commercialized, allowing patients to continuously measure and manage blood glucose without pain. However, there are several drawbacks such as that medical staff has to help attach the blood glucose meter, and side effects such as inflammatory reactions can be caused by the use of metal needles. In this work, we present a painless, lightweight, and small

patch-type wearable glucometer made of polydimethylsiloxane (PDMS) microneedle and a self-powered supercapacitor. The principle of self-powering of this patch-type glucose sensor is to charge the supercapacitor by generating a potential difference of the supercapacitor with electrons generated by the oxidation reaction of glucose. Due to this potential difference, ions present in the electrolyte are adsorbed on the surface of each electrode, and charging begins. Herein, the supercapacitor consists of polymeric thin films, which makes it mechanically flexible. We coated the electrode layer and enzyme layer by dip-coating method to form the glucose sensor on the uneven microneedle surface. The PDMS microneedle-type blood glucose sensor can penetrate the skin without pain and detect the blood glucose in the interstitial fluid (ISF). The experimental verification of the glucose-sensing by the microneedle-type sensor was done with an artificial skin immersed in the solution with glucose. The glucose concentration varies from the pre-diabetes level to diabetes, and the levels between the two. As glucose concentration increases, more electrons are produced by glucose oxidation. The potential difference between the supercapacitor electrodes increases, which gives the driving force for more electrolyte ions to move towards the electrodes. As a result, we confirmed that the supercapacitor was charged with more energy as the glucose concentration was increased through cyclic voltammetry. Finally, the self-powered patch-type glucose sensor is combined with a light-emitting diode (LED) on-off system to inform users of blood glucose levels easily and quickly. When the glucose concentration increased from the pre-diabetic to the diabetic level, the light turned on because enough energy was delivered to the connected LED.

7:30 PM SB08.13.04

Self-Folding Graphene-Based Electrode Array for Long-Term Monitoring of Interconnected 3D Neuronal Culture [Koji Sakai](#), Tetsuhiko F. Teshima, Toichiro Goto, Hiroshi Nakashima and Masumi Yamaguchi; NTT Corporation, Japan

Single-layer graphene (SLG) is an ideal material for neuronal interfaces such as electrodes and cell scaffolds thanks to its high biocompatibility, transparency, and electro-conductivity. Despite these useful properties, conventional SLG-based neuronal interfaces involve constraints related to a mismatch between the 2D SLG surface and the complex structure of 3D neuronal tissues. Self-folding with SLG-based film has recently emerged as a method to encapsulate cells for both constructing 3D-shaped tissues and sensing molecules from the encapsulated cells. This suggests it could be applied for electrophysiology from a 3D-shaped neuronal construct. The approach with a foldable electrode has recently attracted a great deal of interest in 3D-spatio electrophysiology of single neural spheroids. However, it is still challenging to investigate the firing dynamics exhibited by networks of interconnected neuronal constructs because the multiple neuronal constructs need to be in contact with each electrode. In this work, we propose a foldable SLG-based electrode array that allows for producing 3D-shaped neuronal constructs within the folded electrodes while recoding firing dynamics from neuronal constructs simultaneously.

To encapsulate cultured cells within an SLG surface, we modified our previous method to induce self-folding with SLG-based film. A previous report showed that this method causes a SLG/parylene-C bilayer to spontaneously roll up into a folded cylindrical structure (micro-roll), with the SLG formed on the outer face, so we need to modify it such that the SLG forms on the inner face. We transferred another SLG to the opposite side of the parylene-C layer, and the SLG-sandwiched parylene-C film formed a micro-roll that allowed us to encapsulate cells within the inner SLG surface. We applied the self-folding to an electrode array by incorporating the SLG-sandwiched parylene-C film as an electrode. To investigate whether the electrode allows for both creating cellular constructs and electrophysiology, dissociated hippocampal neurons were encapsulated by the self-folding electrodes. Immunocytochemical images indicated that the encapsulated neurons formed a neuronal construct within the folded SLG and interconnected between each neuronal construct via axons. Spontaneous activities of neurons were continuously recorded for 70 days from the folded electrodes, whereas the signals disappeared at 28 days in recordings of an aggregated culture by unfolded electrodes. These long-term recordings were possible because the confined structure provides a firm contact between the neuronal construct and the electrode. To take advantage of the long-term recording, we further investigated a development of functional networks in the interconnected neuronal constructs (clustered culture). The clustered culture exhibited synchronous bursting activities from nine days in culture, which is consistent with a homogenous culture. On the other hand, fewer electrodes participated in the synchronized activities in the clustered culture (40% of all electrodes) than in the homogenous culture (>90%), suggesting that the clustered culture contained the rich pattern repertoires of smaller networks. These results demonstrate that our method for self-folding graphene-based electrode arrays allows us to characterize the firing dynamics exhibited by interconnected neuronal constructs for a long culture period.

7:45 PM SB08.13.05

Organic Mixed Ionic-Electronic Conductor-Based Sub-1V Signal Rectifying Electrochemical Device Operated with Aqueous Electrolytes [Youngseok Kim](#)¹, Gunwoo Kim¹, Bowen Ding², Martin Heeney² and Myung-Han Yoon¹; ¹Gwangju Institute of Science and Technology, Korea (the Republic of); ²Imperial College London, United Kingdom

Owing to outstanding electrical/electrochemical performance, device operational stability and solution processability, organic mixed ionic-electronic conductors (OMIECs) have been researched for their applications to flexible biosensors, bioelectronics interfaces, neuromorphic devices, etc. Considering essential device modalities in the modern electrical circuit architecture, not only transistors but also diodes are needed for many purposes such as signal processing and device protection. Herein, we report OMIEC-based electrochemical diodes operated with aqueous electrolytes. By designing an active layer asymmetrically patterned on source and drain electrodes, the channel could be electrochemically doped/dedoped under opposite bias polarity of the applied signal, and the unprecedented current density over 30 kAcm^{-2} could be achieved by using high-transconductance OMIECs. The resultant device architecture was utilized to realize two-terminal rectifying electrochemical devices. Furthermore, not only analog signal rectification but also digital logic processing could be demonstrated by employing a simple circuitry based on the multiple number of organic electrochemical diodes.

8:00 PM SB08.13.06

Flexible, Stretchable and Self-Adhesive Biopotential Electrodes Using Silver Nanorods Embedded PDMS Microstructures [Yogita Maithani](#)¹, Bijit Choudhuri², Bodh Raj Mehta¹ and Jitendra P. Singh¹; ¹Indian Institute of Technology Delhi, India; ²NIT Silchar, India

Biopotential signals are extremely useful in assessing organ function and diagnosing diseases. In order to measure and record biopotentials, biopotential electrodes act as an interface between the biological tissue and the electronic circuit. The electrical and mechanical characteristics of the electrodes used for biopotential measurements significantly influence the measured signal quality.

This work proposes a highly flexible, conductive, antibacterial, and self-adhesive silver nanorods (AgNRs) embedded polydimethylsiloxane (PDMS) based dry electrode for biopotential measurements. We have used a unique glancing angle deposition method to fabricate aligned AgNRs and embedded them in a biocompatible PDMS matrix. These electrodes do not cause skin irritation even after several hours of use and work efficiently even without prior skin preparation. These AgNRs-PDMS electrodes have an electrical resistivity of $10^{-7} \Omega\text{-m}$ and a skin contact impedance of $93.9 \pm 0.7 \text{ k}\Omega$ to $6.2 \pm 3.7 \text{ k}\Omega$ for frequencies ranging from 40 Hz to 1 kHz, which is comparable to the most conventional Ag/AgCl wet electrodes. Furthermore, it maintains its conductivity across various mechanical stress, including bending, twisting, and stretching, as illustrated by a light-emitting diode circuit. Nanoindentation was used to measure the mechanical properties of fabricated AgNRs-PDMS electrodes, which shows the elastic modulus and hardness of the AgNRs-PDMS are increased by 167.6 and 93.3 %, respectively, compared to PDMS film, due to the strong interfacial adhesion of AgNRs embedded in the PDMS matrix.

The proposed AgNRs-PDMS dry electrodes are expected to give greater comfort for use over time due to their flexible nature and a better match to the skin's modulus. Simultaneously, the antibacterial properties of silver make it an attractive candidate for wearable electronics. The fabrication method is simple, cost-effective, and scalable, thus permitting the production of arbitrary-shaped flexible electrodes for long-term biopotential monitoring.

8:15 PM SB08.13.07

Electrical Properties of Free-Standing Conductive Hydrogel Electrode for Autonomous Mobile Biosensors Shogo Himori and Toshiya Sakata; The University of Tokyo, Japan

Electrochemical biosensors directly detect electrical signals based on biomolecular charges or electrical changes in biomolecular recognition events, regardless of their molecular sizes; therefore, such electrochemical methods are suitable for the detection of small biomolecules. In general, carbon and metals such as gold and platinum are used for the electrodes of electrochemical biosensors. On the other hand, considering the development of a novel biosensor in the future, a conductive polymer, which shows a flexibility and then reduces the burden to a body, is a strong candidate for the electrode in an autonomous mobile biosensing system, whereby targeted biomolecules and ions are collected and detected all over in a biological fluid or a sample solution. However, the lack of mechanical strength for the conductive polymer prevents it from maintaining a free-standing state, even when it is coated on a supporting electrode, which is a concern of the conductive polymer for the practical use [1]. That is, the development of free-standing conductive polymer is expected for the autonomous mobile biosensor without the supporting electrode. In this study, we have developed the free-standing conductive hydrogel with a functional monomer that allows biomolecular recognition, and evaluated the electrical properties with the electrochemical setup. In particular, we would like to discuss about the possibility of the functionalized free-standing conductive hydrogel for its application to the autonomous mobile electrochemical biosensor.

As the conductive hydrogel used in this study, polyaniline (PAni) was prepared with self-oxidation of aniline (Ani) monomers in an ammonium persulfate solution. In particular, aminophenylboronic acid (APBA) was copolymerized to obtain the PAni-PBA hydrogel electrode; that is, diol compounds such as glucose bind to PBA on the basis of the equilibrium reaction, which allows the detection of glucose molecules. Furthermore, by adding polyvinyl alcohol (PVA) into the PAni-PBA polymer gel network, the obtained hydrogel showed the free-standing property [1]. This is because PVA also has diol groups and is cross-linked in the PAni-PBA polymer based on the diol binding. The PAni-PBA-PVA free-standing conductive hydrogel was connected to the gate electrode of field-effect transistor (FET) through a platinum wire, and then the change in the surface potential of the hydrogel was measured with varying the glucose concentrations.

As a result, the gate potential of the FET sensor with the PAni-PBA-PVA free-standing conductive hydrogel increased with increasing the glucose concentrations. Because the binding constant of PBA to glucose was higher than that to PVA, the binding of PBA to PVA was replaced by that to glucose in the hydrogel [2]. Therefore, the crosslink density based on PVA decreased with increasing the glucose concentrations in the hydrogel and then the negative charge of PBA was induced by the diol binding with glucose; as a result, the capacitance of the hydrogel increased, which contributed to the FET signals. In this study, we have found the electrical properties of the PAni-PBA-PVA free-standing conductive hydrogel for the glucose detection with the electrochemical setup. Moreover, we would like to discuss about the possibility of the fabricated free-standing conductive hydrogel for the autonomous mobile electrochemical biosensor.

References

[1] W. Li et. al., *Angew. Chemie - Int. Ed.*, 55, 32, 9196–9201, (2016). [2] X. Zhang et.al., *Biomacromolecules*, 13, 1, 92–97, (2012).

SESSION SB08.14: Tissue Engineering/Materials

Session Chairs: Tzahi Cohen-Karni, Nicolette Driscoll, Victor Druet, Sahika Inal, David Ohayon, Jonathan Rivnay, Sneha Shankar and Flavia Vitale
Tuesday Morning, December 7, 2021
SB08-Virtual

8:00 AM SB08.14.01

Multifunctional Polymer Scaffolds for Human Stem Cell Cultures Achilleas Savva and Roisin Owens; University of Cambridge, United Kingdom

Stem cell research has benefitted enormously from a variety of different materials used to create scaffolds to grow stem cells in 3D, however, only few studies report the development of structures that are able to recapitulate 3D tissue-like environments and exhibit multifunctional properties (i.e. electrical and optical). Three-dimensional organic bioelectronic devices proposed to bridge the dimensionality mismatch between 2D/static electronics and 3D/dynamic biology, comprising a versatile platform for hosting and monitoring cells. These devices take advantage of the mixed conduction properties of conjugated polymers (CPs) and enabled the realization of highly biomimetic, electro-active interfaces. Here we show the development of 3D, multifunctional polymer composite structures that exhibit good electrical and optical properties. Water-based solution mixtures of PEDOT:PSS, polythiophene and a polyethylene glycol-based crosslinker are freeze dried, and 3D scaffolds with an average pores size of 50 μm are realized. These structures exhibit lower Young's modulus and higher water swelling capacity compared with pure PEDOT:PSS scaffolds cross-linked with GOPS. Scaffold slices with different thicknesses between 100 μm - 400 μm are attached on flat ITO substrates and their photo-electrochemical properties are measured with electrochemical impedance spectroscopy (EIS) and photo-amperometry. These multifunctional platforms are used to host human adipose derived stem cells (hADCs) and to monitor their proliferation in situ with both EIS and fluorescence microscopy.

8:15 AM *SB08.14.02

In Vitro Biosensing Enhanced by Optically Responsive Nanostructures and Novel Electro-Optical Transduction Approaches Michele Dipalo¹, Sahil Rastogi², Raghav Garg², Andrea Barbaglia¹, Giulia Bruno¹, Rustamzhon Melikov¹, Giuseppina Iachetta¹, Laura Matino¹, Francesco Tantussi¹, Francesca Santoro¹, Tzahi Cohen-Karni² and Francesco De Angelis¹; ¹Istituto Italiano di Tecnologia, Italy; ²Carnegie Mellon University, United States

Over the past decade, nanostructured materials have substantially improved the performance and the capabilities of in-vitro biosensors for cellular analyses. On the one hand, materials with ordered nanostructures or with randomly nanostructured morphology improve adhesion and coupling of cells. On the other hand, these materials enable new effects that are beyond the capabilities of planar interfaces, such as electrical and optical enhancements.

In this talk, I will focus on two recent nanotechnologies: (i) ultrashort pulsed lasers on nanostructured materials for enhancing detection capabilities of electrophysiological sensors, and (ii) novel strategies for electro-optical transduction of action potentials.

The key-enabling factor of ultrashort pulsed lasers in biosensing is the squeezing of high energy in short and sparsely distributed photon packages. Lasers with pulse duration in the picosecond range may reach extremely high peak powers for activating threshold phenomena while maintaining low average irradiation intensities and thus low photocytotoxicity. By proper irradiation with ultrashort pulsed lasers, nanostructured materials immersed in water can emit hot-electrons, which are highly energetic charges that can produce redox reactions and lead to useful effects on adhering cells. In particular, the emission of hot-charges from nanomaterials may result in the non-invasive poration of the cellular membrane or in the photostimulation of action potentials. I will show that such effects can be exploited for enabling intracellular recordings or stimulation of action potentials in electrogenic cells on microelectrode arrays (MEA) decorated with nanomaterials^{1,2}.

In the second part of the talk, I will describe the novel concept of "Virtual mirror Cell" (VICE)³ for monitoring non-invasively the action potentials of

electrogenic cells in-vitro with high spatial resolution. The approach relies on the “mirror charge” effect to transduce transmembrane ionic currents into the motion of fluorophores in a separated microfluidic compartment. The VICE biosensor consists in a thin silicon nitride (Si_3N_4) membrane (thickness 100 - 500 nm) decorated with pass-through gold nanoelectrodes in floating configuration. Electrogenic cells such as neurons or cardiomyocytes are cultivated on the Si_3N_4 membrane and adhere strongly on the gold nanoelectrodes. The other side of the Si_3N_4 membrane is in contact with a microfluidic chamber loaded with charged fluorescent dyes. When cells fire action potentials, the gold nanoelectrodes become polarized and the fluorescent dyes in the microfluidic compartment move according to the generated electric field. Thus, the fluorescent optical intensity under each gold nanoelectrode is directly proportional to variations of the membrane potential of the adhering cell above. By employing high resolution cameras to detect variations of fluorescence intensities under each gold nanoelectrode, the action potentials of thousands of cells can be monitored accurately and non-invasively. In fact, the key advantage of the VICE concept is that the fluorescence dyes are completely separated by the cells thanks to the Si_3N_4 membrane. Thus, cells remain in physiological conditions and can be measured in long-term experiments.

- 1) M. Dipalo et al., Nature Nanotechnol., 2018
- 2) M. Dipalo et al., Science Advances, 2021
- 3) A. Barbaglia et al., Advanced Materials, 2021

8:45 AM SB08.14.03

Crosstalk Studies of Thin Polymer Microelectrode Arrays Yi Qiang and Hui Fang; Dartmouth College, United States

Thin-film polymer microelectrode array (MEA) has emerged as an increasingly significant tool for neuroscience by enabling the measurement of neuronal activities through a more mechanically compliant substrate. The miniaturization of the MEA, which includes high electrode densities and thin encapsulation/substrate layers, is essential for achieving the desired spatial resolution and mechanical compliance. However, the miniaturized MEA sizes, along with the interest of recording neuronal signals in a wide frequency band, lead to the potential frequency-dependent crosstalk among the densely packed microelectrode and interconnects, which can cause severe interference in the signal recording, especially for polymer MEAs. To date, how device parameters affect this crosstalk in polymer MEAs remain poorly studied. In this work, the crosstalk between two adjacent microelectrodes in a thin Kapton thread is modelled using equivalent circuits, then validated with experimental results. Experimentally, crosstalks are measured between two microelectrodes distanced with a different gap, encapsulated by a SU8 layer of different thicknesses and fabricated when placed in different environments (dry, wet, vs. wet with different load resistances). Finite element analysis (FEA) simulation are then utilized to explore the crosstalk in more aggressively scaled polymer electrode threads. This study sheds light on the dependence of the crosstalk in polymer MEAs on a variety of important device parameters and provides the guidelines to the design of thin polymer MEAs for high-quality neural signal recording.

9:00 AM *SB08.14.04

A Look at Resorbable Polymers for Flexible Electronics Kaitlyn E. Crawford; University of Central Florida, United States

Over 200 million wearables were shipped in 2020 with the number of shipped devices likely to increase to over 700 million by 2026 [1]. Wearables are being used for a range of applications from human health monitoring, to lifestyle organizing. The rapidly increasing demand for wearable devices come at a time when environmental and interplanetary pollution are at an all-time high. It is becoming ever-more necessary to consider the sustainability and life-cycle of emerging wearables. To this end, the amount of electronic waste (e-waste) produced in 2020 was ~50 million tons with up to 80% of that waste expected to reach landfills [2]. Other devices such as medical implants remain in patients or require risky second surgeries to remove when their use is complete. The development and integration of degradable materials for wearables can facilitate the decomposition of electronic devices when they are no longer needed. This talk focuses on the use of bioresorbable materials to achieve transient flexible electronics for medical applications, including devices for use underwater and as implants. The talk will include a discussion about the use of natural materials, and resorbable conductive materials for transient electronics. An evaluation of their biocompatibility, moisture permeability, and biodegradation pathways will be presented.

- [1] mordorintelligence.com
[2] thebalancemb.com

SESSION SB08.15: Bioelectronic Devices

Session Chairs: Tzahi Cohen-Karni, Nicolette Driscoll, Victor Druet, Sahika Inal, David Ohayon, Jonathan Rivnay, Sneha Shankar and Flavia Vitale
Tuesday Morning, December 7, 2021
SB08-Virtual

10:30 AM SB08.15.01

Late News: Rapid Single-Molecule Detection of COVID-19 and MERS Antigens via Nanobody-Functionalized Organic Electrochemical Transistors Keying Guo¹, Shofarul Wustoni¹, Anil Koklu¹, Escarlet Díaz-Galicia^{1,1}, Maximilian Moser², Iain McCulloch^{2,1}, Stefan T. Arold^{1,1,3}, Raik Grünberg^{1,1} and Sahika Inal¹; ¹King Abdullah University of Science and Technology, Saudi Arabia; ²University of Oxford, United Kingdom; ³Université de Montpellier, France

The COVID-19 pandemic has highlighted the need for rapid and sensitive protein detection and quantification in simple and robust formats for widespread point-of-care applications. We here introduce a modular nanobody-functionalized organic electrochemical transistors (OECT) architecture that enables rapid quantification of single-molecule-to-nanomolar levels of specific antigens in complex bodily fluids.¹ The sensors combine a new solution-processable organic semiconductor material in the transistor channel and the high-density and orientation-controlled bioconjugation of nanobody-SpyCatcher fusion proteins on disposable gate electrodes. They provide results after 10-min of exposure to 5 μL of unprocessed samples, maintain high specificity and single-molecule sensitivity in human saliva and serum, and can be reprogrammed to detect any protein antigen for which nanobodies exist. We demonstrate the use of this highly modular platform to detect green fluorescent protein (GFP), SARS-CoV-2 and MERS-CoV spike proteins, and for the COVID-19 screening of unprocessed clinical nasopharyngeal swab and saliva samples with a wide range of viral loads.

References

1. Guo, Keying, et al. Rapid single-molecule detection of COVID-19 and MERS antigens via nanobody-functionalized organic electrochemical transistors. *Nature Biomedical Engineering* (2021): 1-12.

10:45 AM SB08.15.02

S-Layer Protein Coated Carbon Nanotubes Dietmar Pum, Andreas Breitwieser and Uwe Sleytr; University of Natural Resources and Life Sciences Vienna, Austria

S-layer proteins form the outermost cell envelope component in a wide range of bacteria and archaea [1]. They can be considered one of the most abundant biopolymers on Earth. In addition to the surface of bacterial cells, S-layer proteins have the natural ability to reassemble into crystalline monomolecular arrays on solid supports, at the air-water interface, on planar lipid films and liposomes. Recently, we have shown that the S-layer protein SbpA from *Lysinibacillus sphaericus* CCM2177 can be used to disperse and functionalize pristine or oxidized multi-walled carbon nanotubes (MWNTs) by fully coating them [2,3].

This presentation summarizes the covalent and non-covalent modification of MWNTs, characterizes the highly ordered helical arrangement of the S-layer proteins, but also lattice defects at kinks and describes the formation of caps on closed nanotubes. In addition, using the recombinant fusion protein rSbpA₃₁₋₁₀₆₈GG (consisting of the SbpA S-layer protein and two copies of the IgG binding region of protein G) as a proof-of-concept, the introduced functionality could be confirmed by visualizing bound gold-labelled antibodies following a helical path around the nanotubes. Moreover, SbpA coated MWNTs were silicified with tetramethoxysilane (TMOS) in a mild biogenic approach. As expected, the thickness of the silica layer could be controlled by the reaction time. Since S-layer proteins have already demonstrated their capability to bind (bio)molecules in dense packing or to act as catalytic sites in biomineralization processes the successful coating of pristine or oxidized MWNTs has the potential for the development of new materials, such as biosensor surfaces. Key to such developments are S-layer fusion proteins, which - as shown here too - have retained the natural self-assembly properties of wild-type proteins, but are additionally equipped with specially tailored bio-reactive domains that enable a highly specific and sensitive functionalization of surfaces.

1. Sleytr, U.B.; Schuster, B.; Egelseer, E.M.; Pum, D. S-layers: principles and applications. *FEMS Microbiol Rev* 2014, 38, 823-864, doi:10.1111/1574-6976.12063.
2. Breitwieser, A.; Siedlaczek, P.; Lichtenegger, H.; Sleytr, B.U.; Pum, D. S-Layer Protein Coated Carbon Nanotubes. *Coatings* 2019, 9, 492, doi:10.3390/coatings9080492.
3. Breitwieser, A.; Sleytr, U.B.; Pum, D. A New Method for Dispersing Pristine Carbon Nanotubes Using Regularly Arranged S-Layer Proteins. *Nanomaterials-Basel* 2021, 11, doi:10.3390/nano11051346.

SESSION SB08.17: Poster Session II: Bioelectronics—Materials and Interfaces

Session Chairs: Tzahi Cohen-Karni, Nicolette Driscoll, Victor Druet, David Ohayon, Jonathan Rivnay, Sneha Shankar and Flavia Vitale
Tuesday Afternoon, December 7, 2021
SB08-Virtual

4:00 PM SB08.17.01

Late News: Quantitative Understanding of Amplification in Organic Electrochemical Transistor-Based Impedance Sensors Filippo Bonafè, Tobias Cramer, Isabella Zironi, Francesco Decataldo and Beatrice Fraboni; University of Bologna, Italy

Organic electrochemical transistors (OECTs) based on the conducting polymer poly(3,4 ethylenedioxythiophene) doped with poly(styrene sulfonate) (PEDOT:PSS) allow for highly efficient bioelectronic interfaces which can transduce biological signals with high gain.¹ Due to their low operation voltage, high transconductance and biocompatibility, ² OECTs have been successfully employed for the detection of biochemical analytes and the impedance sensing of living tissue.³ Despite these promising applications, different studies demonstrate that the OECT gain is limited to the low frequency regime, ⁴ and a quantitative study on the transistor amplification in the frequency spectrum relevant for biosensing is still lacking.

To overcome the issue, we introduce a model experiment where we simulate the detection of a single cell by the impedance sensing of a dielectric microparticle. The microparticle is attached to an atomic force microscopy cantilever to have a refined control of its positioning on the device channel. Measurements are performed with both an OECT and a PEDOT:PSS microelectrode to study the impact of the transistor amplification on the device sensitivity. We interpret the experimental results with a mathematical model which relates the OECT gain to the applied frequency and the device geometry. We use this model as a guideline for the design of an optimized device, and we perform an *in vitro* experiment where we sense the impedance of a single cell with both an OECT and a PEDOT:PSS microelectrode.

By comparing the experimental sensitivities, we observe a significant gain for the transistor structure, thereby demonstrating the advantages arising from the OECT amplification in high precision bioelectronic impedance sensing.

References:

- [1] Khodagholy, D. *et al.* High transconductance organic electrochemical transistors. *Nat. Commun.* (2013) doi:10.1038/ncomms3133.
- [2] Bonafè, F. *et al.* Charge carrier mobility in organic mixed ionic-electronic conductors by the electrolyte gated van der Pauw method, accepted on *Adv. Elect. Mat.* (2021)
- [3] Hempel, F. *et al.* PEDOT:PSS organic electrochemical transistors for electrical cell-substrate impedance sensing down to single cells. *Biosens. Bioelectron.* **180**, 113101 (2021).
- [4] Wang, N., Liu, Y., Fu, Y. & Yan, F. AC Measurements Using Organic Electrochemical Transistors for Accurate Sensing. *ACS Appl. Mater. Interfaces* **10**, 25834–25840 (2018).

4:05 PM SB08.17.02

Nernst-Planck-Poisson Modelling of EGOFET Biosensors Larissa Huetter¹, Adrica Kyndiah² and Gabriel Gomila¹; ¹Institute for Bioengineering of Catalonia (IBEC), Spain; ²Italiano Istituto di Tecnologia (IIT), Italy

Electrolyte-gated organic field-Effect transistors (EGOFETs) are promising electronic devices for application as biosensors. Using organic semiconductors as active materials enables developing biocompatible, low-cost and highly sensitive devices for biorecognition events. Biosensing events modify the charge and/or specific capacitance of the bilayer/electrolyte interface at the gate electrode or semiconductor interfaces, resulting in the alteration of the semiconductor's conductivity, hence the electric current flowing through the device. EGOFETs can also be used to record the electrical activity of excitable cells since a slight potential variation at the gate electrode or semiconductor surface can lead to a shift into the current flowing through the transistor^{1,2}. Despite their wide use and potential, the theoretical modelling of the EGOFET biosensor still lacks a proper understanding of several of the experimental features observed. The main reason is the use of theoretical models borrowed from the analysis of solid-state devices like MOSFETs and TFTs, which lack the physics of liquid electrolytes present in EGOFETs.

In the current work, we present the theoretical modelling of EGO-FET biosensors in the Nernst-Planck-Poisson and drift-diffusion framework. In the present approach, we offer a physical description of the coupling of the electrolyte and the semiconductor through its interface, retaining the entire physics of the formation and evolution of the electrical double layers. We analyze the voltage and charge distributions across the EGO-FET devices and explore how the variations of the interfacial charge or the specific capacitances at the electrolyte interfaces during a biorecognition effect affect them. Moreover, we investigate the current-voltage characteristics of the devices predicted in this framework and propose a generalized phenomenological model for its description. Finally, and based on the phenomenological model proposed, we propose an interpretation technique of experimental biosensor data based on the analysis of the conductivity vs gate voltage function, which offer significant advantages with respect to the analysis of current-voltage transfer curves, common in the field at present.

¹E. Macchia, R. A. Picca, K. Manoli, C. Di Franco, D. Blasi, L. Sarcina, N. Ditaranto, N. Cioffi, R. Österbacka, G. Scamarcio, F. Torricelli and L. Torsi, "About the amplification factors in organic bioelectronic sensors," *Mater. Horizons*, vol. 7, p. 999–1013, 2020.

²A. Kyndiah, F. Leonardi, C. Tarantino, T. Cramer, R. Millan-Solsona, E. Garetta, N. Montserrat, M. Mas-Torrent and G. Gomila, "Bioelectronic Recordings of Cardiomyocytes with Accumulation Mode Electrolyte Gated Organic Field-Effect Transistors," *Biosens. Bioelectron.*, vol. 150, p. 111844, 2020.

4:10 PM SB08.17.03

Development of a Wearable, Ultra-Sensitive and Highly Stable Electrospun Strain Sensor Incorporating Graphene-MXene-CNC Nanohybrids Sara Mohseni Taromsari, Chul B. Park and Hani E. Naguib; University of Toronto, Canada

Wearable strain sensors have long been a prominent member of the biomedical sensing devices, however, their applications are mostly hindered by their low sensitivity (gauge factor of at most 32 at subtle strains as caused by most of the physiological motions), as well as insufficient stability. In order to overcome such shortcomings, we have focused on development of a nanoporous, highly stretchable styrene-butadiene-styrene (SBS) substrate via electrospinning, to provide nanofibrous, interconnected pathway for a conductive network. Further, a novel approach consisting of simultaneous ultrasonic-assisted atomization and vacuum-assisted filtration was taken to carefully deposit suspensions of two types of conductive 2D materials, graphene and MXene with varying ratios, onto the surface of each fiber within the interlocked network. Such approach managed to guarantee fiber decoration, instead of forming a blanket coating on the whole surface of electrospun membranes, and to preserve the nanofibrous network that contributes to both high sensitivity and ultra stretchability. Cellulose nanocrystals (CNC) were used both as a surfactant in the liquid phase to assist 2D materials dispersion and as a compatibilizer in solid phase to act as nano-stitches, consequently enhancing the interfacial bonding between the fillers and the SBS substrate, and providing long-term stability. In the meanwhile, in an optimal concentrations which includes equal contents of graphene and MXene, each of the conductive fillers play a vital role in formation of the conductive network and its ultimate reversible disconnection when exposed to subtle motions; graphene's larger flakes provide mechanical strength by supporting the conductive framework, develop conductive interconnections for smaller MXene flakes, while they contribute to stability and easy slippage of the fillers over one another due to their inborn lubricity effect. On the other hand, smaller, yet metallic conductive MXene flakes form the conductive network at much lower filler contents (3.9 wt.% in total), while their irregular, more brittle nanoparticles with random morphologies contribute to the formation of small brittle structures that can respond to smallest of strains. The chemical, interfacial bonding between CNC, SBS and the conductive fillers were studied and verified by Fourier-transform infrared spectroscopy (FTIR), x-ray photoelectron spectroscopy (XPS) and thermogravimetric analysis (TGA) analyses, while the scanning electron microscopy (SEM) micrographs could prove the formation of a uniform, agglomerate-free, hybrid conductive network on each fiber of the interlocked network. Results of the tensile and dynamic mechanical analysis (DMA) tests, indicated the successful effect of both CNC and graphene in providing a mechanically robust conductive network with up to 171% and 167% increase in yield strength and elastic modulus, respectively. Moreover, the hybrid sensors, especially the one containing the optimal concentrations of fillers, showed the highest reported gauge factor of 68 for small strain regions, while the same factor went up to even 430 for higher strain regions, which is over 50% higher than the best value reported in the literature. Cyclic loading/unloading tests were carried out on the samples, the results of which indicated the effectiveness of CNC and graphene's role in providing low hysteresis and stabilizing the conductive network over the long run. Results of the actual sensing performance of the samples indicated highly sensitive and repeatable detection of phonations, respiration patterns and muscle movement as physiological motions, thanks to the formation of the robust, reversibly disconnectable conductive network and the stabilization provided by the compatibilizer and the processing technique.

4:15 PM SB08.17.04

Automated High Throughput Testing of Organic Electrochemical Transistors (OECT) Ulyana S. Cubeta¹, Lucas Flagg¹, Austin L. Jones², John R. Reynolds² and Lee Richter¹; ¹National Institute of Standards and Technology, United States; ²Georgia Institute of Technology, United States

Because biosensors can be designed with a wide array of materials, device architectures, and used in a wide array of sensing environments, the rapid development and optimization of a biosensors is particularly amenable to automated high throughput testing. We have devised a screening system to rapidly perform electrochemical device testing in an array of sensing environments. Organic mixed electronic/ion conductors are emerging as an important material platform for applications diverse as energy storage, neuromorphic computing and organic electrochemical (OECT) biosensors. Unlike the related organic semiconductors, OECTs typically operate as bulk devices, in intimate contact with electrolyte. Therefore, their electronic and ionic conductivity is intimately linked to their swelling by both electrolyte and compensating ions. Insight into the impact of swelling on the fundamental operation of OECTs can be obtained by varying the polarity or dielectric constant of the solvent and by selecting a different ion from the Hofmeister series; however, these studies are rarely done due to their tedium. As a proof-of-concept we have deployed our automated measurement system to rapidly test OECT devices in multiple electrolytes. We compare the solvent and ion sensitivity of the prototypical PEDOT:PSS polymer semiconductor to a novel oligo(ether)-functionalized propylenedioxythiophene (ProDOT)-based copolymer[1] in a standard OECT architecture. When applied to complete sensors, the system enables testing against multiple analyte concentrations with varied interfering species. When combined with automated device fabrication, automated testing will enable machine-guided optimization of complete sensor architectures.

[1] Savagian et al. *Adv Mater* 2018, doi: 10.1002/adma.201804647

4:20 PM SB08.17.05

Investigation of the Effects of Prednisone on Normal Epithelial Cell and Cancer Cell Attachment Using Electric Impedance Characterization Steffi Kong, Alejandra Martinez and Maddy Behravan; Converse College, United States

This research investigates the effects of Prednisone on the attachment of normal epithelial cells (HaCAT) and cancerous cells (A431) by electric impedance measurement. An alternating signal is applied to a series of electrodes on the bottom of cultureware on which cells were seeded. The impedance (resistance and capacitance) is recorded in real-time and correlated to cell spreading, cell-to-cell, and cell-to-substrate attachment. The real-time resistance and the capacitance were examined to infer the effects of prednisone on HaCAT and A431 cells. In harmony with prior work on these cells, it was observed the resistance increases with time and the capacitance decreases with time for both cell types. And consistently, a larger resistance and smaller capacitance

were measured for A431 cell compared with HaCAT cells. The impedance data analysis indicates that Prednisone at applied doses does not have a significant effect on the impedance of HaCAT cells over a long time. The impedance data exhibits that Prednisone may result in partial detachment and reattachment of A431 cell-to-cell bonds, indicating cellular matrix restructuring.

4:25 PM SB08.17.06

Late News: Understanding the Role of Voltage-Dependent Ion Movement in Organic Electrochemical Transistor Using Equivalent Circuit Modeling [Jaspreet Kaur Pawa](#)^{1,2}, Rachel Owyueung^{1,1} and Sameer Sonkusale^{1,1}; ¹Tufts University, United States; ²Birla Institute of Technology and Science, India

Organic electrochemical transistors (OECTs) are promising devices for a wide variety of biological applications, as they exhibit a high transconductance at low operational regimes, and can mimic ion doping profiles of biochemical signals for artificial synapse applications. However, to our knowledge, the asymmetric nature of an OECTs transient drain current response to a uniform gate voltage pulse has not been addressed adequately, although it is apparent across devices shown in literature. In this work, we seek to analyze this asymmetric transient response, as well as hysteresis in the transistor's characteristic curves, to gain a better understanding of the device physics of OECTs. We fabricated PEDOT:PSS-based OECTs with different configurations and dimensions, and took transfer and output characteristics, as well as tested the transient behavior of the device. The OECT under consideration showed a pinch off voltage of 0.54V, and a process transconductance parameter of 0.89 mA/V². A uniform pulse of 100mHz frequency, alternating between voltages -0.5V and +0.5V was applied to the gate terminal of the OECT with a source-drain voltage of 0.8V. The resulting drain current response was seen to have an asymmetric shape, i.e. for the falling edge of input gate voltage pulse, we witnessed a gradual increase in drain current magnitude (3.0 s), whereas we observed an abrupt decrease in drain current magnitude for the rising edge (0.4 s). This is a landmark observation in most OECTs published in literature, though not thoroughly explored.

We hypothesize that the interplay between concentration gradient (electrolyte to channel) and influence of applied voltage on the dedoping cations, alters the rate of cation movement in and out of the semiconductor channel. This consequently affects the rise and fall time in drain current response, ultimately giving rise to hysteresis in the characteristic curves and an asymmetric transient response. We model the components of the OECT, namely the gate electrolyte, its interface with the active channel (in this case, PEDOT:PSS), and the channel itself using resistances, capacitances, and a diode. Using device equations, characteristics, and dimensions of the devices, we can accurately predict the drain current response for any voltage input or shape (absolute error of 5.35% in simulated output characteristics). We argue this model can be applied to OECTs with different geometries and materials. Further, using discrete electrical elements in the model allows us to isolate how the OECT components affect the overall device performance. This can be a powerful tool for better design of future OECTs, and for more facile implementation of OECTs into more complex, higher order circuitry, which requires knowledge of device behavior at all points of operation.

4:30 PM SB08.17.07

Tailoring the Physicochemistry of SU-8 Polymers to Modulate Bacteria-Surface Interaction Silambarasan Anbumani¹, Aldeliane M. Silva¹, Andrei Alaferdov¹, Marcos Puydinger¹, Mariana S. Silva², Stanislav Moshkalev¹, Hernandes F. Carvalho¹, Alessandra A. de Souza² and [Monica A. Cotta](#)¹; ¹University of Campinas, Brazil; ²Agronomic Institute of Campinas, Brazil

An epoxy polymer, SU-8 shows important potential for fabrication of high aspect ratio of micro/nanostructures scaffolds for lab-on-a-chip devices. In particular, this polymer has been used as an impressive platform for the development of various smart biomedical devices owing to its excellent optical and mechanical properties, as well as chemical stability. Whilst SU-8 properties combined with its biocompatibility facilitate its application in bio-related material interfaces, still, how SU-8 physicochemical properties affect bacteria-surface interaction has not been properly evaluated so far.

In this work, we tailor SU-8 surface properties to investigate single cell motility and adhesion of *Xylella fastidiosa* bacteria. Different SU-8 samples have been prepared using UV illumination, thermal processing and oxygen plasma treatment. Atomic Force Microscopy and X-Ray Photoelectron Spectroscopy were used to determine nanoscale surface properties; in vitro studies at the level from single cell to biofilm formation were carried out with Confocal Laser Scanning Microscopy (CLSM). The mean velocity and displacement of single cells have been extracted from CLSM tracking information data and the architecture of biofilms as well as surface coverage are compared for different samples. We observed significant differences in bacterial cell motility, for both speed and direction, as well as adhesion and biofilm architecture on SU-8 as nanoscale surface property changes. Larger density of carboxyl groups in SU-8 plasma-treated surfaces provide enhanced cell motility, while denser biofilms are found in untreated SU-8. Our results can be interpreted based on how bacterial pili interaction with the surface takes place, therefore providing different bacterial motility and cluster assembly regimes. These results advance our understanding of the role of surface functional groups and wettability on bacteria-surface interaction for biosensing and bioelectronics applications; additionally, they might indicate new strategies to prevent microbial adhesion and, consequently, biofilm development of pathogenic species.

4:35 PM SB08.17.08

Optogenetic Behaviour Control of *Drosophila melanogaster* Using Smartphone Displays [Ilenia Meloni](#)¹, Divya Sachidanandan^{2,3}, Andreas S. Thum^{2,3}, Robert J. Kittel² and Caroline Murawski¹; ¹Kurt-Schwabe-Institut für Mess- und Sensortechnik Meinsberg e.V, Germany; ²Institute of Biology, Universität Leipzig, Germany; ³Carl-Ludwig-Institute for Physiology, Universität Leipzig, Germany

Optogenetics is a powerful method to modulate neuronal activity with light¹. Currently used optogenetic light sources such as lasers, LEDs, and projectors are limited in spatial resolution and typically require sophisticated, bulky and expensive experimental setups. Here, we propose using smartphone displays as simple, low-cost light sources that provide high spatial resolution for optogenetic stimulation of larval and adult stages of *Drosophila melanogaster* (fruit fly)².

We developed a smartphone app that allows spectral, spatial, and temporal control over the light emitted by the display and used this to deliver light patterns to induce activation and inhibition of several sets of neurons, including motoneurons, muscles, all sensory and class IV multidendritic neurons using different light-sensitive proteins (*UAS-CsChrimson*, *UAS-ChR2^{XXL}*, *UAS-GtACR1* and *UAS-GtACR2*). Using, e.g., the green/red light-sensitive CsChrimson expressed in the muscles of *Drosophila* larvae, we detected a strong muscle contraction in response to stimulation with green, red, and white light of around 2-6 $\mu\text{W}/\text{mm}^2$ intensity. We also used fine patterns of light to constrain larval movement within a maze pattern or guide larvae through a disk of light. We demonstrate the suitability of smartphones as a simple testbench for a wide range of standard optogenetic experiments in both flies and larvae. In order to precisely determine the optical power density of the display also for complex light patterns, we developed a routine to simulate the spatial light distribution. This tool improves our understanding of the larvae's light-induced behaviour and leads to enhanced targeting of both individual and groups of larvae. We expect this low-cost test environment may be extended to other invertebrate species or adopted for use in teaching labs.

1. Deisseroth, K. Optogenetics: 10 years of microbial opsins in neuroscience. *Nat. Neurosci.* **18**, 1213–1225 (2015).

2. Meloni, I., Sachidanandan, D., Thum, A. S., Kittel, R. J. & Murawski, C. Controlling the behaviour of *Drosophila melanogaster* via smartphone optogenetics. *Sci. Rep.* **10**, 17614 (2020).

4:40 PM SB08.17.09

Multi-Mechanism Pressure Sensor—Simulation and Fabrication Azmal H. Chowdhury, Borzooye Jafarizadeh, Iman Khakpour, Nezhir Pala and Chunlei Wang; Florida International University, United States

Recently, skin mountable wearable devices have gained much attention due to their non-invasive usage and wearer comfort for health care monitoring. These devices are generally used for applications such as pulse detection and e-skin application. For instance, monitoring pulse waveform detected from the wrist or neck artery can provide information on cardiovascular abnormalities such as arterial fibrosis or hypertension. The requirement for a high-performance flexible pressure sensor is good sensitivity, low power consumption, and instantaneous response for effective human-machine interfacing. In general, pressure sensors can be categorized by types of operations into piezoresistive, capacitive, piezoelectric, triboelectric, etc. Since all of these mechanisms require one flexible substrate, merging different sensing mechanisms into one multi-mechanism sensor can compound the advantages and minimize the shortcomings of these various modes of operation.

In this study, the design parameters were optimized to realize a breathable, multimodal pressure sensor consisting of piezoresistive, capacitive, and strain gauge sensing elements for precise monitoring of arterial pulse waveform. Using finite element analysis (commercial software COMSOL), simulation studies were carried out on micro-feature design parameters, such as pyramid angle, base size, and number density to find the design rules to achieve high sensitivity for the piezoresistive mode of the sensor. Also, based on finite element analysis of structural deformation, the rule for a micropatterned dielectric layer for the capacitive sensor has also been studied. These design rules yield a compact multi-mechanism sensing platform where each part has been fabricated separately. Moreover, fabrication of breathable polymeric substrate has been accomplished by methods such as electrospinning, sacrificial template, and electrostatic spray deposition to ensure long term comfortable wearability of the device. Finally, the conductive sensing material was realized via bi-polar electrochemistry to deposit porous graphene on the polymeric foundation for the piezoresistive sensor. The simulation results state that lower number density, smaller feature size, and an angle of about 50 degrees of microfeatures achieve the highest sensitivity. Furthermore, the fabrication of the multi-mechanism sensor followed the standard microfabrication techniques including photolithography and transfer printing method to integrate heterogeneous elements into the sensor. The detailed results will be discussed during the presentation.

Keywords: Wearable pressure sensor, pulse, simulation, bipolar electrochemistry, graphene, photolithography, transfer printing, finite element analysis, modeling.

4:45 PM SB08.17.10

Late News: Microelectrode Arrays for Simultaneous Electrophysiology and Advanced Brain Imaging Sagnik Midya, Alejandro Carnicer Lombarte, Stephen Sawiak, Sam Hilton, Vincenzo F. Curto, Gabriele Kaminski Schierle and George G. Malliaras; University of Cambridge, United Kingdom

Advanced brain imaging techniques are crucial in neuroscience research as well as in clinical diagnosis. Optical microscopy enables the targeting of specific molecules in the brain and provides a high spatial resolution. On the other hand, spectroscopic techniques like magnetic resonance imaging (MRI) can access deep regions of the brain over a large area and identify their functions. Additionally, electrical readout through neural electrodes is indispensable in measuring their activity. It is important in several applications, for example, in mapping different functions to different regions of the brain. Clinically, it is utilised in studying the initiation and spreading of seizure like activities. Unfortunately, simultaneous brain imaging and electrophysiology is challenging. Firstly, conventional electrodes are non-transparent, thus inhibiting optical imaging. In case of MRI, this is further compounded by the possibility of heating caused by eddy currents in metal electrodes. Mismatch between the magnetic susceptibilities of common electrode materials and the surrounding tissue also results in significant artefacts due to loss of signal. In this regard, conducting polymer electrodes are prospective alternatives since their compositions are closer to biological tissues. PEDOT:PSS, one of the most widely used conducting polymers, has been used in neural electrodes to improve their signal to noise ratio. This can be achieved by virtue of the volumetric capacitance effect in the conducting polymer which significantly reduces the electrode impedance. Here, we present PEDOT:PSS based versatile transparent microelectrode arrays (MEA). The glass substrate-based MEAs are immune to laser-induced artefacts and enable simultaneous Ca^{2+} imaging with electrophysiology in vitro. They are also compatible with the state-of-the-art optical imaging as well as super resolution microscopy techniques. Further, in the form of conformable electrocorticography arrays, the PEDOT:PSS electrodes can be coupled with optical brain imaging techniques. They allow MRI along with simultaneous electrical interrogation through stimulation and recording.

SESSION SB08.19: Poster Session III: Bioelectronics—Materials and Interfaces

Session Chairs: Tzahi Cohen-Karni, Nicolette Driscoll, Victor Druet, David Ohayon, Jonathan Rivnay, Sneha Shankar and Flavia Vitale

Tuesday Afternoon, December 7, 2021

SB08-Virtual

9:00 PM SB08.18.01

Electropolymerized pHEMA coating on Flexible Multichannel Neural Probe for Localized Sensing and Stimulation Gary Kwok Ki Chik^{1,2}, Na Xiao^{3,2}, Gianni Deng², Chung Tin³ and Paddy K. L. Chan^{1,2}; ¹The University of Hong Kong, Hong Kong; ²Advanced Biomedical Instrumentation Centre, Hong Kong; ³City University of Hong Kong, Hong Kong

Miniaturization and minimization of mechanical mismatch in neural probes have been two well-proven directions in suppressing immune response and improving spatial resolution for neural stimulations and recordings. While the high impedance brought by the miniaturization of electrodes have been addressed by using conductive polymers (CPs) coatings in multiple reports, the stiffness of such coatings remains orders of magnitude from the brain tissue. In this study, we present a highly flexible microelectrode array neural probe of 8 gold electrodes with electrodeposited hydrogel coatings poly(2-hydroxyethyl methacrylate) (pHEMA) and conductive polymer poly(3,4-ethylenedioxythiophene) polystyrene sulfonate (PEDOT:PSS), with a cross-section area at only 300 μm x 2.5 μm . The porous and sponge-like pHEMA provided excellent cell adhesion properties and bridged the mechanical mismatch between the probe and the brain tissues. Besides, the PEDOT:PSS coating provides a low interfacial impedance that enhance the signal-to-noise ratio and allow the microelectrodes array to be engineered for both recording and stimulation purposes. The signal-to-noise ratio increases 70% while comparing with bare gold electrodes, and the charge injection capacity of the probe achieved 2.2 mC/cm^2 . In vivo testing of microelectrode arrays implanted in rat hippocampus revealed that the microelectrodes show high signal-to-noise ratio and excellent charge injection capacity, providing a robust and low-cost solution in the brain interfaces problem.

9:05 PM SB08.18.02

Monitoring Cells After Low-Voltage Electroporation Using a Small-Size Multiple-Pulse Framework Denise Lee¹, Sophia Chan¹, Nemanja Aksic¹, J Shamita Naiker^{1,2}, Natasa Bajalovic¹ and Desmond K. Loke^{1,2}; ¹Singapore University of Technology and Design, Singapore; ²Changi General Hospital, Singapore

A long-term, nondestructive monitoring of cells is significant for understanding different cellular processes and functions. However, traditional methods are limited to a certain range of testing conditions and may reduce cell viability. Furthermore, the ability to demonstrate cell recovery and pore resealing after electroporation for long periods remains elusive due to difficulties in cell maintenance. Here, we develop a small-size, multiple-pulse electroporation system for monitoring cell recovery for an extended period of time with the use of low bias voltage pulses. We demonstrate that our system is able to preserve cell viability during the electroporation of cells and achieve real-time cell monitoring during the recovery period. Theoretical studies elucidate the origin of the pulsing-facilitated change in recovery time. Additionally, our method does not require specialized equipment, which allows for easy access across laboratories and medical facilities.

9:10 PM SB08.18.03

Flexible Semi-Transparent Top-Contact Organic Electrochemical Transistors Based on Ultra-Thin Gold-PEDOT:PSS Hybrid Electrode for Human Skin Interfaces Il-Young Jo, Gunwoo Kim, Youngseok Kim and Myung-Han Yoon; Gwangju Institute of Science and Technology, Korea (the Republic of)

In this research, we report ultra-thin gold-conducting polymer hybrid electrodes and their applications to flexible semi-transparent human skin interfaces. Ultra-thin hybrid electrodes were fabricated by thermal evaporation of a very thin gold layer on crystalline poly(3,4-ethylenedioxythiophene):poly(styrene sulfonate) (PEDOT:PSS) film, leading to low sheet resistance (39.13 Ω /sq) as well as substantial optical transparency (56%) at the visible light range. Subsequently, semi-transparent electrodes were realized on flexible top-contact OECT devices which exhibited decent optical transparency, high transconductance (1 mS), and operational stability even at the highly bent state. Finally, it was successfully demonstrated that these semi-transparent flexible OECTs were mounted on human skin for electromyography recording.

9:15 PM SB08.18.04

Doubly Crosslinked Microgel-Based Electrodes Enable Electrically-Controlled Drug Delivery and Biochemical Sensing Applied for Smart Wound Dressing Chi-Yao Ku, Ting-Heng Lu, Liang-Jie Lu, Wei-Chen Huang and Yu-Te Liao; National Yang Ming Chiao Tung University, Taiwan

Smart Wound dressings with electrically controlled drug release and real-time monitoring can accelerate wound healing. Flexible electronics integrated with structurally and mechanically tissue-mimicked electrodes can not only provide high filling space for drug loading, but also can permit a seamless and biocompliant contact with skin to reduce the resistance for drug delivery and electrical signal transduction. Herein, an antibacterial hydrogel electrode is designed and integrated into a wireless system composed of a multimodality readout IC and an electrical current stimulator for electrically-controllable anti-inflammatory drug release and uric acid (UA) detection. The doubly crosslinked microcapsules composed of carboxymethyl-hexanoyl chitosan-doped poly(3,4-ethylenedioxythiophene) and silk, called PEDOT:CHC/silk, are served as hydrogel electrodes to demonstrate tissue-like mechanical properties, electrochemical activity, and antibacterial ability. Active loading of ibuprofen (Ibu) in the PEDOT:CHC microgels allows large amount of drug loading, whereas the incorporation of silk leads to densely crosslinking of the microgels, in turns resulting in a precisely electrically-controlled release under the application of both DC (1-5V) and cyclic voltametric (CV) electrical stimulation. With the integration of hydrogel electrodes into a wireless multimodality chip fabricated in a 0.18 μ m CMOS process, a repeated burst-to-zero-to-burst and UA detection through CA/CV is demonstrated. This smart wound dressing with highly biological and electrical compatibility is expected to provide more precise wound care.

9:20 PM SB08.18.05

Biocompatible Performance Enhancer for Organic Electrochemical Transistors Ting Li, Wei Lin Leong, Xihu Wu and Shuai Chen; Nanyang Technological University, Singapore

Organic electrochemical transistors (OECTs) have attracted attention in recent years due to their high transconductance, low operating voltage, and compatibility with aqueous solutions for broad biosensing applications. Especially, OECT-based biocompatible electronic devices enable the monitoring of physiological signals on human skin. Poly-3,4-ethylenedioxythiophene:poly-4-styrenesulfonate (PEDOT:PSS) is a typical material acting as the active channel layer in OECTs. However, the poor electrical conductivity of pristine PEDOT:PSS diminish the lifetime and restrict the application scope of the electronic device systems. Although some additives in PEDOT:PSS have been proposed to enhance the conductivity, those additives are not proved to be non-toxic or biocompatible. Besides, 4-dodecylbenzenesulfonic acid (DBSA), glycerol, dimethyl sulfoxide (DMSO), and ethylene glycol (EG) have been claimed to be biocompatible and reported to obtain PEDOT:PSS based OECTs with higher performance, however, their contribution to the enhancement of OECT performance is limited. It is worth investigating whether there is any intrinsically biocompatible additive that is more effective. Herein, a biocompatible ionic liquid [MTEOA][MeOSO₃] is proposed as a biocompatible additive to enhance the performance of PEDOT:PSS based OECTs. The influence of [MTEOA][MeOSO₃] on the morphology, conductivity, and the redox process of PEDOT:PSS during electrochemical doping/de-doping processes are explored. The biocompatible P+[MTEOA][MeOSO₃] (PEDOT:PSS mixed with [MTEOA][MeOSO₃]) film as OECT channel layer exhibits enhanced transistor characteristics, including higher transconductance, excellent switching cycling stability, and low energy consumption. The electrophysiological (ECG) signals recording ability of the P+[MTEOA][MeOSO₃] based OECT is explored, ECG signals from the hand and heart of a volunteer are recorded successfully. Further, the P+[MTEOA][MeOSO₃] film is employed as the sensing component of a pressure sensor, and the integration of the pressure sensor with the OECT shows interesting tunable pressure sensitivity by gate bias and is demonstrated to monitor physiological signals on human skin as a wearable electronic device. In addition, the P+[MTEOA][MeOSO₃] film also shows robust resistance to physical deformation and desired compatibility with flexible substrates as the active channel layer of the flexible OECT.

9:25 PM SB08.18.06

Late News: Effect of Additives on the Performance of a p-type Organic Semiconductor Tania C. Hidalgo Castillo¹, Maximilian Moser², Camila Cendra³, Prem Nayak¹, Alberto Salleo³, Iain McCulloch² and Sahika Inal¹; ¹King Abdullah University of Science and Technology, Saudi Arabia; ²University of Oxford, United Kingdom; ³Stanford University, United States

Organic electrochemical transistors (OECTs) transduce ionic fluxes into electronic signals with exceptional performance.^[1] It has been shown that OECTs comprising channels made of poly(3,4-ethylenedioxythiophene)-poly(styrenesulfonate) (PEDOT:PSS) show stable operation up to ~21 days.^[2] These transistors, however, operate in depletion mode, which show inferior ON/OFF ratios at low bias and are always ON, having adverse influence on power consumption. These are drawbacks hindering the practical use of these devices for long-term, biological sensing applications. On the contrary, semiconducting polymers give rise to accumulation (enhancement) mode OECTs with inherently high ON/OFF ratios and low power consumption, and, as such, they are highly sought after. These polymers should however be stable at ambient and aqueous conditions, typical for biological sensing applications.

A good measure for OECT stability is switching the gate between ON and OFF states while biasing the drain electrode. As such, current degradation, and therefore transconductance loss, is probed. Nonetheless, longer term stability measurements, such as shelf-life stability, have often been overlooked. Recently, a p-type diketopyrrolopyrrole-based organic semiconducting polymer was reported to retain more than 85% its initial transconductance value

over ~75 hours exposed to electrolyte.^[3] However, this value was reported for a large radius anion, which is not biologically relevant. We show that by tuning the solvent mixture composition used to cast a thiophene-based p-type semiconducting polymer film, not only the OECT performance is enhanced but also the device shelf-life stability is significantly improved. The same effect is obtained by the use of a strong Lewis acid in the polymer solution. We find that the solvent additive and the acid both change the film morphology and microstructure, leading to such significant improvements in OECT performance and stability. As such, our work provides insights into structure-property relations of semiconducting polymers for applications in bioelectronics that require high performance alongside long shelf-life.

[1] Rivnay, J. *et al.* Organic electrochemical transistors. *Nat. Rev. Mater.* **3**, 17086 (2018)

[2] Kim, S.-M. *et al.* Influence of PEDOT:PSS crystallinity and composition on electrochemical transistor performance and long-term stability. *Nat. Commun.* **9**, 3858 (2018).

[3] Wu, X. *et al.* Enhancing the Electrochemical Doping Efficiency in Diketopyrrolopyrrole-Based Polymer for Organic Electrochemical Transistors. *Adv. Electron. Mater.* **7**, 2000701 (2021).

SESSION SB08.20: Neurotech/Devices

Session Chairs: Tzahi Cohen-Karni, Nicolette Driscoll, Victor Druet, Sahika Inal, David Ohayon, Jonathan Rivnay, Sneha Shankar and Flavia Vitale
Wednesday Morning, December 8, 2021
SB08-Virtual

10:30 AM *SB08.20.01

Skin-Inspired Soft Sensors and High-Density Electrode Arrays for Biointerfaces [Zhenan Bao](#); Stanford University, United States

In this talk, I will present recent development of materials and fabrication for sensors and electrode arrays for biointerfaces and their in vivo applications.

11:00 AM SB08.20.02

Soft, Flexible Cryogel-Based Neurostimulation Electrodes to Promote Neuroplasticity in the Brain [Tianhao Chen](#)¹, Kylie Lau¹, Mary Jiayi Chen¹, Sung Hwa Hong¹, Stephanie Iwasa², HaoTian Shi³, Taylor Morrison¹, Suneil Kalia¹, Milos Popovic¹, Cindi M. Morshead¹ and Hani E. Naguib¹; ¹University of Toronto, Canada; ²University Health Network, Canada; ³University of Cambridge, United Kingdom

Deep brain stimulation (DBS) involves the delivery of electrical pulses to the brain via penetrating electrodes. While the mechanism is not well understood, DBS has proven to be a successful clinical approach to treat a variety of neurological disorders. Most recently, it has been shown that resident neural precursor cells in the brain are electrosensitive cells that expand in number, migrate and differentiate in response to stimulation. As such, the potential for electrical stimulation to promote brain repair by harnessing the regenerative properties of neural precursor cells (NPCs) is an exciting area of research. We have shown that metal-based electrodes with optimized electrical stimulation parameters can activate resident NPCs however, conventional rigid, metal-based materials are suboptimal for clinical application. This is due to the mechanical mismatch with brain tissue, poor biocompatibility and high electrode-tissue impedance that can cause damage to both electrodes and tissue during stimulation. Currently, there are numerous soft electrodes designs with good stimulating capacity and similar modulus with neural tissue in the kilopascal range but these are mostly surface electrodes that require sophisticated fabrication and additional implantation techniques due to low modulus. Here, we report a conductive and biocompatible cryogel electrode that has a simple modulus switching mechanism – high stiffness for penetration to brain tissue when dry, then softening to the kilopascal range in response to the wet environment of brain tissue. The material also exhibits high charge storage and injection capacities in brain electrolyte, reducing the interfacial impedance to deliver the required electrical field with ~7 times lower voltage under charge-balanced current controlled stimulation. We have demonstrated successful NPC stimulation using cryogel electrodes resulting in significant NPC expansion and migration of NPCs in ex-vivo brain tissue models. The cryogel material combined with optimized stimulation parameters is a promising approach to be used in DBS to promote endogenous neural repair.

Key words: deep brain stimulation, galvanotaxis, neural stem cells, conductive polymers, neuromodulation

11:15 AM *SB08.20.03

Flexible Adhesive Electronics for Electrophysiological Monitoring [Chenchen Mou](#)¹, [Jiwoo Song](#)¹, [Charles Horn](#)², [Scott Halbreiner](#)³ and [Christopher J. Bettinger](#)¹; ¹Carnegie Mellon University, United States; ²University of Pittsburgh, United States; ³Allegheny General Hospital, United States

Reliable recording and modulation of excitable tissue using implantable electronic devices have implications in diagnosing and treating many types of diseases. The advent of flexible electronics has enabled new concepts in interfacing devices with soft tissues. However, to date, most flexible electronics achieve mechanical compliance by using substrates composed of thin curable resins or elastomers. These materials are suboptimal for tissue interfacing because they: (1) exhibit Young's moduli that are orders of magnitude larger than many excitable tissues, such as peripheral nerves and vascular structures; (2) are difficult to integrate with hydrated tissue in vivo. Here we present recent advances in materials and fabrication from our lab to address current limitations in flexible electronics. Specifically, the synthesis and formulation of flexible adhesive hydrogels and transfer printing to create ultracompliant devices to interface with peripheral nerves and cardiac tissues will be described. Details regarding the in vitro and in vivo performance of peripheral nerve interfaces and cardiac monitoring devices will be presented. Future prospective applications for this concept will also be highlighted, too.

11:45 AM *SB08.20.04

3D Artificial Dendritic Spines for Engineering Bioelectronic Interfaces [Chiara Ausilio](#), [Sara Grasselli](#), [Anna Mariano](#), [Valeria Criscuolo](#) and [Francesca Santoro](#); Istituto Italiano di Tecnologia, Italy

The interface between biological cells and non-biological materials has profound influences on cellular activities, chronic tissue responses, and ultimately the success of medical implants and bioelectronic devices. The optimal coupling between cells, i.e. neurons, and materials is mainly based on surface interaction, electrical communication and sensing.

In the last years, many efforts have been devoted to the engineering of materials to recapitulate both the environment (i.e. dimensionality, curvature, dynamicity)¹ and the functionalities (i.e. long and short term plasticity)² of the neuronal tissue to ensure a better integration of the bioelectronic platform and cells.

Here, we present how dendritic spine-like structures can be engineered by means of two-photon polymerization in 2.5 and 3D architectures³. In particular, these structures can be functionalized with ECM proteins and artificial lipid bilayers to emulate the composition of living spines in the neuronal tissue. Moreover, the topographical cues at the spine-neuron interface trigger different cell response in terms of neuronal polarization, network development and synaptic formation in primary and differentiated neuronal cultures.

In this way, both the topology and the material functionalities can be exploited for achieving in vitro biohybrid platforms for neuronal network interfacing.

References

- (1) Pennacchio, F. A.; Garna, L. D.; Matino, L.; Santoro, F. Bioelectronics Goes 3D: New Trends in Cell–Chip Interface Engineering. *J. Mater. Chem. B* **2018**, *6* (44), 7096–7101. <https://doi.org/10.1039/C8TB01737A>.
- (2) Lubrano, C.; Matrone, G. M.; Forro, C.; Jahed, Z.; Offenhaeusser, A.; Salleo, A.; Cui, B.; Santoro, F. Towards Biomimetic Electronics That Emulate Cells. *MRS Commun.* **2020**, *10* (3), 398–412. <https://doi.org/10.1557/mrc.2020.56>.
- (3) Pennacchio, F. A.; Caliendo, F.; Iaccarino, G.; Langella, A.; Siciliano, V.; Santoro, F. Three-Dimensionally Patterned Scaffolds Modulate the Biointerface at the Nanoscale. *Nano Lett.* **2019**, *19* (8), 5118–5123. <https://doi.org/10.1021/acs.nanolett.9b01468>.

12:15 PM SB08.04.07

Chronic and Minimally Invasive Subdermally Implantable Neuromodulation and Recording Tools in Freely Moving Subjects Philipp Gutruf; University of Arizona, United States

Materials and fabrication concepts for the creation of soft electronics coupled with miniaturization of wireless energy harvesting schemes enable the construction of high-performance electronic and optoelectronic systems with sizes, shapes and physical properties matched its biological host^[1]. Applications range from continuous monitors for health diagnosis to minimally invasive exploratory tools for neuroscience^[2]. This talk presents science and engineering approaches for the creation of soft devices with near field power transfer and data communication capabilities^[3] and discusses application in devices for the stimulation of the brain and the peripherals in a range of complex 3D environments and contexts (e.g. social interactions) that cannot be explored with conventional technologies. We introduce a series of advances in subdermally implantable device technologies that follow from developments in materials, electronics and operational concepts that enable digitally controllable subdermal platforms with multimodal optogenetic and electrical stimulation capabilities^{[4][5]} with the ability to provide stimulus without the physical penetration of the blood brain barrier. Additional to these stimulation capabilities new developments in low power electronics allow for capabilities in recording genetically encoded calcium indicators and physiological states of organs to enable neuronal modulation with high precision and direct feedback in freely moving subjects.^[6] Because of the minimally invasive nature of these tools we show chronic neuromodulation capabilities over months in freely moving subjects. Combined these capabilities elevate device functionality substantially over current tethered platforms enabling fundamentally new approaches in experimental design to uncover the working principle of the central and peripheral nervous system and show promise to advance digital medicine approaches.

[1] P. Gutruf, J. A. Rogers, *Curr. Opin. Neurobiol.* **2018**, *50*, 42.

[2] P. Gutruf, C. H. Good, J. A. Rogers, *APL Photonics* **2018**, *3*, 120901.

[3] P. Gutruf, V. Krishnamurthi, A. Vázquez-Guardado, Z. Xie, A. Banks, C.-J. Su, Y. Xu, C. R. Haney, E. A. Waters, I. Kandela, *Nat. Electron.* **2018**, *1*, 652.

[4] P. Gutruf, R. T. Yin, K. B. Lee, J. Ausra, J. A. Brennan, Y. Qiao, Z. Xie, R. Peralta, O. Talarico, A. Murillo, S. W. Chen, J. P. Leshock, C. R. Haney, E. A. Waters, C. Zhang, H. Luan, Y. Huang, G. Trachiotis, I. R. Efimov, J. A. Rogers, *Nat. Commun.* **2019**, *10*, 5742.

[5] J. Ausra, S. J. Munger, A. Azami, A. Burton, R. Peralta, J. E. Miller, P. Gutruf, *Nat. Commun.* **2021**, *12*, 1968.

[6] A. Burton, S. N. Obaid, A. Vázquez-Guardado, M. B. Schmit, T. Stuart, L. Cai, Z. Chen, I. Kandela, C. R. Haney, E. A. Waters, H. Cai, J. A. Rogers, L. Lu, P. Gutruf, *Proc. Natl. Acad. Sci.* **2020**, 201920073.

SESSION SB08.21: Biosensing

Session Chairs: Tzahi Cohen-Karni, Nicolette Driscoll, Victor Druet, Sahika Inal, David Ohayon, Jonathan Rivnay, Sneha Shankar and Flavia Vitale
Wednesday Afternoon, December 8, 2021
SB08-Virtual

1:00 PM SB08.21.01

Organic Electronic Ion Pump for Flow-Free Ions Delivery for Controlling Water Transpiration in Intact Arabidopsis and Kalanchoe Plant Models Towards Better Understanding of Drought Tolerance Iwona A. Bernacka-Wojcik¹, Alexandra Sandéhn¹, Loïc Talide², Daniel Cowan-Turner³, Ilaria Abdel Aziz¹, Abdul Manan Dar¹, Totte Niitylä² and Eleni Stavrinidou¹; ¹Linköping University, Sweden; ²Umeå Plant Science Centre, Sweden; ³Newcastle University, United Kingdom

Developments in imaging techniques accounted for unravelling insights in plant signaling at the molecular level, elucidating the role of transporters, proteins and ions during plant growth, development and stress. However, the imaging technological improvements did not go hand in hand with stimulation approaches, as important molecular compounds are currently delivered through low resolution approaches, as foliar spraying or soaking. Therefore, the need of precise and controllable delivery techniques is evident. In this context, we have developed Organic Electronic Ion Pump (OEIP) that enables electrophoretic delivery of ions in a flow-free manner greatly reducing the imposed shear stress. The delivery channel is based on polyelectrolyte of high fixed charge concentration that prevents backflow of ions minimizing the disturbance of the ionic concentrations in the targeted tissue. Previously, we have demonstrated that miniaturized, capillary-based OEIP can be inserted in intact plant with low invasiveness allowing hormone ions delivery at cellular resolution, demonstrating local and precise electronic control of plant physiology. Here, we report the development of OEIP for implantation in hard tissue of plants, such as stem, hypocotyl or succulent leaves. The mechanical properties of the capillary-based OEIPs have been significantly enhanced thanks to the use of thin polyimide coating. These devices were applied in the model plant species Arabidopsis to deliver abscisic acid that controls plant response to environmental stresses. The device targeted the plant vascular tissue for systemic control of plant transpiration. Furthermore, OEIPs were used to gain insight on the high drought tolerance of the tropical plant *Kalanchoe Blossfeldiana*.

1:15 PM *SB08.21.02

Plant Bioelectronics for Real Time Monitoring and dYnamic Regulation of Plant Physiology Eleni Stavrinidou; Linköping University, Sweden

The development of bioelectronic technologies is driven by biomedical applications for new therapeutic and diagnostic tools. However, there are many important questions in plant biology that remain unanswered due to lack of sophisticated tools. Furthermore, the climate change and growing population calls for plants with increased tolerance to biotic and abiotic stress and plants with higher productivity. In my group we are developing organic bioelectronic technologies for sensing and actuation in plants that overcome limitations of conventional methods used in plant science. In my talk I will present our recent advancements of interfacing bioelectronic tools with plant model systems. We demonstrate enhanced plant resistance to drought via

electronically controlled delivery of biomolecules with the organic electronic ion pump. Furthermore, with OECT implantable sensors we reveal previously uncharacterized sugars dynamics in trees and finally we present a novel bioelectronic platform for stimulation of plant growth. Our results highlight the potential of bioelectronics in elucidating and enhancing plant processes but also for their application in agriculture.

1:45 PM SB08.21.03

Electrochemical Detection of Glucose with Highly Conductive PEDOT:PSS:Poly(acrylamide)-Based Hydrogels Containing Phenylboronic Acid Alex C. Tseng and Toshiya Sakata; The University of Tokyo, Japan

Sensors built on smart, functional materials pave the way for democratized health care by providing high quality personal health data at the point-of-care. In the aftermath of the novel coronavirus pandemic, the need for such technologies is salient. The required materials must be mediators of electronic and ionic transport, mechanically compliant and flexible, and crucially, chemically stable and biocompatible. Hydrogels of semiconducting conjugated polymers (CPs) fit this profile exceptionally well.

PEDOT:PSS (poly(3,4-ethylenedioxythiophene) polymerized with poly(styrene sulfonate)) may be readily gelled by various means [1]; however, so-called interpenetrating networks (IPNs), whereby separate conducting and structural polymers form a homogenous phase, are interesting because of the possibility for orthogonal design of electrical and mechanical properties. This allows for the use of optimized CP formulations with sensor functionality governed by the selection of hydrogel monomers, for instance, by including phenylboronic acid moieties to give selective binding towards diol-containing biomolecules [2].

In this study, we take a simple approach of polymerizing acrylamide monomers mixed with equal parts by weight of PEDOT:PSS from ready-made suspensions. Specifically, we took acrylamide (AAm) as the backbone, 2-acrylamido-2-methylpropanesulfonic acid (AMPS) as a polyelectrolytic mediator, 3-(acrylamido)phenylboronic acid (AAPBA) as a complexing site, and *N-N'*-methylenebisacrylamide (MBA) as cross-linker. The resulting PEDOT:PSS:P(AAm-co-AMPS-co-AAPBA) hydrogels, prepared as sheets tens of micrometers thick, (de)swelled reversibly in thickness by a factor of ~5 in phosphate-buffered saline (pH 7.4). Conductivities of ca. 50 (dry) and 10 S/cm (swelled, accumulating) were typical. These results indicate that the formation of IPN did not hinder electrical transport in the CP, and their high values compare favorably with previously reported pure PEDOT:PSS hydrogels [3] considering our CP loading.

Cyclic voltammetry revealed the effect of AAPBA as a secondary dopant, evidenced by the appearance of a redox peak that delayed the onset of PEDOT reduction and hastened its re-oxidation. This extended the range of pseudo-capacitance, giving a value of 2.2 F/cm³. Upon exposure to glucose, AAPBA redox activity is suppressed, suggesting that boronic acid is preferentially reduced to boronate by applied potentials, until the formation of boronate esters with addition of glucose shifts the equilibrium back towards boronic acid. Thanks to the high conductivity of our hydrogels, direct use as the channel of an organic electrochemical transistor is possible and an amplified signal from AAPBA-glucose binding was observed. These results indicate the possibility of using PEDOT:PSS:P(AAm-co-AMPS-co-AAPBA) hydrogels for the direct electrochemical detection of glucose concentration at physiologically-relevant levels.

[1] L. V. Kayser *et al.*, *Advanced Materials*, vol. 31, no. 10, p. 1806133, 2019.

[2] G. Vancoillie *et al.*, *Polym. Chem.*, vol. 7, no. 35, pp. 5484–5495, Aug. 2016.

[3] B. Lu *et al.*, *Nat Commun*, vol. 10, no. 1, p. 1043, Mar. 2019.

SESSION SB08.22: Devices

Session Chairs: Tzahi Cohen-Karni, Nicolette Driscoll, Victor Druet, David Ohayon, Jonathan Rivnay, Sneha Shankar and Flavia Vitale
Wednesday Afternoon, December 8, 2021
SB08-Virtual

4:00 PM SB08.22.01

Surface Characteristics of Polyserotonin Thin Film for Molecularly Imprinted Polymer-Based Electrochemical Biosensors Kanako Ishino, Shoichi Nishitani and Toshiya Sakata; The University of Tokyo, Japan

In developing an electrochemical biosensor, the design and fabrication of the bioelectrical interface is important for transducing the adsorption of a target biomolecule on an electrode to an electrical signal. Recently, a poly-dopamine (pDA) film has been attractive for the bioelectrical interface, because it can be easily synthesized with self-oxidation of DA monomers on an electrode;¹ thus, it has been used for many purposes.² Similarly to the pDA film, serotonin (ST) monomers are simply polymerized on the electrode with its self-oxidation in an alkaline solution; as a result, the pST film shows a good biocompatibility and adhesiveness.³ In particular, pST has been reported to be more slowly polymerized than pDA, which can expectedly lead to a smoother and thinner film formation on the electrode. On the other hand, the pDA film is utilized for a molecularly imprinted polymer (MIP)-based biosensor to detect biomarkers as one of the applications.² Also, considering our previous works,⁴ the MIP-based biosensor can detect target biomolecules with high binding affinities by measuring the change in the molecular charges. However, the surface roughness of pDA film may be too large to properly control the thickness and surface roughness of MIP films suitable for biomolecular sizes; therefore, the thin and smooth surface characteristics of pST film are expected as one of the bioelectrical interfaces for the MIP-based biosensor. In this paper, we show the fundamental surface and electrochemical characteristics of pST film for its application to the MIP-based electrochemical biosensor.

The pST film was coated on a gold electrode or a silicon substrate by the electrochemical deposition or the self-oxidation of ST monomers in the alkaline solution (pH 8.5). After that, the thickness and roughness of pST film were measured by atomic force microscopy (AFM), and cyclic voltammetry (CV) was performed to evaluate electrical properties in buffer solutions containing a redox couple. These fundamental characteristics of pST film were strictly controlled by the CV cycles for the electrochemical deposition or the polymerization time for the self-oxidation.

Not only was the thickness of pST film linearly controlled within 5 to 15 nm, according to the CV cycles or the polymerization time, but also the roughness of pST film was much smaller than that of pDA film. Moreover, the pST film was found to be insulative from the CV curve, the surface charge of which varied with the change in pH of the measurement solutions. The insulative film on the electrode was suitable for the bioelectrical interface to control the electrical conductivities, when including cavities like MIP films. Considering the above, the thinner and smoother pST insulative film, compared to the pDA film, is applied to the MIP-based electrochemical biosensor. In the conference we are going to introduce the results about the detection of biomarkers such as peptides with the pST-MIP-based electrochemical biosensor as well.

References

[1] S. Kim *et al.*, *Scientific Reports* 2016, 6, 1–8. [2] P. Jolly *et al.*, *Biosensors and Bioelectronics* 2016, 75, 188–195. [3] N. Nakatsuka *et al.*, *ACS Nano* 2018, 12, 4761–4774. [4] T. Sakata *et al.*, *RSC Advances* 2020, 10, 16999–17013.

4:15 PM SB08.22.03

Development of the Au-Au Flexible Bonding Without Any Adhesive Masahito Takakuwa^{1,2}, Kenjiro Fukuda², Tomoyuki Yokota³, Daishi Inoue², Daisuke Hashizume², Shinjiro Umezui¹ and Takao Someya^{2,3}; ¹Waseda University, Japan; ²RIKEN, Japan; ³The University of Tokyo, Japan

By using flexible and lightweight electronics such as sensors and energy harvester fabricated on the μm -thick polymer film, developing the next-generation wearable electronics with the excellent conformability of human skin is expected¹. One of the important challenges for fabricating the practical electronics device is how to integrate each electronic such sensor, energy harvester, and control unit. Conductive adhesive such as anisotropic conductive film (ACF) is mainly used as a conventional conductive bonding method for the integration of each ultra-thin electronics now. However, such conventional conductive bonding lost flexibility at the bonding area because flexural rigidity gets large along with an increasing thickness.

This research shows the Au-Au direct bonding method by water vapor plasma activation. In this research, evaporated gold electrodes on 2 μm -thick of parylene substrate were used as a bonding target. A gold surface of a thin-film sample had a rough surface (root-mean roughness of 6.3 nm) compare with metal on a Si wafer. There is a simple bonding procedure: firstly, the gold surface was treated by water vapor plasma treatment. Secondly, treated gold surfaces contacted together, and keeping left several time. Then, we achieved direct bonding in the air at room temperature without any adhesive and post-treatment such as annealing and pressing.

The cross-sections of a bonded gold thin film were observed by scanning electron microscope. In the case of a sample bonded by using water vapor plasma, the bonding interface had disappeared and the gold deposited on the separate films had become one. On the other hand, thin-film samples bonded using conventional Ar plasma bonding^{2,3}, which is used to bond Si wafers, were clearly separated at the interface, and direct bonding of thin-film gold could not be achieved. Therefore, only water vapor plasma bonding achieved direct bonding of gold on thin film.

Moreover, the bonding area maintained excellent flexibility since there is no increase in thickness by the adhesive. In the flexibility test, two kinds of bonding samples were prepared, thin-film samples bonded by using the water vapor plasma and ACF tape. And each bonded sample placed on the plate having a bump of several bending radius. A bonded thin-film sample by water vapor plasma was exhibited excellent conformation even at a 0.5 mm radius, whereas bonded thin-film sample by ACF tape was not conformed at a less than 1 mm radius.

By using a new conductive bonding method using water vapor plasma, we have succeeded in flexibly bonding gold electrodes on a thin film without adhesives. It can be applied to fabricate the integration electronics using the ultra-thin sensor and energy harvester through investigation of the bonding of other metal materials by using water vapor plasma bonding.

1. Y khan, *et al. Adv. Mater.* 32, 1905279 (2020).
2. E. Higurashi, *et al. IEICE Trans. Electron.* E100.C, 156–160 (2017).
3. M. Yamamoto, *et al. Micromachines*, 11, 454 (2020).

4:30 PM SB08.22.04

Highly Flexible Magnetic-Elastomeric Composite Film—Experiments and Modelling Zhi LI^{1,2}, Erwin Alles^{1,2}, Ivan P. Parkin¹, Adrien Desjardins^{1,2} and Sacha Noimark^{1,2}; ¹University College London, United Kingdom; ²Wellcome/ EPSRC Centre for Interventional and Surgical Sciences, United Kingdom

Soft magnetic-elastomeric composites are a class of smart materials formed by embedding magnetic particles into non-magnetic elastomer matrix host materials and curing in the presence or absence of a magnetic field. When fabricated into films, magnetic-elastomeric composites can be readily integrated with micro-scale structures to achieve flexible and compact smart sensors. With respect to their magnetic/mechanical properties, magnetic-elastomeric composite films can exhibit rapid and robust mechanical responses to external magnetic fields, which are enabling for wide biomedical applications such as wireless soft robotics, remotely stimulated magnetic actuators, and medical localisation sensors.

One of the key technical challenges in the development of the magnetic-elastomeric materials is to achieve a strong and reversible magnetic response whilst maintaining high and long-lasting mechanical flexibility. The magnetic response is governed by intrinsic material properties, such as B-H behavior and the Young's elastic modulus. Recent efforts have been centred on the fundamental mechanisms of magneto-mechanical coupling effects (dipole-dipole interactions of isolated magnetic particles) accounting for the static responses subject to external magnetic field, and magnetorheological effects that allow for dynamic changes to the elasticity of the composite material by applying an external magnetic field. It appears that multiple factors could all play vital but sometimes conflicting roles in the material performances, including: (i) the initial properties of magnetic particles and elastomers, (ii) the magnetic conditions for composite curing, (iii) the loading ratio of each component, and (iv) the film thickness. There is a significant need to understand and balance the trade-off effects of each factor to optimize the overall material properties.

Here, we report on the development of a simple, cost-effective, and scalable fabrication method to achieve centimetre-scale, highly flexible magnetic-elastomeric composite films with readily controllable magnetic particle loadings (0- 70 wt%) and film thickness (micron-scale). The composition-dependent magnetic and mechanical properties were explored by investigating a wide range of parameters including magnetic particle loading and film thickness. As a demonstration of their practical value in different applications, the magnetically induced mechanical deformations of the films with different particle loadings, field thickness and external magnetic field were simulated using a computational framework (Ansys Mechanical). Benefiting from their extremely high magnetization and maintained low Young's moduli, magnetic-elastomeric composite films show large deformation and excellent stability in response to magnetic stimuli. We conclude that soft magnetic-elastomeric composites are very promising for a wide range of biomedical devices.

SYMPOSIUM SB09

Biological and Bioinspired Functional Materials—From Nature to Applications
November 30 - December 7, 2021

Symposium Organizers

Guillaume Gomard, Carl Zeiss AG
Mathias Kolle, Massachusetts Institute of Technology
Radwanul Siddique, Samsung Semiconductor, Inc.
Silvia Vignolini, University of Cambridge

Symposium Support

Silver

Samsung Semiconductor Inc

Bronze

ZEISS

* Invited Paper

SESSION SB09.01: Biological Vision and Related Materials
Session Chairs: Benjamin Palmer and Radwanul Siddique
Tuesday Morning, November 30, 2021
Sheraton, 2nd Floor, Republic B

10:30 AM *SB09.01.01

How to See Without Eyes—Lessons Learned from Dissecting Cephalopod Skin Leila Deravi; Northeastern University, United States

Cephalopods, including squid, octopus, and cuttlefish, can rapidly camouflage in different underwater environments by employing multiple optical effects including light scattering, absorption, reflection, and refraction. They can do so with exquisite control and within a fraction of a second—two features that indicate distributed, intra-dermal sensory and signaling components. However, the fundamental biochemical, electrical, and mechanical controls that regulate color and color change, from discrete elements to interconnected modules, are still not fully understood despite decades of research in this space. This talk highlights key advancements in the biochemical and structural analysis of cephalopod skin and discusses compositional connections between cephalopod ocular lenses and skin with features that may also facilitate signal transduction during camouflage.

11:00 AM SB09.01.02

Crystallization Pathways of Biogenic Guanine Crystals Avital Wagner, Gan Zhang and Benjamin A. Palmer; Ben-Gurion University of the Negev, Israel

Guanine crystals are responsible for an extraordinary variety of optical phenomena in animals. The crystals are formed from stacked, planar layers of H-bonded molecules. The optical utility of guanine derives from its extreme refractive index ($n=1.83$) within the H-bonded plane. Little is known about how these crystals form and how the organisms precisely control crystal morphology. Key questions include whether crystallization proceeds via an amorphous precursor phase or whether physical confinement by de-limiting membranes dictates morphology. To illuminate pathways governing the crystallization, we studied model guanine-producing organisms during development, including spiders, lizards, and scallops. The onset of crystallization was determined by the emergence of birefringence in the crystal-forming cells. The tissues were then examined by cryogenic scanning electron microscopy (cryo-SEM) and transmission electron microscopy (TEM). In all three models, crystallization occurs within a spherical, double-membrane delimited vesicle. In white widow spiders, which produce prismatic guanine crystals, the crystals are progressively laid down along the H-bonded direction on parallel fibers which stretch across the length of the vesicle. As crystallization proceeds these 2D sheets of crystals merge along the π -stacking direction to form a single crystal. In lizard tails, vesicles containing very small crystals are observed and grow in all directions to form the final crystal. Evidence of a layered structure is sometimes observed in the side faces of mature guanine crystals in all three models. Though we cannot yet fully describe the crystallization pathway of biogenic guanine, initial observations are consistent with a classical 2D growth model where H-bonded layers of guanine molecules are deposited epitaxially on lipid membranes. Biological crystallization pathways can inspire new ways to synthetically control morphologies of organic crystals which then can be utilized in many optical systems.

11:15 AM SB09.01.03

Cephalopod Protein-Based Materials—Structure, Self-Assembly and Applications Preeta Pratakshya, Nadia Tolouei and Alon Gorodetsky; University of California, Irvine, United States

The study of protein-based materials has enabled the development of several optical, electronic, and medical technologies. Within this context, cephalopod structural proteins called reflectins have recently gained attention due to their demonstrated potential for the development of biophotonic and bioelectronic devices. Moreover, reflectins make up the subcellular structures found in optically active cephalopod skin cells that play a critical role in cephalopods' remarkable camouflage abilities. Given reflectins' significance from both technological applications and fundamental biology perspectives, these proteins have recently emerged as a desirable target for the design of functional biomaterials. However, the development of such materials has been hindered by a lack of complete understanding of their structures and properties. Here we highlight the structure, self-assembly, and multi-faceted applications of reflectin-based materials within the context of biophotonic and bioelectronic platforms. Specifically, we discuss how the structure and assembly of these biomaterials enable their optical and electrical functionalities. Our findings not only underscore the potential of these unique cephalopod proteins as functional biomaterials but also hold relevance for the development of cephalopod-inspired optical and electronic technologies.

11:30 AM SB09.01.04

Crack-Resistant Layered Structure in Coralline Red Algae—Formation Mechanism via Periodic Spinodal Decomposition Alexander Katsman, Nuphar Bianco-Stein and Boaz Pokroy; Technion - Israel Institute of Technology, Israel

Articulated coralline red algae is abundant in the shallow waters of oceans worldwide. Its structure exhibits hierarchical organization from the macro to the nano-scale. We revealed that the high-Mg calcite cell wall nanocrystals of *Jania* sp. are arranged in layers with alternating Mg contents. This non-

homogenous elemental distribution assists the alga in preventing fracture caused by crack propagation. The mechanism of the layered structure formation was proposed as a periodic spinodal decomposition (SD) of the Mg-ACC matrix.

The crystallization in the coralline red algae occurs on an organic template via an amorphous precursor. SD of amorphous precursor to Mg-rich ACC nanoparticles and subcritical Mg-ACC matrix is activated near the cell wall/organic interface and advances to the internal regions. Following crystallization of the subcritical Mg-ACC to Mg-calcite is accompanied by an exclusion of excess Mg ions to the adjacent ACC layer. After a certain time, Mg concentration in this layer exceeds the critical value, and a secondary SD occurs, thus a layer of Mg-ACC with increased density of Mg-rich nanoparticles forms. Parameters of the layered structure were calculated based on the diffusional model developed. Using reasonable values for diffusion coefficient of Mg in gel/liquid ACC, $D \approx 10^{-15} \text{ m}^2/\text{s}$, and crystallization rate $V \approx 10^{-9} \text{ m/s}$, the typical layer thickness $\sim 0.3 \mu\text{m}$ was obtained, which corresponds rather well to experimental data.

11:45 AM SB09.01.05

Functional Biopigment Xanthommatin—Bio-Inspiration and Squid Skin Optics Richard M. Osgood¹, Sean Dinneen¹, Zhuangsheng Lin², Steven Kooi³ and Leila Deravi²; ¹DEVCOM SC, United States; ²Northeastern University, United States; ³Massachusetts Institute of Technology, United States

Biomaterials and bio-inspired materials like biopigments (xanthommatin (Xa), melanin, etc.) are of increasing interest for photonics applications and for basic science to understand how some species create an impressive array of photonic effects, ranging from bright color due to structural coloration or photonic crystals in tropical birds to stunning visible camouflage in underwater animals like the cephalopods, which still partially defies understanding (how can they blend into the background so well?).

Small-molecule biopigments dissolve in polymer hosts and are robust against ultraviolet light and toxicologically benign, and could form optical thin films (e.g., anti-reflective coatings). The chromatophores in squid skin, which contain the biopigment Xa in nanostructured bioparticles (granules) (100-500 nm dia.), influence light scattering and color; they achieve both pancake-like, expanded and spherical, punctate states. The granules are well-sized for nanophotonic scattering of visible light, especially blue-green wavelengths, instead of absorbing it, even in sub-monolayer arrays [1]. Recently, researchers have succeeded in mimicking chromatophore color and the light scattering granules within them, using artificial materials in the laboratory and chemically synthesizing Xa; the latter was produced in large (hundreds of mg) quantities via a straightforward, scalable process, and spraycoated onto surfaces [2]. The chromatophore could be approximated as containing multiple layer of sub-monolayers. Under the chromatophores lie iridocytes; multilayered Bragg reflectors that reflect color iridescently. By understanding how the color of the chromatophore plus iridocyte changes, artificial and novel material platforms will enable more efficient control of light at the nanoscale.

We have discovered that the Xa pigment in cephalopod chromatophores has a high refractive index (RI) ($n > 1.55$) at fixed wavelengths [3]. Recently, we have carried out comprehensive broadband (300 nm – 3200 nm) ellipsometric spectroscopy to determine the UV-to-infrared optical indices (n and k) of Xa pigment, using natural Xa from the squid's chromatophores and forming smooth, high-quality films using a novel method. These broadband measurements of Xa's fundamental optical properties allow the design of new lightweight optical components, such as lenses, that can adaptively change in response to external stimuli.

In this presentation, we will use our new experimental data for a 4-flux model (forward and backwards-propagating specular and diffuse light), to better understand squid skin optics, improving on an earlier analytical model (Kubelka-Munk). An optical model [4] made important discoveries on the optics of combined squid skin organs, but lacked separate experimental data on Xa. We improve this model analytically, coupling the chromatophore and iridocyte and not ignoring the background reflectivity and scattering. Armed with experimental n and k , our model will better assess the optical response (e.g. scattering, reflectivity) of the combined chromatophore-iridocyte to best understand the squid skin optical system. This will enable biopigments and bio-inspired pigments to serve as optically and sensing functional materials (perhaps even with electrical functionality [2]). Such a high-RI material will demonstrate strong and interesting new scattering and coloration functionalities and, when synthesized in large scale in an environmentally-friendly way, may enable new lightweight optical systems that can adapt and change shape, that may aid in underwater detection or imaging. We discuss possible new functional and optical nanophotonic systems, using the interesting biopigments and bio-inspired pigments, and possible applications in optical sensing.

[1] A. Kumar et. al. AOM 6 2018.

[2] A. Kumar et. al., ACS AMI 2018, 10.

[3] S. Dinneen et. al. JPCL 8 2017.

[4] Sutherland, R. L. et al., C. JOSA A 25.

SESSION SB09.02: Novel Biomaterials
Session Chairs: Mathias Kolle and Admir Masic
Tuesday Afternoon, November 30, 2021
Sheraton, 2nd Floor, Republic B

2:00 PM *SB09.02.01

Molecular Crystals in Animal Coloration and Vision Keshet Shavit¹, Avital Wagner¹, Gan Zhang¹, Jayasurya Yallapragada² and Benjamin Palmer¹; ¹Ben-Gurion University of the Negev, Israel; ²Weizmann Institute of Science, Israel

Organic crystals are widely used as the reflective materials in animal coloration and vision [1]. Guanine crystals, for example, have been studied for over 100 years and their role in structural coloration is well-established. Here we focus mainly on the less-studied pteridine molecules which are used, in crystalline form, as colorants and as reflectors in vision. Isoxanthopterin crystals form reflectors in the eyes of decapod crustaceans which are used in image-formation, enhancing photon-capture and camouflage [2]. The isoxanthopterin crystals are arranged in nanoparticles, constructed from a shell of plate-like isoxanthopterin crystals arranged in concentric lamellae around an aqueous core. The reflectors are formed from dense assemblies of nanoparticles. Isoxanthopterin crystals are characterized by layers of planar H-bonded molecules, and the reflectivity of the material derives from the extreme refractive index ($n=1.96$) parallel to these layers. The reflectivity and scattering of the particles are enhanced by the alignment of the crystals and an optimized core-shell ratio [3]. We also present recent insights on the formation of biogenic crystals from cryo-SEM studies of developing organisms. This includes the formation of guanine-based photonic structures in lizards and spiders and the formation of isoxanthopterin crystals in larval crustaceans. The exquisite control organisms exert over formation of these materials provides a wealth of inspiration for the design of new optical materials.

[1] B. A. Palmer, D. Gur, S. Weiner, L. Addadi, D. Oron, Adv. Mater., 30, 1800006 (2018).

[2] B.A. Palmer, A. Hirsch, V. Brumfeld, E.D. Aflalo, I. Pinkas, A. Sagi, S. Rozenne, D. Oron, L. Leiserowitz, L. Kronik, S. Weiner and L. Addadi, PNAS,

115, 10, 2299–2304 (2018).

[3] B.A. Palmer, V.-J. Yallapragada, N. Schiffmann, E. Merary Wormser, N. Elad, E.D. Aflalo, A. Sagi, S. Weiner, L. Addadi, D. Oron, *Nature Nanotechnology* 15, 138–144 (2020).

2:30 PM SB09.02.03

Biomaterialization by Design—Application of *de novo* Proteins for Nanocrystal Synthesis Leah Spangler, Sarangan Chari, Michael Hecht and Gregory Scholes; Princeton University, United States

Biomaterialization – the synthesis of inorganic materials using proteins – has recently gained interest as a low cost, green route for the production of metal chalcogenide semiconductor nanocrystals. Typically, biomaterialized nanocrystals are synthesized using proteins or biomolecules identified from organisms which possess a native biomaterialization response. Natural biomaterialization pathways utilize proteins which either catalyze or template mineralization, but rarely possess a single biomolecule capable of both functions. Here, we demonstrate an alternative biomaterialization approach which uses the artificially designed *de novo* protein, Construct K (ConK), to both catalyze and template metal chalcogenide nanocrystals. ConK was found to catalyze a PLP-dependent reaction which produces H₂S from L-cysteine. In the presence of metal precursors, such as Cd, enzymatically produced H₂S then reacts to form metal sulfide quantum dots in solution. In addition to having enzymatic activity, ConK is also structurally stable and highly tolerant to mutations in amino acid sequence, allowing for facile addition of new functionalities and properties. Using site directed mutagenesis, we selectively modified ConK to contain strong metal binding amino acids, such as histidine and cysteine, which act as stabilizing capping ligands to template nanocrystal populations of various controllable sizes. We characterized the optical properties of the resultant nanocrystal populations using absorbance and fluorescence spectroscopy, and verified the crystal structure using XRD and TEM measurements. Semiconductor nanocrystals synthesized using ConK demonstrate well-controlled growth and high stability when compared to naturally derived biomaterialization pathways, making them ideal for commercial implementation and use.

2:45 PM SB09.02.02

Asymmetric Polymer/Lipid Vesicles Yuting Huang¹, Arash Manafirad², Simon Matoori¹, David Weitz¹, Anthony Dinsmore² and David Mooney¹; ¹Harvard University, United States; ²University of Massachusetts Amherst, United States

Lipid vesicles are aqueous volumes surrounded by a bilayer of lipid molecules, which are amphiphilic molecules with their head groups facing water and tail groups facing oil. These vesicles are simple models for cell membranes and can be used for drug delivery. Similarly, block copolymers are amphiphilic molecules that form vesicles by themselves or with lipids. Like lipid vesicles, polymer vesicles can also be used for drug delivery and cell membrane mimicry. One interesting type of lipid/polymer vesicle is the asymmetric vesicle, in which its bilayer is composed of two dissimilar lipid monolayers or a lipid monolayer and a polymer monolayer. Importantly, all eukaryotic cell membranes exhibit this type of asymmetry and asymmetry is also proposed to enhance mechanical properties of the membrane. Here, we use microfluidics to fabricate mono disperse and highly controllable asymmetric vesicles, which unlike the conventional methods that often end up with highly poly disperse samples. To achieve this, asymmetric vesicles are produced using water/oil1/oil2/water emulsions in a glass capillary device, with different lipids/polymers immersed in two different volatile oil phases. In future, we envision asymmetric lipid/polymer vesicles could open a new door in the drug delivery field.

3:00 PM SB09.02.04

Effects of Lignin on Bacterial Cellulose Nanocomposite Materials Andrew Jimenez¹, Esther Law¹, Mallory Parker¹, Jeremy Fredricks¹, Hareesh Iyer¹, Marissa Nelsen¹, Bichlien H. Nguyen^{1,2}, Karin Strauss^{1,2} and Eleftheria Roumeli¹; ¹University of Washington, United States; ²Microsoft, United States

In recent years, there has been a significant thrust towards the creation of sustainable green polymers and polymer composites^{1,2}. Reductions in manufacturing resources, synthetic polymer waste, and greenhouse emissions are all driving forces for advancements in this area. Cellulose, the world's most abundant polymer, is not only derived from renewable resources, but also combines remarkable specific mechanical properties (comparable to steel wire, Kevlar and carbon fibers^{3,4}) with biodegradability, biocompatibility, and a molecular structure that allows for easy functionalization⁴⁻⁶. Compared to cellulose extracted from wood, nanocellulose secreted from bacterial cultures (also referred to as bacterial cellulose, 'BC') is matrix-free, has high aspect ratio and crystallinity, and can be obtained with minimal processing^{3,4}. Emerging applications of BC include nanopapers and microfibers showing remarkable Young's modulus (~66 GPa³), strength (~1GPa³) and toughness (16.9 MJ/m³) for binder-free, pure nanocellulose materials. The incredible mechanical properties and ability to self-bind without additives stem from the combination of high aspect ratio nanofibrils, vast hydrogen bonding network, high degree of crystallinity, and for the mentioned cases arise from fiber alignment effects that enhance further the hydrogen bonding interactions between the cellulose nanofibrils^{7,8}. However, BC-based materials are naturally brittle and hydrophilic due to the molecular structure of cellulose. In natural wood, phenolic molecules forming large lignin networks, serve, together with other biopolymers, as a binder to the cellulose matrix, tuning mechanical properties, conferring hydrophobicity, and protecting against pathogens⁴. In fact, recent research into sustainable biocomposites has shown significant increases of mechanical properties, thermal stability and hydrophobicity on wood-extracted cellulose-lignin composite papers with hot press treatment, compared to conventional cellulose paper⁹.

In this work, we present an exploration into the development of BC-lignin nanocomposites through a design of experiments approach which allows the systematic investigation of the governing structure-processing-property relationships in these nanocomposites. Specifically, we explore a matrix of hot press processing conditions including time (10-30 minutes), temperature (120-160 °C), and pressure (5-15 MPa) and correlate the performance of those nanocomposites in response to the processing conditions. Our characterization includes scanning electron microscopy, thermogravimetric analysis, X-ray diffraction and nanoindentation tests. Additionally, the effects of lignin binding the cellulose matrix are further examined through contact angle analysis and Fourier-transform infrared spectroscopy.

References

1. Mohanty, A. K., Vivekanandhan, S., Pin, J.-M. & Misra, M. *Science* **362**, 536–542 (2018).
2. Liu, C. *et al. Adv. Mater.* **n/a**, 2001654.
3. Wang, S. *et al. Adv. Mater.* **29**, 1702498 (2017).
4. Moon, R. J., Martini, A., Nairn, J., Simonsen, J. & Youngblood, J. *Chem. Soc. Rev.* **40**, 3941 (2011).
5. Rahman, M. M. & Netravali, A. N. *ACS Macro Lett.* **5**, 1070–1074 (2016).
6. Qiu, K. & Netravali, A. N. *Polym. Rev.* **54**, 598–626 (2014).
7. Zhu, H. *et al. Proc. Natl. Acad. Sci.* **112**, 8971–8976 (2015).
8. Ling, S. *et al. Prog. Polym. Sci.* **85**, 1–56 (2018).
9. Jiang, B. *et al. Adv. Funct. Mater.* **30**, 1906307 (2020).

3:15 PM SB09.02.05

AquaPlastic—A Novel Water-Processable, Coatable and Biodegradable Bioplastic Produced from Genetically Engineered Microbial Biofilms Avinash Manjula Basavanna^{1,2,3}, Anna Duraj-Thatte^{1,2,3}, Noemie-Manuelle Dorval Courchesne¹, Giorgia Cannici¹, Antoni Sanchez-Ferrer⁴,

Benjamin Frank⁵, Leonie van't Hag⁴, Sarah Cotts⁶, Howard Fairbrother⁵, Raffaele Mezzenga⁴ and Neel Joshi³; ¹Wyss Institute Harvard University, United States; ²Massachusetts Institute of Technology, United States; ³Northeastern University, United States; ⁴ETH Zürich, Switzerland; ⁵Johns Hopkins University, United States; ⁶TA Instruments, United States

The non-biodegradability of petrochemical-based plastics has led to its pollution in almost all parts of the globe causing severe damages to our ecosystems, while the recent discovery of microplastics in human gut and lungs, shows alarming signs of the potential health problems. One promising long-term solution to this global problem of plastic pollution is to design and develop novel biodegradable bioplastics that can replace the conventional plastics. In this regard, we have engineered *E. coli* biofilms to produce the world's first water-processable protein nanofiber-based bioplastic termed as AquaPlastic, which biodegrades to ~90% in just 45 days.^[1] AquaPlastic is resistant to organic solvents, strong acid, and base, which can be further utilized to form the protective coatings on various 1D and 2D substrates. Remarkably, AquaPlastic can also be molded, healed, and welded by using water. This work on AquaPlastic paves the way for packaging and coating applications, and to build a sustainable world.
[1] Nature Chemical Biology, 2021, 17, 732.

3:30 PM BREAK

SESSION SB09.03: Characterization of Biomaterials
Session Chairs: Leila Deravi and Radwanul Siddique
Tuesday Afternoon, November 30, 2021
Sheraton, 2nd Floor, Republic B

4:00 PM *SB09.03.01

Contribution of Crystallographic Texture to the Mechanical Properties of Biomineralized Composite Materials Admir Masic; Massachusetts Institute of Technology, United States

Most of the structural materials found in nature are characterized by a complex multi-scale hierarchy, which ultimately contributes to their multiple functions and mechanical properties¹. Recent studies have shown that crystal orientation is yet another element of hierarchical structure that affects the mechanical properties of mineralized biological materials²⁻³. In this talk I will describe how correlative chemical, mechanical, and crystallographic characterization tools can be used to explore structure-property relationships in crystallographically anisotropic biological minerals. I will show how the combination of polarized piezo-Raman and micro-indentation can be used to quantify the residual strain energy in nacreous material. Nacre's work of fracture is approximately 3,000 times that of monolithic aragonite, and its high toughness has been attributed to various chemo-mechanical mechanisms generally related to its hierarchical structure. We show that the cooperative movement of the co-oriented aragonite stacks contributes to the strain hardening of the nacre, defining a new length scale of nacre toughening⁴. In a similar fashion we studied the contributions of the chemical and crystallographic texture in the enameloid and dentin layers to mechanical properties of the drumfish teeth material. We show that the chemical doping of fluoride and zinc on the outer surface, the high crystallinity, and the crystallographic misalignment all contribute to the superior stiffness, hardness, and fracture resistance of the enameloid. The incorporation of these features into the design strategies paves the road for crystal orientation-driven mechanical enhancement of bio-inspired composite materials.

References

Dunlop, JWC, Weinkamer, R, and Fratzl, P. 2011. "Artful Interfaces within Biological Materials." *Materials Today* 14 (3): 70–78.
Beniash, E, Stiffler, CA, Sun, C-Y, Jung, GS, Qin, Z, Buehler, MJ, and Gilbert, PUPA. 2019. "The Hidden Structure of Human Enamel." *Nature Communications* 10 (1): 4383.
Griesshaber, E, Schmahl, WW, Ubhi, HS, Huber, J, Nindiyasari, F, Maier, B, and Ziegler, A. 2013. "Homoepitaxial Meso- and Microscale Crystal Co-Orientation and Organic Matrix Network Structure in *Mytilus Edulis* Nacre and Calcite." *Acta Biomaterialia* 9 (12): 9492–9502.
Loh, H, Divoux, T, Gludovatz, B, Gilbert, PUPA, Ritchie, RO, Ulm, F, and Masic, A. 2020. "Nacre Toughening Due to Cooperative Plastic Deformation of Stacks of Co-Oriented Aragonite Platelets." *Communications Materials* 1 (77): 1–10.

4:30 PM SB09.03.02

Silk Fibroin—A Fundamental Spin to Biomaterials Fabrication Rafael O. Moreno Tortolero¹, Nick Skaer², Robert Walker² and Sean A. Davis¹; ¹University of Bristol, United Kingdom; ²Orthox LTD, United Kingdom

Our current understanding about the seemingly broad range of self-assembly mechanisms involved in natural silk production has been developed predominantly from studies of dragline spider silk. Protein monomeric units (spidroins) polymerize via terminal interactions and allow the material to undergo an orchestrated liquid-to-solid transformation, ultimately resulting in the silk thread. However, despite its widespread availability, there have been limited mechanistic investigations on the analogous protein fibroin, which is the main component in silkworm silk. This is attributed to both its complexity and perceived inferior mechanical properties. Paradoxically, silkworm silks are the most commercially exploited of the natural silks. The inherent biocompatibility has driven applications in biomedicine, where a liquid precursor form of fibroin can be processed into a myriad of materials, from vesicles, nano and microparticles, films, hydrogels, and sponges. To obtain liquid fibroin from the solid fibre, it must first endure a process termed regeneration, where the protein is considered to be returned to a state similar to its pre-spun condition. This work explores fundamental aspects of silkworm silk fabrication that encompasses, simultaneously, a fundamental biophysical understanding of the regeneration process at the molecular scale and its effects. We use the acquired knowledge to exploit the delicate and metastable equilibrium between protein self-assembly and aggregation in a more controlled manner to fabricate complex materials with a special focus on the regeneration of hard tissue.

4:45 PM SB09.03.03

The Rose Petal Surface, a Wonder of Nature—Complexity on the Nanoscale Lisa Almonte¹, Carlos Pimentel², Enrique Rodríguez-Cañas³, Jose Abad⁴, Victoria Fernandez⁵ and Jaime Colchero¹; ¹University de Murcia, Spain; ²Instituto Andaluz de Ciencias de la Tierra, Spain; ³Universidad Miguel Hernández, Spain; ⁴Technical University of Cartagena, Saint Pierre and Miquelon; ⁵Universidad Politécnica de Madrid, Spain

Biological organisms are covered with a cuticle as outermost extracellular material and interface between organs and the environment. A precise understanding of the structure-function relation of these interfaces is still an open issue. In particular for the case of wetting, it is far from clear how nanoscale chemistry and structure determine macroscopic wetting. In our opinion, Nature is still ahead of "first principles calculations": if surfaces with well-defined and robust wetting properties are to be designed, it is still more effective to "look" at what Nature offers, than to rely on theoretical modeling. The Lotus and Rose Petal effect are two striking examples of how Nature fine-tunes nanoscale physics to obtain an appropriate (biological) function on the

macro-scale.

We use Atomic Force Microscopy (AFM) to simultaneously measure nanoscale topography and chemistry of (natural!) Rose Petals. We found two extraordinary features linked to their peculiar wetting properties, namely: (i) surface roughness is concentrated on the nanoscale and fractal-like, and (ii) the surface has an extreme nanoscale chemical variability. While high roughness is generally accepted to be the origin of peculiar wetting (super-hydrophobicity) the role of nanoscale chemical variability is usually not really a topic of discussion; most probably because -up to now- it could not be "seen".

An extreme roughness on the scale from 5 nm to 25 μm was measured. Although the total roughness is very different (25 μm vs. 3 μm), the Power Spectral Density of surface roughness of the upper and lower side are very similar, both surfaces being fractal with $df \approx 2.45$. For water, the contact angle on both surfaces is similar, which proves that rather than total roughness, other parameters -and in particular fractal dimension- are relevant for their wetting behavior. In addition, we find an extreme chemical heterogeneity of the surfaces, with very hydrophilic and very hydrophobic patches being close together. In our opinion, both, extreme roughness and chemical variability are the basis for the Rose Petal Effect.

From our data, we conclude that a liquid drop will strongly adhere to nanoscale hydrophilic patches, and detach from all the other hydrophobic parts of the surface, since the combined effect of roughness and chemical (nanoscale) wetting properties will induce a high effective local contact angle (=nanoscale wetting parameter). This explains the surprising and in principle antagonistic properties associated with the Rose Petal Effect, i.e., high contact angle and high drop adhesion. We are convinced that, although this work has focused on rose petals, the fundamental mechanism by which Nature is able to generate high contact angle and drop adhesion will apply to other surfaces with similar characteristics. In addition, the application of this fundamental mechanism will trigger the development of new functional surfaces by "learning from Nature".

5:00 PM SB09.03.04

Magnetic Nacre—Superior Mechanical and Magnetic Performance of Highly Anisotropic Sendust-Flake Composites Freeze Cast in a Uniform Magnetic Field Kaiyang Yin^{1,2,3}, Bradley A. Reese², Charles R. Sullivan² and Ulrike G. Wegst^{1,2}; ¹Northeastern University, United States; ²Dartmouth College, United States; ³University of Freiburg, Germany

Despite extensive research, the manufacture in the bulk of high-performance flake-based magnetic composites with a highly aligned, nacre-like structure remains challenging. Many challenges can be overcome by freeze casting in an externally applied, uniform magnetic field, which causes both the flakes and the composite walls of the cellular solid to align parallel to the B-field lines. When appropriately sized, the flakes experience a second alignment parallel to the freezing direction because of a shear flow that occurs due to both the volumetric expansion of the ice phase and mold contraction during the directional solidification. The resulting orthotropic structure of the freeze-cast magnetic composite is reflected in orthotropic mechanical and magnetic properties of the material. The magnetic composites manufactured by magnetic-field assisted freeze casting outperform by a factor of 2–4 in terms of stiffness, strength, and toughness materials that are processed in the absence of a magnetic field and do not exhibit a monodomain architecture. Additionally, the anisotropic freeze-cast magnetic composites achieve lower losses in two directions of flux excitation so that they can be used without an additional high permeability flux return path in applications like power transformation. Because of the highly aligned microstructure, it is possible to compact the initially lamellar composite with 90% porosity to at least 80% strain. The results presented in this study illustrate the tremendous potential for magnetic freeze casting of nacre-like magnetic composites for use in power conversion.

SESSION SB09.04: Poster Session I: Biological and Bioinspired Functional Materials—From Nature to Applications

Session Chairs: Mathias Kolle and Radwanul Siddique

Tuesday Afternoon, November 30, 2021

8:00 PM - 10:00 PM

Hynes, Level 1, Hall B

SB09.04.02

Light-Adapted Photosynthetic Membranes from Marine Bacteria and Diatoms for Bio-Electronic and Bio-Photovoltaic Applications [Constantinos A. Varotsis](#), Marios Papageorgiou, Konstantinos Yiannakos, Charalambos Andreou and Charambos Tselios; Cyprus University of Technology, Cyprus

The high quantum efficiency of photosynthetic reaction centers (RCs) makes them attractive for bioelectronics and biophotovoltaic applications. In the bacterial species *Roseobacter denitrificans*, *Roseobacter litoralis* and *Erythrobacter litoralis* the photovoltaic machinery which is located within few nm diameter transmembrane protein can be removed from the cells and interfaced with electrodes. Cytochrome *c* (cyt *c*) has been utilized as an electron-transfer (ET) element between electrodes and RCs. Diatoms are a major group of microalgae ubiquitous in the oceans. They have developed a unique light-harvesting apparatus, the Fucoxanthin Chl *a/c* binding protein (FCP) which shows a sequence similarity to light harvesting complex (LHC II) of higher plants but with pigment composition significantly different. In FCP, Chl *b* is replaced by Chl *c*₂ and Fucoxanthin (Fx) is the major carotenoid instead of lutein in LH II.

In the present work the photodynamics and spectroscopic characterization, including Resonance Raman, FTIR, Fluorescence, light induced adaptations, and Electrochemistry, of membranes from *Roseobacter denitrificans*, *Roseobacter litoralis* and *Erythrobacter litoralis* and from the diatoms *Thalassiosira pseudonana*, *Chaetoceros ceratosporus* and *Chaetoceros sp* will be presented.

References

1. Vincent M. Friebe et al. ACS Appl. Mater. Interfaces 2017, 9, 28, 23379–23388
2. Photonics and Optoelectronics with Bacteria: Making Materials from Photosynthetic Microorganisms Francesco Milano, Angela Punzi, Roberta Ragni, Massimo Trotta, and Gianluca M. Farinola Adv. Funct. Mater. 2019, 29, 1805521
3. Photoreduction of Carotenoids in the Aerobic anoxygenic photoheterotrophs probed by Real time Raman spectroscopy Marios Papageorgiou, Charalambos Tselios, Constantinos Varotsis submitted

SB09.04.03

Multi-Lamellar Structured Ceramide Microparticles Enveloped with a Thin Layer of Bacterial Cellulose Nanofibers [Kyounghee Shin](#), Boryeong Lee and Jin Woong Kim; Sungkyunkwan University, Korea (the Republic of)

Ceramides are the main component of the stratum corneum, the outermost layer of the skin, providing an epidermal barrier against dehydration or external microorganisms. However, much wider application of ceramides has been limited since molecular crystallization readily occurs in aqueous formulations. To solve this problem, this study introduces a practically useful approach to encapsulate ceramide molecules, in which hydrophobically modified bacterial cellulose nanofibers (BCNFs) were employed as a thin film-forming fiber surfactant. We confirmed that the ceramide microparticle core with a multi-lamellar structure could be enveloped with a BCNF wall of which thickness is about hundreds of nanometers. The multi-lamellar structure was

characterized by analyzing the inter-layer distance through small-angle x-ray scattering. The inter-layer distance could be manipulated by using fatty alcohols with different alkyl chain length; 4.3 nm, 4.9 nm, and 5.9 nm for 1-tetradecanol, 1-octadecanol, and 1-docosanol, respectively. Wide-angle x-ray scattering showed that the ceramide exhibited hexagonal lateral packing with 1-tetradecanol and orthorhombic lateral packing with 1-octadecanol and 1-docosanol. These results suggest that the chain length of fatty alcohols critically involved in the process of ceramide molecules forming the multi-lamellar structure. Furthermore, we demonstrated that the longer chain length of fatty alcohols prevented more effectively the microcrystalline phase from penetrating the capsule wall and protruding out due to the formation of thicker hydrophobic lamellar phase. The results obtained in this study highlight that BCNF-based encapsulation technology provides a practical methodology to control the crystallization behavior of ceramide molecules, thus enabling the development of various types of skin-friendly formulations that can strengthen the skin barrier function.

SB09.04.05

***Euglena gracilis*-Derived Exosomal Nanovesicles as Cell Activating Therapeutic Agents** Hwira Baek, Yuri Ko and Jin Woong Kim; Sungkyunkwan University, Korea (the Republic of)

Exosomes, a class of extracellular vesicles secreted by almost eukaryotic cells, are known as an important mediator for signaling in cell-cell communication and cellular processes including immune response and antigen presentation. Since exosomes contain therapeutic proteins, a variety of cell therapeutic strategies are developing while avoiding side effects such as low survival rate and immune rejection response associated with direct use of cells as a therapeutic agent. Most of the exosome studies conducted so far are based on animal-originated cells. Recently, there are challenging attempts to extract exosomes from other types of raw materials such as plant cells and microalgae. The approach to obtain exosomes from microalgae is of special interest, because they have abundant biomolecules such as proteins, vitamins, minerals, and amino acids. Herein, we first propose a microalgae-derived exosomal nanovesicle (ExoNV) system for cellular drug delivery. Our ExoNVs were extracted from *euglena gracilis*, representative microalgae, containing β -glucans, vitamins, and minerals, via cell-extrusion. Extruding *euglena gracilis* through a series of polycarbonate membrane from 5 μ m to 0.2 μ m pores allowed us to produce ExoNVs with a particle size of ~190 nm and the number of 6.55x10⁹ particles/ml. The ExoNVs produced by using this approach encapsulated 14% of β -glucans, which was confirmed by aniline blue fluorescence analysis. In our continued studies, we also confirmed through *in vitro* cellular ROS detection and cell proliferation assays that β -glucans-containing ExoNVs not only exert improved cellular antioxidation activity but also aid dramatically in cell proliferation. These results highlight that our ExoNV system has great potential as an exosome-mimetic therapeutic agent that can activate cells or deliver drugs to cells.

SB09.04.06

A Biomimetic Approach to Improve the Tribological Performance of PVD Coated Surfaces for Automotive Applications SangYul Lee¹ and Jungwan Kim²; ¹Korea Aerospace University, Korea (the Republic of); ²InCheon National University, Korea (the Republic of)

Improvement of tribological properties with the enhancement of lubrication by applying surface texturing has been paid much attention recently in wide ranges of applications. The laser texturing, a surface texturing using a laser has been received lots of attention to improve the tribological performance of various surfaces and this laser surface texturing could be considered in a large extent as one of various biomimetic approaches to improve surface performance. In this work, the surface engineering using bio-inspired patterns had been introduced and the results from the laser texturing on the PVD coated steel substrate were illuminated so that the feasibility of combining surface texturing and hard coating to further improve the tribological properties could be examined. The tribological properties of the surface were evaluated using a ball on disk type tribometer with a 9.25 mm diameter Al₂O₃ ball as a counterpart material. The tests were performed at room temperature in air environment with oil lubrication under an applied normal load of 5.0 N. Our results indicated that laser texturing affected the tribological performance of the surfaces extensively and the size as well as pattern type of laser texturing were critical factors affecting the tribological performance of the coatings. For CrZrSiN coatings applied on the laser textured steel specimens, much improvement of the friction coefficient at room temperature, nearly 10 times depending upon the type of the bio-inspired pattern could be obtained under lubrication condition.

SB09.04.10

Color Pattern Variation with the Control of Multiply Scattered Light in Birds Deok-Jin Jeon¹, Seungmuk Ji¹, Eunok Lee², Jihun Kang¹ and Jong-Souk Yeol¹; ¹Yonsei University, Korea (the Republic of); ²National Institute of Ecology, Korea (the Republic of)

Coloration in nature has evolved for a long time to become biologically diversified for camouflage, predation, signal communication, and mate choice. Birds are representative examples of nature's coloration. More than 10,000 bird species have amazing diversity of colors in their feathers. Nature's coloration methods are mainly divided into two parts: pigments and structural colors. Structural colors are produced by selective light reflection of certain wavelengths from nanostructures, not by light absorption in contrast to pigment-based colors. Birds also show the colors not only with pigments but also with optical nanostructures. The optical nanostructures are highly organized with keratin, melanin, and air in varying refractive indices, thus producing the most brilliant colors in nature through structural coloration. In birds, structural colors are mainly observed in feather barbules and feather barbs.

Avian structural colors are produced by constructive interference of coherent backscattering of light. Although this single-scattering model helps to analyze reflectance peaks, color pattern variations are not well understood due to the limitations of single-scattering model to analyze real structural colors of blue birds. So, we use the theoretical model based on transport length, which provides improved understanding on the multiply scattered light in birds. The transport length in a strongly diffusing medium is the length over which the direction of the photon's propagation is randomized. We select Eurasian jay and Oriental dollarbird as the target species and analyzed the transport length based on the thickness of spongy layer. Eurasian jay and Oriental dollarbird show color pattern variations from white to sky blue, blue, and dark, and the thickness of disordered medium could be defined as thickness of spongy layer in this transport system. We calculate transport length by energy-density coherent-potential approximation (ECPA). From the results, we also observe that light propagation regime is in intermediate state between ballistic and diffusive transport. Therefore, we need to consider color pattern or spectrum variation by the relationship between transport length and thickness of spongy layer. For blue barbs with thin spongy layer, red light that could not be scattered through the layer will be absorbed by basal melanin layer. In the case of white barbs, the spongy layer is sufficiently thick so the multiply scattered light spans from blue to red light, resulting in white. Our results also suggest that the peak broadening by multiple scattering could only occur when spongy layer is sufficiently thick. Based on this knowledge, we develop thickness-dependent bio-inspired structural colors via self-assembly. This enhanced understanding on the nature's coloration has a potential for various biomimetic application to reflective colors such as pigment-free coating materials to digital signage, and deformable display.

SB09.04.12

Photoreactivity and Enhanced Toughness and Stability in Polysaccharide-Based Films Using Vanadium Ion Coordination Carina Haddad, Alexis D. Ostrowski, Kalani D. Edirisinghe and Hope Brown; Bowling Green State University, United States

Strategies such as covalent cross-linking, chemical modification and blending of polymers or nanotechnology can be used to enhance the physicochemical and mechanical properties of soft polysaccharides-based materials. In an alternative approach, we used metal coordination bonding of vanadium ions to

polysaccharides to create strong, and water-stable bio-based films. Two naturally occurring polymers, pectin and chitosan were combined with glycerol to impart stretchability. Vanadium ions were incorporated into the films and the formation of ionic interactions as well as hydrogen bonding and coordinate bonding was confirmed via FT-IR. Scanning electron microscopy showed laminated sheets with intermolecular distance of ~0.16 μm for V(V) containing films as compared to a much larger ~0.75 μm for films without vanadium. Moreover, we showed that V(V) coordinated films possessed higher storage modulus, water and thermal stability than films without vanadium. More interestingly, we observed striking changes in color from yellow to blue inside the V(V)-containing films upon irradiation with blue light. This corresponds to reduction of V(V) to V(IV) according to previous studies. A small change in modulus was observed with light stimulus, with no significant changes in the structure of the film. Based on these results, we can conclude that it is possible to create robust, water-stable and photoresponsive polysaccharides-based materials through the strong supramolecular metal-coordination interactions between metals and polysaccharides.

SB09.04.13

Bioinspired Guanine-Based Photonic Structures—Synthesis and Magnetic Alignment [Natalie Nicolas](#) and Joanna Aizenberg; Harvard University, United States

Guanine crystals are a common natural material used in biological photonic crystals and photonically active structures. Layered guanine crystals produce the characteristic structural colors of iridophores in cephalopods and tree frogs, as well as producing complex optical structures such as the concave mirrors in the eyes of scallops. They can also produce dynamic structural color, as some species of frogs can change the shape and alignment of layered guanine in their iridophores to produce skin colors ranging from yellow-green to dark gray. The production of β phase guanine platelets with various morphologies was achieved by recrystallizing guanine in formamide in the presence of poly(1-vinylpyrrolidone-co-vinyl-acetate) and small organic molecules such as uric acid. The diamagnetic anisotropy of guanine crystals created the opportunity to both align guanine crystals and to affect their morphology to create interesting photonic structures, such as C-shaped crystal stacks, by applying a magnetic field. Magnetically aligned guanine platelets and platelet stacks were then embedded inside a hydrogel or elastomer matrix to create bioinspired photonic crystals with dynamic photonic properties, taking inspiration from the iridophores of tree frogs. By examining the effect of magnetic fields on guanine crystal structure and assembly, we can better understand how magnetic fields affect the crystallization dynamics of diamagnetic molecules and better utilize guanine crystals in applications where alignment is a critical factor, including in the assembly of bioinspired photonic structures.

SESSION SB09.05: Structural Colors and Bioinspired Optical Materials

Session Chairs: Radwanul Siddique and Jan Totz

Wednesday Morning, December 1, 2021

Sheraton, 2nd Floor, Republic B

10:45 AM *SB09.05.01

Harnessing Microstructures for Tunable Structural Color [Lauren Zarzar](#); The Pennsylvania State University, United States

A variety of physical phenomena create color, such as selective absorption by dyes or pigments, optical dispersion, and structural color from light interference. Nature has exquisitely harnessed structural color, with examples including opals, butterfly wings, and iridescent bird feathers, which traditionally exploit nanoscale periodic geometries to create optical interference. Here, we explore an optical mechanism for creating iridescent structural color that is accessible in larger, microscale geometries. In this mechanism, light traveling by different trajectories of total internal reflection along a concave interface interferes to generate patterns of color. The effect is generated at interfaces with dimensions that are orders of magnitude larger than the wavelength of visible light and is readily observed in materials as simple as sessile water droplets. We further exploit this phenomenon in more complex systems, including multiphase droplets, solid micro-particles, and 3D patterned polymer surfaces to create patterns of iridescent color that are consistent with theoretical predictions. Given the ease by which controllable structural coloration is generated at microscale interfaces, we expect that the design principles and predictive theory outlined here will be of interest for fundamental exploration in optics and application in functional colloidal inks and paints, displays, and sensors.

11:15 AM SB09.05.03

Structural Color Production in Melanin-Based Colloidal Assemblies in Spherical Confinement [Anvay A. Patil](#)¹, Christian Heil², Arthi Jayaraman^{2,2} and Ali Dhinojwala¹; ¹The University of Akron, United States; ²University of Delaware, United States

Melanin, a ubiquitous dark pigment present in various living organisms, is well-known for its two unique optical properties - high refractive index (RI) and broadband absorption, that contribute to structural coloration, photoprotection, and thermoregulation in many biological systems. These dark melanin particles self-assemble strategically in many organisms including avian species to produce a wide gamut of structural colors ranging from vibrant iridescent to earthy colors. Nevertheless, little is discussed about how absorbing species like melanin participate in color production. In this work, we perform optical modeling using the finite-difference time-domain (FDTD) method on melanin particle supraballs and binary melanin and silica particle supraballs to elucidate the role of melanin in structural color generation. By filling this void in the literature, we can open exciting avenues to tune structural colors, and these insights are of interest for many applications including cosmetics, paints, inks, and food colorings.

11:30 AM SB09.05.04

Engineering the Self-Assembly of Large Colloidal Crystals With DNA-Programmed Interactions [Alexander Hensley](#)¹, William Jacobs² and Benjamin Rogers¹; ¹Brandeis University, United States; ²Princeton University, United States

Self-assembly is one of the cornerstones of the development of nanometer-scale functional materials in living systems. Inspired by nature, researchers have developed methods that use specific short-range interactions between building blocks made possible by DNA to self-assemble prescribed structures. For example, grafting single-stranded DNA to the surfaces of micrometer-scale particles can direct the particles to self-assemble into a diverse set of crystal structures. However, a relatively poor understanding of the dynamic pathways that lead to crystallization has made it difficult to assemble the types of large, defect-free crystals that are required for practical applications in plasmonics or photonics. In this talk I will present a detailed study of the nucleation and growth of DNA-coated particles. I will show an experiment that uses several droplets containing DNA-coated particles that under specific conditions nucleate and grow a single crystal per droplet due to the crystal's growth depleting monomers from the solution, quickly lowering the supersaturation below where further crystals are likely to form. I will also describe the development of a model, grounded in classical nucleation theory, that predicts the absolute nucleation and growth rates that we observe in experiments. Finally, we apply this knowledge to develop protocols that create colloidal crystals that are large, mono-disperse, faceted, and exhibit pronounced structural coloration using a combination of microfluidics and commercial temperature-

control hardware. These advancements in understanding and controlling the dynamic pathways to crystallization with DNA-coated micrometer-scale particles is a firm foundation for future experiments involving the creation of large crystals of the wide variety of structures that thus far have only been self-assembled in small amounts which is a significant step towards approaching the impressive resourcefulness of the natural world.

11:45 AM SB09.05.05

Reflectin-Based Optical Structures in Human Cells [Georgii Bogdanov](#), Atrouli Chatterjee, Preeta Pratakshya, Nikhil Kaimal and Alon Gorodetsky; University of California, Irvine, United States

Over the last few decades, the camouflage capabilities of cephalopods were extensively studied and shown to be enabled by their unique skin morphology. These capabilities are achieved via the complex optical phenomena that occur within the multiple layers of cephalopod skin. The layers may contain one or more types of cells: pigment-based organs called chromatophores that act like color filters; reflective cells called iridophores that act like Bragg stacks; and scattering cells called leucophores that act like broadband diffusers. Iridophores and leucophores possess reflective and scattering properties due to the presence of unusual proteins known as reflectins, which assemble into high refractive index subcellular ultrastructures. We show that such high refractive index structures can be produced in human cells as well. We discuss optical properties of the human cells with and without high refractive index structures, associated challenges, and future potential. The reproduction of the optical elements within the human cells holds a potential for the development of bio-derived optical living materials.

SESSION SB09.06: Biomaterial Modeling, Characterization and Mechanical Properties
Session Chairs: Mathias Kolle and Radwanul Siddique
Wednesday Afternoon, December 1, 2021
Sheraton, 2nd Floor, Republic B

1:30 PM *SB09.06.01

Butterfly Scale Morphogenesis: Wrinkling on the Micron Scale [Jan F. Totz](#); Massachusetts Institute of Technology, United States

Micron-scale surface modulations such as wrinkles or folds underly a number of modern engineering applications, such as photonic structures in photovoltaics and flexible metasurfaces. Controlled and precise fabrication of these modulations is a challenge for human manufacturing techniques. In stark contrast, biological systems robustly utilize morphological changes in their developmental program to create multi-germ bodies, hairs and scales on spatial scales which would be costly to replicate with human manufacturing. In this talk I will present recent measurements of in-vivo butterfly scale development exhibiting wrinkling. The observations are rationalized with a parsimonious continuum mechanics model.

2:00 PM SB09.06.02

A Geometrical Theory for Edge-Driven Growth of Thin-Walled Materials [C. N. Kaplan](#)¹ and L. Mahadevan²; ¹Virginia Tech, United States; ²Harvard University, United States

Accretion of mineralized thin wall-like structures via localized growth along their edges is observed in a range of physical and biological systems ranging from molluscan and brachiopod shells to carbonate-silica composite precipitates. Controlled self-assembly drawing inspiration from these systems holds great potential for fabrication of functional materials with complex geometries. To understand the shape of these mineralized structures, we develop a mathematical framework that treats the thin walls as a smooth surface left behind an evolving space curve which corresponds to the growth front. Our theory that takes an explicit geometric form indicates that in addition to prescribing the interfacial growth speed, the growth of a non-planar 2D pattern in a 3D domain requires a closure equation related to the nature of surface curling, unlike the growth of a bulk crystal in 3D that solely requires a condition for the surface growth rate. The result is a set of equations for the geometrical dynamics of a curve that leaves behind a compatible surface. Solutions of these equations capture a range of shapes such as those of clam shells, rippled chemical garden tubes, and other curled precipitate patterns. Overall, our theory provides a versatile framework for the practical realization of intricate functional morphologies that harness accretive mineralization.

2:15 PM SB09.06.03

Soft Materials Surface and Interface Characterization Through Multi-Scale Simulations [Francesco M. Bellussi](#), Annalisa Cardellini, Pietro Asinari and Matteo Fasano; Politecnico di Torino, Italy

The surface free energy of soft coatings determines the adhesion, friction, and wettability response of solid surfaces in several applications of engineering and biomedical interest. However, the multiscale nature of these phenomena limits a bottom-up prediction of the resulting surface properties.

In this work we use computational experiments to characterize the surface and solid-fluid interface of low-surface-free-energy coatings and materials [1,2]. In particular, the free energy perturbation approach is first used to evaluate the work of adhesion between polymer surfaces and fluids; then, the Young-Dupré equation is adopted to compute the ideal contact angle [3]. Such molecular dynamics and coarse-grained simulations allow to explore the interfacial properties of soft materials, enabling a more comprehensive understanding of their effect on the adhesion, friction, and wettability of solid surfaces. Differently from standardized experimental approaches, numerical experiments allow to understand and decouple the different mechanisms regulating the wetting properties of soft coatings with atomistic precision. The aim is to propose a first step towards a multiscale standard framework for the computational characterization of surfaces, required for the optimal design of materials with tailored surface properties.

The results obtained in this work are validated against experiments and then used as input parameters for materials modelling at higher scales, such as finite elements simulations, to investigate the contribution of surface topology on wettability, in terms of nano- and micro-roughness or patterning. In perspective, multiscale models linking the chemical and topological characteristics of soft surfaces with their effective response will allow predictive in silico testing of new materials with tunable functionalities.

This work received funding by the European Union's Horizon research and innovation programme under grant agreement No 760827 (OYSTER: OpenCharacterisation and Modelling Environment in Nanoarchitected Hard/Soft Interfaces, www.oyster-project.eu)

[1] Cardellini et al. "Multi-scale approach for modeling stability, aggregation, and network formation of nanoparticles suspended in aqueous solutions". *Nanoscale*, 2019.

[2] De Angelis et al. "Exploring the Free Energy Landscape To Predict the Surfactant Adsorption Isotherm at the Nanoparticle–Water Interface". *ACS*

central science, 2019

[3] Cardellini et al. "Integrated Molecular Dynamics and Experimental Approach to Characterize Low-Free-Energy Perfluoro-Decyl-Acrylate (PFDA) Coated Silicon". *Material & Design*, 2021

2:30 PM SB09.06.04

Bioinspired Materials with Dynamically Adaptable Mechanical Properties and Damage Mitigation Santiago Orrego^{1,2}, Mostafa Omar¹, Bohan Sun¹ and Sung Hoon Kang¹; ¹Johns Hopkins University, United States; ²Temple University, United States

Nature provides inspiration for next-generation materials that can dynamically adapt to the changing environments by modulating their properties such as color, adhesion, and stiffness. Inspired by natural examples, there have been many impressive progresses in synthesizing tunable materials that can either actively or passively switch their properties. However, they usually allow a finite number of (usually two) pre-determined configurations, there are few material systems that can "sense" and adapt their properties in response to a dynamically changing environment.

Inspired by bone mineralization mechanisms, we have investigated a multifunctional material system that "senses" mechanical loading and proportionally triggers mineral formation from media with mineral ions so that the material can adaptably change its mechanical property and mitigate damages. The mineralization rate is autonomously modulated in response to changing loading conditions, for example, resulting in a 30-180% increase in the modulus of the material upon 1 to 5 N cyclic loadings (frequency: 2 Hz). Moreover, the material adds more minerals to the region of high stress and vice versa for that of low stress so that the material can mitigate the damage and enhance its fatigue life. We envision that our findings can open new strategies for synthesizing multifunctional materials with dynamically adaptable mechanical properties and damage mitigation.

Reference: S. Orrego, Z. Chen, U. Krekora, D. Hou, S.-Y. Jeon, M. Pittman, C. Montoya, Y. Chen, S. H. Kang, "Bioinspired materials with self-adaptable mechanical properties," *Advanced Materials*, 1906970 (2020).

Acknowledgments: This work was supported by the Air Force Office of Scientific Research Young Investigator Program Award (Award number: FA9550-18-1-0073, Program manager: Dr. Byung-Lip (Les) Lee), Johns Hopkins University Whiting School of Engineering start-up fund, and Temple University Maurice Kornberg School of Dentistry start-up fund (PI: Orrego). Any opinions, findings, and conclusions or recommendations expressed in this material are those of the author(s) and do not necessarily reflect the views of the United States Air Force.

2:45 PM SB09.06.05

Mechanical Properties and Deformation Behavior of Self-Assembled Nanoparticle Superlattices Daryl W. Yee, Somayajulu Dhulipala, Margaret S. Lee, Carlos Portela and Robert J. Macfarlane; Massachusetts Institute of Technology, United States

Natural materials often exhibit complex material properties due to hierarchically organized structural motifs at the molecular, nano, micro, and macroscopic size regimes. They have inspired a whole generation of advanced multifunctional synthetic materials that utilize structural hierarchy to reach new property spaces. Self-assembly approaches have been heavily utilized to fabricate these hierarchical materials as its ability to build materials via weak, dynamic interactions between nanometer-sized build blocks provides great control over material structure from the molecular to the micro-scale.

In particular, self-assembled nanoparticle superlattices — three-dimensional ordered arrays of nanoparticles — have been the subject of significant interest due to their emergent properties that arise from the ordering of their nanoparticle building blocks. As a result, these nanoparticles superlattices are promising materials for a variety of applications, from optoelectronics to energy storage. While significant efforts have been made on understanding and controlling the formation of these nanoparticle superlattices, investigations on their mechanical properties are scarce. As the mechanical properties of a material impacts its processing and its suitability for a given application, it is critical that we understand the mechanical behavior of these self-assembled nanoparticle superlattices and develop chemistries to control them.

Here, we discuss how the self-assembly chemistry and superlattice structure impacts the mechanical behavior of these nanoparticle superlattices. Nanocomposite tectons (NCTs), a recently developed nanoparticle superlattice system that uses polymer brush particles functionalized with supramolecular binding groups to drive assembly, are ideal for exploring these parameters as the strength of the supramolecular interactions and the superlattice structure can be easily tuned. In-situ uniaxial compression of substrate-grown hydrogen-bonded nanoparticle superlattices show that these materials undergo significant plastic deformation with an associated loss of nanoparticle ordering. Our systematic nanomechanical experiments, performed to various compression states (up to 50% strain), shed light on the mechanisms of deformation as well as the evolution of properties such as Young's modulus and yield strength. By modulating the strength of the nanoparticle interactions, via the use of different supramolecular binding groups or covalent bonds, we show that the mechanical properties and deformation behavior of these nanoparticle superlattices can be controlled. The impact of superlattice crystal structure on the mechanical properties are also discussed. These observations provide a more general understanding of how self-assembly chemistry and superlattice structure can be used to control the mechanical properties of these nanoparticle superlattices.

3:00 PM BREAK

SESSION SB09.07: Self-Assembly of Biological and Bioinspired Materials
Session Chairs: Giulia Guidetti and Lauren Zarzar
Wednesday Afternoon, December 1, 2021
Sheraton, 2nd Floor, Republic B

4:00 PM SB09.07.01

Nanopatterning Surface with a Self-Assemble Protein Depicting a Honeycomb Structure with Tunable Pores—A New Biomaterial for Nanotechnological Field Elise Jacquier^{1,2}, Grégory Si Larbi², Renaud Dumas² and Pierre-Henri Elchinger¹; ¹Univ. Grenoble Alpes, CEA, CNRS, IRIG-DIESE-SYMMES, France; ²Univ. Grenoble Alpes, CEA, CNRS, INRAE, IRIG-DBSCI-LPCV, France

Achieving nanopatterning of a surface is a key point in fields covering microelectronics, photovoltaic, biomedical and biosensors. The purpose of nanopatterning a surface is to increase the surface specificity to improve, for example, nanotechnological devices sensitivity. As cutting-edge technics (e.g. top down methods) are reaching physical limitations and become more and more expensive, light has been put on bottom up methods. This approach relies on the organization of small building blocks to create supramolecular 2D lattices. Nowadays, constructing 2D lattices for nanopatterning is mainly

based on self-assembly process with an emphasis on biological self-assembled building blocks. However, these 2D lattices depict thin height which limits their grafting capability and thereby their wider use in nanotechnological field.

In this work, we present a self-assembled protein oligomerization domain able to create large 3D honeycomb lattice based on the natural ability of the protein to self-assemble through head-tail interaction. With electron microscopy analysis, we showed that the orientation of the honeycomb structure on carbon or SiO₂ surface can be modulated. Atomic force microscopy measurements revealed a height of 30 nm corresponding to 40-stacked protein for one pore of the honeycomb. Furthermore, we showed that the amino acid sequence of the protein can be modulate without altering the honeycomb structure. Noteworthy, depending on the amino acid present inside the honeycomb pores, we also showed a specific metal chelation inside the pore. Altogether, these characteristics make this protein-based 3D lattice a grafting platform never described until now paving the way to design adaptive self-assembled structure for nanotechnological purpose.

4:15 PM SB09.07.02

Microscopic Actuation for Macroscopic Aggregation Mustafa K. Abdelrahman, Lindy Jang, Suitu Wang, Mahjabeen Javed and Taylor H. Ware; Texas A&M University, United States

An important area of materials research is the development of adaptive structures capable of sensing, reconfiguring, and self-healing with minimal intervention. Such structures will enable the realization of a new class of materials capable of on-demand assembly, reorganization, and disassembly. Inspiration for the development of such structures is found in the survival strategies demonstrated by many insects. For example, fire ants quickly organize themselves into a buoyant raft in the presence of floods, and honey bees aggregate to form bivouacs during turbulent weather conditions. Notably, the structures formed demonstrate viscoelastic behavior with one remarkable feature which distinguishes these aggregations from their synthetic polymer counterparts: the aggregate's ability to morph from a fluid-like swarm to a global solid-like material. This dynamic behavior is achieved through each insect's ability to attach and detach to its neighbors. In order to mimic this behavior, liquid crystal elastomer (LCE) rectangular films (strips) (250 μm x 6 mm x 50 μm in cross-section) are programmed to reversibly actuate from a straight to a coiled configuration. By heating these LCE strips and allowing them to aggregate and mechanically interlock with each other, structures capable of reversibly transitioning from a liquid-like state to a solid-like state are achieved. Rheological data of these structures demonstrate an increase in yield stress from 23 Pa at 50 °C to 329 Pa at 150 °C. Along with this increase in yield stress, a reversible negative thermal expansion of 30% is observed. Notably, mechanical properties of the aggregate structure are controlled by tuning individual strip properties. By increasing the length of the individual strips from 3 mm to 12 mm, yield stress increases from 200 Pa to 725 Pa, and by increasing the cutting angle from 0° to 45°, a decrease in yield stress from 459 Pa to 38 Pa is observed. This synthetic aggregate's ability to reversibly transition from low yield stress to high yield stress on-demand enables various functionalities such as clogging, targeting, and self-healing.

4:30 PM SB09.07.03

Photo-Driven Fabrication of Bioinspired Surface Textures with Programmable Anisotropy Marcella Salvatore, Stefano Luigi Oscurato and Pasqualino Maddalena; University of Naples Federico II, Italy

The realization of artificial complex surface pattern, inspired by nature or driven by specific technological needs, requires the use of lithographic techniques which have brought to prominent progress in several fields. However, the standard lithographic techniques are often costly and time-consuming, and do not allow further modification of the pattern once fabricated. The fabrication of superficial micro-textures, in simple and cost-effective way, is highly desirable in this framework. A versatile technique for surface micropatterning is based on surface reconfiguration of photosensitive materials, such as light-responsive polymers containing azobenzene molecules.

Azopolymers are material systems able to be directly structured in a reversible way over large scale in simple fabrication schemes without any further development step. Spatially structured UV/visible light fields generate topographic modulations on the free surface of films of such materials by activating cyclic structural transitions between *trans* and *cis* isomerization states of the azomolecules. The final surface geometry depends on the irradiated intensity pattern and the light polarization state over the sample, which control the degree of the surface deformation and its directionality, respectively. Here we demonstrate several large-scale surface textures, with different degrees of complexity and anisotropy, realized by means of simple illumination schemes based on interference lithography and light-induced reconfiguration of pre-structured azopolymer microtextures. In particular, periodic and aperiodic complex surface textures are obtained by means of multiple exposures steps or multiple beam interference. Furthermore, surfaces with programmable directionality and degree of anisotropy have been achieved by reconfiguring symmetric prepatterned azopolymer films, exploiting the peculiar anisotropic response of the material motion to the polarization distribution of the optical field.

The techniques described here allow the all-optical tailoring of surface functionalities directly affected by relief geometry, including anisotropic wetting effects (such as controlled directionality or unidirectional spreading) and substrate-influenced cell growth that opens to the design of new biomaterials generation with improved functionalities and bioactive properties.

4:45 PM SB09.07.04

Droplet-Assisted Growth and Shaping (DAGS)—A Straightforward Process to Synthesize Bioinspired Nano- and Microstructures with Complex Geometrical Shape and Subnanometer-Confined Reactive Sites Stefan Seeger, Georg Artus, Sandro Oliveira and Kangwei Chen; University of Zurich, Switzerland

The control of shape and intraparticle heterogeneity of nano and microstructures in some cases is extremely complex and often even impossible. However, it is important for practical applications, since complex shapes may have influence on rheology, wetting, coating stability, and mechanical properties of bulk composites. Recently, we described a simple and low-cost approach to synthesize nanoparticles applying a delicate composition of monomer, water, and surface properties. We call this synthesis approach Droplet assisted growth and shaping (DAGS). It has been applied in many variants to synthesize various nano- and microstructures based on polysiloxanes which are applied in industrial products, e.g. filters, insulation materials, etc. Beside the different shapes, e.g. filaments, rods, spirals, stars, and others, subsequently, we have been able to extend the range of structures to other materials, e.g. Germaniumoxide, Aluminum oxide and Al-Si-based structures. These structures are useful as coatings for luminescence and/or wetting control of surfaces. In this presentation we will show that further nano- and micromaterials can easily be created: Ceramic structures with defined shapes as well as nano and microstructures with incorporated ultrasmall reactive sites and other heterogeneities which show new properties and can be used for building highly anisotropic and complex coatings. The sequential use of different chemical entities during the synthesis of the nano and microstructures allows for completely new and highly sophisticated shapes. Using those structures as coatings, a precise tuning of surface properties, i.e. wetting, loading with reactive particles and nanocatalysts, adsorption properties and others more, becomes possible.

Beyond these structural properties and performance tuning, this DAGS chemical synthesis strategy is of interest also because of its simple execution: The process can be executed at room temperature, normal pressure, and with simple equipment and low-cost chemicals. The process execution in gas phase or liquid phase both is possible. We also demonstrate potential for industrial applications.

References:

- /1/ G. Artus, S. Jung, J. Zimmermann, H. P. Gautschi, K. Marquardt, S. Seeger, EP1644450A2 (2003), *Adv. Mater.* (2006),18, 2758
/2/ J. Zhang, S. Seeger, *Angew. Chem.* (2011) 50, 6652
/3/ Stojanovic, S. Oliveira, M. Fischer, S. Seeger, *Chem. Mater.* (2013), 25, 2787
/4/ G Artus, S Oliveira, D Patra, S Seeger, *Macromol. Rapid Comm.* (2017), 38, 1600558
/5/ N. Saddiqi, D. Patra, S. Seeger, *ChemPhysChem* 20, 538–5 (2019)
/6/ N. Saddiqi, S. Seeger, *Adv. Mat. Interfaces*, doi.org/10.1002/admi.201900041 (2019)
/7/ X. Zhang, S. Seeger, *ChemNanoMat* 5 (7), 964-971 (2019)
/9/ K. Chen, S. Seeger, in prep. (2022)

5:00 PM SB09.07.05

Late News: Electric Field Induced Macroscopic Cellular Phase of Nanoparticles [Abigail L. Rendos](#)¹, Wenhan Cao¹, Margaret Chern¹, Marco Lauricella², Sauro Succi², Joerg Werner¹, Allison M. Dennis¹ and Keith A. Brown¹; ¹Boston University, United States; ²Center for Life Nano Science, Italy

Electric fields provide a flexible means to manipulate soft matter, however, they interact with polarizable materials in electrolytic solutions through numerous distinct phenomena making the outcome of field-directed assembly difficult to predict. In this work, a suspension of nanoparticles is found to assemble into a macroscopic cellular phase with particle-rich walls and particle-free voids under the collective influence of AC and DC voltages. This unique, porous structure is observed here at a volume fraction and particle size an order of magnitude smaller than previous examples. Systematic variation of the applied field revealed that the onset of the cellular phase is determined by the volume fraction of the particles, the AC voltage, and the DC voltage. Additionally, a series of control experiments revealed that the complex interactions required to produce a cellular phase in this system include (1) electrochemistry to generate a DC current, (2) electrophoresis to aggregate particles into a 2D arrangement on one electrode, and (3) an instability driven by the long-ranged repulsive and short-ranged attractive electrohydrodynamic interaction that is nucleated at regions on the electrode with high local field enhancement. This mechanistic understanding, along with comparison to prior work, reveals two characteristics needed to observe a cellular phase: a system that is considered two-dimensional and short-range attractive, long-range repulsive interparticle interactions. Furthermore, photolithography was used to localize assembly thus proving the potential to tune the location of the pores in the cellular structure. This understanding paves the way towards electrically-driven assembly of hierarchical porous structures that may impact fields including energy storage and filtration.

5:15 PM SB09.07.06

Late News: Inorganic Phototropism–Biomimetic Mesostructure Growth via Light-Mediated Electrodeposition [Azhar I. Carim](#) and Nathan S. Lewis; California Institute of Technology, United States

Plants exhibit a phototropic growth response and direct the addition of new biomass to optimize collection of solar insolation. Analogous inorganic phototropic growth has been demonstrated via the light-mediated electrodeposition of chalcogen semiconductor materials and can generate highly ordered mesostructures with anisotropic nanoscale features conformally over macroscopic length scales. This process mirrors the phenotypic plasticity exhibited by plants, wherein despite a fixed genotype a wide range of different morphologies can be displayed depending on the environmental conditions: the precise structure produced is determined by the characteristics of the growth illumination and wide array of structures can be despite a consistent material composition and phase. No structured light field (no photomask) and no physical or chemical templates are utilized. The structure pitch is dependent on the spectral distribution of the input light with shorter wavelengths effecting higher feature densities, similar to how blue light effects branching in many shade-intolerant plants. The out-of-plane growth direction is related to the propagation direction of the input light, mirroring the way in which palm trees develop an observable tilt toward the average position of the solar azimuth. In-plane anisotropy is a function of the input polarization. Modeling of the growth using a combination of full-wave electromagnetic simulations of light absorption and scattering coupled with Monte Carlo simulations of mass addition successfully reproduced the experimentally observed morphologies and indicated that morphology development was directed by evolution of the growth interface to maximize anisotropic light collection. The growth process was observed to be a highly emergent phenomenon involving optical communication between neighboring features including cooperative scattering and synergistic absorption and thus is similar to the manner in which neighboring plants exchange information and avoid competition for light resources.

SESSION SB09.08: Poster Session II: Biological and Bioinspired Functional Materials—From Nature to Applications

Session Chairs: Mathias Kolle and Radwanul Siddique

Wednesday Afternoon, December 1, 2021

8:00 PM - 10:00 PM

Hynes, Level 1, Hall B

SB09.08.01

Nanomechanics of Actin Filaments—A Steered Molecular Dynamics Approach [Sharad V. Jaswandkar](#), Kalpana Katti and Dinesh R. Katti; North Dakota State University, United States

Biological systems commonly use complex multiscale and multiphase structures to provide functions that surpass those of artificial systems. Although knowing the chemical makeup of these systems is essential, understanding the passive and active mechanics inside biological systems is critical when examining the various natural systems that reach advanced features like high strength and stimuli-responsive adaptability. Finding out how and why biological systems achieve these desirable mechanical functions frequently exposes concepts that can be used to inform future synthetic designs based on biological systems. In eukaryotic cells, the cytoskeleton is a three-dimensional dynamic structure that helps cells retain their form, internal organization, and mechanical rigidity. The polymer biomolecules in eukaryotic cells that function as structural elements of the cytoskeleton are the actin microfilaments, microtubules, and intermediate filaments. The diseases like cancer transform the cell's cytoskeletal structure. Altered cytoskeletal structures modify cancer cell's ability to contract or stretch by affecting their deformation mechanics. The abnormal cellular motility is a signature characteristic of metastatic cancer cells, promoting tumor cells' spread to both local and distant locations in the body. The dynamic reorganization of the actin cytoskeleton is a fundamental requirement of this process. We have also shown that the cancer cells' altered mechanical properties during disease progression are connected with the actin reorganization. In actin assembly dynamics, actin filaments are severed constitutively by an essential regulatory protein, ADF/Cofilin. Therefore, Several studies were performed to examine the mechanical properties of F-actins. However, the fundamental mechanism that controls F-actin's response to deformation is not understood. In the present study, steered molecular dynamics (SMD) simulation approach has been utilized to understand actin filament mechanics. The work was performed in four computational sets of experiments, namely bending, compression, tension, and torsion simulations. Our findings demonstrate that F-actin's deformation response is regulated by the pattern of dissociation of conformational locks at intra-strand and inter-strand G-actin interfaces. F-actin elongation enabled salt bridge formation at the inter-strand interfaces improving the G-actin-G-actin bond strength. Furthermore,

we noticed an inter-strand serrated locking pattern connecting G-actin subunits, restricting their relative movement, thus enabling F-actin's ability to resist deformation. Additionally, we found ADF/Cofilin to cause structural transmutations in f-actin, thus altering their physical properties. The F-actin mechanics described here are vital for constructing a mechanobiological eukaryotic cell model that mimics cell mechanics with disease progression.

SB09.08.04

Directing Macromolecular Self-Assembly of Graphene Oxide and Silk Fibroin Towards Mesoscale Architectures Catherine Machnicki, Megan Fay, Eric DuBois and Ian Wong; Brown University, United States

Mesoporous, anisotropic architectures that integrate two-dimensional nanomaterials with protein-based polymers are highly promising as biologically-inspired functional materials. In particular, ice-templated freeze-casting offers a facile and economical process to create aligned, nacre-like architectures. Here, we investigated freeze-casting of biologically-inspired composites that incorporate graphene oxide (GO). Silk fibroin, a naturally-occurring polypeptide, forms crystalline β -sheets as a result of hydrogen bonding between repetitive subunits. However, in mesoporous structures, natural polymers like silk fibroin often exhibit limited chemical stability and mechanical strength. We hypothesized that silk fibroin could be reinforced by leveraging the inherent structural stiffness and surface functionalization of GO, a nanomaterial that would readily form hydrogen bonds between silk subunits. By studying the physical, chemical and mechanical properties, we were able to gain insight into the nature of self-assembly of this composite meso-structure.

Our work optimized the freeze-casting process by tuning the pH and freezing direction which resulted in aligned and porous microstructures. Next, we varied the ratio of GO to silk content by weight. We found alterations to the micro-porous structure, mechanical stiffness and uptake of both water and oil with the addition of GO. Moreover, with increasing amounts of GO, there is an increase of stability in water, ionic solutions and oil over relatively long periods of time. Using analytical techniques including FTIR-ATR, Raman, contact angle, compression and other mechanical tests, we were able to deduce structural information and interactions of GO with silk sub-units. Overall, these self-assembled mesoporous materials exhibit outstanding physicochemical properties for extreme mechanics, environmental remediation, and energy storage.

SB09.08.05

Modulating Nanoparticle Size to Understand Factors Affecting Hemostatic Efficacy and Maximize Survival in a Lethal Inferior Vena Cava Injury Model Celestine Hong^{1,1}, Osaid Alser², Anthony Gebran², Yanpu He^{1,1}, Wontae Joo¹, Nikolaos Kokoroskos², George Velmahos², Bradley Olsen¹ and Paula Hammond¹; ¹Massachusetts Institute of Technology, United States; ²Harvard Medical School, United States

Polymeric particle-based hemostats have been demonstrated to be an attractive technology to halt bleeding through extensive testing in animal models, ranging from arterial injury to blast trauma. While the results of these *in vivo* experiments have been well documented and utilized to develop subsequent generations of hemostats, the details of particle-target interactions *in vitro* and their predictive capabilities for *in vivo* performance has yet to be fully explored. In this work, the size of GRGDS-conjugated PEG-b-PLGA nanoparticles was tuned and its effect on platelet binding, particle adherence to wound-mimetic surfaces, aggregation capability, biodistribution, and circulation lifetime were systematically assessed using various *in vitro* and *in vivo* experiments. Smaller and intermediate-sized nanoparticles were all found to specifically bind a larger number of activated platelets when compared to larger (>250 nm) particles, while incubation of these larger particles on collagen and activated platelet-coated surfaces led to a higher total mass of polymer bound. Intermediate particle diameters led to the greatest number of platelets aggregated on a surface relative to agonist-only positive controls. Finally, larger particles experienced faster clearance and higher pulmonary accumulation per organ mass in an uninjured murine model, whereas smaller particles exhibited longer circulation and retention times and increased accumulation in the liver. To assess hemostatic efficacy, these three distinct sizes were challenged with a lethal inferior vena cava (IVC) puncture model. The intermediate nanoparticle size was observed to result in the most significant increase in survival over the course of two hours ($P = 0.0060$), as well as the greatest accumulation at the injury site relative to uninjured vessel controls. These results indicate that tuning particle size provides a key handle for engineering the performance of particle-based hemostat systems, and may influence its efficacy in treating various types of lethal internal hemorrhage.

SB09.08.07

Changes in the Magnetic Properties of Manganese (II) Carbonate Using a Bio-Inspired Route Arad Lang¹, Iryna Polishchuk¹, Ariel Maniv², Elad Caspi² and Boaz Pokroy¹; ¹Technion - Israel Institute of Technology, Israel; ²Nuclear Research Centre, Israel

The creation of inter-crystalline organic inclusions is one of Nature's strategies to enhance the mechanical properties of biominerals. As was shown synthetically for calcite, the most abundant marine biomineral, incorporated pinned organic species act as barriers for dislocations movement. Thus, they increase the hardness of the single-crystalline calcite host.

Inspired by this phenomenon, we showed in the past that a variety of semiconductors, both fully inorganic and hybrid organic-inorganic, are able to incorporate single amino acids. This incorporation induces a measurable increase in the optical band gap of the semiconducting host, which results from charge localization created by the incorporated amino acids.

Here, we decided to study the influence of amino acids incorporation on yet another set of properties, namely the magnetic properties of manganese (II) carbonate (MnCO_3). Similarly to the isostructural calcite, we discovered that certain amino acids can be incorporated into the crystalline structure of the host. Using high-resolution powder X-ray diffraction (HR-PXRD, using synchrotron source), we measured an anisotropic lattice expansion, of both a - and c -parameters, resulting from amino acids incorporation. These induced lattice distortions can be relaxed upon heating and organics decomposition. When we measured the magnetic properties of amino acid-incorporated MnCO_3 , we observed the predicted paramagnetic behavior, namely, a positive and linear relation between the magnetization, M , and the applied magnetic field, H . Nevertheless, the magnetic susceptibility (which was taken as the slope of the M - H curve), was observed to decrease with the increase of incorporated amino acids concentration. This decrease follows the simple rule of mixtures, indicating the creation of a MnCO_3 -amino acid composite.

MnCO_3 is known to possess a Néel temperature of about 32 K. At this temperature, it undergoes a magnetic phase transition, from a paramagnetic to a canted antiferromagnetic phase. When we repeated our M - H measurement at 2 K, we discovered the opposite trend: the increase in magnetic susceptibility upon the increasing amount of incorporated amino acid. Moreover, the Néel temperature itself decreases. During amino acids incorporation, the inter-atomic distances inside MnCO_3 increases. This results in a weakening of the magnetic interaction, which makes the MnCO_3 crystal more sensitive to external changes, such as the applied magnetic field and the changes in temperature.

SB09.08.08

Bioinspired Ion Conducting Membranes for Next-Generation Batteries Ahmet Emre, Emine S. Turali-Emre, Ji-Young Kim, Jinchen Fan, Volkan Cecen and Nicholas Kotov; University of Michigan, United States

Bioinspired ion transport membranes have been widely investigated for energy storage applications. The high theoretical specific energy density (2600Wh/kg) and high specific capacity (1675mA/g) along with the natural abundance and low toxicity of sulfur have been attracting significant attention for the development of an alternative battery system to replace traditional lithium-ion batteries which suffer from safety and capacity/energy density limitations in various applications. However, challenges such as polysulfide dissolution and shuttling prevent the mass commercialization of metal sulfur

batteries. Inspired by biological ion transport mechanisms, we show a practical yet comprehensive approach for the development of high-performance metal sulfur batteries. Aramid nanofiber (ANF) based composite ion transport membranes not only prevent dendrite formation but also confine polysulfides on the cathode side. ANF composite battery separators provide diverse and opposing properties including high mechanical properties, high ionic conductivity, and high thermal/chemical stability. The highly selective ion sieving properties of these biomimetic separators provide safe and high-performance batteries. Fabrication of such biocompatible, affordable, flexible, and high energy density battery is quite crucial in powering next-generation electronics including but not limited to portable, wearable, and implantable biomedical devices.

SB09.08.12

Late News: RNA Chemistry in Multiphase Complex Coacervates as Bioinspired Protocell Models [Saehyun Choi](#), Philip C. Bevilacqua and Christine D. Keating; The Pennsylvania State University, United States

Compartment systems encapsulating RNAs have gained significant interests as artificial cells and drug delivery systems. Cells form liquid membraneless organelles to localize and control RNAs' activities. Specifically, multiphase biomolecular condensates are appealing as material systems to have an impact on functional control of RNA and other biomolecular processes. However, the understanding of the relationship between RNA chemistry and multiphase biomolecular condensates is still lacking that limits the development of such RNA compartments for various applications. Therefore, inspired by these multiphase biomolecular condensates, we investigated complex coacervates composed of simple biomolecules, such as oligopeptides, and their impact on RNA partitioning and hybridization. Complex coacervates are organic-rich phases or droplets, formed by spontaneous liquid-liquid phase separation of mixed oppositely charged molecules. Complex coacervates share similarities to liquid biomolecular condensates in cells and have great encapsulation efficiency of RNAs. Here, we present that coacervates can have different levels of RNA partitioning and hybridization depending upon the length and identity of oligopeptides. We recently found that multiphase complex coacervate droplets can have different RNA partitioning and hybridization levels in each phase due to local differences in RNA-peptide interactions without specific RNA binding motifs. This study aids fundamental understanding of how biocondensates influence RNA localization and function, and points to design strategies for artificial cells construction using coacervate droplets.

SB09.08.13

Functional Active and Adaptive Janus Particles Templated from Responsive Complex Emulsions [Lukas Zeininger](#); Max Planck Institute of Colloids and Interfaces, Germany

Responsive materials capable to autonomously and reversibly adapt to their chemical environment hold great promise in the design of artificial chemo-intelligent life-like soft material platforms. In this context, we are using active complex emulsions, kinetically stabilized multiphase dispersions of fluids, as an intrinsically out-of-equilibrium material platform that can act as structural controlling elements for the generation of a variety of functional intricate, responsive and adaptive, precision objects. The dynamic multiphase emulsion droplets are formed from two or more immiscible fluids that are immiscible at room temperature but exhibit a lower (LCST) or upper critical solution temperature (UCST). Emulsification of the mixture below LCST or above UCST enables a simple one-step generation of complex multicomponent emulsions with highly uniform internal droplet morphologies. The internal droplet geometry of these dynamic liquid colloids is exclusively controlled by the force-balance of interfacial tensions acting at the individual interfaces, which allows altering the droplet geometries also after emulsification.

The complex emulsions can be hardened or gelled, e.g. by using photo-crosslinkable acrylate monomers as the constituent droplet phases. Upon polymerization, the shape of the droplet molds is essentially retained and a compartmentalization of designer surfactants, biologicals, polymer, and nanoparticle solutes enables their use as functional "cytoskeletons" for the generation of Janus particles with tunable shape, functionality and wettability profiles, functional thin-films as well as defined 3D objects and meso- and macroscale assemblies. In addition, as a result of the refractive index contrast of the individual phases, the particles can manipulate the pathway of light passing through these micro-scale colloids. Examples on how an associated understanding of the unique chemical-morphological-optical coupling inside these chemically functionalized active soft matter colloids give rise to a variety of new and improved application concepts, including in biomimicry, (photo-)catalysis, optical imaging platforms, as structural templates for the generation of precision objects, and as chemo-intelligent transducers in chemo- and biosensing applications will be presented.

SESSION SB09.09: Soft Biomaterials, Robots and Applications

Session Chair: Radwanul Siddique

Thursday Morning, December 2, 2021

Sheraton, 2nd Floor, Republic B

10:30 AM *SB09.09.01

Physical Hydrogels from Entropy-Driven Non-Covalent Interactions and Their Applications [Eric A. Appel](#); Stanford University, United States

Physically-crosslinked hydrogels exhibit highly useful properties that are impossible with traditional hydrogels but crucial for a wide variety of emerging applications in industry or biomedicine. Yet, these materials typically employ enthalpy-dominated crosslinking interactions that become more dynamic at elevated temperatures, leading to network softening. Indeed, standard mathematical frameworks typically assume network softening and faster dynamics at elevated temperatures. Yet, deriving a mathematical framework connecting the crosslinking thermodynamics to the temperature-dependent viscoelasticity of physical networks suggests the possibility for entropy-driven crosslinking interactions to provide alternative temperature dependencies. Herein, we will discuss the investigation of a physical hydrogel platform exploiting dynamic multivalent interactions between biopolymers and nanoparticles that are strongly entropically driven. We will discuss the implications of these crosslinking thermodynamics on the observed mechanical properties, demonstrating that tuning the thermodynamics and kinetics of these crosslinking interactions enable broad modulation of the mechanical properties of these materials, including their shear-dependent viscosities, temperature responsiveness, self-healing, and cargo encapsulation and controlled release. In particular, these materials exhibit viscous flow under shear stress (shear-thinning) and rapid recovery of mechanical properties when the applied stress is relaxed (self-healing), affording facile processing through direct injection or spraying approaches, making them well served for applications ranging from wildfire prevention to biomedicine. Overall, this talk will illustrate our recent efforts exploiting dynamic and multivalent interactions between polymers and nanoparticles to generate hydrogel materials exhibiting properties not previously observed in physical hydrogels and affording unique opportunities in industry and biomedicine.

11:00 AM SB09.09.02

Amphiphilic Copolymer Excipients to Enable an Ultrafast Monomeric Insulin Formulation and Ultrastable Insulin Formulation [Caitlin L. Maikawa](#), Joseph Mann and Eric A. Appel; Stanford University, United States

Insulin was first isolated a century ago, yet commercial formulations of insulin and its analogues for hormone replacement therapy falls short of mimicking the endogenous glycemic control that occurs in non-diabetic individuals. Insulin formulations that better mimic secretion from the beta-cells, by enabling more rapid insulin absorption kinetics and/or co-delivering complementary hormones (i.e. amylin), are needed to reduce patient burden and improve glucose management. However, formulation innovation is complicated by the poor stability of insulin monomers and amylin. We have developed a polymeric excipient platform using amphiphilic acrylamide copolymers that can be used to increase the stability of insulin in formulation. Here I will present on the use of these designer excipients, to develop an ultrafast monomeric insulin lispro and an ultra-stable insulin for improved global access.

A formulation of insulin monomers would more closely mimic endogenous postprandial insulin secretion, but monomeric insulin is unstable in solution using present formulation strategies and rapidly aggregates into amyloid fibrils. Amphiphilic acrylamide copolymer (AC/DC) excipients preferentially adsorb to the air-water interface and disrupt interfacial insulin-insulin aggregation events. Combining a AC/DC excipient with monomeric insulin lispro enables stable formulation under stressed-aging conditions for up to 25 hours compared to only 5 hours for commercial fast-acting insulin lispro formulations (Humalog). In a diabetic pig model, our ultrafast monomeric lispro formulation demonstrated unprecedented ultrafast absorption kinetics, exhibiting peak action at 9 minutes, whereas commercial Humalog exhibited peak action at 25 minutes. The more rapid onset and shorter duration of action observed in our monomeric lispro formulation has the potential to better control mealtime glucose excursions.

Moreover, the prevalence of diabetes is rising in middle and low-income countries. Current commercial insulin formulations require costly refrigerated transport and storage to prevent loss of insulin integrity. Our AC/DC excipients can be used as a simple additive to current standard commercial insulin formulations and demonstrated we can extend stability, while maintaining formulation integrity, bioactivity, pharmacokinetics and pharmacodynamics, for over 2 months in stressed aging conditions that cause current formulations to fail in under 2 days. These enhanced insulin formulations are promising candidates for improving glucose control and reducing burden for patients with diabetes.

11:15 AM SB09.09.03

Bioinspired Enzyme-Powered Nano/Nicromotors for Smart Healthcare Applications Hyunsik Choi, Jeeyoon Yi and Sei Kwang Hahn; Pohang University of Science and Technology, Korea (the Republic of)

Self-propelling micro- and nano-motors (MNMs) have been extensively investigated as an emerging oral drug delivery carrier for gastrointestinal (GI) tract diseases. However, the propulsion of current MNMs reported so far is mostly based on the redox reaction of metals (such as Zn and Mg) with severe propulsion gas generation, remaining non-degradable residue in the GI tract. Here, we develop a bioinspired enzyme-powered biopolymer micromotor mimicking the mucin penetrating behavior of *Helicobacter pylori* in the stomach. It converts urea to ammonia and the subsequent increase of pH induces local gel-sol transition of the mucin layer facilitating the penetration into the stomach tissue layer. The successful fabrication of micromotors is confirmed by high-resolution transmission electron microscopy, electron energy loss spectroscopy, dynamic light scattering analysis, zeta-potential analysis. In acidic condition, the immobilized urease could efficiently converted urea to ammonia, comparable with that of neutral condition because of the increase of surrounding pH during propulsion. After administration into the stomach, the micromotors show enhanced penetration and prolonged retention in the stomach for 24 h. Furthermore, histological analysis shows that the micromotors are cleared within 3 days without causing any toxicity in the GI tract. The enhanced penetration and retention of the micromotors as an active oral delivery carrier in the stomach would be successfully harnessed for the treatment of various GI tract diseases.

11:30 AM SB09.09.04

Microstructured Hydrogels via Phase Separation of Elastomeric Resilin-Like Polypeptides Sai Patkar, Cristobal Garcia and Kristi Kiick; University of Delaware, United States

Resilin-like polypeptides (RLPs), bioinspired protein-engineered polymers derived from the elastomeric insect protein resilin undergo phase separation upon cooling below their Upper Critical Solution Temperature (UCST), which can be precisely controlled by altering their amino acid composition. The native extracellular matrix (ECM) is characterized by structural and compositional heterogeneity across varying length scales. Current state-of-the-art soft matter patterning techniques for generating sophisticated ECM mimics are limited due to their reliance on expensive equipment and multiple time- and energy-intensive steps. Therefore, photocrosslinking distinct morphologies of multicomponent RLP solutions undergoing phase separation offers a relatively simple alternative for the fabrication of microstructured hydrogels. RLPs enriched in select aromatic and aliphatic residues were recombinantly produced in bacterial expression hosts and purified via immobilized metal affinity chromatography. Gel electrophoresis and mass spectrometry were used to confirm their composition and purity. The thermal response of distinct RLPs and their multicomponent solutions was investigated via turbidimetry. The RLPs reported in this study fall into two main categories based on their physicochemical properties. Molecules in the first category, defined as phase separating RLPs (psRLPs) demonstrate robust UCST-type behavior, and function as cell-friendly porogens/templating agents. Lysine residues along the polypeptide backbone of the molecules in the second category were modified to produce photocrosslinkable RLP-acrylamide (pcRLP-Ac), which upon UV irradiation in the presence of photoinitiator and psRLPs result in the formation of microporous hydrogels. Confocal microscopy data indicate that harnessing the interplay of inter- and intramolecular interactions between distinct psRLP and pcRLP-Ac molecules allows further control over pore size. The average pore size observed in hydrogels enriched in aliphatic residues was approximately 10 μm , an order of magnitude lower than the average pore size observed in hydrogels enriched in aromatic residues (ca. 100 μm). We report a simple biofabrication method to produce microstructured hydrogels for use as cell-instructive materials to support regenerative medicine applications.

11:45 AM SB09.09.05

High Water-Responsiveness of Peptidoglycan from Gram-Positive *Staphylococcus aureus* and *Saccharomyces cerevisiae* Haozhen Wang, Zhi-Lun Liu, Seungri Kim, Tai-De Li and Xi Chen; ASRC, CUNY, United States

In nature, plants use water-responsive (WR) materials that deform in response to humidity changes to drive their essential movements. Recent studies have shown that such kind of WR actuation could be extremely powerful and hold great potential to be used as actuating components for robotics, shape-morphing, and energy harvesting. Here, we present that peptidoglycan (PG) extracted from gram-positive bacteria *Saccharomyces cerevisiae* and *Staphylococcus aureus* show significant water-responsiveness such that their WR actuation energy density and efficiency reach 39.6 MJ m⁻³ and 38.4%, respectively, surpassing those of frequently used actuator materials. PG is the primary component of gram-positive bacterial cell walls, and it shows distinct architectures and molecular structures across different bacteria species. For example, peptidoglycan extracted from *Saccharomyces cerevisiae* (~2000 nm) is thicker than that from *Staphylococcus aureus* (~500 nm). Moreover, PG of *Staphylococcus aureus* have polysaccharides of alternating N-acetyl-glucosamine and N-acetyl-muramic acid crosslinked by peptide stems, whereas PG of *Saccharomyces cerevisiae* consists of two types of polysaccharides: β -1,3 and β -1,6 linked glucose and β -1,4 linked NAG. Meanwhile, *Saccharomyces cerevisiae* PG is not crosslinked by peptide stems but by the alkali-sensitive bond to mannoproteins or disulfide link to the PIR protein. By using a liquid AFM, we also showed that these PG consist of nanoscale pores with different porosities, pore sizes, and geometries. Using a customized AFM, we characterized WR strain and energy density of *Staphylococcus aureus* PG and *Saccharomyces cerevisiae* PG, and found that *Staphylococcus aureus* PG, with a lower WR strain (11.2 %), exhibits a much higher WR energy density (39.6 MJ m⁻³) than that of *Saccharomyces cerevisiae* PG (6.0 MJ m⁻³). By introducing pressure disturbance on PG's

surface using the AFM, we also measured these two PGs' relaxation dynamics, and found that *Staphylococcus aureus* PG's higher WR energy density strongly correlates to its super viscous nanoconfined water. Our findings suggest that highly viscous confined water resulted from nanoporous *Staphylococcus aureus* PG' plays an important role in the energy conversion from water's chemical potential to PG's mechanical deformations, which could be serving as general criteria for high-efficiency WR structures.

SESSION SB09.10: Wetting Properties and Application of Biological and Bioinspired Materials

Session Chair: Radwanul Siddique
Thursday Afternoon, December 2, 2021
Sheraton, 2nd Floor, Republic B

2:00 PM SB09.10.02

Bioinspired Self-Cleaning Broadband Antireflection Coatings Peng Jiang; University of Florida, United States

Millions of years before people began to generate functional nanostructures, biological systems were using nanometer-scale architectures to produce unique functionalities. Some nocturnal moths use hexagonal arrays of subwavelength nipples as antireflection coatings to reduce reflection from their compound eyes. Similar periodic arrays of nanopillars have also been observed on the wings of cicada to render superhydrophobic surfaces for self-cleaning functionality. Inspired by these natural nanostructures, we have developed various bottom-up nanofabrication technologies for producing wafer-scale, self-cleaning, broadband antireflection coatings on a large variety of technologically important optical substrates, such as crystalline silicon, GaAs, polymer, and glass. These techniques combine the simplicity and cost benefits of bottom-up self-assembly with the scalability and compatibility of standard top-down microfabrication. The resulting subwavelength-structured antireflection coatings can greatly suppress light reflection, promising for a spectrum of applications ranging from highly efficient photovoltaics and light emitting diodes to smart optical devices. By integrating this biomimetic design with smart shape memory polymers, we have demonstrated tunable antireflection coatings with multi-stimuli-responsive optical properties.

2:15 PM SB09.10.03

Bioinspired Translation of Classical Music into *de novo* Protein Structures Markus J. Buehler, Mario Milazzo and Grace I. Anderson; Massachusetts Institute of Technology, United States

Architected biomaterials, as well as sound and music, are constructed from small building blocks that are assembled across time- and length-scales. Here we present a novel deep learning-enabled integrated algorithmic workflow to merge the two concepts for radical discovery of *de novo* protein materials, exploiting musical creativity as the foundation, and extrapolating through a recursive method to increase protein complexity by successively injecting protein chemistry into the process. Indeed, music is able to overcome differences among people and nations, creating bridges between cultures, and to find associations between seemingly unrelated concepts, and can form a novel way to generate bio-inspired designs that derive functions from the imaginations of the creative mind. Earlier work (Buehler et al., ACS Nano, 2019) has offered a pathway to concert proteins into sound, and sound into proteins. Here we build on this paradigm and translate a piece of classical music into matter. Based on a systematic analysis of different pieces including J.S. Bach's Goldberg variations and Leonard Bernstein's Chichester Psalms, we offer a series of case studies to convert the musical data imagined by the composer into protein design, and folded into a 3D structure using deep learning. The quest we seek to address is to identify semblances, or deep-time memories, or information content in such musical creation, that offers new insights into pattern relationships between distinct manifestations of information. The resulting protein forms the basis for iterative musical composition, and an evolutionary paradigm that defines a variational pathway for melodic development, complementing conventional creative or mathematical methods. This paper broadens the concept of what is understood as bio-inspiration to include a broad array of signals and designs created by humans, animals, or complex physical mechanisms.

2:30 PM SB09.10.04

Wafer-Scale Heterostructured Piezoelectric Bio-Organic Thin Films Jun Li; University of Wisconsin--Madison, United States

Piezoelectric biomaterials are intrinsically suitable for coupling mechanical and electrical energy in biological systems to achieve in vivo real-time sensing, actuation, and electricity generation. However, the inability to synthesize and align the piezoelectric phase on a large scale remains a roadblock toward practical applications. We present a wafer-scale approach to creating piezoelectric biomaterial thin films based on γ glycine crystals. The thin film had a sandwich structure, where a crystalline glycine layer self-assembles and automatically aligns between two polyvinyl alcohol (PVA) thin films. The heterostructured glycine-PVA films exhibited piezoelectric coefficients of 5.3 pC/N or 157.5×10^{-3} Vm/N, and nearly an order of magnitude enhancement of the mechanical flexibility compared to pure glycine crystals. With its natural compatibility and degradability in physiological environments, glycine-PVA film may enable the development of transient implantable electromechanical devices

2:45 PM SB09.10.05

A Wearable UV Sensor Based on Unique Features of a Natural Biochrome Daniel Wilson and Leila Deravi; Northeastern University Chemistry & Chemical Biology, United States

The optical properties of the primary pigment that facilitates rapid and precise appearance changes in cephalopods, xanthommatin, have been evaluated for a variety of applications including electrochromic displays and photoprotective films. However, the fundamental mechanisms underlying the optical performance of xanthommatin upon irradiation with solar light remain incompletely characterized. We investigated irradiation-induced color changes of xanthommatin that could be controlled by manipulating the pH of the surrounding environment. Photoreduction of the pigment in acidic conditions was enhanced by incorporating additional ultraviolet (UV)-responsive materials (e.g., disulfides) to generate redox agents upon irradiation. We leveraged these dose-dependent optical changes to create colorimetric UV light sensors, which can be incorporated into a user-friendly microfluidic architecture that can be worn or surface-mounted. These devices provide radiation-driven responses that may be useful for personal solar monitoring, tracking exposure of perishable goods, or verifying UV dose thresholds for germicidal sterilization.

3:00 PM SB09.10.06

Late News: Self-Organized Mycelium Nanocomposites for Sustainable Buildings—From Bioprocessing to Structure and Mechanical Properties Precious O. Etinosa¹, Ali Salifu^{1,1}, Salifu Tahiru Azeko² and Winston W. Soboyejo^{1,1,3}; ¹Worcester Polytechnic Institute, United States; ²Tamale Technical University, Ghana; ³African University of Science and Technology, Nigeria

This work presents the results of a combined experimental and analytical study of the mechanical properties of bioprocessed mycelium nanocomposites

that are reinforced with self-organized cellulosic fibers. The bioprocessed mycelium nanocomposite blocks were composed of cellulose/hemicellulose hemp-duct with varying laterite percentage compositions. The mycelium functions as a supportive matrix holding the reinforcing hemp-duct particles within its filamentous structural network. In-situ studies of the mechanical properties of the composites were conducted to determine the hardness, compression/flexural properties, and fracture toughness/resistance-curve behaviors. For supportive evidence and to gain further insight into the failure mechanism, the microstructure and strain mapping of the resulting composites at relevant stages of compression was characterized using SEM and DIC, respectively. The observed deformation and fracture mechanisms are then used to provide insights for the prediction of the composite strength and resistance-curve behavior. The implications of the results are discussed for the bioprocessing of mycelium-nanocomposite for sustainable building materials.

SESSION SB09.11: Bioinspired Materials I
Session Chairs: Guillaume Gomard and Silvia Vignolini
Tuesday Morning, December 7, 2021
SB09-Virtual

8:00 AM *SB09.11.01

Bioinspired Fabrication of Strong and Tough Hydrogels Esther Amstad; Ecole Polytechnique Federale de Lausanne, Switzerland

Nature produces soft materials possessing exceptional mechanical properties. These properties are to a large extent related to the well-defined structures and locally varying compositions of these natural materials. Key to the excellent control nature possesses over the structure and local composition of its materials is their fabrication: Many of these materials are formed from compartmentalized reagents that are transported to the desired locations where they are released locally. Inspired by nature, we use emulsion drops as compartments to build macroscopic granular hydrogels. In this talk, I will demonstrate how we convert individually dispersed emulsion drops into selectively permeable viscoelastic capsules that enable controlled localized release of reagents. These capsules are most frequently employed as individually dispersed delivery vehicles. In the second part of this talk, I will demonstrate how we go a step beyond the current use of capsules by converting them into inks that can be 3D printed into strong and tough double network granular hydrogels.

8:30 AM SB09.11.02

Multi-Scale Characterisation of the Load-Bearing Shells of the Brachiopod *Disciniscia Tenuis* Johannes Ihli¹, Anna Schenk², Sabine Rosenfeldt², Klaus Wakonig¹, Mirko Holler¹, Giuseppe Falini³, Eugenia Delacou⁴, Jim Buckman⁵, Thomas Kress⁶, Esther Tsai⁷, David Reid⁶, Melinda Duer⁶, Maggie Cusack⁸ and Fabio Nudelman⁴; ¹Paul Scherrer Institute, Switzerland; ²Universität Bayreuth, Germany; ³Università di Bologna, Italy; ⁴University of Edinburgh, United Kingdom; ⁵Heriot-Watt University, United Kingdom; ⁶University of Cambridge, United Kingdom; ⁷Brookhaven National Laboratory, United States; ⁸University of Stirling, United Kingdom

Biominerals are a class of inorganic-organic composite materials that exhibit function-optimized properties. These properties arise from a hierarchical organization of primary building blocks. While some biomineral producing organisms can alter these properties in response to environmental stresses, this generally involves a time-intensive process of resorption and reprecipitation. In this presentation, we show that the load-bearing shells of the brachiopod *Disciniscia tenuis* can dynamically modulate their mechanical properties in response to environmental changes. They gradually transition from hard and stiff to fully malleable as a function of water content in the environment/ their structure. Using a combination of Cryo ptychographic X-ray computed tomography, electron microscopy, spectroscopy, in-situ wide-angle X-ray scattering and mechanical testing, we describe the hierarchical structure and composition of these shells to reveal the structural motifs and deformation mechanism that endow the shells with this adaptability.

8:45 AM SB09.11.03

From Nature to Applications—Self Healing and Breathable Multilayer Composit Materials Thorsten Neumann; Continental SSL / Benecke Kaliko AG, Germany

Continental is widely known as the tire company. However, the company has a wide product range for multiple applications in the automotive industry as well as beyond.

Contitech Business Unit Surface Solutions specializes in innovative and functional films and multilayer textile laminates which are applied in the automotive industry, transportation, and many other business fields e.g. cruise ships, stadiums, and hotels.

In this presentation we describe smart and functional materials that exhibit self-healing properties and breathability for seating applications in the field of artificial leather materials. These materials must fulfill a wide range of specific tests, ranging from flame retardant behavior, stain-, flexibility- and abrasion- resistance as well as decent haptic touch and environmental impact resistance. The breathable material is made by several layers and pores that are generated in situ, allowing the penetration of air and humidity. Furthermore, the hybrid approach of soft PVC and polyurethane allows the free passage of water vapor through the material depending on the relative humidity level. This technology may allow a reduction of energy use (for example by reducing the need for air conditioning), especially in seating applications. Use of upcycling raw materials such as used coffee grounds reduce the CO₂ footprint of the material.

The second topic of self-healing materials is an in situ generated polyurethane system based on a solid phase reaction of a diamine. A chemically controlled reaction allows production of a defined polymer chain length range, which leads to a self-healing coated fabric. Material cuts heal within minutes by the adhesion of small fast migration molecules which tend to concentrate on the surface of the cut material, leading to an initial adhesion similar to the healing process of human skin. Longer chain polymers migrate and stabilize the cut to its full strength. Mechanical tests show no reduction of performance of the healed materials.

9:00 AM SB09.11.04

When and How Self-Cleaning of Superhydrophobic Surfaces Works Doris Vollmer, Florian Geyer, Rüdiger Berger and Hans-Jürgen Butt; Max Planck Institute for Polymer Research, Germany

Self-cleaning is the most prominent feature of superhydrophobic surfaces [1]. Macroscopic contamination such as dust is indeed easily cleaned away by water drops rolling across the superhydrophobic surface. A lot of research went into exploring different strategies to achieve long-lasting and highly liquid-repellent surfaces [2]. Despite the enormous interest in superhydrophobicity, it is still unclear when microscopic and in particular nanoscopic contamination (soot, aerosols, etc.) influences superhydrophobicity and how self-cleaning works in detail.

To gain an in-depth insight into self-cleaning, we monitored self-cleaning at the micron scale using laser scanning confocal microscopy [3]. Aiming to correlate self-cleaning, surface topography and particle size and hydrophilicity, we contaminated different surfaces with particles varying four orders of magnitude and having different polarities. When the drop is moved over the contaminated surface, individual particles were picked up at the advancing edge. Upon further movement of the drop, these particles accumulated at the lower air-water interface of the drop. To design superhydrophobic surfaces that are resistant to hydrophobic as well as hydrophilic particle contamination, the pore size of the superhydrophobic surface needs to be smaller than the contamination particle size. Even smaller nanoscopic contaminants do not necessarily degrade superhydrophobicity.

While the ability to withstand various kinds of contamination is essential, the ease of self-cleaning is equally crucial. To remove particles from a superhydrophobic surface, the capillary force acting on the particle at the rear side of the drop needs to overcome the adhesion force between the particle and the surface. We quantified the forces involved in the self-cleaning process and compared the experimental results with quantitative calculations.

To compare the results based on model contamination to real-world outdoor exposure, we fixed several coated fabrics on a car. These fabrics repelled water and organic liquids and were chosen because of their robustness. They were obtained by coating polyester fabrics silicone filaments. These superhydrophobic surfaces having a nanoscale pore size surfaces are capable of resisting long-term real-world exposure and industrial contamination tests.

[1] Barthlott, W. & Neinhuis, C.: Purity of the sacred lotus, or escape from contamination in biological surfaces. *Planta* **202**, 1–8 (1997).

[2] Bhushan, B. & Jung, Y.C.: Natural and biomimetic artificial surfaces for superhydrophobicity, self-cleaning, low adhesion, and drag reduction. *Prog. Mater. Sci.* **56**, 1–108 (2011).

[3] Geyer F., D'Acunzi M., Sharifi-Aghili A., Saal A., Gao N., Kaltbeitzel A., Slood T.F., Berger R., Butt H.J. & Vollmer D.: When and how self-cleaning of superhydrophobic surfaces works, *Science Adv.*, **2020**, 6: eaaw9727

9:15 AM SB09.11.05

Focusing and Camouflage Mirrors in the Eyes of Decapod Crustaceans Qiang Wen; Ben-Gurion University of the Negev, Israel

Many aquatic animals use reflective optics in their eyes. The nature of the reflective materials underlying these systems is often unknown. A fascinating example is the reflecting superposition compound eye of decapod crustaceans. This eye contains a distal mirror which focusses light across onto the retina and a photon-enhancing tapetum reflector. Previous reports¹ suggested that both the tapetum and distal mirror were formed from high refractive index crystals of isoxanthopterin. We present a comparative study of reflecting optics in the eyes of several decapods to reveal that: (i) the distal mirror is formed from xanthopterin crystals, not isoxanthopterin and (ii) many species contain a third reflector – the 'reflective cap' which underlies the cornea and which appears to function as a camouflage device. Cryo-SEM, TEM in-situ X-ray diffraction studies showed that the distal mirror in the eyes of decapods is formed from polycrystalline rods of xanthopterin crystals. These rods are aligned in a 3-tiered multilayer reflector surrounding the distal portion of the ommatidia. The mirror boosts the reflection of off-axis light at the walls of the ommatidia, enhancing the amount of light of focused on the retina. In several species a third reflector – the reflecting cap resides immediately above the distal mirror. The reflective cap is formed from a dense array of crystalline isoxanthopterin nano-spheres identical to those found in the tapetum². Optical ray-tracing and comparative anatomy of decapods from diverse habitats shows that the reflecting cap is a camouflage device, which deflects light away from the underlying conspicuous screening pigments.

9:30 AM *SB09.11.06

Structural Colour from Plant Waxes Rox Middleton, Sverre A. Tunstad and Heather Whitney; University of Bristol, United Kingdom

Structural colour is a widespread phenomenon in nature, especially well-known in its production of brilliant high intensity hues in insects and feather. More recent developments have demonstrated the sometimes more subtle effects of structural colour in plants, for example fruits [1], leaves [2] and flowers [3]. Epicuticular waxes are well known for their striking hydrophobic qualities [4], and many other potential functions across plant organs. We discuss a previously unreported phenomenon of coloration from natural epicuticular wax crystal surface coatings. Widespread in nature, these offer a new self-assembled avenue to alternative coloration for artificial application without dye molecules. We report on the chemical and mechanical composition of these materials, and their in vitro recrystallisation for use as colorants.

[1] R. Middleton, M. Sinnott-Armstrong, Y. Ogawa, G. Jacucci, E. Moyroud, P. Rudall, P.J. Prychid, M. Conejero, B.J. Glover, M.J. Donoghue, S. Vignolini, *Current Biology*, 2020 *Viburnum tinus* Fruits Use Lipids to Produce Metallic Blue Structural Color

[2] M. Jacobs, M. Lopez-García, O. Phrathep, T. Lawson, R. Oulton, & H. Whitney, H. *Nature Plants*, 2016. Photonic crystal structure of *Begonia* chloroplasts enhances photosynthetic efficiency

[3] E. Moyroud, T. Wenzel, R. Middleton, P.J. Rudall, H. Banks, A. Reed, G. Mellers, P. Killoran, M.M. Westwood, U. Steiner, S. Vignolini, & B.J. Glover, B. J. *Nature*, 2017. 550(7677), 469–474. Disorder in convergent floral nanostructures enhances signalling to bees

[4] K. Koch & W. Barthlott, W. *Natural Product Communications*, 2006 Plant Epicuticular Waxes: Chemistry, Form, Self-Assembly and Function.

SESSION SB09.12: Bioinspired Materials II
Session Chairs: Guillaume Gomard and Silvia Vignolini
Tuesday Morning, December 7, 2021
SB09-Virtual

10:30 AM *SB09.12.01

Control over Chitin Fiber Orientation in the Insect Cuticle Yael Politi¹, Luca Bertinetti¹, Peter Fratzl², Jan-Henning Dirks³ and Bernard Moussian⁴; ¹Technische Universität Dresden, Germany; ²Max Planck Institute of Colloids and Interfaces, Germany; ³Hochschule Bremen, Germany; ⁴Eberhard-Karls Universität Tübingen, Germany

The orientation of fibers in the arthropod cuticle, made of chitin and proteins, strongly affects its physical properties, which in turn determines morphogenesis and functionality. Fiber orientation therefore needs to be spatially and temporally controlled by the animal. The arthropod cuticle is often described as liquid crystal (LC) analogues as it exhibits structural similarity to LC but are solid in its functional state. Using focused ion beam/scanning electron microscopy (FIB/SEM) volume imaging and scanning X-ray scattering, we show that the epidermal cells depositing the cuticle, determine an initial fiber orientation, from which the final architecture emerges by the self-organized co-assembly of chitin and proteins. Fiber orientation in the locust cuticle is therefore determined by both active and passive processes.

11:00 AM SB09.12.02

Spatiotemporal Control of Melanin Synthesis in Liquid Droplets [Ayala Lampel](#); Tel Aviv University, Israel

Melanins are natural biopolymers that have remarkable properties including UV-protection, coloration and antioxidant activity. Their biosynthesis is regulated both spatially and temporally and involves supramolecular templating and compartmentalization of enzymes and reactants within specialized organelles called melanosomes. In contrast, the laboratory-based bulk synthesis of melanin by tyrosine or dopamine oxidation is a poorly controlled process, resulting in materials with undefined properties. Inspired by the pigment's biosynthesis, we developed a methodology to spatiotemporally regulate melanin formation in liquid droplets. The spatial control is achieved by sequestration of the reaction in dextran-rich droplets of a polyethylene glycol/dextran aqueous two-phase system, where the use of a photocleavable protected tyrosine provides a temporal control over its enzymatic oxidation-polymerization. This methodology opens tremendous opportunities for applications in skincare and biomedicine.

11:15 AM SB09.12.03

Extracting Meaningful Structural Information on the Nanometer Scale from Highly Hydrated Materials [Irene U. Wacker](#)¹, Ernest R. Curticean², Willi Wagner², Christine Arndt¹, Christine Selhuber-Unkel¹, Steven J. Mentzer³ and Rasmus R. Schröder^{2,1}; ¹Universität Heidelberg, Germany; ²University Hospital Heidelberg, Germany; ³Brigham & Women's Hospital, Harvard Medical School, United States

Ultrastructural analysis of morphological features of highly hydrated biomaterials is still a difficult task. In structural biology, specifically protein structure determination, cryo-preparation and cryo-imaging have led to a "resolution revolution" [1]. While vitrification – the embedding in amorphous ice – is routinely achievable for concentrated protein solutions, the situation is different for carbohydrates or bio-inspired hydrogels. Their water content can be so high that conventionally used freezing methods – e.g. "flash freezing" followed by lyophilization – may not provide accurate ultrastructural features such as the exact size of pores [2]. For alginate hydrogels the effects on matrix morphology of different freezing techniques - including high-pressure freezing, the gold standard for cellular material – were analyzed in detail using cryo-SEM [3]. Pore sizes varied by two orders of magnitude from micropores in the range of tens of nanometers to macropores in the micrometer range, depending on the freezing method used. Although high pressure freezing was found in this study to be the most suitable freezing method it cannot be applied to large or more complex systems, because sample size is limited to roughly 2x2x0.2 mm. Analyzing e.g. the interaction of a pectin-based pleural sealant with the outer surface of the mammalian lung [4] is not possible with this approach.

Another important aspect when imaging low atomic number Z materials in an electron microscope is the lack of contrast – conventionally this is solved by "staining" materials with high Z metal (Ru, Os, U) compounds. For carbohydrates and many hydrogel materials without reactive groups this procedure is not straightforward.

Due to these numerous limitations and the need for rather sophisticated machinery for cryo-preparation and cryo-imaging we were looking for alternative, more easily accessible methods.

One approach, which has been used in the early days of cryo-preparation, is the replacement of freely diffusible water in a sample by a number of reagents, which either directly dehydrate the sample in a gentle way or help prevent formation of ice-crystals during a sub-optimal freezing regime. We tested partial dehydration with ethanol or tannic acid, and infiltration with trehalose to reduce the amount of free water, which would otherwise be available for crystallization. In combination with osmium tetroxide alone or together with ruthenium red we were able to introduce sufficient contrast to image bulk samples or thin sections from resin-embedded hydrated carbohydrates in an SEM at highest resolution.

For biomaterial films fabricated with pectins from different plant sources we could demonstrate different morphologies – from a more globular aspect for potato pectin to a highly branched network of interconnected carbohydrate chains for lemon and orange pectin. Controlling the degree of dehydration during the initial preparation step allowed us to visualize carbohydrate networks with different pore sizes.

We are currently investigating how to apply our preparation protocols to a number of different hydrogel classes with different pores sizes and validating the effects of the different reagents used on water content and morphology.

[1] Kühlbrandt W. (2014) The Resolution Revolution. *Science* 343, 1443; DOI: 10.1126/science.1251652

[2] Kaberova Z. et al. (2020) Microscopic Structure of Swollen Hydrogels by Scanning Electron and Light Microscopies: Artifacts and Reality. *Polymers* 2020, 12, 578; <https://doi.org/10.3390/polym12030578>

[3] Aston R. et al. (2016) Evaluation of the impact of freezing preparation techniques on the characterisation of alginate hydrogels by cryo-SEM. *European Polymer Journal*, 82, <https://doi.org/10.1016/j.eurpolymj.2016.06.025>

[4] Servais A.B. et al. (2018) Functional Mechanics of a Pectin-Based Pleural Sealant after Lung Injury. *Tissue Eng Part A* 24, 199; DOI: 10.1089/ten.tea.2017.0299

11:30 AM SB09.12.04

Bioinspired Multifunctional Glass Surfaces Through Regenerative Secondary Mask Lithography [Martyna Michalska](#), Sophia K. Laney, Tao Li, Mark Portnoi, Nicola Mordan, Elaine Allan, Manish K. Tiwari, Ivan P. Parkin and Ioannis Papakonstantinou; University College London, United Kingdom

Nature-inspired nanopatterning offers exciting multifunctionality spanning antireflectance and the ability to repel water/fog, oils, and bacteria; strongly dependent upon nanofeature size and morphology [1,2]. Broadly, this multifunctionality is inherent to and bridged by the nanocone structure, yet such patterning in glass (SiO₂) – a material of great practical importance – remains a bottleneck due to its high chemical stability alongside structuring at the nanoscale itself, which becomes increasingly challenging to manage as the pattern resolution advances (pitch <100 nm).

Here, we demonstrate a novel Regenerative Secondary Mask Lithography process which enables customized glass nanopillars through dynamic nanoscale tunability of the side-wall profile and aspect ratio (>7). Our method is facile and versatile, comprising just two steps. Firstly, we generate sub-wavelength scalable soft etch-masks (55-350 nm) through an example of block copolymer micelles or nanoimprinted photoresist. Secondly, we overcome their inherent durability problem – typically addressed by metal/metal oxide incorporation which adds time and complexity – through our innovative cyclic etching. During this etching, the original mask becomes embedded within a protective secondary organic mask, which is tuned and regenerated, permitting dynamic nanofeature profiling with etching selectivity >1:32.

We envision that such structuring in glass will facilitate fundamental studies and be useful for myriad of practical applications – from displays to architectural windows. Providing the highly-tunable nature of our method (size/shape/pitch), we tailor glass features and present excellent broadband omnidirectional antireflectivity, self-cleaning, and unique antibacterial activity towards *Staphylococcus aureus*.

[1] D. P. Linklater, V. A. Baulin, S. Juodkazis, R. J. Crawford, P. Stoodley and E. P. Ivanova, *Nat. Rev. Microbiol.*, 2021, **19**, 8–22.

[2] P. Lecointre, S. Laney, M. Michalska, T. Li, A. Tanguy, I. Papakonstantinou and D. Quéré, *Nat. Commun.*, 2021, **12**, 3458.

11:45 AM SB09.12.05

Droplet Dynamics on Asymmetric Wettability Patterns on Superbiphilic Surfaces [David Feldmann](#) and Bat-El Pinchasik; Tel Aviv University, Israel

A little beetle (*Stenocara Gracilipes*) living in the desert collects water from early morning mist. Nature has equipped its back with a biphilic wettability pattern: small hydrophilic patches embedded into a hydrophobic matrix made of wax. Since the discovery of this wettability pattern, extensive research was conducted to analyze and create biphilic surfaces for various purposes such as boiling heat transfer, and freezing or defreezing, and water collection from air. Hydrophilic surfaces favor nucleation, whereas hydrophobic surfaces favor water transport. The role of surface design is not well elaborated. In most cases, the patches are randomly or circularly shaped. We investigate the effect of patch asymmetry, size, distribution, and surface direction on droplet growth and droplet transport. To achieve efficient water collection, asymmetric patches can induce directional transport in capillary regime, and thus, fast water removal from the surface. Nucleation favors droplet growth in hydrophilic patches, however, for roll-off droplets need to overcome strong adhesion forces due to hysteresis hindering water removal. The influence of area fraction, distribution, and size of asymmetric patches on growth dynamics such as coalescence and droplet motion has been studied. We developed superbiphilic surfaces with isosceles triangular patches with a varying length to width ratio (l/w) from 2.0 to 10 and sizes between $l = 200$ microns and 4 mm. Droplets grow favorably in patches with accumulation on the base of the triangle. Experiments have been conducted in a controlled environment (T, RH) under a tilting angle ($0^\circ - 90^\circ$). A top-down camera records details about droplet distribution and area coverage. A quantitative image analysis reveals droplet dynamics, in which we identify various phases of droplet growth until roll-off. Adhesion forces have been determined depending on the direction of the triangles.

12:00 PM *SB09.12.06

Biomimetic Nano- and Microstructured Polymeric Surfaces Hendrik Hölscher; Karlsruhe Institute of Technology, Germany

Many nano- and microstructured surfaces found in nature can serve as an inspiration for improving technical applications. Although most biomimetic archetypes can be replicated with advanced techniques on a lab-scale, it remains a challenge to develop processes for large-scale fabrication techniques appropriate for commercial applications. Here, I review recent approaches with high potential for up-scaling.

The super-hydrophobic surfaces of water ferns like *Salvinia* and *Pistia* can be mimicked with nanofur, a dense fur of nanoscale hair hot pulled from polymer surfaces. This fractal surface is super-hydrophobic and oleophilic at the same time. With these properties it is the perfect material to separate oil and water and to clean up oil spills [1, 2].

White beetles of the genus *Cyphochilus* are well-known for their scales producing a nearly perfect whiteness in a very efficient way with an astonishing low amount of material. Inspired by this biological architecture, we developed two techniques allowing for the fabrication of ultra-thin, yet highly scattering, white polymer films [3,4]. Both approaches can be utilized for various applications ranging from extremely white but ultra-thin coatings to scattering particles as potential replacements for titanium dioxide.

Many snakes feature nano-scale fibril structures on their scales which are only some 10 nm high and feature a periodicity of some μm . Although they cannot be observed in the visible range and the surfaces appear smooth, these nano-steps cause significant anisotropic frictional properties which are helpful for the locomotion of snakes. These nano-step structures can be copied to artificial polymeric surfaces which can be utilized for the self-cleaning of photo-voltaic modules.

[1] C. Zeiger, I. C. Rodrigues da Silva, M. Mail, M. N. Kavalenka, W. Barthlott, H. Hölscher, *Microstructures of superhydrophobic plant leaves - inspiration for efficient oil spill cleanup materials*, *Bioinspir. Biomim.* **11**, 056003 (2016)

[2] M. N. Kavalenka, F. Vüllers, J. Kumberg, C. Zeiger, V. Trouillet, S. Stein, T. T. Ava, C. Li, Matthias Worgull, *Adaptable bioinspired special wetting surface for multifunctional oil/water separation*, *Sci. Rep.* **7**, 39970 (2017)

[3] J. Syurik, R. H. Siddique, A. Dollmann, G. Gomard, M. Schneider, M. Worgull, G. Wiegand, H. Hölscher. *Bio-inspired, large scale, highly scattering films for nanoparticle-alternative white surfaces*, *Sci. Rep.* **7**, 46637 (2017).

[4] J. Syurik, G. Jacucci, O. D. Onelli, H. Hölscher, S. Vignolini. *Bio-inspired Highly Scattering Networks via Polymer Phase Separation*, *Adv. Funct. Mater.* **28**, 1706901 (2018).

[5] W. Wu, M. Guttman, M. Schneider, R. Thelen, M. Worgull, G. Gomard, H. Hölscher, *Snake-Inspired, Nano-Stepped Surface with Tunable Frictional Anisotropy Made from a Shape-Memory Polymer for Unidirectional Transport of Microparticles*, *Adv. Funct. Mater.* 2009611 (2021)

SESSION SB09.13: Bioinspired Materials III
Session Chairs: Guillaume Gomard and Mathias Kolle
Tuesday Afternoon, December 7, 2021
SB09-Virtual

1:00 PM SB09.13.01

Bioinspired Synthesis of Thermally Stable and Mechanically Strong Nanocomposite Coatings Guangping Xu, Hongyou Fan, Chad A. McCoy, Melissa M. Mills, Jens Schwarz, Tuan A. Ho and Justin Rosenthal; Sandia National Laboratories, United States

The demand for materials with strong thermal and mechanical properties that can withstand harsh environments, such as pulsed power facilities, magnetic fusion reactors and space environments, is rapidly increasing. The ideal materials need to survive a range of individual and combined threats such as mechanical, shock, and x-ray insults. However, such materials are presently not available.

An innovative biomimetic method has been developed to synthesize layered nanocomposite coatings using silica and sugar-derived carbon to mimic the formation of natural seashell structure. The layered nanocomposites are fabricated through alternate coatings of condensed silicate and sugar. Sugar-derived carbon is a cost-effective material due to sugar being abundantly available, making it a relatively inexpensive chemical, as well as environmentally friendly. Pyrolysis of sugar will form polycyclic aromatic carbon sheets, i.e., carbon black.

Each layer is thermally pretreated at $\sim 200^\circ\text{C}$ for 3-5 minutes in order to solidify the composite before coating the next layer. The final nanocomposite coatings are then thermally treated at temperatures higher than 800°C which converts the sugar into carbon black and condenses silicate to form a silica network through cross-linking of carbon with silica. Infrared spectra show chemical crosslinking of Si-O with carbon ring and Si- with carbon ring. Chemical crosslinking between silica and carbon contributes to the enhanced mechanical properties, and thermal pretreatment plays the important role in solidification of the composite coatings while initiating crosslinking. Without this step, the hardness and modulus of the nanocomposite is not enhanced. Molecular dynamics models, incorporating the crosslinking between silica and carbon layers, are conducted to simulate the interfacial bonding energy and shear strength.

The resulting final nanocomposite coatings can survive temperatures of more than 1150°C and potentially up to 1700°C . These coatings have strong mechanical properties, with hardness of more than 23 GPa, elastic modulus of 240 GPa, and yield stress of more than 20 GPa, which are 62 – 94% greater than those of pure silica. The layered coatings have more than 80% transmission for $>10\text{keV}$ x-rays and have many applications besides use in pulsed power facilities, such as shielding in the form of mechanical barriers, body armors, and space debris shields.

SNL is managed and operated by NTESS under DOE NNSA contract DE-NA0003525

1:15 PM SB09.13.02

Coupled Oscillatory Motion of Photothermal Particles Driven by Marangoni Forces [Hyunki Kim](#)^{1,2}, Subramanian Sundaram^{3,4}, Todd Emrick¹ and Ryan Hayward⁵; ¹University of Massachusetts Amherst, United States; ²3M, United States; ³Boston University, United States; ⁴Harvard University, United States; ⁵University of Colorado Boulder, United States

Coupled motions are frequently observed in living systems, such as oscillatory gait patterns of terrestrial animals, flocking behaviors of birds, and oscillatory motion of bacterial flagella. These motions are dynamically reconfigurable, with the possibility to select from multiple oscillatory patterns from a single system. Here, we describe an oscillatory material system, which relies on optically-defined boundary conditions to guide photothermal Marangoni propulsion and coordinate multiple particles. Hydrogel nanocomposite particles containing plasmonic gold nanoparticles are illuminated by patterned light at an air-water interface, leading to coupled oscillatory motions with on-demand reconfiguration through variations in light patterns. This experimental platform may prove useful in understanding oscillatory dynamics in natural and synthetic systems.

Reference : Hyunki Kim, Subramanian Sundaram, Ji-Hwan Kang, Nabila Tanjeem, Todd Emrick, and Ryan C. Hayward. Coupled oscillation and spinning of photothermal particles in Marangoni optical traps, PNAS, 2021, 118 (18)

1:30 PM SB09.13.04

Bioinspired Oil-Infused Elastomers with Excellent Water and Ion Barrier Properties for Flexible Bioelectronic Implants [He Sun](#) and Yi Zhang; University of Connecticut, United States

Implantable bioelectronics have a wide range of applications in basic biomedical research and clinical medicine. The encapsulation of these systems represents a key challenge as they demand perfect isolation of electronics from surrounding biofluids to prevent current leakage and the degradation of underlying devices. To date, all the barrier materials for flexible bioelectronics, including polymer layers, inorganic coatings, and transferred barriers, are *solid* materials. These solid materials suffer from limited barrier lifetime due to pinholes, cracks, and nanopores or from complicated fabrication processes and limited stretchability for interfacing with complex biological tissues. This paper reports a solution to this materials challenge by introducing a bioinspired oil-infused rough silicone elastomer as a transparent, flexible, stretchable, slippery, and damage-tolerant biofluid barrier material. Accelerated lifetime tests suggest robust water barrier characteristics that approach 226 days at 37 degrees, even under severe mechanical damage using a knife. A combination of temperature- and thickness-dependent experimental measurements and reaction-diffusion modeling reveal the key water-proof property. In addition to serving as a barrier to water, oil-infused rough elastomer demonstrates an attractive ion prevention property. All these exceptional properties suggest the potential applications in flexible bioelectronics implants for emerging applications ranging from chronic neural recording to bioelectronic medicine.

1:45 PM *SB09.13.05

Bioceramic Cellular Solids—Structure, Mechanics and Formation [Ling Li](#); Virginia Polytechnic Institute and State University, United States

Cellular solids, or foams, are an important class of structural materials for packaging, transportation, sports, and infrastructure due to their mechanical efficiency. While many current foams are primarily based on metallic and polymeric materials, ceramic foams are usually used for non-mechanical applications, such as filtration, catalysis, thermal insulation, etc. The major limitation of using ceramic cellular solids as structural components are their brittleness and flaw sensitivity. Overcoming the fragile nature of ceramic foams, making them lighter while reaching higher stiffness, strength and energy absorption capability is challenging but critical toward many applications. In this talk, I will present our ongoing work in elucidating the structural design principles in natural ceramic cellular solids from a variety of model systems, particularly echinoderm stereom, cuttlefish bone, and sponges. These structures are characterized by their highly mineralized porous morphology, yet exhibiting remarkable damage tolerance, which is in stark contrast to synthetic ceramic foams. We utilize a combinatorial approach by integrating quantitative 3D structural analysis, 4D in-situ mechanical analysis, theoretical and mechanical modeling in order to establish the structure-property relationship for this unique group of biological materials. In this talk, we demonstrate important microstructural design strategies to overcome the intrinsic brittleness of porous ceramics learned from these model systems, which could inspire novel lightweight ceramic cellular solids. In addition, the formation mechanisms of these complex biomineralized structures will also be briefly discussed.

2:15 PM SB09.13.06

A Camouflage Reflector in the Eyes of Decapod Crustaceans Larvae [Keshet Shavit](#)¹, Avital Wagner¹, Venkata Jayasurya Yallapragada², Bracha V. Farstey³, Amir Sagi¹ and Benjamin A. Palmer¹; ¹Ben-Gurion University of the Negev, Israel; ²Weizmann Institute of Science, Israel; ³The Interuniversity Institute for Marine Sciences in Eilat, Israel

Larval crustaceans use transparency to camouflage themselves in rivers and the open ocean. Many of these animals have evolved an ingenious optical device to conceal the conspicuous screening pigments in their eyes – an ‘eyeshine’ reflector that deflects light away from the opaque pigments [1]. Using cryo-SEM and TEM we show that the eyeshine reflection of larval shrimp is produced by light-scattering from dense arrays of high refractive index, core-shell nanoparticles of crystalline isoxanthopterin. The same nanoparticles were recently found in the tapetum of adult shrimp where they are used in image-formation and enhancing photon-capture [2]. The reflectivity and scattering of the particles are enhanced by their birefringence, which results from the anisotropic arrangement of refractive indexes within the particle shell [3]. These particles are located in specialized cells overlaying the screening pigment and extending down the sides of the rhabdoms. The location of the particles indicates that the reflector has a dual function: camouflaging retinal pigment and preserving visual acuity by preventing crosstalk between neighboring rhabdoms. Reflectivity measurements and optical modeling demonstrate that the color of the scattering is determined by the size of the particles and their degree of short-range ordering. The eyeshine color is spectrally-matched to the watercolor in the native habitat of the shrimp and also changes upon light-dark adaptation. This enables the crustaceans to remain inconspicuous against the background. For example, the prawn *M. rosenbergii* which inhabits yellow/green rivers in the Indo-Pacific exhibits yellow/green eyeshine, produced by 400 nm particles. While Marine shrimp from the gulf of Eilat have blue eyeshine, produced by 220 – 330 nm particles.

[1] K.D. Feller, T.W. Cronin, Journal of Experimental Biology, 217, 18, 3263-3273 (2014).

[2] B.A. Palmer, A. Hirsch, V. Brumfeld, E.D. Aflalo, I. Pinkas, A. Sagi, S. Rozenne, D. Oron, L. Leiserowitz, L. Kronik, S. Weiner and L. Addadi, PNAS, 115, 10, 2299–2304 (2018).

[3] B.A. Palmer, V.-J. Yallapragada, N. Schiffmann, E. Merary Wormser, N. Elad, E.D. Aflalo, A. Sagi, S. Weiner, L. Addadi, D. Oron, Nature Nanotechnology 15, 138–144 (2020).

2:20 PM SB09.13.07

USAXS Study of High Aspect Ratio 2D Clay Nanolayer Suspended in saline Water—Nematic Self-Assembly in the Photonic Range of Interlayer Spacings [Osvaldo Trigueiro Neto](#)¹, Paulo H. Michels Brito¹, Tomás S. Plivelic², Daniel Wagner³, Josef Breu³, Barbara Pacakova¹, Kenneth Knudsen⁴ and Jon O. Fossum¹; ¹Norwegian University of Science and Technology, Norway; ²MAX IV Laboratory, Lund University, Sweden; ³University of Bayreuth, Germany; ⁴Institute for Energy Technology (IFE), Norway

Systems of high aspect ratio of 2D nanolayers of fluorohectorite clay mineral, suspended in saline solutions of various clay and salt concentrations, exhibit a rich nematic phase behavior. This system is studied here using Ultra Small-Angle X-ray Scattering (USAXS): the anisotropy of the obtained images is quantified, and, together with reflective spectrophotometric measurements, this provides a precise determination of the nematic organization and inter-particle distance. In addition, the USAXS analysis provides information about nematic phase order such as misalignment or turbostratic organization. We find that the inter-nanolayer distances can be related to electrostatic interactions combined with osmotic pressure effects.

2:25 PM SB09.13.08

Role of Zn²⁺ Ions in the Folding of Nereis Virens Nvj-1 Folding Jaden Luo¹, Eesha Khare¹, Patrick Dennis², Rajesh Naik² and Markus J. Buehler¹; ¹Massachusetts Institute of Technology, United States; ²Air Force Research Laboratory, United States

Metal-coordination bonds are dative chemical bonds that arise when a ligand donates a lone pair of electrons to a metal ion. These bonds are dynamic, reversible, and easily tunable, allowing them to span a large range of different strengths and timescales. Several biological organisms have been found to utilize metal-coordination bonds to synthesize a wealth of bioinspired materials. One such organism, the *Nereis virens*, is a species of marine worm with a remarkably strong and stiff jaw that owes its strength not to bones or minerals, but to metal-coordination bonds. Understanding how metal-coordination bonds affect the structure and properties of the *Nereis virens* worm jaw Nvj-1 protein would enable the understanding and design of new metal-coordinated materials with complex and optimized mechanical properties.

Nvj-1 contains over 25 mol % of histidine, which is believed to play a key role in the metal-coordinated crosslinking that gives the worm jaw its strength. To understand the nanoscale mechanism behind the crosslinking and its pathway to macroscopic mechanical behavior, we analyze the effect of Zn²⁺ on the form and structure of the Nvj-1 protein. To gain insight into the behavior of the Nvj-1 protein in the presence of metal ions, replica-exchange molecular dynamics (REMD) simulations are run with explicit solvent conditions to investigate the formation of the protein structures in various environments. REMD enables an efficient computational search of likely protein structures by overcoming kinetic trapping in local energy minima during the protein folding simulation of Nvj-1. Metal ions are initiated in different positions of the Nvj-1 protein, previously solved by REMD in Chou et. al (ACS Nano, 2017) to understand how the protein folds in the presence of metal ions and how differing conditions of metal ions impact the strength of the metal-coordination bonds that the Nvj-1 protein forms. We find that the initial location of metal ions has an effect on the resulting protein structure.

Largely, this work helps elucidate further details on the roles of metal-coordination binding in protein structures to lend better insight into how the bonds affect macroscopic mechanical properties. Further, information about Nvj-1 binding with metal ions will enable its broader use in mechanomutable engineering materials. With this information, optimized bioinspired materials could be created for a variety of practical applications.

2:30 PM SB09.13.10

Identifying New Strategies to Promote Polymer Adhesion via Bacterial Surface Display Mark T. Kozłowski, Joshua A. Orlicki, Randall A. Hughes, Rebecca L. Renberg, Randi M. Pullen and Jimmy Gollihar; U.S. Army Research Laboratory, United States

Modern polymers have a wide range of surface characteristics, from polar plastics such as polycarbonate, to highly non-polar plastics such as polystyrene and polypropylene. The poor reactivity of many polymers makes adhesion an ongoing challenge. This challenge is particularly pronounced in hydrophobic polymers, which require extensive pre-treatment, priming, solvent plasticization, or high temperatures to adhere. While adhesion of more-polar polymers is typically easier to achieve, these polymers are susceptible to water infiltration, which can lessen the strength of the adhesive contact in humid environments. New strategies to enable good adhesive bonding would allow for facile repair in the field, and the creation of new types of composites.

The large diversity of peptides in both sequence and functional groups makes them potentially useful to search for strong interactions with polymer substrates. Furthermore, the insights provided by peptide binding may eventually allow the design of more-effective synthetic adhesives. Screening the chemical compositional space afforded by peptides and the natural amino acids would be nearly impossible if undertaken in a serial fashion. Recently, the Army Research Laboratory developed a peptide surface display and high-throughput library screening system to find candidate peptides capable of adhering to polylactic acid [1], and to gold nanoparticles [2]. The on-cell peptide screening has the advantages of easy recoverability, the ability to propagate and sequence the genetic code of the adhesive peptides, and possible further improvements of the peptides by directed evolution. In this presentation, we will provide updates on peptide library construction, screening methods, and initial results of screens against substrates with a range of polarities.

References

- [1] S.D. Stellwagen, D.A. Sarkes, B.L. Adams, M.A. Hunt, R.L. Renberg, M.M. Hurley, D.N. Stratis-Cullum, The next generation of biopanning: next gen sequencing improves analysis of bacterial display libraries, BMC Biotechnol. 19(1) (2019) 12.
- [2] J.P. Jahnke, H. Dong, D.A. Sarkes, J.J. Sumner, D.N. Stratis-Cullum, M.M. Hurley, Peptide-mediated binding of gold nanoparticles to E. coli for enhanced microbial fuel cell power generation, MRS Commun. 9(3) (2019) 904-909.

2:35 PM SB09.13.11

Direct, Real-Time Visualization of Self-Assembly of Lipid Bilayers into Liposomes by Graphene Liquid Cell-Transmission Electron Microscopy Vahid Jabbari and Reza Shahbazian-Yassar; University of Illinois at Chicago, United States

Liposomes, vesicles formed by self-assembly of lipid bilayers, have a similar structure to biological membranes, making them a model system for biotechnological and biomedical purposes. Liposomes are composed of one or more lamellae, consisting of a phospholipid bilayer and enclosing a small volume of aqueous liquid. Liposomes diameter can vary (from tens of nanometers up to tens of micrometers) depending on amphiphilic lipid structure, synthetic procedure and solution properties. Biodegradability, biocompatibility, and ability to encapsulate different substances, to isolate and permit controlled release of drugs make these lipid vesicles attractive drug carriers. Indeed, development of lipid-based formulations to enhance recombinant vaccine antigens immunogenicity is of high interest to modern vaccine research [1].

With a growing interest in high precision drug therapies, it is critical to assess microemulsions in a liquid environment similar to living systems. However, fragile structures and susceptibility to electron beam damage, imaging liposome delivery vehicles is challenging with transmission electron microscope (TEM). Low contrast between lipid-based species and aqueous environment causing liposomes imaging particularly challenging without contrast reagents or staining. Emergence of graphene liquid cell-transmission electron microscopy (GLC-TEM) with ability to attain the lowest possible solvent thickness, mitigation of the electron radiation-induced damage by conductive graphene layers, significantly contributed to attain high-resolution TEM images of dynamic processes in real time [2,3].

In this work, and for the first time, in-situ GLC-TEM is employed to observe liposomes dynamics (nucleation and evolution) in real time. Liposomes are synthesized by using phosphatidylcholine and cholesterol in PBS buffer solution. We were able to visualize some of fundamental and important steps in the formation of liposomes. Based on our observations, liposome formation mechanism can be described by initial amphiphilic lipids assembly into micelles followed by turning into small vesicles (liposomes). Coalescence of small liposomes results in the formation of larger liposomes.

References

- [1] Abolfazl Akbarzadeh et al., Liposome: classification, preparation, and applications, *Nanoscale Research Letters* 2013, 8:102.
- [2] Sarah M. Hoppe, Darryl Y. Sasaki, Aubrianna N. Kinghorn, and Khalid Hattar, In-Situ Transmission Electron Microscopy of Liposomes in an Aqueous Environment, *Langmuir* 2013, 29, 9958–9961.
- [3] Vahid Jabbari, David J. Banner, Abhijit H. Phakatkar and Reza Shahbazian-Yassar, (2020). Nucleation and Growth Visualization of Self-Assembled Polymeric Micelles/Vesicles Using in Situ Liquid Cell-TEM. *Microscopy and Microanalysis*, 26(S2), 2576-2578. doi:10.1017/S1431927620022084.

2:40 PM SB09.05.02

Bright, Non-Iridescent Structural Coloration from Clay Mineral Nanosheet Suspensions Paulo H. Michels Brito¹, Volodymyr Dudko², Daniel Wagner², Josef Breu² and Jon O. Fossum¹; ¹Norwegian University of Science and Technology, Norway; ²University of Bayreuth, Germany

Structural colors originate from the constructive interference by reflection and scattering of light from structures with length scales in the visible region of wavelengths. Structural colors can be iridescent or non-iridescent depending on the degree of disorder in the structures. Bright and non-iridescent structural coloration could not yet be achieved for the most abundant two-dimensional (2D) sustainable material, clay minerals. Recently we have demonstrated that bright non-iridescent structural coloration easily and rapidly can be achieved from nematics of suspended clay mineral nanolayers. We demonstrated how brightness can be enormously improved in this system, and moreover that non-iridescence is readily obtained. The clay nanolayer distances, and thus the structural colors are precisely controlled by clay concentration and water salinity.

SESSION SB09.14: Bioinspired Materials IV
Session Chairs: Mathias Kolle and Radwanul Siddique
Tuesday Afternoon, December 7, 2021
SB09-Virtual

4:00 PM SB09.14.01

Sustained Enzymatic Activity and Flow in Crowded Protein Droplets Andrea Testa¹, Mirco Dindo², Aleksander Rebane¹, Robert Style¹, Paola Laurino² and Eric Dufresne¹; ¹ETH Zürich, Switzerland; ²Okinawa Institute of Science and Technology, Japan

Living cellular systems are active materials typically consisting of an extremely crowded environment, in which millions of different enzyme-catalysed reactions happen any second. The complexity and out-of-equilibrium nature of these systems makes it very hard to comprehend the underlying mechanisms governing their behaviour.

In this work, we present a model system consisting of protein droplets that are driven out of equilibrium by enzymatically catalysed reactions, at activity and crowding levels comparable to the cellular cytoplasm, yet retaining compositional simplicity. The droplets possess remarkable stability, and show a plethora of interesting biomimetic activity driven behaviours. We hope our findings can provide an effective framework to design active systems, study biological and biochemical phenomena in a controllable yet biologically relevant environment, and ultimately design active materials that possess superior properties.

4:03 PM SB09.14.03

Bio-Hybrid White Light-Emitting Devices Using Elastic Fluorescent Proteins Jinyeong Kim¹, Butaek Lim² and Seung Wuk Lee^{2,3}; ¹Samsung Display, Korea (the Republic of); ²University of California, Berkeley, United States; ³Lawrence Berkeley National Laboratory, United States

Fluorescent proteins (FPs) provide a novel opportunity to design highly efficient and eco-friendly display devices and technology. Current organic and inorganic display materials (i.e., fluorescent dyes and quantum dots) are toxic and environmentally harmful. In contrast, nature evolves proteins to produce highly efficient and photostability chromophore, FPs together with intrinsic eco-friendly and biocompatibility features. The integration of FPs into light-emitting devices, however, presents several scientific and technical challenges including stability of chromophores and mechanical rigidity in harsh manufacturing conditions. In this study, we designed a novel bio-inspired functional optical material by combining fluorescent proteins as color down-converters conjugated with elastin-like polypeptide (ELP) to enhance mechanical processability. ELPs are naturally evolved biopolymers in nature to endow the flexibility and rigidity of our body in blood vessels and muscles. Using recombinant DNA technique, we fused FPs and ELP genes and synthesized novel functional proteins, and fabricated a composite material of FP/ELP as a thin film to integrate into a blue-emitting LED chip. The resulting thin FP/ELP film exhibited excellent optical properties as well as mechanical properties such as elasticity, stiffness, and tensile strength. We anticipate that biocompatible and eco-friendly elastic biopolymer coating of FP/ELP onto LED would pave a new way to create robust, biocompatible, and environment friendly display technology and its applications in human-machine interfacing materials in the future.

4:06 PM SB09.14.04

Influence of Carbon Source and Concentration on Microbial Cellulose Biofabrication Romare Antrobus¹, Yueh-Ting Chui¹, Theanne Schiros^{1,2} and Helen H. Lu¹; ¹Columbia University, United States; ²Fashion Institute of Technology, United States

Introduction: The textile industry's linear model of production and reliance upon nonrenewable resources to manufacture synthetic fibers, dyes, and finishing agents make it one of the most polluting industries globally, and the leading source of carbon emissions, global waste water, and microplastic pollution. Similarly, medical textiles fabricated in the tissue engineering field also utilize harsh solvents during development, not only limiting their biocompatibility and scalability, but also creating environmental concern in large, industrial volumes. Consequently, new fabrication strategies are required to design functional biomaterials that support a sustainable and circular material economy. Inspired by the complexity of nature and its robust regenerative potential, we harness microbial biosynthesis of nanocellulose using *Gluconacetobacter xylinus* (*G. xylinus*) bacteria for the synthesis and production of regenerative, high performance biotextiles. A variety of carbon sources can be metabolized by *G. xylinus* to tailor microbial cellulose (MC) for different textile applications, in which changes in bioavailability and molecular weight affect biochemical pathways, production rates and ultimately, structural properties. Here, we evaluate the effect of several carbon sources (mannitol, dextrose, and sucrose) and concentration (2% and 8% w/v), on the production of microbial cellulose. It is hypothesized that both sugar type and dose will regulate cellulose yield, crystallinity, and tensile properties.

Methods: *Fabrication:* Microbial cellulose pellicles were biofabricated by culturing *G. xylinus* (ATCC 31174, Manassas, VA) in Hestrin-Schramm (HS) medium with varying carbon sources. Culture medium pH was adjusted to 4.5 using citric acid (Fisher Scientific, Chicago, IL). Prior to investigating the effects of carbon source and concentration, *G. xylinus* was pre-cultured in HS medium (2% w/v sucrose) at 30°C for 72 hours under static conditions.

Medium prepared with various carbon sources were inoculated with 5% v/v preculture. All cultures were held under static conditions at 30 °C for 14 days. *Media and Cellulose Production Analyses*: pH was assessed at each timepoint with a pH meter (n=3/group). MC samples were weighed before and after freeze drying to obtain wet and dry weights, respectively (n=3/group). Morphology was assessed with electron microscopy (Zeiss Sigma VP, Oberkochen, Germany; 3 kV; n=5/group). The fiber diameter of each sample was measured by analyzing randomly selected fiber segments in SEM images using NIH ImageJ software (Bethesda, MD; n=50/group). For mechanical testing, samples (1 x 5 cm) were mounted in a uniaxial tensile testing machine (Instron, Norwood, MA, USA; n=5/group), equipped with a 100N load cell. Samples were maintained to have a gauge length of 30 mm and were tested to failure. MC Young's modulus, toughness, and ultimate tensile strength were determined from stress-strain curves.

Results/Discussion: Electron microscopy revealed that MC produced from either mannitol, dextrose, or sucrose as carbon sources exhibited a nanofibrous morphology and are comparable in fiber diameter. However, use of dextrose (2% and 8% w/v) resulted in a significant decrease in medium pH, indicative of gluconic acid formation, and is associated with a lower cellulose yield. In contrast, mannitol, a sugar alcohol, added at 2% w/v resulted in significantly higher cellulose production by day 7. Although differences in yield between carbon sources was minimized at higher sugar concentrations, the overall increase in production led to an increase in Young's modulus and ultimate tensile strength. The ability to tailor mechanical properties of MC by altering carbon sources, offers a versatile platform for tailoring material properties during synthesis. Clearly, biofabrication of MC can be readily engineered to meet target material properties, with broad applicability for the production of both medical or non-medical biotextiles.

4:09 PM SB09.14.05

Characterization of Covalently Crosslinked Cellulose Nanocrystals for Multifunctional Materials with Tunable Physicochemical Properties Joseph Batta-Mpouma^{1,2,2}, Joshua Sakon² and Jin-Woo Kim^{1,2,2}; ¹Institute for Nanoscience & Engineering, University of Arkansas, United States; ²University of Arkansas, United States

Biologically extracted cellulose nanocrystals (CNCs) have drawn significant attention for the development of multifunctional materials for many research communities, ranging from bioresorption engineering to materials science and engineering. CNCs are rod-like materials that exhibit unique physicochemical properties such as high surface area, high mechanical strength, high aspect ratio, and unique self-assembly with a rheological and liquid crystalline nature. CNCs not only offer hydroxyl (OH) group-rich surfaces that are amenable and suitable for surface functionalization, but their ability to phase change is also triggered by the formation of self-assembled networks, which are held together by hydrogen (H) bonds. While the intramolecular H-bond interactions in CNCs are responsible for their observed relative stiffness and rigidity, the intermolecular H-bond interactions are the major contributors to the organization of CNC networks, holding the interactions among pristine CNCs as the predominant factor responsible for their assembly through packed units into films or gel-like forms, and leading to a preferential tendency to form ordered structures. However, accessible OH groups of colloidal CNCs at the (10)β/(100)α and (110)β/(010)α facets and their intermolecular H-bonds account for the good water molecule adsorption at their surface, making them structurally instable in moist environment.

In this work, exposed OH groups of CNCs were crosslinked with adjacent ones to develop a hydrogel (crosslinked (x) CNC). The intermolecular H-bond was controlled by the type and concentration of cross-linkers, as well as CNC concentrations. Rheological analyses showed tunable viscoelasticity of formed hydrogels, using loss tangent for the determination of the degree of crosslinking. Fourier transform infrared spectroscopy demonstrated that H-bond intensity (HBI) was inversely proportional to increasing crosslinking degree when using an acid-reactive (i.e., pH<7) crosslinker, but proportional for a base-reactive (i.e., pH>7) crosslinker. Wettability showed that water contact angle (CA) increased with degree of crosslinking by an acidic crosslinker, indicating tunable water stability of CNC network structures from hydrophilic to hydrophobic surfaces. While the diffraction intensity of the crosslinked CNC network varied, the diffraction patterns, as shown by X-ray diffraction, remained identical to that of pristine CNCs, suggesting the interface modification process did not alter the intrinsic molecular crystal structure, and confirming crosslinking was solely achieved from the exposed OH groups. Atomic force microscopy showed images with varied CNC organization and surface roughness inversely proportional to increasing CA when an acidic crosslinker was used, as opposed to a basic one, suggesting cross-linking is related to degree of intermolecular regularity of cellulose chains, which were consistent with observations made with HBI. The technology of crosslinking CNCs does not only generate a potential pathway to fabricate water-stable network of colloidal CNCs, but also provide an alternate approach to integrate CNCs in biological and synthetic nanomaterials, as well as polymer matrices for the development of cutting-edge multifunctional materials. The non-toxic, renewable, and biocompatible nature of x-CNCs could see potential use as building blocks to produce advanced 3D printed scaffolds, beads, and nanofibers for their related functions.

This project is supported by the Center for Advanced Surface Engineering (CASE), under the National Science Foundation (NSF) Grant No. IIA-1457888 and the Arkansas EPSCoR Program, ASSET III.

4:12 PM SB09.14.06

Anisometric Microgels for All-Aqueous Liquid-Liquid Phase Separation Studies Yufan Xu¹, Yi Shen^{1,2} and Tuomas P. Knowles^{1,1}; ¹University of Cambridge, United Kingdom; ²The University of Sydney, Australia

Liquid-liquid phase separation of protein is a burgeoning area that is thought to be related to functional and aberrant biology, and can inspire the conceptualisation and processing of smart and multifunctional materials. Conventionally, fluorescence recovery after photobleaching, the fusion of liquid droplets, and rheology were used to characterise the liquid nature of the phases in liquid-liquid phase-separated systems. Other simple methods can also realise the above-mentioned characterisation, and are expected to be developed.

Recently, we demonstrated that protein microgels, from droplet microfluidics, could function as the precursors of the formation of all-aqueous liquid-liquid phase-separated systems that were two-phase or multiphase. We developed oil-free anisometric protein microgels, such as elongated microgels, hole-shell microgels, and buckled core-shell microgels. More interestingly, we demonstrated that these three forms of anisometric microgels could undergo gel-sol transition and convert into isotropic droplets or isotropic core-shell droplets. In summary, the microgels can be the consequences and the outcomes of liquid-liquid phase separation. The protein microgels and all-aqueous liquid-liquid phase-separated systems are promising candidates for extracellular matrix analogues, tissue engineering scaffolds, as well as implantable or injectable biosensors.

References:

- Xu Y, et al. *Small* 16 (32), 2000432, 2020.
- Xu Y, et al. *Advanced Materials*, 2021. In production.
- Xu Y, et al. arXiv preprint arXiv:2009.13413, 2020. Submitted.

4:15 PM SB09.14.07

The Effect of Chemical Composition on the Morphology and Structure of Biogenic Guanine Crystals Noam Pinski and Benjamin A. Palmer; Ben-Gurion University of the Negev, Israel

Animals use guanine crystals to manipulate light, producing a variety of plate-like habits in which the reflective (100) face is preferentially expressed. These habits differ from the stable prismatic growth-form produced synthetically. How does biology so precisely control crystal morphology? One

hypothesis is that the biogenic guanine contains additives that inhibit crystal growth along certain directions. In the 1960s hypoxanthine was found in guanine-containing tissues in fish but it could not be determined whether this molecule was included within the crystal lattice or was simply a solute in the crystal-forming cells. Our study aims to determine the chemical composition of biogenic guanine in order to support or refute the 'additive hypothesis'. Here we report nine unique guanine crystal morphologies from different animals, characterized by SEM and TEM. These include prisms, regular hexagonal and square plates, irregular hexagonal plates and a variety of irregular polygonal plate habits. We developed an enzymatic/centrifugation method for extracting and purifying the crystals from their surrounding - a key weakness in previous studies. Solid-state Raman spectroscopy and MALDI-TOF analysis on the purified crystals showed that hypoxanthine was present in plate-like crystals but was absent from prismatic crystals. UV-vis analysis of dissolved crystal solutions showed that fish guanine contains approximately 16 mol% hypoxanthine. UV-vis and NMR studies are ongoing to quantify the chemical compositions of the remaining crystal morphologies. Preliminary analysis of synchrotron PXRD data reveals only minute differences in the lattice parameters of guanine crystals with differing compositions, but substantial differences in crystal strain. We show for the first time that 'guanine' crystals are, much like inorganic biominerals, composites. The impact that additives have on crystal structure and morphology remains an intriguing open question we are actively pursuing.

4:18 PM SB09.14.08

Sustainable Anti-Icing on Cilia-Inspired Quasi-Liquid Surface Jyotirmoy Sarma and Xianming Dai; The University of Texas at Dallas, United States

Each year icing significantly impacts energy production, transportation, and human activities. For example, the entire state of Texas came to a standstill in February 2021 due to the unexpected freeze. Typically, active strategies (e.g., electrical heating elements, infrared hangars) and passive strategies (e.g., surface coatings) are used for fighting against icing. However, most of the active approaches are complex and costly. Consequently, passive anti-icing strategies relying on durable surface coatings are highly desired. The current state-of-the-art anti-icing technologies, such as liquid-infused surfaces and superhydrophobic surfaces, dramatically reduce ice adhesion strength. Nevertheless, severe durability challenges of lubricant depletion and coating damage during the ice removal process hinder their practical applications. Taking inspirations from how the mobile cilia in the bronchus of human lungs remove microbes and debris, we developed a quasi-liquid surface (QLS) coating that can effectively reduce the ice adhesion strength. QLS is made by chemically grafting flexible polymer of polydimethylsiloxane on a substrate where one end of the molecular chain is tethered to the solid substrate and the other end is mobile. These highly mobile chains of the flexible polymer with nanometer thickness serve as persistent interfacial lubrication and transfer the steady ice/solid interface to a non-sticky ice/quasi-liquid interface. This dramatically reduces the interfacial shear strength between ice and the substrate as well as provide long-term de-icing even after harsh chemical rinsing when state-of-the-art anti-icing surfaces fail. We envision that the robust QLS with sustainable ultralow shear strength to ice will provide design guidelines to the next generation anti-icing technologies that can be potentially applied on wind turbine blades, aircrafts, power lines, and vehicles.

Keywords: Anti-icing, ultralow ice adhesion, cilia-inspired, quasi-liquid surface, sustainable

4:33 PM SB09.14.09

Microbial Biotextiles for a Circular Materials Economy Theanne Schiros^{1,2}, Romare Antrobus¹, Delfina Farias², Christian Joseph¹, Shanece Esdaille¹, Yueh-Ting Chui¹, Dong An¹, Sebastian T. Russell³, Adrian Chitu¹, Susanne Goetz², Anne Marika Verploegh Chassé², Colin Nuckolls¹, Sanat Kumar¹ and Helen H. Lu¹; ¹Columbia University, United States; ²Fashion Institute of Technology, United States; ³Brookhaven National Laboratory, United States

A circular materials economy can disrupt linear production models while mitigating environmental threats. The linear economy that has been the dominant production model since the Industrial Revolution presents serious ecological and human health concerns and threatens potentially catastrophic climate instability. In particular, the textile industry is reliant on industrial agriculture for cellulosic fibers, and nonrenewable resources and petrochemicals to produce synthetic fibers, dyes, tanning and finishing agents, as well as chemically and energy intensive processing, making it one of the most polluting industries globally. We harness extracellular biosynthesis of microbial nanocellulose (MC), coupled to a protocol inspired by a serendipitous intersection between ancient textile techniques and biobased processing as a route to high-performance bioleather with a circular life cycle. Specifically, we used lecithin phosphocholine as a plasticizer to modify MC's crystallinity and cross-linking, to create a material with excellent mechanical properties and outstanding flame retardance, without introducing toxicity or compromising end of life biodegradability. A broad color palette and controlled color modulation was achieved with cultural heritage dyes and waste-to-resource strategies. Life cycle impact assessment shows up to an order of magnitude reduction in environmental impacts relative to conventional textiles, making MC relevant for widespread application in fashion, interiors, construction and insulating materials. The sustainable development of regenerative, high performance biotextiles shown here highlights how biofabrication and green chemistry can strategically address the most damaging impacts of a linear economy, as encapsulated by the fashion industry.

4:48 PM SB09.14.10

Coarsening Droplet—Hydrophilic Slippery Surface Enabled Coarsening Effect for Rapid Water Harvesting Zongqi Guo¹, Deepak Monga¹, Lei Zhang¹, Howard Stone² and Xianming Dai¹; ¹The University of Texas at Dallas, United States; ²Princeton University, United States

Water harvesting through condensation of water vapor in air has the potential to alleviate water scarcity in arid regions around the globe. When water vapor is condensed on a cooled surface, tiny water droplets are formed on the condensing surface and act as thermal barriers for further vapor condensation. Thus, water droplets must be removed rapidly for efficient water harvesting. State-of-the-art passive technologies for droplet removal rely on in-site growth and direct contact of densely distributed droplets, such as coalescence-induced jumping droplets. However, it is challenging to remove submicrometer droplets that lead to a large area of water coverage and poor water harvesting. There exists a scientific gap of droplet size evolution from nucleated droplet to shedding droplet. Here, we present a meniscus-mediated spontaneous droplet climbing and coalescence, namely a coarsening effect, to rapidly remove water droplets with diameters below 20 μm from the hydrophilic slippery liquid-infused porous surface (SLIPS). The self-propelled microdroplets move along the oil meniscus to approach and coalesce with larger water droplets. This passive droplet movement rapidly reduces the number of droplets below 20 μm and simultaneously increases the number of droplets with diameters above 150 μm . We quantitatively study the driving and drag forces for droplet movement and provide important design rationales to enhance the coarsening effect-enabled rapid droplet size evolution. The self-propelled climbing droplet on hydrophilic SLIPS shows rapid removal of droplets below 20 μm and growth of droplets above 150 μm , showing a promising mechanism compared to hydrophobic SLIPS, PEGylated hydrophilic surface, and superhydrophobic surface in water harvesting.

5:03 PM SB09.14.11

Broadband and Pixelated Camouflage by Pneumatic Actuation of Main-Chain Chiral Nematic Liquid Crystalline Elastomers with Large Poisson Effect Shu Yang, Se-Um Kim, YoungJoo Lee, Jiaqi Liu, Dae Seok Kim and Haihuan Wang; University of Pennsylvania, United States

Fishes, cephalopods, and clams can dynamically change their appearances with a wide range of hues and patterns, closely matching their respective environments for camouflage, signaling, or energy regulation. Structural colors offer many advantages over dye or pigment colors, such as brighter color, longer lifetime, and environmental friendliness. However, their tunable range is often limited by the sample's physical size and geometric constraints, making it difficult to achieve broadband, pixelated color switching. Here, we fabricate thin membranes from the main-chain chiral nematic liquid crystalline elastomers (MCLCEs) with large elasticity anisotropy and Poisson's ratio (> 0.5). We demonstrate pneumatic inflation of the thin membranes

with geometrically patterned air channels to achieve broadband color shift from near-infrared to ultraviolet wavelengths with less than 20 % equi-biaxial transverse strain. Each channel could be individually programmed as a color “pixel” to match with surroundings for on-demand camouflage.

5:18 PM SB09.14.12

Mechanical Function and Multiscale Modeling of Mycelium Based Bio-Composites Libin Yang and [Zhao Qin](#); Syracuse University, United States

Mycelium-based bio-composites materials have been invented and widely applied to different areas including the construction industry, manufacturing industry, agriculture, and biomedical. As the vegetative part of a fungus, mycelium has the unique capability to utilize agricultural crop waste (e.g., sugarcane bagasse, rice husks, cotton stalks, straw, and stover) as substrates for the growth of its network, which integrates the wastes from pieces to continuous composites without energy input nor generating extra waste. Their low-cost and environmentally friendly features attract interest in its research and commercialization. For example, mycelium-based foam and sandwich composites are commonly used for construction structures. We are working toward combining computational simulation and experimental methods to synthesize and optimize the mechanics of lightweight mycelium composites. Our result shows that by growing mycelium in a humid environment and using the heat-press process, we can turn the mixture of hardwood and straws into a lightweight synthetic plate with a strength higher than 10 MPa, the same order as that of medium density fiberboard. It is shown that the material function of these composites can be further tuned by controlling the species of fungus, the growing conditions, and the post-growth processing methods. Our multiscale computational simulations help to explore the interface between mycelium and wood fibers and reveal that the entanglement and binding from mycelium fibers can enhance the composite mechanics and thus yield maximum strength and toughness through structural optimization.

5:33 PM SB09.14.13

Polymorphism in Hierarchical Assemblies of Coiled-Coil Building Blocks [Adam Grosvirt-Dramen](#)¹, Zachary J. Urbach¹, Fengbin Wang², Michal Wierzbicki¹, Paul Hurst¹, Wyeth Gibson¹, Joseph Patterson¹, Edward Egelman² and Allon Hochbaum¹; ¹University of California, Irvine, United States; ²University of Virginia School of Medicine, United States

Nature's vast array of multifunctional proteins and peptides provides inspiration for synthetic stimuli-responsive nanomaterials. Both amino acid sequence and solution environment are key to dynamic protein folding/assembly into these multifunctional materials. Building on this foundation, novel pH-sensitive peptide-based assemblies were designed and synthesized. In this work, the assembly mechanism of a *de novo* class of Phe-Ile zipper coiled-coil peptides were studied through point mutations of the amino acid sequence and varying assembly solution conditions. The resulting structures represent polymorphic assemblies ranging from β -sheet amyloid-like fibers to highly ordered, hierarchical fibers of α -helical peptides in coiled-coil building blocks as analyzed by their cryo-electron microscopy structure. Buffer concentration and pH affect multi-scale aspects of supramolecular assembly, including peptide monomer secondary structure and interactions between hexamer building blocks. Here, the library of self-assembling peptide sequences has been expanded to include new sequences and structures that can be used to create amino acid-based biomaterials that mimic the complexity and stimuli-responsiveness of their natural counterparts.

5:48 PM SB09.14.14

Bioinspired Color-Changing and Morphing Structures with Stiffness Heterogeneity Yi Li and [Xueju Wang](#); University of Connecticut, United States

Three-dimensional (3D) structures that can mimic the characteristics of biological systems such as camouflage, adaptivity to environment, and material heterogeneity are desired for a lot of applications. In this talk, I will discuss our recent effort in designing and fabricating bioinspired multifunctional structures by using liquid crystal elastomers (LCEs) as a platform. Color-changing and adaptive capabilities will be incorporated into LCEs that are capable of large, reversible shape changes. In addition, stiffness heterogeneity in the material will be created by utilizing the different domains of the material. Structures that resemble the shape and the functionality of a butterfly and a chameleon will be presented. The studies would provide important insights for the development of intelligent bioinspired systems.

5:51 PM SB09.14.15

Stimulus-Responsive Microphase-Separation of Resilin/Elastin Block-Copolypeptides in Solution and on Surfaces Luis Navarro¹, Justin Ryan², Michael Dzuricky¹, Ashutosh Chilkoti¹ and [Stefan Zauscher](#)¹; ¹Duke University, United States; ²U.S. Naval Research Laboratory, United States

We investigated the self-assembly of a series of stimulus-responsive block copolypeptides (BCPs) composed of a hydrophobic, resilin-like domain and a hydrophilic, elastin-like domain in the bulk and on surfaces using small-angle X-ray scattering (SAXS) and atomic force microscopy (AFM). We observed classical, microphase-separated nanostructures, such as hexagonally-packed cylinders and alternating lamella, in concentrated solutions of the block copolypeptides. The emergence of these nanostructures was strongly dependent on copolymer composition and temperature. Discrete order-order transitions were observed for higher molecular weight species, and order-disorder transitions were observed with increasing temperature for all species due to the lower-critical solution behavior of the elastin-like block. BCP thin-films also exhibited microphase-separated nanostructures that resembled those in solution and could be further refined by annealing in a high humidity environment, resulting in long-range, periodic nanostructures. Structures that form via microphase-separation of distinct polypeptide blocks can display linear peptide motifs that serve as sites for protein / peptide recognition, or enable the selective and ordered presentation of functional proteins with high spatial density.

5:54 PM SB09.14.16

Facile and Cost-Effective Fabrication of Bio-Inspired Patterned Surfaces for Multiple Applications [Ravi Kant Upadhyay](#) and Chander S. Sharma; Indian Institute of Technology (IIT) Ropar, India

The introduction of bio-inspired patterned surfaces exhibiting wettability gradient has presented a new approach towards enhancing environmental water harvesting from fog and dew. A wide range of multifunctional patterned surfaces has been designed by drawing inspiration from different natural surfaces to outperform conventional surfaces in terms of atmospheric water harvesting capacity. However, intricate and expensive fabrication is a major bottleneck that discourages the large-scale implementation of these surfaces. Therefore, efforts are ongoing to address these challenges to make the use of bio-inspired patterned surfaces more viable for practical applications. In this direction, herein, we introduce a novel facile and cost-effective fabrication approach capable of delivering multipurpose patterned surfaces with millimeter to micrometer-level precision.

Our method involves the controlled deposition of superhydrophobic carbon nanoparticles onto the masked hydrophilic or moderately hydrophobic surface for printing a predefined array of adjacent superhydrophobic and hydrophilic patterns. Unlike conventional methods such as laser engraving and photolithography, the developed method does not require any sophisticated instrumentation or costly masks. Steel mesh and PDMS sheets having carved patterns of desired shapes are successfully used as masks. To demonstrate the flexibility and wide-scale applicability of the method, we have successfully created biomimetic patterns on a wide range of substrates, including polymers and metals. These include surfaces with patterns mimicking the surface textures of Namib Desert beetle, rice leaf, and pitcher plant which have inspired many of the recent studies on water harvesting. Subsequently, we test these patterned surfaces for fog harvesting in a controlled environment to investigate the underlying mechanism of water collection and the influence of the size and shape of the patterns. Through judicious tailoring of the shapes of patterns and careful optimization of their dimensions, we are able to achieve

significantly higher fog harvesting performance compared to several state-of-the-art interfaces.

Apart from fog harvesting, we also demonstrate that the developed method can be utilized for creating channels exhibiting sharp wettability contrast for surface microfluidics applications. We show that these channels can be used for water drop manipulation, storage, and guided fluid transport. Overall, the current study not only reports a versatile method for the fabrication of bio-inspired patterned surfaces but also demonstrates the use of these surfaces for multiple applications.

SESSION SB09.15: Bioinspired Materials V
Session Chairs: Mathias Kolle and Radwanul Siddique
Tuesday Afternoon, December 7, 2021
SB09-Virtual

6:30 PM *SB09.15.01

Bio-Inspired Multifunctional Metaphotonic Devices for Sensing and Imaging Applications Radwanul H. Siddique, Vinayak Narasimhan, Daniel Assumpcao and [Hyuck Choo](#); Samsung Electronics, United States

Recent progress in mobile optoelectronics and machine vision has increased the demand for advanced image acquisition and sensing technologies. Conventional optical imaging and sensing devices require bulky and sophisticated optical systems to obtain high-quality information. Over the last decades, photonic metamaterials have attracted considerable interest in various imaging and sensing applications due to their compactness and on-chip processing capabilities. However, millions of years of evolution in the biological world has developed a plethora of unique micro- and nanoscopic photonic structures to perform versatile vision and sensory functions.

In this talk, I will discuss how the development of metaphotonic devices harnessing bioinspired attributes can provide novel yet highly practical solutions for novel imaging and sensing applications. First, I will present our studies on biophotonic nanostructures found in butterfly wings that show unique optical properties with tailored structural disorder, and their successful replication in laboratories using a self-assembly based scalable nanofabrication technique. We utilize this approach to pattern Si_3N_4 -based metasurfaces onto a Fabry-Perot-resonator-based intraocular pressure (IOP) sensor for glaucoma management. The metasurface integration onto the IOP sensor led to a 2.5-fold improvement in readout angle allowing easy handheld monitoring and in a one-month in vivo study conducted in rabbits, showed a 3-fold reduction in IOP error and 12-fold reduction in tissue encapsulation and inflammation, compared to an IOP sensor without nanostructures.

We will further show its application in optical wearables and contact lenses where, we developed a nanostructured scleral lens with enhanced optical, bactericidal, and sensing capabilities. The bioinspired nanostructures, made on biocompatible parylene thin-films are mounted on the anterior and posterior side of a traditional scleral lens. Compared to a traditional scleral lens, the nanostructured scleral lens minimizes glare at large viewing angles of 80° by 4.3-fold, and block UVA light while offering greater transmission in the visible regime. Furthermore, they display potent bactericidal activity against *Escherichia coli*, killing 89% of tested bacteria within 4 hr in vitro. The same nanostructures conformally coated with gold are used to perform simple, rapid, and label-free multiplex detection of lysozyme and lactoferrin (protein biomarkers of chronic dry eye disease) in artificial and whole human tears using drop coating deposition Raman spectroscopy within their physiological and pathological concentration range of 0-6 mg/mL, each.

I will conclude the talk showing our recent progress on developing an ultracompact optical spectrometer for smartphones using bioinspired tricks with high angular tolerance, resolution and throughput, suitable for realization of high-performance point-of-care biosensing. Using the smartphone spectrometer, we demonstrated sub-5 nm spectral resolution, 30° FOV, and high throughput sensing and detection.

7:00 PM SB09.15.02

A Novel Multi-Function Cylindrical Structure with Donut-Shaped Tips [Hyunjung Kim](#) and Seongmin Kang; Chungnam National University, Korea (the Republic of)

In this paper, a novel multi-functions cylindrical structure with donut-shaped tips was produced inspired from teacup-shaped mushrooms (*Nidula niveotomentosa*) which has a seed carrier function with concave structure and a chamber function with a roof. With unique structural characteristics, a cylindrical column having donut-shaped tips inside and outside the top of it was fabricated using a simple yet robust lithography method. Due to the structural properties of its donut-shaped tips, the surface on which this unique structure was formed has remarkable omniphobic properties without additional chemical surface treatment. By applying the micro-dewetting phenomenon on micro/nano structure surfaces with omniphobic properties, the NOA polymer roof was covered. The stable polymer roof formation was proved in that it has omniphobic properties without additional chemical surface treatment and its micro-chamber function was demonstrated by inserting an average of 1.5 μm nanoparticles into the structure and covering with polymer roof. Consequently, this work introduces a matchless fabrication method for fabricating cylindrical structure with donut-shaped tips and proves its multi-functions of omniphobic properties and particles storage function.

7:04 PM SB09.15.03

A Bioinspired Solar Evaporator for Continuous and Efficient Desalination by Salt Dilution and Secretion [Shuqian Zhang](#); Shanghai Jiao Tong University, China

In recent years, solar interfacial evaporation has been one of the most promising techniques to alleviate freshwater scarcity. However, the salt deposition on the evaporation surface limits the long-term operation of evaporators. Herein, inspired by the salt dilution and secretion mechanisms in halophytes, a solar evaporator with a bundle-cross-layer structured absorber and salt secretion bundles is reported. The unique bundle-cross-layer structure realizes the salt dilution by enhancing the water storage and transport, which enables the absorber a high and stable evaporation efficiency of 90.2% over 60 h in brine. More importantly, the salt secretion bundles can completely separate salt crystallization from the absorber by a humidity-controlled salt creeping mechanism. The solar desalination prototype equipped with this evaporator exhibited a stable water collection rate over 600 h of continuous operation, realizing zero liquid discharge in desalination. The study provides new insights into the solar evaporator design and advances other applications such as sea-salt extract, wastewater treatment, and resource recovery.

7:19 PM SB09.15.04

Energy Dissipation in Composites with Hybrid Nacre-Like Helicoidal Microstructures [Hortense Le Ferrand](#); Nanyang Technological University, Singapore

Natural ceramic composites present complex microstructures that lead to tortuous crack path and confer them high toughness. Current microreinforced composites do not yet reach the level of complexity found in natural microstructures. To achieve this, we developed an automated set up for controlling 2D microplatelet orientation using magnetic fields. The setup has 4 degrees of freedom and allows fine control of platelet angles in 3D as well as position. With our setup, we can thus build microstructured porous ceramic materials (alumina) with local orientation of microplatelets, at a concentration of about 40 vol%. Other work in our group has shown that the same setup can be used to process microstructured ceramics up to 95 vol%.

Among the infinite possible microstructures, a nacre-like helicoidal arrangement was selected due to its ability to tilt and twist the crack path. Indeed, we used an analytical model based on the laminate theory to compare energy dissipation due to mixed modes of failure. Nacre-like helicoidal arrangement was predicted to exhibit the highest energy dissipation. Then, we fabricated the hybrid microstructured porous specimen fabricated and infiltrated them with a silicone matrix. Using compression tests, our hybrid dissipated 1.6 times more energy as compared to nacre-like samples of same composition. The fabrication strategy proposed here could thus be a simple route to increase the toughness of microplatelet reinforced composites.

7:34 PM SB09.15.05

Biomimetic Printing of Thermo-Responsive Shape Memory Polymer via Digital Light Processing (DLP) Hyun Lee and Hyun-do Jung; The Catholic University of Korea, Korea (the Republic of)

Shape memory polymers (SMPs) have been utilized for versatile applications due to their stimuli responsive behavior which recovers its original shape after deformation. Compared to shape memory metals, shape memory polymers have exhibited light weight, larger elastic region, and biocompatibility. However, the fabrication method of shape memory polymers mainly dependent on traditional strategies like molding, casting, and extrusion. Those traditional methods are limited to generate customer specific structure rapidly since additional constraint to hold the shape during hardening process of polymer solution. Regarding that, researches adopted 3D printing techniques such as direct ink writing, polyjet, and fused filament fabrication (FFF) to produce objects consisting of shape memory polymers. On the other hand, challenges in acquiring higher resolution and characteristics of usable material are still remained. Alternatively, researches have considered the utilization photopolymerizable raw materials to digital light processing (DLP) technique. Through DLP technique, layer-by-layer stacking of raw materials are possible with excellent precision and resolution. In this study, we aimed to fabricate shape memory polymers which could be facilitated to biomedical applications with biomimetic structure. Mixture of photopolymerizable soft branching material and hard branching material was cured in the aid of photoinitiator. The systematic analyses of the produced objects were carried out in terms of light power, exposure time, layer thickness, and composition. Printability was firstly assessed to determine possible candidates for printing. And degree of precision, compressive properties, tensile properties, and recovering ability were further examined using produced photopolymerized objects. Additionally, bioinspired design of certain seed was applied to SMP and its biomimetic functions was observed. *In vitro* cell tests using pre-osteoblast cells were carried out to assess feasibility of SMPs to biomedical applications.

7:49 PM SB09.15.07

Magnetic Stepwise-Organization of Periodically Arranged Micropillar Arrays Jeong Eun Park¹, Sei Jin Park², Augustine Urbas³, Zahyun Ku³ and Jeong Jae Wie¹; ¹Inha University, Korea (the Republic of); ²Lawrence Berkeley National Laboratory, United States; ³Air Force Research Laboratory, United States

Self-organization of magnetic composites that mimic the collective swarming of natural living creatures has been explored as potential means of accomplishing more complicated tasks. Micron/submicron-scale composite particles can organize into chain-like morphology which allows for directionality of the magnetic response. However, organized shapes and positions could not be reproduced due to unfixed positions of the composite particles. To develop the programmable and reproducible magnetic organization of microscale objects, we introduce periodically arranged micropillar arrays consisting of elastomeric polymer/magnetic particle composites. The magnetic polarities of embedded particles are arranged from S to N pole when an external magnetic field is applied using two permanent magnets. Accordingly, the micropillars act as individual micromagnets where quadrupolar magnetic interactions occur between two vicinal micropillars. As magnetic flux density increases, two vicinal pillar-tops assemble as a pair. At higher magnetic flux density, the two pairwise-assembled micropillars further assemble into a quad-body, and long-range connectivity is ultimately accomplished. We will delve into the mechanisms and governing parameters of this stepwise magnetic-organization via a thorough look into these micropillars consisting of isotropic/anisotropic cross-sections with the directionality of an external magnetic field relative to the geometry of the micropillars.

7:53 PM SB09.15.08

Agile and Adaptable Swimming of Biomimetic Modular Magnetic Soft Robots Sukyoung Won¹, Hee Eun Lee¹, Young Shik Cho², Jeong Eun Park¹, Seung Jae Yang¹ and Jeong Jae Wie¹; ¹Inha University, Korea (the Republic of); ²Seoul National University, Korea (the Republic of)

In soft robotics, agile and adaptable collective motion has been challenged due to sophisticated path programming of individual soft robots. Herein, we present multimodal collective swimming of musculoskeletal system-mimetic soft robots which can control vorticity of fluids. For agile locomotion with lightweight body, the architecture of soft robot consists of nanoporous carbon nanotube yarn (CNTY) filled with magnetic polymer composites, mimicking spongy bone and surrounding skeletal muscle. Under a pulsed rotating electromagnetic field, single magnetic soft robots swim with rectilinear translational motility or rotational motility according to the rotational frequency of the magnetic field. Multiple soft robots articulate with other soft robots owing to magnetic attraction, enabling the assembled swimming. The multiple soft robots are adaptably organized and competition between magnetic attractive force and fluid drag results in trimodal assembly: assembled rectilinear translational swimming, assembled rotational swimming, and interactive vibrational swimming. We will discuss collective swimming of the modular soft robots which can clean hundreds of microbeads and transport multiple semi-submerged millimeter-scale beads.

7:57 PM SB09.04.11

3D Liquid Collecting Surface Decorated with Hierarchically-Structured TiO₂-Al Flakes Inspired from Plant Tissue System Sun Mi Yoon and Myoung-Woon Moon; Korea Institute of Science and Technology, Korea (the Republic of)

Numerous studies have been conducted on the functional structures of living organisms due to their unique properties derived from their intrinsic topological structures and chemistry, which apply to various applications, including nano-micro robotics, self-cleaning surfaces, and water harvesting. For example, all plants have optimized cellular structures and tissue systems for protective function and water absorption. Additionally, among plants with functional surfaces or structures, some, such as *Mimosa pudica*, exhibit extreme wettability, allowing for a strong self-cleaning against water drops to protect their tiny leaves, which is attributed to the well-distributed microscale clusters composed of nanoscale wax flake.

In this study, we proposed a hybrid nanocomposite of TiO₂ nanoparticle encapsulated Aluminum (Al) flake clusters by mimicking the hierarchically grown flake clusters on the leaf of *Mimosa pudica*. These flake clusters could be produced not only on Al and TiO₂ but also on the various surface including 3D structures such as 3D printed polymer surface. When Al substrate is immersed in a heated TiO₂ nanofluid with a three-dimensional substrate, it reacts with the hydroxyl ion decomposed water in the nanofluid to form a flake-like Al nanostructure, with TiO₂ nanoparticles serving as the nucleus of the Al flakes. Due to the dual scale roughness of hierarchical Al flake clusters and the TiO₂ effect, the TiO₂-Al based flakes exhibit long-term stability (more than 90

days) in superhydrophilicity and underwater oleophobicity, whereas the Al base substrate alone exhibited mild hydrophilicity but did not last as long. Since the method to fabricate the durable superhydrophilicity and anti-oil fouling surface is simple and easy to scale up, it would have a broad range of applications in numerous industrial fields. We were able to apply hierarchical structures with long-lasting superwetting to water-transport structures and oil-collecting systems by developing multi-scale functional structures inspired by plant tissue systems such as leaf vein and xylem.

SESSION SB09.16: Bioinspired Materials VI
Session Chairs: Hyuck Choo and Radwanul Siddique
Tuesday Afternoon, December 7, 2021
SB09-Virtual

9:00 PM *SB09.16.01

Imaging of Biological Bicontinuous Membranes—A New Tool to Learn from Nature's Versatile Membrane Forms Gerd E. Schroeder-Turk^{1,2}, Tobias M. Hain^{3,1}, Michal K. Bykowski⁴, Matthias Saba⁵, Myfanwy E. Evans³ and Lucja M. Kowalewska⁴; ¹Murdoch University, Australia; ²The Australian National University, Australia; ³University of Potsdam, Germany; ⁴University of Warsaw, Poland; ⁵University of Fribourg, Switzerland

Bicontinuous membranes in cell organelles epitomise nature's ability to create complex functional nanostructures. Like their synthetic counterparts, these membranes are characterised by continuous membrane sheets draped onto topologically complex saddle-shaped surfaces with a periodic network-like structure. In cell organelles, their structure sizes around 50–500 nm and fluid nature make Transmission Electron Microscopy (TEM) the analysis method of choice to decipher nanostructural features. Here we present a tool to identify bicontinuous structures from TEM sections by comparison to mathematical “nodal surface” models, including the hexagonal lonsdaleite geometry. Our approach, following pioneering work by Deng and Mieczkowski (1998), creates synthetic TEM images of known bicontinuous geometries for interactive structure identification. We apply the method to the inner membrane network in plant cell chloroplast precursors and achieve a robust identification of the bicontinuous diamond surface as the dominant geometry in several plant species. This represents an important step in understanding their as yet elusive structure-function relationship.

9:30 PM SB09.16.02

Late News: Bioinspired Interfacial Design to Regulate the Electrical and Mechanical Properties of Inorganic Fibers and Their Applications Jing Ren; ShanghaiTech University, China

High-performance polymeric fibers with merit of lightweight, strong and tough are of great interest for various applications from functional textiles to structural composites. Carbon nanotubes (CNTs) fibers have an inherently hierarchical structure with high internal surface area approaching $100 \text{ m}^2 \text{ g}^{-1}$ and provide good thermal and electrical conductivity. However, difficulties remain in the exploitation of these nanomaterials' exceptional properties on a macroscopic length scale. CNTs in a CNT fiber are interconnected by “weak link”, Van der Waals forces, the properties of bare CNT fiber are far below single CNTs. In practice, the imbalance between strength and toughness not only exist in CNT fibers but also widely occurs in engineering materials. The high-strength materials, such as high-performance Kevlar and carbon fibers, are often brittle, whereas the elastic materials, such as rubbers and elastomers, possess low strength. However, certain exceptions can be observed in nature. The alternating organic-inorganic nanostructures of bone, nacre and other biological structures, are the secret to achieve an elegant balance between strength and toughness. The organic-inorganic interfaces, on the other hand, play a crucial role in improving fracture toughness and fracture resistance through energy dissipation due to breaking of mineral bridges, inelastic shear of nano-biomaterials and presence of interlocking nanobuilding blocks during sliding.

Ductile and damage-tolerant CNT fibers were produced at large scale by utilizing conductive ionic silk fibroin (ISF) glue to regulate the CNTs' interface. Benefiting from the low energy barrier of solvent molecules within CNTs, the ISF glue can intercalate between CNTs interfaces and, thereby, form an alternating soft and hard interface. Consequently, the inorganic-organic cooperative interactions enhanced the performance of CNT-ISF fiber, rendering an elongation at break of 14%, toughness of 22 MJ m^{-3} and electrical conductivity of $4.4 \times 10^4 \text{ S m}^{-1}$. Similar to other biological nanocomposites, the CNT-ISF fibers exhibit remarkable damage tolerance behavior due to confined CNT sliding and shearing during tensile fracture, supported by TR-SAXS characterization and MD simulations.

Besides mechanical and electric features, the composite fibers can also achieve fog collecting functions. Similar as the cactus, which uses structures and composites to collect fog and retain the water in the body. The fog first deposits on the barb and spine to form water droplets, and the larger droplets are transported along the gradient microchannel. Mucilage is present in the cells of the cactus stem, which is composed of complex polysaccharides including pectin and calcium ions. The existence of calcium ions allows pectin to form hydrogel molecular networks, capable of retaining a large amount of water to meet life activity under arid environmental conditions. The CNT-ISF yarn can capture water molecules from the surrounding foggy environment, and the spine-like microgroove structure was created on the surface of CNT yarn, which provided the driving forces for the directional movement of water droplets. The chemical and structural synergetic effects allow the fog-collecting yarn to absorb the fog, gather water, and directionally transmit the droplets to the ends of yarn.

These structure, mechanical and electric features of CNT-ISF fibers enable them to be used in functional textiles, and flexible and wearable devices.

Reference

Dong, S.; Gan, Z.; Chen, X.; Pei, Y.; Li, B.*; **Ren, J.***; Wang, Y.*; He, H. Y.; Ling, S.*, **Materials Chemistry Frontiers** 2021, 5,5706-5717
Zhang, W.; **Ren, J.**; Pei, Y.; Ye, C.; Fan, Y.; Qi, Z.; Ling, S.*, **ACS Biomater. Sci. Eng.**2020.<https://dx.doi.org/10.1021/acsbomaterials.0c00892>
Ye, C.; **Ren, J.**; Wang, Y. L.; Zhang, W. W.; Qian, C.; Han, J.; Zhang, C. X.; Jin, K.; Buehler, M. J.; Kaplan, D. L.; Ling, S.*, **Matter** 2019, 1 (5), 1411-1425.

9:45 PM SB09.16.03

Late News: Direct-Writing of Structural-Color 2D Graphics and 3D Architectures with Colloidal Inks Jong Bin Kim¹, Changju Chae², Sang Hoon Han¹, Su Yeon Lee² and Shin-Hyun Kim¹; ¹Korea Advanced Institute of Science and Technology, Korea (the Republic of); ²Korea Research Institute of Chemical Technology, Korea (the Republic of)

Nature has astonishing nanostructures in which periodicity is highly crystalline or amorphous exhibiting brilliant or matte structural colors, respectively. Humans have used colloids to mimic the structural colors in nature, where the periodicity is manipulated to design photonic crystals or glasses. Many researchers have used various strategies for creating structural-color patterns. However, both structures mostly require colloid-wasting, complicated, and

multistep processes, which is time-consuming especially for colloidal crystals. Inkjet printing is one of the most promising methods to solve those limitations, but it does not make monolithic structures so that it shows poor mechanical and optical properties. Furthermore, 3D architectures with structural colors have been rarely explored.

Here, we report a direct writing of two- and three-dimensional structural-color patterns using highly viscoelastic colloidal dispersions, first making their patterning highly customizable. We disperse silica nanoparticles in acrylate polymers, where the particles are repulsive as the overlap of solvation layers exerts disjoining pressure. For 2D patterns, the particle fraction in the dispersion is set right before the solid transition fraction over which the dispersion becomes solid. The high fraction brings about good printability including fluid resistance to a sudden flow and a high resolution along with a high printing speed. The particles are crystallized by a shear force when the polymer viscosity is moderate in a range of a few tens of cps. In contrast, a high polymer viscosity over 1000 cps frustrates the crystallization of particles as the high viscosity prevents particles from being sheared to find the energetically optimal state and just kinetically captured in the amorphous state.

By choosing the polymer viscosity, we can customize a photonic-crystal or -glass line pattern with the highest speed of 15 mm/s in a width-controllable manner. It is outstanding to print a 2D Eiffel tower with a dimension of 13×7 mm² in 10 min, of which color is either iridescent or matte according to the polymer viscosity. The rheological properties of the two kinds of inks are examined for the first time, and the analysis is directly linked to the crystallization aspect and to the final colloidal arrangement that is found to have relations with the shear history. Aside from a line, a face is direct-written by merging individual lines at a rate of 4 cm²/min and shows the highest reflectance over 80% by thermal annealing for 10 min. Additionally, this strategy facilitates a multicolor patterning as different inks are not mixed even after being dispensed adjacently. Finally, we can target any kinds of substrates—including glass, plastic, metal, paper, and fabric—and any kinds of mechanical properties of final patterns—they can be rigid, foldable, and stretchable. Interestingly, the colloidal inks can be piled up when ethanol inhibits the solvation layer formation so that the colloids are linked in the dispersion. The dispersion loses flow resistance and becomes transparent around optimal ethanol content as ethanol disrupts the solvation layer that requires shear force to make particles slip and matches the two refractive indices. The particle content must be higher than a threshold where the colloids are close enough to be linked entirely after the solvation layer disruption, which is still much lower than the solid-transition fraction defined at an ethanol-free basis. However, a higher particle fraction is better in that printed structures retain their morphology better as the overall linkage between particles is sturdy. The matte colors are shown after ethanol evaporation, first realizing the 3D-printable colloidal glasses. To sum, direct-writing of these colloidal systems opens a new avenue for creating customizable structural-color patterns both in 2D and 3D spaces by fast and local deposition of the dispersion with programmable trajectories.

10:00 PM SB09.16.04

Mechanical Properties and Fracture Behavior of Sierpinski Carpet Fractal Composites Ya-Yun Tsai, Yuan Chiang, Jacqueline Buford, Meng-Lin Tsai, Hsien-Chun Chen and Shu-Wei Chang; National Taiwan University, Taiwan

Fractals are ubiquitous in nature. Examples include snowflakes, lightning, clouds, river networks, mountains, trees, and coastlines. Fractal geometry formed by simple components has long been applied to many fields, from physics and chemistry to electronics and architecture. The Sierpinski carpet (SC) has a two-dimensional space-filling ability and therefore provides many structural applications. However, few studies have investigated its mechanical properties and fracture behaviors. Here, to understand how fractal iterations affect their mechanical properties and crack propagation, we utilize the lattice spring model (LSM) to construct SC composites with two base materials and to simulate uniaxial tensile tests. The results show that, for either the soft-base or stiff-base SC composites, the one with two hierarchies has the optimal mechanical performance in the terms of stiffness, strength, and toughness compared to the others with higher hierarchies. The reason behind this surprising result is that the largest stress intensities occur at the corners of the smallest inclusion squares, which consequently induces crack nucleation. We also find that the main crack tends to deflect locally in SC composites with a soft matrix, but in global main crack behavior, SC composites with a stiff matrix have a large equivalent crack deflection. Furthermore, considering the inherent anisotropy of SC composites, we rotate the SC composites by 45°. The tensile strength and toughness of the rotated SC composites are inferior and the crack propagating behaviors are distinct from the standard SC composites. Moreover, the rotated SC composites have notable different crack behaviors between the soft-base and the stiff-base ones. This finding infers advanced engineering for crack control and deflection by adjusting the orientation of SC composites. Overall, our study opens the door for future engineering applications in stretchable devices, seismic metamaterials, and structural materials with tunable properties and hierarchies.

10:15 PM SB09.16.05

Spatiotemporal Matter in Meniscus Splitting of Viscous Fluids for Mathematical Models Yoshifumi Katsushima¹ and Kosuke Okeyoshi²; ¹Aoyama Gakuin University, Japan; ²Japan Advanced Institute of Science and Technology, Japan

‘Viscous fingering’ is an example of fluidic flow, an unstable situation that is widely known as tears of wine. This has been explained through the Marangoni effect, coffee ring effect, Saffman-Taylor instability, etc. However, because of the transitional nature of these phenomena, there are difficulties to utilize such fluidically regulated interfaces for preparation of materials. The interfacial instability is comparable to the mechanical instability of gels at the phase transition or to the skin layer of gel surfaces during shrinking. For establishing a universal model of dissipative structures in nature, investigation of biopolymer’s behaviors in air-water interface is an important practical challenge. Recently, the phenomena have been successfully developed to an ordered structure by controlling the evaporation of an aqueous mixture of polysaccharides.¹ Furthermore, by introducing crosslinking points into the deposited polymer, it has huge potentials to use for uniaxially swellable hydrogels.

In this study, we present a brief discussion of nonequilibrium phenomenon, ‘meniscus splitting’ through mathematical approaches. As an experimental model, when the mixture is dried from a top open cell with a millimeter-scale gap, the polymer forms deposits at specific positions to split the air-water meniscus by bridging the gap. Because water irreversibly evaporates to the air phase through a gap, the air-water interface is in a nonequilibrium state between polymer deposition and water evaporation. As a result, the air-liquid interface is divided into multiple interfaces to partition a space. Based on such facts, the interface from the cross-sectional view are focused for the mathematical modeling. The interfacial curves at the typical times for the meniscus splitting are ideally expressed using catenary curves. By validating the length of the multiple curves, the area of the evaporative interface would be evaluated. We envision that this mathematical approach will help general understandings for the phenomena and design of advanced materials independent from kind of substances.

[1] Okeyoshi, et al, *Sci. Rep.* **7**, 5615 (2017); *Adv. Mater. Inter.* **5**, 1701219 (2018); *Adv. Mater. Inter.* **6**, 1900855 (2019); *Polymer J.* **52**, 1185 (2020); *Sci. Rep.* **11**, 767 (2021).

10:30 PM SB09.16.06

Space-Filling Open Microfluidic Channels with Two-Dimensional Fractal Wettability Patterning for the Efficient Droplet Collection Hiroyuki Kai; Tohoku University, Japan

Fractal structures are ubiquitous in biology, such as blood vessels, plant leaves and roots, etc. They are designed for the efficient contact with a larger volume by a smaller length and fewer branches as well as the efficient transport. In the field of microfluidics, the open microfluidic channel, which is made of a patterned surface with different wettability properties, has been studied for trapping and unidirectional transport of aqueous droplets by capillary force. We developed open microfluidic channels with fractal branching that densely fill a substrate surface (H. Kai et al., *RSC Adv.* 2018, 8, 15985; H. KAI, *MicroTAS* 2020). It can collect water droplets from a wide area of the surface to the center by hierarchically repeated transport and fusion of the droplets.

The developed space-filling open microfluidic channels are reminiscent of fractal biological systems, both of which can efficiently contact a larger volume (or area in the case of two dimensions).

The microfluidic channels were fabricated by coating the substrate surface followed by photolithographic patterning. A film of polyethylene terephthalate was coated with a mixture of titanium oxide nanoparticles and Capstone (R) ST-100 fluoroacrylate copolymer to make the surface superhydrophobic (the contact angle of water droplet > 150°). The coated film was irradiated with 365 nm UV light through a photomask, where the only irradiated area turned superhydrophilic (contact angle ~ 0°), to obtain the open microfluidic channels with wettability patterning.

The droplet collection efficiency of the microfluidic channel was investigated by spraying water droplets into the channel and observing the volume of the water droplets collected in the center of the channel. Various photomasks were designed with the different numbers of branching, and the efficiency of water droplet collection was compared. As the number of repeated branching ("generation number") was increased, the collection efficiency monotonically increased up to the generation number of eight, where the efficiency reached 74%±9%. This indicated the effectiveness of the space-filling structures by fractal branching. In addition to the above experiment, we also conducted the computational fluid dynamics simulation to systematically understand the dynamic behavior. Details of the simulation methods as well as the comparison between the numerical and experimental results will be presented.

SESSION SB09.17: On-Demand
Sunday Morning, December 5, 2021
On-Demand

8:00 AM SB09.04.04

Anisotropic Liquid Sliding Velocity Controllable Surfaces with Bioinspired Nanoparticles Composites [Joon Hyung An](#), Jiseong Choi and Seongmin Kang; Chungnam National University, Korea (the Republic of)

In this work, we fabricated omniphobic structural surface with the property of anisotropic droplet sliding using a composite of nano sized ceramic particles and polymers. Inspired by rice leaves, the micro-scale overhang groove structures exhibit omniphobic property and determines the sliding direction of the droplets. The polymer except for the mineral particles on the prepared surface was selectively etched through UV ozone etching treatment, and as a result, nano-bump morphologies were partially exposed. A reliable criterion was presented for the formation of nano-bumps that control the sliding velocity of droplets. It was confirmed that the sliding velocity of various types of liquid droplets with different surface tensions was also controlled according to the exposure level of nanoparticles.

8:05 AM SB09.08.06

Bacterial Pigments as Potential Photosensitizers for Dye-Sensitized Solar Cells [Arshi Gupta](#)^{1,2}, Mukul Dubey^{2,1}, Wenrong Yang¹, Fred Pfeffer¹, Xavier Conlan¹ and S.V. Eswaran²; ¹Deakin University, Australia; ²TERI Deakin Nanobiotechnology Centre, India

The dye-sensitized solar cells based on synthetic Ruthenium dyes and organic metal-free dyes are widely recognized, however, their toxicity, scarce availability of raw material, high cost, and complex synthesis procedures have been a limitation [1]. This led to the exploration of nature-based dyes. Metabolites from plants such as chlorophyll, carotenoid, flavonoid, and betalains have been tested in dye-sensitized solar cells (DSSC) [2] but their narrow absorption spectrum, absence of functional groups to bind strongly with semiconductor [3], and non-availability of the electron-withdrawing group to achieve efficient intramolecular charge transfer (ICT) [4] resulted in low-efficiency of solar cells, also these metabolites have drawbacks such as low photo and thermal stability [5]. On the other hand, microbial metabolites have additional advantages over plant-based metabolites such as broad sunlight absorption [3], good photostability [6], non-toxic properties [7], and the ability to be produced in bulk through bioreactor approach [8]. There are more than 22000 microbially generated bioactive metabolites reported to date [9] which can be potentially explored for their application in solar cells. However, only a few reports are available on the use of microbial pigments in dye-sensitized solar cells [3] with the highest power conversion efficiency (PCE) of 2.3 % for *Monascus yellow* [10] which is very encouraging. Though this research is in its infancy it shows the promise of these sensitizers for solar cell applications. In our research, purified bacterial cultures were isolated from roots of eggplant, chili, sweet potato, and okra plant, and the extracellular pigments extracted and were characterized for their structural, optical, and electrochemical properties. The initial data showed broad absorption in the range of 350 – 600 nm, presence of functional groups required for binding with the semiconductor, and HOMO-LUMO levels required for favorable charge transport in solar cells. The data clearly indicated the promise of microbial pigment as suitable photosensitizer for solar cell application.

References:

1. Adedokun, O., K. Titilope, and A.O. Awodugba, *Review on Natural Dye-Sensitized Solar Cells (DSSCs)*. International Journal of Engineering Technologies, IJET, 2016. **2**(2).
2. Pandey, A.K., et al., *Natural Sensitizers and Their Applications in Dye-Sensitized Solar Cell*, in *Environmental Biotechnology: For Sustainable Future*. 2019, Springer Singapore. p. 375-401.
3. Maddah, H.A., V. Berry, and S.K. Behura, *Biomolecular photosensitizers for dye-sensitized solar cells: Recent developments and critical insights*. Renewable and Sustainable Energy Reviews, 2020. **121**: p. 109678.
4. Cherepy, N.J., et al., *Ultrafast electron injection: implications for a photoelectrochemical cell utilizing an anthocyanin dye-sensitized TiO2 nanocrystalline electrode*. 1997. **101**(45): p. 9342-9351.
5. Millington, K.R., K.W. Fincher, and A.L. King, *Mordant dyes as sensitizers in dye-sensitized solar cells*. Solar Energy Materials and Solar Cells, 2007. **91**(17): p. 1618-1630.
6. Ordenes-Aenishanslins, N., et al., *Pigments from UV-resistant Antarctic bacteria as photosensitizers in Dye Sensitized Solar Cells*. J Photochem Photobiol B, 2016. **162**: p. 707-714.
7. Kumar, A., et al., *Microbial pigments: Production and their applications in various industries*. 2015. **5**(1).
8. Jayaseelan, S., D. Ramaswamy, and S. Dharmaraj, *Pyocyanin: production, applications, challenges and new insights*. World J Microbiol Biotechnol, 2014. **30**(4): p. 1159-68.
9. Berdy, J.J.T.J.o.a., *Bioactive microbial metabolites*. 2005. **58**(1): p. 1-26.
10. Ito, S., et al., *Fabrication of dye-sensitized solar cells using natural dye for food pigment: Monascus yellow*. Energy & Environmental Science, 2010. **3**(7): p. 905-909.

SYMPOSIUM SB10

Micro- and Nanoengineering of Biomaterials—From Precision Medicine to Precision Agriculture and Enhanced Food Security
November 30 - December 8, 2021

Symposium Organizers

Chiara Ghezzi, University of Massachusetts Lowell
Julie Goddard, Cornell University
Benedetto Marelli, Massachusetts Institute of Technology
Amir Sheikhi, The Pennsylvania State University

* Invited Paper

SESSION SB10.01: Nanostructured and Microstructured Biomaterials
Session Chairs: Chiara Ghezzi and Benedetto Marelli
Tuesday Morning, November 30, 2021
Sheraton, 2nd Floor, Back Bay C

10:30 AM *SB10.01.01

Biomaterial Strategies with Silk Nanoparticles and Nanofibers David L. Kaplan; Tufts University, United States

Silk proteins represent unique protein polymer systems due to their regular peptide repeats with block-copolymer features, along with self-assembly in aqueous, ambient conditions into secondary and higher order structures. In nature, this process leads to unique hierarchically structured and functional fibers with remarkable mechanical properties. Generating insights into the nanoscale features of these systems has generated a new range of material features that can be exploited towards structural and functional biomaterials based on silk. Specific polymer processing paths include exfoliation to generate natural silk nanofibers as building blocks for new materials and generating silk amorphous nanoparticles as feedstocks towards commodity plastics processing using silks. In both cases, the critical features are the silk nanostructures and water content, related to mechanics, processability and functional outcomes. Specific examples will be discussed to highlight these new opportunities with this ancient polymer.

11:00 AM SB10.01.02

Dual-Crosslinked Alginate-Based Hydrogels as Cell Instructive Scaffolds for Cultured Meat Irfan Tahir and Rachael Oldinski-Floreani; The University of Vermont, United States

Introduction: With the rising harmful effects of climate change, a novel, emerging field of technology called cellular agriculture has arisen to explore 'cultured meat', an artificial meat substitute developed *in vitro* using animal cells and bioengineered cell scaffolds. Cultured meat is an advantageous alternative to traditional animal agriculture, which is not sustainable in a world with a rising human population and growing meat consumption rates. Plant-based alginate scaffolds can be used to support the development of cultured meat due to their high degree of chemical and mechanical tunability, which can be optimized by adjusting the hydrogel's molecular weight, chemical composition, and cross-linking process. In this project, our goal was to create a dual-crosslinked alginate-based scaffold with material properties that supported tissue development of primary bovine muscle cells, with the overall goal of achieving a cultured steak for human consumption. **Methods:** Herein, we synthesized: 1) methacrylated alginate (Alg-MA) using aqueous chemistry to enable covalent crosslinking via visible light exposure, and 2) arginine-glycine-aspartic acid (RGD) conjugates (Alg-MA-RGD) using carbodiimide chemistries to provide cell-binding sites onto the material. Alginate-based hydrogels of different concentrations (1% and 3%, w/v) and cross-linking types were created. Ionically crosslinked hydrogels were made by injecting the hydrogel precursor solutions into custom molds of 8-mm diameter. The molds and solutions were frozen for two hours at -20 °C, and then crosslinking by adding 1M calcium chloride (CaCl₂) dropwise onto the mold. Photo-crosslinked alginate-based hydrogels were made by injecting hydrogel precursor solutions premixed with 1mM eosin Y (photo-sensitizer), 125 mM triethanolamine (photo-initiator), and 20 mM 1-vinyl-2-pyrrolidinone (catalyst) in a custom mold and exposed to green light (525 nm, SuperBrightLEDs) for five minutes. Dual cross-linking was achieved by combining the two types where photo-crosslinking preceded ionic crosslinking. The crosslinked alginate scaffolds were characterized using proton nuclear magnetic resonance (¹H-NMR), Fourier transform infrared (FTIR) spectroscopy, rheometry, and unconfined uniaxial compression tests. **Results and Discussion:** We demonstrated that modifying the material structure chemically and physically via different crosslinking techniques resulted in differences in the material properties between groups, such as gelation kinetics, viscosity, and scaffold stiffness. For the alginate precursor solution, we were able to obtain low enough viscosity values (0.02 – 0.06 Pa.s) to enable processing via photolithography. The gelation time of the different materials did not vary broadly, although the shear and compression moduli demonstrated significant differences between groups. Ongoing work includes: 1) scaffold structural analysis via scanning electron microscopy (SEM); 2) murine C2C12 and primary bovine muscle cell response and myogenic differentiation on the alginate scaffolds, and investigating the effects of stiffness, pore size, and chemical composition. **Conclusion:** Our unique method of synthesizing alginate hydrogels and the associated pilot data indicates the efficacy of dual-crosslinked alginate-based hydrogels for the production of cultured meat.

11:15 AM *SB10.01.03

Applications of Nanofibers in Building Biological Tissues Kevin K. Parker; Harvard University, United States

The networked architectures that maintain the structural integrity and function of biological tissues are nanofibrous arrays of proteins. We have developed three manufacturing platforms (rotary jet spinning, immersion rotary jet spinning, and pull spinning) as methods of building nanofiber networks of biological and synthetic polymers to mimic the function of the extracellular matrix. We have used these methods to build 3D tissues for in vitro assays, heart valves for implant, wound dressings for skin, cardiac ventricles, and food. This presentation will review the design principles and lessons learned of these works.

SESSION SB10.02: Design and Nanofabrication of Dynamic Biomaterials
Session Chairs: Chiara Ghezzi and Benedetto Marelli
Tuesday Afternoon, November 30, 2021
Sheraton, 2nd Floor, Back Bay C

1:30 PM *SB10.02.01

Engineering Shape Morphing Biomaterials That Respond to Light Fiorenzo Omenetto; Tufts University, United States

Light and materials interact in natural systems with exquisite precision through a designed interaction between electromagnetic waves and the physical properties of the material, both from the bulk and structural point of view. In particular, structural control over multiple length scales, that span from the nanoscale to the macroscale, defines interesting material responses that enable high-performing functional outcomes in light harvesting, reflection, and thermal management among others. We describe here strategies for light harvesting and optomechanical actuation in hybrid biomaterial-elastomeric composites that leverage rationally designed photonic architectures to obtain wireless, light-responsive material formats. The combination of photonic properties designed at the nanoscale with shaped elastomeric material hosts open opportunities in optomechanical actuators with tunable and complex deformation that respond to simple light illumination. The talk will cover some of the potential opportunities for future development of composite materials that are inspired by Nature's ability to harvest light and explore possible classes of smart optomechanical systems that move with light on demand without the need for external sources of power.

2:00 PM SB10.02.03

Metal Ions Regulated Peptide Self-Assembly as Nanocarriers for Plant Micronutrients Hui Sun, Federica Rigoldi and Benedetto Marelli; Massachusetts Institute of Technology, United States

Metal ions play an essential role in many physiological and pathological processes in living systems. Approximately one-third of all proteins currently known require metal ions as cofactors for their structural integrity and biological function. For example, iron is a cofactor of several metalloproteins involved in chlorophyll synthesis and photosynthetic electron transport. Deficiency in iron therefore induces chlorosis and other plant disorder, lowering crop yields drastically.

Peptides are known to exhibit a variety of interactions with metal ions, due to the wide range of functional groups they possess. Metal-binding peptides then attracted a lot of attention as a potential material platform for nanofabrication of organic-inorganic composites built from the bottom up. Besides, coordination with metal ions may induce peptide association into nanostructures that are conformationally and functionally different from the original peptide assemblies. In this presentation, we show that the self-assembly pathway of a silk fibroin-derived peptide can be regulated through addition of differently charged metal ions. Atomic force microscopy (AFM) in combination with a set of correlative light scattering and spectroscopy techniques are employed to investigate the detailed mechanism of peptide assembly facilitated by different metal ions. Factors including the molar ratio of peptides to metal ions and the charge and type of metal ions are found to largely affect the peptide association kinetics and the size and structure of peptide assemblies at equilibrium. Such understanding can hopefully contribute to the design and development of peptide-based nanocarriers for stabilization and delivery of micronutrients in plants.

2:15 PM SB10.02.04

Innovating and Characterizing Bioinspired Soft Materials—Multiscale Molecular Modelling and Machine-Learned Metamodels Jingjie Yeo, Chenxi Zhai, Tianjiao Li, Haoyuan Shi and Liming Zhao; Cornell University, United States

Globally, rapidly ageing human populations are significantly accelerating the occurrence of non-communicable diseases. Understanding the fundamental mechanisms of tissue damage due to aging can provide predictive capabilities that will inform medical treatments. Coupled with this understanding, nature-inspired dynamically responsive biomedical devices and implants can address this major health crisis due to their excellent environmental adaptability and biocompatibility. Developing such novel biomaterials further necessitates multiscale computational modelling and simulations to fundamentally understand the pertinent physical, chemical, and biological material properties. We apply multiscale molecular modelling and machine-learned metamodels to characterize aging-related diseases and engineer various candidate materials on multiple fronts: (I) collagen-related morbidities, (II) dynamically-responsive silk and silk-elastin-like materials, and (III) viscoelastic mechanical properties of soft polymers. Through this approach, we unveil the myriad material properties of mutant collagens, as well as chemically and physically processed silk-based materials. We also rapidly and efficiently determine the material parameters of constitutive models governing the time-dependent behavior of soft polymers.

2:30 PM SB10.02.05

Compact Peptoid Molecular Brushes for Nanoparticle Passivation Shih-Ting Wang¹, Honghu Zhang¹, Sunting Xuan², Dmytro Nykypanchuk¹, Yugang Zhang¹, Guillaume Freychet¹, Benjamin Ocko¹, Ronald N. Zuckermann², Nevena Todorova³ and Oleg Gang⁴; ¹Brookhaven National Laboratory, United States; ²Lawrence Berkeley National Laboratory, United States; ³RMIT University, Australia; ⁴Columbia University, United States

Controlling the interface of colloidal nanoparticles (NPs) via tethered molecular chains of defined passivation properties is crucial for NP applications in electronics, optoelectronics, catalysis, and nanomedicine. There is an urgent need for a flexible system to vary the chemistry and structure of these interfacial molecules in a systematic and pre-determined way to improve control over NP stability and functionality. Here, we report low molecular weight, bifunctional comb-shaped, and sequence-defined peptoids that effectively passivate gold NPs (AuNPs). Each peptoid (PE) is designed with a multivalent NP-binding domain and a solvation domain consisting of branched oligo-ethylene glycol (EG) and varied in arrangements. We find that a diblock arrangement provides superior colloidal stability in varied salt and ionic aqueous solutions yet form a compact layer on the NP surface only ~1.5 nm thick. We further demonstrate by experiments and molecular dynamics simulations that the PE-coated NPs (PE/NPs) are stable in select organic solvents owing to the strong PE-Au binding and solubility of EG motifs. Finally, the PE/NPs can self-assemble into organized 2D lattices at the air-water interface with small lattice constants (~6 nm) due to the thin PE surface layer. The versatility and designability of peptoid architectures for NP passivation render an

attractive approach for nanomaterial-based (bio)technologies, in which precise control over size, surface property and stability are key.

2:45 PM *SB10.02.06

Dynamic Materials Inspired by Cephalopods Alon Gorodetsky; University of California, Irvine, United States

Cephalopods (e.g., squids, octopuses, and cuttlefish) have captivated the imagination of both the general public and scientists alike due to their sophisticated behavior and stunning camouflage abilities. Given such characteristics, it is not surprising that these marine invertebrates have emerged as exciting models for novel materials and systems. Within this context, our laboratory has focused on the development of cephalopod-inspired biomaterials and platforms with unique electrical and optical properties. Our findings hold implications for next-generation bioelectronic devices and biomedical imaging technologies.

3:15 PM BREAK

SESSION SB10.03: Biomaterials Nanotechnology

Session Chair: Benedetto Marelli

Tuesday Afternoon, November 30, 2021

Sheraton, 2nd Floor, Back Bay C

4:00 PM *SB10.03.01

Sustainable Nanotechnology—Bio-Inspired, Nature Derived and Non Toxic Nanomaterials for Agri-Food Applications Philip Demokritou and Tao Xu; Harvard University, United States

Sustainable nanotechnology is an emerging field of interdisciplinary research that focuses on the development of “green” and non toxic nanomaterials and technologies that can be used to tackle major societal challenges in various fields and applications. Maintaining food safety and security for the increasing global population is one of the most important challenges of the 21st century with major societal, environmental and public health implications.

This seminar will present highlights from our current sustainable nanotechnology research in the agriculture and food domain. Projects include among other the development of green, nano-carrier platforms for targeted precision delivery of nature-derived antimicrobials for food safety applications using engineered water nanostructures (EWNS) synthesized using electrospray and ionization processes. EWNS exhibit unique physicochemical properties, are highly mobile due to their nanoscale size and can interact and inactivate food related pathogenic and spoilage microorganisms on surfaces and in the air. In addition, the development of “smart” or stimuli responsive, non toxic and biodegradable antimicrobial packaging materials will be presented. Food packaging plays a key role as it has a great potential to improve food safety and quality and reduce food waste across the “farm to the fork” continuum.

4:30 PM SB10.03.02

Manipulating the Motion of Discretized Droplets with Laser-Microstructured Copper Substrates Decorated with Nanohair-Like

Texture Athanasios Milionis, Christos Stamatopoulos, Norbert Ackert, M. Donati, Paul Leudet de la Vallée, Philipp Rudolf von Rohr and Dimos Poulikakos; ETH Zurich, Switzerland

Transport of small liquid volumes (few and sub droplets) is a desired functionality for a wide range of applications, such as microfluidics, lab-on-chip devices, water collection from the atmosphere, etc. In general, liquid transport is usually achieved through the use of pumping devices, or external fields (electromagnetic, acoustic, optical, etc.) working collaboratively with special fluid or surface properties to enable fluid motion (e.g. ferrofluids or photosensitive substrates). On the other hand, passive droplet transport methods are more attractive compared to the active ones, due to the absence of the need for energy input and their inherent facility.

In addition, another common problem at small scales is the natural liquid adhesion of droplets on surfaces, which deters motion, induces high variation in the transported fluid mass, while the adhered fluid residues also cause surface contamination. Most of the developed passive fluid transport approaches, fail to resolve this issue, as they typically transport fluid in the form of a liquid film rather than discretized droplets. Therefore, still, significant advancements are needed before devices for passive liquid propulsion, without the input of external energy and unwanted contamination, become a reality in applications. In this work, we present an unexplored, bioinspired by the water strider leg surface architecture, scalable, and facile material design approach based on laser micromachining process of copper in the shape of a backgammon-like pattern, followed by chemical growth of copper hydroxide nanoneedles functionalized with a thiol to impart superhydrophobicity. The combined effect of the Laplace-pressure-imbalance and surface superhydrophobicity is able to passively drive droplet motion while maintaining the limited contact of the Cassie-Baxter state on superhydrophobic surfaces. The backgammon-like micro-topography design naturally deforms asymmetrically the menisci formed at the bottom of a spherical droplet and causes a Laplace pressure imbalance that drives droplet motion. We investigate this effect over a range of opening angles (1°, 5°, and 9°) and develop a model to explain and quantify the underlying mechanism of droplet self-propulsion.

We further implement the developed bioinspired topography for applications relevant to microfluidic platform functionalities. In particular, we explore lateral droplet motion and measure the droplet velocity during its self-propulsion (up to 40 mm/s for opening angle 9°), as well as the force acting on the droplet meniscus as it deforms at the solid-liquid interface (up to $\gg 5 \mu\text{N}$). Additionally, we achieve controlled rebound angles after droplet impact on the substrates up to $\omega = 8^\circ$, droplet merging, and long-distance droplet transport without mass loss. Furthermore, we demonstrate spontaneous droplet merging of droplets that are released simultaneously. The merging occurs very fast (in a few hundreds of ms) and it is aided by the underlying backgammon-like structures. Finally, we achieve horizontal self-transport to distances up to 65 times the droplet diameter and even show significant uphill motion against gravity, which to our knowledge is the longest traveling distance reported for discretized droplets by using fully passive means.

SESSION SB10.04: Poster Session I: Biomaterials in Medicine, Food and Agriculture

Session Chair: Benedetto Marelli

Tuesday Afternoon, November 30, 2021

8:00 PM - 10:00 PM

Hynes, Level 1, Hall B

SB10.04.01

Aptamer-Gold Nanoconstruct Coated with Polymer for Scavenging ROS and Capturing Proinflammatory Cytokine TNF- α [Jinseong Kim](#)¹, Hyeonmok Park¹ and Won Jong Kim^{1,2}; ¹Pohang University of Science and Technology, Korea (the Republic of); ²OmniaMed Co, Ltd., Korea (the Republic of)

In this study, we designed a unique aptamer-gold(Au) nanoconstruct coated with polymer capable of scavenging reactive oxygen species(ROS) and capturing tumor necrosis factor alpha(TNF- α) as anti-inflammatory agent for the treatment of peritonitis. Polymer-coated Au nanoconstruct equipped with TNF- α aptamer and ATP aptamer is constructed by interaction between ATP and both ATP aptamer and polymeric phenylboronic acid (pPBA). The phenylboronic ester formed in the nanoconstruct can scavenge ROS and TNF- α aptamer can capture proinflammatory cytokine TNF- α . ROS-responsive removing of pPBA from nanoconstruct with high ROS scavenging capacity, and high TNF- α capturing ability of nanoconstruct are investigated. Thus, these combined properties enable the nanoconstruct an additive anti-inflammatory effects. We demonstrated the high anti-inflammatory effects of the nanoconstruct in vitro and in vivo peritonitis model by monitoring ROS and pro-inflammatory cytokine levels.

SB10.04.02

Hydrogel-Based Artificial Cell (hAC) for Multipotent Cancer Immunotherapy Yunjin Chae¹, Kang-Gon Lee², Yongdoo Park² and [Jongseong Kim](#)²; ¹Scholar Fox trot, Korea (the Republic of); ²Korea University, Korea (the Republic of)

Cancer immunotherapy is a clinical strategy that acts on antitumor responses by invigorating the immune system to attack cancer cells. In the treatment of cancer, immune checkpoint inhibitors, i.e. mAbs binding to cytotoxic T lymphocyte antigen 4 (CTLA4), programmed cell death 1 (PD-1), or PD-1 ligand (PD-L1), neutralize the evadability of cancer cells against the immune system. However, this powerful therapy is hampered by expensive cost for the treatment, as well as by limited efficacy only responding to some patients. Here we show the development of hydrogel-based artificial cells (hAC) that potentiate cancer treatment by increasing the efficacy of bispecific immunotherapy targeting to CTLA4 and PD-L1 simultaneously. The conformation of hAC is characterized by a responsive soft hydrogel nanoparticle consisting of *N*-isopropylacrylamide-co-acrylic acid, antibody binding protein (protein A), and two immune checkpoint inhibitor mAbs (CTLA4 mAb and PD-L1 mAb, respectively). We demonstrate that the use of hAC significantly decreases the survivability of MCF-7 cancer cells in vitro and suppresses the growth of MCF-7 derived xenografts in vivo in comparison to the mAb treatment by itself. Our result also suggests that the bispecific hAC is more potent to treat cancer cells than monospecific hAC which is conjugated with either CTLA4 mAb or PD-L1 mAb alone. The advantage of hAC over current bispecific antibodies arises from their adaptability to link multiple antibodies in easy and fast, enabling the hAC system for rapid validation of bispecific antibodies in cancer treatment. Our finding has an important implication that hAC-based cancer immunotherapy opens a new paradigm not only to treat cancer but also to evaluate bispecific antibodies.

SB10.04.03

Development of Protein-Based Photo-Electrodes for Retinal Prosthesis [Stephanie Monge](#)¹, Ricardo Starbird², Juan J. Montero², Dariana Aguilar¹, Alexandra Tames¹, Sebastián León¹, Enrique Quiroga-Gonzalez³, Ashok Mulchandani⁴, Renugopalakrishnan Venkatesan^{5,6} and [Claudia Villarreal](#)^{1,7}; ¹Instituto Tecnológico de Costa Rica, Costa Rica; ²Tecnológico de Costa Rica, Costa Rica; ³Benemérita Universidad Autónoma de Puebla, Mexico; ⁴University of California, Riverside, United States; ⁵Harvard Medical School, United States; ⁶Northeastern University, United States; ⁷University of California, United States

Retinal prostheses are a promising technology in the field of visual restorative medicine for the treatment of patients with severe stages of retinal degenerative diseases. The highly stable light-activated proton pump bacteriorhodopsin (bR) has a great potential to be used in the fabrication of electrodes for artificial retinal implants due to its optical and photoelectric properties. Its usage in the generation of a photoelectrical signal can show remarkable performance in responsivity and quantum efficiency. In the present work, it is shown the development of a bR-sensitized photoelectrode for its future application in a retinal prosthesis. The study is aiming at analyzing the photovoltaic performance of a photoreceptor cell fabricated with a bR photoanode integrated with different low-cost and carbon-based cathodes of 3,4-ethylenedioxythiophene (PEDOT), graphene, carbon nanotubes, and their hybrids. The protein is immobilized on ITO covered by TiO₂ by drop-casting and electrophoretic deposition. The cell is tested using a hydroquinone/benzoquinone-based redox electrolyte. Linear sweep voltammetry, open-circuit voltage decay, and electrochemical impedance spectroscopy are measured under dark and illuminated conditions to determine the influence of different parameters in the function of the bR-sensitized photoelectrode. A mathematical model of the bR-cell equivalent circuit is fitted to the experimental data to further elucidate charge transfer resistance and frequency in the different interfaces of the device. The biological photoreceptor could significantly contribute to reduce and replace traditional costly and harmful materials used in conventional photovoltaic technology with renewable carbon-based alternatives; which could decrease the cost, enhance its performance, and improve the device biocompatibility and sustainability.

SB10.04.04

Self-Assembly of Charged Amphiphilic Oligomers at the Liquid-Liquid Interface—Insights from Vibrational Sum Frequency Generation Spectroscopy and Molecular Dynamic Simulation [Zening Liu](#), Lu Lin, Tianyu Li, Jan-Michael Carrillo, Benjamin Doughty, Charles Patrick Collier, Kunlun Hong, John Katsaras and Jesse Labbe; Oak Ridge National Laboratory, United States

Knowing the conformational states of amphiphilic molecules at liquid-liquid interfaces is important for understanding the underlying mechanisms governing interfacial phenomena, including adsorption/desorption dynamics, membrane assembly, and domain formation. Previously, using vibrational sum frequency generation spectroscopy (SFG), we found that a series of simple inorganic anions in aqueous solution at a buried hexadecane-water interface profoundly affected the self-assembly of monolayers of charged, amphiphilic oligomers consisting of ionic liquid (IL) headgroups covalently bonded to hydrophobic tails (oligodimethylsiloxane imidazolium cation (ODMS-MIM⁽⁺⁾), *J. Amer. Chem. Soc.* **142**, 290-299 (2020)). Elucidating how aqueous counterions alter the interfacial density of the charged IL headgroups will be critical for understanding monolayer formation at the interface. This talk will describe our use of a liquid-liquid Langmuir trough for controlling the interfacial pressure of the ODMS-MIM⁽⁺⁾ monolayer at the oil-water interface in conjunction with SFG and molecular dynamic simulations. This enables us to characterize how changes in molecular area correlate with conformational changes of the tails and packing of the oligomers in the membrane during assembly, with and without electrostatic interactions with the counterions. The ability to control the packing of the charged oligomers with compression independently from specific ion effects and ion pairing interactions offers new insight into the mechanisms for amphiphile adsorption, membrane structural changes, and hydrogen bonding at the interface that can inform strategies for controlling chemical reaction dynamics at liquid-liquid interfaces.

SB10.04.05

High-Aspect Ratio Cassettes for Rapid Vitrification of Organisms [Justyna Jaskiewicz](#)¹, Derin Sevenler¹, Denise Dayao², Anisa Sweil¹, Donald Girouard², Giovanni Widmer², Saul Tzipori², Mehmet Toner¹ and Rebecca D. Sandlin¹; ¹Massachusetts General Hospital/ Harvard Medical School, United States; ²Tufts University, United States

Infection with protozoa of the genus *Cryptosporidium* is a leading cause of child morbidity and mortality associated with diarrhea in the developing world.

As a zoonotic pathogen transmitted from cattle it is an important threat to public health with its potential for waterborne and foodborne dissemination. Research on this parasite has been impeded by many technical limitations, including the lack of cryopreservation methods. Consequently, laboratory strains of *Cryptosporidium* must be maintained by propagation in susceptible animals every 6–8 weeks, an expensive and time-consuming process. It is parasite sensitivity to formation of ice and limited permeability to cryoprotectants (CPAs) that precludes utilization of classical methods of slow cooling. To address this gap, a vitrification protocol was considered as an ice-free alternative for cryopreservation. Vitrification, unlike slow cooling, utilizes high intracellular concentrations of cryoprotectants combined with rapid cooling rates to achieve formation of an amorphous glassy solid devoid of ice crystals, thus protects cellular systems during cooling. Because of CPA toxicity, the vitrification field has moved toward the development of containers that enable extremely rapid cooling rates and thus vitrify with lower concentrations of intracellular CPA. In consequence of the reduced thermal mass, these containers are restricted to small volumes limiting widespread implementation of vitrification in clinical and research setting. To address this bottleneck, we developed a cryopreservation protocol that enables increased sample volume through the design and manufacture of a novel polycarbonate high aspect ratio specimen container referred to as 'vitrification cassette'. This strategy increases the volume of a single cryopreserved sample by 50-fold up to 100 μ L compared to the previously reported methods using 2 μ L microcapillaries. The high surface area to volume ratio of vitrification cassettes allows to maintain cooling rate at \sim 10,000 $^{\circ}$ C/min and supports vitrification of 30% DMSO/ 0.8 M trehalose extracellular cocktail solution. Due to the increase of CPA concentration required for glass formation, toxic effects were mitigated by application of step-wise CPA addition protocol. These cassettes were shown to support preservation of viable and infectious *Cryptosporidium* oocysts. Oocysts cryopreserved using cassettes exhibit viability at \sim 75%, maintain in vitro infectivity, and are infectious to interferon-gamma (IFN- γ) knockout mice (*C. parvum*) and gnotobiotic piglets (*C. hominis*). Importantly, the course of the infection is comparable to that observed in animals infected with unfrozen oocysts. Vitrification of *Cryptosporidium* oocysts in larger volumes will expedite progress of research by enabling the sharing of isolates among different laboratories and the standardization of clinical trials. Vitrification cassettes allow to obtain multiple inocula from a single cryopreserved sample thus overcoming a major bottleneck in the development and testing of therapeutics and vaccines for the treatment and prevention of cryptosporidiosis. This technology is readily available for translation to other cellular systems.

SB10.04.06

Late News: Brain Tumor Imaging Using Magnetic Particle Imaging (MPI) Hamed Arami, Chirag Patel, Edwin Chang, Jianghong Rao and Sanjiv Sam Gambhir; Stanford University, United States

Routine glioblastoma multiforme (GBM) imaging in clinics are based on using gadolinium-based magnetic resonance imaging contrast agents. However, using these gadolinium-based contrast agents raises major concerns for GBM patients suffering from chronic kidney disease, which can be resolved by using nanoparticle contrast agents that do not show any renal clearance due to their larger size. Here, we will demonstrate how a new imaging technique, called magnetic particle imaging (MPI) can be used for safer GBM imaging. We have investigated our approach for imaging of several types of brain tumors with different levels of aggressiveness, to identify the feasibility of this method in different brain tumor microenvironments. First, we developed methods for tuning iron oxide nanoparticles (NPs) to generate high resolution (i.e., \sim 600 μ m) MPI images with ultra-high contrast agent mass sensitivity of less than \sim 550pg Fe/ μ L. Then, we used MPI for three-dimensional targeted imaging of the orthotopic brain tumors in mice after intravenous injection of these NPs. Iron oxide nanoparticles have been approved by FDA for several clinical applications and we hope that this method will ultimately find clinical applications for safer GBM imaging.

SB10.04.07

Captured the Biophotons to Precisely Activate Chlorin e6 for Photodynamic Therapy Hao Yan^{1,2} and Seok-Hyun A. Yun^{1,2,3}; ¹Massachusetts General Hospital, United States; ²Harvard Medical School, United States; ³Massachusetts Institute of Technology, United States

The clinic utilization of photodynamic therapy (PDT) to treat cancers and malignant diseases has recently gained increasing attention. However, the shallow penetration of activated light, the concern of biosafety for new light delivery methods, and the risks of stimulating invasion and metastasis because of incomplete phototherapy have limited the further applications of PDT in deep tissues. Here we present a bioluminescence (BL) energy-induced PDT (BL-PDT) platform through conjugating sufficient clinic-approved photosensitizer chlorin e6 (Ce6) into the surface of luciferase, which can capture most of the biophotons and precisely activate Ce6 to produce reactive oxygen species (ROS). After largely entering cells, the conjugate (named Luc8-Ce6) produced very considerable intracellular ROS and induced cancer cell death. At the same time, the therapeutic efficiency is comparable to Laser-PDT using the same PS and moderate power. The further *in vivo* studies showed that the conjugate-based BL-PDT resulted in complete tumor remission, prevented the following metastasis in lymph nodes and lungs, and obtained potent neo-adjuvant antitumor efficacy for triple-negative breast cancer tumor after intra-tumoral injection. Our results offer a way to efficiently harness the low energetic bioluminescence to achieve noninvasive, depth-independent, and widely applicable phototherapy.

SESSION SB10.05: Nanocarriers and Nanosensors

Session Chair: Benedetto Marelli
Wednesday Morning, December 1, 2021
Sheraton, 2nd Floor, Back Bay C

10:30 AM *SB10.05.01

Applications of Nanomaterials for Agriculture and Plant Biology—Nanocarriers and Nanosensors Michael S. Strano; Massachusetts Institute of Technology, United States

Our laboratory at MIT has been interested in exploring the relatively new interface between living plants and non-biological nanostructures to impart the former with new and enhanced functions, which we call Plant Nanobionics. We have developed a theory of subcellular uptake and kinetic trapping of a wide range of nanoparticles, validated *in-vivo* in living plants. Confocal visible and near infrared fluorescent microscopy and single particle tracking of Gold-Cystein-AF405 (GNP-Cys-AF405), Streptavidin-Quantum Dot (SA-QD), Dextran and Poly(acrylic acid) nanoceria, and various polymer-wrapped SWCNT, including lipid-PEG-SWCNT, chitosan-SWCNT and (AT)₁₅-SWCNT, were used to demonstrate that particle size and the magnitude, but not the sign, of the zeta potential are key in determining whether a particle is spontaneously and kinetically trapped within chloroplasts or the cytosol. We develop a mathematical model of this Lipid Exchange Envelope Penetration (LEEP) mechanism, which agrees well with observations of this size and zeta potential dependence. As an application, we rationally designed a chitosan-complexed single-walled carbon nanotube (SWNT) as nanocarriers to selectively deliver plasmid DNA (pDNA) to chloroplasts of different plant species without external biolistic or chemical aid. We demonstrate chloroplast-targeted transgene delivery and expression in living mature arugula (*Eruca sativa*) and watercress (*Nasturtium officinale*) plants *in planta* and in isolated *Arabidopsis thaliana* mesophyll protoplasts. Another application of nanoparticles and nanotechnology to plant sciences is in the form of

biochemical sensors that operate *in planta* and across diverse species. Using non-destructive optical nanosensors, we find that the spatial and temporal H₂O₂ concentration immediately post-wounding follows a simple logistic waveform for six dicot plant species: lettuce (*Lactuca sativa*), arugula (*Eruca sativa*), spinach (*Spinacia oleracea*), strawberry blite (*Blitum capitatum*), sorrel (*Rumex acetosa*), and *Arabidopsis thaliana*, ranked in order of wave speed from 0.44 to 3.10 cm/min. The H₂O₂ wave tracks the concomitant surface potential wave measured electrochemically for the series of plants. We show that the plant NADPH oxidase RbohD, glutamate receptor-like channels (GLR3.3 and GLR3.6) are all critical to the propagation of the H₂O₂ waveform upon wounding. Our findings highlight the utility of a new type of nanosensor probe that is species-independent and capable of real-time, spatial and temporal biochemical measurements in plants.

11:00 AM SB10.05.03

Precise Payloads Delivery to Multi-Tissues of Plants via Microneedles Fabricated from Silk-Based Biomaterial Yunteng Cao^{1,2}, Eugene Lim¹, Menglong Xu³, Jing-Ke Weng^{3,1}, Pil Joong Chung⁴, Nam-Hai Chua^{4,2} and Benedetto Marelli^{1,2}; ¹Massachusetts Institute of Technology, United States; ²Singapore-MIT Alliance for Research and Technology, Singapore; ³Whitehead Institute for Biomedical Research, United States; ⁴TLL Temasek Life Sciences Laboratory, Singapore

New challenges to global food security are posed by rapid population growth, limited access to resources, and changes in climate patterns. Plant engineering is of great significance in current efforts by improving yield and/or resistance to abiotic/biotic stresses. The precise deployment of functional payloads to plant tissues is a new approach to help advance fundamental understanding of plant biology and accelerate plant engineering. However, the morphological and physiological barriers in plants (e.g., epidermis, cuticle) hinder efficient delivery of payloads. Here, a novel silk-based biomaterial is designed to function *in planta*. A microneedle-like device (named “phytoinjector”), bio-inspired by the stylet of psyllids fed by xylem/phloem sap, is then fabricated from this material, capable of delivering a variety of payloads ranging from small molecules to large proteins into specific loci of various plant tissues. It is demonstrated that phytoinjector can be used to deliver payloads into plant vasculature to study material transport in xylem and phloem and to perform complex biochemical reactions *in situ*. Furthermore, it is demonstrated *Agrobacterium*-mediated gene transfer to shoot apical meristem (SAM) and leaves at various stages of growth. In addition, tuning of the material composition enables the fabrication of another device, dubbed “phytosampler”, which is used to precisely sample plant sap. The design of plant-specific biomaterials to fabricate devices for drug delivery *in planta* opens new avenues to bridge the biotic/abiotic interface with plants, enhances plant resistance to biotic and abiotic stresses, provides new tools for diagnostics, and enables new opportunities in plant engineering.

11:15 AM *SB10.05.04

Designing Multifunctional Nanomaterials for Highly Sensitive Biosensors Antje Baeumner, Universität Regensburg, Germany

Biosensors for the rapid detection of low concentrations of pathogens, toxins, contaminants and metabolites in an on-site fashion is of utmost interest for clinical diagnostics, food safety and environmental monitoring. Albeit many differences in these application fields exist, challenges raised for the detection technology are strikingly similar: Low amounts and numbers of analytes have to be specifically identified and quantified within an immensely complex matrix such as blood, saliva, food stuff and environmental samples to name a few. Our research group addresses challenges arising from this complicated task in part through the development of multifunctional nanomaterials that enable significant improvements in signal transduction and enhancement, immobilization, pre-isolation or in-line purification, respectively. In combination with specific biorecognition and signal read-out, on-site biosensor platform technologies are thus developed that provide significantly lower limits of detection while maintaining a focus on low-cost, ease-of-use and high specificity characteristics.

The presentation will focus on nanomaterials designed as functional transducers, i.e. laser-induced graphene (LIG), and nanofibers. We have recently shown that LIG is a superior transducer in comparison to screen-printed electrodes used in most electrochemical on-site biosensors. Since ease and reproducibility-of-fabrication of such transducers are of utmost importance in the point-of-care and on-site sensor fields, we have investigated strategies to generate LIG and carbon nanofibers using laser-induced pyrolysis. Here, polyimide sheets and electrospun polyimide nanofibers are transformed using a CO₂ laser in a simple scribing process under ambient conditions. The resulting 3D LIG structures can be transferred to any other surface or in the case of the nanofibers be used as free-standing transducer, and are therefore very easy to make, to miniaturize, to integrate into sensing platforms including microfluidic systems. In addition, this process also enables straight-forward large-scale production. We will present our most recent work on voltammetric, potentiometric and impedance-based biosensors for medical diagnostics and food safety using these LIG and carbon nanofiber materials. Furthermore, we demonstrate that by doping the nanofiber materials with metal precursors, chemical sensing with most significant sensitivity and specificity can be accomplished. Here, morphological and performance characteristics can be directly influenced by metal content and laser power and hence can be adapted towards desired performance. Most importantly, we can show that this strategy can be adapted to a whole range of metal precursors and hence provide opportunities for such 3D carbon nanofiber nanocatalyst hybrids.

Nanofibers can also be made out of a variety of other polymers for the purpose of analyte capture, pre-concentration or even as optical transducers. We will hence also discuss nanofibers entrapping upconverting nanoparticles and fluorescent dyes, respectively, to demonstrate unique and intricate characteristics applied to food safety testing.

SESSION SB10.06: Micro and Nano Fabrication of Biomaterials for Sensing and Delivery

Session Chair: Benedetto Marelli

Wednesday Afternoon, December 1, 2021

Sheraton, 2nd Floor, Back Bay C

1:30 PM SB10.06.01

Aqueous Dispersions of Biodegradable Polymers for Sustainable Crop Protection Tahira Pirzada, Mariam Sohail, Charles H. Opperman and Saad A. Khan; North Carolina State University, United States

Increased awareness of the long-term impacts of agrochemicals has resulted in the hunt for efficient and sustainable delivery platforms. In order to meet the food demands of an exponentially increasing global population, there is a dire need to establish sustainable technologies for targeted and slow release of agrochemicals with minimal environmental footprints. Furthermore, rising concerns of the global community about the accumulation and environmental effects of microplastics have accelerated the search for alternate delivery vehicles developed from biodegradable polymers. We present a sustainable approach to synthesize aqueous dispersions of biodegradable cellulose derivatives *via* anti-solvent precipitation. We propose the utilization of these dispersions as controlled and targeted release formulations for a pesticide as a model active ingredient (AI). While the biodegradable nature of our polymer particles and use of water as the dispersant medium justify the sustainable nature of these formulations, we have investigated dispersion stability, leaf adhesion, rainfastness and AI release profile of the formulations to ensure their efficacy for foliar application. Additionally, we have used Isothermal

Titration Calorimetry (ITC) to investigate the nature of polymer interactions with the AI to provide a comprehensive picture of the performance and tenability of the formulations.

1:45 PM SB10.06.02

Use of Biopolymer-Based Microneedle Technology for the Sustainable Food Supply Chain Doyoon Kim, Yunteng Cao and Benedetto Marelli; Massachusetts Institute of Technology, United States

Ensuring food safety and security requires improvement of the current food quality monitoring system to mitigate risks of foodborne illness and minimize food wastes. Developing a real-time detection platform for bacterial pathogens and spoilage is a compelling goal to achieve this global mission. Incorporating sensors into packaging is a promising approach, but the lack of proper food contacting materials is challenging to enabling all the functionalities required for the smart-sensing sampling. This study presented a platform for detecting pathogenic bacteria in food using a porous microneedle array by utilizing non-toxic and edible silk fibroins extracted from *Bombyx mori* silkworms. The silkworm fibroins have emerged as promising technical materials for food contact applications due to their non-toxic and edible nature, in addition to their tunable mechanical and chemical properties. The porous microneedle structure allows extraction and delivery of internal food fluid to biosensors on the backside of the needle array by capillary action. We demonstrate food contamination by identifying *E. coli* in fish fillets within 16 h of injection through the unique patterns of the polydiacetylene-based colorimetric biosensors. This response by *E. coli* contamination can be distinct from common food spoilage measured via an increase in sample pH. We also show that the microneedle sensor can pierce commercial food packaging, indicating the feasibility of successfully adapting the technology downstream in current food supply chains. This study will contribute to food quality monitoring, ensuring global food safety, and minimizing food loss and waste.

2:00 PM SB10.06.03

Low-Cost Intelligent Food Packaging Systems via Laser-Assisted Synthesis and Microfabrication of Functional Micro/Nanostructures on Metalized Plastic Films Sarath Gopalakrishnan, Sina Nejati, Krish Gupta and Rahim Rahimi; Purdue University, United States

The food packaging market has become an indispensable aspect of our times as it is estimated to reach 450 billion dollars in revenue by 2027. In accordance with the ramping market projections, there has been an increasing demand for improving food quality and guaranteeing food safety. An intelligent and affordable packaging system that can also act as a tracking platform for food quality is the need of the hour. Since the chemical compounds produced inside a package are good indicators of spoilage of non-perishable foods, several active food quality sensors have been developed. However, active sensors are expensive as they need to carry batteries and electronic chips. Battery-less chipless sensors have gained great attention in food packaging and healthcare because of their low cost and wireless sensing capability and are an ideal candidate for pH sensors in food packaging systems. However, the main obstacles along the progress toward commercializing chipless sensors are the shortcomings in their manufacturing process.

Scalable manufacturing techniques such as printing techniques have been widely used for chipless sensors used in item tracking, gas sensors, and healthcare. While scalable manufacturing techniques offer a significant reduction in the number of processes and resources, it introduces tremendous challenges such as the ink formulation for conductive and functional patterns, the need for custom-made screens, and the time required in the drying and sintering processes. We have identified the roll-to-roll laser processing of metalized films as an economically viable low-cost alternative to conventional printing technologies used for chipless sensor development. This approach offers a one-step process that not only patterns the metallic layer to form predefined traces but also leaves remnant nanostructures in the processed region as thin oxide layers which significantly improves the adhesion between the laser ablated region and the functional material.

We propose a novel approach for laser-assisted manufacturing of chipless sensors that can detect the freshness of fish by sensing the levels of hypoxanthine (HX) released by the fish as it undergoes spoilage. A functional material based on xanthine oxidase (XOD), which is sensitive to the HX levels found in fish products, is developed to be coated on the sensor. HX and XOD are optimized to obtain a quick response from the biosensors. The sensor consists of a spiral pattern made of laser ablated Aluminum-based metalized paper that forms an inductor-capacitor tank circuit. The laser ablation of the metalized paper is done to selectively remove aluminum and expose the paper layer underneath. This process also leads to the formation of thin Al_2O_3 layers of the order of nanometers that can provide substantial adhesion to the functional material. The functional material is deposited on the most sensitive region on the inductive coil so that when the functional material dissolves in response to HX, the resonant peak dampens. The sensors are characterized with the help of a portable reader that sends an interrogation signal in the range of 1 MHz to 100 MHz and detects the amplitude of the resonant peak in the spectrum. Since the amplitude of the resonant peak is a function of the dissolution of the functional material, which is concomitant with the HX levels, this wireless sensing approach is employed in the development of a food quality sensor for fish freshness.

2:15 PM *SB10.06.04

Scalable Fabrication of Flexible Graphene Circuits and Fluidics for Multiplexed Electrochemical Sensing for Agriculture Zachary Johnson, Bolin Chen, Cicero Cardoso-Pola, Nate Garland, Carmen L. Gomes and Jonathan Claussen; Iowa State University, United States

This presentation will demonstrate how low-cost printed and flexible graphene circuits can be tailored for agricultural electrochemical biosensing integrated with open microfluidic devices. The use of inkjet and aerosol printing; spin coating; and laser writing (i.e., laser induced graphene) can be used to create such circuits with high resolution (line widths as low as 20 μm). Moreover, the use of laser scribing of the graphene and/or salt porogens added into graphene inks before printing can be used to further improve the electrical conductivity (< 10 ohms/sq.), electroactive surface area (nano/micro structuring), and surface wettability (hydrophilic to superhydrophobic) of the graphene circuits. These printing and laser fabrication techniques are amenable for use on flexible and chemically/thermally sensitive surfaces including polymers and paper.

The graphene-based sensors are subsequently biofunctionalized with enzymes, ion-selective membranes, and antibodies for pesticide and nitrogen sensing in soil/water samples as well as cytokine and histamine monitoring in cattle serum and fish broth. The detection limits of the biosensors so far have achieved 0.6 nM for organophosphate pesticides; 20 mM for ammonium, potassium, and nitrate ions; 25 pg/mL and 46 pg/mL for IL-10 and IFN- γ in cattle serum; and 3.41 ppm in tuna broth respectively. Moreover, we demonstrate how the hydrophobicity of the graphene can be tuned to create multifurcating wedge channels with hydrophilic paths surrounded by superhydrophobic walls that transport and split fluid to distinct biosensors *via* Laplace pressure. We demonstrate how such open microfluidics can be used to develop multiplexed fertilizer ion and pesticides sensors for the field. Such sensing results demonstrate that such scalable graphene sensor technology is well-suited for in-field, low-cost biosensing that is needed for large scale mapping of contaminants in watersheds and farm fields as well as monitoring large volumes of food products.

2:45 PM BREAK

SESSION SB10.07: Biomaterials for Food and Agriculture I
Session Chair: Benedetto Marelli
Wednesday Afternoon, December 1, 2021
Sheraton, 2nd Floor, Back Bay C

4:00 PM *SB10.07.01

Transitioning Bioactive Excipients from Drug Delivery to Crops Anthony Cartwright and David W. Britt; Utah State University, United States

Pharmaceutical excipients vary widely in function, being used as absorption enhancers, emulsifiers, preservatives, and sustained release matrices. Here the FDA-approved excipient, Poloxamer P188, is explored as a bioactive excipient in the wheat rhizosphere and contrasted with the natural osmolyte, glycine betaine. The P188 triblock copolymer self-assembles into 5.5 ± 0.3 nm micelles whose size does not vary significantly when encapsulating hydrophobic cargo, such as the plant metabolite quercetin. Column transport studies demonstrated loaded P188 micelles delivered cargo intact, supporting assessment in plant studies. Wheat seedlings were grown in a sand matrix for 14 days, subjected to 8 days of simulated drought, and then recovered for 7 days. To better represent wheat grown in drought-prone regions, seeds were inoculated with a model rhizobacterium, *Pseudomonas chlororaphis* O6 (PcO6) which has been shown to improve drought tolerance in winter wheat. Seedlings were treated separately with 0.2 mmol P188 or 10 mmol glycine betaine per kg of sand matrix, or with the combined nano-formulation. The quantum yield of photosystem II, total growth of plant mass, and relative water content under drought were measured. Both P188 and the P188 / betaine nano-formulation increased total above ground plant mass relative to the control, while the inclusion of betaine alone suppressed tissue growth and photosynthetic activity during periods of simulated drought but improved performance during recovery. P188 addition resulted in significantly higher relative water content in wheat under drought, suggesting activity as a synthetic osmolyte that resists sorption to soil components while carrying additional cargo intact through the rhizosphere.

4:30 PM SB10.07.02

Microfabrication of Silk-Based Capsules for Stabilization and Controlled Delivery of Payloads Muchun Liu¹, Pierre-Eric Millard², Rupert Konradi², Ophelie Zeyons², Henning Urch² and Benedetto Marelli¹; ¹Massachusetts Institute of Technology, United States; ²BASF Corporation, Germany

Microcapsules are used in a wide range of products including certain types of fertilizers, plant protection products, leave-on and rinse-off cosmetic products to adjust release profiles, stabilize actives and control environmental fate such as volatilization or wash off. The development of microencapsulation is targeted to minimize active levels and limit negative impact on the environment. However, plastic materials are generally used in manufacturing. There is an increasing concern about microplastics dissemination by the public and legislators due to their potential impacts on environment and human health. Here we demonstrate an approach to fabricate biodegradable microcapsules using silk protein as a sustainable alternative. Silk fibroin is a known natural, proteinaceous fiber that can be tailored into a water-soluble suspension for solution processing. Two fabrication methods are employed to encapsulate different types of payloads, including water-soluble (Vitamin C) and -insoluble actives (agrochemicals). Ultrasonic spraying and freeze drying produce uniform microspheres with controllable porosity. Spray drying produces crumpled, but dense microparticles. Increased crystallinity of silk component is achieved by ethanol-induced beta-sheet transformation. The effects of morphology, loading and crystallinity on release profiles are discussed. The resulting silk-based microcapsules offer a solution to current microplastic pollution while retaining adequate delivery performance.

4:45 PM *SB10.07.04

Graphene and Stimuli-Responsive Brush Sensors for Foodborne Pathogens Detection in Food and Hydroponic Water Carmen L. Gomes¹, Raquel Soares¹, Daniela A. Oliveira², Cicero Cardoso-Pola¹, Robert Hjort¹, Kshama Parate¹, Eric S. McLamore³ and Jonathan Claussen¹; ¹Iowa State University, United States; ²Texas A&M University, United States; ³Clemson University, United States

Food contamination in processing facilities and during fresh produce cultivation can lead to serious public health problems and costly recalls of millions of food units. Currently, rapid sensing technology is lacking for definitive detection of foodborne pathogen in food-processing plants and irrigation water during fresh produce production, which delays initiation of appropriate control measures and increases the likelihood of spreading contamination and foodborne illnesses outbreaks. Herein, we report the fabrication of user-friendly biosensors capable of rapid (17-22 min), enrichment-free detection of foodborne pathogens in food processing facilities and hydroponic systems at levels comparable to current culture based and PCR methods (detection limits ~5 CFU/mL). The sensors are fabricated using graphene or stimuli-responsive polymers, and subsequently functionalized with pathogen-specific antibodies or aptamers. Unique laser processing induces a 3D nanostructured topology in graphene that becomes electroactive and hydrophilic, and polymer actuation protocol, i.e., brushes on the extended conformation for bacteria capture and the collapsed state for electrochemical signal transduction are desirable for enabling high signal-to-noise ratios and test sensitivity. An example for *Salmonella* Typhimurium detection is provided. After functionalization with *Salmonella*-antibodies, the graphene-based biosensors were able to detect live *Salmonella* in chicken broth across a wide linear range (25 to 10^{15} CFU/mL) and with a low detection limit (13 ± 7 CFU/mL; $n = 3$). For *Listeria monocytogenes* and *Escherichia coli* spp. detection the use of stimuli-responsive brush actuation is demonstrated. After functionalization with *Listeria*-aptamer and *E. coli*-antibodies, the stimuli-responsive brush sensors were able to detect live *Listeria monocytogenes* and *E. coli* in vegetable broth and hydroponic water across a wide linear range (10 - 10^{10} CFU/mL) and with a low detection limit (as low as 3.3 ± 0.9 CFU/mL; $n = 3$). These results were acquired using a potentiostat with an average response time of 17-22 minutes without sample pre-concentration or redox labeling techniques. After analyzing nanobrush actuation in stagnant media, we developed a flow through system using a series of pumps that are triggered by electrochemical events at the surface of the biosensor. Sense-Analyze-Respond-Actuate proof of concept may be viewed as a cyber-physical system that actuates nanomaterials using smartphone-based electroanalytical testing of samples. These graphene and stimuli-responsive sensors displayed high selectivity as demonstrated by non-significant response to other bacteria strains. These results demonstrate how graphene and stimuli-responsive electrodes can be used for electrochemical sensing in general and, more specifically, could be used as a viable option for rapid and selective pathogen detection in food processing facilities and hydroponic farms.

SESSION SB10.08: Poster Session II: Biomaterials in Medicine, Food and Agriculture
Session Chair: Benedetto Marelli
Wednesday Afternoon, December 1, 2021
8:00 PM - 10:00 PM
Hynes, Level 1, Hall B

SB10.08.01

Novel Method for Rapid Detection of Neutralizing Antibodies After COVID-19 Vaccination Using Bioresponsive Microgel Based SPR

Biosensor Su-Kyoung Lee¹, Bora Yim², Ara Ko², Yongdoo Park¹ and Jongseong Kim^{1,2}; ¹Korea University, Korea (the Republic of); ²Scholar Fox trot, Korea (the Republic of)

The efficacy of COVID-19 vaccination is closely related with the serum level of the SARS-CoV-2 neutralizing antibodies that bind to the receptor binding domain (RBD) of the SARS-CoV-2 spike protein. Therefore, rapid and quantitative measurement of the SARS-CoV-2 neutralizing antibody (NAb) in the sera of vaccinated people is essential to develop the effective vaccine and further achieve population immunity, i.e., herd immunity. Plaque reduction neutralization test (PRNT), the gold standard of NAb effectiveness in serologic test, is accurate but requiring biosafety facilities due to the use of the virus, which hampers its application for common laboratories and clinical sites. Here, we developed a bioresponsive microgel based surface plasmon resonance (SPR) platform that detects SARS-CoV-2 NAb in clinical samples without complicated pre-treatment. We found that protein multivalent binding (PMB) between microgel conjugated RBD protein and the COVID-19 NA yields significantly enhanced SPR signals than those of nonspecific interference from serum proteins in microgel based SPR assay. The excellence of our microgel based COVID-19 NAb test occurs from its selectivity for the NA only with resistance to all other proteins, allowing rapid detection and quantification of NAb for each individual. Importantly, our results provide that microgel based SPR assay will be considered as a novel NAb detection platform for COVID-19 vaccination strategy in easy and safely.

SB10.08.02

Understanding the Interface Between Macromolecules and Metal-Organic Frameworks in Water Christopher DeRe, Daniel Erdosy, Malia Wenny, Joy Cho, Ricardo Sanchez and Jarad A. Mason; Harvard University, United States

Metal-organic frameworks (MOFs) are porous crystalline solids with the ability to selectively concentrate large quantities of gases, offering significant promise as building blocks for energy and biomedical technologies. The surfaces of MOFs are frequently modified by polymers to ensure good compatibility or dispersibility in functional materials or liquids; however, the vast majority of current studies focus on MOF-polymer interactions in solid plastic matrices or organic solvents. Here we show that noncovalent complexation with biological or synthetic polymers enables control over the MOF-polymer interface in water. By understanding and manipulating the interface, properties such as MOF dispersibility and structural stability can be finely tuned—for instance, the degradation rate of a hydrolytically unstable MOF in water can be controlled over 2 orders of magnitude depending on the polymer selection. Present studies provide a path toward controlling the properties of MOFs in water and using MOFs as a platform to understand the behavior of macromolecules at porous interfaces in aqueous media, a ubiquitous situation in Nature that is difficult to study given the sensitivity and complexity of biological systems.

SB10.08.04

Reduced Oxidation of PDMS by Microparticles of Natural Polyphenols Yunho Cho and Jonghwi Lee; Chungang University, Korea (the Republic of)

Polydimethylsiloxane (PDMS) could be oxidized by the various stresses of electrical devices, such as heat, ozone, electrical and mechanical stress, leading to loss of elastomeric properties and ultimate failure. To reduce oxidation, various antioxidants could be mixed with PDMS during manufacture processes. Since the effective radius of antioxidant molecules is relatively small, the antioxidants need to be mixed in a molecular level. However, the low surface energy of PDMS makes the mixing in a molecular level difficult. In this study, we mixed tannic acid, naringenin and a commercial antioxidant with PDMS and investigated their characteristic changes after thermo-oxidation. We added microparticles of antioxidants to PDMS precursor, and the particles are retained matrix to reduce oxidation effectively. Although antioxidants are mixed in micron-size, the antioxidants in PDMS effectively reduced oxidation. In thermogravimetric analysis, PDMS showed faster mass losses than the samples containing antioxidants under 400 °C. In the tensile tests of dumbbell shape specimens, the antioxidants provided a 3-fold increase in Young's modulus, while neat PDMS showed an 88-fold increase in Young's modulus at the thermo-oxidative condition of 3 days and 250 °C. Even though both the neat PDMS and the PDMS containing antioxidants showed similar values of strain-at-break within the error range before heat treatment, neat PDMS showed a significantly smaller strain-to-break (only 10.2%) than the PDMS with antioxidants (46.8%) after 1 day oxidation at 250 °C. The FT-IR spectroscopy result of PDMS containing antioxidant showed much smaller changes in the peaks of 1060 and 865 than that of neat PDMS after oxidation, which are assigned to Si-R stretching. The Si peak analysis of XPS showed that the bonding of silicon atoms in neat PDMS is more oxidized from SiO₂C₂ to SiO₄ compared to the PDMS containing naringenin. These results offer the effective and nontoxic ways to widen the service conditions of PDMS.

SESSION SB10.09: Fabrication of Biomaterials for Regenerative Medicine and Tissue Models

Session Chair: Chiara Ghezzi

Thursday Morning, December 2, 2021

Sheraton, 2nd Floor, Back Bay C

10:30 AM *SB10.09.01

Hydrogel Materials to Improve Peripheral Nerve Repair Ryan Koppes¹, Abigail Koppes¹, Jonathan Soucy² and Katelyn Neuman¹; ¹Northeastern University, United States; ²Schepens Eye Research Institute, United States

Peripheral nervous system (PNS) injuries often lead to partial or complete loss of sensation, chronic pain, apraxia, and even permanent disability. Current guidelines recommend repairing severed nerves with sutures; however, sutures hinder tissue regeneration and often result in scar tissue formation further preventing functional recovery. To limit the need for sutures, fibrin glue has been proposed as an alternative to reattach severed nerve endings, but current formulations are not mechanically robust to significantly reduce the need for sutures. We have been developing new photocrosslinkable hydrogel systems from bioavailable polymers to be used as a glue for nerve anastomosis. Formulations have been developed to improve mechanical strength, flexibility, biocompatibility, adhesiveness, and electrical conductivity.

Conductive biomaterials can amplify endogenous and exogenous signaling that have been shown to play a crucial role in galvanotropism and galvanotaxis, processes that are crucial for neural repair. However, many of the popular conductive biomaterials are brittle, insoluble, opaque, and non-degradable. Choline acrylate has recently emerged as a biocompatible ionic liquid (IL) that can be incorporated into hydrogels to modify bulk conductivity. This IL is a transparent, degradable alternative to popular conductive materials that are not ideal to be placed as a permanent scaffold in patients. Matching the mechanical properties of the native nerve tissue is a crucial consideration when fabricating a new hydrogel composition. Viscoelastic properties have been demonstrated to play a role in maintaining the extracellular matrix (ECM) and tissue structure during normal movements, as well as cell differentiation. We have investigated the role that the addition of IL has on bulk electrical conductivity, biocompatibility, and dynamic mechanical properties.

Mechanical testing and *in vitro* cell culture demonstrate tunable physicochemical properties of our hydrogel systems, and that these materials support of the

growth of both glial and neuronal cells. Furthermore, results from *in vivo* implantation models demonstrate that the composite is biodegradability and biocompatible. Finally, we have confirmed that a severed nerve anastomosed by this composite has tensile strengths greater than the commercially available fibrin glue. In this talk will discuss our progress and our future work for hydrogel composites for use in nerve repair.

11:00 AM SB10.09.02

***In Vitro* Tissue Models to Study Host-Pathogens Interactions for Preclinical Validation of Medical Devices** Chiara Ghezzi; University of Massachusetts Lowell, United States

Introduction: Upon the recent pandemic, the COVID-19 testing process has been plagued by missing components, including swabs. Multiple companies and researchers have been focusing on the development of new swabs to collect clinical samples for COVID-19 testing. In order to validate new swabs, innovative experimental procedures are needed to streamline this process. Therefore, we have developed an *in vitro* tissue model to mimic nasopharyngeal (NP) and mid-turbinate (MT) nasal passages to perform pick-up and release of biological samples from a physiologically relevant nasal mucosa on the bench. There are currently no tissue models available for this purpose, as companies validate their new swabs by dipping in saline without mimicking any of the physiological aspects of the nasal passage (i.e., architecture, mechanical and physical structures). The tissue model will be used to validate NP and MT swabs and advance the design and optimization of the prototypes before reaching the clinical study stage.

Materials and Methods: A tissue model was generated to mimic the nasopharyngeal and mid-turbinate nasal cavities for the validation of NP and MT injection molded swabs. The physiological architecture was realized by 3D printing the Carleton-Civic Standardized Human Nasal Geometry (from Carleton University's Aerosol Research Lab), with Acrylonitrile butadiene styrene using a Fused Deposition Modeling 3D printer. The nasal mucosa was recreated by a soft tissue structure saturated with a viscous mucous component, to mimic the native tissue. Specifically, lyophilized silk fibroin sponges from Bombyx Mori formed the inner surface of the model to replicate the nasal passage tissue, and saturated with artificial mucus to mimic both symptomatic and asymptomatic conditions, based on Locust Bean Gum (LBG). Both mucus viscosities were measured based on LBG concentration to match previously reported values. The asymptomatic (0.23 w/v%) and symptomatic (0.92 w/v%) mucus displayed viscosities at 13 and 1400 cp, respectively. The mucus were then spiked with heat inactivated SARS-CoV-2 virus (BEI, NR-52286) to achieve a clinically relevant viral concentration. To quantify swab pick-up, gravimetric analysis was performed by collecting samples from the nasal model following CDC guidelines. Samples were collected using NP and MT injection molded swabs in comparison to FDA-approved flocked swab (Obecare # 20200507). Viral loads were then quantified with a qScript XLT 1-Step RT-qPCR against N1 N2 SARS-CoV-2 probes to quantify swab efficacy.

Results and Discussion: We tested standard flocked NP and MT swabs and novel injection molded NP and MT swab using models saturated with asymptomatic and symptomatic mucus containing virus. The gravimetric data indicated that the standard NP, MT swabs with asymptomatic mucus and the standard diseased MT swab picked up significantly more than the injected molded NP and MT swabs for those groups. However, the RT-qPCR data from all swabs demonstrated comparable viral loads.

Conclusions: Despite the reduced pick-up volumes from the injected molded swabs in comparison to standard flocked swabs, the viral detection was comparable. The pick-up and release data from the bench top *in vitro* model are also in agreement with on-going clinical studies, thus, supporting the validation of the *in vitro* model for pre-clinical swab validation.

Acknowledgements: NIH Rapid Acceleration of Diagnostics (RADxSM) program, 3U54HL143541-02

11:15 AM SB10.09.05

Late News: Engineering *In Vitro* Contractile Models of Duchenne's Muscular Dystrophy John Zimmerman, Ziad Al Tanoury, Peyton Nesmith, Jerome Chal, Kevin K. Parker and Olivier Pourquie; Harvard University, United States

Duchenne Muscular Dystrophy (DMD) is a devastating wasting disease that leads to the continual degradation of muscle tissues and eventually premature death. DMD is caused by a rare genetic mutation in the protein dystrophin, which is believed to act as a molecular 'shock absorber', helping stabilize the sarcolemma during muscle contraction. As a rare disease, there are limited curative options available for patients, with current drug trials showing a limited success rate. This is due in part to a lack of viable screening methods, with most pre-clinical testing being done in mdx mouse models, which only partially capture the diseased phenotype. As a result, there is a need for improved model systems using human derived tissues, which can more accurately predict patient outcomes and potentially be used for tailoring individualized treatments. Here we describe how engineered tissue constructs can be used to model the contractile phenotype of diseased and healthy patient cells. Using photolithographically defined muscular thin films, we show that muscle fibers derived from human induced pluripotent stem cell (iPSC) lines exhibit defective contractility when carrying an DMD mutation. This strongly supports the hypothesis that intrinsic contractility defects also contribute to the muscle weakness exhibited in DMD patients, in addition to the classical mechanisms of fibrosis and fatty cell replacement. Additionally, we demonstrate that these contractile defects can be largely rescued using prednisolone treatments, in both patient derived and DMD isogenic cell lines, indicating that prednisolone acts directly on mutant fibers, in addition to its anti-inflammatory or immunosuppressive effects. This work provides an *in vitro* platform for studying the etiology of DMD in human myofibers. Additionally, this study indicates that engineered microphysiological systems can serve as important tools in modeling rare diseases, as these systems are amenable to individualized patient screening and may offer potential insights into the mechanism of pharmaceutical action.

SESSION SB10.10: Biomaterials for Biomedical Nanotechnology

Session Chair: Chiara Ghezzi

Thursday Afternoon, December 2, 2021

Sheraton, 2nd Floor, Back Bay C

1:30 PM SB10.10.01

Inkjet-Patterned Protein Films for Engineering Interactions at the Interface for Size Sorting and Controlled Cell Adhesion Applications Sanjana Gopalakrishnan¹, Shuting Pan^{1,2}, Li-Sheng Wang¹, Ann Fernandez¹, Bradley Duncan¹, Rui Tang¹, S. T. Thayumanavan¹, Xuexin Duan² and Vincent M. Rotello¹; ¹University of Massachusetts Amherst, United States; ²Tianjin University, China

Proteins are attractive precursors for the fabrication of biomaterials due to their inherent biocompatibility, biodegradability, and low toxicity. Moreover, fabrication of protein-based materials can be conducted sustainably due to their ready availability and high aqueous solubility. A wide variety of functional proteins are naturally available with unique properties which may be harnessed to design complex multifunctional materials for several applications including tissue engineering, diagnostic tools, and sensors. However, the high solubility of proteins often results in lower aqueous stability and poor mechanical properties. Protein films must therefore be treated to enhance their stability. However, it is challenging to develop treatment strategies that enhance aqueous stability, are widely applicable to different proteins and preserve their native properties. We developed an additive-free thermal treatment strategy in fluorinated media (hereafter referred to as fluorinated-curing) that enhances aqueous stability of protein films, while preserving native protein

properties such as surface charge and hydrophilicity. In this work, fluorine-curing was utilized in combination with inkjet-printing of proteins to develop patterned protein films with varying surface properties. We investigated the application of these patterned protein films for controlled cellular adhesion and size-based microparticle sorting.

For our study, we utilized two different proteins - anionic bovine serum albumin (BSA) and cationic lysozyme (Lyso). Aqueous protein solutions (protein inks) were loaded into empty cartridges of an inkjet printer to print protein patterns onto a glass surface followed by fluorine-curing. This resulted in patterns of varying charges along the surface. These surface charge patterns were utilized to dictate adhesion of cells on specific regions of the surface with potential applications such as tissue engineering scaffolds and *in vitro* co-culture models.

Charge-patterned protein films were also investigated as a platform to size-sort charged microparticles. Rapid size-based sorting of small volumes of analytes is a crucial first step in biomedical diagnostic tools such as microfluidic devices or point-of-care diagnostic systems. We integrated a hypersound-based acoustic streaming system with our inkjet-patterned protein films to provide efficient sorting of microparticles on the basis of particle charge and size. The hypersonic resonator enabled us to generate microvortices in the fluid that exerts a curvature-dependent drag force on the microparticles adhered to the protein surface. This allowed for the translocation of microparticles based on the strength of their electrostatic interactions with the patterned protein surface and the drag force exerted by the microvortices. As the drag force was curvature-dependent, larger particles experienced stronger forces and translocated further on the patterned protein surface. This difference in translocation allowed for efficient (~95%) sorting of microparticles. The combination of inkjet-patterned protein films and hypersound-based acoustic streaming enables precise manipulation of particle movement at the surface and may be used for sorting a variety of chemical or biological analytes or studying interactions of analytes with protein-based surfaces.

1:45 PM SB10.10.02

Biophysical Properties of Self-Assembled Immune Signals Influence Regulatory Processing and Function Eugene Froimchuk¹, Robert S. Oakes^{1,2}, Senta M. Kapnick¹, Alexis A. Yanes¹ and Christopher Jewell^{1,2,3}; ¹University of Maryland, United States; ²United States Department of Veteran Affairs, United States; ³Robert E. Fischell Institute for Biomedical Devices, United States

Introduction: The immune system evolved mechanisms to respond not only to specific molecular signals, but also to biophysical properties such as binding affinity. Unfortunately, the connections between biophysical parameters and immunological outcomes are poorly understood in the context of disease. Understanding this connection would enable better design and translation of new therapies for autoimmune diseases like multiple sclerosis (MS), where the immune system mistakenly attacks myelin in the central nervous system. We posited that inhibiting inflammatory signaling while myelin self-antigen (MOG) is processed by immune cells could reduce autoimmunity and promote immune tolerance during MS. Here we show electrostatically self-assembling complexes formed from an anionic regulatory ligand (GpG) and a cationic MOG peptide improve paralysis in a mouse model of MS. Because efficacy was dependent on antigen-sequence, we probed how antigen sequence and charge impact electrostatic self-assembly of immune signals and how changes in biophysical features of the complexes link to immune tolerance. We *hypothesized* increasing cationic charge of MOG peptide sequences would increase the affinity with which MOG peptides adsorb to GpG. We speculated if increased affinity would improve uptake efficiency of signals by immune cells and increase polarization of self-reactive T cells to protective regulatory phenotypes.

Methods: To vary the charge of MOG peptides, we anchored MOG with 2, 3, or 9 cationic residues of lysine (K) or arginine (R). We used surface plasmon resonance to measure how binding affinity between MOG peptides and GpG changed as a function of total peptide charge. We measured signal loading by gel electrophoresis to assess how self-assembly of MOG and GpG changed as a function of charge balance in solution. To probe how GpG impacts signaling in dendritic cells (DCs), we stimulated DCs with the inflammatory signal CpG, treated DCs with MOG/GpG complexes, and then analyzed expression of inflammatory markers CD80/86 by flow cytometry and MyD88 by RT-qPCR. To determine if treated DCs could polarize T cells towards regulatory phenotypes associated with immune tolerance, we cultured DCs with MOG-specific T cells and measured expression of regulatory markers FoxP3 and CD25 by flow cytometry.

Results: When anchoring MOG with K or R, the dissociation rate constant (K_D) decreased as the number of anchored residues was increased from 2 to 3. This observation indicates that the binding affinity between MOG and GpG increased when MOG exhibited a more positive charge. Signals were fully loaded into complexes when the charge balance in solution was neutral. If the charge ratio of cationic MOG to anionic GpG skewed towards GpG, GpG remained in solution. If the charge ratio skewed towards cationic MOG, then GpG was fully loaded but MOG remained in solution. When stimulated with CpG, DCs treated with MOG/GpG complexes or soluble GpG significantly reduced CD80/86 and *Myd88* expression. This result indicates that GpG remained active when delivered in complexes. Intriguingly, DCs treated with MOG_{K₂} and MOG_{R₉} complexes expressed significantly more *Myd88* relative to DCs treated with other complex formulations. GpG may not have been as readily available to inhibit inflammatory signaling when complexed with MOG_{K₂} or MOG_{R₉}, possibly due to tighter binding with MOG because of the larger cationic charge per peptide. Furthermore, only MOG_{K₂} and MOG_{R₂} complexes polarized MOG-specific T cells towards regulatory phenotypes.

Conclusions: DCs were most effective in polarizing regulatory T cells when treated with complexes containing peptides of lowest cationic charge. Our results suggest self-antigens designed to self-assemble with tolerizing cues without limiting bioavailability of the signals are most effective in polarizing regulatory T cells. This granular understanding of nanomaterial-immune interactions contributes to more rational immunotherapy design.

2:00 PM SB10.10.03

Kinetics and Thermodynamics of Fibril Elongation and Dissociation of Oxyntomodulin and Aib2-Oxyntomodulin Alireza Mohammad Karim¹, Ana L. Gomes Dos Santos² and Mark E. Welland¹; ¹University of Cambridge, United Kingdom; ²AstraZeneca, United Kingdom

Obesity and its implication on type-2 diabetes (T2D) have reached epidemic proportions worldwide. The urgent need to find a safe and effective therapies for treatment of these chronic disorders has gained tremendous attention in scientific community. Recent studies have shown that peptide hormones such as Oxyntomodulin (Oxm) and its analogue 2-aminoisobutyric acid oxyntomodulin (Aib2-Oxm) are extremely safe and effective for body weight loss and regulating the blood glucose level to treat T2D patients. Despite their promising therapeutic effects they exhibit a short *in vivo* bioactivity in serum due to the enzymatic degradation. To address this challenge, it was reported that when these peptides are packed in fibrillar structures they are much less exposed to any degradation and hence their bioactivity is significantly improved. Therefore, it is essential for developing a systematic approach for explore strategies that control the formation of such fibrils and their subsequent controlled dissociation *in vivo* once injected in patients. An understanding of the fibrillation and dissociation processes of such peptides requires a quantitative knowledge of the kinetics and thermodynamics of fibril formation and disassembly; such measurements that to date have remained elusive for these peptides. In this work we report for the first time a through thermodynamic and kinetic study of fibril formation and fibril dissociation using quartz crystal microbalance with dissipation (QCM-D) and bulk experiments for Oxm and Aib2-Oxm. We investigated the speed of peptide attachment and detachment as well as related thermodynamics processes via the Gibbs free energy change for fibril formation as well as fibril dissociation. Our study showed that Oxm and Aib2-Oxm peptides are spontaneously self-assembling into fibrils whilst Oxm fibrils are more stable than Aib2-Oxm fibrils. Therefore, Aib2-Oxm fibrils are more feasible and faster to dissociate *in vivo* relative to Oxm fibrils which indicates higher bioactivity of Aib2-Oxm in serum relative to Oxm. On the other hand, the higher fibrillation speed of Oxm relative to Aib2-Oxm

highlights higher propensity of Oxm for fibril elongation than Aib2-Oxm.

SESSION SB10.11: Biomaterials for Plants, Food and Agriculture

Session Chair: Benedetto Marelli

Thursday Afternoon, December 2, 2021

Sheraton, 2nd Floor, Back Bay C

4:00 PM SB10.11.01

Bioinspired Seed Coatings to Boost Germination and Mitigate Abiotic Stressor Augustine Zvinvashe¹, Manal Mhada², Lamfeddal Kouisni² and Benedetto Marelli¹; ¹Massachusetts Institute of Technology, United States; ²UM6P, Morocco

Changes in climate patterns and soil depletion are major challenges that agriculture needs to address to build a sustainable food infrastructure that can feed the growing human population. In semi-arid regions, water is the determining factor for crop production and water stress during seed germination and early seedling growth is the highest cause of crop loss, with dramatic impact on food security for 1 billion people that are threatened by desertification. In nature, some seeds (e.g. chia, basil) produce a mucilage-based hydrogel that creates a germination-promoting microenvironment by retaining water, regulating nutrients entry, and facilitating interactions with beneficial microorganisms. Inspired by this strategy, a two-layered biopolymer-based seed coating has been developed to increase germination and water stress tolerance in semi-arid, sandy soils. Seeds are coated with a silk/trehalose inner layer containing *rhizobacteria* and with a pectin/Carboxymethylcellulose (CMC) outer layer that upon sowing reswells and acts as a water jacket. Using *Phaseolus vulgaris* (common bean) cultured under water stress conditions in an experimental farm in Ben Guerir, Morocco, it is demonstrated that the proposed seed coating effectively delivers *rhizobacteria* to form roots nodules, results in plants with better health, and mitigates water stress in drought-prone marginal lands.

4:15 PM SB10.11.02

An Edible Electronic Pill for Tunable and Monitored Drug Release Leonardo Lamanna¹, Pietro Cataldi¹, Marco Friuli², Christian Demitri², Alessandro Luzio¹ and Mario Caironi¹; ¹Istituto Italiano di Tecnologia, Italy; ²Università del Salento, Italy

The use of wearable and implantable devices allows continuous monitoring of physiological metrics, personalized drug treatment and rapid sharing of data between patients and caregivers, offering unprecedented diagnosis and treatment opportunities. In this context, ingestible electronics devices represent a key tool supporting medicine since the '60s [1]. To date, these devices are used mainly in diagnostic and administrated in controlled hospital conditions because of costs, need of recollection, and risk of retention.

Nowadays, the research has a chance to move from ingestible to edible electronics to develop safe and self-administrable edible devices[2]. This transformation requires the introduction of new materials coming from food derivatives or approved by FDA/EFSA. In this context, new communication strategies to deliver diagnostic and treatment progress information are required. The most promising communication strategy is the Intra Body Communication (IBC) [3]. IBC is a wireless bioinspired communication platform that exploits body's ionic conductivity to propagate a signal (e.g. nervous system), generating a body area network (BAN). Such technology has the advantage of low power consumption (<10pJ/bit) and the possibility to employ high impedance conductors[4], compatibles with present edible batteries and conductors[2].

To date, IBC has been mainly exploited for wearable applications. The only example of IBC for an ingestible device was proposed by Proteus Digital Health *Inc.* to monitor the pharmacological adherence[5]. These models of IBC show static systems where the signal is not modulated in time by physiological processes. In this work, we introduce IBC through a fully edible pill employed for tunable and monitored drug release.

In particular a fully organic edible pill is proposed, composed by:

1. A green and large scale processable edible conductor (0.01 S/cm) exploited for the IBC signal transmission;
2. An insulating edible composite, including a transient bioinert matrix and the drug (Metformin and Amoxicillin), enabling erosion triggered drug release mechanism along different parts of gastrointestinal (GI) tract.

Upon ingestion, the IBC signal is triggered by the pill contacts with GI solution. Then, the signal is modulated along the GI tract by the insulating edible composite dissolution and consequent system impedance variation occurring during the drug release. The signal is switched-off by the complete pill dissolution. In combination with a wearable patch the system will provide information on pharmacological adherence and real-time drug release monitoring.

The drug release mechanism has been characterized *in vitro* employing simulated gastric and intestinal fluids. Multiple and controlled drug release along the GI tract has been obtained tuning the dissolution properties of the insulating edible matrix through its composition, resulting in release time tunable between 20 minutes to 3 hours. Meanwhile, the insulating material dissolution leads to an impedance reduction of 3 order of magnitude, which modulate the IBC signal and describe the drug release profile.

This technology could pave the way to higher personalized medicine being tailored by patients needs, response, and risk.

1. Farrar, J.T., V.K. Zworykin, and J. Baum, *Pressure-sensitive telemetering capsule for study of gastrointestinal motility*. Science, 1957. **126**(3280): p. 975-976.
2. Sharova, A.S., et al., *Edible electronics: The vision and the challenge*. Advanced Materials Technologies, 2021. **6**(2): p. 2000757.
3. Zimmerman, T.G., *Personal area networks: Near-field intrabody communication*. IBM systems Journal, 1996. **35**(3.4): p. 609-617.
4. Das, D., et al., *Enabling covert body area network using electro-quasistatic human body communication*. Scientific reports, 2019. **9**(1): p. 1-14.
5. Hafezi, H., et al., *An ingestible sensor for measuring medication adherence*. IEEE Transactions on Biomedical Engineering, 2014. **62**(1): p. 99-109.

SESSION SB10.12: Biomaterials for Drug Delivery, Regenerative Medicine and Tissue Models I

Session Chairs: Chiara Ghezzi and Amir Sheikhi

Monday Morning, December 6, 2021

SB10-Virtual

10:30 AM *SB10.12.01

Molecularly Targeted Polymerized Shell Microbubbles to Treat Abdominal Surgical Adhesions Joyce Y. Wong; Boston Univ, United States

We have developed microbubble ultrasound imaging contrast agents with specific molecularly targeting ligands with the goal of detecting and treating abdominal surgical adhesions. Abdominal surgical adhesions are a major burden to the US healthcare system with estimated annual costs of over \$5 billion. During abdominal surgery, the inflammatory response combined with surgically induced ischemia leads to the formation of a fibrin-rich exudate into the peritoneal cavity which can crosslink apposing tissues. Example complications are small bowel obstruction and female infertility. Current FDA-approved strategies to prevent abdominal surgical adhesions are limited because they are site-specific and require the surgeon to predict a priori where the adhesion will form. Moreover, surgical adhesion removal often involves a second surgery, which ironically can lead to additional adhesions. A desired feature of the ultrasound contrast agent is particle and size stability in physiologically relevant fluids. Specifically, an optimal balance must be struck between microbubble stability (maintaining imaging contrast for diagnosis) and reasonable inertial cavitation thresholds (allowing for fibrin breakup). Moreover, care must be taken to ensure no unwanted damage is done to the underlying mesothelium throughout the process. By tuning the crosslink density of the microbubble shell, we show particle and size stability can be controlled. This finding is important for eventual clinical translation because current microbubble in vivo lifetimes are much too short for targeted imaging applications. We will describe our combined in vitro and in vivo approach toward developing a theranostic agent for detecting and treating nascent abdominal surgical adhesions.

11:00 AM SB10.12.02

Orally Fast-Disintegrating Delivery System of Ferulic Acid/Cyclodextrin Inclusion Complex Nanofibers Asli Celebioglu and Tamer Uyar; Cornell University, United States

The fast-disintegrating oral delivery systems are gaining more interest in the pharmaceutical and food industry [1]. Recently, electrospinning of nanofibrous webs incorporating active agents was shown to be a very favorable approach for the development of fast-disintegrating delivery systems. The very large surface area and highly porous structure along with the amorphous state of the active ingredients make these nanofibrous webs suitable for fast-disintegrating oral delivery systems since they can readily dissolve or disintegrate upon contact with liquid medium [2-4]. Cyclodextrins (CyDs) are classified as cyclic oligosaccharides and they are even being used in drug formulations since hydrophobic drugs become water-soluble by inclusion complexation with the doughnut-shaped cavity of CyD molecules. Moreover, such inclusion complex systems can enhance the bioavailability and stability of drugs [5]. The electrospinning of polymer-free inclusion complex formulations can be yielded into nanofibrous webs with fast-disintegrating character and such electrospun nanofibrous webs would be quite proper for designing fast-disintegrating oral delivery systems for pharmaceutical products and/or dietary supplements [3-4]. Additionally, the electrospinning of nanofibers from aqueous solutions of CyD inclusion complexes has the advantage where it is possible to use only water for the electrospinning without the need of polymeric carrier and without the need of using organic solvents. Moreover, CyDs are highly water-soluble compared to polymeric matrices, hence, CyDs being as a fiber matrix and inclusion complex host, nanofibers solely electrospun from inclusion complexes would dissolve instantly in the oral cavity without the need for water and provide enhanced solubility to active compounds by inclusion complexation. Also, by polymer-free electrospinning of these systems, much higher active compound loadings are possible if needed for the finished dosage forms. In our studies, we have chosen ferulic acid as a model bioactive compound for the electrospinning of polymer-free nanofibrous webs of inclusion complex for the development of orally fast-disintegrating delivery systems [6]. Recent studies have shown that ferulic acid displays a wide range of physiological properties such as antioxidant, anticarcinogen, anti-inflammatory, antimicrobial and neuroprotective. However, the low water solubility and stability of ferulic acid result in a lack of bioavailability and activity which limits further applications. On the other hand, its water solubility and bioavailability can be enhanced by inclusion complexation with CyD. Here, the free-standing inclusion complex nanofibrous webs of ferulic acid were produced using electrospinning technique from two different modified cyclodextrin derivatives of hydroxypropyl-beta-cyclodextrin (HP- β -CyD) and hydroxypropyl-gamma-cyclodextrin (HP- γ -CyD). It has been detected from the *in vitro* release and disintegration tests that, the amorphous state of ferulic acid based on inclusion complex formation, and the highly porous feature and high surface area of nanofibrous mats have ensured the fast dissolution/release of ferulic acid and disintegration of nanofibrous mats into the liquid medium and artificial saliva. The results elucidated that electrospun nanofibrous webs of ferulic acid/CyD could be promising material as a fast disintegrating oral delivery system.

References

- [1] V. A. Saharan, *Current Advances in Drug Delivery Through Fast Dissolving/Disintegrating Dosage Forms.*, Bentham Science Publishers, Sharjah, 2017.
- [2] D. G. Yu, J. J. Li, G. R. Williams, M. Zhao, *J. Control. Release.* 2018, **292**, 91-110.
- [3] A. Celebioglu and T. Uyar, *RSC Med. Chem.*, 2020, **11**, 245-258.
- [4] A. Celebioglu and T. Uyar, *T. Mol. Pharm.*, 2019, **16**, 4387-4398.
- [5] T. Loftsson and M. E. Brewster, *J. Pharm. Pharma.*, 2010, **62**, 1607-1621.
- [6] A. Celebioglu and T. Uyar, *Inter. J. Pharma.*, 2020, **584**, 119395.

11:15 AM SB10.12.03

Cyclodextrin/Prednisolone Inclusion Complex Nanofibers for Fast-Dissolving Drug Delivery Nancy Wang, Asli Celebioglu and Tamer Uyar; Cornell University, United States

Fast-dissolving drug delivery systems are receiving increasing attention lately due to their enhanced bioavailability and physicochemical properties. One technique of such studies is to create an electrospun nanofiber web of an inclusion complex with the drug of study. The porous nature of these electrospun nanofiber webs renders this system readily soluble in liquids, thereby improving the bioavailability of the drug of study. A fast-dissolving system is developed for prednisolone, a drug that is often used to treat allergic reactions [1]. The system aims to create an inclusion complex with hydroxypropyl-beta-cyclodextrin (HP β CD) and generate electrospun nanofibrous webs from this system. Cyclodextrin is a starch derivative often known for its presence in enhancing solubility, shelf life, stability of such products as drugs, essential oils, dietary supplements, flavor/fragrance, etc. [2]. There are mainly three native types of cyclodextrin molecules (α -, β -, and γ -CD) in addition to some engineered varieties, which includes HP β CD [2, 3]. Because HP β CD is a ring-shaped molecule with a cavity in the center [2], it can envelope individual drug molecules, commonly at a CD-to-drug ratio of 1/1 or 2/1 [4]. The usage of HP β CD is known for increasing the physical and chemical properties of various substances [4]. Here, HP β CD is used to improve the aqueous solubility of prednisolone, a drug that is barely soluble in water on its own. The HP β CD/prednisolone inclusion complex allows the drug to dissolve quickly in the presence of saliva so that the consumer does not need to struggle with swallowing a large pill. The inclusion complex with the drug molecules is initially in the form of a spinning dope, which will yield a sheet of flexible, free-standing nanofibers after going through the electrospinning process. By connecting the spinning dope to one end of the circuit and a metal collector on the other end, an application of voltage will create the electromagnetic field that enables the collection of nanofibers [5]. The simple sheet of nanofibers produced here, composed of the inclusion complex, is to be placed on the tongue. The sheet will instantly dissolve when in contact with saliva, thereby eliminating the difficulty of swallowing. On the other hand, pullulan is a common polymer for creating electrospun nanofibers and pullulan/prednisolone nanofibers were produced as a control sample. The use of HP β CD thereby eliminates the need for polymer dopes to provide structural integrity in producing free-standing nanofibers. This fast-dissolving drug delivery system with a freestanding nanofiber web appears favorable and offers new potential for the pharmaceutical industry.

References

- [1] Bashar, T., Apu, M. N. H., Mostaid, M. S., Islam, M. S., & Hasnat, A. (2018). *Dose-Response*, 16, 1559325818783932.
- [2] Del Valle, E. M. (2004). *Process Biochemistry*, 39, 1033-1046.
- [3] Celebioglu, A., & Uyar, T. (2021). *Food Hydrocolloids*, 111, 106264.
- [4] Celebioglu, A., & Uyar, T. (2020). *RSC Medicinal Chemistry*, 11, 245-258.
- [5] Greiner, A., & Wendorff, J. H. (2007). *Angewandte Chemie International Edition*, 46, 5670-5703.

11:30 AM SB10.12.04

Development of Vitamin C Loaded Plant-Based Microfibers for Wound Healing Applications Fabrizio Fiorentini^{1,2}, Giulia Suarato^{1,1}, Maria Summa¹, Rosalia Bertorelli¹ and Athanassia Athanassiou¹; ¹Istituto Italiano di Tecnologia, Italy; ²Università degli Studi di Genova, Italy

The wound healing process is a dynamic and highly regulated series of events, comprising four main steps: hemostasis, inflammation, proliferation and remodeling. Fibroblasts and keratinocytes represent the main cell types involved in the process, as they synthesize cytokines and collagen to regulate the inflammation process and to build the extracellular matrix, respectively. For this reason, tissue repair mechanisms can be improved by stimulating cell proliferation through the employment of microfibrillar scaffolds, that can effectively mimic the 3D conformation of the extracellular matrix, and, when loaded with bioactive molecules, to boost the cellular restoration at the wound area. Nowadays, materials derived from natural resources are becoming an optimal choice to create alternative wound dressing.

In this work we fabricate natural 3D microfibrillar scaffolds loaded with vitamin C for the treatment of skin lesions, by combining four plant-based molecules: zein, an alcohol-soluble protein derived from corn; low-methoxy pectin, the most abundant hydrophilic polysaccharide in the plant cell wall; soy lecithin, used as emulsifier agent; and vitamin C, able to exert antioxidant activity and stimulate collagen synthesis. The polymeric microfibrils were produced via vertical electrospinning of emulsions. Five samples (labeled ZPC0, ZPC1, ZPC2, ZPC3, ZPC4) containing different concentrations of vitamin C (0 – 10 mg/mL) were fabricated and their cross-linking via CaCl₂ was optimized, in order to enhance their water resistance. SEM imaging was conducted to analyze the morphology of the samples and FTIR analysis was carried out for the chemical characterization. An *in vitro* drug release assay was set up by incubating the samples in PBS (pH 7.4) at 37°C for up to 24 hours, while a DPPH assay was performed to test the radical scavenging activity of the VitC released in the PBS from the microfibrils. The antioxidant activity was evaluated *in vitro* on Cultured Human Keratinocyte (HaCaT) cells, testing their response toward H₂O₂ by DCFH-DA assay. Swelling and degradation rate were monitored by immersing at 37°C for a week the fibrous matrices in PBS alone or with a protease. The biocompatibility was evaluated on Human Dermal Fibroblast adult (HDFa) cells and HaCaT cells by MTS assay. SEM micrographs showed bead-less and ribbon-like microfibrils. The increase of vitamin C content in the samples resulted in an expansion in the fiber average diameter, from 0.84 to 1.19 μm and the CaCl₂ cross-linking strategy helped maintaining the microfibrils structure. *In vitro* drug release indicated a burst release of the vitamin C from the microfibrils within 3 hours of immersion. The cross-linking treatment was successful in slowing down the release of the bioactive molecule in the first hour of immersion in PBS. The DPPH assay results indicated that the radical scavenging activity was present both in non-cross-linked and cross-linked microfibrils, even if this propriety was higher for the non-cross-linked ones. The DCFH-DA *in vitro* assay on HaCaT cells showed a response to the H₂O₂ proportional to the amount of VitC loaded inside the samples. Degradation assay showed a higher weight loss of the samples when immersed in PBS with protease, compared to the immersion in PBS alone. *In vitro* MTS assay on HDFa and Keratinocyte cells resulted in good biocompatibility for each sample under study. Taken together, these results confirmed that our designed plant-based electrospun microfibrillar patches represent a suitable, naturally-derived biocomposite for wound healing applications.

11:45 AM SB10.12.05

Griseofulvin/Cyclodextrin Inclusion Complex Nanofibers for Fast-Dissolving Oral Drug Delivery Systems Emmy Hsiung, Asli Celebioglu and Tamer Uyar; Cornell University, United States

Fast-dissolving oral drug delivery systems are gaining more interest in the pharmaceutical industry as a means of administering active pharmaceutical ingredients through tablets, films, and, recently, electrospun nanofibrous webs [1,2]. The large surface area and highly porous structure of nanofibrous webs make nanofibers a promising means of drug delivery, as they readily dissolve in the oral cavity [3-5]. Cyclodextrins (CDs) are classified as cyclic oligosaccharides and are used in drug formulations to increase the water-solubility of hydrophobic drug molecules via inclusion complexation with the doughnut-shaped cavity of CD molecules [2,6]. In this study, an orally fast-dissolving drug delivery system was developed by incorporating inclusion complexes of Griseofulvin/Cyclodextrin with pullulan—a non-toxic, water-soluble biopolymer—to form nanofibrous webs via electrospinning. Griseofulvin is used widely as an antifungal, but it is poorly water-soluble and suffers from low bioavailability. In this study, hydroxypropyl beta cyclodextrin (HPβCD), which have been already used in the pharmaceutical industry due to its high-water solubility, were used to form inclusion complexes [6]. Through inclusion complexation with HPβCD, the water solubility and thus bioavailability of the drug were enhanced. The electrospinning of Pullulan-Griseofulvin/HPβCD solutions yielded defect-free nanofibers collected in the form of self-standing and flexible nanofibrous webs. The formation of inclusion complexes between cyclodextrin and the drug was confirmed using FTIR and XRD analysis, the thermal analysis of the fibers were examined using DSC and TGA, and increased solubility of the drug after complexation was confirmed with UV-Vis spectroscopy. The generated electrospun nanofibrous webs readily disintegrated when wetted with artificial saliva indicating that electrospun Pullulan-Griseofulvin/HPβCD web could be a promising material as a fast-dissolving oral drug delivery system.

References

- [1] Muruganantham, S., Kandasamy, R., & Alagarsamy, S. (2021). *Critical Reviews in Therapeutic Drug Carrier Systems*, 38, 1-35.
- [2] Doderio, A., Schlatter, G., Hébraud, A., Vicini, S., & Castellano, M. (2021). *Carbohydrate Polymers*, 264, 118042.
- [3] Ponrasu, T., Chen, B. -, Chou, T. -, Wu, J. -, & Cheng, Y. -. (2021). *Polymers*, 13, 1-17.
- [4] Gao, S., Liu, Y., Jiang, J., Li, X., Ye, F., Fu, Y., & Zhao, L. (2021). *Colloids and Surfaces B: Biointerfaces*, 201, 11162.
- [5] Celebioglu, A. & Uyar, T. (2020). *RSC Medicinal Chemistry*, 11, 245–258.
- [6] Celebioglu, A. & Uyar, T. (2021). *Materials Science & Engineering C*, 118, 1115142.

12:00 PM *SB10.12.06

Hierarchical Assembly of Podocyte Structures on Fractal Substrates for Kidney-on-a-Chip Engineering Milica Radisic^{1,2} and Anastasia Korolj¹; ¹University of Toronto, Canada; ²University Health Network, Canada

Podocytes are highly branched and specialized epithelial cells in the kidney that wrap around glomerular capillaries to form a filtration barrier for the purification and regulation of blood. Many kidney diseases are related to podocyte dysfunction, and limited treatment options make kidneys the most waitlisted transplant organ around the world. Physiologically relevant tissue-engineered models of podocyte function are thus needed to improve our understanding of kidney disease and discover new treatments.

However, *in vitro*, podocytes have severely limited maturation, reach a plateau of gene expression and morphological development that remains far from native levels, and thus lacks relevance to modeling of the native condition, which is a major bottleneck in research progress. Not only are the cells unable to develop multi-level branching morphology, but there is a lack of reliable read-outs that can assess this complex interdigitating morphology *in vitro* in a way

that cross-references with *in vivo* practices.

We have taken an interest in the role of fractal structures and how they contribute to the development of cells and tissues in which these patterns are so ubiquitous.

Fractals are structures with features that repeat at multiple scales, like the leaves of a fern or a cascading Russian doll. The fractal self-similarity adds complexity to these structures, in the way that makes a mountain different from a simple cone. Our hypothesis was that fractal complexity in shape cues, akin to those of looping glomerular capillaries on which podocytes grow, will trigger fractal complexity in podocyte maturation, leading to more fractal branching, by patterning relevant machinery on multiple scales.

First, biomimetic fractal substrates were designed by tracing native histology cross-sections of glomerular capillaries, patterning the designs onto positive photoresist using direct laser writing lithography, and then reflowing to generate curvature. These patterns were then inverse-molded with PDMS to generate 2.5-D scaffolds which were inserted into well plates to use in standard cell culture techniques. Cells cultivated on fractal scaffolds developed higher expression and localization of integrin, cytoskeletal, glycocalyx, and slit diaphragm proteins compared to flat and non-fractal topographical scaffolds, and revealed greater maturation extent by RNA sequencing results. Cells also grew preferentially on topographic features when present.

Remarkably, we observed that the 2.5-D fractal substrates exhibited curvature-dependent patterning of collagen I molecules overtop of the scaffold topography, in perfect correlation with kelvin probe force microscopy measurements of increased charge density and zeta potential on curved versus flat regions of the material surface.

Thus, we present the notion that fractality induces clustering of proteins by concentrating charge in the material interface, which facilitates hierarchical assembly of cell structures resulting in overall advancement of whole cell branching morphology. We observed that 2.5-D fractal shape patterning was dose-dependent, that cells were more sensitive to stimuli when grown on fractal scaffolds, and the morphology could be directly compared with *in vivo* experiments, thus supporting physiological relevance and reliability. To document platform utility, we demonstrate that this new kidney-on-a-chip model can be used for screening of nephrotoxic drugs, for studies of the effects of coronaviruses on the kidney and screening of factors that lead of kidney rejection in patient serum.

SESSION SB10.13: Biomaterials for Drug Delivery, Regenerative Medicine and Tissue Models II
Session Chairs: Chiara Ghezzi and Amir Sheikhi
Monday Afternoon, December 6, 2021
SB10-Virtual

1:00 PM SB10.13.02

Static and Dynamic Analysis of Naturally-Derived Coatings for Drug-Eluting Stents [Martina Lenzini](#)¹, Giulia Suarato¹, Luigino Criante¹, Silvio Bonfadini¹, Dalila Miele², Marco Ruggeri², Giuseppina Sandri² and Athanassia Athanassiou¹; ¹Istituto Italiano di Tecnologia, Italy; ²Università degli Studi di Pavia, Italy

Over the past few years, naturally-derived polymers are being increasingly considered as promising coating materials to obtain novel drug-eluting devices, such as drug-eluting stents (DES). Natural biodegradable polymers include proteins (e.g. zein), and polysaccharides (e.g. alginate), which are not only biocompatible but also release non-toxic degradation products, easily cleared from the body [1]. Moreover, coatings fabricated with naturally-derived polymers may limit adverse effects such as exaggerated inflammatory response and delayed re-endothelialization, which often occur when residual synthetic polymers remain in place [2].

In our study, we developed novel biodegradable zein-based bilayer coatings on stainless steel with improved biocompatibility with respect to synthetic coatings and bare metal cardiovascular devices. Rutin, a plant-based flavonoid, with several biological properties, including anti-inflammatory and antioxidant potential, was loaded into a zein polymer layer. Experiments were carried out to assess the release profile of rutin from single and bilayer coated substrates (up to 21 days) and the resulting antioxidant activities. The fabricated coated surfaces were subjected to extensive physico-chemical characterizations and *in vitro* biocompatibility testing using human umbilical vein endothelial cells and primary human fibroblasts. To better mimic the physiological conditions and recreate the dynamic release mechanisms that exist *in vivo* in a coronary artery, we studied the behavior of our zein-based coating in contact with a flowing liquid. In particular, for these dynamic analyses, we designed and developed a versatile microfluidic platform, which is modeled to mimic the microenvironment of a coronary DES. Experiments were performed to monitor the degradation behavior and drug release from the coated microfluidic channels in contact with several blood-simulated fluids (differing in terms of viscosity and chemical composition), flowing at various flow rates.

Our findings confirm that the proposed plant-based coatings fulfill the key requirements for successful drug-eluting cardiovascular devices. The exclusive use of green solvents and natural polymers can indeed ensure biocompatibility, promotion of cell proliferation, and sustained release. Moreover, our on-chip platform allowed recapitulating the physiological bloodstream microenvironment. Therefore, we consider this study as an important contribution towards a better understanding of polymer degradation and drug release under static and dynamic conditions, which are critical for developing more efficient and optimized local drug delivery systems featuring naturally-derived polymers.

References

- [1] G. Suarato et al. *Front Bioeng Biotechnol.* (2018) 6:137
- [2] T. Palmerini et al. *J Am Coll Cardiol.* (2014) 63(4):299-307

1:15 PM SB10.13.03

Fluorescent Polymeric Nanoparticles with Unfunctionalized, Inert Surfaces for Nano-Bio Interaction Studies [Leisha M. Martin](#), Jian Sheng and Wei Xu; Texas A&M University, United States

Nanoparticles that can be optically tracked are of interest for cell and organismal biodistribution studies. NPs with surface functionalizations linking or adsorbing dyes or fluorophores may detach or leach, resulting in artifacts. Materials with encapsulated fluorescent molecules or quantum dots (QDs) are of interest for bio tracking while avoiding artifacts due to leaching. NP surfaces altered to carry dyes or fluorophores are also anticipated to affect toxicity profiles, protein interactions, and cell-uptake. We have prepared two types of polymeric nanoparticles with encapsulated quantum dots or fluorescent dyes

in order to characterize cell interactions, uptake, and toxicity of polymeric NPs with inert surfaces. These materials have applications in nanoplastics toxicity as well as other applications in which pristine surfaces are necessary. Transparent polymer encapsulated fluorescent molecules or QDs can also be surface functionalized for cell targeting, drug or protein conjugation, while avoiding steric hindrance, electrostatic compatibility issues, and enhanced hydrodynamic sizes imparted by surface bound fluorescent molecules or QDs.

1:30 PM SB10.13.04

Towards a Sustainable Skin Wound Management—Biomaterials from Biomasses for Novel Nature-Inspired Tissue Regeneration Platforms [Giulia Suarato](#)^{1,1}, [Marco Contardi](#)¹, [Giovanni Perotto](#)¹, [Marco Ruggeri](#)², [Giuseppina Sandri](#)², [Rosalia Bertorelli](#)¹ and [Athanassia Athanassiou](#)¹; ¹Istituto Italiano di Tecnologia, Italy; ²University of Pavia, Italy

The skin wound healing process comprises multiple mechanisms, as a result of intricately biochemical events and external factors. Any impairment within the correct interplay of these events could lead to the onset of chronic lesions, with potential effects on the patient's quality of life. To correctly support the tissue regeneration, the appropriate design of a wound dressing relies on the fine tuning of its mechanical properties and its degradation process, which need to follow the dynamics of the lesion repair, preserve the physiological healing evolution, act as a shield against infections, and release bioactive principles. By providing structural framework and biochemical cues, the extracellular matrix (ECM) is fundamental for cellular organization and tissue formation.

Nature itself can constitute the source of inspiration for the development of fully biodegradable materials, with enhanced bioactive potentialities. In today's World, the use of natural polymers and materials of biomass origin, either of protein derivation or polysaccharide-based, is becoming a pressing need, to meet the demand of environmentally sustainable technologies to support our future challenges, including applications in the fields of healthcare and wound management. Within this frame, keratin from wool (textile waste, animal biomass) and mycelial materials constitute a valuable source of renewable raw materials.

Keratins are characterized by a high content of cysteine residues, which promotes disulfide inter- and intra-molecular bonding and confers chemical stability and mechanical resistance. Moreover, keratin and its derivatives have gained consideration within the biomedical field, thanks to their good cytocompatibility and cell adhesion properties. In our recent studies, keratin has been extracted from wool and characterized analytically. From the extracted protein, keratin-based fibrous biocomposites have been obtained using all water-based approaches, suitable for cell culture applications. Thermal crosslinking greatly affected the electrospun matrices biodegradability and water stability, without altering the 3D fibrous network, crucial for primary human fibroblasts attachment. Moreover, encapsulation of active principles within the keratin fibrous structure enhanced the mechanical compliance of the dressing and conferred bioactive properties to the resulting patch.

Another very promising biomaterial alternative is constituted by mycelia, self-growing materials, composed of elongated cells (hyphae), that penetrate a substrate uptaking nutrients and developing a fibrous, 3D interwoven structure. Their chemical constituents can be finely tuned by changing either strains and growth conditions or the feeding substrates. The distinctive porous architecture and the chemical biofunctional groups elect mycelia as potential candidates for the design of novel bio-scaffolds. We therefore conducted an explorative study on the direct use of two edible fungal mycelia, *Ganoderma lucidum* and *Pleurotus ostreatus*, as sustainable alternative for the controlled fabrication of an all-natural and low-cost biomedical scaffolds. Several physicochemical properties of the inactivated systems were thoroughly investigated, and biocompatibility *in vitro* was tested with primary human dermal fibroblasts, revealing how cells successfully adhered to the 3D matrix. Moreover, in a preliminary *in vivo* study of a chronic wound model, rats treated with mycelial scaffolds showed well-formed granulation tissue, collagen deposition and completely regenerated epithelium.

The above-mentioned biocomposites can be processed using water-based strategies or by simply tuning their self-growth, in a quest of a more environmentally "green" approach in the biomaterial design. More importantly, their physico-chemical properties and morphologies can be customized to design a new generation of scaffolds for skin wound healing.

1:45 PM SB10.13.05

Flexible Multifunctional Titania Nanotube Arrays Platform for Biological Interfacing [Thomas J. Stegall](#)^{1,2}, [Yi Yang](#)¹, [Deepti Naruka](#)¹, [Jeffrey Capadona](#)^{1,2}, [Allison Hess-Dunning](#)² and [Hoda Amani Hamedani](#)^{1,2}; ¹Case Western Reserve University, United States; ²Louis Stokes Cleveland VA Medical Center, United States

Multifunctional nanostructured inorganic materials provide unique advantages in interfaces for applications in medicine and biology. When coupled with organic soft polymer substrates that more closely match the mechanical properties of biological tissues, stable devices can be created for monitoring and maintaining health. This work reports on the growth and integration of self-organized nanotube arrays on biocompatible and bioinspired polymer substrates as a novel drug-eluting platform for controlled drug release from flexible devices. To this end, we developed techniques for the growth as well as the integration of titania nanotube arrays (TNAs) on two types of polymer substrates. Successful growth of TNAs is shown via optimization of electrochemical anodization parameters in anodic oxidation of sputtered coated titanium films to facilitate formation of nanotube arrays on the insulating polyimide substrate. In addition, the microfabrication process for the selective (site-specific) growth of TNAs on the polyimide substrate is discussed. Finally, integration process of TNA membranes with a bioinspired mechanically-compliant polymer nanocomposites (composed of poly vinyl acetate reinforced with cellulose nanocrystals) is demonstrated.

The morphology of the nanotube arrays was investigated using scanning electron microscopy (SEM). By varying the anodization conditions (e.g., applied electrochemical potential and time), we obtained highly-ordered vertically-oriented nanotube arrays with an average pore diameter ranging from ~30 – 100 nm and a length of ~0.5 – 20 μm . The nanotube array geometries were defined using either laser micromachining or by selective anodization. Laser-micromachining employed a picosecond laser operated at low power (<2 mW) as a subtractive fabrication method. Alternatively, we optimized a selective-anodization process in which titanium was anodized through a AZ nLOF 2070 negative-tone photoresist mask. By hard baking the photoresist, we were able to maintain a high degree of selectivity even during anodization times exceeding 5 hours. The photoresist was then removed by oxygen plasma exposure, leaving behind defined regions with titania nanotube arrays surrounded by non-anodized titanium.

To demonstrate use in drug-delivery applications, preliminary release tests for the fabricated devices were performed by filling the nanotubes with the food-coloring dye (for the initial tests) and the anti-oxidant resveratrol. Drug release from the resveratrol/dye-loaded TNAs was measured using UV-VIS spectroscopy at various timepoints. After an initial burst phase, the release of both types of molecules follows a highly controlled linear profile (with 47 ng/day as the release rate of resveratrol from 1 mm² sample area) that extends beyond one month. In conclusion, we have demonstrated a facile approach to achieve nanotubes/non-conducting polymer flexible devices with precisely controlled drug release properties. The nano/microfabrication methods developed in this work will enable the development of novel flexible devices with controlled drug delivery systems for use in precision medicine and biological interfacing applications.

2:00 PM *SB10.13.06

Rapidly Mineralizing Dense Collagen Gels Functionalized with Bioactive Sol-Gel Borate-Glass [Ehsan Rezabeigi](#), [William C. Lepry](#), [Hyerey Park](#), [Qiman Gao](#), [Megan Cooke](#), [Alaa Mansour](#), [Derek H. Rosenzweig](#), [Faleh Tamimi](#) and [Showan N. Nazhat](#); McGill University, Canada

There is a significant need to develop novel scaffolding materials for the repair and regeneration of bone. Ideally, these scaffolds should mimic the mineralized extracellular matrix of bone, which is an organic-inorganic nanocomposite consisting primarily of carbonated hydroxyapatite (CHA) and

fibrous type I collagen. However, reconstituted collagen gel scaffolds lack structure and mechanical integrity. More importantly, they mineralize poorly *in vitro* or *in vivo*.

Our research has shown that bioactive sol-gel derived borate glasses (SGBGs) rapidly convert to CHA, *in vitro*, which can be attributed to their high reactivity and enhanced textural properties. In particular, a boron substituted Bioglass 45S5 formulation: [(46.1)B₂O₃-(26.9)CaO -(24.4)Na₂O-(2.6)P₂O₅; in mol %] with at least two-orders of magnitude greater specific surface area and pore volume values compared to melt-derived equivalents, has demonstrated rapid ion release rates and conversion to CHA. This CHA formation is also associated with an increase in pH upon SGBG dissolution, a feature that can be used to simultaneously fibrilize and functionalize injectable and 3D-printable dense collagen hydrogels.

In this study, we demonstrate a one-step process wherein acid-solubilized collagen molecules self-assemble in the presence of dissolving SGBGs without the use of NaOH, thereby generating highly hydrated collagen gels. These gels were then subjected to the gel aspiration-ejection technique, which imparts both fibrillar compaction and meso-scale anisotropy, thus forming a SGBG-functionalized dense collagen gel. The resulting bone extracellular matrix-mimicking scaffolds exhibited rapid mineralization along the collagen fibrils within 2 hours of immersion in simulated body fluid, and by day 7, CHA formation in dense collagen gels reached native bone levels, *in vitro*.

In order to investigate the potential *in vivo* bone regenerative capability of these rapidly mineralizing scaffolds, they were injected into a critical size defect using a rat tibia model. The short-term mineralization capacity of acellular SGBG-functionalized dense collagen gels was compared to dense collagen gels alone. Micro-CT analysis showed that the bone volume fraction significantly increased in both scaffold implants from weeks 1 to 2. While there was no significant difference between the two scaffolds at week 1, SGBG-functionalized dense collagen gels showed significantly higher bone volume fraction at week 2. In terms of bone microarchitecture, at week 2 of implantation, the SGBG-functionalized dense collagen gels showed less trabecular separation than dense collagen gels alone. These analyses were complemented by histological staining of implants, where Von Kossa, Toluidine blue, alkaline phosphatase, tartrate resistant acid phosphatase, were performed on recovered tissue sectioned samples at weeks 1 and 2 to investigate potential new bone formation in implanted scaffolds. Compared to dense collagen gels alone, the histology of SGBG-functionalized dense collagen gels revealed high levels of positive phosphate staining, suggesting mineralization, and high cellular infiltration with indications of osteoblast and osteoclast activity.

Therefore, the ability to simultaneously fibrilize and functionalize collagen gels via the incorporation of SGBG particles enables the production of injectable scaffolds with promise in bone repair. Moreover, this latest breakthrough allows for the development of bespoke gel bioink formulations, which can be used with a novel biofabrication/3D printing technology based on automated-gel aspiration-ejection. This can facilitate the building of rapidly mineralizable tissue-mimicking structures with varying micro-architectures to mimic native protein fibril density and alignment, as well as cell loading and density according to the intended use.

SESSION SB10.14: Micro and Nanofabrication of Biomaterials

Session Chairs: Chiara Ghezzi and Benedetto Marelli

Monday Afternoon, December 6, 2021

SB10-Virtual

6:30 PM *SB10.14.01

Biomimetic Silk Biomaterials in Cardiovascular Device Development and Tissue Vascularisation [Jelena Rnjak-Kovacina](#); University of New South Wales, Australia

Biomaterials play a central role in modern regenerative medicine and tissue engineering strategies, where they serve as tunable biophysical and biochemical environments that direct cellular behavior and function. However, one of the biggest obstacles in translating the advances in biomaterials/tissue engineering research to clinical applications has been the lack of sufficient vascular tissue regeneration in current synthetic and natural biomaterials. We develop silk fibroin-based biomaterials for cardiovascular applications, including vascular grafts and cardiac patches, with a particular emphasis on enhancing vascular ingrowth and integration of these devices with the host tissue.

Silk fibroin biomaterials serve as a highly versatile biomaterial platform that allows us to study how biomaterial properties drive biological processes and apply these design criteria to cardiovascular device optimization. In this talk I will discuss our work toward (1) development of 3D silk biomaterials with tunable pore morphology/architecture, (2) effect of silk biomaterial architecture and pore morphology on immune responses, tissue integration, and vascularization of implants, including vascular grafts (3) biofunctionalization of silk biomaterials with basement membrane proteoglycan perlecan to create vascular niche-like environments that support growth factor signaling and angiogenesis.

7:00 PM SB10.14.02

Tailor-Made RNA Microneedle System for Subcutaneous Drug Delivery [Dajeong Kim](#)¹, [Hyejin Kim](#)² and [Jong Bum Lee](#)¹; ¹University of Seoul, Korea (the Republic of); ²Harvard Medical School, United States

Microneedles (MNs) are prominent tools for efficient subcutaneous drug delivery in a non-invasive manner. In particular, dissolving MNs have been widely exploited for the rapid transfer of the massive amounts of biomacromolecules from MN to the skin followed by the sustainable release of drugs. However, scaffold materials for dissolving tip should be carefully chosen due to biocompatibility and safety issues. The microfabrication process often needs complicated procedures regardless of the formulation of MNs, limiting the general usage of MNs. Moreover, degradation-susceptible biomolecules such as nucleic acid require careful address and design for intact delivery. Thus, developing a straightforward and universal approach to fabricate MNs to ensure stability of drugs, particularly nucleic acids, with high loading efficiency is inevitable.

To address the concerns, we establish a novel and simple method to fabricate custom-made RNA MNs (RMNs) based on RNA membrane for a universally applicable drug delivery system. The free-standing RNA membrane was fabricated from rolling circle transcription with two complementary circular DNAs, followed by evaporation-induced self-assembly. By coating scaffold MNs with RNA membrane bearing high stability and RNA packing density, RMNs with a large amount of RNA were successfully achieved. RMNs can be customized by controlling material features of the RNA membrane and 3D printer-based fabrication of scaffold MN in a purpose-oriented way. Remarkably, RNA membrane-based fancy coating method enables a full coverage of the scaffold MN regardless of the shape and material. In addition, RMNs facilitate a massive delivery of RNA along with various types of other drugs, demonstrating the universal applicability of RMN-based drug delivery system. Altogether, this novel strategy presents a general platform to fabricate tailor-made MNs for an efficient and universal drug delivery system.

- [1] Han, D., Park, Y., Kim, H., & Lee, J. B., Nature communications, 2014, 1-7.
[2] Kim, D., Kim, H., Lee, P. C., & Lee, J. B., Materials Horizons, 2020, 1317-1326.

7:15 PM SB10.14.03

Novel Exosome-Liposome Hybrid Nanoparticles for Central Nervous System (CNS) Drug Delivery Wisawat Keaswejjareansuk, Katawut Namdee and Mattaka Khongkrow; National Nanotechnology Center, National Science and Technology Development Agency, Thailand

The blood-brain barrier (BBB) is a barrier preventing the influx of compounds to diffuse from the blood to the brain. It prevents macromolecules penetrate the central nervous system (CNS). Hence, the BBB is a major challenge for drug delivery and a factor to limits the development of new pharmaceuticals for CNS. Rabies virus glycoprotein (RVG) is known for the rabies virus infection that targeting the extracellular surface of neuron and microvascular endothelial cells due to the binding with nicotinic acetylcholine receptor (nAChR). Many CNS therapeutic drugs were designed with the conjugation of RVG to transport the CNS drugs across the BBB, non-invasively. Exosomes are the vesicles comprise of lipid bilayers membrane. The exosomes function as nanocarriers that can be easily loaded with different types of biomolecules. However, the loading of the therapeutic agents to the exosomes poses difficulty. Liposomes are spherical artificial vesicles formed by non-toxic phospholipids and cholesterol. Besides different properties that are greatly affected by the size, surface charge, and sources of a phospholipid, the liposomes are showing biocompatible by nature and promising vesicles for drug delivery. In this study, RVG decorated exosomes were mechanically fused with the drug-loaded liposomes to formed exosome-liposome hybrid nanoparticles. The hybrid nanoparticles were designed to cross the BBB due to the RGV decoration and deliver the CNS therapeutic agents that encapsulated in the liposomes. The fusing of exosome and liposome was confirmed by Förster resonance energy transfer (FRET). FRET is a photophysical phenomenon that energy transfers from a donor fluorophore to an acceptor molecule at a distance in a range of 1-10 nm. FRET intensity, transmission electron microscopy (TEM), dynamic light scattering (DLS), and fluorescence microscopy were used for the characterization of the hybrid nanoparticles.

In this presentation, physical and optical characteristics of the exosome-liposome hybrid nanoparticles will be discussed. Biological characterizations and the preliminary results of the delivery of therapeutic agents across the blood-brain barrier in mice will be presented.

7:30 PM SB10.14.04

Enzymatically Generated Elongated siRNA Nano Complex for Cancer Therapy Hyangsu Nam and Jong Bum Lee; University of Seoul, Korea (the Republic of)

Introduction: siRNA has been received great attention as emerging gene therapeutics due to its superior capacity of specific gene silencing on the post-transcription level. However, the clinical application of siRNA is still hampered due to its inherent properties and delivery problems. Herein, we proposed a novel systemic siRNA delivery system. We synthesized elongated siRNA via rolling circle transcription and developed nano complexes with a glycol chitosan derivative to systemically deliver the elongated siRNAs to cancer tissues. These elongated siRNA nano complexes (ENCs) showed the highly enhanced in vivo stability and less cytotoxicity, compared to conventional polyelectrolyte complexes. Because ENCs were designed to release active siRNA in the cytoplasmic region, they showed high gene silencing efficacy with efficient tumor target ability. Overall, the proposed RCT-based elongated siRNA nano complexes can provide a new platform technology for efficient cancer therapy.

Method: 5'-phosphorylated linear single-stranded DNA oligonucleotides were circulated by hybridizing with the T7 promoter sequence. To synthesize 0.5uM of circular DNA, ligated the nick in the circularized DNA with T4 ligase. Then, closed circular DNA templated was incubated with T7 polymerase at 37 C 5h with rNTPs. Elongated siRNA was complexed with thiol glycol chitosan (tGC). GC was modified by sulfhydryl groups. We analyzed the stability of ENCs by heparin competition assay, cellular uptake and intracellular distribution on human prostate cancer cells (PC3). In vivo biodistribution of ENCs was investigated through PC3 cells were subcutaneously inoculated to the left flank of male.

Results: We developed the periodically repeated siRNA through the RCT process band its delivery system using glycol chitosan derivatives. The synthesized ENCs have stable formation and protect the siRNA therapeutics against polyanion and nucleases attack formation in blood circulation.

Conclusion: In this study, we developed elongated nano complexes, which were synthesized by a uniquely designed RCT method, as an RNAi therapeutics platform technology for cancer therapy. The ENCs formulation can be considered as a potential candidate for tumor-targeted siRNA delivery system.

Acknowledgements: This research was supported by the Intramural Research Program of KIST (2E27940) and the 2016 Research Fund of the University of Seoul (J.B. Lee).

References: Lee, J.B., Hong, J., Bonner, D.K., Poon, Z. and Hammond, P.T.) Nat. Mater., 2012, 316-322. Lee, J.B., Peng, S., Yang, D., Roh, Y.H., Funabashi, H., Park, N., Rice, E.J., Chen, L., Long, R. and Wu, M., Nat. Nanotech., 2012, 816-820. Lee, S.J., Huh, M.S., Lee, S.Y., Min, S., Lee, S., Koo, H., Chu, J.-U., Lee, K.E., Jeon, H., Choi, Y. et al. Angew. Chem., 2012, 7203-7207.

7:45 PM SB10.14.05

Late News: Multi-Walled Carbon Nanotube/Cellulose Composite for Phthalate Detection in Solutions Thusitha N. Etampawala^{1,2}, Hansini Abeysinghe¹, Susira Perera³ and Gimhani C. Wickramasinghe³; ¹Faculty of Applied Sciences, University of Sri Jayewardenepura, Sri Lanka; ²Center for Advanced Material Research, Faculty of Applied Sciences, University of Sri Jayewardenepura, Sri Lanka; ³Faculty of Natural Sciences, The Open University of Sri Lanka, Sri Lanka

Phthalates or Phthalic acid esters (PAEs) are one of the most widely used plasticizers in the flexible plastic product manufacturing processes. These chemicals leach, migrate, or evaporate into the surrounding with time, as they do not form chemical interactions with the polymer matrix. As a result, PAEs have become a ubiquitous environmental pollutant that humans and animals could get exposed to and cause health complications even endocrine disruptions. Therefore, qualitative and quantitative detection of PAEs in different environments becomes crucial, especially in water, food, and beverages. Even though there are various PAE detection techniques, the use of complex, time-consuming laboratory processes of advanced technology has emphasized the need for easy, in-situ, and real-time detection technologies. In this study, a Multi-Walled Carbon Nanotube (MWCNT)/Cellulose composite paper was developed as an electrochemical PAE sensing material, where its electric conductivity change after PAE absorption was used as an indicator in qualitatively detecting PAEs in solutions. This technique was developed based on the hypothesis that the absorbed dielectric PAEs would interfere with the electron transfer across the MWCNT network by distancing the MWCNTs due to the presence of their bulky hydrocarbon side chains. The developed sensing material is an electric conductive, flexible, biocompatible, and biodegradable composite paper with potential for recycling and reusing. It was determined that the percolation threshold of MWCNTs in the cellulose composite had to be 250 ppm to form electric conductive papers. These papers were prepared by vacuum filtering an ultrasonicated solution containing MWCNT dispersion in cellulose pulp. The effect of these absorbed PAEs on the electric conductivity of the composite paper was observed using the three-electrode Electrochemical Impedance Spectroscopy (EIS) technique, where the composite paper was used as the working electrode. The electric conductivity of the PAE-absorbed composite paper was analyzed with respect to the pristine composite paper. The reduction in the electric conductivity of the composite paper after PAE absorption was clearly observed through the Nyquist plot, which indicated an increase in the charge transfer resistance between the electrolyte and the electrode, and the Bode magnitude plot, which indicated an increase in the impedance of the composite paper. This novel technique was specifically tested for di(2-propylheptyl) phthalate (DPHP) in methanol solution using a PAE sensing composite paper of 0.001:1 MWCNT:Cellulose composition. The conductivity change of the paper was

tested using EIS over a 0.1 Hz – 1 MHz frequency range. The charge transfer resistance of the pristine composite paper was 6130 Ω . It was increased by 1.15 fold for the PAE-absorbed composite paper, when the DPHP methanolic solution concentration was 1000 ppm, whereas an increase of 1.38 fold was observed when the solution concentration was increased by one order of magnitude. However, the charge transfer resistance of the paper was slightly increased (1.46 fold increase with respect to the pristine paper) when the concentration of DPHP methanolic solution was continued to increase by another order of magnitude. Furthermore, it was discovered that the PAE sensitivity of the composite paper varied with its MWCNT composition, showing potential at developing PAE sensing materials with different sensitivity ranges. More studies are conducting to identify the different PAE detecting ranges for different MWCNT compositions. Based on the experimental results, this qualitative technique shows potential to be developed as a quantitative PAE detection technique. Being able to detect the presence of PAE through the conductivity change of the MWCNT/Cellulose composite paper using EIS shows that this PAE sensing material could be used to develop comparably easy, quick, real-time, and in-situ phthalate detecting sensor.

8:00 PM SB10.09.03

In Situ Assembled Microgel Scaffolds—An Emerging Generation of Injectable Microporous Hydrogels for Accelerated Tissue Regeneration Amir Sheikhi; The Pennsylvania State University, United States

Bulk hydrogels with nanoporous structures have widely been used in tissue engineering and regenerative medicine. These gels are typically made up of randomly crosslinked hydrophilic polymer networks, which have coupled stiffness and porosity. In a simplified model, the stiffer the gel the smaller the pores. Such characteristic limits the applications of bulk hydrogels in 3D cellular engineering wherein stiff scaffolds with large pores are required. In this presentation, we will discuss some of our recent advances in microengineering chemically modified protein microgels based on their orthogonal thermochemical response to fabricate biomimetic microporous hydrogels with decoupled stiffness and porosity. We show how these hydrogels support 3D cell viability and proliferation while their bulk counterparts result in cell death. We further demonstrate how the properties of individual microgels regulate the behavior of self-assembled, macro-scale hydrogel constructs. This technology may be generalized for other polymers, opening a new horizon for converting bulk hydrogels to beaded hydrogels with decoupled porosity and stiffness for a broad range of applications in healthcare.

8:15 PM SB10.02.02

Hairy Cellulose Nanocrystals—An Emerging Class of Nanocelluloses for Advanced Applications Amir Sheikhi; The Pennsylvania State University, United States

For decades, cellulose nanocrystals (CNCs) have been produced by hydrolyzing the amorphous regions of hierarchical cellulose fiber structures. These colloidal particles are made up of highly ordered arrays of cellulose chains, impeding the physicochemical modifications of inner crystalline layers, which in turn result in limited/compromised dispersion stability, functionalizability and charge, response to external fields, and transport. Nanoengineering cellulose fibrils via controlled oxidation partially disintegrates the amorphous cellulose chains attached to the crystalline body, which yields Janus-like nanoparticles with a needle-shaped crystalline body (similar to CNCs) sandwiched between two highly functionalized disordered cellulose regions (hairs). This newly emerged class of nanocelluloses are called hairy cellulose nanocrystals (HCNC). The protruding soft brushes from HCNC poles impart significant modifications to the colloidal properties of HCNCs, enhancing their functionality, charge density, stability, and self-assembly. In this presentation, we will review our recent progress in engineering HCNCs for advanced applications, such as water treatment, scale inhibition, biomimetic mineralization, rheology modification, nanocomposites, hydrogels, and so forth. We will show how HCNCs enable several technologies that would otherwise be impossible to develop using conventional CNCs. The outcome of our research may leverage universal biomass-based sustainable, green solutions for long-lasting industrial challenges in water, healthcare, food, and energy sectors.

SESSION SB10.15: Biomaterials for Food, Agriculture and Aquaculture

Session Chairs: Julie Goddard and Benedetto Marelli

Tuesday Morning, December 7, 2021

SB10-Virtual

8:00 AM *SB10.15.01

Disease Control with Microencapsulated Synbiotics in Shrimp Aquaculture M. B. Chan-Park and Guangmin Wei; Nanyang Technological Univ, Singapore

Bacterial diseases in shrimp aquaculture are the major concern to the industry and are typically controlled by eradication of the pathogen. Treatment with antibiotics is a traditional way but it was banned recently because of the concern of antibiotic resistance. To seek an alternative way to control bacterial diseases in shrimp aquaculture, we developed synbiotic (probiotic and prebiotic) microencapsulated beads. We encapsulated probiotic cells in beads (~ 100 μ m) prepared through co-gelation of matrix and prebiotic. Compared with physical mixture of synbiotic, microencapsulated synbiotic beads can greatly decrease pathogen viability. *In vitro* coculture method indicated that both probiotics and pathogen can use prebiotic as their food source. While synbiotic encapsulation could trap probiotic and prebiotic inside of beads, thus blocking the access of pathogens to prebiotic, leaving pathogen to starve while flourishing encapsulated probiotic only. In addition, co-encapsulation of probiotic and prebiotic would promise more success in terms of viability and stability of probiotic when used in shrimp aquaculture.

8:30 AM SB10.15.02

Electrochemical, Enzymatic, Flexible Sensor for Fatty Acids Detection Jacopo Giaretta, Haowei Duan, Farshad Oveissi, Syamak Farajikhah, Fariba Dehghani and Sina Naficy; The University of Sydney, Australia

Non-esterified fatty acids (NEFA) are carboxylic molecule which is worth detecting in both food and health applications. In food, NEFAs are related to the handling, storing, and cooking condition, making them excellent quality indicators. In health, the NEFA concentration in blood plasma can be related to some metabolic disorders, cardiovascular diseases, cancer mortality, and even sudden death. Hence, detection of NEFA is of the utmost importance in both fields. However, fatty acids are difficult to decompose, which hinders the development of portable sensors.

This research aims to develop an electrochemical, enzymatic, flexible biosensor for fatty acids detection. Filter paper and hydrogels are porous, flexible, and cost-effective substrates which can absorb a conductive ink and can also accommodate enzymes. Poly(3,4-ethylenedioxythiophene) polystyrene sulfonate (PEDOT:PSS) conductive polymer is used due to its biocompatibility and safety for use in health and food application. Regarding the enzyme needed, a multi-enzyme system needs to be designed to detect NEFAs. As mentioned, fatty acids are stable, and their metabolic decomposition is complex. Hence, more than one enzyme is required, obtaining a cascade reaction.

Since many oxidase enzymes produce hydrogen peroxide (H_2O_2) as a by-product, the first step was to be able to detect H_2O_2 . Therefore, the first enzyme

used is horseradish peroxidase (HRP). As part of the peroxidase family, HRP reacts with hydrogen peroxide while oxidizing a substrate. In this case, HRP uses H₂O₂ – possibly the one produced by other enzymes - to react with PEDOT:PSS. Consequently, a hydrogen peroxide chemiresistive sensor based on an HRP-PEDOT:PSS ink was produced. This sensor is simply produced by 3D printing the sensitive ink on a filter paper, making the manufacturing simple and keeping the cost low. The sensor's limit of detection for H₂O₂ in liquid is 61.3 nM, and it shows a linear range from 61.3 nM to 61.3 μM. The sensor is also sensitive to hydrogen peroxide vapors. Despite the limitations, such as sensitivity to humidity and a relatively long response time (≈ 1 hour), this sensor could be used in controlled environment applications – e.g. food packaging and face masks.

To improve the drawbacks observed in the paper-based sensor, paper was replaced with a hydrophilic polyurethane hydrogel (HPU). Given their crosslinked structures, hydrogels are characterized by porous structures which allow them to swell when absorbing water. At the same time, the pores can be filled with other compatible materials. By combining HPU with the optimized HRP-PEDOT:PSS ink, it was possible to trap both the conductive polymer and the enzyme in a biocompatible, elastic hydrogel scaffold. Contrarily to what was achieved with the paper-based sensor, the use of HPU enables continuous monitoring of H₂O₂ in liquid. The sensor shows a limit of detection of 613 nM and a linear range between 613 nM and 6.13 μM. Once developed a suitable mechanism for H₂O₂ detection in two different substrates, lipoxygenase (LOX) was added to the ink. LOX is an enzyme that takes part in the digestion mechanism of polyunsaturated fatty acids (PUFAs). LOX works in the first stage of this process by adding a peroxide group in a specific position of the fatty acid chain. This site is meant to be the position where the carbon backbone is split. However, in the absence of the following enzyme in the sequence, the peroxide group is not consumed and instead is freed as hydrogen peroxide. This hydrogen peroxide is in turn used by HRP as the reagent to interact with PEDOT:PSS, consequently allowing PUFAs detection. This bi-enzymatic system allows the detection of PUFAs in a relatively simple, speedy, and cost-effective way compared to the traditional method of fatty acids detection.

8:45 AM SB10.15.03

Simultaneous Cross-Linking and Cross-Polymerization of Enzyme Responsive Polyethylene Glycol Nanogels in Confined Aqueous Droplets for Reduction of Low-Density Lipoprotein Oxidation Nazila Kamaly; Imperial College London, United Kingdom

A key initiating step in atherosclerosis is the accumulation and retention of apolipoprotein B complexing lipoproteins within artery walls. In this work, we address this exact initiating mechanism of atherosclerosis, which results from the oxidation of low-density lipoproteins (oxLDL) using therapeutic nanogels. We present the development of biocompatible polyethylene glycol (PEG) crosslinked nanogels formed from a single simultaneous cross-linking and co-polymerization step in water without the requirement for organic solvent, high temperature or shear stress. The nanogel synthesis also incorporates *in situ* non-covalent electrostatically driven template polymerization around an innate anti-inflammatory and anti-oxidizing paraoxonase-1 (PON-1) enzyme payload - the release of which is triggered due to matrix metalloproteinase (MMP) responsive elements instilled in the PEG crosslinker monomer. Results obtained demonstrate the potential of triggered release of PON-1 enzyme and its efficacy against the production of ox-LDL and therefore a reduction in macrophage foam cell and reactive oxygen species formation.

9:00 AM SB10.15.04

Hierarchical Nanocomposites for Biocatalysis Julie Goddard; Cornell University, United States

Enzymes enable high specificity in applications such as production of value-added agricultural products, environmental remediation, and diagnostics, but are often limited by challenges in stability and recovery in these complex biological systems. Hierarchical structures, incorporating both macrostructures and nanostructures, can harness the benefits of each size regime for the stabilization of enzymes. Here we describe two case studies. In one, lipase B from *Candida antarctica* was interfacially assembled with iron oxide nanoparticles into hierarchically ordered structures consisting of a cross-linked core of poly(dicyclopentadiene). Microparticles were characterized for performance in extreme environments (low/high pH, high temperature, solvents) which are denaturing for native lipase. Kinetic analysis revealed a significant increase in the turnover rate following immobilization. After two hours exposure to 50% acetonitrile, there was no measurable leaching of enzyme from the microparticles, while Novozym 435 lost 99.8% protein under the same conditions, suggesting robust design for use in solvent applications. Per unit protein, microparticles outperformed Novozym 435 in direct esterification and transesterification. In another study, we demonstrate the synthesis of copper microflowers in which the enzyme β-galactosidase is incorporated with retained activity. We explore the nuance of considering both biological and non-biological system performance in the pragmatic assembly of these hierarchical biocatalytic nanocomposites. Such understanding of hierarchical biocatalytic systems can permit their application in complex biological systems to improve the safety and sustainability of food, bioprocessing, and diagnostic applications.

9:15 AM *SB10.15.05

“Designer” Oral Delivery Systems for Agri-Food to Pharmaceutical Applications Joachim Loo and Kaarunya Sampathkumar; Nanyang Technological Univ, Singapore

Delivery or encapsulation systems can be developed to achieve controlled-, sustained-release and targeted delivery for a myriad of applications, ranging from agri-food, biomedical, nutraceutical to pharmaceuticals applications. In addition, delivery systems simultaneously function as a protective carrier for labile compounds that may otherwise degrade under harsh environments; for instance, when exposed to gastro-intestinal fluids. By incorporating specific design parameters to each functional system, it is hypothesized that bioavailability of drugs or nutrients can be enhanced. In this presentation, we shall first discuss how oral delivery systems can be designed to improve patient compliance in the delivery of pharmaceuticals, using Parkinson's disease as a model. With the current shift in paradigm in disease prevention through better nutrition, there has been immense interest in augmenting health with nutraceuticals. On this note, we will also report the design of food-based, enteric-coated carriers that can target nutraceutical release along specific parts of the gastro-intestinal tract. Using animal models, we will discuss how this targeted delivery system can improve shelf-life, increase bioavailability and enhance efficacy of nutrients and other nature-derived compounds. In addition, we will also explore alternative oral encapsulation technologies for the development of functional foods, e.g. synbiotics, for agri-food applications.

9:45 AM SB10.15.06

Cost-Effective Cultured Meat Developed on Cell Sheets Containing Tunable Microstructured Gelatin Powders Sohyeon Park and Jinkee Hong; Yonsei University, Korea (the Republic of)

Cultured meat is artificial meat produced by culturing cells extracted from living animals based on cell engineering technology which allows a continuous supply of meat without unnecessary slaughter. Recently, this slaughter-free meat is coming into the limelight due to its advantages of lowering environmental pollution, protecting animal ethics, and enhancing the safety of meat. In addition, the hunger for a sustainable form of meat has grown even more as the meat industry has been hit by the import and export suspensions caused by the COVID-19 pandemic. However, the fatal limitations of cultured meat production such as using excessive animal-derived materials and high production costs put the brakes on the popularization of cultured meat. To overcome this limitation, we propose the introduction of well-organized biomaterial science into the cultured meat process.

In this research, we first report on a strategy to develop scaffold-free advanced cultured meat using fish gelatin microsphere (GMS) and myoblast sheet. The GMSs are edible and exhibit various morphologies and binding activities based on the degree of crosslinking. We also select insulin-like growth factor 1 (IGF-1) and C-phycoyanin (C-PC), blue algae extract, as reasonable and eco-friendly nutrients to improve the proliferative activity of myoblasts in fetal

bovine serum (FBS)-reduced growth medium. Each of these nutrients was incorporated into GMSs with different surface properties. The loading and release behaviors of nutrients for each GMS are analyzed, and subsequently the most effective GMSs to improve the proliferation of myoblasts under an FBS-reduced medium are selected.

GMSs applied to cell sheet culture produce more cost- and time-effective meat-like cell sheets than conventional methods by exerting four important functions. Finally, we prepare two types of cost-effective cultured meat with GMS-based cell sheets. We evaluate the quality of the cultured meat by comparing the tissue properties with soy meat and chicken breast. GMS is a versatile functional material that can be applied to both batch and continuous processes as well as cell sheets. This technology can economically produce cultured meat with high cell content by overcoming the low cell content and high production cost of conventional cultured meat. We believe that this material engineering technology will provide a significant contribution to the commercialization of cultured meat.

SESSION SB10.16: Biomaterials for Food and Agriculture II
Session Chairs: Julie Goddard and Benedetto Marelli
Tuesday Morning, December 7, 2021
SB10-Virtual

10:30 AM SB10.16.02

Surfactant-Like Cellulose Nanocrystals to Stabilize Pickering Emulsions for Use in Agricultural Applications Gurshagan Kandhola, Joseph Batta-Mpouma and Jin-Woo Kim; University of Arkansas, United States

Surfactants are materials with hydrophobic and hydrophilic sites that adsorb at the interface between an oil and aqueous phase, allowing immiscible liquids to mix easily and produce stable emulsions. These surface-active materials are of immense significance in the agrochemical industry for the development of adjuvant formulations for pesticides and fertilizers. Surfactants are one of the most commonly used adjuvants that increase the efficacy of crop protection products by enhancing their spreading, sticking and wetting properties. However, most commercially available surfactants in agriculture are derived from petroleum sources, and environmental concerns over toxicity and low degradability are key drivers for the growing market demand of renewable, non-toxic, biodegradable surfactants. Thereby, developing efficient and ecofriendly surfactants is of great interest, particularly in the agricultural sector. Biologically extracted materials, such as cellulose nanocrystals (CNCs), are good candidates to fulfill that need. The surface of CNCs is rich with accessible and hidden hydroxyl groups, lending these renewable, non-toxic and biocompatible nanoparticles, an amphiphilic nature and surfactant-like characteristics. While emulsions stabilized by conventional surfactants have been the norm in most industries for many decades, Pickering emulsions stabilized by solid particles; for example, inorganic particles, such as colloidal silica and graphene oxide, and organic particles, such as nanocellulose, are increasingly becoming favorable choices due to their excellent long-term stability.

In this work, cellulosic Pickering emulsions (CPEs) were developed by blending negatively charged CNCs and cellulosic polymers. The tuning of surfactant-like behavior of CNCs was achieved by salts of magnesium nitrate ($Mg(NO_3)_2$) and zinc nitrate ($Zn(NO_3)_2$), respectively. The emulsions were prepared at varied CNC and salt concentrations, without the use of any petroleum-derived surfactants or prior functionalization of the original CNCs with any hydrophobic molecules. The preparation of CPEs was achieved by mixing colloidal CNCs in aqueous phase with oleic acid in oil phase using high-energy ultrasonication. Various interface parameters were investigated, such as surface tension and surface charge as well as shear viscosity, to understand the effect of CNC and salt concentration on the physicochemical characteristics of the CPEs. In addition, the emulsions were also analyzed under an optical microscope to study droplet coalescence and emulsion stability. Results showed that CNCs in the presence of salts influenced the formation and stabilization of the CPEs and were more effective in emulsifying oleic acid compared to when CNCs were used alone. This study not only showed that CPEs can be stabilized by CNCs in the presence of divalent cations, but also established a platform to produce CNC-based PE with customizable properties and functionalities with new insights into their application as eco-friendly surfactants in agriculture. Such a strategy will be useful to develop advanced products in liquid and solid forms as emulsions and beads not only in agriculture but also in several applications ranging from food and pharmaceutical to paint and coating industries.

This project is supported by the Center for Advanced Surface Engineering (CASE), under the National Science Foundation (NSF) Grant No. IIA-1457888 and the Arkansas EPSCoR Program, ASSET III.

10:45 AM *SB10.16.03

Silk Fibroin as an Edible Food Coating Adam Behrens; Mori, United States

Food waste has far-reaching socioeconomic and environmental impact. Nutrient-rich fresh foods are particularly susceptible to waste resulting from cold chain breaks. Further, the decomposition of wasted food and the subsequent energy and water inputs required for redundant production, processing, and distribution are severely detrimental to the environment. Recent developments have demonstrated the ability of silk fibroin to extend the shelf-life of various classes of foods by minimizing oxidation and dehydration. This work will highlight the physical and chemical features of silk fibroin that allow it to act as a barrier coating as well as discuss the safety and integration requirements for successful scale up and commercialization within the food industry.

11:15 AM *SB10.16.04

Synthetic and Natural Occurring Polymers—Their Blends and Composites with 1D/2D Nanomaterials for Agriculture Applications Tony McNally, Chaoying Wan and Fengwei D. Xie; University of Warwick, United Kingdom

Biodegradable polymers, those synthesized from monomers derived from either the biomass or fossil fuels, or those naturally occurring continue to attract intense research interest given the increased global impetus to address the carbon footprint of plastics and issues around climate change and pollution. The largest single use of plastics is in all forms of packaging, including food packaging and *de facto* aligned with agriculture, although there are numerous other uses of mostly fossil-fuel derived plastics in agriculture, from pipes to mulch film. Here, we describe two approaches to the development of biodegradable polymer blends and composites that critically can be prepared using sustainable, environmentally friendly processes and at scale in high volumes. Firstly, focusing on poly(glycolic acid) or PGA, a polymer with a similar structure to poly(lactic acid)(PLA) minus a methyl side group, with the resulting polymer having crystalline content as high as ~55%, high thermal stability (up to 230°C), excellent gas barrier properties as well as high strength (115 MPa) and stiffness (~7 GPa)[1]. However, PGA is 100% compostable and biodegrades rapidly with a profile similar to cellulose. Despite these useful properties, PGA has a number of intrinsic properties, most notably brittleness which have hindered its application. Classically, this has in part been overcome by co-polymerising glycolic acid with lactic acid (PLGA) or to a lesser extent physically blending PGA with other polymers, with the latter

strategy being more commercially viable. Here, PGA was melt blended with poly(butylene adipate-co-terephthalate)(PBAT) using a terpolymer of ethylene, acrylic ester and glycidyl methacrylate (EMA-GMA) to promote interfacial interactions between the blend components. The resultant blends had improved ductility (strain at break increased from 10.7% to 145%), reduced oxygen permeability, enhanced water vapour barrier performance (improved by 47%) and thermal stability up to 300°C, properties required for hot food packaging. Further improvements in barrier properties were achieved by treating the surface of blown films of these blends with electron beam treatment with, further manipulation possible for controlled agrochemical release. A second approach focused on the blends and composites of natural occurring polymers based on chitosan, carboxymethyl cellulose (CMC) and alginate and, 1D/2D materials, both organic and inorganic, including montmorillonite (MMT) and sepiolite (SPT). Thermo-mechanical kneading is used to prepare blends and composites of chitosan, a cationic polysaccharide, with negatively charged biopolymers such as CMC, allowing for the preparation of films with excellent dimensional stability and structural integrity [2]. This advance in hydrolytic stability is derived from physical crosslinks due to polyelectrolyte complexation between chitosan and CMC. Furthermore, it is possible to manipulate the properties of these films by the addition of naturally occurring negatively charged MMT or SPT for application in food packaging [3]. The properties of these films were further modified by selective plasticisation using natural molecules and ionic liquids and other 2D materials such as graphene oxide [4].

References

- [1] P. Kumar Samantaray, A. Little, D. M. Haddleton, T. McNally, B. Tan, Z. Sun, W. Huang, Y. Ji and C. Wan. *Green Chem.*, 2020, **22**, 4055-4081.
- [2] P. Chen, F. Xie, F. Tan, T. McNally. *Compos. Sci. Technol.*, 2020, **189**, 108031.
- [3] P. Chen, F. Xie, F. Tan, T. McNally. *Eur. Polym. J.*, 2021, **144**, 110225.
- [4] P. Chen, F. Xie, F. Tan, T. McNally. *Carbohydr. Polym.*, 2021, **253**, 117231.

11:45 AM SB10.16.05

Polyethylenimine Based Nanoparticles for Enhancing Photosynthesis in Plants Cyril Routier¹, Lorenzo Vallan², Eric Cloutet² and Eleni Stavrinidou¹; ¹Laboratory of Organic Electronics, Department of Science and Technology, Linköping University, Sweden; ²Laboratoire de Chimie des Polymères Organiques (LCPO-UMR 5629), Université de Bordeaux, Bordeaux INP, CNRS, France

During photosynthesis, plants use light energy to transform carbon dioxide and water into carbohydrates. The photosynthetic process comprises many steps that can in principle be optimized to have higher efficiency. Rubisco (Ribulose 1,5-bisphosphate carboxylase/oxygenase) catalyzes the carboxylation reaction that is the initial reaction for carbon fixation and conversion of CO₂ to sugars. The reaction occurs in organelles called chloroplasts present in leaf cells. However, Rubisco has naturally a poor affinity for CO₂ and the transfer of the atmospheric CO₂ to the Rubisco enzyme is highly limited by the diffusion of CO₂ through the stomata and the intercellular space which ultimately considerably reduces the photosynthesis rate. Polyamines have been shown in-vitro to be able to transfer carbon dioxide to Rubisco for the carboxylation reaction. In this work, we present biocompatible fluorescent polyethylenimine nanoparticles for enhancing the CO₂ transfer to the Rubisco enzyme. With in-vitro studies we evaluated the nanoparticles uptake of atmospheric CO₂ and transfer kinetics to Rubisco for the carboxylation reaction. Then we introduce the nanoparticles in-vivo into the plant apoplast via agroinfiltration. First, we studied the toxicity of the nanoparticles and results showed no evidence of a direct harmful impact. We then investigated their localization within the plant leaf with fluorescent microscopy and preliminary observations indicate that the nanoparticles are present in the intercellular space but also in the direct centers of photosynthetic activity: the chloroplasts. Finally, we investigated the impact of the nanoparticles on the plant photosynthesis.

SESSION SB10.17: Biomaterials for Medicine, Food and Agriculture
Session Chairs: Julie Goddard and Benedetto Marelli
Tuesday Afternoon, December 7, 2021
SB10-Virtual

1:00 PM *SB10.17.01

Role of the Assembly Conditions and Macromolecular Structure on Drug Delivery Properties of Multilayer Thin Films Rogerio A. Bataglioli, João Batista M. Rocha Neto, Mariana C. Costa, Patricia F. Martinez and Marisa M. Beppu; University of Campinas, Brazil

The layer-by-layer technique for film deposition presents several advantages for preparing materials for drug delivery, including the mild chemical conditions for handling therapeutics, simple and scalable processing. However, this technique lacks information describing the role of the deposition parameters and film moieties on the drug release process. This study investigated the influence of the assembly parameters (pH, ionic strength, capping layers, and the loading method) on the drug delivery properties in multilayer films. Hyaluronan/chitosan (HA/CHI) films were assembled at different pH (4.5 and 7.2) chitosans with different degrees of deacetylation (40%, 65%, and 85%) to test their role in the loading and release of ionic Rose Bengal dye in the multilayer films. Films assembled at pH 7.2 were rougher and thicker than those deposited at more acidic conditions, presenting superior drug loading capacity and a more sustained release profile. This result was attributed to the more coiled conformation of chitosan during film deposition, which led to a higher number of free amino groups interacting with rose Bengal during drug loading. Drug release data were fitted to the Higuchi model, indicating an increase in the diffusional coefficient with chitosan deacetylation degree. Ritger and Peppas model demonstrated an anomalous drug release mechanism and the more sustained release profile for films assembled at pH 7.2. This study also investigated the drug delivery properties of the traditional poly (acrylic acid)/poly (allylamine hydrochloride) (PAA/PAH) multilayers, which presented the superior calcein (model drug) loading capacity for films prepared at basic pH (> 8.5) with MgCl₂ or NaCl in the polyelectrolyte solutions. This result was attributed to the higher number of free, no complexed amino groups of the PAH chains in the multilayers, available for interacting with carboxylate groups of calcein molecules via salt bridges. The drug loading method (post- or during-film deposition) also affected the film loading capacity and release mechanism in the PAA/PAH films, leading to the highest drug loading signal in films prepared using the postassembly method. The limited amount of drug in PAA/PAH films using the during-assembly method may be attributed to the washing out of calcein molecules during film deposition, possibly leading to a matrix with tightly bound drug molecules for this condition. Data fitting to Higuchi and Ritger-Peppas models demonstrated an increase in the drug release constant with the number of bilayers deposited for films prepared using the postassembly method, whereas the opposite trend was observed for the during- assembly drug loading method. The Berens-Hopfenberg model enabled the decoupling of the individual contribution of different drug release mechanisms (diffusion and polymer chain relaxation), demonstrating an increase of the chain relaxation contribution with the number of bilayers. The stronger interaction between the polymer and the calcein molecules for samples prepared using the during-assembly method may have hindered the fast, drug diffusion process, enhancing the effect of the matrix swelling in the drug release process and leading to a more sustained drug release profile. PAA/PAH films loaded with calcein were also spin-coated with different capping films (fatty acids and phospholipid monolayers, and ALG/CHI multilayers) to reduce the initial burst release effect. The densely packed phospholipid

monolayers led to the most substantial decrease in the release rate with minimal reduction in the drug cargo during the capping layer deposition, highlighting the importance of single-step methods to avoid the drug leaking. These findings illustrate alternatives to modify the drug release profile of small molecules in nanostructure thin films based on the building blocks, film assembly, and drug loading methods, aiming to design drug delivery devices with precise architecture and performance.

1:30 PM SB10.17.02

Tuning Proton Transport in *m*-Polyaniline Through Chemical Functionalization [Gloria Bazargan](#) and Daniel Gunlycke; U.S. Naval Research Laboratory, United States

Proton transport is essential to many physiological processes. For this reason, devices that deliver a controlled flow of protons to living organisms show promise for advancing medicinal/therapeutic treatments. These bioprotonic devices depend on conductive, biocompatible polymer membranes to facilitate protonic movement. Herein, we present *ab initio* molecular dynamics (AIMD) simulations to quantify proton transport in a candidate polymer for bioprotonic membranes, *m*-polyaniline, and its chemically functionalized derivatives. By demonstrating how polar, acidic, and aromatic chemical groups influence protonic movement, our results show that chemical functionalization can be used as a tool for tuning the transport properties of *m*-polyaniline.

1:45 PM SB10.17.03

Late News: Application of Tn5 Transposases to Surface-Immobilized DNA Adsorbed on Grating Surfaces Jonathan Sokolov¹, Anthony Del Valle¹, Hannah S. Saks², [Junzhi Xie](#)³, Robin Xiong⁴ and Leon L. Zhou⁵; ¹Stony Brook University, The State University of New York, United States; ²Walt Whitman High School, United States; ³Richard Montgomery High School, United States; ⁴Ward Melville High School, United States; ⁵Shenzhen Middle School, China

Recently, modified transposases have been used to both fragment and attach end-groups to DNA molecules in solution and on beads. This process, termed 'tagmentation,' has been commercialized and used to improve library preparation for DNA sequencing. We report the application of transposase tagmentation to DNA linearly stretched and immobilized onto grating surfaces with micron-sized periodicities. The use of gratings is done to prevent the steric hindrance inherent to DNA strongly adsorbed to flat surfaces. The places where the DNA bridges across the grating provide open regions where tagmentation can occur. Gratings were produced using standard integrated circuit lithography techniques on silicon substrates. The gratings were either coated with polymethylmethacrylate (PMMA) thin films or used to produce polydimethylsiloxane (PDMS) replicas. DNA was adsorbed and stretched over the gratings by withdrawing a substrate from DNA-containing solutions, a method called molecular combing. Loaded Tn5 transposase (Diagenode) solutions in tagmentation buffer were applied to the surface-adsorbed DNA via microliter droplets and reacted at 40°C for 10 minutes, followed by soaking in sodium dodecyl sulfate (SDS) for 5 minutes. Fragmentation of the DNA (stained with SyBr Gold dye) was confirmed by fluorescence microscopy. Surface tagmentation has the potential to maintain long-range order of the fragments for sequencing applications.

2:00 PM *SB10.17.04

DNA Nanotechnology—A Promising Tool to Target Cancer [Efrosini Kokkoli](#); Johns Hopkins University, United States

DNA is a popular material for constructing complex, multidimensional nanostructures due to its ability to organize in a precise and predictable manner. Popular approaches to create nanostructures from DNA include DNA origami, DNA tile and DNA brick assembly. An alternate approach to direct the assembly of single-stranded DNA (ssDNA) is to conjugate a hydrophobic moiety (i.e., polymer or lipid-like tail) to the ssDNA to form an amphiphilic molecule that spontaneously self-assembles when added to aqueous solutions. However, the majority of structures created by the assembly of ssDNA-amphiphiles have been spherical and cylindrical micelles. In this presentation I will discuss how we design ssDNA-amphiphiles that self-assemble into supramolecular nanostructures such as nanotubes, and how we use them to target glioblastoma (GBM) in an orthotopic mouse model of GBM.

2:30 PM *SB10.17.05

Nanofibers as Functional Surfaces for Concentration and Capture of Biomolecules in Microfluidic Devices [Margaret Frey](#); Cornell University, United States

Nanofiber membranes can be prepared rapidly and inexpensively using the electrospinning process. These fibers have very high surface to volume ratio and a wide range of surface functionalities have been developed for purifying, capturing and mixing fluids within a microfluidic channel. Specific examples of nanofibers with persistent and switchable positive or negative surface charge and biotinylated surfaces for biotin-streptavidin sandwich style assays and their use in microfluidic devices will be presented. Additionally, two strategies for functionalizing electrospun nanofibers for specific capture of biological molecules will be discussed. First, silver-doped carbon nanofibers (SDCNF) are used as the base material for the selective capture of *Escherichia coli* in microfluidic systems. Polyacrylonitrile nanofibers containing silver nitrate were electrospun and carbonized to form carbon fibers with silver particles at the surface. Antibodies are immobilized on the surface via a three-step process. The negatively charged silver particles present on the surface of the nanofibers provide suitable sites for positively charged biotinylated poly-(L)-lysine-graft-poly-ethylene-glycol (PLL-g-PEG biotin) conjugate attachment. Streptavidin and a biotinylated anti-*E. coli* antibody were then added to create anti-*E. coli* surface functionalized (AESF) nanofibers. Functionalized fibers were able to immobilize up to 130 times the amount of *E. coli* on the fiber surface compared to neat silver doped fibers. To demonstrate selectivity and functionalization with both gram negative and gram-positive antibodies, anti-*Staphylococcus aureus* surface functionalized (ASSF) nanofibers were also prepared. Experiments with AESF performed with *Staphylococcus aureus* (*S. aureus*) and ASSF with *E. coli* show negligible binding to the fiber surface showing the selectivity of the functionalized membranes. Second, biotin-cellulose nanofiber membranes are successfully fabricated via "click" chemistry. Cellulose acetate (CA) is electrospun, deacetylated and substituted with an alkyne group in either a one or two step process. Azide-biotin conjugate is then "clicked" onto the alkyne-cellulose surface via Copper-catalyzed Alkyne-Azide Cycloaddition (CuAAC). FTIR, Scanning Electron Microscopy (SEM), Energy Dispersive X-ray spectroscopy (EDX), and X-ray Photoelectron Spectroscopy (XPS) are used to confirm addition of biotin without damage to the fiber structure. The biotin-cellulose nanofiber membranes are used in example assays (HABA colorimetric assay and fluorescently tagged streptavidin assay) where streptavidin specifically binds to the pendant biotin without requiring blocking agent. Both methods yield durable attachment of the specific capture functionality at the fiber surface.

8:00 AM SB10.18.01

Nanomechanical Analysis of Coronavirus Spike Proteins and Correlation with Infectivity and Lethality Yiwen Hu and Markus J. Buehler; Massachusetts Institute of Technology, United States

The novel coronavirus disease, COVID-19, has spread rapidly around the world. Its causative virus, SARS-CoV-2, enters human cells through the physical interaction between the receptor-binding domain (RBD) of its spike protein and the human cell receptor ACE2. As an increasing number of variants of SARS-CoV-2 circulates globally, estimates of infectiousness and lethality of newly emerging strains are important. Here, we provide a novel way to develop a deeper understanding of coronavirus spike proteins, connecting their nanomechanical features – specifically the vibrational spectrum and quantitative measures of mobility – with virus lethality and infection rate. The key result of our work is that both, the overall flexibility of upward RBD and the mobility ratio of RBDs in different conformations, represent two significant factors that show a positive scaling with virus lethality and an inverse correlation with the infection rate. A quantitative model is presented to make predictions on the infectivity and lethality of SARS-CoV-2 variants based on molecular motions and vibrational patterns of the virus spike protein. Our analysis shows that epidemiological virus properties can be linked directly to pure nanomechanical, vibrational aspects, offering an alternative way of screening new viruses and mutations against high threat levels, and potentially exploring novel ways to prevent infections from occurring by interfering with the nanoscale motions.

8:05 AM SB10.18.02

Potassium Incorporated Titanium Dioxide Nanoparticles Modulate the Production of Immune Mediators Associated with Lepromatous Leprosy by Human Dendritic Cells Upon Infection with *Mycobacterium leprae* So Yoon Lee¹, Sam Warren², Jose Barragan², Ai Serizawa¹ and Jorge Cervantes²; ¹Shibaura Institute of Technology, Japan; ²Texas Tech University Health Sciences Center, United States

Introduction: Leprosy is a chronic infectious disease caused by *Mycobacterium leprae*, which is still endemic in many parts of the world including Southern Texas. The two polar clinical forms of leprosy, termed tuberculoid and lepromatous, have polarized cellular immune responses, with complex immunological distinctions.

Dendritic cells (DCs) are the primary antigen presenting cells in the immune system. TiO₂ nanoparticles have shown to induce maturation of these cells leading to an inflammatory response.

Objective: We aimed to evaluate the effect of potassium incorporated TiO₂ nanostructures, namely KTiOx, in the response of human monocyte-derived-DCs to *M. leprae*.

Methodology: THP-1 human monocytes were differentiated and matured into DCs using commercially available media, and then treated with KTiOx for 24 hours. Following, cells were infected with *M. leprae* at an MOI of 10:1 for 24 hours. Secreted human cytokines were measured in the culture supernatants by a multiplex ELISA system.

Results: We observed an increase in the levels of secreted IFN- α and TNF- β upon *M. leprae* infection in cells treated with KTiOx. IFN- β and its downstream gene IL-10 are preferentially expressed in disseminated and progressive lepromatous lesions, while TNF- β gene is identified as a major risk factor for early-onset leprosy. Interestingly, the levels of cytokine secretion differ comparing 1 M KOH treated Ti and 10 M KOH treated Ti. This can be explained by a wider surface area of the 10M preparation compared to 1 M KOH treated Ti. It is possible that this wider KTiOx area can activate more DCs due to an increase in the contact area.

Conclusion: This study demonstrates the effect of nanostructures of KTiOx and the usefulness of nanoparticle technology in the *in vitro* activation of human DCs against an infectious disease with a puzzling immune spectrum. Our findings may prompt future therapeutic strategies such as DC immunotherapy for disseminated and progressive lepromatous lesions.

8:10 AM SB10.18.03

Enhancing Antibacterial Property of Aluminum Foil by Nanostructuring its Surface through a Simple Hot Water Treatment Quinshell Smith, Kenneth Burnnett, Nawab Ali, John Bush and Tansel Karabacak; University of Arkansas at Little Rock, United States

Foodborne pathogens have led to many hospitalizations and deaths. They have been responsible for several outbreaks in recent years. Bacteria are able to survive on a range of surfaces and environments. The risk of bacterial infection from a contaminated surface has increased exponentially due to the formation of biofilm. Bacteria have been able to form a resistance to the modes of action of current antibacterials. This study utilized a hot water treatment (HWT) method for introducing antibacterial property to aluminum surfaces relevant to food processing and packaging applications. The HWT process produces a nanostructured oxide layer on a wide range of metallic materials by simply immersing the metal in water at relatively low temperatures, which can enhance the antibacterial properties. In this work, aluminum foil was hot water treated at 75°C for 30 minutes. Concentrations of *E. coli* (192 cells) and of *S. epidermidis* (185 cells) were placed on aluminum foil for different times, ranging from 1 minute to 60 minutes. The survival time was measured and the results indicate, the longer the bacteria was on the HWT aluminum foil surface, the more bacteria was killed. As the temperature of the HWT increased to 85°C and 95°C we observed a decrease in bacterial growth, which is consistent with the more pronounced nanostructures at higher HWT temperatures. Overall, the HWT aluminum foils were 95-100% more effective in killing the bacteria within 1-60 minutes than the untreated foil. HWT aluminum oxide nanostructures are believed to utilize multiple mechanisms to deactivate bacteria, ranging from contact killing to the production of reactive oxygen species (ROS), which requires the bacteria to form multiple defenses in order to maintain vitality.

8:15 AM SB10.18.04

Precise Control of RNA Microstructure Fabrication by Viscosity Regulation Moon S. Hyun, Hyejin Kim and Jong Bum Lee; University of Seoul, Korea (the Republic of)

RNA nanotechnology has advanced extensively for its potential biomedical applications by leveraging a wide range of biological functions of RNA. Especially, RNA microstructures fabricated by rolling circle transcription (RCT)-based enzymatic RNA self-assembly has gained much attention as one of the promising approaches to enhancing the loading capacity and delivery of therapeutic RNA. In this respect, we controlled the enzymatic RNA polymerization by regulating viscosity and studied how viscosity affects the RNA microstructures fabrication by altering the enzyme activities and molecular interactions between reaction components. The solution viscosity was manipulated by increasing a glycerol contents. The increment of viscosity in reaction conditions resulted in reduced RNA polymerization rate, which means that the polymerase activity is regulated by viscosity. Furthermore, the inorganic crystallization of magnesium pyrophosphate, which has an important role as a structural basis of RNA microstructures, decreased as the solution viscosity increases. As a results, the size of the RNA microstructure was decreased as the solution viscosity was increased. Also, the flower-like structure was disappeared in highly viscous conditions. Finally, the size of the RNA microstructure was fine-tuned by regulating viscosity with other previously reported size reduction method that modulates template DNA to monomer rNTP ratio. The required size of the RNA microstructures would be different depending on the biomedical application. Therefore, we suggested new approaches to manipulate the size of RNA microstructures to satisfy diverse biomedical demands precisely.

8:20 AM SB10.18.05

Late News: (Garcia High School Student) Designing Chitosan-Cellulose Composites for Heavy Metal Absorption Using Deweaved Cotton

Cloth Ivan J. Yuan¹, Elizabeth Zhang², Jacob T. Zerykier³, Guanchen Zhu⁴, Ayush Agrawal⁵, Tianyu Dong⁶, Haojun Xu⁷, Michael Cuiffo⁸ and Miriam Rafailovich⁸; ¹Shanghai High School International Division, China; ²Phillips Academy, United States; ³Rambam Mesivta-Maimonides High School, United States; ⁴Experimental High School Attached to Beijing Normal University, China; ⁵Canyon Crest Academy, United States; ⁶Northview High School, United States; ⁷The Madeira School, United States; ⁸Stony Brook University, The State University of New York, United States

Chitosan is known to have a high capacity for metal absorption, though it exhibits low mechanical strength. Cellulose, on the other hand, has high mechanical strength but low metal absorption capacity. We propose combining the two materials to form a composite that has both metal-absorbing abilities and high mechanical strength. An abundant source of cellulose is in waste cotton fabric, due to the 10 million tons of fabric the textile industry disposes of each year.^[1] Citric acid was used to deweave cotton fabric into fibers and also to cross-link chitosan and cellulose through esterification, which produces a stronger and more chemically active cotton-chitosan composite while retaining its biodegradability.^[2] One application of cellulose-chitosan composites is the absorption of heavy metals, such as chromium. Chromium pollution is largely caused by industries in energy, mining and metal works, fertilizer, paints, and more. Chromium pollutants, especially chromate, dichromate, and chromium trioxide, have toxic effects on plants, animals, and microorganisms and pose risks to human health ranging from skin irritation to DNA damage and cancer development. Existing methods for removal include chemical reduction, adsorption on porous surfaces with ion exchange, and electrocoagulation, but such methods often produce sludge, require large amounts of chemicals, and pose a risk of secondary pollution.^[3] Cellulose-chitosan composites, being fully biodegradable, provide a greener method for heavy metal cleanup.

A 12.5 g/L solution of chitosan was prepared at a pH of 5 (adjusted by HCl). Pieces of fabric, cut across the weave in a diagonal to maximize the number of fibers exposed, were placed in 40 mL of 0.5 M citric acid and stirred at 800 rpm and 60 °C for 15 minutes. The fibers were then placed in a beaker, mixed with approximately 20 mL of chitosan solution, and cured with two different methods: ultraviolet irradiation for 10 minutes and heat lamp for one hour. The UV-cured composite exhibited gel-like properties, suggesting how it can be used as a hydrogel. The heat lamp-cured composite was a stiff material and far more rigid than both the UV-cured composite and the cotton raw material. Scanning electron microscopy (SEM) of the heat lamp-cured composite showed the cotton fibers supporting the chitosan matrix, suggesting that cross-linking was successful and able to provide mechanical reinforcement.

To test the chitosan composite's ability to absorb heavy metals, the heat lamp-cured composites and a control of untreated fabric were immersed in 15 mL of 0.01 M potassium dichromate solution for one hour. The samples were then retrieved from the solutions and dried overnight. The chromium content of the two samples, before and after absorption, was analyzed with X-ray fluorescence (XRF). XRF showed that the chitosan composite contained 149 900 ppm of chromium, which was significantly higher than the 38 000 ppm in untreated fabric and 50 300 ppm in deweaved fibers. To use the composite as an in-line water filtration system, we demonstrated that it was also possible to grind the material into a fine powder after cooling with liquid nitrogen, which can then be contained in a packed-powder filter or incorporated into a porous nanocomposite membrane.

[1] Mohamed S., et. al, *Polymers*, **2021**, 13, 626

[2] Akpomie, K., et. al, *Ecotoxicol. Environ. Saf.*, **2020**, 201, 110825

[3] Tumolo, M., et. al, *Int J Environ Res Public Health*, **2020**, 17, 5438

8:25 AM SB10.18.06

Late News: Mesoporous Pd@Au Film Integrated with Blood Plasma Separation Membrane for Surface-Enhanced Raman Scattering (SERS) Biosensor Hyun-Jong Kim and Hana Lim; Korea Institute of Industrial Technology (KITECH), Korea (the Republic of)

Surface-enhanced Raman scattering (SERS) sensor has been recognized as one of the most versatile tools for ultrasensitive detection of trace chemical and biological analytes. It is now well understood that the plasmonic coupling effect at the nanometer-sized gap junction between particles, that is so called 'nanogap' or 'hot spot' induces enormous electromagnetic enhancement that allows SERS signal to be detected with single-molecule sensitivity. However, inhomogeneous distributions of the location and intensity of the nanogaps lead to varying and non-uniform Raman intensities over substrate, and consequently provides irreproducible measurements. It seems to be practically impossible to obtain both of high sensitivity and good signal reproducibility in a large area.

Currently, SERS sensor is actively employed for the detection of diagnostic biomarkers which provides information about disease from biological fluids. Blood is the most important biological fluid which stands as the medium for transporting nutrients, oxygen and immune cells throughout the body and also maintains body temperature and pH. Therefore, it is an active indicator of various pathological disorders. For the analysis of blood, however, the separation of blood plasma has to first be accomplished to remove red blood cells. The conventional process of blood plasma separation is performed in macroscale centrifugation which requires several milliliters of blood and bulky and expensive apparatus. For patients, it is quite inconvenient due to the high volume of sample blood and transportation time.

To address this problem, we propose a novel strategy for simultaneous separation and SERS sensing of whole blood without additional blood plasma separation. The SERS-active porous metal film is integrated onto the blood plasma membrane. Then, blood plasma is separated from whole blood through the membrane and reached at the surface of SERS-active porous metal film through its pores. For the SERS-active porous metal film, a commercially available pluronic P123 block copolymer was used as a pore former, and physicochemical properties such as porosity and pore size of the metal thin film were controlled by electrodeposition process. As a result, mesoporous palladium thin film with homogeneously perpendicular 6-nm-sized channels was formed onto the blood Pd separation membrane. The homogeneous and perpendicular nanopores was very advantageous for the reproducibility of SERS signals and the facile diffusion of blood plasma. Also, Au layers with the thickness of 1 nm were carefully deposited on the mesoporous Pd thin film by electroless plating process. The obtained mesoporous Pd@Au film integrated with blood plasma separation membrane successfully detected various chemicals and biomarkers from whole blood without interfering with red blood cells.

8:30 AM SB10.18.08

Modification of Bacteriophage Capsid to Improve Bacteria Separation and Detection in Complex Food and Water Samples Kathryn Hufziger, Emma Farquharson, Sam Nugen and Julie Goddard; Cornell University, United States

The ability to detect bacteria in complex matrices with a rapid, low-cost, and simple method is paramount to improving food and water safety worldwide. Bacteriophages (phages), which are natural predators of bacteria and have been used to detect and treat bacterial infections, are a potential solution for bacteria separation and detection. Phages immobilized on magnetic nanoparticles can separate bacteria from their surroundings and then concentrate and detect low concentrations of bacteria in a short time. Our bacteria separation and detection system consists of T7 phages with modified capsid proteins that give a specific and directional binding to silica-coated magnetic nanoparticles. No modification of the phage genome is required; instead, phage capsid modification was accomplished by modifying the bacterial host, which was confirmed with sequencing. Expression of the modified phage capsid protein and assembly on the phage capsid was confirmed by western blotting. The immobilization of modified phages on the silica-coated magnetic nanoparticles was confirmed by infectivity studies, where the infectivity of the modified T7 was higher than wild-type T7. The phage-nanoparticle construct could then separate and detect bacteria in relevant water conditions. Expanding the range of complex conditions in which phage-based detection platforms can perform is an essential step towards improving food and water safety and, in turn, global public health.

8:35 AM SB10.18.10

Scalable Production of Crosslinked Alginate Microparticles Using Spray Drying for Bioactives Encapsulation in Aquaculture Manish Mahotra, Li Ling Tan, Sharad Kharel, Yu Lin Lim and Joachim Loo; Nanyang Technological University, Singapore

Encapsulation of bioactives like nutrients, probiotics, and drugs is of great interest in the aquaculture industry recently. For oral delivery systems, scalable microencapsulation techniques using food-grade materials, protection of the nutrients against harsh environments, and targeted delivery in a certain portion of the Gastro-Intestinal (GI) tract are considered important. In an aquaculture setting, the nutrient delivery system must be able to prevent the leaching of the nutrient in the water environment and ensure release at the specific site of the fish's GI tract, usually the intestine. Alginate-based microparticles are one of the most studied microencapsulation systems for oral delivery applications. Traditionally, crosslinked alginate microparticles are fabricated using a multi-step technique that involves wet extrusion-gelation using calcium salt solution, followed by additional drying steps. The multistep fabrication makes the process less feasible for large-scale production and application in the food and agriculture industry. In this study, a one-step, and scalable fabrication process was designed using spray drying to fabricate crosslinked alginate microparticles. The presence of the crosslinking between the calcium ion and the alginate polysaccharide network was studied using different material characterization techniques. Additionally, the microparticles were studied for encapsulation of a carotenoid, β -carotene—a vitamin A precursor and an antioxidant. The process enabled a high yield production (~60.0%) of the crosslinked microparticles with high encapsulation efficiency (~50.72%) of β -carotene. The microparticles were found to be stable against disintegration in the aqueous environment due to the crosslinking effect. Additionally, the release studies in the simulated gastric and intestinal fluids showed that the crosslinked microparticles had a minimal release in the gastric fluid (3.42% in 2 hours), while a faster and complete release of the β -carotene in the next 4 hours of dissolution in the simulated intestinal fluid. While typical release behavior comparable to crosslinked alginate microparticles prepared using the traditional extrusion-gelation technique was observed, the optimized process is superior in terms of ease of fabrication, scalability, and cost-effectiveness for the use in bioactives encapsulation in the aquaculture industry.

8:40 AM SB10.18.11

Wireless Monitoring of Polymer Degradation for Noninvasive Assessment of Microbial Metabolic Activity in Food Safety Applications Jose F. Waimin, Sarath Gopalakrishnan and Rahim Rahimi; Purdue University, United States

Bioprocessable and biodegradable polymers can be used as functional material for assessing the metabolic activity of microbes within their environment. Current methods for detecting, assessing, and quantifying microbial activity in soil are limited to time consuming and expensive procedures requiring skilled labor, and can rarely be done directly on site. Simultaneously, as the world faces a growing population, the demand for IoT technology that allows for real-time sensing is crucial in precision agriculture to achieve maximum yields. Previous work has shown the feasibility of using an impedimetric method of detection to monitor the degradation of a cellulose acetate film, cast on interdigitated electrodes (IDEs), to assess the cellulolytic activity of microbes directly in soil. Cellulose degradation, which is a plant product specifically degraded by microbes and fungi in soil, can be directly linked to the metabolic activity of microbes, which has been previously used as a marker for soil health and could provide insight into crop yields and soil performance. Other biopolymers found in soil, such as lignin and chitin, can be used as representative to characterize the diverse metabolic activities of microbes. Similarly, monitoring the degradation of similarly relevant parameters is possible. Materials with pH-dependent solubility, such as cellulose acetate phthalate (CAP) and several methacrylates, can be used to detect sudden changes in pH in several environments. In this new concept, we have developed a wireless method for assessing microbial activity based on the same system of material degradation. Wireless sensing tags based on RF backscattering (0.5 – 1.5 GHz) have been designed using simulations done on CST microwave studio to achieve miniaturized sensing systems that can be buried and monitored directly in soil. In this method, the wireless reader transmits an interrogation signal to the sensor tag buried in the soil and collects the backscattered signal from it. The sensor tag embeds its resonance as an electromagnetic signature on the frequency spectrum of the reflected signal. Since the resonant frequency of the sensor tag is a function of the dielectric constant of the surrounding media, variations in the thickness and dielectric properties of the soil as well as the coatings on the sensor tag influence the resonant frequency. The sensor tag consists of a sensing unit and reference unit of size 2 cm x 2 cm each. By passivating the sensing unit with the biodegradable material, shifts in the resonance frequency as the material is decomposed can be measured and correlated to the microbial metabolic activity within the environment. The reference unit is coated with an anti-microbial film which makes it insensitive to microbial activity but sensitive to all the other environmental stimuli the sensing unit is exposed to. This differential pair configuration helps in extracting microbial activity by eliminating the effects of other soil parameters, such as volumetric water content (VWC) and temperature. These small, low-cost, battery-less sensing tags have been manufactured using scalable processes like 3D printing and laser cutting. By making sensing tags from extruded polylactic acid (PLA) filament, the meander-structured antennas using Zinc tape, and using a biodegradable polymer as functional material, we've achieved a fully biodegradable environmentally-friendly sensing system that can be buried in the soil and left for natural resorption without any concerns. These tags have been successfully used to monitor VWC (5% - 30%) in soil and the decomposition of materials with pH-dependent solubility with applications in food packaging and storage.

SESSION SB10.19: On-Demand
Sunday Morning, December 5, 2021
On-Demand

8:00 AM SB10.08.03

Late News: Thermodynamics of DNA Looping for Origami Folding Jacob M. Majikes, Paul N. Patrone, Michael Zwolak, Anthony Kearsley and Alexander J. Liddle; National Institute of Standards and Technology, United States

DNA-based self-assembly provides an exciting materials platform with which to build composite nanostructures impossible to fabricate with top-down techniques. While biological DNA is well characterized, much work must be done to develop a mature understanding of DNA as a nanoscale construction material.

In metals defects contribute only a small fraction of the system free energy, but control material microstructure and properties. In DNA origami, where the scaffold molecule is forcibly routed into a predetermined shape, conformational energy contributions are small compared to those of base pairing and base stacking but control assembly properties.

By leveraging the high throughput of qPCR equipment, we examine the thermodynamics of single folds *via* van't Hoff analysis of melt curves.

We then examine the effect of staple excess revealing unintuitive results in both cases. In contrast to whole origami, increasing staple excess for a single fold significantly reduces yield. We present these results and show how they can inform an understanding of whole-origami systems.

SYMPOSIUM SB11

Photo/Electrical Phenomena at the Interface with Living Cells and Bacteria
November 30 - December 8, 2021

Symposium Organizers

Herdeline Ardoña, University of California, Irvine
Munehiro Asally, University of Warwick
Daniela Comelli, Politecnico di Milano
Giuseppe Paternò, Istituto Italiano di Tecnologia

Symposium Support

Gold
BBSRC

* Invited Paper

SESSION SB11.01: Bacterial Interfaces
Session Chair: Giuseppe Paternò
Tuesday Morning, November 30, 2021
Sheraton, 2nd Floor, Back Bay A

10:30 AM *SB11.01.02

Rational Design of Phenazine Mediator Promoted Extracellular Electron Transfer in *Escherichia coli* [Shelley Minteer](#); University of Utah, United States

The ability to establish successful and efficient extracellular electron transfer (EET) between bacteria and electrode surfaces is critical for the development of mediated microbial electrochemical technologies. Here, we describe a phenazine-based mediator system to facilitate electron transfer from the model bacterium *Escherichia coli* during glucose metabolism. Phenazine redox mediators were experimentally evaluated, demonstrating distinct mediated currents, dependent on mediator structure. Our results show that the choice of a mediator with the appropriate redox potential is not the single aspect to consider when rationally designing future mediator-based EET systems. We will discuss the use of density functional theory and multivariate linear regression for understanding the structural properties that control phenazine mediated EET.

11:00 AM SB11.01.03

Nanomaterial-Bacteria Ensembles for CO₂ and N₂ Conversion to Tunable Value-Added Products [Stefano Cestellos-Blanco](#) and Peidong Yang; University of California, Berkeley, United States

In order to limit and revert the effects of climate change we must find a strategy to convert nearly inert CO₂ to value-added chemicals to close the carbon loop. CO₂ utilization has been industriously studied resulting in a variety of catalysts aiding to reduce CO₂. One auspicious approach integrating both solar energy generation and CO₂ reduction consists of pairing autotrophic whole-cell bacteria with semiconductor nanomaterials. Nanomaterials at length scales similar to those of bacteria absorb light and provide the microorganisms with the requisite energy to undertake CO₂ reduction. The microorganisms convert CO₂, N₂ and H₂O with unparalleled selectivity and low-substrate activation all while self-repairing and reproducing. We present on the evolution of photosynthetic semiconductor biohybrids and how we have built on the earliest demonstrations of the concept. Our enhanced ability to control the microenvironment in a silicon nanowire array, led to an increase in loading of acetogenic bacteria *S. ovata* which in turn improved CO₂ to acetate conversion. We were able to drive this reaction with solar power resulting in a 3.7% solar-to-chemical conversion. We have also undertaken a process to quicken the autotrophic metabolism of *S. ovata* via methanol adaptation yielding a 50% increase in CO₂ turnover rate. Furthermore, acetate can be upgraded by a secondary biocatalyst. Therefore, we have designed co-cultures to upgrade the acetate to value-added products. We demonstrate a co-culture between acetogenic *Sporomusa ovata* and diazotrophic *Rhodospseudomonas palustris* for tandem CO₂ and N₂ fixation to tunable value-added products including acetate, NH₃, nitrogenous biomass, and biopolyester. The dynamics between these two organisms and the products of the co-culture can be directed by electrochemical inputs. Lastly, we present on a strategy to generate sugars through abiotic CO₂ electrosynthesis. Copper nanoparticles and boron doped diamond electrochemically reduce CO₂ to glycolaldehyde and formaldehyde respectively which together form sugars including glucose. These sugars are used to culture *Escherichia coli* which can be engineered to produce chemicals and materials.

11:15 AM SB11.01.04

Tunable Electrochemical Activity and Conduction in Light-Patterned *Shewanella* Biofilms [Marko Chavez](#), Fengjie Zhao, Christina M. Cole, Kyle Naughton, James Boedicker and Moh El-Naggar; University of Southern California, United States

Electroactive bacteria, such as the model organism *Shewanella oneidensis* MR-1, can couple the oxidation of organic electron donors to the reduction of external solid surfaces, including minerals and electrodes, utilizing outer membrane multiheme cytochromes that carry charge from within the cell to external surfaces. In addition to transporting electrons across the cell envelope, the multiheme cytochromes can also facilitate long-distance (micrometer-

scale) redox conduction along the outer membrane and across multiple cells bridging electrodes. While electroactive bacteria are commonly used in the construction of bioelectrochemical energy technologies, the development of more advanced living electronics has been challenged by the inability to control the size and shape of the conductive biofilms in relation to solid-state components. To overcome this challenge, we developed an optogenetic deposition strategy in which projected blue light patterns control the expression of a cell-surface adhesion protein in *S. oneidensis* and direct cell attachment to the illuminated areas of transparent conductive surfaces. Using this technique, we showed that the electrochemical activity of the engineered light-patterned biofilms remained comparable to that of the wild-type and scaled with controlled biofilm size. Furthermore, by depositing biofilms onto transparent interdigitated electrode arrays and performing electrochemical gating measurements, we confirmed that biofilm conduction current can also be tuned as a function of patterned biofilm size. Precise control of biofilm geometry allowed us to determine the intrinsic conductivity of living *Shewanella* biofilms for the first time. Thus, we have developed a facile technique to direct the deposition of living conductive biofilms; we anticipate that this approach will enable further innovations for both studying and harnessing bioelectronics, akin to the role that traditional photolithography played in the development of solid-state electronics.

SESSION SB11.02: Systems Design
Session Chair: Giuseppe Paternò
Tuesday Afternoon, November 30, 2021
Sheraton, 2nd Floor, Back Bay A

1:30 PM *SB11.02.02

Polydopamine—A Bioinspired Polymer to Interface Photosynthetic Bacteria with Electrodes Gianluca M. Farinola¹, Danilo Vona¹, Rossella Labarile¹, Gabriella Buscemi^{1,2}, Roberta Ragni¹, Maria Varsalona^{1,2}, Francesco Milano³, Matteo Grattieri^{1,2} and Massimo Trotta²; ¹University degli Studi-Bari Aldo Moro, Italy; ²CNR-IPCF Institute for Physical-Chemical Processes (IPCF), CNR, Italy; ³CNR-ISPRA, Institute of Sciences of Food Production, Italy

Photosynthetic microorganisms are capable of interacting with light by specific proteins, called Reaction Centers (RCs), which are located into cell membranes and convert photons into charge separated states, in a process with efficiency close to 100%. Our work has demonstrated that the light harvesting capability of the RC extracted from *Rhodobacter sphaeroides* R26 bacterium can be ameliorated by covalently binding tailored molecular organic antennas [1-3]. RCs have been directly exploited in electronic and electrochemical devices [4], acting as photoactive systems in photoelectrochemical cells [5], photosensors [6] and photoactive transistors [7]. Interestingly, intact living photosynthetic bacteria cells can be also integrated in devices for bioelectronic applications [8]. However, the use of conductive artificial materials, like polymers or inorganic electrode surfaces, could lead to detrimental effects for the bacterial viability. Conversely, adhesive biomimetic polymers such as polydopamine (PDA) are promising biocompatible coating materials for application of *Rhodobacter sphaeroides* R26 bacterial cells in bioelectronics. Here, the approach is based on *in situ* polymerization of dopamine monomer in cell medium, with the PDA polymer self-assembling around cells, allowing them to thrive by light absorption and ensuring their interaction with conductive electrode surfaces. Polydopamine has been already successfully exploited to stabilize the interface between *Rhodobacter sphaeroides* RCs with electrodes, avoiding protein denaturation and facilitating the integration in electronic systems [9-10]. Preliminary electrochemical characterization also unveils that PDA layer around living bacterial cells adhered onto electrodes does not alter their viability and it does not hinder the diffusion of mediators and their capability to react at the electrodes.

- [1] F. Milano, R.R. Tangorra, O. Hassan Omar, R. Ragni, A. Operamolla, A. Agostiano, G.M. Farinola, M. Trotta, *Angew. Chem. Int. Ed.*, **51**(44), 11019-11023 (2012).
- [2] O. Hassan Omar, S. La Gatta, R.R. Tangorra, F. Milano, R. Ragni, A. Operamolla, R. Argazzi, C. Chiorboli, A. Agostiano, M. Trotta, G. M. Farinola, *Bioconjugate Chem.* **27**, 1614-1623 (2016).
- [3] S. la Gatta, F. Milano, G. M. Farinola, A. Agostiano, M. Di Donato, A. Lapini, P. Foggi, M. Trotta, R. Ragni, *Biochimica et Biophysica Acta-Bioenergetics*, **1860** (4), 350-359 (2019).
- [4] A.J. McCormick, P. Bombelli, R. W. Bradley, R. Thorne, T. Wenzel, C. J. Howe *Energy Environ. Sci.*, **8**, 1092-1109, (2015).
- [5] F. Milano, F. Ciriaco, M. Trotta, D. Chirizzi, V. De Leo, A. Agostiano, L. Valli, L. Giotta, M.R. Guascito, *Electrochim. Acta*, **293**, 105-115 (2019).
- [6] M. Chatzipetrou, F. Milano, L. Giotta, D. Chirizzi, M. Trotta, M. Massauti, M.R. Guascito, I. Zergioti, *Electrochemistry Communications*, **64**, 46-50 (2016).
- [7] M. Di Lauro, S. la Gatta, C.A. Bortolotti, V. Beni, V. Parkula, S. Drakopoulou, M. Giordani, M. Berto, F. Milano, T. Cramer, M. Murgia, A. Agostiano, G.M. Farinola, M. Trotta, F. Biscarini, *Adv. Electronic Mater.* **6** (1), 1900888 (2020).
- [8] F. Milano, A. Punzi, R. Ragni, M. Trotta, G. M. Farinola, *Adv. Funct. Mater.*, **29** (21), 1805521, (2019).
- [9] M. Lo Presti, M. M. Giangregorio, R. Ragni, L. Giotta, M. R. Guascito, R. Comparelli, E. Fanizza, R. R. Tangorra, A. Agostiano, M. Losurdo, G. M. Farinola, F. Milano, M. Trotta *Adv. Electron. Mater.* **2000140**, (2020).
- [10] G. Buscemi, D. Vona, R. Ragni, R. Comparelli, M. Trotta, F. Milano, G. M. Farinola, *Adv. Sustain. Syst.*, doi.org/10.1002/adsu.202000303 (2021).

2:00 PM SB11.02.03

P3HT Nanoparticles with Core-Shell Architecture—Tuning the Photophysical Properties Jonathan Barsotti¹, Sara Perotto^{1,2}, Andrea Candini^{3,4}, Elisabetta Colombo^{1,5}, Franco V. A. Camargo³, Stefano Di Marco^{1,5}, Mattia Zangoli^{3,4}, Samim Sardar¹, Alex Baker¹, Cosimo D'Andrea², Giulio Cerullo², Shlomo Rozen⁶, Fabio Benfenati^{1,5}, Francesca Di Maria^{3,4} and Guglielmo Lanzani^{1,2}; ¹Istituto Italiano di Tecnologia, Italy; ²Politecnico di Milano, Italy; ³Consiglio Nazionale delle Ricerche, Italy; ⁴Università di Bologna, Italy; ⁵IRCCS Ospedale Policlinico San Martino, Italy; ⁶Tel Aviv University, Israel

Organic nanoparticles (NPs) are promising functional materials for the development of advanced photonic and biophotonic systems. We already demonstrated that blind laboratory rats treated with P3HT nanoparticles were able to recover vision highlighting the potential biomedical applications in the context of neuronal stimulation and neuroprostheses [1]. Here, we investigated thiophene-based core@shell NPs, made of poly(3-hexylthiophene) (P3HT) in the core and oxygenated P3HT (PTDO) in the shell [2], proving their role as highly effective photon nanotransducers. This structure supports long-lived charge separation, originating from the type II alignment at the core/shell interface. Here we provide a general photophysical picture in accordance with the morphology and the oxidation degree of the nanoparticles. Atomic force microscopy and Kelvin probe force microscopy allowed to characterize the nano-organization within the NPs core@shell configuration and their surface photovoltage characteristics. Steady-state and time-resolved spectroscopic measurements suggest that energy transfer is taking place from the core to the shell, followed by charge separation at the surface. Living cells photostimulation can be achieved exploiting different physical mechanisms such as chemical reaction, current injection, capacitive coupling and thermal effect. Each mechanism can be ascribed to a specific material or a particular geometry [1]. The application of these core@shell systems may

advance our understanding of the coupling mechanism at the biotic/abiotic interface.

References

- [1] Maya-Vetencourt, J.F., Manfredi, G., Mete, M. et al. Subretinally injected semiconducting polymer nanoparticles rescue vision in a rat model of retinal dystrophy. *Nat. Nanotechnol.* 15, 698–708 (2020)
- [2] Di Maria F, Zanelli A, Liscio A, Kovtun A, Salatelli E, Mazzaro R, Morandi V, Bergamini G, Shaffer A, Rozen S, *ACS Nano* 11, 2, 1991–1999 (2017)

2:15 PM SB11.02.04

Shedding Light on Thermal Induced Optocapacitance at the Organic Bio-Interface Gaia Bondelli^{1,2}, Samim Sardar¹, Greta Chiaravalli^{1,2}, Vito Vurro¹, Giuseppe M. Paternò¹, Guglielmo Lanzani^{1,2} and Cosimo D'Andrea^{2,1}; ¹CNST@PoliMI, Italy; ²Politecnico di Milano, Italy

The possibility to control selectively the electrical activity of living cells with low invasiveness has opened up new therapeutic paths in neurodegenerative medicine. Optical technologies are particularly suited for this purpose, as light enables precise and localised perturbation of cell activity in a remote and spatiotemporal precise manner. In particular, cell membrane potential modulation occurs via the photoinduced modification of the membrane electrical properties, either through direct photostimulation or by using selected transducers that are able to convert light into an electrical, mechanical, chemical, or thermal stimulus. In these regards, organic semiconductors have emerged as powerful photoactuators for the development of functional interfaces with living cells and organisms, thanks to their relatively high absorption coefficient and to their bio-mimetic nature. Although many efforts have been dedicated to investigate the biophysics underpinning photostimulation with organic semiconductors, the exact stimulation mechanism is still matter of debate. To shed light into these aspects, we employed an all-optical spectroscopic approach, based on the use of well-established fluorescence probes, to monitor the membrane polarity, viscosity and order directly in living cells under thermal excitation transduced by a photoexcited polymer film. Briefly, our findings demonstrate that the opto-capacitive process induced by temperature is not simply due to a geometrical effect, as it is commonly believed. Indeed, our results suggest that a thermal induced phase transition promotes water penetration into the disordered phase of the plasma membrane. Thus, we speculate that the resulting change in dielectric response of the plasma membrane is the ruling phenomenon explaining the temperature induced enhancement in capacitance. Furthermore, we find experimental evidence that optostimulation mediated by a photovoltaic organic film brings about an additional phenomenon reinforcing the perturbation effect. We tentatively assigned this to the surface charging at the bio interface, suggesting that optostimulation mediated by organic semiconductors is not simply due to thermal effects, but it is also related to the capability of the photogenerated charges to polarize the plasma membrane.

2:30 PM SB11.02.05

Hierarchical Mathematical Models of Polythiophene Devices to Understand the Interaction Occurring at Abiotic/Biotic Interface Greta Chiaravalli^{1,2}, Giovanni Manfredi², Riccardo Sacco¹ and Guglielmo Lanzani^{2,1}; ¹Politecnico di Milano, Italy; ²Istituto Italiano di Tecnologia, Italy

The development of a fully organic photovoltaic prosthesis of poly(3-hexylthiophene) (P3HT) for subretinal implants was proposed to treat degenerative blindness (Maya-Vetencourt et al., 2017 and 2020). Although the efficiency of organic polymer-based retinal devices *in vivo* has been proven, the interpretation of the working mechanisms that grant photostimulation at the polymer/neuron interface is still a matter of debate. In order to contribute solving this issue, we have first focused on the characterization of the interface between P3HT films and watery-electrolytes by the combined use of electrochemistry and mathematical modeling.

In particular, the electric behavior of P3HT is modeled through a system of time dependent Drift-Diffusion non linear partial differential equations. The model takes into account the working principles of the organic semiconductor in contact with the electrolyte solution, with a detailed description of its interaction with the dissolved oxygen. This effect experimentally proved to be crucial in the photoelectrical switch of P3HT.

In order to compare and validate the results of our mathematical model, we have performed several electrochemical measurements of photovoltage on P3HT film deposited onto an ITO substrate samples, in different oxygenating conditions and with active layers of various thicknesses. Mathematical simulations well reproduce the experimental results upon illumination of the device in the various conditions.

Besides validation, the good agreement between measurements and simulations can be used to highlight the main effects, secondary to the illumination of the P3HT device, necessary to reproduce the experimental behaviour. Upon illumination, the essential unipolar transport in the photoexcited film leads in few μs to a drift-diffusion equilibrium associated to a space charge separation, responsible for the initial negative photovoltage. Electron transfer reactions towards oxygen at the polymer/electrolyte interface extract negative charge from the polymer and are responsible for the positive signal that we observe after several *ms*. The quantitative description of the phenomena also permits the estimation of the charge accumulated at the interface, possibly responsible for an electrostatic interaction with a biological system.

In spite of the simple model studied, all these considerations shed light on the possible coupling mechanisms between the polymeric device and the living cell, supporting the hypothesis of pseudo-capacitive coupling arising from an electrostatic interaction between the polymeric film and the watery environment. In addition to this, once the fundamental mechanisms of P3HT have been quantitatively reproduced and formalized, it is possible to start developing models to reproduce the effects of P3HT nanoparticles in a watery-electrolyte, a system whose electric properties are hard to characterize experimentally but which appears to be the new frontier of retinal devices.

2:45 PM SB11.02.06

Optoelectronic Studies of Hydrothermally Grown Microcrystalline ZnO Employed in Antibacterial Assays with Staphylococcus Aureus Dustin Johnson, John Reeks, Iman Ali, Shauna McGillivray, Yuri M. Strzhemechny and Jacob Tzoka; Texas Christian University, United States

Nanoscale and microscale ZnO particles are utilized in a wide variety of applications due to their optoelectronic properties and high biocompatibility. One application is the use of ZnO as an antibacterial agent. Antibacterial action of ZnO is well documented, exhibiting growth inhibition for gram-positive and gram-negative bacteria as well as antibiotic resistant bacterial strains. In spite of considerable amount of research in this field, there is no clear consensus on the fundamental mechanisms behind this phenomenon. Suggested mechanisms include: cell internalization of the ZnO particles, release of Zn ions, generation of different reactive oxygen species, surface-surface interactions, etc. In our work, we address, in conjunction with the antibacterial assays, surface and near-surface optoelectronic properties of ZnO microcrystals participating in those assays. In particular, we look at the influence of crystalline morphology and crystallographic polarity on the interaction between bacterial cells and ZnO surfaces. To produce our antibacterial specimens we utilized a bottom-up hydrothermal growth method to synthesize ZnO microcrystals of tunable morphology and relative abundance of polar and non-polar surfaces. Scanning electron microscopy, energy-dispersive X-ray spectroscopy and surface photovoltage experiments were used to characterize the quality and morphology of the ZnO microcrystals. To establish the antibacterial activity of our particles, we ran minimum inhibitory concentration assays of staphylococcus aureus. By utilizing ZnO crystals larger in size than the *s. aureus* bacteria cells, we confirmed that internalization of the ZnO particles is not necessary to inhibit the growth of the bacteria. The larger microcrystals exhibited inhibition of bacterial growth comparable to that of nanoscale ZnO particles. To determine the influence of structural and surface properties of ZnO on the assay outcomes, we performed a series of optoelectronic experiments using photoluminescence spectroscopy as well as spectroscopic and transient surface photovoltage. These investigations were performed on ZnO crystals prior to and following exposure to *s. aureus*. Our results revealed significant spectral changes due to interactions with bacteria and growth

media. We demonstrated that growth media have a significant impact onto the nature and efficacy of antibacterial activity of ZnO.

3:00 PM SB11.02.07

Photophysical Characterization of Previously Unidentified Intrinsic Charge Transfer States in Proteins Leah Spangler, Michael Hecht and Gregory Scholes; Princeton University, United States

The intrinsic optical properties of proteins (*i.e.*, absorbance at 280 nm and fluorescence around 340 nm) are known to originate from the electronic transitions of aromatic amino acids, such as tryptophan. As aromatic amino acids are present in nearly all proteins, intrinsic absorbance and fluorescence have limited use in protein characterization. Recently however, a new weak intrinsic absorbance signal has been uncovered in the visible region, even in proteins which lack aromatic amino acids. This previously overlooked visible absorbance signal has been theorized to arise from charge transfer states which form between charged amino acids within the protein. The unique interactions between charged amino acids likely affect this new intrinsic absorbance signal, and could be used to identify specific protein structures or sequences. Despite experimental observation of this new optical state, the exact photophysical mechanism has not yet been elucidated spectroscopically. Here, we characterize this newly uncovered optical state using advanced spectroscopy techniques in three highly charged proteins. The absorbance spectra of each protein was carefully measured using an integrating sphere to minimize contributions from scattering. We then used transient absorption spectroscopy to fully characterize the energy transfer within each protein, uncovering states with charge transfer character, consistent with theoretical simulations. By fully understanding this intriguing new charge transfer state, protein absorbance could eventually find use as an intrinsic probe for *in vivo* optical microscopy, or as a new method for the identification of specific protein conformations.

3:15 PM SB11.02.08

Nanosensor Chemical Cytometry to Support Cellular Therapeutics Sooyeon Cho, Xun Gong and Michael Strano; Massachusetts Institute of Technology, United States

Cell therapeutics is a rapidly growing medicinal innovation being applied to cancer immunotherapy and degenerative diseases among others. Conventional pharmaceutical standards dictate a regulatory need to understand each and every cell placed within a patient. Thus, cellular therapeutic elements need to be monitored and assessed through various cell production process step to keep consistent and safe clinical outcome. However, this necessarily requires a new generation of non-destructive and label-free techniques that can characterize a single cell and their product at high-throughput, but otherwise leave it unadulterated before administration to the patient. Such a tool would bring unprecedented spatiotemporal resolution to intracellular and pericellular biochemical interactions at the scale of the fundamental building block of life with significant high-throughput. The scientific challenges include the need to measure at a rate and magnitude commensurate with the size of cell population and this goal has remain elusive over the past decades. In this research, we utilize a power of nanosensor array and develop a new class of cell population monitoring platform that addresses those limitations. An array of near infrared (nIR) fluorescent single walled carbon nanotube (SWNT) nanosensors are integrated along a microfluidic channel through which a population of flowing cells will be guided, using specific integration technique of particulate form of fluorescent nanosensors. We show that one can utilize the flowing cell itself as highly informative Gaussian lenses projecting nIR emission profiles and extract rich information on a per cell basis in real-time and a non-destructive manner. This unique biophotonic waveguide allows users to quantify the cross-correlation of the biomolecular information with physical properties such as cell size, eccentricity and refractive index (RI). We show that it operates as a label-free chemical cytometer for the measurement of cellular heterogeneity with unprecedented precision for various type of cells and their target analytes. Our platform can be exploited to new class of chemical cytometry tools for cell-based therapeutic applications, where there are urgent needs for high-throughput characterization of biochemical properties cellular targets with therapeutic potential for new treatments.

SESSION SB11.04: Biostimulation
Session Chair: Herdeline Ardoña
Wednesday Morning, December 1, 2021
Sheraton, 2nd Floor, Back Bay A

10:30 AM *SB11.04.01

Organic Actuators for Cell Photo Stimulation Guglielmo Lanzani^{1,2}; ¹Italian Inst of Technology, Italy; ²Politecnico di Milano, Italy

The overarching goal of our research is to manipulate the light-bio-matter interaction to obtain control over the functioning of living systems. Light can control cell activity, with high space and time resolution and a virtually infinite number of configurations, free from wiring constrains. We develop and study non-genetic cell opto-stimulation techniques based on artificial light actuators that establish functional abiotic-biotic interfaces able to transduce a light signal into a biological stimulus. This talk reports on the state of our research regarding organic bio interfaces for inducing light sensitivity in cells, both *in vitro* and *in vivo*. Light actuators comes in different shapes: planar patches, nanoparticle, intra-membrane probes. Their coupling mechanism is still far from being understood and attempts to shed light will be introduced. The research aims at a new technological platform for application in life enhancing technologies or new cyborg technologies. One of the most appealing application of this emerging technology is rescue vision in blind people.

11:00 AM SB11.04.02

Cyborg Brain Organoids Paul Le Floch¹, Qiang Li¹, Ren Liu¹, Kazi Tasnim¹, Siyuan Zhao¹, Zuwan Lin^{1,2}, Han Jiang¹ and Jia Liu¹; ¹Harvard University, United States; ²Broad Institute of MIT and Harvard, United States

Human induced pluripotent stem cell-derived brain organoids have shown great potential for studies of human brain development and neurological disorders. However, quantifying the evolution and development of electrical functions in brain organoids is currently limited by measurement techniques that cannot provide long-term stable three-dimensional (3D) bioelectrical interfaces with brain organoids during development. In this lecture, I will present the cyborg brain organoid platform, in which 2D progenitor or stem cell sheets can fold "tissue-like" stretchable mesh nanoelectronics through organogenesis, distributing stretchable electrode arrays across 3D organoids. We previously demonstrated this technique in cardiac organoids, and I now expand it to two types of brain organoids, early-stage brain organoids, where the mesh nanoelectronics is integrated to the tissue culture before differentiation and organogenesis, and more mature brain organoids, where the mesh nanoelectronics is integrated after four months of differentiation. I will demonstrate that the tissue-wide integrated stretchable electrode arrays do not interrupt neuronal differentiation, adapt to the volume and morphological changes during organogenesis, and provide long-term stable electrical contacts with neurons within brain organoids during development. Then, I will show that the seamless and non-invasive coupling of electrodes to neurons enables a 6-month continuous recording of the same brain organoids and captures the emergence of single-cell action potentials from early-stage brain organoid development. The increase of action potential

amplitude, synchrony, and firing rate as well as narrowing of action potential duration suggest changes in neural network connectivity and cellular ion channel expression level. Finally, I will discuss the integration of cyborg brain organoid platform with organoid-wide connectomics and spatial transcriptomics mapping to further test this hypothesis. Furthermore, cyborg brain organoid technology can potentially become a useful tool for quantifying the functional development of brain organoids and standardizing the culture conditions across different types of protocols by tracing organoid-wide tissue and single-cell electrical activity during the entire organoid development. It will also be useful for studies of developmental neuroscience and drug screening.

11:15 AM SB11.04.03

Cardiac Cell Non-Genetic Photostimulation [Vito Vurro](#)¹, Francesco Lodola², Carlotta Ronchi¹, Valentina Sesti^{3,1}, Maria Rosa Antognazza¹, Chiara Bertarelli^{3,1} and Guglielmo Lanzani^{1,3}; ¹Istituto Italiano di Tecnologia, Italy; ²Università degli Studi di Milano-Bicocca, Italy; ³Politecnico di Milano, Italy

Nowadays stimulation and control over cellular activity and physiology is an emerging and hot topic. In particular, contactless and wireless methods are extremely appealing due to their ability to leave unaltered the cell and tissue condition. Following this idea, light represents a clean and spatiotemporal precise tool to achieve effective bio-stimulation. Light-transducers, such as conjugated molecules and macromolecules, have proven their efficacy at the interface with living cells and tissue. This interaction is possible thanks to their high optical absorption/emission, biocompatibility and versatility in chemical synthesis.

In this work, we employ a lipid membrane-targeted photochromic molecule to photomodulate signalling in cardiac cells. We characterized the single cell-molecule interaction, to evaluate its ability to photocontrol electrophysiological and functional behaviours. The ultimate goal of this project is the realization of a bio-hybrid photoresponsive smart tissue for future applications in robotics and pharmacology, as well as for tissue regeneration.

SESSION SB11.05: Imaging and Sensing

Session Chair: Giuseppe Paternò

Wednesday Afternoon, December 1, 2021

Sheraton, 2nd Floor, Back Bay A

1:30 PM *SB11.05.01

Imaging the Resting Membrane Potential and Elongation of Individual Bacteria Cells [Christine Payne](#); Duke University, United States

All cells, including bacteria, maintain an ion gradient across their membrane. This ion gradient results in a resting membrane potential that is essential to cell health. The use of light or electricity to control the resting membrane potential, compared to solution-based reagents, is unique in providing spatial control. We have designed a fluorescence microscopy-based platform to monitor and control membrane potential, while also imaging cell elongation and division. Our recent work has focused on the relationship between resting membrane potential and cellular elongation. Resting membrane potential is controlled by exposing *B. subtilis* cells to blue light, thereby limiting the effect to a subset of cells. Neighboring cells, not exposed to blue light, are used as a control. The elongation rate is measured for each cell, thereby incorporating the heterogeneity of cellular populations into each measurement. Our experiments distinguish two populations of cells with correlated membrane potential and elongation rates. The ability to modulate the resting membrane potential with light, and thereby control the growth of a subset of bacteria within a larger population, provides a method to better understand the fundamentals of bioelectricity and ultimately modulate cellular growth in a spatially-controlled manner.

2:00 PM *SB11.05.02

Conducting Polymer Devices Integrated with Cell Membranes for Diagnostics and Drug Discovery [Roisin Owens](#); University of Cambridge, United Kingdom

In vitro models of biological systems are essential for our understanding of biological systems. Many difficulties exist in interfacing complex, biologically relevant models with technology adapted for monitoring function. Polymeric electroactive materials and devices can bridge the gap between hard inflexible materials used for physical transducers and soft, compliant biological components. In this presentation, I will discuss our recent progress in adapting conducting polymer devices, both OECTs (organic electrochemical transistors) and electrodes, to integrate with both mammalian and bacterial cell membranes supported lipid bilayers, preserving native membrane function. The conducting polymer devices preserve native membrane function, including transmembrane protein function, but also provide a means to readout changes to membrane properties such as permeability or binding or fusion with the membrane. Since the cell membrane is the gateway to the cell, this platform allows monitoring of pathogens such as viruses that may enter the cell, or drugs or toxins that may interact with the membrane compromising normal function (e.g. toxins binding to ion channels in the membrane or antibiotics that disrupt bacterial membranes). In this presentation I will describe the development of this platform and showcase how it may be used as a rapid and highly quantitative method for monitoring events occurring at the membrane in a robust and scalable manner without recourse to live cells.

2:30 PM BREAK

3:30 PM *SB11.05.04

Multimodal Nanoelectronics for Charting Cell Electrophysiological and Molecular Phenotypes in Three-Dimensional Tissues Across Time and Space [Jia Liu](#); Harvard University, United States

Charting single-cell gene expression and electrophysiology in intact three-dimensional (3D) tissues across time and space is crucial to fields ranging from developmental biology to cardiology and neuroscience. Such multimodal methods require stable and continuous recording of individual cell electrical activity with high spatiotemporal resolution across 3D tissue, multiplexed profiling of a large number of genes in electrically recorded cells, and cross-modal computational data integration and analysis. In this talk, I will discuss 1) "tissue-like" electronics that possess tissue-like properties for long-term stable single-cell electrophysiology in tissues, organs, and behaving animals; 2) "cyborg organoids", where stretchable sensor arrays are embedded in 2D sheets of stem/progenitor cells and reconfigured through 2D-to-3D organogenesis, enabling 3D electrophysiology over the time course of organoid development; and 3) "in situ electro-sequencing" that integrates "tissue-like" electronics, *in situ* sequencing, and machine learning to chart cell electrophysiology and gene expression at single-cell resolution across time and space.

4:00 PM SB11.05.05

Direct Measurements of Long Distance Electron Transport in Freshwater Cable Bacteria [Tingting Yang](#), Marko Chavez, Christina M. Cole, Shuai Xu and Moh El-Naggar; University of Southern California, United States

Filamentous multicellular cable bacteria facilitate long distance electron transport (LDET), up to centimeter scales, in vast marine and freshwater sediments, indicating that LDET is an essential process in global geochemical cycling.

Through this process, cable bacteria couple sulfide oxidation by cells that dwell in the deeper sulfidic zone to oxygen reduction by cells near the surface sediment. Recent electronic measurements of cable bacteria enriched from marine sediments demonstrated that the electron transport pathway consists of a network of periplasmic fibers that run along the unique cell envelope of entire cables. Here we focus on demonstrating and understanding the electron transport characteristics through cable bacteria from freshwater sediments.

Long cable bacteria filaments were recovered from incubations of freshwater lake sediments (Ballona pond and Mungi Lake) in Southern California. The Southern California Freshwater cable bacteria share >97% sequence similarity to the 16S rRNA gene sequences from the freshwater cable bacterial genus *Candidatus* Electronema within the Desulfobulbaceae family. Current-voltage measurements of cable bacteria bridging 3-mm gaps between interdigitated electrodes reveal nano- to microampere currents through intact single filaments. A combination of atomic and electrostatic force microscopy measurements revealed the characteristics of the underlying periplasmic fiber network, as previously described in marine cable bacteria. In addition, conductive atomic Force microscopy was used to directly assess the conductivity of locations on individual cells. Using four-probe electronic measurements, the conductivity of single fiber in freshwater cable bacteria filaments is found to be ca. 0.1 S/cm. Our study expands the knowledgebase of centimeter scale LDET in cable bacteria to the freshwater niche and shed light on the mechanisms underlying their remarkable conductivity.

4:15 PM SB11.05.06

Electrical Monitoring of Cell Epithelial-to-Mesenchymal Transition Induced by Tumor-Derived Exosomes Using Bioelectronic

Technologies Walther Traber-Christensen¹, Johana Uribe², Adel Hama³, Miriam Huerta², Victor Druet³, Anna-Maria Pappa¹, Susan Daniel², Sahika Inal³ and Roisin Owens¹; ¹University of Cambridge, United Kingdom; ²Cornell University, United States; ³King Abdullah University of Science and Technology, Saudi Arabia

Exosomes are nanosized, lipid bilayer-delimited particles that act as mediators in cell-cell communication and have the ability to transfer RNAs and proteins between donor and recipient cells to elicit a variety of cellular responses. Tumor cell-derived exosomes (TDEs) have recently been reported to play an active role in tumorigenesis and metastasis owing to their ability to transmit oncogenes. One hypothesis is that TDEs contribute to metastasis by inducing the epithelial-to-mesenchymal transition (EMT), characterized by the loss of barrier function in barrier tissue-forming cells.

This study aims to elucidate the role and mechanisms of TDE uptake by investigating the process by which TDEs “infect” normal cells inducing EMT prior to metastasis. Current strategies for investigating the spatial and temporal aspects of exosome uptake, often optical, lack the ability to obtain quantitative data in real time. We have shown that organic electronic devices based on the conducting polymer poly(3,4-ethylenedioxythiophene):poly(styrenesulfonate) (PEDOT:PSS) can be interfaced with biological systems of varying complexity allowing for quantitative real-time monitoring of biological interactions. The optical transparency of our PEDOT:PSS-based devices provides the unique advantage of dual transduction increasing the credibility of our platform and enriching the biological information obtained. Moreover, their compatibility with microfabrication methods allows for high throughput studies.

We have shown that TDEs derived from the triple-negative breast cancer cell line MDA-MB-231 can induce an EMT-like process in MCF-10A non-tumorigenic breast epithelial cells as demonstrated by changes to cell morphology, loss of apico-basal polarity, reorganization of filamentous actin, and gain of mesenchymal proteins, such as vimentin and N-cadherin. An integral feature of EMT is the dissolution of tight junctions and the consequential loss of lateral cell-cell adhesion leading to a phenotype with increased motility and invasiveness. In ongoing studies, this decrease in barrier integrity of the cell monolayer is monitored electrically using organic electrochemical transistors, gaining of truly quantitative insight into TDE-induced EMT with higher temporal resolution than conventional, orthogonal methods. This data will be further substantiated by monitoring the expression of immunofluorescently labelled barrier-forming tight junction proteins. These combinatorial optical and electrical measurements of TDE interactions with cell monolayers provide invaluable information for developing strategies that may inhibit TDE interactions by e.g. blocking specific surface markers, thereby preventing TDE-induced EMT with implications for preventing cancer metastasis.

4:30 PM SB11.05.07

Azobenzene Photoisomerization Probes Cell Membrane Nanoviscosity Arianna Magni^{1,2}, Gaia Bondelli^{2,1}, Giuseppe M. Paternò¹, Samim Sardar¹, Valentina Sesti^{2,1}, Cosimo D'Andrea^{2,1}, Chiara Bertarelli^{2,1} and Guglielmo Lanzani^{1,2}; ¹Istituto Italiano di Tecnologia, Italy; ²Politecnico di Milano, Italy

The viscosity of cell membranes is a crucial parameter that affects the diffusion of small molecules both across and within the lipidic membrane and that is related to several diseases, such as atherosclerosis, Alzheimer's, diabetes, and cell malignancy. In general, the precise determination of viscosity at the molecular scale represents itself an important issue in cellular biophysics. Despite the great interest of viscosity measurements on the nanoscale, it is still challenging to retrieve reliable values, as the traditional mechanical methods used for probing viscosity are not suitable for living cells.

We investigated the photophysics of a recently synthesized amphiphilic membrane-targeted azobenzene (ZIAPIN2) and we validate its use as viscosity probe for cell membranes. Indeed, we proved that the possibility of ZIAPIN2 of undergoing *trans-cis* photoisomerization depends on the viscosity of the environment. This led to the development of a molecular viscometer based on time-resolved fluorescence spectroscopy, that we used to assess the viscosity of *Escherichia coli* bacteria membranes. Lifetime measurements of ZIAPIN2 in *E. coli* bacteria suspensions correctly indicate that membrane viscosity decreases as the samples were heated up. Our results estimate a membrane viscosity value in living *E. coli* cells going from 10 to 5 cP, increasing the temperature from 22 °C up to 40 °C.

SESSION SB11.06: Poster Session: Photo/Electrical Phenomena at the Interface with Living Cells and Bacteria

Session Chair: Giuseppe Paternò

Wednesday Afternoon, December 1, 2021

8:00 PM - 10:00 PM

Hynes, Level 1, Hall B

SB11.06.02

Monitoring and Modulating Bacterial Electrophysiology at the Single Cell Level: Photolithography for High Throughput Devices Xu Han and Christine Payne; Duke University, United States

The resting membrane potential regulates bacterial division, elongation, and electrical signaling. Use of an external electric field is an effective method to

regulate these properties with the advantage of providing spatial control, altering only a subset of cells. The challenge is to develop devices for precise control of the applied electric field with simultaneous monitoring of membrane potential and bacterial growth. Our initial research developed a device using two gold wires as electrodes to apply an electric field while imaging, with either brightfield or fluorescence microscopy, bacteria, including a control population in the absence of an electric field. Although useful for initial studies of membrane potential-regulated bacterial elongation and division, this device was low throughput. A second-generation device has been designed and fabricated by photolithography. The gap distance between the two electrodes, which determines the electric field, can be controlled from 10 μm to 1 mm, largely expanding the range of electric fields that can be achieved. Three pairs of electrodes with different gap distances can be integrated into the same device, increasing experimental throughput. Multiple electrode materials, including gold and platinum, can be used for these devices. In addition, the shape of the electrodes can be customized to achieve the desired electric field distribution. With this device, we can control the frequencies, amplitudes, and waveforms of applied electric fields while simultaneously imaging bacterial growth and membrane potential. We use this single cell-level imaging to understand and control heterogeneity of bacterial cells. Within any population of cells, individual cells will have different membrane potentials, which change in time, even in the absence of an applied electric field. This device allows us to track the membrane potential of individual cells over hours to address fundamental questions of bacterial electrophysiology.

SB11.06.03

Monitoring the Nanoscale Heat Penetration Profile in Laser-Induced Thermal Therapies with Ultrafast Vibrational Spectroscopy Sara Makarem, John A. Tomko, Kimberly Kelly and Patrick E. Hopkins; University of Virginia, United States

The growing interest in the development of minimally-invasive therapeutic strategies has opened the doors to the introduction of one (or several) therapeutic needle(s) inside the tumor target that aim at inducing a controlled change of tissue conditions and environment to achieve tumor necrosis and apoptosis. Amongst all the treatment methods, ablative photothermal therapies are emerging as potential alternatives for the management and treatment of the tumor of which the laser-induced heated region are enabling the use of even finer 'needles,' where the spatial resolution can exceed the diffraction limit. Thus, studying the nanoscale heat transfer mechanisms within the target tissues and across their respective interfaces to gain a fundamental understanding of the dominant mechanisms within this class of therapies are critical for developing the next-generation of thermal ablation treatments.

In this study, we experimentally investigate these fundamental heat transfer mechanisms that dictate photothermal therapy efficiencies in nanoparticle-mediated systems. In particular, we employ ultrafast time-domain thermo-transmission (TDTT)¹ measurements to monitor the heat flux from heated nanoparticles directly into surrounding biological cells. Further, by implementing a tunable-wavelength mid-infrared probe to these measurements, these measurements can directly resonate with different vibrational modes of interest, thus providing insight to which modes dictate the interfacial heat transfer from nanoparticles into surrounding biological tissues. In this study the biological parameters on the temperature distribution, the heat penetration depth, and degree of irreversible damage as a result of the heat source parameters are investigated. These experimental measurements provide direct insight into the vibrational modes that dictate interfacial heat transfer during photothermal therapies and the means of which material parameters can be tuned to enhance these heat transfer pathways.

1. Jung, H., Szejewski, C. J., Pena-Francesch, A., Tomko, J. A., Allen, B., Ozdemir, S. K., Hopkins, P., and Demirel, M. C., 'Ultrafast laser-probing spectroscopy for studying molecular structure of protein aggregates,' *Analyst* **142**, 1434-1441 (2017)

SB11.06.04

Spin Filtering in Bacterial Periplasmic Electron Carriers Christina M. Cole¹, Debkumar Bhowmick², Ron Naaman², Justus Nwachukwu³, Miyuki Thirumurthy³, Anne Jones³ and Moh El-Naggar¹; ¹University of Southern California, United States; ²Weizmann Institute of Science, Israel; ³Arizona State University, United States

A multitude of microbes have adapted to gain energy by transferring electrons to external abiotic surfaces ranging from minerals to solid-state electrodes. In the model metal-reducing bacterium *Shewanella oneidensis* MR-1, this extracellular electron transfer (EET) is achieved through a network of multiheme cytochromes that span the cell envelope and incorporate along microbial nanowires. Recent studies of biomolecules, including cell surface electron conduits, have shown that electron transport in these proteins is spin selective through the chirality induced spin selectivity (CISS) effect. However, the physiological impact of CISS on electron transfer by living cells remains unclear. To further investigate CISS, we perform Hall effect measurements to screen for spin filtering in the *S. oneidensis* periplasmic Small Tetraheme Cytochrome (STC), which bridges the periplasmic gap between inner-membrane components and the cell surface electron conduits. STC has one of the highest heme-to-volume ratios of any known proteins, resulting in closely packed hemes and fast electron transport rates. By performing spin polarization measurements of an STC variant engineered to better interact with electrodes we show that, similar to previous reports of the cell surface cytochromes MtrF and OmcA, electron transport through STC is also spin selective. Our study provides an improved understanding of the electron transport physics in biomolecules and sheds light on an intriguing phenomenon whereby biology may exploit both electron spin and charge for interacting with abiotic surfaces.

SB11.06.05

Enhanced Cascade Biocatalysis by Enzymes Bound to Multi-Walled Carbon Nanotubes Made from Scalable, One-Step Exfoliation by Simple Stirring on the Benchtop Ankarao Kalluri¹, Mansi Malhotra¹, Prabir Patra^{2,2} and Challa V. Kumar^{1,1}; ¹University of Connecticut, United States; ²University of Bridgeport, United States

Efficient, multi-enzyme cascade biocatalysis is currently an unmet challenge, with a high potential in industrial biofuel cell applications. To address this issue, we developed a single-step exfoliation combined with enzyme binding by simply stirring the enzymes and commercially available, inexpensive, multi-walled carbon nanotubes (CNTs). This resulted in highly active biocatalysts that showed very high activities, greater than those of the free enzymes, under otherwise identical conditions of pH, temperature, and ionic strength. This major breakthrough is reported here, where bovine serum albumin (BSA) is used as a co-exfoliant to assist in the formation of the biocatalytic dispersions of CNT/BSA/glucose oxidase (GoX)/horseradish peroxidase (HRP) complexes. The BSA not only promotes exfoliation of CNTs but also passivates the high energy sites on the CNTs and protects the delicate enzymes from denaturation on the hydrophobic surface. The CNT/BSA/HRP complex showed ~2 times higher activity than that of the free HRP, and the CNT/BSA/GoX/HRP showed 6-times greater activity than that of the corresponding mixture of the free enzymes, under otherwise identical conditions. We hypothesize that the CNT surface couples the active sites of these two redox enzymes, promoting the overall activity of the enzyme cascade events. Hence, the biological CNT enzyme complex forms a complex interface, achieving efficient and robust binding while preserving the biological activities of these delicate enzymes. Further, the cascade enzymes are being developed for the construction of industrial-scale biofuel cells. Thus, an improved, simple method is developed to produce highly active cathodes that can be readily adapted even under resource-limited conditions.

Keywords: Carbon nanotubes, proteins, biocatalysts, biofuel cells

SESSION SB11.07: Device Integration
Session Chair: Herdeline Ardoña
Thursday Morning, December 2, 2021
Sheraton, 2nd Floor, Back Bay A

10:30 AM SB11.07.01

Shaping the Electrical Phenomena at the Interfaces of a Photo-Capacitive Electrode Vedran Derek¹, Aleksandar Opančar¹, Marta Nikić¹, Anja Mioković¹, Nikola Habek², Malin Silvera Ejneby³ and Eric Glowacki^{4,3}; ¹University of Zagreb, Faculty of Science, Croatia; ²University of Zagreb, Croatia; ³Linköping University, Sweden; ⁴Brno University of Technology, Czechia

A highly localized and effective, minimally invasive, physiologically stable and wireless electro-stimulation capability would present an important instrument in the toolbox of bioelectronic and electrophysiological methods. It is a milestone in the development of bioelectronic therapies, neural prostheses such as artificial retinas, artificial limbs and auditory prostheses, and brain-machine interfaces. Photo-capacitive organic electronics-based bioelectronic devices – organic electrolytic photocapacitors (OEPC), have demonstrated effective, chronic and localized in-vivo wireless peripheral nerve electric stimulation¹, as well as in-vitro wireless single cell² and retina electrostimulation³. Planar OEPCs fabricated on micrometer-thin flexible substrates have enabled conformal adhesion of the devices to the target tissue. Furthermore, a choice of organic pigment-based semiconductor PN bilayer has enabled effective and stable long-term operation of the devices in-vivo. The bioelectronic interface of an OEPC consisting of a circular-shaped PN bilayer as the active electrode deposited on top of an extensive, transparent conductor comprising the back electrode has been shown to stimulate peripheral nerves effectively. However, the simple circular shape of the top electrode in conjunction with the planar back electrode disperses the stimulating electric currents radially, which may not present the optimal use of the photogenerated charge in applications where high charge density and spatial localization are essential. Similar reasoning can be applied to various trivial electrode shapes, which are often used elsewhere.

We will show how spatial planar and 3D structuring of the OEPC's PN and back electrode layers affects their optoelectronic, bioelectronic and mechanical properties, simultaneously shaping their functionality. We will demonstrate how a complete 3D numerical model comprising the excitable tissue in contact with the photo-capacitive device can be used to tailor the effects of an optically driven device at the interface with living cells. We have manufactured 3D and planar OEPC devices with spatially optimized interfaces, which showed multifold improvements in performance compared to the trivial geometries previously used.

[1] A chronic photocapacitor implant for noninvasive neurostimulation with deep red light, M. Silvera-Ejneby, M. Jakesova, J. J. Ferrero, L. Migliaccio, Z. Zhao, M. Berggren, D. Khodagholy, V. Derek, J. Gelinan and E. D. Glowacki, *bioRxiv* (DOI: 10.1101/2020.07.01.182113), accepted for publication (*Nature Biomedical Engineering*, June 2021)

[2] Optoelectronic control of single cells using organic photocapacitors, M. Jakesova, M. Silvera-Ejneby, V. Derek, T. Schmidt, M. Gryszel, J. Brask, R. Schindl, D. T. Simon, M. Berggren, F. Elinder, E. D. Glowacki, *Science advances*, **5** (2019) eaav5265

[3] Direct Electrical Neurostimulation with Organic Pigment Photocapacitors, D. Rand, M. Jakesova, G. Lubin, I. Vebraite, M. David-Pur, V. Derek, T. Cramer, N. S. Sariciftci, Y. Hanein, E. D. Glowacki, *Adv. Mater.* **30** (2018), 1707292

10:45 AM SB11.07.03

Real Time Monitoring of Host-Pathogen Interactions Using Cell Membranes on a Chip Konstantinos Kallitsis¹, Anna-Maria Pappa¹, Henry Zixuan Lu¹, Walther Traberg-Christensen¹, Quentin Thiburce², Alberto Salles², Susan Daniel³ and Roisin Owens¹; ¹University of Cambridge, United Kingdom; ²Stanford University, United States; ³Cornell University, United States

Plasma membranes represent a biophysical barrier separating the cytoplasm from the extra cellular matrix across living organisms. Their heterogeneous structure consists of a lipid bilayer embedded with proteins and other vital components, which largely determine the interaction of cells with their environment. Recently our group, in collaboration with the Daniel and the Salles groups, have demonstrated that authentic plasma membranes in the form of supported lipid bilayers (SLBs) can be formed on top of poly(3,4-ethylenedioxythiophene) polystyrenesulfonate (PEDOT:PSS) based transducers. The bilayers were produced by a vesicle fusion process of native extra-cellular components (blebs) combined with synthetic liposomes and polymeric healing agents. Due to the transparent nature of PEDOT:PSS, the occurring biological phenomena were transduced in electronic output in real time, while the results were verified by state-of-the-art optical techniques.

Here, we demonstrate a general surface functionalization approach as a tool to introduce a variety of chemical groups on top of the PEDOT:PSS based electronic transducers. In the context of membrane-on-a-chip devices, our approach was used to tune the electrostatic interaction between the lipid bilayers and their electroactive supports. As a result of the increased affinity, membrane-on-a-chip devices with minimized and even eliminated synthetic component were made possible. Those devices were then used to provide mechanistic insight on biological events such as the binding and fusion of viruses. To demonstrate the capabilities of our platform, we monitored the interaction of a SARS-CoV-2 surrogate virus with a mouse-derived bilayer. When this coronavirus strain gets incubated and the virus fuses with the bilayer, a significant increase in impedance is observed, indicating that real-time electronic monitoring on such interactions is possible using our cell-free approach.

This simple platform has potential in assisting and re-directing drug discovery by providing real-time feedback early in the process, helping to reduce the high attrition rates during later stages when the costs are considerably higher.

SESSION SB11.08: Photo/Electrical Phenomena at the Interface with Living Cells and Bacteria I
Session Chair: Daniela Comelli
Tuesday Morning, December 7, 2021
SB11-Virtual

8:00 AM *SB11.08.01

The Proton Motive Force Determines Escherichia coli's Robustness to Extracellular pH Guillaume Terradot¹, Amritha Janardanan¹, Soner Sonmezoglu², Stefano Soneda³, Michel Maharbiz², Peter Swain¹ and Teuta Pilizota¹; ¹University of Edinburgh, United Kingdom; ²University of California, Berkeley, United States; ³Università degli Studi di Cagliari, Italy

Living cells can maintain their internal properties within a certain range, so-called homeostasis, e.g. intracellular pH. However, pH homeostasis has thus far not been looked at in the context of all the cellular physiological variables that are influenced by it, and the intertwined nature of these variables suggests that we need to so, to understand the homeostasis of even just one of them.

Here we build a simplified mathematical model of cellular electrophysiology. We show that bacteria use proton-ion antiporters to generate an out-of-equilibrium cytoplasmic membrane potential and so maintain the proton motive force (PMF) at the constant levels observed empirically. As a consequence, the strength of the PMF determines the range of extracellular pH over which the cell preserves a near-neutral cytoplasmic pH. We employ assays for time-course, single-cell, concurrent measurements of the PMF and pH and find agreement with our model prediction. We also demonstrate our efforts to measure the PMF in individual cells, but on thousands of them at the same time.

Our results suggest a new perspective on bacterial electrophysiology with cells maintaining their PMF and cytoplasmic pH by actively regulating the plasma membrane potential through changing activities of antiporters.

8:30 AM SB11.08.02

Late News: Understanding Photocapacitive and Photofaradaic Processes at the Organic Semiconductor/Water Interface for Biophotomodulation Luca Bondi, Beatrice Fraboni and Tobias Cramer; University of Bologna, Italy

Photoactive organic semiconductors are envisioned as a novel class of materials able to transduce light into stimulating signals inside biological cells or tissue [1]. The direct interface between the semiconductor and the electrolyte gives rise to different, competing electrochemical phenomena such as the photofaradaic or the photocapacitive processes, depending whether the photogenerated charges get involved in redox processes or accumulate at an interface. A detailed understanding of such chemical and photo-induced interactions is necessary to develop and optimize future devices.

We addressed the problem in organic photoelectrodes considering both polymeric single-layer and organic molecular p/n junction thin-films [2]. Both are material systems that have been recently demonstrated to achieve the photomodulation of cardiac regeneration processes [3] or retinal neurons response [4]. By spectroscopic photovoltage and photocurrent measurements we gain insight into the energetics of the involved processes, while performing transient measurement we are able to identify the kinetics of light stimulated charge transfer processes. By combining these techniques with impedance spectroscopy, electric modelling and kinetic modelling, we identify the role of interfacial energy levels in the photoactivated processes and distinguish photocapacitive and photofaradaic contributions. The findings are further combined with nanoscale morphological investigations and Kelvin-Probe Force Microscopy leading to a quantitative interfacial energy diagram. We highlight how the energy diagram enables a comprehensive understanding of the photoelectrochemical reaction pathways and how the findings can be translated to predict the response of novel materials and devices, such as transducers based on floating semiconducting nanoparticles.

[1] J. Hopkins, L. Travaglini, A. Lauto, T. Cramer, B. Fraboni, J. Seidel, and D. Mawad, "Photoactive Organic Substrates for Cell Stimulation: Progress and Perspectives," *Adv. Mater. Technol.*, vol. 4, no. 5, pp. 1–10, 2019.

[2] T. Paltrinieri, L. Bondi, V. Derek, B. Fraboni, E. D. Glowacki, and T. Cramer, "Understanding Photocapacitive and Photofaradaic Processes in Organic Semiconductor Photoelectrodes for Optobioelectronics," *Adv. Funct. Mater.*, vol. 2010116, 2021.

[3] F. Lodola, V. Rosti, G. Tullii, A. Desii, L. Tapella, P. Catarsi, D. Lim, F. Moccia, and M. R. Antognazza, "Conjugated polymers optically regulate the fate of endothelial colony-forming cells," *Sci. Adv.*, vol. 5, no. 9, 2019.

[4] D. Rand, M. Jakesová, G. Lubin, I. Vebráta, M. David-Pur, *et al.*, "Direct Electrical Neurostimulation with Organic Pigment Photocapacitors," *Adv. Mater.*, vol. 30, no. 25, pp. 1–11, 2018.

8:45 AM SB11.08.03

Late News: (Garcia High School Student) The Influence of TiO₂ and ZnO Nanoparticles on Bacterial Infection of HeLa Cells Joanna Li¹, William Stratton², Emily Zhou³, Fan Yang⁴ and Miriam Rafailovich⁴; ¹Townsend Harris High School, United States; ²Hastings High School, United States; ³The Harker School, United States; ⁴Stony Brook University, The State University of New York, United States

Due to the widespread use of Titanium dioxide (TiO₂) and Zinc oxide (ZnO) nanoparticles (NPs) in products such as sunscreen, cosmetics, and food additives, an improved understanding of their possible negative effects on cells may help to better ensure consumer safety and public health [1, 2]. Previous research showed that TiO₂ NPs in the rutile and anatase forms may impair cell function and defense against bacterial infection in HeLa cells and human dermal fibroblasts [3]. ZnO NPs have also been shown to exhibit cytotoxicity to cancer cells; a recent study found that, when compared to controls, HeLa cells with added ZnOs had significantly lowered cell viability [4].

This study aimed to measure the doubling time of HeLa cells exposed to TiO₂ NPs, ZnO NPs, and lecithin-coated TiO₂ (L-TiO₂) NPs to further the understanding of the effects of different NPs on HeLa cell proliferation. HeLa cells were infected with *Staphylococcus aureus* bacteria at a multiplicity of infection (MOI) of 1000. The cells in each well were counted at both 24 hours and 96 hours after their initial exposure to the NPs to calculate the average doubling time for each condition.

To this end, 6-well plates were used to culture 3-well groups of HeLa cells to which 3 types of NPs were added: TiO₂, lecithin-coated TiO₂ (L-TiO₂), and ZnO NPs. Each type of NP was added at a concentration of 0.1 mg/L, which was determined in an earlier study to be the concentration at which TiO₂ NPs negatively affected cells without killing them [5]. One group serving as the control received no NPs. The cells were plated after reaching 80% confluency, and TiO₂ and L-TiO₂ NPs mixed in cell culture media were added to the wells. Cells were plated and cultured with ZnO later in the study, as there was an initial lack of access to ZnO NPs. The cultured cells were counted at 24 hours and 96 hours after exposure to NPs using a hemocytometer, and the average doubling time of HeLa cells growing under each condition was calculated. There was no significant difference between the average doubling time of the control group and those of the TiO₂ group or L-TiO₂ groups.

The cells were stained with Alexa Fluor 488 Phalloidin and the *S. aureus* bacteria were stained with a live dead stain to count the total number of cells and infected cells and the number of live and dead bacteria, respectively. An EVOS cell imaging system (fluorescence microscopy) was used to produce images for cell and bacteria counting.

For the ZnO sample, bacteria cell counts and doubling time have been obtained, and preliminary data suggests that the bacteria per infected cells count on average for ZnO samples is higher than for the TiO₂ samples. This suggests ZnO NPs may be more nanotoxic than ZnO NPs. Future studies may include other NPs, or additional experiments on the nanotoxicity of ZnO if it is found to significantly more affect the proliferation of HeLa cells or their resistance to *S. aureus* infection.

9:00 AM SB11.08.04

High Resolution Correlative Microscopy for the Characterisation of Gram-Negative Outer Membrane Supported Lipid Bilayers Karan Bali¹, Zeinab Mohamed², Clemens Kaminski¹, Susan Daniel², Roisin Owens¹ and Joanna Mela¹; ¹University of Cambridge, United Kingdom; ²Cornell University, United States

Supported lipid bilayers (SLBs) are a useful tool in the investigation of membrane proteins and their interactions at the single molecule level. Outer membrane vesicles (OMVs) can be combined with synthetic liposomes to form complete SLBs that contain the natural components of the bacterial outer membranes (Hsia *et al.*, 2016). These systems show potential as novel antimicrobial screening platforms especially when integrated with bioelectronic devices. However, to date these hybrid SLBs have not been characterised at the molecular level. We employ correlative atomic force (AFM) with structured illumination microscopy (SIM) to gain detailed structural and functional information on those model systems (Ben-Sasson *et al.*, 2021). SLBs containing OMVs derived from *E. coli* BL21(DE3) are studied to fully characterise the membrane protein, bacterial lipopolysaccharide and synthetic lipid

components of the bilayers. We then increase the complexity of the system by engineering OMVs to contain proteins of interest, in this case a GFP binding nanobody-LppOmpA hybrid protein, and show that lipid patches that contain the overexpressed protein can be specifically identified and characterised. The relevance of these hybrid SLBs to antimicrobial screening applications is then demonstrated by SIM-AFM visualisation of known bacteria-targeting DNA nanostructures (Mela *et al.*, 2020) binding selectively to bacterial components of the bilayers. Our study introduces correlative AFM-SIM as a powerful microscopy technique for the characterisation of lipid bilayers with multiple components and demonstrates the need for reproducible, programmable model systems for antimicrobial screening.

9:15 AM *SB11.08.05

Microscopes on a Chip for Automated 3D Imaging Petra Paiè¹, Federico Sala^{2,1}, Roberto Memeo², Matteo Calvarese¹, Andrea Comi², Gianmaria Calisesi², Alessia Candeo², Roberto Osellame^{1,2}, Andrea Bassi^{2,1} and Francesca Bragheri¹; ¹IFN-CNR, Italy; ²Politecnico di Milano, Italy

Heterogeneity is an omnipresent feature of biological populations, and the possibility to investigate it allows revealing important information that might be hidden otherwise. In this regard, it is fundamental to develop tools and techniques capable to investigate the specimens automatically and at high throughput, without affecting the quality of the analysis.

Among different 3D microscopy techniques, significant advantages in sample investigation are offered by light sheet fluorescence microscopy (LSFM). This method is based on a non-invasive optical sectioning approach that permits to obtain 3D information, by illuminating the sample plane by plane with a sheet of light. Standard implementations foresee the use of a cylindrical lens to focus the light in one direction only, while the excited fluorescence is orthogonally collected by a microscope objective. The specimens are manually positioned in a sample chamber, aligned by the user in the optical system and automatically translated or rotated to allow multiple planes acquisition. This method permits fast image acquisition, low photobleaching and high signal to noise ratio. Nevertheless, the manual sample alignment requires up to several minutes, limiting the throughput of this technique.

The use of microfluidics to perform automatic sample delivery and translation could allow high throughput image acquisition of specimens diluted in a liquid suspension. Nevertheless, the integration of microfluidic channels in LSFM setups is not straightforward. This could introduce aberrations both to the excitation and collection path and it demands a very precise a stable alignment between the optical and fluidic system. Considering these constraints, we propose microfluidic based microscopes on a chip, integrating in a single substrate the optical elements necessary to create the light sheet such as optical waveguides and integrated cylindrical lenses as well as the microfluidic channel for automatic sample delivery. The integration of different components in a single platform guarantees the necessary alignment stability.

These microscopes on a chip have been fabricated in glass substrates by femtosecond laser micromachining (FLM) followed by chemical etching. Indeed, by focusing a pulsed laser beam into a transparent substrate, non-linear absorption processes occur and induce a permanent modification of the focal volume. This can lead to an increased etching selectivity or to a local increase of refractive index with respect to the pristine material, depending on the laser parameters. During sample irradiation, a 3D substrate translation permits to define the custom layout of the different components. Therefore, both microfluidic channels, integrated lenses as well as optical waveguides can be fabricated in the same substrate and within the same irradiation step by FLM. Taking advantage of the versatility and capabilities of this technique, we propose different devices that have been adapted to the specificity of the specimens under investigation, such as cellular spheroids, *Drosophila* embryos and even single cells. Indeed, the sample channel size as well as the optical properties of the light sheets must be tailored considering the different size and shape of these samples in order to guarantee a good optical sectioning and a uniform illumination over the entire sample. Zemax simulations have been used to optimize the lens profile and to reduce both spherical and chromatic aberrations. Dual color and dual side illuminations have been demonstrated, with an image quality comparable of the one of standard LSFM, highlighting the capabilities of these microscopes on chip. In addition, the setup automation and the throughput of these devices have been optimized, proving an image acquisition rate of about 1 cell/second. Recently, by modifying the illumination path we have been able to further improve the image quality, proving a subcellular resolution.

SESSION SB11.09: Photo/Electrical Phenomena at the Interface with Living Cells and Bacteria II

Session Chair: Munehiro Asally

Wednesday Morning, December 8, 2021

SB11-Virtual

8:00 AM *SB11.09.01

A Universal Microfluidic Approach for Quantitative Study of Bacterial Biofilms Jintao Liu; Tsinghua University, China

Bacteria usually live in densely packed communities called biofilms, where the interactions between the bacteria give rise to complex properties. Quantitative analysis is very useful in understanding these properties. However, current biofilm culturing approaches impose various limitations. We developed a microfluidic approach for quantitative study of biofilms, which is universal and can be used to study biofilms of various bacterial species. To demonstrate the utility of this approach, we will present two examples, both of which revealed new biological insights. In the first example, we will explore the response of *Escherichia coli* biofilms to exogenous hydrogen peroxide. We found biofilms gained tolerance to H₂O₂, but their growth was slowed down due to the metabolic cost of maintaining the tolerance; However, under certain conditions, H₂O₂ can anti-intuitively boost growth. In the second example, we will show that in *Pseudomonas aeruginosa* biofilms, the extracellular matrix acts as a diffusion barrier for iron chelator, minimizing its loss into the environment and therefore potentially promoting the sharing of the chelator within the biofilm as a public good.

8:30 AM SB11.09.02

Label-Free Rapid Detection of Biomolecule Using Surface-Enhanced Raman Spectroscopy (SERS) for Point-of-Care Testing Wisawat Keaswejjareansuk, Katawut Namdee and Mattaka Khongkow; National Nanotechnology Center, National Science and Technology Development Agency, Thailand

Exosomes are extracellular vesicles with phospholipid bilayer membrane that carry the encapsulated lipids, proteins, genetic materials and transmit *in vivo*. The exosomes those were secreted by specific cells and tissues show unique biological component and characteristics. Raman spectroscopy is a non-destructive and non-invasive technique that measuring the inelastic scattering of photons. It enables the analysis of the vibration mode of different biomolecules caused by monochromatic laser radiation. Distinguish and analysis of the Raman signal are difficult due to the low signal intensity. To overcome this problem, the surface-enhanced Raman spectroscopy (SERS) technique has been utilized. Gold and silver nanoparticles are typical used to amplify the signals in many systems include biosensing. A variety of SERS chips have been widely developed to obtain the signature spectra of the biomolecules. By using the SERS chip, liquid biological samples are dropped and dried before proceeding with the SERS technique. In this study, the SERS technique was employed in the colloid of the exosome-liquid mixture. Colloidal SERS offers the Raman spectra without the cell disruption and suitable for cells and tissues analysis. The exosomes purified from human embryonic kidney 293 (HEK 293) and rabies virus glycoprotein (RVG) were

used. An only a small volume of exosomes (in a range of microliter) was decorated with silver NPs and diluted with 1 mL of phosphate-buffered saline (PBS). PBS is a water-based salt solution that has a pH similar to that of the human body. It is typically used to prevent the cells rupture and shrivel up. Interestingly, the SERS spectra were obtained with only 15 μ L drop of the exosome-PBS mixture. The goal of this study is to develop a reliable and less complex point-of-care testing for practical usages with a handheld Raman spectrometer.

In this presentation, the colloidal SERS technique for detecting tissue-specific and nonspecific exosomes includes the concentration of the exosome-PBS mixture, the optimal volume of NPs, and the materials characterizations such as transmission electron microscopy (TEM), dynamic light scattering (DLS), and SERS spectra will be discussed.

8:45 AM *SB11.09.03

Electronic Communication Between Catalytic Enzymes and Electron-Transporting Conjugated Polymers Sahika Inal; King Abdullah University of Science and Technology, Saudi Arabia

Establishing close interactions between biological systems and synthetic materials is the key to form biohybrid assemblies that find use in sensors, actuators, and robotics. In this work, I will present an electronic platform based on an n-type conjugated polymer that is tailored to form favorable interactions with catalytic enzymes.^{1,2} When this biohybrid is applied in an enhancement mode organic electrochemical transistor (OECT), the device detects glucose and lactate in blood serum or saliva with excellent sensitivity, and selectivity over six orders of magnitude wide detection range. The same biohybrid serves as the anode of a glucose fuel cell, extracting enough power from bodily fluids to drive the microscale OECT sensors. While showing the unique characteristics of these devices, I will discuss the possible pathways through which the polymer film generates charges as the enzyme reacts with its metabolites.

A. M. Pappa et al *Sci. Adv.* 2018, 4 (6), eaat0911.

D. Ohayon et al *Nat. Mater.*, 2020, 19, 456.

9:15 AM SB11.09.05

Electrically Induced Membrane Potential Dynamics in Yeast Tailise Souza G. Rodrigues, Orkun S. Soyer and Munehiro Asally; University of Warwick, United Kingdom

Membrane potential is known to be important for cross-membrane trafficking of ions and nutrients in all forms of life, but they are not limited to that. New discoveries show that electrophysiology plays a role in broader cellular and organism functions, ranging from antibiotic persistence to wound healing. Electrically induced membrane potential dynamics was recently shown to enable rapid detection of live bacteria with single-cell sensitivity, bridging an electro-bio hybrid system to diagnostics. It is still unclear, however, whether electrical stimulation can be used for the detection of live eukaryotic microbes. Here we show that proliferative and growth-inhibited budding yeast, *Saccharomyces cerevisiae*, exhibit distinct electrically induced membrane potential dynamics, enabling detection of proliferative eukaryotic cells from non-growing ones. When proliferative cells were stimulated by an electrical field, it induced hyperpolarization in plasma membrane. The same electrical stimulus, however, caused depolarisation when the cells were inhibited. The ability to detect not only prokaryotic, but also eukaryotic vital cells at single-cell level shows how promising electro-bio hybrid systems are as a tool for diagnostics. And the possibility to modulate membrane potential by applying an exogenous electrical stimulus sheds light on the potential use of electro-bio hybrid systems to regulate electrophysiology-dependent cellular functions, paving the path for future engineering of environment responding living-materials.

9:30 AM SB11.09.06

Late News: Probing the Electrophysiology of Germinating and Outgrowing Spores of *Bacillus subtilis* Jonatan Benarroch and Munehiro Asally; University of Warwick, United Kingdom

Bacterial spores are highly resistant to many conventional microbial elimination techniques. Their resistances to radiation, extreme temperatures, and bactericidal chemicals are in part due to the spores' unique electrochemical properties: namely, decreased hydration, high cationic concentration, a very negatively charged coat, and low permeability across their membranes. Hence electrochemical perturbation can provide novel approaches to overcoming the extreme resistances of spores.

This has led us to probe deeper into the electrophysiology of spores during germination, when they exit dormancy and lose their resistive properties. However, germination timing and speed is heterogeneous as is time taken to return to a vegetative state. Thus, control of these timings is essential for maximising elimination. We study the model organism *Bacillus subtilis* using time-lapse microscopy with electrochemically sensitive dyes to investigate how spore electrophysiology can change on a cellular level. We have discovered that membrane potential dynamics reveal two phenotypic populations. Their significance is still yet to be determined, however it is controlled by varying media salinity and buffering capacity. Finally, we discovered that outgrowth into vegetative cells could be delayed by use of cationic agents providing an opportunity to kill a large population of spores. This fits in with the exciting and emerging field of bacterial electrophysiology, which has seen recent growth due to research demonstrating how microbes use ion flux and membrane potential for dynamic signalling and environmental sensing.

SESSION SB11.10: Photo/Electrical Phenomena at the Interface with Living Cells and Bacteria III

Session Chairs: Munehiro Asally and Daniela Comelli

Wednesday Afternoon, December 8, 2021

SB11-Virtual

1:00 PM *SB11.10.01

From Single Molecules to Living Electronics—Biophysical Studies of Bacterial Extracellular Electron Transport Moh El-Naggar; University of Southern California, United States

Electronic components that bridge the biotic-abiotic interface will have vast implications for both studying and harnessing the activity of living cells. While much ongoing research focuses on applying traditional rigid electronics to biology, an alternative is to discover bioelectronic solutions that life itself evolved to interact with the abiotic world. Towards realizing this vision, recent studies at the interface of microbiology, electrochemistry, and physics have uncovered metalloprotein electron conduits and nanowires that electronically link bacteria to extracellular surfaces ranging from environmental minerals to

solid-state electrodes. Since this extracellular electron transport naturally evolved to interact with external surfaces, a fundamental understanding has special implications for new bioelectrochemical technologies and living electronics that harness the advantages of microbes in detecting external signals or hosting synthetic genetic circuits.

This talk will describe our group's recent progress in understanding extracellular electron transport at multiple length scales, from the biophysics of individual multiheme cytochromes to the electrophysiology of whole bacteria and multicellular communities ranging from biofilms to cable bacteria. Using single molecule tracking and stochastic simulations of cell surface multiheme cytochromes in the metal-reducing bacterium *Shewanella oneidensis* MR-1, we describe how the interplay of cytochrome dynamics and electron hopping can give rise to long-distance electron conduction along bacterial membrane surfaces. In addition, we describe strategies to characterize and harness the electrochemical activity, spin filtering, and conduction properties of bacterial electron conduits in both synthetic structures and living biofilm materials.

1:30 PM *SB11.10.02

Electrical Control of Nerve Growth on Insulating and Conductive Substrates [Ann M. Rajnicek](#); University of Aberdeen, United Kingdom

Electrical stimulation therapies are increasingly useful for nervous system disorders but even state of the art (metal) electrode materials have limitations, such as unwanted production of heat, free radical species, pH changes and associated tissue necrosis. Implanted electrodes also may need to be hard wired to a power source, though indirect electrostimulation is possible by creating an electrical gradient wirelessly through generation of dipoles at the borders of implanted materials by bipolar electrochemistry. Improved understanding of how neurons and materials interact to influence nerve growth would be valuable for future restorative electro-therapies.

By delivering a voltage gradient through the culture medium in vitro we have explored neuron growth on insulating materials, such as glass or tissue culture plastic, and compared it to conducting materials, such as gold or platinum and also to conducting intercalation materials. Materials were prepared as thin coatings to permit optical transparency and to allow observation of growth dynamics. Neurons from the developing amphibian spinal cord were used, mainly because, unlike mammalian neurons, they do not require any adhesion factors between the cell and the underlying substrate.

Neurons grew faster and more directly toward the external driving cathode when plated onto tissue culture plastic (insulating material) and, when the stimulation was within a safe window, they turned to grow toward the cathode on gold. Differences were apparent between conducting and mixed conducting intercalation materials, with neurons grown on IrOx favouring speed of growth (but no directional growth) and those on PEDOT-SS based materials favoring turning towards the external driving cathode (but not faster growth).

The data suggest that indirect electrical stimulation of neurons can be tuned to achieve specific growth responses by designing implant materials with specific bipolar electrochemical traits, even in challenging situations where transparency is required. This has clear potential to for designing neural prostheses or neural repair strategies but the concepts could also be applied to other wound healing and regeneration situations.

2:00 PM *SB11.10.03

Electrogenetics for Dynamic Bidirectional Communications Between Engineered Cells and Electronics [Tanya Tschirhart](#); U.S. Naval Research Laboratory, United States

One of the ultimate goals of bioelectronics is an ability to electronically access all that biology has to offer - to control and record the myriad of native and engineered biological processes inside of cells and organisms. This could be enabled by seamless and dynamic bidirectional communication between electronic and biological components. As a step towards realizing these capabilities, electrogenetics offers tools to use electrical stimuli to modulate engineered gene expression. Electronic control of the oxidation state of redox molecules modulates redox-sensing proteins and gene expression from the promoters they activate. We have co-opted the SoxR and OxyR redox-sensing proteins from *Escherichia coli* in two distinct electrogenetic systems. These allow us to electronically control the expression of a number of engineered genes and behaviors in various environments and configurations. We developed a multi-functional microbial community, the BioLAN, which reliably facilitates on-demand bioelectronics communication and electrogenetic control of a programmed biological task. The BioLAN also provides electronically-recordable cell-based reporting to allow for feedback control. The electrogenetic systems presented here can be incorporated into genetic circuits and logic gates alongside chemical and light-driven components. They present a melding of synthetic biology and bioelectronics towards building seamlessly-integrated bio-hybrid devices.

2:30 PM *SB11.10.04

Encoding Spatio-Temporal Memory in Bacterial Biofilm Communities [Gurol Suel](#); University of California, San Diego, United States

I will present our recent efforts to understand and manipulate the membrane potential of bacteria that make up biofilm communities. In particular, I will talk about our efforts to encode memory in space and time within biofilms using the membrane potential of bacteria. This work can set the stage to utilize biofilms for performing computations. I will end by showing some new results regarding our ability to control biofilms.

SYMPOSIUM SB12

Biomaterials for Regenerative Engineering
November 30 - December 6, 2021

Symposium Organizers

Richard Benninger, University of Colorado Denver
Gulden Camci-Unal, University of Massachusetts Lowell
Natesh Parashurama, University at Buffalo, State University of New York
Donghui Zhu, Stony Brook University, The State University of New York

Symposium Support
Bronze
Engineered Regeneration | KeAi Publishing

* Invited Paper

SESSION SB12.01: Polymeric Biomaterials for Regenerative Engineering I
Session Chairs: Gulden Camci-Unal and Natesh Parashurama
Tuesday Morning, November 30, 2021
Sheraton, 2nd Floor, Back Bay D

10:30 AM *SB12.01.01

Bone Regenerative Engineering—The First 30 Years of Materials Science Cato T. Laurencin; University of Connecticut Health Ctr, United States

The treatment of bone injuries that necessitate bone regeneration continues to be a major challenge for the orthopaedic surgeon. This burden is compounded by supply constraints and associated morbidity with autograft tissues, the gold standard of repair. The use of allografts, xenografts, or metal and ceramic implants overcomes many of these limitations, but fail to provide a viable solution. Over the past 30 years, we have worked to engineer bone with a focus on biomaterial selection, material matrix development, cell/material interaction studies, and the development of inducible materials.

We have developed poly(ester), poly(anhydride), and poly(phosphazene) biomaterials for bone engineering applications through biocompatibility, degradation, and mechanical analyses. We developed a novel three-dimensional sintered microsphere matrix possessing a pore structure and mechanical strength within the range of human cancellous bone, a version of which is now clinically available. We also reported on attachment, growth, proliferation, and differentiation of osteoblasts, mesenchymal-, and marrow-derived stem cells on several of the material matrices we have developed. We have demonstrated regenerative bone formation *in vivo* using these biomaterial technologies. This entire body of work over more than thirty years has largely been responsible for the awarding of the highest honor for technological achievement in the United States, The National Medal of Technology and Innovation, and the American Association for the Advancement of Science's highest award, the Philip Hauge Abelson Prize for 'signal contributions to the advancement of science in the United States'.

11:00 AM SB12.01.02

Late News: Helically Aligned Biohybrid Models of the Left Ventricle John Zimmerman¹, Huibin Chang¹, Qihan Liu², Keel Y. Lee¹, Michael M. Peters¹, Michael Rosnack¹, Suji Choi¹, Sean L. Kim¹, Herdeline Ardoña³, Luke MacQueen¹ and Kevin Kit Parker¹; ¹Harvard University, United States; ²University of Pittsburgh, United States; ³University of California, Irvine, United States

Human ventricles are made up of helically arranged myofibers, that transition across the ventricle wall from a left- to right-handed helix. For more than fifty years, it has been argued that this helical structure is critical for achieving the large ejection fractions (60-80%) observed during healthy cardiac contraction while maintaining minimal ventricular strain. However, testing this fundamental structure-function relationship has been challenging, as *in vivo* studies are often characterized by concomitant changes in protein expression and metabolism, while *in vitro* studies have difficulty in reproducing the complex three-dimensional (3D) structures of the heart. Addressing this challenge, here we show how additive textile manufacturing approaches, such as Focused Rotary Jet Spinning (FRJS), can be used for the rapid manufacture of micro/nanofibers scaffolds with controlled alignments and helical architectures. As aligned micron-scale fibers can be used to direct tissue orientation and subsequent morphogenesis, we reasoned this approach would allow for the biofabrication *in vitro* models that are reminiscent of early simulations of cardiac contraction. Producing both helically and circumferentially aligned 3D biohybrid models of the left ventricle, we show that helically aligned ventricles displayed increased strain uniformity, axial shortening, cardiac output, and ejection fractions as compared to circumferential models. Additionally, we demonstrate how helically aligned scaffolds preserve some features of ventricle twist, a phenomenon observed in clinical readouts, but not previously reported in engineered biohybrid systems. Overall, this work shows that myofibril alignment plays a critical role in regulating cardiac performance, with important implications towards cardiac disease. Additionally, this approach suggests that additive textile manufacturing may serve as a valuable approach for future biofabrication, which can be used in conjunction with, or as a potential alternative to, more traditional methods such as 3D bioprinting.

11:15 AM *SB12.01.03

Moving Forward on the Engineering of Biomaterials and Optimizing their Interactions with Cells for Specific Regenerative Medicine Application Rui Reis^{1,2}; ¹University of Minho, Portugal; ²ICVS/3B's-PT Government Associate Laboratory, Portugal

The selection of a proper material to be used as a scaffold, as a proper matrix, or as a bioink in 3D bioprinting approaches to support or encapsulate cells is both a critical and a difficult choice that will determine the success or failure of any tissue engineering and regenerative medicine (TERM) strategy.

In our research group we have been mainly using natural origin polymers, including a wide range of marine origin materials, for many different approaches that allow for the regeneration of different tissues. Several innovative bioinks with quite specific properties were developed and proposed for several specific uses. We have also been optimizing the respective formulations for using these novel materials in distinct biomaterial manufacturing strategies. This will be presented and discussed during the present keynote talk.

Furthermore, an adequate cell source should be selected. In many cases efficient cell isolation, expansion and differentiation methodologies should be developed and optimized. We have been using different human cell sources namely: mesenchymal stem cells from bone marrow, mesenchymal stem cells from human adipose tissue, human cells from amniotic fluids and membranes and cells obtained from human umbilical cords.

The potential of each materials/cells combination, as related to different manufacturing technologies, with details when appropriated focusing on bioprinting, to be used to develop novel useful regeneration therapies will be discussed. Several examples of TERM strategies to regenerate different types of tissues will be presented. The use of different cells and new ways to assess their interactions with different natural origin degradable scaffolds and bioinks will be described. A unique high-throughput platform to better understand material/cells interactions and optimise their performance and biological performance will be discussed. This rather innovative platform is based on the use of unique microfluidics-based approaches.

1:30 PM *SB12.02.01

Engineered Extracellular Matrices that Emulate Periosteal-Mediated Bone Healing Yiming Li, Michael Hoffman and Danielle Benoit; University of Rochester, United States

INTRODUCTION: Despite serving as the clinical “gold standard” treatment for critical size bone defects, decellularized allografts suffer from long-term failure rates of ~60% due to the absence of the periosteum. To promote allograft healing, our lab has pioneered the tissue engineered periosteum (TEP) based on poly(ethylene glycol) (PEG) hydrogels. The hydrogels entrap mouse mesenchymal stem cells (mMSCs) and mMSC derived osteoprogenitors (mMSC-OPs) and surround allografts to emulate native periosteum cell populations and subsequent paracrine factor production to coordinate periosteum-mediated healing. Despite robust angiogenic factor production, the TEP showed only modest increases in vascular volume versus unmodified allograft controls. Additionally, even though the maximum torque of TEP modified allografts was 2-fold higher versus unmodified allografts after 9 weeks, it was only ~40% of autografts, indicating delayed healing. These results are attributed to limited vascular recruitment within the hydrolytically degradable TEP (hydro-TEP), as its mesh size (~15 nm) is smaller than that of leading filipodia of migrating cells (0.2-0.4 μm). Therefore, to investigate the hypothesis that the degradation mechanism of the TEP is critical for coordinating host tissue infiltration necessary for successful bone, this study compared healing of Hydro-TEP, which bulk degrades, with that of the matrix metalloproteinase (MMP) degradable TEP (MMP-TEP), which enables host cell-dictated degradation.

MMP-degradable hydrogels supported endothelial cell migration *in vitro* whereas no migration was observed in hydrolytically degradable hydrogels. At week 3 post-implantation, ~2.5 and 1.8-fold, and ~3.5 and 2.6-fold greater vessel and nerve densities with high levels of vessel/nerve co-localization was observed using MMP-TEP-modified allografts versus unmodified and Hydro-TEP-modified allografts, respectively. At 3, 6, and 9 weeks post-implantation, the graft-localized vascular volumes of MMP-TEP-modified allografts (0.22 ± 0.8 , 0.20 ± 0.8 , and 0.17 ± 0.07 mm³) were significantly greater than those of unmodified allografts (0.002 ± 0.0004 , 0.05 ± 0.04 , and 0.12 ± 0.03 mm³) and Hydro-TEP-modified allografts (0.06 ± 0.004 , 0.02 ± 0.001 , and 0.05 ± 0.02 mm³). Furthermore, MMP-TEP-modified allografts showed 4.5, 4.6, and 2.8-fold increase in bone volume versus unmodified allografts after 3, 6, and 9 weeks respectively, and enhanced mineralization density of bone callus after 9 weeks versus unmodified and Hydro-TEP-modified allografts. MMP-TEP-modified allografts exhibited approximately 8 and 2-fold enhancements in maximum torque strength versus Hydro-TEP-modified allografts after 6 and 9 weeks respectively, reaching a comparable maximum torque to that of autografts at 9-week post-surgery.

Bone regeneration is synergistically mediated by angiogenesis and innervation. Consistent with this synergy, endothelial sprouting within MMP-degradable hydrogels *in vitro* paralleled significantly increased and co-localized vessel and nerve densities observed *in vivo*, and longitudinal graft-localized vascularization. Furthermore, the robust early stage neurovascularization of MMP-modified allografts significantly increase bridging endochondral callus formation with greater mineralization versus unmodified and Hydro-TEP modified allografts, leading to enhanced maximum torque, which was comparable to that of autografts at 9 weeks post-surgery. In summary, these data indicate that the MMP-TEP effectively coordinates allograft healing via early stage recruitment and support of host neurovasculature. The MMP-TEP improved allograft healing, while overall outcomes still lagged behind those of autografts. In future studies, additional matrix cues, such as alternative extracellular matrix-derived peptides and MMP-degradable crosslinkers can be explored to further orchestrate improved healing.

2:00 PM SB12.02.02

Tissue Engineered Bone Mimetic Scaffolds as Testbeds for Bone Metastasis of Breast Cancer and Prostate Cancer Kalpana Katti¹, Haneesh Jasuja¹, Sibanwita Mohanty¹, Anu Gaba², Jiha Kim¹, Farid M. Solaymani¹ and Dinesh R. Katti¹; ¹North Dakota State University, United States; ²Sanford Health, United States

According to the World Health organization, there were 2.26 million women diagnosed with breast cancer and 1.41 million men with prostate cancer in 2020. Further, over a million deaths were reported due to breast cancer and prostate cancer globally in 2020. Both breast cancer and prostate cancer have the propensity to metastasize to bone, leading to a terminal prognosis for the patient. As of 2020, breast or prostate cancer that has metastasized to the bone is essentially incurable, and only palliative treatments exist. In the event of bone metastasis, skeletal failures are often the cause of death in patients. The inefficacy of anticancer drugs and failure of animal models necessitates the need for *in vitro* models. We have developed a novel bone mimetic scaffold that uses tissue engineering approaches to generate bone mimetic scaffolds for generation of bone that is in a remodelling stage; a preferred niche to which breast and prostate cancer migrate towards. Thus besides providing valuable opportunities for bone regenerative treatment the tissue engineered bone has additional uses as a testbed to evaluate bone metastasis of cancer. The bone mimetic scaffold utilizes unnatural amino acid modified nanoclays to mineralize hydroxyapatite mimicking the process of biomineralization. We report the generation of bone metastasized tumors at the stage of mesenchymal to epithelial transition on seeding the bone scaffold with commercial cell lines of breast cancer and also prostate cancer. We have developed cell lines from patient derived tissues that are also seeded onto the bone mimetic scaffolds to develop patient derived *in vitro* tumors of breast cancer bone metastasis. Further, we evaluate the mechanisms of influence of cancer cells on osteogenesis pathways (the Wnt/bcatenin pathway) and demonstrate the specific role of cancer cell factors DKK and ET-1 on osteogenesis at the bone site. We have also developed unique mechanics-based biomarkers that use direct nanoindentation to evaluate the change in elastic and viscoelastic properties of cancer cells as a measure of progression of bone metastasis with the use of the testbeds. We also report the use of the testbed to screen new drugs for treatment of bone metastasis as well as report their influence on bone. Overall, the use of tissue engineered constructs present a useful testbed for evaluation of cancer.

2:15 PM SB12.02.03

Late News: Unconventional Biomaterials for Regenerative Engineering Gulden Camci-Unal; University of Massachusetts Lowell, United States

Introduction: Across various areas of regenerative engineering, there have been limitations with controlling cell adhesion, stem cell differentiation, viability, growth, and blood-material compatibility. Conversion of simple and abundant items to advanced cell culture substrates addresses some of the current challenges in regenerative engineering. The departure from complex fabrication processes to the applications of unusual and ubiquitous materials provides another dimension to the engineering of viable multiscale tissue constructs and regenerative technologies.¹⁻⁴ In addition, the use of sustainable constructs and novel fabrication strategies has the potential to increase access to regenerative engineering technologies on a global scale. In this work, we used unconventional biomaterials such as eggshells and paper for tissue repair.

Materials and Methods: We fabricated eggshell micro/nanoparticle (ESP) reinforced gelatin-based hydrogels to obtain mechanically stable and biologically active three-dimensional (3D) constructs that can differentiate stem cells into osteoblasts. The ESP-reinforced gels were then subcutaneously implanted in a rat model to determine their biocompatibility and degradation behaviors. In addition, these composite scaffolds were used to regenerate critical sized cranial defects in a rat model. We also used mineralized paper scaffolds through an origami-inspired approach to test their osteoinductivity and potential for tissue repair in *in vitro* and *in vivo* studies.

Results and Discussion: The ESP-reinforced scaffolds enabled the differentiation of stem cells without the use of specialized osteogenic growth medium. The ESP-reinforced gels exhibited significant enhancement in mineralization by the cells. Our findings indicated that the ESP composites exhibited superior mechanical properties and showed a favorable *in vivo* response by subcutaneous implantation in a rat model. These scaffolds were highly responsive to cells, and did not elicit inflammatory responses *in vivo*. The implants were easily accepted by the host, allowed for cellular infiltration in 3D, and highly vascularized. Implantation of ESP-reinforced scaffolds into critical sized calvarial defects in a rat model resulted in significant bone regeneration in 12 weeks. The resulting bone volume and bone density were as high as the native bone using these composite scaffolds as determined by micro-computed tomography analyses.

We also fabricated origami-inspired paper-based scaffolds for biomineralization. Material properties of the paper-based mineralized scaffolds were determined to be highly tunable. The tensile modulus of the scaffolds increased significantly after the mineralization process. Gene expression results for the osteogenic differentiation markers revealed the osteoinductivity of the mineralized paper scaffolds. Subcutaneous implantation of the samples in rats demonstrated biocompatibility, vascularization, and integration *in vivo*.

Conclusions: Unconventional scaffolds that are readily available and adapted from nature exhibited biomimetic characteristics including porosity, structure, and bioactivity resulting in physiologically relevant constructs. The use of existing naturally derived materials for regenerative engineering provides an inexpensive and sustainable approach that benefits the economy and environment while providing unique solutions to unmet clinical needs. Many of the unconventional biomaterials are overlooked and under-studied for biomedical applications, partially for their simplicity as mundane items.

References: ¹Nguyen, M.A., Camci-Unal, G., Trends in Biotechnology, 38(2): 178-190, 2020. ²Suvarnapathaki, S., Wu, X., Lantigua, D., Nguyen, M.A., Camci-Unal, G., Nature Asia Materials, 11(1): 1-18, 2019. ³Wu, X., Stroll, S.I., Lantigua, D., Suvarnapathaki, S., Camci-Unal, G., Biomaterials Science, 7, 2675-2685, 2019. ⁴Ahmed, A.R., Gauntlett, O., Camci-Unal, G., ACS Omega, 6(1): 46-54, 2021.

2:30 PM SB12.02.04

Combination of Ultrasound Stimulation and 3D Printed Piezoelectric Hydrogel for Skeletal Muscle Tissue Engineering Federica Iberite, Claudia Paci, Lorenzo Vannozzi, Lorenzo Arrico and Leonardo Ricotti; Scuola Superiore Sant'Anna, Italy

Introduction 3D bioprinting has the potential for becoming a breakthrough method in the implementation of skeletal muscle (SM) tissue engineering. Bioink chemical cues and mechanical properties have been widely investigated in the last decade¹. Less explored is the incorporation of exogenous stimulations (e.g. electrical, magnetic, mechanical) to boost cell differentiation. Piezoelectric nanoparticles (NPs) have been used as nanoscale transducers able to convert mechanically-induced deformation into an electrical cue when invested by an ultrasound wave (acting as a wireless source of mechanical energy). This paradigm has shown beneficial effects on different cell types, accelerating the differentiation of neural and muscle precursors^{2,3}. No research groups have yet explored the inclusion of piezoelectric NPs in a bioink for SM cells 3D bioprinting. This work shows preliminary results on the properties of a piezoelectric bioink based on Pluronic/alginate doped with barium titanate NPs (BTNPs) and the biological response of C2C12 cells encapsulated in it.

Methods BTNPs (diameter~60 nm) were added to propylene glycol alginate (PGA, ratio 1:1). A hydrogel of 20% w/w Pluronic F127 and 2% w/w alginate was prepared as described in⁴. Four bioinks (one bare bioink and three ones with BNTPs at 100, 250, 500 µg/mL respectively) were loaded with 2x10⁶ C2C12 cells/mL, printed with a 3D Bioplotter (Envisiontec GmbH) in one layer of parallel fibers (7x7 mm², nozzle diameter=250 µm, 37°C, pressure=0.4 bar, speed=10 mm/s), and then crosslinked (25 mM CaCl₂, 10 min). Hydrogels were characterized through SEM, EDX and rheometry. Viability tests at 72 h were carried out using LIVE/DEAD and PrestoBlue assays. For differentiation experiments, two constructs (non-doped and doped with 250 µg/mL BNTPs) were cultured in growth medium (5 days) and for 4 days in differentiation medium (DM=DMEM, 1% ITS, 1% FBS, 1% P/S). Half of the constructs were treated with low-intensity pulsed ultrasound (LIPUS; frequency=1 MHz; spatial average pulse average intensity=250 mW/cm²; pulse repetition frequency=1 kHz; duty cycle=20%; exposure time=5 min) in DM, through a dedicated setup allowing precise control of the LIPUS dose at the cells⁵, while the other half was not stimulated. After 4 days, the expression levels of *MYOG*, *CSRP3*, *MYH2* and *GAPDH* (reference gene) were assessed through real-time qRT-PCR. Cells stained with TRITC-phalloidin and DAPI were imaged using a confocal microscope. All experiments were performed in triplicate for each condition.

Results and Discussion SEM images and EDX results showed that BNTPs were uniformly dispersed in the printed hydrogels, even at high concentrations of BTNPs. Rheometric results highlighted no significant differences between the different bioinks in terms of storage, loss moduli and viscosity. Viscosity decreased under shear strain, showing a shear-thinning behavior. High cell viability was observed up to a BNTP concentration of 250 µg/mL. Constructs with 500 µg/mL BNTPs showed lower cell viability, therefore were excluded for further studies. Differentiation tests showed that the LIPUS-treated doped bioink (250 µg/mL) promoted a significantly higher expression of *MYOG*, *CSRP3* and *MYH2* (key genes in early myogenesis), with respect to the control (bare bioink).

Conclusion The preliminary results here reported, demonstrate the potential of piezoelectric bioinks for the development of 3D printed SM constructs and the myogenic effect of the interaction between LIPUS stimulation and piezoelectric nanomaterials, in this context.

Acknowledgments This work received financial and technical support by INAIL, in the framework of the project MIO-PRO.

References [1] Zhuang P., et al. (2020). Mater. Des., 108794
[2] Ricotti L., et al. (2013). PLoS one, 8(8), e71707
[3] Marino A., et al. (2015). ACS Nano, 9(7), 7678-7689
[4] Mozetic P., et al (2017). J Biomed Mater Res, Part A, 105(9), 2582-2588
[5] Fontana F., et al. (2021). Ultrasonics, 106495

2:45 PM SB12.02.05

Effect of the Synthesis Route on the Antimicrobial Response of Calcium Phosphates Doped with Magnesium in 3D Printing—Potential Application in Regeneration of Dental Tissue Carlos Paucar¹, Natalia Jaramillo², Ana Moreno¹, Ricardo Sanchez², Alejandro Pelaez³ and Claudia Garcia¹; ¹Universidad Nacional de Colombia, Colombia; ²Fundación María Cano, Colombia; ³Universidad Cooperativa, Colombia

Dental demineralization, tooth resorption and endodontic treatments have a high impact on dentistry. Bioglass and calcium phosphate 3D printed scaffolds with suitable degradability and compatibility characteristics are a suitable choice for your solution. However, due to oral lesions, it is necessary to consider the behavior of these materials against pathogens in the dental area. These effects can be reduced by doping with elements associated with the biological processes of bone repair and / or regeneration such as boron (B) and magnesium (Mg), which also affects the reabsorption process of the material due to the release of ions that they generate, an antimicrobial effect. The objective of this work is to compare the antimicrobial activity of calcium phosphate powders obtained by sol-gel and self-combustion routes and scaffolds formed with these powders by 3D printing against *C. albicans*. and *S. mutans*. Calcium phosphates in sol-gel processes present a mixture of various types of crystalline phases, whereas self-combustion leads to a single β-TCP phase. The *in vitro* antimicrobial activity study showed that calcium phosphate obtained via self-combustion and magnesium doped (β-TCP / Mg) had a better effect than calcium phosphate obtained via sol-gel (CP-S) with and without doping against *C. albicans*. For *S. mutans* no inhibitory effect was found. In addition to the

co-cultivation of these two species, it showed an inhibitory effect on the evaluated materials. These results made it possible to formulate a ceramic paste based on the β -TCP / Mg / bioglass system by Design of Experiment (DOE) to obtain 3D printing scaffolds. These ceramic materials show promise as devices in the regeneration of dental tissues.

3:00 PM SB12.02.06

Primers for the Adhesion of Gellan Gum-Based Hydrogels to Cartilage Laura Riacci^{1,2}, Diego Trucco^{1,2,3}, Lorenzo Vannozzi^{1,2}, Leonardo Ricotti^{1,2} and Gina Lisignoli³; ¹Scuola Superiore Sant'Anna, Italy; ²Scuola Superiore Sant'Anna, Italy; ³IRCSS Istituto Ortopedico Rizzoli, Italy

INTRODUCTION A stable adhesion to the cartilage tissue is a crucial requisite for hydrogels used in the fields of cartilage substitution and regeneration. Indeed, the presence of a weak interface between the cartilage and the implanted material may lead to an early detachment, thus causing the failure of the cartilage repair or regeneration process [1]. Using an adhesive primer, namely a coating applied to the cartilage surface to promote the adhesion of materials, may overcome such an issue. Different primers (fibrin glue (FG) [2], cellulose nanofibers (CNF) [3] and catecholamines (CAT) [4]) have been proposed in the state-of-the-art. However, no studies have systematically compared their performance. This study aims at evaluating the adhesion strength between the cartilage tissue and gellan gum (GG)-based hydrogels, crosslinked using ions or, after methacrylation, through a light source.

METHODS GG was dissolved in d-H₂O at 2 % w/v by stirring for 1 h at 37°C, while gellan gum methacrylate (GGMA) was dissolved in PBS at 2 % w/v for 1 h at 37 °C. Then, ruthenium (Ru) and sodium persulfate (SPS) were added to GGMA at a concentration of 0.2 and 2 mM, respectively.

FG was deposited evaluating different waiting times before hydrogel deposition, namely 30 s, 5 min, 15 min and, 30 min. CNFs, dispersed in d-H₂O, were added to GG and GGMA at two concentrations (0.1 and 0.5% w/v) to form a CNF-based primer to be added before GG and GGMA. CAT-modified gelatin was dissolved in a Tris-buffered saline buffer at two concentrations (100 and 125 mg/mL). Then, the solutions were mixed with 1 mM Ru and 20 mM SPS and then crosslinked through a white LED for 30 s.

Before performing adhesion tests, GG or GGMA were cast on each primer and crosslinked for 10 min with MgCl₂ (1 % w/v in d-H₂O) (GG) or with the LED light (GGMA).

To evaluate the adhesion strength, two cartilage-hosting parts were used to block bovine cartilage samples and a top hydrogel-hosting part allowed pouring the primer and the hydrogel solution onto the cartilage. A traction test was performed through an Instron machine.

RESULTS Results showed that the photo-crosslinked GGMA showed higher adhesion strength than GG in absence of primers. However, the adhesion strength of both GG and GGMA improved in the presence of FG with respect to the control. In particular, the waiting times of 5 min for GGMA (9.80 ± 3.03 kPa for GGMA) and 15 min for both the hydrogels (12.64 ± 0.87 kPa for GG and 10.99 ± 3.14 kPa for GGMA) guaranteed to match the clinical goal (10 kPa) [5]. The adhesion strength using CNFs and GG hydrogels reached a value of 12.13 ± 4.69 kPa (clinically acceptable) in the case of 0.1 % w/v CNFs, while the strength was smaller for the higher concentration of CNFs.

The adhesion strengths obtained with the CAT-based gelatin for GG increased from 6.16 ± 1.87 kPa (100 mg/mL) to 8.85 ± 2.40 kPa (125 mg/mL) and for GGMA from 2.93 ± 1.52 kPa (100 mg/mL) to 8.06 ± 1.38 kPa (125 mg/mL), without reaching the clinically acceptable value.

CONCLUSIONS We found that the use of primers can guarantee an increased adhesion of GG-based hydrogels onto the cartilage. In the case of FG primer the best condition was represented by a waiting time of 15 min between primer pouring and subsequent hydrogel deposition on the cartilage, in all cases. In the case of embedded CNFs, the fiber concentration of 0.1 % w/v considerably increased the adhesion strength of GG and GGMA hydrogels. The CAT-modified gelatin layer was less effective in promoting the adhesion between the hydrogels and the cartilage.

ACKNOWLEDGMENTS This work received funding from the European Union's Horizon 2020 research and innovation program, grant agreement No 814413, project ADMAIORA.

REFERENCES [1] L. Zhang *et al.*, *Crit. Rev. Biomed. Eng.*, 2009

[2] F. Scognamiglio *et al.*, 2016

[3] P. Karami *et al.*, 2018

[4] Y. Liu *et al.*, *Colloids Surfaces B Biointerfaces*, 2018

[5] D. A. Wang *et al.*, *Nat. Mater.*, 2007

3:15 PM BREAK

SESSION SB12.03: Cellular Approaches for Regenerative Engineering I

Session Chair: Natesh Parashurama

Tuesday Afternoon, November 30, 2021

Sheraton, 2nd Floor, Back Bay D

4:00 PM SB12.03.01

Gradual and Distributed Exchange of Cryoprotective Agents with Hydrogel Beads Protects Cells from Osmotic Damage Derin Sevenler^{1,2}, Hailey Bean¹, Mehmet Toner^{1,2} and Rebecca D. Sandlin^{1,2}; ¹Massachusetts General Hospital, United States; ²Harvard University, United States

Cryopreservation of patient immune cells is an essential step in the scaled-up production of cell therapies such as stem cell and T cell therapies. Despite the rapidly expanding importance of cryopreservation for cell therapy, clinical best practices remain inadequate, unreliable, and harmful to patients. Cell recovery remains a critical problem: insufficient T cell yield results in manufacturing failure rates of chimeric antigen receptor T cell therapy (for 13%-20% of patients in recent trials). Also, the co-injection of approx. 10 mL of dimethyl sulfoxide (Me2SO) along with thawed cell therapy product is widely acknowledged to be responsible for the nausea and vomiting experienced by up to 60% of patients and is implicated in sometimes life-threatening neurological complications. Regrettably, this exposure is medically unnecessary and only permitted due to the unacceptably low and unreliable recovery rate of exchanging the cryo media with centrifugal cell washing at the point of care (for hematopoietic stem cells, 60% on average). A central challenge is that cryoprotective agents must be diluted gradually (i.e. over the course of several minutes) to prevent hypotonic shock and cell lysis.

We have recently developed a technology to gradually exchange cryoprotective agents (CPAs) from cell suspensions in a distributed manner based on hydrogel beads. We show that these beads exchange common cell-penetrating cryoprotective agents (CPAs)—glycerol and dimethyl sulfoxide (DMSO)—with the surrounding solution at a rate prescribed by the agent's coefficient of diffusion within the gel and bead size.

Calcium alginate hydrogel beads of uniform controlled size (CV 2%) were synthesized by dripping alginate acid into a calcium alginate bath with an adjustable sheath flow of compressed air. Rates of CPA release with the solution were measured by pre-loading the beads with CPA, then gently mixing them with an agent-free solution and measuring the osmolarity of the solution over time. Rates of CPA uptake from solution were measured similarly. Hydrogel beads with volume 25 μ L had an equilibration rate constant of about 1 minute for both uptake and release of glycerol, and about 45 seconds for

DMSO. The rates of CPA exchange were well described by numerical models of diffusion.

We used these uncoated hydrogel beads to mediate glycerol unloading from Jurkat cells (a CD4 T cell line), in a model system of cryoprotective agent-induced hypo-osmotic damage. In this model system, Jurkat cells were loaded with cryo-media containing 15% glycerol, and then unloaded by either immediate dilution in hypotonic phosphate buffer, or by mixing with hypotonic (i.e., glycerol-free) hydrogel beads. The beads gradually diluted the CPA, preventing hypotonic shock and cell lysis. Altogether cell recovery and viability after 4 hours was increased from about 55% (single-step dilution) to about 90% (hydrogel bead mediated dilution).

We further explored the use of polyelectrolyte multilayer films on the beads to allow controllable permeability independent of bead size. Alternating layers of poly(allylamine) and dextran sulfate were adsorbed onto the negatively charged alginate beads, resulting in films which were less permeable to glycerol and DMSO than to water. These semipermeable membranes resulted in the beads acquiring a characteristic shrink-swell behavior when immersed in hypertonic cryoprotective agent solutions, allowing indirect measurement of membrane permeability to both water and the cryoprotective agent by measurement of the bead size over time and fitting with a two-compartment Kedem-Katchalsky formula.

Altogether, the simplicity and control afforded by this system may provide an attractive alternative to centrifugal cell washing for controlled-rate addition and removal of CPAs for large volumes of fragile and precious cell samples.

4:15 PM SB12.03.02

3D Confinement Regulates Cell Life and Death [Oksana Dudaryeva](#) and Mark W. Tibbitt; ETH Zurich, Switzerland

Cell function is influenced by the biochemical and biophysical cues provided by the extracellular matrix (ECM) and neighboring cells. [1,2] To study the role of geometric and mechanical signals from the ECM on cell fate, we developed a single cell culture platform that offers robust control over properties of the individual cell environments. [3] This microwell platform allowed for a decoupled investigation of geometric and mechanical cues. We used our microwell platform to investigate how niche volume and stiffness affect human mesenchymal stem cell (hMSC) function, with an emphasis on the role of 3D confinement. We found that viability and proliferation of hMSCs were affected by confinement of 3D niches compared with unconfined 2D culture. Observed differences in hMSC fate correlated to YAP localization. These results demonstrate that 3D geometric confinement is an important regulator of cell fate.

Single cell niches with controlled geometry and stiffness were patterned on PEG hydrogels through soft lithography. The patterned hydrogels were formed via thiol-ene photopolymerization between norbornene-functionalized star PEG and thiolated linear monomers. The network was functionalized with the RGD adhesion motifs to enable cell attachment. hMSCs were seeded and cultured in the niches, and their fate was assessed using cell viability and proliferation assays. Mechanical activation in hMSCs was assessed using the primary antibody against YAP.

We investigated cell function in three niche volumes: small, intermediate and large (35, 60, and 125 x 10³ μm³); and three stiffnesses: low, medium and high (5, 16, and 30 kPa, respectively). The cells were cultured in the niches for 24 and 72 h and the viability and proliferation rates were quantified. The cells in small niches expressed high death rates that increased with decreasing elastic modulus of the hydrogel; cells expressed maximum viability at high stiffness. The proliferation rate was markedly low in 3D confinement than for 2D controls. Observed differences in hMSC viability and proliferation correlated to YAP localization. hMSCs displayed primarily cytoplasmic YAP localization [Nuclear/Cytoplasmic ratio (N/C) < 1.7], indicating reduced mechanical activation upon confinement.

3D confinement regulated cell function and the effect was influenced by other biophysical parameters of the niche, such as stiffness. We anticipate that our platform, with defined 3D single cell niche arrays, will provide new insights on the role of microenvironmental control of cell fate.

References:

- [1] V. Vogel et al., Nat. Rev. Mol. Cell Biol., 7, 265, (2006).
- [2] M.W. Tibbitt et al., Biotechnol. Bioeng., 103, 655, (2009).
- [3] O.Y. Dudaryeva et al., bioRxiv, (2021). DOI:10.1101/2021.05.02.442094

4:30 PM SB12.03.03

3D Biofabrication of Human Stem Cell Derived Spinal Cord Motor Circuits [Sudeep Joshi](#), Cathleen Hagemann, Kelly O'Toole, Pacharaporn Suklai and Andrea Serio; The Francis Crick Institute and Kings College, United Kingdom

A bioengineered 3D neural tissue construct mimicking the structural and functional characteristics of native neural tissue offers the possibility of recapitulating biological events in-vitro, and acts as a potential tool to understand basic biology and human disease. A major bottleneck in modelling 3D neural tissues in-vitro is to control the interaction between neuronal cells and ECM within these complex 3D arrangements, both across space and time. As a result, several 3D platforms focus on modelling short range circuitry, which makes them less suited to modelling; for example, spinal cord circuitry, where motor axons span vast lengths and interacts with different environments. Recent advancements in 3D bioprinting offer precise control over direct positioning and timing of the cell-ECM interaction, allowing to create better models of these long-range connections.

In the present work, we introduce a biofabrication technique that combines 3D bioprinting, microfabrication, and human induced pluripotent stem cell (hiPSC) populations. This allows us to engineer a functional in-vitro spinal cord like construct capable of modelling physiological motor axons guidance and development. These spinal cord constructs were fabricated via extrusion-based multi-material 3D bioprinting, wherein aggregates of hiPSC-derived motor neuron progenitors (MNP) were precisely positioned within 3D printed hydrogels. The location for placing these MNPs within a bio-compatible hydrogel construct is controlled using a dot-dispensing printing method, both across space (positional arrangement) and time (different timepoints) within one experiment. Mechanical stability of 3D printed neural construct is ensured by printing MNP-laden hydrogels comprising of biodegradable polymers. Moreover, the biofabricated neural tissue construct facilitated diffusion of essential nutrients and oxygen required for cell survival and differentiation. The optimized 3D printable bio-inks facilitated successful neuronal differentiation and axonal elongation throughout hydrogel-based spinal cord construct, and the activity of these 3D neuronal networks is confirmed by physiological spontaneous calcium flux studies.

Future development of these 3D spinal cord constructs is directed towards modelling complex PNS tissue architectures to address clinically relevant approaches for addressing motor neuron diseases and spinal cord defects. Techniques developed in this research work can also be extended for bioprinting other neuronal and glial cells from CNS and PNS with smart hydrogel materials to determine mutualistic interaction between cells in co-culture and ECM matrix. Taken together, our experimental efforts lead towards better control over complex cell/tissue culture environment for understanding the possibility of recapitulating biological events to answer fundamental questions in neural circuit engineering.

4:45 PM SB12.03.04

Fabrication of Tissue-Engineered Oral Mucosa with Micropatterned Fish Scale-Collagen Scaffold Using 3D Printing Technology and Soft Lithography [Kazuma Kishimoto](#)¹, [Orakarn Suebsamarn](#)², [Yoshihiro Kodama](#)³, [Takafumi Komatsu](#)⁴, [Ayako Suzuki](#)⁵, [Shuichi Shoji](#)¹, [Kenji Izumi](#)² and Jun

Mizuno^{1,6}; ¹Waseda University, Japan; ²Niigata University, Japan; ³Taki Chemical Co., Ltd., Japan; ⁴Komatsuseiki Kosakusho Co., Ltd., Japan; ⁵Niigata University Medical and Dental Hospital, Japan; ⁶Suwa University of Science, Japan

In this study, we developed a novel scaffold for oral mucosa tissue regeneration, which is safer and more biomimetic. Fish scale collagen was used as a scaffold to avoid the risk of transmissible infectious diseases for human clinical use. In order to mimic the unique and complex structure that biomedical tissue possesses, a high-precision 3D printing technology was employed to deliver maximized design flexibility. The results showed that 3D printer was capable of manufacturing micro-sized structure with the error rate less than 10% from the original design. The structure from 3D printed mold was transferred to PDMS with soft lithography, and collagen scaffold was fabricated by molding fish scale collagen solution onto PDMS mold. The histological evaluation of the tissue-engineered oral mucosa confirmed the successful formation of the epithelial layer mimicking oral mucosa *in vivo*. This study not only established a method for fabricating a new type of safe scaffold material, but also showed high potential of 3D printing technology as a tool in tissue engineering. By adjusting the structure's geometry with 3D printer, we believe our scaffold derived from tilapia can be applicable in the area of extraoral grafting such as skin as well.

Collagen derived from human or animal tissues have proved to be a success in healing damaged oral mucosa. However, the use of animal-derived collagen is restricted in many countries due to ethical reasons and the risk of transmitting infectious diseases cannot be ignored. Instead, considerable attention has been drawn to fish-derived collagen as a potential material for biomedical applications because the risk of transmitting zoonotic is considerably low compared with animal-derived collagen. The interface area between epithelial layer and connective tissue has a unique three-dimensional undulated structure, also known as the dermal-epidermal interface (DEJ). A lot of studies have shown that mimicking DEJ is crucial in tissue engineering. In our previous study, micro electro mechanical systems technology was used to mimic this structure. However, the result showed a lack of mechanical stability between epithelial layer and connective tissue due to rectangular configuration. We established a technique for fabricating micropatterned fish scale collagen scaffold using 3D printing technology for achieving safety concerns and structural optimization.

The undulated micro-sized structures were manufactured using 3D printing technology. The 3D printed mold was then exposed to UV-ozone irradiation to improve wettability, and mold release agent was coated on its surface. After applying release agent, liquid polydimethylsiloxane (PDMS) was poured directly onto the mold for soft lithography replication. PDMS was specifically chosen for this process because of its biocompatible and gas permeable properties. Soft lithography was again used to fabricate the structures by molding fish scale collagen solution on the PDMS mold. Finally, to create tissue engineered oral mucosa, human oral keratinocytes were seeded on the micropatterned fish scale collagen and cultured for 11 days.

Scanning electron microscopy (SEM) was used to observe 3D printed molds, PDMS molds, and fish scale collagen scaffolds, and optical coordinate measuring machine (μ CMM, Bruker Alicona) was used to determine geometrical measurements of 3D printed molds and PDMS molds. The measurement of the molds' geometries demonstrated high accuracy with the error rate less than 10% from the original design. In addition, SEM images of PDMS molds and fish scale collagen scaffolds showed the structures of the 3D printed molds were successfully replicated. The histological images of the tissue engineered oral mucosa revealed the successful formation of epithelial cell layer along the undulated structures.

SESSION SB12.04: Poster Session I: Biomaterials for Regenerative Engineering

Session Chairs: Gulden Camci-Unal and Natesh Parashurama

Tuesday Afternoon, November 30, 2021

8:00 PM - 10:00 PM

Hynes, Level 1, Hall B

SB12.04.01

Late News: Self-Assembly of Pro-Angiogenic Anti-miRs on Wound Dressings to Promote Diabetic Wound Regeneration Adam G. Berger¹, Michael G. McCoy², Mark W. Feinberg² and Paula Hammond¹; ¹Massachusetts Institute of Technology, United States; ²Brigham and Women's Hospital, United States

Impaired regeneration of damaged skin tissue is a common complication of diabetes, resulting in decreased quality of life and increased mortality. Despite decades of research, few advances have been made in treating these burdensome wounds. Most current treatments do not address the underlying molecular pathophysiological processes, such as impaired angiogenesis. Adequate vascularization is necessary to bring oxygen and nutrients to the healing wound. Non-coding microRNAs (miRNAs or miRs) play a role in regulating the angiogenic state through post-transcriptional modulation of gene expression, and 4 miRNAs - miRNA-26a, -92a, -135a-3p, and -615-5p - have all been implicated in the anti-angiogenic state. One promising approach to promote the regeneration of non-healing wounds is through delivery of miRNA inhibitors (anti-miRs), which block the effects of these anti-angiogenic miRNAs; however, current application of anti-miRs in pre-clinical studies requires numerous intradermal injections of excessive amounts of anti-miR. A packaging and controlled release strategy could enhance the translational potential of this approach. Specifically, we have investigated the coating of wound dressings with electrostatically assembled thin films containing anti-miRs and cationic transfection polymer to enable anti-miR transfection of endothelial cells (ECs). We have demonstrated the emergence of pro-angiogenic phenotypes in a 3D EC spheroid sprouting assay and an EC scratch assay after treatment with each of the 4 anti-miRs delivered using our cationic transfection polymer. Additionally, we have shown the ability to coat woven Tegaderm wound dressings with anti-miRs and to retain the bioactivity of these anti-miRs coated onto wound dressings. Finally, we have begun to explore potential synergies between these pro-angiogenic anti-miRs when dosed in combinations, which could further enhance wound regeneration. Ultimately, this work will enable translational pro-angiogenic anti-miR delivery to promote the regeneration of non-healing diabetic wounds.

SB12.04.02

Late News: The Characterization of SynOss Putty and Its Impact on Dental Pulp Stem Cells Shi Fu¹, Daniel Xie², Mira Rosovsky³, Sabreen Alam⁴, Prabuddha G. Dastidar⁵, Elizabeth Wang⁶, Marcia Simon¹ and Miriam Rafailovich¹; ¹Stony Brook University, United States; ²Panther Creek High School, United States; ³SAR High School, United States; ⁴Portola High School, United States; ⁵North Carolina School of Science and Mathematics, United States; ⁶BASIS Chandler, United States

SynOss Putty is a biocompatible synthetic calcium phosphate mineral matrix with type I collagen derived from bovine Achilles tendon. SynOss has been associated with the clinic use of regeneration of cell tissue in teeth and bones in periodontal, oral and maxillofacial surgery. Previous studies have determined that a more predictable tissue regeneration was found in the majority of samples using SynOss and blood as a scaffold. However, the mechanism of its properties in reconstruction of teeth and bones remains unknown. Analyzing the impact of SynOss on the proliferation of dental pulp stem cells helps to bring insight into the clinical applications of SynOss such as the recovery of dental pulp after dental surgery. The proliferation assay

shows that the dental pulp stem cells treated with SynOss reduce the cell number initially but have a higher growth rate compare to the control group. This leads to the belief that the SynOss material promotes the proliferation of the cells.

SynOss was then measured using the XRF to decide the elemental content. The spectra from the XRF shows that there is a large quantity of calcium and phosphate which provides a ratio of 2.5 +/- 0.011, higher to that of bones which has a ratio of 2.2. This would help with the mineralization since it has a similar ratio and therefore would provide similar properties to bones. And traces of cadmium and tungsten were also found in the material which may help to explain why the cells with SynOss treatment have lower cell counts than the control group in the day 0 of proliferation. Cadmium and tungsten have properties that are carcinogenic which proves to be detrimental to the survival of the cells. To analyze genetic expression of the dental pulp stem cells with SynOss Putty, a 28-day reverse transcription polymerase chain reaction (RT-PCR) test was performed for the 3 groups: control, SynOss treated and SynOss with fibrin. The cells were lysed and RNA were collected on day-0, day-14, day-21 and day-28.

An acellular test is undergoing with different conditions are made to check the mineralization of SynOss. The conditions are: deionized(DI) water, phosphate buffered saline(PBS), PBS with fibrinogen, osteogenic differentiation medium, osteogenic differentiation medium with fibrinogen, osteogenic differentiation medium with fibrinogen and thrombin to simulate the environment of blood.

Future works will include the Raman spectroscopy test to analyze the chemical structure and morphology of SynOss Putty and the impact of SynOss with different amount on metabolic status of dental pulp stem cells .

SB12.04.03

Late News: The Impact of TiO₂ on the Network Mechanics of HUVECs Shi Fu¹, Elizabeth Wang², Sabreen Alam³, Prabuddha G. Dastidar⁴, Daniel Xie⁵, Mira Rosovsky⁶, Marcia Simon¹ and Miriam Rafailovich¹; ¹Stony Brook University, United States; ²BASIS Chandler, United States; ³Portola High School, United States; ⁴North Carolina School of Science and Mathematics, United States; ⁵Panther Creek High School, United States; ⁶SAR High School, United States

Titanium dioxide(TiO₂) is commonly used in consumer applications such as cosmetics, electronics, and sunscreen. Previous studies have determined that in combination with UV light, titanium dioxide has the capability of killing bacteria and microorganisms Given that endothelial cells aid in angiogenesis which provides nutrients and oxygen to newly formed tissue, evaluating the effect of titanium dioxide on endothelial cells could help to realize the impact on the healing factor in humans. In this study, we aim to investigate the effect of TiO₂ nanoparticles on network formation of endothelial cells. Two types of TiO₂ were used to test the effect of TiO₂ on cellular network formation and cell migration of endothelial cells: regular rutile TiO₂ and lecithin coated rutile TiO₂ to reduce the toxicity. Human Umbilical Vein Endothelial Cells (HUVECs) were treated with rutile TiO₂ and lecithin-coated rutile respectively in a concentration of 0.1mg/mL for 24 hours. The angiogenesis tube formation assay on Matrigel was performed for 16 hours. Timelapses spanning the whole process with time interval of 10 minutes were taken for the both treatment group, along with the control group. Cell migration speed and network quantification by total length of branches and number of nodes were analyzed.

Our assumption was that, TiO₂ nanoparticles may cause tangling of actin fibers, making it difficult for cells to stretch out, make connections and create tubes. However, the results from the network quantification indicate that rutile had significantly more network formation than the lecithin-coated rutile and control at all hours. Next was the lecithin-coated rutile with control having the least amount of networks. This data suggests that TiO₂ might be a pro-angiogenic factor as treating the cells with rutile and lecithin-coated rutile, both containing TiO₂ nanoparticles, resulted in more network formation than the control group. It is very likely that TiO₂ increase the cholesterol level of HUVECs, will in turn soften HUVECs and make the cells easier to migrate and reach out. Future tests will re-run the experiment to make sure that TiO₂ is a pro-angiogenic factor, and have cholesterol test and further investigation of HUVECs' metabolic status under the impact of TiO₂.

SB12.04.04

Late News: Analyzing the Toxicity of Titanium Dioxide and Zinc Oxide on HUVECs and Evaluating the Antibacterial Properties of Titanium Dioxide Shi Fu¹, Daniel Xie², Prabuddha G. Dastidar³, Elizabeth Wang⁴, Sabreen Alam⁵, Mira Rosovsky⁶, Marcia Simon¹ and Miriam Rafailovich¹; ¹Stony Brook University, United States; ²Panther Creek High School, United States; ³North Carolina School of Science and Mathematics, United States; ⁴BASIS Chandler, United States; ⁵Portola High School, United States; ⁶SAR High School, United States

In this study, we aimed to investigate the effect of varying concentrations of titanium dioxide(TiO₂) on the viability of Human Umbilical Vein Endothelial Cells (HUVECs). HUVECs were plated in a 24-well plate. Triplicates were made respectively with Rutile TiO₂ treatment, Lecithin-coated Rutile TiO₂ treatment, and a control group with no treatment was used for comparison. The cells were treated with 4 different concentrations: 0.05 mg/ml, 0.1 mg/ml, 0.2 mg/ml, and 0.4 mg/ml. Afterwards, the cells were left in the incubator at a temperature of 37 °C with 5% CO₂ and 80% humidity for 24 hours. From the test results, 0.05mg/mL has no impact compare to the control group since the concentration is too small. For the other concentrations, the impact of TiO₂ start to become effective at 0.1mg/mL, a decrease in the cell count can be seen as the concentration increases for both treatments. This demonstrates that titanium dioxide nanoparticles inhibit the growth and proliferation of the HUVEC cells to a certain extend.

To test TiO₂'s antibacterial properties, after 24 hours treatment of 0.1 mg/mL rutile TiO₂ and 0.1 mg/mL lecithin-coated rutile TiO₂, along with control group, HUVECs were then infected with Staphylococcus aureus bacteria for another 24 hours in order to determine TiO₂'s effect on the infection. The alive and dead cells and bacteria for the bacteria infection test were analyzed, the results shows that live bacteria per cell for the control is greater than that of the rutile TiO₂ test which shows that TiO₂ may have antibacterial properties.

Future tests will look at the impact of TiO₂ nanoparticles on the doubling time of HUVEC cells, as well as study the cell modulus by atomic force microscope(AFM) to gain further insight on the impact that TiO₂ has on cell survival and proliferation.

SB12.04.05

Late News: Localized Delivery of siRNA from Biodegradable Wound Dressings via Layer-by-Layer Assembly Mariss Haddad, Adam G. Berger and Paula Hammond; Massachusetts Institute of Technology, United States

The delivery of therapeutic short interfering RNA (siRNA) directly into a localized area holds significant potential for the treatment of non-healing, cancerous, and other difficult-to-treat lesions. siRNA has the ability to downregulate genes that may be overexpressed in these disease states; however, its delivery is challenged by the need to enter the cell for bioactivity and its degradation by nucleases. Previously, we have shown that siRNA can be coated onto a non-degradable wound dressing using Layer-by-Layer (LbL) assembly, which creates a thin polyelectrolyte film that directly incorporates siRNA and cationic polymer to aid transfection into cells. We have noted that removal of these dressings upon termination of lesion treatment can lead to destruction of the underlying tissue. Biodegradable scaffolds circumvent the need to remove the dressing and thus the associated local tissue damage. Films containing poly(β-aminoester) (Poly2), siRNA, and other polymer excipients were assembled on Endoform™, a biodegradable dressing comprised of reconstituted ECM and collagen. We show that biodegradable scaffolds can be coated with a thin polyelectrolyte film using LbL technology at an average loading 3.7 times greater than the loading on non-biodegradable scaffolds per layer, depending on assembly and substrate conditions. We have also characterized the coating of Endoform™ with siRNA using surface measurement techniques. Finally, we have demonstrated that fluorescently labeled siRNA released from coated Endoform™ dressings can be taken up by mammalian cells and have begun investigating the bioactivity of delivered siRNA from Endoform™ films. Ultimately, this work will enhance the localized delivery of therapeutic siRNAs to localized lesions while preventing damage to the surrounding tissue caused by dressing removal.

SB12.04.07

Polyvinyl Alcohol/ Graphene Oxide/ Polypyrrole Nanocomposites for Applications in Wound Healing [Shamrock Barrera](#), Ky Duyen Le, Chizimuzo Chibuko and Isaac Macwan; Fairfield University, United States

Graphene oxide (GO), an oxidized form of graphene, a carbon allotrope, is a very attractive nanomaterial with potential biomedical applications in tissue engineering owing to its electrochemical activity. However, it lacks the ability to form freestanding films that can actively function as an electrochemical substrate. To work around its inability to do so, different methods have been reported such as annealing, ultrafiltration, electrophoresis, and mid-infrared polarizers. Two of the popular techniques to synthesize free standing films are electrospinning and electropolymerization through cyclic voltammetry (CV). In recent years nanofibrous substrates have found unique applications in the field of biomedical engineering, especially in wound healing. Nanofibrous films are ideal for preventing bacterial contamination in open wounds and in conjunction with viable materials can serve as biocompatible skins for wound dressings. These films can also be coated or mixed with different antibacterial topical medications that can aid in further protection from infections. Similarly, CV is a popular electrochemical technique that is utilized to investigate the reduction and oxidation processes of a species and to synthesize novel substrates for biomedical applications. This work deals with utilizing these two techniques of electrospinning and CV to synthesize nanocomposite GO films with polyvinyl alcohol (PVA) and polypyrrole (Ppy) polymers acting as scaffolds. PVA, which is a biocompatible, water-soluble, synthetic polymer, is simultaneously electrospun with GO to create a scaffold capable of supporting the GO film. Polypyrrole, which is both chemically and thermally stable and has good biocompatibility both in-vivo and in-vitro, can significantly impact cell adhesion, proliferation and differentiation, as well as tissue regeneration and repair. It is theoretically and experimentally supported that Ppy functionalized GO greatly improves the biocompatibility of GO. First, PVA/GO nanocomposite is electrospun using a 5 wt. % solution of PVA and 0.5mg/ml concentration of GO at 25kV and 0.5 ml/hr flow rate. The obtained GO/PVA nanofibrous film is then used as a substrate for the electropolymerization of pyrrole monomers, thereby forming a PVA/GO/Ppy nanocomposite film. After electropolymerization of pyrrole, the thin films are peeled off to test for impedance using electrochemical impedance spectroscopy (EIS). SEM analysis, together with EIS and CV data agrees well with the molecular understanding of the interactions at the interface of PVA, GO and Ppy from the simulated trajectories. The developed composite improves the mechanical properties of tissue engineering scaffolds and is anticipated to be utilized as a wound dressing material.

SB12.04.08

Micro Patterned Polymer Interfaces for Muscular Cells Alignment and Stimulation [Vito Vurro](#)¹, Alberto Scaccabarozzi¹, Francesco Lodola², Filippo Storti^{3,1}, Fabio Marangi^{1,3}, Aaron M. Ross³, Giuseppe M. Paternò¹, Francesco Scotognella^{3,1}, Luigino Criante¹, Mario Caironi¹ and Guglielmo Lanzani^{1,3}; ¹Istituto Italiano di Tecnologia, Italy; ²Università degli Studi di Milano-Bicocca, Italy; ³Politecnico di Milano, Italy

By and large the research on human machine interface is constantly attracted by the idea to act in a contactless and wireless way. In particular biological and medical areas can benefit from optical method for introducing innovative ways to probe and stimulate the biological matter. Conjugated molecules and polymers offers a promising platform to interface with cells and living organisms thanks to their high optical absorption/emission cross section, chemical synthesis' easiness and relatively low toxicity.

In this work, we developed a simple and fast method to fabricate and a micro-machining technique to pattern an interface with a double functionality made possible by the blend of photoactive poly(3-hexylthiophene) and polyethylene. The pattern on the surface of the film is designed to mimic the physiological condition and to help living cells to organize in a tissue. At the same time, the active component is able to transduce light into a stimulus for excitable cells. The mechanical properties and easiness of process are due to the presence of polyethylene while the optoelectronic properties are given by the poly(3-hexylthiophene).

We demonstrate that the obtained scaffold combines the capability to align with that to photostimulate living cells. The ultimate goal of this project is to produce an artificial tissue for future applications in the robotic, pharmacological and regenerative medicine fields.

SB12.04.09

Mechanical Properties, Translucency and Low-Temperature Degradation (LTD) of Ytria (3–6 mol%) Stabilized Zirconia [Sharon Uwanyuze](#)¹, Sulekha Ramesh², Mark King³, Nathaniel Lawson³ and Manoj Mahapatra³; ¹University of Connecticut, United States; ²Bob Jones School, United States; ³The University of Alabama at Birmingham, United States

The market share of zirconia as metal-free dental restoratives continues to grow globally, especially 3 mol% Y₂O₃ stabilized tetragonal zirconia (3YZ). However, premature failure of zirconia femoral heads and subsequent recall of hip implants by the manufacturers in 2001, triggered concern on whether zirconia dental prosthesis could incur similar failure. Here, we investigate the mechanical properties (hardness and biaxial flexural strength), optical properties (translucency and gloss), and low-temperature degradation (LTD) of 3–6 mol% yttria-stabilized zirconia. The specimens were prepared by conventional solid-state sintering at 1400 °C. The mechanical and optical properties were evaluated for sintered and polished specimens. X-ray diffractometer (XRD) and scanning electron microscope (SEM) were used, respectively, for structural and microstructural investigation. LTD was determined by XRD analysis of the samples aged in a hydrothermal autoclave at 134 °C for 5–108 h. We found the mechanical and optical properties are found to be microstructure sensitive, and the LTD due to tetragonal to monoclinic phase transformation decreased with increasing Y₂O₃ content. The mechanical strength, translucency, and LTD were lowest for 6 mol% Y₂O₃ stabilized zirconia.

SB12.04.10

3D Printing of Silk-Bioceramic Nanocomposites for the Regeneration of Innervated and Vascularized Bone Tissue [Vincent Fitzpatrick](#), Zaira Martin Moldes, Anna Deck, Ruben Torres-Sanchez, Chunmei Li and David L. Kaplan; Tufts University, United States

Bone is a dynamic, innervated and vascularized tissue with the inherent ability to regenerate after injury. Nevertheless, non-union fractures remain a major issue in orthopedic surgery. Autografts and allografts are the gold standard for repair but can be associated to donor site morbidity, donor material availability, and increased operative times. Alternative biomaterial-based solutions are promising, including synthetic bone fillers. However, these fillers do not allow refined control of graft geometry, and seldom offer adequate porosity for rapid cell colonization, efficient nutrient exchange, or implant degradation. Further, these approaches usually do not actively promote bone growth, nor account for the complexity of bone, and in particular the neurovascular network.

We developed a silk-ceramic bioink to 3D print porous constructs for bone regeneration. The resulting material was mechanically close to bone, promoting osseointegration. These structures were biocompatible, their shape well-controlled even for complex geometries, and their porosity could be precisely tuned for efficient osteogenesis.

Our constructs supported osteoblastic differentiation in vitro, and a rapid cell response and efficient neosteogenesis when combined with osteoinductive factors (BMP-2). We further loaded this bioink with angiogenic and neurotrophic morphogens (VEGF and NGF), and precisely patterned these biomolecules, promoting the migration, organization and differentiation of human umbilical vein endothelial cells and human induced neural stem cells,

respectively. Coculture conditions showed that the multiple morphogens and cell types promoted the osteogenic differentiation of human mesenchymal stem cells.

Finally, our bioink could be loaded with antibiotics, providing an encouraging solution for the prophylactic treatment of osteomyelitis in non-union fractures.

SB12.04.11

Porous Collagen-Based Matrices for Embedded Bioprinting Daniel Reynolds, Irene de Lazaro, David Mooney and Jennifer Lewis; Harvard University, United States

Embedded bioprinting can recreate the complexity of the *in vivo* microenvironment by spatially patterning multiple cell types and perfusable vasculature within biological matrices. However, most biological inks and matrices that permit cell growth, spreading, and migration exhibit a narrow “printing window”. Here, we report a new class of porous, printable biological matrices for creating 3D vascularized human tissues and tumor models. These matrices contain sacrificial microparticles that both broaden the printing window and generate microporosity upon their removal after printing. We have demonstrated that this porous collagen-based matrix enables the embedded printing of a murine melanoma cell ink in the form of a 3D tumor model. Confocal microscopy reveals that the resulting collagen network is fibrillar, an important *in vivo* feature of collagen type I. Importantly, we find that melanoma cells readily spread and proliferate, and that effector T cells migrate within this collagen-based matrix. Our biofabrication platform enables the formation of a 3D microenvironment that is conducive to cell growth, spreading, and migration – key cellular processes involved in anti-tumor immunity.

SB12.04.12

Actin Cytoskeletal Structure and the Statistical Variations of the Mechanical Properties of Non-Tumorigenic Breast and Triple-Negative Breast Cancer Cells Killian C. Onwudiwe^{1,2}, Jingjie Hu², Vanessa Uzonwanne², Toyin Aina¹, Josephine C. Oparah¹ and John Obayemi²; ¹African University of Science and Technology, Nigeria; ²Princeton University, United States

This paper explores the actin cytoskeletal structures and the statistical variations in the actin fluorescence intensities and viscoelastic properties of non-tumorigenic breast cells and triple-negative breast cancer cells at different stages of metastases. The actin contents of the cell cytoskeletal structures are shown to decrease significantly with cell progression from non-tumorigenic to more metastatic states. The corresponding viscoelastic properties of the nuclei and the cytoplasm (Young’s moduli, viscosities, and relaxation times) of the cells are also measured using Digital Image Correlation (DIC) and shear assay techniques. These are shown to exhibit statistical variations that are well characterized by normal distributions. The changes in the mean properties of individual cancer cells are tested using Fisher pairwise comparisons and the analysis of variance (ANOVA). The probabilistic implications of the results are then discussed for the development of shear assay techniques and mechanical biomarkers for the detection of triple-negative breast cancer at different stages of progression.

SB12.04.13

Green-Mediated Approaches in the Design of Prostate Cancer Targeted Drug Delivery System—Investigation of Underexplored Prostate Tumor-Specific Biomarkers Using Immunohistochemical Approach Josephine C. Oparah^{1,2,3}, Toyin Aina^{1,3}, Killian C. Onwudiwe^{1,3}, Chukwudi Ezeala^{1,3}, Theresa Ezenwafor^{1,2}, John Obayemi³ and Winston W. Soboyejo^{1,3,3}; ¹African University of Science and Technology, Nigeria; ²National Biosafety Management Agency, Nigeria; ³Worcester Polytechnic Institute, United States

This paper presents results using immunohistochemical techniques for prostate cancer tumor characterization in males of African ancestry using Nigeria as a case study. 100 paraffin-embedded prostate tissues blocks were collected from the tissue repository of National Hospital Abuja, following ethical approval from the Institutional Review Board. Hematoxylin and Eosin staining were carried out to determine tissues with suitable characteristics for inclusion in the study. Benign prostate Hyperplasia tissues were used as control while prostatic adenocarcinomas were studied to identify underexplored biomarkers of interest as drug targets. The tissues were stained with tissue-specific proteins to determine over-expression of selected biomarkers; an investigation as to its use as targeted drug therapy. Comparative analysis of tumour biomarkers were carried out using statistical tools to determine the optimal choice of tissue specific proteins. The results reveal significant differences in the individual intensities that predispose different proteins as tumor specific biomarkers for targeted drug delivery.

SB12.04.14

Synthesis of Nano-Biomaterial and the Study of the Kinetics of Localized Cancer Drug Release from Silica Based Nanoparticles Toyin Aina^{1,2}, Josephine C. Oparah^{1,2}, Killian C. Onwudiwe^{1,2}, Chukwudi Ezeala^{1,2}, John Obayemi¹, Ali Salifu¹ and Winston W. Soboyejo¹; ¹Worcester Polytechnic Institute, United States; ²African University of Science and Technology, Nigeria

This paper presents the synthesis of inorganic mesoporous silica nanobiomaterial functionalized with a boronic group and capped with a polymer. The functionalized duo were then characterized and thereafter loaded with cancer drug (doxorubicin). The kinetics study was carried out using the Zero, First, second order, Higuchi and Korsmeyer and Peppas model in different buffers of pH ranging from 5.00 to 7.40. The drug release profile reveals anomalous transport from nanoparticle and supper case II transport from the polymer capped nanoparticle. The release exponent, *n*, of the silica nanoparticles were found and the diffusion coefficients were also obtained. The suitable phases along the drug release profile was explored in administering the drug loaded silica nanoparticles to act as a drug delivery cargo. Computational models using Comsol multiphysics was carried out to reveal the flux of the doxorubicin from the mesoporous silica nanoparticles. The nanoparticle was characterised using SEM, FTIR, TGA and TEM analysis and the diffusion coefficient. Further test would be carried out to reveal the effect of the nanobiomaterial to inhibit the growth of a prostate cancer cell.

SB12.04.15

High-Plex Profiling Reveals Implants to Drive Spatiotemporal Protein Production and Innate Immune Activation for Tissue Repair Prajan Divakar^{1,2}, Jason Reeves², Jingjing Gong², Fred W. Kolling IV¹, P. Jack Hoopes^{1,1} and Ulrike G. Wegst^{1,3}; ¹Dartmouth College, United States; ²NanoString Technologies, Inc., United States; ³Northeastern University, United States

While reducing foreign body capsule formation and increasing regenerative infiltration are central goals in the development of implants, there is surprisingly little clarity as to the effects of biomaterial properties on spatially localized protein expression, which drives implant success. Desired is that wound healing and tissue regeneration are optimally supported by the implant, adsorbed proteins, innate and adaptive immune cells, and fibroblasts. Cells play a central role in repair and functional recovery through the production and regulation of proteins. It is not fully understood, however, how an implant differentially drives the spatial quantity of individual proteins both in the interior of the implant and in the exterior tissue surrounding it. Here we apply GeoMx® digital spatial profiling to site-specifically investigate protein production in porous implants. Data is collected on the location and quantity of 40+ proteins from formalin-fixed, paraffin-embedded tissue slides of anisotropic tissue scaffolds (n=18) with differing pore sizes (35 µm, 53 µm) and implantation durations (2, 14, 28 days). In parallel, matched bulk high-plex gene expression data (700+ genes) was collected for the identical implant

samples. Notably, we discover fundamental spatial relationships in protein localization in the interior and exterior of implants that are uniquely independent or dependent of implant microstructure. In particular, dendritic cell marker CD11c and fibronectin significantly dominate the scaffold interior of the scaffolds, while cell-to-cell adhesion marker CD34 and anti-inflammatory M2 polarization marker CD163 localize in the scaffold exterior. Lastly, collating spatial and bulk information, we report unique spatiotemporal expression patterns for markers such as fibronectin that were otherwise hidden in differential bulk expression analyses and only uncoverable through spatial profiling. Together, these discoveries motivate the critical importance of quantifying and discovering spatial expression patterns for implants, facilitating a paradigm shift in the iterative design, mechanistic understanding, and rapid assessment of biomaterials.

SB12.04.16

Ultra-High Throughput On-Chip Synthesis of Microgels with Tunable Mechanical Properties Jingyu Wu, Sagar Yadavali, David Issadore and Daeyeon Lee; University of Pennsylvania, United States

Hydrogel particles (microgels) generated using microfluidic methods have superb properties such as high size uniformity and precise control over degradation and release profiles, making them useful for applications in wound healing and injectable drug delivery. However, the throughput of microfluidics is constrained by the physics governing the flow of immiscible fluids confined within microchannels. This throughput tends to be several orders of magnitude lower than what would be necessary for commercial and clinical applications. Here, we demonstrate the scaling up of on-chip synthesis of microgels by parallelizing the microfluidic channels. Taking advantage of the established fabrication technologies developed by the semiconductor industry and a high flow control system, a 4-inch silicon microfluidic chip integrating more than 4,000 microfluidic devices is developed. By incorporating a high energy flood UV source, this chip allows the synthesis of poly (ethylene glycol) diacrylate microgel particles with diameter down to 30 μm at a throughput above 1kg/hr. By using photomasks that enable milli-second scale control of the UV exposure, the stiffness of microgels can be varied between 10^3 to 10^4 Pa. Large-scale production of microgels will enable construction of large-scale tissue scaffold with well-defined physicochemical properties, and will provide scalability for translation to clinical settings.

SB12.04.17

Effect of Surface Modification on Cell Adhesion and Tissue Growth Przemyslaw Kurtyka^{1,2,3}, Roman Major¹, Roman Kustosz², Justyna Wiecek¹, Amanda Bartkowiak¹, Karolina Janiczak², Aniel Grajoszek⁴ and Kamil Jozsko³; ¹Polish Academy of Sciences, Poland; ²Foundation of Cardiac Surgery Development, Poland; ³Silesian University of Technology, Poland; ⁴Medical University of Silesia, Poland

Introduction Recently, the number of patients with heart failure has been increasing. When pharmacological treatment does not bring the expected effects, there may be a need for mechanical circulatory support (MCS). One possible solution is to use blood pumps such as Ventricular Assist Devices (VAD). These devices are nowadays widely used as an effective treatment for patients with advanced heart failure and are the only alternative to heart transplantation. Over the years many new devices were introduced to the clinic. However, based on clinical experience, despite undeniable evidences of VAD effectiveness, many components could still be improved. The ongoing optimization performed by many producers does not concern only improvements in terms of their function, but also in terms of patient comfort and reduced mortality. According to the information provided by INTERMACS, patient survival drops to 50% after four years of support. However, the VADs, are designed to be wear-resistant and in some cases are used as a destination therapy. It is therefore important to further improve the devices biocompatibility in order to reduce the occurrence of complications. One of possible complications may be the pump thrombosis and inflow obstruction, caused by the ingrowth of tissue into the lumen of inflow cannula. According to reports from clinics and literature it seems that the solution to this problem may be the use of surface modification. Appropriate topography allows for controlled scar tissue formation, which results in reduction of inflammatory processes and appearance of thromboembolic events.

Materials and Methods The paper presents surface modification performed using vacuum sintering intended for use in an VAD inflow cannula. The study presents an analysis of the relationship between surface parameters on the susceptibility of cells to proliferate and the strength of their adhesion to the implant. Samples were prepared from titanium alloy Ti6Al7Nb in form of cylinders $\varnothing 14\text{mm} \times H 3\text{mm}$. During the initial research the base material was verified for compliance with the standard including the microstructure study, the chemical composition analysis and the study of mechanical properties. Then samples were subjected to tumbling before performing modification. Roughness was measured with the use of contact profilometry and was characterised by $Ra=1.5\mu\text{m}$ and $Rz=12.5\mu\text{m}$. The sintering process included modifications with the use of Commercially Pure Titanium (Cp-Ti) powder with two different grain morphologies - spherical and irregular. The grain size was changed in range of 50 to 250 μm . The obtained surfaces were then analysed by scanning electron microscope [SEM]. Additionally the porosity of obtained surfaces was determined. All samples revealed high roughness with the potential for cell anchoring and scar tissue formation. Fibroblasts were then applied to the samples for three periods of time. The number of cells was assessed on the basis of the stained cell nuclei and the presence of adhesive molecules. In addition, *in vivo* studies were performed in which samples were implanted into the dorsal muscle of New Zealand rabbits. After 4 and 8 weeks, the specimens were deplanted and the force of detachment of formed tissue from the implant surface was tested.

Results and Discussion The results have shown that surface after powder sintering is characterized by high porosity and complex 3D morphology. The obtained roughness was in range $Ra=21-36\mu\text{m}$. The porosity was in range 27-49% depending on the size and shape of the powder grains. The detachment force differed by 0.5N depending on the shape of used powder grains.

Conclusions The presented modification has the potential to anchor cells and form controlled scar tissue on the surface of the implant, both in the context of cardiac and other medical implants.

Acknowledgments Project supported by:
NCBiR: RH-ROT/266798/STRATEGMED-II
National Science Centre, Poland: 2018/31/N/ST8/01085

SB12.04.18

E-Sutures—Electrical and Ionic Conducting Sutures for Medicine and Bioelectronics Onni Rauhala and Dion Khodagholy; Columbia University, United States

Although advances in wireless signal acquisition systems have reduced the invasiveness of many implantable medical and research devices, wire-based systems continue to be necessary for applications directed at treating or analyzing certain areas of the body that are incompatible with wireless device use or conventional surgical approaches. Traditional metal wires provide the high conductivity that is needed for *in vivo* electrophysiological signal transmission. However, due to their rigidity, metal based wires are susceptible to mechanical damage and discomfort to the subject. The ideal bioelectronic wire is thus both highly conducting as well as mechanically and chemically similar to live tissue. In this work, we transform surgical sutures into conducting and biocompatible wires (e-sutures) that can be concomitantly used for wound suturing, electrophysiological signal acquisition, transmission, and power delivery. We use a solution of the conducting polymer PEDOT:PSS together with solvents and a cross-linking agent to coat surgical sutures and make them electrically conductive. Our coating method increases the e-suture conductivity such that we can record ECG and EMG data from rodents, as well as stimulate muscles and evoke movements. We evaluate additional methods to further increase the conductivity of the e-suture such as acid treatment and nanolayer metal deposition. We develop an insulating layer (wire jacket) for the e-suture using a combination of parylene-C, polyurethane and silicone elastomer and characterize its electrical properties over time in an *in vivo* environment using electrochemical impedance spectroscopy. The resulting e-

suture is highly conductive, electrochemically stable and biocompatible. The high yield and ease of creating e-sutures combined with the widespread use of sutures in medicine suggests high translational potential to a broad range of medical procedures that require surgical intervention and monitoring or electrical modulation of tissue.

SESSION SB12.05: Scaffolds for Regenerative Engineering I
Session Chair: Gulden Camci-Unal
Wednesday Morning, December 1, 2021
Sheraton, 2nd Floor, Back Bay D

10:30 AM SB12.05.01

Development of Tissue Engineered Bioelectronic Implants for Integrating with the Brain [Alexander J. Boys](#), Alejandro Carnicer Lombarte, Damiano G. Barone, Christopher M. Proctor, George G. Malliaras and Roisin Owens; University of Cambridge, United Kingdom

Stable, long-term interfaces between implanted devices and the brain remain a challenge. Properly interfaced neural implants provide the potential for recording brain activity, enabling the generation of neurally-driven prosthetics, treatment of neuroses, and a deeper understanding of brain function, among other applications. One of the major issues inhibiting long-term recordings of the brain is the lack of integration between an implant and surrounding tissue. This lack of integration often results in an inflammatory and subsequent scarring response driven by mechanical mismatches between the probe and adjacent tissue. Tissue engineered implants provide a solution to this problem through their superior integrative capacity *in vivo* but traditionally lack any interactive components. To generate a tissue engineered neural probe, we have combined the recording capabilities of bioelectronic devices with the regenerative capacity of tissue engineered implants to create a new type of device designed for long-term implantation. Here, we discuss the design, development, and testing of a tissue engineered implant with an integrated microscale conducting polymer-based recording system for monitoring in the brain.

We aimed to build a device that contains a series of discrete recording sites within a tissue engineered gel. The active portion of the probe was fabricated to consist of individually articulated electrodes on the scale of single neurons. Implants were microfabricated using photolithographic procedures to produce a flexible bioelectronic recording device. The device consists of gold tracks, insulated with parylene-C, which terminate in exposed pads with poly(ethylene dioxythiophene):poly(styrene sulfonate) (PEDOT:PSS)-based coatings to enhance recording efficacy. To embed these devices in gels, a mold was produced to encompass the entirety of the active portion of the device. Collagen was then injection molded around the device, resulting in a three-dimensional spread of the recording sites within the gel. To test the integrative capacity of these implants, we chose a subcutaneous intramuscular model to examine the ability of tissue to grow between the individual leads. Initially, implants without gels were positioned within the musculature of rats. Rats were sacrificed at days 3, 7, and 14 post-implantation to examine the healing response around the implant. By day 14, tissue was observed growing between the individual leads, and tissue around the probes appeared indistinguishable from tissue elsewhere at the insertion site. This result indicates excellent potential for widespread recording at the implantation site and for integration of these implants into the body.

In this study, we have developed a tissue engineered neural implant to promote integration with surrounding tissue. Our next step will be the implantation of gel-based probes to examine the ability of the tissue engineered probe body to promote tissue ingrowth. Ultimately, we will incorporate cells into these devices and move towards intracortical implantations in the brain. Overall, we have generated a new type of neural implant, utilizing tissue engineering and bioelectronic principles, to enhance regeneration at the implantation site and enable long-term recordings of the nervous system.

10:45 AM SB12.05.02

Antioxidant Microreactors as Supports for HepG2 Cells in 3D Cell Aggregates [Stefan Pendlmayr](#), Xiaomin Qian, Noga Gal and Brigitte Städler; Aarhus University, Denmark

In the field of cell mimicry, bottom-up approaches are explored to resemble cells, organelles and enzymes using both natural and synthetic materials. Micro/Nanoreactors that can perform encapsulated catalysis are popular examples for the former cases. However, the first examples of their integration with mammalian cells only start to emerge. For instance, we recently demonstrated that microreactors loaded with catalase could support HepG2 cells in 3D cell aggregates when stressed with hydrogen peroxide. The artificial moieties did only their task for only up to 24 h because the encapsulated enzyme lost its activity.

Here, we use the superoxide dismutase/catalase mimetic Eukarion (EUK) as the active unit in alginate-based microreactors to alleviate the oxidative pressure in 3D cell aggregates. To this end, we first synthesized an EUK derivative that was water-soluble and could be conjugated to alginate resulting in EUK-Alg. Droplet microfluidics was used to fabricate microreactors with incorporated EUK-Alg. Then, the long-term activity of molecular EUK, EUK-Alg and the microreactors was assessed considering both, the catalase- and superoxide dismutase activity. The microreactors were coated with e.g., poly(L-lysine) or cell membrane vesicles, to facilitate integration in 3D cell aggregates with HepG2 cells. The viability of these bionic tissues was followed over time and the integration of the natural and synthetic units was visualized. Finally, bionic tissues could tolerate higher levels of hydrogen peroxide over longer times compared to pristine HepG2 cell spheroids.

Taken together, we advanced the concept of bionic tissue by illustrating the benefits the integration of the biological and synthetic world could have.

11:00 AM SB12.05.03

Material Defects in the Fetal Membrane's Role in Immunomodulation of pre-Term Premature Rupture of the Membrane (pPROM) [Joshua M. Grolman](#); Technion-Israel Institute of Technology, Israel

Preterm labour, representing nearly 20% of births in the United States, is one of the leading and rising causes of infant mortality and nearly 40% of these cases are linked with preterm premature rupture of membrane (pPROM). Despite this, there are no treatments currently available aside from antibiotics, which do not address the cause of pPROM. This is a life-threatening condition that can sometimes be reversed by spontaneous sealing of the membrane, suggested recently to be mediated by fetal macrophage recruitment and polarization. However, the role in the recruitment and polarization of macrophages of amnion-derived mesenchymal stem cells (MSCs), a major constituent of the most loadbearing part of the fetal membrane, is not well understood. We demonstrate that understanding the mechanics of fetal membranes with regard to rupture and repair can drive secretion of proteins from MSCs. This in turn affects recruitment and programming of macrophages, and as a result, pPROM healing. Collecting patient samples from both full-term and pre-term birth patients, we demonstrate we can make large-scale physical property maps of the amnion such as dynamic rheological maps of Storage and Loss Modulus,

as well as millimeter-scale topographical maps to characterize defects in the fetal membrane. We characterized of both sides of the fetal membrane (chorion and amnion), as the intrinsic mechanical cues and resident mechanosensitive resident cells differed. We found that there were substantial topological differences in the amnion due to embrittlement of the fetal membrane, and the viscoelastic properties varied depending on the delivery mechanism. These viscoelastic properties had significant immunomodulatory effects on resident macrophages, responsible for inflammation and overall remodeling in the fetal membrane during birth.

11:15 AM SB12.05.04

Correlating Rheology and Printability of Silk-Hydroxyapatite-Based Inks for Micro-Prosthetic Applications Mario Milazzo^{1,2}, Vincent Fitzpatrick², Crystal Owens¹, Igor Carraretto¹, Gareth H. McKinley¹, David L. Kaplan² and Markus J. Buehler¹; ¹Massachusetts Institute of Technology, United States; ²Tufts University, United States

Devices for micro-prosthetic applications must maintain a reduced footprint in small implant sites while still repairing or restoring a specific function lost following trauma or pathology. We focus on the prosthetic for the middle ear, for which piston-like struts replace the complex arrangement of bones and soft tissues to recover hearing. The selection of a suitable material for such applications is critical in order to generate devices that meet stringent mechanical and biological requirements. Silk-Hydroxyapatite (S-HA) composites have been extensively used in the biomedical field as materials to replace bone-like structures, due to their mechanical properties, biocompatibility, and fabrication versatility via additive manufacturing. Most current medical applications have employed compositions with high percentages of HA over S, leading to stable constructs that, however, have limited toughness. Our study aimed at unveiling correlations between S-HA compositions, rheology, and printability to improve the final part properties with this composite system, in view of micro-prosthetic applications for which geometrical precision and accuracy play a key role in the final device functions.

Two batches of composite materials with different compositions were prepared and studied. The first consisted of HA microspheres (diameter less than 1 μm) with different contents of water, between 1:1 and 1:2 (w/v). The second was composed of S-HA, using silk extracted for 60 min and concentrated to 15% (w/v). In this case, the ratio of solid/liquid was held constant and values of S and W varied from 1:0.8:0.4 up to a ratio of 1:1:1 (w/v/v). Rheology was performed with a parallel plate geometry to mimic forces exerted during printing. In particular, we evaluated the elastic (G') and viscous (G'') moduli across strain to find the main mechanical parameters (yield stress and strain) of the inks. We further monitored the evolution of moduli in a recovery step after the strain was removed. The same inks were printed with a displacement-driven 3D extrusion printer and printed parts were imaged and analyzed to quantify feature fidelity.

The results showed a reduction of elastic properties of the inks with increased water content. The HA showed values of G' above those having S in the composition, up to three orders of magnitude. Yield stresses were also higher, with associated strains two orders of magnitude lower than those of the S-HA composites. This difference highlights the higher toughness for the HA-S composite inks, an important factor for customizations of the constructs. All inks showed a recovery over time for the main viscoelastic parameters (G' , G''), resulting in a stable solid-like behavior when the solid/liquid ratio was below 1:2 (w/v).

Linking rheology and printability, we observed a direct relationship between the main rheology outcomes and the geometric quality of the constructs. Specifically, high printability with high yield stress independently of the concentration of S was observed. Moreover, increasing the concentration of S reduced the elastic moduli of the inks, making them more extrudable through fine nozzles at achievable pressures. In addition, while large amounts of S reduced the stability of the final products, compositions with about 0.13 ml/ml (dry silk/total water) show geometric precision comparable to those of HA alone, but with significantly higher toughness. In addition, this analysis allowed us for the first time to assess printability for ceramic-polymeric inks with varied critical yield strains.

These results provide an insightful picture of the relationships between rheology and printability of S-HA composites, drawing clear relationships about the influence of S on the composition of the ink in view of micro-prosthetic applications.

This work has received funding from the European Union's Horizon 2020 research and innovation program under the Marie Skłodowska-Curie grant agreement COLLHEAR No 794614.

11:30 AM SB12.05.05

Biodegradable poly(vinyl alcohol) Hydrogels as a Temporary Retinal Tamponade MIMOZA XHEKA¹, Veronica Holmes¹, Marsela Deshnic¹, Demetrios Vavvas² and Gavin Braithwaite¹; ¹Cambridge Polymer Group, United States; ²Massachusetts Eye and Ear, United States

Retinal detachment is a serious condition where the thin retina separates from the back of the eye causing immediate vision problems and permanent issues if left untreated. Treatment is aimed at relieving the retina traction and sealing the causative tears. Often this is achieved surgically by removing the existing vitreous from the eye and reattaching the retina into place by drainage of the subretinal fluid through a fluid air exchange and sealing the tears with laser induced retinopexy. However, the sealing of retinopexy is not instant and the retina needs to be supported during healing by an agent commonly referred to as "tamponade". Tamponades have been used since 1911, and today both gas and liquid materials are used. Gas tamponades reabsorb over time in the eye, replaced with fluid spontaneously. For liquid tamponades, silicone oil is most commonly used but requires surgically removal. Neither material is density matched and patients are therefore often required to maintain a face-down prone position for weeks to maintain contact of the tamponade against the retina tear and prevent fluid migration in the subretinal space.

The fluid that comprises the majority of the volume of the eye is known as the vitreous humor. This material is a colorless, transparent crosslinked viscoelastic hydrogel. It is ~99% water, the rest composed largely of collagen, proteoglycans and proteins. If vitreous is removed in patients, the natural fluid turnover in the eye gradually refills the vitreal cavity. The ideal device for support of the healing retina would be one that mimics the properties of the healthy vitreous, at least over the time required to successfully heal. Although a number of attempts to developed permanent replacement vitreous materials have been tried, few have tried to develop a material that will only be present long enough to aid healing. Here we describe a degradable hydrogel for support of the healing retina during recovery from detachment surgery. The added benefit of a designed temporary residence is that regulatory approval is simpler if the device is not considered permanent.

We present work on the development of a thiolated PVA utilizing a polyethylene glycol diacrylate (PEG-DA) crosslinker. This system (termed a Thiogel) reacts through Michael addition, without heat release and formation of by-products, and does not require use of toxic initiators or a UV source. This system is therefore amenable to a mix-and-gel strategy in the operating room and has very low potential toxicity. We will discuss two Design of Experiments (DoE) structured to first screen for an optimal functionalization level, and then to determine the optimal composition for transparency, refractive index, gelation time and tuned degradation kinetics.

Finally, we will describe a pilot rabbit study (New Zealand White (NZW) Rabbits) to examine safety and degradation kinetics of the material *in vivo*. Animals received a vitrectomy using a conventional three port vitrectomy with either Thiogel or control air in the right eye while the left eye was left as the non-surgical control. Full ophthalmic exams, gross ocular exams, Intraocular pressure (IOP), and fundus images were performed to document the response at timepoints out to 8 weeks. Both test and controls exhibited expected IOP reductions immediately following surgery, with the IOP levels returning close to baseline by 3 weeks and thereafter statistically similar.

To attempt to determine the clearance rate of the gel we developed a liquid chromatography based technique to allow us to track the components over time in the excised tissue. This involves separation of the components from the physiological tissue through a purification step, followed by analysis on a liquid chromatography system. These data demonstrate that the gel is almost completely degraded at 14 days and is almost entirely cleared by 28 days.

SESSION SB12.06: Scaffolds for Regenerative Engineering II
Session Chairs: Gulden Camci-Unal and Natesh Parashurama
Wednesday Afternoon, December 1, 2021
Sheraton, 2nd Floor, Back Bay D

1:30 PM SB12.06.01

Incorporation of Glycyl-L-Histidyl-L-lysine (GHK) with Metalized Halloysites for Tissue Regeneration Chris Miller and David K. Mills; Louisiana Tech University, United States

Human adipose stem cells (hASCs) provide a research tool for regenerative medicine in various capacities. There are major research needs for new therapies for bone-related diseases such as osteoporosis, osteomyelitis, and severe trauma. Human ASCs can self-renew for extended durations outside of the body and provide an ideal platform to study therapeutics for the formation of bone-specific modalities or wound healing applications.

Combining hASCs with nanomaterials is a growing area of research that requires additional studies. Halloysites (HNTs) are hollow aluminosilicate nanotubes with an exterior negative charge and a positively charged lumen. These nanoparticles range between 100-900 nanometers and the lumen spanning roughly 20 nanometers across. HNTs have demonstrated biocompatibility in cell and animal-based studies, with additional capabilities for vacuum loading of drugs and coating metal ions such as silver, zinc, strontium, and copper (mHNTs). Metal ions provide synergistic antimicrobial effects on prokaryotes, allowing healthy cells to form in infection risk areas. These unique properties allow a varying of methods to be developed in cell-based therapeutics at the tissue level.

The primary focus of my research is to investigate the therapeutic potential of metalized HNTs with a linked tripeptide; GHK (glycyl-L-histidyl-L-lysine) is known to be essential in the wound healing process. Ultimately, studying these interactions will lead to better bandages to be hemostatic, alleviate pain and inflammation, and cost-effectively possess antimicrobial features. Enhanced wound healing can have drastic implications on military personnel and people without proper medical access. Bone and wound analysis studies were conducted on hASCs after the incorporation of such nanoparticles. Results introducing GHK with metalized HNTs showed increased proliferation of hASCs, collagen production, and an increase in the genes *ki67* and *runx2*, a proliferation and bone marker, respectively. Strontium-coated HNTs increased osteochondral differentiation after analysis by phase-contrast imaging, gene expression, and unique morphological changes of hASCs exhibiting trabecular-like bone formations in culture.

Copper-coated HNTs coupled with GHK increased wound closure after artificial wound analysis, further validating gene expression and proliferation studies. Human ASCs were additionally encapsulated in alginate hydrogels with GHK and mHNTs that increased cell viability and collagen production, leading to differentiated fibroblast clusters within the hydrogel constructs. Given these results, expanding the use of mHNTs with GHK in animal wound healing studies can profoundly impact wound healing if incorporated into FDA-approved materials.

1:45 PM SB12.06.02

Injectable Cellulase-Encapsulated PLGA Microspheres for Degrading Decellularized Bamboo Scaffolds for Bone Tissue Engineering Ali Salifu¹, John Obayemi¹, Chukwudalu Nwazojie^{1,2}, Sophia Silkaitis¹, Precious O. Etinosa¹, Joshua Gershlak^{1,3}, Glenn Gaudette^{1,4} and Winston W. Soboyejo¹; ¹Worcester Polytechnic Institute, United States; ²African University of Science and Technology, Nigeria; ³Massachusetts General Hospital, United States; ⁴Boston College, United States

Many of the proposed alternative strategies to bone grafts for the repair of non-union bone defects rely on the development of synthetic scaffolds for bone regeneration. However, these scaffolds are limited by their structure and scale-up/cost implications. With its well-organized, hierarchical, and functionally graded structure, mechanical strength, and potential for large-scale cultivation for bone tissue engineering applications, decellularized bamboo offers a cost-effective, scalable alternative for scaffold development. In the first part of this work, we demonstrate that decellularized bamboo scaffolds can support the growth of human fetal osteoblasts and the regeneration of bone tissue *in vitro*. "Lucky" bamboo stems are decellularized into scaffolds using detergents (sodium dodecyl sulfate and Triton X-100), washed with deionized water and Tris buffer, and functionalized with dopamine-conjugated RGD peptides (RGDOPA). Human fetal osteoblast (hFOB) cells are cultured for 28 days on the scaffolds, and cell proliferation is evaluated through DNA content and alamar blue assays. Alkaline phosphatase (ALP) activity is used as an early marker of osteogenesis, while ECM production is quantified by estimating the *de novo* total protein contents using the BCA protein assay. Mineralization is detected through measurements of *de novo* calcium contents (calcium colorimetric assay) followed by alizarin red S staining. Scanning electron microscopy is used to visualize the morphologies of the cell-scaffold constructs. However, the major drawback of using decellularized bamboo scaffolds for bone tissue engineering is their limited biodegradability when implanted into a patient, since human enzymes outside the digestive system have limited ability to break down the cellulose, hemicellulose, and lignin macromolecules found in bamboo. Hence, in the second part of this work, we present injectable cellulase-encapsulated poly(lactic-co-glycolic acid) (PLGA) microspheres as a strategy to facilitate the degradability of the decellularized bamboo scaffolds. The cellulase-encapsulated PLGA microspheres are synthesized via the single emulsion solvent evaporation technique. These microspheres are then characterized using scanning electron microscopy, dynamic light scattering, Fourier-transform infrared spectroscopy, thermogravimetric analysis, and differential scanning calorimetry. The amounts of cellulase enzyme released from the PLGA microspheres over a period of 50 days are monitored using the BCA protein assay. Degradation of the decellularized bamboo scaffolds in phosphate-buffered saline (pH 7.4, 37°C) containing the cellulase eluting PLGA microspheres is assessed via changes in weight, compressive mechanical properties, and glucose content due to enzymatic breakdown of the cellulosic macromolecules by cellulase. Strain mapping is also used to study the local strain distributions in the scaffolds under compressive deformation. The implications of the results are then discussed for the production of these sophisticated, and yet, readily-available decellularized bamboo scaffolds to circumvent the challenges associated with conventional bone tissue engineering scaffolds in an environmentally and economically sustainable way.

2:00 PM SB12.06.03

Effect of Fluid Derived Shear Stress on Bone Metastasized Prostate Cancer Evaluated Using Perfusion Bioreactor and Nanoclay Based Testbed Haneesh Jasuja, Dinesh R. Katti and Kalpana Katti; North Dakota State University, United States

The International Agency for Research on Cancer (IARC) of the World Health Organization reports 1,276,106 incidences and 358,989 fatalities resulting from prostate cancer worldwide in 2018. Prostate cancer is the second leading cause of cancer death among men in the United States. Prostate cancer has the propensity to migrate to or metastasize to bone. Although curative treatments are available for primary prostate cancer tumors, advanced-stage prostate cancer that has metastasized to bone often results in a poor prognosis. The primary cause of morbidity due to prostate cancer is the metastasis to bone. The effects of various biochemical factors in the bone microenvironment have been demonstrated in the disease progression to metastasis; however, the role of physical factors such as mechanical cues induced by the interstitial fluid flow around the bone is poorly explored. It has been established that interstitial flow has a pro-migratory and biomechanical stimulatory effect on cancer cell invasion. To address this issue, we designed a 3D *in-vitro* model to evaluate

the progression of prostate cancer cells at metastasis condition, colonizing the bone site under dynamic conditions. In this study, we developed a 3D dynamic *in-vitro* model employing nanoclay-polycaprolactone-hydroxyapatite scaffolds and a specially designed perfusion bioreactor. Initially, we differentiated human mesenchymal stem cells (hMSCs) on scaffolds under dynamic culturing conditions to duplicate an accurate bone-like microenvironment. Next, we utilized these bone mimetic scaffolds to grow prostate cancer cells under identical dynamic conditions to recapitulate prostate cancer metastasis to bone. Finally, we performed various cellular assays and immunocytochemistry studies to establish the feasibility of dynamic culture. We observed a significant increase in bone growth under dynamic culture conditions evaluated by bone-related biomarkers (ALP, RUNX2, and OCN) compared to static culture. We also noticed upregulation in E-cadherin and downregulation of vimentin levels under dynamic conditions that confirms the occurrence of mesenchymal to epithelial (MET) transition of prostate cancer cells at the metastatic bone site. We further examined the influence of fluid-induced mechanical cues on cells by monitoring alteration in orientation and morphology of hMSCs and prostate cancer cells. Overall, we observed significant differences in cellular morphology and gene expressions of bone cells and prostate tumors grown under flow conditions. The established perfusion bioreactor based 3D dynamic *in-vitro* model can be further utilized to elucidate the mechanisms of prostate cancer metastasis and screen novel drug therapies geared towards bone metastatic prostate cancer.

2:15 PM SB12.06.04

Silica-based Nanoparticle Infused Polymeric Microfibers Enhance Mineral Deposition Michael Ming Chau Chan and Helen H. Lu; Columbia University, United States

Bioactive glass nanoparticles have been used for a wide range of biomedical applications including bone regeneration due to its high specific surface area and reactivity. Inspired by the composite nature of bone, bioactive glass nanoparticles (nBG) derived from a $\text{SiO}_2\text{-CaO-P}_2\text{O}_5$ ternary system may be incorporated into polymer blend (PLGA:PCL) fibers, and this study explore nBG synthesis and evaluates the bioactivity and osteogenic potential of this composite fiber platform. The development of a Ca-P phase on the polymer-nBG fibers were monitored longitudinally under physiological conditions using FTIR-ATR, XRD and SEM. It is hypothesized that the nanoparticle infused polymeric fibers will be bioactive, and provide structural template for mineralization *in situ*. Here, A coprecipitation sol-gel method was used to fabricate the nBG (55% SiO_2 -40% CaO -5% P_2O_5 , wt%). For the fabrication of polymer-nBG fibers, 5 wt% of nBG were added to a polymeric blend of PLGA:PCL (5:1) and electrospun at 10 kV. To test the bioactivity and mineralization potential of the composite fibers, the samples with corresponding controls were immersed in DMEM (1mg/mL) and collected at Day 0, 1, 3, 7 and 14. One-way ANOVA and Tukey-Kramer HSD post-hoc tests were used to study significant differences ($p < 0.05$) of pH levels between different experimental groups.

The nBG appeared globular and are 10 – 20 nm in diameter under SEM. The fibers with or without nBG were $2.21 \pm 0.64 \mu\text{m}$ and $2.24 \pm 0.58 \mu\text{m}$ in diameter, respectively. FTIR analysis reveals a peak at 1100 cm^{-1} representing the Si-O bond of the silica network. After immersion in DMEM for 14 days, pH level remained similar across all experimental groups except for day 14 where particle-free control measured significantly lower pH compared to all other groups, indicative of polymer degradation. Coupling the polymer fiber with nBG served to neutralize the negative impact on pH and allow maintenance of physiological pH. XRD patterns showed crystallization peaks at 31.8° and 45° suggesting crystallization of phosphate and the early formation of carbonated apatite. This was confirmed by FTIR spectra showing growing peaks at 603 and 568 cm^{-1} and 960 cm^{-1} suggesting dissociation of Si-O bonds and mineral crystal formation by day 14. These bulk and surface characterization analysis confirm the bioactivity and mineralized in this novel composite system. Future studies will assess both osteoconductive and osteoinductive potential of these composites for bone regeneration.

2:30 PM SB12.06.05

Late News: (Garcia High School Student) F127-DMA—A Reverse Thermo-Responsive Liquid Embolic Agent as a Promising Treatment for Brain Aneurysms Jessica Guo¹, Maya Vendhan², Hannah Tao³, Ifeoluwatobi Alao⁴, Chiara Mosca⁵, Robert Wong⁶, Megha Gopal⁶, Nakisa Dashti⁶, Aryan Roy⁷, Wenxu Xu⁸, Matthew Lim⁹, Tyler Shern¹⁰, Varun Nimmagadda¹¹, Chandramouli Sadasivan⁶, Aaron Sloutski¹², Daniel Cohn¹² and Miriam Rafailovich⁶; ¹Ward Melville High School, United States; ²Colorado Academy, United States; ³Academy for Information Technology, United States; ⁴High Technology High School, United States; ⁵East Islip High School, United States; ⁶Stony Brook University, The State University of New York, United States; ⁷Cherry Creek High School, United States; ⁸High School Affiliated to Renmin University of China, China; ⁹Plainview-Old Bethpage JFK High School, United States; ¹⁰Columbia University, United States; ¹¹University of Michigan—Ann Arbor, United States; ¹²The Hebrew University of Jerusalem, Israel

Brain aneurysms are weak-walled pathological dilations occurring at cerebral vasculatures. If left untreated, they can easily rupture, resulting in stroke or even death. Current prominent treatment methods involve the permanent implantation of metallic devices, flow diversion, and liquid embolic agents (LEA). However, unfavorable primary outcomes occur in 20% to 30% of the treated cases, and the success rate can even be significantly lower depending on the type and location of the aneurysms. This project aims to improve patient outcomes through the development of a novel LEA that is injectable, visible under angiography, has proper mechanical strength, promotes cell adhesion, and is stable within an aneurysm sac. To achieve these properties, the LEA was comprised of the hydrogel F127-DMA, a reverse thermo-responsive, easily injectable, cross-linkable, and shape-conforming polymer system with proper mechanical strength; the catalyst FeCl_2 , which gives the polymer long term stability by allowing chemical crosslinking; and the biocompatible contrast agent iohexol.

To determine the mechanical strength of the LEA, rheology tests (single-frequency time sweeps and amplitude sweeps) were performed using a Bohlin Gemini 150 HR Nano rheometer. The tests showed that 29% F127-DMA hydrogel exhibited an elastic modulus of 202.1 kPa after chemical crosslinking, and the average wall shear stress of the carotid artery— $0.85 \pm 0.2 \text{ Pa}$ —was within the gel's linear viscoelastic region[1]. These results prove that the LEA will be able to withstand pressure from blood flow.

Differential Scanning Calorimetry (DSC) is traditionally used to measure phase transitions, where energy is absorbed or released by a substance. Here, it is shown that DSC can also accurately measure the ordering temperature of the micelles in the gel. This corresponds to the gelation temperature of the F127-DMA polymer, in which the micelles were found to form an FCC lattice. This lattice formation found through DSC corresponds to the drastic rise in modulus found through rheology. In this manner, the LEA composition could be tailored to achieve the desired modulus and viscosity during the injection. Additionally, both DSC and rheology confirmed that the contrast agent iohexol did not interfere with the gel's phase transition ability or lattice formation.

Experiments were also conducted to determine the extent to which cells adhered to the LEA. While F127 alone has been shown by multiple authors not to be cell adhesive, it was found that once cross-linked, the F127-DMA was able to support cell adhesion[2]. This indicates that the LEA can support the migration of endothelial cells, which is required for the healing of aneurysms. Ongoing experiments are being conducted to pinpoint how the hydrogel system acquires its cell adhesive properties once crosslinked. This includes testing samples of F127-DMA with F127, F127-DMA with FeCl_2 and F127, F127-DMA alone, F127 alone, and F127-DMA with FeCl_2 .

The radiopacity of F127-DMA was also tested in animal injection experiments (with IACUC approval). The iohexol contrast agent was visible through angiography, and current testing is focused on determining gel stability *in vivo*.

In addition to the aforementioned ongoing experiments, future development of the LEA will involve monitoring the long-term performance of the agent within animals, enabling the LEA to promote endothelialization, and implementing biodegradability. The results obtained thus far indicate that Pluronic polymers are successful candidates for designing LEAs by meeting the requirements of injectability, radiopacity, and promotion of neointimal layer regrowth.

[1] Sui, B., et al. "Assessment of Wall Shear Stress in the Common Carotid Artery of Healthy Subjects Using 3.0-Tesla Magnetic Resonance." *Acta Radiologica*.

[2] Rodriguez, Natalia M., et al. "Micropatterned Multicolor Dynamically ADHESIVE Substrates to Control Cell Adhesion and Multicellular Organization." *Langmuir*.

SESSION SB12.07: Biomaterials for Regeneration of Tissues
Session Chairs: Richard Benninger and Gulden Camci-Unal
Monday Morning, December 6, 2021
SB12-Virtual

8:00 AM *SB12.07.01

Engineering Bioactive Material Platforms for the Cell-Based Treatment of Type 1 Diabetes [Cherie Stabler](#); University of Florida, United States

Clinical islet transplantation, the intrahepatic infusion of allogeneic islets, has the potential to provide physiological blood glucose control for insulin-dependent diabetics. The success of clinical islet transplantation, however, is hindered by the location of the implant site, which is prone to mechanical stresses, inflammatory responses, and exposure to high drug and toxin loads, as well as the strong inflammatory and immunological responses to the transplant in spite of systemic immunosuppression. To address these challenges, our research has focused on three primary strategies: the development of scaffolds to house islets at alternative transplant sites; the fabrication of encapsulation protocols for the immuno-camouflage of the transplant; and the production of bioactive biomaterials for the local delivery of oxygen and immunomodulatory drugs and/or cells. Three-dimensional scaffolds can serve to create a more favorable islet engraftment site, by ensuring optimal distribution of the transplanted cells, creating a desirable niche for the islets, and promoting vascularization. Encapsulation can substantially decrease the need for systemic immunosuppression of the recipient, by preventing host recognition of surface antigens. Finally, localization of supportive agents to the site of the transplant can serve to enhance efficacy, while minimizing the side effects commonly observed with systemic delivery. Success in these strategies should increase the efficacy of islet transplantation for the treatment of Type 1 Diabetes, whereby the long-term survival and engraftment of the transplanted islets are significantly improved.

8:30 AM *SB12.07.02

Modular Hydrogels Reveal Impact of Type I Innate Lymphoid Cells on Intestinal Organoids Geraldine M. Jowett, Michael D. Norman, Joana F. Neves and [Eileen Gentleman](#); King's College London, United Kingdom

Pathological matrix remodelling plays a central role in many human diseases, but is challenging to study as *in vitro* models often cannot replicate the complex 3D cell-matrix interactions that drive pathologies. Here, we describe a 3D model of the human gut that allowed us to uncover an unexpected role for a rare immune cell type called Type-1 innate lymphoid cells (ILC1) in driving gut fibrosis in patients with inflammatory bowel diseases. ILC1 are enriched in patient mucosa with active inflammatory bowel disease (IBD), but the impact of this accumulation remains elusive, and therapeutics against ILC1's signature cytokine IFN γ lack clinical efficacy.

We used molecular dynamics simulations to design tetra-PEG hydrogels that cross-link quickly, but can still mimic the stiffness of normal intestinal tissue. We then co-cultured encapsulated human intestinal organoids with ILC1, and using a combination of atomic force microscopy force spectroscopy and multiple particle tracking microrheology, found that ILC1 drive intestinal matrix remodelling through a balance of MMP9-mediated matrix degradation and TGF β 1-driven fibronectin deposition. Our findings demonstrate the potential of using hydrogels in disease modelling, and open the possibility of unravelling how pathological matrix remodelling contributes to disease.

Aims and Hypothesis: We hypothesized that ILC1 accumulation in IBD is not simply a driver of inflammation, but rather that ILC1 play a role in driving disease pathology itself. Therefore, the aim of this work was to use reductionist models based on intestinal organoid-ILC1 co-cultures to uncover how ILC1 impact the intestinal epithelium and matrix.

Methods: We established co-cultures of murine small intestinal organoids (SIO) with ILC1, and human induced pluripotent stem cell (iPSC)-derived intestinal organoids (HIO) with patient-derived ILC1. We also developed a functionalized, PEG-based synthetic hydrogel system designed to form efficient networks at low polymer concentrations.

Results: Pico-SMARTSeq2 transcriptomics on SIO co-cultures revealed that IFN γ sensitizes epithelial cells to Fas-mediated apoptosis. However, ILC1 also drive expansion of the epithelial stem cell crypt through p38 γ phosphorylation and aberrant Cd44v6 expression, which is unexpectedly regulated by ILC1-derived TGF β 1, not IFN γ . We next established that human ILC1 also secrete TGF β 1, and drive CD44v6 expression in both HIO epithelium and the surrounding mesenchyme, though notably this phenotype is only recapitulated by ILC1 from patient biopsies with active inflammation. As TGF β 1 is a master regulator of fibrosis, the leading indicator for surgery in IBD, we next characterized the ability of ILC1 to regulate matrix remodelling. We created modifiable PEG hydrogels that cross-link quickly but at low stiffnesses and harnessed this platform to perform multiple particle tracking microrheology and atomic force microscopy force spectroscopy on encapsulated HIO. We show that ILC1 drive matrix stiffening and degradation, which we posit occurs through a balance of MMP9 degradation and TGF β 1-induced fibronectin deposition.

Conclusion: Our synthetic organoid co-culture system enabled us to tease apart an important role for intestinal ILC1 in epithelial and matrix remodelling, which may drive either wound healing, tumor formation or fibrotic pathologies in IBD. Moreover, this controlled 3D microenvironment provides a broader platform for dissecting interactions between complex human iPSC-derived tissues and rare cell subtypes in development and disease.

9:00 AM *SB12.07.03

Investigation of Parameters Influencing Molecule Delivery Efficiency of Multifunctional Glycan-Based Materials—An Artificial Neural Network

Model Approach Syeda R. Batool, Ismail C. Karaoglu, Fusun S. Murat, Anwaar Nazeer and Seda Kizilel; Koç University, Turkey

Current clinical translation of molecule delivery strategies requires distinctive design of materials that can offer innovative solutions to address the limitations associated with biomedical problems. Glycan-based hydrogels are of great promise in terms of creating new vehicles with responsive behavior and tunable properties for various clinical applications. For example, we developed anthracene-functionalized alginate to create both chemically and physically crosslinked polymer networks. Due to reversible dimerization of anthracene in response to light with alternate wavelengths, where we were able to tune the mechanical properties of the hydrogels precisely, while controlling the gelation behaviour in a light-responsive manner. The same approach can be applied to chitosan, another promising glycan-based polymer, where chitosan was used for dual-crosslinking with the anthracene and photopolymerization was carried out in the absence of a toxic photoinitiator. The nature of dual-crosslinking was modulated to adjust the visco-elastic modulus of both hydrogels. Furthermore, it was shown that alterations on moduli significantly influenced the morphology of seeded cells in a 3D environment. Finally, chitosan can be crosslinked through ionic gelation with negatively charged DNA to produce nanoparticles with gene delivery potential. In summary, glycan-based materials hold significant potential for tunable, reproducible, and responsive biomaterials, which can then be utilized as robust systems to be used in drug delivery applications.

9:30 AM SB12.07.04

Late News: Evaluation of LTL Nanozeolite as Doxorubicin Carrier Adriana Medina Ramírez¹, Daniela F. Rodriguez-Chavez², Georgina Garcia-Ruiz² and Jesus I. Minchaca Mojica¹; ¹Universidad de Guanajuato, Mexico; ²Universidad de la Ciénega del Estado de Michoacán Ocampo, Mexico

The specific properties of the zeolites such as their nanoporous structure, stability in biological environments, textural properties and high adsorption capacity made them useful as drug carrier. The performance as carrier mainly depends on zeolite framework, affinity zeolite - drug molecule and the pH of the media. For these reasons in the present work it was evaluated the behavior of LTL nanozeolite as doxorubicin carrier. The LTL nanozeolite was synthesized by hydrothermal method. The performance as nanocarrier was evaluated at different concentrations of doxorubicin in order to evaluate the doxorubicin adsorption capacity on the nanozeolite. In a second step, the doxorubicin-loaded nanozeolite was submitted to a releasing process at two different pH conditions. The nanozeolite was characterized by XRD, SEM and FT-IR techniques. The concentration of doxorubicin was monitored by UV-Vis spectroscopy at wavelength of 480 nm. The LTL nanozeolite was obtained as unique crystalline phase and presented a rod-like morphology. By FT-IR was evidence the loading of doxorubicin on the LTL nanozeolite. The LTL nanozeolite exhibited a high doxorubicin adsorption capacity at all the concentrations evaluated. The doxorubicin releasing rate was influenced by the pH of the media, a faster releasing was observed at pH of 7.4 while a slower and controlled doxorubicin releasing was reached at pH of 5.5. These findings allow to infer that LTL nanozeolite has the potential to be used as doxorubicin nanocarrier.

9:45 AM SB12.07.05

Immobilized Gradients of Biomolecules on Conjugated Polymer Substrates for Nerve Regeneration Omid Dadras-Toussi, Milad Khorrami, Sheereen Majd and Mohammad Reza Abidian; University of Houston, United States

Functional nerve recovery following substantial injury is crucial in the field of neural regeneration. Even though various microfluidics and printing techniques have been established, effective axonal guidance over long distances has still remained challenging. Among numerous biomaterials, conjugated polymers such as poly(3,4-ethylenedioxythiophene) (PEDOT) have demonstrated promising results in engineered scaffolds due to their soft mechanical properties, mixed electronic / ionic conductivity, and excellent chemical stability in physiological environment. Laminin, a substrate-bound protein in the extracellular matrix, is a well-known chemoattractant which fosters neurite outgrowth. In this work, we introduce a novel technique to fabricate various profiles of laminin gradients on thin PEDOT films.

To fabricate the device, first a layer of gold (thickness: 150 nm) was deposited on silicon wafers via electron beam evaporation and laser-cut masks. Using AUTOLAB, a thin layer of PEDOT was then electropolymerized gold-coated silicon substrates at charge deposition density of 0.18 C cm⁻². Surface of PEDOT films was treated with Poly (L, Lysine) to improve laminin adhesion. Laminin gradients were first printed on the surface of a 2 wt% agarose hydrogel slab (thickness: 10 mm), using micro-scale motorized X-Y-Z stages and a nano-syringe pump. The droplets of laminin solutions with different laminin concentrations were deposited at injection volume of 17.5 nl next to each other (vertical and horizontal distances were 400 μm and 800 μm, respectively). Finally, the printed laminin pattern was transferred onto the PEDOT film using molecular stamping. Laminin was fluorescently tagged via immunohistochemistry; and fluorescent imaging was utilized to visualize and quantify various laminin gradients.

To showcase the potential of the developed methodology, linear and hill gradients were created and quantified. The linear gradient consisted of 10 lines (8 mm-long) with a solution concentration range of 10-55 μg ml⁻¹. In the hill gradient (7.2 mm-long, 9 deposited lines), initially the solution concentration was 10 μg ml⁻¹ which linearly increased until it reached a maximum value of 90 μg ml⁻¹, then symmetrically decreased. Measured fluorescent intensity followed a linear trend (R-square= 0.99) with respect to laminin concentrations in the linear gradient. Similarly, both symmetrical sides of the hill gradient showed a good linear fit (R-square= 0.98 and 0.99, respectively) with almost equal absolute slope values.

We aim to assess the neurite response to various gradients and find the optimum gradient type and concentration range for effective axonal regeneration. The outcome of this study will pave the way towards development of more effective engineered conduits for nerve regeneration and will help us unravel fundamental questions of axonal regeneration in the nervous system.

SESSION SB12.08: Scaffolds for Regenerative Engineering III
Session Chairs: Natesh Parashurama and Donghui Zhu
Monday Morning, December 6, 2021
SB12-Virtual

10:30 AM *SB12.08.01

Adaptable, Protein-Engineered Hydrogels for Organoid Culture Sarah C. Heilshorn; Stanford University, United States

While organoid culture has the potential to revolutionize our understanding of human biology, current protocols rely on the use of Matrigel, a complex, heterogeneous material with large batch-to-batch variations that hinder reproducibility. In response, several groups have begun designing synthetic hydrogel systems to enable the reproducible culture of organoids. Recently, the matrix stress relaxation rate (i.e. the ability of a hydrogel to remodel its network connectivity in response to an applied stress) has been demonstrated to have profound effects on encapsulated cells. To date, the role of matrix

stress relaxation on organoid cultures has not been explored. Here we present the design of a family of double-network hydrogels that undergo two stages of crosslinking: the first stage uses reversibly dynamic covalent chemistry bonds, while the second stage reinforces the hydrogel through thermal-induced protein-polymer aggregation. This double-network of physical interactions results in a gel with a broad dynamic range of tunable mechanical properties, where the gel stiffness is set by the number of crosslinks and the gel stress relaxation rate is independently set by the kinetics of the crosslink binding and unbinding. These novel, double-network hydrogels have been used to study the role of mechanotransduction in the culture of patient-derived, human intestinal organoids. In this system, we find that the organoid cultures display strong phenotypic responses to matrix stress relaxation, which are dependent on cell-matrix interactions with both CD44 and integrin cell-surface receptors.

11:00 AM *SB12.08.02

Engineering Porous Scaffolds for Regenerative Medicine Vasiliki Kolliopoulos, Marley Dewey, Aleczandria Tiffany and Brendan A. Harley; University of Illinois at Urbana Champaign, United States

Defects in craniofacial bones of the skull occur congenitally, after high-energy impacts, and during the course of treatment for stroke and cancer. They affect a broad segment of the US population, are large and irregularly shaped, and heal poorly. Autologous bone or alloplastic implants are the clinical gold-standards for repair. However, limited quantities and the need for time-intensive intraoperative fitting of autologous bone, the non-regenerative nature of alloplastic implants, and surgical challenges that stem from irregular defect margins and the quality of the surrounding bone all contribute to poor healing and high complication rates. Advances in the fields of tissue engineering and regenerative medicine require biomaterials that instruct, rather than simply permit, a desired cellular response. Contemporary tissue engineering efforts combining exogenous mesenchymal stem cells (MSCs), morphogens, and biomaterials have not attained wide clinical use due to the cost and time for *in vitro* MSC expansion and MSC-biomaterial culture as well as the need for supraphysiological morphogen doses. A unique opportunity exists to develop degradable biomaterials that actively instruct, rather than passively permit, osteogenic differentiation and subsequent bone regeneration. Our laboratory has developed a class of mineralized collagen scaffold to promote MSC osteogenic differentiation and subsequent CMF bone regeneration in the absence of exogenous growth factor supplements. I will describe recent advances to our collagen scaffold system to address barriers preventing regeneration of craniomaxillofacial bones and orthopedic insertions. Ongoing efforts are developing platform technologies to address challenges such as poor biomaterial-defect contact, inflammatory response and reduced cell bioactivity in large defects, and poor matrix remodeling. We are using selective alteration to scaffold structural alignment and proteoglycan content as well as the incorporation of bioinspired structural motifs to create composite biomaterials able to improve cell bioactivity and mechanical competence in order to address mechanistic and translational challenges.

11:30 AM *SB12.08.03

Engineering Tissue-Informed Cell Culture Platforms for Pulmonary Regenerative Medicine Thomas Caracena¹, Rachel Blomberg¹, Predrag Šerbedzija¹, Donald R. Campbell¹ and Chelsea M. Magin^{1,2,2}; ¹University of Colorado Denver, Anschutz, United States; ²University of Colorado, Anschutz Medical Campus, United States

Chronic respiratory disease is the third leading cause of death worldwide. Prevalence of respiratory conditions is rising and expected to increase further as a direct result of lung damage sustained by COVID-19. Unfortunately, there are currently no effective treatments for the majority of advanced lung diseases. Biomaterials engineered to replicate the intricate geometry and dynamic mechanical properties of the lung could accelerate discovery of new treatments based on pulmonary regenerative medicine.

Toward this goal of engineering tissue-informed models for lung disease and regeneration research we have employed a photopolymerizable poly(ethylene glycol)-norbornene (PEG-NB) hydrogel and new microfabrication techniques to create geometrically accurate 3D lung models that closely mimic the mechanical properties of native lung tissue. Briefly, eight-arm PEG-NB macromers were crosslinked with an MMP3-degradable dithiol crosslinker via emulsion polymerization to create hydrogel microspheres. A design of experiments approach determined the optimal emulsion conditions to achieve a median microsphere diameter ($d=180.8 \mu\text{m}$) that approximates the size of a human lung alveolus ($d\sim 200 \mu\text{m}$). Bioactive peptide sequences mimicking fibronectin and laminin were incorporated into the microspheres to promote cell attachment and magnetic nanoparticles were included to enable magnetic aggregation into structures replicating distal lung architecture. The microspheres were seeded with magnetically labeled primary murine primary alveolar epithelial type II (ATII) cells and aggregated with a magnetic levitating drive to resemble an alveolar air sac. These aggregates were coated with primary murine fibroblasts to replicate interactions between epithelial cells and fibroblasts that drive many chronic pulmonary diseases. These acinar structures were next embedded in a PEG-NB hydrogel that mimics the mechanics of healthy or diseased lung parenchyma to create a robust, physiologically relevant acinar model.

We envision that ongoing work to incorporate patient-derived induced-pluripotent stem cells (iPSCs) into tissue-informed lung models could lead to pulmonary regenerative medicine advances that bridge the gap between outputs measured in traditional *in vitro* models and outcomes in human clinical trials.

12:00 PM SB12.08.04

Injectable, Pore-Forming, Perfusable Double-Network Hydrogels Resilient to Extreme Biomechanical Stimulations Guangyu Bao^{1,2}, Sareh Taheri^{1,2}, Zixin He¹, Sepideh Mohammadi¹, Hossein Ravanbakhsh^{1,2}, Jianyu Li^{1,1} and Luc Mongeau^{1,2}; ¹McGill University, Canada; ²Centre for Interdisciplinary Research in Music Media and Technology, Canada

Injectable hydrogels can be delivered via needle-syringe injection into the human body with low invasiveness. They have found significant use in many branches of medicine. Despite extensive efforts in the field, there remain long-lasting challenges concerning the mass transport and mechanical properties of injectable hydrogels. First, most existing injectable hydrogels are not perfusable. This issue limits the rapid transport of oxygen and nutrients (diffusion depth $\sim 600 \mu\text{m}$), as well as the trafficking of native or transplanted cells. Immediate vascularization is therefore imperative but difficult to realize through injection. Second, injectable hydrogels show limited mechanical toughness and robustness. They tend to crack and fail under large or repeated force excitation. An extreme case is the vocal folds, where implants in the vocal fold lamina propria are exposed to up to 50% strains at a fundamental frequency that is on the order of 10^2 Hz . Currently, patients with vocal fold injuries suffer from repeated hydrogel injections, due in part to the fracture-induced short lifetime of the hydrogel implants under the dynamic loadings. By contrast, many biological tissues are perfusable and yet tough to tolerate extreme biomechanical stimulations as part of their normal functions, as exemplified by the vocal fold and heart. To close the gap between injectable hydrogels and biological tissues, strategies to achieve a combination of high permeability and mechanical toughness are highly desired.

Here, we describe a design and methodology to fabricate new injectable hydrogels featuring *in-situ* pore formation, strengthened mechanical performance, and excellent cytocompatibility. We achieved this by orchestrating stepwise gelation and phase separation processes. The resulting hydrogels contain porous double-networks, thereby termed PDNs, which differ from previously reported injectable hydrogels that consist of either nanoporous or preformed porous networks. PDNs can form interconnected cell-sized pores *in-situ* upon injection. The highly porous matrices enable rapid media perfusion and support cell spreading and trafficking. The permeability of PDNs was at least 2 to 4 order of magnitudes greater than that of most existing hydrogels and

comparable to many biological tissues. Such perfusable hydrogels were demonstrated to support cell survival in organ-sized scaffolds with a dimension beyond 60 mm. To our knowledge, this is the first material reported to support cell viability in centimeter-scale avascular constructs. Meanwhile, unlike many porous hydrogels that are weakened by their pores, PDNs are tough and resist the propagation of moderately-sized cracks below 500 μm . Their fracture toughness was up to 40-fold greater than those of commonly used nanoporous or porous single-network hydrogels. They can be stretched more than 200% of strain without failure. The stiffness of PDNs is tunable between ~ 3 to 10 kPa, which spans the range of various soft biological tissues such as the vocal folds, lungs, heart, and gastrointestinal tract. They also exhibited a fast stress relaxation response within 10 to 100 seconds similar to organs and extracellular matrix.

Thanks to the facile injectability, PDNs can be easily delivered through fine needles and incorporated into 3D cell culture perfusion systems with complex mechanical loadings, such as microfluidic chips and bioreactors. We demonstrated that PDNs can withstand over 6,000,000 cycles of high-frequency (~ 120 Hz) biomechanical stimulations without rupture. Our method is also generalizable to commonly used material systems, such as chitosan and gelatin. With the unparalleled combination of interconnected pores, toughness, cytocompatibility, and injectability, the described material systems and method may open new opportunities for regenerative medicine and serve as biomimetic *in vitro* 3D cell culture platforms for a broader range of applications.

12:15 PM SB12.08.05

Late News: A Sprayable and Antimicrobial Dressing for Treatment of Burn Wounds [Ilayda Firlar](#)^{1,1}, Sanika Suvamapathaki^{1,1} and Gulden Camci-Unal^{1,2}; ¹University of Massachusetts Lowell, United States; ²University of Massachusetts Medical School, United States

Introduction: Wound healing is a highly regulated complex biological process that includes homeostasis, inflammation, proliferation, and maturation stages to regenerate damaged tissue. The coverage of the open wound by a dressing is the general treatment to prevent bacterial invasion and possible further injuries. Recent wound dressings have been improved by providing multifunctional features to better control the wound and the healing process. There are various key features of wound dressings such as retention of wound exudate, creation of a moist environment around the wound, and prevention of inflammation by anti-inflammatory components. Hydrogels have been widely used in wound dressings due to their ability to retain high amounts of water. For practical and rapid wound treatments, conventional dressings demonstrate limitations with inadequate amounts of oxygen, poor fitting onto the wound, and additional need for antimicrobial treatment. To address these issues, we have developed a sprayable hydrogel dressing with antimicrobial properties using naturally-derived materials and inexpensive components.

Methods: In this work, sprayable, antimicrobial, and cost-effective hydrogel wound dressings were developed for rapid treatment of burn wounds. These hydrogels are composed of photocurable gelatin, which is hydrolyzed collagen (GelMA) as the bioactive component and solid peroxide microparticles as the oxygen forming antimicrobial component. GelMA was synthesized and composite hydrogels were fabricated using 5-10% (w/v) GelMA and different concentrations of peroxide microparticles (0-15 mg/mL). The physical characteristics of the composite hydrogels were investigated by mechanical testing, swelling, degradation, and porosity analyses. The oxygen formation kinetics were measured using an oxygen sensing probe. The antimicrobial capabilities of composite hydrogels were tested against the growth of *Escherichia coli* bacteria. The cellular responses were evaluated by performing viability, adhesion, proliferation, metabolic activity, and cytotoxicity assays upon culturing human dermal fibroblasts with the composite hydrogels.

Results: We developed practical, sprayable, and antimicrobial composite wound dressings. 10% (w/v) of GelMA concentration was chosen as an optimum concentration. The composite prepolymer solutions with 10% (w/v) GelMA have shown less hydrophilic characteristics compared to the 5% (w/v) concentration when they were sprayed on an *ex vivo* pig skin model. The gelatin and peroxide containing composite hydrogels have shown tunability in physical and biological properties. The composite hydrogels have generated oxygen up to two weeks which was beneficial to the *in vitro* cell culture. The metabolic stress of human dermal fibroblast cells was relieved by the sustained formation of oxygen from the peroxide microparticles. The generation and supply of additional oxygen reduced cell death as well as providing antimicrobial properties in this novel sprayable wound dressing.

Conclusion: The sprayable, antimicrobial, and composite hydrogels that are composed of GelMA and solid peroxide microparticles were successfully fabricated. Their physical, chemical, and biological characteristics including swelling, degradation, porosity, mechanical strength, oxygen formation kinetics, antimicrobial activities against bacteria, and cytocompatibility with human dermal fibroblasts were evaluated. Our sprayable hydrogel wound dressings can be applied on wounds without contact, eliminating the risk of infection via handling, and are easily conformable to the morphology of the wound allowing for generation of personalized dressings. The fabricated composite hydrogel dressing will not require a frequent change due to its stability on the wound. In addition to pre-treatment of burn wounds, the developed sprayable and antimicrobial hydrogel dressing can be useful in plastic surgery and dermatology, applications.

SESSION SB12.09: Cellular Approaches for Regenerative Engineering II
Session Chairs: Gulden Camci-Unal and Donghui Zhu
Monday Afternoon, December 6, 2021
SB12-Virtual

1:00 PM *SB12.09.01

Controlling Vascular Smooth Muscle Cell Phenotype in Pediatric Vascular Tissue Engineering [Joyce Y. Wong](#); Boston Univ, United States

Our long-term goal is to tissue engineer and build pediatric vascular patches that will grow with a child to address unmet needs of surgical solutions for children with congenital heart defects. A major cell type of blood vessels are vascular smooth muscle cells (VSMCs) which largely comprise the medial layer of blood vessels. Vascular smooth muscle cell behavior is modulated by various physicochemical factors and their phenotype changes during normal developmental processes and during pathophysiology. Examples of vascular smooth muscle cell phenotype involve differences in extracellular matrix molecule production, cell migration, cell proliferation, contractility.

Our laboratory has investigated the effects of a variety of physicochemical stimuli on vascular smooth muscle cell behavior with the goal of understanding key relationships between VSMC phenotype and the underlying substrate. Using these model systems, we have elucidated the effects of substrate mechanical, chemical, and topographical properties on VSMC phenotype. Furthermore, to better represent physiological and pathophysiological conditions, we have investigated the interplay of multiple stimuli on VSMC phenotype.

From this information, we have developed several technologies such as micropatterned cell sheet engineering to form stacked VSMC patches and have assessed their mechanical strength. We have validated computational modeling of these stacked cell sheets in which we investigate the role of structural orientation on their mechanical properties. Computational modeling enables us to interrogate a large experimental variable space *in silico*. Finally, we are developing several strategies for using different stem cell sources from patients with clinical translation in mind.

1:30 PM *SB12.09.02

hPSC Derived Pancreatic Islet Organoids Bioengineered for Regenerative Engineering and Disease Modeling Applications Ipsita Banerjee; University of Pittsburgh, United States

Type 1 diabetes results from the auto-immune destruction of insulin secreting cells of the pancreas – the beta cells within Islets of Langerhans. Exogenous supply of insulin is a commonplace procedure in regulating blood glucose levels in diabetic patients. Alternately, cell replacement therapies such as pancreas and islet transplants offer a more permanent solution to maintain blood glycaemic control. However cell therapy is restricted by the availability of donor tissue, which can be overcome by deriving insulin producing cells from a regenerative cell source, like pluripotent stem cells (PSCs). With the current advancement of PSC-derived cell therapy from the laboratory to Phase 1 clinical trials, there is an enhanced emphasis on deriving mature and functional islets from hPSCs in a robust and reproducible manner. In parallel to regenerative therapy, there is also a strong emphasis to reproduce disease phenotypes *in vitro*, using microphysiology systems (MPS) models in tissue chip platforms. Once developed and validated, these models will be invaluable platforms for interrogating disease mechanisms as well as supplementing drug discovery and drug testing activities. Appropriate functioning of the MPS models, however, will largely rely upon successful derivation of mature and functional cells/ tissues/ organs from hPSCs.

Our research focuses on a range of biomaterial strategies for deriving pancreatic islet like cells from hPSCs. We have developed cell encapsulation strategies for scalable culture of hPSCs and its subsequent differentiation to islet like clusters. We have introduced systems engineering techniques to identify robust biophysical conditions for hPSC propagation. In a collaborative team we have developed biomaterial substrate to synthesize controlled, multicellular organoids from hPSCs resembling pancreatic islets. We are currently developing strategies to induce *in-vitro* microvascular network formation within the stem cell derived islet organoids. This talk will highlight ways in which our laboratory has integrated natural and synthetic materials to engineer the cellular environment to closely mimic the natural islet environment. Our current efforts on integrating islet organoid with microfluidic device towards developing Diabetes MPS models for Diabetes will also be discussed.

2:00 PM *SB12.09.03

Alternative Approaches to Mediate Cell Behaviour Sedat Odabas; Ankara University, Turkey

Cells can sense the physical stimuli that may arise from the composition of the material, from the extracellular matrix (ECM) that they surrounded, or the topography and the stiffness of the surface that they interact with. Cells respond to these stimuli by triggering certain metabolic pathways and altering their metabolic activities, which may lead to a change in gene expression and protein synthesis as well as promoting growth and differentiation.

Generally, the transformation of these physical stimuli into biochemical signals is called “mechanotransduction”. There are several methods and mediators to create physical stimuli and induct cells. Magnetic particles and magnetic scaffolds are one of the most convenient methods to construct a mechano-sensitive system as these scaffolds can respond to external magnetic fields. Our research on magnetic cryogels reveal that these scaffolds can induce bone and cartilage differentiation of mesenchymal stem cells both in low and high magnetic strength.

Conductive scaffolds are one of the other alternatives to use as a mechano-sensitive system. Our research on electrically conductive decellularized muscle/polyaniline/ polycaprolactone blend scaffolds possess favorable properties to serve as a matrix for the regeneration of skeletal muscle tissue. Surface modification is also a very convenient method to obtain desirable surfaces and topography. Polydimethylsiloxane (PDMS) is a widely used polymer due to its biocompatibility, high oxygen permeability and ease of fabrication. Our research on protein-modified PDMS and bone surface mimicked PDMS shows enhanced bone cell-related metabolism.

Cells are surrounded by their own ECM. Therefore, the composition of this ECM may contain several important cues to regulate or affect cell behavior. Engineered decellularized matrices are one of the latest approaches, as decellularization aims to preserve the structural and functional biomacromolecules of ECM while removing the cellular components. We reported both animal and plant derived modified decellularized matrices can provide a suitable biomechanical microenvironment for better cell attachments and proliferation.

Whether using a mechano-sensitive system, modified bio-mimicked surface, or even a decellularized matrices, cells will sense and alter their metabolism as they always do. It should be also noted that tracking and exploring the mechanistic pathways will help us to better explain these behavioral changes.

2:30 PM SB12.09.04

Plasma Immersion Ion Implantation (PIII) in Porous Mesenchymal Stem Cells Expansion Platforms Anyu Zhang, Kuan U. Wong, Giselle Yeo, Behnam Akhavan and Marcela Bilek; The University of Sydney, Australia

Rapidly developing tissue engineering treatment methods address the need to develop three dimensional (3D) porous scaffolds with biofunctionality to promote tissue ingrowth and regulate cell behaviours. Current biofunctionalization strategies rely on wet chemistry to immobilize biomolecules onto the internal complicated porous networks of the 3D porous scaffolds. However, wet chemistry approaches are limited with complicated and time-consuming process, and toxic residues. This project successfully surface-engineered three-dimensional (3D) porous tissue engineering scaffolds using plasma immersion ion implantation (PIII) technology in a customized plasma reactor. The surface-biofunctionalized scaffolds were validated by mesenchymal stem cell (MSC) expansion. PIII is a surface engineering technology that can embed highly reactive radicals in polymeric substrates surface via energetic ion bombardment. Through these radicals, biomolecules can be covalently bonded to the plasma-treated substrates and provide high level bio-functionality for tissue engineering

scaffolds. The PIII modification is typically low cost, versatile, and environmentally friendly compared to wet-chemistry-based covalent immobilization processes.¹ However, conventional plasma treatment strategies are not suitable for uniform surface treatment of porous scaffolds, because the directional approach of these methods relies on diffusion of reactive species into the pores, which has a limited penetration depth.² Therefore, there is a strong demand for a new plasma-based method suitable for homogenous plasma activation of porous 3D scaffolds. Here we report the development of a new approach in which a high voltage electrode surrounds the polymeric scaffolds for their homogenous PIII activation. Voltages in the range of 4- 8 kV and working pressures in the range of 1-3 Torr were tuned to optimize the PIII activation high impact PS scaffolds with pore sizes of 300 µm. Using micro-Fourier-transform infrared spectroscopy (micro-FTIR), the homogeneous surface modification of the PIII-treated scaffolds was confirmed by evaluating the relative concentrations of R-OH groups generated throughout the scaffolds by the interaction between the embedded radicals and oxygen in the atmosphere. FGF2 with an optimized concentration were covalently immobilized to partially cover the surfaces of the scaffolds, promoting both MSC adhesion and MSC proliferation. These results show that porous network of the scaffolds can be PIII-treated with using this new strategy, providing an excellent bio-functional platform for MSC expansion.

REFERENCES

- [1] Wong KU, Biomimetic Culture Strategies for the Clinical Expansion of Mesenchymal Stromal Cells. ACS Biomaterials Science & Engineering, 2021
- [2] Zelzer M, “Influence of the plasma sheath on plasma polymer deposition in advance of a mask and down pores”, The Journal of Physical Chemistry B, 113(25):8487-94 2009.

2:45 PM SB12.09.05

Effect of Fullerenol on Physical Properties and Biocompatibility of Calcium Phosphate Cements Ilayda Duru¹, Nisa I. Büyük², Gamze Torun Köse² and Duygu Ege¹; ¹Boğaziçi University, Turkey; ²Yeditepe University, Turkey

In this study, physical properties and biocompatibility of polymer/calcium phosphate cement (CPC) bone substitutes are improved with incorporation of fullerenol (Ful) which is a cutting-edge carbon nanomaterial due to its biocompatibility and specific physical and chemical features. The main characteristic of Ful is that it is a powerful scavenger for radical oxygen species (ROS) and some studies suggest that it enhances osteogenic differentiation via scavenging ROS and upregulating the expression of osteogenic markers. However, the data presenting the effect of Ful on the characteristics of bone substitutes is scarce. CPCs are the most dominantly used clinical bone substitutes since they possess a similar structure to natural bone and can easily be applied due to their moldability. CPCs are commercially available in pure form and in a compound with polymers because their drawbacks including low degradability, macroporosity and wash-out resistance can be addressed via degradable polymers, such as carboxymethyl cellulose (CMC) and gelatin (Gel). Then finally, Ful is incorporated to the bone substitutes.

In this study, tetracalcium phosphate (TTCP)/dicalcium phosphate dihydrate (DCPD) particles were ball-milled to obtain particles with diameters of less than 20 µm. The powder phase of CPC consisted of TTCP and DCPD in equivalent mass was used to produce Ca-deficient hydroxyapatite. The liquid phase of control CPC was 0.4 M Na₂HPO₄ solution with a pH of 7.4. CMC, Gel and Ful were homogenized in Na₂HPO₄ solution to synthesize the liquid phase of other CPC groups. The specimens were named control, CMC1/Gel1.5, Ful0.02, Ful0.04, Ful0.1. Gum-like consistency was obtained by mixing powder and liquid in 55.56/44.44 ratio by weight, respectively. Particles and CPCs were characterized by scanning electron microscopy (SEM) and X-ray diffraction (XRD). Setting time of specimens were measured by Gilmore test. Moreover, compressive strength and modulus were measured after their incubation at 37°C in phosphate buffered saline (PBS) for 24h. pH change was also analyzed after the incubation at 37°C in PBS. Finally, % cell viability was measured via Alamar Blue reduction.

The results so far show the beneficial effect of Ful on setting time and compressive strength of CPCs, and % cell viability on CPCs. According to the results of Gilmore test, 0.1 wt/v% Ful significantly decreased the initial setting time of CMC1/Gel1.5 CPCs from 20.78 minutes to 16.18 minutes (p<0.05) and final setting time from 27.94 minutes to 18.19 minutes (p<0.01). XRD analysis of CPCs at different time intervals reveals that total reaction of Ful containing CPCs took less than 5 hours since all TTCP and DCPD were consumed, and the only phase was apatite at 5th hour. Compression test shows that 0.1 wt/v% Ful significantly increased the compressive strength of control CPCs to 3.68 MPa from 2.14 MPa (p<0.05) and modulus of control CPCs to 213.09 MPa from 152.08 MPa (p<0.05). pH measurements show that 6.9 was the lowest pH for the groups at the end of the first week. After the first week, the pH of the CPCs raised and remained constant between 7.0-7.4 for one month. Finally, pre-results of Alamar Blue assay demonstrates that Ful significantly increased the cell adhesion on CPCs. % cell viability on CMC1-Gel1.5 CPCs enhanced with the addition of 0.02 wt/v% Ful (p<0.05) and 0.04 wt/v% Ful (p<0.05) in 24h. The results of this study are considered to enlighten the studies on CPCs which are the main elements of orthopedic, maxillofacial, and craniofacial applications.

SESSION SB12.10: Material-Based Approaches for Regenerative Engineering
Session Chairs: Richard Benninger and Natesh Parashurama
Monday Afternoon, December 6, 2021
SB12-Virtual

4:00 PM SB12.10.01

Late News: Mineralized Hydrogels for Regeneration of Critical Size Bone Defects Xinchen Wu and Gulden Camci-Unal; University of Massachusetts-Lowell, United States

Bone regeneration is crucial to repair critical sized bone defects that jeopardize the quality of life. Bone tissue is regenerated by intramembranous and endochondral ossification physiologically, however, a critical sized bone defect without remaining bone pieces or periosteum can be challenging to repair on its own. Allo- and auto-grafts have been developed to enhance bone regeneration. However, the risk of infection, the need of secondary surgery, and high cost limit the use of such grafts. In clinical practice, cranial defects are often caused by surgery to release the intracranial pressure, and the defect is subcutaneously covered by non-degradable implants. Biocompatible and biodegradable biomaterials can repair critical sized bone defects and degrade while the bone tissue is regenerated. Protein-based hydrogel scaffolds are suitable for critical size cranial defects regeneration due to their tunable and pliable physical properties as well as their osteoinductivity. We hypothesized that sequential mineralization process can enhance the mechanical properties of the hydrogel scaffolds while rendering the scaffolds more bioactive, osteoinductive, and osteoconductive.

In this work, we developed sequentially mineralized gelatin-based (GelMA) scaffolds to obtain mechanically stable and biologically active three-dimensional (3D) gels that allow for osteogenesis both *in vitro* and *in vivo*. The GelMA hydrogels were mineralized for 10 cycles in which one cycle is defined as an incubation period in calcium chloride dihydrate that is followed by incubation in sodium phosphate dibasic dihydrate. The mineralized scaffolds were characterized by Dynamic Mechanical Analysis (DMA) and Scanning Electron Microscopy (SEM), Thermogravimetric analysis (TGA), and Fourier Transform Infrared (FTIR). Pre-osteoblast cells were seeded on the scaffolds for 14 days and the expression of osteogenic differentiation maker genes were determined by quantitative reverse transcription polymerase chain reaction (RT-qPCR). The scaffolds were then used to repair critical size cranial defects in a rat model.

The mineralized GelMA hydrogel scaffolds have shown outstanding tunability and pliability in physical and biological properties for bone regeneration. The mechanical properties significantly enhanced for the mineralized hydrogels (125 kPa) compared with the pristine hydrogels (4.25 kPa). The 3D scaffolds induced osteogenic differentiation of pre-osteoblasts without the use of osteogenic growth medium or growth factors. The critical sized cranial defects in a rat model were repaired after 12 weeks by the mineralized scaffolds (55.4 mm³ regenerated bone volume) while no bone regeneration was observed with the use of pristine hydrogel controls or blank control groups. Overall, the findings suggest that our mineralized hydrogel scaffolds show superior mechanical properties and indicate favorable *in vivo* bone regeneration through regeneration of critical sized cranial defects in a rat model. In conclusion, sequentially mineralized hydrogels were fabricated and characterized for their chemical, physical, and biological properties. They were also evaluated for their osteoinductivity *in vitro* and osteoconductivity *in vivo*. The *in vivo* experiments showed that the scaffolds could simply be applied on top of the dura without causing an increase in cranial pressure. The implants were easily accepted by the host, highly vascularized, and biodegradable. We anticipate that our mineralized hydrogels will be useful for regeneration of mineralized tissues in new biomedical applications.

4:15 PM SB12.10.02

Structure-Function Relationships in Biomaterials Surface Science Fabio Variola; University of Ottawa, Canada

In the quest for the next generation of functional biomaterials and new solutions in health-related research, investigators have sought inspiration from

nature by developing better performing bioderived materials (e.g. chitosan, polydopamine) and architectures (e.g. nanoporosity), reproducing naturally occurring micro and nanostructures to control cellular response at the material-host tissue interface. In this context, our team has focused on understanding the effects on cells of poly(dopamine), an adhesive polymer derived from mussels, as a multifunctional layer for direct cueing to osteoblastic and mesenchymal stem cells. In addition, we have employed anodization to create reproducible patterns of nanotubes on titanium surfaces, demonstrating their role in controlling osteoblastic and mesenchymal stem cell activities. In parallel, our work has also contributed to the development of collagen-, agarose- and chitosan-based materials for applications in neuronal tissue engineering and disease modelling. For example, we focused on the creation of micro-engineered chitosan substrates for neuronal guidance and on 3D scaffolds to support neuronal adhesion and network formation.

4:30 PM SB12.10.03

Cells Encapsulated Degradable Alginate Hydrogel Microfibers Fabricated by Microfluidic Aqueous Two-Phase System (ATPS) Wisawat Keaswejjareansuk, Katawut Namdee and Mattaka Khongkow; National Nanotechnology Center, National Science and Technology Development Agency, Thailand

Cells encapsulated hydrogels are a promising material system that immobilizes and protect the cells in porous matrices. Hydrogel allows nutrient and oxygen exchanges between the cells and the matrices, which suitable for tissue engineering and cell therapy. Alginate is a natural anionic polymer that has been used in biomedical applications due to its excellent *in vivo* compatibility and low toxicity. Alginate hydrogels have been utilized for microfibers and implant scaffolds. However, an important limitation of the alginate hydrogels is the gradual degradation in a physiological environment that greatly affects the cell-cell interaction and tissue formation. In this study, microfluidic aqueous two-phase system (ATPS) was employed to fabricate the cell encapsulated hydrogel microfibers. In comparison with other techniques, the ATPS is a less complex and straightforward method to creates continuous microfibers. The microfibers then formed into a bulk mass and called hydrogel microfibers. In the material development, the concentration of the alginate-Dulbecco's Buffered Saline (DPBS) mixture was varied. The corresponding structure, morphology, swelling behavior, elastic modulus, and degradation of the alginate hydrogel microfibers were characterized to determine the optimal concentration. Fibroblast was selected in the biological study. Alginate lyase-loaded poly(lactide-co-glycolide) PLGA nanoparticles (NPs) were fabricated by a double emulsion/solvent evaporation technique. The NPs were then incorporated into the cell-laden alginate to accelerate the degradation and promote cell proliferation. NPs loaded and pristine hydrogel microfibers were studied for comparison. Cell viability, cell toxicity, and cell proliferation in the hydrogel microfibers were tested and observed at the day 1, 3, 7, and 14. Various characterization methods include SEM, DLS, AFM, degree of swelling, degradation, assays include cell proliferation, MTT, cell viability, and micro BCA were used.

In this talk, controls of the laminar flow ATPS to create continuous microfibers will be presented. The physical behavior, structure, and elastic modulus of the hydrogel microfibers will be discussed. The cell viability, toxicity, and proliferation will be reported.

4:45 PM SB12.10.04

Late News: Materials that Breathe for Tissue Engineering Sanika N. Suvarnapathaki and Gulden Camci-Unal; University of Massachusetts--Lowell, United States

Introduction: Oxygen is critical for ensuring cell survival and proliferation. Inadequate oxygen in the cellular microenvironment can trigger cell damage and hypoxia induced necrosis¹. Tissue constructs of physiologically relevant scale (in cm sizes) face diffusion limitations and are unable to translate into clinics successfully. Biomaterials that can release oxygen over time, for up to 4-5 weeks, can fulfill this oxygen demand of physiological scale tissue constructs for clinical applications². To yield biomaterials with high oxygen content, solid peroxides can be encapsulated within hydrophobic polymers. This novel approach can produce oxygen generating biomaterials that can release oxygen over a 5-week period in a controlled, sustainable manner, and augment cell viability and function².

Materials and Methods: We engineered the oxygen-generating microparticles by encapsulating calcium peroxide (CaO₂) within a hydrophobic biopolymer polycaprolactone (PCL). An emulsification technique was used to prepare composite microparticles with 2-10% (w/v) CaO₂ in PCL. The CaO₂ was added to a PCL solution and the blend of CaO₂ and PCL was micro pipetted dropwise to a Polyvinyl alcohol (PVA) solution under constant magnetic stirring at 720 rpm. This process produced CaO₂-PCL composite microparticles which were 100µm in diameter. These microparticles were subsequently encapsulated in gelatin methacrylate (GelMA) hydrogels to engineer the oxygen-generating scaffolds. The oxygen release kinetics of these scaffolds were recorded, and the corresponding cellular viability, metabolic activity, cytotoxicity, and apoptosis of the encapsulated primary cardiac fibroblasts were studied. The cellular studies were performed by microencapsulating primary cardiac fibroblasts within the oxygen-generating hydrogels at a cell density of 5 x 10⁶ cells/mL over a 5-week culture period under induced hypoxia.

Results and Discussion: We developed the oxygen-generating scaffolds and characterized their material properties. This was followed by measuring the oxygen release kinetics, and monitoring the cell behavior (viability, growth, and proliferation) and metabolic function *in vitro*. Our results revealed that the scaffolds sustained release of oxygen for up to 35 days under induced hypoxia with primary cardiac fibroblasts microencapsulated. The cellular metabolic activity over these 35 days reported an increasing trend over 14-days and continued to rise up to day 35 in culture. We achieved a precise control over the oxygen release kinetics by varying the CaO₂ concentration within PCL. The negative controls devoid of the oxygen-generating microparticles, were also tested simultaneously and they resulted in no improvement in cell growth and function.

Conclusions: Primary cardiac fibroblasts are high oxygen consuming cells, and they use oxygen at higher rates under hypoxic environments. Our results validated that the oxygen-generating microparticles enabled the maintenance of high cell viability and metabolic activity under induced hypoxia for up to 5 weeks. We demonstrated that tunable oxygen release kinetics can be obtained by altering the CaO₂ concentration, PCL concentration, and the quantity of the CaO₂-PCL microparticles within the hydrogel matrices. To customize the oxygen-release kinetics for culturing cells from different lineages having varying oxygen demands, these parameters can be easily modified. This approach could be used as a scalable, tunable platform for the development of functional off-the-shelf tissue constructs which could be used to surmount hypoxia-induced necrosis.

References: ¹Suvarnapathaki, and Camci-Unal, G. *et al.*, 2021. Engineering calcium peroxide-based oxygen generating scaffolds for tissue survival. *Biomaterials Science*, 9(7), pp.2519-2532. ²Suvarnapathaki, S., and Camci-Unal G. *et al.*, 2019. Breathing life into engineered tissues using oxygen-releasing biomaterials. *NPG Asia Materials*, 11(1), pp.1-18.

5:00 PM SB12.10.06

Bioactive Tissue Derived Nanocomposite Gel for Permanent Arterial Embolization and Enhanced Vascular Healing Jingjie Hu; North Carolina State University, United States

Transarterial embolization is a minimally invasive procedure to selectively deliver embolic agents using a catheter into arteries to occlude diseased or injured vasculature for therapeutic intent under real-time X-ray guidance. It can be used to treat vascular malformations, aneurysms, and hypervascular

tumors. A variety of embolic agents such as coils, beads, and liquids are currently used in the clinic; though their effectiveness is limited by non target embolization, failure in coagulopathic patients, high cost, and toxicity. In this study, a decellularized cardiac extracellular matrix (ECM) based nanocomposite gel is developed to provide outstanding mechanical stability, catheter injectability, retrievability, antibacterial properties, and biological activity to prevent recanalization. The malleable and shear-thinning nature of the nanocomposites gel allows the formation of an impenetrable solid cast to fill various vessel geometries and sizes, avoiding recurrent bleeding, and provides the versatility that cannot be achieved by clinically used agents. The embolic efficacy of gel is shown in a porcine survival model of embolization in the iliac artery and the renal artery. The ECM based nanocomposite promotes arterial vessel wall remodeling and a fibroinflammatory response while undergoing significant biodegradation such that only 25% of the embolic material remains at 14 days. With its unprecedented proregenerative, antibacterial properties coupled with favorable mechanical properties, and its outstanding performance in anticoagulated blood, the bioactive ECM based nanocomposite gel enables wide tunability providing a platform technology for the next-generation *in vivo* embolic agents to treat a broad range of vascular diseases.

5:15 PM *SB12.10.07

Polypeptide Biomaterials for Photothermal Tissue Repair and Wound Healing Kaushal Rege; Arizona State University, United States

Repair of wounds and surgical incisions is facilitated by primary intention with devices including sutures and staples. However, lack of immediate tissue approximation, high potential for scarring, including in visible areas of the body, propensity for tissue trauma and infection, and long procedure times necessitate new approaches for tissue repair. Light-activated tissue sealing is an emerging strategy that facilitates rapid fluid-tight approximation of ruptured tissues, but the lack of effective biomaterials compromises efficacy. I will discuss our advances in the generation, characterization and evaluation of laser-activated polypeptide biosealants and nanofibers in which, molecular or nanoparticle chromophores are embedded within natural polypeptide matrices and fibers. Irradiation of these biosealants and nanofibers with near infrared light facilitated a photothermal response, which, in turn, engendered rapid, fluid-tight sealing and accelerated repair of soft tissues both *ex vivo* and in live animals. I will also discuss a new approach in which biomaterials alone can be used for simultaneous photothermal conversion of non-ionizing light as well as concomitant tissue sealing, thus dispensing the need of nanoparticles or dyes. In addition to acute wounds, slow-healing and chronic wounds, including in diabetic and obese patients, place an enormous burden on the healthcare system. Advanced treatments, including biologicals, have shown promise but have largely not succeeded in intractable pathologies likely because of poorer stabilities. I will describe our new findings on the delivery of immune-modulating bioactives molecules and polypeptide biomaterials (e.g. silk) in combination with growth factor nanoparticles with an eye towards modulating different stages of tissue repair, leading to accelerate healing and repair. We describe evaluation of these new combination treatments, including using temporal delivery strategies in immunocompetent, and obese, diabetic mice. Taken together, our studies demonstrate that polypeptide biomaterials, in concert with delivery of light, show strong translational promise for accelerating wound healing, and efficacious tissue sealing and repair.

SESSION SB12.11: Biomaterials for Regenerative Engineering and Poster Session
Session Chairs: Richard Benninger and Natesh Parashurama
Monday Afternoon, December 6, 2021
SB12-Virtual

6:30 PM SB12.11.01

Binary Zinc Alloy-Based Biomaterials for Tissue Regeneration Yingchao Su and Donghui Zhu; Stony Brook University-SUNY, United States

Introduction: Zinc (Zn) has been recently proposed as a novel biodegradable metal thanks to its essential physiological and biological roles and its promising *in vivo* degradation rate [1, 2]. Compared to Mg alloys and Fe alloys, the degradation behavior of Zn alloys is more likely in line with clinical demand. One of the main factors limiting the extensive clinical application of Zn and its alloys is their lower mechanical strength [3]. While it can be improved through alloying with different elements (such as Mg, Ca, Mn, Cu, or Li), and plastic deformation processing techniques [34], low mechanical strength still remains an important challenge, and more effort is required to obtain a series of alloys with reproducible mechanical strength and ductility. **Methods:** A series of Zn-0.5X and Zn-3X alloys (X = Cr, Fe, Sr, Zr, V, at.%) were prepared and extruded from $\Phi 28$ mm down to $\Phi 10$ mm cylinder. Mechanical property was measured at a strain rate of 0.04/min using a universal material test machine (Instron 5969, USA) according to ASTM-E8M-09 and ASTM E9-89a (2000) standards. For the cell viability test, extract media was prepared by incubating samples in the corresponding cell culture media at a ratio of 1.25 mL/cm² for 3 days. Afterward, the collected extract solution was diluted with culture media to specific concentrations of 25%. The cell viability of human endothelial cells (EA.hy926, ATCC CRL-2922, US) was measured with the MTT assay. A rabbit abdominal aorta model was used for *in vivo* implantation. Different wire samples with dimensions of $\Phi 0.25 \times 20$ mm were implanted in the abdominal aorta of each rabbit under angiography.

Results & Discussion: All the alloys showed improved mechanical strengths when compared to pure Zn, especially the Zn-0.5Cr, 0.5Zr, 0.5 and 3V alloys have significantly improved mechanical strengths and elongation. The endothelial cells cultured with Zn-0.5Zr, 0.5Sr, 0.5 and 3 Fe and V alloys showed much better cell viability than pure Zn. The *in vitro* and *in vivo* degradation tests of different materials showed similar corrosion behaviors with pure Zn, which is helpful for their potential clinical applications.

Conclusions: Collectively, these data clearly illustrate the different mechanical properties and cell viability on these Zn based materials, which could potentially provide various choices for the tissue regeneration.

References:

1. Bowen PK, Drelich J, Goldman J. Zinc exhibits ideal physiological corrosion behavior for bioabsorbable stents[J]. *Advanced materials*, 2013, 25(18):2577-2582.
2. Su, Y., Cockerill, I., Wang, Y., et. al. Zinc-based biomaterials for regeneration and therapy[J]. *Trends in biotechnology*, 2019, 37(4): 428-441.
3. Bowen PK, Shearier ER, Zhao S, et. al. Biodegradable metals for cardiovascular stents: from clinical concerns to recent Zn Alloys[J]. *Advanced healthcare materials*, 2016, 5(10):1121-40.

6:45 PM SB12.11.02

***In Vivo* Studies of Additive Manufactured Bioabsorbable Magnesium Scaffolds in a Rabbit Femur Model** Juncen Zhou and Donghui Zhu; Stony Brook University, United States

Introduction: Additive manufacturing (also called 3D printing) techniques have been utilized and developed in the field of orthopedic implants, and various materials, fabrication methods, geometry design were studied. When an implant aims to regenerate bone, the porous structure will be beneficial for mass transfer and cell migration, leading to enhanced angiogenesis and new bone growth. Even though many bioabsorbable materials, including polymers and ceramics, have been applied in 3D-printing scaffolds, their mechanical strength is still considered insufficient, especially in the case of load-bearing

applications. Bioabsorbable metals, such as magnesium and its alloys, have shown great potential as the next generation of biomaterials, thanks to their decent mechanical properties, biodegradation, and biocompatibility. Here, we use additive manufacturing to fabricate porous magnesium scaffolds, the degradation behavior and biological response of which are studied in vivo with a rabbit femur model.

Methods and Materials: Magnesium scaffolds are composed of WE43 magnesium alloy. Titanium scaffolds made of Titan-Grade 1 are used as a benchmark group. Laser Powder Bed Fusion is facilitated for the manufacturing of different scaffolds. The scaffold is in the shape of a cylinder with both diameter and height of 4 mm. The pore size of all scaffolds is around 500 μm . Before the implantation, the compression test is performed on different scaffolds. The rabbit femur defect model is used in this study. Two circular defects with a diameter of 4mm are created by the drill in the distal femur, and then two scaffolds made of the same material are inserted into these two defects separately. Two collection time points are set to 5 and 25 weeks. The collected femur bones with scaffolds are analyzed with the Micro CT scanning. Meanwhile, the blood and internal organs, including the heart, liver, spleen, kidney, and lung, are collected for biotoxicity analysis.

Results: In terms of the compression strength and modulus, the titanium scaffold exhibit a higher value, while the value of WE43 scaffold is more close to the natural human bones. All scaffolds can properly fit into defects and hold well. No systematic toxicity is found for all scaffolds based on the analysis of blood and internal organs. The degradation rate of WE43 scaffolds is derived from the volume change in the Micro CT. For all scaffolds, the new growth of bone into the pores can be observed. Interestingly, neither the degradation behavior nor the new bone ingrowth is homogeneous for the whole scaffold. Different sections of the scaffold show various degradation tendencies due to the local physiological environment (contacted with cortical bones or the marrow cavity) and mass permeation. Furthermore, degradation behavior causes an influence on the new bone growth. Meanwhile, the geometry of scaffolds also has an impact on the local biological response.

Conclusion: Compared to titanium scaffolds, WE43 scaffolds present acceptable biological response, and their biodegradation feature exhibit great potential for bone regeneration application.

7:00 PM SB12.11.03

Late News: The Anti-Aging Effects of Polydopamine Particles in Human Skin Epithelial Keratinocytes Yan Nie^{1,2}, Xun Xu¹, Weiwei Wang¹, Barbara Bellomo¹, Nan Ma^{1,3} and Andreas Lendlein^{1,2,3}, ¹Institute of Active Polymers - Helmholtz-Zentrum Hereon, Germany; ²Institute of Biochemistry and Biology, University of Potsdam, Germany; ³Institute of Chemistry and Biochemistry, Free University of Berlin, Germany

Skin aging is a multisystem degenerative process, which is characterized by the accumulation of senescent keratinocytes. The exposure of reactive oxygen species (ROS) is one of the major causes that induce growth arrest and cellular senescence in those cells. The preparation of polydopamine (PDA) intended for biomedical applications typically comprises oxidative self-polymerization of dopamine (DA) in a weak alkaline solution [1, 2]. PDA can be deposited as a biofunctional coating on cell culture substrates acting as a ROS scavenger [3]. However, the role of PDA particles, which are formed during the PDA coating formation, is not yet fully explored. This motivated us to investigate the multiple functions of PDA particles, especially its antioxidant and anti-senescence effect, in cultures of human skin epithelial keratinocytes, HaCaT cells. The PDA particles were synthesized through the self-polymerization of DA in a 50 mM Tris(hydroxymethyl)aminomethane hydrochloride (Tris-HCl) solution at pH 8.8. The PDA particles were filtered through Millipore® Stericup® filter units to control the diameter in the range of 220-450 nm. The uptake of PDA particles by HaCaT cells exhibited a dose-dependent manner in control and PDA groups (0, 10, 20, 30, 40, and 50 $\mu\text{g}/\text{ml}$), while the cell viability was not affected by the PDA uptake as no loss of membrane integrity and inhibition of cell growth were observed. The PDA uptake decreased the oxidative stress provoked by ROS. It also decreased the activity of the senescence-associated β -galactosidase in HaCaT cells by ~10%, where a plateau was reached when the PDA-dosage exceeded 30 $\mu\text{g}/\text{ml}$. Conclusively, these findings demonstrate that PDA particles could effectively decrease the level of cellular senescence, highlighting its potential to be translated into a medicine strategy for preventing skin aging.

Reference

1. H. A. Lee, Y. Ma, F. Zhou, S. Hong and H. Lee, *Accounts of chemical research* **52** (3), 704 (2019).
2. H. A. Lee, E. Park and H. Lee, *Advanced Materials* **32** (35), 1907505 (2020).
3. Z. Deng, W. Wang, X. Xu, Y. Nie, Y. Liu, O. E. Gould, N. Ma and A. Lendlein, *ACS Applied Materials & Interfaces* **13** (9), 10748 (2021).

7:05 PM SB12.11.04

Late News: (Garcia High School Student) The Effect of Surface Chemistry on Neurogenic Differentiation in Dental Pulp Stem Cells Andrew Yuen¹, Layla Shaffer², Leigh Baratta³, Claire Richter⁴, Nikhil Mehta³, Kathryn Rosshirt⁵, Kuan-Che Feng⁶, Haijiao Liu⁶, Marcia Simon⁶ and Miriam Rafailovich⁶, ¹Jericho High School, United States; ²The Lawrenceville School, United States; ³Smithtown High School East, United States; ⁴South Side High School, United States; ⁵University of Notre Dame, United States; ⁶Stony Brook University, United States

Neurodegenerative diseases represent a major incapacitating health problem that has been proven to be difficult to treat. If the nervous system is injured, neurons are unable to regenerate efficiently. Importantly, a variety of stem cells have been determined as a possible treatment provided that they can be induced to differentiate along neurogenic lineage. Here we present research on the factors which can determine neurogenic differentiation of Dental Pulp Stem Cells (DPSCs). DPSCs are pluripotent stem cells that have been shown to differentiate in vitro along neurogenic, odontogenic, or adipogenic lineage depending on the media in which they are cultured. We have previously shown that odontogenic differentiation of the DPSC is highly dependent on the properties of the substrate, where both chemistry and mechanics combine to determine the differentiation lineage. Here we present a study aimed at determining the optimal material's scaffold for implementing neurogenic differentiation.

Polymer films were spun cast onto HF etched flat Si wafers from solutions of 3% PVDF with Dimethylformamide (DMF), 20 mg/ml PB with toluene, 7 mg/ml P4VP with DMF, and 30 mg/ml RDP/clay with PLA in Chloroform were spun cast onto cleaved silicon wafers, and annealed at 150C overnight to remove residual solvent and stresses, as well as to sterilize the substrates. The quality of the films, as well as the surface roughness or crystallinity, was assessed using scanning force microscopy in lateral and friction modes. The cells were plated on these substrates, as well as on tissue culture plastic (TCP) in alpha MEM with 10% FBS and 1% pen strep, where they were cultured for three days. Subsequently, this media was replaced with neurobasal media and changed twice a week. The neurobasal A media was composed of 100 $\mu\text{g}/\text{mL}$ penicillin, 1X B27 supplement, 100 $\mu\text{g}/\text{mL}$ streptomycin, 20 ng/mL epidermal growth factor (EGF), and 40 ng/mL fibroblast growth factor (FGF). We then performed EVOS imaging to acquire cell morphology on day 0, day 7, and day 28. Moreover, the degree of neuronal differentiation was investigated using Real-Time Polymerase Chain Reaction (RT-PCR) on day 0, day 14, day 21, and day 28. The neuro markers are Nestin(early), β -Tubulin-III (intermediate), and NEFM (mature). The AFM film topography images provided a measure of surface roughness and revealed that the surface of P4VP and PB films had a smoother surface while PVDF and RDP/Clay films had rougher surface topographies. The aspect ratio of the cells was quantified on the different substrates at day 28, where it was found that the cells on the RDP clay had the largest value. RT-PCR indicated that the P4VP and RDP/clay with PLA substrate had downregulation of neuro markers Nestin and β -Tubulin-III and upregulation of NEFM which confirmed neurogenic differentiation. Unfortunately, differentiation was poor on the PB and most cells died on the PB+tio2 even though these substrates were shown to be very effective in induction of odontogenic differentiation in osteogenic media. It is interesting to note that the PB substrates had much lower moduli than the PLA/RDP substrate confirming that chemical composition was more important than the mechanical response in neurogenic differentiation. Further work is in progress using electrospun fibers of the same polymer composition to determine the role of substrate morphology.

Keywords: Dental Pulp Stem Cells; Neurogenic differentiation; P4VP; PVDF; RDP/Clay; PLA; PB; RT-PCR

7:10 PM SB12.11.05

Digital Light Processing (DLP) Based 3D Printing of Polytetrafluoroethylene (PTFE) Scaffolds for Vascular Applications Hyun Lee and Hyun-do Jung; The Catholic University of Korea, Korea (the Republic of)

As entering ageing society, cardiovascular diseases have become highly increasing treats to human life with their fatality. Several efforts using organism derived grafts (autografts, allografts, and xenografts) have been adopted to replace the malfunctioning vessels. However, the use of abovementioned grafts is challenging due to their limited sources. Thus, numerous researches have been conducted to fabricate artificial vascular grafts with non-cytotoxicity and sufficient mechanical properties to withstand blood pressure. Polymeric matrices consisting of polytetrafluoroethylene (PTFE), polyethylene terephthalate (PET), or polyurethane (PU) have been most widely utilized for vascular grafts because of their biological stability. Especially for PTFE, it has been clinically utilized to substitute vessels or bypass blood flow to healthy tissues. Generally, PTFE vascular grafts have been fabricated in the form of tube and it should be cut to fit into the surgical sites. Therefore, creation of PTFE vascular grafts with patient specific structure has been challenging. As a solution for that, we are aiming to adopt digital light processing (DLP) based 3D printing technique to fabricate artificial PTFE vascular grafts with complicated branched structure. Through incorporating photocrosslinking agents and photoinitiator to sustain structural integrity of PTFE emulsion, channel structures of PTFE were successfully produced. After sequential heat treatment to eliminate supplemented materials and sinter the PTFE particles, PTFE tubes with distinctive mesh structure were obtained. Since the purpose of this research is to apply PTFE tubes to vascular grafts, evaluation of mechanical properties (tensile property, elasticity, and suture retention ability) and biological properties using endothelial cells and fibroblasts was performed.

7:15 PM SB12.11.06

Molecular Origin of the Effect of Mutation on the Structure and Mechanical Properties of Human Epithelial Keratin K5/K14 Chien-Yu Pan and Chia-Ching Chou; National Taiwan University, Taiwan

Epithelial keratin, a type of intermediate filament (IF) protein, is one of the key components in maintaining the stability of the cell nucleus in the epidermis of the skin, the largest organ in the human body. It absorbs water and withstands external pressure, affecting the structural stability and mechanical properties of the skin. Epidermolysis bullosa simplex (EBS) is a rare genetic skin disease related to genetic mutations in epithelial keratin K5/K14. The resulting structural defects can cause keratinocytes in the basal layer to become fragile and rupture when subjected to mechanical stress. Its pathological feature is that the skin and mucous membranes are extremely fragile, and wounds and blisters occur even under slight external force. In this study, we focused on the amino acid sequence of the wild-type human keratin K5/K14 and sequences with point mutations, beginning with a full atomistic model of the K5/K14 heterodimer and proceeding to the higher hierarchical structure of the tetramer model. For the heterodimer, the structures of the wild type and the mutants share a high degree of similarity, and the helical structure is preserved. Then, based on the heterodimer model, we considered the keratin tetramer model with ID-1 contact from previous experimental observations. Our results suggested that in the wild-type tetramer, the hydrogen bonds formed in the middle and contact regions provide extra stability to tetramer 2B-2B interactions during IF assembly. The probabilities of hydrogen bond formation are lower in the mutant tetramers than in the wild-type tetramer in the contact region; the point mutations do not necessarily affect the structure for dimer formation, but changes in the interactions of amino acids may affect the higher-order assembly of IFs. We observed that, the structures of the tetramers with point mutations were loosely stacked, and the mechanical properties were weaker than those of the wild-type tetramer. We further compare our results with the latest experimental measurements and discuss the relationship between the genotype of EBS disease and the atomic-level mutated structures. The atomistic model allowed us to study point mutations at the molecular level. The results can be further applied to reveal the effect of point mutations on EBS diseases.

7:20 PM SB12.11.07

Late News: Synthesis and Design of PCL-PLA-HAp and PCL-BG-HAsG 3D-Scaffolds for Bone Tissue Applications Nancy Nelly Zurita Méndez, Georgina Carbajal de la Torre, Marco Antonio Espinosa Medina, María de Lourdes Ballesteros Almanza, Citlali Wendolin Rodríguez Páramo and Javier Ortiz-Ortiz; Universidad Michoacana de San Nicolás de, Mexico

Throughout history, human beings have faced the problems of wear and tear of the tissues that compose them, so the need arises to find an alternative to the regeneration, repair, or replace damaged tissues to continue performing their physiological functions; this has led us to the use of materials to help these procedures through the so-called Tissue Engineering, dedicate to the application of chemical and biological principles in the development of substitutes that restore, maintain or improve the function of living tissues through biomaterials. Currently, the bioglass (BG) and hydroxyapatite (HA) are object of study for their high bioactivity, osteoconductivity, biodegradability and because they possess compositional and structural similarities with bone mineral, nevertheless, these biomaterials are relatively brittle and for diminishing this property, they are embedded into polymers. The use of polylactic acid (PLA) had demonstrated a great potential for load-bearing applications when is used as a polymeric matrix with the HAp particles. On the other hand, polycaprolactone (PCL) has been also extensively applied in regenerative medicine applications, among all desirable properties as biocompatibility and flexibility because of its ester bonds, PCL also had shown that enhance the osteogenic differentiation of mesenchymal stem cells, and the incorporation of HAp particles modify its hydrophobic nature, stimulating the cell interaction. In the present study, the synthesis of BG, PLA, hydroxyapatite by sol-gel method (HAsG), and hydroxyapatite by precipitation method (HAp) were performed. Subsequently, those biomaterials were complemented with polycaprolactone (PCL) to elaborate 3D porous scaffolds by the solvent-casting/salt-leaching technique. The PCL-PLA-HAp and PCL-BG-HAsG scaffolds were designed at two weight proportions each. 1. 40%-10%-50% and 2. 40%-50%-10% respectively. The scaffolds were analyzed by infrared spectroscopy (FTIR), X-ray diffraction (XDR), and scanning electron microscopy (SEM) by observing their composition and morphology, besides, as known; the surface reactions of materials with their biological environment occur a few seconds after they are implanted in the body interacting with proteins present in the physiological environment, in this fact lies the importance of evaluating the in-vitro biological behavior of the biomaterials. Simulated body fluid (SBF) and Hank's saline solution at 37 C are the aqueous media that allow us to get closer to the understanding of the biodegradation and bioactivity mechanism of composite biomaterials since their ionic compositions are very close to those of human plasma.

7:25 PM SB12.11.09

Thermosetting and Mechanical Property of poly(2-methoxyethyl acrylate)-Based Polyurethane Synthesized by RAFT Polymerization and Polyaddition Shunsuke Tazawa¹, Tomoki Maeda^{1,2} and Atsushi Hotta¹; ¹Keio University, Japan; ²Ibaraki University, Japan

Poly(2-methoxyethyl acrylate) (PMEA) is one of the well-known antithrombogenic materials [1,2]. Because of its low glass transition temperature around -30°C, PMEA is a liquid-like polymer at room temperature and thus its usage is limited to antithrombogenic coating. Therefore, solidifying PMEA is important to enhance its biomedical applications as a bulk material. In this study, thermally stable poly(2-methoxyethyl acrylate)-based polyurethane (thermoset PMEA-based PU), chemically crosslinked by covalent bonds, was synthesized through reversible-addition fragmentation transfer (RAFT) polymerization and polyaddition with diisocyanate.

In detail, to obtain thermoset PMEA-based PU, hydroxyl-terminated PMEA with 4 hydroxyl groups (PMEA-(OH)₄) was synthesized by RAFT

polymerization, and PMEA-(OH)₄ was then reacted with diisocyanate to form urethane bonding acting as chemical crosslinkings in the material. In fact, PMEA-(OH)₄ synthesized by RAFT polymerization was a viscous liquid-like polymer. After the polyaddition using diisocyanate, a solid standing film of thermoset PMEA-based PU was obtained. The existence of urethane bonds was confirmed by FTIR.

Thermal and mechanical properties of thermoset PMEA-based PU were evaluated through dynamic mechanical analysis (DMA) and tensile testing. From the DMA results, it was found that the storage modulus (E') of thermoset PMEA-based PU was higher than the loss modulus (E'') at the temperature range between 25°C and 110°C. According to the results of tensile testing, it was also found that E' was almost constant at $\sim 7.0 \times 10^5$ Pa in the same temperature range. The Young's modulus, the fracture strain, and the tensile strength of thermoset PMEA-based PU were calculated as 574 ± 54 kPa, $212 \pm 78\%$, and 581 ± 90 kPa, respectively. It was, therefore, confirmed that the synthesized thermoset PMEA-based PU was a thermally-stable solid material.

Intermediate water is a group of water molecules interacting with PMEA molecules, largely contributing to the high antithrombogenicity of PMEA.

Therefore, intermediate water was also analyzed by differential scanning calorimetry (DSC). The DSC curves of the hydrated samples of thermoset PMEA-based PU exhibited cold crystallization around -27°C, deriving from the intermediate water, whereas the DSC curves of dried samples of thermoset PMEA-based PU only showed the glass transition. The ratio of intermediate water to all water in thermoset PMEA-based PU was calculated as 2.1 ± 0.03 wt%, high enough to display antithrombogenicity, considering the ratio of other conventional highly antithrombogenic polymers [3]. It was concluded that the newly synthesized thermoset PMEA-based PU effectively possessed intermediate water for antithrombogenicity.

References

- [1] C. Sato, M. Aoki and M. Tanaka, *Colloids Surf., B*, 2016, 145, 586–596.
- [2] K. Akamatsu, T. Furue, F. Han and S. Nakao, *Sep. Purif. Technol.*, 2013, 102, 157–162.
- [3] S. Kobayashi, M. Wakui, Y. Iwata and M. Tanaka, *Biomacromolecules*, 2017, 18, 4214–4223.

7:30 PM SB12.11.10

'Sporulation' Cytoprotective Strategy for Room-Temperature Cell Logistics Lydia Chong^{1,2}, Derrick Yong² and Juha Song¹; ¹NTU, Singapore; ²A*STAR, Singapore

Considering the time- and temperature-sensitive nature of cell therapeutic products (CTPs), additional protection is important in cell therapy manufacturing where cells are exposed to harsh environmental stressors (i.e. temperature fluctuation) during logistical activities. As market for these products continue to expand rapidly, it is thus critical to look into improved methods of storing and transporting these products to hospitals while ensuring that their standards (i.e. quality, stability) are strictly met via the use of diagnostic tools. Chemically-induced cell 'sporulation' has been recently demonstrated by our group as a bioinspired cell protection strategy for maintaining cell viability in biofabrication, where cells are exposed to UV irradiation during photocrosslinking process. Tapping on the success of this strategy, we proposed its application as a practical solution for room-temperature shipping and short-term storage of CTPs during cell logistics. Herein, plant seed-inspired 'sporulation' of L929-laden alginate microspheres (AlgMS) were induced through the coating of pyrogallol (PG), a plant-derived polyphenol. Thereafter, both 'sporulated' and non-'sporulated' encapsulated cells were subjected to temperature conditions that the CTPs could potentially be exposed to during 3 days of transportation and/or short-term storage. These conditions include, (i) **ET**: extreme temperature increment as a result of heat accumulation in confined storage spaces (e.g. when transportation vehicles with malfunctioned reefers are parked under the sun for a while) – room temperature throughout with temperature increment from 30 to 50°C over 1h at day 2; (ii) **CT**: cyclic temperature simulation based on real-life temperature profile from cell logistics company when CTPs are transported across countries of different seasons – 30°C (day 1), 17°C (day 2), 27°C (day 3). After which, 'germination'/restoration of cell metabolism was achieved by degrading the microspheres and releasing the cells via mild EDTA treatment. The 'germinated' cells were subsequently re-incubated for 72h before cell viability was assessed with LIVE/DEAD cell assay. Regardless of the temperature conditions, majority of cells released from PG-AlgMS remained viable (> 80%), in contrast with those released from AlgMS (< 30%). This suggested the potential of cell 'sporulation' in enhancing protection of encapsulated cells when temperature fluctuation is involved. As expected, when the two temperature conditions were compared, more cells managed to survive when subjected to CT (~91%) than ET (~80%) condition whereby the cells were exposed to much higher temperatures known to cause irreversible cellular damage. Although the viability of cells released from AlgMS was severely compromised (~10%) for ET, a relatively high cell viability (~72%) is still achievable when exposed to the CT condition. This thus, implied the capability of cell encapsulation alone in providing certain degree of protection that could suffice in less harsh temperature fluctuation conditions. Taking into consideration of unforeseen delays that could happen during cell logistics, longer duration room-temperature cell storage and transportation for up to 10 days was also proven to be possible with this bioinspired cell protection strategy, whereby majority of released cells remained viable (>85%). In conclusion, we have demonstrated the potential of translating 'sporulated' encapsulated cells into a cell storage and handling platform that can maintain the quality of CTPs despite the harsh environment that these temperature-sensitive products could be exposed to during cell logistical activities. We envisage that this cell-encapsulated microsphere platforms have great potential for short-term cell storage, cell-involved biofabrication and cell logistics.

7:35 PM SB12.11.11

Design and Development of Inorganic Nanoparticles for Radioenhancement Therapy Lukas Gerken^{1,2}, Anna Neuer^{1,2}, Pascal Gschwend¹, Fabian Starsich^{1,2}, Alexander Gogos², Ludwig Plasswilm³ and Inge K. Herrmann^{1,2}; ¹ETH Zürich, Switzerland; ²Empa-Swiss Federal Laboratories for Materials Science and Technology, Switzerland; ³Cantonal Hospital St. Gallen (KSSG), Switzerland

Nanoparticle-based radio-enhancement has the prospect to improve cancer cell eradication by amplifying the damage caused by (X-ray) irradiation through ejection of secondary particles (electrons) leading to further oxidative stress. Gold nanoparticles are a natural choice because of their high atomic number and biological compatibility and are therefore most researched nanoparticles. However, due to the heterogeneous results and the lack in mechanistic understanding, these particle systems have not yet entered clinics. Recently, nanoparticles based on more exotic hafnium dioxide have shown promising results in clinical studies. There is increasing evidence that radio-enhancement efficacy does not solely dependent on high atomic numbers but involves a complex cascade of secondary reactions.

Here, we will present a comprehensive nanoparticle-based radio-enhancement study including a selection of inorganic oxide nanoparticles with comparable morphologies, sizes and surface chemistries. Liquid flame spray pyrolysis as synthesis technique allows effective scale up to meet clinical and industrial demands. We will bridge physical and chemical nanoparticle-radiation interactions with biological radio-enhancement effects in a radio resistant tumor cell line using clinically relevant exposure settings. We also show how the nanoparticles can be tailored to incorporate multimodal imaging possibilities for a theranostic approach. Our comprehensive analysis will pave the way for a more rationalized nanoparticle design and development for nanoparticle-based radio-enhancement studies.

7:40 PM SB12.11.12

Osteogenic Potential of a Hematene Reinforced Monetite Cement for Bone Regeneration Rachel Monk, Daniela Vieira, Geraldine Merle and Edward Harvey; McGill University, Canada

Introduction: Autografts presently remain the gold standard for bone growth and regeneration. Associated complications such as their limited availability, increased surgical time, blood loss, and donor site morbidity has urged the exploration of other alternatives. Particularly, non-resorbable graphene-family

nanomaterials combined with calcium phosphate has generated notable findings. However recently, hematene, a 2D nanomaterial of iron oxide has been discovered with rather extraordinary properties. This novel bioresorbable nanomaterial with its physicochemical, optical, magnetic, electrical, and mechanical properties shows a promising osteogenic potency for bone regeneration. Nevertheless, the bioactive potential of hematene combined with calcium phosphate (i.e. monetite) remains to be explored. Here, hematene-monetite nanocomposites were synthesized for the first time and their potentials to stimulate osteogenesis were showcased.

Methods: 2D hematene was synthesized by ultrasonic exfoliation from natural iron hematite ($\alpha\text{-Fe}_2\text{O}_3$) and confirmed with bright-field transmission electrical microscope (TEM). Monetite was composed of β -tricalcium phosphate (β -TCP) and monocalcium phosphate monohydrate (MPCM) and subjected to hydrothermal treatment. Monetite implants were decorated with hematene nanocomposites of different concentrations using centrifugal force. The two-dimensional morphology, crystallinity, thermal behaviour, and compressive strength of the scaffolds were confirmed by Scanning electron microscopy (SEM), X-ray diffraction (XRD), Thermogravimetric analysis (TGA), and a high-precision testing system (EZ test), respectively. Cytotoxicity and gene expression profiles of bone specific markers of RUNX2, ALP, BGLAP, and SPARC, were evaluated over 21 days within pre-osteoblastic MC3T3-E1 cells.

Results: TEM imaging confirmed the successful exfoliation of ultrathin mono- and bi-layer hematene sheets with a mean lateral size of 200nm. Nanocomposites at different hematene to monetite ratios were successfully prepared with good thermal stability and decomposition profiles. Physicochemical characterization and SEM imaging confirmed the presence and homogenous distribution of the 2D nanomaterials over the monetite implant without affecting its crystallinity. Furthermore, our findings indicate that the mechanical integrity was significantly enhanced when reinforced with hematene nanocomposites of higher concentrations compared to monetite alone. *In vitro* testing demonstrated that gene expression profiles of alkaline phosphatase (ALP), osteocalcin (BGLAP), osteonectin (SPARC), and RUNX2, were significantly elevated over the 21 days when compared to controls. These findings indicate that osteogenesis of MC3T3-E1 cells was accelerated by the hematene-monetite nanocomposites with and without osteoinductive agents.

Conclusions: For the first time, we showcase the osteogenic potency of hematene-monetite nanocomposites and the abilities to enhance cell proliferation and osteogenic differentiation in pre-osteoblastic MC3T3-E1 cells. We demonstrate the simplicity of obtaining ultrathin 2D hematene sheets through ultrasonic exfoliation to decorate monetite implants without affecting crystallinity or thermal stability within or between treatment conditions. Assuring both properties remain unaffected is of special importance to maintain implant consistency, as variations can vastly contribute to differences in physicochemical properties. Excitingly, these preliminary *in vitro* results suggest that hematene derivatives could be the next big candidate as a scaffold for bone tissue regeneration. Furthermore, the highly unique thermal behaviour of hematene derivatives prompts its potential to open further avenues for therapeutic agents. Future works include the study of this osteoinductive potential on a stem cell culture model, and potentially corroborate those results by an animal study.

7:45 PM SB12.11.14

Long-Term *In Vitro* Degradation Kinetics of Novel Drug-Loaded poly(ϵ -caprolactone) Implants for Contraception and HIV Pre-Exposure Prophylaxis Archana Krovi¹, Christine Areson¹, Guadalupe Arce Jimenez¹, Pafio Johnson¹, Chasity Norton¹, Zach Demkovich¹, Ellen Luecke¹, Linying Li¹, Daniela Cruz¹, Ariane van der Straten^{2,3} and Leah Johnson¹; ¹RTI International, United States; ²Center for AIDS Prevention Studies, United States; ³ASTRA Consulting, United States

Introduction: Most subdermal implants for long-acting (LA) drug delivery for contraception and HIV pre-exposure prophylaxis (PrEP) comprise non-biodegradable materials. The development of new biodegradable subdermal implants can advantageously eliminate the requirement of a second medical procedure to remove the devices at the end of use when drugs are depleted. One slowly degrading polymer, poly(ϵ -caprolactone) (PCL), is established as a prominent and suitable material for various biomedical applications. While the general mechanism of PCL degradation is understood and documented, we uniquely explore the biodegradation profiles of PCL in novel LA reservoir-biomedical implants for contraception and HIV PrEP, showing the influence of excipients and drug formulations on polymer degradation kinetics.

Methods: Different molecular weights of medical-grade PCL (PC-12 M_n 35 kDa, PC-17 M_n 55 kDa) were extruded into cylindrical tubes with an outer diameter of 2.5 mm and wall thicknesses of 70, 100 or 200 μm . Implants were prepared by loading excipients (castor oil, sesame oil) or drug-excipient formulations (contraceptive hormones or antiretrovirals) into an extruded tube and then enclosing the tubes via heat sealing. Unsealed empty tubes, excipient- and formulation-filled implants were sterilized via gamma irradiation at 18-24 kGy. Implants were submerged in phosphate buffered saline (PBS, pH 7.4) at 37 °C to mimic physiological conditions. Polymer properties were analyzed each month via gel permeation chromatography (GPC) and differential scanning calorimetry (DSC). *In vitro* exposure conditions were also varied to accelerate polymer degradation.

Results: Overall, the degradation rates were faster for PCL with a higher starting molecular weight (MW) (5 kDa/month), as compared to PCL of a lower initial MW (1.5 kDa/month). The presence of an excipient affected the rate of degradation; implants containing castor oil degraded slower than implants containing sesame oil. Implants with thinner walls were more susceptible to larger changes in MW when filled with sesame oil. Implants containing drug formulations degraded at similar rates, but underwent faster degradation than implants filled with excipient alone. Additionally, when the drug was formulated with sesame oil as opposed to castor oil, the polymer degradation rate was faster. For the same MW PCL, the degradation rates of empty tubes were independent of the wall thickness. Implants subjected to accelerated conditions yielded faster degradation kinetics. For instance, PCL MW at the 3-month timepoint under accelerated conditions was comparable to the PCL MW achieved at the 1-year timepoint under simulated physiological conditions. The development of this accelerated model can support rapid screening of degradation profiles for the new polymers.

Conclusions/Implications: In this long-term study, we explored novel biodegradable implants designed for contraception and HIV PrEP that comprise extruded tubes of medical grade PCL filled with relevant drugs. We studied the influence of excipients and drug formulations on the polymer degradation rate, in real time and under accelerated conditions. Next steps include evaluating the biodegradation profiles of the implants in preclinical studies and correlating the *in vitro*-*in vivo* degradation kinetics. An in-depth understanding of the degradation characteristics of this polymer platform will enable new implant designs for varied medical indications that might require tailored degradation timeframes.

Acknowledgements: This research is made possible by the generous support of the American people through the U.S. President's Emergency Plan for AIDS Relief (USAID Cooperative Agreement numbers AID-OAA-A-14-00012 and AID-OAA-A-17-00011). The contents are the responsibility of the authors and do not necessarily reflect the views of USAID, PEPFAR, or the United States Government.

7:48 PM SB12.11.15

Late News: The Effects of Hypochlorous Acid on Dental Pulp Stem Cells Shi Fu¹, Mira Rosovsky², Sabreen Alam³, Elizabeth Wang⁴, Daniel Xie⁵, Prabuddha G. Dastidar⁶, Marcia Simon¹ and Miriam Rafailovich¹; ¹Stony Brook University, United States; ²SAR High School, United States; ³Portola High School, United States; ⁴BASIS Chandler, United States; ⁵Panther Creek High School, United States; ⁶North Carolina School of Science and Mathematics, United States

The objective of this study is to investigate the effect of hypochlorous acid (HOCl) on dental pulp stem cells (DPSCs). Analyzing the cytotoxicity of hypochlorous acid contributes important information on the safety and effectiveness of using this compound in root canal irrigation. In addition, examining

the migration and differentiation of dental pulp stem cells in response to hypochlorous acid can provide insight into whether the solution will stimulate mineralization if leakage occurs on live cells around the root. HOCl was mixed with carbon dioxide enriched DPSCs growth medium to make the HOCl solution in the certain concentrations. The HOCl solution were then applied to DPSCs in the incubator for 5 minutes. The viability test result shows that DPSCs cannot survive in the HOCl solutions with the concentration greater than 30%. Proliferation assay was made in 3 different concentration sets: 10%, 20% and 30% respectively. The readout indicates that all 3 concentration groups showed no significant difference in proliferation rate compare to the control group. To analyze genetic expression of the cell abnormalities after HOCl treatment, a 28-day reverse transcription polymerase chain reaction (RT-PCR) test was performed for the 3 concentrations groups as well as the control group. The cells were lysed and RNA were taken on day-0, day-14, day-21 and day-28. Future directions would include additional trials of the different concentrations of HOCl on DPSCs migration, observing the effects of HOCl on scaffolds with DPSCs and relevant growth factors, and analyzing the long-term effects of HOCl compared to alternative root canal irrigation solutions on differentiation and dentine-pulp complex regeneration.

7:51 PM *SB12.11.16

Genes that Escape X-Chromosome Inactivation Modulate Sex Differences in Valve Myofibroblasts Brian Aguado; University of California, San Diego, United States

Introduction: Patients with aortic valve stenosis (AVS) can have fibrosis and/or calcification in valve tissue, which leads to heart failure if left untreated. Emerging clinical evidence suggests aortic valve stenosis (AVS) is a sexually dimorphic disease. Characterization of valve tissue from male and female AVS patients reveals that the aortic valve fibrosis to calcification ratio is significantly higher in women relative to men. Surgical valve replacements remain the gold standard of treatment, yet patients experience various post-surgical complications. Non-surgical approaches would be desirable, but no known biomolecular treatment exists to slow or halt progression of AVS in patients of either sex. Here, we developed an *in vitro* hydrogel culture platform for culture of male and female valvular interstitial cells (VICs) and characterized the sex-specific effects of microenvironmental cues on myofibroblast activation.

Materials and Methods: VICs were isolated from porcine aortic valves and seeded on soft RGD-functionalized PEG hydrogels (elastic modulus, $E \sim 6$ kPa) known to maintain the quiescent VIC phenotype and stiff hydrogels ($E \sim 41$ kPa) known to activate VICs to a myofibroblast state. Male and female VICs were cultured separately and seeded on hydrogels for 3 days. VICs were immuno-stained for the myofibroblast marker alpha smooth muscle actin (α -SMA) and imaged to quantify the percentage of cells with α -SMA stress fibers. Myofibroblast transcriptomes were analyzed using the HISAT2-Rsubread-EdgeR differential gene expression pipeline, and pathway enrichment analysis was performed in Ingenuity Pathway Analysis (IPA).

Results and Discussion: Our data suggest male and female VICs exhibit sex-specific myofibroblast responses to hydrogel substrates at day 3 in culture. We consistently observed female VICs to have elevated myofibroblast activation on soft gels that mimics the stiffness of healthy valves ($E \sim 6$ kPa) and stiff gels that recapitulate fibrotic valve stiffness ($E \sim 40$ kPa). Our transcriptomic data suggest hundreds of sex-specific gene expression differences between male and female myofibroblasts, and we identified the RhoA/ROCK signaling pathway to have increased activity in female VICs using IPA. Indeed, *in vitro* validations revealed female VICs to be less sensitive to RhoA/ROCK inhibition relative to male VICs on stiff hydrogels. Recognizing that sex-dependent variability in cellular phenotypes is attributed to the 15-25% of genes that escape X-chromosome inactivation (XCI) in women, we also found 28 genes differentially expressed in female myofibroblasts that are also known to escape X-chromosome inactivation. Two of these genes, *BMX* and *STS*, which encode for the BMX non-receptor tyrosine kinase and steroid sulfatase and necessary for cardiac hypertrophy and integrin expression, were validated as key genes that regulate RhoA/ROCK activity in female VICs. Using ibrutinib and irosustat to inhibit *BMX* and *STS*, respectively, we observed increased female VIC deactivation in response to RhoA/ROCK inhibition. Collectively, we suggest genes that escape X-chromosome inactivation uniquely regulate myofibroblast activation processes in female myofibroblasts.

Conclusions: Our data support the importance of (1) sex-separating cells and (2) engineering the appropriate culture microenvironment to understand how male and female cells interpret microenvironmental cues. We suggest female VICs are more susceptible to myofibroblast activation due to increased expression of key XCI genes, which may contribute to increased fibrosis found in valve leaflets from female AVS patients. We envision future *in vitro* disease models to appreciate the potent effects of cell sex, which may impact how diseases are understood and treated as a function of sex.

SYMPOSIUM SF01

Advanced Atomic Layer Deposition and Chemical Vapor Deposition Techniques and Applications
November 30 - December 8, 2021

Symposium Organizers

Noa Lachman, Tel Aviv University
Graziella Malandrino, Univ di Catania
Kevin Musselman, University of Waterloo
Wyatt Tenhaeff, University of Rochester

Symposium Support

Bronze
Waterloo Institute for Nanotechnology

SESSION SF01.01: 2D Materials
Session Chairs: Gilbert Nessim and Wyatt Tenhaeff
Tuesday Morning, November 30, 2021
Sheraton, 3rd Floor, Berkeley

10:30 AM *SF01.01.01

The Versatility of CVD to Synthesize 1D and 2D Nanostructures—Carbon Nanotubes and Transition Metal Chalcogenides for Electronic and Electrochemical Applications [Gilbert D. Nessim](#); Bar Ilan University, Israel

1D Nanosynthesis

Despite the massive progress achieved in the growth of carbon nanotube (CNT) forests on substrate, apart from lithographic patterning of the catalyst, little has been done to selectively (locally) control CNT height. Varying process parameters, gases, catalysts, or underlayer materials uniformly affects CNT height over the whole substrate surface. We show here how we can locally control CNT height, from no CNTs to up to 4X the nominal CNT height from iron catalyst on alumina underlayer by patterning reservoirs or by using overlayers during annealing or growth.

We show how we can lithographically pattern the reservoir material and obtain four different CNT heights during a unique growth process: no growth (Cu/Ag reservoir), nominal growth (no reservoir), 2X growth (Fe reservoir), and 4X growth (Mo reservoir).

Using a complementary technique, we show how a copper or nickel overlayer (stencil or bridge) placed above the catalyst surface during pre-annealing or during CNT growth deactivates the catalyst. We showed how we could pattern regions with CNTs and without CNTs by simply annealing the sample with a patterned overlayer positioned above its surface. We thus synthesized patterned CNT forests using a simple process, without the need for lithography.

We can combine the overlayer technique with one of the above-mentioned reservoirs (no reservoir, Cu/Ag reservoir, Fe reservoir, or Mo reservoir) to further modulate CNT growth by offsetting some or all of the growth enhancements achieved using the reservoirs. This modulation of the CNT height is a significant improvement compared to the "CNTs (one height) / no CNTs" patterning that has been achieved using lithography of the catalyst, and moves us closer to building 3D architectures of CNTs that could be useful for future electronic devices or sensors.

2D Nanosynthesis

Since the excitement about graphene, a monolayer of graphite, with its 2010 Nobel Prize, there has been extensive research in the synthesis of other non-carbon few/mono-layers exhibiting a variety of bandgaps and semiconducting properties (e.g., n or p type). The main approaches to deposit few/monolayers on a substrate are: (a) bottom-up synthesis from precursors using chemical vapor deposition (CVD) or (b) top-down exfoliation (liquid or mechanical) of bulk layered material. Using a Lego approach of superposing monolayers, we can envisage the fabrication of heterojunctions with original electronic behavior.

Here we show a combined bottom-up and top-down approach where (a) we synthesize in one step high yields of bulk layered materials by annealing a metal in the presence of a gas precursor (sulfur, phosphorous, or selenium) using chemical vapor deposition (CVD) and (b) we exfoliate and deposited few/mono-layers on a substrate from a sonicated mixture of our material in a specific solvent. It is interesting to note that, besides the structure being 2D layered, the properties of the nanomaterials synthesized slightly differ from the materials with the same stoichiometry synthesized using conventional chemical methods (e.g., solvothermal).

In this talk, we will discuss the chemical synthesis, the very extensive characterizations, and the lessons we learned in making multiple metal sulfides (Cu-S, Ag-S, Ni-S), metal phosphides (Ni-P, Cu-P), and metal selenides (Ag-Se, Cu-Se, W-Se, Mo-Se). We will see how we integrated these new materials into electrochemical devices and sensors.

11:00 AM SF01.01.02

Fluid Guided Chemical Vapor Deposition of Large-Scale Monolayer Two-Dimensional Materials [Bo Li](#), Qianhong Wu, Dong Zhou and Ji Lang; Villanova University, United States

Chemical vapor deposition (CVD) has been used extensively for synthesizing two-dimensional (2D) materials. Among various CVD methods, atmosphere pressure CVD is of great interest due to its low cost and promise for high-quality monolayer 2D materials. Despite extensive efforts, the understanding of the reaction mechanism and the key controlling parameters is still in its embryonic stage. Hence, it is extremely challenging to achieve large-scale continuous films. Here, we present a fluid-guided growth strategy and use MoSe₂ as a model system for understanding and controlling the growth of 2D materials. We have integrated experiment and computational fluid dynamics (CFD) analysis in the full-reactor scale. We have identified three key parameters in obtaining large-scale continuous film: good precursor mixing, low fluid velocity, and low shear rate near the substrate. Following these principles, we modified the geometry of the growth setup and successfully obtained inch-scale monolayer MoSe₂. This unprecedented integration of fluid design and simulation lays the foundation for designing new CVD systems to synthesize 2D materials and other thin-film nanomaterials.

11:15 AM SF01.01.03

Polymer Compatible Low Temperature Plasma-Enhanced Chemical Vapor Deposition of Graphene on Electroplated Cu for Flexible Hybrid Electronics [Chen-Hsuan Lu](#)¹, [Chyi-Ming Leu](#)² and [Nai-Chang Yeh](#)¹; ¹California Institute of Technology, United States; ²Industrial Technology Research Institute, Taiwan

Flexible Hybrid Electronics (FHE) and the Fan-Out redistribution layer (RDL) rely on electroplated Cu. In this work, we demonstrate direct low-temperature (~ 100 °C) plasma enhanced chemical vapor deposition (PECVD) of graphene on electroplated Cu over polyimide substrate, which passivates and strengthens the electroplated Cu circuit on polyimide. We investigate the effect of the H₂/CH₄ ratio on PECVD graphene growth and find that not only the quality of graphene but also the durability of Cu are affected. Folding for 100,000 cycles with a bending radius of 2.5 mm and the corresponding resistance tests show that the Cu circuit when covered with graphene grown with higher H₂/CH₄ ratios could sustain many more bending cycles. In addition, we find that graphene coverage could suppress the formation of Cu oxide under ambient environment for at least 8 weeks after the PECVD process.

11:30 AM SF01.01.04

Evolution of the Graphene-Metal Interface During Chemical Vapor Deposition [Mitisha Surana](#)¹, [Ganesh Ananthkrishnan](#)¹, [Matt Poss](#)¹, [Jad Yaacoub](#)¹, [Tusher Ahmed](#)¹, [Nikhil Chandra Admal](#)¹, [Pascal Pochet](#)², [Harley Johnson](#)¹ and [Sameh Tawfik](#)¹; ¹University of Illinois at Urbana-Champaign, United States; ²Université Grenoble Alpes, France

Chemical vapor deposition (CVD) is the most widely used process to synthesize graphene for device applications. In this process, the interaction between graphene and the metal catalyst plays a critical role in the properties and quality of graphene, producing strains, wrinkles, moiré patterns, and in some cases an electronic bandgap in graphene. A very robust and repeatable phenomenon observed after graphene CVD is the modification of the substrate's surface topography. Orientation-dependent large, faceted morphologies have been observed under graphene on all metal substrates. These facets grow by step-

bunching and have a typical size of 50-100 nm. Previous studies are limited to a qualitative description of step bunching, and model the phenomenon as a bending energy-driven process. In this presentation, we present an approach to quantitatively characterize and analyze the facets' orientation. We use electron backscatter diffraction (EBSD) in conjunction with atomic force microscopy to calculate the crystallographic orientation of facets that have step-like and pyramid-like topologies. We will present new approaches to visualize the crystallographic evolution of these steps using inverse pole figures (IPF). We carry statistical analysis on the observed step sizes and orientations on various catalyst grain orientations. We correlate the geometrical facet characterization method to measurements made by Transmission Electron Microscopy. Our studies reveal that the step-like facets comprise a high-symmetry low-index surface on one side and a vicinal surface on the other side, showing that system energy minimization is not the only driving force of the phenomena. We believe that faceting occurs as a result of a trade-off between the diffusion kinetics and the interfacial energy of the complete system which includes van der Waal's interaction, the thermal strains in addition to the bending energy of graphene. MD simulations also show suppression of the substrate's melting under graphene, which we believe plays a role in the kinetics of the faceting process. Our studies provide insights into metal-graphene interfaces that will enable us to better control graphene during synthesis.

SESSION SF01.02: Modeling and Novel Precursors, Mechanisms
Session Chairs: Bo Li and David Munoz-Rojas
Tuesday Afternoon, November 30, 2021
Sheraton, 3rd Floor, Berkeley

1:30 PM SF01.02.01

Applications of a Combined Approach of Kinetic Monte Carlo Simulations and Machine Learning to Model Atomic Layer Deposition (ALD) of Metal Oxides [Emily Justus](#)¹, David Magness¹, Bikash Timalisina¹, Judy Z. Wu² and Ridwan Sakidja¹; ¹Missouri State University, United States; ²The University of Kansas, United States

Metal-oxides such as ZnO or Al₂O₃ synthesized through Atomic Layer Deposition (ALD) have been of great research interests as the candidate materials for ultra-thin tunnel barrier layers is. In this study, we have applied a 3D on-lattice Kinetic Monte Carlo (kMC) code developed by Timo Weckman's group to simulate the growth mechanisms of the tunnel barrier layer and to evaluate the role of various experimentally relevant factors of the ALD processes. We have systematically studied the effect of a wide range of ALD parameters such as the chamber pressure and temperature, pulse/purge times, as well as the coverage of wetting layers on the substrate. The database generated from the kMC simulations was subsequently used as descriptors in the subsequent analyses via Machine Learning (ML) algorithms to gain more insights into the dynamics of the deposition processes. The results of a combined approach of kMC and ML were then compared to the experimental results. The support from NSF (EPMD Division) Award No. 1809284 is gratefully acknowledged. We also thanks to NERSC for the computational support.

1:45 PM SF01.02.02

Modeling Atomic Layer Deposition of Alumina as an Ultra-Thin Tunnel Barrier Using Reactive Molecular Dynamics [Devon T. Romine](#)¹, Yuxuan Lu¹, Judy Z. Wu² and Ridwan Sakidja¹; ¹Missouri State University, United States; ²University of Kansas, United States

In this study, we have utilized the reactive molecular dynamics (MD) simulations to model the Atomic Layer Deposition (ALD) process that forms an ultra-thin film of a tunnel barrier made of amorphous alumina. We chose the reactive MD approach over the ab-initio molecular dynamics simulation used in previous studies due to its lower computational cost, its ability to model over a relatively longer simulation period and its capability to assess atomistic-based dynamics for a larger substrate. To further refine and parameterize the existing ReaxFF potentials, we used the Density Functional based Tight Binding (DFTB) -based in conjunction with the Python toolkit as implemented in the Amsterdam Modeling Suite (AMS) program package. The additional training sets were made from evaluations of the potential energy surface (PES) scans of various ALD-relevant species including H₂O, OH, and the ALD precursors trimethylaluminum (TMA) and Bis(20ethyl-1,3-cyclopentadien-1-yl) magnesium (C₁₄H₁₈Mg), as well as the bond-dissociation energies during the reactions that occur when they interact. We systematically evaluated the role of the various ALD precursors including the TMA and C₁₄H₁₈Mg and the water pulse toward the chemical reactions that take place on the surface during ALD. We additionally evaluated the role of experimentally- observable parameters including the operating temperature and precursor concentrations for the internal structure of the amorphous alumina/magnesium as the final deposition products. Lastly, we assessed the role of wetting layers as the means to improve the quality and performance of the tunnel barrier. The support of NSF (Grant No. 1809284) from the Electronics, Photonics and Magnetic Devices (EPMD) Program is gratefully acknowledged. We also thanks to NERSC for the computational support.

2:00 PM SF01.02.03

Thermal Decomposition of Titanium(IV) Isopropoxide Studied by Reactive Force-Field Molecular Dynamic Simulations [Benazir Fazlioglu Yalcin](#), Dundar E. Yilmaz, Adri van Duin and Roman Engel-Herbert; The Pennsylvania State University, United States

The thermal decomposition process of metalorganic precursors, which are frequently used in various thin film deposition techniques, can have a governing effect on the overall growth and reaction kinetics of the thin film deposition methods employed. Particularly in cases of more complex thin-film synthesis schemes, such as combinatorial approaches employing molecular beam epitaxy and chemical vapor deposition, or for the deposition of films with multi-elemental composition, such as ternary and quaternary complex oxide thin films with perovskite structure, a quantitative understanding of reaction pathways, activation energies, and by-product formation at the atomic scale are becoming key towards an improved understanding of the reaction kinetics, as well as providing insights towards tailoring ligand chemistry of the metalorganic precursor employed.

A recently proposed thin film growth technique, dubbed hybrid molecular beam epitaxy,¹ has shown dramatic improvement in the film quality of complex perovskite oxide films in general and SrTiO₃ in particular, attributed to the accessibility of a self-regulated growth mechanism enabled by the volatility and decomposition characteristics of metalorganic precursors involved in the growth. Despite remarkable advancements in material quality, no clear understanding of the underlying atomic-scale growth mechanism has been achieved. For the particular case of SrTiO₃, where Sr is supplied by a thermal effusion cell and Ti using the metalorganic precursor titanium tetraisopropoxide (Ti(OiPr)₄, TTIP), the relatively complex thermal decomposition process of TTIP has thus far prevented a detailed understanding of the growth kinetics at play.

In this talk, we will discuss the first steps towards resolving the mystery of the hybrid MBE growth process by studying the thermal decomposition of TTIP using reactive force field molecular dynamics (ReaxFF-MD) simulations.² We find that the total thermal decomposition takes place via multiple steps and is typically initiated by bond breaking between C-O bonds rather than Ti-O bonds without additional hydrogen abstraction, followed by multiple ligand bond breaking steps, all with hydrogen abstraction. Metadynamics simulations were in excellent agreement with the ReaxFF-MD, revealing that the energy barriers to break Ti-O bonds (237-451 kcal/mol) were 4-5 times higher compared to breaking C-O bonds instead (53-119 kcal/mol). Nevertheless, ligand bond breaking subsequent to the first C-O bond breakage can also involve Ti-O bonds, which is attributed to the over coordination of Ti with oxygen.

Performing the ReaxFF-MD simulation in the presence of TiO₂ and SrO terminated SrTiO₃(001) surfaces revealed that the particular surface chemistry of SrTiO₃ growth front dramatically affected the initialization of the TTIP decomposition process. While the metalorganic was found to be rather stable with a pronounced tendency to thermally desorb from TiO₂ terminated SrTiO₃(001) surfaces, its decomposition on SrO terminated surfaces was much pronounced, providing first insights into the intricacies of the hybrid MBE growth process.

¹ M. Brahlek, A. Sen Gupta, J. Lapano, J. Roth, H. T. Zhang, L. Zhang, R. Haislmaier, R. Engel Herbert, Adv. Funct. Mater. **28**, 1702772 (2018).

² T.P. Senftle, S. Hong, M.M. Islam, S.B. Kylasa, Y. Zheng, Y.K. Shin, C. Junkermeier, R. Engel Herbert, M.J. Janik, H.M. Aktulga, T. Verstraelen, A. Grama, A.C.T. Van Duin, npj Comp.Mater. **2**, 15011 (2016).

2:15 PM SF01.02.04

Plasma-Enhanced Atomic Layer Deposition of Titanium Nitride—Impact of the N-Reactant on the Growth, Conformality and Quality of the Film Badie Clemence¹, Maissa Barr², Julien Bachmann^{2,3}, Thomas Defforge⁴, Gael Gautier⁴, Héloïse Tissot¹ and Lionel Santinacci¹; ¹Aix-Marseille Université, France; ²Friedrich-Alexander-Universität Erlangen-Nürnberg, Germany; ³Saint-Petersburg State University, Russian Federation; ⁴Tours Université, France

Titanium nitride thin films can be fabricated by both thermal and Plasma-Enhanced Atomic Layer Deposition (ALD and PE-ALD, respectively). The prevalent precursor couple is TDMAT as Ti-source and NH₃ as co-reactant. This combination is suitable for both routes. Nevertheless, PE-ALD recipes found in the literature exhibit a slower growth rate compared to thermal ALD (see e.g. Ref [1]). This can be disadvantageous for industrial development. However, in addition to NH₃, PE-ALD offers a larger palette of nitrating agent such as N₂, H₂ and N₂/H₂. This work compares therefore the PE-ALD of TiN using NH₃ and N₂, both combined with Ar, to evidence their influence on the final film properties and to maximize the growth rate. Parameters impacting the growth are monitored by in situ characterizations (ellipsometry, OES) while ex situ techniques (TEM/SEM/AFM, XPS, XRD, 4-probes measurements) are used to assess the morphology, the composition, the crystalline structure and the electric properties of the films. A similar approach is applied to the thermal route taken as reference.

To optimize the initial PE-ALD recipe, a set of parameters are investigated: the pulse and purge durations as well as the dilution of the N-sources within Ar and the plasma power. Those parameters are adapted to limit recombination reactions of the generated reactive species between the remote plasma source and the substrate. A large Ar dilution of both N₂ and NH₃ limits the film growth, while a 1:1 gas ratio for N-source and Ar leads to the optimal values. The pulse duration is set at 2 and 5 s for NH₃- and N₂-based plasmas, respectively. The purge duration is also optimized to shorten the ALD cycle duration. The applied plasma power (from 50 to 300 W) has no significant impact on the growth per cycle (GPC) with NH₃ while, using N₂, the GPC is maximum at the highest power. This is consistent with the expected low reactivity of N₂ (inert without plasma activation) regarding to highly reactive NH₃. These measurements are correlated to the plasma signals observed by OES. This indicates that producing less active species enhances their transport by limiting their recombinations. The films grown from both N-sources have a similar roughness, composition and morphology. However, the conductivity and the GPC are superior using NH₃-based plasma. In addition, this process exhibits a remarkable conformality on high aspect ratio Si substrate for a PE-ALD route. The N₂ plasma process presents an acceptable film quality, it can be considered as well since it is more affordable, and it uses a non-harmful gas.

[1] L. Assaud et al. Highly-Conformal TiN Thin Films Grown by Thermal and Plasma-Enhanced Atomic Layer Deposition, *ECS J. Solid State Sci. Technol.*, 2014, **3**, 7, 253–258.

SESSION SF01.03: Poster Session: Advanced Atomic Layer Deposition and Chemical Vapor Deposition Techniques and Applications

Session Chairs: Bo Li and Wyatt Tenhaeff

Tuesday Afternoon, November 30, 2021

8:00 PM - 10:00 PM

Hynes, Level 1, Hall B

SF01.03.01

Growth of SiO₂ by SMFD-ALD and Its Application in Thin-Film Capacitor Mahesh Nepal, Wendifer R. Ramos and Tara P. Dhakal; Binghamton University, United States

We report uniform film growth of SiO₂ on a large surface area (8-inch wafer) using synchronous modulated flow draw ALD (SMFD-ALD) technique. This technique allows greater precursor utilization and shorter deposition cycles time by modulating a pressure gradient between the reaction space and the pumping system. SiO₂ thin films are grown using BDEAS, ozone, and MMH precursors, wherein MMH acts as a catalyst. The use of catalyst is very important in SiO₂ film growth because without catalyst, surface reactions are generally very slow and occur at exceptionally high temperature. This SiO₂ film will be used as a capping layer in Al₂O₃/TiO₂ based nanolaminate capacitors to reduce the leakage current thereby improving working potential. We have already been able to fabricate capacitors with multi-stacked Al₂O₃/TiO₂ nanolaminate (~150 nm) with 4 nm of Al₂O₃ capping layer deposited by SMFD-ALD technology on both rigid and flexible substrates. The stacking of thin layers of these oxides results in a dielectric constant value that is one or two orders of magnitude higher than the individual oxides used due to a process known as Maxwell Wagner relaxation. On a planar substrate, these capacitors have the specific capacitance of ~1.6 /cm² and breakdown voltage of 3 V (~2 x10⁵ V/cm) with 10 leakage current. To lower the leakage and increase the breakdown voltage, SiO₂ will be employed as a capping layer and new capacitors will be fabricated on both planar and nano-structured high surface area electrodes, and the results will be presented. Since ALD technique is proved to produce uniform and conformal coating on high aspect ratio structures, it allows us to coat these dielectric nanolaminates in high surface area electrodes to further increase the energy density. As we have a well-established process for ZnO nanorods growth, nanostructured capacitors will be fabricated by coating Al₂O₃/TiO₂/SiO₂ nanolaminate on ZnO nanorods.

SF01.03.02

Correlation Between Plasma Etching Behavior of Silicon Carbide and Micropipe Defects Je Hoon Oh, Jongbeom Kim, Je Jun Jeong and Kyu Hwan Oh; Seoul National University, Korea (the Republic of)

Silicon carbide (SiC) is a remarkable semiconductor material for high-temperature and high-voltage applications. It is also used as a material for a focus ring in etching process of silicon wafers, due to its high plasma resistance. SiC is commonly fabricated via chemical vapor deposition (CVD) or physical vapor transport (PVT) methods, and CVD-SiC is widely used as a material for the focus ring to protect the electrostatic chuck and create a uniform plasma condition during the plasma etching process of a silicon wafer. It is well known that a defect typically found in SiC known as a micropipe degrades the material's quality. A micropipe density is an important characteristic in SiC quality through SiC development due to the problem of reduced electron mobility.

Currently, CVD-SiC is widely used because it is favorable for manufacturing SiC with a low micropipe density. However, CVD-SiC has an issue in that the unit cost is high. PVT-SiC, on the other hand, offers the advantage of a cheap production cost despite the difficulty of reducing micropipe density. While it has been reported that micropipes reduce electron mobility in SiC, no specific influence on plasma resistivity has been identified. In this study, we investigated the etching rate of CVD-SiC with small grain size and PVT-SiC with large grain size when SiC crystals grown by PVT and CVD methods are etched by reactive ion etching (RIE) under severe etching circumstances. In addition, we compared the etching behavior of micropipes and other sections.

As a result, the etching behavior in the micropipe was revealed to differ from that at the grain boundary. CVD-SiC with a small grain size has a problem in that SiC particles are peeled off grain by grain during the etching process, affecting the Si wafer quality. In the case of PVT SiC, however, the etching resistance was found to be higher due to lower grain boundary density. We also observed that, despite its relatively high micropipe density, PVT-SiC could be used as a focus ring material due to its high plasma resistance. The lower unit cost of the SiC focus ring, which is required as a consumable in the semiconductor process, is expected to increase production efficiency.

SESSION SF01.04: Organic and Hybrid Materials
Session Chairs: Emily McGuinness and Wyatt Tenhaeff
Wednesday Morning, December 1, 2021
Sheraton, 3rd Floor, Berkeley

10:30 AM *SF01.04.02

Topologically Controlled Surfaces via Chemical Vapor Deposition Polymerization Joerg Lahann; University of Michigan, United States

There is a broad and increasing interest in chemically controlled surfaces. Potential applications span from biotechnological and medical to antifouling and adhesive coatings. Chemical vapor deposition (CVD) polymerization of substituted [2.2]paracyclophanes is a versatile method that can result in a wide spectrum of functionalized surface coatings [1-3]. Emerging research involves the design of topologically controlled surfaces using templated CVD polymerization. Controlled deposition into thin liquid crystalline films resulted in supported polymer nanofiber arrays where intrinsic properties of the LC phase dictate the lengths, shapes and diameters of the nanofibers [3]. Building upon these earlier efforts, we explored the LC-templated CVD polymerization of chiral [2.2]paracyclophanes for the synthesis of nanohelices with superhierarchical chirality. Intrinsic properties of the precursors such as the side group chemistry and enantiomeric excess critically influence the properties of the resulting enatiomorphic polymer coatings. A more detailed understanding of the underlying mechanisms contributing to the chirality transfer from molecular to meso- and macroscopic scales is emerging and will inform the controlled synthesis of chiral interfaces for biomedical, optical and electronic properties.

[1] H.Y. Chen, J. Lahann, Designable Biointerfaces Using Vapor-Based Reactive Polymers, *Langmuir* **2011**, 27(1), 34–48.

[2] X. Deng, C. Friedmann, J. Lahann, Bio-Orthogonal “Double-Click” Chemistry Based on Multifunctional Coatings, *Angewandte Chemie International Edition* **2011**, 50, 6522-6526.

[3] A. Ross, H. Durmaz, K. Cheng, X. Deng, Y. Liu, J. Oh, Z. Chen, J. Lahann, Selective and reversible binding of thiol-functionalized biomolecules on polymers prepared by chemical vapor deposition polymerization, *Langmuir* **2015**, 31, 5123-5129.

[4] K.C.K. Cheng, M.A. Bedolla-Pantoja, Y.-K. Kim, J.V. Gregory, F. Xie, A. de France, C. Hussal, K. Sun, N.L. Abbott, J. Lahann, Templated Nanofiber Synthesis via Chemical Vapor Polymerization into Liquid Crystalline Films, *Science* **2018**, 362, 804–808.

11:00 AM SF01.04.03

In Situ Synthesis of Ni₃S₂ Nanowires Filled Carbon Nanotubes and Study of Their Electrical Properties Yuba R. Poudel and Wenzhi Li; Florida International University, United States

Filled carbon nanotubes (CNTs) possess unique physical properties which arise because of the combined effects of the host CNTs and the guest fillers. Until now, many inorganic and organic materials have been successfully encapsulated inside CNTs, however, there is still a lack of a reliable method to achieve a complete filling of CNT cores with transition metal sulfide nanowires. Unlike the conventional ex-situ filling techniques which primarily lead to a partial filling, an in-situ filling method can be used to achieve a continuous and complete filling of the CNT channels. We have developed for the first time, a simple and reliable in-situ method to synthesize the Ni₃S₂ nanowires filled CNTs (Ni₃S₂@CNTs) directly on different substrates such as silicon, nickel foam, and carbon cloth using nickel salt and nickel nanoparticles as the catalyst precursor in a chemical vapor deposition system. The samples have been characterized using SEM, TEM, EDX, Raman spectroscopy, XRD, UV-Vis, TGA, and FTIR. The electron microscopy results show a linear and a tapering structure of Ni₃S₂@CNT completely filled with a continuous and single-crystalline Ni₃S₂ nanowire up to several micrometers in length whereas the Raman spectroscopy indicates a highly graphitized multi-walled CNT system ($I_D/I_G = 0.26$). The intrinsic I-V characteristics of individual Ni₃S₂@CNTs were studied using both two probe and four-point probe methods which reveal the metallic properties of Ni₃S₂@CNTs with a mean resistivity of $6.1 \times 10^{-5} \Omega m$. Also, it was observed that an individual Ni₃S₂@CNT having a small diameter (below 150 nm) can undergo an electrical breakdown at a higher current causing the encapsulated Ni₃S₂ nanowire to extrude out from the breakdown region whereas the Ni₃S₂@CNT with a bigger diameter can be emptied by pushing out the Ni₃S₂ nanowire along the direction of the current. Given the high quality and metallic behavior of Ni₃S₂@CNTs, they can find potential applications in future nanoelectronics devices and systems.

This work is supported by the National Science Foundation under Grant DMR- 1506640.

11:15 AM SF01.04.04

Halogenated Polymer Thin Film with Ultra-High Refractive Index Ni Huo; University of Rochester, United States

High refractive index polymers (HRIP) are an incredibly important class of materials given their potential applications in optoelectronic devices, such as anti-reflective components for displays, encapsulants for light-emitting diodes, and optical sensors. Because typical commodity polymers possess refractive indexes (RI) in the range 1.3 – 1.7, obtaining polymers with RI greater than 1.8 while maintaining high optical transparency is an important challenge. Halogen atoms such as chlorine, bromine, and iodine have high atomic refractivity ranging from 5.97 to 13.90, making them useful components in the development of HRIPs.

In this work, a series of halogenated polymer thin films with high refractive indexes ($n = 1.7 - 2.0$) and outstanding optical transparency in the visible range, were prepared via a unique vapor phase process – initiated chemical vapor deposition (iCVD). iCVD is a versatile technique that has been used to fabricate a wide range of polymer coatings for many applications. In this study, poly(4-vinylpyridine) (P4VP) films with thickness ranging from 100nm to 600nm were prepared using iCVD, then treated by halogen vapor to form halogen-containing polymer thin films with high RI. The charge-transfer complex (CTC)

formed between P4VP and halogen compounds, prepared by a simple vapor phase infiltration of halogen compounds, increases the RI of the P4VP thin film from 1.58 to 2.0 or higher, while maintaining the conformal and smooth nature of as-deposited thin films. Specifically, the P4VP-I₂ complex is demonstrated to have an RI of 2.0 and is transparent above a wavelength of 600nm. In another formulation, P4VP complexed with ICl achieved an RI up to 1.77, while still retaining the outstanding optical transparency throughout visible range. The RI of the halogenated polymer films can be further fine-tuned by controlling the concentration of CTC in the polymer film via copolymerization with other monomers that are inert to halogen compounds. In this work, a series P4VP thin films copolymerized with ethylene glycol dimethacrylate (EGDMA) with RI ranging from 1.50 to 1.98 were prepared. The formation of charge-transfer complex (CTC) in halogenated polymer thin film was confirmed via both Fourier-transform infrared and UV-Vis spectroscopies. The optical performance of these coatings was characterized by spectroscopic ellipsometer and specular reflectometry. The thermal resistance and environmental stability of these films were also investigated as a function of temperature. The refractive index (RI) of P4VP-I₂ film decreased by 7.9% after 24 hours at 20°C. In comparison, the RI of P4VP-ICl film decreased by 0.41% over 24 hours at 20°C. These halogenated polymer thin films are expected to have wide applications in sensors and optoelectronic devices.

SESSION SF01.05: Devices and Applications I
Session Chairs: Eran Edri and Andrew Meng
Wednesday Afternoon, December 1, 2021
Sheraton, 3rd Floor, Berkeley

1:30 PM SF01.05.01

Late News: Area Selective Plasma Enhanced Chemical Vapor Deposition of Silicon using a Fluorinated Precursor Ghewa Akiki; Ecole Polytechnique, France

Area-selective deposition (ASD) is a process that controls where the deposition takes place through the underlying surface rather than through any masking step. This process can be achieved by either Atomic Layer Deposition (ALD) or Chemical Vapor Deposition (CVD) techniques [1]. In previous work, we studied area selective plasma enhanced CVD or PECVD using Ar/SiF₄/H₂ plasma chemistry [2]. For specific plasma parameters, a microcrystalline silicon film is selectively grown on a SiO_xN_y area while the AlO_x adjacent area remains pristine (see figure 1). This effect was then attributed to the formation of Al-F bonds that blocks the deposition of silicon on top of the AlO_x area [3].

However, when the plasma conditions are slightly changed or when those two materials are patterned, the selectivity is lost. Each case will be discussed and presented based on in-situ ellipsometry, atomic force microscopy and x-ray photoelectron spectroscopy analyses.

[1] G. N. Parsons and R. D. Clark, *Chem. Mater.* 32, 4920 (2020).

[2] G. Akiki, D. Suchet, D. Daineka, S. Filonovich, P. Bulkin, and E. V. Johnson, *Appl. Surf. Sci.* 531, 147305 (2020).

[3] G. Akiki, M. Fregnaux, I. Florea, P. Bulkin D. Daineka, S. Filonovich, M. Bouttemy and E. V. Johnson, *J. Vac. Sci. Technol. A* 39, 013201 (2021)

1:45 PM SF01.05.02

Using Molecular Layer Deposition to Instill Monovalent Selectivity in Cation Exchange Membranes Without Compromising Resistivity Eran Edri, Oded Nir and Eyal Wormser; Ben-Gurion University of the Negev, Israel

Desalination is becoming a vital part of the solution to water scarcity with a current worldwide desalination capacity of approx. 100 million m³/day, which is expected to grow by 40% by 2030. In 2019, 29% of the global desalination capacity was of brackish and river water (500-20000 ppm TDS). Most (98%) of the brackish water nowadays is desalinated by reverse osmosis (RO) which completely deprives the permeate of Mg²⁺ and Ca²⁺. Both are critical nutrients needed to sustain human health and agriculture. Replenishing these divalent ions to the desalinated water increases the cost and complexity of the overall process and decreases its sustainability and economic attractiveness. Electrodialysis is energetically more efficient than RO for desalination of brackish water and using monovalent selective membranes—membranes that enable monovalent ions passage, but retain divalent ions—offer a potential solution to preserve the nutrients in the permeate. However, current methods for instilling ion selectivity use large macromolecular building blocks to form the selective layer, which increases ion transport resistance and hence the energy demand and cost of selective electrodialysis. To disrupt the resistance-selectivity trade-off, a method for uniformly depositing an ultrathin and highly charged selective layer is needed.

While low-temperature atomic layer deposition is a suitable method for depositing ultrathin metal oxides on membranes, the elastic mismatch between metal oxides and polymers hinders the stability of the selective layer. Instead, we used molecular layer deposition of alucones to resolve the elastic mismatch. We show that the electrostatic charge of alucone surface leads to monovalent selectivity values on par with commercial membranes, but with only a marginal increase in resistivity. We further investigate the resistance-selectivity trade-off using electrodialysis simulation and suggest “guidelines” for further improvement of performance.

2:00 PM SF01.05.03

Multiscale Materials Bear Multiscale Challenges—Why Bridging the Length Scales is Important for Developing New, Multifunctional, Bulk Nanocomposites. Alexander Plunkett¹, Berta Domènech¹, Diletta Giuntini^{2,1} and Gerold A. Schneider¹; ¹Hamburg University of Technology, Germany; ²Eindhoven University of Technology, Netherlands

Nanomaterials, in which nanoparticle size-dependent properties are maintained, but also new collective properties derived from the synergy between their individual building blocks emerge, gained significant interest in recent decades. However, the lack of structural integrity when the dimensions are upscaled still limits them to microscale applications. The lack of control over larger length scales when nanomaterials are processed usually leads to defects which scale with the dimensions of the specimen. A promising strategy to overcome this issue is inspired by nature. Nature in fact evolved hard, strong, and tough materials-like bone, teeth, and nacre- by hierarchically structuring nano building blocks with soft interfaces on different length scales.

The synthetic emulation of these multiscale, hierarchical structures based on hard minerals combined with soft biopolymers with structural features down to the nanoscale bears tough practical challenges on each length scale. These challenges start at the atomic level, and expand up to the final macroscopic material and its application. Therefore the cooperation from different scientific disciplines ranging from chemistry and physics to material science and engineering becomes crucial.

This talk will discuss how these different hurdles can be addressed via a bottom-up approach using organo-functionalized ceramic nanoparticles. It will be shown how the quest begins on the atomistic scale, aiming to boost and control the materials' strength by a crosslinking reaction of the nano-building blocks as well as their self-assembly at the nanoscale level. At the microscale, it will be shown how emulsion-based approaches allow to control the shape of nano- to micro-architected suprastructures. These ceramic nanocomposite suprastructures can be afterwards functionalized in order to process them on the mesoscale with polymers ultimately leading to robust macroscale materials in which nano- and micro-features are maintained.

2:15 PM SF01.05.04

Compliant and Transparent Polymer Barrier Layer for Flexible Optics Yineng Zhao, Ni Huo and Wyatt E. Tenhaeff; University of Rochester, United States

Flexible optics and optoelectronics are becoming increasingly desirable in many advanced technologies. One example is varifocal liquid lenses mimicking the mechanism of a human eye, where transparent fluid is encapsulated between two flexible membranes. Varifocal liquid lens is particularly useful in volume-limited applications, such as miniature medical devices, smartphone cameras, and wearable augmented reality equipment. The focal length is modulated by mechanically actuating the membrane—similar to the ciliary muscle in the human eye. These optical devices present significant material design challenges; flexible, transparent coatings are required to inhibit the diffusion of high-index fluids (optical oil) into the elastomeric membrane, which would otherwise degrade the optical quality of the lens. Conventional optical coatings based on inorganic compounds, such as silica and alumina, can provide the required barrier performance but their intrinsic brittleness limit compatibility with polymer-based flexible optics/optoelectronics. Herein, a flexible and transparent polymer barrier layer was created by initiated chemical vapor deposition (iCVD) of a highly crosslinked and fluorinated diacrylate—poly(1H,1H,6H,6H-perfluorohexyl diacrylate) (pPFHDA). The deposition was realized by a bubbler-enhanced iCVD which enables vapor delivery of nonvolatile monomers such as PFHDA. During the deposition, the monomer and the substrate were kept at around room temperature, and the deposited coating showed high uniformity and conformality. This was believed to be the first report of vapor deposition of pPFHDA. The pPFHDA coating has no optical absorption from the wavelength of 300 nm to 1690 nm and is thermally stable to 300°C. Coatings with thicknesses in hundreds of nanometers were found to be impermeable to high-index optical fluid for more than two months at 70°C, which is equivalent to a four-year lifetime at room temperature. Such barrier performance was achieved even after the layer was subject to equi-biaxial strain, which demonstrated that the pPFHDA barrier layer was able to accommodate mechanical deformation, making it a compelling solution for flexible optics/optoelectronics.

SESSION SF01.06: Advanced Processing Characterization
Session Chairs: Ni Huo and Mitisha Surana
Thursday Morning, December 2, 2021
Sheraton, 3rd Floor, Berkeley

10:30 AM *SF01.06.01

The Triumphs and Tragedies of Spatial Atomic Layer Deposition David Munoz-Rojas; LMGP Grenoble INP/CNRS, France

Spatial Atomic Layer Deposition (SALD) is a recent variant of ALD that offers fast processing, even at atmospheric pressure, while preserving the unique assets of ALD, namely, precise thickness control down to the nanometer, high-quality films even at low temperatures, and unique conformality. As a result, SALD is ideal for applications requiring high throughput at low cost, such as new generation photovoltaics, LEDs or packaging. In particular, the SALD approach based on close-proximity deposition heads is highly versatile since it can be easily customized by proper design of the deposition heads and because the deposition takes place in the open air without the need of any deposition chamber.

In my talk, I will first present the developments on close proximity SALD we are currently carrying out at LMGP. In particular, I will illustrate how 3D printing can be used to prototype and customize the deposition heads, and how in so doing SALD can indeed be tuned to deposit custom patterns without the need of pre-patterning steps. This approach represents a new versatile way of printing functional materials and devices with spatial and topological control, thus extending the potential of SALD, and of ALD in general.

I will then present recent studies showing the effect of air-processing on the properties of the thin films deposited with our close-proximity system, and how the choice of precursor can have a huge impact on the final properties of the materials deposited.

The potential of SALD will be illustrated through different examples of applications of the thin films developed in our group.

11:00 AM SF01.06.02

Area-Selective Atomic Layer Deposition on Graphene Substrates Gordon L. Koerner¹, Quinton Wyatt¹, Nikhila Paranamana¹, Brady Bateman², Matthias Young¹ and Matthew Maschmann¹; ¹University of Missouri, United States; ²Berea College, United States

In this work we report a new area-selective atomic layer deposition (AS-ALD) approach enabled by a spatially controlled hydroxylation process. The processing occurs within a low-pressure water vapor ambient established within an environmental scanning electron microscope (ESEM). The ESEM electron beam interacts with the water vapor and generates a local region of reactive species (e.g. hydroxyl radicals) in the neighborhood of the focused electron beam. Here, we functionalize exfoliated graphene substrates with a surface hydroxyl layer by selectively scanning the electron beam within the region to be patterned. The electron-beam generates reactive hydroxyls that then dock on the graphene surface. We emphasize that graphene is natively resistant to surface hydroxylation using conventional exposure to water vapor at elevated temperature. As a result, conventional ALD deposition on graphene is limited to defects and edges where functional groups may take root. Our area-selective hydroxylation technique produces dense and well-patterned hydroxylation on a graphene surface, resulting in high-quality patterned ALD deposition.

In the current study, hydroxyl functionalization and ALD deposition occur within 2 x 2 micron patterned regions on the surface of graphene flakes exfoliated from HOPG. A nominal 10 nm layer of alumina and zinc oxide is then deposited using conventional ALD methods. The hydroxylated regions are sufficiently stable to withstand the ALD deposition temperature of 200 °C. We show that the hydroxyl functionalization and resulting ALD deposition efficacy is highly dependent on electron beam dwell time, electron beam current, pressure, and electron beam acceleration voltage. These processing factors have previously been shown to direct the radiolysis reaction products formed during electron collisions with water vapor. Importantly, all successful hydroxylation experiments required an electron beam dwell time that far exceeds conventional SEM imaging parameters. The patterned hydroxyl functionalization and resulting ALD coatings are characterized using scanning electron microscopy, energy dispersive spectroscopy (EDS) mapping, atomic layer deposition, and Raman spectroscopy. We foresee that this technique may be used to deposit high-quality oxides to traditionally ALD-resistant materials to form field-effect transistor devices, metamaterials, and other nanoscale or microscale devices.

11:15 AM SF01.06.03

In Situ Atmospheric Pressure Chemical Vapor Deposition of Carbon Nanofibers in the TEM Andrew C. Meng¹, Peifu Cheng², Piran Ravichandran Kidambi², Yuyang Song³, Nikhilendra Singh³ and Eric A. Stach¹; ¹University of Pennsylvania, United States; ²Vanderbilt University, United States; ³Toyota Research Institute of North America, United States

Although carbon nanotubes have a wide variety of uses in electronics, structural composites, and energy storage, questions remain regarding specific growth mechanisms. The interactions between the carbon precursor, the metal catalyst, and the substrate are complex and involve the evolution of the metal catalyst oxidation state under hydrogen and hydrocarbon reductants. As carbon nanotube growth yield is often less than 10%, understanding the growth mechanism may provide insights for more efficient synthesis. We study chemical vapor deposition of carbon species *in-situ* in the transmission electron microscope (TEM) at atmospheric pressure in order to better understand the parameters that most strongly influence the morphology of carbon grown. Recent studies have shown that Na-based catalysts were observed to exhibit significantly reduced growth temperatures for carbon nanotubes. Here we report the influence of alkali metal salts on Fe and Ni based catalysts for carbon fiber growth. *In-situ* chemical vapor deposition experiments in the TEM with ethylene hydrocarbon precursors showed that Na₂CO₃ led to significantly increased yield in carbon nanofiber growth, which we hypothesize to be related to a desiccating effect. We combine these *in-situ* growth experiments in the TEM with *ex-situ* growth experiments on the influence of Na₂CO₃ additive on *ex-situ* carbon nanofiber growth using various substrates and carbon precursors. *In-situ* chemical vapor deposition in the TEM is promising for insights into the growth mechanism for carbon based materials, which exhibit a wide range of structures.

11:30 AM SF01.06.04

Late News: Using *In Situ* Quartz Crystal Microbalance Gravimetry to Explore the Temperature Dependent Vapor Phase Infiltration of Trimethylaluminum into Poly(methyl methacrylate) and the Solvent Stability of the Resulting Hybrid Films Emily K. McGuinness and Mark Losego; Georgia Institute of Technology, United States

Vapor phase infiltration (VPI) infuses the bulk of polymers with vapor phase metalorganic precursors which are often co-reacted with an oxidant to form air stable hybrid materials. Due to its vapor phase nature, the VPI process can be utilized as for post-fabrication modification of a wide range of polymeric forms (thin films, fabrics, etc.) without significantly modifying the material's macroscale shape. To date, VPI has shown promise in several industrially relevant areas including: the creation of solvent stable hybrid membranes for chemical separations, the modification and stabilization of mechanical properties for polymer and biomaterial-based fibers, and the creation of nanoscale metal oxide structures from block copolymer templates. The properties of these hybrid materials have shown significant dependence on both their chemical and physical structure. This structure is determined by inherent properties of the polymer and precursor system in addition to the processing parameters employed during VPI. Developing a complete understanding of the process-structure-property relationships for hybrids created via VPI is necessary for specific application design and scale-up. In this talk, we will understand the temperature dependent property of solvent stability by exploring changes in the chemical and physical structure of AlO_x / poly(methyl methacrylate) [PMMA] hybrid materials. *In situ* quartz crystal microbalance gravimetry (QCM) will be leveraged to study the long-term mass change behavior of precursor sorption and desorption. Specifically, this work explores the role of temperature on the total mass sorption of TMA into PMMA with insight into contributions from the free diffusing and chemically interacting species. Consistent with literature reports, we find the total precursor uptake for this VPI system displays a complex dependency on temperature with an increase in quantity from 70 °C to 90 °C followed by a continuous decrease with further increasing temperature. Using QCM experimentation, we determine that the initial increase is driven by reaction kinetics where the reacted quantity increases with temperature and then saturates at approximately 110 °C. However, we find the quantity of free diffusing species decreases continuously with temperature and drives the decrease in uptake at higher temperatures. This information is used to explain quantitatively the temperature dependent property of solvent stability observed in this VPI system as well as provide a framework for studies of this nature. Additionally, we extract kinetic behaviors of this VPI system as a function of infiltration temperature for use in scaling the VPI process to industrial levels.

SESSION SF01.07: New Precursors and Reaction Mechanisms; Simulation and Modelling
Session Chairs: Anna Maria Coclite and Kevin Musselman
Monday Morning, December 6, 2021
SF01-Virtual

10:30 AM *SF01.07.01

Inorganic-Organic Materials and Interfaces through ALD/MLD for Emerging Energy Technologies Maarit Karppinen; Aalto University, Finland

The ALD/MLD (atomic/molecular layer deposition) technique allows us to fabricate novel hybrid materials not readily accessible through any other fabrication route. These include exciting in-situ crystalline metal-organic framework (MOF) like materials and inorganic-organic interfaces and superlattice (SL) structures in which ultra-thin organic layers are introduced periodically between nm-scale metal oxide layers to e.g. enhance mechanical flexibility, block phonon conduction, or bring photoactivity.^[1,2] In this presentation I will briefly discuss exciting examples of properties/functionality realized for these materials: (i) electroactive lithium-organic thin films for battery components (electrodes, solid electrolytes) and artificial solid electrolyte interphase (SEI) layers;^[3,4] (ii) lanthanide-organic upconverting layers for solar cells;^[5] (iii) ZnO-based oxide:organic SL films for textile-integrated thermoelectrics;^[6] (iv) ε-Fe₂O₃:azobenzene SL films for flexible and photo-responsive room-temperature magnets.^[7]

References

- [1] A. Khayyami, A. Philip, M. Karppinen (2019) 13400.
- [2] R. Ghiyasi, M. Milich, J. Tomko, P.E. Hopkins, M. Karppinen, Appl. Phys. Lett. 118 (2021) 211903.
- [3] J. Multia, J. Heiska, A. Khayyami, M. Karppinen, ACS Appl. Mater. Interfaces 12 (2020) 41557.
- [4] J. Heiska, M. Madadi, M. Karppinen, Nanoscale Adv. 2 (2020) 2441.
- [5] A. Ghazy, M. Safdar, M. Lastusaari, A. Aho, A. Tukiainen, H. Savin, M. Guina, M. Karppinen, Sol. Ener. Mater. Sol. Cells 219, 110787 (2021).
- [6] G. Marin, R. Funahashi, M. Karppinen, Adv. Eng. Mater. 22 (2020) 2000535.
- [7] A. Philip, J.-P. Niemelä, G.C. Tewari, B. Putz, T.E.J. Edwards, M. Itoh, I. Utke, M. Karppinen, ACS Appl. Mater. Interfaces 12 (2020) 21912.

11:00 AM SF01.07.02

On the Synthesis of ALD Complex Oxides for Flexible Magnetic Devices Pengmei Yu¹, Pol Sallés Perramon¹, Sebastian Beer², Anjana Devi² and Mariona Coll¹; ¹ICMAB-CSIC, Spain; ²Ruhr-Universität Bochum, Germany

The growth of complex oxide thin films with atomic precision offers bright prospects to study new physics emerging from the films and at their interfaces. Unfortunately, the ALD synthesis of a ternary oxides is, in most of the cases, not a simple addition of the corresponding binary oxide processes. The compatibility of different chemical precursors confined under similar deposition conditions together with a varying surface species after every precursor dose increase considerably the level of intricacy. As a case example, here we will present the challenging synthesis of Gd₄Fe₃O₂ phase by combining two homometallic Gd and Fe compounds using an ALD-type approach. We investigate the use of tailor-made metalorganic precursors, designed to provide similar thermal behavior, (bis(*N*-isopropyl ketoiminate) iron(II), [Fe([⋄]pki)₂] and tris(*N,N'*-diisopropyl-2-dimethylamido-guanidinato)gadolinium(III),

[Gd(DPDMG)₃]). The deposited films resulted in cation ratio close to nominal stoichiometry with negligible amount of organic species according to the RBS/NRA analysis. Upon thermal treatment, XRD and SQUID measurements confirmed the formation of the garnet Gd₃Fe₅O₁₂ phase coexisting with GdFeO₃, Gd₂O₃ and Fe₂O₃. [1]

Additionally, when epitaxial growth is pursued for enhanced physical properties, the growth is further limited to specific fragile and expensive substrates hindering the opportunity to integrate such materials into polymeric and silicon substrates. To broaden the applicability of these materials we went one step further developing an all-chemical deposited route based on the use of a water-soluble sacrificial layer, to manipulate complex crystalline oxides as free-standing membranes and integrate them on polymer substrates such as PDMS and PET. [2] As a case example, we will present the synthesis of ALD-CoFe₂O₄ membranes followed by the structural and magnetic characterization by means of STEM and SQUID, respectively.

This is a robust chemical and low-cost methodology that could be adopted to prepare a wide variety of complex oxide films to fabricate artificial heterostructures to go beyond the traditional electronic, spintronic, and energy storage and conversion devices.

[1] P. Yu, M. Coll et al. *CrystEngComm*, 2021, 23, 730-740

[2] P. Salles, M. Coll et al. *Adv. Mater. Interfaces* 2021, 8, 2001643

11:15 AM SF01.07.04

Plasma-Enhanced Chemical Vapor Deposition of P-Type Cu₂O from Metal Organic Precursors [Daisy Gomersall](#)^{1,2} and Andrew J.

Flewitt¹; ¹Electrical Engineering, University of Cambridge, United Kingdom; ²EPSRC CDT in Integrated Photonic and Electronic Systems, United Kingdom

Although n-type amorphous metal oxide semiconductors have received commercial traction, and particularly amorphous indium gallium zinc oxide (a-IGZO), large-area electronics is still largely dominated by silicon-based technologies. The advance and development of both display and solar cell technologies is limited by the relatively poor performance or high temperature processing conditions of amorphous silicon or polycrystalline silicon devices. The commercial success of metal oxide semiconductors would be significantly enhanced if there was a good p-type metal oxide material which could complement a-IGZO in low power circuits based on thin film transistors (TFTs) and p-n junctions as required by the display and solar cell industries respectively.

Cuprous oxide (Cu₂O) is a non-toxic, low cost metal oxide that exists naturally as a p-type semiconductor due to intrinsic copper vacancies [1]. Reported Hall mobilities of ~10² cm²V⁻¹s⁻¹ suggest potential as a good thin film electronic material [2], but with sputter-deposited Cu₂O TFT field-effect mobilities of ~10⁻¹ cm²V⁻¹s⁻¹ and high off-state currents widely reported [3], further research is required to optimise the deposition and device fabrication.

This work looks at the deposition of Cu₂O films using plasma enhanced chemical vapor deposition (PECVD) with pulsed liquid injection of metal-organic precursors. PECVD is used for large-area amorphous silicon growth and has the advantage over physical vapor deposition techniques, such as sputtering, of allowing chemical control of the deposition process and hence potentially the oxidation state of the copper oxide thin film. The pulsed liquid injection is achieved with a Kemstream Vapbox liquid precursor delivery system and Cupraselect (Cu(hfac)(TMVS)) is used as the copper precursor with oxygen as the oxidising agent.

Existing literature using Cupraselect is primarily focussed on CVD of copper films and the presence of a significant incubation period is widely reported, with film deposition delayed by as much as 50 minutes depending on process conditions [4]. However, using PECVD and pre-treating the substrates with oxygen plasma, this work reports the deposition of 20nm thick Cu₂O films from a single 1 ms injection of precursor. Such film thicknesses would be ideal for deployment in TFT structures.

References

[1] H. Raebiger, S. Lany and A. Zunger, *Phys. Rev. B*, 76, 2007.

[2] B. S. Li, K. Akimoto and A. Shen, *J. Cryst. Growth*, 311, 2009.

[3] S. Han, et al., *Appl. Phys. Lett.*, 109, 2016.

[4] S. Kim, J. M. Park, and D. J. Choi, *Thin Solid Films*, 315, 1998.

Acknowledgement - The authors thank EPSRC for providing the funding for this work through grant numbers EP/M013650/1, EP/P027032/1 and the EPSRC Centre for Doctoral Training in Integrated Photonic and Electronic Systems.

11:30 AM SF01.07.06

Theoretical-Computational Study of the Nucleation Process of TiO₂ on Carbon Nanostructures [Jonathan E. Rodríguez Hueso](#), Hugo A. Borbon and Jonathan Guerrero; CNyN-UNAM-CICESE, Mexico

There are many fields within the physical and engineering sciences, where the key to scientific and technological progress is the understanding and control of the properties of matter at the scale of individual atoms and molecules, so conducting a study of the mechanisms that occur within the processes that allow us to manipulate matter on this scale; which has become a fundamental part of scientific development in its different areas. However, to carry out the study of nucleation and growth of matter at the atomic-molecular scale few techniques allow us to carry out the growth of materials with such precise control, and in techniques that are capable of doing it, there is a great ignorance of all the phenomena and interactions that occur in them due to the complexity involved in the study at this scale. ALD is one of the few techniques that provide control of film growth at the molecular atomic scale and a high precision of synthesis of nanocomposites, which makes ALD the ideal method to carry out the study of nucleation and growth of the different nanocomposite. Where one of the approaches of greatest interest within the field is the area of functional hybrid materials at the nanoscale since it is one of the most promising and emerging research areas in materials chemistry. This is because the limitless possible combinations of the different properties of inorganic, organic, or even bioactive components in a single material, in nanometric dimensions, have attracted considerable attention. This approach provides the opportunity to create a host of novel and advanced materials with well-controlled structures and multiple functions. Where the TiO₂ / graphene hybrid stands out, which is a new group of nanomaterials whose use and performance are tested with greater thanks to its improved properties and possible applications, which, compared to pure materials, this composite material exhibits improved activities due to the synergistic effect of the GR and TiO₂ components. This material is widely used in the area of thin films, so the ideal technique for its growth is ALD thanks to the properties it has and allows the TiO₂ / graphene hybrid to grow in a very controlled and precise way, but most of the information on the growth mechanisms is very little known, and to have a greater efficiency of the technique and the materials, it is very important to know all the factors that involve the growth of the material. However thanks to the self-limiting nature of the chemisorption reactions during the ALD growth of the film, allows us to carry out a theoretical study through calculations using density functional theory (DFT) to develop a model of the chemistry involved in the reactions that occur in the ALD process during the early stages of growth of TiO₂ on graphene for each grown film. Theories of the electronic structure of matter have become a very useful and powerful tool for understanding the chemistry involved in the early stages of the ALD process. In this work, we have used DFT calculations to present a complete reaction mechanism between OH-functionalized graphene and the 3 main Ti precursors (TDMAT, TIP, TiCl₄) using water as the

oxidizing gas. We have studied the ligand exchange reactions. A theoretical-computational study of the initial stages of ALD growth of the TiO₂-GR hybrid was carried out from graphene functionalized with hydroxyl (OH) groups as growth sites for the interaction with the main titanium precursors in ALD. It was demonstrated how the chemical nature of the precursor directly affects the reaction mechanism to be carried out, reflecting on the energy required to invest in the system to overcome the barriers and for the reaction to take place. Additionally, we obtained the secondary products that the system produced when carrying out the growth of the film, with which a reaction mechanism was proposed for each ALD half cycle.

11:45 AM SF01.07.07

Late News: Large Single-Crystal Monolayer MoS₂ Growth with Halide Activation and Its Mechanism Cong Su^{1,2,3}, Qingqing Ji^{4,3}, Nannan Mao³, Xuezheng Tian⁵, Juan C. Carlos⁶, Jianwei (John) Miao⁷, William Tisdale³, Alex Zettl^{1,2}, Ju Li³ and Jing Kong³; ¹University of California, Berkeley, United States; ²Lawrence Berkeley National Laboratory, United States; ³Massachusetts Institute of Technology, United States; ⁴ShanghaiTech University, China; ⁵Institute of Physics, Chinese Academy of Sciences, China; ⁶Oak Ridge National Laboratory, United States; ⁷UCLA, United States

Two-dimensional (2D) semiconductors such as monolayer MoS₂ are essential building blocks for next-generation ultrathin flexible and low-power electronics. A recent study using semimetal Bi as the electrical contact to monolayer MoS₂ has improved the on-current and contact resistance of the monolayer transistor to be on par with traditional Si-based transistors. As a premise for large-scale electronics, batch production of the 2D semiconductors requires large domain size, large-area continuity, and thickness uniformity. These are difficult tasks in particular for synthetic MoS₂ and other transition metal dichalcogenides (TMDs), considering the less controllable mass flux from solid metal precursors in chemical vapor deposition (CVD), as compared to the case of graphene growth with gaseous hydrocarbons. One recent advance to mitigate this is the use of alkali metal halide salts [*e.g.*, NaCl, KI, and NaBr], which, in conjunction with transition metal or metal oxide powders, could increase the mass flux of metal precursors and accelerate the 2D growth of TMDs. Various research efforts have been made to explain the mechanism, in terms of these metal halides as a molten salt to facilitate the evaporation of the metal oxide precursor, or as a surfactant to modify the substrate surface and the MoS₂ edge. Both the alkali metal ions and the halogens have been proposed to play an important role in the promoted growth. Continued endeavors are being devoted to bringing further lights in understanding the detailed mechanism.

In this work, we provide unambiguous experimental evidence that halogens are closely related to MoS₂ growth dynamics. To achieve this, post-growth Arrhenius analysis is implemented without any involvement of *in-situ* characterizations. We find that within the same reaction family, the halide-assisted growths conform to Brønsted-Evans-Polanyi (BEP) relation, where their reaction barriers are linearly correlated to the Mo-X (X = I, Br, Cl, F, and O) bond dissociation energies (E_b), suggesting the substitution of Mo-X bonds by the Mo-S bonds to be the rate-limiting step for the CVD growth. Based on this, we propose a theoretical growth model that not only reproduces the BEP relation but also explains the sulfur concentration-dependent growth dynamics observed in our experiments. By harnessing the synergistic effect of the KI promoter and the sulfur supply, we can reproducibly and rapidly synthesize near millimeter-sized 2D MoS₂ crystals dispersed over the entire SiO₂/Si substrates. These results not only shed lights on the detailed mechanism of TMD growth activated by the halide salts, but also guide the designer growth towards larger domain sizes that should enable practical applications.

SESSION SF01.08: Organic, Hybrid, and 2D Materials
Session Chairs: Maarit Karppinen and Graziella Malandrino
Monday Afternoon, December 6, 2021
SF01-Virtual

1:00 PM *SF01.08.01

From Functional Polymers to Functional Devices Based on Nanofilms Anna Maria Coclite; Graz University of Technology, Austria

Functional and responsive surfaces have been successfully deposited by initiated Chemical Vapor Deposition (iCVD) on a variety of substrates. Such method allows the full retention of the functional groups of the monomer structure, including, but not limited to, C-/N- containing ones. The high versatility of iCVD in driving application-specific properties into the material, creating a platform for the implementation of polymeric coatings into device fabrication, will be discussed.

A case study will be presented in the field of stimuli-responsive materials, in particular, hydrogels whose size and shape change when stimulated by light, humidity, temperature and aqueous environments. iCVD allows to obtain stimuli-responsive thin films with high chemical specificity and this is important to obtain a large responsiveness amplitude. In addition, the thin film form allows obtaining fast response.

Fast response and large signal amplitude are fundamental requirements for good sensors. Fast and ultra-fast humidity sensors based on the optical detection of the change in thickness of the iCVD hydrogels will be shown. The implemented sensor prototype delivered reproducible relative humidity values and the achieved response time for an abrupt change of the humidity was about three times faster compared to one of the fastest commercially available sensors on the market.

This presentation will focus on the applications of stimuli-responsive nanofilms for drug delivery devices, sensors and actuators. Their combination with piezoelectric/piezoresistive materials will also be discussed for innovative device geometries.

1:30 PM SF01.08.02

ALD Growth of High-κ Dielectrics on Monolayer MoS₂—The Role of the Substrate Emanuela Schilirò¹, Raffaella Lo Nigro¹, Salvatore Ethan Panasci², SimonPietro Agnello³, Franco Gelardi³, Fabrizio Roccaforte¹ and Filippo Giannazzo¹; ¹CNR-IMM of Catania, Italy; ²University of Catania, Italy; ³University of Palermo, Italy

Two-dimensional materials (2DM), such as graphene and transition metal dichalcogenides (TMDs), always achieve great interest for future applications in electronics, optoelectronics and sensing. The atomic layer deposition (ALD) of ultra-thin high-κ dielectrics (among which Al₂O₃ and HfO₂) on the 2DM materials is an essential requirement to realize some high performance electronic devices, including lateral field effect transistor (FETs) and/or hot electron transistors (HETs). However, the lack of out-of-plane bonds in the 2DM makes that seeding-layers and/or pre-functionalization treatments are necessary to promote the ALD growth, despite the possible adverse impacts on the carrier mobility and the dielectric quality. In some special cases, the peculiar interaction between 2DM and the underlying substrate proved to be beneficial to achieve a direct ALD growth, such as in the case of monolayer (1L) CVD graphene residing on catalytic-metals (Cu, Ni-Au) [1,2], or 1L epitaxial graphene on 4H-SiC [3,4]. So far, similar substrate effects have not been explored in the ALD deposition of dielectrics on TMDs.

In this work, large area (in the order of cm) and high quality monolayer-MoS₂ were exfoliated from the bulk molybdenite on a gold layer and successively

transferred onto Al₂O₃/Si substrate [5]. Hence, the direct ALD growth of ultra-thin (about 4 nm) Al₂O₃ and HfO₂ films was investigated on MoS₂ residing on these two different substrates. Employing the same deposition conditions, an optimal ALD-coverage has been obtained for monolayer-MoS₂ on gold (see Fig. 1(a) for 80 cycles of Al₂O₃ deposition), while a highly inhomogeneous coverage was observed for monolayer-MoS₂ on the Al₂O₃/Si substrate (see Fig. 1(b)). The beneficial effect of the gold substrate on the ALD growth has been correlated to the strong van-der-Waals interaction between the MoS₂ and Au, resulting in a tensile strain and p-type doping of the MoS₂ membrane, as shown by Raman mapping [5]. Good insulating properties of the compact ~4 nm thick Al₂O₃ membrane on Au-supported monolayer-MoS₂ have been found by conductive atomic force microscopy.

These results can have an important impact in the realization of devices based on large area MoS₂ membranes produced by gold assisted exfoliation.

This work has been supported by the FLAG-ERA JTC2019 project "ETMOS"

[1] B. Dlubak, et al., *Appl. Phys. Lett.* **100**, 173113 (2012).

[2] A. I. Aria, et al., *ACS Appl. Mater. Interfaces* **8**, 30564 (2016).

[3] E. Schilirò, R. Lo Nigro, S.E. Panasci, F.M. Gelardi, S. Agnello, R. Yakimova, F. Roccaforte, F. Giannazzo, *Carbon* **169**, 172-181 (2020).

[4] E. Schilirò, R. Lo Nigro, F. Roccaforte, I. Deretzi, A. La Magna, A. Armano, S. Agnello, B. Pecz, I.G. Ivanov, R. Yakimova, F. Giannazzo, *Adv. Mater. Interfaces* **1900097** (2019).

[5] S.E. Panasci, E. Schilirò, G. Greco, M. Cannas, F. M. Gelardi, S. Agnello, F. Roccaforte, F. Giannazzo, *ACS Applied Materials & Interfaces* (2021). DOI: acsami.1c05185.

1:45 PM *SF01.08.03

Hybrid Chemical Vapor Deposition of Heterogeneous Thin Films Yu Mao; Oklahoma State University, United States

The technique of initiated chemical vapor deposition (iCVD) is gaining increasing interest in the fabrication of various polymer thin films. By implementing the chemistry of radical polymerization under the condition of vapor-based deposition, iCVD provides fine control of coating composition and functionality as well as adaptability and conformality to complex substrates. While the uniformity of polymer thin films is pursued in many fabrications, thin films with heterogeneous composition and morphology can provide high level of versatility, especially when holistic solutions are desired. We report our exploration of heterogeneous film fabrication using hybrid chemical vapor deposition with multiple film growth steps in one deposition. Besides changing process variables (such as vapor pressure and temperature) during iCVD, we introduced other fabrication procedures *in situ* to create polymer films with multi-scale heterogeneity in vertical and planar dimensions. We will discuss three hybrid deposition process and the composition, structure, interfacial strength, surface property, and biocompatibility of the resultant thin films. The technical challenges encountered in the hybrid deposition process will also be discussed. We will conclude by demonstrating our recent work of implanted drug delivery, smart textiles, and sustainable water solutions enabled by fabricating heterogeneous thin films on three-dimensional substrates.

2:15 PM SF01.08.04

Development of Hybrid Organic-Inorganic Nanocomposites via the Atomic Layer Deposition of Nanoscale Metal Oxides Inside SU-8 Negative Photoresist Zhongyuan Li¹, Nikhil Tiwale², Ashwanth Subramanian², Ying Li¹, Chang-Yong Nam² and Seok-Woo Lee¹; ¹University of Connecticut, United States; ²Brookhaven National Laboratory, United States

It has been extremely challenging to achieve the uniform distribution of a large volume fraction (>50%) of nanoscale fillers in a polymer matrix because the nanoscale fillers tend to agglomerate, and this agglomeration almost always degrades the mechanical properties of polymer nanocomposites. In this presentation, we show that it is possible to overcome this issue by using the modified atomic layer deposition that deposits metal oxides inside the polymer matrix instead of depositing them on the polymer surface. We use a SU-8 negative photoresist, which has a large-sized free volume due to its cage-like structure of the repeating molecular unit, so both the precursors (trimethylaluminum and diethylzinc) and water molecules can diffuse into SU-8 matrix during the atomic layer deposition process. Compared to the conventional atomic layer deposition, we intentionally used the longer purging time of precursor and water molecules to allow them to diffuse into SU-8 matrix. By repeating the infiltration process several times, it is also possible to control the volume fraction of nanoscale metal oxides. Transmission electron microscopy revealed that the infiltration depth is dependent on the type of precursor, and we obtained the ~50 nm thick infiltration depth of Al₂O₃ and over 150 nm thick infiltration depth of ZnO under the similar deposition condition. The high-resolution composition mapping showed that Al₂O₃ formed the particulate-like structure, but ZnO seemed to form the unique organic-inorganic interpenetrating network structure. We obtained the volume fraction of oxides by using the quartz crystal microbalance measurement, and both cases showed the uniform distribution of nanoscale oxides with ~44 vol.% of Al₂O₃ and ~24 vol.% of ZnO. Therefore, our synthesis technique enabled us to achieve the ideal microstructure of polymer nanocomposite successfully.

To evaluate the mechanical performance of our SU-8 nanocomposites, we performed in-situ nanomechanical testing on polymer nanocomposite nanopillars, which were fabricated by the e-beam lithography followed by the modified atomic layer deposition. Mechanical data revealed that our polymer nanocomposites exhibit metal-like strength (~400 MPa) but still polymer-like Young's modulus (~8 GPa). This unusual combination of strength and Young's modulus results in the giant modulus of resilience (~24 MJ/m³), the orders of magnitude higher than the modulus of resilience of most engineering materials. Modulus of resilience, the measure of a material's ability to store and release elastic strain energy, is critical for realizing advanced mechanical actuation technologies in micro-/nano-electro-mechanical systems and in robotics. Our hybrid polymer nanocomposite features lightweight, ultrahigh tunable modulus of resilience, and versatile nanoscale lithographic patternability with potential for application as nanomechanical components, which require ultrahigh mechanical resilience and strength such as flexible display or durable three-dimensional structures in SU-8-based micro-electro-mechanical-systems (MEMS).

2:30 PM SF01.08.05

Progress in Growth of Carbon Nanotubes from Catalyst Particles Incorporating Diffusion Inhibitors Michael J. Bronikowski; University of Tampa, United States

Results will be presented of our most recent studies of growth of Carbon Nanotubes (CNTs) by Chemical Vapor Deposition (CVD) from catalyst metals combined with heavy refractory diffusion inhibitor metals. The carbon source gas used in these studies is ethylene, C₂H₄, and various combinations of catalysts and diffusion inhibitor metals are investigated. The key concept is the inhibition of high-temperature erosion and Ostwald ripening of the catalyst particles by inclusion of the diffusion inhibitors, allowing the catalyst particles to have a longer lifetime and thus grow longer CNTs. We have previously demonstrated this effect using carbon monoxide (CO) as a carbon source gas, and we present here the extension of these studies to CNT growth using C₂H₄ as the source gas. Implications will be discussed for the growth of ultra-long (tens of cm or more) CNTs.

2:45 PM SF01.08.06

Probing the Growth of Inorganic Clusters in Polymer Templates During Sequential Infiltration Synthesis Xiang He, Ruben Waldman, David Mandia, Nari Jeon, Nestor Zaluzec, Olaf Borkiewicz, Uta Ruett, Seth Darling, Alex Martinson and David Tiede; Argonne National Laboratory, United States

States

Sequential infiltration synthesis (SIS) is a modified atomic layer deposition process to precisely grow inorganic solids in soft material templates (e.g., polymers). Removal of the template via annealing results in the formation of polycrystalline inorganic thin films that inherit the morphology of the template matrix, offering opportunities to create a variety of nanostructured inorganic solid thin films. The properties of the resultant inorganic thin films rely heavily on the growth of the inorganic clusters in the template matrix. Therefore, to gain full control of the final inorganic thin films, it is of great importance to map out how the inorganic clusters grow inside the polymer templates.

In this work, structures of SIS-derived initial nucleating and final annealed indium-based inorganic materials with a PMMA template were systematically investigated as a function of SIS cycles using multiple tools, such as high-energy X-ray scattering (HEX) with pair distribution function (PDF) analysis, extended X-ray absorption fine structure, and transmission electron microscopy (TEM). The results resolved structures for the initial nucleating InO_xH_y clusters in PMMA as a function of the number of SIS cycles, which were found to exhibit similar local structures of cubic In_2O_3 and $\text{In}(\text{OH})_3$ crystals. PDF analysis demonstrated that the SIS-derived InO_xH_y clusters in the first SIS cycle are characterized by a combination of mono-, di-, and tri-nuclear structures which and grow to larger clusters with higher aspect ratios during subsequent SIS cycles. Further extended SIS cycles lead to the increased number density of InO_xH_y clusters, which then condense to form larger and three-dimensional networks in the PMMA matrix. Annealing in air removes the PMMA template and converts the amorphous InO_xH_y clusters into crystalline In_2O_3 particles, which also show SIS-cycle-dependent properties.

Overall, this work contributes to the fundamental understanding of how inorganic clusters grow inside polymer matrices during the early stages of the SIS process.

SESSION SF01.09: ALD/CVD General I
Session Chairs: Noa Lachman and Kenneth Lau
Monday Afternoon, December 6, 2021
SF01-Virtual

6:30 PM *SF01.09.01

A Chemical Vapor Deposition of High Refractive Index ($n > 1.9$) Functional Polymer Films with Full Transparency in Whole Visible Region [Sung Gap Im](#); KAIST, Korea (the Republic of)

High refractive index polymers (HRIPs) have recently emerged as an important class of materials for use in a variety of optoelectronic devices including image sensors, lithography, and light-emitting diodes. However, achieving polymers having refractive index exceeding 1.8 while maintaining full transparency in the visible range still remains formidably challenging. Here, we present a unique one-step vapor-phase process, termed sulfur chemical vapor deposition, to generate highly stable, ultrahigh refractive index ($n > 1.9$) polymers directly from elemental sulfur. The deposition process involved vapor-phase radical polymerization between elemental sulfur and vinyl monomers to provide polymer films with controlled thickness and sulfur content, along with the refractive index higher than 1.95. Notably, the HRIP thin film showed unprecedented optical transparency throughout the visible range, attributed to the absence of long polysulfide segments within the polymer, which will serve as a key component in a wide range of optical devices.

7:00 PM SF01.09.02

Late News: Atomic Layer Deposition of c-Axis-Oriented GeTe/Sb₂Te₃ Superlattice for Low-Power and Large-Capacity Phase Change Memory [Chanyoung Yoo](#)¹, [Woohyun Kim](#)¹, [Jeong Woo Jeon](#)¹, [Wonho Choi](#)¹, [Byongwoo Park](#)¹, [Gwangsik Jeon](#)¹, [Yoon Kyeong Lee](#)² and [Cheol Seong Hwang](#)¹; ¹Seoul National University, Korea (the Republic of); ²Jeonbuk National University, Korea (the Republic of)

Despite the extensive research and available commercial memory products based on the phase-change-material (PCM), the Ge-Sb-Te alloy-based PCM's full functionality for low-power and high-density memory has not been accomplished. This is mainly due to the lack of conformal film growth techniques, such as atomic layer deposition (ALD), of the chalcogenide-based PCM. The current PCM architecture relies on the crossbar arrays (CBA) structure due to its condensed and straightforward architecture. However, the CBA cannot keep up with the ultra-high density demands due to the increased fabrication cost of lithography steps and masks required for each stacking layer. It can be best addressed by the state-of-the-art vertical NAND architecture, proven technology with a stack of more than 150 layers. To fabricate highly integrated vertical-type crossbar array (V-CBA) memory, the Ge-Sb-Te phase change layer should be uniformly deposited in the inner surface of the deep etched holes vertical architectures, which could be accomplished only by ALD. Meanwhile, the high power consumption of the Ge-Sb-Te PCM during the write operation also poses another severe drawback.

This work demonstrates the development of GeTe/Sb₂Te₃ superlattice film utilizing ALD to achieve a high-performance V-CBA memory device. The chemical affinity of the ALD precursor to the substrate surface and the two-dimensional nature of the Sb₂Te₃ enabled to achieve the *in-situ* crystallized superlattice film where the out-of-plane directions of the two-component layers precisely matched the *c*-axis, while the in-plane directions were random. Such a *c*-axis-oriented Sb₂Te₃ could serve as the seed for the *in-situ* crystallized 111-direction aligned GeTe layer, which would have been either amorphous or randomly oriented polycrystalline layer if it was directly grown on a SiO₂ or TiN surfaces. The peculiar alignment method can be applied to deposit other van der Waals films such as transition metal chalcogenides and topological insulators with such alignments for future electronic device applications. The well-aligned and crystallized GeTe/Sb₂Te₃ superlattice film showed a RESET current of $\sim 1/7$ of randomly oriented Ge₂Sb₂Te₅ alloy films grown by the identical ALD process. The fluent improvement in the resistance switching performance from this GeTe/Sb₂Te₃ superlattice originates from the pressure-induced solid-state amorphization by the well-oriented superlattice films. The reduction of RESET current with the aligned GeTe/Sb₂Te₃ superlattice film was also feasible in the vertical structures, showing a step forward improvement for fabricating the futuristic V-CBA memory with low operating power and high density.

7:15 PM SF01.09.04

Synthesis of Magnesium-Doped Hexagonal Boron Nitride Films By Chemical Vapor Deposition [Ranjan Singhal](#), [Elena Echeverria](#), [Dave N. McIlroy](#) and [Raj N. Singh](#); Oklahoma State University, United States

Hexagonal boron nitride (h-BN) is of great interest and potential due to its excellent electrical, optical, and mechanical properties and is isostructural to graphene. hBN is also a wide bandgap semiconductor with an optical bandgap of ~ 6 eV. To be used in the semiconductor industry, wide-area processing and engineering the bandgap is of utmost importance. As of now, chemical vapor deposition (CVD) is the most promising method to synthesize h-BN as it

provides great control over the thickness of the deposited films and is the best candidate for the industrial scale-up process. To engineer the bandgap, in-situ doping is the most convenient and the most effective way, as it offers great control over the dopant material in terms of selection, introduction into the chamber, controlling the dopant concentration. Synthesizing hBN with in-situ doping directly on silicon, which is the most commonly used substrate in the semiconductor industry, eliminates the need for a post-synthesis transfer process and the employment of another process for doping. In this presentation, we have shown the direct synthesis of Mg-doped hBN films on silicon by chemical vapor deposition. XPS analysis confirmed the incorporation of Mg in hBN films. UV-vis spectroscopy was utilized to find the bandgap of the doped hBN films. As expected, it was concluded that the bandgap of the Mg-doped hBN films was less than the bandgap of the undoped hBN films.

7:30 PM *SF01.09.05

Rapid and Accurate Prediction of the Volatility of Organometallic Precursor Complexes [Simon D. Elliott](#), Asela Chandrasinghe, Anand Chandrasekaran, Yuling An and Mathew D. Halls; Schrödinger Inc, United States

Despite its importance for many industries, a quantitative model for the volatility of inorganic compounds has remained elusive. Vapor-based deposition technologies, including CVD and ALD, make use of certain metalorganic complexes and related compounds that show appreciable vapor pressure under moderate heating. However the rational discovery of new complexes is hindered by a lack of detailed understanding to link chemical identity with the conditions for evaporation or sublimation. To overcome these issues, we present a model for volatility and discuss its accuracy and scope.

We have assembled experimental pressure-temperature data from the literature for over 1,000 inorganic complexes, featuring 70 metal centers and 400 different ligands. We use machine learning (ML) approaches to train surrogate models for the dependence of evaporation, boiling or sublimation temperature on chemical identity and pressure. A variety of ML algorithms (Random Forest, Neural Networks etc) are studied in conjunction with different chemoinformatic descriptors and fingerprints. When supplied with the chemical identity and topology of a candidate inorganic compound, the trained ML model is capable of predicting the evaporation temperature at a specified pressure with a mean error of 10 degrees C for the most common metals. The speed with which the model is evaluated makes this approach suitable for screening thousands of candidate complexes, as one step within computational and/or experimental discovery of new precursors.

SESSION SF01.10: Devices and Applications II
Session Chairs: Sung Gap Im and Kevin Musselman
Tuesday Morning, December 7, 2021
SF01-Virtual

10:30 AM *SF01.10.01

Importance of the Substrate on CVD Polymerization [Kenneth K. Lau](#); Drexel University, United States

Polymer thin films can be formed conformally on a substrate by chemical vapor deposition (CVD). Specifically, initiated and oxidative chemical vapor deposition (iCVD and oCVD) can easily form nanometer-thin polymer films conformally on a wide range of substrate topologies and materials, from planar silicon, glass or metal to microporous membranes, fabric and paper to nanoporous particle networks, tubes and fibers. In fact, one of the major advantages of iCVD and oCVD is that they are able to use mild reaction conditions, including mild substrate temperatures (at or near room temperature) and mild vacuum (using only a roughing pump), to conformally deposit on such a varied range of substrate geometries and materials. As such, the solid substrate itself on which the polymer film is deposited has generally not been considered an important or determinant factor in influencing the quality and characteristics of the deposited film.

Here, in this talk, the role of the substrate in influencing the deposition behavior and characteristics of the polymer films, particularly for depositing nanometer-thin films by iCVD and oCVD, will be scrutinized more carefully. Specifically, we will present evidence that indicate the surface energy of the substrate can have a profound impact on the resulting conformality of the deposited polymer film. In addition, we will present results that further indicate the substrate temperature can yield different rate-limiting regimes that impact polymer growth rates, where previously it has generally been considered that deposition rate is only limited by monomer adsorption or availability of the monomer reactant at the substrate surface. These new insights challenge our current understanding and notion of iCVD and oCVD polymerization, and can offer new avenues and opportunities for iCVD and oCVD processing and their applications.

11:00 AM SF01.10.02

MOCVD Fabrication and Downconversion Luminescence of Eu-Doped BaF₂ Thin Films for Photovoltaic Applications [Francesca Lo Presti](#)^{1,2}, Anna L. Pellegrino^{1,2}, Adolfo Speghini^{3,4} and Graziella Malandrino^{1,2}; ¹University of Catania, Italy; ²INSTM Udr Catania, Italy; ³Università di Verona, Italy; ⁴INSTM Udr Verona, Italy

In recent years, considerable efforts have been done in the development of new functional materials for the fabrication of increasingly sophisticated and advanced photovoltaic devices (PV) that can ensure an efficient exploitation of solar spectrum. An advanced approach used to enhance the efficiency of PV systems, is based on the conversion of photons with energies outside the absorption range of the photoactive material (usually silicon) into a more suitable optical region. In this context, lanthanide (Ln)-doped fluoride materials are considered particularly promising for energy conversion (EC) applications due to their unique luminescent properties under light irradiation. The EC process can be achieved by simply integrating, into the PV layers, a material able to host an active luminescent Ln element. Upconversion (UC) and downconversion (DC) are the main luminescence mechanisms used for EC applications which increase the efficiency of photovoltaic devices. Concerning different Ln elements used for DC processes, europium has attracted great attention from the scientific community, thanks to its high peculiar chemical properties, especially in the oxidation state +3. Up to now, for EC processes it has been demonstrated that fluorides, compared to other inorganic matrices are more efficient inorganic hosts. In particular, BaF₂ is considered a suitable host for the UC and DC luminescence of Ln³⁺ ions because of its low phonon energy (similar or even lower than the extensively used hosts such as NaYF₄), high chemical stability, wide transparency (i.e. BaF₂ is transparent from 150 nm to 15 μm) and versatile synthetic strategies. It is important to stress that host materials require lattice matches with Ln³⁺ dopant ions. Trivalent lanthanide ions can be well incorporated into crystal structure of alkaline-earth fluorides due to the similar coordination sphere. However, a charge compensation mechanism is required to balance the additional charge introduced after the replacement of divalent alkaline-earth ions with trivalent Ln dopants.

In the present study, we report the synthesis of Eu³⁺-doped BaF₂ thin films on silicon and quartz substrates, using metalorganic chemical vapor deposition technique (MOCVD) focusing the attention on the fabrication process and the DC luminescence properties. The advantages of the MOCVD approach includes simplified instrumental apparatus, high deposition rate, high purity and easy industrial scale-up. For the fabrication of BaF₂ thin films doped with

Eu³⁺, a multicomponent mixture of metalorganic adducts in an appropriate molar ratio is used as a single molten source. It is possible to easily tune the chemical compositions of the films, to tailor the energy transfer processes, by changing the composition of the precursor mixture, that is the Ba:Eu ratio in the multicomponent source. X-ray diffraction analysis (XRD), field-emission scanning electron microscopy (FE-SEM) and energy dispersive X-ray analysis (EDX) allowed a structural, morphological and compositional characterization of the films. Finally, the film functional properties have been assessed through luminescence spectroscopy.

11:15 AM SF01.10.03

Nanoscale Investigation of Al₂O₃ Thin Layers by Thermal- and Plasma-Enhanced Atomic Layer Deposition for Power Devices Raffaella Lo Nigro¹, Emanuela Schilirò¹, Patrick Fiorenza¹, Filippo Giannazzo¹, Guido G. Condorelli², Marzia Monforte² and Fabrizio Roccaforte¹; ¹CNR, Italy; ²Università degli Studi di Catania, Italy

The scientific research activity on AlGaN/GaN-based high-electron-mobility-transistors (HEMTs) is always under continuous and progressive development because of their promising performances for future electronic devices [1,2]. However, the conventional HEMTs with Schottky contact between the metal gate and AlGaN exhibits some reliability issues related to leakage current and current collapse phenomena, but also to limited gate voltage swings and possible metal inter-diffusion phenomena during the high temperature device processing. In this context, the realization of Metal-Insulator-Semiconductor (MIS)-HEMTs structure, with high- κ insulator integration between the metal gate and AlGaN, is the most favorable method to solve these issues [3]. Among the different kinds of high- κ dielectrics (Al₂O₃, HfO₂, ZrO₂, AlN), the aluminum oxide (Al₂O₃) is the most widely reported for the GaN focused technology. The large Al₂O₃ implementation is closely related to the excellent physical properties as insulator, namely high permittivity ($\kappa \sim 9$), high critical electric field (10 MV/cm), large band gap (~ 8.9) and advantageous conduction band alignment with AlGaN/GaN structure. The ALD is the growth technique of choice for microelectronics high- κ gate insulators, and in particular, in the case of Al₂O₃ thin film growth on AlGaN/GaN heterostructures a debate aspect is related to the ALD growth modes to be implemented [4,5]. In fact, some works reported on quite promising physical properties by thermal ALD process, while many others claimed the best choice is the plasma enhanced-ALD approach. In this context, we compared the ALD growth modes of Al₂O₃ on AlGaN/GaN by both thermal (ALD) and plasma (PE-ALD) approaches. In particular, the deposition very thin Al₂O₃ layers have been investigated since the early growth stages (about ~ 1 nm thick layers) and upon increasing thickness up to 6 nm. Investigation has been carried out by both X-ray photoelectron spectroscopy (XPS) and Conductive- Atomic Force Microscopy (C-AFM), in order to correlate the physical covering upon film growth to the insulating properties of the growing Al₂O₃ layers. Two different growth mechanisms have been found, i. e. a quite ideal "layer-by-layer" growth in the case of PE-ALD process, while the thermal ALD process is quite consistent with an "island growth modes". C-AFM can also provided nano-scale electrical information on the intimate electrical properties of the ultra-thin dielectrics and besides the standard imaging, it has been used for statistical study on Al₂O₃ thin films reliability upon stressing applied voltages on nanoscale matrix of punctual I-V measurements. The best performance has been entirely obtained for PE-ALD grown Al₂O₃ films both for the complete covering of the substrate surface and for the total and homogeneous insulating properties.

[1] U. K. Mishra, P. Parikh, and Y. F. Wu, Proc. IEEE 90, 1022 (2002)

[2] K. J. Chen and C. Zhou, Phys. Sta. Sol. (a), vol. 208, no. 2, 434–438, (2011)

[3] F. Roccaforte, P. Fiorenza, G. Greco, R. Lo Nigro, F. Giannazzo, F. Iucolano, M. Saggio, Microelectronic Engineering 187–188, 66–77, (2018)

[4] E. Schilirò, R. Lo Nigro, P. Fiorenza, F. Roccaforte, AIP ADVANCES 6, 075021 (2016)

[5] E. Schilirò, P. Fiorenza, C. Bongiorno, C. Spinella, S. Di Franco, G. Greco, R. Lo Nigro, F. Roccaforte, AIP Advances 10, 125017 (2020)

11:30 AM SF01.10.04

Comparison of ALD grown AZO and ZnO Thin Film Heater Performances Deniz Tugrul, Doga Doganay, Husnu E. Unalan and Bilge Imer; Middle East Technical University / Metallurgy and Materials Engineering, Turkey

Ideal properties for transparent thin film heaters (TTFHs) can be summarized as low sheet resistance, high transmittance in visible range and high thermal stability. Generally, the material of choice converts the electrical energy into heat by "Joule Heating Mechanism". Therefore, achieved maximum temperature is related with applied voltage, sheet resistance and heat loss. Also, uniformity of such material is important due to heating consistency and stability of the entire film. Oxide films grown by atomic layer deposition (ALD) has advantages such as high uniformity, thickness control at angstrom level and excellent step coverage due to its self-limiting growth mechanisms¹. Aluminum doped zinc oxide (AZO) thin films growth by ALD expected to show ideal properties for a TTFH. The studies suggest that the AZO thin films are suitable to be used as heater on different substrates with different production methods, reason being chemical and thermal stability of AZO²⁻³.

In this work, Al doped and undoped ZnO thin films grown by ALD were demonstrated as TTFH. The growth of the thin films were done on quartz substrates. Growth temperature for AZO was varied between 175 and 225 °C, Al doping was kept between 2–4 atomic percent, and thickness was kept constant as 100 nm for all samples. The varying temperature and doping levels were utilized to establish relation between doping concentration of aluminum on the performance of the thin films. The variables for ZnO were pulse/purge variations, and growth temperatures. Growth temperature for ZnO was in between 125 and 150 °C, and DI water pulse and Diethylzinc (DEZ- Zn(C₂H₅)₂) pulse was selected as 15 ms and purge time was kept at 10s. Different growth temperatures were chosen to vary stoichiometry of ZnO. Different temperatures were utilized to establish relation between ZnO thin films. Also, one of the main purposes was comparing Al doped and undoped ZnO thin films with similar sheet resistance to display Al effect to TTFH performance such as maximum temperature and overall responsiveness. The lowest resistivity values achieved with AZO sample with 3.5 Al atomic percent as 3.3 10⁻³ Ω.cm while the each produced thin films transparency were over 85% in spectral range. The expected maximum temperature values were over 70°C with applied fairly low voltage (≤ 10 V) with heating rate of 20 °C/s.

1. George SM. Atomic layer deposition: An overview. *Chem Rev.* 2010;110(1):111-131. doi:10.1021/cr900056b

2. Ke S, Xie J, Chen C, et al. Van der Waals epitaxy of Al-doped ZnO film on mica as a flexible transparent heater with ultrafast thermal response. *Appl Phys Lett.* 2018;112(3). doi:10.1063/1.5010358

3. Tonbul B, Can HA, Ozturk T, Akyildiz H. Solution processed aluminum-doped ZnO thin films for transparent heater applications. *Mater Sci Semicond Process.* 2021;127(February). doi:10.1016/j.mssp.2021.105735

11:45 AM SF01.10.05

Chemical Vapor Deposition of Cu₂O Thin Films—Optimization of the Process and Applications as Photodetectors and HTL for Solar Cells Anna L. Pellegrino, Francesca Lo Presti and Graziella Malandrino; Università degli Studi di Catania, Italy

In recent years, copper-oxide compounds represent one of the most studied classes of semiconducting materials due to their main advantages of easily tuning the optical and electronic properties within the semiconducting behavior. For this reason, copper oxide materials play a significant role in many technological applications, ranging from batteries to catalysis, from photodetectors to solar cell devices. In particular, among the three most common and stable copper oxide phases, Cu₂O, Cu₄O₃, and CuO, named cuprite, paramelaconite and tenorite, respectively, the cuprite phase (Cu₂O) has been intensively studied and applied as p-type semiconducting material in many technological fields. In fact, Cu₂O represents an attractive material, due to

copper abundance, nontoxicity, a wide variety of synthetic strategies and low-cost production.

Herein, we report an in-depth study of the metalorganic chemical vapor deposition (MOCVD) process for the fabrication of both cuprite Cu_2O and tenorite CuO copper oxide thin films starting from β -diketonate copper (II) precursor, i.e. $\text{Cu}(\text{tmhd})_2$ bis(2,2,6,6-tetramethyl-3,5-heptanedionate). Operative conditions of fabrication strongly affect both composition and morphologies of the copper oxide thin films. Deposition temperature has been accurately monitored in order to stabilize and to produce selectively and reproducibly the two phases of cuprite Cu_2O and/or tenorite CuO . The present approach represents a simple, easily scalable and industrially appealing process for the production of compact and homogeneous copper oxide films at relatively low temperature. X-ray diffraction (XRD), field-emission scanning electron microscopy (FE-SEM) and atomic force microscopy (AFM) analyses allowed an accurate determination of the physico-chemical properties of deposited layers.

Moreover, as preliminary studies, two main applications have been tested: i) the use of Cu_2O thin films as hole transporting layer for the hybrid perovskite (methylammonium lead iodide, MAPI) based solar cell devices; ii) a core-shell system of all-oxide $\text{ZnO-Cu}_2\text{O}$ n-p junction as fast and stable self-powered photodetectors. Morphology, crystalline and electronic structure of the Cu_2O thin films materials play a crucial role in determining the main functional parameters of both applications.

12:00 PM SF01.10.06

Design of Functional Composite and All-Inorganic Nanostructures via Polymer Infiltration Using ALD Technique Elena Shevchenko^{1,2} and Diana Berman³; ¹Argonne National Laboratory, United States; ²The University of Chicago, United States; ³University of North Texas, United States

Infiltration of polymer templates with inorganic precursors using ALD technique enables the design of composite and all-inorganic structures for a broad range of applications. We will present the strategies for fabrication of conformal coatings with tunable thicknesses and porosities that reveal promising antireflective properties,[1] thermally stable multifunctional catalysts[2] and highly sensitive sensing layers.[3] We will present a systematic study on the conditioning of the polymer templates for its effective use for targeted applications. We will show that combining the infiltration of the polymer template from solution and from gas phase can significantly expand the compositional diversity of the structures that can be generated via ALD processes. We will discuss the perspectives of using plasma and thermal ALD for polymer infiltration. We will show that the choice for postpreparative polymer removal techniques can affect the dimensions, structure and composition of deposited all-inorganic heterostructures.[4]

[1] D. Berman, S. Guha, B. Lee, J.W. Elam, S.B. Darling, E.V. Shevchenko, Sequential Infiltration Synthesis for the Design of Low Refractive Index Surface Coatings with Controllable Thickness, ACS Nano 11 (2017) 2521-2530.

[2] Y. She, E.D. Goodman, J. Lee, B.T. Diroll, M. Cargnello, E.V. Shevchenko, D. Berman, Block-Co-polymer-Assisted Synthesis of All Inorganic Highly Porous Heterostructures with Highly Accessible Thermally Stable Functional Centers, ACS Applied Materials & Interfaces 11 (2019) 30154-30162.

[3] D. Berman, E. Shevchenko, Design of functional composite and all-inorganic nanostructured materials via infiltration of polymer templates with inorganic precursors, Journal of Materials Chemistry C (2020).

[4] D. Berman, Y. Sha, E.V. Shevchenko, Effect of Polymer Removal on the Morphology and Phase of the Nanoparticles in All-Inorganic Heterostructures Synthesized via Two-Step Polymer Infiltration, Molecules 26 (2021) 679.

12:15 PM SF01.10.07

Multiferroic BiFeO_3 Films Grown by MOCVD for Hybrid Energy Harvesters Quentin Micard, Guglielmo G. Condorelli and Graziella Malandrino; Univ di Catania, Italy

Multiferroics are materials in which at least two of the three ferroic orders, ferroelectricity, ferromagnetism or antiferromagnetism and ferroelasticity coexist. Among multiferroics, perovskite bismuth ferrite (BiFeO_3) and its derived systems are of special interest for keeping their properties in extreme temperature environments because of their Curie ($T_C = 1103$ K) and Neel temperatures ($T_N = 643$ K) well above room temperature. A lot of research has been devoted to the optimization of BiFeO_3 as ceramics, thin films and nanostructures. The interest in BFO is also boosted by it being a lead-free perovskite since the rising importance of environmental issues and questions of process sustainability have contributed to the prominence of lead-free perovskite systems. Photoelectric, pyroelectric, and piezoelectric properties are the most studied and appealing characteristics, which make BiFeO_3 an important material for energy harvesting applications. The possibility of combining the above-mentioned properties in a single device, a hybrid energy harvester, makes BiFeO_3 one of the most promising materials for the next generation of lead-free harvesters. The main deposition techniques applied to the production of BFO films are chemical solution deposition (CSD), pulsed laser deposition (PLD), sputtering and sol-gel. So far, compared to other methods, Metal-Organic Chemical Vapor Deposition (MOCVD) has been relatively unexplored and never used to develop BiFeO_3 deposition on silicon to fit the standard of the MEMs industry. MOCVD deposition technique offers a large number of advantages compared to other thin-film production methods with a wide choice of industrial precursors, high-quality substrates, and upscale opportunities.

In this presentation, a simple synthetic strategy based on MOCVD for the fabrication of pure and doped BiFeO_3 perovskite thin films on Si/IrO_2 and STO:Nb (100) substrates will be presented. The carried work aims to bring a methodology for the synthesis of BiFeO_3 systems thin films that are compatible with conventional industrial processes. The MOCVD approach proved a powerful tool for the fabrication of Dy-doped BiFeO_3 films. An accurate control of the processing parameters, in particular the multicomponent source mixture ratio, resulted selectively and reproducibly in the formation of $\text{Bi}_{1-x}\text{Dy}_x\text{FeO}_3$ ($x = 0, 0.06, 0.08$ and 0.11) thin films. Ferroelectric, dielectric and pyroelectric properties of $\text{Bi}_{1-x}\text{Dy}_x\text{FeO}_3$ ($x = 0, 0.06, 0.08$ and 0.11) thin films have been investigated showing that this films may be integrated as lead-free pyroelectric energy harvesters.

As material chemical composition has a critical influence on its properties, precursor thermal behavior has been checked by thermogravimetric analysis (TGA) for complex doped systems. The understanding of the films chemical compositions and homogeneity has been obtained by energy-dispersive X-ray analyses (EDX) and X-ray photoelectron spectroscopy (XPS). The polycrystalline or epitaxial nature of the films has been controlled by X-ray diffraction (XRD) and transmission electron microscopy (TEM) in the case of intricate nanostructures. Morphological study of the materials has been done by field emission scanning electron microscopy (FE-SEM) and atomic force microscopy (AFM). Coupled to the AFM, piezoresponse force microscopy (PFM) and piezoresponse force spectroscopy (PFS) have permitted the imaging of ferroelectric domains and the confirmation of the films piezoelectric properties.

This work was supported by the European Community under the Horizon 2020 Programme in the form of the MSCA-ITN-2016 ENHANCE project, Grant Agreement N.722496.

1:00 PM *SF01.11.01

Rapid, Low-Temperature Growth of *p*-type Oxides by Atmospheric Pressure Chemical Vapor Deposition for Photovoltaics and Field-Effect Transistors Rob Jagt¹, Tahmida N. Huq¹, Mari Napari², Maung Thway³, Tianyuan Liu³, David J. Meeth¹, Kham M. Niang¹, Andrew J. Flewitt¹, Fen Lin³, Judith L. MacManus-Driscoll¹ and Robert Hoye⁴; ¹University of Cambridge, United Kingdom; ²University of Southampton, United Kingdom; ³National University of Singapore, Singapore; ⁴Imperial College London, United Kingdom

Oxides are widely appealing, owing to their high mobility (compared to organic materials) and robust electronic properties. Whilst less common than their *n*-type counterparts, *p*-type oxides are needed as hole transport layers in photovoltaics, as well as for CMOS. For next-generation applications, it is critical to deposit *p*-type oxides at low temperature in order to be compatible with thermally-sensitive underlayers, such as flexible substrates (*e.g.*, for wearable electronics) and photovoltaic device stacks (*e.g.*, based on lead-halide perovskites).

This talk explores the use of atmospheric pressure chemical vapor deposition (AP-CVD) for the growth of *p*-type cuprous oxide (Cu₂O) at low temperature for photovoltaic and field-effect transistor (FET) applications.

In the first part, the deposition of uniform Cu₂O by AP-CVD at temperatures down to 100 °C is developed. The growth rate is 1.3 nm s⁻¹, which is an order of magnitude larger than conventional atomic layer deposition. This is used to create the *p*-type buffer layers on *n-i-p* structured perovskite photovoltaics. We show that owing to the high density of the Cu₂O films grown, a 3 nm layer of Cu₂O is sufficient to mechanically protect the perovskite device stack from damage when sputter depositing a transparent indium tin oxide electrode on top. The Cu₂O layer has minimal parasitic optical absorption (with >95% transmittance) and hole mobilities of 4±2 cm² V⁻¹ s⁻¹, which is orders of magnitude larger than that of the PTAA hole transport layer in the perovskite device stack. This leads to semi-transparent perovskite photovoltaics with state-of-the-art efficiencies of 16.7%. By stacking these semi-transparent devices over silicon bottom cells made with industrially-relevant processes, four-terminal tandems with efficiencies up to 24.4% are achieved.^[1]

In the second part of the talk, AP-CVD Cu₂O is developed into FETs. The switching characteristics of the devices are examined and compared against Cu₂O grown by atomic layer deposition under comparable processing conditions.^[2] The effect of Al₂O₃ passivation on the performance of the FETs is investigated, coupled with in-depth photoemission spectroscopy and transmission electron microscopy to understand the cause of changes in performance.

References

[1] Jagt, ..., Hoye, *ACS Energy Lett.*, **2020**, *5*, 2456

[2] Napari, *et al.*, *ACS Appl. Mater. Interfaces*, **2021**, *13*, 4156

1:30 PM SF01.11.02

ALD-Grown IrO_x-TiO₂ Oxygen Evolution Reaction Electrocatalyst Alloys and Multilayers for Enhanced Stability and Performance Aein Babadi¹, Scott Monaghan², Christopher O'Rourke³, Michael Braun¹, Paul Hurley², Andrew Mills³ and Paul McIntyre¹; ¹Stanford University, United States; ²Tyndall National Institute, University College Cork, Ireland; ³Queens University Belfast, United Kingdom

Low temperature electrolysis of water as a source of protons and electrons for electrochemical synthesis of hydrogen, liquid fuels and chemicals is an essential approach for decarbonization of the global economy. Water electrolysis is heavily reliant on highly active and stable electrocatalysts, and the most challenging step, from the perspective of electrochemical kinetics and catalyst stability is the oxygen evolution reaction (OER). High-rate water oxidation leads to acidic conditions in the electrolyte near the anode surface in electrolyzers. Among the highly active OER catalysts, only iridium oxide is relatively stable at acidic pH. However, the efficient utilization of IrO_x-based catalysts is essential for a cost-effective and scalable implementation of water electrolysis systems. The IrO_x catalyst layers need to be mechanically robust and stable during water oxidation and remaining highly active over long time periods.

Atomic layer deposition (ALD) is well-suited for the deposition of ultra-thin catalysts and support materials, and for catalysts surface functionalization to promote stability and enhance catalytic performance. We have synthesized stable nanoscale metal oxide alloys in the IrO_x-TiO₂ system that catalyze water oxidation while achieving high electronic conductivity. Thin TiO₂-IrO_x alloy films were grown by a super-cycle ALD process consisting of alternative cycles of TiO₂ and IrO₂ ALD processes. ALD TiO₂ films were grown using tetrakis(dimethylamido)titanium (TDMAT) and water vapor. IrO₂ ALD was performed by using ethyl cyclopentadienyl cyclohexadiene iridium (I) ((EtCp)Ir(CHD)) and ozone as the oxidant. The alloy compositions were controlled by varying the ALD cycle ratio. X-ray photoelectron spectroscopy (XPS) determined that the Ir/(Ir+Ti) compositions were reproducible and varied in a range from 0.13 to 0.51. Hall-effect analysis exhibits an overall decrease in the resistivity of the TiO₂-IrO_x alloys with increasing the iridium content, and *p*-type conduction for ALD-IrO₂ films.

Another approach to stabilize the catalyst layers is the application of overlayer coating for corrosion protection. The coating can be an electrochemically active overlayer or a combination of overlayer and catalyst material, which induces activity for catalyst reactions on the surface. It may also be a nominally inactive material, which allows the correct reaction species to come to the catalyst/electrolyte interface, while preventing other components poisoning the surface of the catalyst. We observed coating of ALD-IrO_x catalyst layers with very thin layers (< 1 nm) of TiO₂ which is normally an inactive material for water oxidation, enhances its activity by reducing the activation overpotential for OER. The current associated with water oxidation (electron transfer in OER) at a given potential was higher when we had a thin TiO₂ coating with a thickness on the order of less than one nanometer. We report on possible chemical modification of the IrO_x surface caused by the TiO₂ coating and how this correlates with the observed overpotential and Tafel behavior for OER.

1:45 PM SF01.11.03

Late News: Atomic Layer Deposition of Nickel Nanoparticles on Boron Nitride Nanotubes for Plasma-Assisted Catalysis Elham Kamali Heidari, Ania Sergeenko and Ken Bosnick; National Research Council Canada, Canada

Boron nitride nanotubes (BNNTs) are a new type of one-dimensional material that is similar to carbon nanotubes. BNNTs have recently attracted attention due to their desirable physical, thermal, and mechanical properties. Due to the high surface area and stability under harsh conditions, BNNTs can be a suitable substrate supporting catalyst particles, including for use in harsh, plasma-assisted reactors. In this research, Ni nanoparticles are deposited on BNNT papers via plasma enhanced atomic layer deposition (PEALD) using bis ethylcyclopentadienyl nickel (Ni(EtCp)₂) as the precursor and N₂/H₂ plasma. Scanning Electron Microscopy (SEM) and Helium Ion Microscopy (HIM) studies show BNNTs to be well covered with Ni particles after 150 cycles of ALD at 350 °C. Elemental analysis (EDS) proves the existence of Ni on the BNNT papers after the ALD process. According to the Transmission Electron Microscopy (TEM) observations, Ni nanoparticles are uniformly distributed over the BNNTs and have a diameter of about 4 nm. The synergy arising from the catalytic nature of the Ni nanoparticles and the high surface area, porosity, and stability of the BNNT substrates makes this

material system a perfect candidate for catalysis applications such as for the plasma-assisted production of ammonia.

2:00 PM SF01.11.04

Atomic Layer Deposition of the Alkali Polyphosphazene Electrolytes to Enable Solid-State Batteries [Alexander C. Kozen](#), R. B. Nuwayahid, Daniela Soltano, Keith Gregorczyk, Sang Bok Lee and Gary Rubloff; University of Maryland, United States

Solid state batteries (SSBs) are considered the most promising next-generation energy storage technology both due to their increased safety over conventional wet Li-ion cells and their ability to fabricate novel architectures with simultaneous high energy and power density. However, the ionic conductivities of many solid electrolyte materials are orders of magnitude lower than liquid carbonate-based electrolytes. In order to offer SSBs with competitive charge/discharge rates, SSB layers need to be thin (for fast ion diffusion) but have a large surface area (to enable large ion flux from anode to cathode). These geometric constraints establish the need for 3D electrode (and solid electrolyte) structures for a high performance battery architecture. Atomic layer deposition (ALD) is ideally suited to fabricate such devices due to its low deposition temperature, highly conformal nature, and Angstrom-scale thickness control, however many challenges remain with materials fabrication and process integration.

We have developed both plasma-enhanced ALD (PEALD) and thermal ALD processes for the Li, Na, and K alkali polyphosphazene (A*PON) electrolytes^{1,2,3,4}. The PEALD A*PON processes, by virtue of their 4-precursor synthesis route, allow some degree of chemical composition tuning. The thermal A*PON processes, unlike their PEALD counterparts, have a predetermined P-N ratio fixed by use of the precursors, however there is a tradeoff between the low temperature deposition enabled using plasma-based A*PON processes, and the conformality offered using the thermal A*PON processes. I will discuss and compare the reaction mechanisms and growth behavior among the entire family of A*PON solid electrolyte thin films, as well as discuss the integration challenges on the path to developing all-ALD planar and 3D SSBs.

1. Pearse, A.; Schmitt, T.; Sahadeo, E.; Stewart, D. M.; Kozen, A.; Gerasopoulos, K.; Talin, A. A.; Lee, S. B.; Rubloff, G. W.; Gregorczyk, K. E., Three-Dimensional Solid-State Lithium-Ion Batteries Fabricated by Conformal Vapor-Phase Chemistry. *ACS Nano* **2018**, *12* (5), 4286-4294.
2. Pearse, A. J.; Schmitt, T. E.; Fuller, E. J.; El-Gabaly, F.; Lin, C.-F.; Gerasopoulos, K.; Kozen, A. C.; Talin, A. A.; Rubloff, G.; Gregorczyk, K. E., Nanoscale Solid State Batteries Enabled by Thermal Atomic Layer Deposition of a Lithium Polyphosphazene Solid State Electrolyte. *Chemistry of Materials* **2017**, *29* (8), 3740-3753.
3. Nuwayahid, R. B.; Jarry, A.; Rubloff, G. W.; Gregorczyk, K. E., Atomic Layer Deposition of Sodium Phosphorus Oxynitride: A Conformal Solid-State Sodium-Ion Conductor. *ACS Applied Materials & Interfaces* **2020**, *12* (19), 21641-21650.
4. Kozen, A. C.; Pearse, A. J.; Lin, C.-F.; Noked, M.; Rubloff, G. W.; Atomic Layer Deposition of the Solid Electrolyte LiPON. *Chemistry of Materials* **2015**, *27* (15), 5324-5331.

2:15 PM SF01.11.05

Ceramic Nanocomposites Through Pressureless Sintering of CVD-Produced Hybrid Ceramic Powders [Ken Bosnick](#), Serguei Koutcheiko, Jennifer Bruce, Ruilin Liang and Syed Bukhari; National Research Council Canada, Canada

Theoretically, the integration of nanomaterials, such as carbon nanotubes (CNT), into a continuous matrix will produce a nanocomposite material with new and exciting properties. However, problems with the dispersion of the nanomaterials in the matrix have greatly hindered the realization of this opportunity. For example, mixing a bulk sample of CNTs with a polymer matrix often requires shear forces high enough to damage the CNTs and the polymer in order to be able to get reasonable dispersion. Mixing a bulk sample of CNTs with a ceramic matrix, in order to make a ceramic nanocomposite, would be even more difficult. Fortunately, unlike polymers, ceramics can easily survive at the temperatures needed for chemical vapour deposition (CVD) of CNTs (and other nanomaterials). In this work, CNTs are deposited onto ceramic (alumina) powder by CVD after staining with catalyst precursor and jet milling. The CNTs are well separated from each other and immobilized on the powder. This hybrid CNT-ceramic powder is mixed with a binding agent, pressed into a green body, and pressurelessly sintered to fabricate the nanocomposite. Physicochemical characterization reveals the CNTs to have survived the sintering process. The nanocomposite is characterized for its mechanical properties and the process optimized. A "floating-catalyst", plasma CVD reactor is under construction that will produce 1 kg/h of sinterable hybrid ceramic powder from a jet of neat alumina powder and a ferrocene / xylene solution, eliminating the need to deposit catalyst precursor and jet mill the powder.

2:30 PM *SF01.11.06

Tuning Conformality in Templated Initiated Chemical Vapor Deposition for Fabrication of Functional Nanostructures [Gozde Ince](#)^{1,2}; ¹Sabancı University, Turkey; ²Sabancı University Nanotechnology Research and Application Center, Turkey

Recent advances in technology accomplished by operating at nanoscale, require surface modification and functionalization for improved performance. However, functionalization of patterned surfaces or surfaces that are not directly exposed, present significant challenges in homogeneity and conformality. Functionalization of surfaces with highly conformal and homogenous coatings can be achieved via vapor deposition methods. Initiated chemical vapor deposition (iCVD) as a polymer thin film deposition technique provides conformal coatings of functional polymers on patterned surfaces.

In this talk, methods to obtain conformal iCVD coatings in confined spaces by optimizing the process parameters will be introduced and studies on one dimensional nanostructures and hybrid membranes prepared by templated iCVD method will be presented. The templated iCVD method involves conformally coating the pore walls of a sacrificial porous template with functional polymers. Stimuli responsive polymer nanotubes as nanocarriers for controlled release and biosensor applications, are successfully fabricated by templated iCVD method.

In the second part of this talk, smart membranes, which have tunable pore sizes that depend on the pH or temperature will be presented. Smart membranes are fabricated using the templated iCVD method and the conformality of the coatings are controlled by tuning the process parameters. The performance of these hybrid membranes are optimized for macromolecular separation and for protein gating applications.

SESSION SF01.12: Advanced ALD/CVD Processing
Session Chairs: Robert Hoye and Graziella Malandrino
Wednesday Morning, December 8, 2021
SF01-Virtual

10:30 AM *SF01.12.01

Understanding and Tuning Surface Chemistry to Achieve Area Selective ALD [Stacey F. Bent](#); Stanford University, United States

With the growing interest in nanoscale materials for applications such as electronics, catalysts, and batteries, methods for fabricating materials with precise control are becoming increasingly important. Area selective atomic layer deposition (AS-ALD) is gaining attention as an important process to achieve spatial control of materials deposition down to the nanometer length scale. AS-ALD is a bottom-up patterning process in which material is deposited only where desired. This talk will describe how control over the chemical properties of the substrate surface can be used to achieve AS-ALD. A deep understanding of the gas-surface chemistry behind ALD can be critical toward developing area selective processes. Research into the fundamental chemical mechanisms of ALD will be illustrated, including studies into both ALD precursor design and surface treatments that can enhance or inhibit nucleation. The development of inhibitory or enhancing layers to alter the native surface reactivity will be described. We will show that this process provides good selectivity in the deposition of thin films ranging from inorganic to organic on a variety of substrate materials, including dielectrics and metals.

11:00 AM *SF01.12.02

Atomic Layer Deposition of Cobalt Phosphate as Electrocatalyst for the O₂ Evolution Reaction—Process Characterization and Mechanism of Electrochemical Activation [Mariadriana Creatore](#); Eindhoven University of Technology, Netherlands

Storage of electricity into molecules is the most viable answer to the intermittency of renewable sources. In this respect, H₂O splitting to H₂ and O₂ is key to enable the usage of H₂ as fuel for transport, as well as building block together with CO for the electrosynthesis of hydrocarbons. For the O₂ evolution half reaction (OER), cobalt phosphate-based materials (CoPi) are interesting because they are based on earth-abundant elements and behave as bulk electro-catalysts, with Co³⁺ being the electro-chemically active centers.

Atomic Layer Deposition (ALD) is gaining major attention in the field of (electro-)catalysis because of its merit of control over conformality, uniformity, film growth (from nano-particles to thin films) and stoichiometry. Recently, we have contributed to this exciting field by demonstrating the synthesis of amorphous CoPi films by ALD [1]. CoPi is prepared by combining ALD of CoO_x from cobaltocene (CoCp₂) and O₂ plasma, with cycles of (CH₃O)₃PO (TMPO) and O₂ plasma, according to an ABCD recipe scheme [1]. The process shows a GPC of 1.12 ± 0.05 Å at 300°C, linear growth and no nucleation delay. Insights into the surface reactions occurring during the ALD process are inferred by mass spectrometry [1]. The CoCp₂ dosing is characterized by the absence of by-products, suggesting that the adsorption of the precursor on the surface is likely to occur without ligand exchange. The subsequent O₂ plasma exposure promotes the combustion of the Cp ligands, as supported by the detection of CO₂⁺, CO⁺ and H₂O⁺ species. The presence of C₄H₄⁺ and C₂H₂⁺ species in the initial stages of the plasma step, provides indirect evidence that cyclopentadienone (C₅H₄O) is an intermediate product in the Cp oxidation process. Then, C₅H₄O dissociates, generating C₄H₄, C₂H₂ and CO. The TMP dosing is characterized by chemisorption accompanied by abstraction of one methanol molecule. Finally, the conversion of the remaining ligands occurs through the O₂ plasma exposure.

Next to the above-mentioned CoPi growth studies, we have also shown that tuning the Co-to-P ratio, by combining this recipe with extra cycles of CoO_x, leads to the increase in OER performance [2], beyond that achieved by traditional electro-deposited films.

Moreover, we have investigated the mechanism behind the enhancement of the catalytic activity of ALD CoPi when tuning the Co-to-P ratio. We have found that ALD CoPi thin films progressively undergo activation under alkaline conditions with increasing number of cyclic voltammetry (CV) cycles. During this activation process induced by the infiltration of the electrolyte in the bulk of the film, the current density increases in parallel with the leaching of phosphorus out of the electro-catalyst and the shift of the oxidation state of Co from Co²⁺ to Co³⁺ [3]. CV analysis combined with Rutherford backscattering measurements indicate that after activation, as much as 22% of all Co atoms become accessible to the electrolyte and are activated. The electrochemical surface area (ECSA), i.e. the surface area accessible to promote H₂O splitting, increases up to a factor of 30. The increase in ECSA is strongly dependent on the composition of the pristine CoPi films: while the aforementioned increase holds for CoPi films with a Co-to-P ratio of 1.6, for films with a Co-to-P ratio of 1.9 the ECSA only increases by a factor 3.6. We find that for all investigated Co-to-P ratios, the electrochemical activity scales linearly with ECSA upon activation. Thus, the pristine composition indirectly affects the activity of the electro-catalyst by guiding its restructuring during activation.

It can be concluded that the digital control over the chemical composition of ALD CoPi enables to unravel the mechanism behind its electrochemical activation.

[1] V. Di Palma *et al.*, *J. Vac. Sci. Technol.* **38**,022416 (2020)

[2] V. Di Palma *et al.*, *Electrochem. Commun.* **98**, 73 (2019)

[3] R. Zhang *et al.*, *ACS Catal.* **11**, 2774 (2021)

11:30 AM SF01.12.04

Atomic Layer Deposition of Epitaxial Perovskite Nickelates [Tae Joon Park](#), Zhen Zhang and Shriram Ramanathan; Purdue University, United States

Atomic layer deposition (ALD) of correlated oxides is an emerging field. With limited data available in literature on thermodynamics of precursors to deposit rare-earth metals, significant experimental effort and instrumental optimization is essential for robust formation of crystalline phases of complex oxides such as rare-earth nickel oxides. ALD of such complex semiconductors could make them directly relevant to electronic technologies as well as enabling high quality ultra-thin films necessary for electric field control of various physical properties. In this work, we will discuss ALD processing of epitaxial NdNiO₃ thin films. By controlling various deposition parameters including precursor pulsing time, deposition temperature, we have successfully optimized the growth conditions to obtain stoichiometric NdNiO₃ thin films grown epitaxially on LaAlO₃. We will then discuss their excellent functional properties such as large electrically tunable opacity to realize electrochromic window coatings on glass and highly responsive hydrogen gas sensors for environmental monitoring. Finally, we will critically compare these functional properties to those of similar thickness epitaxial NdNiO₃ films grown by RF-sputtering.

11:45 AM SF01.12.05

Tuning the Electrochemical Properties of Multifunctional Catalyst Layers by Plasma-Enhanced Atomic Layer Deposition [Matthias Kuhl](#), Alex Henning, Lukas Haller, Laura I. Wagner, Chang-Ming Jiang, Verena Streibel, Ian Sharp and Johanna Eichhorn; TU Munich, Germany

Photoelectrochemical (PEC) energy conversion is a promising route for synthesis of storable chemical fuels from sunlight, thereby providing a route to overcome the current global reliance on fossil fuels. One of the major challenges in such artificial photosynthetic systems are the poor efficiency and material instability of semiconductor photoelectrodes under harsh PEC operating conditions. One strategy to overcome this limitation is to interface the semiconductor light absorber with conformal and ultra-thin catalytic layers, which promote the desired chemical reaction, while permitting efficient interfacial charge transport, maintaining chemical stability, and minimizing parasitic light absorption. In this regard, plasma-enhanced atomic layer deposition (PE-ALD) is a powerful tool for designing surface layers and interfaces with tailored functionality and precise thickness control.

Recently, it was demonstrated that PE-ALD can be used to fabricate conformal, biphasic Co₃O₄/Co(OH)₂ catalyst layers on semiconductor photoelectrodes, which are simultaneously robust and electrochemically active¹. In this system, the nanocrystalline Co₃O₄ layer forms a durable interface to the substrate and the disordered Co(OH)₂ surface layer significantly improves the electrocatalytic oxygen evolution reaction (OER) activity. Here, we leverage the

precise control of PE-ALD to further tailor the thickness ratio of the surface and interface layers of the $\text{Co}_3\text{O}_4/\text{Co}(\text{OH})_2$ bilayer by tuning the plasma pulse time during growth. Short pulses lead to the formation of porous, unstable $\text{Co}(\text{OH})_2$ layers, while long pulses reduce the thickness of the surface layer and form stable, inactive Co_3O_4 layers. Furthermore, we show that the underlying mechanism for the formation of the $\text{Co}(\text{OH})_2$ surface layer is the incomplete decomposition of the precursor at short pulse durations. This work highlights the use of PE-ALD as a promising approach for engineering catalyst/semiconductor interfaces to create efficient and stable photoelectrodes.

1. Yang, J. *et al.* A multifunctional biphasic water splitting catalyst tailored for integration with high-performance semiconductor photoanodes. *Nat. Mater.* **16**, 335–341 (2017).

12:00 PM SF01.12.06

Development of Strained-Germanium Based Light-Emitting Microstructures via Liquid Phase Epitaxy Buse Unlu¹, Milad Ghasemi¹, Selcuk Yerci^{1,1} and Cicek Boztug²; ¹Middle East Technical University, Turkey; ²TED University, Turkey

Germanium (Ge) is a promising candidate to serve as an infrared light emitter in the fully integrated, miniaturized biosensing systems where electronic and photonic components are realized on the same silicon (Si) chip in a CMOS-compatible fashion. Despite the inherently indirect band structure of Ge, its bandgap can be engineered to convert it into an efficient light emitter with the emission wavelength tuned into the mid-infrared range of the spectrum, which is suitable for biosensing applications. Among various techniques utilized to enhance the light emission efficiency of Ge, such as Sn alloying, n-type doping, and application of tensile strain, the latest one provides an additional advantage by enabling the development of the room-temperature-operated infrared light source with a predefined emission wavelength, where the emission wavelength is simply a function of the strain. In this work, we introduce a CMOS-compatible fabrication technique that allows obtaining single-crystalline tensilely-strained germanium microstructures, where both crystallization and tensile strain induction is achieved through a single annealing process. The fabrication procedure of the structures relies on the deposition of the germanium, silicon nitride, and silicon dioxide films all by using a physical vapor deposition, namely sputtering, technique, which is a room-temperature-operation, environmentally-friendly deposition technique as opposed to the chemical vapor deposition methods. The crystallization of the sputtered amorphous germanium is achieved via liquid phase epitaxy following a single rapid thermal annealing process, during which tensile stress is also introduced into the silicon nitride film capping the germanium. A subsequent photolithography process allows the strain transfer from the tensilely-stressed nitride film to the lithographically defined germanium microstructure. Strain, and therefore the emission wavelength, can simply be adjusted by varying the duration of the final wet etching process. The method is suitable for both the fabrication of uniaxially and biaxially tensile-strained germanium microstructures, where uniaxial and biaxial strain levels of around 3% and 1.5%, respectively, have been demonstrated and verified by Raman spectroscopy and micro-photoluminescence (micro-PL) measurements, as well as the finite element method (FEM) simulations. Overall, our results show that infrared light emitters based on tensilely-strained germanium microstructures suitable for the biochemical sensing applications can be realized on Si chips in a CMOS-compatible fashion utilizing cost-efficient and easy-to-use deposition (sputtering) and crystallization (liquid phase epitaxy) methods.

SESSION SF01.13: ALD/CVD General II

Session Chair: Kevin Musselman

Wednesday Afternoon, December 8, 2021

SF01-Virtual

1:00 PM SF01.13.02

Controlling Reaction Paths for Growth of Inorganic Nanowires Floating in the Gas Phase Richard S. Schaeufele^{1,2}, Juan J. Vilatela¹ and Miguel Vazquez-Pufleau¹; ¹Imdea Materials Institute, Spain; ²Universidad Autónoma de Madrid, Spain

Synthesis of inorganic nanowires/nanotubes suspended in the gas through floating catalyst chemical vapour deposition (FCCVD) produces exceptional growth rates of 500 - 1000 micron/second, more than two orders of magnitude faster than conventional substrate processes. It leads to nanowire lengths > 100 microns and thus to the possibility of direct assembly into freestanding macroscopic networks as a continuous process. This work studies the different reaction paths controlling conversion and crystallinity in FCCVD applied to the synthesis of silicon nanowires (SiNW) from silane, grown through an aerosol of gold catalyst nanoparticles. There are two main competing reactions: catalysed growth of SiNW and nucleation of amorphous Si nanoparticles. The two populations can be conveniently distinguished for high-throughput screening by their colour and Raman spectra. Their balance is kinetically controlled by the ratio of precursor/hydrogen carrier gas, through its inhibition of the pyrolysis of silane into silylene. This role of hydrogen is common to other nanomaterials grown by FCCVD, but differs with respect to carbon and boron nitride in having little influence on the nucleation stage of 1D nanomaterial growth. As a consequence, we were able to identify effective process conditions for producing large free-standing and pristine SiNW sheets. These yield highly promising results when exploited as active material in lithium ion battery anodes.

1:15 PM SF01.13.03

Atmospheric-Pressure Spatial Atomic Layer Deposition (AP-SALD) Of Metal Oxides for Gravimetric Gas Sensing Applications Masoud Akbari¹, Viet Huong Nguyen², Gaëtan Debontride³, Martial Defoort¹, Skandar Basrouf¹, Kevin Musselman⁴ and David Munoz-Rojas¹; ¹University of Grenoble Alpes, France; ²Phenikaa University, Viet Nam; ³CIME Nanotech/Grenoble INP, France; ⁴University of Waterloo, Canada

Metal oxides are commonly used as sensing material for gas detection applications. The surface of the metal oxide is covered with oxygen ions (ion adsorbed) in presence of air, and these ions act as electron acceptors [1]. Metal oxides have mostly been used in resistive or conductive gas sensors, where electronic events in the material generate a detection signal. However, they are also promising as sensing layer in gravimetric micro-electromechanical systems (MEMS). MEMS-based gravimetric sensors are ultra-fast and highly sensitive and the sensing mechanism is related to mass change. Upon exposure of the metal oxide-coated sensor to a gas, the surface oxygen ions react with the gas molecules, which results in lowering or increasing the sensor mass [2]. The sensing performance of the sensor is highly dependent on the chemical and structural properties of the sensing layer. Recently, Atmospheric-Pressure Spatial Atomic Layer Deposition (AP-SALD) has proven to be an excellent deposition technique that is capable of producing high quality metal oxide thin films with precision control, while being up to 2 orders of magnitude faster than conventional ALD, and working at atmospheric pressure [3][4]. Recently, we developed ZnO-based transparent conductive films deposited with our home-made AP-SALD for resistive gas sensing [5]. In this research, we employed AP-SALD for deposition of different metal oxides for gravimetric gas sensing. We present a complete study on deposition of tin oxide (SnO_2), as a common sensing material, and structural, optical, chemical and electrical properties of the SnO_2 thin films will be shown. Gas sensing properties of SnO_2 , ZnO, Al-ZnO, etc. deposited by AP-SALD and effect of annealing and doping on sensing behavior will be investigated and discussed in detail. The gas sensors functionalized by metal oxides showed fast response and high sensitivity toward humidity, ethanol and acetone.

References:

1. M. E. Franke, T. J. Koplin, and U. Simon, *Small* **2**, 36 (2006).
2. K. M. Goeders, J. S. Colton, and L. A. Bottomley, *Chem. Rev.* **108**, 522 (2008).
3. D. Muñoz-Rojas and J. Macmanus-Driscoll, *Mater. Horizons* **1**, 314 (2014).
4. K. P. Musselman, C. F. Uzoma, and M. S. Miller, *Chem. Mater.* **28**, 8443 (2016).
5. V. H. Nguyen, D. Bellet, B. Masenelli, and D. Muñoz-Rojas, *ACS Appl. Nano Mater.* **1**, 6922 (2018).

1:30 PM SF01.13.04

P-Type Cu₂O Thin Films Deposited via Atmospheric-Pressure Spatial Atomic Layer Deposition—A Step Towards Low-Cost Photovoltaic Solar Harvesters Abderrahime Sekkat^{1,2,3}, Viet Huong Nguyen⁴, Daniel Bellet¹, Anne Kaminski-Cachopo², Guy Chichignoud³ and David Munoz-Rojas¹; ¹LMGP, France; ²IMEP-LaHC, France; ³SIMaP, France; ⁴Faculty of Materials Science and Engineering, Phenikaa University, Viet Nam

Cuprous oxide (Cu₂O) is a non-toxic and abundant p-type semiconductor with a direct band gap around 2.1 eV and a large visible absorption coefficient. It has been studied and developed for several devices such as solar cells, thin film transistors or batteries. In this work, Cu₂O thin films with thickness below 100 nm and record mobilities up to 92 cm²V⁻¹s⁻¹ have been obtained. The films have been deposited via AP-SALD (Atmospheric-Pressure Spatial Atomic Layer Deposition) at low temperatures (up to 260 °C), under atmospheric pressure. AP-SALD is an alternative approach to conventional ALD in which the precursors are separated in space rather than in time, allowing fast deposition rates as compared to conventional ALD (up to nm/s in some cases). The impact of the deposition parameters on the growth rate and transport properties (mobility and concentration of carriers) has been studied, and different Cu precursors have been evaluated. The high mobility values obtained, which are close to values associated to epitaxial Cu₂O thin films or Cu₂O single crystals, have been rationalized based on Raman data. Optimized Cu₂O thin films, combined with n-type ZnO also deposited by AP-SALD, lead to all-oxide solar harvesters with efficiency values rivaling similar devices made with high temperature and/or vacuum approaches, thus opening the door to efficient semitransparent solar harvesters.

1:45 PM SF01.13.05

Bandgap and Defect States Analysis Using Spectroscopy of Chemical Vapor Deposition (CVD) Grown Cu₂O Vivek Singh, Jyoti Sinha and Sushobhan Avasthi; Indian Institute of Science Bangalore, India

Cuprous oxide (Cu₂O) is a promising material for emerging electronics. Bandgap and defect states estimation of Cu₂O film grown by chemical vapor deposition (CVD) technique on SiO₂/Si substrate at 600 °C was performed in this work using various spectroscopies. XRD and XPS confirmed the phase purity of deposited film. The optical bandgap of Cu₂O was 2.35 eV which was calculated from absorption spectroscopy (UV-Vis). Using ultraviolet photoelectron spectroscopy (UPS) and absorption spectroscopy (UV-Vis), the nature of deposited Cu₂O was confirmed as a p-type semiconductor. Using UPS, the energy level of the valence band and Fermi level of the intrinsically p-doped Cu₂O film were determined as 6.02 eV and 5.62 eV respectively from the vacuum level. The temperature dependence photoluminescence spectra of these films exhibited emission peaks at ~1.4 eV and ~1.72 eV which corresponds to energy states of copper and oxygen vacancies level in the bandgap. Photoluminescence spectra also show a peak at ~2 eV which is due to the relaxation of free excitons to the valence band.

2:00 PM SF01.13.06

A Synchrotron-Assisted Investigation of the Thermal Decomposition of Zirconium Acetylacetonate—Pathways to the Formation of Metal-Containing Intermediates in the Gas Phase Sebastian Grimm¹, Seung-Jin Baik¹, Patrick Hemberger², Andreas Kempf^{1,3}, Tina Kasper^{1,3} and Burak Atakan^{1,3}; ¹University of Duisburg-Essen, Germany; ²Paul Scherrer Institute, Switzerland; ³Center for Nanointegration Duisburg-Essen (CENIDE), Germany

Solid layers^{1,2} of ZrO₂ are often deposited by chemical vapor deposition (CVD), where a metal-containing precursor is evaporated and forms a film in a surface reaction. To design such a process, the gas phase reactions, especially their temperature-dependent kinetics, should be known, which is seldom the case. Intermediates, formed in the gas phase can lead to film formation or to a depletion of the precursor and therefore a reduction in growth rate. The analysis of these early stages of growth requires fast and sensitive analytical techniques with sufficiently low detection limits for elusive gas phase species. Experimental limitations precluded the detection of most of the postulated intermediate species, and reaction mechanisms are predominantly hypothetical so far.^{3,4} An experimental approach to enlighten the gas phase chemistry of an often used precursor, zirconium acetylacetonate, is presented here, using a microreactor coupled to a mass spectrometer with mild ionization from a synchrotron source. This was demonstrated previously, to be an effective way to detect and characterize gas phase intermediates with short lifetime.^{5,6}

A combined numerical and experimental study of the vacuum pyrolysis of zirconium acetylacetonate, Zr(C₅H₇O₂)₄, in a microreactor at short residence times of < 60 μs was carried out. The precursor is sublimed, subsequently transported by argon or helium carrier gas, and expanded through a pinhole into a resistively heated 1 mm inner diameter SiC-microreactor. Products leaving the reactor are expanded and ionized by tuneable vacuum ultraviolet (VUV) synchrotron radiation and characterized by imaging photoelectron photoion coincidence spectroscopy (i²PEPICO) and mass spectrometry at the Swiss Light Source in Switzerland. From the temperature-dependent photoionization mass spectra between 130 and 650 °C, two initial decomposition steps were identified and temperature regimes for the following pathways of thermal decomposition at higher reactor temperatures were determined. In addition, we recorded photoionization efficiency curves and threshold photoelectron spectra (TPES) at photon energies of 6.5–11.5 eV, which gave us direct evidence about the intermediates and products formed. Six important Zr-intermediates were identified for the first time, as for example Zr(C₅H₇O₂)₂(C₅H₆O₂), and ZrO(C₅H₇O₂)₂, together with several organic products, which aided us to describe the predominant thermolysis pathways in the temperature range of 130–650 °C. In conjunction with the simultaneous numerical simulation of the flow field in the microreactor, the application of synchrotron radiation coupled to the i²PEPICO experimental apparatus is a promising way to enlighten pyrolysis pathways and kinetics of metal-organic precursors.

References

1. A. Méndez-López, O. Zelaya-Ángel, M. Toledano-Ayala, I. Torres-Pacheco, J.F. Pérez-Robles and Y.J. Acosta-Silva, *Crystals*, 2020, **10**(6), 454.
2. J.G. Thakare, C. Pandey, M.M. Mahapatra and R.S. Mulik, *Met. Mater. Int.*, 2020, **366**, 338.
3. M.V.F. Schlupp, J. Martynczuk, M. Prestat and L.J. Gauckler, *Adv. Energy Mater.*, 2013, **3**(3), 375.
4. H.M. Ismail, *Powder Technology*, 1995, **85**(3), 253.
5. Z. Zhang, Y. Pan, J. Yang, Z. Jiang and H. Fang, *Journal of Crystal Growth*, 2017, **473**(12), 6.
6. P. Hemberger, J.A. van Bokhoven, J. Pérez-Ramírez and A. Bodi, *Catal. Sci. Technol.*, 2020, **10**(7), 1975.

SYMPOSIUM SF02

Additive Manufacturing—From Material Design to Emerging Applications
November 29 - December 7, 2021

Symposium Organizers

Kun Fu, University of Delaware
Sung Hoon Kang, Johns Hopkins University
Yayue Pan, University of Illinois at Chicago
Jordan Raney, University of Pennsylvania

* Invited Paper

SESSION SF02.01: Additive Manufacturing Methods, Characterizations, and Mechanics I

Session Chairs: Kun Fu and Yayue Pan
Monday Morning, November 29, 2021

Hynes, Level 3, Room 309

8:30 AM SF02.01.01

Mechanical Characterization of Elastomeric Lattice Parts Produced by Continuous Liquid Interface Production Roozbeh Neshani¹, Davis J. McGregor², Sameh Tawfik², William P. King² and Sezer Ozerinc¹; ¹Middle East Technical University, Turkey; ²University of Illinois at Urbana-Champaign, United States

Additive manufacturing of elastomeric parts has become increasingly important due to unique opportunities in biomedical and vibration isolation applications. Continuous liquid interface production (CLIP) is a recently developed technique that addresses some major limitations in this route by providing fast production of high-resolution features in a repeatable and reliable fashion. In this study, we report on the mechanical properties of CLIP-produced parts made of EPU 41, an elastomeric polyurethane developed specifically for CLIP.

Mechanical characterization studies employed a wide range of techniques, including tensile and compression testing and stress relaxation measurements. Tensile strength of EPU 41 exceeds 10 MPa with an elongation at break reaching 175%. A 2-term Ogden model accurately predicts the tensile response. Compressive stress relaxation measurements provided a compressive set of 13% after a 48-hour constant-strain loading. A three-term Prony series based on the generalized Maxwell model fits the experimental results accurately.

The study also considered the compressive response of a series of lattice parts, including octet, cubic, and BCC-based geometries. The structures fully recover after loading to a strain of 75%. The critical densification strain varies in the range of 0.5 – 0.9, and the corresponding plateau stress exhibits a wide range of values in the range of 0.01 – 0.30 MPa. Tuning of the geometry and the strut thickness enables structures to exhibit a wide range of load absorbing characteristics. The results show the great potential of the CLIP process in manufacturing new generation lattice structures and load-bearing components with optimized compliance and absorbance characteristics.

8:45 AM SF02.01.02

Additive Manufacturing of Colloidal Suspensions—Printing Broadband Omnidirectional Reflectors on Surfaces for High Temperature Applications Benedikt F. Winhard, Gerold A. Schneider and Kaline Furlan; Institute of Advanced Ceramics, Germany

Photonic glasses may yield a new class of thermal barrier coatings, due to their broadband omnidirectional reflection capabilities. To apply such photonic structures, precise deposition even on complex substrate geometries is mandatory. However, conventional techniques, like spin coating, are not capable to form homogenous coatings on curved surfaces. Therefore, we combine an additive manufacturing technique, direct writing, with colloidal self-assembly (AMCA) to deposit polystyrene (PS) colloidal suspensions onto metallic and aluminum oxide surfaces, which subsequently assemble into PS-templates. The inverse opal photonic coatings are then formed via ALD infiltration and subsequent burn-out.

When printing low viscosity suspensions by direct writing, the contact line must remain pinned during solvent evaporation to prevent split up of the filament. However, such pinning also enhances capillary flow, usually leading to a coffee ring effect (CRE). In this work, we performed a parameter study varying both writing velocity v_w and dispense velocity v_d , as well as particle loading. We show that increasing the particle loading enhances the self pinning effect, thus enhancing printability, while the CRE can be suppressed by increasing the velocity ratio v_w/v_d . To ensure coverage of large areas, single lines must be connected, however the conventional line-by-line approach is insufficient for low viscosity colloidal suspensions due to capillary penetration of the previously printed line. Hereby, we present a “comb”-printing approach to overcome this issue and print coherent colloidal layers. Finally, we demonstrate that ceramic-based inverse opal photonic coatings are produced when the optimized templates are infiltrated via ALD, showing broadband omnidirectional reflection properties.

9:00 AM SF02.01.03

Energy Absorption Properties of 3D Printed Lattice Structures Ryan Nam¹, Michael Jakubinek² and Hani E. Naguib¹; ¹University of Toronto, Canada; ²National Research Council Canada, Canada

Novel lattice structure designs fabricated by additive manufacturing are promising in aerospace development in terms of lightweight alternatives to the current solutions. Cellular core sandwich structures offer many multifunctional advantages, such as high specific energy absorption capabilities and

flexural stiffness, and can be further tailored to enhance specific properties. Fused deposition modeling (FDM) of functionally graded lattices shows the potential to be used as a lightweight cellular core for sandwich structures due to their high specific energy absorption in quasi-static compression. Variations in the structural configuration and material composition of an architected core structure are performed to observe the differences in compressive behavior. By FDM printing a lattice composed of repeating unit cells with rows differing in the wall thickness and, consequently, the filled cell volume, the structural grading effects in the direction of compression is explored. Both discrete and continuous grading of the wall thickening were applied from the top to bottom lattice rows along the direction of applied compressive force and display differences in energy absorption properties. The material grading effects are characterized by using two distinct filaments to vary composition of the core structure and hence the material density and tensile modulus properties between the layers. The stress-strain behavior and values of the specific energy absorbed were calculated by examining the printed samples during a quasi-static compression load test. Greater specific energy absorption (energy per mass) was seen in the graded layer by layer design compared to the non-graded octet lattices. The multi-material grading arrangements significantly modified the onset location of structural collapse to influence the layer compression order. These behaviors demonstrate the possibility of 3D printing a lightweight sandwich core with tailorable compressive properties using a combination of material and structural grading.

9:15 AM SF02.01.05

Late News: Micro/Nanofibers-Based 3D Fibrous Scaffolds Using Additive Textile Manufacturing Huibin Chang, Qihan Liu, John Zimmerman, KeelYong Lee, Qianru Jin, Michael M. Peters, Michael Rosnach, Suji Choi, Sean L. Kim, Herdeline Ardoña, Luke MacQueen, Christophe Chantre, Sarah Motta, Elizabeth Cordoves and Kevin K. Parker; Harvard University, United States

There is growing interest to develop next generation of additive manufacturing platform that can rapidly produce micro/nanofibers and precisely control of the fiber alignment in fibrous 3D complex structure, which allows biomimetic materials for next generation philologically assays or customized fiber reinforced composite materials. However, reproducing micro/nano sized fibrous structure is difficult using existing technologies. For instance, approaches such as 3D printing are generally considered too slow for producing fibers in micro/nano size, while high-throughput nonwoven fiber deposition methods provide poor control over structural alignment and 3D geometry. Here we report a new form of additive textile manufacturing platform termed focused rotary jet spinning (FRJS) where micro/nanofiber formation and patterning process are independently controlled. We show that these deposited fibers can conform to various 3D geometries with controllable fiber alignment. This technology has potential in a range of applications, reaching from biomedical applications, fashion design to next-generation food packaging.

9:30 AM SF02.01.06

Probing Polycarbonate Welds Using a Novel Fracture Induced Test Method Ojaswi Agarwal¹, Zheliang Wang¹, Jonathan Seppala², Edwin P. Chan², Thao (Vicky) Nguyen¹ and Kevin Hemker¹; ¹Johns Hopkins University, United States; ²National Institute of Standards and Technology, United States

The Razorblade Induced Fracture Test (RIFT) is a mechanical test method in which a sharp blade is pressed into a sample to initiate and propagate a crack and used to determine the energy release rates (G_C) of soft polymers such as gels or food products [1, 2]. Its use in measuring G_C of stiffer polymers has been limited as the frictional component of the measurement becomes significant [3-5]. In this study we develop a cyclic RIFT test that can easily and repeatedly probe narrow regions of the sample and simultaneously account for the frictional contribution to the measurement. We use this method to determine the strength of polycarbonate (PC) welds made using Fused Filament Fabrication (FFF). In conjunction with geometry and thermal characterization using micro-computed tomography (μ -CT) and infrared imaging (IR), we undertake a parametric study of how the thermal and flow history of the print affects the measured strength of the welds in the printed material. This information is compared to bulk PC made by injection molding [6-8].

In-situ birefringence measurements of the sample have shown a concentration of plastic deformation at the crack tip, and a non-negligible strain due to bending which is accounted for through parallel FE modelling. Ex-situ birefringence measurements have shown a small region around the crack tip where the plastic deformation localizes. The width of this region is limited to a single layer on either side of the strongest tested welds, decreasing in size as the welds get weaker. The radius of the region is approximately 0.3 mm while the calculated elastofracture length is much smaller at 11.8 μ m. Preliminary results suggest that the frictional force component ranges from 35% to 45% of the measured cutting force. As expected, measured values of G_C for PC welds vary with printing conditions and with the measured thermal and flow history of the print. Increasing the welding increases the measured strength of the weld. The G_C for samples with longer welding times (printed at higher temperatures), approach that of injection molding bulk PC.

- [1] T. Brown, S.J. James, G.L. Purnell, Journal of food engineering 70 (2005) 165-170.
- [2] T.T. Duncan, J.M. Sarapas, A.P. Defante, K.L. Beers, E.P. Chan, Soft Matter 16 (2020) 8826-8831.
- [3] A. Gent, C. Wang, Journal of Polymer Science Part B: Polymer Physics 34 (1996) 2231-2237.
- [4] H. Uete, R.M. Caddell, International Journal of Mechanical Sciences 25 (1983) 87-92.
- [5] B. Zhang, C.-S. Shiang, S.J. Yang, S.B. Hutchens, Experimental Mechanics 59 (2019) 517-529.
- [6] L. Fang, Y. Yan, O. Agarwal, J.E. Seppala, K. Migler, T.D. Nguyen, S.H. Kang, Additive Manufacturing (2021) 101983.
- [7] J.E. Seppala, S.H. Han, K.E. Hillgartner, C.S. Davis, K.B. Migler, Soft Matter 13 (2017) 6761-6769.
- [8] J.E. Seppala, K.D. Migler, Additive manufacturing 12 (2016) 71-76.

9:45 AM SF02.01.07

Decoupling the Effect of Geometry and Microtexture on the Mechanical Response of Additively Manufactured IN625 Thin-Walled Elements Arunima Banerjee¹, Jeff Rossin², William Musinski³, Paul Shade³, Marie Cox³, Tresa Pollock² and Kevin Hemker¹; ¹Johns Hopkins University, United States; ²University of California, United States; ³Air Force Research Laboratory, United States

Additively manufactured (AM) metallic components have highly anisotropic microstructures spanning multiple length scales. The relationship between microstructure and mechanical properties of printed structures is complicated by the introduction of additional design parameters, such as build orientation and geometric variations. This study was undertaken to decouple the contribution of microstructure and geometry on the mechanical response of thin-walled Inconel 625 T-elements fabricated by laser powder bed fusion. The T-elements were printed at either 40° or 90° inclinations from the build plate resulting in a 10% difference in the ligament widths. Milli-scale tests indicate that the 90° T-elements are stiffer in both the stress-relieved and the fully recrystallized states. However, the modulus along the loading direction determined from EBSD maps suggest the 40° T-elements to be stiffer in the stress-relieved case. The measured yield load difference between the recrystallized samples was in better agreement with the values predicted from beam theory.

10:00 AM BREAK

10:30 AM SF02.01.08

Late News: In Situ Evolution of Microtribology in Additively Manufactured 316L Steel by Selective Laser Melting Mohanad Bahshwan^{1,2}, Mark Gee³, John Nunn³, Connor Myant¹ and Tom Reddyhoff¹; ¹Imperial College London, United Kingdom; ²University of Jeddah, Saudi Arabia; ³National

Physical Laboratory, United Kingdom

Consensus on the wear and friction performance of additively-versus-conventionally manufactured components has not been achieved; mainly because the tribological test set-ups thus far were not suited for investigating the underlying microstructure's influence on the tribological properties. As a result, utilization of additive manufacturing techniques, such as selective laser melting (SLM), for sliding components remains questionable. Here, we investigate the anisotropic microtribology of SLM 316L stainless steel via in situ SEM reciprocating scratch testing to highlight the microstructure's role. As-built 316L SLM specimens were compared against annealed wire-drawn 316L. We found that: (i) microgeometric conformity was the main driver for achieving steady-state friction, (ii) the anisotropic friction of the additively manufactured components is limited to the break-in and is caused by the lack of conformity, (iii) the cohesive bonds, whose strength is proportional with frictional forces, are stronger in the additively manufactured specimens likely due to the presence of dislocations and/or cellular structures, (iv) low Taylor-factor grains with large dimension stimulate microcutting in the form of long, thin sheets with serrated edges. These findings uncover some microstructurally driven tribological complexities when comparing additive to conventional manufacturing.

10:45 AM SF02.01.09

Assembly, Sintering and Characterization of III-V Nanoparticles for Electronics Applications [Anthony S. Childress](#), Jared Cohen and Ahmed Busnaina; Northeastern University, United States

Additive manufacturing has the potential to make nanoscale electronics at a fraction of the cost required by current conventional fabrication. Through the directed assembly-based printing of nanomaterials, hundreds of steps of deposition and etching can be removed from the fabrication process. Previous research conducted at the NSF Center for High-rate Nanomanufacturing and other works have shown the effectiveness of the directed assembly processes that allow for high throughput and high precision at comparatively low cost. However, the assembly and sintering of semiconducting nanomaterials such as InP and GaAs poses a significant challenge to this endeavor. In this talk I will outline our recent results in the processing, assembly, and annealing of III-V semiconducting nanoparticles. Through high-speed ball milling, bulk particles of III-V semiconductors have been reduced to dimensions of less than 30 nm, after which they were formulated into a stable ink suitable for printing. A silicon wafer with a functionalized surface allows the precise assembly of nanoparticles through preferential adhesion of the ink. The particles are assembled as structures suitable for making transistors and measuring Hall and other electronics characteristics. Annealing the particles to make a continuous structure is critical for fabricating practical electronics, and it is this aspect which poses one of the greatest challenges due to the loss of the lighter elements (P and As) during annealing. This barrier is overcome through the use of small amounts of sacrificial particles during annealing, resulting in a continuous structure. Once the assembled particles are sintered, gold contacts (source and drain) are deposited for electronic characterization. The results from our work demonstrate the feasibility of printing III-V semiconductors for electronics applications.

11:00 AM SF02.01.10

Differences in Microstructures and Mechanical Properties of Ti-6Al-4V Fabricated by Selective Laser Melting with Pulse Width Modulation Under the Same Volumetric Energy Density and Duty Cycle [Seunghwan Moon](#), Seungmuk Ji, Young-Shik Yun and Jong-Souk Yeo; Yonsei University, Korea (the Republic of)

Metal Additive Manufacturing (AM) is drawing attention to the application of biomedical implants because of its ability to fabricate customized precise structures readily than conventional casting methods. Powder Bed Fusion (PBF), which is implemented by irradiating powder particles with a heat source, provides sufficient mechanical property without post-processing in contrast to the other AM technologies. There are two types of heat sources that are used for PBF; laser and electron beam. The former is known as Selective Laser Melting (SLM) and the latter is Electron Beam Melting (EBM). Especially for SLM, a pulse laser can be used by modulating the power signal of a continuous-wave laser into a pulse shape. This process is called Pulse Width Modulation (PWM), which allows additional process control compared to a continuous-wave laser.

Volumetric Energy Density (VED), calculated by dividing laser power by the product of scan speed, layer thickness, and hatch spacing, is a concept that expresses the applied average energy on the unit volume of the specimen. In many cases, microstructures and mechanical properties of fabricated specimens with SLM can be described by VED, but there exist exceptions. This is because the degree that each process parameter contributes to the properties of the specimen is different.

In this study, we focus on the differences in microstructures and mechanical properties of the specimen fabricated using the same VED conditions, especially with PWM laser. Even if all the process parameters composing the concept of VED and the duty cycle (DC) of the PWM laser are the same, the microstructure and mechanical properties are still very different depending on the pulse width. The surface roughness is also changed according to the pulse width. Mechanical properties are measured by using the Vickers hardness test, and the porosity and roughness are compared using an optical micrograph. For microstructural analysis, electron back-scattered diffraction is measured on the transverse section of specimens. Based on the results from these measurements and the simulation of the thermal distribution obtained through the finite element method, the causes leading to the differences in microstructures and mechanical properties of specimens fabricated under the same VED and DC are analyzed.

This research was supported by the Ministry of Trade, Industry and Energy (MOTIE) and Korea Institute for Advancement of Technology (KIAT) through the International Cooperative R&D program (N0002624) and was also supported by the National Research Foundation (NRF) of Korea under the "Korean-Swiss Science and Technology Program" (2019K1A3A1A1406720011).

SESSION SF02.02: Additive Manufacturing Methods, Characterizations, and Mechanics II
Session Chairs: Kun Fu and Yayue Pan
Monday Afternoon, November 29, 2021
Hynes, Level 3, Room 309

1:30 PM SF02.02.01

Late News: A Study of Microstructure and Mechanical Properties in Additively Manufactured AlCuFeNiTi High Entropy Alloy [Sandeep Khadka](#) and Philip Yuya; Clarkson University, United States

An equiatomic AlCuFeNiTi high entropy alloy (HEA) was synthesized using pre-alloyed powder by direct energy deposition (DED) on a Ti6Al4V substrate and characterized to provide

insight into its microstructural and nanoscale mechanical properties. Scanning electron microscope (SEM) and energy-dispersive X-ray spectroscopy (EDS) were performed to characterize the alloy's microstructure. Also, electron backscatter diffraction (EBSD) and X-ray diffraction (XRD) were carried out to understand the crystallographic information of the alloy. Nanoindentation technique was used to determine the reduced modulus and hardness. Microstructural characterization results show three distinct regions as Cu-rich, Fe-rich, and Al-Ti-Ni rich regions. The presence of these regions shows the variance of local composition within the alloy that influences its mechanical properties. The dendritic regions rich in Al, Ni, and Ti presented a hard zone, whereas the inter-dendritic regions rich in Cu and Fe showed a soft zone. XRD and EBSD analysis confirmed that the regions are a mixture of BCC and FCC phases. The alloy was determined to have a reduced modulus and hardness of 181 ± 14.26 GPa and 9.03 ± 2.42 GPa, respectively.

1:45 PM SF02.02.02

Late News: An Alternative Method for Accident Tolerant Fuel Cladding Using Swaging and Drawing Process at Room Temperature Jong Woo Kim¹, Young Ah Park¹, Jisu Na¹, Hyeongwoo Min¹, Yong Hee Kim² and Young Soo Yoon¹; ¹Gachon university, Korea (the Republic of); ²Korea Advanced Institute of Science and Technology, Korea (the Republic of)

At the time of the nuclear power plant accident in Fukushima of Japan, zirconium alloy (Zr-alloy) cladding reacted with high-temperature steam in Loss of Coolant Accident (LOCA) and a large amount of hydrogen gas was generated. [1] In order to solve these problems, the Accident-Tolerant Fuel (ATF) cladding is inevitably a hot topic, led to innovative designs, such as coated Zr-alloy, ceramic cladding and advanced steels. [2] Among others a variety of coating technology have been studied to satisfy the goal of improving ATF in a short term without replacing the existing Zr based alloys. However, it's not easy to deposit coating materials on long cladding, almost 4-meters. The development of the multi-walled swaging & drawing process using Stainless Steel 316 (SS316) tube on Zr-alloy cladding is very simple and can be performed at room temperature which can be mass-produced. However, thermal conductivity of SS316 is low and the thermal neutron absorption cross-section is more than 10 times larger than Zr-alloy. [3] Therefore, it should be used as thin as possible in SS316 tube. The SS316 tube about 100 μ m thickness was overlapped inside and outside of the Zr-alloy cladding and adhered using drawing process. The multi-walled cladding specimen was oxidized at 1200 $^{\circ}$ C for 600s, in conditions of LOCA, and test shown increase the resistance to oxidation compared to commercial Zr-based alloy cladding. The interface between SS316 tube and Zr-alloy cladding was investigated by Optical Microscope (OM) and Scanning Electron Microscope (SEM). The multi-walled cladding was successfully fabricated using a drawing process, and it was proved that oxidation resistance was excellent through Energy Dispersive Spectroscopy (EDS) and mass change results. Based on the results, it is expected that better Accident-Tolerant Fuel (ATF) can be derived with the thin SS316 tube swaging and drawing process.

[1]ZINKLE, Steven J., et al. Accident tolerant fuels for LWRs: A perspective. *Journal of Nuclear Materials*, 448.1-3: 374-379, 2014

[2]DUAN, Zhengang, et al. Current status of materials development of nuclear fuel cladding tubes for light water reactors. *Nuclear Engineering and Design*, 316: 131-150, 2017

[3]AZEVEDO, CRDF. Selection of fuel cladding material for nuclear fission reactors. *Engineering Failure Analysis*, 18.8: 1943-1962, 2011

2:00 PM SF02.02.03

Late News: Effect of CrN Thin Layer Deposited by Sputtering Method on SS316L Structural Material for PMFR Unho Lee, Young Ah Park, Jisu Na, Jeong Hye Jo and Young Soo Yoon; Gachon University, Korea (the Republic of)

Recently, 4th generation nuclear power generator for Distributed Energy Resources (DERs) in Passivation Molten salt Fast Reactor (PMFR). However, the interface of reactor vessel materials occurs corrosion by molten salt with Nuclear Fission Product (NFP) at operating temperature. Generators under conventional operating conditions have overcome their limitations and current models at 600 K to 700 K, 46 KCl-54 UCl (mol%) or 17.8 KCl-68.2 MgCl₂-14 NaCl (mol%) salts. Materials that overcome chemical stability, high corrosion, and temperature resistance for semi-permanent use should be selected. (NFP: Te, Nb, Zr). Penetrates into the grain boundary of the base material and acts fatally. Therefore, a non-reactive material, CrN, is coated to prevent corrosion decay accidents. The integrity behavior was confirmed through the combined Cr and CrN layer by PVD RF-Sputtering system. NFP adsorption and penetration analysis were performed by heating the specimen at the misch metal jig at 930.15K with 1atm. Through the nano-indenter-based scanning electron microscope (SEM) analysis, the adhesive strength of the 3 μ m thin film was confirmed, and the elastic modulus of 160GPa was confirmed. A corrosion current density plot was obtained through an immersion test to confirm the chemical stability of the grain boundary. Corrosion voltage section is improved over 0.5V. These results suggested that CrN as a Passivation Molten salt Fast Reactor (PMFR) base material with secured lifetime promises to be a suitable candidate.

2:15 PM SF02.02.04

Customizable Digital Manufacturing Method for Silicon Carbide Jatinder Sampathkumar¹, Nik Ninoss², Gregory L. Whiting¹ and Nicole J. Labbe¹; ¹University of Colorado Boulder, United States; ²Calix Ceramics, United States

Silicon carbide (SiC) is a desirable ceramic for a wide range of applications due to its ability to withstand very high temperatures (>1500K), resistance to thermal shock, and inertness in corrosive environments. These characteristics make the material ideally suited for heat transfer devices, which often require small feature sizes such as aviation engine components and microfluidic devices. For these types of applications, conventional manufacturing processes are primarily used and involve rigid tooling and expensive fabrication techniques. These methods have limited small component silicon carbide manufacturing to relatively simple geometries, with more intricate configurations requiring specialized modifications which can be cost-prohibitive for low volume production and one-off prototype manufacturing. Furthermore, these processes are not amenable to iterative design changes. Additive manufacturing for silicon carbide, while presenting a more flexible processing method compared to other orthodox manufacturing routes, continues to be challenged by smaller form factors or with high feature resolution due to constraints imposed by the slurry and powder composition. High aspect ratio configurations with small feature sizes in the range of 100 to 500 microns prove particularly difficult with these manufacturing methods, requiring numerous post-sinter processing steps or bespoke tooling implements.

To address these shortcomings, this work describes a novel processing route that is iterable, has a high throughput, and is inexpensive for manufacturing small, high aspect ratio silicon carbide geometries. This fabrication sequence utilizes a hybrid manufacturing technique that harnesses the rapid iterability of additive manufacturing and combines it with the knowledge base that exists for conventional ceramic processing. This novel method involves a unique SiC precursor composition that is tailored to be compatible with multiple compaction techniques. The flexibility of polymer and metallic additive manufacturing is utilized to create multiple variants of the tooling required to produce these intricate high aspect ratio geometries at scale and reliably. Specialized compaction tooling to achieve the required green-state strength for compatibility with these small volumes is detailed. The capability of this processing technique is extended to other high aspect ratio structures and ceramic types, showcasing its broad applicability. Material characterization studies are presented to compare features of the sintered SiC geometries constructed using this process to typical fabrication methods.

A use case for this manufacturing technique is presented in the development and production of microfluidic reactor devices. SiC reactors that are straight

tubes with a 1mm inner diameter and 3cm in length featuring an internal constriction of 300 microns to stabilize the fluid flow were manufactured with our process, replacing the current tubular reactors of similar size produced using an extrusion process. An experimental evaluation of this new design in a combustion pyrolysis experiment is presented compared to the currently used SiC reactor geometry, highlighting improvements in material performance and the variation in results obtained due to the presence of an internal taper which stabilizes fluid flow within the reactor. This specific application showcases the adaptability of this method in producing small devices which can be iteratively modified based on the experimental requirement to meet the needs of small-scale experimental facilities.

2:30 PM SF02.02.05

Surface Force-Driven Direct Ink Writing of Polyelectrolyte Membranes [Guy J. Cordonier](#), KmProttoy S. Piash, Oishi Sanyal and Kostas Sierros; West Virginia University, United States

A direct ink writing method for 3D printing low-viscosity inks has been developed and used to fabricate polyelectrolyte membranes. Poly(allylamine hydrochloride) and poly(acrylic acid) inks are deposited in a meandering pattern in a layer-by-layer fashion, forming films with thickness up to hundreds of nanometers. Additionally, films are formed using a traditional layer-by-layer dip coating methodology for comparison. The molecular weight of each polyelectrolyte and post-treatment is varied to change the properties of the resulting films. The films are characterized with scanning electron microscopy, atomic force microscopy, optical profilometry, contact angle, and water filtration.

2:45 PM SF02.02.06

Long-Term Stabilized Amorphous Calcium Carbonate—An Ink for Bio-Inspired 3D Printing Hadar Shaked and [Boaz Pokroy](#); Technion-Israel Institute of Technology, Israel

Biomaterials formed by organisms in the course of biomineralization often demonstrate complex morphologies despite their single-crystalline nature. This is achieved owing to the crystallization via a predeposited amorphous calcium carbonate (ACC) phase, a precursor that is particularly widespread in biomaterials. Inspired by this natural strategy, we utilized robocasting, an additive manufacturing 3D-printing technique, for printing 3D objects from novel long-term, Mg-stabilized ACC pastes with high solids loading. We demonstrated, for the first time, that the ACC remains stable for at least a couple of months, even after printing. Crystallization, if desired, occurs only after the 3D object is already formed and at temperatures significantly lower than those of common post-printing sintering. We also examined the effects different organic binders have on the crystallization, the morphology, and the final amount of incorporated Mg. This novel bio-inspired method may pave the way for a new bio-inspired route to low-temperature 3D printing of ceramic materials for a multitude of applications.

3:00 PM SF02.02.08

Voxel 3D Printing and Computer Simulations to Prototype Bimaterial Attachments Based on Local Interface Patterning [Quentin Grossman](#)¹, Peter Varga² and Davide Ruffoni¹; ¹University of Liège, Belgium; ²AO Research Institute Davos, Switzerland

Joining materials with dissimilar properties is a challenging but ubiquitous task for load-bearing engineering and biological materials. Bimaterial interfaces are prone to stress concentration, which may trigger failure upon loading. Nature's materials feature several strategies to mitigate stresses at bimaterial junctions, making soft-to-hard attachments long lasting. Some biological materials, such as squid beak and byssus thread, display a gradual change in mechanical properties over a region spanning up to several millimeters, which is a length scale much larger than the soft and hard elementary constituents. Other biological interfaces, like the bone-tendon junction, lack long-range property gradients and the transition in mechanical behavior occurs over a micrometer-sized region. Here, failure resistance is obtained by introducing local interface patterning. Advances in multimaterial manufacturing are opening unprecedented possibilities to prototype new bioinspired solutions for bimaterial attachments. Using 3D printing is nowadays possible to assign location-specific material properties to individual voxels within a macroscopic object, enabling the fabrication of complex centimeter-sized heterogeneous structures, referred to as voxel-based materials, with properties tuned at the micrometer level. In this work, we combined voxel 3D printing and computer simulations to prototype bimaterial attachments based on local interface patterning at the mesoscale. We used a polyjet printer (Object 260, Stratasys), which deposits and UV-cures photopolymer droplets in a layer-by-layer fashion. Using different inks, the printer allows fabricating structures composed of individual stiff or compliant cuboid voxels having minimum dimensions of 40 x 80 x 30 μm . In a previous work we have shown that, owing to the printing process, the spatial transition in elastic properties across bimaterial interfaces can be fairly broad (around 150 μm) and larger than voxel size [1]. Here, we manufactured centimeter-sized bimaterial samples featuring voxels having side length of 420 μm . This dimension, higher than printer resolution, is chosen to minimize the impact of the interface, such that a voxel can retain its mechanical character. Samples were fabricated by assigning to the stiff voxels a rigid glassy polymer (Young's modulus of 2 GPa) and to the soft voxels a rubber-like material (Young's modulus of 40 MPa). We architected bimaterial interfaces based on the general idea of introducing minimal interface patterning, i.e. the width of the perturbed region at the interface between stiff and compliant materials (mesoscale) was at least one order of magnitude smaller than sample length (macroscale). Stiff and compliant voxels were rearranged to form either geometrical patterns or compositional gradients. Starting from a flat interface, we considered chessboard, rectangular and triangular designs as well as gradients with different slopes. We performed failure tests to measure strength and fracture toughness. Our results indicated that minimal interface perturbation in the form of triangular patterns outperformed compositional gradients to enhance failure resistance. Finite element simulations were done to characterize stress concentration and spatial distribution of strain energy density (SED). Firstly, a mesh analysis underlined that at least 4 hexahedral elements were necessary to model individual voxels in case the two materials were assigned very dissimilar properties. More relevant, simulations highlighted that while a flat interface led to the smallest stress concentration in a defect-free case, in the presence of a locally damaged interface triangular patterns minimized stress localization and helped to redistribute SED away from the damaged region. Our results shall provide guidelines to improve failure resistance of bimaterial junctions using voxel-based interface patterning.

[1] Zorzetto et al., Scientific Reports 2020; 10: 22285.

3:15 PM SF02.02.09

Functionally Graded Materials Fabricated by Site-Specific Texture Control During Laser Powder Bed Fusion [Karl Sofinowski](#), Mallory Wittwer and Matteo Seita; Nanyang Technological University, Singapore

Due to the unique ability to manipulate the local solidification conditions point by point, additive manufacturing makes it possible to design materials with spatially varying microstructures. By controlling the distribution of these microstructures, we can design components with enhanced structural and functional properties. In this work, we use our recently published layerwise engineering of grain orientation (LEGO) technique to design functionally graded materials using blocks of discrete near-single crystal and gradient crystallographic textures. We apply our LEGO technique during laser powder bed fusion of stainless steel 316L to demonstrate the potential of site-specific texture control with two applications. In the first, we leverage the anisotropic chemical properties of 316L to create a new, high-throughput method for encoding data in metals. In the second, macro-scale "metamaterial" specimens that mimic grain-scale structures such as grain boundaries, twin boundaries, and triple junctions are examined with in situ mechanical testing. The techniques presented in this work may be further extended to control any material properties affected by crystallographic texture.

3:30 PM BREAK

4:00 PM SF02.02.10

Late News: Mechanical Evaluation of Laser Powder Bed Fusion (LPBF) Process Based 3D Printed Parts Using Partially Pre-Alloyed Water-Atomized Iron Powder (Fe-1.50Cu-1.75Ni-0.50Mo) Taehyeob Im¹, Huengseok Oh¹, Jai-Sung Lee¹, Sebastian Meyers², Kopila Gurung², Brecht V. Hooreweder² and Caroline S. Lee¹; ¹Hanyang university, Korea (the Republic of); ²KU Leuven, Belgium

The demand for metal based additive manufacturing (AM) is exponentially increasing in the field of aerospace, automotive, medical, and other sectors. Accordingly, the metal 3D printing market is also increasing, while steel is the most used material among them. In metal 3D printing, the most widely used technology is laser powder bed fusion (LPBF) for which typically expensive gas-atomized (GA) powders are used due to their high quality, flowability, and purity, which enables the production of high quality parts. On the other hand, water-atomized (WA) powders with their irregular shape causing low powder flowability, with poor layer deposition quality and forming defects in final parts, generally are not favorable in metal AM. However, due to its economic advantage and straightforward fabrication process, vigorous research has recently been carried out to prove its applicability to 3D printing. In this study, low alloyed steel powder inspired by the 'Distaloy series' of Hoeganaes was fabricated for AM part production and for evaluating the resulting mechanical properties. Nano-sized Cu-Ni-Mo metal compound was mixed with WA iron powder for low alloy steel powder fabrication. Here, the nano-sized metal alloy elements were homogeneously milled and mixed, to be added to the concave part of the WA iron powder while the commercial powder (Distaloy series) uses only micro-sized alloy elements. It was found that the developed partially pre-alloyed powder showed better flow properties than those of commercial powder.

This powder was used to produce cuboids by applying LPBF with a varying energy density window from 90 to 124 J/mm³. The parts which had the relative density values of over 99 % can be obtained at a feasible range of laser power from 150 W to 225 W. Especially, the maximum relative density of 99.79% was achieved when producing parts at its laser power of 175 W, scan speed of 700 mm/s (108 J/mm³) while observing pore structure and the melt pool structure. Moreover, hardness of the parts was measured to find out that the 3D printed parts under that processing window show uniform hardness values (217.1±4.7 HV) among parts with no pores observed while other parts which were manufactured outside the processing window showed non-uniform hardness values (210.0±15.2 HV). Finally, the tensile strength measurement results compared the sample fabricated using partially pre-alloyed WA iron powder with the parts made by raw WA iron powder. The tensile bars made by pre-alloyed powder had two times higher yield stress values [points of yield (pre-alloyed powder: 372.4 MPa, raw WA powder: 167.0 MPa), two times higher ultimate tensile stress (pre-alloyed powder: 460.9 MPa, raw WA powder: 207.3 MPa)] and three times higher strain values [points of ultimate tensile strength (pre-alloyed powder: 7.0%, raw WA powder: 2.6%), three times higher elongation to fracture (pre-alloyed powder: 11.7%, raw WA powder: 3.0%)] compared to those made by raw WA powder. Finally, it was found that the fabricated parts achieved their tensile test results which are comparable to the values [the yield stress (357.4 MPa), the ultimate tensile stress (459.6 MPa), the strain at the ultimate tensile strength (6.5%), the elongation to fracture (7.0%)] of the sample proceeded by GA stainless-steel powder. Therefore, the results show that the pre-alloyed WA iron powder can potentially be a promising material suitable for the LPBF process used for various applications.

SESSION SF02.03/SF03.01: Joint Session: Multifunctional Soft Composites

Session Chairs: Stephanie Flores-Zopf and Javier Morales

Tuesday Morning, November 30, 2021

Sheraton, 3rd Floor, Commonwealth

10:30 AM SF02.03/SF03.01.01

Temperature-Responsive Multistable Metamaterials Rui Yin, Lucia Korpas, Hiromi Yasuda and Jordan R. Raney; University of Pennsylvania, United States

The ability for materials to adapt their shape and mechanical properties to their environment is useful in a variety of applications, such as soft robotics and deployable structures. Liquid crystal elastomers (LCEs) have been widely explored in recent years due to their ability to controllably actuate in response to multiple external stimuli, such as heat and light. In this work we integrate LCEs with multistable structures to allow autonomous reconfiguration in response to temperature changes. To accomplish this, we integrate LCE-silicone bilayers as hinges in a kirigami-inspired multistable material based on a rotating squares mechanism. The bilayer hinges bend and soften as the temperature increases. By choosing geometric parameters for the hinges such that bifurcation points in the stability exist, a transition from mono- or tristability to bistability can be triggered by a sufficient increase in temperature, forcing rearrangements of the structural configuration in the heat-affected area as minima in the energy landscape are removed. Depending on the choice of energy landscape, these local structural reconfigurations may or may not propagate to the rest of the structure, analogous to the propagation of a phase transformation. These effects are relevant to applications smart interfaces, reconfigurable structures, and soft robotics.

10:45 AM SF02.03/SF03.01.02

Cellular Fluidics: Using Architected Lattices to Tune Multiphase Interfaces in 3D Nikola Dudukovic, Erika Fong, Hawi Gameda, Joshua DeOtte, Maira Cerón, Bryan Moran, Jonathan Davis, Sarah Baker and Eric Duoss; Lawrence Livermore National Laboratory, United States

We present a novel platform based on capillary fluid flow in ordered three-dimensional open-cell lattices: cellular fluidics [1]. By designing the cell and lattice architecture, combined with additive manufacturing methods that provide access to length scales below 100 μm, we can fabricate complex polymeric 3D structures with deterministic porosity and advanced functionalities. This approach enables selective placement and direction of liquid flow into predetermined continuous paths through the structure and optimization of gas-liquid and liquid-liquid interfaces for multiphase processes. We demonstrate the application of such cellular fluidic devices for processes such as transpiration cooling and CO₂ capture. Further, we show that flowing the appropriate electroless plating solutions through the predetermined paths allows selective metallization in regions of interest in three dimensions, resulting in multimaterial heterostructures that can further be electroplated with different materials. Hence, this new platform is a promising tool for designing novel 3D microfluidic devices such as electrochemical reactors with control over multiphase transport processes.

[1] N.A. Dudukovic, E.J. Fong, H. B. Gameda, J.R. DeOtte, M.R. Cerón, B.D. Moran, J.T. Davis, S.E. Baker, E.B. Duoss, "Cellular Fluidics", Nature 2021 (accepted)

*This work performed under the auspices of the U.S. Department of Energy by Lawrence Livermore National Laboratory under Contract DE-AC52-07NA27344 within the LDRD program 19-SI-005. LLNL-ABS-810682.

11:00 AM SF02.03/SF03.01.03**Tissue-Adhesive and Stretchable Liquid Metal Antennas by Direct Silicone Printing on Elastomeric Thin-Film Substrates** Kento Yamagishi, Wenshen Zhou, Terry T. Ching, Shao Ying Huang and [Michinao Hashimoto](#); Singapore University of Technology and Design, Singapore

Flexible and stretchable antennas are important for devices that use wireless communication to address mechanical mismatches at the tissue-device interface. To mechanically comply with the curvature of the organs and match their motion, such devices typically featured thin designs to ease bendability and elastomer encapsulations to enhance stretchability. Emerging technologies of liquid metal-based stretchable electronics are promising approaches to improve the flexibility and stretchability of conventional metal-based antennas. However, existing methods to encapsulate liquid metal requires monolithically thick (at least 100 μm) substrates and the resulting devices are limited in deformability and tissue-adhesiveness. To overcome this limitation, we demonstrated fabricating microchannels by direct ink writing on a 7 μm -thick elastomeric substrate, referred to as Ecoflex microsheet, to obtain liquid metal microfluidic antennas that exhibited unprecedented deformability. The fabricated wireless light-emitting device was powered by a standard near-field-communication system (13.56 MHz) and retained a consistent operation under deformations including stretching (> 200% uniaxial strain), twisting (180° twist), and bending (3.0-mm radius of curvature) while maintaining a high Q factor (> 20). We also demonstrated suture-free conformable adhesion of the polydopamine-coated device to *ex vivo* animal tissues under mechanical deformations. This technology offers a new capability for the design and fabrication of wireless biodevices, which require conformal tissue-device integration. Liquid metal antennas would be used as a platform for various multifunctional wireless biodevices. DIW 3D printing technology can also offer integration of other functional components such as physical sensors, electrochemical sensors, and drug delivery systems. This technology paves the way towards minimally invasive, imperceptible medical treatments.

11:15 AM SF02.03/SF03.01.04**Innervated, Self-Sensing Liquid Crystal Elastomer Actuators with Closed Loop Control** [Arda Kotikian](#)¹, Javier Morales², Aric Lu¹, Jochen Mueller¹, Zoey Davidson¹, John W. Boley² and Jennifer Lewis¹; ¹Harvard University, United States; ²Boston University, United States

Soft materials that exhibit self-sensing and programmable actuation are of great interest for applications ranging from robotics to adaptive structures. Liquid crystal elastomers (LCEs) are an emerging class of soft materials that exhibit reversible and large deformations with high energy density. These materials have been patterned into shape-morphing architectures with programmed director alignment via HOT-DIW, an extrusion-based 3D printing method (Kotikian et al, *Adv. Mater.* 2018; Kotikian & McMahan et al, *Sci. Rob.* 2019). Recently, we have further demonstrated the fabrication of innervated LCEs (iLCEs) composed of liquid metal (LM) cores surrounded by LCE shell features via core-shell 3D printing. iLCE actuation is programmed by Joule heating power and thermal response is measured and modeled. Importantly, iLCEs self-sense their own deformation during actuation, as strain correlates with resistance in unidirectional and 3D morphing structures. Due to their large concomitant changes in length and resistance and their high energy density, iLCE fibers and spiral architectures are capable of closed loop control, with regulation of actuation sequences even with large bias loads. Our multi-material 3D printing platform enables the rapid design and fabrication of soft functional materials with exquisite control over their composition, architecture, and performance.

11:30 AM *SF02.03/SF03.01.05**3D Printing of Dynamic Liquid Metals and Liquid Metal Composites** [Michael Dickey](#); North Carolina State University, United States

This talk will discuss the use of liquid metals for 3D printing. Gallium-based metal alloys have interesting properties including low-viscosity, low melting point, low toxicity, and negligible volatility. Despite the large surface tension of the metal, it can be molded, patterned and printed into non-spherical shapes due to the presence of a native oxide skin that is only a few nanometers thick. We have harnessed these properties to form a number of electronic devices encased in polymer matrices. The resulting structures take on the mechanical properties of the polymer and can therefore be soft, self-healing, and ultra-stretchable. The metal can be printed and then withdrawn from 3D printed structures as a sacrificial, fugitive ink to create microvasculature in polymer monoliths. In addition, it is possible to 3D print vasculature within polymeric materials printed using conventional 3D printing, and then back-fill the structures with liquid metal to add function in a post-processing step. The metals can be used for adding electrical conductivity as well as toughening. In addition, liquid metal can be mixed with uncured elastomers to tune the rheology to create printable inks. These inks can be cured to create self-encapsulated, stretchable conductors. Finally, we have recently demonstrated ways to treat 3D printed polymeric structures so that liquid metal can be injected and withdrawn on demand. This allows for reconfigurable and dynamic structures in which the conductors can be fully recovered. The challenge is to create a coating that can be deposited on the walls inside 3D printed parts without damaging the part. To address this, we have create a solvent-based coating that uses fumed silica to create slightly roughened surface to which the liquid metal does not adhere. This talk will discuss the key processing parameters to enable printing of metal, the applications of such printing, as well as future opportunities and challenges.

SESSION SF02.04: Multifunctional Soft Composites

Session Chairs: Kun Fu and Jordan Raney

Tuesday Afternoon, November 30, 2021

Sheraton, 3rd Floor, Commonwealth

1:30 PM *SF02.04.01**Additive Manufacturing of 3D Nano-Architected Metals, Oxides and Multifunctional Gels via Vat Polymerization** [Julia R. Greer](#)^{1,2}, Amylynn Chen¹, Max Saccone¹, Carlos Portela³, Daryl W. Yee³ and Ryan Ng¹; ¹California Institute of Technology, United States; ²Kavli Nanoscience Institute, United States; ³Massachusetts Institute of Technology, United States

Additive manufacturing (AM) represents a set of processes that enable layer-by-layer fabrication of complex 3D structures, with some advanced methods attaining nanometer resolution and the creation of unique, multifunctional materials and shapes derived from a *photoinitiation-based chemical reaction* of custom-synthesized resins and thermal post-processing. A type of AM, vat polymerization, has allowed for using hydrogels as precursors, and exploiting novel material properties, especially those that arise at the nano-scale and do not occur in conventional materials. The development of small-scale AM has revolutionized the production of complex parts for aerospace, military, automotive and medical applications, and is enabling major innovations in these areas. Shapes as complex as fractal trusses and as simple as cubes, with vastly multi-scale dimensions, from nanometers for nanophotonics to millimeters for sensors to centimeters for space-relevant technologies been demonstrated.

We present synthesis and fabrication of nano- and micro-architected materials using vat polymerization and 3D (two-photon and interference) lithography, and characterize their properties as a function of architecture, constituent materials, and microstructural detail. We focus on specific materials and architectures with unique properties: (1) Impact resistant nano-architected carbon, (2) Hydrogel-enabled AM of pure metals and alloys with micron and sub-micron dimensions, (3) Ligand exchange-based fabrication of 3D TiO₂ photonic crystals (PhCs), with critical feature dimensions between 150 and 600

nm, and (4) AM of Metallo-polyelectrolyte Complexes with stretchability up to 1000% and full recoverability, and (5) Hydrogels moisture-harvesting properties.

2:00 PM SF02.04.03

Tough, Fatigue-Resistant Soft Composites via Controlled Spatial Variation of Fiber Alignment Using Direct Write 3D Printing [Chengyang Mo](#), Haiyi Long and Jordan R. Raney; University of Pennsylvania, United States

Stretchable electronics, tissue engineering, and soft robotics are a few of the many examples in which engineers require soft materials with higher toughness and better fatigue-resistance in order to prevent premature failure during demanding, repeated mechanical loading. One effective method to improve the toughness of soft materials is to embed stiff fibers in a soft matrix. We 3D print soft composites using direct ink writing (DIW). The composite material consists of polydimethylsiloxane (PDMS) reinforced with glass fibers (with diameter roughly 15 μ m). DIW processes result in alignment of fibers during printing, due to the shear field in the deposition nozzle. Hence, parts can be 3D printed with controlled spatial variations in fiber alignment, based on the print path and other parameters that affect the shear field in the nozzle. In this work, we first consider how the fiber-matrix bond influences the failure properties of the printed composite. We show that if the glass fibers are treated with acid prior to formulating the ink, the fiber-matrix bond is strengthened, and the toughness of the composite is greatly improved. Additional experiments are conducted to quantify the intrinsic toughness of the composite, and the effect of mechanical dissipation resulting from fiber-matrix debonding. We also measure the fatigue properties, which also show significant improvement after fiber treatment. Finally, we show that using bioinspired spatial variations in fiber alignment, such as in skin and artery, the composites are tougher and more fatigue resistant without further stiffening the material.

2:15 PM SF02.04.04

Freeform Polymer Precipitation (FPP) on Thermoplastics in Non-Newtonian Support Gels [Rahul Karyappa](#) and [Michinao Hashimoto](#); Singapore University of Technology and Design, Singapore

Embedded 3D printing (e3DP) has demonstrated fabricating freeform structures of curable polymer resins in microparticulate hydrogels. This method is, however, not compatible with thermoplastics extruded at high temperature. This communication presents a unique approach to 3D-print thermoplastics in embedding media, termed freeform polymer precipitation (FPP). FPP is based on spatially controlled immersion precipitation of polymer inks patterned in microparticulate gels for various thermoplastics with additives. The embedding media offers unique dual functions: Bingham plastic to maintain printed structures, and nonsolvent for *in situ* precipitation of polymer inks. Polymer inks with a wide range of vapor pressure (0.04 – 60 kPa) and viscosity (0.1 – 1000 Pa.s) were demonstrated for FPP. Using acrylonitrile butadiene styrene (ABS) dissolved in acetone (20 – 60 w/w%) as a model ink, we identified the printing conditions to ensure vertical and lateral attachments of printed inks. The fabricated 3D objects were porous due to rapid phase separation induced by nonsolvent, which was controlled by the concentration of the polymer and the porogens in the inks. FPP offers a simple route to fabricate 3D freeform structures of thermoplastics with controlled internal porosity and should serve as a useful toolkit to 3D-print multi-functional materials such as polymer nanocomposites.

2:30 PM SF02.04.05

Metallizing Complex 3D-Printed Polymers with Electroless Deposition—The Design Rule Toolbox of Pretreatment Steps [Megan Ellis](#)¹, [Shohini Sen-Britain](#)¹, [Jonathan Davis](#)¹, [Rohan Akolkar](#)², [Christine Orme](#)¹ and [Nikola Dudukovic](#)¹; ¹Lawrence Livermore National Laboratory, United States; ²Case Western Reserve University, United States

Recent advances in additive manufacturing have allowed fabrication of high resolution, complex geometries with fine features from UV-curable acrylated polymers. Utilizing electroless deposition in conjunction with these manufacturing techniques allows us to leverage the aforementioned benefits and impart electrical and thermal conductivity, a basis for catalytic activity, and improved mechanical properties. Electroless deposition onto 3D-printed polymer acrylates is not well understood and frequently demands a trial-and-error approach to successful metallization of the surface. Plating of these polymer surfaces requires pretreatment steps; there is a lack of knowledge surrounding how these steps affect the coating adhesion and uniformity. Here, we present a systematic investigation into these pretreatment steps with the aim of leveraging quantifiable data to establish best practices. We characterize the effects of alkaline etching on surface roughness and surface chemistry through the use of optical surface topography measurements and ToF-SIMS, respectively. We utilized Quartz Crystal Microbalance to examine the absorption of Tin (sensitizer) and Palladium (activator) species on the polymer surface. The resulting adhesion strength of the plated metal was measured through peel testing and the coating uniformity was quantified with a coverage fraction parameter. We show that changes in surface roughness of the polymers during the etching step occur at several length scales and time scales, associated with uneven curing degrees in regions of oxygen-inhibited polymerization. We find that the surface concentration of adsorbed sensitizer and activator species is related to the surface concentration of hydrophilic groups produced in the alkaline etching step. We show that the adhesion and uniformity are a function of both surface roughness and surface chemistry. These findings facilitate design guidelines for electroless deposition on 3D-printed polymers, specifically UV-cured acrylates. Further, these design rules allow for a deeper understanding of the role mass transport plays in the metallization of multiscale three-dimensional architectures. This work performed under the auspices of the U.S. Department of Energy by Lawrence Livermore National Laboratory under Contract DE-AC52-07NA27344 within the LDRD program 20-ERD-056. LLNL-ABS-821864.

2:45 PM SF02.04.06

On-the-Fly Modulation of Grain Size in Sub-Micrometer Copper Wires Deposited by Electrohydrodynamic Redox 3D Printing [Maxence Menétrey](#)¹, [Alain Reiser](#)², [Lukas Koch](#)¹, [Alla Sologubenko](#)¹, [Stephan Gerstl](#)¹ and [Ralph Spolenak](#)¹; ¹ETH Zürich, Switzerland; ²Massachusetts Institute of Technology, United States

Additive manufacturing at the micro-/nano-scale has the potential of revolutionizing the conception of small-scale devices. Yet, a major challenge is currently encountered: combining high-resolution, geometry control, high-throughput together with multi-materials printing. Even more crucial towards real applications is the ability to synthesize device-grade materials [1].

In this contribution, we will show that electrohydrodynamic redox 3D printing (EHD-RP) can be used to locally optimize grain size in 3D printed wires, changing mechanical strength by a factor of 2. EHD-RP is an ink-free AM technique with multi-metal capabilities and offering sub-micron spatial and chemical resolution [2]. A unique feature of this synthesis technique (and all synthesis techniques in comparison to transfer techniques) is the possibility to locally tune microstructure by adjusting growth parameters. In this work, we show the different microstructures accessible by EHD-RP, showing potential for material optimization. To this end, we first map the microstructure and morphology of wires as a function of printing voltage. We then use detailed microstructure and elemental analysis by TEM and APT to elucidate the causal relationship between the printing voltage and the grain size, adding important understanding to the formation of the microstructure. The influence on materials properties is illustrated by micro-compression experiments showing the relationship between the grain size distribution and the materials' strength—the so-called Hall-Petch strengthening. Finally, we demonstrate the fast switching between the different regimes by fabricating nano-wires with sub-micrometer modulation in grain size, and thus local strength. Our work opens the door to the fabrication of small-scale metal 3D geometries with optimized microstructural distributions..

- [1] A. Reiser, et al. *Adv. Funct. Mater.* 30, 1910491 (2020).
[2] A. Reiser, et al. *Nat. Commun.* 10, 1853 (2019).

3:00 PM BREAK

SESSION SF02.05/SF03.03: Joint Session: Multi-Scale Enabled Material Properties
Session Chairs: Chengyang Mo and Rui Yin
Tuesday Afternoon, November 30, 2021
Sheraton, 3rd Floor, Commonwealth

4:00 PM SF02.05/SF03.03.01

Additively Manufactured Spinodoid Metamaterials with Enhanced Toughening Mechanisms [Somayajulu Dhulipala](#) and Carlos Portela;
Massachusetts Institute of Technology, United States

Research in the field of additively manufactured (AM) architected materials has enabled engineered materials with mechanical properties that were previously thought unattainable. For instance, a large part of the research has focused on the linear properties of truss-based lattices, demonstrating high stiffness- and strength-to-weight ratios. However, most truss-based lattice structures suffer from a bending-dominated response and stress concentrations at the sharp joints, the latter of which results in initiation and propagation of fracture. Spinodoid metamaterials have been proposed as an alternative to combat these stress concentrations due to their finite (low) curvature and bicontinuous morphologies. Furthermore, the mechanical properties of these spinodoid metamaterials can be tuned by introducing preferential interface directions which results in tailorable anisotropy. In this study, we explore the effect of curvature and anisotropy on the strength and toughness of spinodoid metamaterials. The spinodoid morphologies are generated using a computational spinodal decomposition framework where tunable anisotropy is introduced by energetically penalizing preferential directions for interface formation, resulting in a mean curvature and Gaussian curvature distribution that is dependent on the direction of the surface normal. Using a two-photon lithography process we fabricate prototypes of these 50%-relative-density (i.e., fill fraction) anisotropic spinodoid morphologies, containing spatially varying curvature distributions, and perform in-situ nanomechanical uniaxial compression and bending experiments to determine their curvature-dependent stiffness, strength, and toughness. Complemented by finite element models of the as-fabricated morphologies, we demonstrate a relation between curvature distributions, the stress distribution, and the toughness of these metamaterials. Our findings present the potential of architected spinodoid metamaterials as a new class of additively manufactured lightweight materials with widely tunable properties such as fracture resistance, which may expand the property space of classical lattice-based AM materials.

4:15 PM SF02.05/SF03.03.02

StructureD Electrode Additive Manufacturing for Lithium-Ion Batteries [Kun Fu](#); University of Delaware, United States

Current battery electrode manufacturing using slurry coating and drying to produce electrode films is energy and time-intensive, containing significant quantities of environmentally toxic solvents, and lacks processability that controls electrodes' thickness and geometric complexity. New manufacturing processes have been developed to produce electrodes with increased thicknesses and complex physical structures with improved performance and safety characteristics. A growing trend to rapidly create structured electrodes with programmable geometries, improved thickness, and multiscale structural details is using additive manufacturing, also known as 3D printing, as replacements for typical state-of-the-art ink casting. However, existing 3D printing strategies can only fabricate electrodes using ink-based slurries, which lack the capability of forming complex geometries or use a narrow range of UV-curable resins with insufficient ionic and electric transport capabilities. Therefore, a new electrode fabrication route is needed to improve structured electrode design and manufacturing flexibility.

In this talk, I will present a novel electrode processing route, Structured Electrode Additive Manufacturing (SEAM), which can rapidly fabricate ultra-thick structured electrodes with low tortuosity, mechanical robustness, and complex geometry, enabling LIBs to achieve high power and high energy at a low production cost. SEAM involves two innovations of dry electrode formation and the debinding/sintering process. The innovation in dry electrode formation is enabled by a high-loading dry-extrusion technique called Shear Assisted Particle Extrusion (SHAPE). SHAPE can manufacture thick electrodes using compositions close to commercial electrodes without using any solvents or the drying process, and it can orient geometrically anisotropic active materials (e.g., graphite flakes) along their longitudinal directions at high-pressure induced shear flow and deposition. The debinding/sintering process can remove polymer components in the electrode while retaining the original printed "green" geometry without structural collapse or failure. SEAM leverages the dry-extrusion additive manufacturing combined with a rapid debinding/sintering process to meet the geometric design and cost requirements for replacing slurry coating and drying techniques.

4:30 PM SF02.05/SF03.03.03

Bulk Ferroelectric Metamaterial with Enhanced Piezoelectric and Biomimetic Mechanical Properties from Additive Manufacturing [Jun Li](#);
University of Wisconsin--Madison, United States

Three-dimensional (3D) ferroelectric materials are promising electromechanical building blocks for achieving human-machine interfacing, energy sustainability, and enhanced therapeutics. However, current natural or synthetic materials cannot offer both high piezoelectric responses and desired mechanical toughness at the same time to meet the practicality. Here, a nacre-mimetic ferroelectric metamaterial was created with a ceramic-like piezoelectric property and a bone-like fracture toughness through a novel low-voltage-assisted 3D printing technology. The one-step printed bulk structure, consisting of periodically intercalated soft ferroelectric and hard electrode intercalated layers, exhibited a significantly enhanced longitudinal piezoelectric charge coefficient (d_{33}) of over 150 pC N^{-1} , as well as a superior fracture resistance of $\sim 5.5 \text{ MPa m}^{1/2}$, more than three times higher than conventional piezo-ceramics. The excellent printability together with the unique combination of both high piezoelectric and mechanical behaviors allowed us to create bone-like structure with tunable anisotropic piezoelectricity and bone-comparable mechanical properties, marking a cornerstone toward manufacturing practical, high-performance, and smart biological systems.

4:45 PM SF02.05/SF03.03.04

Experimental and Numerical Investigation of Impact Absorbing Viscoelastic Truss Metamaterials [Raphael N. Glaesener](#), Jan-Hendrik Bastek and Dennis M. Kochmann; ETH Zurich, Switzerland

Recent advances in the additive manufacturing of trusses made from viscoelastic base materials have created new opportunities for the design of time-

dependent metamaterial properties. Using compliant polymers as base material [1] to fabricate 3D periodic architected metamaterials facilitates high energy absorption capabilities and allows the engineering and tailoring of the topology to a specific impact situation. Such structures facilitate shock and impact absorbing capabilities that have great potential in blast-protection applications but also as protective sports gear. The dissipation of energy is induced solely by the viscous base material model instead of layer-wise plastic deformation and failure of beams [2], coming with the advantage of shape-recoverability [3] and thereby also reusability of the lattice after impact.

We use a linear viscoelastic constitutive model along with the co-rotational beam description by Crisfield [4], which captures large rotations. We solve linear momentum balance in a time-discrete fashion, based on a variational formulation employing variational constitutive updates for the viscoelastic material model, which results in a rate-dependent material response to be explored. In addition to performing discrete numerical beam calculations, we include the viscoelastic beam model into the generalized continuum description of Glaesener et al. [5] and show a good match with the discrete formulation. The closed-form solution for the incremental update formulation, combined with the first-order homogenization approach at the microscale allows for an efficient computation of initial boundary value problems. Applying the linear viscoelastic material model to the investigation of non-catastrophic impact combines the study of history-dependent constituents with time-dependent load scenarios. We show that, for a given viscous base-material behavior, truss topology, and known impact velocity, the magnitude of damping (coefficient of restitution) upon impact can be computed. We present calculations for both the discrete and continuum framework, reporting good agreement with experimental observations.

[1] Gibson, I., D. W. Rosen, and B. Stucker, 2010. Additive Manufacturing Technologies: Rapid Prototyping to Direct Digital Manufacturing. Boston, MA: Springer Science+Business Media LLC.

[2] Mueller, J., Matlack, K.H., Shea, K. and Daraio, C., 2019. Energy absorption properties of periodic and stochastic 3D lattice materials. Adv. Theory Simul., 2 (10), 1900081.

[3] Meza, Lucas R and Zelhofer, Alex J and Clarke, Nigel and Mateos, Arturo J and Kochmann, Dennis M and Greer, Julia R, 2015. Resilient 3D hierarchical architected metamaterials. PNAS 112 (37), 11502 - 11507.

[4] Crisfield, M., 1990. A consistent co-rotational formulation for non-linear, three-dimensional, beam-elements. CMAME 81 (2), 131 – 150.

[5] Glaesener, R., C. Lestringant, B. Telgen, and D. M. Kochmann 2019. Continuum models for stretching- and bending-dominated periodic trusses undergoing finite deformations. IJSS, 171, 117 - 134.

5:00 PM *SF02.05/SF03.03.05

Additive Manufacturing of Architected and Functional Materials [Christopher M. Spadaccini](#); Lawrence Livermore National Laboratory, United States

In this presentation, we will cover some of the latest work in advanced and custom additive manufacturing processes for the fabrication of architected materials and functional devices. The concept of architected materials revolves around the notion that material properties are traditionally governed by the chemical composition and spatial arrangement of constituent elements at multiple length-scales. This usually limits material properties with respect to each other creating trade-offs when selecting materials for specific applications. For example, strength and density are inherently linked so that, in general, the more dense the material, the stronger it is in bulk form. We will review the latest in design methods such as topology optimization, as well as advanced additive micro- and nanomanufacturing techniques to create new material systems with previously unachievable property combinations. These processes include projection microstereolithography (PuSL), direct ink writing (DIW), and electrophoretic deposition (EPD) as well as new advanced concepts such as volumetric additive manufacturing (VAM), computed axial lithography (CAL), parallel two-photon polymerization, liquid metal jetting, and diode-based additive manufacturing of metals (DiAM). The performance of the resulting material constructs is fundamentally controlled by geometry at multiple length-scales, from the nano- to the macroscale, rather than chemical composition alone. We have fabricated and will review the resulting properties of these mechanical metamaterials in polymers, metals, ceramics, and combinations thereof. These new processes and concepts can also be applied to functional materials such as those for supercapacitor electrodes, optical components, and even for fluidic system such as the recently published cellular fluidics concept. A review of these functional systems will be followed by a brief discussion of future directions.

SESSION SF02.06: Poster Session: Additive Manufacturing—From Material Design to Emerging Applications

Session Chair: Kun Fu

Tuesday Afternoon, November 30, 2021

8:00 PM - 10:00 PM

Hynes, Level 1, Hall B

SF02.06.02

Multifunctional Artificial Artery from Direct 3D Printing with Built-in Ferroelectricity and Tissue-Matching Modulus for Real-Time Sensing and Occlusion Monitoring [Jun Li](#); University of Wisconsin--Madison, United States

Treating vascular grafts failure often requires complex surgery procedures and associates with a high mortality rate. Real-time monitoring vascular system could enable quick and reliable identification of complications and initiate safer treatments in the early stage. In this work, electric field-assisted 3D printing technology was developed to fabricate *in situ*-poled ferroelectric artificial arteries that offered battery-free real-time blood pressure sensing and occlusion monitoring capability. The complex functional artery architecture was made possible by the development of a printable ferroelectric bio-composite which could be quickly polarized during printing and reshaped into devised objects. Synergistic effect from the ferroelectric potassium sodium niobate (KNN) particles and the ferroelectric polyvinylidene fluoride (PVDF) polymer matrix yielded a superb piezoelectric performance (bulk-scale $d_{33} > 12 \text{ pC N}^{-1}$, confirmed by piezometer) on a par with that of commercial ferroelectric polymers. The sinusoidal architecture brought the mechanical modulus down to the same level of human blood vessels. The desired piezoelectric and mechanical properties of the 3D-printed artificial artery provided an excellent sensitivity to pressure change (0.306 mV/mmHg, $R^2 > 0.99$) within the range of human blood pressure (11.25 to 225.00 mmHg). The high pressure sensitivity and the ability to detect subtle vessel motion pattern change enabled early detection of partial occlusion (e.g., thrombosis), allowing for preventing grafts failure. This work demonstrated a promising strategy of incorporating multi-functionality to artificial biological systems for smart healthcare systems.

SF02.06.03

Directed Assembly, Annealing and Characterization of III-V Semiconductors Jared Cohen, Anthony S. Childress and Ahmed Busnaina; Northeastern University, United States

As the demand for smaller feature size and lower cost integrated circuits, printed circuit boards, and other micro and nano-scale devices increases, newer and faster printing methods that retain the accuracy of previously used methods must be developed in order to address such challenges. Previous research conducted at the NSF Center for High-rate Nanomanufacturing and others have shown the effectiveness of directed assembly processes which allow for highly precise and comparatively low cost manufacturing. However, the printing of single crystals using nanoparticles for making semiconducting devices, such as transistors and diodes, has proven to be a significant challenge. We report in this poster experimental efforts to print III-V semiconductors that show promising results. The particle size was significantly reduced to the nanoscale utilizing both physical milling and chemical synthesis techniques. Nanoparticle suspensions were formulated to be used in our fast fluidic directed assembly printing process. We have shown that indium phosphide and gallium arsenide nanoparticles can be reliably and accurately assembled. After printing, the printed structures are annealed and the crystalline structure, material properties, and electrical properties are measured. This poster shows the results of sintering the printed semiconductor devices along with their electrical characterization to demonstrate the effectiveness of the methods developed. Our directed assembly method allows for reliable and accurate assembly of these semiconducting devices. This will enable faster, lower cost, and more sustainable prototyping and production of micro and nanoscale electronic devices which could revolutionize semiconductor fabrication as we know it.

SF02.06.05

Evaluation of Additively Printed Dielectrics for Fully Printed Carbon Nanotube Thin-Film Transistors Brittany N. Smith, Hope Meikle, Shiheng Lu and Aaron D. Franklin; Duke University, United States

Carbon-nanotube thin-film transistors (CNT-TFTs) have the potential for a wide variety of applications, such as chemical sensors and digital logic circuits, due to their high field-effect mobility and compatibility with versatile fabrication approaches. Aerosol jet printing is an additive, direct-write approach for integrating CNT-TFTs onto various substrates. Among all the layers making up a CNT-TFT, the gate dielectric is the most difficult to additively print owing to challenges in thickness scaling, pinhole formation, and reliance on high sintering temperatures. The most commonly used printed dielectrics include electrolytes and ion gels due to their high specific capacitance and compatibility with solution-phase dispersion into inks. Recently, crystalline nanocellulose (CNC) has been utilized as an electrolyte gate dielectric to realize a fully recyclable, printed CNT-TFT. In this work, we present a detailed evaluation and benchmarking of three additively printed gate dielectrics for fully printed, top-gated CNT-TFTs that operate at low voltage: an electrolyte consisting of elastomer PVDF-HFP; CNC with varying salt concentrations from 0% up to .5%; and an ion gel consisting of triblock polymer PS-PMMA-PS, ionic liquid EMIM-TFSI, and ethyl acetate in a 1:9:90 w/w ratio. Using a surface map of the transistor on/off-current ratio, we evaluate the dependence of gate location on device performance. Because electrolyte dielectrics are performance-limited by ionic diffusion rates, the impact of voltage sweep rate on switching characteristics, such as threshold voltage, subthreshold slope, and hysteresis, is examined. Further, electrical bias and mechanical stress testing are performed to determine the resilience of these dielectrics. This extensive evaluation of three leading options for additively printed dielectrics will aid in moving the field of printed electronics closer to application-ready devices with stable, low-voltage operation TFTs.

SF02.06.06

Controlled Nano-Porosity in Additively Manufactured Micro-Scale Ag Structures Nikolaus Porenta¹, Mirco Nydegger¹, Souzan Hammadi² and Ralph Spolenak¹; ¹ETH, Switzerland; ²Uppsala University, Sweden

For many industrial applications such as catalysis, sensing, optical elements and many more, complex three-dimensional micro-scale porous metal structures with pore sizes in the sub-micron scale are desirable. However the fabrication of such sophisticated small-scale structures is not an easy task. In recent years the field of additive manufacturing (AM) has received more and more interest as a very powerful tool for the production of complicated three-dimensional structures^[1] One AM technique that has been shown to be able to produce complex structures with sub-micron resolution is electrohydrodynamic redox printing (EHD-RP)^[2]. EHD-RP furthermore has multi-metal and multi-material capabilities.

In this contribution, we will describe a fabrication process that can be used to readily produce nano-porous Ag structures on the micro-scale utilising the multi-metal capabilities of EHD-RP. Aqueous Ag-Cu salt solutions were used as printing solutions to produce small-scale metallic structures. Porosity in these structures was then achieved by selectively etching away Cu. In this work we show that by varying the composition of the printing solutions used, precise control over the ratio of Ag to Cu in the as-printed structures was achieved. Utilising this control of the chemical composition we were able to tune the porosity as well as the pore size of the dealloyed structures. Being able to precisely tune the porosity of micro-scale three-dimensional structures, as demonstrated in this work, opens up many new possibilities in the field of optical meta-materials especially focused on sensing applications. The high local control given by EHD-RP combined with the porosity control described here could also be used to fabricate structures with locally varying mechanical properties.

[1] Hirt L. et al., *Adv. Mater.* **2017**, *29*, 1604211

[2] Reiser A. et al., *Nat. Commun.* **2019**, *10*, 1853

SF02.06.07

Modification of Regolith for Lunar Habitat Development—A Preliminary Assessment of Novel Additives for NASA Formulated Simulants to Generate 3D Printable Concrete K. Shipp¹, B. Chadwick², M. Tittermore³, B. Wan¹, C. Dilman¹, T. Trinh¹, L. Baglio¹, H. Talbot³, M. McCuish¹, A. Perticone¹, D. Rodriguez¹, A. DaSilva¹, S. Abbas¹, Douglas X. Shattuck^{4,3} and Markus J. Buehler⁴; ¹Malden Catholic High School, United States; ²Concord-Carlisle High School, United States; ³St. Joseph School, United States; ⁴Massachusetts Institute of Technology, United States

In 2015 NASA began issuing challenges for the development of innovative technologies that would support human colonization of the moon and Mars by 2050. Subsequently, our students began with concepts and images developed at MIT as part of the initial Habitat Challenge [1]. From there, the team, including middle and high school students, their advisors, MIT researchers, and grad students, hypothesized that the most efficient and sustainable means of structural development would be to use the indigenous materials: silicon-rich basaltic and calcium-rich plagioclase regolith with water-ice discovered at the poles. In addition, we assume NASA's Challenge to biologically harvest solar energy to produce organic binders will be successful and provide additional structural constituents.

Our research focused on evaluating the structural capacity of a lunar regolith analogs [2] and their ability to withstand compression and impact forces. For this work we evaluated Lunar Highland Simulant (LHS-1) and Lunar Mare Simulant (LMS-1) prepared by Exolith Lab at the University of Central Florida. Commercially available stone-dust with similar geologic properties was also used as a lunar analog. Published works suggests that albumin may serve as an effective binder while other authors suggest chitin may be effective [3,4]. For this investigation commercially available chicken egg albumin (egg white) and chitosan (commercially available chitin) were among the materials evaluated. Water was used as a non-binding control. In addition, samples of fine

fractions were vitrified using a glass-manufacturing kiln.

Each regolith sample was mixed with varying amounts of binding agent, formed in 5 cm cube molds, pressed, smoothed, and allowed to cure for 24 hours, 7 or 14 days. Afterward, each sample was non-destructively tested with commercial compression hammers. The results were compared to terrestrial construction standards and are being presented.

Based on our observations, we believe lunar regolith may become a viable construction material, but additional work will be necessary to produce a binding material that will be suitable for building sound, impact-resistant dwellings. In addition to reinforcing concepts developed during research, this activity dramatically demonstrates the links among elementary and secondary school learning, academic research, and the private sector that supports them.

References

[1] <http://news.mit.edu/2017/mars-city-living-designing-for-the-red-planet-1031>

[2] <https://sciences.ucf.edu/class/exolithlab/>

[3] https://chemrxiv.org/articles/preprint/Blood_Sweat_and_Tears_Extraterrestrial_Regolith_Biocomposites_with_in_Vivo_Binders/14769369/1

[4] <https://www.constructionspecifier.com/building-on-mars-chitin-may-help/>

SF02.06.08

Printing of Flexible Electronic Components Using Directed Fluidic Assembly [Jonah Yu](#)^{1,2}, Ahmed Abdelaziz^{1,2} and Ahmed Busnaina^{1,2}; ¹Northeastern University, United States; ²Nano OPS Inc., United States

As the demand for smaller and more reliable mass-produced electronic devices grows, the directed assembly of electronic devices as additive manufacturing technique provides a promising potential solution to achieve mass production with low fabrication costs. This technique is proved to be capable of directly printing conducting, semi-conducting, as well as insulating materials using variety of liquid dispersions within micro to nano-scale resolution. Moreover, this technique is additive, more efficient, and cheaper than many other conventional subtractive techniques. Conventionally, in order to print basic electronic components such as resistors, capacitors and inductors on different substrates, high vacuum vapor deposition, ink jet printing, and etching techniques are implemented. However, these techniques require high energy consumption, poor printing resolution, and incompatibility with many substrates. Here, we utilized the directed fluidic assembly technique to monolithically print basic electronic components on a large scale with high printing resolution and large production throughput. Using this technique, we tackled different obstacles simultaneously. First, the process can be applied to wide range of substrates, which allows these circuit components to be dynamically integrated into other systems that may have not been previously compatible. Second, unlike other traditional printing processes, this process is considered conservative, thus minimizing the fabrication cost significantly. Third, basic electronic components can be easily controlled by adjusting thickness and structure dimensions down to several microns. Our results, show two basic printed electronic components, these are thin film resistors and micro-scale capacitors, which're printed monolithically on a flexible PET substrate. The resistors values showed wide resistance range of 1-10 K Ω using metallic conducting ink and 10 K Ω to 25 M Ω using ceramic composite dispersion. The achieved capacitance of the printed capacitors was between 80-100 pF which can be adjusted by varying the electrodes surface area and the spacing between the printed electrodes. We believe that this fluidic directed assembly will pave the way for the mass production of basic circuit components at lower time and energy costs than normally possible with conventional fabrication techniques.

SF02.06.12

Late News: An Automated Process for Eliminating Racial and Gender Bias in Respiratory Protective Equipment Enabled by Additive Manufacturing [Shiya Li](#)¹, [Samuel Willis](#)¹, [Mohanad Bahshwan](#)^{1,2}, [Jacob Tan](#)¹, [Joseph Folkes](#)¹, [Livia Kalossaka](#)¹, [Usman Waheed](#)¹ and [Connor Myant](#)¹; ¹Imperial College London, United Kingdom; ²University of Jeddah, Saudi Arabia

Various studies highlighted the failure of generically designed respiratory protective equipment (RPE) in fitting female and black, asian, and minority ethnic (BAME) users. As a result, many of those users' lives were put at risk during the COVID-19 pandemic. Employing additive manufacturing (AM) techniques for producing custom-fit RPE may overcome this problem if the laborious barriers in computer-aided design (CAD) creation can be overcome. Here we propose a process for producing custom fit RPE based on a single input containing the user's 3D facial scan captured via smartphone depth-sensitive camera. Through a combination of rigid and non-rigid iterative close point transformations, the coordinates of key landmarks were extracted to generate a custom-fit RPE via a CAD API. Subsequently, the goodness of fit was measured between each of the generated RPE and the raw facial scan using Euclidean distance. We evaluated the process for 207 submissions from users of different demographics, out of which 180 submissions were successfully processed (87.0%) with an average runtime of 3.33 minutes per scan. Furthermore, it was found that goodness of fit from the process-generated RPE was independent of age, race, gender, and Body Weight Index. The results demonstrate the viability of combining automated CAD generation with AM for producing inclusive wearable devices.

SESSION SF02.07/SF03.05: Keynote Session: Emerging Areas In Additive Manufacturing: Artificial Intelligence Tools and Translation to Medicine
Session Chairs: Nicole Bacca and Rui Yin
Wednesday Morning, December 1, 2021
Sheraton, 3rd Floor, Commonwealth

10:30 AM *SF02.07.05

Keynote: Machine Learning-Based Design of Metamaterials and Soft Robots [Xuanhe Zhao](#); Massachusetts Institute of Technology, United States

How to design metamaterials and soft robots to achieve a set of specific properties is an inverse problem facing the challenges of non-existent or non-unique solutions. The design of extreme properties such as the Hashin-Shtrikman (H-S) bounds of moduli and strengths makes the challenges even more daunting. Existing methods such as the trial-and-error approach have proven to be inefficient for such designs. Here we propose an initio approach to the design of metamaterials and soft robots to achieve multiple extreme properties simultaneously. The ab initio method is based on a combination of crystallography for structural symmetries, simulations to generate data, and machine-learning algorithms to exploit the data for designs. We demonstrate the concurrent designs of multiple extreme properties of architecture materials such as moduli, strengths, negative Poisson's ratios, and thermal conductivity. We will further discuss the implications of our ab initio method for material and structural designs in general.

11:00 AM SF02.07.01

Explainable AI for Investigating Replication of Subject Expertise in AM (A Quantitative Approach to Explainable AI in AM) [Jennifer Ruddock](#)^{1,2}, [Robert Weeks](#)³, [Ezra Ameperosa](#)², [Jeannette Geisler](#)^{1,2}, [James Hardin](#)², [J. D. Berrigan](#)² and [Jennifer Lewis](#)³; ¹UES, Inc, United States; ²Air Force Research Laboratory, United States; ³Harvard University, United States

With the growth of machine learning techniques and their more direct societal use, the need for interpretability and transparency of how these algorithms make their decisions also grows. This understanding instills trust and helps to engineer more robust algorithms and data treatments by ensuring that the algorithm is picking up on features that a human would deem important, as opposed to correlated or contextual features, or even machine-specific features that would not transfer across users and systems. Here, we use Layerwise Relevance Propagation (LRP) to examine the results of convolutional neural networks used to estimate the rheological properties of inks printed by direct ink write 3D printing. LRP is often used to assign relevance to pixels in image classification. In this study, we look at the changes in relevance for image regression analysis. In particular, ink properties such as the yield stress, rate index, and consistency index of an ink can be determined from the sharpness of printed corners and the width of deposited filaments. We determine how well these algorithms predict these properties and compare them to direct measures of width and curvature, while also drawing relations to the pixel relevancy values and locations. We bring a quantitative approach to LRP in understanding print morphologies in AM.

11:15 AM SF02.07.02

Topology Optimization of a Bi-Material Composite Using Genetic Algorithm-Augmented Finite Element Method (GA-AFEM) Mehrzad Soltani, Yunwei Xu and Yijie Jiang; University of North Texas, United States

These days, topology optimization designs via pixelized/voxelized heterogeneous material programming to achieve desired mechanical properties are of interest. Synergy between soft and stiff components in heterogeneous materials leads to delocalization of stress field throughout the composite and thus advanced mechanical properties, such as high toughness and damage tolerance. The enormous possible combinations of two materials and design of crack path via displacing fracture-prone stress concentration areas make finding the optimum designs challenging, where advanced computer-aided and machine learning-aided designing strategies are needed. In this study, we investigate a genetic algorithm (GA) guided material programming strategy to get a robust model with optimum toughness to moderate catastrophic failure of bi-material systems. The GA is a stochastic global search algorithm mimicking biological evolution. In GA, the design space is pixelized and each pixel is treated as a gene by assigning one type of materials. An augmented finite element method (A-FEM), which is a numerical efficient cohesive zone model (CZM) type method, is used to perform the tensile and fracture simulations to evaluate fitness score of each design. We leverage the GA operator of crossover to create a new generation of designs by switching parts of pixels based on the objective function of previous generation. A mutation ratio, which randomly changes pixels, is used to avoid local maximum to find the global optimization. We develop a dynamic selection of the mutation ratio regarding the fitness scores by generations to further enhance the efficiency of GA searching. Finally, samples are fabricated by 3D printing and tested by tensile experiments to validate the materials designs. The GA-AFEM method can be further applied for different loading conditions (impact, bending) and combinations of other materials.

11:30 AM SF02.07.03

Programmable Microbial Ink for 3D Printing of Functional Living Materials Avinash Manjula Basavanna^{1,2,3}, Anna Duraj-Thatte^{1,2,3}, Jarod Rutledge¹, Jing Xia⁴, Shabir Hassan⁴, Arjrios Sourlis¹, Andrés Rubio⁴, Ami Leshia⁴, Michael Zenkl¹, Anton Kan¹, David Weitz⁴, Yu Shrike Zhang⁴ and Neel Joshi³; ¹Wyss Institute Harvard University, United States; ²Massachusetts Institute of Technology, United States; ³Northeastern University, United States; ⁴Harvard University, United States

3D printing technology has been recently utilized to print microbial cells for biotechnological and biomedical applications. Typically, microbes are embedded in well-established bioinks to print 3D architectures. In contrast to existing approaches, we have designed and developed the world's first bioink, termed as Microbial Ink that is produced entirely from the genetically engineered microbes by a bottom-up approach. The shear-thinning property of the Microbial Ink coupled with its high viscosity, high yield-stress and shape fidelity facilitated the extrusion-based 3D printing into multi-layered architectures. The Microbial Ink was further programmed by using rationally designed genetic circuits in microbial cells to produce: 1) Therapeutic Living Material – On demand secretion of an anticancer drug, 2) Sequestration Living Material – Selective removal of toxic moieties and 3) Regulatable Living Material – To control the number of cells by inducing cell death. This work enables unprecedented avenues to manufacture macroscopic Functional Living Architectures and showcases advanced capabilities of Living Materials Technology.

11:45 AM SF02.07.04

Conformable and Robust Force Sensors to Enable Precision Joint Replacement Surgery Liam Ives¹, Alizée Pace¹, Fabian Bor¹, Qingshen Jing¹, Thomas Wade¹, Jehangir Cama², Vikas Khanduja³ and Sohini Kar-Narayan¹; ¹University of Cambridge, United Kingdom; ²University of Exeter, United Kingdom; ³Addenbrookes Hospital, United Kingdom

The correct balance of forces on weight-bearing joints such as the hip and knee during joint replacement surgeries is essential for implant longevity. Minimising implant failure and the corresponding need for expensive and difficult revision surgery is vital to both improve patient quality of life and lighten the burden on overstretched healthcare systems. This is increasingly important, for example, in total hip replacements, where the average age of patients is decreasing; these implants must survive greater activity levels and correspondingly higher stresses than those typically found in older, less active patients. However, force balancing during total hip replacements is presently entirely dependent on surgical skill, as there are no sensors capable of providing quantitative force feedback within the small and complex geometry of the hip joint. Here, we solve this clinical unmet need by presenting a thin, conformable and flexible microfluidic force sensor, whose use can be easily incorporated into the standard surgical process. Such sensors were fabricated using a combination of stereolithography 3D printing and aerosol-jet printing. Using precise mechanical testing and finite element modelling, we calibrate the sensors and optimise their design and materials choices. We incorporated our novel sensor into a model hip implant geometry and, with a bespoke mechanical testing rig, determined that these sensors are operational and highly sensitive at force ranges typically achieved during hip implant positioning in surgery. We anticipate that these sensors will be used in the clinic to guide implant positioning and thereby increase the lifetime of existing hip replacements, and more generally represent a powerful new surgical aid for a range of orthopaedic procedures where force balancing is crucial.

SESSION SF02.08/SF03.06: Joint Session: Biomimicry, Bioinspirations, and Bioelectronics

Session Chairs: Stephanie Flores-Zopf and Ramon Sanchez Cruz

Wednesday Afternoon, December 1, 2021

Sheraton, 3rd Floor, Commonwealth

1:30 PM SF02.08/SF03.06.01

3D-Printed “Growing” Cardiovascular Implants for Pediatric Patients with Congenital Heart Defects Fanzhen Ding¹, Runhan Tao¹, Emilio Bachtiar^{1,2} and Sung Hoon Kang¹; ¹Johns Hopkins University, United States; ²Duke University, United States

3D printing has been actively studied for patient-specific devices due to its advantage for low-cost customization and rapid prototyping. However, most 3D printed devices have fixed shapes and properties, which are not suitable for situations where we need dynamic changes, especially medical implants that require surgery for replacement. Right ventricle-to-pulmonary artery (RV-PA) conduits are used as a surgical palliative treatment for various congenital heart diseases. Due to the growth of the infant or child, these conduits require replacement as they cannot grow, which involves several major open-heart surgeries.

To address this issue, we have investigated 3D-printed RV-PA conduits that “grow” through self-unfolding mechanisms triggered by flow and pressure change associated with growth so that fewer surgeries are required from infancy to adulthood. We will present our results for design of self-adaptable implants, followed by experimental results of testing 3D printed implant devices using an in-vitro testing set-up. The results showed that our self-adaptable implants can autonomously change shapes to accommodate the growth of children. We anticipate that our approaches and findings can contribute to improving patient welfare by customized designs with growth potential based on patient anatomy, which can minimize the number of required surgeries and associated danger, trauma, and expenses.

Acknowledgments: The research was supported by the Eunice Kennedy Shriver National Institute of Child Health & Human Development of the National Institutes of Health under Award Number R21HD090663 and the Johns Hopkins University Whiting School of Engineering Start-Up Fund. E. O. Bachtiar was supported by the Indonesian Endowment Fund for Education. The content is solely the responsibility of the authors and does not necessarily represent the official views of the funding agencies.

1:45 PM SF02.08/SF03.06.02

Molecular Engineering of Liquid Crystalline Elastomer Inks for Additive Manufacturing of Biologically Relevant Actuators Grant E. Bauman, Joselle M. McCracken and Timothy White; University of Colorado Boulder, United States

Recent innovations in additive manufacturing of liquid crystalline elastomer (LCE) inks via direct ink write (DIW) have produced actuators capable of programmable performance based on the tailorable actuation temperatures of their constituent inks. Approaches to date utilize polymer network optimization to control actuation onset temperatures and overall strain of DIW LCE. Here, we describe a molecular engineering approach to 3D printed LCE devices that are capable of producing high strains at or below body temperature and room temperature. To do so, we utilize the LCE mesogen C6BAPE in DIW LCE formulations, which we have previously shown to substantially reduce actuation temperature (T_N) and increase rate of actuation. The rheological and phase transition properties of C6BAPE-based DIW LCE inks are explored to minimize smectic character conferred by C6BAPE and to maximize actuation output across a range of low temperatures. Resulting materials have been demonstrated with T_N that are responsive across biological temperature ranges that may enable numerous biomaterial application opportunities.

2:00 PM SF02.08/SF03.06.04

Additive Manufacturing of Hydrogel Bioelectronic Interfaces Tao Zhou, Hyunwoo Yuk and Xuanhe Zhao; Massachusetts Institute of Technology, United States

Bioelectronic interfaces require intimate and prolonged functional communication with soft, wet, and dynamic biological tissues or organs. However, conventional bioelectronic devices based on engineering solids are dissimilar to biological tissues in their mechanical and chemical properties, and therefore, can face limitations in long-term functional interfacing and biocompatibility due to unfavorable foreign body responses. Clearly noticeable in the progressive advances in bioelectronic interfaces in the recent decades, bioelectronic interfaces have been continuously innovated in both designs and materials to achieve tissue-matching properties to minimize foreign body responses while providing desired electrophysiological functionalities such as recordings and stimulations. Owing to the unique tissue-matching properties, hydrogels have been one of the most promising materials to provide biocompatible long-term interfacing with biological tissues. In this talk, we introduce our recent advances on the 3D-printed hydrogel bioelectronic interface consists of highly stretchable and soft hydrogels. The unique set of 3D-printable hydrogel inks allows facile and flexible one-step additive manufacturing of bioelectronic interfaces with diverse designs. To validate tissue-matching properties and biocompatibility of the 3D-printed hydrogel bioelectronic interfaces, we perform systematic mechanical and electrical characterizations and *in vivo* evaluations based on rat models. The resulted hydrogel bioelectronic interfaces will not only provide a promising platform for bioelectronic devices and treatments but also inspire the future development of functional hydrogel devices and machines.

2:15 PM SF02.08/SF03.06.05

3D Printed Porous Molds for the Fabrication of Biomimetic Vascular Constructs Terry T. Ching^{1,2}, Jyothsna Vasudevan^{1,2}, Shu-Yung Chang¹, Hsieh Yin Tan², Chwee Teck Lim², Javier Fernandez¹, Jun Jie Ng², Yi-Chin Toh³ and Michinao Hashimoto¹; ¹Singapore University of Technology and Design, Singapore; ²National University of Singapore, Singapore; ³Queensland University of Technology, Australia

Anatomically and biologically relevant vascular models are critical to progress our understanding of cardiovascular diseases (CVDs) that can lead to effective therapeutics. Recent advances in 3D printing employ techniques such as sacrificial molding, direct ink writing, coaxial bioprinting, embedded bioprinting to 3D-print the intricate vascular architecture. Despite advances in the 3D-bioprinting, however, there is yet a single fabrication technique that (1) enables a wide array of anatomical mimicry (*i.e.*, freestanding, branching, multilayered, perfusable, mechanically stretchable), and (2) enables customizability of the employed bioinks (*i.e.*, improving compatibility with relevant cell types and mimicking the mechanical properties of native vessels). In this work, we highlight a technique capable of fabricating anatomical accurate vascular models (*i.e.*, freestanding, branching, multilayered, perfusable, mechanically stretchable) with the option of customizing the bioink blend to improve compatibility with relevant cells and the mechanical properties. Briefly, this fabrication technique relies on a two-part mold that was 3D-printed using porous hydrogels (*i.e.*, poly(ethylene glycol) diacrylate (PEGDA) hydrogel). These molds can be designed with desired shape (*i.e.*, bifurcating, construction) or derived from computerized tomography (CT) scan of native vasculatures. Before casting, the molds were then soaked in calcium chloride solution to allow the calcium ions to diffuse into the PEGDA matrix. When alginate-containing precursor solution was perfused into the mold cavity, the calcium ions in the PEGDA matrix diffused radially inwards. The diffusion of calcium ions into the mold cavity prompted ionic crosslinking of the alginate in the precursor, forming a tubular construct. To prevent the further curing of alginate, a buffer solution was perfused through the mold to remove the uncrosslinked alginate-containing precursor. Finally, the vessel construct was removed from the mold and exposed to ultraviolet (UV) light to photo-crosslink the photocurable monomer (*e.g.*, gelatin-methacryloyl (GelMA)) present in the precursor. Applying our proposed technique, vessel constructs with anatomically accurate geometries (*i.e.*, constructions, bifurcation) and mechanical stress (*i.e.*, cyclical motion) were readily fabricated. Our technique also permitted the fabrication of multilayered architecture mimicking native blood vessels. Importantly, we successfully fabricated cell-laden vessel constructs with smooth muscle cells and endothelial cells in a multilayer arrangement. Lastly, we demonstrate the capability of our platform to simulate the insertion of a drug-eluting stent, highlighting a possible preclinical model to test future percutaneous coronary interventions. Overall, we developed a fabrication technique capable of fabricating a freestanding cell-laden hydrogel vascular model with high anatomical relevance: freestanding, branching, multilayered, perfusable, mechanically stretchable. Furthermore, the hydrogel composition of the vessel wall can be specifically tuned for mechanical and biological functions. We believe that these vasculature models with increases biomimicry can benefit future research in mechanistic understanding of CVD progress and the development of therapeutic intervention.

2:30 PM *SF02.08/SF03.06.06

3D Printing Bionic Devices Michael C. McAlpine; University of Minnesota, United States

The ability to three-dimensionally interweave biological and functional materials could enable the creation of devices possessing personalized geometries and functionalities. Indeed, interfacing active devices with biology in 3D could impact a variety of fields, including biomedical devices, regenerative biomedicines, bioelectronics, smart prosthetics, and human-machine interfaces. Biology, from the molecular scale of DNA and proteins, to the macroscopic scale of tissues and organs, is three-dimensional, often soft and stretchable, and temperature sensitive. This renders most biological platforms incompatible with the fabrication and material processing methods that have been developed and optimized for functional electronics, which are typically planar, rigid, and brittle. A number of strategies have been developed to overcome these dichotomies. Our approach is to utilize extrusion-based multi-material 3D printing, which is an additive manufacturing technology that offers freeform, autonomous fabrication. This approach addresses the challenges presented above by (1) using 3D printing and imaging for personalized device architectures; (2) employing 'nano-inks' as an enabling route for introducing a diverse palette of functionalities; and (3) combining 3D printing of biological and functional inks on a common platform to enable the interweaving of these two worlds, from biological to electronic. 3D printing is a multiscale platform, allowing for the incorporation of functional nanoscale inks, the printing of microscale features, and ultimately the creation of macroscale devices. This blending of 3D printing, functional materials, and 'living' inks may enable next-generation 3D printed devices.

3:00 PM BREAK

SESSION SF02.09: Emerging Area in Additive Manufacturing

Session Chairs: Sung Hoon Kang and Yayue Pan

Wednesday Afternoon, December 1, 2021

Sheraton, 3rd Floor, Commonwealth

4:00 PM SF02.09.01

Versatile Additive Manufacturing of Metals and Alloys via Hydrogel Infusion Max Saccone¹, Daryl W. Yee², Rebecca Gallivan¹, Kai Narita¹ and Julia R. Greer¹; ¹California Institute of Technology, United States; ²Massachusetts Institute of Technology, United States

Additive manufacturing (AM) of metal components has emerged as a uniquely powerful tool for rapid prototyping and creating parts with complex geometries. We explore AM enabled by vat polymerization, typically used to produce polymers and ceramics, for the fabrication of metals and metal alloys. This technique can simultaneously achieve high resolution and high throughput, making it a promising candidate for practical industrial use.

We developed a general method for the fabrication of a wide variety of metals and alloys with complex shapes and overall dimensions of several mm via vat polymerization AM and subsequent post-processing and thermal treatment. This streamlined technique makes use of a single resin composition and a single set of processing conditions during the vat polymerization process, followed by infusion of appropriate metal precursors into a hydrogel structure. Heat treatment in oxidizing followed by reducing atmospheres converts the polymer/precursor matrix into the target metal. Unlike previous vat polymerization strategies which have target materials or precursors incorporated into the resin during the printing process, this method does not require re-optimization of resins and resin curing parameters when the target material is changed.

We report photoresin design and post-processing strategies to show how to use this technique to easily fabricate a range of AM metal and alloy structures. As a proof of concept, we fabricated octet lattice architectures with beam diameters on the order of 50 μm from several materials including copper, nickel, silver, cobalt, cupronickel alloys, and tungsten. We characterize these materials to show the unique microstructures enabled by our technique and link them to mechanical properties measured by nanoindentation. Our approach represents a paradigm shift in vat polymerization AM of functional materials by reducing the experimental burden on resin design and allowing the target material to be selected after the structure is fabricated.

4:15 PM SF02.09.02

Multimaterial Rotational Direct Ink Writing Natalie Larson¹, Jochen Mueller¹, Alex Chortos², Zoey Davidson¹ and Jennifer Lewis¹; ¹Harvard University, United States; ²Purdue University, United States

Patent Pending

4:30 PM SF02.09.03

Expanding Available Polymeric Materials for Powder Bed Fusion via Rational Control of Liquid-Liquid Phase Separation Kaizhong Guan, Akan George and Mark Dadmun; University of Tennessee, United States

Powder Bed Fusion (PBF) is an important process in polymeric additive manufacturing. However, there exist limited polymers available for PBF, where most efforts use nylon to create object using PBF. In an effort to expand the polymers available for PBF and to provide additional insight into the sintering process, we have utilized a relatively facile method, thermally induced phase separation (TIPS), to synthesize polypropylene (PP) powders for PBF. More specifically, using TIPS, polymeric microspheres from PP with molecular weights of 12k, 250k and 340k, and their blends, have been formed. Specific conditions of the TIPS process, including polymer concentration and precipitation temperature were controlled to fabricate spherical PP powders with smooth surface morphologies, and appropriate particle size that is suitable for PBF (between 45 μm and 100 μm). Interpretation of the temperature, solution concentration, and molecular weight dependence of particle size that emerge from the TIPS process provides important fundamental understanding into the phase separation processes that govern particle formation. This in turn offers insight that will enable the rational design of thermodynamic conditions required to create polymer powders that are suitable for powder bed fusion for a broad range of polymers using the TIPS process.

At the same time, coalescence in PBF occurs in stationary particles, and thus the rate of weld formation is related to the zero-shear viscosity of the polymer melt. Given the fundamental importance of polymer diffusion in particle coalescence in PBF, we are interested in examining the impact of polymer molecular weight, and thus zero-shear viscosity, on the success of the fabrication of structures by PBF. The production of PP powder that is suitable for PBF with varying molecular weight provides an experimental system to examine this relationship, which is underway. Thus, we will discuss how the TIPS process opens clear routes to fabricate PBF powders with controlled zero-shear viscosity, providing pathways to examine and more thoroughly optimize the complexities of the coalescence process in PBF printing.

4:45 PM SF02.09.04

Additive Solution-Processed Iridescent Metal-Dielectric-Metal Structural Color [Weijie Feng](#) and L.Jay Guo; University of Michigan, United States

Thin metal-dielectric-metal (MDM) structure, a simple Fabry-Perot cavity, is highly desirable for structural color applications due to its simple structure and ability to reflect strong visible colors. However, conventional fabrication methods typically require high vacuum processes such as physical vapor deposition, magnetron sputtering, which significantly limits their practical use, especially for large-scale production due to the high cost and long processing time. Herein, we developed a series of solution-based methods for thin layer deposition of MDM structural color aiming at similar quality to cost-ineffective vacuum processes. We chose Cu-SiO₂-Cu as our model system due to its easy accessibility and low cost. Electroless plating of copper is implemented for the top and bottom metal while an electrochemical-assisted sol-gel process is adopted for the middle silica deposition. A systematic investigation is carried out for each deposition layer to ensure good film quality as well as its compatibility with all previous layers. Precise control of the silica precursor concentration, deposition time, deposition potential, and pH allow for a wide dielectric (SiO₂) thickness range, from sub-100nm up to 400nm thickness. Due to the low refractive index of silica, attractive iridescent structural colors are produced. The spectroscopic and morphological qualities of these solution-deposited structural colors are then compared with conventional vacuum-deposited samples for color performance. Subsequent work will utilize solution-based thin film deposition methods to deposit conformal thin-film structural color on curved surfaces, which is considered difficult for conventional deposition methods. Further exploration of solution-based deposition of other thin metals and dielectrics depositions will be carried out to expand the material library. We believe that these solution-based thin film-based methods can advance practical implementations of structural color fabrication.

5:00 PM SF02.09.05

Manifold Learning Between Geometric Defects and Electromagnetic Performance in Additively Manufactured Devices Deanna Sessions¹, Venkatesh Meenakshisundaram², Andrew Gillman³, Alexander Cook⁴, Kazuko Fuchi⁵, Gregory Huff¹ and [Phil Buskohl](#)³; ¹The Pennsylvania State University, United States; ²UES, Inc., United States; ³Air Force Research Laboratory, United States; ⁴NextFlex, United States; ⁵University of Dayton Research Institute, United States

Additive manufacturing enables game-changing fabrication capabilities for customized, low-cost, and multi-functional devices. However, process-specific fabrication anomalies can result in non-intuitive variations in geometry and function, especially for electromagnetic applications. To address this challenge, we implemented a machine learning methodology to map between geometric variances and their impact on electromagnetic performance, and further characterized the underlying defect mechanisms of the print. Using a direct-write additive manufacturing approach with a conductive Ag thermoplastic polyurethane ink, we printed a frequency selective surface (FSS) consisting of ~4000 Archimedean spirals in a hexagonal-packed array. Each spiral was optically imaged and then simulated as a FSS in a computational electromagnetic solver, which resulted in a paired geometric and electromagnetic performance dataset. Dimensionality reduction was applied to both datasets, which revealed 6 distinct classes of geometry defects and a strong dependence of the electromagnetic data manifold on the resonance frequency of the FSS. To map between the two domains – geometry and electromagnetic performance – convolutional neural networks were used to predict electromagnetic performance from images of the spiral geometry. Two convolutional neural networks (CNN) were explored: one using the image-derived geometric description, and one using the geometric description plus surface current information from the simulation. Network latent space dimensional analysis showed that the neural networks organized the geometric input information according to both geometric and electromagnetic values even in the case with no seeded electromagnetic information. Collectively, these results highlight the potential of CNNs to serve as low-cost surrogate models for in-line feedback predictions of electromagnetic performance from as-printed geometry, and highlight the utility of manifold learning techniques to provide a lens into the mechanisms and distribution of defects in additive manufacturing processes.

5:15 PM SF02.09.06

Extreme Mechanics Enabled by Additive Manufacturing—From Extreme Extensibility to Supersonic Impact Mitigation [Carlos Portela](#)¹, Widiyanto Moestopo², Julia R. Greer², Dennis M. Kochmann³ and Keith Nelson¹; ¹Massachusetts Institute of Technology, United States; ²California Institute of Technology, United States; ³ETH Zürich, Switzerland

Advances in additive manufacturing (AM) have enabled the fabrication of novel materials with high stiffness & strength and simultaneously low weight, but realizations of these lightweight materials beyond this quasi-static and small-deformation regime have remained scarce. For instance, few additively manufactured materials can achieve extreme deformations without accumulating permanent damage, and their stiff mechanical properties prevent their application in regimes where compliance is required (e.g., tissue engineering). At the other extreme, little is known about these materials' performance under dynamic stimuli such as impact. To enable emerging applications of additively manufactured materials, new design and fabrication paradigms are required to achieve materials beyond the classical small-deformation parameter space.

To this end, we employ a two-photon lithography process to fabricate two types of material systems that independently achieve (i) extreme extensibility (and compliance), and (ii) extreme impact mitigation. First, we present a novel design paradigm for AM-materials that consists of 'woven' monolithic fibers which bypasses the need for nodes or joints between structural elements. Performing in situ nanomechanical experiments, we demonstrate that woven architecture gives rise to compliant mechanical properties, extensibility of up to twice the elastic strain limit of the constituent material, and cyclic compression to 35% strain with minimal damage accrual. Second, we present additively manufactured carbon materials with nanoscale features (consisting of 13,500 unit cells) that attain extreme energy dissipation upon supersonic microparticle impact. Here, we subject polymeric precursor micro-architected materials to a pyrolysis process of 900C in vacuum, resulting in isotropically shrunk carbon nano-architected materials. Using a laser-induced particle impact technique, we showcase the potential for architected materials at the nanoscale to serve as lightweight shielding materials, dissipating up to 70% more energy than Kevlar for the same mass-normalized impact conditions. Together, these works showcase new design paradigms and mechanical property spaces capable of opening new frontiers for additively manufactured materials.

SESSION SF02.10: Multifunctional Structures I

Session Chairs: Kun Fu and Yayue Pan

Thursday Morning, December 2, 2021

Sheraton, 3rd Floor, Commonwealth

10:30 AM SF02.10.01

Two-Photon Fabrication of 3D Nanoporous Structures with Enhanced Mechanical Properties Using Nanocluster-Based Photoresists [Qi Li](#), John Kulkwsk, David Doan and Wendy Gu; Stanford University, United States

Currently there is still a pressing need to develop new printable resins which are comparable with the state-of-the-art micro-/nano- printing techniques for a fast 3D fabrication of desired structures (for example, hierarchical nanoporous structure) with high shape-fidelity and improved properties. Herein, we report a new type of resin solution for the efficient fabrication of 3D metal-carbon hierarchical nanoporous structures which utilizes the atomically precise metal nanoclusters as two-photon initiators, nano-porogens and Reinforcing fillers for enhanced mechanical properties. Our resin shows high fabrication efficiency and high shape fidelity for various complex 3D metal structures with line widths down to ~200 nm can be obtained. Furthermore, 3D nanoporous metal-carbon structures are obtained after annealing and improved mechanical properties are obtained based on the nanoindentation and micro-compression testing. Overall, this work provides a new resin solution which utilizes the unique light-matter interactions and intrinsic chemical physics properties of ultrasmall metal nanoclusters for the efficient nanoscale 3D printing with high-fidelity and improved properties achieved in the final structures.

10:45 AM SF02.10.02

Additive Manufacturing of 3D Micro-Scaffolds with Computationally-Predicted Anisotropic Stiffnesses [Weiting Deng](#)¹, Siddhant Kumar², Alberto Vallone³, Dennis M. Kochmann³ and Julia R. Greer¹; ¹California Institute of Technology, United States; ²Delft University of Technology, Netherlands; ³ETH Zürich, Switzerland

Cell viability, proliferation, and tissue formation are significantly influenced by the physical cues of local microenvironments, i.e., extracellular matrix (ECM) elasticity directs stem cell differentiation. Proper scaffold design would help identify the mechanisms of cell-ECM interactions in three-dimensional environments. A key unsolved challenge has been the lack of quantifiable mechanical cues that could guide the fabrication of physiologically relevant scaffolds with high architectural complexity and anisotropy. To date, matching the mechanical property landscape within a scaffold has relied on trial-and-error techniques and topology optimization, which are computationally and experimentally expensive, sensitive to the initial guess, and incapable to explore the entire design space.

In this work, we fabricated and characterized biomimetic 3D scaffolds with tunable anisotropic stiffness predicted by an artificial intelligence-enabled model. We generated spinodal-like topologies via a machine learning-based technique and fabricated the computed structures out of IP-Dip photoresist with critical dimensions of 2.3 μm and overall sample dimensions of 70 μm \times 70 μm \times 70 μm using two-photon lithography (TPL). The SEM images of the samples showed that they could geometrically resemble the porous structure of natural tissue environments, for example trabecular bone. Quasi-static uniaxial compression experiments, conducted at a strain rate of to a strain of 10⁻³ s⁻¹, revealed the normalized elastic moduli of the samples in e₁, e₂, and e₃ directions as 1.000 \pm 0.097, 0.354 \pm 0.042, and 0.619 \pm 0.100, respectively. The results matched closely with the numerically computed prediction that the normalized elastic moduli of the sample in e₁, e₂, and e₃ would be 1.000, 0.360, and 0.621.

Through these experiments and computations, we successfully demonstrate that this spinodoid model can accurately predict direction-dependent stiffnesses, with high tunability and flexibility, rendering it possible to systematically investigate ECM environments in various tissues. This approach could help expand the parameter space of mechanobiology research.

11:00 AM SF02.10.03

Additively Manufactured Complex Reactors for Carbon Utilization [Jacquelynn Garofano](#)¹, Mehdi Mortazavi², Seyed Niknam² and Dongsheng Li³; ¹Connecticut Center of Advanced Technology Inc, United States; ²Western New England University, United States; ³Advanced Manufacturing LLC, United States

The objective of this research work is to design, develop and fabricate microchannel reactor with complex features using additive manufacturing (AM) for carbon capture and utilization. Fabrication parameters of selective laser melting were optimized to improve fabrication quality. The designs were optimized based on simulation results from computational fluid dynamics. AM technologies will provide an opportunity for enhanced design and superior heat transfer performance. In this study, innovative Manifold-microchannel reactor or heat exchanger (MMHX) are designed and fabricated starting from the study of fluid flow in single channel reactor to multichannel with complex features and configurations. An experimental instrument was designed to measure pressure drop and heat transfer in AM designed MMHXs with a wide range of Reynolds numbers. Measurement results demonstrated that in some scenarios adding more internal features, i.e. increasing design complexity, does not necessarily improve the MMHX performance. This fluid flow study provides a guidance for additively manufactured MMHXs design optimization from experimental perspective. The reactors were loaded with catalyst to hydrogenate carbon dioxide into methanol. The effect of twist angle of the channels on carbon utilization efficiency and selectivity were investigated preliminarily. Further study on balancing conversion efficiency with pressure drop due to complexity will be investigated. MMHX studied here has become a favorite topic in various fields ranging from air conditioning to aircraft gas turbine engines. In essence, high manufacturing cost has emerged as the major drawback in broad applications of MMHXs. The possibility of cost-effective manufacturing has generated wide interest in applying additive manufacturing (AM) for fabricating MMHXs. The methodology established in this study will contribute to the development of other reactors using similar additive manufacturing methods.

11:15 AM SF02.10.04

Failure Mechanisms of Nano-Architected Nanocrystalline Zinc Oxide [Rebecca A. Gallivan](#)¹, Zachary Aitken², Yong-Wei Zhang² and Julia R. Greer¹; ¹California Institute of Technology, United States; ²Institute of High Performance Computing, A*STAR, Singapore

The advances in additive manufacturing at the nanoscale drive the need to understand the role of microstructure and size effects in mechanical properties of constituent solids. Nanomechanical studies have shown the emergence of size effect in mechanical properties of materials, with small-is-stronger behavior in single crystals, smaller-is-weaker in nanocrystalline metals, and suppression of brittle failure in amorphous metallic glasses. In addition to this size effect that emerges in samples with sub-micron extrinsic dimensions, the intrinsic length scale of material microstructure also dictates the dominance of different deformation and failure mechanisms. While heavily studied in metallic systems, a dearth of studies exists on the contribution of nanocrystallinity and nanostructuring in ceramics.

Using a Photopolymer Complex Synthesis additive manufacturing technique, we created nanocrystalline zinc oxide (ZnO) pillars with diameters ranging from 250nm to 3 μm and heights of 600nm to 9 μm . We achieve these structures by first patterning zinc ion-containing aqueous photoresins using two-photon lithography and subsequently calcining them at 500°C to produce pure nanocrystalline ZnO. Through in-situ micro-compression experiments we show three distinct failure behaviors based on structure size: 1) splitting via crack propagation 2) shear off events and 3) non-catastrophic deformation of the structures. These three regions can be described through the energetic competition of different failure mechanisms, similar to those in metal and metallic glasses. TEM analysis of the microstructure and Molecular Dynamics simulations of nanocrystalline ZnO provide insights into the deformation mechanisms and help establish the link between the microstructural features and failure behavior. Investigation of this system highlights the interplay between traditional weakest link failure theory and stochastic localization of stress within the microstructure. Through these studies we show the effect of extrinsic size on failure behavior in nanocrystalline ZnO, reveal the role of intrinsic length scales in deformation and failure mechanisms, and lay the foundation for fundamental insight to designing metal oxide nano-architectures from a microstructural viewpoint, as well as emphasize the importance of microstructural investigation in micro- and nano-sized additively manufactured materials.

11:30 AM SF02.10.05

Multimaterial Design of Programmable Shape Memory Alloy-Based Smart Structures via Topology Optimization Ziliang Kang¹, Pascal Zehnder², Felix Jensch³, Markus Bambach² and Kai James¹; ¹University of Illinois at Urbana-Champaign, United States; ²ETH Zürich, Switzerland; ³Brandenburg University of Technology Cottbus - Senftenberg, Germany

Shape memory alloy (SMA)-based smart structures have been long-awaited for comprehensive computational design tools. Generally, SMA-based smart structures are developed based on experimental or empirical designs. Their configurations vary drastically from application to application, and are limited in ability to achieve multifunctionalities with simple, generic geometries. Via the technique of topology optimization, we propose a computational design framework that enables programming the stimuli-responsive behaviors of SMA-based smart structures with multiple material candidates. Specifically, the proposed framework is able to program the target thermomechanical performance of the structure into its material distribution, by modeling nonlinear phase transformation of SMAs coupled with transient thermal conduction. The proposed design framework allows for achieving multifunctionalities such as bending, inchworm-like crawling, and twisting with simple geometries. Further, we study laser powder bed fusion (LPBF)-based 3D printing techniques to realize our designs. A series of 3D printed sample designs enabled by the framework including SMA-based stents and grippers are then discussed.

11:45 AM SF02.10.06

Transforming 3D-Printed Mesostructures with Nanoscale Conductive Metal Oxides Julia Huddy, Md Saifur Rahman, Andrew B. Hamlin, Youxiong Ye and William J. Scheideler; Dartmouth College, United States

Additive manufacturing (AM) excels at fabricating structural materials in complex geometries, but electronics integration could transform these parts into sensors and systems, expanding 3D printing far beyond prototyping. Here we present a method for engineering conductive 3D mesostructures via low-temperature atomic layer deposition (ALD) and industrial microstereolithography (μ SLA). μ SLA was used to produce a range of 3D structures (cubes, spheres, etc.) composed of internal octet lattices (10 - 200 μ m critical features) having ultrasoft surface morphology, ($r_q < 40$ nm) enabling 3D deposition of ZnO, ZnO:Al, and SnO₂ films leveraging an Al₂O₃ seed layer to prevent growth inhibition.

Uniform growth of ultrathin layers (7 nm – 100 nm) was achieved over a wide range of temperatures up to the polymer T_g , allowing control of the films' semiconducting or degenerate behavior and yielding resistance from 100 Ω to 100 k Ω per dimensionless cubic volume. XRD studies of the 3D oxide coatings reveal the ability to grow both amorphous and crystalline films matching those of 2D ALD films. Similarly, XPS and EDS studies indicate the similar atomic composition of coatings on 3D polymers and 2D substrates. However, despite their similar material characteristics these 3D networks show significantly enhanced conduction vs. 2D films, stemming from their high surface area and parallel 3D conduction paths. This allows precision geometrical manipulation with μ SLA to enhance volumetric conductance and engineer electronic transport in novel 3D devices. This process has significant and broad implications for designing 3D electronics that bridge the gap between nanoscale materials and 3D-printed mesostructures.

SESSION SF02.11: Multifunctional Structures II

Session Chair: Sung Hoon Kang

Thursday Afternoon, December 2, 2021

Sheraton, 3rd Floor, Commonwealth

1:30 PM SF02.11.01

Custom 3D Beauty Masks—An Additive Technology Approach to Deliver Fully Tailored Consumer Goods Products Scott Stanley; The Procter & Gamble Company, United States

We have been investigating additive manufacturing across a range of applications in the consumer goods space at P&G. One commercial interest lies in creating tailored, personalized products. In this talk, I will review additive manufacturing technology approaches we have explored in the beauty products category, specifically, custom 3D beauty masks. I will cover scanning approaches, resolution requirements, a manufacturing path for creating custom shaped objects, application of custom chemistries and the benefits associated with custom shape applicators and chemistries. Our approach utilizes a combination of 3D scanning, additive manufacturing (3D printing) of disposable molds, thermoforming replicates, custom laser cutting, and custom application of chemistries to create a scaled approach of creating fully tailored, customized offerings. I also will cover business model considerations for offering such products and share some future directions of this research. I hope that this work serves as an example and case study of how additive manufacturing technologies can be applied in the consumer goods space and open the door for partnerships.

1:45 PM SF02.11.02

Hierarchical Co-Assembly-Enabled 3D-Printing of Porous Materials Chenfeng Ke; Dartmouth College, United States

Natural materials are inherently constructed hierarchically from the molecular-level to the macroscale, which often possess light-weight porous scaffolds (e.g. bone), outstanding mechanical properties (e.g. shells and skins), as well as stimuli-responsive behaviors (e.g. muscles). My research group aims to develop 3D-printing materials that emulate natural systems' multiscale and multifunctional integration across the nano-to-macroscale. Currently, there is an emerging need to introduce smart molecular systems that lack the necessary molecular features for direct ink writing technique. This roadblock severely limits the number of smart materials available for 3D printing. To address this problem, my research group has developed a general method to integrate a variety of inorganic and organic molecules as functional 3D-printing inks through the introduction of micellar-based supramolecular templates.[1] In our hierarchical co-assembly enhanced direct ink writing design, molecular monomers and supramolecular templates co-assembled via multivalent noncovalent interactions to form a viscoelastic ink. After 3D printing, the molecular monomers and supramolecular templates in the 3D-printed monolith co-assembled in a holistic manner, affording monoliths with hierarchically ordered superstructures. In this process, a localized re-configuration of monomer and template was critical to maintaining the self-standing macroscale structure. Subsequent chemical crosslinking and template removal stapled these assembled molecular monomers together at the macroscale to afford the desired functional monoliths. 3D-printed mesoporous silica monoliths with a surface area of 304 m²/g were successfully fabricated. We further demonstrated that a molecular pillar insertion resulted in a macroscopic size expansion in the 3D-printed BTA monolith. The co-assembly process not only enhances the printing resolution by up to one order of magnitude but also enables precise spatial control of nanoscale features, such as molecular assembly, over a large scale. In the next step, we expanded this co-assembly-enabled 3D-printing method to fabricate highly ordered covalent organic frameworks (COFs) with imine and β -ketoenamine linkages.[2] The supramolecular template was introduced to coassemble with imine precursors in an aqueous environment. By limiting the degree of imine polycondensation during COF formation, co-assembled 3D-printable hydrogels were formed. After the removal of the template followed by an amorphous-to-crystalline transformation, the assemblies

were converted to the first set of single- and multi-component 3D-printed covalent organic framework monoliths, possessing high crystallinity and large surface areas, as well as robust mechanical stability.

Reference:

- [1] L. Li, P. Zhang, Z. Zhang, Q. Lin, Y. Wu, A. Cheng, Y. Lin, C. M. Thompson, R. A. Smaldone, and C. Ke, *Angew. Chem. Int. Ed.* 2018, 57, 5105 – 5109.
- [2] M. Zhang, L. Li, Q. Lin, M. Tang, Y. Wu, and C. Ke, *J. Am. Chem. Soc.*, 2019, 141, 5154–5158.

2:00 PM SF02.11.03

Mechanical Properties of Micrometer-Size Foam-Like Auxetic Structures Ming Wang and David Harding; University of Rochester, United States

Applications for polymer structures made using the two-photon polymerization additive manufacturing method, which produces structures with submicrometer resolution, are primarily optical or biological. Mechanical applications are less prevalent, partially because the structures' properties depend on the processing parameters and structural design, and these are less extensively studied. This study investigates the performance of millimeter-size cellular auxetic structures ($\sim 0.2 \text{ g/cm}^3$) subjected to impulse loadings at room and cryogenic temperatures (295 K and 130 K, respectively). Auxetic structures are an example of a metamaterial that is ideally suited for the deterministic production methods of additive manufacturing and can be purposely designed for specific applications.

The stress-strain relationship, creep behavior, and recovery response of structures made from a proprietary thermoset acrylate resin (IP-STM) under static and dynamic loading is reported. Different auxetic structures were designed using two finite-element programs, NX7.5 and ANSYS, to calculate the stress/strain distribution in the structure for different loads and to produce stereolithographic files for use with a commercial laser writer (Nanoscribe GmbH). These structures were tested using a thermal mechanical analyzer (PerkinElmer) at 295 K and 130 K, at loads ranging from 10^5 to 10^6 Pa, and at different cyclic frequencies. The compression modulus and strength of the best-performing structure were 2.5X and 2X higher, respectively, at 130 K and at 295 K. The maximum strain the structure could withstand under cyclic loading and recover was 2% and 0.8% at 295 K and 130 K, respectively; the maximum strain it could withstand before crushing irretrievably was 18%. The corresponding energy dissipated as strain is calculated to be $\sim 86 \text{ J/kg}$.

This material is based upon work supported by the Department of Energy National Nuclear Security Administration under Award Number DE-NA0003856, the University of Rochester, and the New York State Energy Research and Development Authority.

2:15 PM SF02.11.04

Additive Manufacturing and Characterization of Microstructures Using Two-Photon Polymerization for Use in Cryogenic Applications Sherman Peek, Jacob Ward, Stephen Bankson, Archit Shah, John Sellers, Mark Adams and Michael Hamilton; Auburn University, United States

Additive manufacturing technologies and techniques are becoming a more mainstream approach to prototyping, small-scale manufacturing, and one-off manufacturing especially in microelectronics and medical sciences. Two primary criteria are necessary for implementation of additive manufacturing techniques: resolution and scalability. One method of additive manufacturing that addresses these criteria is direct writing of three-dimensional structures by way of two-photon polymerization. Two-photon polymerization has the potential of being an incredibly useful tool for micro/nanofabrication due to the ability to fabricate with sub-wavelength resolution; however, the technique requires additional exploration. The equipment required to achieve two-photon polymerization provides the benefit of high resolution and is becoming more accessible for research groups lending to scalability through parallelization.

In this work, we demonstrate a process to additively fabricate microstructures on diced silicon chips with oxide. We describe the process of creating the polymerized resin as well as its application onto the target substrate. Parameters of the laser system are described. Pre-fabrication adhesion layers are also discussed and post-write procedures are described. Characterizations of the load shear failure mode at room temperature and post cryogenic thermal cycling at temperatures as low as 77 K are presented. Cryogenic thermal cycling shown in this work was accomplished by direct submersion in liquid nitrogen to assess the worst-case degradation due to thermal shock. A discussion of experimental results and a comparison of room temperature and thermal cycle data is provided. The reliability of the structures demonstrated in this work show promise for additional exploration for more complex structures at cryogenic temperatures.

2:30 PM SF02.11.05

Inkjet-Printed Polymeric Dampers for MEMS Application Prisca Viviani¹, Martina Scolari², Ilaria Gelmi², Laura Castoldi² and Luca Magagnin¹; ¹Politecnico di Milano, Italy; ²STMICROELECTRONICS, Italy

Over years, additive manufacturing has gained growing interest and attention in applications where customization and cost-effectiveness are strategic features. In this frame, Ink-jet printing (IJP) has emerged as a potential process to be flanked by traditional microelectronics material deposition method, where less exigent restraints on resolutions are required. However, high resolution in the micrometric range can be achieved, making this technique attractive for microfabrication. Indeed, many devices feature microfabricated parts, as Micro-electro-mechanical systems (MEMS). Compared to more traditional surface patterning techniques, IJP is a contact-less, mask-less droplet-based technique able to deposit functional materials onto specific substrates. The possibility to finely control the thickness, by tuning the number of printed layers, combined with minimum material waste reveal the great versatility of this fabrication technique. However, major challenges of IJP are found on two levels. One is the long-term cartridges durability, as nozzle clogging is prone to occur. On the other hand, IJP requires precise ink rheological properties to guarantee flow under the application of a shear stress: low viscosity (i.e. 2-20 cP) and surface tension (i.e. 25-50 mN m⁻¹)^[1,2].

IJP is also considered to be a key technology regarding polymers deposition. In particular, polymers are optimal candidate materials for vibration damping applications. Vibrations often represent a problem due to undesired motions and stresses, that can lead to fatigue, failure, degradation and reliability loss for a wide range of structures in microelectronics. As MEMS devices consist of mechanical parts, they are prone to experience harsh undesired vibrations too. There are two material classes for vibration control mechanism: active and passive damping. The most common passive damping material are Viscoelastic materials (VEMs), combining properties of elastic and viscous materials, where damping occurs by energy dissipation due to friction among oligomers chains under cyclic deformation. VEMs may be used as discrete dampers, absorbers or the surface of the structure can be fully or partially covered. As a matter of fact, a common viscoelastic treatment to control vibrations in a structure is the Free-layer damping (FLD) approach. The damping material is deposited on the structure surface, creating a damping layer. When the structure is deflected, vibrations are damped because of the energy dissipated following of the compression/extension of the damping material^[3,4].

The aim of this work is to propose a simple VEM deposition through IJP on top of a spring in the MEMS device, exploiting the FLD approach. First, an extensive material selection has been performed to individuate an adequate polymeric material, with low elastic modulus that would not alter spring properties. The characterization of the optimized ink in terms of physical properties, to understand ink printability through considerations regarding the

Ohnesorge diagram, will be presented. A jetting characterization will also be presented, evaluating the printability assessment as a function of the ink droplet speed. Eventually printed pattern characterization will be discussed either in terms of surface profilometry, microscopy and vibration damping ability.

[1] R. Bernasconi, M. C. Angeli, F. Mantica, D. Carniani, L. Magagnin, *Polymer* **2019**, *185*, 121933.

[2] E. P. Furlani, in *Fundamentals of Inkjet Printing*, John Wiley & Sons, Ltd. **2015**, pp. 13–56.

[3] N. Choudhary, D. Kaur, *J Nanosci Nanotechnol* **2015**, *15*, 1907.

[4] R. Singh, A. Ghosh, R. Kant, M. Asfar, B. Bhattacharya, P. Panigrahi, S. Bhattacharya, *Journal of Microelectromechanical Systems* **2013**, *22*, 695.

2:45 PM SF02.11.06

Large-Scale Transparent and Flexible Electronics Based on SWCNTs Enabled by Directed Fluidic Assembly Ahmed Abdelaziz, Jonah Yu and Ahmed Busnaina; Northeastern University, United States

Over the past two decades, single-walled carbon nanotubes (SWCNTs) attracted a lot of interests due to their outstanding electronic, physical, and structural properties. Which make them extremely promising candidates for high performance integrated circuits. On the other hand, the expanding of microelectronic large area sensors arrays, smart labels, and RFID tags enhanced the motivation of implementing these SWCNTs integrated circuits onto flexible and transparent substrates. However, large scale SWCNT development has been facing numerous challenges attributed to the difficulty of achieving homogeneously distributed nanotubes across large substrate surface area, as well as the complexity of the fabrication process, that in many cases affects the nanotubes stability as well as the maximum fabrication yield. Here, we report the fabrication of transparent large scale SWCNTs transistors and logic circuits on a four-inch scale wafer flexible substrate. Our approach implements directed fluidic assembly method to directly print SWCNTs over large scale on flexible and transparent substrates. This facilitates the fabrication of SWCNTs with high device density and yield without affecting the nanotubes stability compared to other fabrication techniques such as transfer printing or dry etching. Following this approach, the field effected transistors are fabricated with density of 1250 transistors per cm², with a yield of 97 %, whereas the on/off ratios for the fabricated devices was 0.5x10⁵ in average. This technique also allows the fabrication of various flexible integrated logic circuits using SWCNTs such as NOR gates, NAND gates, and inverters. We believe that this fabrication approach will be of a significant value in the development of flexible electronics for different application such as sensing, computing, and communications.

3:00 PM SF02.11.07

Dynamic Behavior of Additively Manufactured Polymeric Microlattices Thomas Butruille and Carlos Portela; Massachusetts Institute of Technology, United States

Ultralight mechanical metamaterials enabled by additive manufacturing (AM) have previously achieved density-normalized strength and stiffness properties that are inaccessible to monolithic materials, but the majority of this work has focused on static loading while the mechanical properties of these metamaterials under extreme dynamic loading conditions has remained largely unexplored. Properties such as energy absorption and the ballistic limit of these additively manufactured materials are of high interest for protective applications and recent works on their dynamic response have demonstrated the benefit of architecture for impact mitigation. Despite these promising results, limitations of current additive manufacturing processes at the macroscale have made thorough investigations of impact both time- and cost-inefficient, particularly if separation of scales between the periodic building block and the impactor is required.

Here, we use two-photon lithography as a rapid prototyping technique for microscopic polymeric microlattices, to systematically study their response to projectile impact. We fabricate lattice architectures of different morphologies (i.e., kinematically rigid and non-rigid architectures), with beam diameters ranging from ~1.0 to ~1.5 μm and unit cells of 7.5 μm, and we qualitatively and quantitatively characterize their response to microparticle impact. We employ the laser-induced particle impact test (LIPT) method to accelerate ~30 μm-diameter microparticles to velocities of up to 800 m/s, and use ultra high-speed imaging of the impact process to measure impact energetics. To isolate the effect of architecture, we maintain a constant relative density (i.e., fill fraction) across prototypes and probe them with a range of impact energies. Lastly, we analyze our experiments in a dimensionless framework that allows application of these results to metamaterials at larger scales. This investigation provides a framework for the rapid design and characterization of future AM metamaterials for a variety of energy mitigation applications.

SESSION SF02.12: Additive Manufacturing Techniques, Characterizations, and Applications III

Session Chair: Kun Fu

Monday Morning, December 6, 2021

SF02-Virtual

8:00 AM *SF02.12.01

High-Area Rapid Printing (HARP)—A Dead Layer-Free Approach to High Throughput 3D Printing Chad Mirkin, David Walker and James Hedrick; Northwestern University, United States

We report a stereolithographic three-dimensional printing approach for polymeric components that uses a mobile liquid interface (a fluorinated oil) to reduce the adhesive forces between the interface and the printed object, thereby allowing for a continuous and rapid print process, regardless of polymeric precursor. The bed area is not size-restricted by thermal limitations because the flowing oil enables direct cooling across the entire print area. Continuous vertical print rates exceeding 430 millimeters per hour with a volumetric throughput of 100 liters per hour have been demonstrated, and proof-of-concept structures made from hard plastics, ceramic precursors, and elastomers have been printed. This novel High-Area Rapid Printing (HARP) methodology works in the presence or absence of O₂, which expands the scope of resin materials that can be utilized for both prototyping and manufacturing.

8:30 AM SF02.12.05

Designing Direct-Ink-Write Structures for Specific Mechanical Responses Ilse Van Meerbeek, Todd H. Weisgraber, Ward Small and Jeremy Lenhardt; Lawrence Livermore National Laboratory, United States

This talk presents a method that uses simulation to explore the large design space of direct-ink-write (DIW) structures. Research has shown that we can design porous, elastomeric structures whose mechanical responses are specifically tailored to a given application; however, without complete information

about the design space, we are limited in what mechanical responses we can achieve. We used this method to expand our knowledge of the DIW design space by examining helicoidal structures in compression. We defined a parameter set and performed 90 simulations. The results suggest that changing the angle of rotation between layers (while keeping other parameters fixed) can increase the stress in compression by up to 300%. This raises the question: what other parameters can we define, and what effect will they have on the stress response? Porous elastomers are used for stress mitigation, in medical devices, and in soft robotics, all of which could benefit from precisely tuned mechanical responses. This method can facilitate optimizing for such applications.

This work was performed under the auspices of the U.S. Department of Energy by Lawrence Livermore National Laboratory under Contract DE-AC52-07NA27344. LLNL-ABS-823652

8:45 AM SF02.12.04

Late News: Enhancement of Tensile Toughness of poly(lactic acid) (PLA) Through Blending of an Alkyl-Branched Polydecalactone-Grafted Cellulose Graft Copolymer Woojin Lee¹, Jinsu Park¹, Jae W. Chung² and Seung-Yeop Kwak^{1,3,4}; ¹Seoul National University, Korea (the Republic of); ²Soongsil University, Korea (the Republic of); ³Research Institute of Advanced Materials (RIAM), Seoul National University, Korea (the Republic of); ⁴Institute of Engineering Research, Seoul National University, Korea (the Republic of)

Bio-polymers and bio-degradable plastics have attracted a considerable attention in scientific and industrial fields as a solution for alleviating pending issues regarding petrochemical-based plastic wastes, carbon dioxide emissions, and depletion of fossil resources. Poly(lactic acid) (PLA), an aliphatic polyester generally derived from bio-resources such as plant starches including corn, cassava, and sugarcane, is one of the most essential bio-polymers for various industrial applications. However, it is well known that the applications of PLA are considerably limited when compared to the typical petrochemical-based polymers owing to its inherent characteristics such as brittleness. Accordingly, increasing the toughness of PLA, i.e., concurrently increasing both the tensile stress and elongation at break, remains as a major challenge. In this present study, the fully bio-based PLA blends with polydecalactone (PDL)-grafted cellulose copolymer (CgPD) were fabricated to enhance the tensile toughness of the PLA matrix. As a toughness enhancer, the CgPD was synthesized via the direct ring-opening polymerization (ROP) of ϵ -decalactone (ϵ -DL), which is known as renewable and bio-degradable alkyl-branched lactone derivatives. The blending ratio was controlled by varying the amount of CgPD from 1 wt% to 10 wt% relative to that of PLA matrix, and the formation of thermoplastic film was performed by solution casting and subsequent melt-quenching methods under 4500 psi at 190 °C. The prepared bio-blends were found by FT-IR and solid-state ¹H NMR to be physically intact and miscible at the sub-twenty-nanometer scale. The WAXRD and DSC analyses indicated that the addition of the alkyl-branched CgPD imparts a more structurally disordered PLA mesophase state to the prepared PLA_CgPD bio-blends. UTM analysis was used to characterize the macroscopic mechanical properties of the PLA_CgPD bio-blends. Both the tensile strength and elongation properties were simultaneously improved with the addition of 1 wt% CgPD loading amount to PLA (PLA_CgPD1). This study experimentally demonstrates that the enhanced mechanical properties of PLA_CgPD1 are closely related to the existence of more ordered PLA mesophases induced by the introduction of an optimal amount of CgPD additive into the PLA matrix. Consequently, the proposed strategy in this study presents the possibility of designing a fully bio-based polymeric blend materials with exceptionally improved mechanical properties.

9:00 AM SF02.12.06

Recycling of Additively Manufactured Bio-Based Composites Katherine E. Copenhaver, Xianhui Zhao, Tyler Smith, Matthew Korey, Meghan Lamm and Soydan Ozcan; Oak Ridge National Laboratory, United States

As demand for high-performance composite materials rises, their management at end-of-life (EOL) must be considered more carefully. Bio-based polymers and composites have gained interest as global environmental awareness has heightened and governments and industries alike have put forth efforts to lower their carbon footprint. Identifying efficient routes for recycling of bio-based composites and establishing their application space after reprocessing will make these materials even more environmentally friendly. Additive manufacturing (AM) has also gained attention as a low-waste and highly flexible technique in which bio-based polymers and composites can be readily used. High-throughput, large area AM is a relatively new and fast-growing area of research, and the recyclability of these parts is important to establish considering the scale of parts and amount of material used. As such, the effect of recycling on additively manufactured poly(lactic acid) (PLA)/wood flour (WF) composites was studied. Parts were printed on the Big Area Additive Manufacturing (BAAM) system at Oak Ridge National Laboratory. The parts were size reduced using a water jet cutter and fed into a shredder/granulator. The obtained granulate was then fed directly back into the BAAM for reprinting without the need for repelletization. The thermomechanical performance of virgin and recycled parts was then characterized and compared in order to determine the impact of mechanical recycling on PLA/WF parts produced by AM. Mechanical recycling and direct reprinting of EOL AM parts was demonstrated as a cost-effective pathway for converting used bio-based composites into new products.

9:15 AM SF02.12.07

Late News: Fabrication of a Stretchable Cellulosic Material with Internally- and Externally Dual-Plasticized Structure Woojin Lee¹, Jinsu Park¹, Jae W. Chung² and Seung-Yeop Kwak^{1,3,4}; ¹Seoul National University, Korea (the Republic of); ²Soongsil University, Korea (the Republic of); ³Research Institute of Advanced Materials (RIAM), Seoul National University, Korea (the Republic of); ⁴Institute of Engineering Research, Seoul National University, Korea (the Republic of)

In recent years, environmental issues regarding the disposal of conventional synthetic plastics derived from petrochemical resources have emerged as a major issue. Thus, the development of bio-based plastics has received significant scientific interest over the past decades. Among the various natural resources, cellulose, which constitutes the main skeletal component of plants, is the most abundant natural polymer on the planet. However, it is well known that cellulose has a low solubility in most organic solvents, in addition to a poor melt processability owing to their intrinsic supramolecular hydrogen bonding properties and chain rigidity. Therefore, it is necessary to the develop of methodology capable of controlling molecular structure, flexibility, and stretchability of cellulose by imparting an effective plasticizing structure. In this study, we developed a highly stretchable internally- and externally-plasticized (i.e., dually-plasticized) cellulose, which is composed of a polydecalactone-grafted cellulose copolymer (CgPD) and a hyperbranched polycaprolactone external plasticizing additive (HPC). To investigate the effect of branching structures of polycaprolactone-based external plasticizing additives on the plasticization capability, a linear polycaprolactone (LPC) and a star-shaped polycaprolactone (SPC) plasticizing additives were prepared as control groups to HPC. It is observed that dipolar interactions existed between CgPD and external plasticizing additives in the dually-plasticized cellulosic materials (i.e., CgPD_LPC, CgPD_SPC, and CgPD_HPC). Especially, among the dually-plasticized cellulose samples, the CgPD_HPC exhibited the lowest apparent activation energy ($E_a = \sim 128.8 \text{ kJ mol}^{-1}$) required to achieve the sufficient plasticizing behavior, which resulted in an enhanced elongation at break value ($\epsilon = \sim 136\%$) compared to those of the CgPD ($\epsilon = \sim 75\%$), whereas CgPD_LPC and CgPD_SPC displayed severely deteriorated values ($\epsilon = \sim 25$ and $\sim 59\%$). This deterioration of mechanical properties may be attributed to the induction of structural discontinuity derived from the recrystallized polycaprolactone in the dually-plasticized celluloses. Therefore, it can be concluded that the highly-branched architectures as well as the structural uniformity between the internal- and external-plasticizing components play a critical role in determining the plasticization behavior.

9:30 AM SF02.02.07

Morphological Simulation for Material Design of Uniform Droplet-Sprayed Mg Alloys in Additive Manufacturing Charalabos C. Doumanidis¹, Yiliang Liao², Nikolaos Kostoglou³, Hiroki Fukuda⁴ and Claus Rebholz⁵; ¹BRAC University, Bangladesh; ²Iowa State University, United States; ³Montanuniversitat Leoben, Austria; ⁴Fukuda Metal Foil & Powder Co Ltd, Japan; ⁵University of Cyprus, Cyprus

This work introduces a morphological simulation of rapid solidification process deposited structures on 2-D planar sections, modeled as Apollonian packs of generalized ellipsoidal domains growing out of nuclei and dendrite arm fragments. The model employs descriptions of the dynamic thermal field based on superposed Green's/Rosenthal functions with source images for initial/boundary effects, along with alloy phase diagrams and classical solidification theory for nucleation and fragmentation rates. Initiation of grains is followed by their free and constrained growth by adjacent domains, represented via potential fields of level set methods, for effective mapping of the solidified topology and its metrics, i.e. apparent grain size and fractal dimension of densely-packed domains. The model parameters are calibrated and its predictions are validated against micrographs of three Mg-Zn-Y alloys deposited by uniform droplet spraying for additive manufacturing.

Further evolution of this real-time computational model and its application as a process observer for feedback control in 3D printing processes, as well as for off-line material design and optimization, is also summarized.

SESSION SF02.13: Additive Manufacturing Techniques, Characterizations, and Applications IV
Session Chair: Ketki Mahadeo Lichade
Monday Morning, December 6, 2021
SF02-Virtual

10:30 AM SF02.13.01

Impact of Novel Post-Processing Techniques on the Corrosion Response of L-PBF 316L Stainless Steels Stephanie Prochaska^{1,2} and Owen Hildreth¹; ¹Colorado School of Mines, United States; ²US Bureau of Reclamation, United States

Post-processing of additively manufactured (AM) 316L stainless steel parts printed via laser powder bed fusion (L-PBF) is required for removing support structures and to improve surface finish. Various novel processes have been recently developed to remove supports and/or improve surface finish on the entire part without requiring intensive manual labor. One technique, a self-terminating etching process, removes supports and smooths surfaces; another technique that improves surface finish involves a stepwise application of a chemical conversion coating and subsequent mechanical removal of material. The corrosion response of AM 316L stainless steel parts having undergone these novel processes is not fully understood. This puts into question their ability to be reliably used in real-world environments and limits their practical application. To date, most corrosion studies of L-PBF 316L materials have been limited to parts in the as-built condition, with preliminary data showing that L-PBF 316L stainless steel's corrosion response differs significantly from conventionally manufactured counterparts. Additionally, the corrosion response of L-PBF specimens has been found to change based on print orientation with respect to the build platform and also vary with post-processing heat treatments that impact microstructure. This work evaluates AM 316L stainless steel samples in the as-built condition and after they have undergone post-processing techniques to show how printing parameters, build orientation, and novel post-processing treatments impact corrosion response. Electrochemical data was combined with metallographic analysis to connect corrosion mechanisms to the underlying microstructure and, ultimately, the processing conditions.

10:45 AM SF02.13.02

Ultra-Sonic Fatigue Testing—A Rapid Testing Method for Additively Manufactured Metal Alloys Christopher Macey, Jarid Barthold-Robinson and William Gabler; Shimadzu Scientific Instruments, Inc., United States

Rapid prototyping using additive manufacturing techniques has increased the need for faster methods to characterize the fatigue behavior of 3D-printed alloys. Fatigue testing instruments utilizing ultra-sonic (20kHz) sample resonance enable testing to 10^7 cycles in about 10 minutes versus over 10 hours using standard instrument designs. Ultra-sonic fatigue measurements also allow sample testing to extremely high cycles (10^{10}) in a reasonable timeframe allowing insight to material failure behavior beyond the traditional "fatigue limit" of 10^7 cycles.

This paper reviews the experimental considerations necessary for successful USF measurements and provides examples of USF measurements of 3D printed alloys.

11:00 AM SF02.13.03

3D and 4D Printing of Smart and Nanostructured Polymer Thermosets—Shape Memory and Light-Weighting Properties Rigoberto C. Advincula^{1,2,3}; ¹Case Western Reserve University, United States; ²The University of Tennessee, Knoxville, United States; ³Oak Ridge National Laboratory, United States

There is high interest in smart and nanostructured materials based on the use of chemical and nanoparticle additives that enable structure-composition-property correlation towards their targeted application. 3D printing enables a convergence of optimized materials and geometrical design which can be further fine-tuned by the effective use of the 3D printing parameters: flow, slicing, temperature, adhesion, etc. There is the possibility of using artificial intelligence and machine learning (AI/ML) methods including simulation to optimize these properties such that valuable feedback can be obtained for optimized processing both during and post-printing. Herein, we focus on developing thermoset polymer materials to enable high performance for thermo-mechanical properties and eventual light-weighting applications. These include the following projects: 1) Thermoset elastomers based on VSP process emulsions, 2) Shape-memory polybenzoxazine materials that are highly stable, and 3) High-performance epoxy-carbon fiber materials and ideal light-weighting properties. The focus on thermosets enables materials development independent of melt-processability and using of photo-curing methods enabling the use of both chemical and physical crosslinking for curing modes. The VSP methods when applied at room temperature followed by post-printing curing methods including thermal treatment enable a more versatile method compared to high-performance polymer (HPP) FDM 3D printing methods.

11:15 AM SF02.13.04

Irregular Mechanical Metamaterials Using Liquid-Solid Scaffolds for Enhanced Impact Energy Absorption Zongling Ren¹, Robert Green-Warren², Assimina Assimina Pelegri², Jonathan Singer² and Jae-Hwang Lee¹; ¹University of Massachusetts Amherst, United States; ²Rutgers, The State University of New Jersey, United States

Disordered or irregular microstructures may demonstrate extraordinary mechanical characteristics when short-range phenomena, including interfacial (2D)

and nanoscale confined (3D) interactions, are tailored to govern the overall collective characteristics. Since the lack of lattice symmetry and statistical isotropy can allow scalable additive manufacturing as well as defect insensitivity in manufacturing, irregular metamaterials have been gaining greater attention in recent years. Because the range of mechanical exchanges is highly localized for the mechanical stimuli of high strain rates (HSRs), the irregular mechanical metamaterials can be more effective compared to ordinary regular mechanical metamaterials. In this respect, we have investigated irregular solid-liquid hierarchical structures having characteristic lengths ranging from micro to nanometers. In their two-step additive manufacturing processes, first, polystyrene spherical nano-shells are stacked with uniform thicknesses using self-limiting electrospray deposition (SLED). Second, the nanoscale interstitial space of the PS structure are subsequently backfilled with weakly-crosslinked polydimethylsiloxane to introduce nanoscale interactions found between solid and viscous liquids to the system. To observe HSR viscoelastic responses of the microstructures, a single silica microsphere (approximately 20 μm diameter) is accelerated up to 500 m/s incident to the sample using laser-induced projectile impact test (LIPIT). Kinetic energy dissipation of the speeding microsphere during its collision with the metamaterial is quantified from the ultrafast stroboscopic microscopy. The correlations of the energy dissipation with a projectile's impact energy and viscoelasticity of the PDMS filler are demonstrated and compared with low-strain-rate indentation results. This study provides an understanding of the role of solid-liquid interactions within irregular solid nano-scaffolds materials under HSR inelastic deformation conditions.

11:30 AM SF02.13.05

Role of Substrate Surface Oxide and Temperature on the Bonding Characteristics of Al6061 Microspheres at Ultra-High Strain Rates in Cold Spray Process Swetaparna Mohanty¹, Carmine Taglienti¹, David L. Arellano¹, Victor K. Champagne² and Jae-Hwang Lee¹; ¹University of Massachusetts Amherst, United States; ²United States Army Research Laboratory, United States

Cold spray is a deposition process of solid powders and is employed in the additive manufacturing process to fabricate parts and structures below the powders' melting temperatures. Supersonic velocity impacts of microparticles to target substrates in this process results in the microparticles experiencing high-strain-rate microscopic ballistic collisions. At these high speeds, the kinetic energy of the particles leads to extreme plastic deformation of the interface of the microparticle and the target substrate, which eventually enables solid-state consolidation. Study of impact dynamics, bonding mechanism, and critical velocities of these microparticles helps us better understand the cold spray process. It has been generally understood that the parameters influencing the critical velocity and bonding mechanism include the presence of an oxide layer and the temperature at which the collision events take place. In this study, as a model system, the dynamic behavior of polycrystalline aluminum 6061 T6 alloy (Al 6061) microparticles (~ 20 μm diameter) after impact on a target substrate at ultra-high strain rates are quantified by using a micro-ballistic method: advanced laser induced projectile impact test (α -LIPIT). The controlled parameters in these highly controlled experiments are impact speed (0-1,000 m/s), temperature (room temperature-300°C), and substrate oxide film thickness (10-20 nm additional oxide layer prepared using atomic layer deposition). Individual particle's deformation characteristics are systematically studied with electron microscopy and focused ion beam milling. The precisely simulated microscopic collision events establish a quantitative relationship between the high-strain-rate dynamic response of the microparticles and the control parameters.

*This work was sponsored by the U.S. Department of Defense under Cooperative Agreement Award No. HQ0034-15-2-0007 and W911NF-15-2-0024.

11:35 AM SF02.13.06

Toward Optimum Processing Parameters for Direct Laser Writing—A Molecular Dynamics Simulation Approach Elaheh Sedghamiz, Modan Liu and Wolfgang Wenzel; Karlsruhe Institute of Technology, Germany

Three-dimensional direct laser writing (3D-DLW) is an indispensable tool to high accuracy structuring and fabricating of 3D micro- and nano-objects via polymerization processes induced by direct laser writing. Over the past decade, this technology has become a well-established lithography tool for fabricating 3D geometries directly on functional substrates. This capability provided the possibility for a wide range of applications in photonics, microfluidics, mechanical microstructures, and cell scaffolds.

As the dimensions of the printed structures shrink, it remains a challenge to control the stiffness and resolution of the fabricated structure by changing the many conditions influencing direct laser writing. We, therefore, developed a nanoscale simulation approach as an alternative to physical experiments to optimize the 3D writing process and reduce the number of experiments. This approach enables a systematic study of how various writing parameters affect the structure and stiffness of the fabricated polymer network. We employ a coarse-grained molecular dynamics (CG-MD) approach to simulate direct laser writing of 3D polymer networks from a monomer pool, where monomers react irreversibly according to reaction rate constants, which results in 3D objects being printed voxel by voxel.

Simulations show that the degree of monomer conversion increases with higher laser power or, correspondingly, higher exposure times and saturates towards high writing powers/ high exposure times. Nonetheless, the laser power has a more pronounced effect on the degree of monomer conversion and mechanical properties than the exposure time. Furthermore, we study the relationship between mechanical strength, the porosity of the polymer network, and the mixture ratio of the radical quencher into the resins. We propose the optimum writing condition including the oxygen quenching effect to fabricate polymer networks of high resolution with acceptable mechanical stability. This approach allows us to tune the writing conditions of the 3D printed objects exploiting the fine interplay between laser power, exposure time, oxygen quenching to meet the requirements for different applications.

11:40 AM SF02.06.11

Late News: (Garcia High School Student) Optimizing the PP/PS Blends for Polymer 3D Printing Forest Ho-Chen¹, Emma Savov², Shuhe Liu², Yu-Chung Lin³ and Miriam Rafailovich³; ¹George school, United States; ²Mainland Regional High School, United States; ³SUNY Stony Brook University, United States

Polypropylene (PP) is a widely used plastic, due to its superior mechanical properties and resistance to corrosion. Processing of PP using classical extrusion is well established but using PP as filaments for 3D printing has proven challenging. One problem, common in general to semi-crystalline polymers, is warpage which is exacerbated by the lack of adhesion to the base plate and makes printing of larger structures difficult. Polystyrene is another common polymer with good chemical corrosion resistance, which is easy to extrude, but very difficult to print. Its high melting point, makes it brittle, resulting in filament breakage and clogging of the nozzle mechanism during printing. Here we demonstrate that blends of PP and PS can overcome these problems to produce filaments that are ductile and print structures that resist warping and maintain structural accuracy. Furthermore, it has been shown that PP allows high loading of graphene nanoplatelets, GNP, while still retaining ductility [kai]. Printing with PP/GNP produced highly oriented layers, with high electrical conductivity, but the warpage persisted, and only narrow interconnects were easily produced.

Here we show that blends of these polymers could be made, extruded into filaments, which are then easily printed and could produce large multilayer structures. Blends of PP and PS, with 80/20, 70/30, and 60/40 ratios, were produced via melt mixing in a Brabender twin-screw extruder, where torque was monitored, and drawn into filament using a Filabot extruder. Samples were printed for tensile and Izod impact testing, as well as temperature and frequency rheological measurements. Measurement of G' and G'' at $T=200\text{C}$, showed shear thinning behavior, which is advantageous for nozzle extrusion followed by rapid thickening to maintain accuracy. Tensile data indicates that the impact toughness of 80/20 PP/PS was significantly higher than the rest. Filaments were also produced where the PP phase was loaded with up to 20 weight percent GNP, and the electrical and thermal conductivity properties were compared to those obtained from pure PP with comparable loading, where large differences were observed between the perpendicular and parallel

orientations relative to the extruded control samples. Correlation with TEM images of the blend morphology and in operando x-ray scattering of the printing process will be presented.

SESSION SF02.14: Additive Manufacturing Techniques, Characterizations, and Applications V
Session Chair: Rui Yin
Monday Afternoon, December 6, 2021
SF02-Virtual

1:00 PM *SF02.14.01

Emergence of Multi-Material Volumetric Additive Manufacturing—Overprinting and Particle Inclusion Hayden Taylor, Joseph Toombs, Chi Chung Li, Sui Man Luk, Weisa Wang, Ingrid Shan, Vishal Bansal and Alexander Watson; University of California, Berkeley, United States

Volumetric additive manufacturing (VAM) describes a developing class of 3D printing methods in which a photosensitive precursor material is transformed into a solid object via highly parallelized illumination. Computed axial lithography (CAL) is a specific VAM process in which a rotating volume of material is illuminated with a time-evolving light pattern such that the cumulative light dose is tomographically synthesized and can be controlled in three dimensions. Where the light dose exceeds a material-dependent threshold, the material is transformed into a solid object. Unlike conventional photopolymer additive manufacturing, CAL is layer-free, which brings several advantages. Here, we describe two ways in which the unique characteristics of CAL are enabling multimaterial objects to be prototyped.

Firstly, because the entire volume of the target object is exposed simultaneously, pre-existing solid objects can be immersed in the precursor material and “overprinted” with a polymeric geometry, analogously to overmolding or insert molding in thermoplastic injection molding. We have evaluated ways of strengthening the bond between CAL-printed polymer geometries and metallic objects, including silane-based coupling agents and cross-pattern knurling, the latter of which was found to increase the shear strength of the printed bond by approximately a factor of two. We also describe a specialized algorithm to generate illumination patterns that compensate for the occlusion of light by the object. This algorithm is shown to improve the accuracy of 3D dose reconstruction during overprinting, compared to ignoring the occlusion of light. We discuss the application of overprinting to microfluidic devices incorporating CAL-printed hydrogels.

Our second multimaterial process innovation exploits the fact that in CAL there is no relative motion between the precursor material and the fabricated object during printing. Thus freed of the limitations of hydrodynamic stresses, CAL can access a wider range of higher-viscosity or thermally pre-gelled precursor materials without sacrificing processing speed. We can harness this advantage to process dispersions of solid particles with exceptionally high volume fractions and associated high viscosities. We discuss approaches to modeling the propagation of light through these precursor materials, and the prospects for processing dispersions of fibers using CAL.

1:30 PM SF02.14.03

Three-Dimensional Printing of Glass Micro-Optics Using Liquid Precondensed Tetramethoxysilane Oligomers Piaoran Ye¹, Zhihan Hong¹, Rongguang Liang¹ and Douglas A. Loy^{2,1}; ¹The University of Arizona, United States; ²University of Arizona, United States

To meet the increasing needs of high-precision glass micro-optics and address the major limitations of current three-dimensional (3D) printing optics, we have developed a liquid, solvent-free, silica precursor and two-photon 3D printing process. The printed optical elements can be fully converted to transparent inorganic glass at the temperature as low as 600 °C with the shrinkage of 17%. We demonstrate the complete process chain, from material development, printing process, and performance evaluation of the printed glass micro-optics. 3D printing of glass micro-optics with isotropic shrinkage, micrometer resolution, low deviation peak-to-valley value (<100 nm), and low surface roughness (< 6 nm) is achieved. The reported technique will enable the rapid fabrication of complex glass micro-optics previously impossible using conventional glass optics fabrication processes.

1:45 PM SF02.14.04

BCC High Entropy Alloy with High Strength in High Temperature Environments for Additive Manufacturing Kazuhiro Abe, Tomonori Kimura and Kazuya Shinagawa; Materials Processing Research Department CTI - Production Engineering and MONOZUKURI, Japan

New high temperature materials exceeding Ni-base superalloys are highly demanded because it can realize higher burning efficiency in turbines or internal combustion engines by improving temperature resistance of heat resistant parts. Although Ni-base superalloys has excellent high temperature properties up to 1000°C, improvement is needed for their use at higher temperatures due to their melting temperatures and γ' -solvus. As a breakthrough solution, high entropy alloys (HEAs), which are composed of multi-principal elements, are highly attracted because of their several unique properties [1]. Among them, refractory high entropy alloys (RHEAs), which are based on refractory metals such as WNbMoTaV and WNbMoTa, are known as alloys with excellent high-temperature strength because of high melting temperature [2]. Also, additive manufacturing for RHEAs has been reported, and thus they are promising for new structure materials [3]. However, most of RHEAs with outstanding high-temperature strength are low ductility at room temperature and they have higher density than conventional Ni-based alloys. They are large obstacles to make RHEAs in practical use.

The purpose of this study is development of alloys with both high strength and low density for additive manufacturing. We focused on the elements with both high melting temperature and low density compared with Ni, and the properties of VNbMoCrTi alloys and VNbMoCrTiC alloys were investigated. VNbMoCrTi alloys and VNbMoCrTiC alloys ingots were prepared by arc-melting under an Ar atmosphere. Specimens cut from the ingots were solution treated at 1300°C for 24 hours under vacuum followed by furnace cooling. All ingots were characterized by scanning electron microscopy (SEM) and energy dispersive X-ray spectroscopy (EDX). The phase structure was analyzed by X-ray diffractometer (XRD). Density of each specimen were measured by Archimedes method. The high-temperature strength was evaluated by the compressive test.

From the SEM observation of VNbMoCrTiC alloys, homogenized body centered cubic (BCC) matrix phase with carbide were confirmed after heat treatment. Also, EDX results indicated that carbide is mainly composed of TiC. XRD pattern showed the peak derived from BCC phase and carbide, and these results agree with EDX results. Besides, VTiNbMoCrC alloy showed the yield stress of 780MPa at 1000°C regardless of lower density compared with Ni-based alloys.

2:00 PM SF02.14.05

Self-Terminating Etching Method for Support Removal of Additively Manufactured GRCop Sanaz Yazdanparast, Subbarao Raikar and Owen Hildreth; Colorado School of Mines, United States

Selective Laser Melting (SLM) is an emerging manufacturing technique that enables fabrication of parts with complex geometries and excellent mechanical properties. However, metal SLM components require expensive and difficult post-processing steps to remove supports and improve surface finish. To address this issue, this work presents a new self-terminating etching process to simplify the post-processing of copper alloy components fabricated using SLM. This process was performed on two advanced copper alloys; GRCo-84 and GRCo-42 that are interesting materials in aerospace applications due to their excellent thermal and mechanical properties. The self-terminating etching process contains two main steps: 1) altering the chemical composition of the outer surface of a metal by a proper sensitizing agent, and 2) dissolution of the resultant corrosive region by wet chemical etching. We demonstrate that iodine can be used to "sensitize" the surface of copper alloy components by forming soluble metal iodide salts that can be then dissolved in acetonitrile. Using this technique, a pre-defined amount of copper is removed from all interior and exterior surfaces resulting in separation of the component from the support. In addition, the surface roughness measurement shows an improvement of surface finish of GRCo by 70 % after 4 iodization-dissolution cycles.

2:15 PM SF02.14.06

Evaluation of the Infill Design on the Tensile Response of Metal Parts Produced by FFF Process Using Digital Twin Reconstruction Method Saleh Atareh, Mozah Alyammahi, Hayk Vasiyan, Rahmat Agung Susantyoko, Tawaddod Alkindi and Oginne Lapuz; Dubai Electricity & Water Authority, United Arab Emirates

Additive Manufacturing (AM) technologies have evolved significantly. The applications of AM have expanded from rapid prototyping to a larger scale, such as the construction of buildings and the mass production of spare parts. The world's first 3D-printed laboratory has been constructed in Dubai in 2017, aligned with Dubai's strategy to be a leading hub of 3D printing technologies by 2030. AM has various advantages, such as reduced material usage, geometric freedom, and automation that will shape the future of the manufacturing industries.

AM technologies can be classified into material extrusion, binder jetting, and powder bed fusion (PBF), direct energy deposition (DED), and other technologies. Each of the above classifications can be sub-categorized based on feedstock material and sub-processes. With the rapid expansion of AM applications, feedstock materials have developed noticeably: from polymers and ceramics to metals and composites. Selective Laser Melting (SLM) is the most common method within PBF to fabricate metal parts. Electron Beam Additive Manufacturing (EBAM) is adopted for DED of metals.

The progress in developing new AM feedstock material has empowered the exploration of other technologies to manufacture metal parts, such as Material Extrusion. The flexibility in choosing the feedstock material is an advantage for the technology that facilitated its growth by users around the globe in research and industry. Fused Filament Fabrication (FFF) is one of the most common and cost-effective material extrusion AM technologies. FFF applications include rapid prototyping and the production of high-performance functional parts. The feedstock material is shaped in a wire form that is utilized through a filament. It passes through a nozzle that heats and extrudes it layer by layer over the print bed, following a predefined path determined by the G-code. Different terms have been used in the industry and literature that refer to metal fabrication through FFF, such as metal FFF, Bound Powder Extrusion (BPE), Atomic Diffusion Additive Manufacturing (ADAM), and Metal Fused Filament Fabrication (MF³). The process of manufacturing metal parts with FFF consists of 3 main steps: printing, de-binding, and sintering.

It is critical to understand how different printing parameters and other factors along the process of metal FFF can affect the mechanical properties of the parts. Understanding the different characteristics of such parts is considered essential to expand the applications of this process and understand the economic and environmental impacts.

This paper attempts to explore the different characteristics of the parts produced via metal FFF, which includes the mechanical properties of two metals: 17-PH stainless steel and copper. The study will also investigate the porosity of these parts, cost analysis, weight, and environmental impact.

Two comparison models are designed to validate the results: experimental 3D Printed and numerical Finite Element Analysis (FEA) for the same. For the experimental test, two sets of each metal material are manufactured using FFF through the Markforged Metal X system. One set is fabricated with solid infill, while the other has triangular infill. Each set consists of four identical "dog bone" specimens. The dimensions and test conditions were set according to ASTM F3122 and ASTM-E8 standard. A uniaxial tension test will be conducted using Instron 3367 tensile testing machine. For the numerical FEA Analysis, the Digital Twin reconstruction method will be used where an explicitly generated CAD Model is made using an Additive Reconstruction Tool with the G-Code as input to simulate the solid layer by layer and obtain a digital equivalent of the 3D Printed part in CAD Software. A Scanning Electron Microscope (SEM) will be used to investigate the parts' internal structure and average pore size. The porosity will be characterized through density comparison and analyzing pore distribution.

2:30 PM SF02.01.04

Analysis of Additively Manufactured Material Using Thermomechanical Simulation and X-Ray Diffraction Trupti S. Mali, Todd Letcher and Anamika Prasad; South Dakota State University, United States

Additive Manufacturing (AM) is an emerging and highly promising technology for manufacturing metal-based complex geometries for specialized applications such as aerospace, defense, medical implants, and in-space manufacturing, among others. However, the structural and property impact of additive manufacturing processes on manufactured parts remains to be fully explored. For example, the repeated thermal cycles during layer-by-layer deposition can create uneven material properties and residual stresses. These localized residual stresses may result in material failure during use. Also, minor changes in input parameters such as powder size, laser power, and laser scan speed can significantly impact the final quality of the deposit. A critical study of the relationship of input parameters with residual stresses and part performance is necessary for designing post-processing heat treatment and broader acceptance of AM process.

The finite element analysis (FEA) is an effective tool to analyze the impact of AM input parameters on the final performance of manufactured parts, resulting in a significant saving on cost and time compared to production and experimental analysis. Hence, to generate design guidelines for AM processes, we analyze residual stress patterns on the directed energy deposited (DED) thin-wall structure in as-built and post-treated conditions. The computational results are compared and contrasted against the X-ray diffraction (XRD) study of AM. The simulation is performed in ABAQUS (Dassault Systemes, USA) using an integrated thermomechanical analysis step with temperature-dependent material properties. The materials properties for the simulation were used from tensile and fatigue tests data available in literature for AM copper alloy (GRCo-42), a material developed for NASA rocket propulsion application. A plot of the effect of input parameters such as laser power and scan speed on the residual stress changes is presented, along with simulation validation through comparison with the experimental residual stresses XRD data. The simulation stress distribution implicates the agreement with experimental analysis. Also, it exemplifies the use of the thermomechanical model to guide parameter space for the AM.

4:00 PM SF02.15.01

Optimization of Additive Manufactured Housings for IoT Devices in an Alpine Environment [Thomas Schmiedinger](#), Markus Ehrlenbach and Christian Schmid; University of Applied Sciences Kufstein, Austria

Common housings for Internet of Things (IoT) sensors consist of a polymer like acrylonitrile butadiene styrene (ABS). The primary function of these objects is to protect the electronics from environmental influences e.g., water. Due to the exposed location of IoT sensors, especially in alpine regions, the housings are important for a proper and long-term function of the sensor. Beside protection, additional features like insulation properties are important too, for ensuring sensor functionality. The insulation aspect of common IoT housings has been realized by adding insulation material in addition to the housings. Additive manufacturing may enable a combined design approach in fulfilling mechanical and thermodynamical requirements at the same time. The aim of the paper is to describe and investigate different designs for additive manufacturing which combine insulation properties without affecting structural stability of housings for IoT devices in alpine regions.

Finite element analysis simulation models for IoT housings are used to determine the thermodynamical and structural properties of different materials and designs. Selected designs are fabricated and tested in a climate chamber regarding insulation and mechanical properties.

The approach of design for additive manufacturing enables an integration of different functionality (e.g., thermal and mechanical function) into the designed part. The insulation property of additive manufactured housings for IoT devices exhibit a significantly higher insulation ability in comparison to common housings of IoT devices. This approach enables highly innovative housings which can withstand the harsh environment in alpine region.

4:15 PM SF02.15.02

Additive Manufacturing of Thermosetting Resins via Direct Ink Writing and Radio Frequency Heating and Curing [Anubhav Sarmah](#), Ava Crowley, Suchi K. Desai, Gabriel Zolton and Micah J. Green; Texas A&M University, United States

Direct Ink Writing (DIW) is an extrusion-based additive manufacturing method where the print medium is a liquid-phase 'ink' dispensed out of small nozzles and deposited along digitally defined paths. Conventional DIW methods for thermosetting resins rely on the use of viscosifiers, novel crosslinking chemistries, and/or long curing schedules in an oven. Here, we demonstrate the use of a co-planar radio frequency applicator to generate an electric field which can be used to rapidly heat and cure DIW-printed, nano-filled composite resins. This method avoids the need of an oven or post-curing step. The proposed process consists of a layer-by-layer, print-and-cure cycle which allows for printing of high-resolution, multi-layer structures. Every extruded layer is partially cured using RF before depositing the next layer; this allows the printed part to maintain structural integrity without buckling under its own weight. The process enables both increased throughput and decreased touch time relative to traditional part manufacturing. Commercial epoxy resin with varied nano-filler loadings were examined as DIW candidates. Rheological characterization was used to assess both curing kinetics and printing behavior. After printing, the thermo-mechanical properties, surface finish, and shape retention of RF-cured samples were evaluated and found to be comparable against samples conventionally cured in an oven. This method of manufacturing establishes RF heating as a suitable alternative to conventional methods, facilitating rapid, free-form processing of thermosetting resins without a mold.

4:30 PM SF02.15.04

Additive Manufacturing of a Superhydrophobic/Superoleophilic Fluoropolymer Nanocomposite Membrane for Oil/Water Separation [Lucas Kilpatrick](#)^{1,2}, Eugene Caldoni^{1,2}, Zane J. Smith^{1,2} and Rigoberto C. Advincula^{1,2,3}; ¹Joint Institute for Advanced Materials, United States; ²The University of Tennessee, Knoxville, United States; ³Case Western Reserve University, United States

Lucas L. Kilpatrick^{a,b}, Eugene B. Caldoni^{a,b}, Zane J. Smith^{b,c}, and Rigoberto C. Advincula^{a,b,d,e}

^aDepartment of Chemical and Biomolecular Engineering, University of Tennessee, Knoxville, TN 37996, USA

^bJoint Institute for Advanced Materials, University of Tennessee, Knoxville, TN 37996, USA

^cDepartment of Materials Science and Engineering, University of Tennessee, Knoxville, TN 37996, USA

^dDepartment of Macromolecular Science and Engineering, Case Western Reserve University, Cleveland, OH 44106, USA

^eCenter for Nanophase Materials and Sciences, Oak Ridge National Laboratory, Oak Ridge, TN 37830, USA

Abstract

This study focuses on the fabrication of a porous superhydrophobic membrane for oil/water separation. The membrane, made from nanosilica-containing poly(vinylidene fluoride-co-hexafluoropropylene) (PVDF-HFP), was prepared by direct ink writing. The as-prepared membrane displayed anti-wetting property and superoleophilicity, allowing oil to pass, but not water, through its openings. Such surface characteristics are mainly attributed to the synergistic effect of hierarchical surface roughness created by the silica nanoparticles and low surface energy inherent to PVDF-HFP. Combined with mechanical robustness and high thermal stability, the nanosilica-filled fluoropolymer membrane is practically useful in solving industrial problems concerning water contamination and oil spill response.

Keywords: superhydrophobicity; superoleophilicity; fluoropolymer; silica; oil/water separation

4:45 PM SF02.15.05

Operando X-Ray Characterization of Temperature Profiles and Phase Evolution Along Building Direction During Laser 3D Printing of Ti Alloys [Ming Chen](#)¹, Marco Simonelli², Steven Van Petegem¹, Yau Yau Tse³, Dario Ferreira Sanchez¹ and Helena Van Swygenhoven-Moens¹; ¹Paul Scherrer Institute, Switzerland; ²The University of Nottingham, United Kingdom; ³Loughborough University, United Kingdom

The high temperatures and rapid cooling rates during laser powder bed fusion make it difficult to characterize the thermal cycles the material undergoes during printing. Such information is however crucial for understanding the evolving microstructures, especially, when the material undergoes phase transformations during thermal cycling. We recently demonstrated an *operando* X-ray diffraction technique to measure temperature and phase evolutions in a newly deposited layer during laser powder bed fusion (L-PBF) of Ti-6Al-4V (*Hocine et al., Materials Today, 34, 2020*). Here, the *operando* X-ray diffraction experiments are carried out on thin walls of Ti-6Al-4V-3Fe and Ti-6Al-4V. Temperature profiles and cooling rates are derived from X-ray diffraction patterns measured in transmission mode for multiple layers below the surface while the laser rescans the surface. Microstructures are further characterized by transmission electron microscopy (TEM) and energy dispersive X-ray (EDX) spectroscopy. The powders used were prepared by

decorating a pre-alloyed Ti-6Al-4V powder with pure Fe particles using a simple mixing method (Simonelli *et al.*, *Materials Characterization*, 143, 2018). It is known that minor addition of Fe can stabilize the β -Ti phase at ambient temperature. The present study shows that Fe is heterogeneously distributed after printing and that the β -Ti phase is stabilized where the Fe concentration is highest. During remelting the surface layer, temperatures above the β transus (1252 K) are reached in at least 3 layers below that newly printed layer. Furthermore, during remelting of the upper layer, the Fe distribution is homogenized. The evolution of the β phase during thermal cycling is discussed in terms of the temperature profiles and cooling rates in multiple layers along the building direction.

5:00 PM SF02.15.06

Shape-Reconfigurable and Recyclable 4D Plastics for Wearable and Adaptive Device Platforms Kiesar Sideeq Bhat, Wen See Tan, [Amelia Lee](#), Rui Yuan Han, Mike Regan and Juha Song; Nanyang Technological University, Singapore

The increased demand for wearable devices such as smartwatches, shoes, and even masks, amid the pandemic, has led to an increased demand for customized and adaptive materials, specifically for use on the human body. One such material is smart materials with an intrinsic shape memory effect to morph into another shape when an external stimulus is applied. The fabrication of such materials through additive manufacturing is known as 4D printing. However, such 4D printing is limited to materials with intrinsic shape memory effects, which are usually expensive and limited. Thus, herein, we proposed a new smart material platform where a conventional non-smart thermoplastic material with pre-programmed structure induces reversible 4D effect through local heat generation associated with selective Joule heating mechanisms. Through multi-material printing capability of a Multi-Jet Fusion printer, we successfully fabricated polyamide-12 (PA-12) with embedded heat channels. Through a designed 3D structure and silver-polymer composition variation, resistance gradient was induced at selective local regions where Joule heating considerably occurred. 3D finite element analysis (FEA) modeling was conducted in parallel to experiments, and the simulation results showed good agreement with the experimental observation, validating the underlying mechanism of this 4D system. Through parametric studies with various structural and material parameters, those 4D systems can be tuned depending on operation conditions. We also demonstrated the applicability of this system through a proof-of-concept product, adaptive mask frames that could be conformed depending on the contour of a human face. This 4D system was also durable and reversible, showing consistent performance over multiple loading cycles. In conclusion, this study demonstrated that common thermoplastics with embedded heat channels can be used as a new type of smart material systems, creating a new material category, "4D plastics". We envisage that this system can be applied to build wearable devices, customized clothing and shoes, military weapons, and medical instruments where adaptability, conformity and rigidity are required.

5:15 PM SF02.15.07

Effect of Laser Remelting Processing on Microstructure and Mechanical Properties of 17-4 PH Stainless Steel During Laser Direct Metal Deposition Zhiyuan Yu; Shanghai Jiao Tong University, China

Laser direct metal deposition (DMD) is an efficient and flexibility additive manufacturing technique which has broad application prospects, but limited due to varieties of defects and anisotropy. Laser remelting (LR) is a process that the same slice data is scanned secondly without powder deliver after each layer is deposited, and it is often used during selective laser melting. Herein, LR process has been applied during the DMD process of a 17-4 PH steel to enhance the densification level and relieve the mechanical anisotropy. It is found that thermal history, porosity and microstructural evolution are shown to be dependent on the LR energy density. Moreover, the roughness of top surface of the deposited layer and intralayer porosity decrease with increase of laser remelting energy density. While for interlayer defects, there is an optimal LR energy density corresponding to the lowest interlayer porosity. Furthermore, LR process can enhance the holding time at high temperature, even sometimes heat the sample above A_{c1} , resulting in change in contents of austenite and carbide. In addition, LR process greatly dilutes the pre-solidified texture. It was also proved that the flat defects in-plane to the interlayer and the anisotropy of the crystallographic orientations are extremely harmful for the mechanical isotropy of the DMDed samples. Finally, sample manufactured with laser remelting at 15.0 J/mm^2 has the lowest porosity and random crystallographic orientations resulting in near isotropous tensile strength, but the contribution of laser remelting to eliminate anisotropy in elongation is limited because of the interlayer defects.

5:30 PM SF02.15.08

Development of a Nanocomposite Conductive Photocurable Resin for the Production of MEMS Through Stereolithography [Raffaella Suriano](#), Filippo Iervolino and Marinella Levi; Politecnico di Milano, Italy

In recent years, additive manufacturing has become an attractive technology that offers many advantages over the other widespread subtractive methods. The most evident advantage is the possibility to make any object, virtually without any geometrical limitations.[1] Among the additive manufacturing processes, stereolithography enables the manufacturing of small items with miniaturized features and extraordinary precision. For these reasons, the production of MEMS (microelectromechanical system)-based sensors by stereolithography could be a valid alternative to the existing silicon-based technologies, even though it is diametrically opposite to current technologies, which allow the production of huge amounts of identical objects, i.e. mass production. Oppositely, stereolithography enables mass customization thanks to the production of objects which can be different from each other and completely customizable.[2]

In this work, a commercial resin was used and fully characterized, because its formulation, as well as its physical and mechanical properties, were unknown. The high precision of stereolithography, together with the thermal stability of the resin, were exploited to produce customized MEMS-like sensors. However, stereolithography is suitable only for photo-curable materials called photopolymers. They are usually insulating materials, which should be coated with metallic layers either by inkjet printing or by electroless deposition and subsequent wet metallization, to add electrically conductive patterns to the 3D printed objects.[3] In this work, carbon nanotubes (CNTs) were added to the photocurable resin to obtain a photocurable conductive nanocomposite aiming to create electrically active parts in MEMS-like sensors. Furthermore, different types of CNTs were investigated: (i) pristine CNTs; (ii) amino-functionalized CNTs; and (iii) silver-decorated ones. The addition of CNTs to obtain an electrically conductive photocurable material has been revealed to be effective. The enrichment of the matrix with a CNT content greater than 0.1 wt% led to improve the conductivity of the material by 5-to-6 orders of magnitude. Using a 0.5 wt% CNT concentration, the material showed a conductivity equal to $3.9 \cdot 10^{-4} \text{ S/cm}$. This result could be increased by 2.4 times using CNTs functionalized with NH_2 due to their more homogenous dispersion in the matrix and by 10.8 times by using CNTs decorated with silver nanoparticles. Even higher values could be obtained by better controlling the synthesis of Ag-MWCNTs to deposit much smaller nanoparticles. However, a custom-made formulation for the resin can be developed in the future to tune some properties such as stiffness and viscosity.

[1] I. Gibson, D. Rosen, B. Stucker. Additive Manufacturing Technologies: 3D Printing, Rapid Prototyping and Direct Digital Manufacturing, 2015, Springer, New York.

[2] P.F. Jacobs, Rapid Prototyping & Manufacturing, 1999, Society of Manufacturing Engineers, Dearborn.

[3] L. Gaffuri Pagani, P. Carulli, V. Zega, R. Suriano, R. Bernasconi, A. Frangi, M. Levi, L. Magagnin, G. Langfelder, "The First Three-Dimensional Printed and Wet-Metallized Coriolis Mass Flowmeter," in IEEE Sensors Letters, vol. 4, no. 6, pp. 1-4, June 2020, Art no. 2500604, doi:

5:45 PM SF02.06.10

A Fabrication Method of 3D Printing Alumina Ceramic with Complex Structure Yiran Ma and Yuxiang Zhang; Northwestern Polytechnical University, China

Ceramics are characterized with high hardness, brittleness and heat resistance, the applications of which are restricted by traditional fabrication processes. Additive Manufacture (AM) can be innovatively applied to direct manufacture of ceramic structures, hence the relatively labour-saving fabrication of 3D ceramic parts in contrast with the conventional methods. DLP (Digital Light Processing), as one of the AM techniques, is capable to fabricate alumina ceramics with complex structures through mask-image-projection, which ensures the precision and improves the efficiency of manufacture. In this research, alumina ceramic with complex structures was obtained by DLP with a high resolution and applicable mechanical properties. A long-time stable ceramic suspension with high ceramic powder content was firstly obtained, which achieved the mass fraction of 70%. Then optimized parameters of the UV-curing process ensured the resolution of the complex structure. The two-step sintering method was adopted to optimize the sintering process in order to reduce defects and improve density. The complex ceramic structure with high resolution showed an average flexural strength of 220MPa and a relative high density, with potential applications of aerospace, tissue engineering, machinery manufacture and so on.

Yuxiang Zhang and Yiran Ma contributed equally to this work.

SESSION SF02.16: Additive Manufacturing Techniques, Characterizations, and Applications VII
Session Chair: Ketki Mahadeo Lichade
Tuesday Morning, December 7, 2021
SF02-Virtual

8:00 AM SF02.16.01

Preventing Premature Failure and Circumventing the Strength-Ductility Trade-Off of Additively Manufactured Materials Jurgen H. Eckert^{1,2}, Zhi Wang³ and Konda Gokuldoss Prashanth^{4,1}; ¹Austrian Acad of Sciences, Austria; ²Montanuniversitaet Leoben, Austria; ³South China University of Technology, China; ⁴Tallinn University of Technology, Estonia

Additively manufactured metallic materials exhibit excellent mechanical strength. However, they often fail prematurely owing to external defects that act as sites for crack initiation. Cracks then propagate through grain boundaries and/or cellular boundaries that may contain brittle second phases. In this work, the premature failure mechanisms in selective laser melted (SLM) materials are studied. A submicron structure is introduced containing semicoherent precipitates distributed in a discontinuous but periodic fashion along the cellular boundaries. Alternatively, martensitic phases are used to create alloys with modulation of phases and different strengthening mechanisms. The observed hierarchical microstructure combining different phases spanning over different length scales, consisting of remelted zones and track core regions at the macro-scale, regions with elongated columnar grains and equiaxed grains at the micro-scale, martensitic laths at the submicron-scale, and a high density of dislocations and stacking faults at the nano- and atomic scale leads to outstanding tensile properties of as-prepared and annealed samples. The mechanisms determining the strength and ductility are discussed in terms of the hierarchical microstructure and internal defects. The cellular structure with a high density of dislocations along their boundaries and the martensitic structure are the reasons for strengthening, while the hierarchical microstructure helps to obtain appropriate ductility. Furthermore, martensitic transformation induced plastic bending of residual FCC plates helps to balance the different plastic strains within the heterogeneous structure. This work provides a material design approach for creating hierarchically structured additively manufactured materials with improved strength-ductility tradeoff provided that premature failure is alleviated.

8:15 AM SF02.16.02

Development and Characterization of a Personalized 3D-Printable Bioactive Splint Christian Schmid¹, Leif Steuernagel², Markus Ehrleben¹ and Thomas Schmiedinger¹; ¹University of Applied Sciences Kufstein Tirol, Austria; ²Clausthal University of Technology, Germany

A challenge of combined traumata is, that these situations may require contradictory interventions. Open fractures or fractures in combination with burns requires on one hand a stabilization of the fracture and on the other hand a treatment of the superficial injury. Common therapeutical approaches may lack the ability, to fulfill both requirements at the same time.

The aim of the paper is to develop and characterize a 3D-printable bioactive splint. This bioactive device ensures splintage in combination with the healing stimulation of superficial injuries (e.g. skin abrasion, burn). By creating a digital model of the affected body part, an individualized splint can be realized. Stimulants for healing support are transported through a permeable membrane. This membrane enables an exchange of stimulants to the affected region. The University of Applied Sciences Kufstein develop the design of the splints. A digital model of the affected body part is generated by 3D-scanning. The resulting point cloud of the surface is used for designing the splint. Reservoirs for healing stimulants are added at the individual positions. Standardized connectors are used for enabling the application of standardized medical devices. Polymeric filament blends are fabricated by Technical University of Clausthal. The filaments are processed on a material extrusion machine.

The fabricated bioactive splint enables a personalized design. This approach can support the therapy of combined traumata by resolving contradictory requirements, thus, the approach may have a positive effect on the healing duration.

8:30 AM SF02.16.03

Tailoring Thermal Post-Treatments for Additively Manufactured Nickel Superalloy Alloy 718 Sneha Goe^{1,2}, Uta Klement³ and Shrikant Joshi²; ¹Paul Scherrer Institute, Switzerland; ²University West, Sweden; ³Chalmers University of Technology, Sweden

Electron beam melting (EBM) is a powder bed fusion (PBF) based additive manufacturing technology which has been gaining increased popularity for manufacturing complex customized parts for various sectors such as aerospace, medical etc. An interesting candidate to process using EBM technique is Alloy 718, which is a nickel-based superalloy extensively used in aerospace sector. Irrespective of the choice of processing conditions, EBM processed Alloy 718 is almost always subjected to thermal post-treatments to resolve challenges associated with formation of detrimental defects and/or phases, microstructural inhomogeneity, as well as to achieve the required mechanical response for demanding applications. However, the post-treatment (hot isostatic pressing, HIP and heat treatment, HT) procedures employed are those typically used for castings. This is also reflected in the ASTM F3055 standard for PBF Alloy 718, which appears to adopt the long time-temperature schedules applied for castings. However, this procedure might not be most appropriate and perhaps excessive for EBM Alloy 718 builds.

Therefore, the objective of this study was to investigate the possibility of shortening the duration of post-treatment from the typically long protocols suggested in the above ASTM standard. Results from a detailed study of microstructure evolution during post-treatment revealed possibility of significantly reducing the time for post-treatment. A pathway for further shortening the post-treatment by combining different post-treatment steps into one uninterrupted HIP cycle was also explored. The above results were further substantiated by the mechanical response of EBM Alloy 718 builds subjected to varied post-treatment protocols. Furthermore, such a shortened protocol was found to be robust when applied to EBM builds with distinctly different starting microstructures.

8:45 AM SF02.16.05

Quantitative Percussion Diagnostics for Evaluating Porosity and Roughness of Cold Sprayed and Laser Deposited Materials Mahsa Amiri¹, Grant A. Crawford² and James C. Earthman¹; ¹University of California, Irvine, United States; ²South Dakota School of Mines and Technology, United States

Quantitative percussion diagnostics (QPD) has been used successfully in a number of applications for non-destructive evaluation of structural integrity. This technique involves a rod that is actuated to tap on a specimen with a given kinetic energy. The resulting mechanical response of the specimen as a function of time is measured using a piezoelectric force sensor and the mechanical energy returned to the rod is then analyzed. Because contact with the specimen is on the order of a few hundred microseconds, QPD can be used in situations and for specimen conditions (e.g. high temperature) that are not feasible for other nondestructive testing methods. The objective of the present study was to evaluate the use of QPD for characterization of defects in specimens fabricated using two additive manufacturing methods, i.e. cold spray deposition and laser powder directed energy deposition (LPDED). Cold spray specimens were produced using commercially pure nickel with varied process conditions including gas type (i.e. helium and nitrogen) and deposition rate. In addition, a Ti-6Al-4V specimen was manufactured using LPDED with varying porosity content. All specimens were characterized using both QPD and destructive methods (i.e. cross-sectional metallography) to compare results for observed defect characteristics. Cold spray specimens exhibited a lower energy return when they contained more porosity and/or surface roughness. Microscopic plastic deformation at highly porous surfaces was indicated during percussion testing that reached a saturation level after repeated percussion. Overall, the results showed that QPD can effectively evaluate cold spray and LPDED specimens for porosity and surface roughness.

9:00 AM SF02.16.07

Direct Observation of Crack Formation Mechanisms with *Operando* Laser Powder Bed Fusion X-Ray Imaging Steven Van Petegem¹, Hossein Ghasemi Tabasi², Charlotte de Formanoir², Jamsap Jhabvala², Samy Hocine¹, Eric Boillat², Navid Sohrabi², Federica Marone¹, Helena Van Swygenhoven¹ and Roland Logé²; ¹Paul Scherrer Institute, Switzerland; ²EPFL, Switzerland

Laser powder bed fusion (L-PBF) is a versatile additive manufacturing process that can print geometrically complex metal parts for a variety of applications. However, poor control of defect formation during processing hampers its widespread industrial adoption. Many materials suffer from a high crack susceptibility during L-PBF, which results in degraded mechanical properties, and is an obstacle to the certification of critical parts.

The CM247LC nickel-based superalloy is a gamma-prime-strengthened Ni superalloy, which is of particular interest due to its excellent mechanical, creep, wear, and oxidation properties at both ambient and elevated temperatures. However, this alloy contains high amounts of Al and Ti and is considered vulnerable to cracking due to L1₂ Ni₃ (Al, Ti) precipitation. In literature, several mechanisms are reported to be responsible for cracking during the manufacturing of CM247LC alloy.

In order to unveil those cracking mechanisms, we employ, for the first time, high-speed synchrotron X-ray imaging in combination with a miniaturized L-PBF set-up that reproduces real processing conditions (Hocine et al. *Materials Today* 34 (2020) 30-40). This unique setup provides *operando* imaging of crack formation during L-PBF. These measurements are complemented by post-mortem inspection of crack morphology and analysis of the chemistry around the cracks. Furthermore, finite elements simulations were performed to obtain the evolution of the local temperature during printing. The simulations are validated by *operando* X-ray diffraction-based measurements (Hocine et al. *Additive Manufacturing* 24 (2020) 101194). The results provide, for the first time, direct evidence of the occurrence of solidification and liquation cracking in CM247LC.

9:15 AM SF02.16.08

Changes on Textural Properties of Additively Manufactured IN718 During High Temperature Homogenization Process Selda Navir¹, Bertrand Max², Simon Perusin² and Todd A. Palmer¹; ¹The Pennsylvania State University, United States; ²IRT Saint Exupéry, Institut de Recherche Technologique, France

Heat flow direction during Additive manufacturing plays an important role while shaping the textural properties of the build samples. The grain structure of nickel-base alloys fabricated using powder bed fusion additive manufacturing processes display a preferred orientation along heat flow direction that usually overlaps with building direction. These highly oriented grains with strong orientational dependencies can cause anisotropy in the properties of the final components. Age-hardenable nickel base alloys, such as IN718, undergo a series of high-temperature post-process heat treatments in order to obtain their strength. However, the effectiveness of these high-temperature heat treatments in altering the grain structures and removing the preferential grain orientations is not well established. Through a series of high-temperature heat treatments at temperatures between 1050C and 1200C, the evolution of the as-deposited grain structure across different orientations with respect to the build direction was evaluated. Surface textures along the build direction rotated from a prominent [001] to [011] direction while the texture perpendicular to build direction remained unchanged along the [011] with increasing temperatures and times. At the same time, the grain sizes and morphologies changed along this same direction transitioned from elongated to equiaxed grains, matching those observed on the plane normal to this orientation.

9:30 AM SF02.01.11

3D Printed Surface Topography to Achieve On-Demand Wettability and Separation Bingchen Wang^{1,2}, Cliff Kowall¹ and Lei Li¹; ¹University of Pittsburgh, United States; ²University of Wisconsin–Madison, United States

The biomimetic superhydrophobic and superoleophobic surfaces require the microscale and nanoscale hierarchical surface textures, combined with coatings with low surface energy. While it has always been difficult and expensive to fabricate the superwetting surfaces with well-controlled textures via conventional manufacturing techniques, 3D-printing serves as a time-efficient and cost-efficient alternative. Here, a novel microscale re-entrant surface topography is successfully fabricated by two-photon polymerization (2PP) 3D-printing. On-demand wettability of various liquids has been achieved on the single re-entrant surface. For a given liquid, the re-entrant angle can be precisely manipulated to be either smaller than the liquid CA on the flat surface to achieve dewetting, or larger than the liquid CA on the flat surface to achieve wetting. The 3D-printable microscopic repeating re-entrant surface, which is difficult to make by conventional techniques, has been demonstrated to further enhance the desired on-demand surface wettability. Moreover, efficient on-demand separations of liquid mixtures with high flux are enabled by the 3D-printed separation membranes with the repeating re-entrant structures, which is critical for wastewater treatment in the chemical industry.

SESSION SF02.17: Additive Manufacturing Techniques, Characterizations, and Applications VIII
Session Chair: Kun Fu
Tuesday Morning, December 7, 2021
SF02-Virtual

10:30 AM SF02.17.01

FFF 3D Printing of Filled Thermoplastics and Thermoreversible Thermosets Luis Arciniaga, Piaoran Ye, Krishna Muralidharan, Barrett G. Potter, David S. Margolis, John A. Szivek and Douglas A. Loy; The University of Arizona, United States

In order for 3d printing to realize its potential for distributed manufacturing, it must be possible to make parts with acceptable mech. properties, use local materials, and recycle or rework printed materials. Fused Filament Fabrication (FFF) printing of thermoplastics is generally limited by poor adhesion between layers in prints. Composite filaments for FFF are difficult to make and use due to the challenges in mixing highly viscous molten thermoplastics with filler and the inflexibility of the resulting filled filaments. Soln. processing of thermoplastics facilitates homogeneous incorporation of filler, but introduces addnl. process steps, creates a solvent waste stream and potentially degrades composite performance through plasticization by residual solvent. Thermoreversible thermosets provides a soln. to all of these problems. These highly cross-linked resins have thermal weak-links that break apart at higher temps. and can reform to re-establish crosslinks once the temp. is reduced. The most common weak-link is the Diels-Alder cycloadduct of maleimides and furans that form at room temp. and exhibit a reversion temp. of 100°C. In our study, we have prepd. and mech. tested composites based on PLA, ABS, TPU, and bismaleimide-tetrafurfuryl thermoreversible thermosets with silica, silicate minerals, and tricalcium phosphate.

10:45 AM SF02.17.02

Design of Soft Homocomposite Silicone Gels for 3D Printed Architectures with Magneto-Capillary Reconfiguration Lilian B. Okello¹, Sangchul Roh², Joseph B. Tracy¹ and Orlin D. Velev¹; ¹North Carolina State University, United States; ²Cornell University, United States

This talk will present the design of a new class of smart elastomeric architectures that undergo complex reconfiguration and shape change in applied magnetic fields. These magnetoactive soft actuators are fabricated by 3D printing with Homocomposite Thixotropic Pastes (HTPs) of capillary ink consisting of silicone microbeads, liquid silicone and water [1,2] Superparamagnetic and ferromagnetic nanoparticles are embedded inside the microbeads before curing to render the resulting ink magnetically active without compromising its mechanical properties. The mechanical stability of the printed and cured structures as well as their extensibility to attain maximum possible actuation distance is achieved by optimizing the HTPs material moduli. We will discuss how the magnetic particle loading into the microbeads, volume of liquid polymer precursor used for capillary bridging and controlled level of polymer crosslinking, can be adjusted to fabricate 3D printed structures which are very soft, yet strong enough to withstand many cycles when actuated by external magnetic fields. We will show that the printed meshes and strands are much softer and more flexible than those fabricated by merely reducing crosslink density of bulk PDMS. This ultrasoft material is biocompatible and has tunable mechanical characteristics, which make it suitable for biomedical and soft robotics applications. The HTP 3D printing method makes possible the fabrication of soft architectures with different actuation modes, such as isotropic/anisotropic contraction and multiple shape changes [3]. The cyclic actuation of these objects can be modulated to mimic the pumping mechanism like that seen in heart and lung muscles, while the moduli can be tuned by design to match that of live tissues. Specifically, magneto-capillary actuators can be reversibly laterally contracted and expanded by controlling the normal magnetic field applied from below the vessel. Similar architectures that reconfigure in magnetic fields in response to external stimuli could find a broad range of applications, such as making 2D auxetic materials, soft actuators and soft robots with non-contact actuation.

[1] S. Roh, D. P. Parekh, B. Bharti, S. D. Stoyanov and O. D. Velev, *Adv. Mater.* **29**, 1701554, 1 (2017).

[2] S. Roh and O. D. Velev, *AIChE J.* **64**, 3558-3564 (2018).

[3] S. Roh, L. B. Okello, N. Golbasi, J. P. Hankwitz, J. A.-C. Liu, J. B. Tracy and O. D. Velev, *Adv. Mater. Technol.* **1800528**, 1 (2019).

11:00 AM SF02.17.03

Hierarchically Structured Composite Fiber for Thermal Regulated Textiles and Beyond Weiheng Xu, Dharneedar Ravichandran, Sayli Jambhulkar, Yuxiang Zhu and Kenan Song; Arizona State University, United States

Multilayered polymer nanoparticle composite (PNC) has shown potential in enhancing thermal and electrical properties. Most widely used manufacturing techniques include layer-by-layer coating, filtration, and ice-templating. Here, we introduce a new scalable manufacturing technique including both forced assembly and dry-jet-wet fiber spinning processes. Multipliers were designed and fabricated with metal 3D printing. The resulting continuous fiber, approximately 100 μm in diameter, consists of 4 to 512 alternating layers of composite A and composite B. Depending on the fabrication process, each layer's thickness can be controlled from a few micrometers to hundreds of nanometers. To demonstrate the fiber's potential as a thermally regulated textile, boron nitride (BN) and polyvinyl alcohol (PVA) were chosen as materials A and B. The alternating structure enabled continuous pathways of confined BN for high thermal conduction within flexible PVA matrices. By changing A and B materials, alternating layers of porous structure also showed excellent mechanical stability and thermal insulating behavior. Through varying the material selection for A and B, including nanoparticle and polymer, this fabrication technique can be applied to numerous applications with multilayered structures.

11:15 AM SF02.17.04

Multichannel-Electrochromic Data Transmission Analyzed by Computer Vision for Smart Contact Lens on 3D Printed Template Moobum Kim, Jeonghun Yun, Jia Li, Yeongae Kim and Seok Woo Lee; Nanyang Technological University, Singapore

In the 4th industrial revolution, the market size of wearable devices is growing dramatically with the recent advances in the smart healthcare system. Users receive the notification from the device by sound or vibration when the real-time sensor detects a sudden change in vital signal or danger from the surrounding. In the wearable device market, wristwear and eye-headwear take more than 60% of the whole market of wearable devices. Among them, the market size of the smart contact lens can be extended with the advantage of important and diverse vital signs from eye and tear. Examples of those elements involve ions, such as sodium and potassium, organic molecules, such as glucose, and biomolecules. However, in the past research, wireless communication was used to transfer the data from the sensor in the smart contact lens. Also, it required a complex circuit containing an antenna and receiver inside and outside. In previous our group's research, the only single channel was suggested with a limited amount of data transmission for electrochromic data transmission.

Here, a multi-channel electrochromic data transmission system on the 3D printed template is suggested. 3D printer was used to manufacture the template

having eight channels in one procedure instead of a complicated and multi-step process. A 3D printed template provided more strength to sustain unintended bending or folding of contact lenses. The device was made with eight electrochromic channels and one reference electrode. The color of each electrode was changed between blue and transparent. Electrochromic channels were used to transfer the diverse and complex signals to the user. 256 (28) different signals can be expressed theoretically at least, and the number of signals has the potential to be increased by controlling the color change in three or four steps. Also, the Prussian Blue (PB)'s electrochromic performance was characterized, and various color-changing combinations were realized as an 8-bit barcode pattern by controlling each channel's voltage. For example, 10110001 was changed to 11110001 for transferring different signals to the user. Furthermore, the video of eight-channel color change was taken, and color change patterns were recognized by video processing using Python with OpenCV, one of the libraries in Python to solve the computer vision problems.

11:30 AM SF02.17.05

Polymer-Assisted 3D Printing of Magnetocaloric Cooling Devices Vaibhav Sharma, Lilly Balderson, Radhika Barua, Ravi L. Hadimani and Hong Zhao; Virginia Commonwealth University, United States

As the key component of a magnetic refrigerator, magnetocaloric regenerators (also known as heat exchangers) consist of magnetocaloric materials (MCM) with voids and channels to enable efficient heat transfer to a heat-exchanger fluid. To date, research efforts to produce magnetocaloric regenerators are mainly focused on packed particle beds and plane plates that can be stacked and separated by spacers to provide channels for the heat-exchanger fluid. Both structures possess inherent processing challenges that reduce their performance once integrated into a device. Powder bed fusion-based additive manufacturing methods, such as selective laser sintering, on the other hand, are expensive; and the melting and re-crystallizing of the magnetic particles changes the magnetic and crystalline phases and induces defects in the printed structures.

To address these unique challenges, in this work, we have fabricated magnetocaloric cooling devices using a polymer-assisted 3D printing process followed by a two-stage sintering post-treatment. The printing ink consists of magnetocaloric particles, a sacrificial polymer binder, and a tri-solvent system. Preliminary experiments were conducted using magnetocaloric nanoparticles of nominal composition, $\text{La}_{0.6}\text{Ca}_{0.4}\text{MnO}_3$. The solvents modulate the rheology of the printing ink to facilitate the 3D printing process. The polymer binder (polyethylene glycol or PEO) holds the 3D printed magnetic materials in place after solvent removal. A low-temperature sintering process removes the polymer binder, and a high-temperature sintering process fuses/bonds the magnetic particles inside the printed 3D architectures. Thermogravimetric analysis (TGA) is used to determine the processing condition of the sintering. Results indicate that the magnetocaloric response, i.e., the magnetic entropy change upon application or removal of a magnetic field, exhibits a small difference between the unprocessed MCM powders and the 3D printed devices, which demonstrates the effectiveness of this fabrication process. Compared to other metal additive manufacturing methods, this approach eliminates the complexity of powder handling, expensive laser or e-beam systems, and extremely delicate green parts for powder removal (e.g., binder jet 3D printing). With the inherent advantage of creating spatially designed channels and structures, this polymer-assisted 3D printing scheme provides a promising additive manufacturing platform for high-performance magnetocaloric cooling devices.

11:45 AM SF02.17.06

Late News: In Operando X-Ray Diffraction Studies of Metal Additive Manufacturing Adrita Dass and Atieh Moridi; Cornell University, United States

Understanding the dynamic solidification behavior during metal additive manufacturing (AM) is essential as it directly influences final microstructures, defects and therefore mechanical properties of the part. Many efforts in this domain are based on numerical and computational approaches. Some studies focus on experimental determination of these parameters using in operando monitoring including pyrometry or IR imaging, which fail to provide sub-surface information.

Novel in-operando synchrotron x-ray experiments at different spatial and temporal resolutions provide an unprecedented opportunity to develop a new understanding of the underlying physics of the AM process and solidification in cooling rates applicable to beam-based AM. Here we demonstrate a novel approach using in operando synchrotron x-ray diffraction to analyze the solidification process by tracking the evolution of the mushy zone during a single line scan of Inconel 625. Using this approach, we calculate the melt pool and mushy zone dimensions, along with real-time cooling rates, all by virtue of tracking real-time changes in lattice parameters. Finally, our work aims to establish a link between the transient 'mushy zone' formed during solidification for prediction of defects inside the final microstructure of the AM parts. Results are corroborated with microscopy analysis of the printed structures and show good agreement. Future experiments to study material behavior during extreme heating and cooling rates of AM process will be discussed as a tool to develop new materials for AM.

12:00 PM SF02.17.07

Late News: 3D- Printing of Li-Ion Conductive Oxide Solid Electrolytes Erika Ramos; Lawrence Livermore National Laboratory, United States

Significant advances in battery technology requires electrochemistry that goes beyond conventional Li-ion batteries to further boost energy density and increase safety. All-solid-state lithium battery (ASSLB) technology, with the integration of solid-state electrolytes (SSEs), has the potential to provide higher energy density, better safety, and longer cycle life. Significant progress has been made for ASSLBs by the development and optimization of SSEs that can provide efficient Li-ion conduction while mitigating the problems of leakage and high flammability associated with the organic liquid electrolytes currently used in commercial Li-ion batteries. Among the different chemistries employed as inorganic SSEs, e.g., sulfides and halides, oxides are considered promising SSE candidates for ASSLBs due to their chemical stability and ionic transport properties. Among the reported inorganic solid Li-ion conductive oxides, the garnet-like $\text{Li}_{6.4}\text{La}_3\text{Zr}_{1.4}\text{Ta}_{0.6}\text{O}_{12}$ (LLZTO) cubic structure has received increasing attention due to its chemical stability against lithium metal, high lithium ion conductivity (10^{-3} S/cm at 25°C) and wide electrochemical window.

ASSLBs are difficult to process by traditional manufacturing strategies due to the brittleness of SSE ceramic materials, poor solid-solid contact (SSE/electrodes), and electrolyte-electrode stability issues; as a result, battery performance is far from ideal. The advancement in novel manufacturing techniques such as 3D printing has enabled the assembly of electrodes and SSE materials in more complex geometry configurations, with intimate solid-solid contact and lower interfacial resistance. Particularly, direct ink writing (DIW), is the most widely used additive manufacturing method due to its low cost, easy operation, and broad applicability. Here, we developed different ink formulations with desired rheological properties that enable DIW 3D printing of the LLZTO solid electrolyte with varying features. Different additives such as Al_2O_3 , SiO_2 , and Li_3BO_3 and post-sintering approaches were investigated to boost the LLZTO's density and improve battery performance. These inks were used to 3D-print different patterns, which after sintering revealed thin, nonplanar, intricate architectures composed of LLZTO SSE. Using the herein developed 3D-printing ink formulations to further study and optimize electrolyte structure and properties could lead to the advance of batteries with low cell resistance and higher energy and power density.

12:15 PM SF02.17.08

Automated Support Removal and Surface Finishing for Additively Manufactured Ti-6Al-4V Subbarao Raikar, Steven DiGregorio, Robert Hoffman and Owen Hildreth; Colorado School of Mines, United States

The advent of 3D printing has widened the design space and complexity of parts/assemblies manufactured using Ti-6Al-4V (Ti64) alloy. The complex designs manufactured using additive manufacturing (AM) inevitably have sacrificial support structures that are challenging or inaccessible to remove using traditional methods, i.e., milling, electrical discharge machining, or using a rotary tool. The removal of supports accounts for almost 50 percent of the post-processing cost. With a high demand for one-of-a-kind parts in the medical and aerospace industries, there is a need to develop faster, cheaper, and scalable ways to remove supports. This work introduces a novel, self-terminating etching process for support removal for AM Ti64 parts. During heat treatment, a corrosion agent is diffused into the part to a depth equal to at least half of the support thickness. The corrosion products formed during the heat treatment are then dissolved chemically. The etching solution dissolves only the corrosion products and not the base metal. The effect of the process on the surface finish and the mechanical properties is studied in this work, along with the process kinetics. This work also describes a COMSOL Multiphysics simulation developed to study the impact of part geometry and position on the support removal process. In summary, a novel approach to remove supports from additively manufactured Ti64 parts is demonstrated to decrease costs and further expand the design space for additively manufactured Ti64 parts.

12:20 PM SF02.17.10

3D Printed Schwarzites for Nanoplastics Water Remediation Raphael M. Tromer¹, Bramha Gupta², Rushikesh Ambekar², Partha Ghosal², Rupal Sinha², Abhradeep Majumder², Partha Kumbhakar², Pulickel Ajayan³, Douglas S. Galvao¹, Ashok Gupta² and C S. Tiwary²; ¹Universidade Estadual de Campinas, Brazil; ²Indian Institute of Technology Kharagpur, India; ³Rice University, United States

Nanoplastics contamination has increasingly become one important environmental problem because of their presence in rivers and oceans, toxicity and difficulty in separation and removal. Here we report the development of a 3D printed water filter system [1], which is topologically based on schwarzites, which can perform as an efficient nanoplastic scavenger. Schwarzites are mathematical, 3D porous solids with periodic minimal surfaces having negative Gaussian curvatures. The atomic-scale models obtained from molecular dynamics simulations are converted into .stl format. This approach has been proved effective to other classes of 3D printed materials [2-4]. The FlashForge Adventure 3 Printer (Fused Deposition Modeling) was used to fabricate the water filters. The ABS (acrylonitrile butadiene styrene) filament used to print the filter was melted in the extruder at 210 °C and extruded through a nozzle onto the heated bed. The proposed filtration mechanism of surface-charge-based water cleaning was further validated using ab initio and molecular dynamics simulations. The fabricated filters proved to be effective in removing nanoplastics from samples from various sources, such as sea, river, and pond. These new classes of 3D printed water filters represent a significant low-cost, energy-efficient, and feasible advanced system to address the problem of nanoplastics water remediation.

[1] B. Gupta, R. S. Ambekar, R. M. Tromer, P. S. Ghosal, R. Sinha, A. Majumder, P. Kumbhakar, P. M. Ajayan, D. S. Galvao, A. K. Gupta, C. S. Tiwary, RSC Advances 11, 19788 (2021).

[2] S. M. Sajadi, P. S. Owuor, S. Schara, C. F. Woellner, V. Rodrigues, R. Vajtai, J. Lou, D. S. Galvão, C. S. Tiwary, and P. M. Ajayan, Adv. Mater. 30, 1704820 (2018).

[3] S. M. Sajadi, C. F. Woellner, P. Ramesh, S. L. Eichmann, Q. Sun, P. J. Boul, C. J. Thaelmlitz, M. M. Rahman, R. H. Baughman, D. S. Galvao, C. S. Tiwary, and P. M. Ajayan, Small 15, 1904747 (2019).

[4] R. S. Ambekar, E. F. Oliveira, B. Kushwaha, V. Pal, L. D. Machado, M. Sajadi, R. H. Baughman, P. M. Ajayan, A. K. Roy, D. S. Galvao and C. S. Tiwary, Addit. Manuf. 101628 (2020).

12:25 PM SF02.06.01

Textile Force Sensitive Resistors by Inkjet Printing for Wearable Tactile Sensors Beomjun Ju, Inhwon Kim, Braden Li, Caitlin Knowles, Amanda Mills, Landon Grace and Jesse Jur; North Carolina State University, United States

Pressure sensors for wearable healthcare devices, particularly force sensitive resistors (FSRs) are widely used to monitor physiological signals and human motions. However, current FSRs are not suitable for integration into wearable platforms and are expensive to process. This work presents a novel technique for developing textile force sensitive resistors (TFSRs) using a combination of inkjet printing of metal-organic decomposition silver inks and heat pressing for facile integration into textiles. The TFSR structure consists of a thermoplastic polyurethane (TPU) membrane sandwiched between two nonwoven textiles with inkjet printed electrodes. The insulating void between the top and bottom electrodes creates an architected piezoresistive structure. The structure functions as a simple logic switch where under a threshold pressure the electrodes make contact to create conductive paths (on-state) and without pressure returns to the prior insulated condition (off-state). The TFSR can be controlled by arranging the number of layers and hole diameters of the TPU spacer to specify a wide range of activation pressures from 4.9 kPa to 7.1 MPa. For a use-case scenario in wearable healthcare technologies, the TFSR connected with a readout circuit and a mobile app shows highly stable signal acquisition from finger movement. According to the on/off state of the TFSR with LED bulbs with different weights, it can be utilized as a textile switch showing tactile feedback. When integrated with a physical device or object, the sensor design has a high potential for registering tactile interaction as a means to quantify health-related behaviors such as medication adherence or use of a self-monitoring device.

SESSION SF02.18: Additive Manufacturing Techniques, Characterizations, and Applications IX

Session Chair: Kun Fu

Tuesday Afternoon, December 7, 2021

SF02-Virtual

1:00 PM *SF02.18.01

Robotic Metamaterials: Additive Fabrication for Multi-Materials and Multi-Functionalities Xiaoyu Zheng; University of California, Los Angeles, United States

Material properties are governed by their chemical composition and intrinsic crystalline structures. This fundamentally limits material properties and their applicability creating trade-offs for selecting materials for product applications, from structural components to antennas and robots.

Metamaterials represent the concept of utilizing artificial material building blocks to create desirable properties and behaviors derived from three-dimensional architectures and compositions. Additive manufacturing is widely used to construct complex 3D objects and architectures made of metal, plastic, or ceramics from a digital computer model. However, it is presently difficult to combine different materials (structural, dielectric, conducting and ferroelectrics) to create a complex device with multiple functionalities.

In this talk, I will outline a suite of new material processing and additive fabrication routes to rapidly assemble complex topology, multi-scale features and multi-material attributes. I will present high speed printing techniques that enable the rapid patterning of a variety of structural, electronic and ferroelectric materials into complex architectures, not limited by tool-path, embedding and wiring requirement. Attention is focused on how these additive manufacturing techniques, combined with computations and artificial intelligence, unlock new material discovery and design freedoms, which leads to new classes of structural and ferroelectric materials, where presently unachievable mechanical and energy conversion behaviors can be created. Next, I will present future device architectures derived from these artificial building blocks, from materials for energy absorption, wave guiding, to smart transducers and autonomous micro-robots.

1:30 PM SF02.18.02

Adaptive Auger Extrusion-Based 3D Printing of Ceramics with In-Line Viscosity Monitoring [Chao Liu](#) and Junjun Ding; New York College of Ceramics at Alfred University, United States

Ceramics are extensively used in applications due to their excellent mechanical and chemical performance, such as outstanding compressive mechanical strength, high thermal stability, and corrosion resistance. Extrusion-based 3D printing methods are promising for digitally manufacture ceramics due to ease of use, good adaptability to different materials, and high solid loading of slurries. The auger extrusion method, extruding the slurry by a screw, not only provides accurate control of the slurry flow including consistent flow rate and precise start and stop, but also possesses the ability of mixing multi feedstocks into a homogeneous slurry before being extruded. The viscosity of the slurry determines the printability of the slurry in the auger extrusion-based 3D printing process. However, little research has focused on the in-line measurement of the slurry viscosity and a feedback system to self-control the viscosity of the slurry. In this work, we fabricate alumina parts using an adaptive auger extrusion-based 3D printing system with an in-line viscosity monitoring and feedback system. A high viscous alumina feedstock and a low viscous ink are fed into the barrel and mixed by the auger screw. The viscosity of the mixed slurry is calculated with an in-line capillary rheometer using measured pressure drop after extrusion. Based on the measured in-line viscosity, the slurry is adaptively controlled by adjusting the feeding ratio of two ceramic feedstocks with different rheological properties. This work enables a speedy development of printable ceramic slurries and provides a quality control in the extrusion-based 3D printing of ceramics.

1:45 PM SF02.18.03

Flexible Core-Shell Fiber Supercapacitors Manufactured by Coaxial Extrusion Printing [Yuqi Gao](#) and Junjun Ding; New York State College of Ceramics, United States

Energy storage devices have a spreading application in various fields, such as soft robotics, human motion monitoring, and smart textiles. Fiber-shaped supercapacitors are especially attractive as an energy storage unit in these applications due to their excellent flexibility. However, fabricating robust fibers with large yields remains a challenge.

In this work, we prepare flexible core-shell fibers via coaxial extrusion printing. Specifically, an extrusion system with a custom-designed core-shell nozzle is used to extrude two separate slurries at the same time. Carboxymethylcellulose sodium salt (CMC) slurry with controlled rheological properties is extruded from the outer channel, while the graphene oxide (GO) slurry is extruded from the inner channel simultaneously. The freeze-drying processing protects GO sheets from agglomeration, providing more efficient chemical reduction. The reduced GO (rGO) sheets are separated and expanded to fill in the CMC sheath, which eliminates the shrinkage of the shell structure and delamination between the CMC sheath and rGO core after drying. CMC is designed as a sheath to package the inner conductive rGO core, as well as a separator to avoid short circuits between two electrodes. We study the influences of the freeze-drying process on the fiber microstructures, and explore the slurry design, fiber quality, reduction condition, and electrochemical performance. The core-sheath structure endows the fiber-shaped supercapacitors with robustness and flexibility. The fabrication method realizes more efficient conducting networks, allowing scalable manufacturing of the core-shell microfiber electrodes.

2:00 PM SF02.18.05

Late News: Exploiting Lack of Fusion Defects for Microstructural Engineering in Additive Manufacturing Jennifer Bustillos and [Atieh Moridi](#); Cornell University, United States

Rapid cooling rates and stochastic interactions between the heat source and feedstock in additive manufacturing (AM) result in strong anisotropy and process-induced defects deteriorating the tensile ductility and fatigue resistance of printed parts. We show that by deliberately introducing a high density of lack of fusion (LoF) defects, a processing regime that has been avoided so far, followed by hot isostatic pressing, we can print Ti-6Al-4V with reduced texture and exceptional properties surpassing that of wrought, cast, forged, annealed, and solution-treated and aged counterparts. Such improvement is achieved through the formation of low aspect ratio α -grains around LoF defects upon healing, surrounded by α -laths. This occurrence is attributed to surface energy reduction and recrystallization events taking place during healing of LoF defects. Using an adaptive domain misorientation approach of electron backscattered diffraction, we resolve the heterogenous distribution of strains in the duplex microstructure in the form of complex dislocation cells, and sub-grains. Our approach to design duplex microstructures is applicable to a wide range of AM processes and alloys and can be used in the design of damage tolerant microstructures.

2:15 PM SF02.18.06

Late News: Fabrication of Nanostructured, Phase Separated, Liquid Crystal-Silicone Polymer Networks Using Direct Ink Writing [Jay M. Taylor](#), Paul V. Braun and Ralph Nuzzo; University of Illinois at Urbana-Champaign, United States

The ability to control the nanoscale internal structures of soft polymers networks during fabrication is challenging. When done, these materials have interesting mechanical, optical, and physical properties. Herein, using direct ink writing, phase separated liquid crystalline networks are 3D printed that exhibit oriented, phase-separated molecular structure. The liquid crystalline domains within the printed material are aligned in the print direction and feature a nanoscale lamellar structure that impacts the materials mechanical and optical properties. At temperatures above the phase transition of the liquid crystal, its nanostructure deteriorates resulting in material softening and loss of optical birefringence. Upon cooling, the nanostructure reforms and its properties return. As a result of the oriented structure, when the printed material is submerged in solvents that swell the liquid crystalline phase, the material expands preferentially in its printed direction. This expansion results in a reconfiguration of the materials structure that can be controlled by adjusting its print direction and orientation during fabrication. The results and strategies presented herein, will be of interest to those studying how additive manufacturing can be used to design polymers with aligned and oriented structures.

2:30 PM SF02.18.07

Late News: Direct Ink Writing of TiO₂-based Foams in Microgravity Conditions for Lunar Habitation Applications [Ellena D. Gemmen](#), Samuel

Cyphert, Guy J. Cordonier and Kostas Sierros; West Virginia University, United States

With the increasing interest in long-term human habitation of space on the lunar and Martian surfaces for both research and commercial interests, there is a growing need for cutting-edge, versatile materials that can be modified to be used for more than a single purpose. TiO₂ based foam and microemulsion inks have been shown to have many advantageous properties, including: photocatalyzation with the UV spectra, filtration, habitat repair/reinforcement, and solar cell creation.

In this report, the first successful 3D printed metal oxide nanoparticles aqueous-based foams performed in microgravity are recorded. While undergoing parabolic flight and simulating microgravity in an aircraft, a Direct Foam Writing (DFW) method was used to print TiO₂ foam in line patterns onto glass substrates. Initial characterization of the foam's properties is stated. The printed foam's cross-sectional area, contact angle of DI water, and surface roughness is affected by microgravity as compared to Earth gravity, displaying less deflation and lower amount of spread after being deposited on the substrate.

As a result of the experiment's success, the WVU Microgravity Research Team plans to test the viability of two additive manufacturing techniques; Cold Spray Additive Manufacturing (CSAM) and spray atomization of a TiO₂-based foaming microemulsion.

SESSION SF02.19: On-Demand
Sunday Morning, December 5, 2021
On-Demand

8:00 AM *SF02.04.02

Grayscale Digital Light Processing 3D/4D Printing—A Novel Method to Create Functional Parts Liang Yue, Xiao Kuang, Xiaohao Sun, Stuart M. Montgomery and Hang (Jerry) Qi; Georgia Institute of Technology, United States

Digital light processing (DLP) based 3D printing is an additive manufacturing method that utilizes light patterns to photopolymerize a liquid resin. Typical DLP method uses a digital micromirror device (DMD) to control light pattern at the resolution around 20-50 microns and cure a thin resin in 1-5s. DLP thus has the advantage of high speed and high resolution. However, conventional DLP method is not suitable for multimaterial printing because it uses a single vat of resin. In recent years, our group has explored using light grayscale (or light intensity) to control local properties of printed parts to achieve multimaterial-like printed parts. The advantage of this grayscale DLP (g-DLP) method is that it still uses a single resin vat and thus retains the advantages of conventional DLP printing. In this talk, we will first present a few examples of how to use grayscale light together with novel resins to achieve multimaterial functional parts, including 4D printing of inflatable structures, 3D printing of cold-draw shape memory polymers, etc. Second, As the graded light intensity can create concentration gradients of the different chemical species during photocuring, the spatial resolution as well as the physical property resolution in g-DLP printing can be affected. We will briefly present a reaction-diffusion model coupled with radiative transfer to analyse the effects of component diffusion and its impact upon the resulting mechanical property resolution on a sub-pixel and macro scale. Third, the capability of spatially control mechanical properties offers a vast design space for 4D printing to create shape-changing devices. We present our recent efforts of using evolutionary algorithm and machine learning to rapidly explore the design space and to obtain optimized design. This new design paradigm seamless connects design concepts to the 3D printed shape changing devices. Finally, we will briefly discuss the future work in the g-DLP method.

SYMPOSIUM SF03

3D Printing of Functional Materials and Devices
November 30 - December 8, 2021

Symposium Organizers

John Boley, Boston University
Sohini Kar-Narayan, University of Cambridge
Ethan Secor, Iowa State University of Science and Technology
Yanliang Zhang, University of Notre Dame

* Invited Paper

SESSION SF03.02: Soft Robotic Matter
Session Chairs: Arda Kotikian and Ryan Truby
Tuesday Afternoon, November 30, 2021
Sheraton, 3rd Floor, Fairfax

2:00 PM SF03.02.01

Stretchable HAXEL Arrays Made by Multi-Material Additive Manufacturing [Giulio Grasso](#)¹, Samuel Rosset² and Herbert Shea¹; ¹EPFL, Switzerland; ²The University of Auckland, New Zealand

Soft electrostatic actuators stand out from other classes of compliant transducers thanks to their combination of fast response, high strain, and high power density. Hydraulically-Amplified Taxels (HAXELs) consist of planar polymer pouches filled with dielectric oil, with electrodes patterned on the periphery of both surfaces, and a central stretchable region. Applying a voltage between the electrodes generates an electrostatic pressure that pulls the electrodes together in a zipping motion, thus displacing the fluid towards the center of the actuator, creating a raised bump.

We present the design, fabrication and characterization of stretchable, ink-jet printed, HAXEL arrays. Using additive manufacturing (AM) allows the fabrication of fully-integrated actuators whose design can be rapidly changed. Three inks were developed for a commercially available printer (Jetlab 4XL from MicroFab Inc.). A solution of polydimethylsiloxane (PDMS) and solvent is dispensed in order to deposit 30 μm thick stretchable dielectric layers. 5 μm thick electrodes are patterned by using a suspension of carbon black particles combined with silicone polyglucoside. Fluidic channels and cavities are obtained by printing sub-3 μm thick sacrificial layers from ethyl cellulose. Printing HAXELs requires patterning a stack of at least 6 layers. The sacrificial layer, which defines the fluidic circuit, extends to the edge of the printed structure, where PDMS tubes are temporarily connected. The sacrificial material is removed by injecting ethanol, which is then replaced by a dielectric oil (Envirotemp FR3) at the desired pressure. The HAXELs are finally sealed, and the filling tubes removed.

We printed and tested 2x2 arrays of 5 mm wide square HAXELs. Each actuator is obtained by printing a 100 μm thick stack of the functional materials on a 150 μm thick PDMS substrate. Actuators are less than 1 mm thick after filling with dielectric fluid. We observe 250 μm of free displacement and 30 mN blocked force at 4 kV voltage. These actuators will be integrated into stretchable haptic feedback systems. Inkjet printing enables easily tailoring the geometry of the device to adapt to different location on the body, and to different morphologies between users.

2:15 PM SF03.02.02

Fluidically Innervated Architected Materials for Soft Robot Proprioception [Ryan L. Truby](#), Lillian Chin and Daniela Rus; Massachusetts Institute of Technology, United States

Designing soft sensorized robots with distributed sensing capabilities is essential for addressing long-standing challenges in soft robot control. However, progress in designing soft sensorized robots has been limited due to the inherent multi-material manufacturing challenges of fabricating such devices and the disadvantages posed by many sensing strategies with soft conductive materials. We present a strategy for creating soft sensorized robots through the fabrication of fluidically innervated, architected materials. These structures are 3D printed with distributed, embedded networks of open fluidic channels. The fluidic channels are connected to pressure transducers, which provide an analog voltage corresponding to changes of pressure within the deforming networks. Importantly, our manufacturing method involves one single material: structure, actuation, and sensing capabilities are seamlessly integrated through printed architecture. Here, we first demonstrate our methods for fluidic sensing on well-studied lattices printed from elastomeric and flexible polyurethanes. We then design and characterize fluidically innervated handed shearing auxetics (HSAs), which we use in examples of electrically-driven soft sensorized robots. Finally, we showcase the importance of robust, reliable sensory feedback in an HSA-based soft robotic system that learns its configuration via deep learning. Overall, our methods represent a simple, single-material strategy for sensorizing soft robotic materials that we anticipate will help expedite efforts in the design, fabrication, and control of autonomous soft machines.

2:30 PM SF03.02.04

Late News: On-Board Timing, Memory, and Sensing in Autonomous Cell-Sized Robots Enabled by a Simple Memristor-Based Circuit Friendly to Additive Manufacturing [Jingfan Yang](#)¹, Albert T. Liu^{2,1,3}, Thomas A. Berrueta⁴, Ge Zhang¹, Allan M. Brooks¹, Volodymyr Koman¹, Sungyun Yang¹, Xun Gong¹, Todd Murphey³ and Michael Strano¹; ¹Massachusetts Institute of Technology, United States; ²Stanford University, United States; ³University of Michigan–Ann Arbor, United States; ⁴Northwestern University, United States

Micrometer-scale robots capable of navigating enclosed spaces and remote locations are approaching reality, with a rich literature emerging on externally actuated and supervised agents. To accelerate the advancement of micron-sized robots with greater autonomy, alternatives to conventional top-down lithography, particularly those amenable to assembly by additive manufacturing, are desired for rapid prototyping and access to novel materials. Building upon experimental findings that memristive networks can be rapidly printed on substrates and lifted-off as single, intact microparticles, we herein introduce an alternative design paradigm based on arrays of two-terminal memristive elements that enables autonomous use of memory, sensing, and actuation in robots at the micron scale. The design's simple circuit topology permits the use of facile technologies – such as printing, stamping, and colloidal self-assembly – as well as diverse materials including polymers, bio- and nanomaterials. We validate several memristor-based designs representing key building blocks towards robot autonomy: tracking elapsed time, detecting and timestamping a rare event, continuously cataloguing time-indexed data, as well as accessing the collected information for a feedback-controlled response as in a robotic glucose-responsive insulin for diabetes treatment, as a test problem. Our computational results establish a novel actionable framework for microrobotic design whereby tasks that normally require complex microelectronic circuits can be achieved with self-assembled and printed memristor arrays within single microparticles.

2:45 PM SF03.02.05

Late News: Silicone-Based Support Material for Precision 3D Printing of Soft Silicone [Senthilkumar Duraivel](#) and Thomas E. Angelini; University of Florida, United States

Soft silicone structures are difficult to fabricate using the conventional FDM approach to 3D printing. Without adding rheological modifiers silicone inks, printed features will sag and spread upon deposition from the nozzle. Embedded printing into jammed support materials helps to overcome this challenge by trapping the silicone ink in space as it is printed, eliminating the need for ink additives. However, previously developed support materials for 3D silicone printing exhibit a large interfacial tension against silicone inks, creating instabilities that break up fine features and setting a minimum feature size. These instability-driven breakups can be prevented by developing a jammed support material that is chemically similar to silicone oil. Such a material would enable 3D printing of high-resolution structures having fine feature sizes. In the work presented here, we developed a silicone oil-based support material having tunable rheological properties that can be optimized for embedded 3D printing of soft silicone. We show that by practically eliminating interfacial tension between silicone ink and the silicone-based support material, features as small as 8 microns in diameter can be fabricated; these fine features are indefinitely stable over time. Using this new material we are able to fabricate robust, accurate, and complex structures like a model brain aneurysm for surgical simulation and a functional tri-leaflet heart valve model for potential biomedical applications.

3:00 PM *SF03.02.06

Scalable and Printable Granular Actuators Sophia Eristoff, Sang Yup Kim, Lina Sanchez-Botero, Trevor Buckner and [Rebecca Kramer-Bottiglio](#); Yale University, United States

Soft robots have garnered interest due to their potential ability to change shape in response to changing tasks or environments, be robust to impacts and

falls, conform to the human body without restriction on the natural mechanics of motion, and grasp delicate and diverse objects. Fluidic actuators, which are controlled by the influx of circulating fluids, are the most common artificial muscle technology employed in the soft robotics literature. However, fluidic actuators typically require actuator-source tethering, limiting the mobility of the robot, especially for micro-scale systems. Alternatively, stimuli-responsive materials have been proposed to realize untethered, micro-scale actuation. Such stimuli-responsive materials include hydrogels and shape-memory polymers, among others. However, these material-based actuators are often slow or only expand or contract axially, preventing use in applications that require volumetric expansions.

To address such limitations of existing actuating materials, actuators based on the liquid-to-gas phase change of solvent inclusions encapsulated in a hyperelastic matrix have been realized. These phase-changing inclusion composites fill a gap in the field of material-based actuators by inducing rapid volumetric expansion similar to fluidic actuators, without being tethered to an external fluid source. However, phase-changing inclusion composites have never been demonstrated in micro-scale actuation spaces and generally are not amenable to printing, given the high content of low-viscosity liquid solvent in the mixtures.

In this talk, we will present granular actuators composed of volumetrically expanding grains as a new class of actuator to unlock scalable and printable actuation. A single grain consists of multiple solvent cores encapsulated in a hyperelastic silicone shell (Ecoflex 00-30). At elevated temperatures, the encapsulated solvent vaporizes and increases the internal pressure of the hyperelastic shell, inducing volumetric expansion of the grain. The grains are independently capable of rapid, high-force actuation, and are also easily arranged into granular assemblies to form larger-scale bulk actuators. Finally, the use of grains suspended in a carrier solvent or resin enables compatibility with granular self-assembly and 3D printing techniques, offering the potential to print volumetrically expanding actuators into freeform patterns across scales.

3:30 PM BREAK

SESSION SF03.04: Poster Session: 3D Printing of Functional Materials and Devices
Session Chairs: Stephanie Flores-Zopf, Ramon Sanchez Cruz and Ryan Truby
Tuesday Afternoon, November 30, 2021
8:00 PM - 10:00 PM
Hynes, Level 1, Hall B

SF03.04.01

Ductile All-Ceramic Composites with High Thermal Shock Resistance [Jason Hoffman-Bice](#), Grace Goddard and Randall M. Erb; Northeastern University, United States

Ductile all-ceramics composite materials are at the forefront of the next generation of materials. Typically, engineering ceramics are brittle across working temperatures and do not allow for any deformation, let alone extreme ductility. The ability to have an all-ceramic, with typical ceramic characteristics, that can have ductile behavior, under relatively low temperatures, and maintain structural integrity without catastrophic failure is a unique characteristic that is experimentally explored in this work. Further, thermally conductive filler particles in a ceramic matrix has the potential to provide unique thermal management opportunities for high-powered electronics or hypersonic aircraft. In order to fabricate these materials, a previously developed 3D printing technique is used to align the micro-particles to produce the green-body part, and then run through a sintering process to produce the all-ceramic composite. This work also explores the materials thermal shock resistance that is believed to be directly correlated to the alignment patterns of the microstructure, and the thermal conductivity of the platelets distributed throughout the dominant ceramic matrix. Therefore, the work presented here demonstrates the feasibility of a highly-ductile all-ceramic composite, at relatively low temperatures, that demonstrates good thermal shock resistance.

SF03.04.02

Coaxial Core-Shell Direct Ink Writing of Flexible Sensors [Derrick Banerjee](#)¹, John Burke¹, Han Mei², Chih-Hung Chang², Edward M. Sabolsky¹ and Kostas Sierros¹; ¹West Virginia University, United States; ²Oregon State University, United States

Direct ink writing of 3D structures has many advantages, specifically in this study is the ability to print multiple materials with tailored functionalities in a controllable and single-step process. It further allows for net shape printing in ambient conditions of a wide range of materials normally incompatible with each other or with other printing systems. In this work, custom-designed coaxial nozzles have been 3D printed using a stereolithography printer. These nozzles were then used to co-extrude conductive ink cores within shells of ambient or UV-cured elastomeric shells. Initially, conductive fibers were printed to study the interfaces, curing, and electro-mechanical properties of the dual ink system. Further, the core-shell fibers were printed into strain gages and incorporated within direct ink written 3D soft robotic pneumatic actuators. Infrared spectroscopy, nuclear magnetic resonance, and optical and electron microscopy were performed to further characterize the printed structures.

SF03.04.03

Development of Nanocoated Filaments for 3D Fused Deposition Modeling of Antibacterial and Antioxidant Materials [Adnan Memic](#), Rayan Qurban, Tuerdimaimaiti Abudula, Mazin Zamzami, Ammar Melaibar, Numan Salah and Mohammed Shaaban Abdulwahab; King Abdulaziz University, Saudi Arabia

There is a technological need for materials with improved functionalities to propel new biomedical applications. Some of the outstanding challenges could be solved using three dimensional (3D) printing. However, there is a pressing need for new generation of biomaterials that have unique properties. Combining nanomaterials with natural and synthetic polymers could yield biomaterials with improved properties including the ability to better recapitulate complex architecture, better match native mechanical properties of tissues and even guide the formation of functional tissues. To accomplish some of these goals we have engineered dual nanocoated (Zinc and Silver) filaments using polybutylene succinate (PBS) and lignin as the base polymer blend. We show that this combination of polymers and coating provides strain specific antibacterial activity and antioxidant properties while improving the rheological and physical properties of the composites filaments. Taken together these nanocoated filaments could propel several biomedical applications including aiding design of bracing materials.

SF03.04.04

High Resolution 3D Printed Anion Exchange Membranes—Expanding the Design Space of Electrochemical Reactors [Auston Clemens](#), Megan Ellis, James S. Oakdale, Nikola Dudukovic, Sarah Baker and Eric Duoss; Lawrence Livermore National Laboratory, United States

Electrochemical reactors and separation devices are predominantly planar in nature and limited to basic design space and inability to optimize complex

reactor designs. An explicit limiting component are ion exchange membranes (IEMs) that control transport of selective ions across a physical boundary. IEMs are typically manufactured by evaporation casting ionomers into thin flat sheets; however, three-dimensional ion exchange membranes have the potential for significant improvement in optimized mass transport properties, antifouling capabilities, as well as increasing active interfacial surface areas for membrane electrode assemblies. Here, we present a photocurable anion exchange membrane (AEM) formulation that can be 3D printed with ~100 nm resolution using micro-stereolithography. We optimize the printable formulation by characterizing the ion exchange capacity, ion conductivity, water uptake and dimensional stability as a function of the composition. Printed 3D structures are investigated and operated in diffusion dialysis acid recovery flow cells for continuous recycling of metal contaminated acid. This technology has the potential to enable customizable manufacturing of membrane electrode assemblies for CO₂ electrolysis, unlocking control over structures across multiple length scales to optimize for desired reduction products. This work is performed under the auspices of the U.S. Department of Energy by Lawrence Livermore National Laboratory under Contract DE-AC52-07NA27344 within the LDRD program 19-SI-005. LLNL-ABS-823498.

SF03.04.05

Designing 3D Printed Micro-Actuators for Functionalized Fiber Optics Adia Radecka¹, Alyssa Bradshaw¹, Georgia Kaufman², Rebecca R. Tafoya², Michael Gallegos³, Tim Dallas³, Holly Golecki¹ and Bryan Kaehr^{2,4}; ¹University of Illinois at Urbana-Champaign, United States; ²Sandia National Laboratories, United States; ³Texas Tech University, United States; ⁴Center for Integrated Nanotechnologies, United States

The ability to capture, manipulate and release microscale objects using autonomous systems can enable widespread applications—from microsurgery and selective cell extraction to the assembly of complex microdevices. Microelectromechanical (MEMs) grippers fabricated using semiconductor techniques provide precise and reliable gripping mechanisms but are intrinsically planar and require direct electrical contacts for operation. With continuing development of smart and environmentally responsive materials compatible with 3D printing, cue-driven micro-grippers with high spatial and temporal precision can give rise to biocompatible devices. In this work, we investigate 3D printing of microgrippers based on traditional MEMs designs as well as non-planar, bioinspired architectures. Our aim is to develop robust micro-grippers integrated into imaging/optogenetic devices at the scale of single fiber optics and individual biological cells to enable micro-surgical applications. Using multiphoton lithography, we fabricate multimaterial actuators that incorporate inert skeletal components with hydrogel actuators. We evaluate the response time, accuracy and cyclability of grippers that use temperature and pH responsive hydrogels. Following this optimization, we designed microgrippers that incorporate a photothermal transducer within a thermally responsive gel actuator fabricated on the tip of a 200-micron diameter core fiber. By incorporating 3D printed micro-optics (lenses and reflectors), we show that gripper components can be actuated individually via site-specific photothermal transduction. This work provides a foundation to integrate stimuli responsive mechanical functions with micro-scale optical devices.

SF03.04.06

Hybrid Fabrication of Multimodal Intracranial Probes for Neural Recording and Local Drug Delivery Johannes Gurke¹, Alejandro Camicer Lombarte¹, Tobias Nägele¹, Sam Hilton¹, Roberto Pezone^{1,2}, Emil J. W. List-Kratochvil³ and George G. Malliaras¹; ¹University of Cambridge, United Kingdom; ²Delft University of Technology, Netherlands; ³Humboldt-Universität zu Berlin, Germany

New fabrication approaches for mechanically flexible materials hold the key to advancing the applications of bioelectronics in fundamental neuroscience and the clinic. By combining the high precision of thin film microfabrication with the versatility of additive manufacturing, we demonstrate a straightforward approach for the prototyping of intracranial probes capable of multichannel local field recordings and convection-enhanced drug delivery. The process makes use of parylene-based arrays of neural recording electrodes and a commercial vat polymerizable elastomer, combining to produce a flexible implant. The mechanical and electrical properties of the implant are characterized, and its function is validated in an in vivo rodent model. We show that the implant can modulate neuronal activity in the hippocampus through local drug delivery, while simultaneously recording brain activity by its electrodes. Chronic implantation tests show good implant stability and minimal tissue response one week post-implantation. Our work shows the potential of hybrid neuronal probes combining different manufacturing technologies and paves the way for a new approaches to the development of multimodal probes.

SF03.04.07

High Conductivity Copper Ink-Based 3D Printed Flexible Sensors Saurabh V. Khuje and Shenqiang Ren; University at Buffalo, United States

Recent advancements in the field of flexible electronics, for instance, smart wearables, soft robotics and health monitoring devices has garnered immense attention in the domain of stretchable chemical and physical sensing methods. Amongst the plethora of sensors available, temperature and pressure sensors have been extensively investigated for fulfilling the demand of flexible, light-weight and disposable sensors demonstrating high sensitivities. The sensors of the former category can be utilized for structural-health monitoring, whereas sensors from the latter category can be utilized for pulse monitoring and provide vital information regarding the arterial physical situation of the body in a non-invasive way. A printed and built-in geometry with a capability of detecting stimuli such as temperature, pressure, etc. over a wide range are highly sought-after characteristics for any sensor. These smart components are manufactured using a combination of conductive copper inks and an extrusion-based direct-ink writing technique, onto flexible substrates. The sensors exhibit high sensitivities and show resistance to mechanical stimuli of bending. These demonstrations enunciate the capability of additive manufacturing techniques for flexible electronics.

SF03.04.08

Towards Multi-Material Small-Scale Additive Manufacturing—Fabrication of Semiconducting ZnO and Insulating MgO Microstructures and Their Integration with Metallic Cu by Electrohydrodynamic Redox 3D Printing Mirco Nydegger¹, Alain Reiser² and Ralph Spolenak¹; ¹ETH Zürich, Switzerland; ²Massachusetts Institute of Technology, United States

Combining the unprecedented design freedom in microscale additive manufacturing with the ability to control the chemical nature of each printed voxel could unlock unique possibilities for tailoring mechanical, chemical, electrical, optical and magnetic properties of inorganic microstructures. A current challenge in the field of micro- and nanoscale additive manufacturing is to provide what microfabrication needs: the fast and reliable deposition of a wide range of device-grade materials, from insulators to semiconductors and metals [1]. In addition, on-the-fly switching between different materials classes remains a crucial, yet unsolved problem. Electrohydrodynamic redox 3D printing (EHD-RP) is a novel small-scale additive manufacturing technique, that offers a resolution of 250 nm with feature sizes down to 120 nm [2]. The ink-free approach, based on the on-demand generation of metal ions, enables the local modification of the chemical composition in a voxel-by-voxel fashion. However, so far only the deposition of metals was demonstrated.

We will focus on the challenges involved in expanding the materials range of EHD-RP from Cu and Ag to a wide range of metals, semiconductors and insulators. In particular, the deposition of Zn structures and their subsequent thermal oxidation to semiconducting ZnO will be presented. Together with an analysis of its structure, its optical properties will be assessed by photoluminescence spectroscopy. In addition, the direct deposition of insulating structures will be demonstrated on the example of MgO and first results towards their integration with printed metal conductors will be shown.

In summary, we outline a route towards establishing electrohydrodynamic redox 3D as a toolbox for the manufacturing of multi-material microelectronic devices.

- [1] L. Hirt et al., Additive Manufacturing of Metal Structures at the Micrometer Scale, *Adv. Mater.*, 29(17), 2017.
[2] A. Reiser et al., Multi-metal electrohydrodynamic redox 3D printing at the submicron scale, *Nat. Comm.*, 10(1):1-8, 2019.

SF03.04.10

A Thin-Film Flexible Inkjet Printed Lithium-Ion Battery Exploiting Innovative MXene Material as Current Collector Prisca Viviani, Eugenio Gibertini and Luca Magagnin; Politecnico di Milano, Italy

The Internet of things (IoT) market is a new groundbreaking field that has gained great attention both from the academic and industrial point of view. Progress in this field is deeply interconnected to the possibility of integrating smart devices with everyday objects and instruments, so that they are able to collect process and elaborate data without the need of human input. Therefore, always more demanding energy storage devices able to power such smart objects are needed. However, rigid, conventional batteries, as well as their respective fabrication processes, find limited applications when dealing with wearable electronics. Specifically, one of the major limitations of conventional batteries is, indeed, their rigidity and inadequate mechanical. When patterned electrodes or unconventional substrates are involved, new fabrication strategies are required to overcome limitations of traditional slurry coating electrode processing^[1,2].

In this context, printing of batteries can be framed as a potentially innovative fabrication technique able to combine the benefits of thin-film technology, as for the lightness, mechanical flexibility, easiness of integration, and those typical of Additive manufacturing (AM), as for the long-term production low costs, scalability and versatility, easy processability and reproducibility. Among the technologies belonging to the AM class, Inkjet printing (IJP) is a solution-based mask-less additive technique able to deposit layers of different materials by propelling droplets of ink onto various substrates. When dealing with thin-film batteries, IJP is preferable over other printing techniques for several reasons, above all the limited material waste, as it is possible to finely control the position of the droplets, and the higher resolution this technique can provide^[3]. However, a challenging aspect is related to the material processing, as specific ink physical properties need to finely be tuned to achieve a printable suspension.

Despite being a strategic solution for patterned flexible electrodes fabrication, to date poor attention has been driven toward a systematic study of how IJP could be possibly applied to Lithium-ion batteries (LIB) fabrication. In addition to this aspect, printing current collectors represents the main obstacle to obtain a fully inkjet printed LIB. An emerging class of material with outstanding electrical, electrochemical and rheological properties is represented by 2D transition metal carbides/nitrides, known as MXenes. $Ti_3C_2T_x$ is the most studied, due to its extremely high conductivity ($> 15 \text{ kS cm}^{-1}$) and hydrophilicity, allowing to produce a safe, non-toxic aqueous ink, without the need of any surfactant or additive to control the stability^[4]. The combination of these properties allows to easily print an extremely conductive current collector.

The aim of the work is the fabrication of a thin-film flexible inkjet printed battery exploiting aqueous-based LTO and LMO inks, used as anode and cathode, respectively, and MXene-based current collector. An extensive inks characterization will be presented in terms of viscosity, surface tension and mean zeta potential, to understand the inks stability and printability. Morphological and electrical analysis of the printed substrates, combined with an in-depth electrochemical characterization in order to understand the battery performance, will be discussed.

- [1] K.-H. Choi, D. B. Ahn, S.-Y. Lee, *ACS Energy Letters* **2018**, 3, 220.
[2] W. B. Hawley, J. Li, *Journal of Energy Storage* **2019**, 25, 100862.
[3] S. Lawes, Q. Sun, A. Lushington, B. Xiao, Y. Liu, X. Sun, *Nano Energy* **2017**, 36, 313.
[4] S. Uzun, M. Schelling, K. Hantanasirisakul, T. S. Mathis, R. Askeland, G. Dion, Y. Gogotsi, *Small* **2021**, 17, 2006376.

SF03.04.11

Direct Handwriting of High-Performance Perovskite/Polymer Composite-Based Optoelectronic Devices on Paper, Textile and Other Unconventional Substrates Junyi Zhao¹, Li-Wei Lo¹, Haochuan Wan¹, Zhibin Yu² and Chuan Wang¹; ¹Washington University in St. Louis, United States; ²Florida State University, United States

Owing to its unique properties such as tunable bandgap and strong optical absorption, perovskite material holds great potential and has drawn extensive research interest for a wide range of optoelectronic applications including solar cells, photodetectors (PDs), and light-emitting diodes (LEDs). In most reported work, the perovskite-based optoelectronic devices are constructed in a multilayer structure on rigid indium-tin-oxide (ITO) glass substrate with a vacuum-evaporated metal top electrode. In this work, we report a unique approach for direct handwriting of high-performance hybrid organic-inorganic perovskite LEDs and PDs on unconventional substrates (paper, textile, three-dimensional surfaces) using a regular ballpoint pen filled with formulated electronic inks. This novel and alternative fabrication strategy allows high-performance LEDs and PDs to be easily fabricated by any untrained individuals in a time-efficient (the whole device can be made within a few minutes) and cost-effective manner. This is especially useful for early-stage demonstrations or application with less stringent requirement on resolution, as well as science popularization and education purposes.

More specifically, the fully-handwritten perovskite LEDs and PDs employs a simple sandwich structure, consisting of a composite transparent bottom electrode of poly(3,4-ethylenedioxythiophene) polystyrene sulfonate (PEDOT:PSS) and poly(ethylene oxide) (PEO), a composite active layer of methylammonium lead tribromide ($CH_3NH_3PbBr_3$) and PEO, and a silver nanowire (AgNW) top electrode. With the addition of polymer into the perovskite precursor, the voids between crystals can be eliminated to obtain a uniform and compacted functional layer. The multicolor perovskite-LEDs exhibit emission covering the whole visible range, especially the green emission with a low turn-on voltage of 2.3 V and high brightness of greater than $600,000 \text{ cd m}^{-2}$. Furthermore, this direct handwriting approach is also extremely versatile for use on various cellulose and fabric substrates and on curved and irregular surfaces that cannot be accomplished via conventional coating and deposition approaches. By integrating the perovskite-based LEDs and PDs, a handwritten sensor patch capable of measuring photoplethysmogram (PPG) waveforms from humans has also been demonstrated. This work demonstrates the great promise of using handwritten perovskite optoelectronic devices for emerging wearable health-monitoring applications.

SF03.04.13

Late News: Stencil Printed Micro Li-Ion Batteries for Autonomous Microsystems Anju Toor and Ana C. Arias; University of California, Berkeley, United States

The rapid growth of the electronics industry has resulted in a sustained need for portable electronics. Significant effort has been directed towards developing miniaturized devices for applications in wireless sensor networks, biomedical sensors, actuators, and wearables. Due to a rise in the popularity of the Internet of Things (IoT), demand for "autonomous wireless sensors" has increased. These devices can be used for smart building control, industrial process automation, factory automation, and many other applications. Such devices require integrated power sources to provide stable current supply and to deliver high peak currents on the order of $\sim 1\text{-}10 \text{ mA}$ while occupying small areas ($< 1 \text{ cm}^2$). Recent work has shown that except for the power supply, all the components needed for standards-compatible wireless communication can be integrated onto a single silicon chip with a wirebond antenna. Printing the

power supply directly on such a chip at wafer-scale would be a low-cost, small-volume solution.

For miniature or scaled-down Li-ion batteries, there are three key battery configurations that have been adopted, thin-film, thick-film, and 3D architectures. Typically, thin-film batteries suffer from insufficient power and capacity per unit footprint area to allow the operation of microelectronic devices. Thick-film battery configurations employ printing processes such as stencil printing[1], laser-direct write technique (LDW)[2,3] etc. to allow the fabrication of porous structured thick-film electrodes without requiring any lithographic patterning. 3D battery architectures involve 3D electrodes in several forms such as arrays of microrods/microtubes synthesized by templating method, honeycomb-like and sponge-like. However, the fabrication of 3D battery architectures is often quite complex and restricted to very few cathode and anode materials. One promising approach to develop high capacity miniature/micro Li-ion batteries is to employ printing methods such as stencil and screen printing to deposit thick, high capacity electrodes[1]. Printing methods also provide the flexibility to customize battery active area as per the device layout and size requirements.

This work demonstrates stencil-printed high-capacity Li-ion micro-batteries fabricated in Silicon for IoT applications. The battery consists of synthetic graphite and lithium cobalt oxide (LCO) as the respective anode and cathode layers printed on thin evaporated current collectors. For the fabrication of batteries, LCO is printed in a 225 μm deep, 25 mm^2 Si cavity and the graphite electrode is printed on a glass substrate. Once printed, the batteries are assembled and packaged using an airtight seal (Torr Seal) in a glovebox and tested in air. This work investigates the electrochemical limitations of Li-ion batteries as the active areas are scaled-down. The influence of the electrode film thickness on the battery performance is studied. The batteries demonstrate an areal capacity as high as ~ 7.2 mAh/cm^2 , capacity retention $>80\%$ and columbic efficiency $>97\%$ under 30 charge/discharge cycles. Our experiments show that a 25 mm^2 battery can power a wireless transceiver chip, SC μM [7] that consumes a baseline current of 650 μA with a peak current as high as ~ 4 mA.

- [1] R. Kumar, K. M. Johnson, N. X. Williams, V. Subramanian, *Adv. Energy Mater.* 2019.
- [2] H. Kim, J. Proell, R. Kohler, W. Pflöging, A. Pique, J. Laser Micro Nanoeng. 2012.
- [3] J. Pröll, H. Kim, A. Piqué, H. J. Seifert, W. Pflöging, J. Power Sources 2014.
- [4] A. M. Gaikwad, A. C. Arias, D. A. Steingart, *Energy Technol.* 2014.
- [5] R. E. Sousa, C. M. Costa, S. Lanceros-Méndez, *ChemSusChem* 2015.
- [6] K. H. Choi, D. B. Ahn, S. Y. Lee, *ACS Energy Lett.* 2018.
- [7] F. Maksimovic, B. Wheeler, et al, in *IEEE Symp. VLSI Circuits, Dig. Tech. Pap.*, 2019.

SF03.04.14

Jet Printing of Benzocyclobutene-Based Inks as Polymeric Adhesive Materials Filippo Iervolino¹, Raffaella Suriano¹, Martina Scolari², Ilaria Gelmi², Laura Castoldi² and Marinella Levi¹; ¹Politecnico di Milano, Italy; ²STMICROELECTRONICS, Italy

Polymeric adhesive materials are widely used in the electronic industry for applications such as wafer bonding, 3D integration and packaging. One of the most used materials is benzocyclobutene (BCB). BCB is a thermosetting polymer that can be processed as polymer solution, also called ink. Usually, BCB is processed with spin-coating. However, spin-coating alone does not allow to fabricate complex patterns and it needs to be coupled with a lithographic process. Moreover, lithography is challenging when high topographies need to be fabricated¹.

To overcome this issue, jet printing technologies can be used. Jet printing is a direct ink writing additive manufacturing technology based on the emission of material in form of droplets². It is a non-contact and maskless technology. Two of the most used jet printing technologies are drop-on-demand inkjet printing and aerosol jet printing. Inkjet printing is characterized by the selective emission of droplets obtained by a thermal or a piezoelectric actuator³. Aerosol jet printing, instead, is based on the emission of a focused nebulized ink, i.e., the aerosol, onto a substrate⁴. Both inkjet and aerosol jet printing present common advantages, such as the high versatility, high scalability, and the possibility of printing a wide variety of functional inks, e.g., polymeric, metallic and ceramic inks⁵. The main advantage of aerosol jet printing over inkjet printing is the possibility of using inks with a much wider range of viscosity, i.e., up to 1000 mPas instead of 20-30 mPas. However, aerosol jet printing has some drawbacks such as overspray and ink stability⁶.

Here, we present the fabrication of BCB-based inks by inkjet printing and aerosol jet printing. For inkjet printing, we use a drop-on-demand system with a piezoelectric actuator. For aerosol jet printing, a pneumatic system is used allowing to print inks with a relatively high viscosity. Careful ink formulation is carried out for inkjet printing to have printable inks. Indeed, inks having a viscosity of ~ 5 mPas exhibit a stable jetting. For aerosol jet printing, instead, we evaluate the effect of different polymer dilutions. We show aerosol formation and printing of BCB-based inks with a viscosity up to ~ 400 mPas. Moreover, the other physical properties of the inks that have an influence on the printing process are characterized. Then, we print simple geometries to perform an in-depth characterization of the printing parameters. The feasibility of printing complex patterns is also presented. A comparison between inkjet printing and aerosol jet printing is proposed, with particular interest in the difference of the morphology of the printed patterns. On one hand, we observe that aerosol jet printing exhibit a higher versatility being possible to print pattern having a thickness ranging from 1 μm to 30 μm . On the other hand, inkjet printing shows a better reproducibility for complex geometries and better edge sharpness. Finally, adhesive properties of the printed materials are characterized.

1. Iervolino, F. *et al.* Inkjet Printing of a Benzocyclobutene-Based Polymer as a Low-k Material for Electronic Applications. *ACS Omega* **6**, 15892–15902 (2021).
2. Shao, F. & Wan, Q. Recent progress on jet printing of oxide-based thin film transistors. *J. Phys. Appl. Phys.* **52**, (2019).
3. Nayak, L., *et al.* A review on inkjet printing of nanoparticle inks for flexible electronics. *J. Mater. Chem. C* **7**, 8771–8795 (2019).
4. Secor, E. B. Principles of aerosol jet printing. *Flex. Print. Electron.* **3**, (2018).
5. Seifert, T. *et al.* Additive Manufacturing Technologies Compared: Morphology of Deposits of Silver Ink Using Inkjet and Aerosol Jet Printing. *Ind. Eng. Chem. Res.* **54**, 769–779 (2015).
6. Abdolmaleki, H. *et al.* S. Droplet-Based Techniques for Printing of Functional Inks for Flexible Physical Sensors. *Adv. Mater.* **33**, 2006792.

SESSION SF03.07: Electronics and Sensors
Session Chairs: Nicole Bacca, Yanliang Zhang and Tao Zhou
Wednesday Afternoon, December 1, 2021
Sheraton, 3rd Floor, Fairfax

4:00 PM *SF03.07.01

Design and Applications of Printable Two-Dimensional Material Inks Mark C. Hersam; Northwestern University, United States

Two-dimensional (2D) materials have emerged as promising candidates for next-generation electronics [1] and quantum technologies [2]. With properties ranging from insulating (e.g., hexagonal boron nitride) to semiconducting (e.g., transition metal dichalcogenides) to conducting (e.g., graphene), nearly any electronic device can be fabricated by properly assembling 2D materials into heterostructures [3]. While device prototypes have been demonstrated on idealized research-scale samples, scalable manufacturing remains a challenge for 2D materials. In parallel, the field of printed electronics has made significant progress towards roll-to-roll additive manufacturing based on organic and nanoparticle inks. This talk will explore recent work aimed at uniting these efforts by designing electronic inks that combine the superlative electronic properties of 2D materials with the scalable manufacturing of printed electronics. To achieve this objective, multiple design goals have been concurrently pursued including exfoliation (i.e., optimizing yield, throughput, and flake size), ink formulation (i.e., engineering solvents and stabilizing surfactants and polymers for aerosol, inkjet, gravure, screen, and 3D printing), printed structure morphology (i.e., controlling film morphology and microstructure following printing via solvent evaporation, solvent additives, and curing conditions), and control of interfacial properties (i.e., minimizing interfacial resistance in conductive inks, maximizing capacitance in dielectric inks, and maximizing mobility for semiconductor inks). By achieving high levels of 2D material ink homogeneity and printing fidelity, a variety of high-performance applications have been achieved including photodetectors, optical emitters, supercapacitors, batteries, and sensors [4-7].

[1] V. K. Sangwan and M. C. Hersam, *Nature Nanotechnology*, **15**, 517 (2020).

[2] X. Liu and M. C. Hersam, *Nature Reviews Materials*, **4**, 669 (2019).

[3] M. E. Beck and M. C. Hersam, *ACS Nano*, **14**, 6498 (2020).

[4] J.-W. T. Seo, *et al.*, *ACS Appl. Mater. Interfaces*, **11**, 5675 (2019).

[5] K. Parate, *et al.*, *2D Materials*, **7**, 034002 (2020).

[6] K.-Y. Park, *et al.*, *Advanced Energy Materials*, **10**, 2001216 (2020).

[7] W. J. Hyun *et al.*, *Advanced Materials*, **33**, 2007864 (2021).

4:30 PM SF03.07.04

3D Printing Glass with Metastable Silicates Devon Beck, Paul Miller, James Mcrae, Bradley Duncan and Melissa Smith; Lincoln Laboratory, Massachusetts Institute of Technology, United States

Additive manufacturing of glass allows the fabrication of complex structures and geometries that traditional approaches cannot achieve. However, current strategies for 3D printing glass require thermal processes over 1000 °C to produce functional parts. We describe the development of low temperature process to 3D print glass and multimaterial composite glasses based on metastable silicate chemistry. The direct-write deposition process occurs at room temperature and the curing process only requires 250 °C to achieve a stable glass structure. The properties of the printed glass can further be tailored in a plug-and-play fashion by introducing functional filler materials such as conductive particles. This straight-forward strategy will enable the fabrication of a wide variety of microfluidic, electronic, and radio frequency devices with higher thermal stability without the need for extensive thermal processing.

4:45 PM SF03.07.05

3D-Enhanced Multimodal Sensing with Ultrathin Conductive Oxides on Polymer Scaffolds Md Saifur Rahman, Julia Huddy, Andrew B. Hamlin and William J. Scheideler; Dartmouth College, United States

We present a strategy for transforming 3D-printed polymer lattices into a versatile technology platform for multimodal electronic sensing. This method exploits nanometric ALD coatings of ZnO and ZnO:Al deposited directly onto the 3D printed polymer scaffold structures. We demonstrate that these conductive octet lattices can be designed for electronic multifunctionality, demonstrating 3D-enhanced chemical, thermal, mechanical, and fluid sensing. These applications leverage the synergistic effects of ultrathin semiconducting and conducting coatings with an increased surface-to-volume ratio due to the microscale pores of the 3D lattice.

The 3D sensors show a 100X enhanced response over 2D films when applied as low power, (10-50 nW) room temperature gas sensors for volatile organic compounds (VOCs). Leveraging the ultrathin deposition capability, 3D sensors with varying ZnO coatings (11 - 60 nm) were fabricated to enhance sensitivity, achieving thicknesses near the Debye Length to induce surface-dominated electrostatic interactions with physisorbed gas molecules. The tunable electrical conductivity of these structures also facilitates a variety of thermophysical response mechanisms, including rapid air temperature sensing enabled by the low thermal mass resulting in millisecond response time. We explore self-heating functionality at the mW level and utilize geometric control of convective heat transfer to perform thermal anemometry over a 100X range of air velocities. Finally, the 3D scaffolds were also implemented using deformable polymer lattices that allow these oxide-coated structures to function as kPa-level mechanical pressure sensors operating up to 3% overall strain, overcoming the inherent mechanical limitations of ceramic materials.

This ability to engineer electronic transport in additive manufactured mesoscale structures offers huge potential for microelectronics integration and provides a glimpse of how 3D design can fundamentally enhance the performance of biosensors, actuators, and microelectromechanical systems.

5:00 PM SF03.07.06

Quantum Tunneling of Charge Carriers in 3D Printed Graphene Functional Devices Jonathan H. Gosling^{1,1}, Feiran Wang¹, Gustavo Trindade^{1,1}, Graham Rance¹, Oleg Makarovskiy¹, Nathan Cottam¹, Zakhar Kudrynskiy¹, Alexander Balanov², Mark Greenaway², Ricky Wildman¹, Richard Hague¹, Christopher Tuck¹, T. Mark Fromhold¹ and Lyudmila Turynska¹; ¹The University of Nottingham, United Kingdom; ²Loughborough University, United Kingdom

The unique structural and electronic properties of 2D materials can be exploited for use in transformative optoelectronic applications. However, devices are usually bespoke structures that require the sequential deposition of exfoliated 2D layers. Therefore, there is a need for scalable manufacturing techniques capable of producing high-quality large-area devices comprising multiple 2D materials. The 3D printing of inks containing 2D material flakes provides a promising solution. It has been demonstrated that inkjet-printing can be used to manufacture devices incorporating 2D materials. However, a greater understanding of the electronic transport phenomena and structural properties of such devices is still needed. Here, detailed electrical and structural characterization is reported and explained by comparison with charge transport modeling which includes inter-flake tunneling transport and percolation network dynamics. Results reveal that the electrical properties are strongly influenced by flake density and complex meandering electron trajectories, which form in the presence of disorder and can traverse several printed layers. Controlling such trajectories is essential for printing high-quality devices that exploit the properties of 2D materials. We use inkjet-printed graphene to form the conductive channel of a fully inkjet-printed field effect transistor and to provide Ohmic contacts on an InSe phototransistor. This is the first time that inkjet-printed graphene has successfully replaced single layer graphene as a contact material for 2D metal chalcogenides.

10:30 AM SF03.08.01

Interfacial Photopolymerization (IPP) Additive Manufacturing of Linear Chain Polymers [Cecile Chazot](#)¹, Megan A. Creighton² and John Hart¹; ¹Massachusetts Institute of Technology, United States; ²Drexel University, United States

Photopolymerization additive manufacturing (AM), particularly stereolithography (SLA) and Digital light processing (DLP) is widely adopted due to its high resolution, simplicity, and the broad range of mechanical properties available from photopolymer resins. However, the technique is currently restricted to crosslinked polymers, resulting in challenges in both post-processing and recycling of printed parts that are absent when considering thermoplastic AM techniques. Here, we present a new process called interfacial photopolymerization (IPP) which enables photopolymerization AM of linear chain polymers. In IPP, a polymer film is formed at the interface between two immiscible liquids, each containing one type of reactive species. We demonstrate the integration of IPP in a proof-of-concept projection system and discuss how the reaction parameters affect printing resolution and final polymer properties. We also present a macrokinetics model to deepen understanding of the transport and reaction rates involved in IPP and evaluate the resolution of the printing process.

10:45 AM SF03.08.02

Late News: Integrating Non-Transparent Materials with Direct Laser Writing to Create Functional Microdevices [Meng Li](#)¹, Zemin Liu¹, Xiaoguang Dong¹, Ziyu Ren¹, Wenqi Hu¹ and Metin Sitti^{1,2,3}; ¹Max Planck Institute for Intelligent Systems, Germany; ²ETH Zürich, Switzerland; ³Koç University, Turkey

The development of miniaturized 3D devices with programmability and high performance is key in paving the way towards building next-generation smart micro-systems to revolutionize healthcare, data storage, and human-machine interface. Integrating advanced functionalities, heterogeneous properties and complex 3D geometries is challenging in the micro-scale. Among all the fabrication techniques, 3D printing is the most advantageous in shaping 3D geometries with automated processes of large flexibility and design freedom. Two photon polymerization direct laser writing (2PP-based DLW) has risen as a promising technique for printing arbitrary 3D architectures with a resolution down to hundreds of nanometers.

However, functional composite inks that are compatible with 2PP-based DLW usually suffer from poor performance, due to their low loading fractions of the functional dopants. Because of the intense near-infrared laser beam needed for the 2PP 3D lithography, highly light absorptive materials are intrinsically not suitable for the DLW process—bubbles generated locally will destruct the printed structure, and not enough transmitted light can reach the desired printing depth. Such exemplary materials are composites doped with micrometer-size particles and non-transparent particles (such as carbon nanomaterials, magnetic particles, metallic particles) and highly photoactive materials (such as gold nanoparticles, photothermal dyes). Researchers have used different methods to incorporate DLW-incompatible materials with printed 3D architectures, such as coating, electroplating, surface modification, and molding. Every fabrication technique has its own advantages to meet the requirements of specific applications, but it also has its own limitations. For example, the coating method functionalizes the architectures in a 2D manner, lacking 3D space selectivity; electroplating and surface modification have a limited selection of compatible materials; molding a single material gives an isotropic property lacking advanced programmability.

We present here multistep-molding-integrated direct laser writing that is able to integrate those incompatible functional materials into high-resolution and complex 3D geometries, to create various microdevices with unique functionalities. Metachronal wave motion, fluid mixing, function reprogramming, structural reconfiguring, multiple degrees-of-freedom rotations, and stiffness-tunable double-layer mechanical bits are exemplary demonstrations of the versatility of this fabrication routine.

11:00 AM *SF03.08.03

Conformal Geometry and Multi-Material Additive Manufacturing Through Freeform Transformation of Building Layers Jigang Huang, Henry O. Ware, Rihan Hai, Guangbin Shao and [Cheng Sun](#); Northwestern University, United States

3D printing or additive manufacturing is the process for building complex geometries via successive addition of materials based on a digital model. However, the traditional 3D printing processes employing planar-layer printing strategy have rather limited flexibility in customization and multi-materials integration. Originally developed for the sole purpose of rapid prototyping, the planar-layer printing process slices the digital models along the z-axis to generate a set of horizontal build layers in x-y plane. Those layers are sequentially stacked from bottom-up to create the physical replica of the digital model. After more than three decades, this standard procedure remains the would-be choice in most of the commercial 3D printers possessing 3-Degree of freedom (DOF) Cartesian motion. Despite its popularity, the limited 1-DOF stage motion along z-axis imposes serious constraints in 3D printing complex geometries. Recognizing how multi-axis machines are capable of producing freeform geometries with better quality and efficiency as compared to the 3-axis machines, there is a growing interest in exploring the new slicing and printing strategy beyond the 3-DOF Cartesian motion. Methods that employed high-DOF stage motion have also investigated in enabling conformal 3D printing on non-planar surfaces and support-free 3D printing. Recently reported computed axial lithography (CAL) method prints entire complex objects via angular accumulation of dynamically evolving light pattern in a cylindrical coordinate system. All these methods demonstrated the ability to handle complex geometries with improved speed and surface finishing. Inspired by these most recent studies, we went a step further by allowing freeform manipulation of each build layer during the layered manufacturing process.

We show here untethering the build layer fabrication from unidirectional stage motion unlocks the means to reconstitute the 3D objects with added manufacturability such as custom design transformations, conformal geometry, and multi-material integration. The newfound fabrication flexibility allows us to execute full degree-of-freedom (DOF) transformation (translating, rotating, and scaling) of each individual building layer while utilizing continuous fabrication techniques. Transforming individual building layers within the sequential layered manufacturing process enables dynamic transformation of the 3D printed parts on-the-fly, eliminating the time-consuming redesign steps. Preserving the locality of the transformation to each layer further enables the discrete conformal transformation, allowing objects such as vascular scaffolds to be optimally fabricated to properly fit within specific patient anatomy obtained from the Magnetic Resonance Imaging (MRI) measurements. The manufacturability of the 3D printing process is further augmented with the use of the high-precision 6-axis robotic arm. It allows us to perform manufacturing tasks other than 3D printing, such as rinsing the samples mid-printing process. Finally, exploiting the freedom to control the orientation of each individual building layer, we further establish multi-materials, multi-axis 3D printing capability for integrating functional modules made of dissimilar materials in 3D printed devices. This final capability we demonstrate through 3D printing a soft pneumatic gripper via heterogeneous integration of rigid base and soft actuating limbs. Although the reported method primarily focusing on the continuous stereolithography process, the underlying principle can be applied to other 3D printing process, with the potential to ease the burden towards the envisioned multi-process 3D printing.

11:30 AM SF03.08.04

Gas-Phase 3D Printing of Functional Materials David Munoz-Rojas; LMGP Grenoble INP/CNRS, France

Spatial Atomic Layer Deposition (SALD) is a recent approach 100 times faster than conventional ALD, even at atmospheric pressure. Previous works exploited these assets focussing on high-rate, large-area deposition for scaling-up into mass production. Conversely, this work shows that SALD indeed represents an ideal platform for area-selective deposition of functional materials by proper design and miniaturization of close-proximity SALD heads. In particular, the potential offered by 3D printing is used to fabricate low-cost customized close-proximity heads, which can be easily designed and modified to obtain different deposition areas, free-form patterns, and even complex multimaterial structures. Finally, by designing a miniaturized head with circular concentric gas channels, 3D printing of functional materials can be performed with nanometric resolution in Z. This constitutes a new gas-phase 3D printing approach. Because the process is based on ALD reactions, conformal and continuous thin films of functional materials can be printed at low temperatures and with high deposition rate in the open air. Our approach represents a new versatile way of printing functional materials and devices with spatial and topological control, thus extending the potential of SALD and ALD in general, and opening a new avenue in the field of area-selective deposition of functional materials.

SESSION SF03.09: Energy Materials and Devices

Session Chair: John Boley

Thursday Afternoon, December 2, 2021

Sheraton, 3rd Floor, Fairfax

1:30 PM *SF03.09..01

3D Printing of Inorganic Thermoelectric Materials Jae Sung Son, Fredrick Kim, Seungjun Choo, Jungsoo Lee and Seong Eun Yang; Ulsan National Institute of Science and Technology, Korea (the Republic of)

Heat is omnipresent in natural and artificial environments, more than 60% of which is dissipated. Thermoelectric (TE) power generation can provide a unique solution to convert this dissipated, wasted heat into useful energy, that is, electricity. Generally, TE conversion efficiency depends on the material properties and design of the module structure. However, despite the development of highly efficient TE materials, module engineering is rather less advanced and is still fabricated by the traditional multi-step process of materials synthesis, dicing, and assembly, restricting the available design of modules to that of planar structures. At this moment, three-dimensional (3D) printing technology can maximize the flexibility in the design and fabrication of TE modules into more efficient structures. Furthermore, the printing process can significantly reduce the processing cost for the fabrication of TE modules owing to lower energy input and a simplified assembly process. Herein, I present the development of the 3D printing process applied to a range of different TE materials of Bi₂Te₃, BiSbTe, PbTe, and Cu₂Se-based inorganic alloys. Surface states of TE particles were precisely optimized with the controllable charge states in the presence of anionic inorganic binders, achieving the suitable viscoelasticity of the TE inks to the extrusion-based 3D printing. The geometrically designed 3D-printed TE materials were assembled into power generating systems, in which high efficiencies of energy conversion were achieved by the optimization of heat transfer.

2:00 PM SF03.09..02

High-Throughput Additive Manufacturing Toward Material Design and Discovery Minxiang Zeng and Yanliang Zhang; University of Notre Dame, United States

The discovery of new materials and their compositional/microstructural optimization holds the key to next-generation technologies in areas such as sustainable energy and environmental mitigation. Highly universal, fast, and controllable manufacturing method with the ability to generate a large number of sample features is therefore becoming progressively more important. Here we report a high-throughput combinatorial printing (HTCP) technique capable of integrating multiple nanoscale materials in a single nozzle and varying the material compositions on the fly, generating chemically heterogeneous films in a gradient manner (compositional density > 10⁴/cm³). Leveraging aerosol-based mixing and deposition, the proposed HTCP approach demonstrates the on-demand control on the compositional/structural arrangements with programmable accuracy. Due to the vast tolerance of ink particle size and morphology, the HTCP successfully fabricates intriguing matter with gradient compositions and complex structures by integrating a wide range of nanoparticles, including 0D nanosphere, 1D nanowire/nanorods, and 2D nanoplates/nanosheets. Furthermore, we demonstrate a fascinating variety of printing strategies including combinatorial doping, alloying, chemical reaction, and compositional microstructuring, expanding the application space for the HTCP method. As a proof of concept, HTCP has been used to investigate the role of doping level in thermoelectric (TE) materials, which helps to identify a high-performance n-type TE composite. The ability to combine the top-down designing freedom of additive manufacturing with bottom-up molecular control over material composition and structure promises almost infinite possibility of heterogeneous material library which is inaccessible from conventional manufacturing approaches, offering a new pathway toward the design and discovery of next-generation materials and composites for broad applications.

2:15 PM SF03.09..03

Inkjet Printing of Organic Electronics on 3D Objects Marc Steinberger, Andreas Distler, Hans Joachim Egelhaaf and Christoph J. Brabec; I-Meet Institute Materials for Electronics and Energy Technology, Germany

Inkjetprinting of organic electronics is an emerging field of interest in current research. The flexibility of the production process allows the production of organic photovoltaic with different shapes, colors and on several different 2D substrates. Here we show the first time all inkjet printed organic solar cells and OLEDs on a 3D object using a 5-Achs automated robot system. The ink engineering process was guided by the optimization towards stable inks that can be deposited on curved substrates with different printing distances. To overcome shunting issues a method for planarizing different substrates on 3D was developed using different polymer coatings. A successive study on performance dependence of print distance was performed in order to achieve full automation of the printing process. On top live time studies of fully printed solar cells on 2D and 3D were performed.

2:30 PM SF03.09..04

In Situ Materials Synthesis for Vat Photopolymerization of Functional Metal Oxides and Metals Daryl W. Yee¹ and Julia R. Greer²; ¹Massachusetts Institute of Technology, United States; ²California Institute of Technology, United States

Additive manufacturing (AM) is one of the most powerful manufacturing tools available today. Its layer-by-layer approach to fabrication enables greater flexibility in the use of topology to design functional materials with significant improvements in performances and/or previously impossible functionalities. Vat photopolymerization (VP) stands out amongst the various AM techniques as its ability to achieve high volumetric throughputs and resolutions allows it

to be applied in a variety of different settings, from fabricating nanophotonic devices to shoe soles. However, a key limitation of VP is the limited number of functional inorganic materials that are compatible with it. While composite resins with inorganic fillers and hybrid inorganic-organic resins have been developed to allow VP of these inorganic materials, they are often challenging to use, have poor resolutions, or are limited in the compositions achievable.

In this presentation, we will discuss the use of in-situ materials synthesis as an alternative materials development approach for VP that can address some of the current challenges associated with VP of functional inorganic materials. By printing a 3D object that contains the necessary reagents for the in-situ synthesis of the desired material, i.e. printing a “chemical reactor”, we can adapt the extensive materials synthesis reactions already developed for use with VP. As a demonstration of this “chemical reactor” framework, we show how in-situ combustion synthesis can be used with various VP processes for the fabrication of various functional metal oxides and metals.

Central to this approach is the fabrication of metal-ion containing 3D hydrogels which are then thermally treated to yield either 3D metal oxide or metal structures. These homogenous hydrogels are facile to prepare and compositionally versatile, circumventing the issues associated with the state of the art in metal oxide and metal VP. Using this system, we fabricated zinc oxide structures with sub-micron features using two-photon lithography and demonstrated their piezoelectric properties via in-situ compression experiments. Lithium cobalt oxide materials were also fabricated using digital light processing (DLP) printing and showed efficient performance as a lithium ion battery cathode over greater than 100 cycles. An array of micro-architected metals such as copper, silver, and cupronickel alloys were also fabricated with DLP printing, which could be used for thermal management applications.

This work highlights the use of polymer chemistry and materials science in expanding the range of materials that can be made via additive manufacturing. The ability to fabricate these functional 3D materials in a facile and versatile way has the potential to open up the field of smart devices and change how we design them.

2:45 PM SF03.09..05

3D Printing of the Half-Heusler Alloy $Nb_{1-x}CoSb$ —A Case for Ternary Thermoelectric Materials Muath Al-Malki, G. J. Snyder and David C. Dunand; Northwestern University, United States

The continuous development of thermoelectric materials in the past decades led to the improvement of the dimensionless figure of merit and ultimately the overall device efficiency. However, synthesis and manufacturing of electronic materials in general, and thermoelectric materials particularly, requires delicate attention to attain the planned electronic and thermal properties. Furthermore, most of the conventional synthesis techniques, such as the hot pressing, limit the shape of the synthesized material; restricting them from being used in wide range of applications, including wearable devices. The literature of 3D printing of thermoelectric materials, so far, is limited to binary materials ($Bi_2Te_3, PbTe, \dots$). We are showing here the case for 3D printing of the half-Heusler alloy $Nb_{1-x}CoSb$, in which we tackle the problems of secondary phases formation, porosity control and the relation of all that to the transport properties. This should bridge the gap towards printing other ternary and quaternary thermoelectric materials.

3:00 PM *SF03.09..06

Printable Energy Storage and Soft Robotic Components for Soft Electronics Andrew Fassler^{1,2}, Ryan Kohlmeyer^{1,3}, Greg Horrocks¹, Eliot Gomez^{1,2}, Shiwanka Wanasinghe⁴, Alex Flynn^{1,2}, Obed Dodo⁴, Jessica Sparks⁴, Luke A. Baldwin¹, Christopher Tabor¹, Dominik Konkolewicz⁴, Carl Thrasher¹ and Michael F. Durstock¹; ¹Air Force Research Laboratory, United States; ²UES, Inc., United States; ³Xerion Advanced Battery Corp., United States; ⁴Miami University, United States

Soft electronics and soft robotics aim to bridge the gap between functional, high performance, electronic devices & systems and our compliant, organic, human-centric environment. It involves the development of active and responsive electronic materials, devices, and systems in a form factor that is soft, flexible, stretchable, and mechanically robust. The use of 3D printing and direct write techniques offers some distinct advantages with respect to the fabrication of soft robotic components of increasing size and complexity, as well as in the heterogeneous integration of functional components such as distributed power sources and electronic components and interconnects. In particular, the development of flexible, printable, and mechanically robust energy storage devices is a key and oftentimes limiting requisite for many of these applications due to the fact that common battery materials and manufacturing methods are often incompatible with 3D printing and soft electronics. We demonstrate control of 3D printed batteries and energy storage components using a variety of printing approaches, including aerosol jet and direct ink write, combined with a mixed solvent, phase inversion approach to deliver porosity control, high resolution feature sizes, and high temperature performance. Additionally, advances in materials and design approaches are propelling the field of soft robotics at an incredible rate, however current methods of fabrication remain cumbersome and struggle to incorporate desirable geometric complexity at large scale. By developing a 3D printable, tunable, self-healing elastomer system, we demonstrate a soft robotic manufacturing approach that combines the advantages of 3D printing (e.g. vat photopolymerization) together with modular soft robotics whereby smaller subcomponents can be printed and subsequently self-healed together to form integrated parts.

SESSION SF03.10: Liquid-Phase Patterning of Electronics
Session Chairs: Sohini Kar-Narayan and Ethan Secor
Tuesday Morning, December 7, 2021
SF03-Virtual

8:00 AM SF03.10.01

3D Printing of Perovskite Nanopixels for Ultrahigh-Resolution, Multi-Level Anticounterfeiting Displays Mojun Chen and Ji Tae Kim; The University of Hong Kong, Hong Kong

The manufacture of pixels is a core task in optoelectronics and hybrid perovskites are emerging as a promising material candidate due to their strong, tunable, and high-color-purity luminescence. A number of lithographic or printing methods have been devised to fabricate perovskite pixels in thin-film forms. However, downsizing a thin-film pixel to the nanoscale loses its brightness, which remains a longstanding issue. Here, we show that 3D layout of perovskite nanopixels offers an effective route to improve the brightness without sacrificing the lateral resolution [1]. Our nanoscale 3D printing approach that is based on femtoliter meniscus-guided crystallization [2] enables the fabrication of freestanding metal halide perovskite color nanopixels with programmed dimensions and placements. This approach provides outstanding lateral pixel dimensions such as a diameter of ~ 550 nm and a pitch of ~ 1.3 μm (pixel density > 19,500 ppi). Furthermore, on-demand control of the vertical pixel dimension by our 3D printing enables a couple of remarkable achievements: (1) enhancement and balancing of nanopixel brightness (tens of times brighter than a thin-film pixel) and (2) data encryption into nanopixel height for multi-level anticounterfeiting which is not easily accessible by high-magnification optical microscopy with

limited depth-of-field. This 3D printed nanopixel scheme is general and could be applied to diverse optoelectronic materials. In this talk, we will present our results and discuss the prospects of our work for potential applications in smart optoelectronic devices.

Corresponding author. Email: jtkim@hku.hk

References

- [1] Chen M., Hu S., Zhou Z., Huang N., Lee S., Zhang Y., Cheng R., Yang J., Xu Z., Liu Y., Lee H., Huan X., Feng S.-P., Shum H.C., Chan B.P., Seol S.K., Pyo J.*, Kim J.T.*, Three-Dimensional Perovskite Nanopixels for Ultra-High-Resolution Color Displays and Multi-Level Anticounterfeiting. *Nano Letters* (2021) <https://pubs.acs.org/doi/10.1021/acs.nanolett.1c01261>
- [2] Chen M., Yang J., Wang Z., Xu Z., Lee H., Lee H., Zhou Z., Feng S.-P., Lee S., Pyo J., Seol S.K., Ki D.-K., Kim J.T.*, 3D Nanoprinting of Perovskites. *Advanced Materials* **31**, 1904073 (2019)

8:15 AM *SF03.10.02

Water-Based and Defect-Free 2D Material Inks for Printed Electronics Cinzia Casiraghi; University of Manchester, United Kingdom

Solution processing of 2D materials [1] allows simple and low-cost techniques, such as ink-jet printing, to be used for fabrication of heterostructure-based devices of arbitrary complexity. However, the success of this technology is determined by the nature and quality of the inks used. Our group has developed highly concentrated, defect-free, printable and water-based 2D crystal formulations, designed to provide optimal film formation for multi-stack fabrication [2]. I will give examples of all-inkjet printed heterostructures, such as large area arrays of photosensors on plastic [2], programmable logic memory devices [2], capacitors [3] and transistors on paper [3,4]. Furthermore, inkjet printing can be easily combined with materials produced by chemical vapor deposition, allowing simple and quick fabrication of complex circuits on paper, such as high-gain inverters, logic gates, and current mirrors [5].

- [1] Coleman et al, *Science* **331**, 568 (2011)
- [2] McManus et al, *Nature Nano*, **12**, 343 (2017)
- [3] Worsley et al, *ACS Nano*, 2018, DOI: 10.1021/acsnano.8b06464
- [4] Lu et al, *ACS Nano*, **13**, 11263 (2019)
- [5] Conti et al, *Nature comms*, **11** (1), 1-9 (2020)

8:45 AM SF03.10.03

Impact of Complexing Agent Evaporation on the Morphology and Media Resistivity of Printed Reactive Silver Inks Steven DiGregorio¹, Michael Martinez-Szewczyk², Subbarao Raikar¹, Avinash Mamidanna¹, Mariana Bertoni² and Owen Hildreth¹; ¹Colorado School of Mines, United States; ²Arizona State University, United States

3D printing of conductive inks is poised to revolutionize the microelectronics industry. However, some new technologies use thermally sensitive substrates that are not compatible with the high sintering temperatures (~ 200 °C) of metal nano-particle conductive inks. Reactive inks are an emerging technology that can solve this problem due to their ability to form highly conductive features at low temperatures (~ 90 °C). The underlying kinetics of reactive inks systems is crucial for designing high-performance inks but is not well understood. This work elucidates the impact of reaction kinetics on the morphology and the media resistivity of reactive silver inks (RSI) printed via direct ink writing. We introduce a new RSI system consisting of silver acetate, formic acid, and ethylamine, whose silver reduction mechanism is predominantly thermal. Comparing this new ink to an ink whose reduction mechanism is predominantly evaporative shows that thermal reduction produces dense bottom-up silver growth, and evaporative reduction produces highly porous silver morphologies. Decreasing the vapor pressure of the complexing agent or increasing the substrate temperature leads to more thermal reduction and, therefore, denser morphologies with lower media resistivities.

9:00 AM SF03.10.04

Inkjet-Printed Functionalized Surface Enhanced Raman Scattering (SERS) Sensors for Improved Detection of Narcotics Li-lin Tay and John Hulse; National Res Council Canada, Canada

Recent advances in Inkjet-printing of advanced materials have provided a versatile platform for the rapid development and prototyping of sensor devices. We have recently demonstrated inkjet-printed surface enhanced Raman scattering (SERS) sensors on flexible substrates for the detection of small chemical molecules. (Tay et al., *J Raman Spectrosc.*, 2021, **52**, 563-572) These flexible SERS sensors have good batch-to-batch uniformity and many advantages for performing point-of-sampling testing such as liquid or aerosol filtration and swabbing capabilities. These simple sampling and separation attributes make these inkjet-printed paper-based sensors ideal for field applications. The SERS effect relies upon the electromagnetic field enhancement that results from coupling of plasmonic nanostructures (e.g. silver or gold nanoparticles). SERS exploits the unique vibrational signature of an analyte molecule and in practice, it is often coupled with spectral recognition software for the detection of molecules of interest. Most SERS sensors are fabricated as non-functionalized plasmonic nanostructures in a single device. Because SERS is an optical near-field effect, it works best with molecules that have good binding affinity towards the plasmonic surfaces (such as thiols). SERS detection of non-binding molecules such as cannabinoids or other narcotics with poor affinity towards the plasmonic surfaces performs poorly. This can be improved through the use of surface functionality to help sequester or attract the molecules of interest to the plasmonic surfaces. The functionalization concept has been applied in SERS detection for a number of years. However, its applications have been limited typically to optimization of functional groups to target one particular chemical analyte, for example, the use of alkylthiol to improve glucose SERS sensing. (Lyandres et al., *Anal. Chem.*, 2005, **77**, 6134-6139) Once the surface has been functionalized and tailored for one specific analyte, it can often render the entire surface inaccessible for other molecular analytes. For example, a gold nanoparticle surface functionalized by halide ions (Cl⁻ or I⁻) is often no longer active for detection of thiol species, despite the strong affinity of thiolated species towards gold surfaces. This problem can be overcome through the use of inkjet-printed SERS devices. With inkjet printing, multi-functionalized SERS active surfaces can be prepared in a single device thus retaining the performance of multiple types of functionalization in a single device. In this presentation, we will demonstrate the optimization of functionalized plasmonic ink formulation, inkjet-printing conditions and integration of multi-functional SERS active sites in a single sensing device. We will discuss the performance of differently functionalized SERS devices for the detection of narcotics.

9:05 AM *SF03.10.06

In-Space Manufacturing to Support Human Spaceflight Jessica Koehne; NASA Ames Research Center, United States

As human spaceflight pushes beyond Low Earth Orbit (LEO), resupply of consumables becomes a significant challenge. One solution to this problem is In-Space Manufacturing (ISM), the capability to perform on-demand manufacturing and repair of consumables in an in-space environment. ISM offers significant flexibility to missions as it allows for a high degree of tailorability and reduction in launch mass. Leveraging advancements in fabrication, repair and recycling, ISM provides a highly sustainable and affordable solution to exploration mission operations and logistics. In this talk, advances in printed

electronics and sensors, ranging from nanomaterial ink development and hands-free fabrication methodologies to devices will be presented. Applications presented will include sensors for crew health monitoring along with supporting electronics. In the future, these devices will be fabricated and characterized on the International Space Station and the approach will be evaluated for future in-space manufacturing to support human spaceflight.

SESSION SF03.11: Engineering Complex Structures by 3D Printing
Session Chairs: Sohini Kar-Narayan and Ethan Secor
Tuesday Morning, December 7, 2021
SF03-Virtual

10:30 AM SF03.11.01

Stereolithography-3D Printed Hierarchically Porous Carbon Microarchitectures for Structurally Robust Energy Storage Akira Kudo¹, Jihui Han¹ and Mingwei Chen^{2,1}; ¹Tohoku University, Japan; ²Johns Hopkins University, United States

3D printing has become one of the most attractive fabrication techniques in materials science and engineering, offering its immense degree of freedom in designing complicated architectures with feature sizes smaller than millimeters or even micrometers. As the designed architectures can control the physical and chemical properties of the materials, 3D printing thrives creating innovative multifunctional materials.

In this presentation, we employed stereolithography (SLA) 3D printing to fabricate hierarchically porous carbon microarchitectures that integrate structural robustness and energy storing functionality. By using photocurable resin mixed with magnesium oxide (MgO) nanoparticles as a porogen, an LCD (liquid crystal display)-SLA 3D printer successfully replicated the 3D-modeled microarchitectures. After pyrolysis in vacuum at 1000degC and removal of MgO nanoparticles in heated hydrochloric acid, we obtained fully-carbonized simple cubic lattices that retained the architected micropores (<200µm) and stochastic nanopores (<40nm) developed in the individual structural elements. While showing ~300m²/g of the specific surface area, supercritical liquid or other complicated setups were not required for drying. The obtained structures demonstrated a combination of mechanical robustness and functionality as a supercapacitor in a single body. Further optimization of both microarchitectures and nanoporosity will lead to a highpower energy device embedded in structural components.

Our results can present a novel configuration of structural capacitors and/or batteries different than ones using carbon fibers, benefitting from the capability of 3D printing.

10:45 AM SF03.11.02

Direct 3D Printing of High-Aspect-Ratio Metallic Nanoprobes for Scanning Microscopy Heekwon Lee and Ji Tae Kim; The University of Hong Kong, Hong Kong

Over the past 40 years, the scanning probe microscope (SPM), a class of Nobel-Prize-winning techniques, has become a routine and essential imaging tool for exploring not only surface topography but also material properties at the nanoscale. The core feature of SPM is a “nanoprobe” typically made up of a sharp tip mounted on a cantilever.

Recently, high-aspect-ratio (HAR) nanoprobes have ushered in a new era in SPM characterization. First, the HAR probe enables full-profile topography of deep and narrow 3D nanodevices, e.g., fin-based multigate transistors (FinFETs), photonic metamaterials, and neuromorphic circuitries. Second, the HAR probe geometry is quite effective in amplifying the chemical imaging contrast in tip-enhanced-Raman spectroscopy (TERS), as it provides enough space to separate the light excitation region from the Raman scattered region on the probe. However, the technological challenges associated with the fabrication of HAR nanoprobes such as high-cost, labor-intensive, and low-throughput remain unresolved.

Here, we have developed a one-step, on-demand, material-saving benchtop 3D printing method to fabricate metallic HAR atomic force microscope (AFM) probes for deep 3D imaging [1]. This method exploits electrohydrodynamic (EHD) nano-dripping to fabricate a freestanding silver nanowire (AgNW) with an aspect ratio over 30 directly on a cantilever. Our 3D printing approach offers the benefits associated with unprecedented simplicity in the probe’s dimension control, material selection, and regeneration, which are not easily attainable in the traditional lithographic approach. Moreover, our 3D printed tip delivers a high fidelity in deep-trench imaging better than a standard pyramidal tip and comparable to commercial HAR probes, yet at a fraction of their cost.

Furthermore, 3D printing has the potential to produce/customize diverse classes of functional nanoprobes, as recently demonstrated scanning 3D thermocouple networks for mapping microscale temperature fields in three-dimensions [2]. In this talk, we will present the experimental results including 3D printing of functional nanoprobes and discuss prospects of our work for potential applications in nanomaterial characterization and sensing.

KEYWORDS:3D printing; electrohydrodynamic nano-dripping; nanowire probe; 3D deep AFM imaging

[1] Lee H., Gan Z., Chen M., Min S., Yang J., Xu Z., Shao X., Lin Y., Li W.-D., Kim J.T., On-Demand 3D Printing of Nanowire Probes for High-Aspect-Ratio Atomic Force Microscopy Imaging. *ACS Appl. Mater. Interfaces*, **12**, 46571 (2020).

[2] Lee H. and Kim J.T. (in preparation)

11:00 AM SF03.11.03

BackBot—Insect Inspired Underwater Miniature 3D printed Robot with Self-Regulation of Catalytic Driven Buoyancy Dror Kobo and Bat-El Pinchasik; Tel Aviv University, Fleischman Faculty of Engineering, Israel

Backswimmers (family Notonectidae) are aquatic insects known for their ability to hang upside-down at the water-air interface, due to their superhydrophobic legs.¹ They can, however, also regulate their buoyancy underwater through controlling the size of a bubble attached to their abdomen.^{2,3} They do that by controlling the amount of oxygen attached to haemoglobin cells. In this way, they reach neutral buoyancy without the need to swim actively.

With the miniaturization of robots, interfacial phenomena become prominent in terms of stability, adhesion and arts of locomotion.⁴ While interfacial phenomena may hinder locomotion and complicate the development of small robots, it can also be used in order to facilitate the performance of specific tasks, as exhibited in nature, and promote the development of robotic insects and insect-inspired devices. This is especially important in underwater robotics, where energy consumption and hydrodynamics challenge the miniaturization of robots.

In this study, a 3D printed backswimmer-inspired miniature robot is developed. A mat of gas bubbles is created and autonomously controlled, in order to

regulate the buoyancy of the robot. The bubbles nucleate and grow using a catalytic mechanism underwater. Water from the environment split into oxygen and hydrogen micron-sized bubbles on small (2 cm) comb-like electrodes, in response to voltage. In order to release bubbles and regulate the buoyant forces, three mechanisms for bubble release are investigated: rotational, linear and pulse mechanism. An undesirable outcome of the bubble release rotational mechanism is rotational motion of the robot to the opposite direction, due to conservation of angular momentum. In the case of the pulse driven release mechanism, high-energy consumption is recorded, in comparison to the other release mechanisms. Therefore, the linear mechanism is the most useful for bubble release in terms of power consumption and motion control. Through a control loop, the nucleation, growth and release of bubbles are self-regulated, allowing the robot to achieve neutral buoyancy without any further energy consumption, in an autonomous fashion. The development of this device lays the ground for investigating interactions between autonomously moving underwater miniature robotic swimmers.

11:15 AM SF03.11.05

Direct Printing of Functional 3D Objects [Bhavana Deore](#)¹, Katie Sampson¹, Thomas Lacelle¹, Rony Amaya², Joseph Hyland², Hendrick W. de Haan³, Patrick Malenfant¹ and Chantal Paquet¹; ¹National Research Council Canada, Canada; ²Carleton University, Canada; ³University of Ontario Institute of Technology, Canada

3D printing is an emerging additive manufacturing technology poised to transform both design and manufacturing due to its ability to customize design and generate structural complexity not possible using traditional manufacturing processes. Commercial examples of 3D printed objects using monolithic materials, such as GE's fuel nozzle, illustrate early success of this technology by enabling new designs and significantly reducing the number of parts and supply chain required for manufacturing. However, only marginal progress has been made to demonstrate multi-material printing and as such it remains a low technology readiness level research endeavour at the moment with enormous potential for innovation and commercial impact. Multi-material 3D-printing would increase the complexity and enable the fabrication of complete devices in a single printing process combining materials with different properties (structural, functional, conductive, etc.). Through novel chemistries, and the exploitation of controlled self-assembly, various functions (e.g. electrical, optical, magnetic, mechanical) may be introduced into objects as they are being constructed/printed. 3D spatial segregation of materials within the object will be controlled from the nano-scale to the macro-scale, carefully tuning bulk and surface properties, yet breakthroughs in many aspects of material science will be required to achieve this level of control. These "smart multifunctional objects" are intended to be adaptive and responsive (i.e. intelligent) and enable applications that cannot be easily addressed using other forms of fabrication. This is a leap beyond traditional assembly. Success will provide breakthroughs in robotics and IoT via new form factors with optimized mechanical properties, embedded sensors and antennas for wireless communication. In this presentation, we demonstrate a strategy to generate functional objects by vat polymerization 3D printing that relies on controlled phase separation. Using photoresins comprising of judiciously selected components, the diffusion of phase separating components are modulated via the kinetics of gelation and network entrapment to yield spatial control over material placement. This methodology yields a rich selection of morphologies with distinct functional surfaces that provide direct access to 3D printed smart objects such as sensors and wireless applications.

11:30 AM SF03.11.06

Microextrusion of Energy Storage Materials for Custom-Form Lithium Batteries [Jorge A. Cardenas](#), John P. Bullivant, David Ashby, Eric Allcorn, A. A. Talin, Adam W. Cook and Katharine L. Harrison; Sandia National Laboratories, United States

Additively manufactured custom-form batteries can maximize practical energy densities in applications where power sources must be more efficiently packed into a given space. Conversion cathodes paired with lithium metal further enable high energy density batteries. Carbon monofluoride (CF_x) and iron disulfide (FeS₂) are two conversion cathode materials of broad interest where little to no work has been carried out on the development of microextrusion methodologies for these materials. Meanwhile, silica sol based ionogels have been shown as a promising solution-deposited solid-state electrolyte, though no work has been carried out on the printing of this material for custom-form cells. In this work we demonstrate and optimize the printing of CF_x and FeS₂ cathode systems in custom-form lithium batteries, where the impact of ink solid composition on rheology, custom-form shape retention, cell capacity, rate, and cyclability is investigated. Additionally, the microextrusion of silica-based ionogels is demonstrated for the first time, where it is used with conversion or intercalation chemistries in custom-form cells. For the FeS₂ material system, it is found that ink solid compositions between 40-50% w/w are needed to adequately retain shape in custom-form configurations while maintaining up to 450 mAh/g cell capacity over 10 charge/discharge cycles. For the CF_x material system, ink solid compositions between 30-40% w/w are needed for shape retention in custom-forms and low process variance while cells discharge at capacities above 600 mAh/g at rates greater than C/25. Overall, this work demonstrates the microextrusion of energy storage materials for custom-form lithium batteries, which are of broad interest generally and for Sandia related applications where practical energy densities in a given system must be maximized. Sandia National Laboratories is a multimission laboratory managed and operated by National Technology & Engineering Solutions of Sandia, LLC, a wholly owned subsidiary of Honeywell International Inc., for the U.S. Department of Energy's National Nuclear Security Administration under contract DE-NA0003525.

11:45 AM *SF03.11.07

Next Generation Bioelectronic and Biosensing Devices via Nanoparticle 3D Printing [Rahul Panat](#)¹, Azahar Ali¹, Sandra Ritchie¹, Hailey Gordon¹, Chunshan Hu¹, Mark Nicholas¹, Bin Yuan¹, Sanjida Jahan¹, Sadeq Saleh¹, Eric Yttri¹ and S.J. Gao²; ¹Carnegie Mellon University, United States; ²University of Pittsburgh Medical Center, United States

In this research, we develop a nature-inspired droplet-based nanoparticle 3D printing method that creates highly complex three-dimensional architected structures and use them to make a new class of biomedical devices. Fluid dynamics of aerosol microdroplets is used to stack nanoparticles in 3D space without any support materials to create such structures. First, we use this technique to realize a regenerable biosensor that detects COVID-19 antibodies and antigens within 10 seconds! This is the fastest detection time yet reported in literature and will have a significant positive impact on the course of the current pandemic. Several fundamental problems related to deformation during nanoparticle sintering were solved during this research. Second, we use 3D printing to create fully customizable brain-computer interfaces (BCIs) having recording densities of thousands of electrodes/cm², which is 5-10x higher than the current state-of-the-art BCI technologies. Recording of action potentials from the brain of anesthetized mice was achieved with a high signal to noise ratio. Lastly, we also demonstrate highly flexible 3D printed cardiac biomonitors that lead to minimal patient discomfort. Our research thus focuses on advancing microfabrication via 3D printing and using the same to realize next-generation biomedical devices for the benefit of public health.

8:00 AM SF03.12.01

Freeform Embedded 3D Printing and Pressurized Thermo-Curing Platform for Customized Acrylic Biomedical Implants Qian Shi^{1,2}, Wen See Tan¹ and Juha Song¹; ¹Nanyang Technological University, Singapore; ²Xi'an Jiaotong University, China

Poly (methyl methacrylate) (PMMA) is a synthetic polymer commonly used for medical implants in cranioplasty and orthopaedic surgery owing to its good mechanical properties, optical transparency, and minimal inflammatory responses. Recently, the development of 3D printing opens new avenues in fabrication of patient-specific PMMA implants for personalized medicine. However, challenges are confronted when introduction of medical-grade PMMA resins to a conventional 3D printing process due to its dynamic viscosity and poor self-supportability during printing. In addition, the intrinsically exothermic polymerization of PMMA creates voids and pores within the printed product due to locally trapped MMA gas to which is often attributed poor mechanical performance and resultant opaqueness. Therefore, in this study, a freeform embedded 3D printing platform is proposed, followed by the pressurized thermo-curing for fabrication of customized PMMA implants with improved strength and transparency. An alginate-based supporting matrix is used to structurally support the extruded liquid acrylic resin during both 3D printing and post-curing processes; moreover, the autoclave reactor enclosing the alginate matrix and as-printed PMMA is utilized to generate temperature-dependent hydrostatic pressure, which serves for suppressing bubble formation and densifying polymerised PMMA during the post-curing. The 3D printed PMMA shows almost comparable mechanical behavior to that of PMMA from a conventional casting method because of well-densified uniform microstructures. Also, *in vitro* cytotoxicity results confirm that 3D-printed PMMA is as biocompatible as casted PMMA. As proof-of-concepts, various complex structures are also fabricated through this 3D printing and post-curing platform. We envisage that the proposed freeform 3D printing platform in conjunction with the pressurized post-curing method can also allow fabrication of various liquid resins such as epoxy resins and their composites besides acrylic resins.

8:05 AM SF03.12.02

3D Printed Magneto-Active Fibrous Scaffolds for Skeletal Muscle Regeneration and Stimulation Miguel Castillo^{1,2}, Ouafa Dahri³, Gerardo Cedillo¹, Joost van Duijin¹, Joao Meneses⁴, Joana Silva⁴, Andre Pereira⁴, Fernao Magalhaes⁴, Jos Malda¹, Niels Geijsen³ and Artur Pinto⁴; ¹UMC Utrecht, Netherlands; ²Technische Universiteit Eindhoven, Netherlands; ³Leiden University Medical Center, Netherlands; ⁴Faculdade de Engenharia da Universidade do Porto, Portugal

Introduction

Skeletal muscle comprises the majority of tissue in the human body. It is essential to keeping posture, balance and mobility but also has crucial functions in many physiological and metabolic processes. Gene mutations leading to muscular dystrophies, such as Duchenne Muscular Dystrophy (DMD), have a major impact on patients' lives causing progressive disability and, ultimately, death due to cardiac or respiratory failure. Current therapeutic methods against DMD are very limited, including corticosteroids with severe side effects and experimental stem cell based therapies [1]. Despite great promise, this latter method has been restricted by the absence of 3D matrices that promote myofiber alignment and, importantly, support and stimulate muscle contractile force during regeneration. Furthermore, magnetic fillers embedded into 3D matrices can be used to externally induce cyclical deformation over implanted scaffolds to activate mechanotransduction pathways that will improve tissue regeneration. [2] In this work, we hypothesized that iron-modified reduced graphene oxide (rGO-Fe) with magnetic responsive properties can be processed by melt electrowriting (MEW) – a unique technique for the fabrication of highly ordered scaffolds with ultra-fine fibers – once mixed with polycaprolactone (PCL), and that well-organized fiber scaffold architectures can guide myofiber growth and remotely stimulate muscle contraction.

Materials and Methods

Composites of medical grade PCL and rGO-Fe were prepared by melt blending (rGO-Fe loadings between 2-20 wt%), and their processing compatibility was systematically investigated according to key MEW parameters. Fabrication of well-organized fibrous scaffolds with different laydown microstructures (square, hexagonal and auxetic) and macrostructures (straight and circular) was explored. The effect of rGO-Fe content and MEW processing parameters on fiber scaffold morphology, magnetic properties and mechanical performance was studied. Finally, fiber scaffolds were seeded with an immortalized mouse myoblast cell line (C2C12), encapsulated in an extracellular matrix-like hydrogel, to ensure uniform cell distribution within the fiber scaffold. Cell survival, morphology, tissue structure and functionality were studied after 7 and 14 days in culture.

Results and discussion

Well-organized scaffolds (microfiber diameter=10-15 µm) composed of rGO-Fe/PCL blends with square, hexagonal and auxetic microstructures were successfully manufactured for the first time using MEW. The smallest pore resolution achievable was 300 µm, for a scaffold thickness of 300 µm and 2 wt% rGO-Fe. Both hexagonal and auxetic architectures allowed for better deformation recoverability and approximately a 10-fold increase in applied strain with respect to conventional square fiber architectures. Additionally, above a rGO-Fe content of 10 wt%, scaffolds allowed for in-plane and out-of-plane deformation of near to 10% in the presence of magnetic stimulation. All scaffolds were cytocompatible, and hexagonal constructs showed enhanced myofiber alignment and organization with respect to square fiber architectures.

Conclusion

In summary, the present study demonstrated for the first time that highly ordered microfiber scaffolds based on rGO-Fe/PCL blends can be reproducibly produced and that these organized constructs are promising candidates to guide skeletal cell growth, stimulate contraction and (potential) regeneration under externally controllable magnetic triggering.

References

- [1] Sun et al., *Exp Neurol* 323 (2020) 113086.
- [2] Vining & Mooney, *D. Nat Rev Mol Cell Biol* 18 (2017) 728–742.

8:10 AM SF03.12.03

3D Printing of Antibacterial Polymer Devices Based on Nitric Oxide Release from Embedded S-nitrosothiol Crystals Wuwei Li¹, Yuanhang Yang¹, Christopher Ehrhardt¹, Nastassja Lewinski¹, David Gascoyne², Gary Lucas², Hong Zhao¹ and Xuewei Wang¹; ¹Virginia Commonwealth University, United States; ²Momentive Performance Materials, United States

Drug-eluting polymer devices play a pivotal role in combating foreign body reactions and infections associated with the functional devices. We report here a one-step 3D printing strategy to create drug-eluting polymer devices with a drug-loaded bulk and a drug-free coating. The spontaneously formed drug-free coating is crucial to biomedical applications because it drastically reduces the surface roughness and also functions as a protective layer to suppress the burst release of drugs. A moisture cured silicone is used as the printing ink that can be extruded based on its shear-thinning property and quickly vulcanize upon exposure to ambient moisture to retain the fidelity of the 3D printed patterns. S-nitrosothiol type nitric oxide (NO) donors in their crystalline forms are selected as model drugs because of the potent antimicrobial, antithrombotic, and anti-inflammatory properties of NO. Direct ink writing of the homogenized polymer-drug mixtures results in devices with very rough and ill-defined surfaces because of the exposed S-nitrosothiol microparticles. By further addition of a low-viscosity silicone (polydimethylsiloxane) into the ink, the low-viscosity silicone diffuses outwards upon deposition to form a drug-free outermost layer without compromising the printing integrity. S-nitroso-N-acetylpenicillamine (SNAP) embedded in the printed silicone matrix releases NO under physiological conditions from days to about one month. The micro-sized drug crystals are well preserved during the ink preparation and printing processes, which is one reason of the sustained NO release. Preliminary biofilm and cytotoxicity experiments confirm the antibacterial property and safety of the printed NO-releasing devices. This additive manufacturing platform does not require dissolution of drugs and involve no thermal or UV

curing processes, and therefore, offers unique opportunities to produce drug-eluting silicone devices in a customized manner.

8:15 AM SF03.12.04

Cellulose Nanocrystals-Based All-3D Printed Piezoelectric Nanogenerator for Mechanical Energy Harvesting Application Kuntal Maity, Anirban Mondal and Mrinal Saha; University of Oklahoma, India

Rapid development of wearable electronics, accessible and environmentally sustainable energy generation has attracted an extensive attention in next generations. In this context, piezoelectric materials have the ability of generating electric signal when it is subjected to certain mechanical stimuli, such as stress, elongation, tension, vibration, etc.^[1] It has been found that different types of piezoelectric materials are reported so far, for example, as a semiconductor (ZnO, ZnS, GaN, etc.), ceramics (PZT, BaTiO₃, NaNbO₃, KNbO₃, KNN, ZnSnO₃, etc.), polymers (PVDF and its copolymers, polyamides, etc.) and some natural materials (bones, hairs, collagen fibrils, peptide, cellulose, sugar cane, etc.).^[2] Among them, natural piezoelectric materials possess several advantages over the other class of piezoelectric materials. For example, cellulose, a novel piezoelectric polymer is almost endlessly available polymeric raw material that exhibits fascinating natural structure and also treated as eco-friendly and biocompatible product. In addition, cellulose is also utilized for versatile sensing applications and easily obtained from various plants as micro-fibrils consist of glucose-glucose linkages with linear chains. On the other hand, the advancement of three-dimensional (3D) printing technology has recently attracted a great deal of attention as the 3D printing enables the fabrication of materials with intricate macroscopic shapes and controlled microstructures and properties.^[3] Cellulose nanocrystals (CNCs) have recently received significant attention due to its high Young's modulus, high strength, light weight, low density, sustainability, biocompatibility, biodegradability, recyclability, and abundance nature. As a result, it is conceivable and advantageous to substitute traditional 3D printing thermoplastics with cellulosic materials such as CNCs. In addition, the choice of electrodes and their compatibility with 3D printed surface remain challenging tasks, particularly when device performance, durability and implant ability are considered.

Here we present an all-3D printed piezoelectric nanogenerator (PNG) based on CNCs by direct-ink write (DIW) process for energy harvesting from various types of mechanical vibrations. We achieved the all-3D printed multilayer structure where active piezoelectric ink CNC is printed in between two printed electrodes (top and bottom). For electrode printing, the conductive ink is developed using the carbon nanotube (CNT) into CNCs matrix. Interestingly, we address the electrode compatibility issue by keeping the same polymer matrix (CNCs here) through the whole structure and subsequently enhancing the interface compatibility of the piezoelectric active layer and the electrode layers. Noteworthy that, for distinct electrode and piezoelectric material, mechanical pressure imparting leads to the delamination of the interfacial layer due to the mismatch of Young's modulus, and results in the degradation of PNG performance. The crystallinity of the printed CNC was determined from X-ray diffractometry (XRD) spectra. The Fourier transform infrared spectroscopy (FT-IR), Raman spectroscopy are used to examine the vibrational bands of CNC and CNT. The surface morphology is characterized by Field emission scanning electron microscope (FE-SEM) images. The mechanical properties are done by stress-strain testing. Owing to excellent electrode contact-adherence, the PNG exhibits an effective conversion of mechanical energy of human finger movements into electrical energy (~10 V). Importantly, the fatigue test under continuous mechanical impact (over 1000 cycles) shows great promise as a highly durable mechanical energy harvester. Thus the all-3D printed PNG will play an essential role in future self-powered electronics.

References:

- [1] Wang et al., *Science* **2006**, 312, 242.
- [2] Maity et al., *ACS Appl. Mater. Interfaces* **2018**, 10, 44018.
- [3] Davidson et al., *Adv. Mater.* **2019**, 1905682.

8:20 AM *SF03.12.05

3D Printing of Living Materials Andre R. Studart; ETH Zurich, Switzerland

Exploiting microorganisms to fabricate engineered living materials has gained impulse in recent years due to the sustainable nature of biological processes and the possibility to add living functionalities to synthetic materials, including self-healing, self-regeneration and adaptation. In this talk, I will show how 3D printing can be used to leverage the metabolic activity of microorganisms and create a new generation of complex-shaped living materials. To this end, biocompatible hydrogels are thoroughly designed to enable loading with selected microorganisms and printing using the extrusion-based Direct Ink Writing technique. By formulating inks with suitable rheological properties and appropriate culture media, it is possible to control the geometry of the printed object and promote the proliferation and growth of material-forming microorganisms within the deposited structures. Using selected examples, I aim to demonstrate that the achieved shape programmability and tailored spatial distribution of microorganisms makes 3D printing a powerful tool for the manufacturing of functional living materials.

8:50 AM SF03.12.06

All-Organic Flexible Nanogenerator with 3D Printed Ferroelectrets and Fabric Electrodes Ningzhen Wang¹, Kerry L. Davis¹, Robert Daniels¹, Mohamadreza Arab Baferani¹, Michael Sotzing¹, Chao Wu¹, Reimund Gerhard², Gregory Sotzing¹ and Yang Cao¹; ¹University of Connecticut, United States; ²University of Potsdam, Germany

Ferroelectrets with internal polarized pores are an appealing solution for self-powered sensors and wearable energy harvesting devices due to its flexibility and strong piezoelectric response. Additive manufacturing, or 3D printing, enables the designability of pore structures and the piezoelectric performance of ferroelectrets to be optimized further than traditional manufacturing methods. Our previous investigation found that the compressible fabric-based electrodes and the outer surface of the ferroelectret film can form an additional electro-electret and can significantly contribute to the overall piezoelectric performance. In this work, polypropylene (PP) ferroelectrets with different kinds of porous structures (ellipsoid, hexagon, triangle, spherical protrusions) were fabricated by 3D printing and polarized through corona discharge. The all-organic ferroelectret nanogenerator (FENG) was then assembled after applying the electrodes of poly(3,4-ethylenedioxythiophene):poly(styrene sulfonate) (PEDOT:PSS)-coated Spandex fabric. It was found that the PP ferroelectret with spherical protrusions on the surface, which is the optimal balancing in film thickness, porosity and elastic modulus, shows the best short-circuit current and open-circuit voltage under the same compressive condition. The performance of the all-organic FENG was demonstrated by charging several capacitors and lighting up the light emitting diodes (LEDs) successfully. The 3D-printed porous structures would be conducive for studying the charge storage mechanism of ferroelectrets due to the pores' regularity and designability. Moreover, because of its easy integration with clothing, shoes, carpets, etc., the all-organic FENG with fabric electrodes would be a competitive candidate in wearable electronics field.

9:05 AM SF03.12.07

3D Bioprinted Functional Surgical Mesh for Soft Tissue Repair Crystal S. Shin¹, Apam Adumbukulath², Remya Ammassam Veetil¹, Richard Lee¹, Pulickel Ajayan² and Ghanashyam Acharya¹; ¹Baylor College of Medicine, United States; ²Rice University, United States

A hernia is a common soft tissue injury resulting from a weak or defective abdominal wall, causing protrusion of the intra-abdominal contents. Surgical implantation of a prosthetic mesh is the most common hernia repair technique to support and reinforce the abdominal wall. Over 400,000 incisional hernia repair surgeries are performed annually in the US. However, surgeries involving prosthetic meshes induce local inflammatory responses leading to the

formation of visceral adhesions, hardening, and gradual shrinking of the implanted meshes, which require additional surgeries. Hence, there is a critical need for a soft tissue repair scaffold to minimize post-surgical complications.

This study presents the development of a 3D-bioprinted functional biomaterial-based surgical mesh (Biomesh) that modulates local inflammation. We designed and fabricated Biomesh to yield a soft, pliable, and mechanically strong mesh by in situ phosphate crosslinking of polyvinyl alcohol. The crosslinking of hydroxyl groups with phosphate groups gives a negative surface zeta potential of Biomesh. We showed that the negatively charged Biomesh “captured” positively charged pro-inflammatory cytokines such as IL-1 β , IL-6, and TNF- α via electrostatic interactions. We also reported that in a rat ventral hernia model, the implantation of Biomesh modulated inflammation in the surgical site and prevented visceral adhesions even after 8 weeks compared to the polypropylene mesh implant. Thus, this study successfully demonstrated the therapeutic efficacy of Biomesh as an intrinsically inflammation-modulating surgical mesh without the need for anti-inflammatory agents for soft tissue repair surgery.

9:20 AM SF02.08/SF03.06.03

Wearable, 3D Printed, Personalized, Wireless and Battery-Free Tools for Chronic Recording of Biosignals Philipp Gutruf; University of Arizona, United States

The concept of digital medicine, which broadly deals with streams continuous information from the body to gain insight into health status, manage disease and predict onset health problems, is currently only gradually developing.^{[1][2]} Key technological hurdles that slow the proliferation of this approach are means by which clinical grade biosignals are continuously obtained without frequent user interaction.^[3] To overcome these hurdles, solutions in power supply and interface strategies that maintain high fidelity readouts function chronically are critical. Current approaches for high fidelity recordings typically rely on adhesive interfaces that are subject to epidermal turnover, limiting sensor lifetime. Additionally, they rely on electrochemical power supplies which are subject to frequent recharge, add bulk and weight, require user interaction and introduce motion artefacts. Here we introduce a new class of devices that overcomes the limitations of current approaches by utilizing digital manufacturing to tailor geometry, mechanics, electromagnetics, electronics, and fluidics to create unique personalized devices optimized to the wearer. These elastomeric, 3D printed and laser structured constructs, called biosymbiotic devices, enable adhesive-free interfaces and the inclusion of high performance, far field energy harvesting to facilitate continuous wireless and battery-free operation of multimodal and multi device, high-fidelity biosensing in an at-home setting without user interaction.

References

- [1] T. R. Ray, J. Choi, A. J. Bandodkar, S. Krishnan, P. Gutruf, L. Tian, R. Ghaffari, J. A. Rogers, *Chem. Rev.* **2019**, *119*, 5461.
- [2] J. Heikenfeld, A. Jajack, J. Rogers, P. Gutruf, L. Tian, T. Pan, R. Li, M. Khine, J. Kim, J. Wang, *Lab Chip* **2018**, *18*, 217.
- [3] T. Stuart, L. Cai, A. Burton, P. Gutruf, *Biosens. Bioelectron.* **2021**, 113007.

SESSION SF03.13: 3D Printing Functional Composites and Devices

Session Chairs: Sohini Kar-Narayan and Ethan Secor

Wednesday Morning, December 8, 2021

SF03-Virtual

10:30 AM SF03.13.02

Additive Manufacturing of Functional Emulsions Aaron Haake¹, Ravi Tutika², Michael D. Bartlett² and Eric Markvicka¹; ¹University of Nebraska Lincoln, United States; ²Virginia Tech, United States

Elastomer composites with embedded liquid phase fillers are an emerging material architecture for creating highly functional elastomer composites that are soft, elastically deformable, and exhibit unique combinations of electrical, thermal, and mechanical properties. The material architecture consists of a functional emulsion of liquid phase fillers, such as liquid metal microdroplets, dispersed in an uncured hyperelastic polymer that can be cured into an elastomer composite. These functional emulsions are typically manufactured in bulk using replica molding or soft lithography techniques that results in primarily spherical inclusions with little control of shape, orientation, or spatial placement. Here, we will introduce a new additive manufacturing process to actively tailor the liquid inclusion microstructure of functional emulsions throughout a manufactured part to control the electrical, thermal, and mechanical properties of soft elastomeric composites of complex geometry. The material microstructure is actively tailored through a direct ink write alignment processing technique and the creation of a new emulsion ink that is suitable for additive manufacturing. The programmed inclusion shape and orientation is characterized as a function of material properties and processing parameters. Individual printed filaments and printed sheets are experimentally characterized for mechanical and functional properties. Finally, the ability to print sheets and multilayer parts with varying material microstructure is demonstrated. This manufacturing method for processing functional emulsions provides new opportunities to create soft elastomer composites with directly tunable and addressable material properties and performance.

10:35 AM SF03.13.04

Effects of Extrusion-Based Additive Manufacturing on Thermoelectric Transport in Elemental Ni and Bi Victoria J. Stotzer, Christian Apel, Ashley Paz y Puente and Sarah J. Watzman; University of Cincinnati, United States

Conventional synthesis and manufacturing of thermoelectric materials is often tedious, time-intensive, and expensive with severe limitations in terms of resultant sample geometry and size. While traditional growth techniques have been used for many years in the field, as the interest in thermoelectric devices and environmental efficiency has increased, the wastefulness of the process has become abruptly apparent. Recently, popularity has grown for using additive manufacturing methods in materials science fields, offering the potential to decrease fabrication time and cost for both samples and devices. Nevertheless, success in additive manufacturing has been majorly limited to metals and polymers, while the manufacture of thermoelectric semiconductors has identified current limitations [1]. These limitations include the need for post-processing that often leads to pore formation and decreased adhesion [1]. Additionally, current work has not extensively studied how additive manufacturing techniques alter thermoelectric transport. In this work, we approach the problem starting with Ni, whose thermoelectric properties are well known [2], albeit less compelling than those of Bi₂Te₃ and other conventional thermoelectric materials. Specifically, we focus on the particle-laden ink extrusion printing process, which has proven successful with producing bulk Ni samples [3]. This process contributes to the formation of micro and macro cracks and pores in bulk samples. Through altering printing parameters and sintering techniques, we study the microstructure of printed samples with a specific focus on densification, composition, and pore and crack concentration. Then through comparison of the temperature dependence of thermopower, electrical resistivity, and thermal conductivity in the printed samples to those made using traditional crystal growth techniques, including dense and porous polycrystalline samples, the effects of the particle-laden ink extrusion printing processing on thermoelectric transport properties can begin to be made clear. This information is then used to inform the extension of the particle-laden ink extrusion printing technique to more efficient thermoelectric materials, in this case starting with Bi, which are more demanding in their

manufacturing requirements. Bi makes an ideal starting point due to the well-known transverse thermoelectric transport properties. Pure Bi has also not previously been printed using extrusion based additive manufacturing; therefore, we present a newly-developed low-temperature method.

[1] A. El-Desouky et al. *Mater. Lett.* 185, 598-602 (2016).

[2] S. J. Watzman et al. *Phys. Rev. B* 94, 144407 (2016).

[3] S. L. Taylor et al. *Adv. Eng. Mater.* 19 (11), 1600365 (2017).

10:40 AM SF03.13.05

Smart Viscoelastic Materials via Viscous Solution 3D Printing (VSP) Methods—From Elastomers to Metals Fabrication Rigoberto C.

Advincula^{1,2,3}; ¹Case Western Reserve University, United States; ²The University of Tennessee, Knoxville, United States; ³Oak Ridge National Laboratory, United States

3D Printing methods have enabled rapid prototyping and production of parts and OEMs that have been considered a paradigm shift in several industries. In the area of polymers, thermoplastics, thermosets, and elastomers based on their thermo-mechanical properties have been matched with their processability. However, it is not as simple as the classification into these groups when it comes to their intended applications and the development of new properties.

There are a number of choices for 3D printing methodologies (FDM, SLA, SLS, VSP)

which can make use of blended or formulated compositions. However, this talk will focus on a class of viscoelastic materials that can be 3D printed even at room temperature. This will be exhibited in the following examples: 1) Elastomeric foam materials from plastics based on polyurethane, 2) Silicone materials with high electrical and thermal conductivity, and 3) Metals from bio-based sustainable viscoelastic materials. The design of the materials and the geometry are very important and must be matched with the 3D printing parameters. The utilization of rheological and viscoelastic materials studies is important prior to the study as these emphasize shear thinning behavior, sufficient yield stress, and thixotropic behavior to achieve high fidelity with the CAD design.

10:55 AM *SF03.13.06

Printing Methods for Flexible and Conformal Wearable Sensors Ana C. Arias; University of California, Berkeley, United States

Wearable sensors are increasingly prevalent in health monitoring and human-machine interface applications as a result of improvements in their size and comfort. Flexible and printed electronics have enabled the fabrication of wearable sensors that can mechanically bend and conform to non-planar and dynamic surfaces of the human body, allowing physiological signals of low bandwidth to be measured. Hybrid systems that combine flexible sensors with rigid computational components on a separate substrate have also been developed. To provide a real-time analysis of physiological signals, wearable biosensors can implement machine-learning models for signal processing. Traditionally, skin bioelectrodes have relied on wet electrodes, metal or composite electrodes coated in an electrolytic gel, applied by trained professionals. These wet electrodes ensure consistent electrode-skin contact but are susceptible to impedance mismatch related noise and interference as they dry out. In addition, the skin preparation required for wet electrodes (often lead to skin-irritation and hair loss). We have developing methods for 3D printed dry electrodes that are optimized for different sensing locations. In this talk I will discuss several fabrication methodologies and materials used for skin conformal sensors, including dry electrodes. These electrodes exhibit high effective surface areas and when compared to wet electrodes of the same area, they express comparable electrode-skin impedances. Applications in electrocardiography (ECG), electromyography (EMG), and electroencephalography (EEG) will also be discussed.

11:25 AM SF03.13.07

Polymer and Nanoparticle Composites in Layered Nanostructures Kenan Song, Weiheng Xu, Sayli Jambhulkar, Dharnedar Ravichandran and Yuxiang Zhu; Arizona State University, United States

Layer-structured composites have broad applications in structural systems, thermal insulation, microelectronics, optics, and biomedical devices. The design and assembly of layered structures containing polymer and particle materials have been challenging in sub-microscale. The bottleneck is the lack of appropriate manufacturing compatible with soft matter and nanomaterials. This research will demonstrate three examples in 1D, 2D and 3D structures containing polymer and nanoparticle layers for different applications.

The first example was the use of polymer-nanoparticle interphase design to achieve 1D fibers. As well known that polymer fibers of microscale with continuous nanoparticle distribution are difficult to process due to the stiffness mismatching between polymers and nanoparticles. This example will demonstrate unique fiber spinning that blends polymers and nanoparticles at different layers. The soft macromolecules and rigid particles will be stacked along the radial or the fiber axis for enhanced mechanical, electrical, and thermal properties. The unique material system of composite fibers were used as piezo- and chemi-resistive sensors.

The second example exhibited a thin composite film on compliant structures for thermoelectric generators (TEGs). The stacking of 2D films contained conjugating polymers in-situ polymerized at the presence of nanoparticles. During the processing, the polyaniline molecules were found to coat evenly on carbon nanotubes and led to high electrical conductivity, power factor, and enhanced mechanics. Thus, these compressed films were exhibited on compliant structures and used as wearable devices for human body heat collection. The generated electricity was for powering wearable sensors in detecting human movement and health conditions.

The third demonstration utilized layer-by-layer-based deposition techniques. Both additive manufacturing (e.g., 3D printing) and coating methods were used on the same processing platform. One dimensional carbon nanofibers (CNF) and 2D MXene particles were used as examples to be selectively deposited on polymer surfaces with pre-printed patterns. The control of the surface patterns and the nanoparticle assembly conditions (e.g., thermodynamic parameters, nanoparticle interactions, solid-liquid-air contact lines, etc.) led to selective deposition and preferential alignment of nanoparticles. As a result, the conductive paths on the substrate were developed to be anisotropic; following this characterization, the multifunctional sensitivity to strain, temperature, chemical liquids and volatile organic compounds (VOCs) were also displayed.

11:40 AM SF03.13.08

Hybrid Printing of Wearable Piezoelectric Sensors Yipu Du¹, Ruoxing Wang², Minxiang Zeng¹, Mortaza Saeidi-Javash¹, Wenzhuo Wu² and Yanliang Zhang¹; ¹University of Notre Dame, United States; ²Purdue University, United States

Piezoelectricity provides an ideal electromechanical mechanism with emerging applications in wearable devices due to its simplicity and self-powered nature. However, the 3D printing of piezoelectric devices still faces many challenges, including material printability, high energy poling process, and low dimensional accuracy. This study demonstrates, for the first time, a tellurium nanowire-based poling-free piezoelectric device fabricated by a hybrid printing method. The home-built hybrid printer consists of an extrusion printing head for structural material fabrication and an aerosol jet printing head for functional material fabrication. The aerosol jet printed tellurium nanowire demonstrates piezoelectric properties without the need for any poling or post-

printing processing due to the unique properties of the tellurium nanowires coupled with the aerosol jet printing process. The silver nanowire electrodes printed by aerosol jet printing demonstrate excellent conductivity and stretchability without the need of sintering. The extrusion method is employed to print the silicone films which serve as the stretchable substrate and the electrical insulation layers between the printed tellurium and silver. The fully printed, sintering-free and poling-free, and stretchable piezoelectric device opens enormous opportunities for facile integration with a broad range of printed electronics and wearable devices.

SESSION SF03.14: On-Demand
Sunday Morning, December 5, 2021
On-Demand

8:00 AM SF03.04.09

Customized 3D Printer Filament with Metalized Ceramics [Antwine McFarland](#), Anusha Elumalai and David K. Mills; Louisiana Tech University, United States

Halloysite nanotubes (HNTs) are naturally occurring clay nanotubes having 50 nm external diameters, 15 nm luminal diameters, and 500-1500 nm lengths on average. *Halloysite* is a two-layered aluminosilicate, chemically similar to kaolin, and has a predominantly hollow nanotubular structure in the submicron range. HNTs typically display an inner diameter ranging from 15–50 nm, an outer diameter from 30–50 nm, and a length between 100–2000 nm. HNTs exhibit vigorous activity, especially when coated with metal, and have found industrial uses due to their properties as a filler leading to strength reinforcements. We created a new nanocomposite 3D printer filament designed to manufacture replacement parts in a matter of hours, not days, using a 3D scanner and a commercially available 3D printer. Our composite consists of HNTs and nylon (6 and 12). Our lab analysis (3-point bed test, crystallinity measurements, elasticity, hardness tests) of this printer filament products showed significant increases in mechanical strength. In addition, DSC analyses showed enhancement of the nanocomposite filament's thermal resistance. Fused depositional modeling (FDM) or high-intensity laser-powered projector printing (LAPS) were used to design and print high-end, high-performance devices, parts, and tools. Regardless of which nylon type or a blend of nylon, the addition of HNTs significantly reinforced the material properties of 3D printed parts and tools. 3D printed constructs showed a higher bend capacity, increased hardness, and elasticity while keeping the inherent native properties of nylon. The filaments are the most costly to produce. The application of nylon with additives 3D printing will enable 3D printed devices, and parts produced on-site. Examples include anti-icing gasket, O-rings, sump cover, non-critical components, and standard requirements such as surface toilet cover, door handles, and light switches. These devices can be custom-fitted, produced on-demand, and in a rapid manner. The complexity of design, internal or external architectures, does not significantly challenge the fabrication of high-quality finished parts. Accordingly, this technology can move beyond its original low-volume, high-value market niches toward economical and sustainable manufacturing on an industrial scale.

8:05 AM *SF03.02.03

Printing Programmable Materials [Skylar Tibbitts](#); Massachusetts Institute of Technology, United States

Programmable Materials are physical materials that can be embedded with information and capabilities like logic, actuation, or sensing. We are now able to design and fabricate these material compositions through new forms of 3D and 4D printing. In this talk we will present the fundamental principles for programmable materials through material properties, geometry, activation energy and physical transformation. We will then explore various material properties and fabrication processes that enable new programmable behaviors and functionality in our built environment. By taking advantage of these new material behaviors and emerging fabrication processes we are now able to create higher performing products which tap into natural forces like moisture, light, temperature, or pressure to become highly active and tuned to their environment.

SYMPOSIUM SF04

New Types of Polymers, Composites and Hybrid Materials for Additive Manufacturing
November 30 - December 6, 2021

Symposium Organizers

Susmita Bose, Washington State University
Richard Hague, University of Nottingham
Jayme Keist, The Pennsylvania State University
Roger Narayan, North Carolina State University

Symposium Support

Silver
Eastman Chemical Company

* Invited Paper

SESSION SF04.01: New Types of Polymers, Composites and Hybrid Materials for Additive Manufacturing I
Session Chairs: Anne Arnold, Douglas Chrisey and Kalpana Katti
Tuesday Afternoon, November 30, 2021
Sheraton, 3rd Floor, Beacon A

1:30 PM SF04.01.02

3D Printing of Corn-Based Natural Fiber Composites via Direct Ink Writing Md Nurul Islam and Yijie Jiang; University of North Texas, United States

Natural materials and composites are receiving increased attention for sustainable manufacturing. They are renewable, biodegradable, and inexpensive. Manufacturing using natural resources into mechanically-robust materials alleviates environmental concerns associated with the use of petroleum-based materials. Cellulose fibers have been used as fillers in polymer matrices to make composites. However, the hydrophilic cellulose fibers are incompatible with synthetic hydrophobic polymers¹, leading to poor interfaces between fillers and matrix. In addition to traditional manufacturing, additive manufacturing enables the customized and precision fabrication of composites with the control of internal microstructures^{2,3}. Although there are emerging researches using natural materials into 3D printing^{4,5}, limitations on printable materials and their mechanical robustness exist. In this study, we develop 3D printable biocomposites entirely from corn byproducts and waste. We extract cellulose microfibrils from corn husks by alkalization, delignification and high-speed homogenization. FTIR spectrum reports the effective removal of hemicellulose and lignin from corn husk. The extracted cellulose fibers (60 µm in length and 10 µm in diameter) are distributed into compatible matrices derived from corn starch to formulate 3D printable biocomposites. Ink preparation is tailored with water content and thermal treatment to achieve desired rheological properties for direct ink writing (DIW) 3D printing and tunable mechanical properties for the printed samples. The printed triangular cellular architectures using composites (10 wt% fiber) show 2 and 1.5 times increase in stiffness and strength, respectively, over the pure starch. Besides, preheating time substantially affects the mechanical properties of the printed biocomposites. The specific young's modulus and specific strength increase 159.8% and 160% for 14 minutes preheating at 120°C compared to 6 minutes preheated samples, correlating to the microstructures evolution at different preheating times. The results indicate a comparable mechanical performance compared with other 3D printed thermoplastics. The manufactured biocomposites consist of purely natural components will have potential applications in medical and food area.

References:

1. Mohanty, A. K., Misra, M. & Hinrichsen, G. Biofibres, biodegradable polymers and biocomposites: An overview. *Macromol. Mater. Eng.* 276–277, 1–24 (2000).
2. Compton, B. G. & Lewis, J. A. 3D-printing of lightweight cellular composites. *Adv. Mater.* 26, 5930–5935 (2014).
3. Raney, J. R. *et al.* Rotational 3D printing of damage-tolerant composites with programmable mechanics. *Proc. Natl. Acad. Sci. U. S. A.* 115, 1198–1203 (2018).
4. Nguyen, N. A. *et al.* A path for lignin valorization via additive manufacturing of high-performance sustainable composites with enhanced 3D printability. *Sci. Adv.* 4, 1–16 (2018).
5. Jiang, Y. & Raney, J. R. 3D Printing of Amylopectin-Based Natural Fiber Composites. *Adv. Mater. Technol.* 1900521, 1–8 (2019).

1:45 PM SF04.01.03

Multifunctional Polyethylene Based Composite Material for Space Applications Lembit Sihver^{1,2,3}, Cody Alison Paige⁴ and Svetlana V. Boriskina⁴; ¹Cosmic Shielding Corporation, United States; ²Technische Universität Wien, Austria; ³Chalmers University of Technology, Sweden; ⁴Massachusetts Institute of Technology, United States

To enable the planned rapid growth of both government and private operators in space, including satellites, space tourism and manned missions to the Moon and to Mars, a realistic and holistic approach to radiation risk reduction is needed. In deep space, ionizing radiation from Galactic Cosmic Rays (GCRs) and Solar Energetic Particles (SEPs) from the sun pose a critical threat to both humans and electronic equipment. GCRs provide a chronic, slowly varying, highly energetic background source of High-Z high-Energy (HZE) particles, while the Sun's activity varies with an 11-year cycle during which the Sun produces Solar Wind (SW) at varying intensities and unpredictable bursts of Solar Particle Events (SPEs). SPEs can be a nightmare for the astronauts and cause acute radiation damage, while GCRs can cause long term damage including cancer, cataracts, central nervous system and cardiovascular system damage, fibrosis, neurodegeneration, digestive diseases, and immunological, endocrine, hereditary effects, and cognitive impairment.

The GCRs and SPEs can also cause degradation of micro-electronics, optical components and solar cells. Spacecraft electronics are especially susceptible to radiation effects that emerge from interactions with HZE particles, but highly energetic gamma photons, neutrons and protons can also damage electrical components. Since the exposure of humans and electronics to GCRs and SPEs in deep space, and on the surface of the Moon and Mars, will cause huge radiation risks, it is very important to apply the best possible protection for both humans and electronics. Currently, the only proven and practical countermeasure to reduce the exposure to GCRs and SEPs is passive shielding. It is well known that low atomic number (Z) materials are most effective for shielding in space, and liquid hydrogen has the maximum theoretical performance as a shielding material. Hydrogen is not, however, a practical shielding material, being a low temperature liquid associated with practical handling problems and explosion risks. Hydrogen concentrated in specially engineered and doped polyethylene based composites, however, is ideal for stopping primary cosmic and solar radiation, as well as secondary neutrons created when the primary particles are impinging on the spacecraft. Low atomic number (Z) materials also produce less electron-positron pairs and Bremsstrahlung than materials with higher Z, such as aluminum alloys, which are used in conventional satellites and spacecraft. Additives can improve the flame retardancy and inhibit the release of toxic gases as well as absorption of neutrons created when HZE particles hit the shielding and other components of the spacecraft. The material can also be produced for protection against micrometeoroids, debris, extreme temperature variations and protection against atomic oxygen present at low Earth orbit (LEO).

We will present the basic physics, as well as simulated and experimental properties of a 3D printed specially engineered and doped polyethylene based composite, which can be manufactured with different degrees of flexibility, stiffness and thermal conductivity. We have demonstrated that hierarchical engineering of PE materials and composites enables drastic modification of their light absorption, thermal emission, heat, and moisture transport properties [1,2]. The material can therefore be used for many different applications, ranging from radiation shielding of components inside a satellite or spacecraft, to a construction material for satellites, to spacecraft and space habitats, and components in intravehicular (IVA) and extravehicular (EVA) spacesuits.

1. S.V. Boriskina, An ode to polyethylene, *MRS Energy & Sustainability*, 6, E14, 2019.

2. M. Alberghini, et al. Sustainable polyethylene fabrics with engineered moisture transport for passive cooling, *Nature Sustainability*, 2021, doi: 10.1038/s41893-021-00688-5.

2:00 PM SF04.01.04

Fatigue Damage Reversal in Self- Healing Vitrimer and Its Composites Mithil Kamble, Nikhil Koratkar and Catalin R. Picu; Rensselaer Poly Institute, United States

Thermosetting polymeric composites which are ubiquitous in structural applications due to their superior strength and stiffness compared to their thermoplastic counterparts. These superior properties are principally imparted by dense and permanent crosslinking present at the molecular network level. However, as thermosets are subjected to fatigue loading, they accumulate damage in terms of ruptured crosslinks which eventually result in catastrophic failure. Vitrimers provide an advantage relative to the standard thermosets in that the network is transient and damage introduced by excessive loading may heal. In this work we explore the ability of the vitrimer to repair damage introduced during fatigue loading. We work with a vitrimeric system based on epoxy resin and adipic acid, with a suitable catalyst. The system has stiffness and strength comparable to those of conventional epoxies. We demonstrate that the vitrimer can be periodically healed by heating at temperature between T_g and T_v . Further, we develop and test a carbon fiber vitrimer composite which can be similarly healed by periodic healing. Such composites can pave the way for next generation of structural components which are recyclable and have longer service lifespans.

2:15 PM *SF04.01.05

The Role of Pulsed Lasers in Progress of 3D Assembly and the Materials Used Jayant Saksena¹, Binod Subedi¹, Roger Narayan² and Douglas B. Chrisey¹; ¹Tulane University, United States; ²North Carolina State University, United States

Direct writing describes any technique or process capable of depositing, dispensing, or processing, including removal of, different types of materials over various surfaces following a present computer-generated pattern. Indeed, 3D assembly involves the confluence of information, energy, and materials in different and often novel platforms. This presentation will describe the unique role that materials play in present day pulsed laser and photonic processing of 3D hierarchical assemblies ranging from mesoscopic passive and active electronics and engineered tissue constructs to nanometric control of surfaces for energy storage and conversion. In all cases there is a need to refine and optimize the aforementioned confluence to have better control over the function of the final product. The energy supplied by pulsed lasers and photonic processing can be used to simply heat materials to high temperatures almost instantaneously allowing for rapid synthetic transformations or to initiate photolytic processing such as in Click Chemistry. In all cases there is the absorption of light, electronic excitation, and followed by the relaxation of excited states into the desired material phases as well as shapes and sizes. Therein the photon-material interaction plays a paramount role and the energy attributes of intensity, wavelength, pulse width, and repetition rate make this route to processing very powerful. The distinctive control of pulsed lasers and photonic processing make this approach to processing materials for 3D assembly especially enabling and amenable to roll-to-roll manufacturing.

2:45 PM *SF04.01.06

Polymeric Nanoclay Scaffold Blocks with BMP Coatings for Enhanced Long-Term Bone Regeneration Kalpana Katti, Krishna Kundu and Dinesh R. Katti; North Dakota State University, United States

Often, the time required to regenerate bone in nonunion bone defects using tissue-engineered scaffolds is too long for practical clinical relevance. Hence we have designed novel interlocking blocks using 3D printed miniature molds to fill large bone defects. The scaffold blocks are fabricated using nanocomposite polymer materials with amino acid-modified nanoclays. In addition, these blocks are coated with bone morphogenic proteins (BMP-2 and BMP-7) to initiate and speed up bone growth. On seeding the scaffolds with a combination of human mesenchymal stem cells and osteoblasts, the BMP-coated scaffolds exhibit a much higher formation of the extracellular matrix formed within three days. We also observe enhanced osteogenic differentiation of MSCs at the interfaces between the blocks and the formation of bone mimetic fibril-like collagen. We also observe that the interlocked assembly of the scaffold blocks maintains the mechanical integrity of a single cylindrical scaffold. We also report long-term bone growth over a period of up to 9 weeks on the scaffolds. The coating of scaffolds with BMP-2 and BMP-7 increases cell viability on the scaffold interlocking blocks. We also observe increased intracellular ALP levels in interlocking blocks coated with BMPs indicating enhanced osteogenic differentiation of MSCs. Further immunocytochemistry and FTIR experiments indicate the formation of bone mimetic fiber-like collagen formation and increased ECM formation in the BMP-coated scaffolds. The role of BMPs on long-term bone growth is significant. The degradation in material properties of a hydrated scaffold over a period of 0 to 9 weeks is compared with increasing mechanical properties of the cell-seeded scaffold with the formation of ECM using the nanomechanical investigation of elastic modulus of the scaffolds. The changes in mechanical properties are consistent with the gene expressions indicative of enhanced osteogenesis in the scaffold blocks. Thus, here a novel BMP-coated interlocking blocks system is presented for accelerated bone growth.

3:15 PM SF04.01.07

Late News: 3D Printable PLA/PP/WO₃ Nanocomposites Mohammed L.M.Shaath¹ and Mohamed Ansari Mohamed Nainar^{1,2}; ¹Universiti Tenaga Nasional, Malaysia; ²Institute of Power Engineering, UNITEN, Malaysia

3D printable materials reinforcement and fabrication processes have attracted many scientists and researchers, as most industries and consumers require tailored materials specifically suitable for their needs. These materials are usually chosen for their specific characteristics and attributes, which can enhance the desired characteristics or reinforce the polymer, while fabricating the materials by physical blending then by extruding it into filaments with a specific dimensions. In this study a method for the preparation of 3D printing wire rods of Poly (lactic acid) (PLA) / polypropylene (PP) / Tungsten tri-oxide (WO₃) nanocomposite with up to 10wt% of WO₃ constitution was developed. The results showed that the interfacial compatibility of WO₃ and PLA was improved by adding 20wt% of PP. The addition of nano sized WO₃ with PLA greatly increased the tensile strength of the PLA composites and addition of PP has enhanced the elasticity of the composites. Moreover, morphological studies revealed the brittle behaviour of the PLA/WO₃ composites has shifted to ductile behaviour by the influence of PP phase in the nanocomposite.

Keywords: Poly (lactic acid) (PLA), Tungsten-trioxide (WO₃), polypropylene (PP), nanocomposites, 3D printing (3DP)

3:30 PM BREAK

8:00 PM - 10:00 PM
Hynes, Level 1, Hall B

SF04.02.02

Magnetorheological Elastomers Using Hybrid Magnetic Particulate and Magnetic Annealing for Fused Deposition Modeling Sarah Ziemann, Nathan Fischer, Jimmy Lu, Alex Robinson, Thomas J. Lee and Brittany Nelson-Cheeseman; University of St. Thomas, United States

Magnetorheological elastomers are smart materials that are magnetoactive, meaning they can deform and change shape based on the application of a magnetic field. These magnetic elastomers perform best in soft robotics and biomedical applications when they have increased anisotropy, or different properties along different axes. Magnetic annealing and the use of hard magnetic particulate are common ways to increase the anisotropy- and thus performance- of magnetic elastomers. To further increase this anisotropy, one can utilize fused deposition modeling (FDM), also known as 3D printing. FDM generates different underlying infill patterns within the sample, creating meso-scale anisotropy [1]. FDM of magnetic elastomers has recently been shown to control the magnetic anisotropy within these materials [2]. To create added micro-scale anisotropy by aligning magnetic particulate within the sample, magnetic annealing is used during extrusion of the elastomer filament. Hard or permanent magnets can be oriented using an external alignment field, and strontium ferrite is particularly interesting because it costs less than other rare-earth magnets (or materials). Previous studies in this group have focused on carbonyl iron, a soft or impermanent magnet that showed a large amount of magneto-action, though small changes in its properties after magnetic annealing. Strontium ferrite shows a smaller magnitude of magneto-action in comparison to carbonyl iron, but it has more distinct anisotropy effects after magnetic annealing. Combining these two magnetic particulates into one hybrid composite elastomer filament leverages these trade-offs, creating innovative and emergent mechanical, magnetic, and magnetoactive properties. Our thermoplastic magnetic elastomer composite is created using solvent-casting techniques with 15 vol% SrFe₁₂O₁₉ particulate, 10 vol% SrFe₁₂O₁₉/5 vol% carbonyl iron, and 5 vol% SrFe₁₂O₁₉/10 vol% carbonyl iron. The material is then extruded into FDM filaments. During the extrusion process, some filament of each different chemical composition is magnetically annealed in an axial applied field created by NdFeB magnets, while other filament extruded without magnetic annealing acts as the control. Mechanical stress vs. strain curves of the extruded filaments are acquired using an MTS tensile testing machine. Magnetic hysteresis loops are measured using a vibrating sample magnetometer (VSM). In order to determine the relative level of magnetic anisotropy within the samples due to these factors, hysteresis loops with the field applied parallel and perpendicular to the axis of extrusion are compared to one another. Magnetoactive testing is used to measure the mechanical deflection angle as a function of the strength of a transverse applied magnetic field. Understanding the mechanical, magnetic, and magnetoactive properties of these magnetorheological elastomers provides insight into how magnetic anisotropy can be controlled by a combination of hard and soft magnetic particulate, magnetic annealing, and FDM for optimized performance.

SF04.02.03

Tuning the Mechanical Properties of Nanoglass-Metallic Glass Composites with Brick-and-Mortar Designs Suyue Yuan and Paulo Branicio; University of Southern California, United States

We use molecular dynamics simulations to characterize the mechanical behavior and failure mechanisms of Cu₆₄Zr₃₆ metallic glass-nanoglass (MG-NG) composites. The composites are designed with a brick-and-mortar arrangement consisting of a soft and highly ductile NG matrix and a strong MG second phase. The results show that the best compromise of mechanical properties is reached at a 30/70% volume fraction of the MG/NG phases, when the ultimate strength of the NG is distinctly improved from ~1.8 to ~2.0 GPa without inducing localized plasticity. In addition, MG bricks arranged in a staggered way can further synergize the mechanical properties of the two phases by effectively distributing the stress load, hindering the buildup of local stress hotspots, and preventing the generation of critical shear bands.

SF04.02.04

Composite Aerogels of Cellulose/Poly(Lactic Acid)(PLA) Made by Directional Freezing Yejin Park and Jonghwi Lee; Chungang University, Korea (the Republic of)

Cellulose is the most abundant natural polymer on the planet. Despite its high heat resistance and high toughness, it is insoluble in many solvents, making its fabrication process difficult. Poly(lactic acid) (PLA), a biodegradable polymer made from corn or sugar cane, is made by polycondensation of lactic acid or ring-opening polymerization of lactide. PLA has poor foam processability because of its low melt viscosity. In this study, a cellulose/PLA composite is prepared with wood-like vertically aligned pore structures to overcome the weak mechanical properties of foam. Cellulose was dissolved in an alkaline solution of NaOH and urea at a low temperature. This solution is frozen by a liquid nitrogen reservoir followed by ice removal with cryogenic ethanol. Cellulose aerogel is made by exchanging solvents from ethanol to water and then freeze drying. Finally, PLA solution is infiltrated into the dried cellulose aerogel to create PLA-cellulose aerogel composite. NaOH-urea solution can be frozen at low temperatures, especially using the liquid nitrogen reservoir. Etching ice with ethanol retains the cellulose structure created during freezing. The temperature gradient freezing method creates honeycomb-shaped holes aligned vertically like a tree. The aerogel composite is made of cellulose and PLA using infiltration method. The porosity of aerogel is calculated by the ethanol replacement method. In this way, the porosity of cellulose and cellulose/PLA is about 80% similar. Cellulose/PLA aerogel composite has a higher modulus and stress-to-break than the control cellulose aerogel in compression tests, due to the thin PLA continuous phase. Because both PLA and cellulose are biodegradable, cellulose/PLA composites have great potential to be used in future eco-friendly applications.

SESSION SF04.03: New Types of Polymers, Composites and Hybrid Materials for Additive Manufacturing II
Session Chair: Roger Narayan
Monday Morning, December 6, 2021
SF04-Virtual

8:00 AM SF04.03.01

Design and Fabrication by 4D Printing of Multilayered Tissue Engineering Scaffolds with High Elasticity and Good Shape-Morphing Ability Shangsi Chen and Min Wang; Department of Mechanical Engineering, The University of Hong Kong, Hong Kong

The injuries and defects of uterus, especially impaired endometrium, can cause abnormal menstruation, recurrent miscarriage and pregnancy complications and may lead to absolute uterine factor infertility (AUF). The inability to achieve pregnancy usually has a severe impact on couple's physical and mental health. Conventional gynecological treatments including hysteroscopic adhesiolysis, intrauterine devices (IUDs) intervention and hormone therapy can relieve patients' symptoms to some extent and partially restore uterine structure but they do not recover the function of fertility for patients. The anatomical

structure of the uterus consists of three layers: perimetrium, myometrium and endometrium. The myometrium comprising smooth muscle cells is very elastic and the endometrium has a significant regeneration capability. Current studies start to employ tissue engineering scaffolds to repair uterine defects. For example, natural polymers such as collagen, hyaluronic acid and gelatin and synthetic polymers such as poly(lactic acid) (PLA) and poly(lactic-co-glycolic acid) (PLGA) have been used for uterine scaffolds. Although, those biomaterials are biocompatible and biodegradable and have been widely used in the tissue engineering field, their lack of good elasticity restricts their ability to simulate myometrium functions. In this study, a multilayered scaffold with high elasticity and good shaping-morphing ability was designed to mimic the anatomical structure of the uterus and was fabricated by combining 3D printing and electrospinning techniques. First, highly elastic thermoplastic urethane (TPU) and poly(D,L-lactide-co-trimethylene carbonate) (PDLLA-co-TMC) were melted and blended at high temperature. The blends were then 3D printed into scaffolds with different hierarchical structures in accordance with a CAD model. The TPU/PDLLA-co-TMC scaffolds were prepared to as a substitute for the uterine myometrium layer. Therefore, the elastic properties of printed scaffolds were studied through tensile testing. Additionally, the glassy transition temperature of TPU/PDLLA-co-TMC blends was investigated. The shape-morphing ability of 3D printed TPU/PDLLA-co-TMC scaffolds was investigated by immersing the scaffolds in a water bath at 37 degrees Celsius. Subsequently, a layer of electrospun PLGA/polydopamine (PDA) hybrid fibers was fabricated on the surface of 3D printed TPU/PDLLA-co-TMC. In this electrospun nanofibrous layer, 17beta-estradiol (E2) was loaded in PDA particles. The incorporation of E2 in PDA particles could solve the E2 insoluble problem and also preserve its bioactivity. Previous studies showed that E2 could promote endometrium regeneration by augmenting the function of angiogenic growth factors, e.g., vascular endothelial growth factor (VEGF) and human basic fibroblast growth factor (hFGF). The controlled and sustained E2 release was studied in different pH solutions (pH4.5, 7.4 and 9.0) and under different NIR laser (808nm) irradiation energy. Finally, the last layer from a gelatin methacryloyl (GelMA)/gelatin (Gel) bioink encapsulated with human bone marrow derived mesenchymal stem cells (hBMSCs) was printed on the electrospun PLGA/PDA layer. *In vitro* biological behaviors such as cell viability and cell proliferation on 3D printed GelMA/Gel were evaluated. The effects of released E2 on cell survival and differentiation were also studied. The multilayered tissue engineering scaffolds made by 4D printing and electrospinning possess hierarchical structures to bio-mimic native structures of the uterus and have the potential for uterine regeneration.

8:15 AM *SF04.03.02

3D Printing of Hard Materials for Surfboards [Marc In het Panhuis](#); University of Wollongong, Australia

Surfing is an iconic sport that is extremely popular in coastal regions. Current surfboard fin manufacturers produce high end products using an expensive injection moulding process to create hydro-foil shaped fins. This process, however, does not allow for easy customisation or rapid prototyping.

I will discuss the development of surfboard fins (a hard material) using a performance feedback loop. This loop involves the unique combination of computational fluid dynamics, computer aided design, 3D printing of hard materials, stiffness/flex testing, ocean testing (surfing the waves), embedded sensors / wearables and surfers' perceptible experiences.

I will finish my talk with our progress on measuring the mechanical flex behaviour of surfboards, including modal (vibration) analysis and (what we call) 'fingerprint' analysis.

8:45 AM SF04.03.03

Graphene-Based Nanocomposite Materials and 3D Printing—Nanostructuring for Improved Mechanical Properties and Electronic

Applications [Rigoberto C. Advincula](#)^{1,2,3}, ¹Case Western Reserve University, United States; ²The University of Tennessee, Knoxville, United States; ³Oak Ridge National Laboratory, United States

The use of 2D nanomaterials including graphene for improving electrical and thermal conductivity properties in thin-film devices and sensors is well-studied. There is also high interest in using these materials for anti-microbial properties in coatings and formulations. However, there is high interest in the use of these materials in fabrication methods based on 3D printing. The 2D and high aspect nature of the nanomaterials enable nanostructuring of the nanocomposites for improved transport and stress or residual stress mitigation. Other than their known contribution to electrical and thermal conductivity they also enable stimuli-responsive properties in 3D fabricated objects and function. To this goal, this talk will focus on emphasizing the unique properties of graphene materials and their incorporation in 3D printed materials using FDM, VSP, SLA, and SLS Methods. In this talk, we will demonstrate the nanostructuring of graphene materials for 3D printing in the following projects: 1) FDM of polyurethane nanocomposites, 2) SLA 3D printing, and the use of post-processing thermal curing for highly improved thermo-mechanical properties, 3) Plastic motor based on emulsions coating on SLS 3D printed powders. On these demonstrated projects it is important to emphasize the use of integrated spectroscopic and microscopic characterization to correlate with structure-composition-property relationships.

9:00 AM SF04.03.05

3D Printing DIY Thermoset Elastomeric Adhesives and Formulated Nanocomposites [Fazley Elahee](#)¹, Chase P. Breting¹, Matthew Yang¹, Zane J. Smith², Lihan Rong¹, Tania E. Ceniceros³, José B. Cruz³ and Rigoberto C. Advincula¹; ¹Case Western Reserve University, United States; ²The University of Tennessee, Knoxville, United States; ³CIMAV-Unidad Monterrey, Mexico

Commercial thermoset elastomers are widely available at lower costs compared to prepolymer formulations. They are classified as do-it-yourself (DIY) home improvement and repair materials. They are based on a wide array of chemistries and have been found to have rheologies very suitable for AM. We hereby investigated their 3D printability using direct ink writing (DIW) methods. The materials are divided into two main classes: silicone (three materials) and non-silicone (six materials) with hybrid chemistries and composites. They were characterized by: functional identification using GC-MS pyrolysis, rheology, cure behavior, cured Shore A hardness, 3D printability, TGA, thermal conductivity, dielectric, and mechanical properties. Corresponding ASTM standard test methods were also used and the results are reported. We also investigated the addition of nanoparticles to develop new properties out of the typical DIY function. Dispersion of nanoparticles is achieved using high-frequency ultrasonication techniques. Methods to incorporate nanoparticles into commercial thermoset elastomers is described. Nanoparticles include carbon nanotubes (CNT), graphene oxide (GO) and a 50/50 composite blend of CNT and GO up to 2% by weight. Reported results highlight the advantage in thermal and electrical conductivity.

9:15 AM SF04.03.06

Development of Highly Conductive Printable Material by the Combination of Fused Filament Deposition and Laser Sintering [Remi Rafael](#) and Paddy K. L. Chan; Hong Kong University, Hong Kong

3D printing has significantly participated to a general acceleration of research activities by providing a rapid and economical source of completely personalized parts. Besides being the central focus of some publications thanks to the novel design strategies enabled by additive manufacturing technologies, the holders, adaptors and other mechanical supports are innumerable. However, printed parts are often relegated to purely mechanical functions due to the difficulties to print multi-materials and the restrictions associated with functional (and in particular conductive) material. In this work, we aim at developing a hybrid 3D printer and a new composite material to print both conventional Fused Filament Deposition (FFD) filaments and a highly conductive material. FFD of conductive materials is limited by the necessarily thermoplastic properties of the filament used. Since

no currently existing material is at the same time highly conductive and thermoplastic, a trade-off is obtained with composite materials using conductive particles inside a thermoplastic matrix. The composites use high aspect ratio particles to form conductive path by percolation, but the maximal particle loading is limited by the mechanical properties of the filament. As a result, the high loading leads to embrittlement and lowers the printability of the filament. Furthermore, the matrix material present at the junction between particles strongly impacts the contact resistance. Electrify, the most conductive filament currently available on the market still has a conductivity of $0.006 \Omega \text{ cm}$ (too high for advanced PCB applications) and suffers from high contact resistance and high price (196USD/100g).

To remedy this limitation of the maximal loading of particles in the printed material, here we propose a two-step printing process comprised of the FFD of a composite material, followed by a step of laser sintering to remove (evaporate) the thermoplastic matrix material and sinter the conductive particles together. This process is repeated for each layer to produce fully 3D PCB-like structures. To achieve this, we developed both a hybrid 3D printer based on economical desktop 3D printer and laser engraver parts, and a composite filament based on PLA and copper microparticles. The detailed electrical and mechanical characterizations of the printed conductive materials will be presented.

9:30 AM SF04.03.07

Late News: Two Photon Polymerization of Micronstructured and Nanostructured Medical Devices [Roger Narayan](#); North Carolina State University, United States

Two photon polymerization involves the use of ultrashort (e.g., femtosecond) laser pulses to selectively polymerize photosensitive resins; this technique has been used for 3D printing of medical devices with microscale and/or nanoscale features. The two photon polymerization technique involves near simultaneous absorption of two or more photons from a Ti:sapphire or fiber laser within a small volume over a short time period. The nonlinear nature of two photon absorption enables 3D printing of structures, including medical devices, which contain features below the diffraction limit. Several kinds of photosensitive resins, including polymers and polymer-ceramic hybrid materials, may be processed into medical devices with two photon polymerization. Recent medical uses of two photon polymerization have included processing of drug delivery devices, scaffolds for tissue engineering, and transdermal sensors. In vitro and in vivo evaluation of two photon polymerization-fabricated medical devices will be considered. Our results indicate that two photon polymerization is an important technique for creating microstructured and nanostructured medical devices.

SESSION SF04.04: New Types of Polymers, Composites and Hybrid Materials for Additive Manufacturing III

Session Chairs: Shuji Ogata and Min Wang

Monday Morning, December 6, 2021

SF04-Virtual

10:30 AM SF04.04.01

Influence of Sintering Temperature and Print Orientation on Copper Printed with an FDM Printer Using Bound-Metal Filament [Ahron Wayne](#); Lawrence Technological University, United States

3D printing of thermoplastics has become a mainstay of modern engineering research and development, enabling industry, universities, and even individuals the ability to rapidly manufacture and iterate upon computer-aided designs. 3D printing of metals, however, has continued to remain out of reach except for those able to bear the exceptional start-up and operational costs of existing solutions, such as powder bed fusion or metal injection molding (MIM). One solution that has the potential to reduce costs is the MIM-like process of using an organic binder mixed with powdered metal to produce a feedstock (filament) that can be printed using any conventional fused-deposition-modeling (FDM) 3D printer; the result after debinding and sintering is a pure metal part. We report here an even more accessible variant of this process we have improved upon to create 3D-printed copper parts. The process utilizes a purely thermal, as opposed to chemical debinding step, and the addition of carbon produces a locally favorable gaseous environment during sintering without the use of vacuum or outside injection of protective gas. The influence of printing orientation and sintering temperature on the microstructure and mechanical properties of printed and sintered copper parts was investigated. Higher sintering temperatures resulted in stronger and denser parts but with increasingly anisotropic shrinkage. Parts sintered at 1074 C showed comparable tensile strength and ductility as copper produced using the powder bed fusion process. Printing orientation was found to play a major role in the strength of unsintered parts, but this effect diminished to undetectable levels after sintering. Microstructural analysis showed the presence of carbon in both the printed part interior and exterior; this presence of carbon and its role in the densification process was discussed. The process shows promise for rapid, inexpensive turnaround of 3D printed copper parts for applications without the strict requirements of both strength and 3D intricacy.

10:45 AM SF04.04.01

Enhancing Strength and Ductility of AlSi10Mg Fabricated by Selective Laser Melting by TiB₂ Nanoparticles [Yakai Xiao](#), Yi Wu, Zhe Chen and Haowei Wang; Shanghai Jiao Tong University, China

Nanoparticles are known to play a crucial role in helping achieve excellent mechanical properties in advanced metal matrix composites fabricated by emerging selective laser melting (SLM) technology. Despite this, the understanding of their impacts on the evolution of microstructure and mechanical properties remains nebulous. In the present study, we adopted the SLM process to fabricate *in-situ* nano-TiB₂ decorated AlSi10Mg composites with alternative TiB₂ nanoparticle contents (0, 0.5, 2, 5, 8 wt.%) to investigate the effects of introduced nanoparticles on the SLM processability, microstructures, texture evolution and mechanical properties. Results show that nearly fully-dense TiB₂/AlSi10Mg composite samples can be manufactured at the optimized SLM processing parameter due to the enhancing SLM processability by nano-TiB₂ particles. Besides, increasing the nano-TiB₂ addition can gradually transform the coarse columnar grain structure with <100> fiber orientation texture to fine equiaxed grain structure without preferred crystallographic texture due to the heterogeneous nucleation effect of nano-TiB₂ particles. The elongated cellular sub-structure transforms to the equiaxed cellular sub-structure without obvious directionality. The dislocation density of the TiB₂/AlSi10Mg composites is higher than that of the alloy due to the mismatch of the thermal expansion coefficient between TiB₂ particles and α -Al matrix. Additionally, the microhardness, tensile strength and ductility can be improved simultaneously by the addition of nano-TiB₂ particles. With increasing TiB₂ nanoparticles content, the tensile strength and microhardness increased in a stepwise manner while the ductility increased first and then decreased. Moreover, the SLMed TiB₂/AlSi10Mg composites have superior tensile properties comparing to the previous SLMed AlSi10Mg alloy and their composites with the addition of other particles. The underlying mechanisms of strengthening are mainly attributed to grain boundary strengthening, dislocation density strengthening, load-bearing transformation strengthening, and Orowan strengthening. Meanwhile, the enhancing ductility in the composites is mainly attributed to higher relative density due to better SLM processability, less strain localization due to modified grain structure, high dislocation plasticity due to the intragranular nanoparticles. This study sheds light on SLM-produced nanoparticles decorated aluminium composites for the production of advanced materials.

11:00 AM SF04.04.02

Protonation and Weakening of Epoxy Resin Under Wet Conditions from First-Principles Calculations [Shuji Ogata](#) and Masayuki Uranagase; Nagoya Institute of Technology, Japan

Adhesive bonding using epoxy resin is a key industrial manufacturing process of joining materials. Recently, advanced technologies requiring extensive use of adhesive bonding, such as multi-material design with proper mixing of metals and polymers for lightweight automobile bodies, tight packing of electronic components requiring rapid heat dissipation, and additive manufacturing for novel materials, have become increasingly popular. However, a significant challenge facing adhesive bonding is the weakening or loss of adhesion under damp conditions. For instance, the adhesion strength between aluminum and epoxy resin decreases by 30–50% under wet conditions. This study proposes, for the first time, a proton-related mechanism for the moisture-induced breaking of epoxy resin from the extensive first-principles calculations.

We investigated the cohesive failure of epoxy resin prepared using amine-based curing agents by DFT-based free energy calculations. To this end, we performed the thermodynamic integration of the DFT energy difference between the deprotonated and original states through the artificial process of gradually transformation of the target proton into a dummy atom having zero charge to calculate the free energy of protonation. We thereby found that the amine group of the epoxy resin is protonated at equilibrium depending on the location of the amine group when the epoxy resin is embedded in water under standard conditions.

Next, we calculated the bond breaking barrier energies of the principal groups of the epoxy resin under both dry and wet conditions. Concerning the ether group, the energy barrier to C-O bond breaking is reduced from 2.86 eV under dry conditions to 2.30 eV under wet conditions because of the dissociation of H₂O. The energy barrier for breaking the amine group decreases from 2.30 to 1.94 eV under dry and wet conditions, respectively, because of the protonation of the amine group, but the dissociation of H₂O does not lower the transition state barrier energy further. We thereby show that the bond breakage of the protonated amine groups is the principal process causing the weakening of epoxy resins under wet conditions.

11:15 AM *SF04.04.03

Composites and Hybrids for 3D Printing in Tissue Engineering [Min Wang](#); Department of Mechanical Engineering, The University of Hong Kong, Hong Kong

3D printing provides a powerful manufacturing platform for different industries and has been increasingly used in the tissue engineering field. 3D printing technologies includes an array of technologies: liquid-based, filament- or paste-based, and powder-based technologies. Using smart materials and with innovative designs, 4D printing produces dynamic structures that can change their shape, property, and/or function under external stimulus/stimuli. Using inks that contain living cells, 3D/4D bioprinting creates living structures for different purposes (cancer tissue models, tissue engineering, organ-on-a-chip, etc.) in the biomedical field. 3D printing technologies greatly improve our ability to fabricate a variety of complex and customized biomedical products accurately, efficiently, economically and with high reproducibility. However, finding or developing suitable biomaterials appears to be a bottleneck for the advancement of 3D/4D printing in biomedical engineering (J.Lai, C.Wang, M.Wang, “3D Printing in Biomedical Engineering: Processes, Materials and Applications”, *Applied Physics Review*, Vol.8 (2021), DOI:10.1063/5.0024177). Different 3D printing technologies have different requirements for the materials/inks to be used, and in most situations these requirements are highly demanding. The requirements for 3D printing materials/inks in tissue engineering include printability, biocompatibility, biodegradation properties, and mechanical properties of printed products. Biocompatibility is of paramount importance for a material in tissue engineering applications but it becomes highly important only when the material can be 3D printed where 3D printing is employed for structure formation. We have investigated / are investigating several 3D printing technologies, such as selective laser sintering (SLS), cryogenic extrusion 3D printing, and digital light projection (DLP), for fabricating advanced tissue engineering scaffolds and cell/scaffold constructs for the regeneration of bone, osteochondral tissue, blood vessel, etc. For example, for 3D printing of bone tissue engineering scaffolds via SLS, calcium phosphate (Ca-P) poly(hydroxybutyrate-co-hydroxyvalerate) (PHBV) nanocomposite was developed (B.Duan, *et al.*, “Three-dimensional Nanocomposite Scaffolds Fabricated via Selective Laser Sintering for Bone Tissue Engineering”, *Acta Biomaterialia*, Vol.6 (2010), 4495–4505). For cryogenic extrusion 3D printing of scaffolds for osteochondral tissue regeneration, beta-tricalcium phosphate (beta-TCP)/poly(lactic-co-glycolic acid) (PLGA) nanocomposite was used (C.Wang, *et al.*, “Cryogenic 3D Printing of Heterogeneous Scaffolds with Gradient Mechanical Strengths and Spatial Delivery of Osteogenic Peptide/TGF-beta1 for Osteochondral Tissue Regeneration”, *Biofabrication*, Vol.12 (2020), 025030). For shape-morphing scaffolds, beta-TCP/poly(D,L-lactide-co-trimethylene carbonate) (PDLLA-co-TMC) nanocomposite was developed (C.Wang, *et al.*, “Advanced Reconfigurable Scaffolds Fabricated by 4D Printing for Treating Critical-size Bone Defects of Irregular Shapes”, *Biofabrication*, Vol.12 (2020), 045025). For obtaining complex shape-morphing structures, alginate (Alg) and methylcellulose (MC) blends were investigated (J.Lai, *et al.*, “4D Printing of Highly Printable and Shape-morphing Hydrogels Composed of Alginate and Methylcellulose”, *Materials & Design*, Vol.205 (2021), 109699). This talk will give an overview of our work in developing different materials for 3D/4D printing in tissue engineering. It will provide design guidelines and practical approaches in developing composites and hybrids for biomedical 3D/4D printing.

11:45 AM SF04.04.04

Design and Fabrication by Digital Light Processing of Biphasic Calcium Phosphate Tissue Engineering Scaffolds Yue Wang^{1,2}, Jiaming Bai² and [Min Wang](#)¹; ¹Department of Mechanical Engineering, The University of Hong Kong, Hong Kong; ²Department of Mechanical and Energy Engineering, Southern University of Science and Technology, China

Tissue engineering provides new vital means for human body tissue/organ repair. Tissue engineering scaffolds give temporary structural support to cells for their attachment, growth, and proliferation until the body has restored the mechanical and biological properties of the host tissue. However, the fabrication of tissue engineering scaffolds with controlled porous structures (pore shape, pore size, porosity, etc.) and desired external morphologies (shape, dimensions, etc.) is still a challenge. Digital light processing (DLP) is now recognized as a powerful 3D printing technology which can process ceramics into complex and interconnecting porous structures with high precision and resolution. Biphasic calcium phosphate (BCP), a physical mixture of hydroxyapatite (HAp) and beta-tricalcium phosphate (beta-TCP), is a promising bioceramic for bone tissue regeneration owing to its proven biocompatibility, osteoconductivity, possible osteoinductivity, and controllable biodegradation rates. But fabrication of BCP bioceramic scaffolds via DLP is rarely reported. In this study, a comprehensive investigation was conducted to assess and optimize DLP fabrication to produce high-performance porous BCP scaffolds. First, equal amounts of nano-sized HAp and beta-TCP powders were mixed using a planetary mill. The BCP powders were then formulated with photosensitive resins to prepare BCP slurries. In this step, different dispersants were used and compared for powder surface modification, aiming to decrease bioceramic nanoparticle agglomeration and to achieve stable BCP slurry with high solid loading and low viscosity. The relationships between solid loading and slurry viscosity, DLP energy dose and cure depth and the optimal concentration of photo-initiator were systematically investigated so as to obtain the optimal processing parameters. Second, thermogravimetric analysis (TGA) was performed on DLP-formed green bodies to determine the debinding and sintering strategy for obtaining crack-free BCP porous scaffolds with desired biological and mechanical properties. Furthermore, the effects of sintering temperature (1100 - 1300 degree Celsius) on the shrinkage, phase stability, mechanical properties and biological properties of BCP scaffolds were investigated. Fourier transformed infrared spectroscopy (FTIR), X-ray diffraction (XRD), mechanical testing (compression tests and hardness testing) and surface roughness measurement were conducted for scaffold samples. Finally, BCP scaffolds with different designed pore morphologies, pore sizes

and porosities were made via DLP and sintering using optimized processing parameters. The results showed that scaffolds sintered at 1300 degree Celsius had the best mechanical properties and the lowest surface roughness. Cell attachment and proliferation experiments indicated that DLP-formed BCP scaffolds had good cell viability. Also, the optimized DLP process demonstrated the DLP capability to fabricate complex tissue engineering scaffolds with great freedom and high accuracy. This study has therefore shown great potential of DLP for constructing complex bioceramic scaffolds and possibly other devices for biomedical applications.

12:00 PM SF04.04.05

Late News: Fabrication, Processing and Characterization of Copper Nanoparticle Deposited Graphene Sheet Embedded Carbon Fiber Composite Vishwas S. Jadhav and Ajit Kelkar; North Carolina Agricultural and Technical State University, United States

Due to high stiffness and strength per unit mass, carbon fiber composite became more popular during the last few decades. The low conductivity of carbon fiber composite made aeronautical structures more vulnerable to withstand lightning strikes and unable to prevent electrostatic accumulation. To overcome this, typically different nanofiller are used in conjunction with conventional carbon fiber composites. Due to the high aspect ratio, extraordinary mechanical and electrical properties of nanomaterials, nanoengineered composites are becoming popular. In the present research work Graphene sheet (GS) of 120 μm thick, fabricated from 2D Graphene nanoplatelets, was incorporated into carbon fiber composites to enhance the electrical and mechanical properties of the composite laminate. Preliminary studies indicated that GS embedded composite laminates degraded the mechanical properties instead of enrichment due to weak graphene epoxy bonding. To improve the bonding in addition to vertical, horizontal, and square grids spiked roller was used to make holes in the GS. The utilization of the graphene grid helped to boost the graphene-epoxy bonding as well as mechanical properties. GS added at the mid-plane was expected to send the strong electric signal but in reality, the strength of the signal was not strong. To overcome the issue of weak bonding and electrical conductivity, a chemical deposition method was used to deposit copper nanoparticles on a Graphene sheet. The electrical conductivity of copper deposited GS was evaluated using Jandel four-point tester. Dynamic Mechanical Analysis (DMA) was carried out to evaluate and compare thermomechanical properties of copper deposited Graphene, plain graphene sheet reinforced composite and bare composite. Fragile interface observed due to weak plain GS- epoxy bonding resulted in degraded mechanical properties. The effect of copper nanoparticles deposited on the GS helped to enhance the bonding. Glass transition temperature (T_g), storage, and loss modulus, in addition to Electrical conductivity, were evaluated and compared. Scanning electron microscopy was used to evaluate and compare bonding at the mid-plane of the laminate. Overall study indicates that the copper deposited GS into carbon fiber composites would help to enhance the strength, stiffness, and conductivity of the carbon fiber-reinforced composite laminate.

SESSION SF04.05: New Types of Polymers, Composites and Hybrid Materials for Additive Manufacturing IV

Session Chair: Xianhui Zhao

Monday Afternoon, December 6, 2021

SF04-Virtual

1:00 PM SF04.05.01

Light-Induced Levitation of Ultralight Carbon Aerogels via Temperature Control Reo Yanagi, Ren Takemoto, Kenta Ono and Tomonaga Ueno; Nagoya University, Japan

The weight reduction of materials is crucial for building a resource- and energy-conscious society, realizing comfortable living spaces, and space exploration. Porous materials, such as aerogels, facilitate the fabrication of materials with density less than that of air. Owing to their high electrical, thermal, and mechanical properties, carbon aerogels have been studied for use in many applications. The lightest carbon aerogel, discovered to date, has a density of 0.16 mg cm^{-3} , as reported by Sun et al. in 2013 [1]. The density of this aerogel is approximately 1/6 of the density of air at room temperature; however, it does not levitate in air. This is because there are many pores in the ultralight aerogel that are filled with air, and therefore the apparent density is the sum of those of the material and inner air, thereby making it heavier than air. Many studies have been conducted on ultra-lightweight materials; however, the attempts to make them levitate in air have been very few and limited. If ultralight materials can levitate in air, they will behave as if they are defying gravity, providing new values to our lives. In recent years, research on carbon aerogels with a three-dimensional geometric structure designed using 3D printing technology has also been conducted to expand the applications of carbon aerogels further. This technology makes it possible to create aerogels that retain specific mechanical properties in a density range approaching air density by realizing complex geometric structures.

In this study, we show ultralight carbon aerogels that can intermittently levitate in air for a long time according to Archimedes' principle. Ultralight carbon aerogels fabricated with CNTs can be easily heated by light, and the temperature can be controlled. A carbon aerogel, with density that is less than that of air, is heated using a halogen lamp. As a result, the air inside expands to reduce the air density inside the aerogel, thereby creating a state in which the sum of the densities of the aerogel and inner air is less than that of the surrounding air. This allows the material to levitate due to buoyancy.

Ultralight aerogels, composed of CNTs and cellulose nanofibers (CNFs), were produced with a prepared density of 0.25, 0.50, 0.75, and 1.0 mg cm^{-3} . UV-visible/near-infrared spectroscopy (UV-vis/NIR) measurements using an integration sphere show that the diffuse reflectance of all samples is between 0 % and 4 % in the wavelength range of 350–2500 nm. The ultralight aerogel fabricated showed a heat capacity of approximately 9.3×10^{-4} to $2.7 \times 10^{-3} \text{ J K}^{-1} \text{ cm}^{-3}$ per unit volume in the temperature range of 20–200 °C. The small heat capacity across the entire temperature range suggests that the aerogel could be heated instantaneously using a small amount of energy.

The levitation experiment was conducted by heating the ultralight aerogel with a 90 W halogen lamp in an acrylic cylinder whose bottom was covered with an aluminum lid placed in a container filled with liquid nitrogen. When the lamp was turned on, the aerogel was heated and began to levitate. A cylinder surrounded the aerogel, and the bottom was covered with an aluminum lid such that it was not affected by the updraft caused by the liquid nitrogen. The aerogel levitated as long as it remained exposed to light from the lamp. To confirm that the ultralight aerogel was heated by the halogen lamp and levitated via buoyancy according to Archimedes' principle, the densities of the aerogel (ρ_a) and ambient air (ρ_m) during levitation were calculated and compared. All the data obtained from the calculation results are near the line where $\rho_a = \rho_m$, indicating that air buoyancy levitates the ultralight aerogel, according to Archimedes' principle, when heated by the halogen lamp.

[1]. Sun, H., Xu, Z. & Gao, C. Multifunctional, ultra-flyweight, synergistically assembled carbon aerogels. *Adv. Mater.* **25**, 2554–2560 (2013).

1:15 PM SF04.05.02

Engineering Bottom-up Fabrication of Functional Multi-Material Nanostructures Created Through Evaporation Induced Self-Assembly of Nanocolloidal Droplets Shadi Shariatinia, Dorrin Jarrahbashi and Amir Asadi; Texas A&M University, United States

Achieving desired performance from self-assembly of nanoparticles (NPs) is very challenging due to the stochastic nature of interactions among the constituent building blocks. Self-assembly of Nano-colloids through evaporation of particle-laden droplets can be exploited to fabricate tailored nanostructures that add functionality and engineer the properties of the manufactured components. The particle-particle and particle-solvent interactions, as

well as the forces arising from the evaporation of the solvent are the main driving factors that define the formation of the final nanostructure. In this study, we introduce a nanoparticle-agnostic approach that allows the fabrication of multi-material nanostructures with precisely engineered patterns. Evaporative droplets of aqueous suspensions of Carbon Nanotubes (CNTs), Graphene Nanoplatelets (GNPs), and Boron Nitride Nanotubes (BNNTs) representing NPs of different elemental composition (i.e., carbonaceous and ceramic) with different sizes and shapes (i.e., Nanotube, Nanoplatelets) are investigated. We utilize cellulose nanocrystals (CNCs) as a platform to make hybrid systems of CNC and the secondary NP (i.e., CNC-CNT, CNC-GNP, and CNC-BNNT). We then capitalize on fundamentally understanding the repulsive-attractive interactions in this hybrid system and their effects on the final pattern that is created. It is shown that the formation and thickness of deposited patterns of CNC-bonded CNTs, GNPs, and BNNTs after evaporation of nano-colloidal droplets depends only on the concentration and mass ratio of the NPs and not their shape and size or material that is utilized. This system involves non-toxic, abundant, and biocompatible agents such as water and CNC that promote its scalability. The proposed method enables new capabilities in the precisely controlled fabrication of engineered nanostructures, and programming smart self-assembly systems.

1:30 PM SF04.05.03

Fused Filament Fabrication Using a Diels-Alder Reversible Thermoset—Novel Isotropic 3D Printable Material with High Filler Content Piaoran Ye¹, Douglas A. Loy^{2,1}, Krishna Muralidharan² and Barrett G. Potter²; ¹University of Arizona, United States; ²The University of Arizona, United States

A thermoreversible thermoset formed by Diels-Alder (DA) chem. was used in Fused Filament Fabrication (FFF) 3D printing to obtain a printable, elastic thermoset with isotropic mech. properties. FFF additive manuf. typically uses thermoplastics that are limited in the amt. of filler that can be incorporated in composite prints due to their high melt viscosities and often exhibit anisotropic strengths according to the print geometry. Thermoreversible thermosets with weak links based on cycloadducts between maleimide and furan groups can revert from crosslinked network to liq. oligomeric resins with heating above 100 °C. In this study, filaments with up to 60wt% tricalcium phosphate and silica particles were prep'd. and used in FFF printing. Thermoreversible resins were prep'd. by reacting 1,1'-(methylenedi-4,4'-phenylene)bismaleimide (MPB) with furfuryl group functionalized oligomeric Jeffamines. The resulting resins were then heated to mix with particle filler and extruded to afford 1.75 mm filament. Tensile test specimens were printed between 130-150 °C with varying printing geometries to establish that the thermoreversible thermosets displayed isotropic strength relative to print orientation. The resulting printed structures were readily recyclable by chopping into fragments and re-extruding as filament for addnl. printing. The resins can be recycled back into filament and then printed up to five times. Irreversible crosslinking, through reaction of free maleimides, occurs after 5 h at 140 °C but could be used to prevent thermoreversion. Properties of the resins could be tuned with filler content and with the mol. wt. of the jeffamine.

1:45 PM SF04.05.04

Highly Loaded Wood Flour Biocomposites for Large-Scale 3D Printing Xianhui Zhao¹, Katie Copenhaver¹, Yousoo Han², Lu Wang², Sanjita Wasti³, Halil Tekinalp¹, Uday Vaidya³, Douglas Gardner² and Soydan Ozcan¹; ¹Oak Ridge National Laboratory, United States; ²University of Maine, United States; ³The University of Tennessee, Knoxville, United States

Biomass natural fibers have been commonly used for reinforcing polymers (e.g., polylactic acid [PLA]) because of their low cost, low density, abundance, and biodegradability. In this study, PLA/wood flour composites were produced with wood flour loading between 30 and 60 wt% to investigate the effect of wood flour loading on the composite performance. The composites obtained were characterized using dynamic mechanical analysis (DMA), tensile testing, thermogravimetric analysis (TGA), differential scanning calorimetry (DSC), scanning electron microscopy (SEM), and rheology. The rheological properties of these highly loaded composites were then modified using various coupling agents and viscosity modifiers to optimize the composites for large-scale additive manufacturing applications. The mechanism of the viscosity modification in the PLA/wood flour composites was investigated, and the chemical treatments were found to be effective in tuning the properties of the biocomposites for specific applications.

SESSION SF04.06: Poster Session II: New Types of Polymers, Composites and Hybrid Materials for Additive Manufacturing
Session Chairs: Susmita Bose, Richard Hague, Jayme Keist and Roger Narayan
Monday Afternoon, December 6, 2021
SF04-Virtual

9:00 PM SF04.06.01

4D Printed Shape-Morphing Tissue Engineering Scaffolds with Enhanced Biocompatibility Xiaodie Chen, Jiahui Lai and Min Wang; Department of Mechanical Engineering, The University of Hong Kong, Hong Kong

3D printing is very attractive for fabricating tissue engineering scaffolds because it can produce either simple or complex scaffolds precisely and rapidly according to the scaffold design and custom-make scaffolds to meet the requirements for individual patients. However, 3D printed structures have static shapes and properties during their application and hence do not accurately imitate the dynamic nature of body tissues. Shapes, properties or functions of tissue engineering products should evolve along with the dynamic tissue regeneration process. Therefore, 4D printing, an emerging manufacturing platform through the integration of time with 3D printing, is now hotly pursued for fabricating dynamic structures which can change the shape, properties or functions over time under appropriate stimulus/stimuli such as temperature, pH, humidity, light, electricity, magnetic field, sound, or a combination of these stimuli. Currently, shape memory polymers are the most popular responsive materials for 4D printing in tissue engineering. However, most of them are synthetic polymers whose biocompatibility is not as desired. Combining a synthetic shape memory polymer with a biocompatible natural hydrogel is an effective way for obtaining a polymer blend with both shape memory ability and enhanced biocompatibility for 4D printing in tissue engineering. Poly(D,L-lactide-co-trimethylene carbonate) (PDLLA-co-TMC) is a popular synthetic shape memory polymer. Structures made of PDLLA-co-TMC with a DLLA-to-TMC ratio of 80:20 respond at 37 degrees Celsius for shape memory, suggesting its potential for shape-morphing scaffolds for human bodies. Gelatin methacryloyl (GelMA), a photopolymerizable hydrogel composed of natural gelatin functionalized with methacrylic anhydride, retains the functional amino acid sequence of gelatin and hence exhibits good biological activity. It is shown to promote cell adhesion and proliferation. In this study, 4D printing of shape-morphing scaffolds with improved biocompatibility was investigated using polymer blends of PDLLA-co-TMC (80:20) and GelMA. The 4D printing process involved four steps: (1) Pure PDLLA-co-TMC and PDLLA-co-TMC/GelMA blends at 1:1, 2:1 and 3:1 blend ratios were printed into planar structures; (2) the planar structures were shaped into tubes by using a glass rod at 80 degree Celsius; (3) the tubular structures were flattened at 25 degree Celsius; (4) the flattened scaffolds could self-fold into tubular structures at 37 degree Celsius within a minute in an aqueous environment. The influence of blend ratio on the shape memory ability and printability was studied and compared with pure PDLLA-co-TMC. Surface morphologies of the 4D printed pure PDLLA-co-TMC and PDLLA-co-TMC/GelMA scaffolds were observed under SEM. Also, the mechanical properties of pure PDLLA-co-TMC and PDLLA-co-TMC/GelMA blends were assessed via tensile tests. Finally, the viability, attachment and proliferation of cells seeded on 4D printed pure PDLLA-co-TMC scaffolds and PDLLA-co-TMC/GelMA scaffolds were studied. It was found that the addition of GelMA into PDLLA-co-TMC improved printability, stretchability, and biocompatibility while maintaining the shape memory property. 4D printed PDLLA-co-TMC/GelMA scaffolds

with desired functionalities such as biocompatibility and shape memory property have great potential for tissue engineering applications, especially for tubular tissues such as vasculature and gastrointestinal tract.

9:05 PM SF04.06.02

3D-Printed Monolithic Porous CO₂ Adsorbents from a Solution-Processible, Hypercrosslinkable, Functionalizable Polymer Junghyun Lee¹, Chong Yangh Chuah¹, Wen See Tan¹, Juha Song¹ and Tae-hyun Bae²; ¹Nanyang Technological University, Singapore; ²Korea Advanced Institute of Science and Technology, Korea (the Republic of)

In recent several decades, the global warming has been accelerating due to increasing carbon dioxide emissions, and accordingly various environmental problems are newly raised. Among the solutions to reduce CO₂ emissions, the adsorptive approaches have been actively progressing. Research on CO₂ adsorbent using 3D printing technology which is one of the most focused issues in the scientific community has been conducted recently, however, the approaches using the existing traditional concept using clay as a binder can cause limitation of adsorption capacity and preparation of feed for 3D printing. Herein, we present a new unconventional processable adsorbent fabrication method using 3D printing technology which starts with a widely used printable polymer. CO₂ adsorption capacity of 3D-printed polymers is imposed by post-treatment processes such as hypercrosslinking and amine-grafting. 3D-printed monolithic adsorbents showed significantly improved CO₂ adsorption capability and CO₂/N₂ selectivity due to the presence of microporosity and amine-functionality, compared with their original polymer form. Moreover, tests under dynamic flow in dry and humid condition demonstrated that the 3D monolithic adsorbents effectively captured CO₂ at an extremely low flow rate, while possessing good stability and regenerability. Based on the promising results presented in this proof-of-concept study, we are aiming to further improve the CO₂ capture capacity by increasing both porosity and amine loading in future work.

9:10 PM SF04.06.03

Hydrothermal Processing of Solid Waste Materials Shengfei Zhou, Sabrina Shen and Markus J. Buehler; Massachusetts Institute of Technology, United States

Hydrothermal processing (HTP) is a green method to convert biomass (such as algae) and solid waste into valuable materials. In this study, HTP is conducted to treat and valorize sewage sludge and food wastes into biocrude oil and biochar. The effects of process parameters including feedstock, solids load, HTP temperature, and reaction time, are investigated. Statistical model is created to predict the yields of the HTP products. A techno-economic analysis (TEA) of a continuous HTP process is developed, assuming the biocrude oil is used as asphalt binder additive. Biochar is characterized and assembled with fiber materials into composites, which might be used as electrodes for energy storage. Activated carbon is also prepared from the biochar, then used for 3D printing.

9:15 PM SF04.06.04

FDM 3D Printing of Epoxy-Polybenzoxazine Thermoset Composite E. A. Dineshi A. Peiris and Douglas A. Loy; The University of Arizona, United States

Fused Deposition Modeling (FDM) is the cheapest 3D printing technique centered around thermoplastic printing. However, the current usage of FDM 3D printing has been limited, especially in the applications where mechanical strength becomes crucial. The main reason for this limitation is the inherent anisotropic nature of the layered prints. Epoxy-benzoxazine based filaments can reduce this anisotropy effect by forming covalent crosslinking during the print. Polybenzoxazine and epoxies are major thermoset classes with excellent thermomechanical properties and rich molecular design flexibility. Blends of benzoxazine and epoxy resins exhibit a long shelf life at room temperature but will react at elevated temperatures to afford copolymers with superior properties. Here, thermoplastic filaments were prepared from epoxy-benzoxazine blends for FDM 3D printing that cure during printing to afford robust thermoset prints. The benzoxazine can polymerize by a base-catalyzed condensation reaction with itself and with the bisphenol A-based epoxide resin. Benzoxazine's tertiary amine group can also catalyze the reaction of alcohol hydroxy groups with epoxides in the epoxide resin. The thermoplastic blend was formulated from poly(bisphenol A glycidyl ether end-capped), a bisphenol A-based benzoxazine, and fumed silica. DSC analysis of the blend revealed that its cure temperatures are higher than the softening points of the epoxy polymer and the benzoxazine monomer, permitting the filament to be extruded below the cure temperature with no crosslinking. Printing of the blend-based filament at higher temperatures initiates the curing reactions that ultimately lead to 3D filament printed thermosets.

9:20 PM SF04.06.05

Topological Structure Enhanced Nanostructure of High Temperature Polymer Exhibiting Giant Dielectric Response Xin Chen and Qiming Zhang; The Pennsylvania State University, United States

Nanofillers in polymer composites will induce interface regions in the polymer with non-uniform nanostructures which can be approximated as multilayer shells surrounding nanofillers. This work studies topological nanostructures in polymers that interface with one-dimensional (1-D) and zero-dimensional (0-D) nanofillers. This new class of dielectric polymer nanocomposites involves nanofillers at ultra-low volume loading (< 1 volume percent) that generate large dielectric enhancement. The results show that the dipolar response of polyetherimide, a high temperature dielectric polymer, is increased by more than ten times with ultra-low (0.75 vol%) loading of 1-D nanofillers. The results reveal that 1-D nanofillers induce cylindrical shell-topology in the polymer matrix which is more effective in enhancing the high dielectric constant interfacial region than the spherical shell-topology generated by 0-D fillers. The cylindrical shells generated by 1-D fillers provide much higher dielectric enhancement over a broader interfacial region in the polymer matrix, as compared to the spherical shells induced by 0-D nanofillers.

9:25 PM SF04.06.06

Late News: A Flame Resistant, 3D Printed polyhydroxyalkanoate/ammonium Phosphate Biodegradable Polymer Blend Yiwei Fang¹, Ethan Zuo², Abhishek Vangipuram³, Katerina Popova⁴, Miffy Liu⁵, Joshua Kaplan⁶, Anna Cho¹, Krish Patel¹, Vikash Persaud¹ and Miriam Rafailovich¹; ¹Stony Brook University, United States; ²Saratoga High School, United States; ³Novi High School, United States; ⁴Hackley School, United States; ⁵Shenzhen Middle School, China; ⁶The Frisch School, United States

Polyhydroxyalkanoate (PHA), synthesized by certain bacteria like Cupriavidus necator, is an environmentally sustainable polymer that can be degraded by enzymes and microorganisms. As PHA has good processing property and biocompatibility, PHA is favored in many areas such as food packaging, biomedical engineering and 3D printing. However, the flammable nature of PHA limits its potential of being a substitute of conventional petroleum-based polymer. Ammonium polyphosphate (APP) is an effective flame retardant additive for polymer such as polylactic acid and polypropylene, which creates char layers as a physical barrier could stop the combustion. While the effect of APP in PHA has rarely been investigated yet. Here we combined APP and resorcinol bis(diphenyl phosphate) (RDP), which acts as a surfactant, with PHA by melt blending technique to enhance the flame resistance of PHA. The dense char formation shown in Thermogravimetric analysis (TGA) could possibly explain that even with a low loading of 5wt%APP and RDP could make PHA V-0 grade in UL-94 flame test. The fact that RDP as a surfactant

could increase the dispersion of APP in PHA is proven by SEM-EDS analysis. Heat effect and crystallization behavior was investigated by Differential Scanning Calorimetry (DSC). The chemical composition of the blend and char was investigated by Fourier Transform Infrared Spectroscopy (FTIR). As the Izod impact test and tensile test showed that APP reduces the strength of PHA due to its rigidity, it's essential to minimize the usage of APP to increase the 3D printing quality of PHA. Fiber drawing and comparison of the combustibility upon FDM printing will be discussed.

We gratefully acknowledge support from the Louis Morin Charitable Trust.

9:30 PM SF04.06.07

Cost-Effective Fabrication of High-Performance 3D Printed Composites Using Continuous Fiber by Modified Fused Deposition Modeling (FDM) Technology Patrapee Kungsadalpipob, Mostakima M. Lubna and Philip Bradford; North Carolina State University, United States

Additive manufacturing which is also known as Three-dimensional printing (3D printing) has become the most promising material fabrication approach for academic, R&D and industrial use. Among various types of 3D printing technology, Fused Deposition Modeling (FDM) is currently the most popular category because of its cost-effectiveness, high scalability and flexibility as well as minimal post-processing required. Unfortunately, it is still challenging to print continuous fiber reinforced structures due to various issues such as complex machine design, fiber flexibility and durability, as well as fiber-matrix incompatibility. Some companies have developed alternative 3D printers capable of printing carbon fiber composite, but the machine cost is still a hindrance for small scale use. Moreover, 3D printing with other types of continuous fibers has not been explored.

Our research aims to develop and modify a commercial desktop 3D printer to be capable of printing continuous carbon nanotubes (CNT) assemblies. In our lab we grow vertically aligned multiwalled carbon nanotubes (CNTs) using Chemical Vapor Deposition process (CVD). The resulting CNTs are called "Spinnable CNTs" because they can be spun continuously as yarns, sheets, and fibers which can be incorporated in other matrices. With their inclusion in polymers, CNT reinforcement not only leads to mechanical strength improvements, but also results in unique multi-functionalities such as electrical conductivity. We successfully impregnated CNT yarns onto the surface of the polylactic acid (PLA) filament. The binary solvent system with 2 %w/v of PLA has been used as a binder during filament feeding without applying additional pull forces. Moreover, different types of commodity and industrial yarns such as cotton, polyester as well as Zylon yarns have been printed and studied. The 3D printed composites are fabricated by ROBO 3D R1 plus FDM printer. The structure-property relationship of the printed parts were investigated by varying layer thickness, fill density, infill type, printing temperature, printing speed, and delay time.

Results revealed that a 210°C extruder temperature leads to the best printability in comparison against 190-205°C. Minimizing printing speed also results in better printability as it prevents the dragging and the peeling off of the reinforcement yarns. Mechanical performance is investigated through measuring the tensile strength. At the same fiber volume fraction, the 1 mm thickness 3D printed part containing Zylon yarn shows the highest tensile strength of 45MPa and modulus of 1.40 GPa, followed by the CNT yarn as reinforcement which presents tensile strength of 39 MPa and modulus of 1.27 GPa. Results showed that 3D printed PLA reinforced Zylon yarn has 7.1% higher in tensile strength and 0.72% higher in tensile modulus than 3D printed neat PLA. This demonstrated that different yarn strengths lead to varying degree of the printed composite strength.

Morphology, fiber orientation, and void formation of the printed parts were characterized by SEM, electrical properties, and thermal properties by DSC and TGA. For future work, we aim to modify commercial desktop 3D printer for more seamless integration of the continuous fiber with high fiber volume fraction. Enhancing printing productivity and broadening various types of continuous fiber also need to be developed. Successful development of this hybrid 3D printing technology will be useful in a broad range of applications such as electronics, automotive, and aerospace.